ANGEWANDTE CHEMIE
International Edition in English
Volume 26 · Number 1
January 1987
Pages 1–92

Unsaturated Molecules Containing Main Group Metals

By Michael Veith*

Molecules in which there are neighboring electrophilic and nucleophilic centers are unusually reactive. Oligomerization can be prevented only by bulky groups attached to the main group metal atom that would act as electron pair acceptor, or to the basic non-metal atom. The basic and the acid centers behave as a single unit in chemical reactions; the system is similar to a "double bond" whose π-electron density is largely concentrated at one atom. The unsaturated nature of these molecules can be seen in (for example) their addition reactions with hydrogen compounds of non-metals, or in reactions that are distantly related to cycloadditions at homopolar double bonds. The selection of suitable reaction partners leads to polycyclic, cage-like molecules containing metal atoms. If these atoms possess lone pairs (as is usual in the lower oxidation states of the third and fourth main groups), these can be utilized to form bonds to further (Lewis acid) metal centers. In some cases large assemblies can be built up from polycyclic systems in this way; a characteristic of these assemblies is a one-dimensional array of metal atoms. Commonly occurring structural features of the polycyclic species are tetrahedra, trigonal bipyramids and cubes.

1. Introduction

Two properties of metallic elements are particularly conspicuous on their incorporation into molecules: their low electronegativity (compared with the ligands) and their marked tendency to maximize their coordination number. The resulting electrophilicity at the metal atom causes nucleophiles to attack this part of the molecule preferentially and the first reaction step is thus coordination. Such an intermolecular reaction can lead to a stable compound that is generally described as a Lewis acid/Lewis base complex.[1]

Here we wish to consider only those Lewis acids in which one or more non-metal atoms bearing lone pairs are bound to the electrophilic main group metal. Such compounds thus formally contain neighboring Lewis acid and Lewis base centers, which can lead to intra- or intermolecular interactions. The compounds are generally unstable with respect to oligomerization because of the marked heteropolar contribution to the metal/non-metal bond. An expansion of the coordination at the metal atom results, which can be interpreted as filling an electron vacancy.[1] Although this model may seem very primitive and superficial (it is concerned largely with "counting electrons") it should nevertheless be noted that parallels between the oligomerization of such special Lewis acid/Lewis base systems and of element-element double bonds do exist. This can be illustrated by a comparison of the reactivity of the aluminum compound **1** with that of the isosteric or (in the broader sense) isoelectronic molecules **2**, **3** and **4** (Scheme 1).

A common property of compounds **1**–**4** is that they oligomerize or polymerize under suitable (generally different)

[*] Prof. Dr. M. Veith
Institut für Anorganische Chemie der Universität
Im Stadtwald, D-6600 Saarbrücken (FRG)

 © VCH Verlagsgesellschaft mbH, D-6940 Weinheim, 1987 0570-0833/87/0101-0001 $ 02.50/0

conditions. Compound **1** reacts instantaneously to form four- or six-membered rings (depending on the substituent R) that do not decompose to the monomers even at high temperatures.[2,3] Compound **2** is also converted spontaneously into the corresponding oligomer; it can be obtained as a monomer only by the use of sterically demanding substituents R (kinetic stabilization).[4-6] Compound **3** possesses a completely non-polar double bond (in contrast to **1** and **2**), but here again the monomer is only stable when such kinetic effects are exploited.[7] Monomers of **2** and **3** are obtained as extremely short-lived intermediates when suitable precursors are photolyzed or thermolyzed; they can be chemically identified by trapping reactions.[8,9] The ethene derivatives **4**, on the other hand, are kinetically especially stable with respect to their oligomers and polymers and can only be converted into these photochemically or catalytically.[10,11]

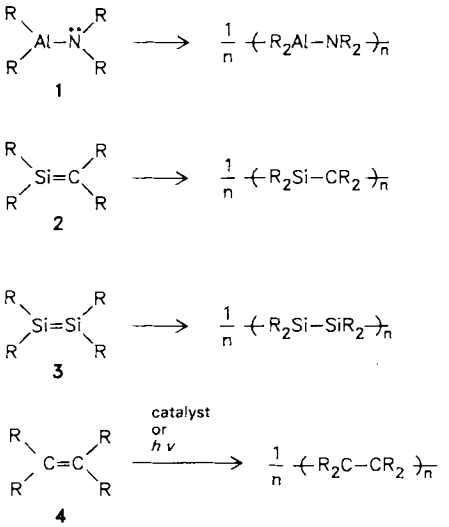

R = organic or inorganic substituent

Scheme 1.

It is apparent from this comparison of the compounds **1**–**4** that the tendency to oligomerize is correlated with the polarity of the relevant bond and that heavy elements (because of their reluctance to form π-bonds[12]) amplify this effect. Compounds such as **1**, which contain a Lewis acid and a Lewis base, can be classified on the basis of a simple model as "unsaturated" and represent, at least formally, a limiting case of the double bond. Irrespective of the contributions of the individual mesomeric forms **5a** and **5b**, this can be represented as follows for a main group metal M and a non-metal X:

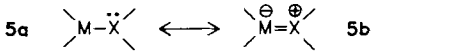

In this review we have not considered it important to present evidence for the existence of one or the other mesomeric form (there are incidentally other possible formulations, e.g. as an ion pair); we prefer to show how this model can be exploited synthetically. The reactivity of the compounds is best represented, not by treating M and X in **5** separately as acid and base but by considering the cooperation of both centers—*similarly* to the behavior of double bonds. We concern ourselves with compounds of type **5** that either exist as monomers under normal conditions or can be assumed as intermediates. After considering the general principles we present examples that are mostly drawn from our own work.

2. The Synthesis of Metallacycles with Lewis Acid and Lewis Base Centers

2.1. The Choice of Ligand at the Metal Atom

As already explained, compounds that, like **1**, contain a Lewis acid and a Lewis base center are unstable with respect to oligomerization. Apart from the use of sterically demanding groups (to reduce the tendency to intermolecular reactions), one further important point should be considered; this will be discussed with respect to **1** as an example. An intramolecular stabilization of the aluminum atom (by a contribution from limiting structure **5b**) is only possible if the occupied orbital on the N atom possesses the same symmetry as the acceptor orbital (p_z on the Al atom); this would require an sp^2 hybridization of the nitrogen. An additional requirement, however, is that both p orbitals are parallel (**6a**). It can be shown, for an open chain system with free rotation about the bond joining the Lewis acid to the Lewis base, that both conditions presented here (steric requirements, electronic effects) tend to compete with, rather than reinforce, each other.

In tris(bis(trimethylsilyl)amino)aluminum (R = $SiMe_3$, R′ = $N(SiMe_3)_2$ in **6**), which indeed contains three-coordinate aluminum,[13,14] the R_2N-moiety is however rotated by 50° from the $(R')_2Al$ moiety (as depicted in **6b**). Because of this large dihedral angle between the p_z orbitals, there can only be a weak donor-acceptor interaction between the two atoms.

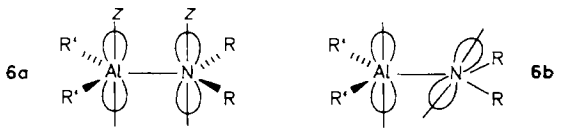

If the aluminum and nitrogen atoms are incorporated in a small ring system, however, such a rotation is no longer possible. This consideration prompted us to incorporate electrophilic metal atoms in ligand systems derived from the donor-substituted silanes **7**[15] and **8**,[16] which should lead to high stabilization. Starting from **7** and **8**, we can in

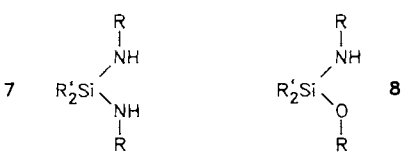

principle construct compounds containing any metallic element (see formulas **9**–**15**; the Roman subscripts refer to the main group number. For examples see also Table 1). All the molecules **9**–**15** share the common feature that the

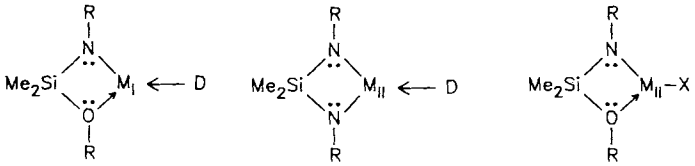

9 10 11

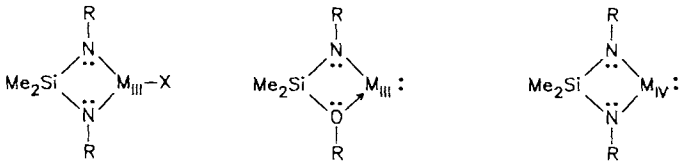

12 13 14

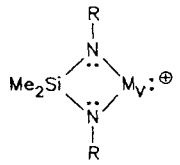

15 D = donor molecule; R = organic substituent

Table 1. Metallacycles **9**–**15** synthesized so far [19–24]. R = *t*Bu; high yields with the exception of **10a**.

Cpd.	M	D/X	Cpd.	M	Cpd. [a]	M
9a	Li	$\frac{1}{2}$THF [b]	**13a**	Tl^{I}	**15a**	P
9b	Li	$\frac{1}{2}$dioxane	**14a**	Ge^{II}	**15b**	As
9c	Li	$\frac{1}{2}C_5H_5N$	**14b**	Sn^{II}	**15c**	Sb
10a	Mg	THF [b]	**14c**	Pb^{II}	**15d**	Bi
12a	Al	Me				
12b	Al	Ph				
12c	In	Me				

[a] $AlCl_4^{\ominus}$ as counterion. [b] THF = tetrahydrofuran.

metal atom (Lewis acid) formally possesses six outer electrons and is adjacent to two non-metal atoms with "non-bonding" electron pairs.

The ring structure and the stabilizing effect of silicon on the sp^2 hybridization at the nitrogen or oxygen atom should ensure the coplanarity of the generally trigonal planar ligand spheres at the metal and the non-metal atom (assuming monomeric structures). The metal atoms can display either their maximum oxidation state or an oxidation state two units lower (**13**, **14**); they may be present as metal cations (**15**). Any organic group R may be chosen, but the principle of "kinetic stabilization" should be borne in mind; *tert*-butyl groups have proved especially useful. The completion of the outer electron complement and the coordinative saturation of the metal atom in **9** and **10** are achieved by bonds from donor molecules.

2.2. Synthesis of the Metallacycles

The metallacycles **9**–**15** can be synthesized by a variety of methods,[18] some of which are presented as examples in Eqs. (a)–(f). Corresponding syntheses can be carried out with compound **8**. The most important and generally applicable syntheses are (a), which proceeds with "salt formation", and the redox or metal exchange reactions (d) and (e), respectively. The amine transfer reaction (b), the direct hydrogen–metal exchange (c) and the thermolysis (f) are of more specialized interest.[19,24] We have so far succeeded in preparing the compounds listed in Table 1. Attempts to prepare a compound corresponding to formula **11** led (for magnesium) only to $[Me_2Si(NtBu)(OtBu)]_2Mg$.[22]

3. Properties and Structures of the Metallacycles 9–15

Mass spectrometry in the gas phase, molecular weight determinations in solution and X-ray structure analyses in the solid state all show that the compounds **9**–**15** are

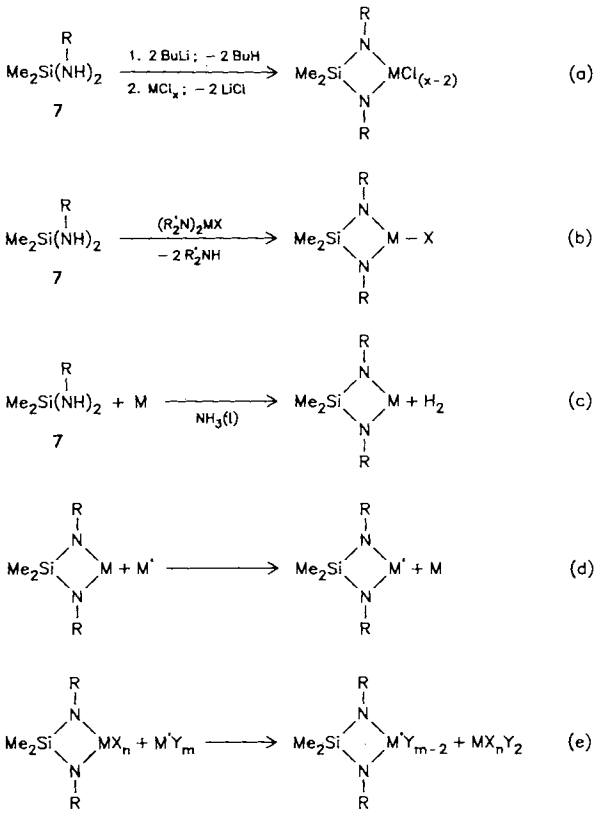

(a) (b) (c) (d) (e) (f)

Table 2. Structures of some metal-containing cyclic molecules in different states of matter. E.N. = electronegativity.

Compound	M	E.N. [25] of the metal atom	Degree of association: Gas phase	Benzene soln.	Crystal
9a, 9b	Li	0.98	—	dimeric	dimeric
10a	Mg	1.31	—	dimeric	dimeric
12a	Al	1.61	dimeric	dimeric	dimeric
12c	In	1.78	monomeric	dimeric	dimeric
13a	Tl^{I}	1.62	monomeric	monomeric	—
14a	Ge^{II}	1.85	monomeric	monomeric	—
14b	Sn^{II}	1.80	monomeric	monomeric	monomeric/dimeric
14c	Pb^{II}	1.87	monomeric	monomeric	—

either monomeric or dimeric; none of them forms a "coordination polymer". Table 2 shows that physical conditions (e.g. the state of matter) and the electronegativity of the metal atom both have a direct influence on the tendency to dimerize; as expected, the tendency to coordinative saturation at the metal is greater for more electropositive metals and for more closely neighboring molecules. The indium derivative **12c**, for example, is monomeric in the gas phase but dimeric in benzene solution and in the solid state. Interesting results have been obtained for the tin derivative **14b**; crystallization from hexane yields a monoclinic modification in which monomers and dimers are both present in the lattice,[26] but crystallization from molten material gives a second, triclinic, modification that only contains dimers.[27]

All the compounds that contain lower valent metals and are monomeric are also colored; the heavier the metal atom, the further the light absorption is shifted to the red (**14a** is yellow, **14b** red, **14c** dark red). Dimerization is accompanied by a marked change in color; molten **14b** (containing only monomers) is red, the monoclinic modification (1:1 monomer:dimer) orange, the triclinic modification (only dimers) pale yellow.[27] The differing coordination numbers at the metal are obviously reflected in the color of the compounds, as is also the case for tin(II) amides.[28] The cations containing elements of the fifth main group (**15a–d**), like the corresponding isoelectronic compounds **14**, are also colored.[24]

Figures 1–3 show the results of X-ray structure analyses of the compounds **14b** and **15c** (as examples of monomeric units) and of **12c** and **9a** (as examples of different types of dimers). In **14b** and **15c** the four-membered ring is almost planar and the N-atoms trigonal planar coordinated. As discussed in Section 2, this causes the empty p orbitals on the metal atoms[30] and the filled p orbitals on the nitrogen atoms to be parallel. A resonance formula corresponding to **5b** is possible from strictly geometric considerations but does not appear to lead to a noticeable shortening of the M–X bond. The molecule $Sn[N(SiMe_3)_2]_2$ is, like **14b**, monomeric in the gas phase; electron diffraction studies show that the Si_2N planes are not coplanar with, but are instead orthogonal to, the SnN_2 plane; however, the Sn–N bond length is identical to that in **14b**.[31]

The dimeric **12c** (Fig. 2) can be considered as a cycloadduct of two monomeric units. The dimer of **14b**[27] and the magnesium compound **10a**[20] display a similar structural type. Common to all three molecules is a polycyclic structural element consisting of three edge-bridged perpendicular four-membered rings ("step structure"). The electron transfer from the λ^4-N atom to the In atom is reflected in the drastically lengthened bonds to this atom, compared with the λ^3-N atom.[29] As in [2+2]-cycloaddition reactions of ethene derivatives,[32] the bond lengths in the addition product are all increased with respect to those in the starting materials. The structural data for **10a**, **12c** and **14b** can be transcribed as the chemical formulas **16a–c** (R = *t*Bu; M = Mg, In, Sn; X = THF, Me or lone pair).

There is however a danger of reading too much into the formulas **16a–c** as regards the real electronic states; the formal charges in **16a** might be taken to indicate a high electron density at the metal atom, which would be incon-

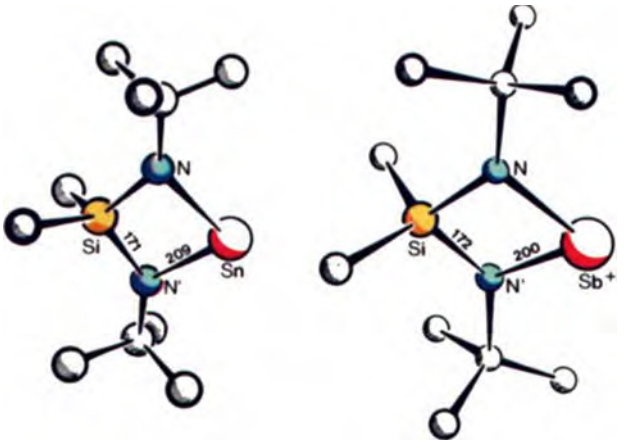

Fig. 1. Molecular structures of **14b** [27] (left) and **15c** (without counterion) [28] (right). Here and in the following figures, the metal atoms (acceptors) are colored red or orange, the donor atoms blue or green; C-bonded H-atoms omitted (distances in pm).

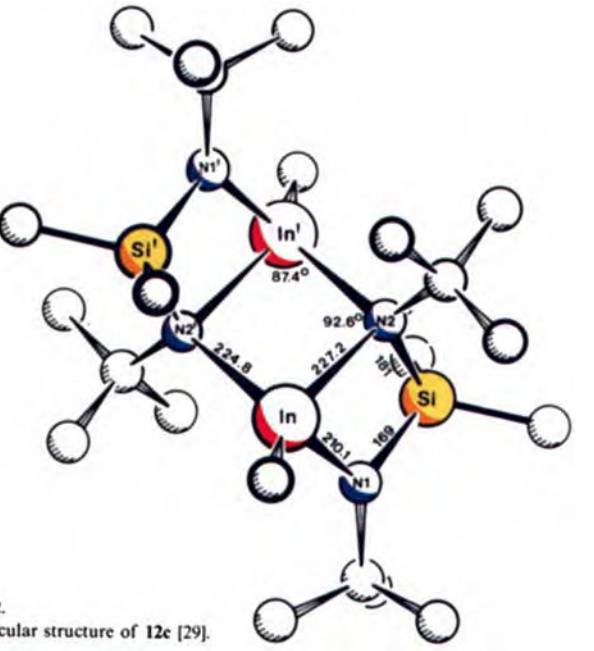

Fig. 2.
Molecular structure of **12c** [29].

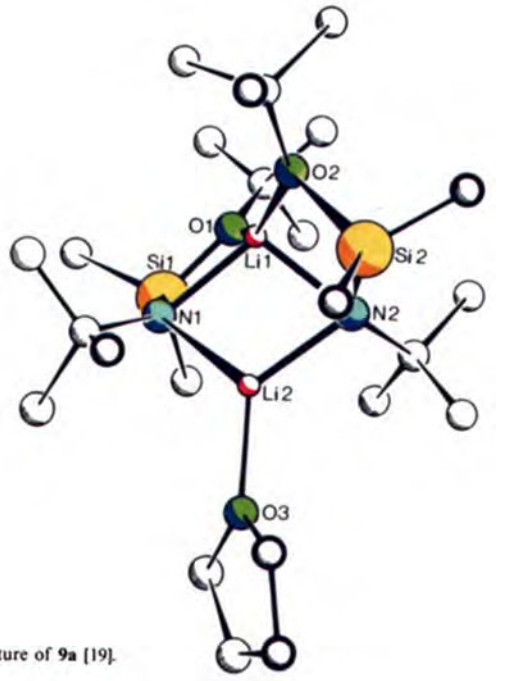

Fig. 3.
Molecular structure of **9a** [19].

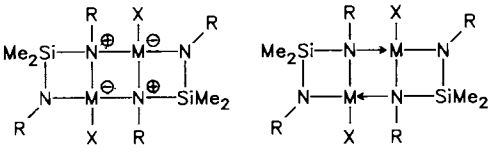

16a

16b

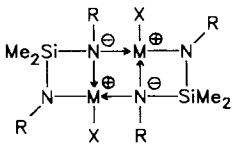

16c

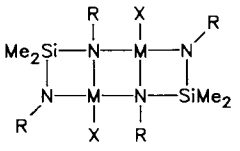

16d

sistent with the electronegativities of the elements M and N.[25] The donor-acceptor bond shown by an arrow in **16b** should differ appreciably in length from the N–M single bond; this is indeed the case for dimeric **14b**,[27] but not for dimeric **12c**.[29] Finally, there are formulations such as **16c** with ionic charges, which are structurally difficult to distinguish from **16a**. Although the formulas **16a–c** are fairly readily comprehensible for the molecules discussed here, more complicated systems are more difficult to formulate in a similar manner and are thus more liable to misinterpretation. To avoid this problem, it is often more sensible to dispense with the formulas with formal charges and arrows, as in **16d**; each line represents an electron pair, irrespective of the nature of the bond (2-center 2-electron or donor-acceptor). The reader will be able to interpret the particular bonding implied by, for instance, the four-coordinate nitrogen atom.

In contrast to the compounds **10a**, **12c** and **14b** (dimer), in which all metal atoms are coordinatively saturated (which usually implies a noble gas configuration), dimeric **9a** (Fig. 3) contains two lithium atoms, only one of which is four-coordinate; the other is bonded to two nitrogen atoms and the oxygen of a donor tetrahydrofuran molecule, resulting in the unusual coordination number three.[33] The point symmetry of **9a** is close to C_2 symmetry, the twofold axis passing through both lithium atoms and the donor oxygen. This oxygen displays trigonal planar coordination, and is thus, like the λ^3-lithium atom, sp^2 hybridized. It can be shown that the dihedral angle between the p orbitals of both atoms (ca. 45° in **9a**) results from steric effects that make a parallel arrangement impossible. It is not clear why the structure of the lithium derivative **9a**[19] is so different from that of the isoelectronic magnesium derivative **10a**; **9a** does not react with excess tetrahydrofuran. As for **16**, different representations of the formula are possible; we prefer **17**, corresponding to **16d** (cf. lithium compounds in Ref. [34]). The structural type **9a**

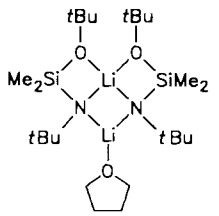

17 [= (9a)$_2$]

(Fig. 3) is preserved in exchange reactions of the donor THF (as shown by X-ray structure determinations of **9b** and **9c**); this feature is however restricted to lithium compounds.[19]

4. Reactions of Monomeric Metallacycles

The concept advanced in Sections 1 and 2, of regarding the Lewis acid/Lewis base systems defined at the outset as limiting cases of molecules with a π double bond, can be tested by methods other than structural analysis. Unsaturated molecules are expected, in particular, to undergo addition reactions. We shall here analyze selected reactions of the monomeric metallacycles to see if this expectation is borne out in practice. We restrict ourselves to the addition of hydrogen compounds of non-metals and their derivatives to the molecules **14** and to reactions that may by extended analogy be regarded as cycloadditions (for further examples see, e.g., Refs. [35, 36]).

4.1. Addition of Hydrogen Compounds of Non-Metals to 14

The tin(II) compound **14b** (monomeric in solution) reacts with hydrogen compounds H–X (X = halogen, C_5H_5) according to the general equation (g).[37,38] The germanium compound **14a** also reacts in this way.[39] The ad-

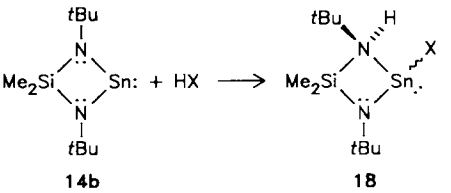

(g)

14b 18

18a–d: X = C_5H_5, Cl, Br, I

dition products **18a–d** can be isolated and characterized; Figure 4 shows the result of an X-ray structure determination of **18b**.[38] As expected, the λ^4-N–Sn bond is appreciably longer than λ^3-N–Sn ($\Delta = 40$ pm). The *cis* position of the hydrogen and chlorine atoms (with respect to the ring plane) is caused by steric effects. Molecules of the type **18**

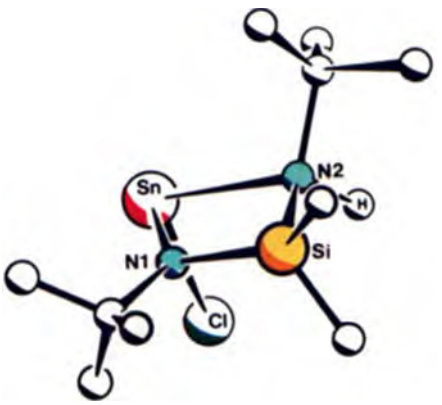

Fig. 4. Molecular structure of **18b** [37].

are conformationally unstable in solution (as shown by temperature-dependent NMR studies); equation (h) shows the equilibrium involved[37–39] (only two of the four possible isomers are represented (cf. Ref. [37])). **18A** and **18B** are mirror images; each contains two chiral centers (λ^4-N and Sn). The formal replacement of the SnX group in **18** by ElX_2 (El = Al, Ga, In, Tl; X = Me or halogen) leads to compounds that are similar to **18** in many respects, especially with regard to temperature-dependent "ligand redistribution" within the molecule.[21,29]

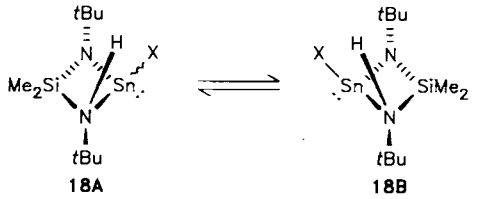

18A **18B** (h)

Apart from the explicitly mentioned hydrogen compounds in Eq. (g), alcohols, thiols and secondary amines can also react in a similar manner with **14b**; the difference is that the intermediate **18** cannot be isolated. The reaction continues by further addition of HX and breaking of both Sn–N bonds, leading to the bis(amino)silane **19** and derivatives **20** of divalent tin [Eq. (i)].[37–39] Dihalides of tin are

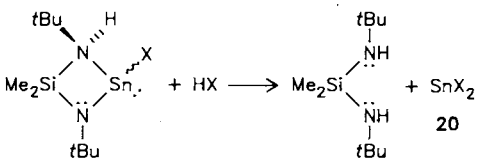

18 **19** **20** (i)

20a–d: X = C_5H_5, NMe_2, O*t*Bu, S*t*Bu

also obtained when compounds **18** are allowed to react with a further mole equivalent of hydrogen halide, but interesting side reactions also take place [Eq. (j)] for compound **18b**.[37] The ratio of products $SnCl_2$ and **22** can be influenced by temperature and concentration.

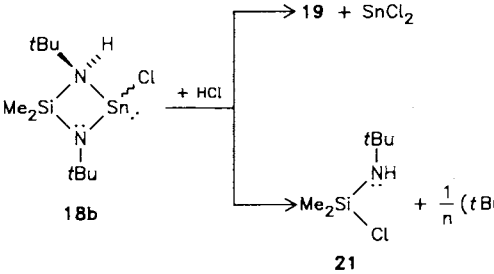

18b **21** **22** (j)

Whereas alternative methods of preparing **20a–d**[40] are available, the addition reaction (g) is particularly suitable for preparing asymmetrically substituted germanium(II) or tin(II) compounds[41] such as **23** [Eq. (k)], which are otherwise obtainable only with difficulty or not at all.[39] The cyclic species **14a**, **b** function in Eq. (k) in two separate reaction steps as formally unsaturated systems; the Lewis acid/base adduct **24** is obviously unstable [Eq. (l)]. The

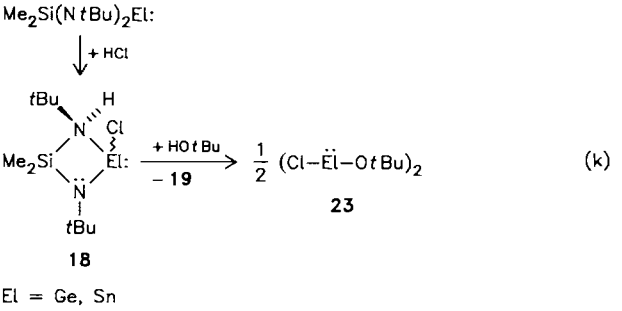

18 **23** (k)

El = Ge, Sn

bis(amino)silane **19** is, for a coordinating molecule, extremely bulky (because of the *tert*-butyl groups on the nitrogen atoms) and thus dissociates readily from the metal

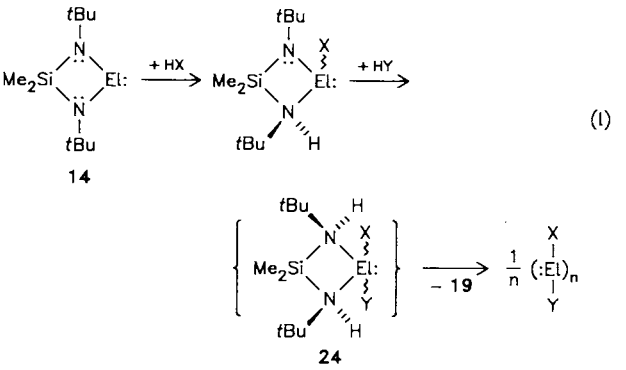

14 **24** (l)

atom. A detailed consideration of the reaction sequence (l) raises the question whether two hydrogen atoms can be simultaneously transferred to **14**, rather than in two separate steps. Such a reaction could be expected with hydrogen compounds that contain two element–hydrogen bonds, such as primary amines or water. Since the basic group X is only available for reaction once (in contrast to the successive reactions (l)), double bonds should be formed in the product after addition of the hydrogen, as shown in Eq. (m). The intermediates **25** and **26** are hypothetical and serve only to demonstrate the analogy to reaction (l).

The experimental test of this idea indeed shows that the reaction of compound **14** with primary amines (and in principle also with water) leads, apart from to the quantitatively generated bis(amino)silane **19**, to a compound whose empirical composition corresponds to formula **27**[23a,42] or that contains **27** as a constituent of a larger molecule.[43] The product should however not be repre-

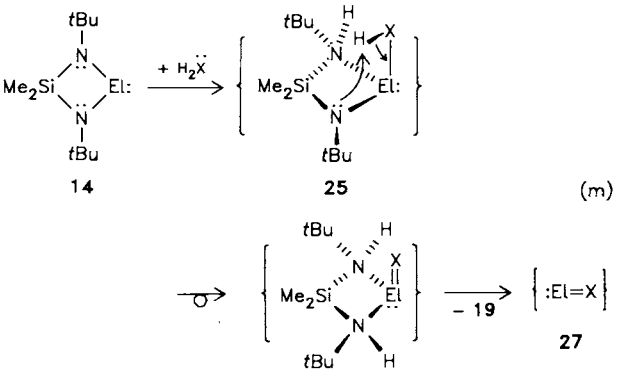

14 **25** **26** **27** (m)

X = NR, O

sented as a monomer containing a double bond, but rather as a tetramer. Figure 5 shows the molecular structure of $(SnNtBu)_4$, which contains a central Sn_4N_4 cube.[44] All the "bond lines" between tin and nitrogen atoms can be interpreted as σ bonds. A more detailed discussion of this and related bonding systems is presented in Section 4.2.

Fig. 5. Molecular structure of $(SnNtBu)_4$ [44].

Equation (m) could be formally classified as a simple substitution reaction, where the element El in **14** is replaced by two hydrogen atoms. A thorough analysis of the reaction of *tert*-butylamine with the bis(amino)stannylene **14b** shows that the first step should be formulated as an addition reaction.[45] The unstable intermediate **28** was successfully characterized by a low temperature X-ray structure determination. The nitrogen of the *tert*-butylamine in **28** interacts not only with the tin atom, but also via hydrogen bonds with the nitrogen atoms of the diazasilastannetane ring. The N_2Sn group of **14b** thus functions as a "trihapto" ligand with respect to the NH_2 group of the primary amine; this is an attractive confirmation of the concept that both Lewis bases and the Lewis acid act together as one unit. In this connection the *formal* similarity between the N_2Sn system and an allyl anion should be noted,[46] since both are equipped with 4π electrons distributed (localized or delocalized) over three atoms.

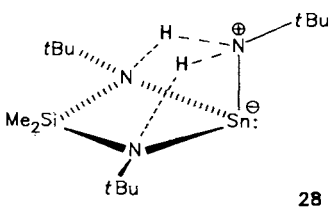

28

A similar formal analogy seems to exist between the formation of isocyanides (isonitriles)[46] and the formation of tetrameric iminogermylenes, -stannylenes and -plumbylenes[42] [Eq. (n)]. However, whereas the reaction of the heavy carbene analogues takes place by an addition mechanism, the reaction of carbenes with primary amines has as its first step the insertion of $:CX_2$ into the N–H bond; a base-induced elimination of HX follows.[47] The special stability of the "inert electron pair" of the heavy main group element is obviously an important factor in determining the differing reactivities of $:EIX_2$ and $:CX_2$.[48a]

$$:CX_2 + R{-}NH_2 \xrightarrow{OH^{\ominus}} 2\,HX + :\overset{\ominus}{C}{\equiv}\overset{\oplus}{N}{-}R$$
$$:EIX_2 + R{-}NH_2 \longrightarrow 2\,HX + \tfrac{1}{4}(:EIN{-}R)_4 \qquad (n)$$

El = Ge, Sn, Pb; X = basic substituent

Methylene phosphoranes are, in the broader sense, isoelectronic with primary amines (cf. formulas **29**, **30**) (for the similar relationship between phosphorus ylides and silylamines see Ref. [48b]). It is therefore not surpris-

$H_2\overset{\ominus}{C}{-}P^{\oplus}R_3$ **29** $\qquad$ $H_2\ddot{N}{-}CR_3$ **30**

ing that methylene phosphoranes also react with the stannylene **14b**, the addition and subsequent thermolysis leading to the bis(amino)silane **19** and the product **31** [Eq. (o)].[49] Compound **31** can be isolated in the form of

$$Me_2Si(N\,tBu)_2Sn \xrightarrow[2)\ \Delta T]{1)\ +\ H_2CPR_3} \mathbf{19} + \frac{1}{n}\,[SnCPR_3]_n \qquad (o)$$

14b $\qquad$ **31**

red crystals for R = Ph. The X-ray structure analysis shows that **31** does not contain a central tin-carbon cube (analogous to the iminostannylenes) but instead is a polycyclic compound (**32**).

Clearly a phenyl ligand is involved in the reaction of **14b** with the phosphorane. The reactive intermediate can be isolated and structurally characterized (as in the reaction of **14b** with *tert*-butylamine). It is an addition product that contains a tin–carbon bond and a $N\cdots H{-}C$ bridge[49] (**33**). The carbanion, stabilized at the *o*-carbon of the phenyl ring, can then displace the λ^4-N atom at tin; this explains the formation of the five-membered ring in **32** (for the experimental verification and the further reaction steps cf. Ref. [49]).

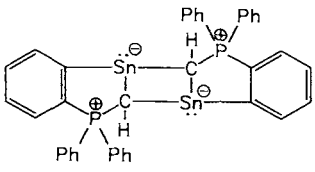

32

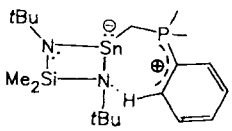

33

4.2. Reactions between Unsaturated Element–Metal Compounds

Ethene and acetylene and their derivatives are generally stable with respect to oligomerization to cyclobutanes, tetrahedranes or cubanes; this stability is primarily kinetic[50] (see e.g. tetra-*tert*-butyltetrahedrane[51]). As mentioned in the introduction, molecules with a polar "double bond"

(e.g. **1** and **2**) are appreciably more reactive and therefore easily convertible into oligomers; this property can be utilized to prepare cyclic and polycyclic molecules containing metal atoms. The use of sterically demanding ligands (either on the metal or the non-metal atom) largely avoids the formation of polymers.

The polycyclic compounds described below arise from multiple acid-base reactions of unsaturated starting materials containing metal atoms. In some cases the starting materials are only obtainable as intermediates because of their high reactivity; the comments on the mechanisms involved should therefore be interpreted with caution. With this reservation we present a simple model with which the formation of the compounds can be formally described:

1) The starting materials always come together in such a manner that the nucleophilic and electrophilic centers are adjacent; in other words, the arrangement of atoms in the polycyclic products is such as to neutralize the polarity of the starting materials.

2) The metal atoms tend, by increasing their coordination number, to acquire an electron configuration corresponding (at least) to the next noble gas. They can act as multiple acceptors to several donors.

In our classification of these reactions, we consider the number of atoms involved; this is a loose analogy to cycloaddition reactions of unsaturated hydrocarbons.[32b] As an example, see Eq. (p); this can be described as a [2+2]-cycloaddition involving the interaction of a Lewis acid/base pair **34** with a second pair **35**. An important differ-

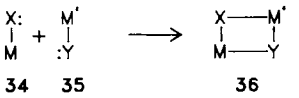

34 **35** **36** (p)

ence from the hydrocarbon reactions is that the size of the new ring is not necessarily given by the number of interacting centers in the reaction; for instance, the three centers of **37** react with the two centers of **35** to give not a simple ring system but the polycyclic compound **38**. The reason for this is the multiple acceptor nature of the metal atom M′ in **35** towards the two bases X of **37**.

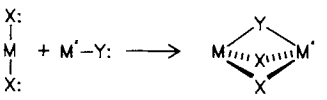

37 **35** **38**

4.2.1. [2+2]-Additions

As already mentioned, the dimers described in Section 3 can be considered to arise from [2+2]-additions of the monomeric Lewis acid/base systems. Further examples of this reaction type are given in Scheme 2.

The reaction of the bis(amino)stannylene **14b** with the asymmetrically substituted tin(II) compound **23** proceeds by dissociation of dimeric **23** and addition of the resulting monomer to one of the tin–nitrogen bonds of **14b**, leading to **39**, which has been characterized by X-ray structure determination.[39] For steric reasons the molecule **40**, which is equipped with two acid and two basic centers, cannot

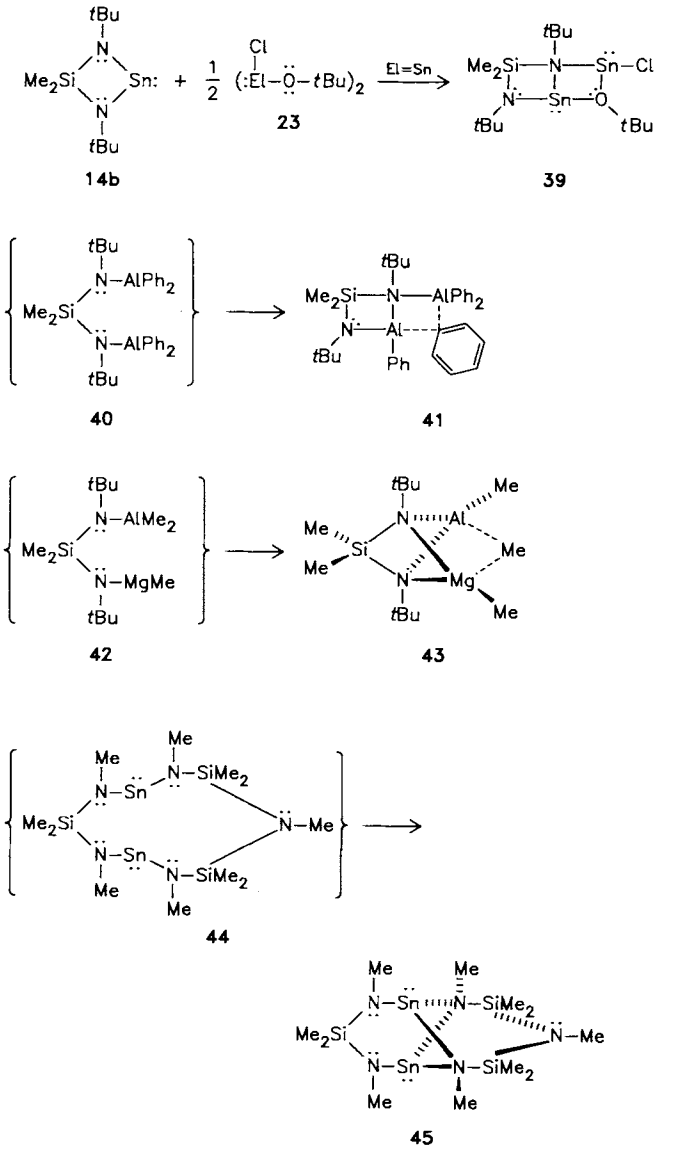

Scheme 2.

"react" intramolecularly to give a tricyclic product in which both nitrogen atoms function as bases. In **41** a three-center, two-electron bond, in which the carbon atom of a phenyl group and two aluminum atoms take part, serves to complete the coordination of the metal atoms.[29] The tricyclic product just mentioned *is* obtained, however, if an atomic arrangement as in **42** is provided. A three-center two-electron bond must also be assumed in **43** to complete the coordination at magnesium.[52] Another intramolecular double addition enables the tricyclic **45** to be "constructed" from **44**.[53]

4.2.2. [3+2]-Additions

The ability of the SnN_2 group in **14b** to coordinate through all three centers, rather than just two, has been discussed in Section 4.1. This property is particularly marked when **14b** comes into contact with extremely reactive molecules containing metal atoms with unusually low coordination number (Scheme 3).

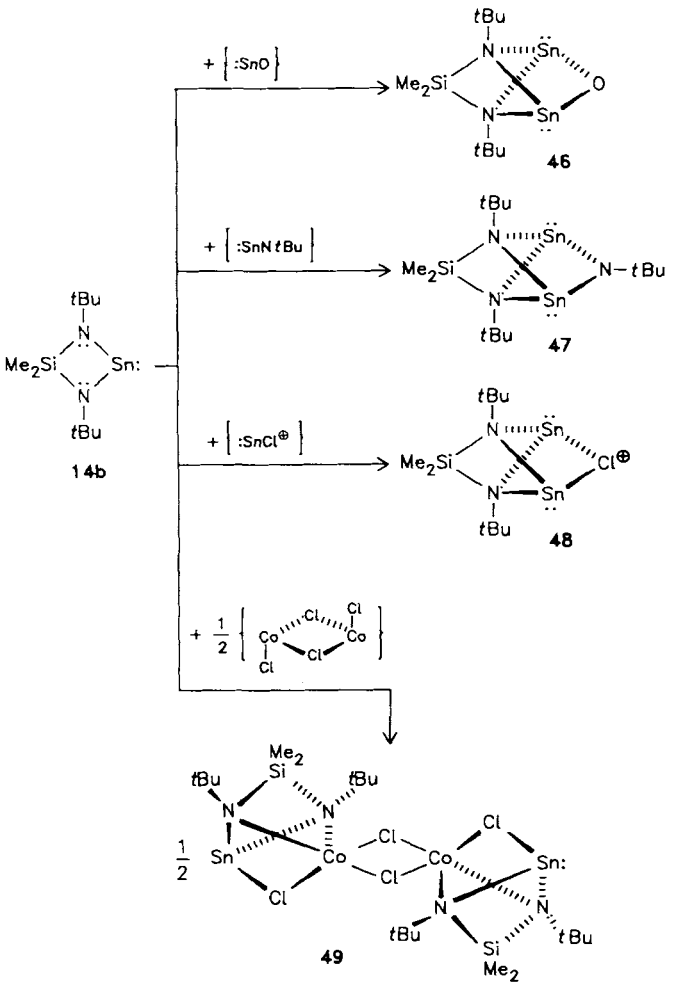

Scheme 3.

The reaction product in each case is a hexatomic system of three rings containing as a structural element a distorted tetrahedron, two opposite edges of which are bridged by one atom each (Fig. 6). The products **46**–**49** all contain the starting molecule **14b**; it coordinates via both nitrogen atoms to the metal atom (Sn or Co) and its tin atom functions as acceptor. The recently discovered molecule **49** shows that transition metals can also function as acceptors.[55] SnO and SnN–*t*Bu are probably generated as reactive intermediates in the hydrolysis[43] or *tert*-butylaminolysis[42] of **14b**, respectively, and are then trapped by excess **14b** to give **46** and **47**. The latter decomposes irreversibly at 210 °C by a first-order reaction to give **14b** and $(SnNtBu)_4$[4a]—evidence for the existence of an SnN–*t*Bu intermediate. The polycyclic compound **48** is formed, together with the anion $SnCl_3^{\ominus}$, in the reaction of **14b** with two mol equivalents of tin(II) chloride.[56]

Fig. 6. Structure of **46** as a structural unit in the compounds $Me_2Si(NtBu)_2Sn_2O \cdot SnCl_2$ [43] and $[Me_2Si(NtBu)_2Sn_2O]_2 \cdot Me_2Si(NtBu)_2Sn(O)_2Sn(NtBu)_2SiMe_2$ [45].

The intermediates SnO and SnN–*t*Bu can be regarded as heavy homologues of carbon monoxide or *tert*-butyl isocyanide respectively[36] (see Ref. [57] concerning the existence of Ph–NSi). However, whereas the limiting structures **50b** and **50c**, involving multiple bonds, are clearly

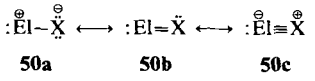

50a **50b** **50c**

El = C, Si, Ge, Sn, Pb; X = O, N*t*Bu

dominant for carbon, the structure **50a**, which involves a single bond, is probably more important for the heavier homologues.[36] The differing bonding schemes are reflected in the properties of the compounds. Carbon monoxide and organic isocyanides are monomeric; the corresponding compounds of the higher homologues, where existent, are tetrameric (see next Section). In the compounds **46**–**48**, several such tin species form part of the respective molecules.

The isoelectronic substitution of the low-valent main group element and of the nitrogen in ElN–R leads formally to alkoxides of univalent elements of the third main group, which have been known for a long time.[58] These alkoxides should correspond electronically to the iminocarbene analogues (see e.g. formula **50a**). As expected, thallium(I) *tert*-butoxide reacts smoothly with tin(II) *tert*-butoxide in a [3+2]-addition [Eq. (q)].[59] The distorted trigonal bipyramidal structure of the SnO_3Tl framework of **52** is easily recognized in Figure 7.

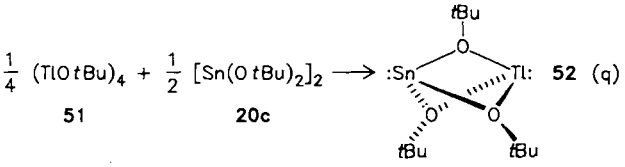

51 **20c** **52** (q)

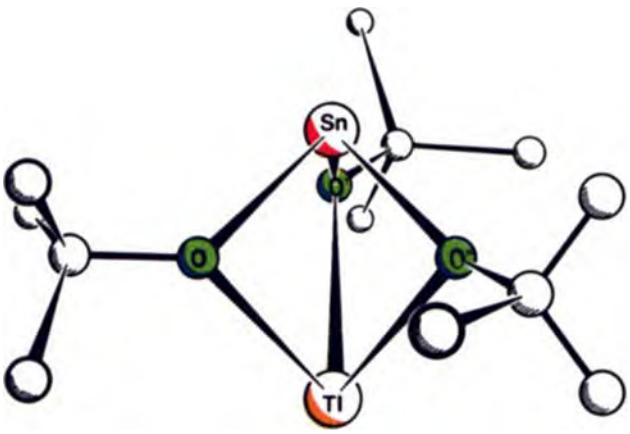

Fig. 7. Molecular structure of **52** [59].

4.2.3. [3+3]- and [3+4]-Additions

Trifunctional systems containing one acid and two base functions react with the same compounds, but in a manner depending on the strength of the base. Whereas **14b**, for example, reacts with one equivalent of SnN-*t*Bu to give stable polycyclic **47**, **20c** reacts with two equivalents of SnN-*t*Bu. From these two equivalents one can construct the four-membered ring **53**, which formally displays two acid and two basic functions and is isoelectronic with a cyclobutadiene. As can be seen from Scheme 4, this ring can be trapped by reactions with various trifunctional molecules. The reaction of **53** with the equally unstable **54** is a [3+3]-addition resulting in a seco-norcubane skeleton **55**;[42a,60] all four centers of **53**, however, react with the three centers of **20c**, and this causes one of the tin atoms of the product **56** to be four-coordinate.[61] The structural difference between **56** (with a central seven-atom framework consisting of two bipyramids with a common face) and **55** may be attributed to the three-coordinate oxygen and four-coordinate nitrogen respectively. The preparation of **57** also depends on a [4+3]-addition.[36,56] An X-ray structure

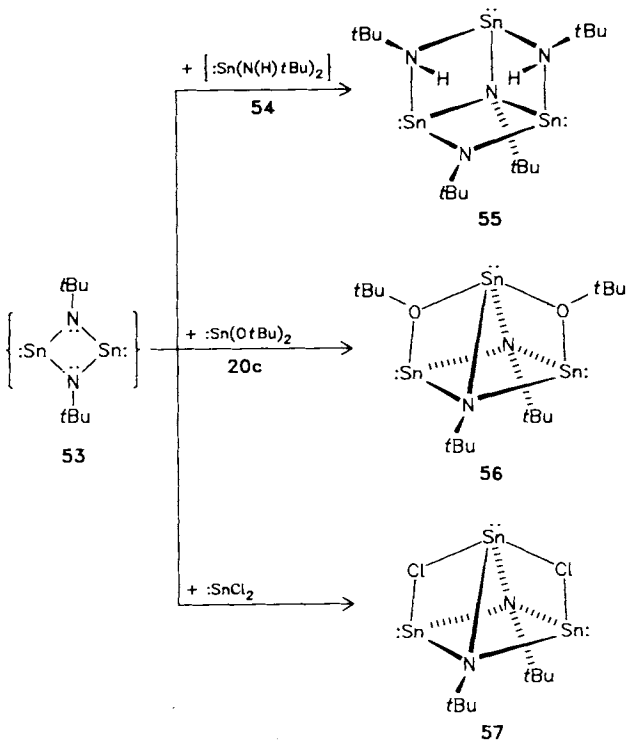

Scheme 4.

analysis has shown that the molecular units **57** link to form a polymer; one of the chlorine atoms acts as a bridge to two adjacent λ^3-tin atoms, itself acquiring square planar coordination (Fig. 8).

4.2.4. [2+2+2+2]- or [4+4]-Additions

There are a large number of molecules with the cubane structure whose formation can in general be attributed

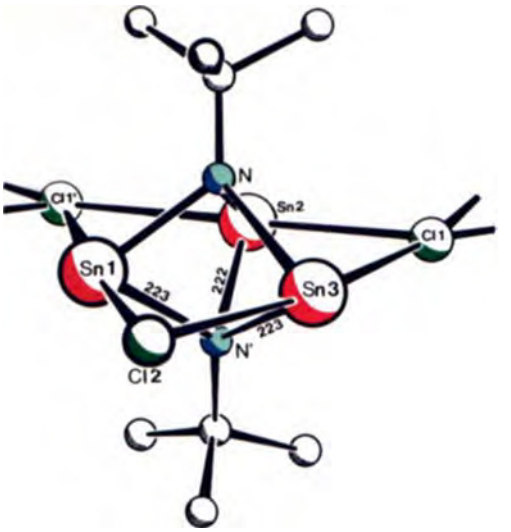

Fig. 8. Section of the crystal structure of **57** [36, 57]. The local symmetry of the $Sn_3(NtBu)_2Cl_3$ unit is close to D_{3h}.

to the reaction of doubly unsaturated acid-base systems. Examples are organoberyllium alkoxides $(RBeOR')_4$,[62] iminoalanes $(RAlNR)_4$,[63] and thallium(I) alkoxides $(TlOR)_4$,[58] to name only three typical representatives. Retrosynthetic considerations lead to the assumption that monomeric units first come together in pairs to form four-membered rings, pairs of which then mutually complete their coordination spheres by forming a cubane system **58** [Eq. (r)].

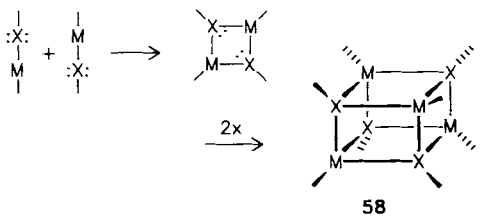

(r)

With light elements and less bulky substituents, higher oligomers than tetramers can be formed,[64] whereas with heavy elements (in particular low-valent metals with an "inert" s-electron pair) the preferred use of pure p orbitals leads exclusively to cubane-type arrangements.[35b,36] The formation of tetrameric iminogermylenes (e.g. $(GeN\text{-}tBu)_4$[23a,65]), iminostannylenes $(SnNR)_4$ (R = isopropyl, 1,1-dimethylhydrazyl,[42b] *tert*-butyl,[42a,44] benzyl[44]) and iminoplumbylenes (e.g. $(PbNtBu)_4$[23a]) can be described in an analogous manner (cf. also Fig. 5).

Apart from these "homogeneous" oligomers of doubly unsaturated acid-base systems, there are also a series of compounds that are formed from non-identical starting materials (e.g. by "scrambling" reactions) or that formally arise from an intramolecular [4+4]-cycloaddition (e.g. to give **64**). Some of these compounds are presented in Scheme 5; for the exact preparative details the reader should consult the original references (**59**,[44,66,67] **60**–**63**,[23a] **64**[53]). Figure 9 shows the structure of the molecule **64**, which is analogous to basketane.[68]

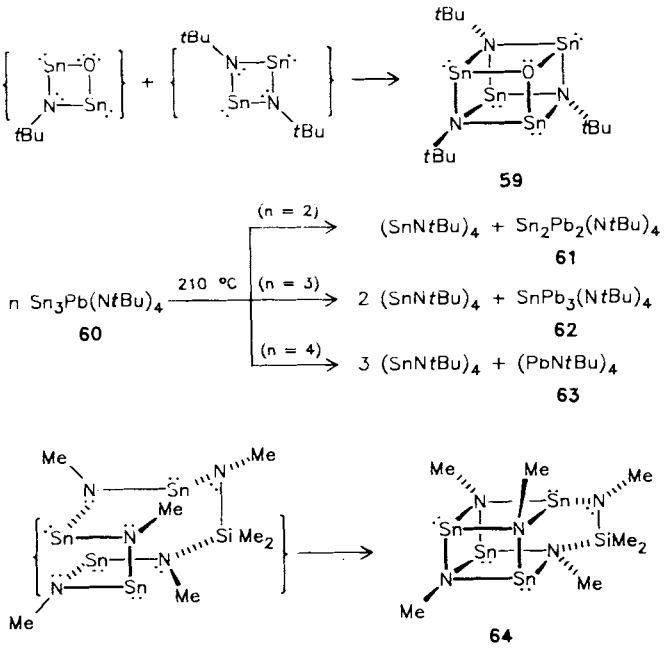

Scheme 5.

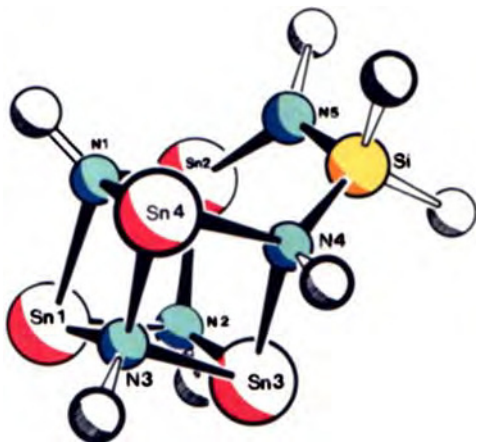

Fig. 9. Molecular structure of **64** [53].

4.2.5. Additions Involving Several Acid and Base Centers

Metal alkoxides of the first and second main groups form oligomeric, in some cases molecular, compounds in which the metal atoms tend to compensate for their lack of electrons by acquiring as many oxygen donors as possible;[69,70] they should therefore be ideal starting materials for addition reactions with trifunctional acid-base systems. This is indeed confirmed in the reactions of metal *tert*-butoxides with tin di-*tert*-butoxide (Scheme 6). An X-ray structure determination shows that the metal atoms Li and Na in molecule **65**[71] are four-coordinate, the tin atoms three-coordinate and the oxygen atoms three- or four-coordinate. The polycyclic unit $Sn_2O_6M_2$ is composed of two seco-norcubane-analogous subunits that share a common face. The reaction of **20c** with the alkoxides of the heavy alkali metals leads to polymeric arrangements of trigonal bipyramidal cages $Sn(OtBu)_3M$ (**66**), in which the alkali metal atom is coordinated by five oxygens and forms the link between the cages (cf., on the other hand, **52**).[71] The larger radius (and possibly the accessibility of d orbitals) is associated with a larger coordination number for K, Rb and Cs. The alkoxides of the alkaline earth elements strontium and barium react with the tin alkoxide **20c** to form the molecules **67**, which contain six-coordinate alkaline earths (the reaction corresponds to a [3+3+3]-addition; $Mg(OtBu)_2$ and $Ca(OtBu)_2$ do not react).[72]

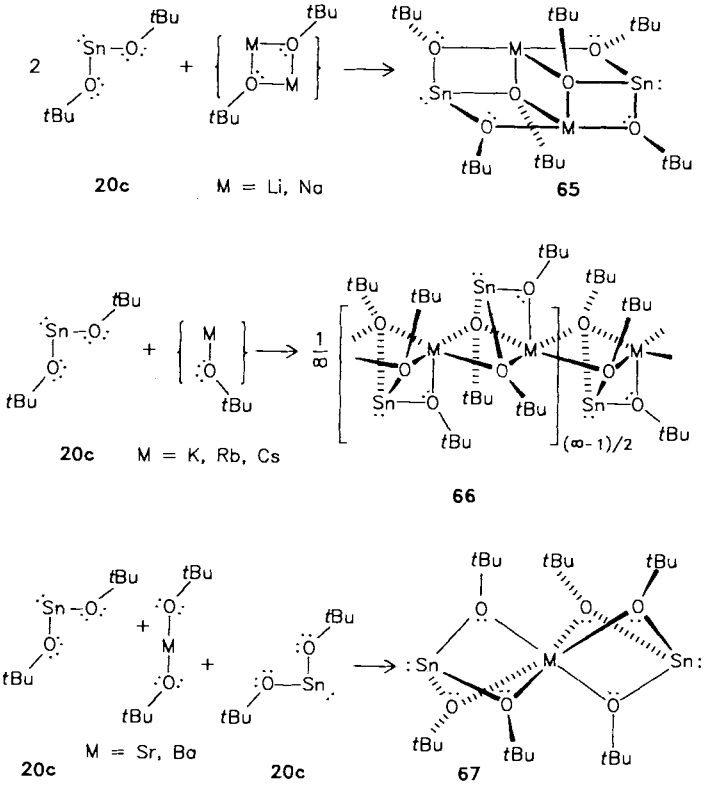

Scheme 6.

5. Properties of Metallapolycycles

The polycyclic species described in Section 4 are thermally more stable when the point symmetry of the central framework is high and the distribution of the peripheral ligands is isotropic. Whereas $(SnNtBu)_4$, for example, can be heated to above 250°C without decomposing, **47** decomposes within a few hours at 210°C to **14b** and $(SnNtBu)_4$.[42a] Molecules that possess, in addition to the donor and acceptor functions that are bound to each other, further coordinatively unsaturated bases (e.g. the three-coordinate nitrogen atoms in **39**, **41**, **55** and **64**) can display intramolecular valency fluctuation; this is shown here for molecule **41**. The temperature-dependent ^{1}H-NMR spectrum shows that there is an equilibrium between **41A** and **41B** [Eq. (s)]. The fluctuation within compound **41** is

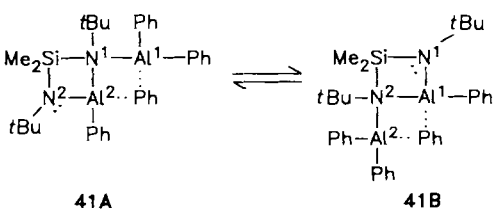

(s)

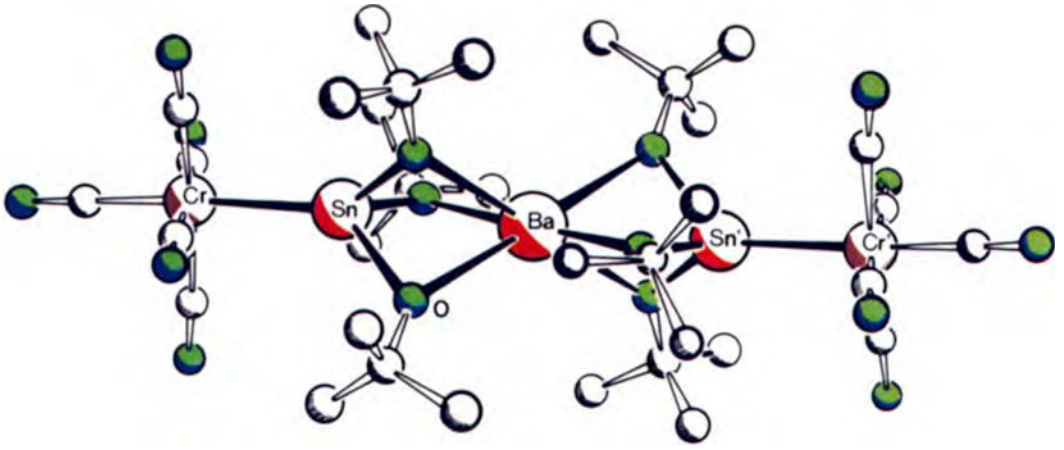

Fig. 10. Molecular structure of **70** [78].

caused by the competition between the donors N2 and N1 for a coordination site at a further aluminum atom (for a more detailed discussion see Ref. [29]). Similar competition leads to intramolecular dynamic exchange of formal donors in molecules **39**,[39] **55**,[60] and **64**.[53]

Our description of the compounds presented in Section 4 as polycyclic molecules is a necessary consequence of the model we use to interpret their formation. If, on the other hand, the accumulation of metal atoms in these compounds is accentuated, then an alternative bonding model arises in which the metal cluster[73] of the central framework is described, the non-metal ligands serving only to neutralize its charge. There is however neither structural nor spectroscopic evidence[44] to give this model particular support.

Polycyclic compounds that contain low-valent metal atoms with lone pairs should be able to utilize these to act as electron donors. Since the heavy metals can additionally function as electron acceptors, it is conceivable that, under special conditions, the molecules may aggregate to form "coordination polymers" with metal-metal interactions. We have only found one compound in which different tin atoms act as acceptors and donors (in the crystal). The crystal structure of $(SnNNMe_2)_4$[42b] involves an undulating ribbon of approximately equidistant tin atoms—irrespective of whether the contacts are intra- or intermolecular. The compound is a red solid (in contrast to the colorless iminostannylenes that only involve van der Waals contacts between molecules); it decomposes above 50°C to β-tin, nitrogen, methane, ethane and dimethylamine.

Compounds **68**, **69** and **70**, synthesized as shown in Scheme 7, confirm that the low-valent metal atoms can react as bases with strong Lewis acids such as $AlCl_3$ or with transition metal fragments (the intermolecular interactions in $(SnNNMe_2)_4$ have been discussed in terms of other models too[42b]). Compound **68** is the first chemically and structurally characterized example of an adduct of a tin(II) compound and a main group Lewis acid; the synthesis is strikingly simple considering that the compound contains a new type of metal-metal bond. The tin-chromium bond in **69**, however, is already familiar from other examples.[75,76] In both **68** and **69**[77] it is only possible to add two metal fragments to the tetrameric iminostannylene. We have not succeeded in synthesizing a molecule

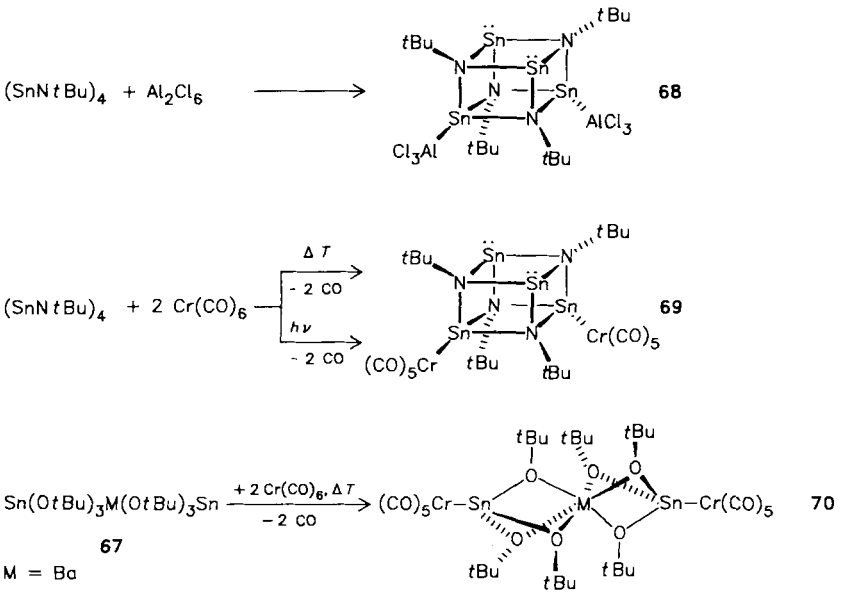

Scheme 7.

in which all four tin atoms are bound to metal fragments, either by using drastic conditions or by substituting $Mo(CO)_6$ or $W(CO)_6$ for $Cr(CO)_6$.[77]

The reaction that leads to the polycyclic compound **70** (Fig. 10) seems particularly promising as a pointer to future research. The addition of two metal fragments to **67** converts the linear arrangement of three metal atoms to a chain consisting of five metal atoms.[78] Preliminary studies suggest that this principle can be arbitrarily extended.

6. Concluding Remarks

The technical interest in main group metals is mainly concerned with the elements themselves or with metal ions in solution or in the solid state. Except for organometallics[79] and other specialized compounds such as alkoxides[69] and metal amides,[18,69] molecular compounds of these elements play only a modest role. The cyclic and polycyclic metal compounds described in this review are noteworthy because they allow the transfer of the metal atoms to nonpolar solvents and thus satisfy one condition necessary for homogeneous reactions with other species. The synthetic potential of these compounds is illustrated in Scheme 8 by some reactions of **14b** with organic molecules; the low oxidation state of the metal atom permits both addition and redox reactions (for further redox reactions see Ref. [80]).

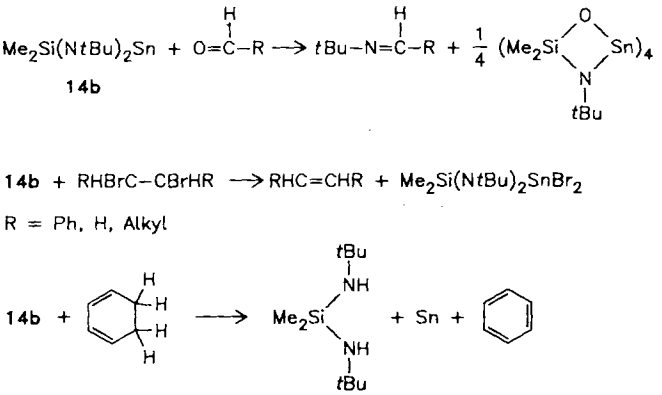

Scheme 8.

Aliphatic or aromatic aldehydes are converted into *tert*-butylimines;[81] the initial step in this quantitative reaction is the [2+2]-addition of the polar C-O bond to one of the ring tin-nitrogen bonds of **14b**.[81] The tin atom acts as a halogen acceptor (and is thus oxidized) in the conversion of bromoalkanes to ethenes.[82] The possibility of using **14b** as an oxidizing agent has been realized only in the conversion of hexadiene to benzene.[37a]

I am grateful to my co-workers for their valuable contributions to the work described here (see References). Financial assistance was generously given, at various times, by the Fonds der Chemischen Industrie, the Deutsche Forschungsgemeinschaft, the State of Lower Saxony, and by Hoechst AG.

Received: June 6, 1986;
revised: August 11, 1986 [A 591 IE]
German version: *Angew. Chem. 99* (1987) 1

[1] a) Holleman-Wiberg: *Lehrbuch der Anorganischen Chemie*, 33rd Edit., de Gruyter, Berlin 1985, p. 239; b) V. Gutmann: *The Donor-Acceptor Approach to Molecular Interactions*, Plenum, New York 1978.

[2] Four-membered rings: a) A. Ahmed, W. Schwarz, H. Hess, *Acta Crystallogr. Sect. B 33* (1977) 3574; b) *Z. Naturforsch. B 33* (1978) 43; c) H. Hess, A. Hinderer, S. Steinhauser, *Z. Anorg. Allg. Chem. 377* (1970) 1; d) T. C. Barthe, A. Haaland, D. P. Novak, *Acta Chim. Scand. Ser. A 29* (1975) 273; e) K. Onzonnis, H. Riffel, H. Hess, U. Kohler, J. Weidlein, *Z. Anorg. Allg. Chem. 504* (1983) 67; f) W. E. Dorogy, E. P. Schramm, *Inorg. Chim. Acta 72* (1982) 187.

[3] Six-membered rings: a) K. N. Semenenko, E. B. Lobkovskii, A. L. Dorosinskii, *J. Struct. Chem. Engl. Transl. 13* (1972) 696; b) G. M. McLaughlin, G. A. Sim, J. O. Smith, *J. Chem. Soc. Dalton Trans. 1972*, 2197; c) J. L. Atwood, G. D. Stucky, *J. Am. Chem. Soc. 92* (1972) 285.

[4] a) A. G. Brook, F. Abdesaken, B. Gutekunst, G. Gutekunst, R. K. Kallury, *J. Chem. Soc. Chem. Commun. 1981*, 191; b) A. G. Brook, S. C. Nyburg, F. Abdesaken, B. Gutekunst, G. Gutekunst, R. K. M. R. Kallury, Y. C. Poon, Y.-M. Chang, W. Wong-Ng, *J. Am. Chem. Soc. 104* (1982) 5667.

[5] a) N. Wiberg, G. Wagner, G. Müller, *Angew. Chem. 97* (1985) 220; *Angew. Chem. Int. Ed. Engl. 24* (1985) 229; b) N. Wiberg, K. Schurz, G. Reber, G. Müller, *J. Chem. Soc. Chem. Commun. 1986*, 581.

[6] A. G. Brook, J. W. Harris, I. Lennon, M. J. ElSheikh, *J. Am. Chem. Soc. 101* (1979) 83.

[7] a) R. West, M. J. Fink, J. Michel, *Science (Washington) 214* (1981) 1343; b) R. West, *ibid. 225* (1984) 1109; c) S. Masamune, S. Murakami, J. T. Snow, H. Tobita, D. J. Williams, *Organometallics 3* (1984) 333; d) J. C. Dewan, S. Murakami, J. T. Snow, S. Collins, S. Masamune, *J. Chem. Soc. Chem. Commun. 1985*, 892.

[8] a) L. E. Gusel'nikov, M. C. Flowers, *J. Chem. Soc. B 1968*, 419; b) C. M. Golino, R. D. Bush, D. N. Roark, L. H. Sommer, *J. Organomet. Chem. 66* (1974) 29; c) P. Boudjouk, L. H. Sommer, *J. Chem. Soc. Chem. Commun. 1973*, 54.

[9] a) R. P. Gaspar, *React. Intermed. 3* (1985) 333; b) M. Weidenbruch, K. Kramer, A. Schäfer, J. K. Blum, *Chem. Ber. 118* (1985) 107; and references cited therein.

[10] J. March: *Advanced Organic Chemistry*, 3rd Edit., Wiley, New York 1985, p. 745-779; and references cited therein.

[11] G. Odian: *Principles of Polymerisation*, McGraw-Hill, New York 1970.

[12] a) P. Jutzi, *Angew. Chem. 87* (1975) 269; *Angew. Chem. Int. Ed. Engl. 14* (1975) 232; b) *Chem. Unserer Zeit 15* (1981) 149; c) B. Coleman, M. Jones, Jr., *Rev. Chem. Intermed. 4* (1981) 297.

[13] Preparation: a) J. Pump, E. G. Rochow, U. Wannagat, *Angew. Chem. 75* (1963) 374; *Angew. Chem. Int. Ed. Engl. 2* (1963) 364; b) D. Ya. Zhinkin, G. K. Korneeva, N. N. Korneev, M. V. Sobolesskii, *J. Gen. Chem. USSR Engl. Transl. 36* (1966) 360.

[14] Structure: G. M. Sheldrick, W. S. Sheldrick, *J. Chem. Soc. A 1969*, 2279.

[15] W. Fink, *Helv. Chim. Acta 47* (1964) 498.

[16] a) R. Parker, L. H. Sommer, *J. Am. Chem. Soc. 98* (1976) 618; b) M. Veith, R. Rösler, *J. Organomet. Chem. 229* (1982) 131.

[17] J. E. Huheey: *Inorganic Chemistry: Principles of Structure and Reactivity*, 3rd Edit., Harper & Row, New York 1983, p. 824-836.

[18] Review article on preparation of metal amides: M. F. Lappert, P. P. Power, A. R. Sanger, R. C. Srivastava: *Metal and Metalloid Amides*, Horwood, Chichester 1980.

[19] **9a-c**: M. Veith, J. Böhnlein, unpublished.

[20] **10a**: a) F. Töllner, *Dissertation*, Technische Universität Braunschweig 1985; b) M. Veith, F. Töllner, H. Feuerhake, unpublished.

[21] **12a-c**: M. Veith, H. Lange, A. Belo, O. Recktenwald, *Chem. Ber. 118* (1985) 1600.

[22] **13a**: see Ref. [16b]; the yield can be increased to 95% according to: J. Pöhlmann, *Dissertation*, Saarbrücken 1986.

[23] a) **14a, c**: M. Veith, M. Grosser, *Z. Naturforsch. B 37* (1982) 1375; b) **14b**: M. Veith, *Angew. Chem. 87* (1975) 287; *Angew. Chem. Int. Ed. Engl. 14* (1975) 263.

[24] **15a-d**: a) B. Bertsch, *Dissertation*, Saarbrücken 1986; b) M. Veith, B. Hoppe, V. Huch, 20. GDCh-Hauptversammlung, Heidelberg 1985, Referat D 2.10.

[25] Definition of electronegativity after L. Pauling; numerical values according to L. Allred, *J. Inorg. Nucl. Chem. 17* (1961) 215.

[26] M. Veith, *Z. Naturforsch. B 33* (1978) 7.

[27] M. Veith, *Z. Naturforsch. B 33* (1978) 1.

[28] P. J. Corvan, J. J. Zuckerman, *Inorg. Chim. Acta 34* (1979) L255.

[29] M. Veith, H. Lange, O. Recktenwald, W. Frank, *J. Organomet. Chem. 294* (1985) 272.

[30] In the crystal structures of **14b** [27] and **15c** [24] there are additional weaker coordinative bonds to the two-coordinate elements Sn and $Sb^{\oplus}$ respectively; these can however be neglected to a first approximation.

[31] M. F. Lappert, P. P. Power, M. J. Slade, L. Hedberg, K. Hedberg, V. Shomaker, *J. Chem. Soc. Chem. Commun. 1979*, 369.
[32] a) D. N. Reinhoudt, *Adv. Heterocycl. Chem. 21* (1977) 253; b) R. Huisgen, *Angew. Chem. 80* (1968) 329; *Angew. Chem. Int. Ed. Engl. 7* (1968) 321.
[33] J. L. Atwood, R. Shakir, *J. Am. Chem. Soc. 102* (1980) 2086.
[34] D. J. Brauer, H. Bürger, G. R. Liewald, *J. Organomet. Chem. 308* (1986) 119.
[35] a) M. Veith, *J. Organomet. Chem. Libr. 12* (1981) 319; b) M. Veith, O. Recktenwald, *Top. Curr. Chem. 104* (1982) 1; c) M. Veith, *Nachr. Chem. Tech. Lab. 30* (1982) 940; d) *Nova Acta Leopold. 264* (1985) 321.
[36] M. Veith, *Comments Inorg. Chem. 4* (1985) 179.
[37] a) M. Veith, F. Töllner, *J. Organomet. Chem. 246* (1983) 219; b) unpublished.
[38] M. Veith, M. Jarczyk, V. Huch, unpublished.
[39] M. Veith, P. Hobein, unpublished.
[40] a) **20a**: E. O. Fischer, H. Gruber, *Z. Naturforsch. B11* (1956) 423; b) **20b**: P. Foley, M. Zeldin, *Inorg. Chem. 14* (1975) 2264; c) **20c**: see [37a]; d) **20d**: W.-W. du Mont, M. Grenz, *Chem. Ber. 118* (1985) 1045.
[41] a) K. D. Bos, E. J. Bulten, J. G. Noltes, *J. Organomet. Chem. 39* (1972) C52; b) A. Meller, C. P. Gräbe, *Chem. Ber. 118* (1985) 2020.
[42] a) M. Veith, M.-L. Sommer, D. Jäger, *Chem. Ber. 112* (1979) 2581; b) M. Veith, G. Schlemmer, *Chem. Ber. 115* (1982) 2141.
[43] M. Veith, *Chem. Ber. 111* (1978) 2536.
[44] M. Veith, O. Recktenwald, *Z. Naturforsch. B38* (1983) 1054.
[45] M. Veith, G. Schlemmer, M.-L. Sommer, *Z. Anorg. Allg. Chem. 497* (1983) 157.
[46] T. Kauffmann, *Top. Curr. Chem. 92* (1980) 109.
[47] M. P. Periasamy, H. M. Walbersky, *Org. Prep. Proced. Int. 11* (1979) 293.
[48] a) See [17], S. 843; b) H. Schmidbaur, *Fortschr. Chem. Forsch. 13* (1969) 167.
[49] M. Veith, V. Huch, *J. Organomet. Chem. 293* (1985) 161; *ibid. 308* (1986) 263.
[50] K. Fukui, *Angew. Chem. 94* (1982) 852; *Angew. Chem. Int. Ed. Engl. 21* (1982) 801.
[51] a) G. Maier, S. Pfriem, U. Schäfer, K.-D. Malsch, R. Matusch, *Chem. Ber. 114* (1981) 3965; b) H. Irngartinger, A. Goldmann, R. Jahn, M. Nixdorf, H. Rodewald, G. Maier, K.-D. Malsch, R. Emrich, *Angew. Chem. 96* (1984) 967; *Angew. Chem. Int. Ed. Engl. 23* (1984) 993.
[52] M. Veith, W. Frank, F. Töllner, H. Lange, *J. Organomet. Chem.*, in press.
[53] M. Veith, M. Grosser, O. Recktenwald, *J. Organomet. Chem. 216* (1981) 27.
[54] M. Veith, O. Recktenwald, *Z. Anorg. Allg. Chem. 459* (1979) 208.
[55] M. Veith, A. Müller, V. Huch, unpublished.
[56] V. Huch, *Dissertation*, Braunschweig 1984.
[57] a) H. Bock, R. Dammel, *Angew. Chem. 97* (1985) 128; *Angew. Chem. Int. Ed. Engl. 24* (1985) 111; b) J. Michl (Austin, TX (USA)), private communication.
[58] a) L. F. Dahl, G. L. Davis, D. L. Wampler, R. West, *J. Inorg. Chem. 24* (1962) 52; b) H. Schmidbaur, M. Bergfeld, F. Schindler, *Z. Anorg. Allg. Chem. 363* (1968) 73.
[59] M. Veith, R. Rösler, *Angew. Chem. 94* (1982) 867; *Angew. Chem. Int. Ed. Engl. 21* (1982) 858.
[60] M. Veith, *Z. Naturforsch. B35* (1980) 20.
[61] M. Veith, W. Frank, *Angew. Chem. 96* (1984) 163; *Angew. Chem. Int. Ed. Engl. 23* (1984) 158.
[62] G. E. Coates, A. H. Fishwick, *J. Chem. Soc. A 1968*, 477.
[63] a) S. Cucinella, G. Dozzi, C. Busetto, A. Mazzei, *J. Organomet. Chem. 113* (1967) 233; b) H. Nöth, P. Wolfgardt, *Z. Naturforsch. B31* (1976) 697; c) G. Del Piero, M. Cesari, G. Dozzi, A. Mazzei, *J. Organomet. Chem. 129* (1977) 281.
[64] a) P. B. Hitchcock, J. D. Smith, K. M. Thomas, *J. Chem. Soc. Dalton Trans. 1976*, 1433; b) G. Del Piero, M. Cesari, G. Parego, S. Cucinella, E. Cernia, *J. Organomet. Chem. 129* (1977) 289; c) S. Amirkhalili, P. B. Hitchcock, J. D. Smith, *J. Chem. Soc. Dalton Trans. 1979*, 1206.
[65] The tetrameric structure of $(GeN^tBu)_4$ has been confirmed by an independent X-ray study: G. M. Sheldrick, A. Meller (Göttingen), private communication.
[66] M. Veith, H. Lange, *Angew. Chem. 92* (1980) 408; *Angew. Chem. Int. Ed. Engl. 19* (1980) 401.
[67] M. Veith, O. Recktenwald, *Z. Naturforsch. B36* (1981) 144.
[68] S. Masamune, H. Cuts, M. G. Hogben, *Tetrahedron Lett. 1966*, 1017.
[69] D. C. Bradley, R. C. Mehrotra, D. P. Mehrotra, D. P. Gaur: *Metal-Alkoxides*, Academic Press, New York 1978.
[70] *tert*-Butoxides: a) G. E. Hartwell, T. L. Brown, *Inorg. Chem. 5* (1966) 1257; b) E. Weiss, H. Alsdorf, H. Kühr, *Angew. Chem. 79* (1967) 816; *Angew. Chem. Int. Ed. Engl. 6* (1967) 801; c) E. Weiss, H. Alsdorf, H. Kühr, H. F. Grützmacher, Chem. Ber. 101 (1968) 3777.
[71] M. Veith, R. Rösler, *Z. Naturforsch. B41* (1986) 1071.
[72] M. Veith, D. Käfer, V. Huch, *Angew. Chem. 98* (1986) 367; *Angew. Chem. Int. Ed. Engl. 25* (1986) 375.
[73] a) H. G. von Schnering, *Angew. Chem. 93* (1981) 44; *Angew. Chem. Int. Ed. Engl. 20* (1981) 33; b) D. Fenske, J. Hachgenei, J. Ohmer, *Nachr. Chem. Tech. Lab. 34* (1986) 432.
[74] M. Veith, W. Frank, *Angew. Chem. 97* (1985) 213; *Angew. Chem. Int. Ed. Engl. 24* (1985) 223.
[75] M. D. Brice, F. A. Cotton, *J. Am. Chem. Soc. 95* (1973) 4529.
[76] a) D. Uhlig, H. Behrens, E. Lindner, *Z. Anorg. Allg. Chem. 401* (1973) 233; b) W. Petz, *J. Organomet. Chem. 165* (1979) 199; c) W. W. du Mont, B. Neudert, *Chem. Ber. 111* (1978) 2267; d) A. B. Cornwell, P. G. Harrison, *J. Chem. Soc. Dalton Trans. 1975*, 1486.
[77] M. Veith, J. Fischer, V. Huch, unpublished.
[78] M. Veith, D. Käfer, V. Huch, unpublished.
[79] a) T. L. Brown, *Adv. Organomet. Chem. 3* (1965) 365; b) J. P. Oliver, *ibid. 15* (1977) 235; c) E. Ashby, *Q. Rev. Chem. Soc. 21* (1967) 256; d) R. Köster, P. Binger, *Adv. Inorg. Radiochem. 7* (1965) 263; e) E. W. Colvin, *Chem. Soc. Rev. 7* (1978) 15; f) I. Fleming, *ibid. 10* (1981) 83; g) A. G. Davies, P. J. Smith, *Adv. Inorg. Radiochem. 23* (1980) 1.
[80] a) M. Veith, *Z. Anorg. Allg. Chem. 446* (1978) 227; b) M. Veith, O. Recktenwald, E. Humpfer, *Z. Naturforsch. B33* (1978) 14; c) M. Veith, V. Huch, J. P. Majoral, G. Bertrand, G. Manuel, *Tetrahedron Lett. 24* (1983) 4219; d) M. Veith, M. Grosser, V. Huch, *Z. Anorg. Allg. Chem. 513* (1984) 89.
[81] M. Veith, M. Grosser, *J. Organomet. Chem. 229* (1982) 247.
[82] M. Veith, A. Müller, unpublished.

Totally Synthetic Routes to the Higher Monosaccharides

New Synthetic Methods (63)

By Samuel J. Danishefsky and Michael P. DeNinno

The evolution of a strategy to synthesize the title compounds is described. Three principal developments allowed realization of this goal: (1) the attainment of high margins of diastereofacial selectivity and regioselectivity in the construction of pyranoid systems via the Lewis acid-catalyzed cyclocondensation reaction of activated dienes and aldehydes; (2) the exploitation of stereoselective reactions for functionalization of the pyranoid matrix; and (3) the discovery of stereoselective reactions for extending the chiral biases of pyranoid systems to newly emerging stereogenic centers on side chains. The coordination of these components in the synthesis of target systems of high biological interest is described.

1. Introduction

The vast majority of monosaccharides of biological interest have continuous networks of five (pentoses) or six (hexoses) carbon atoms.[1,2] Among the most widely known monomeric sugars are the pentoses, ribose and arabinose, and the hexoses, glucose, mannose, and galactose. While such monosaccharides are found in free form, they are more widely encountered as integral units of biooligomers and biopolymers. Thus, phosphodiester bonds at the 3- and 5-positions of ribose provide the connectivity for ribonucleotides in RNA. L-Arabinose is found in conjugated form in various glycoproteins. Homopolymers of simple hexoses (e.g., cellulose, glycogen, and starch) provide invaluable support material and energy storage depots. In addition, simple hexoses are often covalently linked to other natural products as glycoconjugates (e.g., macrolide antibiotics and glycolipids).

The existence of a few naturally occurring C_7 monosaccharides has been known for some time.[3] In the past thirty years, however, a group of natural products of broadly varied biological function has been shown to contain monosaccharide arrangements containing eight to eleven consecutive carbon atoms. We refer to such compounds as "complex" monosaccharides or as "higher" monosaccharides. Ordinarily, the compounds are not present in free form, but exist as substructural units in glycoconjugates or as the sugar unit in novel nucleosides.[4] Often the compounds in which these higher monosaccharides are found have valuable biological properties. A partial listing of these systems is given in Figure 2.

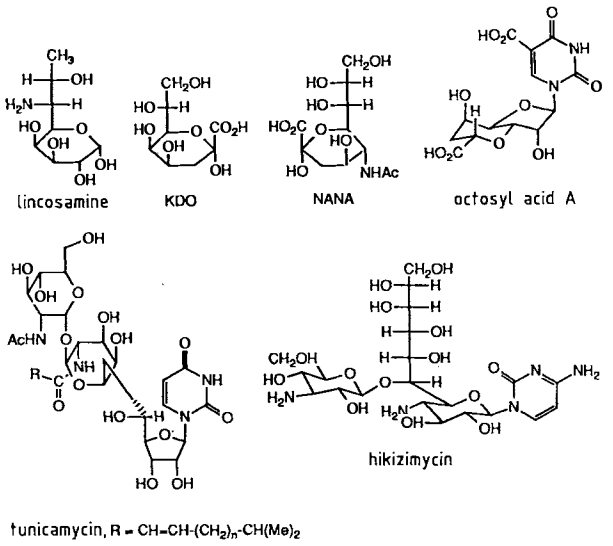

Fig. 2. Examples of higher (complex) monosaccharides. KDO = 3-deoxy-D-*manno*-2-octulosonic acid; NANA = N-acetylneuraminic acid.

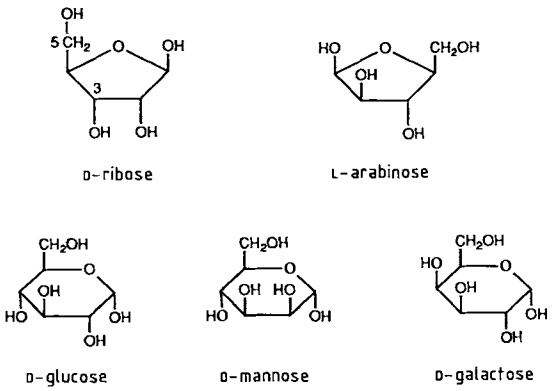

Fig. 1. Frequently occurring pentoses and hexoses.

Lincosamine, an amine octose (cf. Fig. 16), is a component of the commercially important antibiotic lincomycin.[5] Another octose, KDO (cf. Fig. 17),[6] is an important connecting link in the membrane structures of Gram-negative bacteria. The octosyl acids (cf. Fig. 11) are unusual eight-carbon bicyclic sugars which are *N*-glycosidically linked to novel pyrimidine bases.[7] Certain octosyl acids are powerful phosphodiesterase inhibitors,[8] presumably because of their rough structural similarity to cyclic AMP.

Various neuraminic acids[9,10] are encountered as sialic acid residues in glycoconjugates: *N*-acetylneuraminic acid (NANA) is a prime example (cf. Fig. 18). The extent of "sialidation" of oligosaccharides and glycoproteins has vast consequences ranging from influence on the viscosities of various biological fluids to the governance of immunogenic responses.

[*] Prof. S. J. Danishefsky, M. P. DeNinno
Department of Chemistry, Yale University
New Haven, CT 06511 (USA)

 © VCH Verlagsgesellschaft mbH, D-6940 Weinheim, 1987 0570-0833/87/0101-0015 $ 02.50/0

A C_{11} complex monosaccharide substructure is found in the antihelminthic nucleoside hikizimycin.[11] The mechanism of action of hikizimycin is not presently known. By contrast, a great deal of study and progress has been realized in understanding the mode of action of the bacterially derived tunicamycins (cf. Fig. 12).[12, 13] These compounds have become valuable resources for studying the fine details of the bioprocessing of complex polysaccharides. The tunicamycins apparently function by inhibiting the enzyme UDP-galactose transferase.

Another unusual type of complex monosaccharide is one where there is a carbon glycosidic bond connecting a simple hexose or pentose system with an aromatic framework. Intriguing examples of such linkages are found in the vineomycins[14] and in the papulacandins (Fig. 3).[15] Antitumor activity has been ascribed to both systems.

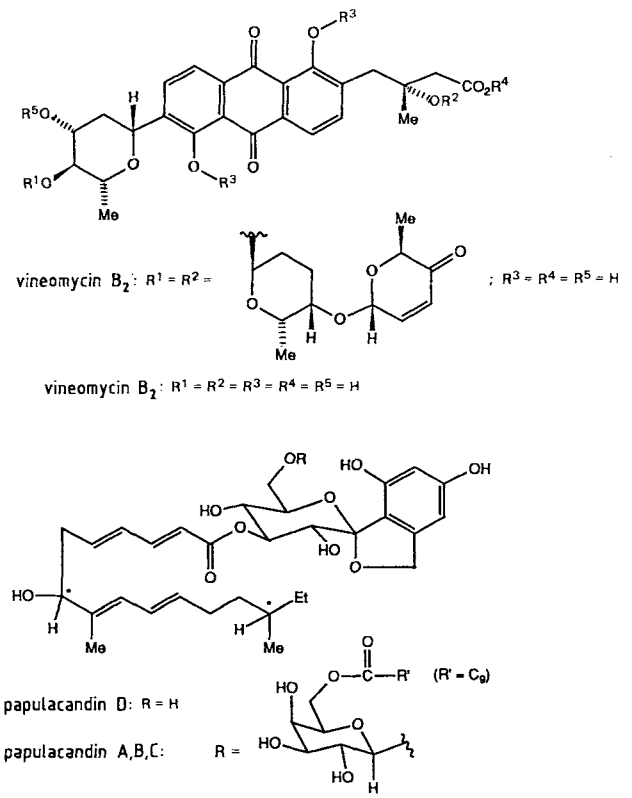

Fig. 3. Monosaccharides with aromatic groups.

As part of a broader effort to identify new reactions and new strategies that might be of utility in organic synthesis, we undertook an exploration into the possibilities for the total synthesis of target systems of the types described above. Our hope was that some new chemistry could be learned as we struggled with these formidable synthetic problems.

2. An Early Discovery

In formulating a program designed to achieve totally synthetic routes to these natural products, we were guided by several considerations. From a biological standpoint, total synthesis appeared to provide possibilities for the assessment of the consequences of structural modification on activity. In many instances, de novo synthesis rather than "retro-fitting" of the natural product offered the most attractive possibility for achieving subtle changes in stereochemistry.

Of course, the motivation from the standpoint of pure chemistry was the challenge of generating such highly oxygenated structures in the laboratory and in coping with the stereochemical subtleties posed by these targets. Serious chemical issues would inevitably be confronted in addressing such challenges. It seemed not unlikely that a successful solution to these problems could have broader implications for synthesis.

The development of a new synthetic reaction type encouraged our entry into this field. In the classical Diels–Alder reaction, the dienophilic framework is comprised of two carbon centers connected by either a double or a triple bond. In connection with the classical "all carbon" Diels–Alder reaction, we had developed access to a new class of highly activated and highly functionalized siloxydienes.[16] These systems, of which compound **1** is prototypical, emerged as very valuable reagents. They are readily prepared from the corresponding α,β-unsaturated ketones. The electron-donating effects of the 1- and 3-oxygen functions are synergistic, thus serving to endow such dienes with a high degree of reactivity and apparently total regiospecificity vis à vis electron-withdrawing dienophiles. Moreover, the functionality endowed by such dienes to their corresponding cycloadducts can be very nicely exploited in the synthesis of polyfunctional target systems. Several total syntheses of biologically active natural products were achieved in our laboratory via recourse to the activated diene concept in the all-carbon Diels–Alder reaction.[16] Happily, the broad potential of the method has not escaped the attentions of many other laboratories in the pursuit of worthy target systems.[17]

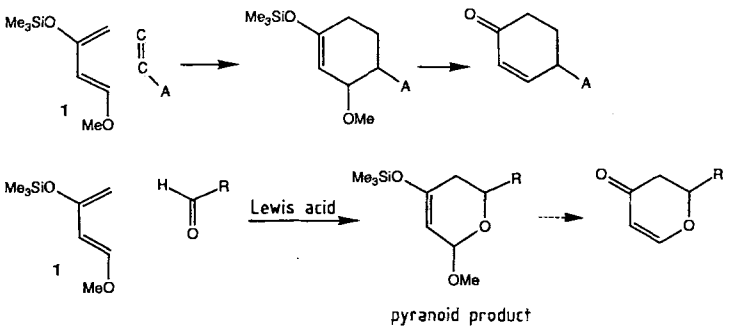

Fig. 4. Above: All-carbon Diels–Alder reaction with siloxydienes; A = activating group (CO, C≡N, NO_2). Below: Lewis acid–catalyzed ring formation of dienes with aldehydes. The overall reaction giving the dihydropyranone is formally a cyclocondensation.

In connection with a fully synthetic route to saccharides, including the higher carbon sugars of the type shown in Figure 2, it was of great interest to investigate the possibility that oxygenated dienes would furnish cycloaddition

products with carbonyl groups, particularly those contained in aldehydes.[18,19] Initial results indicated that such reactions could not be readily effected by strictly thermal means.

However, *James Kerwin*, then a graduate student in our laboratory, found that under the influence of Lewis acids, cyclocondensation of diene **1** with aldehydes can be realized.[20] Other research in our laboratory indicated that, under appropriate catalysis, a remarkably broad range of siloxydienes will react with virtually any aldehyde.[21,22] We had thus developed a concise synthetic entry to pyranoid systems which might serve as intermediates in the synthesis of the pyranose segment of sugars, including complex monosaccharides. Moreover, by exploiting well-known principles and mechanisms of carbohydrate chemistry, the pyranose systems could be converted into furanoses.

3. Stereoselective Routes to Functionalized Pyrans

With a sound route to the basic carbohydrate matrix available, reliable methods were developed to elaborate the interior structure and to incorporate the oxidation and stereochemical patterns found in the monosaccharides of interest. The availability of diverse options proved to be most helpful in being able to approach virtually every member of the series. It was possible to use very heavily oxygenated dienes (e.g., compound **2**), thus producing in the cyclocondensation product the functionality necessary to obtain galactosyl types of sugars.[21] Alternatively, methodology was developed to introduce the oxygen function subsequent to cyclocondensation by oxidation with manganese(III) acetate.[23] In this way, glucose-like stereochemistry is generated at C-4.

Another important reaction was the reduction of the keto group at C-3. When carried out with the reagent system sodium borohydride–Ce(III) chloride (Luche reagent), equatorial alcohols are obtained.[24] Thus, very rapid and highly stereoselective routes to the "glucal" and "galactal" families were available (Fig. 5).

The CC double bond of the galactal and glucal precursors can be functionalized either equatorially or axially at C-2 with high stereoselectivity. Thus, the reaction of *meta*-chloroperbenzoic acid (MCPBA) on the free alcohol (OH unprotected) in the glucal-type system leads to incorporation of a β-hydroxyl group at C-2 (i.e., mannose-like configuration). However, if the hydroxyl group at C-3 is first blocked, MCPBA introduces an α-hydroxyl group (such as is encountered in glucose) at this center. The same stereochemical flexibility is available in the galactal series, thus providing fully synthetic access to either galactose or talose stereochemistry (Fig. 6).

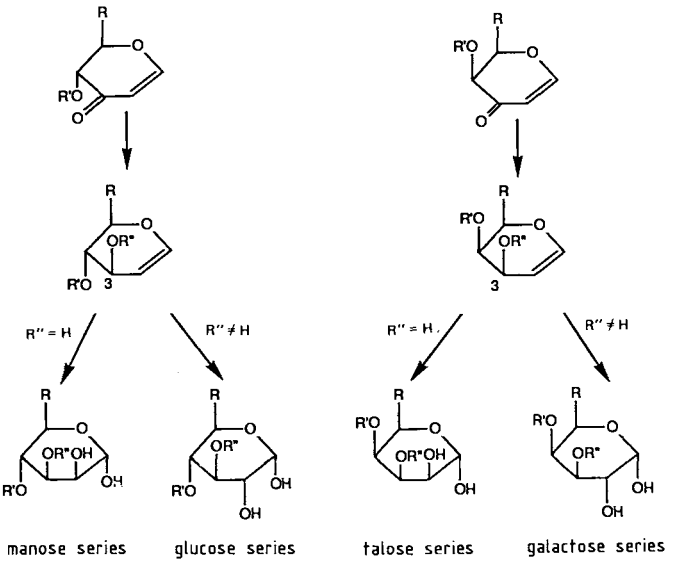

Fig. 6. Totally synthetic approach to some hexoses (for the initial steps, see Fig. 5).

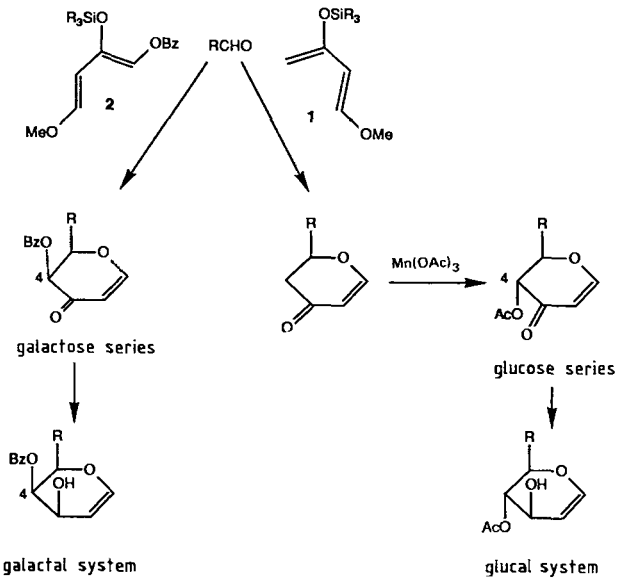

Fig. 5. Syntheses of the galactal and glucal systems. Bz = benzoyl.

As a result of these and other reactions, we had reached the stage where the pyranose (as well as the furanose) rings of the simple sugars could be synthesized in virtually any stereochemical pattern. It also proved possible to delete oxygen atoms and to replace certain oxygen-based centers with nitrogen-based functions. This methodology was used in the synthesis of several novel C_6 monosaccharides such as daunosamine and fucose.[21] Daunosamine is the sugar component of the antitumor agents daunorubicin and adriamycin.[25]

Two applications of the synthesis of aromatic *C*-glycosides are seen in the synthetic routes to the papulacandins[26] (Fig. 7) and the vineomycins[27] (Fig. 8). In the case of the papulacandins, the cyclocondensation of diene **1** with aldehyde **3** generated dihydropyranone **4**. A vinyl group was then introduced by conjugate addition. Product **5** was eventually converted into **6**, setting the stage for an oxidative spiroketalization leading to aglycone **7**.

The route to vineomycin B_2 aglycone passed through ketoaldehyde **8**. Cycloaddition with diene **9** was specific at the aldehyde group. The silyl enol ether functionality of the intermediate cycloadduct **10** was then exploited in a

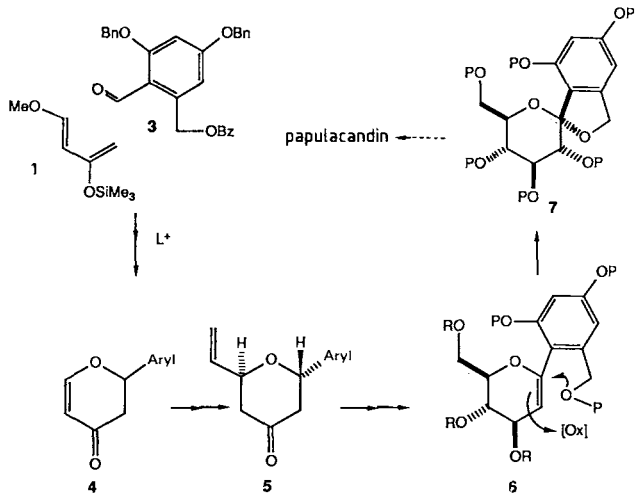

Fig. 7. Syntheses of papulacandins (cf. Fig. 3). Bn = benzyl, P = protecting group, L^+ = Lewis acid ($Yb(fod)_3$).

achieve control over the relationship of the newly emerging stereogenic centers with those present in the original ring. It was through the development of a "menu" of stereoselective reactions to accomplish these chirality extensions that the goal of total synthesis of the complex monosaccharides was furthered.

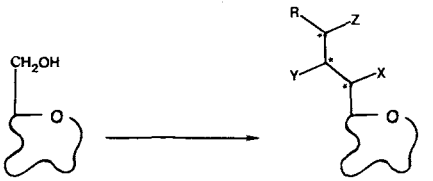

Fig. 9. Generation of chiral centers on the side chain.

One particularly attractive approach focused on a reiterative sequence (Fig. 10). Cyclocondensation of aldehyde

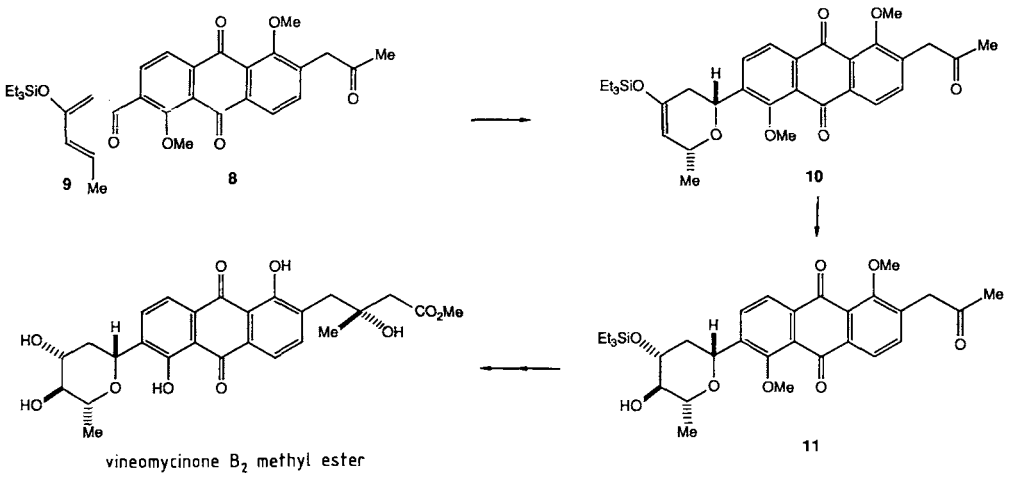

Fig. 8. Synthesis of the aglycone of vineomycin B_2 as its methyl ester (cf. Fig. 3).

hydroboration reaction. *Thus, in two steps (cycloaddition and hydroboration) the entire stereochemistry of the aryl C-glycoside was established (see compound 11).*

4. Chirality Extensions and Reiterative Cyclocondensation

At this juncture, we had reached the stage of a general synthesis of pyranosides, including those linked to an aromatic residue. We could install in the ring virtually any pattern of oxygenation and stereochemistry of interest. However, to make more progress, it would be necessary to move outward from the relatively safe matrix of the pyranoid ring to its less charted side-chain periphery. The challenge lay in developing "lines of communication" between the dissymmetric ring systems and the stereogenic centers that would have to be elaborated on the side chain. This prognosis is set forth in Figure 9, wherein the goal is that of installation of stereogenic centers on a side chain of a pyran ring. Needless to say, it would be necessary to

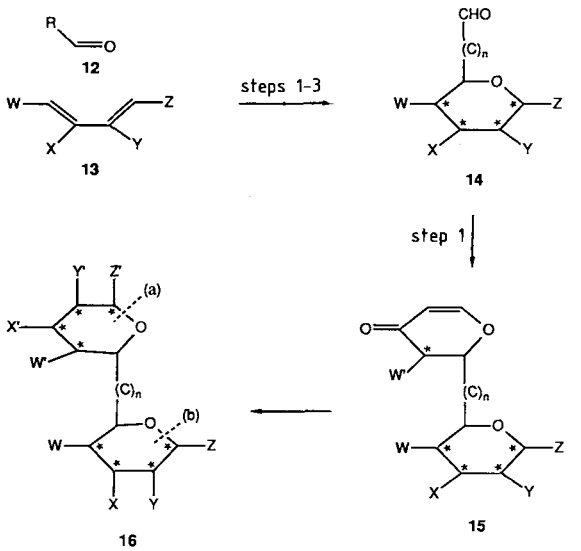

Fig. 10. Iterative cyclocondensation. 1. Cyclocondensation; 2. generation of stereochemistry; 3. formation of an aldehyde group on the side chain.

12 with diene **13** under Lewis acid catalysis would establish the pyranoid matrix. This stage would be followed by the sorts of stereochemical adjustments discussed above. The third stage of the plan called for the unveiling of a new aldehyde on the side chain (see compound **14**). There would then follow another cyclocondensation reaction to give compound **15**. Further adjustments of functionality and stereochemistry would generate a bis-pyranoid system, **16**. In principle, cleavage of either the "a" or "b" bond, or neighboring bonds thereof, might be part of the scheme.

For this program to be attractive, a high degree of diastereofacial selectivity would have to be realized. *The dissymmetric array present in the aldehyde must guide the sense of the subsequent cyclocondensation reaction* (see step **14** → **15**).

This reiterative cyclocondensation strategy was applied to the total syntheses of octosyl acid A,[28] peracetyltunicaminyluracil,[29] and peracetyl-β-methylhikosamide.[30] We first describe the synthesis of octosyl acid A (Fig. 11). The "ribose aldehyde" **18** is itself available by total synthesis[29] via benzoyloxydihydropyranone **17**,[31] which in turn is prepared by cyclocondensation of diene **2** with formaldehyde. For practical purposes, however, we prepared **18** from D-ribose. Cyclocondensation of aldehyde **18** with the parent diene **1** under various forms of Lewis acid catalysis afforded, with very high stereoselectivity, the bis-saccharide **19**.[32] Thus, the ribose ring had induced the sense of chirality at C-1 in the newly fashioned pyranone. The stereogenic center at C-3′ was formed through simple Luche reduction (see compound **20**). At this stage the derived pyranoid ring was cleaved, exposing the octose **21**. After suitable functional group adjustments, the mesyl-substituted cyclic stannane **22** was generated. Fortunately, the otherwise difficult ring closure of the 3-hydroxyl group of the ribose with the C-7 center of the side chain proved to be possible via the tin derivative.[28]

The same dihydropyranone **19** was employed in a total synthesis of peracetyltunicaminyluracil[29] (Fig. 12). In this case, a different pathway was employed. The dihydropyranone ring was cleaved by ozonolysis (bond "a") and subsequent treatment with alkaline hydrogen peroxide (bond "b"). The resultant β-hydroxyacid **23** was converted into the protected aldehyde **24**. Under the influence of the novel binary catalyst system, boron trifluoride etherate-

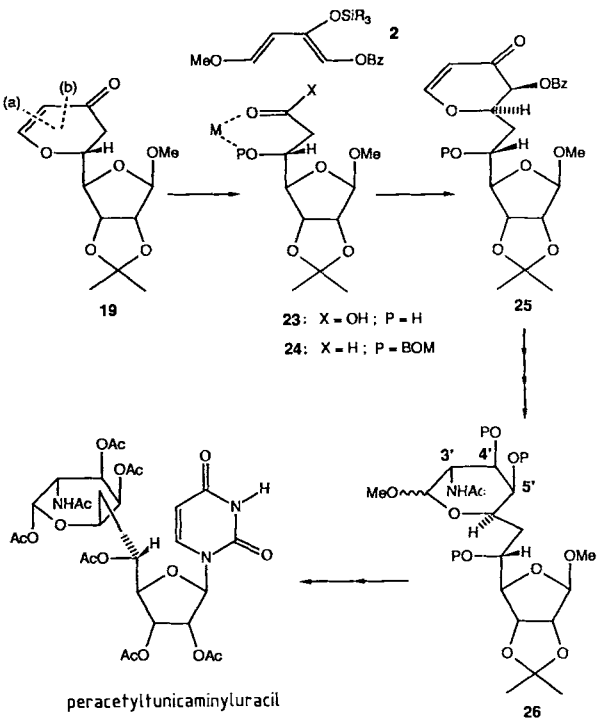

Fig. 12. Synthesis of peracetyltunicaminyluracil. BOM = benzyloxymethyl, M = metal.

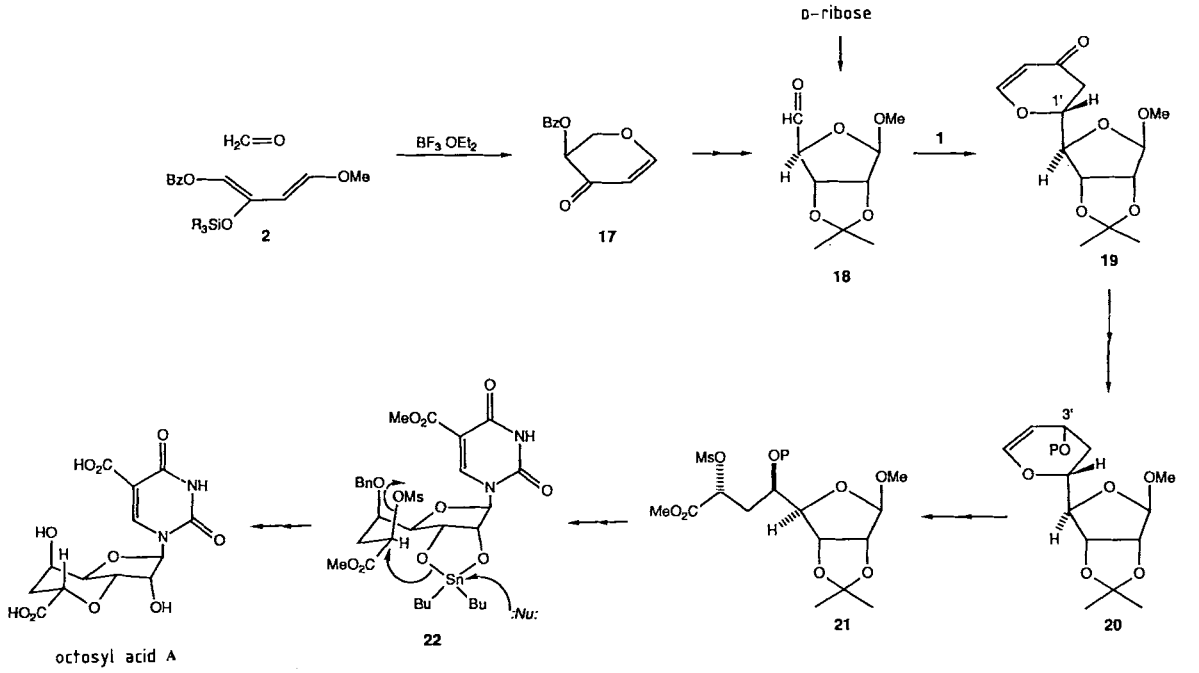

Fig. 11. Synthesis of octosyl acid. Ms = methanesulfonyl.

Ce(III) acetate, the cyclocondensation of aldehyde **24** with diene **2** was highly stereoselective. The sense of the reaction can be rationalized by postulating the chelated conformer of **24** shown in Figure 12. Attack of the diene **2** occurs from the less hindered face. The newly fashioned dihydropyranone ring of **25** was advantageously employed for incorporation of the required functionality and stereochemistry at C-3′ and C-4′ (see compound **26**). Installation of the uracil function in the ribose ring proved to be the most difficult phase of the effort, but eventually was accomplished.[29]

A striking application of this strategy was achieved in the total synthesis of peracetyl-β-methylhikosamide, **36** (see Fig. 13). Cyclocondensation of furfural with diene **2** was followed by highly stereoselective ring functionalization reactions, leading to compound **28**. The furan ring was degraded to eventually produce aldehyde **29**. This same aldehyde, in optically active form, is much more readily obtained from D-galactose.

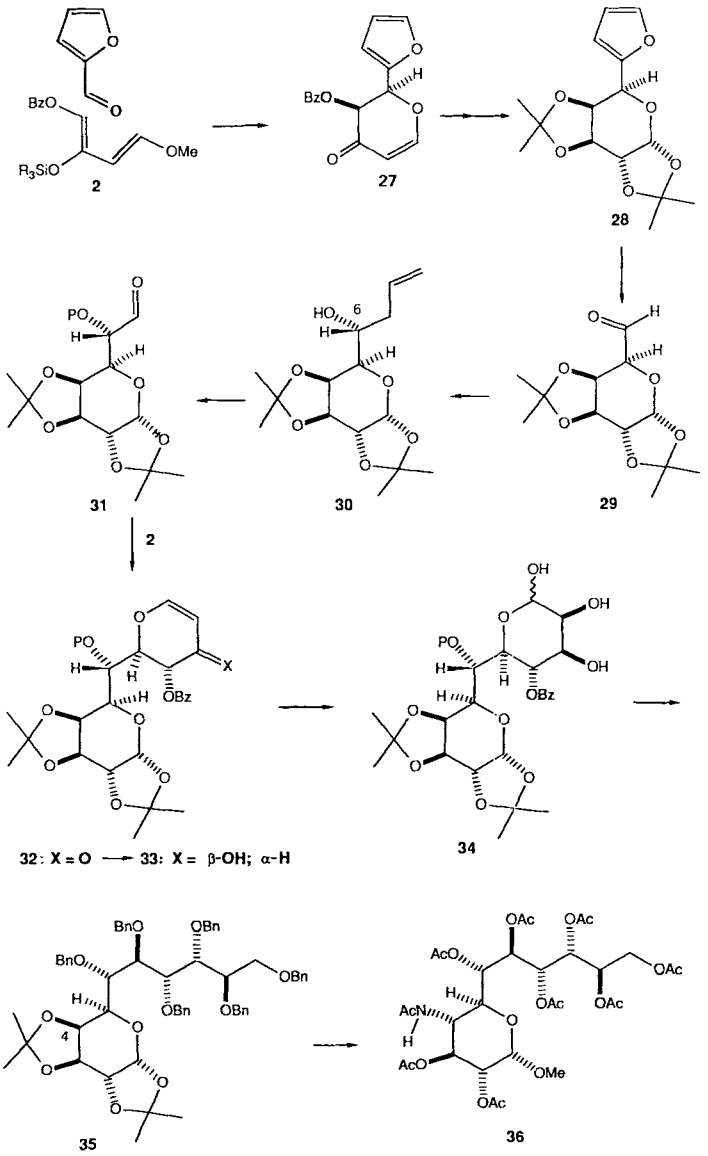

Fig. 13. Synthesis of peracetyl-β-methylhikosamide **36**. P = benzyl.

In the next step, the configuration of C-6 was properly adjusted, taking advantage of a very stereoselective addition of allyltrimethylsilane to the aldehyde function under the influence of boron trifluoride etherate (cf. Fig. 14). The homoallylic alcohol functionality of compound **30** was converted into the α-benzyloxyaldehyde system **31**. Cyclocondensation of this aldehyde with diene **2** via magnesium bromide catalysis under apparent chelation control afforded the *trans*-disubstituted dihydropyranone **32**. Reduction of this compound with $NaBH_4$–$CeCl_3$ led to the glucal-like system **33**. Because of the influence of the free 3-hydroxyl group, epoxidation occurs via *syn* attack on the double bond leading to the D-*manno* configuration in the newly fashioned pyranose system (see compound **34**). Reductive cleavage of the hemiacetal linkage, followed by protection gave the hexabenzyl system **35** with *the proper configuration at nine contiguous oxygenated carbon atoms.* By suitable manipulations, the axial 4-hydroxyl group was selectively exposed. Inversion of the derived mesylate with sodium azide set the stage for completion of the synthesis of system **36**.

It is appropriate to point out that in both the tunicaminyluracil and hikosamine syntheses we were exploring new notions concerning the transmission of stereochemical information. In these syntheses all stereochemical relationships were achieved by inductions, which were accomplished without recourse to artificial auxiliaries. There is also no recourse to coupling of components with prearranged chirality. All stereochemistry flows from the mechanistic character of the carbon–carbon bond forming and oxidation-reduction reactions (see Section 5).

We have also explored another type of chirality extension reaction involving nucleophilic addition of allyltrimethylsilane to several dialdoses under the influence of various Lewis acids. Some remarkable discoveries were registered[33] (Fig. 14). First, this Sakurai[34] reaction is highly stereoselective. Thus, with the ribose aldehyde **18**, either the (5*R*) epimer **37a** or the (5*S*) epimer **37b** can be ob-

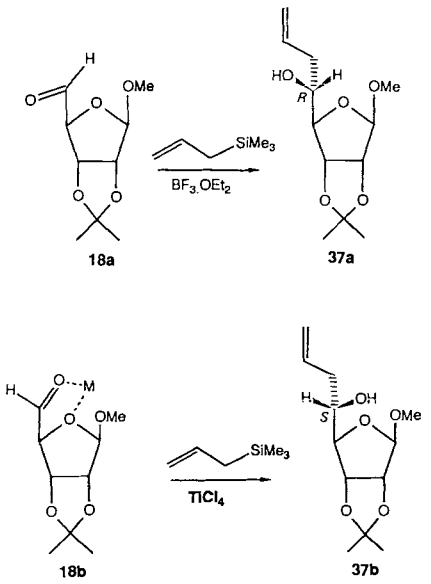

Fig. 14. Influence of the catalyst on the configuration at C-5 of compound **37**.

tained with high stereoselectivity (> 10 : 1) through the simple expedient of changing the Lewis acid catalyst from boron trifluoride etherate to titanium tetrachloride. Product **37a** corresponds to that expected from attack in the Cram-Felkin[35a,b] sense, while **37b** would be the one produced by attack of the allyl group from the less hindered face of the *syn*-conformer **18b**. That titanium tetrachloride should favor the reactive *syn*-conformer **18b** seems reasonably ascribable to chelation. Similar selectivities have been observed with the galactose aldehyde (see **29**→**30**). It should be noted that the product **37a** has the configuration at C-5 that is appropriate for reaching intermediate **23** used in the tunicaminyluracil synthesis. This conversion has in fact been accomplished.[36]

5. Applications to Lincosamine, KDO, and NANA

We turned next to the total syntheses of lincosamine,[37] KDO,[38] and NANA[39] (see Fig. 2) from non-carbohydrate sources. Our strategy at the outset was to concern ourselves with issues of functionality and relative stereochemistry. These matters have now been solved in the context of our syntheses of the racemates. It is not difficult to imagine how the chemistry described below can be applied to the preparation of the required enantiomers by starting with naturally derived, optically pure starting materials.

In the first stage of these syntheses (Fig. 15), suitable aldehydes were combined with appropriate dienes to afford dihydropyranones which were already well advanced toward the target systems. The pyranoids were subsequently

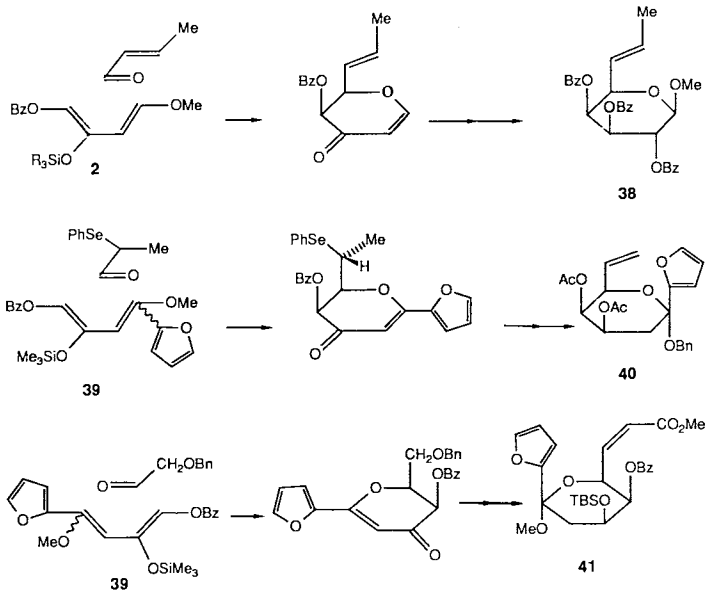

Fig. 15. Synthesis of the enepyranosides **38**, **40**, and **41**. TBS = *tert*-butyldimethylsilyl.

functionalized using stereoselective reactions of the type previously discussed, thereby affording the enepyranosides **38**, **40**, and **41**. We now addressed the question of stereoselectivity in the attack of various electrophiles on these enepyranosides.

Fortunately, in each case we were able to find highly stereoselective reactions of these olefinic linkages with electrophiles. These findings are part of a broader investigation of this type of stereochemical question.[40] Pending accumulation of a more comprehensive collection of data and a satisfactory correlative theory, extrapolations beyond the cases shown here are not without risk.

Two highly stereospecific reactions were observed upon treatment of enepyranoside **38** with osmium tetroxide and with aqueous *N*-bromosuccinimide (Fig. 16). The former

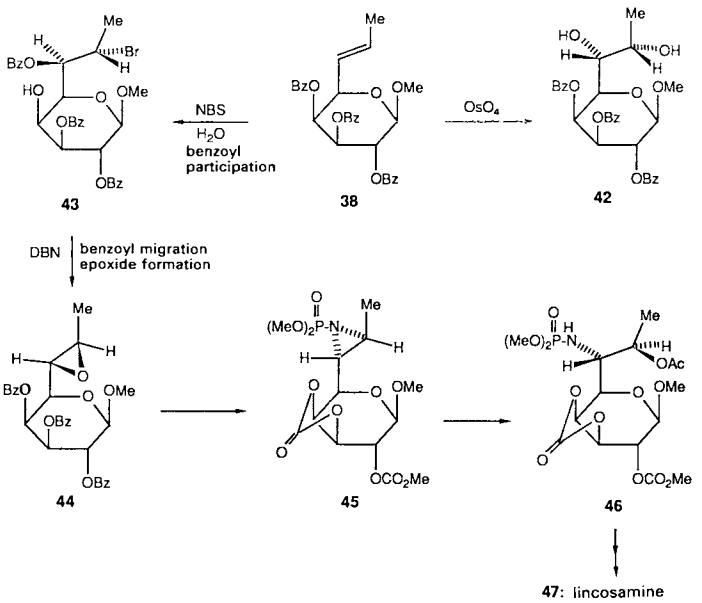

Fig. 16. Synthesis of lincosamine **47** (see Fig. 2 for formula). NBS = *N*-bromosuccinimide; DBN = diazabicyclononane.

reaction gave quite cleanly compound **42**. The latter reaction, proceeding in the same stereochemical sense, afforded the rearranged hydroxybenzoate **43**. Conversion of diol **42** into the lincosamine series proved to be unattainable. However, success was achieved via compound **43**, which reacts with diazabicyclononane to afford, by another rearrangement, the epoxide **44**. The latter was converted into the phosphoaziridine **45** by a lengthy but logical series of transformations. Solvolytic inversion of **45** at C-7 afforded **46** and, eventually, fully synthetic access to α-methyllincosamide.[37]

We turn now to the synthesis of KDO (Fig. 17). Hydroxylation of the vinylpyranoside **40** with osmium tetroxide afforded, in a highly stereoselective reaction, the diol **48** with the side-chain stereochemistry corresponding to

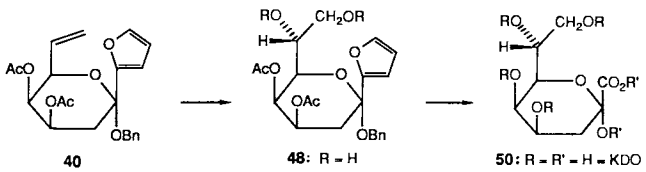

Fig. 17. Synthesis of *rac*-3-deoxy-*manno*-2-octulosonic acid (KDO) **50**.

KDO. The furan surrogate had served us well. It had conferred high reactivity to diene **39** in the cyclocondensation reaction, facilitated construction of the benzylketosidic linkage en route to compound **40**, and withstood a variety of transformations which might have been problematic with a carboxyl (or alkoxycarbonyl) group at C-1.

In the terminal phase of the KDO synthesis, compound **49**, readily derived from diol **48**, underwent oxidation and deacetylation through the action of ruthenium dioxide and sodium metaperiodate. Racemic KDO, **50**, was thereby obtained.[38]

To reach NANA (Fig. 18), the sense of the hydroxylation reaction required was opposite to that observed in the case of pyranosides **38** and **40**. The α,β-unsaturated ester **41** was employed for two reasons. It was conjectured that the steric consequence of the (*Z*) configuration and the electronic effect of sharply attenuating the nucleophilicity of the alkene would converge to change the diastereofacial sense of attack of the osmium tetroxide. Fortunately, this turned out to be the case, in that a virtually stereospecific reaction took place, affording diol **51**. Shortly thereafter, through a sequence that included reduction of the ester group at C-9 and oxidation of the furyl group, compound **52** became available to us.

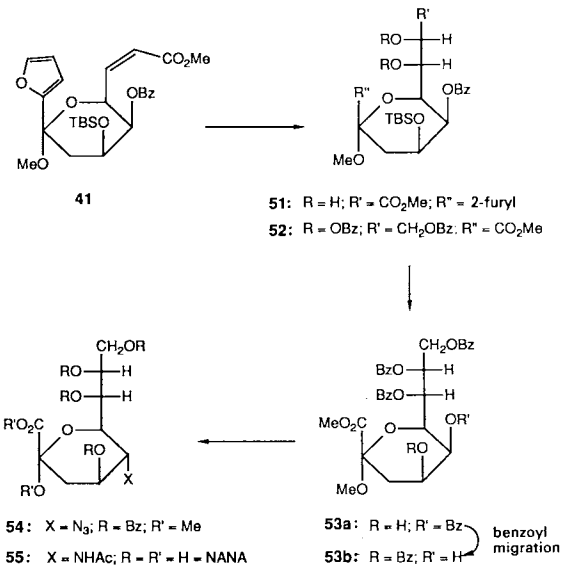

Fig. 18. Synthesis of *rac-N*-acetylneuraminic acid (NANA) **55**.

It was not purely by chance that we now found ourselves with a *tert*-butyldimethylsilyl-protected oxygen at C-4 (equatorial) and a benzoyloxy group at C-5 (axial). *Cleavage of the silyl function from C-4 set into motion the expected migration of the benzoyl group from the C-5 oxygen to the C-4 oxygen, thus specifically liberating the axial 5-OH group.* After suitable activation (by mesylation) and displacement (by azidolysis) the equatorial azide **54** was in hand. Shortly thereafter, fully synthetic NANA **55** took up its place of honor in our collection of fully synthetic complex monosaccharides.

6. Outlook

As indicated above, our involvement with the higher carbon monosaccharides was spurred by the challenges associated with synthesizing such compounds and by the opportunities that they presented to develop new chemistry. Of course, many of the syntheses leave unexplored significant issues of process improvement. Moreover, in some instances we have left unaddressed the matter of synthesizing the biologically active enantiomer rather than the racemate. We do not view this as posing a particularly difficult problem. There are available for this purpose many enantiomerically pure aldehydes of relevance. Since a great deal has been learned about the facial selectivity of the cyclocondensation reaction, some excellent prospects can be pursued for communicating the dissymmetry of the chirons to the emerging saccharide.

The really serious challenge that engages our attentions involves building upon the chemistry learned in this program to produce new compounds of value. It is likely that this goal would be served by inserting the complex monosaccharides into oligosaccharide settings similar to those in which they are housed in nature. Particularly fascinating possibilities in this regard present themselves in the KDO and NANA areas. Our further research in the carbohydrate domain will attempt to deal with this type of problem and opportunity.

Support for this program was provided by various grants from the U. S. Public Health Service and from the Merck Foundation. A special sense of gratitude and indebtedness is extended to the creative and resourceful colleagues in our laboratory at Yale. Some worked out the chemistry of the cyclocondensation reactions. Others worked on particular total syntheses. Their names are individually identified in the various publications cited above. It is to their vision and meticulous experimentation that we dedicate this article.

Received: August 14, 1986 [A 602 IE]
German version: *Angew. Chem. 99* (1987) 15

[1] J. F. Kennedy, C. A. White: *Bioactive Carbohydrates*, Ellis Horwood, Chichester, England 1983.
[2] N. Sharon, *Sci. Am. 243* (1980) No. 11, p. 80; *Specktrum Wiss. 1981*, No. 1, p. 70.
[3] See, for example: D. A. L. Davies, *Biochem. J. 67* (1957) 253; S. Umezawa, *Adv. Carbohydr. Chem. Biochem. 20* (1974) 111.
[4] R. J. Suhadolnik: *Nucleosides as Biological Probes*, Wiley, New York 1979.
[5] B. J. Magerlein in D. Pearlman (Ed.): *Structure Activity Relationships Among the Semisynthetic Antibiotics*, Academic Press, New York 1977, p. 601-650.
[6] a) F. M. Unger, *Adv. Carbohydr. Chem. Biochem. 38* (1981) 323; b) L. Anderson, F. M. Unger: *Bacterial Lipopolysaccharides: Structure, Synthesis and Biological Activities (ACS Symp. Ser. No. 231)*, American Chemical Society, Washington, DC 1983.
[7] K. Isono, P. F. Crain, J. A. McCloskey, *J. Am. Chem. Soc. 97* (1975) 943.
[8] a) T. Azuma, K. Isono, *Chem. Pharm. Bull. 25* (1977) 3347; b) A. Bloch, *Biochem. Biophys. Res. Commun. 64* (1975) 210.
[9] A. Gottschalk, *Nature (London) 167* (1951) 845; b) E. Klenk, *Hoppe Seylers Z. Physiol. Chem. 268* (1941) 50.
[10] a) R. Schauer, *Adv. Carbohydr. Chem. Biochem. 40* (1982) 131; b) R. Schauer: *Sialic Acids*, Springer, Vienna/New York 1982.

[11] a) R. L. Hamill, M. H. Hoehn, *J. Antibiot. Ser. A 17* (1964) 100; b) M. Vuilhorgne, S. Ennifar, B. C. Das, J. W. Paschal, R. Nagarajan, E. W. Hagaman, E. Wenkert, *J. Org. Chem. 42* (1977) 3289; c) K. Uchida, H. Wolf, *J. Antibiot. 27* (1974) 783; d) A. Gonzalez, G. D. Vazquez, A. Jimenez, *Biochem. Biophys. Acta 561* (1979) 403; e) K. Uchida, *Agric. Biol. Chem. 40* (1976) 395.

[12] a) A. Takatsuki, K. Arima, G. Tamura, *J. Antibiot. 24* (1971) 215; b) A. Takatsuki, G. Tamura, *ibid. 24* (1971) 224, 232, 785; c) T. Ito, A. Takatsuki, K. Kawamura, K. Sato, G. Tamura, *Agric. Biol. Chem. 44* (1980) 695, and references cited therein.

[13] a) A. D. Elbein, *Trends Biochem. Sci. Pers. Ed. 6* (1981) 219; b) R. T. Schwarz, R. Datema, *ibid. 5* (1980) 65; c) K. Eckardt, *J. Nat. Prod. 46* (1983) 544; d) M. J. Morin, R. J. Bernacki, *J. Cancer Res. 43* (1983) 1669.

[14] a) S. Omura, H. Tanaka, R. Oieva, J. Awaya, R. Masura, K. Tanaka, *J. Antibiot. 30* (1977) 908; b) N. Imamura, K. Kakinuma, N. Ikekawa, H. Tanaka, S. Omura, *ibid. 34* (1981) 1517; c) K. Ohta, K. Kamiya, *J. Chem. Soc. Chem. Commun. 1981*, 154.

[15] a) P. Traxler, H. Fritz, W. F. Richter, *Helv. Chim. Acta 60* (1977) 578; b) P. Traxler, H. Fritz, H. Fuhrer, W. J. Richter, *J. Antibiot. 33* (1980) 967; c) G. Rommele, P. Traxler, W. Wehrli, *ibid. 36* (1983) 1539.

[16] S. J. Danishefsky, *Acc. Chem. Res. 14* (1981) 400.

[17] M. Petrzilka, J. I. Grayson, *Synthesis 1981*, 753.

[18] For cyclocondensations of the specially activated glyoxylates, see: H. C. J. G. Van Balen, A. A. Broekhuis, J. W. Scheeren, R. J. F. Nivard, *Recl. Trav. Chim. Pays Bas 98* (1979) 36; R. W. Aben, J. W. Scheeren, *J. Chem. Soc. Perkin Trans. 1* 1979, 3132.

[19] For the application of high pressure to the cycloaddition reaction, see: J. Jurczak, M. Chmiekwski, S. Filipek, *Synthesis 1979*, 41.

[20] S. J. Danishefsky, J. F. Kerwin, Jr., S. J. Kobayashi, *J. Am. Chem. Soc. 104* (1982) 358.

[21] S. J. Danishefsky, C. J. Maring, *J. Am. Chem. Soc. 107* (1985) 1269.

[22] M. Bednarski, S. J. Danishefsky, *J. Am. Chem. Soc. 105* (1983) 3716.

[23] S. J. Danishefsky, M. Bednarski, *Tetrahedron Lett. 26* (1985) 3411.

[24] J. L. Luche, A. L. Gemal, *J. Am. Chem. Soc. 101* (1979) 5848.

[25] F. Arcamone, *Lloydia 40* (1977) 45.

[26] S. J. Danishefsky, G. B. Phillips, M. Ciufolini, *Carbohydr. Res.*, in press.

[27] S. J. Danishefsky, B. J. Uang, G. Quallich, *J. Am. Chem. Soc. 107* (1985) 1285.

[28] S. J. Danishefsky, R. Hungate, *J. Am. Chem. Soc. 108* (1986) 2486.

[29] S. J. Danishefsky, M. R. Barbachyn, *J. Am. Chem. Soc. 107* (1985) 7761.

[30] S. J. Danishefsky, C. J. Maring, *J. Am. Chem. Soc. 107* (1985) 7762.

[31] The synthesis of racemic ribose was carried out by *J. Y. Lee* of our laboratory.

[32] S. J. Danishefsky, C. J. Maring, M. R. Barbachyn, B. E. Segmuller, *J. Org. Chem. 49* (1984) 4564.

[33] S. J. Danishefsky, M. P. DeNinno, *Tetrahedron Lett. 26* (1985) 823.

[34] A. Hosomi, H. Sakurai, *Tetrahedron Lett. 1976*, 1295.

[35] a) D. J. Cram, F. A. A. Elhafez, *J. Am. Chem. Soc. 74* (1952) 5828; b) M. Cherest, H. Felkin, N. Prudent, *Tetrahedron Lett. 1968*, 2199.

[36] M. P. DeNinno, unpublished results.

[37] S. J. Danishefsky, E. Larson, J. P. Springer, *J. Am. Chem. Soc. 107* (1980) 1274.

[38] S. J. Danishefsky, W. H. Pearson, B. E. Segmuller, *J. Am. Chem. Soc. 107* (1985) 1280.

[39] S. J. Danishefsky, M. P. DeNinno, *J. Org. Chem. 51* (1986) 2615.

[40] S. J. Danishefsky, M. P. DeNinno, G. B. Phillips, R. E. Zelle, P. A. Lartey, *Tetrahedron 42* (1986) 2809.

Stereoselective Aldol Reactions with α-Unsubstituted Chiral Enolates

New Synthetic Methods (64)

By Manfred Braun*

Dedicated to Professor George Büchi on the occasion of his 65th birthday

The aldol reaction is among the most important methods of forming carbon-carbon bonds. The addition of an enolate to an aldehyde leads to the formation of at least one chiral center. In the case of α-substituted enolates it has to a large extent been possible to control the product stereochemistry, while the aldol reaction of α-unsubstituted chiral enolates was for many years a "problem child" for synthetic chemists because of its insufficient stereoselectivity. Progress in this area has only been made in the last few years using either new chiral auxiliaries or alternatives to the aldol reaction.

1. Introduction

The aldol reaction, the classical method for the construction of carbon chains with oxygen functionality in 1,3-positions,[1] has undergone a remarkable renaissance in the last twenty years. The impulse for this development was given by the increasingly ambitious synthetic goals which were provided in particular by the macrolide and polyether antibiotics with their many functional groups. New and particularly *stereoselective* variants of the aldol reaction have proved to provide the key to success.[2]

On the assumption that a carbonyl compound **1a** with a substituent Y in the α-position functions solely as the C–H acid component (forming the enolate **2a**), and that an aldehyde RCHO functions only as the carbonyl-active component,[3] the four stereoisomeric adducts **3a**, **b** and **4a**, **b** can be formed. Using suitable metals M and optimized reaction conditions, the preparation of either the *syn*- or *anti*-diastereomers[4] **3** or **4** is possible. In addition, the use of chiral auxiliaries X* permits further differentiation between **3a** and **3b** or **4a** and **4b**, so that each of the products **3a**, **3b**, **4a** and **4b** can be obtained as an almost pure enantiomer.[2,5]

When instead of the reagents **2a** the α-unsubstituted enolates **2b** (which can be obtained by deprotonation of acetyl derivatives **1b**) are used, the situation is apparently simplified in that now only one new chiral center is formed, so that the problem of *syn-anti* isomerism ("simple diastereoselection"[2c]) is no longer present. However, the transition from the α-substituted enolate **2a** to the unsubstituted chiral reagent **2b** is unexpectedly accompanied by the almost total loss of the ability of the latter to discriminate between the two enantiotopic sides of an aldehyde ("enantiofacial differentiation"[6]), so that the specific preparation of one of the diastereomers **5a** and **5b** is not possible. While for example the boron enolate **6a** reacts with isobutyraldehyde to give almost solely the product **7**, the amount of the other three isomers being in total less than one percent, the addition of the α-unsubstituted enolate

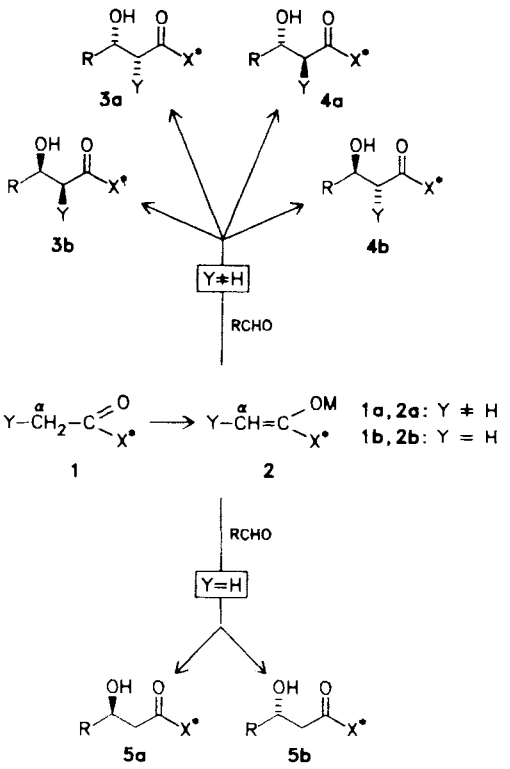

6b, using the same metal and the same chiral auxiliary, to the same aldehyde gives a 52:48 mixture of the hydroxyketones **8** and **9**.[7,8] Similar observations have been made with chiral ketone and amide enolates[9–13] and with deprotonated dihydrooxazoles[14] and hydrazones.[15]

The key role played by the α-substituent in enantiofacial differentiation is not easily understood. In the case of the kinetically controlled aldol reaction of the boron enolates **6a** and **6b**, an interpretation has been provided by *Evans* et al.[2d,e] It is based on the Zimmerman-Traxler model[16] of a six-membered transition state with a chair conformation, the aldehyde substituent R occupying an equatorial position. It appears plausible that the approach of the aldehyde to the enolate takes place from that side which faces away from the isopropyl residue of the oxazolidone, so that of the four diastereomeric transition states **10**–**13**

[*] Prof. Dr. M. Braun
Institut für Organische Chemie der Universität
Universitätsstrasse 1, D-4000 Düsseldorf (FRG)

 © VCH Verlagsgesellschaft mbH, D-6940 Weinheim, 1987 0570-0833/87/0101-0024 $ 02.50/0

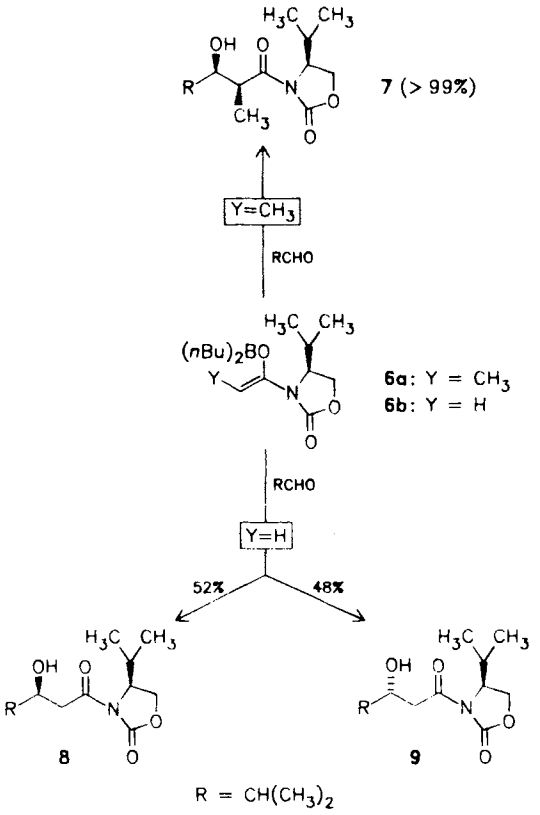

only the two (**10** and **13**) with the isopropyl group in "*exo*" position must be taken into consideration. Stereoselectivity is only observed when one of them is clearly favored. In the case of the propionic enolate **6a** this seems to

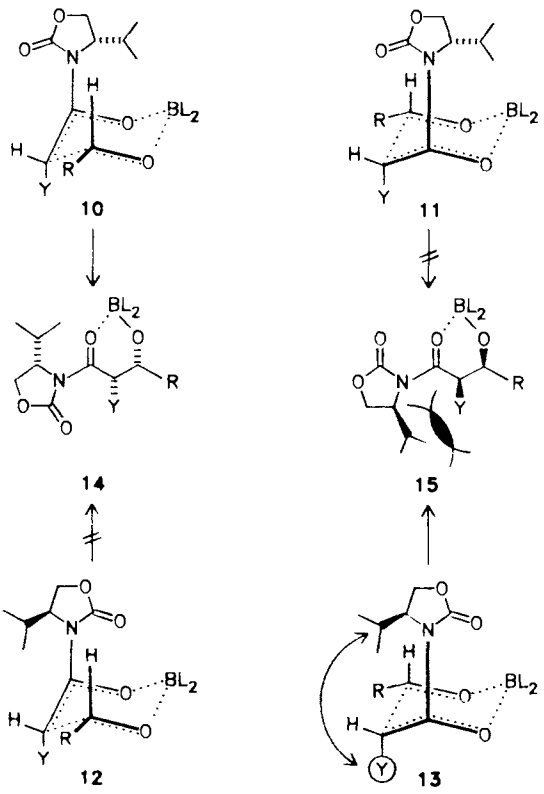

L = *n*-C_4H_9; **a**: Y = CH_3; **b**: Y = H

be the case: the mutual repulsion of the isopropyl group and the substituent Y must be responsible for the fact that the transition state **10a** is favored, so that the borinate **14a** is formed. In contrast, starting from the unsubstituted enolate **6b** no appreciable steric hindrance is present in the chair form **13b**, so that neither of the transition states **10b** and **13b** is particularly favored; thus the chelates **14b** and **15b** are formed in almost equal amounts.

Another explanation for the non-existent enantiofacial selectivity of α-unsubstituted chiral carbonyl compounds, which can also be extended to include ketone and ester enolates, takes into account that boat- or twist-shaped transition states can successfully compete with the chair model.[2c,e] *Hoffmann*, *Cremer* et al. have recently pointed out that a twist boat **17b** can easily be formed from the U-configuration of the enolate **16b**, while the intermediate with the zigzag conformation **16a** is the suitable precursor for the chair-type transition state **17a**.[17]

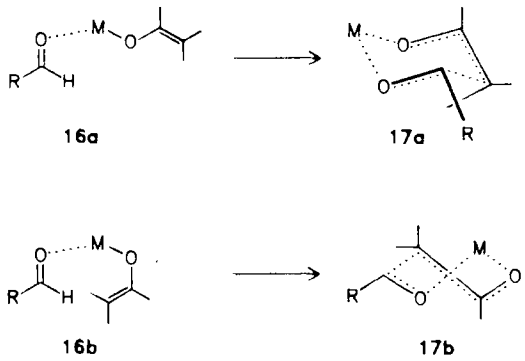

STO-3G calculations for the boron enolates **18** and **19** show that for the (*Z*)-enolate of butanone the W-form **18b** is clearly more stable (by 3–5 kcal/mol) than the U-conformation **18a**. In the case of the acetone derivative **19** the α-substituent is not present, and as a result the corresponding arrangement **19b** is no longer favored, but is in fact somewhat less stable (by 1–2 kcal/mol) than the U-conformer **19a**.[17,18]

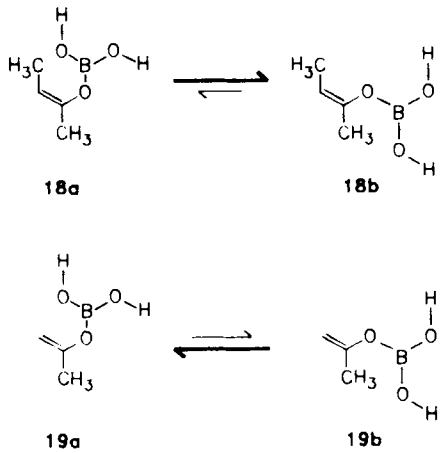

Thus it is conceivable that in aldol additions of α-unsubstituted enolates both the chair and the twist transition states are involved, as they have almost the same activation

energy. When, as indicated in formulas **20a** and **20b**, the enantiotopic faces of an aldehyde are in each case attacked preferably, product mixtures result in which the diastereomers **5a** and **5b** are formed in almost equal proportions.

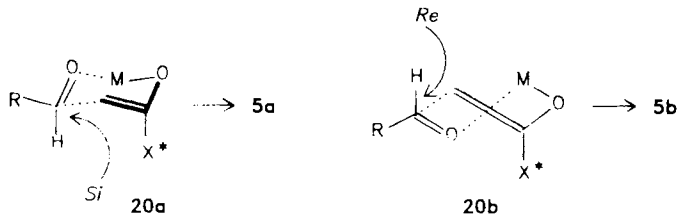

Further investigations on the structure and reactivity of these metal enolates are however necessary in order to support such interpretations of the non-existent stereodifferentiation. Here we shall discuss the progress which has recently been made in the directed *synthesis* of enantiomerically pure β-hydroxycarbonyl compounds of the type **21** and *ent*-**21** using new modifications of the aldol reaction.[19]

2. The Addition of Chiral Metal Enolates to Aldehydes and Unsymmetrical Ketones

2.1. Reversible Introduction of an α-Substituent

The incorporation of an α-substituent which serves to guarantee good stereoselectivity and which can be removed after carrying out the aldol addition is an obvious solution. Thus when the derivative **22** of (methylthio)acetic acid is converted into its boron enolate and allowed to react with aldehydes, the main products are the *syn*-diastereomers **23** (in analogy to the corresponding reaction of the propionic reagent **6a**). Desulfurization using Raney nickel, followed by saponification, gives β-hydroxycarboxylic acids **24** with an optical purity of 85-99%; the chemical yields are reported to be good.[7]

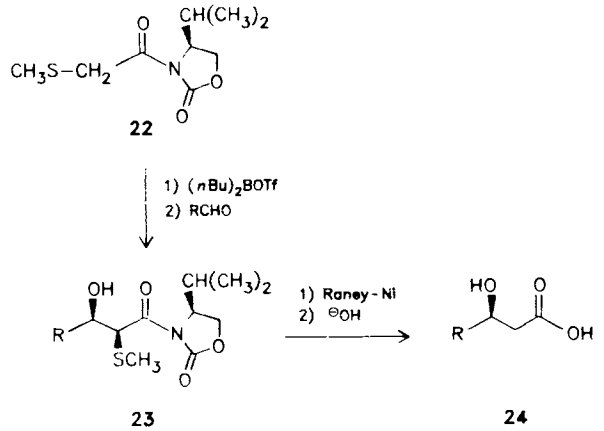

R = $(CH_3)_2CH$, n-C_3H_7, CH_3, C_6H_5; Tf = CF_3SO_2

Furthermore, an α-substituent can also serve as a carrier of the chiral information. Thus *Solladié* and *Mioskowski* observed several years ago[20] that the α-sulfinic ester **26** adds (after deprotonation by a Grignard reagent) diastereoselectively to aldehydes. Reductive removal of the sulfinyl function from the crude products gives the β-hydroxyesters **28** in chemical yields of 50-85% (enantiomeric excess as shown).[21-23]

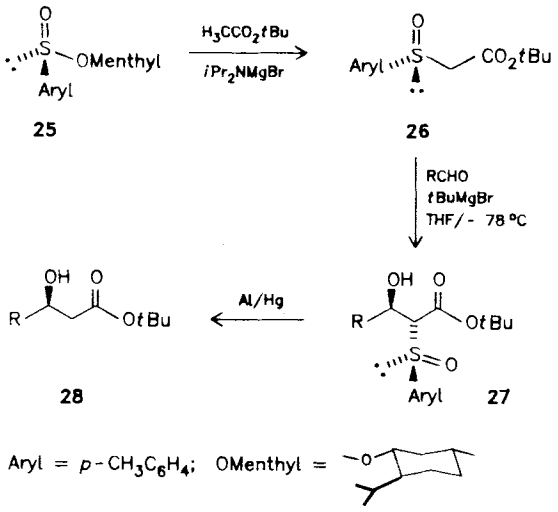

Aryl = p-$CH_3C_6H_4$; OMenthyl =

R = C_6H_5, 91% *ee*; R = n-C_7H_{15}, 86% *ee*; R = n-C_8H_{17}, 87% *ee*; R = n-$C_{11}H_{23}$, 80% *ee*; R = nPr–C≡C, 80% *ee*; R = nBu–C≡C, 84% *ee*; R = C_6H_5–C≡C, >90% *ee*. THF = tetrahydrofuran

The favored formation of the excess diastereomer **27** is explained by the transition state model **30**, in which the magnesium atom is chelated by the enolate, sulfoxide and carbonyl oxygens. It appears plausible that the approach of the aldehyde to the enolate **29**[24] occurs from the side of the non-bonding electron pair of the sulfur atom (opposite to the aryl residue) and that the group R of the aldehyde occupies a position *anti* to the sulfinyl substituent.[21]

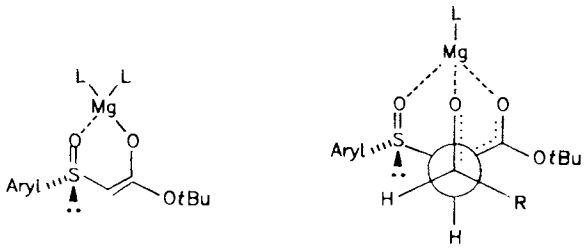

Aryl = p-$CH_3C_6H_4$; L = Ligand

The ester **26** can also be added to unsymmetrical ketones, whereby the degree of stereoselectivity varies greatly from substrate to substrate.[22,23]

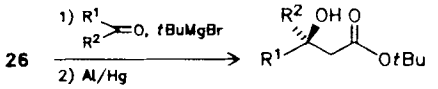

R^1 = C_6H_5, R^2 = CH_3, 68% *ee*; R^1 = CF_3, R^2 = C_6H_5, 20% *ee*; R^1 = *cyclo*-C_6H_{11}, R^2 (in this case and in the following compounds) = CH_3, 95% *ee*; R^1 = $CO_2C_2H_5$, 8% *ee*; R^2 = CH_2CH_2OAc, 40% *ee*; R^1 = nPr–C≡C, 48% *ee*; R^1 = n-C_5H_{11}–C≡C, 36%

This method has also been used successfully in a total synthesis of maytansin **33**:[25] when the carbon chain of the aldehyde **31** is lengthened by introducing an acetate residue, a 92:8 mixture of the diastereomers **32a** and **32b** is obtained. The main product **32a** can then be converted in several steps into the macrocycle **33**.

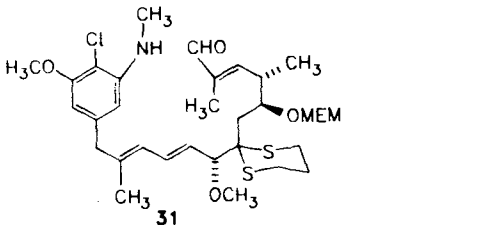

31

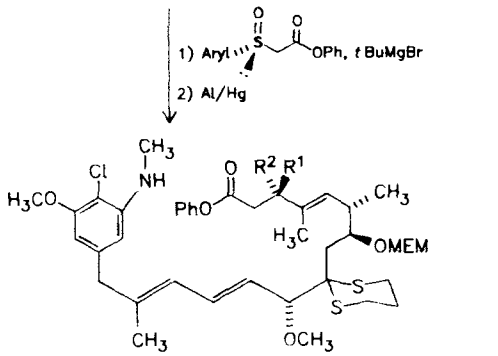

32a: R^1 = H, R^2 = OH; **32b**: R^1 = OH, R^2 = H

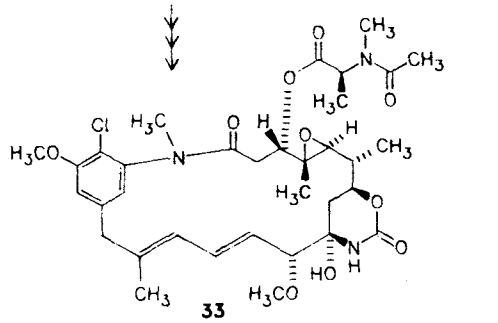

33

Aryl = *p*-$CH_3C_6H_4$
MEM = $CH_2O(CH_2)_2OCH_3$

The stereoselectivity of the Solladié-Mioskowski reagent **26**, which can be prepared from the enantiomerically pure menthyl sulfinate **25**, is impressive. This method has, however, the disadvantage that the chirality of the auxiliary reagent is destroyed subsequent to carbon–carbon bond formation. Utilizing the same concept, sulfinyl-substituted acetamides **34a**,[26] dihydrooxazoles **34b**[27] and hydrazones **34c**[28] can be converted with varying degrees of stereoselectivity into the corresponding β-hydroxycarbonyl compounds.

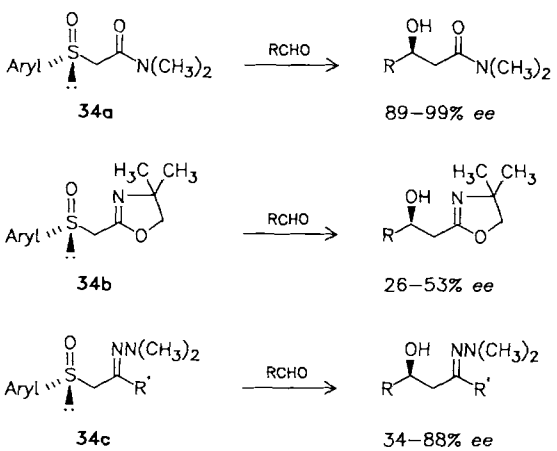

34a 89–99% *ee*

34b 26–53% *ee*

34c 34–88% *ee*

Two additional reaction steps, those involving introduction and removal of the α-substituent, are the price paid for the often remarkable chemical and in particular optical yields which can be attained using this method.

2.2. Enolates without an α-Substituent

2.2.1. Chiral Complexing Agents

Chiral auxiliaries which are not covalently bonded are often used in asymmetric syntheses, since they can normally be readily separated from the product.[29] Thus *Guetté* et al. studied the Reformatsky reaction in the presence of the bidentate ligand (−)-sparteine.[30] Depending on the type of carbonyl-active component used, large variations in the enantioselectivity are observed, as shown by the examples cited (benzaldehyde and acetophenone); a further disadvantage is that the chemical yields are low (21 and 16% respectively).

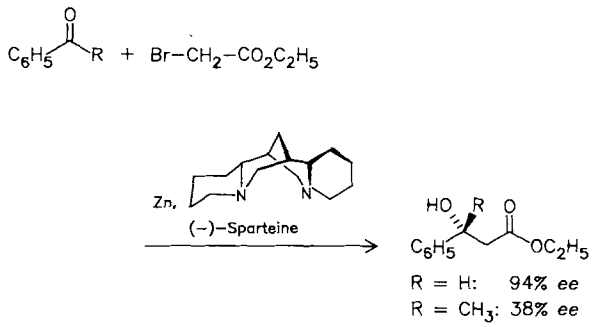

R = H: 94% *ee*
R = CH_3: 38% *ee*

The proline derivative **36** appears to be superior to the alkaloid sparteine: when the tin enolate of the *N*-acetylthiazolidine thione **35** is added to aldehydes in the presence of the diamine **36**, the products **37** can be obtained with enantiomeric excesses between 65 and over 90%. Their hydrolysis to β-hydroxycarboxylic acids **24** in corresponding optical purity is possible.[31] Similarly, thioesters of acetic acid can (also via tin enolates) be added enantioselectively to aldehydes (58–80% *ee*).[32]

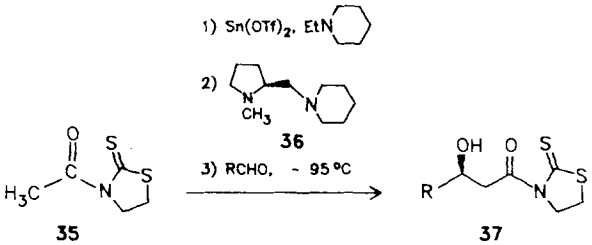

R = C_6H_5, 65% *ee*; R = $(CH_3)_2CH$, >90% *ee*; R = $C_6H_5CH_2CH_2$, >90% *ee*; R = C_2H_5, 90% *ee*; R = *cyclo*-C_6H_{11}, 88% *ee*; R = *n*-C_6H_{11}, 90% *ee*

In contrast to some of the methods presented in Section 2.2.2, the use of chiral complexing agents gives *enantiomerically pure* end products only in exceptional cases (e.g. after enrichment via crystallization[33]).

2.2.2. *Covalently Bonded Chiral Auxiliaries*

In a fundamental investigation on the addition of the chiral lithium enolate **38** to propanal, *Seebach* et al. observed only poor diastereoselectivity (57 : 43).[34] The reagents **39** and **40** show absolutely no enantiofacial differentiation with respect to aldehydes.[10,11]

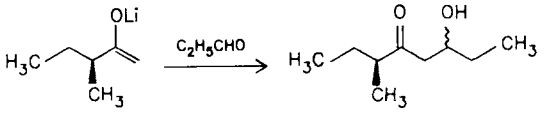

38

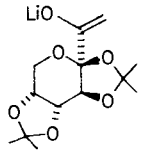

39

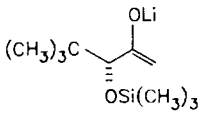

40

Reaction of the proline derivative **41** with benzaldehyde, on the other hand, yields the adducts **42a** and **42b** in the ratio of 83 : 17. However, this is also an "immolative" method, since the removal of the heterocycle by Baeyer-Villiger oxidation causes the chirality of the auxiliary reagent to be "sacrificed".[9]

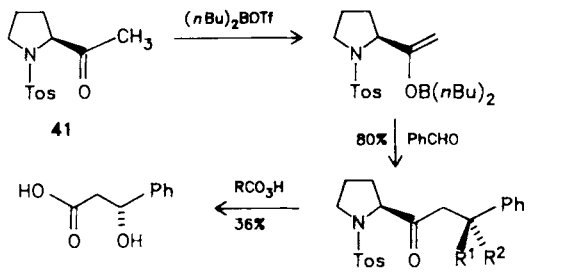

41

42a: R^1 = H, R^2 = OH
42b: R^1 = OH, R^2 = H

Comparable stereoselectivity is also obtained in the aldol reaction between the two enantiomerically pure partners **43** and **44**. Here, however, the chiral auxiliary of the methyl ketone **44** is incorporated into the target molecule (+)-latrunculin B.[35]

Even using "RAMP"- and "SAMP"-hydrazones, reagents which have proved themselves in the stereoselective α-alkylation of carbonyl compounds, the β-hydroxyketones **45** can be obtained only with enantiomeric excesses between 31 and 62%. The total chemical yields lie between 51 and 82%.[15]

An increase in selectivity is however observed using the enamide (azaenolate) **47**, an intermediate which is formed in the deprotonation of the oxazolidine **46** ($R^1 = CH_3$).[36]

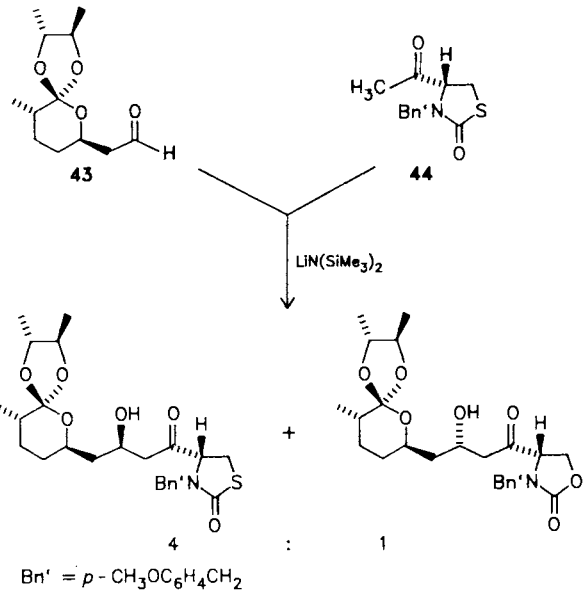

43 **44**

4 : 1

Bn' = *p*-$CH_3OC_6H_4CH_2$

The optical purity of the ketones **48** obtained (in ca. 60% chemical yield) after transmetalation, aldehyde addition and removal of the auxiliary reagent norephedrine is 58–86%. If acetophenone or *tert*-butyl methyl ketone is used instead of acetone, values of 70 to 95% *ee* are obtained.

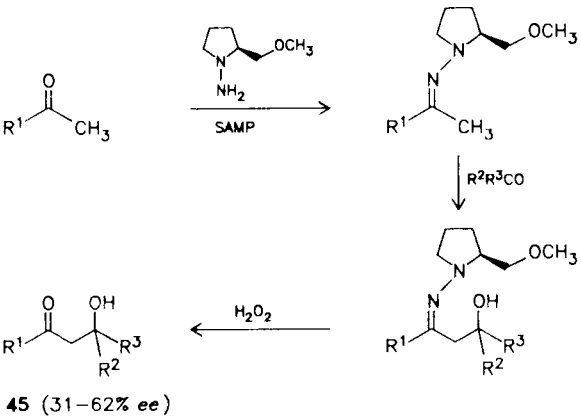

45 (31–62% *ee*)

Many attempts have been made to prepare non-racemic β-hydroxycarboxylic acids **24** by the addition of chiral derivatives of acetic acid to aldehydes or unsymmetrical ketones.[37] Sufficient stereoselectivity, combined with acceptable chemical yields, were however obtained neither

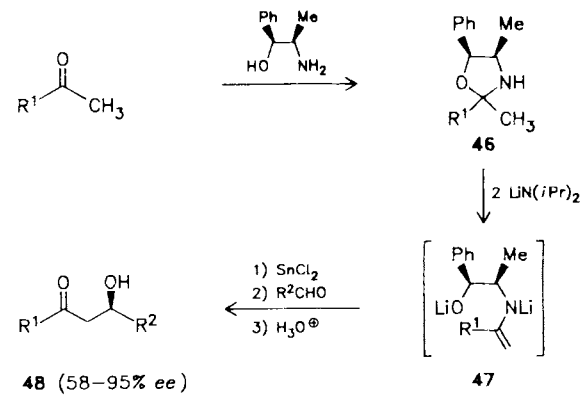

46

47

48 (58–95% *ee*)

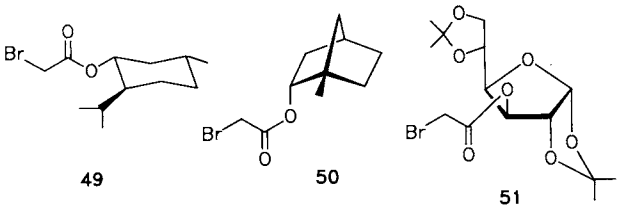

49 50 51

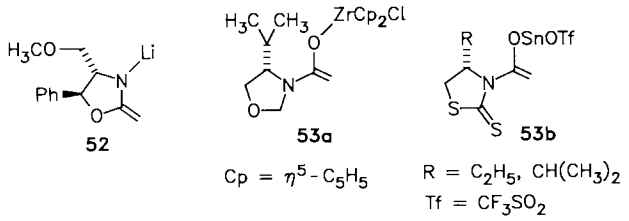

52 53a 53b

Cp = η^5-C_5H_5 R = C_2H_5, $CH(CH_3)_2$ Tf = CF_3SO_2

from the Reformatsky reaction of esters of bromoacetic acid **49**–**51**[38] (in part in the presence of chiral amines[39]) nor using the lithiated oxazolidine **52**[14] or the amide enolate **53a**.[12] The tin derivative **53b**, structurally related to the latter, however reacts with α,β-unsaturated aldehydes to give products with diastereomer ratios of ca. 95 : 5.[40]

A report by *Mitsui* et al.[41a] of an unusually high stereoselectivity (93% *ee*) in the addition of menthyl acetate **54** to acetophenone was later corrected by the Solladié group:[41b] the real *ee* value is 58% for acetophenone and propiophenone, the chemical yields being ca. 50%. The latter fall in the reactions of **54** with methyl cyclohexyl ketone and with benzaldehyde to 30 and 6% respectively, although the optical purities are 66 and 82%.[42]

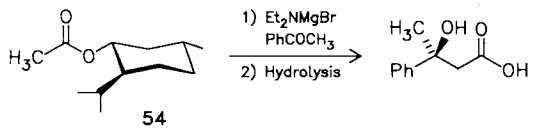

54

The use of the acetamide **55**, which has been added (after conversion to the zirconium enolate) to benzaldehyde in the presence of various amines, also does not permit the simultaneous achievement of sufficient stereoselectivity and good chemical yields of the product **56a**/**56b**.[13]

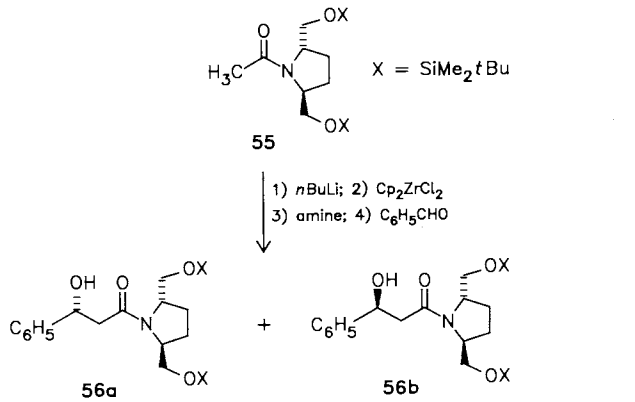

55

56a + 56b

Amine	56a : 56b	Yield [%]
$[(CH_3)_2CH]_2NH$	3.7 : 1	97
$(C_2H_5)_2NH$	5.3 : 1	62
n-$C_4H_9NH_2$	8.5 : 1	20

A considerable improvement was made by *Helmchen* et al. with the $TiCl_4$-catalyzed addition of the ketene acetal **57** to aldehydes, whereby diastereomer ratios **58a** : **58b** of better than 93 : 7 can be obtained.[43] The preferred attack of the reagent **57** at the *Re*-side of the aldehyde is in agreement with the model **59**. The excess diastereomers **58a** can be obtained in a pure state by recrystallization; hydrolysis leads to β-hydroxycarboxylic acids *ent*-**24**. Enantiomeric end products **24** can similarly be formed from the ester **60**.

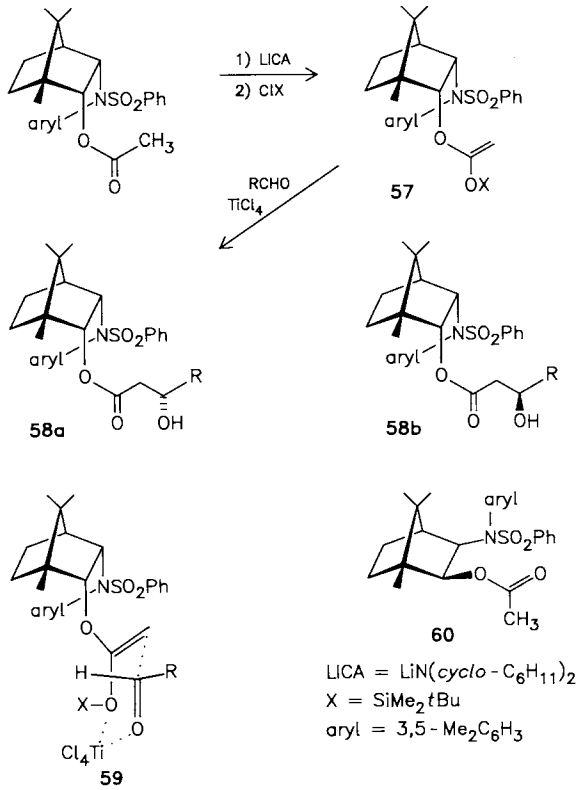

57 58a 58b 59 60

With the motivation that chiral α-unsubstituted enolates **2b** should be available in simple ways starting from enantiomerically pure auxiliary reagents which in turn should be as cheap as possible, we recently studied the reaction of (*R*)-*N*-acetyl-α-phenylglycinol **64** (see Scheme 1).[44,45] With *n*-butyllithium the triple deprotonation to the enolate **65** is possible; this adds to aldehydes or to acetophenone, forming the isomers **66a**/**66b**. The diastereomer ratios are given in Scheme 1. Alkaline hydrolysis of the adducts **66a**/**66b** leads to the corresponding carboxylic acids *ent*-**24**. The preparation of the chiral amide **64** is carried out as follows: (−)-phenylglycine **61** is first reduced by lithium aluminum hydride to the aminoalcohol **62**, which is *N*- and *O*-acylated by acetyl chloride to give **63**. Heating with one equivalent of potassium hydroxide in aqueous methanol leads to selective hydrolysis[46] of the ester **63**, yielding the amide **64**. Phenylglycinol **62** is liberated during the hydrolysis of the adducts **66a**/**66b** and can be reused. The product mixtures **66a**/**66b** afford after only a single recrystallization the pure excess diastereomers **66a** in yields between 25 and 43% (with respect to the amide **64**); hydrolysis of these gives enantiomerically pure β-hydroxycarbox-

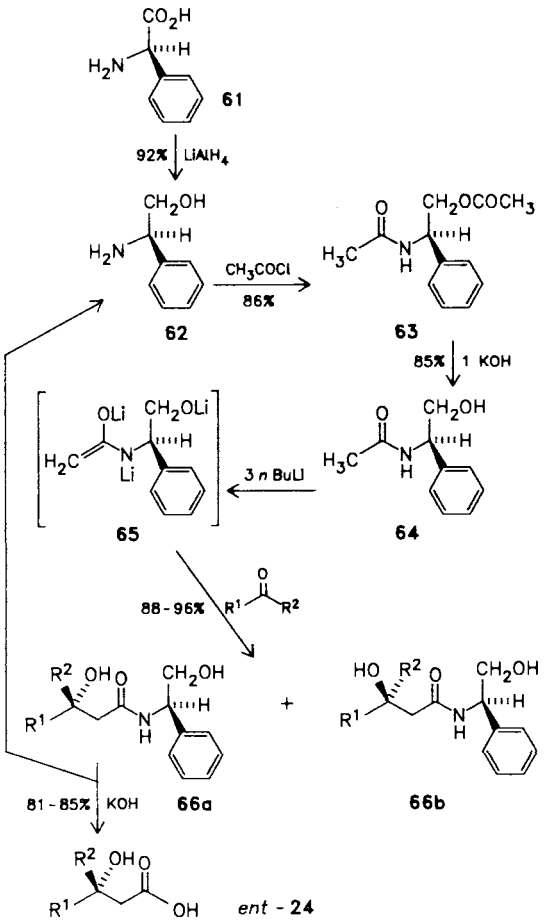

Scheme 1. Addition of (*R*)-**64** to achiral aldehydes and to acetophenone. Examples:

R^1	R^2	**66a** : **66b**	**66a** + **66b** [%]
C_6H_5	H	80 : 20	96
$(CH_3)_3C$	H	83 : 17	95
$(CH_3)_2CH$	H	78 : 22	93
n-C_3H_7	H	78 : 22	93
C_6H_5	CH_3	82 : 18	88

ylic acids *ent*-**24**. Both (*R*)- and (*S*)-phenylglycine are commercially available.

The hydroxymethylene group of the *N*-acetylphenylglycinol **64** shows itself not only to be useful in the amide hydrolysis, but (in the form of the deprotonated alkoxide in **65**) it also has a positive influence on the stereoselectivity of the addition: the lithium enolate **68** of the *N*-acetyl-α-phenylethylamine **67** reacts with benzaldehyde to give

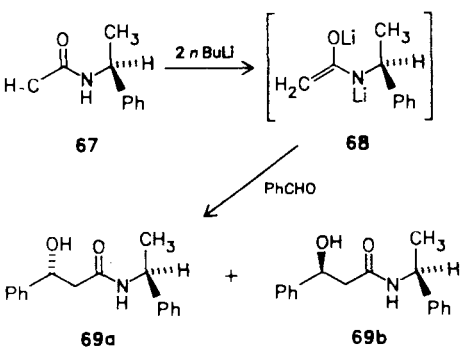

the diastereomers **69a**/**69b** only in the ratio 60 : 40. In addition, alkaline hydrolysis of the adduct does not occur.[47]

With the goal of improving the diastereoselectivity, we then studied the aldol reaction of (*R*)- and (*S*)-2-acetoxy-1,2,2-triphenylethyl acetate **72** (cf. Scheme 2).[48] In the light of our experience with the phenylglycine derivative **75**, we expected that the hydroxyl group (deprotonated to the alkoxide) in the ester **72** would also have a positive influence on the enantiofacial differentiation with respect to aldehydes. When a suspension of the acetic acid derivative **72** is treated in THF with two equivalents of lithium diisopropylamide, a clear solution of the enolate **73** (M = Li) is formed; this, after transmetalation with magnesium bromide or iodide, is reacted with aldehydes at −120 to −135 °C using the cosolvents dimethyl ether or isopentane. The diastereomers **74a**, **b** are formed in the proportions shown in Scheme 2. Mild alkaline hydrolysis leads to β-hydroxycarboxylic acids *ent*-**24** in corresponding optical purity. The chemical yields of the products **24** lie between 76 and 85% overall (2 steps). The chiral reagent **72** can readily be prepared from methyl mandelate **70**: this is first converted by phenylmagnesium bromide into the

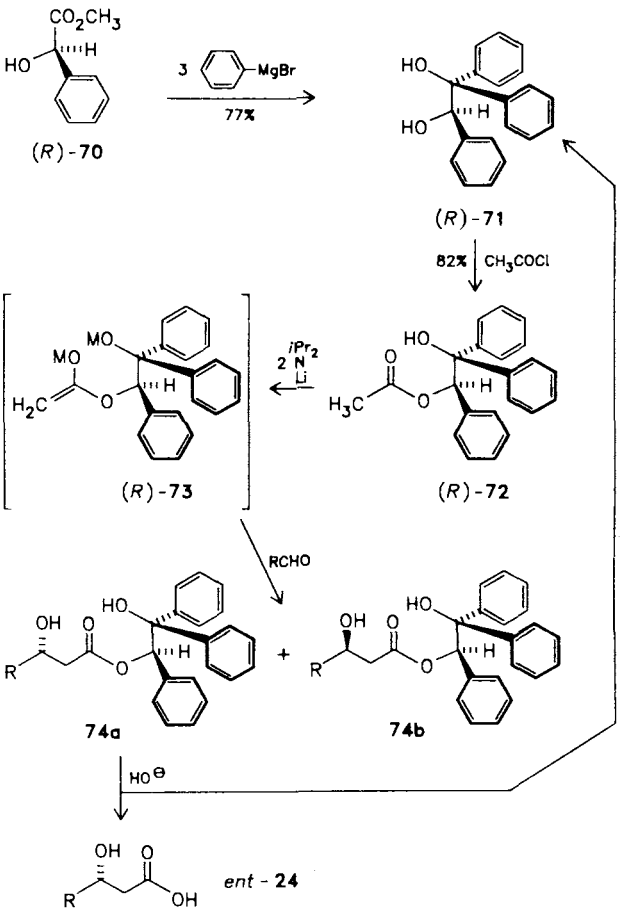

Scheme 2. Addition of (*R*)-**72** to achiral aldehydes. Examples:

R	**74a** : **74b**
C_6H_5	50 : 1
$(CH_3)_2CH$	25 : 1
n-C_3H_7	11 : 1

diol **71**,[49,50] which can then be converted into the ester **72** by acetyl chloride in the presence of pyridine (selective esterification of the secondary hydroxyl group). Both enantiomers of the reagent **72** are easily available, since both (*R*)- and (*S*)-mandelic acid are inexpensive commercial products. In this method the chiral auxiliary is also recovered from hydrolysis of the adducts **74a**, **b** in an unracemized state as the diol **71**.

In all cases which we have so far studied, the (*R*)-configurated reagent **73** attacks the aldehyde from the *Re*-side, the (*S*)-enolate correspondingly from the *Si*-side.[51]

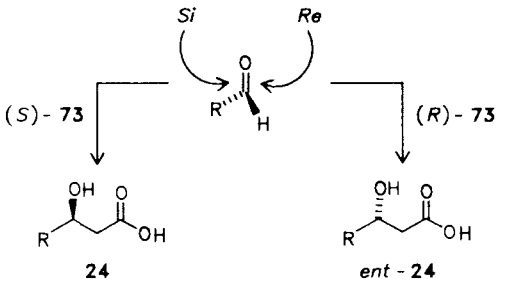

If however homochiral aldehydes **75** (see Scheme 3) are allowed to react with both enantiomers of an enolate **2b**, it must be expected that the diastereofacial selectivities of aldehyde and enolate will work together in one of the combinations ("matched pair"), but be opposed in the other ("mismatched pair").[2f] Thus, after hydrolysis, differing product ratios **76** : **77** will be observed in the two cases: the matched pair gives a larger, the unmatched pair a smaller diastereomer excess.

One possibility of controlled and predictable synthesis of both the *anti* and the *syn* isomers **76** or **77** occurs when the reagent selectivity of the enolates (*R*)- or (*S*)-**73** dominates, so that it is able to overcompensate the diastereofacial ("inherent") selectivity of the aldehydes **75**. It can be seen from Scheme 3 that the selective synthesis of *anti* or *syn*-configured carboxylic acids is actually possible in the cases **76a/77a** and **76b/77b**.[52,53] As in the case of the achiral aldehydes, the deprotonated ester (*R*)-**72** here also attacks (independent of the chirality of the substrates **75a** and **75b**) mainly from the *Re*-side (→**76a**, **b**), while the (*S*)-reagent **72** attacks preferably from the *Si*-side (→**77a**, **b**) with comparable stereoselectivity. The diastereofacial selectivity of the aldehydes **75a**, **b** towards lithium and magnesium enolates of *achiral* acetates is low, so that *anti*- and *syn*-products **76a**, **b** or **77a**, **b** are formed in approximately equal amounts.[53,54] In the $TiCl_4$-catalyzed addition of silyl enol ethers and in reactions with several organometallic reagents (particularly those containing boron and titanium) the stereochemistry can be controlled by the chirality of the substrate in the sense of "chelate control".[55] A recent review article contains a detailed treatment of this concept for stereoselective synthesis.[56]

In contrast to β-alkoxy-substituted aldehydes such as **75a** and **75b**, the isopropylidene glycerinaldehyde **75c** also exhibits a clear inherent selectivity towards organolithium compounds.[57] Thus the diastereomers **76c/77c** (R = CH_3) are formed from the lithium enolate of methyl acetate in the ratio of 85 : 15.[58] An increase in the *anti*-selectivity can be attained using the (*S*)-reagent **72**, which here also attacks preferably from the *Si*-side. The *lk*-topicity does in fact also dominate in the addition of the (*R*)-ester **72**, but in this mismatched pair the preference for the *syn* isomer **77c** is only low.[53]

Joullie et al.[59] recently reacted (*S*)-**72** with the (racemic) aldehyde **78**; after removal of the minor diastereomer, they obtained (−)-detoxinine **80** via the lactone **79**.

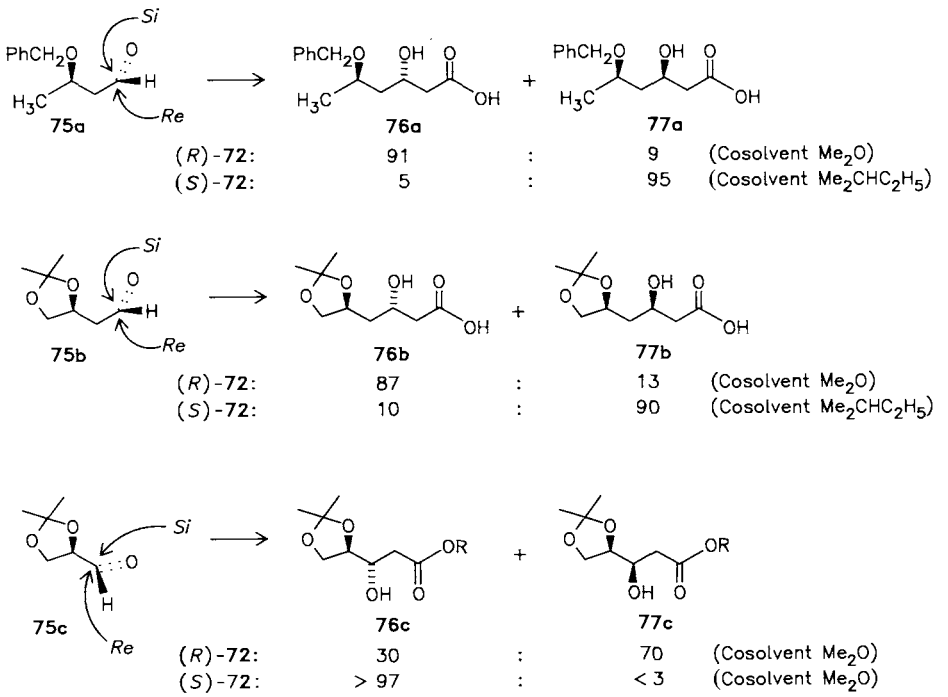

Scheme 3. Reaction of (*R*)- and (*S*)-**72** with chiral aldehydes **75** in tetrahydrofuran.

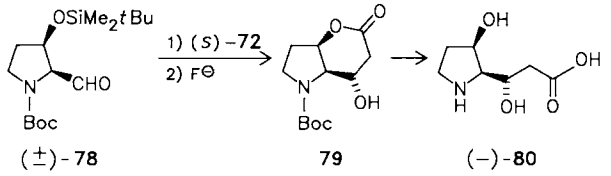

2.2.3. *Metal Atoms as Chiral Centers*

The creative idea of using a transition metal as a chiral auxiliary was realized almost simultaneously by the groups of *Liebeskind*[60] and *Davies*.[61] The acetyliron complex **81** adds (after deprotonation and transmetalation) to aldehydes at $-100\,^{\circ}C$ with a very high diastereoselectivity to give the products **82a/82b**. Removal of the iron complex gives the corresponding β-hydroxycarboxylic acids **24**. Enantiomerically pure starting material is however not very readily available, since it must be prepared by resolution of a racemate.[62] Thus until now all aldol reactions have also been carried out using the racemic acetyl derivative **81**. The *lk*-configuration of the excess diastereomer **82a** ($R=C_2H_5$) was demonstrated by an X-ray structure analysis.[63]

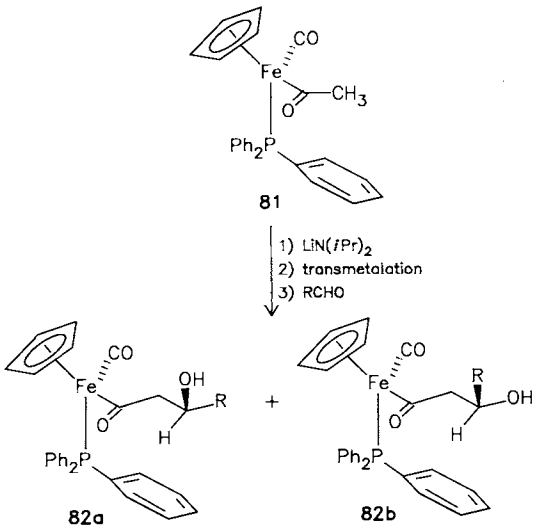

R	Transmetalation with	82a : 82b	Ref.
Ph	iBu_2AlCl	3.7 : 1	[60]
Ph	Et_2AlCl	20 : 1	[61]
Ph	$SnCl_2$	1 : 12	[60]
*i*Pr	iBu_2AlCl	8.2 : 1	[60]
*i*Pr	Et_2AlCl	> 100 : 1	[61]
Et	iBu_2AlCl	5.2 : 1	[60]
Et	Et_2AlCl	> 100 : 1	[61]
*t*Bu	Et_2AlCl	> 100 : 1	[61]

The inadequate enantiofacial selectivity of α-unsubstituted enolates **2b** towards aldehydes has thus very recently been improved with the help of new chiral reagents. For a longer time prior to this, attempts had been made to bypass the problematic aldol reaction in such cases and to seek a route to enantiomerically pure β-hydroxycarbonyl compounds such as **21** or **24** using alternative methods. The following section contains a short account of such attempts.

3. Alternatives to the Aldol Reaction

3.1. Allylmetal Reagents as Masked Enolates

Since carbon–carbon double bonds can generally be readily cleaved to give ketones, aldehydes or carboxylic acids, a homoallyl alcohol **84** can serve as precursor for a β-hydroxycarbonyl compound; thus an organometallic reagent **83** with a σ-bonded allyl residue can be regarded as a masked enolate.[64]

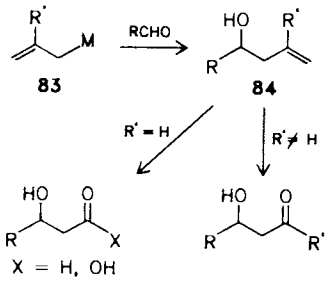

The silane **87** can be added enantioselectively to aldehydes in the presence of $TiCl_4$; the alcohols **88** thus obtained can be cleaved to β-hydroxycarboxylic acids *ent*-**24** without any decrease in optical purity.[65] The allylsilane **87** is formed in 95% enantiomeric excess by coupling the Grignard reagent **85** with vinyl bromide in the presence of the chiral catalyst **86**.[66]

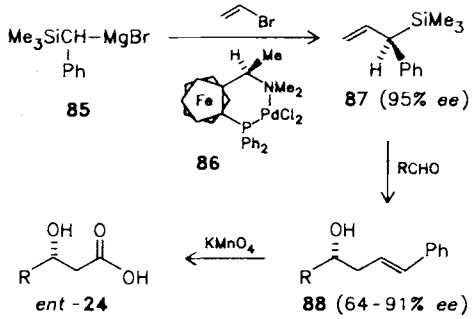

Chiral allylboron reagents have been used (particularly in the groups of *Hoffmann*,[67] *Midland*,[68] and *Brown*[69]) as substitutes for enolates:[70] thus, the boronic ester **89** obtained from (+)-camphor adds to aldehydes and gives (after cleavage of the borate intermediate with nitrilotriethanol) the alcohols **90** in ca. 70% enantiomeric excess.[67]

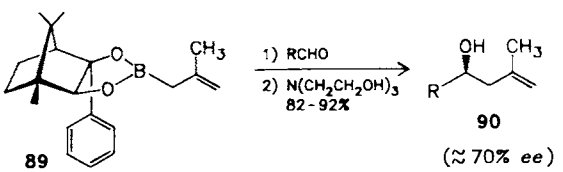

An increase in the selectivity can be obtained with the help of the allylborane **92**, which can be obtained in almost 99% optical purity from α-pinene. Apparently the hydroboration of α-pinene affords predominantly that diastereomer of diisopinocamphenylborane which contains the same enantiomers of α-pinene. Thus, the borane **91** is obtained as a crystalline product with a higher enantiomeric excess than that of the starting terpene.[71] It is thus possible to start from commercial (+)- or (−)-α-pinene of about 91% optical purity. After introduction of the allyl substituent, the addition of the borane **92** to aldehydes and to unsymmetrical ketones gives the alcohols **93** or **94** with in some cases excellent enantioselectivity.[69]

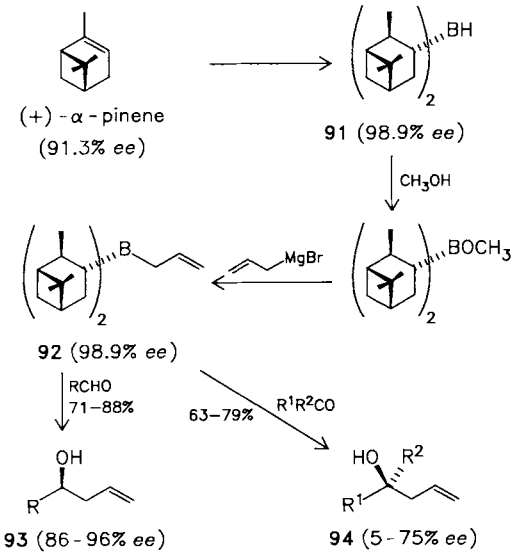

Esterification of the propadienylboronic acid **95** with tartaric acid derivatives also yields an effective transmitter of chirality: the homopropargyl alcohols **96** are obtained in 92–99% *ee*; the chemical yields are between 78 and 90%.[72] Since carbon-carbon triple bonds can be transformed into carbonyl compounds using known methodology,[73] this method can also be considered to be equivalent to the aldol reaction.

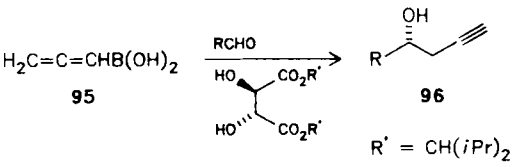

Addition reactions of the analogous allylboronic esters **97** to aldehydes have recently been described (79–87% *ee*).[74]

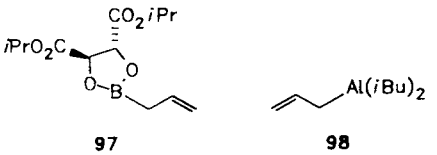

As a last example, the transfer of the allyl residue from the organoaluminum compound **98** to aldehydes occurs in an enantioselective manner (53–84% *ee*) when the chiral complexing agent **36** is added.[75]

3.2. The Use of Chiral Acetals and Lactones

A further concept which by-passes the aldol reaction of α-unsubstituted enolates **2b** is the following: the aldehyde itself is converted temporarily into the chiral partner and then allowed to react (as diastereoselectively as possible) with an achiral enol ether or enolate equivalent (see Section 3.1).[76] *Johnson* et al.[77] chose the 1,3-dioxanes **99**, which can readily be obtained by acetalization using enantiomerically pure 2,5-pentanediol, as chiral aldehyde derivatives. The ring opening reaction with a nucleophile, catalyzed by Lewis acids MX_n, should occur in an S_N2 manner and will then lead (depending whether the bond a or b is broken) to the diastereomer **101a** or **101b**. The hindrance to the axial substituents in 2- and 4-position ($CH_3 \leftrightarrow H$) which is present in the ground state is reduced when the bond a is broken. Since this is not the case when the bond b is lengthened, the transition state **100a** should be favored over **100b**.

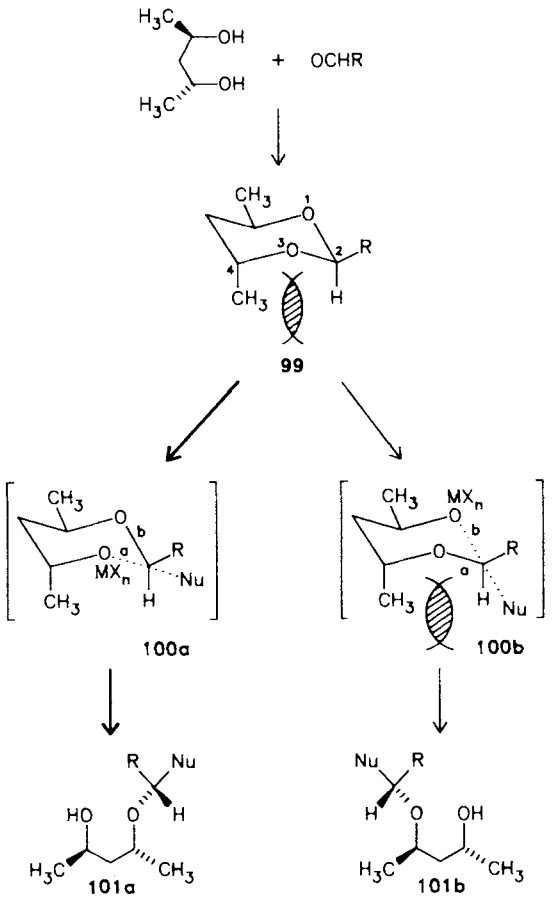

It is indeed the case that when allylsilanes,[78] allylmagnesium bromide[79] or silyl enol ethers[80] are added to dioxanes **99** the products **102** and **103** are formed in excess, with an average diastereoselectivity of 95 : 5. The removal of the chiral auxiliary is carried out by oxidation with pyridinium chlorochromate to the ketones **104** and **105**, from

which in turn homoallyl alcohols or β-hydroxyketones are liberated by base-catalyzed β-elimination of methyl 1-propenyl ketone ("retro-Michael addition").

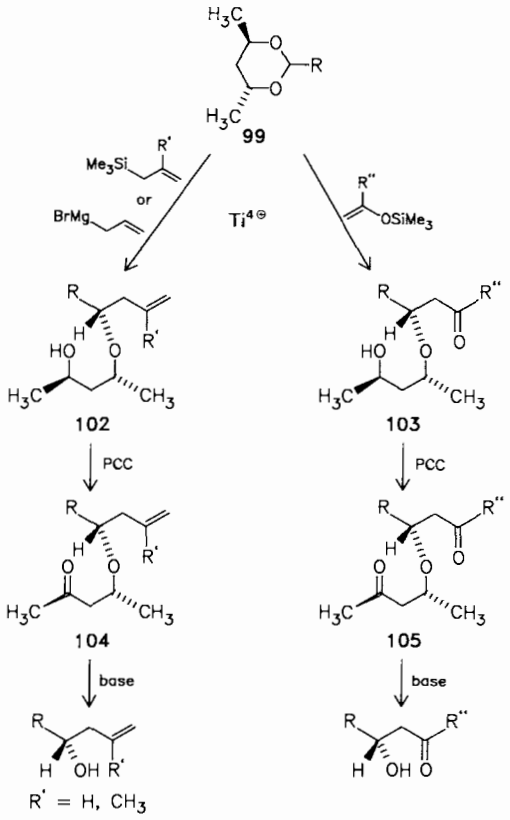

A similar diastereoselective ring opening of the chiral dioxolanes **106** occurs with the α-silyl ketone **107**: the adducts **108a/108b** are formed in a ratio of up to 16:1. In this case the chiral auxiliary is removed by oxidation to the diketone **109** followed by a Baeyer-Villiger rearrangement

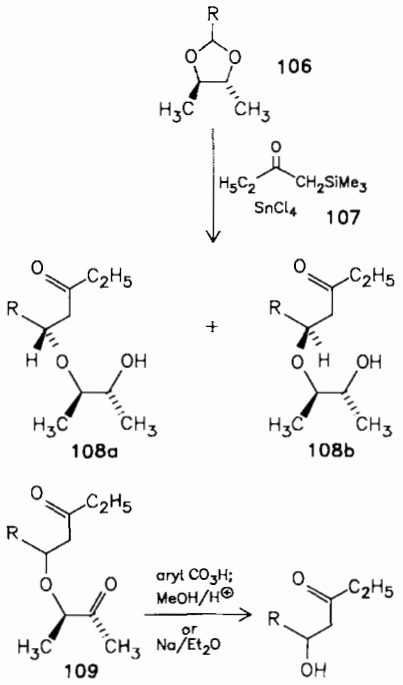

and transesterification with methanol.[81] Reductive cleavage of the α-alkoxyketones of type **109** is also possible.[82]

With the help of this method *Kishi* et al.[81] were able to synthesize aclavinone **111** starting from the acetal **110**; a diastereoselectivity of 10:1 is attained in the key step.

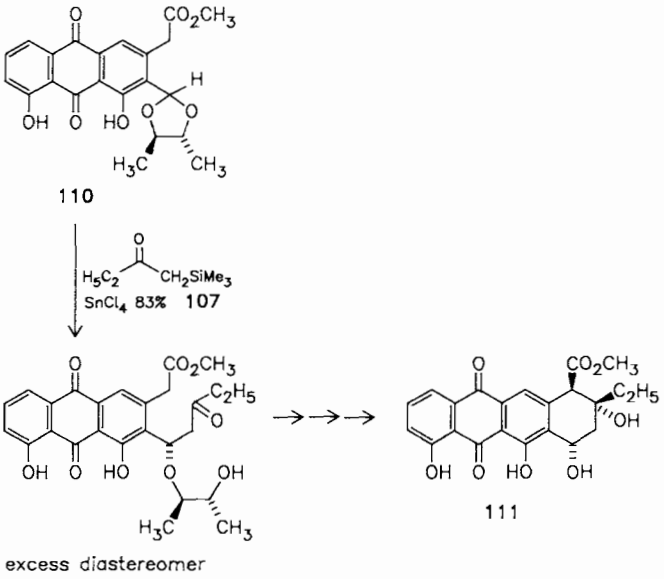

In the nucleophilic opening of the lactones **112** and **114**, the carboxylate functions as the leaving group rather than the alkoxide; this is to be expected on the basis of the acidities of the corresponding conjugate acids. Thus, when the dioxolanones **112** are reacted with allyltrimethylsilane or with silyl enol ethers in the presence of BF_3-etherate or $SnCl_4$ the carboxylic acids **113a/113b** are formed, the diastereomers **113a** being in excess (ratio 63:37 to 93:7).[83] The heterocycles **112** obtained from the condensation of aldehydes with mandelic acid are mainly *cis*-configurated.[84] In this case the cleavage of the chiral reagent occurs by means of oxidative decarboxylation using lead tetraacetate.

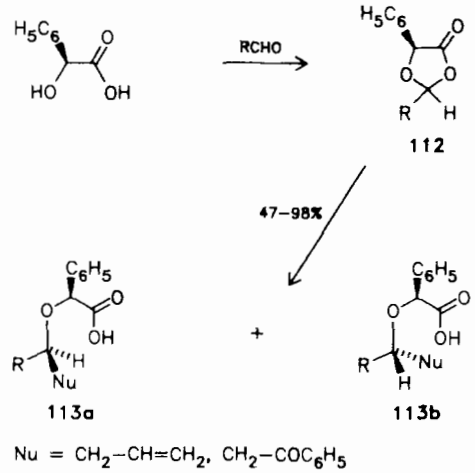

The reaction of aldehydes with 3-hydroxybutyric acid, which is readily available in both enantiomeric forms (see

Section 3.3), gives mainly the *cis*-dioxanones **114**, which can usually be obtained in a pure state by recrystallization. As shown by *Seebach* et al.,[76,85] these heterocycles also react diastereoselectively with allylsilanes; the ratios of the products **115a** and **115b** are ca. 97:3. Treatment with lithium diisopropylamide liberates the homoallyl alcohols **93**.

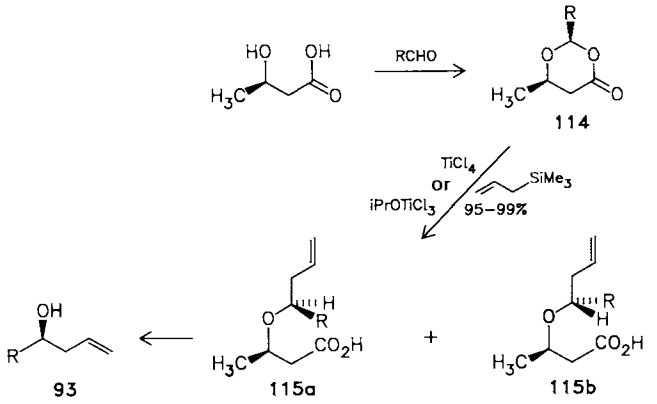

The common feature of all these methods for nucleophilic substitution at acetals is that the chirality of the auxiliary reagent is eventually destroyed.

3.3. Further Methods for the Preparation of Enantiomerically Pure β-Hydroxycarboxylic Acids

Enantioselective reduction permits the conversion of the often readily available β-ketocarboxylic acids or their esters into the corresponding alcohols. Besides the use of chirally modified hydride transfer reagents,[86] microbial methods are continually becoming more popular.[87] An example of the latter is the reduction of ethyl acetoacetate to (*S*)-3-hydroxybutyric acid ethyl ester in the presence of bakers' yeast.[88] The (*R*)-enantiomer can easily be obtained by depolymerization of the commercially available polyhydroxybutyric acid ("PHB").[89]

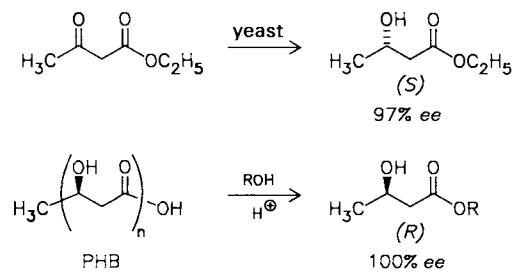

The diastereoselective reduction of the β-ketoester **116** gives (after reductive cleavage of the chiral auxiliary) the (*R*)-diol **117** with a maximum of 43% *ee*.[90]

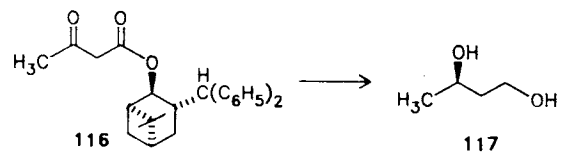

In the approach used by *Masamune*,[2f] 1,3-diols with a high degree of optical purity are obtained by stereoselective epoxidation of allyl alcohols using the Katsuki-Sharpless reagent,[91] followed by regioselective opening of the oxirane ring.

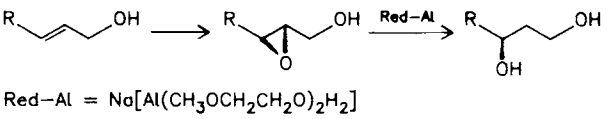

A review of the use of the Paterno-Büchi reaction as an alternative to the aldol reaction has appeared recently.[92] Thus, while the reaction of 1,1-diethoxyethylene with the chiral phenylglyoxylic ester **118** gives mainly the unwanted regioisomer **119**, the oxetane **120** is formed in an almost diastereomerically pure state and can undergo ring opening to give the hydroxy ester.[93]

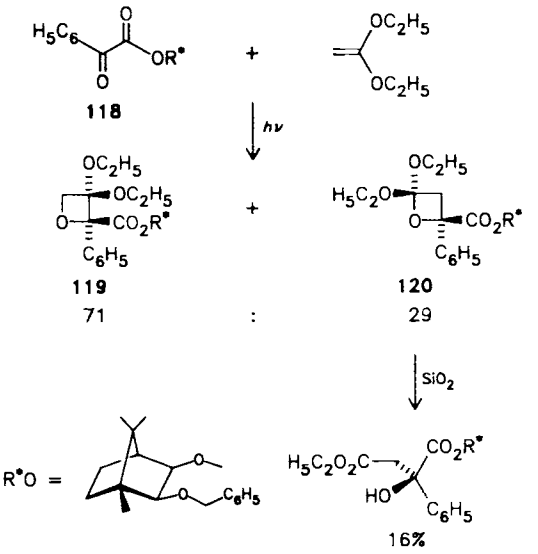

4. Future Prospects

Today various reliable methods are available which make possible a stereoselective addition of chiral α-unsubstituted enolates **2b** to aldehydes. Several alternatives to the aldol reaction also provide effective routes to almost enantiomerically pure β-hydroxycarbonyl compounds **21** or **24**. The future is likely to bring further developments and applications in this area, one which had for an astonishingly long time resisted the attempts of synthetic chemists.

Note added in proof (November 21, 1986): Reetz et al. have succeeded in carrying out the enantioselective addition of ketene acetals to aldehydes with a chiral Lewis acid.[94] A further acetic ester derived from camphor has found application in aldol reactions after conversion into the corresponding silylketene acetal.[95] Finally, *Seebach* et al. have recently described a new route to almost enantiomerically-pure β-hydroxycarboxylic acids with "self-reproduction of the stereogenic center."[96]

I thank the Deutsche Forschungsgemeinschaft, the Fonds der Chemischen Industrie, and the Karl Winnacker and Konrad Adenauer Fundations for their support of our work.

We are also grateful to BASF AG and Hoechst AG for generous gifts of (R)- and (S)-mandelic acid. The results from our own group which are presented here were obtained by my co-workers Dr. Ralf Devant and Dipl.-Chem. Ulrike Mahler, to whom my sincere thanks are due.

Received: July 14, 1986 [A 603 IE]
German version: *Angew. Chem. 99* (1987) 24
Translated by Prof. *T. N. Mitchell*, Dortmund (FRG)

[1] Review: A. T. Nielsen, W. J. Houlihan: *Organic Reactions, Vol. 16*, Wiley, New York 1968.

[2] a) C. H. Heathcock, *Science 214* (1981) 395; b) C. H. Heathcock in E. Buncel, T. Durst (Eds.): *Comprehensive Carbanion Chemistry, Part B*, Elsevier, Amsterdam 1984, Chap. 4; c) C. H. Heathcock in J. D. Morrison (Ed.): *Asymmetric Synthesis, Vol. 3, Part B*, Academic Press, New York 1984, Chap. 2; d) D. A. Evans, J. M. Takacs, L. R. McGee, M. D. Ennis, D. J. Mathre, J. Bartroli, *Pure Appl. Chem. 53* (1981) 1109; e) D. A. Evans, J. V. Nelson, T. R. Taber, *Top. Stereochem. 13* (1982) 1; f) S. Masamune, W. Choy, J. S. Petersen, L. R. Sita, *Angew. Chem. 97* (1985) 1; *Angew. Chem. Int. Ed. Engl. 24* (1985) 1.

[3] "Directed aldol reaction"; cf. G. Wittig, H. Reiff, *Angew. Chem. 80* (1968) 8; *Angew. Chem. Int. Ed. Engl. 7* (1968) 7; G. Wittig, *Top. Curr. Chem. 67* (1976) 1; T. Mukaiyama, *Org. React. N. Y. 28* (1982) 203.

[4] S. Masamune, S. A. Ali, D. L. Snitman, D. S. Garvey, *Angew. Chem. 92* (1980) 573; *Angew. Chem. Int. Ed. Engl. 19* (1980) 557; the *syn-anti* nomenclature suggested therein appears to be increasingly accepted by other authors, see, e.g., Refs. [2d, 17, 56]. - In addition this review uses the *lk*(like)-*ul*(unlike)-nomenclature for the description of the topicity of the approach of reagent and substrate: D. Seebach, V. Prelog, *Angew. Chem. 94* (1982) 696; *Angew. Chem. Int. Ed. Engl. 21* (1982) 654.

[5] High *anti*-selectivity is in general more difficult to achieve than *syn*-selectivity (compare Ref. [2]). For more recent approaches to the solution of this problem see: A. I. Meyers, Y. Yamamoto, *Tetrahedron 40* (1984) 2309; C. Palazzi, L. Colombo, C. Gennari, *Tetrahedron Lett. 27* (1986) 1735 and Ref. [43].

[6] Having regard to the diastereomeric transition states which are involved in these reactions, several authors use the term "diastereofacial selectivity" (cf. [2c]).

[7] D. A. Evans, J. Bartroli, T. L. Shih, *J. Am. Chem. Soc. 103* (1981) 2127.

[8] An increase in the selectivity can however also be attained using other counterions. Thus the addition of the lithium enolate **6b** (Li instead of $B(n\mathrm{Bu})_2$) to benzaldehyde yields the diastereomers **8/9** in the ratio of 87:13, while this ratio can be reversed to 25:75 when $Ti(O\mathrm{i}Pr)_3Cl$ is used (R = Ph): M. Nerz-Stormes, E. R. Thornton, *Tetrahedron Lett. 27* (1986) 897.

[9] D. A. Evans, J. V. Nelson, E. Vogel, T. R. Taber, *J. Am. Chem. Soc. 103* (1981) 3099.

[10] C. H. Heathcock, C. T. White, J. J. Morrison, D. VanDerveer, *J. Org. Chem. 46* (1981) 1296.

[11] C. H. Heathcock, M. C. Pirrung, J. Lampe, C. T. Buse, S. D. Young, *J. Org. Chem. 46* (1981) 2290.

[12] D. A. Evans, L. R. McGee, *J. Am. Chem. Soc. 103* (1981) 2876.

[13] T. Katsuki, M. Yamaguchi, *Tetrahedron Lett. 26* (1985) 5807.

[14] A. I. Meyers, G. Knaus, *Tetrahedron Lett. 1974*, 1333; A. I. Meyers, P. J. Reider, *J. Am. Chem. Soc. 101* (1979) 2501.

[15] D. Enders in J. D. Morrison (Ed.): *Asymmetric Synthesis, Vol. 3, Part B*, Academic Press, New York 1984, Chap. 4.

[16] H. E. Zimmerman, M. D. Traxler, *J. Am. Chem. Soc. 79* (1957) 1920.

[17] R. W. Hoffmann, K. Ditrich, S. Froech, D. Cremer, *Tetrahedron 41* (1985) 5517.

[18] The U-conformation is also the one most favored by (*E*)-enolates which, according to MNDO calculations, react with aldehydes preferably via a twist-boat transition state: C. Gennari, R. Todeschini, M. G. Beretta, G. Favini, C. Scolastico, *J. Org. Chem. 51* (1986) 612.

[19] In this article we use the term "aldol reaction" to include additions of enols and enolates and their hetero-analogues to aldehydes and ketones; cf. Ref. [2b], footnote on p. 178.

[20] C. Mioskowski, G. Solladié, *J. Chem. Soc. Chem. Commun. 1977*, 162.

[21] G. Solladié in J. D. Morrison (Ed.): *Asymmetric Synthesis, Vol. 2, Part A*, Academic Press, New York 1983, Chap. 6; G. Solladié, *Chimia 38* (1984) 233.

[22] C. Mioskowski, G. Solladié, *Tetrahedron 36* (1980) 227.

[23] G. Solladié, C. Frechou, G. Demailly, *Nouv. J. Chim. 9* (1985) 21.

[24] For ^{13}C-NMR investigations on the enolate **29** see: A. Solladié-Cavallo, C. Mioskowski, *Org. Magn. Reson. 16* (1981) 273.

[25] E. J. Corey, L. O. Weigel, A. R. Chamberlin, H. Cho, D. H. Hua, *J. Am. Chem. Soc. 102* (1980) 6613.

[26] R. Annunziata, M. Cinquini, F. Cozzi, F. Montanari, A. Restelli, *J. Chem. Soc. Chem. Commun. 1983*, 1138.

[27] R. Annunziata, M. Cinquini, A. Gilardi, *Synthesis 1983*, 1016; cf. also: R. Annunziata, M. Cinquini, F. Cozzi, A. Restelli, *J. Chem. Soc. Chem. Commun. 1984*, 1253.

[28] L. Colombo, C. Gennari, G. Poli, C. Scolastico, R. Annunziata, M. Cinquini, F. Cozzi, *J. Chem. Soc. Chem. Commun. 1983*, 403.

[29] Cf. D. Valentine, Jr., J. W. Scott, *Synthesis 1978*, 329; J. W. ApSimon, R. P. Seguin, *Tetrahedron 35* (1979) 2797.

[30] M. Guetté, J. Capillon, J.-P. Guetté, *Tetrahedron 29* (1973) 3659.

[31] N. Iwasawa, T. Mukaiyama, *Chem. Lett. 1983*, 297; T. Mukaiyama, N. Iwasawa, R. W. Stevens, T. Haga, *Tetrahedron 40* (1984) 1381.

[32] T. Mukaiyama, N. Yamasaki, R. W. Stevens, M. Murakami, *Chem. Lett. 1986*, 213.

[33] See textbooks on stereochemistry such as: *E. L. Eliel: Stereochemie der Kohlenstoffverbindungen*, Verlag Chemie, Weinheim 1966.

[34] D. Seebach, V. Ehrig, M. Teschner, *Justus Liebigs Ann. Chem. 1976*, 1357.

[35] R. Zibuck, N. J. Liverton, A. B. Smith III, *J. Am. Chem. Soc. 108* (1986) 2451.

[36] K. Narasaka, T. Miwa, H. Hayashi, M. Ohta, *Chem. Lett. 1984*, 1399.

[37] For a review of older publications in this area see: J. D. Morrison, H. S. Mosher: *Asymmetric Organic Reactions*, American Chemical Society, Washington, DC 1976, p. 142ff.

[38] M. H. Palmer, J. A. Reid, *J. Chem. Soc. 1960*, 931; *1962*, 1762.

[39] S. Brandänge, S. Josephson, L. Mörch, S. Vallén, *Acta Chem. Scand. Ser. B 35* (1981) 273.

[40] Y. Nagao, Y. Hagiwara, T. Kumagai, M. Ochiai, T. Inoue, K. Hashimoto, E. Fujita, *J. Org. Chem. 51* (1986) 2391, and references cited therein.

[41] a) S. Mitsui, K. Konno, I. Onuma, K. Shimizu, *Nippon Kagaku Zasshi 85* (1964) 437; b) E. B. Dongala, D. L. Dull, C. Mioskowski, G. Solladié, *Tetrahedron Lett. 1973*, 4983.

[42] Y. Kudo, M. Iwasawa, K. Kobayashi, Y. Senda, S. Mitsui, *Tetrahedron Lett. 1972*, 2125.

[43] G. Helmchen, U. Leikauf, I. Taufer-Knöpfel, *Angew. Chem. 97* (1985) 874; *Angew. Chem. Int. Ed. Engl. 24* (1985) 874.

[44] M. Braun, R. Devant, *Angew. Chem. 95* (1983) 802; *Angew. Chem. Int. Ed. Engl. 22* (1983) 788.

[45] R. Devant, M. Braun, *Chem. Ber. 119* (1986) 2191.

[46] M. Kuna, G. Ovakimian, P. A. Levene, *J. Biol. Chem. 137* (1941) 337; G. Ovakimian, M. Kuna, P. A. Levene, *ibid. 135* (1940) 91.

[47] In this special case the hydrolysis can be carried out with N_2O_4; cf. Ref. [45].

[48] M. Braun, R. Devant, *Tetrahedron Lett. 25* (1984) 5031.

[49] A. McKenzie, H. Wren, *J. Chem. Soc. 97* (1910) 473.

[50] R. Roger, W. B. McKay, *J. Chem. Soc. 1931*, 2229.

[51] In view of the paucity of information available on the structure of enolates such as **65** or **73** it appears too early to propose a model for the transition states which takes into account both the extent of the stereoselectivity and the *lk*-topicity.

[52] R. Devant, *Dissertation*, Universität Karlsruhe 1985.

[53] U. Mahler, unpublished results, Universität Düsseldorf.

[54] Cf. A. I. Meyers, J. Lawson, R. A. Amos, D. G. Walker, R. F. Spohn, *Pure Appl. Chem. 54* (1982) 2537; H. Redlich, B. Schneider, R. W. Hoffmann, K.-J. Geueke, *Liebigs Ann. Chem. 1983*, 393.

[55] M. T. Reetz, A. Jung, *J. Am. Chem. Soc. 105* (1983) 4833. - Using other Lewis acids, the non-chelate-controlled reaction is also possible; however, the selectivity in favor of the *syn*-diastereomer is only low: S. Kiyooka, H. Sasaoka, R. Fujiyama, C. H. Heathcock, *Tetrahedron Lett. 25* (1984) 5331.

[56] M. T. Reetz, *Angew. Chem. 96* (1984) 542; *Angew. Chem. Int. Ed. Engl. 23* (1984) 556.

[57] Review: J. Jurczak, S. Pikul, T. Bauer, *Tetrahedron 42* (1986) 447; J. Mulzer, *Nachr. Chem. Tech. Lab. 32* (1984) 146.

[58] C. H. Heathcock, S. D. Young, J. P. Hagen, M. C. Pirrung, C. T. White, D. VanDerveer, *J. Org. Chem. 45* (1980) 3846.

[59] W. R. Ewing, B. D. Harris, K. L. Bhat, M. M. Joullie, *Tetrahedron 42* (1986) 2421.

[60] L. S. Liebeskind, M. E. Welker, *Tetrahedron Lett. 39* (1984) 4341.

[61] S. G. Davies, I. M. Dordor, P. Warner, *J. Chem. Soc. Chem. Commun. 1984*, 956.

[62] H. Brunner, E. Schmidt, *J. Organomet. Chem. 21* (1970) P53; *36* (1972) C18; see also S. G. Davies, I. M. Dordor-Hedgecock, K. H. Sutton, J. C. Walker, C. Bourne, R. H. Jones, K. Prout, *J. Chem. Soc. Chem. Commun. 1986*, 607.

[63] S. G. Davies, I. M. Dordor-Hedgecock, P. Warner, R. H. Jones, K. Prout, *J. Organomet. Chem. 285* (1985) 213; for a conformational analysis of the acetyliron complex **81** see: S. G. Davies, J. I. Seeman, I. H. Williams, *Tetrahedron Lett. 27* (1986) 619.
[64] Cf. R. W. Hoffmann in W. Bartmann, B. M. Trost (Eds.): *Selectivity - a Goal for Synthetic Efficiency*, Verlag Chemie, Weinheim 1984, p. 87; see also [56].
[65] T. Hayashi, M. Konishi, M. Kumada, *J. Org. Chem. 48* (1983) 281.
[66] T. Hayashi, M. Konishi, H. Ito, M. Kumada, *J. Am. Chem. Soc. 104* (1982) 4962.
[67] R. W. Hoffmann, T. Herold, *Chem. Ber. 114* (1981) 375.
[68] M. M. Midland, S. B. Preston, *J. Am. Chem. Soc. 104* (1982) 2330.
[69] P. K. Jadhav, K. S. Bhat, P. T. Perumal, H. C. Brown, *J. Org. Chem. 51* (1986) 432.
[70] Review: M. Braun, *Nachr. Chem. Tech. Lab. 33* (1985) 504.
[71] H. C. Brown, P. K. Jadhav in J. D. Morrison (Ed.): *Asymmetric Synthesis, Vol. 2, Part A*, Academic Press, New York 1983, Chap. 1.
[72] N. Ikeda, I. Arai, H. Yamamoto, *J. Am. Chem. Soc. 108* (1986) 483; cf. also: N. Ikeda, K. Omori, H. Yamamoto, *Tetrahedron Lett. 27* (1986) 1175.
[73] See textbooks of organic chemistry, e.g.: J. March: *Advanced Organic Chemistry*, 3rd Edit., Wiley, New York 1985.
[74] W. R. Roush, A. E. Walts, L. K. Hoong, *J. Am. Chem. Soc. 107* (1985) 8186.
[75] T. Mukaiyama, N. Minowa, T. Oriyama, K. Narasaka, *Chem. Lett. 1986*, 97.
[76] A detailed discussion of this concept has been provided: D. Seebach, R. Imwinkelried, T. Weber in R. Scheffold (Ed.): *Modern Synthetic Methods*, Springer, Berlin 1986, p. 125.
[77] V. M. F. Choi, J. D. Elliott, W. S. Johnson, *Tetrahedron Lett. 25* (1984) 591.
[78] W. S. Johnson, P. H. Crackett, J. D. Elliott, J. J. Jagodzinski, S. D. Lindell, S. Natarajan, *Tetrahedron Lett. 25* (1984) 3951; W. S. Johnson, M. F. Chan, *J. Org. Chem. 50* (1985) 2598.
[79] S. D. Lindell, J. D. Elliott, W. S. Johnson, *Tetrahedron Lett. 25* (1984) 3947.
[80] W. S. Johnson, C. Edington, J. D. Elliott, I. R. Silverman, *J. Am. Chem. Soc. 106* (1984) 7588.
[81] J. M. McNamara, Y. Kishi, *J. Am. Chem. Soc. 104* (1982) 7371.
[82] P. A. Bartlett, W. S. Johnson, J. D. Elliott, *J. Am. Chem. Soc. 105* (1983) 2088.
[83] S. H. Mashraqui, R. M. Kellogg, *J. Org. Chem. 49* (1984) 2513.
[84] The diastereomer ratio **113a** : **113b** is almost independent of the configuration of the dioxolanones **112**.
[85] D. Seebach, R. Imwinkelried, G. Stucky, *Angew. Chem. 98* (1986) 182; *Angew. Chem. Int. Ed. Engl. 25* (1986) 178.
[86] M. Nakahata, M. Imaida, H. Ozaki, T. Harada, A. Tai, *Bull. Chem. Soc. Jpn. 55* (1982) 2186; K. Soai, T. Yamanoi, H. Hikima, H. Oyamada, *J. Chem. Soc. Chem. Commun. 1985*, 138.
[87] Review: C. J. Sih, C.-S. Chen, *Angew. Chem. 96* (1984) 556; *Angew. Chem. Int. Ed. Engl. 23* (1984) 570.
[88] R. U. Lemieux, J. Giguere, *Can. J. Chem. 29* (1951) 678; B. S. Deol, D. D. Ridley, G. W. Simpson, *Aust. J. Chem. 29* (1976) 2459; K. Mori, *Tetrahedron 37* (1981) 1341; B. Wipf, E. Kupfer, R. Bertazzi, H. G. W. Leuenberger, *Helv. Chim. Acta 66* (1983) 485; D. Seebach, M. A. Sutter, R. H. Weber, M. F. Züger, *Org. Synth. 63* (1985) 1.
[89] D. Seebach, M. Züger, *Helv. Chim. Acta 65* (1982) 495.
[90] S. Takano, M. Morimoto, K. Ogasawara, *Yakugaku Zasshi 103* (1983) 1257; see also: T. Oishi, T. Nakata, *Acc. Chem. Res. 17* (1984) 338.
[91] T. Katsuki, K. B. Sharpless, *J. Am. Chem. Soc. 102* (1980) 5974.
[92] Review: M. Braun, *Nachr. Chem. Tech. Lab. 33* (1985) 213.
[93] H. Koch, J. Runsink, H.-D. Scharf, *Tetrahedron Lett. 24* (1983) 3217; see also: H. Gotthardt, W. Lenz, *Angew. Chem. 91* (1979) 926; *Angew. Chem. Int. Ed. Engl. 18* (1979) 868.
[94] M. T. Reetz, F. Kunisch, P. Heitmann, *Tetrahedron Lett. 27* (1986) 4721.
[95] W. Oppolzer, J. Marco-Contelles, *Helv. Chim. Acta 69* (1986) 1699.
[96] D. Seebach, J. Zimmermann, *Helv. Chim. Acta 69* (1986) 1147.

Laser Chemistry—What is Its Current Status?

By Karl Kleinermanns and Jürgen Wolfrum*

In recent years, various methods have been developed to observe and to influence the course of chemical reactions using laser radiation. By selectively increasing the translational, rotational, and vibrational energies and by controlling the relative orientation of the reaction partners with tunable infrared and UV lasers, direct insight can be gained into the molecular course of the breaking and re-forming of chemical bonds. Examples for the application of lasers include the synthesis of monomers such as vinyl chloride and polymers such as polyethylene, the synthesis of biologically active substances such as vitamin D_3, the separation of isotopes, the removal of impurities, the production of catalysts, glasses, and ceramics, and the deposition and ablation of material on surfaces. Finally, several applications of lasers in medicine are discussed.

1. Introduction

Irradiation with light can strongly affect the course of chemical reactions. The best known example is photosynthesis in plants. In addition, electromagnetic radiation is the most important aid in determining the structure, properties, and chemical behavior of molecules. In spite of great successes, spectroscopy with conventional light sources has not been able to answer many interesting questions. Only the practical realization of the principle of stimulated emission (first formulated by *Einstein*[1]), in the microwave region in 1955[2] and in the visible spectral region in 1960,[3] led to a decisive advance. As in many other areas of science and technology, the laser has also created numerous new possibilities for chemistry.[4] Particularly the introduction of tunable laser light sources, such as the dye laser,[5] and the development of linear and nonlinear optical techniques, such as laser-induced fluorescence (LIF), resonant multiphoton ionization (REMPI), coherent anti-Stokes Raman scattering (CARS), laser Raman spectroscopy on surfaces (SERS), photoacoustic spectroscopy (PAS), laser magnetic resonance spectroscopy (LMR), and Doppler-free absorption spectroscopy, allow virtually every spectroscopic state of an atom or molecule to be observed with high resolution, from the far infrared with wavelengths of several millimeters to the vacuum ultraviolet with wavelengths in the nanometer range.[6] The higher sensitivity allows observation of single atoms in ultramicroanalysis. Further, laser spectroscopy allows nonintrusive observation of rapidly changing chemical processes, such as combustion with high temporal, spectral, and spatial resolution.[7]

The high power of laser light sources within a narrow spectral region allows specific degrees of freedom of molecules to be excited in order to initiate or to influence reactions and to investigate the reaction products state-selectively. In this way, the relative velocity of reaction partners can be adjusted very precisely over a wide region, molecules allowed to rotate faster or slower, and bonds in a molecule stretched to various degrees; with polarized laser light, the mutual orientation of chemical species during the course of a reaction can be specified. Moreover, short-lived "transition states" of chemical reactions can be observed. In the first part of this article, the selective excitation and observation of chemical transformations with the aid of laser radiation is exemplified by reactions in the gas phase.

The progress achieved in laboratory investigations in controlling the course of reactions by excitation with laser light suggests that the newly developed methods could also be used for the production of new products or the improvement of syntheses. However, it was found that, for large-scale reactions performed in chemical reactors, the energy exchange between molecules and the deactivation of excited molecules take place very quickly and that "memory" effects with respect to the initially prepared state only rarely influence the reaction. In spite of these limitations, a number of interesting laser-induced chemical processes have been described in recent years. In the second part of this article, selected examples of the application of high-power lasers for initiating chemical transformations are presented.

2. Influence of the Specific Excitation of Molecular Degrees of Freedom on the Course of Chemical Reactions

The dependence of the rate of chemical reactions on the energy supplied is daily laboratory experience for the chemist. Often, the energy of the reaction partners can be represented by a temperature and the dependence of the reaction rate on temperature by a simple Arrhenius equation. The Arrhenius parameters obtained in this way do not, however, provide any information on the contribution of specific degrees of freedom of the reaction partners to overcoming the energy barrier of the reaction. In the following examples, reactions in the gas phase are used to show how information on the molecular course of reaction can be obtained in experiments with lasers.

[*] Prof. Dr. J. Wolfrum, Dr. K. Kleinermanns
Physikalisch-Chemisches Institut der Universität
Im Neuenheimer Feld 253, D-6900 Heidelberg (FRG)

 © VCH Verlagsgesellschaft mbH, D-6940 Weinheim, 1987 0570-0833/87/0101-0038 $ 02.50/0

2.1. Translational Excitation

Chemical reactions of fast ("hot") atoms from nuclear recoil and photolysis processes have long been investigated by analysis of their stable end products.[8] On bombarding ^{6}Li with neutrons, for example, tritium (^{3}H) atoms with a recoil energy of 2.7 MeV are formed. Collisions then retard these fast ^{3}H atoms to the "chemical" energy range around 20 eV to give a broad, continuous distribution of velocities. Thus the reaction energy cannot be controlled directly. Narrow-bandwidth laser light of high intensity and short pulse length (10^{-8} s), on the other hand, allows high concentrations of atoms with defined velocities to be produced by photodissociation (Fig. 1).

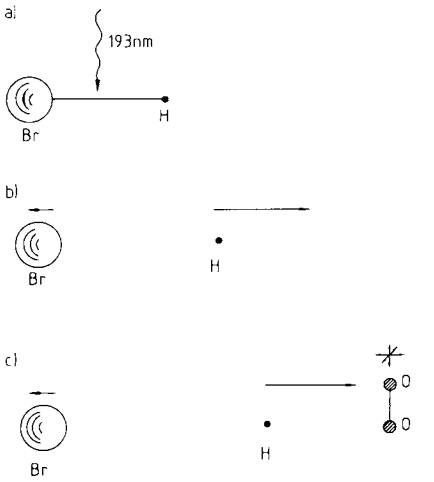

Fig. 1. Production of fast hydrogen atoms by photolysis with short-wavelength laser radiation. a) The ArF excimer laser photolyzes a suitable hydrogen-atom precursor such as HBr. b) The photolysis energy $h\nu$ is considerably greater than the dissociation energy of HBr and is more than 98% converted into the translational energy of the hydrogen atom, because the heavy bromine atom is more or less stationary compared with the light hydrogen atom. The hydrogen atom then passes with a velocity of 23 km s^{-1} through the reactor until it collides with an oxygen molecule. The average velocity of the oxygen molecule at room temperature is more than two orders of magnitude smaller than that of the hydrogen atom, so that, to a good approximation, the velocity of H relative to O_2 is the same as the velocity of the hydrogen atom. In this way, a collision energy of 251 kJ mol^{-1} is obtained. By changing the photolysis wavelength and the hydrogen-atom precursor, the velocity of the hydrogen atom can be set over a wide range and collision energies from 80 kJ mol^{-1} to over 400 kJ mol^{-1} can be attained.

As an example, the reaction (a) of translationally excited hydrogen atoms H^T with oxygen is examined. This endothermic reaction leads to the formation of two reactive radicals and is the most important chain-branching step in numerous oxidation and combustion processes.[9, 14]

$$H^T(^2S) + O_2(^3\Sigma_g^-) \longrightarrow OH(^2\pi, v, J, f) + O(^3P) \qquad (a)$$

$\Delta H_0 = 69.9$ kJ/mol

v = vibrational quantum number,
J = rotational quantum number,
f = fine structure quantum number

One experimental setup that can be used to investigate reaction (a) and other reactions of fast atoms with molecules is shown in Figure 2. It consists of a flow system

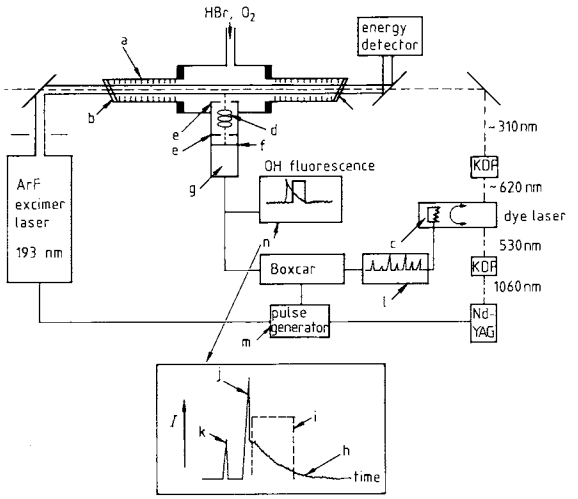

Fig. 2. Setup for state-specific and time-resolved investigation of reactions of fast atoms with molecules. The photolysis pulse of the ArF excimer laser (193 nm, 200-mJ pulse energy, 15-ns pulse length) and the analysis pulse of the Nd-YAG laser-pumped dye laser pass through the flow reactor coaxially. The reactor is equipped with collimators (a) in the side-arms, which partially remove the laser light scattered at the quartz windows (b). The analysis laser (0.2-cm^{-1} spectral band width, 12-ns pulse length and 0.1-1-mJ pulse energy) employs the laser dye Rhodamine 640. After frequency doubling (potassium diphosphate crystal), the OH radicals can be excited between 306 and 311 nm (tuning by a "grating" (c)). If the wavelength of the analysis laser is changed, the OH radicals absorb and fluoresce at different excitation wavelengths with varying strength, depending on how favorably the corresponding vibrational-rotational fine-structure state is populated by reaction (a). The fluorescence intensity is detected by a photon detector (g) after passing a lens system (d), collimators (e), and a filter (f). This intensity is a measure of the probability with which a particular OH state is excited by the chemical reaction. The signal current (h) released by the fluorescence at the photomultiplier is summed over many laser pulses using a "boxcar" system in an adjustable time region ("box") (i) beyond the interferring stray light (j, k) and then plotted against the analysis laser wavelength on a recorder (l). The analysis time is varied by starting the two lasers with two trigger pulses, time-delayed with respect to each other. Typical analysis times are 40-100 ns at a partial pressure of 5 mbar HBr and 50 mbar O_2. Owing to the short analysis times and the low concentrations of species, one avoids secondary reactions and deactivation of the fast hydrogen atoms and the excited OH radicals by collisions.

combined with a photolysis laser for producing hot hydrogen atoms and a frequency-doubled dye laser for state-specific, time-resolved detection of the OH radical by means of laser-induced fluorescence (LIF). The measurements show that the OH radicals formed in reaction (a) are rotationally very highly excited[10] (Fig. 3).

In order to compare the experimental rotational distribution with a calculated rotational distribution, the motion of the three atoms over a quantum-mechanically (ab initio) calculated H-O_2 potential hypersurface[11] is followed by stepwise integration of the classical equations of motion for various initial conditions (relative velocities, orientation of the collision partners, rotational and vibrational states of O_2).[12] The greater part of the relative translational energy of the reactants is converted into rotational energy of the product OH, in qualitative agreement with experimental results. However, careful quantitative comparison still shows distinct discrepancies (Fig. 3). For a collision energy of 251 kJ/mol (ca. 60 kcal/mol), the theoretical cross section, i.e., the reaction probability integrated over the collision parameters and other initial conditions, is a factor of 3 smaller than the experimental value. This discrepancy is particularly disturbing because the absolute

rate constant of reaction (a) at high temperatures, a sensitive parameter, for example in the mathematical modeling of combustion processes,[9] needs to be known exactly. The larger cross section found experimentally has been confirmed by more recent measurements[13] of the thermal rate constants $k_1(T)$ at higher temperatures (1500–2500 K); thus, the values calculated using the quantum-mechanical potential hypersurface are much too low.

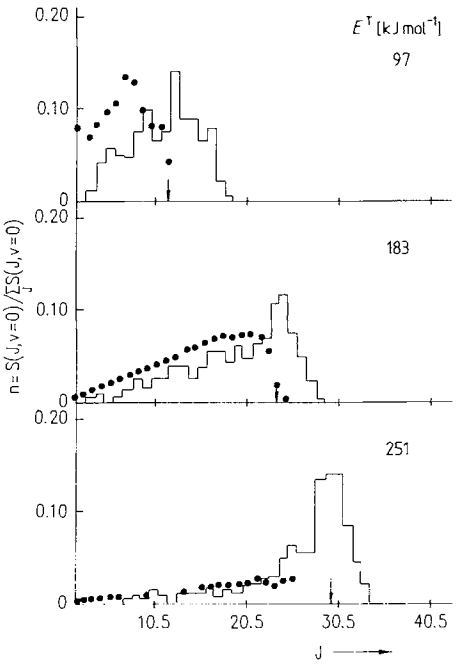

Fig. 3. Rotational excitation of OH (v=0) produced by reaction (a). The points show the experimental, the curve (histogram) the calculated distribution at collision energies of 97, 183, and 251 kJ mol^{-1}. At very high excitation (J > 23.5), OH (v=0) predissociates from the $^2\Sigma$ state and no longer fluoresces. The arrows show the maximum rotational excitation obtainable for complete conversion of the reaction energy into rotational energy. The collision energies E^T given here have an uncertainty of ± 10%.

The fine structure distribution also provides interesting information on reaction dynamics. For instance, the OH λ-doublet excitation shows that the π^+ components are favored.[10,15] As explained in Figure 4, this means that, at high collision energies, the H^T–O_2 reaction proceeds mainly on the initial plane. By using polarized photolysis and analysis laser light, the flight direction of the photolytically produced hydrogen atoms can be specified and the orientation of the OH product radicals relative to the flight direction of the hydrogen atoms measured. Strong polarization effects were found experimentally[16]—the OH angular momentum vector, J_{OH}, lies perpendicular to the velocity vector of the hydrogen atoms, v_H (Fig. 5).

2.2. Rotational Excitation

Because rotational states are energetically very close together and can be rapidly deactivated, the influence of reactant rotation on the course of reactions is investigated using an arrangement with crossed molecular beams to avoid interfering collision processes. Infrared transitions of an HCl or HF molecular laser are used for selective excitation of rotational states in HCl and HF molecules. Typ-

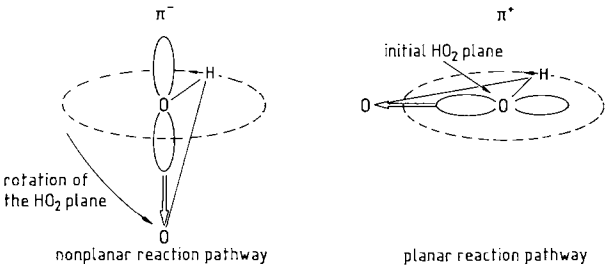

Fig. 4. The physical difference between the two λ-doublet components π^+ and π^- arises from interaction of the electronic spin-orbit momentum with the rotation of the molecule. For fast rotation of the OH radical, the unpaired electron in the p orbital on oxygen is no longer able to follow the movement of the atomic nuclei. If the p orbital lies in the OH rotational plane, the electron distribution on the oxygen atom changes, becoming increasingly spherical. In contrast, for a π^- configuration, the oxygen atom moves in the nodal plane of the p orbital and thus continues to "see" a dumbbell-shaped electron environment, even for fast rotation. This leads to a splitting of the energies of the π^+ and π^- configurations, which increases with increasing rotational energy. Experimentally, at 183 kJ mol^{-1} collision energy, three OH radicals were found in the π^+ state for each OH radical in the π^- state [15]. This shows that the unpaired electron formed after bond cleavage of O_2 stays in an orbital in the rotational plane of the OH radical. During the reaction, most of the HO_2 complexes do not rotate out of the initial plane, because of the short reaction time at high collision energies.

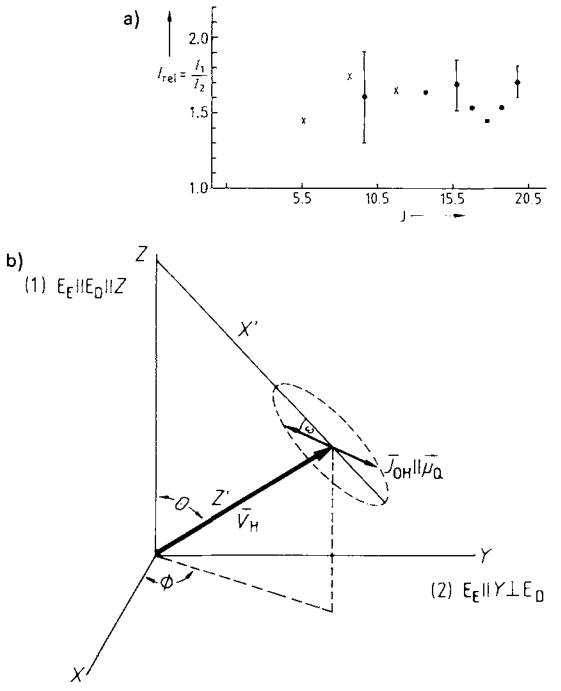

Fig. 5. a) Experimental polarization effects at 251-kJ mol^{-1} collision energy. J is the rotational quantum number; the ordinate is the polarization ratio, I_{rel}, the ratio of the fluorescence signal intensity for polarization of the photolysis laser E_D parallel to the analysis laser E_E and perpendicular to it. The electric vectors of the laser radiation at 193 (×) and 307 nm (•) are rotated independently. b) The laser beams lie parallel to the laboratory X axis, the detector parallel to the Y axis. The molecular coordinates are X′ and Z′; $\vec{v}_H$ is the velocity vector of the hydrogen atoms, and J_{OH} the angular momentum vector in the molecular coordinate system. On excitation of a Q transition (ΔJ = 0) of the OH radical, fluorescence intensities and polarization ratio can be calculated from the projection of the Q transition moments μ_Q ($\| J_{OH}$ for high rotational states) on the laboratory axis [16]. For the orientation $J_{OH} \perp v_H$, the calculation is in agreement with the experimental polarization ratio of 1.60.

ical results are shown in Figure 6. Initially, a decrease in the reaction probability with increasing degree of rotational excitation is observed. A possible explanation is that a particular orientation of the reaction partners, e.g., colinear, often gives the reaction path of lowest energy. With increasing rotation of the molecule, however, the potential forces are less and less able to orient the reaction partners satisfactorily with respect to one another and the reacting atom is increasingly "protected" from the reaction partner. If the rotational excitation is further increased, the steric hindrance plays a lesser role as a result of the rapidly increasing total energy, i.e., the "cone of acceptance" rapidly expands. In addition, because of the higher total energy, more states become accessible on the product side, which leads to a further increase in the reaction probability.

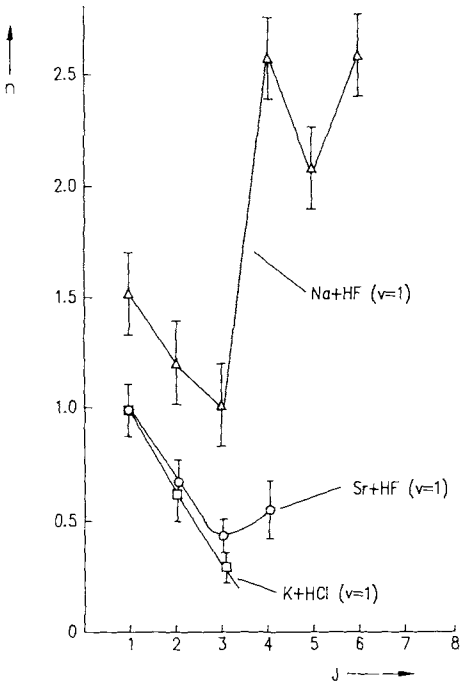

Fig. 6. Investigation of the dependence of the reaction cross section on rotational excitation in the following reactions: K + HCl (v = 1, J) ⟶ KCl + H, Sr + HF (v = 1, J) ⟶ SrF + H, and Na + HF (v = 1, J) ⟶ NaF + H. n = relative reaction cross section; J = rotational quantum number.

If a long-lived intermediate complex is formed during the reaction, the additional rotational energy is distributed statistically over the various degrees of freedom of the product; i.e., "memory" of the energy form of the original excitation is largely lost. Thus, in the reaction

$$Ca(^1S) + HF(X\,^1\Sigma^+_g, v = 1, J = 0\text{-}7) \longrightarrow CaF(X\,^2\Pi, v', J') + H(^2S)$$

X = electronic ground state

Zare et al.[18] observed statistical vibrational excitation of CaF following selective rotational-vibrational excitation of HF.

With the laser-induced fluorescence technique described in Section 2.1, the rotational states of the products could be investigated for a large number of reactions. For instance, the reactions of $O(^3P)$ atoms with saturated and unsaturated hydrocarbons, amines, and aldehydes lead to OH product radicals with low rotational excitation, which can be attributed to the weak rotary torque involved in the almost colinear, direct abstraction of the hydrogen atom.[19] In contrast, the rotational excitation of OH produced by reaction of excited oxygen atoms $O(^1D)$ with H_2 and HCl is extremely high. With saturated hydrocarbons, one observes overlapping of two distributions. This can be traced to a direct, colinear abstraction path (low rotational excitation) and a parallel reaction path with insertion of $O(^1D)$ into the C–H bond (high rotational excitation via decay of a highly excited "alcohol").[20]

2.3. Vibrational Excitation

A connection between chemical reactivity and the efficiency of the vibrational energy exchange between molecules was first postulated by *Franck* and *Eucken* more than 50 years ago.[21] However, systematic investigations in this area only became possible through the development of powerful and tunable infrared lasers.[22,23] The reaction of hydrogen molecules with hydrogen atoms or their isotopes, as the simplest example of a bimolecular reaction of neutral species, is particularly suitable for a theoretical investigation of the influence of selective vibrational excitation of reacting species (see energy diagram, Fig. 7). The energy required for vibrational excitation of the hydrogen molecule considerably exceeds the Arrhenius activation energy (E_a), the threshold energy (E_0), and the height of the energy barrier (E_c) of the reaction in the vibrational ground state.

E_c was first calculated quantum mechanically by *London*[24] more than half a century ago. The value he obtained is not very different from the results of modern ab initio calculations.[25] This good agreement disappears, however, when a more exact calculation is performed according to *London*'s valence bond method.[26] The classical methods for the study of reaction kinetics are difficult to apply to this reaction, because known concentrations of vibrationally excited hydrogen molecules have to be produced and detected. Only the application of CARS spectroscopy has allowed direct, quantitative detection of hydrogen molecules in selected vibrational and rotational states. It was shown that when the H_2 molecule is excited to the first vibrational state, only about a third of the vibrational energy is used to overcome the energy barrier E_c.[27] Thus, the reaction of vibrationally excited hydrogen molecules still shows an energy barrier, whose height can be predicted both from classical and from quantum-mechanical calculations of the course of reaction on the ab initio potential hypersurface, in good agreement with the experiments.[28] More recent measurements of the absolute value of the rate constant by CARS spectroscopy[29] agree well with the results of quasi-classical trajectory calculations.[30] This is also the case for the results of experiments with translationally excited hydrogen atoms.[31]

The results obtained from study of the hydrogen exchange reaction on the efficiency of a selective vibrational excitation cannot be simply transferred to similar reac-

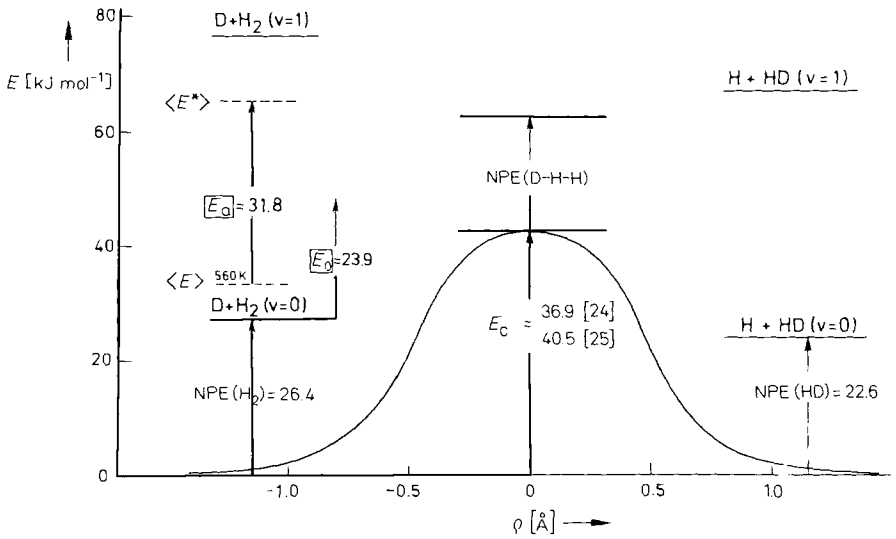

Fig. 7. Characteristic energy requirements of the hydrogen exchange reaction. E_a is the Arrhenius activation energy, E_0 the minimum collision energy that leads to reaction (threshold energy), and E_c the height of the potential energy barrier of the reaction in the vibrational ground state. $\langle E \rangle$ is the average thermal energy of all binary collisions per unit time and $\langle E^* \rangle$ the average kinetic energy of all collisions per unit time that lead to reaction. NPE is the zero point energy of vibration, ρ the reaction coordinate.

tions. Thus, investigations of the also thermoneutral reaction

$$^{37}Cl + H^{35}Cl\,(v=1) \longrightarrow H^{37}Cl\,(v=1,0) + {}^{35}Cl$$

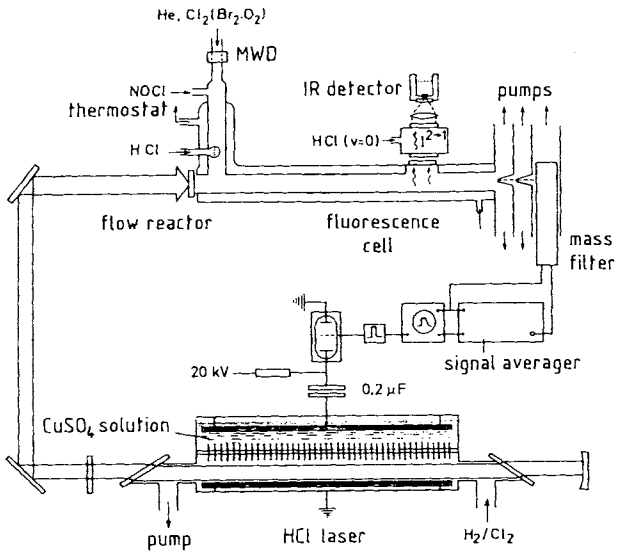

Fig. 8. Experimental setup for the investigation of reactions of vibrationally excited hydrogen halide molecules with the aid of time-resolved molecular-beam mass spectrometry. A discharge flow reactor is coupled through a molecular beam sampling system directly to the ion source of a quadrupole mass spectrometer. The HCl molecules are vibrationally excited isotope selectively by the infrared radiation of an HCl laser. The degree of the vibrational excitation is determined from the intensity of the infrared emission. A filter cell with cold HCl absorbs the infrared radiation of the transition HCl (v = 1) → HCl (v = 0) resonantly and transmits the wavelengths of the transition HCl (v = 2) → HCl (v = 1). From the ratio of the infrared intensity with and without the HCl cell, the degree of excitation of the HCl molecules can be determined directly. Chlorine, bromine, or oxygen atoms, which are produced by dissociation in a microwave discharge (MWD), react in the flow system with the vibrationally excited HCl molecules. The reaction products are detected mass spectrometrically.

demonstrate very effective use of the vibrational energy for overcoming the energy barrier.[32] The experimental setup for investigation of the reaction is shown schematically in Figure 8. The experimental rate constants of the reaction in the states HCl (v = 0) and HCl (v = 1) are given in Figure 9. The high efficiency with which the vibrational energy is used to overcome the energy barrier causes the chemical reaction, with increasing temperature, to proceed preferentially via the excited vibrational states. Thus, the temperature dependence of the reaction deviates significantly from that predicted by an Arrhenius equation. The dynamics of the reaction have been simulated by classical, semiclassical, and quantum-mechanical calculations.[33] Particularly

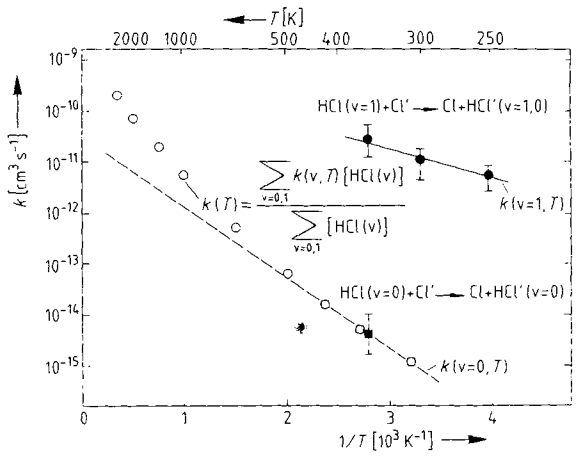

Fig. 9. Contributions of the vibrational ground state (v = 0) and the first excited state of HCl (v = 1) to the rate constant of the reaction Cl + HCl(v) → Cl + HCl(v'). The strong rise in reaction rate after vibrational excitation has the effect that, at higher temperatures ($T > 500$ K), marked deviations from the Arrhenius line are observed. Measured rate constants: □, ■ for HCl (v = 0), ● for HCl (v = 1); ○, calculated rate constants from the contributions of HCl (v = 0) and HCl (v = 1).

in very strongly endothermic reactions can vibrational excitation be used effectively for increasing the rate of reaction. Thus, in the reaction[34]

$$Br + HCl(v) \longrightarrow HBr(v=0) + Cl$$

an increase in the reaction rate constant by more than ten orders of magnitude can be obtained by vibrationally exciting the HCl molecule from $v=0$ to $v=2$. This dramatic increase in the rate constant can be used to separate chlorine isotopes (Fig. 10). ^{35}Cl atoms from HCl can be transformed in this way into $Br^{35}Cl$, which because of its different chemical and physical properties can be readily separated from the reaction mixture.

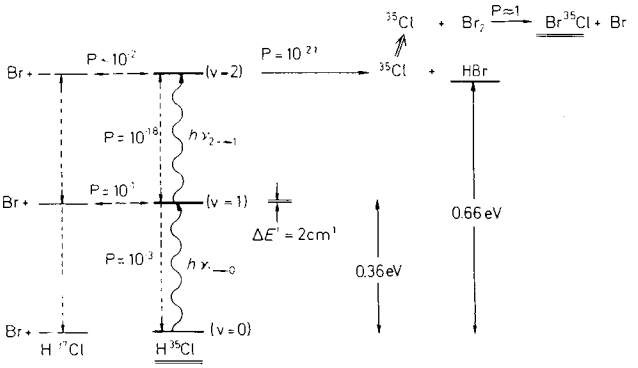

Fig. 10. Energy diagram for the reaction of Br atoms with isotope-selectively excited HCl molecules. P gives the probability for the transfer of vibrational energy between laser-excited $H^{35}Cl$ and $H^{37}Cl$ and for the course of a reaction in the various collision processes, respectively. The Br atoms react preferentially with $H^{35}Cl$ ($v=2$). The resulting ^{35}Cl atoms further react with molecular bromine to give easily separated $Br^{35}Cl$. $\Delta E'$ is the energy difference between $H^{35}Cl$ ($v=1$) and $H^{37}Cl$ ($v=1$).

Investigations of the reactions of polyatomic molecules in specifically excited vibrational states are much more difficult to perform. One main problem is the decoupling of the vibrational energy-transfer processes from the processes leading to reaction. Interesting model molecules are substituted methanes.[35] For example, Figure 11 shows the energy flow in CH_3F after excitation of the CF stretching vibration ν_3 with a CO_2 laser. By almost resonant vibrational energy transfer, subsequent collisions rapidly populate higher states ($2\nu_3$, $3\nu_3$) of this stretching vibration, resulting in a "metastable," mode-selective excitation of the CF stretching vibration. Through local Coriolis resonance between the third overtone of ν_3 and the CH stretching vibration ν_4, part of the energy can be channeled into this CH stretching vibration. Simultaneously, depending on pressure, CH bending vibrations (ν_6, ν_2, ν_5) are excited by collisions with further molecules, the excitation energy being provided by the thermal energy of the surrounding gas. In the subsequent resonant vibrational energy transfer, higher states of these vibrations can be populated, from which the CH stretching vibration ν_1 is reached by Fermi resonance. Examples of reactions of vibrationally excited polyatomic molecules are the reaction of laser-excited ozone molecules with nitric oxide[23,36] and that of fluorine with unsaturated hydrocarbons in a low-temperature matrix.[37]

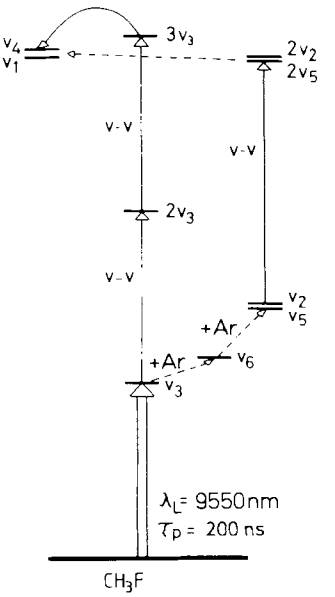

Fig. 11. Paths for the collision-induced intramolecular vibrational energy transfer in CH_3F. Laser radiation with wavelength λ_L and pulse length τ_p.

2.4. Electronic Excitation

In the following, no attempt is made to give a detailed overview of the reaction behavior of electronically excited atoms and molecules. Rather, using selected examples, it is shown how reactants can be selectively oriented with respect to one another, regions of "transition states" probed, and reaction rate constants for high excitation far above the reaction threshold investigated using electronic excitation with laser light.

At some stage in the course of a chemical reaction, new bonds are formed and old bonds broken, so that neither "reactants" nor "products" are in effect present. The direct investigation of such "transition states" has long been the chemist's dream. Figure 12a shows that a range of such transition states can be excited with laser light having a wavelength that is nonresonant with the reactant or product states. Among the reactions investigated[38] was that of $K(4s^2S)$ atoms with NaCl using excitation with laser light in a crossed molecular beam experiment (Fig. 12b).[39] As the reaction partners approach, the states of the species mutually "perturb" each other and their energy changes. When the wavelength of the laser light is finally resonant with the $Na^*(3p^2P)$-KCl state, excitation to this state occurs and light emission at $\lambda = 589$ nm ($Na^*(3p^2P) \rightarrow Na(3s^2S)$ transition, sodium D-line) is observed, as shown in Figure 13 as a function of excitation wavelength. Emission at 589 nm occurs even on excitation with longer-wavelength light. The missing energy comes from the exothermicity of the reaction and thermal energy of the reactants. By improving the signal-to-noise ratio of the measurements, it should be possible to recognize structures in the spectrum and identify areas of longer residence time of the complex on the ground-state hypersurface from the intensity maxima.

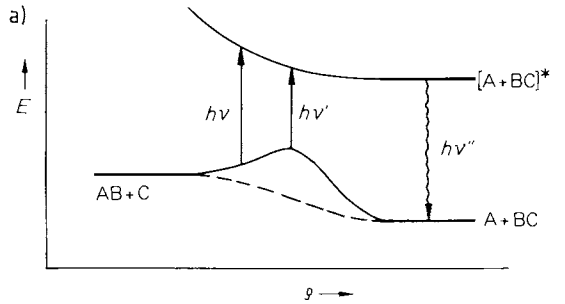

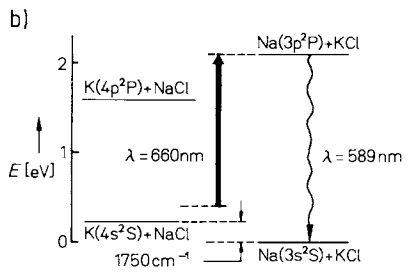

Fig. 12. a) "Transition state" spectroscopy of an exothermic reaction. The emitted frequency ν'' is higher than the radiated frequencies ν or ν'. The missing energy comes from the heat of reaction and the thermal energy of the reactants. b) Energy level diagram of the K-NaCl reaction. 1750 cm^{-1} corresponds to the heat of reaction.

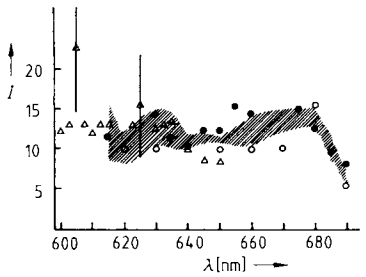

Fig. 13. Luminescence signal from the reaction K $(4s^2S)$ + NaCl → $Na^*(3p^2P)$ + KCl, occurring in crossed molecular beams, as a function of the excitation wavelength. Only when all three beams are present *simultaneously* (K, NaCl, and laser beam) is intense luminescence at 589 nm observed. The dotted area in the diagram gives the average of two or more measurements. The differently marked data points refer to measurements on different days.

In addition to emission from laser-excited "transition states," emission from *chemically* excited intermediate complexes also has been observed. As Figure 14 shows, *Polanyi* and co-workers[40] were still able to detect fluorescence from the reaction

$$F + Na_2 \longrightarrow FNaNa^{+*} \longrightarrow NaF + Na^*(3p^2P)$$

far from the sodium D-line. This "wing" fluorescence originates from Na* near NaF (and hence also from $FNaNa^{+*}$). The higher intensity of the long-wavelength "wing" is due to the fact that the upper and lower potential surfaces tend to lie closer together at intermediate configurations (cf. Fig. 12a).

Following excitation into "repulsive states," structured emission spectra were observed, even though a rapid dissociation follows the excitation.[41,42] These fluorescence

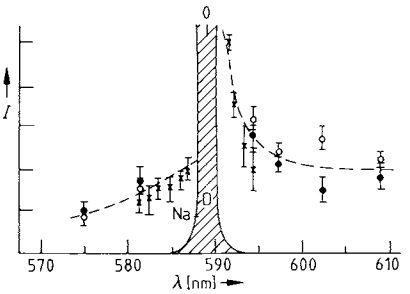

Fig. 14. Emission of the "intermediate complex" $FNaNa^{+*}$ formed in the reaction F + Na_2 → NaF + Na*.

spectra provide information on the previously inaccessible temporal course of a bond rupture. From the frequency shift of the emission lines relative to the excitation wavelength, the vibrational frequency in the electronic ground state is obtained up to the vicinity of the dissociation limit (Fig. 15). Fluorescence occurs when the continuum wave function of the upper (repulsive) potential surface overlaps favorably with vibrational wave functions of the lower (bonding) electronic ground state. In a direct dissociation, later times in the course of photodissociation correspond to more elongated bonds and hence emission to higher vibrational states of the electronic ground state (cf. Fig. 15, vertical optical transition). For example, following excitation at $\lambda = 266$ nm, CH_3I dissociates within femtoseconds to CH_3 and I. Although the dissociation is about six orders of magnitude faster than the spontaneous emission, fluorescence is still observed. Optical transitions to highly excited states of the CH_3 "umbrella vibration" of CH_3I are only observed in combination with excited C-I stretching vibrations.[42] This behavior can be attributed to the fact that the C-I bond has to be elongated considerably before the methyl group opens from the tetrahedral geometry in CH_3I to the planar form in the CH_3 product radical.

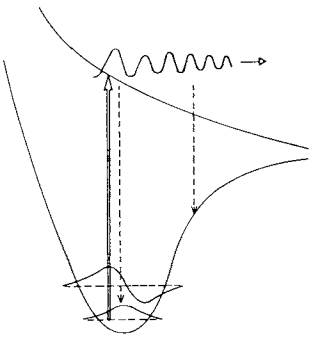

Fig. 15. Scheme for laser-induced fluorescence spectroscopy on repulsive surfaces. A molecule is excited by a UV laser into a dissociative state. In spite of rapid decay, fluorescence (dotted line) occurs when continuum wave functions and vibrational wave functions favorably overlap.

The influence of the orientation of the reaction partners with respect to one another, observed indirectly in experiments involving rotational excitation of the reactants, can also be observed directly using laser techniques. With polarized laser light, molecules having a particular orientation can be selectively excited, since the probability for ab-

sorption of light is at a maximum when the transition dipole moment is parallel to the electric field vector. With this method, *Zare* and co-workers[17b,43] were able to show that the reaction of polarized, excited iodine molecules with indium atoms occurs faster in "head-on" collisions than in a "side-on" attack (Fig. 16).

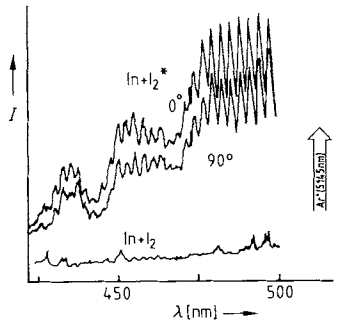

Fig. 16. LIF spectrum of InI from the reaction $In + I_2^* \rightarrow InI + I$. Iodine was excited into the $B(^3\Pi)$ state with a linearly polarized $Ar^{\oplus}$ ion laser at 514.5 nm. The transition moment here lies parallel to the iodine molecular axis. On orienting the electrical vector parallel to the In beam (0°), the reaction proceeds more rapidly ("head-on" collisions) than for perpendicular orientation (90°). The lowest curve gives the fluorescence measured upon switching off the laser.

Different wavelengths of light can be employed to selectively excite molecules having different orientations. Thus, SrF from the reaction of strontium atoms with vibrationally excited HF (excitation to v = 1, J = 1 by a polarized HF infrared laser) is more highly vibrationally excited after a side-on than after a head-on collision. Calculations show[44] that when the reaction occurs at the energetically more favorably angled alkali-metal–HF orientation, energy is preferentially transferred to the internal degrees of freedom of the product molecule.

Polarized laser light can also be used to influence the orientation of the electron orbitals in atoms. The excitation of $Ca(^1S_0)$ to $Ca(^1P_1)$ results in transfer of charge from a spherical s orbital to a dumbbell-shaped p orbital. The transition moment lies in the direction of the Ca p orbital, so that this orbital is aligned with the electrical vector of the laser light. In the reaction of $Ca(^1P_1)$ with HCl, the CaCl $A(^2\Pi)$ state is formed preferentially when the calcium p orbital is aligned perpendicular to the calcium beam. In contrast, the CaCl $B(^2\Sigma^+)$ state is excited preferentially when the Ca p orbital lies parallel to the calcium beam (formation of a σ_p orbital in CaCl).[45] "Memory effects" on the initial state have also been observed in the reaction of $O(^3P)$ atoms with saturated hydrocarbons. *Luntz* and *Andresen*[19a] showed that $O(^3P_2)$ atoms give rise preferably to the $^2\Pi_{3/2}$ spin-orbit states of the OH radical for symmetry reasons.

By electronic excitation of molecules with lasers, specific rate constants, $k(E)$, for unimolecular reactions can be measured directly. *Troe* and co-workers have investigated the isomerization of various cycloheptatrienes in their electronic ground states by means of thermal isomerization[46] as well as stationary[47] and direct, time-resolved[48] photoisomerization. On excitation of cycloheptatriene molecules in the ultraviolet spectral region, light absorption ($S_0 + h\nu \rightarrow S_1$) is followed by rapid internal conversion to vibrationally highly excited levels of the electronic ground state (S_0^*, Fig. 17). The hot cycloheptatriene molecules isomerize faster with decreasing wavelength. From the increase in the absorption signal with time, the specific rate constants could be determined directly. Figure 18 shows that a statistical model of $k(E)$ is in good agreement with the experimental results.

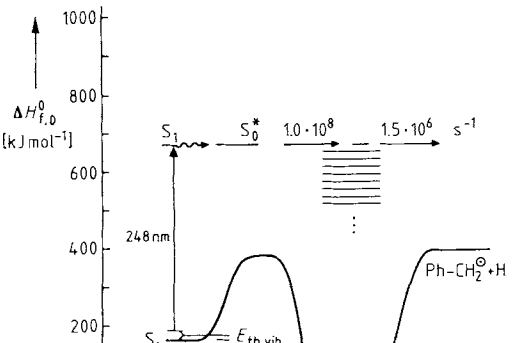

Fig. 17. Potential energy scheme for the photoisomerization of cycloheptatrienes. Electronic excitation into the S_1 state is followed by rapid internal conversion to vibrationally excited CHT in the electronic ground state (S_0), which with rising excitation energy isomerizes increasingly faster to toluene.

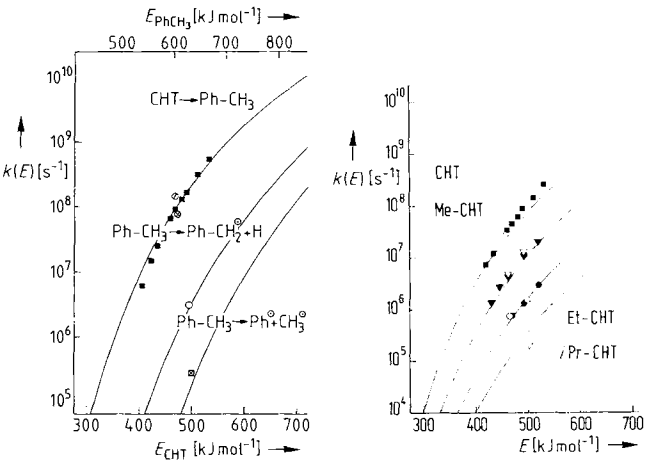

Fig. 18. Specific rate constants, $k(E)$, for the unimolecular isomerization of cycloheptatriene. ○, ∅, ⊗, ▽, ⊠, direct, time-resolved measurements by excitation with laser light; ●, ▼, ■, stationary photoisomerization experiments (Stern-Volmer extrapolation); solid line, statistical calculation according to RRKM theory.

3. Lasers in Synthesis

It would seem obvious to use the methods described for the selective control of chemical reactions for making new products or improving synthetic procedures. Under the typical conditions of industrial chemical processes (high pressures, reactions in the liquid phase, large molecules), however, a selected molecular state cannot, in most cases,

be held stable until the actual reaction stage. The exchange of energy between the degrees of freedom within a molecule and between various molecules usually occurs on a time scale of 10^{-13} to 10^{-10} s, whereas the reaction times themselves are considerably longer. On the other hand, nonthermal isomer and isotope distributions as well as nonthermal radical concentrations from laser-induced dissociation and isomerization processes can readily be maintained under industrial chemical conditions and used for producing new or appreciably purer products or for producing products with lower energy consumption. Here, the use of the laser offers a number of advantages over conventional light sources: (1) extension of the available range of wavelengths; (2) the selective excitation of just one kind of molecule (e.g., for isotope separation or ultrapurification), because of the narrow spectral bandwidth of the laser light; (3) spatially and temporally controllable, homogeneous excitation of the reaction volume, because of the possibilities of pulsed operation and strong collimation; (4) the possibility of multiphoton excitation, because of the high power density.

As shown in Figure 19, Hg or Xe lamps are preferable as light sources for industrial photochemistry both in terms of investment and operational cost as well as in terms of maintenance expenditure, long-term power, and lifetime. For economic application of lasers in this area, the effective cost of the photons must lie considerably below that of the desired product (Fig. 20). One should remember that, generally, the product price is determined only to a small extent by the photochemical step involved in the production process and that techniques employing lasers have to compete not only with conventional photochemical processes, but also with other routes of synthesis. Optimally, the use of lasers should result in several improvements simultaneously, such as cheaper starting materials, fewer or more valuable side products, and fewer or cheaper process steps. In particular, the production of cheap mass-produced chemicals by the use of lasers is only worthwhile if very high quantum yields (number of product molecules produced per photon generated) can be achieved in radical chain reactions.

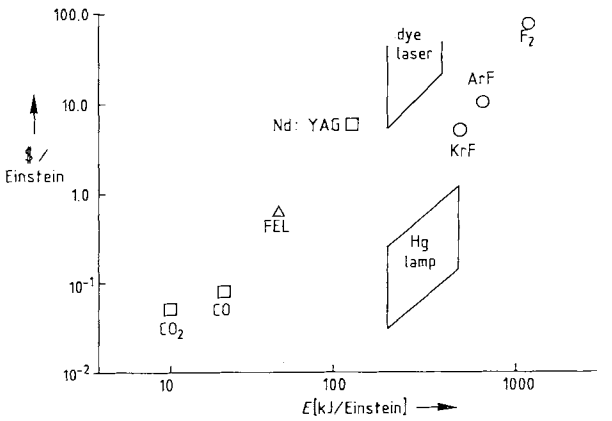

Fig. 19. Photon costs for laser light as a function of photon energy. 1 Einstein is 1 mole of light quanta. FEL = free electron laser. Conventional lamps are at present considerably more inexpensive as light sources than lasers.

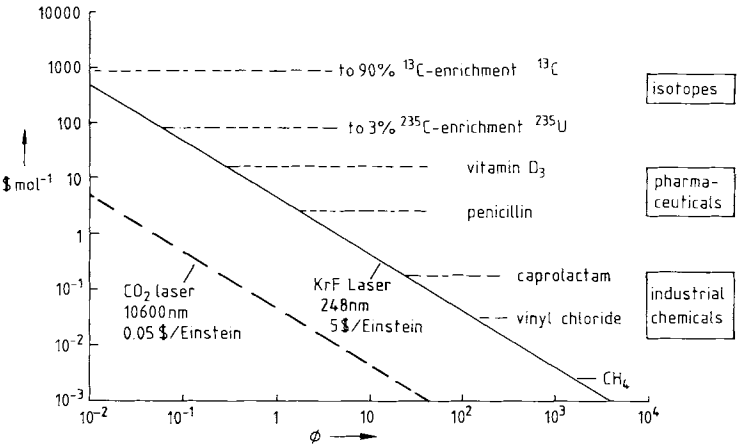

Fig. 20. Influence of quantum yield on product cost. The ordinate gives the cost in dollars per mole of product for conventional chemical syntheses. The application of lasers for production of cheap mass-produced chemicals is only economical at very high quantum yields, Φ.

3.1. Laser-Induced Radical Chain Reactions

Vinyl chloride (VC), the monomer of PVC, is produced industrially mainly by thermal cleavage of HCl from 1,2-dichloroethane (DCE) in a chain reaction. With a worldwide production of over 25×10^6 metric tons per year, VC is one of the leading products of chemical industry in terms of quantity. The advantage of photolytic over thermal initiation of the chain reaction is that the unimolecular process

$$C_2H_3Cl_2 \xrightarrow{+\text{inert gas}} C_2H_3Cl^{\circ} + Cl^{\circ}$$

is rate-determining with a low energy barrier. This leads to a low activation energy for the overall reaction and hence to lower reactor temperatures, higher conversions, and fewer side products. The use of laser radiation to initiate the chain reaction also permits detailed investigations of the reaction kinetics. Radicals may thereby be produced in

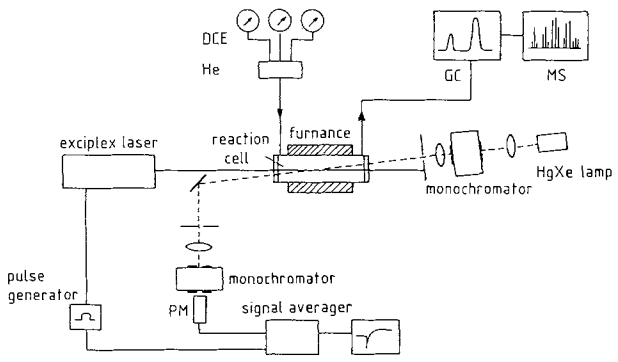

Fig. 21. Experimental setup for the investigation of laser-induced radical chain reactions for the synthesis of VC. The products are detected by time-resolved UV spectroscopy, gas chromatography (GC), and mass spectrometry (MS). PM = photomultiplier.

a wide concentration range and the reactions followed as a function of time. Figure 21 shows the experimental setup required. The formation of vinyl chloride can be followed

directly by time-resolved UV spectroscopy. The entire spectrum of products is recorded with the aid of a GC-MS system. The experimental data can be compared with those obtained from a kinetic model, which for a given temperature and pressure, simulates the whole course of the reaction (Fig. 22) by using a system of coupled differential equations for the elementary chemical steps. From a comparison of the experimental data with the predictions of

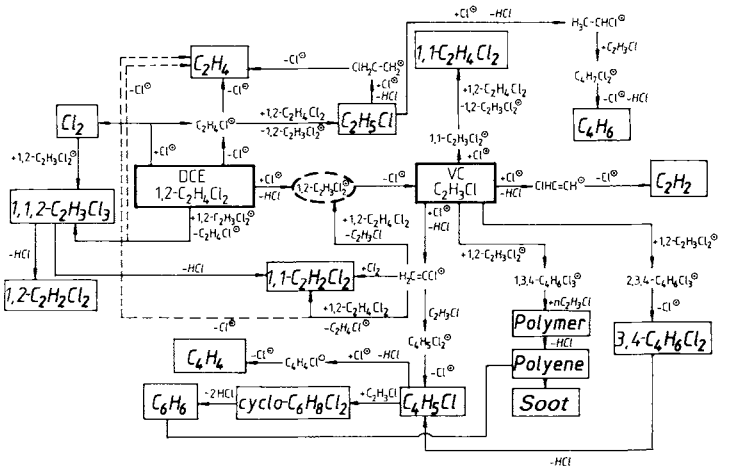

Fig. 22. Reaction paths for the cleavage of hydrogen chloride from dichloroethane, $1,2\text{-}C_2H_4Cl_2$, in a laser-induced chain reaction.

the model, missing rate constants of selected elementary steps can be determined. The pressure and temperature dependence of the laser-induced VC formation can then be used to predict the efficiency of conversion of DCE to VC for industrial conditions. The calculations show that laser photocatalysis results in a clear increase in the efficiency. The addition of chain carriers such as chlorine can increase the quantum yields by over 10^5. A pilot plant for the laser-induced conversion of DCE to VC, which is presently under construction, is shown schematically in Figure 23. DCE is first heated in a tubular reactor. A segment of the reactor is then irradiated with a powerful excimer laser, which is tuned to a wavelength at which the absorption by the medium is as small as possible. Owing to the high parallelism of the laser beam, a steady, small concentration of active chlorine atoms can be generated in a very large volume and hence long chains are produced. At the same time, irradiation of the wall and hence the initiation of heterogeneous processes is to a large extent avoided. With laser radiation, faster conversion at lower temperatures can be achieved compared with other processes. Thus, both higher total conversions and reduced formation of side products are possible simultaneously. Like the thermally initiated process, the laser-induced production of vinyl chloride consumes energy. Therefore, besides the radiation intensity, the rate of heat transport from the walls into the gas is a limiting factor for the shortening of the reaction times. In addition, the interactions between the laser radiation and the reaction medium, which arise from the density and concentration gradients in flow reactors and can lead to undesired beam divergence and focusing,

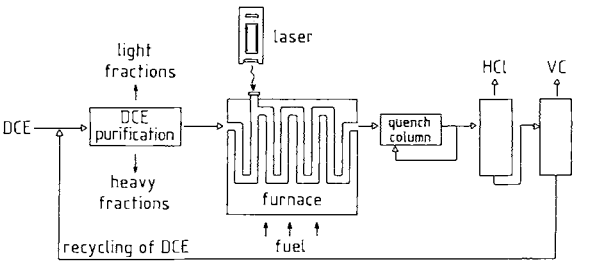

Fig. 23. Pilot plant for the production of vinyl chloride using an excimer laser.

have to be investigated in detail. A further problem in the industrial application of laser photolysis is the contamination of the windows through which the laser beam is admitted to the chemical reactor. One possibility is to flush the window with inert gas or cold DCE, which has a much lower absorption owing to the strong temperature dependence of the UV absorption of DCE. Under certain conditions, the laser itself can "burn" the windows clean by virtue of its high intensity. Compared with conventional photolysis setups, the required transmission surface is considerably smaller here. Overall, the use of high-power UV lasers in synthesis remains to be explored. Compared with the discharge lamps employed to date, the good spatial and spectral collimation of the laser radiation is particularly advantageous. This avoids too high radical concentrations in the vicinity of the light source and allows the required production of reactive radicals under the extreme conditions of pressure and temperature often encountered in large-scale industrial processes.

In the chlorination of 1,1-dichloroethane [Eq. (b)], hydrogen atoms can be replaced at two different positions. The desired α-substitution product, 1,1,1-trichloroethane, is employed as a metal degreaser in place of the more poisonous trichloroethylene. The maximum value of the α:β ratio is 9:1 using lasers compared with 1:1 for the classical thermal method and ca. 4:1 using a Hg lamp. The maximum selectivity is obtained when low-energy chlorine atoms, produced by the photolysis of ICl (from a mixture of iodine and chlorine) at 450 nm, are used as chain carriers.[49]

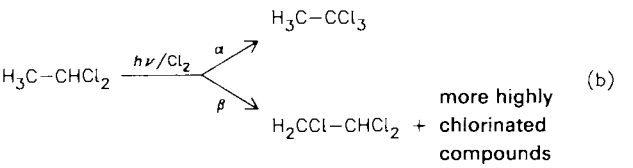

(b)

Ethylene can be produced from methane in the presence of chlorine at high pressure and temperatures around 900 °C via a chain reaction [Eq. (c), (d)].[50] Under these

$$CH_4 + Cl_2 \longrightarrow CH_3Cl + HCl \quad (c)$$

$$2\,CH_3Cl \longrightarrow C_2H_4 + 2\,HCl \quad (d)$$

conditions, however, numerous undesired side products are formed. The methyl chloride produced in the first step [Eq. (c)] can alternatively be obtained in high quantum yield (ca. 10^4) at 200°C using a KrF laser (248 nm). The second step [Eq. (d)] can be initiated by an ArF laser (193 nm), although with a quantum yield of only 1.[51]

The dehydration of ethylbenzene to styrene [Eq. (e)] is catalyzed by OH initiator radicals obtained by photolysis (193 nm) of water vapor at 1 atm with an ArF laser; O_2 is added to prevent premature styrene polymerization.[52] Quantum yields of 10^5 at 500°C and 10^3 at 300°C were attained.

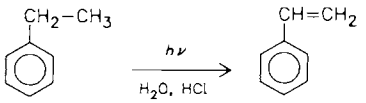

(e)

The photooxidation of cumene to cumene hydroperoxide [Eq. (f), (g)], a precursor of methylstyrene, is another example of a laser-induced chain reaction. In the thermal oxidation with air, numerous undesired side products are formed, whose amount can be reduced by lowering the temperature. By using photoinitiation, the reduction in reaction rate that occurs can be compensated for. At 351 nm (XeF laser), a quantum yield of approximately 500 is attained.[53] At shorter wavelengths (249 nm, KrF laser), the yield is reduced owing to photolysis of the product, cumene hydroperoxide.

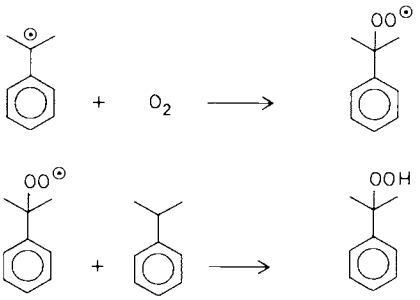

In the photooxidation of isobutane to *t*-butyl hydroperoxide, irradiation (351 nm) with a XeF laser also leads, on addition of chain carriers (HBr), to higher quantum yields, and higher selectivity is attained compared with thermal reactions.[54]

The ketene produced by rapid pyrolysis of acetone at 700°C can only be obtained in relatively small yields (ca. 20%) because of the rapid thermal decomposition that follows. By starting the chain reaction photochemically using a KrF laser (248 nm), higher conversions can be achieved. As in the production of VC, the quantum yield falls with increasing irradiation intensity.[55]

3.2. Laser-Induced Polymerization

Conventional light sources for photopolymerization in layers for reprographic technology as well as for curing synthetic insulating materials have already been applied in industry. Because only the initiator needs to be excited for photopolymerization, large quantum yields can, in principle, be achieved. As an example, the laser-induced, high-pressure polymerization of ethylene is considered in more detail. Numerous investigations have provided information on chemical and phase equilibria as well as kinetic parameters.[56] Thermally induced radical polymerization of ethylene has a number of disadvantages. Long induction periods result from the need to heat the monomer/initiator mixture. Also, the use of a multicomponent mixture (monomer/initiator/regulator) is usually necessary. Polymerization requires initiation by means of heat transfer, initially from the walls. The polymer coating so formed raises the heat transfer resistance of the reactor walls considerably. In the exothermic polymerization process, however, the removal of heat from the reactor is also an important parameter. Indeed, on exceeding a critical temperature, explosive decomposition of the monomers can occur. In contrast, providing the necessary initiation energy with the aid of laser radiation allows controlled and homogeneous initiation of the polymerization process. Figure 24 shows an experimental setup for investigating the UV laser-induced polymerization of ethylene at pressures up to 3000 bar and temperatures up to 300°C in the fluid phase. By means of quantitative infrared and near-infrared spectroscopy, the quantum yields and time course of the polymerization process as a function of pressure, temperature, and laser intensity can be studied directly over a wide range of conversions. Figure 25 shows the time course of the polymer formation as monitored by measuring the absorption of the second overtone of the C–H stretching vibration following initiation of the polymerization with a KrF laser (248 nm). As with the irradiation of DCE, one can work in a region of low absorption and hence achieve very large penetration depths in the starting material. However, the weak ethylene absorption at 248 nm (absorption cross section $\sigma = 2 \times 10^{-4}$ m^2 mol^{-1} at 100°C) is strongly influenced by impurities such as O_2. The absorption of the reaction product, polyethylene, at these wavelengths can be neglected. In the above experiments, quantum yields of 10^4 could be achieved and rate constants for the propagation and termination reactions of polymeriza-

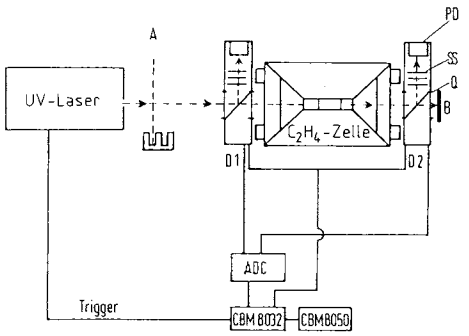

Fig. 24. Experimental setups for the investigation of the laser-induced high-pressure polymerization of C_2H_4. PD, photodiode; SS, scatterer; Q, quartz plate; B, pinhole; D1(2), detector 1(2); A, absorber; ADC, analog-digital converter.

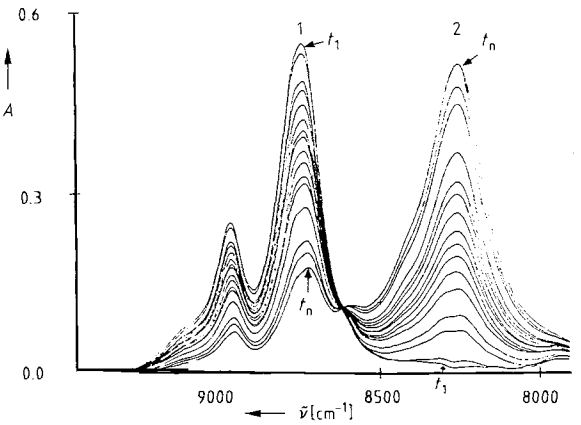

Fig. 25. Observation of polymer formation in C_2H_4 using the overtone spectrum of the CH stretching vibration after irradiation with a KrF laser. 1 = monomer band; 2 = polymer band; A = absorption. t_1 = start, t_n = termination of spectral recording.

tion could be measured directly as a function of pressure and temperature.[56]

Polymerization by photochemical activation has also been achieved with infrared lasers[57] and continuously operating ion lasers; the laser-initiated copolymerization of cyclohexene oxide with maleic anhydride is two orders of magnitude more efficient than is the case for irradiation with conventional UV lamps.[58] On introducing a suitable photoinitiator, very rapid cross-linking in epoxy acrylate layers can be obtained by irradiation with an N_2 laser (337 nm). Up to 450 cross-link points are produced per absorbed photon. About 10^3 double bonds are polymerized for each initiator radical produced.[59] However, polymerization can also be initiated by laser photoionization. Cations can thereby be generated either from suitable, thermally stable salts[60] or by direct photoionization of the monomer via multiphoton processes.[61] The high temporal resolution feasible with laser photolysis also allows detailed investigations of the elementary processes involved in radical polymerization.[62] By introducing photochemically active catalysts, polymerization of acetylene and ethylene can be achieved in 3-μm-thick layers within the irradiation zone of an $Ar^{\oplus}$ ion laser (257.2 nm).[63] Interesting insight into the kinetics of the polymerization process can also be obtained using holographic techniques.[64,65]

The irradiation of varnish coatings with excimer and dye lasers allows, even at very low intensities, very rapid polymerization without the use of solvents or heat. In this way, transparent coatings of 200-μm thickness and pigmented coatings of 20-μm thickness can be produced more than an order of magnitude faster than by the processes used previously.[66]

Laser-induced polymerization allows three-dimensional structures to be produced with high spatial resolution. To this end, two different laser beams are focused simultaneously on a point in a monomer solution, so that polymerization is initiated by two-photon excitation of the monomer or of the cross-linker. By controlling computationally the spatial position of the laser overlap zone of several micrometers diameter, one aims to produce complex, highly precise plastic prototypes and raw forms.[67]

3.3. Organic Photochemistry with Lasers

The photolytic ring opening of 7-dehydrocholesterol (7-DHC) (Fig. 26) to give vitamin D_3, via previtamin D_3 (P_3), has long been employed for the large-scale synthesis of vitamin D_3.[68] The three isomers lumisterol (L_3), tachysterol (T_3), and P_3 can be interconverted by irradiation with UV light, whereby the photostationary composition depends strongly on wavelength. Table 1 and Figure 26 show that the use of two laser wavelengths rather than irradiation with a Hg lamp leads to a considerable improvement in the yield of the desired vitamin D_3 precursor P_3.[69,70] Irradiation with short UV light pulses in the picosecond range decreases the photolysis of P_3 and improves the ratio of P_3 to the undesired T_3 by another factor of 3.[71]

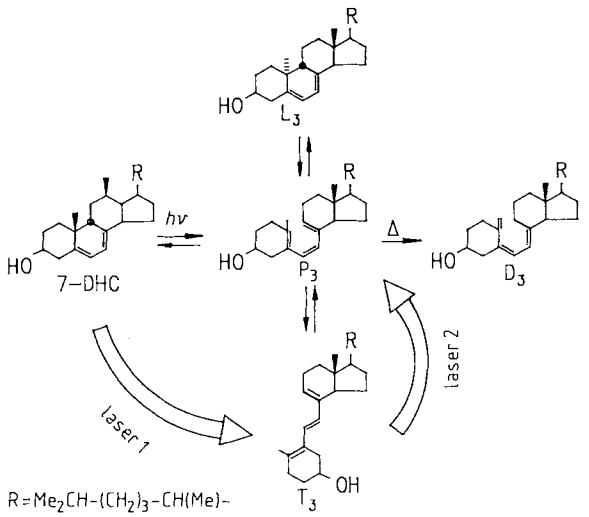

Fig. 26. Synthesis of vitamin D_3.

Table 1. Photostationary composition of the mixture upon irradiation of the vitamin D_3 precursor [69].

Light source	% 7-DHC	% T_3	% L_3	% P_3
Low-pressure Hg lamp	1.5	75.0	2.5	20.0
Medium-pressure Hg lamp	3.4	26.0	17.0	53.0
KrF laser (248 nm)	2.9	71.0	—	26.0
XeCl laser (308 nm)	13.0	3.4	42.0	35.0
KrF + N_2 laser (334 nm)	0.1	11.0	9.0	80.0

The results of the laser experiments allow improvements in the conventional photochemical process: namely, the KrF laser (248 nm) and the N_2 laser are replaced by a low-pressure Hg lamp (254 nm) and a medium-pressure Hg lamp equipped with a suitable filter, respectively. In the production of special vitamin D_3 metabolites for medical diagnostics, an increase in yield by a factor 5 is achieved by the use of lasers.[72]

Peroxides, which are produced from azoalkanes, are important intermediates in the synthesis of the beetle attractant pheromone frontalin.[73] Alone in North America, the beetles *Dendroctonus brevicomis* and *D. frontalis* cause more than a billion dollars worth of damage to wood annually. Frontalin (Fig. 27) can be produced from the azoalkane **1** via the endoperoxide **2**. The 364-nm line of the $Ar^{\oplus}$ laser is particularly suitable for this synthesis, since this

wavelength is absorbed sufficiently by the sensitizer benzophenone but not by the azoalkane **1**. In contrast, direct light absorption by the azoalkane results in loss of N_2 and formation of a singlet diradical which undergoes C–C bond closure to give an undesired product.

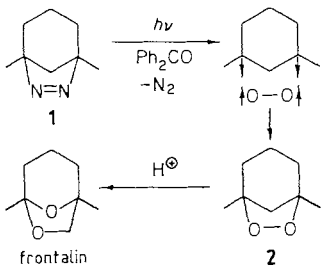

Fig. 27. Synthesis of frontalin. Direct photolysis of **1** results in the formation of a triplet diradical which reacts with O_2.

Similarly, certain azoalkanes can be converted into endoperoxides by laser photolysis followed by scavenging of the resulting diradicals with O_2. From those endoperoxides, substances for preventing (prostacyclins) or promoting (thromboxane) blood clotting can also be produced.[73] The photodecomposition of vitamin K, **3**, which leads to termination of respiration in living cells, can be traced back to the reaction of the preoxetane diradicals **4** with O_2.[73] By using high O_2 partial pressures (>10 bar) and photosensitization with benzophenone, the diradicals **5** and **6** can be scavenged in high yields as the corresponding peroxides.[74]

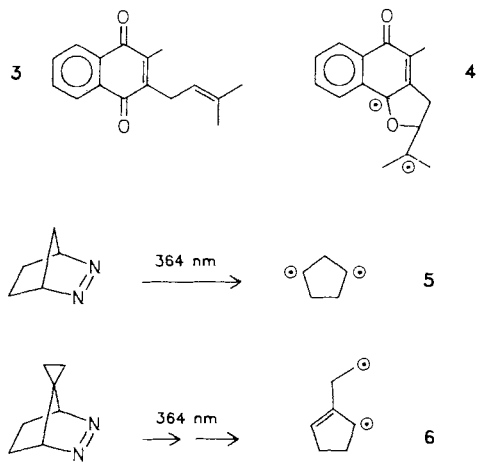

With high-power pulsed lasers, sufficiently high concentrations of radicals can be produced for direct spectrally and temporally resolved detection.[75] Also, higher triplet and singlet states can be reached by successive absorption of laser pulses in the nanosecond and picosecond range (Fig. 28).[76] For a triplet-state lifetime of 10^{-4} to 10^{-7} s, laser intensities of 10^4–10^7 W cm^{-2} are sufficient and are easily attainable using excimer lasers at pulse lengths around 10^{-8} s. In this way, the quantum yield of the photocyclization of carvone **7** to carvone camphor **8** [Eq. (h)] in ethanol can be increased 70-fold compared with the single-

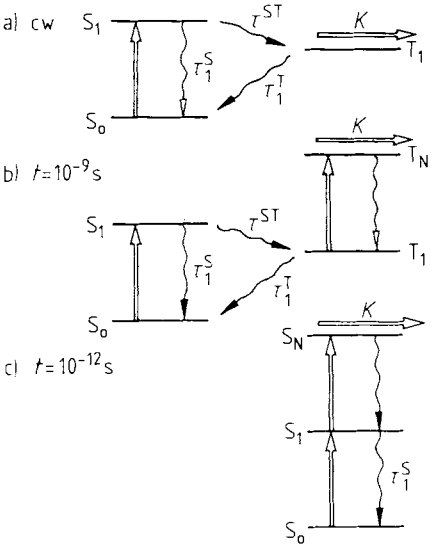

Fig. 28. Reaction possibilities of polyatomic molecules after single-photon and multiphoton excitation by laser pulses of differing duration. a) The relatively small intensity of the continuous (CW) laser leads to excitation only of the S_1 or T_1 state. b) With laser intensities of 10^4–10^7 W cm^{-2} and pulse lengths in the nanosecond range, higher states can also be reached by successive absorption of photons. c) The direct excitation into higher singlet states requires intensities of 10^9–10^{10} W cm^{-2} and pulse lengths of 10^{-12} s. Molecules in higher singlet or triplet states can undergo new reactions (K). τ_1^S, τ_1^T, and τ^{ST} are the characteristic lifetimes of the S_1 state, the T_1 state, and the transition from the S_1 to the T_1 state.

photon excitation.[77] The direct excitation to give higher singlet states requires laser pulses of around 10^{-12} s, since, for the intensities of 10^9–10^{10} W cm^{-2} required for pulses of 10^{-8} s, the damage threshold of the condensed phase is considerably exceeded. Excitation of maleic acid with pi-

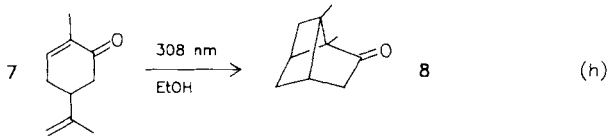

Fo. 5

Angew. Chem. A 601 Fo. 4 + 5 WERK FACHA A60102

cosecond pulses at 265 nm results not only in photodimerization, but, with increasing intensity, also in addition of water to the double bond.[76] Here, the direct cleavage of water by multiphoton excitation apparently plays an important role.[79] The use of ultrashort light pulses of high intensity could open interesting new approaches to the photochemistry of energy-rich double bonds: for example, in the development of optical switches, the construction of organic molecules for energy and information storage, and the synthesis of active substances. Still little used is the selective production of enantiomers by photolysis with polarized light, already described in the 1930s by *W. Kuhn* et al.[80]

The intensive efforts to apply organic glasses and polymers to optical storage of data[81] have already been reported in detail.[65,82] More recently, both for inorganic[83] and for organic[84] materials, interesting results have been achieved by "multicolor" photoionization (simultaneous irradiation with photons of various wavelengths).

3.4. Separation of Isotopes with Lasers

The high frequency sharpness of the electromagnetic radiation possible with the laser has given new impetus to investigations of the photochemical separation of isotopes, which was first attempted over half a century ago.[85] A specific isotope of an element (either in the elemental state or in a molecule) is excited selectively by narrow-band laser light and converted into an ion, isomer, or dissociation or reaction product that can be more readily separated chemically or physically (Fig. 29). The focus of interest was initially the uranium isotope ^{235}U.[86] The most developed process for this so far, AVLIS (*a*tomic *v*apor *l*aser *i*sotope *s*eparation), employs the selective multiphoton ionization of uranium atoms (Fig. 29a) with dye lasers, pumped by powerful copper vapor lasers with high repetition frequency (10 kHz).[87] Besides uranium and plutonium, numerous other elements can be isotope-selectively enriched by this method.[88]

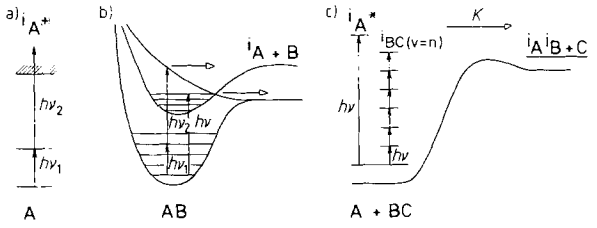

Fig. 29. Possibilities for photochemical separation of isotopes with the laser. ^{i}A represents a particular isotope of the element A. For details, see text.

Following the observation of isotope-selective, infrared multiphoton dissociation of SF_6 with the aid of CO_2 lasers,[22] analogous experiments were performed with UF_6. The radiation required for excitation of the fundamental vibrations of UF_6 at 16 μm can be obtained by rotational Raman scattering of CO_2 laser radiation on para-hydrogen.[89] However, the UF_6 gas beam has to be strongly cooled to obtain the necessary differences in absorption between $^{238}UF_6$ and $^{235}UF_6$. By further selective vibrational excitation of UF_6, clear differences are obtained in the UV absorption spectra[90] of $^{238}UF_6$ and $^{235}UF_6$, which can be used for the isotope-selective dissociation shown in Figure 29b. The laser powers at 308 nm required for industrial application are in the 100-kW range.[91] Besides UF_6, other uranium compounds, such as $UO_2(OCH_3)_6$[92] and uranium complexes[93] were investigated. The technique was also applied successfully for the enrichment of plutonium isotopes by selective excitation of PuF_6.[94] In nuclear power reactors, zirconium is used as a containment material for fuel rods. Isotope separation is of interest since ^{91}Zr has a neutron-capture cross section more than an order of magnitude larger than the other isotopes. Indeed, the selective ionization of ^{91}Zr was reported recently.[95] Because the economic use of nuclear fission is developing more slowly and with more difficulty than was originally assumed, the requirement for additional capacity for isotope separation of uranium is smaller than predicted. This is also true for deuterium,[96] which is required for reactors using natural uranium. Tritium can be enriched (e.g., for experiments in controlled nuclear fusion) by multiphoton excitation of $^3HCCl_3$[97] and $^3HCF_3$[98] with an IR laser.

The isotope-selective dissociation by one-photon excitation (Fig. 29b) can also be achieved by selective excitation of predissociative states, as for isotopes of carbon in formaldehyde.[99] ^{13}C-labeled compounds can be used in medical diagnostics, for example, in metabolic investigations in place of radioactive ^{14}C-labeled compounds, and in NMR tomography. An annual requirement of several hundred kilograms of ^{13}C is to be expected. An industrially relatively well developed process for laser-induced production of carbon isotopes is presented schematically in Figure 30.[100] Laser-induced multiphoton dissociation (Fig. 29c) of Freon 22 (CF_2HCl) results in the formation of C_2F_4, from which ^{13}C-enriched CF_2HCl can be obtained by thermal addition of HCl.[101] The cost of the CO_2-laser photons required for this process can be reduced still further by employing a continuous-discharge CO_2 laser.[102] Enrichment of ^{13}C-isotopes via multiphoton dissociation of CF_3Br[103] is more expensive, because of the considerably higher cost of the starting material. Isotopes can also be enriched by selective excitation of bimolecular exchange[34, 104] or addition reactions.[105]

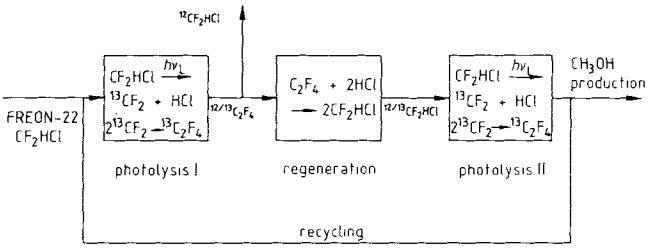

Fig. 30. Production of ^{13}C-enriched compounds by multiphoton dissociation of Freon-22. Photolysis I ($\lambda = 9.5$ μm) leads to a mixture of $^{12/13}C_2F_4$ and $^{12}CF_2HCl$. After separation of $^{12}CF_2HCl$, the remaining $^{12/13}C_2F_4$ is reconverted into $^{12/13}CF_2HCl$ and further enriched with the ^{13}C-isotope by photolysis II ($\lambda = 9.5$ μm).

3.5. Photochemical Purification with Lasers

The selective photochemical removal of impurities with lasers is exemplified by the purification of gaseous SiH_4 (the starting material for the preparation of pure silicon for semiconductor production) from compounds such as AsH_3, PH_3, and B_2H_6, which are difficult to remove chemically. Contamination of such p- and n-charge carriers, even at a ratio of $1:10^9$, can negatively influence the functioning of integrated circuits. Whereas in conventional methods the entire material is subjected to the purification process, the laser acts only on the impurities. Thus, laser irradiation at $\lambda = 193$ nm is absorbed four orders of magnitude more strongly by PH_3 and by AsH_3 and two orders of magnitude more strongly by B_2H_6 than by SiH_4. For an impurity of 1%, more than 99% of the AsH_3 and 40% of the PH_3 and B_2H_6, but only 1% of the SiH_4 is photolyzed.[106] The end products of this photolysis are readily separable solid polymers or gaseous compounds. Laboratory experiments show that the purification process even proceeds ef-

ficiently at atmospheric pressure, so that, for impurities of several ppm, typical absorption cross sections of 10^{-17} cm^2 and reactor lengths of several meters, more than 50% of the laser light is absorbed. Extremely high-purity silane is important for the economic production of electricity from sunlight, since the efficiency of silicon solar cells depends strongly on the impurities present. Further examples of efficient purification of gases are the separation of $COCl_2$ from BCl_3[107] and of CCl_4 from $AsCl_3$[108] and the destruction of dioxin.[109]

Lanthanoids and actinoids can be efficiently separated and purified by exciting the narrow absorption bands of their compounds in the visible and UV.[110] The excitation is still selective even for higher absorber densities in the liquid phase. The new oxidation states formed by the photoredox processes enable the compounds to be readily separated. Figure 31 shows the separation of europium [Eq. (i)] as an example, whereby the hydroxyl radical has to be scavenged, e.g., by isopropanol, to avoid the reverse reaction. The quantum yield for $Eu^{3\oplus}$ photoreduction at

$$Eu^{3\oplus} + H_2O \xrightarrow{193\ nm} Eu^{2\oplus} + H^{\ominus} + OH^{\circ} \quad (i)$$

$$Eu^{2\oplus} + SO_4^{2\ominus} \longrightarrow EuSO_4\downarrow$$

193 nm was given as 5% at 90% conversion, whereby up to a three-hundred-fold enrichment of europium was measured in the precipitate after irradiation of binary europium/lanthanoid mixtures. H_2S in CO/H_2 synthesis gas was photolyzed selectively with an ArF laser and the sulfur released was removed by adsorption on a metal surface.[111] In this way, sulfur impurities could be reduced from 10 ppm to 1 ppm. A spectroscopic selectivity (excitation only of H_2S in the synthesis gas) of 10^7 was measured in the wavelength range 210–220 nm. Quantum yields (H_2S molecules removed per absorbed photon) of 0.4 (1 atm) to 1.0 (10 torr) were achieved. In particular, the use of a laser is interesting for the removal of "fine impurities" (< 1 ppmH_2S), since catalysts based on copper (e.g., those used for production of methanol from synthesis gas) have lifetimes of about one year if the H_2S impurities in the CO/H_2 mixture can be reduced to less than 1 ppm.

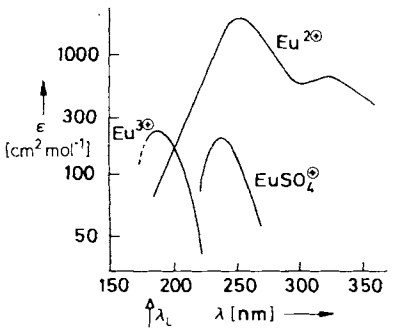

Fig. 31. Laser-induced separation of lanthanoids. The absorption spectra of europium in various oxidation states show that the $Eu^{3\oplus}$ ions can be selectively reduced in the liquid phase with the aid of an ArF excimer laser ($\lambda_L = 193$ nm). The $Eu^{2\oplus}$ ions formed are precipitated as $EuSO_4$ after reaction with sulfate ions.

3.6. Synthesis of Defined Solids and Catalysts with Lasers

Pyrolysis of gas mixtures with laser radiation can be used to produce catalytically active solids of variable composition (Fig. 32). After complete mixing of the gaseous starting materials and their rapid heating in the laser beam,

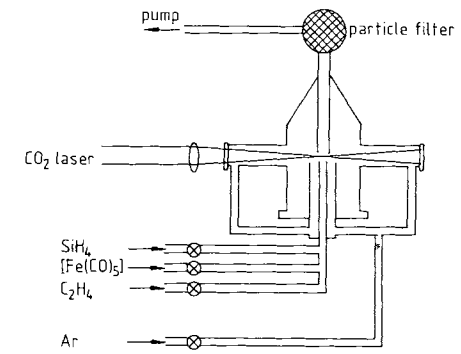

Fig. 32. Synthesis of Fe/Si/C catalysts by CO_2 laser pyrolysis of gaseous starting materials. By varying the partial pressures of the components and the laser intensities, catalysts with varying properties can be produced.

very small solid particles with homogeneous structure and large surface area are obtained. Figure 33 shows the yield of alkanes and alkenes obtained from the Fischer–Tropsch synthesis with laser-synthesized Fe/Si/C catalysts. Whereas with saturated hydrocarbons mainly methane is formed, with olefins considerably longer chains are obtained. By optimizing the composition of the laser-synthesized catalysts, higher selectivity and preferential formation of the valuable light olefins (C_2–C_4) can be achieved.[112] By a similar process to that described in Figure 32, powders of defined composition can be obtained for the production of specialty ceramics.[113] Irradiation of $[Fe(CO)_5/SiH_4$,[114] NH_3/SiH_4,[115] $(Me_3Si)_2NH$,[116] or $SiH_4/NH_3/CH_4$[117] gas mixtures with a CO_2 laser leads to particularly fine, pure, spherical, relatively non-clumping, and almost identically sized Si/Fe, Si_3N_4, and Si/C/N grains for the production of special ceramics.

Metal carbonyl catalysts can be UV-photoactivated instead of thermally activated. Active centers are formed by cleavage of one or more CO ligands, often resulting in ca-

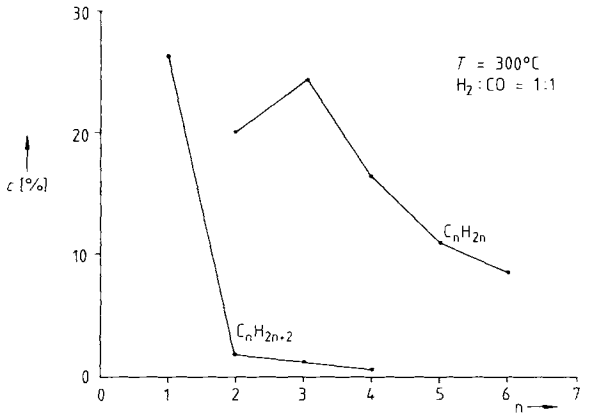

Fig. 33. Fischer–Tropsch synthesis with laser-produced Fe/Si/C catalysts. n = number of C atoms; c = amount of product in %.

talytic activity even at room temperature. Besides polymerization (Section 3.2), the isomerization and hydration of alkenes with $[Fe(CO)_5]$ catalysts[118,119] and the silylation of alkenes and aldehydes[118,130] with $[Co_4(CO)_{12}]$ catalysts upon irradiation with a XeF laser or a frequency-doubled Nd-YAG laser have been investigated. For the isomerization of 1-pentene, quantum yields of 10^3 and "turn-over" rates (quantum yield per average lifetime of the catalyst) of 4×10^3 s^{-1} at 50% conversion of 1-pentene can be achieved. Broad-band light sources such as flash lamps lead more readily to direct photolysis and to undesired side products.

Metallic glasses having unusual compositions and properties and other metastable phases can be produced by irradiation with intense laser pulses. Short laser pulses lead here to extremely rapid heating and melting, followed by very rapid cooling and solidification. Cooling rates of up to 10^{12} K s^{-1} have been obtained for alloy films after heating by means of picosecond laser pulses.[121]

3.7. Laser-Induced Deposition of Materials on Surfaces

In conventional, thermally induced deposition of materials from the gas phase (*c*hemical *v*apor *d*eposition, CVD), relatively high temperatures (600–900 °C) are required. The temperature can be reduced to 350–450 °C by employing electrical discharges in plasma CVD. However, undesired species can be formed in wall reactions and interfere with the process, and radiation damage can be induced in the deposited films; moreover, in order to ensure the stability of the discharge, only a restricted range of pressures is available and the reaction volume can only be controlled to a very limited extent. The LICVD method (*l*aser-*i*nduced *c*hemical *v*apor *d*eposition) for controlled deposition of selected species offers many advantages: control of the irradiation area from μm^2 to cm^2 and of the irradiation time from 10^{-14} s to continuous operation, no wall effects, and independent control of the substrate temperature for production of layers with extremely high purities.

Figure 34 shows schematically three possibilities for the LICVD method.[122] In the pyrolytic process (I), the laser light is generally not absorbed by the reaction gas, but is used instead to produce strong localized heating at the substrate surface. Because of the strong temperature gradient formed, the material is deposited in a narrowly defined region, so that transport from the gas phase can occur from various directions. The pyrolytic method can be applied over a wide range of pressures and allows deposition rates on the order of 1 to 10^2 $\mu m\ s^{-1}$, a factor of 10^2 to 10^4 higher than with a conventional CVD process.[123] In process II, a better directed and more homogeneous beam of the material to be deposited is obtained than in the ion vaporization technique otherwise generally employed.[124] In the photolytic process (III), selective excitation of dissociating states is employed. The products of laser dissociation can either be condensed directly on the surface or allowed to react chemically with other species present in the surface layer. As shown in Figure 35 III, the laser can also be focused directly on the surface and moved over it.

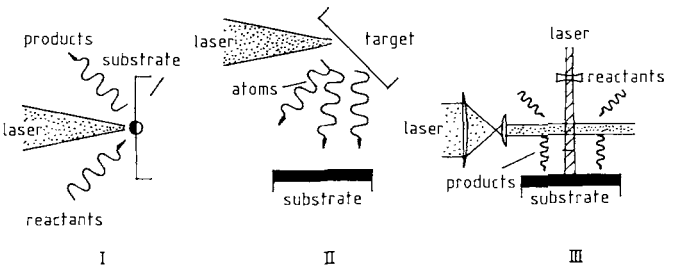

Fig. 34. Possibilities for the photochemical deposition of materials from the gas phase by means of IR or UV lasers. For details, see text.

Frequency-doubled $Ar^{\oplus}$ lasers ($\lambda = 257$ nm) can be used to deposit Cd from $Cd(CH_3)_2$,[125] Zn from $Zn(CH_3)_2$,[126] and Ni from $[Ni(CO)_4]$.[127] Because of the nonlinearity of the grain-formation process, spatial resolution of 0.2 to 0.5 μm is obtained. In conjunction with computer control of the laser beam, it is therefore possible to "draw" complex electronic circuits directly onto a substrate.[128] Besides metallic conducting layers, insulators and semiconductor layers can also be deposited. In addition to continuously operating ion lasers, CO_2 and UV-excimer lasers can be employed, which permit the production of large-surface-area, thin layers, e.g., amorphous Si layers for the production of cheap solar cells.[129] The rate of deposition can be increased considerably by the participation of the photoelectrons produced by the UV excimer laser.[130] Information on the primary processes occurring on applying the radiation of a UV-excimer laser for the deposition of metals from organometallic compounds (MOCVD) can be obtained using multiphoton mass spectrometry with time-of-flight analysis. This technique allows the production of an entire mass spectrum with high sensitivity by using a single laser pulse.[131] The species involved can be identified from both their absorption spectra and their masses. In this way, the formation of tellurium atoms and dimers upon photolysis of $Te_2(CH_3)_2$ at two different laser wavelengths, the energy states of the Te atoms formed, and the energy distribution within the molecular fragments can be determined directly. Use of ultrashort light pulses appreciably facilitates the detection of unstable parent ions.[132] Further, the deposition and dissolution rate of metals at liquid/solid boundaries can be increased considerably ($> 10^3$) by the use of laser radiation. The laser beam is directed onto the cathode in an electrolyte solution and the laser wavelength chosen so that the electrolyte absorbs as little as possible.[133,134] Metal deposition without electric current is also feasible.

4. Ablation and Processing of Materials with Lasers

Two types of material processing with lasers can be distinguished: thermal, nonreactive processing and chemical processing. In thermal processing, the sample is heated locally and brought to melting and evaporation. Welds and cuts can be made on the sample. This method is applied in a modified form to anneal defects on surfaces, to recrystallize, to harden materials, or to alloy locally. In chemical processing, chemical reactions are initiated by the laser radiation.

4.1. Processing of Polymer and Semiconductor Materials

In principle, any laser with sufficient power density is suitable for processing of polymer materials and substrates for microchips. Recently, however, several significant advantages of UV lasers have become apparent,[134] particularly when microscopically fine and precise work with clean edges is required. These types of requirements arise especially in the production of chips of very high information density (microlithography), but also in "microwriting" on polymer materials and in micromanipulation of biological objects. A significant advantage of UV light is that at wavelengths below ca. 350 nm the energy of single photons is sufficient to break chemical bonds. In contrast to IR lasers, whose radiation can penetrate more deeply and excite vibrations in polymer molecules, leading to thermal decay, the use of UV lasers results in cleavage of bonds where the photon density is highest, i.e., on the surface. This leads predominantly to monomer fragments and very clean ablation edges.[135] By laser decomposition of halogen compounds adsorbed on surfaces, fine patterns can be etched in semiconductors, glasses, metals, ceramics, and other materials.[136]

The following processes occur in etching:

Photodissociation	CH_3Br	$\longrightarrow CH_3^{\odot} + Br^{\odot}$	
Chemisorption	n(Br)	$\longrightarrow$ (nBr):(GaAs)	$\Delta H < 0$
Surface erosion	(nBr):(GaAs)	$\longrightarrow GaBr_n + As$	
Evaporation	GaBr (solid)	$\longrightarrow$ gallium bromide (g)	

Free halogen atoms are removed from the gas phase by radical scavengers, so that the etching process occurs only in the direct vicinity of the laser beam. The method is also applicable to liquid/solid boundaries.

5. Application of Lasers in Medicine

Most of the laser applications described below are not yet accepted in routine clinical practice. The application of the laser in surgery offers a number of advantages: stypsis, precise work, reduction in the number of instruments required, contact-free tissue ablation, asepsis, minimal damage to the surrounding tissue.[137] In respiratory tract or gynecological operations, the laser light can be led directly to the site of operation via light guides.

For laser light to interact with tissue, it must first be absorbed. Several simple observations can be made:

1. The interaction with IR radiation is best described in terms of absorption by water. The interaction is predominantly thermal in nature.
2. The absorption properties with respect to visible light are determined by the pigmentation of the tissue in question.
3. The further one goes into the UV, the more important photochemical effects become. At wavelengths below 200 nm, photoablation occurs almost exclusively. Here, the interaction of light with polymers (Section 4.1) can serve as a model.

This overview says nothing about the influence of power density on the interaction of laser light with tissues. Table 2 shows the variety of interactions possible and how they can be applied in medicine. The data in Table 2 are collected mostly from ref. [137, 138]. Table 3 gives an overview of the lasers used in medicine and their applications, which will be illustrated below with no attempt at completeness.

The aim of *angioplasty* with lasers is to open sclerotic blood vessels.[140] The use of lasers operating in the visible or infrared, however, results in carbonized edges and bubblelike lesions in the vessel tissues, which remain after removal of the stenosis.[141] Thrombocytes attach themselves to such edges and are the starting point for a new stenosis. Very recently, it was shown that these problems do not arise when ArF excimer lasers are used.[142] The edges of the recanalized tissue are smooth (Fig. 35).[143]

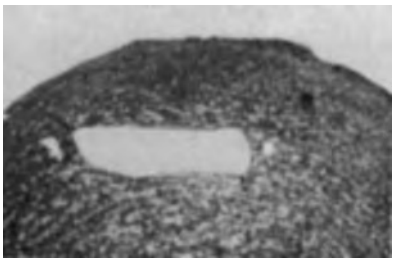

Fig. 35. Histological section through aorta tissue that has been recanalized using an ArF laser. Enlargement ca. 100-fold; laser power ca. 50 J cm^{-2} [143].

Table 2. Medically useful interactions of light and matter.

Power density	Type of interaction	Mechanism	Application
mW/cm^2	Biostimulation [139]	Influencing certain parts of metabolism	Healing of inflammations and wounds
kW/cm^2	Coagulation	Denaturation and resulting clotting of proteins, etc., at local temperatures of 40–80 °C	"Glueing" of tissue parts; clotting of bleeding
MW/cm^2	Evaporation	Water evaporates (partly explosively) from the tissue; breakdown of tissue structure	Cutting of tissues analogous to the surgical knife but contact-free.
GW/cm^2	Photoablation Photodisruption	Individual bonds are broken	Cold evaporation of tissue parts
TW/cm^2	Formation of microplasms	Molecules are ionized so that electron avalanches occur	Destruction of "hard" materials such as gallstones

Table 3. Possibilities for application of material processing in medicine

Laser type	Working wavelength [nm]	Presumed nature of interaction with tissue	Penetration depth into the skin	Main use following interaction [a]						Areas of medical application [b]				
				A	B	C	D	E	U	V	W	X	Y	Z
ArF excimer	193		Surface				×	×	×					
KrF excimer	248		Very small			(×)	×	×	×					
XeCl excimer	308		Small			×	×	×	×					
$Kr^{\oplus}$ ion	407		Deep	×	×	×				×				
$Ar^{\oplus}$ ion	516		Very deep	×	×	×				×	×	×	×	
Nd-YAG, frequency-doubled	532		Very deep		×	×	(×)			×				
He-Ne	620		Very deep	×						×				×
Semiconductor	780–1200		Deep	×										×
Nd-YAG	1064		Deep		×				×		×	×	×	
Er-YAG	2936		Small										×	
CO_2	10000		Small			×			×		×	×		

[a] A = biostimulation; B = coagulation; C = evaporation, cutting; D = photoablation, photodisruption; E = formation of microplasms. [b] U = angioplasty, V = photodynamic therapy, W = urology - gynecology, X = gastroenterology, Y = ophthalmology, Z = dental medicine.

In *tumor therapy with lasers*, two methods are being explored. One attempts to coagulate tumors directly[144] and the other uses the laser for photodynamic therapy (PDT).[145] In PDT, dyes are employed that absorb light of a particular wavelength preferentially and are either incorporated selectively in the tumor tissue or are more slowly degraded by the tumor tissue. An example is provided by the hematoporphyrin derivatives (HpD), which are incorporated selectively by the vessel tissue of tumors. If the tumor is irradiated with a red laser (e.g., He-Ne laser), the HpD-labeled tumor tissue absorbs selectively. HpD is decomposed photolytically, so that oxygen radicals are formed, which as strong cytotoxins interfere with the blood vascular system of the tumor and hence cut off its supply of nutrients. Other dyes, such as phthalocyanines, are incorporated preferentially in the mitochondria of cancer cells and after laser irradiation interfere with the metabolism of these cells.

Numerous tumors can be temporarily degraded by use of PDT. Nevertheless, baring individual exceptions, cancers cannot be cured in this way, since the metastases are not treatable and the effects of PDT on various tumors vary greatly.[146]

PDT is still being investigated to some extent in animal experiments for the treatment of bladder tumors,[147] breast cancer,[148] gynecological tumors,[149] intestinal cancer[150] and lung tumors. The selectivity for certain tumors might be increased by coupling monoclonal antibodies to HpD.[151]

A very attractive application of lasers in *gastroenterology* could be in the destruction of gallstones. In contrast to kidney stones, 90% of which can be destroyed by a lithotripter without an operation, gall stones are insensitive to fluid shock waves. In contrast, laser pulses of high power density destroy gall stones, probably after forming microplasms which break the stones from within. For this type of application, the excimer laser is probably the most suitable.

All *lasers* that are suitable for coagulation of tissue can also be applied to *stop stomach hemorrhages* by thermally clotting the blood. In contrast to drug therapies to stop hemorrhages, one can work very well locally with the laser and thereby avoid irritating the neighboring tissue.

In *neurosurgery*, lasers have long been used to treat tumors in the brain.[152] In particular, the possibility of precise, contact-free operation is made use of since in brain surgery, even more than for other parts of the body, it is important to protect healthy neighboring tissue. Most recently, first results on the application of lasers in microsurgery were reported.[153] Here, the coagulating action of a focused laser was used to reconnect interrupted nerve connections very precisely.

In *dermatology*, hemorrhages that form in the skin by perforation of capillary vessels can be treated by the green light of the $Ar^{\oplus}$ laser[154] and the frequency-doubled Nd-YAG laser. In this way, blood clots are destroyed and simultaneously capillary vessels are closed. Less specific is work with the CO_2 laser, whose thermal effect is used, for example, to remove warts or tatoos.[155]

The development of laser treatment methods in ophthalmology is the most advanced and illustrates clearly how completely different results can be achieved by choosing a suitable laser wavelength. With an Nd-YAG laser, one can reach areas just behind the eye lens on account of the shallow penetration depth of IR light. Membranes can therefore be opened, through which intraocular overpressure

can be released. The green light of the $Ar^{\oplus}$ laser,[156] the frequency-doubled light of the Nd-YAG laser,[157] or the blue light of the $Kr^{\oplus}$ laser can be used to reach the fundus of the eye, the retina, through the transparent eye lens and the transparent vitreous humor, for example to "weld" (coagulate) detached areas of the retina. For corrections of curvature defects of the cornea, on the other hand, wavelengths that are absorbed by the cornea, such as those of excimer laser light, are needed.[158] With the aid of cylindrical lenses, excimer laser pulses are imaged to a streak-formed cross section, which is used to change the radius of curvature in the desired manner.

In treatment of opthalmic disorders, another important advantage of the laser is apparent: often, the laser, which is required for material processing, i.e., operational tasks, can be employed by means of a suitable regulation technique for diagnosis and analysis of the operation results. This not only reduces the number of instruments required for the operation but but also reduces the irritation to which the eye is exposed.[159]

6. Summary and Outlook

Twenty-five years after its discovery, the laser is irreplaceable in many areas of basic chemical research. The use of lasers provides a direct approach to the investigation of the molecular details of chemical reactions. The results can be compared directly with predictions based on quantum-mechanical calculations. The data so obtained on reaction cross sections and rate constants of elementary chemical processes can be used as a basis for detailed mathematical modeling of chemical reactions, which in the future will have the same significance that tables of thermodynamic values have at present. Investigations with lasers will increasingly provide information on numerous kinetic processes in gases, liquids,[160, 161] and solids as well as in biological systems. A significant breakthrough in the investigation of changes in molecular structures in the course of chemical and biological processes is to be expected from the extension of the laser principle to the X-ray region. Although stimulated emission has been observed down to wavelengths of 21 nm, for the region of several nm considerable difficulties still have to be overcome,[6b, 161] because extremely high pumping efficiencies are required owing to the short lifetimes of excited states in the X-ray region.

Although the cost of laser photons is at present markedly above that of photons from conventional light sources, photochemical synthesis with lasers can afford a number of interesting results. In particular, the laser-photochemical production of thin layers of metal, insulators, and semi- and superconductors will acquire increasing technological importance, not only for newer processing techniques for semiconductor components and circuits, but also particularly for the development of integrated sensors for controlling automated finishing processes. The application of lasers for the production of larger quantities of isotopically pure compounds, specific pharmaceuticals, initiation of chain reactions in the production of monomers or the polymerization of coating layers, and the production of powders for ceramics and catalytically active material will depend on how far the costs of laser photons can be further reduced and whether lasers with higher powers and lifetimes become available. For some technical applications, such as laser printers and material processing using CO_2 lasers, these requirements have already been met. For excimer lasers, systems with powers in the kW range will be realized in the near future. It is at present hard to estimate how far new laser principles, such as the free electron laser (FEL), will allow high powers and efficiencies in a wide range of wavelengths from the infrared to the ultraviolet to be attained. So far, FEL systems have only been operated in the infrared and visible spectral regions, whereby extreme demands on the quality of the electron beam are made.

It is assumed that, besides the production of chemical products and the processing of technical materials, high-power lasers will be of particular interest for applications in medicine. A significant advantage of the laser is that one can penetrate inside the body using light guides. However, for this purpose, very high laser powers often have to be transported if specific photochemical effects, and not just thermal effects, are desired in the processing of biological material. Suitable optical materials still need to be developed for this purpose.

We thank numerous colleagues for sending material for the review and Dr. K. O. Greulich (Heidelberg) for compiling the section on the application of lasers in medicine. Financial support for our work was received from the Fonds der Chemischen Industrie, the Deutsche Forschungsgemeinschaft, the Stiftung Volkswagenwerk, and the Bundesministerium für Forschung und Technologie.

Received: June 27, 1986 [A 601 IE]
German version: *Angew. Chem. 99* (1987) 38
Translated by Dr. *Penelope Monkhouse*, Heidelberg

[1] A. Einstein, *Phys. Z. 18* (1917) 121.
[2] J. P. Gordon, C. H. Townes, *Phys. Rev. 99* (1955) 1264.
[3] T. H. Maiman, *Nature (London) 187* (1960) 493; P. J. Collins, D. F. Nelson, A. L. Schawlow, W. Bond, C. G. B. Garrett, W. Kaiser, *Phys. Rev. Lett. 5* (1960) 303.
[4] J. Wolfrum, *Nachr. Akad. Wiss. Göttingen Math. Phys. Kl. 2 1973*, No. 5.
[5] F. P. Schäfer, W. Schmidt, J. Volze, *Appl. Phys. Lett. 9* (1966) 306; P. P. Sorokin, J. R. Lankard, *IBM J. Res. Dev. 10* (1966) 162.
[6] a) W. Demtröder, *Laser Spectroscopy Springer Ser. Chem. Phys. 5* (1981); b) F. P. Schäfer, *Phys. Bl. 42* (1986) 283.
[7] D. R. Crosley (Ed.): *Laser Probes for Combustion Chemistry (ACS Symp. Ser. 134)*, Washington 1980.
[8] H. A. Schwarz, R. R. Williams, Jr., W. H. Hamill, *J. Am. Chem. Soc. 74* (1952) 6007; R. M. Martin, J. E. Willard, *J. Chem. Phys. 40* (1964) 3007.
[9] J. Warnatz, *Ber. Bunsenges. Phys. Chem. 87* (1983) 1008; J. Wolfrum, *XXth Symp. (Int.) Combust.* (The Combustion Institute, 1985) 64.
[10] K. Kleinermanns, J. Wolfrum, *J. Chem. Phys. 80* (1984) 1446.
[11] C. F. Melius, R. J. Blint, *Chem. Phys. Lett. 64* (1979) 183.
[12] K. Kleinermanns, R. Schinke, *J. Chem. Phys. 80* (1984) 1440.
[13] T. Just, P. Frank, *Ber. Bunsenges. Phys. Chem. 89* (1985) 1981.
[14] C. Cobos, H. Hippler, J. Troe, *J. Phys. Chem. 89* (1985) 342.
[15] K. Kleinermanns, E. Linnebach, *J. Chem. Phys. 82* (1985) 5012.
[16] K. Kleinermanns, E. Linnebach, *Appl. Phys. B 36* (1985) 203.
[17] a) H. H. Dispert, M. W. Geis, P. R. Brooks, *J. Chem. Phys. 70* (1979) 5317; b) Z. Karny, R. C. Estler, R. N. Zare, *ibid. 69* (1978) 5199; c) C. Man, R. C. Estler, *ibid. 75* (1981) 2779; d) F. Heismann, H. J. Loesch, *Chem. Phys. 64* (1978) 5199; e) M. Hoffmeister, L. Potthast, H. J. Loesch, *ibid. 78* (1983) 4376.
[18] R. Altkorn, F. E. Bartoszek, J. Dehaven, G. Hancock, D. S. Perry, R. N. Zare, *Chem. Phys. Lett. 98* (1983) 212.

[19] a) P. Andresen, A. C. Luntz, *J. Chem. Phys. 72* (1980) 5842; b) K. Kleinermanns, A. C. Luntz, *ibid. 77* (1982) 3533, 3774.
[20] A. C. Luntz, R. Schinke, W. A. Lester, Jr., S. H. Günthard, *J. Chem. Phys. 70* (1979) 5908; A. C. Luntz, *ibid. 73* (1980) 1143, 5393.
[21] J. Franck, A. Eucken, *Z. Phys. Chem. Abt. B 20* (1933) 460.
[22] V. S. Letokhov, *Annu. Rev. Phys. Chem. 26* (1975) 133.
[23] M. Kneba, J. Wolfrum, *Annu. Rev. Phys. Chem. 31* (1980) 47.
[24] F. London, *Z. Elektrochem. Angew. Phys. Chem. 35* (1929) 552.
[25] P. Siegbahn, B. Liu, *J. Chem. Phys. 68* (1978) 2455; *80* (1984) 581.
[26] J. Wolfrum in W. Jost (Ed.): *Atom Reactions in Physical Chemistry - an Advanced Treatise*, Academic Press, New York 1975.
[27] U. Wellhausen, J. Wolfrum, *Ber. Bunsenges. Phys. Chem. 89* (1985) 314.
[28] J. Wolfrum, *J. Phys. Chem. 90* (1986) 375.
[29] T. Dreier, J. Wolfrum, *Int. J. Chem. Kinet. 18* (1986) 919.
[30] H. R. Mayne, J. P. Toennies, *J. Chem. Phys. 75* (1981) 1754.
[31] D. D. Gerrity, J. J. Valentini, *J. Chem. Phys. 79* (1983) 5202; C. T. Rettner, E. E. Marinero, R. N. Zare, *ibid. 80* (1984) 4142; R. Götting, H. R. Mayne, J. P. Toennies, *ibid. 80* (1984) 2230.
[32] M. Kneba, J. Wolfrum, *J. Phys. Chem. 83* (1979) 69.
[33] D. K. Bondi, J. N. L. Connor, J. Manz, J. Römelt, *Mol. Phys. 50* (1983) 467.
[34] D. Arnoldi, K. Kaufmann, J. Wolfrum, *Phys. Rev. Lett. 34* (1975) 1597.
[35] R. S. Sheorey, G. W. Flynn, *J. Chem. Phys. 72* (1980) 1175; M. Kneba, R. Stender, U. Wellhausen, J. Wolfrum, *J. Mol. Struct. 59* (1980) 207.
[36] H. Frei, G. C. Pimentel, *J. Phys. Chem. 85* (1981) 3355.
[37] H. Frei, G. C. Pimentel, *J. Chem. Phys. 78* (1983) 3698; A. Knudsen, G. C. Pimentel, *ibid. 78* (1983) 6780.
[38] P. Hering, P. R. Brooks, R. F. Curl, R. S. Judson, R. S. Lowe, *Phys. Rev. Lett. 44* (1980) 687; H. P. Grieneisen, J. Xue-Jing, K. L. Kompa, *Chem. Phys. Lett. 82* (1981) 421; C. Jouvet, B. Soep, *ibid. 96* (1983) 426.
[39] T. C. Maguire, P. R. Brooks, R. F. Curl, Jr., *Phys. Rev. Lett. 50* (1983) 1918.
[40] P. Arrowsmith, P. E. Bartoszek, S. H. P. Bly, T. Carrington, P. E. Charters, J. C. Polanyi, *J. Chem. Phys. 73* (1980) 5895; P. Arrowsmith, S. H. P. Bly, P. E. Charters, J. C. Polanyi, *ibid. 79* (1983) 283.
[41] D. G. Imre, J. L. Kinsey, R. W. Field, D. H. Katayama, *J. Phys. Chem. 86* (1982) 2564.
[42] D. G. Imre, J. L. Kinsey, A. Sinha, J. Krenos, *J. Phys. Chem. 88* (1984) 3956.
[43] R. C. Estler, R. N. Zare, *J. Am. Chem. Soc. 100* (1978) 1323.
[44] G. G. Balint-Kurti, R. N. Yardley, *Faraday Discuss. Chem. Soc. 62* (1977) 77.
[45] C. T. Rettner, R. N. Zare, *J. Chem. Phys. 75* (1981) 3636.
[46] D. Astholz, J. Troe, W. Wieters, *J. Chem. Phys. 70* (1979) 5107.
[47] J. Troe, W. Wieters, *J. Chem. Phys. 71* (1979) 3931.
[48] H. Hippler, J. Troe, H. J. Wendelken, *J. Chem. Phys. 78* (1983) 6709; H. Hippler, K. Luther, J. Troe, H. J. Wendelken, *ibid. 79* (1983) 239.
[49] D. J. Perettie, J. C. Stevens, J. B. Clark, *NATO ASI Ser. Ser. B 105* (1984) 239.
[50] S. W. Benson, US-Pat. 4 199 533 (1980).
[51] K. V. Reddy, *Proc. SPIE Int. Soc. Opt. Eng. 458* (1984) 53.
[52] A. Kaldor, *NATO Adv. Study Inst.* (San Miniato, Italy 1982) lecture.
[53] D. J. Perettie, *NATO Adv. Study Inst.* (San Miniato, Italy 1982) lecture.
[54] R. G. Bray, M. S. Chou, *Proc. SPIE Int. Soc. Opt. Eng. 458* (1984) 75.
[55] Zhang Yunwu, W. Fuß, K. L. Kompa, F. Rebentrost, *Laser Chem. 5* (1985) 257.
[56] P. Ehrlich, R. N. Pittilo, *Hochpol. Forsch. 7* (1970) 386; G. Luft, *CZ Chem. Tech. 2* (1973) 89; M. Buback, H. Lendle, *Makromol. Chem. 184* (1983) 193; M. Buback, H. Hippler, J. Schweer, H. P. Vögele, *Makromol. Chem. Rapid Commun. 7* (1986) 261; H. Brademann, M. Buback, H. P. Vögele, *Makromol. Chem. 187* (1986) 1977.
[57] S. G. Il'Yasov, I. N. Kalvina, G. A. Kyulyan, V. F. Moskalenko, E. P. Ostapchenko, *Sov. J. Quantum Electron. (Engl. Transl.) 4* (1975) 1287; J. P. Fouassier, P. Jaques, D. J. Lougnot, T. Pilot, *Polym. Photochem. 5* (1984) 57.
[58] R. K. Sadhir, J. D. B. Smith, P. M. Castle, *J. Polym. Sci. Polym. Chem. Ed. 23* (1985) 411.
[59] C. Decker, *J. Polym. Sci. Polym. Chem. Ed. 21* (1983) 2451.
[60] S. P. Pappas, B. C. Pappas, L. R. Gatechair, W. Schnabel, *J. Polym. Sci. Polym. Chem. Ed. 22* (1984) 69.
[61] R. Bussas, K. L. Kompa in *Max-Planck Inst. Quantenopt. (Ber.) 1984.*
[62] G. Amirzadeh, W. Schnabel, *Makromol. Chem. 182* (1981) 2821; T. Sumiyoski, W. Weber, W. Schnabel, *Z. Naturforsch. A 40* (1985) 541; C. E. Hoyle, R. D. Hensel, M. B. Grubb, *J. Polym. Sci. Polym. Chem. Ed. 22* (1984) 1865.
[63] D. J. Ehrlich, J. Y. Tsao, *Appl. Phys. Lett. 46* (1985) 198.
[64] H. Niederwald, K. H. Richter, W. Güttler, M. Schwörer, *Mol. Cryst. Liq. Cryst. 93* (1983) 247.
[65] C. Bräuchle, D. M. Burland, *Angew. Chem. 95* (1983) 612; *Angew. Chem. Int. Ed. Engl. 22* (1983) 582.
[66] G. L. Paul, *Conf. Lasers Electroopt.* (San Francisco 1986) p. 48.
[67] R. E. Schwerzel, V. E. Wood, V. D. McGiuniss, C. M. Verber, *Proc. SPIE Int. Soc. Opt. Eng. 458* (1984) 90; F. Nakai, Y. Marutani, *Conf. Lasers Electroopt.* (San Francisco 1986) p. 42.
[68] M. Fischer, *Angew. Chem. 90* (1978) 17; *Angew. Chem. Int. Ed. Engl. 17* (1978) 16.
[69] V. Malatesta, C. Willis, P. A. Hackett, *J. Am. Chem. Soc. 103* (1981) 6781.
[70] W. G. Dauben, R. B. Phillips, *J. Am. Chem. Soc. 104* (1982) 858.
[71] N. Gottfried, W. Kaiser, M. Braun, W. Fuss, K. L. Kompa, *Chem. Phys. Lett. 110* (1984) 335.
[72] P. A. Hackett, C. Willis, M. Gauthier, A. J. Alcock, *Proc. SPIE Int. Soc. Opt. Eng. 458* (1984) 65.
[73] R. M. Wilson in A. Padwa (Ed.): *Organic Photochemistry, Vol. 7*, Dekker, New York 1985, Chap. 5; *Proc. SPIE Int. Soc. Opt. Eng. 458* (1984) 58.
[74] W. Adam, K. Hannemann, R. M. Wilson, *J. Am. Chem. Soc. 108* (1986) 929; see also W. Adam, M. Dörr, P. Hössel, *Angew. Chem. 98* (1986) 820; *Angew. Chem. Int. Ed. Engl. 25* (1986) 818.
[75] D. H. R. Barton, B. Chapiot, K. U. Ingold, L. J. Johnston, W. B. Motherwell, J. C. Scaniano, S. Stanforth, *J. Am. Chem. Soc. 107* (1985) 3607; N. Bischofberger, B. Frei, J. Wirz, *Helv. Chim. Acta 66* (1983) 2485; E. F. Hilinski, D. Huppert, D. F. Kelley, S. V. Milton, P. M. Rentzepis, *J. Am. Chem. Soc. 106* (1984) 1951; C. V. Kumar, D. Ramaiah, P. K. Das, M. V. George, *J. Org. Chem. 50* (1985) 2818.
[76] V. S. Letokhov in H. Grünewald (Ed.): *Chemistry for the Future*, Pergamon, New York 1984, p. 253.
[77] U. Brackmann, F. P. Schäfer, *Chem. Phys. Lett. 87* (1982) 579.
[78] V. S. Letokhov, Y. A. Matveetz, V. A. Semchishen, E. V. Khoroshilova, *Appl. Phys. B 36* (1985) 243.
[79] D. N. Nikogosyan, *VII. USSR-BRD Laser Spectrosc. Semin.* (Baku, UdSSR 1985).
[80] W. Kuhn, E. Knopf, *Z. Phys. Chem. Abt. B 7* (1930) 292.
[81] L. A. Rebane, A. A. Gorokhovskii, J. V. Kikas, *Appl. Phys. B 29* (1982) 235; M. Eich, J. H. Wendorff, H. Ringsdorf, H. W. Schmidt, *Makromol. Chem. 186* (1985) 2639.
[82] J. Friedrich, D. Haarer, *Angew. Chem. 96* (1984) 96; *Angew. Chem. Int. Ed. Engl. 23* (1984) 113.
[83] A. Winnacker, R. M. Shelby, R. M. Macfarlane, *Opt. Lett. 10* (1985) 350.
[84] H. W. H. Lee, M. Gehrtz, E. E. Marinero, W. F. Moerner, *Chem. Phys. Lett. 118* (1985) 611.
[85] W. Kuhn, H. Martin, *Z. Phys. Chem. Abt. B 21* (1933) 93; C. B. Moore (Ed.): *Chemical and Biochemical Applications of Laser*, Academic Press, New York 1977.
[86] F. S. Becker, K. L. Kompa, *Nucl. Technol. 58* (1982) 329.
[87] J. I. Davis, J. Z. Holtz, M. L. Spaeth, *Laser Focus Fiberopt. Technol. 18* (1982) 49; *Conf. Lasers Electroopt.* (San Francisco 1986) p. 89.
[88] R. W. Solarz, GRA *85* (1985) 24; R. L. Byer, *IEEE J. Quantum Electron. QE 12* (1976) 732.
[89] P. Rabinowitz, A. Stein, R. Brickman, A. Kaldor, *Appl. Phys. Lett. 35* (1979) 793.
[90] K. C. Kim, S. M. Freund, M. S. Sorem, D. F. Smith, *J. Chem. Phys. 83* (1985) 4344.
[91] H. J. Circel in W. Waidelich (Ed.): *Optoelectronics in Engineering*, Springer, Heidelberg 1986, p. 706.
[92] S. S. Miller, D. D. DeFord, T. J. Marks, E. Weitz, *J. Am. Chem. Soc. 101* (1979) 1036.
[93] A. Kaldor, R. L. Woodin, *Proc. IEEE 70* (1982) 565.
[94] R. Cunningham, *Lasers and Applications 4* (1985) 11.
[95] M. R. Humphries, O. L. Boarne, P. A. Hackett, *Chem. Phys. Lett. 118* (1985) 134; A. V. Evseev, V. S. Letokhov, A. A. Puretzky, *Appl. Phys. B 36* (1985) 93.
[96] Zhang Linyang, Zhang Yunwu, Ma Xingxiao, Yuan Peng, Xu Yan, Gong Mengxiong, W. Fuß, *Appl. Phys. B 39* (1986) 117.
[97] F. Magnotta, I. P. Herman, *J. Chem. Phys. 81* (1984) 2363.
[98] K. Takendu, S. Satooka, Y. Makide, *Appl. Phys. B 33* (1984) 83; F. Magnotta, I. P. Herman, *ibid. 36* (1985) 207.
[99] J. H. Clark, Y. Haas, P. L. Houston, C. B. Moore, *Chem. Phys. Lett. 35* (1975) 82; R. E. M. Hedges, P. Ho, C. B. Moore, *Appl. Phys. B 23* (1980) 25; L. Mannik, S. K. Brown, *ibid. 37* (1985) 75.
[100] A. Outhouse, P. Lawrence, M. Gauthier, P. A. Hackett, *Appl. Phys. B 36* (1985) 63; R. J. Nadalin, R. G. Charles, U.S. Pat. 4496495 (1985), Westinghouse Electric Corp.
[101] J. Moser, P. Morand, R. Duperrex, H. van den Bergh, *Chem. Phys. 79* (1983) 277.
[102] W. Fuss, W. E. Schmidt, K. L. Kompa, *Verh. Dtsch. Phys. Ges. 20* (1985) 1056.

[103] O. N. Avatkov, A. B. Bakhtadze, V. Yu. Baranov, V. S. Doljikov, I. G. Gverdsiteli, S. A. Kazakov, V. S. Letokhov, V. D. Pismmenyi, E. A. Ryobov, V. M. Vetsko, *Appl. Opt. 23* (1984) 26.
[104] T. J. Manuccia, M. D. Clark, E. R. Lory, *J. Chem. Phys. 68* (1978) 227.
[105] M. Stuke, *Spektrum Wiss. 1982*. No. 4, p. 76.
[106] J. H. Clark, R. G. Anderson, *Appl. Phys. Lett. 32* (1978) 46; A. Hartford, *J. Appl. Phys. 51* (1980) 4471.
[107] J. A. Merritt, L. C. Robertson, *J. Chem. Phys. 67* (1977) 3545.
[108] R. V. Ambartzumyan, *Sov. J. Quantum Electron. (Engl. Transl.) 6* (1977) 96.
[109] E. M. Geiser, R. W. Johnson, U.S. Pat. 4287038 (1981).
[110] T. Donohue, *J. Chem. Phys. 67* (1977) 5402; *Conf. Lasers Electroopt.* (Phoenix, AZ, 1982) p. 95.
[111] H. L. Chen, C. Borzileri, *IEEE J. Quantum Electron. QE 16* (1980) 1229.
[112] A. Gupta, J. T. Yardley, *Proc. SPIE Int. Soc. Opt. Eng. 458* (1984) 131.
[113] W. M. Shaub, S. H. Bauer, *Int. J. Chem. Kinet. 7* (1975) 509.
[114] D. J. Frurip, P. R. Staszak, M. Blander, *J. Non-Cryst. Solids 68* (1984) 1.
[115] Y. Kizaki, T. Kandori, Y. Fujitani, *Jpn. J. Appl. Phys. 24* (1985) 806.
[116] G. W. Rice, R. L. Woodin, *Proc. SPIE Int. Soc. Opt. Eng. 458* (1984) 98.
[117] W. R. Cannon, S. C. Danforth, J. H. Flint, J. S. Haggerty, R. A. Marra, *J. Am. Ceram. Soc. 65* (1982) 324; W. R. Cannon, S. C. Danforth, J. S. Haggerty, R. A. Marra, *ibid. 65* (1982) 330; J. H. Flint, J. S. Haggerty, *Proc. SPIE Int. Soc. Opt. Eng. 458* (1984) 108.
[118] J. C. Mitchener, M. S. Wrighton, *J. Am. Chem. Soc. 103* (1981) 975.
[119] R. L. Whetten, K. J. Fu, E. R. Grant, *J. Am. Chem. Soc. 104* (1982) 4270.
[120] D. J. Perettie, M. S. Paquette, R. L. Yates, H. D. Gafne, *NATO ASI Ser. Ser. B 105* (1984) 259.
[121] E. Huber, M. von Allmen, *Phys. Rev. B Condens. Matter 28* (1983) 2979; M. von Allmen, *Mater. Res. Soc. Symp. Proc. 13* (1983) 691; K. Attolter, M. von Allmen, *Appl. Phys. A 33* (1984) 93.
[122] S. D. Allen, *J. Appl. Phys. 52* (1981) 6501; D. Bäuerle, P. Irsingler, G. Leyendecker, H. Noll, D. Wagner, *Appl. Phys. Lett. 40* (1982) 819.
[123] G. D. Davis, C. A. Moore, R. A. Goltscho, *J. Appl. Phys. 56* (1984) 1808.
[124] R. Solanki, W. H. Ritchie, G. J. Collins, *Appl. Phys. Lett. 43* (1983) 454.
[125] T. F. Deutsch, D. J. Ehrlich, R. M. Osgood, *Appl. Phys. Lett. 35* (1979) 381.
[126] D. J. Ehrlich, R. M. Osgood, T. F. Deutsch, *J. Vac. Sci. Technol. 21* (1982) 23.
[127] W. Kräuter, D. Bäuerle, F. Fimberger, *Appl. Phys. A 31* (1983) 13.
[128] D. J. Ehrlich, J. Y. Tsao, *J. Vac. Sci. Technol. B 1* (1983) 969; D. J. Ehrlich, J. Y. Tsao, *Springer Ser. Chem. Phys. 39* (1984) 386.
[129] R. Bilinchi, I. Gianinoni, M. Musci, R. Murri, S. Tacchetti, *Appl. Phys. Lett. 47* (1985) 279; H. M. Branz, S. Fan, J. H. Flint, D. Adler, J. S. Haggerty, *ibid. 48* (1986) 171.
[130] H. Schröder, K. L. Kompa, D. Musci, I. Gianinoni, *Appl. Phys. A 38* (1985) 227.
[131] W. G. Hollingsworth, V. Vaida, *J. Phys. Chem. 90* (1986) 1235.
[132] R. Fantoni, M. Stuke, *Appl. Phys. B38* (1985) 209; *Verh. Dtsch. Phys. Ges. 21* (1986) 657.
[133] R. J. von Gutfeld, E. E. Tynan, R. L. Melcher, S. E. Blum, *Appl. Phys. Lett. 35* (1979) 651.
[134] H. Pummer, *Phys. Bl. 41* (1985) 199.
[135] R. Srinivasan: *Photophysics and Photochemistry above 6 eV*. Elsevier, Amsterdam 1985, p. 595; G. Gorodetsky, T. G. Kazyaka, R. L. Melcher, R. Srinivasan, *Appl. Phys. Lett. 46* (1985) 828.
[136] F. Friedrich, Ch. J. Raub, *Metalloberfläche 38* (1984) 237; R. J. von Gutfeld, D. R. Vigliotti, *Appl. Phys. Lett. 46* (1985) 1003.
[137] G. J. Müller, P. Berlien, C. Scholz, *Umschau (1982) 86* (1986) 233.
[138] A. Anders, *Proc. SPIE Int. Soc. Opt. Eng. 236* (1980) 160; V. S. Letokhov, *Nature (London) 316* (1985) 327.
[139] T. I. Karu, G. S. Kalendo, V. S. Letokhov, V. V. Lobko, *Sov. J. Quantum Electron. (Engl. transl.) 13* (1983) 1169.
[140] J. M. Isner, R. H. Clarke, *IEEE J. Quantum Electron. QE 20* (1984) 1406; R. Thull, *Herz und Gefäße 5* (1985) 179.
[141] G. S. Abela, S. Normann, D. Cohen, R. L. Feldmann, E. A. Geiser, C. R. Conti, *Am. J. Cardiol. 50* (1982) 1199; D. S. J. Choi, S. Stertzer, H. Rotterdam, M. S. Burns, *ibid. 50* (1982) 1209.
[142] D. Muller, *Lasers and Applications 5* (1986) 85.
[143] F. W. Mohr, K. O. Greulich, R. Weller, J. Wolfrum, W. Lenz, S. V. Kuserow, P. G. Kirchhoff, *3. Jahrestag. Dtsch. Ges. Lasermedizin*, Lübeck-Travemünde 1986.
[144] E. M. H. Mathus-Vliegen, G. N. J. Tytgat, *Cancer (Philadelphia) 57* (1986) 396.
[145] J. C. van Gemert, M. C. Berenbaum, G. H. M. Gijsers, *Br. J. Cancer 52* (1985) 43.
[146] J. S. Nelson, W. H. Wright, M. W. Berns, *Cancer Res. 45* (1985) 5781.
[147] D. A. Bellnier, C. W. Lin, G. R. Prout, Jr., *JNCI J. Natl. Cancer Inst.*, in press.
[148] R. Hilf, R. S. Murant, U. Narayanan, S. L. Gibson, *Cancer Res. 46* (1986) 211.
[149] G. S. Lin, A. A. Al Dakan, D. P. Gibson, *Br. J. Cancer 53* (1986) 265.
[150] L. Herrera-Ornelas, N. J. Petrelli, A. Mittelman, T. J. Dougherty, D. B. Boyles, *Cancer (Philadelphia) 57* (1986) 677.
[151] M. Moretti, *Lasers and Applications 4* (1985) 46.
[152] O. J. Beck, F. Frank, E. Keiditsch, F. Wondrazek, *Laser 1* (1985) 13.
[153] R. Schober, F. Ulrich, T. Saner, H. Dürselen, S. Hessel, *Science (Washington) 232* (1986) 1421.
[154] D. Katalinic, *Laser 1* (1985) 57.
[155] J. Kaplan, S. Giler (Eds.): *CO_2 Laser Surgery*, Springer, Berlin 1984.
[156] C. A. Puliafito, R. F. Steinert, *Laser Focus (Littleton Mass.) 1985*, September issue p. 84.
[157] C. A. Puliafito, R. F. Steinert, *IEEE J. Quantum Electron. QE 20* (1984) 1442.
[158] J. Marshall, S. Trokel, S. Rothery, R. R. Krueger, *Lasers Ophthalmol. 1* (1986) 1; R. Scinivasan, *Science 234* (1986) 559.
[159] U. Klingbeil, A. Plesch, J. Bille, O. Käfer, *Fortschr. Ophthalmol. 79* (1982) 275.
[160] J. Troe, *J. Phys. Chem. 90* (1986) 357.
[161] W. Kaiser, *Phys. Bl. 41* (1985) 370.

When submitting manuscripts, authors of articles intended for publication as "Communications" are requested to read the "Notice to Authors" reproduced in the January issue of the journal following the list of contents; upon request, a copy can be obtained from the editorial office.

$[(\eta^5\text{-}P_5)Fe(\eta^5\text{-}C_5Me_5)]$, a Pentaphosphaferrocene Derivative**

By *Otto J. Scherer** and *Thomas Brück*

After having demonstrated that *cyclo*-P_5 could be stabilized as bridging ligand in the mixed-valence triple-decker complex **1**,[17] we then attempted to realize the classical

$[(\eta^5\text{-}C_5Me_5)Cr(\mu,\eta^5\text{-}P_5)Cr(\eta^5\text{-}C_5Me_5)]$

1

sandwich coordination of this ligand (cyclo-$P_5^{\ominus}$ as 6π electron donor). Success was achieved upon cothermolysis of **2** with white phosphorus.

Pentamethylpentaphosphaferrocene **3** forms sublimable, green crystals which can be handled in the presence of air and which begin to melt (with partial sublimation and slight decomposition) at 270°C when heated in a sealed tube. **3** is very soluble in dichloromethane, readily soluble in benzene and toluene, and moderately soluble in pentane.

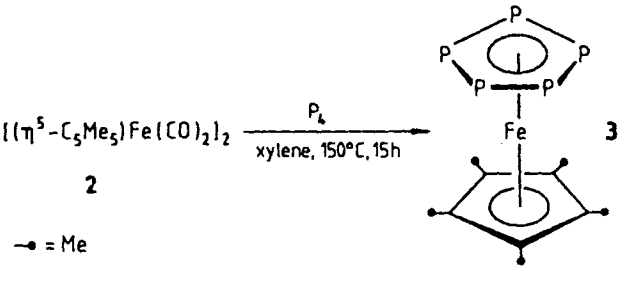

In the ^{1}H-NMR spectrum (200 MHz, 293 K, C_6D_6, TMS int.) of **3** a sharp singlet is observed at $\delta = 1.08$ which is shifted 0.6 ppm upfield compared to that of decamethylferrocene $[(\eta^5\text{-}C_5Me_5)_2Fe]$ **4**.[3] In comparison to the $^{13}C\{^1H\}$-NMR signals of **4**,[2,3] those of **3**[2] are shifted slightly downfield. The $^{31}P\{^1H\}$-NMR signal shows a continuous downfield shift within the series triple-decker **1** ($\delta = -290.5$[1]), monophosphaferrocene $[(\eta^5\text{-}C_5H_5)Fe(\eta^5\text{-}PC_4H_4)]$ **5** ($\delta = -67.5$[4]), **3** (81.01 MHz, C_6D_6, 85% H_3PO_4 ext., $\delta = 153.0$ (s)), and $Li(P_5)$ ($\delta = 470$[5]). In the mass spectrum,[2] the most intense peak is the molecular peak of **3**, followed by the peak for $M^{\oplus} - P_2$. So far, all attempts to prepare a single crystal suitable enough for an X-ray structure analysis have failed, both by sublimation as well as recrystallization. *cyclo*-$P_5^{\ominus}$ is probably formed from $P_3^{\ominus}$ and P_2.[6]

Experimental

A mixture of **2** [7] (980 mg, 2.3 mmol) and P_4 (1500 mg, 12.1 mmol) in xylene (80 mL) was stirred under reflux for 15 h and the insoluble material removed by filtration on a D3 frit and extracted three times with 80 mL each of CH_2Cl_2 (393 mg of residue after drying under high vacuum). The solvent was removed from the combined extracts under oil-pump vacuum. After three extractions with 50 mL each of pentane there remained 726 mg of a brown solid whose composition could not be unequivocally established. After removal of the solvent from the green extracts (oil-pump vacuum), the residue remaining behind was sublimed. At 60°C/0.01 torr, excess phosphorus was removed; between 90° and 110°C, green needles sublimed on the wall of the glass vessel. Recrystallization from pentane furnished 175 mg of **3** (yield 11%). Correct elemental analysis.

Received: October 20, 1986;
supplemented: November 7, 1986 [Z 1957 IE]
German version: *Angew. Chem. 99* (1987) 59

[1] O. J. Scherer, J. Schwalb, G. Wolmershäuser, W. Kaim, R. Gross, *Angew. Chem. 98* (1986) 349; *Angew. Chem. Int. Ed. Engl. 25* (1986) 363.
[2] $^{31}C\{^1H\}$-NMR (50.28 MHz, C_6D_6, TMS intern) **3**: $\delta = 90.6$ (s; C_5Me_5), 10.6 (s; CH_3); **4**: $\delta = 78.5$ (s; C_5Me_5), 9.8 (s; CH_3). EI-MS (70 eV) of **3**: *m/z* 346 ($M^{\oplus}$, $I_{rel} = 100\%$), 284 ($M^{\oplus} - P_2$, 91%), P_4 (19.8%), P_3 (7.9%), P_2 (53%), P (7.8%) and further, weak intensity lines.
[3] Cf. : J. L. Robbins, N. Edelstein, B. Spencer, J. C. Smart, *J. Am. Chem. Soc. 104* (1982) 1882.
[4] F. Mathey, *Struct. Bonding (Berlin) 55* (1983) 153.
[5] M. Baudler, *Phosphorus Sulfur*, in press; M. Baudler, D. Düster, D. Ouzounis, *Z. Anorg. Allg. Chem.*, in press.
[6] Cf. also the theoretical studies on $N_3^{\ominus}$ and its complex stabilization. M. T. Nguyen, M. Sana, G. Leroy, J. Elguéro, *Can. J. Chem. 61* (1983) 1435; M. T. Nguyen, M. A. McGinn, A. F. Hegarty, J. Elguéro, *Polyhedron 4* (1985) 1721.
[7] D. Catheline, D. Astruc, *Organometallics 3* (1984) 1094, and references cited therein.

$(Me_3Si)_2N-P=NSiMe_3$ as Educt for Electron-Rich Phosphorus-Nitrogen Ligands**

By *Otto J. Scherer,** *Karin Göbel*, and *Jürgen Kaub*

Of the tervalent phosphorus double bond systems described so far, the amino(imino)phosphanes in particular display an unusual diversity of coordination properties.[1] We have now found that reaction of $[Fe_3(CO)_{12}]$ **1** with $(Me_3Si)_2N-P=NSiMe_3$ **2** not only leads to formation of the unusual tridentate 6e-donor ligand **B** (stabilized in the cluster **3**) but also gives the phosphanediyl (phosphini-

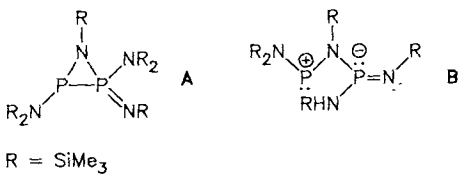

R = $SiMe_3$

[*] Prof. Dr. O. J. Scherer, Dipl.-Chem. T. Brück
Fachbereich Chemie der Universität
Erwin-Schrödinger-Strasse, D-6750 Kaiserslautern (FRG)

[**] This work was supported by the Fonds der Chemischen Industrie.

[*] Prof. Dr. O. J. Scherer, Dipl.-Chem. K. Göbel, Dr. J. Kaub [+]
Fachbereich Chemie der Universität
Erwin-Schrödinger-Strasse, D-6750 Kaiserslautern (FRG)
[+] X-ray structure analysis.

[**] This work was supported by the Fonds der Chemischen Industrie.

dene) $(Me_3Si)_2NP$ and the first hydroxy(imino)phosphane derivative $Me_3SiO-P=NSiMe_3$ (both stabilized in the cluster **4**). A conceivable route to **B** is the heterolytic opening of the PP bond of **A**, which itself can be formed by [2+1] cycloaddition of **2**.[2a,b] Probably $Me_3SiO-P=NSiMe_3$ is formed from $(Me_3Si)_2N-P=O$ by Me_3Si migration (cf. the conversion of complexed $iPr_2N-P=NtBu$ into complex-stabilized $iPr_2N-P=O$[2c] as well as the reaction of $Ph_3P=NR'$ with $Fe(CO)_5$ and R''NCO, which gives, inter alia, Ph_3PO[3]; Me_3SiNCO could be detected in the solution by IR spectroscopy). Nothing is as yet known about the mechanism of formation of $(Me_3Si)_2NP$.

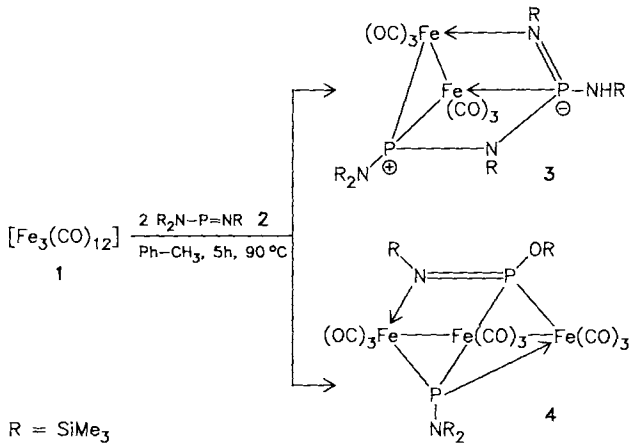

From the complex reaction mixture ($^{31}P\{^1H\}$-NMR control) obtained on reaction of **1** and **2**, it has so far been possible to isolate, in addition to **3** and **4**, also black **5a** and **5b** as derivatives of the intensively studied phosphanediyl-Fe_3 clusters.[4]

$[Fe_3(CO)_9(\mu\text{-}CO)\{\mu_3\text{-}PNR'(SiMe_3)\}]$ **5a**, R'=H; **5b**, R'=$SiMe_3$

3 and **4** form respectively orange and dark-red crystals which are readily soluble in ether, pentane, benzene, and toluene. The NMR and IR data of **3**–**5** (Table 1) show no unusual features (cf. Refs. [1, 4, 7]). In **3**, (Fig. 1) the tripod-like 6e-donor ligand **B**, attaches to the $Fe_2(CO)_6$ fragment in such a way that a polycycle is formed whose skeletal unit is a strongly distorted trigonal prismatic array with an open edge (N1N3). From the crystal structure analysis[5] it follows that the P1–N1 bond length of 1.605(5) Å is the shortest endocyclic P–N bond of this molecule. In contrast to the trigonal planar coordinated N4 (sum of angles 359.3°), N1 (353.3°) and N3 (346.1°) are slightly pyramidally configurated. The skeletal geometry requires a very short P1···P2 distance of 2.430(3) Å (cf. Ref. [6]).

Table 1. NMR and IR data of **3**–**5** (δ, J [Hz], $\tilde{\nu}$ [cm^{-1}]).

	^1H [a]	$^{31}P\{^1H\}$ [b]	$\tilde{\nu}$ (CO) [c]
3	Diastereomer I [d] 0.56 (s, 9H), 0.37 (s, 9H), 0.28 (s, 9H), 0.21 (s, 9H), 0.20 (s, 9H), 2.16 (d, 1H, ^2J(PH) = 16.6)	74.0 (d; P1), 201.5 (d; P2), ^2J(PP) = 153	2045 (s), 2010 (vs), 1985 (s), 1970 (m), 1940 (w, br)
	Diastereomer II [e]	67.0 (d), 197.9 (d), ^2J(PP) = 147	
4	Diastereomer I [d] 0.50 (s, 9H), 0.37 (s, 9H), 0.31 (s, 9H), 0.25 (s, 9H)	188.2 (d), 518.6 (d), ^2J(PP) = 12.2	2048 (w), 2024 (vs), 1994 (vs), 1982 (s), 1963 (s)
	Diastereomer II 0.52 (s, 9H), 0.40 (s, 9H), 0.29 (s, 9H), 0.19 (s, 9H)	187.5 (d), 531.1 (d), ^2J(PP) = 24.4	
5a	[f] 0.06 (s, 9H), 3.54 (d, 1H, ^2J(PH) = 11.6)	488.3 (s)	2079 (m), 2042 (vs), 2032 (vs), 2000 (s), 1993 (sh), 1964 (w,
5b	[f] 0.29 (s, 18H)	493.7 (s)	br), 1838 (m, br)

[a] 200 MHz, 293 K, C_6D_6, TMS int. [b] 81.01 MHz, 293 K, C_6D_6, 85% H_3PO_4 ext. [c] Toluene. [d] X-ray structure analysis. [e] Only ^{31}P-NMR data measured because of too small amount of this diastereomer. [f] 3:1 mixture of **5a** and **5b**.

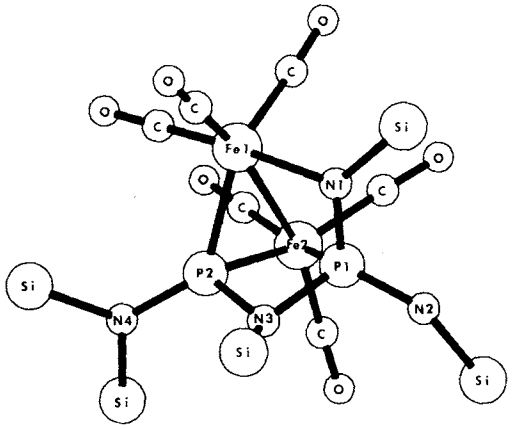

Fig. 1. Crystal structure of **3** (methyl groups omitted for clarity). Selected bond lengths [Å] and angles [°] (see also text): Fe1-Fe2 2.616(1), Fe1-P2 2.250(2), Fe2-P1 2.227(2), Fe2-P2 2.210(2), Fe1-N1 2.123(5), P1-N1 1.605(5), P1-N3 1.742(5), P2-N3 1.730(5), P1-N2 1.659(5), P2-N4 1.692(6); Fe2-Fe1-P2 53.37(5), Fe2-Fe1-N1 80.4(1), Fe1-Fe2-P1 68.78(6), Fe1-Fe2-P2 54.81(6), P1-Fe2-P2 66.41(7), Fe2-P1-N1 106.0(2), Fe2-P1-N3 96.2(2), N1-P1-N3 105.8(3), Fe1-P2-Fe2 71.82(6), Fe1-P2-N3 104.8(2), Fe2-P2-N3 97.1(2), Fe1-N1-P1 94.2(3), P1-N3-P2 88.8(2); N1···N3 2.671(7) Å.

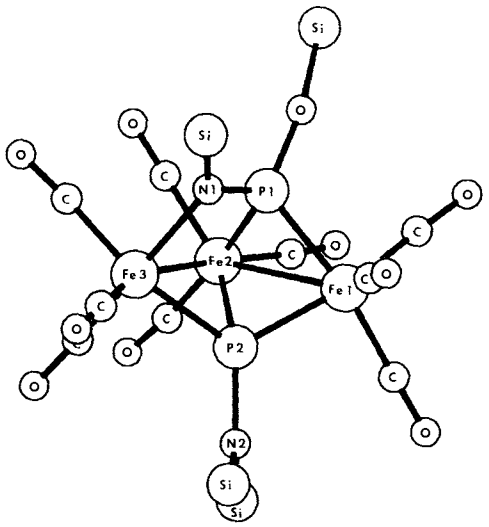

Fig. 2. Crystal structure of **4** (methyl groups omitted for clarity). Selected bond lengths [Å] and angles [°] (see also text): Fe1-Fe2 2.736(2), Fe2-Fe3 2.672(2), Fe1-P2 2.183(3), Fe2-P2 2.278(3), Fe3-P2 2.250(3), Fe1-P1 2.198(3), Fe2-P1 2.233(3), Fe3-N1 2.072(9), P1-N1 1.597(8), P1-O 1.553(7), O-Si 1.684(7), P2-N2 1.710(6); N1-P1-Fe1 117.7(3), N1-Fe3-P2 90.1(2), P1-Fe1-P2 79.3(1), P1-Fe2-P2 76.6(1), Fe1-Fe2-Fe3 88.05(7), Fe1-P2-Fe3 116.0(1), P1-O-Si 157.8(6); P1···P2 2.800(9), Fe1···Fe3 3.775(2) Å. The angles of the Fe_2P triangle and of the Fe_2PN square differ only slightly from those in **3**.

The skeleton of **4** (Fig. 2)[5] can be imagined as being built up of an Fe_3P "butterfly" (angle between the Fe1Fe2P2 and Fe3Fe2P2 planes = 123.9°), bridged by $Me_3SiO-P=NSiMe_3$ in the *cis* form as μ_3-PN ligand (dihedral angle OP1N1Si = 32.1°). Both nitrogen atoms (N1 359.9°, N2 359.8°) are trigonal planar coordinated, and the length of the P1–N1 bond (1.597(8) Å) lies in the expected range (cf. Ref. [1]). The P2–N2 bond length (1.710(6) Å) is comparable with the P–N bond length in the phosphanediyl complex $[\mu\text{-}(Me_3Si)_2NP\{Cr(CO)_5\}_2]$ (1.697(3) Å).[7]

Experimental

3 and **4**: A suspension of **1** (755.5 mg, 1.5 mmol) in toluene (7 mL) was treated with 835.7 mg (3 mmol) of **2** [8]. The mixture was stirred for 5 h at 90°C. After removal of the solvent (oil-pump vacuum), the dark-red, oily residue was taken up in 3 mL of acetonitrile and stored in the refrigerator for 2 d. The precipitate that formed was separated from the mother liquor and then re-cooled (2 d, refrigerator). Altogether three crops of a red precipitate were obtained; these were combined and taken up in 20 mL of pentane. After filtration over filter flocks and evaporation of the filtrate to 1 mL, dark-red **4** crystallized at −30°C as a mixture of diastereomers (I : II ≈ 2 : 1); yield 100 mg (8.2% referred to **1**). Repeated recrystallization from ether at −30°C furnished pure **4** I (X-ray structure analysis). On storing the combined acetonitrile filtrates in a refrigerator for three weeks an orange precipitate separated out, which upon recrystallization from a little pentane at −30°C furnished 5 mg (0.3%) of **3** (exclusively diastereomer I, X-ray structure analysis) as orange crystals.

5: The oily residue obtained after removal of toluene from the reaction solution of **1** and **2** was taken up in ether and cooled to −75°C for ca. 12 h; **5** separated as a black precipitate. This was dissolved in 30 mL of ether. After filtration through filter flocks and evaporation of the filtrate to 3 mL, 193 mg (22%) of **5** crystallized out on cooling to −75°C as a 3 : 1 mixture of **5a** and **5b**. The yield could be increased to 290 mg (33%) by allowing **1** and **2** to react in a molar ratio of 1 : 1 in benzene for 1 h at 75°C.

Received: August 19, 1986;
supplemented: September 11, 1986 [Z 1907 IE]
German version: *Angew. Chem. 99* (1987) 59

[1] Review: O. J. Scherer, *Angew. Chem. 97* (1985) 905; *Angew. Chem. Int. Ed. Engl. 24* (1985) 924.

[2] a) E. Niecke, R. Rüger, W. W. Schoeller, *Angew. Chem. 93* (1981) 1110; *Angew. Chem. Int. Ed. Engl. 20* (1981) 1034; b) E. Niecke, D. Gudat, W. W. Schoeller, P. Rademacher, *J. Chem. Soc. Chem. Commun. 1985*, 1050; c) E. Niecke, M. Engelmann, H. Zorn, B. Krebs, G. Henkel, *Angew. Chem. 92* (1980) 738; *Angew. Chem. Int. Ed. Engl. 19* (1980) 710.

[3] E. W. Abel, S. A. Mucklejohn, *Phosphorus Sulfur 9* (1981) 235, and references cited therein.

[4] See, e.g., M. O. Albers, D. J. Robinson, N. J. Coville, *Coord. Chem. Rev. 69* (1986) 127; K. Knoll, G. Huttner, L. Zsolnai, I. Jibril, M. Wasiucionek, *J. Organomet. Chem. 294* (1985) 91; D. J. Brauer, S. Hietkamp, H. Sommer, O. Stelzer, G. Müller, C. Krüger, *J. Organomet. Chem. 288* (1985) 35; R. Lal De, H. Vahrenkamp, *Z. Naturforsch. B41* (1986) 273.

[5] **3**: monoclinic, $P2_1/n$, $a = 12.585(2)$, $b = 18.331(5)$, $c = 17.111(6)$ Å, $\beta = 108.66(3)°$, $Z = 4$, $V = 3740.0$ Å^3, $\rho_{calc} = 1.36$ g cm^{-3}. 5564 measured reflections, 3163 observed ($Mo_{K\alpha}$, $F_0^2 \geq 2.0\sigma(F_0^2)$, $2\theta \leq 47°$), $R = 0.059$, $R_w = 0.050$. **4**: triclinic, $P\bar{1}$, $a = 12.649(3)$, $b = 13.120(2)$, $c = 12.187(4)$ Å, $\alpha = 108.55(2)$, $\beta = 107.65(2)$, $\gamma = 83.55(2)°$, $Z = 2$, $V = 1826.8$ Å^3, $\rho_{calc} = 1.49$ g cm^{-3}. 4599 measured reflections, 2655 observed ($Mo_{K\alpha}$, $F_0^2 \geq 2.0\sigma(F_0^2)$, $2\theta \leq 45°$), $R = 0.091$, $R_w = 0.080$. Further details of the crystal structure investigation are available on request from the Fachinformationszentrum Energie, Physik, Mathematik GmbH, D-7514 Eggenstein-Leopoldshafen 2 (FRG), on quoting the depository number CSD-52 124, the names of the authors, and the journal citation.

[6] O. J. Scherer, H. Sitzmann, G. Wolmershäuser, *J. Organomet. Chem. 309* (1986) 77; diazadiphosphetidines: R. Keat, *Top. Curr. Chem. 102* (1982) 82, and O. J. Scherer, R. Anselmann, W. S. Sheldrick, *J. Organomet. Chem. 263* (1984) C 26.

[7] K. M. Flynn, B. D. Murray, M. M. Olmstead, P. P. Power, *J. Am. Chem. Soc. 105* (1983) 7460; cf. also $[(iPr_2NP)_2Fe_3(CO)_9]$: R. B. King, F.-J. Wu, E. M. Holt, *Inorg. Chem. 25* (1986) 1733.

[8] O. J. Scherer, N. Kuhn, *Chem. Ber. 107* (1974) 2123.

Total Synthesis of the Pseudoguaianolide (+)-Confertin**

By *Gerhard Quinkert,* Hans-Günther Schmalz, Egon-Walzer, Teresa Kowalczyk-Przewloka, Gerd Dürner,* and *Jan W. Bats*

The three-membered ring compounds **1a** (preparation, see ref. [1a]; absolute configuration, see ref. [1b]) or *ent*-**1a** (preparation, see ref. [1b, 2]) serve as enantiomerically pure building blocks in the synthesis of (+)-estrone,[1a] (−)-norgestrel,[3] or (−)-methyl jasmonate.[1b,2] They are accessible by chirality-inducing cyclopropanation and can be transformed by stereospecific ring expansion into the 2-alkyl-3-vinyl-substituted cyclopentanone derivatives **2a/3a**, **2b/3b**, or *ent*-**2c**/*ent*-**3c**[4] (see Scheme 1).

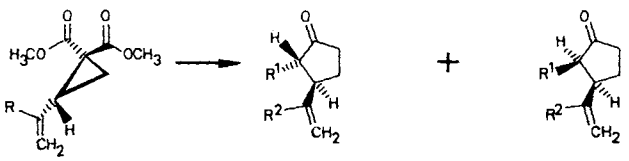

1 **2** **3**

a: R = H
b: R = CH_3

a: $R^1 = CH_3$; $R^2 = H$
b: $R^1 = C_2H_5$; $R^2 = H$
c: $R^1 = CH_2-C\equiv C-C_2H_5$; $R^2 = H$
d: $R^1 = R^2 = CH_3$

Scheme 1. Stereospecific ring expansion of enantiomerically pure three-membered ring building blocks of type **1** (preparation, see ref. [1a, 5]).

We have now employed the enantiomerically pure diastereomers **2d/3d**, prepared from dimethyl (*R*)-2-isopropenylcyclopropane-1,1-dicarboxylate **1b** (preparation and absolute configuration, see ref. [5]), for the synthesis of the sesquiterpene lactone (+)-confertin **14** (see Scheme 2).

In order to construct the hydroazulene system, we utilized an intermolecular Michael addition of the thermodynamically more stable enolate anion of **2d/3d** onto acrylonitrile, which results in exclusive formation of the *trans*-adduct **4**, and a Lewis-acid-catalyzed intramolecular hetero-ene reaction of **7** to give a mixture of isomers **8** and **9**, which were not separated, but rather directly converted via the constitutional isomers **10/11** into **12**.

The ketone **12**, whose structure was established by single-crystal X-ray diffraction analysis,[6] reacts, under conditions of kinetic control, regioselectively at C7 and stereoselectively from the α side with ethyl α-bromoacetate (93%).[7] The resulting alkylation product was transformed via **13** into (+)-confertin **14** in analogy to the synthesis of (±)-confertin *rac*-**14**[8] by *Schlessinger* et al.[9d] and *Heathcock* et al.[9f] This represents the first total synthesis of an enantiomerically pure pseudoguaianolide and makes accessible once again another cyclopentanoid target compound from a chiral cyclopropane derivative. Physical

[*] Prof. Dr. G. Quinkert, Dr. H.-G. Schmalz, Dipl.-Chem. E. Walzer, Dr. T. Kowalczyk-Przewloka, Dr. G. Dürner, Dr. J. W. Bats
Institut für Organische Chemie der Universität
Niederurseler Hang, D-6000 Frankfurt am Main 50 (FRG)

[**] This work was supported by the Deutsche Forschungsgemeinschaft (Project 15/2), the Bundesminister für Wirtschaft (Project AIF No. 5811), the Fonds der Chemischen Industrie, and Hoechst AG.

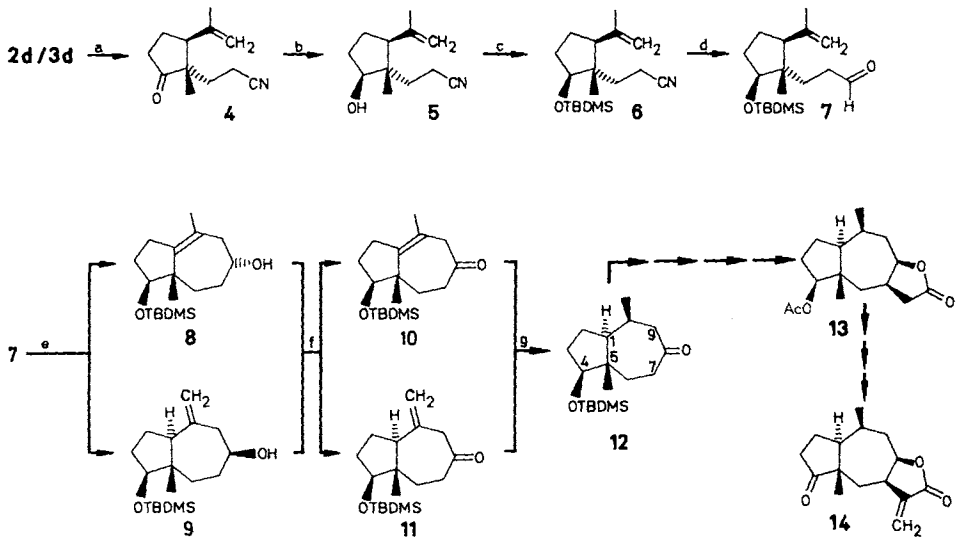

Scheme 2. Synthesis of (+)-confertin **14** from **2d/3d**: a) acrylonitrile, NaOMe, ether, room temperature (RT), 2 h, kugelrohr distillation (67%); b) $NaBH_4$, MeOH, 0°C, 1.5 h (97%), product contains 5% of the OH epimer; c) *tert*-butyldimethylsilyl chloride (TBDMSCl), imidazole, dimethylformamide (DMF), 60 h, RT, kugelrohr distillation (93%); d) diisobutylaluminum hydride (DIBAH), hexane, −60°C to 10°C, 4 h; then HCl, H_2O/Et_2O, 30 min, filtration through SiO_2; e) Me_2AlCl, CH_2Cl_2, 0°C, 15 min, chromatography on SiO_2, product contains **8** and **9** in the ratio 1.7:1 (62% based on **6**); f) $CrO_3 \cdot 2py$, CH_2Cl_2, RT, 2 h, filtration through SiO_2; g) H_2, Rh (5% on Al_2O_3), ethyl acetate/AcOH = 98/2, 4.5 bar, RT, 16 h; then $CrO_3 \cdot 2py$, CH_2Cl_2, RT, 2 h (60% based on a mixture of **8** and **9**).

Table 1. Physical data for selected synthetic intermediates as well as the product.

1b: IR (film): $\tilde{\nu}$ = 3080 (w), 1725 (s), 1650 (w), 890 cm^{-1} (m); ^{1}H-NMR ($CDCl_3$): δ = 1.47 (dd, 1H), 1.80 (s, 3H), 1.87 (dd, 1H), 2.49 (t, 1H), 3.68 (s, 3H), 3.75 (s, 3H), 4.71 (s, 1H), 4.87 (s, 1H); $[\alpha]_D^{20}$ = +128.0° (c = 1.113 in $CHCl_3$); $\theta(\lambda)$: −4870 (227 nm) (CH_3OH)

2d: IR (film): $\tilde{\nu}$ = 3080 (w), 1740 (s), 1645 (m), 890 cm^{-1} (m); ^{1}H-NMR ($CDCl_3$): δ = 1.03 (d, 3H), 1.61–1.79 (m, 1H), 1.76 (s, 3H), 2.01–2.46 (m, 5H), 4.81 (m, 1H), 4.86 (m, 1H); $[\alpha]_D^{20}$ = +137.6° (c = 0.864 in $CHCl_3$); $\theta(\lambda)$: +12450 (295), +12010 (303 nm) (dioxane)

4: IR (film): $\tilde{\nu}$ = 3080 (w), 2240 (m), 1735 (s), 1645 (m), 895 cm^{-1} (m); ^{1}H-NMR ($CDCl_3$): δ = 0.87 (s, 3H), 1.77–2.64 (m, 12H), 4.81 (s, 1H), 5.01 (s, 1H); $[\alpha]_D^{20}$ = +81.5° (c = 0.8899 in $CHCl_3$); $\theta(\lambda)$: +5360 (300), +5630 (308 nm) (dioxane)

8: IR (film): $\tilde{\nu}$ = 3630–3100 (m), 1255 (s), 1115 (s), 830 (s), 770 cm^{-1} (s); ^{1}H-NMR ($CDCl_3$): δ = 0.02 (s, 3H), 0.03 (s, 3H), 0.87 (s, 9H), 0.88 (s, 3H), 1.44–1.95 (m, 10H), 2.01–2.32 (m, 3H), 2.62 (d, 1H), 3.61 (dd, 1H), 4.03 (m, 1H); $[\alpha]_D^{20}$ = +51.4° (c = 1.068 in $CHCl_3$)

9: IR (film): $\tilde{\nu}$ = 3590–3020 (m), 3080 (w), 1630 (m), 1250 (s), 1120 (s), 880 (s), 830 (s), 770 cm^{-1} (s); ^{1}H-NMR ($CDCl_3$): δ = 0.00 (s, 3H), 0.01 (s, 3H), 0.63 (s, 3H), 0.87 (s, 9H), 1.08–1.26 (m, 1H), 1.36–1.51 (m, 2H), 1.54–1.91 (m, 6H), 2.11 (t, 1H), 2.41–2.54 (m, 1H), 2.81 (d, 1H), 3.58 (t, 1H), 3.77–3.87 (m, 1H), 4.75 (s, 1H), 4.92 (s, 1H); $[\alpha]_D^{20}$ = −5.5° (c = 0.728 in $CHCl_3$)

12: M.p. = 48–49°C (hexane); IR (KBr): $\tilde{\nu}$ = 1695 (s), 1255 (s), 1240 (s), 1115 (s), 870 (s), 830 (s), 770 cm^{-1} (s); ^{1}H-NMR ($CDCl_3$): δ = 0.02 (s, 3H), 0.03 (s, 3H), 0.69 (s, 3H), 0.88 (s, 9H), 0.95 (d, 3H), 1.39–1.55 (m, 3H), 1.64–1.98 (m, 4H), 2.04–2.14 (m, 1H), 2.40–2.58 (m, 3H), 2.79 (dd, 1H, 3.54 (t, 1H); $[\alpha]_D^{20}$ = −34.6° (c = 0.521 in $CHCl_3$); $\theta(\lambda)$: −3960 (288 nm) (dioxane)

13: M.p. = 116–117°C (ether/pentane); IR (KBr): $\tilde{\nu}$ = 2960 (m), 2875 (m), 1765 (s), 1730 (s), 1245 (s), 1170 cm^{-1} (s); ^{1}H-NMR ($CDCl_3$): δ = 1.00 (s, 3H), 1.03 (d, 3H), 1.36–1.59 (m, 4H), 1.61–1.87 (m, 3H), 1.99 (m, 1H), 2.07 (s, 3H), 2.08–2.23 (m, 3H), 2.70 (m, 1H), 2.90 (dd, 1H), 4.63 (t, 1H), 4.72 (ddd, 1H); $[\alpha]_D^{20}$ = +52.7° (c = 0.621 in $CHCl_3$)

14: M.p. = 144–145°C (acetone/hexane); IR (KBr): $\tilde{\nu}$ = 3090 (w), 1760 (s), 1730 (s), 1660 (m), 1270 (s), 1140 (s), 1005 (s), 985 cm^{-1} (s); ^{1}H-NMR ($CDCl_3$): δ = 1.02 (s, 3H), 1.13 (d, 3H), 1.64 (dd, 1H), 1.78 (dd, 1H), 1.80–2.01 (m, 3H), 2.10–2.28 (m, 3H), 2.43 (dd, 1H), 2.48–2.59 (m, 1H), 3.05 (m, 1H), 4.69 (ddd, 1H), 5.67 (d, 1H), 6.29 (d, 1H); $[\alpha]_D^{20}$ = +176.0° (c = 0.374 in $CHCl_3$); $\theta(\lambda)$: −2940 (257), +5290 (298, sh), +5810 (303), +4135 (312 nm, sh) (dioxane)

data for some of the synthetic intermediates as well as the product are presented in Table 1.

Received: September 10, 1986 [Z 1926 IE]
German version: *Angew. Chem. 99* (1986) 82

[1] a) G. Quinkert, U. Schwartz, H. Stark, W. D. Weber, F. Adam, H. Baier, G. Frank, G. Dürner, *Liebigs Ann. Chem. 1982*, 1999; b) G. Quinkert, H.-G. Schmalz, E. M. Dzierzynski, G. Dürner, J. W. Bats, *Angew. Chem. 98* (1986) 1023; *Angew. Chem. Int. Ed. Engl. 25* (1986) 992.

[2] G. Quinkert, F. Adam, G. Dürner, *Angew. Chem. 94* (1982) 866; *Angew. Chem. Int. Ed. Engl. 21* (1982) 856; *Angew. Chem. Suppl. 1982*, 1777.

[3] H. Baier, G. Dürner, G. Quinkert, *Helv. Chim. Acta 68* (1985) 1054.

[4] a) G. Quinkert, H. Stark, *Angew. Chem. 95* (1983) 651; *Angew. Chem. Int. Ed. Engl. 22* (1983) 637; b) G. Quinkert in W. Bartmann, B. M. Trost (Eds.): *Selectivity—a Goal for Synthetic Efficiency*, Verlag Chemie, Weinheim 1984.

[5] G. Quinkert, H.-G. Schmalz, E. Walzer, S. Gross, G. Dürner, *Angew. Chem. 98* (1986) 732; *Angew. Chem. Int. Ed. Engl. 25* (1986) 732.

[6] *rac*-**12**: ρ_{calcd} = 1.047 g/cm^3; triclinic, space group $P\bar{1}$; a = 7.0418(7), b = 11.829(2), c = 12.783(1) Å, α = 71.00(1), β = 78.21(1), γ = 85.35(1)°; V = 985.4(3) Å^3; Enraf-Nonius CAD4 diffractometer; $Cu_{K\alpha}$ radiation; half-circle to 2θ = 120°, 2838 unique reflections with $I > \sigma(I)$; structure determination by direct methods; $R(F)$ = 0.053, $wR(F)$ = 0.047; SDP program system. Further details of the crystal structure investigation may be obtained from the Fachinformationszentrum Energie, Physik, Mathematik GmbH, D-7514 Eggenstein-Leopoldshafen 2 (FRG), on quoting the depository number CSD-51895, the names of the authors, and the journal citation.

[7] Of the four C–H bonds in neighboring positions to the keto group, Hα-C7 undergoes preferential heterolysis for stereoelectronic reasons; the resulting enolate is attacked rapidly from the α side for both stereoelectronic and steric reasons.

[8] Concerning syntheses of *rac*-**14**, see [9].

[9] a) J. A. Marshall, R. H. Ellison, *J. Am. Chem. Soc. 98* (1976) 4312; b) M. F. Semmelhack, A. Yamashita, J. C. Tomesch, K. Hirotsu, *ibid. 100* (1978) 5565; c) P. A. Wender, M. A. Eisenstat, M. P. Filosa, *ibid. 101* (1979) 2196; d) G. J. Quallich, R. M. Schlessinger, *ibid. 101* (1979) 7627; e) F. E. Ziegler, J.-M. Fang, *J. Org. Chem. 46* (1981) 825; f) C. H. Heathcock, E. G. DelMar, S. L. Graham, *J. Am. Chem. Soc. 104* (1982) 1907; g) A. G. Schultz, L. A. Motyka, M. Plummer, *ibid. 108* (1986) 1056; h) H.-G. Schmalz, *Dissertation*, Universität Frankfurt am Main 1985.

Control of the Molecular Weight of Polyethene in Syntheses with Bis(ylide)nickel Catalysts

By *K. Alexander Ostoja Starzewski** and *Josef Witte*

We recently reported on highly active Ni-catalyst systems for ethene polymerization. These were generated from bis(cyclooctadiene)nickel(0), $Ni(cod)_2$, a carbonyl-stabilized and a non-stabilized ylide, $Ph_3PCR^1C(O)R^2$ and $R^3_3PCR^4R^5$, respectively.[1] In the catalytically active, square-planar nickel complex, the non-stabilized ylide is structurally intact C-coordinated, whereas the stabilized ylide is PO-coordinated due to rearrangement. The activity of the catalyst can be optimized by variation of the intact ylide ligand; but modification of the substituent R^2 in the carbonyl-stabilized ylide ligand also increases the catalytic activity in the $Ni(cod)_2/Ph_3PCHC(O)R^2/Me_3PCH_2$ system: On going from the formylmethylene(triphenyl)phosphorane **1a** via the acetyl derivative **1b** to the benzoylmethylene(triphenyl)phosphorane **1c** (R^2 = H, Me, Ph) the turnover number increases to ca. 0.5×10^5 moles ethene per mole of nickel.[1]

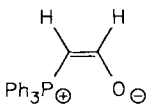

1a

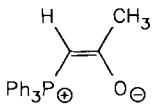

1b

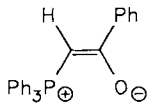

1c

Characterization of the polymers showed that the average chain length of the ethene polymerizates also increases with increasing catalyst activity. The intrinsic viscosities in tetralin at 140 °C do not, however, exceed 0.2 dL/g, which corresponds to molecular weights M of about 5×10^3 g/mole.[2] We have therefore tried to noticeably increase the range of molecular weights accessible with this Ni-catalyst system by further variation of the carbonyl-stabilized ylide ligand.

With the three ligands **2a**–**2c**, we have indeed been able to obtain novel, very active bis(ylide)nickel polymerization catalysts, which afford access to polyethene (PE) in practically all molecular weight ranges from PE waxes and hard waxes through high molecular weight high-density polyethene (HDPE) to ultrahigh molecular weight polyethene (UHMW-PE) with $M \geq 10^6$ g/mole (Table 1).

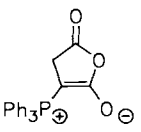

2a

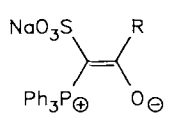

2b

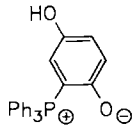

2c

The new catalysts are obtained in situ by stoichiometric reaction of the three components in toluene at 40–60 °C (cf. Ref. [1]). The triphenylphosphane-maleic anhydride adduct **2a**[3] has so far found no use as ligand; the sulfonated benzoylmethylene(triphenyl)phosphorane **2b**, R = C_6H_5, and the triphenylphosphane-benzoquinone adduct **2c**,[3] on the other hand, have already been employed successfully in combination with nickel(0) complexes and triphenylphosphane as catalysts for the synthesis of low-molecular weight PE waxes (α-olefins),[4,5] but nothing was known about the formation of high molecular weight PE in this connection.

The **2a**-catalysts are soluble in non-polar solvents, whereas the **2b**- and **2c**-catalysts are nearly insoluble. The **2b**-catalysts are soluble in dimethylformamide (DMF), and polymerizations can be initiated with DMF/toluene solutions; the resulting polyethene, however, has a relatively low molecular weight (Table 1); the intrinsic viscosities usually lie below 1 dL/g, i.e. the molecular weights are below 5×10^4 g/mole.

Regarding molecular weight control,[6] the **2c**-catalyst system is the most versatile. Depending upon which non-stabilized ylide is used, the intrinsic viscosities of the PE samples in tetralin at 140 °C reach values of up to 10 dL/g and more, from which molecular weights of $\geq 10^6$ g/mole can be calculated. In these catalyst systems, which are free of alkylaluminum compounds,[7] termination and transfer reactions can accordingly be suppressed as a function of the ligand in favor of an uninterrupted growth of the polymer chains. The second ylide ligand[8] and the polarity

Table 1. Polyethene synthesis with bis(ylide)nickel catalysts prepared from $Ni(cod)_2$, $Ph_3PCR^1C(O)R^2$ ("$R_3\overset{\oplus}{P}\!-\!\overset{\ominus}{O}$") and $R^3_3PCR^4R^5$ ("$R_3\overset{\oplus}{P}\!-\!\overset{\ominus}{X}$"). (For experimental details see Ref. [1].)

$R_3\overset{\oplus}{P}\!-\!\overset{\ominus}{O}$	$R_3\overset{\oplus}{P}\!-\!\overset{\ominus}{X}$	Catalyst injection [a]	Solvent [g]	Polymerization temperature [b] [°C]	Intrinsic viscosity in tetralin at 140 °C [dL/g]	PE molecular weight M [g/mole] [c]
1b	iPr_3PCH_2	m.p.i.	cyclohexane	125 ± 5	0.07	1.3×10^3
1c	iPr_3PCH_2	m.p.i.	cyclohexane	130 ± 10	0.10	2.1×10^3
2a	Ph_3PCHMe	s.p.i.	cyclohexane	ca. 100	0.5	1.87×10^4
2b	Ph_3PCH_2	m.p.i. [d]	cyclohexane	ca. 110	0.7	2.97×10^4
2b	$Ph_3P(CH)_3Ph$ [e]	s.p.i. [f]	cyclohexane	ca. 110	1.5	8.44×10^4
2c	Ph_3PCHMe	s.p.i.	cyclohexane	ca. 100	2.1	1.34×10^5
2c	Ph_3PNiBu	s.p.i.	cyclohexane	ca. 100	3.2	2.38×10^5
2c	$(PhO)_3PO$	s.p.i.	cyclohexane	60–100	5.8	5.38×10^5
2c	Ph_3PO	s.p.i.	cyclohexane	65–85	9.6	1.07×10^6
2c	Ph_3PCHMe	s.p.i.	ethyl acetate	ca. 100	0.21	5.7×10^3
2c	Ph_3PCHMe	s.p.i.	acetone	ca. 100	0.16	3.9×10^3
2c	Ph_3PCHMe	s.p.i.	DMF	ca. 100	0.12	2.7×10^3

[a] m.p.i. = multi-pulse injection, 2 mmol in 200 mL of toluene; s.p.i. = single-pulse injection, 2 mmol in 50 mL of toluene. [b] Polymerization pressure ca. 10^2 bar. [c] The PE molecular weight was estimated using the η/M relationship for linear PE: $\eta = 3.8 \times 10^{-4} \times M^{0.73}$ (see Ref. [9]). [d] In toluene/DMF. [e] $Ph_3P(CH)_3Ph$ denotes $Ph_3P{=}CH{-}CH{=}CH{-}Ph$. [f] 1 mmole of catalyst. [g] 1 L.

[*] Dr. K. A. Ostoja Starzewski, Dr. J. Witte
Bayer AG, Zentrale Forschung und Entwicklung
Wissenschaftliches Hauptlaboratorium
D-5090 Leverkusen 1 (FRG)

of the solvent provide chemical means for tuning the **2c**-catalyst system.

Received: August 19, 1986;
revised: October 2, 1986 [Z 1906 IE]
German version: *Angew. Chem. 99* (1987) 76

[1] K. A. Ostoja Starzewski, J. Witte, *Angew. Chem. 97* (1985) 610; *Angew. Chem. Int. Ed. Engl. 24* (1985) 599.
[2] The polymers with a molecular weight M of ca. 10^3 g/mole are PE waxes. Higher molecular weight types are hard waxes ($M \leq 10^4$ g/mole), HDPE ($M \approx 10^5$ g/mole), and UHMW-PE ($M \approx 10^6$ g/mol).
[3] a) A. Schönberg, A. F. A. Ismail, *J. Chem. Soc. 1940*, 1374; b) R. F. Hudson, P. A. Chopard, *Helv. Chim. Acta 46* (1963) 2178; c) G. Aksnes, *Acta Chem. Scand. 15* (1961) 692.
[4] a) D. L. Beach, J. J. Harrison, US-Pat. 4293727 (October 6, 1981), Gulf Research and Development Company. b) Y. V. Kissin, D. L. Beach, *J. Polym. Sci. Polym. Chem. Ed. 22* (1984) 333.
[5] P. Häussle, DOS 2923206 (December 11, 1980), Chemische Werke Hüls AG.
[6] HDPE molecular weights are usually catalyst-specifically regulated down to the desired level. This is usually achieved by increasing the temperature or by use of hydrogen, comonomers, or a second metal component, i.e. generally by termination or transfer agents. Cf., e.g., a) K.-Y. Choi, W. H. Ray, *J. Macromol. Sci. Rev. Macromol. Chem. Phys. C25* (1985) 1; b) W. Kaminsky, K. Külper, S. Niedoba, *Makromol. Chem., Macromol. Symp. 3* (1986) 377; c) J. Boor: *Ziegler-Natta-Catalysts and Polymerizations*, Academic Press, New York 1979, Chap. 10.
[7] We obtain modified catalysts with organoaluminum compounds.
[8] For a comparison of the electronic structure of R_3PCH_2 ligands with R_3PNX ligands and R_3PO ligands, cf. also K. A. Ostoja Starzewski, H. tom Dieck, *Inorg. Chem. 18* (1979) 3307, and references cited therein.
[9] R. Kuhn, H. Krömer, G. Rossmanith, *Angew. Makromol. Chem. 40/41* (1974) 361.

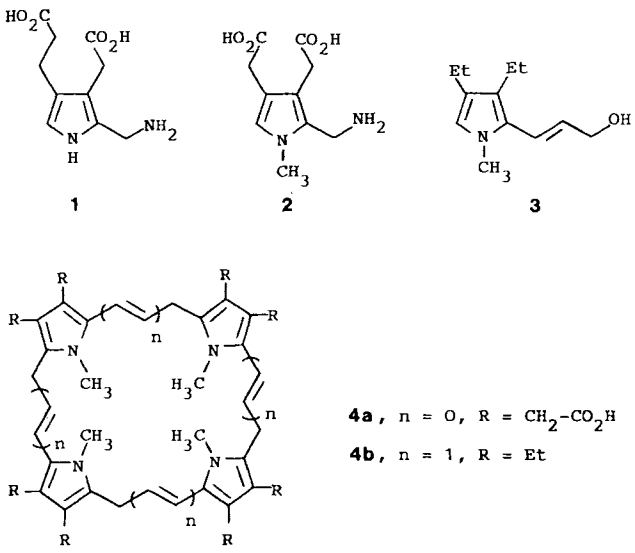

reactive dialcohol **7**, which was allowed to react in situ (see Scheme 1) at −60 °C. Work-up and chromatographic purification furnished the 21,24:22,23-bis-trimethylene-2,3,7,8,12,13,17,18-octaethylporphyrinogen **8** as the tetrahydrate in the form of fine needles that are stable on drying (m.p. 109 °C).[10] According to spectroscopic data, especially MS and ^{1}H-NMR data, **8** is a dimeric condensation product of **7**.

Biomimetic Synthesis of a Twofold *N,N'*-Bridged Porphyrinogen**

By *Ralf Timmermann, Rainer Mattes,* and *Burchard Franck**

Among the reactions of heme biosynthesis,[1,2] the cyclizing condensation of four molecules of the monopyrrole precursor porphobilinogen **1** is of particular significance for the development of biomimetic syntheses. **1** and structurally related pyrrole derivatives undergo highly selective acid-catalyzed condensation to give the porphyrinogens, the cyclic tetrapyrrole precursors of the porphyrins.[3,4] In continuation of our studies on the practicability of this *biomimetic*[5] *cyclotetramerization* we were able to synthesize novel, non-planar and fourfold expanded porphyrinogens **4a**[6] and **4b**[7] by acid-catalyzed condensation of the monopyrroles **2** and **3**, respectively, and to convert them into the corresponding porphyrins. We now report on the use of this biomimetic principle for the synthesis of the twofold *N,N'*-bridged porphyrinogens **8** from the trimethylenedipyrrole **7**, which can be regarded as a simplified *N,N'*-bridged dimer of porphobilinogen **1**.

The readily accessible[8] 3,4-diethyl-2-formylpyrrole **5** was alkylated in the form of its potassium salt with 1,3-dibromopropane to the dialdehyde **6** using a method described by *Burger* and *Dreier*.[9] For activation prior to acid-catalyzed condensation, **6** was reduced to the very

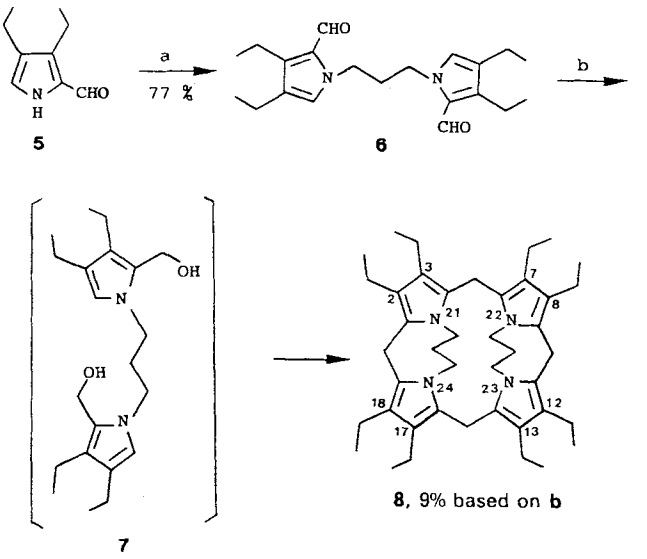

Scheme 1. Synthesis of **8** from **5** [8]. Reaction conditions: a) KOH/dimethyl sulfoxide, 1,3-dibromopropane, room temperature, 14 h; chromatography on silica gel (Merck 0.063–0.2 mm), petroleum ether/ether 4:1. b) $NaBH_4$/MeOH, room temperature, 20 min; *p*-TosOH/AcOH/MeOH, −60 °C; chromatography on Al_2O_3, Activity III (Woelm), petroleum ether/ether 95:5 [10].

An isomeric structure with crossed trimethylene bridges, the 21,23:22,24-bis-trimethylene derivative, could be ruled out on the basis of the MS and ^{1}H-NMR data and by the isolation and structural elucidation of a condensation intermediate. Thus, as expected for **8**, preferred splitting of the molecule into two halves took place in the mass spectrometer; in the case of crossed coupling this would re-

[*] Prof. Dr. B. Franck, Dipl.-Chem. R. Timmermann
Organisch-chemisches Institut der Universität
Orléansring 23, D-4400 Münster (FRG)
Prof. Dr. R. Mattes
Anorganisch-chemisches Institut der Universität
Corrensstrasse 36, D-4400 Münster (FRG)

[**] This work was supported by the Deutsche Forschungsgemeinschaft and the Fonds der Chemischen Industrie.

quire the very unlikely cleavage of four bonds. A crossed condensation product is also irreconcilable with the ^{1}H-NMR data, because, in contrast to **8**, it would be centrosymmetric and would not exhibit splitting of the methyl and methylene signals of the ethyl side chains into two triplets and quadruplets, respectively. Furthermore, it can be assumed that the acid-catalyzed condensation of **6** first leads intramolecularly to **9b**, from which only **8** can be formed.

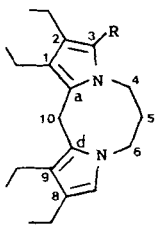

9a, R = H

9b, R = CH_2OH

If the condensation is carried out with suppression of the intermolecular reaction (dilution, high temperature, and large amounts of catalyst) a crystalline product is obtained as well-formed needles in 12% yield (m.p. 92°C). From a crystal structure analysis (Fig. 1) it followed that the product was the tetrahydrodipyrrolo-1,5-diazocine **9a**, formed from the initial hydroxymethylene product **9b** by elimination of formaldehyde.

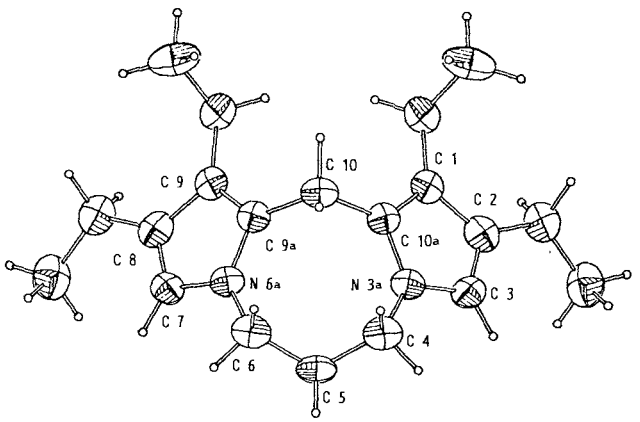

Fig. 1. Crystal structure of **9a**. Selected bond lengths [pm]: C(10a)-N(3a) 137.4(3), N(3a)-C(3) 138.3(3), C(3)-C(2) 135.9(5), C(2)-C(1) 142.4(3), C(1)-C(10a) 138.1(4). Interplanar angle between the pyrrole rings: 111° [10].

In **9a** the pyrrole rings are tilted at 111° to each other in a roof-like fashion. Assuming that **9a** is a structural element of **8**, only **8a** and **8b** of the four possible configurations of **8** come into question, of which, according to model considerations, the cage-like configuration **8a** is sterically favored.

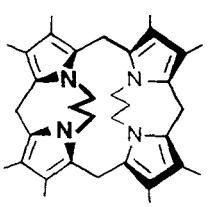

8a

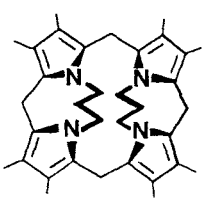

8b

In contrast to the unbridged *N,N',N'',N'''*-tetramethylporphyrinogen **4a**,[6] in the new porphyrinogens **8a** and **8b** there are strong steric interactions in the center of the molecule, thus rendering a planarization of the molecule difficult. As a consequence, **8** cannot be dehydrogenated like **4a** to the corresponding porphyrin.

Received: September 23, 1986 [Z 1930 IE]
German version: *Angew. Chem. 99* (1987) 74

[1] B. Franck, *Angew. Chem. 94* (1982) 327; *Angew. Chem. Int. Ed. Engl. 21* (1982) 343.
[2] M. Akthar, P. M. Jordan in D. H. R. Barton, W. D. Ollis (Eds.): *Comprehensive Organic Chemistry, Vol. 5*, Pergamon, Oxford 1979, p. 1121.
[3] G. H. Cookson, C. Rimington, *Biochem. J. 57* (1954) 476.
[4] B. Franck, G. Bringmann, C. Wegner, U. Spiegel, *Liebigs Ann. Chem. 1980*, 263.
[5] R. Breslow, *Q. Rev. Chem. Soc. 1* (1972) 553: "Biomimetic chemistry is the branch of organic chemistry which attempts to imitate natural reactions and enzymatic processes as a way to improve the power of organic chemistry".
[6] B. Franck, C. Wegner, *Angew. Chem. 87* (1975) 419; *Angew. Chem. Int. Ed. Engl. 14* (1975) 424.
[7] M. Gosmann, B. Franck, *Angew. Chem. 98* (1986) 1107; *Angew. Chem. Int. Ed. Engl. 25* (1986) 1100.
[8] A. W. Johnson, I. T. Kay, *J. Chem. Soc. 1965*, 1620; B. Fietzke, *Dissertation*, Universität Münster 1986.
[9] U. Burger, F. Dreier, *Tetrahedron 39* (1983) 2065.
[10] The new compounds **6**, **8**, and **9a** have been completely characterized by elemental analyses and spectroscopic data.—**6**: m.p. = 69–71°C, ^{1}H-NMR ($CDCl_3$): $\delta = 1.17$ (t, $J = 7.6$ Hz, 6H, ethyl-CH_3 at C-4/C-4'), 1.18 (t, $J = 7.6$ Hz, 6H, ethyl-CH_3 at C-3/C-3'), 2.40 (q, $J = 7.6$ Hz, 4H, ethyl-CH_2 at C-4/C-4'), 2.69 (q, $J = 7.6$, 4H, ethyl-CH_2 at C-3/C-3'), 9.65 (s, 2H, 2 aldehyde-H).—**8**: m.p. = 109°C, MS (EI): *m/z* 620 (52%, $M^{\oplus}$), 310 (28, $M^{\oplus}/2$), 162 (100, diethyl pyrrole + $3CH_2$); ^{1}H-NMR ($CDCl_3$): $\delta = 1.10$ (t, $J = 7.4$ Hz, 12H, 4CH_3), 1.17 (t, $J = 7.4$ Hz, 12H, 4 CH_3), 2.27 (m, 4H, 2 CH_2 in the middle of the two bridges), 2.42 (q, $J = 7.4$ Hz, 8H, CH_2 in 4 ethyl groups), 2.44 (q, $J = 7.4$ Hz, 8H, CH_2 in 4 ethyl groups), 3.89 (t, $J = 6.7$ Hz, 8H, 4 N-CH_2 groups), 4.45 (s, 8H, 4 *meso*-CH_2).—**9a**: m.p. = 92°C, crystallizes in the space group $P2_1/m$, with two formula units per unit cell and has a crystallographic mirror symmetry. $a = 924.5(8)$, $b = 2236(4)$, $c = 468.4(4)$ pm, $\beta = 116.8(1)°$; Syntex $P2_1$ diffractometer, 1057 independent reflections with $F_0 \geq 3.92\sigma(F_0)$, 167 parameters, $R = 0.0561$, $R_w = 0.0522$. Further details of the crystal structure investigation are available on request from the Fachinformationszentrum Energie, Physik, Mathematik GmbH, D-7514 Eggenstein-Leopoldshafen 2 (FRG), on quoting the depository number CSD-52163, the names of the authors, and the full citation of the journal.—MS (EI): *m/z* 298 (55%, $M^{\oplus}$), 269 (100, $M^{\oplus}$ – Ethyl), 162 (66, diethylpyrrole + 3 CH_2); ^{1}H-NMR ($CDCl_3$): $\delta = 1.15$ (t, $J = 7.5$ Hz, 6H, 2 CH_3), 1.16 (t, $J = 7.5$ Hz, 6H, 2 CH_3), 2.26 (m, $J = 6.8$ Hz, 2H, CH_2 in the middle of the trimethylene bridge), 2.40 (q, $J = 7.5$ Hz, 4H, ethyl-CH_2), 2.53 (q, $J = 7.5$ Hz, ethyl-CH_2), 3.86 (t, $J = 6.8$ Hz, 4H, N-CH_2), 4.33 (s, 2H, H at C-10), 6.28 (s, 2H, H at C-3/C-7).

Nickel Complexes with a Propellane Structure**

By *Harald Schwager, Carl Krüger, Richard Neidlein,* and *Günther Wilke**

Stable complexes of low-valent transition metals with fluorine-substituted hydrocarbons have been the subject of numerous studies over the past 20 years.[1] Of particular interest is the nature of the bonding in these complexes compared to that in non-fluorinated systems. The observa-

[*] Prof. Dr. G. Wilke, Dr. H. Schwager, Prof. Dr. C. Krüger [+]
Max-Planck-Institut für Kohlenforschung
Kaiser-Wilhelm-Platz 1, D-4330 Mülheim a. d. Ruhr (FRG)
Prof. Dr. R. Neidlein
Pharmazeutisch-chemisches Institut der Universität
Im Neuenheimer Feld 364, D-6900 Heidelberg (FRG)

[+] X-ray structure analysis.

[**] This work was supported by the Deutsche Forschungsgemeinschaft and the Fonds der Chemischen Industrie.

tion that the reactivity of cyclopropabenzene towards nickel(0) depends drastically on the other ligands, as demonstrated for example in the transition from trimethylphosphane to triethylphosphane,[2] directed our interest to the reaction behavior of the difluorocyclopropabenzene **1**[3] toward nickel(0) compounds. We report here a facile entry to the novel class of compounds of the nickelatricyclo-[4.1.1.0^{1,6}]octadienes **5** having a propellane structure.

Reaction of **1** with the nickel(0) complexes **2** or **3**, or with a 1 : 1 mixture of tris(ethene)nickel(0) **4** and a nitrogen chelate ligand leads in high yields to nickel compounds of type **5** (Scheme 1).[4, 5] **5** is the product of removal of the olefin and phosphane ligands and addition of the central three-membered ring double bond of **1** to the nickel atom. The compounds **5**[6] are stable at room temperature, but decompose however on exposure to atmospheric oxygen. In solution, the complexes—with exception of **5c** and **5d**—slowly eliminate **1** at temperatures below −20°C.

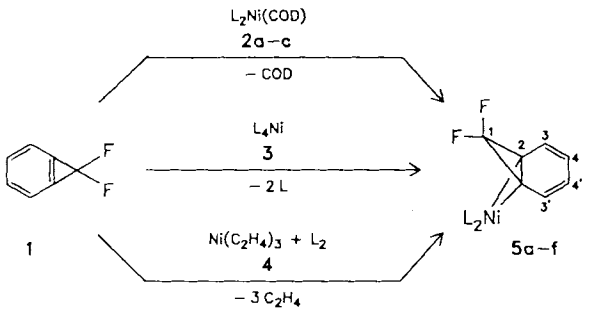

Product	Ligand	Educt	Solvent	T [°C]	t [h]	Yield [%]
5a	L = PMe_3	**2a**	pentane	−30	0.1	93
5b	L = PEt_3	**2b**	pentane	−20	3	61
5c	L_2 = dcpe	2c	toluene	+25	20	68
5d	L = PPh_3	3	toluene	+25	6	92
5e	L_2 = TMEDA	**4**	Et_2O	−78 to +25	1	87
5f	L_2 = bpy	**4**	Et_2O	−78 to +25	1	84

Scheme 1. Synthesis of **5a–f** (unsystematically numbered). COD = *cis,cis*-1,5-cyclooctadiene; dcpe = ethylenebis(dicyclohexylphosphane); TMEDA = tetramethylethylenediamine; bpy = 2,2′-bipyridyl.

The nuclear resonance spectra[7] are reconcilable with the given propellane structure. In the ^{31}P-NMR spectra of **5a–d** a double doublet is observed which results from the coupling of the equivalent phosphorus atoms with the two ^{19}F nuclei. Considering only homonuclear couplings in the ^{1}H-NMR spectra of **5**, the non-equivalent protons H-3, H-3′, H-4, and H-4′ show the splitting pattern of an AA′BB′ system (δ_A = 5.6–6.5 and δ_B = 5.3–5.8). The norcaradiene partial structure of the difluorosubstituted ligand follows from the ^{13}C-NMR spectra. The chemical shift of the carbon atom C-2 bonded to the nickel atom (δ = 33–52) (see Table 1) supports the given structure, since a chemical shift of $\delta \approx 100$–120 would be expected for a cycloheptatriene partial structure. The C-2 signal of **5** is shifted more than 80 ppm upfield compared to the corresponding signal of **1**.[8] This upfield shift confirms the loss of aromaticity due to complexation in **1**. As a result of the deshielding effect of the fluorine atoms, the C-1 singlet of **5** is observed at relatively low field.

Table 1. ^{13}C-NMR data of the nickelatricyclooctadiene moiety of **5a–e** (75.5 MHz, [D$_8$]THF, δ referred to TMS, J in Hz) [a]. For numbering see Scheme 1.

	5a	**5b**	**5c**	**5d**	**5e**
Temperature [°C]	−80	−50	+40	−30	−40
δ(C-1)	103.7 s	102.7 s	103.6 s	102.7 s	113.3 s
J(C-1,F)	284.6	285.3	282.5	287.9	285.5
δ(C-2)	49.0 s	48.4 s	51.2 s	52.3 s	33.1 s
J(C-2,F)	56.0	54.9	57.0	52.1	45.5
	7.0	6.6	7.1	7.3	18.7
δ(C-3)	124.1 d	124.2 d	123.4 d	125.4 d	122.1 d
J(C-3,F)	7.3	7.9	8.3	7.1	6.8
	—	—	—	—	1.9
δ(C-4)	123.0 d	123.2 d	125.9 d	122.8 d	120.4 d

[a] Due to the poor solubility of **5f**, a detailed analysis was not possible; the observed signals, however, lie in the expected region.

In the case of **5b**, the structure type derived from NMR spectra was confirmed by an X-ray structure analysis.[9] The carbon atoms bound to the nickel atom have a bond length of 1.514(9) Å, significantly longer than an aromatic CC bond.

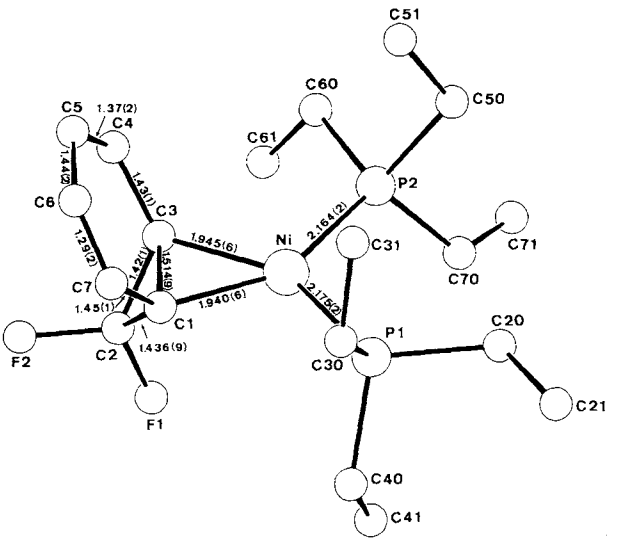

Fig. 1. Crystal structure of 8,8-difluoro-7,7-bis(triethylphosphane)-7-nickelatricyclo[4.1.1.0^{1,6}]octa-2,4-diene **5b**. Important bond lengths in Å.

The X-ray structure analysis of **5b** and the ^{1}H- and ^{13}C-NMR spectra suggest that **1** reacts with nickel(0) complexes by a formal oxidative addition.

Received: July 31, 1986 [Z 1883 IE]
German version: *Angew. Chem.* 99 (1987) 72

[1] C. S. Cundy, M. Green, F. G. A. Stone, *J. Chem. Soc. A 1970*, 1647, and references cited therein.

[2] a) R. Mynott, R. Neidlein, H. Schwager, G. Wilke, *Angew. Chem.* 98 (1986) 374; *Angew. Chem. Int. Ed. Engl.* 25 (1986) 367; b) R. Neidlein, A. Rufińska, H. Schwager, G. Wilke, *ibid.* 98 (1986) 643 and 25 (1986) 640.

[3] a) S. Korte, *Dissertation*, Universität Köln 1968; b) E. Vogel, S. Korte, W. Grimme, H. Günther, *Angew. Chem.* 80 (1968) 279; *Angew. Chem. Int. Ed. Engl.* 7 (1968) 289.

[4] Typical procedure: **5a**: A solution of **2a** (380 mg, 1.19 mmol) in pentane (50 mL) was treated with 0.3 mL (2 mmol) of **1** under argon at −30°C. A yellow microcrystalline solid immediately separated out. The reaction mixture was stirred for 2 h at −20°C and then cooled to −78°C. The precipitate was recovered by suction on a cooled frit, washed twice with

cold pentane, and then dried under high vacuum at −20°C. Yield: 374 mg (93%) yellow crystals, correct elemental analysis. ^{1}H-NMR (400 MHz, [D$_8$]THF, 27°C): δ = 6.21 (m, 1 H, H-3), $^3J(3,4)$ = 8.8 Hz, $^4J(3,4')$ = 0.2 Hz, $^5J(3,3')$ = 2.2 Hz, $^4J(P,3)$ = 4.1 Hz, $^4J(F,3)$ = 4.1 Hz); 5.72 (m, 1 H, H-4, $^3J(4,4')$ = 5.7 Hz, $^5J(P,4)$ = 1.7 Hz, $^5J(F,4)$ = 1.8 Hz); 1.26 (d, 9 H, PCH$_3$, $^2J(P,H)$ = 6.9 Hz). ^{31}P-NMR (32 MHz, [D$_8$]THF, −20°C): δ = −10.8 (dd). MS (CI-NH$_3$): *m/z* 337 (M+H$^{\oplus}$). IR (KBr): $\tilde{\nu}$ = 1659 (m) (C=C) cm^{-1}.

[5] Typical procedure: **5e**: A solution of tris(ethene)nickel(0) **4** (freshly prepared from 850 mg (3.6 mmol) of cyclododecatrienenickel) in ether (30 mL) was treated at −78°C with 0.54 mL (3.6 mmol) of TMEDA and then 0.6 mL (4.0 mmol) of **1**. The reaction mixture was warmed to room temperature for 30 min and then slowly cooled to −78°C; yellow crystals separated out. These were removed from the mother liquor by filtration, washed with cold ether, and dried under high vacuum. ^{1}H-NMR (200 MHz, [D$_8$]THF, 27°C): δ = 5.89 (m, 1 H, H-3); 5.54 (m, 1 H, H-4); 2.65 (s, 3 H, NCH$_3$); 2.59 (s, 3 H, NCH$_3$); 2.15 (s, 2 H, NCH$_2$−). MS: *m/z* 300 ($M^{\oplus}$); IR (KBr): $\tilde{\nu}$ = 1659 (w) (C=C) cm^{-1}.

[6] The values obtained in the elemental analysis are consistent with the empirical formula.

[7] NMR data collection, NMR-Labor, Max-Planck-Institut für Kohlenforschung, Kaiser-Wilhelm-Platz 1, D-4330 Mülheim a. d. Ruhr (FRG).

[8] B. Halton, H. M. Huegel, D. P. Kelly, P. Mueller, U. Burger, *J. Chem. Soc. Perkin Trans. 2 1976*, 258.

[9] X-ray structure analysis: cell data: a = 11.075(3), b = 14.599(4), c = 14.343(2) Å, β = 101.15(2)°, V = 2275.3 Å, ρ_{calc} = 1.23 g cm^{-3}, μ = 10.09 cm^{-1}, Z = 4, space group $P2_1/n$; total number of reflections 5137, 2686 observed, 217 refined parameters, R = 0.056, R_w = 0.064. Further details of the crystal structure analysis are available on request from the Fachinformationszentrum Energie, Physik, Mathematik GmbH, D-7514 Eggenstein-Leopoldshafen 2 (FRG), on quoting the depository number CSD-51931, the names of the authors, and the full citation of the journal.

Reactions of (η^3-Allyl)(η^5-cyclopentadienyl)palladium with Cyclopropabenzenes

By *Harald Schwager, Reinhard Benn,* and *Günther Wilke**

We have recently described[3–6] the reactions of nickel(0) complexes with cyclopropabenzene **1**,[1] difluorocyclopropabenzene **2**,[2] and bis(trimethylsilyl)cyclopropabenzene **3**.[3] Irrespective of the ligands on the nickel(0) and of the substitution at the methano bridge of the respective cyclopropabenzene, these reactions lead either to a bismethano-bridged nickel[13]annulene,[4] to nickeltricyclooctadienes,[5] or to nickelacyclobutabenzenes.[3,6] The cyclopropabenzenes behave both in a similar manner as well as in a completely different manner towards (η^3-allyl)(η^5-cyclopentadienyl)palladium **4**.[7]

Reaction of cyclopropabenzene **1** with the palladium(II) complex **4** and trimethylphosphane (Scheme 1) affords, in almost 80% yield, the compound **5**, which is a red oil stable at room temperature, and which can be obtained in pure form by crystallization at low temperature. According to an elemental analysis, **5** has the composition $C_{18}H_{25}PdP$, i.e. the allyl- and the cyclopentadienyl-ligand are not removed: this is in contrast to the reaction of **4** with 3,3-dimethylcyclopropene and trimethylphosphane.[8] The NMR data indicate the presence of a σ-bonded benzyl moiety.

The complex **5** stabilized by trimethylphosphane[9] can be formed by alkylation of the cyclopentadienyl moiety by the allyl ligand, addition of a cyclopropabenzene molecule with opening of one of the two CC single bonds of the three-membered ring, and hydrogen migration to the cyclopropabenzene. A metallacycle is presumably involved as an intermediate (Scheme 1).

2 reacts smoothly with **4** in the presence of trimethylphosphane (Scheme 1) with preservation of the three-membered ring and loss of aromaticity to give the palladatricyclooctadiene complex **6** with a propellane structure, i.e. the central three-membered ring double bond of **2** adds to the palladium atom with loss of the allyl and cyclopentadienyl ligands. **6** is sensitive to oxidation and is also thermally labile (for analogous nickel complexes see Ref. [5]). The nuclear magnetic resonance spectra are consistent with the proposed propellane structure.[10] In the ^{31}P-NMR spectrum, a signal with triplet-like splitting of 7.6 Hz is observed at δ = −22.2. The signals of the non-equivalent protons H-3, H-3′, H-4, and H-4′ in the ^{1}H-NMR spectrum show the splitting pattern of an AA′BB′ system (δ_A = 6.42 and δ_B = 5.85); considering only homonuclear couplings.

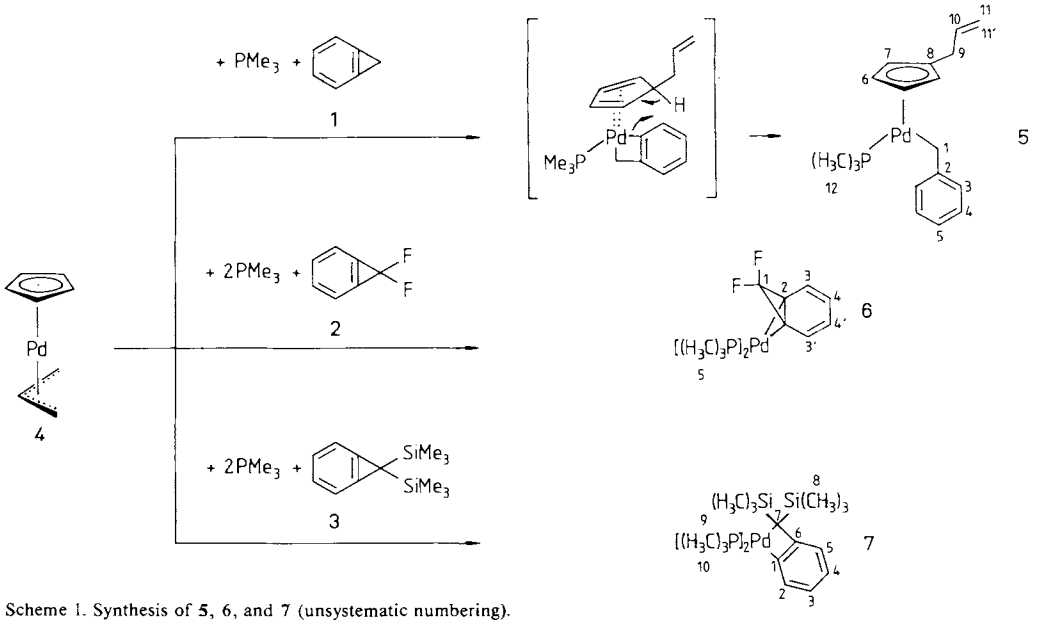

Scheme 1. Synthesis of **5**, **6**, and **7** (unsystematic numbering).

Reaction of **3** and **4** and trimethylphosphane leads in high yields to the palladacyclobutabenzene **7** (Scheme 1).

[*] Prof. Dr. G. Wilke, Dr. H. Schwager, Dr. R. Benn [+]
Max-Planck-Institut für Kohlenforschung
Kaiser-Wilhelm-Platz 1, D-4330 Mülheim a. d. Ruhr (FRG)
[+] NMR investigations.

7 is also the product of the displacement of the allyl- and cyclopentadienyl-ligands and insertion of the palladium into one of the two CC single bonds of the three-membered ring of **3**. The complex **7** is stable at room temperature, but decomposes on exposure to atmospheric oxygen. The nuclear resonance spectra[10] confirm the proposed structure. The ^{31}P-NMR spectrum is that of an AX spin system ($\delta = -22.0/-29.9$, $J(P,F) = 25.3$ Hz). The different P-C-7 coupling constants (70.7 and 4.6 Hz) rule out a quasi square-planar arrangement at the palladium. Moreover, the NMR data of **7** are consistent with those for the analogous nickel(II) complex.[3, 6]

Thus, with the synthesis of the compounds **5**, **6**, and **7** it has been possible for the first time to obtain well defined products by reaction of palladium complexes with cyclopropabenzenes. In analogy to the reactions with nickel(0) complexes,[3–6] reaction of **2** and **3** with the palladium(II) complex **4** leads to formation of a metallatricyclooctadiene **6** and a metallacyclobutabenzene **7**, respectively. In contrast, the parent compound **1** reacts with **4** to give a benzyl complex **5**. An analogous compound could not be obtained with nickel.

Received: July 31, 1986 [Z 1884 IE]
German version: *Angew. Chem. 99* (1987) 73

CAS Registry numbers:
1, 4646-69-9; **2**, 18238-55-6; **3**, 103322-20-9; **4**, 1271-03-0; **5**, 105858-64-8; **6**, 105882-00-6; **7**, 105858-65-9.

[1] W. E. Billups, A. J. Blakeney, W. Y. Chow, *Org. Synth. 55* (1976) 12.
[2] a) S. Korte, *Dissertation*, Universität Köln 1968; b) E. Vogel, S. Korte, W. Grimme, H. Günther, *Angew. Chem. 80* (1968) 279; *Angew. Chem. Int. Ed. Engl. 7* (1968) 289.
[3] a) H. Schwager, *Dissertation*, Universität Bochum 1986; b) H. Schwager, C. Krüger, K. Laakmann, G. Schroth, G. Wilke, *Chem. Ber.*, in press.
[4] a) R. Mynott, R. Neidlein, H. Schwager, G. Wilke, *Angew. Chem. 98* (1986) 374; *Angew. Chem. Int. Ed. Engl. 25* (1986) 367; b) H. Schwager, R. Neidlein, G. Wilke, Deutsch-Österreichisches Chemikertreffen 1986, Vortragsbd. p. 68.
[5] H. Schwager, C. Krüger, R. Neidlein, G. Wilke, *Angew. Chem. 99* (1987) 72; *Angew. Chem. Int. Ed. Engl. 26* (1987) 65.
[6] R. Neidlein, A. Rufińska, H. Schwager, G. Wilke, *Angew. Chem. 98* (1986) 643; *Angew. Chem. Int. Ed. Engl. 25* (1986) 640.
[7] Y. Tatsuno, T. Yoshida, *Inorg. Synth. 19* (1979) 220.
[8] a) H. M. Büch, *Dissertation*, Universität Kaiserslautern 1982; b) P. Binger, H. M. Büch, R. Mynott, *Angew. Chem. 94* (1982) 66; *Angew. Chem. Int. Ed. Engl. 21* (1982) 62; *Angew. Chem. Suppl. 1982*, 153.
[9] Procedure for **5**: A solution of **4** (890 mg, 4.19 mmol) [7] in pentane (50 mL) was treated at −30°C with 0.84 mL (8.38 mmol) of trimethylphosphane and 0.87 mL (8.38 mmol) of **1**. The orange-colored suspension that was formed initially gradually changed to a clear red solution upon stirring at room temperature. After removal of the remaining insoluble material by filtration through a D_4 frit, the filtrate was evaporated down to 20 mL and slowly cooled to −78°C. After 2 d, the red crystals that separated out were recovered from the mother liquor by filtration and dried under high vacuum. At room temperature the crystals give a red oil. Yield: 1.26 g (3.33 mmol, 79%) as a red oil. Correct elemental analysis.—MS (70 eV): *m/z* 378 ($M^{\oplus}$, 27%). IR (KBr): $\tilde{\nu}$ = 1486, 1593 (C=C); 3019, 3070 (=C−H) cm^{-1}. ^{1}H-NMR (400 MHz, [D$_8$]THF, TMS, 27°C): δ = 2.64 (d, 2H, H-1, $^3J(1,P) = 5.5$ Hz); 7.13 (dd, 2H, H-3); 6.97 (br. t, 2H, H-4); 6.79 (br. t, 1H, H-5); 5.20 (m, 2H, H-6), $^3J(6,7) = 4.8$ Hz, $^3J(6,P) = 1.1$ Hz); 5.07 (m, 2H, H-7, $^3J(7,P) = 1.5$ Hz); 2.86 (br. d, 2H, H-9, $^3J(9,10) = 6.7$ Hz, $^4J(9,11) = -1.3$ Hz, $^4J(9,11') = -1.6$ Hz, $^4J(9,P) = 1.9$ Hz); 5.83 (m, 1H, H-10, $^3J(10,11) = 10.0$ Hz, $^3J(10,11') = 17.1$ Hz); 4.83 (m, 1H, H-11, $^2J(11,11') = 2.3$ Hz); 4.92 (m, 1H, H-11'); 1.33 (d, 9H, H-12, $^2J(12,P) = 10.2$ Hz). ^{31}P-NMR (32 MHz, [D$_8$]THF, TMS, 37°C): $\delta = -6.6$ (s). ^{13}C-NMR (75.5 MHz, [D$_8$]THF, TMS, 38°C): δ = 7.68 (t, C-1, $^2J(P,C) = 8.1$ Hz); 154.10 (s, C-2); 128.68 (d, C-3); 128.20 (d, C-4); 122.51 (d, C-5); 97.62 (d, C-6, $^2J(P,C) = 3.1$ Hz); 95.94 (d, C-7, $^2J(P,C) = 1.8$ Hz); 115.94 (s, C-8, $^2J(P,C) = 2.7$ Hz); 33.57 (t, C-9); 139.8 (d, C-10); 113.5 (t, C-11); 18.86 (q, C-12, $^1J(P,C) = 29.3$ Hz).
[10] NMR data collection, NMR-Labor, Max-Planck-Institut für Kohlenforschung, Kaiser-Wilhelm-Platz 1, D-4330 Mülheim a. d. Ruhr (FRG).

A Triple Decker Sandwich Structure by Reaction of Cyclopentadienylbis(ethylene)cobalt with Carbodiimides: an Unusual Cyclopentadienylcobalt Oligomer**

By *Sergio Stella, Carlo Floriani,* Angiola Chiesi-Villa,* and *Carlo Guastini*

A variety of metal-mediated organic reactions, including insertion, cycloaddition, reductive coupling, C–H bond cleavage, lead to C–C bond formation. These reactions are usually performed by potentially coordinatively unsaturated species, a prototype of which is the [CpCo] (Cp = η^5-C_5H_5) fragment, which forms a variety of $CpCoL_2$ derivatives.[1] Two general aspects of the reactivity of the [CpCo] unit are relevant: the metal can promote reactions between functional groups; moreover it can react with a preformed organometallic species. The latter reaction usually leads to some unpredictable polymetallic structures. We wish to report here the reaction of cyclopentadienylbis(ethylene)cobalt **1**[2] with carbodiimides which emphasizes both the above mentioned aspects of [CpCo] reactivity.

Carbodiimides undergo reductive disproportionation[3] to alkyl isocyanide and the dianion *N,N',N''*-trialkylguanidinediide upon reaction with **1**, which, however, is able to elaborate a quite unusual transformation of the isocyanide fragment.[4]

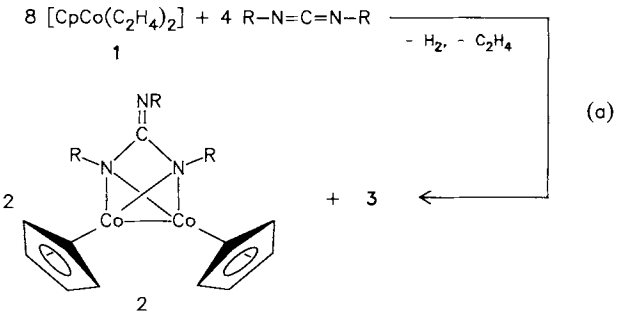

R = *cyclo*-C_6H_{11}

Two crystalline solids, **2** and **3**, are formed according to reaction (a).[5] The complex **2**[5] is a diamagnetic dinuclear complex, the structure of which has been confirmed by an X-ray analysis. Figure 1 shows the structure of **3**,[6] with selected bond distances and angles. The molecule can be viewed as a triple-decker sandwich in which Co1 and Co3 share a quite unusual organometallic fragment. This consists of two fused five-membered rings, each one containing a cobalt atom. Such a fragment is almost planar, with Co2 and Co4 deviating by only 0.094(1) and 0.329(1) Å, respectively, from the C27, C28, C29, C30, N1, N2 plane. The structural data are consistent with both delocalized (**3A**) as well as with localized double bonding (**3B**).

[*] Prof. Dr. C. Floriani [+], S. Stella
Chemistry Department, Columbia University
New York, NY 10027 (USA)
Dr. A. Chiesi-Villa, Dr. C. Guastini
Istituto di Strutturistica Chimica
Centro di Studio per la Strutturistica Diffrattometrica del CNR
Università di Parma, I-43100 Parma (Italy)
[+] Present address:
Institut de Chimie Minérale et Analytique, Université de Lausanne
3 Place du Chateau, CH-1005 Lausanne (Switzerland)

[**] This work was supported by the U. S. Office of Naval Research (Columbia University Grant No. N-00014-86-K-0380) and by the Italian CNR (Università di Parma).

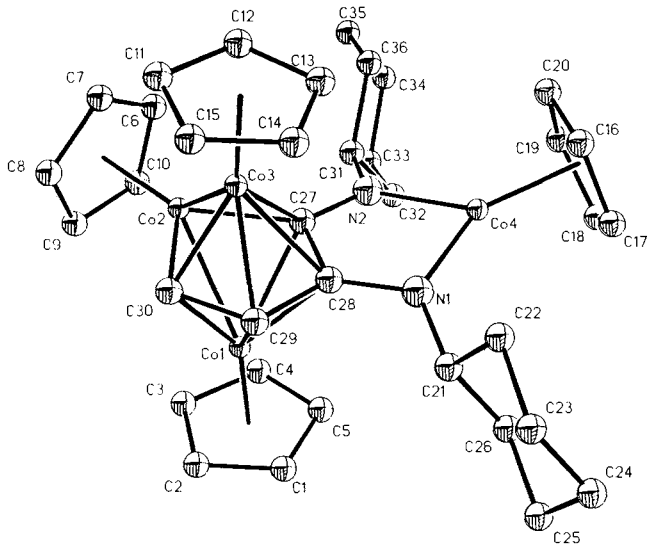

Fig. 1. Crystal structure of the complex **3**. Bond distances [Å]: Co2-C27, 1.963(6); Co2-C30, 1.914(7); C29-C30, 1.457(8); C28-C29, 1.438(9); C27-C28, 1.502(8); C28-N1, 1.358(8); C27-N2, 1.316(9); Co4-N1, 1.913(6); Co4-N2, 1.946(5); Co1-Cp1, 1.704(6); Co2-Cp2, 1.749(6); Co3-Cp3, 1.704(8); Co4-Cp4, 1.736(7); Co1-S, 1.686(2); Co3-S, 1.700(2). Cp1, Cp2, Cp3, Cp4 refer to the centroids of the rings C1···C5; C6···C10; C11···C15; C16···C20, S refers to the centroid of the ring C27, C28, C29, C30, Co2.

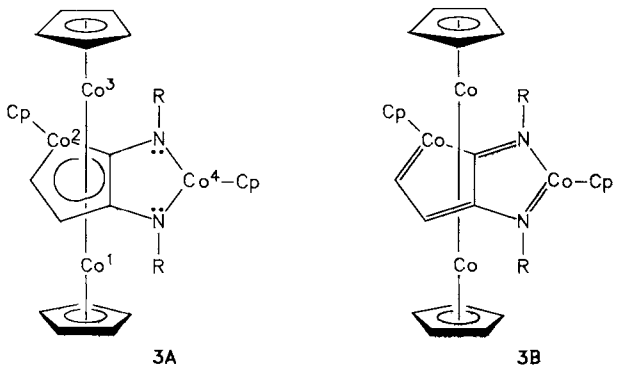

It should be mentioned that there are in each case significant differences between the two Co2–C bonds and the two Co4–N bonds (see Fig. 1). A length of Co–C 1.902(3) was recently reported for the double bond in the carbene complex **4**.[7]

[CpCo=C–N(Me)–CH_2–CH_2–N(Me)(SPh)] **4**

The planarity of the ring system, however, allows for a certain amount of electron delocalization over the two rings. The cyclopentadienyl rings bonded to Co1 and Co3 are almost parallel to the common five-membered ring; the dihedral angles are 4.9(2) and 3.5(2)°, respectively. The distances of Co1 and Co3 from the plane of this ring are very similar to the distances from the Cp rings; in contrast, the Co2-Cp and Co4-Cp distances are significantly longer. The structure **3A** (delocalized) can be described as a triple decker sandwich having 32 valence electrons, while the structure **3B** (localized) requires 33 valence electrons for the triple decker; Co4 has 19 valence electrons. Although the 32e configuration, in which Co4 has 16 valence electrons is more likely, since CpCo and RB are isolobal, the spin distribution in complex **3** must be known before one of the hypotheses can be ruled out. Complex **3** is paramagnetic (two unpaired electrons), as expected for both configurations ($\mu = 2.69$ BM at 292 K).[8]

The diazadimetallapentalene-type fragment is formally formed by co-oligomerization of ethylene with two isocyanide molecules, which are set free during the reductive dimerization of dicyclohexylcarbodiimide in reaction (a). In order to ascertain whether **3** can be formed from cyclohexyl isocyanide and **1**, we carried out reaction (b).[9]

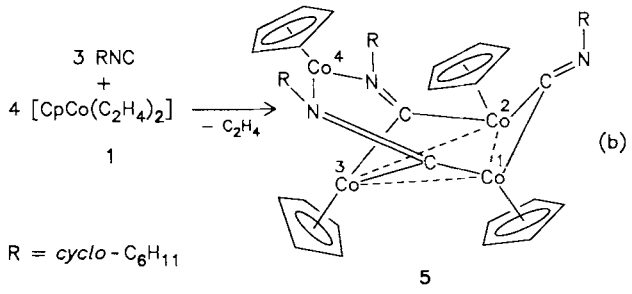

The resulting tetranuclear complex **5** contains only [CpCo] and cyclohexyl isocyanide units, and no ethylene. The structure is shown in Figure 2 with selected bond distances and angles.[10] The $Cp_3Co_3(RNC)_3$ core can be depicted as a six-membered ring with a chair conformation in which two nitrogens bind a fourth [CpCo] unit. The Co···Co distances compare with those commonly found in $[CpCo]_n$ clusters like $Cp_3Co_3(CO)_3$,[11a] $Cp_4Co_4(CO)_2$,[11b] and $[Cp_3Co_3(COTiCp_2)_2]$.[11c] The Co–C bond distances,

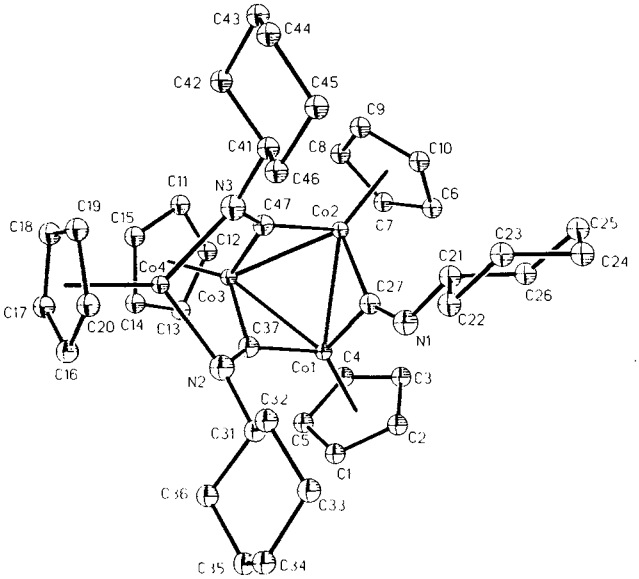

Fig. 2. Crystal structure of the complex **5**. Bond distances [Å]: Co1-C27, 1.91(1); Co1-C37, 1.85(1); Co1-Cp1, 1.77(1); Co2-C27, 1.90(1); Co2-C47, 1.83(1); Co2-Cp2, 1.76(1); Co3-C37, 1.84(1); Co3-C47, 1.87(1); Co3-Cp3, 1.76(1); Co4-N2, 2.038(9); Co4-N3, 2.022(9); Co4-Cp4, 1.91(2); C27-N1, 1.21(1); C37-N2, 1.30(1); C47-N3, 1.32(2); Co1-Co2, 2.513(2); Co1-Co3, 2.457(2); Co2-Co3, 2.483(2).

though significantly different from each other, vary within the range of lengths found for $Co–C_{(\mu\text{-}CO)}$ bonds in the known $[CpCo]_n$ clusters.[11] The C–N bond distances including the distance to Co4 are significantly longer than C27–N1. The proximity of C37 and C47 [2.42(1) Å] would

indicate that the diazadimetallapentalene skeleton can be formed by such a structure. This result, however, seems to rule out the preliminary stage of the reaction between **1** and carbodiimides serving for the generation of isocyanides only. The reaction must be much more complex.

Received: August 5, 1986;
revised: October 16, 1986 [Z 1892 IE]
German version: *Angew. Chem. 99* (1987) 84

[1] H. Bönnemann, *Angew. Chem. 97* (1985) 264; *Angew. Chem. Int. Ed. Engl. 24* (1985) 248; *ibid. 90* (1978) 517 and *17* (1978) 505; H. Werner, *ibid. 95* (1983) 932 and *22* (1983) 927; K. Jonas, *ibid. 97* (1985) 292 and *24* (1985) 295; K. P. C. Vollhardt, *Acc. Chem. Res. 10* (1977) 1; *Angew. Chem. 96* (1984) 525; *Angew. Chem. Int. Ed. Engl. 23* (1984) 539; B. C. Berris, G. H. Hovakeemian, Y. H. Lai, H. Mestdagh, K. P. C. Vollhardt, *J. Am. Chem. Soc. 107* (1985) 5670; B. Eaton, J. M. O'Connor, K. P. C. Vollhardt, *Organometallics 5* (1986) 394.

[2] K. Jonas, E. Deffense, D. Habermann, *Angew. Chem. 95* (1983) 729; *Angew. Chem. Int. Ed. Engl. 22* (1983) 716; *Angew. Chem. Suppl. 1983*, 1005.

[3] N. J. Bremer, A. B. Cutcliffe, M. F. Farona, W. G. Kofron, *J. Chem. Soc. A 1971*, 3264; D. M. Duggan, *Inorg. Chem. 18* (1979) 903; J. D. Cotton, S. D. Zornig, *Inorg. Chim. Acta 25* (1977) L133; M. Pasquali, S. Gambarotta, C. Floriani, A. Chiesi-Villa, C. Guastini, *Inorg. Chem. 20* (1981) 165.

[4] Dicyclohexyl- and di-*p*-tolyl-carbodiimides gave the same results. Details will be given only for reactions with dicyclohexylcarbodiimide.

[5] Procedure for **2**: **1** (1.03 g, 5.7 mmol) was added to a solution of dicyclohexylcarbodiimide (1.45 g, 7.0 mmol) in hexane (50 mL). The dark solution obtained was heated at 50°C for 10 min, then evaporated to 30 mL and allowed to stand for ca. 12 h. A mixture of green, **2**, and red, **3**, crystalline solids was removed by filtration. On storing the mother liquor at room temperature for two days, 0.65 g of complex **2** (41%) separated out. IR (nujol): $\tilde{\nu}$(C=N) = 1638 cm^{-1}. ^{1}H-NMR (300 MHz, C_6D_6): δ = 4.72 (s, 10H); 2.7-1.1 (m, 33H); MS: m/z = 551.—Procedure for **3**: **1** (2.38 g, 13.3 mmol) was added to a solution of dicyclohexylcarbodiimide (2.74 g, 13.3 mmol) in hexane (50 mL). The resulting solution was kept at −20°C for ca. 12 h and then filtered. The filtrate, after standing at room temperature for two days, yielded a mixture of crystalline **1** and **2**, which was removed by filtration. The mother liquor, after standing for ca. 12 h, furnished 0.40 g of **3** as a red crystalline solid (yield 32%). MS: m/z = 740. The results were independent of the Co/carbodiimide molar ratio used. Compounds **2** and **3**, R = *p*-tolyl instead of cyclohexyl, crystallized simultaneously, and could only be separated mechanically under the microscope. The elimination of hydrogen, as required from the stoichiometry, was not proven.

[6] **3** is triclinic, space group $P\bar{1}$, a = 11.118(3), b = 14.696(5), c = 9.804(3) Å; α = 97.78(3), β = 98.93(3), γ = 93.65(2)°; V = 1562.0(8) Å^3, Z = 2; ρ_{calcd} = 1.574 g cm^{-3}; $\lambda(Mo_{K\alpha})$ = 0.7107 Å), $\mu(Mo_{K\alpha})$ = 21.1 cm^{-1}; crystal dimensions 0.32 × 0.48 × 0.66 mm^3. The intensities of 4882 reflections were measured at room temperature (3° < θ < 24°) on a Philips PW 1100 diffractometer using $Mo_{K\alpha}$ radiation. The structure was solved by the heavy-atom method and refined anisotropically (full-matrix least squares). All calculations were carried out using the SHELX-76 program. For 3591 unique observed reflections [$I > 3\sigma(I)$], the final R value was 0.052 [12].

[7] D. W. Macomber, R. D. Rogers, *Organometallics 4* (1985) 1485.

[8] J. Edwin, M. Bochmann, M. C. Böhm, D. E. Brennan, W. E. Geiger, C. Krüger, J. Pebler, H. Pritzkow, W. Siebert, W. Swiridoff, H. Wadepohl, J. Weiss, U. Zenneck, *J. Am. Chem. Soc. 105* (1983) 2582; W. Siebert, *Angew. Chem. 97* (1985) 924; *Angew. Chem. Int. Ed. Engl. 24* (1985) 943.

[9] Procedure for **5**: A solution of **1** (1.12 g, 6.25 mmol) in hexane was treated with cyclohexyl isocyanide (1.36 g, 12.5 mmol). The oily product formed showed two CN bands at $\tilde{\nu}$ = 2090 and 1975 cm^{-1} (hexane). On addition of a further amount of **1** (1.00 g, 5.60 mmol) a maroon solution was obtained, which on standing for two days gave crystals of **5** (1.1 g; 60%). IR (nujol): $\tilde{\nu}$(C≡N) = 1765 and 1710 cm^{-1}. ^{1}H-NMR (300 MHz, C_6D_6): δ = 4.84 (s, 20H), 2.1-1.3 (m, 33H); MS: m/z 824.

[10] **5**: monoclinic, space group $P2_1/c$, a = 13.620(3), b = 13.533(3), c = 20.567(6) Å; β = 93.03(3)°; V = 3786(2) Å^3, Z = 4; ρ_{calcd} = 1.445 g cm^{-3}; $\lambda(Mo_{K\alpha})$ = 0.7107 Å, $\mu(Mo_{K\alpha})$ = 17.5 cm^{-1}; crystal dimensions 0.25 × 0.45 × 0.59 mm^3. Data collection and solution of structure as in the case of **3**. 7028 reflections measured at room temperature (6° < 2θ < 47°), 2407 independent reflections with $I > 3\sigma(I)$; R = 0.052 [12].

[11] a) W. I. Bailey, F. A. Cotton, J. D. Jamerson, B. W. S. Kolthammer, *Inorg. Chem. 21* (1982) 3131; b) S. Gambarotta, C. Floriani, A. Chiesi-Villa, C. Guastini, *J. Organomet. Chem. 296* (1985) C6; c) S. Gambarotta, S. Stella, C. Floriani, A. Chiesi-Villa, C. Guastini, *Angew. Chem. 98* (1986) 283; *Angew. Chem. Int. Ed. Engl. 25* (1986) 254.

[12] Further details of the crystal structure investigation are available from the Director of the Cambridge Crystallographic Data Centre, University Chemical Laboratory, Lensfield Road, Cambridge CB2 1EW (England) on quoting the full journal citation.

A New Class of Organozirconium(IV) Compounds: Alkyl Derivatives of Tetramethyltetraazadibenzo[14]annulenatozirconium(IV)**

By *Carlo Floriani,* Stefano Ciurli, Angiola Chiesi-Villa, and Carlo Guastini*

Zirconium-carbon functionalities are prototypes for studying fundamental organometal reactions.[1] Such functionalities are stabilized by ancillary ligands, normally by cyclopentadienyl- and substituted cyclopentadienyl-,[1,2] but also by a few alkoxo- and amido-ligands.[3,4] Macrocyclic and polydentate square planar ligands are very well known stabilizers for metal-carbon functionalities in iron and cobalt chemistry.[5] Apart from one exception, nothing has been reported about such a stabilizing effect in the chemistry of the early transition metals.[6] We now report on easily accessible zirconium compounds which can serve for the preparation of electron-rich complexes and organozirconium derivatives. For this purpose we used the ligand tetramethyltetraazadibenzo[14]-annulene, (H_2TMTAA).[7]

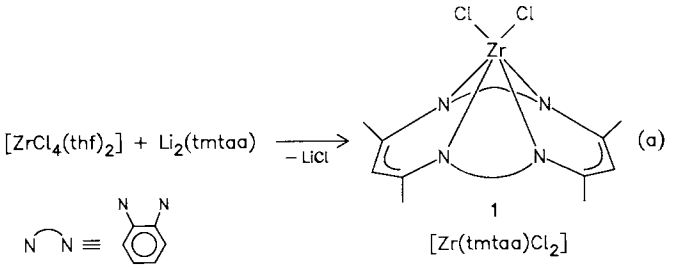

The complex **1** was prepared according to reaction (a) in tetrahydrofuran.[8] **1** crystallizes with two molecules of THF. The ligand has the usual saddle-shape conformation with the metal atom located 1.070(2) Å above the N_4 plane and the chlorine atoms arranged *cis* to each other [Cl-Zr-Cl, 85.6(1)°]. A similar structure was reported for the analogous titanium derivative.[9] Complex **1** could be alkylated with Grignard reagents as shown in reactions (b) and (c).[10,11]

The complex **2** obtained according to reaction (b) is stable in the solid state, while in solution it undergoes a rather complex, and not yet clarified, transformation. Such

[*] Prof. Dr. C. Floriani [+], S. Ciurli
Chemistry Department, Columbia University
New York, NY 10027 (USA)
Dr. A. Chiesi-Villa, Dr. C. Guastini
Istituto di Strutturistica Chimica,
Centro di Studio per la Strutturistica Diffrattometrica del CNR
Università di Parma, I-43100 Parma (Italy)
[+] Present address:
Institut de Chimie Minéral et Analytique, Université de Lausanne
3 Place du Chateau, CH-1005 Lausanne (Switzerland)

[**] This work was supported by the National Science Foundation (Grant CHE-8512660, Columbia University) and the Italian CNR (Università di Parma).

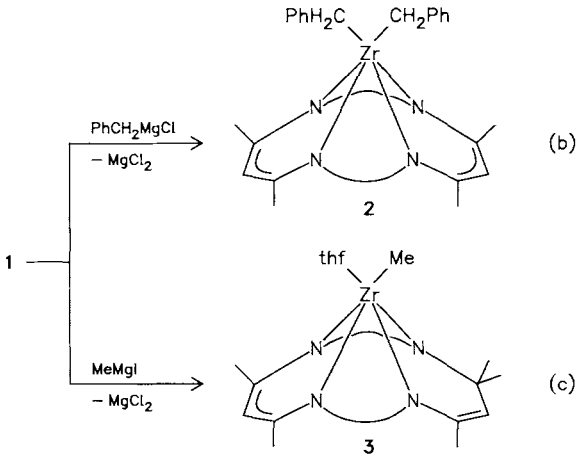

a transformation may involve some alkyl migration to the ligand, as observed in the synthesis of **3**. Although reaction (c) was carried out at low temperature, the only identified product was **3**,[11] which does not undergo any further transformation even in boiling THF.

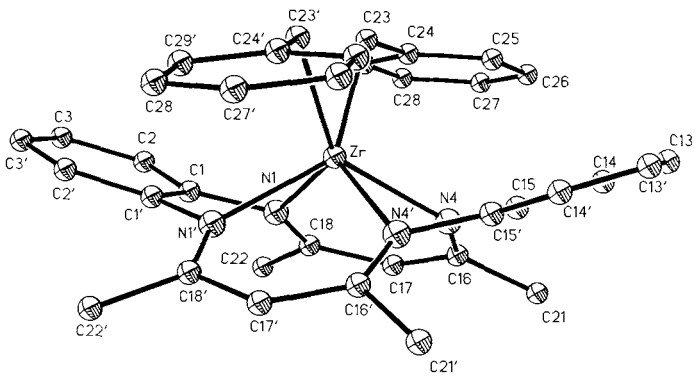

Fig. 1. Crystal structure of the complex **2**. Bond distances [Å]: Zr-N1 2.195(8), Zr-N4 2.184(8), Zr-C23 2.371(12); bond angles [°]: C23-Zr-C23' 80.1(4), N1-Zr-N1' 72.6(3), N1-Zr-N4 82.6(3), N1-Zr-N4' 124.5(3).

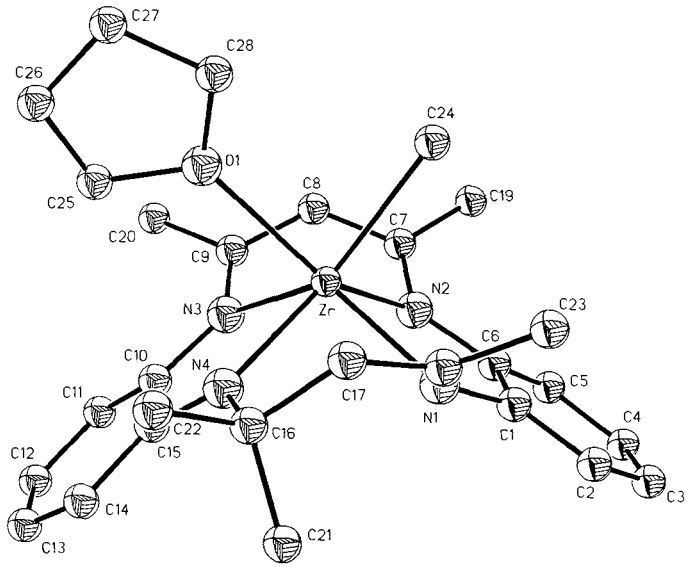

Fig. 2. Crystal structure of the complex **3**. Bond distances [Å]: Zr-N1 2.135(5), Zr-N2 2.188(5), Zr-N3 2.191(4), Zr-N4 2.129(6), Zr-C24 2.418(6), Zr-O1 2.387(5); bond angles [°]: C24-Zr-O1 80.3(2), N1-Zr-N2 70.7(2), N1-Zr-N4 85.2(2), N3-Zr-N4 71.5(2), N2-Zr-N3 77.8(2).

The structures of **2**[12] and **3**[13] are shown in Figures 1 and 2, respectively. Complex **2** has C_m symmetry with the TMTAA ligand in a saddle shape conformation. The zirconium atom lies 1.019(2) Å above the N_4 plane. The Zr-N bond distances are about the same as in complex **1**. The Zr-C bond distance [2.371(12) Å] lies in the upper range of Zr-C bond distances, as is usually found in the case of sterically demanding substituents.[14] The two benzyl groups are arranged *cis* to each other and form an angle of 80.1(4)°, which compares with the mean value for the Cp_2ZrR_2 series.[14] There is nothing unusual in the structural parameters of the TMTAA ligand,[15] excepting the slight modification of bond distances and angles close to the metal because of the large displacement of zirconium from the N_4 plane.

In complex **3** the overall geometry of the ligand is strongly altered by the methylation, while the zirconium atom maintains a comparable coordination geometry; it protrudes from the N_4 plane by 1.049(1) Å and binds THF and the methyl group in a *cis* arrangement [C24-Zr-O1, 80.3(2)°]. The Zr-C distance [2.418(2) Å] is significantly longer than in the corresponding cyclopentadienyl derivatives.[14] TMTAA is transformed into a threefold negatively charged ligand by the methylation at one of the C=N groups. The two Zr bonds to the nitrogens of the more saturated part of the ligand [Zr-N1 and Zr-N2] become significantly shorter than the other two. Alkylation of the ligand diminishes the electron delocalization within the carbon chain linking N1 and N4, and two of the C-N bonds, namely C16-N4 [1.430(1) Å] and to a lesser extent C18-N1 [1.361(8) Å], approach the length of a C-N single bond.

A significant structural difference between **2** and **3** is the orientation of the plane defined by the L_2Zr moiety. In **2**, the C23-Zr-C23' plane is parallel to the N1-N1' and N4-N4' vectors, whereas in **3** the O1-Zr-C24 plane is essentially perpendicular to the N1-N2 and N3-N4 vectors. The structure of **3** poses the question of how the alkylation of the ligand occurs. It could be a case of either a direct alkylation at the imino group or of a methyl migration from the metal to the ligand. The insertion of a C=N group into a M-C bond is known;[16] in the present case, however, the imino carbon atom and metal are too far apart.

The organometallic compounds **2** and **3** should make it possible to establish a chemistry comparable with that of the corresponding cyclopentadienyl derivatives as regards the zirconium-carbon functionalities.

Received: August 11, 1986;
revised: October 16, 1986 [Z 1901 IE]
German version: *Angew. Chem.* 99 (1987) 86

[1] G. Erker, *Acc. Chem. Res. 17* (1984) 103; P. T. Wolczanski, J. E. Bercaw, *ibid. 13* (1980) 121; J. Schwartz, F. T. Dayrit, J. S. Temple in B. M. Trost, C. R. Hutchinson (Eds.): *Organic Synthesis—Today and Tomorrow*, Pergamon Press, Oxford 1981; J. Schwartz, J. A. Labinger, *Angew. Chem. 88* (1976) 402; *Angew. Chem. Int. Ed. Engl. 15* (1976) 333; B. Weidmann, D. Seebach, *ibid. 95* (1983) 12 and *22* (1983) 31; H. Sinn, W. Kaminsky, *Adv. Organomet. Chem. 18* (1980) 99.

[2] D. J. Cardin, M. F. Lappert, C. L. Raston: *Chemistry of Organo-Zirconium and -Hafnium Compounds*, Ellis Horwood, Chichester 1986; P. C. Wailes, R. S. P. Coutts, H. Weigold: *Organometallic Chemistry of Titanium, Zirconium, and Hafnium*, Academic Press, New York 1974; D. J. Cardin, M. F. Lappert, C. L. Raston, P. I. Riley in G. Wilkinson, F. G. A. Stone, E. W. Abel (Eds.): *Comprehensive Organometallic Chemistry, Vol. 2*, Pergamon Press, Oxford 1982, pp. 549-646; R. R. Schrock, G. W. Parshall, *Chem. Rev. 76* (1976) 219; P. J. Davidson, M. F. Lappert, R. Pearce, *Acc. Chem. Res. 7* (1974) 209.

[3] T. V. Lubben, P. T. Wolczanski, G. D. van Duyne, *Organometallics 3* (1984) 977; T. V. Lubben, P. T. Wolczanski, *J. Am. Chem. Soc. 107* (1985) 701; A. K. McMullen, I. A. Rotwell, J. C. Huffman, *ibid. 107*

(1985) 1072; S. L. Latesky, A. K. McMullen, G. P. Niccolai, I. P. Rothwell, *Organometallics 4* (1985) 902, 995.
[4] R. P. Planalp, R. A. Andersen, *J. Am. Chem. Soc. 105* (1983) 7774; M. Fryzuk, H. D. Williams, S. J. Rettig, *Inorg. Chem. 22* (1983) 863.
[5] J. M. Pratt, P. J. Craig, *Adv. Organomet. Chem. 11* (1973) 404; V. L. Goedken, S. M. Peng, Y. Park, *J. Am. Chem. Soc. 96* (1974) 284.
[6] S. Gambarotta, M. Mazzanti, C. Floriani, A. Chiesi-Villa, C. Guastini, *J. Chem. Soc. Chem. Commun. 1985*, 829.
[7] A. R. Cutler, C. S. Alleyne, D. Dolphin, *Inorg. Chem. 24* (1985) 2276, and references therein.
[8] Procedure for **1**: A solution of H_2TMTAA (32.7 g, 95.0 mmol) in THF (300 mL) was treated with a solution of LiMe (190.0 mmol) in ether. After removal of the ether a solution of $ZrCl_4(thf)_2$ (35.8 g, 95.0 mmol) in THF (250 mL) was added. The suspension, which contained a yellow crystalline solid, was refluxed for twelve hours; yield of **1**·2THF 46.6 g (75.0%). ^{1}H-NMR ($CDCl_3$, 300 MHz): δ = 1.78 (m, 8H), 2.44 (s, 12H), 3.68 (m, 8H), 5.59 (s, 2H), 7.45 (m, 4H), 7.56 (m, 4H). The structure of **1** was confirmed by an X-ray analysis.
[9] V. L. Goedken, J. A. Ladd, *J. Chem. Soc. Chem. Commun. 1982*, 142.
[10] Procedure for **2**: A suspension of **1** (2.10 g, 3.24 mmol) in ether (500 mL) was treated at −50°C with 6.53 mmol of $PhCH_2MgCl$. The mixture was stirred for 36 h at −20°C. Dioxane (1.2 mL) was added to the resulting red-orange solution, which was stirred for two hours and then evaporated to dryness. The residue was taken up in toluene (200 mL) at −20°C and the resulting solution filtered and cooled to −50°C. After two days, 0.46 g (23%) of orange-red crystals of **2** separated out. ^{1}H-NMR (C_6D_6, 300 MHz): δ = 1.88 (s, 4H), 1.89 (s, 12H), 4.77 (s, 2H), 6.85 (m, 10H), 7.12 (m, 4H), 7.25 (m, 4H).
[11] Procedure for **3**: The synthesis was carried out as reported for **2**; **3** was obtained (62%) as a red-orange crystalline solid. ^{1}H-NMR (C_6D_6, 300 MHz): δ = −0.39 (s, 3H), 1.53 (s, 3H), 1.93 (s, 3H), 2.02 (s, 3H), 2.13 (s, 3H), 2.16 (s, 3H), 4.58 (s, 1H), 5.10 (s, 1H), 6.68-7.16 (m, 8H), 1.35 (m, 4H), 3.54 (m, 4H).
[12] **2**, space group *Pnma*, a = 16.028(3), b = 20.666(4), c = 9.018(2) Å, V = 2987(1) Å^3, Z = 4, ρ_{calcd} = 1.37 g cm^{-3}; $F(000)$ = 1280, $\lambda(Mo_{K\alpha})$ = 0.71069 Å, $\mu(Mo_{K\alpha})$ = 3.91 cm^{-1}. The structure was solved by the heavy atom method and refined anisotropically for all non-hydrogen atoms. All the hydrogen atoms were located by difference methods and introduced into the final refinement as fixed contributors (U_{iso} = 0.10 Å^2). 1063 unique observed reflections [$I > 3\sigma(I)$] collected at room temperature (6° < 2θ < 45°) were used, R = 0.063. The intensities were corrected for absorption [17].
[13] **3**: space group $P2_1/n$, a = 19.895(5), b = 14.771(5), c = 9.072(4) Å, β = 93.85(3)°, V = 2655(2) Å^3, Z = 4, ρ_{calcd} = 1.34 g cm^{-3}; $F(000)$ = 1120, $\lambda(Mo_{K\alpha})$ = 0.71069 Å, $\mu(Mo_{K\alpha})$ = 4.32 cm^{-1}. Solution of structure as in the case of **2**. 2430 unique observed reflections [$I > 3\sigma(I)$] collected at room temperature (6° < 2θ < 48°) were used, R = 0.044 [17].
[14] W. E. Hunter, D. C. Hrncir, R. V. Bynum, R. A. Penttila, J. L. Atwood, *Organometallics 2* (1983) 750; G. Erker, U. Dorf, P. Czisch, J. L. Petersen, *ibid. 5* (1986) 668, and references therein; S. Gambarotta, S. Strologo, C. Floriani, A. Chiesi-Villa, C. Guastini, *Inorg. Chem. 24* (1985) 654.
[15] M. C. Weiss, B. Bursten, S. M. Peng, V. L. Goedken, *J. Am. Chem. Soc. 98* (1976) 8021; V. L. Goedken, J. J. Pluth, S. M. Peng, B. Bursten, *ibid. 98* (1976) 8014; V. L. Goedken, S. M. Peng, J. Molin-Norris, Y. Park, *ibid. 98* (1976) 8391; M. C. Weiss, V. L. Goedken, *Inorg. Chem. 18* (1979) 819.
[16] M. Bottrill, P. D. Gavens, J. M. Kelland, J. McEaking in G. Wilkinson, F. G. A. Stone, E. W. Abel (Eds.): *Comprehensive Organometallic Chemistry, Vol. 3*, Pergamon Press, Oxford 1982, pp. 271-279.
[17] Further details of the crystal structure investigation are available from the Director of the Cambridge Crystallographic Data Centre, University Chemical Laboratory, Lensfield Road, Cambridge CB2 1EW (England) on quoting the full journal citation.

Unusual 1,6-Addition of a Carbenoid**

By *Michael Birkhahn, Eckehard V. Dehmlow,** and *Hartmut Bögge*

Tetracyclo[4.4.2.0^{2,10}.0^{5,7}]dodeca-3,8,11-triene **1** is a highly symmetric but as yet unknown representative of the $(CH)_{12}$ hydrocarbons. A conceivable entry to compounds of this type would be via intramolecular carbenoid addition in a suitably substituted bicyclo[6.1.0]nonatriene. As a model reaction we have investigated the decomposition of the diazoketone **3**.

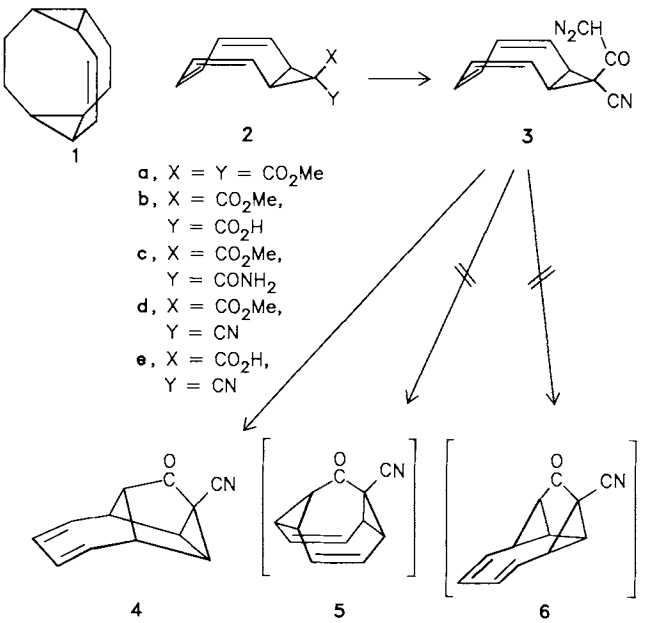

Reaction of cyclooctatetraene with dimethyl diazomalonate in CCl_4 in the presence of $[Rh_2(OAc)_4]$ affords **2a**, together with small amounts of bis- and tris-adducts. Selective hydrolysis of the *exo* ester group to give **2b** (3 h boiling of **2a** with KOH/MeOH), followed by conversion into the amide **2c**, then into the nitrile **2d**, and finally hydrolysis, affords **2e** (1 h boiling of **2d** with KOH/MeOH) (Table 1). The relative position of the acid group and the nitrile group follows from analogous reactions in the bicyclo[4.1.0]heptane series[1] and from the fact that tetrahydro-

Table 1. Yields, melting points and spectral data of the new compounds [a].

Cpd.	Yield [%] (M.p. [°C])	Spectral data
2a	32 (47)	6.05 (br. s, 4H), 5.90 (br. s, 2H), 3.76 (s, 6H), 2.39 (s, 2H) [b]
2b	86 (115-118)	10.7 (br. s, 1H), 6.2-5.8 (m, 6H), 3.77 (s, 3H), 2.72 (s, 2H) [b] 3400-2400, 1740, 1690 [c]
2c	97 (177-180)	3420, 3180, 1705, 1680, 1575 [c]
2d	88 (114-115)	6.25-5.65 (m, 6H), 3.81 (s, 3H), 2.72 (s, 2H) [b] 2260, 1730 [c]
2e	95 (206 (dec.))	3200-2400, 2260, 1700 [c]
3	84 (133 (dec.))	6.3-5.5 (m, 7H), 2.7 (s, 2H) [b] 3120 (w), 2260 (w), 2110, 1700 (w), 1600, 1380, 1350, 700 [c]
4	65 (151-152)	5.96-5.84 (m, 4H), 3.07-3.00 (m, 4H), 2.02 (t, J = 1.2 Hz, 1H) [b] 2240, 1750, 1270, 1080, 860, 710, 690 [c] 202.5 (C8), 131.0 (C3, C4), 128.5 (C2, C5), 114.6 (C12), 42.7 (C1, C6), 38.3 (C10, C11), 36.9 (C7), 17.5 (C9) [d]

[a] Correct C,H,N analyses for all the new compounds. [b] ^{1}H-NMR ($CDCl_3$, internal TMS, δ values). [c] IR ($\tilde{\nu}$ cm^{-1}). [d] ^{13}C-NMR ($CDCl_3$, internal TMS, δ values), for numbering see Figure 1.

[*] Prof. Dr. E. V. Dehmlow, Dipl.-Chem. M. Birkhahn, Dr. H. Bögge [+]
Fakultät für Chemie der Universität
D-4800 Bielefeld 1 (FRG)

[+] X-ray structure analysis.

[**] This work was supported by the Fonds der Chemischen Industrie and by BASF AG (supply of cyclooctatetraene).

2e (prepared from 1,5-cyclooctadiene) forms a bromolactone. The diazoketone **3**, which is readily accessible from **2e**, is undoubtedly present in the given stretched conformation.[2,3] Planarization of the eight-membered ring in the transition state of a carbenoid addition, and probably also intermediary complex formation with the transition metal employed, could facilitate cyclopropanation of the distant double bond (to give **5**) or of a proximal double bond (to give **6**). However, 11-oxotetracyclo[5.4.0.0^{2,9}.0^{8,10}]undeca-3,5-diene-10-carbonitrile **4** was actually formed in the Rh^{II}-catalyzed decomposition of **3** (boiling in CH_2Cl_2 in the presence of $[Rh_2(OAc)_4]$. Whereas the NMR spectra only ruled out **6** and other unsymmetrical products, the X-ray structure analysis (Fig. 1)[4] ruled out **5**, **6**, and other conceivable rearrangement products. Wolff rearrangement of **3** (Ag_2O/CH_3OH) afforded the chain-expanded ester ($R-CO-CHN_2$(**3**)$\rightarrow R-CH_2-CO_2CH_3$) in 34% yield together with 3% of **4**. Vacuum pyrolysis of **3** (350°C/0.3 mbar) without metal compound led predominantly to resinification; **4** was detectable in traces. **4** itself is stable up to 500°C/0.1 mbar.

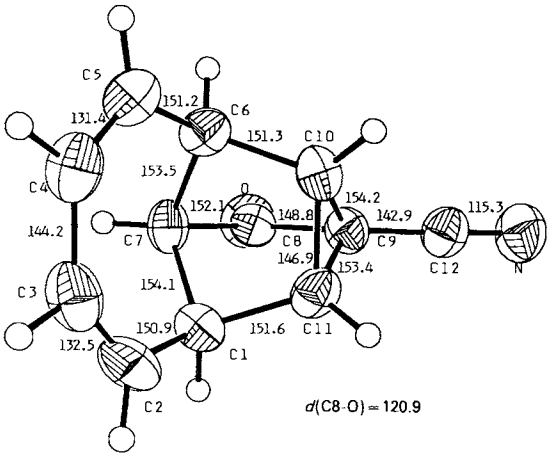

Fig. 1. Crystal structure of **4**. Bond lengths in pm (standard deviations 0.3–0.5 pm).

The basic carbon skeleton of **4** is present in the tetracyclic sesquiterpene longicyclene, whose total synthesis involves a "normal" carbene addition to a double bond.[5] The 1,6-addition to a triene described in this communication is to the best of our knowledge novel. It is apparently enforced by steric compression in the transition states, which would lead to the products "actually expected".

Received: September 2, 1986;
revised: October 29, 1986 [Z 1917 IE]
German version: *Angew. Chem. 99* (1987) 80

[1] H. Musso, U. Biethan, *Chem. Ber. 97* (1964) 2282; D. S. Wulfman, B. McGiboney, B. W. Peace, *Synthesis 1972*, 49.

[2] C. J. Cheer, W. Rosen, J. J. Uebel, *Tetrahedron Lett. 1974*, 4045.

[3] S. W. Staley, T. J. Henry, *J. Am. Chem. Soc. 91* (1969) 1239.

[4] **4** crystallizes in the monoclinic system ($P2_1/c$), $a=860.3(2)$, $b=633.2(1)$, $c=1684.1(4)$ pm, $\beta=90.47(2)°$, $V=917.3\times10^6$ pm^3, $Z=4$, $\rho_{calc}=1.33$ g cm^{-3}. The structure was determined by direct methods: $R=0.067$, $R_w=(\Sigma w(|F_o|-|F_c|)^2/\Sigma w|F_o|^2)^{1/2}=0.059$ ($1/w=\sigma^2(F)\pm0.0001F^2$) for 1229 independent reflections ($F_o>2.5\sigma(F_o)$); Syntex $P2_1$ diffractometer; $Mo_{K\alpha}$ radiation, graphite monochromator. Further details of the crystal structure investigation are available on request from the Fachinformationszentrum Energie, Physik, Mathematik GmbH, D-7514 Eggenstein-Leopoldshafen 2 (FRG), on quoting the depository number CSD-52 168, the names of the authors, and the full citation of the journal.

[5] S. C. Welch, R. L. Walters, *J. Org. Chem. 39* (1974) 2665.

First Four-Membered Metallacycles of Rhenium**

By *Henricus J. R. de Boer, Bartholomeus J. J. van de Heisteeg, Martina Flöel, Wolfgang A. Herrmann,* Otto S. Akkerman,* and *Friedrich Bickelhaupt**

Four-membered metallacycles of rhenium were hitherto unknown. The smallest stable ring system of this metal documented so far is the rhenacyclopentane $[(\eta^5-C_5H_5)(CO)_2Re(CH_2)_3CH_2]$;[1] its lower homologue $[(\eta^5-C_5H_5)(CO)_2Re(CH_2)_2CH_2]$ has been postulated as an unstable intermediate, but has not been unequivocally characterized.[1a] This gap in the large and rapidly growing number of metallacyclobutanes[2,3] is all the more striking as oxidic rhenium compounds belong to the most active catalysts of olefin metathesis besides those of molybdenum and tungsten if the metals are present in higher oxidation states.[4] According to the generally accepted mechanism of this industrially valuable reaction, rhenacyclobutanes must play an important role as intermediates (Scheme 1), particularly if they carry an oxo function at the metal atom. We now wish to report the first stable four-membered ring compounds of rhenium: the rhena(v)cyclobutane **3a** and the rhena(v)cyclobutabenzene **3b**, as derivative of a (previously unknown) rhena(v)cyclobutene.

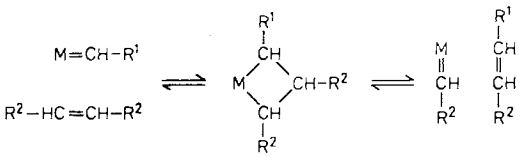

Scheme 1.

As indicated in Scheme 2, for the synthesis of the rhenacycles **3a** and **3b** we chose the route via 1,3-di-Grignard compounds, which has already proven useful for metallacyclobutanes of the main group and transition metals.[4,5] A simple method has recently been developed for the synthesis of the dichloride **1**, the substance we required as precursor for **3a**, **b**.[6] **3a** is best prepared by reaction of **1** with the 1,3-di-Grignard reagent **2a**[7] in diethyl ether at room temperature. After work-up as usually employed in Grignard chemistry (cf. *Experimental*), a dark-red powder was obtained which dissolved in benzene to give a violet-red solution. On the basis of spectroscopic data[8] the product was characterized as **3a**, which still contained ca. 7% of an impurity.[9] Particularly characteristic is the AX pattern for the diastereotopic geminal methylene protons on α- and γ-C ($\delta(A)=3.42$, $\delta(X)=1.08$; $^2J(AX)=11.2$ Hz). Due

[*] Prof. Dr. F. Bickelhaupt, Dr. H. J. R. de Boer,
Dr. B. J. J. van de Heisteeg, Dr. O. S. Akkerman
Scheikundig Laboratorium, Vrije Universiteit
De Boelelaan 1083, NL-1081 HV Amsterdam (The Netherlands)
Prof. Dr. W. A. Herrmann, M. Flöel
Anorganisch-chemisches Institut der Technischen Universität München
Lichtenbergstrasse 4, D-8046 Garching (FRG)

[**] Multiple Bonds between Main Group Elements and Transition Metals, Part 35. This work was supported by the Netherlands Foundation for Chemical Research (SON) (financial support for *H. J. R. de B.*), by the Netherlands Organization for the Advancement of Pure Research (ZWO), by the Deutsche Forschungsgemeinschaft, and by the Bundesministerium für Forschung und Technologie (Bonn).—Part 34: W. A. Herrmann, E. Herdtweck, M. Flöel, U. Küsthardt, J. Kulpe, J. Okuda, *Polyhedron*, in press.

to the two different substituents on the rhenium (C_5Me_5 and O) the two sides of the four-membered ring are not equivalent.

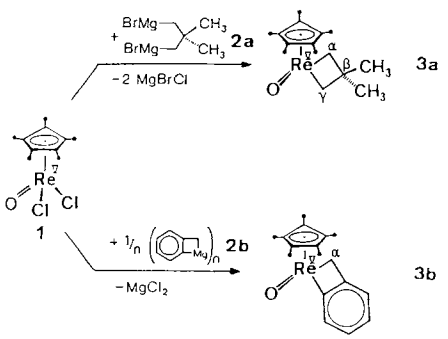

Scheme 2.

Compound **3b** was obtained analogously as a slightly impure brown powder by reaction of **1** with the organomagnesium reagent **2b**[5] in tetrahydrofuran (THF) at −78 °C. Once again, the constitution follows conclusively from the spectroscopic data,[8] especially from the AX pattern for the geminal methylene protons on C_α ($\delta(A)=3.61$, $\delta(X)=1.88$; $^2J(AX)=13.9$ Hz).

The new rhenacycles are thermally stable; in particular, the high stability of **3a** is surprising: no decomposition was observed to take place after 3 h at 80 °C or after 1.5 h at 100 °C. In the mass spectrometer, on the other hand, metathetical degradation of **3a** took place with formation of isobutene. The stability of rhenacycles of type **3** would suggest that such rhenium(v) complexes may be accessible via alternative routes. From the point of view of future catalytic studies, likely alternatives of interest are the metal-centered opening of cyclopropabenzene and its derivatives[10] and the [2+2] addition of olefins to intermediate fragments such as $[(\eta^5\text{-}C_5Me_5)Re(=O)(=CH_2)]$.

Experimental

3a: A solution of **2a** [7] (0.25 mmol) in diethyl ether (35 mL) was added to **1** (101.8 mg, 0.25 mmol) in a closed high-vacuum system at room temperature. The precipitate of magnesium salts was filtered off and the filtrate evaporated to dryness. The resulting dark-red residue was dissolved in C_6D_6; the product yield (determined by quantitative ^{1}H-NMR spectroscopy ($C_6(CH_3)_6$ as internal standard), was 50% [8].

3b: A suspension of **2b** [5] (0.278 mmol) in THF (60 mL) was added to a suspension of **1** (113.1 mg, 0.278 mmol) in THF (50 mL) in a closed high-vacuum system at −78 °C. The mixture was stirred for 1/2 h at −78 °C, 2 h at −20 °C and 1/2 h at room temperature. After subsequent removal of ca. 90 mL of THF by distillation at room temperature, the residue was treated with 20 mL of dioxane. The precipitate of magnesium salts was filtered off and the filtrate evaporated to dryness. The resulting brown residue was dissolved in C_6D_6 and analyzed by quantitative ^{1}H-NMR spectroscopy (see **3a**). Yield of pure **3b**: 60% [8].

Received: August 6, 1986;
revised: September 15, 1986 [Z 1893 IE]
German version: *Angew. Chem. 99* (1987) 88

[1] a) G. K. Yang, R. G. Bergman, *J. Am. Chem. Soc. 105* (1983) 6500; b) *Organometallics 4* (1985) 129.
[2] G. Wilkinson, F. G. A. Stone, E. W. Abel (Eds.): *Comprehensive Organometallic Chemistry*, Pergamon, Oxford 1982.
[3] a) J. W. F. L. Seetz, B. J. J. van de Heisteeg, G. Schat, O. S. Akkerman, F. Bickelhaupt, *J. Mol. Catalysis 28* (1985), and references cited therein; b) F. Bickelhaupt, *Pure Appl. Chem. 58* (1986), and references cited therein.
[4] K. J. Ivin: *Olefin Metathesis*, Academic Press, London 1983.
[5] H. J. R. de Boer, O. S. Akkerman, F. Bickelhaupt, G. Erker, P. Czisch, R. Mynott, J. M. Wallis, C. Krüger, *Angew. Chem. 98* (1986) 641; *Angew. Chem. Int. Ed. Engl. 25* (1986) 639.
[6] W. A. Herrmann, U. Küsthardt, M. Flöel, J. Kulpe, E. Herdtweck, *J. Organomet. Chem. 314* (1986) 151.
[7] J. W. F. L. Seetz, B. J. J. van de Heisteeg, G. Schat, O. S. Akkerman, F. Bickelhaupt, *J. Organomet. Chem. 275* (1984) 173.
[8] **3a**: MS (70 eV): *m/z* 408 (3%, $M^{\oplus\oplus}$; referred to ^{187}Re), 352 (28%, $(C_5Me_5)ReOCH_2$), 135 (5%, C_5Me_5). High-resolution MS for $C_{15}H_{25}ReO$: calc. 408.1475; found 408.1485.—^{1}H-NMR (C_6D_6, 250 MHz, 28 °C): $\delta=3.42$ (d, $^2J(HH)=11.2$ Hz, 2H; 1H each of α- and γ-CH_2), 1.57 (s, 15H; C_5Me_5), 1.08 (d, $^2J(HH)=11.2$ Hz, 2H, 1H each of α- and γ-CH_2), 0.96 (s, 6H; CMe_2).—^{13}C-NMR (C_6D_6, 63.7 MHz, 28 °C): $\delta=97.3$ (C_5Me_5), 32.6 (β-C), 11.7 (q, $^1J(CH)=127$ Hz; C_5Me_5), 11.4 (q, $^1J(CH)=129$ Hz; CMe_2), −6.1 (t, $^1J(CH)=136$ Hz; α- and γ-CH_2). **3b**: MS (70 eV): *m/z* 428 (100%, $M^{\oplus\oplus}$), 398 (44%). High-resolution MS for $C_{15}H_{21}ReO$: calc. 428.1152; found 428.1156.—^{1}H-NMR (C_6D_6, 250 MHz, 28 °C): $\delta=7.55$ (m; 1H of C_6H_4), 7.16 (m; 2H of C_6H_4), 6.77 (m; 1H of C_6H_4), 3.61 (d, $^2J(HH)=13.9$ Hz; 1H of CH_2), 1.88 (d, $^2J(HH)=13.8$ Hz; 1H of CH_2), 1.51 (s, 15H; C_5Me_5).
[9] The impurity was found to be the dinuclear complex $[Me_2C(CH_2Re(=O)(\eta^5\text{-}C_5Me_5)Cl)_2]$.
[10] R. Neidlein, A. Rufinska, H. Schwager, G. Wilke, *Angew. Chem. 98* (1986) 643; *Angew. Chem. Int. Ed. Engl. 25* (1986) 640.

$[CH_3C_6H_5BiCl_2][AlCl_4]$ and $[(CH_3)_6C_6BiCl_2][AlCl_4]$—Compounds containing η^6-Arene-Complexed $BiCl_2^{\oplus}$ Units

By *Walter Frank,* Jürgen Weber,* and *Elisabeth Fuchs*

It has been known for more than a century, i.e. since the discovery of the Menshutkin complexes, that element(III) halides of the 5th main group of the periodic system form arene complexes.[1] Results of X-ray structure investigations are available, e.g., for the compounds **1**–**4**.

$C_6H_6(SbCl_3)_2$[2a] **1** $1,3\text{-}(CH_3)_2C_6H_4(SbCl_3)_2$[2b] **2**

$1,3,5\text{-}(CH_3)_3C_6H_3BiCl_3$[3] **3** $(CH_3)_6C_6(BiCl_3)_2$[3] **4**

Many aspects of interest to structural chemists and theoretical chemists should emerge from a comparison of these compounds with arene complexes of cationic species such as $SbCl_2^{\oplus}$ or $BiCl_2^{\oplus}$. Nevertheless, the η^6-arene complexation of such units has so far never been systematically studied. A first attempt in this direction was undertaken by *Amma* et al., who were able to characterize, albeit only incompletely, a compound of the composition $C_6H_6AlBiCl_6$.[4]

In the course of our studies on the ability of aluminum trichloride to abstract chloride ions from bismuth(III) chloride in the presence of toluene or hexamethylbenzene, we isolated the extremely hydrolysis-sensitive title compounds **5** (yellow, "soft" crystals, m.p. 83 °C) and **6** (orange crystals, m.p. 180 °C), respectively.[5] (The compositions (elemental analyses) are given in the reaction equations.)

$$BiCl_3 + \tfrac{1}{2}Al_2Cl_6 \xrightarrow[CH_3C_6H_5]{\Delta} CH_3C_6H_5AlBiCl_6 \quad \mathbf{5}$$

$$BiCl_3 + \tfrac{1}{2}Al_2Cl_6 + (CH_3)_6C_6 \xrightarrow[CH_3C_6H_5]{\Delta} (CH_3)_6C_6AlBiCl_6 \quad \mathbf{6}$$

[*] Dr. W. Frank, J. Weber, E. Fuchs
Anorganische Chemie der Universität
Im Stadtwald, D-6600 Saarbrücken (FRG)

In each case, twinned crystals were obtained; splitting of these, for preparation of samples for a structure analysis, was possible only in the case of the hard compound **6**. According to a crystal structure analysis[6] **6** exists as a centrosymmetric dimer (point symmetry $\bar{1}$ (C_i)) (cf. Fig. 1). Two

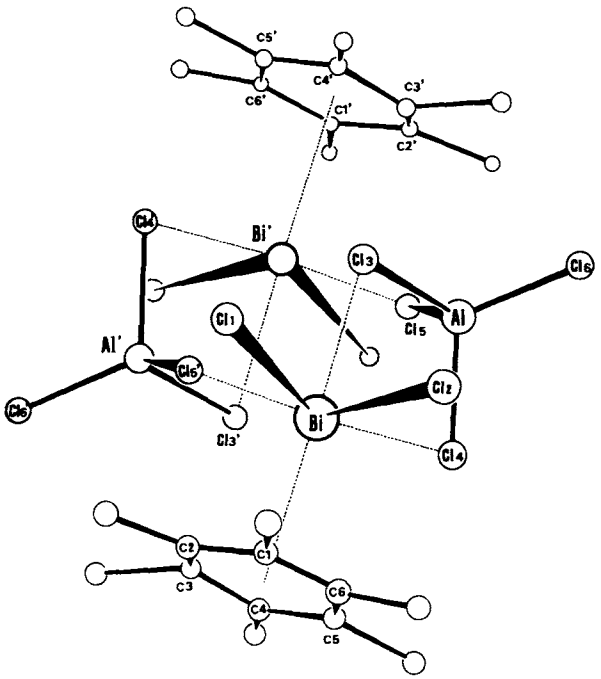

Fig. 1. Crystal structure of the dimeric unit of **6**. The carbon atoms of the methyl groups are not marked, and the hydrogen atoms have been omitted. Selected bond lengths [pm] and angles [°] (for further details see Fig. 2 and caption thereto): Al-Cl3 215.8(4), Al-Cl4 211.9(4), Al-Cl5 210.1(4), Al-Cl6 207.9(4); Cl-Al-Cl 105.2(1)–112.2(2); mean values: C_{arene}-C_{arene} 139(1), C_{arene}-C_{methyl} 152(1), C_{arene}-C_{arene}-C_{arene} 120.6(7).

$AlCl_4$ groups are arranged between two η^6-arene-complexed $BiCl_2$ units. Two Cl atoms are bound to the one Bi atom, and a third Cl atom is bound to the other Bi atom—similarly to the situation in the bis(benzene)gallium(I) tetrachlorogallate(III) dimer.[7] As expected, the $AlCl_4$ "tetrahedra" show a distinct deviation from the $\bar{4}3m$-(T_d) symmetry (cf. caption to Fig. 1), which is found in $Na[AlCl_4]$.[8] The bismuth atom has in addition to two short Cl-contacts, three other Cl-contacts (cf. Fig. 2). As shown by an analysis of the Bi–C distances (caption to Fig. 2) the planar aromatic ring is tilted with respect to the central atom. This is revealed by an observed angle of 10° between the line connecting the bismuth atom and the center of the aromatic ring and the normal to the best C1–C6 plane. As expected, the Bi-$arene_{center}$ distance of 272 pm in **6** is markedly shorter than in **3** (311 pm) or **4** (307 pm).[3] No unusual bonding situation is observed within in the hexamethylbenzene ligand. If the center of the aromatic ring is regarded as a coordination site, a strongly distorted octahedron results as coordination figure for the bismuth atom. In the crystal lattice, only van der Waals forces are effective between the dimers of **6**.

$[\{[(CH_3)_6C_6BiCl_2][AlCl_4]\}_2]$ **6**

Collectively, the structural parameters justify **6** being regarded as arene-stabilized $[\{[BiCl_2][AlCl_4]\}_2]$.

All attempts to synthesize $(CH_3)_6C_6BiCl_3$ led instead to the already well-known compound **4**.[3] In comparison, suitable crystals of $CH_3C_6H_5BiCl_3$[1b] are easily accessible;

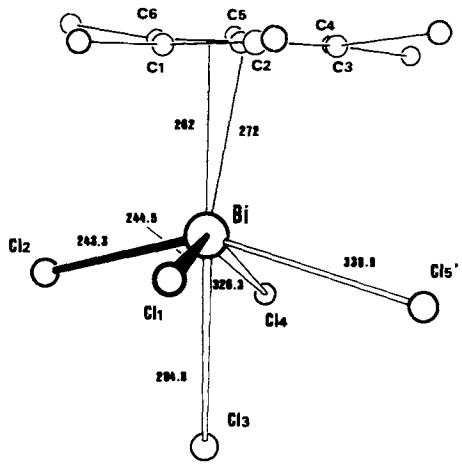

Fig. 2. Coordination figure of the bismuth atom, viewed parallel to the best plane of the six carbon atoms of the aromatic ring. Selected bond lengths [pm] and angles [°]: Bi-C1 275.2(9), Bi-C2 295.2(8), Bi-C3 317.6(9), Bi-C4 321.5(9), Bi-C5 308.0(9), Bi-C6 285.8(8); Cl1-Bi-Cl2 92.8, Cl1-Bi-Cl3 85.3, Cl1-Bi-Cl4 151.4, Cl1-Bi-Cl5′ 86.5, Cl2-Bi-Cl3 84.2, Cl2-Bi-Cl4 83.2, Cl2-Bi-Cl5′ 154.4, Cl3-Bi-Cl4 66.1, Cl3-Bi-Cl5′ 70.2, Cl4-Bi-Cl5′ 85.2. The standard deviations of the Bi-Cl distances and Cl-Bi-Cl angles are 0.3 pm and 0.1°, respectively.

an X-ray study of this compound, as well as further attempts at elucidating the structure of **5**, are presently under way.

Received: August 18, 1986;
revised: September 19, 1986 [Z 1904 IE]
German version: *Angew. Chem. 99* (1987) 68

[1] a) W. Smith, *J. Chem. Soc. 35* (1879) 309; b) G. Peyronel, S. Buffagni, M. Vezzosi, *Gazz. Chim. Ital. 98* (1968) 147; for further literature references see [2a].

[2] a) D. Mootz, V. Händler, *Z. Anorg. Allg. Chem. 533* (1986) 23; b) R. Hulme, D. J. E. Mullen, *J. Chem. Soc. Dalton Trans. 1976*, 802.

[3] A. Schier, J. M. Wallis, G. Müller, H. Schmidbaur, *Angew. Chem. 98* (1986) 742; *Angew. Chem. Int. Ed. Engl. 25* (1986) 757.

[4] T. Auel, E. L. Amma, *J. Am. Chem. Soc. 90* (1968) 5941.

[5] Procedure for **5** [6]: A mixture of freshly sublimed bismuth(III) chloride (0.631 g, 2.00 mmol) and freshly sublimed aluminum trichloride was treated with 20 mL of anhydrous toluene [a solution of 0.325 g (2.00 mmol) hexamethylbenzene (melted in presence of $LiAlH_4$ and sublimed) in 20 mL of anhydrous toluene]. By briefly heating to 80°C, an orange-red [red] solution was obtained, from which yellow [orange colored] crystals of **5** [6] precipitated upon slowly cooling the solution when all operations were carried out in the strict absence of moisture.—Yield: 0.76 g (77%) of **5** [1.02 g (83%) of **6**]. Correct analytical data were obtained for **5** and **6**.

[6] **6**: monoclinic, space group $P2_1/n$, $a=906.1(7)$, $b=1545(1)$, $c=1461(1)$ pm, $\beta=93.14(6)°$, $Z=4$, four-circle diffractometer, empirical absorption correction, $R=0.046$ with a reflection parameter ratio of 15.6:1. Further details of the crystal structure investigation are available on request from the Fachinformationszentrum Energie, Physik, Mathematik GmbH, D-7514 Eggenstein-Leopoldshafen 2 (FRG), on quoting the depository number CSD-52117, the names of the authors, and the full citation of the journal.

[7] H. Schmidbaur, *Angew. Chem. 97* (1985) 893; *Angew. Chem. Int. Ed. Engl. 24* (1985) 893.

[8] N. C. Baenzinger, *Acta Crystallogr. 4* (1951) 216.

High-Pressure LiGe with Layers Containing Two- and Four-Coordinate Germanium Atoms**

By *Jürgen Evers,* Gilbert Oehlinger, Gerhard Sextl,* and *Hans-Otto Becker*

LiGe is unique among the monogermanides of the alkali metals. Whereas the germanium atoms in LiGe form a three-dimensional network at normal pressure (NP),[1] they form discrete tetrahedra in NaGe,[2] KGe,[3] RbGe,[3] and CsGe.[3] More densely packed high-pressure (HP) phases can be prepared for the monogermanides with M = Na–Cs, but these still contain discrete Ge_4 tetrahedra[4,5] and, therefore, like the NP phases, they are Zintl phases (formally M^+Ge^-).[6] We have now found that LiGe can also be transformed into an HP phase in which, surprisingly, layers containing two- and four-coordinate germanium atoms are present.

NP LiGe is obtained by fusion of a stoichiometric mixture of lithium (m3N) and germanium (semiconductor quality) under argon at 650 °C in a molybdenum crucible. In order to prevent evaporation of lithium during the synthesis, the molybdenum crucible was heated in a closed system (iron crucible with conical sealing edges and a copper gasket). A copper trace analysis carried out by atomic absorption spectroscopy on NP LiGe showed that, under the preparation conditions, the copper gasket is sufficiently inert (< 50 ppm Cu). All operations with the open iron crucible were performed under purified argon in a glove box. NP LiGe was transformed in a belt-type apparatus at 4 GPa and 500 °C in 10 min in boron nitride or iron crucibles. By rapid cooling to room temperature and releasing the pressure, the HP phase can be metastably quenched to ambient conditions.

The HP phase is about 7% more densely packed than the NP phase. Heating to approximately 200 °C at normal pressure results in quantitative transformation of the HP phase into the NP phase in an exothermic reaction. Weissenberg and precession photographs of an HP LiGe crystal reveal the Laue symmetry *4/mmm* with systematic extinctions, leading directly to the space group $I4_1/amd$. Patterson and Fourier syntheses give the approximate positional parameters. The quality of the crystal was not sufficiently good for a measurement on a four-circle diffractometer. For this reason, the positional parameters of the HP phase were refined by a profile analysis of the Guinier powder diffractogram (computer-controlled Huber G644, capillary with 0.3-mm ∅, $Cu_{K\alpha 1}$ radiation) according to the Rietveld method. The diffractogram was recorded from 14 to 94° (2θ-range) in steps of 0.02° (4000 data) and corrected for absorption ($\mu \cdot r = 1.78$). The program of *Young*[7,8] with a modified PL factor[9] was used for the profile analysis, taking into account the Guinier geometry. An R value of 4.8% was obtained for 52 reflections using a Lorentz function. The occupation of the Ge and Li sites is ordered and stoichiometric within the limits of error. The observed and calculated diffractograms are shown in Figure 1. (In the measured diffractogram, an additional reflection at $2\theta = 26.38°$ with an intensity of $0.06 \cdot I_{max}$ is obtained, due to another HP phase with approximately 1:1 stoichiometry.) The crystallographic data for the phases NP LiGe[1] and HP LiGe are shown in Table 1.

Table 1. Crystallographic data for NP LiGe [1] and HP LiGe [a].

	Normal-pressure phase [1]	High-pressure phase
Space group	$I4_1/a$	$I4_1/amd$
Lattice parameters [pm]	$a = 975(2)$	$a = 405.29(1)$
	$c = 578(2)$	$c = 2328.2(3)$
Formula unit per unit cell	16	12
Volume of the unit cell [pm^3]	549.5×10^6	382.4×10^6
ρ_{calcd} [g/cm^3]	3.85	4.14
ρ_{exp} [g/cm^3]	3.75	4.1
Positions	16 Li in 16f;	4 Li_I in 4a
	x = 0.150, y = 0.100,	8 Li_{II} in 8e;
	z = 0.820	z = 0.713(1)
	16 Ge in 16f;	4 Ge_I in 4b
	x = 0.199, y = 0.106,	8 Ge_{II} in 8e;
	z = 0.269	z = 0.5486(1)

[a] The numbers in parentheses give the standard deviations.

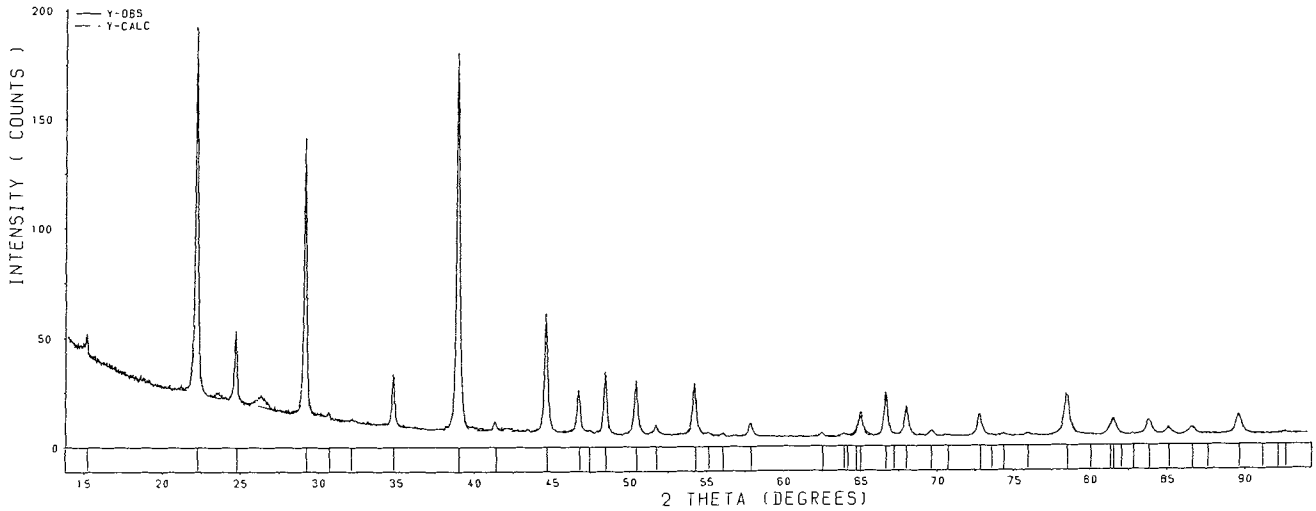

Fig. 1. Observed and calculated Guinier powder diffractogram of HP LiGe ($Cu_{K\alpha 1}$ radiation).

[*] Dr. habil. J. Evers, G. Oehlinger, Dipl.-Chem. G. Sextl, Dr. H.-O. Becker
Institut für Anorganische Chemie der Universität
Meiserstrasse 1, D-8000 München 2 (FRG)

[**] This work was supported by the Deutsche Forschungsgemeinschaft and the Fonds der Chemischen Industrie.

HP LiGe crystallizes in a new type of structure. The number of neighbors, the distances, and the germanium bond angles for the NP and the HP phase are summarized in Table 2. In both phases, the Ge atoms have eight Li neighbors and vice versa. The eight Li–Ge distances in the HP phase consist of only four different values (from 270 to 288 pm), whereas in the NP phase eight different values are found (from 264 to 324 pm). Therefore, the Li–Ge distances show less variation in the HP phase and, on average, they are shorter than in the NP phase. Furthermore, the Li atoms in the HP phase have one more Li neighbor up to 288 pm than those in the NP phase.

Table 2. Number of neighbors, distances, and germanium angles for NP LiGe [1] and HP LiGe.

Normal pressure phase [1]	High-pressure phase [a]	
Ge neighbors	*Ge_I neighbors*	*Ge_{II} neighbors*
- 8 Li: 264, 266, 272, 281, 299, 317, 322, 324 pm	- 4 Li_I: 287 pm - 4 Li_{II}: 288 pm	- 2 Li_I: 270 pm - 2 Li_{II}: 284 pm - 4 Li_{II}: 288 pm
- 3 Ge: 255 (2×), 260 pm	- 4 Ge_{II}: 270 pm	- 2 Ge_I: 270 pm - 2 Ge_{II}: 304 pm
∢GeGeGe: 105, 109, 118°	∢GeGeGe: 97 (2×), 116° (4×)	∢GeGeGe: 97°
Li neighbors	*Li_I neighbors*	*Li_{II} neighbors*
- 8 Ge: 264, 266, 272, 281, 299, 317, 322, 324 pm	- 4 Ge_{II}: 270 pm - 4 Ge_I: 287 pm	- 2 Ge_{II}: 284 pm - 4 Ge_{II}: 288 pm - 2 Ge_I: 288 pm
- 3 Li: 283, 288 pm (2×)	- 4 Li_{II}: 288 pm	- 2 Li_{II}: 266 pm - 2 Li_I: 288 pm

[a] Maximum error for HP phase: Ge-Ge, Li-Ge, ±1 pm; Li-Li, ±2 pm; ∢GeGeGe, ±0.1°.

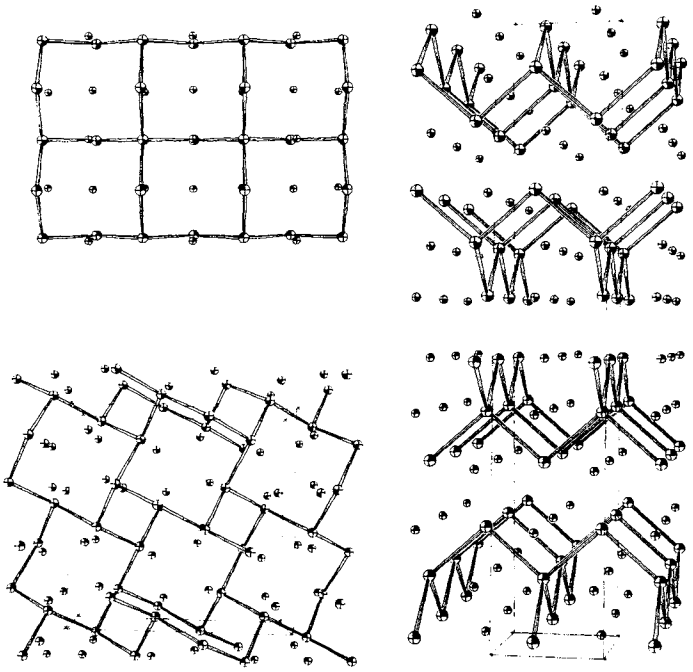

Fig. 2. Left above: View along [001] at a layer of puckered eight-membered rings in HP LiGe. The Li_I atoms lie at the centers of the eight-membered rings, the Li_{II} atoms alternately above and below the two-coordinate bridging atoms. Left below: View along [001] at the network formed by eight-membered rings in NP LiGe. The Li atoms lie, as distorted Li_4 tetrahedra, in the cavities of the eight-membered rings. Right: View along [100] at the layer structure of two-coordinate and four-coordinate germanium in the sequence ABCDA in HP LiGe.

On the other hand, the Ge–Ge distances slightly increase from 257 pm in the NP phase to 270 pm in the HP phase. The germanium bond angles in the HP phase are decreased by approximately 8° in comparison to the NP phase. In HP LiGe, the Ge_I atoms are bonded to four other germaniums, the Ge_{II} atoms to two others. They are present in a 1 : 2 ratio and form puckered eight-membered rings (Fig. 2, left above). The Li_I atoms lie in the centers of the eight-membered rings, the Li_{II} atoms alternately above and below the Ge_{II} atoms. In the NP phase, puckered eight-membered rings are also found, but they are shifted by one edge against each other and form a network of three-coordinate germanium atoms (Fig. 2, left below). Here, the Li atoms are arranged as distorted Li_4 tetrahedra in the cavities of the eight-membered rings. In the HP phase, the eight-membered rings are linked with common edges in layers (Fig. 2, left above), which are stacked in the order ABCDA... (Fig. 2, right). Connection of the two-coordinate Ge_{II} atoms with the two neighboring Ge_{II} atoms in a neighboring layer leads to a planar arrangement. However, the resulting distances of 304 pm (Table 2) are 13% longer than the Ge_I–Ge_{II} bonds (270 pm). Therefore, a network containing only four-coordinate Ge atoms is not formed.

In accordance with the Zintl–Klemm model,[6] four-coordinate Ge atoms have no formal negative charges, three-coordinate have one, and two-coordinate Ge atoms have two negative charges. Therefore, NP LiGe (formally Li^+Ge^-) is a Zintl phase, and HP LiGe (formally $(Li^+)_3Ge^0(Ge^{2-})_2$) is no longer a Zintl phase owing to the lack of charge balance.

It is worthwhile to compare HP LiGe with its analogues formed from heavy elements of group IV of the periodic table. In LiSn,[10] a layer structure composed of four-coordinate Sn atoms with 8 : 8 coordination is formed, which is therefore no longer a Zintl phase. Apparently, the lithium compounds are no longer Zintl phases if, on the one hand, germanium is replaced by the more metallic tin at normal pressure or, on the other hand, germanium becomes more metallic owing to a high-pressure treatment, for example in HP LiGe. The last member of this class of 1 : 1 compounds with 8 : 8 coordination is LiPb. The ideal CsCl-type structure is found in the high-temperature modification ($T > 214$°C); in the low-temperature modification, a slightly distorted rhombohedral structure is found ($\alpha = 89.5$°).[11] The structural units in LiPb are centered cubes, which are uniformly stacked. In LiSn, the cubes are distorted but stacking remains unchanged. Finally, in HP LiGe uniform stacking is also absent: in this case, distorted cubes form blocks which are twisted by 90° against each other.

LiGe is the first compound of a strongly electropositive metal with an electronegative element to the right of the Zintl boundary in which the NP phase still belongs to the Zintl phase but the HP phase no longer. Other promising candidates for such pressure-induced transitions are NaGe, NaSn, and NaPb.

Received: August 29, 1986;
revised: October 28, 1986 [Z 1916 IE]
German version: *Angew. Chem. 99* (1987) 69

[1] E. Menges, V. Hopf, H. Schäfer, A. Weiss, *Z. Naturforsch. B24* (1969) 1351.
[2] J. Witte, H. G. von Schnering, *Z. Anorg. Allg. Chem. 327* (1964) 260.
[3] E. Busmann, *Z. Anorg. Allg. Chem. 313* (1961) 90.

[4] J. Evers, G. Oehlinger, G. Sextl, A. Weiss, *Angew. Chem. 96* (1984) 512; *Angew. Chem. Int. Ed. Engl. 23* (1984) 528.
[5] J. Evers, G. Oehlinger, G. Sextl, A. Weiss, *Angew. Chem. 97* (1985) 499; *Angew. Chem. Int. Ed. Engl. 24* (1985) 500.
[6] H. G. von Schnering, *Nova Acta Leopold. 264, Bd. 59* (1985), S. 165.
[7] R. A. Young (School of Physics, Georgia Institute of Technology, Atlanta, GA 30332, USA): *Program for Rietveld-Analysis of X-Ray and Neutron Powder Diffraction Patterns by D. B. Wiles, 1982.*
[8] Program inplemented on a Cyber 875 by Dr. *H.-O. Becker*, Munich 1986.
[9] Change of the PL factor for Guinier geometry by *G. Sextl*, Munich 1986.
[10] W. Müller, H. Schäfer, *Z. Naturforsch. B28* (1973) 246.
[11] A. Zalkin, W. J. Ramsey, *J. Phys. Chem. 61* (1957) 1413.

Crystal Structure of [α-Nitrobenzyllithium · Ethanol]$_n$; A Lithium Nitronate-Ethanol Interaction**

By *Gerhard Klebe, Karl Heinz Böhn, Michael Marsch,* and *Gernot Boche**

Ninety-three years ago, *Holleman*[1a] described the conversion of phenylnitromethane **1** into the sodium salt ("nitronate") **2**-Na. Shortly thereafter, *Hantzsch* et al.[1b] found that protonation of **2**-Na leads to an isomer of **1**, the phenylmethanenitronic acid **3**, which is slowly transformed into **1** in solution (see also ref. [1c]).

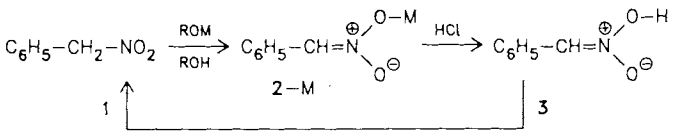

Numerous applications have been reported for nitronates in synthesis.[2] Nitronates are of particular interest in substitution reactions that proceed through electron transfer.[3] Here we report on the crystal structure of a lithium nitronate, the title compound [**2**-Li · C_2H_5OH]$_n$ (see Fig. 1a).[4]

2-Li, which is prepared from **1** with lithium ethoxide in ethanol,[5] crystallizes with ethanol in a molar ratio of 1 : 1 as a polymeric aggregate. Two **2**-Li · C_2H_5OH species are present in the asymmetric unit of the unit cell. Each lithium atom is bound to three oxygen atoms of three different nitronate ions and to an oxygen atom of an ethanol molecule, resulting in the formation of Li-O-N-O-Li-O six-membered rings. These "annelated" rings are connected through Li and O atoms forming an infinite, ribbonlike structure, which is further stabilized by internal hydrogen bonds. As a part of this framework, three six-membered rings are shown in Figure 1b. The conformation of these rings is close to a boat form. With respect to a "best" plane through the four basal atoms (Li1, N8, O9, O29) of this boat, the planes through the atoms of two neighboring phenyl rings (Fig. 1a) are oriented nearly parallel whereas those through the atoms of the two remaining phenyl rings are arranged nearly perpendicular. In the $C_6H_5CHNO_2$ moiety, the "best" plane through C7, N8, O9, O10 is twisted by 15.2° with respect to a plane through C1 to C6. This twisting and the significant expansion of the bond angles to values larger than 120° indicate a reduction of the van der Waals repulsion between H1 and O10 (distance 236 pm). Related bond angles were found for **2**-Si(*t*-Bu)Me_2.[6] The C7-N8 bond (129 pm) is significantly shorter and the N8-O9 and N8-O10 bonds (133 and 130 pm, respectively) are significantly longer compared with similar bonds in uncharged nitro compounds.[7]

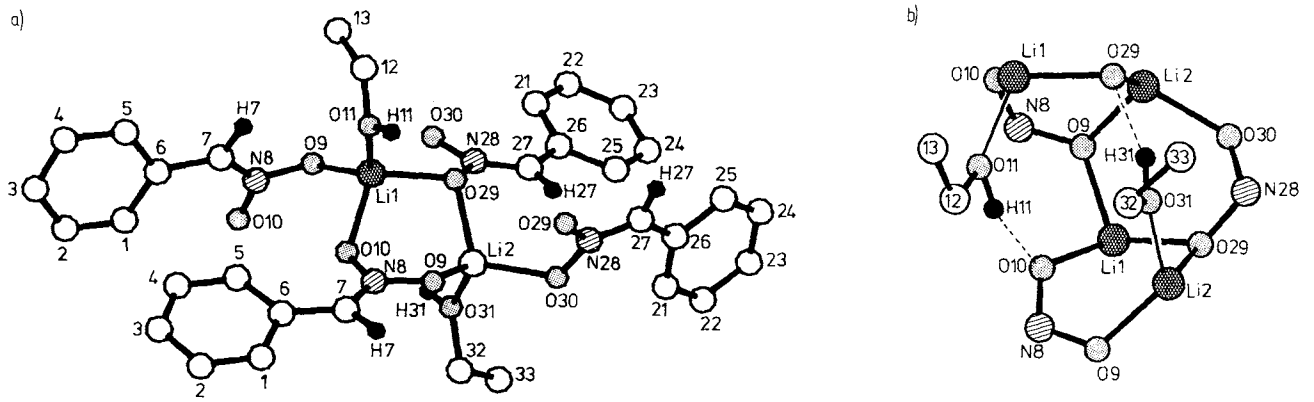

Fig. 1. a) Crystal structure of [**2**-Li · C_2H_5OH]$_n$. The H atoms on the phenyl ring and the ethyl moiety have been omitted; the C atoms are only labeled by numbers. A Li-O-N-O-Li-O six-membered ring is shown which has been extracted from the infinite, ribbonlike framework of "annelated" six-membered rings. The additional rings are connected through the oxygen atoms of the NO_2 groups (cf. Fig. 1b). As indicated by the numbering scheme, the part shown in Fig. 1a is built up from two Li atoms, two ethanol molecules, and four $C_6H_5CHNO_2$ moieties, of which two are related by a symmetry operation.—Space group $Pna2_1$, selected by means of intensity statistics; $a = 732.4(1)$, $b = 1703.6(3)$, $c = 1640.8(4)$ pm, $Z = 8$ (2 formula units per asymmetric unit). Data collection at ca. 230 K with monochromated $Cu_{K\alpha}$ radiation, profile analysis, structure solution by direct methods; refinement with 1351 reflections with $F > 4\sigma(F)$ leads to $R = 0.054$, SHELXTL program [12]. The alkyl moiety of one of the ethanol molecules is disordered over two positions (C32, C32', C33, C33'); only one arrangement is shown in the figure. The positions of the H atoms on the anions and the ordered atoms of ethanol were determined by difference Fourier synthesis. Important distances [pm] and angles [°] (average values or ranges): Li-O 191.9(10)-197.9(10); C-C(phenyl) 136.3(9)-141.5(8); C7-N8 129.3(7); N8-O9 133.2(6); N8-O10 130.1(5); O-Li-O 99.7(4)-122.3(4); C1-C6-C7 126.8(5); C6-C7-N8 126.5(5); C7-N8-O10 124.7(5).—b) Three "annelated" Li-O-N-O-Li-O six-membered rings of the infinite structure of [**2**-Li · C_2H_5OH]$_n$. For clarity, except for the C atoms of ethanol, all atoms that are not directly involved in the ring structure have been omitted: OH···O hydrogen bonds of ethanol to the nitro group: O11···O10 272.6(10) pm; O31···O29 281.6(10) pm; O-H···O (averaged) 158°.—Further details of the crystal structure investigation may be obtained from the Fachinformationszentrum Energie, Physik, Mathematik GmbH, D-7514 Eggenstein-Leopoldshafen 2 (FRG), on quoting the depository number CSD-52057, the names of the authors, and the journal citation.

Ethanol, which is used as solvent and which is formed as reaction product from lithium ethoxide, is incorporated into the crystal.[8] In spite of the fact that for one of the

[*] Prof. Dr. G. Boche, M. Marsch
Fachbereich Chemie der Universität
Hans-Meerwein-Strasse, D-3550 Marburg (FRG)
Dr. G. Klebe, K. H. Böhn
BASF AG, D-6700 Ludwigshafen (FRG)

[**] This work was supported by the Fonds der Chemischen Industrie and the Deutsche Forschungsgemeinschaft.

ethanol molecules a disordered arrangement of the carbon atoms on two positions is found, the difference Fourier synthesis reveals two peaks in the neighborhood of O11 and O31 which can be assigned to two protons on the ethanolic oxygens. Furthermore, these maxima are suitably oriented for a hydrogen-bond formation to the oxygen atoms of the vicinal nitro groups. The geometry of these hydrogen bonds matches that normally found for such bonds (Fig. 1b).[9]

The presence of an OH···O hydrogen bond in the crystal structure of $[\mathbf{2}\text{-Li}\cdot C_2H_5OH]_n$ is in agreement with the findings for nitronates taken from acidity measurements on nitro compounds in protic solvents.[10] For example, in alcohol or water nitromethane is appreciably more acidic ($pK_a(H_2O) = 10.21$)[11] than in aprotic dimethyl sulfoxide ($pK_a = 17.2$).[10] In the protic solvent the nitronate form is stabilized by the formation of OH···O hydrogen bonds.

As mentioned earlier, the nitronate **2**-Na is protonated to form the nitronic acid **3** and not the nitro compound **1**. Accordingly, it might be tempting to use the structure correlation principle to assign the geometry of the fragment formed by the phenylmethylnitronate and the ethanol to an incipient step of such a protonation reaction. However, it has to be kept in mind, that any conclusion taken from structure correlations gain their significance and reliability from the statistical evaluation of a large data set containing the fragment under consideration embedded in various environments. Thus, to support the outlined assumption, the results for $[\mathbf{2}\text{-Li}\cdot C_2H_5OH]_n$ have to be completed by further examples.

Received: August 1, 1986;
supplemented: September 4, 1986 [Z 1885 IE]
German version: *Angew. Chem. 99* (1987) 62

[1] a) A. F. Holleman, *Recl. Trav. Chim. Pays-Bas 13* (1894) 403; b) A. Hantzsch, O. W. Schultze, *Ber. Dtsch. Chem. Ges. 29* (1896) 699; c) A. T. Nielsen in H. Feuer (Ed.): *The Chemistry of the Nitro and Nitroso Group, Part 1*, Wiley, New York 1969, p. 349.

[2] a) D. Seebach, E. W. Colvin, F. Lehr, T. Weller, *Chimia 33* (1979) 1; b) M. Eyer, D. Seebach, *J. Am. Chem. Soc. 107* (1985) 3601; c) M. Braun, *Nachr. Chem. Tech. Lab. 33* (1985) 598.

[3] a) N. Kornblum, R. E. Michel, R. C. Kerber, *J. Am. Chem. Soc. 88* (1966) 5660, 5662; b) G. A. Russell, W. C. Danen, *ibid. 88* (1966) 5663; c) N. Kornblum, *Angew. Chem. 87* (1975) 797; *Angew. Chem. Int. Ed. Engl. 14* (1975) 734.

[4] Crystal structures of nitronates that contain several acceptor substituents are known; see, e.g., a) $2\,K^{\oplus}[O_2CCHNO_2]^{2\ominus}$, D. J. Sutor, F. J. Llewellyn, H. S. Maslen, *Acta Crystallogr. 7* (1954) 145; b) $NH_4^{\oplus}(K^{\oplus})[(H_2NCO)_2CNO_2]^{\ominus}$, O. Simonsen, *ibid. B37* (1981) 344; c) $2\,Rb^{\oplus}[(O_2N)_2C{-}C(NO_2)_2]^{2\ominus}$, B. Klewe, *Acta Chem. Scand. 26* (1972) 1049; d) $K^{\oplus}(Rb^{\oplus},Cs^{\oplus})[(O_2N)_2CH]^{\ominus}$, N. V. Grigor'eva, N. V. Margolis, I. N. Shokhor, I. V. Tselinski, V. V. Mel'nikov, *Zh. Strukt. Khim. 9* (1968) 475 (engl. translation); e) $K^{\oplus}(Rb^{\oplus},Cs^{\oplus})[(O_2N)_3C]^{\ominus}$, N. V. Grigor'eva, N. V. Margolis, I. N. Shokor, V. V. Mel'nikov, I. V. Tselinski, *ibid. 7* (1966) 272 (engl. translation).

[5] Preparation of $[\mathbf{2}\text{-Li}\cdot C_2H_5OH]_n$: **1** (100 mg, 0.73 mmol) in 2 mL of ethanol was treated at 20°C with 0.87 mmol of lithium ethoxide. After 2 h, the solution was concentrated in vacuum to ca. 1 mL. After 12 h, it was possible to free the colorless, needle-shaped crystals from the solvent using a syringe; yield 0.11 g (78%).

[6] E. W. Colvin, A. K. Beck, B. Bastani, D. Seebach, Y. Kai, J. D. Dunitz, *Helv. Chim. Acta 63* (1980) 697.

[7] Examples: a) 2,3-dimethyl-2,3-dinitrobutane: C–N 154.7, N–O 122.1 and 122.7 pm; Y. Kai, P. Knochel, S. Kwiatkowski, J. D. Dunitz, J. F. M. Oth, D. Seebach, *Helv. Chim. Acta 65* (1982) 137; b) 1,2-diphenyl-3-nitrocyclopropene: C–N 151.8, N–O 121.4 and 121.7 pm; M. Marsch, W. Massa, G. Boche, unpublished results.

[8] T. Laube, J. D. Dunitz, D. Seebach, *Helv. Chim. Acta 68* (1985) 1373, reported on the interaction between lithium enolates and secondary amines in the crystal (and in solution).

[9] Similar distances and bond angles have been found for other O–H···O hydrogen bonds; see, e.g., a) I. Olovsson, P.-G. Jönsson in P. Schuster, G. Zundel, C. Sandorfy (Eds.): *The Hydrogen Bond, Vol. 2*, North Holland, Amsterdam 1976, S. 393; b) F. A. Allen, O. Kennard, R. Taylor, *Acc. Chem. Res. 16* (1983) 146; c) H. B. Bürgi, J. D. Dunitz, *ibid. 16* (1982) 153; d) R. Taylor, O. Kennard, *ibid. 17* (1984) 320.

[10] F. G. Bordwell, J. C. Branca, D. L. Hughes, W. N. Olmstead, *J. Org. Chem. 45* (1980) 3305, and references cited therein.

[11] See [1c], p. 373.

[12] G. M. Sheldrick, SHELXTL Program Package, Universität Göttingen 1983.

Synthesis of Nitriles via the Ylide Anion of Sodium Cyanotriphenylphosphoranylidenemethanide

By *Hans Jürgen Bestmann** and *Martin Schmidt*

In phosphonium ylides, the phosphorus atom is capable of stabilizing quasi two negative charges.[1] For this reason, anionic compounds of type **2** may be generated from ylides **1** that have an H atom in the α position to phosphorus.[2–5]

We have now been able to deprotonate cyanomethylenetriphenylphosphorane **3** with a benzene solution of sodium bis(trimethylsilyl)amide **4** to give the salt **5** having an ylide anion.

Compound **5** is isolated, upon evaporation of the solvent, as a yellow, air- and moisture-sensitive powder, thus allowing the first spectroscopic investigation of such a species. In the IR spectrum of **5**, the nitrile band appears at $\tilde{\nu} = 2000\ cm^{-1}$; in comparison, $\tilde{\nu} = 2130\ cm^{-1}$ in the case of **3**.[6] Whereas the ^{31}P-NMR signal of **3** appears at $\delta = 23.2$ (H_3PO_4 as external standard), that of **5** occurs at $\delta = 2.5$, a value that is similar to that found for the *N*-substituted triphenylphosphoranylidene ketenimines ($\delta = 2.3$–5.0).[7] We conclude from this that the resonance structure **5b** strongly contributes to the electron distribution in **5**. The ^{13}C-NMR signal of the ylidic C atom appears at $\delta = 6.60$; $J_{PC} = 94.6$ Hz. The coupling constant shows that the anion **5** has a smaller $P\text{-}C_\alpha\text{-}C_\beta$ angle than open-chain phosphacumulene ylides.[7,8]

Compound **5** reacts with halogen compounds **6** to give the cyanomethylenetriphenylphosphoranes **7**, which are thereby accessible more readily in greater variety than previously. Examples are listed in Table 1.[9]

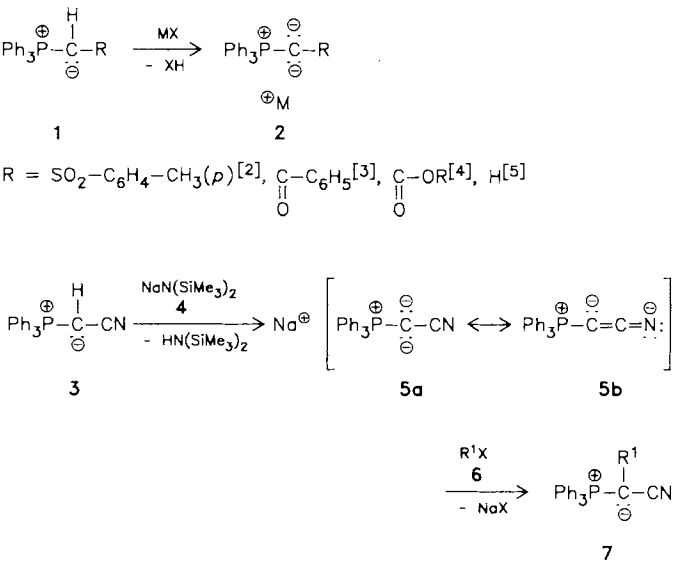

[*] Prof. Dr. H. J. Bestmann, Dipl.-Chem. M. Schmidt
Institut für Organische Chemie der Universität Erlangen-Nürnberg
Henkestrasse 42, D-8520 Erlangen (FRG)

Table 1. Cyano ylides **7** prepared from **5** and the halogen compounds **6**.

	X	R^1	**7** Yield [%]	M.p. [°C]
a	Cl	$CH_2-C_6H_5$	74	124
b	Br	$CH_2-CH=CH_2$	72	101-102
c	I	CH_3	93	171-172 [a]
d	I	$n-C_4H_9$	78	71-72
e	Cl	$CH_2-Si(CH_3)_3$	73	125-127
f	Br	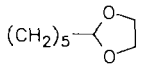	88 (crude)	oil
g	Cl	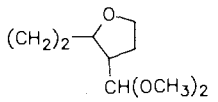	51	103-105
h	Cl	$Si(CH_3)_3$	86	142-144
i	Br	Br	85	164 [b]

[a] M.p. = 172-173 °C [6]. [b] M.p. = 162.5-164.5 °C [10].

The cyano ylides **7** react in the usual way with aldehydes to give α,β-unsaturated nitriles.[6] Of particular preparative interest appears to us to be the following possibility for the construction of cyclic compounds of this kind. Treatment of **7f** with 0.1 N HCl results in cleavage of the acetal groups to give the phosphonium chloride **8**. When a solution of **8** in dichloromethane is added to a solution of imidazole in the same solvent at reflux temperature, the ylide **9** is formed as the primary product. Intramolecular Wittig reaction results in conversion of **9** into the cycloheptenecarbonitrile **10** (yield 52%, b.p. = 95 °C/15 torr). The synthetic potential of this reaction sequence is demonstrated by the analogous transformation of **7g**[11] via **11** into the bicyclic nitrile **12** (yield 71%, b.p. = 58-59 °C/0.01 torr).

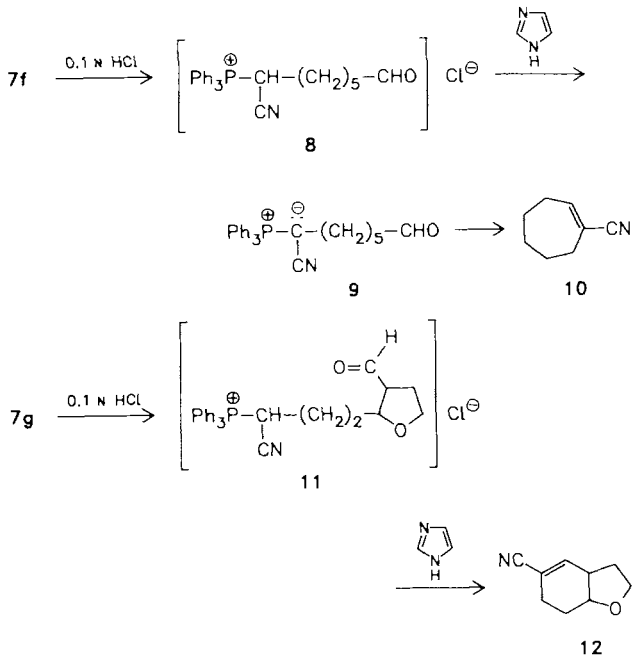

The reaction of **5** with aliphatic aldehydes and subsequently with trimethylchlorosilane **14** opens up a flexible approach to 2-cyano-1,3-dienes such as **19**, which are of interest for syntheses involving dienes with inverse electron demand.

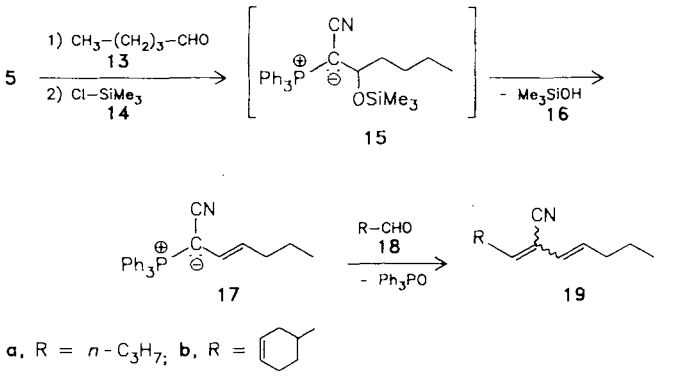

a, R = $n-C_3H_7$; **b**, R =

When **5** is allowed to react first with valeraldehyde **13** and subsequently with trimethylchlorosilane **14**, not the expected product **15** but rather the α,β-unsaturated cyano ylide **17** (yield 58%, m.p. = 97-99 °C), formed by loss of trimethylsilanol **16**, is isolated. Compound **17** can react with aldehydes **18** to give 2-cyano-1,3-dienes **19** (**19a**, yield 48%, b.p. = 60-64 °C/0.3 torr (kugelrohr distillation); **19b**, yield 72%, b.p. = 94 °C/0.05 torr).

Reaction of **5** with the carboxylic esters **20** in benzene results in formation of the insoluble sodium alkoxides **21**. After removal of the solvent, the acyl cyano ylides **22** are obtained. They can undergo thermolysis to give the alkyne carbonitriles (cyanoacetylenes) **23**.[12] Nonoptimized results are shown in Table 2, in which example **c** shows that chiral carboxylic esters can also be employed.

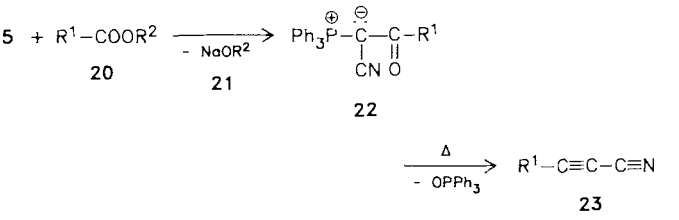

Table 2. Acyl cyano ylides **22** prepared from **5** and the carboxylic esters **20**; alkyne carbonitriles **23** prepared by thermolysis of **22**.

R^1	**22** Yield [%]	M.p. [°C]	**23** Yield [%]	B.p. [°C/torr]
a C_6H_5	78	207 [a]	84 [b]	[b, c]
b $(CH_2)_8-CH=CH_2$	65	95	21	76-77/0.07
c 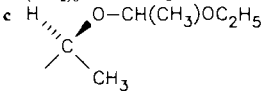	72	137-148 [d]	26	42-50/0.05 [e]

[a] M.p. = 208 °C [12]. [b] According to [12]. [c] M.p. = 38-39 °C. [d] Melting range of the mixture of diastereomers. [e] Bath temperature, kugelrohr distillation ($[\alpha]_D^{20} = -3.1°$, $c = 1.4$ ($CDCl_3$)); mixture of diastereomers.

Experimental Procedure

A) Synthesis of **7**: **3** (9.03 g, 30 mmol) and **4** (5.49 g, 30 mmol) were stirred together in 150 mL of dry benzene at room temperature, until a clear, orange-yellow solution of **5** was obtained (ca. 1 h). Compound **6** (30 mmol) was then added to this cooled, stirred solution. After addition, the reaction mixture was allowed to stir for 20 h at room temperature (**7f** and **7g**: 3 d at 40-50 °C), and the inorganic salt was filtered off under suction. Removal of

the solvent gave a usually oily residue, which was dissolved in ca. 50 mL of ethyl acetate. Addition of hexane until the solution became cloudy resulted in the crystallization of the compounds **7** at −20°C (cf. Table 1).

B) Synthesis of **22**: **20** (30 mmol) was added to a solution of **5** (30 mmol) in benzene prepared according to A above, and the reaction mixture was heated at reflux for 2 h. After cooling to room temperature, the reaction mixture was worked up as described under A (cf. Table 2).

Received: July 21, 1986;
revised: October 6, 1986 [Z 1864 IE]
German version: *Angew. Chem. 99* (1987) 64

[1] H. J. Bestmann, A. J. Kos, K. Witzgall, P. von R. Schleyer, *Chem. Ber. 119* (1986) 1331.
[2] A. M. van Leusen, B. A. Reith, A. J. W. Iedema, J. Strating, *Recl. Trav. Chim. Pays-Bas 91* (1972) 37.
[3] C. Brouquet, M. Simalty, *Tetrahedron Lett. 1972*, 933; C. Broquet, *Tetrahedron 29* (1973) 3595.
[4] H. J. Bestmann, R. Besold, D. Sandmeier, *Tetrahedron Lett. 1975*, 2293; H. J. Bestmann, D. Sandmeier, *Angew. Chem. 87* (1975) 630; *Angew. Chem. Int. Ed. Engl. 14* (1975) 634; *Chem. Ber. 113* (1980) 274.
[5] E. J. Corey, J. Kang, *J. Am. Chem. Soc. 104* (1982) 4724; cf., however, B. Schaub, T. Jenny, M. Schlosser, *Tetrahedron Lett. 25* (1984) 4097; E. J. Corey, J. Kang, K. Kyler, *ibid. 26* (1985) 555; B. Schaub, M. Schlosser, *ibid. 26* (1985) 1623.
[6] H. J. Bestmann, S. Pfohl, *Justus Liebigs Ann. Chem. 1974*, 1688.
[7] H. J. Bestmann, G. Schmid, *Chem. Ber. 113* (1980) 3369.
[8] T. A. Albright, P. Hofmann, A. R. Rossi, *Naturforsch. B 35* (1980) 343.
[9] Correct elemental analyses and spectroscopic data were obtained for all new compounds.
[10] A. J. Speziale, K. W. Ratts, *J. Am. Chem. Soc. 85* (1963) 2790.
[11] Synthesis of **6g**: cf. H. Frauenrath, T. Philipps, *Tetrahedron 42* (1986) 1135. We thank Dr. *Frauenrath* for a large amount of **6g**.
[12] S. T. D. Gough, S. Trippett, *J. Chem. Soc. 1962*, 2333.

Magnesium Phosphides—Synthesis and Structure of [Mg(PHPh)$_2$(tmeda)]**

By *Evamarie Hey, Lutz M. Engelhardt, Colin L. Raston,** and *Allan H. White*

The synthesis of organomagnesium reagents and their utility in organic and organometallic chemistry is well known.[1] Inorganic magnesium reagents, however, remain largely unexplored. For example, little is known about magnesium phosphides[2,3] and their use as transfer agents of $PR_2^{\ominus}$ has not been investigated. We now report the synthesis and spectroscopic properties of the magnesium phosphides **1**[3,4] and **2**,[5] and the X-ray crystal structure determination of **2**, which to our knowledge represents the first crystallographic study of a magnesium phosphido complex.

The relatively new reagent *n*Bu*s*BuMg, whose potential is slowly being realized,[6] was found to selectively metalate PH_2Ph in heptane under mild conditions. The product, **1**, is assumed to have a polymeric structure containing bridging $PHPh^{\ominus}$ groups which are cleaved by tetramethylethylenediamine (TMEDA) to yield a monomeric hydrocarbon-soluble bis(phosphido) complex, **2**.

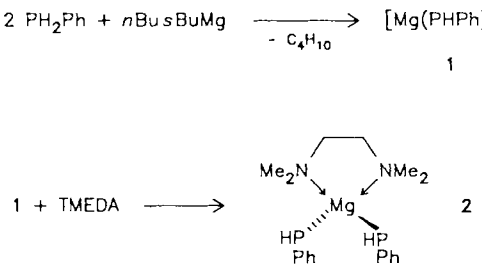

Compounds **1** and **2** show characteristic ν(P–H) absorptions at 2280 and 2262/2250 cm^{-1}, respectively. The ^{31}P-NMR spectrum of **2** shows two virtual triplets centered at $\delta = -123.65$ and -123.70 ppm in a ratio of ca. 2:1 ($(^1J + {}^3J)/2 = 198.5$ Hz, both triplets), corresponding presumably to coupling to two protons in each of the *meso* and *rac* diastereoisomers that are possible for two chiral P centers attached to magnesium. No ^{25}Mg–^{31}P coupling was evident and we were unable to obtain a ^{25}Mg-NMR spectrum,[7] probably because of the low site symmetry at the quadrupolar ^{25}Mg nuclei.

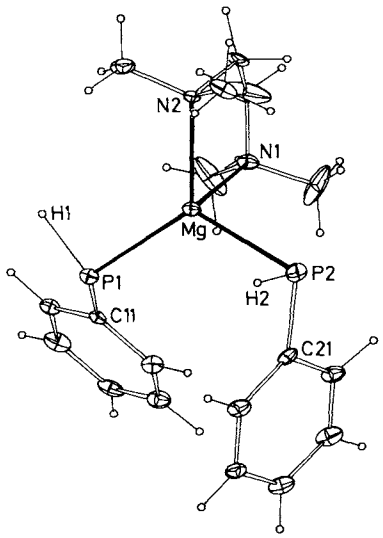

Fig. 1. Crystal structure of **2** showing 20% thermal ellipsoids. Hydrogen atoms have arbitrary radii of 0.1 Å; H1 and H2 were located in a difference map but not refined. Selected bond lengths [Å] and bond angles [°]:Mg-P1, Mg-P2 2.592(5), 2.587(5); Mg-N1, Mg-N2 2.306(8), 2.226(8); P1-C11 1.822(8), P2-C21 1.821(10); P1-Mg-P2 122.5(1), P1-Mg-N1, P1-Mg-N2 100.9(3), 126.0(3), P2-Mg-N1, P2-Mg-N2 100.1(3), 110.1(3), N1-Mg-N2 79.9(3), Mg-P1-C11 122.6(4), Mg-P2-C21 98.4(5).

The X-ray structure of **2** (Fig. 1),[8] obtained from a crystal selected from a bulk sample of inseparable isomers, was of the *rac* isomer. The magnesium centers have a distorted tetrahedral environment with the P1–Mg–P2 angle (122.5(1)°) greater than the N1–Mg–N2 angle (79.9(3)°). The Mg–P distances are virtually equivalent (2.592(5) and 2.587(5) Å) and compare with those in MgP_4 (2.608–2.862 Å);[9] the P–C distances are also equivalent. However, the Mg–P–C angles differ considerably (122.6(4) and 98.4(5)°). The associated hydrogen atom positions, although not satisfactorily resolved beyond difference map artifacts, suggest pyramidal dispositions. Interestingly, the nitrogen centers of monodentate amido ligands bound to magnesium are trigonal.[6]

The only other X-ray structures of phenylphosphido complexes, namely, **3**[10] and **4**,[11] and the results of other investigations[12] show that the properties and reactivity of the $PHPh^{\ominus}$ group are largely dependent on the nature of the metal and coligands.

[*] Dr. C. L. Raston, Dr. E. Hey, Dr. L. M. Engelhardt, Dr. A. H. White
Department of Physical and Inorganic Chemistry,
University of Western Australia
Nedlands 6009 (Australia)

[**] We thank the Verband der Chemischen Industrie für a habilitation grant for *E. H.*, and the Deutsche Forschungsgemeinschaft and the Australian Research Grants Scheme for supporting this work.

$[Os(CO)_2Cl(PHPh)(PPh_3)_2]$ $[W(\equiv CCMe_3)Cl_2(PHPh)(PEt_3)_2]$

3 **4**

The synthetic utility of magnesium phosphido reagents in gaining access to other metal phosphido complexes is being investigated. Interestingly, reaction of **5** with **1** gave the known diphosphene complex **6**[13] rather than the expected phosphido complex.[14]

$[NiCl_2\{(PR_2CH_2)_2\}] + [Mg(PHPh)_2] \longrightarrow$

5 **1**

$[Ni(\eta\text{-}Ph{-}P{=}P{-}Ph)\{(PR_2CH_2)_2\}]$

6

$R = c\text{-}C_6H_{11}$

Received: July 28, 1986;
revised: November 3, 1986 [Z 1879 IE]
German version: *Angew. Chem. 99* (1987) 61

[1] W. E. Lindsell in G. Wilkinson, F. G. A. Stone, E. W. Abel (Eds.): *Comprehensive Organometallic Chemistry, Vol. 1*, Pergamon Press, Oxford 1982, p. 155; M. S. Vharasch, O. Reinmuth: *Grignard Reactions of Nonmetallic Substances*, Constable, London 1954.

[2] A. Job, G. Dussolier, *C. R. Hebd. Séances Acad. Sci. 184* (1927) 1454; *Chem. Abstr. 21* (1927) 3049; F. G. Mann, I. T. Millar, *J. Chem. Soc. 1952*, 3039; K. Issleib, C. Rock Stuoh, I. Duchek, E. Fluck, *Z. Anorg. Allg. Chem. 360* (1968) 77.

[3] K. Issleib, H. J. Deylig, *Chem. Ber. 97* (1964) 946.

[4] *Experimental procedure* for **1** (exclusion of air and water): To $PhPH_2$ (3.03 g, 27.5 mmol) in pentane (30 mL) was added a 0.7 M solution of *n*BusBuMg in heptane (88 mL, 61.6 mmol). In an exothermic reaction a white precipitate formed. The solution was then stirred at 25°C for 2 h. The product (6.34 g, 95%) was collected, washed with pentane, and dried in vacuo. **1** is pyrophoric, insoluble in pentane, hexane, and toluene, and soluble in donor solvents. IR: ν(P-H) = 2280 (w), ν(Mg-P) = 510–300 cm^{-1} (br, structured).

[5] *Experimental Procedure* for **2**: **1** (2.03 g, 8.37 mmol) was dissolved in TMEDA (4 mL). The resulting pale yellow solution was stirred for 1 h at 25°C, then pumped dry. The product was recrystallized from toluene/pentane. Yield: 2.33 g (78%); white crystals, m.p. = 115–120°C (dec.). ^{1}H-NMR (C_6D_6, 25°C, TMS): δ = 7.66–6.97 (m, Ph), 5.05, 2.57 (d, $J(^1H\text{-}^{31}P)$ = 198.6 Hz, P-H), 1.94 (s, CH_3), 1.86 (s, CH_2). ^{31}P-NMR (C_6D_6, 25°C, 85% H_3PO_4): $\delta(^1H$ decoupled) = −123.64 (s), $\delta(^1H$ coupled) = −123.65 (t), −123.70 (t, $J(^{31}P\text{-}^1H)$ = 198.5 Hz). IR: ν(P-H) = 2262 (m), 2250 (m) cm^{-1}.

[6] J. J. Eisch, R. Sanchez, *J. Organomet. Chem. 296* (1985) C27; A. W. Duff, P. B. Hutchcock, M. F. Lappert, R. G. Taylor, *ibid. 293* (1985) 271; M. Henderson, R. I. Papasergio, C. L. Raston, A. H. White, M. F. Lappert, *J. Chem. Soc. Chem. Commun. 1986*, 672.

[7] R. Benn, H. Lehmkuhl, K. Mehler, A. Rufińska, *Angew. Chem. 96* (1984) 521; *Angew. Chem. Int. Ed. Engl. 23* (1984) 534.

[8] **2**, triclinic, $P\bar{1}$ (C_i^2, No. 2), a = 11.916(6), b = 11.612(7), c = 9.080(6) Å, α = 68.42(4), β = 85.11(5), γ = 62.39(4)°, V = 1030(1) Å^3, Z = 2, ρ_{calcd} = 1.16 g·cm^{-3}, $F(000)$ = 384, monochromatic $Mo_{K\alpha}$ radiation, λ = 0.71079 Å, μ_{Mo} = 2.5 cm^{-1}, specimen size ≈ 0.2 mm (capillary); Syntex-$P\bar{1}$ diffractometer, ≈ 20°C, $2\theta_{max}$ = 45°, 2024 reflections, 1276 with $I > 2\sigma(I)$, direct methods, full matrix refinement, R, R' = 0.076, 0.057 (statistical weights). Further details of the crystal structure investigation may be obtained from the Fachinformationszentrum Energie, Physik, Mathematik GmbH, D-7514 Eggenstein-Leopoldshafen 2 (FRG), on quoting the depository number CSD-52260, the names of the authors, and the journal citation.

[9] H. G. von Schnering, G. Menge, *Z. Anorg. Allg. Chem. 422* (1976) 219.

[10] D. S. Bohle, T. C. Jones, C. E. T. Richard, W. R. Roper, *J. Chem. Soc. Chem. Commun. 1984*, 865.

[11] S. M. Rocklage, R. R. Schrock, M. R. Churchill, H. J. Wasserman, *Organometallics 1* (1982) 1332.

[12] D. S. Bohle, W. R. Roper, *J. Organomet. Chem. 273* (1984) C7.

[13] H. Schäfer, D. Binder, D. Fenske, *Angew. Chem. 97* (1985) 523; *Angew. Chem. Int. Ed. Engl. 24* (1985) 522.

[14] *Experimental procedure* for **6**: **5** (0.23 g, 0.42 mmol) was allowed to react with **1** (0.10 g, 0.41 mmol) in 20 mL of tetrahydrofuran at ca. 20°C. Cooling of the mixture to ca. −30°C afforded green crystals of **6** [13] (0.15 g, 53% yield), which were washed with hexane and dried in vacuo.

$As_4S_5N_{10}$—A Diaminosulfane Derivative with Two Bicyclic Arsino Sulfur Diimides**

By *Max Herberhold,* Karlheinz Guldner, Alfred Gieren, Catalina Ruiz-Pérez,* and *Thomas Hübner*

The reaction of the salt K_2SN_2 with organoarsenic chlorides has proved useful for the synthesis of the arsenic-substituted sulfur diimides **1** and **2**.[1,2] According to the X-ray structure analysis of **1** (R = Ph), the sulfur diimide skeleton in the bis(diorganoarsino) sulfur diimides **1** has the *Z/Z* configuration;[2] the eight-membered ring in **2** (R = *t*Bu) has the boat form.[2] Compounds of type **1** were first described in 1984;[1] eight-membered ring compounds of type **2** with R = Me,[3] Ph,[4] and Mes[4] had been obtained previously.

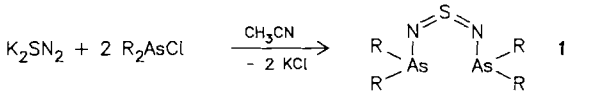

$K_2SN_2 + 2\ R_2AsCl \xrightarrow[-\ 2\ KCl]{CH_3CN}$ **1**

R = Me, *t*Bu, *cyclo*-C_6H_{11}, Ph

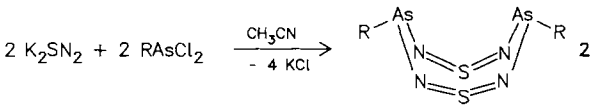

$2\ K_2SN_2 + 2\ RAsCl_2 \xrightarrow[-\ 4\ KCl]{CH_3CN}$ **2**

R = *t*Bu

Surprisingly, the corresponding reaction of K_2SN_2 with arsenic halides AsX_3 (X = Cl, Br, I) does not lead to the expected cage compound $As(NSN)_3As$, even though the analogous silicon compound, $MeSi(NSN)_3SiMe$,[5] is known. Instead, **3** is formed preferentially in the course of a redox reaction.

Starting from $AsBr_3$, compound **3** is obtained in about 40% yield as red, moderately air-stable crystals, which are poorly soluble in hydrocarbons and diethyl ether, moderately soluble in acetonitrile, and very soluble in dichloro-

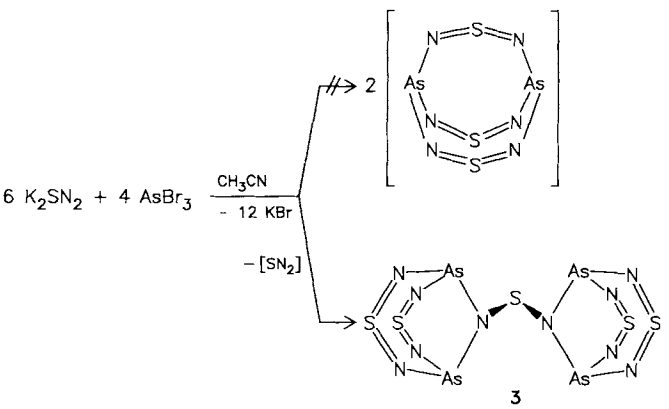

$6\ K_2SN_2 + 4\ AsBr_3 \xrightarrow[-\ 12\ KBr]{CH_3CN}$ // → 2 [ ] ; $-[SN_2]$ → **3**

[*] Prof. Dr. M. Herberhold, Dr. K. Guldner
Laboratorium für Anorganische Chemie der Universität
Universitätsstrasse 30, D-8580 Bayreuth (FRG)
Prof. Dr. A. Gieren [+], Dipl.-Phys. C. Ruiz-Pérez, Dr. T. Hübner
Max-Planck-Institut für Biochemie
D-8033 Martinsried (FRG)

[+] Present address:
Institut für Anorganische und Analytische Chemie der Universität
Innrain 52a, A-6020 Innsbruck (Austria)

[**] This work was supported by the Deutsche Forschungsgemeinschaft and the Fonds der Chemischen Industrie.

methane. In the mass spectrum, the peaks for the molecular ion $As_4S_5N_{10}^{\oplus\oplus}$ (m/z 600) and for $As_2SN_3^{\oplus}$ (m/z 224) are very intense. In the IR spectrum, the two bands at 1143/1119 (vs) can be tentatively assigned to the ν_{as}(NSN) stretching mode, and the bands at 1069/1039 (s) to the ν_s(NSN) stretching mode of the sulfur diimide units in the bicyclic moieties.

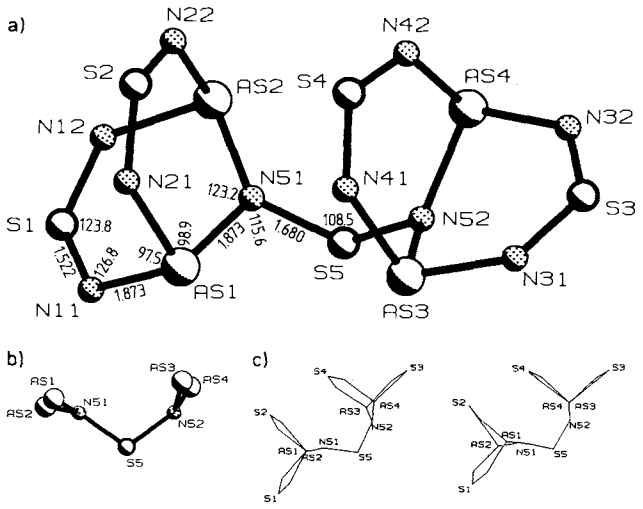

Fig. 1. Crystal structure of **3**. a) Bond lengths [Å] and angles [°] averaged over *mm*2 symmetry. b) Diaminosulfane moiety projected onto N-S-N. c) Projections in the directions As1-As2 and As3-As4.

The structure of **3** (Fig. 1) was determined by X-ray structure analysis of $3 \cdot 0.5CH_2Cl_2$.[7] A diaminosulfane derivative is found in which two bicyclic [$As_2S_2N_5$] units are coupled through a sulfur atom. In both the entire molecule and the two cages, the highest possible symmetry *mm*2 is reduced to 2. However, even this symmetry is not strictly imposed. The structure of the As(NSN)$_2$As eight-membered rings is comparable to that in compounds of the type **2**[2,4] and in $[Os_3(CO)_{10}\{\mu\text{-}(t\text{Bu})As(NSN)_2As(t\text{Bu})\}]$.[8] The N=S=N groups have the geometry characteristic of sulfur diimides[9] (S=N bonds: 1.522 Å) and are nearly coplanar with the directly bonded As atoms. The As···As distance (3.295 Å) in **3** is significantly smaller than that in comparable compounds[2,4,8] and even shorter than that in **1** (R = Ph) (3.379 Å).[2] The shorter As···As distance is accompanied by a reduction of the As-N=S, N-As-N, and N=S=N angles in the eight-membered rings. The diaminosulfane moiety $As_2N-S-NAs_2$ has the geometry[10,11] characteristic of this structural unit with the lone pairs of electrons on the N atoms in the N-S-N plane; the N atoms are situated 0.16(2) Å (N51) and 0.32(3) Å (N52) outside of the plane of their three binding partners ("transoid arrangement of electron pairs"[10]); the S-N bonds (1.680 Å) are somewhat shorter than a S-N single bond.

Experimental Procedure

A suspension of K_2SN_2 (0.58 g, 4.2 mmol) [6] in acetonitrile (100 mL) was allowed to react at −40°C with a solution of $AsBr_3$ (0.88 g, 2.8 mmol) in ether (20 mL). After thawing, the orange-brown mixture was stirred for 2 h, filtered through Na_2SO_4 (anhydrous), concentrated to half of the original volume, and cooled to −30°C. The crude product **3** separated out as an orange-red powder (0.17 g, 40%), which can be recrystallized from CH_2Cl_2 or ether/CH_2Cl_2 (5/1). Red crystals ($3 \cdot 0.5CH_2Cl_2$), dec. above 138°C. IR (Nujol): $\tilde{\nu}$ [cm^{-1}] = 1143 (vs), 1119 (vs), 1069 (s), 1039 (s), 1027 (vs), 966 (w), 912 (w), 805 (w), 722 (w), 662 (s), 632 (m), 590 (s), 495 (vs), 470 (sh), 457 (s), 410 (s), 391 (w).

Received: September 12, 1986;
revised: October 21, 1986 [Z 1927 IE]
German version: *Angew. Chem. 99* (1987) 81

[1] M. Herberhold, W. Ehrenreich, K. Guldner, *Chem. Ber. 117* (1984) 1999.
[2] A. Gieren, H. Betz, T. Hübner, V. Lamm, M. Herberhold, K. Guldner, *Z. Anorg. Allg. Chem. 513* (1984) 160.
[3] O. J. Scherer, R. Wies, *Angew. Chem. 83* (1971) 882; *Angew. Chem. Int. Ed. Engl. 10* (1971) 812.
[4] N. W. Alcock, E. M. Holt, J. Kuyper, J. J. Mayerle, G. B. Street, *Inorg. Chem. 18* (1979) 2235.
[5] H. W. Roesky, M. Witt, B. Krebs, G. Henkel, H.-J. Korte, *Chem. Ber. 114* (1981) 201.
[6] M. Herberhold, W. Ehrenreich, *Angew. Chem. 94* (1982) 637; *Angew. Chem. Int. Ed. Engl. 21* (1982) 633; *Angew. Chem. Suppl. 1982*, 1346.
[7] X-ray structure analysis of $3 \cdot 0.5CH_2Cl_2$: monoclinic, space group *C*2/*c*, $a = 16.523(4)$, $b = 16.790(3)$, $c = 11.458(3)$ Å, $\beta = 97.03(2)°$, $Z = 8$, $\rho_{calcd} = 2.528$ g cm^{-3}, $\rho_{obs} = 2.525$ g cm^{-3}. CAD4, $Mo_{K\alpha}$, graphite monochromator, 2761 unique reflections observed ($I > 2\sigma(I)$, $1.5° \leq \theta \leq 28°$), Patterson, Fourier, difference Fourier syntheses. $R = 0.038$ ($R_w = 0.041$; $w = k/(\sigma^2(|F_o|) + 0.0003|F_o|^2)$. CH_2Cl_2 in a special site at 2. Further details of the crystal structure investigation may be obtained from the Fachinformationszentrum Energie, Physik, Mathematik GmbH, D-7514 Eggenstein-Leopoldshafen 2 (FRG), on quoting the depository number CSD-52091, the names of the authors, and the journal citation.
[8] A. Gieren, T. Hübner, M. Herberhold, K. Guldner, G. Süss-Fink, *Z. Anorg. Allg. Chem.* (1986), in press.
[9] A. Gieren, B. Dederer, *Z. Anorg. Allg. Chem. 467* (1980) 68.
[10] V. Lamm, M. Rabben, A. Gieren, *Z. Anorg. Allg. Chem. 507* (1983) 100.
[11] H. W. Roesky, W. Clegg, J. Schimkowiak, M. Schmidt, M. Witt, G. M. Sheldrick, *J. Chem. Soc. Dalton Trans. 1982*, 2117.

Imino-, Phosphoranylidene-, and Sulfuranylidenephosphanes by 1,3-Silyl Migration**

By *Frank Zurmühlen* and *Manfred Regitz**

Compounds containing λ^3 phosphorus with coordination number 2, such as methylenephosphanes ("phosphaalkenes") **1**,[1,2] iminophosphanes **2**,[3] and phosphanylidenephosphanes ("diphosphenes") **3**,[4] play an important role in current developments in phosphorus chemistry. We describe here the preparation of low-coordinate phosphorus compounds of types **2**, **4**, and **5** from silylated phosphides and acid chlorides, the P/X double bond being introduced by 1,3-silyl migration.[5]

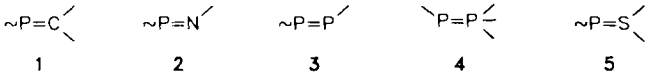

1 **2** **3** **4** **5**

Iminophosphanes **2** are known[3] (albeit without the =NOR structural unit); phosphoranylidenephosphanes **4** are largely uninvestigated;[6] sulfuranylidenephosphanes were up to now completely unknown.

The reaction of nitrosyl chloride **7a** with the lithium phosphide **6a**[7] in pentane at −50°C affords, after distillative workup (200°C, kugelrohr) the thermally extremely stable iminophosphane **9a**; the conceivable dimerization

[*] Prof. Dr. M. Regitz, Dipl.-Chem. F. Zurmühlen
Fachbereich Chemie der Universität
Erwin-Schrödinger-Strasse, D-6750 Kaiserslautern (FRG)

[**] Phosphorus Compounds with Unusual Coordination, Part 14. This work was supported by the Fonds der Chemischen Industrie and the Landesregierung of Rheinland-Pfalz. — Part 13: R. Hussong, H. Heydt, M. Regitz, *Z. Naturforsch. B41* (1986) 915.

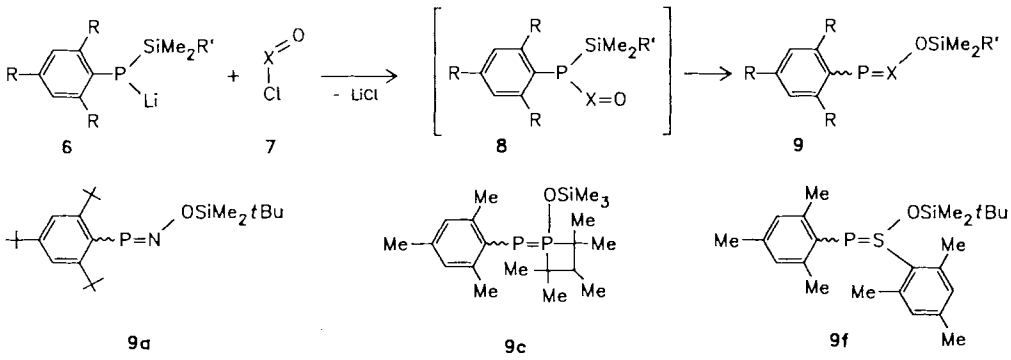

Table 1. Reaction conditions, yields, melting points, isomeric ratios, and NMR data of the phosphanes **9a–g**. THF = tetrahydrofuran.

Starting material	Product	R from 6	R′	X from 7	Reaction conditions [a]	Yield [%]	M.p. [°C]	*E*:*Z*	^{31}P-NMR [b]	^{1}H-NMR [c] Si–Me	Si–*t*Bu
6a, **7a**	**9a**	*t*Bu	*t*Bu	N	pentane, −50°C	58	76	—	315 (−)	0.11	0.79
6b, **7b**	**9b**	Me	Me	P(*t*Bu)$_2$	ether/THF, 1:1	38	44 [d]	—	96, −213 [e]	0.29	—
6b, **7c**	**9c**	Me	Me	[f]	ether/THF, 1:1	25	39 [d]	—	78, −209 [e]	0.31	—
6c, **7d**	**9d**	Me	*t*Bu	S-1-adamantyl	pentane	61	oil	22:78	121, 118	0.27/0.09	1.07/0.84
6b, **7d**	**9e**	Me	Me	S-1-adamantyl	pentane	54	42	40:60	121, 115	0.38/0.27	—
6c, **7e**	**9f**	Me	*t*Bu	S-mesityl	pentane	68	88	12:88	145, 140	0.20/−0.08	1.04/0.89
6b, **7e**	**9g**	Me	Me	S-mesityl	pentane	48	57	51:49	139 (0.8), 139 (0.2)	0.35/0.29	—

[a] At 20°C, unless otherwise given. [b] C_6D_6, 85% H_3PO_4 (ext.). [c] $CDCl_3$, TMS (int.). [d] Decomposition. [e] Sequence λ^5,λ^3-phosphorus. [f] See formula.

does not occur for steric reasons. The corresponding reactions of phosphinic chlorides **7b**, **c** with **6b**[8] and of sulfinic chlorides **7d**, **e** with **6b**[8] and **6c**[9] afford the phosphoranylidene and sulfuranylidenephosphanes **9b**, **c** and **9d–g**, respectively.[10] Except for the oil **9d**, all these compounds are crystalline and sensitive to moisture; in addition, **9b**, **c** are thermally labile. The silyl migration **8** → **9** is apparently so fast that **8** cannot be detected by ^{31}P-NMR spectroscopy.

The elemental analyses and the ^{31}P-NMR spectroscopic data support the constitution of the two-coordinate phosphanes and exclude the possibility of isomers of type **8**. Moreover, in no case is the splitting of the silyl methyl signals by the phosphorus, which is expected for **8**, observed.

The strongly low-field shifted ^{31}P-NMR resonance of **9a** (Table 1) is characteristic of iminophosphanes.[11] In the case of **9b**, **c**, the λ^3 phosphorus appears at remarkably high field (Table 1), which points to the ylide character of this compound. The $^{1}J_{P,P}$ coupling constants are 429 and 433 Hz, respectively.[12] For **9d–g**, two phosphorus resonances having different intensities but relatively large chemical shifts were found in each case (Table 1); this can be ascribed to the presence of *E*/*Z* isomers. The same distribution of isomers is also revealed by ^{1}H-NMR spectroscopy (silyl methyl signals).[13] The positions of the ^{31}P-NMR resonances are in good agreement with those of methylenephosphanes having similar patterns of substitution.[1]

Experimental Procedure

9f: A 1.45 M solution of methyllithium in ether (15 mL) was added at 20°C to a solution of the phosphane **6c** (5.8 g, 21.8 mmol) (H instead of Li) [9] in diethyl ether (20 mL) and the reaction solution was evaporated to dryness. The residue was dissolved in pentane (50 mL) and the resulting suspension added to a solution of **7e** (4.4 g, 21.8 mmol) in pentane (50 mL). After 12 h, the lithium chloride was removed by centrifugation, the solution was evaporated, and the residue was distilled at 160–170°C (oven temperature)/10^{-3} torr in a kugelrohr apparatus. Yield 5.8 g (68%) colorless oil, which crystallizes from pentane at −76°C. M.p. = 88°C.

Received: August 5, 1986;
revised: September 10, 1986 [Z 1891 IE]
German version: *Angew. Chem. 99* (1987) 65

[1] Review: R. Appel, F. Knoll, I. Ruppert, *Angew. Chem. 93* (1981) 771; *Angew. Chem. Int. Ed. Engl. 20* (1981) 731.
[2] Review: B. Weber, M. Regitz in *Houben-Weyl: Methoden der Organischen Chemie, Bd. E1*, Thieme, Stuttgart 1982, p. 28ff.
[3] E. Niecke, O. J. Scherer, *Nachr. Chem. Tech. 23* (1975) 395; see also [2], p. 56ff.
[4] M. Yoshifuji, N. Inamoto, K. Ito, S. Nagase, *Chem. Lett. 1985*, 437; A. H. Cowley, *Polyhedron 3* (1984) 389.
[5] For corresponding reactions for the synthesis of *C*-siloxyphosphaalkenes, see G. Becker, *Z. Anorg. Allg. Chem. 430* (1977) 66.
[6] Trimethylphosphoranylidenetrifluoromethylphosphane: A. B. Burg, W. Mahler, *J. Am. Chem. Soc. 83* (1961) 2388; A. B. Burg, *J. Inorg. Nucl. Chem. 33* (1971) 1575; (triethyl- and tributylphosphoranylidene)diethoxyphosphorylphosphane: D. Weber, E. Fluck, *Z. Anorg. Allg. Chem. 424* (1976) 103; for triphosphenium salts of similar structure, see A. Schmidpeter, S. Lochschmidt, *Angew. Chem. 98* (1986) 271; *Angew. Chem. Int. Ed. Engl. 25* (1986) 253.
[7] M. Yoshifuji, K. Toyota, K. Shibayama, N. Inamoto, *Chem. Lett. 1983*, 1653.
[8] G. Becker, W. Uhl, H. J. Wessely, *Z. Anorg. Allg. Chem. 479* (1981) 41.
[9] Reaction analogous to **6b** [8].
[10] Thioxophosphanes R–P=S are short-lived, but may be detected by trapping reactions: R. Hussong, H. Heydt, M. Regitz, *Phosphorus Sulfur 25* (1985) 201.
[11] Trimethylsilylimino[bis(trimethylsilyl)amino]phosphane: $\delta = 326$; O. J. Scherer, N. Kuhn, *Chem. Ber. 107* (1974) 2123; review: E. Fluck, *Top. Phosphorus Chem. 10* (1980) 193.
[12] For comparison (triethylphosphoranylidene)diethoxyphosphorylphosphane: $\delta = 44$ and -218, $^{1}J_{P,P} = 444$ Hz [6].
[13] The tentative *E*/*Z* assignment is based on observations on the two geometric isomers of a methylenephosphane (**9**, X = CPh, R = R′ = *t*Bu), for which both the silyl substituents (^{1}H-NMR) and the phosphorus of the *E* isomer absorb at lower field.

 © VCH Verlagsgesellschaft mbH, D-6940 Weinheim, 1987 0570-0833/87/0101-0084 $ 02.50/0

Isomerization Reactions in the System Dewar-Phosphinine/Phosphaprismane/ Phosphabenzvalene/Phosphinine**

By *Karsten Blatter, Wolfgang Rösch, Uwe-Josef Vogelbacher, Jürgen Fink,* and *Manfred Regitz**

Of the classical valence isomers of the phosphinines **1**, only the 2-Dewar-phosphinines **2** have been described to date.[1] Starting from these compounds, we have now synthesized the 1-Dewar-phosphinines **3**, the phosphaprismanes **4**, and the phosphabenzvalenes **5** having a $\lambda^3\sigma^3$ phosphorus. The isomers **6**, with two-coordinate phosphorus, still remain unknown.

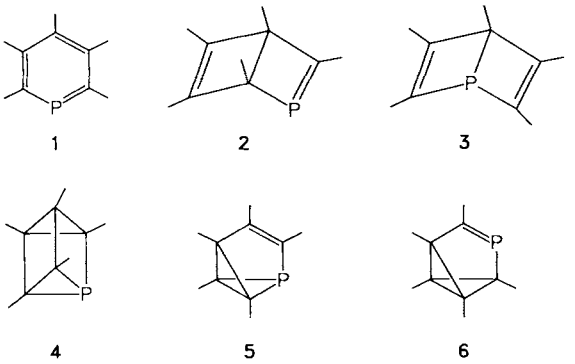

Heating of the 2-Dewar-phosphinine **7** for four days in the absence of solvent at 160 °C and subsequent workup of the crude product by kugelrohr distillation (165 °C/10^{-3} torr) followed by chromatography[2] gave the 1-Dewar-phosphinine **9** (m.p. = 39 °C; colorless crystals; yield 44%). The change in the coordination of the phosphorus upon the isomerization **7** → **9** is accompanied by a strong high-field shift of the ^{31}P resonance (Table 1). Furthermore, in contrast to **7**, the bicyclic compound **9** shows four olefinic carbon atoms in the ^{13}C-NMR spectrum (Table 1).

It is logical to postulate the existence of the phosphinine **8** as the intermediate in the Dewar-phosphinine/Dewar-phosphinine rearrangement **7** → **9**.[3] Indeed, the phosphinine **8** (for preparation from **13** and structure, see below) produced photochemically from **9** ($\lambda \geq 280$ nm, $CDCl_3$) can undergo reverse isomerization under authentic, thermal conditions.

Irradiation of the bicyclic compound **7** for 4 h at −40 °C[4] results in relatively fast intramolecular [2 + 2] cycloaddition to form, as the main product, the phosphaprismane **10** (m.p. = 71 °C; colorless crystals; yield 40%); in addition, the phosphinine **8** and the phosphabenzvalene **14** (each 10%) are formed. The NMR data of **10** confirm its tetracyclic structure (Table 1): no signals are found in

Table 1. ^{1}H- [a], ^{13}C- [b], and ^{31}P-NMR data [c] for the phosphinine **8** and for the valence isomers **9**, **10**, **13**, and **14** as well as the derivative **15**.

8: ^{1}H-NMR: δ = 1.23, 1.26 (2s, 9H, *t*Bu), 1.36, 1.60 (2d, ^4J(P/H) = 1.8 Hz, 9H, *t*Bu), 3.83 (s, 3H, OMe); ^{13}C-NMR: δ = 133.8 (d, ^2J(P/C) = 13.8 Hz, C-3), 150.2 (d, ^3J(P/C) = 11.9 Hz, C-4), 157.0 (d, ^2J(P/C) = 11.7 Hz, C-5), 170.9 (d, ^1J(P/C) = 51.2 Hz, C-2), 173.5 (d, ^1J(P/C) = 55.3 Hz, C-6); ^{31}P-NMR: δ = 188.0, 188.9 (ratio 2 : 1) [d]

9: ^{1}H-NMR: δ = 1.10 (d, ^4J(P/H) = 1.0 Hz, 18H, *t*Bu), 1.15, 1.13 (2d, ^4J(P/H) = 1.5 Hz, 9H, *t*Bu), 3.70 (s, 3H, OMe); ^{13}C-NMR: δ = 47.5 (d, ^1J(P/C) = 47.6 Hz, C-4), 139.2 (d, ^2J(P/C) = 5.0 Hz, C-3), 160.2 (d, ^1J(P/C) = 21.9 Hz, C-6), 162.6 (d, ^2J(P/C) = 15.0 Hz, C-5), 177.1 (d, ^1J(P/C) = 32.6 Hz, C-2); ^{31}P-NMR: δ = −19.0 [e]

10: ^{1}H-NMR: δ = 1.06, 1.11 (2s, 9H, *t*Bu), 1.16 (s, 18H, *t*Bu), 3.66 (s, 3H, OMe); ^{13}C-NMR: δ = 34.6 (s, C-3), 46.0 (s, C-5), 64.8 (d, ^1J(P/C) = 19.5 Hz, C-2), 67.2 (d, ^1J(P/C) = 11.8 Hz, C-6), 68.8 (s, C-4); ^{31}P-NMR: δ = −130.2

13 [f]: ^{1}H-NMR: δ = 1.10, 1.23 (2s, 9H, *t*Bu), 1.33 (d, ^4J(P/H) = 1.2 Hz, 18H, *t*Bu), 3.63 (s, 3H, OMe); ^{13}C-NMR: δ = 71.6 (d, ^2J(P/C) = 6.7 Hz, C-5), 93.4, 94.3 (2d, ^1J(P/C) = 35.4 and 36.5 Hz, C-1/C-6) [g], 142.3 (s, C-4), 157.0 (d, ^1J(P/C) = 41.9 Hz, C-3); ^{31}P-NMR: δ = −89.8

14: ^{1}H-NMR: δ = 1.17 (s, 9H, *t*Bu), 1.19 (d, ^4J(P/H) = 1.1 Hz, 18H, *t*Bu), 1.32 (d, ^4J(P/H) = 1.6 Hz, 9H, *t*Bu), 3.65 (s, 3H, OMe); ^{13}C-NMR: δ = 61.2 (s, C-5), 84.9 (d, ^1J(P/C) = 34.9 Hz, C-1/C-6), 149.3 (d, ^1J(P/C) = 40.3 Hz, C-3), 156.2 (d, ^2J(P/C) = 2.3 Hz, C-4); ^{31}P-NMR: δ = −83.3

15: ^{1}H-NMR: δ = 1.39, 1.44 (2s, 18H, *t*Bu), 3.76 (s, 3H, OMe); ^{13}C-NMR: δ = 65.0 (d, ^1J(P/C) = 60.1 Hz, C-4), 158.2 (d, ^1J(P/C) = 36.2 Hz, C-2/C-6), 165.8 (d, ^2J(P/C) = 15.4 Hz, C-3/C-5); ^{31}P-NMR: δ = 39.3

[a] 90 MHz, $CDCl_3$, TMS (int.). [b] 50.2 MHz, $CDCl_3$, TMS (int.). [c] 80.8 MHz, $CDCl_3$, 85% H_3PO_4 (ext.). [d] Presumably a conformational problem is involved. [e] **7** (for comparison): δ = 314.8. [f] Measurement at −40 °C. [g] The phenomenon may be explained by rotational hinderance of the ester group: this results in loss of the mirror plane in **13**, so that C-1 and C-6 are no longer equivalent.

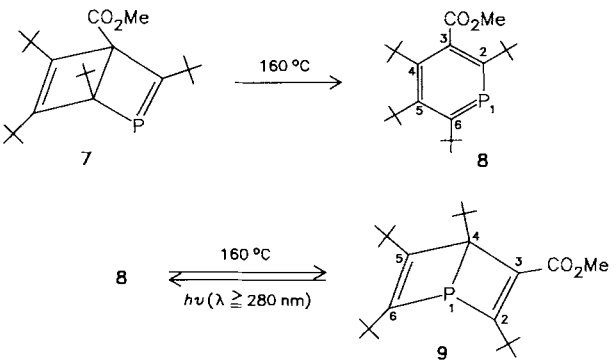

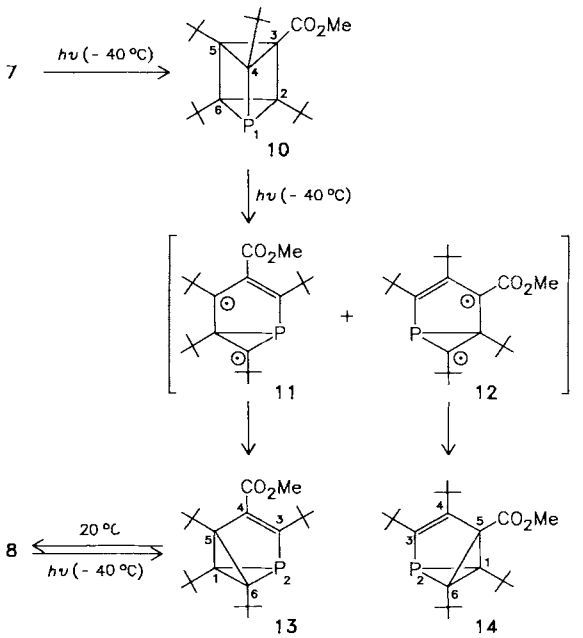

[*] Prof. Dr. M. Regitz, Dipl.-Chem. K. Blatter, Dipl.-Chem. W. Rösch, Dipl.-Chem. U.-J. Vogelbacher, Dr. J. Fink
Fachbereich Chemie der Universität
Erwin-Schrödinger-Strasse, D-6750 Kaiserslautern (FRG)

[**] Phosphorus Compounds with Unusual Coordination, Part 16. This work was supported by the Fonds der Chemischen Industrie and the Deutsche Forschungsgemeinschaft. — Part 15: M. Regitz, W. Rösch, T. Allspach, U. Annen, K. Blatter, J. Fink, M. Hermesdorf, H. Heydt, U. Vogelbacher, O. Wagner, *Phosphorus Sulfur*, in press.

the region of olefinic carbon atoms and the phosphorus resonance exhibits the expected diamagnetic shift ($\delta = -130.2$) relative to **7** ($\delta = 314.8$).

The mixture of products formed under the same conditions upon "prolonged" photolysis (13 h)[4] of **7** demonstrates that the two isomers **8** and **14** are the photochemical secondary products of the phosphaprismane **10**, which is the primary product formed upon irradiation of **7**. Chromatographic separation of the products affords only **8** (m.p. = 71 °C; yellow crystals) and **14** (m.p. = 76 °C; colorless crystals; ratio ≈ 1 : 1). Observation of this reaction by ^{31}P-NMR spectroscopy reveals that, in the photolysis solution maintained at −40 °C, only **14** ($\delta = -83.3$) and apparently another phosphabenzvalene **13** ($\delta = -89.8$) are present, but no **8**. Upon workup (20 °C), the isomer **13** is transformed thermally into the phosphinine **8**. A clear picture of the reaction is afforded by irradiation of **8** at −40 °C,[4] which gives only **13** (^{31}P-NMR); upon thawing of the solution, the heteroaromatic compound **8** is formed once again.

The formation of the phosphabenzvalenes **13** and **14** from **10** can be explained as follows: either the C-2/C-3 and the C-4/C-5 bonds (→ **11**) or the C-5/C-6 and C-4/C-3 bonds (→ **12**) are broken and the diradicals thus formed lead to product formation [**11** → **13** (→ **8**) and **12** → **14**].

The constitution of the phosphabenzvalenes is in accord with their NMR spectra (Table 1). An X-ray crystal structure analysis was carried out for the phosphinine **8**; it reveals a twisted boat form, which is due to steric factors; the atoms C-2 and C-5 correspond to the "stern" and the "bow," respectively. The angles formed with the idealized plane of the base are 17.9° (twisting around the P1/C3 axis) and 33.7° (twisting around the C4/C6 axis). To the best of our knowledge, this is the largest deviation of an aromatic or heteroaromatic ring from planarity observed so far.[5]

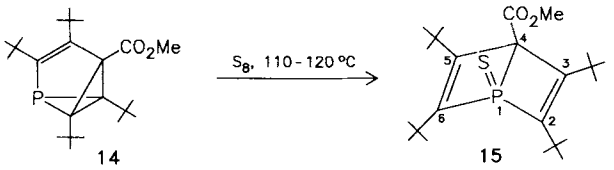

Finally, heating of the phosphabenzvalene **14** with sulfur in the absence of solvent (12 h, 110–120 °C) results in formation of the 1-Dewar-phosphinine sulfide **15** (m.p. = 107 °C, colorless crystals, yield 65%). The ^{1}H- and ^{13}C-NMR spectra reveal the consequences of the resulting C_s symmetry (Table 1). The chemical shift of the phosphorus ($\delta = 39.3$) corresponds to that found for 1-methyl-1-phosphacyclohexane 1-sulfide ($\delta = 33.9$).[6] Furthermore, a crystal structure analysis of **15** is available.[7]

Received: September 15, 1986 [Z 1930 IE]
German version: *Angew. Chem. 99* (1987) 67

[1] J. Fink, W. Rösch, U.-J. Vogelbacher, M. Regitz, *Angew. Chem. 98* (1986) 265; *Angew. Chem. Int. Ed. Engl. 25* (1986) 280.

[2] Büchi MPLC system 681, column: 46 × 2.6 cm, Merck silica gel (15–25 μm), petroleum ether/ether 30 : 1.

[3] Dewar benzene/Dewar-benzene isomerization: G. Maier, K. A. Schneider, *Angew. Chem. 92* (1980) 1056; *Angew. Chem. Int. Ed. Engl. 19* (1980) 1022; H. Wingert, M. Regitz, *Chem. Ber. 110* (1986) 244; Dewar-pyridine/Dewar-pyridine isomerization: J. Fink, M. Regitz, *Bull. Soc. Chim. Fr. 1986*, 239.

[4] Philips HPK 125-W high-pressure mercury lamp, Pyrex filter, $CDCl_3$.

[5] The sterically bulky substituents of **8** result in C-C-C and P-C-C interior angles (116.8–124° and 118.4–119.8°, respectively) that deviate from the normal values, as well as a small increase in the bond lengths of the six-membered ring (P-C distances: 1.730 and 1.758 Å; C-C distances: 1.402–1.437 Å). For further details, see G. Maas, J. Fink, H. Wingert, K. Blatter, M. Regitz, *Chem. Ber. 120* (1987), in press.

[6] L. D. Quinn: *The Heterocyclic Chemistry of Phosphorus*, Wiley, New York 1981, p. 204.

[7] The bond lengths and angles of **5** are in the usual range and exhibit no unusual features. The two phosphacyclobutene structural units P1,C2,C3,C4 and P1,C4,C5,C6 are planar within five and three standard deviations, respectively; the puckering angle is 117.1°. J. Fink, M. Regitz, unpublished results, Universität Kaiserslautern 1986.

New $AuPt_2$ A-Frame Cluster Complexes**

By *Gilles J. Arsenault, Ljubica Manojlović-Muir,* Kenneth W. Muir, Richard J. Puddephatt,** and *Ilse Treurnicht*

The chemistry of the metal-metal bond in diplatinum(I) complexes such as **1** and in analogous gold(II) complexes has been developed rapidly, and many fundamental reaction pathways of binuclear complexes have been found.[1,2] Although many unsaturated and electrophilic reagents add to the metal-metal bond of **1**, no direct additions of electrophilic metal fragments to form cluster complexes have been found.[3] For example, whereas "CH_2," from CH_2N_2, adds to the metal-metal bond of **1**, the isolobal $SnCl_2$ inserts into a Pt-Cl bond instead.[4,5] We report here that electrophilic gold fragments, AuX or $AuPPh_3^{\oplus}$, add to the Pt-Pt bond of **1** whereas similar copper or silver fragments do not.

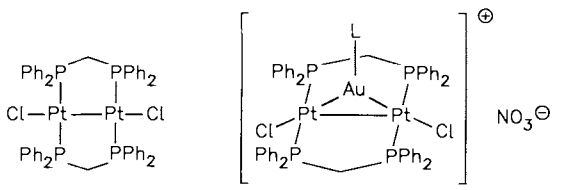

1

2a, L = PPh_3
2b, L = $Ph_2PCH_2PPh_2AuCl$
2c, L = $Ph_2P(CH_2)_2PPh_2AuCl$

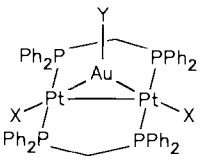

3a, X = Y = Cl
3b, X = Y = C≡C*t*Bu
3c, X = C≡C*t*Bu, Y = Cl
3d, X = C≡C*t*Bu, Y = I

Reaction of **1** with $[Au(NO_3)(PPh_3)]$ or $[AuCl(SMe_2)]$ gave the cationic **2a** or neutral **3a**, respectively, in nearly quantitative yields. They have NMR spectra typical of A-frame complexes.[4,6] The complex **3b**,[6] prepared by reaction of $[Pt_2(\mu\text{-dppm})_3]$[7] (dppm = $Ph_2PCH_2PPh_2$) with

[*] Dr. Lj. Manojlović-Muir, Dr. K. W. Muir
Department of Chemistry, University of Glasgow
Glasgow G12 8QQ, Scotland (U. K.)
Dr. R. J. Puddephatt, Dr. G. J. Arsenault, Dr. I. Treurnicht
Department of Chemistry, University of Western Ontario
London N6A 5B7 (Canada)

[**] This work was supported by N.S.E.R.C. (Canada) and S.E.R.C. (U.K.).

$AuC{\equiv}CtBu$,[8] reacted with CH_2Cl_2 to give **3c**. Complex **3c** reacted with NaI to give **3d**,[6] whose structure was determined crystallographically (Fig. 1).[9]

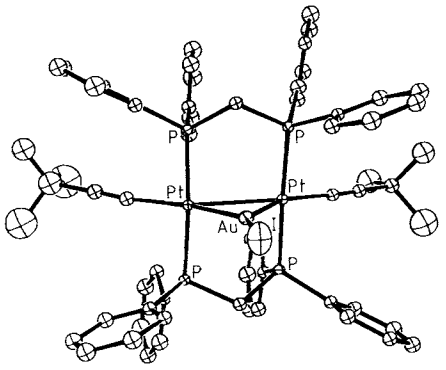

Fig. 1. The molecular structure of **3d**, with carbon atoms not labeled and the atomic thermal ellipsoids displaying 20% probability. Selected bond lengths [Å] and angles [°] are: Au-I 2.580(2), Pt-P 2.274(5)–2.289(6), Pt-C 2.01(3), 2.02(3); Pt-Au-Pt 64.5(1), Au-Pt-C 151.0(7), 151.7(6), Pt-C-C 172(2), 177(2). Further details of the crystal structure investigation are available on request from the Director of the Cambridge Crystallographic Data Centre, University Chemical Laboratory, Lensfield Road, Cambridge CB2 1EW (U.K.), upon quoting the names of the authors and the journal citation.

In contrast to the ease of formation of Pt_2Au clusters as described above, it has not yet been possible to prepare derivatives of silver or copper. Thus, reaction of **1** with $[M(NO_3)(PPh_3)]$, M = Cu or Ag, gave **4** and MCl (replacement of $Cl^{\ominus}$ by PPh_3). Similarly, reaction of **1** with one or two equivalents of $[Cu(MeCN)_4]^{\oplus}$ gave **5a** or **5b**, respectively, and CuCl. Reaction of **1** with excess CuCl gave a 1 : 1 adduct; however, it was not an A-frame complex but was tentatively assigned the unusual structure **6**, involving the addition of CuCl to a chloride ligand of **1**. Complex **6** was fluxional in solution, and solutions slowly deposited CuCl. A useful citerion of structure of **6** was the low-tem-

$[Pt_2Cl(PPh_3)(\mu\text{-dppm})_2](NO_3)$ **4**
$[Pt_2Cl(MeCN)(\mu\text{-dppm})_2]^{\oplus}$ **5a**
$[Pt_2(MeCN)_2(\mu\text{-dppm})_2]^{2\oplus}$ **5b**

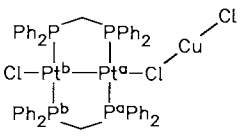

6

perature ^{195}Pt-NMR spectrum,[6] which gave two signals due to nonequivalent Pt atoms, and the coupling constant ^1J(PtPt) (10334 Hz), which was greater than in the parent **1** (8145 Hz[10]); the A-frame clusters have lower ^1J(PtPt) values: 6980 ± 50 Hz and 6200 ± 100 Hz for complexes **2a** and **3a**, respectively.

Some digold reagents gave behavior of both gold and copper/silver reagents. Thus reaction of **7**, n = 1 or 2, with two equivalents of **1** gave **2b** or **2c** respectively, and $[Pt_2Cl(NO_3)(\mu\text{-dppm})_2]$. The first gold atom adds to the Pt–Pt bond of **1**, while the second gold abstracts chloride from the second molecule of **1**. We believe that steric hindrance prevents the expected formation of bridged bis(A-frame) complexes in these cases.

$[(NO_3)Au(\mu\text{-}Ph_2P(CH_2)_nPPh_2)Au(NO_3)]$ **7**

The structure of **3d** (Fig. 1) shows that the AuI fragment symmetrically bridges the Pt_2 unit to form a triangular Pt_2Au cluster. The PtAu [2.656(2) and 2.661(2) Å] and PtPt [2.837(1) Å] separations are all indicative of bonding interactions. The clusters **2** and **3** are therefore considered to contain a 3-center-2-electron Pt_2Au group, in which the platinum and gold atoms have 16e and 14e configurations, respectively. These complexes are the first examples of 42e Pt_2Au clusters. The only other known trinuclear Pt–Au cluster is the 40e cluster complex **8**.[11]

$[PtCl(PEt_3)_2(AuPPh_3)_2]^{\oplus}$ **8**

Within the coinage metals, it is clear that gold has by far the greatest ability to form heteronuclear PtM (M = Cu, Ag, Au) bonds.

Received: September 1, 1986;
revised: October 13, 1986 [Z 1913 IE]
German version: *Angew. Chem. 99* (1987) 79

[1] R. J. Puddephatt, *Chem. Soc. Rev. 1982*, 99, and references cited therein.
[2] a) H. Schmidbaur, C. Hartmann, *Angew. Chem. 98* (1986) 573; *Angew. Chem. Int. Ed. Engl. 25* (1986) 575; b) H. Schmidbaur, T. Pollok, R. Herr, F. E. Wagner, R. Bau, J. Riede, G. Müller, *Organometallics 5* (1986) 566; c) H. H. Murray, J. P. Fackler, Jr., A. M. Mazany, *ibid. 3* (1984) 1310; d) S. L. Schiavo, G. Bruno, P. Piraino, F. Faraone, *ibid. 5* (1986) 566; e) W. A. Herrmann, W. Kalcher, *Chem. Ber. 118* (1985) 3861; f) R. Uson, A. Laguna, *Coord. Chem. Rev. 70* (1986) 1.
[3] Y. Yamamoto, K. Takahashi, H. Yamazaki, *J. Am. Chem. Soc. 108* (1986) 2458.
[4] K. A. Azam, A. A. Frew, B. R. Lloyd, Lj. Manojlović-Muir, K. W. Muir, R. J. Puddephatt, *Organometallics 4* (1985) 1400.
[5] M. C. Grossel, R. P. Moulding, K. R. Seddon, *Inorg. Chim. Acta 64* (1975) L275.
[6] **2a**: yellow needles, m.p. = 182–220°C (dec.); NMR spectra in CD_2Cl_2: ^{1}H: δ = 3.56 [m, 2H, $^2J(H^aH^b)$ = 14, ^2J(PH) = 5, ^3J(PtH) = 20 Hz; 2 × CH^aH^b], 5.02 [m, 2H, $^2J(H^aH^b)$ = 14, ^3J(PtH) = 112 Hz; 2 × CH^aH^b]; ^{31}P: δ = 8.3 [^1J(PtP) = 2400, ^3J(PtP) = −100, ^2J(PP) = 62, ^4J(PP) = 26 Hz; P of dppm], 36.5 [^2J(PtP) = 600 Hz; PPh_3]. **3a**: red platelets, m.p. = 235–245°C; NMR spectra in CD_2Cl_2: ^{1}H: δ = 4.10 [m, 2H, $^2J(H^aH^b)$ = 14, ^2J(PH) = 5, ^3J(PtH) = 20 Hz; 2 × CH^aH^b], 4.69 [m, 2H, $^2J(H^aH^b)$ = 14, ^2J(PH) = 2, ^3J(PtH) = 112 Hz; 2 × CH^aH^b]; ^{31}P: δ = 9.1 [^1J(PtP) = 2410, ^3J(PtP) = −78, ^2J(PP) = 59, ^4J(PP) = 25 Hz; P of dppm]. **3b**: NMR spectra in C_6D_6: ^{1}H: δ = 0.89 [s, 18H; 2 × tBuCCPt], 1.69 [s, 9H; tBuCCAu], 4.93 [m, 2H, $^2J(H^aH^b)$ = 13, ^2J(PH) = 5 Hz; 2 × CH^aH^b], 5.26 [m, 2H, $^2J(H^aH^b)$ = 13, ^2J(PH) = 2, ^3J(PtH) = 97 Hz; 2 × CH^aH^b]; ^{31}P: δ = 8.71 [^1J(PtP) = 2556, ^3J(PtP) = −45, ^2J(PP) = 69, ^4J(PP) = 25 Hz; P of dppm]. **3d**: NMR spectra in CD_2Cl_2: ^{1}H: δ = 0.58 [s, 18H; 2 × tBuCCPt], 4.62 [m, 2H, $^2J(H^aH^b)$ = 13, ^2J(PH) = 6 Hz; 2 × CH^aH^b], 5.48 [m, 2H, $^2J(H^aH^b)$ = 13, ^2J(PH) = 2, ^3J(PtH) = 90 Hz; 2 × CH^aH^b]; ^{31}P: δ = 8.90 [^1J(PtP) = 2509, ^3J(PtP) = −18, ^2J(PP) = 64, ^4J(PP) = 25 Hz; P of dppm]. **6**: orange prisms, m.p. = 195–240°C (dec.); NMR spectra in CD_2Cl_2 at −70°C: ^{31}P: δ = 11.9 [m, ^1J(PtP) = 2860; P^a], −4.3 [m, ^1J(PtP) = 2760; P^b]; ^{195}Pt ($K_2[PtCl_4]$ as standard): δ = 652.9 [m, ^1J(PtP) = 2270, ^2J(PtP) = 105, ^1J(PtP) = 10334 Hz; Pt^a], 314.5 [m, ^1J(PtP) = 2860, ^2J(PtP) = 153, ^1J(PtPt) = 10334 Hz; Pt^b]. Good analytical data have been obtained for all new complexes (**2**, **3**, and **6**).
[7] M. C. Grossel, M. P. Brown, C. D. Nelson, A. Yavari, E. Kallas, R. P. Moulding, K. R. Seddon, *J. Organomet. Chem. 232* (1982) C13.
[8] G. E. Coates, C. Parkin, *J. Chem. Soc. 1962*, 3220.
[9] Orthorhombic, space group $Pna2_1$ (No. 33), a = 29.053(4), b = 16.131(3), c = 13.956(3) Å, V = 6540.5 Å^3, Z = 4, ρ_{calcd} = 1.671 g cm^{-3}; $F(000)$ = 3128, $Mo_{K\alpha}$, λ = 0.71069 Å, $\mu(Mo_{K\alpha})$ = 71.4 cm^{-1}. Intensity data were measured at room temperature on an Enraf-Nonius CAD4 diffractometer. The structural model included dppm hydrogen atoms in calculated positions (d(CH) = 1.0 Å); the phenyl rings were constrained to $6/mmm$ symmetry with d(CC) = 1.38 Å. Only Au, Pt, P, and I atoms were assigned anisotropic thermal parameters. The least-squares refinement gave R = 0.040 and R_w = 0.050 for 4442 unique, absorption-corrected reflections with $I \geq 3\sigma(I)$.
[10] M. C. Grossel, J. R. Batson, R. P. Moulding, K. R. Seddon, *J. Organomet. Chem. 304* (1986) 391.
[11] P. Braunstein, H. Lehner, D. Matt, A. Tiripicchio, M. Tiripicchio-Camellini, *Angew. Chem. 96* (1984) 307; *Angew. Chem. Int. Ed. Engl. 23* (1984) 304.

 © VCH Verlagsgesellschaft mbH, D-6940 Weinheim, 1987 0570-0833/87/0101-0087 $ 02.50/0

Mixed-Metal Cluster Formation by Carbonylmetalate-Induced Pt–P Bond Cleavage in $[PtCl_2(Ph_2PCH_2PPh_2]$**

By *Pierre Braunstein,* Nicolas Guarino, Claude de Méric de Bellefon,* and *Jean-Luc Richert*

The synthesis and structural characterization of the first mixed-metal clusters containing the $Ph_2PCH_2PPh_2$ (dppm) ligand [Eq. (a)][1] showed that the mobility of this ligand, i.e., the lability of the Pd–P bond, is greater than expected from previous studies carried out on $Pd(\mu\text{-dppm})_2Pd$ systems.[2] In the case of $Pd(\mu\text{-dppm})_2Pt$ systems, we found that regioselective insertion of the metal carbonyl fragment takes place into the Pd–P bond,[3] although evidence for Pt–P lability could also be found in the isomerization of **1**.[4] The $Pd(\mu\text{-dppm})_2Pt$ system is usually rigid,[5] with only few exceptions.[6]

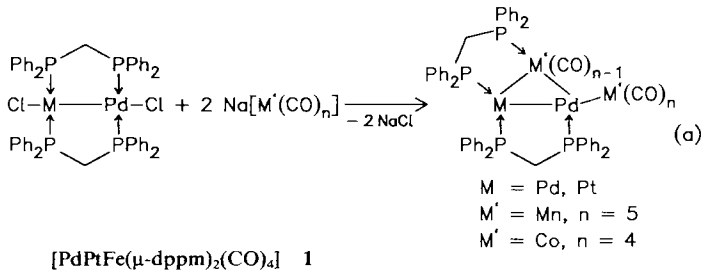

(a)

[PdPtFe(μ-dppm)$_2$(CO)$_4$] **1**
trans-[Pt{Mn(CO)$_5$}$_2$(CO)$_2$] **2**
[PtCl$_2$(Ph$_2$PCH$_2$PPh$_2$)] **3**

We thought that reaction (a) could perhaps be extended to simple mononuclear complexes, such as **3**, containing a chelating dppm whose opening could result in new dppm-bridged mixed-metal clusters (Scheme 1). The features that all reactions of Scheme 1 have in common are the formation of one or more Pt–M bonds and the retention of at least one Pt–P bond. The differences observed in either the nature or the reactivity of the new complexes depend on the nature of the carbonylmetalate anion.

The complex **4** results from the replacement of only one chloride ligand in **3** by $[Mn(CO)_5]^{\ominus}$ (reaction 1) and represents a rare example of a heterobimetallic complex containing a chelating dppm ligand.[7] **4** reacts further with a second equivalent of $[Mn(CO)_5]^{\ominus}$, affording the trinuclear complex **5**. This suggests that **4** could be an intermediate in the direct synthesis of **5** from **3** (reaction 2). The crystal structure of the linear trinuclear complex **2**, which is related to **5**, has been previously determined.[8]

Reaction of **3** with two equivalents of $[Co(CO)_4]^{\ominus}$ (reaction 3) or of $[M(CO)_3Cp]^{\ominus}$ (M = Mo, W; Cp = η^5-C_5H_5) (reaction 4) results in formation of the heterotrinuclear clusters **6** or of **7** (M = Mo) and **8** (M = W), respectively. In these cases, no intermediate species corresponding to **4** could be detected when only one equivalent of these anions was used: the clusters **6**, **7**, and **8** were the only products isolated, along with 50% of the starting material **3**. Clusters **7** and **8** reversibly add CO under ambient conditions with selective opening of the M–M bond, affording **9** and **10**, respectively (reactions 5, 6). The more strongly Mn-bound

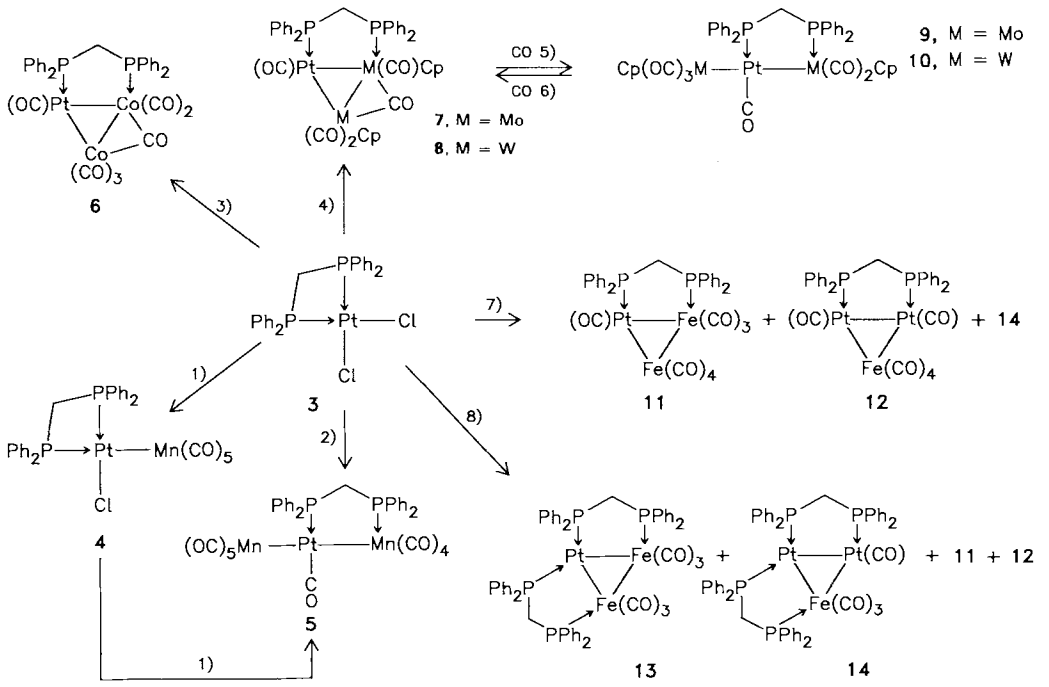

Scheme 1. 1) 1 equivalent Na[Mn(CO)$_5$], tetrahydrofuran (THF), 20°C, 3 h. 2) 2 equivalents Na[Mn(CO)$_5$], THF, 20°C, 3 h. 3) 2 equivalents Na[Co(CO)$_4$], THF, in 1 h from 0 to 20°C, then 3 h at 40°C. 4) 2 equivalents Na[M(CO)$_3$Cp]·2DME (dimethoxyethane), THF, 50°C, 4 h. 5) 1 atm CO, THF, 0.1 h. 6) Dry at 20°C in vacuum. 7) 10 equivalents [Fe$_2$(CO)$_9$], THF, 20°C, 12 h. 8) 1 equivalent Na$_2$[Fe$_2$(CO)$_8$], THF, 0–20°C, 5 h.

carbonyls do not allow a reversible CO elimination to occur with **5**. The transoid M–Pt–M arrangement in **5**, **9**, and **10** is suggested by the ^1J(PtP) values (not consistent with a phosphorus *trans* to a M–Pt bond[7d]) and by steric considerations.

The selectivity of formation of the iron–platinum clusters was found to depend on the iron carbonyl reagent.

[*] Dr. P. Braunstein, N. Guarino, Dr. C. de Méric de Bellefon, J. L. Richert
Laboratoire de Chimie de Coordination, UA 416 CNRS,
Université Louis Pasteur
4 rue Blaise Pascal, F-67070 Strasbourg Cédex (France)

[**] We thank Atochem for a grant to *J.-L. R.*, the CNRS for financial support (ATP Chimie Fine 4384), and Johnson-Matthey Co. Ltd. for a generous loan of $PtCl_2$.

Thus, with $[Fe_2(CO)_9]$ (reaction 7), a known dehalogenating reagent, the new clusters **11** and **12** and the known **14**[6c] were formed and could be separated by column chromatography. With $Na_2[Fe_2(CO)_8]$ (reaction 8), the new cluster **13** was isolated, together with the clusters **11**, **12**, and **14** (30% yield). The complex redox reactions encountered particularly in the Pt–Fe systems involve ligand migrations that occur under very mild conditions. Thus, CO migration from M to Pt occurs during the synthesis of **5**–**8**, **11**, and **12**, while one of the phosphorus atoms of the chelated dppm becomes attached to M or to a second Pt atom in **5**–**8** and **11**–**14**. In the case of **13**, moreover, complete transfer of a dppm ligand has occurred since this cluster contains two dppm ligands but only one Pt atom.

These types of mixed-metal clusters are of particular interest because of the dppm-assisted metal–metal bond formation and the recent use of the palladium analogue of **14** as a precursor for a heterogeneous carbonylation catalyst which selectively transforms *o*-nitrophenol into benzoxazol-2-one.[4] The reactions reported here involve the opening of a P–M bond of a chelating dppm ligand, which is also observed with other reagents.[6, 7c, 9] The products **5**–**14** contain at least one Pt(μ-dppm)M five-membered ring, which is more stable than the Pt(η^2-dppm) four-membered ring in **3** and **4**. The general applicability of this method, which employs readily available precursors, is being further evaluated.

Experimental Procedure and Spectroscopic Data

All new compounds isolated gave satisfactory elemental analyses. The ^{1}H-, ^{31}P{^{1}H}-, and ^{195}Pt{^{1}H}-NMR spectra were recorded on an FT-Bruker WP 200 SY spectrometer at 200.13, 81.02, and 42.95 MHz, respectively. TMS, 85% H_3PO_4 in H_2O, and 0.3 M $K_2[PtCl_4]$ in D_2O were used as standards.

4: 65% yield after recrystallization from THF/hexane at 20°C.—IR (THF): $\tilde{\nu}$(CO) [cm^{-1}] = 2056 (vs), 1976 (s, br), 1954 (vs, br), 1933 (vs, br).—^{31}P{^{1}H} (THF/C_6D_6): $\delta = -36.2$ (d with Pt satellites, ^2J(PP) = 60, ^1J(PtP) = 2241 Hz, 1 P; P *trans* to Mn), −47.4 (d with Pt satellites, ^2J(PP) = 60, ^1J(PtP) = 3364 Hz, 1 P; P *trans* to Cl).

5 (from reaction 2): 90% yield after recrystallization from THF/hexane at −30°C.—IR (THF): $\tilde{\nu}$(CO) [cm^{-1}] = 2073 (m), 2022 (s), 1996 (m), 1966 (s, br), 1923 (m, br).—^{1}H ($CDCl_3$): $\delta = 4.28$ (t with Pt satellites, ^2J(PH) = 10.3, ^3J(PtH) = 50.8 Hz, 2 H; CH_2).—^{31}P{^{1}H} (THF/C_6D_6): $\delta = 57.5$ quadrupole-broadened signal, not resolved, 1 P; MnP), 19.3 (d with Pt satellites, J(PP) = 79, ^1J(PtP) = 3515 Hz, 1 P; PtP).

6: 81% yield after recrystallization from THF/pentane at −30°C.—IR (THF): $\tilde{\nu}$(CO) [cm^{-1}] = 2052 (vs), 2017 (vs), 1995 (s, br), 1988 (s, br), 1757 (m, br).—^{1}H ($CDCl_3$): $\delta = 4.63$ (t with Pt satellites, J(PH) = 10.7, ^3J(PtH) = 48.0 Hz, 2 H; CH_2).—^{31}P{^{1}H} ($CDCl_3$): $\delta = 22.2$ (quadrupole-broadened signal, not resolved, 1 P; CoP), −1.5 (d with Pt satellites, ^2J(PP) = 26, ^1J(PtP) = 3295 Hz, 1 P; PtP).—^{195}Pt{^{1}H} ($CDCl_3$): $\delta = -2502$ (dd, ^1J(PtP) = 3294, ^2J(PtP) = 47 Hz).

7: 71% yield after recrystallization at −30°C.—IR (THF): $\tilde{\nu}$(CO) [cm^{-1}] = 1921 (s), 1901 (vs), 1849 (s), 1778 (s).—^{1}H ($CDCl_3$): $\delta = 5.32$ (s, 5 H; Cp), 5.24 (s, 5 H; Cp), 4.13 (t with Pt satellites, ^2J(PH) = 9.5, ^3J(PtH) = 55 Hz, 2 H; CH_2).—^{31}P{^{1}H} ($CDCl_3$): $\delta = 46.3$ (d with Pt satellites, J(PP) = 45, ^2J(PtP) = 118 Hz, 1 P; MoP), 27.3 (d with Pt satellites, J(PP) = 45, ^1J(PtP) = 4062 Hz, 1 P; PtP).

8: 47% yield after extraction with CH_2Cl_2/hexane = 1/1 and recrystallization from THF/Et_2O at −30°C.—IR (THF): $\tilde{\nu}$(CO) [cm^{-1}] = 1918 (s), 1895 (vs), 1838 (s), 1776 (s).—^{1}H ($CDCl_3$): $\delta = 5.41$ (s, 5 H; Cp), 5.27 (s, 5 H, Cp).—^{31}P{^{1}H} ($CDCl_3$): $\delta = 15.3$ (d with W and Pt satellites, J(PP) = 53, ^1J(WP) = 327, ^2J(PtP) = 114 Hz, 1 P; WP), 21.6 (d with Pt satellites, J(PP) = 53, ^1J(PtP) = 3936 Hz, 1 P; PtP).

9 and **10**: Characterized in solution only; spectroscopic yield 100%.—**9**: IR (THF): $\tilde{\nu}$(CO) [cm^{-1}] = 1935 (s), 1899 (vs), 1832 (s).—^{31}P{^{1}H} ($C_6D_5CD_3$): $\delta = 42.8$ (d with Pt satellites, J(PP) = 71, ^2J(PtP) = 213 Hz, 1 P; MoP), 6.6 (d with Pt satellites, J(PP) = 71, ^1J(PtP) = 3445 Hz, 1 P; PtP).—**10**: IR (THF): $\tilde{\nu}$(CO) [cm^{-1}] = 1932 (s), 1900 (vs), 1822 (s).

11 (from reaction 7): 65% yield after purification by column chromatography (silica gel, CH_2Cl_2/hexane = 35/100 v/v).—IR (THF): $\tilde{\nu}$(CO) [cm^{-1}] = 2054 (s), 2019 (s), 1979 (s, br), 1960 (s, br), 1930 (w, sh), 1908 (w).—^{1}H (C_3D_6O): $\delta = 5.12$ (dd with Pt satellites, $^2J(P_PH) = 12.0$, $^2J(P_{Fe}H) = 10.6$, J(PtH) = 45.1 Hz, 2 H; CH_2).—^{31}P{^{1}H} (THF/C_6D_6): $\delta = 53.9$ (d with Pt satellites, J(PP) = 49, ^2J(PtP) = 12 Hz, 1 P; FeP), 14.7 (d with Pt satellites, J(PP) = 49, ^1J(PtP) = 3151 Hz, 1 P; PtP).—MS (CI): m/z 915 ($M^{\oplus}$), successive loss of eight CO molecules. This cluster was also characterized by X-ray analysis: P. Braunstein et al., unpublished results.

12 (from reaction 8): 19% yield after purification by column chromatography (silica gel, CH_2Cl_2/hexane = 70/100 v/v).—IR (THF): $\tilde{\nu}$(CO) [cm^{-1}] = 2047 (s), 2018 (s), 1994 (s), 1942 (s), 1909 (s).—^{1}H (C_3D_6O): $\delta = 6.14$ (t with Pt satellites, ^2J(PH) = 11.5, ^3J(PtH) = 68.0 Hz, 2 H; CH_2).—^{31}P{^{1}H} (THF/C_6D_6): $\delta = -2.4$ (s with Pt satellites, ^1J(PtP) = 3187, ^2J(PtP) = −74, ^1J(PtPt) = 1373, J(PP) = 30 Hz; the parameters were determined using the spin simulation program PANIC (Bruker).—MS (CI): m/z 998 ($M^{\oplus}$), successive loss of six CO molecules. This cluster was also characterized by X-ray analysis: P. Braunstein et al., unpublished results.

13 (from reaction 8): 1% yield after purification by column chromatography (silica gel, CH_2Cl_2/hexane = 70/100 v/v).—IR (THF): $\tilde{\nu}$(CO) [cm^{-1}] = 1991 (s, br), 1941 (s, br), 1928 (s, br), 1858 (w, br).—^{1}H (C_3D_6O): $\delta = 4.28$ (t with Pt satellites, ^2J(PH) = 9.7, ^3J(PtH) = 37.8 Hz, 2 H; CH_2).—^{31}P{^{1}H} (THF/C_6D_6): $\delta = 56.6$ (m, 2 P; FeP), 21.7 (m with Pt satellites, ^1J(PtP) = 3250 Hz, 2 P; PtP).—MS (FD): m/z 1215 ($M^{\oplus} - CO$), 1075 ($M^{\oplus} - 6CO$).

Received: August 8, 1986;
supplemented: October 6, 1986 [Z 1897 IE]
German version: *Angew. Chem. 99* (1987) 77

[1] a) P. Braunstein, J.-M. Jud, Y. Dusausoy, J. Fischer, *Organometallics 2* (1983) 180; b) P. Braunstein, J.-M. Jud, J. Fischer, *J. Chem. Soc. Chem. Commun. 1983*, 5.
[2] A. L. Balch, *Adv. Chem. Ser. 196* (1982) 243.
[3] P. Braunstein, C. de Méric de Bellefon, M. Ries, *J. Organomet. Chem. 262* (1984) C 14.
[4] P. Braunstein, J. Kervennal, J.-L. Richert, *Angew. Chem. 97* (1985) 762; *Angew. Chem. Int. Ed. Engl. 24* (1985) 768.
[5] R. J. Puddephatt, *Chem. Soc. Rev. 12* (1983) 99.
[6] a) R. J. Puddephatt, K. A. Azam, R. H. Hill, M. P. Brown, C. D. Nelson, R. P. Moulding, K. R. Seddon, M. C. Grossel, *J. Am. Chem. Soc. 105* (1983) 5642; b) R. J. Blau, J. H. Espenson, *Inorg. Chem. 25* (1986) 878; c) M. C. Grossel, R. P. Moulding, K. R. Seddon, *J. Organomet. Chem. 253* (1983) C 50.
[7] a) G. Smith, D. J. Cole-Hamilton, A. C. Gregory, N. G. Gooden, *Polyhedron 1* (1982) 97; b) K. A. Mead, I. Moore, F. G. A. Stone, P. Woodward, *J. Chem. Soc. Dalton Trans. 1983*, 2083; c) M. R. Awang, J. C. Jeffery, F. G. A. Stone, *ibid. 1983*, 2091; d) P. Braunstein, C. de Méric de Bellefon, M. Lanfranchi, A. Tiripicchio, *Organometallics 3* (1984) 1772; e) B. Delavaux, B. Chaudret, F. Dahan, R. Poilblanc, *ibid. 4* (1985) 935.
[8] O. Bars, P. Braunstein, J.-M. Jud, *Nouv. J. Chim. 8* (1984) 771.
[9] See, e.g., a) M. M. Olmstead, C.-L. Lee, A. L. Balch, *Inorg. Chem. 21* (1982) 2712; b) C. R. Langrick, D. M. McEwan, P. G. Pringle, B. L. Shaw, *J. Chem. Soc. Dalton Trans. 1983*, 2487; c) C. R. Langrick, P. G. Pringle, B. L. Shaw, *ibid. 1984*, 1233; d) B. R. Lloyd, R. J. Puddephatt, *Inorg. Chim. Acta 90* (1984) L-77; e) S. W. Carr, B. L. Shaw, M. Thornton-Pett, *J. Chem. Soc. Dalton Trans. 1985*, 2131; f) S. Sabo, B. Chaudret, D. Gervais, *J. Organomet. Chem. 292* (1985) 411; g) M. C. Grossel, J. R. Batson, R. P. Moulding, K. R. Seddon, *J. Organomet. Chem. 304* (1986) 391, and references cited therein; h) B. Delavaux, B. Chaudret, J. Devillers, F. Dahan, G. Commenges, R. Poilblanc, *J. Am. Chem. Soc. 108* (1986) 3703.

The Poisonous Cloud, Chemical Warfare in the First World War. By *L. F. Haber*. Clarendon Press, Oxford 1986. xiv, 415 pp., hardcover, £ 35.00.—ISBN 0-19-858142-4

The cloud of poisonous gas that settled over the British and French trenches at Ypres on 23 April 1915 was considered by some people to mark a turning point in the technological conduct of war and by most people as an act of barbarism and a violation of the Hague Convention. *Fritz Haber* (1886–1934), the German chemist and Nobel laureate (for the "synthesis of ammonia from air"), is generally regarded, and probably rightfully so, as the inventor of gas warfare. Since then, an immense amount of writing has been devoted to this topic from a variety of standpoints: neutral and purely technological, nationalistic and glorifying, humanistic and condemnatory, hateful and damning. The most recent work is a monograph by *L. F. Haber*.

Who is *L. F. Haber*? He is the son of *Fritz Haber*, Reader in Economics at the University of Surrey, and a prominent scholar of the history of industrial chemistry. We do not wish to ask why *L. F. Haber* has written this book. Beyond doubt, however, he has presented us with a superb, exceedingly objective work, based in part on new sources of information.

After a personal and historical introduction, the events surrounding the first chlorine gas attack at Ypres are described. In the following chapters, the author shows how reaction and counterreaction led to an escalation of chemical warfare on both sides and how chemical warfare underwent technological development without, however, becoming a decisive factor in the First World War. The threat posed by this new weapon was greatly overestimated by both sides, in part because of the ignorance of the general public and the helplessness of the military in coming to terms with technological and scientific matters. The sources of information are excellently documented. Both the author's personal knowledge of the subject matter and the collaboration of *Fritz Haber*'s English counterpart, the chemist Sir *Harold Hartley*, proved very useful in this respect. The two scientists met in 1921 after *Fritz Haber* had been awarded the Nobel prize and subsequently developed a relationship verging on friendship. With *Hartley*'s support, *Fritz Haber* was offered a laboratory at the Chemical Institute in Cambridge after he was forced to leave Germany in 1933. *L. F. Haber* presumably met *Hartley* through his father.

A few words need to be said about the "prostitution of science" for the purpose of gas warfare. It is nearly impossible for us, in 1987, to morally judge the way researchers thought and acted in 1914. In any case, the prostitution did not involve money. We Germans today, morally drained by the period of National Socialist rule and grown lazy by current prosperity, are hardly capable of imagining what national spirit and patriotism meant at that time. It is even harder for a younger generation in Germany to grasp that Jewish Germans were then involved in military research for their beloved mother country. In this connection, the biography of the mathematician *Richard Courant* (1888–1972), who worked in Göttingen and was also forced to leave Germany in 1933, is of particular interest (Constance Reid: *Richard Courant - Der Mathematiker als Zeitgenosse*, Springer, Heidelberg 1979). During the First World War, *Courant* invented the "ground telegraph," which was clearly a less inhuman discovery, if war inventions can be measured at all in such terms. In *Haber*'s book, we encounter such names as *Herbert B. Baker, J. B. Conant, Karl Duisberg, James Franck, Herbert Freundlich, Fritz Haber, Otto Hahn, Sir Harold Hartley, Walter Nernst*, Sir *William Pope*, and *J. F. Thorpe*, and even the famous correspondence between *Fritz Haber* and *Hermann Staudinger* is mentioned. "Staudinger replied placatingly, and his dignified pacifism contrasts sharply with *Haber*'s intemperate self-justification. The correspondence ended inconclusively but it showed that the Chemical Warfare controversy cut across professional lines." Such personal remarks, however, occur only seldomly in the book. Overall, the book presents an exact technological and historical account of gas warfare in 1914–1918.

Little mention is made of why chemical warfare did not take place during the Second World War. And completely unaddressed is the issue of the nerve gases stored at present in the arsenals of the superpowers, the effect of which would be to kill people like flies are killed with insect spray: shaking, vomiting, foaming at the mouth, while fully conscious—this is the vision of "Chemical Warfare" in the second half of the 20th century. Let us hope that the poisonous cloud remains history.

Friedrich Cramer [NB 816 IE]
Max-Planck-Institut für experimentelle Medizin,
Göttingen (FRG)

Frontiers in Bioinorganic Chemistry. By *A. V. Xavier*. VCH Verlagsgesellschaft, Weinheim 1986. xiii, 736 pp., bound, DM 185.00.—ISBN 3-527-26460-4

This book contains the texts of the papers presented by the invited speakers at the 2nd International Conference on Bioinorganic Chemistry, held in Portugal in April 1985. The 69 papers are contained in 12 chapters, with more than 700 pages. Owing to the interdisciplinary nature of bioinorganic chemistry, there is some degree of unavoidable overlapping between the papers, e.g. when iron–sulfur proteins are discussed from the standpoint of the kineticist or that of the spectroscopist.

Iron is the dominant transition metal in the living world, and for that reason it is not surprising that the lion's share of the contributions (more than a third) are concerned either directly or indirectly with that element. In addition to the permanent oxygen carrier hemoglobin (and myoglobin), which has recently been studied with particular regard to electron transfer reactions between the heme group and a redox-active metal (ruthenium, iron or copper) at the protein surface, much attention is also given to progress in understanding the action of hemerythrin, the second most important oxygen carrier after hemoglobin. Other iron-related topics treated here are the transport and storage of iron, and cytochromes.

The emphasis on iron in this book does, however, reflect to some extent a difficulty that besets research in bioinorganic chemistry, namely that elements whose electronic, optical, or other properties are favorable for spectroscopic measurements receive more intensive study than those which are more difficult to observe. For example, zinc, which is the second most abundant transition metal in nature, is treated in only one paper.

Topics concerned with the biochemistry of nickel (methanogenic bacteria, toxicity, carcinogenicity) form a sec-

ond major theme. Other contributions are concerned with molybdenum, with trace elements in general, with biominerals, and with environmental aspects (with regard to Ni, Al, As, and Pu). Quite a long chapter is devoted to the use of spectroscopic methods in bioinorganic chemistry.

The chapter entitled "Nucleic Acid-Metal Ion Interactions" contains two excellent contributions on the reactions of metals with nucleosides and nucleotides and on the structure and stability of metal-nucleotide complexes. However, there is also a regrettably much too short "abstract" on the very interesting topic of the role of metals in the replication and transcription of nucleic acids and their translation into proteins, which also contains too few references.

A further chapter is headed "Metals in Medicine". The choice of topics here does not seem entirely a happy one. There are two good contributions on the nature and treatment of metabolic disturbances caused by zinc, and on the use of gold compounds in arthritis therapy, but also one on the development of a pharmaceutical product from the initial idea to its application, which seems out of place, having no obvious connection with bioinorganic chemistry. One looks in vain here for a paper reporting on new developments in the area of platinum cytostatics, which seems a bad omission in view of the current importance of this class of compounds in the treatment of various cancers.

Apart, however, from these few criticisms, "Frontiers in Bioinorganic Chemistry" succeeds well as a presentation of the current situation in this field.

Bernhard Lippert [NB 773 IE]
Institut für Anorganische und Analytische Chemie
der Universität Freiburg (FRG)

Plasma Polymerization. By *H. Yasuda*. Academic Press, New York 1985. x, 432 pp., bound, $ 62.00.—ISBN 0-12-768760-2

Plasma polymerization means the formation of polymeric substances from organic vapors in low temperature plasmas (i.e. electrical discharges in gases). The polymers are formed at pressures between 10^{-2} and 10 mbar and near-ambient temperatures, usually as thin films on glass, metal or polymer substrates. Although the effect has been known for many years (the earliest paper cited is that by *P. de Wilde*, published in 1874 in Ber. Dtsch. Chem. Ges.), its existence had not been much noticed up to about 1960. Attention was first drawn to this particular type of synthesis and its potential technical importance in a publication by *J. Goodman*. Since 1970 the American Chemical Society has held regular symposia on the topic, so contributing appreciably to the spreading of interest in the technique.

Plasma polymerization is an interdisciplinary topic, which is best approached from the background of thin-film technology in association with high-vacuum preparative techniques. The author begins with some introductory chapters which cover the fundamental basis of plasma polymerization, the kinetic theory of gases and the theory of plasmas, dealing with the ionization of molecules by electron impact, ion-molecule reactions, reactions of excited molecules, and also the effects of the accompanying UV radiation. This is followed by a summary of the kinetics of polymerization, with particular emphasis on polymerization by free radicals, ionic polymerization, and radiation-induced polymerization. While plasma polymerization has little in common with addition polymerization, it is closely related to radiation-induced polymerization; on the other hand, it is a particular type of vacuum polymerization.

It is not until Chapters 6 and 8 that the author comes to the central theme and the main part of the book, namely the reaction kinetics and mechanisms of plasma polymerization. To systematically describe the enormous variety of reactions, which is a consequence of the varied and multifunctional nature of the building blocks and the smallness of many of these, is a daunting task. The products are for the most part highly branched and cross-linked, and often differ from conventional polymers. The methods for analyzing them are also discussed here.

An intermediate chapter deals with the opposite process which accompanies plasma polymerization, whereby material is removed in the plasma (etching process), and with the deposition of material by sputtering which also occurs. This is followed by a detailed chapter on the experimental arrangements used, and the effects of the many experimental variables which critically influence the results obtained.

As a result of their molecular structures the polymers deposited often show unusual properties, which can give them some technological importance. In particular they show extremely strong adhesion to the support, and are highly resistant chemically. These and other characteristics, along with their electrical properties, especially their conductivities and dielectric constants, are the subject of the last two chapters of the book.

Eleven years have passed since the publication of the last monograph dealing with this topic (Hollahan and Bell: *Techniques and Applications of Plasma Chemistry*), and books such as that of *Baddour* and *Timmins*, and that of *McTaggart*, are already as old as 18 years. For this reason alone the publication of the present book is to be welcomed. It contains so many new results, in a concise and readable form, that it must be recommended for reading by specialists in the field. In interpreting experimental results the author has tended to disregard alternative explanations proposed by others; such a bias can be accepted in view of the author's competence.

Ernst-Günther Schlosser [NB 778 IE]
Hoechst Aktiengesellschaft, Frankfurt/Main (FRG)

Metalloproteins. Pt. 1: Metal Proteins with Redox Roles. Pt. 2: Metal Proteins with Non-Redox Roles. Edited by *P. Harrison*. VCH Verlagsgesellschaft, Weinheim 1985. Pt. 1: xi, 256 pp., bound, DM 138.00.—ISBN 3-527-26136-2; Pt. 2: xii, 339 pp., bound, DM 166.00.—ISBN 3-527-26137-0

Volumes 6 and 7 of the series *Topics in Molecular and Structural Biology* deal with the enormous progress that has occurred in inorganic biochemistry (also called bioinorganic chemistry) in the last twenty years. This is quite a demanding task, since the questions surrounding the role of metal ions in living organisms cross the conventional boundaries of research specialisms, and the multidisciplinary nature of the undertaking stretches the holistic point of view to its limits. There are already several series of progress reports in green, orange or blue covers, which for more than ten years have been presenting bioinorganic matters. Is this an opportune time to extend the range of colors? The editor *Pauline Harrison* and the publishers are to be congratulated on the idea of presenting the current

state of knowledge, in the form of twelve articles whose topics have all been treated previously in various monographs, such as that on cytochrome P-450 which was recently reviewed (*Angew. Chem. 98* (1986) 195; *Angew. Chem. Int. Ed. Engl. 25* (1986) 294). It is an advantage for both the already involved and the uncommitted reader to be able to absorb in a condensed form, and in comparatively few pages, twelve topical and representative pieces of work on which current ideas and activity in the bioinorganic field are based. Of course, the authors had to be selective in presenting examples rather than reviews of an encyclopedic nature.

Part 1 deals with proteins in which transition metal atoms are the functional centers. Recent results on blue copper proteins are discussed in the light of known structures *(Elinor T. Adman)*. Under the heading cytochrome C the main topics discussed by *C. Greenwood* are cytochrome C peroxidase, and nitrate reductase with the redox processes on which its action depends. Under iron-sulfur proteins *(A. J. Thomson)*, those treated as examples of this group are the aconitase and nickel-containing hydrogenases, the latter being especially topical as new territory. In the discussion of superoxide dismutases *(A. E. G. Cass)*, the emphasis is on reaction kinetics and mechanism. The camphor-5-exo-hydrolyase derived from *Pseudomonas putida* is discussed in a particularly instructive way in the chapter on the structure and chemistry of cytochrome P-450 *(R. I. Murray, M. T. Fisher, P. G. Debrunner, S. G. Sligar)*. Thanks are due to the well-known Sussex group *(D. J. Lowe, R. N. F. Thorneley, B. E. Smith)* for a short contribution on the virtually never-ending story of nitrogenase.

Part 2 is devoted to fragmentation, regulation, transport and storage phenomena in proteins. In the chapter *Metalloproteinases (T. Hofmann)*, the emphasis is on new structural data for carboxypeptidase A (bovine pancreas) and on microbial thermolysin. The abundance, structure, and function of troponin C and calmodulin are discussed from a comparative point of view *(R. J. A. Grand)*. *M. Forgac* and *G. Chin* give a concise account of the ($Na^{\oplus}$,$K^{\oplus}$)- and ($Ca^{2\oplus}$)-ATP-ases, whose structural geometries have not yet been clarified. In the sections on metallothioneins *(P. E. Hunziger, J. H. R. Kägi)*, transferrins *(J. H. Brook)* and oxygen-carrying proteins *(M. Brunori, M. Coletta, B. Giardina)*, the material has been summarized very successfully from a learning standpoint, as the presentation is easy to read, explicit, and not spoiled by too great an urge to show the authors' detailed knowledge of the literature.

This bold undertaking deserves one's goodwill. It might also effect a "metal catalyzed reaction" in promoting a greater appreciation of the art of good presentation!

Walter Schneider [NB 771 IE]
Laboratorium für Anorganische Chemie
der Eidgenössischen Technischen Hochschule
Zürich (Switzerland)

Hopping Conduction in Solids. By *H. Böttger* and *V. V. Bryksin*. VCH Verlagsgesellschaft, Weinheim 1985. 398 pp., bound, DM 140.00.—ISBN 3-527-26451-5

The subject matter of the book is undergoing an explosive growth, as is well-documented by some thousand references, of which around 400 are from the period 1983–1985. The authors have succeeded in tracing shortcuts through the sometimes densely proliferating original literature. At times, the presentation attains the clarity of textbooks for well-established fields of research; that is not always the case, but no blame for it may be put on a work which impressively summarizes such a wealth of material.

The first chapter discusses basic elements in the theory of hopping transport. Following a historical survey, the presentation (for which only standard notions of solid state physics are required) highlights the Kubo-formula, the polaron canonical transformation, the Hartree-Fock-decoupling and the generalized master equation. The second chapter is devoted to the small polaron. The extensive third chapter (more than half of the book) deals with hopping conduction in disordered systems, the main subjects being DC- and AC-hopping conductivity, non-ohmic hopping conduction and the Hall-effect. Here the physical principles of the theory of random media are also discussed: Anderson- and Mott-transitions, percolation, fractals, continuous-time random-walks, and effective-medium theories. The following short fourth chapter deals with diffusive atomic (or ionic) motion classically, a topic which might well have been treated at an earlier stage. The fifth and final chapter is the mixing-pot for extensive results of recent developments, and is a rich mine of interesting, in some cases not yet solved, research problems.

Under the cover of a textbook, the work also displays many facets of a review article and can be recommended both to graduate students and to specialists in the field. Reading is rendered easy by adequate author and subject indexes, by very good cross references and by judicious repetitions in the text. Disregarding its price, the book is well-suited as a basis for lectures and seminars.

Alexander Blumen [NB 777 IE]
Physikalisches Institut
der Universität Bayreuth (FRG)

Registered names, trademarks, etc. used in this journal, even when not marked as such, are not to be considered unprotected by law.

© VCH Verlagsgesellschaft mbH, D-6940 Weinheim, 1987. - Printed in the Federal Republic of Germany by Zechnersche Buchdruckerei, Speyer/Rhein.

All rights reserved (including those of translation into foreign languages). No part of this issue may be be reproduced in any form – by photoprint, microfilm, or any other means – nor transmitted or translated into a machine language without written permission from the publishers. Only single copies of contributions, or parts thereof, may be made for personal use.

Valid for users in the USA: The appearance of the code at the bottom of the first page of an article in this journal (serial) indicates the copyright owner's consent that copies of the article may be made for personal or internal use, or for the personal or internal use of specific clients. This consent is given on the condition, however, that the copier pay the stated per-copy fee through the Copyright Clearance Center, Inc., for copying beyond that permitted by Sections 107 or 108 of the U.S. Copyright Law. This consent does not extend to other kinds of copying, such as copying for general distribution, for advertising or promotional purposes, for creating new collective works, or for resale. For copying from back volumes of this journal see 'Permissions to Photo-Copy: Publisher's Fee List' of the CCC.

Editorial office: Pappelallee 3, D-6940 Weinheim, Federal Republic of Germany, Telephone (06201) 602315, Telex 465516 vchwh d, Telefax (06201) 602328.

Editor: *P. Gölitz.*

Associate editors: *D. I. Loewus, A. Stimson.* **Editorial assistant:** *E. Schweikart*

Publishers: VCH Verlagsgesellschaft mbH. (Managing Directors: *Prof. Dr. Helmut Grünewald* and *Hans Dirk Köhler*), Pappelallee 3, D-6940 Weinheim, Federal Republic of Germany. Correspondence concerning advertisements should be addressed to VCH Verlagsgesellschaft mbH. (Advertising Manager *R. J. Roth*), Boschstr. 12, P.O. Box 1260/1280, D-6940 Weinheim, Federal Republic of Germany, Telephone Weinheim (06201) 602-0, Telex 465516 vchwh d, Telefax (06201) 602328.

ANGEWANDTE CHEMIE

Volume 26 · Number 2
February 1987
Pages 93–160

Difficulties in the Emergence of the Polymer Concept—an Essay**

By Herbert Morawetz*

1. Introduction

The inauguration of the Max-Planck-Institut für Polymerforschung is a milestone in the long and tortuous road over which the study of polymers emerged as a scientific discipline and gained recognition by the scientific establishment.[***] It is hard to believe that *Partington*'s monumental "History of Chemistry"[1] published in 1964 does not refer to "polymers" in the index, refers to *Staudinger* only in connection with his work on diazomethane and ketene, and still refers to polystyrene as "metastyrol." Yet, we should remember that students of polymers are not unique in being victims of such glaring prejudice. In his inaugural address as rector of the University of Bonn, a little over a hundred years ago, *Kekulé*[2] complained that "one-sided representatives of so-called humanistic studies, who also confuse the application of chemistry with its scientific work, tend towards the unjustified view that chemistry ought to be taught at polytechnic schools and not at universities."

2. Three Early Experiments

What should we regard as the earliest significant polymer experiment? I shall suggest three that come to mind. The first could be the demonstration by the blind *John Gough* in 1805[3] that natural rubber heats up when stretched and contracts when a loaded sample is heated. *Gough* interpreted his results in a rather fanciful way. For instance, the contraction of a stressed rubber specimen on heating "is occasioned by the absorption of caloric fluid in the same manner that ropes are obliged to contract by absorption of water." Yet, the phenomena he described were real and it took more than a century to formulate their interpretation. The second choice might be *Faraday*'s analysis of rubber latex in 1826.[4] He showed that the aqueous phase contains protein and he gave a reasonably accurate figure for the elemental composition of the rubber. It is little known that he also recorded in his notebook an experiment in which he heated rubber with sulfur. All he observed was hydrogen sulfide generation and he concluded that heating organic compounds with sulfur might be a novel way to reduce their hydrogen content![5] This may surely be regarded as one of the great missed opportunities in the history of science!

My third choice is the 1839 report by *Simon*, a Berlin pharmacist, who first isolated styrene from a natural resin and noted that styrene distillation left a residue whose amount increased with the time the styrene was stored.[6] He assumed that the product was styrene oxide. A few years later, *Simon*'s experiment was repeated by *Blyth* and *Hofmann*[7] who showed conclusively that no oxidation was involved. To determine the nature of the transformation, they nitrated the styrene and the residue remaining after distillation and characterized them by the N/C ratio. They reported that this ratio changed from 1/8 to 1/7 and concluded that the original substance, C_8H_8, had been transformed into C_7H_7.

3. The Origin of the Term Polymer

The origin of the term "polymer" is rather curious. It was the result of the isolation, by *Faraday*, of butene for which he found a gas density twice as high as that of ethy-

[*] Pof. H. Morawetz
Polytechnic University
333 Jay Street, Brooklyn, NY 11201 (USA)

[**] Lecture presented at the inauguration of the Max-Planck-Institut für Polymerforschung on March 11, 1986, in Mainz.

[***] Note added by the editorial staff: The author of this article has written a history of macromolecular chemistry (H. Morawetz: *Polymers. The Origins and Growth of a Science*, Wiley, New York 1985), which was reviewed in this journal (*Angew. Chem. 98* (1986) 1039).

 © VCH Verlagsgesellschaft mbH, D-6940 Weinheim, 1987 0570-0833/87/0202-0093 $ 02.50/0

lene, although the two substances had the same elemental composition.[8] This puzzled *Faraday*, since he believed that the elemental composition defines a chemical compound. He was clearly unaware of a paper by *Gay-Lussac*,[9] who had pointed out as early as 1814 that "the composition of acetic acid does not differ significantly from that of ligneous matter.[*]... This is a new proof that the atomic arrangement in a compound has great influence on its character."[**] But this paper was also unknown to *Berzelius*, who was astounded by *Faraday*'s finding[10] and suggested that his new gas be referred to as a "polymer" of ethylene. According to *Berzelius*' definition, a polymer had to have the same elemental composition as a reference substance and this criterion was used rigorously a century later by *Staudinger*, who objected, therefore, to the application of this term to the products of polycondensations. *Berzelius*' definition paid no attention to molecular structure, so that all through the nineteenth century we may find statements describing, for example, styrene, C_8H_8, as a polymer of acetylene, C_2H_2, or even lactic acid, $C_3H_6O_3$, as a polymer of formaldehyde, CH_2O. Our current usage of the term was defined by *Carothers*,[11] who called polymers substances whose "structure may be represented by $-R-R-R-$ where "$-R-$" are bivalent radicals which, in general, are not capable of independent existence."

4. The Second Half of the 19th Century—Important Experiments and Misconceptions

In spite of the mistaken characterization of "metastyrol" by *Blyth* and *Hofmann*, this and similar products of transformation were soon considered to be "polymeric." We may well wonder how this concept could have arisen at a time when gas densities were the only reliable measures of molecular size. An increasing molecular weight was then estimated from a rising boiling point or inferred from an increasing density and the softening temperature of solids, which was not differentiated from a melting point. Considering the crudity of such methods, it is remarkable that *Berthelot* arrived at an understanding of the conversion of vinyl compounds into polymeric chain molecules. He reasoned[12] that on addition of an olefin to a chain with a terminal double bond, the unsaturation would be retained, so that there was no reason why very long chains should not be produced, although, as he stressed, the possibility of the formation of such chains did not ensure that they would be produced under some given conditions. *Berthelot* isolated the dimer, trimer, and tetramer of pentene and estimated from their heat of combustion the heat of polymerization. His long lecture on "la polymérie" presented to the Chemical Society of Paris in 1863 may well be regarded as the first intensive treatment of the subject. We should admire his insight and not stress unduly some of his more extravagant theories on the nature of catalysis or his cautious suggestion that the principle of polymerization may perhaps also apply to atoms, so that sulfur might be viewed as the dimer of oxygen and tellurium its tetramer.

A considerable number of vinyl monomers were polymerized before the end of the nineteenth century although the nature of the process was generally not understood. We should not be misled by the expression "hochpolymer" in the German literature of that time, which could refer to association complexes of small molecular species as well as to large molecules. The nature of polycondensation was understood by *Lourenço*,[13] who, between 1859 and 1863, studied the condensation of ethylene glycol and described the products up to the hexamer. He should also be given credit for having understood the concept of copolymerization—something which seemed surprisingly difficult when it was considered again sixty years later. There were, of course, other results which obviously involved polycondensation, but they were misunderstood mainly for two reasons: (1) Nothing was known about the constraints on molecular geometry, so that there was no hesitation in assigning to the products of ester interchange of resorcinol or hydroquinone with diphenyl carbonate[14] the structures **1** and **2**, respectively.

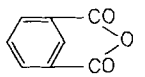

1

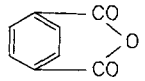

2

(2) There was a strong bias toward assigning a unique structure to a reaction product, particularly if it appeared to be crystalline. Thus, the condensation of salicylic acid was represented as leading to a cyclic tetramer[15] and the product of the condensation of succinic acid with ethylene glycol was thought to be the cyclic dimer.[16]

5. The Early 20th Century—New Arguments against the Existence of Polymers

The strong resistance to the concept of long-chain molecules involving only normal chemical bonds had several causes. The major opposition was due to the emergence of the concept of colloids as aggregates of a large number of small molecules. This "colloidal state" was supposed to be responsible for a high solution viscosity, low diffusion rate, gelation, and the failure of substances such as "metastyrol" to crystallize. Most important, it was frequently stated that "colloid solutions" cannot be expected to follow the laws of physical chemistry which were supposed to be restricted to "true solutions." It was also widely believed that solubility decreases necessarily with molecular size, so that the solubility of substances such as "metastyrol" seemed incompatible with a polymeric nature. Later, with the introduction of X-ray crystallography, the small

[*] His analysis was inaccurate. Cellulose was isolated from wood only 25 years later. However, he also pointed out that starch, which could be obtained pure at that time, has the same elemental composition.

[**] "Cette composition de l'acide acétique ne differe pas sensiblement de celle de la matière ligneuse qui ne jouit en aucune manière des propriétés acides. Voilà donc deux corps composés de carbon, d'oxigène et d'hydrogène, en même proportions, dont les propriétés sont eminemment differentes. C'est une nouvelle preuve que l'arrangement de molécules dans un composé a la plus grande influence sur le caractère neutre, acide ou alcalin de ce composé. Le sucre, la gomme et l'amidon conduisent encore a la même conclusion ..."

size of the unit cell of substances such as cellulose and *Hevea* rubber seemed to suggest a small molecular size. It is true that *Polanyi*[17] wrote in 1921 that the unit cell of cellulose allows two alternative interpretations: It could contain either two disaccharide segments of long polysaccharide chains, or two cyclic disaccharides. But he never returned to this argument, which seems to have been generally overlooked at the time. *Polanyi* wrote ruefully forty years later:[18] "Unfortunately I lacked the chemical sense to eliminate the second alternative—I should have been better occupied in establishing definitely the chain structure." We may also refer to some rather quaint arguments against the existence of long-chain molecules: The influential organic chemist *Karrer* ridiculed in 1921[19] the notion that starch could consist "of dozens or hundreds of glucose molecules joined by glucosidic bonds" since "it is improbable that a plant in converting sugar to a reserve substance from which it might soon have to be recovered would perform such complex work." Finally, *Hermann Mark* recalls that at a tempestuous farewell lecture given by *Staudinger* at the ETH in Zürich in 1925, one of the speakers compared *Staudinger*'s championship of long-chain molecules to the report of some traveler in Africa that he had seen a zebra which was 400 meters long. Who could believe such nonsense!

6. *Staudinger*'s Decision to Concentrate on Polymer Studies

Staudinger's conviction that "hochmolekular" compounds consist of covalently bonded long-chain molecules was first expressed in a paper published in Switzerland in 1919[20] and elaborated at some length in Berichte der Deutschen Chemischen Gesellschaft during the following year.[21] *Staudinger* cited three examples, polyoxymethylene (then called paraformaldehyde), "metastyrol," and *Hevea* rubber, for which, as he acknowledged, *Pickles*[22] had previously proposed a linear structure. It is fair to say that at that time *Staudinger*'s view was largely intuitive with little experimental evidence, but he was determined to prove his point and he had the courage to concentrate henceforth on a field which was viewed with undisguised contempt by many of the leading organic chemists of that time. As for this first communication on high-polymeric compounds, four features deserve our attention: It contained a clear description of the concept of polydispersity. It also contained a statement that "it makes no sense to carry out molecular weight determinations on such substances," justified by the observation that ebullioscopic and cryoscopic data would only reflect the presence of low-molecular-weight impurities. It raised the question of the chemical nature of the ends of chains formed by the addition of unsaturated monomers: Here *Staudinger* observed that with sufficiently long chains the concentration of these reactive sites would be reduced to a point where their presence would not be significant. Similar arguments, claiming that reactivities of chemical structures decrease with the length of chains to which they are attached may strike us today as farfetched, but such arguments were commonly accepted for a long time. Finally, *Staudinger* believed that "hundreds of molecules will add to each other until equilibrium, which may depend on temperature, concentration, and solvent, has been attained."

In view of *Staudinger*'s eminent role in establishing the polymer concept, it is of some interest to inquire what may have been the influences which induced him, a man with a solid reputation in classical organic chemistry, to concentrate after 1920 on a field which appeared so unpromising at the time. While the answer is necessarily speculative, there are some pointers worth considering. In his memoir,[23] *Staudinger* writes warmly about the "outstanding personality" of *Carl Engler*, in whose chemical institute at Karlsruhe he spent the five years 1907-1912 as "Extraordinärer Professor." It is, therefore, of some interest that *Engler* wrote as early as 1897,[24] in speculating about the origin of petroleum, that molecules with double bonds may undergo "slow addition to complex structures" and that "one need not assume that only similar molecules assemble." (It may even be significant that *Engler*'s wording "lagern sich zusammen" was adopted by *Staudinger* in his 1920 paper). *Engler* was well ahead of his time in speculating as early as 1904 about the relationship between autoxidation and polymerization,[25] and *Staudinger* became involved for the first time with polymerization when he advised *Engler*'s student *Lautenschläger* on his thesis dealing with "Autoxidation and polymerization of unsaturated hydrocarbons,"[26] *Staudinger* became involved for the first time with polymerization processes.

7. 1920–1940: The Classical Age of Polymer Science

A number of experimental results that were incompatible with the view of the colloid school made surprisingly little impression on the scientific community. *Duclaux* and *Wollman*[27] carried out a fractional precipitation of cellulose nitrate solutions and found that the fractions differed in their solution viscosities. This result would have been clearly incomprehensible if cellulose were an aggregate of small molecular species. In 1925 *Hock*[28] found that when a stretched rubber specimen was frozen in liquid air and shattered, it broke up into fibers—a result which certainly suggested a fibrous structure for the constituent molecules. During the same year *Katz*[29] published his finding that *Hevea* rubber, amorphous in the relaxed state, yields a sharp X-ray diffraction diagram when stretched. In reporting this sensational observation, he wrote that "molecules or parts thereof" are being oriented, but although he was unhappy with the notion that the small unit cell signifies that rubber is composed of small molecules, he did not dare to conclude that it is composed of molecular chains.

In 1926, *Sponsler* and *Dore*[30] published their interpretation of the X-ray diffraction by cellulose. It is important to note that they started with the observation that "a satisfactory formula for cellulose must account for its physical properties." Thus, they were clearly predisposed to reject the notion that cellulose represents an aggregate of small molecules or that "lattice forces are here comparable in their magnitude and nature to the valence forces: The whole crystallite appears as a large molecule."[31] They proposed a chain structure on the basis of rather limited data, but their result had the fateful flaw that it contra-

dicted solid chemical evidence that cellulose is composed of cellobiose residues. This tended to reinforce the skepticism of organic chemists regarding the utility of the crystallographic method.

One of *Staudinger*'s most fruitful ideas was the concept of model chain molecules, analogous to natural macromolecules but offering experimental advantages for their study. He reasoned that since studies of *Hevea* rubber are complicated by the chemical sensitivity due to its unsaturation, polystyrene, an amorphous synthetic polymer, would be a suitable analogue. In the case of cellulose, a highly crystalline material, he proposed to study the polymers of formaldehyde, since here the properties of a continuous series of oligomers could be compared with those of the high polymer. The results of this study showed quite unambiguously that the polymer is built up on the same principle as the oligomers which could be characterized by standard chemical techniques.[32] It contained another most important generalization: The ends of long-chain molecules are randomly distributed in the crystallites, so that X-ray diagrams cannot be used for an estimation of molecular weights.

The paper on formaldehyde polymers by *Staudinger* and his students may be said to have provided for the first time incontrovertible evidence on the chain structure of a high polymer. The crystallographic method was soon to be applied successfully by *Meyer* and *Mark* to cellulose, silk fibroin, chitin, and *Hevea* rubber.[33] In the case of cellulose, a correction of the interpretation by *Sponsler* and *Dore* showed that the X-ray data were fully compatible with the chemical evidence that the chains are composed of repeating cellobiose units. In the case of rubber, the crystal structure was shown to indicate a *cis*-1,4 enchainment of isoprene residues, contrary to the *trans* structure championed by *Staudinger*. It is remarkable that these papers were submitted from an industrial laboratory which was sufficiently farsighted to realize that such structural studies would form the basis for the development of successful artificial fibers.

At about the same time, *Staudinger* proposed a method by which the molecular weight of polymers could be deduced from their solution viscosity.[34] Although his theory assumed a rigid rodlike structure for chain molecules and was incorrect even on this basis, the use of the parameter that became known as the "Staudinger index" provided for the first time a cheap and convenient method for the characterization of the molecular size of polymers. In that way it advanced polymer science even though it led to incorrect values for molecular weights.

However, *Staudinger*'s solution viscosity theory had also an unfortunate side effect in that it contributed to the bad relations between the *Staudinger* school and the polymer chemists emphasizing physico-chemical techniques, particularly *Meyer, Mark,* and *Kuhn*. These men listed incontrovertible arguments for the flexibility of chain molecules, but *Staudinger* and his students chose to disregard them. It is hard for us today to understand that even phenomena such as rubber elasticity, the swelling of cross-linked polymer gels, and the dramatic increase in the viscosity of poly(acrylic acid) solutions when they are neutralized were not considered by *Staudinger* as incompatible with the model of rigid rodlike polymer chain molecules. On the other hand, two of *Staudinger*'s arguments must have seemed convincing:[35] (1) He felt that the easy crystallization of chain molecules could not be understood if randomly coiled chains had to assume extended shapes in the crystal. (2) He believed that the small volume change when crystalline polymers melt implied a packing efficiency in the melt which could not be achieved with randomly coiled chains. My conversations with *Staudinger*'s widow have indicated to me that there was also possibly a deeper psychological cause for these controversies: *Staudinger* seems to have been haunted by the conviction that physical chemists looked down on organic chemistry and that they expected, in particular, physical chemistry to provide all significant progress in the understanding of polymers. Since he believed that the study of macromolecules was opening a vast new area of activity for organic chemistry, he reacted to the perceived slight with passionate emotion.

8. Macromolecular Chemistry and Molecular Biology—Little Interaction despite Common Methods

Finally, I should like to comment briefly on the relation between the development of synthetic macromolecular science and the rise of molecular biology. The idea that very large molecular structures are involved in the life process was expressed already by *Kekulé* in his inaugural address at the University of Bonn, referred to above.[2] He cited *Pflüger* as believing that "these mass molecules ... through constant change of position of polyvalent atoms change the connection between individual molecules so that the whole ... is in a sort of living state." Later, colloid chemists were fascinated by the idea that their field played a central role in explaining the life process. This may be exemplified by *Pauli*[36] writing that "the colloid chemistry of proteins provides an approach to the obscure region which scientists contemplate today only with the silent longing for the promised land—the physical chemistry of living matter." *Staudinger* expressed a similar sentiment when he wrote in his memoir that he had chosen as a young man "to study chemistry in order to enter more readily into the problems of botany" and he concluded his Nobel Prize lecture in 1953 with some speculations concerning macromolecules and life.[23]

Clearly, a number of experimental techniques are equally applicable to the study of synthetic polymers and the investigation of proteins and nucleic acids with which molecular biology is concerned. Let us see then how the developments of the macromolecular concept in these two fields compared with each other.

For a long time, protein chemistry was just as influenced by the skepticism concerning the possible existence of very large covalently bonded molecules as the chemistry of synthetic polymers—particularly since the great *Emil Fischer*[37] had expressed his doubt of the existence of proteins with molecular weights exceeding 4000. It was only when *Svedberg*'s ultracentrifuge study of hemoglobin showed that it consisted of particles with a discrete molecular weight, that he abandoned his preconception that proteins

are aggregates of small molecules with a variable particle size, such as he had observed with inorganic colloidal dispersions.[38] Yet, *Svedberg* told his student, *B. G. Rånby* that he was completely unaware of *Staudinger*'s existence at the time he developed the ultracentrifuge. The study of globular proteins, which have a uniquely defined sequence of a relatively large number of comonomers and a unique conformation in their "native state" and which exhibit denaturation phenomena, raised obviously different problems compared with polystyrene or rubber. Crystallographic data on synthetic polypeptides were useful in confirming the structure of the α-helix[39] as one of the structural elements of proteins, and studies of helix-coil transitions in polypeptide solutions[40] continue to be motivated by the hope that they might lead to a full understanding of the principles governing chain folding in globular proteins. The utility of this approach is yet to be proved.

Nucleic acids were assigned for a long time a tetranucleotide structure.[41] The realization of their high molecular weight was probably delayed owing to difficulties in their isolation, which led to various degrees of degradation. This made *Feulgen*[42] refer in 1935 to the "bad reputation" of DNA. He showed that an enzyme can convert a gelling preparation "a" into a non-gelling product "b." Study of these two materials in the ultracentrifuge led *Schmidt* and *Levene*[43] to conclude that the preparation "a" with a molecular weight of 200000-1000000 was depolymerized by *Feulgen*'s enzyme to the tetranucleotide. But what did they mean by depolymerization? As late as 1938 they referred[44] to the "dissociation of the tetranucleotides of high molecular weight to those of lower molecular weight," suggesting that they viewed the heavy particles as loose aggregates. Only the flow birefringence study of *Signer*, *Caspersson*, and *Hammarsten*,[45] published during the same year, established the rodlike nature of the DNA particle.

We can see from the examples detailed above that the interaction between polymer chemists and the practitioners of molecular biology was minimal. Most of the time they went their separate ways with little awareness of each other.

Received: June 26, 1986 [A 605 IE]
German version: *Angew. Chem. 99* (1987) 95

[1] J. R. Partington: *A History of Chemistry*, Macmillan, London 1964.
[2] A. Kekulé, *Nature (London) 18* (1878) 210; R. Anschütz: *August Kekulé*, Verlag Chemie, Berlin 1929, Vol. 2, p. 903.
[3] J. Gough, *Mem. Lit. Phil. Soc. Manchester (2) 1* (1805) 288.
[4] M. Faraday, *Quart. J. Sci. Arts 21* (1826) 19.
[5] T. Martin (Ed.): *Faraday Diary*, Bell, London 1932.
[6] E. Simon, *Ann. Pharm. (Lemgo, Ger.) 31* (1839) 265.
[7] J. Blyth, A. W. Hofmann, *Ann. Chem. Pharm. 53* (1845) 289.
[8] M. Faraday, *Phil. Mag. 66* (1826) 180.
[9] M. Gay-Lussac, *Ann. Chim. (Paris) 91* (1814) 149.
[10] J. Berzelius, *Fortschr. Phys. Wissensch. 6* (1827) 98; *11* (1832) 44; *12* (1833) 63.
[11] W. H. Carothers, *J. Am. Chem. Soc. 51* (1929) 2548.
[12] M. Berthelot: *Leçons de chimie professées en 1864 et 1865*, Societé Chimique de Paris, Paris 1866, pp. 18-65 and 148-167.
[13] A. V. Lourenço, *Ann. Chim. Phys. (3) 67* (1863) 257.
[14] C. A. Bischoff, A. von Hedenström, *Ber. Dtsch. Chem. Ges. 35* (1902) 3431.
[15] R. Anschütz, *Justus Liebigs Ann. Chem. 273* (1893) 73; R. Anschütz, G. Schröter, *ibid. 273* (1893) 97.
[16] D. Vorländer, *Justus Liebigs Ann. Chem. 280* (1894) 267.
[17] M. Polanyi, *Naturwissenschaften 9* (1921) 288.
[18] M. Polanyi in P. P. Ewald (Ed.): *Fifty years of X-ray diffraction*, N.V.A. Oosthoek Uitgeversmaatshapij, Utrecht 1962, p. 631.
[19] P. Karrer, C. Nägeli, *Helv. Chim. Acta 4* (1921) 263.
[20] H. Staudinger, *Schweiz. Chem. Z. 3* (1919) 1-5, 28-33, 60-64.
[21] H. Staudinger, *Ber. Dtsch. Chem. Ges. 53* (1920) 1073.
[22] S. S. Pickles, *J. Chem. Soc. 97* (1910) 1085.
[23] H. Staudinger: *Arbeitserinnerungen*, Hüthig, Heidelberg 1961.
[24] C. Engler, *Ber. Dtsch. Chem. Ges. 30* (1897) 2358.
[25] C. Engler, J. Weissberg: Kritische Studien über die Vorgänge der Autoxydation, Vieweg, Braunschweig 1904, p. 179.
[26] L. Lautenschläger, *Dissertation*, Technische Hochschule Karlsruhe 1913.
[27] J. Duclaux, E. Wollman, *Bull. Soc. Chim. Fr. 27* (1920) 414.
[28] L. Hock, *Z. Elektrochem. 31* (1925) 404.
[29] J. R. Katz, *Kolloid-Z. 36* (1925) 300; *37* (1925) 19.
[30] O. L. Sponsler, W. H. Dore, *Colloid Symp. Monogr. 4* (1926) 174.
[31] H. Mark, *Ber. Dtsch. Chem. Ges. 59* (1926) 2982.
[32] H. Staudinger, H. Johner, H. Signer, G. Mie, J. Hengstenberg, *Z. Phys. Chem. Stöchiom. Verwandtschaftsl. 126* (1927) 425.
[33] K. H. Meyer, H. Mark, *Ber. Dtsch. Chem. Ges. 61* (1928) 593, 1932, 1936, 1939.
[34] H. Staudinger, W. Heuer, *Ber. Dtsch. Chem. Ges. 63* (1931) 222.
[35] H. Staudinger, *Z. Elektrochem. 40* (1934) 434.
[36] W. Pauli, *Kolloid-Z. 3* (1908) 2.
[37] E. Fischer, *Ber. Dtsch. Chem. Ges. 40* (1907) 1754.
[38] T. Svedberg, *Kolloid-Z. 51* (1930) 10.
[39] L. Pauling, R. B. Corey, *Proc. Natl. Acad. Sci. USA 37* (1951) 235, 241.
[40] M. Sueki, S. Lee, S. P. Powers, J. B. Denton, Y. Konishi, H. A. Scheraga, *Macromolecules 17* (1984) 148.
[41] P. A. Levene, *J. Biol. Chem. 40* (1919) 415; *48* (1921) 119.
[42] R. Feulgen, *Hoppe-Seyler's Z. Physiol. Chem. 227* (1935) 261.
[43] G. Schmidt, P. A. Levene, *Science 88* (1938) 172.
[44] P. A. Levene, G. Schmidt, *J. Biol. Chem. 126* (1938) 423.
[45] R. Signer, T. Caspersson, E. Hammarsten, *Nature (London) 141* (1938) 122.

Sulfur Oxides as Ligands in Coordination Compounds

By Wolfdieter A. Schenk*

Donor molecules undergo dramatic changes in their chemical properties on coordination to a transition-metal atom. Highly reactive species can be trapped and studied as ligands. Conversely, stable compounds can be activated to undergo novel reactions. Sulfur dioxide complexes have generally been studied from a structural viewpoint, their reactivity having been somewhat neglected. The unstable sulfur oxides SO, S_2O, and S_2O_2 are still often regarded as laboratory curiosities. Their successful stabilization in transition-metal complexes has now made them accessible to detailed study, in the course of which many relationships to the chemistry of SO_2 complexes have become apparent.

1. Introduction

The first complexes with SO_2 were reported in 1938 by *Gleu* and co-workers.[1,2] However, only when spectroscopic and structural studies revealed the versatility of the SO_2 ligand did the interest in this class of compounds become widespread.[3,4] Investigation of their chemical reactivity was essentially confined to studies of SO_2 dissociation from the complexes and of the "sulfate reaction," i.e., the oxidation with O_2 to give sulfate complexes.[4]

SO is in equilibrium with SO_2 at high temperatures; it is an intermediate in the combustion of compounds containing sulfur.[5] Early reports of the isolation of SO[6] and of the investigation of its properties[7] had to be revised on the basis of mass-spectrometric evidence;[8] SO disproportionates extremely rapidly, mostly according to Equation (1),

$$3\,SO \longrightarrow S_2O + SO_2 \qquad (1)$$

with the dimer S_2O_2 (also highly unstable) as an intermediate.[5,9] Under pressures of a few millibars, the S_2O polymerizes to form polysulfur oxides of variable composition, SO_2 being given off.[5] Many sulfoxides decompose thermally[10-21] or photochemically[22] with elimination of SO, which can be identified spectroscopically[21] or by trapping reactions.[10,12,13,16,18,20] The thermolysis of thiirane 1-oxides, in particular, has proved to be a useful method of generating SO in solution [Eq. (2)].[10,11,16,19]

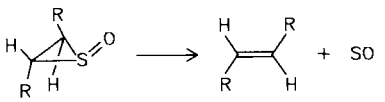

$$+ \; SO \qquad (2)$$

R = H, Ph

Further possible sources of SO and S_2O are represented by reactions (3) and (4).[23] SO and S_2O have also been postulated as short-lived intermediates in the electrolytic reduction of SO_2[24] and in the $Li/SOCl_2$ battery.[25]

$$RSO_2N{=}S{=}O + Ph_3P \longrightarrow RSO_2N{=}PPh_3 + SO \qquad (3)$$

$$RSO_2N{=}S{=}O + Ph_3PS \longrightarrow RSO_2N{=}PPh_3 + S_2O \qquad (4)$$

[*] Prof. Dr. W. A. Schenk
Institut für Anorganische Chemie der Universität
Am Hubland, D-8700 Würzburg (FRG)

The lower sulfur oxides also include the compounds S_nO (n = 6–10) and S_7O_2, which have been obtained by oxidation of the corresponding sulfur homocycles with peracids. Recent reviews of these compounds are available.[26]

2. Complexes with SO_2

2.1. Structure and Bonding

The small molecule SO_2 displays a fascinating variety of bonding modes (Fig. 1), which can be understood in terms

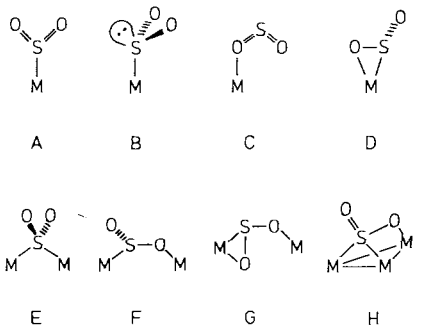

Fig. 1. Types of SO_2 complexes.

of the frontier orbitals shown in Figure 2.[3-5] The HOMO and LUMO are symmetry-equivalent to the frontier orbitals of a carbene, and complexes of type A (Fig. 1) are thus closely related in structure to carbene complexes; repre-

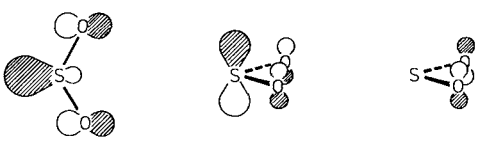

Fig. 2. The frontier orbitals of SO_2 and their energies [eV].

 © VCH Verlagsgesellschaft mbH, D-6940 Weinheim, 1987 0570-0833/87/0202-0098 $ 02.50/0

sentative examples are shown in Figure 3. SO_2 coordinates to electron-rich transition-metal fragments to form complexes of type B (Fig. 1). *Vaska*'s SO_2 complex **4**[31,32] and

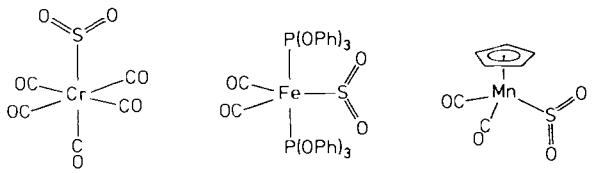

1a[27] **2**[28,29] **3**[30]

Fig. 3. η^1-SO_2 complexes with planar-coordinated sulfur (type A in Fig. 1).

the platinum complex **5**[33] can be cited as examples (Fig. 4). Compounds such as **4** and **5** may be viewed as analogues of the amine adducts of SO_2,[34,35] since the bonding electron pair is formally provided by the transition metal.

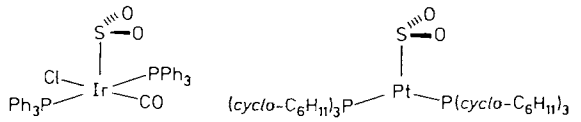

4[32] **5**[33]

Fig. 4. η^1-SO_2 complexes with pyramidally coordinated sulfur (type B in Fig. 1).

A more detailed analysis shows that, as in nitrosyl complexes, a bent (here pyramidal) geometry (A→B) can be expected when the σ^* orbital, which is antibonding with respect to the M–S bond, and the b_1 orbital of the SO_2 are of similar energy and one of them is occupied.[36] The nickel complexes **6**,[37] **7**,[38] and **8**[39] (Fig. 5) demonstrate especially clearly the transition from planar to pyramidal geometry. Complex **7** is the only known example of an SO_2 complex that is comparable structurally to slightly bent nitrosyl complexes.[40]

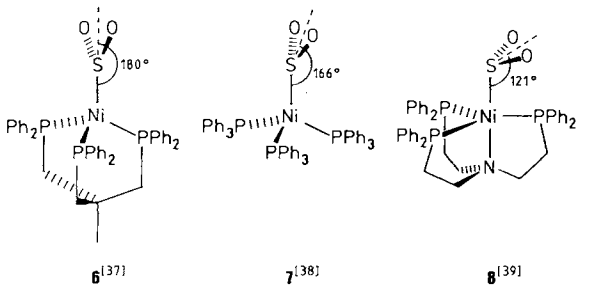

6[37] **7**[38] **8**[39]

Fig. 5. Transition from planar-coordinated to pyramidally coordinated sulfur.

Hard Lewis acids coordinate preferentially to the oxygen (type C in Fig. 1). The adduct $SO_2 \cdot SbF_5$[41] is the prototype of such systems, but several transition-metal complexes of this sort have been recently isolated.[42,43] Since the LUMO of SO_2 has an appreciable coefficient at the oxygen atom, SO_2 can also coordinate side-on to a transition metal (type D in Fig. 1). The energetically unfavorable and poorly polarizable a_2 orbital then serves as the donor orbital. This type of coordination is therefore also limited to electron-rich complexes such as **9**,[44] **10**,[45] and **11**[46] (Fig. 6).

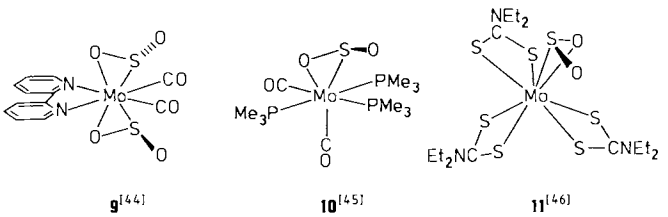

9[44] **10**[45] **11**[46]

Fig. 6. η^2-SO_2 complexes (type D in Fig. 1).

In polynuclear complexes, SO_2 is, almost without exception, a carbene-type 2-electron bridging ligand (type E in Fig. 1); the close analogy between CR_2 and SO_2 is illustrated by the complexes **12a** and **12b**[47] (Fig. 7). In contrast to the corresponding carbonyl complexes, SO_2-bridged complexes are characterized by severely limited or even nonexistent intramolecular CO exchange.[47,48] This is due to the great preference of the "single-faced" π-acceptor SO_2 for the bridging position; indeed, no polynuclear SO_2 complex with terminal SO_2 is known.

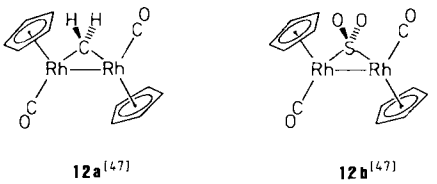

12a[47] **12b**[47]

Fig. 7. Analogy between μ-CH_2 and μ-SO_2 complexes.

The structural types F,[49] G,[50] and H[51] (Fig. 1) are each represented by one X-ray crystal structure. They may be considered as products of an electrophilic attack on the oxygen atoms of complexes of types B, D, and E, respectively; the SO_2 in F, G, and H functions as a 4-electron donor.

The structural variety that has been briefly discussed here makes SO_2 complexes an ideal model for studying the relationship between the nature of the transition-metal fragment L_nM, the nature of the ligand coordination, and reactivity.

2.2. Synthesis

2.2.1. Mononuclear Compounds

Because of its ready accessibility and ease of manipulation, almost all syntheses start from free SO_2, which is added to either isolable complexes or to coordinatively unsaturated complex fragments generated in situ. Reactions (5)[31] and (6)[52] are typical examples. Complexes **1a** and **1c** were first observed in solution by *Strohmeier* et al.,[53] but only with the discovery of reaction (6) did the highly substitution-labile pentacarbonyl complexes become accessible. Analogous methods led to the synthesis of a series of phosphane-substituted complexes, *cis*-

$[M(CO)_4(PR_3)(SO_2)]$[52] (M = Cr, Mo, W), and of the cations $[M(CO)_5(SO_2)]^{\oplus}$ (M = Mn, Re),[54] $[CpCr(NO)_2(SO_2)]^{\oplus}$, and $[CpFe(CO)_2(SO_2)]^{\oplus}$[55] (Cp = η^5-C_5H_5). The phosphane-substituted derivatives are markedly more stable than the parent compounds **1a–c**, since the replacement of one CO group by a donor ligand raises the energy of one of the three t_{2g} orbitals of the metal and thus strengthens the back-bonding into the b_1 orbital of the SO_2.

$$[Ir(PPh_3)_2(CO)Cl] \overset{SO_2}{\rightleftharpoons} [Ir(PPh_3)_2(CO)(Cl)(SO_2)] \quad (5)$$

4

$$[M(CO)_5Cl]^{\ominus} \xrightarrow[-NaCl]{NaBPh_4} \{M(CO)_5\} \xrightarrow{SO_2} [M(CO)_5(SO_2)] \quad (6)$$

1a–c

M = Cr (**1a**), Mo (**1b**), W (**1c**)

The chromium triad provides a large number of SO_2 complexes of various substitution types; these have revealed relationships between the arrangement of donor and acceptor ligands and the nature of the SO_2 coordination (η^1 planar or η^2). The complexes were obtained by replacement of labile neutral ligands such as tetrahydrofuran, acetone, or acetonitrile by SO_2.[52,56,57] The oxidative cleavage of M–M bonds with AsF_5 in liquid SO_2 provides another interesting synthetic route.[58]

$$[Ru(NH_3)_4(SO_3H)_2] \xrightarrow{HCl} [Ru(NH_3)_4Cl(SO_2)]^{\oplus} \quad (7)$$

13

$$[Ru(NH_3)_5(SO_3)] \xrightarrow{H^{\oplus}} [Ru(NH_3)_5(SO_2)]^{2\oplus} \quad (8)$$

14

The SO_2 complexes isolated by *Gleu* and co-workers in 1938 also represented the first examples of the generation of SO_2 at a metal complex. The two ruthenium complexes **13** and **14** were formed by acid hydrolysis [Eq. (7)[1] and (8)[2]]. Later, the manganese complex **3**[59] and the square-planar compounds **15a,b** and **16a,b**[60] were also synthesized [Eq. (9) and (10)]. *Kubota* and *Loeffler* reported the thermally induced rearrangement of sulphinato complexes

$$[CpMn(CO)_2\{OS(NEt_2)_2\}] \xrightarrow{H_2O} [CpMn(CO)_2(SO_2)] \quad (9)$$

3

$$[M(PR_3)_2Cl(OSNR')] \xrightarrow{H_2O} \begin{matrix} R_3P & SO_2 \\ & M \\ Cl & PR_3 \end{matrix} \quad (10)$$

M \ R	*i*Pr	*cyclo*-C_6H_{11}
Rh	**15a**	**15b**
Ir	**16a**	**16b**

$$\begin{matrix} L & N_2 \\ & Ir \\ Cl & L \end{matrix} + RSO_2Cl \longrightarrow \begin{matrix} L & SO_2R \\ & Ir \\ Cl & L \end{matrix} Cl \longrightarrow \begin{matrix} L & SO_2 \\ & Ir \\ Cl & L \\ & R \end{matrix} Cl \quad (11)$$

L = PPh_3; R = Me, Et, Pr, Ph, ...

[Eq. (11)].[61] The spectroscopic data, particularly ν(SO), cannot however be reconciled with the formulation of the products as octahedral Ir^{III} complexes. The iron complex **2** is formed in surprisingly good yield according to Equation (12).[29] Complexes **2**, **15a**, and **16a** can also be obtained by oxidation of the corresponding SO complexes (see Section 3.3).

$$[FeH_2(CO)_2\{P(OPh)_3\}_2] + SO_2Cl_2 \xrightarrow[-2\,Et_3N\cdot HCl]{2\,Et_3N} [Fe(CO)_2\{P(OPh)_3\}_2(SO_2)] \quad (12)$$

2

The reactions (7) to (12) are of minor importance as synthetic routes to SO_2 complexes but they demonstrate the diverse reactivity of sulfur–oxygen compounds with respect to transition-metal centers.

2.2.2. *Polynuclear Compounds*

The isolobal relationship between SO_2 and CR_2 leads one to expect that SO_2 can coordinate to complexes with metal–metal bonds, the process being accompanied by a lowering of the metal–metal bond order. Examples are provided by the reactions (13)[62–64] and (14).[65] The well-known insertion of SO_2 into nonbridged M–M single bonds can also be included here.[66,67] Coordinatively unsa-

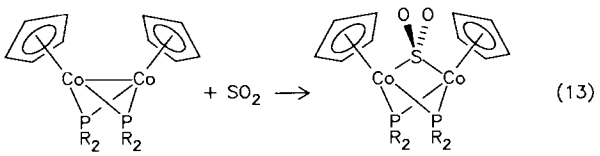

(13)

R = Me, Ph

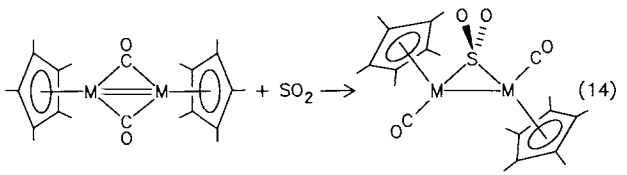

(14)

M = Co, Rh

turated polynuclear complexes add SO_2 readily [Eq. (15)].[68] Equation (16)[74,75] is a typical example of the (often reversible) coordination of SO_2 to an A-frame complex.[69–75] The enormous versatility in the reactivity of

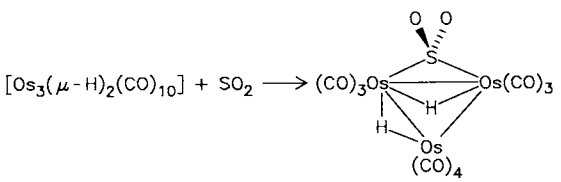

(15)

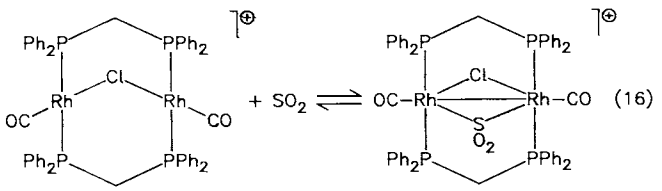

(16)

polynuclear systems is revealed in numerous further reaction types : ligand substitution at μ-SO_2 complexes,[70,75-77] uptake of SO_2 with bridge cleavage,[78,79] cluster formation from smaller units,[51,80-84] and replacement of labile ligands by SO_2.[48] Even CO can often be easily replaced by SO_2.[47,51,73,76,79,85,86] This method was used to prepare **17**, an SO_2-bridged heterometallic complex [Eq. (17)].[87,154]

$$[MoRhCl(dppm)_2(CO)_4] + SO_2 \longrightarrow \textbf{17} + CO \quad (17)$$

17

$$[Mo_2(\mu\text{-}S)_2(CN)_8]^{6\ominus} \xrightarrow{O_2} \textbf{18} \quad (18)$$

18

Reaction (18) is worthy of mention in connection with the oxidation of sulfur by microorganisms; an SO_2 bridge is formed from a μ-sulfido ligand, but the mechanism is unknown.[88,89] Closely related reactions are the formation of thiosulfito and dithiosulfato complexes by air oxidation [Eq. (19)[90] and (20)[91]].

$$[Co_2(CN)_{10}(\mu\text{-}S_2)]^{6\ominus} \xrightarrow{O_2} [(NC)_5Co\text{-}S\text{-}S(O)_2\text{-}Co(CN)_5]^{6\ominus} \quad (19)$$

$$MoS_4^{2\ominus} \xrightarrow{O_2} \left[\begin{array}{c} S \\ O \\ S \end{array}\!\!>\!Mo\!<\!\begin{array}{c} S \\ O \\ S \end{array}\!\!>\!Mo\!<\!\begin{array}{c} S \\ S \\ O \end{array}\right]^{2\ominus} \quad (20)$$

2.3. Reactivity

2.3.1. Loss or Substitution of SO_2

The SO_2 complexes of type A or D (Fig. 1) that were discovered before 1980 were nearly all stable with respect to loss of SO_2. This led to the assumption that SO_2 ligand lability was diagnostic for type-B coordination.[4,92] The concept of "lability" was interpreted as ready, reversible loss of SO_2 [Eq. (21)][92] or as ready substitution of SO_2 [Eq. (22)].[4] Reaction (21) can obviously be reversible on a preparative scale only when $[ML_n]$ is a stable, isolable compound; the reversibility of SO_2 loss is therefore a consequence of the properties of the $[ML_n]$ moiety and not necessarily of the SO_2 complex itself. It is clear why type-B complexes lose SO_2 readily; the pyramidality results from an antibonding interaction between the a_1 orbital of the SO_2 and an occupied metal orbital of σ symmetry. However, a series of type-A SO_2 complexes have now been prepared that also lose SO_2 readily, even if the process is not macroscopically reversible. These are exemplified by the pentacarbonyls **1a–c**, which decompose in the solid state at 0°C with loss of SO_2 or exchange the coordinated SO_2 within seconds even with weak donor ligands.[52] The SO_2 is probably lost by a dissociative mechanism, the first step of which is represented by Equation (21).

$$[ML_n(SO_2)] \rightleftharpoons [ML_n] + SO_2 \quad (21)$$

$$[ML_n(SO_2)] + L' \longrightarrow [ML_nL'] + SO_2 \quad (22)$$

For SO_2 substitution, however, there are several further possible mechanisms, which make the usefulness of a simple reactivity criterion for the nature of the SO_2 coordination seem questionable. For example, the square-planar d^8-complexes **15a,b** and **16a,b**, which are thermally extremely stable, react smoothly with CO, CO/SO_2 exchange taking place.[60] A detailed examination revealed an associative mechanism; the pentacoordinate intermediates **19a,b** could be spectroscopically identified at low temperature [Eq. (23)].[93] In this case the ease of substitution of the SO_2 is clearly dependent on the nature of the attacking ligand.

$$\textbf{16a, b} + CO \longrightarrow \textbf{19a, b} \rightleftharpoons \textbf{20a, b} + SO_2 \quad (23)$$

a, R = *i*Pr; **b**, R = *cyclo*-C_6H_{11}

SO_2 substitution at electron-deficient complexes could be induced (similarly to CO substitution at metal carbonyls[94]) by nucleophilic attack on the sulfur. Several examples of this reaction type are indeed known (see Section 2.3.4).

2.3.2. Substitution of Other Ligands in the Complex

Electron-rich SO_2 complexes whose M–S bond is not labile to substitution may sometimes undergo substitution of other ligands. *Gleu* and co-workers reported the reversible aquation of the complex **13** [Eq. (24)].[1] The cationic rhodium complexes $[RhLL'(SO_2)]^{\oplus}$ (L = PEt_3, PMe_2Ph; L' = bis(3-diphenylphosphinopropyl)phenylphosphane) release the monodentate phosphane ligand reversibly in solution.[95] The substitution of acetonitrile and triphenylphosphane in $[Mo(PPh_3)_2(MeCN)(CO)_2(SO_2)]$ made accessible a series of dicarbonylmolybdenum complexes of types A and D (Fig. 1).[45,96] Such ligand substitutions are also possible at polynuclear complexes; examples have been found for A-frame complexes[70,74,75] and for the trinuclear platinum complexes $[Pt_3L_3(\mu\text{-}SO_2)_3]$.[77]

$$[Ru(NH_3)_4Cl(SO_2)]^{\oplus} + H_2O \longrightarrow \underset{\textbf{13}}{} \quad (24)$$

$$\underset{\textbf{21}}{trans\text{-}[Ru(NH_3)_4(H_2O)(SO_2)]^{2\oplus}} + Cl^{\ominus}$$

2.3.3. Coordinative and Oxidative Addition

Coordinatively unsaturated SO_2 complexes (exemplified by the d^8-compounds **15a,b** and **16a,b**) should readily undergo addition reactions. Indeed, **16a,b** react not only with CO (see Section 2.3.1) but also with H_2 and HCl [Eq. (25) and (26)].[93] Reaction (25) is reversible; the dihydridoiridium(III) complexes **22a,b** lose H_2 slowly in solution at room temperature, and **23a,b** eliminate HCl on treatment with base.[93] Complexes **16a,b** are thus surprisingly similar to compounds of the Vaska type. This underlines the close relationship between CO and SO_2 complexes and may serve as a basis for future reactivity studies.

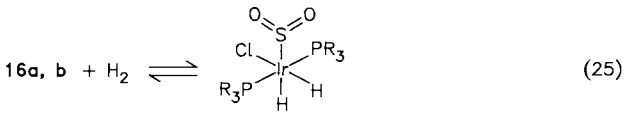

16a, b + H_2 ⇌ **22a, b** (25)

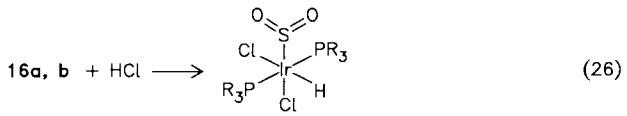

16a, b + HCl ⟶ **23a, b** (26)

a, R = *i*Pr; **b**, R = *cyclo*-C_6H_{11}

2.3.4. Reactions at Coordinated SO_2

The first example of a nucleophilic attack at the sulfur atom was again presented by *Gleu* et al.[2] The reversible transformation of the SO_2 ligand into an $SO_3H^{\ominus}$ ligand [Eq. (27)] clearly occurs by attack of H_2O or $OH^{\ominus}$, facilitated by the positive charge of the complex. To the best of our knowledge, there is only one further example of attack on sulfur by a base; in this reaction, a μ-SO_2 ligand is converted into a terminal $SO_3R^{\ominus}$ ligand [Eq. (28)].[48]

$$[Ru(NH_3)_5(SO_2)]^{2\oplus} + H_2O \rightleftharpoons [Ru(NH_3)_5(SO_3H)]^{\oplus} + H^{\oplus} \quad (27)$$

14

$$[Ir_4(CO)_9(\mu\text{-}CO)_2(\mu\text{-}SO_2)] + MeO^{\ominus} \longrightarrow [Ir_4(CO)_8(\mu\text{-}CO)_3(SO_2OMe)]^{\ominus} \quad (28)$$

In principle, type-B SO_2 complexes (Fig. 1) should undergo electrophilic attack at sulfur. Reaction of $[Pt(PPh_3)_2(SO_2)]$ with MeI and $MeOSO_2F$ have indeed been mentioned,[3] but no details were given. The anionic complex **24**, obtainable at low temperature according to Equation (29)[67] and isolable as the potassium salt,[97] can be smoothly alkylated at sulfur with a variety of reagents RX.[67,97,98] Sulfinato complexes with unsaturated substituents R ($CH_2CH{=}CMe_2$, $CH_2C{\equiv}CMe$) can thus be obtained that are inaccessible by insertion of SO_2 into the Fe-C bond of the corresponding organoiron complex $[CpFe(CO)_2R]$ because of competing rearrangement reactions.[98] The loss of optical activity on reacting **24** with (*R*)-PhMeCHBr,[99] and also the formation of side products such as $[Cp_2Fe_2(CO)_4]$ and $[CpFe(CO)_2X]$, indicate that radical intermediates play a role in reaction (29).[67]

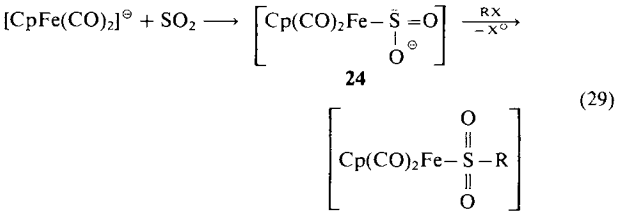

24

(29)

Examples of electrophilic attack at oxygen are more numerous. The compound $[Ru(CO)_2(PPh_3)_2(\eta^2\text{-}SO_2\cdot SO_2)]$ arises by attack by the Lewis acid SO_2 on the *exo* oxygen of an η^2-SO_2 ligand.[100] The formation of the binuclear complex $[Mo(CO)_2(py)(PPh_3)(\mu\text{-}SO_2)]_2$ (py = pyridine) may also be interpreted as the attack of a coordinatively unsaturated metal fragment on the *exo* oxygen.[50,96] However, attempted addition of BF_3, protonation, or methylation have been unsuccessful.[45,96] The high energy of the Si–O bond has been exploited in many cases for facile electrophilic attack at oxygen [Eq. (30)]. Competition studies indicate that η^2-coordinated SO_2 is much more easily silylated than η^1-coordinated.[57]

$$[\{M\}(SO_2)] + Me_3SiOSO_2CF_3 \longrightarrow [\{M\}(SO_2SiMe_3)]^{\oplus}SO_3CF_3^{\ominus} \quad (30)$$

{M} = metal fragment of the type $M(PR_3)_n(CO)_{5-n}$ with M = Cr, Mo, W; n = 2, 3

Numerous SO_2 complexes of the platinum metals react with molecular oxygen to give sulfato complexes; an example is given in Equation (31).[101] This reaction is considered as diagnostic for η^1-pyramidal coordination of SO_2,[4]

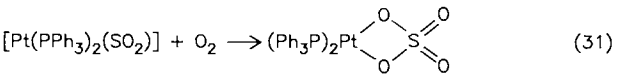

(31)

but some exceptions are known.[33,95,102] Recent studies show that the first step is the replacement of complexed SO_2 by O_2,[33] followed by electrophilic attack by the free SO_2 on the coordinated O_2.[103]

2.3.5. Reduction, SO_2 Insertion, and Related Reactions

This Section reports some further reactions that are important with respect to transition-metal-mediated transformation of SO_2. The reduction of $[Ru(NH_3)_5(SO_2)]^{2\oplus}$ **14** with zinc amalgam gives $[(NH_3)_5Ru{-}S{-}S{-}Ru(NH_3)_5]^{4\oplus}$.[104] The reduction of $[MoCl(S_2CNEt_2)_3]$ with zinc amalgam in CH_2Cl_2/SO_2 results in the formation not only of the Mo^{III}-complex $[Mo(S_2CNEt_2)_3(SO_2)]$ **11**, but also of the analogous $SOCl_2$ complex $[Mo(S_2CNEt_2)_3(SOCl_2)]$.[46] The reactions of $[Pt(PPh_3)_2(SO_2)]$ with CS_2 and of $[Pt(PPh_3)_2(CS_2)]$ with SO_2, which both lead to the dithiocarbonate complex $[Pt(PPh_3)_2(S_2CO)]$,[105] also proceed by unknown mechanisms. The sterically more protected complex **5** and its analogue with CS_2 instead of SO_2 as ligand undergo only

CS_2/SO_2 exchange. This may indicate that the formation of the dithiocarbonate complex can only occur when CS_2 and SO_2 are simultaneously coordinated to platinum.[33]

Innumerable examples of the insertion of SO_2 into transition-metal-carbon σ bonds are known.[4,5,106] SO_2 can react with terminal or bridged methylene complexes by insertion[65] or [2+2] cycloaddition[107] [Eq. (32) and (33)].

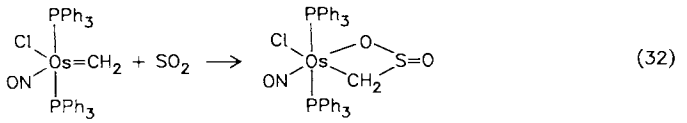

(32)

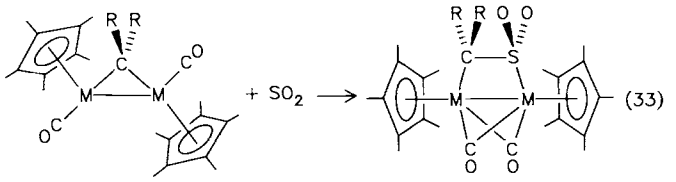

(33)

M = Co, Rh; R = H, Ph

A report of a rapid tautomerism in the hydrido-SO_2 complexes $[MH(CO)(PPh_3)_2(SO_2)]$ (M = Rh, Ir) [Eq. (34)][108] could not be substantiated.[109]

$$[MH(CO)(PPh_3)_2(SO_2)] \rightleftharpoons [M(CO)(PPh_3)_2(SO_2H)] \quad (34)$$

The first authentic example of insertion of SO_2 into a metal-hydrogen bond is shown in Equation (35).[110] The X-ray structure analysis of **25a**, in which all hydrogen

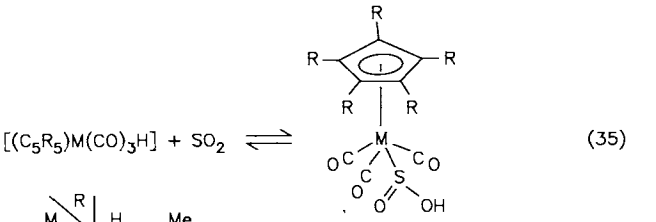

(35)

M \ R	H	Me
Mo	**25a**	**25b**
W	**26a**	**26b**

atoms could be located, unambiguously proves the pyramidal coordination at sulfur; both S-O bonds are distinctly longer (d(S=O) 151.5(6), d(S–OH) 163.7(6) pm) than those in SO_2 complexes. Reaction (35) is reversible, but over longer periods of time reduction products such as **27a** (from **25b**) or **27b** (from **26b**)[110] and μ-sulfido complexes[111] are formed. One μ-sulfido complex, $[Cp_2Mo_2(\mu\text{-}S)_2(\mu\text{-}S_2)]$, is known to catalyze the reduction of SO_2 to sulfur with H_2.[112] An insertion analogous to Equation (35) may be the first step in the formation of the thiosulfato complexes **28a**, **b** from $[Cp_2MH_2]$ and SO_2.[113]

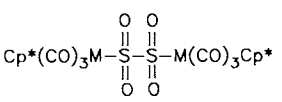

27a, b

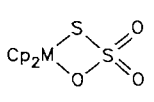

28a, b

Cp* = η^5-C_5Me_5; a, M = Mo; b, M = W

Light-induced insertion of SO_2 has been used to obtain μ-dithionite complexes [Eq. (36)].[114] Reaction (36) is reversible; the radicals $[L_nM]^{\ominus}$ and $[L_nMSO_2]^{\ominus}$ are probably intermediates. This type of intermediate is probably responsible also for the formation of **29**, which is obtained along with **24**, on reaction of $[CpFe(CO)_2]^{\ominus}$ with SO_2 (see Section 2.3.4).[67,114]

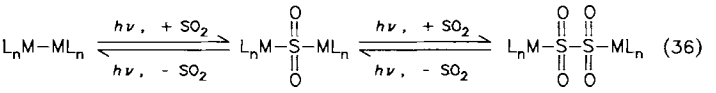

(36)

29, 30a, b

L_nM = $CpFe(CO)_2$ **(29)**, $Mn(CO)_5$ **(30a)**, $Re(CO)_5$ **(30b)**

The well-known reduction of SO_2 to the radical anion $SO_2^{\odot\ominus}$ can also occur with organometallic compounds. One example is the reaction with dibenzenechromium, in which, as shown by ESR spectroscopy, a radical pair is generated [Eq. (37)].[115] The ensuing disproportionation to the salt $[(C_6H_6)_2Cr]_2(S_4O_{10})$ is not well understood. An X-ray structure analysis shows that the anion is a bis-SO_2 adduct of dithionate.[115]

$$[(C_6H_6)_2Cr] + SO_2 \longrightarrow [(C_6H_6)_2Cr]^{\oplus} + SO_2^{\odot\ominus} \quad (37)$$

The examples presented here demonstrate the versatile reactivity of SO_2 in combination with transition metals. The task of fitting together the isolated reaction patterns so far discovered in order to form a complete picture will have to be left to future studies.

3. Complexes with SO

3.1. Synthesis

Attempts to trap SO with reactive transition-metal complexes cannot be regarded as promising because of its extremely rapid disproportionation [Eq. (1)].[9] *Agarwala* et al. reported that thermolysis of *trans*-2,3-diphenylthiirane 1-oxide in the presence of $[Rh(PPh_3)_3X]$ (X = Cl, Br) afforded products $[Rh(PPh_3)(SO)(\mu\text{-}X)]_2$, but these were identified solely on the basis of IR spectra and PPh_3-induced degradation.[116] The analogous reaction with $[Ir(dppe)_2]^{\oplus}$ (DPPE = 1,2-bis(diphenylphosphino)ethane), however, gave complex **31**. The disproportionation of SO

$[Ir(dppe)_2(S_2O)]^{\oplus}$ **31**

obviously competes successfully with its complexation.[117] This problem can be avoided if reaction (2) is transferred to the coordination sphere of a transition metal. The first unambiguously characterized complexes with terminally bound SO were indeed obtained in this way [Eq. (38)].[118,119] Reaction (38) proceeds smoothly at temperatures below 0°C, whereas free thiirane 1-oxide decomposes to SO and C_2H_4 only above 100°C.[11,12,16,19] The coordination to a transition metal thus lowers the activation energy for ring opening by an appreciable amount. Reaction (38) cannot be automatically extended to other

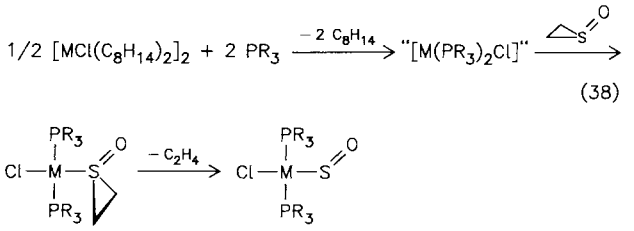

(38)

M \ R	*i*Pr	*cyclo*-C_6H_{11}
Rh	**32a**	**32b**
Ir	**33a**	**33b**

systems[120] (see Section 4.1); the only comparable reaction is the generation, in moderate yield, of the SO-bridged complexes **34a**, **b**

$[\{(RC_5H_4)Mn(CO)_2\}_2(\mu\text{-SO})]$ **34a**, R = H; **b**, R = Me

by the photochemical reaction between $[(RC_5H_4)Mn(CO)_3]$ and thiirane 1-oxide (R = H,[121] Me[119]) or diphenylthiirene 1-oxide (R = Me[122]).

Polynuclear complexes with bridging SO are readily accessible by the oxidation of sulfido complexes. The known examples of this reaction type are summarized by Equations (39)–(41). The formation of complexes **36b**,**c** is supported only by spectroscopic evidence.

$$[\{(C_5R_5)Mn(CO)_2\}_2(\mu\text{-S})] \xrightarrow{O_2} [\{(C_5R_5)Mn(CO)_2\}_2(\mu\text{-SO})] \quad (39)$$

34a, **c**

a, R = H[123]; **c**, R = Me[124]

$$[\{Fe_3(CO)_9\}(\mu\text{-S})_2] + \text{CPBA} \longrightarrow [\{Fe_3(CO)_9\}(\mu\text{-S})(\mu\text{-SO})] \quad (40)$$

35[117, 125]

CPBA = 3-chloroperbenzoic acid

$$[\{Fe_2Pt(CO)_6(PPh_3)_2\}(\mu\text{-E})_2] + \text{CPBA} \longrightarrow [\{Fe_2Pt(CO)_6(PPh_3)_2\}(\mu\text{-E})(\mu\text{-EO})] \quad (41)$$

36a-c[117]

a, E = S; **b**, E = Se; **c**, E = Te

Three related reactions probably proceed similarly, but are less well understood: the synthesis of **35** from $[Fe(CO)_5]/NaOH/Na_2SO_3/H_2O_2$,[126] of **37** from $[p_3Rh(S_2CO)]^{\oplus}$[127] (P_3 = 1,1,1-tris(diphenylphosphinomethyl)ethane), and of **38** from cobalt sulfide and cyanide by air oxidation.[128] Attempts to prepare the μ-SeO complex analogous to **37** led instead to the μ-Se_2 complex.[129]

$[(p_3Rh)_2(\mu\text{-SO})_2]^{2\oplus}$ **37** $[Co_4(CN)_{12}(\mu\text{-S})_3(\mu\text{-SO})]^{8\ominus}$ **38**

As a preparative method, the oxidation of sulfido ligands has its limits. It proved impossible to oxidize the second chalcogen atom of the cluster **35**;[117, 125] the electron-withdrawing SO group apparently makes further electrophilic attack more difficult. *Balch* et al. have reported that the A-frame complex $[\{Pd_2(dppm)_2Cl_2\}(\mu\text{-S})]$ (DPPM = bis(diphenylphosphino)methane) is oxidized to the μ-SO_2 complex even when only one equivalent of CPBA is used.[130]

In two cases thionyl chloride proved a suitable reagent for the introduction of an SO ligand: namely, the preparation of **35** from $[Fe_3(CO)_9(\mu\text{-S}t\text{Bu})]^{\ominus}$[131] and the synthesis of **39**[29] by a reaction analogous to Equation 12. *Vanderpool* and *Abrahamson* reinvestigated the oxidative addition

$[Fe\{P(OPh)_3\}_2(CO)_2(SO)]$ **39**

of thionyl chloride to the Vaska complex[132, 133] and found that the expected product $[Ir(PPh_3)_2(CO)Cl_2(SOCl)]$ is only formed when $SOCl_2$ is always in excess; otherwise, the SO_2 adduct **4** (Fig. 4) is formed, possibly by a second addition step followed by decomposition of the intermediate μ-SO complex.[134]

3.2. Structure and Bonding

The frontier orbitals of SO are largely similar in energy and size to those of CO (Fig. 8);[119] the two extra valence electrons occupy the antibonding 3π orbital and are responsible for the $^3\Sigma^-$ ground state of SO. On coordination to an $[M(PR_3)_2Cl]$ fragment (M = Rh, Ir), these electrons bring about the bending of the M–S–O unit; spin pairing takes place, resulting in a lone pair localized at the sulfur.[119] The coordination of diatomic molecules in linear, bent, or side-on geometry has been thoroughly analyzed by *Hoffmann*.[135] According to his analysis, the compounds **32a**,**b** and **33a**,**b**, like $[Rh(PiPr_3)_2Cl(O_2)]$,[136] should prefer the η^2 coordination, but the electronic asymmetry of the SO ligand makes the bent η^1 coordination more favorable. Less electron-rich systems would have to be employed to realize linear coordination.[137]

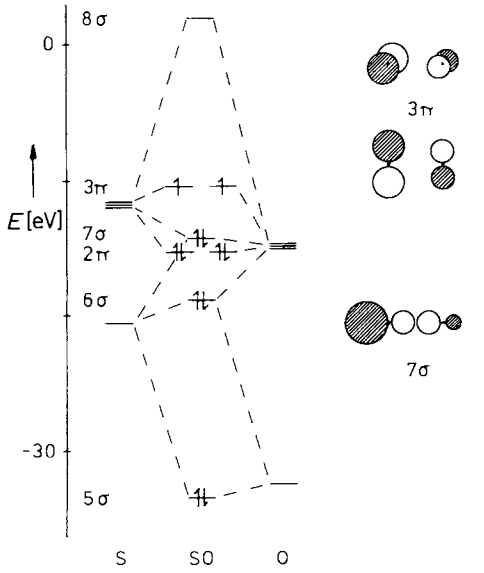

Fig. 8. MO diagram and frontier orbitals of SO [119].

Each known coordination mode of SO has been confirmed by one X-ray structure analysis (Fig. 9). Disorder of Cl and SO in the crystal of **33a** allowed only a rough de-

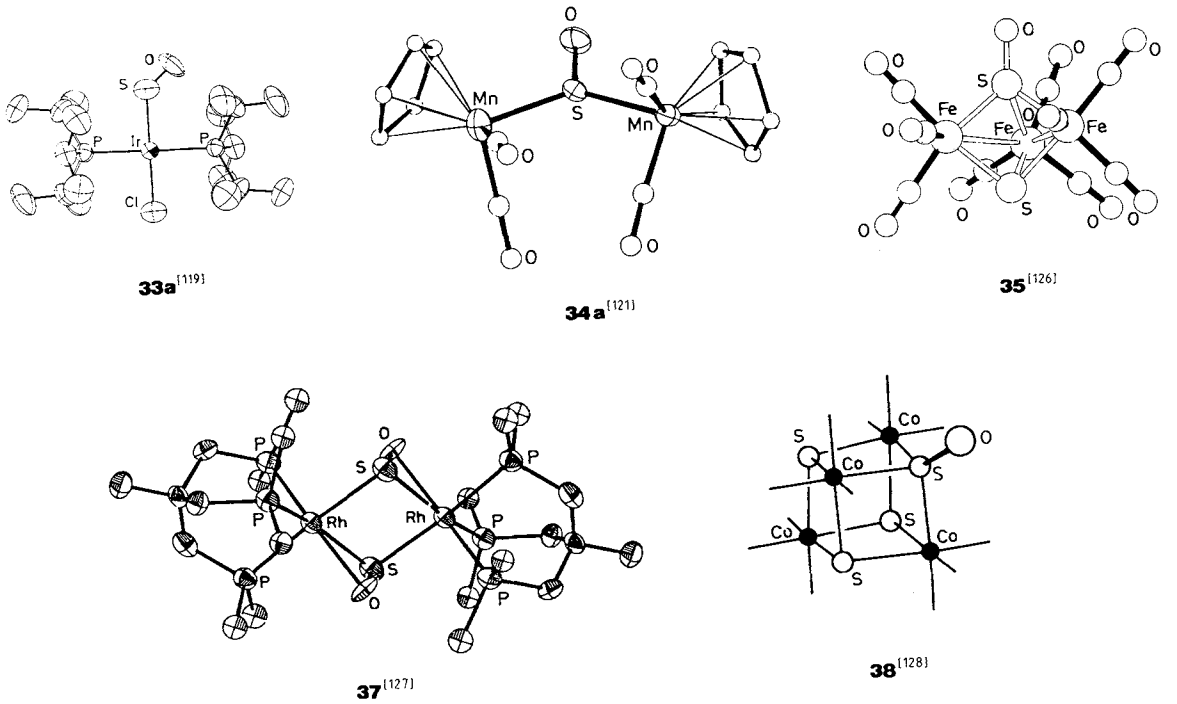

Fig. 9. Structures of the SO complexes **33a**, **34a**, **35**, **37**, and **38** in the crystal. (The unlabeled atoms are carbon atoms.)

termination of the S–O bond length (139 pm),[119] some 9 pm shorter than in free SO.[5] However, the SO stretching frequency of **32a,b** and **33a,b** (ca. 1070 cm^{-1}) is markedly lower than in free SO (1136.7 cm^{-1}[5]), which unambiguously indicates a weakening of the S–O bond on coordination.

The accommodation of a further metal fragment at the lone pair of a bent M–SO group leads to μ^2-bridged complexes of the type **34**. The long Mn–Mn distance of 386.2(1) pm in **34a** rules out metal–metal bonding,[121] and SO thus functions here as a 4-electron donor (Scheme 1, **A**). A conceivable alternative would be the valence tautomer **B** with Mn–Mn bonding and a bent SO unit as 2-electron donor. The same tautomerism is seen in the isoelectronic stibinidene (stibanediyl) complexes (Scheme 1,

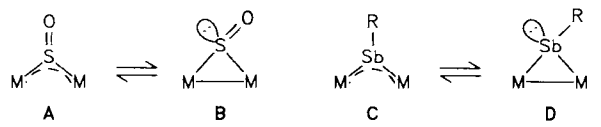

Scheme 1.

C and **D**) and is responsible for the amphoteric behavior toward Lewis acids and bases.[138] The μ-SO complexes **34a–c** should show similar chemical properties. SO also contributes four electrons to the bonding in the *nido*-cluster **35** and in the binuclear complex **37**. Noteworthy in the structure of **35** is the S–S contact of 272 pm, which could indicate a weakly bonding S–S interaction.[126] Complex **37** is the only known example of side-on coordination of SO. The S–O bond is lengthened to 168(1) pm,[127] which is approximately equal to the sum of the single-bond radii of S and O (175 pm). The cobalt cluster **38** can be better described as containing $S^{2\ominus}$ and $SO^{2\ominus}$ (rather than SO) ligands, each acting as a 6-electron donor.[128] The very low S–O stretching frequency (995 cm^{-1}) supports this view.

3.3. Reactivity

The most extensively studied compounds are the square-planar d^8-complexes **32a,b** and **33a,b**. Whereas the rhodium complexes **32a,b** react with CO, even at −70 °C, with displacement of the SO ligand, the analogous iridium complexes **33a,b** form the pentacoordinate intermediates **40a,b** [Eq. (42)]. These decompose in solution at 0 °C but in the solid state only at room temperature; the SO given off can be identified by mass spectrometry.[119] Complexes **32a,b** and **33a,b** are thus promising new reagents, from

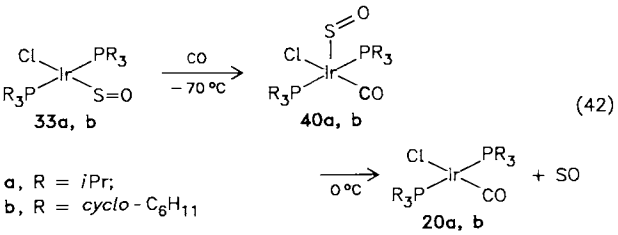

(42)

which SO can be released under much milder conditions than, for example, those of Equation (2). Complex **33a** undergoes oxidative addition with H_2 and HCl [Eq. (43) and (44)].[139] The products, **41** and **42**, respectively, correspond to the $Ir^{[1]}$–SO_2 complexes **22a** and **23a**, respectively. The reactions (42)–(44) thus demonstrate the close analogy between SO and SO_2 complexes.

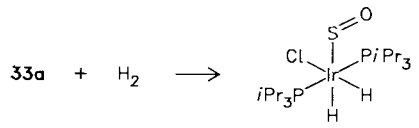

(43)

41

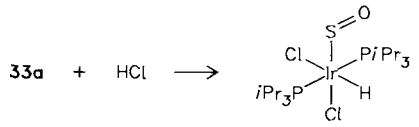

(44)

42

Another typical property of η^1-bonded SO is that it is easily oxidized. For example, CPBA converts **32a** and **33a** into the SO_2 complexes **15a** and **16a**, respectively.[119] Oxygen in the air is sufficient to oxidize the iron complex **39** to **2** (Fig. 3).[29] Bridging SO, however, is not easily oxidized, which is consistent with its role as a 4-electron donor.

4. Complexes with S_2O and S_2O_2

4.1. Synthesis

Almost all known syntheses of S_2O and S_2O_2 complexes are based on the oxidation of S_2 units bound to metal centers. *Schmid* et al. succeeded in preparing the first complexes of unstable sulfur oxides in this way [Eq. (45)].[140, 141] CPBA has proved once again to be a useful

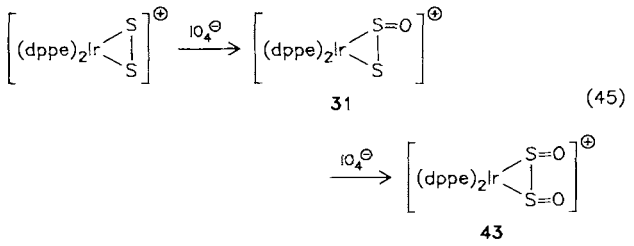

(45)

31

43

electrophilic oxygen-transfer reagent; apart from **31** and **43**, the mononuclear compounds **44**–**48** were synthesized.

$[Cp_2NbCl(S_2O)]$ **44**[116] $[Cp^*Mn(CO)_2(S_2O)]$ **45**
$[Cp^*Mn(CO)_2(S_2O_2)]$ **46** $[Cp^*Re(CO)_2(S_2O)]$ **47**
$[Cp^*Re(CO)_2(S_2O_2)]$ **48**[124]

The synthesis of the first Se_2O complex by oxidation with peracetic acid [Eq. (46)][117] is particularly worthy of

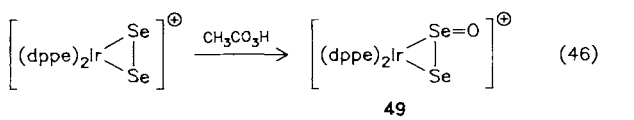

(46)

49

mention. Occasionally the oxidizing power of atmospheric oxygen has proved sufficient; **45**[142] and (in low yield) the S_2O-bridged complex **50** [Eq. (47)][143] were prepared in this way.

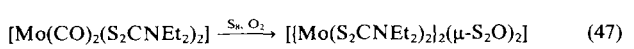

(47)

50

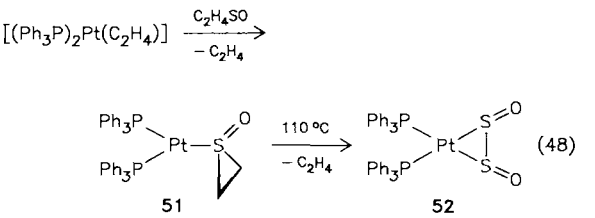

(48)

51 52

Lorenz and *Kull* have recently reported the synthesis of a thiirane 1-oxide complex of platinum, **51**, which is converted into the S_2O_2 complex **52** at 110°C [Eq. (48)].[144] Complex **51** is unusual in several respects (apart from its stability): its phosphorus atoms are nonequivalent in the ^{31}P-NMR spectrum and its SO stretching frequency (953 cm^{-1}) lies well outside the expected range for *S*-coordinated sulfoxides.[145] An η^2-SO coordination has also been considered for **51**, which would however be without precedent.[145] Three-membered rings bearing electronegative substituents usually undergo insertion reactions with Pt^0 complexes, forming platinacyclobutanes,[146] but the authors rule out this possibility for **51**. The SO frequencies given for **52** are also unusual; they lie ca. 200 cm^{-1} lower than for **43**,[117] **46**, and **48**.[124]

4.2. Structures

X-ray structure determinations have been reported for three compounds; relevant details are summarized in Figure 10. On coordination to a $[Cp^*(CO)_2Mn]$ fragment, the S–S bond length, in particular, increases appreciably (free S_2O: *d*(S-S) 188.2 pm, *d*(S-O) 146.4 pm, ∢(SSO) 118.3°[5]).[142] This is attributable to charge transfer from the HOMO of the metal fragment to the π^* orbital of S_2O. The high π-acceptor capability of the S_2O ligand is also reflected in the CO force constant (15.83 N cm^{-1}), which is significantly greater than in the starting material $[Cp^*Mn(CO)_3]$ (15.30 N cm^{-1}).[124] The S–O bond also is weakened on coordination, as can be seen from the increased bond length and the reduced stretching frequency (1156 to 1056 cm^{-1}).[142] In the binuclear complex **50**, the S–S bond is longer than a normal single bond.[143] This presumably corresponds to the first stages of breaking the S–S bond, a process that is complete in the cluster **35** (Fig. 9).

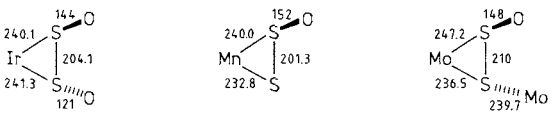

43[140] **45**[142] **50**[143]

Fig. 10. Part of the structure of the S_2O_2 complex **43** and the S_2O complexes **45** and **50** in the crystal. Bond lengths in pm.

The oxidation of $[Ir(dppe)_2(S_2)]^{\oplus}$ to the S_2O_2 complex **43** leaves the geometry of the IrS_2 ring practically unchanged. The S–S bond length, which in free S_2O_2 also corresponds to a single bond (202.5 pm),[5] is only marginally increased. However, the S_2O_2 ligand in **43** displays a torsion angle of 68°,[140] whereas the free molecule is planar. Complexes **46** and **48** are formed as mixtures of two isomers; presuma-

bly one is the *anti* isomer corresponding to **43** and the other is the *syn* isomer.[124]

4.3. Reactivity

S_2O_2 complexes are characterized by ease of reduction. In solution the complexes **46** and **48** undergo spontaneous conversion to the S_2O complexes **45** and **47**, respectively;[124] **43** can be deoxygenated to **31** with PPh_3.[141] More reactive still is the Se_2O compound **49**, which, for example, oxidizes thiols to disulfides.[117]

With excess PPh_3 the S_2O and S_2O_2 complexes are reduced to various products. Complex **44** gives $[Cp_2Nb(O)Cl]$ and Ph_3PS.[117] Complex **43** is broken down completely to $[Ir(dppe)_2]^{\oplus}$, Ph_3PO and Ph_3PS being formed in a 1 : 1 ratio.[140]

The attempt to convert **31** into an η^2-SO complex, by analogy with the abstraction of sulfur from CS_2 complexes [Eq. (49)],[147] was unsuccessful [Eq. (50)].[117] Nucleophilic attack on the endocyclic sulfur is successful, however, if the oxygen is first methylated [Eq. (51)].[148]

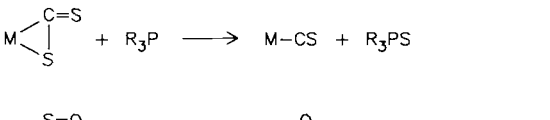

(49)

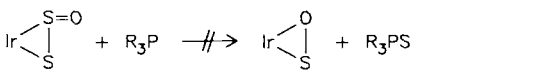

(50)

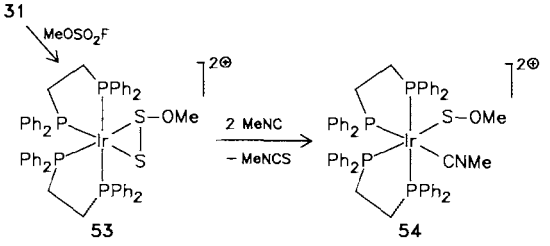

(51)

Complex **53** was characterized by X-ray structure determination; a comparison with the S_2O complex **45** shows a conspicuously (10 pm) longer S–O bond. The end product **54** can be considered as an Ir^{III} complex of the *O*-methylsulfenate ligand $MeOS^{\ominus}$.

5. Complexes with SO_3 and with Cyclic Sulfur Oxides

SO_3 is a strong Lewis acid and therefore reacts with a variety of bases to form adducts having tetracoordinated sulfur.[5] (Transition-metal complexes of the form $[L_nM(SO_3)]$ can, consistent with their chemical properties, be regarded as sulfito complexes; i.e., the bonding electron pair is, as usual, considered to originate from the ligand.) A coordination at oxygen is only conceivable with the strongest Lewis acids. Examples are the adducts with $SbCl_3$ and $SbCl_5$,[149] which, however, have also been formulated as chlorosulfates.[150] No structure determinations have been performed.

The compounds **55**[151] and **56**[152] have been unambiguously demonstrated to be *O*-adducts. On coordination, the conformation of the S_8O ring undergoes reversible change, the oxygen changing its position from axial to equatorial. The S–O bond in **55** is longer than that in free S_8O by 7 pm and the neighboring S–S bonds shorter by 9 pm. Similar bond lengths are found in the adduct **56**, in which the $OSbCl_5$ groups, however, are axial. Complex **56** is notable in particular for its formation from S_6O.[152]

$S_8O \cdot SbCl_5$ **55** $S_{12}O_2 \cdot 2SbCl_5$ **56**

Sulfur rings are easily opened and broken down to smaller units by transition-metal complexes; the only example of an intact S_n molecule as a ligand is in the compound $[Ag(S_8)_2]AsF_6$.[153] In view of the lability of cyclic sulfur oxides, it is likely to be difficult to obtain transition-metal complexes containing them as ligands. They may, however, be suitable sources of smaller S_nO units.

6. Summary and Prospects

Many preparative and structural studies have demonstrated the versatility of SO_2 as a ligand. Correlations between structure and reactivity are beginning to be recognized. Future studies will be able to build on these results and to develop the chemistry of coordinated SO_2. The chances of generating otherwise unstable compounds in the protecting environment of a transition metal seem particularly promising.

The unstable lower sulfur oxides SO, S_2O, and S_2O_2 can be stabilized in mono- and polynuclear metal complexes. Preliminary results show that the analogous selenium and tellurium compounds are also accessible, but studies of the reactivity of these compounds are still in their infancy. The experience gained with SO_2 complexes should be transferable to such systems and should thus help to exploit the lower sulfur oxides as synthetic "building blocks."[155]

I should like to thank Prof. Dr. M. Herberhold and Prof. Dr. E. Weiss for making unpublished results available, my co-workers, in particular Dr. Franz-Erich Baumann and Dipl.-Chem. Johanna Leissner, for carrying out much of our own work that has been described here, Dr. Christian Burschka for X-ray structure determinations, and the Deutsche Forschungsgemeinschaft, the Fonds der Chemischen Industrie, and Degussa AG for generous financial assistance.

Received: April 9, 1986;
revised: July 24, 1986 [A 607 IE]
German version: *Angew. Chem. 99* (1987) 101
Translated by Dr. *Peter G. Jones*, Göttingen

[1] K. Gleu, W. Breuel, K. Rehm, *Z. Anorg. Allg. Chem. 235* (1938) 201.
[2] K. Gleu, W. Breuel, *Z. Anorg. Allg. Chem. 235* (1938) 211.
[3] D. M. P. Mingos, *Transition Met. Chem. (Weinheim Ger.) 3* (1978) 1.
[4] R. R. Ryan, G. J. Kubas, D. C. Moody, P. G. Eller, *Struct. Bonding (Berlin) 46* (1981) 47.
[5] *Gmelin Handbuch der Anorganischen Chemie*, 8th ed. *(Schwefel, Ergänzungsband 3)*, Springer, Berlin 1980.
[6] P. W. Schenk, *Z. Anorg. Allg. Chem. 211* (1933) 150.
[7] P. W. Schenk, R. Steudel, *Angew. Chem. 77* (1965) 437; *Angew. Chem. Int. Ed. Engl. 4* (1965) 402.

[8] D. J. Meschi, R. J. Myers, *J. Am. Chem. Soc. 78* (1956) 6220.
[9] J. T. Herron, R. E. Huie, *Chem. Phys. Lett. 76* (1980) 322.
[10] G. Maccagnani, *Org. Sulfur Chem. Invited Lect. Int. Symp. 9th 1980 (1981)* 123.
[11] G. E. Hartzell, J. N. Paige, *J. Am. Chem. Soc. 88* (1966) 2616.
[12] R. M. Dodson, R. F. Sauers, *Chem. Commun. 1967*, 1189.
[13] Y. L. Chow, J. N. S. Tam, J. E. Blier, H. H. Szmant, *Chem. Commun. 1970*, 1604.
[14] J. E. Baldwin, G. Höfle, S. C. Choi, *J. Am. Chem. Soc. 93* (1971) 2810.
[15] D. C. de Jongh, R. Y. van Fossen, *J. Org. Chem. 37* (1972) 1129.
[16] P. Chao, D. M. Lemal, *J. Am. Chem. Soc. 95* (1973) 920; D. M. Lemal, P. Chao, *ibid. 95* (1973) 922.
[17] K. Torssell, *Acta Chem. Scand. Ser. B30* (1976) 353; R. H. Kellog, W. L. Prins, *J. Org. Chem. 39* (1974) 2366; C. L. Gajurel, S. R. Vaidya, K. B. Shrestha, *Indian J. Chem. Sect. B18* (1979) 361.
[18] B. F. Bonini, G. Maccagnani, G. Mazzanti, *J. Chem. Soc. Chem. Commun. 1976*, 431.
[19] W. G. L. Aalbersberg, K. P. C. Vollhardt, *J. Am. Chem. Soc. 99* (1977) 2792.
[20] B. F. Bonini, G. Maccagnani, G. Mazzanti, P. Pedrini, P. Picinelli, *J. Chem. Soc. Perkin Trans. 1 1979*, 1720.
[21] R. Schulz, A. Schweig, *Angew. Chem. 93* (1981) 603; *Angew. Chem. Int. Ed. Engl. 20* (1981) 570.
[22] L. A. Carpino, H. W. Chen, *J. Am. Chem. Soc. 101* (1979) 390; S. Ito, J. Mori, *Bull. Chem. Soc. Jpn. 51* (1978) 3403; F. H. Dorer, K. E. Salomon, *J. Phys. Chem. 84* (1980) 3024.
[23] A. Senning, *Acta Chem. Scand. 19* (1965) 1755.
[24] D. Knittel, *J. Electroanal. Chem. Interfacial Electrochem. 195* (1985) 345.
[25] W. K. Istone, R. J. Brodd, *J. Electrochem. Soc. 129* (1982) 1853; *131* (1984) 2467.
[26] R. Steudel, *Comments Inorg. Chem. 1* (1982) 313; in A. Müller, B. Krebs (Eds.): *Studies in Inorganic Chemistry: Sulfur, Vol. 5*, Elsevier, Amsterdam 1984, p. 3; *Phosphorus Sulfur 23* (1985) 33.
[27] C. Burschka, F. E. Baumann, W. A. Schenk, *Z. Anorg. Allg. Chem. 502* (1983) 191.
[28] P. Conway, S. M. Grant, A. R. Manning, F. S. Stephens, *Inorg. Chem. 22* (1983) 3714.
[29] I. P. Lorenz, W. Hiller, M. Conrad, *Z. Naturforsch. B40* (1985) 1383.
[30] C. Barbeau, R. J. Dubey, *Can. J. Chem. 51* (1973) 3684.
[31] L. Vaska, S. S. Bath, *J. Am. Chem. Soc. 88* (1966) 1333.
[32] S. J. la Placa, J. A. Ibers, *Inorg. Chem. 5* (1966) 405.
[33] J. M. Ritchey, D. C. Moody, R. R. Ryan, *Inorg. Chem. 22* (1983) 2276.
[34] D. van der Helm, J. D. Childs, S. D. Christian, *Chem. Commun. 1969*, 887.
[35] J. D. Childs, D. van der Helm, S. D. Christian, *Inorg. Chem. 14* (1975) 1386.
[36] R. R. Ryan, P. G. Eller, *Inorg. Chem. 15* (1976) 494.
[37] P. Dapporto, S. Midollini, A. Orlandini, L. Sacconi, *Inorg. Chem. 15* (1976) 2773.
[38] D. C. Moody, R. R. Ryan, *Inorg. Chem. 18* (1979) 223.
[39] C. Mealli, A. Orlandini, L. Sacconi, P. Stoppioni, *Inorg. Chem. 17* (1978) 3020.
[40] J. E. Huheey: *Inorganic Chemistry: Principles of Structure and Reactivity*, 2nd ed., Harper & Row, New York 1978, p. 534; F. A. Cotton, G. Wilkinson: *Advanced Inorganic Chemistry*, 4th ed., Wiley, New York 1980, p. 90.
[41] J. W. Moore, H. W. Baird, H. B. Miller, *J. Am. Chem. Soc. 90* (1968) 1358.
[42] R. Hoppenheit, W. Isenberg, R. Mews, *Z. Naturforsch. B37* (1982) 1116.
[43] G. A. Gott, J. Fawcett, C. A. McAuliffe, D. R. Russell, *J. Chem. Soc. Chem. Commun. 1984*, 1283.
[44] G. J. Kubas, R. R. Ryan, V. McCarty, *Inorg. Chem. 19* (1980) 3003.
[45] F. E. Baumann, *Dissertation*, Universität Würzburg 1985; F. E. Baumann, C. Burschka, W. A. Schenk, *Z. Naturforsch. B41* (1986) 1211.
[46] J. A. Broomhead, N. S. Gill, B. C. Hammer, M. Sterns, *J. Chem. Soc. Chem. Commun. 1982*, 1234.
[47] W. A. Herrmann, J. Planck, M. L. Ziegler, P. Wülknitz, *Chem. Ber. 114* (1981) 716.
[48] D. Braga, R. Ros, R. Roulet, *J. Organomet. Chem. 286* (1985) C8.
[49] C. E. Briant, G. R. Hughes, P. C. Minshall, D. M. P. Mingos, *J. Organomet. Chem. 224* (1982) C21.
[50] G. D. Jarvinen, G. J. Kubas, R. R. Ryan, *J. Chem. Soc. Chem. Commun. 1981*, 305.
[51] C. E. Briant, B. R. C. Theobald, D. M. P. Mingos, *J. Chem. Soc. Chem. Commun. 1981*, 963.
[52] W. A. Schenk, F. E. Baumann, *Chem. Ber. 115* (1982) 2615.
[53] W. Strohmeier, J. F. Guttenberger, G. Popp, *Chem. Ber. 98* (1965) 2248.
[54] R. Mews, *Angew. Chem. 87* (1975) 669; *Angew. Chem. Int. Ed. Engl. 14* (1975) 640.
[55] G. Hartmann, R. Froböse, R. Mews, G. M. Sheldrick, *Z. Naturforsch. B37* (1982) 1234.
[56] W. A. Schenk, F. E. Baumann, *J. Organomet. Chem. 256* (1983) 261.
[57] W. A. Schenk, F. E. Baumann, *J. Organomet. Chem. 260* (1984) C6.
[58] G. Hartmann, R. Mews, *Chem. Ber. 119* (1986) 374.
[59] M. Höfler, A. Baitz, *Chem. Ber. 109* (1976) 3147.
[60] R. Meij, D. J. Stufkens, K. Vrieze, W. van Gerresheim, C. H. Stam, *J. Organomet. Chem. 164* (1979) 353.
[61] M. Kubota, B. M. Loeffler, *Inorg. Chem. 11* (1972) 469.
[62] W. Hofmann, H. Werner, *Angew. Chem. 93* (1981) 1088; *Angew. Chem. Int. Ed. Engl. 20* (1981) 1014.
[63] H. Werner, W. Hofmann, R. Zolk, L. F. Dahl, J. Kocal, A. Kühn, *J. Organomet. Chem. 289* (1985) 173.
[64] L. Chen, D. J. Kountz, D. W. Meek, *Organometallics 4* (1985) 598.
[65] W. A. Herrmann, C. Bauer, J. Weichmann, *Chem. Ber. 117* (1984) 1271.
[66] J. K. Ruff, *Inorg. Chem. 6* (1967) 2080.
[67] P. Reich-Rohrwig, A. C. Clark, R. L. Downs, A. Wojcicki, *J. Organomet. Chem. 145* (1978) 57.
[68] G. D. Jarvinen, R. R. Ryan, *Organometallics 3* (1984) 1434.
[69] J. T. Mague, A. R. Sanger, *Inorg. Chem. 18* (1979) 2060.
[70] M. Cowie, S. K. Dwight, *Inorg. Chem. 19* (1980) 2500.
[71] M. Cowie, R. S. Dickson, B. W. Hames, *Organometallics 3* (1984) 1879.
[72] M. L. Kullberg, C. P. Kubiak, *Organometallics 3* (1984) 632; *Inorg. Chem. 25* (1986) 26.
[73] J. Ellermann, G. Szucsányi, *Chem. Ber. 118* (1985) 1868.
[74] M. Cowie, S. K. Dwight, A. R. Sanger, *Inorg. Chim. Acta 31* (1978) L407.
[75] M. Cowie, S. K. Dwight, *Inorg. Chem. 19* (1980) 209.
[76] M. Angoletta, L. Malatesta, G. Caglio, *J. Chem. Soc. Dalton Trans. 1977*, 2131.
[77] M. F. Hallam, N. D. Howells, D. M. P. Mingos, R. W. M. Wardle, *J. Chem. Soc. Dalton Trans. 1985*, 845.
[78] T. W. Turney, *Inorg. Chim. Acta 64* (1982) L141.
[79] P. Thometzek, K. Zenkert, H. Werner, *Angew. Chem. 97* (1985) 520; *Angew. Chem. Int. Ed. Engl. 24* (1985) 516.
[80] J. M. Ritchey, D. C. Moody, *Inorg. Chim. Acta 74* (1983) 271.
[81] C. S. Browning, D. H. Farrar, R. R. Gukathasan, S. A. Morris, *Organometallics 4* (1985) 1750.
[82] D. G. Evans, G. R. Hughes, D. M. P. Mingos, J. M. Bassett, A. J. Welch, *J. Chem. Soc. Chem. Commun. 1980*, 1255.
[83] S. Otsuka, Y. Tatsuno, M. Miki, T. Aoki, M. Matsumoto, H. Yoshioka, K. Nakatsu, *J. Chem. Soc. Chem. Commun. 1973*, 445.
[84] D. M. P. Mingos, R. W. M. Wardle, *J. Chem. Soc. Dalton Trans. 1986*, 73.
[85] F. Faraone, G. Bruno, S. lo Schiavo, G. Bombieri, *J. Chem. Soc. Dalton Trans. 1984*, 533.
[86] D. M. P. Mingos, R. W. M. Wardle, *Transition Met. Chem. (Weinheim Ger.) 10* (1985) 441.
[87] W. A. Schenk, *Z. Naturforsch. B41* (1986) 663.
[88] C. Potvin, J. M. Brégault, J. M. Manoli, *J. Chem. Soc. Chem. Commun. 1980*, 664.
[89] J. M. Manoli, J. M. Brégault, C. Potvin, G. Chottard, *Inorg. Chim. Acta 88* (1984) 75.
[90] F. R. Fronczek, R. E. Marsh, W. P. Schaefer, *J. Am. Chem. Soc. 104* (1982) 3382.
[91] A. Müller, U. Reinsch-Vogell, E. Krickemeyer, H. Bögge, *Angew. Chem. 94* (1982) 784; *Angew. Chem. Int. Ed. Engl. 21* (1982) 790.
[92] G. J. Kubas, *Inorg. Chem. 18* (1979) 182.
[93] W. A. Schenk, J. Leißner, *J. Organomet. Chem. 311* (1986) C27.
[94] F. Basolo, *Inorg. Chim. Acta 100* (1985) 33.
[95] P. R. Blum, D. W. Meek, *Inorg. Chim. Acta 24* (1977) L75.
[96] G. J. Kubas, G. D. Jarvinen, R. R. Ryan, *J. Am. Chem. Soc. 105* (1983) 1883.
[97] C. R. Jablonski, *J. Organomet. Chem. 142* (1977) C25.
[98] J. E. Thomasson, P. W. Robinson, D. A. Ross, A. Wojcicki, *Inorg. Chem. 10* (1971) 2130; R. L. Downs, A. Wojcicki, *Inorg. Chim. Acta 27* (1978) 91.
[99] J. J. Alexander, A. Wojcicki, *Inorg. Chim. Acta 5* (1971) 655.
[100] D. C. Moody, R. R. Ryan, *J. Chem. Soc. Chem. Commun. 1980*, 1230.
[101] D. C. Moody, R. R. Ryan, *Inorg. Chem. 16* (1977) 1052.
[102] T. E. Nappier, D. W. Meek, R. M. Kirchner, J. A. Ibers, *J. Am. Chem. Soc. 95* (1973) 4194; J. Terheijden, G. van Koten, W. P. Mul, D. J. Stufkens, F. Muller, C. H. Stam, *Organometallics 5* (1986) 519.
[103] J. Valentine, D. Valentine, J. P. Collman, *Inorg. Chem. 10* (1971) 219; S. P. Mehandru, A. B. Anderson, *ibid. 24* (1985) 2570.
[104] C. R. Brulet, S. S. Isied, H. Taube, *J. Am. Chem. Soc. 95* (1973) 4758; R. C. Elder, M. Trkula, *Inorg. Chem. 16* (1977) 1048.

[105] I. Ghatak, D. M. P. Mingos, M. B. Hursthouse, P. R. Raithby, *Transition Met. Chem. (Weinheim Ger.) 1* (1976) 119.
[106] A. Wojcicki, *Adv. Organomet. Chem. 12* (1974) 31; T. C. Flood, *Top. Stereochem. 12* (1981) 37; J. J. Alexander in F. R. Hartley, S. Patai (Eds.): *The Chemistry of the Metal-Carbon Bond. Vol. 2*, Wiley, New York 1985, p. 339.
[107] W. R. Roper, J. M. Waters, A. H. Wright, *J. Organomet. Chem. 276* (1984) C 13.
[108] J. J. Levison, S. D. Robinson, *J. Chem. Soc. Dalton Trans. 1972*, 2013.
[109] L. K. Bell, D. M. P. Mingos, *J. Chem. Soc. Dalton Trans. 1982*, 673.
[110] G. J. Kubas, H. J. Wasserman, R. R. Ryan, *Organometallics 4* (1985) 2012.
[111] G. J. Kubas, H. J. Wasserman, R. R. Ryan, *Organometallics 4* (1985) 419.
[112] G. J. Kubas, R. R. Ryan, *J. Am. Chem. Soc. 107* (1985) 6138.
[113] G. J. Kubas, R. R. Ryan, *Inorg. Chem. 23* (1984) 3181.
[114] C. A. Poffenberger, N. H. Tennent, A. Wojcicki, *J. Organomet. Chem. 191* (1980) 107.
[115] C. Elschenbroich, R. Gondrum, W. Massa, *Angew. Chem. 97* (1985) 976; *Angew. Chem. Int. Ed. Engl. 24* (1985) 967.
[116] K. S. Arulsamy, K. K. Pandey, U. C. Agarwala, *Inorg. Chim. Acta 54* (1981) L 51.
[117] J. E. Hoots, D. A. Lesch, T. B. Rauchfuss, *Inorg. Chem. 23* (1984) 3130.
[118] W. A. Schenk, J. Leißner, C. Burschka, *Angew. Chem. 96* (1984) 787; *Angew. Chem. Int. Ed. Engl. 23* (1984) 806.
[119] W. A. Schenk, J. Leißner, C. Burschka, *Z. Naturforsch. B40* (1985) 1264.
[120] J. Messelhäuser, I.-P. Lorenz, K. Haug, W. Hiller, *Z. Naturforsch. B40* (1985) 1064.
[121] I.-P. Lorenz, J. Messelhäuser, W. Hiller, K. Haug, *Angew. Chem. 97* (1985) 234; *Angew. Chem. Int. Ed. Engl. 24* (1985) 228.
[122] E. Weiß (Hamburg), private communication; K.-J. Jens, *Dissertation*, Universität Hamburg 1983.
[123] M. Höfler, A. Baitz, *Chem. Ber. 109* (1976) 3147.
[124] M. Herberhold, B. Schmidkonz, *J. Organomet. Chem. 308* (1986) 35.
[125] I.-P. Lorenz, J. Messelhäuser, *Z. Naturforsch. B39* (1984) 403.
[126] L. Markó, B. Markó-Monostory, T. Madach, H. Vahrenkamp, *Angew. Chem. 92* (1980) 225; *Angew. Chem. Int. Ed. Engl. 19* (1980) 226.
[127] C. Bianchini, C. Mealli, A. Meli, M. Sabat, *J. Chem. Soc. Chem. Commun. 1985*, 1024.
[128] A. Müller, E. Krickemeyer, R. Jostes, H. Bögge, E. Diemann, U. Bergmann, *Z. Naturforsch. B40* (1985) 1715.
[129] C. Bianchini, C. Mealli, A. Meli, M. Sabat, *J. Am. Chem. Soc. 107* (1985) 5317.
[130] A. L. Balch, L. S. Benner, M. M. Olmstead, *Inorg. Chem. 18* (1979) 2996.
[131] A. Winter, L. Zsolnai, G. Huttner, *J. Organomet. Chem. 234* (1982) 337.
[132] G. Schmid, G. Ritter, *Z. Anorg. Allg. Chem. 415* (1975) 97.
[133] S. J. Markham, Y. L. Chung, G. D. Branum, D. M. Blake, *J. Organomet. Chem. 107* (1976) 121.
[134] R. A. Vanderpool, H. B. Abrahamson, *Inorg. Chem. 24* (1985) 2985.
[135] R. Hoffmann, M. M.-L. Chen, D. L. Thorn, *Inorg. Chem. 16* (1977) 503.
[136] C. Busetto, A. d'Alfonso, F. Maspero, G. Perego, A. Zazzetta, *J. Chem. Soc. Dalton Trans. 1977*, 1828.
[137] For analogous considerations of phosphinidene complexes, see G. Trinquier, G. Bertrand, *Inorg. Chem. 24* (1985) 3842.
[138] U. Weber, G. Huttner, O. Scheidsteger, L. Zsolnai, *J. Organomet. Chem. 289* (1985) 357; H. Lang, G. Huttner, B. Sigwarth, U. Weber, L. Zsolnai, I. Jibril, O. Orama, *Z. Naturforsch. B41* (1986) 191; G. Huttner, *Pure Appl. Chem. 58* (1986) 585.
[139] W. A. Schenk, J. Leißner, unpublished results.
[140] G. Schmid, G. Ritter, T. Debaerdemaeker, *Chem. Ber. 108* (1975) 3008.
[141] G. Schmid, G. Ritter, *Angew. Chem. 87* (1975) 673; *Angew. Chem. Int. Ed. Engl. 14* (1975) 645.
[142] M. Herberhold, B. Schmidkonz, M. L. Ziegler, T. Zahn, *Angew. Chem. 97* (1985) 517; *Angew. Chem. Int. Ed. Engl. 24* (1985) 515.
[143] J. Dirand-Colin, M. Schappacher, L. Ricard, R. Weiss, *J. Less-Common Met. 54* (1977) 91.
[144] I.-P. Lorenz, J. Kull, *Angew. Chem. 98* (1986) 276; *Angew. Chem. Int. Ed. Engl. 25* (1986) 261.
[145] J. A. Davies, *Adv. Inorg. Chem. Radiochem. 24* (1981) 115.
[146] J. K. Stille in F. R. Hartley, S. Patai (Eds.): *The Chemistry of the Metal-Carbon Bond. Vol. 2*, Wiley, New York 1985, p. 625.
[147] I. S. Butler, A. E. Fenster, *J. Organomet. Chem. 66* (1974) 161; P. V. Yaneff, *Coord. Chem. Rev. 23* (1977) 183; I. S. Butler, *Acc. Chem. Res. 10* (1977) 359; J. A. Ibers, *Chem. Soc. Rev. 11* (1982) 57; H. Werner, *Coord. Chem. Rev. 43* (1982) 165; P. V. Broadhurst, *Polyhedron 4* (1985) 1801.
[148] J. E. Hoots, T. B. Rauchfuss, S. R. Wilson, *J. Chem. Soc. Chem. Commun. 1983*, 1226.
[149] H. A. Lehmann, L. Riesel, *Z. Anorg. Allg. Chem. 371* (1969) 274, 281; L. Riesel, *Z. Chem. 9* (1969) 129.
[150] C. L. Arora, R. Kumar, B. B. Sandhir, *Ann. Chim. 1977*, 219; R. C. Paul, R. C. Kumar, R. D. Verma, *Indian J. Chem. Sect. A 16* (1978) 695.
[151] R. Steudel, T. Sandow, J. Steidel, *J. Chem. Soc. Chem. Commun. 1980*, 180.
[152] R. Steudel, J. Steidel, J. Pickardt, *Angew. Chem. 92* (1980) 313; *Angew. Chem. Int. Ed. Engl. 19* (1980) 325.
[153] H. W. Roesky, M. Thomas, J. Schimkowiak, P. G. Jones, W. Pinkert, G. M. Sheldrick, *J. Chem. Soc. Chem. Commun. 1982*, 895.
[154] Besides **17**, a heterometallic Pd-Pt complex with SO_2 bridge is known: P. G. Pringle, B. L. Shaw, *J. Chem. Soc. Dalton Trans. 1983*, 889.
[155] Since completion of this manuscript the following publications have appeared. SO_2 complexes of Ni and Pd: E. Wenschuh, T. Hoffmann, K. Handtke, *Z. Chem. 26* (1986) 212; P. Zdunneck, A. Häusler, E. Wenschuh, *ibid. 26* (1986) 302. Reactions of $[(R_3P)MnX_2]$ (X = Cl, Br, I) with SO_2: D. S. Barratt, C. G. Benson, G. A. Gott, C. A. McAuliffe, S. P. Tanner, *J. Chem. Soc. Dalton Trans. 1985*, 2661; W. E. Hill, S. D. Worley, D. K. Paul, V. F. Newberry, *Inorg. Chem. 24* (1985) 4429; V. F. Newberry, W. E. Hill, S. D. Worley, *Phosphorus Sulfur 27* (1986) 253. Pt clusters with SO_2 bridges: C. E. Briant, D. G. Evans, D. M. P. Mingos, *J. Chem. Soc. Dalton Trans. 1986*, 1535. Me_3NO-promoted SO_2 dissociation: M. F. Hallam, D. M. P. Mingos, *J. Organomet. Chem. 315* (1986) C 35. Kinetics of the insertion of SO_2 into the Pt-Pt bond: S. Muralidharan, J. H. Espenson, S. A. Ross, *Inorg. Chem. 25* (1986) 2557. Heterobimetallic Pd-Pt complexes with SO_2 bridges: J. Fornies, F. Martinez, R. Navarro, A. Redondo, M. Tomas, A. J. Welch, *J. Organomet. Chem. 316* (1986) 351. Formation of **37** from $[(p_3Rh)_2(\mu\text{-}S)_2]^{2\oplus}$: C. Bianchini, C. Mealli, A. Meli, M. Sabat, *Inorg. Chem. 25* (1986) 4617. Synthesis and structure of $[(S_8O)_2SnCl_4]$: R. Steudel, J. Steidel, T. Sandow, *Z. Naturforsch. B41* (1986) 951.

Nuclear Quadrupole Interaction and Time-Resolved Perturbed γ-γ-Angular Correlation Spectroscopy: Applications in Chemistry, Materials Science, and Biophysical Chemistry

New Analytical Methods (31)

By Anton Lerf* and Tilman Butz

The study of nuclear quadrupole interactions, i.e. of the strength, symmetry, and orientation of the electric field gradient tensor, yields valuable information on charge density distributions on an atomic scale. Apart from the nowadays "conventional" methods of NMR and Mössbauer spectroscopy there is yet another technique: time-resolved perturbed γ-γ-angular correlation spectroscopy. This technique is very well suited for applications in chemistry (e.g. comparative studies of bond conditions of inorganic complexes in the solid and in solution or in the melt), in molecular biology (e.g. intramolecular dynamics in biomolecules), and in materials science (e.g. investigation of catalyst surfaces) because of, inter alia, the extremely small sample requirements and the temperature independence of the sensitivity. The variation of the electric field gradient tensor (strength, symmetry, possibly orientation) is observed as a function of external parameters or, in the case of reactions, as a function of the degree of reaction. The interpretation of results requires the assignment of observed signals to known species or configurations. In this progress report we review modern areas of application of perturbed angular correlation spectroscopy.

1. Introduction

NMR and Mössbauer (ME) spectroscopy are well established techniques that have become indispensable in chemical laboratories. In contrast, a further hyperfine spectroscopic technique, namely perturbed angular correlation (PAC), is practically unknown to chemists. The reasons for this are that the technique requires the use of radioactive material, and that its application was for decades almost exclusively confined to the domains of the nuclear physicist.[1-8] Only since about 1970 has it been applied to any notable extent to problems in solid state physics, chemistry, and biology.

The method relies on the fact that, due to conservation of angular momentum, the direction of emission of a particle in a nuclear decay is strictly correlated with the orientation of the nuclear spin. Since the nuclear spins are normally randomly oriented, "information" on the spatial correlation is lost. If, on the other hand, the nuclei are oriented in an applied external magnetic field at very low temperatures, different count-rates can be measured with detectors positioned at 0° and 90° with respect to the axis of orientation; this difference is called anisotropy. Since orientation of the nuclei[6] usually requires temperatures in the mK range, such a method of measurement is not suitable for chemical applications. There is, however, a further method for the detection of anisotropy: angular correlation (theoretically predicted in 1940,[9] first demonstrated experimentally in 1947[10]). For this, excited nuclei, which decay via a particle cascade (see Fig. 1), are used. With the observation of the first particle, a sub-ensemble of the ensemble of randomly oriented nuclei is selected. By measuring in coincidence, only those second particles which are emitted by this sub-ensemble are detected. This leads, irrespective of the nature of the particles (α,β,γ-particles or CE[*]), to different coincidence count-rates in detectors positioned at 90° and 180°. However, the measurement of α- and β-particles is less suited for applications in chemistry, as these particles are easily absorbed in the reaction vessel. The nuclear orientation can also be achieved by nuclear reactions via particle bombardment in accelerators. If the

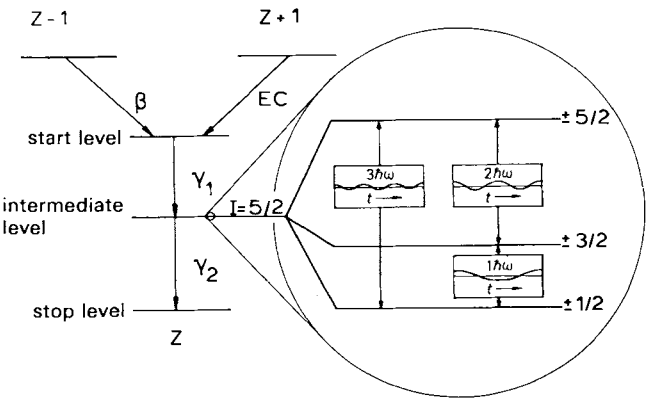

Fig. 1. Left: Schematic description of the decay of an excited nucleus with nuclear charge Z via a γ-γ-cascade. The start level can be populated via β-decay (mother isotope with nuclear charge Z−1) or via an EC-process (EC = electron capture; mother isotope with nuclear charge Z+1). If the start level itself is sufficiently long-lived ($\tau_{1/2} \geq 1$ h), one speaks of an isomeric decay. Right: Magnified presentation of the intermediate I = 5/2 level, split by NQI. If the lifetime τ_N of this state is sufficiently long ($\tau_N = 1$ ns–1 μs) the nuclear spin precession frequencies $n\omega$ (or their superposition) corresponding to the energy differences can be observed (see also Section 2).

[*] Dr. A. Lerf
Walther-Meissner-Institut für
Tieftemperaturforschung der Bayerischen Akademie der Wissenschaften
Walther-Meissner-Strasse 8, D-8046 Garching (FRG)

Dr. T. Butz
Physik-Department E15 der Technischen Universität München
D-8046 Garching (FRG)

[*] CE = conversion electrons: Instead of γ-emission, a shell electron can be emitted during the transition from one excited state to another.

angular distribution of the emitted particles is referred to the direction of the beam the "perturbed angular distribution" (PAD)[11] is obtained. A large number of isotopes are available for PAD studies,[11] of which ^{19}F[12] is very promising for applications in chemistry, provided the problems associated with radiation damage in the sample are brought under control. Until now, almost exclusively γ-γ-angular correlation spectroscopy has found applications in chemistry. The angular correlation can be perturbed via the interaction of nuclear moments with extranuclear fields,[13-15] provided the nucleus remains in the intermediate excited state for a sufficiently long time. Perturbations by magnetic interactions, especially by hyperfine fields in magnetically ordered systems, have been studied extensively and are well documented in Tables[16] and review articles by *Rinneberg*[17] and *Forker* and *Vianden*.[18] A second way to perturb the angular correlation is based on the interaction of the nuclear quadrupole moment with electric field gradients (EFG). These result from the charge density distribution, which, in turn, reflects the nature of the chemical bond. The investigation of the nuclear quadrupole interaction (NQI) by PAC was boosted when time integral PAC was superseded by the time differential method (TDPAC spectroscopy).[*] Since the latter technique yields much more detailed information (e.g. it resolves sites differing in charge density distribution in the same material) we restrict ourselves to this method in this article. The application of TDPAC spectroscopy to chemically oriented questions is reviewed in several articles.[17-22] *Vargas*[19] and *Adloff*[20] concentrate on chemistry after nuclear decays ("hot atom chemistry", "after-effects", see also *Thun*[23]).

Here, we report on modern TDPAC spectroscopic investigations which open a wider area of applications in chemistry. A brief introduction to NQI and to the theory of TDPAC spectroscopy is followed by a description of experimental aspects (instrumentation, data treatment, sample preparation). Further, we discuss the advantages and disadvantages of this technique compared to NMR and Mössbauer spectroscopy. In the subsequent overview of areas of application of TDPAC spectroscopy in the border region between chemistry, physics and biology we select examples to show how this technique is capable of yielding new information that cannot be obtained otherwise. Apart from some studies on liquids, the examples from the area of materials science form the largest part of the article (amorphous solids, surfaces, probe-specific interactions on an atomic scale, structural phase transitions, and solid state reactions). Biological applications of TDPAC spectroscopy are discussed only briefly, since they are reviewed extensively in a recent article by *Bauer*.[24]

2. Theory of Nuclear Quadrupole Interactions

A non-spherical nucleus, when subjected to an inhomogeneous electric field, adopts certain orientations with respect to the gradient of this field,[25-27] i.e. it behaves similarly to a magnetic dipole in a magnetic field. The quantum-mechanical description yields for an axially symmetric EFG the energy eigenvalues

$$E_m = e^2 q Q \frac{3m^2 - I(I+1)}{4I(2I-1)} \quad \text{with } m = -I, -I+1, \ldots, I-1, I \qquad (1)$$

Here, eQ denotes the nuclear quadrupole moment, eq the largest component of the EFG tensor ($= V_{zz}$), I the nuclear spin, and m the quantum number which describes the possible orientations. For example a nuclear state with spin $I = 5/2$ splits into 3 substates (cf. Fig. 1), whose energy differences are

$$\Delta E_{m,m'} = E_m - E_{m'} = 3e^2 q Q(m^2 - m'^2)/40, \qquad (2)$$

i.e. $\Delta E_{\pm 3/2, \pm 1/2} = 6e^2 qQ/40 \equiv \hbar\omega_0$,
$\Delta E_{\pm 5/2, \pm 3/2} = 12e^2 qQ/40 \equiv \hbar 2\omega_0$,
$\Delta E_{\pm 5/2, \pm 1/2} = 18e^2 qQ/40 \equiv \hbar 3\omega_0$

In analogy to the Larmor precession one can imagine a nuclear spin precession with frequencies ω_0, $2\omega_0$, and $3\omega_0$. The EFG is defined as a traceless tensor, which in the principal coordinate system can be written as

$$\begin{pmatrix} V_{xx} & 0 & 0 \\ 0 & V_{yy} & 0 \\ 0 & 0 & V_{zz} \end{pmatrix} \quad \text{with} \quad V_{xx} + V_{yy} + V_{zz} = 0 \qquad (3)$$

The components are ordered in such a way that $|V_{zz}| \geq |V_{xx}| \geq |V_{yy}|$, and one defines the asymmetry parameter as follows:

$$\eta = |(V_{xx} - V_{yy})/V_{zz}| \qquad (4)$$

If $V_{xx} = V_{yy}$, then $\eta = 0$ and there is axial symmetry; otherwise one obtains $0 < \eta \leq 1$. A deviation from axial symmetry modifies the splitting of energy levels and, hence, the precession frequencies.

The relation between the charge distribution $\rho(r)$ and the EFG tensor can be written:

$$V_{\kappa\nu}(r) = \int \rho(r') \frac{(3\kappa\nu - \delta_{\kappa\nu} r'^2)}{|r - r'|^5} dx'dy'dz' \qquad (5)$$

$\kappa, \nu = x, y, z$; $\delta_{\kappa\nu}$ = Kronecker symbol (= 1 for $\kappa = \nu$; = 0 otherwise)

If a multipole expansion of the charge distribution is carried out, one notes that only the $l = 2$ multipole components contribute to the EFG. In principle one can deduce the EFG from point charge models or semi-empirical binding models,[24-28] from ab initio calculations of the charge distribution,[29,30] or from experimentally determined charge distributions.[31] Generally, the agreement between experiment and theory is poor. The main problem is the exact description of the quadrupolar core polarization—especially for the heavy elements—which is caused by an external EFG ("Sternheimer-effect"[32]). Despite these problems in the theoretical treatment of the EFG tensor, the experimental determination of its orientation, symmetry and magnitude provides very useful information for the chemist where other techniques fail.

[*] In integral PAC spectroscopy the coincidence count-rate is measured as a function of angle between detector without any time resolution. In contrast, in TDPAC spectroscopy the events are resolved in the time elapsed between the arrival of the first particle in one detector and the arrival of the second particle in the other detector.

3. TDPAC—A Short Introduction

3.1. Theory of TDPAC

The theory of time differential perturbed angular correlation[33, 34] will be outlined here only inasfar as it is relevant to the contents of this article.

The angular correlation can be written

$$W(\theta) = 1 + A_2 P_2(\cos\theta) + \ldots^{[*]} \tag{6}$$

Here, $W(\theta)$ denotes the coincidence count-rate between the two quanta which are detected at an angle θ with respect to each other. P_2 is a Legendre-polynomial. A_2 is the anisotropy of the cascade, which depends exclusively on nuclear properties.

If the nucleus remains for a period of time τ_N in the intermediate state (Fig. 1), the coincidence count-rate for samples without preferred orientation can be written as a function of θ and the time t as follows

$$W(\theta,t) = \exp(-t/\tau_N)(1 + A_2 G_2(t) P_2(\cos\theta) + \cdots) \tag{7}$$

$G_2(t)$ is the so-called perturbation function. In the case of an axially symmetric, static[**] EFG one obtains, e.g., for $I = 5/2$:

$$G_2(t) = \sum_{n=0}^{3} a_n \cos(n\omega_0 t) \tag{8}$$

$a_0 = 0.2;\ a_1 = 0.371;\ a_2 = 0.286;\ a_3 = 0.143$

Here, ω_0 denotes the precession frequency [cf. Eq. (2)]. This perturbation function contains all information on the NQI. The following modifications occur in practice:

(1) The finite solid angle of the detectors reduces the observable anisotropy A_2.

(2) Inequivalent probe sites in the unit cell or inequivalent sites due to the coexistence of several phases in the sample lead to a superposition of perturbation functions, e.g. for a two-phase system

$$G_2(t) = \alpha G_2^{I}(t) + (1-\alpha) G_2^{II}(t) \tag{9}$$

(3) A finite frequency distribution around a mean precession frequency ω_0 due to inhomogeneities yields, e.g., for a Lorentzian frequency distribution with a half width at half maximum δ, damped oscillations or line-broadening of the Fourier-transformed $G_2(t)$:

$$G_2(t) = \sum_{n=0}^{3} a_n \exp(n\delta\omega_0 t)\cos(n\omega_0 t) \tag{10}$$

(4) The finite time resolution of the spectrometer suppresses higher frequencies progressively. A crude approximation of the convolution of $\exp(-t/\tau_N)G_2(t)$ with the time resolution function of the spectrometer, which frequently is assumed to be Gaussian with a width ($\sim$HWHM) τ_{res}, yields

$$G_2(t) = \sum_{n=0}^{3} a_2 \exp\left(-\frac{1}{2}\tau_{res}^2 n^2 \omega_0^2\right)\cos(n\omega_0 t) \tag{11}$$

Note that the finite time resolution does not yield damped oscillations, but rather modified amplitudes of the cosine terms.

(5) The above Equations (6)–(11) have to be modified for samples with texture or oriented crystals. It is still possible, however, to use perturbation functions of the type described in Eq. (8). The intensities of the cosine terms then depend on the crystal orientation.

(6) If the EFG tensor deviates from axial symmetry, then the intensities and precession frequencies are also functions of the asymmetry parameter η.

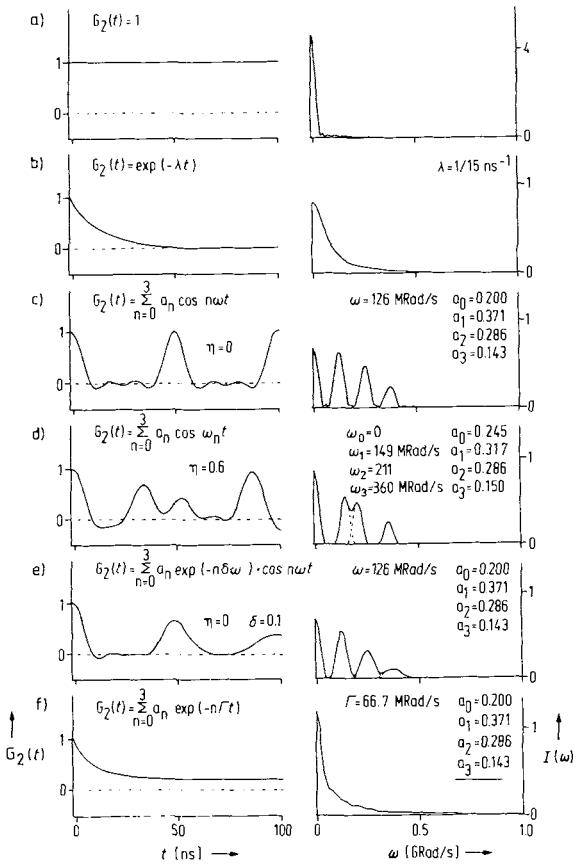

Fig. 2. Various typical perturbation functions $G_2(t)$ (left) and their Fourier-transforms (right, intensity $I(\omega)$ in arbitrary units) for pure NQI ($I = 5/2$, samples without preferred orientation). a) Absence of a perturbation, e.g. $V_{zz} = 0$ or extremely fast relaxation (decoupling of the nuclear spin from the environment). The width of the peak at $\omega = 0$ results from the time interval and the window function used (Kaiser-Bessel, $\beta = 4$). b) Fast relaxation (isotropic rotator) [33, 34]. The decay constant is proportional to the product of the mean square of the precession frequency and the reorientational correlation time. The Fourier transform is a Lorentzian, convoluted with the instrumental resolution function (cf. a). c) Time-independent NQI with axial symmetry ($\eta = 0$). d) Time-independent NQI with axial asymmetry ($\eta = 0.6$). e) As c), but with an additional frequency distribution $\delta = 0.1$ around the mean precession frequency ω. f) Time-independent NQI with a half width $\Gamma = 66.7$ Mrad/s centered around a mean frequency zero. The Fourier transform consists of three Lorentzians and a delta-function, convoluted with the instrumental resolution function (cf. a).

[*] Higher terms of the form $A_4 P_4(\cos\theta)$ are frequently neglected.

[**] Here, "static" means that, on the one hand, the variation of the EFG is very slow compared to the precession period $2\pi/\omega_0$, but, on the other, that the fluctuations (e.g. due to lattice vibrations) are so fast that the nucleus is unable to follow them and "feels" the time average only.

For illustration we show in Figure 2 a few important perturbation functions with their corresponding Fourier transforms.

3.2. Instrumental

Any TDPAC measurement requires the detection of a pair of γ-quanta which are characterized by their energy. Moreover, the time between the emission of the first and the second quantum has to be measured as accurately as possible. Finally, the detection efficiency per detector should be as close as possible to 100%, because the detection probability for a delayed coincidence is the product of two individual probabilities and would otherwise become excessively small.

Our TDPAC spectrometer (Fig. 3) consists of four detectors arranged in one plane. Each detector consists of a scintillation crystal (e.g. NaI(Tl), 1.75″×2″ ∅) with optical coupling to a photomultiplier. The information obtained from the detectors is processed in two different ways and analyzed independently. In the so-called "slow" circuit the signals are analyzed with respect to their γ-energies (proportional to the pulse area) and coincidences of suitable pulses from two detectors are formed (here, time resolution plays no role!). In the so-called "fast" circuit the time difference between two pulses is accurately analyzed, irrespective of the pulse height (energy). For this, the time of arrival in a detector is determined by a "constant-fraction trigger" (CFT) (rise of the pulse) and fed into a time-to-amplitude converter (TAC). The analog output signal of this TAC is stored in a multichannel analyzer (MC) via an analog-to-digital converter (ADC), provided a valid coincidence for one of the possible detector combinations was found in the "slow" circuit. According to the detector combination the corresponding subgroup of the multichannel analyzer is addressed via a "routing" unit. The activity of the sample must be kept sufficiently low (~ 10 μC) as to ensure that no further nuclear decay takes

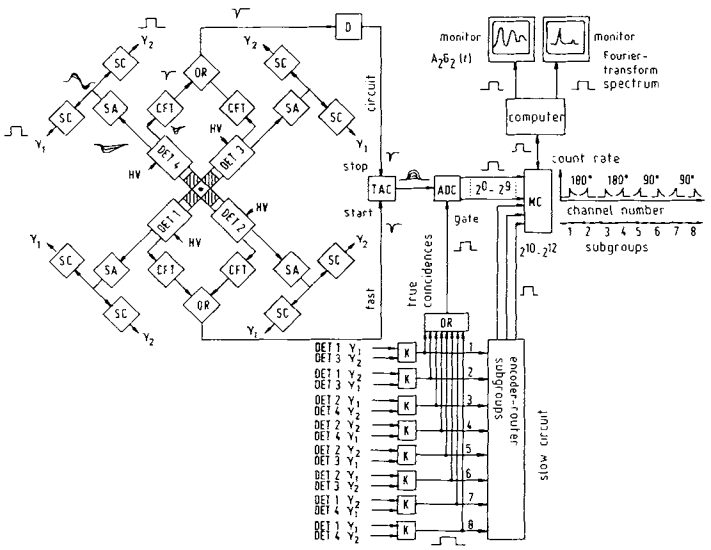

Fig. 3. Block diagram of a four-detector TDPAC spectrometer. DET = detector, HV = high voltage supply, OR = or gate, D = delay, SA = spectroscopy amplifier, SC = single-channel discriminator, K = coincidence, ● = sample. For details see text.

place during the pulsed operation of both circuits and the data storage in the multichannel analyzer (typically 10–20 μs). In this way, eight (out of 12 possible) coincidence spectra are stored simultaneously. Aside from a constant background, which results from chance coincidences (two nuclei decay at approximately the same time and the corresponding γ-quanta hit by chance two detectors and imitate a coincidence), one obtains an exponentially decaying curve of "true" coincidences; the precession signal $A_2G_2(t)$ is superimposed onto this curve (lifetime of the intermediate state!). The exponential curve decays to the right, if the start detector detects γ_1, and to the left if it detects γ_2. The zero time is shifted to the center of a multichannel subgroup by a delay line in the stop line. Further details on the "fast-slow" principle are given in Refs. [17, 35].

3.3. Data Processing

The data reduction starts with the substraction of the chance coincidence background in each subgroup. This background is determined from that part of the spectrum which contains no "true" coincidences, i.e. the range of "negative" time. Then all spectra decaying to the left are inverted, and all eight spectra are shifted to a common zero time t_0. This t_0 of each subgroup is predetermined by measuring prompt coincidences, e.g. using a ^{22}Na source. At the same time, the instrumental time resolution τ_{res} is also determined. We can now write the following ratio

$$R(t) = 2\,\frac{\sqrt[4]{W_{13}W_{31}W_{24}W_{42}} - \sqrt[4]{W_{14}W_{41}W_{23}W_{32}}}{\sqrt[4]{W_{13}W_{31}W_{24}W_{42}} + 2\sqrt[4]{W_{14}W_{41}W_{23}W_{32}}} \qquad (12)$$

where, W_{ij} denotes the "true" coincidence count rate between the detectors i (γ_1) and j (γ_2). The exponential decay factors cancel (exactly for $\tau_{res} = 0$). Moreover, the efficiencies of the detectors also cancel. This ratio is commonly presented as the so-called TDPAC spectrum, and for a powder sample we have $R(t) = A_2G_2(t)$ (A_4G_4-term neglected). Since the number of "true" coincidences decreases with time, the statistical accuracy also decreases with increasing delay time between the emission of γ_1 and γ_2 (error bars increase).

In many cases computer fits of appropriate theoretical functions [e.g. Eq. (10)] are performed. For this, complete analytical expressions for the effect of finite time resolution, as described in Ref. [36], are used. In addition to these fits, Fourier transforms of the reduced data $R(t)$ are very useful. In order to suppress side lobes we use a Kaiser-Bessel weighting function and implement the data set with an appropriate number of zeros to reduce truncation effects and to provide the required 2^N data points for the "fast Fourier transform routines". The calculation of $A_2G_2(t)$ and its corresponding Fourier-transformed spectrum is performed on a desk computer connected directly to the spectrometer, quasi on-line.

3.4. Isotopes and Sample Preparation

The radioactive isotopes are produced either in nuclear reactors (neutron capture), or in accelerators or cyclotrons

Table 1. Isotopes suitable for TDPAC spectroscopy according to [17]: The isotopes marked with an asterisk have been the most frequently used until now; mother isotope with half-life $\tau_{1/2}$; type of decay to the daughter isotope (cf. also Fig. 1); γ energies of the cascade; spin I and half-life $\tau_{1/2}$ of the intermediate state, and the anisotropy A_2 of the cascade.

Mother-isotope	$\tau_{1/2}$	Decay	Daughter-isotope	γ-Energy [keV]	I	$\tau_{1/2}$ [ns]	A_2 [%]
^{99}Mo	2.75 d	β^-	^{99}Tc	739, 181	5/2	3.6	+ 9.5(4)
				739 (40) 141 [a]	5/2	3.6	−12
^{99}Rh	15 d	EC, β^+	^{99}Ru	528, 90	3/2	20.7	−22.1
				353, 90	3/2	20.7	−13.1
^{100}Pd	3.6 d	EC	^{100}Rh	84, 75	2	214.5	+17.3
^{111m}Cd*	48.6 min	IT	^{111}Cd	151, 245	5/2	84.1	+17.5(1.4)
^{111}In*	2.8 d	EC	^{111}Cd	171, 245	5/2	84.1	−18.0(2)
^{116m}Sb	60.4 min	EC, β^+	^{116}Sn	543, 1072	5	370	+13
^{117}Cd	2.4 h	β^+	^{117}In	90, 345	3/2	58.7	−36
^{118m}Sb	5 h	EC, β^+	^{118}Sn	254, 1092	5	21.7	+10.7
^{140}La	40.3 h	β^-	^{140}Ce	329, 487	4	3.5	− 9.2(1.2)
^{155}Tb	5.3 d	EC	^{155}Gd	180, 87	5/2	6.4	−12.7(2.2)
^{172}Lu	6.7 d	EC	^{172}Yb	91, 1094	3	7.8	+38(1)
^{181}Hf*	42.4 d	β^-	^{181}Ta	133, 482	5/2	10.8	−25.8(3)
^{187}W	23.9 h	β^-	^{187}Re	480, 72	9/2	563	−12
^{199m}Hg	42.6 min	IT	^{199}Hg	374, 158	5/2	2.45	+25
^{204m}Pb	67 min	IT	^{204}Pb	911, 375	4	270	+24(1)

[a] Triple cascade (40 keV unobserved).

(nuclear reactions by particle bombardment). Table 1 gives a list of isotopes which are well suited for TDPAC spectroscopy according to the following criteria: Long lifetime of the mother isotope (or of the isomeric state); large anisotropy of the cascade; not too low γ-energies (absorption!); low degree of conversion of transitions (emission of conversion electrons instead of γ-quanta); suitably long lifetime of the intermediate state; large nuclear quadrupole moments.

The choice of isotope may present problems but should be guided by the following criteria: (1) In the ideal case one of the constituents of the sample under investigation has an isotope with an isomeric decay (no nuclear transmutation), i.e. there are neither problems with the sample preparation nor with "hot atom chemistry" (chemical or electronic after-effects[23,37]). (2) If the mother isotope is a constituent of the sample, there are no preparation difficulties, but one must bear in mind that, since the measurement is carried out on a foreign atom (impurity atom), chemical after-effects, e.g. the breaking of weak bonds,[37] can occur; electronic after-effects can occur if the rearrangement of the electron shell (for EC there is an Auger-cascade!) proceeds too slowly compared to the lifetime of the start level. This problem will not be encountered with metals, but may be with semiconductors and insulators. (3) If the daughter isotope is a constituent of the sample under investigation, there can be impurity-specific problems during sample preparation only. (4) If neither the mother nor the daughter isotope is a constituent of the substance of interest, there can be impurity-specific problems both during preparation and in the measurement.

It is not suggested that all of these problems will always be encountered. However, they should be considered before starting an investigation. After all, for a whole series of interesting applications an impurity probe is an absolute requirement (e.g. for nuclear transmutation doping, and for impurity-defect complexes). Generally, a substutional incorporation of the probe is desirable. This is best achieved when mother/daughter isotopes and the host material under investigation form isomorphous compounds or alloys with complete miscibility. In principle, two sample preparation procedures can be distinguished: (1) The radioactive probe is introduced into the substance under investigation during preparation. (2) The probe is produced in the ready-made sample through a nuclear reaction (irradiation with neutrons or ions), provided only negligible amounts of another radioactive isotope are produced besides the desired isotope. In the second case (but not in the first) one generally has to remove simultaneously produced radiation defects by annealing. In principle, 10^{10}–10^{12} probe atoms suffice, so only very small amounts of substance are required for an investigation. However, the preparation of a sample without an inactive carrier, i.e. without other, non-radioactive isotopes of the same element, is frequently difficult.

3.5. Comparison of Methods

In this section the advantages and disadvantages of TDPAC compared to the other better-known hyperfine spectroscopic techniques NMR/NQR and ME will be discussed. The main disadvantage of TDPAC is that one has to work with radioactive material. However, the activity levels required are very low (10–100 μC). In contrast thereto there are enormous advantages:

(1) The sample quantities can be very small (typically 1...100 mg).
(2) There is essentially no limitation to the choice of reaction vessel material because of the high energies of the γ-rays used (contrary to ME).
(3) The sensitivity is independent of temperature (no Debye-Waller factor as in ME; no Boltzmann factor as in NMR).
(4) Insensitivity to vibrations (contrary to ME): one can use, e.g. a stirred bath.
(5) No magnetic field is required and no radio frequency field (as in NMR).
(6) Small NQI's are more easily resolved then in ME.
(7) Contrary to NMR and ME it is practically impossible, for instrumental reasons, to detect only a part of the entire hyperfine spectrum (velocity range or field variation too small); moreover, the signal (= anisotropy) is a constant, which depends on nuclear properties only. This means that the sum of all observed spectral components of a TDPAC spectrum is constant. Therefore the sum of all inequivalent probe sites must always add up to 100%, even in heterogeneous systems (although problems can arise due to insufficient time resolution).
(8) Other than in the case of ME and NMR, there is practically no way in which the observed linewidth in the Fourier-transformed spectra (damping of the oscillations in the A_2G_2-spectrum) can be influenced by instrumental means; this means that small site inhomogeneities can be detected with high reliability.
(9) Reorientational motions of the EFG can generally be identified unequivocally and are easily distinguished from static inhomogeneous EFG-distributions.

(10) Finally, the isotopes that are suitable for TDPAC spectroscopy complement those amenable for ME and NMR in a useful way.

4. Applications to Solutions and Melts

For solutions and melts one normally obtains TDPAC spectra similar to those in Figure 2b, i.e. an exponential decay of the anisotropy with a decay constant[33,38]

$$\lambda_k = k(k+1)\tfrac{3}{5}\tau_c\langle\omega^2\rangle(4\cdot I(I+1)-k(k+1)-1) \quad k=2,4^{[*]} \qquad (13)$$

where $\langle\omega^2\rangle$ denotes the average squared NQI-frequency and τ_c the reorientational correlation time (tumbling motion). An estimate of $\langle\omega^2\rangle$ can be made by freezing the solution. If the value in the frozen solution agrees with that of the solid starting material which is to be dissolved, we have in both cases the same complex or the same ion complex. (If this is not the case then depolymerization or ligand exchange reactions must have taken place during dissolution.) One then assumes that the species in frozen solution are identical to those in the liquid state. This assumption is most likely justified for shock-freezing. When $\langle\omega^2\rangle$ is known, one can derive from λ_k the correlation time τ_c, which itself depends on the volume V of the tumbling species, on the temperature T, and on the viscosity η[**] of the solution, via the Debye-formula[40]

$$\tau_c = \frac{\eta V}{k_B T} \quad (k_B = \text{Boltzmann's constant}) \qquad (14)$$

Normally, the volume of the dissolved species is derived from the correlation time. By comparing measured values for $\langle\omega^2\rangle$ and τ_c for two different species one can distinguish between ligand exchange and polymerization processes: if the values for τ_c are comparable, but those for $\langle\omega^2\rangle$ differ, both species have a comparable size but differ in coordination or ligation, respectively; if the values for $\langle\omega^2\rangle$ are comparable, but those for τ_c differ, we have the same coordination, but a different degree of polymerization.

Despite the fact that the sensitivity of TDPAC spectroscopy is well demonstrated by a large range of observed decay constants,[41,42] only very few systematic studies have so far been carried out on solutions, the substances to be dissolved, and the frozen solutions. Examples are Hf-complexes[39] and $Cd(CH_3)_2$[22] in non-aqueous solvents. These complexes retain their integrity upon dissolution and, with the exception of Hf(tropolone)$_4$, are unsolvated in dimethylformamide and chloroform, where ligand exchange reactions occur and where associates are formed. With $^{99}Mo(^{99}Tc)$ the molybdate polymerization was studied as a function of pH.[43] Further studies, partly incomplete, have been carried out on In-porphyrins,[44] on aqueous In-solutions over the entire pH range,[45] and on Hf-solutions in HCl (0.01-9 M).[46-48] Further, the kinetics of $OH^{\ominus}/F^{\ominus}$ exchange in aqueous Hf-solutions[49] and of In-binding to AMP, ATP and other biomolecules has been investigated.[50]

Similar studies have been carried out on metal melts[51,52] and chalcogenide melts[*][53] with special emphasis on precursors of compound and associate formation. Such associates (discrete coordination sphere!) occur whenever heteroatomic interactions dominate over homoatomic interactions.

5. Applications in the Border Region of Solid State Chemistry/Physics

5.1. Amorphous Solids

In contrast to diffraction techniques and EXAFS studies, which in amorphous systems yield radical distributions of the nearest neighborhood only,[**] the determination of the NQI (tensor rank 2!) yields information on both the radial *and* angular distribution. From the hyperfine spectra, a V_{zz},η-distribution can be derived which serves to characterize the short range order.[54] The great advantage of TDPAC is that recrystallization processes and molecule and compound formation are observable at an extremely early stage. Here, the NQI parameters are assumed to be known and serve for an identification of intermediates and final products.

Despite the high sensitivity of TDPAC spectroscopy to variations in charge distribution in the near neighborhood of the probe atoms, and despite its virtual independence of long-range order, only a few TDPAC investigations have so far been carried out on amorphous systems. In the case of amorphous Ga[55] and Bi[56] [probe: $^{111}In(^{111}Cd)$], the model of "random dense packing of hard spheres" yields, in the point charge approximation, a V_{zz},η-distribution in good agreement with the observed spectra. In Figure 4 the time spectra and the corresponding Fourier transforms are shown for $^{111}In(^{111}Cd)$ in amorphous $In_{80}Ag_{20}$ and in the fully crystallized final state.[56] In accord with the composition and the In-Ag phase diagram, chiefly In_2Ag is formed, apart from metallic In-segregations. There is no short range order in the amorphous state, which can also be well described in the model of "random dense packing of hard spheres".

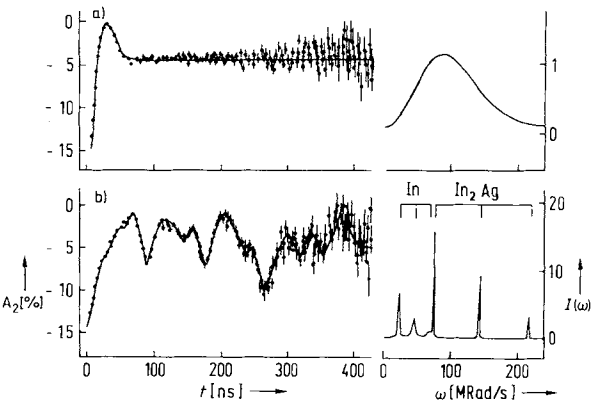

Fig. 4. TDPAC spectra (left) and corresponding Fourier transforms (right) of $^{111}In(^{111}Cd)$ (a) in amorphous $In_{80}Ag_{20}$ and (b) after recrystallization [56].

[*] For the case where $\eta \neq 0$ see Ref. [39].

[**] Not to be confused with the asymmetry parameter η.

[*] Investigated TDPAD-spectroscopically.

[**] Exception: "near edge structure" in EXAFS [57].

In a further investigation with $^{111}In(^{111}Cd)$, simultaneous compound formation (Ni-phosphides) and annealing of defects was observed in nickel amorphized by phosphorus-ion implantation.[58]

It should be emphasized that in the few TDPAC studies that have been carried out on solidified solutions, there is a wide temperature range below the solidification temperature in which molecules exhibit dynamics similar to that observed in the fluid phase ("superviscous state"[59-61]).

5.2. Surfaces

One can distinguish two extreme types of surface: The "perfect" surface (single crystals, ultra-high-vacuum!) and the "technical" surface with fractal dimension[62] (porous materials). For TDPAC spectroscopy, the radioactive probe is applied in atomic form in the first case (due to the small surface area in carrier-free form!), and in molecular form in the second case.

In the case of nearly perfect surfaces the identification of atomic configurations requires NQI parameters (V_{zz}, η, orientation) sufficiently different from each other and from the bulk values. It is also possible to monitor surface reactions identifying product species via the hyperfine parameters of already known species. Such studies are of great interest, especially for technical surfaces, where many of the conventional surface-sensitive techniques can only be used with difficulty, if at all. This is especially true for in situ studies, e.g. in the presence of reactive gases.

Up to now, only one study with $^{111}In(^{111}Cd)$ on an epitaxially grown In(111) surface has been reported in the literature.[63,64] The surface NQI was found to be roughly twice as large as the bulk value. In order to demonstrate that a probe at the surface was observed and not a probe-gas complex, a monolayer of non-radioactive indium was deposited. Then, only the bulk signal was observed, demonstrating the extremely short-range nature of the NQI in this system. Above 150 K, diffusion from the surface into the bulk was observed. Both the EFG orientation as well as the measured asymmetry parameter show that the probe environment is not that of a perfect (111) surface.

TDPAC investigations of reactions on technical surfaces have only been carried out on supported molybdenum catalysts (on Al_2O_3).[65] Figure 5a shows the TDPAC spectrum of $^{99}Mo(^{99}Tc)$ in a 0.24 M ammonium paramolybdate (APM) solution (case of fast relaxation, cf. Fig. 2b). When Al_2O_3 (surface area $\sim 150\ m^2/g$) is impregnated with this solution the tumbling motion of molybdate ions is stopped by adsorption and, hence, a static NQI (cf. Fig. 2c/d) is observed (see Fig. 5b). From a comparison of the V_{zz}- and η-values with those for crystalline APM (Fig. 5c), one can conclude that preferentially heptamers (or higher polymolybdates) are adsorbed. These polymolybdates remain intact after drying and calcination up to approximately 773 K. They can be completely decondensed by post-impregnation with K_2CO_3, which leads to a loss of catalytic activity for hydrodesulfurization.

Treatment of the calcined oxidic precursor with H_2/H_2S does not yield MoS_2, as commonly assumed, because the observed hyperfine interaction is about 30% higher than for crystalline MoS_2.[66] The discrepancy most likely results from hydrogen uptake during reduction/sulfidation, as has been shown by in situ studies on highly disperse "H_xMoS_2".[66] The proton uptake is hardly detectable by EXAFS, since it does not lead to an appreciable change in the Mo-S distance; however, it drastically modifies the charge balance and, hence, the NQI.

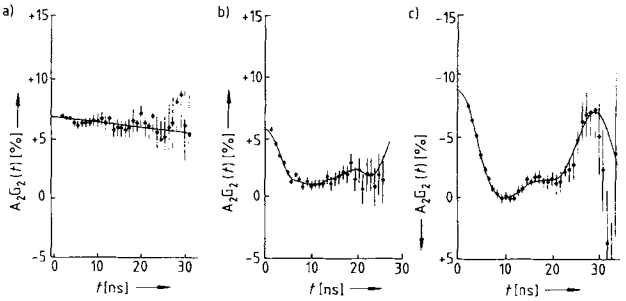

Fig. 5. TDPAC Spectra of $^{99}Mo(^{99}Tc)$ at 300 K. a) $(NH_4)_6[Mo_7O_{24}]$(APM) in aqueous solution; b) Al_2O_3 support impregnated with this solution, moist; c) crystalline APM·$4H_2O$, dissolved after irradiation, precipitated with EtOH. The spectra a) and b) were recorded with the 739 keV–181 keV cascade, the spectrum c) with the 739 keV (40 keV)–141 keV cascade. With $\omega = 230$ Mrad/s for crystalline APM·$4H_2O$ and a reorientational correlation time $\tau_c = 140$ nsec (derived from the spectra of solutions) a volume of 220 ± 50 Å^3 is determined, comparable to that of the $[Mo_7O_{24}]^{6\ominus}$ ion. The spectrum of the impregnated Al_2O_3 consists of a static contribution and a contribution with fast relaxation (the anisotropy does never reach or fall below zero, as in Figs. 2c–e). From this the degree of adsorption can be determined.

5.3. Probe-Atom-Specific Interactions on an Atomic Scale

5.3.1. Probe Atom–Defect Interactions

Usually,metals are irradiated at low temperatures (e.g. 4.2 K) with high energetic particles (photons, electrons, protons, neutrons, ions) in order to create defects (radiation damage). If the host metal has not been previously doped with probe atoms (= impurity atoms), the radiation damage can be at the same time as probe-ion implantation. In addition, vacancies can be frozen out by quenching the melt. Plastic deformation at room temperature, on the contrary, produces mainly extended defects (e.g. dislocations).[*]

The annealing of defects is usually carried out by isochronous tempering: the samples are kept for a fixed time (e.g. 10 min) at consecutively increasing temperatures and then cooled down to one and the same low measuring temperature. The defects—mainly interstitial atoms and vacancies—can be observed by TDPAC spectroscopy because they are in many cases trapped by the probe atoms during annealing and thus form probe atom-defect complexes. Otherwise they would be "invisible" due to their low concentration. Different complexes usually have different values for V_{zz} and η and, above all, differ in their EFG-tensor orientation. By the determination of these quantities—single crystal measurements are required to determine the orientation—the complexes can be charac-

[*] For compounds there are in addition defects due to non-stoichiometry or due to incorporation of components of another valency. The only TDPAC-example up to now for the latter case is the Ca- or Y-substitution in ZrO_2, in which the oxygen diffusion was studied [67].

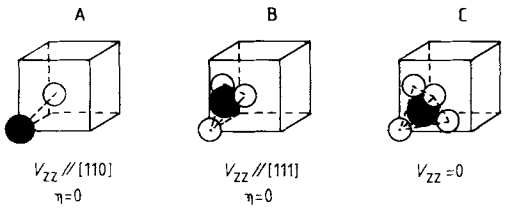

Fig. 6. Three different impurity-vacancy complexes in fcc lattices after [68]; ● = impurity atom, ○ vacant site. The first two complexes **A** and **B** can be distinguished according to the orientation of V_{zz}. The complex **C** (one impurity atom 4 vacant sites) shows no NQI and hence cannot be distinguished from a substitutional impurity without vacancies (these two types of coordination can be distinguished via the magnetic interaction [69]).

terized on an atomic scale. Figure 6 shows a selection of simple impurity-vacancy complexes. Defect production by various particle beams (and various particle energies!) and quench experiments are helpful for complex identification. The potential of PAC is recognized in the case of two or more coexisting complexes; the variation of the individual fractions with temperature yields information on the formation and dissociation enthalpies of the coexisting complexes and on their sequence during annealing. Usually, the *quantitative* interpretation of the individual fractions, including the "nearly unperturbed" fraction, and of the V_{zz} and η values still presents some problems. For the latter, however, there are now theoretical approaches.[70]

Since there are several review articles on the investigation of radiation damage in cubic (bcc, fcc) metals[71–76] we shall quote but a single example here. Gold, an fcc metal, was doped with ^{111}In(^{111}Cd), irradiated with 3 MeV electrons at 4.2 K, and isochronously annealed.[74,77,78] Figure 7 shows that at an annealing temperature $T_A = 77$ K there are

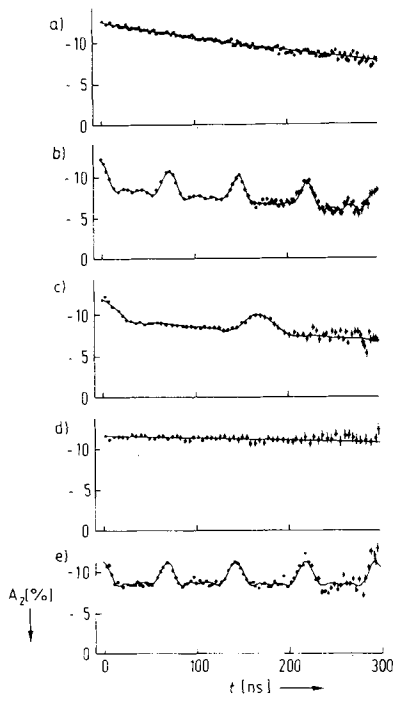

Fig. 7. TDPAC spectra of ^{111}In(^{111}Cd) in gold, irradiated with e^- at 4.2 K, and measured at 4.2 K after isochronous annealing at T_A = a) 77, b) 257, c) 320, d) 873 K. e) Spectrum of melt-quenched gold (T_A = 257 K) a) no impurity-defect complexes. b)+c) At first a discrete high-frequency component is observed (rapid sequence of signal maxima in b), and then a low-frequency component (in c) on top of a slowly decreasing background. d) All probes are in an unperturbed cubic environment.

defects present (slight decrease of the anisotropy with time), but they are not yet "trapped" by probe atoms. At $T_A = 257$ K about 30% of the probe atoms form a complex of type **A**. This is verified by comparison with a melt-quenched sample (cf. Fig. 7e) and above all by the determination of the EFG orientation. At $T_A = 320$ K a probe atom/3-vacancies complex (or a dislocation loop) is formed.

Investigations have likewise been carried out on the hcp-metals Cd[79,80] and Zn[81] and the compounds InSb,[84] InP[84,85] and $CdSiP_2$[86] [probe always ^{111}In(^{111}Cd)],[*] for which, because of the variety of possible defect types (differences in the sub-lattices?!), the interpretation of the TDPAC data becomes progressively more difficult. Interestingly, it is possible to "decorate" probe atom-vacancy clusters with atoms such as He,[87,88] C,[89] and O.[90] This leads to a shift of the NQI to higher V_{zz}-values. Such processes are of technical importance, since they, e.g., contribute to material embrittlement in reactors, above all in fusion reactors.

5.3.2. *Probe Atom–Impurity Atom Interactions*

Metal–Metal Interactions: In all the TDPAC studies thus far undertaken, noble metals were used as the reaction media for studying attractive interactions between probe atoms and impurity atoms, which are frequently also added in a high dilution.[91–93] The methodology is as described in Section 5.3.1 with the exception that, instead of defects, impurity atoms are introduced.

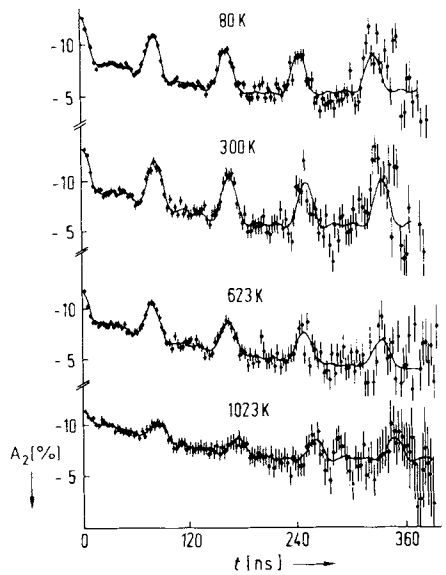

Fig. 8. TDPAC spectra of ^{111}In(^{111}Cd) in $Rh_{0.005}Cu_{0.995}$ at various temperatures, after [91].

Figure 8 shows an example for an attractive interaction between ^{111}In(^{111}Cd) and Rh in a copper matrix. The discrete frequency component, which is due to In–Rh pairs, progressively vanishes with increasing temperature as a result of pair dissociation.[**]

[*] Investigations of defects in semiconductors like Si [82] and Ge [83] and in insulators, respectively, are still at an exploratory stage [71, 72].

[**] For higher impurity concentrations higher aggregates of the type $In-Rh_n$ ($n > 1$) are formed [91].

From the temperature dependence of this discrete component one can derive the formation enthalpy. For the probe atom-impurity atom complexes in various metallic matrices thus far investigated, this enthalpy frequently agrees with the heat of formation calculated according to *Miedema*[94] for an intermetallic phase of the corresponding combination of elements and corrected for the coordination number.[95] If there is a pronounced tendency for the probe atom and impurity atom to form intermetallic phases, one should not overlook the possibility of molecule formation, even at very low concentrations. If these molecules are insoluble in the host matrix, aggregation and segregation occurs, in analogy to binary systems.[*] This, of course, poses the question of how many formula units of this aggregate are necessary in order to identify it as a "segregation" in the host matrix. It is suggested that one can speak of compound formation whenever all the NQI parameters (V_{zz}; η) of this probe atom-impurity atom complex are essentially identical to those of the pure intermetallic phase, even in the extreme case of a complex consisting of atoms of a single formula unit only.[**]

Metal-nonmetal interactions: An interesting example of the formation of a A_2B_3-type compound is the oxidation of In in a silver matrix.[101-104] Already at an In-concentration of 0.25 atom-%, two In-sites are observed with an ^{111}In(^{111}Cd) probe with V_{zz}- and η-values characteristic of In_2O_3, provided the oxidation temperature and the oxygen supply are sufficiently high. Parameters of the reaction kinetics can be derived from the "In_2O_3" fractions as a function of reaction time.[101, 103] Another example is the trapping of hydrogen at impurity atoms in metals.[105]

A remarkable special case is the conversion of a probe atom into a host atom by nuclear transmutation. Here, the probe atom-impurity atom interaction is so to speak "switched off" and the subsequent temporal evolution of the system is observed. However, a sufficiently long-lived start level of the γ-γ cascade (see Fig. 1) is required in order to allow sufficient time for the impurity atom to diffuse away. The only examples for this so far are the systems ^{181}Hf(^{181}Ta) in a Ta-matrix with oxygen,[106] hydrogen,[107] and oxygen and hydrogen simultaneously bound to it.[108]

5.4. Structural Phase Transitions

At structural phase transitions not only the lattice positions of the constituents change, but also, of course, the electron density distributions. This is usually easily detected via a variation of the NQI parameters. Despite the superiority of diffraction techniques to hyperfine techniques for the investigation of structural phase transitions, there are, nevertheless, cases where the structural changes are minute, despite large variations of the electron density distribution. Then, in contrast to diffraction techniques, there is no problem in determining the number and population of inequivalent sites by hyperfine spectroscopy. Furthermore, information on dynamic processes in the time window of hyperfine spectroscopy can be gained, e.g. fluctuations, and rotation and diffusion processes, which can be inferred only indirectly from diffraction data.[*]

Since the measurements are usually carried out with impurity probes, it is necessary to consider carefully for each system to what extent the dynamic processes are impurity-atom-specific.

5.4.1. *Displacive Phase Transformations*

Antiferroelectric Phase Transitions: Yeshurun et al.[108] have investigated the NQI at ^{181}Hf(^{181}Ta) probes in antiferroelectric $PbHfO_3$ and observed a critical behavior in the immediate vicinity of both phase transitions: on the one hand, the EFG diverges in a dispersion-like manner and additional high frequency spectral components show up, while on the other, one observes temperature-dependent linewidths. All observed effects are correlated with the sublattice polarization and the sublattice susceptibility, respectively. Apparently there are fluctuations in the vicinity of the phase transition, which slow down sufficiently to become noticeable in the NQI parameters.

"Charge-Density-Wave" Systems:[**] Among the "charge-density-wave" (CDW) systems the transition metal dichalcogenide 2H-$TaSe_2$ has been the most extensively studied.[110] This is built up from hexagonal layers with the sequence Se-Ta-Se Se-Ta-Se ... (in the 2H-modification the Ta has a trigonal prismatic coordination and the repetition length comprises two Se-Ta-Se sandwiches). The symmetry breaking at the onset of the CDW manifests itself in a redistribution of electron density, which is revealed in a dramatic way by the deviation of the EFG tensor from axial symmetry. In fact, this effect is much more pronounced than the changes in the electronic transport properties or in the associated lattice distortions. It is known from electron diffraction experiments that the commensurate superstructure is formed by three identical wave vectors, 120° apart from each other. Thus the two-dimensional unit cell with the dimensions $3a \times 3a$ (a = lattice constant in the hexagonal plane) comprises nine Ta-atoms. The phase between the charge density maximum/minimum and the Ta-lattice is virtually indeterminable from these measurements. From TDPAC measurements with ^{181}Hf(^{181}Ta) probes in this material (as for 2H-TaS_2; see Fig. 9) the number and population of inequivalent Ta-sites can be measured immediately.[112] One finds three sites with equal populations (A, B, C), one of which exhibits an extremely large asymmetry parameter ($\eta_A = 0.64$ for 2H-$TaSe_2$ and

[*] An example for this is the segregation of In dissolved in Al [96].

[**] The question of compound formation also arises in several very dilute binary systems, provided the probe and matrix exhibit a pronounced tendency towards compound formation. Whether this actually happens, or whether the impurity atoms are indeed highly diluted and on substitutional sites, could easily be decided by comparing NQI data of the dilute system with those of the relevant intermetallic phases for the corresponding element combination. With the exception of a few studies [97, 98], no attention has been paid to this problem in discussing the huge amount of data for EFG values in metals [99, 100].

[*] Dynamic processes in the GHz to THz-range can be investigated by inelastic diffraction methods.

[**] In CDW systems we have a static modulation of the conduction-electron density. With such, *Wilson* et al. [109] explained the formation of superstructures in some transition-metal chalcogenides with layer structures. Meanwhile CDW phenomena have been observed in several quasi one- and two-dimensional, metallic conducting compounds [111].

$\eta_A = 0.35$ for 2H-TaS_2, both at 10 K). At this lattice site $|V_{zz}|$ decreases compared to the unperturbed system above the CDW onset temperature; at the other two sites $|V_{zz}|$ slightly increases. Together with the orientation of the EFG-tensor determined on single crystals, it follows that the electron density maximum is centered *between* three Ta atoms and that the electron density must be fairly concentrated because of the relatively small perturbation of the peripheral Ta atoms (B, C) (formation of "Ta_3-clusters").

5.4.2. *Polymorphic Phase Transitions*

Besides the 2H-modifications of TaS_2 and $TaSe_2$, which are stable at room temperature, there is a high-temperature modification for both compounds with octahedrally coordinated Ta and a repetition length 1 (1T-TaX_2: CdI_2 structure type), which can be retained as a metastable phase by quenching rapidly to room temperature. Furthermore, there are modifications with alternating layers of both coordinations ($4H_b$, 6R). In Figure 10 the observed precession frequencies with $^{181}Hf(^{181}Ta)$ probes in TaS_2[113] and $TaSe_2$ during heating and cooling cycles are shown. In both systems, below 600 K and 500 K respectively, irreversible transitions from the 1T- to the 2H-structure take place, which are "smeared" over a broad temperature range and proceed via shear-transformations.[114] In this range, broad frequency distributions are observed rather than a superposition of 1T- and 2H-modifications.

For $TaSe_2$, the frequency jumps in the high-temperature range are exactly at those temperatures where structural transformations from the 2H to the mixed coordination phase and ultimately to 1T and back to 2H (with a large hysteresis) were observed according to X-ray data;[114] for TaS_2 there are no X-ray data available. In the mixed coordination phase, upon heating there is a *unique* well-defined precession frequency despite the simultaneous occurrence

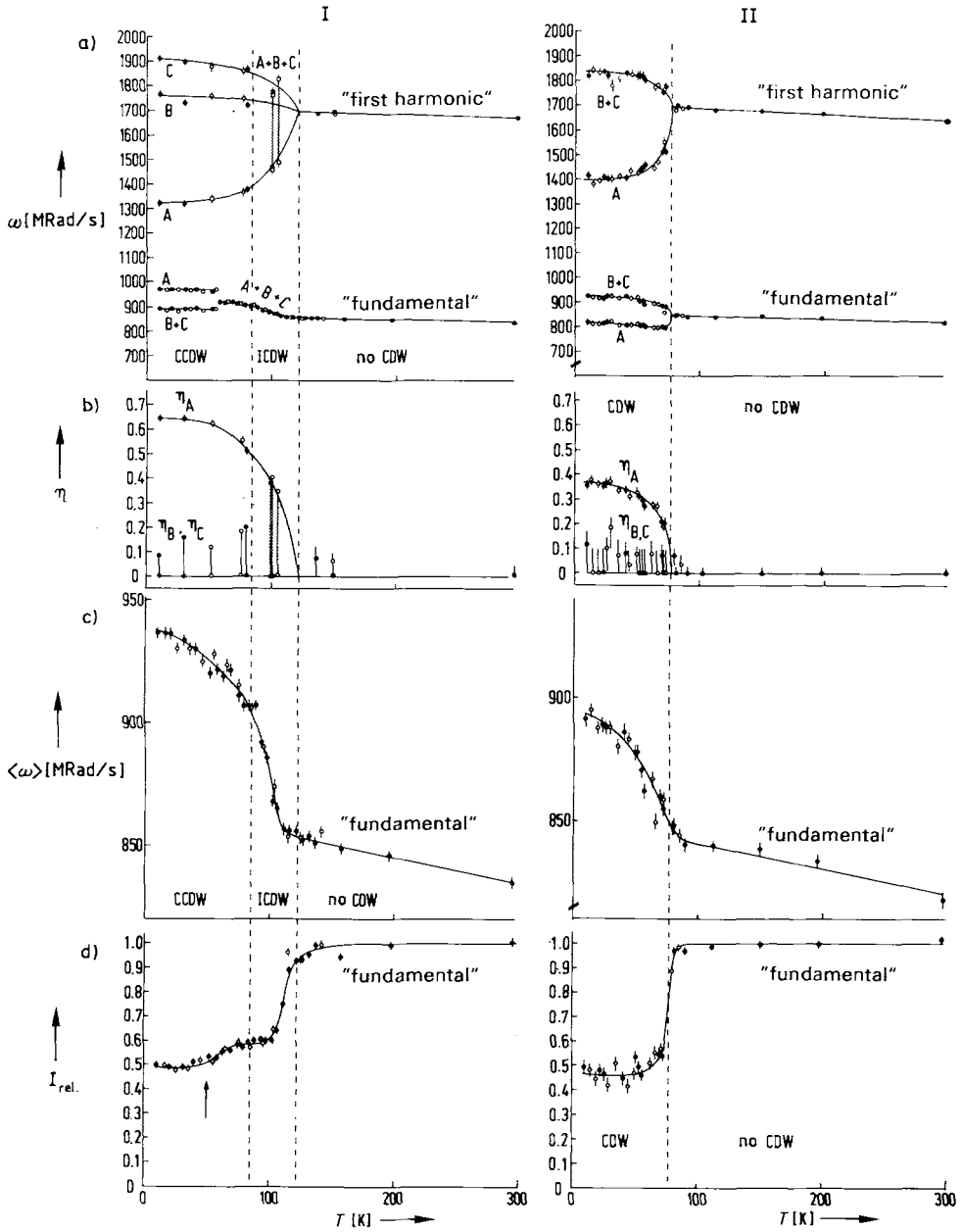

Fig. 9. NQI parameters versus temperature for the CDW phase of 2H-$TaSe_2$ (I) and 2H-TaS_2 (II) from TDPAC measurements with $^{181}Hf(^{181}Ta)$ probes (CCDW: commensurate CDW; ICDW: incommensurate CDW). a) Precession frequencies ω for fundamental (observable when the crystal is oriented with V_{zz} perpendicular to the detector plane) and first harmonic (observable when V_{zz} is in the detector plane midway between two detectors); the latter is resolved for 2H-$TaSe_2$ into three inequivalent Ta-sites (A, B, C) with equal population. Note, that in both cases V_{zz} at the A-site decreases at the CDW onset due to the development of η_A, despite an increase of ω_A (fundamental) in the case of 2H-$TaSe_2$. b) Asymmetry parameter: η_A increases at the CDW onset as for a second order phase transition; η_B and η_C are both small and can not be separated. c) Average precession frequency (fundamental): for 2H-$TaSe_2$ a small change in slope is observed when passing from the ICDW to the CCDW. ● = Measurement point on cooling, ○ = measurement point on heating. d) Relative peak-height (fundamental): for 2H-$TaSe_2$ the peak-height drops slowly at the CDW onset, but rapidly for 2H-TaS_2. This points to the absence of an ICDW in 2H-TaS_2. In addition, there is for 2H-$TaSe_2$ in the CCDW region a further small step (arrow), which is related to a change in the CDW stacking perpendicular to the layers.

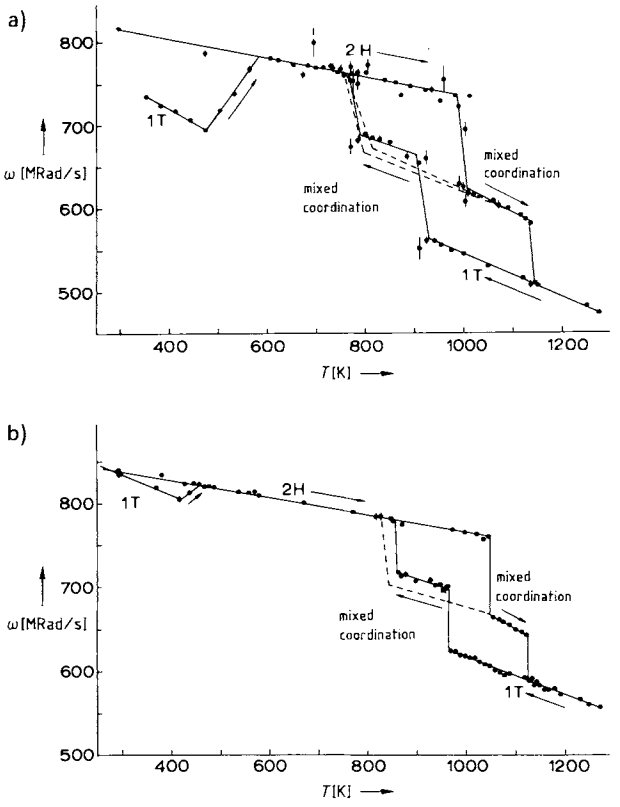

Fig. 10. Precession frequencies ω (fundamental) for $^{181}Hf(^{181}Ta)$ probes a) in TaS_2, b) in $TaSe_2$ versus temperature. The heating and cooling cycles are indicated by arrows. One clearly observes the polymorphic phase transitions with the sequence: 1T→2H – mixed coordination → 1T → mixed coordination → 2H with an extremely large hysteresis. The dashed lines represent measurements (no data points are shown for the sake of clarity), where the sample was cooled starting from the mixed coordination phase. It is clear that the two mixed coordination phases are not identical. In contrast to the low-temperature form, in the high-temperature form a unique sharp frequency is observed, despite the coexistence of Ta-atoms with trigonal-prismatic and octahedral coordination. The linear temperature dependence of the EFG over a wide temperature range is remarkably identical for 2H-TaS_2 and 2H-$TaSe_2$.

of two different metal coordinations, whose frequencies are markedly different in the pure modifications. A possible explanation would be a rapid coordination fluctuation at the Ta, as one would expect for Ta diffusion (within and perpendicular to the layers). The mixed coordination phase achievable upon cooling differs from that obtained upon heating mainly by the occurrence of substantial line-broadening, which could be a consequence of incomplete averaging by diffusion. This "diffusion picture" is further substantiated by the fact that in the case of TaS_2 the static TDPAC signal already begins to disappear several 100 K below the transition from the 2H- to the mixed coordination phase.[113] This is only possible if motional processes occur, e.g. the melting of the Ta sublattice or, at least, a "bound diffusion" of Ta without macroscopic transport.

5.4.3. Order-Disorder Transitions

So far only two types of such transitions have been investigated: the reorientational motion in ion-complexes and the sublattice melting in ion conductors. In the TDPAC spectra of many salts of $HfF_6^{2\ominus}$ and $HfF_7^{3\ominus}$, [probe: $^{181}Hf(^{181}Ta)$] one mostly observes a sharp transition from a static to a dynamic behavior (cf. Fig. 2c and b).[115–123] The analysis of the relaxation spectra yields the reorientational correlation time. In the case of the hexafluorides the $TaF_6^{\ominus}$ (nuclear transition!) complex rotates, whereas, in the case of the heptafluorides it is not clear what sort of a coordination $TaF_7^{2\ominus}$ has,[124] nor whether the observed dynamics results from coordination fluctuations[124] or from $TaF_7^{2\ominus}$ rotations.

Sublattice melting has been observed, e.g., in Ag_2S and Ag_2Se with a $^{111}In(^{111}Cd)$ probe.[125] At high temperatures the static interaction disappears, thus indicating that the $In^{3\oplus}$ ions become highly mobile. The activation energy for the motion of the $In^{3\oplus}$ ions was derived from the temperature dependence of the correlation times and this compares well with the activation energies for $Ag^{\oplus}$ ions. The diffusion constants for $Cd^{2\ominus}$ and $In^{3\oplus}$ in Ag_2S, determined with radioactive tracers, are only about a factor of 3 smaller than that for the $Ag^{\oplus}$ ion. Both facts suggest that the rapidly diffusing Ag ions, being present in excess, carry the $In^{3\oplus}$ ions along with them.[*]

Phase transitions in metal-hydrogen systems as well as hydrogen diffusion processes have been investigated in the metals Pd, Hf, Ta and Nb [probes: $^{99}Rh(^{99}Ru)$, $^{100}Pd(^{100}Rh)$, $^{181}Hf(^{181}Ta)$] and are described in a review article by *Weidinger*.[128]

5.4.4. Other Lattice Instabilities

In the following we briefly present a few systems which exhibit lattice instabilities, although at present there is no reliable evidence for the presence of a structural phase transition. In $HfTe_5$, a compound consisting of $HfTe_3$ chains, in which the Hf is surrounded trigonal-prismatically by Te atoms, and which are interconnected via Te chains, one observes [$^{181}Hf(^{181}Ta)$ probes] with decreasing temperature (starting from 300 K) an increase in η from 0.25 to 1, a characteristic V_{zz}-η distribution, and, below about 80 K, a complete collapse of the static TDPAC spectrum (see Fig. 11).[129]

This anomaly is very likely related to the anomaly observed in electronic transport properties at 75 K. Interestingly, this "collapse" of the spectrum is essentially suppressed by very small concentrations of radiation defects (displacements) produced by neutron activation.[129, 130]

Finally, we refer to materials with electric switching properties: $^{111}In(^{111}Cd)$ in InSe[131] and $^{181}Hf(^{181}Ta)$ in HfS_2.[130, 132] In both cases one observes the occurrence of an additional NQI frequency, which is exactly twice the normal component. In the case of InSe it was shown that this additional component could be switched on and off. At present, it is unclear whether this is structure related or of dynamic origin.

[*] The investigation of diffusion mechanisms is more interesting than the determination of the diffusion constant by TDPAC. So far only investigations using $^{111}In(^{111}Cd)$ in Ag and Zn have been carried out[126, 127].

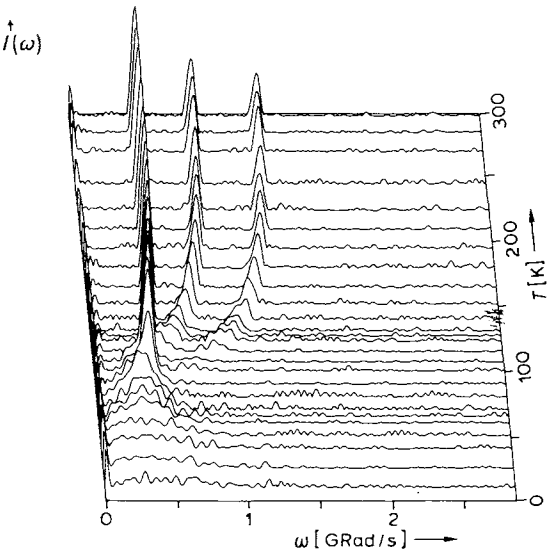

Fig. 11. Fourier-transformed TDPAC spectra of ^{181}Hf(^{181}Ta) probes in a $HfTe_5$ single crystal versus temperature. Upon cooling, the first harmonic shifts towards the fundamental (i.e. the asymmetry parameter becomes $\eta = 1$); simultaneously, the harmonics broaden considerably without a significant broadening of the fundamental. Starting at 90 K the fundamental also "melts away". This scenario is characteristic for critical fluctuations in the vicinity of an incompletely developed phase transition which "freeze out" on the hyperfine time scale.

5.5. Solid State Reactions

The application of TDPAC to the investigation of solid state reactions is based on the possibility of determining individual constituents of phase mixtures *quantitatively* with the help of known hyperfine parameters of the individual phases. The separation of various species is the more successful the more different the associated NQI parameters (V_{zz}, η, orientation). Substances, which do not lead to a NQI of the probe due to symmetry, are absolutely indistinguishable. Generally speaking, the identification of the initial and final products presents no problems, especially if phases with high quality are prepared efficiently (adequate preparation and reaction performance). The identification of intermediate products becomes problematic whenever they cannot be produced separately and as single phases, or when they are, e.g., highly disordered or non-stiochiometric despite an adequate reaction performance. An essential advantage of TDPAC over many other spectroscopic techniques is that the sensitivity of detection is largely sample-independent, i.e. the relative fractions of the observed spectral components are identical with the mole fractions of the individual phases. The efficacy of TDPAC fully emerges only in in-situ applications. Thus, it is possible to monitor the temporal evolution of the different mole fractions non-destructively under practically all reaction conditions, provided the reaction can be slowed down sufficiently or—better—provided the data collection times can be drastically shortened by multi-detector systems with high efficiency.

In the field of solid state reactions there have been isolated studies of the dehydration/rehydration reaction of $HfF_4 \cdot 3H_2O$,[133] the thermal decomposition of $(NH_4)_2ZrF_6$,[134] the formation of $CuIn_2$ at interfaces,[135] the oxidation of Hf metal,[113] internal oxidation processes in silver alloys[101-104] (cf. Section 5.3.2), and of gas-phase transport reactions in-situ.[113, 136]

Systematic investigations of solid state reactions have thus far only been made on intercalation reactions in the layered compound 2H-TaS_2, and these will now be discussed in more detail.

Metal ions and molecular ions can be intercalated both chemically and electrochemically between neighboring sulfur layers.[137, 138] The radioactive probe ^{181}Hf(^{181}Ta) resides on Ta-sites. During the intercalation the NQI is modified by a charge transfer from the intercalate to the host in the immediate vicinity of the intercalate and registered by the probes in the metal plane.[139][*]

In Figure 12 the Fourier-transformed TDPAC-spectra during the electrochemical intercalation of $Li^{\oplus}$ ions close to equilibrium, i.e. at very low surface current densities, are shown.[139, 140] It can be clearly seen, that the signal of the empty host material decreases with increasing Li uptake, while a new component shows up on the low-frequency side. Beyond an uptake of $Li/TaS_2 \approx 1/3$ a single-phase region is observed. The average precession frequency $\langle\omega\rangle$ depends approximately linearly on the charge transfer.[139] The variation of the linewidth in the single-phase range shows that the mobility of the Li ion is not sufficient to average out site inequivalences completely. One should not conclude from the two-phase region at the beginning of the reaction that a miscibility gap in the Li/TaS_2 phase diagram actually exists. Rather, this apparent miscibility gap is related topologically to the lattice expansion due to the intercalation and the associated coherent intercalation front and disappears after homogenization at high temperatures.[140]

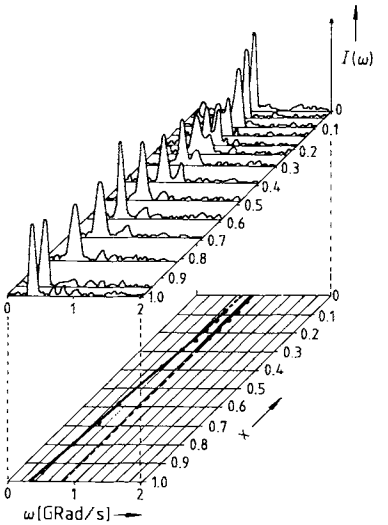

Fig. 12. Fourier-transformed TDPAC spectra (top) of ^{181}Hf(^{181}Ta) probes in 2H-TaS_2 as a function of the electrochemical lithium intercalation for near-equilibrium conditions and the projection of the peak positions (bottom) connected by solid lines (dashed lines: extrapolation) after [139]. At the beginning one observes a lithium-deficient phase apart from the unreacted 2H-TaS_2; above a lithium content of $x \approx 0.3$ there is a single phase with continuously increasing lithium content (continuously decreasing precession frequency). The variation of the linewidth is attributed to ordering phenomena at $x \approx 2/3$ and, by definition, at $x = 1$).

[*] If the intercalate diffuses rapidly enough the probes register a unique, time-averaged charge transfer (proportional to the intercalate packing density). Otherwise there are, for intercalate/Ta ratios < 1, inequivalent Ta-sites, depending on the intercalate arrangement, which, however, are very similar due to the large Ta-intercalate distance.

The creation of non-equilibrium structures, i.e. of coexisting phases with different Li content, at high prism surface current densities and the subsequent monitoring of their equilibration is shown in Figure 13.[140] It is possible to assign phases with a well-defined Li content to the different spectral components in the TDPAC spectra. Studies of this kind can only be performed in situ. Here, metastable non-equilibrium structures in an electrode material were successfully revealed for the first time. These can be detected only in an integrated way in macroscopic parameters such as, e.g., the electrochemical potential.

The electrochemical intercalation of hydrated metal ions such as, e.g., $K^{\oplus}_{aq}$ proceeds similarly to that of unsolvated $Li^{\oplus}$, with the following exceptions (Fig. 14):[139] (a) due to the high intercalate mobility the reaction proceeds always close to equilibrium; (b) at the beginning of the reaction one observes an additional intermediate phase (two successive two-phase regions); (c) the single-phase range terminates already at $x \approx 0.42$ due to the onset of water decomposition.

In contrast to Li_xTaS_2, where all interlayer gaps are uniformly filled (such compounds are called first stage), we have here the possibility of filling only every second interlayer gap at the beginning of the reaction (2nd stage),[*] and the formation of a coherent intercalation front is avoided. The intermediate phase described above is identified as a second stage with the same intercalate packing density (per intercalated layer!) as in the subsequent first stage at the onset of the single phase region.[*] As soon as the formation of the first stage sets in ($x \approx 0.13$), small temporary shifts of the characteristic precession frequencies are observed. In the case of the more strongly hydrated $Gd^{3\oplus}$ ions these effects are more pronounced.[142] The intercalate packing density enhancements which are correlated with these peak migrations are related to stacking faults due to the uncorrelated nucleation.[141] Apparently, it is energetically favorable to tolerate packing density pile-ups temporarily at the formation of the first stage. Such details of the intercalation process are difficult to observe or to interpret with macroscopic techniques.

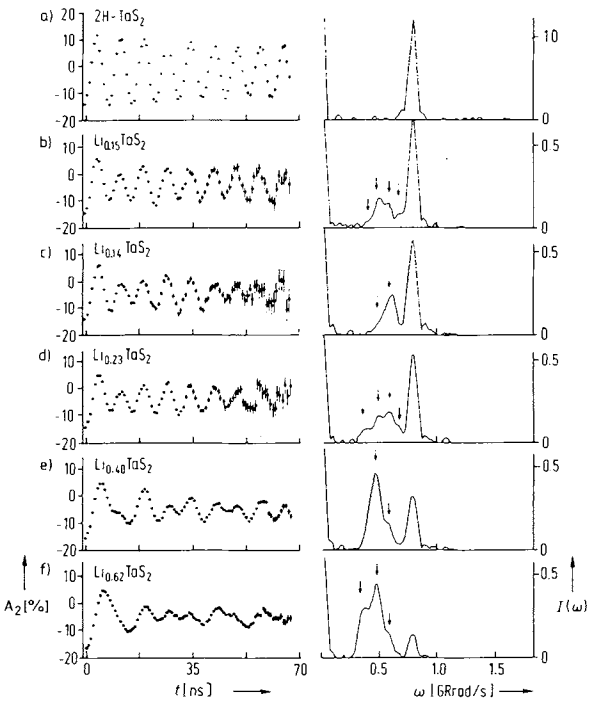

Fig. 13. TDPAC spectra (left) and corresponding Fourier transforms (right) of $^{181}Hf(^{181}Ta)$ probes in a 2H-TaS_2 crystal during electrochemical lithiation under extreme non-equilibrium conditions [140]. a) Empty host material. b) Reduction at 200 μA (prism surface current density ca. 5000 μA/cm²) until a lithium uptake of $\langle x \rangle \approx 0.15$; one observes four different phases (arrows) which differ in the lithium concentration. c) Subsequent oxidation at 100 μA until $\langle x \rangle \approx 0.14$; the most lithium-rich phase (lowest frequency) disappears and the inner-crystalline equilibration superimposes the deintercalation, as shown by the decrease in the peak of the empty host material. d) Subsequent reduction at 100 μA; again, four different phases are produced. e) When the current is reduced to 20 μA, the most lithium-rich phase disappears. f) At an uptake of $\langle x \rangle \approx 0.62$, a large fraction of the phase with maximum lithium content is already formed; here, the intercalation slows down very much, i.e. even at 25 μA there is essentially lithium metal deposition.

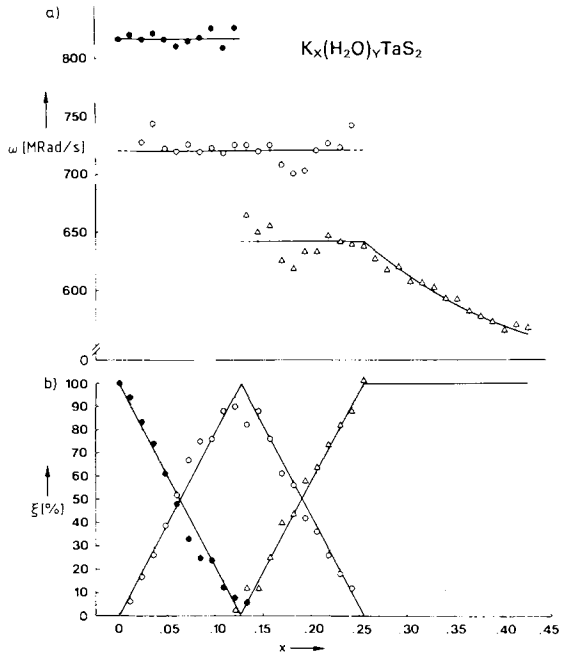

Fig. 14. a) Precession frequencies ω of $^{181}Hf(^{181}Ta)$ probes in 2H-TaS_2 during electrochemical intercalation of hydrated $K^{\oplus}$ ions; b) corresponding mole fractions (ξ) versus charge transfer [139]. There are two consecutive two-phase regions, and then starting from $x = 0.26$ there is a single-phase range. ● = TaS_2, ○ = second stage, △ = first stage.

Further studies deal with the chemical intercalation of Li (via *n*-butyllithium),[139, 143] In, Ga, Sn, Cd (all thermally),[144] GaIn-eutectic (room temperature),[144] and the electrochemical intercalation of unsolvated Ag[113] and hydrated $Fe^{2\oplus}$.[145] In the latter case the oxidation of $Fe^{2\oplus}$ to $Fe^{3\oplus}$ enables the formation of new and interesting compounds.

6. Applications in the Border Region between Physics and Biology

Since there are extremely few isotopes of elements suitable for TDPAC spectroscopy which have a physiological function in biomolecules, it is understandable that this spectroscopic technique has hitherto played only a very

[*] Instead of the formation of higher stages [138] the fully uncorrelated intercalation with near neighbor layer exclusion is discussed as well [141].

[*] Based on TDPAC spectra alone the intermediate phase could also be a first stage with half the intercalate packing density.

minor role in biology. There are two ways of labeling the probes: (1) The unspecific labeling of the biomolecule. Here, the dissolved probe is added to the biomolecule in solution and the binding can be recorded quantitatively by comparing spectra of the dissolved probe (cf. Fig. 2b) with that of the bound probe (cf. Fig. 2c-f); (2) the specific labeling of the biomolecule and the metal substitution in metalloenzymes. The "label" can be offered as free ions or "packed", as, e.g., in EDTA or serum albumin.

For the TDPAC measurements the labeled biomolecules can be present in solution, immobilized in highly viscous solutions, as polycrystals (precipitates, lyophilized) or as single crystals. The last case often presents difficulties due to prolonged crystallization times, especially when using isomeric isotopes, which generally have lifetimes of one hour or less. Provided the radioactive isotope can be separated from the inactive carrier there are no problems with regard to sample quantities.

One can roughly distinguish two areas of applications of TDPAC spectroscopy in biology: (1) Coordination studies. Here, nonequivalent sites are identified and characterized according to their different NQI parameters (V_{zz}, η). (2) Molecular dynamics. Here, on the one hand, the tumbling motion of the biomolecule in solution is studied, on the other, one can investigate the intramolecular dynamics provided the molecules are immobilized.

6.1. Coordination Studies

The only systematic investigations have been carried out by *Bauer* et al.[24] on Zn-containing enzymes in highly viscous solutions, in which Zn was substituted by ^{111m}Cd ($\tau_{1/2}=48$ min). *Bauer* et al.[146] demonstrated that although the isotope ^{111}In(^{111}Cd) would appear much more suitable for the spectroscopic examination due to its longer lifetime ($\tau_{1/2}=2.8$ d) it was, in fact, not practical for this purpose, the reasons being that In-chemistry is radically different from that of Zn-chemistry, that aqueous In-solutions tend to precipitate as hydroxides at physiological pH values,[147] and that after-effects due to nuclear transmutation can be problematic. The loss of enzymatic activity due to the Zn/Cd-exchange can be recovered partly or fully by adjusting the pH.[148] An impressive example of how sensitively different Cd-ligations in various enzymes are reflected in different NQI parameters is illustrated in Figure 15. *Bauer* tried to correlate absolute values of V_{zz} and η with different coordinations and different ligands.[24] In this way changes in the coordination at substrate or inhibitor binding were investigated in various systems as a function of pH. Of particular interest is the study of carboxypeptidase,[24] which shows that there are different conformations in the crystalline state and the highly viscous solution. In the case of carboanhydrase one observes a significant "site heterogeneity" despite the immobilization, which possibly is caused by ligand exchange not yet fully stopped, or by slow internal molecular dynamics which is still occurring.

Relatively new are the first investigations of the Cd-binding in metallothioneines[149] which play an essential role in heavy metal detoxification of organisms.

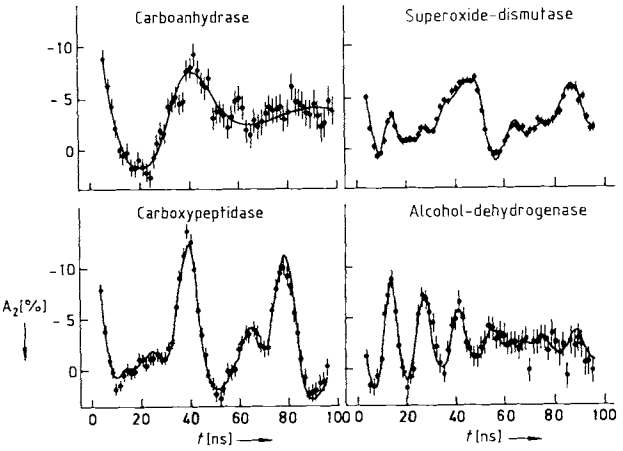

Fig. 15. TDPAC spectra of specifically bound ^{111m}Cd probes in four different metalloenzymes (Cd/Zn substitution) in highly viscous solutions [24].

6.2. Molecular Dynamics

For the investigation of the tumbling motion of biomolecules in solution,[150-152] almost without exception ^{111}In(^{111}Cd) was bound unspecifically to the biomolecule. The determination of the reorientational correlation time from the spectra is problematic, since the few available spectra of immobilized molecules are very featureless and indicate an extreme site heterogeneity.

This could be a consequence of the unspecific binding of the "labels". However, investigations of specifically bound ^{111}In(^{111}Cd) in serum albumin[152] and in porphyrins[44] in the immobilized state also showed very featureless spectra, thus suggesting more fundamental problems, e.g. chemical after-effects. Finally, the investigation of the macromolecular dynamics with "packed labels" such as ^{111}In(^{111}Cd) in serum albumin is problematical, because a molecular "label" can exhibit its own dynamics. Apart from very indirect hints towards *intramolecular* dynamics in hemoglobin compared to myoglobin,[153] there is only one direct indication of intramolecular reorientational motion,[154] in the system trypsinogen/trypsinogen-pancreatic trypsin inhibitor (PTI). Here, the disulfide bridge between cysteine 191 and cysteine 220 in the so-called activation domain of trypsinogen, which can be selectively reduced, was labeled with ^{199m}Hg ($\tau_{1/2}=43$ min) and the NQI was studied as a function of temperature between 195 K and 319 K (see Fig. 16). At 195 K one observes several discrete Hg-sites which can be assigned to different conformations of the active center. The flexibility of the activation domain of trypsinogen, which is considered to cause the blocking of the enzymatic activity, is clearly revealed in a temperature-dependent reorientational correlation time. In this way an activation enthalpy of 8 kcal/mol and a correlation time of about 10 ns at room temperature were determined. The use of an atomic label, which is extremely small compared to the total mass of the activation domain and therefore does not influence the flexibility of the activation domain, promises to yield system-specific results rather than results that reflect the local dynamics of the label. A control experiment with the trypsinogen-PTI complex at 300 K and 320 K did not reveal any intramolecular

reorientational motion within the easily accessible time range from about 1 ns to 200 ns. This is consistent with the fact that this complex has a rigid activation domain[155].

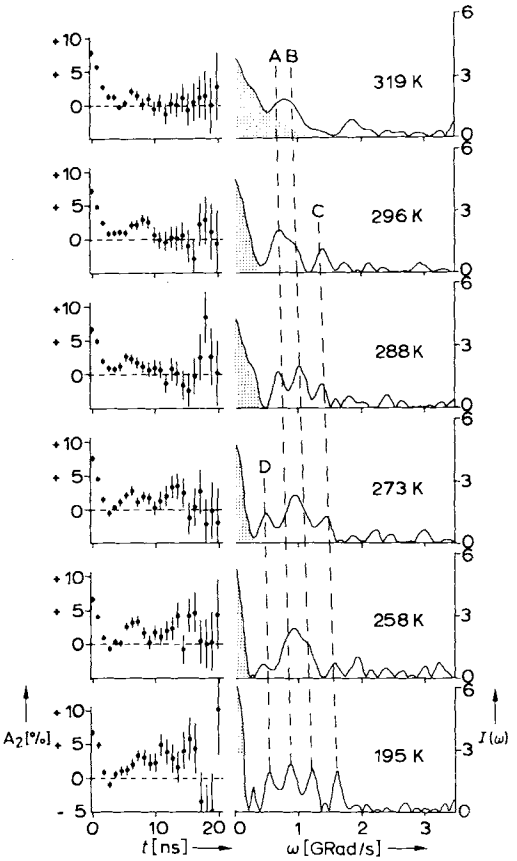

Fig. 16. TDPAC spectra (left) and corresponding Fourier transforms (right) of ^{199m}Hg labels specifically bound between cysteine-191 and cysteine-220 in precipitated trypsinogen versus temperature [154]. The dashed lines represent various Hg-conformations (A-D) of the active center of trypsinogen. The width of the dotted area at $\omega = 0$ is a measure of the intramolecular reorientational motion in the activation domain of trypsinogen.

7. Outlook

Since TDPAC spectroscopy always requires radioactive samples, this technique presumably will never become as widespread as NMR/NQR or ME. However, a great deal would be gained if the existing facilities of TDPAC spectroscopy, which are excellent in Germany, were jointly used and further developed by chemists, physicists and biologists to a much larger extent. Prerequisite for this are the willingness to cooperate, the encouragement of such a cooperation by moral and financial support, the readiness to learn the "language" of the respective partner (whether a colleague from a different faculty or an expert from a related discipline), and, most important, the intensified development of existing spectrometers, all of which must be regarded as inefficient. For example, only 1% of all γ-γ-coincidences is actually recorded, and on-line data analysis is seldom possible. Here, multi-detector systems (e.g. 6 instead of the usual 4 detectors) with high acceptance and optimized scintillator geometry (e.g. conical), an improved time resolution at unchanged high detection efficiency (e.g. BaF_2 crystals instead of NaI(Tl) or plastic scintillators), and a massive computer support can help a great deal (such a spectrometer is presently under construction in the physics department at the Technische Universität, München). The data collection time per spectrum can easily be reduced to one hour or a few minutes compared to the currently typical times of the order of one day. "Armed" in such a way, the new applications listed in Table 2 ("authors desire") seem to be within reach. One should not, of course, restrict oneself to the description of the stationary state, but rather study the processes in situ.

Table 2. Future areas of application of TDPAC spectroscopy in the border region of physics/chemistry/biology.

Field of Research	Examples
Liquids/ Solutions	Polymetalate chemistry (e.g. of Zr, Mo, Hf, Ta, Pb), Lewis Acid-Base reactions (charge redistribution), crystallization in metal melts
Cryochemistry	Matrix isolation, "low temperature chemical vapor deposition"
Glasses/ Amorphous systems	hydrogels, oxide gels (kinetics of recrystallization, structure); halogenide glasses (kinetics of recrystallization, structure, hydrolysis); metallic glasses (kinetics of recrystallization, oxidation)
Surfaces	Ideal: growth processes, reactions; fractal: reactions, catalysis
Electrochemistry	Electrochromic displays, battery electrodes, Ionic conductors (also based on polymers); electrocrystallization (non-equilibrium processes during dendritic crystal growth)
Phase transitions	Incommensurate structures, lattice instabilities ("turbulent crystal", chaos), switching behavior (optic, electronic), "memory-effects"
Solid state reactions/ Metallurgy	In situ studies of solid state reactions [corrosion (oxidation, sulfidation), sintering, reactions in crystals of organometallic complexes] and preparation methods [ion implantation (also "ion-mixing"), laser treatment (metastable phases, "non-equilibrium solidification")], first steps of compound formation on an atomic level, segregation (also spinodal decompositon), annealing of defects in compounds, defect aggregation in non-stoichiometric phases
Polymers	Metal polymers, polymer dynamics, switching behavior
Biochemistry/ Biophysics	Intramolecular dynamics, membrane dynamics, toxicology of heavy metals

We are greatly indebted to Prof. Dr. K. Andres and Prof. Dr. G. M. Kalvius for the excellent research facilities they put at our disposal in their institutes, and gratefully acknowledge the enthusiastic cooperation of the following diplomands, Ph.D-students and guests: Dr. H. Ernst, Dr. W. Biberacher, R. Mühlberger, A. Hübler, H. Gierisch, C. Vogdt, S. Saibene, U. Klapp, Dr. A. Vasquez, Dr. H. Saitovitch. We are also indebted to Prof. Dr. J. O. Besenhard, Prof. Dr. R. Huber, and Prof. Dr. H. Knözinger for their kind cooperation in solving the mainly interdisciplinary problems. Our work was generously supported through funds for material and personnel by the Bundesministerium für Forschung und Technologie and the Deutsche Forschungsgemeinschaft.

Received: August 19, 1985;
revised: May 20, 1986 [A 604 IE]
German version: *Angew. Chem. 99* (1987) 113

[1] H. Frauenfelder, *Annu. Rev. Nucl. Sci. 2* (1953) 129.
[2] R. M. Steffen, *Adv. Phys. 4* (1955) 293.
[3] S. Devons, L. J. B. Goldfarb, *Encycl. Phys. 42* (1957) 362.
[4] E. Heer, T. B. Novey, *Solid State Phys. 9* (1959) 199.
[5] E. Karlsson, E. Matthias, K. Siegbahn (Eds.): *Perturbed Angular Correlations*, North-Holland, Amsterdam 1964.
[6] K. Siegbahn (Ed.): *Alpha-, Beta-, Gamma-Ray-Spectroscopy*, North-Holland, Amsterdam 1965.
[7] A. J. Freeman, R. B. Frankel (Eds.): *Hyperfine Interactions*, Academic Press, New York 1967.
[8] H. van Krugten, B. van Nooijen (Eds.): *Angular Correlations in Nuclear Disintegration*, Rotterdam University Press, Groningen 1971.
[9] D. R. Hamilton, *Phys. Rev. 58* (1940) 122.
[10] E. L. Brady, M. Deutsch, *Phys. Rev. 72* (1947) 870; *74* (1948) 1541; *78* (1950) 559.
[11] H. Haas in J. J. Bara, K. Ruebenbauer, Z. Stachura (Eds.): *Condensed Matter Studies by Nuclear Methods* (Proc. XX Winter School on Physics, Zakopane 1985), Vol. 2, p. 453.
[12] H. Barfuss, G. Böhnlein, P. Freunek, R. Hofmann, H. Hohenstein, W. Kreische, H. Niedrig, A. Reimer, *Hyperfine Interact. 10* (1981) 1051, and references cited therein; K. Bonde Nielsen, B. Toft, *ibid. 10* (1981) 747.
[13] G. Goertzel, *Phys. Rev. 70* (1946) 897.
[14] K. Alder, *Helv. Phys. Acta 25* (1952) 235.
[15] H. Frauenfelder, *Phys. Rev. 82* (1951) 549; H. Aeppli, A. S. Bishop, H. Frauenfelder, M. Walter, W. Zünti, *ibid. 82* (1951) 550.
[16] K. S. Krane, *Hyperfine Interact. 15/16* (1983) 1069.
[17] H. H. Rinneberg, *At. Energy Rev. 17* (1979) 477.
[18] M. Forker, R. J. Vianden, *Magn. Reson. Rev. 7* (1983) 275.
[19] J. I. Vargas, *MTP Int. Rev. Sci. Inorg. Chem. Ser. One 8* (1972) 45.
[20] J. P. Adloff, *Radiochim. Acta 25* (1978) 57.
[21] D. A. Shirley, H. Haas, *Annu. Rev. Phys. Chem. 23* (1972) 385.
[22] H. Haas, D. A. Shirley, *J. Chem. Phys. 58* (1973) 3339.
[23] R. Thun in [8], p. 78.
[24] R. Bauer, *Q. Rev. Biophys. 18* (1985) 1.
[25] M. H. Cohen, F. Reif, *Solid State Phys. 5* (1957) 321.
[26] T. P. Das, E. L. Hahn, *Solid State Phys. Suppl. 1* (1958) 1.
[27] E. A. C. Lucken: *Nuclear Quadrupole Coupling Constants*, Academic Press, London 1969.
[28] C. H. Townes, B. P. Dailey, *J. Chem. Phys. 17* (1949) 782; G. M. Bancroft, *Coord. Chem. Rev. 11* (1973) 247; S. Vega, *J. Chem. Phys. 60* (1974) 3884.
[29] S. Nagel, *J. Phys. Chem. Solids 46* (1985) 743; *J. Phys. C 18* (1985) 3673; D. E. Ellis, D. Guenzburger, H. B. Jansen, *Phys. Rev. B Condens. Matter 28* (1983) 3697.
[30] A. C. Beri, T. Lee, T. P. Das, R. M. Sternheimer, *Phys. Rev. B Condens. Matter 28* (1983) 2335; P. Blaha, K. Schwarz, P. Herzig, *Phys. Rev. Lett. 54* (1985) 1192; K. D. Sen, *J. Phys. C 18* (1985) 3153.
[31] R. F. Stewart, *J. Chem. Phys. 57* (1972) 1664; D. Schwarzenbach, *Chimia 35* (1981) 100; P. Coppens, L. Li, *J. Chem. Phys. 81* (1984) 1983; E. D. Stevens, M. L. DeLucia, P. Coppens, *Inorg. Chem. 19* (1980) 813.
[32] R. M. Sternheimer, *Phys. Rev. 130* (1963) 1423.
[33] R. M. Steffen, H. Frauenfelder in [5], p. 3.
[34] H. Frauenfelder, R. M. Steffen in [6], Vol. 2, p. 997.
[35] K. E. G. Löbner in W. D. Hamilton (Ed.): *The Electromagnetic Interaction in Nuclear Spectroscopy*, North-Holland, Amsterdam 1975, p. 173.
[36] J. D. Rogers, A. Vasquez, *Nucl. Instrum. Methods 130* (1975) 539.
[37] H. Müller, *Angew. Chem. 79* (1967) 128; *Angew. Chem. Int. Ed. Engl. 6* (1967) 133; G. Harbottle, A. G. Maddock (Eds.): *Chemical Effects of Nuclear Transformations in Inorganic Systems*, North-Holland, Amsterdam 1979.
[38] A. Abragam, R. V. Pound, *Phys. Rev. 92* (1953) 943.
[39] A. Baudry, P. Boyer, J. D. Fabris, P. Vulliet, *Hyperfine Interact. 10* (1981) 1057, and references cited therein.
[40] N. Bloembergen, E. M. Purcell, R. V. Pound, *Phys. Rev. 73* (1948) 679.
[41] H. F. Wagner, M. Popp, M. Forker, *Z. Phys. 248* (1971) 195.
[42] B. K. Sinha, R. Bhattacharyya, *Nucl. Instrum. Methods 143* (1977) 583.
[43] A. Lerf, C. Vogdt, T. Butz, A. M. M. Eid, H. Knözinger, *Hyperfine Interact. 15/16* (1983) 921.
[44] O. C. Mullins, M. Kaplan, *J. Chem. Phys. 79* (1983) 4475.
[45] G. R. Demille, D. L. Livesey, K. Mailer, S. P. Turner, *Chem. Phys. Lett. 44* (1976) 164.
[46] A. Boussaha, J. C. Abbe, A. Haessler, *J. Inorg. Nucl. Chem. 39* (1977) 853.
[47] M. E. Phillips, F. A. Smith, *Hyperfine Interact. 10* (1981) 1063.
[48] R. M. Alcock, F. A. Smith, *Radiochem. Radioanal. Lett. 41* (1979) 197.
[49] M. de Bruin, R. W. Hollander, J. van der Plicht, *J. Inorg. Nucl. Chem. 38* (1976) 2149.
[50] K. S. R. Sastry, G. J. Hallee, M. E. Ottlinger, E. W. Westhead, *Hyperfine Interact. 4* (1978) 891.
[51] M. von Hartrott, D. Quitmann, J. Rossbach, E. Weihreter, F. Willeke, *Hyperfine Interact. 10* (1981) 1027.
[52] P. Maxim, R. Brinkmann, M. Elwenspoek, M. von Hartrott, M. Kiehl, C. A. Paulik, D. Quitmann, *Hyperfine Interact. 15/16* (1983) 573.
[53] D. K. Gaskill, J. A. Gardner, K. S. Krane, K. Krusch, R. L. Rasera, *Hyperfine Interact. 10* (1981) 1023.
[54] G. Czjzek, *Hyperfine Interact. 14* (1983) 189.
[55] P. Heubes, D. Korn, G. Schatz, G. Zibold, *Phys. Lett. A 74* (1979) 267.
[56] P. Heubes, D. Korn, G. Schatz, G. Zibold in E. N. Kaufmann, G. K. Shenoy (Eds.): *Nuclear and Electron Resonance Spectroscopies Applied to Material Science*, Elsevier, North-Holland, New York 1981, p. 385.
[57] K. O. Hodgson, R. Hedman, J. E. Penner-Hahn (Eds.): *EXAFS and Near Edge Structure III*, Springer, Berlin 1984.
[58] L. Thomé, H. Bernas, P. Heubes, M. Deicher, E. Recknagel, *Nucl. Instrum. Methods 199* (1982) 431.
[59] J. A. Cameron, P. R. Gardner, L. Keszthelyi, W. V. Prestwich, *Chem. Phys. Lett. 4* (1969) 229.
[60] J. S. Barrett, J. A. Cameron, P. R. Gardner, L. Keszthelyi, W. V. Prestwich, *J. Chem. Phys. 53* (1970) 759.
[61] J. A. Martinez, I. J. R. Baumvol, F. Sanchez, E. F. Fraga, A. Vasquez, *Chem. Phys. Lett. 67* (1979) 168.
[62] D. Avnir, D. Farin, P. Pfeifer, *Nature (London) 308* (1984) 261.
[63] W. Körner, W. Keppner, B. Lehndorff-Junges, G. Schatz, *Phys. Rev. Lett. 49* (1982) 1735.
[64] W. Körner, W. Keppner, T. Klas, B. Lehndorff-Junges, G. Schatz, *Hyperfine Interact. 15/16* (1983) 993.
[65] C. Vogdt, T. Butz, A. Lerf, H. Knözinger, *Proc. VIIIth Int. Congr. Catal.* (Berlin 1984) Vol. III, p. 117.
[66] C. Vogdt, T. Butz, A. Lerf, H. Knözinger, *Polyhedron 5* (1986) 95.
[67] A. Baudry, P. Boyer, A. L. de Oliveira, *J. Phys. Chem. Solids 43* (1982) 871.
[68] F. Pleiter, K. G. Prasad, *Hyperfine Interact. 20* (1984) 221.
[69] F. Pleiter, *Hyperfine Interact. 5* (1977) 109; C. Hohenemser, A. R. Arends, H. de Waard, H. G. Devare, F. Pleiter, S. A. Drentje, *ibid. 3* (1977) 297.
[70] M. J. Ponnambalam, P. Jena, *Phys. Rev. B Condens. Matter 31* (1985) 5680.
[71] H. de Waard, *Phys. Scr. 11* (1975) 157.
[72] H. Bernas, *Phys. Scr. 11* (1975) 167.
[73] A. Perez, R. Coussement (Eds.): *Site Characterization and Aggregation of Implanted Atoms in Materials*, Plenum, New York 1980.
[74] E. Recknagel, T. Wichert, *Nucl. Instrum. Methods 182/183* (1981) 439.
[75] F. Pleiter, C. Hohenemser, *Phys. Rev. B Condens. Matter 25* (1982) 106.
[76] E. Recknagel, G. Schatz, T. Wichert in J. Christiansen (Ed.): *Hyperfine Interactions of Radioactive Nuclei*, Springer, Berlin 1983, p. 133.
[77] M. Deicher, E. Recknagel, T. Wichert, *Hyperfine Interact. 10* (1981) 675.
[78] M. Deicher, O. Echt, E. Recknagel, T. Wichert, *Hyperfine Interact. 10* (1981) 667.
[79] W. Witthuhn, A. Weidinger, W. Sandner, H. Metzner, W. Klinger, R. Böhm, *Z. Phys. B 33* (1979) 155.
[80] R. Keitel, W. Engel, S. Hoth, W. Klinger, R. Seeböck, F. Simonato, R. Böhm, W. Witthuhn, *Hyperfine Interact. 10* (1981) 681.
[81] R. Seeböck, F. Simonato, R. Keitel, W. Witthuhn, *Hyperfine Interact. 10* (1981) 695.
[82] K. Bonde Nielsen, H. K. Schou, T. Lauritzen, G. Weyer, I. Stensgard, J. W. Petersen, S. Damgaard, *J. Phys. C 17* (1984) 3519.
[83] M. Behar, G. Garcia Bermudez, A. Filevich, R. P. Livi, F. C. Zawislak, *Phys. Lett. A 60* (1977) 250.
[84] K. Matsui, T. Shoji, *Conf. Ser. Inst. Phys. 31* (1977) 379.
[85] F. Schneider, S. Unterricker, *Phys. Status Solidi A 85* (1984) 455.
[86] S. Unterricker, J. Hausbrand, *Phys. Status Solidi A 46* (1978) 125.
[87] F. Pleiter, A. R. Arends, H. de Waard, *Phys. Lett. A 77* (1980) 81; A. R. Arends, F. Pleiter, *Hyperfine Interact. 10* (1981) 651; H. de Waard, F. Pleiter, L. Niesen, D. W. Hafemeister, *ibid. 10* (1981) 643.
[88] M. Deicher, G. Grübel, T. Wichert, *Nucl. Instrum. Methods 209/210* (1983) 817; M. Deicher, G. Grübel, W. Reiner, T. Wichert, *Hyperfine Interact. 15/16* (1983) 467.
[89] U. Pütz, A. Hoffmann, K. Freitag, R. Vianden, *Radiat. Eff. 69* (1983) 253.
[90] W. Bolse, P. Wodniecki, H. Schröder, M. Uhrmacher, K. P. Lieb, *Phys. Lett. A 93* (1983) 429.
[91] I. J. R. Baumvol, M. Behar, J. A. H. da Jornada, R. P. Livi, K. W. Lodge, A. Lopez-Garcia, F. C. Zawislak, *Phys. Rev. B Condens. Matter 22* (1980) 5115.

[92] K. Krolas, B. Wodniecka, P. Wodniecki, *Acta Phys. Pol. A 58* (1980) 605.
[93] K. Krolas, P. Heubes, G. Schatz, *J. Phys. F 13* (1983) 291; A. Z. Hrynkiewicz, K. Krolas, *Phys. Rev. B Condens. Matter 28* (1983) 1864.
[94] A. R. Miedema, R. Boom, F. R. de Boer, *J. Less-Common Met. 41* (1979) 283.
[95] K. Krolas, *Phys. Lett. A 85* (1981) 107.
[96] G. J. Kemerink, F. Pleiter, *Scr. Metall. 19* (1985) 881.
[97] B. D. Sawicka, *Nucl. Instrum. Methods 182/183* (1981) 1039.
[98] E. N. Kaufmann, R. Vianden, J. R. Chelikowsky, J. C. Phillips, *Phys. Rev. Lett. 39* (1977) 1671; E. Gerdau, H. Winkler, W. Gebert, B. Giese, J. Braunsfurth, *Hyperfine Interact. 1* (1976) 459.
[99] E. N. Kaufmann, R. Vianden, *Rev. Mod. Phys. 51* (1979) 161; R. Vianden, *Hyperfine Interact. 15/16* (1983) 1081.
[100] W. Witthuhn, W. Engel in J. Christiansen (Ed.): *Hyperfine Interactions of Radioactive Nuclei*, Springer, Berlin 1983, p. 205.
[101] A. F. Pasquevich, A. G. Bibiloni, C. P. Massolo, F. H. Sanchez, A. Lopez-Garcia, *Phys. Lett. A 82* (1981) 34.
[102] P. Wodniecki, B. Wodniecka, *Hyperfine Interact. 12* (1982) 95.
[103] J. Desimoni, A. G. Bibiloni, L. Mendoza-Zelis, A. F. Pasquevich, F. H. Sanchez, A. Lopez-Garcia, *Phys. Rev. B Condens. Matter 28* (1983) 5739.
[104] A. F. Pasquevich, F. H. Sanchez, A. G. Bibiloni, J. Desimoni, A. Lopez-Garcia, *Phys. Rev. B Condens. Matter 27* (1983) 963; M. Uhrmacher, W. Bolse, *Hyperfine Interact. 15/16* (1983) 445.
[105] J. Trager, M. Karger, T. Butz, F. E. Wagner, *Hyperfine Interact. 15/16* (1983) 795.
[106] A. Weidinger, M. Deicher, T. Butz, *Hyperfine Interact. 10* (1981) 717.
[107] A. Weidinger, R. Peichl, *Phys. Rev. Lett. 54* (1985) 1683; R. Peichl, A. Weidinger, E. Recknagel, J. M. Gil, P. J. Mendes, N. Ayres de Campos, *Hyperfine Interact. 15/16* (1983) 463.
[108] Y. Yeshurun, S. Havlin, Y. Schlesinger, *Solid State Commun. 27* (1978) 181; Y. Yeshurun, Y. Schlesinger, S. Havlin, *J. Phys. Chem. Solids 40* (1979) 231.
[109] J. A. Wilson, F. J. DiSalvo, S. Mahajan, *Phys. Rev. Lett. 32* (1974) 828; *Adv. Phys. 24* (1975) 117.
[110] J. A. Wilson, *J. Phys. F 15* (1985) 591.
[111] R. L. Withers, J. A. Wilson, *J. Phys. C 19* (1986) 4809; J. Rouxel (Ed.): *Crystal Chemistry and Properties of Materials with Quasi-one-dimensional Structures*, Reidel, Dordrecht 1986.
[112] T. Butz, A. Hübler, A. Lerf, W. Biberacher, *Mater. Res. Bull. 16* (1981) 541; T. Butz, K. H. Ebeling, E. Hagn, S. Saibene, E. Zech. A. Lerf, *Phys. Rev. Lett. 56* (1986) 639; T. Butz, S. Saibene, A. Lerf, *J. Phys. C 19* (1986) 2675.
[113] T. Butz, A. Lerf, A. Hübler, H. Gierisch, S. Saibene, J. O. Besenhard, *Hyperfine Interact. 15/16* (1983) 925.
[114] R. Huisman, F. Jellinek, *J. Less-Common Met. 17* (1969) 111; J. van Landuyt, G. van Tendeloo, S. Amelinckx, *Phys. Status Solidi A 26* (1974) 585.
[115] J. A. Martinez, A. M. Rodriguez, M. C. Caracoche, R. C. Marcader, A. Lopez-Garcia, P. C. Rivas, *Hyperfine Interact. 13* (1983) 307.
[116] A. M. Rodriguez, J. A. Martinez, M. C. Caracoche, P. C. Rivas, A. Lopez-Garcia, *Hyperfine Interact. 14* (1983) 227.
[117] M. C. Carocoche, A. Lopez-Garcia, J. A. Martinez, L. A. Mendoza-Zelis, R. C. Mercader, *Phys. Rev. B Condens. Matter 25* (1982) 5972.
[118] A. Vasquez, J. D. Rogers, A. Maciel, *Phys. Lett. A 45* (1973) 253.
[119] A. Vasquez, J. D. Rogers in E. Karlsson, R. Wäppling (Eds.): *Hyperfine Interaction Studied in Nuclear Reactions and Decay (Contributed Papers)*, Upplands Grafiska AB, Uppsala 1974, p. 54.
[120] P. Boyer, O. de O. Damasceno, J. D. Fabris, J. R. F. Ferreira, A. L. de Oliveira, J. de Olivero, *J. Phys. Chem. Solids 37* (1976) 1019.
[121] W. V. Prestwich, I. A. Cunningham, T. J. Kennett, *Hyperfine Interact. 12* (1982) 329.
[122] P. da R. Andrade, A. Vasquez, J. D. Rogers, E. R. Fraga, *Phys. Rev. B Solid State 1* (1970) 2912.
[123] E. Gerdau, J. Birke, H. Winkler, J. Braunsfurth, M. Forker, G. Netz, *Z. Phys. 263* (1973) 5.
[124] M. G. B. Drew, *Prog. Inorg. Chem. 23* (1977) 67; D. L. Kepert, *ibid. 25* (1979) 41.
[125] I. Seguchi, M. Mekata, *J. Phys. Soc. Jpn. 54* (1985) 3454.
[126] A. Lopez-Garcia, A. G. Bibiloni, M. C. Caracoche, J. A. Martinez, L. A. Medoza-Zelis, R. C. Mercader, A. F. Pasquevich, F. Dyment, *J. Phys. F 9* (1979) 1283.
[127] M. Rots, L. Hermans, J. van Cauteren, P. Put, *J. Phys. C 17* (1984) L261.
[128] A. Weidinger, *J. Less-Common Met. 103* (1984) 285.
[129] S. Saibene, T. Butz, A. Lerf, *Hyperfine Interact.*, in press.
[130] T. Butz, A. Lerf, S. Saibene, A. Hübler, *Hyperfine Interact. 20* (1984) 263.
[131] L. Amaral, M. Behar, A. Maciel, L. S. de Oliveira, W. H. Schreiner, *J. Phys. C 16* (1983) L1039; M. Behar, E. R. Fraga, A. Maciel, W. H. Schreiner, H. Saitovitch, *ibid. 18* (1985) 5863.
[132] T. Butz, A. Hübler, A. Lerf, *Phys. Rev. B Condens. Matter 26* (1982) 3973.
[133] M. C. Caracoche, J. A. Martinez, P. C. Rivas, A. Lopez-Garcia, *Hyperfine Interact. 23* (1985) 221.
[134] A. M. Rodriguez, J. A. Martinez, M. C. Caracoche, P. C. Rivas, A. Lopez-Garcia, S. Spinelli, *J. Chem. Phys. 82* (1985) 1271.
[135] W. Keppner, T. Klas, W. Körner, R. Wesche, G. Schatz, *Phys. Rev. Lett. 54* (1985) 2371.
[136] T. Butz, A. Lerf, S. Saibene, H. Gierisch, unpublished; A. Hübler, *Diplomarbeit*, Technische Universität München, 1982.
[137] G. V. Subba Rao, M. W. Shafer in F. Levy (Ed.): *Intercalated Layered Materials (Physics and Chemistry of Materials with Layered Structures, Vol. 6)*, Reidel, Dordrecht 1979, p. 99.
[138] R. Schöllhorn, *Angew. Chem. 92* (1980) 1015; *Angew. Chem. Int. Ed. Engl. 19* (1980) 983.
[139] T. Butz, A. Lerf, *Rev. Chim. Miner. 19* (1982) 496.
[140] T. Butz, A. Lerf, J. O. Besenhard, *Rev. Chim. Miner. 21* (1984) 556.
[141] W. Biberacher, A. Lerf, J. O. Besenhard, H. Möhwald, T. Butz, *Mater. Res. Bull. 17* (1982) 1385.
[142] T. Butz, A. Hübler, J. O. Besenhard, A. Lerf, W. Biberacher, *Nuovo Cimento Soc. Ital. Fis. D 2* (1983) 1971.
[143] T. Butz, H. Saitovitch, A. Lerf, *Chem. Phys. Lett. 65* (1979) 146.
[144] T. Butz, A. Lerf, *Ber. Bunsenges. Phys. Chem. 90* (1986) 638.
[145] A. Lerf, T. Butz in P. Barret, L.-C. Dufour (Eds.): *Reactivity of Solids*, Elsevier, Amsterdam 1985, p. 473.
[146] R. Bauer, J. Johansen, P. Limkilde, *Hyperfine Interact. 4* (1978) 906.
[147] G. R. Demille, K. Larlee, D. L. Livesey, K. Mailer, *Chem. Phys. Lett. 64* (1979) 534.
[148] R. Bauer, P. Limkilde, J. Johansen, *Biochemistry 15* (1976) 334.
[149] M. Vasak, R. Bauer, *J. Am. Chem. Soc. 104* (1982) 3236; A. Bakka, D. Ø. Eriksen, H. E. Rugsted, R. Bauer, *FEBS Lett. 139* (1982) 57.
[150] C. F. Meares, R. G. Bryant, J. D. Baldeschwieler, D. A. Shirley, *Proc. Natl. Acad. Sci. USA 64* (1969) 1155.
[151] R. D. Vis, A. J. J. Bos, S. Idzenga, H. Verheul, *Nucl. Instrum. Methods 163* (1979) 265.
[152] P. W. Martin, S. El-Kateb, U. Kuhnlein, *J. Chem. Phys. 76* (1982) 3819, and references cited therein.
[153] A. G. Marshall, K. M. Lee, P. W. Martin, *J. Chem. Phys. 78* (1983) 1528.
[154] T. Butz, A. Lerf, R. Huber, *Phys. Rev. Lett. 48* (1982) 890; *Hyperfine Interact. 15/16* (1983) 869.
[155] R. Huber, W. Bode, *Acc. Chem. Res. 11* (1978) 114; J. Walter, W. Steigemann, T. P. Singh, H. D. Bartunik, W. Bode, R. Huber, *Acta Crystallogr. Sect. B 38* (1982) 1462.

When submitting manuscripts, authors of articles intended for publication as "Communications" are requested to read the "Notice to Authors" reproduced in the January issue of the journal following the list of contents; upon request, a copy can be obtained from the editorial office.

Conversion of η^4-Bound Cyclopentadiene into the Complexed Carbene Cyclopentadienylidene

By *Hubert Wadepohl** and *Hans Pritzkow*

The activated *exo* CH bond of η^5-cyclopentadienyl-η^4-cyclopentadienecobalt **1** readily undergoes reactions such as hydride abstraction[1] or addition to activated alkynes.[2] We now report a reaction in which *both* CH bonds of the methylene group are cleaved and a novel, binuclear carbene complex of cyclopentadienylidene is formed.

Complex **1** reacts at 50°C with the Jonas reagent $[CpCo(C_2H_4)_2]$ **2** (Cp = cyclopentadienyl)[3] to form the turquoise, very air-sensitive binuclear complex **3a**, which is poorly soluble in nonpolar solvents. The ethylene ligand in **3a** readily undergoes substitution by CO and PMe_3 to give **3b** and the extremely air-sensitive **3c**, respectively.

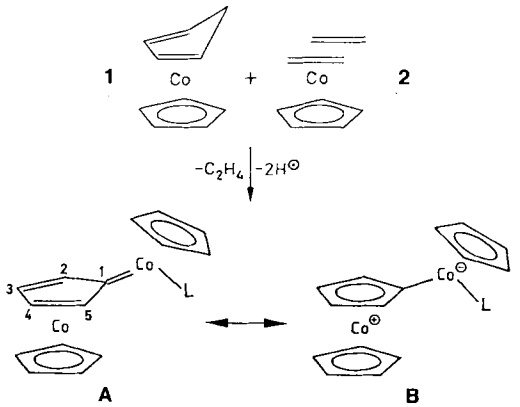

3a, L = C_2H_4; **3b**, L = CO; **3c**, L = PMe_3

According to MO calculations, free cyclopentadien-1-ylidene is expected to be bent (18°) and to exhibit alternation of the CC bond lengths (C2(4)–C3(5) short, C1–C2(5) medium, C3–C4 long).[4] Complex **3** can be represented formally by the resonance structures **A** and **B**. Examples of μ-η^4,η^1 coordination of cyclopentadienylidene (**A**) were previously unknown. In this case, we expect to find a geometry of the bridging ligand characteristic of η^4-cyclodiene complexes: CC bond alternation (C3–C4 short, C2(4)–C3(5) medium, C1–C2(5) long) and puckering around C2···C5 away from the metal atom. In an η^5,η^1 bridge (**B**), the bonds are expected to be nearly equal in length and only minor deviations from planarity (for steric reasons) are expected to be observed. In the binuclear complexes with η^5,η^1-C_5H_4 bridges[5] that have been studied by X-ray diffraction, the picture is complicated by the presence of a metal–metal bond. In those cases, the ligand is bent toward the π-bonded metal atom; C3–C4 is shorter than the other bonds in the ring.[5]

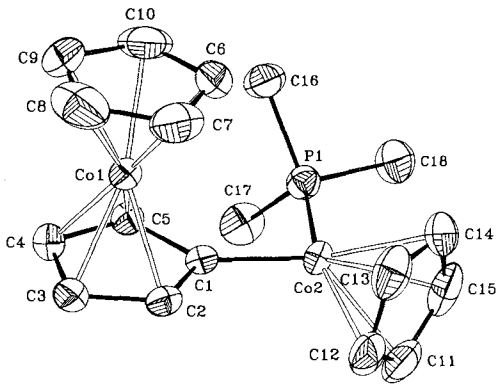

Fig. 1. Structure of **3c** in the crystal. Important bond lengths [Å] and angles [°] (standard deviation 0.004–0.006 Å, 0.3°): Co1–(C2···C5) 2.029···2.056, Co1–(C6···C10) 2.039···2.097, Co2–P1 2.150, Co2–C1 1.881, Co2–(C11···C15) 2.073···2.119, C1–C2(5) 1.447 (1.441), C2(5)–C3(4) 1.411 (1.418), C3–C4 1.406; Co2–C1–C2 125.2, Co2–C1–C5 133.9, P1–Co2–C1 97.0.

According to X-ray structure analysis,[6] **3c** adopts the μ-(η^4-diolefin, η^1-carbene) structure **A** (Fig. 1). The bridging ligand is coordinated through its diene moiety to a CpCo group. The CC bond lengths in the planar diene moiety (C2···C5, plane E1) are equal, and the bonds to the carbene carbon atom C1 are somewhat longer. C1 is bonded to the $CpCo(PMe_3)$ fragment by a very short bond (1.881(4) Å),[7] and is located 0.12 Å off E1 on the side opposite to Co1. The corresponding bond in the μ-(η^5,η^1-cyclopentadienylidene) complexes is surprisingly long; its length corresponds to that of metal–alkyl bonds.[5] The dihedral angle E1/E2 (E2: C2,C1,C5) is 7.7° in **3c**. In the crystal, the plane passing through Co2, P1 and the center of the Cp ring C11 to C15 is perpendicular to E1. However, the conformation is more symmetric on the NMR time scale in solution (only two ^{13}C-NMR signals for C2–C5). Considering the isolobal relationship[8] $CH_2 \leftrightarrow CoCp(L)$ [ML_4, Co^I, d^8], complex **3** is analogous to mononuclear complexes with pentafulvene as ligand. Typical diene systems are present in the η^4-pentafulvene complexes of type **4** with dihedral angles E1/E2 of 22.3° for **4a** and 8.0° and 10.4° for **4b** (cod = 1,5-cyclooctadiene).[9] No bond exists between the ring carbon atom C1 and the metal atom in **4**.[10] On the other hand, the Co1–C1 distance in **3c** (2.240 Å) still indicates the existence of a bonding interaction. In summary, the structural findings for **3c** indicate a small contribution of the dipolar "ylide" resonance structure **B** to the actual structure. The situation is similar in the cationic fulvene complexes **4c** (angle E1/E2 4.4°) and **4d** (angle E1/E2 8.8°).[11]

[*] Dr. H. Wadepohl, Dr. H. Pritzkow
Anorganisch-chemisches Institut der Universität
Im Neuenheimer Feld 270, D-6900 Heidelberg (FRG)

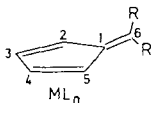

a, R = Ph, ML_n = $Fe(CO)_3$
b, R = Ph, ML_n = Ni(cod)
c, R = Ph, ML_n = $Rh(cod)^{\oplus}$
d, R = Ph, ML_n = $Rh\{P(OPh)_3\}_2^{\oplus}$

4

The solution chemistry of cyclopentadienylidene reveals it to be an electrophilic singlet carbene.[12] This behavior is due to the interaction of the carbene orbitals with the antiaromatic 4π-electron ring system.[4, 13] The very low frequency of the carbonyl band[14] of **3b** ($\tilde{\nu}$(CO) = 1903 cm^{-1} (THF)), on the other hand, indicates that the carbene ligand is an extremely good σ-donor. The resulting high electron density at Co2 exerts a destabilizing effect on the Co–P bond in **3c**, which reacts smoothly with CO to give **3b**. Complex **3** is an example of the reversal of the Lewis acid–base properties of a carbene upon complexation. This may be ascribed to the fact that the diene π^* orbital involved in the bond to Co1 is no longer available for an interaction with the electron pair of the carbene carbon atom.

Experimental Procedure

3a: **2** (1.60 g, 8.88 mmol) in 50 mL of petroleum ether (PE) was added to **1** (1.57 g, 8.26 mmol) in 50 mL of PE at 50°C. The dark solution was then concentrated under vacuum to ca. 70 mL. After standing at room temperature for 24 h, the solution was decanted from the precipitated crystals, which were washed with PE and recrystallized from toluene. Green platelets (700 mg **3a**, 2.06 mmol, 25% yield). M.p. = 146°C (dec.).—^{1}H-NMR (300 MHz, C_6D_6): δ = 4.75 (s, 5H; Cp), 4.44 (m, 2H; 2 × CH), 4.2 (m, 7H; Cp + 2 × CH), 3.63 (*m*; 2H of C_2H_4), 2.10 (m; 2H of C_2H_4).—^{13}C-NMR (75.5 MHz, C_6D_6): δ = 85.0 (d), 81.6 (d), 81.0 (d), 78.7 (d), 35.0 (t); the signal for C1 could not be observed for any of the compounds **3**.

3b, **3c**: **3a** was allowed to react with 1 bar CO (−60°C to room temperature) or with excess PMe_3 (room temperature), respectively, in toluene. After removal of the solvent from the filtered, deep green solution, analytically pure **3b** (L = CO, 97%) was obtained; **3c** (L = PMe_3) was recrystallized from toluene (68%). **3b**: green needles (dec. above 200°C). Correct C,H analyses.—^{1}H-NMR (90 MHz, C_6D_6): δ = 4.85 ("s," 7H; Cp + 2 × CH), 4.5 (m, 2H; 2 × CH), 4.23 (s, 5H; Cp).—^{13}C{^{1}H}-NMR (75.5 MHz, C_6D_6): δ = 87.3, 83.7, 82.2, 79.9. **3c**: green platelets (dec. above 170°C).—^{1}H-NMR (90 MHz, C_6D_6): δ = 5.0 (m, 2H; 2 × CH), 4.54 (s, 5H; Cp), 4.32 (s, 5H; Cp), 3.87 (m, 2H; 2 × CH), 1.40 ("s," 9H; PMe_3).—^{13}C{^{1}H}-NMR (75.5 MHz, C_6D_6): δ = 92 (br), 80.1, 78.6, 75.9, 21 (br).

Received: September 8, 1986;
revised: October 15, 1986 [Z 1924 IE]
German version: *Angew. Chem. 99* (1987) 132

[1] E. O. Fischer, G. E. Herberich, *Chem. Ber. 94* (1961) 1517; Reactions of the *endo* CH bond of several *exo*-substituted complexes are known: N. El Murr, *J. Organomet. Chem. 208* (1981) C9, and references cited therein.

[2] G. R. Knox, M. Nutley, P. L. Pauson, S. Toma, W. E. Watts, P. A. Elder, R. Griffiths, *J. Chem. Res. Miniprint 1981*, 1901.

[3] a) K. Jonas, C. Krüger, *Angew. Chem. 92* (1980) 513; *Angew. Chem. Int. Ed. Engl. 19* (1980) 520; b) K. Jonas, E. Deffense, D. Habermann, *ibid. 95* (1983) 729 and *22* (1983) 716; *Angew. Chem. Suppl. 1983*, 1005.

[4] M. Z. Kassaee, M. R. Nimlos, K. E. Downie, E. E. Waali, *Tetrahedron 41* (1985) 1579.

[5] W. A. Herrmann, G. Kriechbaum, C. Bauer, E. Guggolz, M. L. Ziegler, *Angew. Chem. 93* (1981) 838; *Angew. Chem. Int. Ed. Engl. 20* (1981) 815, and references cited therein.

[6] Monoclinic, space group $P2_1/a$, a = 12.40(1), b = 8.105(6), c = 16.81(1) Å, β = 93.61(5)°, μ = 20.5 cm^{-1}, Z = 4, STOE-two-circle diffractometer ($Mo_{K\alpha}$ radiation, ω-scan), 2583 reflections with $I > \sigma(I)$, all non-hydrogen atoms anisotropic, R = 0.051, R_w = 0.052, $w = 1/\sigma^2(F)$. Further details of the crystal structure investigation may be obtained from the Fachinformationszentrum Energie, Physik, Mathematik GmbH, D-7514 Eggenstein-Leopoldshafen 2 (FRG), on quoting the depository number CSD-52127, the names of the authors, and the journal citation.

[7] Crystallographically determined Co=C bond lengths are: 1.913(11) Å in [$(Ph_3Ge)(CO)_3Co\{C(OEt)Et\}$]: F. Carre, G. Cerveau, E. Colomer, R. J. P. Corriu, J. C. Young, L. Ricard, R. Weiss, *J. Organomet. Chem. 179* (1979) 215; 1.974(15) Å in [$(Ph_3P)(CO)(NO)Co\{(S)$-1,3,4-trimethylimidazolidin-2-ylidene}]: A. W. Coleman, P. B. Hitchcock, M. F. Lappert, R. K. Maskell, J. H. Müller, *J. Organomet. Chem. 250* (1983) C9; 1.902(3) Å in [Cp(SPh)Co(1,3-dimethylimidazolidin-2-ylidene)]: [15].

[8] R. Hoffmann, *Angew. Chem. 94* (1982) 725; *Angew. Chem. Int. Ed. Engl. 21* (1982) 711.

[9] Calculated from data in [10].

[10] F. Edelmann, B. Lubke, U. Behrens, *Chem. Ber. 115* (1982) 1325.

[11] Z. Dauter, L. K. Hansen, R. J. Mawby, E. J. Probitts, C. D. Reynolds, *Acta Crystallogr. Sect. C41* (1985) 850.

[12] H. Dürr, F. Werndorff, *Angew. Chem. 86* (1974) 413; *Angew. Chem. Int. Ed. Engl. 13* (1974) 483.

[13] R. Gleiter, R. Hoffmann, *J. Am. Chem. Soc. 90* (1968) 5457.

[14] Comparable values of $\tilde{\nu}$(CO): 1923 cm^{-1} in [$CpCo(CO)(PMe_3)$]: A. Spencer, H. Werner, *J. Organomet. Chem. 171* (1979) 219; 1915 cm^{-1} in [$(C_5Me_5)Co(CO)(PMe_3)$]: H. Werner, B. Heiser, B. Klingert, R. Dölfel, *ibid. 240* (1982) 179; 1915 cm^{-1} in [CpCo(CO)(1,3-dimethylimidazolidin-2-ylidene)]: [15].

[15] D. W. Macomber, R. D. Rogers, *Organometallics 4* (1985) 1485.

A Biocatalyst for the Preparation of (*R*)- and (*S*)-2-Hydroxycarboxylic Acids**

By *Haike Skopan, Helmut Günther,* and *Helmut Simon**

We have reported several times on the use of *Proteus vulgaris* in the presence of a catalytic amount of methyl- or benzylviologen to reduce structurally diverse 2-oxomono- and 2-oxodicarboxylates to (*R*)-2-hydroxycarboxylates, such as (*R*)-**1** (R = alkyl, arylalkyl, etc.) of very high enantiomeric purity [reaction (a)]. Possible electron donors include hydrogen, formate, and the cathode of an electrochemical cell (for electron flow and conditions, see ref. [1]). Productivity numbers are thereby attained that are approximately one to three orders of magnitude larger than those obtained in, for example, the reduction of carbonyl groups with yeast.[1–3] The reductase catalyzing these reactions does not employ NADH or NADPH;[3] its natural electron donor is still unknown. We have not been able to effect reversal of reaction (a) using methyl- ($MV^{2\oplus}$) or benzylviologen, even when we employed, for example, hexacyano-

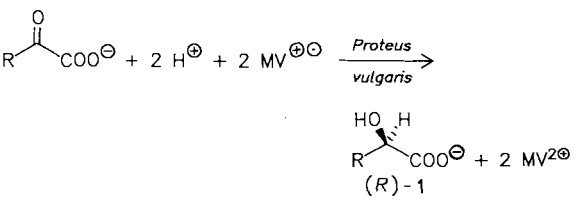

(a)

[*] Prof. Dr. H. Simon, Dipl.-Chem. H. Skopan, Dr. H. Günther
Lehrstuhl für Organische Chemie und Biochemie
der Technischen Universität München
Lichtenbergstrasse 4, D-8046 Garching (FRG)

[**] This work was supported by the Deutsche Forschungsgemeinschaft (Sonderforschungsbereich 145) and the Fonds der Chemischen Industrie. We thank *C. Frank* and *L. Riesinger* for dedicated and skilled work. We thank Dr. *P. Rauschenbach* and *F. Wendling* for working out the conditions of the HPLC analyses.

ferrate(III) or other electron acceptors with a relatively positive redox potential, which should remove every trace of reduced viologen and thereby make the overall reaction exergonic.

However, the dehydrogenation of (*R*)-2-hydroxycarboxylates, (*R*)-**1**, with carbamoylmethylviologen [$CAV^{2\oplus}$ = 1,1'-bis(carbamoylmethyl)-4,4'-bipyridinium dication] is possible. This viologen, which may be prepared by reaction of 4,4'-bipyridine with chloroacetamide,[2] exhibits a redox potential E_0' of -295 mV, which is thus 145 and 70 mV less negative than those of methyl and benzylviologen, respectively.

The kinetic parameters are of considerable importance for the preparative application of enzymes. The K_M values for the dehydrogenation reaction [cf. reaction (b)], carried out with crude extracts of *Proteus vulgaris* are 0.05 for $CAV^{2\oplus}$, 0.76 for (*R*)-lactate, 0.15 for (*R*)-3-phenyllactate, and 0.58 mM for (*R*)-2-hydroxy-4-methylpentanoate. These values are rather favorable for attaining complete conversions.

The dehydrogenation of (*R*)-2-hydroxycarboxylates, (*R*)-**1**, is also possible in the presence of (*S*)-2-hydroxycarboxylates, (*S*)-**1**. The K_i values, also determined with crude extracts, are 33, 77, and 100 mM for the (*S*) enantiomers of lactate, 3-phenyllactate, and 2-hydroxy-4-methylpentanoate, respectively. Thus, in the case of racemic mixtures of 2-hydroxycarboxylates, *rac*-**1**, the (*R*) enantiomer is selectively converted into the 2-oxocarboxylate, the (*S*) enantiomer remaining unchanged. To date, we have found no 2-oxomono- or 2-oxodicarboxylate that cannot be reduced with *Proteus vulgaris*. Since reaction (a) can now be carried out in reverse [reaction (b)], it is possible to obtain (*S*)-2-hydroxycarboxylates, (*S*)-**1**, starting from *rac*-**1**. The pH optimum of reaction (b) is in the range of 8.5 to 9.0.

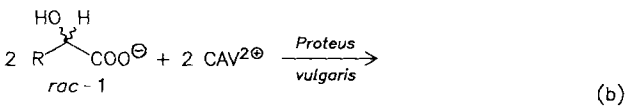

(b)

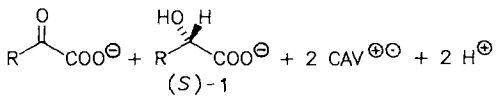

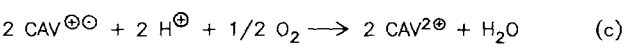

(c)

For preparative purposes, the $CAV^{\oplus\odot}$ produced in reaction (b) must be converted back into $CAV^{2\oplus}$. $CAV^{\oplus\odot}$ undergoes ready oxidation in an electrochemical cell at a carbon electrode (glassy carbon or carbon felt) at about -400 mV (versus a standard calomel electrode). Since the rate of reaction is proportional to the amount of current, this method has the advantage that the conversion is given by the product of current × time.

Surprisingly, regeneration of $CAV^{2\oplus}$ is also possible by shaking with air, without fast loss of enzyme activity [reaction (c)]. As a reductase, the enzyme is very sensitive toward oxygen; as a dehydrogenase, it is not. With *Proteus vulgaris* cells it is possible to carry out reactions (b) and (c) for 10–20 hours. During the regeneration of $CAV^{2\oplus}$ with O_2, we have not observed even traces of H_2O_2.[4]

Examples for the preparation of (*S*)-2-hydroxycarboxylates from racemic mixtures are given in Table 1. Analysis of the products is carried out enzymatically with (*R*)- and (*S*)-lactate dehydrogenase and NAD or by HPLC on RP-18 phases or on Chiral-I columns.[5]

Since carboxyl groups can be transformed in a variety of ways, it is possible to prepare numerous chiral compounds starting from the two enantiomers of 2-hydroxycarboxylic acids and 2-hydroxydicarboxylic acids. Although there have been recent reports of the use of pyridine-nucleotide-dependent 2-oxoacid reductases for the preparation of (*R*)- and (*S*)-2-hydroxycarboxylic acids,[6,7] their scope of application is narrower than that for the oxidoreductase from *Proteus vulgaris*. For example, no 2-oxodicarboxylates are accepted as substrates, and the specific activity in the crude extract of the organism is at least one order of magnitude smaller. There has been no report so far whether these pyridine-nucleotide-dependent reductases can be used in the form of whole cells.

Table 1. Preparation of (*S*)-2-hydroxycarboxylates, (*S*)-**1**, from racemic mixtures of 2-hydroxycarboxylates, R–CHOH–$COO^{\ominus}$, *rac*-**1**, by dehydrogenation of the (*R*)-2-hydroxycarboxylates, (*R*)-**1**.

R in *rac*-**1**	Mixture employed		Procedure	Result
CH_3	lactate	300 μmol	In 30 mL of 0.1 M phosphate buffer (pH 8.5) with 2 mM $CAV^{2\oplus}$ and 10 mg of *P. vulgaris*. In electrochemical cells (graphite electrode at -440 mV versus standard calomel electrode), 47% of the lactate had been dehydrogenated by the time the current had fallen to zero. After thermal deactivation of the microorganism, the product pyruvate was reduced to (*S*)-lactate in the same cell in the presence of (*S*)-lactate dehydrogenase and with regeneration of NADH [8].	252 μmol of (*S*)-lactate [a]. No (*R*)-lactate detected enzymatically.
$(CH_3)_2CHCH_2$	2-hydroxy-4-methylpentanoate	3.3 mmol	As above in 55 mL of anolyte with 1.5 mM $CAV^{2\oplus}$ and 32 mg of *P. vulgaris*. No current after 5 h.	After HPLC, 1.62 mmol of oxocarboxylate and 1.57 mmol of hydroxycarboxylate. According to analysis on a Chiral-I column, the (*S*) enantiomer had >95% *ee*.
CH_3	lactate	100 μmol	Each racemate was dissolved in 3.0 mL of Tris-HCl (pH 8.5) containing 2 mM $CAV^{2\oplus}$ and 20 mg of *P. vulgaris* and the mixture was shaken under air for 4 h at 35°C.	No (*R*) compound detected enzymatically. Pyruvate and 2-oxoglutarate were metabolized. In the other cases, 50–51 μmol of 2-oxocarboxylate and the same amount of (*S*)-hydroxycarboxylate were present.
$PhCH_2$	3-phenyllactate	100 μmol		
C_2H_5	2-hydroxybutyrate	100 μmol		
$(CH_3)_2CH$	2-hydroxy-3-methylbutyrate	100 μmol		
$^{\ominus}OOC-(CH_2)_2$	2-hydroxyglutarate	100 μmol		

[a] The pyruvate formed as an intermediate is partly degraded by the cells.

The findings presented here also demonstrate that, by using viologen-dependent enzymes and by selecting viologens having different redox potentials, it is possible to shift at will the equilibrium position of a reaction. An example is the equilibrium constant for reaction (a): $K = 2.8 \times 10^{10}$ for methylviologen ($E_0' = -440$ mV) at pH 6.0; $K = 3.5$ for $CAV^{\oplus\oplus}$ ($E_0' = -295$ mV) at pH 8.5. Of these ten orders of magnitude, five are due to the difference in pH (the hydrogen ion concentration is squared in the expression for the mass action law) and five are due to the difference in redox potential of methyl- and carbamoylmethylviologen.

This is not possible for pyridine-nucleotide-dependent oxidoreductases, because the enzymatically active pyridine nucleotide analogues so far known differ only slightly in their redox potentials.

Received: September 23, 1986;
revised: November 18, 1986 [Z 1933 IE]
German version: *Angew. Chem. 99* (1987) 139

[1] H. Simon, J. Bader, H. Günther, S. Neumann, I. Thanos, *Angew. Chem. 97* (1985) 541; *Angew. Chem. Int. Ed. Engl. 24* (1985) 539.
[2] H. Günther, S. Neumann, H. Simon, *J. Biotechnol.*, in press.
[3] S. Neumann, H. Günther, H. Simon: *European Congress on Biotechnology (Third). Proceedings*, Verlag Chemie, Weinheim 1984.
[4] Tests carried out with the diammonium salt of 2,2'-Azino-di-3-ethyl-2,3-dihydrobenzothiazole-6-sulfonic acid (ABTS) according to the method of J. Pütter, R. Becker in H. U. Bergmeyer, J. Bergmeyer, M. Grassl (Eds.): *Methods of Enzymatic Analysis, Vol. 3*, 3rd ed., Verlag Chemie, Weinheim 1983, p. 291.
[5] Macherey & Nagel Chiral-I column. The analyses were carried out by elution with 3 mM copper sulfate solution.
[6] W. Hummel, H. Schütte, M.-R. Kula, *Eur. J. Appl. Microbiol. Biotechn. 21* (1985) 7.
[7] H. Schütte, W. Hummel, M.-R. Kula, *Eur. J. Appl. Microbiol. Biotechn. 19* (1984) 167.
[8] The viologen-dependent pyridine-nucleotide oxidoreductase was used for regeneration: see H. Simon, H. Günther, I. Thanos in M. P. Schneider (Ed.): *Enzymes as Catalysts in Organic Synthesis*, D. Reidel, Dordrecht 1986, p. 35.

Heptacyclo[19.3.0.0^{1,5}.0^{5,9}.0^{9,13}.0^{13,17}.0^{17,21}]-tetracosane([6.5]coronane)**

By *Detlef Wehle* and *Lutz Fitjer**

Polycyclic hydrocarbons in which a central m-membered ring ($m = 4, 6, 8 \ldots$) is coupled to m peripheral n-membered rings ($n = 3, 4, 5 \ldots$) such that each edge of the central ring is simultaneously an edge of a peripheral ring ([m.n]coronanes[1]) were previously unknown. They have an unusual topology and should exhibit interesting chemical and physicochemical properties. Examples are the [6.4]coronane **1** and the [6.5]coronane **2**, whose synthesis should be possible via cascade rearrangements of pentaspiranes.[2,3] We report here on the use of such a cascade for the synthesis of the coronane **2** and of its incomplete analogue **3**.

We explored two possibilities for the synthesis of **2**: first, addition of allylmagnesium bromide to **4**,[3] rearrangement of the expected homoallyl alcohol **5a** (OH_{axial}) to **6**, and cyclization with diisobutylaluminum hydride (DIBAH)[4] to give **2** and/or **7** (see Scheme 1); second, hydrozirconization[5] followed by bromination[5] of **6** to give **10** and cyclization with tri-*n*-butyltin hydride[6] to give **2** (see Scheme 2). These approaches led not only to the synthesis of **2** and **3** but also to several surprising results.

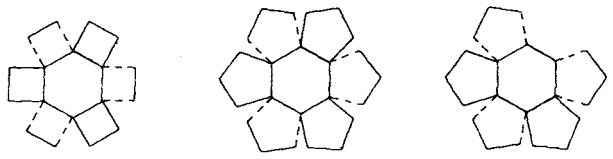

1 **2** **3**

Thus the addition of allylmagnesium bromide to **4**[3] afforded not only the homoallyl alcohol **5a** (m.p. = 145 °C) but also its conformational isomer **5b** (m.p. = 154–156 °C) with an equatorial OH group. Both alcohols have such high barriers to inversion [$\Delta G^{\ddagger}_{413} = 134.9$ kJ/mol (**5a**) and 136.9 kJ/mol (**5b**)][7] that they can be studied separately. In order to induce the rearrangement, we took advantage of the antiperiplanar arrangement of the hydroxyl group and the axial bonds of the neighboring cyclobutane rings in **5a**, which favors the 1,2-shifts. Reaction with thionyl chloride in pyridine afforded the expected[3] hexacyclic diene **6** (m.p. = 189–196 °C),[8a] whose cyclization with DIBAH was then studied. Only at 160 °C and upon addition of six molar equivalents of DIBAH did the reaction proceed beyond simple addition of the hydride to the vinyl group and hence formation of **8** (glassy solid),[8] which had already been observed at 80 °C. However, GC/MS analyses provided no evidence for a cyclization with formation of **2** and/or **7**. Instead, after 72 h at 160 °C, the reaction mixture consisted of 49% **8** and 26% **9** (m.p. = 24–27 °C),[8a]

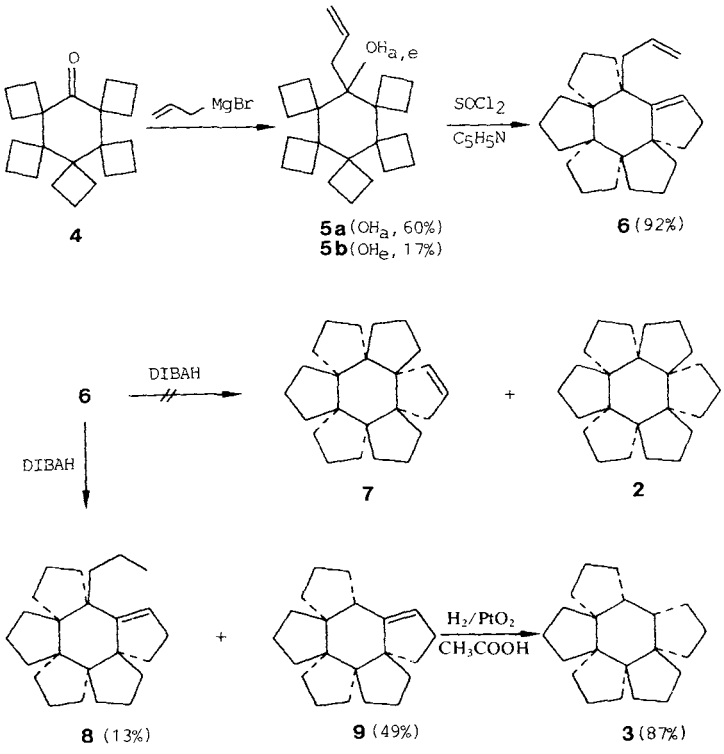

Scheme 1.

[*] Prof. Dr. L. Fitjer, Dipl.-Chem. D. Wehle
Institut für Organische Chemie der Universität
Tammannstrasse 2, D-3400 Göttingen (FRG)

[**] Polyspiranes, Part 12; Cascade Rearrangements, Part 7. This work was supported by the Deutsche Forschungsgemeinschaft (project Fi 191/6-3/7-2) and the Fonds der Chemischen Industrie. *D. W.* thanks the Fonds der Chemischen Industrie für a Chemiefonds fellowship.—Parts 11 and 6, respectively: L. Fitjer, M. Majewski, A. Kanschik, E. Egert, G. M. Sheldrick, *Tetrahedron Lett. 27* (1986) 3603.

and after 11 d at 160°C, 13% **8** and 49% **9** were present. The mechanism of the fragmentation remains to be explored.

Compound **9** was separated by gas chromatography and hydrogenated over platinum dioxide in glacial acetic acid to give **3** (glassy solid).[8a] We have studied this incomplete [6.5]coronane in order to gain insight into the properties expected for **2**. Its ^{13}C-NMR spectrum (50.3 MHz, $CHFCl_2$[9]) exhibits only eleven signals at −78°C [δ = 21.50, 21.81, 23.21, 30.23, 37.14, 38.29, 39.55, 45.42 ($C_{sec.}$), 48.57 ($C_{tert.}$), 53.27, 55.98 ($C_{quart.}$)], which are only in accord with a rapidly inverting species in the all-*cis* configuration (effective symmetry: C_s). At −130°C, 21 signals are observed [δ = 20.35, 20.84, 21.81, 22.20, 25.52, 28.94, 31.60, 35.46, 36.60, 37.37, 37.63, 39.26, 40.49, 45.45, 45.82, 47.58, 50.49, 52.21, 53.26, 55.51, 55.83] which must be ascribed to a fixed conformation having C_1 symmetry. Which of the five conceivable conformations (one chair, two twist-boat, and two boat conformations) is involved must remain an open question, although force field calculations[10] support a flattened chair conformation ($\Sigma|\omega|_{central\ ring} = 245°$). In order to estimate the barrier to inversion, we followed the coalescence of the resonance lines of the quaternary carbon atoms at δ = 52.21 and 53.26. From the frequency difference ($\Delta\nu$ = 52.7 Hz) and the coalescence temperature (−115 ± 5°C) and using the Gutowsky-Holm relation and the Eyring equation, an extremely low value of $\Delta G^{\neq}_{153} = 31.3 \pm 1.1$ kJ/mol for the free energy of activation resulted. It thus appeared certain that the [6.5]coronane **2** would be characterized by a similar low barrier to inversion.

We then investigated the synthesis of **2** via the second approach outlined above (Scheme 2). For this purpose the diene **6** was first hydrozirconized with zirconocene chloride hydride[5] and then brominated with *N*-bromosuccinimide (NBS).[5] Chromatography on silica gel with hexane afforded pure **10** (m.p. = 35–37°C).[8a] In order to carry out the cyclization, a solution of **10** in benzene was heated with 2.0 equivalents of tri-*n*-butyltin hydride and 0.2 equivalents of azobisisobutyronitrile for 38 h at 80°C. Complete consumption of **10** led to the formation of at least eight products, including, as main product, the heptacyclic **13** (m.p. = 164°C)[8a] and, as side products, the already known **8** and the sought [6.5]coronane **2** (m.p. = 222–224°C).[8a] Separation was achieved by a combination of column and gas chromatography.[8b]

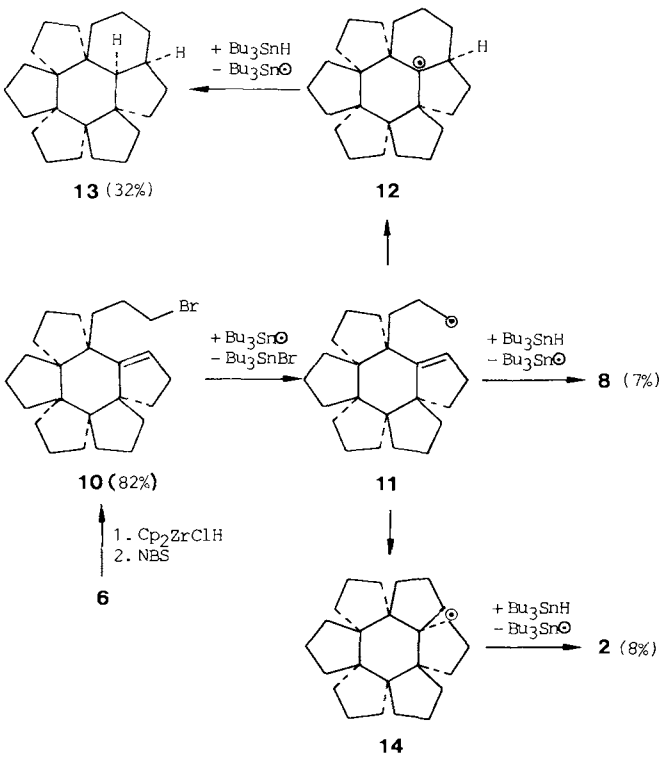

Scheme 2.

The structural assignment of **13** is based on the available spectroscopic data,[8a] especially on the number, position, and multiplicity of the signals in the ^{13}C-NMR spectrum. The configuration results from the fact that the radical **11** can only attack the double bond from the side shown and the resulting **12** should be configuratively stable. It is not surprising that **13** is preferentially formed although it is the product of an unfavorable *endo-trig* ring closure according to *Baldwin*'s rules.[11, 12]

The structure and configuration of the title compound **2** could be assigned unequivocally. The ^{13}C-NMR spectrum (50.3 MHz, CD_2Cl_2) shows only three signals at 20°C at δ = 21.24, 40.07 ($C_{sec.}$), and 56.80 ($C_{quart.}$), which are only in accord with a rapidly inverting species in the all-*cis* configuration (effective symmetry: D_{3d}). On account of the extremely low solubility of **2**,[13] we had to always use [D_2]dichloromethane for the low-temperature ^{13}C-NMR investigations. At −80°C, the signal at δ = 40.07 clearly began to broaden, until, at −94°C, the lowest temperature attainable in [D_2]dichloromethane, it exhibited a halfwidth (12 Hz) five times that of the still sharp signals at δ = 21.24 and 56.80. We are therefore certain that this signal will be split at lower temperature into two resonances, as expected for a fixed chair conformation. Even the most careful estimate of the coalescence temperature (−100°C) and the frequency difference (20 Hz) gives the expected low value, $\Delta G^{\neq}_{173} = 36$ kJ/mol, for the corresponding barrier to inversion.

Most interesting is the finding that the barriers to inversion of **5a** and **5b** are extremely high, whereas those of **2** and **3** are extremely low. This clearly indicates that on going from spiroannelation, as in **5a,b**, to edge-annelation, as in **2** and **3**, the central ring is flattened in the ground state[14] and the 1,2-interactions are reduced in the transition state. Both effects should be even more pronounced in the [6.4]coronane **1**.[14] Therefore, we expect the barrier to inversion for **1** to be even smaller than that for **2**.

Received: September 29, 1986;
revised: November 17, 1986 [Z 1941/1942]
German version: *Angew. Chem.* 99 (1987) 135

[1] L. Fitjer, D. Wehle, *Angew. Chem. 91* (1979) 927; *Angew. Chem. Int. Ed. Engl. 18* (1979) 868. Recently, it was suggested [J. A. Marshall, J. C. Peterson, L. Lebioda, *J. Am. Chem. Soc. 106* (1984) 6006], that [m.n]coronanes should be regarded as members of a more inclusive family, the perannulanes. Accordingly, the [6.5]coronane would be called all-*cis*-[3.3.3.3.3.3]hexannulane.

[2] L. Fitjer, D. Wehle, M. Noltemeyer, E. Egert, G. M. Sheldrick, *Chem. Ber. 117* (1984) 203.

[3] L. Fitjer, M. Giersig, W. Clegg, N. Schormann, G. M. Sheldrick, *Tetrahedron Lett. 24* (1983) 5351.

[4] The use of DIBAH to effect spiroalkylation to give a derivative of the spiro[4.4]nonane is known: P. W. Chum, S. E. Wilson, *Tetrahedron Lett. 17* (1976) 1257. Our own studies with 1-(3-butenyl)cyclopentene, using DIBAH in excess, led to high yields of spiro[4.4]nonane itself: L. Fitjer, D. Wehle, unpublished results.

[5] J. Schwarz, J. A. Labinger, *Angew. Chem. 88* (1976) 402; *Angew. Chem. Int. Ed. Engl. 15* (1976) 333.

[6] A. L. J. Beckwith, K. U. Ingold in P. de Mayo (Ed.): *Rearrangements in Ground and Excited States, Vol. 1*, Academic Press, New York 1980, p. 161.
[7] D. Wehle, L. Fitjer, *Tetrahedron Lett. 27* (1986) 5843.
[8] a) All new compounds (**2**, **3**, **6**, **8**, **9**, **10**, and **13**) gave correct elemental analyses and/or high-resolution mass spectra. The IR, ^{1}H-NMR, and mass spectra are in accord with the given structures. ^{13}C-NMR data: **2** ($CDCl_3$): δ=21.16, 40.30 ($C_{sec.}$), 57.33 ($C_{quart.}$); **3** ($CDCl_3$, −39°C): δ=21.70, 21.83, 23.27, 30.17, 37.58, 38.49, 39.80, 45.11 ($C_{sec.}$), 47.90 ($C_{tert.}$), 53.52, 56.05 ($C_{quart.}$); **6** (C_6D_6): δ=21.38 (two signals overlap), 21.69, 24.07, 29.44, 36.71, 37.14, 38.25, 39.37, 39.45, 39.61, 40.09, 40.21, 40.73, 42.09 ($C_{sec.}$), 48.57, 57.09, 58.40, 58.58, 59.11 ($C_{quart.}$), 115.75 ($C_{sec.}$), 125.10, 137.17 ($C_{tert.}$), 150.66 ($C_{quart.}$); **8** ($CDCl_3$): δ=14.80 ($C_{prim.}$), 18.90, 21.20, 21.26, 21.44, 23.64, 29.17, 36.39, 36.62, 38.07, 39.03, 39.25, 39.48, 39.69, 39.71, 39.99, 40.38 ($C_{sec.}$), 49.25, 56.88, 58.17, 58.42, 58.89 ($C_{quart.}$), 124.16 ($C_{tert.}$), 150.38 ($C_{quart.}$); **9** ($CDCl_3$): δ=21.00, 21.21, 21.67, 23.28, 26.05, 29.99, 34.11, 37.64, 37.73 (two signals overlap), 38.18, 38.42, 39.28, 40.02 ($C_{sec.}$), 41.73 ($C_{tert.}$), 56.86, 56.98, 58.84, 60.04 ($C_{quart.}$), 119.80 ($C_{tert.}$), 150.60 ($C_{quart.}$); **10** ($CDCl_3$): δ=21.14 (two signals overlap), 21.44, 23.58, 29.20, 29.57, 34.94, 36.27, 36.40, 36.86, 38.16, 39.01, 39.34, 39.56 (two signals overlap), 39.63, 40.38 ($C_{sec.}$), 48.76, 56.97, 58.18, 58.61, 58.98 ($C_{quart.}$), 124.96 ($C_{tert.}$), 149.88 ($C_{quart.}$); **13** ($CDCl_3$): δ=21.36, 21.51, 21.57, 22.04, 23.89, 28.68, 30.38, 31.47, 32.95, 34.88, 36.33, 37.11, 37.15, 38.54, 38.94, 39.00, 39.28, 40.72 ($C_{sec.}$), 46.43 ($C_{quart.}$), 47.12 ($C_{tert.}$), 53.86, 57.69, 59.36, 59.52 ($C_{quart.}$). b) Preparative glc on column A [0.6 m × 1/4" all-glass system, 12% FFAP on chromosorb W AW/DMCS, 60/80 mesh, 210°C, 200 mL H_2/min; relative retention times: 0.76, 0.87, 1.00 (**8**), 1.11, 1.75, 2.00, 2.45 (**2**/**13**), 3.53] yielded pure **8** and an impure mixture of **2** and **13**. This mixture was purified on silica gel (0.1–0.2 mm) with hexane [R_F=0.61 (**2**/**13**)] and then separated on column B [1.6 m × 1/4" all-glass system, 2% GE SE30 on chromosorb W AW/DMCS, 60/80 mesh, 200°C, 130 mL H_2/min; relative retention times: 1.00 (**2**) and 1.10 (**13**)].
[9] δ_C ($CHFCl_2$) = 100.95 and 106.82; these values were measured for a saturated solution of dichlorofluoromethane in $CDCl_3$/TMS (95:5 v/v).
[10] Program MM2: N. L. Allinger, *J. Am. Chem. Soc. 98* (1977) 8127; D. Wehle, L. Fitjer, unpublished results.
[11] J. E. Baldwin, *J. Chem. Soc. Chem. Commun. 1976*, 734.
[12] An *endo-trig* ring closure was also observed for 7-bromo-3-methyl-*trans*-2-heptene, which is similar to **10** in terms of substitution pattern and stereochemistry: M. Julia, C. Decoins, M. Baillarge, B. Jaquet, D. Uguer, F. A. Groeger, *Tetrahedron 31* (1975) 1737.
[13] 1.5 mg of **2** in 500 μL of dichlorofluoromethane (m.p. = −135°C) could be maintained in solution only down to 0°C; at −40°C, most of the substance had precipitated.
[14] According to force field calculations (MM 2) **2** has a significantly flattened chair conformation [$\Sigma|\omega|_{central\ ring}$ = 237°] [10, 15]. This effect is still more pronounced for **1** [$\Sigma|\omega|_{central\ ring}$ = 136°] [15].
[15] H. Dodziuk, *Bull. Chem. Soc. Jpn.*, in press; we thank Dr. *Dodziuk* for a preliminary copy of her article.

Oxidative Addition of Hydrogen Telluride to Organometallic Fragments**

By *Wolfgang A. Herrmann,* Christian Hecht, Eberhardt Herdtweck,* and *Heinz-Josef Kneuper*

A large number of reports have appeared recently concerning the advantages of using simple binary hydrides, such as GeH_4, SnH_4, AsH_3, and TeH_2, to incorporate unsubstituted main-group elements into organometallic complexes.[1] Examples of compounds thus formed under mild conditions and usually in good yields, are the tin and tellurium compounds $L_XM{=}Sn{=}ML_X$ (linear) and $L_XM{=}Te{=}ML_X$ (bent), respectively ($L_XM = (\eta^5\text{-}C_5R_5)Mn(CO)_2$; R = H, CH_3).[2,3a] The star-shaped complex $[(\mu_3\text{-Te})\{(\eta^5\text{-}C_5H_5)Mn(CO)_2\}_3]$ was also obtained in this way.[3b] The working hypothesis that is used to explain the formation of these unusual complexes involves an initial oxidative addition of the element hydride to the reactive complex fragment L_XM according to Equation (a), followed by coupling with elimination of H_2.[1,4j] This suggestion, which so far has remained more or less speculative, is now supported by the first successful oxidative addition of hydrogen telluride to a transition metal.

$$L_XM + EH_a \longrightarrow L_XM\begin{matrix}\diagup EH_{a-1}\\ \diagdown H\end{matrix} \quad \cdots\cdots \text{(a)}$$

A

Treatment of the substitution-labile solvent complex **2**, generated by photolysis, with externally generated, acid-free hydrogen telluride in tetrahydrofuran at room temperature in the dark (!) affords, after column-chromatographic workup of the crude product at low temperature, the four new organorhenium complexes **1** and **3**–**5** (Scheme 1). The components of the hydride TeH_2 are completely maintained only in the mononuclear complex **1**. According to ^{1}H- and ^{125}Te-NMR spectroscopy and an X-ray diffraction study, **1** is a TeH/H complex of type **A** with nearly square-pyramidal coordination around the transition-metal atom and a *trans* arrangement of the ligands TeH and H (Fig. 1a, Table 1).

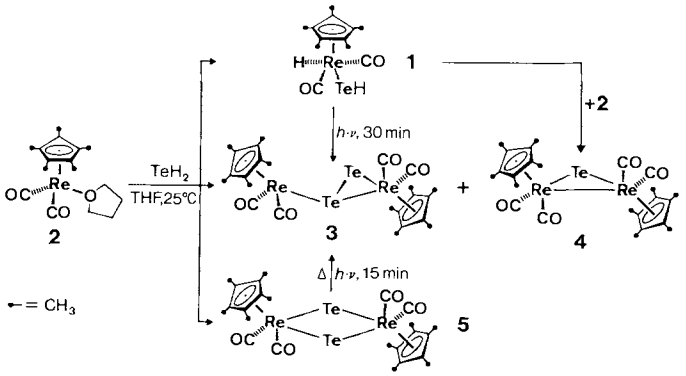

Scheme 1.

Isolated **1**, a dark red-brown solid, is thermally stable under inert atmosphere but remarkably photolabile. Irradiation with UV light, filtered through Duran glass, results in the nearly quantitative transformation of **1** to **3** with elimination of H_2; **3** is the most stable of the four complexes. This complex contains an unsymmetrical Te_2 bridge (Fig. 1b, Table 1), which until now had only been observed in organometallic compounds containing sulfur or selenium.[6,7] The bond lengths in the Re_2Te_2 skeleton are in accord with the number of electrons in this fragment. Thus, the Re2-Te2/1 distances [279.3(<1)/280.6(<1) pm] are consistent with a π-type side-on complexation of a Te_2 fragment,[8] and the Re1–Te1 distance [263.2(<1) pm] is not inconsistent with the postulated ReTe double bond. By way of contrast, ReTe single bonds are estimated to have lengths of ca. 285 pm.[9]

Complex **3** can also be obtained from the isomeric complex **5** either photochemically (irradiation with UV light in THF) or thermally (refluxing THF). This unusual isomerization reaction is restricted to the constitution of the Re_2Te_2 skeleton.

The red-brown complex **4**, which contains a Re_2Te three-membered ring and is formed in only small amounts,

[*] Prof. Dr. W. A. Herrmann, Dr. C. Hecht, Dr. E. Herdtweck, Dr. H.-J. Kneuper
Anorganisch-chemisches Institut der Technischen Universität München
Lichtenbergstrasse 4, D-8046 Garching (FRG)

[**] Multiple Bonds between Main-Group Elements and Transition Metals, Part 33. This work was supported by the Fonds der Chemischen Industrie, Hoechst AG, and the Bundesministerium für Forschung und Technologie. — Part 32: [7].

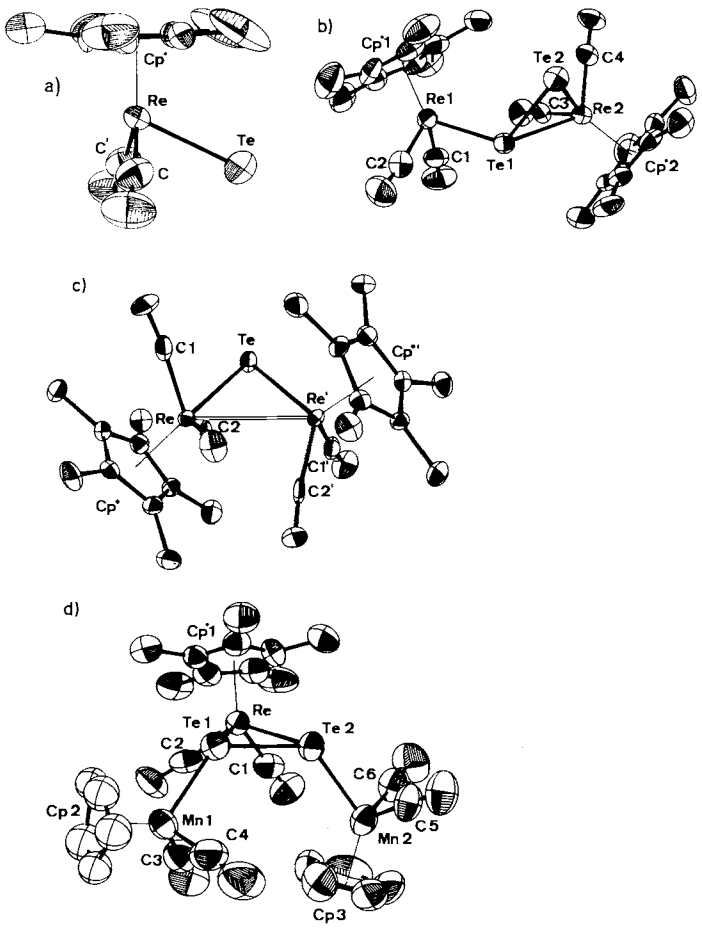

Fig. 1. Crystal structures of the new complexes (hydrogen atoms omitted) [5]. Selected bond lengths [pm] and angles [°]. Cp = center of a η^5-C_5H_5 ligand. Cp* = center of a η^5-C_5Me_5 ligand. a) **1**: Re-Te 274.3(1), Re-C 191.6(6), Re-Cp* 193.8(-); C-Re-C' 100.9(3), Te-Re-C 79.2(2), Te-Re-Cp* 116.5(-), C-Re-Cp* 129.0(-). b) **3** (crystallizes with 1/2 molecule of THF): Te1-Te2 270.3(1), Re1-C1 189.9(7), Re1-C2 189.1(9), Re1-Cp*1 195.8(-), Re2-C3 191.7(7), Re2-C4 190.9(7), Re2-Cp*2 195.5(-); Re1-Te1-Re2 121.45(2), Re2-Te1-Te2 60.90(1), Re1-Te1-Te2 117.45(2), Re2-Te2-Te1 61.37(1). c) **4**: Re-Re' 314.0(< 1), Re-Te 267.9(< 1), Re-C1 190.0(6), Re-C2 190.7(5), Re-Cp* 197.1(-); Re-Te-Re' 71.76(1), Re-Re'-Te 54.12(1). d) **8** (the C_5H_5 ligand Cp2, which is disordered on two positions, is shown in ball-and-stick form): Re-Te1 282.7(1), Re-Te2 280.7(1), Te1-Te2 273.2(1), Mn1-Te1 253.0(1), Mn2-Te2 252.0(1), Re-C1 186.3(9), Re-C2 187.2(9), Re-Cp*1 194.7(-), Mn1-C3 172.0(10), Mn1-C4 165.8(10), Mn1-Cp2 175.1(-), Mn2-C5 175.9(9), Mn2-C6 173.7(9), Mn2-Cp3 177.9(-); Re-Te1-Mn1 122.10(4), Re-Te2-Mn2 121.54(3), Te1-Te2-Mn2 126.23(4), Te2-Te1-Mn1 125.04(4), Re-Te1-Te2 60.62(2), Re-Te2-Te1 61.37(2).

Table 1. Selected X-ray diffraction data for the new complexes.

	1	**3**	**4**	**8**
a [pm]	746.7(1)	858.9(1)	1319.2(2)	1116.1(2)
b [pm]	1320.8(5)	1289.4(2)	1402.1(1)	1183.1(2)
c [pm]	757.0(1)	1446.7(5)	1341.6(2)	1328.6(3)
α [°]	90	77.41(2)	90	109.79(2)
β [°]	99.48(1)	74.01(2)	101.11(1)	94.41(2)
γ [°]	90	89.67(2)	90	114.43(1)
Z	2	2	4	2
ρ_{calcd} [g cm^{-1}]	2.287	2.315	2.407	2.230
space group	$P2_1/m$	$P\bar{1}$	$C2/c$	$P\bar{1}$
measured reflections	1448	4056	2337	3546
unique reflections	1216	3468	1863	2465
intensity	$>3\sigma(I)$	$>1\sigma(I)$	$>1\sigma(I)$	$>1\sigma(I)$
parameters	80	294	141	329
R	0.051	0.027	0.031	0.031
R_w	0.058	0.030	0.032	0.022

has C_2 symmetry in the solid (Fig. 1c, Table 1). Whereas the analogous manganese compound $[(\mu\text{-Te})\{(\eta^5\text{-}C_5Me_5)Mn(CO)_2\}_2]$ exhibits no bonding interactions between the manganese atoms on account of the MnTe double bond, with the MnTeMn angle being expanded to 124° [d(Mn···Mn) = 421 pm], the ReTeRe angle in **4** is only 72° and the (bonding) ReRe distance (314 pm) is comparable to that of $[Re_2(CO)_8(\mu\text{-}C_4H_6)]$ (311.4 pm).[10]

Even though the ReTe bonds (267.9(< 1) pm) may have some double bond contributions, the electron density at the tellurium bridge is still sufficient to make this atom nucleophilic. Thus, **4** can be protonated or methylated at −78°C with HBF_4 or $CF_3SO_2OCH_3$, respectively. The product of protonation is not only thermally labile, but can also be readily deprotonated reversibly, even with weak bases. The methylation product **6** is isolable in pure form.

$[(\mu\text{-}TeCH_3)\{(\eta^5\text{-}C_5Me_5)Re(CO)_2\}_2]^{\oplus}PF_6^{\ominus}$ **6**

According to the results presented here, it would appear that the hydridotellurium complex **1** should play a key role in the construction of multinuclear organometallic complexes containing "naked" tellurium. Complex **1** reacts with excess solvent complex **2** with elimination of H_2 to give the Re_2Te compound **4** in good yield (70% based on **1**) (Scheme 1). Complex **1** also readily loses hydrogen in the presence of other organometallic complexes and is therefore suitable for the construction of heteronuclear tellurium complexes. For example, **1** reacts at room temperature in the dark with the solvent complex **7**, which is known to be substitutionally labile, to give, in a straightforward reaction, the novel Mn_2Te_2Re complex **8**, which, according to a single-crystal X-ray structure analysis, may be regarded as an organometallic isolobal analogue of *cis*-1,2-dimethylcyclopropane (Scheme 2, Fig. 1d, Table 1).

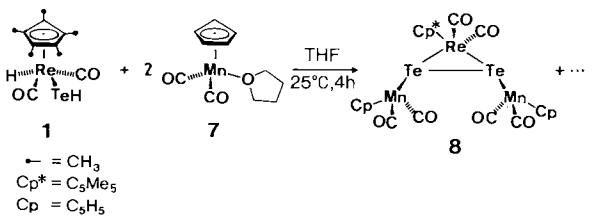

Scheme 2.

^{125}Te-NMR spectroscopy, which has hardly been used so far, proved to be a quick and highly sensitive method for determining the constitution of the new complexes (shift range ca. 1800 ppm; Table 2), especially for locating the hydrogen atoms, which are difficult to find by X-ray diffraction analysis. The key compound **1** furnishes an excellent example for the use of this method (Fig. 2).

Experimental Procedure

A solution of $[(\eta^5\text{-}C_5Me_5)Re(CO)_3]$ (1.00 g, 2.47 mmol) in 250 mL of THF was irradiated at 15°C in a quartz-glass immersion-lamp apparatus. The irradiation was carried out for approximately 90 min, during which time the liberated CO was repeatedly pumped out of the apparatus. The brownish yellow solution of **2** was transferred to a Schlenk tube fitted with a glass inlet, and excess TeH_2 (generated externally from Al_2Te_3/4 N HCl) was then admitted. The reaction mixture was allowed to stir for 4 h in the dark and then evaporated; the residue was chromatographed on a Florisil (100-200 mesh) column at −20°C. *n*-Hexane, colorless $[(\eta^5\text{-}C_5Me_5)Re(CO)_3]$; *n*-hexane/toluene (5/1), **1** as an extended yellow band; *n*-hexane/toluene (3/1), **4** as a

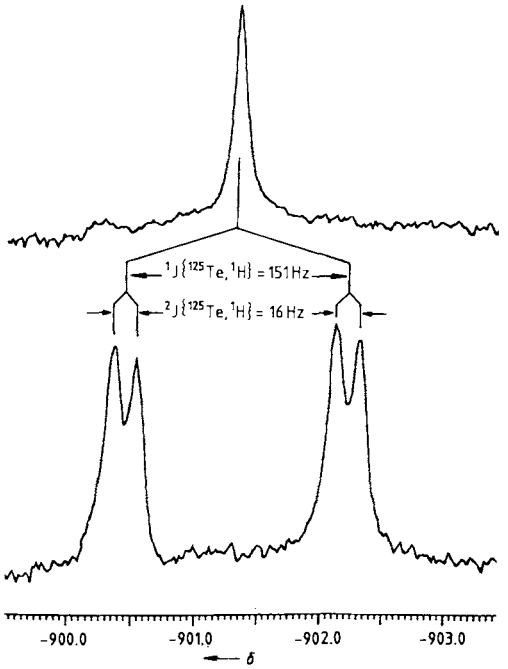

Fig. 2. ^{125}Te-NMR spectrum of **1**. Above: ^{1}H-broadband-decoupled. Below: ^{1}H-coupled. Shown are the couplings to the two metal-bound hydrogen atoms.

Table 2. ^{1}H- and ^{125}Te-NMR data for the new rhenium-tellurium complexes **1**, **3**–**6**, and **8** [a].

Compound	$\delta(^1H)$	$\delta(^{125}Te)$
[Cp*Re(CO)$_2$H(TeH)] **1** (*trans*)	−11.34 [TeH, 1H] −10.60 [ReH, 1H] 1.71 [C_5Me_5, 15H]	−901.3 $^1J(^{125}Te,^1H) = 151$ Hz $^2J(^{125}Te,^1H) = 16$ Hz
[(μ,η^1:η^2-Te$_2$){Cp*Re(CO)$_2$}$_2$] **3**	1.85 [C_5Me_5, 15H] 1.60 [C_5Me_5, 15H]	−200.3 434.4
[(μ-Te){Cp*Re(CO)$_2$}$_2$] **4**	1.89 [C_5Me_5]	613.7
[(μ-Te)$_2$}Cp*Re(CO)$_2$}$_2$] **5**	1.85 [C_5Me_5]	−510.0
[(μ-TeCH$_3$){Cp*Re(CO)$_2$}$_2$]$^{\oplus}$PF$_6^{\ominus}$ **6**	2.14 [C_5Me_5, 30H] 2.57 [CH_3, 3H]	568.4
[{μ-(η^1,η^1:η^2)-Te$_2$}-{CpMn(CO)$_2$}$_2$Cp*Re(CO)$_2$] **8**	4.52 [C_5H_5, 10H] 1.50 [C_5Me_5, 15H]	848.0

[a] ^{1}H-NMR: JEOL JNM-GX-270 (270 MHz); solvent: **1**, **3**–**5**, **8** C_6D_6, **6** CD_2Cl_2, measuring temperature 25 °C, δ values relative to internal TMS. ^{125}Te-NMR: JEOL JNM-GX-270 (85.2309 MHz); solvent: **1**, **3**–**5**, **8** [D_8]toluene, **6** [D_6]acetone, measuring temperature: **1** −30 °C, **3**–**6**, and **8** 30 °C, δ values relative to external $(CH_3)_2Te$/15% [D_8]toluene.—Cp = η^5-C_5H_5; Cp* = η^5-C_5Me_5.

short, bright red band; *n*-hexane/toluene (1/1), **5** as a red-brown band; toluene/diethyl ether (3/1), **3** as a violet band. The products were further purified by crystallization.—**1**: orange-yellow, light-sensitive microcrystals; yield 120 mg (10%). **4**: bright red rods; 20 mg (2%). **5**: red-brown, intergrown needles; 300 mg (24%). **3**: black platelets; 110 mg (9%).

Received: October 24, 1986;
supplemented: November 24, 1986 [Z 1966 IE]
German version: *Angew. Chem. 99* (1987) 158

[1] Review: W. A. Herrmann, *Angew. Chem. 98* (1986) 57; *Angew. Chem. Int. Ed. Engl. 25* (1986) 56.
[2] W. A. Herrmann, H.-J. Kneuper, E. Herdtweck, cited in [1]; H.-J. Kneuper, *Ph.D. Thesis*, Technische Universität München 1986.
[3] a) W. A. Herrmann, C. Hecht, M. L. Ziegler, B. Balbach, *J. Chem. Soc. Chem. Commun. 1984*, 686; b) M. Herberhold, D. Reiner, D. Neugebauer, *Angew. Chem. 95* (1983) 46; *Angew. Chem. Int. Ed. Engl. 22* (1983) 59; *Angew. Chem. Suppl. 1983*, 10.
[4] Cf. I. M. Blacklaws, E. A. V. Ebsworth, D. W. H. Rankin, H. E. Robertson, *J. Chem. Soc. Dalton Trans. 1978*, 753.
[5] Further details of the crystal structure investigation of complexes **1**, **3**, **4**, and **8** may be obtained from the Fachinformationszentrum Energie, Physik, Mathematik GmbH, D-7514 Eggenstein-Leopoldshafen 2 (FRG), on quoting the depository number CSD-52224, the names of the authors, and the journal citation.
[6] W. A. Herrmann, J. Rohrmann, H. Nöth, C. K. Narula, J. Bernal, M. Draux, *J. Organomet. Chem. 284* (1985) 189.
[7] W. A. Herrmann, J. Rohrmann, E. Herdtweck, C. Hecht, M. L. Ziegler, O. Serhadli, *J. Organomet. Chem. 314* (1986) 295.
[8] O. Scheidsteger, G. Huttner, K. Dehnicke, J. Pebler, *Angew. Chem. 97* (1985) 434; *Angew. Chem. Int. Ed. Engl. 24* (1985) 428.
[9] W. Beck, W. Sacher, U. Nagel, *Angew. Chem. 98* (1986) 280; *Angew. Chem. Int. Ed. Engl. 25* (1986) 270.
[10] E. Guggolz, F. Oberdorfer, M. L. Ziegler, *Z. Naturforsch. B36* (1981) 1060.

Sulfur Pentafluoride Cyanate, $F_5S-O-C\equiv N$**

By *Arno Schmuck* and *Konrad Seppelt**

Sulfur pentafluoride isocyanate, $F_5S-N=C=O$, is a long-known, chemically and structurally investigated compound.[1–3] The analogous tellurium compound, $F_5Te-N=C=O$, has been synthesized by three routes: in two of these, the cyanate formed as an intermediate undergoes immediate rearrangement to the isocyanate.[4,5] However, one of these reactions, when applied to selenium, afforded the cyanate, $F_5Se-O-C\equiv N$, which could only be identified as such after laborious physical investigation.[5,6]

We have now succeeded in augmenting the series of known isomers, $F_5S-N=C=O$, $F_5Se-O-C\equiv N$, and $F_5Te-N=C=O$, by synthesis of $F_5S-O-C\equiv N$ (Scheme 1). $F_5S-O-Cl$[7] reacts with $Cl_2C=NCl$[8] ("cyano trichloride") to give **1**. Compound **1** eliminates chlorine spontaneously in the presence of mercury to give the isomers **2a** and **2b**, which can be separated by gas chromatography on Chromosorb on a 2-m halocarbon column. The structural assignment of the two isomers can be made on the basis of the nuclear magnetic resonance data in analogy to the isomers of $F_5S-O-CF=NCl$.

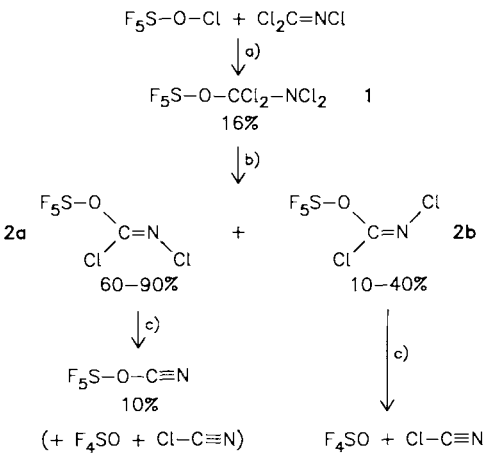

Scheme 1. a) Reaction in $C_2F_4Cl_2$ (Freon 114) at −120 to −70 °C; b) Hg, −20 °C, 4 h stirring; c) Hg, 25 °C, ultrasound.

[*] Prof. Dr. K. Seppelt, Dipl.-Chem. A. Schmuck
Institut für Anorganische und Analytische Chemie
der Freien Universität
Fabeckstrasse 34-36, D-1000 Berlin 33

[**] This work was supported by the Deutsche Forschungsgemeinschaft and the Fonds der Chemischen Industrie. We thank Prof. Dr. *F. Seel* (Saarbrücken/Munich) for the loan of his Cady codistillation apparatus.

Only the (*Z*) isomer **2a** undergoes further elimination of chlorine in the presence of mercury at room temperature to afford the desired $F_5S-O-C\equiv N$ as a colorless liquid (b.p. = 5 °C) in 10% yield. The product always contains $Cl-C\equiv N$ as a contaminant, which can only be removed with difficulty by codistillation.

The differentiation between the cyanate $F_5S-O-C\equiv N$ and the isocyanate $F_5S-N=C=O$ is based on two observations: (1) Like $F_5Se-O-C\equiv N$ (1104 cm^{-1}), $F_5S-O-C\equiv N$ exhibits a strong IR absorption at $\tilde{\nu}=1111$ cm^{-1}, which is assigned to ν(CO) and is characteristic of cyanates.[9] (2) With respect to chemical shift and line halfwidth, the ^{14}N-NMR spectra of $F_5S-O-C\equiv N$ and $F_5Se-O-C\equiv N$ are in close agreement ($\delta=-194$ and -189.2; $\nu_{1/2}=57$ and 60 Hz) and differ strongly from those of $F_5S-N=C=O$[6] and $F_5Te-N=C=O$[6] ($\delta=-271.8$ and -303.9; $\nu_{1/2}=120$ and 160 Hz). Physical data for **1**, **2a**, **2b**, and $F_5S-O-C\equiv N$ are summarized in Table 1.

Table 1. Physical data for **1**, **2a**, **2b**, and $F_5S-O-C\equiv N$.

	1	**2a**	**2b**	$F_5S-O-C\equiv N$
B.p.[°C]	dec.	85.8	85.8	5
M.p. [°C]	−39	−77.5	−87.0	−60
^{19}F-NMR ($CFCl_3$) ab_4 spectra				
δ_a	64.2	63.1	62.5	51.7
δ_b	71.1	67.6	70.2	66.5
J_{ab} [Hz]	159	158.7	158.7	157
^{14}N-NMR, δ				−194 ($\nu_{1/2}=57$ Hz)
IR (gas) [cm^{-1}]	1120 (m), 990 (s), 885 (s), 800 (m), 690 (m)	1600 (m), 1158 (m), 1120 (m), 940 (vs), 900 (s), 845 (s), 610 (s)		2283 (m), 1111 (m), 944 (vs), 879 (vs), 847 (w), 736 (w), 607 (s)
Raman (liq.) [cm^{-1}]		1587 (w), 1562 (w), 1140 (w, b), 952 (w), 884 (w), 832 (w), 737 (vs), 704 (w), 668 (m), 640 (m), 615 (s)		2284 (vs, p), 1118 (w, dp), 945 (w, p), 875 (w, p), 845 (w, p), 736 (vs, p), 643 (m, p), 605 (w, p)
MS (80 eV), base peak (m/z)	239 M^+-Cl_2	239 M^+		150 M^+-F

The complicated method of preparation cannot be simplified. $F_5S-O-Cl$ reacts with $Cl-C\equiv N$ to give **3**,[10] which reacts with zinc to give **4a** and **4b**[11] (ca. 1.3 : 1). Apart from traces of $F_5S-N=C=O$, **4a**, and **4b**, they afford only decomposition products upon reaction with zinc at 250 °C (Scheme 2).

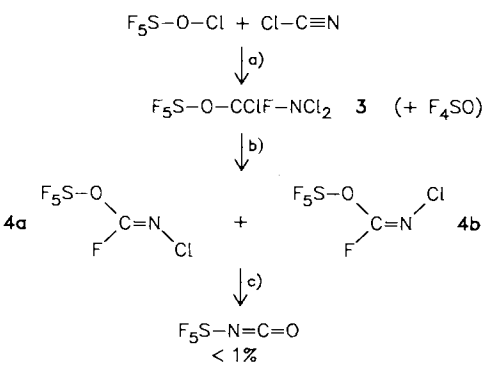

Scheme 2. a) −196 to +25 °C; b) Zn, 50 °C; c) Zn, 250 °C.

From these results, we conclude that at high temperatures $F_5S-O-C\equiv N$ undergoes rearrangement to give $F_5S-N=C=O$, accompanied by decomposition products. Of the six possible chalcogen pentafluoride cyanates and isocyanates, four are now known. It should be possible to synthesize $F_5Se-N=C=O$ as well; the synthesis of $F_5Te-O-C\equiv N$, on the other hand, will be difficult.

Received: October 2, 1986;
revised: November 14, 1986 [Z 1945 IE]
German version: *Angew. Chem. 99* (1987) 138

[1] C. W. Tullock, D. D. Coffmann, E. L. Muetterties, *J. Am. Chem. Soc. 86* (1964) 357.
[2] J. S. Thrasher, J. L. Howell, A. F. Clifford, *Chem. Ber. 117* (1984) 1707.
[3] H. Oberhammer, K. Seppelt, R. Mews, *J. Mol. Struct. 101* (1983) 325.
[4] H. Hartl, P. Huppmann, D. Lentz, K. Seppelt, *Inorg. Chem. 22* (1983) 2183.
[5] P. Huppmann, G. Klöter, J. S. Thrasher, K. Seppelt, D. D. DesMarteau, *Inorg. Chem. 23* (1984) 2217.
[6] K. Seppelt, H. Oberhammer, *Inorg. Chem. 24* (1985) 1227.
[7] a) K. Seppelt, *Z. Anorg. Allg. Chem. 428* (1977) 35; b) C. J. Schack, R. D. Wilson, J. S. Muirhead, S. N. Cohz, *J. Am. Chem. Soc. 21* (1969) 2907.
[8] H. Hagemann, D. Arlt, J. Ugi, *Angew. Chem. 81* (1969) 572; *Angew. Chem. Int. Ed. Engl. 8* (1969) 606.
[9] J. Weidlein, U. Müller, K. Dehnicke: *Schwingungsspektroskopie*, Thieme, Stuttgart 1982, p. 83.
[10] **3**: Colorless liquid after treatment with mercury, yield 20%. MS (80 eV): m/z 258 (M^+-Cl, 5.6%), 127 (SF_5^+, 100%) and further fragments; IR (gas): $\tilde{\nu}$ [cm^{-1}] = 1160 (s), 1100 (s), 1070 (m), 1010 (s), 928 (s), 909 (s) cm^{-1}; Raman (liq.): 1160 (w), 1100 (w), 1070 (w), 935–885 (w, very broad), 813 (m), 774 (m), 736 (vs), 722 (vs), 681 (m), 662 (w), 636 (w), 594 (w); ^{19}F-NMR ($CFCl_3$): ab_4x-spectrum, $\delta_a=62.7$, $\delta_b=71.2$, $\delta_x=53.1$, $J_{ab}=154$, $J_{ax}=1$, $J_{bx}=15$ Hz.
[11] **4**: Colorless liquid, yield 79% (both isomers). MS (80 eV): m/z 223 (M^+, 10%), 162 (SF_5Cl^+, 96.7%), 127 (SF_5^+, 100%) and further fragments; IR (gas): $\tilde{\nu}$ [cm^{-1}] = 1690 (m), 1280 (m), 1020 (m), 940 (vs), 880 (vs), 810 (w), 610 (m); ^{19}F-NMR ($CFCl_3$): two ab_4x spectra, integration ratio $E:Z=1.3:1$; (*E*) isomer **4a**: $\delta_a=58.9$, $\delta_b=65.4$, $\delta_x=-28.8$, $J_{ab}=151.7$, $J_{ax}=1$, $J_{bx}=6.8$ Hz; (*Z*) isomer **4b**: $\delta_a=58.6$, $\delta_b=68.4$, $\delta_x=-51.3$, $J_{ab}=151.5$, $J_{ax}=1$, $J_{bx}=10.2$ Hz.— When the fluorine atom at carbon and the lone electron pair of nitrogen are on the same side of the double bond [(*Z*) isomer **4b**], the CF signal is at higher field and is broader (cf. D. Lentz, H. Oberhammer, *Inorg. Chem. 24* (1985) 4665).

Heterometallic Polyhydride Raft Formation: A Comparison of Syntheses using Alkoxides of Copper and Gold**

By *Bruce R. Sutherland, Douglas M. Ho, John C. Huffman,* and *Kenneth G. Caulton**

There has been much recent interest in the formation of mixed transition-metal/coinage-metal complexes, particularly those containing hydride ligands.[1,2] The usual strategy for the formation of such compounds involves the reaction of reagents such as $ML_x^{\ominus}$ (M = Cu, Ag, Au; L = PPh_3, CH_3CN) with previously formed metal hydrides.[3–5] Recently, we reported an alternative method involving the reaction of $[CuO\mathit{t}Bu]_4$ with $[OsH_4(PMe_2Ph)_3]$ to give the Cu_3Os_3 cluster $[CuOsH_3(PMe_2Ph)_3]_3$ with elimina-

[*] Prof. K. G. Caulton, Dr. B. R. Sutherland, Dr. D. M. Ho, Dr. J. C. Huffman
Department of Chemistry and Molecular Structure Center, Indiana University Bloomington, IN 47405 (USA)

[**] This work was supported by the U.S. National Science Foundation (Grant No. 83-05281) and by the Canadian Natural Sciences and Engineering Research Council. We thank Johnson Matthey, Inc. and Rhenium Alloys, Inc. for material support and *Scott Horn* for skilled technical assistance.

tion of *t*BuOH.[6] We report here a comparative study of the reaction of the dinuclear polyhydride complex $[Re_2H_8(PMe_2Ph)_4]$ **2** with either $[Ph_3PCuO\mathit{t}Bu]_2$ **1** or its gold analogue $[Ph_3PAuO\mathit{t}Bu]$ **6**.[7]

$$1/2[Ph_3PCuO\mathit{t}Bu]_2 + [Re_2H_8(PMe_2Ph)_4] \xrightarrow{C_6H_6} 1/2[Re_2CuH_7(PMe_2Ph)_4]_2 + \mathit{t}BuOH + PPh_3 \quad (a)$$

1 **2** **3**

The reaction of $[Ph_3PCuO\mathit{t}Bu]_2$ **1**[8] with the rhenium complex **2** is complete within the time of mixing [Eq. (a)].[9] The dark brown product can be isolated in essentially quantitative yield by removing the solvent and volatile by-products. Neither evolution of H_2 nor deposition of elemental copper is observed. These results, the ^{1}H-NMR spectrum, and an X-ray diffraction study[11] of crystals of **3** grown from toluene/hexane confirm the structure. The tetradecahydrido complex **3** is the most hydride-rich neutral cluster yet reported. The six metal atoms are arranged in a centrosymmetric, nearly planar parallelogram (Fig. 1) reminiscent of the structures found for clusters **4** and **5**.

$[Re_4Cu_2H_{16}(PMe_2Ph)_8]^{2\oplus}$ **4**[12]

$[Mn_4Cu_2H_6(CO)_{12}\{(EtO)_2POP(OEt)_2\}_2]$ **5**[13]

The 14 hydride ligands adopt four different modes of bonding in **3**: six hydrides bound to only Re (two terminal, four Re-Re bridging) and eight hydrides bound to Re and Cu (six Re-Cu bridging, 2 Re_2Cu bridging). Solution molecular-weight measurements indicate that this aggregate is maintained in solution.[14] The ^{1}H-NMR spectrum of **3**[15] shows a quintet for the hydride resonances (i.e., coupling to four P spins), indicating that although significant scrambling is occurring, the hydrides never move past the copper to the other Re_2P_4 unit in this rapid migration. At -80°C, the hydride resonance resolved into two broad peaks with an intensity ratio of 3:4, indicating that the ligation to copper has significantly hindered hydride mobility compared with that in $[Re_2H_8(PMe_2Ph)_4]$ **2**, which is still fluxional at -80°C. At -80°C, the ^{31}P{^{1}H}-NMR spectrum of **3** shows two signals, corresponding to the inequivalence of Re1 and Re2.

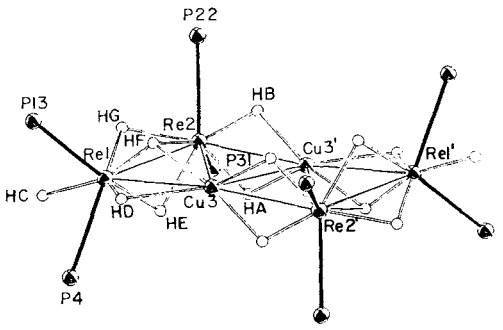

Fig. 1. ORTEP drawing of the crystal structure of **3**, omitting the methyl and phenyl groups. Primed metals and all unlabeled atoms are related to those labeled by a center of symmetry. Selected structural parameters: Re1-Re2 2.5683(7), Re1-Cu3 2.6258(10), Re2-Cu3, 2.6517(10), Cu3-Cu3' 2.5267(14) Å, Re-H distances range from 1.31(8) to 1.81(8) Å, Cu-H distances from 1.93(8) to 2.00(7) Å. Re2-Re1-Cu3 65.05(3), Re1-Re2-Cu3' 113.26(3), Re1-Cu3-Re2' 173.15(3), Re1-Cu3-Cu3' 115.57(4), Re2-Cu3'-Cu3 65.23(3)°.

The close stoichiometric and structural similarity of **3** and $[Re_4Cu_2H_{16}(PMe_2Ph)_8]^{2\oplus}$ (synthesized by very different procedures[3]) raises the question of their interconvertibility [Eq. (b)]. Indeed, the two compounds have been shown to be related by a Brønsted acid/base equilibrium, an interesting contrast to the H_2 elimination which follows protonation of early-transition-metal or main-group-metal hydrides.

$$[Re_4Cu_2H_{14}(PMe_2Ph)_8] \underset{KH}{\overset{2H^\oplus}{\rightleftharpoons}} [Re_4Cu_2H_{16}(PMe_2Ph)_8]^{2\oplus} \quad (b)$$

3

In order to determine the influence of the coinage metal on this cluster condensation synthesis, the reaction of **2** with $[Ph_3PAuO\mathit{t}Bu]$ **6** was also examined. The Re_2 complex **2** reacts rapidly (< 1 min) at room temperature with two equivalents of $[Ph_3PAuO\mathit{t}Bu]$ **6**[16] to give a mixture of two black isomers, which, on the basis of spectroscopy, can be formulated as **7** [Eq. (c)].

$$2[Ph_3PAuO\mathit{t}Bu] + [Re_2H_8(PMe_2Ph)_4] \xrightarrow{C_6H_6} [Re_2H_6(AuPPh_3)_2(PMe_2Ph)_4] + 2\mathit{t}BuOH \quad (c)$$

6 **2** **7**

The two isomers can be readily separated based on their differing solubilities in benzene.[17] For the major isomer, **7a**, ^{31}P{^{1}H}-NMR[18a] indicates that the two $AuPPh_3$ units are inequivalent at room temperature as are the two rhenium centers of the dimer (two PMe_2Ph phosphorus resonances are observed). This, coupled with the observation of three distinct hydride resonances in the ^{1}H-NMR, suggests a configuration as shown in Scheme 1, where $AuPPh_3$ replaces one terminal and one bridging hydride in the $Re_2H_8P_4$ structure. An Au-Au bond is suggested in **7a** based on comparison with analogous complexes.[1,2]

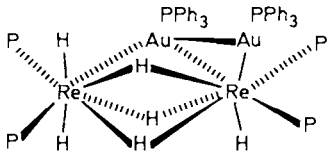

7a

Scheme 1. Proposed structure of **7a**. P = PMe_2Ph.

Spectroscopic data[18b] on the minor isomer, **7b**, suggests a symmetric configuration (i.e., the two $AuPPh_3$ units are equivalent). This was confirmed by an X-ray diffraction study[19] on a crystal grown from tetrahydrofuran (THF)/ether. The structure of **7b** consists of a centrosymmetric (planar rhomboidal) arrangement of four metal atoms with the Au atoms symmetrically bridging the two Re atoms (Fig. 2). Surprisingly, this isomer does *not* have proximate gold centers. The overall geometry of **7b** bears a strong resemblance to the structure of the parent compound $[Re_2H_8(PMe_2Ph)_4]$ **2**,[20] except that a *trans* pair of bridging hydrides have been replaced by $AuPPh_3$ units. The remaining six hydrides are bound only to Re and show no interaction with the Au atoms in contrast to the case with Cu (compound **3**).

 © VCH Verlagsgesellschaft mbH, D-6940 Weinheim, 1987 0570-0833/87/0202-0136 $ 02.50/0

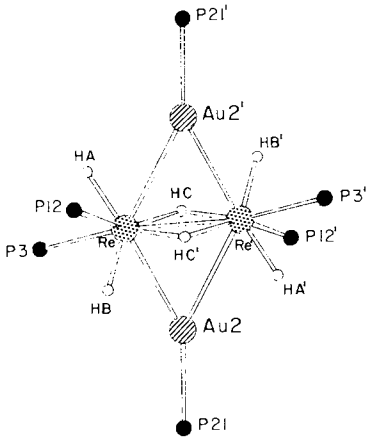

Fig. 2. ORTEP drawing of the crystal structure of **7b**, omitting methyl and phenyl groups for clarity. Primed and unprimed atoms are related by a crystallographic center of symmetry. Selected structural parameters: Au-Re 2.7625(9), Au-Re' 2.7725(10), Re-Re' 2.5644(10), Au-P 2.270(2), Re-P3 2.343(2), Re-P12 2.334(2), Re-HA 1.52(6), Re-HB 1.51(7), Re-HC 1.56(8), Re'-HC 1.90(8) Å; P3-Re-P12 99.40(7), Re-Au-Re' 55.20(2), Au-Re-Au' 124.80(2)°.

Both **7a** and **7b** are remarkable in that—in contrast to **2** and **3**—neither shows any evidence for fluxional behavior of hydride at 25°C. It is likely that the H/AuPPh$_3$ exchange impedes the interchange of hydrides from one end of the dimer to the other. The static character of the gold centers can be confirmed since the two isomers **7a** and **7b** do not interconvert in solution, even upon extended heating (90°C, 24 h). Compound **7a** is the first example of a gold/transition-metal complex that contains stereochemically rigid AuPPh$_3$ groups at 25°.

In addition to demonstrating the versatility of alcohol elimination as a rational route to mixed-metal clusters, the present work reveals that gold tenaciously retains phosphane ligands and thus phosphane-gold fragments serve as capping groups in cluster growth reactions. Copper, on the other hand, exhibits a tendency to be a linking group, thus promoting cluster growth to higher aggregates. This also explains the surprisingly different stoichiometries of the reactions of [Ph$_3$PCuO*t*Bu]$_2$ **1** and [Ph$_3$PAuO*t*Bu] **6** with [Re$_2$H$_8$(PMe$_2$Ph)$_4$] **2**. At the heart of these differences is the apparently greater affinity of copper for Cu–H and perhaps even Cu–Cu interactions; note that in [Re$_4$Cu$_2$H$_{14}$(PMe$_2$Ph)$_8$] **3**, copper is surrounded by four hydride ligands.

Received: October 7, 1986;
revised: November 26, 1986 [Z 1949 IE]
German version: *Angew. Chem. 99* (1987) 147

[1] P. Braunstein, J. Rose, *Gold Bull. 18* (1985) 17.
[2] K. P. Hall, D. M. P. Mingos, *Progr. Inorg. Chem. 32* (1984) 237.
[3] L. F. Rhodes, J. C. Huffman, K. G. Caulton, *J. Am. Chem. Soc. 107* (1985) 1759, and references cited therein.
[4] F. Bachechi, J. Ott, L. M. Venanzi, *J. Am. Chem. Soc. 107* (1985) 1760.
[5] B. D. Alexander, B. J. Johnson, S. M. Johnson, A. L. Casalnuovo, L. H. Pignolet, *J. Am. Chem. Soc. 108* (1986) 4409, and references cited therein.
[6] T. H. Lemmen, J. C. Huffman, K. G. Caulton, *Angew. Chem. 98* (1986) 267; *Angew. Chem. Int. Ed. Engl. 25* (1986) 262.
[7] B. R. Sutherland, K. R. Folting, W. E. Streib, J. C. Huffman, K. G. Caulton, *J. Am. Chem. Soc.*, in press.
[8] G. V. Goeden, J. C. Huffman, K. G. Caulton, unpublished.
[9] The liberated PPh$_3$ slowly reacts with **2** to give [Re$_2$H$_6$(PMe$_2$Ph)$_4$(PPh$_3$)] + H$_2$ [10]. Consequently, isolation of product **3** is easier from the reaction of **2** + 1/4[CuO*t*Bu]$_4$ in benzene; this latter reaction is an order of magnitude slower than the reaction in Equation (a). Thus, reaction of **2** with [CuO*t*Bu]$_4$ (Re : Cu = 2 : 1) in a minimum amount of benzene on a 20-mmol scale is complete (^{1}H-NMR) after 48 h to give **3** in 90% isolated yield after removal of the solvent.
[10] M. A. Green, J. C. Huffman, K. G. Caulton, *J. Am. Chem. Soc. 103* (1981) 695.
[11] Crystallographic data for **3** (−158°C): a = 12.791(3), b = 13.904(3), c = 11.676(2) Å; α = 105.04(1), β = 93.97(1), g = 63.39(1)°, Z = 1, space group $P\bar{1}$. $R(F)$ = 0.0248 for 7496 absorption-corrected reflections with $F > 3\sigma(F)$, using anisotropic thermal parameters for non-hydrogen atoms. All hydrogens were refined isotropically [21].
[12] L. F. Rhodes, J. C. Huffman, K. G. Caulton, *J. Am. Chem. Soc. 105* (1983) 5137.
[13] V. Riera, M. A. Ruiz, A. Tiripicchio, M. Tiripicchio-Camellini, *J. Chem. Soc. Chem. Commun. 1985*, 1505.
[14] The molecular weight of **3** was determined by the isopiestic method to be > 1800 in toluene (calcd 1991).
[15] a) ^{1}H-NMR (360 MHz, 21°C, C$_6$D$_6$): δ = −6.95 (quint., J(P-H) = 8.5 Hz); (−80°C, C$_7$D$_8$): δ = −6.3 (br., 8H), −7.2 (br., 6H). b) ^{31}P{^{1}H}-NMR (40.5 MHz, 30°C, C$_6$D$_6$): δ = −9.6 (s); (−80°C, C$_7$H$_8$): δ = −6.9 (s, 2P), −9.0 (s, 2P).
[16] Reaction of **2** with an equimolar amount of **6** gives only a 50% yield of **7**, together with unreacted **2**.
[17] Reaction of **2** with **6** (Re : Au = 1 : 1) on a 0.2-mmol scale in a minimum amount of benzene is complete in less than 1 min (^{1}H-NMR) to give a mixture of **7a** and **7b**. Upon standing overnight, **7a** precipitates, leaving only **7b** in solution. Filtration and removal of solvent gives pure **7b**.
[18] a) Major isomer **7a**: ^{1}H-NMR (360 MHz, 21°C, [D$_8$]THF): δ = −3.63 (s, br., 1H), −5.04 (tdd, J(H-PRe) = 34.6 Hz, J(P-PAu1) = 14.5 Hz, J(H-PAu2) = 14.8 Hz, 2H), −6.41 (s, br., 3H). ^{31}P{^{1}H}-NMR (40.5 MHz, 30°C, THF): δ = 75.2 (s, br., 1P[AuP]), 70.9 (s, br., 1P[AuP]), −9.4 (s, 2P, [ReP$_2$]), −9.6 (s, 2P, [ReP$_2$]); b) **7b**: ^{1}H-NMR (360 MHz, 21°C, C$_6$D$_6$): δ = −4.58 (t, J(PRe-H) = 33.9 Hz, 4H), −2.8 (s, br., 2H). ^{31}P{^{1}H}-NMR (40.5 MHz, 30°C, C$_6$H$_6$): δ = 72.5 (s, br., 2P, [AuP]), −10.4 (s, 4P, [Re$_2$P$_4$]).
[19] Crystallographic data for **7b** (−160°C): a = 13.366(5), b = 14.832(6), c = 17.225(7) Å; β = 107.18(2)°, Z = 2, space group $P2_1/n$. $R(F)$ = 0.0270 for 3872 absorption-corrected reflections with $F > 3\sigma(F)$, using anisotropic thermal parameters for non-hydrogen atoms. All hydrogens except the bridging hydride were refined isotropically. The latter (HC) would not refine satisfactorily, but is reported here as the coordinates of a peak in the final difference Fourier map [21].
[20] R. Bau, W. F. Carroll, R. G. Teller, T. F. Koetzle, *J. Am. Chem. Soc. 99* (1977) 3872.
[21] Further crystallographic details are available from the Cambridge Crystallographic Data Centre, University Chemical Laboratory, Lensfield Road, Cambridge CB2 1EW (England), by quoting the names of the authors and the journal citation.

The Copolymer of 2,6-Pyridinedimethanethiol and 1,4-Benzenedimethanethiol**

By *Giovanni Modica, Silvia Maffi, Enzo Montoneri,* Luigi Giuffré,* and *Antonio Grassi*

Aromatic polymers containing sulfur in the backbone chain (e.g., polyarylene sulfides, $+C_6H_2X_2S+_n$, X = H or Me) are commercially available[1] as non-cross-linked, melting, and highly stable materials which are insoluble at room or medium temperature. Such polymers with pyridine rings in the chain are not known. Yet polypyridinediyl sulfides would be desirable alternatives to cross-linked, insoluble, nonmelting polyvinylpyridines,[2] which cannot be processed to obtain technologically useful products (e.g., membrane sheets or films). The thermal stability and an-

[*] Dr. E. Montoneri, Dr. G. Modica, Dr. S. Maffi, L. Giuffré
Dipartimento di Chimica Industriale e Ingegneria Chimica G. Natta
Politecnico di Milano
Piazza L. da Vinci 32, I-20133 Milano (Italy)
Dr. A. Grassi
Cattedra di Chimica Generale, Facoltà di Farmacia
Dipartimento di Scienze Chimiche
Università di Catania
Viale A. Doria 8, I-95125 Catania (Italy)

[**] This work was supported by the Ministero della Pubblica Istruzione (art. 65, DPR 382/80 (40%), 1983).

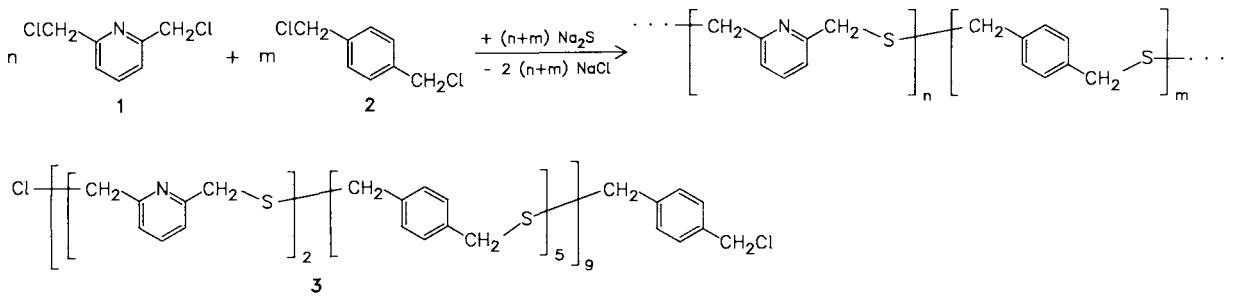

ion-exchange potential of polyvinylpyridines are exploited by manufacturing composite structures.[3]

With the aim of obtaining polymers that contain nucleophilic pyridine rings and are at the same time insoluble, melting, and processable (e.g., in the form of free-standing films), we have carried out the reaction between bis(chloromethyl) aromatic derivatives and sodium sulfide.[4] The reaction occurs readily at moderate temperature (78 °C) and with high conversion ($\geq 89\%$ (mol/mol)). The selectivity and the product molecular weight, however, vary significantly depending on the reacting monomers.

2,6-Bis(chloromethyl)pyridine **1**[5] and 1,4-bis(chloromethyl)benzene **2** reacted with sodium sulfide to give the copolymer **3** in high yields (100 **1***/**1** = 88.8 and 100 **2***/**2** = 99.8, **1** and **2** are the initial molar amounts of the monomers, **1*** and **2*** are the moles of monomers found as repeating units in the copolymer **3**). The copolymer **3** is insoluble in all common solvents, does not undergo significant weight loss up to 200 °C, melts at 177 °C, and yields a free-standing film upon melt pressing.

The IR spectrum (KBr pellet or neat) did not change after heating the product: its most intense bands are at 1580, 1540, and 1455 cm^{-1} (stretching vibrations of the 2,6-disubstituted pyridine ring) and at 1510 and 1420 cm^{-1} (stretching vibrations of the 1,4-disubstituted benzene ring). The X-ray diffraction powder pattern exhibits six very broad, poorly resolved bands in the 2θ range from 16 to 30 (centered at 20.87, 17.79, 23.29, 16.58, 27, and 19 in order of decreasing intensity).

The formation of the copolymer **3** is surprising since an analogous elimination reaction between the sodium salt of 1,4-benzenedimethanethiol and 2,5-bis(bromomethyl)pyridine in ethanol[6] has been reported to yield **4**, which is soluble in chloroform.

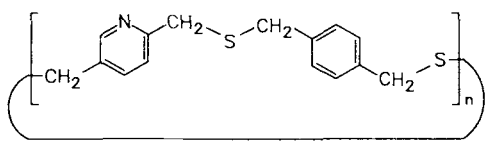

4, n = 1, 2

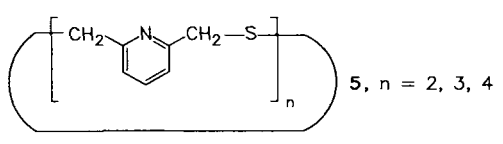

5, n = 2, 3, 4

Contrary to the synthesis of **3** but similarly to that of **4**, the reaction of **1** with Na_2S in the absence of **2** failed to yield a polymer. The sharp peaks in the X-ray diffraction pattern of the reaction product (Fig. 1) reveal a high degree of crystallinity such as found in low-molecular-weight compounds.[7] The elemental analysis corresponds to the

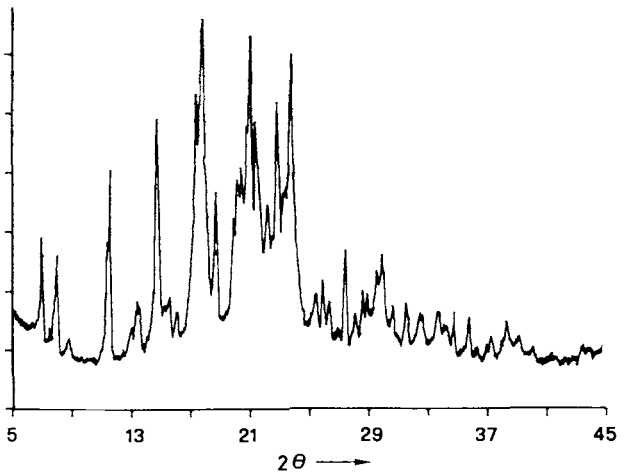

Fig. 1. X-ray powder diffraction pattern of poly(2,6-pyridinediylmethylene-thiomethylene) **5**.

formula CH_2-pyridinediyl-CH_2-S after allowing for 2% water content (confirmed by thermogravimetric analysis up to 120 °C); the absence of chlorine (unlike the case of the copolymer **3**) can only be interpreted on the basis of the cyclic structure **5**. The highest mass spectrum peak at *m/z* 548 indicates n = 4; no chlorine mass peaks were observed. However, peaks at 411 and 274 either could be interpreted as fragments of the tetramer **5** or, more in line with the NMR data, indicate the presence of other oligomers (the trimer and dimer) in the product. Indeed, the product was found to melt over a wide temperature range (128–180 °C) and differential scanning calorimetry showed a series of endothermic, broad, and poorly resolved bands with maxima at 124.5, 157 and 173 °C, and no weight loss.[8] Contrary to the copolymer **3**, the low-molecular-weight product **5** is soluble in chloroform. Its NMR spectrum ($CDCl_3$, int. TMS) shows a complex aromatic multiplet pattern at $\delta = 6.96$–7.56 (3 H) and three main singlets at $\delta = 3.97$, 3.79, and 3.74 (1.76, 1.56, and 0.68 H). The same resonances were reported for the protons of the *ortho* methylene group in the CH_2-pyridinediyl-CH_2-S unit in **4**:[6] 3.70 for **4**, n = 1, and 3.94 for **4**, n = 2.[9]

The results show that the possibility of obtaining high-molecular-weight polymers from bis(chloromethyl) aromatic derivatives and sodium sulfide strongly depends on the starting monomers. It appears that oligomerization of disubstituted pyridines can be inhibited and the formation of high-molecular-weight polymers containing pyridine rings in the backbone chain can be accomplished by reacting the pyridine reagent with an excess of the *p*-disubstituted benzene.

Received: October 20, 1986;
revised: November 24, 1986 [Z 1956 IE]
German version: *Angew. Chem.* 99 (1987) 149

[1] W. H. Hill, Jr., D. G. Brady in: *Kirk-Othmer, Encyclopedia of Chemical Technology, Vol. 18*, Wiley, New York 1982, p. 793; A. B. Port, R. H. Still, *J. Appl. Polym. Sci. 24* (1979) 1145.
[2] S. Tazuke, S. Okamura in F. H. Mark, N. G. Gaylord (Eds.): *Encyclopedia of Polymer Technology, Vol. 14*, Interscience, New York 1971, p. 637.
[3] G. Modica, L. Giuffré, E. Montoneri, H. Wendt, H. Hofmann, *Polymer 25* (1984) 1513; R. A. Wallace, N. V. Vijayaraghavan, *Polym. Eng. Sci. 14* (1974) 674.
[4] *Experimental procedure* for **3** and **5**: $Na_2S \cdot 9H_2O$ (Fluka, 10% mole excess), $AcONa \cdot 3H_2O$ (C. Erba) (0.12 g), EtOH (250 mL), and toluene (145 mL) were dried by azeotropic distillation at ca. 73 °C. When the temperature had risen to 78 °C, **1** (8 g), prepared from 2,6-pyridinedimethanol (Ega-Chemie), or a mixture of **1** (4 g) and **2** (9 g, Fluka) were added and the solution was refluxed under N_2 for 16 h; a solid formed after 90 min. The product **5** (from **1**) was then filtered, washed with hot water, and dried overnight at 60 °C under vacuum; yield 5.65 g. The product **3** (from **1** and **2**) was treated as above, but washed with hot water, toluene, acetone, and finally with hot chloroform; yield 9.5 g.
[5] W. Baker, K. M. Buggle, J. F. M. McOhmie, D. A. M. Watkins, *J. Chem. Soc. 1968*, 3594.
[6] J. Bruhin, W. Jenny, *Tetrahedron Lett. 1973*, 1215.
[7] The presence of small amounts of low-molecular-weight compounds in the product **3** was excluded on the basis of the absence of their characteristic X-ray pattern, particularly in the low-angle portion ($7 \leq 2\theta \leq 15$), which (for **3**) was totally free of bands.
[8] Weight loss (34%) occurred between 210 and 350 °C.
[9] By analogy, the three CH_2 proton resonances are tentatively assigned to the di-, tri-, and tetramers **5**, n = 2, 3, and 4, respectively. The proton shielding with increasing ring size could be reasonably accounted for by a corresponding decrease of steric hindrance, which makes likely intramolecular shielding of the CH_2 fragment: these groups, as shown by inspection of molecular models, can fall within the shielding cones of the pyridine rings, owing to increased conformational flexibility.

The Crystal Structure of Mn_2O_7

By *Arndt Simon,* Richard Dronskowski, Bernt Krebs,** and *Bernhard Hettich*

Dedicated to Professor Oskar Glemser on the occasion of his 75th birthday

Mn_2O_7 was first studied by *Aschoff*[1] in 1860. Important insights into the synthesis and properties of the compound were provided by the work of *Glemser* and *Schröder*[2] (cf. also ref. [3]). At room temperature, Mn_2O_7 is a volatile, dark red oil, which solidifies at 5.9 °C to give red crystals with green reflectance. The compound detonates when it is warmed to above 55 °C, when it is struck, or when it comes into contact with organic compounds.

The properties of Mn_2O_7 support a molecular structure for the solid state consisting of corner-sharing pairs of MnO_4 tetrahedra.[4] The initially suggested average distance $d(Mn-O) = 165$ pm[4] has been replaced by the newer values $d(Mn=O) = 158$ pm and $d(Mn-O) = 176$ pm for terminal and bridging O atoms, respectively, which were predicted by *Trömel*[5] on the basis of bond length-bond strength considerations. The IR spectra of Mn_2O_7, condensed from the gas phase at 12 K, indicate an Mn-O-Mn angle of 150 to 160°.[6]

Single crystals of Mn_2O_7 for X-ray diffraction analysis could be grown on a diffractometer, using a *Bridgman* technique,[7] by immediately cooling the X-ray capillary after filling it with liquid Mn_2O_7. The results of the X-ray crystal structure analysis are shown in Figures 1 and 2.

[*] Prof. Dr. A. Simon, R. Dronskowski, B. Hettich
Max-Planck-Institut für Festkörperforschung
Heisenbergstrasse 1, D-7000 Stuttgart 80 (FRG)
Prof. Dr. B. Krebs
Anorganisch-chemisches Institut der Universität
Corrensstrasse 36, D-4400 Münster (FRG)

Mn_2O_7 forms monoclinic crystals in the space group $P2_1/c$ with eight formula units per unit cell.[8] The density calculated from the X-ray data at -30 °C, $\rho_{-30} = 2.79$ g cm^{-3}, is considerably larger than the measured density of the liquid, $\rho_{+20} = 2.396$ g cm^{-3}.[2]

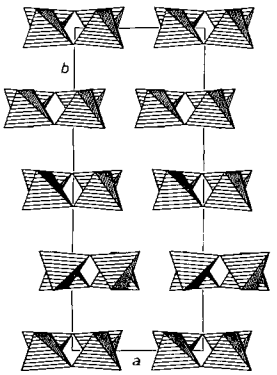

Fig. 1. Projection of the crystal structure of Mn_2O_7 along [001] with representation of the molecules as polyhedra [12].

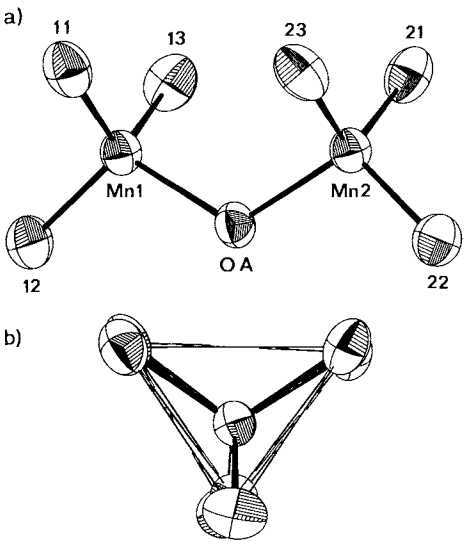

Fig. 2. Molecular structure of Mn_2O_7 (ORTEP II, ellipsoids with 50% probability). a) Viewed as in Fig. 1. b) Newman projection along the Mn1-Mn2 axis. The Mn-O bond lengths [pm] (standard deviation 0.3 pm), corrected for libration of the MnO_4 tetrahedra, for the Mn1/Mn2- and Mn3/Mn4-containing, symmetry dependent molecules are: Mn1-OA 177.0, Mn1-O11/13 160.5, Mn1-O12 158.9, Mn2-OA 177.0, Mn2-O21/23 159.6, Mn2-O22 158.4, Mn3-OB 177.3, Mn3-O31/33 160.0, Mn3-O32 158.4, Mn4-OB 176.6, Mn4-O41/43 159.9, Mn4-O42 158.2. The Mn-O-Mn angles at OA and OB are 120.7(2)°. Those angles that involve bridging atoms lie between 107.8 and 108.4°, the remaining between 110.3 and 111.3 °C.

The distances between the Mn atoms and the bridging O atoms are 177.0(3) pm, in excellent agreement with the previously estimated bond lengths.[5] The average value of the distance between the Mn and the terminal O atoms (159.5(8) pm), is also in agreement with predictions. More careful examination reveals that the bonds between the Mn atoms and the terminal O atoms, which lie in the Mn1-OA-Mn2 plane, are slightly shorter (158.5(3) pm) than those between the Mn atoms and the remaining terminal O atoms (160.0(4) pm). This difference in lengths can be easily explained in terms of the electrostatic repulsion between the Mn atoms.

 © VCH Verlagsgesellschaft mbH, D-6940 Weinheim, 1987 0570-0833/87/0202-0139 $ 02.50/0

The Mn-O-Mn bond angle (120.7°) is considerably smaller than that measured for (amorphous?) Mn_2O_7 films.[6] However, it is possible that the two findings are not in contradiction. In the crystal, the small angle leads to the intramolecular formation of a nido-octahedral arrangement for the bridging and the four terminal O atoms (cf. Fig. 2b), which is augmented to form an octahedron by a further O atom from an adjacent molecule.

This indicates that the Mn_2O_7 molecules are packed in a way to yield a close-packed arrangement of all O atoms. Indeed, the Mn_2O_7 structure can be described in terms of an fcc lattice of the O atoms; the actual positions of the O atoms deviate, on the average, by 24 ± 5 pm (contraction of the neighboring tetrahedral voids occupied by Mn) from the ideal lattice positions. The formation of a close-packed structure explains the unusual increase in the density of Mn_2O_7 upon crystallization.

Comparison of the crystal structures of Mn_2O_7, Tc_2O_7, and Re_2O_7 reveals interesting similarities and differences: In Tc_2O_7,[10] discrete M_2O_7 molecules with tetrahedrally surrounded M atoms also occur, but the M-O-M angle is 180°. The molar volume of Tc_2O_7 (86.5 $cm^3\ mol^{-1}$) is considerably larger than that of Mn_2O_7 (79 $cm^3\ mol^{-1}$). In contrast, for the three-dimensional network of Re_2O_7,[11] with tetrahedrally and octahedrally surrounded Re atoms, a molar volume of 78 $cm^3\ mol^{-1}$ is found, which is close to that of Mn_2O_7. This comparison shows that Tc_2O_7 occupies a special position in the series of compounds, indicating, for example, that transformations under pressure might take place.

Experimental Procedure

$KMnO_4$ (ca. 50 mg) was treated with H_2SO_4 (+20% SO_3). After a short period of time, Mn_2O_7 separated out as a dark, oily ring around the reaction mixture and was sucked into a carefully cleaned capillary (0.2-mm Ø, 20-mm continuous column of liquid). The (open) capillary was cooled immediately with liquid N_2 in order to prevent interruptions of the column of material by the formation of O_2 bubbles, and it was then mounted at −10°C on a four-circle diffractometer. Suitable crystals, which were nearly aligned along [001] in the direction of the axis of the tube, were obtained in a temperature gradient of $-10/+20$°C [7] and improved by variation of the temperature between ca. 0 and 5°C, continuously monitoring via X-ray diffraction.

Received: October 30, 1986;
revised: November 12, 1986 [Z 1974 IE]
German version: *Angew. Chem. 99* (1987) 160

[1] H. Aschoff, *Ann. Phys. Chem. Ser. 2 111* (1860) 217, 224.
[2] O. Glemser, H. Schröder, *Z. Anorg. Allg. Chem. 271* (1953) 293.
[3] A. Simon, F. Feher, *Z. Elektrochem. Angew. Phys. Chem. 38* (1932) 137.
[4] B. Krebs, *Z. Anorg. Allg. Chem. 380* (1971) 146.
[5] M. Trömel, *Acta Crystallogr. Sect. B 39* (1983) 664; the bond length-bond strength relationship was derived from structure data, which were not corrected for errors in the distance (bond shortening) due to vibrations of the atoms. The corresponding, uncorrected distances in Mn_2O_7 are $d(Mn-O) = 176.2(3)$, 157.5(3), and $2 \times 158.8(3)$ pm for the MnO_4 tetrahedra.
[6] W. Levason, J. S. Ogden, J. W. Turff, *J. Chem. Soc. Dalton Trans. 1983*, 2699.
[7] A. Simon, H.-J. Deiseroth, E. Westerbeck, B. Hillenkötter, *Z. Anorg. Allg. Chem. 423* (1976) 203.
[8] Space group $P2_1/c$ (No. 14); $Z = 8$, $a = 679.56(4)$, $b = 1668.68(16)$, $c = 945.39(29)$ pm, $\beta = 100.20(1)$° (from modified Guinier-diffractograms [9] at −30°C); 3325 reflections, 2310 with $F_0 \geq 3\sigma(F_0)$ (CAD4 diffractometer, −30°C); structure solved by direct methods in *Pc*, refinement in $P2_1/c$ (SHELXTL); $R_{aniso} = 0.043$, $R_w = 0.039$, $R' = 0.065$. Further details of the crystal structure investigation may be obtained from the Fachinformationszentrum Energie, Physik, Mathematik gmbH, D-7514 Eggenstein-Leopoldshafen 2 (FRG), on quoting the depository number CSD-52 169, the names of the authors, and the journal citation.
[9] A. Simon, *J. Appl. Crystallogr. 3* (1970) 11; *ibid. 4* (1971) 138.
[10] B. Krebs, *Z. Anorg. Allg. Chem. 380* (1971) 146.
[11] B. Krebs, A. Müller, H. H. Beyer, *Inorg. Chem. 8* (1969) 436.
[12] R. X. Fischer, *J. Appl. Crystallogr. 18* (1985) 258.

CO_2 Elimination from Vinylene Carbonate Radical Anions and Charge Reversal in $C_2H_2O^{\odot\ominus}$: Reactions Involving the Radical Anion and Cation of Oxirene?**

By *Ben L. M. van Baar, Nikolaus Heinrich, Wolfram Koch, Ron Postma, Johan K. Terlouw,* and *Helmut Schwarz**

Vinylene carbonate **1** reacts with low-energy electrons in the gas phase to give, via elimination of CO_2, a metastable radical anion $C_2H_2O^{\odot\ominus}$, which loses an electron to form C_2H_2O.[1] It has not been possible so far to elucidate the structures of the intermediate radical anions or of the neutral molecules of empirical formula C_2H_2O (**2a**–**5a** and **2b**–**5b**, respectively). This is not surprising in view of the confusing chemistry of this small species.[2, 3]

We report here on gas-phase experiments, supplemented by extensive ab initio MO calculations, that show that

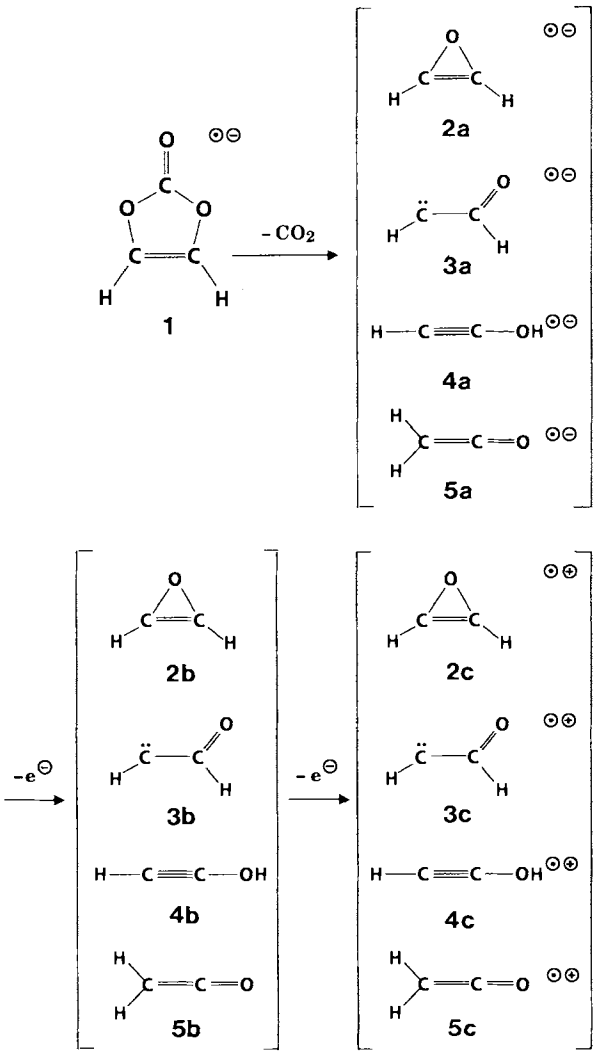

[*] Prof. Dr. H. Schwarz, N. Heinrich, Dr. W. Koch
Institut für Organische Chemie der Technischen Universität
Strasse des 17. Juni 135, D-1000 Berlin 12
B. L. M. van Baar, R. Postma, Dr. J. K. Terlouw
Laboratory for Analytical Chemistry, Utrecht University
Croesestraat 77 A, NL-3522 AD Utrecht (Netherlands)

[**] This work was supported by the Fonds der Chemischen Industrie, the Deutsche Forschungsgemeinschaft, and the Gesellschaft von Freunden der Technischen Universität Berlin.

elimination of CO_2 from $\mathbf{1}^{\odot\ominus}$ results in the formation of **3a**, the radical anion of the ketocarbene **3b**. Spontaneous loss of an electron from the metastable **3a** affords the ketene **5b**. Charge reversal[4] via collision-induced 2-electron loss from **3a** results mainly in formation of the ketocarbene radical cation **3c**. Depending on its internal energy, it undergoes decomposition or isomerization to the long-sought and theoretically predicted[5] oxirene radical cation **2c**.

Electron attachment to **1** in a ZAB-2F mass spectrometer results in loss of CO_2 and formation of $C_2H_2O^{\odot\ominus}$ ions, which were mass-selected by employing tandem mass spectrometry (MSMS).[6] The collisional activation (CA)[7] spectra were then recorded. The CA spectrum of $C_2H_2O^{\odot\oplus}$ formed by spontaneous loss of an electron from $C_2H_2O^{\odot\ominus}$, followed by collisional reionization mass spectrometry,[8] is identical in all respects with the CA spectrum of **5c** produced from **5b**.[9] This indicates that spontaneous electron loss from $C_2H_2O^{\odot\ominus}$ leads to **5b**. However, the following experiment and ab initio results (described below) strongly suggest that $C_2H_2O^{\odot\ominus}$ is not present as **5a** but rather as **3a**. If charge reversal is allowed to take place in a collision experiment of the $C_2H_2O^{\odot\ominus}$ ions (vertical removal of two electrons), the CA spectrum shown in Figure 1 is obtained. This spectrum cannot be simulated by a linear combination of the CA spectra of **5c** and **4c**. In contrast, more detailed comparison with the CA spectra of these ions[9] indicates that only a few percent of **4c** and **5c** are formed upon generation of "reactive" $C_2H_2O^{\odot\oplus}$ ions from $C_2H_2O^{\odot\ominus}$. On the basis of the spectrum, therefore, the intermediacy of at least one, previously unknown, $C_2H_2O^{\odot\oplus}$ species is suggested. We propose formation of **3c**, the radical cation of ketocarbene **3b**, the most important ionic fragmentation products of which are the ion at *m/z* 29 ($HCO^{\oplus}$), produced by loss of CH, and that at *m/z* 26 ($C_2H_2^{\odot\oplus}$), produced by deoxygenation. *m/z* 41 corresponds presumably to the ion $H-\overset{\oplus}{C}=C=O$, which can also arise directly from **3c**.

According to ab initio calculations,[5] **3c** is not stable. The radical cation undergoes decomposition (see preceding paragraph) or isomerizes to **2c** (via ring closure) and **4c** or **5c** (via H migration). The reaction **3c**→**4c** is unlikely for energetic reasons.[5] The spontaneous process **3c**→**5c** should, on account of the large enthalpy of formation of **3c**,[5] yield highly excited **5c**, which, in turn, should decompose spontaneously into CO and $CH_2^{\odot\oplus}$. Indeed, we believe that the signal at *m/z* 14 (Fig. 1) may originate from the reaction **3c**→**5c**→$CH_2^{\odot\oplus}$ + CO. However, what is the explanation for the observation that the vertical removal of two electrons from **3a** does not only lead to fragments but also to a *stable* ion at *m/z* 42 ($C_2H_2O^{\odot\oplus}$), which has a lifetime $t > 10^{-5}$ s? The only possible explanation is that the radical cation **3c**, generated with only a small amount of excess energy, undergoes isomerization to **2c**, the radical cation of oxirene **2b**. **2c** is theoretically predicted[5] to reside in a sufficiently deep potential well so that fragmentation processes are not favored.

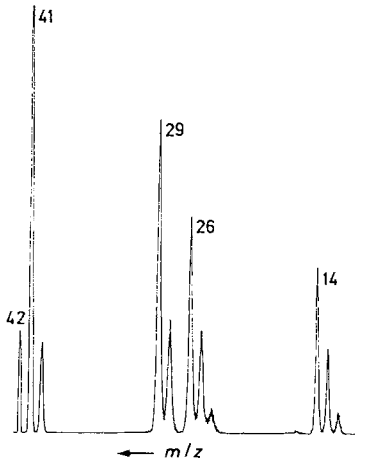

Fig. 1. CA spectrum of $C_2H_2O^{\odot\oplus}$ ions generated by charge reversal from $C_2H_2O^{\odot\ominus}$.

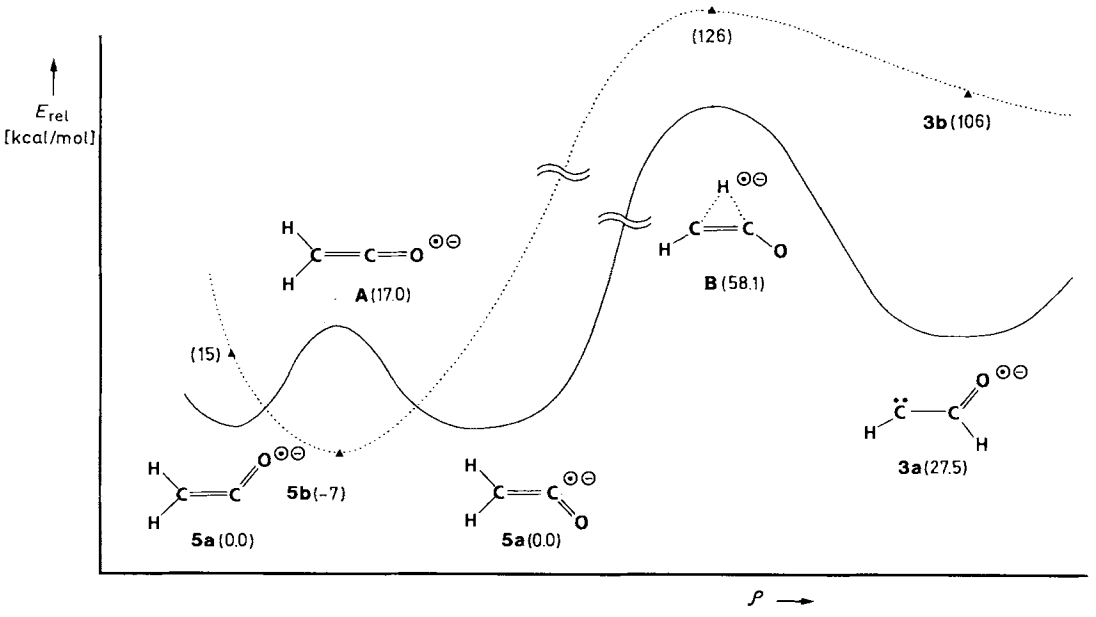

Fig. 2. Schematic potential hypersurface for species of empirical formula $C_2H_2O^{\odot\ominus}$ (——) and C_2H_2O (-----). The calculations were carried out at the MP3/6-311++G(d,p)//6-31+G(d) level. ρ = reaction coordinate; **A**, **B** = transition states; relative energies in parentheses.

Let us return to the initially posed question as to the structure of the $C_2H_2O^{\oplus\ominus}$ ions. Supplementing and supporting the results of the experiments, ab initio calculations (performed at the MP3/6-311++G(d,p)//6-31+G(d) level) yielded the following results:[10] **3a** (and several of its conformers), like the bent form of **5a**,[12] exist in potential minima (Fig. 2). **3a** is about 27.5 kcal/mol less stable than **5a**; the barrier for the isomerization **3a** → **5a** is 30.6 kcal/mol. Positive electron affinities are predicted for both species. The experimental observation that electron loss nonetheless occurs from **3a** must be due to the fact that **3a** is generated with excess energy upon electron attachment to vinylene carbonate **1**. If this amount of energy is large enough to overcome a barrier of about 30 kcal/mol (or less, if tunnel effects play a role), then the reaction **3a** → **B** → **5a** ⇄ **A** results necessarily in electron loss to form ketene **5b**; the latter is identified in the experiment. The radical anion of oxirene, **2a**, plays no role in the chemistry of the $C_2H_2O^{\oplus\ominus}$ species. **2a**, which is about 100 kcal/mol less stable than **3a**, corresponds, moreover, to a saddle point of second order (two imaginary frequencies).

Received: November 4, 1986;
revised: November 25, 1986 [Z 1980 IE]
German version: *Angew. Chem. 99* (1987) 153

[1] R. N. Compton, P. W. Reinhardt, H. C. Schweinler, *Int. J. Mass Spectrom. Ion Phys. 49* (1983) 113.
[2] Further discussions of C_2H_2O and, in particular, of oxirene: a) G. Maier, H. P. Reisenauer, T. Sayraç, *Chem. Ber. 115* (1982) 2192; b) W. J. Bouma, R. H. Nobes, L. Radom, C. E. Woodward, *J. Org. Chem. 47* (1982) 1869; c) E. G. Lewars, *Chem. Rev. 83* (1983) 519.
[3] To the best of our knowledge, neither theoretical nor other experimental results are available for the $C_2H_2O^{\oplus\ominus}$ species.
[4] J. L. Holmes, *Org. Mass Spectrom. 20* (1985) 169.
[5] W. J. Bouma, P. M. W. Gill, L. Radom, *Org. Mass Spectrom. 19* (1984) 610.
[6] F. W. McLafferty (Ed.): *Tandem Mass Spectrometry*, Wiley, New York 1983.
[7] Review: K. Levsen, H. Schwarz, *Mass Spectrom. Rev. 2* (1983) 77.
[8] Selected references: a) P. O. Danis, D. Wesdemiotis, F. W. McLafferty, *J. Am. Chem. Soc. 105* (1983) 7454; b) P. C. Burgers, J. L. Holmes, A. A. Mommers, J. K. Terlouw, *Chem. Phys. Lett. 102* (1983) 1.
[9] The CA spectra of **4c** and **5c** are found in B. van Baar, T. Weiske, J. K. Terlouw, H. Schwarz, *Angew. Chem. 98* (1986) 275; *Angew. Chem. Int. Ed. Engl. 25* (1986) 282.
[10] The notation MP3/6-311++G(d,p)//6-31+G(d) means that the calculation of individual points for the geometries optimized at a 6-31+G(d) level [11a] was carried out with the 6-311++G(d,p) basis set [11c], which is more than sufficient for anions. The effects of electron correlation were taken into consideration by perturbation calculations (according to Møller-Plesset [11d,e]) up to third order (MP3). The extended (+) basis sets are described in [11f]. Minima and maxima were unequivocally located by an analysis of the force-constant matrix. Complete data for geometries and energies of the structures reported here (and their conformers) are available on request.
[11] a) P. C. Hariharan, J. A. Pople, *Theor. Chim. Acta 28* (1973) 213; b) J. Chandrasekhar, J. G. Andrade, P. von R. Schleyer, *J. Am. Chem. Soc. 103* (1981) 5609, 5612; E. R. Davidson, D. Feller, *Chem. Rev. 86* (1986) 681; R. H. Nobes, D. Poppinger, W.-K. Li, L. Radom in E. Buncel, T. Durst (Eds.): *Comprehensive Carbanion Chemistry*, Part C, Elsevier, Amsterdam 1987; c) R. Krishnan, J. S. Binkley, R. Seeger, J. A. Pople, *J. Chem. Phys. 72* (1980) 650; d) C. Møller, M. S. Plesset, *Phys. Rev. 46* (1934) 618; e) R. Krishnan, M. J. Frisch, J. A. Pople, *J. Chem. Phys. 72* (1980) 4244; f) T. Clark, J. Chandrasekhar, G. W. Spitznagel, P. von R. Schleyer, *J. Comput. Chem. 4* (1983) 294.
[12] The fact that ketene has a negative electron affinity [Prof. E. Illenberger (Berlin), Prof. N. M. M. Nibbering (Amsterdam), private communication] does not contradict the ab initio results. Vertical electron attachment to **5b** yields the transition state **A**, corresponding to the topomerization of **5a**. In the process **A** → **5a** crossing with the hypersurface of the neutral C_2H_2O molecule (broken line in Fig. 2) occurs; this results in spontaneous electron loss with re-formation of **5b**.

Stereoselective Alkylation of Aromatic Compounds with Threonine Trifluoromethanesulfonates**

By *Franz Effenberger** and *Thomas Weber*

Dedicated to Professor Rudolf Gompper on the occasion of his 60th birthday

Alkyl trifluoromethanesulfonates (alkyl triflates) have only been used in special cases for the alkylation of aromatic compounds.[1] We have now succeeded in synthesizing the *N*-protected triflates of (*S*)- and (*R*)-serine methyl ester as well as the *N*-protected triflates **1** of all diastereomeric threonine methyl esters in very good yields and with complete retention of configuration. This was accomplished by treating the *N*-phthaloyl-protected amino acid esters with trifluoromethanesulfonic anhydride in the presence of pyridine. With the triflates of the serine and threonine esters, it was possible to alkylate benzene and benzene derivatives to obtain phenylalanine and β-methylphenylalanine esters **2**, respectively.

These reactions proceed with retention of configuration at C-2 of the amino acid ester under all conditions employed. Of particular interest but difficult to predict was the stereochemistry at C-3 of the β-methylphenylalanine esters **2**. The Friedel-Crafts alkylation of aromatic compounds with optically active alkylating agents usually proceeds with extensive racemization.[2] However, *Suga* et al., in particular, have shown that alkylation with optically active compounds can also be carried out without significant racemization if special structural properties are fulfilled.[3] In general, these alkylations occur with inversion of confi-

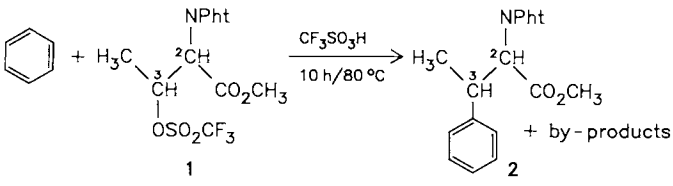

1 **2**

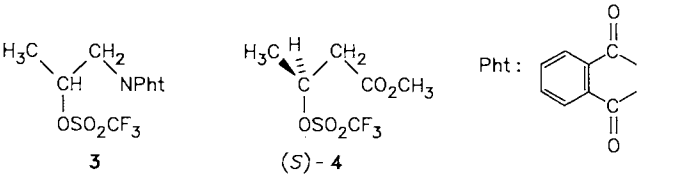

3 (*S*)-**4**

Table 1. Changes in configuration upon alkylation of benzene with the diastereomeric threonine derivatives **1** to give the phenylalanine derivatives **2** [a].

	Educt		Product		Relative amounts
1a	(2*S*,3*R*)	**2a**	(2*S*,3*S*)	+ **2c**	97 : 3
1b	(2*R*,3*S*)	**2b**	(2*R*,3*R*)	+ **2d**	98 : 2
1c	(2*S*,3*S*)	**2c**	(2*S*,3*R*)	+ **2a**	40 : 60
1d	(2*R*,3*R*)	**2d**	(2*R*,3*S*)	+ **2b**	40 : 60

[a] 3*R* in **1** and 3*S* in **2** correspond to the same configuration at C-3.

[*] Prof. Dr. F. Effenberger, Dipl.-Chem. T. Weber
Institut für Organische Chemie der Universität
Pfaffenwaldring 55, D-7000 Stuttgart 80 (FRG)

[**] Electrophilic Aromatic Substitution, Part 32. This work was supported by the Deutsche Forschungsgemeinschaft and the Fonds der Chemischen Industrie. *T. W.* thanks the Fonds der Chemischen Industrie for a doctoral fellowship.—Part 31: F. Effenberger, F. Reisinger, K. H. Schönwälder, P. Bäuerle, J. J. Stezowski, K. H. Jogun, K. Schöllkopf, W. D. Stohrer, *J. Am. Chem. Soc.*, in press.

guration of the attacking C atom of the alkylating agent. Retention was observed for alkylation with β-phenylalkyl halides: in the first step, intramolecular alkylation with inversion results in the formation of a cyclohexadienylium intermediate, which, in the second step, again with inversion, reacts with the aromatic compound.[4]

In the alkylation of benzene with the triflates of the *N*-phthaloylthreonines **1a,b** and the *N*-phthaloylallothreonine methyl esters **1c,d**, we obtained in every case the β-methyl-*N*-phthaloyl phenylalanine methyl esters **2**. The overall yields of **2** are between 20 and 40%, because, in addition to the substitution of **1** to give **2**, substantial elimination occurs to give α,β- (25–30%) and β,γ-dehydroamino acid esters (35–40%).

Whereas the configuration at C-2—as previously mentioned—is maintained upon the reactions of **1a–d** to give **2**, the threonine (**1a,b**) and allothreonine (**1c,d**) derivatives show diverse behavior upon alkylation with respect to the stereochemistry at C-3.

The threonine derivatives **1a,b** react largely with retention at C-3, whereas the allothreonine derivatives **1c,d** afford diastereomeric mixtures in the ratio of 2:3. The characterization and structural assignments of the four diastereomers **2a–d** were determined by comparison of their optical rotations and ^{1}H-NMR data with literature values.[5] For **2a**, we confirmed the configuration by carrying out an X-ray structure analysis.[6] Furthermore, we were able to show that the product obtained by acid hydrolysis of **2a**, removal of the phthaloyl protecting group, and acetylation is identical with the reported (2*S*,3*S*)-*N*-acetyl-β-methylphenylalanine.[7]

The high stereoselectivity observed in the alkylation of benzene with **1a, b** and the different behavior of **1c, d** can be explained in terms of the different conformations of the carbenium ions **B** and **D**, which are formed as intermediates in the alkylation.

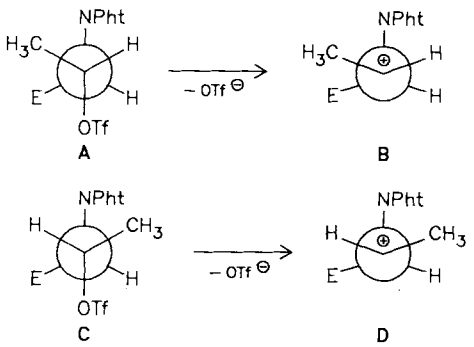

E = CO_2CH_3; Tf = SO_2CF_3

Alkylation of benzene with (*S*)- and (*R*)-1-methyl-2-phthaloylaminomethyl triflate **3** results in partial retention, whereas with methyl (*S*)-3-trifluoromethanesulfonyloxybutyrate, (*S*)-**4**, complete racemization is observed. We conclude from this that, in the dissociation step, the threonine derivatives **1a,b** prefer conformation **A**, whereas the allothreonine derivatives **1c,d** prefer conformation **C**. In the carbenium ion **B** formed from **A**, rotation is rendered difficult by the two large neighboring substituents (CH_3, CO_2CH_3); moreover, the aromatic compound can react only from the bottom side with **B**, because the cationic center is blocked from above by the *N*-phthaloyl group. This explains the retention observed in the reactions of **1a,b**. For the cationic intermediate **D**, on the other hand, no or at most only a small hindrance to rotation is expected, which is confirmed by the results of the reactions of **1c,d**.

In analogy to the reactions of benzene, alkyl- and alkoxybenzenes can also undergo reaction with the triflates **1** of the threonine ester. In a one-pot procedure, it is also possible to synthesize phenylalanines and β-methylphenylalanines such as **2** from the corresponding aromatic compounds, the *N*-protected esters of serine and threonine, and trifluoromethanesulfonic anhydride (without isolation of the triflates of type **1**). Trifluoromethanesulfonic acid can be precipitated as its barium salt and thus recovered.

Experimental Procedure

2a: *N*-phthaloyl-*O*-(trifluoromethanesulfonyl)-(2*S*,3*R*)-threonine methyl ester **1a** (1.58 g, 4 mmol) and trifluoromethanesulfonic acid (0.61 g, 4 mmol) were stirred in 8 mL of benzene for 10 h at 80°C under dry atmosphere. The excess benzene was then removed in vacuo. After addition of water to the residue, the mixture was extracted with chloroform. The combined organic phases were dried over $MgSO_4$ and evaporated; the residue was chromatographed on silica gel with petroleum ether/ethyl acetate (9:1). Yield 300 mg (24%) **2a**, m.p. = 107°C (petroleum ether), $[\alpha]_D^{20}$ = −139.1° (*c* = 1, $CHCl_3$) and 10 mg (0.77%) **2c**, oil, $[\alpha]_D^{20}$ = −120.5° (*c* = 0.6, $CHCl_3$).

One-pot procedure: *N*-phthaloyl-(2*S*,3*R*)-threonine methyl ester (0.53 g, 2 mmol) and trifluoromethanesulfonic anhydride (0.56 g, 2 mmol) were allowed to react as described above. Yield 0.15 g (23%) **2a**, $[\alpha]_D^{20}$ = −138.3° (*c* = 1, $CHCl_3$).

Received: October 6, 1986;
revised: November 17, 1986 [Z 1947 IE]
German version: *Angew. Chem. 99* (1987) 146

[1] a) F. Effenberger, *Angew. Chem. 92* (1980) 147; *Angew. Chem. Int. Ed. Engl. 19* (1980) 151, and references cited therein; b) B. L. Booth, R. N. Haszeldine, K. Laali, *J. Chem. Soc. Perkin Trans. 1 1980*, 2887.
[2] a) C. C. Price, M. Lund, *J. Am. Chem. Soc. 62* (1940) 310; b) A. Streitwieser, Jr., P. J. Stang, *ibid. 87* (1965) 4953.
[3] a) T. Nakajima, S. Suga, T. Sugita, K. Ichikawa, *Bull. Chem. Soc. Jpn. 40* (1967) 2980; b) T. Nakajima, S. Masuda, S. Nakashima, T. Kondo, Y. Nakamoto, S. Suga, *ibid. 52* (1979) 2377; c) O. Piccolo, F. Spreafico, G. Visentin, E. Valoti, *J. Org. Chem. 50* (1985) 3945.
[4] M. Shinji, T. Nakajima, S. Suga, *Bull. Chem. Soc. Jpn. 56* (1983) 1089.
[5] Y. Kataoka, Y. Seto, M. Yamamoto, T. Yamada, S. Kuwata, H. Watanabe, *Bull. Chem. Soc. Jpn. 49* (1976) 1081.
[6] We thank Prof. Dr. *John J. Stezowski* for the X-ray structure analysis.
[7] a) H. Arold, M. Eule, S. Reissmann, *Z. Chem. 9* (1969) 447; b) G. I. Tsuchihashi, S. Mitamura, K. Ogura, *Bull. Chem. Soc. Jpn. 52* (1979) 2167.

Asymmetric Synthesis of Cyclic α-Amino Acids by the Bislactim Ether Method**

By *Ulrich Schöllkopf,** *Rolf Hinrichs*, and *Ralph Lonsky*

Dedicated to Professor G. Quinkert on the occasion of his 60th birthday

Optically active α-methylproline **10a** and its analogues **10b** and **11** are of interest because of their potential biological activity as competitive enzyme inhibitors.[2] (*S*)-α-Methylproline (*ent*-**10a**) was prepared by *Seebach* et al.[3] from naturally occurring L-proline in an asymmetric synthesis. This synthesis, although elegant, has the disadvantage that it cannot be applied to ring homologues without modification, because homologues of proline do not exist in the "chiral pool" of nature. We report here a very flexible asymmetric synthesis of 2-methyl-1-azacycloalkane-2-

[*] Prof. Dr. U. Schöllkopf, Dipl.-Chem. R. Hinrichs, Dr. R. Lonsky
Institut für Organische Chemie der Universität
Tammannstrasse 2, D-3400 Göttingen (FRG)

[**] Asymmetric Syntheses via Heterocyclic Intermediates. Part 32.—Part 31: [1].

carboxylic acids of the types **10** and **11** according to the bislactim ether method.[4] The cyclic amino acid is constructed during the synthesis by diastereoselective alkylation (**2** + **3/4** → **5/6**).

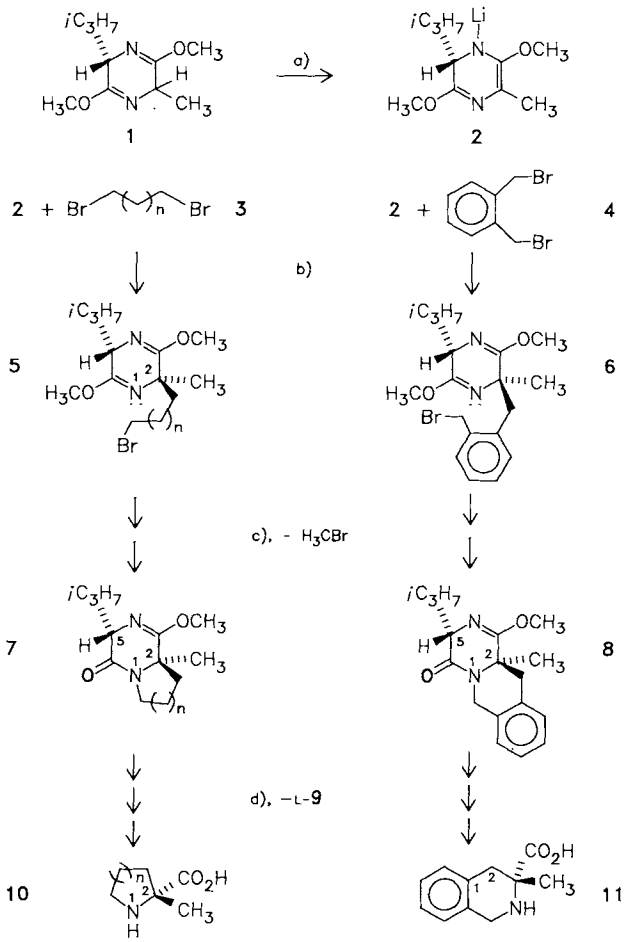

3, 5, 7, 10: a, n = 1: b, n = 2

	7a	7b	8
Yield [%]	81[a]	76[b]	75[a]
(2*R*,5*S*) : (2*S*,5*S*)[8]	97:3	97.5:2.5	98.5:1.5

[a] Based on **1**. [b] Based on **5b**.

Scheme 1. Synthesis of cyclic amino acids. a) BuLi, tetrahydrofuran (THF), −78°C, 2 equivalents *N,N'*-dimethyl-2-imidazolidinone (*N,N'*-dimethylethyleneurea, DMEU). b) 3.0 equivalents **3** or **4**, 12 h at −78°C, then warming to room temperature [7]. c) **7a**: distillation of **5a**; **7b** and **8**: dimethylformamide (DMF), 1 equivalent NaI, reflux 2 h or 1 h, respectively [9]. d) 20 mL conc. HBr (2.0 mmol), reflux 18 h for **7a**, **b**, 40 h for **8**, concentration in vacuo, heating with propene oxide in ethanol [10]. The (nonsystematic) numbering is given for configurational assignment and assignment of the NMR signals.

The synthesis starts from **1**, the commercially available bislactim ether of *cyclo*-(L-Val-Ala) [or *cyclo*-(D-Val-Ala)].[5,6] Compound **1** was lithiated to give **2**, which was allowed to react with the dihalide **3** or **4** to give the intermediates **5** or **6**, respectively, which, in turn, gave **7** or **8** in a thermal reaction. Compounds **5** and **6** are formed with high asymmetric induction.[8] In the case of **5b** and **6**, the cyclizations **5** → **7** and **6** → **8** require heating in DMF in the presence of sodium iodide.[9] Compound **5a**, on the other hand, cyclizes already upon distillation. When the compounds **7** and **8** are heated with hydrobromic acid, they undergo hydrolysis to valine **9** and to the (*R*)-2-methyl-1-azacycloalkane-2-carboxylic acids **10** and **11**, respectively. From the mixture of the amino acid hydrobromides remaining after removal of the excess hydrobromic acid, the amino acids may be isolated by short heating (15 min) in ethanol with propene oxide. Compound **9** may easily be separated from the target molecules **10** and **11**, either by chromatography or by crystallization.[10,12] The ^{1}H-NMR data for compounds **5**, **7**, **8**, **10**, and **11** are collected in Table 1.

Table 1. δ(^{1}H) values of **5**, **7**, **8**, **10**, and **11** from 200 MHz spectra.

5a: ($CDCl_3$) 0.71 and 1.10 (2d, J=7 Hz, 6H; $CH(CH_3)_2$), 1.38 (s, 3H; 2-CH_3), 1.50-2.05 (m, 4H; 2-$(CH_2)_2CH_2Br$), 2.10-2.45 (d sept, J=3 and 7 Hz, 1H; $CH(CH_3)_2$), 3.35 (t, J=6 Hz, 2H; CH_2Br), 3.62 and 3.65 (2s, 6H; 3- and 6-OCH_3), 3.96 (d, J=3 Hz, 1H; 5-H)

5b: ($CDCl_3$) 0.69 and 1.09 (2d, J=7 Hz, 6H; $CH(CH_3)_2$), 1.34 (s, 3H; 2-CH_3), 1.48-2.00 (m, 6H; 2-$(CH_2)_3CH_2Br$), 2.10-2.45 (d sept, J=3 and 7 Hz, 1H; $CH(CH_3)_2$), 3.34 (t, J=6 Hz, 2H; CH_2Br), 3.68 (s, 6H; 3- and 6-OCH_3), 3.97 (d, J=3 Hz, 1H; 5-H)

7a: ($CDCl_3$) 0.97 and 1.15 (2d, J=7 Hz, 6H; $CH(CH_3)_2$), 1.40 (s, 3H; 2-CH_3), 1.75-2.40 (m, 5H; $CH_2CH_2CH_2N$ and $CH(CH_3)_2$), 3.20-3.51 (m, 1H; N−C*H*H), 3.75 (s, 3H; OCH_3), 3.80-4.11 (m, 1H; N−CH*H*), 3.91 (d, J=3 Hz, 1H; 5-H)

7b: ($CDCl_3$) 0.70 and 1.08 (2d, J=7 Hz, 6H; $CH(CH_3)_2$), 1.22-1.84 and 1.96-2.08 (m, 6H; $(CH_2)_3CH_2N$), 1.49 (s, 3H; 2-CH_3), 2.47 (d sept, J=3.5 and 7 Hz, 1H; $CH(CH_3)_2$), 2.70 (ddd, $^2J = {}^3J_{trans} = 13.5$ Hz, $^3J_{gauche} = 3$ Hz, 1H; N−C*H*H), 3.68 (s, 3H; OCH_3), 4.00 (d, J=3.5 Hz, 1H; 5-H), 4.65-4.78 (m, 1H; N−CH*H*)

8: ($CDCl_3$) 0.77 and 1.15 (2d, J=7 Hz, 6H; $CH(CH_3)_2$), 1.45 (s, 3H; 2-CH_3), 2.57 (d sept, J=3 and 7 Hz, 1H; $CH(CH_3)_2$), 3.10 (br., 2H; 2-CH_2), 3.81 (s, 3H; OCH_3), 4.09 (d, J=3 Hz, 1H; 5-H), 4.17 and 5.56 (AB, J=18 Hz, 2H; N−CH_2), 7.05-7.25 (m, 4H; aryl H)

10a: (D_3COD) 1.60 (s, 3H; 2-CH_3), 1.80-2.50 (m; 4H; 3-H and 4-H), 3.25-3.50 (m, 2H; N−CH_2)

10b (D_2O) 1.18-2.18 (m, 6H; $(CH_2)_3CH_2N$), 1.35 (s, 3H; 2-CH_3), 2.95-3.16 (m, 2H; N−CH_2)

11: (D_2O) 1.40 (s, 3H; 3-CH_3), 2.85 and 3.18 (AB, J=16 Hz, 2H; 2-H), 4.12 and 4.37 (AB, J=18 Hz, 2H; N−CH_2), 6.95-7.25 (m, 4H; aryl H)

Received: May 7, 1986;
revised: September 29, 1986 [Z 1765 IE]
Publication delayed at the authors' request
German version: *Angew. Chem. 99* (1987) 137

[1] U. Schöllkopf, U. Busse, R. Hinrichs, R. Lonsky, *Liebigs Ann. Chem. 1987*, in press.
[2] G. C. Barrett, *Amino Acids Pept. Proteins 10* (1979) 11.
[3] D. Seebach, M. Boes, R. Naef, W. B. Schneider, *J. Am. Chem. Soc. 105* (1983) 5390.
[4] Reviews of the bislactim ether method for the asymmetric synthesis of amino acids: U. Schöllkopf in J. Streith, H. Prinzbach, G. Schill (Eds.): *Organic Synthesis: An Interdisciplinary Challenge*, Blackwell, Oxford 1985, p. 101; U. Schöllkopf, *Pure Appl. Chem. 55* (1983) 1799; *Chem. Scripta 25* (1985) 105.
[5] **1** and *ent*-**1** may be obtained from Merck-Schuchardt, Hohenbrunn (FRG).
[6] Synthesis of **1**: U. Schöllkopf, U. Groth, K. O. Westphalen, C. Deng, *Synthesis 1981*, 969.
[7] Workup: The solvent and excess **3/4** were removed under vacuum, the residue was dissolved in ether, and DMEU was removed by washing with water. **5a**: b.p. = 90°C/0.01 torr (cyclization occurs to give **7a**); **5b**: b.p. = 120°C/0.05 torr; **6**: converted into **8** without purification.
[8] Determined by capillary gas chromatography: quartz column, CPSil5CB, 0.22 mm, 50 m, H_2 as carrier gas; Carlo-Erba-Fraktovap. 2300.
[9] Workup: The solvent was removed under vacuum, the residue was dissolved in ether, and the ether phase was washed three times with water. **7b**: Purified by low-pressure chromatography (silica gel, ether, R_F = 0.45); m.p. = 53-55°C; **8**: purified by distillation; b.p. = 170°C/0.05 torr.

[10] (*R*)-**10a**: (*R*)-**9** precipitates from ethanol. **10a** is precipitated from methanol/ether; yield: 81%; m.p. = 330 °C (dec.); $[\alpha]_D^{20} = +75.3$ ($c = 1.0$ g/100 mL, methanol); reported value: $[\alpha]_D^{20} = +77.8$ ($c = 1.0$ g/100 mL, methanol) [11]. (*R*)-**10b** and (*R*)-**11**: The mixture of **9** and **10** or of **9** and **11** is separated by low-pressure chromatography (20 g of silica gel per 1.0 mmol of the mixture. Chloroform/methanol/conc. aqueous ammonia = 30/10/1; R_f values refer to tlc); **10b**: $R_F = 0.12$; yield 74%; $[\alpha]_D^{20} = +7.7$ ($c = 1.0$ g/100 mL, 6 N HCl); m.p. > 330 °C; **11**: $R_f = 0.33$; yield 73%; $[\alpha]_D^{20} = +31.6$ ($c = 1.0$ g/100 mL, 6 N HCl); m.p. = 327 °C (dec.).

[11] C. G. Overberger, Y. S. Yong, *J. Polym. Sci. Polym. Chem. Ed. 15* (1977) 1413.

[12] Correct C,H analyses were obtained for all compounds reported herein.

$[Ag_4(SCH_2C_6H_4CH_2S)_3]^{2-}$, a Novel Polynuclear Silver Thiolate with Trigonal-Planar Coordination of All Silver Atoms and a Central $[Ag_4S_6]$-Cage**

By *Gerald Henkel,* Peter Betz,* and *Bernt Krebs*

Parallel with the increasing interest being shown in transition metal-sulfur chemistry, numerous complexes with thiolate ligands have been synthesized in the past few years. These include, inter alia, the anions **1**–**4**,[1–4] which, because of similar coordinative properties, are formed both by monovalent copper (M = Cu) as well as by monovalent silver (M = Ag).

$[M_5(S\,t\mathrm{Bu})_6]^-$ **1**

$[M_5(SPh)_7]^{2-}$ **2**

$[M\{SC_6H(CH_3)_4\}_2]^-$ **3**

$[AgM_8(SCH_2CH_2S)_6]^{3-}$ **4**

Surprisingly, however, all attempts to isolate a silver thiolate complex containing the $[M_4S_6]$ center that is quite common in copper thiolate chemistry and has been found for example in the compounds **5**–**8**[5–8] have so far been unsuccessful, even though the existence of $[Ag_4(SPh)_6]^{2-}$ has already been speculated upon in the literature.[9]

$[Cu_4(SCH_3)_6]^{2-}$ **5**

$[Cu_4(SPh)_6]^{2-}$ **6**

$[Cu_4(SCH_2CH_2S)_3]^{2-}$ **7**

$[Cu_4(SCH_2C_6H_4CH_2S)_3]^{2-}$ **8**

We now report on the synthesis and structure of the anion **9**, the first compound with a tetrahedro-Ag_4-octahedro-$(\mu\text{-}S)_6$ cage; with tetraphenylphosphonium bromide in methanolic solution, **9** forms pale yellow prisms of the salt **10**.

$[Ag_4(SCH_2C_6H_4CH_2S)_3]^{2-}$ **9**

$[Ph_4P]_2[Ag_4(SCH_2C_6H_4CH_2S)_3]\cdot 6\,MeOH$ **10**

[*] Priv.-Doz. Dr. G. Henkel, Dr. P. Betz, Prof. Dr. B. Krebs
Anorganisch-chemisches Institut der Universität
Corrensstrasse 36, D-4400 Münster (FRG)

[**] This work was supported by the Bundesminister für Forschung und Technologie, by the Minister für Wissenschaft und Forschung des Landes Nordrhein-Westfalen, and by the Fonds der Chemischen Industrie.

The tetranuclear cluster **9** is, moreover, the only silver thiolate complex known so far in which all silver atoms are surrounded by a trigonal planar array of sulfur atoms. It is formed upon reaction of 10 mmol of $AgNO_3$ with 10 mmol of $Na_2(SCH_2C_6H_4CH_2S)$ in 100 mL of methanol. According to the results of an X-ray structure analysis (Fig. 1),[10] crystals of **10** contain, besides Ph_4P^+ ions and discrete cluster anions **9**, also ordered and disordered methanol molecules in the ratio 2:1, which are not bound to metal atoms and presumably contribute to the stability of the crystal lattice.

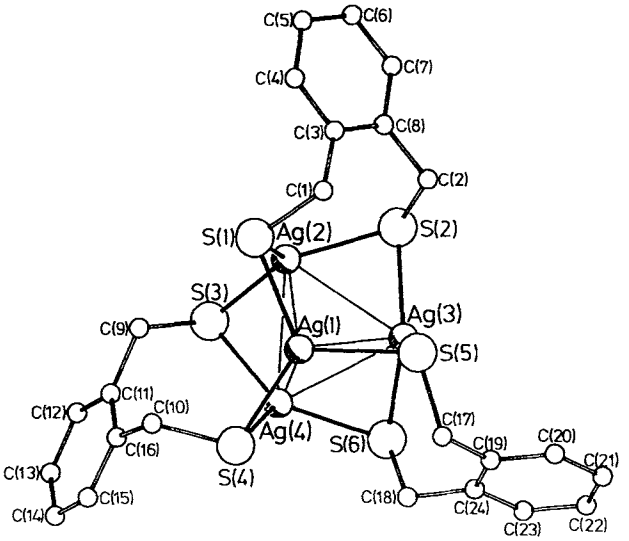

Fig. 1. Structure of the dianion **9** in crystals of **10** (without hydrogen atoms). Bond length ranges [Å]: Ag···Ag 2.998(1) to 3.085(1) (mean value 3.044), Ag-S 2.449(1) to 2.588(1) (mean value 2.505), S-C 1.835(5) to 1.844(5) (mean value 1.840). Angle ranges [°]: Ag-S-Ag 73.56(3) to 76.45(4) (mean value 74.82), S-Ag-S 112.26(4) to 132.88(4) (mean value 119.84), Ag-S-C 100.1(2) to 109.4(2) (mean value 104.8).

All six sulfur atoms of the *o*-xylene-α,α′-dithiolate ligands bridge two silver atoms each with Ag-S-Ag bridge angles in the range of 73.56(3) to 76.45(4)° (example: S(1) bridges Ag(1) and Ag(2)); the silver has a distorted trigonal-planar sulfur coordination. Ag(2), Ag(3), and Ag(4) are each chelated by one ligand (example: Ag(2) is chelated by S(1) and S(2)), while Ag(1) is surrounded by three sulfur atoms of three ligands.

The central $[Ag_4S_6]$ unit of **9** is in its idealized form an octahedron whose vertices are formed by sulfur atoms; half of its faces are occupied by silver atoms, constructed as shown schematically in Figure 2.

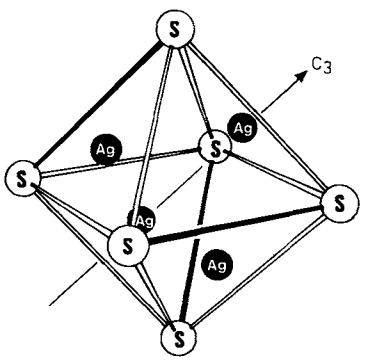

Fig. 2. The $[Ag_4S_6]$ cage as idealized center of **9** with edges of the octahedron (without silver-sulfur bonds). Sulfur atoms that belong to the same ligand are those connected by bold-face edges.

Thereby, the resulting silver tetrahedron and the sulfur octahedron have a common centroid. Although the anion **9** is chiral because the six sulfur atoms are functional groups of bidentate ligands, both enantiomers occur with equal abundance in the centrosymmetric crystals of **10** (cf. Ref. [10]). In Figure 2 the sulfur atoms which belong to the same ligands are connected by filled edges of the octahedron.

In its idealized form **9** has C_3 symmetry, whereby the threefold axis passes through Ag(1) and the center of the Ag(2)-Ag(3)-Ag(4) triangle. The mean S-Ag-S valence angle is 119.84° and thus indicates that the AgS_3-coordination centers are not completely planar. The S-Ag-S chelate angles, with an average value of 112.62°, are very small. Compared to the corresponding copper compound,[8] the larger metal-sulfur bond lengths lead to a diminution of the angle in the chelate ring of about 5°. In addition to the small angle in the chelate ring, the atoms Ag(2), Ag(3), and Ag(4) are each characterized by a somewhat larger (example: S(1)-Ag(2)-S(3); mean value 115.20°) and a very much wider valence angle (example: S(2)-Ag(2)-S(3); mean value 131.58°). Moreover, there are two shorter (mean value 2.468 Å) and one somewhat longer Ag-S bond (mean value 2.572 Å) around each of the atoms Ag(2), Ag(3), and Ag(4). Interestingly, there are differences in the bond lengths within the S-Ag-S chelate fragments, the longer bonds being formed to the sulfur atoms that are also bound to Ag(1) (example: Ag(2)-S(1)). Compared to this, valence angles of 113.30(4), 122.77(4), and 123.78(4)° and Ag-S bond lengths of 2.475(1), 2.521(1), and 2.532(1) Å are observed at Ag(1). Thus, the distortion of the real molecule is clearly documented, since C_3 symmetry requires equal valence angles and equal bond lengths.

Received: September 5, 1986 [Z 1921 IE]
German version: *Angew. Chem. 99* (1987) 131

[1] G. A. Bowmaker, G. R. Clark, J. K. Seadon, I. G. Dance, *Polyhedron 3* (1984) 535.
[2] I. G. Dance, *Aust. J. Chem. 31* (1978) 2195.
[3] S. A. Koch, R. Fikar, M. Millar, T. O'Sullivan, *Inorg. Chem. 23* (1984) 121.
[4] G. Henkel, P. Betz, B. Krebs, *Proc. Int. Conf. Coord. Chem. 24* (1986) 737 (Chimika Chronika New Series, Special Issue, August 1986).
[5] I. G. Dance, G. A. Bowmaker, G. R. Clark, J. K. Seadon, *Polyhedron 2* (1983) 1031.
[6] a) I. G. Dance, J. C. Calabrese, *Inorg. Chim. Acta 19* (1976) L41; b) D. Coucouvanis, C. N. Murphy, S. K. Kanodia, *Inorg. Chem. 19* (1980) 2993.
[7] G. Henkel, K. H. Saatkamp, P. Betz, B. Krebs, unpublished.
[8] a) J. R. Nicholson, I. L. Abrahams, W. Clegg, C. D. Garner, *Inorg. Chem. 24* (1985) 1092; b) P. Betz, Dissertation, Universität Münster 1986.
[9] I. G. Dance, *Inorg. Chem. 20* (1981) 1487.
[10] Crystal data: Syntex $P2_1$ four-circle diffractometer, $Mo_{K\alpha}$ radiation, graphite monochromator, scintillation counter, $2\theta-\theta$ scan, $T = 150$ K, empirical absorption correction. **10** is triclinic, $a = 13.959(3)$, $b = 14.272(3)$, $c = 22.868(5)$ Å, $\alpha = 76.10(2)$, $\beta = 87.68(2)$, $\gamma = 60.96(2)$°, space group $P\bar{1}$, $Z = 2$, $\rho_{calc} = 1.56$ g cm^{-3}, $\mu(Mo_{K\alpha}) = 12.3$ cm^{-1}, crystal size $0.28 \times 0.18 \times 0.17$ mm^3, $2\theta_{max} = 48$°, 11996 independent reflections, $R(R_w) = 0.034$ (0.048) for 10845 reflections with $F_0 > 3.92\sigma(F_0)$, 825 variables (hydrogen atoms at idealized positions with isotropic temperature factors [$B(H) = 4$ Å^2], all other atoms refined with anisotropic (anions and cations) and isotropic (methanol molecules) temperature factors, respectively; one scaling factor). Further details of the crystal structure investigation are available on request from the Fachinformationszentrum Energie, Physik, Mathematik GmbH, D-7514 Eggenstein-Leopoldshafen 2 (FRG), on quoting the depository number CSD-52209, the names of the authors, and the full citation of the journal.

Unusual Photoisomerization of a Cyclic Sulfonamide**

By *Dietrich Döpp,* Carl Krüger,* Peter Lauterfeld,* and *Eleonore Raabe**

Dedicated to Professor Howard E. Zimmerman on the occasion of his 60th birthday

The light-induced cleavage of the R-S, S-N, and N-R′ bonds in open-chain sulfonamides $R-SO_2-NH-R'$ has already been well documented and it has been demonstrated that the resulting fragments undergo radical-type reactions.[1] We have now found that 3,3-dimethyl-2,3-dihydro-1,2-benzothiazole 1,1-dioxide **1a** (readily accessible in two steps from saccharin[2]) is rapidly and completely converted into its isomer 2-hydroxy-3,3-dimethyl-2,3-dihydro-1,2-benzothiazole 1-oxide **2a** upon irradiation in methanol with the quartz-glass filtered light of a low-pressure mercury vapor lamp ($\lambda = 254$ nm).[3] Crystalline **2a** can be stored for long periods; in solution, however, it notably isomerizes back to **1a** (especially under influence of acid).

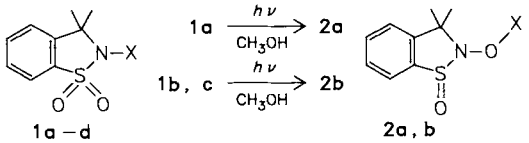

a, X = H; **b**, X = CH_2OCH_3
c, X = $CH_2OCH(CH_3)_2$; **d**, X = CH_3

The crystal structure analysis[4] of **2a** (Fig. 1) clearly shows the distorted and folded five-membered ring with trigonal-pyramidal N and S atoms. The hydroxyl H atom (H2) is bound by an almost linear intermolecular hydrogen bridge to the sulfoxide O atom (O1′) of a neighboring molecule (Fig. 2).

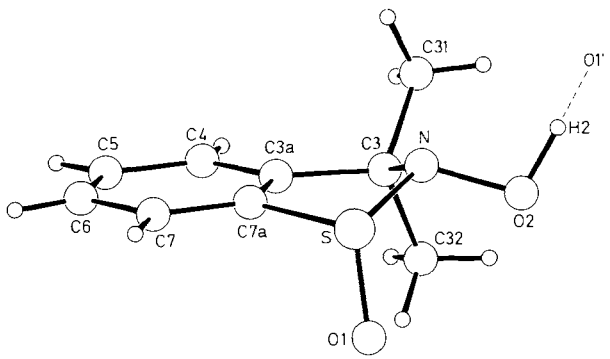

Fig. 1. Crystal structure of **2a**. Important bond lengths [Å] and angles [°]: S-N 1.695(1), N-C3 1.499(2), C3-C3a 1.504(2), C3a-C7a 1.386(2), C7a-S 1.786(2), S-O1 1.492(1), N-O2 1.418(2), O2-H2 1.03(3), H2···O1′ 1.68(3); C7a-S-N 86.9(1), S-N-C3 115.5(1), N-C3-C3a 100.7(1), C3-C3a-C7a 114.4(1), C3a-C7a-S 112.3(1), C7a-S-O1 106.7(1), O1-S-N 113.5(1), S-N-O2 109.0(1), O2-N-C3 113.4(1), C31-C3-C32 111.4(2).

[*] Prof. Dr. D. Döpp, Dipl.-Chem. P. Lauterfeld
Fachgebiet Organische Chemie der Universität-Gesamthochschule
Lotharstr. 1-21, D-4100 Duisburg 1 (FRG)
Prof. Dr. C. Krüger, Dr. E. Raabe
Max-Planck-Institut für Kohlenforschung
Kaiser-Wilhelm-Platz 1, D-4330 Mülheim (FRG)

[**] We thank Prof. *R. S. Givens* (Lawrence, KS) and Prof. *J. P. Pete* (Reims) for stimulating discussions. This work was supported by the Fonds der Chemischen Industrie.

2a is to our knowledge the first example of a sulfinohydroxamic acid.[5] A color formation with iron(III) ions, as found in the case of the hydroxamic acids, is not observed. Reduction of **2a** with potassium iodide solution 0.2 N in hydrochloric acid afforded about equal amounts of the expected 3,3-dimethyl-2,3-dihydro-1,2-benzothiazole 1-oxide and **1a**.[3] Upon gas-phase pyrolysis (600 °C, 10^{-3} torr) **2a** is rearranged into **1a**, which is stable at this temperature.[3]

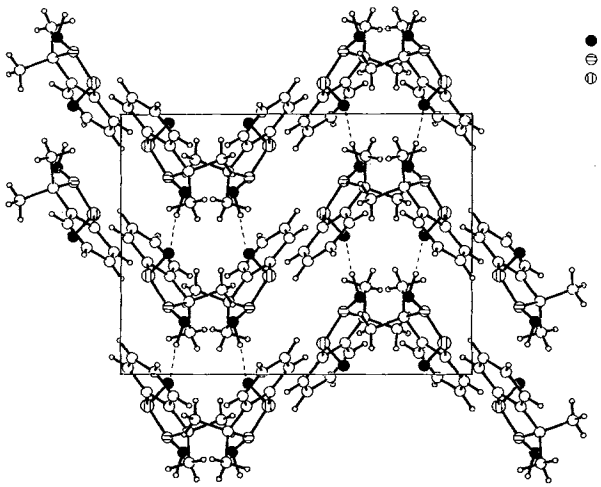

Fig. 2. Packing of racemic **2a** in the crystal.

Under the same conditions, the dihydrobenzothiazoles **1b**, **c** are converted into **2b**; in the case of **1c** this additionally implies replacement of the isopropoxy group by a methoxy group. Thus, in the course of the isomerization, not only an H atom but also a group with a sufficiently electrophilic C atom can be transferred from the N atom to the O2 atom. 2,3,3-Trimethyl-2,3-dihydro-1,2-benzothiazole 1,1-dioxide **1d**, on the other hand, is photolyzed only slowly and gives a complex product mixture.

We are at present directing our efforts towards clarification of the course of both the photochemical forward (**1** → **2**) and the thermal or acid-catalyzed reverse reaction (**2** → **1**). It is highly unlikely that either of the reactions does not involve intermediates. Our working hypothesis is that the photoisomerization of **1a**, **b** is initiated by a cleavage of the S-N bond, and that **3** is then transformed via the conceivable intermediates **4** and **5** into **2a**, **b**.

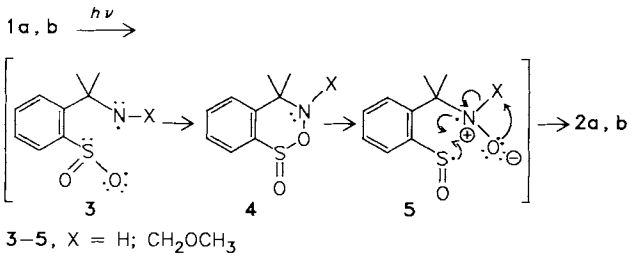

Experimental

2a: A solution of **1a** (1.00 g, 5.08 mmol) in anhydrous methanol (140 mL) was irradiated with a Hanau-TNN-15 lamp (15 W) through a water-cooled immersion well for 2.5 h with N_2-purging. The oily residue obtained upon concentration immediately crystallized and, after washing with acetone furnished 710 mg (71%) of colorless crystals, m.p. 112 °C.

Received: September 15, 1986;
supplemented: November 11, 1986 [Z 1928 IE]
German version: *Angew. Chem. 99* (1987) 142

[1] H. Dürr in *Houben-Weyl-Müller: Methoden der Organischen Chemie, Vol. IV/5b*, 4th edit., Thieme, Stuttgart 1975, especially pp. 1047–1049, and references cited therein; F. Golpasphin, B. Weiss, H. Dürr, *Arch. Pharm. (Weinheim Ger.) 317* (1984) 906; see also M. Z. A. Badr, M. M. Aly, A. M. Fahmy, *J. Org. Chem. 46* (1981) 4784; J. A. Pincock, A. Jürgens, *Tetrahedron Lett. 1979*, 1029.

[2] A. Mustafa, M. K. Hilmy, *J. Chem. Soc. 1952*, 1339.

[3] All the compounds gave correct elemental analyses; the spectroscopic data are in full agreement with the proposed structures.

[4] Crystal structure analysis of **2a**: space group *Pbcn* (No. 60), $a = 14.801(1)$, $b = 12.035(1)$, $c = 11.048(2)$ Å, $V = 1968$ Å^3, $Z = 8$, $\rho_{calc} = 1.33$ g cm^{-3}, $\mu(Mo_{K\alpha}) = 2.82$ cm^{-1}. Structure solution by direct methods (SHELX 84) from 2010 reflections with $I \geq 2\sigma(I)$; $R = 0.035$, $R_w = 0.043$. Further details of the crystal structure analysis are available on request from the Fachinformationszentrum Energie, Physik, Mathematik GmbH, D-7514 Eggenstein-Leopoldshafen 2 (FRG), on quoting the depository number CSD-52094, the names of the authors, and the journal citation.

[5] In earlier attempts to synthesize sulfinohydroxamic acids from sulfinates and hydroxylamine, only sulfonamides were formed: H. Metzger in *Houben-Weyl-Müller: Methoden der Organischen Chemie, Band X/4*, Thieme, Stuttgart 1968, especially p. 217 and references cited therein. Even a computer-controlled substructure search in the CA Registry File gave no positive result.

Azulene as Unusual η^6-Ligand and as η^6:η^4-Bridge in Mo-Complexes**

By *Susanne Töfke* and *Ulrich Behrens**

Investigations of the structure of transition metal-azulene complexes show a preferred coordination of the metal atom to the five-membered ring with formation of a π-cyclopentadienyl system. In addition, there is a tendency for dinuclear complexes to be formed.[1, 2]

We have now found a novel type of η^6-coordination of azulene, namely in the mononuclear complex $[(C_{10}H_8)(C_6H_6)Mo]$ **1** (Fig. 1).[3]

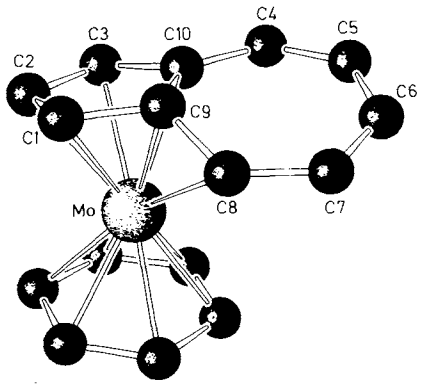

Fig. 1. Crystal structure of **1** [3]. Selected bond lengths [Å]: Mo-center of five-membered ring 1.898(1), Mo-center of benzene ring 1.758(1), Mo-C1 2.231(6), Mo-C2 2.342(6), Mo-C3 2.346(5), Mo-C9 2.125(5), Mo-C10 2.257(5), Mo-C8 2.447(6), C1-C2 1.380(9), C2-C3 1.405(8), C3-C10 1.416(7), C10-C4 1.442(7), C4-C5 1.349(8), C5-C6 1.410(9), C6-C7 1.342(9), C7-C8 1.457(10), C8-C9 1.422(8), C9-C10 1.454(7), C1-C9 1.443(8).

[*] Prof. Dr. U. Behrens, Dr. S. Töfke
Institut für Anorganische und Angewandte Chemie der Universität
Martin-Luther-King-Platz 6, D-2000 Hamburg 13 (FRG)

[**] Transition Metal-Fulvene Complexes, Part 30. This work was supported by the Deutsche Forschungsgemeinschaft and the Fonds der Chemischen Industrie. Part 29: F. Edelmann, O. Koch, U. Behrens, *J. Organomet. Chem. 311* (1986) 111.

The azulene molecule is coordinated via the fulvene system formally contained in it to the [(benzene)Mo] fragment. Similarly as in η^6-coordinated mononuclear fulvene complexes,[4] the "exocyclic" double bond is markedly bent (33°) with respect to the five-membered ring. The bonds in the azulene ligand have very different lengths; they approximate to a system of alternating double and single bonds. In non-coordinated azulene[5] and in the η^5-bonded mononuclear [(azulene)$Cr(CO)_3$] complexes,[2] on the other hand, no bond length alternance occurs. Other than in the case of **1**, the azulene ligand is planar in such complexes.

Metal-ligand fragments of the type $M(CO)_3$ (M = Cr, Mo, W) can add to **1** with formation of dinuclear complexes **2**. Surprisingly, the azulene in them is $\eta^6:\eta^4$ coordinated – a hitherto unknown form of coordination for azulene.[6] In contrast, in the case of the dinuclear complexes of the type [(μ-azulene)$M_2(CO)_6$] (M = Cr, Mo), which are isoelectronic with **2**, the metal atoms are $\eta^5:\eta^5$-coordinated.[7]

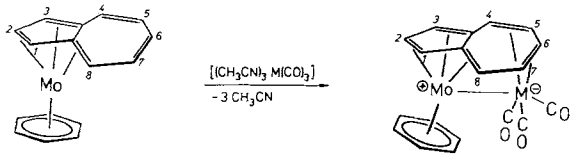

1 **2**

a, M = Cr; **b**, M = Mo; **c**, M = W

All azulene complexes have fluxional behavior in solution: The coordination of the C-atoms 4 and 8 interchanges rapidly. As a consequence, only five signals are observed for the eight azulene protons in the ^{1}H-NMR spectra.[8] The same holds true for the ^{13}C-NMR spectra.[8] In all complexes the region of slow exchange is not reached on cooling to 193 K.

Experimental

All operations were carried out under N_2.

1: A suspension of dibenzenemolybdenum (1.64 g, 6.5 mmol) and azulene (0.92 g, 7.2 mmol) in toluene (60 mL) was stirred for 5 d at 95°C. The blue solution slowly turned reddish violet. The solution was filtered off and evaporated to dryness. Excess azulene was removed by washing with 10 mL of cold pentane and the residue was recrystallized from toluene/hexane. On cooling to −78°C reddish-violet crystals were formed. Yield 1.22 g (62%); m.p. 250°C (dec.); correct elemental analysis.

2: A solution of **1** (310 mg, 1.0 mmol) and [$(CH_3CN)_3M(CO)_3$] (M = Cr, Mo, W) in THF (30 mL) was boiled under reflux for 5 h. The mixture was then filtered and the filtrate evaporated to dryness. The red residue was dissolved in CH_2Cl_2, covered with the same volume of hexane, and stored at −30°C. After a few days the complexes **2** crystallized out. Yields, m.p. (dec.). $\tilde{\nu}$(CO) in CH_2Cl_2: **2a**: 220 mg (50%) of dark red needles; 210°C; 1921, 1853, 1820 cm^{-1}.—**2b**: 410 mg (85%) of dark brown crystals; 185°C; 1935, 1859, 1824 cm^{-1}.—**2c**: 100 mg (18%) of a red crystalline powder: 175°C; 1931, 1853, 1815 cm^{-1}.

Received: September 25, 1986;
supplemented: October 31, 1986 [Z 1936 IE]
German version: *Angew. Chem. 99* (1987) 134

[1] M. R. Churchill, *Prog. Inorg. Chem. 11* (1970) 54; M. R. Churchill, R. A. Lashewycz, F. J. Rotella, *Inorg. Chem. 16* (1977) 265, and references cited therein; O. M. Valderrama, P. Cifuentes, C. Foces-Foces, F. H. Cano, *J. Organomet. Chem. 276* (1984) 67.

[2] O. Koch, F. Edelmann, U. Behrens, *J. Organomet. Chem. 168* (1979) 167; F. Edelmann, U. Behrens, *ibid. 232* (1982) C24.

[3] Syntex-AED, $Mo_{K\alpha}$: orthorhombic *Pbca*, $Z = 8$, $a = 7.913(2)$, $b = 13.319(6)$, $c = 22.928(6)$ Å, $V = 2416(1)$ Å, $5 < 2\theta < 60°$, 3550 independent reflections, 1962 observed with $F > 4\sigma(F)$, $R = 0.048$, $R_w = 0.046$. Further details of the crystal structure investigation are available on request from the Fachinformationszentrum Energie, Physik, Mathematik GmbH, D-7514 Eggenstein-Leopoldshafen 2 (FRG), on quoting the depository number CSD-52157, the names of the authors, and the full citation of the journal.

[4] J. A. Bandy, V. S. B. Mtetwa, K. Prout, J. C. Green, C. E. Davies, M. L. H. Green, N. J. Hazel, A. Izquierdo, J. J. Martin-Polo, *J. Chem. Soc. Dalton Trans. 1985*, 2037; F. Edelmann, S. Töfke, U. Behrens, *J. Organomet. Chem. 309* (1986) 87, and references cited therein.

[5] H. N. C. Wong, K. P. So, T. C. W. Mak, *Z. Kristallogr. 169* (1984) 117.

[6] An X-ray structure analysis was carried out on **2a**: length of Mo–Cr bond 3.178(1) Å.

[7] M. R. Churchill, P. H. Bird, *Inorg. Chem. 7* (1968) 1545; F. Edelmann, S. Töfke, U. Behrens, *J. Organomet. Chem. 308* (1986) 27.

[8] ^{1}H-NMR data (360 MHz, 20°C): **1** ($CDCl_3$): $\delta = 4.26$ (s; C_6H_6), 4.88 (d, $J = 2.8$ Hz; H 1/3), 5.56 (t, $J = 2.8$ Hz; H2), 5.69 (d, $J = 9.3$ Hz; H4/8), 6.15 (t, $J = 9.3$ Hz; H5/7), 5.70 (t, $J = 9.3$ Hz; H6).—**2a** (CD_2Cl_2): $\delta = 5.36$ (s; C_6H_6), 4.31 (d, $J = 2.9$ Hz; H1/3), 5.30 (t, $J = 2.9$ Hz; H2), 3.65 (d, $J = 7.6$ Hz; H4/8), 4.63–4.76 (m; H5/6/7).—**2b** (CD_2Cl_2): $\delta = 5.36$ (s; C_6H_6), 4.31 (d, $J = 3.1$ Hz; H1/3), 5.23 (t, $J = 3.1$ Hz; H2), 3.75 (d, $J = 7.5$ Hz; H4/8), 4.66 (t, $J = 7.5$ Hz; H5/7), 4.88 (t, $J = 7.5$ Hz; H6).—**2c** (CD_2Cl_2): 5.38 (s; C_6H_6), 4.34 (d, $J = 3.1$ Hz; H1/3), 5.21 (t, $J = 3.1$ Hz; H2), 3.76 (d, $J = 7.6$ Hz; H4/8), 4.59 (t, $J = 7.6$ Hz; H5/7), 4.82 (t, $J = 7.6$ Hz; H6).—^{13}C{^{1}H}-NMR data (20.15 MHz, 25°C): **1** (C_6D_6): $\delta = 74.4$ (C_6H_6), 84.3 (C1/3), 90.5 (C2), 101.2 (C4/8), 124.8 (C5/7), 118.6 (C6), 96.5 (C9/10).—**2b** ($CDCl_3$): 227.6 (CO), 81.3 (C_6H_6), 62.7 (C1/3), 85.9 (C2), 79.9 (C4/8), 73.8 (C5/7), 87.4 (C6), 87.8 (C9/10).

Novel Ni-Clusters with Se and PR_3 (R = Ph, Et) as Ligands**

By *Dieter Fenske** and *Johannes Ohmer*

Dedicated to Professor Gerhard Quinkert on the occasion of his 60th birthday

Reaction of [$MCl_2(PPh_3)_2$] (M = Co, Ni) with $E(SiMe_3)_2$ (E = S, Se) in tetrahydrofuran (THF) or toluene leads to the formation of metal-rich clusters.[1] So far we have been able to characterize the following compounds:[2]

$[Co_4E_4(PPh_3)_4]$ $[Co_6E_8(PPh_3)_6]$ $[Co_7S_6(PPh_3)_5Cl_2]$ $[Co_9Se_{11}(PPh_3)_6]$

$[Ni_8S_6Cl_2(PPh_3)_6]$ $[Ni_8S_5(PPh_3)_7]$ $[Ni_{34}Se_{22}(PPh_3)_{10}]$

The structures of the complexes are apparently dependent upon the ratio $MCl_2:PPh_3:E(SiMe_3)_2$ and on the solvent used. For this reason we have now examined the reaction of $Se(SiMe_3)_2$ with [$NiCl_2(PR_3)_2$] (R = Ph, Et) and $(NBu_4)[NiCl_3(PPh_3)]$ in MeCN or toluene. Within a few minutes a crystalline, black precipitate is formed which consists of Ph_3PSe and several cluster compounds. In the case of the complexes with PPh_3 ligands, only a small fraction of the residue can be dissolved upon extraction with solvents such as THF, toluene, $C_2H_4Cl_2$ and CH_2Cl_2. If these solutions are covered with a layer of hexane, **1**–**3** are obtained in crystalline form. The yields are small (10–20%). From the elemental analyses of the insoluble residues it

$[Ni_6Se_5(PPh_3)_6]$ **1** $[Ni_{12}Se_{11}(PPh_3)_8Cl][NiCl_3(PPh_3)]_2$ **2**

$[Ni_{15}Se_{15}(PPh_3)_6]$ **3** $[Ni_{12}Se_{12}(PEt_3)_6]$ **4**

[*] Prof. Dr. D. Fenske, Dipl.-Chem. J. Ohmer
Institut für Anorganische Chemie der Universität
Niederurseler Hang, D-6000 Frankfurt/Main 50 (FRG)

[**] This work was supported by the Deutsche Forschungsgemeinschaft and the Fonds der Chemischen Industrie. We thank the Institut für Kristallographie der Universität Karlsruhe for help with the measurements of the crystal structure data.

follows that they also consist of metal-rich clusters; their structures, however, are as yet unknown.

In contrast only a small amount of insoluble residue is obtained upon reaction of $[NiCl_2(PEt_3)_2]$ with $Se(SiMe_3)_2$ in toluene. When the filtrate is covered with a layer of hexane, black **4** crystallizes. **1**, **3**, and **4** are diamagnetic, whereas **2** is paramagnetic. All four complexes are practically insoluble in organic solvents; consequently, a characterization of the complexes by means of NMR spectroscopy is very difficult. The IR spectra of **1**–**4** are very similar, they differ only below $\tilde{\nu}=750\ cm^{-1}$.

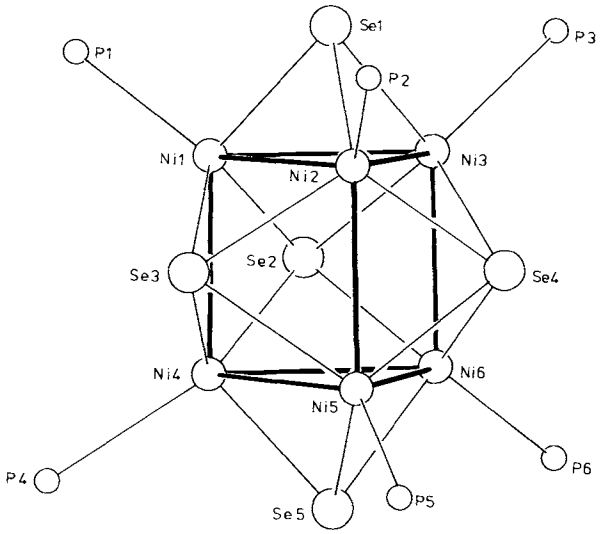

Fig. 1. Crystal structure of **1** (without phenyl groups) [3]. Important bond lengths [pm] (±0.3 pm) and angles [°] (±0.1°). Ni1-Ni3 273.0, Ni1-Ni2 277.4, Ni2-Ni3 276.8, Ni4-Ni5 273.0, Ni5-Ni6 275.2, Ni4-Ni6 279.8, Ni1-Ni4 260.6, Ni2-Ni5 263.3, Ni3-Ni6 266.3, Ni-P 217.9-219.4, (μ_3-Se)-Ni 226.4-227.2, (μ_4-Se)-Ni 237.2-241.9; Ni-Ni-Ni 59.0-61.4 (in the Ni_3-faces), 89.2-91.9 (in the Ni_4-faces), Ni-(μ_3-Se)-Ni 74.0-76.2, Ni-(μ_4-Se)-Ni 66-71.6 and 104.7-106.3.

Crystal structure analyses of **1**–**4**[3] revealed the following: **1** (Fig. 1) contains a trigonal-prismatic Ni_6 cluster in which each Ni atom is coordinated in a distorted tetrahedral fashion to three Se atoms and to the P atom of a PPh_3 ligand. The lengths of the (μ_3-Se)-Ni and (μ_4-Se)-Ni bonds are different. In the Ni_6 cluster the Ni-Ni bonds within the triangular faces (Ni1-Ni3 and Ni4-Ni6) are significantly longer than the distances between these faces. A cluster of similar structure is present in the $[Pt_3(CO)_3(\mu_2\text{-}CO)_3]_2^{2\ominus}$ ion.[4] However, in this instance the bonds in the Pt_3 faces (266 pm) are shorter than the distances between these faces (304 pm). The 92e-cluster **1** contains two electrons more than one would expect according to the 18-electron rule and the topological electron counting rules.[5]

Although octahedral Ni_6 clusters, e.g. $[Ni_3(CO)_3(\mu_2\text{-}CO)_3]_2^{2\ominus}$, are well known,[6] we have so far been unable to isolate any compounds of this structure type. The structures of **2**–**5**, however, show that the synthesis of face-to-face linked Ni_6 octahedra is possible. Figure 2 shows the structure of the $[Ni_{12}Se_{11}(PPh_3)_8Cl]^{2\oplus}$ ion (cation of **2**) which formally consists of bound Ni_9Se_9- (Ni1-Ni9,Se1-Se9) and Ni_3Se_2-clusters (Ni10-Ni12, Se10, Se11). These fragments have already been found in $[Ni_9S_9(PEt_3)_6]^{2\oplus}$ **5**, $[Ni_3Se_2(PEt_3)_6]^{2\oplus}$ **6**, and $[Ni_3S_2Cp_3]$ ($Cp=\eta^5\text{-}C_5H_5$).[7] In the dioctahedron of **2** there are three planes (●, ◍, ◎), each of which is formed from three Ni(Δ) atoms and three Se atoms. Within these layers the Ni-Ni bonds are longer than the corresponding distances between the layers.

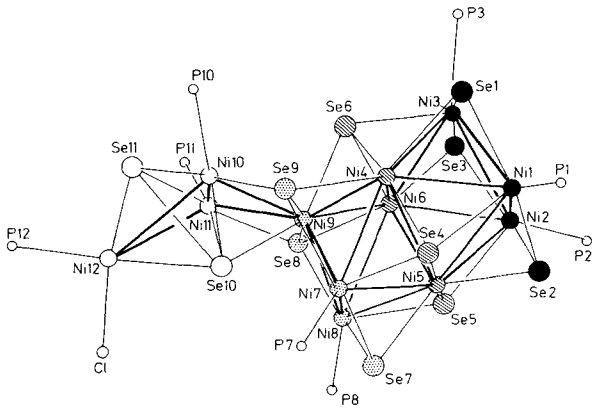

Fig. 2. Structure of the cation **2** in the crystal (without phenyl groups) [3]. Important bond lengths [pm] (±0.4 pm) within the polyhedral faces of 3 Ni atoms (Δ): Δ[Ni1-Ni2-Ni3] 296–299, Δ[Ni4-Ni5-Ni6] 289-308, Δ[Ni7-Ni8-Ni9] 268-313, Δ[Ni5-Ni7-Ni8] 273-313, Δ[Ni4-Ni6-Ni9] 253-308, Δ[Ni3-Ni4-Ni6] 279-308, Δ[Ni1-Ni2-Ni5] 276-296, Δ[Ni9-Ni10-Ni11] 261-283, Δ[Ni10-Ni11-Ni12] 283-311, and between the Ni_3 planes: Ni1-Ni4 266, Ni2-Ni6 277, Ni4-Ni7 289, Ni6-Ni8 289; (μ_3-Se)-Ni 225-232, (μ_4-Se)-Ni 229-246, Ni-P 217-220, Ni12-Cl 220; and bond angles [°] (±0.2°): Ni-(μ_3-Se)-Ni 71-82, Ni-(μ_4-Se)-Ni 66-72 and 120-135.

The polyhedral surfaces of the dioctahedron in **2**, like those in **5**, are capped by μ_3-Se- (Se1-Se3, Se7) and μ_4-Se-ligands (Se4-Se6). Se8 and Se9 are bound to three Ni atoms of the dioctahedron (Ni-Se: 233-245 pm) and at the same time act as bridges to Ni10 and Ni11, respectively (Ni-Se: 230-233 pm). The Ni-Ni bonds from Ni9 are relatively short, while those within the Ni10-Ni12 cluster are rather long (283-311 pm). This points to weak interactions between the atoms Ni10-Ni12, which are bound to a μ_3-Se- (Se11) and a μ_4-Se-ligand (Se10, Ni-Se: 229-232 pm). The distance between Se10 and Se11 is very short (311 pm) and thus compares with the corresponding distance in **6**. With exception of Ni4-Ni6 and Ni9 all the Ni atoms are bound to the P atom of a PPh_3 ligand. Ni12 is additionally coordinated to a $Cl^{\ominus}$ ligand. This Ni-Cl bond is the reactive site of the molecule, at which the clusters can grow by reaction with $Se(SiMe_3)_2$ and $NiCl_2$. On the basis of the topology of the Ni and Se atoms, **2** could be regarded as an intermediate en route to higher condensed clusters with *trans*-face-coupled octahedra.

Comparable structures occur in molybdenum-rich chalcogenides. Here, compounds could be isolated which are formed by "condensation" of M_6E_8 units (E = S, Se)[8] and, e.g., contain $[Mo_{12}Se_{14}]^{2\ominus}$, $[Mo_{18}Se_{20}]^{4\ominus}$, $[Mo_{24}Se_{26}]^{6\ominus}$, and $[Mo_{30}Se_{32}]^{8\ominus}$ clusters.[9] The molecular structures of **3** (Fig. 3) and **4** (Fig. 4) clearly indicate that such cluster structures can also be formed in the case of nickel. **3** and **4** respectively consist of four and five coupled, slightly distorted Ni_6 octahedra.

In contrast to the Chevrel phases and to $[(Co_9Se_{11}(PPh_3)_6]$ the basal faces (**3**: Ni1-Ni3, Ni13-Ni15; **4**: Ni1-Ni3) are not occupied by Se ligands. All other polyhedral faces are capped by μ_3-Se- (**3**: Se1-Se3, Se13-Se15, Ni-Se: 226-231; **4**: Se1-Se3, Ni-Se 227-234 pm) or μ_4-Se-ligands (**3**: Se4-Se12, Ni-Se: 231-249, **4**: Se4-Se6, Ni-Se: 232-244 pm). Most remarkable in **4** is that the distance of the μ_4-Se-ligands to N1, Ni2, Ni3, with a value of 244-246 pm, is ca. 12 pm greater than that to the other Ni atoms. A similar behavior is also found in **3** with the Se-ligands Se4-Se6 and Se10-Se12. In contrast, the (μ_4-Se)-

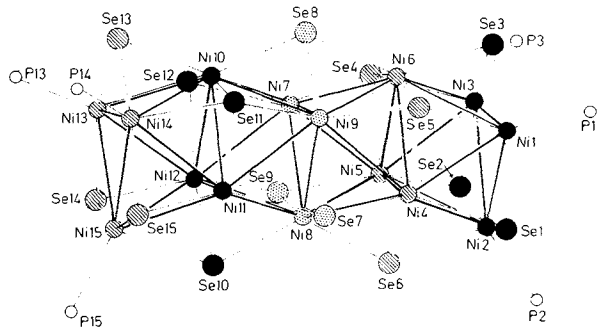

Fig. 3. Crystal structure of **3** (without phenyl groups) [3]. Important bond lengths [pm] (±0.6 pm) within the polyhedral faces of 3 Ni atoms: Δ[Ni1-Ni3] 296–301, Δ[Ni4-Ni6] 288–291, Δ[Ni7-Ni9] 282–291, Δ[Ni10-Ni12] 288–290, Δ[Ni13-Ni15] 295–302, and between the Ni_3 faces: Δ[Ni1-Ni3]-Δ[Ni4-Ni6] 275–288, Δ[Ni4-Ni6]-Δ[Ni7-Ni9] 270–275, Δ[Ni7-Ni9]-Δ[Ni10-Ni12] 271–277, Δ[Ni10-Ni12]-Δ[Ni13-Ni15] 270–278; (μ_3-Se)-Ni 226–231, (μ_4-Se)-Ni 231–249, Ni-P 218–221; and bond angles [°] (±0.2°): Ni-(μ_3-Se)-Ni 70.6–83.3, Ni-(μ_4-Se)-Ni 66.8–78.0 and 130.5–133.5.

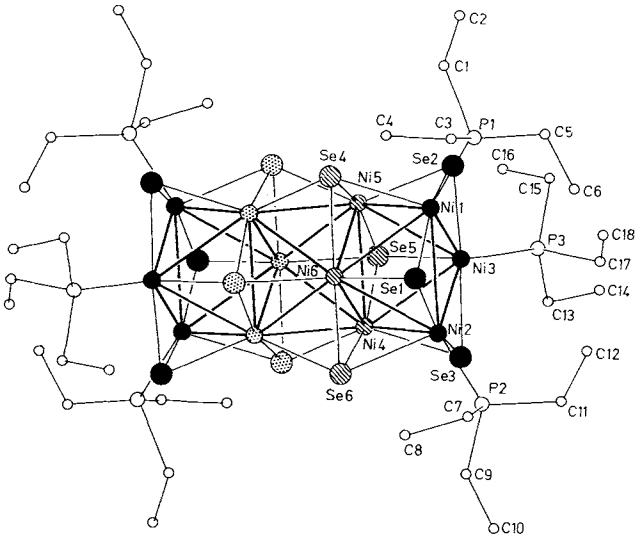

Fig. 4. Crystal structure of **4** (without H atoms) [3]. Important bond lengths [pm] (±0.6 pm): Δ[Ni1-Ni3] 295–297, Δ[Ni4-Ni6] 288–293, Ni1-Ni6 276, Ni1-Ni5 278, Ni2-Ni4 277, Ni2-Ni6 278, Ni3-Ni4 272, Ni3-Ni5 275, (μ_3-Se)-Ni 227–234, (μ_4-Se)-Ni 232–246, P-C 180–184, C-C 151–154, Ni-P 216–217. The bond angles of the cluster are of the same order of magnitude as those for **3**.

Ni bonds from Se7–Se9 can be divided into two short (231–233 pm) and two long bonds (238–240 pm). Both **3** and **4** contain Ni atoms in different bond situations:

1) Ni atoms of the basal faces are each bound to two μ_3-Se-, one μ_4-Se- and one PR_3-ligand as well as to four Ni atoms.
2) Ni atoms inside the octahedra chain are either coordinated to one μ_3-Se- and three μ_4-Se-ligands (**3**: Ni4–Ni6, Ni10–Ni12; **4**: Ni4–Ni6) or to four μ_4-Se-ligands (**3**: Ni7–Ni9). These metal atoms are each bound to six further Ni atoms.

3 and **4** contain parallel layers (distance 216(3) pm, deviation from the plane ±10 pm), each of which is formed from three Ni atoms and three Se atoms. Within these layers, the Ni–Ni bonds have different lengths. The longest are found in the external Ni_3 faces (**3**: Δ[Ni1-Ni3], Δ[Ni13-Ni15], **4**: Δ[Ni1-Ni3], i.e. between the atoms which are bound to PR_3.

Markedly shorter are the Ni–Ni bonds in the inner layers (**3**: Δ[Ni4-Ni6], Δ[Ni7-Ni9], Δ[Ni10-Ni12]; **4**: Δ[Ni4-Ni6]). As in the case of **5**, the shortest Ni–Ni distances are observed between the layers (**3**: 270–288; **4**: 272–278 pm). These values are relatively large compared to those found in other complexes with Ni_3 faces.[10]

The 222e- and 180e-clusters **3** and **4** contain respectively 30 and 24 electrons more than would be expected according to the 18-electron rule. Apparently, increasingly more antibonding states are occupied in **3** and **4**. This is also evident from the fact that **3** and **4** have eight valence electrons per Ni atom, whereas the Chevrel phases contain 3.33–4.33 valence electrons per metal atom.[11] We can conclude therefore that even still larger clusters are formed in the reactions described here. Their characterization however is problematic owing to decreasing solubility. The composition of these compounds should correspond to the formula $[Ni_{3n+3}Se_{3n+3}(PR_3)_6]$ (n = number of coupled octahedra).

Experimental

1: A solution of $(NBu_4)[NiCl_3(PPh_3)]$ (10.03 g, 0.015 mmol) in toluene (100 mL) was treated with 3.2 mL (0.015 mol) of $Se(SiMe_3)_2$. The solution immediately turned black. After 5 days reaction time the fine crystalline precipitate was filtered off. On treatment with THF, 4 g of precipitate dissolved. After covering the solution with a layer of heptane, dark brown crystals of **1** were isolated. Yield 20%.

2: A suspension of $[NiCl_2(PPh_3)_2]$ (15.03 g, 0.023 mol) in MeCN (150 mL) was treated with 10.0 mL (0.047 mol) of $Se(SiMe_3)_2$. After 5 days reaction time the precipitate was filtered off (6 g). This was first treated with 100 mL of toluene and then recrystallized from 100 mL of THF. Upon covering the THF solution with a layer of hexane, **2** separated out at the interface. Yield 10%.

3: A solution of $(NBu_4)[NiCl_3(PPh_3)]$ (8.08 g, 0.012 mol) in MeCN (100 mL) was treated with 5.4 mL (0.025 mol) of $Se(SiMe_3)_2$. After 5 days reaction time about 6 g of a fine crystalline precipitate separated out. For removal of the Ph_3PSe the precipitate was treated with 50 mL of toluene. After addition of 100 mL of CH_2Cl_2 (to the insoluble residue) 1.2 g of **3** dissolved. Upon covering the solution with a layer of hexane, black crystals of **3** separated out at the interface. Yield 10%.

4: A solution of $[NiCl_2(PEt_3)_2]$ (5.6 g, 0.023 mol) in toluene was treated with 5.0 mL (0.023 mol) of $Se(SiMe_3)_2$. After 4 days reaction time ca. 100 mg of a fine crystalline precipitate separated out. This was filtered off and the filtrate was covered with a layer of heptane. Black crystals of **4** could be isolated. Yield 20%.

Received: October 1, 1986;
revised: November 10, 1986 [Z 1944 IE]
German version: *Angew. Chem. 99* (1987) 155

[1] D. Fenske, *Nachr. Chem. Tech. Lab. 34* (1986) 432.
[2] D. Fenske, J. Hachgenei, J. Ohmer, *Angew. Chem. 97* (1985) 684; *Angew. Chem. Int. Ed. Engl. 24* (1985) 706; D. Fenske, J. Ohmer, J. Hachgenei, *ibid. 97* (1985) 993 and *24* (1985) 993.
[3] Further details of the crystal structure investigations are available on request from the Fachinformationszentrum Energie, Physik, Mathematik GmbH, D-7514 Eggenstein-Leopoldshafen 2 (FRG), on quoting the depository number CSD-52170, the names of the authors, and the journal citation.—**1**: **1** crystallizes with 2 molecules of THF, space group $P2_1/a$, lattice constants (180 K): $a = 2710.1(13)$, $b = 1444.8(6)$, $c = 2926.4(14)$ pm, $\beta = 94.86(2)°$. $Z = 4$. Data collection: Syntex-R3, $2\theta \leq 52°$, $Mo_{K\alpha}$, 21809 reflections, 12046 with $I > 2\sigma(I)$, absorption correction. Structure solution: Patterson methods, Ni, Se, P anisotropic. $R_1 = 0.096$, $R_2 = 0.089$.—**2**: space group $P\bar{1}$, lattice constants (180 K): $a = 2074.9(13)$, $b = 2184.3(14)$, $c = 2486.6(15)$ pm, $\alpha = 63.79(4)$, $\beta = 69.19(4)$, $\gamma = 88.00(4)°$. $Z = 2$. Data collection: Syntex-R3, $Mo_{K\alpha}$, $2\theta \leq 48°$, 27116 reflections, 12463 with $I > 2\sigma(I)$, absorption correction. Structure solution: due to a disorder of the PPh_3 ligand in the $[NiCl_3(PPh_3)]^{\ominus}$ ion not all the C atoms of the anion could be located. MULTAN-80, Patterson methods, Ni, Se, Cl anisotropic, C isotropic Ph rings refined as rigid groups (C–C: 139.5 pm). $R_1 = 0.082$, $R_2 = 0.086$.—**3**: **3** crystallizes with 2 molecules of CH_2Cl_2, space group $P2_1/c$, lattice constants (140 K): $a = 2059.2(10)$, $b = 2244.0(9)$, $c = 2659.8(13)$ pm, $\beta = 103.55(4)°$. $Z = 4$. Data collection: Siemens-AED2, $2\theta \leq 46°$, $Mo_{K\alpha}$,

15115 reflections, 6239 with $I > 2\sigma(I)$, absorption correction. Structure solution: Patterson methods, all atoms isotropic. $R_1 = 0.073$, $R_2 = 0.074$.—**4**: Space group $C2/c$, lattice constants (170 K): $a = 3166.8(23)$, $b = 1381.7(10)$, $c = 2319.7(15)$ pm, $\beta = 136.26(4)°$, $Z = 4$. Data collection: Siemens-AED2, $2\theta \leq 52°$, $Mo_{K\alpha}$, 10213 reflections, 6964 with $I > 2\sigma(I)$, absorption correction $\mu(Mo_{K\alpha}) = 95.04\ cm^{-1}$. Structure solution: Patterson methods, Ni, Se, P anisotropic, C isotropic, H positions calculated and refined as rigid CH_2/CH_3 groups. $R_1 = 0.071$, $R_2 = 0.060$.

[4] J. C. Calabrese, L. F. Dahl, A. Cavalieri, P. Chini, G. Longoni, S. Martinengo, *J. Am. Chem. Soc. 96* (1974) 2614.

[5] B. K. Teo, G. Longoni, F. R. K. Chung, *Inorg. Chem. 23* (1984) 1257.

[6] J. C. Calabrese, L. F. Dahl, A. Cavalieri, P. Chini, G. Longoni, S. Martinengo, *J. Am. Chem. Soc. 96* (1974) 2618.

[7] C. A. Ghilardi, S. Midollini, L. Sacconi, *J. Chem. Soc. Chem. Commun. 1981*, 47; F. Cecconi, C. A. Ghilardi, S. Midollini, *Inorg. Chem. 22* (1983) 3802; H. Vahrenkamp, V. A. Uchtmann, L. F. Dahl, *J. Am. Chem. Soc. 90* (1968) 3272.

[8] A. Simon, *Angew. Chem. 93* (1981) 23; *Angew. Chem. Int. Ed. Engl. 20* (1981) 1.

[9] R. Chevrel, M. Sergent, *Top. Curr. Phys. 32* (1982) 25; R. Chevrel, P. Gougeon, M. Potel, M. Sergent, *J. Solid State Chem. 57* (1985) 25; M. Potel, R. Chevrel, M. Sergent, M. Decroux, Ø. Fischer, *C. R. Hebd. Seances Acad. Sci. Ser. C 288* (1979) 429; R. Chevrel, M. Sergent, B. Seeber, Ø. Fischer, A. Grüttner, K. Yvon, *Mater. Res. Bull. 14* (1979) 567; A. Grüttner, K. Yvon, R. Chevrel, M. Potel, M. Sergent, B. Seeber, *Acta Crystallogr. Sect. B 35* (1979) 285.

[10] S. Otsuka, A. Nakamura, T. Yoshida, *Inorg. Chem. 7* (1968) 261; J. C. Calabrese, L. F. Dahl, A. Cavalieri, P. Chini, G. Longoni, S. Martinengo, *J. Am. Chem. Soc. 96* (1974) 2616; L. R. Byers, V. A. Uchtmann, L. F. Dahl, *J. Am. Chem. Soc. 103* (1981) 1942; J. J. May, A. D. Rae, L. F. Dahl, *J. Am. Chem. Soc. 104* (1984) 3045.

[11] W. Hönle, H. G. von Schnering, A. Lipka, K. Yvon, *J. Less-Common Met. 71* (1980) 135.

Chromatographic Separation of Higher Polythionates $S_nO_6^{2\ominus}$ (n = 3...22) and Their Detection in Cultures of *Thiobacillus ferrooxidans*; Molecular Composition of Bacterial Sulfur Secretions**

By *Ralf Steudel,** *Gabriele Holdt, Thomas Göbel,* and *Willem Hazeu*

The exact analytical characterization of polythionates[1] is difficult,[2] since such compounds readily decompose and interconvert, especially in solution; they are therefore also formed along with each other in many reactions, and, moreover, form a long homologous series $S_nO_6^{2\ominus}$, where, according to *Weitz* et al.,[3] n can assume values of up to ca. 40. Hydrophilic sulfur sols after *Oden*,[4] are said to contain even polythionic acids with up to 140 S atoms;[5] such acids are then water-insoluble and form fine globules. *Weiss* and *Göbl*[6] recently reported on the ion-pair chromatography of sulfur-oxygen anions ($S_2O_4^{2\ominus}$, $S_2O_3^{2\ominus}$, $S_2O_6^{2\ominus}$, $S_4O_6^{2\ominus}$), which we have been able to extend to polythionate ions containing up to 13 S atoms.[7] The anions are separated on an organic stationary phase with aqueous acetonitrile containing some sodium carbonate and tetra-*n*-butylammonium hydroxide or dihydrogenphosphate. Since the retention times of the $S_nO_6^{2\ominus}$ ions increase with the square of n,[7] we have now used a concentration gradient for the two ionic components of the eluent, whereby all members up to $S_{22}O_6^{2\ominus}$ are separated and individually detected in the UV detector (215 nm). Figure 1 shows the chromatogram of an $S_nO_6^{2\ominus}$ solution (n = 4...18) that was prepared from S_7Cl_2 and $Na_2S_2O_3$ according to Equation (a),[7] and which, because of the other chlorosulfanes contained in the S_7Cl_2[8] and because of concomitant disproportionation reactions, also contained numerous polythionates other than $S_{11}O_6^{2\ominus}$.

$$2\,Na_2S_2O_3 + S_7Cl_2 \longrightarrow Na_2S_{11}O_6 + 2\,NaCl \qquad (a)$$

During the elution with an acetonitrile-water mixture (30/70 v/v) the concentrations of $(NBu_4)H_2PO_4$ and Na_2CO_3 in the mixture were lowered linearly within 10 min from 2 and 1 mmol/L, respectively, to zero. Under these conditions (flow rate 1 mL/min), $S_{11}O_6^{2\ominus}$ appeared in the detector after 12.3 min, and $S_{18}O_6^{2\ominus}$ after 28.4 min.[9]

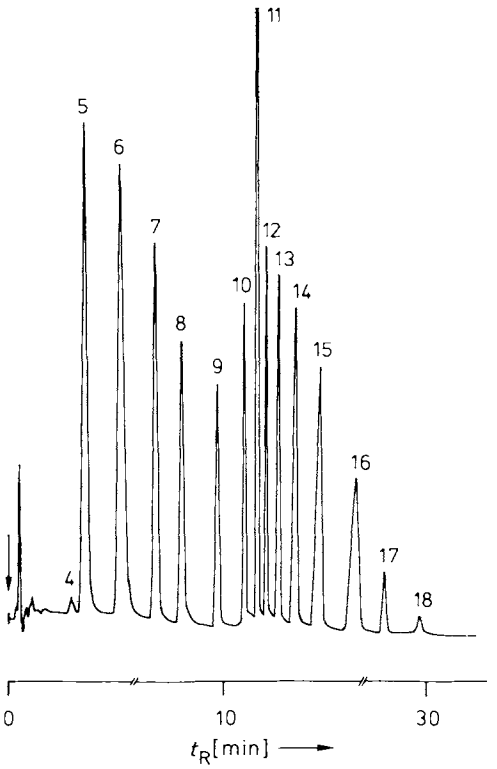

Fig. 1. Chromatogram of a polythionate mixture on octadecylsilane (C18) with a linear concentration gradient for the counterion ($NBu_4^{\oplus}$) and the inorganic "modifier" (Na_2CO_3). The scale for the retention time t_R is not linear; ordinate: UV detector signal. The arrow marks the injection point. The numbers relate to the number of sulfur atoms in the molecule.

In order to separate still higher polythionates, the concentration of the organic "modifier" acetonitrile was increased from 30 to 40% and the linear concentration gradient of the two salts shortened to 5 min (2→0 mmol/L). Under these conditions, however, the lower polythionates were no longer separated. In the chromatogram of a mixture of $Na_2S_nO_6$, which was prepared according to *Weitz* et al.[3c] by reaction of $K_2S_2O_3$ with S_2Cl_2 in concentrated hydrochloric acid and subsequent ion exchange with NaCl, and which, according to a sulfur analysis, contained anions with up to 40 S atoms,[3c] the members up to $S_{22}O_6^{2\ominus}$ were recognizable; by further modification of the chro-

[*] Prof. Dr. R. Steudel, G. Holdt, Dipl.-Chem. T. Göbel
Institut für Anorganische und Analytische Chemie
der Technischen Universität, Seks. C 2
Strasse des 17. Juni 135, D-1000 Berlin 12

Ir. W. Hazeu
Laboratory of Microbiology, Delft University of Technology
Julianalaan 67a, NL-2826 BC Delft (The Netherlands)

[**] Sulfur Compounds, Part 106. This work was supported by the Deutsche Forschungsgemeinschaft and the Fonds der Chemischen Industrie.—Part 105: R. Steudel, D. Jensen, B. Plinke, *Z. Naturforsch. B 42* (1987), in press.

matographic conditions probably even higher anions could have been separated. The concept of a very long homologous series of the polythionic acids is therefore justified.

Thiobacillus ferrooxidans (*T.f.*) is a chemolithotrophic bacterium which participates in the sulfur cycle in nature and plays an important role in the bacterial leaching of mineral ores. *T. f.* thrives at low pH value and draws energy from the oxidation of $Fe^{2\oplus}$ ions or from sulfur in lower oxidation states (sulfide, elemental sulfur, thiosulfate, polythionates).[10] These compounds are oxidized, in part, via unknown intermediates to sulfate;[11, 12] with an oversupply of substrate, *T. f.* oxidizes a part of the educt to elemental sulfur (S^0), which is deposited extracellularly as minute globules and is degraded again as required;[11, 12] with other thiobacilli, even polythionates up to $S_8O_6^{2\ominus}$ have been detected in the culture medium.[11] The molecular nature of the S^0, which is present in liquid form, is still unclear.

We have treated suspensions of *T. f.*[13] (150 mL with ca. 200 mg of dry mass per liter) at 30°C with a tetrathionate solution (100 mL; 5–10 mmol/L) under vigorous passage of air and taken samples after definite time intervals; these samples were cooled rapidly to 0°C, centrifuged, and the aqueous phase tested for polythionates (1). The centrifugate (cells and S^0) was extracted with various solvents and the extracts were examined by reversed phase HPLC[14] on elemental sulfur (2). During the oxidation the increasing turbidity due to S^0 formation was also measured by the absorbance at 430 nm.

1. In the aqueous phases (pH ca. 3) all polythionates up to $S_{13}O_6^{2\ominus}$ were detected; on using pentathionate as substrate and previously deep-frozen cells, even all anions up to $S_{17}O_6^{2\ominus}$ were detectable (Fig. 2). The concentrations of the individual polythionates passed through a maximum during the oxidation, while the turbidity continually increased.
2. Extraction of the cells (containing S^0) with CS_2 furnished solutions, which besides containing S_8 (ca. 98%) also contained small amounts of S_6, S_7, S_9, and S_{12} (Fig. 3); extraction with a methanol-water mixture (95/5 v/v) yielded solutions of $S_nO_6^{2\ominus}$ and sulfur, which consisted of 96–98% of S_8 and 2–4% of S_7 and S_6. Repeated extraction continually afforded further S_n solutions independent of the solvent used; this indicates that S^0 is either also deposited intracellularly and then only slowly extracted, or that the hydrophilic surface of the S^0 globules (vide infra) hinders the extraction of S_n. The S_8 concentration increased with increasing turbidity.

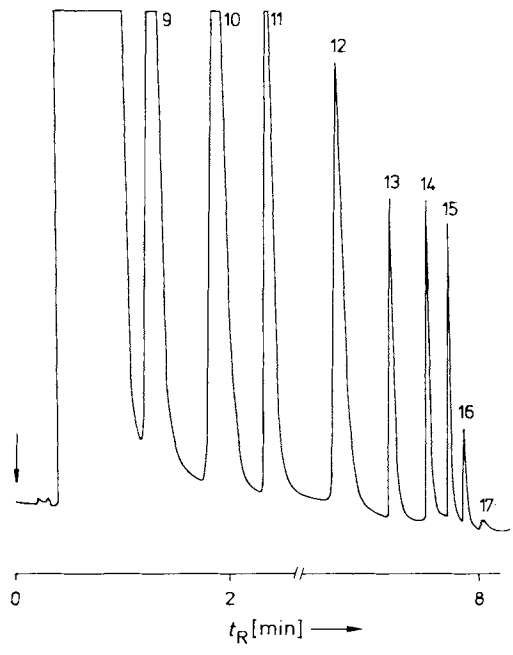

Fig. 2. Chromatogram of the polythionates which were formed in a culture of *Thiobacillus ferrooxidans* after incubation with $K_2S_5O_6$.

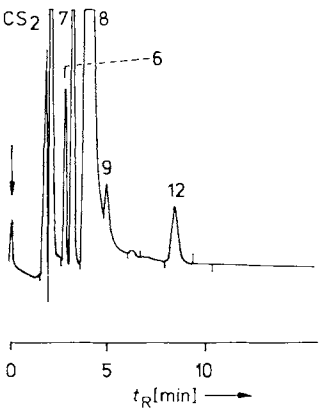

Fig. 3. Chromatogram of the CS_2 extract of *Thiobacillus ferrooxidans* after incubation with tetrathionate (column: Radial-Pak 10C18 (Waters), eluent: methanol; cf. Ref. [14]).

When the cells were extracted before addition of tetrathionate, neither polythionates nor sulfur rings were detectable. Our results can be explained in terms of the following (and analogous) reactions:

$$S_4O_6^{2\ominus} + H_2O \longrightarrow HS_2SO_3^{\ominus} + HSO_4^{\ominus} \quad (b)$$

$$2\,HS_2SO_3^{\ominus} \rightleftharpoons HS_4SO_3^{\ominus} + HSO_3^{\ominus} \quad (c)$$

$$2\,HS_4SO_3^{\ominus} \rightleftharpoons HS_8SO_3^{\ominus} + HSO_3^{\ominus} \quad (d)$$

$$HS_8SO_3^{\ominus} \rightleftharpoons S_8 + HSO_3^{\ominus} \quad (e)$$

$$HSO_3^{\ominus} + 1/2\,O_2 \longrightarrow HSO_4^{\ominus} \quad (f)$$

$$2\,HS_2SO_3^{\ominus} + 1/2\,O_2 \longrightarrow S_6O_6^{2\ominus} + H_2O \quad (g)$$

$$2\,HS_2SO_3^{\ominus} \rightleftharpoons S_5O_6^{2\ominus} + H_2S \quad (h)$$

The availability of enzymes for the catalysis of reactions such as (b), (f), and (g) in thiobacilli is well known;[11, 12] the other reactions are known from laboratory experiments.[15] The irreversible oxidation of sulfite to sulfate as in Eq. (f) drives the equilibrium reactions (c)–(e) to the right. Instead of the hydrolysis (b), a reduction of tetrathionate to thiosulfate followed by a disproportionation of the thiosulfate analogously to (c), is also conceivable as primary step.[16]

The first detection of polythionates containing more than 10 sulfur atoms and unstable sulfur rings S_n ($n \neq 8$) in a biological system demonstrates the importance of the sulfanemonosulfonic acids HS_nSO_3H[17] as intermediates, since polysulfur compounds can be rapidly and reversibly synthesized and degraded and transported only via these highly reactive and readily soluble substances in a strongly acidic, aqueous medium. The hydrophilic S^0 globules most likely consist of a hydrophobic nucleus of mainly S_8 (with traces of other S_n-rings, which hinder crystallization) on whose surface long-chain polythionate ions[18] are deposited by hydrophobic interaction with the aqueous medium such that the droplet as a whole becomes hydrophilic (Fig.

4); the approximate "formula" for S^0 is therefore: $x S_8 \cdot y H_2S_nO_6 \cdot z H_2O$.—$S_8$, which is very sparingly soluble in water (solubility of α-S_8 at 25 °C: 5 μg/kg[19]), can, e.g., be rapidly reactivated[20] via reactions such as (e) and, in this way, can even be transported through membranes.

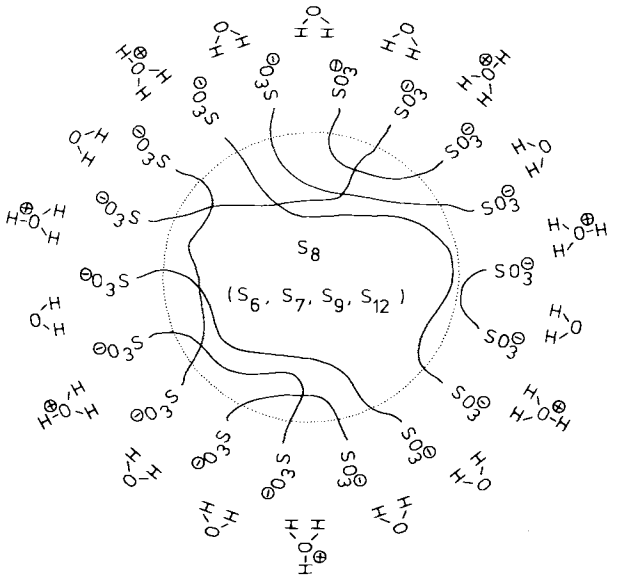

Fig. 4. Simplified model of a sulfur globule as is formed extracellularly by *Thiobacillus ferrooxidans*. It consists mainly of S_8 and small amounts of other compounds (S_6, S_7, S_9, and S_{12}) which impede crystallization, as in globules of supercooled liquid sulfur. Long-chain polythionate ions are deposited on the surface and make the globule hydrophilic. Hence it is surrounded by a hydrate-sheath in which cations are possibly also present. The average density of such a micelle must be significantly smaller than that of liquid sulfur (1.85 g/cm³).

The chromatographic detection of polythionates as described here, which, e.g., requires a concentration of only 5 μg/mL in the case of the tetrathionate, should now be extended to a systematic search for these compounds in the culture media of other sulfur bacteria.

Received: October 3, 1986 [Z 1946 IE]
German version: *Angew. Chem. 99* (1987) 143

[1] *Gmelin, Handbuch der Anorganischen Chemie, 8th edition, Schwefel, Teil B2*, Verlag Chemie, Weinheim 1960, p. 969-1046.
[2] L. Szekeres, *Talanta 21* (1974) 1; E. Blasius, E. Thiele, *Z. Anal. Chem. 197* (1984) 347.
[3] a) E. Weitz, K. Spohn, *Chem. Ber. 89* (1956) 2322; b) E. Weitz, F. Becker, K. Gieles, *ibid. 89* (1956) 2345; c) E. Weitz, F. Becker, K. Gieles, B. Alt, *ibid. 89* (1956) 2353.
[4] S. Odén, *Nova Acta Regiae Soc. Sci. Upsaliensis Ser. IV 3* (1913) No. 4, *Z. Phys. Chem. 80* (1912) 709.
[5] E. Weitz, K. Gieles, J. Singer, B. Alt, *Chem. Ber. 89* (1956) 2365.
[6] J. Weiss, M. Göbl, *Fresenius Z. Anal. Chem. 320* (1985) 439.
[7] R. Steudel, G. Holdt, *J. Chromatogr. 361* (1986) 379.
[8] R. Steudel, R. Strauss, D. Jensen, *Chem. Ztg. 109* (1985) 349.
[9] Varian 5000 chromatograph with microcomputer-controlled gradient adjustment, Rheodyne loop injector (10 μL), Chrompack cartridge glass column (CT™SpherC18; l = 10 cm), Varian UV5 detector (215 nm), Hewlett-Packard 3390A integrator, Knauer recorder. For further experimental details see Ref. [7].
[10] See e.g. M. Eccleston, D. P. Kelly, *J. Bacteriol. 134* (1978) 718, and references cited therein.
[11] P. A. Trudinger, *Rev. Pure Appl. Chem. 17* (1967) 1.
[12] D. P. Kelly, *Philos. Trans. R. Soc. London Ser. B 298* (1982) 499; *Microbiol. Sci. 2* (1985) 105.
[13] W. Hazeu, W. Bijleveld, J. T. C. Grotenhuis, E. Kakes, J. G. Kuenen, *Antonie van Leeuwenhoek 52* (1986) 507; the bacteria were cultivated in Delft by *W. H.* and transported by express mail to Berlin for the oxidation and extraction experiments.
[14] R. Steudel, H.-J. Mäusle, D. Rosenbauer, H. Möckel, T. Freyholdt, *Angew. Chem. 93* (1981) 402; *Angew. Chem. Int. Ed. Engl. 20* (1981) 394; R. Strauss, R. Steudel, *Fresenius Z. Anal. Chem.*, in press.
[15] R. E. Davis, *J. Am. Chem. Soc. 80* (1958) 3565; R. Steudel, H.-J. Mäusle, *Z. Anorg. Allg. Chem. 457* (1979) 165.
[16] P. A. Trudinger, *Aust. J. Biol. Sci. 17* (1964) 446.
[17] M. Schmidt, *Z. Anorg. Allg. Chem. 289* (1957) 158.
[18] In the case of those phototrophic and chemolithotrophic sulfur bacteria, which likewise form "S^0 globules" (some extra-, some intracellular), probably other compounds with polar groups instead of polythionates can cover the surface of the hydrophobic S_8 globule and thus make them hydrophilic; cf., e.g., the stabilization of sulfur particles in water by adsorption of organic carboxylic acids (e.g. polyacrylic acid): A. Asanov, A. Il'yasov, K. S. Akhmedov, *Dokl. Akad. Nauk UzSSR 1985*, 35 (*Chem. Abstr. 104* (1986) 136611), and references cited therein.
[19] J. Boulege, *Phosphorus Sulfur 5* (1978) 127.
[20] G. W. Donaldson, F. J. Johnston, *J. Phys. Chem. 73* (1969) 2064; R. H. Dinegar, R. H. Smellie, *J. Colloid Sci. 7* (1952) 370.

CC-Linkages of Ethene with CO_2 on an Iron(0) Complex—Synthesis and Crystal Structure Analysis of $[(PEt_3)_2Fe(C_2H_4)_2]$

By *Heinz Hoberg,* Klaus Jenni, Klaus Angermund,* and *Carl Krüger*

We recently reported the 1/1 CC-linkage of CO_2 with 1,3-butadiene on an iron(0) system.[1] We have now extended our investigations to reactions of ethene on iron(0) complexes. CC-linkages between ethene and CO_2 can be controlled on nickel(0) in such a way that, depending on the ligand, either propionic acids[2] or *n*-pentenoic acids[3] are formed in the course of acid hydrolysis. On molybdenum(0) or tungsten(0) complexes acrylic acid is formed.[4]

We have now found that the iron(0) system induces further unexpected CC-coupling steps between CO_2 and ethene. The π-bonded ethene in the well already known 18e-complex ethenebis[*P,P'*-ethylenebis(diphenylphosphane)]-iron(0)[5] does not react with CO_2 (5 bar, 80 °C) to give the carboxylate. However, we have been able to prepare a novel ligand-Fe^0-C_2H_4 complex on which the desired CC couplings are possible for the first time.

In the reduction of $FeCl_2$ with Mg*[6] in tetrahydrofuran (THF) in the presence of ethene and PEt_3 the 16e-complex bis(ethene)bis(triethylphosphane)iron(0) **1** is formed in 72% yield [m.p. 16 °C (dec.), paramagnetic, black crystals].[7]

$$FeCl_2 + Mg^* + 2\,C_2H_4 + 2\,PEt_3 \xrightarrow[-30\,^\circ C]{THF} (PEt_3)_2Fe(C_2H_4)_2 + MgCl_2$$

1

The structure of **1** (Fig. 1) was determined by a crystal structure analysis. In the crystalline state the complex has C_2 symmetry, with the symmetry axis passing through the Fe atom and bisecting the P1-Fe-P1* angle. The metal atom is surrounded pseudotetrahedrally by two ethene molecules and two triethylphosphane molecules (angle between the plane through the atoms Fe, P1 and P1* and the plane through the iron atom and the midpoints of the C1-C2 and C1*-C2* bonds: 89.9°); the ethene ligands, however, form an angle of 35.8° with respect to each other (torsion angle C1-C2-C1*-C2*).

[*] Prof. Dr. H. Hoberg, Dipl.-Chem. K. Jenni,
Dr. K. Angermund [+], Prof. Dr. C. Krüger [+]
Max-Planck-Institut für Kohlenforschung
Kaiser-Wilhelm-Platz 1, D-4330 Mülheim a. d. Ruhr 1 (FRG)
[+] Crystal structure analysis.

For investigating the behavior of **1** towards CO_2 the complex was first dissolved in THF at $-78\,^{\circ}C$ and treated with a stream of CO_2 (1 bar). This, however, merely resulted in "reductive disproportionation" to iron carbonate and carbon monoxide,[10] and not in the desired formation of carboxylate. Apparently, the molar ratio PEt_3/Fe of 2:1 asserted for **1** is too small for this.

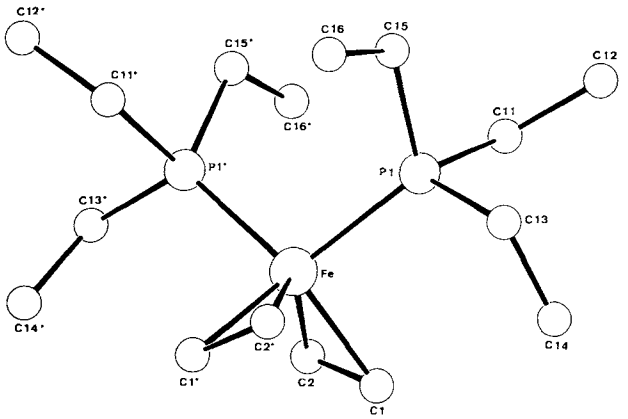

Fig. 1. Crystal structure of **1** [8], $a=14.572(6)$ Å, $b=7.314(3)$ Å, $c=18.487(8)$ Å, $\beta=98.13(3)^{\circ}$, $V=1950.6$ Å^3, $T=100$ K, $\lambda=0.71069$ Å, $C2/c$, $Z=4$, $\rho_{calc}=1.19$ g cm^{-3}, $\mu_{(Mo)}=9.23$ cm^{-1}, empirical absorption correction (0.911 min., 1.135 max.), 2658 reflections measured ($\pm h \pm k + l$), 1347 independent reflections, 1271 observed reflections ($I \geq 2\sigma(I)$), H-atom positions found but not refined, 87 refined parameters, $R=0.028$, $R_w=0.036$ ($w=1/\sigma^2(F_0)$), maximum residual electron density 0.27 e/Å^3). Selected bond lengths [Å] and angles [°]: Fe-P1 2.267(1), Fe-C1 2.083(2), Fe-C2 2.105(3), P1-C11 1.854(2), P1-C13 1.855(3), P1-C15 1.850(2), C1-C2 1.382(4); P1-Fe-P1* 106.2(1), P1-Fe-C1 98.0(1), P1-Fe-C2 120.0(1), C1-Fe-C2 38.5(1), C1-Fe-C1* 100.4(1), C1-Fe-C2* 103.3(1), C2-Fe-C2* 128.9(1) [9].

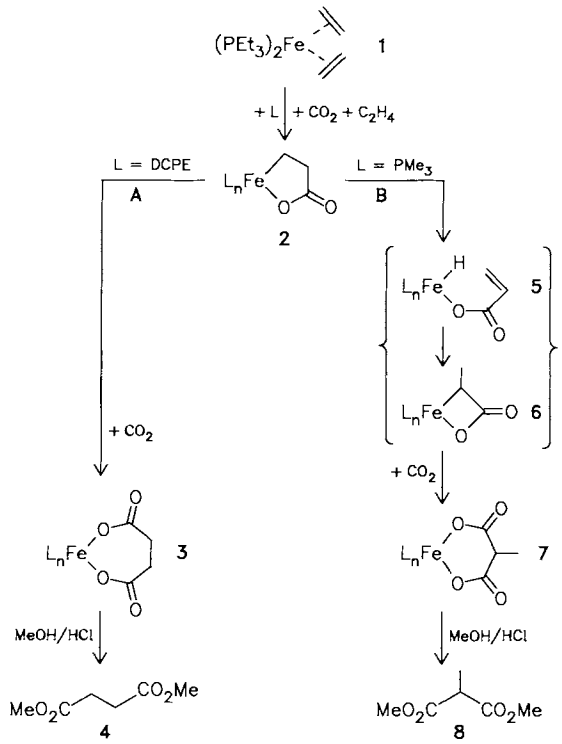

Table 1. Influence of ligands on the yield and molar ratio of the dicarboxylic acids **4** and **8** in the reactions of **1** with CO_2.

L	Molar ratio L/**1**	Yield [%]	Molar ratio **4/8**
PMe_3	3/1	60	1/400
$[Me_2P-CH_2-]_2$ (DMPE)	1/1	57	1/7
$[(c\text{-}C_6H_{11})_2P-CH_2-]_2$ (DCPE)	2/1	49	10/1

A CC-linkage between ethene and CO_2 is achieved on iron(0) when the reaction is carried out after addition of further ligands such as, e.g., PMe_3, *P,P'*-ethylenebis(dicyclohexylphosphane) (DCPE), or *P,P'*-ethylenebis(dimethylphosphane) (DMPE).[11] The iron carboxylates formed thereby could be recognized by the C=O stretching vibration bands at 1580 cm^{-1} in the IR spectrum. The type of carboxylate formation that had taken place was determined by acid-hydrolysis of the complex mixture in methanol on the basis of the methyl ester that was formed (Table 1). Surprisingly, no monocarboxylic acids but exclusively dicarboxylic acids, namely succinic acid **4** and the isomeric methylmalonic acid **8**, are formed.

As can be seen from Table 1 the ligands have a significant influence on the course of the CC coupling reaction. Whether this is of a steric or electronic nature or due alone to the chelate-effect of the bidentate phosphanes cannot be inferred from the present observations. Apparently the iron carboxylates **3** and **7** derive from a common unstable intermediate, the oxaferracyclopentanone **2**.

Whereas the formation of **4** (insertion of CO_2 into the Fe-C σ-bond of **2** to give **3**, Route **A**) is comparable with the corresponding reaction sequences in the reaction of 1,3-butadiene on nickel(0)[12] and iron(0) systems,[1] the reaction course **B** is postulated for the unexpected formation of **8**: β-H elimination leads to **5**; renewed hydrometalation affords the methyloxyferracyclobutanone **6**,[13] from which **7** is formed by CO_2 insertion. Finally, the diester **8** is liberated from **7** by methanolic HCl.

Received: October 17, 1986;
revised: November 17, 1986 [Z 1954 IE]
German version: *Angew. Chem. 99* (1987) 141

[1] H. Hoberg, K. Jenni, C. Krüger, E. Raabe, *Angew. Chem. 98* (1986) 819; *Angew. Chem. Int. Ed. Engl. 25* (1986) 810.
[2] H. Hoberg, D. Schaefer, *J. Organomet. Chem. 251* (1983) C51.
[3] H. Hoberg, Y. Peres, A. Milchereit, *J. Organomet. Chem. 307* (1986) C41.
[4] R. Alvarez, E. Carmona, D. J. Cole-Hamilton, A. Galindo, E. Gutierrez-Puebla, A. Monge, M. L. Poveda, C. Ruiz, *J. Am. Chem. Soc. 107* (1985) 5529.
[5] G. Hata, H. Kondo, A. Miyake, *J. Am. Chem. Soc. 90* (1968) 2278.
[6] Mg* signifies a suspension of Mg powder, particle size 50 mesh, in THF with addition of 0.5 mL of ethyl bromide.
[7] *Procedure* for **1**: A mixture of Mg* (3.20 g, 131.69 mmol) in THF (20 mL) was cooled to $-78\,^{\circ}C$ and saturated at this temperature with ethene. The resulting mixture was then combined with an ethene-saturated suspension of $FeCl_2$ (15.83 g, 125 mmol) and PEt_3 (36.4 mL, 250 mmol) in THF (240 mL), likewise cooled to $-78\,^{\circ}C$. After 36 hours' stirring at $-40\,^{\circ}C$ the THF was distilled off at $-15\,^{\circ}C$ (10^{-5} bar), the residue taken up in 1 L of cold pentane ($-30\,^{\circ}C$), filtered, washed several times with cold pentane, and the combined filtrate and washings cooled to $-78\,^{\circ}C$. The large needles of **1** that subsequently crystallized out were isolated and dried. Yield 31.45 g (90.36 mmol, 72%); m.p. 16 °C (dec.); IR (KBr, $-55\,^{\circ}C$): $\tilde{\nu}$ [cm^{-1}] = 3040, 1194, 1178 (C_2H_4), 2961, 1458, 1417, 1373, 1039/1028, 763, 724 (PEt_3); correct elemental analysis.
[8] The calculations were carried out on VAX-11/780, VAX-11/730, and MicroVAX-II computers. In addition to some self-written programs, the following software was used: TRACER by S. L. Lawton and R. A. Jacobson, SHELX-76 by G. M. Sheldrick, FMLS, a modified version of the ORFLS by W. R. Busing and H. A. Levy, XANADU by P. Roberts and G. M. Sheldrick, DAESD by R. E. Davis, and ORTEP by C. Johnson.

[9] Further details of the crystal structure investigation are available on request from the Fachinformationszentrum Energie, Physik, Mathematik GmbH, D-7514 Eggenstein-Leopoldshafen 2 (FRG), on quoting the depository number CSD-52153, the names of the authors, and the journal citation.
[10] H. H. Karsch, *Chem. Ber. 110* (1977) 2213.
[11] *Typical procedures* for **4** and **8**: 1.48 g (4.25 mmol) of **1** and 0.97 g (1.29 mL, 12.76 mmol) of PMe_3 were dissolved in 70 mL of THF (−78 °C); the solution was then treated, via a buret, first with 286 mL (12.76 mmol) of ethene, and then with 286 mL (12.76 mmol) of CO_2. With careful equalization of built-up pressure, the solution was slowly warmed (6 h) to room temperature, whereupon a dark brown precipitate separated out. This was filtered off and dried. Yield: 1.12 g; IR (KBr): $\tilde{\nu}$ [cm^{-1}] = 1580 (C=O). The dried solid was treated at −30 °C with 4 mL of 6 N methanolic HCl. After 24 hours' stirring the solution was neutralized with $NaHCO_3$. The volatile components were distilled off under vacuum (2×10^{-4} bar). According to a GC analysis the distillate contained 0.93 mg (6.36×10^{-3} mmol, 0.15%) of **4** and 370.84 mg (2.54 mmol, 59.76%) of **8**. The products were identified by comparison of the MS spectra obtained after combined GC-MS with literature data and quantitatively determined by calculation from the GC curves taking into consideration the response factors referred to isopentyl acetate as internal standard. The reactions of **1** in the presence of the ligands DMPE and DCPE in the molecular ratios given in Table 1 were carried out analogously.
[12] H. Hoberg, B. Apotecher, *J. Organomet. Chem. 270* (1984) C15.
[13] Ring contractions have also been observed on platinacyclopentane complexes (cf. G. B. Young, G. M. Whitesides, *J. Am. Chem. Soc. 100* (1978) 5808), tantalacyclopentane complexes (cf. S. L. McLain, J. Sancho, R. R. Schrock, *ibid. 101* (1979) 5451), and oxanickelacyclohexanone complexes (cf. K. Sano, T. Yamamoto, A. Yamamoto, *Chem. Lett. 1982*, 695).

Isolation and Photoisomerization of Simply Substituted Nitrile Oxides**

By *Günther Maier** and *Joaquim Henrique Teles*

The haloformonitrile oxides **2** and **5** should, according to *Wieland*,[1] be formed as intermediates upon reaction of the mercury salt of fulminic acid (formonitrile oxide) with chlorine and bromine to give the respective dihalofuroxanes [Eq. (a)]. The in situ generation of **2** and **5** from the

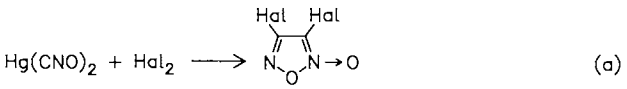

(a)

corresponding hydroximic acid halides by HHal-elimination with bases[3] has attracted renewed interest in connection with the synthesis of the antitumor reagent acivicin.[2] Furthermore, molecules such as **2**, **5**, **8**, and in particular their photoisomers, could perhaps occur in interstellar space.[4] Both aspects have prompted us to attempt the direct detection of such species.

When the fragments formed in the gas-phase pyrolysis (600 °C, 10^{-5} torr) of the dihaloformoximes **1** and **4** are condensed with argon on a cold window ($T = 10$ K) the halonitrile oxides of interest, namely **2** and **5**, can be detected as main products on the basis of their typical IR bands[5] (Table 1). Of the five fundamental vibrations to be expected for a linear atomic arrangement[6] only two are intense enough for observation.[7] Besides these, the IR absorptions of the respective hydrogen halides and, to a lesser extent, those of the corresponding haloisocyanates **3** and **6**, respectively, are also observed.

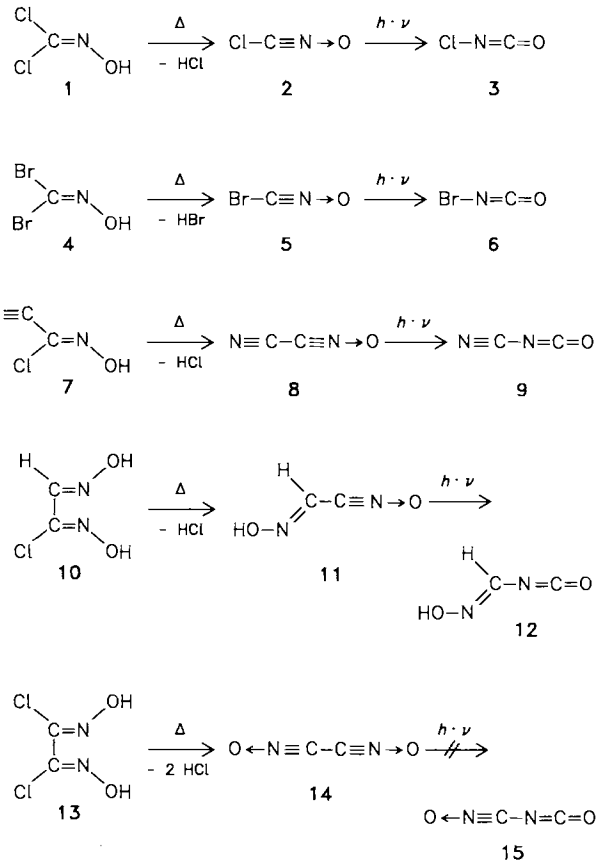

The structures of **2** and **5** follow also from the fact that these compounds are smoothly converted into the haloisocyanates upon irradiation in the matrix ($\lambda = 254$ nm, 10 min),[8] as shown by a comparison with the spectra of authentic samples[9] of **3** and **6**. Vacuum pyrolysis of chlorocyanoformoxime **7** at 400 °C leads to formation of cyanogen mono-*N*-oxide **8**, which can be isolated as the only product besides HCl in the argon matrix.[10] In the case of a linear structure, seven bands should occur in the IR; five were observed (Table 1). Irradiation in the matrix ($\lambda = 254$ nm, $t = 20$ min) affords cyanogen isocyanate **9**[11] and C_2O.[12] Gas-phase pyrolysis of chloroglyoxime **10** analogously afforded the nitrile oxide **11**. Its constitution follows, once again, from the IR spectrum (Table 1); irradiation of **11** in the matrix at 10 K affords the isocyanate **12** (IR bands at 3638, 2276, 1646, and 976 cm^{-1}) within 2 min.

Table 1. IR spectra [Ar matrices, 10 K, $\tilde{\nu}$ [cm^{-1}] (relative intensity)] of the nitrile oxides **2**, **5**, **8**, and **11**.

Assignment	**2**	**5**	**8** [b]	**11** [c]
ν_s(CNO)	1326.3 (100)	1305.6 (100)	1445 (25)	1453 (34)
ν_{as}(CNO)	2261.7 (21) [a]	2252.5 (19) [a]	2356 (100)	2301 (100)
	2281.4 (31)	2271.3 (34)		
$2\nu_s$(CNO)	2643.5 (11)	2602.1 (10)		

[a] Splitting due to matrix effects. [b] Additional bands: 407 (2), 717 (1), 2192 (9). [c] Additional bands: 423 (30), 425 (63), 914 (28), 940 (21), 989 (55), 1241 (11), 1258 (30), 1346 (9), 3621 (83).

[*] Prof. Dr. G. Maier, Dipl.-Chem. J. H. Teles
Institut für Organische Chemie der Universität
Heinrich-Buff-Ring 58, D-6300 Giessen (FRG)

[**] This work was supported by the Deutsche Forschungsgemeinschaft and the Fonds der Chemischen Industrie.

As expected, flash vacuum pyrolysis of dichloroglyoxime **13** leads to smooth formation of the well-known cyanogen di-*N*-oxide **14**, which is stable up to $-45\,^{\circ}C$.[13] A special feature of this series is that photoexcitation of **14** ($\lambda = 254$ nm) does not lead to the isocyanate **15**, but to nitrosyl cyanide **18**.[14] This photoreaction is to be seen in

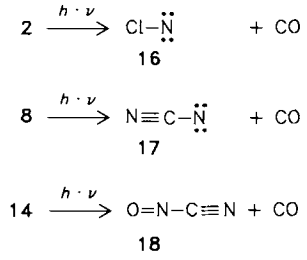

context with the observation that the bands of chloronitrene **16**[15] also appear in the IR spectrum after prolonged irradiation of the nitrile oxide **2** in argon at 10 K and that not only the photostable isocyanate **9** but also C_2O is obtained upon photochemical excitation of **8**. This reaction is probably best explained in terms of the formation of cyanonitrene **17** (detectable on using light of wavelength 229 nm), from which nitrogen is split off. The atomic carbon formed thereby is finally trapped by the carbon monoxide that is still present in the argon cage (the intensity of the CO band decreases upon prolonged irradiation).

The "breakaways" in the photochemically-induced nitrile oxide-isocyanate rearrangement can be accounted for in terms of a theoretically justifiable mechanism[6, 16] if one assumes that the nitrile oxides **19** are converted via the oxazirenes **20** into the acylnitrenes **21**. The latter can subsequently rearrange to the isocyanates **23** or be cleaved in a second photo-step to give nitrene **22** and carbon monoxide. Since it has been confirmed experimentally, at least in the case of R = CN, that the carbon monoxide does not originate from the isocyanate, a process **23** → **22** is also not very likely in the case of other residues R.

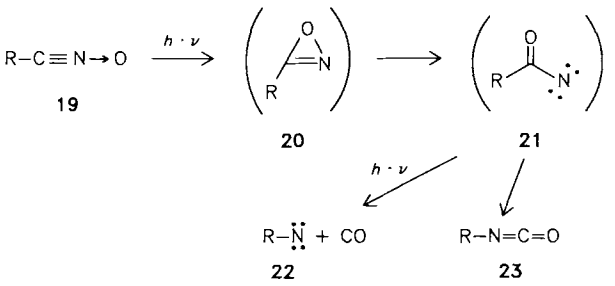

Summary: Simple nitrile oxides are readily accessible by gas-phase pyrolysis of the corresponding hydroximic acid halides. We are confident that this method will prove advantageous in the preparative use of simply substituted nitrile oxides.

Received: October 30, 1986;
supplemented: November 24, 1986 [Z 1973 IE]
German version: *Angew. Chem. 99* (1987) 152

[1] H. Wieland, *Ber. Dtsch. Chem. Ges. 42* (1909) 4192.
[2] J. E. Baldwin, C. Hoskins, L. Kruse, *J. Chem. Soc. Chem. Commun. 1976*, 795; A. A. Hagedorn, B. J. Miller, J. O. Nagy, *Tetrahedron Lett. 21* (1980) 229; P. A. Wade, M. K. Pillay, S. M. Singh, *ibid. 23* (1982) 4563; R. V. Stevens, R. P. Polniaszek, *Tetrahedron 39* (1983) 743.
[3] Survey: C. Grundmann, P. Grünanger: *The Nitrile Oxides*, Springer, New York 1971.
[4] Review: G. Winnewisser, E. Herbst, *Top. Curr. Chem.*, in press. The list of detected interstellar molecules includes, inter alia, HCl and isocyanic acid HNCO.
[5] Aromatic nitrile oxides show two intense bands at ca. 2330 and 1370 cm^{-1}: [3], p. 24ff.
[6] D. Poppinger, L. Radom, J. A. Pople, *J. Am. Chem. Soc. 99* (1977) 7806; D. Poppinger, L. Radom, *ibid. 100* (1978) 3674.
[7] MNDO calculations [M. J. D. Dewar, W. Thiel, *J. Am. Chem. Soc. 99* (1977) 4899] gave the following absorption values for the most intense IR bands [cm^{-1}] (relative intensities): **2**: 2674 (100), 1766 (70); **5**: 2654 (100), 1751 (46); **8**: 2695 (100), 2535 (15), 1824 (27).
[8] Irradiation of fulminic acid HCNO in the matrix leads, in the same unusual reaction, to isocyanic acid: V. E. Bondybey, J. H. English, C. W. Mathews, R. J. Contolini, *J. Mol. Spectrosc. 92* (1982) 431.
[9] E. Nachbaur, W. Gottardi, *Monatsh. Chem. 97* (1966) 115; W. Gottardi, *ibid. 103* (1972) 1150.
[10] For the in situ preparation of **8** and **11** and their application in 1,3-dipolar cycloadditions cf. C. Grundmann, H.-D. Frommeld, *J. Org. Chem. 31* (1966) 4235; M. Christl, R. Huisgen, *Tetrahedron Lett. 1968*, 5209.
[11] E. Mayer, *Monatsh. Chem. 101* (1970) 834.
[12] M. E. Jacox, D. E. Milligan, N. G. Moll, W. E. Thompson, *J. Chem. Phys. 43* (1965) 3734.
[13] C. Grundmann, V. Mini, J. M. Dean, H.-D. Frommeld, *Justus Liebigs Ann. Chem. 687* (1965) 191.
[14] E. A. Dorko, L. Buelow, *J. Chem. Phys. 62* (1975) 1869.
[15] D. E. Milligan, M. E. Jacox, *J. Chem. Phys. 40* (1964) 2461.
[16] A. Rauk, P. F. Alewood, *Can. J. Chem. 55* (1977) 1498.

$^2H,^2H$-COSY and $^2H,^2H,^{13}C$-RELAY NMR Experiments for the Analysis of Deuteriated Compounds**

By *Detlef Moskau* and *Harald Günther**

The homonuclear shift correlation technique (COSY[1c]) introduced by *Jeener*[1a] and *Ernst* et al.[1b] is one of the most important 2D-NMR spectroscopic methods. The cross peaks occurring between anisochronous nuclei are due to scalar spin-spin coupling, which generally leads to characteristic line splittings in a one-dimensional spectrum. COSY-NMR spectra therefore afford immediate structural information and are indispensable, in particular, for the detection of connectivities in complicated NMR spectra.

An attractive aspect of the COSY-NMR experiment is that cross peaks can even be obtained when the coupling between two nuclei is not resolved in a one-dimensional spectrum because of line broadening.[2] Such situations are encountered with quadrupolar nuclei whose lines are usually strongly broadened by fast relaxation, so that line splittings due to homonuclear spin-spin couplings are not observed.[3] Consequently, line assignments in the 1D-NMR spectrum are rendered difficult or impossible. Although even the COSY-NMR experiment is not unproblematical for such nuclei because of the dependence of the cross-peak intensities on the magnitude of the scalar coupling and the relaxation time T_2[4], successful $^{11}B,^{11}B$-,[5] $^{51}V,^{51}V$-,[6] and $^6Li,^6Li$-correlation experiments[7] show that COSY-NMR spectroscopy is possible with quadrupolar nuclei and is most useful for the elucidation of structures.

We now report on the COSY- and RELAY-NMR spec-

[*] Prof. Dr. H. Günther, Dipl.-Chem. D. Moskau
FB 8, OC II der Universität-Gesamthochschule
Postfach 10 12 40, D-5900 Siegen (FRG)

[**] This work was supported by the Minister für Wissenschaft und Forschung des Landes Nordrhein-Westfalen.

troscopy of the quadrupolar nucleus deuterium. Figure 1 shows the homonuclear two-dimensional $^2H,^2H$-shift cor-

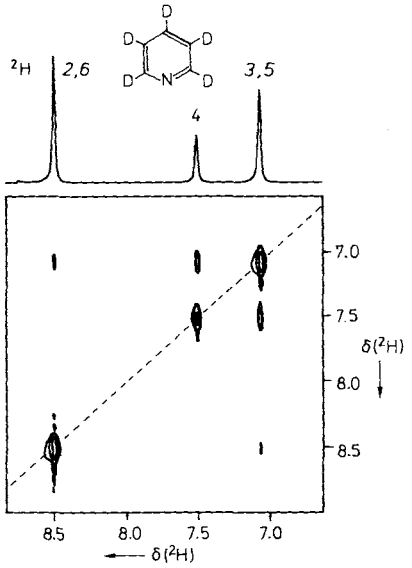

Fig. 1. $^2H,^2H$-COSY-NMR spectrum of [D_5]pyridine (in C_6F_6 3 : 1) with pulse sequence (a); cross peaks for vicinal deuterons. Spectral window 300 Hz, 64 t_1 increments of 3.3 ms, relaxation interval 5 s, $\Delta = 0.4$ s, $t_2 = 1.71$ s, 32 accumulations, phase cycle of the Bruker standard software, data processing with sine functions, measurement time 4.3 h. From the width of the signals in the 1D spectrum one gets $T_2^*(^2H) = 0.3$ s; the cross signal intensities are respectively 3 and 25% of the diagonal signal intensity.

relation for [D_5]pyridine. As can be calculated from the vicinal $^1H,^1H$-coupling constants of pyridine ($J(2,3) = 4.88$, $J(3,4) = 7.67$ Hz[8]) and the ratio $\gamma(^1H)/\gamma(^2H) = 6.51$,[9] the corresponding $^2H,^2H$-couplings are only 0.1 and 0.2 Hz, respectively. Since they are not resolved in the 1D-NMR spectrum the recommended modification of the Jeener pulse sequence with a constant interval Δ before and after the mixing pulse was used for accentuating smaller couplings. Furthermore, the COSY-45 variant[4] for the reduction of diagonal signal intensities also proved useful:

$$^2H:\ 90°/\text{---}t_1\text{---}/\text{-}\Delta\text{-}/45°/\text{-}\Delta\text{-}/\mathrm{FID}(t_2) \qquad (a)$$

For perdeuteriated compounds of unknown constitution, this assignment method is the method of choice, since geminal and vicinal interactions are detected.

A homonuclear polarization transfer is also a component of the RELAY method,[10] which enables a correlation of neighboring ^{13}C nuclei via vicinal protons. The pulse sequence for the analogous $^2H,^2H,^{13}C$-RELAY-NMR experiment, in which smaller couplings are likewise preferably detected by a suitable choice of the intervals $t_1(0)$ and Δ_1, and the $^2H,^2H,^{13}C$-RELAY-NMR spectrum of [D_5]pyridine are shown in Figure 2. The assignment of the ^{13}C-signals is documented by the corresponding cross peaks. The experiment extends the earlier described $^2H,^{13}C$-shift correlation,[11] but, since it necessitates long measuring times, it is only of interest when $^2H,^{13}C$ correlation experiments and $^2H,^2H$-COSY-NMR spectroscopy fail because of signal overlap.

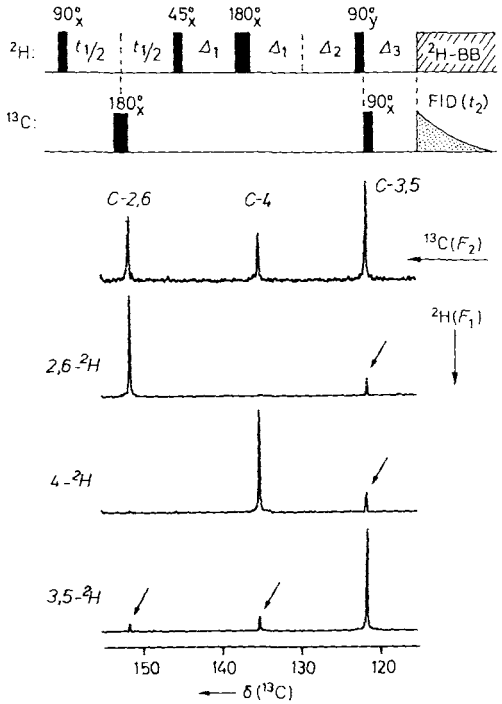

Fig. 2. Pulse sequence for the $^2H,^2H,^{13}C$-RELAY-NMR experiment and the result obtained for [D_5]pyridine. The traces of the two-dimensional data matrix parallel to the ^{13}C-shift axis (F_2) are shown. Besides the RELAY signals (arrows) there also appear the intense signals of the $^2H,^{13}C$-shift correlation over the direct $^1J(^{13}C,^2H)$ coupling. Spectral window 300 (F_1) and 3500 Hz (F_2), 64 t_1 increments of 3.3 ms with $t_1(0) = 0.4$ s, relaxation interval 4 s, $\Delta_1 = 0.2$ s, polarization transfer interval $\Delta_2 = 1/2J(^{13}C,^2H) = 20$ ms, refocusing interval $\Delta_3 = 5$ ms, $t_2 = 0.14$ s, 160 accumulations, phase cycle of the Bruker standard software, data processing with sine function in F_1 and exponential multiplication in F_2, measuring time 14.1 h.

Received: October 23, 1986;
supplemented: November 26, 1986 [Z 1963 IE]
German version: *Angew. Chem.* 99 (1987) 151

[1] a) J. Jeener, Ampère Int. Summer School (Basko Polje, Yugoslavia 1971), unpublished; b) W. P. Aue, E. Bartholdi, R. R. Ernst, *J. Chem. Phys. 64* (1976) 2229; c) reviews: R. Benn, H. Günther, *Angew. Chem. 95* (1983) 381; *Angew. Chem. Int. Ed. Engl. 22* (1983) 350; H. Günther, D. Moskau, *Kontakte 1986*, No. 2, S. 41; G. A. Morris, *Magn. Reson. Chem. 24* (1986) 371.
[2] W. Peters, M. Fuchs, H. Sicius, W. Kuchen, *Angew. Chem. 97* (1985) 217; *Angew. Chem. Int. Ed. Engl. 24* (1985) 231.
[3] Exception $^{11}B,^{11}B$-couplings: C. Brevard, P. Granger: *Handbook of High Resolution Multinuclear NMR*, Wiley, New York 1981, p. 89.
[4] A. Bax, R. Freeman, *J. Magn. Reson. 44* (1981) 542; A. Bax: *Two-Dimensional Nuclear Magnetic Resonance in Liquids*, Reidel, Dordrecht 1982.
[5] T. L. Venable, W. C. Hutton, R. N. Grimes, *J. Am. Chem. Soc. 104* (1982) 4716; *ibid. 106* (1984) 29.
[6] P. J. Domaille, *J. Am. Chem. Soc. 106* (1984) 7677.
[7] H. Günther, D. Moskau, R. Dujardin, A. Maercker, *Tetrahedron Lett. 27* (1986) 2251.
[8] S. Castellano, C. Sun, R. Kostelnik, *J. Chem. Phys. 46* (1967) 327.
[9] T. F. Wimett, *Phys. Rev. 91* (1953) 499; P. Diehl, T. Leipert, *Helv. Chim. Acta 47* (1964) 545.
[10] G. Eich, G. Bodenhausen, R. R. Ernst, *J. Am. Chem. Soc. 104* (1982) 3731; P. H. Bolton, G. Bodenhausen, *Chem. Phys. Lett. 89* (1982) 139; P. H. Bolton, *J. Magn. Reson. 48* (1982) 336.
[11] J. R. Wesener, P. Schmitt, H. Günther, *Org. Magn. Reson. 22* (1984) 468; J. R. Wesener, H. Günther, *J. Am. Chem. Soc. 107* (1985) 1537.

 © VCH Verlagsgesellschaft mbH, D-6940 Weinheim, 1987 0570-0833/87/0202-0157 $ 02.50/0

Has Quantum Chemistry Grown Up?

This question is prompted by the appearance of the following two new books:

A Handbook of Computational Chemistry. By *T. Clark*. Wiley, Chichester 1985. 332 pp., bound, £ 35,80.—ISBN 0-471-88211-9.

Semi-empirical Methods of Quantum Chemistry. By *J. Sadlej*. Ellis Horwood, Chichester 1985. 386 pp., bound, £ 42.50.—ISBN 0-85312-167-2

Instead of giving a conventional review of these books, I shall try here to examine the development of quantum chemistry since its emergence, and to consider its present state and its continually changing relationship to "established" chemistry.

Quantum chemistry is the application of quantum mechanics to chemistry, even though the activities in which quantum chemists are engaged can vary quite widely. Does a theoretical statement become a useful contribution to our knowledge only when it is expressed as a mathematical formula, or do numbers that are arrived at by less explicit methods, and yet are real in terms of our observations, also have a knowledge value? This question can be put more succinctly as follows: do we want quantum chemistry to provide generalized statements, or are its most useful results those that are more specific to particular substances? At present quantum chemistry is well on the way to adopting a more sceptical attitude towards broad generalizations. Thus, for example, benzene now seems to be the only molecule which is truly aromatic, although some definitions of aromaticity are quite unrelated to material properties, but are of a topological nature, and are therefore shown to be inadequate. Again, the *Hückel* $4n+2$ and $4n$ rules now show more exceptions than regular cases, and elements which are said to be homologous are often radically different. Quantum chemistry today ought not to impose limitations on the scope of its applications, e.g. by avoiding the study of compounds not yet prepared synthetically, but instead should test familiar general statements more widely and, where necessary, re-express them in a more restricted form. Theory is thus approaching closer to chemical reality, as it concerns itself more with statements related to particular substances, and rejects over-generalized statements when required. These observations allow us to formulate an up-to-date definition of applied quantum chemistry as the application of computational methods, with the help of a computer, to give data on structures and energies.

We can now see that the question posed in the title can hardly be answered by a simple yes or no. What criteria can be used to judge the development progress of this scientific discipline?

● In the preface to *Clark*'s book *Paul von Ragué Schleyer* writes: "The chemist now has incredibly powerful mathematical tools at his disposal. These tools are simple to use. ... The future directions of chemical research are already programmed!" The physicist *Dirac* was moved to express a rather similar hymn of praise in 1929 when he first encountered the Schrödinger Equation. Predictions of this sort were also made during the sixties, when quantum chemistry had passed through its critical first phase of development and become established as a chemical discipline. The essential difference now, though, is that the statements come from chemists, showing that one of the aims of quantum chemistry, namely to become accepted as an integral part of chemistry, has been achieved.

● The first book published on quantum chemistry—and in fact the expression itself—came in 1937 from *Hans Hellmann* (H. Hellmann: *Einführung in die Quantenchemie*, Deuticke, Vienna 1937). If one could ask the author for his view of quantum chemistry today, one might expect a reply something like the following: quantum chemistry is now in its adolescence—much grown in size, enormously powerful, but intellectually immature. Thus, for example, a chemist using a computer program for configurational interaction (CI) calculations, which relies on Brillouin's theorem, does not need to have this theorem in mind each time he does so, nor even ever to know that he is using the theorem. In its application quantum chemistry today is for that very reason a matter of volition rather than of knowledge and ability. Is this a situation that is appropriate to the academic ideal?

● This criticism of the process of growing up can, however, be seen in a different way. In the book by *Clark* an attempt is made for the first time to separate science from technology. From being originally the preserve of a few physicists with a mathematical background, the application of quantum chemistry now no longer calls for an expensive mathematical training, and it is therefore accessible to the whole of the chemical community. This situation reminds one of *Coulson*, who several decades ago was bold enough to venture into chemistry, and successfully replaced the mathematical formalism of quantum mechanics by "primitive patterns of understanding" (C. A. Coulson: *Valence*, Clarendon Press, Oxford 1952).

Clark mainly sticks to his stated intention of not writing a book for theoreticians, which is fortunate, since those brief attempts at theoretical explanations that have been inserted into the text have a confusing effect. Not much can be made of statements like "the Walsh orbitals in cyclopropane are responsible for much of the unusual chemistry of three-membered ring systems", "the Born-Oppenheimer approximation is a very good one, except in the case of extremely flat potential surfaces", or "in the CI treatment there is mixing of electronic states". The section on electron correlation, though, is unforgivable, where it is stated, and illustrated by a diagram, that in the CI treatment the wave function of a singly excited singlet state is mixed with that of the SCF ground-state! What has become of Brillouin's theorem in this case? Inevitably at this point one has misgivings that the knowledge of technology alone might open the way to its misuse.

How do the facilities available for applying quantum chemistry now look? Essentially three programs are described, for which the manner of feeding in the input and the interpretation of the output are described with numerous examples, namely:

1) classical force field calculations (molecular mechanics);

2) semi-empirical MO procedures (MINDO and MNDO);
3) ab initio procedures (GAUSSIAN 82).

The fact that such a wide range of possibilities exists may be taken as an indication of the increasing maturity of quantum chemistry, for only a few years ago it would not have been possible to bring together in a single book computational procedures based on such differing philosophies. The book will be of interest to all chemists who are interested in molecular structure and energetics.

Semi-empirical methods of calculation have made a contribution to the development of quantum chemistry whose importance can scarcely be overestimated. The great heyday of semi-empirical methods occurred in the sixties, and therefore it is hardly to be noticed that the second of the books under review, by *Joanna Sadlej*, should describe the state of the topic in 1978. It has apparently taken seven years for the book to be translated from Polish into English. During that time the following developments have occurred:

1) the CNDO method, and the procedures derived from it, apart from MNDO, have practically disappeared from the journals;
2) studies of molecular structures and energies of reactions have become much more common than the 40 pages here would suggest;
3) semi-empirical calculations of spectroscopic quantities have declined to such an extent that the 95 pages occupied in the book now seem far too many;
4) CNDO calculations on hydrogen bonding are now recognized to be basically incorrect, so that the chapter of 38 pages is now superfluous;
5) the size of compounds for which semi-empirical calculations are indispensable is now considerably larger.

Unhappily the one method which might have been kept unaltered from 1952, and still retains its standing today, namely the extended Hückel theory (EHT), is given only one page in the appendix.

Despite these deficiencies, however, *Joanna Sadlej* shows in her book in a very impressive way the importance of semi-empirical methods in the development of quantum chemistry, particularly through the many examples and their associated literature references. Whereas many of the early books on semi-empirical methods reflect mainly the personal views of their authors, *Sadlej* has tried—successfully for the most part—to remain objective, so as to produce as complete a work as can be achieved by a single author. It is unfortunate that this care is to some extent wasted, since all that this book contains; and a great deal more besides, is contained in volumes 7 and 8, both edited by *G. A. Segal*, in the series *Modern Theoretical Chemistry* (*Semiempirical Methods of Electronic Structure Calculations*, Plenum Press, New York 1977).

The relationship of quantum chemistry to physics and chemistry, and that between the alternative approaches of ab initio and semi-empirical methods, can best be discussed by considering Table 1, which lists the annual totals of papers on quantum chemistry in several journals; the figures in parentheses give the number of papers on ab initio methods included in the total.

Table 1.

Year	*J. Chem. Phys.*	*J. Am. Chem. Soc.*	*Angew. Chem.*
1960	88	1	0
1961	136	0	1
1962	217	1	0
1963	244	14	1
1964	292	7	2
1965	288	19 (1)	3
1966	209	23	2
1967	252	18 (4)	2
⋮	⋮	⋮	⋮
1985	60	145 (121)	6

In the years after 1960 the numbers of quantum chemistry papers in physics journals increased sharply as a result of computer developments. They reached a maximum in the middle of the sixties, and at the same time papers on these topics began to appear in chemical journals, even in those published in countries where a strong traditionalism in chemistry is said to exist. This breakthrough was mainly due to the work of *Dewar* and *Hoffmann*. Quantum chemistry was at that time divided into two camps, the physical (ab initio methods) and the chemically oriented (semi-empirical methods). Papers giving results obtained by ab initio methods were accepted only hesitantly in the chemical literature from the mid-sixties. Now, twenty years later, quantum chemistry work is carried out to a considerably greater extent in chemical than in physical research groups, and semi-empirical methods play only a secondary role, the only appreciable contributions in 1985 for the three journals of Table 1 being 17 on MNDO and 7 on EHT methods. Two of the arguments put forward in the past for using semi-empirical methods, now becoming less valid, are that "qualitative results are often sufficient", and that "calculations on large molecules call for drastic approximations". Meanwhile ab initio calculations have been successfully applied to the spherical C_{60} molecule and to a DNA fragment with three stacked base pairs. The trend in quantum chemistry is plainly towards obtaining numerically reliable results from ab initio calculations.

The development of quantum chemistry is undoubtedly closely linked to that of computers. However, to avoid the possibility of any misunderstanding with regard to quantum chemistry reaching its maturity, this attempt at a study of its historical development will conclude with a quotation from *Coulson:* "Our understanding ... must be in terms of simple physical models which can readily be visualized, and not in terms of numbers gushing from a computer. If our concepts and patterns of understanding are sound they will be supported by rigorous calculation; if not they must be rejected."

Rudolf Janoschek [NB 775 1E]
Institut für Theoretische Chemie
der Universität Graz (Austria)

Medicinal Chemistry Research in India. By *H. Singh, A. S. Chawla,* and *V. K. Kapoor.* National Information Centre for Drugs and Pharmaceuticals, Lucknow (India) 1985. 184 pp., bound, Rs. 150.00/$ 35.00.—ISBN 81-85042-00-4

Medicinal chemistry is a line of research which has been pursued more intensively in India since independence. This book gives a survey of Indian research in this field, in twenty concise chapters which cover published work up to 1985.

An introductory chapter describes the achievements of Indian pharmaceutical research, six of its drugs having come on to the market. The following sixteen chapters are

devoted to the treatment of specific conditions. The lengths of the various chapters show which are the main areas of emphasis in the research. It will come as no surprise to discover that these areas are the control of fertility, the central nervous system, and the cardiovascular system. On the other hand, the search for an antimalarial drug, which would certainly be of importance to India, appears to receive less attention. Also one looks in vain for papers on antibiotics of the β-lactam type. In contrast to this, there is considerable emphasis on the isolation and structure determination of natural products.

Five chapters deal with chemotherapeutic compounds: anthelmintics, antiprotozoics, fungicides and antibacterial substances, and antiviral and cytostatic agents. Pharmacologically active substances are divided into psychotropic and other drugs which affect the central nervous system, anti-inflammatory agents, local anesthetics, neuromuscular and ganglionic blocking agents, antihistaminics, cardiovascular drugs, diuretics, and agents affecting hyperglycaemia or fertility. Information is given on the effectiveness, state of development, and origin of each pharmacological substance. Descriptions of syntheses and detailed pharmacological information are not included. Regrettably too, structural formulas have often been omitted in favor of systematic chemical names, so as to save space, and the readability of the text has consequently suffered in places.

There is a further chapter dealing with structure-activity relationships and drug design. The references given are mainly to studies which aim to establish quantitative structure-activity relationships (QSAR). The book concludes with two brief chapters describing research on prostaglandins and peptides.

The authors have evidently been concerned to make this as complete a survey as possible, and to include references to all the relevant papers. Accordingly the bibliography, containing more than 1100 references and occupying two-fifths of the text, is very comprehensive. The book is rounded off by a subject and an author index.

Harald Burghard [NB 781 IE]
Hoechst Aktiengesellschaft, Frankfurt/Main (FRG)

Geschichte der Elektrochemie. By *L. Dunsch.* VEB Deutscher Verlag für Grundstoffindustrie, Leipzig 1985. 145 pp., paperback, DM 14.00.—Order no. 5478814

As one scans through the latest issues of scientific journals on display in the library, wondering how valuable this host of publications really is, it is occasionally quite useful to take a look back at the history of one's own particular field. For electrochemists I can recommend for that purpose this little book by *L. Dunsch,* which presents a brief history of the subject. It starts with the mysterious monocell of the Parthians, and continues up to the beginnings of electrode kinetics in the 1940's.

The accounts of the earliest attempts to understand electrical phenomena, of "animal electricity", and of the "glass" and "amber" types of electricity, make enjoyable reading. But while one may smile at some of the misconceptions, or nod one's approval for a brilliant idea, suddenly one asks oneself: why in fact did the frog's leg muscles twitch in the experiments of *Galvani*?—what actually happens at a molecular level within the nerves? To some extent one is annoyed that one still does not know the precise answer, but is comforted on the other hand, by knowing that *Galvani*'s contemporaries would not even have understood the question.

It is exciting to see how concepts have gradually emerged; how, for example, the earliest electrochemical series were established, or when the idea of an ion first appeared. On many of the topics, especially on the great disputes that have occurred, one would like a more detailed account. On what grounds did the respective adversaries base their views? What experimental evidence did they rest on? When was the controversy finally settled, and why? Answers to these questions would of course have expanded the text beyond the bounds of this little volume, but one would nevertheless like to see a fuller account published, perhaps from this same author!

Towards the end of the book we arrive at those questions and techniques which are familiar to us now. We learn something about the beginnings of kinetic studies and pulse techniques, but these developments are not followed up further. It is understandable that the author has refrained from writing the history of an area of research which is still incomplete, but I wish that he had been bold enough to bring us closer to the present situation in electrochemistry.

However, this is on the whole a very successful book. It is nicely illustrated with pictures of apparatus and scientists, and is rounded off by a table of dates, some well chosen literature references, and a list of relevant people with biographical notes which is quite detailed for such a small book.

Wolfgang Schmickler [NB 762 IE]
Institut für Physikalische Chemie
der Universität Bonn (FRG)

Registered names, trademarks, etc. used in this journal, even when not marked as such, are not to be considered unprotected by law.

© VCH Verlagsgesellschaft mbH, D-6940 Weinheim, 1987. - Printed in the Federal Republic of Germany by Zechnersche Buchdruckerei, Speyer/Rhein.

All rights reserved (including those of translation into foreign languages). No part of this issue may be be reproduced in any form - by photoprint, microfilm, or any other means - nor transmitted or translated into a machine language without written permission from the publishers. Only single copies of contributions, or parts thereof, may be made for personal use.

Valid for users in the USA: The appearance of the code at tbe bottom of the first page of an article in this journal (serial) indicates the copyright owner's consent that copies of the article may be made for personal or internal use, or for the personal or internal use of specific clients. This consent is given on the condition, however, that the copier pay the stated per-copy fee through the Copyright Clearance Center, Inc., for copying beyond that permitted by Sections 107 or 108 of the U.S. Copyright Law. This consent does not extend to other kinds of copying, such as copying for general distribution, for advertising or promotional purposes, for creating new collective works, or for resale. For copying from back volumes of this journal see 'Permissions to Photo-Copy: Publisher's Fee List' of the CCC.

Editorial office: Pappelallee 3, D-6940 Weinheim, Federal Republic of Germany, Telephone (06201) 602315, Telex 465516 vchwh d, Telefax (06201) 602328.

Editor: *P. Gölitz.*

Associate editors: *D. J. Loewus, A. Stimson.* **Editorial assistant:** *E. Schweikart*

Publishers: VCH Verlagsgesellschaft mbH. (Managing Directors: *Prof. Dr. Helmut Grünewald* and *Hans Dirk Köhler*), Pappelallee 3, D-6940 Weinheim, Federal Republic of Germany. Correspondence concerning advertisements should be addressed to VCH Verlagsgesellschaft mbH. (Advertising Manager *R. J. Roth*), Boschstr. 12. P.O. Box 1260/1280, D-6940 Weinheim, Federal Republic of Germany, Telephone Weinheim (06201) 602-0, Telex 465516 vchwh d, Telefax (06201) 602328.

ANGEWANDTE CHEMIE
International Edition in English
Volume 26 · Number 3
March 1987
Pages 161–274

Electrodes for Potential Measurements in Aqueous Systems at High Temperatures and Pressures

By Leonard W. Niedrach*

The measurement of pH, redox potentials, and corrosion potentials at high temperatures and pressures is often desirable for the control and monitoring of industrial processes; e.g., for controlling water chemistry in conventional and nuclear power generators, for process control in the chemical industry, and for monitoring performance in petroleum extraction and refining. Such measurements are also needed for research on the thermodynamics of high-temperature aqueous solutions including those associated with geothermal and hydrothermal reactions. Zirconia electrodes for these purposes are described, and their application is illustrated with examples. While not yet routinely available on a commercial basis, useful versions can be readily fabricated in the laboratory. Some of the pitfalls encountered in making such measurements at elevated temperatures are also discussed because great care is often required to assure that valid and useful data are being obtained.

1. Introduction

Of considerable concern in the operation of high-temperature aqueous systems is the control of pH and the redox potential because of their importance as process variables in such areas as paper manufacturing, catalysis, polymerization, and petroleum refining. While in some cases adequate information can be obtained from measurements on cooled side streams, it is often more useful to perform the measurements at the process temperature. Under such conditions less time lag is involved, and, more important, unpredicted shifts in equilibria are avoided. The importance of making measurements under process conditions is particularly evident in the case of corrosion potentials. In the nuclear industry, for example, it has been demonstrated that maintaining the corrosion potential of stainless steel below a critical value can be effective in mitigating stress corrosion cracking. For adequate control such measurements must be made under the process conditions.

In recent years much work has been published aimed at the development of suitable electrodes for such measurements. As might be expected, much of the impetus has come from the nuclear industry through a widespread interest in mitigating corrosion problems through an understanding of the theoretical principles and thermodynamic parameters involved. This article reviews some of these developments and describes some of the more useful electrodes. Their applications are illustrated with examples.

2. Description of Electrodes

2.1. Conventional Reference Electrodes

In thinking of a reference electrode one normally focuses on a type that is essentially insensitive to the environment being monitored. Such electrodes are generally fabricated with a highly reversible couple such as the mercury/mercury(I) chloride (calomel) couple or the silver/silver chloride couple in contact with a stable, aqueous po-

[*] Dr. L. W. Niedrach
General Electric Company
Corporate Research and Development
P.O. Box 8, Schenectady, NY 12301 (USA)

 © VCH Verlagsgesellschaft mbH, D-6940 Weinheim, 1987 0570-0833/87/0303-0161 $ 02.50/0

tassium chloride solution, and they are capable of establishing a liquid junction with the environment being monitored with only a minor offset or liquid-junction potential at the interface. For applications at ambient temperature the saturated or 3 M calomel and silver/silver chloride electrodes are classical examples. Such high concentrations of KCl cannot be employed at high temperatures, however, because of the strong complexing action on mercury(I) and silver chlorides and the ensuing changes in chloride activity. It has been found, however, that lower concentrations of KCl do function satisfactorily at elevated temperatures, and considerable effort has been devoted to the development of practical reference electrodes based upon the silver/silver chloride couple.

Two variants of the silver/silver chloride electrode have proven most popular for high-temperature applications. One, the *isothermal type*, operates entirely at the temperature and pressure of the environment being monitored. The other, the *thermal junction type*, operates with a thermal junction across the electrolyte bridge, and the reference couple itself is held at ambient temperature. Both have proven quite satisfactory in practice.

Numerous investigators have described a variety of versions of the isothermal-type electrode.[1-4] That of *Indig* et al.[3] will serve as an example for more detailed discussion. As shown in Figure 1, a silver wire coated with silver chloride is contained within a Teflon housing adapted to a Conax pressure fitting. The filling solution of 0.01 M KCl communicates with the external environment through a porous plug. Related structures employing only water as the internal filling solution have been found to perform satisfactorily for measurements in the high-purity water employed in nuclear reactors.[4,5] In this case an excess of silver chloride is added to the Teflon housing and its dissolution in the water within the housing establishes a steady reference potential.

The thermal-gradient-type electrode has also been investigated by a number of workers.[6-8] An example, as described by *Danielson*,[6] is shown in Figure 2. It is assembled within a Teflon tube, which also serves as the electrolyte bridge to the point of interest within the environment being monitored. To permit operation in pressurized systems, the Teflon bridge is retained within metal tubing. The potential offset resulting from the temperature gradient is a function of the temperature difference between the solution and the reference couple as well as the concentration of the salt in the bridge. These effects have been studied by *Macdonald* et al.,[7] who have tabulated relevant offset data.

In our experience, both types of reference electrode function quite satisfactorily. It must be emphasized, how-

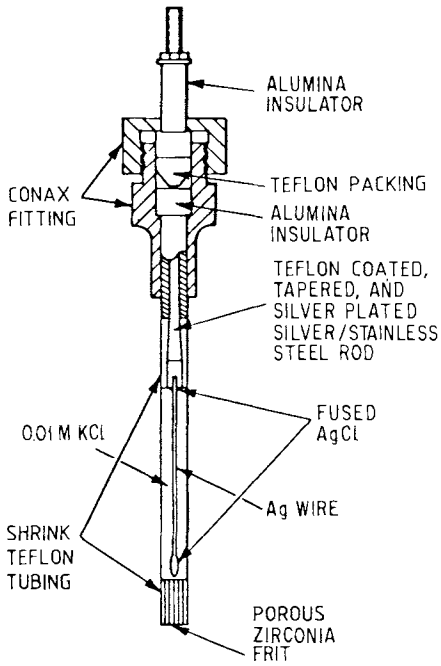

Fig. 1. Isothermal-type reference electrode after *Indig* et al. [3]. Standard Conax fittings establish the pressure boundary. Care must be exercised that the porous zirconia frit forms the only junction with the environment being monitored.

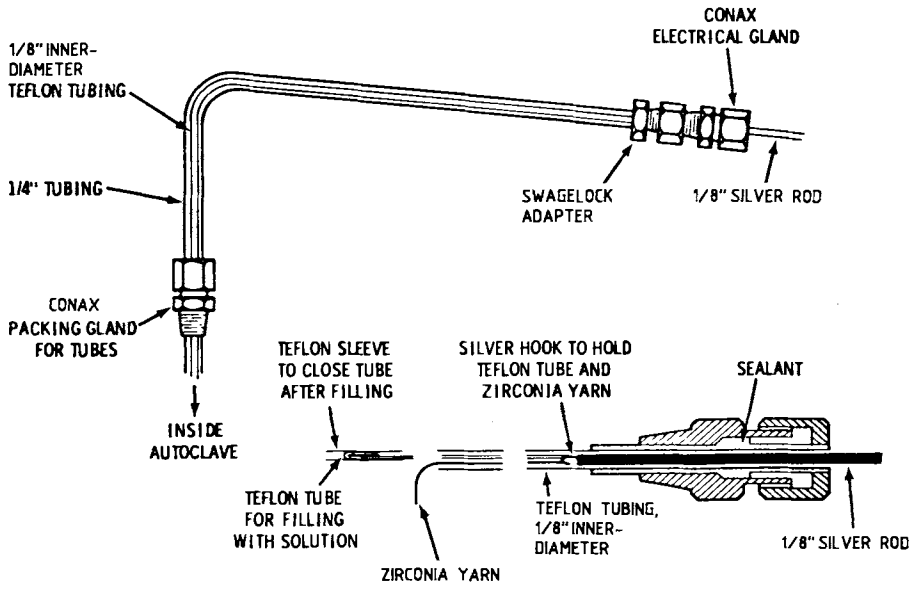

Fig. 2. Thermal-gradient-type reference electrode after *Danielson* [6]. A porous zirconia plug (not shown) forms the junction with the environment being monitored. The zirconia yarn serves to bridge any gaps in the electrolyte that may form during operation without an overpressure.

ever, that both do involve porous junctions between the reference couple and the environment being monitored. In principle, then, exchange of solutes can occur between the two and this can result in drift in the reference potential as chloride is lost or gained by the filling solution. The rate of such drift is dependent upon the magnitude of the concentration gradients and the porosity of the junction.[5] It is also important to consider the expansion of water upon heating to higher temperatures. Thus, upon cooling after use at a high temperature, water will be drawn in from the external environment to further change the chloride concentration within the electrode chamber. This effect is smaller with a thermal-gradient electrode than with an isothermal electrode because less of the filling solution goes through the temperature cycle in the former case.

Another possible source of drift is associated with perfusion of dissolved hydrogen or oxygen into the reference chamber from the environment. Hydrogen can reduce silver chloride to release hydrochloric acid into the solution, thereby contributing to drift by increasing the chloride ion concentration. Conversely, oxygen can oxidize silver in the presence of chloride to form silver chloride and thereby cause drift in the opposite direction. Perfusion is markedly limited by the outer steel tubing employed with the Danielson electrode. A variant of the Indig electrode, in which the Teflon housing is replaced with a zirconia tube, reduces perfusion with that type of electrode.[9]

2.2. Indicator Electrodes

For the monitoring of the redox potential of an environment, a platinum electrode can be used in conjunction with an appropriate reference electrode. Design can vary significantly, the major concern being a reliable seal against the pressure and adequate insulation of the support so that the working area is reasonably well defined. An example is shown Figure 3. A Conax compression seal with a Teflon insert is used to penetrate the pressure barrier and Teflon is used to insulate all but the area designed to contact the environment. Alternatively, a flag-type electrode supported by a Teflon-insulated wire passing through the compression seal may be used.

2.3. pH Electrodes

A wide variety of electrodes have been investigated in order to measure pH at elevated temperatures. They include the classical hydrogen electrode,[10, 11] the palladium hydride electrode,[12, 13] the glass electrode, and metal–metal oxide couples.[14] For general application, the first suffers from a need to know the concentration of dissolved hydrogen in the environment being monitored and from interference from other redox-active species. Metal oxide and palladium hydride electrodes also suffer from interference from other redox-active species. Up to temperatures of about 150 °C the glass electrode can be employed, but at higher temperatures it is severely attacked even by high-purity water. This electrode, however, responds through changes in a membrane potential rather that through the response of electron-transfer couples and is therefore independent of redox-active species in the solution.

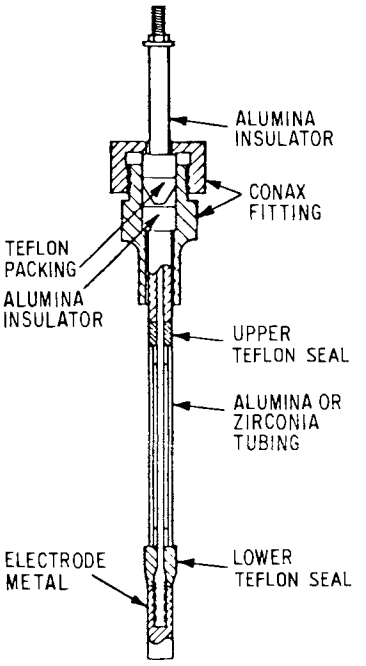

Fig. 3. Metal electrode after *Indig* et al. [3]. The stainless steel support rod is threaded on the lower end to accept the metal electrode. Care must be exercised to assure a tight seal of the metal electrode against the Teflon.

It was more recently found that stabilized zirconia can serve as a membrane-type electrode, much like the glass electrode,[15, 16] but without the major disadvantage of the latter (excessive solubility at high temperatures). This has proven to be the most satisfactory type of pH sensor available for high-temperature studies. Representative designs are shown in Figure 4. In early work sensors were fabricated in a fashion somewhat akin to that of the conventional glass electrode in that a buffered saline solution in contact with a silver wire coated with silver chloride served as the internal element within the membrane sheath[15, 16] (cf. Fig. 4a). Although this type of internal element has been used by others,[17] it has been observed that a dry mix of a metal and its oxide—or two oxides of the same metal in different valence states—is preferable.[18] Such a design, in which the copper–copper(I) oxide couple serves as the internal element, is shown in Figure 4b. Mercury/mercury(II) oxide has also served satisfactorily[16, 19] and the use of silver/silver oxide has also been reported.[19] In another satisfactory approach the internal element has been prepared with platinum left exposed to air.[20]

In the design shown in Figure 4b, a 1/4-in.-outer-diameter tube[*] consisting of zirconia stabilized with yttria (8 wt-%) is retained in a Conax type EG-125 fitting with a seal consisting of Teflon, Vespel, silver, and alumina elements as shown. The dry mix of copper and copper(I) oxide powders (1 : 1 by weight) is packed around a copper wire in a one to two inch long section near the closed end of the zirconia tube. This defines the active region of the

[*] Obtainable from Corning Glass Works/Zircoa, Solon, OH (USA).

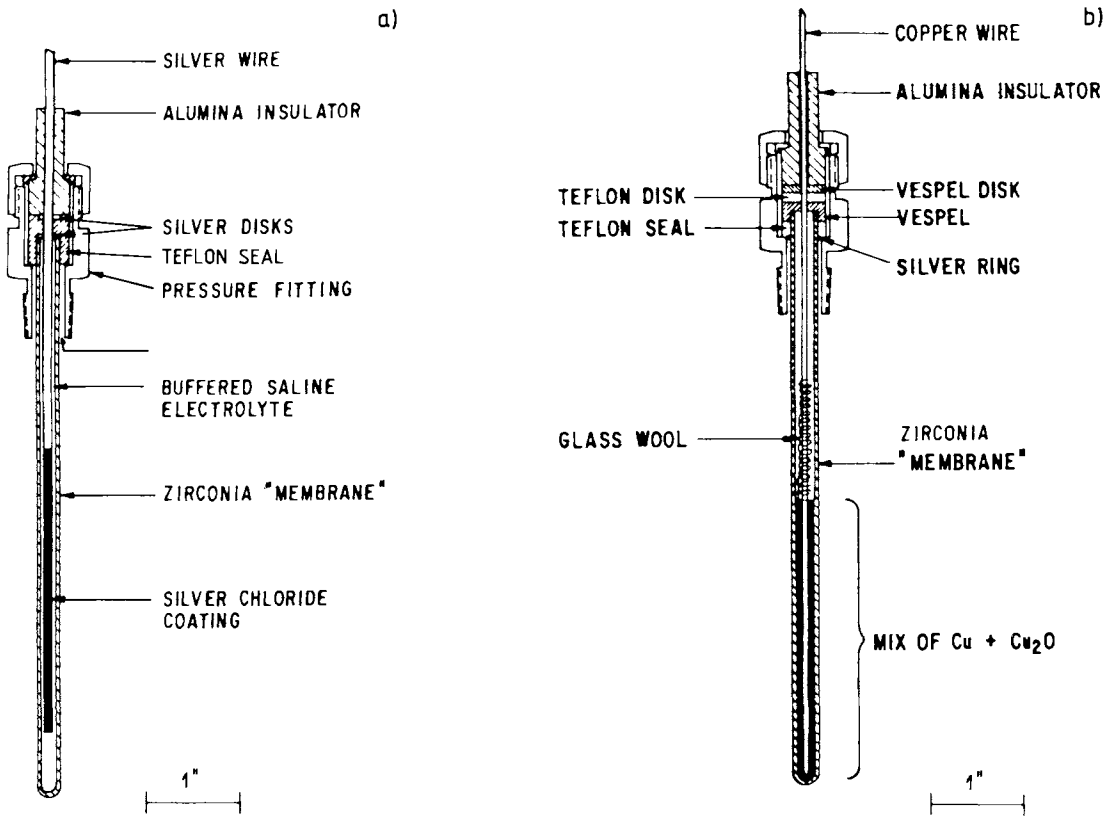

Fig. 4. Schematic diagrams of pH sensors with zirconia "membranes." The diagrams are essentially to scale and none of the dimensions are critical. Clearance between the zirconia tube and the lower portion of the Conax fitting must be provided, if necessary, by enlarging the bore of the fitting. The Teflon and Vespel contacting the zirconia must be machined to fit the outside diameters of the individual tubes, which show considerable variation. For a) and b), see text.

sensor. A backing of glass wool is then added to help confine the powder. Finally, the seal is assembled and tightened with a torque of about 5.7 Nm. This design offers several advantages over the earlier aqueous system: (1) it can be readily prepared by simple mixing of the powders and packing into the tube; (2) it is extremely stable and reproducible; (3) it permits ready designation of the active region of the sensor because the wall is not wetted with a conducting film; and (4) seal fabrication is simplified because of the absence of an internal aqueous phase.

This arrangement has proven highly satisfactory for laboratory work, but because of the thermal properties of the polymeric elements and their tendencies to flow and/or relax, care must be taken to keep them thoroughly confined. For this reason a modification with a brazed metal-to-ceramic seal has been devised.[21]

Because it is relatively new, a brief discussion of the operation of the zirconia pH sensor is perhaps in order. For the sensor shown in Figure 4b, several interphase potentials are involved in series between the external terminal (copper wire) and the solution being monitored. These and the thermodynamic balances involved in the potential-determining reactions at the various interfaces are summarized in Figure 5 according to the approach of *Vetter*.[22] The balances are derived from the fact that at equilibrium the algebraic sum of the electrochemical potentials (${}_i\eta_s$) of the reacting species is zero:

$$\Sigma\ {}_i\nu_s \cdot {}_i\eta_s = 0 \tag{1}$$

where

$${}_i\eta_s = {}_i\mu_s + {}_iz_s \cdot F \cdot {}_i\phi \tag{2}$$

and where ${}_i\mu_s$ is the chemical potential of reacting species s in phase i, ${}_iz_s$ is the charge on the species, ${}_i\phi$ is the Galvani (inner) potential in phase i, ${}_i\nu_s$ is the stoichiometric factor of the species involved in the potential-determining reaction, and F is Faraday's constant.

In summing the interphase potentials between phases 1 and 4, the net change is equivalent to that for the simple copper/copper(I) oxide couple (see Fig. 5):

$$2Cu + H_2O \longrightarrow Cu_2O + 2H^+ + 2e^- \tag{3}$$

The thermodynamics of this reaction is well established.

The membrane may therefore be looked upon as a protective sheath that prevents the metal and its oxide from interacting directly with the solution or redox-active species in the solution. Whereas a copper/copper(I) oxide mix could be exposed to water and dilute acids and bases without significant attack, such would not be the case with strongly acidic or basic solutions. Under any conditions, use of the unsheathed metal/metal oxide mix would necessitate alternative protection from direct interaction with hydrogen or oxygen.

Phases	Thermodynamic balances	Interface potentials
1-2	${}_1\mu_{Cu^0} - ({}_1\mu_{e^-} - F_1\phi) - ({}_2\mu_{Cu^+} + F_2\phi) = 0$	$\Delta\phi_{1-2} = 1/F({}_2\mu_{Cu^+} + {}_1\mu_{e^-} - {}_1\mu_{Cu^0})$
2-3	$({}_2\mu_{O^{2-}} - 2F_2\phi) - ({}_3\mu_{O^{2-}} - 2F_3\phi) = 0$	$\Delta\phi_{2-3} = 1/F(\frac{1}{2}{}_2\mu_{O^{2-}} - \frac{1}{2}{}_3\mu_{O^{2-}})$
1-3		$\Delta\phi_{1-3} = 1/F({}_2\mu_{Cu^+} + \frac{1}{2}{}_2\mu_{O^{2-}} + {}_1\mu_{e^-} - \frac{1}{2}{}_2\mu_{O^{2-}} - {}_1\mu_{Cu^0}) = 1/F(\frac{1}{2}{}_2\mu_{Cu_2O} + {}_1\mu_{e^-} - \frac{1}{2}{}_3\mu_{O^{2-}} - {}_1\mu_{Cu^0})$
3-4	${}_4\mu_{H_2O} - ({}_3\mu_{O^{2-}} - 2F_3\phi) - 2({}_4\mu_{H^+} + F_4\phi) = 0$	$\Delta\phi_{3-4} = 1/F(-\frac{1}{2}{}_4\mu_{H_2O} + \frac{1}{2}{}_3\mu_{O^{2-}} + {}_4\mu_{H^+})$
1-4		$\Delta\phi_{1-4} = 1/F(\frac{1}{2}{}_2\mu_{Cu_2O} + {}_4\mu_{H^+} - {}_1\mu_{Cu^0} - \frac{1}{2}{}_4\mu_{H_2O} + {}_1\mu_{e^-})$

This is thus equivalent to the potential of the following half couple: $Cu^0 + \frac{1}{2}H_2O = \frac{1}{2}Cu_2O + H^+ + e^-$

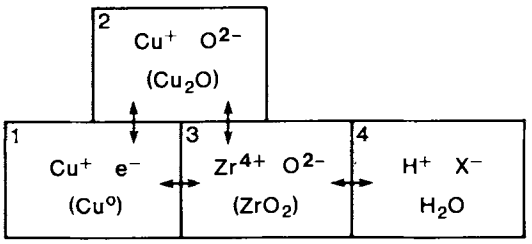

Fig. 5. Interphase potentials and related thermodynamic data for the zirconia pH sensor.

3. Applications

3.1. Measurement of pH

Zirconia sensors are particularly of interest for the measurement of pH at relatively high temperatures and pressures; e.g., 285 °C at 83 bar. When used under these conditions with an appropriate silver/silver chloride reference electrode, they have invariably performed well in both pure water and simulated brines for as long as 40 days. Such performance has been thoroughly documented elsewhere,[18,23] and representative response data obtained in conjunction with a reference electrode of the isothermal type are shown in Figure 6.

Also shown in Figure 6 are the pH responses of a hydrogen electrode and an oxygen electrode under the same conditions. In the latter two cases the same platinized platinum flag was used; however, the redox status of the solutions was changed by equilibrating with either a hydrogen–nitrogen or oxygen–nitrogen mixture. With the hydrogen electrode the response paralleled that of the zirconia electrode since both electrodes are nearly reversible. The response of the oxygen electrode deviates from the theoretically predicted values because of its poorer kinetic behavior.

The data in Figure 7 further emphasize that the zirconia electrode, like the glass electrode, does *not* respond to changes in the redox potential of the environment. These data were obtained while 0.0005 M sulfuric acid, initially aerated, was being fed to the stainless steel autoclave.[16] On switching to a nitrogen purge of the feed stream, the potentials of the autoclave and the platinum flag (oxygen electrode) immediately started to fall while that of the zirconia pH sensor remained constant. After several hours a more rapid drop occurred in the potentials of the autoclave and the platinum electrode. This is attributed to a change in the passivation reaction for the stainless steel autoclave. Instead of the passive film being maintained by the reduction of oxygen to water, water is reduced to liberate hydrogen. The platinum flag then clearly showed its sensitivity to this change in the redox environment. The oxygen-ion-conducting ZrO_2 membrane, however, retained an essentially constant potential. The small, transient increase in potential is believed to have been a response to a real transient in pH associated with the change in the passivation reaction on the stainless steel.

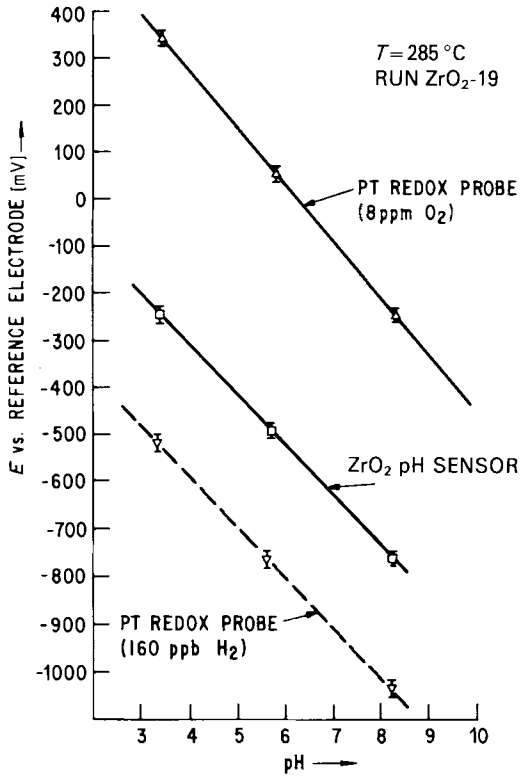

Fig. 6. Variations in the potentials of several electrodes with pH. Reference electrode: silver/silver chloride.

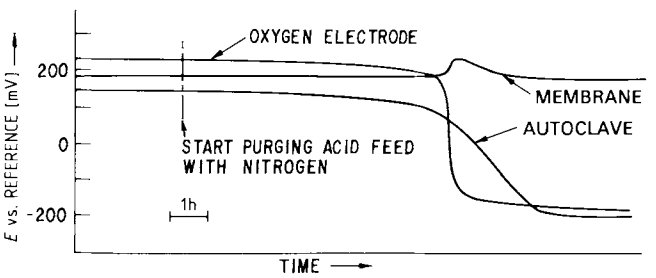

Fig. 7. Behavior of a ZrO_2 pH sensor, the oxygen electrode, and the stainless steel autoclave as the redox potential of the environment is changed at 285 °C. The transient perturbation of the membrane potential at the ZrO_2 pH sensor is believed to reflect a real pH transient associated with a change in the corrosion film on the steel autoclave as the corrosion potential changes. Reference electrode: silver/silver chloride.

An additional example demonstrating the versatility of the zirconia pH sensor is the collection of data in Figure 8 obtained by monitoring pH changes in simulated geothermal brines upon changing the carbon dioxide content and upon introducing hydrochloric acid or base into the solution. The upper portion of the figure shows the changes observed in the solution at 25 °C as measured with a commercial glass electrode (Ingold) while the lower portion shows the measurements at 285 °C. For the latter, two reference electrodes, 13RR and 14RR, of the thermal-gradient type were employed. As much as 100 ppm of sulfide ion (as sodium sulfide) was also introduced into the solution at various times. This had no effect on the instrumentation or the electrodes apart from that caused by the pH changes.

Further examples of the performance of this combination of zirconia pH electrode with a thermal-gradient-type reference electrode are shown in Figure 9 where measured pH values are compared with calculated values for 0.2- and 20-percent brine solutions. In both cases the agreement is excellent.

As noted above, in experiments of this type there is always some chance for bias to creep into the measurements through offsets in either the sensing or reference electrode. It is therefore desirable to calibrate the combination of sensor electrode and reference electrode with known standards. In the brine work, for example, slow drift in the calibration always occurred. Upward displacement of the calibration curve occurred with a 20-percent brine and

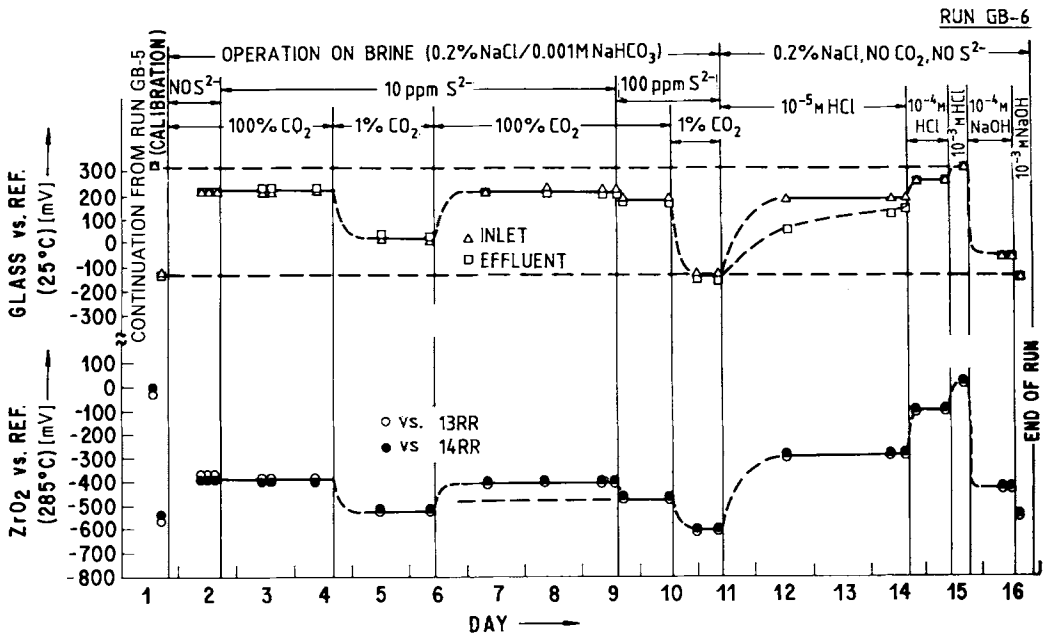

Fig. 8. Potentials of the zirconia pH sensor at 285 °C and glass electrodes at 25 °C versus silver/silver chloride as reference electrode during run GB-6. Two high-temperature reference electrodes, 13RR and 14RR, were used.

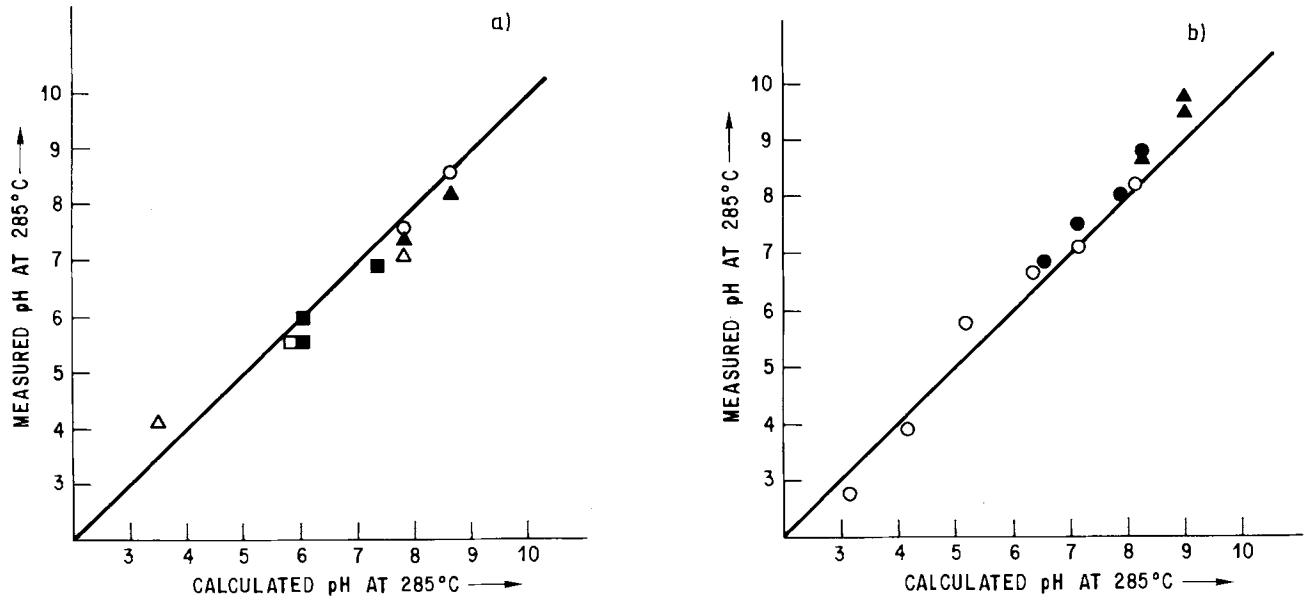

Fig. 9. Correlation between measured and calculated pH at 285 °C for brines. White symbols, no sulfide; black symbols, 10 or 100 ppm sulfide. a) 20% NaCl/0.001 or 0.1 M $NaHCO_3$; circles, triangles, and squares represent runs GB1, GB3, and GB4, respectively. b) 0.2% NaCl/0, 0.001, or 0.1 M $NaHCO_3$; triangles and circles represent runs GB5 and GB6, respectively (cf. Fig. 8).

downward displacements with a 0.2-percent brine. Since the original filling solution in the reference electrode was 0.1 M KCl in all cases, the displacements reflected diffusion of chloride into or out of the reference electrode as a result of the concentration gradients between the internal filling solution and the environment being monitored. This suggests that selection of a filling solution having a chloride concentration close to that of the brine should minimize drift of this type.

3.2. Measurement of Corrosion and Redox Potentials

Corrosion or redox potentials are often measured in order to maintain their values within some favored range. Often these limits are specified in terms of potentials relative to that of the standard hydrogen electrode (SHE). Such values can be derived from measurements against any of the above electrodes, which may serve as reference electrodes when sufficient ancillary information is available. For the conventional type of reference electrode, such as the silver/silver chloride electrode, only the chloride ion content within the electrode chamber must be known. With a knowledge of the pH of the environment, a pH electrode may also serve as a reference electrode. If, in addition, the hydrogen or oxygen activity of the environment is known, the Pt/H_2 (or Pt/O_2) electrode may also serve.

In principle the problem of measuring corrosion or redox potentials should equate with that of measuring the pH. In each case one is interested in the potential between a sensing electrode and a reference electrode. A fundamental difficulty arises, however, in that a convenient, definitive means of calibrating the measurement is available only when measuring pH. In that case a conventional scale has been adopted and convenient standard buffers are available for frequent calibrations to assure the accuracy of the potential measurement even though the reference and/or the sensing electrodes may have suffered drift.

Such standards are not available for corrosion and redox potential measurements. In particular, corrosion potentials are expected to vary considerably with the experimental conditions, the age of the corrosion film, the composition of the metal, etc. For this reason the most stable reference electrode available should be employed for such measurements. If one wishes to be more conservative, at least one additional reference electrode *of another type* should be employed as a check. To underscore this point further, two reference electrodes of the same type cannot be considered as reliable checks upon one another; both could respond to the environment in identical, erroneous ways, or exhibit essentially identical drifts with time.

In connection with the stability of reference electrodes, we have made a number of intercomparisons of the relative stabilities of silver/silver chloride electrodes, zirconia pH sensors, and Pt/H_2 and Pt/O_2 electrodes.[18] As noted in Section 2.1, silver/silver chloride electrodes must be expected to show some drift with time because of their diffusion junctions, especially if temperature cycling of the solution occurs. Such drift has clearly been demonstrated with fillings of 0.01 and 0.1 M KCl.[5] In agreement with *Leibovitz* et al.,[4] we have found that elimination of the KCl and resorting to only the dissolution of an excess of silver chloride gave a more stable potential.[5,24]

Even under these conditions the zirconia pH sensor and the Pt/O_2 electrode[8] have been shown to provide the most stable potential. Figures 10 and 11 show that the most stable correlations are obtained for the potential of the oxygen electrode vs. the ZrO_2 pH sensor. The stability of the Pt/H_2 electrode also falls into this category and in addition is more reliable in establishing a predictable potential.[25] Several types of reference electrode are thus available that can be used as cross-checks on one another if sufficient environmental information is available (namely, the pH and the concentration of dissolved hydrogen or oxygen).

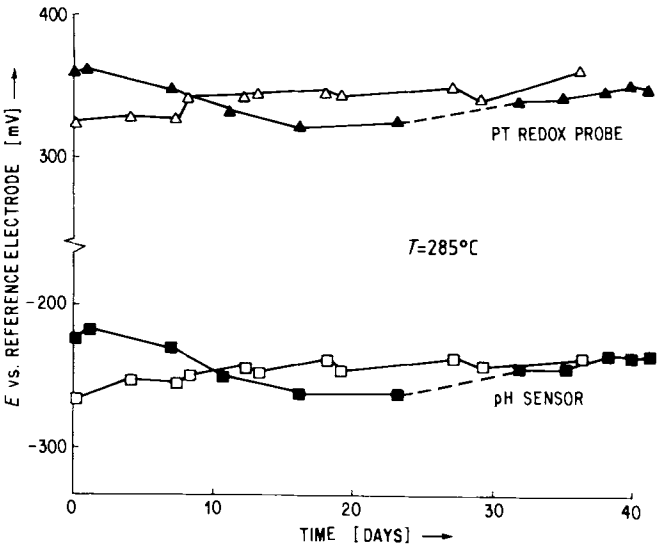

Fig. 10. Potentials of the platinum electrode and the zirconia pH sensor (reference electrode: silver/silver chloride). The solution was aerated so that the platinum was functioning as an oxygen electrode. The silver chloride electrode contained no KCl. The similar temporal changes shown by the platinum and zirconia electrodes suggest that the major cause of the variations lies with the silver/silver chloride electrode. White symbols: Run ZrO_2-19; black symbols: Run ZrO_2-20.

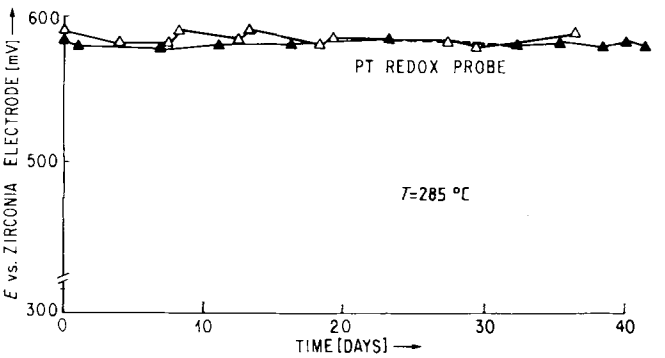

Fig. 11. Potential of the platinum electrode in the aerated solution (reference electrode: zirconia pH sensor). The excellent stability implies that both electrodes are very stable. White triangles: Run ZrO_2-19; black triangles: Run ZrO_2-20.

The focus of interest to date has been in measuring corrosion potentials of stainless steel and other structural materials in the high-purity cooling water of boiling-water

reactors at about 285 °C. Routine measurements of conductivity and pH at ambient temperature assure that the water is indeed pure and therefore has a pH value close to the theoretical neutral point of 5.65 at 285 °C. Routine monitoring of hydrogen and oxygen concentrations—which are the redox-potential-determining species in this case—then permit the calculation of the potential of the hydrogen or oxygen electrode.

The potentials of the various electrodes under consideration vs. the SHE potential at 285 °C have been calculated. With freshly prepared reference electrodes, satisfactory agreement can be obtained with measurements between various pairs of reference electrodes, generally to within ±20–30 mV. With the passage of time, however, drift will sometimes be encountered, especially in measurements involving the silver/silver chloride electrode with the KCl filling.

Based upon our experience, the zirconia pH electrode is preferred for measurements with such relatively pure water systems as the cooling water of boiling-water reactors. This has indeed been our choice for studies of corrosion potentials of stainless steel under so-called normal and hydrogen water conditions. Under normal water conditions, oxygen tends to be somewhat in stoichiometric excess of hydrogen and the platinum electrode behaves much as an oxygen electrode. Under hydrogen water conditions, hydrogen is in excess and the platinum electrode behaves as a hydrogen electrode. The behavior of stainless steel is more complicated.[25] These conditions are of practical interest because the more reducing conditions result in suppression of stress corrosion cracking[26] and much present work is aimed at establishing the value of a critical potential as well as electrochemical means for monitoring the reactor piping.

The data in Figure 12, obtained during studies of crack growth rates of 304 stainless steel under hydrogen water conditions,[24] illustrate the way the corrosion potential responds to changes in the water chemistry. The data were obtained using a zirconia pH electrode, with a copper/copper(I) oxide internal element[24] as the reference electrode. The water chemistry was also followed continuously by analyses of pH, hydrogen and oxygen concentration, and conductivity of the effluent from the autoclave at ambient temperature. Because of the reversibility of the Pt/H_2 electrode, its behavior under changing conditions provided a check on the zirconia electrode during operation under hydrogen water conditions. A silver/silver chloride reference electrode was not used in the work.

In this case the potential measurement was employed as a routine process-control monitor. Shown in Figure 12 are corrosion potentials measured at 285 °C for water nominally containing 160 ppb dissolved hydrogen and no oxygen. At one point, immediately following replacement of a tank of forming gas (nominally 10 percent H_2 in N_2) used to maintain the hydrogen level in the feed stream, the corrosion potential began to rise significantly. Subsequent analysis indicated that the drift had resulted from oxygen contamination in the forming gas to a sufficient extent to introduce 50 ppb into the feedwater. Since the observed effect possibly reflected an influence of the hydrogen–oxygen recombination reaction on the mixed potential of the corroding specimen, additional studies were undertaken.

These examples, drawn from the area of nuclear reactor technology, are perhaps representative of somewhat ideal conditions for such measurements coupled with relatively straightforward means for checking on the validity of the measurements. In situations where complex solutions at high ionic strength are involved, the required additional information concerning pH and redox activity may be too difficult to obtain and correlate to permit valid intercomparisons of the various potential measurements. Under such circumstances extreme caution is required in the interpretation of measured values.

4. Summary and Outlook

Electrodes have been described for the measurement of pH and of redox and corrosion potentials at elevated temperatures. While not yet routinely available on a commercial basis, useful versions can be readily fabricated in the laboratory. In making such measurements at elevated temperatures many pitfalls can be encountered, and great care is required to assure that valid and useful data are being obtained. When possible, direct calibrations to check performance, such as the measurement of pH, should be

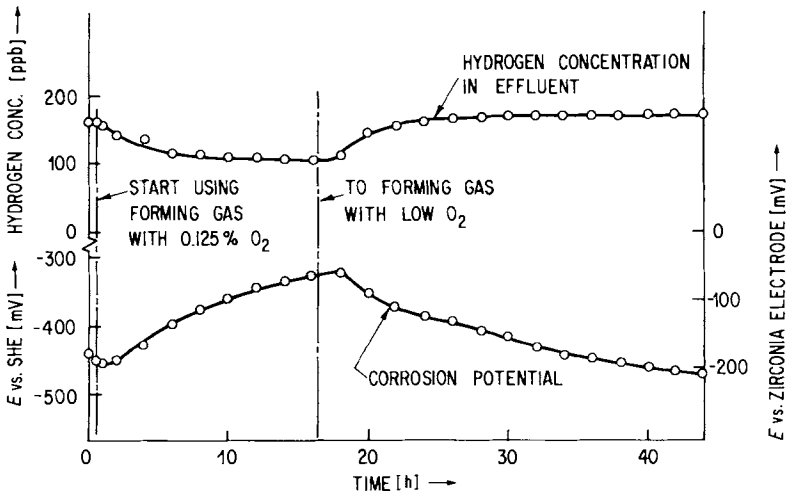

Fig. 12. Transients in the corrosion potential of stainless steel caused by forming gas (N_2 containing 10% H_2) contaminated with 0.125% oxygen. The oxygen content of the gas would introduce 50 ppb O_2 into the water. This amount is stoichiometrically equivalent to only 4 ppb H_2 and would not be expected a priori to have such pronounced effects on the corrosion potential of steel.

made. When such calibration is not possible, it is desirable to employ at least two reference electrodes of different types as a means of protection against undetected, insidious drift of a single reference electrode.

The customized electrodes of today are providing a basis for establishing instrumentation and procedures for their more routine application in the future. As their usefulness becomes more established, commercial versions should become more readily available, and general application should expand.

Received: November 22, 1985;
revised: April 28, 1986 [A 606 IE]
German version: *Angew. Chem. 99* (1987) 183

[1] M. Indig, D. A. Vermilyea, *Corrosion (Houston) 27* (1971) 312.
[2] A. K. Agrawal, R. W. Staehle, *Corrosion (Houston) 33* (1977) 418.
[3] M. Indig, A. R. McIlree, *Corrosion (Houston) 35* (1979) 288.
[4] J. Leibovitz, W. R. Kassen, W. L. Pearl, S. G. Sawochka: *Improved Electrodes for BWR In-Plant ECP Monitoring, EPRI Report No. NP-2524,* Research Project 706-1, July 1982.
[5] L. W. Niedrach, W. H. Stoddard: *The Development of a High-Temperature pH Electrode for Geothermal Fluids. Final Report-Task I,* Report No. PNL 3857 UC-66, März 1981. This report was prepared for the Pacific Northwest Laboratory, which is operated by the Battelle Memorial Institute under contract for the United States Department of Energy, Division of Geothermal Energy (prime contract No. DE-AC-06-76-RLO-1830).
[6] M. J. Danielson, *Corrosion (Houston) 35* (1979) 200.
[7] D. D. Macdonald, A. C. Scott, P. Wentrcek, *J. Electrochem. Soc. 126* (1979) 908.
[8] P. Andresen, M. E. Indig: *Investigation of Benefits of BWR Oxygen Control, EPRI Report No. NP-2424-LD,* Research Project T115-3, June 1982.
[9] D. F. Taylor, C. A. Caramihas, *J. Electrochem. Soc. 129* (1982) 2458.
[10] R. S. Greeley, W. T. Smith, R. W. Stoughton, M. H. Lietzke, *J. Phys. Chem. 64* (1960) 652, 1445.
[11] R. E. Mesmer, C. F. Baes, F. H. Sweeton, *J. Phys. Chem. 74* (1970) 1937.
[12] J. V. Dobson, B. R. Chapman, H. R. Thirsk in R. W. Staehle, D. de G. Jones, J. E. Slater (Eds.): *High Temperature, High Pressure Electrochemistry in Aqueous Solutions,* National Association of Corrosion Engineers (NACE), Houston, TX 1973, p. 341.
[13] D. D. Macdonald, P. R. Wentrcek, A. C. Scott, *J. Electrochem. Soc. 127* (1980) 1745.
[14] J. V. Dobson, P. R. Snodin, H. R. Thirsk, *Electrochim. Acta 21* (1976) 527.
[15] L. W. Niedrach, *Science 207* (1980) 1200.
[16] L. W. Niedrach, *J. Electrochem. Soc. 127* (1980) 2122.
[17] T. Tsuruta, D. D. Macdonald, *J. Electrochem. Soc. 129* (1982) 1221.
[18] L. W. Niedrach, *J. Electrochem. Soc. 129* (1982) 1445.
[19] S. Hettiarachchi, P. Kedzierzawski, D. D. Macdonald, *J. Electrochem. Soc. 132* (1985) 1866.
[20] M. J. Danielson, O. H. Koski, J. Myers, *J. Electrochem. Soc. 132* (1985) 2037.
[21] L. W. Niedrach, W. H. Stoddard, *Ind. Eng. Chem. Prod. Res. Dev. 22* (1983) 594.
[22] K. J. Vetter: *Elektrochemische Kinetik,* Springer, Berlin 1961, p. 16.
[23] L. W. Niedrach, W. H. Stoddard, *J. Electrochem. Soc. 131* (1984) 1017.
[24] L. W. Niedrach, W. H. Stoddard, *Corrosion (Houston) 41* (1985) 45.
[25] L. W. Niedrach, W. H. Stoddard: *Corrosion (Houston) 42* (1986) 696.
[26] R. L. Jones, A. Machiels, M. Naughton, J. T. A. Roberts, *Corrosion '84, Paper No. 167,* March 1984.

Neutral and Charged Biradicals, Zwitterions, Funnels in S_1, and Proton Translocation: Their Role in Photochemistry, Photophysics, and Vision

By Vlasta Bonačić-Koutecký,* Jaroslav Koutecký,* and Josef Michl*

A knowledge of the geometries at which excited molecules return to the electronic ground state (S_0) is essential for the understanding of the structures of photoproducts. Particularly good candidates are geometries corresponding to local minima on the S_1 (lowest excited singlet) and T_1 (lowest triplet) surfaces, as well as S_0–S_1 conical intersections (funnels). Given sufficient effort, such geometries can nowadays be found numerically for small enough molecules. Still, it is interesting to ask whether more approximate, but also more general, statements can be made concerning the geometries at which the S_0 and S_1 surfaces closely approach each other. Since many of these are biradicaloid geometries, it is logical to examine the properties of biradicals and related species at some length. After reviewing the two-electron two-orbital model for molecules at biradicaloid geometries, we formulate the conditions under which the S_0 and S_1 surfaces touch. The results obtained for the simple model are supported by ab initio large-scale configuration interaction (CI) calculations for the twisting of ethylene in the polarizing field of a positive charge and for the twisting of charged double bonds and π-donor-to-π-acceptor single bonds, and by similar calculations for "push-pull" perturbed cyclobutadienes, some of which are predicted to have nearly degenerate S_0, S_1, and T_1 states. The likely consequences of these results for the detailed description of the mechanisms of *cis–trans* isomerization, the formation of *t*wisted *i*nternal *c*harge-*t*ransfer (TICT) states, proton translocation, and possibly of the initial step in vision, as well as for the understanding of the regiospecificity of singlet photocycloaddition, are summarized.

1. Introduction: S_0–S_1 Surface Touching

The 3 × 3 CI description of the two-electron two-orbital model for biradicals has been in common use in organic chemistry for over a decade.[1–4] We shall use it to identify the conditions under which the S_0 and S_1 surfaces of a biradical-like species touch or nearly touch. The corresponding regions in the nuclear configuration space have long been recognized[5–13] as important in determining the geometry a molecule will have as it returns to the electronic ground state after the initial excitation in a photochemical event. Although the simple Hückel description leads one to expect an S_0–S_1 "touching" whenever orbital degeneracy in a biradical-like species occurs (e.g., in orthogonally twisted ethylene or in square cyclobutadiene), this is quite unrealistic, and most such touchings are strongly avoided in better approximations. A better tool than inspection of orbital crossings is therefore needed to answer the question, what structural and geometric features are required for the S_0 and S_1 surfaces of a biradical-like species to touch or nearly touch?

[*] Prof. V. Bonačić-Koutecký, Prof. J. Koutecký
Institut für Physikalische und Theoretische
Chemie der Freien Universität
Takustrasse 3, D-1000 Berlin 33
Prof. J. Michl [+]
Department of Chemistry, University of Utah
Salt Lake City, UT 84112 (USA)
[+] Present address:
Department of Chemistry, University of Texas at Austin
Austin, TX 78712 (USA)

In this article, we first review the 3 × 3 CI model for a perfect (homosymmetric[1]) biradical for the reader unfamiliar with prior literature[1–4] on the subject and provide further details that do not seem to have appeared in print before.

After this introduction, we address the case of a perturbed biradical in terms of wave functions based on the most localized pair of orbitals. The two orbitals are allowed to differ in energy (heterosymmetric biradicaloid, a concept that is similar to but not identical with the heterosymmetric diradical category as defined in ref. [1]), to interact (homosymmetric biradicaloid), or to do both (nonsymmetric biradicaloid). We find that the S_0–S_1 touching or near touching occurs when the electronegativity difference of the two localized orbitals just balances the effects of electronic repulsion which tend to keep the S_0 and S_1 surfaces apart.

Although the 3 × 3 CI model serves as a useful initial description of the electronic structure of molecules at biradicaloid geometries, it is far from exact. In particular, the energetic order of closely spaced states obtained from the model can be incorrect. Examples are the change in the order of the S_0 and T_1 states due to dynamic spin polarization[3,14] in twisted double bonds[15] and in disjoint alternant biradicals[16,17] and the reversal of the character of the S_1 and S_2 states in twisted ethylene[18] and along pericyclic reaction paths in systems such as H_2+H_2.[19] Still, those aspects of the results of the 3 × 3 CI model that do not depend on small energy differences are generally correct.

Subsequently, we consider the likely effects of improvements in the theoretical description and find that the con-

clusions concerning S_0–S_1 touching obtained from the 3×3 CI model should remain qualitatively correct. These conclusions are tested by ab initio large-scale CI calculations for two series of examples: polar twisted double bonds and push-pull perturbed cyclobutadienes. As expected from the simple model, in both instances a suitable degree of polarity results in S_0–S_1 touching or near touching (and in S_0–T_1 crossing).

Finally, we discuss briefly the implications of the resulting improvements in the understanding of S_0–S_1 surface touching in the areas of organic and bioorganic photochemistry.

2. The Two-Electron Two-Orbital Model

2.1. General

When two localized orbitals A and B interact weakly or not at all, the single-configuration description of the resulting two-electron states becomes inadequate. This happens in some molecules at all geometries (e.g., O_2, CH_2) and in all molecules at biradicaloid geometries, such as those in which a σ bond has been stretched or a π bond twisted. In this case, since the two electrons do not contribute much, if at all, to covalent bonding in any of the electronic states of the system, all three possible singlet configurations need to be considered on equal footing, hence the term 3×3 configuration interaction. Since there is only one triplet configuration within this model, no configuration interaction is needed for the triplet state.

Biradicals of real interest typically contain many more than two electrons, and these have many more than two orbitals available to them. Nonetheless, it is often possible to describe them more or less successfully by concentrating on only two electrons in two approximately nonbonding orbitals ("active space") and representing the others by a fixed core. This model is adopted throughout Section 2. Illustration is provided by ethylene twisted by 90°, **1**, in which the two localized orbitals A and B are the nonbonding 2p orbitals on the two carbon atoms, and square cyclobutadiene **2**, in which they are the two nonbonding orbitals shown (Scheme 1).

The quantities that characterize the interactions involved when two electrons are contained in two general orbitals $\mathscr{A}$ and $\mathscr{B}$ are collected in Table 1. $\mathscr{A}$ and $\mathscr{B}$ are chosen

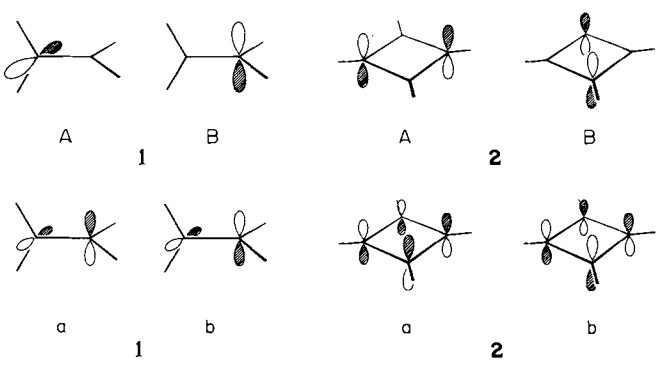

Scheme 1. Localized (A, B) and delocalized (a, b) orbitals in twisted ethylene **1** and cyclobutadiene **2**.

Table 1. The quantities characterizing the interactions involved in the 3×3 CI model description of two electrons contained in two orthogonal orbitals $\mathscr{A}$ and $\mathscr{B}$.

Hamiltonian matrix

$$\begin{array}{l} {}^1|\mathscr{A}^2-\mathscr{B}^2\rangle \\ {}^1|\mathscr{A}^2+\mathscr{B}^2\rangle \\ {}^1|\mathscr{A}\mathscr{B}\rangle \\ {}^3|\mathscr{A}\mathscr{B}\rangle \end{array} \begin{pmatrix} E(\mathrm{T})+2K'_{\mathscr{A}\mathscr{B}} & \delta_{\mathscr{A}\mathscr{B}} & \gamma_{\mathscr{A}\bar{\mathscr{B}}} & 0 \\ \delta_{\mathscr{A}\mathscr{B}} & E(\mathrm{T})+2(K'_{\mathscr{A}\mathscr{B}}+K_{\mathscr{A}\mathscr{B}}) & \gamma_{\mathscr{A}\mathscr{B}} & 0 \\ \gamma_{\mathscr{A}\bar{\mathscr{B}}} & \gamma_{\mathscr{A}\mathscr{B}} & E(\mathrm{T})+2K_{\mathscr{A}\mathscr{B}} & 0 \\ 0 & 0 & 0 & E(\mathrm{T}) \end{pmatrix}$$

One-electron integrals

$$S_{\mathscr{A}\mathscr{B}} = \int \mathscr{A}^*(1)\mathscr{B}(1)\,d\tau = 0 \quad \text{(overlap)}$$
$$h_{\mathscr{A}\mathscr{B}} = \int \mathscr{A}^*(1)\mathrm{H}(1)\mathscr{B}(1)\,d\tau \quad \text{[a]}$$

Two-electron integrals

$$J_{\mathscr{A}\mathscr{B}} = \iint \mathscr{A}^*(1)\mathscr{B}^*(2)\frac{e^2}{r_{12}}\mathscr{A}(1)\mathscr{B}(2)\,d\tau_1 d\tau_2 \quad \text{(Coulomb)}$$
$$K_{\mathscr{A}\mathscr{B}} = \iint \mathscr{A}^*(1)\mathscr{A}^*(2)\frac{e^2}{r_{12}}\mathscr{B}(1)\mathscr{B}(2)\,d\tau_1 d\tau_2 \quad \text{(exchange)}$$
$$(\mathscr{A}\mathscr{A}|\mathscr{A}\mathscr{B}) = \iint \mathscr{A}^*(1)\mathscr{A}^*(2)\frac{e^2}{r_{12}}\mathscr{A}(1)\mathscr{B}(2)\,d\tau_1 d\tau_2 \quad \text{(hybrid)}$$

Secondary quantities

$$\gamma_{\mathscr{A}\mathscr{B}} = 2h_{\mathscr{A}\mathscr{B}} + (\mathscr{A}\mathscr{A}|\mathscr{A}\mathscr{B})^* + (\mathscr{B}\mathscr{B}|\mathscr{B}\mathscr{A})$$
$$\gamma_{\mathscr{A}\bar{\mathscr{B}}} = (\mathscr{A}\mathscr{A}|\mathscr{A}\mathscr{B})^* - (\mathscr{B}\mathscr{B}|\mathscr{B}\mathscr{A})$$
$$\delta_{\mathscr{A}\mathscr{B}} = h_{\mathscr{A}\mathscr{A}} - h_{\mathscr{B}\mathscr{B}} + (J_{\mathscr{A}\mathscr{A}} - J_{\mathscr{B}\mathscr{B}})/2$$
$$K'_{\mathscr{A}\mathscr{B}} = [(J_{\mathscr{A}\mathscr{A}} + J_{\mathscr{B}\mathscr{B}})/2 - J_{\mathscr{A}\mathscr{B}}]/2$$
$$E_0 = h_{\mathscr{A}\mathscr{A}} + h_{\mathscr{B}\mathscr{B}} + (J_{\mathscr{A}\mathscr{A}} + J_{\mathscr{B}\mathscr{B}})/4 + J_{\mathscr{A}\mathscr{B}}/2$$
$$E(\mathrm{T}) = E_0 - K'_{\mathscr{A}\mathscr{B}} - K_{\mathscr{A}\mathscr{B}}$$

[a] H(1) is the one-electron part of the Hamiltonian.

to be orthogonal ($S_{\mathscr{A}\mathscr{B}} = 0$). The physical significance of $J_{\mathscr{A}\mathscr{B}}$ is the repulsion between the charge density due to an electron in orbital $\mathscr{A}$ and that due to one in orbital $\mathscr{B}$. The physical significance of $K_{\mathscr{A}\mathscr{B}}$ is the repulsion between the overlap charge density due to the first electron, $e\mathscr{A}^*(1)\mathscr{B}(1)$, and an identical charge density due to the second electron, $e\mathscr{A}^*(2)\mathscr{B}(2)$. The overlap density is large only in those parts of space in which $\mathscr{A}$ and $\mathscr{B}$ both have a large amplitude simultaneously. Thus, $K_{\mathscr{A}\mathscr{B}}$ is a measure of the degree to which the two electrons get in each other's way. For real orbitals $\mathscr{A}$ and $\mathscr{B}$, $J_{\mathscr{A}\mathscr{B}}$ and $K_{\mathscr{A}\mathscr{B}}$ cannot be negative.

The secondary quantities listed in Table 1, $\gamma_{\mathscr{A}\mathscr{B}}$, $\gamma_{\mathscr{A}\bar{\mathscr{B}}}$, and $\delta_{\mathscr{A}\mathscr{B}}$, contain information on the degree to which a two-electron two-orbital system deviates from an "ideal" biradical: $\gamma_{\mathscr{A}\mathscr{B}}$ provides a measure of the interaction between $\mathscr{A}$ and $\mathscr{B}$ and corresponds roughly to twice the resonance integral of semiempirical theories, $\gamma_{\mathscr{A}\bar{\mathscr{B}}}$ is related to the degree of localization of orbitals $\mathscr{A}$ and $\mathscr{B}$, and $\delta_{\mathscr{A}\mathscr{B}}$ provides a measure of the electronegativity difference between $\mathscr{A}$ and $\mathscr{B}$. Specifically, $\delta_{\mathscr{A}\mathscr{B}}$ is equal to the energy difference between the two-electron configuration $\mathscr{A}^2$, in which both electrons reside in $\mathscr{A}$, and the configuration $\mathscr{B}^2$, in which both reside in $\mathscr{B}$. We shall always choose the higher energy orbital as $\mathscr{A}$, so that $\delta_{\mathscr{A}\mathscr{B}} \geq 0$.

The choice of orbitals $\mathscr{A}$ and $\mathscr{B}$ (see Appendix 1). Since we work with the full CI solution within the function space defined by the model, the results must be independent of

any transformation of the orbital basis set. The condition $\gamma_{\mathscr{A}\bar{\mathscr{B}}}=0$ is satisfied by two pairs of real orbitals $\mathscr{A}$ and $\mathscr{B}$: the most localized possible set A, B and the most delocalized possible set a, b. These are related by (1).

$$\begin{aligned} a&=(A-B)/\sqrt{2}\\ b&=(A+B)/\sqrt{2}\end{aligned} \tag{1}$$

The exchange and Coulomb integrals, $K_{\mathscr{A}\mathscr{B}}$ and $J_{\mathscr{A}\mathscr{B}}$, between the two orbitals acquire their minimum values, K_{AB} and J_{AB}, for the most localized choice and their maximum values, K_{ab} and J_{ab}, for the most delocalized choice. This makes physical sense, since the localized orbitals A and B avoid each other in space to the maximum degree possible, while the opposite is true for a and b (Scheme 1). Both integrals, $K_{\mathscr{A}\mathscr{B}}$ and $J_{\mathscr{A}\mathscr{B}}$ are maximized or minimized simultaneously, since their difference is invariant with respect to orbital transformations.

The Appendix also describes an algorithm for finding the most localized and the most delocalized orbital sets starting with an arbitrary real orthogonal set $\mathscr{A}$, $\mathscr{B}$. The values of E_0, $(K'_{\mathscr{A}\mathscr{B}}+K_{\mathscr{A}\mathscr{B}})$, $[(K'_{\mathscr{A}\mathscr{B}}-K_{\mathscr{A}\mathscr{B}})^2+(\gamma_{\mathscr{A}\bar{\mathscr{B}}})^2]$, and $(\delta^2_{\mathscr{A}\mathscr{B}}+\gamma^2_{\mathscr{A}\mathscr{B}})$ are invariant with respect to orthogonal orbital transformations.

2.2. Perfect Biradicals

A perfect (homosymmetric[11]) biradical is one in which the real and orthogonal ($S_{\mathscr{A}\mathscr{B}}=0$) orbitals $\mathscr{A}$ and $\mathscr{B}$ can be chosen in such a way that $h_{\mathscr{A}\mathscr{A}}=h_{\mathscr{B}\mathscr{B}}$, $J_{\mathscr{A}\mathscr{A}}=J_{\mathscr{B}\mathscr{B}}$, and $\gamma_{\mathscr{A}\bar{\mathscr{B}}}=\delta_{\mathscr{A}\mathscr{B}}=\gamma_{\mathscr{A}\mathscr{B}}=0$. Such orbitals have equal energies and do not interact. As shown in the Appendix, the condition $\gamma_{\mathscr{A}\bar{\mathscr{B}}}=0$ implies that the orbitals chosen in this way are either fully localized ($\mathscr{A}=A$, $\mathscr{B}=B$) or fully delocalized ($\mathscr{A}=a$, $\mathscr{B}=b$).

The states and their energies (see Fig. 1). If spin is ignored for the moment, two electrons can be accommodated in two orbitals $\mathscr{A}$ and $\mathscr{B}$ in four ways to produce four configurations: $\mathscr{A}^2=\mathscr{A}(1)\mathscr{A}(2)$, $\mathscr{B}^2=\mathscr{B}(1)\mathscr{B}(2)$, $\mathscr{A}\mathscr{B}=\mathscr{A}(1)\mathscr{B}(2)$, and $\mathscr{B}\mathscr{A}=\mathscr{B}(1)\mathscr{A}(2)$. In the absence of electron repulsion (Hückel approximation), all four wave functions would have the energy $2h_{\mathscr{A}\mathscr{A}}=2h_{\mathscr{B}\mathscr{B}}$. If electron repulsion is taken into consideration, the energy expressions become more complicated. For the choices $\mathscr{A},\mathscr{B}=A,B$ or a, b, we obtain a symmetric split by $\pm K'_{\mathscr{A}\mathscr{B}}$ [Eq. (2)] with respect to E_0 [Eq. (3)].

$$2K'_{\mathscr{A}\mathscr{B}}=(J_{\mathscr{A}\mathscr{A}}+J_{\mathscr{B}\mathscr{B}})/2-J_{\mathscr{A}\mathscr{B}} \tag{2}$$

$$E_0=h_{\mathscr{A}\mathscr{A}}+h_{\mathscr{B}\mathscr{B}}+(J_{\mathscr{A}\mathscr{A}}+J_{\mathscr{B}\mathscr{B}})/4+J_{\mathscr{A}\mathscr{B}}/2 \tag{3}$$

The equivalence of $\mathscr{A}$ and $\mathscr{B}$ demands the use of the combinations $\mathscr{A}^2\pm\mathscr{B}^2$ and $\mathscr{A}\mathscr{B}\pm\mathscr{B}\mathscr{A}$. The in-phase combinations are destabilized and the out-of-phase ones stabilized by $K_{\mathscr{A}\mathscr{B}}$, resulting in four levels at $E_0\pm K'_{\mathscr{A}\mathscr{B}}\pm K_{\mathscr{A}\mathscr{B}}$. The three symmetric spatial wave functions need to be multiplied by the singlet spin wave function, Σ, and the antisymmetric one by one of the three triplet wave functions Θ_i ($i=-1,0,1$), to produce a total of six wave functions that satisfy the Pauli principle and represent a complete basis in a two-electron space. The normalized wave functions S_0, S_1, S_2, and T are the energy eigenstates of a perfect biradical (cf. the Hamiltonian matrix in Table 1). The wave functions and their energies are listed in (4); the expressions for the energies of S_0 and S_1 apply only if the orbitals $\mathscr{A},\mathscr{B}$ are chosen to be equal either to A, B or to a, b. For a general choice, they are $E_0\pm[(K'_{\mathscr{A}\mathscr{B}}-K_{\mathscr{A}\mathscr{B}})^2+(\gamma_{\mathscr{A}\bar{\mathscr{B}}})^2]^{1/2}$.

$$\begin{array}{lll}
S_2 & {}^1|\mathscr{A}^2+\mathscr{B}^2\rangle=(1/\sqrt{2})[\mathscr{A}(1)\mathscr{A}(2)+\mathscr{B}(1)\mathscr{B}(2)]|\Sigma\rangle & E_0+K'_{\mathscr{A}\mathscr{B}}+K_{\mathscr{A}\mathscr{B}}\\
S_0,S_1 & \left\{\begin{array}{l}{}^1|\mathscr{A}\mathscr{B}\rangle=(1/\sqrt{2})[\mathscr{A}(1)\mathscr{B}(2)+\mathscr{B}(1)\mathscr{A}(2)]|\Sigma\rangle\\ {}^1|\mathscr{A}^2-\mathscr{B}^2\rangle=(1/\sqrt{2})[\mathscr{A}(1)\mathscr{A}(2)-\mathscr{B}(1)\mathscr{B}(2)]|\Sigma\rangle\end{array}\right. & \begin{array}{l}E_0-K'_{\mathscr{A}\mathscr{B}}+K_{\mathscr{A}\mathscr{B}}\\ E_0+K'_{\mathscr{A}\mathscr{B}}-K_{\mathscr{A}\mathscr{B}}\end{array}\\
T & {}^3|\mathscr{A}\mathscr{B}\rangle_i=(1/\sqrt{2})[\mathscr{A}(1)\mathscr{B}(2)-\mathscr{B}(1)\mathscr{A}(2)]|\Theta_i\rangle,\ i=-1,0,1 & E_0-K'_{\mathscr{A}\mathscr{B}}-K_{\mathscr{A}\mathscr{B}}
\end{array} \tag{4}$$

Since both $K_{\mathscr{A}\mathscr{B}}$ and $K'_{\mathscr{A}\mathscr{B}}$ are nonnegative, T is the most stable of all four states. The wave function ${}^1|\mathscr{A}^2+\mathscr{B}^2\rangle$ represents S_2, the least stable of the four states. The order of the two singlet states that are represented by the wave functions ${}^1|\mathscr{A}\mathscr{B}\rangle$ and ${}^1|\mathscr{A}^2-\mathscr{B}^2\rangle$, and thus their assignment as S_0 and S_1, depends on the relative magnitudes of $K'_{\mathscr{A}\mathscr{B}}$ and $K_{\mathscr{A}\mathscr{B}}$, which, in turn, are determined by the choice of $\mathscr{A}$, $\mathscr{B}$ as either A, B or a, b.

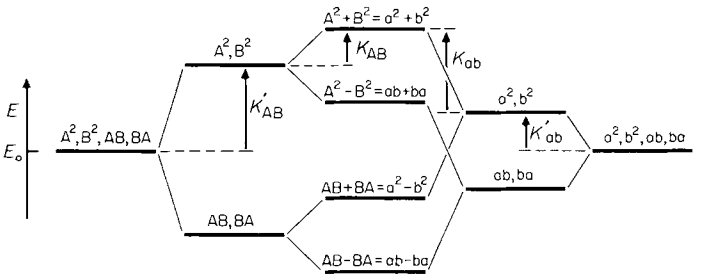

Fig. 1. 3×3 CI model: construction of the energies and wavefunctions of a perfect biradical (center), starting with localized (left) or delocalized (right) orbitals. See also text.

The three simple choices of the orbitals $\mathscr{A}$, $\mathscr{B}$. In Figure 1, the form of the wave functions and the energies associated with them are shown once for the pair A, B and once for the pair a, b. For the localized orbitals A and B, $K'_{AB}\geq K_{AB}$, for the delocalized orbitals a and b, $K'_{ab}\leq K_{ab}$, and the two sets are related by Equation (5).

$$K'_{AB}=K_{ab},\quad K'_{ab}=K_{AB} \tag{5}$$

The different ways in which the same final state wave functions can be expressed in terms of orbital pairs A, B and a, b are shown in Table 2. In terms of A and B, S_0 is given by ${}^1|AB\rangle$ and S_1 by ${}^1|A^2-B^2\rangle$, while in terms of a and b, S_0 is given by ${}^1|a^2-b^2\rangle$ and S_1 by ${}^1|ab\rangle$. It is important to note that for a general choice of the real orbitals $\mathscr{A}$ and $\mathscr{B}$, the wave functions S_0 and S_1 are given by mixtures of contributions from ${}^1|\mathscr{A}\mathscr{B}\rangle$ and ${}^1|\mathscr{A}^2-\mathscr{B}^2\rangle$. However, for

Table 2. State wave functions and energies of a perfect biradical [a].

State	Wave functions: Localized orbitals [b]	Delocalized real orbitals	Delocalized complex conjugate orbitals	Energies
S_2	$(1/\sqrt{2})[A^2+B^2]\|\Sigma\rangle$	$=(1/\sqrt{2})[a^2+b^2]\|\Sigma\rangle$	$=(1/\sqrt{2})[cc^*+c^*c]\|\Sigma\rangle$	$K'_{AB}+K_{AB}=\ K_{ab}+K'_{ab}=\ K_{AB}+K_{ab}$
S_1	$(1/\sqrt{2})[A^2-B^2]\|\Sigma\rangle$	$=(1/\sqrt{2})[ab+ba]\|\Sigma\rangle$	$=(1/\sqrt{2})[c^{*2}+c^2]\|\Sigma\rangle$	$K'_{AB}-K_{AB}=-K'_{ab}+K_{ab}=-K_{AB}+K_{ab}$
S_0	$(1/\sqrt{2})[AB+BA]\|\Sigma\rangle$	$=(-1/\sqrt{2})[a^2-b^2]\|\Sigma\rangle$	$=(i/\sqrt{2})[c^{*2}-c^2]\|\Sigma\rangle$	$-K'_{AB}+K_{AB}=-K_{ab}+K'_{ab}=\ K_{AB}-K_{ab}$
T_i	$(1/\sqrt{2})[AB-BA]\|\Theta_i\rangle$	$=(1/\sqrt{2})[ab-ba]\|\Theta_i\rangle$	$=(i/\sqrt{2})[cc^*-c^*c]\|\Theta_i\rangle$	$-K'_{AB}-K_{AB}=-K_{ab}-K'_{ab}=-K_{AB}-K_{ab}$

[a] Energies are relative to E_0 given by Equation (3). The localized and the delocalized orbitals are related by Equations (1) and (6). For the triplet wave functions, $i=-1, 0, 1$. [b] The four wave functions based on the localized orbitals are used as the basis set in Section 2.3.

any choice of real orbitals $\mathscr{A}$ and $\mathscr{B}$, the forms of $S_2(^1|\mathscr{A}^2+\mathscr{B}^2|)$ and of $T(^3|\mathscr{A}\mathscr{B}|)$ remain the same.

Biradicals with $K_{AB}=0$, and therefore $K'_{ab}=0$, will be referred to as *pair biradicals* since the condition can be strictly satisfied only if the separation between the orbitals A and B is infinite so that the biradical consists of a pair of distant radical centers. In practice, this condition is nearly satisfied already in biradicals **1** and **2**, and very well satisfied in **3** (Scheme 2). We shall refer to systems such as these as pair biradicals as well. In pair biradicals, S_0 and T as well as S_1 and S_2 are pairwise degenerate.

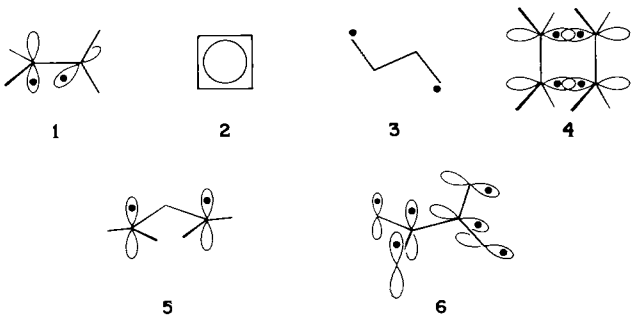

Scheme 2. Pair biradicals.

Biradicals for which $K'_{\mathscr{A}\mathscr{B}}=K_{\mathscr{A}\mathscr{B}}$ will be referred to as *axial biradicals*.[20] This condition is normally enforced by symmetry (Scheme 3). In axial biradicals, S_0 and S_1 are degenerate.

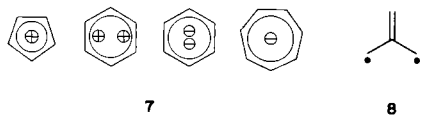

Scheme 3. Axial biradicals.

Since the S_0 and S_1 wave functions can equally well be written in a form that contains two singly occupied orbitals ("open-shell"), it is natural to ask whether S_2 should not be an equally open-shell state. In fact, S_2 can also be written in the open-shell form if the condition that $\mathscr{A}$ and $\mathscr{B}$ be real is relaxed. In terms of the pair of delocalized, orthogonal, complex conjugate orbitals c and c* given by (6), the wave function for S_2 is $^1|cc^*\rangle$, and $\gamma_{cc^*}=0$.

$$\begin{aligned} c &= (A+iB)/\sqrt{2} \\ c^* &= (A-iB)/\sqrt{2} \end{aligned} \qquad (6)$$

The full set of relations between the three different forms in which the wave functions can be written under the condition $\gamma_{\mathscr{A}\mathscr{B}}=0$ is summarized in Table 2.[20] The threefold symmetry in the stepwise derivation of state energy splittings and wave functions starting with the three sets of orbitals is displayed in Figure 2. It is obvious from the form of the wave functions that all three singlet states can be labeled *open-shell* with equal justification. This becomes particularly clear in the language of natural orbitals.

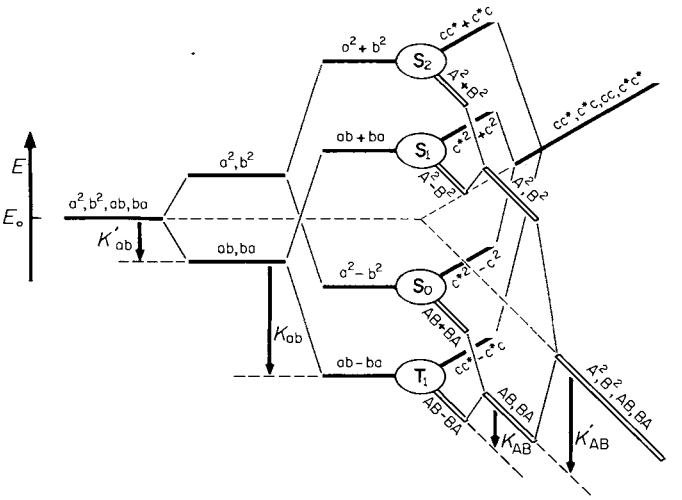

Fig. 2. 3×3 CI model: construction of the energies and wavefunctions of a perfect biradical (center), starting with localized (front right) delocalized (left), or complex (back right) orbitals. See also Figure 1 and text.

Natural orbital occupancies—a measure of biradicaloid character. Natural orbitals (NOs) of an electronic system are defined as those orbitals that diagonalize its exact first-order density matrix (the bond-order and charge-density matrix). These orbitals thus have fractional occupancies n_i (orbital "charge densities") and vanishing interactions ("bond orders" between orbitals). The NOs of a state are uniquely defined once its exact wave function is known. All one-electron properties of a system are additive when expressed in terms of the NOs, $|i\rangle$ [Eq. (7)].

$$\langle\psi|\hat{A}|\psi\rangle = \sum_i n_i\langle i|\hat{A}|i\rangle \qquad (7)$$

In the ground states of ordinary "closed-shell" molecules, all NO occupancies are either close to two, describing a nearly perfectly coupled electron pair, or close to zero. In biradicals and biradicaloids, this is true for all

but two of the NOs, whose occupancies are close to one, describing a nearly perfectly uncoupled electron pair (open shell). This feature has been proposed as a measure of biradicaloid character.[17,22]

Any pair of orthogonal real orbitals $\mathscr{A}$ and $\mathscr{B}$ represents the NOs of the S_0, S_1, S_2, and T states of a perfect biradical in the 3×3 CI model (see Appendix). The density matrices are given by Equation (8).

$$\rho(S_0)=\rho(S_1)=\rho(S_2)=\rho(T)=\begin{pmatrix}1 & 0\\ 0 & 1\end{pmatrix} \tag{8}$$

The occupation number of unity for both NOs displays nicely the open-shell, or "perfectly biradical," nature of all four states. The exact equality of the occupation numbers of the two NOs is responsible for the total freedom of choice of the NOs $\mathscr{A}$ and $\mathscr{B}$.

S_0–S_1 surface touching in perfect biradicals. The condition for degeneracy of the S_0 and S_1 states in perfect biradicals is $K'_{\mathscr{AB}}=K_{\mathscr{AB}}$; i.e., S_0 and S_1 touch only in axial biradicals. Examples are atoms such as O and S, linear molecules such as O_2, NH, or B_2H_2, cyclic molecules with $4N$ π electrons in a charged perimeter shaped as a regular polygon, **7**,[21] and other highly symmetric biradicals such as trimethylenemethane **8** (Scheme 3).

In nonlinear molecules, Jahn–Teller distortion will prevent the equilibrium geometry in the S_0 state from coinciding exactly with the high-symmetry geometry considered here. However, we are primarily interested in the S_1 surface, for which just this geometry will be very favorable.

In most perfect biradicals the equality $K'_{\mathscr{AB}}=K_{\mathscr{AB}}$ is not enforced by symmetry so that S_0 and S_1 are split by $2(K'_{AB}-K_{AB})$, typically several dozen kcal/mol. Examples are **1**–**3** and the "antiaromatic" biradicaloid geometries, such as **4**, occurring along ground-state forbidden pericyclic reaction paths (see Scheme 2). Although the S_1 surface still lies relatively low in energy at these geometries, it does not even come close to touching the S_0 surface.[6–13,19,23] The largest S_0–S_1 energy gap is found for pair biradicals formed by stretching a single bond to infinity (e.g., H + H). This gap is equal to J_{AA}, typically hundreds of kcal/mol. On the other hand, K_{AB} vanishes and S_0 is then degenerate with T. A comparison of such "loose" geometries, in which A and B are far separated, with their "tight" counterparts, in which they are close, is of importance in photochemistry as well (e.g., the pair **3** and **4**).[2,10,24] At a loose geometry, E_0 is more negative and J_{AB} is smaller, so that K'_{AB} is larger. If nothing else changes, S_0 and T of a perfect biradical are favored at loose geometries, while the S_1 and S_2 states are not. In the latter states, cyclic conjugation then often favors a tight geometry.

As we shall see in the following, degeneracy of the S_0 and S_1 states is usually far more readily reached or at least approached in biradicaloids than in perfect biradicals.

2.3. Biradicaloids

2.3.1. General

We use the noun "biradicaloid" for all imperfect biradicals;[25] i.e., those in which the real orthogonal orbitals $\mathscr{A}$ and $\mathscr{B}$ either interact ($\gamma_{\mathscr{AB}}\neq0$) or have different energies ($\delta_{\mathscr{AB}}\neq0$) or both, no matter how they are chosen. In the complete basis set of wave functions that has already been used for the perfect biradical (Table 2) the singlet part of the Hamiltonian matrix (Table 1) is given by (9), where $E(T)$, the energy of the triplet state, stands for $E(T)=E_0-K'_{\mathscr{AB}}-K_{\mathscr{AB}}$. Its value may change as various perturbations are introduced, but this is immaterial for the consideration of energy differences.

$$\begin{matrix}{}^1|\mathscr{A}^2-\mathscr{B}^2\rangle\\ {}^1|\mathscr{A}^2+\mathscr{B}^2\rangle\\ {}^1|\mathscr{AB}\rangle\end{matrix}\begin{pmatrix}E(T)+2K'_{\mathscr{AB}} & \delta_{\mathscr{AB}} & \gamma_{\bar{\mathscr{A}}\mathscr{B}}\\ \delta_{\mathscr{AB}} & E(T)+2(K'_{\mathscr{AB}}+K_{\mathscr{AB}}) & \gamma_{\mathscr{A}\bar{\mathscr{B}}}\\ \gamma_{\bar{\mathscr{A}}\mathscr{B}} & \gamma_{\mathscr{A}\bar{\mathscr{B}}} & E(T)+2K_{\mathscr{AB}}\end{pmatrix} \tag{9}$$

The wave functions $|S_0\rangle$, $|S_1\rangle$, and $|S_2\rangle$ obtained by diagonalization have the form shown in Equation (10), and the density matrices are given by Equation (11). For their derivation, see Appendix 2; Appendix 3 shows how the state energies can be found graphically.

$$|S_i\rangle=C_{i,-}\,{}^1|\mathscr{A}^2-\mathscr{B}^2\rangle+C_{i,+}\,{}^1|\mathscr{A}^2+\mathscr{B}^2\rangle+C_{i,0}\,{}^1|\mathscr{AB}\rangle \qquad i=0,\,1,\,2 \tag{10}$$

$$\rho(S_i)=\begin{pmatrix}1+2C_{i,+}C_{i,-} & 2C_{i,0}C_{i,+}\\ 2C_{i,0}C_{i,+} & 1-2C_{i,+}C_{i,-}\end{pmatrix} \tag{11}$$

Diagonalization of $\rho(S_i)$ yields the occupation numbers n_I and n_{II} for the two natural orbitals [Eq. (12)].

$$n_{I,II}=1\pm2C_{i,+}\sqrt{1-C_{i,+}^2} \tag{12}$$

As we have seen already, in a perfect biradical ($\delta_{\mathscr{AB}}=\gamma_{\mathscr{AB}}=0$), $n_I=n_{II}=1$ holds for any choice of orbital basis (for any value of $\gamma_{\bar{\mathscr{A}}\mathscr{B}}$). With increasing perturbation $\delta^2_{\mathscr{AB}}+\gamma^2_{\mathscr{AB}}$, one can approach the limiting case of a closed shell, for which $n_I=2$, $n_{II}=0$.[26] The gradual change from the perfect biradical situation to the ordinary closed-shell situation illustrates very nicely the continuous nature of the conversion of a biradical into a biradicaloid and eventually into an ordinary molecule by the introduction of a suitable perturbation. The physical significance of the parameters $\delta_{\mathscr{AB}}$ and $\gamma_{\mathscr{AB}}$, which describe the perturbation, needs to be discussed next.

According to the definitions given in Table 1, $\delta_{\mathscr{AB}}$ is a measure of the energy difference of orbitals $\mathscr{A}$ and $\mathscr{B}$ while $\gamma_{\mathscr{AB}}$ is a measure of the degree to which they interact. The significance of these quantities depends on the choice of the orbital pair $\mathscr{A},\mathscr{B}$. We have already noted that $\delta^2_{\mathscr{AB}}+\gamma^2_{\mathscr{AB}}$ is invariant to this choice. For any perturbation there is a choice that makes $\delta_{\mathscr{AB}}$ vanish and another choice that makes $\gamma_{\mathscr{AB}}$ vanish, but, in general, these choices correspond neither to the localized orbitals A, B nor to the delocalized orbitals a, b.

Since we wish to work with either the A, B or the a, b orbital set, we must accept the existence of two independent perturbation parameters, δ and γ, but matters simplify in that $\gamma_{AB}=\gamma_{ab}=0$ holds. As shown in the Appendix, the parameters in the two orbital bases are related by (13).

$$\delta_{AB}=\gamma_{ab},\quad \gamma_{AB}=\delta_{ab} \tag{13}$$

To illustrate the physical significance of these quantities, we select orthogonally twisted ethylene as an example of a perfect biradical and consider two types of perturbation: return to planarity and pyramidalization on one of the carbon atoms.

The orbital sets A, B and a, b are shown in **1** (Scheme 1) for the geometry of a perfect biradical. The energies of the two localized orbitals are equal ($\delta_{AB}=0$) and the orbitals cannot interact ($\gamma_{AB}=0$). The same is true of the delocalized orbitals ($\delta_{ab}=\gamma_{ab}=0$). When **1** is distorted toward planarity, the energies of the localized orbitals A and B remain equal ($\delta_{AB}=0$), but the orbitals begin to interact ($\gamma_{AB}\neq 0$). The energies of the delocalized orbitals a and b are no longer equal ($\delta_{ab}\neq 0$)—one orbital eventually becoming the HOMO and the other the LUMO of planar ethylene—but the orbitals do not interact ($\gamma_{ab}=0$).

In contrast, when one of the carbons in **1** is pyramidalized, the energies of the localized orbitals begin to differ ($\delta_{AB}\neq 0$), but symmetry still prevents them from interacting ($\gamma_{AB}=0$). The energies of the delocalized orbitals remain the same, $\delta_{ab}=0$ (since the orbitals are equally distributed over both carbon atoms). However, now we have $\gamma_{ab}\neq 0$, since a and b are not the usual canonical orbitals for **1** pyramidalized on one carbon, which have unequal coefficients on the two carbon atoms. Upon simultaneous planarization and pyramidalization, δ_{AB}, γ_{AB}, δ_{ab}, and γ_{ab} all become nonzero.

In the perfect biradical **1**, and in its partly planarized form, the delocalized orbitals a, b are identical with the usual canonical MOs. At singly pyramidalized geometries, however, the canonical MOs correspond to the localized orbitals A, B if the geometry is still orthogonal and to neither a, b nor A, B if it is not. Since computer programs normally produce canonical MOs, the algorithm described in Appendix 1 is then needed to convert them into the set A, B or a, b.

It is useful to distinguish three types of biradicaloids:

1. *Homosymmetric biradicaloids*, for which $\gamma_{AB}=\delta_{ab}\neq 0$ and $\delta_{AB}=\gamma_{ab}=0$; i.e., the localized orbitals have equal energies but interact. An example is ethylene at a twist angle other than 90°.
2. *Heterosymmetric biradicaloids*, for which $\delta_{AB}=\gamma_{ab}\neq 0$ and $\gamma_{AB}=\delta_{ab}=0$; i.e., the localized orbitals have different energies but do not interact. Examples are orthogonally twisted, singly pyramidalized ethylene and orthogonally twisted propene.
3. *Nonsymmetric biradicaloids*, for which both $\delta_{AB}=\gamma_{ab}\neq 0$ and $\gamma_{AB}=\delta_{ab}\neq 0$; i.e., the localized orbitals have different energies and interact as well. An example is propene at a double-bond twist angle other than 90°.

These definitions are compatible with the more usual definition of biradicaloids as biradical-like species in which the canonical nonbonding MOs have different energies. It is important to recall that the use of the terms homosymmetric and heterosymmetric proposed in ref. [1] is similar to ours but not identical.

It is obvious that for large enough perturbations the two-electron two-orbital system in question may deviate so much from a perfect biradical that its ground-state NO occupation numbers are close to $n_I=2$, $n_{II}=0$, so that ordinarily it would no longer be considered a biradicaloid. Examples are twisted aminoborane **9**, in which δ_{AB} is large, planar ethylene **10**, in which γ_{AB} is large, and planar aminoborane **11**, in which both δ_{AB} and γ_{AB} are large (Scheme 4). Sometimes species such as these are viewed as biradicals when they are in their S_1 or T_1 electronic states, for which $n_I\approx n_{II}\approx 1$.

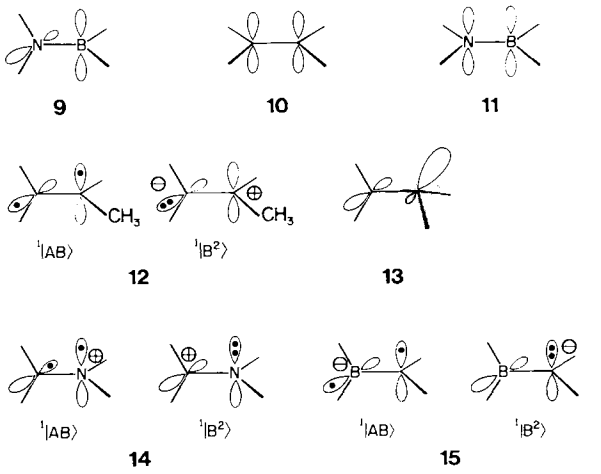

Scheme 4. Biradicaloids.

In the following, we shall use exclusively the basis of localized orbitals A, B, but the subscripts A, B will no longer be explicitly indicated. The wave functions $^1|A^2\rangle$ and $^1|B^2\rangle$ will be referred to as "hole-pair" configurations and $^1|AB\rangle$ and $^3|AB\rangle$ as "dot-dot" configurations (Scheme 4). When A, B are each localized on a single center, as in **1**, these wave functions actually correspond very closely to valence-bond (VB) structures and would traditionally be referred to as "structures" rather than "configurations." Since we include cases in which A, B are delocalized over several centers, as in **2**, we use the term "configurations."

All results can be transformed to the delocalized basis a, b, which is more convenient in the case of homosymmetric biradicaloids, by making the substitutions $^1|A^2-B^2\rangle\rightarrow{}^1|ab\rangle$, $^1|AB\rangle\rightarrow K\,{}^1|a^2-b^2\rangle$, $K_{AB}\rightarrow K'_{ab}$, $K'_{AB}\rightarrow K_{ab}$, $\delta_{AB}\rightarrow\gamma_{ab}$, and $\gamma_{AB}\rightarrow\delta_{ab}$ (compare matrices (14) and (19)).

2.3.2. Homosymmetric Biradicaloids

When two interacting orbitals ($\gamma\neq 0$) are orthogonal, they generally cannot be perfectly localized. Typically, they correspond to Löwdin-orthogonalized orbitals, each of which is localized mostly on one, but also partly on the other partner atom or atoms.

The Hamiltonian matrix for the singlet states of a homosymmetric biradicaloid has the block-diagonal form (14).

$$\begin{array}{l} {}^1|A^2-B^2\rangle \\ {}^1|A^2+B^2\rangle \\ {}^1|AB\rangle \end{array}\begin{pmatrix} E(T)+2K' & 0 & 0 \\ 0 & E(T)+2(K'+K) & \gamma \\ 0 & \gamma & E(T)+2K \end{pmatrix} \qquad (14)$$

The antisymmetric wave function $^1|A^2-B^2\rangle$ remains as an eigenstate. It corresponds to $^1|ab\rangle$ and therefore to a

"singly excited" S_1 state. The symmetric functions $^1|AB\rangle$ and $^1|A^2+B^2\rangle$ mix to produce the ground state S_0 and the "doubly excited" state S_2. If the phases of the orbitals are so chosen that $\gamma<0$, S_0 is represented by the in-phase combination of the functions and S_2 by their out-of-phase combination. The energies of the singlet states are given by (15) and an example of their dependence on γ is shown in Figure 3a. The resulting wave functions are listed in (16), where the parameter α, given by Equation (17), describes the mixing of $^1|AB\rangle$ and $^1|A^2+B^2\rangle$ as a result of the perturbation by γ (note that the strength of the perturbation is given by the ratio $|\gamma/K'|$). For $\gamma=0$, the states $|S_0\rangle=(^1|AB\rangle$ and $|S_2\rangle=^1|A^2+B^2\rangle$ are those of a perfect biradical. In the limit of very large negative γ, we have $\alpha=-\pi/4$, and the wavefunction of the S_0 state goes to $(^1|AB\rangle+{}^1|A^2+B^2\rangle)/\sqrt{2}$. This can be rewritten in terms of delocalized orbitals as $|S_0\rangle=^1|b^2\rangle$; i.e., in this limit the simple MO description of the ground state of an ordinary molecule is correct, both electrons occupying the bonding MO.

$$\begin{aligned} E(S_2) &= E(T)+K'+2K+\sqrt{K'^2+\gamma^2} \\ E(S_1) &= E(T)+2K' \\ E(S_0) &= E(T)+K'+2K-\sqrt{K'^2+\gamma^2} \end{aligned} \tag{15}$$

$$\begin{aligned} |S_2\rangle &= \cos\alpha\ {}^1|A^2+B^2\rangle+\sin\alpha\ {}^1|AB\rangle \\ |S_1\rangle &= {}^1|A^2-B^2\rangle \\ |S_0\rangle &= -\sin\alpha\ {}^1|A^2+B^2\rangle+\cos\alpha\ {}^1|AB\rangle \end{aligned} \tag{16}$$

$$\alpha=\frac{1}{2}\tan^{-1}\frac{\gamma}{K'} \tag{17}$$

In all four states of the homosymmetric biradicaloid, the natural orbitals coincide with the delocalized orbitals a and b. Their occupation numbers are obtained from Equation (12). Assuming $\gamma<0$, they are given by (18), which clearly shows the gradual transition from a perfect biradical ($n_a=n_b=1$) to an ordinary molecule ($n_b\approx 2$, $n_a\approx 0$) with increasing perturbation $|\gamma/K'|$ as well as the open-shell nature of the singly excited S_1 state. Clearly, the perturbation γ can only increase the S_0–S_1 gap relative to that for a perfect biradical. Indeed, the gap increases rapidly upon motion away from a 90° twist in **1** or from a square toward a rectangular geometry in **2** and upon decrease of the separation between the radical centers in a radical pair.

$$\left.\begin{aligned} n_a(S_0)=n_b(S_2)= \\ n_b(S_0)=n_a(S_2)= \end{aligned}\right\} = 1\pm\sin 2\alpha = 1\pm[1+(K'/\gamma)^2]^{-1/2} \tag{18}$$
$$n_a(S_1)=n_b(S_1)=n_a(T)=n_b(T)=1$$

As $|\gamma|$ increases, S_0 is stabilized relative to T. When $|\gamma|=2\sqrt{K(K+K')}$ is attained, the two states become degenerate. For even larger values of $|\gamma|$, S_0 lies below T. Instructive examples of the effect of the variation of γ on the S_0–T gap are the π,π 1,3-biradicals **5** (Scheme 2). In these species, γ contains two opposed contributions that nearly cancel and whose relative weight depends critically on the CCC valence angle.[27] Once S_0 drops significantly below T_1, a species is created which most chemists would no longer call a biradicaloid, at least not in its ground state.

2.3.3. *Heterosymmetric Biradicaloids*

The Hamiltonian matrix for singlets has the block-diagonal form (19). $^1|AB\rangle$ remains as an eigenstate and corresponds to the dot-dot configuration with one electron in each of the two localized orbitals. The hole-pair functions $^1|A^2-B^2\rangle$ and $^1|A^2+B^2\rangle$ mix out-of-phase to produce a lower-energy state $|1\rangle$ and in-phase to produce an oppositely polarized higher-energy state $|2\rangle$ (20). Here, β given by Equation (21), is a parameter describing the mixing of $^1|A^2-B^2\rangle$ and $^1|A^2+B^2\rangle$ as a result of the perturbation δ/K (recall that δ is always nonnegative). The singlet state energies are given by (22) and an example of their dependence on the perturbation parameter δ is shown in Figure 3b.

$$\begin{array}{c} \\ {}^1|A^2-B^2\rangle \\ {}^1|A^2+B^2\rangle \\ {}^1|AB\rangle \end{array} \begin{array}{c} \begin{array}{ccc} {}^1|A^2-B^2\rangle & {}^1|A^2+B^2\rangle & {}^1|AB\rangle \end{array} \\ \begin{pmatrix} E(T)+2K' & \delta & 0 \\ \delta & E(T)+2(K'+K) & 0 \\ 0 & 0 & E(T)+2K \end{pmatrix} \end{array} \tag{19}$$

$$\begin{aligned} |2\rangle &= \cos\beta\ {}^1|A^2+B^2\rangle+\sin\beta\ {}^1|A^2-B^2\rangle \\ |1\rangle &= -\sin\beta\ {}^1|A^2+B^2\rangle+\cos\beta\ {}^1|A^2-B^2\rangle \end{aligned} \tag{20}$$

$$\beta=\frac{1}{2}\tan^{-1}\frac{\delta}{K} \tag{21}$$

$$\begin{aligned} E(S_2) &= E(T)+2K'+K+\sqrt{K^2+\delta^2}=E(|2\rangle) \\ E(S_0),E(S_1) &= \begin{cases} E(T)+2K'+K-\sqrt{K^2+\delta^2}=E(|1\rangle) \\ E(T)+2K \end{cases} \end{aligned} \tag{22}$$

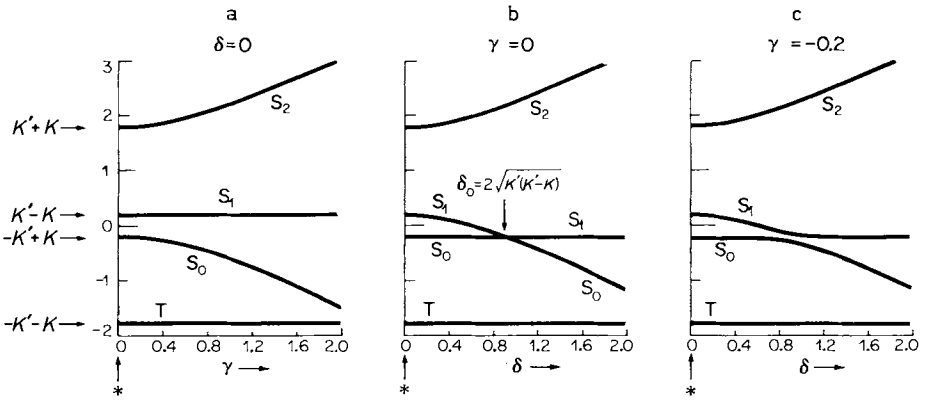

Fig. 3. 3 × 3 CI model: Energies of the singlet and triplet states of a biradicaloid as a function of δ and γ. In the arbitrary energy units chosen, $K=0.8$ and $K'=1.0$. The asterisks indicate the perfect biradical limit ($\delta=\gamma=0$). a) Homosymmetric, b) heterosymmetric, c) nonsymmetric biradicaloid.

In addition to the wave function $^1|AB\rangle$, which represents S_0 or S_1, we thus have the two functions $|2\rangle$ and $|1\rangle$, the latter of which represents either S_1 or S_0. For $\delta=0$, we have $\beta=0$; i.e., the functions $^1|A^2-B^2\rangle$ and $^1|A^2+B^2\rangle$ are not mixed, and the state wave functions remain those of a perfect biradical. As δ grows very large, one obtains $\beta=\pi/4$; the wave function $|1\rangle$ goes from $^1|A^2-B^2\rangle$ to $(^1|A^2-B^2\rangle-{}^1|A^2+B^2\rangle)/\sqrt{2}$, i.e., $^1|B^2\rangle$ and the wave function $|2\rangle$ goes from $^1|A^2+B^2\rangle$ to $^1|A^2\rangle$. This process can be described as a polarization of the hole-pair wave functions $^1|A^2+B^2\rangle$ and $^1|A^2-B^2\rangle$ into the individual hole-pair configurations $^1|A^2\rangle$ and $^1|B^2\rangle$. In this limit, the simple MO description of the ground state of an ordinary molecule is correct, both electrons occupying the lower-energy orbital B; the simple MO and VB descriptions are identical. Note that only the ratio δ/K counts; i.e., the magnitude of δ required for a given degree of polarization increases as K increases.

In all four electronic states of the heterosymmetric biradicaloid, the natural orbitals coincide with the localized orbitals A and B. Their occupation numbers are obtained from Equation (12). The results are given in (23), are analogous to (18), and show clearly the gradual transition from a perfect biradical ($n_B=n_A=1$) to an ordinary molecule ($n_B\approx 2$, $n_A\approx 0$) with increasing perturbation (δ/K), as well as the open-shell nature of the state described by $^1|AB\rangle$, even in strongly perturbed systems (cf. "charge-transfer" biradicals and "TICT" states, Section 4.3).

$$\left.\begin{aligned} n_B(|1\rangle)=n_A(|2\rangle)=\\ n_A(|1\rangle)=n_B(|2\rangle)=\end{aligned}\right\}=1\pm\sin 2\beta=1\pm[1+(K/\delta)^2]^{-1/2}$$
$$n_A(^1|AB\rangle)=n_B(^1|AB\rangle)=n_A(T)=n_B(T)=1 \qquad (23)$$

In biradicals with small K, and therefore nearly degenerate S_1 and S_2 states according to (4), such as **1** twisted by 90°, even a weak polarizing perturbation δ, such as pyramidalization on one center or the presence of a nearby charge, causes an essentially complete polarization of $^1|A^2+B^2\rangle$ and $^1|A^2-B^2\rangle$ toward $^1|A^2\rangle$ and $^1|B^2\rangle$. The very high polarizability of twisted ethylene in its S_1 state has been recognized for a long time.[28] In a biradical with a large K, a much larger orbital energy difference between A and B will have to be introduced in order to produce a similar degree of polarization. In an axial biradical with $K=K'$, and therefore degenerate S_0 and S_1 states according to (4), the polarization of $^1|A^2+B^2\rangle$ and $^1|A^2-B^2\rangle$ toward $^1|A^2\rangle$ and $^1|B^2\rangle$ tends to be incomplete even when the energies of A and B are quite different. Thus, the bending of linear carbene leaves the p orbital A intact but strongly stabilizes B by giving it s character; yet, it is known[29] that $|A^2\rangle$ and $|B^2\rangle$ are still fairly extensively mixed in the description of the S_0 state of even strongly bent CH_2.

Several isolated instances of S_0–S_1 surface touching in biradicaloids at geometries of relatively low symmetry, resulting from a suitable choice of perturbation δ/K in the present terminology, have already been described.[17a,30] The realization that, starting with any general perfect biradical with $K'>K$, a suitable choice of δ will force S_0–S_1 degeneracy opens the way for the rational design of a large number of systems in which the S_0 and S_1 surfaces touch or nearly touch. The significance of this fact in photochemistry has only been recognized relatively recently.[31]

$$\delta_0=2\sqrt{K'(K'-K)} \qquad (24)$$

The point at which the S_0–S_1 degeneracy occurs is given by Equation (24), which clearly displays the limiting cases of a perturbed axial biradical ($K=K'$, $\delta_0=0$) and of a perturbed pair biradical ($K=0$, $\delta_0=2K'=J_{AA}$). Accordingly, it is useful to distinguish three classes of heterosymmetric biradicaloids: (1) weakly heterosymmetric, in which $\delta<\delta_0$, (2) strongly heterosymmetric, in which $\delta>\delta_0$, and (3) critically heterosymmetric, in which $\delta=\delta_0$. We shall now consider the three cases individually (Fig. 3b).

(1) *Weakly heterosymmetric biradicaloids.* For $\delta<\delta_0$, the lowest singlet S_0 is represented by $^1|AB\rangle$, similarly as in a perfect biradical, and S_1 by a mixture of the "hole-pair" configurations $^1|A^2\rangle$ and $^1|B^2\rangle$, with $^1|B^2\rangle$ dominating. This situation is usually encountered in uncharged biradicaloids, where the "dot-dot" configuration $^1|AB\rangle$ involves no formal separation of charges (and is often called covalent), while the hole-pair configurations $^1|A^2\rangle$ and $^1|B^2\rangle$ do (and are often called "zwitterionic"). Examples are 90°-twisted unsymmetric double bonds, such as twisted propene **12** or twisted ethylene pyramidalized at one carbon atom, **13** (Scheme 4).

(2) *Strongly heterosymmetric biradicaloids.* For $\delta>\delta_0$, $^1|AB\rangle$ describes S_1 and the lowest singlet S_0 is represented by a mixture of the hole-pair configurations $^1|A^2\rangle$ and $^1|B^2\rangle$, with $^1|B^2\rangle$ now much more stable than $^1|A^2\rangle$ and usually strongly dominating. If the heterosymmetry is very pronounced (δ large), both electrons are thus kept virtually exclusively in orbital B in S_0, often as a "lone pair." Once δ has exceeded the value $2\sqrt{K'(K'+K)}$, S_0 lies below T, often far below it. For both reasons, strongly heterosymmetric biradicaloids are normally considered not to be biradicaloids at all, at least not in their ground state. If the hole-pair configuration $^1|B^2\rangle$ involves formal separation of charge, such species are usually referred to as zwitterions or ion pairs, with a positive charge on A and a negative charge on B. However, really large δ values are normally reached in systems in which it is the dot-dot configuration $^1|AB\rangle$ that is zwitterionic in that it carries separated formal charges, negative on A and positive on B, while the hole-pair configuration $^1|B^2\rangle$ does not. It is then the excited state S_1 that has both the charge separation and the spatially separated odd electrons and is sometimes referred to as a charge-transfer biradicaloid. Examples of strongly heterosymmetric biradicaloids are molecules containing a noninteracting donor-acceptor pair, such as the 90°-twisted aminoborane **9** and the TICT states of compounds such as *p-N,N*-dimethylaminobenzonitrile, discussed in Section 4.3.

(3) *Critically heterosymmetric biradicaloids.* The case $\delta=\delta_0$, for which we expect S_0–S_1 degeneracy from the simple model, is by far the most interesting for the photochemistry and photophysics of such systems. At this value of δ, the dot-dot configuration $^1|AB\rangle$ has the same energy as the out-of-phase combination of the hole-pair wave functions $^1|A^2+B^2\rangle$ and $^1|A^2-B^2\rangle$, which can usually already be quite well approximated by $^1|B^2\rangle$ alone. This situ-

ation is most readily obtained if neither $^1|AB\rangle$ nor $^1|B^2\rangle$ involves formal charge separation. Then, these structures need to differ in translocation of a formal charge, either positive as in **14** or negative as in **15**. Charged biradicaloids thus have a particularly good chance of exhibiting S_0–S_1 degeneracies.

The prescription for causing the S_0–S_1 gap in a perfect biradical to vanish, exactly or nearly, is therefore simple: destabilize the orbital A or stabilize the orbital B to such a degree as to make the energies of the configurations $^1|AB\rangle$ and $^1|B^2\rangle$ approximately equal.

2.3.4. *Nonsymmetric Biradicaloids*

The Hamiltonian matrix for the singlet states is given by (25). Although the expressions for state energies can be written explicitly, they are not instructive. It is preferable to find the solutions for E graphically by use of Equation (26) (see Appendix 3). It then becomes clear by inspection that S_0 and S_1 can only be degenerate when γ vanishes and that the general shape of the $E(S_i)-E(T)$ surfaces is as shown in Figure 4 for one particular choice of constant values for K' and K.

$$\begin{array}{c} \\ ^1|A^2-B^2\rangle \\ ^1|A^2+B^2\rangle \\ ^1|AB\rangle \end{array} \begin{pmatrix} E(T)+2K' & \delta & 0 \\ \delta & E(T)+2(K'+K) & \gamma \\ 0 & \gamma & E(T)+2K \end{pmatrix} \qquad (25)$$

$$[E-E(T)-2K'-K]^2-\delta^2-K^2=2(K-K')\gamma^2/[E-E(T)-2K]+\gamma^2 \qquad (26)$$

The one case of a nonsymmetric biradicaloid in which a solution can be written simply is a perturbed axial biradical ($K=K'$). In this limit, the state energies are given by (27), from which it is seen that the perturbation lifts the degeneracy of S_0 and S_1. The wave functions are given by (28) where α and β are defined by (29).

$$\begin{aligned} E(S_2) &= E(T)+3K+\sqrt{K^2+\delta^2+\gamma^2} \\ E(S_1) &= E(T)+2K \\ E(S_0) &= E(T)+3K-\sqrt{K^2+\delta^2+\gamma^2} \end{aligned} \qquad (27)$$

$$\begin{pmatrix} |S_2\rangle \\ |S_1\rangle \\ |S_0\rangle \end{pmatrix} = \begin{pmatrix} \cos\alpha\sin\beta & \cos\beta & \sin\alpha\sin\beta \\ -\sin\alpha & 0 & \cos\alpha \\ \cos\alpha\cos\beta & -\sin\beta & \sin\alpha\cos\beta \end{pmatrix} \begin{pmatrix} ^1|A^2-B^2\rangle \\ ^1|A^2+B^2\rangle \\ ^1|AB\rangle \end{pmatrix} \qquad (28)$$

$$\begin{aligned} \alpha &= \tan^{-1}\frac{\gamma}{\delta} \\ \beta &= \frac{1}{2}\tan^{-1}\frac{\sqrt{\delta^2+\gamma^2}}{K} \end{aligned} \qquad (29)$$

In the limit $\delta=0$ (homosymmetric biradicaloid), the S_1 and S_2 states remain perfectly balanced with respect to charge when γ is changed from large negative to large positive values (say, by twisting ethylene from the *cis* to the *trans* configuration). As soon as $\delta\neq 0$ (nonsymmetric biradicaloid), this balance is lost since $^1|A^2+B^2\rangle$ and $^1|A^2-B^2\rangle$ mix. If δ is comparable to the S_1–S_2 separation at the point $\gamma=0$ (i.e., to $2K$ in the present model) or smaller, a large charge imbalance appears only for very small values of γ.

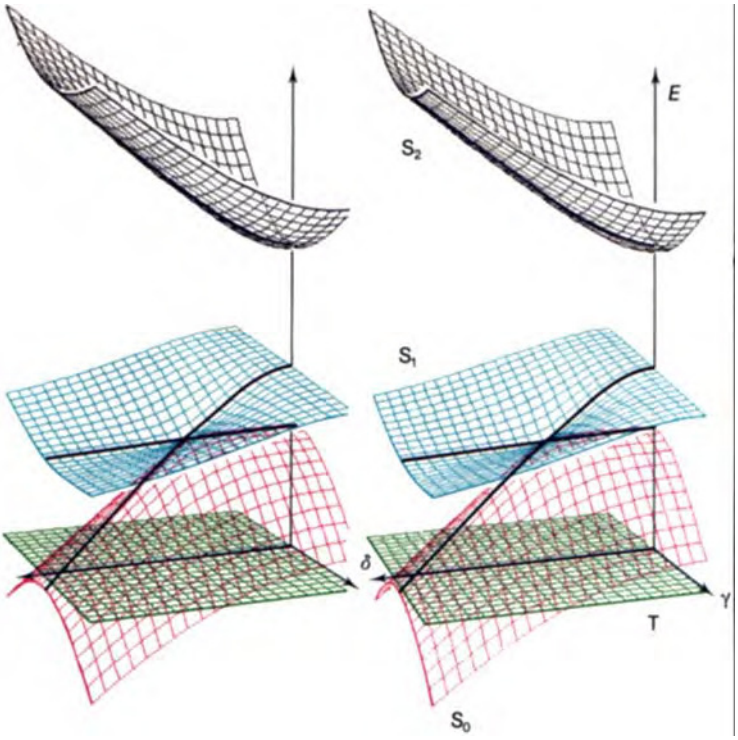

Fig. 4. Excitation energies from the T state (green) to the S_0 (red), S_1 (blue), and S_2 (black) states of a biradicaloid as a function of δ and γ, based on the 3×3 CI model. The origin of the coordinate system corresponds to the perfect biradical limit. In the energy units chosen, $K=1.0$ and $K'=1.5$.

In ethylene, the S_1–S_2 energy gap is very small at orthogonal twist ($K\approx 0$). Therefore, as long as δ is small, this polarization of the S_1 and S_2 states appears and disappears quite suddenly as γ sweeps through zero (sudden polarization[28]). For larger values of δ in pair biradicals and for all values of δ in biradicals with large K values, this polarization develops and disappears much more gradually as the value of γ is changed.

The conclusion to be drawn from Figure 4 is that the choice $\delta\rightarrow\delta_0$ and $\gamma\rightarrow 0$ is optimal when biradicaloids with a small S_0–S_1 energy gap are sought.

2.4. Potential Energy Surfaces

While inspection of the energy differences $E(S_i)-E(T)$ displayed in Figure 4 is useful for classification and comparison of various types of biradicals for any particular choice of K' and K, it does not in itself provide a useful guide for the shape of the potential energy surfaces of a biradicaloid as a function of its geometry and environment, which is of prime interest for a photochemist. In order to obtain such guidance it is necessary to express the reference energy, $E(T)$, as a function of molecular geometry and environmental effects. This will be illustrated for a twisted double bond, starting from nonorthogonal atomic orbitals A, B. Within the two-electron two-orbital model, one obtains Equation (30) for $E(T)$, where E_T^0, given by Equation (31), is the triplet energy at the orthogonal reference geometry ($\gamma=0$) and K'^0_{AB}, K^0_{AB} are also evaluated at this geometry (see Appendix 3).

$$E(\mathrm{T}) = \frac{1}{1-S_{AB}^2}(h_{AA}+h_{BB}+\frac{J_{AA}+J_{BB}}{2}-2K'_{AB}-K_{AB}-2h_{AB}S_{AB})$$

$$= E_{\mathrm{T}}^0 + \frac{1}{1-S_{AB}^2}[(h_{AA}-h_{AA}^0)+(h_{BB}-h_{BB}^0)+(J_{AB}-J_{AB}^0) \quad (30)$$

$$-(K_{AB}-K_{AB}^0)+S_{AB}^2E_{\mathrm{T}}^0-2h_{AB}S_{AB}]$$

$$E_{\mathrm{T}}^0 = h_{AA}^0+h_{BB}^0+J_{AB}^0-K_{AB}^0 \quad (31)$$

For the purposes of qualitative discussion, the difference terms in parentheses can be neglected. Since h_{AB} is approximately proportional to S_{AB}, it is reasonable to approximate $E(\mathrm{T})$ by Equation (32), where c is a constant which reflects the average electronegativity of orbitals A and B. Its value must be positive if a deviation from the perfect biradical geometry produces bonding between orbitals A and B in the ground state, as would ordinarily be the case (e.g., in **1**).

$$E(\mathrm{T}) = E_{\mathrm{T}}^0 + cS_{AB}^2/(1-S_{AB}^2) \quad (32)$$

Since the resonance integral between Löwdin-orthogonalized, localized orbitals A, B is approximately proportional to the overlap between the atomic orbitals A, B, Equation (32) can be transformed into Equation (33), where the constants f and g are both positive.

$$E(\mathrm{T}) = E_{\mathrm{T}}^0 + f[\gamma_{\mathrm{AB}}^2/(1-g\gamma_{\mathrm{AB}}^2)] \quad (33)$$

The shape of the T surface obtained from Equation (33) is shown in Figure 5. Thus, $E(\mathrm{T})$ equals E_{T}^0 if γ vanishes and it increases gradually as $|\gamma|$ increases. This result reproduces the well-known general fact that triplet-state energies are particularly low at geometries at which the two singly occupied orbitals do not interact; after all, upon such interaction the antibonding combination is destabilized more than the bonding one is stabilized.

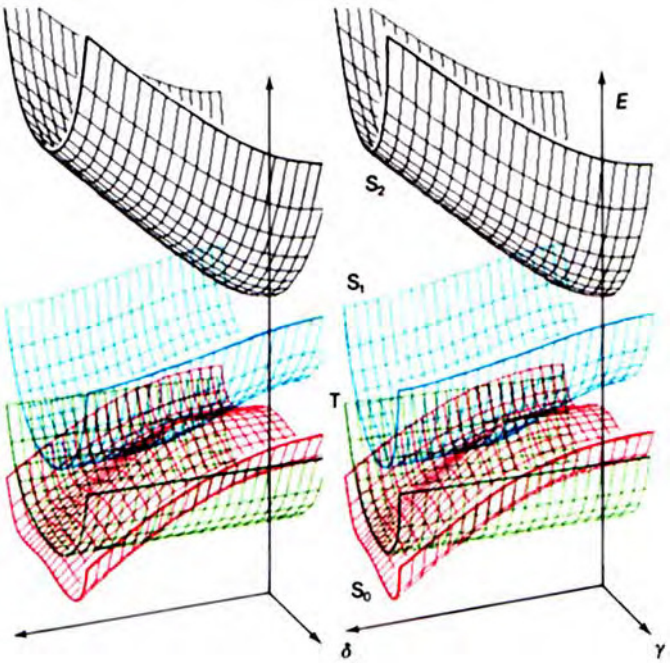

Fig. 5. Energies of the singlet [S_0 (red), S_1 (blue), S_2 (black)] and triplet (green) states of a twisted double bond as a function of δ and γ, based on the 3×3 CI model and Equation (33) for $E(\mathrm{T})$. Core energy, E_{T}^0, K', and K are assumed constant.

The last item to consider is the effect of changes in geometry and solvent environment on δ_{AB} and on E_{T}^0. To a first approximation, the value of δ_{AB} is determined by the value of δ_{AB}, which, in turn, depends primarily on the nature of the atoms on which A and B are located and on the substituents they carry (Table 1). In the following, the appropriate value is labeled δ'. Figure 6 shows the shapes of the singlet potential energy surfaces for a series of such choices of δ. The changes in geometry can be grouped into three categories: (1) those that cause the orbitals A and B to interact (twisting), (2) those that cause changes in δ, and (3) those that change the average electronegativity of the orbitals A and B and thus E_{T}^0. Category (2) includes variations due to the charge-stabilizing or charge-destabilizing effects of the solvent environment. Categories (2) and (3) are normally associated with rehybridization at the centers that carry orbitals A and B. A given geometry change may contribute in more than one category.

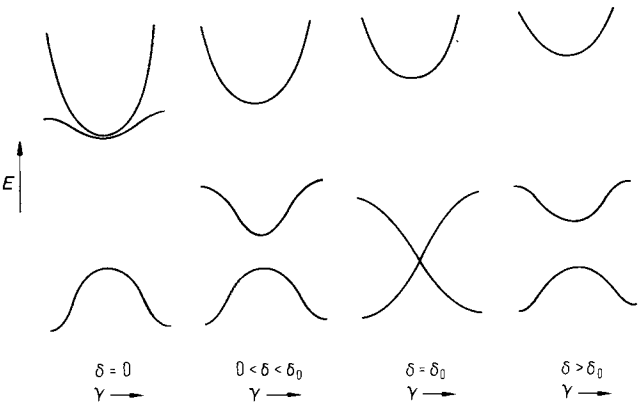

Fig. 6. Schematic representation of the energies of the singlet states of a twisted double bond as a function of γ for four choices of δ.

The effect of the changes of type 1 is already incorporated into Figure 5 in the form of the dependence on γ. The effects of the changes of types 2 and 3 are limited by the steric and other problems that other bonds in the molecule experience upon excessive atom rehybridization or solvent displacement. Their effects on the potential energy surfaces of Figure 5 can then be simulated by adding suitable empirical potentials such as $(\delta-\delta')^4$. This was done in Figure 7, which displays the energies as a function of γ and δ for propene ($\delta' \approx 0$), protonated formaldimine ($\delta' \approx \delta_0$), and aminoborane ($\delta' > \delta_0$). Only in the second case is the S_0–S_1 touching point accessible. The effects of the variations in the average electronegativity could be represented similarly but call for the use of yet another dimension in the graph.

3. Ab Initio Models

3.1. General

Emerging from the netherworld of simple but more or less exactly soluble models to the real world often amounts to a rude awakening. Are actual biradical-like species really described by the simple equations that have been de-

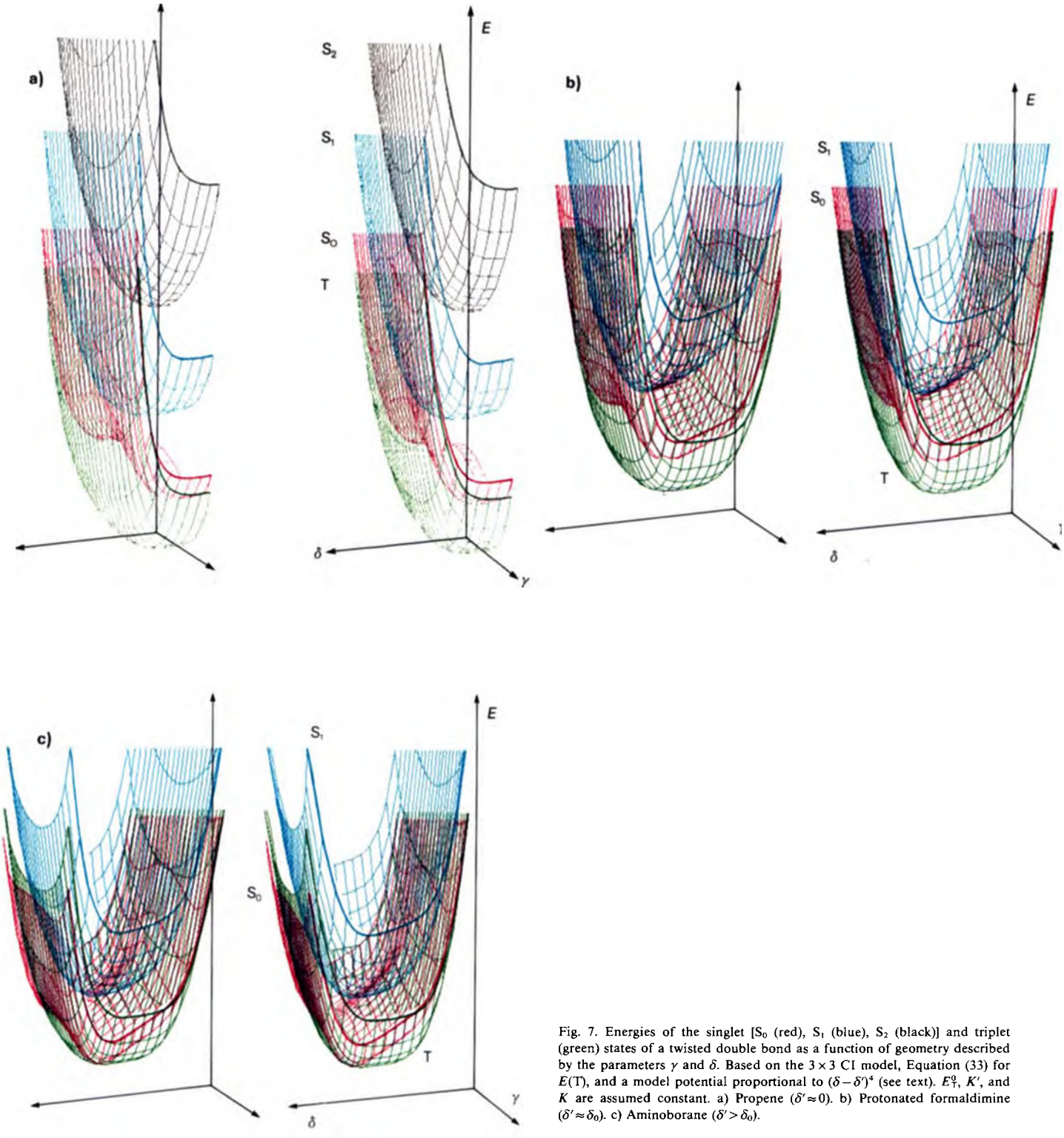

Fig. 7. Energies of the singlet [S_0 (red), S_1 (blue), S_2 (black)] and triplet (green) states of a twisted double bond as a function of geometry described by the parameters γ and δ. Based on the 3×3 CI model, Equation (33) for $E(T)$, and a model potential proportional to $(\delta-\delta')^4$ (see text). E_T^0, K', and K are assumed constant. a) Propene ($\delta'\approx0$). b) Protonated formaldimine ($\delta'\approx\delta_0$). c) Aminoborane ($\delta'>\delta_0$).

rived for the two-electron two-orbital case with a fixed core? Surely they are not, at least not exactly, but perhaps they at least exhibit the predicted behavior qualitatively? Whether an S_0–S_1 degeneracy in a heterosymmetric biradicaloid occurs precisely at $\delta_0=2\sqrt{K'(K'-K)}$ or just close to δ_0 is less important than that it should occur at all as δ is increased from zero.

In order to evaluate the performance of a simple model, one can rely on experiments or on more accurate calculations, i.e., better models. Since we are aware of essentially no experimental information on the main subject of interest here, S_0–S_1 near degeneracies and degeneracies that are not imposed by symmetry (as they are in axial biradicals), we shall take the latter route. We shall select two classes of perfect biradicals, a twisted double bond and square cyclobutadiene, and introduce $\delta\neq0$ either by replacing carbon by heteroatoms or by placing a point charge next to the molecule. Ab initio calculations for these systems at the CI level will then be examined for the expected qualitative effects.

Shortcomings of the simple model. Although ample experimental and theoretical evidence has already estab-

lished that the model is quite adequate in many applications, two well-recognized shortcomings of the model should be mentioned, both having to do with states predicted to be split by $2K$ when K is a small number. These shortcomings are characteristic of the 3×3 CI approximation for singlet states even at the ab initio level.

In perfect biradicals that approach the pair biradical limit of $K=0$, T_1 is expected to lie only a little below S_0 since $2K$ is small. It is now well recognized[3, 14] that, in the presence of additional electrons in the molecule, mechanisms exist for the preferential stabilization of S_0 relative to T_1. These often lead to the reversal of their order. This happens in both examples of interest here, twisted double bonds and square cyclobutadiene. The prediction of an S_0–T_1 crossing, which should occur at $\gamma = 2\sqrt{K(K'+K)}$ in homosymmetric biradicaloids and at $\delta = 2\sqrt{K'(K'+K)}$ in heterosymmetric biradicaloids according to the simple model, is therefore worthless in these cases, although it may still be of some use in biradicals in which K is larger.

While this first shortcoming of the model has no impact on our present interests, the second shortcoming is potentially more serious. When K is small, the S_1–S_2 gap in a perfect biradical is expected to be small, with the $^1|A^2-B^2\rangle$ state below $^1|A^2+B^2\rangle$. Once again, it is now well recognized[18, 19] that other electrons present in real molecules provide mechanisms for a differential stabilization of $^1|A^2+B^2\rangle$ relative to $^1|A^2-B^2\rangle$, so that their order may be reversed. This happens both in twisted double bonds and in square cyclobutadiene. In a sense then, the examples we have selected for testing are such that the simple model is not at its best.

The mechanism provided by the simple model for reaching S_0–S_1 degeneracy in heterosymmetric biradicaloids by polarization of the $^1|A^2+B^2\rangle$ and $^1|A^2-B^2\rangle$ states toward states described approximately by the $^1|A^2\rangle$ and $^1|B^2\rangle$ configurations and by preferential stabilization of the latter configuration should of course be independent of the initial order of the $^1|A^2+B^2\rangle$ and $^1|A^2-B^2\rangle$ states. For large values of δ, the memory of their initial order at $\delta=0$ will long since have been lost, and δ_0 should be quite large, since K' is large in both reference systems selected for study, as judged by the large S_0–S_1 gap present for $\delta=0$.

3.2. Twisted π Bonds

3.2.1. Ethylene in the Field of a Charge

The simplest test of the proposal that introduction of a sufficient orbital energy difference between A and B will reduce the S_0–S_1 gap and eventually produce an S_0–S_1 touching is offered by a calculation of the electronic states of ethylene in the field of a strong nearby charge. We have performed such calculations using a multireference double (MRD) CI treatment[32, 33] for the simultaneous description of the singlet states of interest.

Figure 8 shows the energies of the two lowest singlet states of orthogonally twisted ethylene in the presence of a positive charge of magnitude q located on the C–C axis at a distance of 1.85 Å from the midpoint of the C–C bond. The large S_0–S_1 gap of 70 kcal/mol present in the absence of the external charge is reduced to zero when the charge is increased, as expected from the simple model considerations (cf. Fig. 3), and the nature of the wave functions changes as predicted. The S_0–S_1 touching occurs when $q = 1.735\,|e|$.

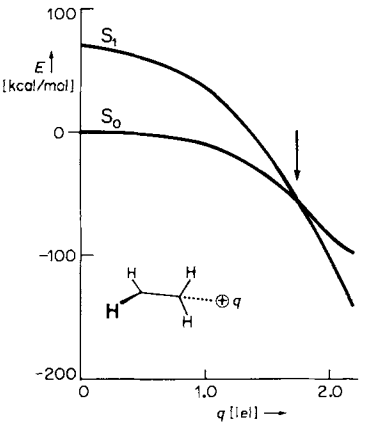

Fig. 8. Ab initio MRD CI calculation of singlet state energies of orthogonally twisted ethylene located next to a positive charge of magnitude q. Bond lengths: C–C 1.416, C–H 1.09 Å; bond angles 120°. The charge lies on the C–C axis 1.85 Å from the midpoint of the bond. Huzinaga double zeta quality basis set, nine reference configurations, except for $q = 1.735\,|e|$ where fourteen were used. (The diagonalized CI spaces contain approximately 5000 configurations. The extrapolated energies toward the full MRD CI space are plotted.)

Figure 9 shows the ethylene S_0, S_1, and S_2 energies as a function of the twist angle for three selected values of the external charge. It displays clearly the gradual transformation of an S_1 minimum into a conical intersection with a vanishing S_0–S_1 gap and then again into an S_1 minimum as the external field effect increases further. The behavior is that expected from the simple model (cf. Fig. 6).

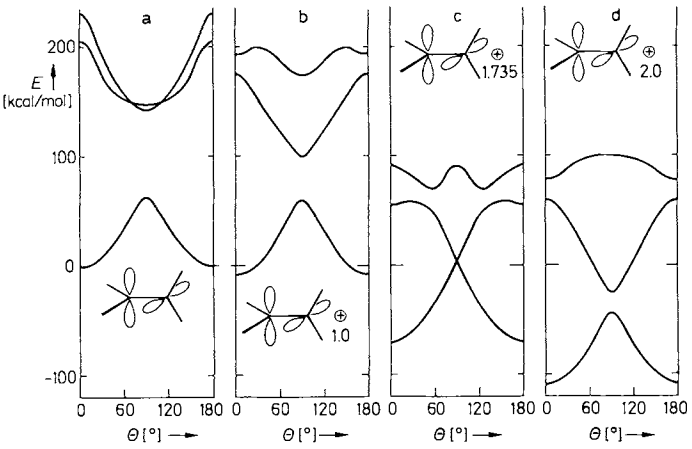

Fig. 9. Ab initio MRD CI calculation of singlet state (S_0, S_1, S_2) energies of ethylene located next to a positive charge $q[|e|]=0$ (a), 1.0 (b), 1.735 (c), and 2.0 (d), as a function of the twist angle (rigid rotation). For details of calculations, see caption to Figure 8.

3.2.2. Polar π Bonds

A more realistic modeling of the effect of increasing electronegativity difference between orbitals A and B on

the S_0–S_1 energy gap is provided by calculations for actual polar molecules. These were performed at a similar level as those described above and have already been published.[31] Figure 10 collects the plots of S_0, S_1, and S_2 energies as a function of the twist angle for ethylene, propene, protonated formaldimine, and aminoborane, providing four examples nicely illustrating the behavior expected from the simple model (Fig. 6): The S_0–S_1 gap is large in the perfect biradical (twisted ethylene), and not much smaller in a weakly heterosymmetric biradicaloid (twisted propene). It is reduced approximately to zero in a critically heterosymmetric biradicaloid (twisted formaldiminium ion) and is again large in a strongly heterosymmetric biradicaloid (twisted aminoborane). With this type of computational example it is difficult to provide a continuous plot such as that of Figure 5; on the other hand, the example illustrates the expected phenomena on real molecular systems.

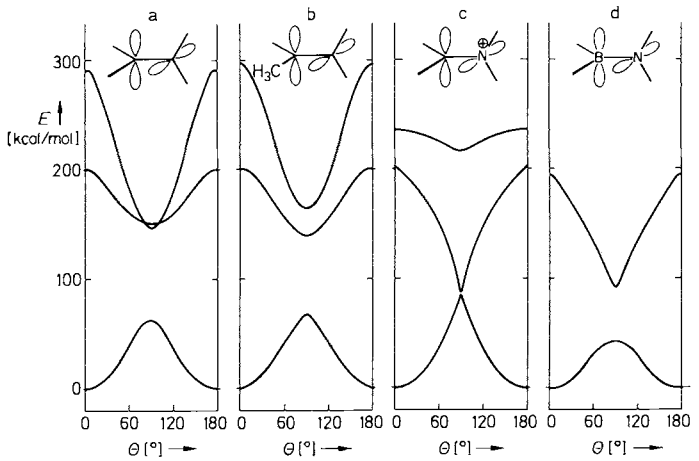

Fig. 10. Ab initio MRD CI calculation of singlet state energies of a) ethylene [31a], b) propene [28e], c) formaldiminium ion [31a], and d) aminoborane [31b] as a function of the twist angle.

We believe that the ab initio calculations discussed here clearly verify the qualitative concepts derived from the simple model, with respect to both energies and wave functions.

3.3. Push-Pull Perturbed Cyclobutadienes

Cyclobutadienes perturbed by increasing the electronegativity of carbons 1 and 3 and/or decreasing the electronegativity of carbons 2 and 4 provide a second class of examples. This type of substitution pattern is required in order to induce an energy difference between the localized orbitals A and B of **2** (Scheme 1).[34,35a] The relative energy of the hole-pair configurations $^1|A^2\rangle$ and $^1|B^2\rangle$ can be modified either by the introduction of substituents such as CN or $N(CH_3)_2$, or by the replacement of carbon atoms by heteroatoms such as nitrogen or boron. When sufficiently strong, either of these perturbations leads to push-pull stabilized cyclobutadienes, such as **16**[35] and **17**[36] (Scheme 5). Unlike the parent cyclobutadiene and weakly perturbed cyclobutadienes, these molecules are quite stable, with four equal bond lengths in the ring; in their singlet ground state, the configuration $^1|B^2\rangle$ dominates by far.[36,37] While square cyclobutadiene is an archetypical example of a perfect biradical, the known strongly push-pull perturbed cyclobutadienes are so strongly heterosymmetric biradicaloids that one could be reluctant to label them biradicaloids at all.

We are interested in critically heterosymmetric biradicaloids of this type as another illustration of the general principle deduced from the simple model. No such species appear to be known experimentally.

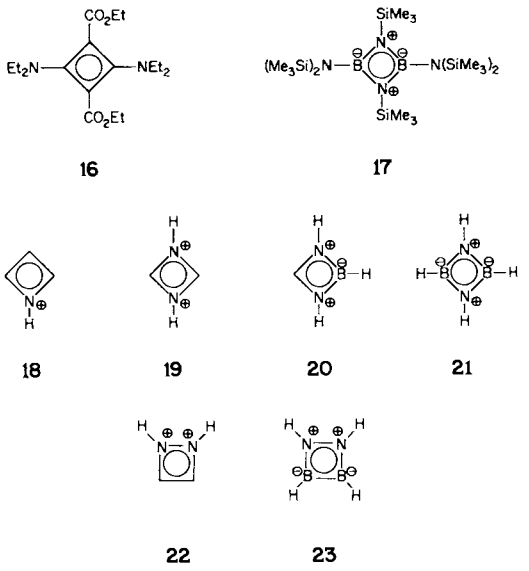

Scheme 5. Perturbed cyclobutadienes.

Figure 11 shows the state energies for a series of perturbed square cyclobutadienes, calculated using the method described in Section 3.2. The geometries have not been optimized but this is not essential to the argument. The energies and wave functions behave just as expected from the simple model. The S_0–S_1 splitting is large in the perfect biradical **2** (ca. 46 kcal/mol); as a result of the gradual stabilization of orbital B relative to A, the splitting vanishes almost completely in the critically heterosymmetric biradicaloids **18** and **19** and is again large in the strongly heterosymmetric biradicaloids **20** (ca. 52 kcal/mol) and particularly **21** (ca. 89 kcal/mol). The triplet lies close to the singlet $^1|AB\rangle$; i.e., close to S_0 in **2** and **18** and close to S_1 in **18**–**21** (the simple model predicts exact singlet–triplet degeneracy in the zero-differential overlap approximation).

The S_1 and T_1 states of the perturbed cyclobutadienes should have minima at square or rhombic geometries, but we expect this to be true of the S_0 state only for sufficiently large values of δ, say in **21** (the work is in progress to verify this computationally). For critically heterosymmetric cyclobutadienes such as **18**, and certainly for weakly heterosymmetric ones, a geometric distortion toward nonzero γ takes place in S_0 (pseudo Jahn–Teller effect, Fig. 7), leading to bond-length alternation.

The results for push-pull perturbed square cyclobutadienes ($\delta_{AB} \neq 0$) can be contrasted with those computed for the opposite substitution pattern ($\delta_{AB} = 0$). In **22** and **23**, the localized orbitals A,B remain degenerate, while the

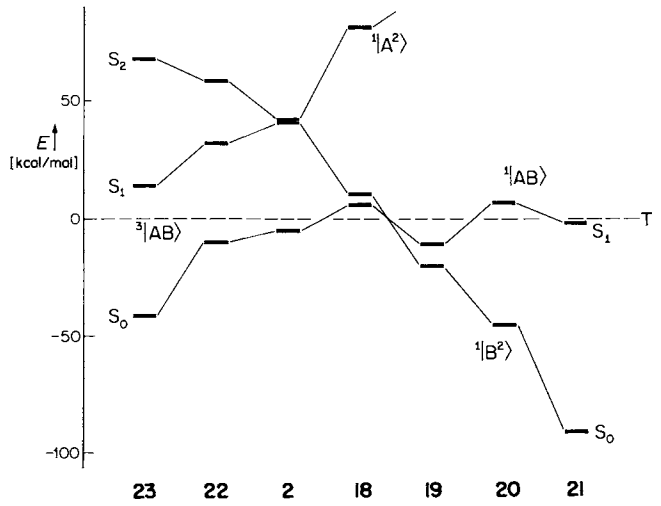

Fig. 11. Ab initio MRD CI calculation of singlet and triplet state energies of square-planar 1,2,3,4-diazadiborete **23**, doubly protonated 1,2-diazete **22**, cyclobutadiene **2**, protonated azete **18**, doubly protonated 1,3-diazete **19**, protonated 1,3,2-diazaborete **20**, and 1,3,2,4-diazadiborete **21**. Bond lengths [Å]: 1.456 Å (all C-C, C-N, and N-B bonds), 1.09 (C-H), 0.985 (N-H), 1.178 (B-H), 4-31G basis. The CI calculation was performed in two steps, using between five and fourteen reference configurations. At first, these were constructed from triplet SCF MOs. For each state, natural orbitals were then computed and used as the basis set for a final MRD CI calculation. (The diagonalized CI spaces contain approximately 10000 configurations. The extrapolated energies toward the full MRD CI space are plotted.)

delocalized orbitals a,b are split ($\gamma_{AB}=\delta_{ab}\neq 0$). The ab initio CI results (Fig. 11, left) show the anticipated behavior: there is no S_0–S_1 crossing, but rather a strong stabilization of S_0 and destabilization of S_2. The decrease in the S_1–T_1 gap is due to the increasing localization of the orbital a (LUMO) on atoms 2 and 3 and of the orbital b (HOMO) on atoms 1 and 4, which gives the $^1|ab\rangle$ configuration considerable charge-transfer character.

4. Conjectures for Photochemical Mechanisms

4.1. General

The general conclusions concerning the conditions for minimal S_0–S_1 gaps and for the location of S_1 minima in biradicaloids that were reached from the simple model and confirmed on a limited number of examples by large-scale CI calculations suggest certain general consequences for singlet photochemical processes. In general, the quantum yield of a particular photoproduct can be viewed as a function of the likelihood that an appropriate funnel leading to S_0 is reached and used and of the likelihood that return to S_0 through that funnel leads to eventual formation of the product. The former is related to the presence and height of the barriers that may separate the funnel geometry from the geometry reached initially after excitation. A complicated series of barriers may have to be overcome and a kinetic description will be correspondingly complex. All else being more or less equal, one might hope that making the funnel deeper will reduce the barriers around it, enhancing the photoprocesses that proceed through it.

In the absence of more detailed information on the shapes of the potential energy surfaces and on the nature of the rate-determining step in reaching the funnel, this statement is no more than a conjecture which will require considerable testing before it can be accepted as valid for any particular class of photochemical reactions. In the following we illustrate the application of the ideas outlined above to a few selected problems in organic photochemistry, without attempting a comprehensive coverage of the literature.

4.2. *cis–trans* Isomerization

There are three ways in which the present results could be pertinent to the mechanism of photochemical *cis–trans* isomerization about double bonds.

1. If twisting about several such bonds is possible in a molecule, according to the above conjecture the twist leading to the deepest funnel should occur preferentially. Other factors such as steric constraints being the same, the simple model suggests that this will be the twist that produces localized orbitals A and B in such a way that the energies of the configurations $^1|AB\rangle$ and $^1|B^2\rangle$ are comparable.

An example is provided by $CH_2{=}CH{-}CH{=}\overset{\oplus}{N}H_2$, which, according to calculations[38] and the above conjecture, should preferentially twist about the C=N and not the C=C bond. The C=N twist is calculated to produce an S_0–S_1 near touching[31,38] since the $CH_2{=}CH{-}\overset{\oplus}{C}H{-}$ + $-\ddot{N}H_2$ and $CH_2{=}CH{-}\overset{\odot}{C}H{-}$ + $-\overset{\odot}{\ddot{N}}H_2^{\oplus}$ structures are of comparable energy (the ionization potential of the allyl radical is 8.13 eV,[39] that of methylamine 9.64 eV[40]). The C=C twist does not produce an S_0–S_1 near touching since $CH_2^{\oplus}-$ + $-CH{=}CH{-}\ddot{N}H_2$ is a much less stable combination than $\overset{\odot}{C}H_2-$ + $-CH{=}CH{-}\overset{\odot}{\ddot{N}}H_2^{\oplus}$.

In the presence of an even larger number of double bonds available for isomerization, the situation becomes more complicated. Also, the relative energies of the various neutral and charged fragment combinations will respond differently to the presence of a polar solvent and to changes in the environment. It is conceivable that a particular combination of molecular structure and organized surrounding is responsible for the specificity of *cis–trans* photoisomerization about only one particular bond in both rhodopsin and bacteriorhodopsin (see Section 4.4).

2. Those twisting motions that lead to a funnel in which the S_0–S_1 gap vanishes may induce an $S_1 \rightarrow S_0$ jump the very first time the funnel region is reached. Dynamical memory ("momentum effect") in the sense that has been discussed in photochemistry repeatedly[9,10,41,42] but, to our knowledge, not actually demonstrated experimentally in a convincing manner, except perhaps in rhodopsin,[43] could then lead to extraordinarily high (or low) quantum yields. In this case, the sum of the quantum yields of processes proceeding through the same funnel could actually exceed unity.

3. As discussed in more detail in Section 4.4, critically heterosymmetric biradicaloids of the protonated Schiff base type could exist in two isomeric ground-state forms, which differ, first, in the location of the positive charge and, second, by an interchange of positions of single and

double bonds. Rotation around formally single bonds is usually easily induced thermally. Thus, *cis-trans* photoisomerization about a formal double bond in one of the forms could proceed by an initial phototransformation into the other form accompanied by a bond shift and subsequent rotation around the now formally single bond in the ground state.

4.3. Twisted Internal Charge-Transfer (TICT) Zwitterionic Excited States

It is of interest to point out the connection between the *cis-trans* isomerization about double bonds and the existence of twisted internal charge-transfer (TICT) zwitterionic excited states[44] in molecules such as **9**, which contain a π-donor moiety (orbital *B*) coupled by a formal single bond to a π-acceptor moiety (orbital *A*). The electronegativities of *A* and *B* differ greatly, and in the S_0 state the wave function is almost exactly of the hole-pair type, $^1|B^2\rangle$. Geometries for which $S_{AB}=\gamma_{AB}=0$ are preferred in the S_1 state (Fig. 7c), which corresponds to the dot-dot configuration $^1|AB\rangle$ and thus is of zwitterionic character, with the donor positively and the acceptor negatively charged. If the donor and the acceptor are connected by a formally single bond, the S_0 state favors a planar geometry (large γ_{AB}). The geometry that is optimal for S_1 can be reached by twisting around this bond to make *A* and *B* orthogonal, hence "twisted internal charge-transfer" ("twisted zwitterion") states.

The spatial separation of *A* and *B* and the large geometry difference between S_0 and S_1 make optical transitions into TICT states from S_0 weak and hard to observe. These states are normally populated by internal conversion from other excited states and observed in emission. The energy of such dipolar states depends sensitively on the polarity of the environment, and they are therefore most readily detected by characteristic solvent shifts of fluorescence.

Although the above description is adequate for a simple donor-acceptor combination such as **9**, in most of the compounds in which TICT emission has been observed the two-electron two-orbital representation of excited states is inadequate in that the donor or the acceptor or both are complicated structures with low-lying locally excited electronic states, such as substituted benzene rings. A typical example is *p-N,N*-dimethylaminobenzonitrile, in which the NMe_2 group acts as the donor and the C_6H_4CN group as the acceptor. These additional locally excited states typically favor planar geometries and thus impose barriers to the twisting motion. Only if the TICT state represents the S_1 surface at least in the vicinity of orthogonal twist does it have a chance to be detected in fluorescence (Fig. 12). Since this highly polar state is preferentially favored by a polar environment, TICT emission is usually though not always observed only in polar solvents.

Also other donor-acceptor systems with zwitterionic excited states can be discussed in terms of the two-electron two-orbital model. Examples are species in which the donor and the acceptor are not attached to each other at all (radical ion pairs) and those in which they are linked by a saturated hydrocarbon chain.[45] Thus, the category of zwitterionic biradicaloid states is more general than the category of TICT states.

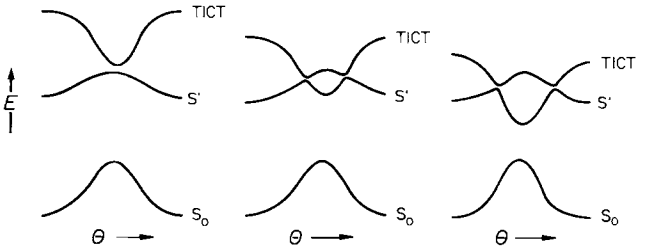

Fig. 12. Schematic representation of three typical cases for the relative energies of a locally excited state (S') and a TICT state as a function of twist angle. From left to right the TICT state is lowered due to variation of donor-acceptor groups and/or polar solvents.

4.4. Proton Translocation and Vision

In charged biradicaloids such as **14** and **15**, the dot-dot $^1|AB\rangle$ and hole-pair $^1|B^2\rangle$ configurations are related by a charge displacement rather than charge separation as was the case in the species discussed in Section 4.3. In order to distinguish between the two cases clearly, such transport of a positive or a negative charge is referred to as charge translocation. In critically heterosymmetric biradicaloids the two configurations are degenerate, and already a relatively small change in the electronegativity difference δ will remove the degeneracy. A small increase in δ, due perhaps to some environmental effect that stabilizes positive charge in the localized orbital A or negative charge in B, will cause the hole-pair configuration $^1|B^2\rangle$ to represent a nondegenerate ground state S_0. A small decrease in δ, such as might be caused by solvent rearrangement that stabilizes positive charge in B or negative charge in A, will cause the dot-dot configuration $^1|AB\rangle$ to represent a nondegenerate ground state S_0. These effects are shown for rhodopsin in Figure 13. Solvated, charged biradicaloids such as these clearly have the potential to be bistable, i.e., to exist in two ground-state isomeric forms that differ by charge translocation and by some perturbation external to the biradicaloid proper. Typically, in the ground state the geometries of these biradicaloids will be distorted so as to make not only δ but also γ different from zero. If this can occur both toward a *cis* and a *trans* geometry in **14** or **15**, up to four separate minima in S_0 may result.

However, if the distortion toward large $|\gamma|$, i.e., toward planarity in **14** or **15**, is excessive, the configurations $^1|AB\rangle$ and $^1|B^2\rangle$ will interact and the charge will become delocalized. In a fluid environment, the system will then most likely end up with a single "*cis*" and a single "*trans*" minimum. As Figure 13 shows, electronic excitation, either $S_0 \rightarrow S_1$ or $S_0 \rightarrow S_1 \rightarrow S_1$, has the potential for isomerizing each form of the solvated biradicaloid into the others via the funnel in S_1 located at the critical value of δ_0 where S_1 and S_0 touch (or nearly touch if γ is small but not zero). The motions required for such isomerization are, first, a geometry change in the biradicaloid that causes γ to vanish, such as a twist of a double bond to orthogonality, and,

second, a change in the rest of the molecule or in the environment that brings δ to the critical value δ_0.

It is interesting to speculate that such bistable charged biradicaloids might be involved in the photobiological mechanism of operation of the visual pigment, rhodopsin. The chromophore is **24**, the protonated Schiff base of 11-*cis*-retinal (Scheme 6), presumably embedded in a relatively rigid environment. The primary event is believed to consist of its excitation to the S_1 state **24***, followed by twisting around the *cis* double bond (and possibly other chain motions, such as those involved in the "hula twist") to produce a charged biradicaloid species and eventually to yield the S_0 state of the *trans* isomer **26**, protonated bathorhodopsin (=prelumirhodopsin), which is 35 kcal/mol higher in energy than rhodopsin.[46] This process occurs on a picosecond time scale; much slower subsequent changes in the ground state modify the conformation of the protein, leading eventually to the production of a nerve impulse.

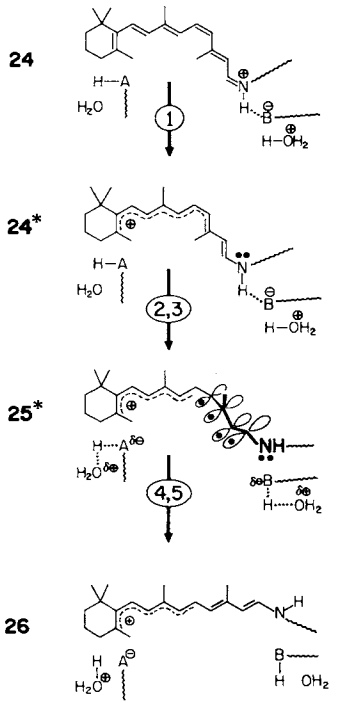

Scheme 6. Phototransformation of rhodopsin to bathorhodopsin. 1) Vertical excitation. 2) Twist to orthogonality. 3) First half of proton motion. 4) Twist to planarity. 5) Second half of proton motion.

In the initial photoproduct **26**, the nitrogen atom of the Schiff base is still protonated. It has therefore been somewhat of a puzzle that a replacement of exchangeable protons of the protein by deuterium slows down bathorhodopsin formation by a factor of seven; at very low temperatures proton tunneling seems to be involved.[47]

This coupling of the twisting motion with motions of protons in the environment and the large amount of energy stored are naturally accounted for by the reaction scheme proposed in Scheme 6 (Fig. 13), based on the concept of bistability for charged biradicaloids as outlined above. For the purposes of this illustration, we have chosen specific locations for acidic and basic groups in the environment of the chromophore, but other locations and more complicated acidic and basic centers can be envisaged readily. We have chosen a particularly simple chain conformation for bathorhodopsin, but others such as 10-*s-cis* are equally compatible with our proposal.

There is little doubt that a transfer of positive charge from the protonated nitrogen to the polyene chain occurs upon vertical excitation; it has been proposed to be particularly complete in the orthogonally twisted molecule **25***.[48] This translocation of positive charge will change the acid-base properties of protein groups on both ends of the chromophore. A more or less simultaneous protonation of a base near the nitrogen end and deprotonation of an acid near the ionone ring end will change the energy order of the $^1|AB\rangle$ and $^1|B^2\rangle$ configurations, taking the system through the S_0–S_1 touching point at δ_0. As shown in Figure 13, it is then the proton motion coordinate that is responsible for the return to S_0, accounting for the effects of deuteration and the low-temperature tunneling behavior. In this picture, **26** differs from **24** not only in the geometry around the $C_{11}=C_{12}$ double bond and possibly one or more single bonds, but also in the location of charges in the environment; these factors account for the much higher energy content and shifted absorption spectrum of **26**. It is proposed that the new charge positions, along with the presumably poorer mechanical fit of the all-*trans* chromophore into its pocket, then lead to changes in hydrogen bonding and protein conformation.

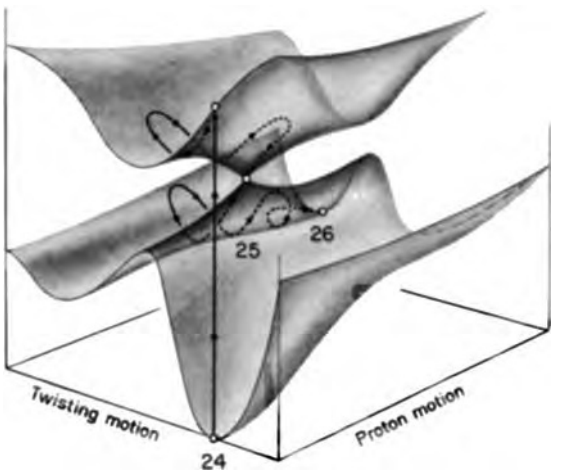

Fig. 13. A schematic representation of the conjectured energies of the S_0 and S_1 states of rhodopsin as a function of twist angle and proton motion in the environment (see also text).

Thermal return from **26** to **24** by deprotonation of the newly formed acid near the nitrogen atom and by reprotonation at the newly formed base near the ionone ring is presumably hindered by the final all-*trans* geometry of the polyene chain, which no longer provides for a close proximity between the nitrogen atom and the newly formed acidic group, so that other processes occur faster.

The proposal that some change in protein environment causes an interchange of the nature of the S_0 and S_1 wave functions has been made before;[28c,49] the present formulation is more specific and accounts for the observed effects

of deuteration. It is possible that a similar mechanism with coupled twisting and proton translocation applies in the case of bacteriorhodopsin even though the deuteration effect there is much smaller.[47]

If the present understanding of the basic principles is correct and bistable (or tetrastable) charged critically heterosymmetric biradicaloids can be designed and built into a membrane in proper orientation, it should be possible to construct an artificial charge-pumping photosystem that responds to irradiation at one wavelength by lowering the pH on one side and by increasing it on the other side of the membrane and does the opposite upon irradiation at another wavelength.

4.5. Singlet Photocycloaddition

The following mechanistic scheme has been proposed[19] for singlet photocycloadditions that are ground-state forbidden and excited-state allowed, such as the [2s + 2s] photocycloaddition of two olefins (Fig. 14):

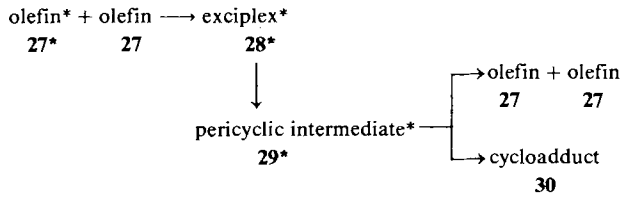

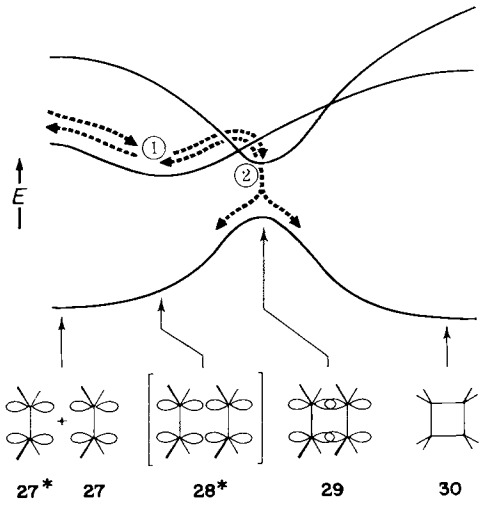

Fig. 14. Schematic representation of the energies of the S_0, S_1, and S_2 states for a concerted cycloaddition of two olefins. ① = excimer or exciplex minimum, ② = pericyclic minimum.

The return from the S_1 to the S_0 state occurs at the geometry of the pericyclic intermediate, which is isoconjugate with an antiaromatic annulene such as square cyclobutadiene and in which there is cyclic bonding between the four centers involved in the photocycloaddition. This preserves stereochemical information, so that the cycloaddition is stereospecific.

This process is of considerable mechanistic and synthetic interest. It is therefore important to develop a predictive capability when more than one regiochemical (head-to-head, head-to-tail) and stereochemical (*exo, endo*) possibility exists for the product structure. Three of the many factors that are likely to affect the outcome are the energies of **28*** and **29*** and the height of the barrier between them.

Simple perturbation theory considerations[50] show that electronic factors always favor the head-to-head regiochemistry and *syn* or *cis* stereochemistry in an excimer. Such considerations, along with an estimate of the energy of the pericyclic intermediate from triplet energies of the two reaction partners, have been used to estimate which cycloadditions will and which ones will not proceed.[51] The *syn* or *cis* adducts are indeed generally formed in the singlet photodimerization of olefins. However, it is known experimentally that some singlet cycloadditions, for instance those of substituted acenaphthylenes and anthracenes, yield head-to-tail products even though no steric or other reasons for this are readily apparent.[52]

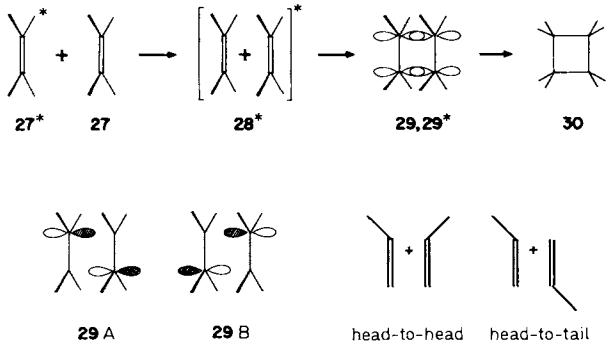

Scheme 7. Regiochemistry in [2 + 2] photocycloaddition.

The results described here, in particular the analogy to the isoconjugate perturbed cyclobutadienes, suggest a resolution of the dilemma (Scheme 7): The localized nonbonding orbitals of the pericyclic intermediate, **29** A and **29** B, will have equal energies ($\delta_{AB} = 0$) in head-to-head cyclodimerization but different energies ($\delta_{AB} > 0$) in head-to-tail cyclodimerization. The latter should stabilize the S_1 state of the biradicaloid and produce a deeper pericyclic minimum. If our initial conjecture is correct, this should in turn reduce the barriers around the minimum and thus fa-

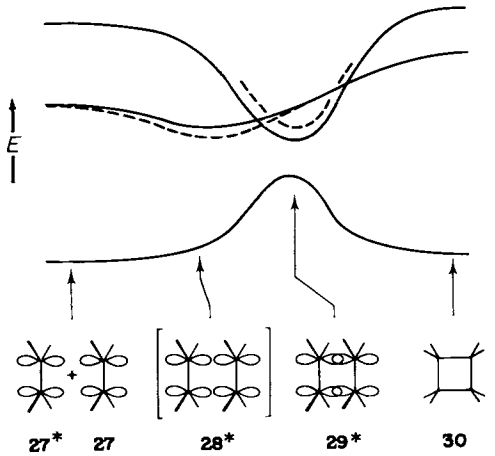

Fig. 15. Regiochemistry in a concerted singlet photocycloaddition. A schematic representation of the singlet energy surfaces S_0, S_1, and S_2 for a head-to-head (---) and head-to-tail coupling (——).

vor the formation of **29*** from the excimer. Thus, the head-to-head geometry is favored by the excimer **28*** and the head-to-tail geometry by the pericyclic intermediate **29*** (Fig. 15); either **28*** or **29*** can dictate which product is formed preferentially.

Similar considerations suggest that excited singlet-state pericyclic reactions hardly ever favor the most symmetrical paths for which most calculations have been done so far (e.g., butadiene $\rightleftarrows$ cyclobutene[7,23]), even though, unlike their triplet counterparts, they develop and preserve cyclic bonding along the reaction path.

5. Summary

We have attempted to formulate a systematic overview of the whole range of biradical-like species, from perfect biradicals to nonpolar, polar, or charged covalent and dative bonds, based on a simple two-electron two-orbital model and on comparison with ab initio calculations for a selected series of examples. Particular attention was paid to identifying the conditions for S_0-S_1 surface touching, which is believed to be of key importance in photochemistry. Several conjectures concerning photophysical and photochemical mechanisms, including that of the primary process in vision, have been formulated.

Appendix

1. Orbital Transformations

A general unitary transformation of the orbitals $\mathscr{A}$ and $\mathscr{B}$ to some new orbital pair $\mathscr{A}_{\omega\phi}$, $\mathscr{B}_{\omega\phi}$ is characterized by a rotation angle ω and complex phase ϕ [Eq. (A1)]. The state wave functions in the new and old orbital bases are related by Equation (A2). For $\mathscr{A}=\mathrm{A}$ and $\mathscr{B}=\mathrm{B}$, special cases of interest are $\phi=0$, $\omega=\pi/4$ ($\mathscr{A}_{\omega\phi}=\mathrm{a}$, $\mathscr{B}_{\omega\phi}=\mathrm{b}$) and $\phi=\pi/2$, $\omega=\pi/4$ ($\mathscr{A}_{\omega\phi}=\mathrm{c}^*$, $\mathscr{B}_{\omega\phi}=i\mathrm{c}$).

$$(\mathscr{A}_{\omega\phi},\mathscr{B}_{\omega\phi})=(\mathscr{A},\mathscr{B})\begin{pmatrix}\cos\omega & -e^{-i\phi}\sin\omega\\ e^{i\phi}\sin\omega & \cos\omega\end{pmatrix}=(\mathscr{A},\mathscr{B})\cup(\omega,\phi) \tag{A1}$$

$$\begin{pmatrix}{}^3|\mathscr{A}_{\omega\phi}\mathscr{B}_{\omega\phi}\rangle\\ {}^1|\mathscr{A}_{\omega\phi}^2+\mathscr{B}_{\omega\phi}^2\rangle\\ {}^1|\mathscr{A}_{\omega\phi}\mathscr{B}_{\omega\phi}\rangle\\ {}^1|\mathscr{A}_{\omega\phi}^2-\mathscr{B}_{\omega\phi}^2\rangle\end{pmatrix}=\begin{pmatrix}1 & 0 & 0 & 0\\ 0 & 1-2\sin^2\phi\sin^2\omega & i\sin\phi\sin 2\omega & -i\sin 2\phi\sin^2\omega\\ 0 & i\sin\phi\sin 2\omega & \cos 2\omega & -\cos\phi\sin 2\omega\\ 0 & i\sin 2\phi\sin^2\omega & \cos\phi\sin 2\omega & \cos 2\omega+2\sin^2\phi\sin^2\omega\end{pmatrix}\begin{pmatrix}{}^3|\mathscr{A}\mathscr{B}\rangle\\ {}^1|\mathscr{A}^2+\mathscr{B}^2\rangle\\ {}^1|\mathscr{A}\mathscr{B}\rangle\\ {}^1|\mathscr{A}^2-\mathscr{B}^2\rangle\end{pmatrix} \tag{A2}$$

In the following, we limit our attention to orthogonal transformations of orbitals ($\phi=0$). These have the effect of mixing only ${}^1|\mathscr{A}\mathscr{B}\rangle$ and ${}^1|\mathscr{A}^2-\mathscr{B}^2\rangle$. The transformations given by (A3) then occur.

$$\begin{aligned}&[(K'_\omega-K_\omega),\gamma^-_\omega]=[(K'-K),\gamma^-]\cup(4\omega,0)\\ &(\delta_\omega,\gamma_\omega)=(\delta,\gamma)\cup(2\omega,0)\end{aligned} \tag{A3}$$

Here and in the following, unsubscripted quantities refer to the original orbital choice $\mathscr{A}$, $\mathscr{B}$ ($\omega=0$) and subscripted ones to the rotation angle ω. The repulsion integrals J and J_ω stand for $J_{\mathscr{A}\mathscr{B}}$ and $J_{\mathscr{A}_\omega\mathscr{B}_\omega}$, respectively. E_0, $(K'+K)$, $(J-K)$, $(\gamma^2+\delta^2)$, and $[(K'-K)^2+(\gamma^-)^2]$ are invariant to the rotation. The derivatives with respect to ω are given by (A4). The derivatives $\mathrm{d}K_\omega/\mathrm{d}\omega$ and $\mathrm{d}J_\omega/\mathrm{d}\omega$ vanish when $\gamma^-_\omega=0$, showing that the most localized orbital set A, B (J_ω and K_ω minimized) and the most delocalized one a, b (J_ω and K_ω maximized) fulfill the condition $\gamma^-=0$. Also the set c, c* fulfills it.

$$\begin{aligned}&\frac{\mathrm{d}K'_\omega}{\mathrm{d}\omega}=-\frac{\mathrm{d}K_\omega}{\mathrm{d}\omega}=-\frac{\mathrm{d}J_\omega}{\mathrm{d}\omega}=2\gamma^-_\omega\\ &\frac{\mathrm{d}\gamma^-_\omega}{\mathrm{d}\omega}=4(K_\omega-K'_\omega)\\ &\frac{\mathrm{d}\gamma_\omega}{\mathrm{d}\omega}=-2\delta_\omega\\ &\frac{\mathrm{d}\delta_\omega}{\mathrm{d}\omega}=2\gamma_\omega\end{aligned} \tag{A4}$$

The rotation angle ω needed to produce either A, B or a, b from an arbitrarily chosen initial set $\mathscr{A}$, $\mathscr{B}$ is given by Equation (A5). This equation has a positive root ω_+ and a negative root ω_- in the range of interest, $-\pi/4\le\omega\le\pi/4$. They are related by $\omega_+-\omega_-=\pi/4$. Since Equation (A6) holds, one of the roots transforms $\mathscr{A}$, $\mathscr{B}$ into the localized orbitals A, B ($K'_\omega\ge K_\omega$) and the other into the delocalized orbitals a, b ($K'_\omega\le K_\omega$).

$$\omega=\frac{1}{4}\tan^{-1}\frac{\gamma^-}{K'-K} \tag{A5}$$

$$\frac{\mathrm{d}^2K_\omega}{\mathrm{d}\omega^2}=8(K'_\omega-K_\omega) \tag{A6}$$

Considering the sign of $[\mathrm{d}K_\omega/\mathrm{d}\omega]_{\omega=0}=2\gamma^-$, we see that ω_- yields A, B and ω_+ yields a, b if $\gamma^->0$, and that the opposite holds if $\gamma^-<0$. If $\gamma^-=0$ and $K'>K$, the orbitals $\mathscr{A}$, $\mathscr{B}$ are already equal to the sought orbitals A, B ($\omega=0$). If $\gamma^-=0$ and $K'<K$, $\mathscr{A}$ and $\mathscr{B}$ are equal to a, b and a rotation by $\omega=\pm\pi/4$ is needed to produce A, B. Finally, if $\gamma^-=K'-K=0$, all orbital choices are equally localized or delocalized by our criteria since $[(K'-K)^2+(\gamma^-)^2]$ is an invariant.

2. Density Matrices and Natural Orbitals

In an arbitrary orthonormal basis set $\mathscr{A}$, $\mathscr{B}$, the elements E^Q_P of a one-electron excitation operator E are defined by Equation (A7).[53] Its effect on the wave functions ${}^1|\mathscr{A}^2\pm\mathscr{B}^2\rangle$ and ${}^{1,3}|\mathscr{A}\mathscr{B}\rangle$ is given in Table 3, so that for this singlet basis the diagonal density matrices have the form given in Equation (8) and the transition density matrices are given by Equations (A8) to (A10).

$$E^Q_P=|Q(1)\rangle\langle P(1)|+|Q(2)\rangle\langle P(2)| \quad P,Q=\mathscr{A},\mathscr{B} \tag{A7}$$

$$\langle\mathscr{A}^2+\mathscr{B}^2|E|\mathscr{A}^2-\mathscr{B}^2\rangle=\langle\mathscr{A}^2-\mathscr{B}^2|E|\mathscr{A}^2+\mathscr{B}^2\rangle=\begin{pmatrix}1 & 0\\ 0 & -1\end{pmatrix} \tag{A8}$$

$$\langle \mathscr{A}\mathscr{B}|E|\mathscr{A}^2+\mathscr{B}^2\rangle=\langle \mathscr{A}^2+\mathscr{B}^2|E|\mathscr{A}\mathscr{B}\rangle=\begin{pmatrix}0 & 1\\ 1 & 0\end{pmatrix} \quad (A9)$$

$$\langle \mathscr{A}\mathscr{B}|E|\mathscr{A}^2-\mathscr{B}^2\rangle=-\langle \mathscr{A}^2-\mathscr{B}^2|E|\mathscr{A}\mathscr{B}\rangle=\begin{pmatrix}0 & 1\\ -1 & 0\end{pmatrix} \quad (A10)$$

Table 3. The action of the E operator on the four two-electron basis functions of the 3 × 3 CI model.

	$^1\|\mathscr{A}^2+\mathscr{B}^2\rangle$	$^1\|\mathscr{A}^2-\mathscr{B}^2\rangle$	$^1\|\mathscr{A}\mathscr{B}\rangle$	$^3\|\mathscr{A}\mathscr{B}\rangle$
E:	$\sqrt{2}\|\mathscr{A}^2\rangle$	$\sqrt{2}\|\mathscr{A}^2\rangle$	$^1\|\mathscr{A}\mathscr{B}\rangle$	$^3\|\mathscr{A}\mathscr{B}\rangle$
E:	$\sqrt{2}\|\mathscr{B}^2\rangle$	$-\sqrt{2}\|\mathscr{B}^2\rangle$	$^1\|\mathscr{A}\mathscr{B}\rangle$	$^3\|\mathscr{A}\mathscr{B}\rangle$
E:	$^1\|\mathscr{A}\mathscr{B}\rangle$	$^1\|\mathscr{A}\mathscr{B}\rangle$	$\sqrt{2}\|\mathscr{B}^2\rangle$	0
E:	$^1\|\mathscr{A}\mathscr{B}\rangle$	$-^1\|\mathscr{A}\mathscr{B}\rangle$	$\sqrt{2}\|\mathscr{A}^2\rangle$	0

Note that Equation (A10) guarantees that all linear combinations of the configurations $^1|\mathscr{A}\mathscr{B}\rangle$ and $^1|\mathscr{A}^2-\mathscr{B}^2\rangle$ yield the same diagonal density matrix. For any two singlet states $|S_i\rangle$ and $|S_j\rangle$ defined by Equation (10), the transition density matrix is given by Equation (A11). The expressions for one-electron density matrices for perfect biradicals [Equation (8)] and for biradicaloids [Equation (11)] follow.

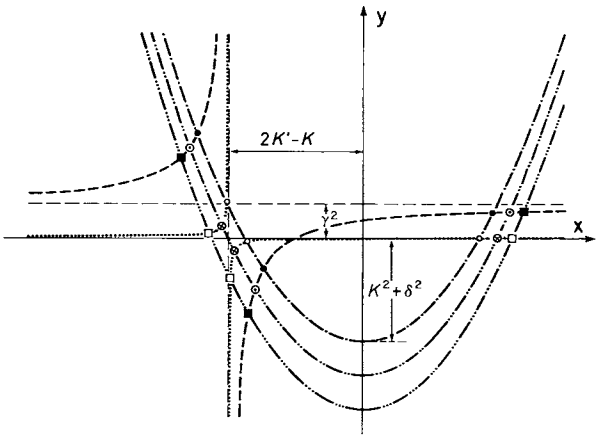

Fig. 16. Graphical solution of Equation (26). Two choices of γ^2 (0 and $\neq 0$; two hyperbolas) and three choices of δ^2+K^2 (three parabolas) are displayed. The three solutions for each of the six cases are obtained as the x coordinates of the points indicated by circles or squares.

$$\langle S_i|E|S_j\rangle=\begin{pmatrix}\langle S_i|S_j\rangle+(C_{i,+}C_{j,-}+C_{i,-}C_{j,+}) & C_{i,+}C_{j,0}+C_{i,0}C_{j,-}+C_{i,0}C_{j,+}-C_{i,-}C_{j,0}\\ C_{j,+}C_{i,0}+C_{j,0}C_{i,+}+C_{j,0}C_{i,+-}-C_{j,-}C_{i,0} & \langle S_i|S_j\rangle-(C_{i,+}C_{j,-}+C_{i,-}C_{j,+})\end{pmatrix} \quad (A11)$$

where $\langle S_i|S_j\rangle=C_{i,+}C_{j,+}+C_{i,-}C_{j,-}+C_{i,0}C_{j,0}$

3. *State Energies of a Nonsymmetric Biradicaloid*

1. *Orthogonal orbitals* $\mathscr{A},\mathscr{B}$. Graphical solutions for E in Equation (26) are found from the x coordinates of the points in which the parabola $y=x^2-(\delta^2+K^2)$ cuts the two branches of the hyperbola $y=2(K-K')\gamma^2/(x-K+2K')+\gamma^2$, where E is given by Equation (A12).

$$E=x+E(T)+2K'+K \quad (A12)$$

As shown in Figure 16, the S_0 root lies below the asymptote $x=K-2K'$ and the S_1 and S_2 roots lie above. The S_0 and S_1 roots approach each other as the product $(K-K')\gamma^2$ goes to zero, provided that the parabola cuts the horizontal line $y=\gamma^2$ near the asymptote. The two roots can coincide only if two conditions are fulfilled simultaneously: (1) the hyperbola degenerates into a pair of lines and (2) the parabola cuts the line $y=\gamma^2$ at $x=K-2K'$. The former condition demands $\gamma=0$ or $K=K'$ or both and the latter condition demands $4K'(K'-K)=\delta^2+\gamma^2$. If $K=K'$, both conditions are satisfied by $\delta=\gamma=0$ (perfect axial biradical). If $K\neq K'$, both conditions are satisfied by $\gamma=0$, $\delta=\delta_0=2\sqrt{K'(K'-K)}$ (critically heterosymmetrical biradicaloid).

2. *Nonorthogonal orbitals* A,B. The expression for the triplet energy E_T^0 is given by Equation (31). The Hamiltonian matrix for the sinjglets is given by (A13) where κ and γ' are given by Equations (A14) and (A15).

$$\begin{matrix}{}^1|A^2-B^2\rangle\\ {}^1|A^2+B^2\rangle\\ {}^1|AB\rangle\end{matrix}\begin{pmatrix}(1-S_{AB}^2)^{-1}E_T^0+2K'_{AB} & (1-S_{AB}^4)^{-1/2}\delta_{AB} & (1-S_{AB}^4)^{-1/2}\gamma_{AB}\\ (1-S_{AB}^4)^{-1/2}\delta_{AB} & (1+S_{AB}^2)^{-1}E_T^0+2(K'_{AB}+\kappa_{AB}) & (1+S_{AB}^2)^{-1}\gamma'_{AB}\\ (1-S_{AB}^4)^{-1/2}\gamma_{AB} & (1+S_{AB}^2)^{-1}\gamma'_{AB} & (1+S_{AB}^2)^{-1}E_T^0+2\kappa_{AB}\end{pmatrix} \quad (A13)$$

$$\kappa_{AB}=K_{AB}+2h_{AB}S_{AB} \quad (A14)$$

$$\gamma'_{AB}=\gamma_{AB}+S_{AB}(h_{AA}+h_{BB})/2 \quad (A15)$$

V. B.-K. and J. K. thank the Deutsche Forschungsgemeinschaft and the Fonds der Chemischen Industrie for support. J. M. thanks the National Science Foundation for support and gratefully acknowledges the award of a Guggenheim fellowship.

Received: December 19, 1985 [A 593 IE]
German version: *Angew. Chem. 99* (1987) 216

[1] L. Salem, C. Rowland, *Angew. Chem. 84* (1972) 86; *Angew. Chem. Int. Ed. Engl. 11* (1972) 92.
[2] J. Michl, *Mol. Photochem. 4* (1972) 257.
[3] W. T. Borden (Ed.): *Diradicals*, Wiley, New York 1982.
[4] L. Salem: *Electrons in Chemical Reactions*, Wiley, New York 1982.
[5] G. Herzberg, H. C. Longuet-Higgins, *Discuss. Faraday Soc. 1963*, 77.

[6] H. E. Zimmerman, *J. Am. Chem. Soc. 88* (1966) 1566; *Acc. Chem. Res. 15* (1982) 312.
[7] W. T. A. M. van der Lugt, L. J. Oosterhoff, *J. Am. Chem. Soc. 91* (1969) 6042.
[8] R. C. Dougherty, *J. Am. Chem. Soc. 93* (1971) 7187.
[9] J. Michl, *Mol. Photochem. 4* (1972) 243.
[10] J. Michl, *Top. Curr. Chem. 46* (1974) 1.
[11] M. J. S. Dewar, R. C. Dougherty: *The PMO Theory of Organic Chemistry*, Plenum, New York 1975.
[12] W. G. Dauben, L. Salem, N. J. Turro, *Acc. Chem. Res. 8* (1975) 41.
[13] N. J. Turro: *Modern Molecular Photochemistry*, Benjamin/Cummings, New York 1978.
[14] H. Kollmar, V. Staemmler, *Theor. Chim. Acta 48* (1978) 223.
[15] R. J. Buenker, S. D. Peyerimhoff, *Chem. Phys. 9* (1975) 75.
[16] W. T. Borden, E. R. Davidson, *J. Am. Chem. Soc. 99* (1977) 4587.
[17] a) D. Döhnert, J. Koutecký, *J. Am. Chem. Soc. 102* (1980) 1789; b) J. Koutecký, D. Döhnert, P. E. S. Wormer, J. Paldus, J. Čížek, *J. Chem. Phys. 80* (1984) 2244.
[18] C. M. Meerman-van Benthem, H. J. C. Jacobs, J. J. C. Mulder, *Nouv. J. Chim. 2* (1978) 123.
[19] W. Gerhartz, R. D. Poshusta, J. Michl, *J. Am. Chem. Soc. 98* (1976) 6427; J. Michl, *Photochem. Photobiol. 25* (1977) 141; *Pure Appl. Chem. 41* (1975) 507.
[20] The use of complex orbitals is advantageous in the case of axial biradicals. These belong to a point symmetry group with a threefold or higher axis of symmetry and their characteristic property is $K'_{AB}=K_{AB}$. If the orbitals A and B are members of a degenerate pair, c and c* will transform according to the representations ε_n and ε_n^*. When $\varepsilon_{2n}\neq\varepsilon_{2n}^*$, it is immediately obvious that the configurations $|c^{*2}\rangle$ and $|c^2\rangle$ cannot interact. Instead, they form two members of a degenerate pair of states, S_0 und S_1 (Table 2). For instance, in molecular oxygen, O_2, $c=\pi_+$, $c^*=\pi_-$, and c^2 and c^{2*} together describe the degenerate state $^1\Delta$. Similarly, in methylnitrene, CH_3-N with $c=2p_+$ and $c^*=2p_-$, c^{*2} and c^2 form the degenerate S_0, S_1 state ^1E. The complex MOs of the π system of regular 4N-electron [n]annulenes of D_{nh} symmetry (7) have served as the starting point for a recently developed classification of the electronic excited states of cyclic π systems derivable from such perimeters [21] (e.g., biphenylene, 9b-azaphenalene, heptalene), similar in spirit to the classical L_b,L_a,B_b,B_a nomenclature for the excited states of aromatic π systems; cf. *Platt's* perimeter model for (4N+2)-electron perimeters: J. R. Platt, *J. Chem. Phys. 17* (1949) 484; W. Moffitt, *ibid. 22* (1954) 320, 1820; E. Heilbronner, J. N. Murrell, *Mol. Phys. 6* (1963) 1; M. Gouterman, *J. Mol. Spectrosc. 6* (1961) 138; J. Michl, *J. Am. Chem. Soc. 100* (1978) 6801, 6812.
[21] U. Höweler, J. Michl, unpublished results.
[22] C. R. Flynn, J. Michl, *J. Am. Chem. Soc. 96* (1974) 3280.
[23] D. Grimbert, G. Segal, A. Devaquet, *J. Am. Chem. Soc. 97* (1975) 6629.
[24] K. Fukui, *Acc. Chem. Res. 4* (1971) 57; H. E. Zimmerman, G. A. Epling, *J. Am. Chem. Soc. 94* (1972) 8749; H. E. Zimmerman, D. Armesto, M. G. Amezua, T. P. Gannett, R. P. Johnson, *ibid. 101* (1979) 6367.
[25] The adjective "biradicaloid," as in "a biradicaloid geometry," is used at times, and stands for "of a biradical" or "of a biradicaloid" (as in "a geometry at which the molecule is a biradical or a biradicaloid").
[26] This result is obtained readily from the form which the S_0 wave function takes when $(\delta^2_{\mathscr{A}\mathscr{B}}+\gamma^2_{\mathscr{A}\mathscr{B}})$ grows beyond all bounds. Note that this quantity as well as $C_{0,+}$ are invariant to rotations within the orbital basis set according to Equations (A2) and (A3). Choosing a rotation [Eq. (A1)] by an angle $\omega=(1/2)\tan^{-1}(\gamma_{AB}/\delta_{AB})$ that converts the localized orbital pair A, B into the pair $\mathscr{A}_\omega$, $\mathscr{B}_\omega$ for which $\gamma_{\mathscr{A}_\omega\mathscr{B}_\omega}$ vanishes, and noting that $\gamma_{\mathscr{A}_\omega\mathscr{B}_\omega}$ and $2K_{\mathscr{A}_\omega\mathscr{B}_\omega}$ can be neglected next to $\delta_{\mathscr{A}_\omega\mathscr{B}_\omega}$ in the limit, we see that $C_{0,+}$ approaches $1/\sqrt{2}$, $C_{0,-}$ goes to $-1/\sqrt{2}$, and $C_{0,0}$ goes to zero, so that the S_0 wave function goes to $^1|\mathscr{B}_\omega^2\rangle$. If $\gamma_{AB}=0$, this is $^1|B^2\rangle$, and both electrons are in the more stable localized orbital B. If $\delta_{AB}=0$, this is $^1|b^2\rangle$, and both electrons are in the bonding delocalized orbital b.
[27] C. Doubleday, Jr., J. W. McIver, Jr., M. Page, *J. Am. Chem. Soc. 104* (1982) 6533; A. H. Goldberg, D. A. Dougherty, *ibid. 105* (1983) 284.
[28] a) C. E. Wulfman, S. Kumei, *Science 172* (1971) 1061; b) V. Bonačić-Koutecký, P. Bruckmann, P. Hiberty, J. Koutecký, C. Leforestier, L. Salem, *Angew. Chem. 87* (1975) 599; *Angew. Chem. Int. Ed. Engl. 14* (1975) 575; c) L. Salem, *Acc. Chem. Res. 12* (1979) 87; d) R. J. Buenker, V. Bonačić-Koutecký, L. Pogliani, *J. Chem. Phys. 73* (1980) 1836; e) V. Bonačić-Koutecký, L. Pogliani, M. Persico, J. Koutecký, *Tetrahedron 38* (1982) 741.
[29] C. F. Bender, H. F. Schaefer III, D. R. Franceschetti, L. C. Allen, *J. Am. Chem. Soc. 94* (1972) 6888.
[30] W. Gerhartz, R. D. Poshusta, J. Michl, *J. Am. Chem. Soc. 99* (1977) 4263; E. R. Davidson, W. T. Borden, J. Smith, *ibid. 100* (1978) 3299.
[31] a) V. Bonačić-Koutecký, J. Köhler, J. Michl, *Chem. Phys. Lett. 104* (1984) 440; b) V. Bonačić-Koutecký, J. Michl, *J. Am. Chem. Soc. 107* (1985) 1765.
[32] R. J. Buenker, S. D. Peyerimhoff, *Theor. Chim. Acta 35* (1974) 33; R. J. Buenker, S. D. Peyerimhoff, W. Butscher, *Mol. Phys. 35* (1978) 771; the calculations have been carried out with the Bonn-Wuppertal MRD CI package using the Table CI algorithm for computing Hamiltonian matrix elements: R. J. Buenker in R. Carbo (Ed.): *Studies in Physical and Theoretical Chemistry* (Current Aspects of Quantum Chemistry Vol. 21), Elsevier, Amsterdam 1982, pp. 17–34; *Proc. Workshop Quantum Chem. Mol. Phys.* (Wollongong, Australia 1980); R. J. Buenker, R. A. Phillips, *J. Mol. Struct. THEOCHEM 123* (1985) 291.
[33] V. Bonačić-Koutecký, M. Persico, *J. Am. Chem. Soc. 105* (1983) 3388.
[34] R. Hoffmann, *Chem. Commun. 1969*, 240.
[35] a) R. Gompper, G. Seybold in T. Nozoe, R. Breslow, K. Hafner, S. Ito, I. Murata (Eds.): *Topics in Non-benzenoid Aromatic Chemistry, Vol. II*, Hirokawa, Tokyo 1977; b) R. Gompper, J. Kroner, G. Seybold, H. U. Wagner, *Tetrahedron 32* (1976) 629.
[36] V. H. Hess, *Acta Crystallogr. Sect. B 25* (1969) 2342.
[37] N. C. Baird, *Inorg. Chem. 12* (1973) 473.
[38] V. Bonačić-Koutecký, J. Köhler, unpublished results.
[39] F. A. Houle, J. L. Beauchamp, *J. Am. Chem. Soc. 100* (1978) 3290.
[40] S. Katsumata, T. Iwai, K. Kimura, *Bull. Chem. Soc. Jpn. 46* (1973) 3391.
[41] E. Teller, *J. Phys. Chem. 41* (1937) 109.
[42] R. M. Weiss, A. Warshel, *J. Am. Chem. Soc. 101* (1979) 6131; H. E. Zimmerman, R. E. Factor, *ibid. 102* (1980) 3538; V. Bonačić-Koutecký, J. Michl, *Theor. Chim. Acta 68* (1985) 45.
[43] T. Suzuki, R. H. Callender, *Biophys. J. 34* (1981) 261.
[44] Z. R. Grabowski, J. Dobkowski, *Pure Appl. Chem. 55* (1983) 245; W. Rettig, M. Zander, *Ber. Bunsenges. Physik. Chem. 87* (1983) 1143; review: W. Rettig *Angew. Chem. 98* (1986) 969; *Angew. Chem. Int. Ed. Engl. 25* (1986) 971.
[45] A. Weller, H. Staerk, R. Treichel, *Faraday Discuss. Chem. Soc. 78* (1984) 271, 332; H. Staerk, W. Kühnle, R. Treichel, A. Weller, *Chem. Phys. Lett. 118* (1985) 19.
[46] M. Ottolenghi, *Adv. Photochem. 12* (1980) 97; W. Stoeckenius, R. A. Bogomolni, *Annu. Rev. Biochem. 52* (1982) 587; A. G. Doukas, M. R. Junnarkar, R. R. Alfano, R. H. Callender, T. Kakitani, B. Honig, *Proc. Natl. Acad. Sci. USA 81* (1984) 4790; R. R. Birge, A. F. Lawrence, T. M. Cooper, C. T. Martin, D. F. Blair, S. I. Chan in W. R. Adey, A. F. Lawrence (Eds.): *Nonlinear Electrodynamics in Biological Systems*, Plenum, New York 1984; R. S. H. Liu, A. E. Asato, *Proc. Natl. Acad. Sci. USA 82* (1985) 259; R. S. H. Liu, D. T. Browne, *Acc. Chem. Res. 19* (1986) 42; J. K. Lanyi, *Annu. Rev. Biophys. Biophys. Chem. 15* (1986) 11; R. A. Mathies, S. O. Smith, I. Palings in T. G. Spiro (Ed.): *Biological Applications of Raman Spectroscopy*, Wiley, New York, in press.
[47] P. M. Rentzepis, *Prog. Clin. Biol. Res. 102 B* (1982) 461.
[48] L. Salem, P. Bruckmann, *Nature (London) 258* (1975) 526; L. Salem, *Science 191* (1976) 822.
[49] A. Lewis, *Proc. Natl. Acad. Sci. USA 75* (1978) 549.
[50] W. C. Herndon, *Top. Curr. Chem. 46* (1974) 141.
[51] R. A. Caldwell, *J. Am. Chem. Soc. 102* (1980) 4004; R. A. Caldwell, K. Mizuno, P. E. Hansen, L. P. Vo, M. Frentrup, C. D. Ho, *ibid. 103* (1981) 7263.
[52] a) J.-P. Desvergne, C. Courseille, *Mol. Cryst. Liq. Cryst. 50* (1979) 59; b) H. Bouas-Laurent, A. Castellan, J.-P. Desvergne, *Pure Appl. Chem. 52* (1980) 2633; c) J. Bendig, J. Fischer, D. Kreysig, *Tetrahedron 37* (1981) 1973; d) T. Wolff, N. Müller, G. von Bünau, *J. Photochem. 22* (1983) 61.
[53] J. Koutecký, A. Laforgue, *Int. J. Quantum Chem. 11* (1977) 505; F. A. Matsen, *Int. J. Quantum Chem. Symp. 8* (1974) 379.

Directed Homogeneous Hydrogenation

New Synthetic Methods (65)

By John M. Brown*

Stereochemical control is a major concern in the application of homogeneous catalysis to organic chemistry. In this context, the directed hydrogenation of olefins employing cationic rhodium or iridium catalysts has considerable potential, for very high selectivity can be attained under mild reaction conditions. The only requirement is a polar functional group in proximity to the double-bond which remains bound to the metal during the catalytic cycle and thereby controls the stereochemical course of hydrogen delivery through the constraints of chelation. The substituent is most frequently a hydroxy group OH but can also be an ester, amide or carbamate group; other groups remain to be scrutinized. In cyclic compounds, directed hydrogenation can lead to face-selectivity, and the polar substituent may be in the β-, γ-, or δ-position to the double-bond. Acyclic stereoselection ensues with β- or γ-substituents in appropriate compounds, and the configuration of reduced product is predictable on the basis of simple rules. The application of optically active rhodium complexes leads to useful kinetic resolution procedures.

1. Introduction

The potential of homogeneous hydrogenation for organic synthesis became clear in the 1960's following the demonstration of its feasibility by *Halpern* et al.[1] and the development of effective rhodium and ruthenium catalysts, largely by *Wilkinson*'s group.[2,3] Major advances since then include the development of highly active iridium catalysts[4] and the utilization of cyclopentadienyllanthanoid complexes.[5] Simple olefins can be hydrogenated very readily, and catalyst turnover rates in excess of $1\ s^{-1}$ are attainable.

In modern synthetic chemistry, the need is not so much for high reactivity but rather selectivity in functionally diverse molecules. The simplest manifestation is *site selectivity*, and homogeneous hydrogenation affords a degree of control which is generally unattainable with heterogeneous catalysts. For example, the disubstituted double-bond in carvone is completely hydrogenated in the presence of $[ClRh(PPh_3)_3]$, while the trisubstituted double-bond remains intact.[6] An exceptionally high *enantioselectivity* has been achieved in the catalytic hydrogenation of dehydroamino acids and their esters,[7] but this required the development of optically active chelating bisphosphanes.[8]

When a tertiary center is generated by hydrogenation of an appropriate di- or trisubstituted olefin, two diastereomers may be formed. The potential of homogeneous hydrogenation regarding *diastereoselectivity* had hardly been broached until fairly recently, and earlier efforts tended to concentrate on unsaturated hydrocarbons. When using $[ClRh(PPh_3)_3]$ as catalyst, the extent of stereochemical control is generally small for both *exo*- and *endo*cyclic olefins. In those cases where significant differentiation was observed, the major epimer was formed by approach of hydrogen to the less encumbered face, even when this gave rise to the thermodynamically less favored product.[9]

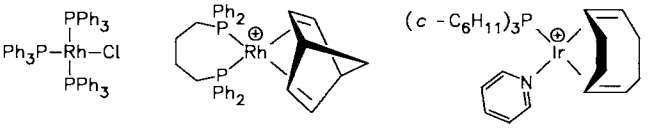

Fig. 1. Structures of the main catalysts used for directed hydrogenation in the homogeneous phase. *Wilkinson*'s catalyst, **A**, is commercially available from a number of sources. The cationic complexes **B** and **C** are readily prepared, and indefinitely stable at room temperature if maintained in an inert atmosphere. Synthesis of **B** (as trifluoromethanesulfonate) according to *Phillip L. Evans* [59]: To a yellow solution of bicyclo[2.2.1]heptadiene-2,4-pentanedionatorhodium (0.093 g, 0.32 mmol) [60] in THF (2 mL) was added trimethylsilyl trifluoromethanesulfonate (67 μL, 0.37 mmol) with stirring. The color changed to orange. Solid *P,P'*-tetramethylenebis(diphenylphosphane) (0.135 g, 0.32 mmol) was then added under Ar with continued stirring. The resulting orange-red suspension was stirred for 1 h and then rapidly transferred to vigorously agitated hexane (50 mL). The product was then filtered and dried in vacuo. Yield 0.224 g (92%) of catalyst **B** as an orange powder, m.p. 211–212°C (dec.), ^{31}P-NMR (CH_2Cl_2): $\delta = 23.6$ ($J_{PRh} = 154$ Hz).—Synthesis of **C** according to *Crabtree* and *Morris* (cf. Ref. [12]): Potassium hexafluorophosphate (0.8 g, 4.3 mmol) and di-μ-chlorodi(1,5-cyclooctadiene)diiridium (1.4 g, 4.2 mmol) were added with stirring to a degassed mixture of pyridine (3 mL), acetone (20 mL), ethanol (10 mL), and H_2O (2 mL). The solvent was removed in vacuo and the resulting yellow solid was washed with degassed H_2O and dried. The 1,5-cyclooctadienebis(pyridine)iridium hexafluorophosphate thus obtained (2.4 g, 96%) was stirred with tricyclohexylphosphane (1.2 g, 4.3 mmol) in dichloromethane for 10 min. The solvent was removed in vacuo and the residue was recrystallized from dichloromethane/ether, filtered, and dried *in vacuo* overnight. Yield of catalyst **C** 3.0 g (92%).

In the ensuing discussion three catalysts will be referred to repeatedly. They are *Wilkinson*'s catalyst, **A**, the cationic rhodium complex **B** derived from *P,P'*-tetramethylenebis(diphenylphosphane), and *Crabtree*'s iridium catalyst **C** (Fig. 1).

Hydrogenations are best carried out using standard inert atmosphere techniques, since the catalyst is sensitive to oxidation once the diolefin ligand has itself been hydrogenated and displaced. If the reaction is slow, traces of metal may be produced, particularly for catalyst **B** in dichloromethane. Addition of one drop of mercury in such cases suppresses any competing heterogeneous hydrogenation.[15] For slow reactions it is better to work at elevated

[*] Dr. John M. Brown
The Dyson Perrins Laboratory, University of Oxford
Oxford OX1 3QY (UK)

 © VCH Verlagsgesellschaft mbH, D-6940 Weinheim, 1987 0570-0833/87/0303-0190 $ 02.50/0

pressures[17] and small-scale equipment suitable for this purpose is readily available.[61]

An explicit procedure for a rapid hydrogenation requiring only a small quantity of catalyst is given in Table 3.

2. Selectivity in the Hydrogenation of Cyclic Alcohols with Endo- or Exocyclic Double Bond

The key factor in asymmetric hydrogenation of dehydroamino acids is the formation of a chelate rhodium enamide complex in which olefin and amide carbonyl group are bound to the metal.[7] This suggests that any functionality in proximity to the olefin which is capable of binding to rhodium is capable of exerting stereochemical control over the course of hydrogenation. *Facial selectivity*, whereby a polar substituent directs the course of hydrogen addition to a cyclic olefin, illustrates the general principle. If the polar group remains bound to the metal center, then *cis*-delivery of hydrogen is enforced.

Indeed, the potential of directed hydrogenation in this manner was indicated as long ago as 1974 in an experiment by *Thompson* and *McPherson*.[10] The tricyclic unsaturated alcohol **1** was unreactive towards hydrogenation

Table 1. Catalytic hydrogenation of cyclic alcohols with endo- or exocyclic double bonds in dichloromethane (**1** and **11** in benzene). Catalysts **A**, **B**, **C** see Figure 1. Bz = benzoyl.

	Educt	Main product		Conditions	Main isomer [%]	Ref.
1	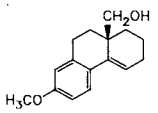	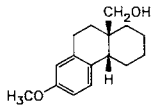		3.6 mol-% **A**, 50 °C, 3.5 bar [a]	> 98	[10]
2	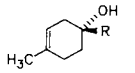	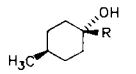	**a**, R = H	20 mol-% **C**	97	[12]
				< 20 mol-% **B**, 45 bar	98.5	[17]
			b, R = CH_3	20 mol-% **C**	> 99	[12]
			c, R = *i*Pr	2.5 mol-% **C**, 0 °C	99.9	[11]
3	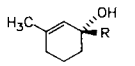	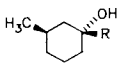	**a**, R = H	20 mol-% **C**	98.5	[12]
				< 20 mol-% **B**, 45 bar	99.7	[17]
			b, R = CH_3	20 mol-% **C**	> 99	[12]
4	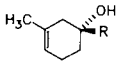	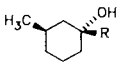	**a**, R = H	20 mol-% **C**	96.5	[12]
			b, R = CH_3	20 mol-% **C**	> 99	[12]
5	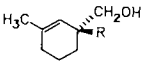	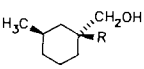	**a**, R = H	20 mol-% **C**	85	[12]
			b, R = CH_3	20 mol-% **C**	90	[12]
6	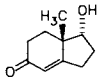	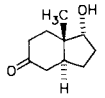		20 mol-% **C**	96	[12]
7	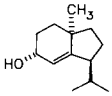	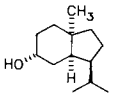		20 mol-% **C**	high	[14]
8	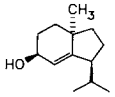	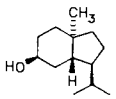		30 mol-% **C**	high [b]	[14]
				5 mol-% **B**, 69 bar	98.5	[17]
9	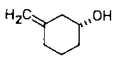	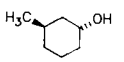		2 mol-% **B**	99	[15]
10	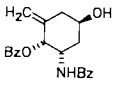	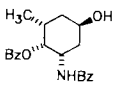		35 mol-% **B**	> 95	[16]
11	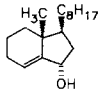	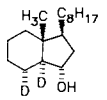		**A**, reaction with D_2	97	[19]
12	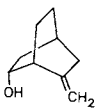	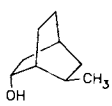		2 mol-% **B**, 5 h	98.5	[20]
				2 mol-% **C**, 2 min	99.8	[20]
13	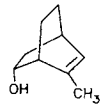	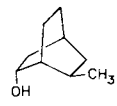		2 mol-% **B**	> 99.5	[20]
				2 mol-% **C**	> 99.5	[20]

[a] 68% yield; **1** is employed as potassium alkoxide. [b] Yield < 20%.

and catalyst **A** even under forcing conditions. However, up to 20 turnovers can be achieved by first converting the alcohol into the potassium alkoxide; the *cis*-product is then formed exclusively (Table 1). *Thompson* and *McPherson* proposed, very reasonably, that the alkoxide displaces chloride from the coordination sphere and thereby controls the stereochemistry of hydride delivery.

Cationic iridium complexes are catalytically active in non-coordinating solvents but their reactivity is slowly dissipated through the formation of inert dimers. Reduction of 4-terpineol **2c** in dichloromethane occurs slowly (relative to 1-methylcyclohexene) but the catalyst **C** is indefinitely stable and the *trans*-product is formed with 1000:1 selectivity—clear evidence for coordination of the hydroxy group to iridium during the hydrogen-transfer step.[11] Again using catalyst **C** but at rather higher relative concentrations, *Stork* and *Kahne* examined directing effects in the hydrogenation of cyclohexenes such as **1**, **2a–c**, **3a,b**, **4a,b**, **5a,b**, and **6** bearing allylic or homoallylic hydroxyl substitution.[12] In all cases the *trans*-product predominated. Some general trends are apparent from the data which suggest that the order of effectiveness is *tert* > *sec* > *primary* OH; all examples in the first category are stereospecific within experimental error. The high ratio of catalyst to substrate employed in these experiments is probably unnecessary, since rapid hydrogenation was observed for the reactant **3b** employing <2 mol-% of catalyst **B**.[13] The utility of directed hydrogenation as a route to *trans*-hydrindanones was confirmed by *Corey* and *Engler*, with the reaction of **8**.[14]

The reactivity of rhodium complexes in homogeneous hydrogenation diminishes markedly as the degree of substitution on the olefin increases. For this reason directed hydrogenation was examined by employing exocyclic disubstituted olefinic alcohols.[15] 2-Methylenecyclohexanol proved uninteresting, since (unselective) hydrogenation was overridden by isomerization to 2-methylcyclohexanone. For the 3-isomer **9**, catalyst **B** gives exclusively the *trans*-isomer of the hydrogenation product, whilst the bis(triphenylphosphane)-analogue of **B** gave only 91% of the *trans*-isomer. In similar vein a carbocyclic relative of daunosamine was formed with excellent stereoselectivity using catalyst **B**, albeit at 35 mol-%![16] The unreactivity of trisubstituted olefins in Rh-complex-catalyzed hydrogenation can be overcome by working at high pressures, and the stereoselectivity observed is comparable to or better than in iridium-catalyzed reactions at ambient pressure.[17] For catalyst **C**, the stereochemical course of hydrogenation is insensitive to pressure change, even though the catalyst concentration is a significant but undefined variable.[18] There is even one case, the hydrogenation of **8**, where the iridium catalyst fails but the rhodium catalyst **B** succeeds at high pressure. Deuterated *trans*-hydrindanone is readily obtainable from **11** with catalyst **A**.[19]

The parallel development of cationic rhodium and iridium cationic complexes for directed hydrogenation prompted a comparison of their effectiveness using 6-methylenebicyclo[2.2.2]octan-2-ol **12**, where the hydroxy group perturbs an otherwise symmetrical environment.[20] Hydrogenation with catalyst **C** was very rapid, and stereospecific. In contrast, rhodium catalyst **B** effected a much more sluggish reaction in which 1.5% of *cis*-product was formed, and here competitive isomerization to the endocyclic isomer **13** occurred. This trisubstituted olefin was itself reduced rapidly and stereoselectively and accounted for 75% of the total reduction pathway via **12**. This result raises interesting questions about the spatial orientation of the hydroxy group and olefin which are addressed in Section 7.

3. Other Directing Groups for the Hydrogenation of Cyclic Olefins

Acetates of allylic or homoallylic alcohols invariably exhibit poor stereochemical control in hydrogenation.[12] A better result was obtained with the bicyclic ether **14** and the catalyst **B** (Table 2) but substantially lower selectivity was observed, although it proved a more reactive substrate than the parent alcohol. These observations indicate that the nature of the directing group is critical; ethers are inferior to alcohols in their coordinating ability towards iridium(I) ions,[21] and acetates prefer to bind through the more basic carbonyl oxygen, which is not well-disposed for chelate formation in the preferred s-*cis*-conformation.[22]

The OH group has a Brønsted pK_a value of about -2, whilst amides typically have a pK_a of -1 (for *O*-protonation) and esters are in the range of -4 to -7.[23] This encouraged a survey of the directed hydrogenation of the unsaturated esters **15–17**. With rhodium catalyst **B**, reactions were rather sluggish and the iridium catalyst **C** was much more effective. The allylic ester **15** was reduced with essentially complete stereoselectivity.[24] *Schultz* and *McCloskey* have demonstrated that amides are superior to esters in directing power.[25] This result might have been anticipated given the general effectiveness of dehydroamino acids in asymmetric hydrogenation and the mandatory requirement for amide coordination in the catalytic cycle.[26] A series of cyclohexene and cyclohexadienecarboxamides with the amide group attached to a quaternary allyl center were reduced with a selectivity of 100:1 or better using catalyst **C**. All the starting materials **22a,b**, and **23** are readily available by alkylative Birch reduction;[27] in the case of **23**, the *O*-methylprolinamide of *o*-toluic acid, this reaction is enantioselective. Direction by the amide group remains effective as it is attenuated from the double bond whilst the influence of an ester group diminishes (cf. **18**, **20** *versus* **17**, **19**).

These observations have immediate synthetic potential, for an intermediate (**25**) in the total synthesis of pumiliotoxins was exclusively hydrogenated from the amide-bearing face. The unwanted diastereomer predominated in the reduction catalyzed by Pd/C.

4. Selective Hydrogenation of Acyclic Allylic Alcohols

In these face-selective hydrogenations the stereochemical outcome is predictable, since the directing-group must be *cis*-related to the new C–H bonds. The outcome is less certain for acyclic substrates, but it is serendipitous that

Table 2. Catalytic hydrogenation of cyclic compounds with diverse directing groups and endo- or exocyclic double-bond(s) in dichloromethane. Catalysts **A**, **B**, **C** see Figure 1.

	Educt	Main product		Catalyst	Main isomer [%]	Ref.
14	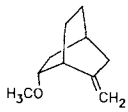	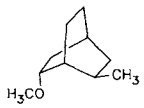		2 mol-% **B** 2 mol-% **C**	86.5 97.4	[20] [20]
15	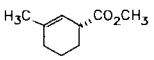	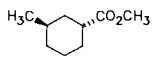		2 mol-% **B** 2 mol-% **C**	97 99.9	[24] [24]
16	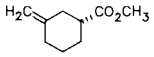	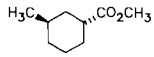		2 mol-% **B** 2 mol-% **C**	90.5 81.5	[24] [24]
17	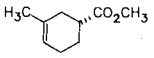	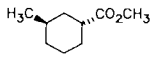		2 mol-% **C**	89	[24]
18	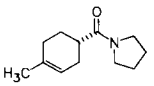	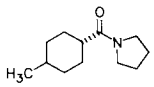		5 mol-% **C**	99	[25]
19	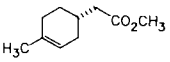	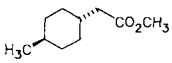		5 mol-% **C**	55	[25]
20	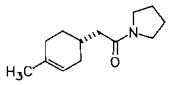	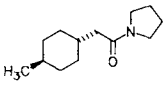		5 mol-% **C**	99	[25]
21	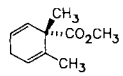	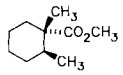		5 mol-% **C**	99	[25]
22	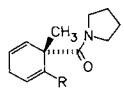	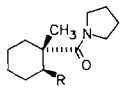	**a**, R = CH_3 **b**, R = OCH_3	5 mol-% **C** 5 mol-% **C**	99.4 99.4	[25] [25]
23	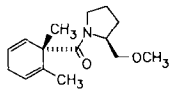	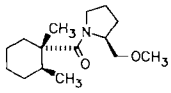		5 mol-% **C**	99.8	[25]
24	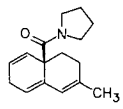	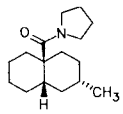		5 mol-% **C**	99.9	[24]
25	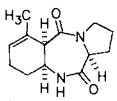	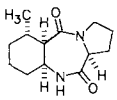		5 mol-% **C**	99	[25]

many reductions can be carried out with high stereoselectivity.

Kinoshita and co-workers planned an allyl alcohol hydrogenation in a synthetic route to the rifamycin backbone. The first hint of selectivity came when a mixture of the diastereomeric alcohols (23*R*)-**26** and (23*S*)-**26** (Fig. 2) was reduced with hydrogen and a *stoichiometric* quantity of $[ClRh(PPh_3)_3]$ (catalyst **A**). Each component of the mixture gave rise to 95% of a single product.[28] A more clear-cut result was later obtained in the case of the alcohol (21*R*)-**27a** upon employing 24 mol-% of catalyst **A** — almost 100% stereoselectivity. The corresponding TBDMS-ether (21*R*)-**27b** was hydrogenated slowly with 150 mol-% **A** in the same stereochemical sense. The diastereomer (21*S*)-**27a** was reduced without selectivity although its TBDMS-ether (21*S*)-**27b** gave mainly the *syn* product.[29] In a more recent synthesis, compound **28** was hydrogenated in the presence of 25 mol-% **A** to the *anti*-products (selectivity 20 : 1).[30]

Although interesting regarding their stereoselectivity it is not certain whether these hydrogenations arise from coordination of the allylic hydroxy group to rhodium, since its relative configuration with respect to the polyol chain is crucial in determining the stereochemical outcome (cf. the

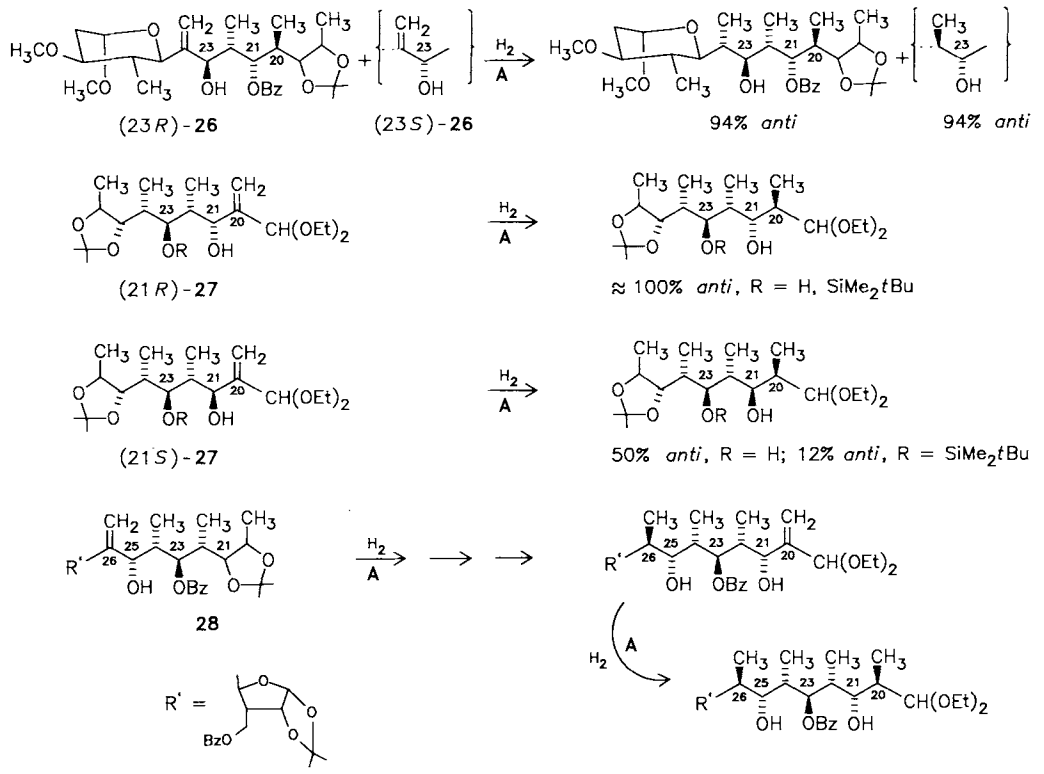

Fig. 2. Reduction steps in *Kinoshita*'s synthesis of the ansa-chain of rifamycin. The numbering scheme is that conventionally applied to rifamycin S. In **27a** R = H, in **27b** R = *tert*-butyldimethylsilyl.

hydrogenation of (21*R*)-**27a** and (21*S*)-**27a**). There is less ambiguity when the *cationic* rhodium complex **B** is employed where there are well-established precedents for hydroxyl-coordination.[21] Under optimum conditions hydrogenation of the disubstituted allylic alcohol **29** proceeds with 97% *anti*-selectivity using 2 mol-% of catalyst **B** (Table 3).[31] The yield is lowered by about 20% because of competing isomerization to the methyl ketone. In the case of the more highly functionalized reactants examined by *Evans* and *Morrissey*, it was found necessary to work at high H_2-pressures and high catalyst loading; but under these conditions isomerization was effectively suppressed.[17] This is probably due to the fact that reduction is first-order in [H_2] but the competing isomerization reaction has a lesser pressure dependence. Note that the disubstituted olefin **30** and its trisubstituted isomer **31** give *syn* and *anti*-isomers of an otherwise identical product.

Electron-withdrawing groups enhance the binding of olefins to rhodium[32] and in consequence of this may also augment their reactivity towards homogeneous hydrogenation.[33] α-(Hydroxyalkyl)acrylates such as **32** are very easily obtained by condensation of aldehydes and acrylates in the presence of tertiary amines:[34] they are hydrogenated rapidly and with extremely high stereoselectivity using catalyst **B**, whereas both catalysts **A** and **C** give slow and ineffective reactions.[35] In the case of compounds **32a–c**, the reaction is even stereoselective in protic solvents such as MeOH which generally override intramolecular hydroxyl-direction. Starting from a given aldehyde, the reaction provides an equivalent to an *anti*-selective aldol-condensation with two straightforward steps. It is both simple and competitive in stereoselectivity to present alternatives (cf. Fig. 3).[36] As shown in Table 3 the α,β-unsaturated γ-hydroxy-ester **33** is again hydrogenated with reasonable selectivity, although its reactivity is much reduced.[37]

In all these examples *anti*-stereoselectivity of the reduction product predominates and it might be thought desirable to provide the equivalent of a *syn*-selective aldol condensation.[36] This objective has been achieved, albeit indirectly. There were a few examples of homogeneous hydrogenation of allenes indicating that the double bond with lesser terminal substitution is reduced regioselectively.[38] It has now been observed that the allenic alcohol **34** is exclusively reduced at the double bond adjacent to the OH-group. Ozonolysis of the product (O_3 then Ph_3P) gave only the *syn*-aldehyde.[39]

5. Kinetic Resolution in Homogeneous Hydrogenation[40]

The best substrates for asymmetric hydrogenation are α,β-unsaturated acids or esters with a chelating group attached to the α-position.[41] This is precisely what the α-(hydroxyalkyl)acrylates **32** have to offer, and what made their reduction with H_2 and asymmetric catalysts of direct interest. The starting material is of course racemic, and in such cases enantioselection leads to kinetic resolution. A general feature of such experiments is that the optical purity of the product diminishes with time, whereas that of the starting material becomes enhanced, particularly so in the latter stages of reaction. In a kinetically well-behaved process, the sharpness of differentiation between the fast and slow reactant enantiomers increases with the relative

Table 3. Catalytic hydrogenation of alkyl alcohols and comparable compounds. Catalysts **A**, **B**, **C** see Figure 1. THF = tetrahydrofuran. R in **30** and **31** = CH_3; X in **30** and **31** = 4-methyl-2-oxo-5-phenyl-3-oxazolidinyl.

	Educt	Main product		Conditions	Main isomer [%]	Ref.
29				2 mol-% **B**, 0°C, CH_2Cl_2	97	[31]
30	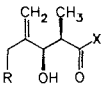	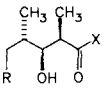		> 2 mol-% **B**, CH_2Cl_2, 44 bar	93	[17]
31	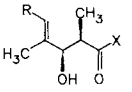	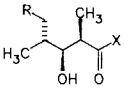		> 2 mol-% **B**, CH_2Cl_2, 44 bar	91	[17]
32	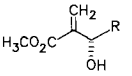	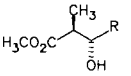	**a**, R = CH_3 [a]	0.5 mol-% **B**, 0°C, THF	99	[35]
			b, R = Ph	0.5 mol-% **B**, CH_2Cl_2	99	[35]
				0.5 mol-% **B**, MeOH	97	[35]
			c, R = 2-furyl	0.5 mol-% **B**, THF	99	[35]
33	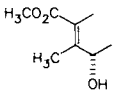	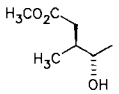		10 mol-% **B**, CH_2Cl_2	97	[37]
34	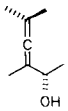	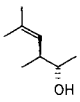		5 mol-% **B**, THF	> 95	[39]
35	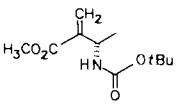	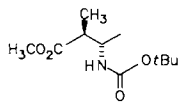		5 mol-% **B**, CH_2Cl_2	99	[45]
36	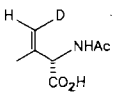	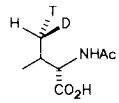		**A**	95	[46]
37	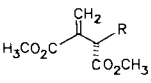	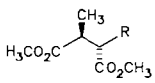	**a**, R = CH_3	2 mol-% **B**, MeOH	99	[47]
			b, R = C_2H_5	2 mol-% **B**, MeOH	99	[47]
			c, R = Ph	2 mol-% **B**, MeOH	99	[47]
			d, R = OCH_3	2 mol-% **B**, MeOH	> 98	[47]

[a] Procedure for the hydrogenation of *rac*-**32a**, ethyl instead of methyl ester, to *rac*-ethyl *anti*-3-hydroxy-2-methylbutyrate: To a solution of *rac*-ethyl 3-hydroxy-2-methylenebutyrate (5.00 g, 3.47 mmol) in dichloromethane (40 mL) was added catalyst **B** (0.050 g, 0.2 mol-%, BF_4-salt) under argon, with shaking to complete dissolution. The solution was cooled to −80°, thoroughly degassed by three evacuation/argon atmosphere cycles and then argon replaced by H_2, with the vessel connected to a burette line. The temperature was allowed to rise to ambient (< 20°C, cold water bath) and equilibrated. Stirring was commenced and continued until the theoretical amount of H_2 had been adsorbed (840 mL, ca. 4 h), whereupon gas-chromatographic analysis (180-cm column of Carbowax 20M, 120°C) showed complete reduction. The reaction was then stopped, the catalysts removed by filtration through a short plug of silica gel (Merck 60H), and the solvent removed below 20°C on a rotary evaporator. The residue was distilled in a trap-to-bucket apparatus (40°, 0.1 mm) giving *rac*-**32a** (4.7 g, 93%), 99% isomerically pure by gas-liquid chromatography.—The *anti-syn* ratio increased with decreasing reaction temperature.

reaction rate; Figure 4 shows calculated curves for 5 : 1, 15 : 1 and 35 : 1 ratios.

For the resolution of *ent*-**32b** and **32b** (*R*- and *S*-form, respectively, Fig. 5) the DIPAMP-Rh catalyst is more effective than other asymmetric complexes, a property consistent with the general superiority of such catalysts in the hydrogenation of unsaturated esters.[42] Under optimum conditions, reaction was carried out with 0.5—1 mol-% of catalyst in THF at 0°C to around 70% completion. Starting material and product were then separated by standard chromatographic methods, whereupon the former was obtained with > 90% optical purity.[35] The diastereoselectivity (*anti* : *syn*) observed with the DIPAMP-rhodium catalyst was very high, being 99.6 : 0.4 in a reaction run to 65% completion. The recovered starting material, essentially optically pure (*S*)-enantiomer (**32b**), is hydrogenated much more slowly than the (*R*)-enantiomer *ent*-**32b** and the *anti* : *syn* ratio in the hydrogenation product is 97.4 : 2.6. This means that the sense of enantioselectivity is the same for both *syn* and *anti*-isomer formation (and independent

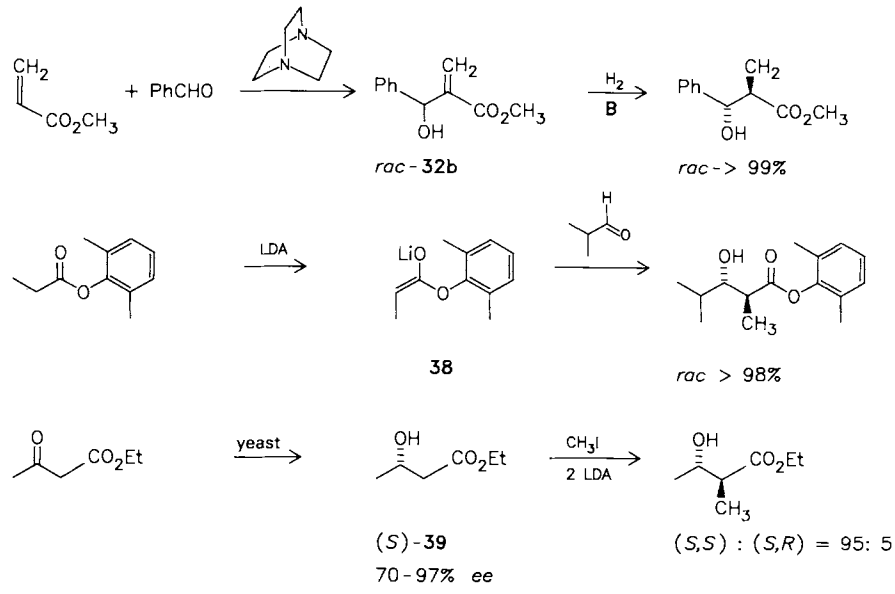

Fig. 3. Comparison between directed hydrogenation (of *rac*-**32b**) of the aldol reaction of the ester **38** lithiated with lithium diisopropylamide (LDA) and the alkylation of the optically active β-hydroxyester (*S*)-**39** generated with yeast enzymes.

of the process leading to *anti*-dominance) with *R*- configuration of the new asymmetric center being preferred.[43]

Double asymmetric induction is evident in the hydrogenation of L- or D-menthyl α-(hydroxyethyl)acrylate.[43,44]

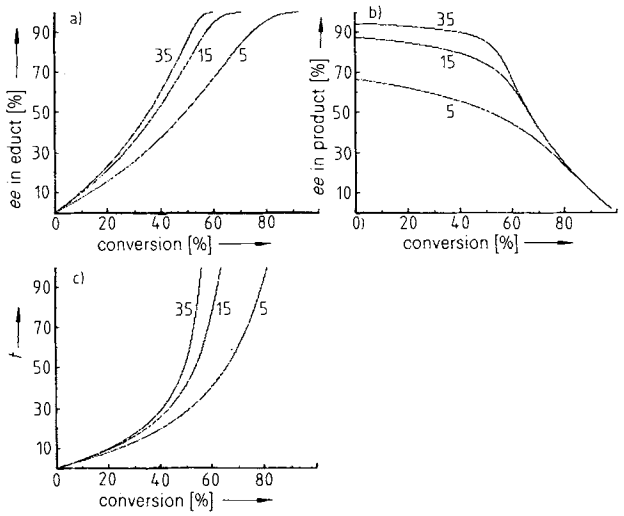

Fig. 4. a), b) Change of enantiomeric purity in a kinetic resolution experiment; c) time conversion diagram; the relative reaction rates of the enantiomers are 5 : 1, 15 : 1 and 35 : 1 (calculated curves). The time in c) is given in arbitrary units.

This leads to greater enantioselectivity (up to 8 : 1) in the reduction of the L-isomer.

These examples extend hydroxyl-directed hydrogenation in a useful way, but what of the effect of other substituents? The *tert*-butoxycarbonyl (Boc) functionality (see **35** in Table 3) is superior to OH in its *anti*-selectivity, and a kinetic resolution of 15 : 1 is observed in the—albeit rather slower—hydrogenation of *rac*-**35** with [(DIPAMP)-Rh]$^{\oplus}$ as catalyst.[45] There are good precedents for anticipating the effectiveness of carbonyl-derived functionalities, as exemplified in Table 2. In an acyclic case, the specifically deuterated dehydrovaline **36** (Table 3) is reduced by HT (H_2 diluted) and catalyst **A** from the direction which indicates participation of the carbonyl group.[46] The 3-substituted dimethyl itaconates **37** could be hydrogenated with high *anti*-selectivity in methanol employing catalyst **B**.[47] When [(DIPAMP-Rh]$^{\oplus}$ was employed as catalyst, kinetic resolution with up to 20 : 1 rate discrimination between enantiomers was obtained, with starting material enriched in the slow-reacting *S* enantiomer remaining. The ready availability of the 3-methoxyitaconate **37d** permitted a test of the relative efficiency of OCH_3 and CO_2CH_3 as directing groups. With catalyst **B**, more than 98% of the (*S,S*)-diastereomer (Table 3) was obtained from the (*S*)-configurated **37d**, indicating that the stereochemical course of reaction is dominated by the CO_2CH_3-group.

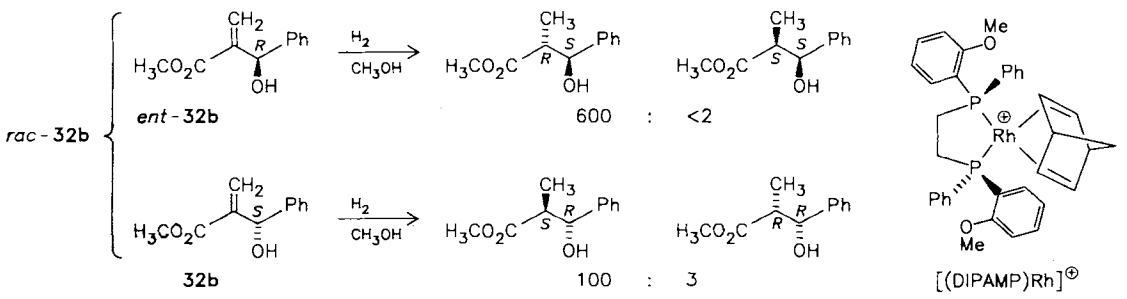

Fig. 5. Estimated initial relative rates of hydrogenation of racemic methyl 2-(α-hydroxybenzyl)acrylate *rac*-**32b** with the (optically active) rhodium complex of (*R,R*)-*P,P'*-ethylenebis[*o*-methoxyphenyl(phenyl)phosphane] (DIPAMP).

The reaction sequence makes a number of unsaturated esters available in good enantiomeric purity (>95% *ee*). The racemate is reduced to the extent of 60–65% with hydrogen in CH_3OH using [(DIPAMP)-Rh]$^{\oplus}$ as catalyst (Fig. 6, step ①). Recovered starting material is then enriched in the (*S*)-enantiomer. Since *anti*-selective hydrogenation is readily achieved, a further reduction employing catalyst **B** (step ②) affords a route to (*S,S*)-2-alkyl 3-methylsuccinates.

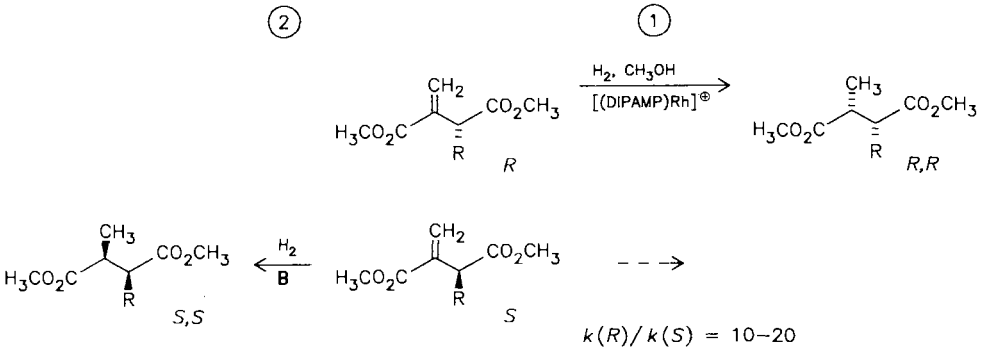

Fig. 6. Step ①: Kinetic resolution in the reduction of 3-alkyl itaconates of type **37** in the presence of (*R,R*)-[(DIPAMP)Rh]$^{\oplus}$ as catalyst. Step ②: Hydrogenation of the enriching enantiometer.

6. Selective Hydrogenation of Acyclic Homoallylic Alcohols

Methods for remote asymmetric induction are far less common than for vicinal asymmetric induction, providing an incentive to discover examples in directed hydrogenation. A simple case for remote induction (hydrogenation of **40** in Table 4) demonstrates the general principle.[31] The diastereoselectivity is only moderate with catalyst **B**, but still rather better than the related case with **41**, where the hydroxyl group has reduced basicity.[48] When a carbonyl group intervenes between the secondary alcohol and disubstituted olefin as in **42**, catalyst **A** gives the most satisfactory result.[49] All these reactions occur in the same stereochemical sense, but in the last one *Evans* et al.[49] suggest that intramolecular H-bonding (CHOH···O=C) is the controlling factor which makes approach to the double bond diastereoselective in the preferred conformation.

Stereospecific hydrogenation of trisubstituted double bonds is an important goal in synthesis, since it provides access to many desirable targets, for example in polyether and macrolide antibiotics. *Evans* et al. have discovered a general method employing directed hydrogenation which has wide applicability.[48] Figure 7 shows a key compound (**50**) for the synthesis of the C1–C10 fragment of ionomycin. The desired stereochemistry at C6 was obtained by directed hydrogenation. This atom is remote from the other chiral centers and hence incorporation by other methods of synthesis would be very difficult. A number of related examples have been described (**43**–**49**) and inspection of the first two of these makes it clear that the allylic alkyl group controls the stereochemical course of the reaction. The same pattern is observed for **45** and **46**, and comparison between **47** and **48** makes it clear that the configuration of the secondary homoallylic alcohol plays only a minor part, overridden by the configuration of the adjacent allylic center (see Section 7). Enantiomerically pure **48** and more particularly **49** illustrate the potential for double asymmetric induction using an optically active catalyst, since the starting materials are homochiral. In both cases the reduction catalyzed by [((+)-BINAP)Rh]$^{\oplus}$[50] was substantially more successful than hydrogenation with catalyst **B** or with [((−)-BINAP)Rh]$^{\oplus}$. The hydroxy ester **49** is an important intermediate in the synthesis of premonensin.[51]

7. Mechanistic Considerations

The wide-ranging applicability of directed hydrogenation suggests that a common principle or set of principles may be involved. A majority of the examples cited are unsaturated alcohols, and in cyclic cases the face-selective hydrogenation observed requires that the hydroxyl group is bound to rhodium or iridium during hydrogenation of the double bond. The only direct evidence for this is in the NMR-characterization of an iridium complex derived from *endo*-bicyclo[2.2.1]hept-5-en-2-ol,[11] although alcohol-bound cationic complexes are known in other cases.[21,52]

For acyclic allylic alcohols, the reaction is invariably *anti*-selective, and this may be rationalized by consideration of non-bonded interactions in the two diastereomeric

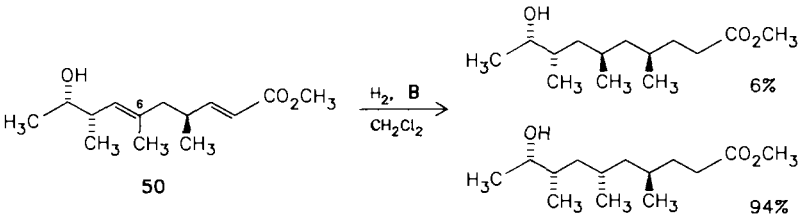

Fig. 7. Hydrogenation of **50** to give the fragment C1–C10 of ionomycin according to *Evans* using the catalyst **B** in the key step of the reaction [48].

Table 4. Catalytic hydrogenation of homoallyl alcohols in dichloromethane (**40** in THF, **42** in benzene). Catalysts **A**, **B**, **C** see Figure 1. BINAP = *P,P'*-(1,1'-binaphthyl-2,2'-diyl)bis(diphenylphosphane). *OSi* denotes *tert*-butyldimethylsilyloxy.

	Educt	Main product	Conditions	Main isomer [%]	Ref.
40	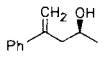	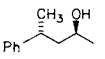	2 mol-% **B**, 0 °C	88	[31]
41	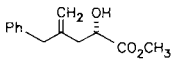	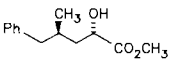	2.5 mol-% **C**	79	[48]
42	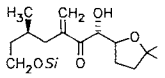	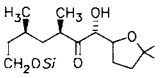	**A**	94	[49]
43	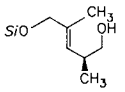	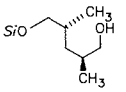	> 5 mol-% **B**	95	[48]
44	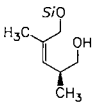	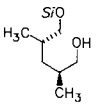	> 5 mol-% **B**	91	[48]
45	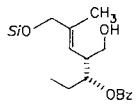	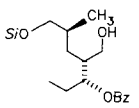	> 5 mol-% **B** 2.5 mol-% **C**	97 97	[48] [48]
46	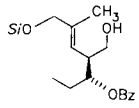	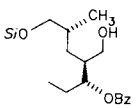	> 5 mol-% **B** 2.5 mol-% **C**	99 97	[48] [48]
47	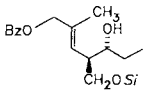	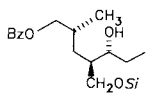	> 5 mol-% **B** 2.5 mol-% **C**	97 94	[48] [48]
48	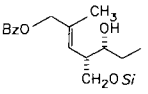	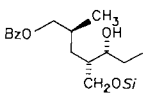	> 5 mol-% **B** [((+)-BINAP)Rh]$^{\oplus}$, 69 bar [((−)-BINAP)Rh]$^{\oplus}$, 69 bar	89 97 92	[48] [48] [48]
49	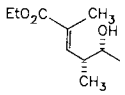	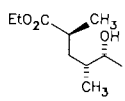	> 5 mol-% **B** [((+)-BINAP)Rh]$^{\oplus}$, 69 bar [((−)-BINAP)Rh]$^{\oplus}$, 69 bar	83 98 67	[48] [48, 51] [48, 51]

chelate complexes of **32a** (Fig. 8). The precursor of the *syn*-product engenders a strongly perturbing 1,2-interaction between the methyl group of the substituent $CH(CH_3)OH$ and the other substituents of the double-bond. This does not arise in the *anti*-precursor, where it is only an hydrogen atom which interacts with the substituents. If correct, this analysis implies that stereoselectivity arises from torsional and non-bonding interactions within the substrate and does not involve the phosphane ligands. The magnitude of discrimination which arises can be quite large since the 300 : 1 diastereoselection observed in α-(hydroxyalkyl)acrylates corresponds to a difference in free energy of 14 kJ mol^{-1} between the transition-states of competing pathways.

In a model for the hydrogenation (Fig. 8, bottom) where the allylic C–H eclipses the neighboring vinyl group (*anti*), the H–C–C=C torsion angle is 180°. This is at variance with models which explain the stereochemical course of hydroboration and other electrophilic additions to double bonds.[53] Here the C–H eclipses C=C (*syn*), so that the torsion angle is 0° (Fig. 8, bottom), in accord with the theoretically derived[54] or spectroscopically observed[55] ground-state conformation of allylic alcohols. This indicates that the geometrical constraints which accompany

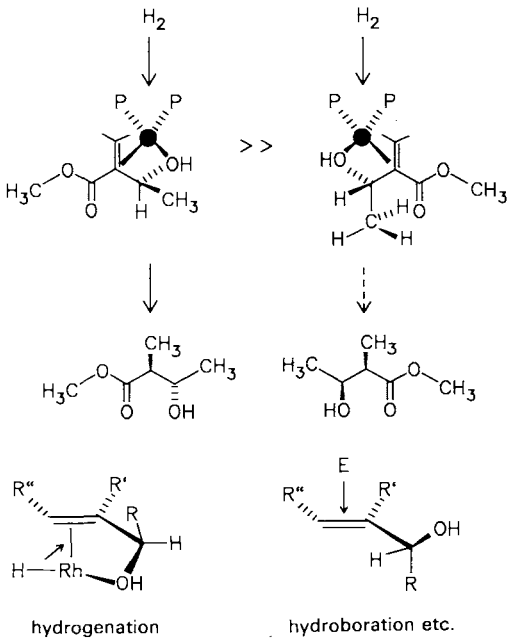

Fig. 8. The origin of *anti*-selectivity in the hydrogenation of allylic alcohols (cf. **32a**)—a comparison between the stereochemical course of hydrogenation and that of other electrophilic additions is also given.

chelate formation are quite stringent and impose a higher energy conformation on the reactant. In the metal-promoted epoxidation of chiral allylic alcohols, the oxygen is coordinated to Mo, V or Ti prior to peroxide delivery from the metal[56] to olefin; in this case, the *syn* isomer is preferred, but of course there is no direct metal-olefin binding.

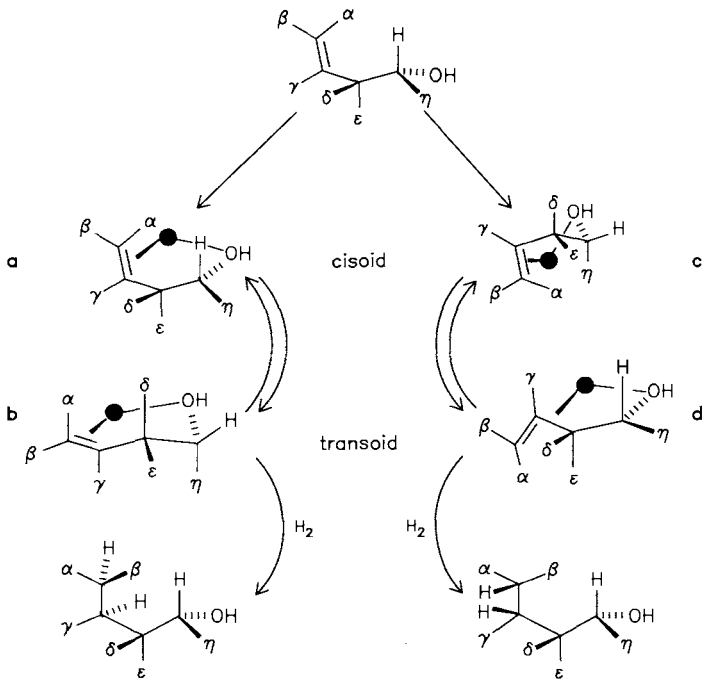

Fig. 9. Pathways for the stereochemical course of directed hydrogenation of homoallylic alcohols. When $\delta = \varepsilon = H$, the preferred intermediates have cisoid structure **a**. When α, $\delta \neq H$, $\varepsilon = H$ the transoid form **d** is preferred, and when α, $\varepsilon \neq H$, $\delta = H$ the transoid form **b** is preferred.

For simple homoallylic alcohols, where a CH_2-group is situated between the double bond and C–O bond, the results are less clear-cut. Additional flexibility in the chelate ring permits two distinct conformers for each configurational isomer. These are designated cisoid (Fig. 9, **a** and **c**) or transoid (Figure 9, *2* and *4*) depending on whether the torsion-angle (HO–C–C–C=) in the chelate ring is around 30° or around 150°. An observed 7:1 preference (as in **40**) corresponds to the major part of reaction proceeding via the cisoid form **a**. (In **40**, γ = phenyl and η = methyl.) In **a**, hydrogen as the smaller substituent in the homoallyl position interacts with the double-bond and particularly with the hydrogen at position α. In the alternative cisoid form **c**, the larger substituent η at the hydroxy-site experiences an unfavorable non-bonded interaction with the hydrogen at position α. There is an interesting corollary in the hydrogenation of exocyclic and endocyclic olefins of the bicyclo[2.2.2]octane series (cf. **12** and **13**). With catalyst **B**, the *di*substituted exocyclic olefin **12** in fixed transoid conformation is hydrogenated more sluggishly and less selectively than the *tri*substituted endocyclic olefin **13** in fixed cisoid conformation.

Nevertheless, *Evans* et al. have demonstrated convincingly that the stereochemical course of hydrogenation can be controlled by allylic substitution at sites δ or ε (Fig. 9). Their examples invariably possess a *Z* alkyl substituent at site α, which will be expected to destabilize the cisoid chelate **a** (and **c**) in favor of the transoid isomers **b** and **d**.[48] Reaction proceeds through the pathway which engenders less allylic 1,3-strain in the coordinated intermediate. If α and δ are alkyl groups and ε is hydrogen, then the chelate **d** is preferred since the interaction between α and ε is less destabilizing than that between α and δ. This correctly predicts the outcome of all their examples (see **43**–**49** in Table 4 and Fig. 7).

For cationic rhodium complex **B**, the catalytic cycle of directed hydrogenation appears straightforward. Although competitive olefin isomerization may occur, all product molecules are dideuterated when reduction is carried out with D_2. Not so for iridium catalyst **C**! Reduction of methyl 3-methyl-2-cyclohexenecarboxylate **15** with D_2 gave a stereoisomerically pure product which, according to the ^1H-, ^2H- and ^{13}C-NMR spectra was evidently a mixture of several isotopomers. Figure 10 shows the ^2H-NMR spectrum of the product, assigned by comparison with cross-sections of the ^{13}C-^1H-NMR shift correlation spectrum.[13] This demonstrates incorporation of deuterium only at C3, and at the C2 and C4 equatorial sites (i.e. exclusively *cis* to the methoxycarbonyl group). This is consistent with isomerization processes which occur during the catalytic cycle of hydrogenation *without* release of the substrate.

In the reduction of *endo*-6-methylenebicyclo[2.2.2]octan-2-ol **12** with D_2 and catalyst **C**, deuterium appears at the methyl group and at the 5-*endo* and 6-position, with all possible D_0–D_3 isotopomers, but dideuteration overall. The ^{13}C-NMR spectrum can be analyzed and computer modelling employed to derive a mechanism which fits the isotopic distribution; it is necessary that each molecule of reactant encounters more than one D_2 as it passes through the catalytic cycle.[56] The pathway delineated in Figure 11 best fits the experimental data. Its novel feature is the ad-

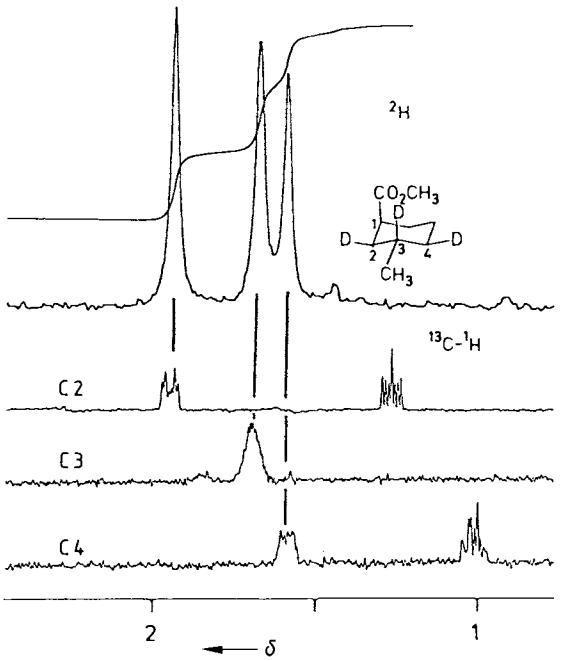

Fig. 10. ^2H-NMR spectrum of the reduction product from methyl 3-methyl-2-cyclohexenecarboxylate **15** and D_2 using catalyst **C**; comparison with the relevant cross-sections of the ^{13}C-^1H-2D-NMR correlation spectrum of the *hydrogenation* product of **15**.

dition of hydrogen to the chelate-stabilized alkyliridium hydride, which can have an appreciable lifetime at room temperature.[57] A number of groups have recently isolated iridium trihydride complexes, the work of *Crabtree* and *Lavin* being particularly pertinent.[58]

These mechanistic subtleties are not perceived without isotopic labeling, but they may help to explain why olefins with varying torsion angles about C=C–C–COH are readily reduced—compare **2a** and **6** (Table 1). Internal isomerization *via* an allyliridium hydride or by Ir-H addition/elimination can provide chelated intermediates of optimum geometry.

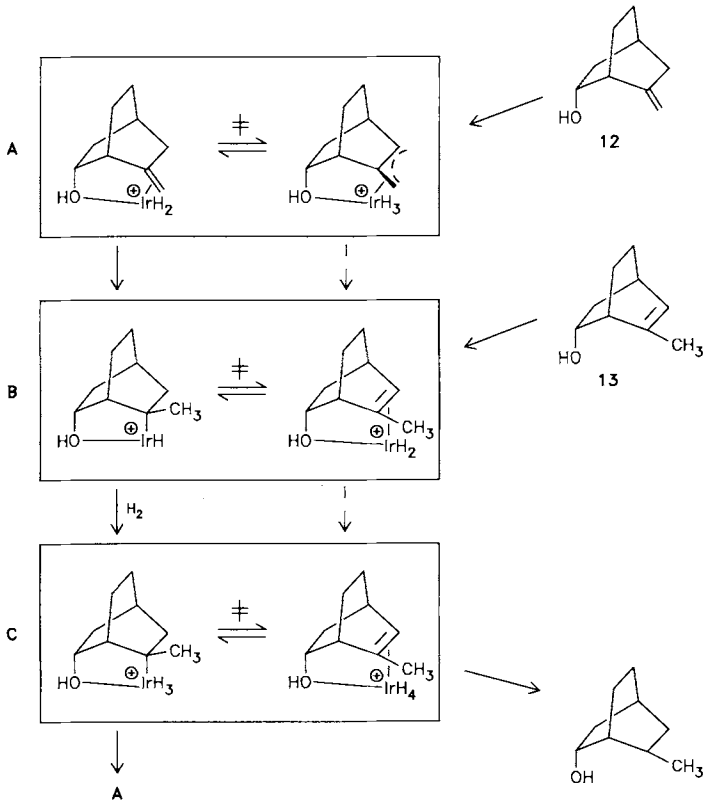

Fig. 11. A pathway for directed hydrogenation of the bicyclo[2.2.2]octanol derivatives **12** and **13** in the presence of the catalyst **C**. This reaction pathway explains the deuterium distribution in the product. (Ligands omitted for clarity.)

8. Comparison of Homogeneous and Heterogeneous Catalysis

An advantage of homogeneous catalysts is, in general, that every batch has identical and predictable reactivity, and poisoning is never a problem.

It has been known for over thirty years that polar groups, particularly the hydroxy group, can influence the stereochemical course of catalytic hydrogenation over metals. Since a book dealing with this topic has recently been published,[62] the discussion that follows will be selective rather than exhaustive.

The choice of metal, support, and solvent are all crucial in heterogeneous hydrogenation, and often all three must be varied before optimum stereocontrol is achieved. Early workers did this in a fairly empirical way. Thus, 2-butylidene-1-cyclopentanol **51a** (Table 5) is reduced most selectively with Raney Ni in ethanol,[63] whilst the corresponding benzylidene derivative **51b** gave little indication of stereochemical control by the hydroxy group because aryl-coordination competed successfully for surface sites.[64] Increasing the ring size diminished stereoselectivity since the relative disposition of hydroxy group and double bond is then less favorable.[65] For the cyclopentylidene analogue **52a**, Raney nickel gave selective hydrogenation but the related tertiary alcohol **52b** added H_2 (in the presence of Pd/C) from the opposite face, reflecting greater steric hindrance to the developing alkyl group along the OH-directed path.[66]

Among cyclohexenol reductions the example **53** is notable, since OH-direction provides the less stable epimer with an axial methyl group.[67] *Kishi* et al. discovered that alumina-supported catalysts were much more responsive to hydroxyl-direction (cf. **54**).[68] With Pd/C the unwanted stereoisomer predominated, whereas Pt on alumina gave 93% of the desired product.

The critical importance of solvent effects was demonstrated during a systematic survey of direction in heterogeneous hydrogenation.[69] In the case of **55a**, the proportion of *syn*-isomer increased from 39% in hexane to 94% in ethanol on using Pd/C; a very similar trend was observed with Pt/C. By comparing substitution effects under standard conditions—see **55a–e** and **56a–d**—an order of haptophilicity towards the catalyst surface was derived with $CH_2NH_2 > CH_2OH \gg CO_2^{\ominus}M^{\oplus} > CO_2H > CO_2Me$.[70] For 2-substituted-7-methylenenorboranes only the CH_2NH_2 group gave any semblance of a directing effect.

Finally, there is an interesting recent example of diastereoselectivity in the hydrogenation of α,β-unsaturated amides in presence of Pd/C using a chiral auxiliary derived from camphor,[71] a system where reduction by H_2 and catalyst **C** gave poor stereochemical control. The success of this hydrogenation of the amides **58** is attributed to coordination of the SO_2-group of the acylsultam to the metal surface, and steric constraints then favor hydrogen delivery to the α-*re*-face of the olefin.

9. Summary

In the context of directed hydrogenation it was stated as recently as 1983 that "only scattered reports have appeared which suggest the possibility of this kind of control in a hydrogenation reaction."[12] Three years later it is fair to say that the method is well-established and affords a particularly simple route to diverse types of structure with

Table 5. Catalytic hydrogenation of cyclic allyl alkohols and related compounds in the presence of heterocatalysts. Solvent: ethanol (**54**: ethyl acetate).

	Educt	*syn*-Product [a]		Conditions	Yield [%]	Ref.
51			**a**, R = *n*Pr	Raney-Ni, 69 bar	96	[63]
			b, R = Ph	Raney-Ni, 69 bar	51	[65]
52			**a**, R = H	Raney-Ni, 69 bar	98	[65]
			b, R = CH_3	Raney-Ni	91	[66]
				Pd/C	45	[66]
53	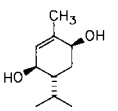	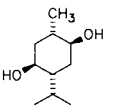		Raney-Ni, 2 bar	90	[67]
54	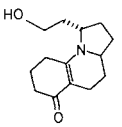	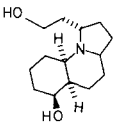		5% Pt/Al_2O_3, 4 bar	92	[68]
55	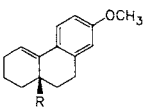	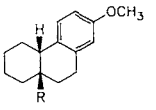	**a**, R = CH_2OH	5% Pd/C	94	[69]
			b, R = CH_2NH_2	5% Pd/C	100	[70]
			c, R = CO_2K	5% Pd/C	75	[70]
			d, R = CO_2H	5% Pd/C	26	[70]
			e, R = CO_2Me	5% Pd/C	9	[70]
56	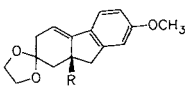	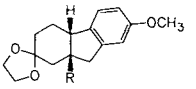	**a**, R = CH_2OH	5% Pd/C	95	[70]
			b, R = CO_2Na	5% Pd/C	55	[70]
			c, R = CO_2H	5% Pd/C	18	[70]
			d, R = CO_2Me	5% Pd/C	15	[70]
57	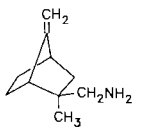	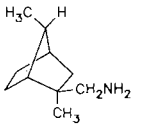		5% Pd/C	63	[70]
	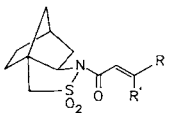	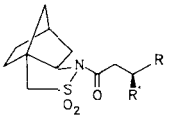				
	58a, R = 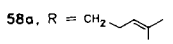 R' = CH_3	**59a**, R = 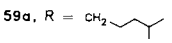 R' = CH_3		10% Pd/C, 7 bar	95	[71]
	58b, R = CH_3 R' = 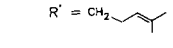	**59b**, R = CH_3 R' = 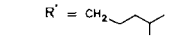		10% Pd/C, 7 bar	96	[71]

[a] *syn* refers to the added hydrogen.

high and predictable diastereoselectivity. Figure 12 shows some of the more successful variants.

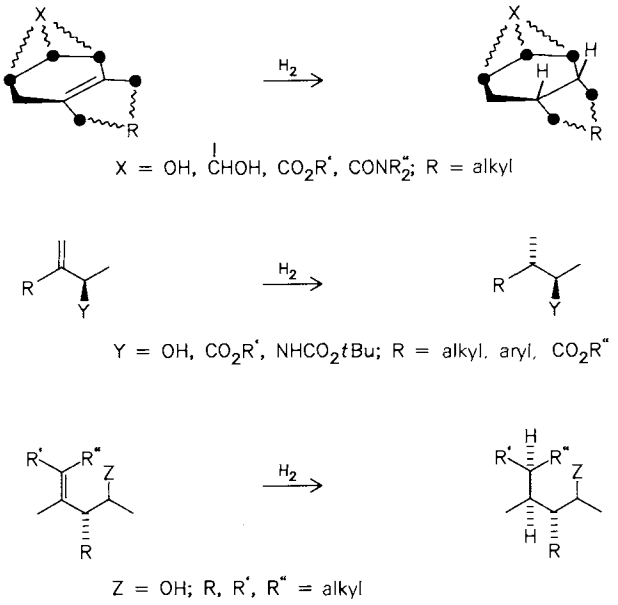

Fig. 12. Substructures of successful substrates for directed hydrogenation with cationic rhodium and iridium catalysts.

Much of the authors' research presented here was conducted with SERC support, which is gratefully acknowledged. Enthusiastic co-workers have contributed greatly to the development of the project, especially Dr. Ian Cutting, Mr. Phillip L. Evans, Dr. Stephen A. Hall, Dr. Alun P. James, Mr. Peter Maddox and Dr. Ramachandra Naik. Dr. Naik made the early observations on which subsequent work was based.

Received: February 10, 1986;
revised: July 14, 1986 [A 608 IE]
German version: *Angew. Chem. 99* (1987) 169

[1] J. Halpern, J. F. Harrod, B. R. James, *J. Am. Chem. Soc. 83* (1961) 753.

[2] F. H. Jardine, *Prog. Inorg. Chem. 28* (1981) 63, and references therein.

[3] F. H. Jardine, *Prog. Inorg. Chem. 31* (1984) 265, and references therein.

[4] R. H. Crabtree, H. Felkin, G. E. Morris, *J. Organomet. Chem. 141* (1977) 205; R. H. Crabtree, *Acc. Chem. Res. 12* (1979) 331.

[5] G. Jeske, H. Lauke, H. Mauermann, H. Schumann, T. J. Marks, *J. Am. Chem. Soc. 107* (1985) 8111.

[6] R. E. Ireland, P. Bey, *Org. Synth. 53* (1973) 63.

[7] J. D. Morrison (Ed.): *Asymmetric Synthesis, Vol. 5*, Academic Press, New York 1985, esp. Ch. 1, 2, 3, 5.

[8] T. P. Dang, H. B. Kagan, *J. Am. Chem. Soc. 94* (1972) 6429; B. D. Vineyard, W. S. Knowles, M. J. Sabacky, G. K. Bachman, D. J. Weinkauff, *ibid. 99* (1977) 5946; M. D. Fryzuk, B. Bosnich, *ibid. 99* (1977) 6262.

[9] A. S. Hussey, Y. Takeuchi, *J. Org. Chem. 35* (1970) 643; C. Rousseau, M. Evrard, F. Petit, *J. Mol. Catal. 5* (1979) 163.

[10] H. W. Thompson, E. McPherson, *J. Am. Chem. Soc. 96* (1974) 6232.

[11] R. H. Crabtree, M. W. Davis, *Organometallics 2* (1983) 681; fuller account: R. H. Crabtree, M. W. Davis, *J. Org. Chem. 51* (1986) 2655.

[12] G. Stork, D. E. Kahne, *J. Am. Chem. Soc. 105* (1983) 1072.

[13] S. A. Hall, *D. Phil. Thesis*, Oxford 1985.

[14] E. J. Corey, T. A. Engler, *Tetrahedron Lett. 25* (1984) 149.

[15] J. M. Brown, S. A. Hall, *Tetrahedron Lett. 25* (1984) 1393.

[16] A. S. Machado, A. Olesker, S. Castillon, G. Lukacs, *J. Chem. Soc. Chem. Commun. 1985*, 330.

[17] D. A. Evans, M. M. Morrissey, *J. Am. Chem. Soc. 106* (1984) 3866.

[18] D. A. Evans, M. M. Morrissey, *Tetrahedron Lett. 25* (1984) 4637.

[19] C. A. Hoeger, W. H. Okamura, *J. Am. Chem. Soc. 107* (1985) 268.

[20] J. M. Brown, S. A. Hall, *Tetrahedron 41* (1985) 4639.

[21] For Ir: R. H. Crabtree, P. C. Demou, D. Eden, J. M. Mihelcic, C. A. Parnell, J. M. Quirk, G. E. Morris, *J. Am. Chem. Soc. 104* (1982) 6994; for Rh: J. Halpern, D. P. Riley, A. S. C. Chan, J. J. Pluth, *ibid. 99* (1977) 8055; J. M. Brown, P. A. Chaloner, A. G. Kent, B. A. Murrer, P. N. Nicholson, D. Parker, P. J. Sidebottom, *J. Organomet. Chem. 216* (1981) 263.

[22] J. Auffret, P. Courtot, R. Pichon, R. Runin, J. Y. Salaun, *J. Organomet. Chem. 262* (1984) C 19.

[23] E. M. Arnett, G. Scorrano, *Adv. Phys. Org. Chem. 13* (1976) 84; J. Hine, *Structural Effects on Equilibria in Organic Chemistry*, Wiley, New York 1975, pp. 188, 189.

[24] J. M. Brown, S. A. Hall, *J. Organomet. Chem. 285* (1985) 333.

[25] A. G. Schultz, P. J. McCloskey, *J. Org. Chem. 50* (1985) 5905.

[26] J. M. Brown, P. A. Chaloner, *J. Am. Chem. Soc. 102* (1980) 3040; A. S. C. Chan, J. J. Pluth, J. Halpern, *ibid. 102* (1980) 5952.

[27] A. G. Schultz, P. Sundaraman, M. Macielag, F. P. Lavieri, M. Welch, *Tetrahedron Lett. 26* (1985) 4575.

[28] M. Nakata, H. Takao, Y. Ikeyama, T. Sakai, K. Tatsuta, M. Kinoshita, *Bull. Chem. Soc. Jpn. 54* (1981) 1749.

[29] M. Nakata, H. Enari, M. Kinoshita, *Bull. Chem. Soc. Jpn. 55* (1982) 3283.

[30] M. Nakata, K. Toshima, T. Kai, M. Kinoshita, *Bull. Chem. Soc. Jpn. 58* (1985) 3457; for a similar approach to erythromycin see: M. Kinoshita, M. Arai, N. Ohsawa, M. Nakata, *Tetrahedron Lett. 27* (1986) 1815.

[31] J. M. Brown, R. G. Naik, *J. Chem. Soc. Chem. Commun. 1982*, 348.

[32] F. R. Hartley, *Chem. Rev. 73* (1973) 163; cf. V. Schurig, *Inorg. Chem. 25* (1986) 945.

[33] C. R. Landis, J. Halpern, *J. Organomet. Chem. 250* (1983) 485.

[34] S. E. Drewes, N. D. Emslie, *J. Chem. Soc. Perkin Trans. 1 1982*, 2079; H. M. R. Hoffmann, J. Rabe, *Angew. Chem. 95* (1983) 795; *Angew. Chem. Int. Ed. Engl. 22* (1983) 795; cf. DBP 2 155 113; *Chem. Abstr. 77* (1972) 34 174.

[35] J. M. Brown, I. Cutting, *J. Chem. Soc. Chem. Commun. 1985*, 578.

[36] Extensively reviewed in recent years, for example: a) C. H. Heathcock: *Comprehensive Carbanion Chemistry, Vol. 5B*, Elsevier, Amsterdam, 1984, p. 177; b) C. H. Heathcock in J. D. Morrison (Ed.): *Asymmetric Synthesis, Vol. 3*, Academic Press, New York 1984, p. 111ff; c) D. A. Evans in [36b], p. 2ff.

[37] T. C. Smith, *Part II Thesis*, Oxford 1986.

[38] M. M. Bhagwat, D. Devaprabhakara, *Tetrahedron Lett. 1972*, 1391.

[39] J. M. Brown, A. P. James, M. Wali, S. Wilkie, unpublished.

[40] V. Schurig, unpublished work, quoted in J. D. Morrison (Ed.): *Asymmetric Synthesis, Vol. 1*, Academic Press, New York 1983, Ch. 4.

[41] Dehydroamino acids and esters: see Ref. [7]; enol esters: M. D. Fryzuk, B. Bosnich, *J. Am. Chem. Soc. 101* (1979) 3043; itaconates: W. C. Christopfel, B. D. Vineyard, *ibid. 101* (1979) 4408; S. Saito, Y. Nakamura, Y. Morita, *Chem. Pharm. Bull. 33* (1985) 5284 and references cited therein; enol phosphinates: T. Hayashi, K. Kanehira, M. Kumada, *ibid. 22* (1981) 4417.

[42] J. W. Scott, D. D. Keith, G. Nix, Jr., D. R. Parrish, S. Remington, G. P. Roth, J. M. Townsend, D. Valentine, Jr., R. Yang, *J. Org. Chem. 46* (1981) 5086.

[43] J. M. Brown, I. Cutting, P. L. Evans, P. J. Maddox, *Tetrahedron Lett. 27* (1986) 3307.

[44] S. Masamune, W. Choy, J. S. Petersen, L. R. Sita, *Angew. Chem. 97* (1985) 1; *Angew. Chem. Int. Ed. Engl. 24* (1985) 1.

[45] L. Prior, *Part II Thesis*, Oxford 1986.

[46] D. H. G. Crout, M. Lutstorf, P. J. Morgan, R. M. Adlington, J. E. Baldwin, M. J. Crimmin, *J. Chem. Soc. Chem. Commun. 1981*, 1175; D. H. G. Crout, M. Lutstorf, P. J. Morgan, *Tetrahedron 39* (1983) 3457.

[47] J. M. Brown, A. P. James, *J. Chem. Soc. Chem. Commun. 1987*, in press.

[48] D. A. Evans, M. M. Morrissey, R. L. Dow, *Tetrahedron Lett. 26* (1985) 6005.

[49] D. A. Evans, S. L. Bender, *Tetrahedron Lett. 27* (1986) 799.

[50] A. Miyashita, H. Takaya, T. Souchi, R. Noyori, *Tetrahedron 40* (1984) 1245.

[51] D. A. Evans, M. di Mare, *J. Am. Chem. Soc. 108* (1986) 2476.

[52] B. R. Stults, R. M. Friedman, K. Koenig, W. S. Knowles, R. B. Greegor, F. W. Lytle, *J. Am. Chem. Soc. 103* (1981) 3235.

[53] K. N. Houk, N. G. Rondan, Y.-D. Wu, J. T. Metz, M. N. Paddon-Row, *Tetrahedron 40* (1984) 2257; A. R. Chamberlin, R. L. Mulholland, Jr., *ibid. 40* (1984) 2297; I. Fleming, J. J. Lewis, *J. Chem. Soc. Chem. Commun. 1985*, 149; G. J. McGarvey, J. M. Williams, *J. Am. Chem. Soc. 107* (1985) 1435.

[54] S. D. Kahn, W. J. Hehre, *Tetrahedron Lett. 26* (1985) 3647.

[55] E. B. Wilson, K. M. Marstokk, H. Mollendal, Z. Smith, N. Carballo, *J. Am. Chem. Soc. 107* (1985) 1951.

[56] V. S. Martin, S. S. Woodward, T. Katsuki, Y. Yamada, M. Ikeda, K. B. Sharpless, *J. Am. Chem. Soc. 103* (1981) 6237.

[57] Cf. M. Basato, B. Longato, F. Morandini, S. Bresadola, *Inorg. Chem. 23* (1984) 3972; B. Longato, S. Bresadola, *ibid. 21* (1982) 168; N. W. Alcock, J. M. Brown, A. E. Derome, A. R. Lucy, *J. Chem. Soc. Chem. Commun. 1985*, 575.

[58] R. H. Crabtree, M. Lavin, *J. Chem. Soc. Chem. Commun. 1985*, 794; T. M. Gilbert, R. G. Bergman, *J. Am. Chem. Soc. 107* (1985) 3502.

[59] P. L. Evans, *D. Phil. Thesis*, Oxford 1987.

[60] F. Bonati, G. Wilkinson, *J. Chem. Soc. 1964*, 3156.

[61] Pressure vessels of 22 mL and 45 mL capacity are available from Charles Cook Ltd., Birmingham BI3DS (UK).

[62] M. Bartok, J. Czombos, K. Felfoldi, L. Gera, Gy. Gondos, A. Molnar, F. Notheisz, I. Palinko, Gy. Wittmann, A. G. Zsigmond: *Stereochemistry of Heterogeneous Metal Catalysis*, Wiley, Chichester 1985.

[63] R. K. Sehgal, R. U. Koenigsberger, T. J. Howard, *J. Org. Chem. 40* (1975) 3073.

[64] R. K. Sehgal, R. U. Koenigsberger, T. J. Howard, *J. Chem. Soc. Perkin Trans. 1 1976*, 191.

[65] T. J. Howard, *Recl. Trav. Chim. Pays-Bas 83* (1964) 992; *Chem. Ind. (London) 1963*, 1899.

[66] S. Mitsui, K. Hebiguchi, H. Saito, *Chem. Ind. (London) 1967*, 1746.

[67] R. D. Stolow, K. Sachdev, *J. Org. Chem. 36* (1971) 960; S. Mitsui, M. Ito, A. Nanbu, Y. Senda, *J. Catal. 36* (1975) 119.

[68] R. Fujimoto, Y. Kishi, J. F. Blount, *J. Am. Chem. Soc. 102* (1980) 7154.

[69] H. W. Thompson, E. McPherson, B. L. Lences, *J. Org. Chem. 41* (1976) 2903.

[70] H. W. Thompson, J. K. Wong, *J. Org. Chem. 50* (1985) 4270.

[71] W. Oppolzer, R. J. Mills, M. Réglier, *Tetrahedron Lett. 27* (1986) 183.

New Reductive Transformations of Unsaturated Cyclic Hydrocarbons

New Synthetic Methods (66)

By Klaus Müllen*

The successive reduction of fully conjugated cyclic hydrocarbons leads to singly and multiply charged ions with unusual bonding. The charge distribution in these ions can be determined spectroscopically, and the information so obtained is then used in kinetically-controlled trapping reactions for the regioselective introduction of electrophilic groups. When non-benzenoid substrates are used, syntheses become possible which can either not be carried out or can only be carried out with great difficulty in other ways. Examples of new preparative applications are cycloannelation and bridging reactions as well as polymerization reactions. The ion pair structure of the intermediate and the type of electrophile used are of paramount importance in controlling the mechanism of these reductive transformations.

1. Formation and Reactions of Charged Hydrocarbons

The carbanions arising from electron transfer reactions of fully conjugated cyclic hydrocarbons can readily be trapped by electrophiles. Depending on the type of reagent used, the overall reaction can be a reduction or reductive alkylation,[1,2] but arylation,[3] acylation,[4] silylation[5] or cyanation[6] is also possible.[7] The preparative importance of such reactions lies in the fact that unsaturated hydrocarbons can be modified in a highly selective manner under mild conditions. The selectivity includes not only the position of attack, but also the number of electrophilic reagents which are introduced. There is a large number of experimental possibilities for the reduction of the unsaturated starting material and also for the trapping of the ionic intermediate;[8-14] variation of the method used is well known to change the product spectrum, often radically. However, because factors such as counterion, solvent and temperature have a determining influence on the structure and stability of the ion pairs which are the primary products, it should be useful for the control of the trapping reaction to characterize the labile carbanions in situ using spectroscopic techniques.[15]

It must first be determined which carbanion in the complex overall reaction is actually trapped. Electron transfer can convert the substrate A into a radical anion $A^{\odot\ominus}$ or a dianion $A^{2\ominus}$, and both ions can then react with an electrophile RX (see Scheme 1). However, in liquid ammonia both species can first be protonated by the solvent, so that the types of product and the mechanisms of their formation can vary.[16]

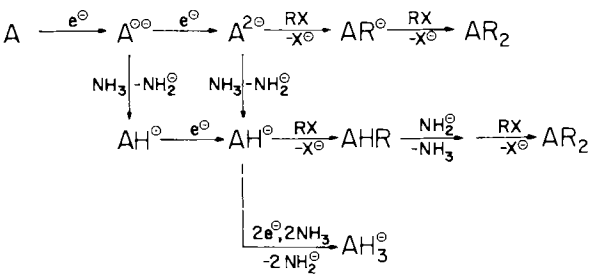

Scheme 1. Mechanisms of the reductive alkylation of a cyclic conjugated hydrocarbon in liquid ammonia.

[*] Prof. Dr. K. Müllen
Institut für Organische Chemie der Universität
Johann-Joachim-Becher-Weg 18-20, D-6500 Mainz 1 (FRG)

The second important piece of information is the charge distribution in the π-delocalized carbanions, since the kinetically controlled attack of an electrophile will occur preferentially at the position of highest electron density.[16-18] The synthetic applications of reductions in liquid ammonia have been described in several review articles.[2,9,19-21] The correlation between preparative and mechanistic results which is intended here has three advantages over empirical procedures:

1) Only the knowledge of the π-charge distribution in the ionic intermediate makes it possible to forecast the regioselectivity of the trapping reaction.
2) Such structural information can be taken as a basis for attempts to use new hydrocarbons as substrates for unconventional reductive transformations.
3) When a dianion $A^{2\ominus}$ is dialkylated to AR_2, the intermediate $AR^{\ominus}$ can also be observed spectroscopically. The preparative importance of the separate control of the first and second alkylations will make itself particularly felt when dianions are reacted with bifunctional electrophiles.

The present paper can thus be divided into a section dealing with the structure determination of π-delocalized paramagnetic and diamagnetic carbanions (Section 2) and further sections (Sections 3-6) dealing with preparative applications resulting from the structural information.

2. The Structures of Charged π-Systems

2.1. Highly Charged Ions

The "combined" approach assumes the formation under mild conditions and the detailed spectroscopic characterization of charged hydrocarbons.[22-25] The experimental description of an extended redox sequence is shown in

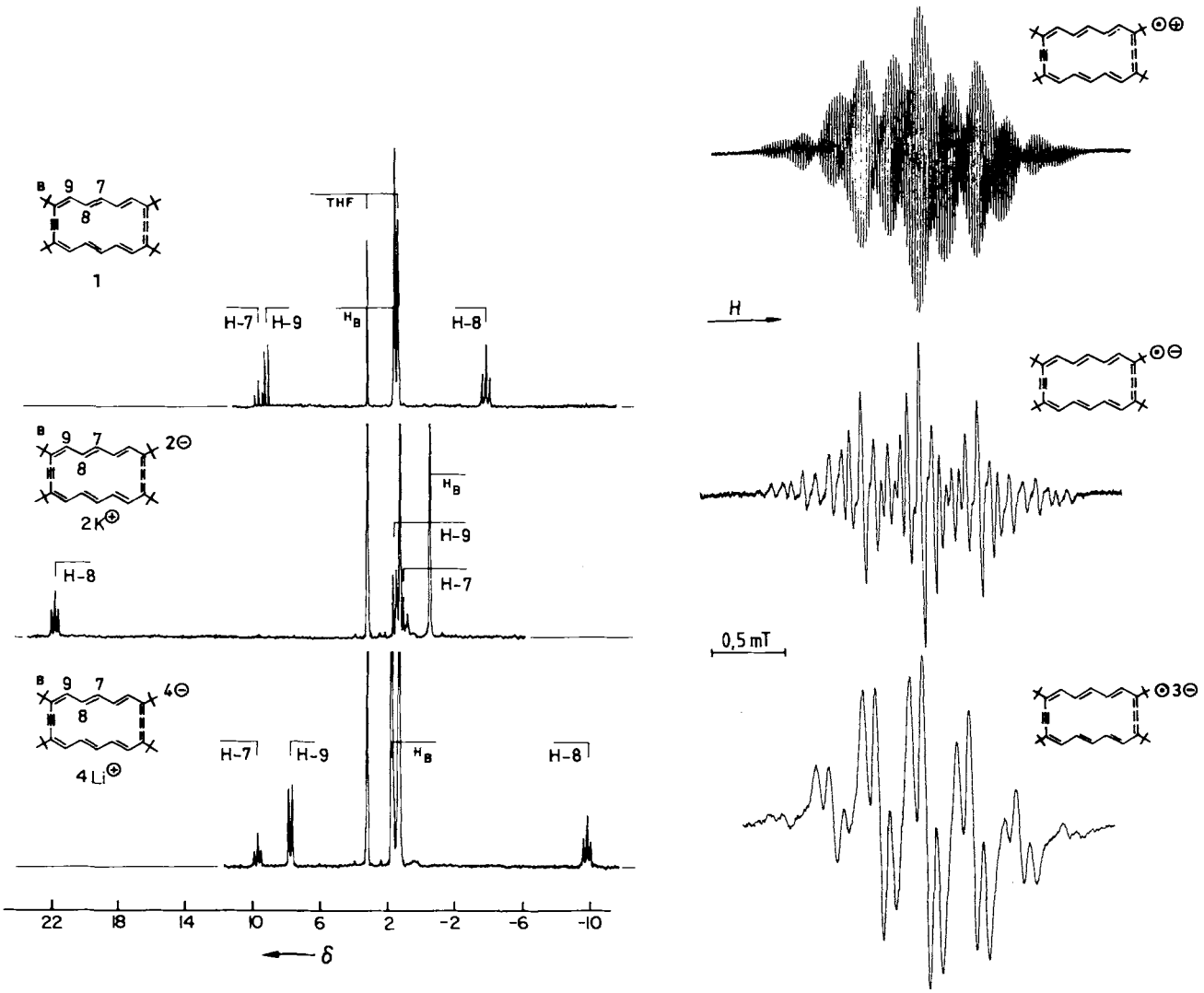

Fig. 1. Ionic species of the [18]annulene derivative **1**. The diamagnetic systems (neutral compound, dianion, tetraanion) are characterized by ^{1}H-NMR spectroscopy (on the left), the paramagnetic systems (radical cation, radical anion, radical trianion) by ESR spectroscopy. The reduction was carried out using lithium or potassium in tetrahydrofuran, the oxidation with aluminum(III) chloride in dichloromethane.

Figure 1 for the example of [18]annulene **1**. Careful control of the redox process makes it possible to characterize the diamagnetic systems (neutral starting material, dianion, tetraanion) as well as the paramagnetic systems (radical cation, radical anion, radical trianion) by means of well-resolved proton NMR or ESR spectra.

The formation of tetraanions from the hydrocarbons **2**,[26] **3**,[27] or **4**[28] appears plausible, since they are built up from separate π-systems and since the monomeric units can form dianions. The selectivity of the protonation of, for example, $2^{4\ominus}$ and $3^{4\ominus}$ to **5** or **6** corresponds to that found for anthracene. In the case of the annulenoannulenes **7**[29] and **8**,[30] which consist of two condensed rings, the formation of stable tetraanions can be explained by the particular redox properties of the sub-rings. In contrast, the formation of a tetraanion from [18]annulene **1**[31,32] can only be explained by assuming that the increase in the electron-electron repulsion is compensated not only by ion-pair effects[32,34] but also by a conjugative stabilization of the π-system.[33,35,36] Cyclovoltammetric studies show that the reduction of the radical anion $1^{\odot\ominus}$ to the di-, tri-

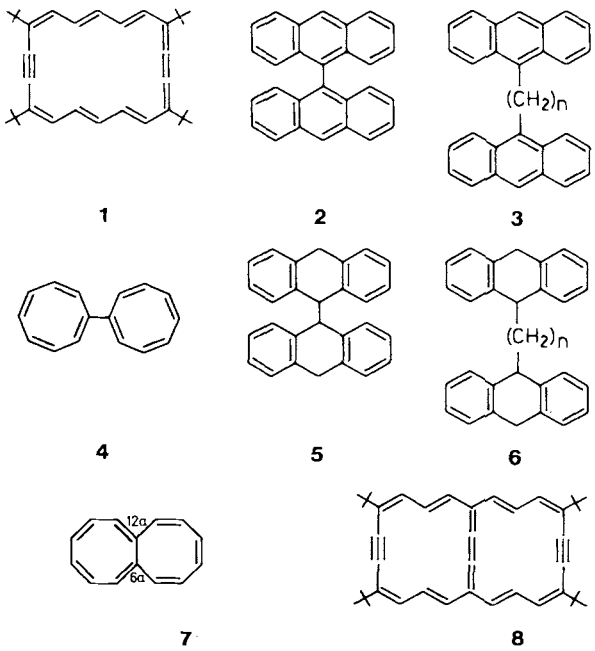

1 2 3 4 5 6 7 8

and tetraanions occurs over a very small total potential range of less than 0.1 V.[31] Electrostatic considerations alone would have led us to expect considerably larger potential differences when the charge is increased; in the case of reduction of benzenoid compounds, the mono- and dianions are indeed separated by about 0.5 V.[24] Thus if during the annulene reduction the ion pair energies do not change drastically, it follows that the increase in the electron-electron repulsion is partially compensated by conjugation.[29,35]

2.2. Charge Distribution and Ion Pair Structure

The ESR spectroscopy of paramagnetic π-systems (e.g. of the mono- and trianions formed in a reduction process) allows us to determine proton hyperfine coupling constants, with the help of which the local spin density at the neighboring π-center can be estimated.[37] Similarly, the NMR treatment of diamagnetic ions often shows a linear correlation between proton or carbon-13 chemical shifts and local π-charge densities.[39,40,44] There is no cogent theoretical justification for this correlation; furthermore, its application requires that other effects such as ring current and ion pair phenomena or the structure dependence of the proportionality constant K_c[45] be taken into account. In spite of this, the NMR-spectroscopic determination of local π-densities (particularly in a series of structurally related systems) can be considered to be a reliable method in the sense of a heuristic principle.

Using a simple MO model, the spin density at the π-center of a paramagnetic π-system is calculated from the square of the AO coefficient in the singly occupied molecular orbital and thus from the π-charge density.[37] The practical result of such a procedure is that the symmetry of the newly occupied frontier orbital in the monoanion can be estimated from spectroscopic parameters, or that vice versa the expected spin or charge density can be estimated from a knowledge of the MO's involved.[38] Making the plausible assumption that the doubly occupied HOMO in $A^{2\ominus}$ is identical to the singly occupied HOMO in $A^{\odot\ominus}$, the spin density distribution in $A^{\odot\ominus}$ can also be used to estimate the expected charge density distribution in $A^{2\ominus}$.[24,41-43]

The total range of the carbon-13 NMR signals of the anthracene dianion $\mathbf{9}^{2\ominus}$[46,47] (lithium salt, tetrahydrofuran [THF]) is much larger than that in the neutral compound, and suggests an inhomogeneous charge distribution in the ionic π-system. The sequence of the charge densities resulting from the relative ^{13}C-NMR chemical shifts q_π(C-9) $> q_\pi$(C-1) $> q_\pi$(C-2) agrees with the sequence of the spin densities for the corresponding radical anion determined by ESR spectroscopy and corresponds to the AO coefficients in the newly-occupied frontier orbital. The existence of a positive partial charge at the quaternary positions in the dianion is indicative of the character of the charge distribution.[48,49]

In the case of benzenoid substrates, it has been predicted from MO models that the excess charge is localized at certain positions; this has been demonstrated by ^{13}C-NMR spectroscopy, since the corresponding signals are shifted to higher field. This is also observed for the non-benzenoid octalene dianion $\mathbf{7}^{2\ominus}$;[29] here the highest local

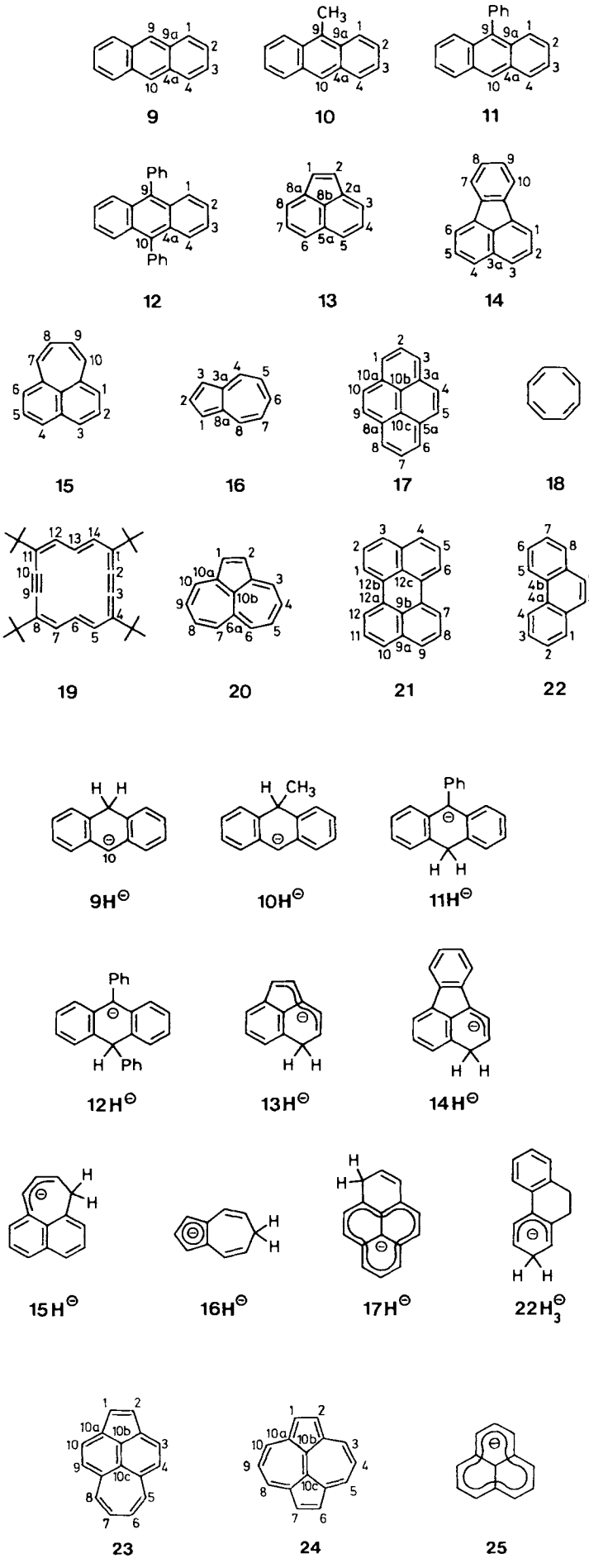

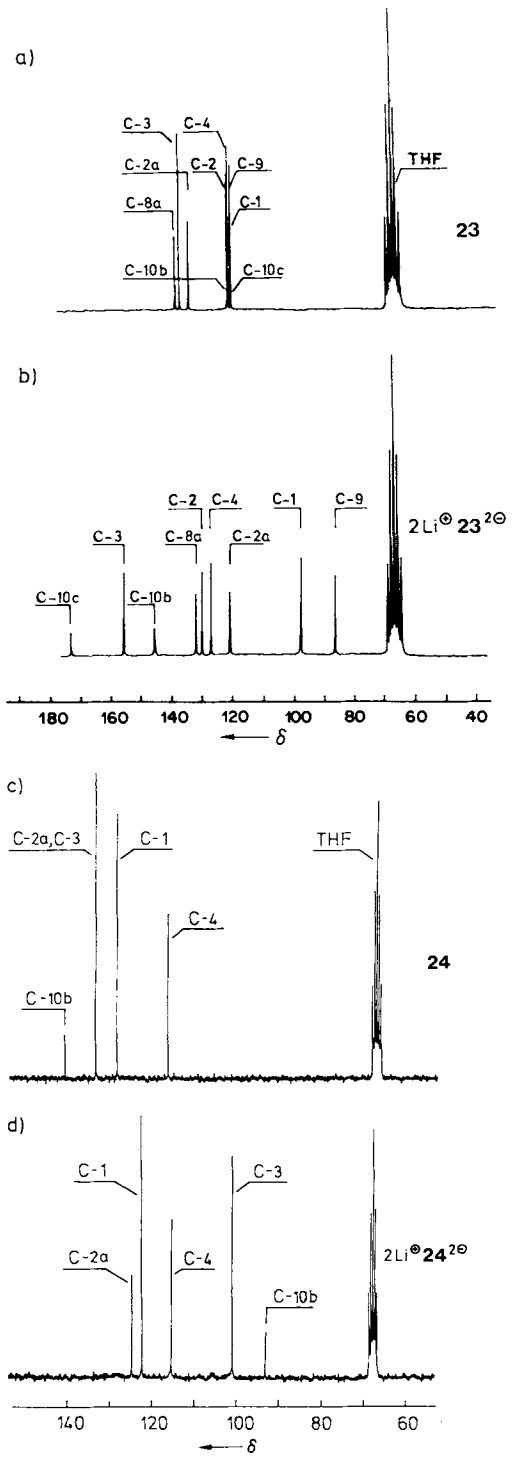

Fig. 2. ^{13}C-NMR spectra of a) cyclohepta[*de*]cyclopenta[*ij*]naphthalene (**23**) and b) its dianion ([D$_8$]THF, lithium salt); c) ^{13}C-NMR spectra of dicyclopenta[*ef*,*kl*]heptalene (**24**) and d) its dianion ([D$_8$]THF, lithium salt).

charge density is to be found at the two neighboring quaternary centers C-6a and C-12a.

The radical anions and dianions of pyrene (**17**) and its isomers **23**[50] and **24**[51] differ considerably in the distribution of their spin and charge.[17,52–54] A simple MO model predicts a high charge density at the "inner" ethylene group only for $24^{2\ominus}$, while in $17^{2\ominus}$ and $23^{2\ominus}$ this bridge is not expected to accommodate any excess charge. This difference, which results from the nodal properties of the frontier orbitals, is confirmed by the high-field shift $\Delta\delta_c = -47$ ppm in $24^{2\ominus}$ and the low-field shift $\Delta\delta_c = +50$ ppm in $23^{2\ominus}$ (see Fig. 2) observed on the formation of the dianions.[15,33]

The tricyclic compound aceheptylene (**20**)[55] is structurally related to **24**. From the nature of the LUMO we expect that the reductive formation of a dianion will lead to a pronounced accumulation of charge at the inner angular center. This prediction can be experimentally verified by the drastic high-field shift of the corresponding ^{13}C-NMR signal of more than 60 ppm.[56,57] The charge distribution in $20^{2\ominus}$ is different from that in a related tricyclic compound, the phenalene anion **25**: in **25** there is *no* excess charge at the central position, as can readily be predicted from the nature of the frontier orbital.

The description of π-delocalized anions[59] must also take into account the structure of the ion pair and thus the role played by the counterion and the solvent.[60] Crystal structures of the alkali metal salts show that the counterions are located above or below the systems; in the case of polycyclic substrates they lie preferentially above certain rings.[61–64] A further complication to be considered is that the ion pairs may form aggregates in solution, and that the π-charge distribution predicted by a frontier orbital treatment can be modified by the effects of the counterions. The polarizing effect of the counterions leads to a further increase in the *a priori* high local charge density (see Scheme 2),[15] the influence of the small lithium cation in a contact ion pair being the largest. Even more drastic is the effect of the counterion on going from dilithium to magnesium anthracenediide, as can be shown by ^{13}C-NMR spectroscopy[65]. While $2\,Li^{\oplus}/9^{2\ominus}$ can be described as an ionic system, the corresponding magnesium derivative has a stronger covalent bond between the metal and the centers C-9 and C-10. The result is a considerably smaller excess charge at the terminal benzene rings than in the dilithium salt.

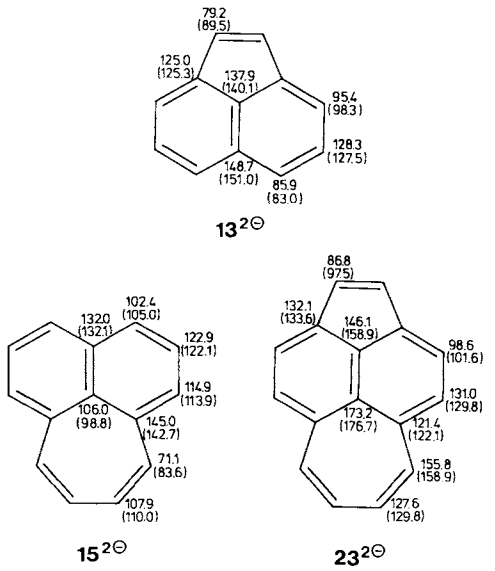

Scheme 2. ^{13}C-NMR chemical shifts (δ_c) of the polycyclic dianions $13^{2\ominus}$, $15^{2\ominus}$, and $23^{2\ominus}$ as lithium and (in brackets) potassium salts ([D$_8$]THF, −30°C).

The structure of the ion pair also influences the reactivity of the substrate, as can readily be shown by the protonation of certain dianionic π-systems occurring in liquid ammonia (see Section 1.3). The acenaphthylene dianion ($\mathbf{13}^{2\ominus}$) is stable in NH_3 as its dipotassium salt.[16] However, the dilithium salt is converted quantitatively into the monoanion $\mathbf{13H}^{\ominus}$, as can be shown spectroscopically. Because of the stronger eigensolvation of $Li^{\oplus}$, the amount of solvent-separated ion pairs increases, and as a result the basicity of the dianion is also increased. The frequently observed temperature dependence of reductive transformations can be interpreted in a similar way as a change in the structure of the ion pair.[66-68] It is generally true that the existence of free ions or of solvent-separated ion pairs is favored at lower temperatures.

2.3. Electron Transfer and Protonation in Liquid Ammonia

The NMR- and ESR-spectroscopic observation of their reduction in liquid ammonia shows[16] that a certain group of unsaturated hydrocarbons, **9**–**17** (group 1), are rapidly protonated subsequent to the electron transfer and thus converted into monoanions; in contrast, the dianions $\mathbf{18}^{2\ominus}$–$\mathbf{21}^{2\ominus}$ of another group, **18**–**21** (group 2) remain unchanged. The following observations should be noted:

1) In each case only one single hydroproduct, $\mathbf{9H}^{\ominus}$–$\mathbf{17H}^{\ominus}$, is formed. The constitution of these anions can be determined from spectroscopic measurements.

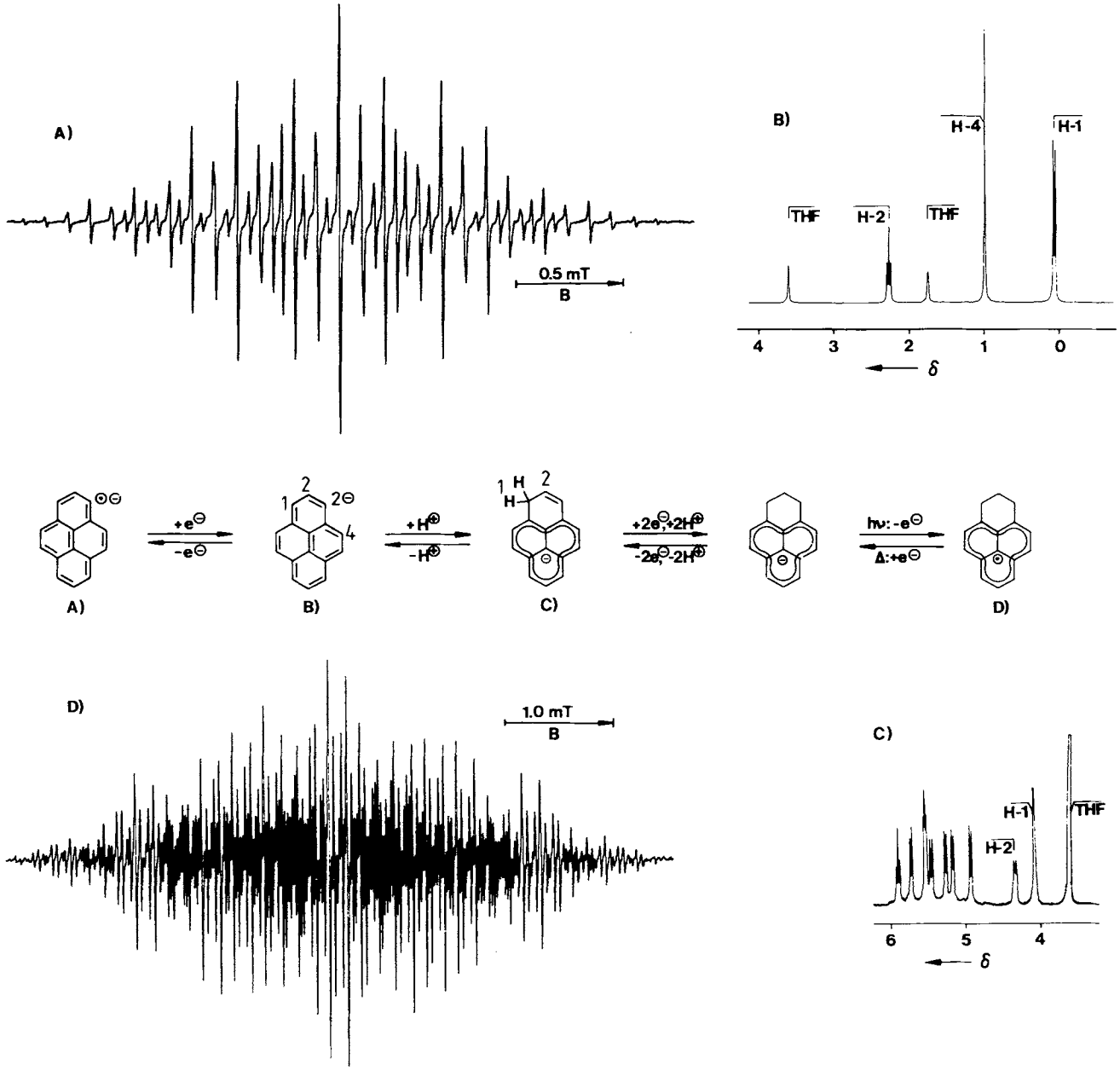

Fig. 3. ESR and ^{1}H-NMR spectroscopic monitoring of the reduction of pyrene (**17**) in liquid ammonia.

2) If there is an equilibrium between monoanion and dianion, the concentration of the latter is too low for it to be detected.
3) The protonation observed is that of the dianion: the corresponding radical anions are stable under the reaction conditions.

Figure 3 demonstrates the spectroscopic observation of the reduction using pyrene (**17**) as an example.

Phenanthrene (**22**) shows a third type of behavior, since in liquid ammonia it forms the trihydro-monoanion $\mathbf{22H_3^{\ominus}}$, even when only two equivalents of alkali metal are used.[18]

The basicity of the dianions can be assessed from the atom localization energies,[69] which result from the difference between the π-energy of the dianion and of the monoanion formed by its protonation. The experimental results can be explained on the basis of the difference between the types **9**-**17** and **18**-**21**; this difference can also be used to predict the behavior of other substrates.

3. Reductive Alkylations using Monofunctional Reagents

3.1. Benzenoid Hydrocarbons

When hydrocarbons of group 1 (substrates **9**-**17**) are alkylated in liquid ammonia, the protonation (with formation of $\mathbf{9H^{\ominus}}$-$\mathbf{17H^{\ominus}}$) always occurs at the position of highest charge density. In the case of pyrene (**17**) this is position 1. The dianion $\mathbf{17^{2\ominus}}$ is also attacked in this position in non-protic solvents.[16,17,90,91] When **17** is reductively alkylated in NH_3, however, the substrate to be alkylated is no longer $\mathbf{17^{2\ominus}}$ but $\mathbf{17H^{\ominus}}$. As the constitution of the products shows, the electrophile attacks at position 5 in the second ring. Such possibilities of controlling the regioselectivity of the reductive alkylation simply by the choice of solvent also occur in other cases, azulene (**16**) being a typical example.[70-72]

Anthracene (**9**) is a special case: preliminary considerations would indicate that the dianion $\mathbf{9^{2\ominus}}$ and the protonated monoanion $\mathbf{9H^{\ominus}}$ should both be attacked at C-10 of the central benzene ring, so that the choice of solvent will not be relevant to the constitution of the monoalkylhydro derivative produced. In fact, however, only $\mathbf{9H^{\ominus}}$ is attacked at C-10 with high selectivity;[3,23,73-75] the dianion $\mathbf{9^{2\ominus}}$ (THF) is in contrast attacked at C-9(10) as well as at C-1.[76-81]

26

27

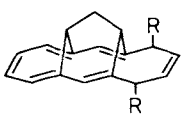

28

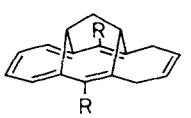

29

a: R = CH_3 ; **b**: R = $COOCH_3$

ESR[83] and NMR[84,85] spectroscopic results show that the radical ions and dianions of anthracene (**9**) and the bridged [14]annulene **26**[82] have frontier orbitals of the same symmetry type. Reductive alkylation of **26** (NH_3, Li, CH_3Br) gives a 3:1 mixture of the dimethyl adducts **27a** and **28a** in nearly quantitative yield.[84] The positions of attack are as expected, though the regioselectivity of the reaction is apparently less than for anthracene. This can be explained by the fact that $\mathbf{26^{2\ominus}}$, in contrast to $\mathbf{9^{2\ominus}}$, is not protonated by ammonia (see Section 2.3). If a solution of $2\,Li^{\oplus}/\mathbf{26^{2\ominus}}$ in tetrahydrofuran is treated with methyl chloroformate, the products **28b** and **29b** are formed. **29b** is apparently formed from **27b** by a base-induced hydrogen shift. The dihydro derivatives **27**-**29** can be readily dehydrogenated to the corresponding annulenes. This type of reaction is worthy of note, since the direct alkylation and acylation of the annulene is not possible.

The limits of the use of spectroscopic information are evident from the example of acenaphthylene (**13**). Doubly negatively charged ions $A^{2\ominus}$ react much more rapidly with an electrophile than do singly charged ions such as $AH^{\ominus}$ or $A^{\odot\ominus}$. It is thus in principle possible that $A^{2\ominus}$, although present in a much smaller equilibrium concentration which cannot be detected by spectroscopic means, is the substrate for the primary alkylation step. When **13** is reductively dialkylated in THF, the product formed is as expected **30**, which readily rearomatizes to **31** by means of a proton shift.[86-88] When NH_3 is used as the solvent, the products

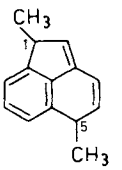

30

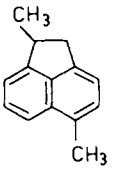

31

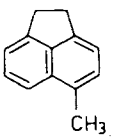

32

obtained are those of a primary alkylation at C-1 as well as at C-5.[89] The formation of **32** observed when methyl iodide is used as the trapping reagent cannot be explained as being due to alkylation of the monoanion $\mathbf{13H^{\ominus}}$ which is the only species observed spectroscopically, but indicates the participation of $\mathbf{13^{2\ominus}}$.[89]

The conclusions from a mechanistic consideration of reductive transformations force a reinterpretation of a number of preparative results.[20,90,91] We shall now proceed to consider new reductive alkylations using *non-benzenoid* starting materials.

3.2. Octalene

The highest charge density in the octalene dianion ($\mathbf{7^{2\ominus}}$) is at the two bridgeheads.[29] The attack of the electrophile in methylation (dimethyl sulfate, −78°C) also occurs at these positions. However, the primary bicyclic diadduct **33** is not isolated, but instead a [14]annulene, **34**, is obtained; this is formed by an electrocyclic ring-opening (see Scheme 3).[92] In spite of the difficult synthesis of **7**, this route to **34** is useful, even though the yield of the trapping reaction is only 25%. In addition, the formation of the dial-

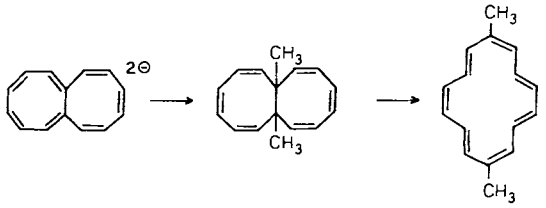

$7^{2\ominus}$ 33 34a

Scheme 3. The reductive alkylation of octalene 7 via the dianion $7^{2\ominus}$.

kyl derivative (see isomers **34a–34d**), which is not obtainable by other routes, gives us information on the much-discussed[93,94] conformational transformations in annulenes.[92]

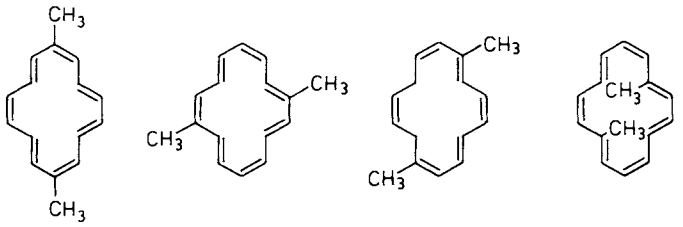

34a 34b 34c 34d

3.3. Pyrene Isomers

Pyrene (**17**) and its isomers **23** and **24** can formally be described as ethylene-bridged 14-center perimeters. The products of the reductive alkylation of pyrene (**17**) mentioned above do not indicate any attack at the inner double bond, a result which is not surprising in view of the charge distribution in $17^{2\ominus}$. The "adduct" **35**[95–97] can only be obtained from a completely different multi-step synthesis. The dimethylation of the isomeric dianion $23^{2\ominus}$ leads to the adduct **36**.[15,33] The kinetically-controlled primary attack occurs at the quaternary position C-4a, the π-conjugation of the naphthalene moiety being destroyed. The reductive formation of **36** corresponds exactly to the conversion of acenaphthylene (**13**) into the diadduct **30**.[86,87] In contrast, the derivative **15**,[15,98] which is structurally related to **23** undergoes alkylation in its seven-membered ring during the reductive transformation, giving products **37** and **38**. These results can readily be explained on the basis of the frontier orbitals involved: the LUMO's of **13** and **23** have the same symmetry, with a nodal plane passing through the central quaternary C-atoms; the LUMO of **15** is different (see Scheme 4).[15,53]

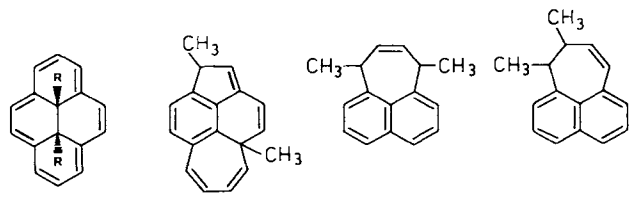

35 36 37 38

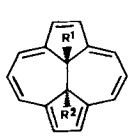

39

a: $R^1 = R^2 = CH_3$

b: $R^1 = R^2 = (CH_2)_nX$; n = 2, 3, 8; X = Hal

c: $R^1 = CH_3$, $R^2 = H$

d: $R^1 = CH_3$, $R^2 = (CH_2)_3CH_3$

e: $R^1 = CH_3$, $R^2 = (CH_2)_3CH_2Br$

If however the charge distribution in the dianion controls the attack of the electrophiles, then the system $24^{2\ominus}$ (isomeric with $17^{2\ominus}$ and $23^{2\ominus}$) should be suitable for the direct synthesis of a bridged 14π-perimeter, since the highest charge density is localized at C-10b and C-10c. The reaction with alkylating agents gives adducts of type **39** in 60–80% yield.[99–101] This simple annulene synthesis, which starts from a readily prepared material,[51] can be easily modified by varying the electrophile since linear alkyl groups, acyl residues, hydrogen or functionalized alkyl groups can be introduced.[99–101]

In this way it is possible to synthesize substrates which are "tailor-made" for investigating questions on the theory of bonding.[100] From a preparative point of view it is important that the method of reductive alkylation permits an easy manipulation and functionalization of the bridging groups in annulenes, thus paving the way for other synthetic applications (see Sections 5 and 6).

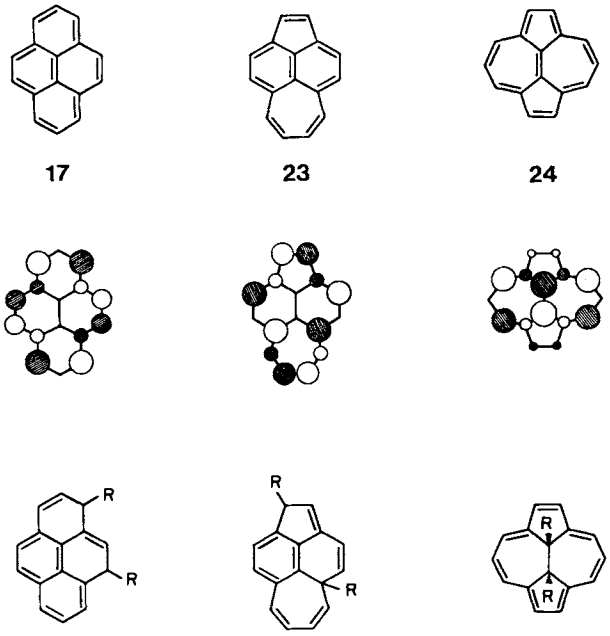

17 23 24

Scheme 4. The reductive alkylation of the pyrene **17** and its isomers **23** and **24**. Top: starting material; center: schematic representation of the LUMO; bottom: products.

3.4. Aceheptylene

The method described above for choosing new substrates for unconventional alkylations leads from the use of a simple MO model via the spectroscopic characterization of the ionic intermediates to preparative applications. This procedure will now be applied to the tricyclic compound aceheptylene (**20**). According to predictions based on spectroscopic measurements $20^{2\ominus}$ should be attacked electrophilically at the central position 10b (in contrast to, say, the phenalene anion **25**[102]). The reaction of $20^{2\ominus}$ with dimethyl sulfate at −20°C in THF does indeed give a

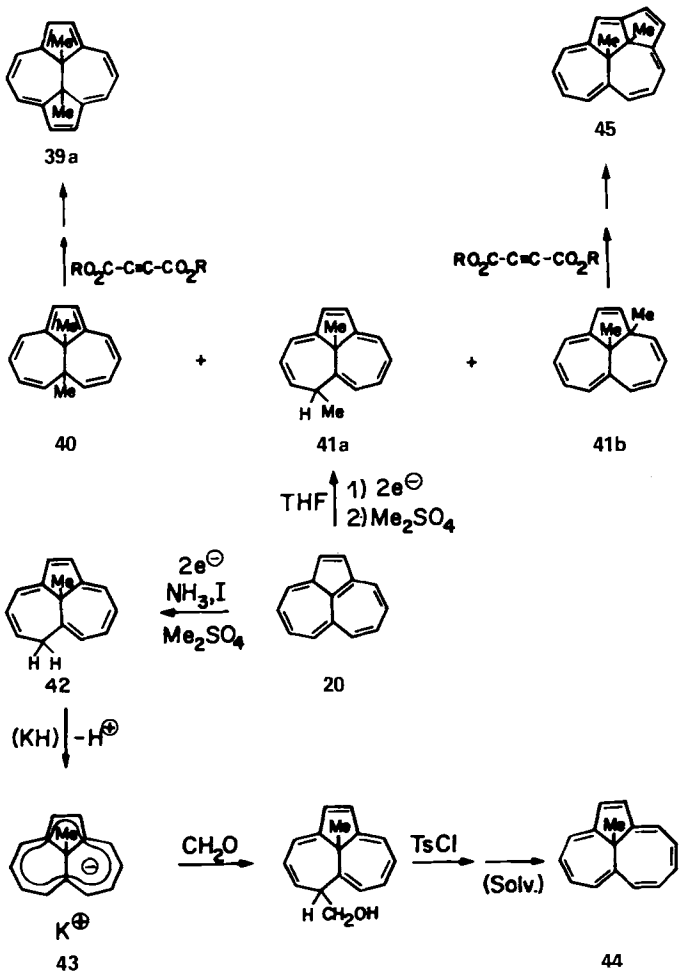

Scheme 5. The reductive alkylation of aceheptylene (**20**) and the further chemical transformations of the trapping products.

mixture of the three dimethyl adducts **40**, **41a**, and **41b** (which can be separated chromatographically); in each case one methyl group has been introduced at the central position (see Scheme 5).[56] If $\mathbf{20}^{2\ominus}$ is trapped with dimethyl sulfate in liquid ammonia instead of in THF, the monomethylation is followed by a rapid protonation, due to the ammonolysis of the dimethyl sulfate occurring in the reaction medium.[103]

The sole product (89% yield) of this reaction is the derivative **42**, which can now be used for further synthetic transformations. Thus its deprotonation gives the strongly diatropic monoanion **43**, the first 14π-homologue of the cyclopentadienide anion.[104] Hydroxymethylation of **43** with formaldehyde and solvolytic ring-expansion of the corresponding tosylate yield a new methine-bridged [14]annulene **44**,[98,105,106] which is an extension of the series of structurally related 10π-[107] and 12π-systems[108] (though the latter were prepared in completely different ways). Finally, **40** and **41b** react with the diester of acetylenedicarboxylic acid[109] by a [12+2]-cycloaddition process, giving (after decarboxylation) the π-systems **39a** and **45**.[106] Common to these new systems is that they can all be derived from a readily-available trapping product and that, as originally intended, angular positions have been substituted by means of reductive alkylations.[110,111]

4. The Multistep Mechanism of Reductive Alkylations

When a dianion $A^{2\ominus}$ is converted into a diadduct AR_2, only the entry of the first electrophile can be described on the basis of the charge distribution in $A^{2\ominus}$: the second attack is determined by the charge distribution in the intermediate anion $AR^{\ominus}$. It is thus advisable to include the spectroscopic characterization of this species in the study of the two-step mechanism. The anion $AR^{\ominus}$ can be obtained either directly by monoalkylation of $A^{2\ominus}$ or by deprotonation of a monoalkyldihydro derivative AHR. Comparable studies have been carried out for deprotonation and alkylation reactions starting from the dihydroanthracene derivatives **46** and **47** as well as from the analogous phenanthrene systems.[18,22,73,75,112–114]

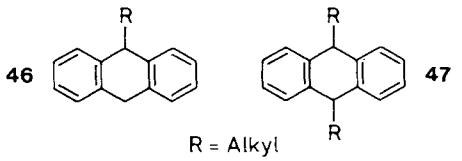

The formation of **40**, **41a**, and **41b** in the methylation of $\mathbf{20}^{2\ominus}$ demonstrates that the monoanionic intermediate **43**, which can also be obtained by deprotonation of **42**, is no longer attacked regioselectively.[56] However, starting from $\mathbf{24}^{2\ominus}$ we obtain only a single diadduct in good yield, via the lithium salt of the monoanion **48**. The analysis of the ^{13}C-NMR spectra of the monoanions **43** and **48** shows the charge distribution to be such that this apparent discrepancy is explained:[115] in the anion **48**, which is readily prepared by deprotonation of **39c** (see Scheme 6), the excess charge is clearly localized at the central position C-10c, so that the selective conversion into the diadducts **39d** or **39e** is to be expected. Since the dianion $A^{2\ominus}$ reacts

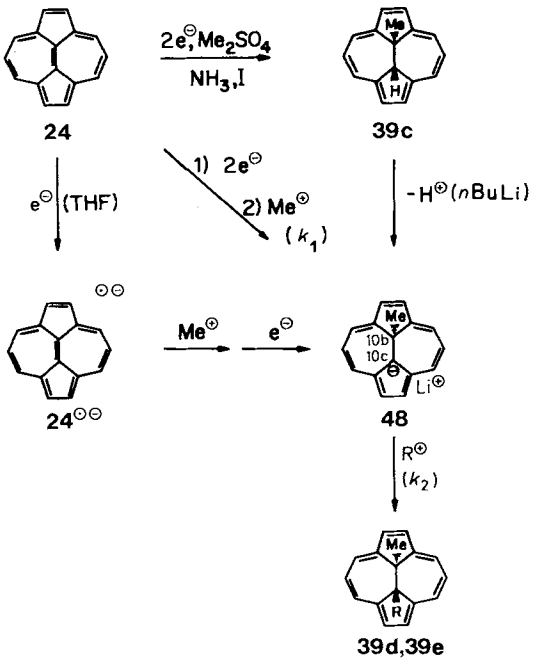

Scheme 6. The two-step mechanism of the reductive alkylation, illustrated for the example of dicyclopenta[*ef*,*kl*]heptalene (**24**).

much faster with the electrophile than do either the monoanion $AR^{\ominus}$ or the paramagnetic radical anion $A^{\odot\ominus}$, $AR^{\odot}$ = **48** can be obtained directly from the dianion by using one equivalent of the alkylating agent and then characterized spectroscopically. The consequence for preparative applications (see Section 6) is that diadducts can readily be obtained using two *different* electrophiles.

The in-situ characterization of the monoalkylated ionic species leads to the question of the configuration of the diadduct and thus to the stereochemical course of the second alkylation step. It is known that the reductive alkylation (R = CH_3, C_2H_5) of anthracene gives *cis*-dialkyldihydroanthracenes **47**.[73] However, the diadducts **39**, **40**, and **41b** are *trans*-configurated (the formation of a *cis*-1,2-diadduct is only possible when a bifunctional electrophile is used (see Section 5).[100, 101, 115] The question as to how the course of the trapping reaction is influenced by the structure of the ion pair **48** and by steric hindrance between the electrophile and the alkyl group already present cannot presently be answered decisively.

Any discussion of the two-step mechanism of the reductive alkylation must include the radical anions $A^{\odot\ominus}$ which are formed as intermediates in the production of dianions $A^{2\ominus}$.[8, 80, 117, 118] Reactions of radical anions with electrophiles have in particular been studied in connection with the electrochemical reduction of benzenoid hydrocarbons, whereby the neutral radical $AR^{\odot}$ primarily formed from trapping of $A^{\odot\ominus}$ is at once reduced further at the reduction potential of A to give the anion $AR^{\ominus}$.[8] When the pyrene isomer **24** is reduced electrochemically (acetonitrile, tetra-*n*-butylammonium chloride as supporting electrolyte) in the presence of dimethyl sulfate to the radical anion, the product **39a** (which also results from the alkylation of the dianion in THF) is obtained in 75% yield.[119] One could argue that the generation of a high charge density at the central carbon atoms C-10b/C-10c of the dianion $\mathbf{24}^{2\ominus}$ and at C-10c of the corresponding monoanion **48** is due to the strong polarizing effect of the lithium counterion in a contact ion pair. However, the same regioselectivity is observed when instead of the dianion $\mathbf{24}^{2\ominus}$ the radical anion $\mathbf{24}^{\odot\ominus}$ is used and instead of the small lithium cation the more voluminous, but only weakly polarizing, tetrabutylammonium ion.[119]

5. Cyclization Reactions using Bifunctional Alkylating Agents

The key ionic intermediate produced in a trapping reaction using *bi*functional alkylating agents can be described by structure **49** (see Scheme 7). The monoanion **49** can undergo a "second alkylation" either at a neighboring position or at a position further removed. In the case of 1,2-attack the result is cycloannelation (product **50**); when the attack is 1,n a bridged product is formed (product **51**).[105] The best-known examples of this type of alkylation come from the chemistry of cyclooctatetraene,[120–122] the dianion $\mathbf{18}^{2\ominus}$ of which gives bicyclo[6.n.0]alkatrienes of the type **54** when allowed to react with 1,n-dihalogenoalkanes.[123–126] 1,4-Attack is not observed, but has been realized for the

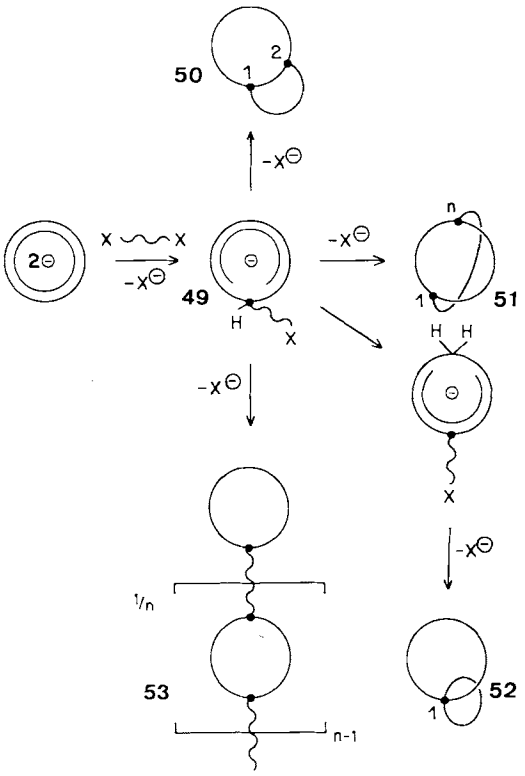

Scheme 7. Reaction between a dianion and a bifunctional electrophile, schematic.

reaction of $\mathbf{18}^{2\ominus}$ with acid chlorides and anhydrides, which give (among other products) bicyclic compounds of the type **55**.[127, 128]

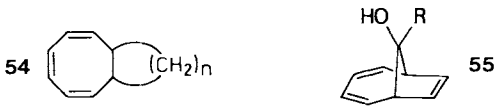

It would be desirable to be able to cyclooctannelate the dianion $\mathbf{18}^{2\ominus}$, giving synthons for new conjugated cyclic π-systems containing a cyclooctatetraene unit. This requires a 1,2-attack by a 1,6-difunctionalized electrophile. The reaction between $\mathbf{18}^{2\ominus}$ and 2,2′-bis(bromomethyl)biphenyl (**56**) does in fact give the desired adduct **57**.[120] While short-chain alkylating agents such as 1,2-dibromoethane give, as expected, only *cis*-configurated products, an X-ray structural analysis of compound **57** shows it to

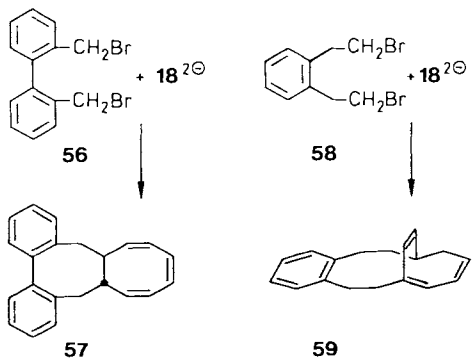

be *trans*. However, when instead of **56** 1,2-bis(2-bromoethyl)benzene (**58**) is used as the alkylating agent, 1,4-attack (followed by a hydrogen shift) occurs, giving **59**.[129]

Reductive alkylations occurring by means of 1,2-attack have also proved themselves useful in the cycloannelation of polycyclic benzenoid compounds: examples are provided by the formation of **60a**, **60b**, and **61** from acenaphthylene[89] and of **62** from pyrene.[90] The syntheses of compounds such as **61** by means of reductive alkylation are clearly superior to other methods for their preparation. Hydrogenated arenes such as **61** and **62** can readily be converted into acephenanthrylene (**63**) or the benzo[*e*]pyrene **64** by dehydrogenation using quinones;[89,90] **63** or **64** are much more readily obtained in this way than for example by means of Friedel-Crafts acylations.

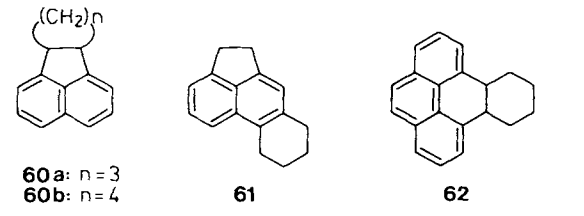

While the adduct **65** is readily cyclized to **62** on the addition of a base, the intermediates produced when the 1-position of acenaphthylene is attacked cannot be detected: only the cyclized products **60a** and **60b** are isolated. In contrast, the primary products **66** and **67** cannot be cyclized, even after addition of base; ring closure can only be carried out starting from **67** by means of a subsequent Friedel-Crafts alkylation.[89]

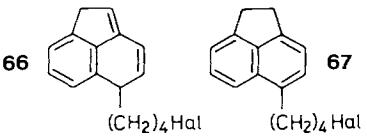

The monoanion **68** which is formed by the attack of a 1,n-dihalogenoalkane on the dianion of anthracene $\mathbf{9}^{2\ominus}$ is a derivative of the diphenylmethyl anion; as such it has the largest π-charge density at C-10. 1,4-Attack leading to bridged dihydroanthracenes of type **69** is thus favored. In the case of longer-chain bridges (e.g. n = 10), the dihydroanthracenes **69** undergo dehydrogenation to the bridged anthracenes **70**,[130] which are thus readily obtainable via reductive alkylation.

Monofunctional alkylating agents convert the dianion $\mathbf{24}^{2\ominus}$ only into 1,2-adducts with *trans*-geometry. However, when 1,3-dihalogenopropanes are used, the lithium salt of the monoanion **71** (n = 3, Hal = Br) is converted into to the cyclization product **72**.[100] With short-chain alkylating agents ring closure is strongly favored over the formation

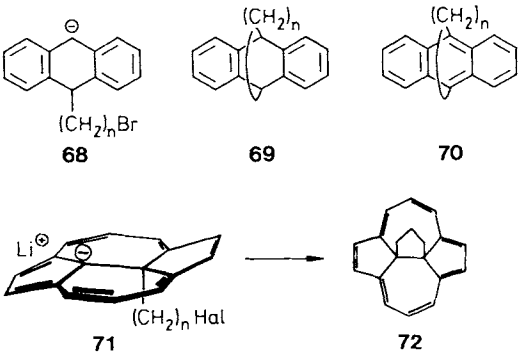

of the diadduct **39**; thus the product ratio **72** : **39b** (n = 3, Hal = Cl) is still 2 : 1 even under conditions of inverse addition.[101] Alkylating agents with longer carbon chains (e.g. n = 8) give only the diadduct. If the diadduct is desired as the main product of the reaction with short-chain dihalogenoalkanes (this is important for the formation of functionalized bridging groups), the intermolecular trapping reaction must be drastically accelerated in comparison with the intramolecular process. Thus 3-chloropropyltrifluoromethanesulfonate does indeed give only the diadduct **39b** (n = 3, Hal = Cl).[131]

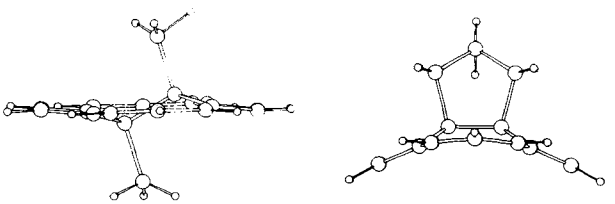

Fig. 4. The crystal structures of the alkylation products **39a** and **72**.

Crystal structures (see Fig. 4) indicate that only the *trans*-bridged annulene **39a** is nearly planar.[100,102] It is thus not surprising that, as shown by NMR, ESR and UV measurements,[100,132,133] compound **72** shows a stronger tendency to double bond fixation. It is important for preparative applications that the preparation of *trans*- and *cis*-bridged perimeters does not require a completely new synthetic approach, but can be made possible by a minor modification of a trapping reaction.

6. Formation of Polymers during Reductive Alkylation

A bifunctional electrophile can attack a dianion in a 1,2- or a 1,n-manner (to give **50** and **51**); apart from spiroannelation (to give **52**) (see Scheme 7),[134,135] the intermediate monoanion **49** has yet another possibility for reaction. If the nucleophilic substitution of the haloalkyl residue by the carbanionic unit occurs intermolecularly rather than intramolecularly, polymers will be formed. In products **53**, dihydro derivatives of the substrate are bridged by polymethylene chains.[79,105,136,137] In the sense of the cycloannelations described previously, this is an unwanted side reac-

tion; however, it can in fact be made useful for preparative purposes. The synthetic possibilities available will be described below taking anthracene (**9**) and dicyclopenta[*ef*,*kl*]heptalene (**24**) as examples.

The complexity of the processes occurring during the reductive alkylation of **9** with bifunctional alkylating agents is shown in Scheme 8. The key intermediates are the 9-(n-bromoalkyl)-9,10-dihydroanthracene **75** and the monoanion **68** formed by its deprotonation. Both species can be produced from anthracene or 9,10-dihydroanthracene in three different ways. When 1,n-dibromoalkane is added to the monoanion $\mathbf{9H}^{\ominus}$, the tetrahydrodianthrylalkanes **74** are formed. As expected, the substituted dihydroanthracenes **75** can be formed by means of inverse addition, i.e. by adding $\mathbf{9H}^{\ominus}$ to a large excess of the alkylating agent.[81] The isolated products **75** can now be converted into the

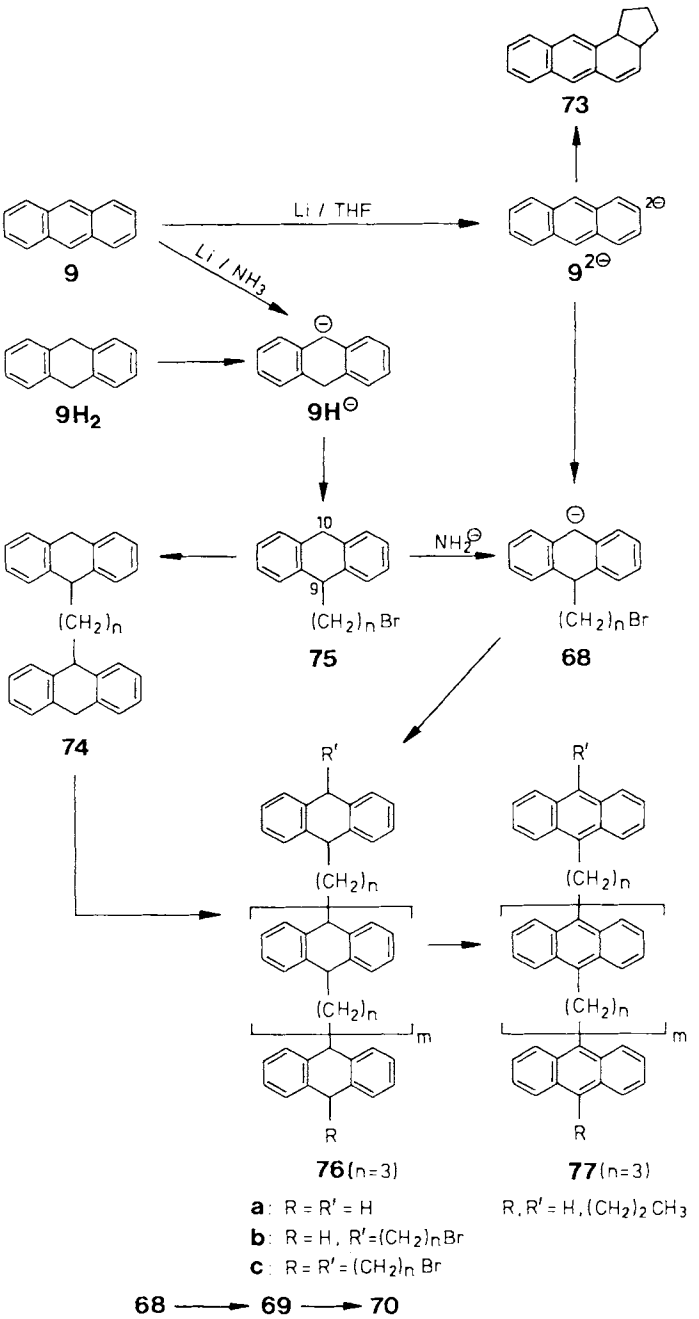

Scheme 8. The reductive transformations of anthracene (**9**).

monoanions **68** by deprotonation. The subsequent reaction of **68** is strongly dependent on the chain length n and the concentration in the reaction medium.[81] As already mentioned, the cyclization products **69**[78,79,81] can readily be obtained under conditions of extreme dilution. The third reaction possibility for **68** and **75** is that of the "polyreaction" to form **76**. Chain formation can be initiated by the linking of two molecules of **68** or by the attack of the nucleophiles $\mathbf{9H}^{\ominus}$ or $\mathbf{9}^{2\ominus}$ on the bromoalkyl residues of **68** or **75**. We have been able to show[81] that **76** is mainly formed via the latter mechanism. A sufficient concentration of the nucleophiles $\mathbf{9H}^{\ominus}$ or $\mathbf{9}^{2\ominus}$ is obtained when **68** or **75** are produced reductively from anthracene.

If the dianion $\mathbf{9}^{2\ominus}$ ($2\,Li^{\oplus}$, THF) is trapped by 1,3-dibromopropane, compounds **9**, **69**, **73** (n = 3) and polymeric material are obtained in yields of 33, 42, 20 and < 5% respectively. Reduction of **9** in NH_3 and alkylation of $\mathbf{9H}^{\ominus}$ give in contrast poly(9,10-dihydroanthrylenetrimethylene) of type **76** in yields up to 90%.[81]

The structures of the polymers of type **76** can be established NMR-spectroscopically. The structural homogeneity of **76** implies that the anthracene systems are linked only at positions 9 and 10. This is due to the extreme selectivity of the reductive alkylation in NH_3 (alkylation of $\mathbf{9H}^{\ominus}$), which is not observed in THF (see above). The fact that the polymer **76** (n = 3) can also be formed by treating the tetrahydrodianthrylpropane **74** (n = 3) with lithium amide and dibromopropane[81] is in agreement with the reaction sequence described here.

A fascinating aspect of the formation of polymers by means of reductive alkylation (which can also be carried out on a large scale) is provided by the fact that the nature of the unsaturated substrate and of the linking group can be varied, so that polymers of many different types result. The dehydrogenation of **76** gives compounds in which the properties of the original π-system, for example its redox activity, are restored.[81] Spectroscopic and cyclovoltammetric studies show that **77** and lower oligomers such as **78** can serve as "electron stores" and that doping of the hydrocarbons with electrons induces a through-space conjugative interaction between the electroactive units.[138,139]

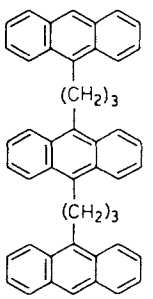

78

In the case of the pyrene isomer **24**, the bifunctional species which is analogous to the anthracene derivative **68** is the monoanion **71**. If, apart from the intramolecular cyclization described above, **71** were capable of polymer formation as in the anthracene case, a new type of multilayer π-system with variable interlayer distance would be

formed. In contrast to the structure of the phanes, the subunits would here be linked by bridging groups "inside" the π-systems and not by external "clamps". The reaction of **48** and **39e** (analogous to that used for linking $\mathbf{9H}^{\ominus}$ and **68**) to give the double layer **79** occurs almost quantitatively in an inert atmosphere (see Scheme 9).[115] We were also able to prepare "stacked" annulenes with three and more layers.[113] Multilayer hydrocarbons such as **79** have shown themselves to be suitable model compounds for studying successive electron transfer processes, just as is for example **77**:[115,116] with them it is also possible to realize the complete redox sequence from the radical anion to the tetraanion.

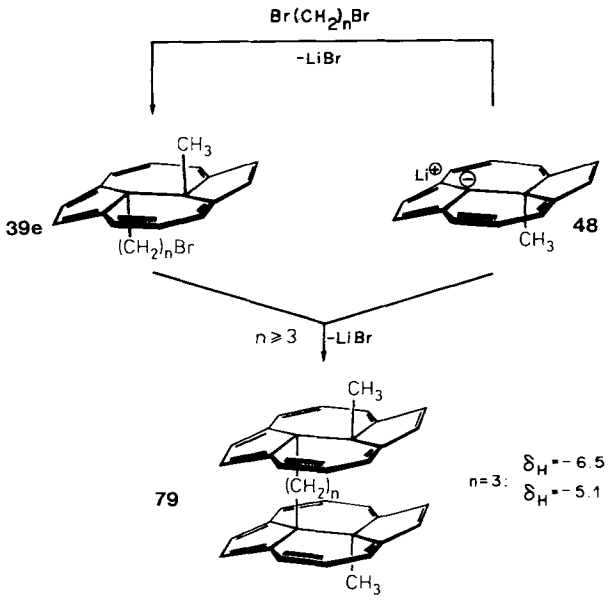

Scheme 9. Construction of double layer annulenes (**79**) from the products of reductive alkylation.

The linking reactions mentioned as examples in this section document the fact that the reductive alkylation of readily available unsaturated derivatives provides a simple method for the synthesis of higher molecular redox-active substances with separate electrophoric groups.[81,136,139]

7. Complications

It is not surprising that reductive conversions of unsaturated hydrocarbons are often accompanied by side reactions.[140,141] A typical example is provided by azulene (**16**), the radical anion of which dimerizes to give **80**. Only the further reduction of **80** causes bond breakage to give the azulene dianion. Depending on the point of the reduction process at which electrophiles are introduced to carry out the trapping reactions, either monomeric or dimeric products are formed.[70,71]

The anions formed in the reductions can attack ethereal solvents such as THF at room temperature in a nucleophilic manner: thus the lithium salt of the pyrene dianion $\mathbf{17}^{2\ominus}$ is converted into an adduct which after dehydrogenation was identified as **81**.[17] The dianions are however not only nucleophiles, but also strong reducing agents, so that electron transfer is able to dominate the planned S_N2-

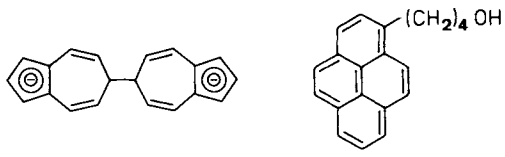

80 **81**

type alkylation. The following examples of attempted alkylations using 1,2-dibromoethane are typical: the cyclooctatetraenediide $\mathbf{18}^{2\ominus}$ is converted into a bicyclic compound of type **54** (n=2),[124] the dianion $\mathbf{24}^{2\ominus}$ is almost quantitatively reoxidized to the neutral compound, and in the system $Li/NH_3/THF$ anthracene is converted via oxidative coupling of the monoanion $\mathbf{9H}^{\ominus}$ into the tetrahydrodianthryl **5**.[18] It is known that a single electron transfer (SET) can also play a role in the actual S_N-reaction.[142] The rate constants k_{SET} and k_{S_N} for the reaction between π-delocalized carbanions and alkyl halides are known in only a few cases.[143] In addition, it is not clear whether the SET- and S_N-mechanisms really involve two separate processes or only a single process in which the position of the transition state on the reaction coordinate can differ.[143] A final example of side reactions is provided by hydrocarbons such as octalene (**7**)[29] or biphenylene,[111] the reductive conversion of which (just as for example the reaction of the cyclooctatetraenediide $\mathbf{18}^{2\ominus}$ with carbon dioxide[144]) is accompanied by a skeletal rearrangement.[145,146]

The realization of regioselective reductive alkylations finds its limits in cases where several positions in either the dianion $A^{2\ominus}$ or the monoalkylated monoanion $AR^{\ominus}$ have comparable electron densities. Typical examples for the first case are the anthracene dianion $\mathbf{9}^{2\ominus}$ and the acenaphthylene dianion $\mathbf{13}^{2\ominus}$, for the second the monocyclic anions **43**, **82**, and **83**. The latter two species have an allyl

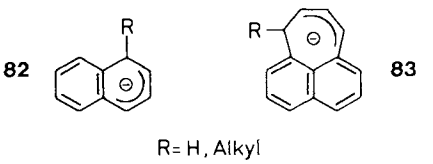

82 **83**

anion structure, further reaction of which can lead to 1,2- and 1,4-diadducts.[147] It is not possible to predict the position of the second alkylation without taking into account additional factors influencing the energy profile of the trapping reaction such as ion pair effects or the soft/hard character[148] of the electrophile and the nucleophile.

8. Summary and Outlook

Reductive transformations of unsaturated hydrocarbons show themselves to be ideal examples for the combined use of preparative, spectroscopic and bond-theoretical methods. Synthetic results can be given a clear mechanistic interpretation, and the spectroscopically established structural information on π-delocalized carbanions can indicate unconventional, simply realizable synthetic routes. A rational selection of starting materials with a suitable topology of the π-system will lead to the synthesis of hydrocar-

bons which are at present unknown but which are ideally suited for reductive transformations.

Finally, it should be emphasized that the mechanistic aspects valid for such reductive transformations are in principle also valid for the attack of nucleophilic reagents on cations produced by oxidation of unsaturated substrates. Preparative applications of this reaction are much more unusual,[42] but are to be recommended in particular for cases in which a regioselectivity different to that observed in reduction is to be expected.

This article is dedicated to my co-workers, since they have made it possible. I thank the Deutsche Forschungsgemeinschaft, the Volkswagenwerk Foundation, and the Fonds der Chemischen Industrie for financial support.

Received: January 13, 1986 [A 611 IE]
German version: *Angew. Chem. 99* (1987) 192
Translated by Prof. *T. N. Mitchell*, Dortmund (FRG)

[1] M. Smith in R. L. Augustine (Ed.): *Reduction*, Marcel Dekker, New York 1968.
[2] H. O. House: *Modern Synthetic Reactions*, Benjamin, Menlo Park, CA 1972.
[3] R. A. Rossi, C. C. Camusso, O. D. Madoery, *J. Org. Chem. 39* (1974) 3254.
[4] W. Reppe, O. Schlichting, K. Klager, T. Toepel, *Justus Liebigs Ann. Chem. 560* (1948) 1.
[5] H. Cho, R. G. Harvey, *J. Org. Chem. 40* (1975) 3097.
[6] J. M. Bellama, J. B. Davison, *J. Organomet. Chem. 86* (1975) 69; G. Märkl, B. Alig, E. Eckl, *Tetrahedron Lett. 24* (1983) 1955.
[7] E. J. Eisenbach, R. C. Bansal, D. V. Hertzler, W. P. Duncan, P. W. K. Flanagan, M. C. Hamming, *J. Org. Chem. 35* (1970) 1265.
[8] R. Dietz in M. M. Baizer, H. Lund (Eds.): *Organic Electrochemistry*, Marcel Dekker, New York 1983.
[9] H. Muth, M. Sauerbier in *Houben-Weyl-Müller: Methoden der Organischen Chemie, Bd. IV/1c*, Thieme, Stuttgart 1980, p. 613.
[10] R. A. Benkeser, F. G. Belmonte, J. Kang, *J. Org. Chem. 48* (1983) 2796.
[11] E. M. Kaiser, *Synthesis 1972*, 391.
[12] P. J. Grisdale, T. H. Regan, J. C. Doty, J. Figueras, J. L. R. Williams, *J. Org. Chem. 33* (1968) 1116.
[13] J. L. Dye, *Acc. Chem. Res. 1* (1968) 306.
[14] R. A. Benkeser, R. K. Agnihotri, M. L. Burrous, E. M. Kaiser, J. M. Mallan, P. W. Ryan, *J. Org. Chem. 29* (1964) 1313.
[15] B. C. Becker, W. Huber, C. Schnieders, K. Müllen, *Chem. Ber. 116* (1983) 1573.
[16] K. Müllen, W. Huber, G. Neumann, C. Schnieders, H. Unterberg, *J. Am. Chem. Soc. 107* (1985) 801.
[17] C. Schnieders, K. Müllen, W. Huber, *Tetrahedron 40* (1984) 1701.
[18] P. W. Rabideau, R. G. Harvey, *J. Org. Chem. 35* (1970) 25.
[19] A. J. Birch, G. Subba Rao, *Adv. Org. Chem. Vol. 8* (1972) p. 1.
[20] R. G. Harvey, *Synthesis 1970*, 161.
[21] H. Smith: *Chemistry in Non-aqueous Ionizing Solvents, Vol. 1, Part 2*, Wiley, New York 1963.
[22] P. W. Rabideau, D. M. Wetzel, C. A. Histud, J. R. Lawrence, *Tetrahedron Lett. 25* (1984) 31.
[23] M. Daney, H. Bouas-Laurent, B. Calas, L. Girol, N. Platzer, *J. Organomet. Chem. 188* (1980) 277.
[24] K. Müllen, *Chem. Rev. 48* (1984) 603.
[25] M. Rabinovitz, I. Willner, A. Minsky, *Acc. Chem. Res. 16* (1983) 298.
[26] W. Huber, K. Müllen, *J. Chem. Soc. Chem. Commun. 1980*, 698.
[27] W. Huber, H. Unterberg, K. Müllen, *Angew. Chem. 95* (1983) 239; *Angew. Chem. Int. Ed. Engl. 22* (1983) 242; *Angew. Chem. Suppl. 1983*, 288.
[28] L. A. Paquette, G. D. Ewing, S. D. Traynor, *J. Am. Chem. Soc. 98* (1976) 279.
[29] K. Müllen, J. F. M. Oth, H.-W. Engels, E. Vogel, *Angew. Chem. 91* (1979) 251; *Angew. Chem. Int. Ed. Engl. 18* (1979) 229.
[30] W. Huber, C. Schnieders, K. Müllen, M. Iyoda, M. Nakagawa, *Helv. Chim. Acta 69* (1986) 949.
[31] K. Müllen, W. Huber, M. Nakagawa, M. Iyoda, *J. Am. Chem. Soc. 104* (1982) 5403.
[32] K. Müllen, W. Huber, T. Meul, M. Nakagawa, M. Iyoda, *Tetrahedron 39* (1983) 1575.
[33] B. C. Becker, W. Huber, K. Müllen, *J. Am. Chem. Soc. 102* (1980) 7803.
[34] U. Edlund, *Org. Magn. Reson. 12* (1979) 661; U. Edlund, B. Eliasson, J. Kowalewski, L. Trogen, *J. Chem. Soc. Perkin Trans. 2 1981*, 1260.
[35] W. Huber, K. Müllen, R. Busch, W. Grimme, J. Heinze, *Angew. Chem. 94* (1982) 294; *Angew. Chem. Int. Ed. Engl. 21* (1982) 301; *Angew. Chem. Suppl. 1982*, 566.
[36] W. Huber, K. Müllen, O. Wennerström, *Angew. Chem. 92* (1980) 636; *Angew. Chem. Int. Ed. Engl. 19* (1980) 624; K. Müllen, H. Unterberg, W. Huber, O. Wennerström, U. Norinder, D. Tanner, *J. Am. Chem. Soc. 106* (1984) 7514.
[37] F. Gerson: *Hochauflösende ESR-Spektroskopie*, Verlag Chemie, Weinheim 1967.
[38] K. Müllen, *Helv. Chim. Acta 57* (1974) 2388.
[39] H. Spiesecke, W. G. Schneider, *Tetrahedron Lett. 1961*, 468.
[40] R. N. Young, *Prog. NMR Spectrosc. 12* (1979) 261, and references cited therein.
[41] W. Huber, *Helv. Chim. Acta 66* (1983) 2582.
[42] H. M. Deger, K. Müllen, E. Vogel, *Angew. Chem. 90* (1978) 990; *Angew. Chem. Int. Ed. Engl. 17* (1978) 957.
[43] K. Müllen, *Helv. Chim. Acta 61* (1978) 1296.
[44] D. H. O'Brien, A. J. Hart, C. R. Russel, *J. Am. Chem. Soc. 97* (1975) 4410.
[45] B. Eliasson, U. Edlund, K. Müllen, *J. Chem. Soc. Perkin Trans. 2 1986*, 937.
[46] K. Müllen, *Helv. Chim. Acta 59* (1976) 1357.
[47] V. J. Mamatyuk, V. A. Koptyug, *Zh. Org. Khim. 13* (1977) 818.
[48] Similar examples of dianionic hydrocarbons in which a charge distribution which is electrostatically apparently unfavorable can be explained on the basis of the frontier orbitals have been described; see A. Minsky, M. Rabinovitz, *J. Am. Chem. Soc. 106* (1984) 6755.
[49] A. Minsky, Y. Cohen, M. Rabinovitz, *J. Am. Chem. Soc. 107* (1985) 1501; A. Minsky, A. J. Meyer, M. Rabinovitz, *ibid. 104* (1982) 2475.
[50] V. Boekelheide, G. K. Vick, *J. Am. Chem. Soc. 78* (1956) 653.
[51] A. G. Anderson, Jr., G. M. Masada, A. F. Montana, *J. Org. Chem. 38* (1973) 1439; C. Jutz, E. Schweiger, *Synthesis 1974*, 193; K. Hafner, H. Diehl, W. Richarz, *Angew. Chem. 88* (1976) 125; *Angew. Chem. Int. Ed. Engl. 15* (1976) 108; K. Hafner, G. Knaup, unpublished.
[52] T. D. Alger, D. M. Grant, E. G. Paul, *J. Am. Chem. Soc. 88* (1966) 5397; R. B. Turner, W. S. Lindsay, V. Boekelheide, *Tetrahedron 27* (1971) 3341; A. J. Jones, P. D. Gardner, D. M. Grant, W. M. Litchman, V. Boekelheide, *J. Am. Chem. Soc. 92* (1970) 2395; A. DasGupta, N. K. DasGupta, *Theor. Chim. Acta 33* (1974) 177.
[53] K. Müllen, *Helv. Chim. Acta 61* (1978) 2307.
[54] B. Eliasson, T. Lejon, U. Edlund, *J. Chem. Soc. Chem. Commun. 1984*, 591.
[55] K. Hafner, *Pure Appl. Chem. 28* (1971) 153; K. Hafner, H. Pelster, J. Schneider, *Justus Liebigs Ann. Chem. 650* (1961) 62; K. Hafner, A. Stephan, C. Bernhard, *ibid. 650* (1961) 42.
[56] B. C. Becker, G. Neumann, H. Schmickler, K. Müllen, *Angew. Chem. 95* (1983) 238; *Angew. Chem. Int. Ed. Engl. 22* (1983) 241; *Angew. Chem. Suppl. 1983*, 282.
[57] A. Minsky, A. Y. Meyer, K. Hafner, M. Rabinovitz, *J. Am. Chem. Soc. 105* (1983) 3975.
[58] H. Prinzbach, V. Freudenberger, U. Scheidegger, *Helv. Chim. Acta 50* (1967) 1087.
[59] W. Huber, A. May, K. Müllen, *Chem. Ber. 114* (1981) 1318.
[60] M. Szwarc: *Ions and Ion Pairs in Organic Reactions*, Wiley-Interscience, New York 1974; T. E. Hogen-Esch, *Adv. Phys. Org. Chem. 15* (1977) 153; J. Smid, *Angew. Chem. 84* (1972) 127; *Angew. Chem. Int. Ed. Engl. 11* (1972) 112.
[61] J. J. Brooks, W. Rhine, G. D. Stucky, *J. Am. Chem. Soc. 94* (1972) 7346; W. E. Rhine, J. Davis, G. Stucky, *ibid. 97* (1975) 2079; W. E. Rhine, J. H. Davis, G. Stucky, *J. Organomet. Chem. 134* (1977) 139.
[62] J. J. Stezowski, H. Hoier, D. Wilhelm, T. Clark, P. von R. Schleyer, *J. Chem. Soc. Chem. Commun. 1985*, 1263; P. von R. Schleyer, *Pure Appl. Chem. 55* (1983) 355; *56* (1984) 151; W. Setzer, P. von R. Schleyer, *Adv. Organomet. Chem. 24* (1985) 353.
[63] G. Boche, H. Etzrodt, W. Massa, G. Baum, *Angew. Chem. 97* (1985) 858; *Angew. Chem. Int. Ed. Engl. 24* (1985) 863.
[64] R. J. Bushby, M. P. Tytko, *J. Organomet. Chem. 270* (1984) 265.
[65] B. Bogdanovic, S. Liao, R. Mynott, K. Schlichte, U. Westeppe, *Chem. Ber. 117* (1984) 1378.
[66] D. F. Lindow, C. N. Cortez, R. G. Harvey, *J. Am. Chem. Soc. 94* (1972) 5406.
[67] P. W. Rabideau, E. G. Burkholder, *J. Org. Chem. 43* (1978) 4283.
[68] R. G. Harvey, P. P. Fu, P. W. Rabideau, *J. Org. Chem. 41* (1976) 2706.
[69] E. Heilbronner, H. Bock: *Das HMO-Modell und seine Anwendung*, Verlag Chemie, Weinheim 1968.
[70] G. Neumann, *Diplomarbeit*, Universität Köln 1982.
[71] U. Edlund, B. Eliasson, *J. Chem. Soc. Chem. Commun. 1982*, 950.
[72] K. Hafner, private communication; W. Klinner, *Dissertation*, Technische Hochschule Darmstadt 1966.
[73] R. G. Harvey, L. Arzadon, *Tetrahedron 23* (1969) 4887.

[74] R. G. Harvey, C. C. Davis, *J. Org. Chem. 34* (1969) 3607.
[75] P. W. Rabideau, E. G. Burkholder, *J. Org. Chem. 44* (1979) 2354.
[76] H. Unterberg, *Dissertation*, Universität Köln 1985.
[77] R. Gerdil, E. A. C. Lucken, *Helv. Chim. Acta 44* (1961) 1966.
[78] D. Lipkin, G. J. Divis, R. W. Jordan, *Am. Chem. Soc. Div. Pet. Chem., Prepr. 13* (1968) D 60.
[79] F. J. Burgess, A. V. Cunliffe, D. H. Richards, P. Shadbolt, *Eur. Polym. J. 10* (1974) 193; F. J. Burgess, A. V. Cunliffe, D. H. Richards, *ibid. 10* (1974) 665.
[80] E. Hobolth, H. Lund, *Acta Chem. Scand. B 31* (1977) 395.
[81] D. Bender, H. Unterberg, K. Müllen, *Angew. Chem. 98* (1986) 446; *Angew. Chem. Int. Ed. Engl. 25* (1986) 444.
[82] E. Vogel, A. Vogel, H. K. Kübbeler, W. Sturm, *Angew. Chem. 82* (1970) 512; *Angew. Chem. Int. Ed. Engl. 9* (1970) 514.
[83] F. Gerson, K. Müllen, E. Vogel, *J. Am. Chem. Soc. 94* (1972) 2924.
[84] T. Meul, *Dissertation*, Universität Köln 1982.
[85] K. Müllen, T. Meul, E. Vogel, U. Kürschner, H. Schmickler, O. Wennerström, *Tetrahedron Lett. 26* (1985) 3091; K. Müllen, T. Meul, P. Schade, H. Schmickler, E. Vogel, unpublished.
[86] L. D. Kershner, J. M. Gaidis, H. H. Freedman, *J. Am. Chem. Soc. 94* (1972) 985.
[87] C. V. Ristagno, R. G. Lawler, *Tetrahedron Lett. 1973*, 159.
[88] R. G. Harvey, D. F. Lindow, P. W. Rabideau, *Tetrahedron 28* (1972) 2909.
[89] G. Neumann, K. Müllen, *Chimia 39* (1985) 275.
[90] C. Tintel, J. Lugtenburg, G. A. J. van Amsterdamm, C. Erkelens, J. Cornelisse, *Recl. J. R. Neth. Chem. Soc. 102* (1983) 228.
[91] R. Brandsma, C. Tintel, J. Lugtenburg, J. Cornelisse, *Synth. Commun. 15* (1985) 91.
[92] E. Vogel, H.-W. Engels, W. Huber, J. Lex, K. Müllen, *J. Am. Chem. Soc. 104* (1982) 3729.
[93] F. Sondheimer, *Pure Appl. Chem. 7* (1963) 363.
[94] J. F. M. Oth, *Pure Appl. Chem. 25* (1971) 573.
[95] V. Boekelheide, J. B. Phillips, *J. Am. Chem. Soc. 89* (1967) 1695.
[96] R. H. Mitchell, V. Boekelheide, *J. Am. Chem. Soc. 96* (1974) 1547; V. Boekelheide, *Pure Appl. Chem. 44* (1975) 751.
[97] R. H. Mitchell, W. Anker, *Tetrahedron Lett. 22* (1981) 5139.
[98] G. Neumann, *Dissertation*, Universität Köln 1985.
[99] W. Huber, J. Lex, T. Meul, K. Müllen, *Angew. Chem. 93* (1981) 401; *Angew. Chem. Int. Ed. Engl. 20* (1981) 391.
[100] W. Huber, W. Irmen, J. Lex, K. Müllen, *Tetrahedron Lett. 1982*, 3889.
[101] W. Irmen, *Dissertation*, Universität Köln 1984.
[102] V. Boekelheide, C. E. Larrabee, *J. Am. Chem. Soc. 72* (1950) 1240; D. H. Reid, *Q. Rev. Chem. Soc. 19–20* (1965–66) 274; I. Murata, *Top. Non-Benzenoid Aromatic Chem. 1* (1976) 159.
[103] H. Glaser in *Houben-Weyl-Müller: Methoden der Organischen Chemie, Bd. XI/1*, Thieme, Stuttgart 1957.
[104] P. J. Garratt in D. Barton, W. D. Ollis (Eds.): *Comprehensive Organic Chemistry, Vol. 1*, Pergamon Press, Oxford 1971, p. 361; Z. Yoshida, M. Shibata, A. Sakai, T. Sugimoto, *J. Am. Chem. Soc. 106* (1984) 6383.
[105] K. Müllen, *Pure Appl. Chem. 58* (1986) 177.
[106] G. Neumann, K. Müllen, *J. Am. Chem. Soc.*, 108 (1986) 4105.
[107] T. L. Gilchrist, D. Tuddenham, R. McCague, C. J. Moody, C. W. Rees, *J. Chem. Soc. Chem. Commun. 1981*, 657; Z. Lidert, C. W. Rees, *ibid. 1982*, 499.
[108] K. Hafer, V. Kühn, *Angew. Chem. 98* (1986) 648; *Angew. Chem. Int. Ed. Engl. 25* (1986) 632.
[109] K. Hafner, M. Goltz, *Angew. Chem. 94* (1982) 711; *Angew. Chem. Int. Ed. Engl. 21* (1982) 695; K. Hafner, H. Diehl, H. U. Süss, *ibid. 88* (1976) 121 and *15* (1976) 104; K. Hafner, H. J. Lindner, W. Ude, *ibid. 91* (1979) 175; *18* (1979) 162; H. Diehl, K. Hafner, *ibid. 88* (1976) 124 and *15* (1976) 107.
[110] B. Eliasson, *Dissertation*, Universität Umeå 1983.
[111] A comparable result is the attack of electrophiles at the quaternary positions in the reductive transformations of biphenylene; see M. E. Günther, R. Aydin, W. Buchmeier, B. Engelen, H. Günther, *Chem. Ber. 117* (1984) 1069.
[112] S. Bank, J. Bank, M. Daney, B. Latrande, H. Bouas-Laurent, *J. Org. Chem. 42* (1977) 4058.
[113] M. Daney, R. Lapouyade, *J. Organomet. Chem. 172* (1979) 385.
[114] M. Daney, R. Lapouyade, M. Mary, H. Bouas-Laurent, *J. Organomet. Chem. 92* (1975) 267.
[115] W. Irmen, W. Huber, J. Lex, K. Müllen, *Angew. Chem. 96* (1984) 800; *Angew. Chem. Int. Ed. Engl. 23* (1984) 818.
[116] A. J. Fry, T. A. Powers, K. Müllen, W. Irmen, *Tetrahedron Lett. 26* (1985) 4879.
[117] G. J. Hoytink, *Adv. Electrochem. Electrochem. Eng. 7* (1970).
[118] T. Troll, M. M. Baizer, *Electrochim. Acta 19* (1974) 951; B. S. Jensen, V. D. Parker, *J. Am. Chem. Soc. 97* (1975) 5211.
[119] K. U. Klabunde, T. Troll, K. Müllen, unpublished.
[120] G. I. Fray, R. G. Saxton: *The Chemistry of Cyclooctatetraene and its Derivatives*, Cambridge University Press, Cambridge (England) 1978.
[121] L. A. Paquette, *Tetrahedron 31* (1975) 2855.
[122] G. Schröder: *Cyclooctatetraen*, Verlag Chemie, Weinheim 1965.
[123] T. J. Katz, P. J. Garratt, *J. Am. Chem. Soc. 86* (1964) 5194.
[124] S. W. Staley, T. J. Henry, *J. Am. Chem. Soc. 91* (1969) 1239.
[125] F. A. Cotton, G. Deganello, *J. Am. Chem. Soc. 95* (1973) 396.
[126] J. F. Monthony, W. H. Okamura, *Tetrahedron 28* (1972) 4273.
[127] T. A. Antkowiak, H. Shechter, *J. Am. Chem. Soc. 94* (1972) 5361.
[128] V. D. Azatyan, *Dokl. Akad. Nauk SSSR 98* (1954) 403; *Chem. Abstr. 49* (1955) 12318i.
[129] G. Krummel, J. Lex, K. Müllen, unpublished.
[130] F. Vögtle, P. Koo Tze Mew, *Angew. Chem. 90* (1978) 58; *Angew. Chem. Int. Ed. Engl. 17* (1978) 60.
[131] J. Fiedler, K. Müllen, unpublished.
[132] E. Vogel, *Isr. J. Chem. 20* (1980) 215.
[133] W. Huber, *Helv. Chim. Acta 67* (1984) 625.
[134] K. Alder, H.-J. Ache, F. H. Block, *Chem. Ber. 93* (1960) 1888; C. F. Wilcox, Jr., R. R. Craig, *J. Am. Chem. Soc. 83* (1961) 3866; A. de Meijere, L.-U. Meyer, *Angew. Chem. 85* (1973) 908; *Angew. Chem. Int. Ed. Engl. 12* (1973) 858.
[135] P. Baierweck, D. Hoell, K. Müllen, *Angew. Chem. 97* (1985) 959; *Angew. Chem. Int. Ed. Engl. 24* (1985) 972.
[136] F. J. Burgess, A. V. Cunliffe, D. H. Richards, P. Shadbolt, *Eur. Polym. J. 10* (1974) 939.
[137] F. J. Burgess, A. V. Cunliffe, D. H. Richards, N. F. Scilly, Brit. Pat. 1403791 (1975).
[138] J. Fiedler, W. Huber, K. Müllen, *Angew. Chem. 98* (1986) 444; *Angew. Chem. Int. Ed. Engl. 25* (1986) 443.
[139] J. Fiedler, J. Heinze, K. Müllen, unpublished.
[140] R. G. Harvey, P. W. Rabideau, *Tetrahedron Lett. 1970*, 3695.
[141] A. Streitwieser, S. Suzuki, *Tetrahedron 16* (1961) 153.
[142] N. Kornblum, *Angew. Chem. 87* (1975) 797; *Angew. Chem. Int. Ed. Engl. 14* (1975) 734.
[143] T. Lund, H. Lund, *Tetrahedron Lett. 227* (1986) 95; H. Lund, J. Simonet, *J. Electroanal. Chem. 65* (1975) 205.
[144] G. Kaupp, K. Rösch, *Angew. Chem. 88* (1976) 185; *Angew. Chem. Int. Ed. Engl. 15* (1976) 163.
[145] K. Müllen, W. Huber, *Helv. Chim. Acta 61* (1978) 1310.
[146] F. Gerson, W. Huber, K. Müllen, *Angew. Chem. 90* (1978) 216; *Angew. Chem. Int. Ed. Engl. 17* (1978) 208.
[147] See [2], p. 192–194.
[148] G. Klopman in G. Klopman (Ed.): *Chemical Reactivity and Reaction Paths*, Wiley-Interscience, New York 1974, Chapter 5; R. F. Hudson, G. Klopman, *Tetrahedron Lett. 1967*, 1103; I. Fleming: *Grenzorbitale und Reaktionen organischer Verbindungen*, Verlag Chemie, Weinheim 1979, Chapter 3.1.

Transcription in Eukaryotes— The Role of Transcription Complexes and Their Components

By Edgar Wingender* and Klaus H. Seifart

The fact that DNA is transcribed into RNA has long been known and has become part of the "central dogma" of molecular genetics. The mechanisms responsible for controlling this process at the individual genes of higher cells (eukaryotes), however, are still not completely understood. RNA polymerases apparently require a number of auxiliary factors (transcription factors) for gene recognition. These factors combine with the enzyme at the gene to form a transcription complex. The structures of these complexes are starting to become clearer; most is known about the control of RNA polymerase III, the enzyme responsible for the synthesis of certain small RNA molecules. The model character of the results obtained with this system is clearly underlined by a series of recent publications. TFIIIA is an especially intensively studied protein, which is a positive regulator for the expression of ribosomal 5S RNA and possesses structural properties that were previously unknown in DNA-binding proteins. It is becoming increasingly evident that the "architecture" of TFIIIA is not an exotic curiosity but probably exemplifies a general structural plan.

1. Introduction

In order to make use of the information set down in the DNA of the chromosomes, the living cell transcribes its genes into RNA (transcription). Regulated gene expression is one of the keys to the differentiation of cells in a multicellular system. The synthesized RNA is then used for its intended purpose: it is incorporated into ribosomes as ribosomal RNA (rRNA) or is translated into proteins on the ribosomes in the form of messenger RNA (mRNA) or is charged with activated amino acids as transfer RNA (tRNA), which plays a key role in protein biosynthesis. There are, in addition, other RNA molecules which have very specialized functions, some of which will be discussed in this article.

Whereas bacterial cells only have one DNA-dependent RNA polymerase, plant and animal cells possess three such enzymes, which are specially adapted for the synthesis of different groups of RNA and have their own transcription systems. RNA polymerase I (or A) transcribes the genes for the large ribosomal RNA molecules (5.8S, 18S, and 28S rRNA), or, more precisely, the gene for their common precursor (45S RNA). RNA polymerase II (or B) synthesizes mRNA. RNA polymerase III (or C) is responsible for the transcription of genes encoding a series of relatively small RNA molecules which consist mainly of tRNA but also include the smallest ribosomal RNA species, 5S rRNA, and certain virus-associated RNAs (e.g., VA_I and VA_{II} RNA of the adenovirus).

None of these polymerases, however, directly recognizes the genes it transcribes; several auxiliary proteins, termed transcription factors (TF), are also required. These factors are divided into initiation, elongation, and termination factors. The initiation factors are of critical importance for the regulation of gene expression and will therefore be the focus of attention in this article. They combine with the enzyme at the gene to form a functional unit—the transcription complex. Electron micrographs of prokaryotic transcription complexes were published a few years ago. Information on the structure and mode of formation of eukaryotic transcription complexes, however, has only been obtained comparatively recently. This progress was made possible by the development of appropriate eukaryotic in vitro systems. Results obtained for polymerase III systems are particularly advanced, because these systems possess certain properties that make them easier to study: (1) in vitro transcription yields a correct product, i.e., initiation and termination both occur; (2) the complexes remain stable for several cycles of transcription, i.e., effective reinitiation takes place and there is a readily measurable accumulation of product; (3) in many cases the product is not subjected to significant post-transcriptional processing; (4) the concentration of transcription factors required is relatively high in comparison with the polymerase II systems. This article will therefore deal mainly with the polymerase III transcription complexes; regulatory elements at the DNA and protein levels will be discussed first before proceeding to consider some functional properties of these complexes. In a short summary, an attempt will finally be made to review present knowledge of polymerase I and II systems in order to describe some general structural properties of eukaryotic gene-regulating proteins that have recently become apparent.

2. Structure of Polymerase III Transcription Complexes

2.1. Promoter Structures

The known genes that are transcribed by RNA polymerase III (pol III genes) share an unusual property: their

[*] Dr. E. Wingender
Gesellschaft für Biotechnologische Forschung mbH
Mascheroder Weg 1, D-3300 Braunschweig (FRG)
Prof. Dr. K. H. Seifart
Institut für Physiologische Chemie I der Universität
Lahnberge, D-3550 Marburg (FRG)

promoters on the DNA are located not in front of but in the middle of the gene. Detailed studies on genes coding for various tRNA species have yielded a clear picture of the structure and function of their promoters. In these investigations, sections were deleted from the ends of the isolated, cloned genes and replaced by bacterial vector DNA. In addition, particular regions within the gene were replaced by foreign DNA. The transcription capability of these genes was then studied either in vivo by means of microinjection into *Xenopus* oocytes or in vitro by incubating cell extracts in the presence of radioactively labeled nucleoside triphosphates. The newly synthesized and thus radioactively labeled RNA formed in these experiments was subsequently isolated, separated by gel electrophoresis, and visualized with the aid of autoradiography.

These studies showed that, in the case of the gene for initiator methionine tRNA ($tRNA_i^{Met}$), any base may occupy positions 1–7; the same applies to positions from 73 onward and to a region in the middle of the gene (14–50). Changes in bases 8–13 or 51–72, however, led to a considerable reduction or even complete loss of transcription.[1] Similar results were obtained with other tRNA genes.[2,3] It was therefore concluded that tRNA genes have a split promoter whose two parts were then denoted as box (or block) A and box B (Fig. 1). "Consensus sequences" acting as general polymerase III promoters were deduced for both parts of the promoter (Fig. 1) and have since been confirmed by chemical synthesis.[4] Analysis of other genes transcribed by RNA polymerase III have shown that, for instance, the genes for adenovirus VA_I and VA_{II} RNA also have a split promoter structure.[5] The sequences of the two boxes correspond to those of the general scheme (Fig. 1). It was discovered, moreover, that this scheme also applies to genes of the so-called Alu family, which are highly repetitive sequences in the human genome (analogues are found in other species) that can be transcribed to some extent by RNA polymerase III in vitro; their function within the cell, however, is still unknown.[6]

The gene for ribosomal 5S RNA is somewhat different. An internal control region was again identified by deletion experiments performed from both ends of the gene.[7] More recent, detailed investigations, moreover, also indicated the existence of a split promoter.[8,9] However, whereas the first part of the promoter is homologous with box A of the tRNA genes, the second block is not related to box B and has therefore been denoted as box C.

Noteworthy is the distance between the beginning of the gene and box A in the 5S RNA gene, which is much greater than in the other genes—50 base pairs compared with about 10. Experiments in which the combinations of the three different boxes and the distances between them were varied helped to elucidate the function of these promoter elements in the initiation of transcription.[10] Box A is apparently the element from which the transcription machinery determines the starting point for RNA synthesis. Boxes B and C determine whether transcription begins 10 or 50 base pairs, respectively, in front of box A.

It should finally be noted that cases have been reported in which the 5′-flanking sequences of the pol III genes play an essential or modulating role in their transcription. This does not, however, seem to be a general property of these genes.[11]

2.2. Recognition of Genes by Transcription Factors

If purified RNA polymerase III is incubated with DNA in the presence of the four nucleoside triphosphates, a mixture of completely random RNA products is obtained. The polymerase initiates statistically regardless of whether the DNA contains defined genes or not[12] and terminates at one of the following clusters of at least four thymidines.[13] If, on the other hand, purified RNA polymerase is replaced by a suitably prepared cell extract, a defined transcript is produced, which is governed by the correct promoter structures found on the DNA.[12,14] The cell extract evidently contains other transcription factors (TFIII) that are needed for specific gene recognition. They can be separated from one another by fractionation on phosphocellulose and are named according to the order in which they are eluted—TFIIIA, TFIIIB, and TFIIIC.[14] The information so far obtained indicates that factors B and C are required for the transcription of all pol III genes and, in most cases, are sufficient. The additional factor, TFIIIA, is only needed for the synthesis of ribosomal 5S RNA.[8,14]

The function of TFIIIC in tRNA synthesis is analogous to that of TFIIIA in 5S RNA transcription, these factors being the primary proteins responsible for gene recognition and binding. Various methods have been employed to analyze the binding of protein to specific DNA sequences. The "footprinting" experiments are the most important, the principle of which is illustrated in Figure 2. They are usually conducted with endonuclease DNase I, but the methidiumpropyl-EDTA·Fe^{II} complex[15] is being used increasingly as a cleaving agent. An alternative approach is

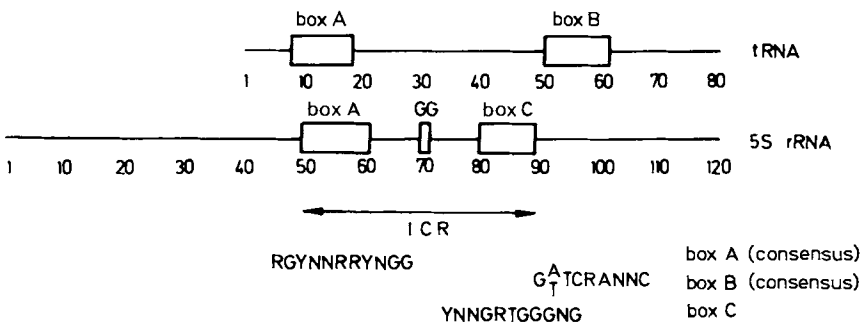

Fig. 1. Promoter structures for RNA polymerase III. tRNA genes, like the majority of other pol III genes, possess a split promotor consisting of two boxes (A and B), which are to a large extent homologous in these genes. The derived consensus sequences are given below. Box A is also found in the internal control region (ICR) of the gene for ribosomal 5S RNA. In addition, this internal control region contains at least two guanine residues (G) and a region referred to as box C. The ribonucleosides are given by the one-letter code described in *Eur. J. Biochem. 15* (1970) 205.

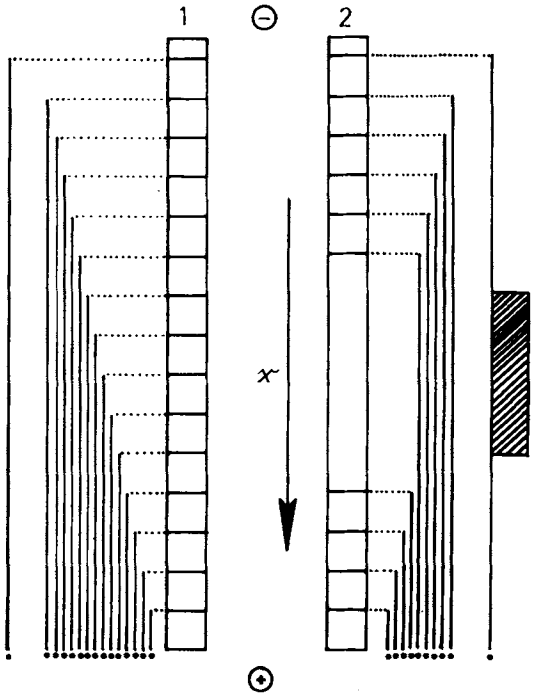

Fig. 2. Footprinting to determine protein binding sites on DNA employs a double-stranded DNA fragment that contains the suspected binding region, the end of one strand being radioactively labeled (—●). Statistical cleavage of a large number of identical fragments yields a mixture of smaller segments of varying lengths. Only those segments that are radioactively labeled (i.e., those derived from one and the same strand) can later be identified; ideally, their lengths will differ by a single nucleotide. The segments can be separated by gel electrophoresis (x = direction of migration) and visualized by autoradiography (1). If the DNA subjected to cleavage is associated with a protein, it will not be fragmented at the protein binding site (▨), the corresponding cleavage products will not be formed, and a "window" then appears in the autoradiogram, which is called the "footprint" (2).

to degrade a DNA-fragment-protein complex from both 3′ ends (with exonuclease III) up to the protected region. The binding position can then be deduced from the size of the remaining fragment. Another method for localizing specific DNA-protein contacts consists in modifying specific bases of the DNA, e.g., in methylating the DNA guanine residues with dimethyl sulfate or ethylating the DNA phosphate residues with *N*-ethyl-*N*-nitrosourea. Investigations are then performed to see how these modifications interfere with the binding of the protein or how binding of the protein protects the DNA against these modifications. Finally, the importance of individual bases in specific protein binding can be established by replacing or deleting the base in question and then carrying out tests of binding or function.

TFIIIA was found to bind specifically to the entire internal control region of the 5S rRNA gene, i.e., to boxes A and C and the region between them;[8] however, protection of the intervening region—apart from two guanine residues—may possibly only be due to steric factors.[14] Contacts in the box C region are particularly strong.[16] The published results are all based on experiments with TFIIIA from the oocytes of *Xenopus laevis*, in which this protein also adopts a storage function for 5S RNA and accounts for 15% of the total cell protein.[17] It still remains to be shown whether these findings are valid for analogous factors in, for example, human cells.

The binding properties of human TFIIIC and a yeast protein that presumably corresponds to TFIIIC to pol III promoters in tRNA and VA RNA genes have been characterized.[18–22] As is the case with the interactions between TFIIIA and the 5S RNA gene described already, the yeast TFIIIC protects the region between the boxes against degradation by DNase I.[21] Some authors have discussed a model which proposes that TFIIIC binds alternately to boxes A and B on passage of the polymerase during transcription.[21] Subsequent binding of other factors or RNA polymerase, however, has not yet been shown to produce any changes (e.g., extension) in the protected DNA regions in any of the cases cited.

2.3. Formation of Transcription Complexes

For a functional transcription complex to be formed at a pol III gene, the gene has to be recognized first. If TFIIIC is allowed to come into contact with the gene for VA RNA, for instance, it binds to the gene promoter so tightly that it is incapable of binding to a subsequently added tRNA gene. In the presence of the other transcription components (TFIIIB, polymerase III, nucleoside triphosphates), only VA RNA is synthesized.[23,24] Evidently, the VA RNA gene forms a stable preinitiation complex with TFIIIC (Fig. 3). Although this factor alone also binds to the tRNA gene it yields a metastable associate from which it can be removed.[23] In this case, TFIIIB is also required in order to produce a complex that is stable against competitive DNA (Fig. 3).

A metastable complex is also formed when TFIIIA binds to the gene for 5S rRNA and becomes stable on association of TFIIIC.[23] TFIIIB combines with this complex in a relatively slow process and is followed by RNA polymerase III (Fig. 3).[26] One of these two last steps is energy-dependent; i.e., it requires ATP. The incorporation of TFIIIB into a stable transcription complex for 5S RNA

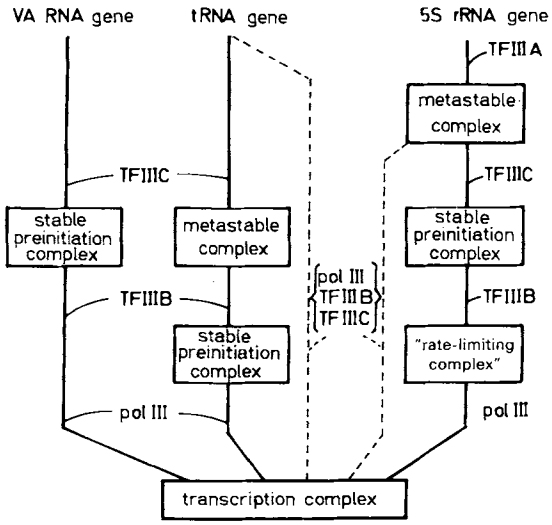

Fig. 3. Formation of transcription complexes at the genes for VA RNA, tRNA, and ribosomal 5S RNA. The steps involved in the successive binding of the individual factors and the alternative, hypothetical pathway in which preformed protein associates are bound (----) are described in the text. TF, transcription factor; pol III, RNA polymerase III.

is time-dependent; transcription begins after a lag phase of approximately 15 minutes.[17] According to recent studies, however, transcription of tRNA and VA RNA with extracts of HeLa cells (a special strain of human cancer cells) starts immediately.[24] This difference may be due to the fact that the factors TFIIIB and TFIIIC needed for tRNA and VA RNA synthesis can exist in association with RNA polymerase III;[26] association of TFIIIA has not yet been detected. These preformed protein–protein associates may possibly initiate and elongate more rapidly, for example, at tRNA genes, than does a mixture of previously separated transcription components (Fig. 3). On the 5S RNA genes, on the other hand, TFIIIA and then a polymerase complex must first assemble, a process that may account for the approximately 15-minute lag phase that is characteristic of 5S RNA.

The functions of the factors that do not initially bind to DNA are still not known. Hitherto, there was no experimental evidence to explain the role that TFIIIC may play in the transcription of 5S RNA genes (e.g., recognition of box A), nor are there any definitive findings relating to the function of TFIIIB. Recent studies, however, strongly suggest that TFIIIC binds to box A of the promoter in 5S RNA genes.[27] Moreover, TFIIIB has recently been purified from yeast and some of its molecular properties have been characterized. It is apparently a protein with a molecular weight of about 60 kDa, but proteins of lower molecular weight are also found in the preparation.[28] Protein kinase activity may be associated with TFIIIB.[28] Our own results indicate that, in any case, TFIIIB may exist as a "polymorphic" protein; the same possibly applies to TFIIIC. The properties of TFIIIA have been studied intensively and will be discussed in Section 5.

3. Properties of Polymerase III Transcription Complexes

3.1. Isolation

Because of the numerous complications encountered in the isolation and characterization of the individual transcription factors in their native forms, it seemed advantageous to develop alternative strategies for studying polymerase III transcription components. Attempts were made to isolate complete, intact transcription complexes as well as to characterize their functions and analyze their composition.

Isolation of functional transcription complexes was achieved by centrifuging complete in vitro transcription systems through glycerol gradients. All the components required for transcription of the genes for 5S rRNA[29] (Fig. 4), tRNA, and VA RNA[25,30] have now been isolated in the form of functional complexes. Kinetic studies on this material revealed that all of the RNA syntheses started without any delay (i.e., 5S RNA transcription no longer displayed a lag phase).[29]

These complexes were isolated not only by centrifugation on glycerol gradients but also by gel electrophoresis.[29] Although the polymerase II complexes isolated by the latter method[31] were inactive, nascent RNA was detected in them in the form of ternary complexes. The isolated polymerase III complexes, in contrast, are active but

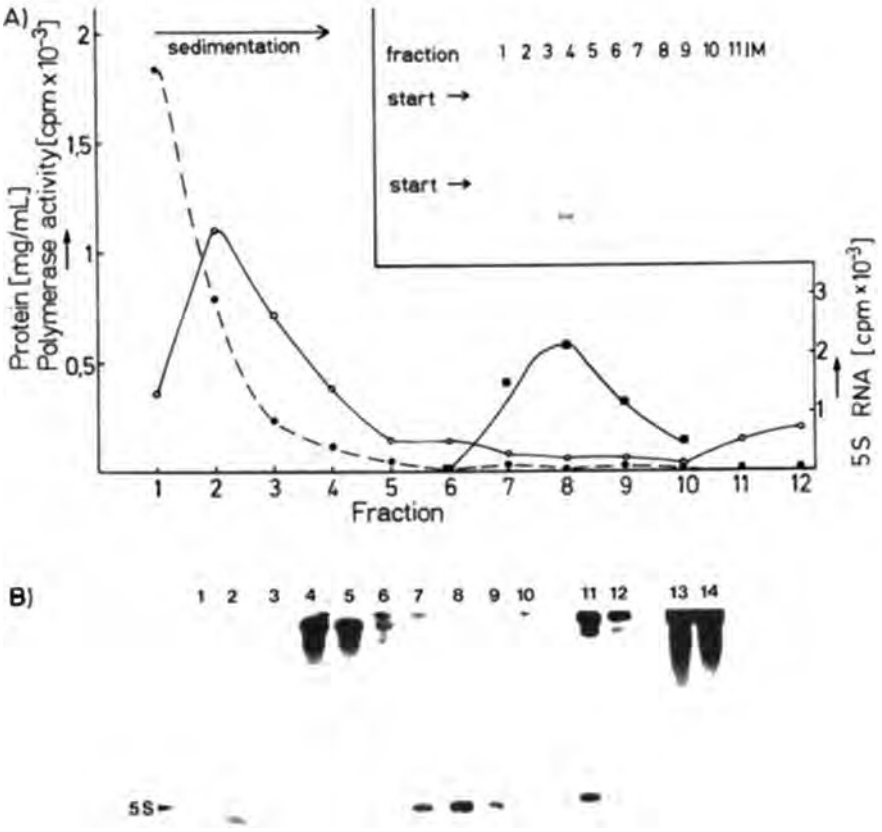

Fig. 4. Isolation of transcription complexes for ribosomal 5S RNA. A) Cytoplasmic extract from human HeLa cells was incubated with plasmid DNA containing the genes for 5S rRNA. The system was then loaded onto a glycerol gradient (20–45%) and centrifuged. After fractionation, the protein profile (---•-), the total polymerase activity (in cpm = counts per minute) (——o——), and the ability to specifically synthesize 5S RNA (——■——, see B) were analyzed. In the insert in the upper right-hand corner, the sedimentation positions of complex-bound (above) and free DNA (below) are shown after electrophoretic analysis on agarose gels; the different mobilities of the free and bound DNA in the gel are clearly visible (M, free DNA on the top gel for comparison). B) The abilities of fractions 1–10 to synthesize 5S RNA on incubation with radioactively labeled nucleoside triphosphates are shown in the correspondingly numbered lanes. The transcripts were separated on polyacrylamide gel and visualized by autoradiography. The position of 5S RNA is given; the bands in fractions 2 and 3 are of nontranscriptive origin. The band in fractions 7–9, however, is due to 5S RNA produced by RNA polymerase III, since it is no longer observed after addition of 200 μg/mL of the mushroom toxin α-amanitin (bands 11 and 12). Lane 13 shows that a specific transcript is not produced if DNA is omitted from the preincubation stage; subsequent addition of DNA does not remedy this (lane 14).

do not contain detectable quantities of the transcript.[29] The transcript appears to be rapidly released in the form of a nucleoprotein particle, as has been demonstrated in the case of 5S RNA.[32]

3.2. Stability of Transcription Complexes

Information about the nature of the interactions responsible for maintaining the structure of a transcription complex can be obtained by studying its stability at high ionic strengths. Comparison with other well-investigated DNA–protein complexes, such as the nucleosomes, can be instructive. These associates are mainly held together by salt bridges between the phosphate groups of the DNA and the basic amino-acid residues of the histones—primarily arginine and lysine side chains. The most stable of these bonds, those between histones H3 and H4 and DNA, are disrupted by salt concentrations slightly higher than 1 M NaCl.[33,34]

We showed that the salt stabilities of 5S RNA and tRNA transcription complexes far surpassed those of the nucleosomes.[24,35] The relevant experiments are presented in Figure 5; transcription components were tested to see whether they could "transfer" from transcription complexes to free, competitive genes or partial complexes. All of the transcription complexes investigated proved to be stable up to at least 1 M KCl, only the polymerase being reversibly released.[24] The complexes for 5S RNA and tRNA can even tolerate KCl concentrations of 2.5 M or more without losing the transcription factors. This property indicates the highly specific nature of the interactions existing in transcription complexes and which must therefore involve other forces besides ionic bonds between basic amino acids and the DNA phosphate backbone.

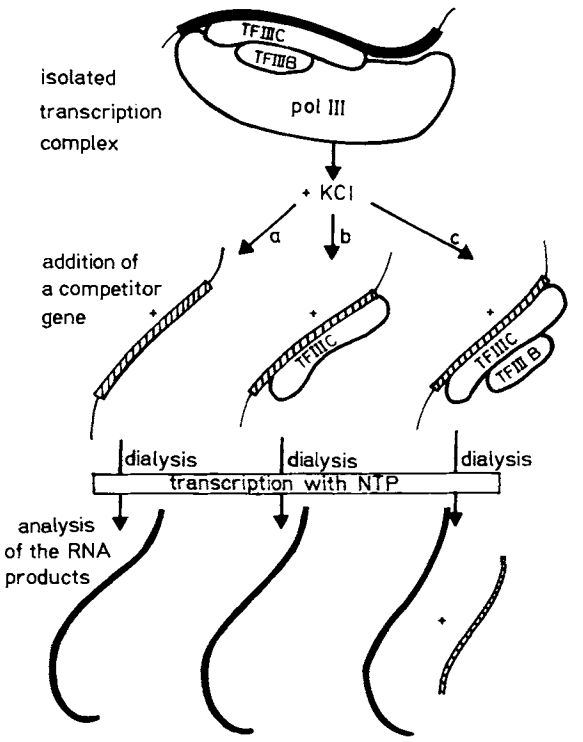

Fig. 5. Stability of transcription complexes at high ionic strengths. Isolated transcription complexes formed, for example, at a VA RNA gene (black) are adjusted to a high salt concentration (e.g., 1 M KCl) and mixed with a functionally equivalent but structurally different gene (e.g., for tRNA, hatched in the diagram) (a), which may also be loaded with TFIIIC (b) or TFIIIC + TFIIIB (c). The preparation is then dialyzed against a solution of low ionic strength, mixed with the four nucleoside triphosphates (NTP), and tested for transcription. RNA is synthesized from the first gene in all cases (black), but the second gene is only recognized if it is loaded with the necessary transcription factors (c): RNA polymerase can "shuttle" from one gene to another at high ionic strengths.

The pronounced stability of the transcription complexes at high ionic strengths encouraged us to attempt their purification by equilibrium centrifugation in cesium sulfate gradients. As expected, the RNA polymerase dissociated from all of the complexes studied but the transcription factors remained partly bound to their respective genes.[24] The resulting purified partial complexes are active on addition of RNA polymerase III; they can be examined by electron microscopy and their composition can be analyzed. Experiments of this kind are currently in progress.

4. Transcription Factors of the Other RNA Polymerases

4.1. RNA Polymerase I

RNA polymerase I transcribes the gene for 45S RNA, the precursor of the larger ribosomal RNA molecules; this precursor is then processed to yield mature 5.8S, 18S, and 28S rRNA. This means that RNA polymerase I is exclusively responsible for the transcription of a single, albeit repeated, transcription unit. Although it only has to recognize one promoter, RNA polymerase I, like all other RNA polymerases, can only do this with the help of transcription factors.

The promoter structures recognized by these factors have been elucidated in a number of organisms by using the methods described in Section 2.1. Unlike the polymerase III promoters, however, the polymerase I promoters vary considerably between different species, the differences reflecting the closeness of the biological relationships between the species in question (for a review see ref. [36]). In simplified terms it can be concluded that the promoter structures for RNA polymerase I lie within the 40 base pairs "upstream" from the rRNA genes and possibly extend to include a few base pairs in the transcribed region. The sequences within these blocks can be further differentiated into those whose deletion reduces transcription efficiency and those that are absolutely essential for transcription.[37] Finally, the thymidine found at position -1 and the guanine at position -16 in front of the gene are highly conserved, suggesting that these bases are of particular importance. Beyond this region there is an "upstream element" from about position -40 to -169 which still requires further investigation and is apparently capable of modulating transcription efficiency.[38]

In accordance with the evolutionary divergence displayed by the promoter structures of the rRNA genes, the transcription factor binding to these genes—the transcription initiation factor (TIF)-IB[39]—also varies between species; it is only exchangeable in comparatively closely re-

lated species, e.g., rat and mouse.[36] This factor, which recognizes the mouse rRNA promoter, has been purified from Ehrlich ascites cells, and digestion with exonuclease III has shown that its binding site is limited to positions -21 to -7.[39] In contrast, the analogous protein from *Acanthamoeba castellanii* protects the region of the homologous rRNA gene from positions -69 to -12 against degradation by DNase I (see Section 2.1 and Fig. 2).[40] It is especially noteworthy that the subsequent binding of RNA polymerase was visualized for the first time in a footprint experiment using this system. The protected region then extends beyond position $+20$; this is not observed with purified polymerase alone.[40]

A second transcription factor is required in addition to TIF-IB for rRNA synthesis, namely, TIF-IA (designated as TFIC by other authors).[41] TIF-IA is closely associated with polymerase I and does not display any DNA-binding properties. Its intracellular concentration varies greatly depending on the physiological state of the cells concerned. Cells in the resting phase do not contain detectable quantities of TIF-IA, and extracts from these cells are accordingly inactive as far as transcription is concerned; they can, however, synthesize rRNA on addition of the isolated factor from exponentially growing cells.[41] Only factor-associated enzyme molecules are probably capable of interacting with TIF-IB and the gene to form a transcription complex. As is the case in the polymerase III system (see Section 2.3), it is evident that protein–protein interactions are of importance for the formation of transcription complexes.

RNA polymerase I transcription complexes have also been detected[42] and isolated[43] by means of ultracentrifugation in a similar fashion to the procedure described in Section 3.1. Their properties (e.g., stability toward competitive genes or at high ionic strengths) are consistent with those of the polymerase III complexes described previously. Study of their composition could reveal, for instance, whether the modulating sequences further "upstream" are still occupied by factors. Glucocorticoid receptors are conceivable in this context because several steroid hormones have been shown to stimulate rRNA synthesis; this effect may possibly be coupled to an increased rate of cell division.[44,45] Furthermore, the region in question has been found to contain sequences that are homologous with the already known receptor binding sites in front of structural genes (cf. Section 4.2).[46]

4.2. RNA Polymerase II

Whereas the polymerase I and III systems and their regulation was relatively easy to elucidate, the RNA polymerase II system is much more complicated. This is easily understood because polymerase II transcribes the large number of protein-coding genes, which are subjected to very subtle regulatory mechanisms, e.g., during cell differentiation. As is to be expected, it appears that there are exceptions to every apparent rule.

The reader is referred to other review articles for a more detailed description of the promotor structures of structural genes.[47,48] In simplified terms, they can be outlined as follows: The "TATA box" ($TATA^{A}_{T}A^{A}_{T}$) is located about 30 base pairs upstream from the starting point of transcription. Many genes possess an additional homologous region further upstream called the "CAAT box" ($GG^{C}_{T}CAATCT$). Additional modulating/activating and regulating sequences may exist even further in front of the transcription start site, some of these being enhancers. The enhancers exert a stimulating effect even if they are positioned downstream from the gene on the DNA or are in the opposite orientation to the gene. According to present knowledge, they are responsible for binding species-, cell- or gene-specific factors. Their effects are counteracted by silencers[49] or dehancers,[50] which will not, however, be discussed in any further detail here. An interesting observation will merely be noted whose significance is still not understood: many of the known enhancers contain sequences that are homologous with the polymerase III promoters (box A and box B) described above.[51]

The subject of polymerase II control is further complicated by the fact that many genes are subjected to hormonal regulation. Special sequences are again involved which will be dealt with in more detail later on in this Section in connection with the hormone receptors that bind to them.

The "mosaic" of polymerase II transcription factors still seems to be rather fragmentary, because it very much depends on the system under investigation. It can therefore only be described with the aid of selected examples. *Roeder*'s group conducted the first systematic studies on polymerase II transcription factors (TFII),[52] the approach used being in principle the same as that described in Section 2.2 for RNA polymerase III and its factors. A transcriptionally active cell extract (from HeLa cells) is fractionated on phosphocellulose and partly on other columns, and the transcription system is then reconstituted by recombination.

These experiments were performed on the major late promoter of adenovirus 2 (AdML). At least three factors were found to be necessary for the transcription of the genes controlled by this promotor: TFIIB, TFIID, and TFIIE.[52] There is also an upstream sequence binding factor (USF) which binds specifically to sequences further upstream and strongly stimulates AdML transcription.[53] No information is so far available as to the functions of TFIIB and TFIIE. It still remains to be established whether they correspond to some of the general transcription factors (e.g., "A factor",[54] "Sp2"[55]) described by other authors. Both factors, but especially TFIIE, can associate with RNA polymerase II.

TFIID appears to be identical with the protein binding to the TATA box.[56,57] Footprint experiments with methidiumpropyl-EDTA·Fe^{II} showed that TFIID bound over a stretch of about 10 base pairs around the TATA box.[53] A protein from *Drosophila* (the "B factor") may be analogous to this factor and prevents DNase I from degrading a 65-base-pair region surrounding the TATA boxes of the histone H3 and H4 genes and the actin 5C gene.[54,58] Interestingly, this TATA-box binding factor is unnecessary in the case of the heat-shock proteins; the A factor and a special heat-shock transcription factor (HSTF) are sufficient for transcription of their genes. The HSTF binds to a region

that is directly upstream from the sequence protected by the TATA binding protein.[58] It thus does not interfere with the binding of the B factor; in fact, simultaneous binding of the two proteins can be demonstrated, but the B factor is apparently without function. HSTF is inactive, however, at the histone genes (for H3 and H4) and the actin 5C gene.[58] Therefore, HSTF is evidently not a general factor but a specific regulator protein with binding affinity for upstream activating sequences.

Sp1 is another protein that binds to a special site; it is a cellular factor that specifically activates several viral promoters; e.g., the early promoters of the SV40 and BK viruses and the promoter of the thymidine kinase gene of the *Herpes simplex* virus (HSV TK).[59] Sp1 has also been shown to bind to cellular promoters. All DNA sequences recognized by this protein contain the common sequence GGGCGG; this base sequence is usually repeated several times in succession but its orientation with respect to the starting point of transcription is not important. It has recently been demonstrated that Sp1 also activates the promoter of the AIDS retrovirus.[60]

The product of the GAL4 gene in yeast *(Saccharomyces cerevisiae)* is a further example of a positive regulatory factor. This protein binds to the upstream activating sequences (UAS) of some galactose-inducible genes via one to four binding sites.[61] Pairs of binding sites display the highest affinities if they are separated by 82–87 base pairs. This form of positive regulation can be counteracted by negative regulation, due to the product of the GAL80 gene. This negative regulation is particularly effective at the dimeric binding sites for the transcription activator.

At this point a proposal concerning the functional mechanism of certain transcription factors will be mentioned. *Di Mauro* et al. showed that even purified RNA polymerase II could recognize a number of yeast promoters, including the regulatory sequences of the GAL1–GAL10 genes or the alcohol dehydrogenase 2 gene (ADH2), when these sequences were made to adopt an optimal topological conformation.[62] These authors recently demonstrated that single-stranded stretches are formed in regulatory regions.[63] One of the functions of transcription factors thus could be to induce a DNA topology that is suitable for transcription.

Finally, hormone-induced gene regulation will be briefly dealt with; this regulation is usually positive as well. In the past few years, particular attention has been paid to the investigation of the mechanism of action of the steroid hormones. These substances bind to "their" receptors in the cytoplasm of the target cell. The resulting hormone–receptor complex then recognizes regulatory sequences in the chromatin, binds to them, and activates the relevant gene. The receptors can thus also be conceived as transcription factors. The binding regions and binding sequences of the glucocorticoid receptors in the 5′-flanking regions of several genes have now been elucidated with the aid of the previously described methods (e.g., deletions, footprint experiments): they are located upstream from certain genes of the MMTV (mouse mammary tumor virus),[64] the uteroglobin gene,[65] the lysozyme gene of the chicken,[66] and the metallothionein genes.[67] Interestingly, the latter genes can bring about induction in another way: their control regions contain metal-responsive elements which increase transcription in response to elevated intracellular concentrations of metal ions. The binding sites are also known for the progesterone receptor in front of the genes for lysozyme[66] and ovalbumin as well as for the estrogen receptor in front of the vitellogenin genes[69] (all in the chicken).

Methods have been developed for the isolation of intact transcription complexes in RNA polymerase II systems. They partly involve electrophoretic procedures or the centrifugation techniques described earlier (see Section 3.1).[43] Purification has not yet reached a stage, however, that allows analysis of the composition of these complexes.

5. Structural Properties of Transcription Factors

5.1. Structure of TFIIIA

TFIIIA requires zinc ions as a cofactor in order to recognize the 5S RNA genes. This was first demonstrated in footprint experiments with *Xenopus* factor A.[70] It was later shown that the human A factor likewise needs zinc in order to function.[34]

The cDNA of TFIIIA was sequenced at about the same time, which meant that its amino-acid sequence was also known.[71] TFIIIA is a basic protein containing 344 amino acids. Computer-aided analysis of its primary sequence showed that, starting at its *N*-terminus, TFIIIA consists of nine repetitions of a specific sequence;[72] the remaining *C*-terminal sequence may be viewed as being composed of three degenerate units of the same structural element.[73] The main feature of this motif is the constant arrangement of a pair of cysteine residues and a pair of histidine residues (Fig. 6), which are assumed to bind a zinc ion by means of tetrahedral coordination. The intervening sequence generally consists of twelve amino acids and is en-

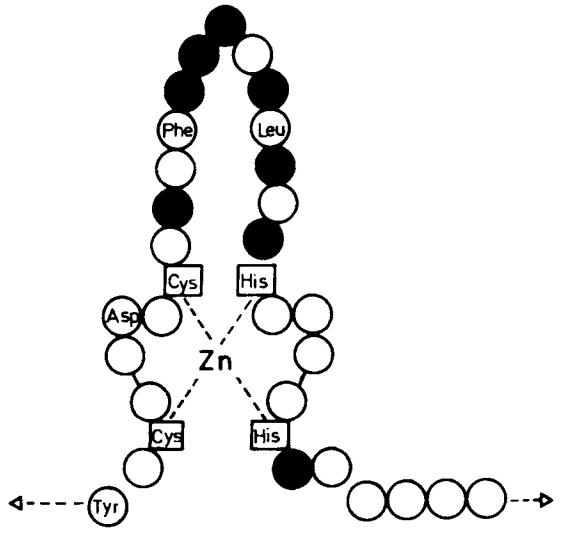

Fig. 6. The finger structure of gene-activating proteins. A metal ion (in TFIIIA, $Zn^{2\oplus}$) is tetrahedrally coordinated by two cysteine thiol groups and two imidazole groups belonging to two histidine residues; in some cases the ion is coordinated by four cysteine SH groups (cf. Table 1, Section 5.2). The intervening and neighboring amino-acid residues are denoted by circles; the names of particularly well conserved amino acids are given and the solid circles represent potential DNA-binding amino-acid residues [72].

visaged as a type of "finger" (Fig. 6) which establishes contact with a specific sequence of DNA bases.[72] Two positions, a phenylalanine and a leucine residue, are highly conserved in this finger.

Since experimental data on the three-dimensional folding of TFIIIA are not yet available, one has to rely on predictions of secondary structure. Predictions have been made by *Brown* et al.[73] and by the present authors using calculations based on the models proposed by *Chou* and *Fasman*[74] and *Robson* et al.[75] These studies indicate that an α-helix consisting of two to three turns is formed in the second half of the finger sequence. This helix includes the amino acids between the conserved phenylalanine and leucine residues but can extend as far as the two histidine residues. The cysteine residues, on the other hand, are located in regions that are less structurally organized or are characterized by a higher β-turn probability, so that they can adopt an arrangement that is suitable for binding zinc.

Helices of similar length, which embed themselves in the major groove of the DNA helix, are also responsible for establishing specific contacts between DNA and bacterial or viral repressors. The "recognition helix" of these proteins also has polar amino acids on the side facing the DNA. The hydrophobic side chains, on the other hand, are found on the other side facing the rest of the protein.[76] Stabilizing contact is thus established with a second α-helix, which is connected to the first by a turn (helix-turn-helix motif).

The TFIIIA structure, in contrast, is stabilized by the presence of a zinc ion; at any rate the structural prediction models do not suggest the existence of other regions with significant α-helix probabilities. The hydrophobicity of the "back," therefore, does not need to be very pronounced and is often restricted to the conserved leucine residue.

5.2. Other "Finger Proteins"

TFIIIA is the first example of a protein that needs metal ions for specific binding to DNA. Discovery of this property raised the question whether TFIIIA is merely an "exotic" protein or whether it conforms to a structural plan that is more generally applicable. A number of protein sequences have since been published that fit in well with the scheme derived from TFIIIA. Their "finger sequences" are compiled in Table 1. The Krüppel (Kr) gene product of *Drosophila* will be dealt with first.[77] This protein is of critical importance for the development and organization of the larval segments; mutations in its gene can produce severe malformations. The gene has been sequenced and four consecutive finger motifs were identified in the subsequently deduced amino-acid sequence—cysteine, histidine, phenylalanine, and leucine residues being located in the expected positions.

Two other *Drosophila* gene products were found to contain mutually homologous regions in which a specific consensus sequence is repeated six or seven times. It was not recognized until later that these sequences were related to the finger motifs of TFIIIA. These proteins are encoded by the serendipity locus (sry) (β- and δ-sry polypeptides);[79] their biological significance is still not clear. However, since their expression is specifically associated with certain stages of development, their functions may be connected with gene regulation.

Finally, a few proteins from yeast cells remain to be mentioned. Two consecutive, partial sequences of ADR1, which activates transcription of the gene for alcohol dehydrogenase 2,[79] fit into the "finger" scheme perfectly. Discrepancies are found, however, in other gene-regulating yeast proteins, namely, GAL4,[80] PPR1,[81] and ARG RII,[82] in which the pair of histidine residues is replaced by a second pair of cysteine residues. Phenylalanine and leucine residues, moreover, are not found in the expected positions, so that the question of homology cannot be answered with certainty.

Nevertheless, the picture of transcription-activating proteins is rounded off by the recently published finding that the finger motif also occurs in the DNA-binding domains of the glucocorticoid and estrogen receptors as well as in the v-erbA gene product. The latter is a virus-encoded protein that is involved in the oncogenic transformation of chicken cells.[83]

5.3. Importance of the Finger Structure

It would certainly be stressing the matter too far to expect all eukaryotic gene activators to contain a finger structure. First of all it must be established whether the proposed model is indeed correct. In addition, it has to be demonstrated whether proteins other than TFIIIA also bind metal ions (presumably zinc) and whether they require them to perform their functions. If this model is assumed to be correct, however, the question is raised as to the specific functions of the finger structure.

The authors of the model suggest that binding of the individual fingers to the DNA is to some extent independent and results in successive, temporary dissociation on passage of RNA polymerase III.[72] These proteins could thus bind to DNA without blocking it, as is the case, for example, with histones. Furthermore, interesting evidence indicating that DNA topology is of importance for transcription relates particularly to TFIIIA.[84,85] By analogy, it could be speculated that the binding of these proteins to RNA will prove to be another of their common features. The binding of TFIIIA to RNA has been intensively investigated; it forms a 7S-RNP particle with 5S rRNA[17] and thus contributes to feedback regulation of the expression of this gene. There is also good reason to believe that the Kr protein binds to its own mRNA or that of another control gene.[77] At any rate it is likely that this extremely interesting class of regulatory proteins will provide further surprising discoveries.

6. Summary and Outlook

The expression of specific genes is controlled by a multitude of components. The promoter structures and regulatory elements of the DNA must be recognized by transcription factors (in the broadest sense of the word). Other factors and RNA polymerase have to be firmly anchored to the gene by means of protein-protein contacts and must

Table 1. Known finger sequences. The amino-acid residues shown in boldface are essential for the finger structure and are thus particularly well conserved; other well-conserved residues are written in italics. In regions containing gaps, the amino-acid residues have been arranged so as to maintain a maximum degree of homology. The individual amino acids are designated according to the one-letter code proposed by *Dayhoff* [86].

Gene, gene product	Finger sequences
TFIII A [a]	P V V Y K R *Y* I **C** S F A D **C** G A A *Y* N K N W K *L* Q A **H** L C K **H**
	T G E K P *F* P **C** K E E G **C** E K G *F* T S L H H *L* T R **H** S L T **H**
	T G E K N *F* T **C** D S D G **C** D L R *F* T T K A N M K K **H** F N R F **H**
	N I K I C V *Y* V **C** H F E N **C** G K A *F* K K H N Q *L* K V **H** Q F S **H**
	T Q Q L P *Y* E **C** P H E G **C** D K R *F* S L P S R *L* K R **H** E K V **H**
	A G *Y* P **C** K K D D S **C** S *F* *V* G K T W T *L* Y L K **H** V A E C **H**
	Q D L *A* V **C** D V **C** N R K *F* R H K D Y *L* R D **H** Q K T **H**
	E K E R T V *Y* L **C** P R D G **C** D R S *Y* T T A F N *L* R S **H** I Q S F **H**
	E E Q R P *F* V **C** E H A G **C** G K C *F* A M K K S *L* E R **H** S V V **H**
Kr [b]	S R D K S *F* T **C** K I **C** S R S *F* G Y K H V *L* Q N **H** E R T **H**
	T G E K P *F* E **C** P E **C** D K R *F* T R D H H *L* K T **H** M R L **H**
	T G E K P *Y* H **C** S H **C** D R Q *F* V Q V A N *L* R R **H** L R V **H**
	T G E R P *Y* T **C** E I **C** D G K *F* S D S N Q *L* K S **H** M L V **H**
	T G E K P *F* E **C** E R **C** H M K *F* R R R H H *L* M N **H** K C
β-sry [c]	F T E T T E I P **C** H I **C** G E M *F* S S Q E V *L* E R **H** I K A D T C
	Q K S E Q A T **C** N V **C** G L K V K D D E V *L* D L **H** M N L **H**
	E G K T E L E **C** R Y **C** D K K *F* S H K R N V L R **H** M E V **H**
	W D K K K *Y* Q **C** D K **C** G E R *F* S L S W L M Y N **H** L M R **H**
	D A E E N A L I **C** E V **C** H Q Q *F* K T K R T Y K H **H** L R T **H**
	Q T D R P R *Y* P **C** P D **C** E K S *F* V D K Y T *L* K V **H** K R V **H**
δ-sry [c]	T K K R V K Q E **C** T T **C** G K V *Y* N S W Y Q *L* Q K **H** I S E E **H**
	S K Q P N H I **C** P I C G V I R R D E E Y *L* E L **H** M N L **H**
	E G K T E K Q **C** R Y **C** P K S *F* S R P V N T L R **H** M R S **H**
	W D K K K *Y* Q **C** E K **C** G L R *F* S Q D N L *L* Y N **H** R L R **H**
	E A E E N P I I **C** S I **C** N V S *F* K S R K T F N H **H** T L I **H**
	K E N R P R H Y **C** S V **C** P K S *F* T E R Y T *L* K M **H** M K T **H**
	E G D V V Y G V **C** L I C N T T *F* E N K K E *L* E H **H** L Q F D **H**
	D V S
ADR [d]	S G K L R S *F* V **C** E V **C** R Q E H *L* K R **H** Y R S **H**
	T N E K P *Y* P **C** G L **C** N R C *F* T R R D L *L* I R **H** A Q K I **H**
GAL4 [e]	L L S S I E Q A **C** D I **C** R L K K L K C S K E K P K *C* A K *C*
PPR1 [f]	G I S K S R T A **C** K R **C** R L K K I K C D Q E F P S *C* K R *C*
ARG R II [g]	G R A K T F T G **C** W T **C** R G R K V K C D L R H P H *C* Q R *C*
cER [h]	E S T K E T R *Y* **C** A V **C** N D Y A S G Y H Y G V W S *C* E G *C*
hGR [i]	T T G P P P K L **C** L V **C** S D E A S G C H Y G V L T *C* G S *C*
erbA [j]	S C L D K D E Q **C** V V **C** G D K A T G Y H Y R C I T *C* E G *C*

[a] Transcription factor III A [71, 72]. [b] Gene product of the Krüppel gene in *Drosophila* [77]. [c] Gene product of the *Drosophila* serendipity locus [78]. [d] Alcohol dehydrogenase-regulating protein 1 from yeast [79]. [e] Galactose metabolism-regulating protein [80]. [f] Pyrimidine pathway-regulating protein [81]. [g] Arginine metabolism-regulating protein [82]. [h] Estrogen receptor from the chicken. [i] Human glucocorticoid receptor [83]. [j] v-erbA gene product of avian erythroblastosis virus [83].

then unite to form a functional transcription complex. The necessary components can bind to the DNA successively or in the form of (partly) preformed protein complexes. In any case, the final transcription complex is extremely stable; the stability of its structural core even appears to excel that of the nucleosomes. Further study of the individual components of these complexes will shed considerable light on the mechanisms responsible both for cell differentiation in a given organism and for the regulated interaction between its organs.

Recent preliminary findings concerning the structure of gene-activating transcription factors suggest completely new developments. It seems possible that detailed analysis of the interactions taking place between DNA and proteins containing a "finger motif" may bring us a step forward in deciphering the protein-DNA binding code.

Received: August 6, 1986 [A 612 IE]
German version: *Angew. Chem. 99* (1987) 206
Translated by Dr. *Gail Schulz*, Seeheim-Jugenheim

[1] H. Hofstetter, A. Kressmann, M. L. Birnstiel, *Cell (Cambridge Mass.) 24* (1981) 573.
[2] G. Ciliberto, C. Traboni, R. Cortese, *Proc. Natl. Acad. Sci. USA 79* (1982) 1921.
[3] S. Sharp, T. Dingermann, J. Schaack, D. De Franco, D. Söll, *J. Biol. Chem. 258* (1983) 2440.
[4] M. H. Murphy, F. E. Baralle, *J. Biol. Chem. 259* (1984) 10208.
[5] R. Guilfoyle, R. Weinmann, *Proc. Natl. Acad. Sci. USA 78* (1981) 3378.
[6] G. Paolella, M. A. Lucero, M. H. Murphy, F. E. Baralle, *EMBO J. 2* (1983) 691.
[7] D. R. Engelke, S.-Y. Ng, B. S. Shastry, R. G. Roeder, *Cell (Cambridge Mass.) 19* (1980) 717.
[8] D. F. Bogenhagen, *J. Biol. Chem. 260* (1985) 6466.
[9] T. Pieler, S.-L. Oei, J. Hamm, U. Engelke, V. Erdmann, *EMBO J. 4* (1985) 3751.
[10] G. Ciliberto, G. Raugei, F. Costanze, L. Dente, R. Cortese, *Cell (Cambridge Mass.) 32* (1983) 725.
[11] J. D. Johnson, G. J. Raymond, *J. Biol. Chem. 259* (1984) 5590.
[12] W. Gruissem, M. Kotzerke, K. H. Seifart, *Eur. J. Biochem. 117* (1981) 407.
[13] N. R. Cozzarelli, S. P. Gerrard, M. Schlissel, D. D. Brown, D. F. Bogenhagen, *Cell (Cambridge Mass.) 34* (1983) 829.
[14] J. Segall, T. Matsui, R. G. Roeder, *J. Biol. Chem. 255* (1980) 11986.
[15] M. W. van Dyke, P. B. Dervan, *Nucleic Acids Res. 11* (1983) 5555.
[16] S. Sakonju, D. D. Brown, *Cell (Cambridge Mass.) 31* (1982) 395.

[17] H. R. B. Pelham, D. D. Brown, *Proc. Natl. Acad. Sci. USA 77* (1980) 4170.
[18] A. Ruet, S. Camier, W. Smagowicz, A. Sentenac, P. Fromageot, *EMBO J. 3* (1984) 343.
[19] R. Klemenz, D. J. Stillman, E. P. Geiduschek, *Proc. Natl. Acad. Sci. USA 79* (1982) 6191.
[20] D. J. Stillman, E. P. Geiduschek, *EMBO J. 3* (1984) 847.
[21] S. Camier, O. Gabrielsen, R. Baker, A. Sentenac, *EMBO J. 4* (1985) 491.
[22] R. E. Baker, O. Gabrielsen, B. D. Hall, *J. Biol. Chem. 261* (1986) 5275; S. A. Fuhrman, D. R. Engelke, E. P. Geiduschek, *ibid. 259* (1984) 1934.
[23] A. B. Lassar, P. L. Martin, R. G. Roeder, *Science (Washington D.C.) 222* (1983) 740.
[24] D. Jahn, E. Wingender, K. H. Seifart, *J. Mol. Biol.*, in press.
[25] J. J. Bieker, P. L. Martin, R. G. Roeder, *Cell (Cambridge Mass.) 40* (1985) 119.
[26] E. Wingender, D. Jahn, K. H. Seifart, *J. Biol. Chem. 261* (1986) 1409.
[27] T. Pieler, J. Hamm, R. G. Roeder, *Cell (Cambridge Mass.)*, in press.
[28] M. S. Klekamp, P. A. Weil, *J. Biol. Chem. 261* (1986) 2819.
[29] E. Wingender, X.-P. Shi, A. Houpert, K. H. Seifart, *EMBO J. 3* (1984) 1761.
[30] G. R. Greenberg, D. S. Louis, L. Duncan, R. C. Miller, G. B. Spiegelman, *J. Biol. Chem. 260* (1985) 6248.
[31] S. Ackerman, D. Bunick, R. Zandomeni, R. Weinmann, *Nucleic Acids Res. 11* (1983) 6041.
[32] A. Houpert, E. Wingender, unpublished results.
[33] J. Bode, K. Henco, E. Wingender, *Eur. J. Biochem. 110* (1980) 143.
[34] E. Wingender, K. Maass, J. Bode, *Int. J. Biol. Macromol. 3* (1981) 114.
[35] E. Wingender, D. Dilloo, K. H. Seifart, *Nucleic Acids Res. 12* (1984) 8971.
[36] J. Sommerville, *Nature (London) 310* (1984) 189.
[37] J. A. Skinner, A. Ohrlein, I. Grummt, *Proc. Natl. Acad. Sci. USA 81* (1984) 2137.
[38] I. Grummt, *Proc. Natl. Acad. Sci. USA 79* (1982) 6908.
[39] J. Clos, D. Buttgereit, I. Grummt, *Proc. Natl. Acad. Sci. USA 83* (1986) 604.
[40] E. Bateman, C. T. Iida, P. Kownin, M. R. Paule, *Proc. Natl. Acad. Sci. USA 82* (1985) 8004.
[41] D. Buttgereit, G. Pflugfelder, I. Grummt, *Nucleic Acids Res. 13* (1985) 8165.
[42] C. Wandelt, I. Grummt, *Nucleic Acids Res. 11* (1983) 3795.
[43] V. Cizewski Culotta, R. J. Wides, B. Sollner-Webb, *Mol. Cell. Biol. 5* (1985) 1582.
[44] A. Frey, K. H. Seifart, *Mol. Cell. Endocrinol. 28* (1982) 161.
[45] A. H. Cavanaugh, E. A. Thompson, Jr., *Nucleic Acids Res. 13* (1985) 3357.
[46] M. Beato (Universität Marburg), private communication.
[47] R. Breathnach, P. Chambon, *Annu. Rev. Biochem. 50* (1981) 349.
[48] E. Serfling, M. Jasin, W. Schaffner, *Trends Genet. 1* (1985) 224; S. McKnight, R. Tjian, *Cell (Cambridge Mass.) 46* (1986) 795.
[49] A. H. Brand, L. Breeden, J. Abraham, R. Sternglanz, K. Nasmyth, *Cell (Cambridge Mass.) 41* (1985) 41.
[50] E. F. Remmers, J.-Q. Yang, K. B. Marcu, *EMBO J. 5* (1986) 899.
[51] A. L. Bak, A. L. Jørgensen, *J. Theor. Biol. 108* (1984) 339.
[52] T. Matsui, J. Segall, P. A. Weil, R. G. Roeder, *J. Biol. Chem. 255* (1980) 11992.
[53] M. Sawadogo, R. G. Roeder, *Cell (Cambridge Mass.) 43* (1985) 165.
[54] C. S. Parker, J. Topol, *Cell (Cambridge Mass.) 36* (1984) 357.
[55] W. S. Dynan, R. Tjian, *Cell (Cambridge Mass.) 32* (1983) 669.
[56] B. L. Davison, J.-M. Egly, E. R. Mulvihill, P. Chambon, *Nature (London) 301* (1983) 680.
[57] X.-P. Shi, R. Lee, R. Weinmann, *Nucleic Acids Res. 14* (1986) 3729.
[58] C. S. Parker, J. Topol, *Cell (Cambridge Mass.) 37* (1984) 273.
[59] K. A. Jones, K. R. Yamamoto, R. Tjian, *Cell (Cambridge Mass.) 42* (1985) 559.
[60] K. A. Jones, J. T. Kadonaga, P. A. Luciw, R. Tjian, *Science (Washington D.C.) 232* (1986) 755.
[61] R. J. Bram, N. F. Lue, R. D. Kornberg, *EMBO J. 5* (1986) 603.
[62] E. Di Mauro, M. Caserta, R. Negri, F. Carnevali, *J. Biol. Chem. 260* (1985) 152.
[63] G. Camilloni, F. Della Seta, R. Negri, E. Di Mauro, *J. Biol. Chem. 261* (1986) 6145.
[64] C. Scheidereit, S. Geisse, H. M. Westphal, M. Beato, *Nature (London) 304* (1983) 749.
[65] A. C. B. Cato, S. Geisse, M. Wenz, H. M. Westphal, M. Beato, *EMBO J. 3* (1984) 2771.
[66] R. Renkawitz, G. Schütz, D. von der Ahe, M. Beato, *Cell (Cambridge Mass.) 37* (1984) 503.
[67] M. Karin, A. Haslinger, H. Holtgreve, R. I. Richards, P. Krauter, H. M. Westphal, M. Beato, *Nature (London) 308* (1984) 513.
[68] J. G. Compton, W. T. Schrader, B. W. O'Malley, *Proc. Natl. Acad. Sci. USA 80* (1983) 16.
[69] J.-P. Jost, M. Seldran, M. Geiser, *Proc. Natl. Acad. Sci. USA 81* (1984) 429.
[70] J. S. Hanas, D. J. Hazuda, D. F. Bogenhagen, F. Y.-H. Wu, C.-W. Wu, *J. Biol. Chem. 258* (1983) 14120.
[71] A. M. Ginsberg, B. O. King, R. G. Roeder, *Cell (Cambridge Mass.) 39* (1984) 479.
[72] J. Miller, A. D. McLachlan, A. Klug, *EMBO J. 4* (1985) 1609; S. Böhm, B. Drescher, *Stud. Biophys. 107* (1985) 237.
[73] R. S. Brown, C. Sander, P. Argos, *FEBS Lett. 186* (1985) 271.
[74] P. Y. Chou, G. D. Fasman, *Biochemistry 13* (1974) 222.
[75] B. Robson, R. H. Pain, *J. Mol. Biol. 58* (1971) 237.
[76] R. P. Wharton, M. Ptashne, *Trends Biochem. Sci. Pers. Ed. 11* (1986) 71.
[77] U. B. Rosenberg, C. Schröder, A. Preiss, A. Kienlin, S. Cote, I. Riede, H. Jäckle, *Nature (London) 319* (1986) 336.
[78] A. Vincent, H. V. Colot, M. Rosbash, *J. Mol. Biol. 186* (1985) 149.
[79] T. A. Hartshorne, H. Blumberg, E. T. Young, *Nature (London) 320* (1986) 283.
[80] A. Laughon, R. F. Gesteland, *Mol. Cell. Biol. 4* (1984) 260.
[81] B. Kammerer, A. Guyonvarch, J. C. Hubert, *J. Mol. Biol. 180* (1984) 239.
[82] F. Messenguy, E. Dubois, F. Desamps, *Eur. J. Biochem. 157* (1986) 77.
[83] A. Krust, S. Green, P. Argos, V. Kumar, P. Walter, J.-M. Bornert, P. Chambon, *EMBO J. 5* (1986) 891.
[84] W. F. Reynolds, J. M. Gottesfeld, *Proc. Natl. Acad. Sci. USA 80* (1983) 1862.
[85] E. B. Kmiec, F. Razvi, A. Worcel, *Cell (Cambridge Mass.) 45* (1986) 209.
[86] M. O. Dayhoff: *Atlas of Protein Structure, Vol. 5, Suppl. 3*, National Biomedical Research Foundation, Washington D.C. 1978.

When submitting manuscripts, authors of articles intended for publication as "Communications" are requested to read the "Notice to Authors" reproduced in the January issue of the journal following the list of contents; upon request, a copy can be obtained from the editorial office.

1D and 2D NMR Investigations of the Jump Mechanism of Co^{II} Ions in [12]Crown-4 Stacks**

By *Franz L. Dickert,* Wolfgang Gmeiner, Walter Gumbrecht,* and *Harald Meissner*

Dedicated to Dr. Heinz Kimmel on the occasion of his 60th birthday

The crown ether [12]crown-4 ([12]C4) forms sandwich complexes with divalent metal ions such as Mg^{II}, Co^{II}, Ni^{II}, and Fe^{II},[1,2] which have the composition $[M^{II}([12]C4)_2]^{2\oplus}$. The protons of the CH_2 groups in coordinated [12]C4 are chemically nonequivalent,[2] so that, despite the identical arrangement of the two [12]C4 ligands in complexes such as **1**, two ^{1}H-NMR signals are observed, which, in the case of **1**, have very large chemical shifts on account of the central paramagnetic ion (Fig. 1, signals Ⓐ and Ⓑ). In the ^{13}C-NMR spectrum, on the other hand, only one signal is observed.[2] In order to depict the rapid fluxional processes taking place within the ligands,[2] the chemically equivalent protons in the crown ethers will be symbolized in each case by rings (Fig. 3, rings A and B).

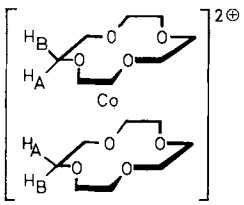

1

Upon addition of free crown ether, [12]C4, to a solution of $[Co^{II}([12]C4)_2][ClO_4]_2$ in deuterated nitromethane, ligand exchange [Eq. (a)] is observed to occur, as revealed by ^{1}H-NMR line broadening (Fig. 1). Coordination of nitromethane is ruled out, because only one ^{1}H-NMR signal is observed for the solvent. As shown by the temperature dependence of the line width of this signal, a more rapid exchange process does not take place.[3] According to conductivity measurements, moreover, no coordination of perchlorate ion occurs.[3]

$$[Co([12]C4)_2]^{2\oplus} + [12]C4^* \rightleftharpoons [Co([12]C4)([12]C4)^*]^{2\oplus} + [12]C4 \quad (a)$$

1 **1'**

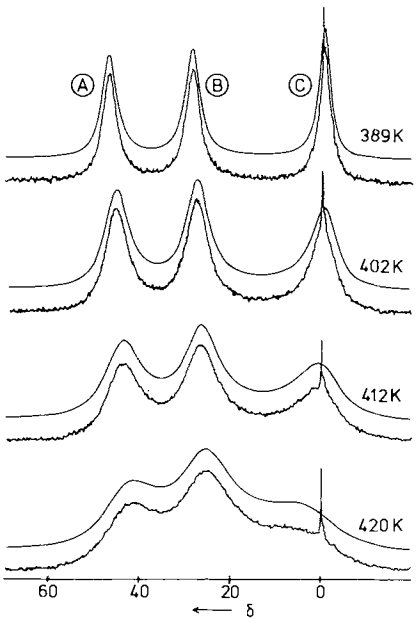

Fig. 1. Experimental and simulated 100-MHz ^{1}H-NMR spectra of 0.4 M $[Co^{II}([12]C4)_2][ClO_4]_2$ and 0.38 M [12]C4 in CD_3NO_2. Ⓐ, Ⓑ, signals of coordinated [12]C4; Ⓒ, signal of free [12]C4.

2D ^{1}H-exchange NMR spectra[4,5] provide information, via cross signals, on the resonance positions undergoing a transfer of magnetization by means of chemical processes (Fig. 2). Such exchange processes are characterized by reciprocal residence times. The "mixing time," the duration

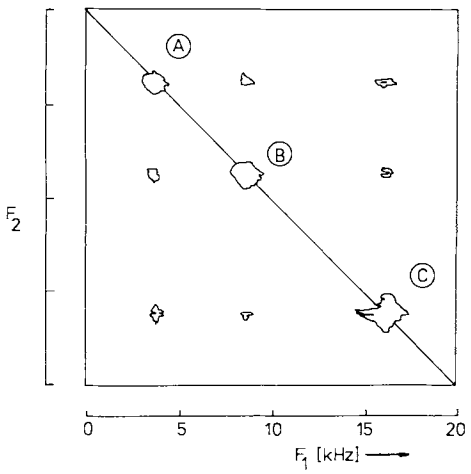

Fig. 2. 2D ^{1}H-exchange NMR spectrum (270 MHz) of 0.4 M $[Co^{II}([12]C4)_2][ClO_4]_2$ and 0.4 M [12]C4 in CD_3NO_2 at 140 °C (pulse sequence, $90°$-t_1-$90°$-t_m-$90°$-t_2; mixing time, $t_m = 1$ ms).

[*] Prof. Dr. F. L. Dickert, Dipl.-Chem. W. Gmeiner, Dr. W. Gumbrecht, Dipl.-Chem. H. Meissner
Institut für Physikalische und Theoretische Chemie
der Universität Erlangen-Nürnberg
Egerlandstrasse 3, D-8520 Erlangen (FRG)

[**] This work was supported by the Deutsche Forschungsgemeinschaft and the Fonds der Chemischen Industrie. We thank Dr. *R. Benn*, Mülheim an der Ruhr, for stimulating discussions.

of magnetization transfer in 2D NMR spectroscopy, must be so chosen that its order of magnitude agrees with the chemical residence times. Cross signals observed upon raising the temperature can thus be distinguished from nuclear Overhauser effect (NOE) signals.[4] In addition, NOE plays no role in paramagnetic complexes such as **1**. Although scalar-correlated cross signals can arise, in principle, even in the case of paramagnetic metal complexes,[6] their intensities decrease with increasing line broadening. For this reason, cross signals arising at high temperatures (Fig. 2) may be ascribed to an exchange process.

Surprisingly, the 2D NMR data (Fig. 2), as well as simulation of the 1D NMR spectra[7,8] (Fig. 1), indicate that, in the system **1**/[12]C4, not only an exchange process between free and coordinated crown ether (A↔C and B↔C) but also one between the magnetization A and B (A↔B) is occurring. The mechanism upon which Equation (a) is based is not so simple, therefore, as might have been expected; namely, replacement of the oxygen atoms of a coordinated [12]C4 consecutively by those of the free crown ether.

The experimental results can be best explained by assuming a stacklike aggregation between the complex **1** and free [12]C4 (Fig. 3). This model is also supported by the first-order rate law for the dissociation of the complex in nitromethane,[2] which is surprisingly observed even for relatively small concentrations (0.1 M) of complex and free crown ether. Accordingly, under the conditions of measurement of the ^{1}H-NMR spectra in Figures 1 and 2, a practically quantitative association of complex and free crown ether is presumably occurring. The structure shown in Figure 3 is most likely from a topological viewpoint, since it guarantees an optimal dispersive interaction between the complex and the free ligand.

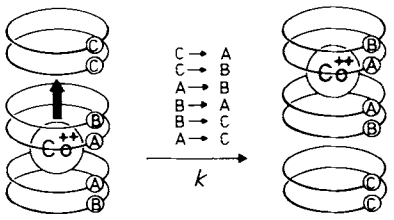

Fig. 3. Stack formation and jump mechanism for the system $[Co^{II}([12]C4)_2]^{2\oplus}$/[12]C4.

The 1D and 2D NMR spectra (Fig. 1 and 2) can be rationalized by assuming that the Co^{II} ion "jumps" through the stack of crown ether rings during the ligand exchange reaction [Eq. (a)]. In this process, the upper, free [12]C4 is bound and the lower, coordinated ligand is released. This also explains the exchange process between the magnetization A and B.

An alternative to this model is the existence of complexes of lower coordination number as intermediates, in which a crown ether is only coordinated through one oxygen atom. It is thereby possible, by flipping the ligand, to achieve likewise an exchange of A and B. A monodentate-bound ligand would undergo ready substitution by free crown ether, however, and magnetization transfer between A and B would no longer occur.

The exact kinetic parameters have been determined by simulation of the spectra (Fig. 1).[7,8] In this way, one obtains rate constants for the jumping of the Co^{II} ions within the [12]C4 stack (110 °C: $k = 105 \pm 10\ s^{-1}$; $\Delta H^{+} = 102 \pm 10$ kJ/mol; $\Delta S^{+} = 57 \pm 20$ J/K mol).

The rate constants or the activation enthalpy of this process provide a very sensitive criterion for the cavity diameter of the macrocycles and the diameter of the ions. A close parallel exists with the pore mechanism[9] in the transfer of ions through biomembranes. In such cases, ions must also pass through channels, e.g., those formed by dimeric gramicidin molecules, the coordinated solvent molecules being removed in the process.

Received: September 1, 1986;
revised: December 30, 1986 [Z 1914 IE]
German version: *Angew. Chem. 99* (1987) 238

[1] K. Meier, G. Rihs, *Angew. Chem. 97* (1985) 879; *Angew. Chem. Int. Ed. Engl. 24* (1985) 858.
[2] F. L. Dickert, W. Gumbrecht, M. Waidhas, *Z. Naturforsch. B39* (1984) 1755.
[3] W. Gmeiner, *Diplomarbeit*, Universität Erlangen-Nürnberg 1985.
[4] J. Jeener, B. H. Meier, P. Bachmann, R. R. Ernst, *J. Chem. Phys. 71* (1979) 4546.
[5] R. Benn, *Angew. Chem. 94* (1982) 633; *Angew. Chem. Int. Ed. Engl. 21* (1982) 626.
[6] W. Peters, M. Fuchs, H. Sicius, W. Kuchen, *Angew. Chem. 97* (1985) 217; *Angew. Chem. Int. Ed. Engl. 24* (1985) 231.
[7] H. M. McConnel, *J. Chem. Phys. 28* (1958) 430.
[8] J. Sandström: *Dynamic NMR Spectroscopy*, Academic Press, London 1982.
[9] E. Bamberg, P. Läuger, *J. Membrane Biol. 11* (1973) 177.

1,1′-Diarsaferrocene**

By *Arthur J. Ashe III,* Samir Mahmoud, Christoph Elschenbroich,* and *Martin Wünsch*

Heterometallocenes of the group 5B elements are of considerable interest for the study of p_π-p_π bonding of main group elements. Although phosphaferrocenes,[1] ring-substituted arsaferrocenes,[2] and stibaferrocenes are known,[3] we wished to obtain the parent 1,1′-diarsaferrocene **1** in order to compare it with bis(arsabenzene)chromium **2**[4] and arsabenzene **3**.[5] Unfortunately, the potential precursor of **1**, 1-phenylarsole **7**, had been available only in low yield through a synthesis involving the explosive 1,4-diiodobutadiyne.[6] We now wish to report on an efficient synthesis of 1-phenylarsole **7** and its conversion to 1,1′-diarsaferrocene **1**.

The readily available mixture of isomeric 1,4-dichloro-1,3-butadienes **6**[7] reacts with dilithiophenylarsane in

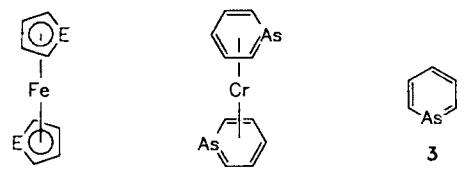

1, E = As
4, E = P
5, E = CH

2

3

[*] Prof. Dr. A. J. Ashe III, S. Mahmoud
Department of Chemistry, University of Michigan
Ann Arbor, MI 48 109 (USA)
Prof. Dr. C. Elschenbroich, Dipl.-Chem. M. Wünsch
Fachbereich Chemie der Universität
Hans-Meerwein-Strasse, D-3550 Marburg 1 (FRG)

[**] This work was supported by the Petroleum Research Fund (administered by the American Chemical Society) and the Horace H. Rackham Fund.

ether at 25 °C to afford 1-phenylarsole **7** (25% yield).[8] The reaction is not stereospecific, since either pure (*Z,Z*)- or (*E,Z*)-1,4-dichloro-1,3-butadiene **6** gives 1-phenylarsole **7** in the same yield. Similarly, dilithiophenylphosphane reacts with the mixed 1,4-dichlorobutadienes **6** to give 1-phenylphosphole in 25% yield, a procedure that offers an alternative to available literature preparations of *C*-unsubstituted phospholes.[9] The reaction of 1-phenylarsole **7** with lithium in tetrahydrofuran (THF) followed by treatment with $FeCl_2$ affords 1,1'-diarsaferrocene **1** in 50% yield as deep red, air-stable, monoclinic crystals (m.p. = 195 °C).[8, 10] NMR, UV, and mass spectra are similar to those of 1,1-diphosphaferrocene **4** (for NMR data see Table 1).

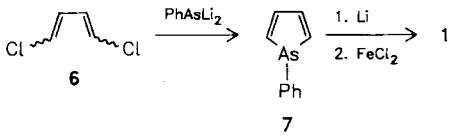

Table 1. ^{1}H- and ^{13}C-NMR chemical shift values (δ values) of **1** and **4** [a].

		1	**4**
^{1}H-NMR	H_α	4.38 [b]	3.79 [c]
	H_β	5.14 [b]	4.88 [c]
^{13}C-NMR	C_α	88.0	79.3 [d]
	C_β	84.0	82.0 [d]

[a] In [D_6]benzene at 300 MHz, δ values relative to TMS. [b] Satisfactory spectral simulation using the Bruker PANIC program is achieved for $J_{2,3}=4.5$ Hz, $J_{2,4}=J_{2,5}=0.9$ Hz, and $J_{3,4}=3.2$ Hz. [c] Satisfactory spectral simulation for $J_{1,2}=37.5$ Hz, $J_{1,3}=5.6$ Hz, $J_{2,3}=4.15$ Hz, $J_{2,4}=J_{2,5}=0.9$ Hz, and $J_{3,4}=2.5$ Hz. [d] See [1a].

Like the parent complex ferrocene **5** and the heteroarene analogue bis(arsabenzene)chromium **2**, **1** may be electrochemically oxidized as well as reduced. Cyclovoltammetry yields the redox potentials $E_{1/2}(\mathbf{1/1}^{\oplus\oplus}) = 0.730 \pm 0.015$ V [−38 °C in 1,2-dimethoxyethane (DME)/tetra-*n*-butylammonium perchlorate (TBAP) versus the saturated calomel electrode (SCE), $v \geq 20$ mV s^{-1}, $I_{pa}/I_{pc} \approx 1.0$] and $E_{1/2}(\mathbf{1/1}^{\ominus\ominus}) = -2.190 \pm 0.01$ V [−40 °C in DME/TBAP vs. SCE, $v \geq 1$ V s^{-1}, $I_{pa}/I_{pc} = 0.98$]. As observed for the couple $[(\eta^6\text{-}C_6H_6)_2Cr]/[\eta^6\text{-}C_5H_5As)_2Cr$ **2**,[4] replacement of two CH units of **5** by two As atoms leads to anodic shifts of the redox potentials (+0.24 V for the oxidation, +0.74 V for the reduction).[11] Obviously, compared with the cyclopentadienyl ring, the arsacyclopentadienyl ring is more effective in withdrawing electron density from the central metal, thereby stabilizing the HOMO of **1**, and in accommodating additional charge into the LUMO. Similar trends are observed in the case of **4**.[12]

Like arsabenzene,[13] 1,1'-diarsaferrocene **1** undergoes rapid acid-catalyzed deuterium exchange. At −20 °C in CF_3CO_2D/CH_2Cl_2, **1** exchanges its four α-protons in 1 min, although heating to 70 °C for 7 h allows only partial exchange at the β-position. In competition experiments, an α-hydrogen undergoes exchange 165 times faster than a hydrogen of ferrocene, while a β-hydrogen exchanges 4 times more slowly than the hydrogen at the 4-position of toluene. Although the scale is only semiquantitative, the relative reactivity of α/β positions must exceed 10^6.[14, 15] Similarly, acetylation with acetyl chloride/$AlCl_3$ in CH_2Cl_2 at 25 °C gives exclusively the α-acetyl derivative of **1**.[16] This large directive effect is much greater than that reported for substituted ferrocenes[17] but is similar to that found for arsabenzene **3**[13] and for metal-complexed heterocycles.[18]

Received: September 24, 1986;
revised: December 11, 1986 [Z 1935 IE]
German version: *Angew. Chem. 99* (1987) 249

[1] a) G. de Lauzon, B. Deschamps, J. Fischer, F. Mathey, A. Mitschler, *J. Am. Chem. Soc. 102* (1980) 994; b) pentaphosphaferrocene was recently described: O. J. Scherer, T. Brück, *Angew. Chem. 99* (1987) 59; *Angew. Chem. Int. Ed. Engl. 26* (1987) 59.
[2] G. Thiollet, F. Mathey, R. Poilblanc, *Inorg. Chim. Acta 32* (1979) L67.
[3] A. J. Ashe III, T. R. Diephouse, *J. Organomet. Chem. 202* (1980) C95.
[4] C. Elschenbroich, J. Kroker, W. Massa, M. Wünsch, A. J. Ashe III, *Angew. Chem. 98* (1986) 562; *Angew. Chem. Int. Ed. Engl. 25* (1986) 571.
[5] A. J. Ashe III, *Top. Curr. Chem. 105* (1982) 125.
[6] A. J. Ashe III, F. J. Drone, *Organometallics 4* (1985) 1478.
[7] R. Criegee, W. Hörauf, W. D. Schellenberg, *Chem. Ber. 86* (1953) 126.
[8] *Experimental procedure*: 7: A solution of **6** (1.58 g, 12.5 mmol) in 50 mL of ether was added dropwise to a solution of dilithiophenylarsane, which had been prepared from 2.0 g (13 mmol) of phenylarsane in 250 mL of ether and 16.3 mL (26 mmol) of 1.6 M *n*-butyllithium in hexane. After 60 min stirring at 25 °C, the solvent was removed and the residue extracted with pentane. Vacuum distillation gave 0.65 g (25%) of 7.—**1**: 7 (0.3 g, 1.27 mmol) and excess lithium wire (0.1 g) in 5 mL of THF were stirred together for 3 h at 25 °C. The deep blue-green solution was decanted into a flask containing 0.06 g (0.45 mmol) of $AlCl_3$ in 30 mL of THF at 0 °C. The solution was then decanted into a flask containing 0.37 g (2.9 mmol) of $FeCl_2$ in 30 mL of THF. After 24 h stirring, the solution was removed and the residue extracted with benzene and purified by chromatography (silica gel, benzene/pentane) to give 200 mg (50%) of red crystals of **1**. For a similar procedure see: F. Mathey, G. DeLauzon, *Organomet. Synth. 3* (1986) 259.
[9] L. D. Quin, J. G. Bryson, *J. Am. Chem. Soc. 89* (1967) 5984; F. Mathey, R. Mankowski-Farelier, *Org. Magn. Reson. 4* (1972) 171.
[10] The crystal packing of disordered crystals of **1** is the same as for **2** (space group $P2_1/n$: $a=628.4(1)$, $b=770.2(2)$, $c=946.9(2)$ pm; $\beta=96.35(2)°$, $Z=2$).
[11] $E_{1/2}(\mathbf{5/5}^{\oplus\ominus}) = 0.49$ V (DME/TBAP vs. SCE) (C. Elschenbroich, E. Bilger, R. D. Ernst, D. R. Wilson, M. S. Kralik, *Organometallics 4* (1985) 2068. $E_{1/2}(\mathbf{5/5}^{\ominus\ominus}) = -2.93$ V (*N,N'*-dimethylformamide/*n*Bu_4NI vs. SCE): Y. Mugnier, C. Moise, J. Tirouflet, E. Laviron, *J. Organomet. Chem. 186* (1980) C49.
[12] P. Lemoine, M. Gross, P. Braunstein, F. Mathey, B. Deschamps, J. H. Nelson, *Organometallics 3* (1984) 1303. Electrochemical measurements on **4** were run in propylene carbonate/tetraethylammonium perchlorate. Owing to the disparity in solvent/electrolyte, a quantitative comparison with our data for **1** is not warranted.
[13] A. J. Ashe III, W.-T. Chan, T. W. Smith, K. M. Taba, *J. Org. Chem. 46* (1981) 881.
[14] At 70 °C in trifluoroacetic acid, pentamethylbenzene undergoes proton isotopic exchange 1.7×10^5 times faster than that measured for the 4-position of toluene [15]. We find that, at −20 °C in mixtures of CH_2Cl_2/CF_3CO_2D, ferrocene **5** undergoes exchange 2.4 times faster than pentamethylbenzene. This allows an approximate comparison between the α and β positions.
[15] K. E. Richards, A. L. Wilkinson, G. J. Wright, *Aust. J. Chem. 25* (1972) 2369.
[16] ^{1}H-NMR (C_6D_6): $\delta = 1.95$ (s, CH_3CO), 4.13, 4.25 (dtt, $J=4.5$, 0.8, 0.8 Hz, H2', H5'), 4.40 (dd, $J=4.5$, 0.8 Hz, H5), 5.03, 5.17 (ddd, $J=4.5$, 3.2, 0.8 Hz, H3', H4'), 5.12 (dd, $J=4.5$, 3.2 Hz, H4), 5.77 (dd, $J=3.2$, 0.8 Hz, H3).
[17] V. N. Setkina, D. N. Kursanov, *Usp. Khim. 37* (1968) 1729.
[18] A. J. Ashe III, E. Meyers, P. Shu, T. Von Lehmann, J. Bastide, *J. Am. Chem. Soc. 97* (1975) 6865.

Synthesis and Structure of $[(C_5Me_5)_2Mo_2S_4 \cdot SO_3]$: Concerning the Oxidation of Sulfur Ligands in Transition-Metal Complexes

By *Henri Brunner, Ulrich Klement, Joachim Pfauntsch,* and *Joachim Wachter**

The oxidation of coordinated sulfur in transition-metal complexes can result not only in the formation of sulfur

[*] Dr. J. Wachter, Prof. Dr. H. Brunner, Dr. U. Klement, J. Pfauntsch
Institut für Anorganische Chemie der Universität
Universitätsstrasse 31, D-8400 Regensburg (FRG)

oxides,[1] which would be highly reactive as free species, but also of sulfur-rich anions such as $S_2O_2^{2\ominus}$ and $S_3O_2^{2\ominus}$.[2] Such reactions are of interest as model systems for the microbiological oxidation of $S^{2\ominus}$ and S^0 in nature.[2a] We report here on the unusual oxidation of an $S^{2\ominus}$ ligand to an $S_2O_3^{2\ominus}$ ligand that is coordinated in a novel fashion.

When a dark blue solution of complex **1** is stirred in toluene while being exposed to air (50 °C, 18 h), **2** precipitates in 17% yield as red-violet crystals. Other sulfur-containing complexes, **3**, which can only be separated with difficulty by column chromatography, remain in solution.[3]

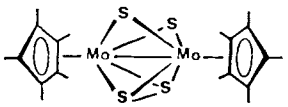

1

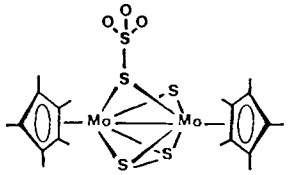

2

$[(C_5Me_5)_2Mo_2O_nS_{4-n}]$

n=1,2

3

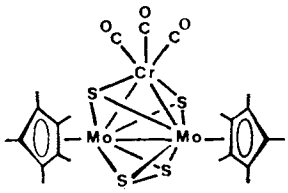

4

Single crystals of **2** suitable for an X-ray structure analysis can be prepared by slow evaporation of a solution of **2** in acetone/CH_2Cl_2 (5:8) exposed to air. The structure of **2** (Fig. 1) is characterized by one each of the following ligands: $S^{2\ominus}$, $S_2^{2\ominus}$, and $S_2O_3^{2\ominus}$, the S atoms of which lie roughly in a plane that is perpendicular to the Mo–Mo axis.[4] The methyl groups of the nearly parallel C_5Me_5 rings are oriented in an eclipsed fashion. This reveals a close structural relationship between **1** and **2**, which is also reflected in their largely similar bonding parameters.[5] A further structural feature, however, is the pseudotetrahedral SO_3 unit fixed at one of the $S^{2\ominus}$ ligands. To the best of our knowledge, thiosulfate ligands bridging two metal centers were previously unknown. Noteworthy, in contrast to the distances in mononuclear, *S*-coordinated thiosulfate complexes, is the very long S4–S5 distance (2.168(2) Å).[6]

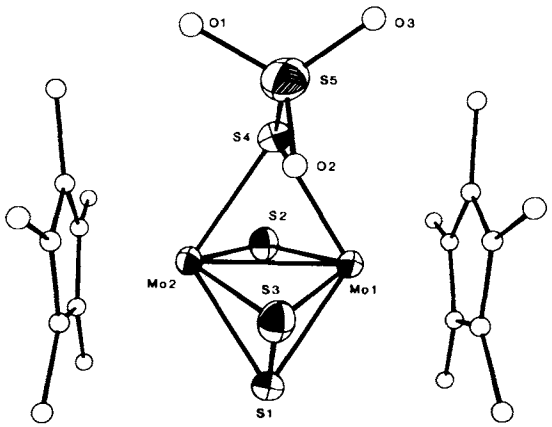

Fig. 1. Structure of **2** in the crystal (ORTEP plot). Selected bond lengths [Å] and angles [°]: Mo1-Mo2 2.628(0), Mo1-S1 2.426(1), Mo1-S2 2.308(1), Mo1-S3 2.432(1), Mo1-S4 2.449(1), S1-S3 2.066(2), S4-S5 2.168(2); Mo1-S1-Mo2 65.50(3), Mo1-S2-Mo2 69.32(3), Mo1-S3-Mo2 65.42(3), Mo1-S4-Mo2 64.91(3), Mo1-S4-S5 113.22(5), Mo2-S4-S5 112.82(5), S4-S5-O 104.4(3) (average).

Significant thermal instability of **2** is indicated by the mass spectra, which only show the molecular ion of **1**, even when the field desorption technique is used. In contrast, the elemental analyses confirm the calculated S/O ratio. The $S_2O_3^{2\ominus}$ ligand is revealed in the IR spectrum (KBr) by the strong $\tilde{\nu}_{SO}$ absorptions at 1246, 1217 (sh), 1207, 1010, and 600 cm^{-1}. A similar pattern is observed for monodentate-bonded sulfate ligands, which is interpreted as being a consequence of local C_{3v} symmetry.[7]

The long S–S distance in the thiosulfate ligand suggests a certain lability of this bond. Indeed, **2** reacts with $[Cr(CO)_5(thf)]$ (CH_2Cl_2/tetrahydrofuran (THF) mixtures, 20 °C) under mild conditions with loss of the SO_3 unit to give the trinuclear cluster **4**,[8] whose structure corresponds to that of the isoelectronic complex **5**[9].

$[(C_5Me_5)_2Mo_2S_4Fe(CO)_2]$ **5**

The formation of **2** may be explained in terms of several steps. Under the reaction conditions, isomerization of **1** to give complexes containing terminal M=S groups[5] precedes the substitution of sulfur by oxygen. The SO_2 thereby formed requires an additional catalytic oxidation, however, by an as yet unidentified complex component. In this way, approximately 37% of the sulfur released from **1** is converted into SO_3, which then adds to **1**.[3] In this connection, it is interesting that the nucleophilic character of the μ-S ligand can already be used to bind SO_2.[10] The simultaneous formation of an SO_2 and an S_2 ligand from an initially sulfur-poor complex by oxidation with air has also been described already.[11] Further experiments are required, however, to elucidate the details of the oxidation mechanism.

Received: November 17, 1986;
revised: December 17, 1986 [Z 1987 IE]
German version: *Angew. Chem.* *99* (1987) 268

[1] Overview of S-O ligands: M. Herberhold, B. Schmidkonz, *J. Organomet. Chem.* *308* (1986) 35; G. A. Zank, C. A. Jones, T. B. Rauchfuss, A. L. Rheingold, *Inorg. Chem.* *25* (1986) 1886.

[2] a) A. Müller, U. Reinsch-Vogell, E. Krickemeyer, H. Bögge, *Angew. Chem.* *94* (1982) 784; *Angew. Chem. Int. Ed. Engl.* *21* (1982) 790; b) F. R. Fronczek, R. E. Marsh, W. P. Schaefer, *J. Am. Chem. Soc.* *104* (1982) 3382.

[3] H. Brunner, H. Kauermann, J. Pfauntsch, J. Wachter, *J. Organomet. Chem.*, in press.

[4] **2**: space group $P2_1/c$, $a=13.813(3)$, $b=10.635(5)$, $c=16.87(2)$ Å, $\beta=93.14(4)°$, $V=2475.1$ Å^3, $Z=4$. Nonius CAD4 diffractometer ($Mo_{K\alpha}$), $2<\theta<29°$, 4577 measured reflections with $I>3\sigma(I)$, Patterson as well as Multan and Fourier methods, anisotropic refinement to $R_w=0.061$. Further details of the crystal structure investigation may be obtained from the Fachinformationszentrum Energie, Physik, Mathematik GmbH, D-7514 Eggenstein-Leopoldshafen 2 (FRG), on quoting the depository number CSD-52226, the names of the authors, and the journal citation.

[5] H. Brunner, W. Meier, J. Wachter, E. Guggolz, T. Zahn, M. L. Ziegler, *Organometallics 1* (1982) 1107.

[6] Examples of *S*-coordinated thiosulfate complexes: $Na_3[Au(S_2O_3)_2]$ (d_{S-S} 2.051(5) and 2.069(5) Å): H. Ruben, A. Zalkin, M. O. Faltens, D. H. Templeton, *Inorg. Chem.* *13* (1974) 1836; $[(NH_3)_5Co(S_2O_3)]Cl$ (d_{S-S} 2.048(2) Å): S. Baggio, *J. Chem. Soc. A 1970*, 2384; R. J. Restivo, G. Ferguson, R. J. Balahura, *Inorg. Chem.* *16* (1977) 167.

[7] R. W. Horn, E. Weissberger, J. P. Collman, *Inorg. Chem.* *9* (1970) 2367.

[8] **4**: ^{1}H-NMR ($CDCl_3$): $\delta=1.86$. IR (CH_2Cl_2): $\tilde{\nu}_{CO}=1937$, 1879, 1823 cm^{-1}. Molecular weight 726 (center of gravity; FD-MS from toluene; corresponds to M^+ of **4**). Correct elemental analyses (C,H,S).

[9] H. Brunner, N. Janietz, J. Wachter, T. Zahn, M. L. Ziegler, *Angew. Chem.* *97* (1985) 122; *Angew. Chem. Int. Ed. Engl.* *24* (1985) 133.

[10] G. J. Kubas, H. J. Wasserman, R. R. Ryan, *Organometallics 4* (1985) 419. These authors reported on SO_2 adducts of $[(C_5H_5)W(CO)_2]_2S_2$, and **1**; however, they could not further characterize the latter.

[11] A. Müller, W. Eltzner, R. Jostes, H. Bögge, E. Diemann, J. Schimanski, H. Lueken, *Angew. Chem.* *96* (1984) 355; *Angew. Chem. Int. Ed. Engl.* *23* (1985) 389.

 © VCH Verlagsgesellschaft mbH, D-6940 Weinheim, 1987 0570-0833/87/0303-0231 $ 02.50/0

[2.2](1,4)Benzo[*g*]chrysenoparacyclophane Dianion: A Novel, Paratropic, Double-Layered Carbanion

By *Ron Frim, Mordecai Rabinovitz,* Henning Hopf,** and *Joachim Hucker*

Dedicated to Professor Heinz A. Staab on the occasion of his 60th birthday

An outstanding characteristic of the [2_n]paracyclophanes is the through-space interaction of the two fully conjugated π-electron systems of the separate layers. As demonstrated by the electronic properties of these compounds,[1] the two layers afford one overall π-electron system.[2] Very little is known, however, about this interaction in charged paracyclophanes. Diatropic anionic [2.2]paracyclophanes have previously been studied,[3–7] but no paratropic [2.2]paracyclophane systems have been reported.

We wish to report the first [2.2]paracyclophane in which a 4nπ paratropic dianion interacts with a virtually neutral benzene moiety. In this case the benzene ring acts as an "observer," which is located in a well-defined position and can be used to probe the spatial interactions due to both charge and anisotropy effects.

The system of choice is [2.2](1,4)benzo[*g*]chrysenoparacyclophane dianion $\mathbf{1}^{2\ominus}$, obtained by metal reduction of [2.2](1,4)benzo[*g*]chrysenoparacyclophane **1** (Scheme 1). To synthesize this hydrocarbon,[8,9] the phosphonate **2** ($R=CH_2PO(OEt)_2$), prepared from 4-bromomethyl[2.2]paracyclophane **2** ($R=CH_2Br$) by the Arbuzov reaction, was coupled with commercially available 9-formylphenanthrene in a Wittig–Horner reaction. The resulting *trans* olefin,[9] formed in 40% yield, was subsequently photocyclized by irradiation (Hanau TQ 150 lamp) in a toluene solution in the presence of iodine, providing the benzochrysenophane **1**[9] (18%, colorless plates, m.p. = 267–269°, dec.). By an analogous route, the chrysenophane **3**[9] was prepared (34%, colorless needles, m.p. = 149–152°C) with a Wittig reaction between 4-formyl[2.2]paracyclophane **2** (R = CHO) and the ylid prepared from 1-naphthylmethylphosphonium bromide serving as the initial step.

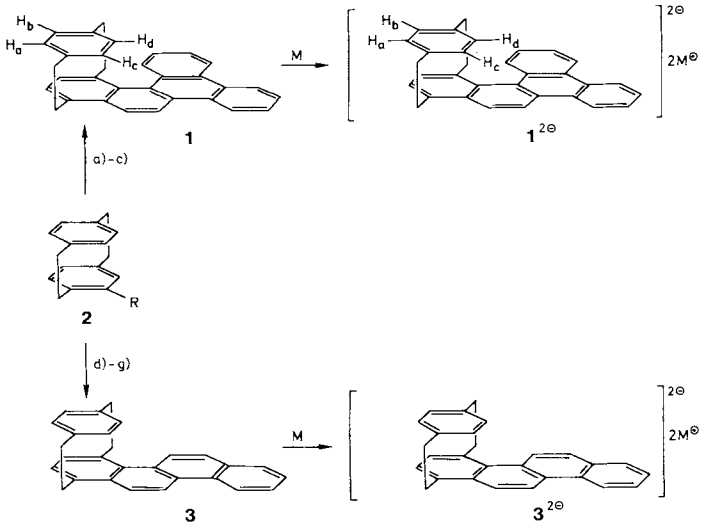

Scheme 1. a) *n*BuLi, THF; b) 9-formylphenanthrene; c) *hν*, I_2, toluene; d) NaH, THF; e) α-naphthyl-CH_2PPh_3Br; f) **2** (R = CHO), THF; g) *hν*, I_2, toluene.

Reaction of **1** with lithium or sodium metal in [D_8]tetrahydrofuran ([D_8]THF) at −78°C afforded deep green solutions, which exhibit well-resolved ^{1}H- and ^{13}C-NMR spectra (Table 1). The ^{1}H-NMR signals appear in the range of $\delta = 10.31$–0.91 for the sodium salt and 9.81–1.14 for the lithium salt. The bridge protons of $\mathbf{1}^{2\ominus}/2\,Li^{\oplus}$ give rise to broad signals at $\delta = 1.14$ (2H), 1.65 (2H), 2.82 (2H), and 3.15 (2H). The dianionic nature of $\mathbf{1}^{2\ominus}/2\,Li^{\oplus}$ and $\mathbf{1}^{2\ominus}/2\,Na^{\oplus}$ is deduced from the general similarity of their spectra to those of other dianionic polycycles which were studied previously.[10] Quenching of $\mathbf{1}^{2\ominus}/2\,Li^{\oplus}$ and $\mathbf{1}^{2\ominus}/2\,Na^{\oplus}$ with oxygen gave **1** in quantitative yield, proving that no skeletal changes had occurred.

The most revealing part of the spectra of $\mathbf{1}^{2\ominus}$ (both lithium and sodium salts) consists of four doublets (one proton each), which are attributed to the atoms H_a, H_b, H_c,

Table 1. ^{1}H- and ^{13}C-NMR data for **1** and $\mathbf{1}^{2\ominus}$ [a].

Compd	^{1}H-NMR	^{13}C-NMR
1 [b]	8.95–8.85 (2H, m, p. [c]), 8.79 (2H, d, $J=9.0$, p.), 8.64 (1H, dd, $J_1=8.2$, $J_2=1.14$, p.), 8.07 (1H, d, $J=8.97$, p.), 7.88–7.77 (2H, m, p.), 7.76–7.54 (2H, m, p.), 7.66 (1H, d, $J=7.36$, p.), 6.95 (1H, d, $J=7.31$, p.), 6.70 (H_a, dd, $J_1=7.9$, $J_2=1.9$, bz. [c]), 6.57 (H_b, dd, $J_1=7.9$, $J_2=1.8$, bz.), 5.92 (H_c, dd, $J_1=7.78$, $J_2=1.8$, bz.), 5.08 (H_c, dd, $J_1=7.8$, $J_2=1.8$, bz.), 4.05–3.97 (1H, m, bridge), 3.63–3.09 (5H, m, bridge), 2.72–2.57 (1H, m, bridge), 2.42–2.31 (1H, m, bridge)	139.7, 139.6, 138.8, 137.0, 136.7, 133.8, 132.9, 132.0, 131.3, 131.2, 131.0, 130.7, 130.4, 129.6, 129.2, 128.5, 128.1, 127.8, 127.7, 127.3, 126.8, 126.3, 124.8, 124.4, 124.2, 124.1, 120.2 (arom. C), 39.0, 35.6, 35.5, 34.3 (bridge C)
$\mathbf{1}^{2\ominus}/2\,Na^{\oplus}$ [d]	10.31 (H_d, d, $J=6.96$, bz.), 8.68 (H_c, d, $J=6.96$, bz.), 7.96 (H_b, d, $J=6.22$, bz.), 6.46 (H_a, d, $J=6.2$, bz.), 4.90 (1H, t, $J=6.5$, p.), 4.76 (1H, t, $J=6.68$, p.), 4.08 (2H, unresolved d, $J=6.7$, p.), 3.93 (1H, d, $J=7.2$, p.), 3.82 (1H, d, $J=7.3$, p.), 3.31 (3H, unresolved d, $J=6.9$, p.), 2.32–2.22 (3H, m, bridge and p.), 1.98 (1H, unresolved t, p.), 1.48 (1H, unresolved m, bridge), 1.27 (1H, d, $J=6.1$, p.), 0.91 (3H, unresolved m, bridge) and protons under THF at 3.67	175.9, 152.7, 148.7, 146.2, 146.0, 143.6, 140.4, 135.2, 134.2, 134.1, 131.8, 131.0, 130.7, 129.4, 127.4, 125.0, 124.3, 124.0, 120.2, 117.4, 117.1, 116.5, 115.2, 114.6, 104.3, 103.5, 100.8 (arom. C), 37.3, 35.5, 33.2, 33.0 (bridge C)
$\mathbf{1}^{2\ominus}/2\,Li^{\oplus}$ [d]	9.81 (H_d, d, $J=6.8$, bz.), 8.40 (H_c, d, $J=6.9$, bz.), 7.54 (H_b, d, $J=6.5$, bz.), 6.49 (H_a, d, $J=7.1$, bz.), 5.27 (1H, t, $J=6.5$, p.), 5.16 (1H, t, $J=6.7$, p.), 4.64 (1H, t, $J=7.2$, p.), 4.59 (1H, d, $J=7.3$, p.), 4.46 (2H, unresolved d, p.), 4.01 (1H, d, $J=6.6$, p.), 3.67 (2H, under solvent signals, p.), 3.15 (1H, unresolved m, bridge), 2.29 (1H, d, $J=8.0$, p.), 2.82 (1H, unresolved d, bridge), 2.16 (1H, unresolved t, p.), 1.65 (1H, unresolved m, bridge), 1.53 (1H, d, $J=6.2$, p.), 1.30 (1H, unresolved m), 1.14 (2H, unresolved m, bridge)	175.5, 151.3, 146.8, 144.8, 144.5, 142.9, 140.6, 133.8, 132.2, 131.6, 130.6, 129.9, 126.6, 125.2, 124.7, 124.1, 123.6, 120.7, 117.4, 116.9, 115.8, 113.7, 104.6, 102.0, 95.0, 70.7 (arom. C), 37.1, 35.5, 33.5, 33.1 (bridge C)

[a] Chemical shifts (δ values) are given relative to TMS (int. standard); coupling constants in Hz. The chemical shifts were calibrated by the THF line at $\delta = 3.67$ ppm. The ^{13}C-NMR spectra are {^{1}H}-broadband decoupled and were measured in [D_8]THF. [b] At room temperature. [c] p = protons of the polycyclic layer; bz. = protons of the benzene ring. [d] At 195°K.

[*] Prof. Dr. M. Rabinovitz, R. Frim
Department of Organic Chemistry,
The Hebrew University of Jerusalem
Jerusalem 91904 (Israel)
Prof. Dr. H. Hopf, Dipl.-Chem. J. Hucker
Institut für Organische Chemie der Technischen Universität
Hagenring 30, D-3300 Braunschweig (FRG)

and H_d of the benzene ring, as deduced from double resonance experiments (Table 1). A conspicuous feature of these spectra is the appearance of extremely low-field bands assigned to H_c and H_d. These signals are registered at $\delta = 10.31$ and 8.68 for $\mathbf{1}^{2\ominus}/2\,Na^{\oplus}$, a very low field indeed for a neutral benzene moiety. Similar reduction experiments carried out on **3** resulted in only very broad ^{1}H-NMR signals in the same region as for $\mathbf{1}^{2\ominus}$, and no well-resolved spectrum could be obtained. Quenching of $\mathbf{3}^{2\ominus}$ with O_2 afforded the neutral hydrocarbon **3** in good yield. Prolonged reaction of **1** and **3** with the alkali metals led to cleavage of the cyclophane bridge, as shown by quenching experiments. A similar cleavage was previously observed by *Müllen* et al. in the case of the nonparatropic anthracenophane dianion.[4]

When a double-deck anion such as $\mathbf{1}^{2\ominus}$ is formed, the following spectral phenomena are expected: (a) a high-field shift of the protons of the charged polycyclic moiety due to the negative charge and even more so to the formation of a paratropic 4nπ species;[11,12] (b) a shift of the signals of the neutral benzene ring due to the through-space interaction between the two conjugated layers.

As expected, the protons of the charged polycyclic layer of $\mathbf{1}^{2\ominus}$ show pronounced high-field shifts. The peculiar and unusually pronounced low-field shift of the uncharged benzene ring layer is caused by the through-space interaction between the two π-electron systems and is attributed to the anisotropy of the 4nπ doubly charged polycyclic moiety of $\mathbf{1}^{2\ominus}$. The extremely low-field signals of one proton of the benzene moiety ($\delta = 10.31$ for $\mathbf{1}^{2\ominus}/2\,Na^{\oplus}$!) show that this interaction is very significant. In the neutral hydrocarbon **1** the benzene protons H_c and H_d are shifted to higher field (Table 1). H_d is presumably shifted more than H_c,[2a] while H_a and H_b appear in the "normal" aromatic region of the ^{1}H-NMR spectrum. In dianion $\mathbf{1}^{2\ominus}$, owing to its different electronic structure and anisotropy, the same arguments should be reversed. The protons H_c and H_d are more influenced by the paratropicity of the charged 4nπ layer, and the H_d signal is most strongly shifted.

The ^{13}C-NMR spectrum for the aromatic carbons of $\mathbf{1}^{2\ominus}/2\,Li^{\oplus}$ and $\mathbf{1}^{2\ominus}/2\,Na^{\oplus}$ are in the range of $\delta = 70$–175 versus a range of $\delta = 120$–140 for **1** (Table 1). The center of gravity of the ^{13}C-NMR spectra of $\mathbf{1}^{2\ominus}/2\,Li^{\oplus}$ and $\mathbf{1}^{2\ominus}/2\,Na^{\oplus}$ did not change significantly. This may arise from the opposing effects of the charge and the anisotropy already mentioned. The failure in observing [2.2](1,4)chrysenoparacyclophane dianion $\mathbf{3}^{2\ominus}$ arises not only from the cleavage of the bridge but also is due to the nature of the dianion.[13] It has been previously demonstrated that the appearance and line shape of polycyclic 4nπ conjugated dianions is a function of several parameters.[12] Similarly, chrysene dianion affords a much less resolved ^{1}H-NMR spectrum than benzo[*g*]chrysene dianion.[10]

From the above it can be concluded that in the first paratropic three-dimensional 4nπ system, $\mathbf{1}^{2\ominus}$, a new aspect of the through-space interaction involves a charged polycyclic layer and a neutral benzene layer, reminiscent of the paracyclophane donor-acceptor systems studied by *Staab* et al.[14]

Received: October 16, 1986;
revised: December 5, 1986 [Z 1953 IE]
German version: *Angew. Chem.* 99 (1987) 243

[1] For recent reviews on the chemistry of [2$_n$]cyclophanes see: a) V. Boekelheide, *Acc. Chem. Res. 13* (1980) 65; b) H. Hopf, J. Kleinschroth, *Angew. Chem. 94* (1982) 485; *Angew. Chem. Int. Ed. Engl. 21* (1982) 469; c) V. Boekelheide, *Top. Curr. Chem. 113* (1983) 87; d) H. Hopf in P. M. Keehn, S. M. Rosenfeld (Eds.): *The Cyclophanes*, Academic Press, New York 1983, p. 521ff; e) E. Heilbronner, Z. Yang, *Top. Curr. Chem. 115* (1984) 1; f) F. Gerson, *ibid. 115* (1984) 57.

[2] a) H. Hopf, C. Mlynek, S. El-Tamany, L. Ernst, *J. Am. Chem. Soc. 107* (1985) 6620; b) R. T. Swann, A. W. Hanson, V. Boekelheide, *ibid. 108* (1986) 3324; c) H. Hopf, *Naturwissenschaften 70* (1983) 349.

[3] M. W. Haenel, *Tetrahedron Lett. 1977*, 1273.

[4] W. Huber, H. Unterberg, K. Müllen, *Angew. Chem. 95* (1983) 239; *Angew. Chem. Int. Ed. Engl. 22* (1983) 242; *Angew. Chem. Suppl. 1983*, 288.

[5] Two *s*-indacenophane dianions have been prepared by *Hafner* and coworkers; see P. Bickert, *Dissertation*, Technische Hochschule Darmstadt 1983.

[6] a) W. Huber, K. Müllen, O. Wennerström, *Angew. Chem. 92* (1980) 636; *Angew. Chem. Int. Ed. Engl. 19* (1980) 624; b) K. Müllen, H. Unterberg, W. Huber, O. Wennerström, U. Norinder, D. Tanner, B. Thulin, *J. Am. Chem. Soc. 106* (1984) 7514.

[7] R. Frim, F.-W. Raulfs, H. Hopf, M. Rabinovitz, *Angew. Chem. 98* (1986) 160; *Angew. Chem. Int. Ed. Engl. 25* (1986) 174.

[8] J. Hucker, *Diplomarbeit*, Technische Universität Braunschweig 1986.

[9] All new compounds were characterized by their NMR, IR, UV, and mass spectra as well as their elemental analyses.

[10] A. Mannschreck, R. Frim, M. Rabinovitz, unpublished results. The ^{1}H-NMR spectrum of 12,14-di-*tert*-butylbenzo[*g*]chrysene dianion shows a very similar spectrum to that ascribed to the benzo[*g*]chrysene moiety in $\mathbf{1}^{2\ominus}$.

[11] H. Günther: *NMR Spectroscopy*, Wiley, New York 1980, p. 63–120.

[12] a) G. Fraenkel, R. E. Carter, A. McLachlan, J. H. Richards, *J. Am. Chem. Soc. 82* (1960) 5846; b) R. Schaefer, W. F. Schneider, *Can. J. Chem. 41* (1963) 966; c) H. Spiesecke, W. F. Schneider, *Tetrahedron Lett. 1961*, 468.

[13] a) A. Minsky, A. Y. Meyer, R. Poupko, M. Rabinovitz, *J. Am. Chem. Soc. 105* (1983) 2164; b) A. Minsky, A. Y. Meyer, M. Rabinovitz, *Tetrahedron 41* (1985) 785.

[14] a) J. Weiser, H. A. Staab, *Angew. Chem. 96* (1984) 602; *Angew. Chem. Int. Ed. Engl. 23* (1984) 623; b) B. Rosenau, C. Krieger, H. A. Staab, *Tetrahedron Lett. 26* (1985) 2081; c) H. Vogler, L. Schanne, H. A. Staab, *Chem. Ber. 118* (1985) 1254.

Synthesis of 2-Deoxy Sugars**

By *Bernd Giese,* Kay S. Gröninger, Tom Witzel, Hans-Gert Korth,* and *Reiner Sustmann*

2-Deoxy sugars, particularly the compounds **1**–**3** (R = H, Ac), which are required for the formation of compactin,[1] olivomycin,[2] and milbemycin,[3] are important

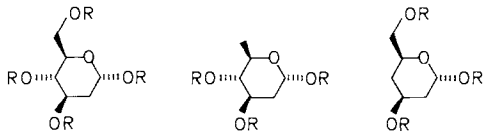

1 **2** **3**

targets of natural product synthesis. However, the syntheses of 2-deoxy sugars reported to date have been laborious; they could be prepared, for example, from glycosyl halides by reductive elimination to give the glycals followed by solvomercuration and subsequent demercuration.[4] We have now developed a new method by which glycosyl halides can be converted directly into the 2-deoxy sugars. The procedure is based on the rapid and irreversible migration of the acyloxy group in the β-acyloxyalkyl radical **4** to give the acyloxyalkyl radical **5**.[5]

[*] Prof. Dr. B. Giese, Dipl.-Ing. K. S. Gröninger, Dipl.-Ing. T. Witzel
Institut für Organische Chemie und Biochemie
der Technischen Hochschule
Petersenstrasse 22, D-6100 Darmstadt (FRG)
Dr. H.-G. Korth, Prof. Dr. R. Sustmann
Institut für Organische Chemie der Universität
Universitätsstrasse 5, D-4300 Essen (FRG)

[**] This work was supported by the Deutsche Forschungsgemeinschaft and the Fonds der Chemischen Industrie.

4 5

When glycosyl radicals are generated by halogen abstraction from the corresponding glycosyl halides,[6] it is possible to trap the rearranged radicals by using low concentrations of Bu_3SnH. Thus, addition of a 0.2-molar solution of Bu_3SnH to 0.05-molar solutions of the glucosyl bromides **6** ($R = CH_3$, C_6H_5) in refluxing benzene in the presence of 10 mol-% azobisisobutyronitrile (AIBN) over 12 hours affords the 2-deoxy sugars **7** in 80–95% yields. Analogously, galactosyl, allosyl, and xylosyl bromides afford 70–85% yields of the rearranged reduction products **8**–**10** (Table 1).[7]

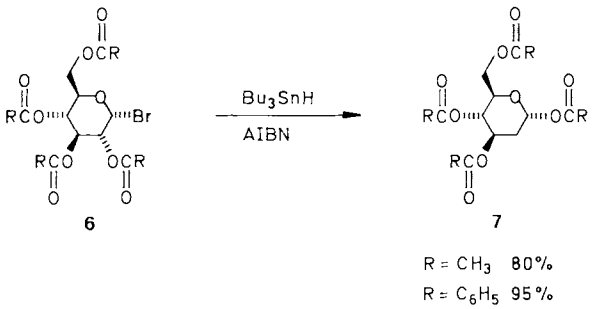

6 7

R = CH_3 80%
R = C_6H_5 95%

Table 1. Synthesis of 2-deoxy sugars from glycosyl bromides.

Glycosyl bromide	2-Deoxy sugar	Yield [%]
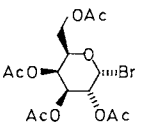	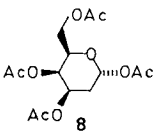 **8**	70
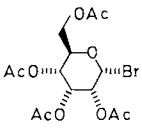	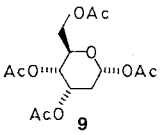 **9**	70
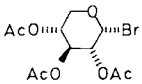	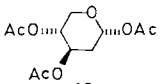 **10**	85

The deoxy sugars **2** and **3** may be prepared from the corresponding dihalides: reduction of the 1,6-diiodide **11**

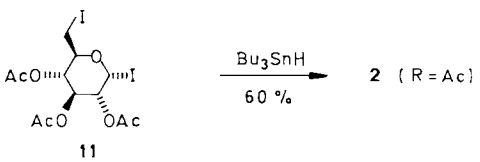

11

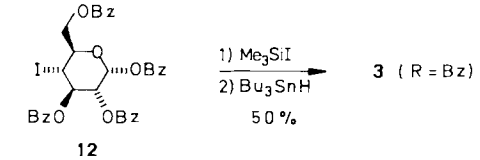

12
Bz = Ph-CO

affords a 60% yield of the deoxy sugar **2** (R = Ac). In order to synthesize **3** (R = Bz), the 4-iodoglucose **12** was subjected to iodination at the anomeric C atom with trimethylsilyl iodide and the product was reduced in situ with Bu_3SnH. Only the acetoxy group on C-2 undergoes migration (to C-1); migration from C-3 to C-4 does not occur.

This new synthetic method opens up a short and general approach to the class of 2-deoxy sugars.

Received: November 7, 1986;
supplemented: December 18, 1986 [Z 1982 IE]
German version: *Angew. Chem. 99* (1987) 246

[1] T. Rosen, M. J. Taschner, C. H. Heathcock, *J. Org. Chem. 49* (1984) 3994; P. A. Grieco, R. Lis, R. E. Zelle, J. Finn, *J. Am. Chem. Soc. 108* (1986) 5908; G. E. Keck, D. F. Kachensky, *J. Org. Chem. 51* (1986) 2487.

[2] W. R. Roush, J. A. Straub, *Tetrahedron Lett. 27* (1986) 3349, and references cited therein.

[3] R. Baker, R. H. O. Boyes, D. M. P. Broom, J. A. Devlin, C. J. Swain, *J. Chem. Soc. Chem. Commun. 1983*, 829, and references cited therein.

[4] This is also part of an industrial synthesis of compactin which is based on the procedure described in [1] and for which large amounts of Zn and Hg are required.

[5] The migration of acyloxy groups in open-chain radicals has been studied by *Ingold* et al. and by *Beckwith* et al.: L. R. C. Barclay, J. Lusztyk, K. U. Ingold, *J. Am. Chem. Soc. 106* (1984) 1793; S. Saebo, A. L. J. Beckwith, L. Radom, *ibid. 106* (1984) 5119. They obtained rearrangement rates of 10^2 to $10^4\ s^{-1}$ (75 °C). Accordingly, the rearrangement occurs at least two orders of magnitude slower than H transfer from Bu_3SnH to alkyl radicals: C. Chatgilialoglu, K. U. Ingold, J. C. Scaiano, *ibid. 103* (1981) 7739. For the migration of the acyloxy group in glucosyl radicals, see B. Giese, J. Dupuis, K. Gröninger, T. Hasskerl, T. Witzel in H. G. Viehe (Ed.): *Substituent Effects in Radical Chemistry*, Reidel, Dordrecht 1986, p. 283.

[6] J. Dupuis, B. Giese, D. Ruegge, H. Fischer, H. G. Korth, R. Sustmann, *Angew. Chem. 96* (1984) 887; *Angew. Chem. Int. Ed. Engl. 23* (1984) 896.

[7] The structures of all new compounds were determined by NMR spectroscopy: ^{1}H-NMR (300 MHz, $CDCl_3$): **2** (R = Ac): $\delta = 1.19$ (d, 3H, $J(5,6) = 6.2$ Hz; H-6), 1.92 (ddd, 1H, $J(1,2a) = 3.6$, $J(2a,2e) = 13.5$, $J(2a,3) = 12.0$ Hz; H-2a), 2.03, 2.07, 2.12 (each s, each 3H; OAc), 2.25 (ddd, 1H, $J(1,2e) = 1.5$, $J(2e,3) = 5.3$ Hz; H-2e), 3.94 (dq, 1H, $J(4,5) = 9.8$ Hz; H-5), 4.80 (t, 1H, $J(3,4) = 9.8$ Hz; H-4), 5.25 (ddd, 1H; H-3), 6.19 (dd, 1H; H-1); **3** (R = Bz): $\delta = 1.86$ (q, 1H, $J(3,4a) = J(4a,5) = J(4a,4e) = 11.2$ Hz; H-4a), 2.19 (ddd, 1H, $J(1,2a) = 3.5$, $J(2a,3) = 11.2$, $J(2a,2e) = 12.5$ Hz; H-2a), 2.42–2.48 (m, 2H; H-2e, H-4e), 4.38–4.48 (m, 3H; H-5, H-6, H-6'), 5.68 (ddt, 1H, $J(2e,3) = J(3,4e) = 4.7$ Hz; H-3), 6.69 (br. d, 1H, $J(1,2e) < 1.0$ Hz; H-1), 8.18–7.28 (m, 15H; 3 OBz); **9**: $\delta = 2.03$, 2.08, 2.11, 2.13 (each s, each 3H; OAc), 2.12–2.38 (m, 2H; H-2), 4.14 (dd, 1H, $J(5,6) = 2.0$, $J(6,6') = 12.2$ Hz; H-6), 4.34 (dd, 1H, $J(5,6') = 4.3$ Hz; H-6), 4.42 (ddd, 1H, $J(4,5) = 10.2$ Hz; H-5), 4.97 (dd, 1H, $J(3,4) = 3.1$ Hz; H-4), 5.40 (q, 1H, $J(2,3) = 3.2$ Hz; H-3), 6.16 (d, 1H, $J(1,2a) = 3.0$, $J(1,2e) < 1.0$ Hz; H-1); **10**: $\delta = 1.91$ (ddd, 1H, $J(1,2a) = 3.3$, $J(2a,3) = 9.8$, $J(2a,2e) = 13.6$ Hz; H-2a), 2.14, 2.09, 2.08 (each s, each 3H; OAc), 2.25 (ddd, 1H, $J(2e,3) = 4.9$, $J(1,2e) = 3.3$ Hz; H-2e), 3.74 (dd, 1H, $J(4,5a) = 9.0$, $J(5a,5e) = 11.6$ Hz; H-5a), 3.94 (dd, 1H, $J(4,5e) = 4.9$ Hz; H-5e), 4.93 (ddd, 1H, $J(3,4) = 8.8$ Hz; H-4), 5.28 (ddd, 1H; H-3), 6.14 (t, 1H; H-1).

Arene Adducts with Weak Interactions: Hexaethylbenzene-bis(tribromoarsane)

By *Hubert Schmidbaur,* Wolfgang Bublak, Brigitte Huber,* and *Gerhard Müller*

The study of arene–metal complexes has expanded in recent years to include the neighboring post-transition metals (Ga, In, Tl;[1] Sn, Pb;[2] Sb;[3] Bi[4]). It appeared that a borderline was reached between Al and Ga, Ge and Sn, and As and Sb, beyond which the interactions between the

[*] Prof. Dr. H. Schmidbaur, Dipl.-Chem. W. Bublak, Dipl.-Chem. B. Huber [+], Dr. G. Müller [+]
Anorganisch-chemisches Institut der Technischen Universität München
Lichtenbergstrasse 4, D-8046 Garching (FRG)

[+] X-ray structure analysis.

components become too weak, and the hapticity is reduced from η^6 to η^3 or η^2. The structures of the Menshutkin complexes of the antimony halides,[5] in particular, show clearly acentric coordination to the arenes,[6] whereas the bismuth halides still prefer hexahapto bonding.[4]

Nonetheless, there is evidence that, at least at low temperatures and for suitably substituted arenes, discrete adducts may even be obtained with *arsenic* halides: for example, *Al. Weiss* et al. used ^{35}Cl-NQR measurements to demonstrate the existence of a phase $C_6H_6 \cdot 2\,AsCl_3$, which is also revealed as a maximum of the liquidus curve (m.p. = −25.5 °C) in the phase diagram.[7] *R. A. Shaw* et al. also showed by means of phase diagrams that hexamethylbenzene forms a 1 : 1 complex with triphenylarsane, which melts as high as 144 °C.[8] The structures of these compounds, however, have remained unknown, and their bonding has been the subject of controversy.[9]

We have now succeeded in synthesizing a complex from hexaethylbenzene and arsenic tribromide and in elucidating its crystal and molecular structure. The adduct is formed from $AsBr_3$ and C_6Et_6 in toluene at room temperature and has a 2 : 1 stoichiometry, in good agreement with the results of *Al. Weiss* et al.[7] The product is easily obtained in the form of large, colorless single crystals, which are only slightly sensitive to air and moisture [Eq. (a)].

$$C_6Et_6 + 2\,AsBr_3 \longrightarrow Br_3As \cdot C_6Et_6 \cdot AsBr_3 \quad \mathbf{1} \qquad \text{(a)}$$

The X-ray structure analysis[10] of the rhombohedral crystals revealed the presence of discrete $Br_3As \cdot C_6Et_6 \cdot AsBr_3$ molecules (Fig. 1) with crystallographic $\bar{3}(S_6)$ symmetry, arranged in strings parallel to the *c* axis. The arsenic atoms are thus strictly η^6-coordinated to the arene. The two independent As–C distances differ by only a negligible amount (Fig. 1). The arsenic atoms are

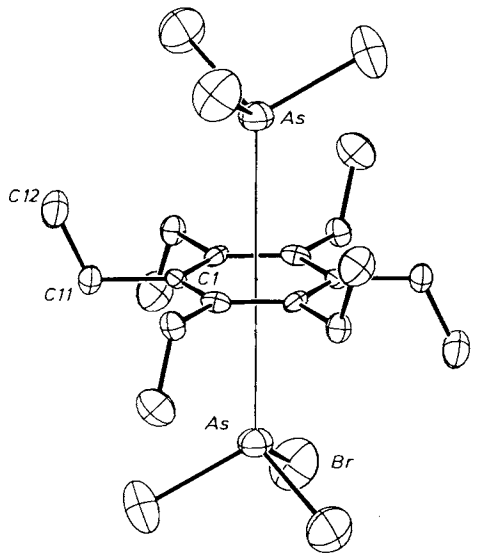

Fig. 1. Crystal structure of **1** (ORTEP plot, thermal ellipsoids at the 50% probability level, without H atoms). Distance [Å] and angles [°]: As-Br 2.322(1), As-C1 3.462(7), 3.456(7), C1-C1 1.412(5), C1-C11 1.521(7), C11-C12 1.509(9); Br-As-Br 98.9(1), C1-C1-C1 120.0(6), C1-C1-C11 120.1(6)/119.9(6), C1-C11-C12 113.3(6).

located at a distance of 3.16 Å from the centers of the aromatic rings. The methyl groups of the ethyl substituents of the arene point alternately up and down and are arranged in a staggered fashion with respect to the bromine atoms of $AsBr_3$. The geometries of the components in **1** differ only slightly from those in free $AsBr_3$[11] and free C_6Et_6.[12] This is also true for the conformation of the ethyl groups. As shown by a space-filling model of the complex (Fig. 2), the η^6-coordination of the $AsBr_3$ unit results in a large number of van der Waals contacts, which probably also contribute appreciably to the stability of **1**, since the arene-arsenic interactions alone—as judged by the distances involved—are quite weak.

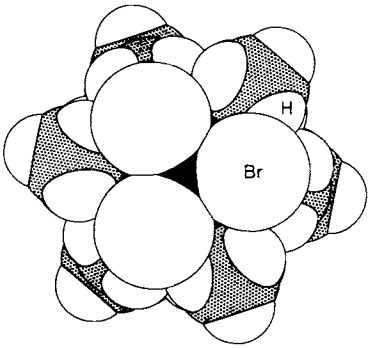

Fig. 2. Space-filling model of **1** as viewed along the $\bar{3}(S_6)$ axis (PLUTO plot), radii [Å]: As 2.0 (black), Br 1.9, C 1.7 (dotted), H 1.2).

The molecules along the string are also related to one another by $\bar{3}(S_6)$ symmetry, i.e., the bromine atoms of neighboring $AsBr_3$ molecules are likewise arranged in a staggered fashion. The intermolecular Br···Br distances (4.373(2) Å) are significantly longer than the typical van der Waals contact of 4.0 Å. Along the *c* axis, the chains are displaced by 1/3 with respect to one another, resulting in an arrangement in which the bromine atoms of one chain and the arene molecules of a neighboring chain lie opposite one another (Fig. 3). Thus, crystalline **1** does not contain the infinite halogen layers that are characteristic of crystalline arsenic trihalides.[11, 13]

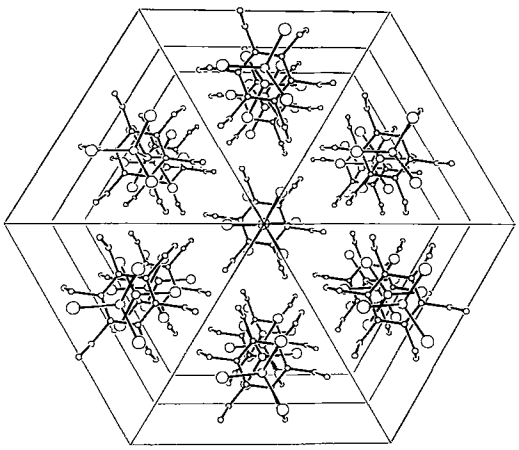

Fig. 3. Perspective view of the crystal structure of **1** along the crystallographic *c* axis (ORTEP plot).

We have been able to show that **1** is only *one* member of a whole series of analogous adducts; their structures, however, need not necessarily be based on the same structural

principle. The NQR data of crystalline $C_6H_6 \cdot 2\,AsCl_3$[7] already reveal that the chlorine atoms exist pairwise at three different sites. Therefore, further details of the structure are necessary before the bonding between the components can be discussed. Only in this way will it be possible to determine whether theoretical concepts based on the structural model derived for one particular species can be extended to other cases. The frequently confirmed observation that the hapticity in the series of As, Sb, and Bi complexes can easily vary between η^6 and smaller η values indicates that the movement of the metal(oid) atoms on the surface of the arenes is characterized by an extremely flat potential energy profile. Accordingly, small perturbations, e.g., steric effects, can have strong effects on the structure.

Experimental Procedure

A solution of C_6Et_6 (0.51 g, 2.07 mmol) in toluene (7 mL) was added to a solution of $AsBr_3$ (1.26 g, 4.00 mmol) in 1.5 mL of toluene at room temperature. The mixture was then cooled to -20°C, which resulted in the formation of large, colorless crystals. The crystals were filtered off, washed with cold toluene (0°C), and dried in vacuo. Yield: 2.34 g (64%); m.p. = 113°C. Correct elemental analyses were obtained. IR (Nujol/CsI): $\tilde{\nu}$ [cm^{-1}] = 1095, 980, 830, 740, 730, 675, 670, 375, 270.

Received: December 1, 1986 [Z 1996 IE]
German version: *Angew. Chem. 99* (1987) 248

[1] H. Schmidbaur, *Angew. Chem. 97* (1985) 893; *Angew. Chem. Int. Ed. Engl. 24* (1985) 893.
[2] M. S. Weininger, P. F. Rodesiler, E. L. Amma, *Inorg. Chem. 18* (1979) 751.
[3] D. Mootz, V. Händler, *Z. Anorg. Allg. Chem. 533* (1986) 23; *521* (1985) 121.
[4] A. Schier, J. M. Wallis, G. Müller, H. Schmidbaur, *Angew. Chem. 98* (1986) 742; *Angew. Chem. Int. Ed. Engl. 25* (1986) 752.
[5] W. Smith, G. W. Davis, *J. Chem. Soc. Trans. 41* (1882) 411; B. N. Menshutkin, *Zh. Russ. Fiz. Khim. Ova. Chast Khim. 43* (1911) 1298, 1786; G. Peyronel, S. Buffagni, I. M. Vezzosi, *Gazz. Chim. Ital. 98* (1968) 147.
[6] See [3] and R. Hulme, J. T. Szymanski, *Acta Crystallogr. Sect. B 25* (1969) 753; G. Bombieri, G. Peyronel, I. M. Vezzosi, *Inorg. Chim. Acta 6* (1972) 349; A. Demaldé, A. Mangia, M. Nardelli, G. Pelizzi, M. E. Vidoni Tani, *Acta Crystallogr. Sect. B 28* (1972) 147; R. Hulme, D. J. E. McMullen, *J. Chem. Soc. Dalton Trans. 1976*, 802; A. Lipka, D. Mootz, *Z. Anorg. Allg. Chem. 440* (1978) 217; *Z. Naturforsch. B 37* (1982) 695.
[7] D. Biedenkapp, A. Weiss, *Z. Naturforsch. B 23* (1968) 174.
[8] R. A. Shaw, B. C. Smith, Ch. P. Thakur, *Justus Liebigs Ann. Chem. 713* (1968) 30.
[9] H. H. Perkampus: *Wechselwirkungen von π-Elektronensystemen mit Metallhalogeniden*, Springer, Berlin 1973.
[10] Crystal structure data: Enraf-Nonius CAD4 diffractometer, $Mo_{K\alpha}$ radiation, $\lambda = 0.71069$ Å, graphite monochromator. Rhombohedral, space group $R\bar{3}$ (No. 148) in hexagonal setting, $a_H = b_H = 13.765(2)$, $c_H = 12.411(2)$ Å, $V = 2036.5$ Å^3, $\rho_{calcd} = 2.142$ g cm^{-3}, $Z = 3$, $T = 22$°C, $\mu(Mo_{K\alpha}) = 112.1$ cm^{-1}, $F(000) = 1242$. 5715 measured reflections to $(\sin\theta/\lambda)_{max} = 0.659$, hkl: -18, ± 18, ± 16 ($(\theta-2\theta)$ scan, $\Delta\omega = 0.85 + 0.35\tan\theta$). Lp, nonlinear, isotropic decay correction (-3.6%) and empirical absorption correction based on ψ scans of six reflections with relative transmission 0.47–1.00; 1094 independent reflections, $R_{int} = 0.03$, solution by Patterson methods (SHELXS-86); $R = 0.055$, $R_w = 0.040$, $w = 1/\sigma^2(F_0)$ for 43 parameters and 731 observables with $F \geq 4.0\sigma(F_0)$ (anisotropic, CH_2 riding, CH_3 as rigid groups). $\Delta\rho_{fin}$(max/min) = $+0.73/-1.03$ e/Å^3. Further details of the crystal structure investigation may be obtained from the Fachinformationszentrum Energie, Physik, Mathematik GmbH, D-7514 Eggenstein-Leopoldshafen 2 (FRG), on quoting the depository number CSD-52230, the names of the authors, and the journal citation.
[11] A. K. Singh, S. Swaminathan, *Z. Kristallogr. Kristallgeom. Kristallphys. Kristallchem. 124* (1967) 375; J. Trotter, *ibid. 122* (1965) 230.
[12] D. J. Iverson, G. Hunter, J. F. Blount, J. R. Damewood, Jr., K. Mislow, *J. Am. Chem. Soc. 103* (1981) 6073.
[13] J. Trotter, *Z. Kristallogr. Kristallgeom. Kristallphys. Kristallchem. 121* (1965) 81; R. Enjalbert, J. Galy, *Acta Crystallogr. Sect. B 36* (1980) 914.

Reaction of Phosphinines with Diazoalkanes: Diphosphachiropteradienes by Intramolecular, Ionic 5s + 5s [6 + 4] Cycloaddition**

By *Gottfried Märkl,* Hans J. Beckh, Klaus K. Mayer, Manfred L. Ziegler,* and *Thomas Zahn*

Compounds containing PC double bonds react with diazoalkanes to give a surprisingly wide spectrum of products, depending on the substituents. Diazomethane and its monosubstituted derivatives react as 1,3 dipoles with acyclic phosphaalkenes, resulting in [3 + 2] cycloaddition[1] to give dihydro-1,2,4-diazaphospholes. Diaryl- and dialkyldiazomethanes react, with elimination of nitrogen, to give phosphiranes.[2] The P=C bond in aza- and diazaphospholes reacts analogously in many cases.[3]

The P=C bond in phosphinines, on the other hand, behaves completely differently. *K. Dimroth* et al.[4] showed that the reaction of 2,4,6-triarylphosphinines with diazoalkanes in the presence of alcohols afforded 1-alkoxy-1-alkyl-λ^5-phosphinines. Analogous behavior was observed by us for the 3,5-diphenylphosphinine **1**, a phosphinine that is unsubstituted in positions 2, 4, and 6 and reacts with all diazoalkanes tested (diazomethane, mono- and disubstituted diazomethanes) in methanol to give the 1-alkyl-1-methoxy-λ^5-phosphinines **2**.[5]

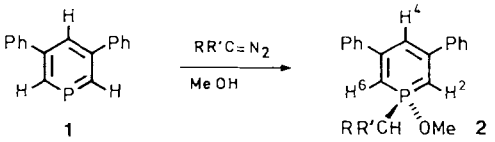

1 **2**

a, R = R' = H; **b**, R = R' = Me; **c**, R = H, R' = Me; **d**, R = H, R' = Et; **e**, R = Me, R' = Ph; **f**, R = R' = Ph; **g**, R = H, R' = CH_2COOMe

In aprotic solvents, on the other hand, **1** exhibits a completely different behavior upon reaction with diazomethane or with mono- and disubstituted diazomethanes. Compound **1** reacts with diazomethane in ether already at 0°C within a few minutes; immediate workup affords **3a**, which is obtained from acetonitrile in 65–70% yield as a colorless, crystalline compound. The X-ray diffraction analysis of **3a** (Fig. 1) revealed a completely unexpected structure,[6] in which two phosphacyclohexene rings are joined through a CH_2 group (between the phosphorus atoms) and three σ bonds to form a system consisting of two five-membered rings and four six-membered rings.

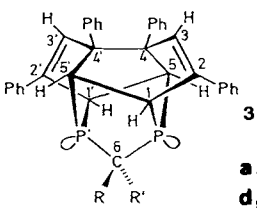

3

a, R = R' = H; **b**, R = R' = Me; **c**, R = H, R' = Me; **d**, R = H, R' = Et; **e**, R = Me, R' = Ph

[*] Prof. Dr. G. Märkl, Dipl.-Chem. H. J. Beckh, Dr. K. K. Mayer
Institut für Organische Chemie der Universität
Universitätsstrasse 31, D-8400 Regensburg (FRG)
Prof. Dr. M. L. Ziegler, Dr. T. Zahn
Anorganisch-chemisches Institut der Universität
Im Neuenheimer Feld 270, D-6900 Heidelberg (FRG)

[**] We propose giving the trivial name "chiropterane" to the saturated hydrocarbon, pentacyclo[7.4.0.0^{2,6}.0^{3,11}.0^{5,10}]tridecane corresponding to **6**, because of their batlike structure (bat: Chiroptera). Compounds **3** are accordingly diphosphachiropteradienes.

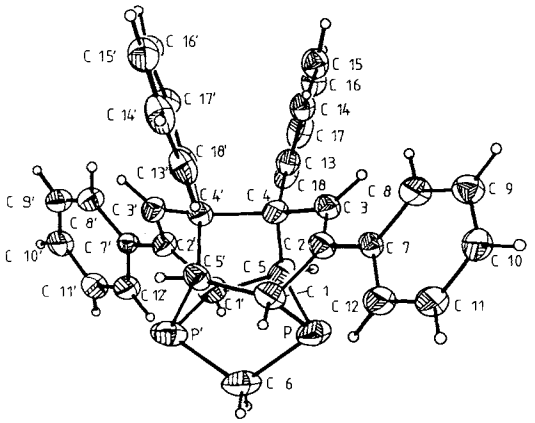

Fig. 1. Crystal structure of **3a**.

Both the ^{1}H-NMR spectrum and the ^{13}C-NMR spectrum[7] of **3a** are in agreement with this structure (Table 1). The ^{31}P-NMR resonance signal ($\delta = 66.8$) is found at unusually low field for tertiary phosphanes. Similar, extremely low-field shifts were previously observed only for *syn*-7-phosphanorbornenes, *syn*-benzo-7-phosphanorbornenes,[8a] and for tBu$_3$P.[8b] The question whether the low-field shift for **3a** is due to the expansion of the C5–P–C6 angle (97.3°)[6] or to the spatial proximity of the lone pair of electrons to the C2=C3 bond or to the phenyl substituents at C2 remains unanswered. Compound **1** reacts analogously with dimethyldiazomethane, diazoethane, diazopropane, and methylphenyldiazomethane to give the compounds **3b–e** (Table 1). In these cases, too, the ^{31}P-NMR signals for the tertiary phosphanes are found at extremely low field ($\delta = 74$ to 94).

The mass spectra of **3** also exhibit unique features. In the 70-eV spectra, only the molecular ion peak of **1** at m/z 248 is observed and, in some cases (with less intensity), also the radical cation of **6** as the ion fragment [phosphinine-CRR']$^{\oplus\ominus}$, e.g., $[C_{17}H_{13}P{-}CH_2]^{\oplus\ominus}$, m/z 262 for **3a**.[9]

The first step in the formation of **3** (shown for **3a**) is the nucleophilic attack of diazomethane on the $\lambda^3\sigma^2$ phosphorus atom of **1** to give the diazonium salt **5** followed by elimination of N_2 to give the dipolar compound **6** (a cyclic derivative of bis(methylene)phosphoranes, first described by *R. Appel* et al.[10]). The existence of the intermediate **6** is supported by its trapping with alcohols to give the λ^5-phosphinines **2**. Nucleophilic attack of **6** on a second molecule of **1**[11] results initially in formation of the adduct **7**, which consists of two phosphinine molecules **1** and a CH_2 fragment and in which a phosphininyl anion and a phosphininium ion are linked by a CH_2 bridge.

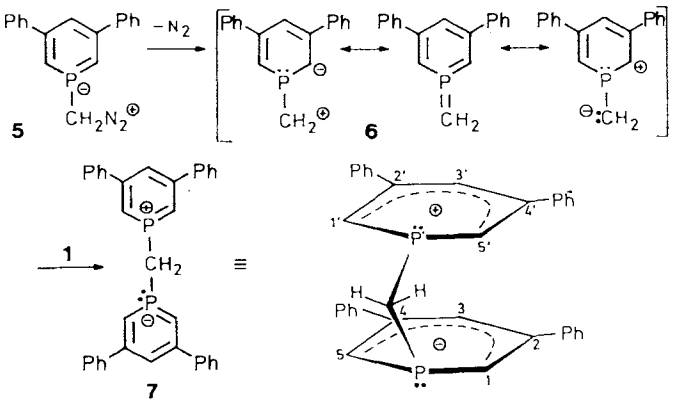

The formation of **7** requires that the diazoalkane employed experience little resonance stabilization, so that the 1,3-dipole **6** is sufficiently nucleophilic to attack a second molecule of **1**. This assumption is supported by the finding that reaction of **1** with diphenyldiazomethane results in formation of the bicyclic phosphirane **9**.[12] In this case, **4**, the intermediate corresponding to **6**, can only undergo stabilization by means of intramolecular ring closure.

Compound **3a** is presumably formed from **7** by ionic, intramolecular [6+4] cycloaddition, resulting in the forma-

Table 1. Physical and spectroscopic data for **3**.

Compound	**3a**	**3b**	**3c**	**3d**	**3e**
M.p. [°C] [a]	146–147 (dec.)	145–146	115–117 (dec.)	102–103 (dec.)	105–107 (dec.)
Yield [%]	65–75	74	86	84	72
^{1}H-NMR (250 MHz, $CDCl_3$, δ, J [Hz]):			[b]	[b]	
H1, H1' [c]	3.13 (t)	3.74 (t)	3.31 (d) [d], 3.57 (d) [d]	3.25 (d), 3.50 (d)	H1 3.84 (dd); H1' 2.96, 2.98
^2J(PH) [e]	7.14	≈6.0	—	—	7.2 (two degenerate
^3J(H1, H5') [f]	7.12	≈6.1	7.20	≈7.0	≈7.0 ABX spectra)
H5, H5'	2.83 (dd) [d]	3.08 (ABX)	2.90 (d), 2.95 (d)	2.86 (d), 2.93 (d)	3.01 (ddd), 3.12 (ddd)
^2J(PH) [g]	28.2	26.0	7.20, 7.04	7.10	24.6, ^3J(PH) = 2.7; ^3J(HH) = 7.1;
H3, H3'	6.05 (dd)	6.06 (dd)	6.02 (d), 6.08 (d)	6.02 (d), 6.07 (d)	6.01 (s), 6.14 (d)
^4J(PH)	5.0	4.8	—	—	—
^4J(H1, H3)	1.6	1.4	1.6	1.5	1.4
R	1.70 (t)	1.62 (t)	2.07 (q)	1.78–1.98 (m)	1.95 (t)
J(PH) [h]	9.72	10.7	J(HH) = 7.6	—	10.1
R'	1.70 (t)	1.62 (t)	1.54 (d)	CH_3: 1.32 (t); CH_2: 1.78–1.98 (m)	C_6H_5
J(PH)	9.72	10.7		J(HH) = 7.2	
^{31}P{^{1}H}-NMR (101.25 MHz, $CDCl_3$, H_3PO_4 as int. standard):					
	66.8 (s)	94.3 (s)	79.0, 89.0	73.6, 74.5	80.8, 91.7
J(PP)			18.9 [i]	17.2 [i]	20.9 [i]

[a] After recrystallization from $CHCl_3$/petroleum ether (40–60°C) or benzene/petroleum ether (40–60°C); all compounds crystallize with one molar equivalent of $CHCl_3$ or benzene, respectively. [b] ^{1}H{^{31}P}-NMR spectra. [c] Pseudo triplet with fine structure due to W coupling. [d] With fine structure. [e] Dihedral angle α(H1–C–P:) ≈ 50° [15]. [f] Identical with ^3J(H1',H5). [g] Dihedral angle α(H5–C–P:) ≈ 10° [15]. [h] Dihedral angle α(R–C–P:) ≈ 50° [15]. [i] AB spectra.

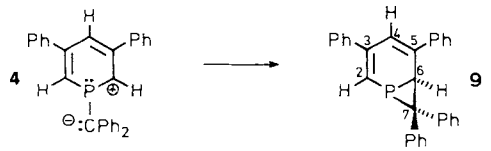

tion of two σ bonds (C1–C5′ and C1′–C5) to give **8**. Intermediate **8**, which consists of an allyl cation moiety and an allyl anion moiety, can undergo stabilization by formation of a (C4–C4′) σ bond to give **3a**.[13]

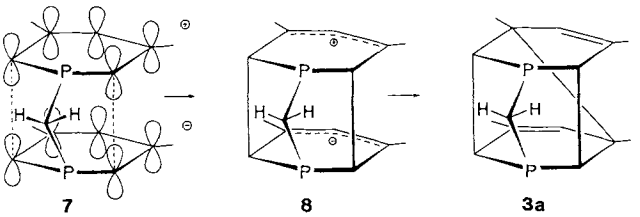

Whereas especially cationic (3s+4s) and, in special cases, (5s+2s) cycloadditions, as well as anionic (5s+4s) and (3s+2s) cycloadditions, have already been reported,[14] the doubly ionic (5s+5s) reaction postulated here is, to the best of our knowledge, the first of its kind. The assumption of a nucleophilic attack of the diazoalkane on the $\lambda^3\sigma^2$ phosphorus atom as opposed to a 1,3-dipolar cycloaddition on the P=C bond is also supported, for example, by the observation that ethyl diazoacetate no longer undergoes reaction with **1** in aprotic solvents. Thus, the electrophilicity of the phosphinine clearly dominates over its dipolarophilicity.[16]

Received: November 13, 1986 [Z 1983 IE]
German version: *Angew. Chem. 99* (1987) 255

[1] T. A. van der Knapp, T. C. Klebach, V. Visser, R. Lourens, F. Bickelhaupt, *Tetrahedron 40* (1984) 991; G. Märkl, I. Troetsch, *Angew. Chem. 96* (1984) 899; *Angew. Chem. Int. Ed. Engl. 23* (1984) 901.

[2] W. Hölzl, *Diplomarbeit*, Universität Regensburg 1986.

[3] B. A. Arbuzov, A. F. Lisin, E. N. Dianova, *Izv. Akad. Nauk SSSR Ser. Khim. 1983*, 2395; B. A. Arbuzov, E. N. Dianova, Yu. Yu. Samitov, *Dokl. Akad. Nauk SSSR 244* (1979) 117; B. A. Arbuzov, E. N. Dianova, *Izv. Akad. Nauk SSSR Ser. Khim. 1977*, 1453; B. A. Arbuzov, E. N. Dianova, S. M. Sharipova, *ibid. 1981*, 1113.

[4] K. Dimroth, W. Städe, *Angew. Chem. 80* (1968) 966; *Angew. Chem. Int. Ed. Engl. 7* (1968) 881; siehe auch G. Märkl, A. Merz, H. Rausch, *Tetrahedron Lett. 1971*, 2989.

[5] The λ^5-phosphinines form colorless crystals or are oily compounds having characteristic spectroscopic data (e.g., ^{1}H-NMR ($CDCl_3$): δ=4.73–5.04 (dd, ^2J(PH)=8.9–10.2 Hz; H2, H6), 6.07–6.11 (dt, ^4J(PH)=2.22–2.35 Hz, ^4J(H4,H2 and H4,H6)=1.26–1.36 Hz; H4)).

[6] Crystal structure data for **3a**·C_6H_6: monoclinic, space group $P2_1/n$, a=7.175(3), b=11.849(4), c=18.293(7) Å, β=96.43(3)°, V=1545.45 Å^3, ρ_{calcd}=1.29 g cm^{-3}, Z=2, F_{000}=552, μ($Mo_{K\alpha}$)=1.57 cm^{-1}. 4508 unique reflections in the measured region (h −11/11, k −17/0, l −26/0; $3<2\theta<60°$), 1982 observed ($\theta/2\theta$ scans) ($I\geq 2.5\sigma(I)$), Lp and absorption correction (empirical, 6 reflections $6\leq 2\theta\leq 20°$), ψ scans), transmission factors: min. 0.672, max. 1.0, $Mo_{K\alpha}$ (λ=0.71069 Å), graphite monochromator, Nicolet-R3. The structure was solved by direct methods (SHELXTL program), H atoms from difference Fourier synthesis. Non-hydrogen atoms anisotropic, H atoms isotropic, R=0.063, R_w=0.056; residual electron density: max. 0.521, min. 0.242 e/Å^3. Selected bond lengths [Å] and angles [°]: P-C1 1.859(3), P-C5 1.891(3), P-C6 1.830(3); C1-P-C6 91.5(1), C5-P-C6 97.3(1), C1-P-C5 90.0(1), P-C6-P′ 102.9(2). Further details of the crystal structure investigation may be obtained from the Fachinformationszentrum Energie, Physik, Mathematik GmbH, D-7514 Eggenstein-Leopoldshafen 2 (FRG), on quoting the depository number CSD-52330, the names of the authors, and the journal citation.

[7] ^{13}C{^{1}H}-NMR ($CDCl_3$) of **3a**: δ=44.3 (d, ^1J(PC)=10.8 Hz; C1, C1′), 37.5 (d, ^1J(PC)=24.4 Hz; C5, C5′), 28.0 (t, ^1J(PC)=25.0 Hz; C6), 59.1 (s; C4, C4′), 143.3 (s; C2, C2′), 137.6, 139.0 (each s; C7, C18, C7′, C18′), 125.9–131.7 (C3, C3′, residual phenyl C).

[8] a) L. D. Quin, K. C. Caster, J. C. Kisalus, K. A. Mesch, *J. Am. Chem. Soc. 106* (1984) 7021; L. D. Quin, F. Ch. Bernhardt, *Magn. Reson. Chem. 23* (1985) 929; b) B. E. Mann, *J. Chem. Soc. Perkin Trans. 2 1972*, 30.

[9] In the FD-MS of **3** (MAT 311A-SS 200, 5.5 kV, immersion method, CH_2Cl_2 solutions), the molecular ion peak and the peak for the protonated molecular ion of **3** ($M^{\odot\oplus}$, $MH^{\oplus}$) are observable for low emitter heating currents (4–5 mA). Between 5 and 10 mA, the molecular ion peak of **1** also appears along with the peak for the [phosphinine-CRR′]$^{\odot\ominus}$ ion belonging to **6**. In addition, the peaks for the molecular ions of the dimers, trimers, and tetramers of **6** are observed. For example, in the FD-MS of **3a**: 4–5 mA: m/z 510 ($M^{\odot\oplus}$), 511 ($MH^{\oplus}$).—5–10 mA: m/z 248 (**1**$^{\odot\oplus}$), 249 (**1**H$^{\oplus}$), 262 (**6**$^{\odot\oplus}$), 510 ($M^{\odot\ominus}$), 511 ($MH^{\oplus}$); 524 (dimer of **6**, $D^{\odot\oplus}$), 525 ($DH^{\oplus}$); 786 (trimer $T^{\odot\oplus}$), 787 ($TH^{\oplus}$), 1048 (tetramer $TE^{\odot\oplus}$), 1049 ($TEH^{\oplus}$).—10–15 mA: m/z 248, 249, 280; 524, 525; 786, 787, 800; 1048, 1049—ca. 20 mA: m/z 248, 249; 524, 525, 535, 552; 786, 787, 788, 800, 814; 1048, 1049.

[10] R. Appel, J. Peters, A. Westerhaus, *Angew. Chem. 94* (1982) 76; *Angew. Chem. Int. Ed. Engl. 21* (1982) 80.

[11] Reaction of phosphinines with the nucleophiles RLi, RMgX: G. Märkl, F. Lieb, A. Merz, *Angew. Chem. 79* (1967) 475; *Angew. Chem. Int. Ed. Engl. 6* (1967) 458; G. Märkl, A. Merz, *Tetrahedron Lett. 1967*, 1755.

[12] **9**: yield 65% yellow crystals, m.p. = 171 °C (dec.; from EtOH), ^{1}H-NMR: δ=3.86 (dd, ^2J(PH)=13.5 Hz, ^4J(H4,H6)=0.7 Hz; H6), 6.43 (d; H4), 6.22 (d, ^2J(PH)=55.1 Hz; H2); ^{31}P{^{1}H}-NMR: δ=−121.3 (s).

[13] In refluxing benzene, **3** already undergoes cycloreversion. After 8 h, 1 molar equivalent of **1** is obtained in approximately 70% yield. In agreement with this finding, FD-MS of CH_2Cl_2 solutions of **3** that have been allowed to stand (2 h, room temperature) give strong signals for **1** as well as for the di-, tri-, and tetramers of **6** (emitter heating current 5–15 mA); correspondingly, the intensities of $M^{\odot\oplus}$ and $MH^{\oplus}$ for M=**3a** are strongly reduced.

[14] See, e.g., Nguyên Trong Anh: *Die Woodward-Hoffmann-Regeln und ihre Anwendung*, Verlag Chemie, Weinheim 1972, p. 154–156, 164.

[15] The observed J values are in agreement with the reported values with respect to the dependence of the PH coupling on the dihedral angle α(H-C-P:): J. P. Albrand, D. Gagnaire, J. Martin, J. B. Robert, *Bull. Soc. Chim. Fr. 1969*, 40.

[16] 1,3-Dipolar cycloadditions to the P=C bond of **1**: G. Märkl, unpublished results.

MNDOC Calculations of the Potential Surfaces for Photochemical α-Cleavage

By *Manfred Reinsch, Udo Höweler,* and *Martin Klessinger**

In contrast to thermal reactions, photochemical reactions have been hardly amenable to semiempirical calculations. There are two reasons for this: the parameters used in semiempirical methods apply only to the ground state, and unacceptably long calculation times are required in order to adequately account for configuration interaction (CI). We show here that it is possible to overcome these difficulties. To accomplish this, the MNDOC method,[1] which is parametrized for explicit calculation of electron correlation and has already been employed for the calculation of excited-state surfaces,[1b] was combined with a CI calculation that was limited by suitable selection criteria, different reference configurations being used for the individual states.[2]

The procedure was applied to formaldehyde, the simplest model compound for studying photochemical α-cleavage. The first three-dimensional potential surfaces of the ground state S_0, the excited (n,π*) states S_a and T_a, and

[*] Prof. Dr. M. Klessinger, Dipl.-Chem. M. Reinsch, Dr. U. Höweler
Organisch-Chemisches Institut der Universität
Orléans-Ring 23, D-4400 Münster (FRG)

[**] This work was supported by the Fonds der Chemischen Industrie. We thank Prof. *W. Thiel*, Universität-Gesamthochschule Wuppertal, for a version of the MNDOC program and for valuable discussions and Dr. *J. Downing*, University of Utah (USA), for the DZDO program.

the excited (π,π^*) state T_s of formaldehyde are depicted in Figure 1. The most important parameters used in calculating the potential surfaces, as well as data required for estimating the accuracy of the results, are summarized in Table 1.

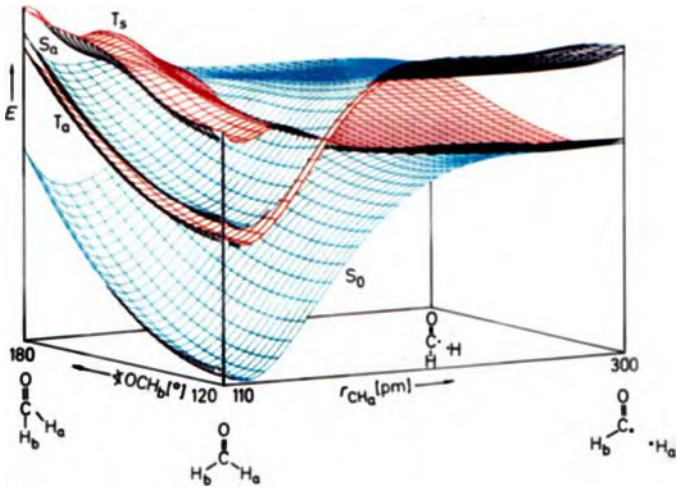

Fig. 1. Potential energy surfaces of the lowest energy singlet and triplet states of formaldehyde as a function of CH_a distance and OCH_b angle. The upper sides of the potential surfaces are blue for singlet states and red for triplet states.

Table 1. MNDOC calculations on formaldehyde (planar conformations). ψ = reference configuration, n_{CI} = number of configurations used in the CI calculation.

State	ψ	n_{CI}	E [kJ mol^{-1}] [a] This study	Values for comparison from the literature [6] [b]	[7] [c]	[8] [c]	[1b] [c]
S_0	GZ [d]	93	348	366	403	425	—
S_a	$^1(n,\pi^*)$	108	275	337	287	282	287 [e]
T_a	$^3(n,\pi^*)$	128	241	301	234	247	264
T_s	$^3(\pi,\pi^*)$	137	425	—	—	—	492

[a] Dissociation energy in the case of S_0, vertical excitation energies in the cases of S_a, T_a, and T_s. [b] Experimental value. [c] Calculated value. [d] Ground state. [e] Calculated at the optimized S_0 geometry.

Plotting of the energies as functions of the distance r_a to the leaving group R_a and the angle φ between the carbonyl group and the substituent R_b in **1** (see Figure 1) clearly reveals which product is produced in which state. This represents a clear advantage over separate correlation of the ditopic reaction to bent and the tritopic reaction to linear primary products, which is usually the case when the α-cleavage is discussed in terms of correlation diagrams.[3]

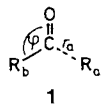

1

According to Figure 1, the energy of the ground state increases along both coordinates, and the ground state correlates with the diradicaloid $^1D_{\sigma\sigma}$ state. The surfaces of the two (n,π^*) states S_a and T_a stay nearly parallel over the entire region and form, after crossing the (π,π^*) state T_s the $^{1,3}D_{\sigma\pi}$ pair of states. Finally, the (π,π^*) state exhibits a barrier, which is due to an avoided crossing with the highly excited $^3(n,\sigma^*)$ state, and becomes the $^3D_{\sigma\sigma}$ state. All four states are degenerate for an OCH_b angle of 180° and a large CH_a distance.

The reaction coordinates corresponding to the minimum energy path, can be determined for the various states from the contour diagrams in Figure 2. For the reaction in the ground state S_0 and in the (π,π^*) state T_s, the bond angle increases by only a small amount from $\varphi = 125°$ to $\varphi = 130°$; the cross section through the potential surfaces of Figure 1, shown in Figure 3a for $\varphi = 130°$, corresponds

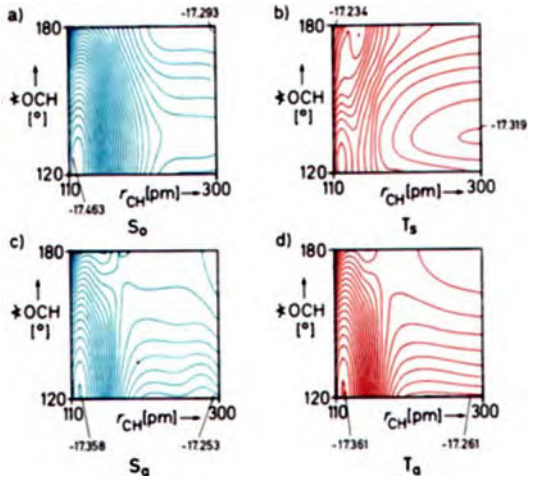

Fig. 2. Contour diagrams of the lowest-energy singlet and triplet states. a) Singlet ground state S_0. b) Symmetric triplet state T_s. c) Antisymmetric singlet state S_a. d) Antisymmetric triplet state T_a. The maximum and the minimum energy value is shown in each diagram. The spacing of the contour lines is 5×10^{-3} a.u.

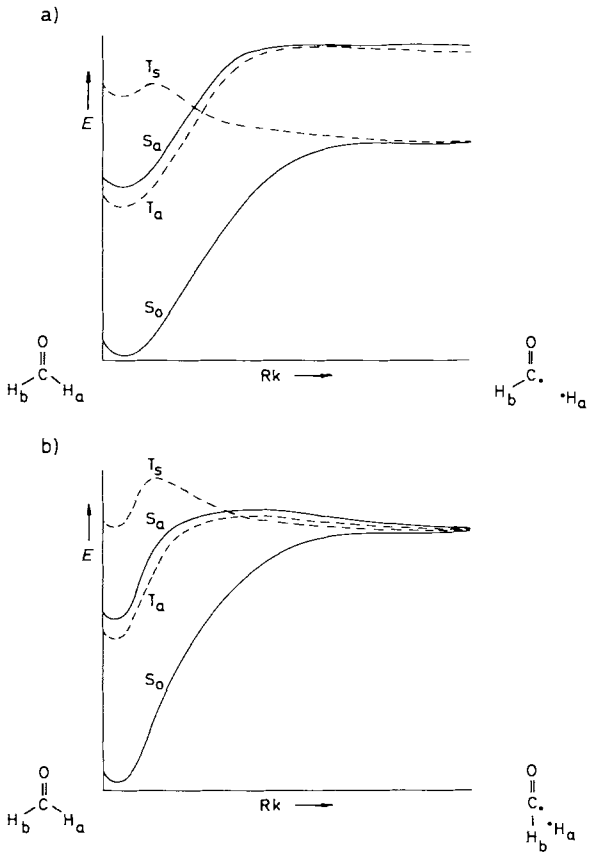

Fig. 3. Potential curves for the ditopic (a) and the tritopic (b) reaction. a) Cross section for an OCH_b angle of 130°. b) Cross section for the minimum energy path in the antisymmetric states. Rk = reaction coordinate.

to the correlation diagram for the ditopic reaction giving the bent acyl radical. On the (n,π*) surface (S_a and T_a), the reaction pathway leads from a point near the ground-state geometry to a linear acyl radical. A cross section through the surfaces of Figure 1 along this pathway is shown in Figure 3b; it corresponds to the correlation diagram for the tritopic reaction giving the linear product. Accordingly, photochemical α-cleavage from the (π,π*) state T_s should lead to bent products and that from the (n,π*) states to linear products. However, it must be noted that the crossing between the triplet states is avoided for a nonplanar conformation. Furthermore, according to Kasha's rule, the reactions arising from the (π,π*) state T_s should have little probability.

In the case of formaldehyde, the barriers in the (n,π*) states are clearly too high for a photochemical reaction,[4] even if the avoided crossing in the case of the nonplanar reaction is taken into consideration. This is in agreement with the experimental results, since in photochemical reactions formaldehyde dissociates mainly into molecular products.[5] Analogous calculations for acetaldehyde and acetone revealed that the general form of the potential surfaces in Figure 1 for α-cleavage is typical, but that the heights of the barriers depend on the molecular structures involved. For instance, the barriers for H cleavage and CH_3 cleavage from the ^{3}(n,π*) state of acetaldehyde are 45 and 80 kJ mol^{-1} greater, respectively, than that for H cleavage from formaldehyde.

Received: September 26, 1986;
revised: November 28, 1986 [Z 1938 IE]
German version: *Angew. Chem. 99* (1987) 250

[1] a) W. Thiel, *J. Am. Chem. Soc. 103* (1981) 1413, 1420; b) A. Schweig, W. Thiel, *ibid. 103* (1981) 1425.
[2] The CI calculations were performed with the corresponding parts of the program DZDO of J. Downing (unpublished); cf. J. Downing, J. Michl, P. Jørgensen, E. W. Thulstrup, *Theor. Chim. Acta 32* (1974) 203. The criteria for the selection of configurations were chosen such that the number of configurations is sufficient to account for the essential contributions to the correlation energy without additional perturbation treatment (U. Höweler, M. Reinsch, M. Klessinger, to be published).
[3] N. J. Turro: *Modern Molecular Photochemistry*, Benjamin/Cummings, Menlo Park, CA (USA) 1978, Chap. 7.
[4] A. Devaquet, A. Sevin, B. Bigot, *J. Am. Chem. Soc. 100* (1978) 2009.
[5] R. D. McQuigg, J. G. Calvert, *J. Am. Chem. Soc. 91* (1969) 1590; J. H. Clark, C. B. Moore, N. S. Nogar, *J. Chem. Phys. 58* (1978) 1264.
[6] P. L. Houston, C. B. Moore, *J. Chem. Phys. 65* (1976) 757.
[7] W. H. Fink, *J. Am. Chem. Soc. 94* (1972) 1073.
[8] D. M. Hayes, K. Morokuma, *Chem. Phys. Lett. 12* (1972) 539.

Photoisomerization of Bis(bipyridyl)rhodium(III) Complexes; Synthesis of *trans*-$[Rh(bpy)_2YCl]^{n\oplus}$, Y = Cl, H_2O**

By *Gerd Krüger, Stefan Wieland,* and *Rudi van Eldik**

Investigations of d^6-transition-metal poly(pyridyl) complexes have contributed to the fundamental understanding of inorganic photochemistry.[1] The nature and arrangement of the ligands can crucially influence their photophysical properties and thereby their photochemical behavior. Thus, in addition to the "tuning" of the ligands,[2] their relative position in the complex with respect to an extension of the π system is of great importance.

In octahedral complexes, $[M(bpy)_2XY]^{n\oplus}$, with bidentate-coordinated 1,4-diazabutadienes of the type 2,2′-bipyridyl (bpy), the *trans* arrangement was long thought to be unlikely because of the spatial proximity of the protons (H-6α, H-6β and H6′α′, H-6′β′) of mutually opposing bpy ligands.[3] The bis(bipyridyl) complexes of the d^8 metal ions $Pd^{2\oplus}$ and $Pt^{2\oplus}$, which have mainly a square-planar environment, overcome this steric hindrance by distortion of either the MN_4 portion of the complex or the ligands.[4]

As observed for the very slow thermal exchange reactions, the early photolyses of rhodium(III) complexes, which led to initial excitation of the intraligand states (**1a** with $\lambda_{max} = 311$ nm), the LF states (**1a** with a shoulder at $\lambda = 380$ nm), or eventually the π*(bpy)←d(Rh) CT states, resulted only in photoaquation with retention of the *cis* configuration.[5] However, in a high-pressure kinetic investigation of the reaction mechanism and the quantum yields of the photolysis of **1a**, the first evidence was obtained for a side or subsequent reaction occurring in addition to the photoaquation and having stereochemical consequences similar to those observed in the *cis–trans* isomerization of $[Ru(bpy)_2(H_2O)_2]^{2\oplus}$.[6]

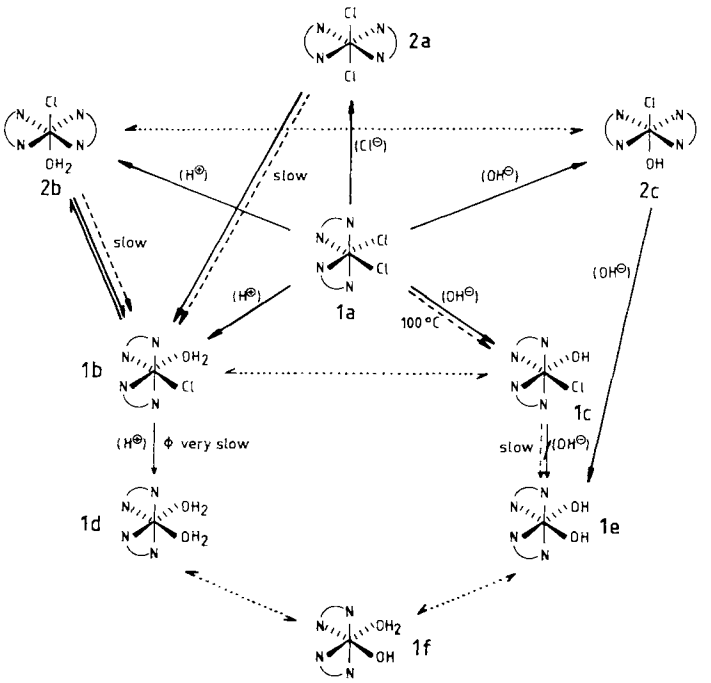

1a: X = Y = Cl
1b: X = Cl, Y = OH_2
1c: X = Cl, Y = OH
1d: X = Y = OH_2
1e: X = Y = OH
1f: X = OH_2, Y = OH

2a: X = Y = Cl
2b: X = Cl, Y = OH_2
2c: X = Cl, Y = OH
2d: X = Y = OH_2

On the basis of UV and ^{1}H-NMR spectroscopic results obtained on photolysis solutions of **1a**–**f**, we now report on the light-induced *cis–trans* isomerization of bis(bipyridyl) complexes and the isolation of the new compounds **2a**Cl and **2b**$(ClO_4)_2$.

cis-$[Rh(bpy)_2Cl_2]^{\oplus}$ $\xrightarrow[\lambda = 313\ nm]{1\ M\ HCl}$ *trans*-$[Rh(bpy)_2Cl_2]^{\oplus}$
1a **2a**

cis-$[Rh(bpy)_2(H_2O)Cl]^{2\oplus}$ $\xrightarrow[\lambda = 313\ nm]{H_2O}$ *trans*-$[Rh(bpy)_2(H_2O)Cl]^{2\oplus}$
1b **2b**

[*] Priv.-Doz. Dr. R. van Eldik, Dipl.-Chem. G. Krüger, Dipl.-Chem. S. Wieland
Institut für Physikalische und Theoretische Chemie der Universität Niederurseler Hang, D-6000 Frankfurt am Main 50 (FRG)

[**] This work was supported by the Deutsche Forschungsgemeinschaft, the Fonds der Chemischen Industrie, and the Max-Buchner-Forschungsstiftung.

The characterization of the isolated *trans* complex salts is based on the significant redshift of the absorption bands of the d-d transitions compared with those of the *cis* complexes and on comparison of the ^{1}H-NMR spectra of the *cis* and *trans* complexes (as well as on elemental analyses). Whereas the four diastereotopic pyridyl rings of the *cis* complexes with X ≠ Y give, in principle, 16 groups of signals, the pattern of signals for the *trans* complexes is reduced to four groups of signals owing to the higher symmetry, similar to the basic arrangement of free 2,2'-bipyridyl. Rhodium is thus the second transition metal preferring an octahedral environment for which photochemistry opens up a preparative route to the *trans*-poly(bipyridyl) complexes.

The results of irradiation of the pure perchlorates of **1a**, **1b**, and **1d** with light of wavelength 313 nm and at pH values between 2 and 13 are summarized in Figure 1. The thermal exchange reactions at 25°C occur much more slowly than the photochemical exchange reactions. The main products resulting from irradiation of **1a** over the entire pH range are the *cis*-monosubstituted products. Whereas a photostationary equilibrium between **1b** and **2b** is attained in acidic medium, **1c** and **2c** are formed in alkaline medium, the latter of which reacts further to give **1e**. The existence of **2b** or **2c** determines in a characteristic way the UV difference spectrum between irradiated and nonirradiated solutions. Photochemical exchange of the chloride ligand in **1c** could not be observed; in the case of **1b**, it occurs with a small quantum yield ϕ.

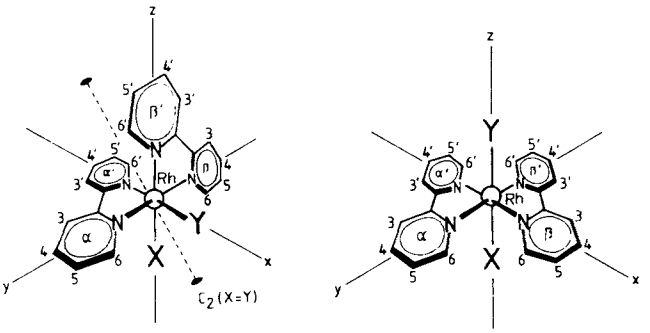

Fig. 1. Reaction scheme for the observed transformations of the rhodium(III) complex ions at 25°C (the charges have been omitted): ——, photochemically at $\lambda = 313$ nm; – – – –, thermally at 25°C unless otherwise noted; · · · · ·, acid-base equilibrium.

The photosubstitution of **2a** to give **1b** and the photoisomerization of **1a** to give **2a** in the presence of an excess of $Cl^{\ominus}$ suggest the existence of a common intermediate, which is formed by light-induced dissociation of a chloride ligand. In accordance with earlier suggestions,[7] this step leads to an equilibrium between two excited square-pyramidal intermediates, which differ in the identity of the ligands in the apical and basal positions. The energetically favored intermediate is that in which the ligands having less σ-donor strength are in the apical position. Since the order of σ-donor strength is $Cl < H_2O < bpy < OH$, this model readily explains the simultaneous formation of **1b** and **2b** and of **1c** and **2c**, respectively, upon photolysis of **1a** in acidic and basic medium. If one assumes that, as in the case of other rhodium complexes, a coordinated water molecule is photolabile, the formation of the photoproduct **2d** only after very long photolysis of **2b** is also understandable.

We thus conclude that inorganic complexes can also be transformed into sterically conjested isomers, which are not available via other routes, by photochemical reactions.

Experimental Procedure

The starting materials afforded correct elemental analyses and appropriate UV and ^{1}H-NMR spectra.

2aCl: **1a**Cl·2 H_2O (1.8 g) was dissolved in 140 mL of 1 M HCl and the resulting, stirred solution was irradiated in a Duran vessel for 110 h with a high-pressure Hg lamp (Hanau TQ 150 Z1) equipped with a filter transparent between 300 and 400 nm. The precipitated, finely divided product was filtered off under suction, recrystallized from 600 mL of 0.01 M HCl, washed with H_2O, EtOH, and Et_2O in that order, and dried in a water-aspirator vacuum over $CaCl_2$. A 36% yield of yellow **2a**Cl was obtained which gave correct C,H,N, and Cl analyses. ^{1}H-NMR (300 MHz, D_2O, standard HDO ($\delta = 4.9$)): $\delta = 9.38$ (d, 4H; H-6), 8.74 (d, 4H, $J(3,4) = 7.5$ Hz; H-3), 8.57 (t, 4H, $J(4,5) = 7.8$ Hz; H-4), 8.10 (t, 4H, $J(5,6) = 5.7$ Hz; H-5); UV/VIS (H_2O): $\lambda_{max} = 250$ (sh) ($\varepsilon = 21200$ M^{-1} cm^{-1}), 307 (sh) (18900), 312.5 (19600), 326 (sh) (8780), 405 (103) nm.

2b $(ClO_4)_2$: As described above, **1b**$(ClO_4)_2 \cdot H_2O$ (1.2 g) was dissolved in 100 mL of H_2O and irradiated for 45 h. The precipitated product was filtered off, recrystallized from 120 mL of 0.01 M $HClO_4$, and washed and dried as described above. A 22% yield of yellow-orange **2b**$(ClO_4)_2$ was obtained, which afforded correct C, H, N, and Cl elemental analyses. ^{1}H-NMR (300 MHz, D_2O, standard HDO ($\delta = 4.9$)): $\delta = 9.43$ (d, 4H; H-6), 8.79 (d, 4H, $J(3,4) = 8.2$ Hz; H-3), 8.64 (t, 4H, $J(4,5) = 7.8$ Hz; H-4), 8.14 (t, 4H, $J(5,6) = 5.5$ Hz; H-5); UV/VIS (0.01 M $HClO_4$): $\lambda_{max} = 248$ (22900), 310 (20000), 323 (sh) (14300), 375 (100) nm.

Received: October 20, 1986;
revised: December 5, 1986 [Z 1955 IE]
German version: *Angew. Chem. 99* (1987) 245

[1] a) M. Kirch, J.-M. Lehn, J.-P. Sauvage, *Helv. Chim. Acta 62* (1979) 1345; b) K. Kalyanasundaram, *Nouv. J. Chim. 3* (1979) 511; c) C. Creutz, A. D. Keller, N. Sutin, A. P. Zipp, *J. Am. Chem. Soc. 104* (1982) 3618.
[2] P. C. Ford, *Rev. Chem. Intermed. 2* (1979) 267.
[3] E. D. McKenzie, *Coord. Chem. Rev. 6* (1971) 187.
[4] A. Hazell, A. Mukhopadhyay, *Acta Crystallogr. Sect. B36* (1980) 1647.
[5] M. Muir, W.-L. Huang, *Inorg. Chem. 12* (1973) 1831.
[6] a) S. Wieland, *Diplomarbeit*, Universität Frankfurt am Main 1984; b) B. Durham, S. R. Wilson, D. J. Hodgson, T. J. Meyer, *J. Am. Chem. Soc. 102* (1980) 600.
[7] L. G. Vanquickenborne, A. Ceulemans, *Coord. Chem. Rev. 48* (1983) 157.

A New Photosynthesis-like System for the Light-induced Reduction of Water to Molecular Hydrogen**

By *Wolfgang Schuhmann,** *Hans-Peter Josel,* and *Harun Parlar*

The conversion of solar energy into electrical current or storable fuels has been the goal of intensive research for several years. Most interesting is the production of molecular hydrogen as a universally employable, environmentally acceptable fuel having high energy density in terms of weight.[1]

Owing to their similarity to chlorophylls, their photostability, and their photoelectrochemical properties, metal porphyrinates are expected to be good photosensitizers.[2] Adsorption of water-insoluble metal porphyrinate layers onto metal electrodes affords photosensitive semiconductor electrodes, whose photoelectrochemical behavior can be described by the band-bending model.[3] The difference between the Fermi level of the metal electrode and that of the applied dye layer results in an equalization of the

[*] Dr. W. Schuhmann, Dr. H.-P. Josel, Priv.-Doz. Dr. H. Parlar
Gesellschaft für Strahlen- und Umweltforschung mbH
Institut für Ökologische Chemie
Schulstrasse 10, D-8050 Freising-Attaching (FRG)

[**] We thank *J. Huber* and *S. Meixner* for their assistance.

chemical potential of the electrons in the contact region and thereby in a bending of the energy bands in the dye layer. The direction and magnitude of this band bending depend only on the relative position of the Fermi levels and largely determine the amount of electron-hole-pair formation and the efficiency of charge separation in the dye layer following excitation with light. In 1978, *Kawai* et al. first described the p-semiconducting behavior of zinc *meso*-tetraphenylporphyrinate adsorbed on platinum electrodes.[4]

We have now investigated the photoelectrochemical behavior of a series of dyes prepared by varying the *meso* phenyl substituents of zinc porphyrinates. These water-insoluble metalloporphyrinates were adsorbed onto platinum electrodes, and their photocurrent properties, i.e., the direction and extent of photoinduced electron-transfer reactions, were examined as a function of the wavelength of the incident light. In contrast to earlier studies,[5] in which exclusively p-type semiconducting behavior was observed with metalloporphyrins adsorbed on aluminum electrodes, the present work shows that several of the metalloporphyrinate layers on platinum electrodes are n-type semiconductors.

The photocurrent spectrum in Figure 1a shows clearly that zinc 5-(4-pyridyl)-10,15,20-tritolylporphyrinate (ZnTTPyP) is n-semiconducting. Excitation with light results in the transfer of an electron from the dye layer to the noble-metal electrode (oxidation of the excited dye molecule). Zinc 5,10,15,20-tetra-(4-pyridyl)porphyrinate (ZnTPyP), on the other hand, is p-semiconducting (Fig. 1b), i.e., the photoexcited electrons are transferred from the dye to acceptors in the surrounding electrolyte.

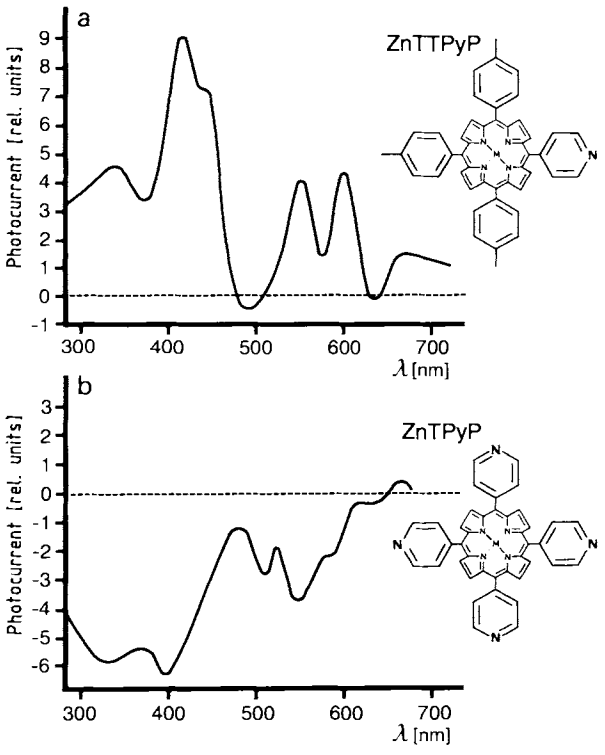

Fig. 1. Photocurrent spectra of a) ZnTTPyP and b) ZnTPyP. Positive values correspond to current flow from the dye layer to the electrode (n-semiconducting, anodic photocurrent); negative values correspond to a current flow from the electrode to the dye (p-semiconducting, cathodic photocurrent). In contrast to the extinction coefficients for the absorption spectrum of metal porphyrinates, the electron transfer appears to occur with greater probability after excitation of the Q band ($\lambda = 500$–600 nm) than after excitation of the Soret band ($\lambda = 425$ nm). The spectra are corrected for the wavelength-dependent intensity of the lamp employed. The experimental setup consists of a xenon lamp, a motor-driven monochromator, and a two-electrode arrangement coupled through a nanoamperemeter. The dye-modified electrode being measured and a platinum counterelectrode are immersed in an aqueous electrolyte containing KCl and the disodium salt of ethylenediaminetetraacetic acid (EDTA). The electrodes are irradiated through a planar polished quartz window.

On the basis of these results, a novel photosynthesis-like system for solar-energy conversion was developed in which the photoinduced reduction of water to molecular hydrogen could be demonstrated upon irradiation with visible light. The potential required for the reduction of water is attained by coupling two a priori independent light-absorption processes at metal porphyrinate-modified platinum electrodes, so that, as in the biological photosynthetic apparatus, two photosystems with different absorption and redox properties work together.

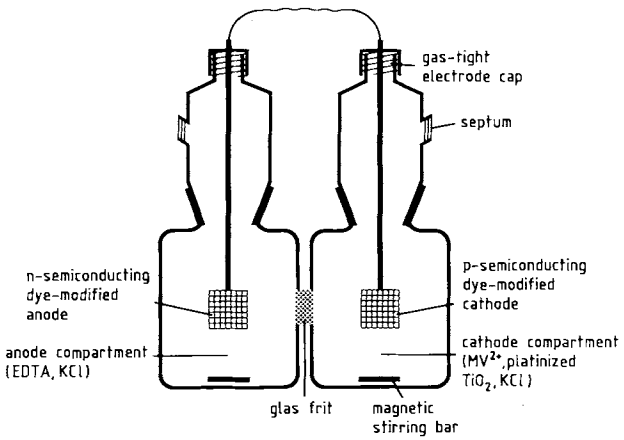

Fig. 2. Photoelectrochemical cell for the reduction of H_2O to H_2.

The results obtained with monochromatic light were verified with polychromatic light that was similar to sunlight by irradiation of dye-modified electrodes in a photoelectrochemical cell with separate anode and cathode compartments (Fig. 2). If a platinum electrode modified with n-semiconducting ZnTTPyP is connected via an external circuit with an electrode modified with p-semiconducting ZnTPyP, polychromatic irradiation of the two electrodes ($\lambda > 455$ nm) results in current flow in the external circuit from the n-semiconducting to the p-semiconducting electrode. The ZnTTPyP anode is immersed in an aqueous electrolyte containing KCl as conducting salt and EDTA as irreversibly oxidizable donor. Dye molecules that undergo oxidation by photoinduced electron transfers are reduced by EDTA and can thus participate again in absorption processes. In the cathode compartment, the ZnTPyP electrode is surrounded by an aqueous electrolyte that contains, in addition to KCl, *N,N*-dimethylbipyridinium dichloride ($MV^{2\oplus}$) as intermediary electron acceptor. Light-induced electron transfer from the irradiated cathode to $MV^{2\oplus}$ is revealed by the formation of the blue radical cation $MV^{\odot\oplus}$. In the presence of a microheterogeneous catalyst—highly disperse, platinized titanium dioxide[6]—$MV^{\odot\oplus}$ is reoxidized to $MV^{2\oplus}$ with simultaneous reduction of water to molecular hydrogen. The formation of hydrogen was monitored quantitatively by subjecting aliquots from the cathode compartment to gas chromatography (Fig. 3).

The electrons that are required in the cathodic dye layer to carry out the reduction are supplied by the photocurrent

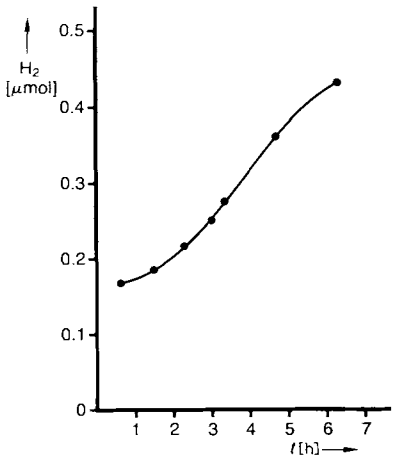

Fig. 3. Time dependence of H_2 formation with the system shown in Figure 2. The system was irradiated with an Osram Ultra-Vitalux lamp (300 W) through a 10-cm water filter and a 455-nm cut-off filter in order to avoid direct band-gap excitation of TiO_2. The quantum yields of H_2 formation were estimated by actinometric experiments with iron oxalate [7]. Taking into consideration the inaccuracy of the quantum current determination for long-wavelength light quanta ($\lambda > 450$ nm), the quantum yield was $< 10^{-3}$.

in the external circuit and are ultimately provided by the irreversible oxidation of the sacrificial electron donor EDTA. This coupling of two a priori independent light-absorption processes is analogous to the light reaction involved in photosynthesis in green plants (Fig. 4). The processes taking place at the anode and cathode compartments are summarized in Scheme 1.

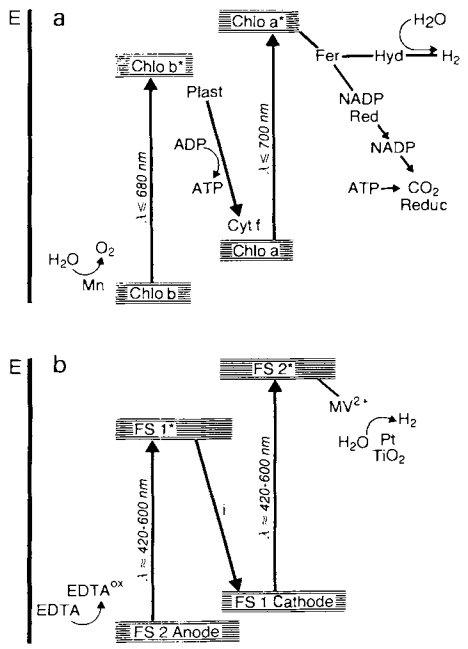

Fig. 4. Schematic comparison of the light reaction involved in the photosynthesis of green plants (a) with the novel photoelectrochemical system (b). The cascadelike sequence of electron-transfer reactions following light excitation of photosystem II in the natural system proceeds from activated chlorophyll to plastoquinone and cytochrome f in analogy to the external circuit of the artificial system. $MV^{2\oplus}$ corresponds to ferrodoxin, and the platinized TiO_2, which serves as reduction catalyst, corresponds to the hydrogenase in photosynthesis. The branch showing CO_2 reduction has no analogy in our artificial solar-energy conversion system.—Mn, manganese complex; Chlo b, chlorophyll b; Chlo a, chlorophyll a; Plast, plastoquinone; Cyt f, cytochrome f; Fer, ferredoxin; Hyd, hydrogenase; NADP Red, NADP reductase; CO_2-Reduct, CO_2 reduction; FS 1, p-semiconducting metal porphyrinate; FS 2, n-semiconducting metal porphyrinate; i, external circuit.

Anode compartment (photosystem II)

$$\text{n-FS} \longrightarrow \text{n-FS}^* \quad \text{(a)}$$

$$\text{n-FS}^* + \text{Pt} \longrightarrow \text{n-FS}^{\oplus} + e^{\ominus}(\text{Pt}) \quad \text{(b)}$$

$$\text{EDTA} + \text{n-FS}^{\oplus} \longrightarrow \text{EDTA}^{ox} + \text{n-FS} \quad \text{(c)}$$

Cathode compartment (photosystem I)

$$\text{p-FS} \longrightarrow \text{p-FS}^* \quad \text{(d)}$$

$$\text{p-FS}^* + MV^{2\oplus} \longrightarrow \text{p-FS}^{\oplus} + MV^{\odot\oplus} \quad \text{(e)}$$

$$2H_2O + 2MV^{\odot\oplus} \xrightarrow{\text{catalyst}} H_2 + 2OH^{\ominus} + 2MV^{2\oplus} \quad \text{(f)}$$

$$\text{p-FS}^{\oplus} + e^{\ominus}(\text{Pt}) \longrightarrow \text{p-FS} \quad \text{(g)}$$

Scheme 1. n-FS = ZnTTPyP; p-FS = ZnTPyP; FS = dye. The reactions described by the equations (a), (b), (d), and (g) take place on the irradiated dye electrodes; reactions (c) and (e) occur in the respective electrode-electrolyte contact regions; and equation (f) represents a reaction in the electrolyte of the cathode compartment. The electron transfer is assumed to take place from the excited triplet states of the porphyrinates. Reductive quenching by EDTA of the dye adsorbed on the anode, with formation of the corresponding dihydroporphyrinate, could be ruled out by observation of the absorption spectrum of dye that was later dissolved from the electrode.

A crucial difference lies in the fact that the efficiency of charge separation following the photosensitization reaction is not determined by a cascade of electron transfer reactions, as in the biological system, but rather by the degree of bending of the energy bands in the dye-noble-metal contact region. This band bending is responsible for the potential gradient that is formed upon irradiation of the electrodes, and thus determines the force applied to the photoexcited electron in the conducting band of the dye semiconductor. This means that the difference between the Fermi levels largely determines the efficiency of charge separation and consequently the efficiency of the conversion of solar energy into chemical energy.

Coupled photosystems such as those described in this communication might be used—after optimization—to convert solar energy into chemically storable energy. This would be an important step toward developing practical solar-energy conversion systems in which hydrogen and oxygen are safely formed from water in separate compartments, all other components of the system being true catalysts.

Received: October 23, 1986;
revised: December 1, 1986 [Z 1964 IE]
German version: *Angew. Chem. 99* (1987) 264

[1] a) A. Fujishima, K. Honda, *Nature 238* (1972) 37; b) K. J. Zamarev, V. N. Parmon, *Catal. Rev. Sci. Eng. 22* (1980); c) K. Kalyanasundaram, M. Grätzel, E. Pelizetti, *Coord. Chem. Rev. 69* (1986) 57; d) J. Kiwi, E. Borgarello, E. Pelizetti, M. Visca, M. Grätzel, *Angew. Chem. 92* (1980) 663; *Angew. Chem. Int. Ed. Engl. 19* (1980) 646.

[2] a) J. A. Shelnutt, *J. Am. Chem. Soc. 105* (1983) 7179; b) G. L. McLendon, D. S. Miller, *J. Chem. Soc. Chem. Commun. 1980*, 553; c) T. A. Moore, D. Gust, P. Mathis, J.-C. Mialocq, C. Chachaty, R. V. Bensasson, E. J. Land, D. Doizi, P. A. Lidell, W. R. Lehmann, G. A. Nemeth, A. L. Moore, *Nature 307* (1984) 630; d) J. R. Darwent, P. Douglas, A. Harriman, G. Porter, M.-C. Richoux, *Coord. Chem. Rev. 44* (1982) 83.

[3] H. Gerischer, *Pure Appl. Chem. 52* (1980) 2649.

[4] T. Kawai, K. Tanimura, T. Sakata, *Chem. Phys. Lett. 56* (1978) 541.

[5] F. J. Kampas, K. Yamashita, J. Fajer, *Nature 284* (1980) 40.

[6] a) B. Kraeutler, A. J. Bard, *J. Am. Chem. Soc. 100* (1978) 4317; b) S. Sato, J. Catal. 92 (1985) 11.

[7] C. G. Matchard, C. A. Parker, *Proc. R. Soc. (London) A 235* (1956) 518.

Synthesis of the Four-Membered Metallacycle $[Cp_2Ti(AsPh)_3]$ via the in situ Reduction of $[Cp_2TiCl_2]$**

By *Paul Mercando, Anthony-Joseph DiMaio*, and *Arnold L. Rheingold**

Bis(cyclopentadienyl)titanium complexes (Cp_2Ti) containing chelating trisulfido,[1a,b] pentasulfido, and pentaselenido ligands ($[Cp_2TiE_5]$, E = S or Se),[1c-f] are well-known and characterized by high reactivity. The isolobal and isoelectronic relationship of a sulfur or selenium atom to a phosphanediyl (phosphinidene) or arsanediyl (arsinidene) fragment prompted us to explore synthetic routes to the analogous $[Cp_2Ti(RE')_n]$ complexes (E' = P or As). *Issleib* et al. prepared $[Cp_2Ti(PPh)_3]$ in moderate yield from $[Na_2(PPh)_4]$ and $[Cp_2TiCl_2]$[1g] and identified the product from its ^{31}P-NMR spectrum, but did not characterize it crystallographically. A related procedure led to the preparation of $[Cp_2Ti(AsEt)_3]$.[1h] The compounds $[Cp_2Ti(PR)_3]$ (R = Ph, Me, Et, and *t*Bu) have been prepared from $[K_2(PR)_n]$ and $[Cp_2TiCl_2]$.[1i] The $(AsPh)_3$ ligand has previously been observed in a late-transition-metal metallacycle, $[(C_5Me_5)Rh(CO)(AsPh)_3]$.[1j]

Following the in situ reduction scheme developed by *Rausch* et al. for the quantitative synthesis of $[Cp_2Ti(PMe_3)_2]$,[2,3] we have obtained good yields of $[Cp_2Ti(AsPh)_3]$ **1** as a moderately air-stable, purple, crystalline product via the reduction of $[Cp_2TiCl_2]$ by magnesium in the presence of *cyclo*-$(AsPh)_6$:

$$[Cp_2TiCl_2] + Mg + 1/2\,cyclo\text{-}(AsPh)_6 \longrightarrow [Cp_2Ti(AsPh)_3] + MgCl_2$$

1

Under the conditions of this reaction, Mg and *cyclo*-$(AsPh)_6$ alone are inert; the apparent ring-opening agent is the reduced Ti species.

Compound **1** has been characterized by ^{1}H-NMR spectroscopy[4] and by an X-ray diffraction study.[5] At room temperature, two singlets for the Cp rings are seen in the ^{1}H-NMR spectrum and no indication of line broadening is seen to 80 °C. In $[Cp_2TiS_5]$, ring conformation flipping produces dynamic effects clearly evident at 80 °C with coalescence occurring at 90 °C.[1c] In $[(Me_5C_5)_2TiS_3]$ only a single methyl peak is seen at room temperature.[1b]

The inequivalence of the Cp rings in **1**, also evident in the solid state, is caused by the arrangement of the phenyl rings (see Fig. 1). Additionally, the bisector of the angle formed by the Ti atom and the centers of the Cp rings is not contained in the As-Ti-As plane. The central $TiAs_3$ rhombus in **1** is essentially flat; the maximum deviation from planarity, which occurs at As2, is 0.018(3) Å. In contrast, the $RhAs_3$ ring in complex **2** is puckered with a dihedral of angle 23.1°.[1i] The TiS_3 ring in $[(Me_5C_5)_2TiS_3]$ is even more puckered, the dihedral angle being 49°.[1a] In **1**, the plane created by the centers of the Cp rings and the Ti atom is perpendicular to the $TiAs_3$ plane (dihedral angle, 89.7(2)°). The angle (133.1(2)°) formed by the Ti atom and the centers of the Cp rings is similar to that found in $[Cp_2Ti(PMe_3)_2]$ (133.2(5) and 134.3(6)° for two independent molecules)[3] and in $[Cp_2TiS_5]$ (average 133.0°).[1d,e] The As1-Ti-As3 angle in **1** (96.8(1)°) is larger than in $[Cp_2Ti(PMe_3)_2]$ (92.9(1)° and 91.5(2)°), but similar to that found in $[Cp_2TiS_5]$ (average 95.0°). The As-Rh-As angle in **2** is considerably more acute (81.41(4)°).[1j]

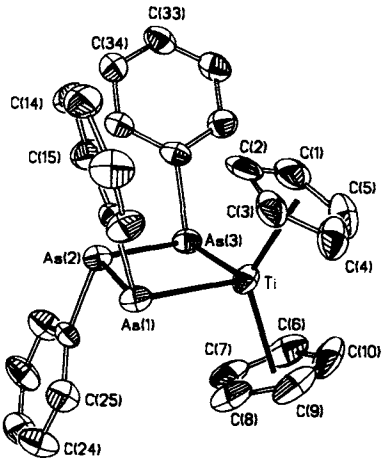

Fig. 1. ORTEP drawing of the crystal structure of **1** (without hydrogen atoms).

$[(C_5Me_5)Rh(CO)(AsPh)_3]$ **2** $[Cp_2Ti{-}CH_2{-}CRR'{-}CH_2]$ **3**

$[\{CpFe(CO)_2\}(AsPh)_2]$ **4**

The Ti-As bond distances (2.668(2) Å to As1 and 2.655(2) Å to As3) appear to be "normal," though little precedent exists: in a bis(dimethylarsino)-*o*-phenylene complex, the average Ti-As bond distance is 2.691 Å;[6] in a 1-diphenylphosphino-2-diphenylarsinoethane complex, it is 2.677(1) Å.[7] The As-As distances (As1-As2 2.431(1) Å and As2-As3 2.442(1) Å) are very similar to a "standard" As-As single bond distance in *cyclo*-$(AsPh)_6$ (average, 2.459 Å).[8] The As1-As2-As3 angle (109.51(6)°) is the largest we have encountered; in *cyclo*-$(AsPh)_6$, the average As-As-As bond angle is 91.1°.[8] The large As-As-As angle is similar to that observed in the isolobal titanacyclobutane complexes **3**: for R = H, R' = Ph, the angle at the central carbon atom is 112.0(3)° and for $R = R' = CH_3$, 110.9(6)°.[9] These complexes also have nearly planar central TiC_3 rhombi. The Ti···As2 distance is correspondingly short (3.173(1) Å), which may signify a weak transannular interaction. In sharp contrast is the As-As-As angle in **2** (82.97(5)°).[1j]

Conventional electron-counting procedures, as applied to **1**, yield a 16-electron Ti environment if the metal is Ti^{IV} and the $(AsPh)_3$ ligand functions as a four-electron donor, or if the metal is Ti^{II} and $(AsPh)_3$ a neutral two-electron donor. The former scheme is preferred if *cyclo*-$(AsPh)_6$ is viewed as an oxidizing agent analogous to *cyclo*-$(S)_8$. The latter becomes credible if **1** is compared to **4**, in which the PhAsAsPh unit functions as a two-electron donor.[10]

If, under similar reaction conditions, *cyclo*-$(AsMe)_5$ replaces *cyclo*-$(AsPh)_6$, the reaction time decreases sharply (1 h vs. 2 d) and the corresponding product, $[Cp_2Ti(AsMe)_3]$, is formed as characterized by ^{1}H-NMR.[11]

Experimental Procedure

To a suspension of pulverized Mg turnings (0.863 g, 35.9 mmol) and *cyclo*-$(AsPh)_6$ (7.321 g, 8.03 mmol) in 50 mL of dry, degassed tetrahydrofuran

[*] Prof. A. L. Rheingold, P. Mercando, A.-J. DiMaio
Department of Chemistry, University of Delaware
Newark, DE 19716 (USA)

[**] This work was supported by the Petroleum Research Fund (administered by the American Chemical Society) and the Center for Catalytic Science and Technology.

(THF) was added [Cp_2TiCl_2] (2.00 g, 8.03 mmol) in 150 mL of THF with stirring. After completion of the addition, the mixture was heated to reflux for 48 h. The reaction mixture slowly turned to a deep blue purple. After cooling and filtering, the solvent was evaporated and the residue dissolved in 400 mL of warm toluene. Following further filtration, the solution was reduced to 200 mL and slowly cooled to −78 °C to provide purple crystals of **1** (60%); m.p. = 212–214 °C (dec.).

Received: November 20, 1986;
revised: December 29, 1986 [Z 1992 IE]
German version: *Angew. Chem. 99* (1987) 252

[1] a) P. H. Bird, J. M. McCall, A. Shaver, U. Siriwardane, *Angew. Chem. 94* (1982) 375; *Angew. Chem. Int. Ed. Engl. 21* (1982) 384; b) A. Shaver, J. M. McCall, *Organometallics 3* (1984) 1823; c) H. Köpf, B. Block, M. Schmidt, *Chem. Ber. 101* (1968) 272; d) E. F. Epstein, I. Bernal, H. Köpf, *J. Organomet. Chem. 26* (1971) 229; e) E. G. Muller, J. L. Peterson, L. F. Dahl, *ibid. 111* (1976) 91; f) C. M. Bolinger, T. B. Rauchfuss, *Inorg. Chem. 21* (1982) 3947; g) K. Issleib, G. Wilke, F. Krech, *Angew. Chem. 84* (1972) 582; *Angew. Chem. Int. Ed. Engl. 11* (1972) 527; h) H. Köpf, U. Görges, *Z. Naturforsch. B36* (1981) 1205; i) H. Köpf, R. Voigtländer, *Chem. Ber. 114* (1981) 2731; j) H. Werner, W. Paul, R. Zolk, *Angew. Chem. 96* (1984) 617; *Angew. Chem. Int. Ed. Engl. 23* (1984) 626.

[2] L. B. Kool, M. D. Rausch, H. G. Alt, M. Herberhold, U. Thewalt, B. Honold, *J. Organomet. Chem. 310* (1986) 27.

[3] L. B. Kool, M. D. Rausch, H. G. Alt, M. Herberhold, U. Thewalt, B. Wolf, *Angew. Chem. 97* (1985) 425; *Angew. Chem. Int. Ed. Engl. 24* (1985) 394.

[4] ^{1}H-NMR (C_6D_6): $\delta = 5.11$ (s, 5H), 5.27 (s, 5H), 7.13 (m, 8H), 7.63 (m, 4H), 8.39 (m, 3H). Mass spectrum (EI): m/z 634 ($M^{\oplus}$, calcd 634).

[5] Crystallographic data (293 K): $a = 10.694(3)$, $b = 15.327(4)$, $c = 15.881(4)$ Å, $\beta = 109.36(2)°$, $V = 2456$ Å^3, $Z = 4$, space group $P2_1/n$, $\rho_{calcd} = 1.715$ g cm^{-3}. Of 4821 independent data collected ($4° \leq 2\theta \leq 52°$), 2927 with $F_0 \geq 3\sigma(F_0)$ were observed. For 290 variables, $R(F) = 0.0498$, $R(wF) = 0.0501$. Further details of the crystal structure determination can be obtained from the director of the Cambridge Crystallographic Data Centre, Lensfield Road, Cambridge CB2 1EW (UK), by quoting the names of the authors and the journal citation.

[6] R. A. Jones, S. T. Schwab, B. R. Whittlesey, *Polyhedron 3* (1984) 505.

[7] L. P. Battaglia, A. B. Corradi, M. Nardelli, *Inorg. Chim. Acta 50* (1981) 125.

[8] A. L. Rheingold, P. J. Sullivan, *Organometallics 2* (1983) 327.

[9] J. B. Lee, G. J. Gajda, W. P. Schaefer, T. R. Howard, T. Ikariya, D. A. Straus, R. H. Grubbs, *J. Am. Chem. Soc. 103* (1981) 7358.

[10] A. L. Rheingold, M. J. Foley, P. J. Sullivan, *Organometallics 1* (1982) 1429.

[11] ^{1}H-NMR (C_6D_6): $\delta = 5.17$ (s, 5H), 5.02 (s, 5H), 1.46 (6H), 1.38 (3H).

Cooperative Effects in the Phase Transformation of Triethylcyclotriboroxane**

By *Roland Boese,* Michael Polk,* and *Dieter Bläser*

In exploratory X-ray structure studies on boron-oxygen and boron-nitrogen compounds we discovered that triethylcyclotriboroxane (**1**)[1] exhibits a reversible first order phase transformation at −82 °C (T_1, heating curves, $\Delta H = 2.88$ kJ/mol) and −89 °C (T_2, cooling curves), respectively.[2] A series of X-ray structure analyses were therefore carried out in the region of the low-temperature (LT) phase[3] and the high-temperature (HT) phase[4] with the aim of clarifying the process of this phase transformation.

Using a computer controlled zone-melting procedure,[5] a cylindrical single crystal of **1** (m.p. −21.5 °C) was grown at −28 °C in a capillary tube mounted on the X-ray diffractometer, viewed with polarized light. The compound **1** crystallizes hexagonally in the space group $P6_3/m$. The single crystal is preserved even on passing through the first order phase transition. On approaching T_2 all reflections hkl with $h-k \neq 3n$ become diffuse and their intensities disappear within a temperature interval of ca. 4 K, i.e. the unit cell reduces to a third of its original volume but still maintaining the space group ($P6_3/m$).

In both phases the molecules of **1** have the same planar conformation with D_{3h} symmetry (Fig. 1a) as well as similar intramolecular bond lengths and angles. In the LT structure the molecules are stacked in columns in such a way that the intermolecular B···O distance is maximally 3.462 Å and 3.410 Å at −90 °C and −160 °C, respectively, when the rings are at their nearest in an eclipsed arrangement. In this arrangement the ethyl groups are equidirectionally oriented (Fig. 1b). In the HT structure there are two different arrangements in the columns: (a) eclipsed stacking with equidirectionally oriented ethyl groups, (b)

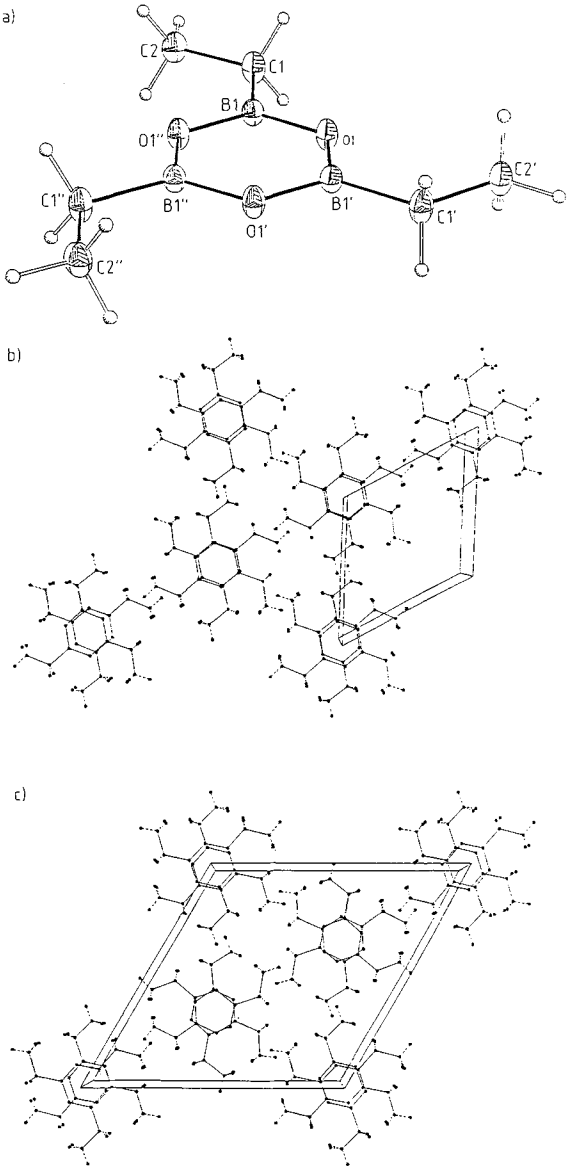

Fig. 1. a) Structure of **1** in the LT phase (−160 °C). Most important bond lengths [Å] and angles [°]: B1-O1 1.380(1), B1-O1'' 1.387(1), B1-C1 1.565(1), C1-C2 1.524(1); B1-O1-B1' 121.6(1), O1-B1-O1'' 118.4(1), O1-B1-C1 121.7(1), O1''-B1-C1 119.7(1), B1-C1-C2 116.8(1). b) Stacking of **1** in the LT phase: view of two layers in the *a*–*b* plane. c) Stacking of **1** in the HT phase: view of two layers in the *a*–*b* plane.

[*] Dr. R. Boese, Dipl.-Chem. M. Polk, Dipl.-Ing. D. Bläser
Institut für Anorganische Chemie der Universität-Gesamthochschule Universitätsstr. 5-7, D-4300 Essen 1 (FRG)

[**] We thank Prof. Dr. *H. G. von Schnering* for stimulating discussions.

slightly staggered with counterdirectionally oriented ethyl groups. In (b) the rings are rotated by 17.5° with respect to each other. This results in two intermolecular B···O distances, 3.519 Å in (a) and 3.535 Å in (b) ($T=-85$°C) (Fig. 1c).

The transition from the LT phase to the HT phase thus corresponds to a reordering of the packing, during which the ethyl groups and the ring rotate in one third of the molecules. The changeover from equidirectionally oriented ethyl groups to counterdirectionally oriented ethyl groups causes a stretching of the *c* axis. It follows that smaller intermolecular B···O interactions are to be expected for the HT phase than for the LT phase. In contrast, the dimensions of the *a* axis and *b* axis are mainly determined by repulsive intermolecular H···H interactions, as shown in Figure 2. The columns in the HT arrangement can come closer together than in the LT phase. Consequently, the influence of the attractive and the repulsive forces on the alteration of the cell dimensions with temperature is clearly separated because of the unique packing of the molecules in the unit cells.

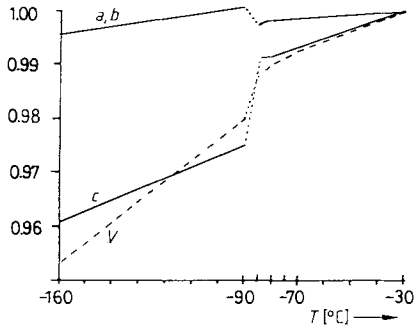

Fig. 2. Change in volume (----) and cell dimensions (——) of **1** with temperature, normalized to the HT phase at −30°C. The volume of the LT phase was multiplied by 3, the *a* and *b* axes were multiplied by $2\cos 30°$.

A comparison with the packing of the molecules of triphenylcyclotriboroxane[6] shows that in this case, intramolecular conjugation (B–C(phenyl)) in the nearly planar system makes an intermolecular B···O interaction unnecessary.[7] No stacking, and, therefore, no corresponding intermolecular interaction of the central benzene ring is even also observed with 1,3,5-trimethylbenzene[8] and 1,3,5-triphenylbenzene.[9] This likewise suggests that the stacking in **1** is effected by the intermolecular B···O interaction.

The course of the phase transformation is best explained using the model in Figure 3 as follows: in the LT phase the heterocycles (ellipses, bodies) are so arranged that the position of the ligands (legs) allow an optimum of B···O interaction (Fig. 3, bottom). Upon heating to above T_1 there is no room in this symmetrical arrangement for thermal motion of the ligands. Therefore, in some molecules at particular points in the crystal (sites of disorder or edges) the ligands start to undergo abrupt changes in their orientation; the heterocycles (bodies) simultaneously rotate somewhat, resulting in less symmetrically oriented ligands. In this way, intermolecular attractive interactions (arms and bodies) are actually reduced, but for the system as a whole this is obviously a more favorable solution than the disruption of the lattice (e.g. melting). The new arrangement (HT structure) finally propagates spontaneously through out the whole crystal (first order transition) and forcibly brings about an increase in volume and, above all, stretching in the direction of the relevant *c* axis which effects the B···O interaction (Fig. 3, top left).

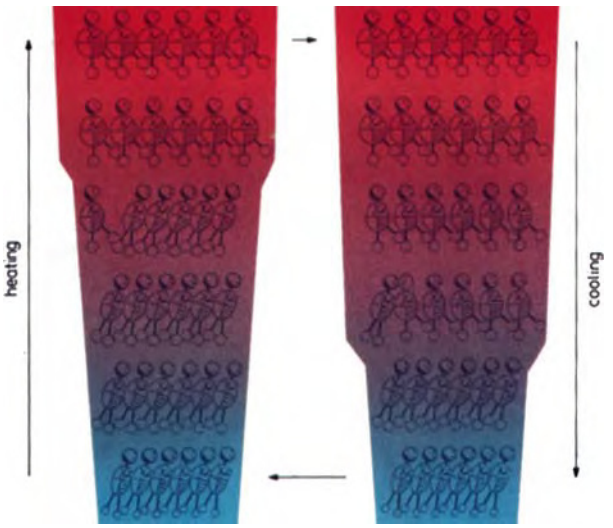

Fig. 3. Models of the phase transition. Left: behavior on heating. Right: behavior on cooling. The volume is represented by the breadth of the rows. The ellipses or bodies represent the heterocycles, the arms correspond to the intermolecular B···O interactions, the legs to the position of the ligands (ethyl groups) and the size of the feet denote their spatial requirement.

On decreasing the temperature to below T_2 (hysteresis) the HT position of the ligands now hinders the thermodynamically more favorable B···O interaction. However there are again molecules at particular points in the crystal whose heterocyclic rings, in order to increase the B···O interaction, overcome the restraints of the wavering ligands and move closer together. This leads to the spontaneous decrease in volume and change to the LT phase.

Received: April 28, 1986;
revised: December 22, 1986 [Z 1747 IE]
German version: *Angew. Chem. 99* (1987) 239

[1] P. A. McCusker, E. C. Ashby, H. S. Makowski, *J. Am. Chem. Soc. 79* (1957) 5179.

[2] R. Köster, W. R. Scheidt (Max-Planck-Institut für Kohlenforschung, D-4330 Mülheim an der Ruhr), unpublished results; *R. B.* thanks Prof. *R. Köster* for supplying a sample of **1**.

[3] LT phase: space group $P6_3/m$, confirmed by parallel refinement in $P6_3$. Cell dimensions [Å]: *a*, $b=9.029(3)$, $c=6.923(3)$ (−90); *a*, $b=8.969(1)$, $c=6.820(1)$ (−160); $Z=2$, ρ_{calc} [g cm^{-3}] = 1.13 (−90), 1.17 (−160); $\mu(Mo_{K\alpha})$ [cm^{-1}] = 0.75 (−90), 0.77 (−160); $2\theta_{max}$ [°] = 75 (−90), 100 (−160); observed reflections 586 (−90), 1411 (−160); *R*, $R_w=0.049$ (−90), 0.035, 0.038 (−160°C). All hydrogen atoms refined isotropically, all non-hydrogen atoms anisotropically with SHELXTL [10].

[4] HT phase: space group $P6_3/m$, confirmed by parallel refinement in $P6_3$. Cell dimensions [Å]: *a*, $b=15.612(11)$, $c=7.101(6)$ (−30); *a*, $b=15.594(5)$, $c=7.056(4)$ (−70); *a*, $b=15.576(4)$, $c=7.038(4)$ (−85); $Z=6$, ρ_{calc} [g cm^{-3}] = 1.11 (−30), 1.12 (−70), 1.13 (−85); $\lambda(Mo_{K\alpha})=0.71069$ Å; $\mu(Mo_{K\alpha})$ [cm^{-1}] = 0.73 (−30), 0.74 (−70), 0.74 (−85); $2\theta_{max}$ [°] = 45 (−30), 40 (−70), 50 (−85); observed reflections ($F_0 \geq 2.5\sigma(F)$), 574 (−30), 481 (−70), 826 (−85); *R*, $R_w=0.064$, 0.056 (−30), 0.044, 0.047 (−70), 0.048, 0.050 (−85°C). All hydrogen atoms refined isotropically, all non-hydrogen atoms anisotropically with SHELXTL [10].

[5] D. Brodalla, D. Mootz, R. Boese, W. Osswald, *J. Appl. Crystallogr. 18* (1985) 316.

[6] Space group $P2_1/c$. Cell dimensions [Å]: $a=10.691(1)$, $b=13.280(2)$, $c=11.583(3)$; $\beta=99.92(2)$ (−150°C); $Z=4$, ρ_{calc} [g cm^{-3}] = 1.29; $\mu(Mo_{K\alpha})$ [cm^{-1}] = 0.77; $2\theta_{max}$ [°] = 55; 2359 observed reflections $F_0 \geq 3.5\sigma(F)$; *R*, $R_w=0.073$, 0.061. Two phenyl rings coplanar with the heterocycle, one phenyl ring together with the boron atom bound to it is inclined at an angle of 10.3° to the rest of the system: B-O 1.382 Å, B-C

1.547 Å, B-O-B 120.3°, O-B-O 119.3° (mean values); shortest intermolecular B···O distance 4.441 Å [10].

[7] During the phase transformation of 2,6-diorgano-1,3,5,7-tetraoxa-2,6-dibora-4,8-octalynediones, a similar effect was observed in the transition from the 2,6-diethyl to the 2,6-diphenyl compound, and was interpreted in the same way. M. Yalpani, R. Boese, D. Bläser, *Chem. Ber. 116* (1983) 3338.

[8] Space group *Pnma*. Cell data (−70°C, m.p. = −65.3°C) [Å]: $a = 8.325(2)$, $b = 15.772(6)$, $c = 8.432(3)$; $Z = 4$, ρ_{calc} [g cm^{-3}] = 0.96; $\mu(Mo_{K\alpha})$ [cm^{-1}] = 0.50; $2\theta_{max}$[°] = 60; 529 observed reflections $F_0 \geq 5.5\sigma(F)$; R, $R_w = 0.086$, 0.099; C_s symmetry of the molecule, two ethyl groups arranged *cis*, one *trans*. Torsion angles C(phenyl)-C(phenyl)-C(ethyl)-C(ethyl) [°] = −90, +97, +88; smallest intermolecular C-C distances are C(ethyl)-C(phenyl) 3.579 Å [10].

[9] Space group $Pna2_1$. $Z = 4$; angle of twist of the phenyl groups [°] = 40.7, −37.2, 36.1; smallest intermolecular C-C distance is C(central benzene ring)-C(phenyl) 3.441 Å: Y. C. Lin, D. E. Williams, *Acta Crystallogr. B31* (1975) 318.

[10] Further details of the crystal structure investigations are available on request from the Fachinformationszentrum Energie, Physik, Mathematik GmbH, D-7514 Eggenstein-Leopoldshafen 2 (FRG) on quoting the depository number CSD-52244, the names of the authors, and the journal citation.

Kinetic ^{15}N-CPMAS-NMR Study of a Double Proton Transfer in a Crystalline Malonaldehyde Diimine Derivative**

By *Hans-Heinrich Limbach,* Bernd Wehrle, Herbert Zimmermann, Ray D. Kendrick,* and *Costantino S. Yannoni**

We report here the rate constants of proton transfer in a strong intramolecularly hydrogen bonded six-membered ring H-chelate of the malonaldehyde type. The data were obtained by dynamic ^{15}N-CPMAS-NMR spectroscopy[1] of crystalline DTAA[2] (Scheme 1). The problem of proton motion in malonaldehyde and its derivatives is a matter of continuing experimental[3-10] and theoretical interest.[11] Evidence for motion along a double minimum potential in these compounds has been obtained using different spectroscopic techniques[3-7] including NMR spectroscopy. Microwave studies[4] indicate a coherent proton tunnel process in gaseous malonaldehyde. So far, these proton transfer processes were found to be so fast that rate constants could not be obtained by NMR or any other method. Using solid state NMR techniques,[12] proton localization was observed for naphthazarine (5,8-dihydroxy-1,4-naphthoquinone)[8,9] and for tropolone[10] at low temperatures, an effect which was, however, caused by intermolecular H-bond formation. This complication does not arise in DTAA. On the other hand, double proton transfers have also been observed in solid porphines.[13,14] However, these compounds are not able to form strong intramolecular H-bonds as do malonaldehyde and its derivatives.

Since solid state proton transfers between nitrogen atoms can be conveniently studied by ^{15}N-CPMAS-NMR spectroscopy of ^{15}N-enriched compounds[13] we have synthesized DTAA-$^{15}N_4$ by slight modifications of the procedures published for the unlabeled compound.[15] The ^{15}N-CPMAS-NMR spectra of DTAA consist of two lines at all temperatures as shown in Figure 1. At low temperature, both the high-field line (which we signify as a), characteristic for an NH environment, and the low-field line (b), characteristic for an sp^2 nitrogen,[16] are sharp. As the temperature is increased, the lines broaden, sharpen again, and move towards each other, but never coalesce. Such line-shape changes are typical for the presence of two un-

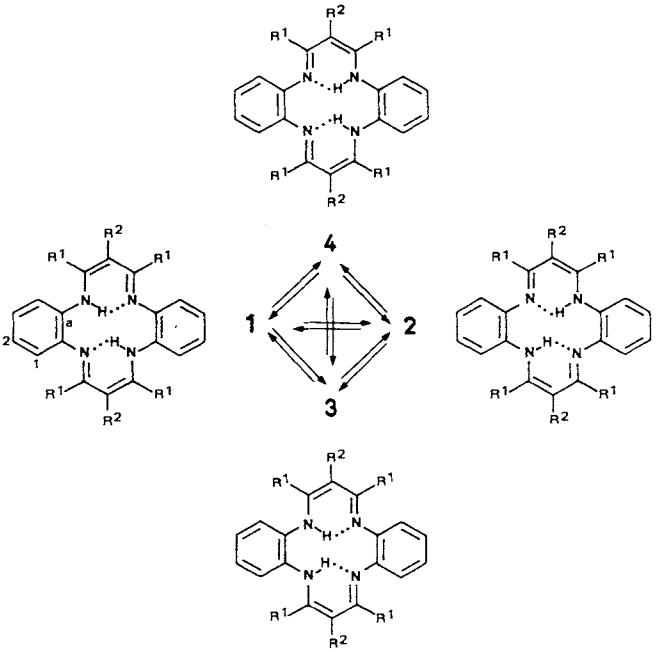

Scheme 1. DTAA: $R^1 = H$, $R^2 = CH_3$; TTAA: $R^1 = CH_3$, $R^2 = H$. N 95% for ^{15}N.

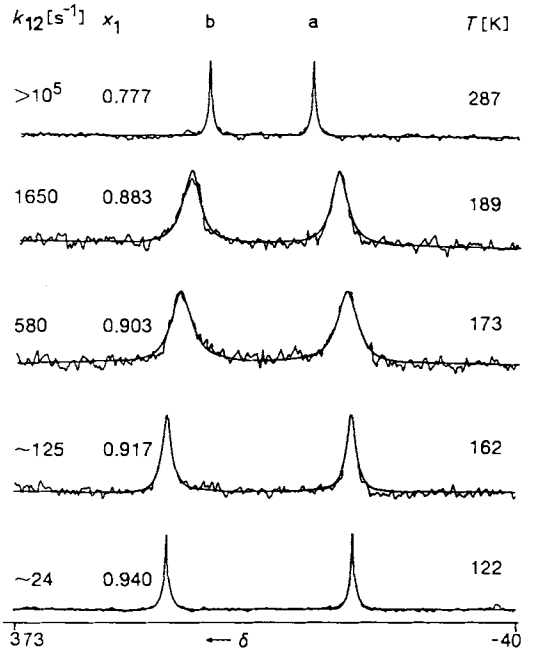

Fig. 1. Superposed experimental and calculated ^{15}N-CPMAS-NMR spectra of enriched DTAA (95% ^{15}N) at 6.082 MHz as a function of temperature. 5 ms cross polarization time, 4 kHz sweep width, 1 s repetition time. Number of scans from 122 to 287 K: 1640, 1770, 6048, 10464, 10464. Reference: external $^{15}NH_4NO_3$. x_1 is the probability of the dominant tautomer **1**, k_{12} the forward rate constant. The linewidth in the absence of exchange was taken from the spectra at 122 and 287 K.

[*] Priv.-Doz. Dr. H.-H. Limbach, Dipl.-Chem. B. Wehrle
Institut für Physikalische Chemie der Universität
Albertstr. 21, D-7800 Freiburg (FRG)
H. Zimmermann
Max-Planck-Institut für Medizinische Forschung
Jahnstrasse 29, D-6900 Heidelberg (FRG)
Dr. C. S. Yannoni, R. D. Kendrick
IBM Almaden Research Center
650 Harry Road, San Jose, California 95120-6099 (USA)

[**] This work was supported by the Deutsche Forschungsgemeinschaft, the Stiftung Volkswagenwerk, and the Fonds der Chemischen Industrie.

equally populated interconverting tautomeric states $\mathbf{1} \rightleftharpoons \mathbf{2}$ of the structure $N_aH\cdots N_b \rightleftharpoons N_a\cdots HN_b$.[13, 14] The lineshapes were simulated in terms of two superposed single-spin systems each of which exchanges between the states **1** and **2** shown in Scheme 1. In addition, it was assumed that for the chemical shifts

$$\delta_a(\mathbf{1})=\delta_b(\mathbf{2}) \quad \text{and} \quad \delta_b(\mathbf{1})=\delta_a(\mathbf{2}).$$

In the fast exchange limit, the equilibrium constant K_{12} of the tautomeric process can be calculated according to equation (a), where δ is the line separation at temperature

$$\delta/\Delta = (1-K_{12})/(1+K_{12}), \qquad \text{(a)}$$

T and $\Delta=\delta_a(\mathbf{1})-\delta_b(\mathbf{1})$ is the intrinsic chemical shift difference obtained at low temperatures.[14] The observation of two ^{15}N lines in the fast exchange regime indicates that the degeneracy of the two tautomers **1** and **2** is lifted due to a solid state effect. Approximatively 20% of the minor tautomer **2** is found at room temperature. A reaction enthalpy of $\Delta H_{12}=3.8\pm0.4$ kJ mol^{-1}, a reaction entropy of $\Delta S_{12}=2\pm0.4$ J K^{-1} mol^{-1} and, as rate constant for the forward reaction

$$k_{12}(T)=10^7\exp(-14.7\pm4.2 \text{ kJ mol}^{-1}/RT) \text{ s}^{-1}$$

were found by spectral simulation.

In view of the small temperature range between 160 K and 220 K, over which rate constants could be obtained so far, the temperature dependence of k_{12} given above is tentative and might be subject to a large error. Deuteration of the molecule in the NH sites resulted in dramatic spectral changes. At 210 K, the deuteron transfer is about 10 times slower than the proton transfer. Whereas the entropy difference between the two tautomeric states **1** and **2** found here for crystalline DTAA is negligible, the energy difference is considerable. This inequivalence is absent in solution and arises, therefore, from a solid state effect. Unfortunately, a crystal structure of DTAA, which might suggest the reason for this inequivalence, has not yet been obtained. In accordance with the literature[15, 18, 19] we assign the structures shown in Scheme 1 to the interconverting states **1** and **2**, where a possible van der Waals interaction between the inner protons is minimized. The fact that we find only two ^{15}N lines in the fast exchange regime indicates that the four nitrogen atoms in solid DTAA are pairwise equivalent, i.e. that the two proton transfer units are characterized by the same equilibrium constants (K_{12}) of tautomerism. In other words, both protons jump in concert or one immediately after the other, i.e. the tautomeric states **3** and **4** in Scheme 1 are not significantly populated. This result is in contrast to solid TTAA (Scheme 1), where all four tautomers **1** to **4** were observed.[17] These tautomers interconvert rapidly on the NMR time scale and are characterized by different energies i.e. different temperature dependent populations.

Our working hypothesis as to why the proton transfer in DTAA is much slower than in TTAA is that in TTAA the protons move independently from each other,[17] whereas in DTAA the two proton transfer units are more or less coupled together. Independent support for this idea comes from the observation that tetraaza[14]annulenes such as DTAA are dark red due to an electronic absorption band in the 450-nm region.[19] This band is absent in the yellow TTAA,[18] which correlates with the fact that the four methyl groups of TTAA sterically hinder a coplanar arrangement of the two chelate subunits in the crystal.[20] Thus, the two H-chelate subunits in TTAA are, to a crude approximation, decoupled electronically leading to independent proton motion, in contrast to DTAA. Since malonaldehyde derivatives also show phototautomerism,[21] we would expect a different behavior of DTAA and TTAA when exposed to light.

In summary, we have found evidence not only for a double minimum potential in solid DTAA for the proton motion $\mathbf{1} \rightleftharpoons \mathbf{2}$, but also for a measurable rate process which involves a kinetic isotope effect.

Received: October 1, 1986;
revised: January 21, 1987 [Z 1943 IE]
German version: *Angew. Chem. 99* (1987) 241

CAS Registry number:
DTAA, 22119-35-3.

[1] CP = cross polarization, MAS = magic angle spinning. Recent review of ^{15}N-NMR spectroscopy: W. von Philipsborn, R. Müller, *Angew. Chem. 98* (1986) 381; *Angew. Chem. Int. Ed. Engl. 25* (1986) 383.
[2] DTAA ≡ [$^{15}N_4$]-5,14-dihydro-7,16-dimethyl-6,9,14,18-tetraazadibenzo-[*a,h*]cyclotetradecene (dimethyldibenzotetraaza[14]annulene).
[3] B. Bock, K. Flatau, H. Junge, M. Kuhr, H. Musso, *Angew. Chem. 83* (1971) 239; *Angew. Chem. Int. Ed. Engl. 10* (1971) 251.
[4] S. L. Baugham, R. W. Duerst, W. R. Rowe, Z. Smith, E. B. Wilson, *J. Am. Chem. Soc. 103* (1981) 6296.
[5] H. H. Limbach, W. Seiffert, *Ber. Bunsenges. Phys. Chem. 78* (1974) 532, 641.
[6] L. J. Altmann, D. Laungani, G. Gunnarsson, H. Wennerström, S. Forsén, *J. Am. Chem. Soc. 100* (1978) 8264.
[7] R. S. Brown, A. Tse, T. Nakashima, R. C. Haddon, *J. Am. Chem. Soc. 101* (1979) 3157.
[8] J. R. Lyerla, C. S. Yannoni, C. A. Fyfe, *Acc. Chem. Res. 15* (1982) 208.
[9] W. I. Shiau, E. N. Duesler, I. C. Paul, D. Y. Curtin, W. G. Blann, C. A. Fyfe, *J. Am. Chem. Soc. 102* (1980) 4546.
[10] N. M. Szeverenyi, A. Bax, G. E. Maciel, *J. Am. Chem. Soc. 105* (1983) 2579.
[11] J. Bicerano, H. F. Schaefer III, W. H. Miller, *J. Am. Chem. Soc. 105* (1983) 2250.
[12] C. A. Fyfe, H. Mossbrugger, C. S. Yannoni, *J. Magn. Reson. 36* (1979) 61.
[13] H. H. Limbach, J. Hennig, R. D. Kendrick, C. S. Yannoni, *J. Am. Chem. Soc. 106* (1984) 4059, and references cited therein.
[14] H. H. Limbach, D. Gerritzen, H. Rumpek, B. Wehrle, G. Otting, H. Zimmermann, R. D. Kendrick, C. S. Yannoni in H. Sixl, J. Friedrich, C. Bräuchle (Eds.): *Photoreaktive Festkörper*, M. Wahl, Karlsruhe 1985, p. 19-43.
[15] E. Lorch, E. Breitmaier, *Chem. Ztg. 99* (1975) 87.
[16] E. Breitmaier, *Pharm. Unserer Zeit 6* (1983) 161.
[17] H. H. Limbach, B. Wehrle, H. Zimmermann, R. D. Kendrick, C. S. Yannoni, *J. Am. Chem. Soc. 109* (1987) 929.
[18] F. A. L'Eplattenier, A. Pugin, *Helv. Chim. Acta 58* (1975) 917.
[19] H. Hiller, P. Dimroth, H. Pfitzner, *Justus Liebigs Ann. Chem. 717* (1968) 137.
[20] V. L. Goedken, J. J. Plutz, S. M. Peng, B. Bursten, *J. Am. Chem. Soc. 98* (1976) 8014.
[21] J. A. Pardoen, J. Lugtenburg, G. W. Canters, *J. Phys. Chem. 89* (1985) 4272, and references cited therein.

A Novel Route to Azaalkenylidene-Metal Complexes**

By *Helmut Werner,** *Wolfgang Knaup,* and *Michael Dziallas*

In contrast to the well-documented alkenylidenemetal complexes [L_nM=C=CRR'], which have been the subject

[*] Prof. Dr. H. Werner, W. Knaup, Dipl.-Chem. M. Dziallas
Institut für Anorganische Chemie der Universität
Am Hubland, D-8700 Würzburg (FRG)

[**] This work was supported by the Deutsche Forschungsgemeinschaft, the Fonds der Chemischen Industrie, and Degussa AG. We thank Prof. Dr. *G. Erker* for very valuable discussions.

of intensive studies in recent years,[1] very little is known about the isoelectronic analogues $[L_nM{=}N{=}CRR']^{\oplus}$ with nitrogen instead of carbon in the α-position of the unsaturated ligand. Hitherto, ketimino derivatives such as, e.g., $LiN{=}CRR'$ or $Me_3SiN{=}CRR'$,[2,3] alkylimido complexes $[L_nM{=}NR]$ (R = Me, Et, Pr),[4] 2-substituted azirines,[5] and nitriles[6,7] have been used as building blocks for the M=N=CRR′ unit. *Erker* et al. have recently obtained zirconocene compounds of the type $[(C_5H_5)_2Zr(N{=}CHR)Cl]$ in a very elegant way by hydrozirconation of RCN with $[\{(C_5H_5)_2Zr(H)Cl\}_x]$ and have also characterized the representative with R = Ph by an X-ray structure analysis.[6a]

An attempted direct extension of the *Erker* method to a d-electron-rich transition metal such as osmium met without success. The complex **3**, which can be obtained in very good yields via **2** from the already known complex $[(C_6H_6)OsI_2]_2$ **1** (Scheme 1),[8] reacts with acetonitrile or benzonitrile in the presence of $AgPF_6$ to give the $PF_6^{\ominus}$ salts of the cations $[(C_6H_6)(PMe_tBu_2)OsH(NCR)]^{\oplus}$, R = CH_3, C_6H_5, but these do not rearrange to $[(C_6H_6)(PMe_tBu_2)Os(N{=}CHR)]^{\oplus}$. Far more suitable than nitriles as synthons are the oximes **4**, which on reaction with **3** (and $AgPF_6$) afford the corresponding azaalkenylidene complexes **6** in good yields. In the case of cyclohexanone oxime **4a** and acetone oxime **4b** it was possible by workup at temperatures below −20 °C to isolate the intermediates **5a** and **5b** and to characterize them spectroscopically.[9] Subsequent chromatography on Al_2O_3 led to abstraction of water and formation of **6a** and **6b**, respectively.

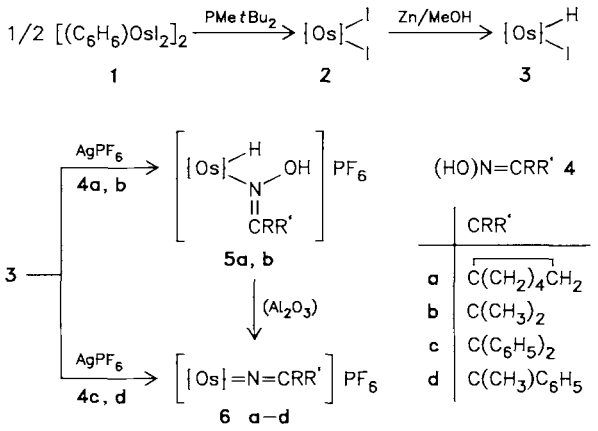

Scheme 1. [Os]=$(C_6H_6)(PMe_tBu_2)Os$.

Figure 1 shows the result of the crystal structure analysis of **6c**.[10] The cation contains a trigonal planar coordinated metal atom (with the midpoint of the benzene ring at one edge of the plane) and structurally corresponds to the alkenylidenerhodium complex $[(C_5H_5)(PiPr_3)Rh{=}C{=}CHPh]$.[11] The Os, N, and C7 atoms are almost linear and form a plane with C8 and C14 which is perpendicular (angle 89.9°) to the best plane of P1, Os and the midpoint of the benzene ring. The orthogonality is consistent with the formation of a $d_{\pi}p_{\pi}$ bond between Os and N and concomitantly also explains the short Os-N distance of 188.2(6) pm. A value of 202.4(10) pm is found for an Os-N *single* bond such as in $[Os(NCMe)(PPh_3)_2Br_3]$.[12] The N-C7 distance (127.0(9) pm) is very similar to that in other azaalkenylidene complexes[2b,3,6a] and also agrees with the N-C distances found in 2-azaallenium ions.[13]

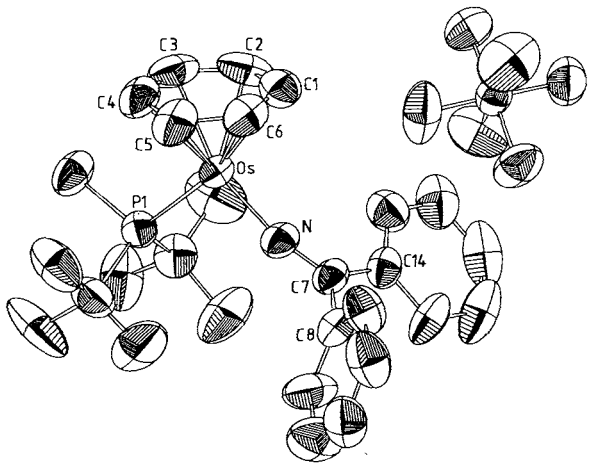

Fig. 1. Structure of **6c** in the crystal. Selected bond distances [pm] and angles [°]: Os-P1 239.2(2), Os-N 188.2(6), Os-C1 222.5(8), Os-C2 215.9(7), Os-C3 221.9(9), Os-C4 223.9(9), Os-C5 219.0(7), Os-C6 222.7(8), N-C7 127.0(9), C7-C8 150(1), C7-C14 147(1); P1-Os-N 92.9(2), Os-N-C7 168.8(5), N-C7-C8 118.5(6), N-C7-C14 121.0(6), C8-C7-C14 120.4(6).

The results of the present study are remarkable in two ways: 1) With the synthesis of **6a–d** it has now been possible for the first time to obtain *azaalkenylidene*metal compounds isoelectronic with a known *alkenylidene*metal complex ($[(C_6H_6)(PiPr_3)Os(C{=}CHPh)]$[14]) with respect to the metallaheteroallene unit M=E=CRR′. 2) The complexes **6a–d** could be prepared very easily by using oximes (HO)N=CRR′ as starting materials, which to our knowledge have so far never been used as building blocks for organometallic complexes.[2b] Since not only numerous oximes but also various halogeno(hydrido)metal compounds $[L_nM(H)X]$ are available, it is conceivable that the method described here opens up a general entry to complexes containing the M=N=CRR′ structural unit.

Experimental

A mixture of **3** (0.085 g, 0.15 mmol) and $AgPF_6$ (0.038 g, 0.15 mmol) was treated with a solution of 0.15 mmol of **4** in 5 mL of CH_2Cl_2 and stirred for a few minutes. After warming to room temperature the mixture was filtered, the filtrate was brought to dryness and the residue chromatographed on Al_2O_3 (Woelm, neutral, activity grade III) with CH_2Cl_2. After removal of the solvent, washing of the residue with pentane, and recrystallization from CH_2Cl_2/pentane, orange-red to red crystals were obtained. Yield 60–70%, correct elemental analyses; equivalent conductivity (in CH_3NO_2): **6a** 69.9, **6b** 69.8, **6c** 73.9, **6d** 71.5 $cm^2\,\Omega^{-1}\,mol^{-1}$. Workup of the reaction mixture obtained from **3**, $AgPF_6$ and **4a** or **4b** below −20 °C afforded, after removal of AgI, yellow solids of the composition **5a** and **5b**, respectively.

Received: October 20, 1986 [Z 1959 IE]
German version: *Angew. Chem.* 99 (1987) 277

[1] a) M. I. Bruce, A. G. Swincer, *Adv. Organomet. Chem. 22* (1983) 59; b) recent publications: F. J. Garcia Alonso, A. Höhn, J. Wolf, H. Otto, H. Werner, *Angew. Chem. 97* (1985) 401; *Angew. Chem. Int. Ed. Engl. 24* (1985) 406; K. R. Birdwhistell, T. L. Tonker, J. L. Templeton, *J. Am. Chem. Soc. 107* (1985) 4474; D. P. Pourreau, G. L. Geoffroy, A. L. Rheingold, S. J. Geib, *Organometallics 5* (1986) 1337; A. van Asselt, J. Burger, V. C. Gibson, J. E. Bercaw, *J. Am. Chem. Soc. 108* (1986) 5347.

[2] a) M. Kilner, C. Midcalf, *J. Chem. Soc. A 1971*, 292; b) M. Kilner, *Adv. Organomet. Chem. 10* (1972) 115.

[3] I. A. Latham, G. J. Leigh, G. Huttner, I. Jibril, *J. Chem. Soc. Dalton Trans. 1986*, 377.

[4] J. Chatt, R. J. Dosser, F. King, G. J. Leigh, *J. Chem. Soc. Dalton Trans. 1976*, 2435.

[5] M. Green, R. J. Mercer, C. E. Morton, A. G. Orpen, *Angew. Chem. 97* (1985) 422; *Angew. Chem. Int. Ed. Engl. 24* (1985) 422.

[6] a) G. Erker, W. Frömberg, J. L. Atwood, W. E. Hunter, *Angew. Chem. 96* (1984) 72; *Angew. Chem. Int. Ed. Engl. 23* (1984) 68; b) W. Frömberg, G. Erker, *J. Organomet. Chem. 280* (1985) 343.

[7] J. E. Bercaw, D. L. Davies, P. T. Wolczanski, *Organometallics 5* (1986) 443.

[8] **2** and **3** were prepared analogously to $[(C_6H_6)(PiPr_3)OsI_2]$ and $[(C_6H_6)(PiPr_3)Os(H)I]$; see H. Werner, K. Roder, *J. Organomet. Chem. 281* (1985) C38; yield for **2** (from **1**) 60%, for **3** (from **2**) 62%.

[9] Selected NMR data (without data for the signals of the phosphane ligand; **3** in $CDCl_3$, otherwise in CD_3NO_2): **3**: ^{1}H-NMR: $\delta = 5.41$ (s; C_6H_6), -10.30 (d, $J(PH) = 42.8$ Hz; OsH); **5a**: ^{1}H-NMR: $\delta = 5.99$ (d, $J(PH) = 0.4$ Hz; C_6H_6), 2.47 and 1.78 (each m; $(CH_2)_5$), -11.36 (d, $J(PH) = 36.0$ Hz; OsH), signal of NO*H* in CH_2Cl_2 at $\delta = 8.21$ (br); **5b**: ^{1}H-NMR: $\delta = 5.88$ (d, $J(PH) = 0.5$ Hz; C_6H_6), 2.03 (d, $J(PH) = 3.2$ Hz; $(CH_3)_2$), -11.27 (d, $J(PH) = 36.4$ Hz; OsH), signal of NO*H* in CH_2Cl_2 at $\delta = 8.18$ (br); **6a**: ^{1}H-NMR: $\delta = 6.09$ (s; C_6H_6), 3.13, 2.93 and 1.57 (each m; $(CH_2)_5$); ^{13}C{^{1}H}-NMR: $\delta = 161.78$ (d, $J(PC) = 4.6$ Hz; N=*C*), 80.36 (d, $J(PC) = 2.6$ Hz; C_6H_6), 28.41, 27.00, 26.93 and 26.09 (each s; $(CH_2)_5$); **6b**: ^{1}H-NMR: $\delta = 6.05$ (s; C_6H_6), 2.67 (d, $J(PH) = 1.9$ Hz; $(CH_3)_2$); **6c**: ^{1}H-NMR: $\delta = 7.49$ (m; $(C_6H_5)_2$), 6.30 (s; C_6H_6); ^{13}C{^{1}H}-NMR: $\delta = 159.89$ (d, $J(PC) = 3.1$ Hz; N=*C*), 132.35, 131.05, 130.25 and 129.41 (each s; $(C_6H_5)_2$), 81.35 (d, $J(PC) = 2.2$ Hz; C_6H_6); **6d**: ^{1}H-NMR: $\delta = 7.42$ (m; C_6H_5), 6.20 (s; C_6H_6), 2.58 (d, $J(PH) = 1.6$ Hz; CH_3).

[10] Crystals from CH_2Cl_2/pentane; dimensions of measured crystal $0.2 \times 0.3 \times 0.2$ mm; monoclinic, space group $P2_1/n$, $Z = 4$; $a = 1089.8(6)$, $b = 1596(1)$, $c = 1819(1)$ pm, $\beta = 107.02(5)°$, $V = 3026.9 \times 10^6$ pm^3; $\rho_{calc} = 1.65$ g/cm^3; $5° \leq 2\theta \leq 50°$ ($Mo_{K\alpha}$, $\lambda = 71.069$ pm, ω scan); 5308 independent reflections, Lorentz and polarization corrections, Patterson method (Syntex-XTL), positions of the hydrogen atoms partly from difference Fourier syntheses, partly calculated; $R_1 = 0.032$, $R_2 = 0.036$ for 4216 structure factors ($F_0 \geq 5.92\sigma(F_0)$). Further details of the crystal structure analysis are available on request from the Fachinformationszentrum Energie, Physik, Mathematik GmbH, D-7514 Eggenstein-Leopoldshafen 2, on quoting the depository number CSD-52217, the names of the authors, and the journal citation.

[11] J. Wolf, H. Werner, O. Serhadli, M. L. Ziegler, *Angew. Chem. 95* (1983) 428; *Angew. Chem. Int. Ed. Engl. 22* (1983) 414.

[12] F. A. Cotton, S. A. Duraj, C. C. Hinckley, M. Matusz, W. J. Roth, *Inorg. Chem. 23* (1984) 3080.

[13] M. Al-Talib, I. Jibril, E.-U. Würthwein, J. C. Jochims, G. Huttner, *Chem. Ber. 117* (1984) 3365.

[14] R. Weinand, H. Werner, *J. Chem. Soc. Chem. Commun. 1985*, 1145.

Synthesis and Crystal Structure of the Homoleptic Thioether Ruthenium Complex $[Ru(1,4,7\text{-trithiacyclononane})_2](BPh_4)_2 \cdot 2Me_2SO$**

By *Michael N. Bell, Alexander J. Blake, Martin Schröder,* Heinz-Joseph Küppers,* and *Karl Wieghardt**

Several recent reports have focused on the binding of 1,4,7-trithiacyclononane **1** to transition-metal ions.[1-3] Of particular interest have been the stereochemical and electronic effects of the homoleptic coordination of six sulfur atoms to these metal centers. As a continuation of this work, we have been investigating the coordination and redox chemistry of **1** with the platinum metals and report herein the synthesis, the single-crystal X-ray structure analysis, and the redox properties of the highly stable bis-sandwich ruthenium(II) complex $[Ru(\mathbf{1})_2]^{2\oplus}$.

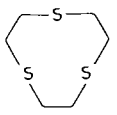

1

The complex cation $[Ru(\mathbf{1})_2]^{2\oplus}$ could be prepared by reaction of $RuCl_3 \cdot 6H_2O$ with an excess of **1** in Me_2SO at elevated temperatures,[4] or by reaction of $[RuCl_2(C_6H_6)]_2$ with an excess of **1** in methanol at room temperature.[3] Recrystallization of the complex in Me_2SO in the presence of $NaBPh_4$ yielded white crystals of **2**, the X-ray crystal structure of which was undertaken.[5]

$[Ru(\mathbf{1})_2](BPh_4)_2 \cdot 2Me_2SO$ **2**

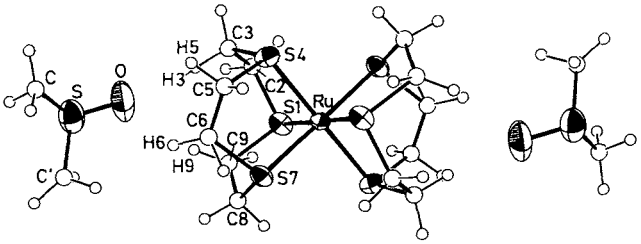

Fig. 1. Crystal structure of the cation and the coordinated Me_2SO molecule in **2**. Bond lengths [Å] and angles [°] around ruthenium: Ru-S1 2.3272(14), Ru-S4 2.3357(14), Ru-S7 2.3331(14); S1-Ru-S4 87.87(5), S1-Ru-S7 88.09(5), S4-Ru-S7 88.26(5). There is no significant interaction between the $BPh_4^{\ominus}$ ions and the cation or the solvent molecules.

The structure analysis (Fig. 1) shows a centrosymmetric cation with the Ru^{II} ion at the inversion center of the molecule; the sulfur macrocycles are each bound to the Ru^{II} center to give an overall octahedral stereochemistry. Only one of the possible conformers is present in the crystal. The two mole equivalents of Me_2SO present in the crystal lattice are well ordered and have full site occupancy. The oxygen atoms of the Me_2SO solvates are slightly closer to S4 than to S1 or S7 and each approaches the outer face of a coordinated sulfur ligand [O···H3 = 2.201(8), O···H6 = 2.419(8), O···H9 = 2.790(8), O···H5 = 3.291(8) Å]. This supplementary interaction is particularly intriguing since it suggests that inclusion of Me_2SO is occurring into the rear cone/cavity formed by **1** on coordination to the metal center (Fig. 2). This is supported by the observation that each Me_2SO molecule can be replaced by a CH_3CN or CH_3NO_2 molecule on recrystallization from these solvents.

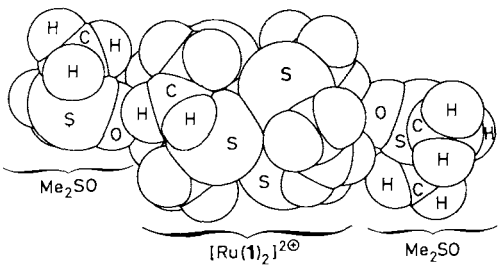

Fig. 2. Space-filling model of $[Ru(\mathbf{1})_2]^{2\oplus}$ showing interactions with two molecules of Me_2SO.

$[Ru(\mathbf{1})_2]^{2\oplus}$ represents the first example of homoleptic thioether coordination to ruthenium and is therefore an important compound with which to probe the electronic properties of thioether ligands in general. $[Ru(\mathbf{1})_2]^{2\oplus}$ is electrochemically inactive between -2.2 and $+1.3$ V vs. $Cp_2Fe/Cp_2Fe^{\oplus}$ ($Cp = \eta^5\text{-}C_5H_5$). Cyclic voltammetry in dried CH_3CN at platinum electrodes shows a quasi-reversible oxidation at $E_{1/2} = +1.41$ V ($\Delta E = 95$ mV, scan

[*] Dr. M. Schröder, M. N. Bell, Dr. A. J. Blake
Department of Chemistry, University of Edinburgh
West Mains Road, Edinburgh EH9 3JJ (Scotland)
Prof. Dr. K. Wieghardt, Dipl.-Chem. H.-J. Küppers
Lehrstuhl für Anorganische Chemie I der Universität
Postfach 102148, D-4630 Bochum (FRG)

[**] We thank the University of Edinburgh (*M. N. B.*), the Science and Engineering Research Council (UK), and the Fonds der Chemischen Industrie for support and Johnson-Matthey for generous loans of platinum metals.

rate = 100 mV s^{-1}), which we tentatively assign to a Ru^{II}/Ru^{III} redox couple, although oxidation of the ligand at these potentials cannot be ruled out. An irreversible reduction is also observed at $E_{pc} = -2.25$ V, leading to the breakdown of the complex, presumably via an unstable Ru^{I} intermediate. The free ligand thereby released can be detected on the return scan as an irreversible oxidation at +0.98 V. The high redox stability of $[Ru(\mathbf{1})_2]^{2\oplus}$ is remarkable and reflects a matching of stereochemical and electronic features of the macrocyclic ligands with those of d^6 Ru^{II} (Table 1).

Table 1. Voltammetric data for the bis-sandwich complexes $[M(\mathbf{L})_2]^{2\oplus/3\oplus}$, M = Fe, Ru.

L	$Fe^{2\oplus}/Fe^{3\oplus}$	$Ru^{2\oplus}/Ru^{3\oplus}$
TACN [a]	+0.13 V [9]	+0.37 V [10]
1 [b]	+0.98 V [2]	+1.41 V

[a] vs. the normal hydrogen electrode in aqueous solution; TACN = 1,4,7-triazacyclononane. [b] vs. $Cp_2Fe/Cp_2Fe^{\oplus}$ in CH_3CN.

We have also prepared the analogous osmium complex $[Os(\mathbf{1})_2]^{2\oplus}$ by reaction of $[OsCl_2(arene)]_2$ with an excess of **1**.[3] The ruthenium complex $[Ru(\mathbf{1})(Me_2SO)_2Cl]^{\oplus}$ can be prepared by reaction of $RuCl_3 \cdot 2H_2O$ with one equivalent of **1** in Me_2SO.[6] We are currently investigating the synthesis of 1:1 platinum-metal complexes of **1** and related tridentate macrocycles and the incorporation of organic and small molecule ligands.

Experimental Procedure

$[Ru(\mathbf{1})_2](ClO_4)_2 \cdot H_2O$: $RuCl_3 \cdot 6H_2O$ (0.1 g, 0.32 mmol) was dissolved in Me_2SO (15 mL) at 200°C. The solution was concentrated to 7 mL and cooled to 20°C, and **1** (0.22 g, 1.2 mmol) was added. The reaction mixture was heated to 140°C for 3 h; on cooling to room temperature a white solid precipitated. This product was dissolved in water and recrystallized by addition of $NaClO_4$ to give $[Ru(\mathbf{1})_2](ClO_4)_2 \cdot H_2O$. Correct elemental analyses (C,H,S).

2: $[RuCl_2(C_6H_6)]_2$ (0.05 g, 0.1 mmol) was treated with **1** (0.08 g, 0.44 mmol) in methanol (15 mL) for 30 min at 20°C. Addition of $NaBPh_4$ afforded a white precipitate, which was recrystallized from Me_2SO to give **2** in 60% yield. Correct elemental analyses (C,H). Recrystallization from CH_3CN or CH_3NO_2 afforded crystals of the corresponding disolvate. Correct elemental analyses (C,H,N). The presence of two equivalents of solvent was confirmed also by ^{1}H-NMR and infrared spectroscopy.

$[Ru(\mathbf{1})(Me_2SO)_2Cl](PF_6)$: $RuCl_3 \cdot 2H_2O$ (0.25 g, 1.01 mmol) was dissolved in Me_2SO (20 mL) and the solution was heated to 160°C for 1.5 h. To the cooled solution was added **1** (0.19 g, 1.05 mmol) and the reaction mixture heated to 60°C for 2 h. To the resulting yellow solution was added $NaPF_6$ and after several days yellow crystals of $[Ru(\mathbf{1})(Me_2SO)_2Cl](PF_6)$ had precipitated. Correct elemental analysis (C,H,S).

Received: October 20, 1986 [Z 1958 IE]
German version: *Angew. Chem.* 99 (1987) 253

[1] W. N. Setzer, C. A. Ogle, G. S. Wilson, R. S. Glass, *Inorg. Chem.* 22 (1983) 266; A. J. Blake, R. O. Gould, A. J. lavery, M. Schröder, *Angew. Chem.* 98 (1986) 282; *Angew. Chem. Int. Ed. Engl.* 25 (1986) 274; A. J. Blake, R. O. Gould, A. J. Holder, T. I. Hyde, M. O. Odulate, A. J. Lavery, M. Schröder, *J. Chem. Soc. Chem. Commun. 1987*, 118; H.-J. Küppers, A. Neves, C. Pomp, D. Ventur, K. Wieghardt, B. Nuber, J. Weiss, *Inorg. Chem.* 25 (1986) 2400.

[2] K. Wieghardt, H.-J. Küppers, J. Weiss, *Inorg. Chem.* 24 (1985) 3067.

[3] M. N. Bell, A. J. Blake, T. A. Stephenson, M. Schröder, *J. Chem. Soc. Chem. Commun. 1986*, 471.

[4] $[Ru(\mathbf{1})_2](ClO_4)_2 \cdot H_2O$ Electronic spectrum: $\lambda_{max}(\varepsilon) = 341$ (160), 293 (183), 220 nm (20040 M^{-1} cm^{-1}); ^{1}H-NMR (80 MHz, 293 K) in $[D_6]Me_2SO$: $\delta = 2.90$ (s); in D_2O: $\delta = 2.78$ (s).

[5] Crystal data of **2**: monoclinic, space group $P2_1/c$, $a = 14.134(3)$, $b = 11.0963(19)$, $c = 19.743(4)$ Å, $\beta = 94.497(16)°$, $V = 3087$ Å^3, $Z = 2$, $\rho_{calcd} = 1.315$ g cm^{-3}, 3762 data measured to $\theta = 22.5°$. Refinement based on 2936 data with $F \geq 6.0\sigma(F)$. $R = 0.0431$, $R_w = 0.0590$ for 322 parameters. Structure solution: The ruthenium atom lies on a special position (½, 0, ½), a center of inversion, and from this starting point DIRDIF [7] located all remaining non-solvent and non-hydrogen atoms. Successive least-squares cycles and difference Fourier syntheses [8] yielded the positions of the solvent atoms. For refinement [8] the methylene hydrogens were included at fixed, calculated positions and the methyl groups of the solvent were treated as rigid groups. The molecules of Me_2SO were completely ordered, with full site occupancy. Further details of the crystal structure investigation may be obtained from the Director of the Cambridge Crystallographic Data Centre, University Chemical Laboratory, Lensfield Road, Cambridge CB2 1EW (England), upon quoting the journal citation.

[6] $[Ru(\mathbf{1})(Me_2SO)_2Cl](PF_6)$: IR: $\tilde{\nu}$ [cm^{-1}] = 1070–1080 ν(S=O), 1020 ν(Ru–O) in addition to bands for **1** and $PF_6^{\ominus}$. Electronic spectrum: $\lambda_{max}(\varepsilon) = 377$ (450), 307 nm (428 M^{-1} cm^{-1}).

[7] P. T. Beurskens, W. P. Bosman, H. M. Doesbury, T. E. M. van den Hark, P. A. J. Prick, J. H. Noordik, G. Beurskens, R. O. Gould, V. Parthasarathai, DIRDIF, *Applications of Direct Methods to Difference Structure Factors*, University of Nijmegen, The Netherlands 1983.

[8] G. M. Sheldrick, SHELX76, Program for Crystal Structure Refinement, University of Cambridge, England 1976.

[9] K. Wieghardt, W. Schmidt, W. Herrmann, H.-J. Küppers, *Inorg. Chem.* 22 (1983) 2953.

[10] K. Wieghardt, W. Herrmann, M. Köppen, I. Jibril, G. Huttner, *Z. Naturforsch. B39* (1984) 1335.

Tetranuclear Mixed-Valence Manganese Complexes with Reduced TCNE or TCNQ as η^4-Bridging Ligands**

By *Renate Gross* and *Wolfgang Kaim**

The concept of single electron transfer (SET) has recently contributed a great deal to an understanding of the reactions of inorganic[1a,b] and organometallic[1c,d] compounds. In most studies reported so far attention has been centered on the mechanistic aspects of known reactions.[1] We now show that application of this concept can also lead to the synthesis of new, unexpected coordination compounds with unusual properties.

When the photolytically generated tetrahydrofuran(THF)-solvate of the organometallic fragment [Mn] (see Scheme 1) is allowed to react with an equimolar amount of tetracyanoethylene (TCNE) or 7,7,8,8-tetracyano-*p*-quinodimethane (TCNQ), a spontaneous (!) oxidative addition

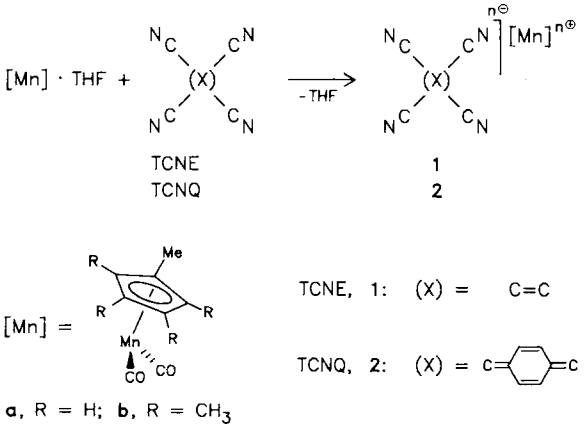

Scheme 1. Formation of the TCNE complex **1** and the TCNQ complex **2**; in each case n = 1. For [Mn]·THF, R = H, $E_{ox}^{\ominus} = +0.3$ V [3]; for TCNE and for TCNQ $E_{red} = +0.33$ V vs. SCE.

[*] Priv.-Doz. Dr. W. Kaim, Dipl.-Chem. R. Gross
Institut für Anorganische Chemie der Universität
Niederurseler Hang, D-6000 Frankfurt am Main 50 (FRG)

[**] This work was supported by the Deutsche Forschungsgemeinschaft, the Fonds der Chemischen Industrie, the Stiftung Volkswagenwerk, the Hermann-Willkomm-Stiftung, and the Flughafen Frankfurt/Main AG. We thank Dr. *J. Pohl* and Prof. Dr. *K. Wieghardt* (Bochum) for the NIR absorption measurements.

takes place to give isolable 1:1 products **1** and **2**, respectively.[2, 3]

The driving force behind the electron transfer is, in the first instance, the ratio of the redox potentials of the two reactants; there are, however, other arguments for a formulation according to Scheme 1:

- In the complexes **1** and **2** the IR vibration frequencies of the organometal fragments ($\tilde{\nu}_{CO}$) are shifted to higher energies, while those of the coordinated ligands ($\tilde{\nu}_{CN}$ and $\tilde{\nu}_{C\text{-}C}$) are shifted to lower energies[4] (Table 1); the position and intensity of the strong C=C(TCNE)-stretching bands at 1420 cm^{-1}, as also the ^{13}C-NMR data (see *Experimental*), indicate unsymmetric complexes with σ-coordinated organometal fragments[2] and radical anion ligands.[4–7]
- With the electron-rich $C_5(CH_3)_5$-ligands on the metal fragment (**1b**, **2b**), the charge transfer absorption band is shifted to *higher* energies (Table 1); accordingly,[5a] to a first-approximation we have a ligand-to-metal charge transfer (LMCT) transition in which the destabilization of the metal levels primarily affects the target orbital (cf. A) in Scheme 3).
- The reduction potentials of the complexes **1** and **2** are more *negative* than those of the free ligands (Scheme 1, Table 1), reduction potentials of ligands without prior electron transfer generally become more *positive* through coordination.[6]
- The complexes **1** with reduced TCNE are stable and, due to spin–spin coupling (cf. A) in Scheme 3),[7] display narrow NMR signals, whereas the TCNQ complex **2b** dissociates in solvents with higher dielectric constants, for example THF, to give ESR spectroscopically detectable low-spin Mn^{II} species[5b] and free $TCNQ^{\odot\ominus}$.[8]

By far the most impressive consequence of single electron transfer is the increase in the ability to coordinate at the three other σ-coordination centers of the potential μ,η^4-ligands TCNE and TCNQ. As a result of the "cyanophilicity" of the [Mn] fragments[5c] further complexation of **1** and **2** takes place to give the compounds **3** and **4**, respectively, with maximum coordinative saturation (Scheme 2).

The composition of the unexpectedly stable tetranuclear complexes **3** and **4** was confirmed analytically (Table 1);

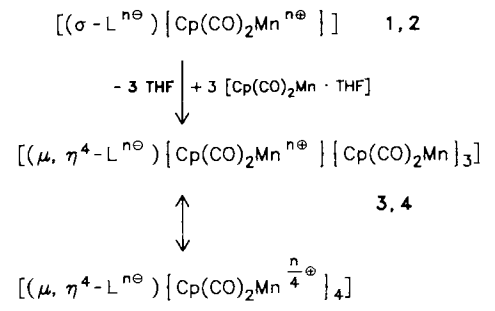

Scheme 2. Formation of the TCNE complex **3** and the TCNQ complex **4**. L=TCNE or TCNQ; Cp=η^5-$C_5H_4CH_3$ or η^5-$C_5(CH_3)_5$; $Cp(CO)_2Mn$=[Mn].

equivalence of the cyclopentadienyl groups (NMR) and the absence of the C=C stretching band in the IR spectrum indicate inversion symmetry of the tetranuclear complexes. The compounds can therefore be regarded, in the first instance, as mixed valence metal arrangements[5d, 9, 10] with delocalized charge and reduced η^4-bridging ligands, for which the relatively sharp NMR signals indicate considerable spin pairing in the ground state.

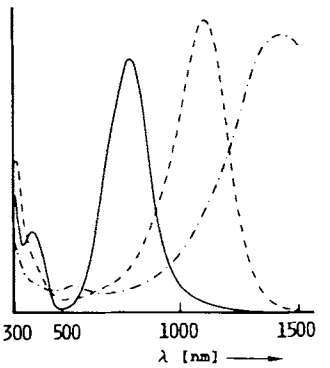

Fig. 1. Absorption spectra of the complexes [(σ-TCNE)|[Mn]|] **1b** (——), [(μ,η⁴-TCNE)|[Mn]|$_4$] **3b** (– – – –), and [(μ,η⁴-TCNQ)|[Mn]|$_4$] **4b** (– · – ·) in toluene (band intensities not to scale, [Mn] = [(η^5-C_5Me_5)$(CO)_2$Mn]). Due to the absorption window in the visible region the tetranuclear complexes have only a slightly green color.

Table 1. IR vibration frequencies $\tilde{\nu}$, charge transfer absorption maxima $\tilde{\nu}_{max}$ and redox potentials E of the complexes [L{[Mn]}$_k$] = [L{(C_5MeR_4)$(CO)_2$Mn}$_k$] **1–4**.

	L	R	k	ν(CN)	$\tilde{\nu}$(CO) [cm^{-1}] [a]	$\tilde{\nu}$(CC)	$\tilde{\nu}_{max}^{LMCT}$ [cm^{-1}] [b]	$\tilde{\nu}_{max}^{MMCT}$ [cm^{-1}] [b]	E_{red} [V] [c]	E_{ox}^{p} [V] [c]
1a	TCNE	H	1	2230(vw) 2205 (m) 2130 (m)	1975 (vs) 1905 (s)	1415 (s)	12150	—	[d]	[d]
1b	TCNE	Me	1	2230 (vw) 2205 (s) 2125 (m)	1985 (vs) 1950 (s)	1420 (s)	12660	—	−0.05	+0.9 (irr.)
3a	TCNE	H	4	2175 (m) 2130 (s)	1970 (w) 1915 (vs)	[e]	15500 (sh)	9050	−0.11	+0.5 (irr.)
3b	TCNE	Me	4	2160(m) 2110 (s)	1950 (w) 1890 (vs)	[e]	15500 (sh)	9050	−0.26	+0.4 (irr.)
2b	TCNQ	Me	1	2200(m) 2110 (w)	1970 (s) 1935 (s)	[e]	9520	—	[d]	[d]
4b	TCNQ	Me	4	2170 (w) 2105 (s)	1950 (m) 1915 (vs) 1885 (s) 1860 (vs)	[e]	[e]	7050	−0.08	+0.2 (irr.)

[a] In THF solution. [b] In toluene solution. [c] In dimethylformamide/0.1 M $Nu_4N^{\oplus}ClO_4^{\ominus}$, potentials versus saturated calomel electrode, cyclovoltammetry at glassy carbon electrodes. E_{ox}^{p}: anodic peak potential at 100 mV/s. [d] Not measured because of dissociation in solution. [e] Not observed.

 © VCH Verlagsgesellschaft mbH, D-6940 Weinheim, 1987 0570-0833/87/0303-0252 $ 02.50/0

Particularly informative with regard to this unique electronic structure are the electronic spectra (Fig. 1) of the tetranuclear complexes **3** and **4**: aside from the weak LMCT bands, extraordinarily intense ($\varepsilon > 50000\ M^{-1}\ cm^{-1}$) metal-metal charge transfer (MMCT) bands $[Mn^{n\oplus}] \leftarrow [Mn]$[5d] are observed in the IR region; a qualitative orbital level diagram (cf. B) in Scheme 3) allows this to be rationalized in terms of multiple degeneration of the Mn^{I} metal level according to the resonance structure with localized charge (Scheme 2), mixed valence complexes of class III-A[9]).

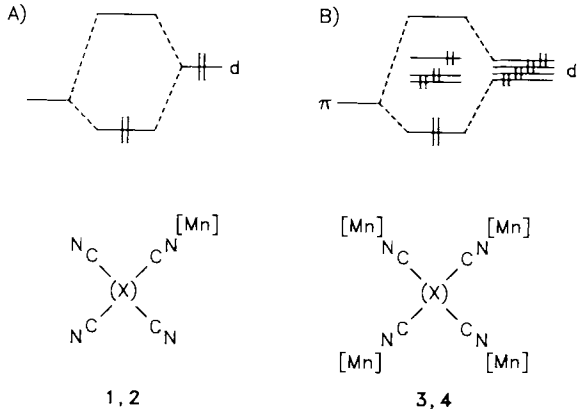

1, 2 3, 4

Scheme 3. Qualitative orbital level diagrams for the complexes **1**, **2**, and **3**, **4**.

Consistent with the very small transition energies, one observes a striking convergence of the oxidation and reduction potentials (Table 1); all the more surprising is the stability of these compounds, which can *only* be understood considering intramolecular metal-ligand electron transfer with additional contributions from the metal–metal delocalization.[5d]

Experimental

Solutions of photochemically generated [Mn]·THF [11] were treated with the appropriate amount of acceptor ligand, whereupon a momentary (cf. [5a]) color change from red to green or blue occurred. After several hours' stirring the solvent was removed and the residue was subjected to low temperature column chromatography under argon (−20°C; Florisil; eluents: hexane, toluene, ether, THF). The main fractions, after evaporation to dryness, were recrystallized from THF/hexane; some di- and trinuclear complexes were also obtained [12].— **1a**: shiny golden needles (dark green solution), yield 26%, correct C,H,N analysis.— **1b**: shiny golden needles, 58%, correct C,H,N, Mn analysis. ^{1}H-NMR (C_6D_6): $\delta = 1.21$. ^{13}C-NMR (C_6D_6): $\delta = 232.2$ (CO), 117.7, 112.2 (C≡N), 104.6, 104.5 (C=C), 88.7 (CCH_3), 11.1 (CH_3).— **3a**: dark powder, 20% correct C,H,N,Mn analysis. ^{1}H-NMR ([D$_8$]THF): $\delta = 4.70$, 4.51 (CH), 1.83 (CH_3). ^{13}C-NMR (THF): $\delta = 232.2$ (CO), 132.3 (C≡N), 107.6 (C=C), 85.0, 84.0 ($C_5H_4CH_3$), 13.3 (CH_3).— **3b**: dark powder, 24%, correct C,H,N analysis.— **4b**: olive-green platelets, 30%, correct C,H,N analysis. MS (FD): molecular peak at m/z 1189; ^{1}H-NMR (C_6D_6): $\delta = 1.65$ (CH_3), TCNQ-C*H* not observed.

Received: November 4, 1986 [Z 1977 IE]
German version: *Angew. Chem. 99* (1987) 257

[1] a) K. Wieghardt, *Chem. Unserer Zeit 13* (1979) 118; b) H. Taube, *Angew. Chem. 96* (1984) 315; *Angew. Chem. Int. Ed. Engl. 23* (1984) 329; c) J. K. Kochi: *Organometallic Mechanisms and Catalysis*, Academic Press, New York 1978; d) W. Kaim, *Acc. Chem. Res. 18* (1985) 160.

[2] One compound $[(C_5H_5)(CO)_2Mn(tcne)]$ was described as a π-complex: M. Herberhold, *Angew. Chem. 80* (1968) 314; *Angew. Chem. Int. Ed. Engl. 7* (1968) 305; *ibid. 84* (1972) 773 and *11* (1972) 730. Cf., however, σ-complexes of 1,2-dicyanoethene: M. Herberhold, H. Brabetz, *Chem. Ber. 103* (1970) 3896, 3909.

[3] J. W. Hershberger, R. J. Klingler, J. K. Kochi, *J. Am. Chem. Soc. 105* (1983) 61.

[4] Dinuclear σ-complexes of the TCNE dianion: W. Beck, R. Schlodder, K. H. Lechler, *J. Organomet. Chem. 54* (1973) 303.

[5] a) R. Gross, W. Kaim, *Inorg. Chem. 25* (1986) 498; b) *Angew. Chem. 97* (1985) 869; *Angew. Chem. Int. Ed. Engl. 24* (1985) 856; c) *J. Organomet. Chem. 292* (1985) C21; d) *Inorg. Chem. 25* (1987) 4865.

[6] W. Kaim, *Coord. Chem. Rev. 76* (1987) 187.

[7] Spin coupling was reported for the σ-coordinated complexes $[(C_5H_5)_2XV^{\oplus}][TCNE^{\odot\ominus}]$, X = halogen: M. F. Rettig, R. M. Wing, *Inorg. Chem. 8* (1969) 2685.

[8] Solvent-separated radical ion pairs with $TCNQ^{\odot\ominus}$: a) W. Kaim, *Angew. Chem. 96* (1984) 609; *Angew. Chem. Int. Ed. Engl. 23* (1984) 613; b) H. G. Fitzky, J. Hocker, *Synth. Met. 13* (1986) 335.

[9] M. B. Robin, P. Day, *Adv. Inorg. Chem. Radiochem. 10* (1967) 247.

[10] Mixed valence tetramanganese complexes in higher oxidation states of the metals have been discussed for several intermediates of the O_2-producing complex in the photosynthetic membrane: J. C. de Paula, W. F. Beck, G. W. Brudvig, *J. Am. Chem. Soc. 108* (1986) 4002; G. W. Brudvig, R. H. Crabtree, *Proc. Natl. Acad. Sci. USA 83* (1986) 4586.

[11] Preparation of [Mn]·THF: cf. W. A. Herrmann, R. Serrano, J. Weichmann, *J. Organomet. Chem. 246* (1983) C57.

[12] R. Gross, *Dissertation*, Universität Frankfurt 1987.

Two Different Intercalate Structures in the Intercalation Compounds of Graphite with Perfluorobutanesulfonic Acid**

By *Bernd Ruisinger* and *Hanns-Peter Boehm**

In graphite intercalation compounds ("graphite salts") with strong acids, e.g. sulfuric acid, layers of anions, e.g. $HSO_4^{\ominus}$, are inserted between the positively charged sheets of the graphite lattice. The interlayer volume not occupied by the anions is filled with acid molecules. A convenient method for the synthesis of graphite salts is by the anodic oxidation of graphite in pure acids.[1,2] Such an electrochemical intercalation leads to formation of stages, in which an intercalated layer is followed by three carbon layers, two carbon layers or one carbon layer (stage 3, stage 2, stage 1). In the course of intercalation of sulfuric acid by galvanostatic oxidation, a small step in the potential curve was observed within the region of the pure stage 2 compound,[2] corresponding to a small current peak in the cyclovoltammetric current/potential curve. At this point the charge of the carbon layers increases without any noticeable change in the interlayer spacing.

We have now found an analogous step (Fig. 1a) in the region of the second stage during the intercalation of perfluorobutanesulfonic acid, $C_4F_9SO_3H$, and a distinct double peak was observed at the corresponding point in the voltammogram (Fig. 1b).

The additional flow of current in the region of the first stage, which corresponds to a step in the potential curve, has never been observed with other acids. X-ray diffraction studies revealed a marked increase in the interlayer spacing after passing through this peak in the voltammogram (see Table 1). The size of the layer separations clearly indicates an intercalation of bilayers, as has also been observed in sheet silicates with intercalated *n*-alkylammonium ions.[3] The increase of ca. 325 pm in each case upon increasing the layer charge within a stage can only be explained in terms of a change in the arrangement of the perfluoroalkyl chains. In the region between the points F and G (Fig. 1) non-integral (001) reflections occur which were

[*] Prof. Dr. H.-P. Boehm, Dr. B. Ruisinger
Institut für Anorganische Chemie der Universität
Meiserstrasse 1, D-8000 München 2 (FRG)

[**] This work was supported by the Fonds der Chemischen Industrie.

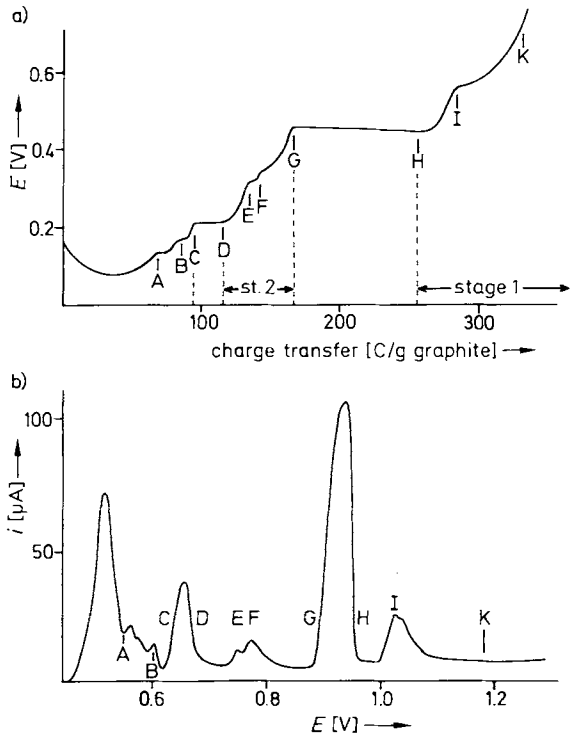

Fig. 1. Electrochemical intercalation of $C_4F_9SO_3H$ in graphite flakes from Madagascar. a) Galvanostatic oxidation: potential E (measured against graphite) as a function of charge transfer in coulomb per gram graphite. In the region of the pure stages the potential increases, in two-phase regions it remains constant. At points B and C stage 3 compounds were observed with similar interlayer spacings; at point A a mixture of stages 4 and 3 was observed. b) Potentiodynamic oxidation: oxidation current i as a function of the potential E (sweep rate 10 μV/s).

shifted in an irregular fashion from the positions for the reflections of the phases with spacings of ≈2100 and ≈2400 pm. This points to structural faults by occasional insertion of thick or thin intercalate layers, respectively.

Table 1. Layer charge and thickness of the layer packets (d_i) in the intercalation compounds of perfluorobutanesulfonic acid in graphite at selected points of the diagram in Figure 1.

Stage	Position in Fig. 1	n in $C_n^{\oplus}$	d_i [pm] [b]
3	C	85	2764 ± 17
2b	E/F [a]	59.5/56	2111 ± 11
2a	G	48	2435 ± 6
1b	I	28	1773 ± 7
1a	K	24	2099 ± 8

[a] A real separation of samples oxidized to points E and F was not possible. [b] The standard deviations are based on an X-ray diffraction diagram with at least ten strictly periodic (00l) reflections. On repeating the intercalation the mean values were within the given standard deviations. Non-integral (00l) reflections appeared in the region between the pure phases. This is not immediately recognized with smaller deviations from the positions of the integral reflections but leads to an increase in the standard deviation.

Such an abrupt change in the structure of the intercalated layers on changing the charge density in the layers of the host lattice has so far never been described in the literature. In contrast, trifluoromethanesulfonic acid behaves like sulfuric acid: It is intercalated in a flat disposition; the interlayer spacing of 804 pm is the same as in graphite hydrogensulfate.[4]

From the results of fluorine determinations, the following formulas can be calculated on the basis of the layer charge:

$C_{28}^{\oplus}(C_4H_9SO_3^{\ominus})\cdot 2.8\,C_4F_9SO_3H$ for phase 1b (1773 pm)

$C_{24}^{\oplus}(C_4F_9SO_3^{\ominus})\cdot 2.5\,C_4F_9SO_3H$ for phase 1a (2099 pm)

The densities of the intercalated layers are calculated to be 1.79 g cm^{-3} and 1.58 g cm^{-3}, respectively. For comparison: the density of the free acid is 1.81 g cm^{-3}. On going from stage 1b to stage 1a very little acid is intercalated, namely 0.1 molecule to one $C_{24}^{\oplus}$ unit.

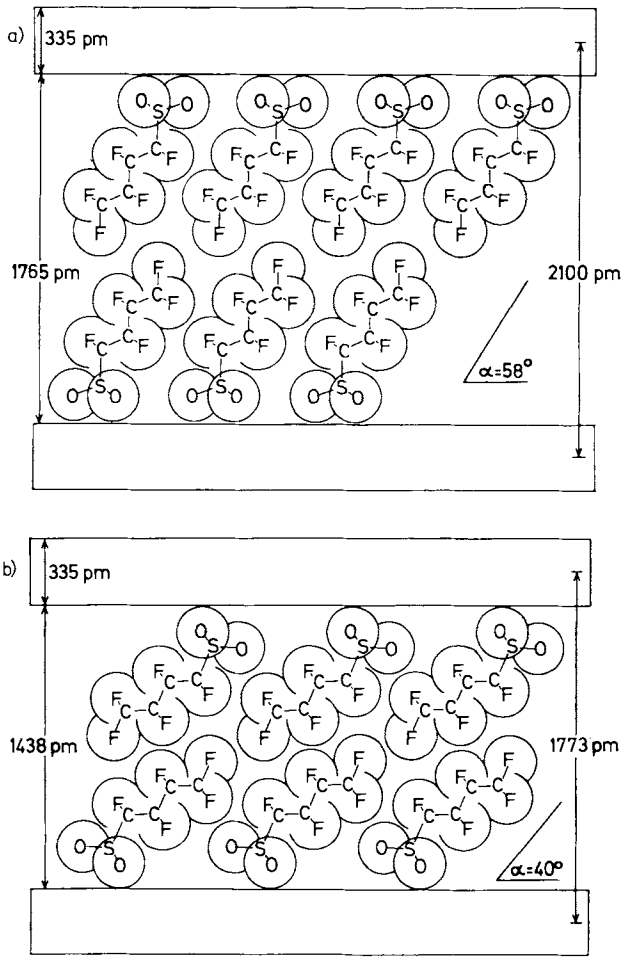

Fig. 2. Model of the phases of the 1st stage of the intercalation compound with $C_4F_9SO_3H$. a) Stage 1a, $d_i = 2100$ pm; b) stage 1b, $d_i = 1773$ pm. The angle α is the angle at which the perfluoroalkyl chains are inclined to the layer planes. The C–C–C bond angle in the chains is 116°. For clarity, the twist of the chains is not taken into consideration.

In the phase with the higher layer charge the carbon layer separation is consistent with the arrangement shown in Figure 2a. The intercalated molecules and ions are oriented with the three oxygen atoms of the sulfonic acid groups on the carbon layers; the C_4F_9 chains are in a slightly distorted *anti* conformation inclined at an angle of 58° to the plane of the layers. In poly(tetrafluoroethylene) the $(CF_2)_n$ chains are twisted into a helix with 15 CF_2 groups in the repeat unit (above 19 °C).[5] Almost the same angle, $\alpha = 56°$, was found in intercalated *n*-alkylammonium ions in layer silicates[3] or metal dichalcogenides, e.g.

TaS_2.[6] Only assumptions can be made about the arrangement of the intercalated molecules in the phases with the smaller interlayer spacing. An undistorted all-*gauche* structure of the C_4F_9 chains is unlikely, because of the size of the fluorine atoms. If, as is assumed, the chains have a twisted *anti* conformation, they must be more strongly tilted at an angle of 40° to the plane of the layers (see Fig. 2b). However, a distorted all-*gauche* conformation or a conformation with *anti* and *gauche* sequences cannot be ruled out. Only one phase was observed for stage 2 as well as stage 1 in the case of the homologous perfluorohexanesulfonic acids. These compounds are not so well ordered; the d_i spacings of ca. 2900 pm and 2620 pm, however, are consistent with the *anti* conformation, analogous to those in Figure 2a.

Experimental

Ca. 4–5 mg of Madagascar graphite (> 99.5% C, flakes of ca. 2 mm diameter) was packed in a platinum gauze pouch and anodically oxidized in perfluorobutanesulfonic acid (liberated from $C_4F_9SO_3K$ [7] with 100% H_2SO_4). Platinum was used as counter electrode; a relatively large piece of graphite foil (Sigraflex) was used as reference electrode. Upon galvanostatic oxidation *well-structured* potential/charge curves were obtained only at a very small current density, e.g. 10 μA with 5 mg of graphite, i.e. less than 500 μA per cm^2 of the prism faces of the graphite flakes. In the potentiodynamic reaction, the current/voltage curves were well-resolved only at a sweep rate below 5–10 μV/s. The use of highly oriented pyrographite (HOPG) gave similar, but not quite so well-structured curves. After a charge transfer corresponding to the selected points of the curves, the oxidation was interrupted and the graphite salt transferred to X-ray capillaries under the acid for taking Debye-Scherrer photographs. For determining the fluorine, the flakes were freed from adhering perfluorobutanesulfonic acid by rinsing with syrupy phosphoric acid and combusted with Na_2O_2/NaOH in a Parr bomb; the fluoride that was formed was determined with an ion-selective electrode by the standard-addition method.

Received: November 17, 1986;
supplemented: December 17, 1986 [Z 1985 IE]
German version: *Angew. Chem. 99* (1987) 266

[1] W. Rüdorff, U. Hofmann, *Z. Anorg. Allg. Chem. 238* (1938) 1.
[2] D. Horn, H. P. Boehm, *Z. Anorg. Allg. Chem. 456* (1979) 117; J. O. Besenhard, H. P. Fritz, *Angew. Chem. 95* (1983) 954; *Angew. Chem. Int. Ed. Engl. 22* (1983) 950.
[3] A. Weiss, *Angew. Chem. 75* (1963) 113; *Angew. Chem. Int. Ed. Engl. 2* (1963) 134.
[4] D. Horn, H. P. Boehm, *Mater. Sci. Eng. 31* (1977) 87.
[5] E. S. Clark, L. T. Muus, *Z. Kristallogr. Kristallgeom., Kristallphys., Kristallchem. 117* (1962) 119.
[6] R. Schöllhorn, E. Sick, A. Weiss, *Z. Naturforsch. B28* (1973) 168.
[7] We thank Bayer AG for a supply of this salt.

Synthesis and Structure of $[(PPh_3)_2N][Fe_3Mn(CO)_{12}(\mu_4\text{-}O)]$: A Butterfly Oxo Cluster**

By *Cynthia K. Schauer* and *Duward F. Shriver**

There has been considerable recent interest in the synthesis of clusters that contain substituent-free main-group elements to provide a conceptual bridge between organometallic chemistry and the areas of inorganic solid-state chemistry and surface chemistry.[1] Among the first-row elements, carbido and nitrido carbonyl clusters are now known which have coordination environments about the main-group atoms ranging from those presumed for surfaces to those observed in solid-state compounds.[2] The synthesis and chemistry of clusters comprised of metal atoms in low oxidation states that contain an oxo ligand is much less well developed. There are only a few examples of clusters containing the μ_3-oxo ligand,[3] a coordination mode common for oxygen atoms bound to surfaces.[4] Additionally, to the best of our knowledge, there are no oxo carbonyl clusters belonging to the interesting class of μ_4-L butterfly clusters, which have been intensely studied recently for L = C and N;[5] nor are there any other higher-nuclearity oxo clusters in which the oxo ligand is bound to more than three metal atoms. We report here on the synthesis and characterization of $PPN[Fe_3Mn(CO)_{12}(\mu_4\text{-}O)]$ **2** (PPN = $[(PPh_3)_2N]^{\oplus}$), a mixed-metal cluster which represents the first butterfly oxo compound and is a step toward building higher-nuclearity oxo clusters.

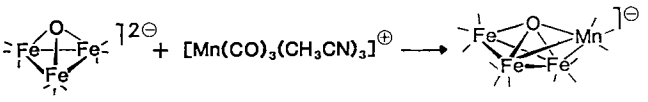

1 **2**

Treatment of the orange-red PPN salt of $[Fe_3(CO)_9(\mu_3\text{-}O)]^{2\ominus}$ **1**[3f] with one equivalent of $[Mn(CO)_3(CH_3CN)_3][PF_6]$[6] in acetone followed by crystallization from Et_2O/pentane gives the dark brown butterfly oxo cluster $PPN[Fe_3Mn(CO)_{12}(\mu_4\text{-}O)]$ **2** in 75% yield.[7] The structure of **2** is shown in Figure 1 (see also Table 1).[8] The

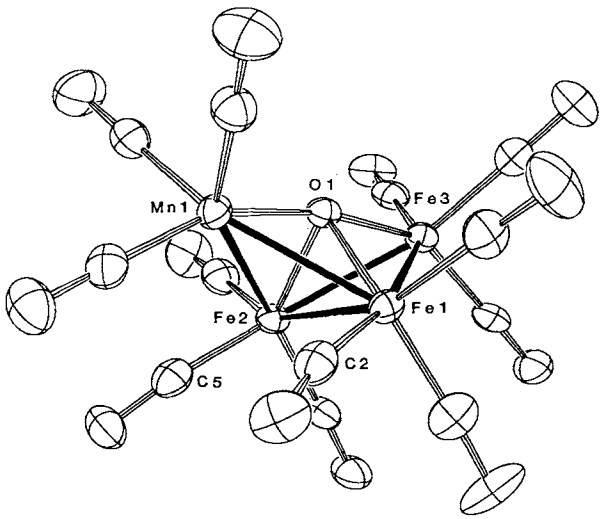

Fig. 1. Crystal structure of **2**. Thermal ellipsoid plot at 40% probability [8].

count of 62 cluster valence electrons, consistent with molecular orbital descriptions of the butterfly carbides,[9] is achieved by counting the oxo ligand as a six electron donor. All oxygen–metal distances are short (average: 1.89(2) Å). The Mn atom occupies a wingtip position in the butterfly arrangement, in contrast to the analogous carbido cluster, $[Fe_3Mn(CO)_{13}(\mu_4\text{-}C)]^{\ominus}$, where the Mn atom occupies a hinge site.[5b] The average Fe–Mn distance (2.61(2) Å) is considerably longer than the average Fe–Fe distance (2.51(1) Å). Two Fe-bound CO ligands form semibridges to the Mn atom (Mn1–C2 = 2.675(5), Mn1–C5 = 2.736(5) Å), consistent with the preference of manganese for a higher coordination number.

$[Fe_4(CO)_{12}(\mu_4\text{-}C)]^{2\ominus}$ **3** $[Fe_4(CO)_{12}(\mu_4\text{-}N)]^{\ominus}$ **4**

[*] Prof. D. F. Shriver, Dr. C. K. Schauer
Northwestern University, Department of Chemistry
Evanston, IL 60201 (USA)

[**] This work was supported by the National Science Foundation through the Synthetic Inorganic and Organometallic Program.

In the homometallic carbido and nitrido clusters, **3** and **4**, the bond distance from the heteroatom to the hinge metal (M_h) atoms is considerably longer than the distance from the heteroatom to the wingtip metal (M_w) atoms (Table 1). Such a distinct bonding preference is not observed for **2**. Additionally, the elongation of the M_h–M_w distance relative to the M_h–M_h distance in **3** and **4** is not observed in **2**. The Fe–Fe distances in **2** are nearly unperturbed from those seen in **1** (C_{3v} symmetry).[3f] As a consequence of these unique structural features, the M_w–L–M_w angle in **2** is more acute than in the nitrido and carbido clusters, **3** and **4**, respectively, and the dihedral angle between the two wings of the butterfly in **2** is approximately 10° larger than in **3** and **4**.

Table 1. Structural parameters of μ_4-L butterfly clusters [a].

	2	**3**	**4**
M_h-L [Å]	1.902(4)	1.96(3)	1.900(6)
M_w-L [Å]	1.872(3), 1.877(3) [b]	1.80(3)	1.771(5)
M_w-M_h [Å]	2.517(2), 2.61(2) [b]	2.64(1)	2.604(7)
M_h-M_h [Å]	2.499(1)	2.533(2)	2.512(1)
M_w-L-M_w [°]	168.3(1)	176.3(4)	179.0(3)
M_w-M_h-M_h-M_w [°]	113	102	102
Ref.	this work	[10]	[11]

[a] M_w, wingtip metal atom; M_h, hinge metal atom. [b] For the first entry, M = Fe; for the second entry, M = Mn.

The oxo clusters **1** and **2** were characterized by ^{17}O-NMR spectroscopy in acetone solution at room temperature on samples enriched with ^{17}O at the oxo ligand. For **1**, the spectrum consists of a resonance for the CO ligands ($\delta = 356$) and one for the μ_3-oxo ligand ($\delta = 107$). For **2**, two distinct resonances are seen for the CO ligands ($\delta = 385$ and 370, intensity ratio 1:3) and the μ_4-oxo ligand resonance is found at $\delta = 93$. The relative positions of the oxo ligand resonances in **1** and **2** is in qualitative agreement with the correlation observed between the oxygen atom coordination number and the ^{17}O chemical shift of the oxygen atom in polyoxometalate systems.[12]

Two resonances for the CO ligands of **2** ($\delta = 214.0$; 225.5; intensity ratio 3:1) were also observed in the ^{13}C-NMR spectrum ($CD_2Cl_2/CHFCl_2$ (1:2), room temperature). These two resonances correspond to the carbonyl ligands bound to the Mn atom and those bound to the Fe atoms. A fluxional process involving equilibration of the hinge and wingtip Fe-bound CO ligands must be occurring at room temperature to account for this pattern. At −50 °C, this equilibration process is not rapid and distinct resonances are seen for the two types of $Fe(CO)_3$ fragments ($Mn(CO)_3$, $\delta = 225.0$; $Fe(CO)_3$, $\delta = 212.1$ and 214.2; intensity ratio 3:3:6).

Unlike the nitrido[5a] and carbido[5b] butterfly clusters and the parent cluster **1**, **2** does not display ready reactivity toward Brønsted acids. Addition of one equivalent of CF_3SO_3H to a CH_2Cl_2 solution of **2** results in only negligible protonation.

The rarity of low-valent oxo clusters seems surprising given the vast chemistry that has been developed for the carbido and nitrido clusters. The apparently facile loss of an oxo ligand as CO_2 in carbonyl-containing complexes may, in part, offer an explanation. For instance, **1** decomposes under CO (1 atm) in acetone over a period of several hours to give CO_2 and lower-nuclearity Fe compounds; such a ready decomposition route is not accessible for nitrido and carbido clusters. If this route for loss of the oxo ligand can be suppressed, higher-nuclearity oxo clusters of low-oxidation-state metals should be accessible utilizing lower-nuclearity oxo clusters as precursors.

Received: November 18, 1986 [Z 1988 IE]
German version: *Angew. Chem. 99* (1987) 275

[1] W. A. Herrmann, *Angew. Chem. 98* (1986) 57; *Angew. Chem. Int. Ed. Engl. 25* (1986) 56, and references cited therein.
[2] a) E. L. Muetterties, M. Tachikawa, *Prog. Inorg. Chem. 28* (1981) 203; b) J. S. Bradley, *Adv. Organomet. Chem. 22* (1983) 1; c) W. L. Gladfelter, *ibid. 24* (1985) 41.
[3] a) A. Colombie, J.-J. Bonnet, P. Fompeyrine, G. Lavigne, S. Sunshine, *Organometallics 5* (1986) 1154; b) C. P. Gibson, J.-S. Huang, L. F. Dahl, *ibid. 5* (1986) 1676; c) A. Bertolucci, M. Freni, P. Romiti, G. Ciani, A. Sironi, V. G. Albano, *J. Organomet. Chem. 113* (1976) C61; d) R. J. Goudsmit, B. F. G. Johnson, J. Lewis, P. R. Raithby, K. H. Whitmire, *J. Chem. Soc. Chem. Commun. 1983*, 246; e) V. A. Uchtman, L. F. Dahl, *J. Am. Chem. Soc. 91* (1969) 3763; f) A. Ceriotti, L. Resconi, F. Demartin, G. Longoni, M. Manassero, M. Sansoni, *J. Organomet. Chem. 249* (1983) C35.
[4] G. A. Somorjai: *Chemistry in Two Dimensions: Surfaces*, Cornell University Press, Ithaca, NY, USA 1981, Chap. 5.
[5] See, for example, a) M. L. Blohm, D. E. Fjare, W. L. Gladfelter, *J. Am. Chem. Soc. 108* (1986) 2301; b) J. A. Hriljac, P. N. Swepston, D. F. Shriver, *Organometallics 4* (1985) 158.
[6] D. Drew, D. J. Darensbourg, M. Y. Darensbourg, *Inorg. Chem. 14* (1975) 1579.
[7] Correct elemental analysis. IR (Et_2O): $\tilde{\nu} = 2057$ (vw), 2007 (s), 1988 (vs), 1963 (m), 1942 (ms), 1917 (w).
[8] **2**: $a = 17.100(2)$, $b = 15.890(1)$, $c = 17.417(2)$ Å, $\beta = 94.90(1)°$ at −120 °C. Space group $P2_1/c$ ($Z = 4$). The full matrix refinement of 613 parameters with 5607 reflections converged at $R = 0.037$, $R_w = 0.044$, GOF = 1.77. Further details of the crystal structure investigation may be obtained from the Fachinformationszentrum Energie, Physik, Mathematik GmbH, D-7514 Eggenstein-Leopoldshafen 2 (FRG), on quoting the depository number CSD-52248, the names of the authors, and the journal citation.
[9] a) S. Harris, J. S. Bradley, *Organometallics 3* (1984) 1086; b) S. D. Wijeyesekera, R. Hoffmann, C. N. Wilker, *ibid. 3* (1984) 962.
[10] R. F. Boehme, P. Coppens, *Acta Crystallogr. Sect. B37* (1981) 1914.
[11] D. E. Fjare, W. L. Gladfelter, *Inorg. Chem. 20* (1981) 3533.
[12] W. G. Klemperer, *Angew. Chem. 90* (1978) 258; *Angew. Chem. Int. Ed. Engl. 17* (1978) 246.

The Diradical 2,3,5,6-Tetramethylene-1,4-cyclohexanediyl ("1,2,4,5-Tetramethylenebenzene")**

By *Wolfgang R. Roth,* Reinhard Langer, Martin Bartmann, Birgitt Stevermann, Günther Maier, Hans Peter Reisenauer, Rainer Sustmann,* and *Wolfgang Müller*

The title compound **10**, a disjoint diradical with conjugated non-Kekulé structure, is of topical interest in discussing the limits of the Hunds rule.[1] High-level ab initio SCF-MO-CI calculations lead one to expect a singlet ground state for **10** which lies about 5–7 kcal/mol below the lowest triplet state.[2] We have now checked this prediction experimentally.

[*] Prof. Dr. W. R. Roth, Dipl.-Chem. R. Langer, Dr. M. Bartmann, Dipl.-Chem. B. Stevermann
Fakultät für Chemie der Universität
Universitätsstrasse 150, D-4630 Bochum 1 (FRG)
Prof. Dr. G. Maier, Dr. H. P. Reisenauer
Institut für Organische Chemie der Universität
Heinrich-Buff-Ring 58, D-6300 Giessen (FRG)
Prof. Dr. R. Sustmann, Dipl.-Chem. W. Müller
Institut für Organische Chemie der Universität
Postfach 103764, D-4300 Essen 1 (FRG)

[**] This work was supported by the Deutsche Forschungsgemeinschaft and the Fonds der Chemischen Industrie.

The synthesis of **10** was accomplished in two ways via the precursors **6** and **9**. Palladium-catalyzed methoxycarbonylation of the Diels-Alder adduct **1** obtained from dimethylfulvene and maleic anhydride afforded the tetracarboxylate **2**, which was found to isomerize under basic conditions to give **3**. Ozonolysis and subsequent reduction furnished the pentaalcohol **4**. Selective substitution of the primary hydroxy groups yielded the tetrahalide, dehydrohalogenation of which afforded access to the tetramethylene compound **5**. Subsequent Swern oxidation led in 25% overall yield to the carbonyl compound **6**[3] (Scheme 1).

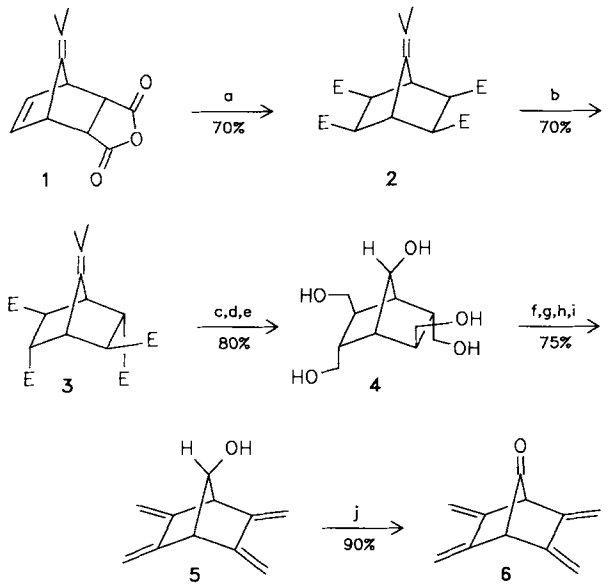

Scheme 1. E=COOMe. a) $CuCl_2$ (anhydrous), Pd/C (10%), CO (5 atm), 60°C, 3 h, MeOH (anhydrous) [4]; b) K_2CO_3, 20°C, MeOH (anhydrous); c) O_3, −78°C, CH_2Cl_2/MeOH (1:1); d) $H_3C-S-CH_3$, −78 to 0°C, CH_2Cl_2/MeOH (1:1); e) $LiAlH_4$, −78 to 60°C, tetrahydrofuran (THF) (anhydrous); f) Ph_3PCl_2/imidazole (1:2), 50°C, 6 h, pyridine/acetonitrile (1:1) [5]; g) ethyl vinyl ether, TsOH, 20°C, 20 min, ether (anhydrous); h) KOH, [18]crown-6, 20°C, 48 h, THF (anhydrous); i) MeOH (anhydrous), TsOH, 20°C, 20 min; j) oxallyl chloride, dimethyl sulfoxide (DMSO), −78°C, CH_2Cl_2 (anhydrous), NEt_3 [6].

A second entry to **10** was possible starting from the dibromide **7**,[7] which can be converted via the diyne **8** into the bisallene **9** (Scheme 2).

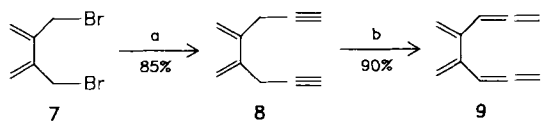

Scheme 2. a) CH≡CMgBr, NaI, Cu_2Cl_2, 60°C, 4 h, THF (anhydrous); b) KO*t*Bu/HO*t*Bu/THF (1:30), −60°C, 20 min.

The diradical **10** can be generated from both precursors **6** and **9** thermally, from **6** also photochemically. When working in the gas phase, **6** and **9** quantitatively rearrange to the tetrahydrodicyclobuta[*a*,*d*]benzene **14**; in solution, exclusively polymerization takes place. If **10** is generated in solution in the presence of a fumarate or oxygen, the Diels-Alder adducts **11** and **12**, or the peroxides **15** and **16**, respectively, are formed. These must be trapping products of **10**, since the dihydrocyclobutabenzene derivatives which are derived from **13** are stable under the reaction conditions (80°C).[8]

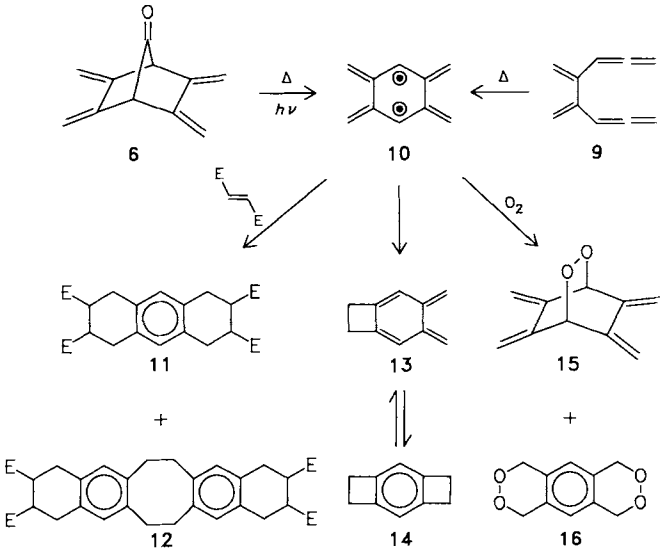

Irradiation[9] of **6** (313 nm) in an argon matrix leads quantitatively in 45 min to a red substance with characteristic IR bands at 854 and 810 cm^{-1}, which we assign, in analogy to the corresponding bands of the allyl radical,[10] to the out-of-plane CH-vibrations of the diradical **10**. The course of the reaction can be monitored by the disappearance of the carbonyl absorption of **6** at 1795 cm^{-1} and the simultaneous appearance of the carbon monoxide band at 2132 cm^{-1}. **10** is stable towards irradiation with light >300 nm, but not towards short-wavelength rays (254 nm), which cause a rearrangement into **14** via an intermediate **13**.[11] The *o*-quinodimethane structure of **13** is not only suggested by the analogous reaction of the parent compound[8] but also by a comparison of the characteristic IR and UV bands of **13** with those of *o*-quinodimethane.[12]

Informative regarding the multiplicity of the diradical **10** is the ESR spectrum. Irradiation[13] of **6** (310 nm) in an adamantane matrix affords the triplet spectrum shown in Figure 1 ($\Delta m=1$ about 3404 G, $\Delta m=2$ about 1693 G),

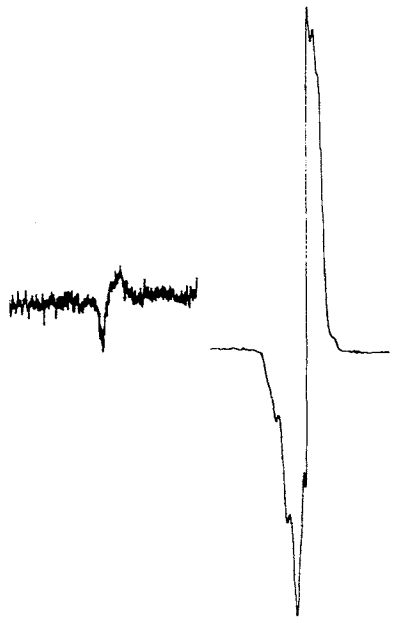

Fig. 1. ESR spectrum of **10** (adamantane matrix, 15 K).
$Hz_1=3351$ G,
$Hx_1=3380$ G,
$Hy_1=3387$ G,
$Hy_2=3419$ G,
$Hx_2=3430$ G,
$Hz_2=3441$ G.

which yields the zero field parameters $|D|/(hc)=0.0042$ and $|E|/(hc)=0.0009$ cm^{-1}. Strict linearity ($r=0.998$) versus $1/T$ was observed for the signal intensity between 15 and 80 K.

Support for this assignment is provided by the UV/VIS spectrum (Fig. 2) with its long-wave bands between 550 and 600 nm ($\lambda_{max}=530$ ($\varepsilon\approx600$), 560 (≈600), 600 (≈400 nm). The position of these bands is in good agreement with the long-wave, forbidden transition at 570 nm calculated for the triplet; these calculations do not lead one to expect any bands for the singlet in this region.[2] Contrary to the theoretical expectations the singlet ground state can accordingly lie 0.02 kcal/mol at most below that of the lowest triplet state, i.e. the states are degenerated, or—what could be more likely—the diradical has a triplet ground state.[14]

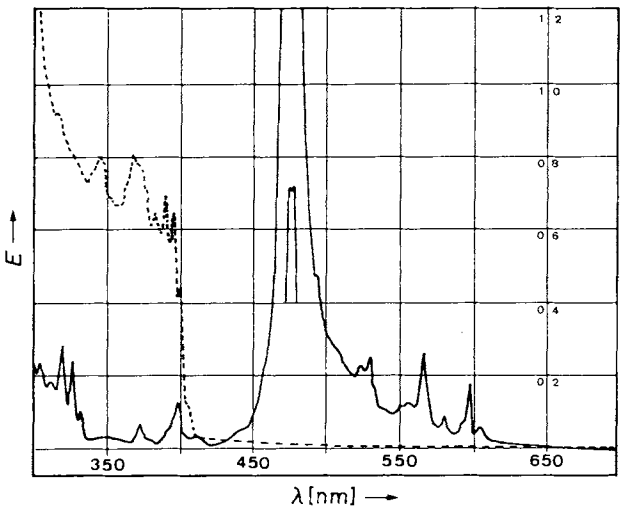

Fig. 2. UV/VIS spectra (argon matrix, 15 K): a) of **10** (——) after 45 min irradiation [9] of **6** at 313 nm; b) of **13** (---) after 15 h irradiation [9] of **10** at 254 nm.

Received: November 24, 1986;
revised: December 19, 1986 [Z 1994 IE]
German version: *Angew. Chem. 99* (1987) 271

[1] W. T. Borden: *Diradicals*, Academic Press, New York 1982, Chapter 1.
[2] P. Du, D. A. Hrovat, W. T. Borden, P. M. Lahti, A. R. Rossi, J. A. Berson, *J. Am. Chem. Soc. 108* (1986) 5072, and references cited therein.
[3] IR (CCl_4): $\tilde{\nu}$(CO) = 1795, $\tilde{\nu}$(=CH_2) = 890 cm^{-1}; ^{1}H-NMR (400 MHz, $CDCl_3$): $\delta=4.4$ (s, 2H), 5.0 (s, 4H), 5.4 (s, 4H); UV/VIS (pentane): $\lambda_{max}=280$ ($\varepsilon=3500$) sh, 256 (9000), 212 (7100), 205 nm (7400).
[4] C. Mahaim, P.-A. Carrupt, J.-P. Hagenbuch, A. Florey, P. Vogel, *Helv. Chim. Acta 63* (1980) 1149.
[5] P. J. Garegg, R. Johansson, B. Samuelsson, *Synthesis 1984*, 168.
[6] A. J. Mancuso, D. Swern, *Synthesis 1981*, 165.
[7] Y. Gaoni, S. Sadeh, *J. Org. Chem. 45* (1980) 870; P. Dowd, L. K. Marwaha, *ibid. 41* (1976) 4035.
[8] W. R. Roth, M. Biermann, H. Dekker, R. Jochems, C. Mosselmann, H. Hermann, *Chem. Ber. 111* (1978) 3892.
[9] Radiation sources: Hg high-pressure lamp Osram HBO 200W with monochromator (halfwidth 10 nm), Bausch and Lomb; Hg low-pressure lamp (spiral lamp, 150 W), Gräntzel; cooling system: Displex Closed Cycle Refrigeration System 202, Air Products.
[10] G. Maier, H.-P. Reisenauer, B. Rohde, K. Dehnicke, *Chem. Ber. 116* (1983) 732.
[11] M. P. Cava, A. A. Deana, K. Muth, *J. Am. Chem. Soc. 82* (1960) 2524; R. Gray, L. G. Harruff, J. Krymowski, J. Peterson, V. Boekelheide, *ibid. 100* (1978) 2892.
[12] K. L. Tseng, J. Michl, *J. Am. Chem. Soc. 99* (1977) 4840.
[13] 1000W Hg/Xe high-pressure lamp (Hanovia: 977B-1); uranium glass filter (Schott: UG5); monochromator (Jobin Xvon: H10-UV).
[14] A similar result was also obtained recently for the diradical tetramethyleneethane (2,3-dimethylene-1,4-butanediyl): P. Dowd, W. Chang, Yi Hyon Paik, *J. Am. Chem. Soc. 108* (1986) 7417.

Dinuclear Complexes of Gold(I) Containing Bridging Cyclometalated Arylphosphane or Arylarsane Ligands

By *Martin A. Bennett,* Suresh K. Bhargava, K. David Griffiths, Glen B. Robertson, Wasantha A. Wickramasinghe,* and *Anthony C. Willis*

Many complexes have been characterized structurally in which two 1,3-difunctional bidentate ligands hold a pair of gold(I) atoms in a dimeric unit in close contact, the metal-metal distances (2.76–3.02 Å) being close to, or even less, than that in metallic gold (2.88 Å).[1,2] Typical are the di-*n*-propyldithiocarbamate complex **1**, complexes of the methylenebis(diphenylphosphane) series such as **2** and **3**, and phosphorus ylide complexes such as **4** and **5** (Table 1).

Table 1. Some Au-Au complexes.

	Complex	τ [Au-Au]	Ref.
1	$[Au_2\{\mu\text{-}S_2CN(n\text{Pr})_2\}_2]$	2.76(1)	[3]
2	$[Au_2Cl_2(\mu\text{-}Ph_2PCH_2PPh_2)_2]$	2.962(1)	[4]
3	$[Au_2(\mu\text{-}Ph_2PCHPPh_2)_2]$	2.888(3)	[5]
4	$[Au_2\{(\mu\text{-}CH_2)_2PEt_2\}_2]$	3.023(1)	[6]
5	$[Au_2\{(\mu\text{-}CH_2)_2PPh_2\}_2]$	2.977(1)	[7]

These results suggest that gold(I)-gold(I) dimers of type **6** containing *ortho*-metalated arylphosphanes or arylarsanes should be stable, especially as the isosteric ligand 2-pyridyldimethylphosphane is known to form stable salts of type **7** in which the gold-gold distance is only 2.776(1) Å.[8] A compound related to **6** is the dimer **8**[9] containing *ortho*-metalated benzyldiphenylphosphane,[9] but its structure has not been determined.

Attempts to synthesize **6a** ($E=PPh_2$) by heating $[Au(O_2CMe)(PPh_3)]$ or $[AuMe(PPh_3)]$, with or without added PPh_3, were unsuccessful.[10] However, reaction of $[o\text{-}LiC_6H_4PPh_2]$ with $[AuBr(PEt_3)]$ in ether at -50 °C gives **6a** in good yield as an air-stable, colorless, crystalline solid which is sparingly soluble in organic solvents except CH_2Cl_2 and $CHCl_3$.[11] The complex AuBr($AsPh_3$) can also

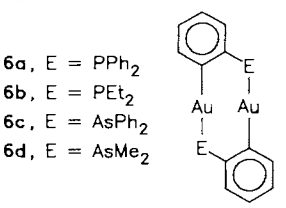

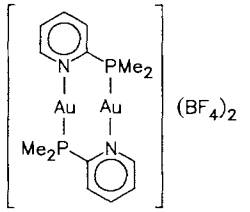

7

$[Au_2(o\text{-}C_6H_4CH_2PPh_2)_2]$

8

$[Au(o\text{-}C_6H_4AsPh_2)(PEt_3)]$

9

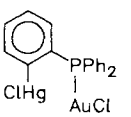

10

[*] Dr. M. A. Bennett, Dr. S. K. Bhargava, K. D. Griffiths [+], Dr. G. B. Robertson [+], Dr. W. A. Wickramasinghe [+], Dr. A. C. Willis [+]
Research School of Chemistry, Australian National University
Canberra, A.C.T. 2601 (Australia)

[+] X-ray structure analysis

be used as a precursor, but there is considerable competing reduction to metallic gold. Reaction of [*o*-$LiC_6H_4PPh_2$] with AuCl complexes containing more labile ligands such as diethyl sulfide or tetrahydrothiophene does not lead to formation of **6a**.

The mass spectrum (70 eV) of **6a** shows a parent ion, the IR spectrum (KBr disk) contains bands typical of *ortho*-metalation at 1563 (w), 1420 (w), and 723 (m) cm^{-1},[12] and there is a singlet in the $^{31}P\{^1H\}$-NMR spectrum at $\delta = 36.2$ (external standard 85% H_3PO_4) arising from equivalent phosphorus atoms.

Molecules of **6a** have exact inversion symmetry in the solid state[13] and the structure of one such molecule (with H-atoms omitted) is shown in Figure 1.[14] The metallacycle has a twist "recliner" conformation with the carbon atoms displaced by 0.40 and 0.25 Å from the Au_2P_2 plane. The gold and phosphorus atoms are displaced to opposite sides of the phenylene ring planes by 0.60 and 0.10 Å respectively. This twisting deformation is probably a consequence of the steric requirements of the fairly bulky phenyl substituents. The P-Au-C angle is 172.8(1)°. The Au···Au distance (2.8594(3) Å) is typical of gold(I) dimers and suggests a substantial bonding interaction between the metal atoms. The Au-P (2.300(1) Å) and Au-C (2.056(3) Å) distances are unexceptional.

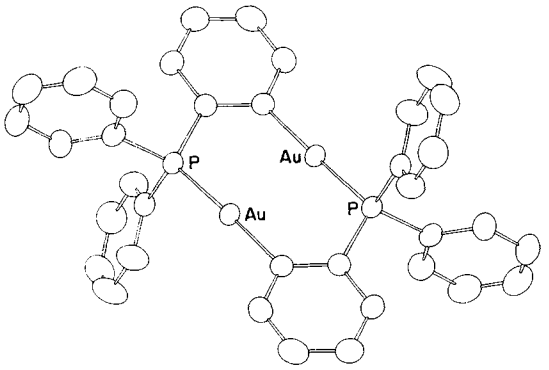

Fig. 1. Crystal structure of **6a** [13, 14].

Other cycloaurated complexes can be made similarly to **6a**, though in generally lower yields; for example **6b** from [AuBr(PEt_3)] and [*o*-$LiC_6H_4PEt_2$] as colorless crystals (ca. 10% yield),[16] **6c** from [AuBr($AsPh_3$)] and [*o*-$LiC_6H_4AsPh_2$] as pale yellow crystals (62% yield), and **6d** from [AuBr(PEt_3)] and [*o*-$LiC_6H_4AsMe_2$], also as pale yellow crystals (18% yield).[17] Treatment of [AuCl(PEt_3)] with [*o*-$LiC_6H_4AsPh_2$] gives the σ-arylgold(I) complex **9** containing an uncoordinated $AsPh_2$ group; the same compound is obtained from **6c** and triethylphosphane. The metallacycle framework in **6b**[18] is very similar to that in **6a**, although it is more nearly planar and the twisting deformation is essentially absent. **6c**[19] is isomorphous with **6a**. Corresponding Au-Au distances are 2.8617(6) and 2.8496(5) Å (**6b**, two independent molecules), and 2.9358(5) Å (**6c**), the longer distance in **6c** reflecting, primarily, the larger covalent radius of arsenic relative to phosphorus.

The new complexes undergo typical oxidative additions with halogens to form dinuclear gold(II) complexes,[20] but an attempt to form a Hg-Au-Au-Hg system by treating **6a** with $HgCl_2$ in THF was unsuccessful. Instead, transmetalation occurred at the σ-aryl group to give the colorless dinuclear complex **10**, which shows a singlet $^{31}P\{^1H\}$-NMR resonance in CD_2Cl_2 at $\delta = 43.2$ with ^{199}Hg satellites ($^3J_{HgP} = 413$ Hz). The Au-Hg distance of 3.112(1) Å in the crystalline mono(tetrahydrofuran) solvate of **10** (Fig. 2)[21] indicates that any metal-metal interaction must be weaker than that in **6a**.

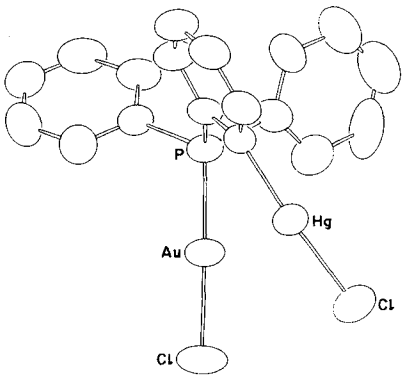

Fig. 2. Crystal structure of **10** [14, 21].

Received: October 29, 1986 [Z 1969 IE]
German version: *Angew. Chem. 99* (1987) 261

CAS Registry numbers:
6a, 106762-23-6; **6b**, 106735-72-2; **6c**, 106735-73-3; **6d**, 106735-74-4; **9**, 106735-75-5; **10**·C_4H_8O, 106735-77-7; *o*-$LiC_6H_4PEt_2$, 106762-24-7; *o*-$LiC_6H_4AsPh_2$, 106762-25-8; AuBr(PEt_3), 14243-60-8; AuBr($AsPh_3$), 25749-30-8; AuCl(PEt_3), 15529-90-5; AuBr(PPh_3), 14243-65-3.

[1] K. P. Hall, D. M. P. Mingos, *Prog. Inorg. Chem. 32* (1984) 238.
[2] Yuanheng Jiang, S. Alvarez, R. Hoffmann, *Inorg. Chem. 24* (1985) 749.
[3] R. Hesse, P. Jennische, *Acta Chem. Scand. 26* (1972) 3855.
[4] H. Schmidbaur, A. Wohlleben, U. Schubert, A. Frank, G. Huttner, *Chem. Ber. 110* (1977) 2751.
[5] C. M. Briant, K. P. Hall, D. M. P. Mingos, *J. Organomet. Chem. 229* (1982) C 5.
[6] H. Schmidbaur, J. E. Mandl, W. Richter, V. Bejenke, A. Frank, G. Huttner, *Chem. Ber. 110* (1977) 2236.
[7] J. D. Basil, H. H. Murray, J. P. Fackler, Jr., J. Tocher, A. M. Mazany, B. Trczinska-Bancroft, H. Knachel, D. Dudis, T. J. De Lord, D. O. Marler, *J. Am. Chem. Soc. 107* (1985) 6908.
[8] Y. Inoguchi, B. Milewski-Mahrla, H. Schmidbaur, *Chem. Ber. 115* (1982) 3085.
[9] H.-P. Abicht, K. Issleib, *J. Organomet. Chem. 149* (1978) 209.
[10] The complex [AuMe(PPh_3)] is known to decompose quantitatively on heating to give ethane, gold, and PPh_3, the process being retarded by added PPh_3: A. Tamaki, J. K. Kochi, *J. Organomet. Chem. 61* (1973) 441.
[11] *Procedure* for **6a**: A solution of *n*-butyllithium in hexane (2.3 ml of a 15% w/w solution) was added to (*o*-bromophenyl)diphenylphosphane (1.16 g, 3.4 mmol) in ether over 0.5 h at room temperature. The resulting precipitate (0.93 g) of (*o*-lithiophenyl)diphenylphosphane containing some ether was washed by decantation with hexane and dissolved in ether (25 mL). This solution was added dropwise to a stirred solution of [AuBr(PEt_3)] (1.1 g, 2.8 mmol) at −70°C. The mixture was stirred for ca. 2 h at −40°C, allowed to come to room temperature, and stirred for a further 1.5 h. The solution was evaporated to dryness in vacuo and the colorless solid residue was washed with ether (3 × 6 mL), methanol (5 × 10 mL), and hexane (3 × 5 mL). It was then extracted with hot dichloromethane (200 mL) to give a purple-tinted solution which was filtered through Celite. Concentration of the colorless filtrate under reduced pressure to ca. 15–20 mL volume gave colorless **6a** (0.8 g, 63%).
[12] M. A. Bennett, D. L. Milner, *J. Am. Chem. Soc. 91* (1969) 6983; D. J. Cole-Hamilton, G. Wilkinson, *J. Chem. Soc. Dalton Trans. 1977*, 797; D. P. Arnold, M. A. Bennett, M. S. Bilton, G. B. Robertson, *J. Chem. Soc. Chem. Commun. 1982*, 115.
[13] **6a**: triclinic, $P\bar{1}$, $a = 9.3653(7)$, $b = 9.7730(9)$, $c = 8.9424(7)$ Å, $\alpha = 109.921(6)°$, $\beta = 87.297(6)°$, $\gamma = 104.186(6)°$, $Z = 1$; Philips PW1100 diffractometer, $\lambda = 0.7107$ Å, $R = 0.018$, $R_w = 0.023$ for 2950 unique reflections [$4 < 2\theta < 55°$, $I \geq 3\sigma(I)$], 181 parameters, H atoms by calculation. Further details of this and the other crystal structure investigations reported herein are available on request from the Director of the Cambridge Crystallographic Data Centre, University Chemical Laboratory, Lensfield Road, Cambridge CB2 1EW (UK).
[14] ORTEP drawing [15], 30% ellipsoids, hydrogen atoms omitted.
[15] C. K. Johnson, ORTEP II, Report ORNL-5138, Oak Ridge National Laboratory Tennessee, 1976.

[16] **6b**: ^{1}H-NMR (CD_2Cl_2): $\delta = 1.5$ [dt, $^3J(PH) = 15$ Hz, CH_3], 2.1 (m, CH_2), 7.1-7.8 (m, C_6H_4). ^{31}P-NMR (CD_2Cl_2): $\delta = 34.6$ (s). MS (70 eV) $m/z = 726$ (calcd. 725).

[17] **6d**: ^{1}H-NMR (CD_2Cl_2): $\delta = 1.65$ (s, CH_3), 7.1-7.8 (m, C_6H_4). MS (70 eV) $m/z = 756$ (calcd. 756).

[18] **6b**: triclinic, $P\bar{1}$, $a = 13.041(2)$, $b = 10.626(1)$, $c = 8.245(1)$ Å, $\alpha = 107.77(1)$, $\beta = 102.22(1)$, $\gamma = 90.90(1)°$, $Z = 2$; Philips PW1100 diffractometer, $\lambda = 0.7107$ Å, $R = 0.032$, $R_w = 0.038$ for 3921 unique reflections [$4 < 2\theta < 55°$, $I \geq 3\sigma(I)$], 431 parameters, H atoms by calculation, absolute configuration.

[19] **6c**: triclinic, $P\bar{1}$ [isomorphous with **6a** [13]], $a = 9.530(2)$, $b = 9.824(1)$, $c = 8.904(1)$ Å, $\alpha = 109.26(1)$, $\beta = 88.01(1)$, $\gamma = 103.96(1)°$, $Z = 1$; PW1100 diffractometer, $\lambda = 0.7107$ Å, $R = 0.017$, $R_w = 0.022$ for 3937 unique reflections [$3 < 2\theta < 60°$, $I \geq 3\sigma(I)$], 181 parameters, H atoms by calculation.

[20] M. A. Bennett, S. K. Bhargava, K. D. Griffiths, G. B. Robertson, *Angew. Chem. 99* (1987) 262; *Angew. Chem. Int. Ed. Engl. 26* (1987) 260.

[21] **10** · THF monoclinic, $P2_1/n$, $a = 15.459(1)$, $b = 13.668(2)$, $c = 10.970(1)$ Å, $\beta = 92.41(1)°$, $Z = 4$; PW1100 diffractometer, $\lambda = 0.7107$ Å, $R = 0.032$, $R_w = 0.037$ for 2433 unique reflections [$3 < 2\theta < 50°$, $I \geq 3\sigma(I)$], 253 parameters, H atoms by calculation.

Coupling of Cyclometalated Phenylphosphanes in Dinuclear Gold(II)-Complexes

By *Martin A. Bennett,* Suresh K. Bhargava, K. David Griffiths,* and *Glen B. Robertson*

Dinuclear complexes in which two gold(I) ($5d^{10}$) atoms are held in close proximity by a pair of bridging ligands[1,2] undergo oxidative addition with halogens to give two types of product, in both of which the bridging framework is retained. For example, depending on the solvent, addition of iodine to the methylenethiophosphinate-gold(I) dimer $[Au_2\{CH_2P(S)Ph_2\}_2]$ can yield either the isovalent gold(II)-gold(II)(d^9-d^9) complex **1** or the isomeric, heterovalent gold(I)-gold(III)(d^{10}-d^8) complex **2**.[3] Halogens add to the phosphorus ylide complexes $[Au_2\{(CH_2)_2PR_2\}_2]$, R = Me, Et, Ph, to form isovalent gold(II)-gold(II) complexes **3a**[4] and **3b**,[5] but **3c** isomerizes in polar solvents to a heterovalent gold(I)-gold(III) dimer **4**, in which one of the ylide ligands is bound terminally to the gold(III) atom[6] (see Scheme 1).

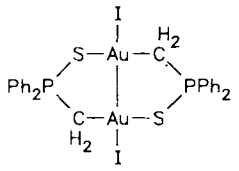

1, r = 2.609(1) Å

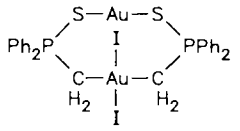

2, r = 3.050(3) Å

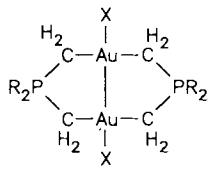

3a, X = Cl, R = Et
r = 2.597(5) Å
3b, X = I, R = Me
r = 2.660 Å
3c, X = Cl, R = Ph

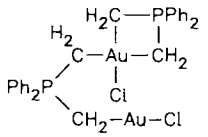

4, r = 3.184(1) Å

Scheme 1. r = gold-gold distance.

The cyclometalated dimer **5**[7] reacts with bromine or iodine in a 1:1 molar ratio at −78 °C to give orange-red crystalline complexes **6** and **7** in good yield.[8] The fact that both show singlet $^{31}P\{^1H\}$-NMR resonances[9] suggests that the compounds have a symmetrical, isovalent structure and this is confirmed by an X-ray structural analysis of **7**[10] (Fig. 1).[11]

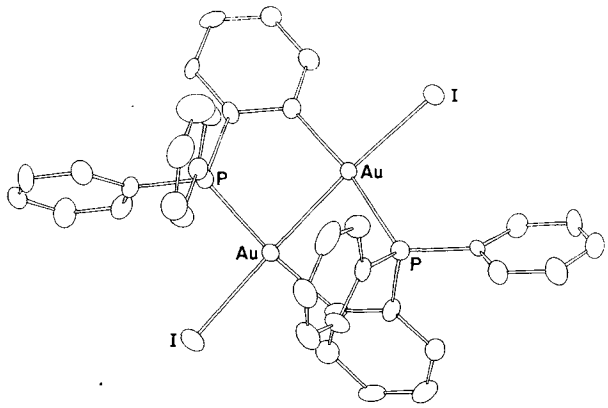

Fig. 1. Crystal structure of **7** [10, 11].

The Au-Au distances in **7** [2.5898(6) Å and 2.5960(7) Å for two independent molecules] are significantly shorter than the corresponding separation in its gold(I)-gold(I) precursor **5** [2.8594(3) Å].[7] Moreover, whereas the metallacycle in **5** has a twist "recliner" conformation, that in **7** adopts a "propeller" conformation in order to reduce nonbonding interactions with the iodine atoms. The basic structure is very similar to that of the cyclometalated platinum(I)-platinum(I) (d^9-d^9) complex **11**[13] in which the axial ligands are phosphanes instead of iodine. The Au-Au distances in **7** are very close to those in the isovalent phosphorus ylide dichloro complex **3a**[4] but are significantly less than those in the diiodo complex **3b**.[5] The Au-I bond lengths in **7** [2.669 Å (av.)] are also significantly shorter than those in **3b** (2.699 Å).[5]

When solutions of **6** and **7** are heated for ca. 12 h in toluene, or are allowed to stand in dichloromethane at room temperature for several days, the color changes from red to pale yellow; the same color change occurs more rap-

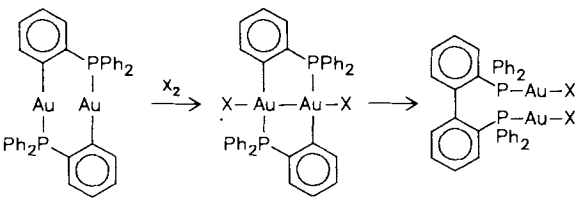

5 → (X_2) → **6**, X = Br; **7**, X = I → **8**, X = Br; **9**, X = I

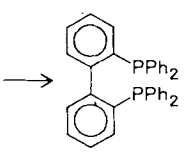

10

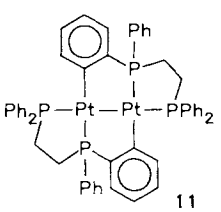

11

[*] Dr. M. A. Bennett, Dr. S. K. Bhargava, K. D. Griffiths [+], Dr. G. B. Robertson [+]
Research School of Chemistry, Australian National University
Canberra, A.C.T. 2601 (Australia)

[+] X-ray structure analysis

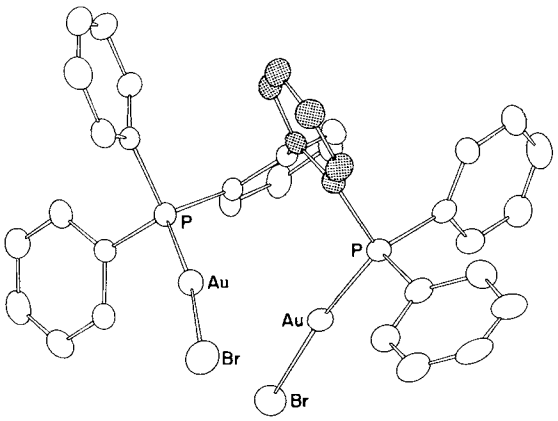

Fig. 2. Crystal structure of **8** [11, 16].

idly on exposure to normal laboratory light. Addition of hexane precipitates colorless, crystalline solids in yields of ca. 70%. The new complexes **8** and **9** are isomeric with their precursors, are dimeric in CH_2Cl_2,[14] and show singlets in their $^{31}P\{^1H\}$-NMR spectra due to equivalent phosphorus atoms.[15] X-ray analysis of the bromo-complex **8**[16] (Fig. 2)[11] shows that it contains a 2,2′-biphenylenebis(diphenylphosphane) ligand.[17] A dihedral angle of 88.6° between the phenyl rings of the biphenyl unit leads to a separation of 3.3013(5) Å between the gold(I) atoms, which are not bound to each other and display their normal linear coordination. The Au–Br and Au–P bond lengths [av. 2.398 and 2.238 Å, respectively] are unexceptional.

Treatment of **9** with aqueous ethanolic NaCN liberates the ligand **10** quantitatively as a white, crystalline solid which melts at 212°C.[18] The value is much higher than the m.p. of 68–70°C reported for a product claimed to be **10** which was isolated in 65% yield from the reaction of Ph_2PCl with 2,2′-dilithiobiphenyl;[19] unfortunately, no spectroscopic data for this compound were reported.

The isomerization of **6** to **8** and of **7** to **9** represents a reductive elimination of two σ-aryl groups at the digold(II) center. The reductive elimination of two σ-alkyl groups at a planar gold(III) center has been studied thoroughly,[20] and the formation of biaryls from aryl-Grignard reagents or aryllithiums in the presence of transition metal halides is well known.[21] The unusual feature in the present case is that the product of reductive elimination is held in the coordination sphere of the metal atoms by the phosphorus donors. This type of behavior has been observed previously only in the case of unsaturated ligands, e.g. in the conversion of the *P,P′*-ethylenebis(dicyclohexylphosphane) tetraphenylnickelacyclopentadiene complex into the corresponding η^4-tetraphenylcyclobutadienenickel compound.[22]

Although the mechanism of the process is as yet unknown, a plausible intermediate in the isomerization could be a heterovalent, salt-like gold(III)–gold(I) species $[\overline{Au^{III}(o\text{-}C_6H_4PPh_2)_2}][Au^IX_2]$, X = Cl, Br. In the cation, the two σ-aryl groups would preferentially occupy *cis* coordination sites,[23] thus favoring reductive elimination and formation of **8** and **9**.

Received: October 29, 1986 [Z 1970 IE]
German version: *Angew. Chem. 99* (1987) 262

[1] K. P. Hall, D. M. P. Mingos, *Prog. Inorg. Chem. 32* (1984) 238.
[2] Y. Jiang, S. Alvarez, R. Hoffmann, *Inorg. Chem. 24* (1985) 749.
[3] A. M. Mazany, J. P. Fackler, Jr., *J. Am. Chem. Soc. 106* (1984) 801.
[4] H. Schmidbaur, J. R. Mandl, A. Frank, G. Huttner, *Chem. Ber. 109* (1976) 466.
[5] J. P. Fackler, Jr., J. D. Basil, *ACS Symp. Ser. 211* (1983) 201.
[6] J. P. Fackler, Jr., B. Trzcinska-Bancroft, *Organometallics 4* (1985) 1891.
[7] M. A. Bennett, S. K. Bhargava, K. D. Griffiths, G. B. Robertson, W. A. Wickramasinghe, A. C. Willis, *Angew. Chem. 99* (1987) 261; *Angew. Chem. Int. Ed. Engl. 26* (1987) 258.
[8] *Procedure* for **7**: A stirred suspension of **5** (300 mg, 0.33 mmol) in toluene (20 mL) contained in a Schlenk flask wrapped in aluminum foil was cooled to −60°C under nitrogen and treated dropwise with a solution of iodine (83 mg, 0.33 mmol) in toluene. The solution was allowed to warm to room temperature and was stirred for a further 1 h. The clear wine-red solution was concentrated in vacuo and hexane (15 mL) was added. On cooling to −10°C, a dark red crystalline solid separated within ca. 12 h. This was filtered in air and washed with hexane (3 × 5 mL) to give **7** (312 mg, ca. 80%), dec. >240°C. Complex **6** was obtained similarly from **5** and bromine. Satisfactory analytical data were obtained for this and other compounds described herein. Both **6** and **7** were found to be dimeric in CH_2Cl_2 by osmometry. **6**: M_r found, 967, calcd., 1076; **7**: found, 1145; calcd., 1170.
[9] $^{31}P\{^1H\}$-NMR (CD_2Cl_2, external standard 85% H_3PO_4): $\delta = -4.6$ (**6**), $\delta = -13.2$ (**7**).
[10] **7**·CH_2Cl_2: triclinic, $A\bar{1}$, $a = 49.572(5)$, $b = 18.859(2)$, $c = 9.394(1)$ Å, $\alpha = 92.550(8)$, $\beta = 88.651(8)$, $\gamma = 54.453(6)°$, $Z = 4$; FACS-1 diffractometer, $\lambda = 1.5418$ Å; $R = 0.033$, $R_w = 0.044$ for 6138 unique reflections [$3 < 2\theta < 100°$, $I \geq 3\sigma(I)$], 784 parameters, H atoms by calculation.
[11] ORTEP drawing [12], 30% ellipsoids, hydrogen atoms omitted.
[12] C. K. Johnson, ORTEP II, Report ORNL-5138, Oak Ridge National Laboratory, Tennessee 1976.
[13] D. P. Arnold, M. A. Bennett, M. S. Bilton, G. B. Robertson, *J. Chem. Soc. Chem. Commun. 1982*, 115.
[14] **9**: M_r (osmometric) 1194, calc. 1169.
[15] ^{31}P-NMR (CD_2Cl_2): $\delta = 28.0$ (**8**), 31.3 (**9**); the isomerizations **6** → **8** and **7** → **9** take place quantitatively, as shown by ^{31}P-NMR monitoring.
[16] **8**: monoclinic, $P2_1/c$, $a = 10.897(2)$, $b = 16.183(3)$, $c = 18.890(4)$ Å, $\beta = 93.72(2)°$, $Z = 4$; FACS-1 diffractometer, $\lambda = 0.7107$ Å; $R = 0.029$, $R_w = 0.031$ for 4082 unique reflections [$3 < 2\theta < 50°$, $I \geq 3\sigma(I)$], 380 parameters, H atoms by calculation. Further details of the crystal structure investigations of **7** and **8** are available on request from the Director of the Cambridge Crystallographic Data Centre, University Chemical Laboratory, Lensfield Road, Cambridge CB2 1EW (UK).
[17] The complex $[Au_2Cl_2(2,2'\text{-}Et_2PC_6H_4C_6H_4PEt_2)]$ has been mentioned briefly, without details: D. W. Allen, F. G. Mann, I. T. Millar, *J. Chem. Soc. C 1967*, 1869.
[18] **10**: $^{31}P\{^1H\}$-NMR (CD_2Cl_2): $\delta = -15.0$ (s).
[19] A. Uehara, J. C. Bailar, Jr., *J. Organomet. Chem. 239* (1982) 1.
[20] A. Tamaki, S. A. Magennis, J. K. Kochi, *J. Am. Chem. Soc. 95* (1973) 6487; S. Komiya, T. A. Albright, R. Hoffmann, J. K. Kochi, *ibid. 98* (1976) 7255.
[21] M. S. Kharasch, O. Reinmuth: *Grignard Reactions of Nonmetallic Substances*, Prentice-Hall, New York 1954, Chapter 5, p. 116; F. A. Cotton, *Chem. Rev. 55* (1955) 551; L. G. Vaughan, *J. Am. Chem. Soc. 92* (1970) 730; *J. Organomet. Chem. 190* (1980) C 56.
[22] H. Hoberg, W. Richter, *J. Organomet. Chem. 195* (1980) 355.
[23] The neutral platinum(II) complex $[\overline{Pt(o\text{-}C_6H_4PPh_2)_2}]$, which is isoelectronic with the postulated gold(III) cation $[\overline{Au(o\text{-}C_6H_4PPh_2)_2}]^{\oplus}$, contains *cis*-aryl ligands: M. A. Bennett, S. K. Bhargava, G. B. Robertson, A. C. Willis, unpublished work.

Chemistry of Pyrrocorphins: Biomimetic Regioselectivity of *C*-Methylation at the Ligand Periphery of Magnesium(II) Uropyrrocorphinate(Type I)-octanitriles**

By *Christian Leumann, Thomas Früh, Michael Göbel,* and *Albert Eschenmoser**

Dedicated to Gerhard Quinkert on the occasion of his 60th birthday

As has recently been shown with octaethylporphyrinogen as a model system, the porphyrinogen → pyrrocor-

[*] Prof. Dr. A. Eschenmoser, Dipl.-Chem. ETH C. Leumann, Dipl. Sc. Nat. ETH T. Früh, Dr. M. Göbel
Laboratorium für Organische Chemie der
Eidgenössischen Technischen Hochschule,
ETH-Zentrum, Universitätstrasse 16, CH-8092 Zürich (Switzerland)

[**] This work was supported by the Schweizerische Nationalfonds zur Förderung der wissenschaftlichen Forschung. *M. G.* acknowledges a Liebig grant from the Verband der Chemischen Industrie (Frankfurt am Main).

phin tautomerization[1] provides an easy synthetic access to pyrrocorphins (see Scheme 1). This novel type of hydroporphinoid ligand system plays an important role in the biosynthesis of vitamin B_{12};[2] its most notable *chemical* characteristic known so far is the ability of its Mg^{II}-complexes to undergo selective *C*-methylation on the ligand periphery when treated with electrophilic methylating reagents.[3] We now report that the peripheral *C*-methylation of Mg^{II}-uropyrrocorphinate-(type I)-octanitriles shows biomimetic regioselectivity; of the two available reaction sites of the pyrrocorphinic pyrrole ring it is the position bearing an acetonitrile side chain which is preferentially methylated.[4]

The metalating tautomerization of uroporphyrinogen-(type I)-octanitrile **1**[5] with ethylmagnesium bromide and 1,5,7-triazabicyclo[4.4.0]dec-5-ene is experimentally more delicate than that of the octaethylporphyrinogen model. This is due both to the propensity of the nitrile groups to undergo side reactions, and to the higher sensitivity of the tautomerized reaction products to oxidation in basic media.

When **1** was subjected to reaction conditions *a* followed by *b* (Scheme 1), chromatographic separation gave, beside starting material **1** and dehydrogenation products **3**, a fraction containing pyrrocorphins **2**. This fraction was further separated by HPLC into two binary (crystalline) mixtures of diastereomers which were characterized by UV/VIS-, ^{1}H-NMR-spectroscopy and FAB-MS, as well as by analytical HPLC separation of all four diastereomers as their Ni^{II}-complexes.[6]

C-Methylation of the Mg^{II}-complexes of the pyrrocorphin fraction **2**[7] required somewhat more severe conditions than for the octaethyl series,[3a] but nevertheless proceeded cleanly to give the corresponding Mg^{II}-corphin complexes as revealed by UV/VIS spectroscopy (steps *c* and *d*).[7] Direct determination of the constitutional course of the reaction (*C*-methylation to products of type **4** as opposed to **5**) was thwarted by the configurational complexity of the system. This difficulty was overcome by conversion of the entire product mixture into the corresponding mixture of Ni^{II}-isobacteriochlorinates (**7** and **8**); HPLC separation[8] and structural identification (^{1}H-NMR) of the

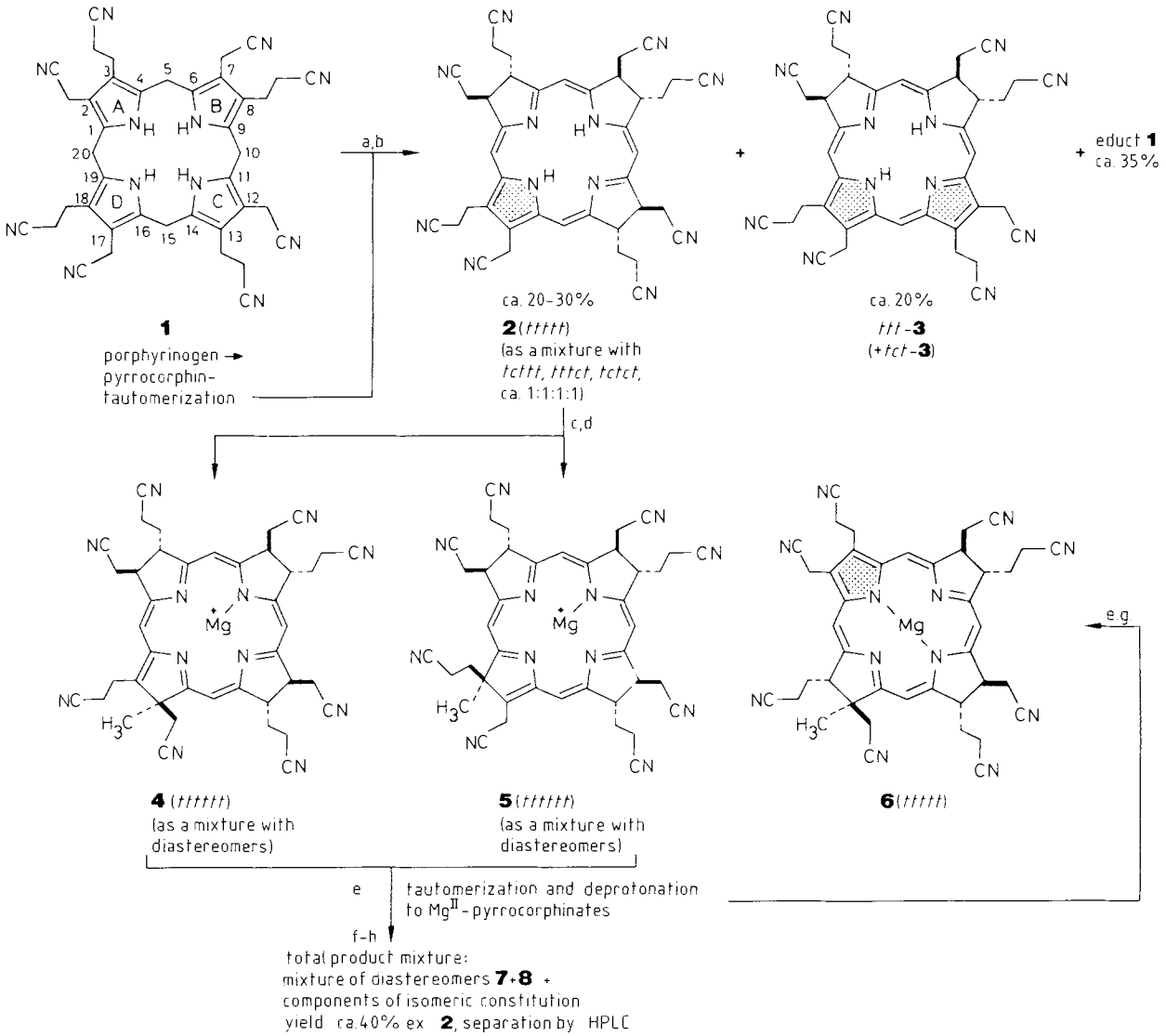

Scheme 1. For the nomenclature of the configuration see ref. [11]; all chiral compounds are racemic. Experimental: a) 9 mol. equiv. 1,5,7-triazabicyclo[4.4.0]dec-5-ene (guanidine base), 5 mol. equiv. C_2H_5MgBr/8 mol. equiv. H_2O, in pyridine ($c = 0.017$ M), 90°C, 4 d. b) $HCOOH/CH_3COOH/CH_3CN$ (1:1:1), 20°C, 5 min. c) 10 mol. equiv. cyclopentadienylmagnesium bromide in tetrahydrofuran (THF) → in CH_3CN, 20°C, 30 min. d) CH_3I/CH_3CN (1:4), 55°C, 66 h, in the dark. e) Pyridine, 80°C, 2 h. f) HCOOH. g) *o*-Chloranil, CH_3CN, 20°C, 5 min. h) $NiCl_2/CH_3CN/CH_3OH$, 60°C, 3 h.—All reactions were conducted in an O_2-free glove box. For separation see Scheme 2.

main components of this latter mixture was then possible. The key step in the overall transformation (steps *e*–*h*) is the conversion of the primary methylation products (Mg^{II}-corphinates **4** and **5**) into the Mg^{II}-pyrrocorphinates **6** (and pyrrocorphinates of isomeric constitution) involving deprotonation and tautomerization in pyridine; dehydrogenation of these Mg^{II}-pyrrocorphinates proceeded with ease. Conditions and results of the two-step HPLC separation of the mixture of Ni^{II}-isobacteriochlorinates are given in Scheme 2 (*i* and *k*). The five isolated components, identified by ^{1}H-NMR spectra and FAB-MS, made up 82% of the total mixture.[9] Four of them were diastereomers of constitution **7** (73% of the total mixture) and just one (9%) of the identified components had the isomeric constitution **8**. The rest of the reaction mixture (18%) contained at least 10 components which were not identified. The conclusion that product type **7** is unequivocally favored over product type **8** in the *C*-methylation step holds even if all the unidentified components of the mixture were of type **8**.[10]

The structures of the five identified Ni^{II}-isobacteriochlorinates were deduced as illustrated in Scheme 3 (in which the *tct*-**7** isomer is used as an example[7]). The ^{1}H-NMR signal of one of the two CH_2CN groups bound to a nonpyrrolic ring has an AB structure (not ABX), as expected for the presence of a methyl group on a carbon atom bearing a CH_2CN side chain. This carbon must be C-17 in ring D, because the methyl group is correlated by an NOE to the bridge proton which resonates at highest field ($\delta = 6.95$ cf. [1a]). The same proton signal exhibits an NOE with an allylic proton ($\delta = 3.88$), thus indicating that the latter sits on C-13 and lies in a quasi-equatorial position. The bridge-proton signals corresponding to CH-20 and CH-10 show an NOE with the signals of the neighboring allylic protons at C-18 and C-12, but not with those of the methylene groups of the neighboring side chains. This shows that the protons at C-12 and C-18 are quasi-equatorial. The conformation of rings C and D of *tct*-**7** thus assigned (Scheme 3) follows the recently established rules for the conformation of corphinoid Ni^{II}-complexes.[11, 1d]

The common constitution of the main components of mixture **7** indicates that, surprisingly, the transformation **4** → **6** after the regioselective methylation step also pro-

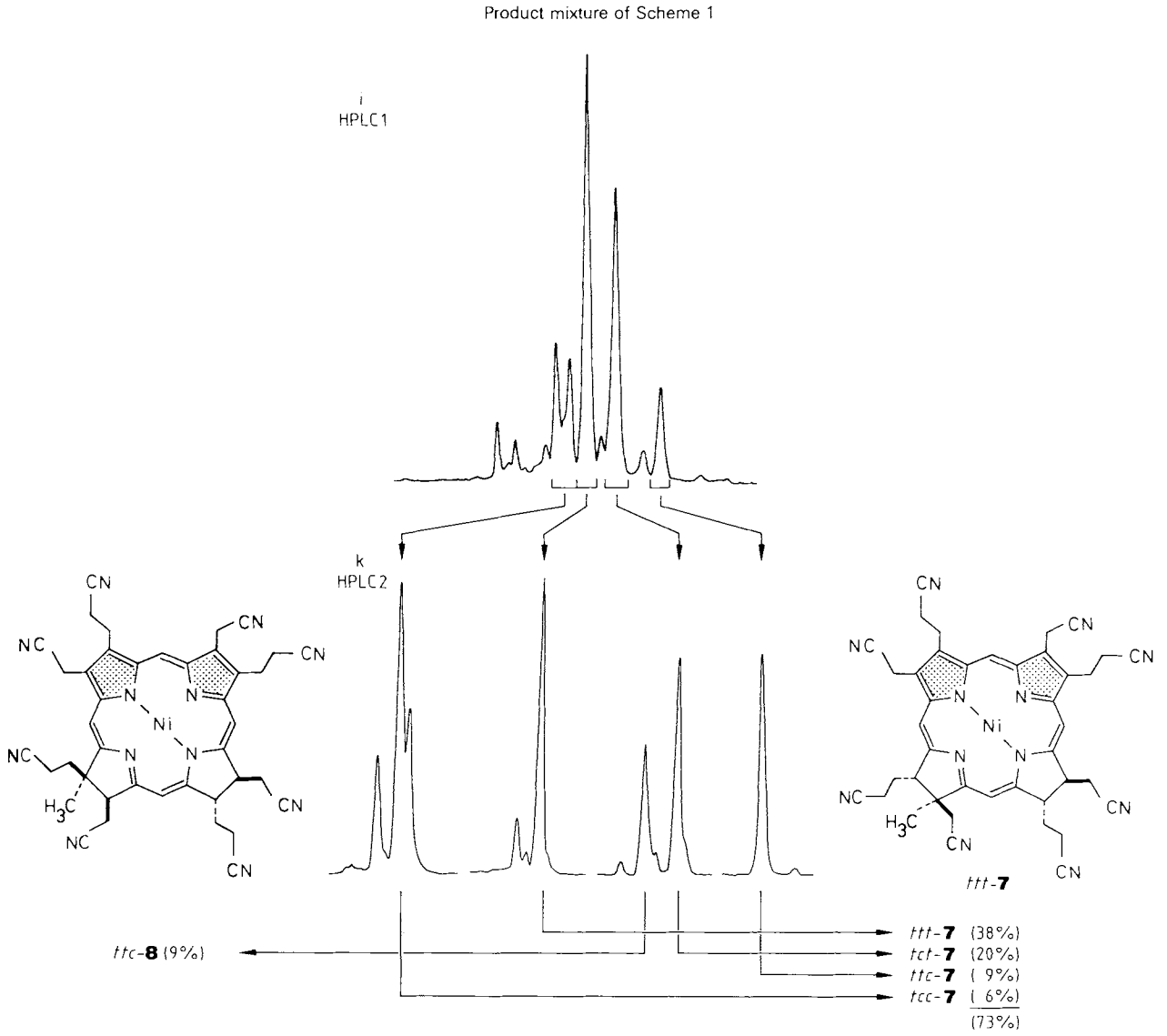

Scheme 2. Experimental: i) HPLC 1: Techsil silica 5 μ/THF-Et_2O 1:2 + 1% H_2O. k) HPLC 2: Techsil silica 5 μ/ethyl acetate-pentane 2:1 + 0.77% H_2O.

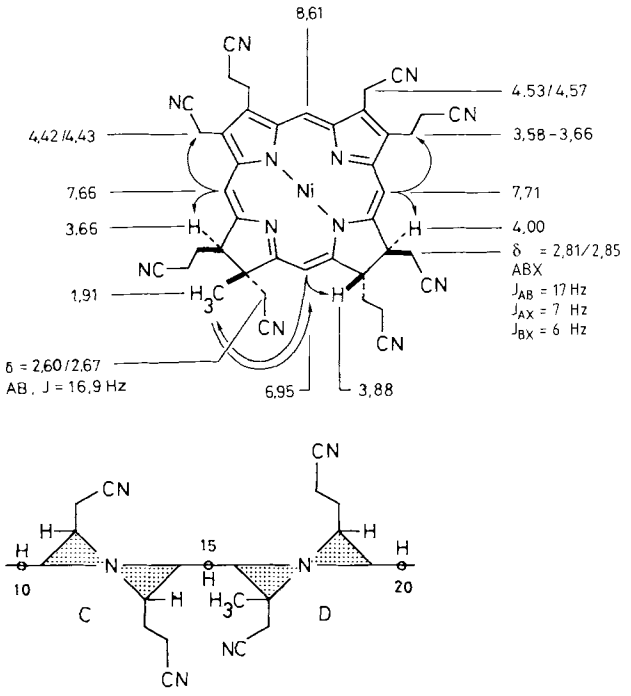

Scheme 3. Top: ^{1}H-NMR data of *tct*-**7**. Bottom: Conformation of rings C and D.

ceeded regioselectively.[12] This implies the possibility that pyrrocorphinates formed in this manner can be further *C*-methylated, and that two repetitions of the methylation-tautomerization procedure should lead to trimethylated pyrrocorphins, among which those of constitution **9** would predominate. Experimentally, trimethylation did indeed prove possible: compound **2** (FAB-MS: $M^+ = 684$), when

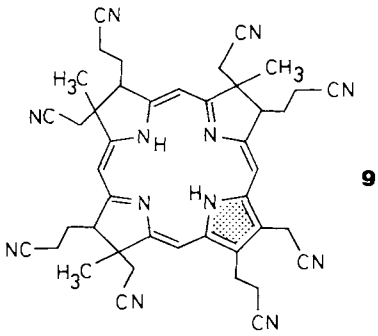

9

subjected three consecutive times to the procedures *c*, *d*, *e*, and *f* (Scheme 1), gave first monomethylated (FAB-MS: $M^+ = 698$), then dimethylated ($M^+ = 712$) and finally trimethylated ($M^+ = 726$) pyrrocorphin fractions[13] in spectroscopically determined yields (UV/VIS) of 75, 70, and 45%, respectively. The composition of the product fractions was found to be complex (HPLC). However, we expect this complexity to be mainly configurational and not constitutional. Apparently, what is needed here is diastereoselectivity in addition to the regioselectivity observed in the *C*-methylation steps.

Received: December 22, 1986 [Z 2018 IE]
German version: *Angew. Chem. 99* (1987) 273

[1] a) J. E. Johansen, V. Piermattie, C. Angst, E. Diener, C. Kratky, A. Eschenmoser, *Angew. Chem. 93* (1981) 273; *Angew. Chem. Int. Ed. Engl. 20* (1981) 261; b) R. Waditschatka, A. Eschenmoser, *ibid. 95* (1983) 639 and *22* (1983) 630; c) R. Waditschatka, C. Kratky, B. Jaun, J. Heinzer, A. Eschenmoser, *J. Chem. Soc. Chem. Commun. 1985*, 1604; d) A. Eschenmoser, "Chemistry of Corphinoids", *Ann. N. Y. Acad. Sci. 471* (1986) 109.

[2] H. C. Uzar, A. R. Battersby, *J. Chem. Soc. Chem. Commun. 1982*, 1204; *1985*, 585; A. I. Scott, N. E. Mackenzie, P. J. Santander, P. E. Fagerness, G. Müller, E. Schneider, R. Sedlmeier, G. Wörner, *Bioorg. Chem. 12* (1984) 356.

[3] a) R. Waditschatka, E. Diener, A. Eschenmoser, *Angew. Chem. 95* (1983) 641; *Angew. Chem. Int. Ed. Engl. 22* (1983) 631; b) C. Leumann, K. Hilpert, J. Schreiber, A. Eschenmoser, *J. Chem. Soc. Chem. Commun. 1983*, 1404; C. Leumann, A. Eschenmoser, *ibid. 1984*, 583.

[4] Sirohydrochlorin, coenzyme F430 and vitamin B_{12} have peripheric methyl groups on the corresponding atoms of rings A and B. See also the recently published work on enzymatic *C*-methylation of uroporphyrinogen type I: G. Müller, J. Schmiedl, E. Schneider, R. Sedlmeier, G. Wörner, A. I. Scott, H. J. Williams, P. J. Santander, N. J. Stolowich, P. E. Fagerness, N. E. Mackenzie, H.-P. Kriemler, *J. Am. Chem. Soc. 108* (1986) 7875.

[5] a) G. Ksander, G. Bold, Y.-B. Xiang, C. Lehmann, T. Früh, R. Lattmann, K. Inomata, E. Zass, J. Schreiber, A. Eschenmoser, *Helv. Chim. Acta 70* (1987), in press; M. Ono, R. Lattmann, K. Inomata, C. Lehmann, T. Früh, A. Eschenmoser, *Croat. Chim. Acta 58* (1985) 627; b) R. Lattmann, Dissertation, ETH Zürich Nr. 7383, 1983; c) C. Lehmann, Dissertation, ETH Zürich (in preparation).

[6] For experimental details see T. Früh, "Zur Chemie der Uroporphyrinogen-octanitrile", *Dissertation*, ETH Zürich No. 8054, 1986.

[7] For experimental details see C. Leumann, "Biomimetische *C*-Methylierungsreaktionen an Corphinderivaten", *Dissertation*, ETH Zürich No. 8064, 1986.

[8] The Ni(II)-complexes of diastereomeric pyrrocorphins and isobacteriochlorins are generally easy to separate by HPLC, in contrast to the metal-free ligands. This difference may be ascribed to the conformational locking of the ligand periphery upon complexation with the nickel ion (see ref. [11]).

[9] Determined by UV/VIS spectroscopy; reference extinction coefficients $\varepsilon_{385} = 52\,700$ and $\varepsilon_{585} = 43\,500$ [6].

[10] We rationalize this regioselectivity by assuming the electron-pair localization energy of the pyrrolic π-system to be lowered at the reacting position through (n→σ*)-conjugation of the lone pair with the C(sp_3)-C(sp)-bond of the (CH_2-CN)-substituent. Steric control can be ruled out (cf. B. Zehnder, *Dissertation*, ETH Zürich No. 7130, 1982).

[11] C. Kratky, R. Waditschatka, C. Angst, J. E. Johansen, J. C. Plaquevent, J. Schreiber, A. Eschenmoser, *Helv. Chim. Acta 68* (1985) 1312.

[12] This becomes comprehensible by supposing that protonation of the position C-20 is a determining step of the tautomerization.

[13] $\lambda_{max}(CH_3CN) \approx 348$ nm (rel. Int. ≡ 1), 356 (0.97), 374 (0.73), 425 (0.10), 460 (0.11), 491 (0.15), 525 (0.13), 566 (0.12) (cf. [1a, 6]).

Structure of Triphenylarsane Diiodide, $[Ph_3As \cdot I_2]$, a Compound Formed in the Thermal Decomposition of $[Mn(OAsPh_3)_3I_2(SO_2)_2]$**

By *Charles A. McAuliffe,* Brian Beagley, George A. Gott, Anthony G. Mackie, Philomena P. MacRory,* and *Robin G. Pritchard*

Our interest in the coordination of small molecules such as sulfur dioxide[1] by $[MnX_2(PR_3)]$ complexes has led us to investigate other manganese(II) systems, and we have recently demonstrated demi-reversible binding of SO_2 in the complex $[Mn(OPPh_3)_4(O_2SI)_2]$ [Eq. (a)].[2]

$$[Mn(OPPh_3)_4(O_2SI)_2] \underset{SO_2}{\overset{129\,^\circ C}{\rightleftharpoons}} [Mn(OPPh_3)_4(O_2SI)I] + SO_2 \qquad (a)$$

1 **2**

$[Mn(OAsPh_3)_3I_2(SO_2)_2]$ **3** $[Ph_3As \cdot I_2]$ **4**

[*] Prof. Dr. C. A. McAuliffe, Dr. B. Beagley, Dr. G. A. Gott, A. G. Mackie, P. P. MacRory, Dr. R. G. Pritchard
Department of Chemistry,
University of Manchester Institute of Science and Technology
Manchester, M60 1QD (UK)

[**] This work was supported by the Science and Engineering Research Council (Research Studentship for *GAG*) and the Northern Ireland Department of Education (Research Studentship for *PPM*).

A similar reaction to that used for the preparation of **1** was carried out using MnI_2 and $OAsPh_3$. Addition of sulfur dioxide to a suspension of the $MnI_2/OAsPh_3$ mixture in propyl acetate resulted in a change of color from beige to orange, and the solid that was subsequently isolated was identified as the SO_2-complex **3** (IR data for **3**: $\tilde{\nu}$(O=As), 875 cm^{-1}; $\tilde{\nu}$(SO) 1248, 1080 cm^{-1}). Heating the complex **3** in a rotaflow tube in vacuo at ca. 100°C to test for reversibility of SO_2 binding resulted in the formation of purple-red crystals on the cool parts of the tube. These were shown, by elemental analysis (C,H,I) and an X-ray structure analysis,[3] to be crystals of the I_2-complex [$Ph_3As \cdot I_2$], **4**, the molecular structure of which is shown in Figure 1.

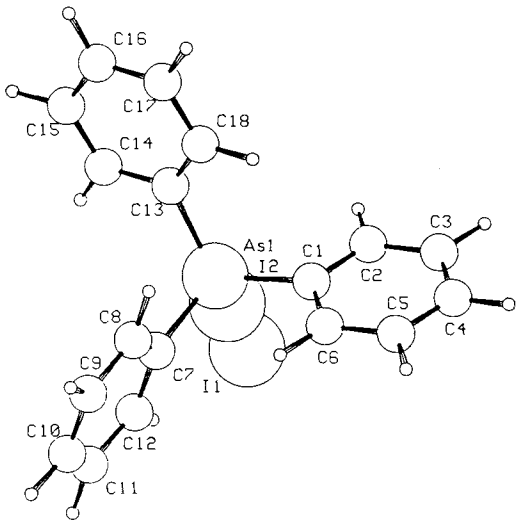

Fig. 1. Molecular structure of [$Ph_3As \cdot I_2$] **4**. Selected bond lengths [Å] and angles [°]: I1-I2 3.005(1), I2-As1 2.64(1); I1-I2-As1 174.8(1), I2-As1-C1-C2 48.5(8), I2-As1-C7-C8 −169.6(7), I2-As1-C13-C14 49.8(9).

Although many other iodine charge transfer complexes are known,[4] [$Ph_3As \cdot I_2$], **4**, is the first compound containing an As-I-I unit that has been crystallographically characterized. The visible spectrum of **4** in toluene solution is typical of other iodine charge transfer complexes, exhibiting absorptions at $\lambda_{max} = 295$ nm ($\varepsilon = 12200$) and 485 nm ($\varepsilon = 850$). Attempts to prepare the complex directly from Ph_3As and I_2 in ethanol, acetone or toluene solutions have been unsuccessful.

The molecule contains a slightly bent As-I-I shaft with three asymmetrically conformed phenyl fins projecting from the arsenic atom (As1-I2-I1) 174.8(1)°). Such a bend is commonly observed in diiodide complexes;[5-9] in this case it is further compounded by an enlarged C13-As1-I2 angle, 119.2(3)°. This is apparently unrelated to intramolecular steric congestion with the shortest non-hydrogen intramolecular contacts involving phenyl rings containing C1 and C7 [I2···C1 3.74(1), I2···C12 3.74(1) Å]. The I-I bond length exceeds that in the uncomplexed I_2 molecule (2.660 Å); this is due to donation of the arsenic's lone pair into the I_2-unit's empty antibonding σ_u orbital and, at 3.005(1) Å, is at the upper limit for uncharged diiodide complexes,[5-9] being surpassed only by some triiodide and pseudotriiodide ions.[10, 11] Some I-I bond lengths are listed in Table 1 for comparison. The weakening of the I-I bond is counterbalanced by an As-I bond which is comparable to those found in other iodoarsane compounds[12-14] with a length, though not the shortest recorded, that is encompassed by the known structures.

Table 1. Comparison of I-I bond lengths in some diiodine compounds.

Compound	I-I [Å]	Ref.
I_2	2.660	
$Ph_3As \cdot I_2$	3.005	
9-cyclohexyladenine $\cdot I_2$	2.764	[5]
1,4-dithiane $\cdot 2I_2$	2.787	[6a]
1,4-diselenane $\cdot 2I_2$	2.870	[6b]
Hexamethylenetetramine $\cdot I_2$	2.830	[7]
Hexamethylenetetramine $\cdot 2I_2$	2.791, 2.771	[7]
N,N'-ethylenethiourea $\cdot 2I_2$	3.147	[8]
$(Dithizone)_2 \cdot 7I_2$	3.215	[8]
$(Ethylenethiourea)_3 \cdot 3I_2$	2.984	[8]
$[Co(C_5H_5N)_4(NCS)_2 \cdot 2I_2]$	2.804	[9]

Several points of interest have emerged from these observations. Firstly, whereas SO_2 will add to $[Mn(OPPh_3)_4I_2]$ to give the bis-adduct $[Mn(OPPh_3)_4(O_2SI)_2]$, **1**, substitution for $OAsPh_3$ occurs in the case of the presumed intermediary $[Mn(OAsPh_3)_4I_2]$ to give "$[Mn(OAsPh_3)_3I_2(SO_2)_2]$", **3**. Of greater importance, however, is the observation that manganese-bound SO_2 appears to be activated and facilely reduces Ph_3AsO to form **4**. Whilst the reduction of organoarsane(v) oxides to organoarsane(III) compounds in strongly acidic media is well known,[15] our present observations suggest that metal-activation of SO_2 greatly assists this process. Further investigations in this connection are currently under way.

Received: August 27, 1986;
supplemented: November 27, 1986 [Z 1909 IE]
German version: *Angew. Chem. 99* (1987) 237

[1] D. S. Barratt, C. G. Benson, G. A. Gott, C. A. McAuliffe, S. P. Tanner, *J. Chem. Soc. Dalton Trans. 1985*, 2661.
[2] G. A. Gott, J. Fawcett, C. A. McAuliffe, D. R. Russell, *J. Chem. Soc. Chem. Commun. 1984*, 1283.
[3] X-ray structure analysis: $C_{18}H_{15}AsI_2$, $M = 560.05$, $T = 293$ K, orthorhombic, space group $P2_12_12_1$ (No. 19), $a = 10.990(4)$, $b = 12.056(4)$, $c = 13.963(3)$ Å, $V = 1850.0$ Å^3, $Z = 4$, $\rho_{calc} = 2.01$ mg m^{-1}, $F(000) = 1048$, Enraf-Nonius CAD4 diffractometer, $Mo_{K\alpha}$ radiation, $\lambda = 0.71069$ Å, $\mu(Mo_{K\alpha}) = 5.04$ mm^{-1}. The structure was solved by normal heavy-atom methods and was refined by full matrix least squares (SHELX). Anisotropic thermal parameters for all non-hydrogen atoms, hydrogen atoms in calculated positions. $R = 0.043$, $R_w = 0.051$ for $w = 0.6584/(\sigma^2(F_0) + 0.0005\ F_0^2)$ for 2880 unique reflections with $F_0 > 3\sigma(F_0)$. Further details of the crystal structure investigation are available on request from the Director of the Cambridge Crystallographic Data Centre, University Chemical Laboratory, Lensfield Road, Cambridge, CB2 1EW (UK) on quoting the names of the authors and the full citation of the journal.
[4] N. N. Greenwood, A. Earnshaw: *Chemistry of the Elements*, Pergamon Press, Oxford 1984, pp. 940-943.
[5] D. Van der Heln, *J. Cryst. Mol. Struct. 3* (1973) 249.
[6] a) G. Y. Chao, J. D. McCullough, *Acta Crystallogr. 13* (1960) 727; b) *14* (1961) 940.
[7] H. Pritzkow, *Acta Crystallogr. B31* (1975) 1589.
[8] F. H. Herbstein, W. Schwotzer, *J. Am. Chem. Soc. 106* (1984) 2367.
[9] H. Hartl, S. Steidl, *Z. Naturforsch. B32* (1977) 6.
[10] J. Runsink, S. Swen-Walstra, T. Migchelsen, *Acta Crystallogr. B28* (1972) 1331.
[11] R. Frölich, K. F. Tebbe, *Z. Kristallogr. 159* (1982) 50.
[12] K. Henrick, C. L. Raston, A. H. White, S. B. Wild, *Aust. J. Chem. 30* (1977) 2417.
[13] J. Willemse, J. A. Cras, W. P. Bosman, J. J. Steggerda, *Recl. J. R. Neth. Chem. Soc. 99* (1980) 65.
[14] R. Kniep, H. D. Reski, *Inorg. Chim. Acta 64* (1982) L83.
[15] See, e.g., E. R. H. Jones, F. G. Mann, *J. Chem. Soc. 1958*, 294.

Energy Transfer Luminescence of Europium(III) and Terbium(III) Cryptates of Macrobicyclic Polypyridine Ligands**

By *Béatrice Alpha, Jean-Marie Lehn,** and *Gérard Mathis*

Dedicated to Professor Gerhard Quinkert on the occasion of his 60th birthday

Cryptate formation by inclusion of a substrate into the intramolecular cavity of a macropolycyclic ligand[1] provides, *inter alia*, an efficient shielding of the bound species from interaction with solvent and other solute molecules. As a consequence the physical and chemical properties of both the included and the external species may be markedly affected.[2] Europium cryptates, e.g., have been found to present a notable emission in aqueous solution at room temperature, whereas simple aqua complexes do not luminesce under the same conditions.[3] This may be attributed to protection of the cryptated europium ions from radiationless deactivation by solvent molecules.[3-6] Similarly, other properties of lanthanoid cryptates, in particular their redox potentials, are also markedly different from those of the aqua complexes.[7,8]

In view of the numerous physical, chemical and biological studies involving luminescent lanthanoid ions, it is of central interest to increase the conversion efficiency of absorbed light into emitted light by making use of energy transfer from excited photosensitive groups of an organic ligand.[9]

We now show that these three features: inclusion, protection, and energy transfer from a ligand group may be combined in a single species: in the photoactive europium and terbium cryptates of macrobicyclic ligands containing α,α′-bipyridine (bpy) and 1,10-phenanthroline (phen) groups as light absorbers (photosensitizers).[10] Cryptates of such ligands with other metal ions are known.[10-12]

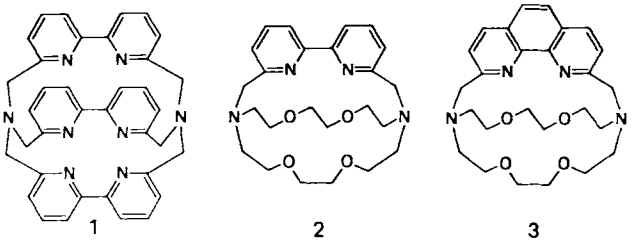

1 2 3

The Eu^{III} and Tb^{III} cryptates of ligands **1** and **2** as well as the Eu^{III} cryptate of **3** can be prepared by adding a solution of the corresponding sodium cryptates (as bromides) in a minimum amount of chloroform to a solution containing 1 equiv. of Eu^{III}- or Tb^{III}-salt (nitrate or chloride) in acetonitrile[14] and heating the mixture under reflux for ca. 24 h. After filtration the solution is concentrated under vacuum until it becomes slightly cloudy; it is then left in the cold and the complex crystallizes slowly. The solvent is removed with a pipette and the solid is washed several times with small amounts of CH_2Cl_2/CH_3OH (98/2) and then with ether. The La^{III} complex of **1** has also been prepared. The complexes obtained may be described as the lanthanoid cryptates $[Ln^{3\oplus} \subset L]$ (where $Ln^{3\oplus} = Eu^{3\oplus}$, $Tb^{3\oplus}$ or $La^{3\oplus}$ and L = **1**-**3**) in which the cation is included in the molecular cavity (see Fig. 1), consistent with the crystal structure of related cryptates.[8,11,15] Lanthanoid cryptates are stable complexes and kinetically very inert.[7,16] Introduction of the rigid bpy and phen groups, should render cation exchange particularly difficult and slow.

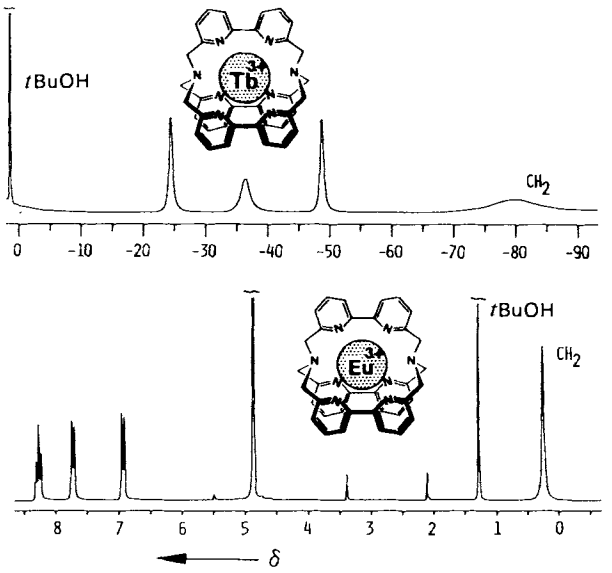

Fig. 1. 200 MHz ^{1}H-NMR spectra of the europium(III) (bottom) and terbium(III) (top) cryptates of the macrobicyclic ligand **1** in D_2O at 20°C; δ values referred to sodium trimethylsilylpropanesulfonate (TMPS); internal reference: *t*BuOH. The peaks between $\delta = 2$-5 in the lower spectrum stem from solvent.

The ^{1}H-NMR spectra of these complexes are highly characteristic, since lanthanoid ions such as $Eu^{3\oplus}$ and $Tb^{3\oplus}$ strongly perturb NMR signals.[17] As illustrated in Figure 1 for ligand **1**, the ^{1}H-NMR spectra of the Eu^{III} and Tb^{III} cryptates of **1**-**3** are very different from those of the corresponding $Na^{\oplus}$ cryptates.[10] For both ions the signals are appreciably shifted; the effect is particularly large for Tb^{III}, which also causes strong line broadening.

Electrochemical studies have shown that the reduction of $[Eu^{3\oplus} \subset \mathbf{1}]$ is reversible (−555 mV, SCE, 0.1 M NMe_4ClO_4); the Eu^{III} state being stabilized with respect to the aqua ion (−625 mV), but much less so than in the case of the Eu^{III} cryptate of the macrobicycle "(2.2.2)".[7]

The photophysical properties of the Eu^{III} and Tb^{III} cryptates of ligands **1**-**3** are of special interest in view of the features discussed above. Some preliminary data are listed in Table 1.[18] Strong red and strong green emissions, respectively, are readily observed for the Eu^{III} and Tb^{III} cryptates of **1**-**3** in aqueous solution at room temperature, whereas the aqua ions do not emit under the same conditions. The excitation spectra are similar to the absorption band of the complexes arising from the ligand groups; the emission spectra are characteristic of Eu^{III} and Tb^{III} luminescence. These data show that in the present cryptates UV light absorbed by the bipy and phen groups is re-emitted as visible light by the complexed lanthanoid ions (see Figure 2 for $[Eu^{3\oplus} \subset \mathbf{1}]$.

These spectral properties may be ascribed to intramolecular energy transfer from the π,π* excited states of the ligand groups to excited levels of the Eu^{III} and Tb^{III} ions,

[*] Prof. Dr. J. M. Lehn, B. Alpha
Institut Le Bel, Université Louis Pasteur
4 rue Blaise Pascal, F-67000 Strasbourg (France)
Dr. G. Mathis,
ORIS LAPAM
Centre de Marcoule,
B.P. 171, F-30205 Bagnols-sur-Cèze (France)

[**] This work was supported by ORIS-Industrie.

which then emit from the $^5D_0$ and $^5D_4$ levels respectively. A contribution from charge-transfer absorption[3b] cannot be excluded, although no such band is observed. The efficiency of conversion is high, probably about unity for $[Eu^{3\oplus} \subset \mathbf{1}]$.[18] The light conversion process absorption-energy transfer-emission, **A-ET-E**, performed by these cryptates, is represented in Figure 2.

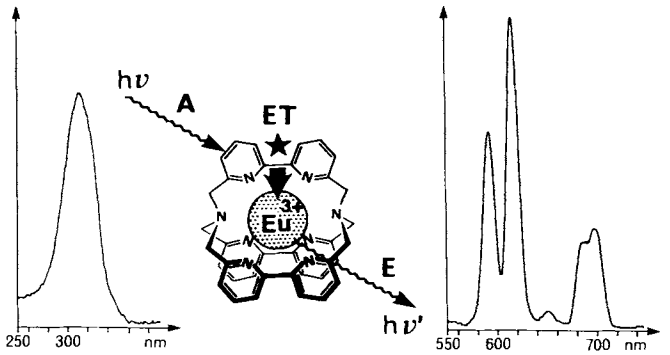

Fig. 2. Illustration of the absorption-energy transfer-emission **A-ET-E** light conversion process performed by the cryptate $[Eu^{3\oplus} \subset \mathbf{1}]$ (center); left: excitation spectrum (emission at 700 nm); right: emission spectrum (excitation at 320 nm); 10^{-6} M aqueous solution of the nitrate at 20°C; uncorrected spectra.

The emission lifetimes of the present europium cryptates (Table 1) are longer than those of the aqua ion (0.11 ms[3b]) and even of the $[Eu^{3\oplus} \subset 2.2.1]$ cryptate (0.215 ms);[3b] this may be due, at least in part, to a better shielding of the included ion by macrobicyclic ligands **1**–**3**. Preliminary measurements gave emission quantum yields above 10^{-2} for the Eu^{III} and Tb^{III} complexes of **1** and **2** (in aqueous solution).[18] This is high for such ions, being in particular at least an order of magnitude higher for $[Eu^{3\oplus} \subset \mathbf{1}]$ than for $[Eu^{3\oplus} \subset 2.2.1]$ (3×10^{-3} in D_2O solution).[3b]

Table 1. Photophysical properties of europium(III) and terbium(III) cryptates of the macrobicyclic ligands **1**–**3** [18] [a].

Cryptate	λ_{exc} [nm]	Lifetime [ms]
$[Eu^{3\oplus} \subset \mathbf{1}]$	300	0.34
$[Eu^{3\oplus} \subset \mathbf{2}]$	310	0.41
$[Eu^{3\oplus} \subset \mathbf{3}]$	280	0.27
$[Tb^{3\oplus} \subset \mathbf{1}]$	302	0.33
$[Tb^{3\oplus} \subset \mathbf{2}]$	310	0.72

[a] All measurements were performed in neutral aqueous solution at 300 K; lifetimes ±20%; the concentrations ranged from 10^{-6} to 10^{-4} M; lifetimes determined at $\lambda_{em} = 619$ nm for Eu^{III} and at $\lambda_{em} = 545.5$ nm for Tb^{III}. Anion: NO_3^-.

The photoactive europium(III) and terbium(III) cryptates described here are efficient luminophores which function as **A-ET-E** light conversion molecular devices, transforming UV light absorbed by ligand groups into visible lanthanoid emission via intramolecular energy transfer. In addition to the interesting photophysical and photochemical features of these and related complexes, a number of potential uses may be envisaged, for instance in the development of luminescent materials and of labels for biological applications[19] such as time-resolved luminescence immunoassays[20] employing monoclonal antibodies.

Received: December 18, 1986;
revised: January 29, 1987 [Z 2016 IE]
German version: *Angew. Chem. 00* (1987) 259

[1] J.-M. Lehn, *Struct. Bonding (Berlin) 16* (1973) 1; *Acc. Chem. Res. 11* (1978) 49.
[2] J.-M. Lehn, *Pure Appl. Chem. 52* (1980) 2303.
[3] a) N. Sabbatini, M. Ciano, S. Dellonte, A. Bonazzi, V. Balzani, *Chem. Phys. Lett. 90* (1982) 265; b) N. Sabbatini, S. Dellonte, M. Ciano, A. Bonazzi, V. Balzani, *ibid. 107* (1984) 212; c) N. Sabbatini, M. Ciano, S. Dellonte, A. Bonazzi, F. Bolletta, V. Balzani, *J. Phys. Chem. 88* (1984) 1534; d) N. Sabbatini, S. Dellonte, G. Blasse, *Chem. Phys. Lett. 129* (1986) 541.
[4] G.-Y. Adachi, K. Sorita, K. Kawata, K. Tomokiyo, J. Shiokawa, *J. Less-Common Met. 93* (1983) 81.
[5] F. Halverson, J. S. Brinen, J. R. Leto, *J. Chem. Phys. 41* (1964) 157.
[6] W. De-W. Horrocks, Jr., D. R. Sudnick, *J. Am. Chem. Soc. 101* (1979) 334; *Acc. Chem. Res. 14* (1981) 384.
[7] O. A. Gansow, A. R. Kausar, K. M. Triplett, M. J. Weaver, E. L. Yee, *J. Am. Chem. Soc. 99* (1977) 7087; E. L. Yee, O. A. Gansow, M. J. Weaver, *ibid. 102* (1980) 2278; J. Tabib, J. T. Hupp, M. J. Weaver, *Inorg. Chem. 25* (1986) 1916.
[8] J.-C. G. Bünzli, D. Wessner, *Coord. Chem. Rev. 60* (1984) 191.
[9] A. Heller, E. Wasserman, *J. Chem. Phys. 42* (1965) 949; R. G. Charles, E. P. Riedel, P. G. Haverlack, *ibid. 44* (1966) 1356; A. Abusaleh, C. F. Meares, *Photochem. Photobiol. 39* (1984) 763.
[10] J.-C. Rodriguez-Ubis, B. Alpha, D. Plancherel, J.-M. Lehn, *Helv. Chim. Acta 67* (1984) 2264.
[11] A. Caron, J. Guilhem, C. Riche, C. Pascard, B. Alpha, J.-M. Lehn, J.-C. Rodriguez-Ubis, *Helv. Chim. Acta 68* (1985) 1577.
[12] The macrobicycle **2** has been obtained as its sodium cryptate in 35% yield by treating the 18-membered N_2O_4 macrocycle with 6,6′-bisbromomethylbipyridine in presence of sodium carbonate following the method described previously for the other ligands [10]. The same sodium cryptate has been prepared in much lower yield by another method [13].
[13] E. Buhleier, W. Wehner, F. Vögtle, *Chem. Ber. 111* (1978) 200.
[14] Anhydrous solutions of the salts were prepared by treating the commercial pentahydrates (Aldrich Chem. Co.) with a large excess (ca. 10×) of trimethylorthoformate in acetonitrile under reflux for about 1–2 h. See also: O. A. Gansow, K. B. Triplett, US Pat. 4257955 (1981).
[15] F. A. Hart, M. B. Hursthouse, K. M. A. Malik, S. Moorhouse, *J. Chem. Soc. Chem. Commun. 1978*, 549; M. Ciampolini, P. Dapporto, N. Nardi, *ibid. 1978*, 788.
[16] a) G. Anderegg, *Helv. Chim. Acta 64* (1981) 1790; b) J. H. Burns, C. F. Baes, Jr., *Inorg. Chem. 20* (1981) 616; c) M.-C. Almasio, F. Arnaud-Neu, M.-J. Schwing-Weill, *Helv. Chim. Acta 66* (1983) 1296.
[17] For NMR spectra of some lanthanoid cryptates see: O. A. Gansow, D. J. Pruett, K. B. Triplett, *J. Am. Chem. Soc. 101* (1979) 4408.
[18] We thank *N. Sabbatini* and *V. Balzani* (Istituto Chimico "G. Ciamician", University of Bologna) for measurements in progress on $[Eu^{3\oplus} \subset \mathbf{1}]$ as well as *F. Grenier* and *P. Bouchy* (UA 328 (Prof. J. C. André) ENSIC, Nancy) for measuring the quantum yields of the Tb^{III} cryptates.
[19] F. S. Richardson, *Chem. Rev. 82* (1982) 541.
[20] See for instance: N. J. Marshall, S. Dakubu, T. Jackson, R. P. Ekins in A. Albertini, R. Ekins (Eds.): *"Monoclonal Antibodies and Developments in Immunoassay"*, Elsevier/North-Holland Biomedical Press, Amsterdam 1981, p. 101.

Diastereoselective Diels–Alder Reaction on Carbohydrate Matrices**

By *Horst Kunz,* Bernd Müller,* and *Dirk Schanzenbach*

Dedicated to Professor Helmut Hoffmann on the occasion of his 60th birthday

Numerous biochemical, immunological and molecular-biological investigations have shown that carbohydrate determinants play an important role in crucial processes of biological selectivity.[1] If one disregards chiral pool-syntheses, in which the carbohydrate itself is substrate, and some chiral hydride carriers, carbohydrates have been used only in isolated cases for the selective control of chemical processes.[2] Stimulated by our synthesis of glycopeptides as biological recognition structures[3] we have

[*] Prof. Dr. H. Kunz, Dipl.-Chem. B. Müller, D. Schanzenbach
Institut für Organische Chemie der Universität
J.-J.-Becher-Weg 18–20, D-6500 Mainz (FRG)

[**] This work was supported by the Fonds der Chemischen Industrie.

now tried to control diastereoselective reactions using the "chiral information" of the carbohydrates, which may be regarded as stereochemical microchips. We describe here the results of Diels-Alder reactions[4] with acrylates which are esterified with carbohydrate matrices. For diastereoselective Diels-Alder reactions with amide-bound[5] or ester-like bound dienophiles,[6] high inductions have been described. This holds true, in particular, for the titanium tetrachloride-catalyzed reactions of the acrylate of (*R*)-pantolactone.[7] We have now exploited the polyfunctionality and chirality of the carbohydrates in analogous Diels-Alder reactions in order to arrange the dienophile and the Lewis acid catalyst on the carbohydrate matrix such that the attack of the diene and the configuration of the main product can be predicted with high probability. For this purpose the 3-*O*-acryloyl-1,2-*O*-isopropylidene-α-D-glucofuranose **1**, which is readily accessible from 1,2,5,6-di-*O*-isopropylidene-α-D-glucofuranose by esterification with acryloyl chloride/triethylamine and selective cleavage of the 5,6-protecting group with 70% acetic acid, is silylated to give **2** in order that the titanium catalyst can be introduced later. **2** reacts with $TiCl_4$ at −78 °C with a change in

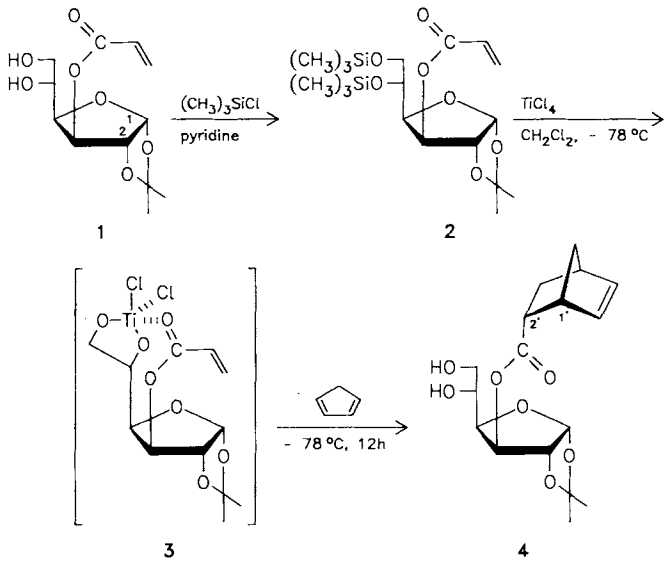

Scheme 1.

color to give **3**; trimethylchlorosilane is formed as a volatile, readily separable by-product. Completion of the exchange can be controlled by thin-layer chromatography. However, because of the instability of the chlorotitanate **3**, its isolation and exact characterization is not possible. The direct reaction of diols such as **1** or their anions with $TiCl_4$, on the other hand, yields HCl- or salt-containing chlorotitanates whose catalytic activity is strongly reduced. In the acrylates **1**–**3**, the α,β-unsaturated carbonyl system is apparently present in the *anti* conformation, since the signals of the vinyl protons appear in the sequence ($\delta_{\beta\text{-}Z} > \delta_{\alpha} > \delta_{\beta\text{-}E}$) characteristic for normal acrylates. This is consistent with the observations made on lactate enoates, in which the Lewis acid catalyst, as here, attacks exclusively at the carbonyl oxygen atom of the enoate.[6] In the reactive complex **3**, the dienophile and the titanium catalyst are so fixed that the *Re* side of the dienophile is shielded, irrespective of which conformation the side chain adopts with respect to the catalyst. The arrangement in which the oxygen atom of the furanose ring can function as sixth ligand for the titanium atom could be especially favorable. Cyclopentadiene can then attack the complex **3** only from the front, and obliquely from above, as shown in Scheme 1. Hence, on preserving the *endo* transition state the (1′*R*,2′*R*)-5′-norbornen-2-ylcarboxylic acid derivative **4** should be formed. The ^{1}H- and ^{13}C-NMR spectroscopic analysis of the adduct, the separation of the diastereomers **4** by flash chromatography,[8] and the reductive cleavage of **4** to give 5-norbornen-2-ylmethanol[9] confirm that the (1′*R*,2′*R*)-diastereomer of the adduct **4** is indeed formed highly selectively (93 : 7). *Exo* configurated isomers could not be detected in the product mixture. The (1′*S*,2′*S*)-diastereomer of **4** formed as by-product presumably arises from the Diels-Alder reaction of the *syn*-rotamer of **3**. The amount of *syn*-rotamer increases with increasing reaction temperature. Reactions of **3** with the less reactive dienes 1,3-cyclohexadiene, 1,3-butadiene and anthracene lead in 12 days at room temperature to formation of the adducts in yields of up to ca. 30%. The diastereoselectivity drops from 82 : 18 (cyclohexadiene) to 78 : 22 to 70 : 30 (anthracene).

We concluded from these findings that the activity of the titanium center should be increased in order to increase the diastereoselectivity. We therefore prepared the 3-*O*-acryloyl-1,2-*O*-isopropylidene-5-*O*-trimethylsilyl-α-D-xylofuranose **5** from 3-*O*-acryloyl-1,2-*O*-isopropylidene-5-*O*-trityl-α-D-xylofuranose by selective acidolytic deblocking in the 5-position and subsequent silylation with trimethylchlorosilane/pyridine. Reaction of **5** with titanium tetrachloride leads to formation of the complex **6** in which the dienophile and the Lewis acid catalyst are arranged similarly as in **3** (Scheme 2). The Lewis acidity in **6**, however, is increased. Cyclopentadiene reacts with **6** to give the adduct **7**, only one diastereomer of which can be detected by chromatography and by 400-MHz ^{1}H- and 100-MHz ^{13}C-NMR spectroscopy.[10] The reduction of **7** to 5-norbornen-2-yl-methanol confirmed that **7** was the expected (1′*R*,2′*R*)-diastereomer.

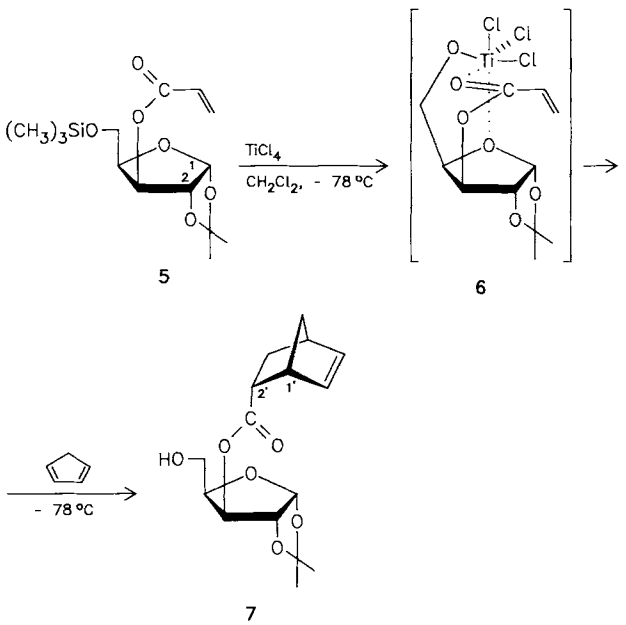

73%, (*R*) : (*S*) > 98 : 2

Scheme 2.

These results show that the chiral information of carbohydrates can be used for directed stereoselective control by binding reversibly several reaction components in a definite way to the functional groups of the carbohydrate matrix.

Received: October 31, 1986;
supplemented: December 5, 1986 [Z 1975 IE]
German version: *Angew. Chem. 99* (1987) 269

[1] Short review, e.g. N. Sharon, *Trends Biochem. Sci. Pers. Ed. 9* (1984) 198.

[2] a) S. Brandänge, S. Josephson, L. Mörch, S. Vallén, *Acta Chem. Scand. Ser. B 35* (1981) 273; b) C. H. Heathcock, C. T. White, J. J. Morrison, D. Van Derveer, *J. Org. Chem. 46* (1981) 1296; c) I. Hoppe, U. Schöllkopf, R. Tölle, *Synthesis 1983*, 789; d) S. Danishefsky, J. Aubé, M. Bednarski, *J. Am. Chem. Soc. 108* (1986) 4145.

[3] Review: H. Kunz, *Angew. Chem.*, in press.

[4] Review on the asymmetric Diels-Alder reaction: W. Oppolzer, *Angew. Chem. 96* (1984) 840; *Angew. Chem. Int. Ed. Engl. 23* (1984) 876.

[5] a) D. A. Evans, K. T. Chapman, J. Bisalia, *J. Am. Chem. Soc. 106* (1984) 4261; b) W. Oppolzer, C. Chapuis, G. Bernardinelli, *Helv. Chim. Acta 67* (1984) 1397.

[6] Recent review: G. Helmchen, R. Karge, J. Weetman: *Modern Synthetic Methods, Vol. 4*, Springer, Berlin 1986, p. 261ff.

[7] T. Poll, A. Sobczak, H. Hartmann, G. Helmchen, *Tetrahedron Lett. 26* (1985) 3095.

[8] (1′*R*,2′*R*)-**4**: ^{1}H-NMR ($CDCl_3$): $\delta = 5.85$ (d, $J(1,2) = 3.7$ Hz; H-1), 2.98 (dt, $J(2',3'\text{endo}) \approx J(2',1') \approx 3.9$ Hz, $J(2',3'\text{exo}) = 9.3$ Hz; H-2′); ^{13}C-NMR: $\delta = 174.8$ (C=O), 138.0 (C-5′), 104.8 (C-1), 83.2 (C-2); $R_f = 0.40$ (petroleum ether 40–70/acetone 1/1). $[\alpha]_D^{22} = +89.5$ ($c = 1$ g/100 mL, $CHCl_3$). (1′*S*,2′*S*)-**4**: ^{1}H-NMR ($CDCl_3$): $\delta = 5.88$ (d, $J(1,2) = 3.7$ Hz; H-1), 3.02 (ddd, $J(2',3'\text{endo}) = 3.85$ Hz, $J(2',1') = 4.0$ Hz, $J(2',3'\text{exo}) = 9.3$ Hz; H-2′); ^{13}C-NMR: $\delta = 175.0$ (C=O), 138.4 (C-5′), 104.9 (C-1), 83.0 (C-2); $R_f = 0.37$ (petroleum ether/acetone 1/1). The product still contains ca. 10% of the (1′*R*,2′*R*) diastereomer.

[9] $[\alpha]_D^{22} = +65.9$ ($c = 1$, ethanol), obtained from the diastereomeric mixture **4**; (2*S*)-*endo*-5-norbornen-2-yl-methanol: $[\alpha]_D = -76.6$ (95% ethanol) according to J. A. Berson, J. Singh Walia, A. Remanick, S. Suzuki, D. Reynolds-Warnhoff, D. Willner, *J. Am. Chem. Soc. 83* (1961) 3986; (2*R*)-*endo*-5-norbornen-2-yl-methanol: $[\alpha]_D^{22} = +76.1$ ($c = 0.9$, EtOH) see E. J. Corey, H. E. Ensley, *ibid. 97* (1975) 6908.

[10] (1′*R*,2′*R*)-**7**: ^{1}H-NMR ($CDCl_3$): $\delta = 5.89$ (d, $J(1,2) = 3.6$ Hz; H-1), 2.95 (m; H-2′). ^{13}C-NMR: $\delta = 174.5$ (C=O), 138.2 (C-5′), 104.6 (C-1), 83.7 (C-2); $[\alpha]_D^{22} = +84.2$ ($c = 0.33$, $CHCl_3$).

BOOK REVIEWS

Chemistry of Hydrocarbon Combustion. By *D. J. Hucknall.* Chapman & Hall, London, New York 1985. viii, 415 pp., bound, £ 39.50.—ISBN 0-412-26110-3

The problems and methods of investigation in the chemistry of hydrocarbon combustion are of an analytical nature. The questions posed are: What types of reactions and intermediates are involved in the combustion? What are the rates of the individual steps in the reaction? How are these steps interconnected with regard to the transfer of matter and energy? The book reviewed here is aimed at obtaining answers to these questions. The treatment of the problem can be divided roughly into three sections:

1. Determining the possible reaction products that can result from oxidation or thermal decomposition under various conditions of combustion (Chapters 1, 2 and part of Chapter 6).
2. A description of the tools used by the combustion chemist, divided into "hardware" (apparatus and investigational techniques), and "software" (information on reaction mechanisms and rate constants).
3. Computer-aided studies which are aimed at simulating and understanding the entire combustion process and the macroscopic observations, starting from reaction mechanisms and kinetic data.

The first group of topics is treated mainly from a historical standpoint. Results obtained for different fuels are followed by a description of theories of hydrocarbon oxidation proposed during the 1920's and 1930's. Similarities of the combustion of various hydrocarbons (induction times, auto-catalytic behavior, negative temperature coefficients, etc.) are outlined, and important stages in the theoretical interpretation (hydroxyl chemistry, branching of reaction chains according to *Semenow*, peroxide theory, etc.) are explained. The development of more sensitive analytical techniques (mass spectrometry, gas chromatography) on the one hand, and the introduction of methods for transient measurements on the other, are reflected in the greater wealth of analytical data and the increasingly detailed reaction mechanisms arising in the 1960's and 1970's (Chapter 2). By this historically oriented treatment, the author puts up with the fact that without a knowledge of the important reaction mechanisms discussed later, the analytical results from early studies and the interpretations based on them appear confusing and lacking an unbroken thread.

Chapters 3 to 5 comprise an excellent review of modern techniques for investigating the basic reactions of combustion processes and measuring their kinetic parameters. This is a critical presentation which also examines theoretical aspects of the interpretation of rate constants and their dependence on temperature and pressure. One chapter is devoted to free radical reactions of the hydrogen-oxygen system and another to those of carbon-containing compounds. It becomes clear how closely related the combustion chemistry of hydrocarbons is to the hydrogen-oxygen system. I enjoyed these chapters the most.

There follows a chapter on the pyrolysis of hydrocarbons, insofar as this is important in relation to combustion reactions, half of this being devoted to soot formation in flames. Here one is a little disappointed at not finding an account of the progress made recently using laser optics methods. Also the fact that soot formation is treated in the chapter on pyrolysis obscures to some extent the important role that oxidation reactions also have in this process.

The book concludes with a briefer survey of methods and progress in modelling complex combustion systems (flames, pyrolyses and oxidations at intermediate temperatures).

Taken as a whole the book mainly has the character of a review. Its strength lies in its concise presentation, limited to the basic essentials, of results from important investigations covering seven decades of combustion research. This is supported by the extremely comprehensive bibliography, containing about 2200 references. Regrettably, though, the author has not quite succeeded in clearly correlating the results of different investigators, nor in reducing complex combustion reactions to their essential features and thereby making them comprehensible to chem-

ists other than combustion specialists. An example is the generalized reaction mechanism for hydrocarbon oxidation on p. 381, which contains reactions such as $R^{\odot} \rightarrow {}^{\odot}R$, and the explanation which follows. Nevertheless, the book is recommended for all combustion chemists, as it will expand their knowledge and thus make their work easier.

Klaus-Heinrich Homann [NB 764 IE]
Institut für Physikalische Chemie
der Technischen Hochschule Darmstadt (FRG)

Olefin Metathesis and Ring-Opening Polymerization of Cyclo-Olefins. By *V. Dragutan, A. T. Balaban,* and *M. Dimonie.* Wiley, Chichester, and Editura Academiei, Bucharest 1985. 544 pp., bound, £ 34.50.—ISBN 0-471-90267-5

Following the publication in 1985 of the revised second edition, in Rumanian, of the book by *V. Dragutan, A. T. Balaban,* and *M. Dimonie,* an English translation has now appeared, making it accessible to a wider range of readers. It is concerned with the scientific and technological aspects of metathesis reactions of linear and cyclic olefins. Since its discovery by *Banks* and *Bailey* in 1964, catalyzed olefin metathesis has quickly attained considerable importance in organic, macromolecular and organometallic chemistry. The main areas of application emphasized are olefin syntheses (triolefin process, Shell higher olefins process and petrochemicals olefin syntheses), and the synthesis of elastomeric polyalkenes. Consequently, there is a large group of interested readers who will welcome a specialist book on this subject.

Dragutan, Balaban, and *Dimonie* present here, in nine chapters, a broad, application-oriented, survey of metathesis reactions. Chapter 1 contains a short historical overview, and definitions of metathesis reactions such as homometathesis, cometathesis and ethenolysis. In Chapter 2 the common heterogeneous and homogeneous catalysts for metathesis are described as well as reaction variables such as temperature, pressure and solvent. In Chapter 3 the metathesis reactions of linear and cyclic olefins and of alkynes are systematically discussed. Ring-opening metathesis of mono-, bi- and polycyclic olefins is described in detail in Chapter 4. Chapter 5 gives a brief examination of the thermodynamic aspects of the metathesis of olefins and the ring-opening polymerization of cyclic olefins. Chapter 6 deals in detail with reaction kinetics and mechanisms. Each of the intermediate steps in the currently favored carbene mechanism for metathesis reactions of linear and cyclic olefins are examined in detail and the effects of different transition metals, ligands and co-catalysts are discussed. Mechanisms for alkyne polymerization are also dealt with. In Chapter 7 an account is given of the stereochemistry of metathesis reactions, with experimental results and theoretical ideas clearly presented alongside each other. Chapter 8 is devoted to practical applications; this includes discussion both of existing technological processes and of further possible applications to the synthesis of organic compounds. The final chapter contains a comprehensive survey of known metathesis reactions in the form of tables, listed both according to catalysts, and the substrate olefins and alkynes.

The literature cited and discussed covers approximately 2000 publications up to 1982. In view of the wealth of published papers in the area of metathesis in recent years, a further new edition or a supplement will presumably appear before very long.

On the whole, this reference book provides a very comprehensive survey (up to 1982) of the metathesis of linear olefins and the ring-opening polymerization of cyclic olefins. The research findings and the reaction mechanisms are discussed in a lucid manner. The figures and tables are clearly set out and easy to understand. A minor fault is the poor quality printing, especially apparent in some of the figures. The book is primarily suited for chemists working in the metathesis field, whether their objectives are mainly of a chemical (organic, macromolecular or organometallic) or technological nature.

Karin Weiss [NB 769 IE]
Laboratorium für Anorganische Chemie
der Universität Bayreuth (FRG)

Polymers. The Origins and Growth of a Science. By *H. Morawetz,* Wiley, Chichester 1985. xvi, 306 pp., bound, £ 54.95.—ISBN 0-471-89638-1

Unlike molecular biology or biotechnology, macromolecular chemistry is not a field of technology that attracts the attention of the public at large. Nevertheless, our industrial civilization has become highly dependent upon polymer science, i.e. upon the synthesis and properties of polymers. Polymers in the form of plastics, synthetic fibers, coatings, adhesives, synthetic rubbers and insulating materials make up one of the most important branches of the chemical industry. The standard of living now enjoyed by Western industrial nations would scarcely be conceivable if the materials provided by macromolecular chemistry did not exist.

Herbert Morawetz's book on the origins and growth of polymer science is a 'must' for all those who wish to come to terms with macromolecular chemistry and physics and who are not merely interested in current facts and figures but also want to find out about the internal structure and concepts of this field of science.

In 25 fascinating chapters *Morawetz* describes the intellectual and experimental difficulties that have had to be overcome since the days of *Berzelius* in order to understand the complexity, diversity and dynamics of macromolecular structures and their properties.

Polymer science has profited from the advances made in general chemistry and physics, yet concomitantly it has stimulated these sciences in certain respects. The interest shown by technology and industry in new materials have done their part to accelerate the progress of research. These considerations run through the whole of the book. *Morawetz* deals with already well known examples—the study of the structure and properties of natural and synthetic rubbers, the controversies concerning the structure and properties of cellulose as a basic material in the textile industry, which finally led to the development of synthetic fibers, and the elucidation of the mechanism for the radical polymerization of olefins, which is basic to the organic chemistry of free radicals and has also enabled the synthesis of important plastics.

The achievements of individual research workers can only be appreciated in the light of the knowledge available to them. The ranges and efficiencies of the methods and techniques at their disposal also have to be taken into consideration. *Morawetz* has successfully managed to relate this in an understandable way, he has made a point of substantiating the concepts of each research worker and his scientific competitors by using original quotations. Al-

though some of these have had to be commented in accordance with modern concepts, this has been done carefully and intelligently.

The book is divided into specialized subjects that are arranged in historical order. The achievements of individual scientists are described within the relevant topic, for example biogenic macromolecules, the importance of X-ray structure analysis, the determination of molecular weights, condensation polymerization, rubber elasticity, properties of polymer solutions. The chapters on the origin and growth of molecular biology and its relationship to macromolecular chemistry are also of interest.

The work has been written at a very high scientific level and thus assumes that the reader already possesses a broad knowledge of macromolecular chemistry and the physical chemistry of the condensed state. This accounts for its great appeal to the expert who wants to obtain a complete grasp of the background on which current knowledge is based, especially since most of the themes that are discussed are still of topical interest.

Gerhard Wegner [NB 751 IE]
Max-Planck-Institut für Polymerforschung Mainz (FRG)

Homogeneous Catalysis with Compounds of Rhodium and Iridium. By *R. S. Dickson*. D. Reidel Publishing Company, Dordrecht 1985. xv, 278 pp., bound, HFl 135.00.—ISBN 90-277-1880-6

In the series *Catalysis by Metal Complexes*, the volume on homogeneous catalysis using compounds of rhodium and iridium has now appeared. This monograph by *Ronald S. Dickson*, containing seven chapters of text, a summary in tabular form of rhodium and iridium catalysts and their applications, as well as nearly 2000 references, gives a detailed survey of the state of research on this topic up to the end of 1982.

After a very brief introduction to catalysis by transition metal compounds in Chapter 1, there follows a chapter on the activation of C–H and C–C bonds (dehydrogenation, H/D isotope exchange, isomerization), then one on C–H bond formation (hydrogenation, hydrosilylation). These are followed by Chapter 4 on carbonylation and hydroformylation reactions, and Chapter 5 on oxidations. Chapter 6 deals with reactions involving functional group removal, and Chapter 7 is devoted to oligomerization, polymerization and cyclization reactions. Within each chapter the reactions discussed are grouped under catalyst types. The appendix contains tables in which the catalyst types dealt with, their applications, and the literature references are collected together.

The author has evidently been concerned to bring order to the flood of detailed information, and has succeeded in providing the reader with a lucid overview of the wealth of studies and results. The summary tables and the literature references (which total 1971) in the appendix make it easier for the reader to get his bearings in this wide ranging field of research, and facilate quick access to the original papers. The alphabetical arrangement of references under first-named authors is especially helpful in that respect. Thus the reader can quickly find information on a particular type of reaction by using the list of contents, on a type of catalyst from the tables in the appendix, or on the work of a particular author from the bibliography. This favorable impression of the book is further reinforced by the inclusion of a carefully compiled subject index.

However, the lucid arrangement of the material is contrasted by a presentation considerably less clear. This is due both to reaction schemes which are not very illustrative, and to the book's catalog-like nature. The readability of the text is also seriously hindered by the monotonous style—for example, almost every section begins with the phrase "... have been used as catalysts for ...". The concern with completeness and clarity has led to a format which does not allow a lively style and terse presentation. Understanding of the reaction schemes, which are thoroughly and critically discussed, is made less easy by unnecessarily adopting a generalized form, and often by a lack of complete stoichiometry, e.g. in Schemes 3.1, 3.3, 3.4, 3.5, and 6.1 the detached ligand (S, CO, or PR_3) is omitted, and in Scheme 2.3 the original complex is ignored.

To summarize, the book is well set out, and the organization of the material is impressive, but it is not easy to read; it will undoubtedly be of considerable value to the specialist, but it will scarcely be attractive for the reader who is looking for an introduction to this field of research.

Georg Süss-Fink [NB 770 IE]
Institut für Anorganische Chemie
der Technischen Hochschule Aachen (FRG)

Organische Chemie. By *S. Hauptmann*. Verlag Harri Deutsch, Frankfurt/M. 1985. 893 pp., bound, DM 48.00.—ISBN 3-87144-902-4

With the appearance in the early sixties of books such as those of *Roberts* and *Caseiro*, *Cram* and *Hammond*, *Morrison* and *Boyd*, and many others, a new sort of textbook was seen to be emerging on to the market. These introductions to organic chemistry were characterized by having their contents arranged according to reaction types (instead of the more traditional arrangement under compound classes), and a thorough discussion of reaction mechanisms, with detailed treatments of, in particular, bonding theory, stereochemistry, and the increasingly important spectroscopic methods. These textbooks were usually also distinguished by their high quality of formula printing, previously unknown in such books, and a clear and concise style. They presented organic chemistry as a well-ordered and systematic branch of science which, even if not fully under our control, is well understood, giving results that generally agree with our predictions. In retrospect it is interesting to note that during those years there were also many other areas of human activity where complicated relationships were accounted for by "theories". Thus, such books were appropriate to the climate of the times, and, first in the USA, then here in Germany, they quickly became the norm. In this country they succeeded to such an extent that textbooks of the more traditional style were no longer used, and furthermore our own authors literally laid down their pens, and soon no competing texts of German language origin were appearing.

Most of us have willingly used and recommended the American textbooks, although really a deficiency ought to have been apparent to us, arising not so much from the books themselves as from their uncritical acceptance into the German educational and training system—more specifically that of the Federal Republic. Textbooks of the sort described above were, and are, written for undergraduates; American students, after taking their bachelor degrees, use textbooks and monographs whose advanced nature is

often evident from their titles. Here, on the other hand, it tends to be assumed that not only undergraduates, but also post-graduate students reading for diplomas and even for doctoral higher degrees can learn about the whole of organic chemistry from books of the former kind. In other words, these books are suited only to a very limited extent for our (present) courses of study; they are too comprehensive for undergraduates, while for post-graduates or for those already in professional jobs they do not go far enough, containing insufficient detailed information for these users.

What, then, are the essential features of an organic chemistry textbook which is better suited to our present time and circumstances? It needs to combine the best characteristics of the two traditions, i.e. it must be up-to-date, lucid, and written from a standpoint of theory and mechanism in the manner of an Anglo-Saxon textbook, while having the encyclopedic and practically-orientated qualities of a traditional German textbook. A hopeless undertaking? Not, it appears, for *Siegfried Hauptman* of the Karl-Marx University, Leipzig, who has attempted singlehandedly to achieve such a synthesis. His "Organic Chemistry" is indeed modern in concept, as is illustrated by the wealth of topics that are treated. These range from the planning of a synthesis to the use of the published chemical literature, from organometallic chemistry to photochemistry and dyestuffs chemistry, from stereochemistry and bonding theory to spectroscopic methods, and many more topics, with nothing of importance omitted. The book is traditional in that it contains a large amount of factual data on substances (melting and boiling points, color, toxicity, etc.), so that one no longer needs to reach for "Karrer" or another classical reference work when these data are needed in a hurry. Many of the old named reactions and historical and biographical details are also referred to. Extensive chapters are given to heterocyclic chemistry, neglected by many other textbooks, and the sections on natural products, with their treatments of the metabolism of carbohydrates, fats and proteins, extend into biochemistry.

Can all this be covered in only 893 pages? It has been helped mainly by the use of a closely spaced text, and by the frequent use of small type and tables. Nevertheless, the question is not so easily dismissed. Covering so many topics incurs risks of a degree of eclecticism, of the bare cataloguing of facts without discussing them, and of underestimating the difficulties faced by the beginner. Thus, for example, the Hückel theory is presented in a way which, though quite correct, is very compressed. I doubt whether the beginner can understand every step of this. In these sections, which come quite early in the book, there is a great risk of encouraging the reader to form habits of blind acceptance and mindless rote learning. Also the pages dealing with the statistical basis of chemistry (Maxwell-Boltzmann statistics, statistical mechanics, etc.) are in my view too much of a good thing—these topics are best left to textbooks on physical chemistry.

The author sometimes falls into the trap of "name-dropping". To mention just two examples, when he mentions spiroconjugation (p. 789) or trimethylsilyl enol ethers in synthesis (p. 551), each in just a single sentence, the reader has encountered a new word but not understood its meaning.

There are remarkably few typographical and factual errors; there is no need to detail them here, as most of them do not confuse the meaning. In future editions no doubt the two pentavalent carbon atoms on p. 501 will disappear. More important, though, is the need to address the book more clearly to an international readership, rather than referring to commercial products only by the names used in the GDR; readers here would prefer to see also names such as nylon, Perlon and aspirin!

On the whole, though, these shortcomings, which are mostly rather better described as aberrations, do not detract significantly from the quality of the book. *Hauptmann* has successfully written a textbook of the eighties which is suited to *our* needs. He is to be congratulated on this achievement, which is in no way diminished by the fact that the book is in many respects similar to the earlier organic chemistry textbook by *Hauptmann, Grafe,* and *Remane,* and owes quite a lot to it. This book, which represents amazingly good value at the price (DM 48.00!) deserves a very wide circulation, amongst students, to learn from it, and amongst lecturers, to teach—and test—from it.

Henning Hopf [NB 774 IE]
Institut für Organische Chemie
der Technischen Universität Braunschweig (FRG)

Methods of Enzymatic Analysis. Volume 8. Metabolites 3: Lipids, Amino Acids, and Related Compounds. Edited by *H. U. Bergmeyer, J. Bergmeyer,* and *M. Grassl.* VCH Verlagsgesellschaft Weinheim 1985. xxx, 629 pp., bound, Price per volume when ordering the complete work DM 285.00; single volumes DM 325.00.—ISBN 3-527-26048-X

Volume 8 is the third volume of the third edition to describe methods of analysis for specific metabolites. Its three chapters cover analyses for lipids, amino acids, and amino acid-related compounds, respectively.

The first chapter, which constitutes half of the volume, comprises six sections covering fatty acids and derivatives, phospholipids, apolipoproteins, cholesterol, steroid hormones, and bile acids. Generally, sections divide further into subsections, each of which discusses assay procedures for a single metabolite. Chapter 1 contains much more material than does the corresponding section of the second edition. It reflects the recent development of powerful enzyme immunoassay (EIA) techniques, especially in determinations of apolipoproteins and steroid hormones. Nicotinamide cofactor-linked assays for prostaglandins, 20-ketosteroids, and steroid alcohols are replaced by more specific EIA methods. Other methods that have been updated since the second edition are those for triglycerides, free fatty acids, D-(−)-3-hydroxybutyrate, acetoacetate, phosphatidylcholine, cholesterol, and bile acids. The discussion of cholesterol is expanded and includes methods for the specific determination of high-density lipoprotein and low-density lipoprotein cholesterol in addition to total cholesterol. The section on bile acids is likewise expanded to include methods specific for 3-α-hydroxy or 7-α-hydroxy bile acids as well as methods for total bile acids. The section on 7-α-hydroxy bile acids includes a description of a continuous-flow assay system using immobilized enzymes. Metabolites covered for the first time in the third edition are thromboxane B_2, succinylacetone, sorbic acid, sphingomyelin, glycerophosphorylcholine, phosphatidylcholine, and apo-lipoproteins.

Chapters 2 and 3 discuss methods of analysis for amino acids and amino acid-related compounds, respectively.

The chapters divide into sections, each of which covers procedures for a single compound or a few related compounds. Two-thirds of the assays of the second edition are repeated in Volume 8. The use of isotope dilution in the tRNA loading test for individual L-amino acids is not repeated, however. Assays revised in Volume 8 are those for branched-chain L-amino acids, L-phenylalanine and tyrosine, L-serine, L-lysine, D-amino acids, carbamoyl phosphate, carnitine and acylcarnitines, glutathione, spermine, and spermidine. Compounds addressed for the first time are 2,6-diaminopimelate, citrulline, octopine, arginine and arginine phosphate, histamine, catacholamines, secretonin, polyamines, *meso*-alanopine and D-strombine, and bilirubin. Volume 8 eliminates discussion of some compounds covered in the second edition—γ-aminobutyric acid, 3-hydroxykynurenine, and 3-hydroxyanthanilic acid—and does not include assays for tryptophan, methionine, threonine, cysteine/cystine, histidine, ornithine, or β-alanine.

As in previous volumes of the third edition, each section on a particular metabolite begins with the compound's structure. A general introduction discusses the occurrence, function, anabolism and catabolism of the compound in vivo, methods available for the compound's determination, substance properties relevant to analysis, applications of the analysis, and international reference standards and methods. The review of other methods of analysis provides a useful evaluation of their advantages and disadvantages. An explicit description of the assay procedure follows. This description includes discussion of the assay design, optimized conditions, equipment (both general and specialized), reagents (including preparation, purity required, and stability), preparation and stability of samples, and calculations. Each section concludes with information on the precision, accuracy, sensitivity, limits of detection, sources of error, and specificity of the method plus reference values for the levels of the metabolite in both normal and abnormal tissues and fluids. Appendices to the sections contain special procedures required for the assay, including the preparation of appropriate antibodies for EIA, isolation and immobilization of certain enzymes, preparation of tissues and other physiological samples, and the preparation of special electrodes.

Volume 8 is devoted to material given only 250 pages in the second edition. It contains more background and explanatory text than corresponding sections of the second edition. Each section contains ten to twenty references, including some as recent as 1983 and 1984. Several appendices provide definitions for common symbols, units, and abbreviations and list helpful constants and formulae. The format is quite convenient and amenable to use by workers unfamiliar with enzymatic analyses. The descriptions of procedures are highly detailed, cookbook-style, sometimes even providing sources of particular reagents. As in previous volumes, a drawback is an incomplete index.

This volume is not a comprehensive text, and is not as extensive in the number of assays contained as some of the previous volumes. Still, it contains assays for approximately seventy compounds, many of which are of great biological significance. The chapter on lipids has more than tripled since the second edition. This volume is recommended as a valuable reference work for those doing analyses of biological materials.

H. Keith Chenault, Alan Akiyama,
and *George M. Whitesides* [NB 779 IE]
Department of Chemistry, Harvard University
Cambridge, MA 02138 (USA)

Instrumentelle Multielementanalyse. Edited by *B. Sansoni.* VCH Verlagsgesellschaft, Weinheim 1985. xviii, 782 pp., bound, DM 160.00.—ISBN 3-527-26255-3

"The analyst's dream of being able to determine in a single operation all the elements present in a sample appears to be coming close to a reality. Instrumental multi-element analysis allows one to determine up to eighty elements simultaneously." So runs the blurb given for the thick volume named above. The reader can learn to what extent that dream has been realized from this book, excellently produced and edited, which contains the 87 papers presented at a conference on the subject held at the KFA (Nuclear Research Center), Jülich, on April 2–5, 1984. Under the auspices of the eight groups which organized the meeting (A.M.S.El., Arbeitskreis Radioanalytik, AFR, VDEh, DPG Mass Spectrometry Group, GDCh, Deutsche Bunsengesellschaft, and the Geochemical Section of the German Mineralogical Society), the delegates reported on research progress and their experiences with the various multi-element techniques.

Following a detailed and critical introductory survey by the editor (including references to the most important works published up to 1984), the introduction continues with contributions on important trends and on practical problems from the standpoint of academic and industrial scientists. The first four chapters describe determination techniques, other procedures involved in analysis, applications, and comparisons of different techniques.

The following analytical methods are covered: nuclear radiation spectrometry (2 papers), activation analysis (13 papers), mass spectrometry (4 papers), ICP mass spectrometry (1 paper), X-ray fluorescence analysis (6 papers), atomic emission spectrometry (9 papers), forward scattering (2 papers), atomic fluorescence spectrometry (1 paper), atomic absorption spectrometry (1 paper), voltammetry (1 paper), and ion chromatography (1 paper). The chapter on "Other Analytical Procedures" contains excellent critical contributions on pre-concentration, standards, and data processing and evaluation, the latter being considered also from the standpoint of industrial practice. The chapter on "Applications" contains informative contributions from the fields of geoscience (10 papers), environmental studies (4 papers), materials science (1 paper), life sciences and food science (3 papers), radiochemistry and nuclear chemistry (4 papers), archeometry (3 papers), and simultaneous elemental analyses by ICP spectrometry as part of a research center's analytical service (1 paper). The book is rounded off by five papers which compare different techniques, including ICP and DCP atomic emission spectroscopies, AA spectroscopy, XRF spectroscopy, synchrotron radiation XRF, FMS, and neutron activation analysis, by a survey of instruments and manufacturers, and by a comprehensive list of abbreviations commonly used in instrumental analysis, and a good subject index.

The satisfaction of reading this book is increased by the fact that it gives a really up-to-date picture of the current state of elemental trace analysis. The organizers of the conference have succeeded in striking a good balance between the monotechnique specialists, who are usually unduly optimistic about "their" method, and the more pessimistically inclined application strategists. To the optimists the search for improvements in detection capability (often confused with limits of detection) appears to result in steady progress, even though one continues to seek to demonstrate also the accuracy of a particular method by analyzing a small number of selected standard materials. However, results which are entirely valid in the ppm range

are often extrapolated into the ppb region, and no mention is made of matrices to which the method cannot be applied, nor of analyses which have failed. Also it is usually not easy to make comparisons on the basis of purely instrumental detection capabilities obtained with "model analyses", since the time intervals for measuring and integration, the amounts of sample needed, or limitations imposed by varying amounts of interfering elements and/or blanks, are not given. The pessimists, on the other hand, point to the results of ring analytical trials for the ppb region, which continue to be disastrous, even when they come from highly respected laboratories engaged in certifying new standard reference materials. *E. Jackwerth* in his paper expresses this very well as follows: "Each type of sample material behaves differently with regard to trace analysis. It is for this reason that trace analysis procedures can hardly ever be carried over from one material to another without problems arising." This fact is borne out in many more of the contributions; it leads *R. Michel, G. V. Iyengar,* and *R. Zeisler,* in their contribution on multi-element analysis in life sciences, to conclude that much more analytical research remains to be done before reliable data can be produced.

Many of the papers clearly show that, particularly in the region of extremely low trace concentrations, the ability and experience of the analyst are much more crucial than the outlay on equipment. In this respect even an experienced analyst can learn from this book. It can be wholeheartedly recommended for everyone who is concerned with techniques for multi-element analysis.

Karl Cammann [NB 772 IE]
Anorganisch-chemisches Institut
Technische Universität München (FRG)

Carbocation Chemistry. By *P. Vogel.* Elsevier Science Publishers, Amsterdam 1985. xiv, 596 pp., bound, HFl 350.00.—ISBN 0-444-42522-5

"Carbocations can be found everywhere, from interstellar space to your glass of wine", runs the beginning of this journey through chemistry, taking carbocations as its guideline. Seventeen years after the appearance of the first volume of the five-part work "Carbonium Ions" by *Olah* and *Schleyer,* we now have a new comprehensive treatment of the chemistry of carbocations.

The reader is taken straight from the anthocyanins present in red wine to free enthalpy diagrams, and is then given, in about fifty pages, a repetition of some of the fundamentals of physical chemistry. Only on page 61 do we arrive at the main theme, with a discussion on nomenclature and an account of gas-phase studies on carbocations. A systematic treatment of methods for generating carbocations in condensed phases is followed by a chapter on NMR spectroscopic studies in super-acidic solvent systems, with particular attention to the use of isotopic perturbation of degeneracy for distinguishing between situations where there is a single or a double potential minimum. The PMO method is discussed in detail, and used to explain substituent effect in carbocations. Solvent effects on equilibria and rate constants are dealt with, as too are the various mechanistic aspects of solvolysis reactions. In the chapter entitled "Rearrangements", the main topic discussed in detail is the behavior of small alkyl cations (C_3-C_6) in super-acidic media, while the studies using nucleophilic solvents, which are mostly early work, are mentioned only in passing. There is a detailed discussion of transition metal complexes of carbocations, with particular emphasis on the importance of carbocations as a link between organic and organometallic chemistry. The final chapter is devoted to the synthetic aspects of carbocations. In addition to the well-known aromatic electrophilic substitutions, the author discusses reactions with aliphatic compounds, carbocationic cyclization and cycloaddition reactions, and the use of transition metal cations. Thus, apart from polymerizations, all the important aspects of carbocation chemistry are covered.

The book offers a unique survey of the present state of this field of research. With an author index containing nearly 3000 entries, it might be described as the "March" of carbocation chemistry. As the examples chosen are mainly from recent papers, and a detailed subject index is also provided, it affords a convenient means of access to the relevant literature. The book, produced by a photoreproduction technique, is reasonably free from errors, and the structural formulas are clear.

The author has succeeded very well in arranging the material in an orderly fashion for easy assimilation, on the basis of a small number of theoretical principles. This is helped particularly by the many cross-references to analogies in other areas of chemistry. Although I very much like the didactic style of the book, I feel that the author, in trying to write a textbook of physical organic chemistry based on the example of carbocations, has taken things a little too far. Presumably, there will only be relatively few readers who will work through the book from beginning to end, since readers whose aim is to study basic principles will in any case use the conventional textbooks. It can only be hoped that the inexplicably high price will not deter even the libraries from buying it, so that it may be followed in a few years time by an extended second edition.

Herbert Mayr [NB 776 IE]
Institut für Chemie
der Medizinischen Universität zu Lübeck (FRG)

Registered names, trademarks, etc. used in this journal, even when not marked as such, are not to be considered unprotected by law.

© VCH Verlagsgesellschaft mbH, D-6940 Weinheim, 1987. - Printed in the Federal Republic of Germany by Zechnersche Buchdruckerei, Speyer/Rhein.

All rights reserved (including those of translation into foreign languages). No part of this issue may be be reproduced in any form - by photoprint, microfilm, or any other means - nor transmitted or translated into a machine language without written permission from the publishers. Only single copies of contributions, or parts thereof, may be made for personal use.

Valid for users in the USA: The appearance of the code at the bottom of the first page of an article in this journal (serial) indicates the copyright owner's consent that copies of the article may he made for personal or internal use, or for the personal or internal use of specific clients. This consent is given on the condition, however, that the copier pay the stated per-copy fee through the Copyright Clearance Center, Inc., for copying beyond that permitted by Sections 107 or 108 of the U.S. Copyright Law. This consent does not extend to other kinds of copying, such as copying for general distribution, for advertising or promotional purposes, for creating new collective works, or for resale. For copying from back volumes of this journal see 'Permissions to Photo-Copy: Publisher's Fee List' of the CCC.

Editorial office: Pappelallee 3, D-6940 Weinheim, Federal Republic of Germany, Telephone (06201) 602315, Telex 465516 vchwh d, Telefax (06201) 602328.

Editor: *P. Gölitz.*

Associate editors: *D. J. Loewus, A. Stimson.* **Editorial assistant:** *E. Schweikart*

Publishers: VCH Verlagsgesellschaft mbH. (Managing Directors: *Prof. Dr. Helmut Grünewald* and *Hans Dirk Köhler*), Pappelallee 3, D-6940 Weinheim, Federal Republic of Germany. Correspondence concerning advertisements should be addressed to VCH Verlagsgesellschaft mbH. (Advertising Manager *R. J. Roth*), Boschstr. 12, P.O. Box 1260/1280, D-6940 Weinheim, Federal Republic of Germany, Telephone Weinheim (06201) 602-0, Telex 465516 vchwh d, Telefax (06201) 602328.

ANGEWANDTE CHEMIE
International Edition in English
Volume 26 · Number 4
April 1987
Pages 275–370

The Development of a Carbene-like Chemistry with Terminal Phosphinidene Complexes**

By François Mathey

When compared to the chemistry of other well-known electron-deficient species such as carbenes, silylenes, and nitrenes, the chemistry of phosphinidenes RP: is extremely underdeveloped. A critical survey of the literature indicates that this state of affairs probably reflects both an inadequate access to these species and an intrinsic lack of reactivity. Theoretical calculations suggest that it is possible to boost the electrophilicity and to stabilize the singlet state of phosphinidenes by complexation with transition-metal moieties such as $M(CO)_5$ (M = Cr, Mo, W). The corresponding terminal phosphinidene complexes [RP=$M(CO)_5$] show a rich and varied chemistry which often parallels the chemistry of singlet carbenes. Phosphinidene complexes are presently easily accessible through thermal decomposition of 7-phosphanorbornadiene complexes, but their stabilization remains a challenge to be met.

1. Introduction

In parallel with the broad development of the chemistry of carbenes, silylenes, and nitrenes,[1] there have been numerous attempts at developing a useful chemistry of the corresponding 6-electron phosphorus species, the so-called phosphinidenes R–P. The early work has been summarized in two interesting reviews by *Schmidt*[2] and *Regitz* et al.[3] In these early experiments, attempts were made to generate the phosphinidenes either by thermolysis of cyclopolyphosphanes, by reduction of dihalophosphanes, or by cycloreversion of phosphorus heterocycles. Tentative physicochemical proofs of the formation of phosphinidenes were provided only in the first case. Using this approach, *Schmidt* carried out the only systematic study of the chemistry of phosphinidenes so far reported. His most significant results are summarized in Scheme 1. Since then, some new phosphinidene precursors have been proposed,[3] but no significant extension of their chemistry has been unveiled.

In view of the poverty of phosphinidene chemistry, one question immediately arises: what is the reason for the apparent lack of reactivity of these species? The absence of reaction with olefins is especially noteworthy, since carbenes, silylenes, and nitrenes readily react with such compounds to give three-membered rings. A clear demonstration of this lack of reactivity was provided recently by *Diemert* et al.[5] Even when the favorable entropy factors associated with intramolecular reactions are exploited, it has not been possible to condense a phosphinidene with a C=C bond as shown in Equation (1) (THF = tetrahydrofuran). Three explanations for this lack of reactivity are conceivable:

[*] Prof. Dr. F. Mathey
Laboratoire de Chimie du Phosphore et des Métaux de Transition
DCPH - Ecole Polytechnique F-91 128 Palaiseau Cédex (France)

[**] According to IUPAC nomenclature, RP: is a phosphanediyl and R_2Si: a silanediyl. The conventional names phosphinidene and silylene are used in this article.

 © VCH Verlagsgesellschaft mbH, D-6940 Weinheim, 1987 0570-0833/87/0404-0275 $ 02.50/0

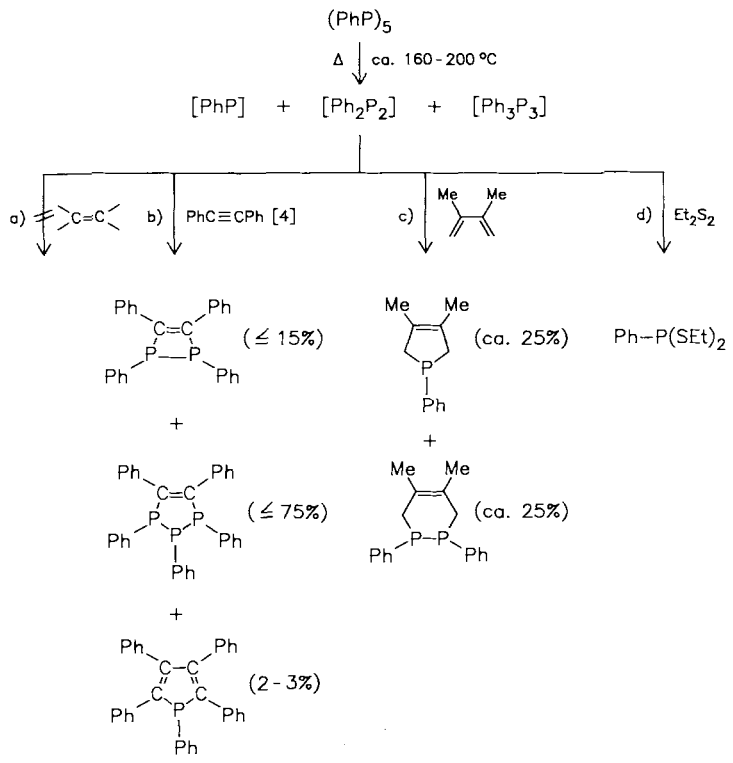

Scheme 1. Reactivity of monomeric and polymeric phosphinidenes.

1. Genuine phosphinidenes have not been generated by the various systems employed so far. For example, although the thermolysis of $(PhP)_5$ at around 400 °C has been demonstrated to produce phenylphosphinidene by mass spectrometric experiments,[2] most of the reactions of pentaphenylcyclopentaphosphane with organic substrates have been carried out at around 160–200 °C, and the products apparently arising from the trapping of phenylphosphinidene might have been formed through different mechanisms. A possible scheme for rationalizing the products obtained from the reaction with conjugated dienes (reaction (c) of Scheme 1) is depicted in Equations (2) and (3). The formation of the phosphorane **2** would be especially favored by the reduction in strain of the three-membered ring of **1** through incorporation into a trigonal-bipyramidal structure.[6] Another example is provided by the thermolysis of 7-phosphanorbornenes containing trivalent phosphorus, an approach initially proposed by *Fluck*[7] and *Quin* et al.[8] The suspected phosphinidene was trapped by conjugated dienes or heterodienes to give dihydrophospholes or dihydroheterophospholes, respectively. Very recently, however, *Quin* et al.[9] demonstrated that this type of reaction does not involve a free phosphinidene (Scheme 2).

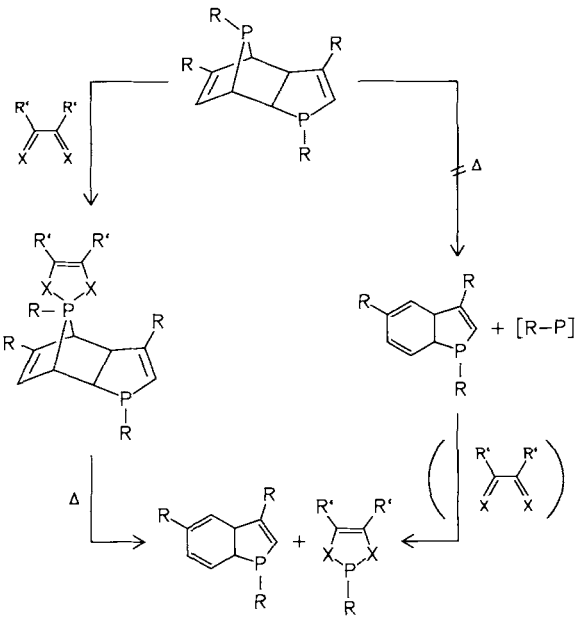

Scheme 2. Mechanism of the reaction of 7-phosphanorbornenes with conjugated dienes [9].

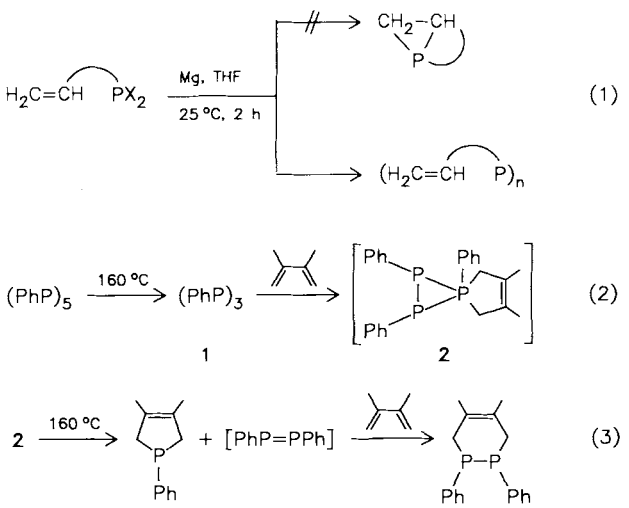

2. The phosphiranes formed according to Equation (1) are expected to exhibit low thermal stability,[10] except when substituted by bulky groups.[11] Thus, any method generating phosphinidenes at high temperatures cannot be used to perform [1+2] cheletropic cycloadditions with C=C bonds.

3. Phosphinidenes themselves might exhibit an intrinsic lack of reactivity. This point will be further discussed below, but the thermodynamic factor can already be stressed. Since P–C bonds are weaker than C–C, Si–C, or N–C bonds,[12] their tendency of formation will be lower. Thus, to say the least, the data concerning the reactivity of phosphinidenes were (and still are today) unsatisfactory and inconclusive. Accordingly, the development of new, reliable ways to generate phosphinidenes remains a logical objective since there is no definitive proof of the effectiveness of the already existing systems. In practice, such a new system must work at a reasonably low temperature (ca. 100 °C). Furthermore, since the ground state of phosphinidenes is a triplet,[13] it would be more interesting (and

hopefully more rewarding!) to generate the phosphinidenes in a singlet excited state in order to achieve higher and cleaner reactivity.

2. Synthesis and Properties of Stable 7-Phosphanorbornadiene Complexes

At the beginning of the 1980s, a quick glance through the literature on phosphinidenes showed that one of the most attractive ways to meet the conditions discussed in Section 1 had not been seriously investigated: namely, the use of 7-phosphanorbornadienes as phosphinidene precursors [Eq. (4)]. This approach offers several potential advantages. The aromaticity of the benzene ring formed could

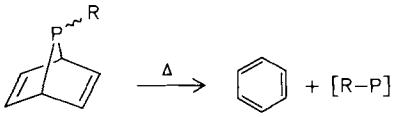

(4)

provide the driving force for a decomposition at low temperatures. Moreover, symmetry reasons suggested that the phosphinidenes thus generated would be singlets if the decomposition followed a concerted mechanism. In fact, similar reasons had previously led to the investigation of 7-silanorbornadienes as precursors of silylenes.[14] However, only two papers[15,17] concerning 7-phosphanorbornadienes are to be found in the early literature. The first report, by *Schmidt* et al.,[15] on the synthesis of a 7-phosphanorbornadiene *P*-oxide was in fact erroneous. Much later, Japanese chemists[16] established that the product of *Schmidt* et al. was a 7-phosphanorbornene and clearly demonstrated that genuine 7-phosphanorbornadiene *P*-oxides had a very low stability; spontaneous decomposition of such a structure was observed at room temperature. The second report, by *Stille* et al.,[17] described the successful synthesis of a benzo-annelated 7-phosphanorbornadiene *P*-oxide by reaction of benzyne with pentaphenylphosphole oxide, but the phosphorus bridge collapsed whenever the reduction of the P=O bond was attempted. A third report, by *Kashman* et al.,[18] again highlighted the low stability of the 7-phosphanorbornadiene structure [Eq. (5)].

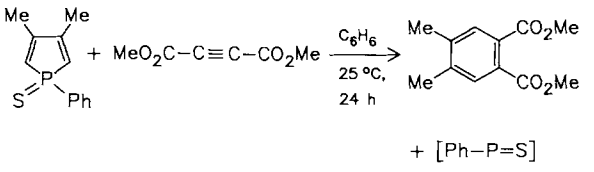

(5)

In spite of these failures, it was quite obvious that the only reasonable way to prepare 7-phosphanorbornadienes remained the [2+4] cycloadditions between electrophilic acetylenic dienophiles and phospholes. The choice of the technique used for masking the phosphorus lone pair, however, remained open. Such a protection is necessary in order to avoid side reactions at phosphorus.[19] Since 7-phosphanorbornadiene *P*-oxides and sulfides appeared unstable, the only practical alternative was to protect phosphorus by complexation. Thus, the reaction of various *P*-coordinated phosphole complexes with dimethyl acetylenedicarboxylate was investigated. It was thereby possible to obtain stable *P*-coordinated 7-phosphanorbornadiene complexes, **4**, with chromium, molybdenum, and tungsten pentacarbonyls as the complexing groups [Eq. (6)].[20]

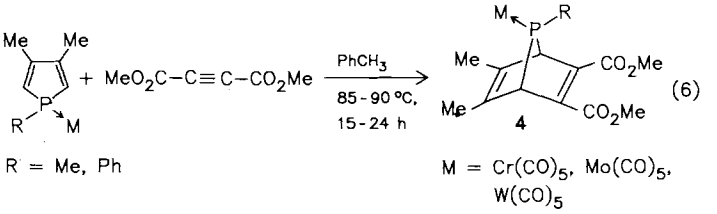

(6)

Other complexing groups such as $Fe(CO)_4$ or CuX are ineffective for the stabilization of the 7-phosphanorbornadiene skeleton. The synthesis of **4** also fails when bulky R groups (e.g., *t*Bu) are used or when the 3,4-dimethyl substitution is not present (fortunately, the corresponding phospholes are especially easy to pepare[21]). The instability of the bicyclic structure is so high that all attempts at decomplexing phosphorus were unsuccessful. Thus, only the chemistry of **4** itself could be studied directly. Mass spectral analysis suggested that **4** might be a convenient precursor of the still unknown terminal phosphinidene complexes [R–P=M] (M = complex fragment).[20] Of the six possible types of phosphinidene complexes (Scheme 3),

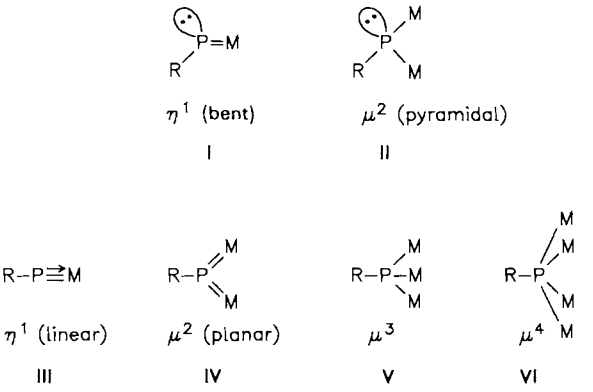

Scheme 3. The various types of phosphinidene complexes. **I** and **II**: phosphinidenes as 2-electron donors; **III**–**VI**: phosphinidenes as 4-electron donors.

the terminal complexes **I** were a priori the most interesting ones as far as phosphorus chemistry was concerned, since the lone pair at phosphorus and the low coordination state of phosphorus are favorable features for a high reactivity. Thus, the thermolysis of **4** was carefully investigated. A kinetic study of the decomposition of **4** with R = Ph, $M = W(CO)_5$[22] in the presence of various trapping reagents clearly demonstrated that the reaction is first order in the concentration of **4** and does not depend on either the nature or the concentration of the trapping reagent. The decomposition starts above 100°C and the activation energy of the rate-determining step is 33 ± 1 kcal mol^{-1}. By analogy with the processes occurring during the thermolysis of norbornadienes,[23] the first-order kinetics can be ra-

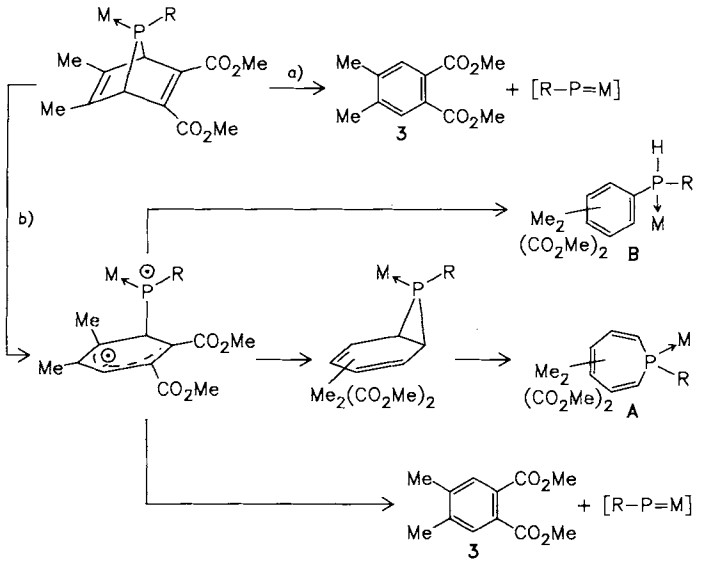

Scheme 4. Possible pathways for the decomposition of 7-phosphanorbornadiene complexes. The postulated intermediates [R–P=M] react with trapping reagents to give the products.

tionalized by the two decomposition paths outlined in Scheme 4 if it is assumed that steps a and b are rate-determining. However, the formation of the phosphepine complex **A** and the secondary arylphosphane complex **B**, which are the expected side products of path b, was never observed. In all cases, the only isolated by-product was the phthalate **3**. Thus, path a remains as the most likely alternative. Before leaving the subject, it must be noted that it is possible to catalyze the decomposition of 7-phosphanorbornadiene complexes by the use of heavy-metal derivatives such as $Cu^{\oplus}$, $Ag^{\oplus}$, and $Pd^{2\oplus}$ salts.[24] The mechanism of this catalysis is unknown. Photochemical decomposition leads to entirely different products including several new polycyclic structures, which, however, are of no interest as far as phosphinidene chemistry is concerned.[25]

3. Chemistry of Terminal Phosphinidene Complexes

Three theoretical studies of terminal phosphinidene complexes have been reported.[26,27,59] In the first study,[26] $Fe(CO)_3$ was found to be the best possible complexing group for stabilizing phosphinidenes in complexes such as $[RP \rightleftarrows Fe(CO)_3]$.[26] Since the phosphinidene here acts as a 4-electron donor (no lone pair at phosphorus), the chemistry of such complexes (type **III**, Scheme 3) has nothing to do with the chemistry discussed in this article. The second study[27] compared the electronic properties of H–P and [H–P=Cr(CO)$_5$]. The structure of the complex was first optimized using extended Hückel (EH) calculations. This led to a P=Cr bond length of 1.90 Å (vs. 2.3–2.4 Å for the bond in R_3P–Cr(CO)$_5$), which indicates a strong double bond character. The phosphorus atom appeared to be sp^2-hybridized with an H–P–Cr bond angle of 125°. Using this optimized geometry, more precise PS HONDO ab initio calculations then predicted a singlet ground state with a singlet–triplet separation of 12 kcal mol^{-1}, a high localization of both the HOMO and the LUMO at phosphorus, and a net charge of +0.41 e at this atom. Since the ground state of H–P is a triplet with a net charge at phosphorus of −0.05 e, the complexation appeared to stabilize the singlet state and to boost the electrophilicity of the phosphinidene. On the basis of these results, some similarities were expected between terminal phosphinidene complexes and phosphenium ions, $R_2P^{\oplus}$, which also exhibit a high electrophilicity and have singlet ground states.[28] Such similarities have indeed been observed in some cases. The last study[59] compared the electronic properties of [H–P=Cr(CO)$_5$] and [H–P=Ni(CO)$_3$]. As expected, the phosphorus atom appeared to be far less electrophilic in the Ni(CO)$_3$ than in the Cr(CO)$_5$ complex. The results concerning [H–P=Cr(CO)$_5$], however, were different from those of the preceding study.[27] The geometry optimization led to an H–P–Cr bond angle of 110° and to a P–Cr bond length of 2.33 Å which implies a single bond character. The ground state was found to remain a triplet and the LUMO to be very low-lying with a high localization at phosphorus. In view of the discrepancies between these last two studies, there is a clear need for additional theoretical work on terminal phosphinidene complexes. A careful optimization of the geometry seems to be a prerequisite for obtaining reliable results concerning the electronic structure of these species.

Using complexes **4** as precursors, the reactions of terminal phosphinidene complexes with substrates containing O–H and N–H bonds, such as water, ammonia, alcohols, and primary and secondary amines, were first investigated. In all cases, an almost quantitative insertion into the O–H or N–H bonds was observed [Eq. (7)].[29] The huge stabiliz-

$$[R\text{–}P{\equiv}M] + A\text{–}H \xrightarrow[\text{or } 55\,^{\circ}C,\ CuCl]{110\text{–}150\,^{\circ}C} R\text{–}\underset{\displaystyle A}{\overset{\displaystyle H}{\underset{|}{\overset{|}{P}}}}\!\rightarrow M \qquad (7)$$

5

A = OH, NH_2, OR', NHR', NR'_2; M = Cr(CO)$_5$, W(CO)$_5$
R = Me, Ph; R' = Me, Et, Ph

ing effect exerted by the complexing groups upon the RP(H)A ligands is noteworthy. When free, such species are normally unstable except if bulky R or A groups are used.[30] Such a stabilizing effect of the complexation had already been noted by *Huttner* et al. with M = CpMn(CO)$_2$.[31]

Interesting results were also obtained with alkynes. Terminal phosphinidene complexes readily react with the C≡C bond to give the phosphirene ring of **6** [Eq. (8)].[32,33,43] This reaction allowed the first unambiguous characterization of this heterocycle. A large variety of al-

$$[R\text{–}P{\equiv}M] + R'\text{–}C{\equiv}C\text{–}R'' \longrightarrow \underset{\displaystyle R}{\overset{\displaystyle R'}{\underset{|}{\overset{|}{C}}}}{=}\underset{\displaystyle M}{\overset{\displaystyle R''}{\underset{|}{\overset{|}{C}}}}\!\!-\!P \qquad (8)$$

6

R = Me, Ph; R', R'' = H, Me, Et, Ph, CO_2Et;
M = Cr(CO)$_5$, Mo(CO)$_5$, W(CO)$_5$

kynes have been used including some electron-poor species such as phenylpropiolates. However, probably owing to their high electrophilicity, terminal phosphinidene complexes are unable to react with acetylenedicarboxylates. Subsequent to these initial investigations, *Hogeveen* et al. demonstrated that chlorophosphenium ions are also able to react with alkynes [Eq. (9)],[34] giving the phosphirenium

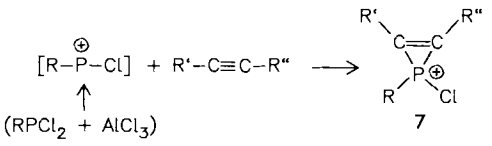

(9)

R = Me, Ph; R', R'' = H, Me

ions **7**. A similar reaction with isolated, stable phosphenium ions was subsequently mentioned by *Cowley* et al.[28] Thus, there is here a clear parallel between the reactivities of terminal phosphinidene complexes and phosphenium ions. However, **7** is only marginally stable at room temperature whereas **6** is almost incredibly stable (when $R = R' = R'' = Ph$ and $M = W(CO)_5$, **6** can be heated at 150°C for 15 h without any noticeable decomposition). This stability is quite striking, because the internal C-P-C bond angle of phosphirenes is around 41–42°, which is by far the lowest value reported for a C-P-C angle in organophosphorus chemistry. The tremendous stabilizing power of $Cr(CO)_5$, $Mo(CO)_5$, and $W(CO)_5$ complexing groups upon tervalent phosphorus derivatives is thus once again highlighted.

Terminal phosphinidene complexes readily react with olefins to give phosphirane complexes **8** [Eq. (10)].[24]

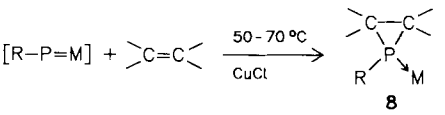

(10)

R = Me, Ph; M = $Cr(CO)_5$, $W(CO)_5$

Complexes **8** are somewhat less stable than complexes **6** and their interconversion is possible in some cases [Eq. (11)].

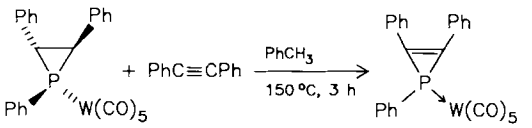

(11)

The condensation of terminal phosphinidene complexes onto olefins represents the first successful synthesis of the three-membered phosphirane ring through cycloaddition of a phosphorus unit with an olefin. It parallels the syntheses of cyclopropanes, siliranes, and aziridines from olefins and carbenes, silylenes, and nitrenes, respectively. It is interesting to note here that the condensation of phosphenium ions onto olefins never leads to stable phosphiranium ions. Experiments conducted with *cis*- and *trans*-stilbenes show that the condensation of terminal phosphinidene complexes takes place with retention of the olefin stereochemistry [Eq. (12)]. This suggests that the reaction is a

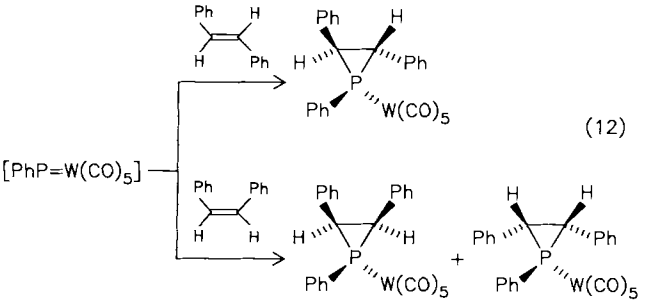

(12)

genuine concerted cheletropic cycloaddition of a singlet terminal phosphinidene complex with a C=C bond, in exact analogy to the reaction between singlet carbenes and olefins. Moreover, experimental data clearly indicate that terminal phosphinidene complexes react better with electron-rich than with electron-poor olefins. Thus, it seems clear that the cycloaddition P+C=C is inter alia governed by the electrophilicity of phosphorus. This observation in turn suggests that the lack of reactivity of free phosphinidenes toward olefins may partly reflect their lack of electrophilicity.

The reaction of terminal phosphinidene complexes with conjugated dienes again underlines their similarity with singlet carbenes. The formation of vinylphosphirane complexes **9**[24] indeed parallels the formation of vinylcyclopropanes from dienes and singlet carbenes. Upon heating, **9** rapidly rearranges to give the corresponding dihydrophosphole complex **10** [Eq. (13)]. *Richter*[35] has observed a

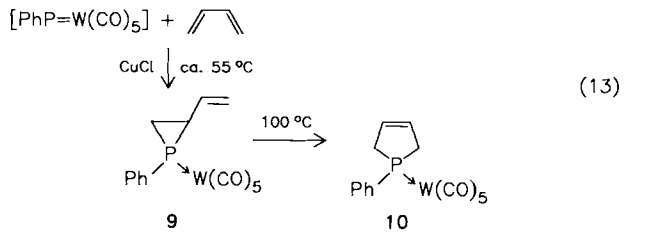

(13)

similar rearrangement of free 2-vinylphosphiranes. According to the Woodward–Hoffmann rules, such a formal [1,3] sigmatropic shift is thermally forbidden, and *Richter* has indeed found that it takes place much more readily upon UV irradiation (25°C) than upon heating (150°C). He has rationalized the results of a kinetic study[36] by a radical mechanism involving the homolytic cleavage of the P–C(vinyl) bond of the phosphirane ring. He has also found that the rearrangement of the free phosphiranes is efficiently catalyzed by transition-metal complexes such as $[Ni(cod)_2]$, $[NiCp_2]$, and $[Pd(allyl)_2]$ (cod = 1,5-cyclooctadiene, $Cp = \eta^5$-cyclopentadienyl).[35] This last result is consistent with Equation (13), which indicates that **9** is more prone to undergo such a transformation. Finally, it is interesting to note here that, contrary to terminal phosphinidene complexes, phosphenium ions seem to give directly the 1,4 adducts with conjugated dienes.[28]

The reactions of terminal phosphinidene complexes with some conjugated heterodienes such as α-enones[24]

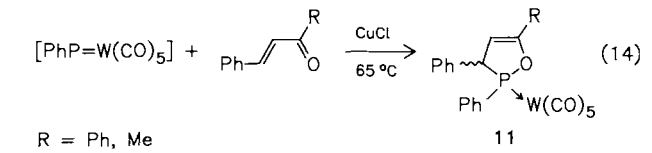

R = Ph, Me

11

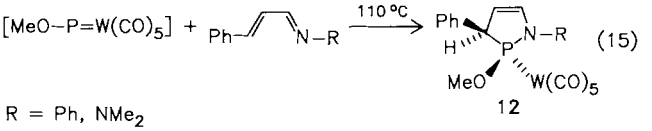

R = Ph, NMe_2

12

and 1-azadienes[37] were also investigated [Eq. (14) and (15)]. In these cases, the 1,4 adducts **11** and **12** are obtained, but this does not exclude the preliminary formation of the 1,2 adducts with the C=C bonds followed by a rapid [1,2]→[1,4] rearrangement, facilitated by the creation of a strong P-O bond in the case of **11**. In the case of **12**, a good steric control was observed during the cycloaddition, which selectively leads to the less hindered isomer.

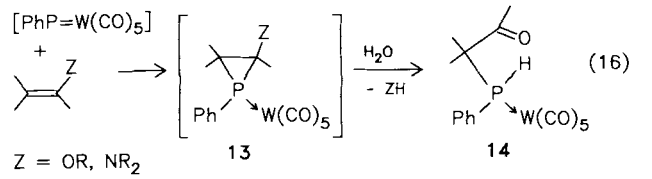

Z = OR, NR_2

13 14

The reaction of terminal phosphinidene complexes with electron-rich olefins such as enol ethers[24] or enamines[38] results in the transient formation of the expected phosphirane complexes **13**, which, however, react very rapidly with water to give functionalized secondary phosphane complexes [Eq. (16)]. The lability of the P-C(Z) bond of **13**

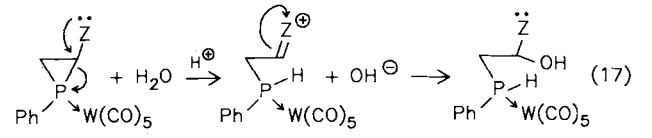

can be related to its polarization. Indeed, theoretical studies have shown that the intracyclic P-C bonds of the phosphirane ring have pronounced π character.[39] As such, they can interact with lone-pair substituents like alkoxy or amino groups in the same way as olefinic π bonds. The normally apolar P-C bonds thus acquire some polarity and become able to react with water [Eq. (17)]. The stability of

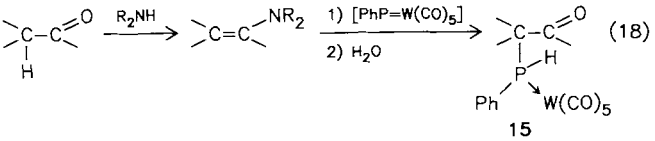

15

14 once again illustrates the protection provided to the P-H bonds by the $W(CO)_5$ complexing group. Using this kind of chemistry, it becomes possible to selectively insert a phosphinidene unit into a carbonyl-activated C-H bond [formation of **15**, Eq. (18)].[38] Finally, the insertion of an activated olefin into the P-C(Z) bond of an activated phosphirane was also observed in one instance [formation of **16**, Eq. (19)].[24]

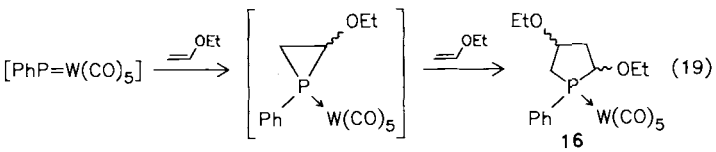

16

The net overall result is a formal carbon-carbon coupling between two molecules of enol ether taking place in the "coordination sphere" of phosphorus.

As mentioned earlier, theoretical calculations[27] indicate that terminal phosphinidene complexes are highly electrophilic species. Therefore, electrophilic insertion of the phosphinidene phosphorus into the C-H bonds of some electron-rich aromatic rings appeared to be a possible reaction. Such an insertion was indeed observed in the case of ferrocene [Eq. (20)].[40] Curiously, the reaction does

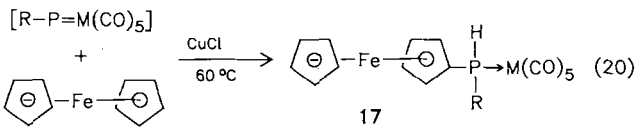

M = Mo, W; R = Me, Ph

17

not work at all in the case of M = Cr, but it is not known at present whether this failure reflects a lack of stability of **17** (M = Cr) or a lack of electrophilicity of the phosphinidene complexes with Cr. Nonetheless, the compounds **17** are particularly interesting since they represent the first known derivatives of this type of secondary phosphane and can serve as a starting material for the synthesis of a wide variety of tertiary ferrocenylphosphanes through metalation of the P-H bond and subsequent reactions.

Rather surprisingly, as shown in Equation (20a), a terminal phosphinidene complex is able to react with an electrophilic Fischer carbene complex to give probably an intermediate σ,π ditungsten complex, which spontaneously loses one metal fragment and then dimerizes to finally yield a single unsymmetrical isomer of a 1,2-diphosphetane. This dimerization is thermally reversible so that it is possible to carry out [4+2] cycloadditions with phosphaalkenes generated only as intermediates. This phosphinidene-carbene coupling offers numerous opportunities for further investigation.

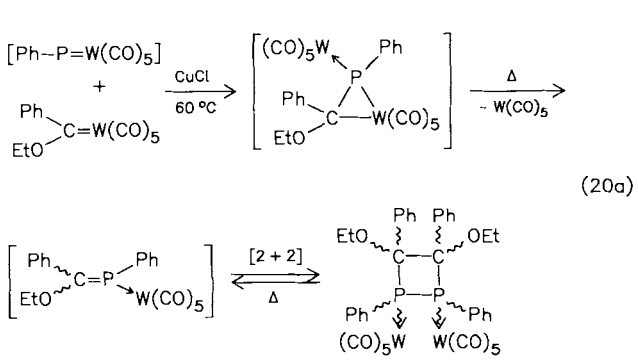

(20a)

It seems appropriate to close this section by some observations concerning the formation of terminal phosphinidene complexes in the absence of trapping reagents. When generated at low temperature, [PhP=W(CO)$_5$] mainly gives the dimer **18** [Eq. (21)].[22]

Complex **18** has also been made by *Huttner* et al.[41] via a different route, which perhaps also involves a transient terminal phosphinidene complex [see Section 6, Eq. (52)]. The formation of **18** means that at least two different decomposition processes of [PhP=W(CO)$_5$] simultaneously take place, the carbene-like dimerization and the cleavage of the P=W bond releasing the third W(CO)$_5$ unit which complexes the P=P bond to give **18**.

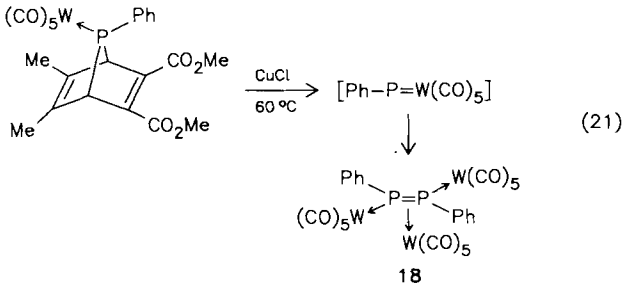

(21)

18

4. Synthetic Equivalency of Free Phosphinidenes and Their Terminal Complexes

From the standpoint of the organophosphorus chemist, the usefulness of terminal phosphinidene complexes is limited since all their chemistry takes place in the coordination sphere of a metal. A prerequisite for exploiting the full potential of these species is a mild technique for decomplexation of the phosphinidene ligand. If such a technique is devised, then terminal phosphinidene complexes become the synthetic equivalents of reactive free phosphinidenes with enhanced electrophilicity. Since the best activating group of phosphinidene appears to be pentacarbonyltungsten, the problem was to find a method for converting a phosphane complex, $R_3P\rightarrow W(CO)_5$, into the corresponding free phosphane or phosphane oxide. It is possible to achieve such a decomplexation in two steps [Eq. (22)]. In the first step, the P–W bond is weakened by selective oxidation of tungsten. Then, the phosphorus ligand is displaced from the tungsten(II) complex by a "hard" ligand such as *N*-methylimidazole or 2,2'-bipyridyl. The

$$R_3P\rightarrow W(CO)_5 \xrightarrow[-\,CO]{X_2} R_3P\rightarrow W(CO)_4X_2 \xrightarrow{R'_3N} R_3P \qquad (22)$$

X = Br, I

use of this method is exemplified by the synthesis of the first known tervalent phosphirene, **19**,[42] and by the synthesis of the first known 2-oxo-1,2-dihydrophosphete *P*-oxide, **20**[43] [Eq. (23) and (24)]. Compound **20** probably results from the bromination of the corresponding free phosphane followed by the hydrolysis of the resulting R_3PBr_2 species. The transition metal ends up in the form of insoluble $[(R_3N)_mW(CO)_nX_p]$ complexes, which have not been characterized. Other unpublished experiments conclusively demonstrate that the applicability of this technique is rather wide.

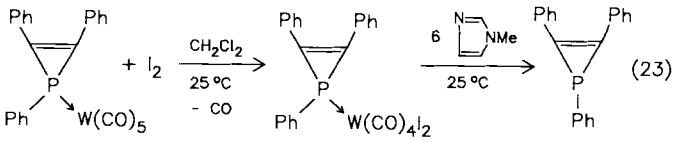

(23)

19

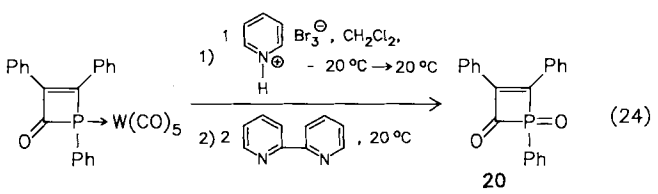

(24)

20

5. Chemistry of Phosphinidene Complexes with Functional Groups

All the chemistry so far described was developed with phenyl- and methylphosphinidene complexes. The extension of these reactions to phosphinidenes bearing functional or heteroatomic groups was necessary in order to expand the synthetic usefulness of terminal phosphinidene complexes in organophosphorus chemistry, to eventually observe novel rearrangements or self-condensations of these new phosphinidenes within the coordination spheres of the complexing metals, and to study the influence of the nature of the substituent on the reactivity of phosphinidenes toward external reagents. For that purpose, the approach via phospholes and 7-phosphanorbornadienes was especially well adapted, since one of the most useful chemical properties of the phosphole ring is the selective cleavage of the external P–C bond of 1-phenylphospholes by alkali metals [Eq. (25), DME = dimethoxyethane].[44]

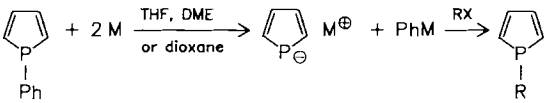

(25)

M = Li, Na, K

Using this kind of chemistry, it is possible to replace the phenyl substituent by almost any type of R group. As a first application of this strategy, the chemistry of ω-chloroalkylphosphinidene complexes was investigated. The necessary 7-phosphanorbornadiene complexes were prepared according to Equation (26) in ca. 20% (**21**) and 40% (**22**) overall yield.[45,46] (β-Chloroethylphosphinidene)pentacarbonyltungsten as generated from **22** using the standard conditions has a normal chemistry. On the contrary, when generated in the presence of CuCl, (chloromethylphosphinidene)pentacarbonyltungsten undergoes a very interesting rearrangement to **23** through migration of chlorine from carbon to phosphorus [Eq. (27)].[45] According to preliminary experiments, the presence of CuCl seems to be necessary for the migration of chlorine, but the precise mechanism of this migration remains unknown at the moment. The π-complex **23** is stable up to +65 °C, whereas

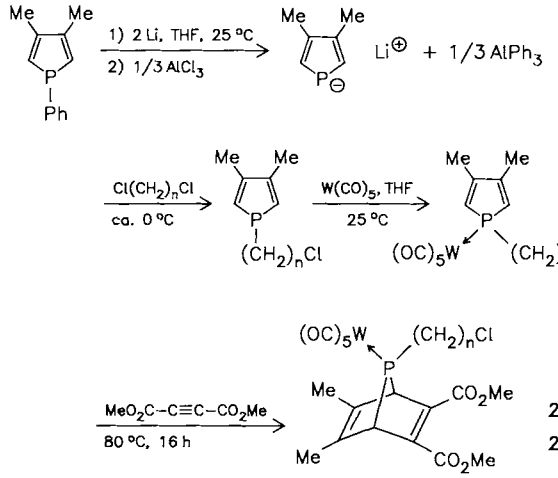

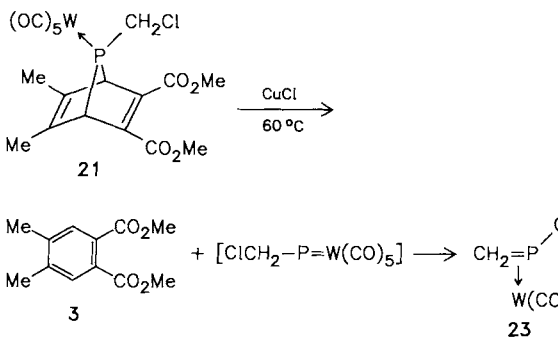

the free phosphane is stable only at low temperatures. The shift of $W(CO)_5$ from phosphorus to the P=C bond is reversible,[47] so that [2+4] cycloadditions with conjugated dienes readily take place [Eq. (28)]. A preliminary study of

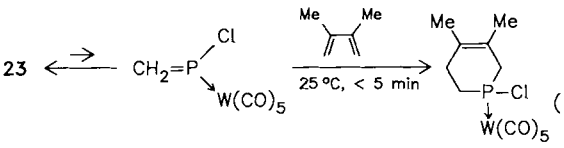

terminal phosphinidene complexes incorporating a C=C bond was also performed. The necessary 7-phosphanorbornadiene complexes were prepared according to Equation (29) in ca. 56% (**24**), 53% (**25**), and 47% (**26**) overall

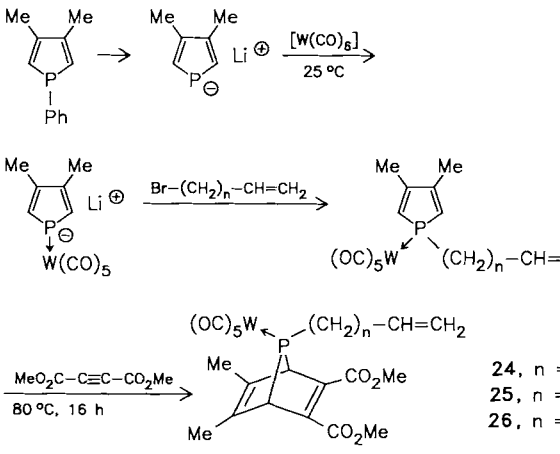

yield.[48] The chemistry of the allyl- and 3-butenylphosphinidene complexes obtained from **24** and **25**, respectively, shows no special features. On the contrary, (4-pentenylphosphinidene)pentacarbonyltungsten undergoes a self-condensation to give **27**; the reaction is so fast that it is practically impossible to trap the phosphinidene with external reagents [Eq. (30)]. The bicyclic structure of **27** is

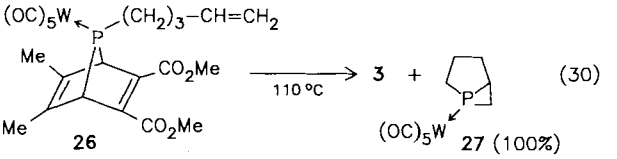

novel. The corresponding free phosphane has recently been obtained by decomplexation of **27** according to Equation (22).[61] This phosphane is especially interesting for the coordination chemist since it has probably the smallest Tolman cone angle so far found.

Finally, a preliminary study of the first chelating bisphosphinidene complex, **30**, was also very recently carried out.[49] The required 7-phosphanorbornadiene complex **29** was prepared as depicted in Equation (31). In **28**, one side

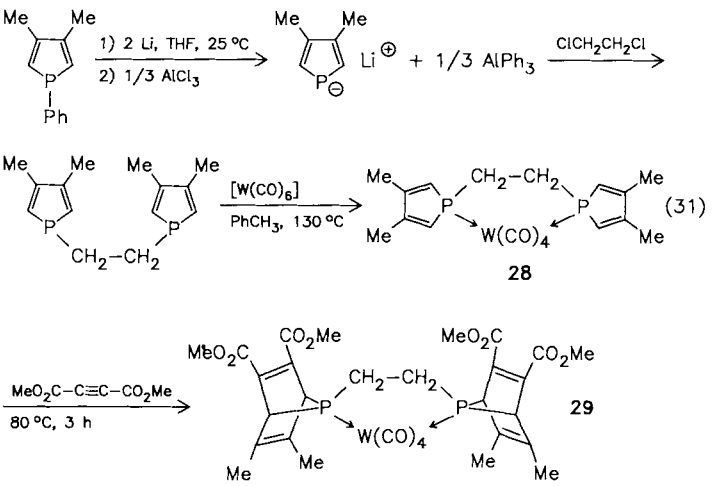

of both dienic systems is well exposed to external attack. Thus, the reaction with acetylenedicarboxylate takes place faster than usual and gives a good yield of **29**. This complex is an efficient generator of **30** as shown in Equations (32)–(35).

All the terminal phosphinidene complexes so far studied incorporate a P–C bond. In the chemistry of carbene complexes, it is well known that alkoxy substituents significantly modify the electrophilicity of the carbenic carbon.[50] For that reason and for expanding once again the applicability of terminal phosphinidene complexes in organophosphorus chemistry, it was interesting to devise an access to alkoxyphosphinidene complexes. The problem was not a trivial one since both 1-halo- and 1-alkoxy-3,4-dimethylphospholes are unknown. The synthesis of the necessary 7-alkoxy-7-phosphanorbornadiene complexes **31** was finally achieved in ca. 25% overall yield via the

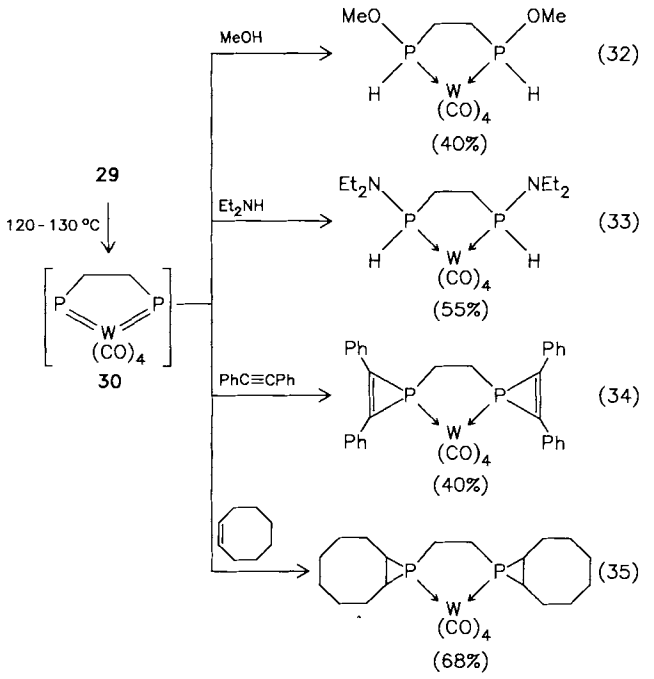

route outlined in Equation (36).[37] Preliminary experiments indicated that the phosphinidene complex **32**, generated from **31**, exhibits completely normal chemical behavior [Eq. (37)-(40)]. In particular, when no trapping reagent is present no rearrangement to give **33** is observed

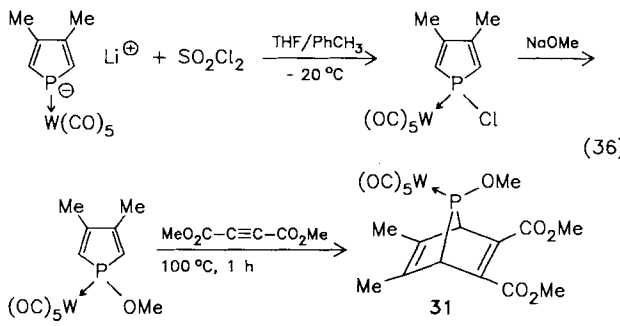

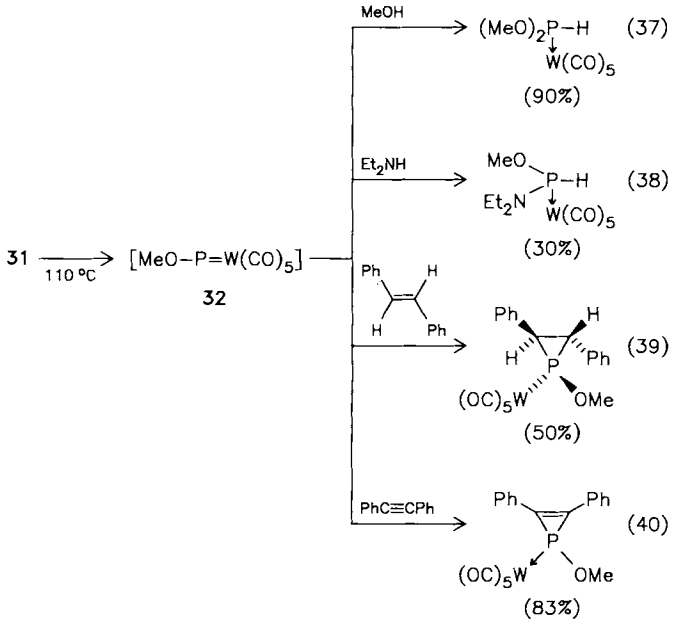

[Eq. (41)], even though similar complexed species are known.[51] In fact, **32** decomposes to give a complicated

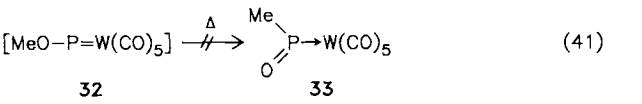

mixture of products from which it has been impossible to isolate a dimer similar to **18**. Additional experiments with azadienes [Section 3, Eq. (15)], however, suggested that **32** has a higher electrophilicity and reactivity than its phenyl-substituted analogue.

In the course of the same study,[37] the generation of [F-P=W(CO)$_5$] was attempted, but it appeared that complex **34**, obtained according to Equation (42), is stable up to 160°C.

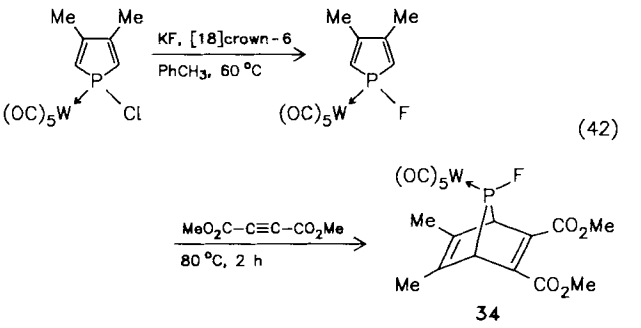

6. Other Routes to Terminal Phosphinidene Complexes and Prospects

As far as organophosphorus chemistry is concerned, the route to terminal phosphinidene complexes via phospholes and 7-phosphanorbornadienes is very satisfactory. The precursor (1-phenyl-3,4-dimethylphosphole) can be made on a large scale[21] (it has been possible to perform its synthesis on a 30-kg scale) and is very easy to handle (low sensitivity to air and low toxicity). Moreover, a large variety of substituents on phosphorus is possible, and the end products can be easily liberated from the corresponding complexes. The most obvious problem that remains to be solved concerns the synthesis of stable terminal phosphinidene complexes. In order to achieve this goal, it is probably necessary to meet two conditions: (1) steric protection of phosphorus by a bulky substituent; (2) the use of a complexing group that imparts less positive charge to phosphorus than either Cr(CO)$_5$, Mo(CO)$_5$, or W(CO)$_5$. Some variations of the complexing group are possible in the phosphole approach. However, the use of bulky substituents at phosphorus is forbidden because such groups block the Diels-Alder cycloaddition which leads to the 7-phosphanorbornadiene skeleton. Thus, it is necessary to devise other routes to terminal phosphinidene complexes. Several such routes have been proposed. The possible intermediacy of a terminal phosphinidene complex was first mentioned by *Huttner* et al.[31] in the chlorination of [CpMn(CO)$_2$(PhPH$_2$)] and [CpMn(CO)$_2$(PhPLi$_2$)] [Eq. (43) and (44)]. However, other mechanisms, which do not imply the intermediacy of [Cp(CO)$_2$Mn=PPh], can explain the

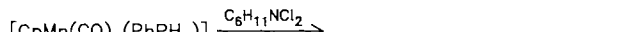

(43)

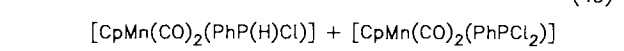

(44)

formation of the observed products. Much more recently, various other approaches have been suggested. One such approach involves the abstraction of a halide ion from a terminal halophosphido complex [Eq. (45)]. The species

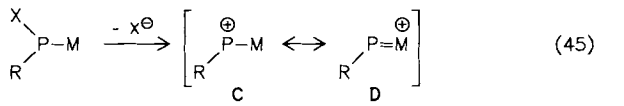

(45)

thus obtained can be viewed either as metallophosphenium cations **C** or as cationic terminal phosphinidene complexes **D**. Their electrophilicity is necessarily very high and it is not surprising to find that this approach has failed to give stable species [Eq. (46)[52] and (47)[53]]. In the

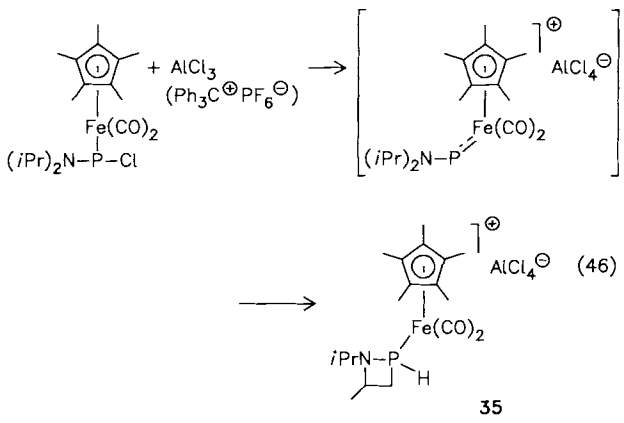

(46)

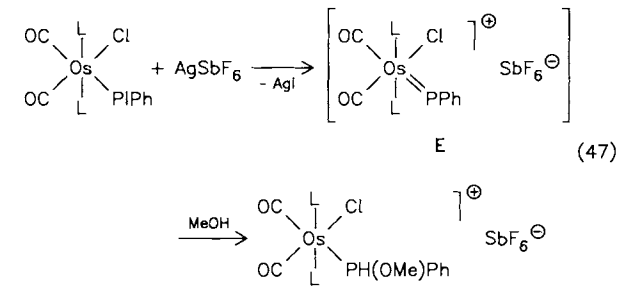

(47)

case of **35**, a novel insertion of the phosphinidene phosphorus into one of the C–H bonds of the diisopropylamino group was observed. On the other hand, attempts to trap the osmium-phosphinidene complex **E** [Eq. (47)] with alkynes and olefins failed to give tractable products.[62] Rather than reflecting the large cone angles of the expected phosphirene and phosphirane ligands,[62] this failure might be due to the reduced electrophilicity of the osmium-phosphinidene complex **E** compared with its Cr, Mo, and W analogues.

Another approach, described by *Roper* et al.,[54] relied upon an H–X elimination as shown in Equation (48).

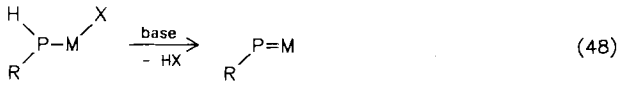

(48)

However, this elimination was only carried out in a special case, which does not necessarily involve a transient terminal phosphinidene complex such as **37** [Eq. (49)]. Indeed,

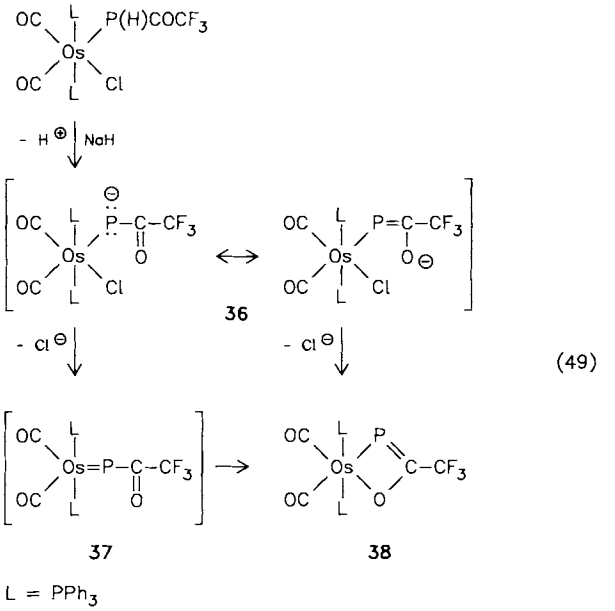

(49)

acylphosphido anions similar to **36** are known to have their negative charge partly localized at oxygen.[55] The end-product **38** was fully characterized by X-ray crystal structure analysis.

A terminal phosphinidene complex was also proposed by *Cowley* et al. as an intermediate in the reaction of phosphaketene **39** with $[Fe_2(CO)_9]$ [Eq. (50)].[56] This last result suggests that steric hindrance alone is not sufficient to stabilize terminal phosphinidene complexes.

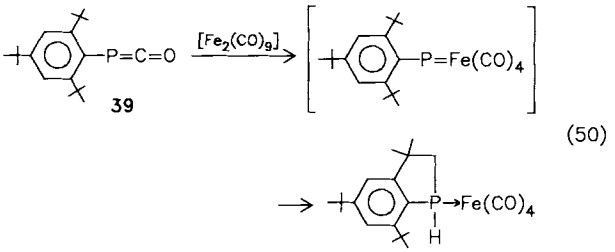

(50)

The search for new syntheses of the phosphirene ring has also led to the discovery of what could be a new route to terminal aminophosphinidene complexes [Eq. (51)].[57] Of course, as in the other examples described here, the intermediacy of the phosphinidene complex is only postulated and not fully proven. Since the attack of bromine can take place either at the P–H bond, at the $W(CO)_5$ complexing group, or at the lone pair on nitrogen, this approach has a limited generality. Replacing one of the dialkylamino

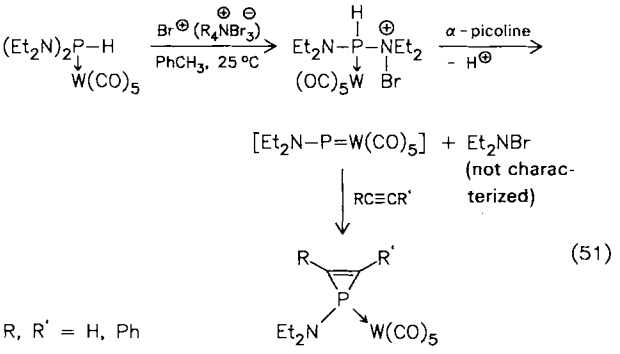

groups by an aryl or alkyl group already suffices to divert the selective attack of bromine at nitrogen. Besides, it seems difficult to generalize this approach to other complexing groups.

Finally, *Huttner* et al.[58] have very recently provided some convincing evidence in favor of the intermediacy of terminal phosphinidene complexes in the reaction of RPX_2 with $Na_2[M_2(CO)_{10}]$ (M = Mo, W). When R = 2,2,6,6-tetramethylpiperidyl, they were able to characterize, among the products of the reaction, the phosphirane complexes **40**, resulting from the trapping of the suspected phosphinidene intermediates by ethylene [Eq. (52)]. Ethylene is thought to be produced by the decomposition of THF after α-metalation. When ethylene is bubbled through the reaction mixture, the formation of **41** (type **IV**, Scheme 3) is suppressed. Complex **40** with M = W was characterized by X-ray crystal structure analysis.

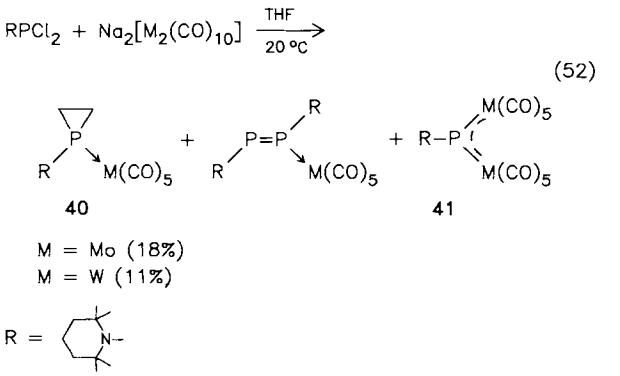

From all the data so far reported, it seems clear that obtaining a stable terminal phosphinidene complex is a difficult task and that success is not granted. However, a lot of useful work remains to be done concerning the chemistry of these species. For example, preliminary experiments indicate that more or less smooth reactions take place with molecules having P-H, P-Cl, and Si-H bonds, as well as with aldehydes, ketones, epoxides, aziridines, trialkylphosphites, etc. Moreover, the use of these complexes as synthetic tools in organophosphorus synthesis looks very promising, especially in the field of potentially biologically active substances containing P-C bonds. Exciting developments are also likely in the field of transition-metal chemistry. It may be possible to use terminal phosphinidene complexes as building blocks for the controlled synthesis of clusters. The reaction of these species with transition-metal multiple bonds also looks promising. Finally, the basic scheme for the activation of a phosphinidene by a transition metal can perhaps be extended to the chemistry of other electron-deficient species such as silylenes, germylenes, and arsinidenes.

The pioneering experiments on terminal phosphinidene complexes were carried out by my co-worker Angela Marinetti. Various aspects of their chemistry have been investigated by my other co-workers J. M. Alcaraz, C. Charrier, B. Deschamps, F. Mercier, N. Maigrot, J. Svara, and N. H. Tran Huy. I owe many thanks to all of them. The help of my colleagues, J. Fischer (X-ray crystal structures, Université Louis Pasteur, Strasbourg), D. Gonbeau, and G. Pfister-Guillouzo (theoretical calculations, Université de Pau et des Pays de l'Adour) is also gratefully acknowledged. Finally, all the work discussed here could not have been carried out without the generous financial support of the Centre National de la Recherche Scientifique and the Société Nationale des Poudres et Explosifs.

Received: May 28, 1986;
revised: October 23, 1986 [A 610 IE]
German version: *Angew. Chem. 99* (1987) 285

[1] For a recent review on carbene chemistry, see: R. A. Moss, M. Jones, Jr. in M. Jones, Jr., R. A. Moss (Eds.): *Reactive Intermediates, Vol. 3*, Wiley, New York 1985, pp. 45–108. This book also contains a review on nitrenes by *W. Lwowski* (pp. 305–332) and a review on silylenes by *P. P. Gaspar* (pp. 333–427). The earlier literature is covered in Vols. 1 and 2.

[2] U. Schmidt, *Angew. Chem. 87* (1975) 535; *Angew. Chem. Int. Ed. Engl. 14* (1975) 523.

[3] B. Weber, M. Regitz in: *Houben-Weyl-Müller, Methoden der organischen Chemie, Vol. E1, Phosphor-Verbindungen*, Thieme, Stuttgart 1982, pp. 15–19.

[4] The quoted results are slightly different from those of *Schmidt*. They come from a more recent and detailed study of the reaction of $(PhP)_5$ with tolan which has been carried out in our laboratory: C. Charrier, J. Guilhem, F. Mathey, *J. Org. Chem. 46* (1981) 3.

[5] K. Diemert, B. Kottwitz, W. Kuchen, *Phosphorus Sulfur 26* (1986) 307.

[6] For a classical discussion on the relationship between cyclic strain and reactivity in phosphorus heterocycles, see: R. F. Hudson, C. Brown, *Acc. Chem. Res. 5* (1972) 204.

[7] E. Fluck, *Chem. Ztg. 105* (1981) 323.

[8] L. D. Quin, K. A. Mesch, K. C. Caster, *Proc. 1981 Int. Conf. Phosphorus Chem. (ACS Symp. Ser. 171)* 623.

[9] K. C. Caster, L. D. Quin, *Tetrahedron Lett. 24* (1983) 5831.

[10] Parent phosphirane decomposes completely in 24 h at room temperature to give ethylphosphane, ethylene, and polymeric by products: R. I. Wagner, L. V. D. Freeman, H. Goldwhite, D. G. Rowsell, *J. Am. Chem. Soc. 89* (1967) 1102.

[11] Recent examples of phosphirane stabilization by bulky substituents include: T. Oshikawa, M. Yamashita, *Synthesis 1985*, 290; M. Baudler, J. Germeshausen, *Chem. Ber. 118* (1985) 4285; M. Yoshifuji, K. Toyota, N. Inamoto, *Chem. Lett. 1985*, 441.

[12] Element-carbon average molar bond enthalpies as measured on gaseous permethylated derivatives are as follows: P 276, N 314, Si 311, C 358 kJ mol^{-1}: M. E. O'Neill, K. Wade in G. Wilkinson, F. G. A. Stone, E. W. Abel (Eds.): *Comprehensive Organometallic Chemistry, Vol. 1*, Pergamon, Oxford 1982, p. 5.

[13] Calculation of the singlet-triplet separation in phosphinidenes: P. E. Cade, *Can. J. Phys. 46* (1968) 1989; A. Mavridis, J. F. Harrison, *J. Am. Chem. Soc. 102* (1980) 7651; G. Trinquier, *ibid. 104* (1982) 6969. An experimental value for the singlet-triplet separation in HP is known: P. F. Zittel, W. C. Lineberger, *J. Chem. Phys. 65* (1976) 1236.

[14] The generation of silylenes from 7-silanorbornadienes has been discussed in a recent paper: T. J. Barton, W. F. Goure, J. L. Witiak, W. D. Wulff, *J. Organomet. Chem. 225* (1982) 87.

[15] U. Schmidt, I. Boie, C. Osterroht, R. Schröer, H. F. Grützmacher, *Chem. Ber. 101* (1968) 1381.

[16] K. Matsumoto, S. Hashimoto, S. Otani, T. Uchida, *Heterocycles 22* (1984) 2713.

[17] J. K. Stille, J. L. Eichelberger, J. Higgins, M. E. Freeburger, *J. Am. Chem. Soc. 94* (1972) 4761.

[18] Y. Kashman, I. Wagenstein, A. Rudi, *Tetrahedron 32* (1976) 2427.

[19] Dimethyl acetylenedicarboxylate reacts with the lone pair of tervalent phospholes: D. G. Holah, A. N. Hughes, D. Kleemola, *J. Heterocycl. Chem. 15* (1978) 1319.
[20] A. Marinetti, F. Mathey, J. Fischer, A. Mitschler, *J. Chem. Soc. Chem. Commun. 1982*, 667.
[21] A. Breque, F. Mathey, P. Savignac, *Synthesis 1981*, 983.
[22] A. Marinetti, C. Charrier, F. Mathey, J. Fischer, *Organometallics 4* (1985) 2134.
[23] R. W. Hoffmann, *Acc. Chem. Res. 18* (1985) 248.
[24] A. Marinetti, F. Mathey, *Organometallics 3* (1984) 456.
[25] A. Marinetti, F. Mathey, J. Fischer, A. Mitschler, *Nouveau J. Chim. 8* (1984) 453.
[26] G. Trinquier, G. Bertrand, *Inorg. Chem. 24* (1985) 3842.
[27] D. Gonbeau, G. Pfister-Guillouzo, A. Marinetti, F. Mathey, *Inorg. Chem. 24* (1985) 4133.
[28] The chemistry of phosphenium cations has been recently reviewed: A. H. Cowley, R. A. Kemp, *Chem. Rev. 85* (1985) 367.
[29] A. Marinetti, F. Mathey, *Organometallics 1* (1982) 1488.
[30] Stable RP(H)A species with bulky R or A groups have been described in the literature; see, for example, E. Niecke, G. Ringel, *Angew. Chem. 89* (1977) 501; *Angew. Chem. Int. Ed. Engl. 16* (1977) 486; A. H. Cowley, J. E. Kilduff, N. C. Norman, M. Pakulski, J. L. Atwood, W. E. Hunter, *J. Am. Chem. Soc. 105* (1983) 4845.
[31] G. Huttner, H.-D. Müller, *Angew. Chem. 87* (1975) 596; *Angew. Chem. Int. Ed. Engl. 14* (1975) 571.
[32] A. Marinetti, F. Mathey, J. Fischer, A. Mitschler, *J. Am. Chem. Soc. 104* (1982) 4484.
[33] A. Marinetti, F. Mathey, *J. Am. Chem. Soc. 107* (1985) 4700.
[34] K. S. Fongers, H. Hogeveen, R. F. Kingma, *Tetrahedron Lett. 24* (1983) 643.
[35] W. J. Richter, *Angew. Chem. 94* (1982) 298; *Angew. Chem. Int. Ed. Engl. 21* (1982) 292; *Angew. Chem. Suppl. 1982*, 739; *Chem. Ber. 116* (1983) 3293.
[36] W. J. Richter, *Chem. Ber. 118* (1985) 1575.
[37] J. M. Alcaraz, J. Svara, F. Mathey, *Nouveau J. Chim. 10* (1986) 321.
[38] A. Marinetti, F. Mathey, *Organometallics 3* (1984) 1492.
[39] D. H. Aue, H. M. Webb, W. R. Davidson, M. Vidal, M. T. Bowers, H. Goldwhite, L. E. Vertal, J. E. Douglas, P. A. Kollman, G. L. Kenyon, *J Am. Chem. Soc. 102* (1980) 5151.
[40] J. Svara, F. Mathey, *Organometallics 5* (1986) 1159.
[41] G. Huttner, J. Borm, L. Zsolnai, *J. Organomet. Chem. 304* (1986) 309.
[42] A. Marinetti, F. Mathey, J. Fischer, A. Mitschler, *J. Chem. Soc. Chem. Commun. 1984*, 45.
[43] A. Marinetti, J. Fischer, F. Mathey, *J. Am. Chem. Soc. 107* (1985) 5001.
[44] E. H. Braye, I. Caplier, R. Saussez, *Tetrahedron 27* (1971) 5523.
[45] B. Deschamps, F. Mathey, *J. Chem. Soc. Chem. Commun. 1985*, 1010.
[46] B. Deschamps, F. Mathey, *Tetrahedron Lett. 26* (1985) 4595.
[47] Equilibria between η^1-P- and η^2-P,C phosphaalkene complexes have been described in the literature: T. A. van der Knaap, F. Bickelhaupt, H. van der Poel, G. van Koten, C. H. Stam, *J. Am. Chem. Soc. 104* (1982) 1756.
[48] J. Svara, A. Marinetti, F. Mathey, *Organometallics 5* (1986) 1161.
[49] C. Charrier, N. Maigrot, F. Mathey, *Organometallics 6* (1978), in press.
[50] The comparison between the chemistry of $[Ph_2C{=}W(CO)_5]$ and $[Ph(EtO)C{=}W(CO)_5]$ is illustrative: C. P. Casey, T. J. Burkhardt, C. A. Bunnell, J. C. Calabrese, *J. Am. Chem. Soc. 99* (1977) 2127.
[51] E. Niecke, M. Engelmann, H. Zorn, B. Krebs, G. Henkel, *Angew. Chem. 92* (1980) 738; *Angew. Chem. Int. Ed. Engl. 19* (1980) 710.
[52] H. Nakazawa, W. E. Buhro, G. Bertrand, J. A. Gladysz, *Inorg. Chem. 23* (1984) 3431.
[53] D. S. Bohle, W. R. Roper, *J. Organomet. Chem. 273* (1984) C4.
[54] D. S. Bohle, C. E. F. Rickard, W. R. Roper, *J. Chem. Soc. Chem. Commun. 1985*, 1594.
[55] See, e.g., G. Becker, M. Birkhahn, W. Massa, W. Uhl, *Angew. Chem. 92* (1980) 756; *Angew. Chem. Int. Ed. Engl. 19* (1980) 741.
[56] D. H. Champion, A. H. Cowley, *Polyhedron 4* (1985) 1791.
[57] F. Mercier, F. Mathey, *Tetrahedron Lett. 27* (1986) 1323.
[58] J. Borm, G. Huttner, O. Orama, *J. Organomet. Chem. 306* (1986) 29.
[59] J.-G. Lee, J. E. Boggs, A. H. Cowley, *Polyhedron 5* (1986) 1027.
[60] N. Hoa Tran Huy, F. Mathey, *Organometallics, 6* (1987) 207.
[61] L. Ricard, unpublished results.
[62] D. S. Bohle, T. C. Jones, C. E. F. Rickard, W. R. Roper, *Organometallics 5* (1986) 1612.

Control of the Electronic Structure of Organic Conductors as Exemplified by [NMP][TCNQ] Charge-Transfer Complexes

By Joel S. Miller* and Arthur J. Epstein

Through replacement of cations with neutral molecules of similar shape and polarizability in a highly conducting "metal-like" change-transfer organic conductor, the deliberate control of the electronic structure from a quarter to a half-filled band is possible. This goal has been achieved with the *N*-methylphenazinium (NMP) salt of the tetracyanoquinodimethane (TCNQ) anion by partial replacement of the cation with phenazine. A detailed study of the optical, electrical, and magnetic properties of these conducting molecular solids has lead to the evolution of a broad understanding of the physics of one-dimensional organic conductors and a reinterpretation of the mechanism of electron transport in such solids. Phenomena such as switching from a low coulomb repulsion two-chain conductor to a high coulomb repulsion one-chain conductor as well as soliton-assisted electron transport are observed.

1. Introduction

New quasi one-dimensional (1-D) materials[1] are required to understand the salient features associated with one-dimensionality. To date a variety of 1-D charge-transfer substances exhibiting high conductivity have been studied: organic, e.g., tetrathiafulvalene (TTF) and 7,7,8,8-tetracyano-*p*-quinodimethane (TCNQ); inorganic, e.g., $K_2Pt(CN)_4Br_{0.3}\cdot 3H_2O$ (KCP); and covalent polymeric, e.g., poly(thiazyl), $(SN)_x$, and doped polyacetylene, $(CH)_x$.[2-7] However, owing to significant differences in the elemental composition, types of bonding, resultant bandwidths (see Table 1), stoichiometries, and crystal structures, detailed comparisons between and within these classes of materials are difficult to make. Therefore, we approached the situation from a different viewpoint, namely, by studying the physical properties solely as a function of band filling, i.e., Fermi energy.

Table 1. Prototype 1-D conductors.

Class of substance (conducting chain)	Type of bonding (orbitals)	Bandwidth [eV]
Organic (based on TCNQ)	$p_z(b_{2g}\text{-}b_{2g})$	0.2-1.0
Inorganic (based on TCP [a])	$d_{z^2}(a_g\text{-}a_g)$	4
Polymeric [$(SN)_x$] or $(CH)_x$] [b]	covalent bonds $sp^2/p_z/d$	5-10

[a] TCP = tetracyanoplatinate. [b] Intermolecular.

In contrast to "classical" semiconductors, e.g., Si, where doping with electron-deficient (e.g., Ga) or electron-rich (e.g., As) atoms (relative to Si) allows the number of electrons in the conduction band to be varied easily, controlled variation of the band filling of molecular-based materials had not been previously reported.

In this article, we summarize the chemical and physical properties of a series of organic compounds containing separate stacks of cations and anions in the crystal with variable band filling. Extensive study of these unusual systems has advanced our understanding of several central issues, including the role of the coulombic interaction between electrons, the effects of structural disorder, the role of soliton defects for nearly commensurate band fillings, and the mechanism of charge transport.

2. Design of an Organic Conductor with Variably Filled Bands

In order to synthesize an isomorphous series of complexes that differ only in the degree of band filling it is necessary to consider the structural aspects of such a system, for example, the segregated 1-D anion (e.g., TCNQ) and cation chains in Figure 1a. If a delocalized valence electron is removed from an anion (Fig. 1b), less than one valence electron, on the average, is present per anion site. This reduces the coulomb repulsion among the valence

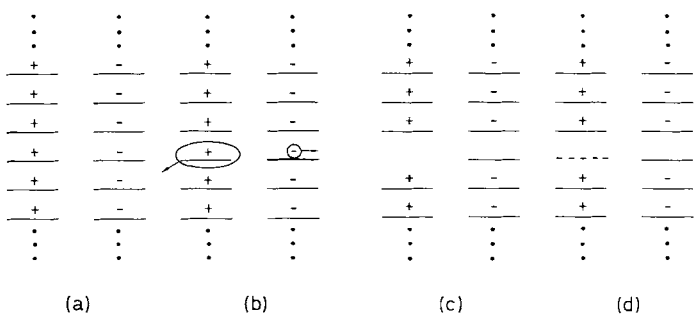

Fig. 1a) Illustration of 1-D charge-transfer salts with segregated cation (e.g., $[NMP]^{\oplus}$) and anion (e.g., $[TCNQ]^{\odot\ominus}$) stacks. b) Removal of an electron from the anion stack and a cation from the cation stack results in less than one valence electron per anion and a void in the cation stack (c). d) Filling the void with a neutral molecule stabilizes the structure.

[*] Dr. J. S. Miller
E. I. du Pont de Nemours and Co., Inc.,
Central Research and Development Department, Experimental Station
Bldg 328, Wilmington, DE 19898 (USA)
Prof. A. J. Epstein
Departments of Physics and Chemistry
Ohio State University
Columbus, OH 43210-1106 (USA)

 © VCH Verlagsgesellschaft mbH, D-6940 Weinheim, 1987 0570-0833/87/0404-0287 $ 02.50/0

electrons and thereby stabilizes the system. To conserve charge, however, a counterion must be removed. The cation loss should result in a crystallographic void (Fig. 1c) and lead to collapse of the unit cell. If, however, a neutral molecule of similar size, shape, and polarizability to the deleted cation were able to fill the cation void (dashed line in Fig. 1d), the structure should be stabilized. Through deliberate variation of the number of neutral molecules replacing cations, the number of electrons in the conduction band could be controlled. This would enable modulation of the Fermi energy and concomitant tuning of the physical properties.

3. Synthesis of an Organic Conductor with Variably Filled Bands

With this paradigm in mind, one of the earliest reported TCNQ salts, [NMP][TCNQ] ([NMP]$^{\oplus}$ = *N*-methylphenazinium, **1**)[8] was selected as the model system. The structure of [NMP][TCNQ] (Fig. 2) shows that the methyl groups have two possible orientations; however, local order exists.[9] Replacing the [NMP]$^{\oplus}$ with phenazine (Phen), **2**, complies with the design criteria outlined above, since phenazine has similar size, shape, and polarizability to [NMP]$^{\oplus}$[10] and possesses a rich donor–acceptor chemistry.[11]

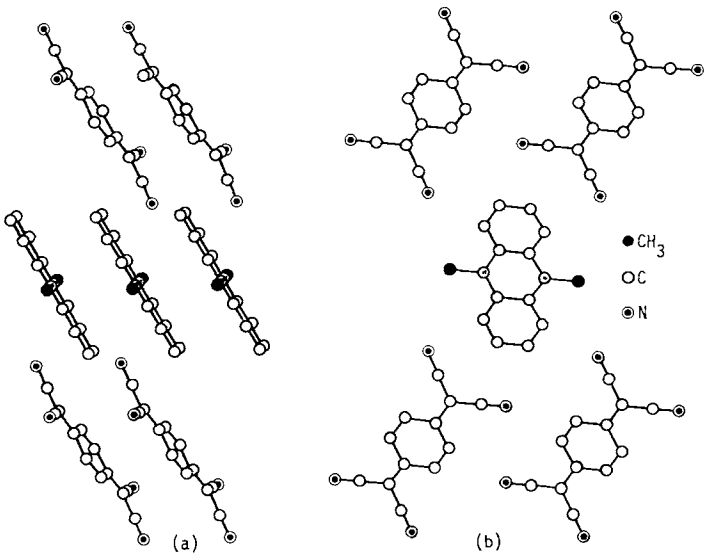

Fig. 2. Crystal structure of [NMP][TCNQ]. a) Side view. b) Top view. Two possible locations for the [NMP]$^{\oplus}$ methyl groups are illustrated by ●.

Reaction of Phen, [NMP]$^{\oplus}$, TCNQ, and [TCNQ]$^{\odot\ominus}$ in acetonitrile resulted in the formation of black needlelike crystals of [NMP]$_{1-x}$[Phen]$_x$[TCNQ], which were characterized by solution absorption spectroscopy and X-ray diffraction. Although the crystals are similar in appearance to [NMP][TCNQ], deconvolution of the solution absorption spectra unambiguously verified the presence of phenazine, **2** (λ_{max} = 347.5 nm), as well as *N*-methylphenazinium, **1** (λ_{max} = 259 nm). The degree of [NMP]$^{\oplus}$/Phen replacement,

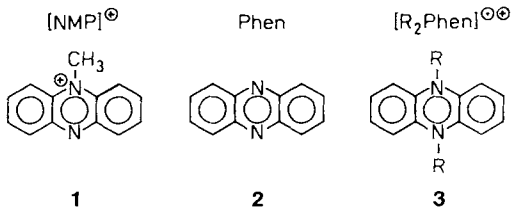

1 **2** **3**

x, could be determined from the 842-nm absorption of [TCNQ]$^{\odot\ominus}$[10] or from a shift in the a_g vibration at 1420 cm^{-1} for [NMP][TCNQ].[11] The unit cell parameters (Table 2) show that for x = 0.26 and 0.46 the substances are isomorphous to the well-characterized [NMP][TCNQ] (x = 0). Thus, an isomorphous series of 1-D materials, which to a first approximation differ only in the degree of band filling, have been prepared and have enabled the detailed study of the physical properties as a function of Fermi energy.

Table 2. Unit cell parameters for [NMP]$_{1-x}$[Phen]$_x$[TCNQ].

Parameter	x = 0.00	x = 0.26	x = 0.46
a [Å]	3.8682(4)	3.890(8)	3.865(7)
b [Å]	7.7807(8)	7.799(3)	7.611(32)
c [Å]	15.735(2)	15.706(6)	16.329(51)
α [°]	91.67(1)	91.75(6)	93.73(49)
β [°]	92.67(1)	92.96(13)	91.53(31)
γ [°]	95.38(1)	95.45(2)	94.65(20)
V [Å^3]	470.7	473.4	477.4

Up to fifty percent of the [NMP]$^{\oplus}$ in [NMP][TCNQ] can be replaced with phenazine. Thus, the physical properties can be studied continuously from nominally the half-filled band case to the quarter-filled band case.[12] We have recently shown that, in addition to phenazine, 9-methylanthracene, 9,10-dimethylanthracene, 9-methylacridine, etc., can replace [NMP]$^{\oplus}$ in [NMP][TCNQ] and thereby be utilized to modulate the degree of band filling. Replacement of [NMP]$^{\oplus}$ with substituted 5,10-dihydrophenazinium, [R$_2$Phen]$^{\odot\oplus}$ (R = Me, Et), **3**, to form [R$_2$Phen]$_{1-y}$[Phen]$_y$[TCNQ] has been reported; however, y could not be varied (i.e., y = 0.50 and 0.45 for R = Me and Et, respectively).[13] The [R$_2$Phen]$_{1-y}$[Phen]$_y$[TCNQ] complexes crystallize with segregated cation ([R$_2$Phen]$^{\odot\oplus}$/Phen) and anion chains, although [R$_2$Phen]$^{\odot\oplus}$[TCNQ]$^{\odot\ominus}$ (i.e., y = 0) possesses an alternating ···DADA··· structure.[14,15] Since y cannot be varied and only limited physical measurements have been reported, we focus primarily on the [NMP]$_{1-x}$[Phen]$_x$[TCNQ] series of charge-transfer salts in this review.

4. Insight into Physical Processes

The availability of [NMP]$_{1-x}$[Phen]$_x$[TCNQ] ($0.5 > x \geq 0$) has enabled an exhaustive study of the electrical, optical, and magnetic properties of this prototype 1-D conductor. The data has led to a broad understanding of the physics of 1-D conductors and to a reinterpretation of the mechanism of electron transport in these materials. Below we re-

view some of the properties and summarize their significance.

4.1. Variation of Electronic Structure with Conduction Electron Density

Prior to discussing the unusual features of the $[NMP]_{1-x}[Phen]_x[TCNQ]$ system, we review the electronic structure of solids.[3a] In an isolated molecule each orbital, which holds two electrons, has a well-defined energy. When two molecules are brought together close enough for their orbitals to overlap, the energy levels split; adding a third molecule splits the levels into three components. In a solid of perhaps 10^{15} molecules the levels are so numerous and closely spaced that they effectively form a continuous band which can hold 2N electrons for an N-molecule system. If each molecule in the solid has only one electron in the highest occupied orbital, the corresponding band will be only half full.[16]

The degree of band filling determines the electrical properties. Conduction cannot take place in an empty band (because it lacks electrons) or in a full band (because the total population of electrons cannot have any net motion). A metal has a partially filled band, where the electrons can be given a net velocity by shifting some of them to infinitesimally higher energies within the band. An insulator has only filled and empty bands separated by a large energy gap. A semiconductor is like an insulator but has a smaller gap and some mobile charge carriers. The carriers are introduced by impurities, defects, deviations from stoichiometry, or the excitation of electrons from the highest filled (valence) band to the lowest empty (conduction) one.

A metal has a degeneracy of empty and filled levels at its highest occupied energy level, the Fermi energy. For a linear arrangement of molecules (stacks or chains), this degeneracy can be removed by changing the uniform spacing of molecules to periodic spacing, e.g., by dimerization. This so-called Peierls distortion lowers the energy of the filled energy levels and raises the energy of the empty ones.[17]

X-ray diffuse scattering[18] enables the observation of the subtle periodicities in the spacing of molecules along a chain that are a consequence of the Peierls distortion. The length of the repeat unit of the distortion provides a direct measure of the number of electrons in the partly filled energy band (the degree of partial oxidation/reduction). For example, the 1-D character of [TTF][TCNQ] with a degree of charge transfer of 0.59 was determined by observing X-ray diffuse scattering.[18] In some materials, the scattering repeat was observed at one-half the repeat length expected for an ordinary Peierls distortion.[19a] This was postulated to occur when the coulomb repulsion, U, between two electrons on the same unit is much greater than the spread of energy levels, i.e., bandwidth, W.[19] The factors determining the relative magnitude of U and W were poorly understood until insights were made available by our detailed study of $[NMP]_{1-x}[Phen]_x[TCNQ]$.

The study of the temperature-dependent dynamical properties of $[NMP]_{1-x}[Phen]_x[TCNQ]$ revealed unique features of the electronic instabilities of 1-D conductors not previously observed.[20] The diffuse X-ray scattering from the "usual" Peierls periodicity and from the one of half the spacing have often been associated with the independent behavior of the donor and acceptor stacks in two-chain materials, e.g., [TTF][TCNQ], but it is conceivable that both anomalies arise in one stack.[19a] The investigations of $[NMP]_{1-x}[Phen]_x[TCNQ]$ demonstrated the latter case to be true for this system.

X-ray diffuse scattering studies established that for [NMP][TCNQ] ($x=0$) there is partial charge transfer with 2/3 electron per TCNQ and 1/3 electron per NMP molecule.[21,22] As $[NMP]^{\oplus}$ is replaced by phenazine, electrons are depleted from the conduction band; the conduction-electron density is thereby reduced and the diffuse X-ray scattering from the $[NMP]^{\oplus}$/phenazine chain is no longer observed. In contrast, scattering from the TCNQ chain is unaffected except for a shift in the superlattice period due to a reduction in conduction-electron density. This important result demonstrates that disorder within the donor stack has little effect upon the electronic properties of the acceptor stack, in contrast to the earlier analysis of the transport[23] and magnetic[24] data, which indicated that $[NMP]^{\oplus}$ orientational (dipolar) disorder induced localization of the conduction electrons on the parallel TCNQ chains. With increased phenazine substitution for $[NMP]^{\oplus}$ a crossover from a two-chain to an one-chain conducting system is observed (at $x \approx 1/3$). This is coincident with a crossover from the usual distortion period ("$2k_F$" regime) to one of half the repeat distance ("$4k_F$" regime) (Fig. 3).

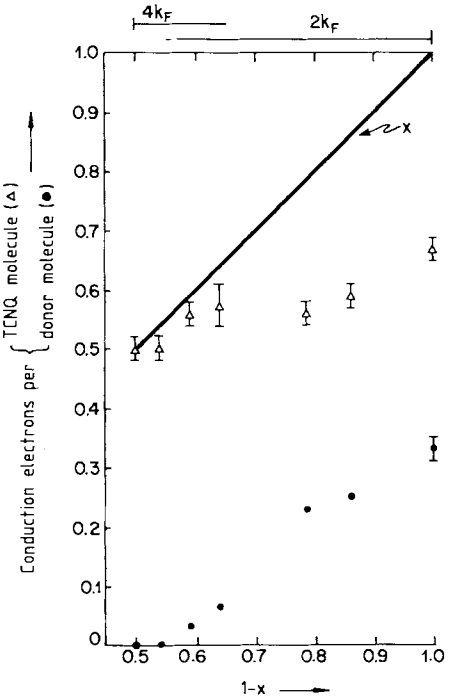

Fig. 3. Number of conduction electrons per TCNQ and per donor molecule vs. NMP concentration, $1-x$, in $[NMP]_{1-x}[Phen]_x[TCNQ]$. The solid line gives the total conduction-electron concentration. The number of conduction electrons per TCNQ is deduced from the periodicity of the Peierls distortion. For $x>0.56$, the additional electrons beyond $x=0.50$ are in soliton states of the TCNQ chain (see text). The concentration ranges where $2k_F$ and/or $4k_F$ are observed are indicated on the top.

There is even a narrow range of electron densities where both types of Peierls distortions are simultaneously observed. There are a comparable number of conduction electrons per TCNQ above and below $x = 1/3$, while the TCNQ bandwidth W remains essentially unchanged. This result confirms the central role of interchain screening in determining the magnitude of U/W.[25] The $4k_F$ anomaly is directly associated with $U/W > 1$; this is revealed by comparing the properties of $[NMP]_{1-x}[Phen]_x[TCNQ]$ samples exhibiting $4k_F$ with those of known large U/W systems and by analysis of other properties of the system, e.g., plasma frequency and magnetic susceptibility.

The crossover from a small to a large U/W regime at $x \approx 1/3$ was predicted from the early spectroscopic studies.[25] The frequency dependence of the polarized reflectivity of $[NMP]_{1-x}[Phen]_x[TCNQ]$ as a function of x (Fig. 4) was the first unequivocal demonstration that the minimum in the reflectivity spectrum (≈ 1 eV), often observed for one-dimensional TCNQ salts, is indeed a collective (plasma) response attributable to the number of charge carriers per unit cell. An anomalous variation in plasma frequency, ω_p, was observed at intermediate n (Fig. 5), which is in remarkable agreement with a change in character of the system from small U/W at high charge density to large U/W at lower charge density.

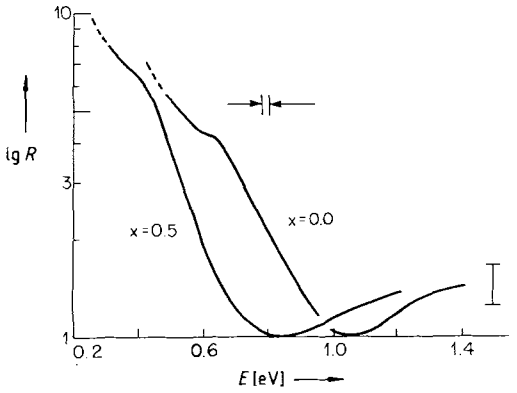

Fig. 4. The logarithm of the reflectivity ($\log R$, arbitrary units) vs. energy of irradiation, E, for $x = 0.0$ and $x = 0.5$; light polarized parallel to the stacking a axis. Note the 0.25-eV redshift on going from $x = 0.0$ to $x = 0.5$. Error bar (right) gives maximum uncertainty; typical spectra were two to three times better. Dashed lines indicate observed rise due (in part) to decrease scattered light (see text).

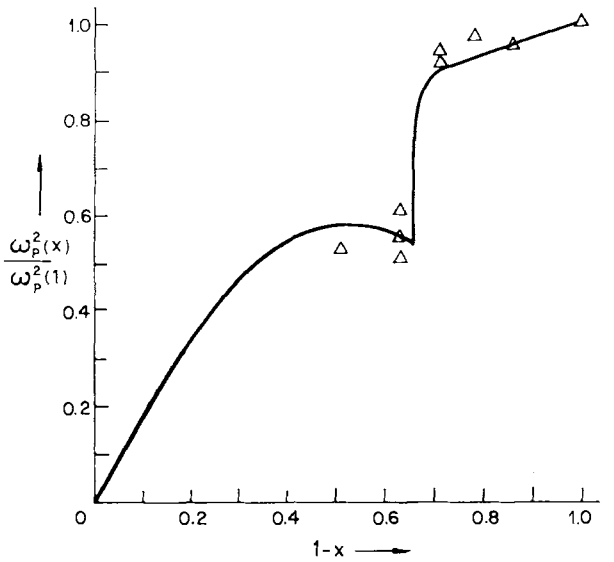

Fig. 5. Normalized plasma frequency as a function of band filling, $1-x$, in $[NMP]_{1-x}[Phen]_x[TCNQ]$. △ : experimental value.

Based on the X-ray diffuse scattering and reflectivity data, a model for the electron energy band structure of $[NMP]_{1-x}[Phen]_x[TCNQ]$ was constructed (Fig. 6). These data indicate that $[NMP]_{1-x}[Phen]_x[TCNQ]$ is a small-bandgap, low-coulomb-repulsion, small-bandwidth semiconductor with conduction bands residing on both donor ($[NMP]^{\oplus}$) and acceptor (TCNQ) stacks (Fig. 6a, $x = 0$). By replacing the $[NMP]^{\oplus}$ with phenazine, conduction electrons are removed from both stacks. Thus, $[NMP]_{0.8}[Phen]_{0.2}[TCNQ]$, like [NMP][TCNQ], is a two-chain conductor. Since conduction electrons reside on both stacks, their coulomb repulsion is reduced and is therefore small relative to the bandwidth (Fig. 6a, $x = 0.2$). Further depletion of conduction electrons leads to an interesting situation at $x \approx 0.33$. For $x < 0.33$, the conduction

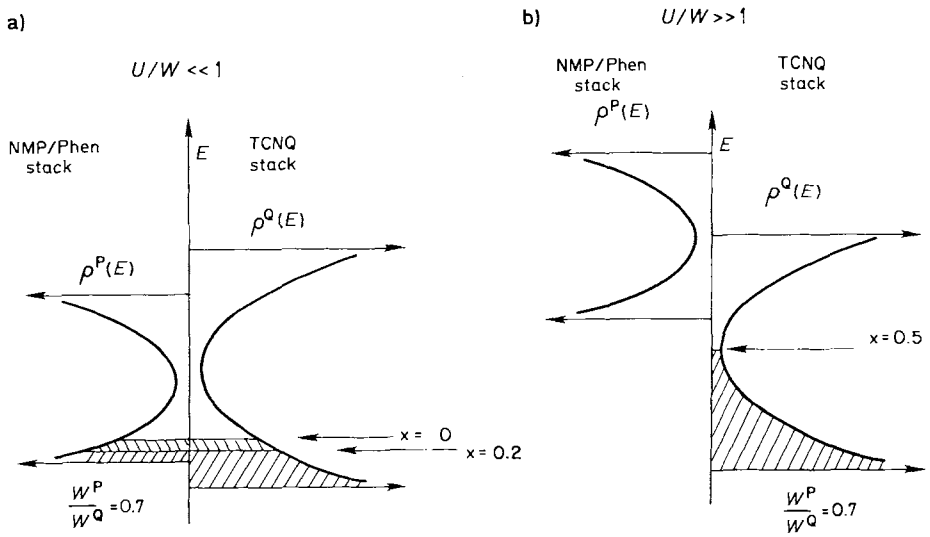

Fig. 6. Electron energy band structure for $[NMP]_{1-x}[Phen]_x[TCNQ]$. a) Small U/W. b) Large U/W. Q = TCNQ; P = NMP/Phen.

electrons are depleted from the donor ([NMP]$^{\oplus}$/Phen) band and the system switches from a two-chain conductor (low coulomb repulsion) to a one-chain conductor (with a relatively high coulomb repulsion relative to W, since all the conduction electrons reside in the TCNQ band); for $x = 0.50$, see Figure 6b. This leads to discontinuities in some of the physical properties (see Fig. 5).

The temperature-dependent magnetic susceptibility, χ,[26] and the results of ESR[27] studies support these conclusions.[26] Below 40 K, $\chi(T) = AT^{-\alpha}$ ($\alpha \approx 0.7$–0.8). This expression is consistent with random exchange among a small number of localized spins.[28] For $x > 1/3$, A decreases owing to the depopulation of the [NMP]$^{\oplus}$/Phen stack such that only unpaired localized spins on the TCNQ chain contribute. For $x < 1/3$, localized spins on both stacks contribute. Above 100 K there are qualitative and quantitative differences in $\chi(T)$ for x greater or less than 1/3. For $x > 1/3$, $\chi(T)$ has a weak maximum near room temperature much like that of [quinolinium][TCNQ]$_2$ with large U/W and an exchange interaction energy of $J \approx 300$ K. For $x < 1/3$, $\chi(T)$ decreases monotonically with increasing temperature. This is consistent with the presence of small U/W on both stacks.

4.2. Solitons in Nearly Commensurate Compositions

The description of the electronic ground state of 1-D conductors with nearly commensurate charge concentration (i.e., number of charges per unit cell being close to a rational fraction) has been a central issue in the field. As noted in Section 4.1, a chain of molecules can undergo a Peierls distortion to lower the system energy leading to a new periodicity of the molecules. For commensurate charge densities, this new periodicity is a small integral number of sites (e.g., for a half-filled band, one electron/site for $U/W \gg 1$; one electron/two sites for $U/W \ll 1$); e.g., for [NMP]$_{0.5}$[Phen]$_{0.5}$[TCNQ], the new periodicity is a dimer (Fig. 7). In Figure 7, the different lengths represent the slightly different molecular shapes that result from the Peierls distortion and the two possible phases of dimerization (shifted by one molecular unit).

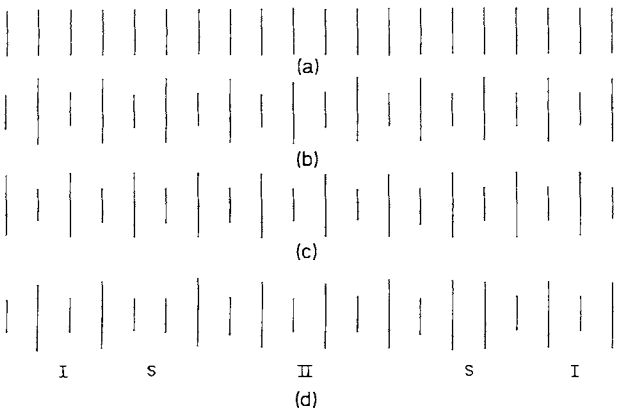

Fig. 7. Schematic illustration of a) uniform chain of molecules, b) dimerized chain of molecules of phase "I," c) dimerized chain of molecules of phase "II,", and d) chain of dimer phase I with segment of dimer phase II within it. The domain walls between phases I and II (and II and I) are the solitons, which can accommodate small numbers of excess charge near the commensurate charge density.

Addition of a few more holes to the TCNQ chain (through Phen replacement of [NMP]$^{\oplus}$) would cause the Peierls distortion to shift to an incommensurate periodicity (nonrational repeat distance). To minimize the reduction in the stabilization energy in going from commensurate to incommensurate structures (for a small charge density range), the system maintains its commensurate structure and accommodates the excess charges in defects (solitons) in the commensurate periodicity (Fig. 7d). The suggestion[29a] that a small excess (or deficiency) of charge relative to the commensurate state is accommodated in polyacetylene, $(CH)_x$, by the formation of spinless solitons of charge $\pm e$ is now well-supported by experimental evidence.[29b] Theoretical studies of highly correlated 1-D charge-transfer salts near the quarter-filled band limit (typified by [NMP]$_{0.5}$[Phen]$_{0.5}$[TCNQ]) have predicted the existence of solitons with quantum observable fractional charges[30] of $\pm e/2$. The results of experimental[31] and theoretical[32] studies of [NMP]$_{1-x}$[Phen]$_x$[TCNQ] ($x \approx 0.5$) as a function of x are a direct demonstration that solitons are experimentally realized in charge-transfer salts. The effects of solitons (and pairs of solitons, or bipolarons) upon the temperature-dependent conductivity,[31,32] $\sigma(T)$, have been observed and can be understood in terms of a model of a decreased gap caused by the presence of the solitons. The concentration regime for soliton formation was identified as $0.50 > x > 0.43$.[31] Additional direct evidence for solitons in the [NMP]$_{1-x}$[Phen]$_x$[TCNQ] system has been obtained by detailed measurements of the optical absorption,[31b,33] thermopower,[31b] X-ray diffuse scattering,[20] and electron spin resonance g value.[27] The role of strong coulomb interactions in stabilizing solitonlike defects in [NMP]$_{1-x}$[Phen]$_x$[TCNQ] has also been suggested.[34]

4.3. A Model for Conductivity

The normalized temperature dependence of the dc conductivity, $\sigma_n(T) \equiv \sigma(T)/\sigma(295\,\mathrm{K})$ (Fig. 8) for [NMP]$_{1-x}$[Phen]$_x$[TCNQ] exhibits several key features: (1) the phenazine-containing samples ($x > 0$) exhibit a similar $\sigma_n(T)$ to [NMP][TCNQ]; (2) the temperature at which the maximum conductivity occurs, T_m, varies with phenazine concentration; and (3) the normalized conductivity, σ_n, varies with phenazine content.

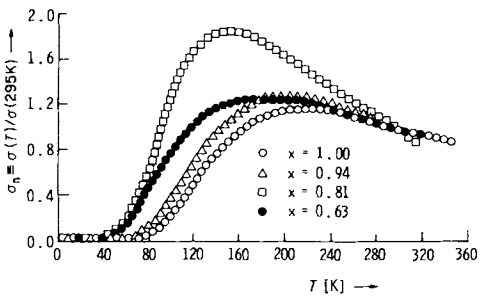

Fig. 8. Temperature dependence of the normalized conductivity for [NMP]$_{1-x}$[Phen]$_x$[TCNQ] (see text).

Conventional wisdom[35] ascribes T_m to a metal–insulator transition temperature such that above T_m metal-like behavior is operative and disorder leading to localization

of conduction electrons and insulating behavior occurs at $T<T_m$.[23] However, the slope ($d\ln\sigma/dT^{-1}$) does not change at T_m, suggesting that one (not two) transport mechanism dominates above 60 K.[36] NMR studies of $[NMP]_{1-x}[Phen]_x[TCNQ]$ confirm that nuclear spin relaxation is not dominated by conduction electrons[37] in contrast to the disorder model prediction.[23b] As confirmed by IR studies,[31b,33] the system is actually a small-bandgap Peierls semiconductor.

To account for the presence of one transport mechanism above 60 K, a new model for the conductivity was developed.[36] For a semiconductor, the conductivity is given by

$$\sigma = ne\mu \qquad (a)$$

where n = number of carriers, e = the fundamental charge of an electron, and μ = mobility. The number of carriers, n, is an exponential function of temperature, T; i.e., $n \propto e^{-E_g/kT}$ (E_g = bandgap), whereas the mobility, μ, is often a power law in temperature, i.e., $T^{-\alpha}$ ($4 \geq \alpha \geq 2$). Thus, Equation (b) is obtained for the conductivity σ (see also Fig. 9).

$$\sigma(\alpha, T) = A\,T^{-\alpha} e^{-E_g/kT} \qquad (b)$$

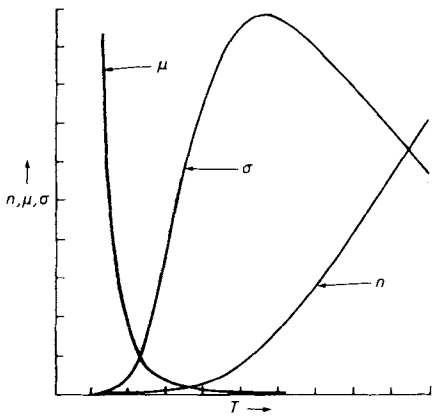

Fig. 9. Schematic temperature dependence of charge-carrier concentration n, the mobility μ, and the conductivity σ.

The conductivity of $[NMP]_{1-x}[Phen]_x[TCNQ]$ ($0.5 < x < 1$; $80\ K < T < 400\ K$) fits Equation (b) very well, although recent IR data indicates that the energy gap is temperature dependent,[31b,33] as expected for a Peierls semiconductor[38] (see below). In general, samples with the same x value may be fit with a relatively unique value of E_g with varying α, reflecting a sample to sample variation in purity (Fig. 10).

Nine of ten a_g TCNQ vibrational modes are found in the absorption spectrum of $[NMP]_{1-x}[Phen]_x[TCNQ]$ ($0.50 \geq x \geq 0.41$).[31] These totally symmetric normally IR-inactive modes become strongly IR active in the presence of oscillations of the phase of the Peierls distortion.[40] Thus, $[NMP]_{1-x}[Phen]_x[TCNQ]$ is a small-bandgap semiconductor at room temperature where it exhibits metal-like conductivity, i.e., $d\sigma/dT < 0$. At low temperatures the optical gaps are in agreement with those calculated in the original semiconductor model.[36]

Direct IR measurements of the bandgap of $[NMP]_{1-x}[Phen]_x[TCNQ]$ are complicated by the polycrystalline nature of the samples necessitated by the small crystal dimensions. Large single crystals of $HNMe_3(I)[TCNQ]$ exhibit a similar $\sigma_n(T)$ dependence near room temperature, enabling verification of these models. The single-crystal reflectivity data for $HNMe_3(I)[TCNQ]$ confirm the presence of a bandgap of 0.16 eV at room temperature where $d\sigma/dT < 0$.[41] Thus, concepts developed during study of $[NMP]_{1-x}[Phen]_x[TCNQ]$ semiconductor systems have been generalized and applied to other 1-D quasi-conductors.

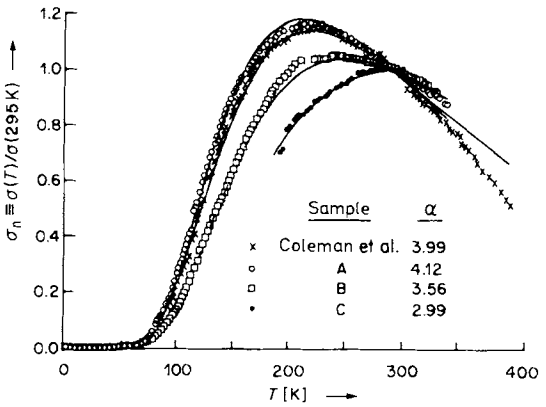

Fig. 10. Normalized four-probe a-axis conductivity versus temperature for representative [NMP][TCNQ] samples. The "Coleman et al." data is from ref. [39]. The solid lines are computer fits to Equation (b) with indicated α.

5. Summary and Outlook

The $[NMP]_{1-x}[Phen]_x[TCNQ]$ "alloy" system has been found to be very rich in physics and chemistry. Through systematic studies several new phenomena have been discovered and new insights into quasi one-dimensional conductors have been obtained:

- The synthesis of an isomorphous series of "metal-like" organic charge-transfer complexes with a variable degree of band filling ("alloying") has been achieved.
- Disorder has been shown to play a secondary role. The electrons are sufficiently delocalized so that the central physics is determined by the Peierls (electron–phonon or Jahn–Teller) interaction and not the disorder.
- The importance of interstack screening in determining the coulomb correlation in 1-D systems has been demonstrated, since we have observed a crossover from small to large U/W regimes with removal of electrons from one of two conducting stacks. Thus, the relative size of U/W is not determined by the charge density of the isolated stacks alone.
- A new model based upon temperature-dependent mobility and carrier concentration for conductivity was developed for $[NMP]_{1-x}[Phen]_x[TCNQ]$. This semiconductor model has been shown to be applicable to a wide range of quasi one-dimensional systems.
- The $[NMP]_{1-x}[Phen]_x[TCNQ]$ system has provided the first direct evidence for solitons in molecular charge-transfer salts. The solitons are predicted to have a fractional charge.

● The presence of a pair of lattice distortions (of $2k_F$ and $4k_F$ periodicities) on the same chain was detected via X-ray diffuse scattering. The coexistence of these two lattice modulations has clarified the understanding of Peierls distortions in two-chain conductors such as [TTF][TCNQ].

The study of $[NMP]_{1-x}[Phen]_x[TCNQ]$ as a function of x has led to the discovery of new phenomena, the development of generalizable physical models, and the better understanding and relative importance of existing concepts. However, with the improved understanding of one-dimensional organic conductors, however, new questions have emerged and are the focus of avid attention in many laboratories throughout the world. The study of variably controlled one-dimensional conductors remains an important aspect of our research. Some of the current topics under investigation include understanding the effects of on-site and near-neighbor coulomb interactions on the simple Peierls and soliton models, together with the related issue of whether the electron-electron or the electron-phonon interaction is the primary driving force for the observed physical properties. Additional effort is still necessary to further quantify the models and concepts presented here and self-consistently fit the myriad data presented. These compounds continue to arouse the curiosity of scientists since they exhibit a wealth of unusual properties of importance to condensed matter physics.

Received: April 4, 1986;
revised: August 18, 1986 [A 609 IE]
German version: *Angew. Chem. 99* (1987) 332

[1] General reviews: K. Menke, S. Roth, *Chem. Unserer Zeit 20* (1986) 1, 33; D. O. Cowan, F. M. Wiygul, *Chem. Eng. News 64* (1986) No. 29, p. 28.
[2] J. Simon, J. J. André: *Molecular Semiconductors*, Springer, New York 1985.
[3] a) J. S. Miller, A. J. Epstein, *Prog. Inorg. Chem. 20* (1976) 1; b) J. M. Williams, *Adv. Inorg. Chem. 26* (1983) 235.
[4] A. J. Epstein, J. S. Miller, *Sci. Am. 241* (1979) No. 10, p. 52; *Spektrum Wiss. 1979*, No. 12, p. 63; K. Bechgaard, D. Jerome, *ibid. 247* (1982) No. 7, p. 52 and *1982*, No. 9, p. 38, respectively.
[5] J. S. Miller (Ed.): *Extended Linear Chain Compounds, Vol. 1-3*, Plenum, New York 1982/1983.
[6] M. M. Labes, P. Love, L. F. Nichols, *Chem. Rev. 79* (1979) 1; J. C. W. Chien: *Polyacetylene*, Academic Press, Orlando, FL, USA 1984; C. B. Duke, H. W. Gibson in Kirk-Othmer: *Encyclopedia of Chemical Technology 18* (1982) 755; G. Wegner, *Angew. Chem. 93* (1981) 352; *Angew. Chem. Int. Ed. Engl. 20* (1981) 361; J. H. Perlstein, *ibid. 89* (1977) 534 and *16* (1977) 519; T. A. Skotheim (Ed.): *Handbook of Conducting Polymers*, Marcel Dekker, New York 1986.
[7] For detailed overviews, see the proceedings of the recent series of international conferences: a) *J. Phys. Colloq.* 44-C3 (1983) (Eds.: R. Comes, P. Bernier, J. J. André, J. Rouxel); b) *Mol. Cryst. Liq. Cryst. 77, 79, 82, 83, 85* (1981) and *86* (1982) (Eds.: A. J. Epstein, E. M. Conwell); c) *Chem. Scr. 17* (1981) (Ed.: K. Carneiro); d) *Lect. Notes Phys. 95, 96* (1979) (Eds.: S. Barisic, A. Bjelis, J. R. Cooper, B. A. Leontic); e) *Ann. N. Y. Acad. Sci. 313* (1978) (Eds.: J. S. Miller, A. J. Epstein).
[8] L. R. Melby, *Can. J. Chem. 43* (1965) 1448.
[9] C. J. Fritchie, *Acta Crystallogr. 20* (1966) 892; J. P. Pouget, S. Megtert, R. Comes, A. J. Epstein, *Phys. Rev. B21* (1980) 486.
[10] J. S. Miller, A. J. Epstein, *J. Am. Chem. Soc. 100* (1978) 1639.
[11] H. J. Keller, Z. G. Soos, *Top. Curr. Chem. 127* (1985) 169.
[12] a) H. Kuzmany, M. Elbert, *Solid State Commun. 35* (1980) 597; b) H. Kuzmany, M. Elbert, B. Kundu, *Chem. Scr. 17* (1981) 33.
[13] K. Dietz, S. Flandrois, H. J. Keller, P. Koch, J. Queckbörner, D. Schweitzer, *Chem. Scr. 17* (1981) 93.
[14] a) H. Endres, H. J. Keller, W. Moroni, D. Nöthe, *Acta Crystallogr. B36* (1980) 1435; b) K. Dietz, H. Endres, H. J. Keller, W. Moroni, D. Wehe, *Z. Naturforsch. B37* (1982) 437.
[15] For R = Me, the complex is isomorphous to [NMP][TCNQ] [14a].
[16] For strong coulomb interaction among the electrons, at most only one electron is allowed per atom. In this case, one electron for every two atoms leads to a half-filled band.
[17] This distortion is similar to the Jahn-Teller distortion for finite-sized molecules with otherwise degenerate ground states.
[18] H. Kobayashi, Y. Kobayashi in J. S. Miller (Ed.): *Extended Linear Chain Compounds, Vol. 2*, Plenum, New York 1982, p. 259; R. Comes, G. Shirane in J. T. Devreese, R. P. Evrard, V. E. van Duven (Eds.): *Highly Conducting One-Dimensional Solids*, Plenum, New York 1979, p. 17.
[19] a) J. P. Pouget, *Chem. Scr. 17* (1981) 85; b) S. Mazumdar, S. N. Dixit, A. N. Bloch, *Phys. Rev. B30* (1984) 4842; S. Mazumdar, A. N. Bloch, *Phys. Rev. Lett. 50* (1983) 207.
[20] A. J. Epstein, J. S. Miller, J. P. Pouget, R. Comes, *Phys. Rev. Lett. 47* (1981) 741.
[21] Transfer of $0.94e^{\ominus}$ was suggested from earlier NMR data (M. A. Butler, F. Wudl, Z. G. Soos, *Phys. Rev. B12* (1975) 4708). An analysis of the Raman frequency shifts supports the $0.67\text{-}e^{\ominus}$ transfer obtained form X-ray diffuse scattering [12].
[22] The $2k_F$ X-ray diffuse scattering from both cation and anion stacks is observed.
[23] a) A. N. Bloch, R. B. Weisman, C. M. Varma, *Phys. Rev. Lett. 28* (1972) 753; A. A. Gogolin, S. P. Zolotukhim, V. I. Melnikov, E. I. Rashba, I. F. Shchegolev, *JETP Lett. Engl. Transl. 22* (1975) 278; C. Papatriantafillou, *Phys. Status Solidi B88* (1978) 663; V. K. S. Shante, *Phys. Rev. B16* (1977) 2597; b) F. Devreux, M. Nechtschein, G. Gruner, *Phys. Rev. Lett. 45* (1980) 53.
[24] G. Theodorou, M. H. Cohen, *Phys. Rev. Lett. 37* (1976) 1014; G. Theodorou, *Phys. Rev. B16* (1977) 2264, 2272.
[25] B. A. Weinstein, M. L. Slade, A. J. Epstein, J. S. Miller, *Solid State Commun. 37* (1981) 643.
[26] A. J. Epstein, J. S. Miller in L. Alcacer (Ed.): *The Physics and Chemistry of Low-Dimensional Solids*, Reidel, Amsterdam 1980, p. 339.
[27] A. Troup, J. S. Miller, A. J. Epstein, unpublished results.
[28] W. G. Clark, J. Hammann, J. Sanny, L. C. Tippie, *Lect. Notes Phys. 96* (1979) 255; Z. G. Soos, S. R. Bondeson, *Mol. Cryst. Liq. Cryst. 85* (1982) 19; W. G. Clark, L. C. Tippie, *Phys. Rev. B20* (1979) 2913.
[29] a) M. J. Rice, *Phys. Lett. A71* (1979) 152; J. R. Schrieffer, *Mol. Cryst. Liq. Cryst. 77* (1981) 201; W. P. Su, J. R. Schrieffer, A. J. Heeger, *Phys. Rev. Lett. 42* (1979) 1698; b) A. J. Heeger, *Handbook of Conducting Polymers 2* (1986) 729; R. R. Chance, D. S. Bourdreaux, J. L. Bredas, R. Sibley, *ibid. 2* (1986) 825.
[30] M. J. Rice, E. J. Mele, *Phys. Rev. B25* (1982) 1339.
[31] a) A. J. Epstein, J. W. Kaufer, H. Rommelmann, I. A. Howard, E. M. Conwell, J. S. Miller, J. P. Pouget, R. Comes, *Phys. Rev. Lett. 49* (1982) 1037; b) A. J. Epstein, R. W. Bigelow, J. S. Miller, R. P. McCall, D. B. Tanner, *Mol. Cryst. Liq. Cryst. 120* (1985) 43.
[32] E. M. Conwell, I. A. Howard, *Synth. Met. 13* (1986) 71; *Mol. Cryst. Liq. Cryst. 120* (1985) 51; I. A. Howard, E. M. Conwell, *Phys. Rev. B31* (1985) 2140.
[33] R. P. McCall, D. B. Tanner, A. J. Epstein, I. A. Howard, E. M. Conwell, unpublished results.
[34] S. Mazumdar, S. N. Dixit, A. N. Bloch, *Mol. Cryst. Liq. Cryst. 120* (1985) 35.
[35] P. Pincus in H. J. Keller (Ed.): *Low-Dimensional Cooperative Phenomena*, Plenum, New York 1974, p. 1; I. F. Shchegolev, *Phys. Status Solidi 12* (1972) 9; A. J. Epstein, S. Etemad, A. F. Garito, A. J. Heeger, *Phys. Rev. B5* (1972) 952.
[36] A. J. Epstein, E. M. Conwell, D. J. Sandman, J. S. Miller, *Solid State Commun. 23* (1977) 355; A. J. Epstein, E. M. Conwell, *ibid. 24* (1977) 627.
[37] L. Z. Azevedo, J. S. Miller, A. J. Epstein, *Mol. Liq. Cryst. 120* (1985) 67.
[38] I. A. Howard, E. M. Conwell, *Phys. Rev. B29* (1984) 6879; E. M. Conwell, I. A. Howard, *J. Phys. Colloq. 44-C3* (1983) 1487.
[39] L. B. Coleman, M. J. Cohen, D. J. Sandman, F. G. Yamagishi, A. F. Garito, A. J. Heeger, *Solid State Commun. 12* (1973) 1125.
[40] M. J. Rice, *Phys. Rev. Lett. 37* (1976) 36.
[41] D. B. Tanner, J. E. Deis, A. J. Epstein, J. S. Miller, *Solid State Commun. 31* (1979) 671.

Synthesis of Glycopeptides, Partial Structures of Biological Recognition Components**

New Synthetic Methods (67)

By Horst Kunz*

Dedicated to Professor Leopold Horner on the occasion of his 75th birthday

Glycopeptides are partial structures of the connecting regions of glycoproteins and, like these, always contain glycosidic bonds between the carbohydrate and peptide parts. Glycoproteins are not only widely distributed but are also decisive factors in post-translational biological selectivity, especially in biological recognition. Targeted syntheses of glycopeptides require stereoselective formation of the glycosidic bonds between the carbohydrate and the peptide parts and protective group methods that enable selective deblocking of only one functional group in these polyfunctional molecules. These heavy demands have been met by the well-established use of benzylic protective groups, which can be removed by hydrogenolysis, combined with the use of base-labile 2-phosphonioethoxycarbonyl (Peoc) or 9-fluorenylmethoxycarbonyl (Fmoc) protective groups or of bromoethyl esters, which can be removed under neutral conditions. The acidolysis of *tert*-butyloxycarbonyl (Boc) groups and of *tert*-butyl esters has also been successfully used, although, under acidic conditions, anomerization or rupture of the glycosidic bonds may occur, especially when nucleophiles are present. The stable, two-stage 2-(pyridyl)ethoxycarbonyl (Pyoc) protective groups allow a more reliable synthesis of complex glycopeptides since they can be removed, after modifications, under mild conditions. Particularly suitable for the synthesis of sensitive glycopeptides are the stable allyl protective groups. They can be removed from the complex glycopeptides in a highly selective and effective manner by means of noble-metal catalysts under practically neutral conditions. These methods have been employed to synthesize glycopeptides corresponding to partial structures of interesting glycoproteins. Deprotected glycopeptides representing tumor-associated antigen structures can be coupled to bovine serum albumin, which serves as a biological carrier molecule, without the necessity of using an artificial coupling component (spacer).

1. Glycoproteins as Carriers of Biological Selectivity on Membranes

The complex molecular processes in a biological system can only take place properly when they are selectively controlled. The best known and probably the best investigated of these control processes is the replication and transcription of the genetic code of the deoxyribonucleic acids and the translation of the genetic information in protein biosynthesis.[1] This regulation ensures that the proteins—e.g., decisive biological catalysts (enzymes)—are always dependably produced, so that they can carry out their often highly selective functions in the cell. As a rule, however, a protein performs its function only in specific areas of the cell. Biological selection processes, which occur predominantly on the intracellular and outer-cell membranes, are responsible for guiding a protein that has been newly synthesized on the endoplasmic reticulum to its "work place." This post-translational biological selectivity is clearly based on a receptor-effector interaction in which—at least in eukaryotic cells—the glycoproteins play a decisive role.[2]

That the carbohydrate part of the glycoprotein can play a key role in this process was first shown by *Ashwell* et al.[3] They found that the copper-transport glycoprotein, ceruloplasmin, has a biological half-life of 54 h in rabbit serum. However, after they had removed the terminal *N*-acetylneuraminic acid (sialic acid) residue from the oligosaccharide chain of ceruloplasmin with neuraminidase and thereby uncovered galactose, they found that the resulting asialoceruloplasmin had a half-life of less than 5 min in rabbit serum. They were able to show that this dramatic biological effect is caused by the recognition of the now terminal galactose residue by a specific receptor in the liver cells of the rabbit, a selection mechanism that holds for many analogous glycoproteins and for mammals in general.[3] This galactose-specific receptor in the hepatocyte membrane, which acts like a lectin, is itself a glycoprotein.[4]

The carbohydrate side chain of a glycoprotein also serves as a recognition signal for the directed transport of lysosomal enzymes into the lysosomes of fibroblasts. In this case, terminal mannose-6-phosphate residues are recognized by specific receptors in the membrane which once again are glycoproteins.[5] If the fibroblasts are treated with the antibiotic tunicamycin, which prevents the connection of the carbohydrate side chain to the asparagine amide function during the biosynthesis of the *N*-glycoproteins, then the carbohydrate-free lysosomal enzymes

[*] Prof. Dr. H. Kunz
Institut für Organische Chemie der Universität
J.-J.-Becher-Weg 16-20, D-6500 Mainz (FRG)

[**] An expanded version of a lecture delivered on October 24, 1985, at the Max-Bergmann Conference in Bozen.

 © VCH Verlagsgesellschaft mbH, D-6940 Weinheim, 1987 0570-0833/87/0404-0294 $ 02.50/0

no longer enter the lysosomes where they carry out their functions.

The importance of glycoproteins in the control of biological processes is clearly demonstrated by the fact that crucial processes, such as cell growth and cell differentiation, are permanently affected when the attachment of carbohydrate side chains to the proteins is blocked.[6] In accord with these results, it has been found that the glycoprotein profiles in the cell membranes of normally growing cells and of tumor cells are very different.[7] The altered glycoprotein structures in the tumor cell membranes appear to be, in part, tumor-associated antigens.[8] The role of the oligosaccharide structures of glycoconjugates as antigen determinants in different blood group systems is well-known.[9] Recent investigations have shown that interactions of the carbohydrate–lectin type are also involved in infection processes. Some bacteria and viruses have surface lectins which bind specifically to carbohydrates on the surface of the host cell and so induce infection.[10]

These results of biochemical, molecular biological, and immunological research open up quite new possibilities for the diagnosis and specific treatment of pathogenic processes. For example, the development of selective chemotherapeutic agents, the delivery of active substances to particular tissues by means of selective signal–receptor interactions,[11] and the production of antibodies active against tumor-associated glycoconjugate structures should be realizable.[7,12] In addition, when one considers that the oligosaccharide portion of the glycoproteins often offers protection against the attack of proteolytic enzymes,[13] it should be possible to design orally applicable, active peptides by incorporation of suitable glycoside portions.

Against this background and in light of the highly developed methods of peptide synthesis,[14] interest in glycopeptide synthesis is increasing.

2. The Carbohydrate–Peptide Connecting Region of Glycoproteins

Despite the large number of natural glycoproteins, the types of covalent bonds between the protein and the saccharide part show relatively little variation.[2] Most common are *N*-glycoproteins, **1**, in which the side chain amide function of an asparagine unit is usually joined to an *N*-acetylglucosamine residue through a β-*N*-glycosidic linkage.[15] To this type of structure, whose biosynthesis has been best investigated,[16] belong serum components such as amylases, plasmaproteins (e.g., fibrinogen and transferrin), immunoglobulins, hormones (e.g., chorionic gonadotropin), hormone precursors (e.g., thyroglobulin), and membrane glycoproteins (e.g., glycosyl transferases, band III glycoprotein, rhodopsin, and receptor glycoproteins, including the galactose-specific receptor of the hepatocyte membrane). The *N*-glycoproteins **1** are characterized, furthermore, by a common sequence in the connecting region: the next but one *C*-terminal amino acid following the *N*-glycosylated asparagine is always serine or threonine. The hydroxy group of this unit appears to be involved catalytically in the glycosyl transfer.[17]

Until recently it was assumed that in nature the type-**1** *N*-glycosidic linkage occurred exclusively.[2] More recent investigations, however, have shown that the cell surface glycoproteins of the halobacteria contain *N*-glucosyl-[18] and *N*-galactosaminylasparagine structures.[19] From the glomerular basal membrane of rats a nephritogenic glycopeptide has been isolated in which an α-*N*-glycosidic bond exists between glucose and the peptide part.[20] Glutamine has been suggested as the binding partner.[21]

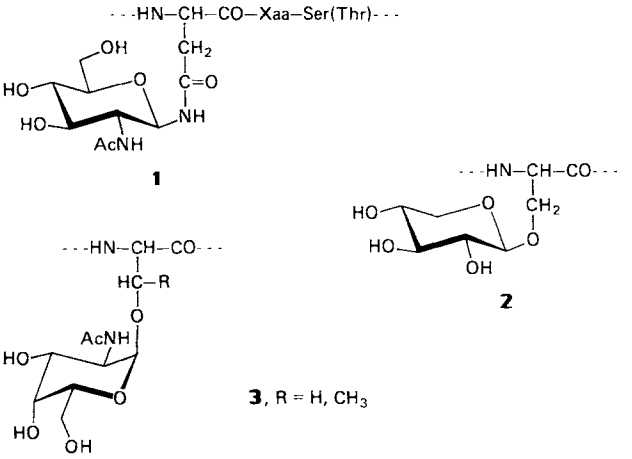

The second important type of connection between the carbohydrate and peptide portions of glycoproteins is the *O*-glycosidic linkage. The β-glycosidic bond between xylose and serine, **2**, is the characteristic connecting element of the proteoglycans of the extracellular matrix and of connective tissue.[22] The α-*O*-glycosidic linkage between *N*-acetylgalactosamine and serine or threonine, **3**, was first found in the mucous glycoproteins (mucins).[2] It is characteristic of many other serum and membrane glycoproteins, including the blood-group glycoproteins,[23] human glycophorin,[24] epiglycanin[25], and the glycoproteins of the tumor-associated T_N and T antigens.[8]

In collagen and collagen-type macromolecules the β-glycosidic bond between galactose and δ-hydroxylysine occurs almost exclusively.[26] Interestingly, this structural element is also thought to occur in the C1q components of the complement system.[27] For further information about other variants of the glycosidic linkage in *O*-glycoproteins, more comprehensive reviews should be consulted.[2]

3. Comparison of Glycopeptide and Peptide Synthesis

Even if one looks only at the partial structures of the connecting regions of glycoproteins of types **1**–**3**, it is quite clear that the problems of peptide and carbohydrate chemistry merge in the chemical synthesis of such polyfunctional molecules. Both branches of preparative natural product chemistry were firmly founded by *Emil Fischer*.[28] However, the analytical techniques then available did not allow the great variety and importance of the protein–carbohydrate conjugates to be recognized. Thus, two separate schools of chemistry stemmed from *Emil Fischer*: that of peptide chemistry, with such names as *Max Bergmann*,

Hans Leuchs, and *Emil Abderhalden*, and that of carbohydrate chemistry, with such names as *Otto Warburg*, *Carl Freudenberg*, and *Burkhard Helferich*. For decades thereafter proteins and carbohydrates were largely dealt with separately.[29]

In comparison with peptide synthesis, glycopeptide synthesis requires the protection of many more functional groups, reversibly and with maximum selectivity. Still more important in compounds of types **1**–**3**, however, is the presence of the glycosidic linkage, which must both be formed stereoselectively[30,31] and be retained unchanged during the course of the synthesis.[32]

The oligosaccharides of the glycoproteins constitute a separate field; their structure and biosynthesis have been dealt with in many reviews.[2,6,16,29,33–35] The chemical synthesis of such oligosaccharides has recently been the subject of extended reviews[36,37] and will not be covered further here.

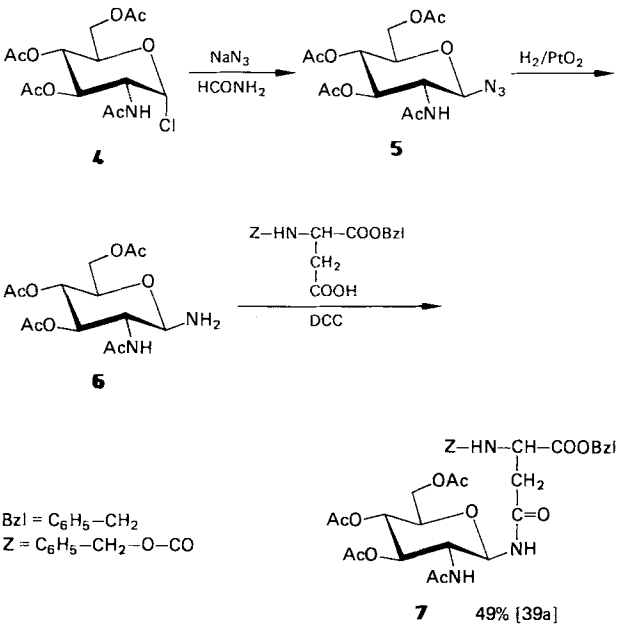

4 **5** **6** **7** 49% [39a]

4. The Formation of Glycosidic Bonds

Until the beginning of the 1980s the formation of glycosidic bonds to specific amino acids was the focal point of glycopeptide chemistry. Of special merit is the work of *Jeanloz* and his co-workers,[38] who have focused their attention on the targeted synthesis of glycopeptides in order to obtain standard compounds for use in studying the degradation of glycoproteins. Since the synthesis of *N*- and *O*-glycosyl amino-acid derivatives was reviewed comprehensively in 1985[30] and 1983,[31] only the more important methods and more recent results will be dealt with here.

4.1. The Asparagine–Glucosamine Linkage

The β-*N*-glycosidic linkage between *N*-acetylglucosamine and asparagine, **1**, which is characteristic of the *N*-glycoproteins that are especially important in cell biology, is formed, e.g., in conjugate **7**, by the condensation of *N*-protected aspartic acid α-monoesters with 2-acetamido-3,4,6-tri-*O*-acetyl-2-deoxy-β-D-glucopyranosylamine **6** (DCC = *N*,*N*′-dicyclohexylcarbodiimide).[39] Compound **6** is prepared,[30,31] in turn, from the glycosyl chloride **4**[40] via the azide **5**.[41] For the conversion of the chloride **4** into the azide **5**, sodium azide in formamide[42] is more suitable than silver azide, which was formerly used exclusively.[39,41] In the more complex chitobiose series, on the other hand, this method was unsuccessful. The unpleasant silver azide[43] could be replaced, however, by a method involving phase-transfer catalysis with sodium azide in chloroform/water.[44] In contrast to the reduction of other carbohydrate azides, the hydrogenation of glycosyl azides in the *N*-acetylglucosamine series has only been satisfactorily accomplished with platinum catalysts.[30] It is accompanied by the formation of bisglycosylamines as by-products.[45] Our recent investigations, however, show that this hydrogenation also proceeds very well with Raney Ni.[46] This method has the advantage that benzylic protective groups are not attacked. In this way, the selective reduction of the azido function in the complex, fully protected trisaccharide **8** was achieved with the nearly quantitative formation of the amine **9**.[47]

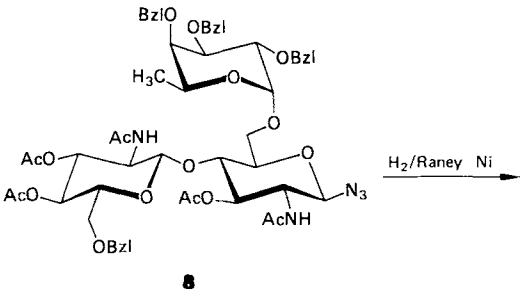

8

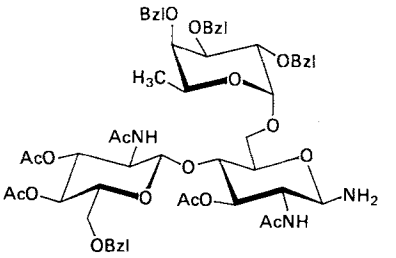

9 92%

For the condensation of glycosylamines of type **6** with *N*-protected aspartic acid α-monoesters to form completely protected *N*-glycosylasparagine derivatives of type **7**, only *N*,*N*′-dicyclohexylcarbodiimide was used at first.[30,31,39] In order to avoid the problem of subsequent selective deblocking, *Garg* and *Jeanloz*[48] studied the reaction of the glucosaminylamine **6**, as well as the corresponding chitobiosylamine, with *N*-benzyloxycarbonyl(Z)aspartic anhydride. However, they always obtained a mixture of the desired *N*-glycosylasparagine derivative and the isomer in which the α-carboxyl group had undergone reaction. Moreover, the method did not afford satisfactory yields of the desired isomer. Of the condensation catalysts employed,[30,31] ethyl 2-ethoxy-1,2-dihydroquinoline-1-car-

boxylate (EEDQ)[49] has proved to be especially effective. For example, the (1,3-dithianyl)methyl (Dim) ester[50] of *tert*-butyloxycarbonylaspartic acid **10** reacts smoothly with **6** in the presence of EEDQ to give the N^4-glucosaminylasparagine ester **11**, which is ready for selective deblocking.[51,82]

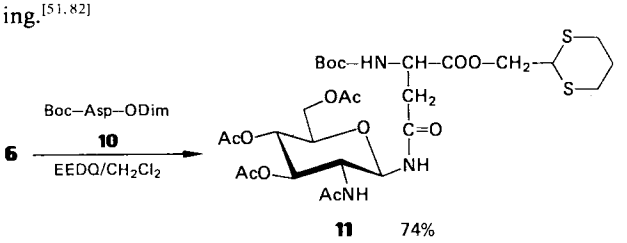

11 74%

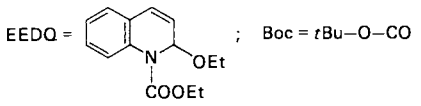

4.2. The β-Glucosyl-Serine Linkage

The β-glycosidic linkage to the serine hydroxyl group, in the form of xylose derivatives of type **2**, is especially characteristic of the proteoglycans in the animal kingdom. In the plant kingdom and in fungi, however, other carbohydrates occur as connecting partners; thus, consideration of this type of linkage should not be confined to xylose. This is further justified by the fact that the chemical properties of this bond are not greatly influenced by the type of carbohydrate involved. The first syntheses of glycosylserine compounds of this sort were carried out by means of dihydrooxazole derivatives of glucosamine.[52] Carbohydrate ortho esters react with *N*-protected serine and threonine esters in a similar fashion to give the corresponding glycosides.[53] Xylosylserine conjugates were obtained by *Lindberg* et al. under the conditions of the Koenigs–Knorr reaction.[54,55]

For details of the large number of other β-glycosylserine or -threonine derivatives that have been prepared under Koenigs–Knorr or Helferich conditions, the reader is referred to the comprehensive reviews already published.[30,31] These methods have also been successfully used in the synthesis of galactosyl-δ-hydroxylysine model compounds.[56]

The modern variants of the Koenigs–Knorr reaction are equally well suited to the glycosylation of the serine hydroxyl group. Z-serine-2-bromoethyl ester,[57] for example, reacts with the α-D-glucopyranosyl bromide **12** in the presence of silver trifluoromethanesulfonate/tetramethylurea[58] to form the completely protected glucosylserine derivative **13**.[59] It is interesting that the halogen in the ester protective group is not attacked under these conditions.

Modern alternatives to the Koenigs–Knorr synthesis[37] have also proved useful in the preparation of *O*-glycosylserine linkages. For example, the xylopyranose **14** was allowed to react with the Z-serine allyl ester **15** by means of the trichloroacetimidate method[37,60] to give, in good yield and with high selectivity, the xylosylserine derivative **16**, in which the hydroxyl groups in the carbohydrate part of the molecule are protected as benzyl ethers.[61]

Compound **16** can also be obtained by reaction of the benzyl-protected xylopyranosyl fluoride **17** with the serine

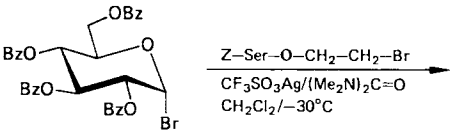

12

Bz = C_6H_5–CO

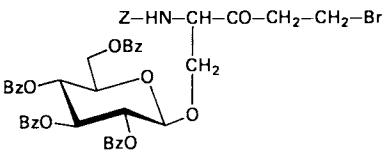

13 53–81%

ester **15** in the presence of boron trifluoride etherate and triethylamine.[62] Both reactions have the advantage that they take place rapidly under homogeneous conditions. In both cases, however, the corresponding α isomer is also formed (ca. 1 : 6) and must be removed chromatographically.

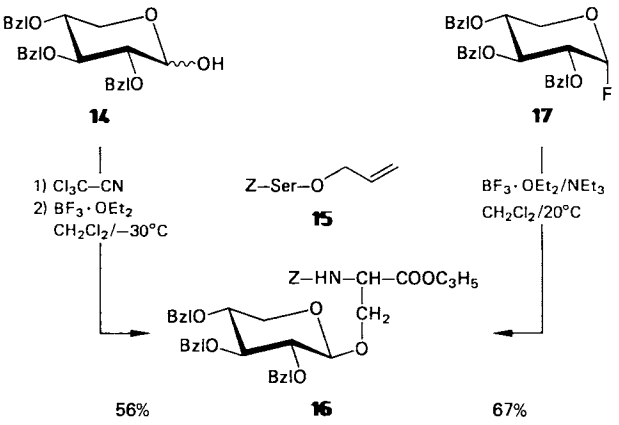

The glycosylation with *O*-acyl-protected glycosyl fluorides is highly stereoselective.[62] The products formed in this way, such as **20**, can also be synthesized effectively and under homogeneous conditions when one starts from the novel ortho ester **18** containing an oxime moiety.[63] Finally, the glycosylation of **15** is very smoothly accomplished by allowing the pentapivaloylglucose **19**,[64] as the 1-*O*-acyl sugar, to react with trimethylsilyl trifluoromethanesulfonate.[65] The glycoconjugate **20** is formed stereoselectively and in almost quantitative yield.[66]

4.3. The α-Glycosidic Serine/Threonine-*N*-Acetylgalactosamine Linkage

The formation of the α-glycosidic linkage between *N*-acetylgalactosamine and serine or threonine (structure type **3**), which is characteristic of many serum and membrane glycoproteins, at first presented great problems. In the corresponding glucose series, substituted glycosyl donors, even with non-neighboring-group-active substituents on C-2, such as the *O*-acetylated 2-deoxy-α-D-glucopyranosyl bromide **21**, reacted with Z-serine methyl ester under Koenigs–Knorr or Helferich conditions to give the β-

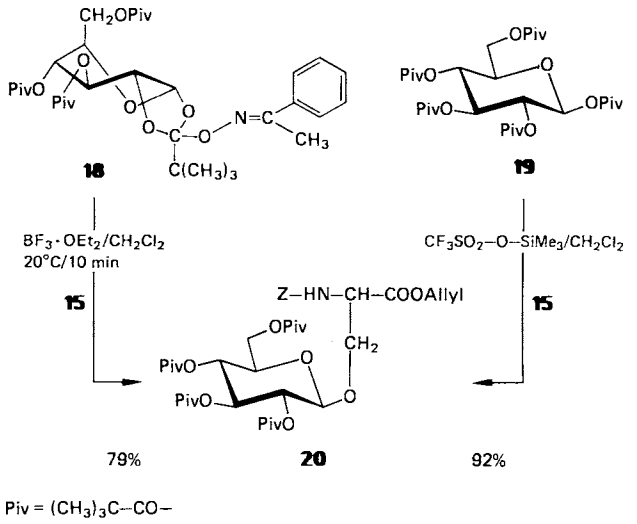

Piv = $(CH_3)_3C$–CO–

glycosyl amino-acid derivative, e.g., **22**,[67] almost exclusively.

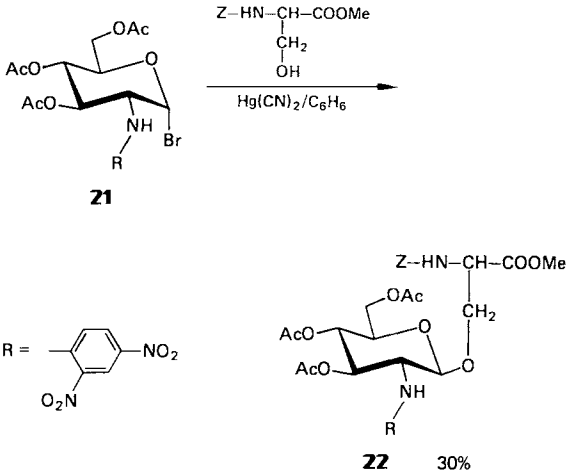

The solution to this problem was found by *Paulsen* et al.[68] Reactive glycosyl chlorides containing the 2-azido function as a non-neighboring-group-active substituent were used as glycosyl donors under the conditions of "in situ anomerization." This method was applied by *Ferrari* and *Pavia*[69] to the glycosylation of serine and threonine. They converted Z-threonine or -serine esters into the desired glycopeptides **24** or **25**, respectively, the precursors

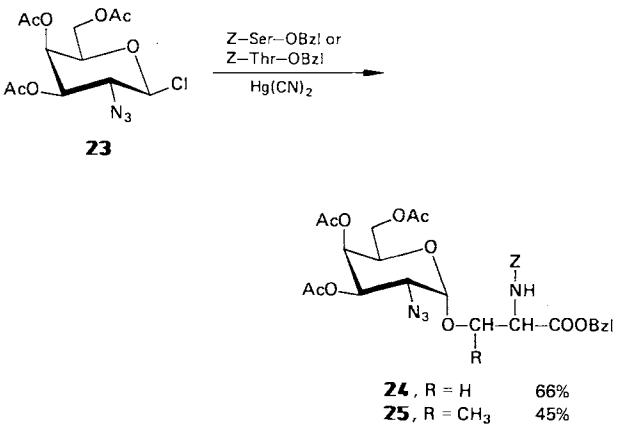

of structures of type **3**, by reaction with the protected 2-azido-β-galactosyl chloride **23**.

The azide method[68] is favored by the fact that 2-azido-glycosyl halides, such as **23**, are readily available by the azidonitration route.[70] In this way, *Paulsen* et al. have worked out an effective α-glycosylation method using the system silver perchlorate/silver carbonate in dichloromethane/toluene.[71] The simultaneous α-glycosidic linking of two disaccharide units to the serylserine derivative **27** by reaction with the glycosyl halide **26** illustrates the power of this method.[72a,b]

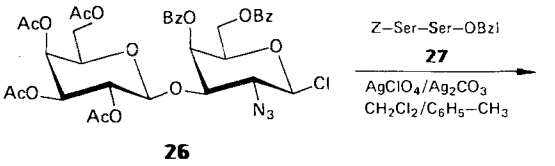

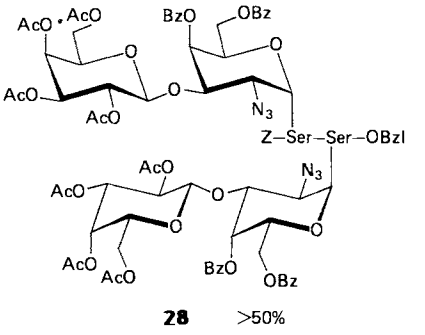

The selective reduction of the azido function in complex glycopeptides, such as **28**, is accomplished with nickel tetrahydroborate.[72] After acetylation of the amino group thus formed, structures of type **3** are obtained which embody partial structures of glycoproteins of T-antigen type associated with tumors. The azido group in compounds such as **24**, **25**, or **28** can also be reduced with hydrogen sulfide.[73,74] With dimethyl(phenyl)phosphane in glacial acetic acid it is possible to convert the azido group in the base-sensitive glycosylserine and -threonine derivatives, e.g., **29**, directly into the acetamido group (e.g., **30**).[75]

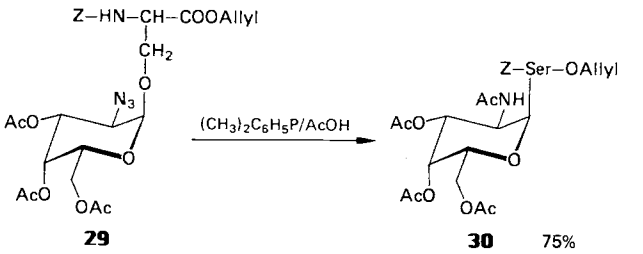

α-Glycosides of 2-azido-2-deoxygalactopyranose with serine derivatives are also available by means of the trichloroacetimidate method.[76] Another α-glycoside synthesis, without mercury or silver reagents, is based on the activation of the free anomeric hydroxyl groups of benzyl-protected carbohydrate building blocks with trifluoromethanesulfonic anhydride.[77] Similarly, by means of the

azido form, the method can be used in the synthesis of the α-galactosaminylserine and -threonine derivatives.[78] In the glycosylation of the threonine derivatives, in particular, significant amounts of the β anomers are formed and must be separated.

5. Selective Deblocking and Peptide Chain Extension on Glycopeptides

The selective removal of protective groups on glycosyl amino acids and glycopeptides remained an unsolved problem until the end of the last decade.[30,31] Only in particular cases was the selective deblocking of a particular functional group on the polyfunctional glycopeptide achieved and then only with considerable material losses.[67] The origin of these difficulties lies in the presence of glycosidic bonds in these molecules (see Section 3). Since the preparative methods for overcoming this problem were developed only recently and, in contrast to oligosaccharide synthesis[36,37] and to the glycosylation of amino-acid derivatives,[30,31] have not been extensively reviewed and since our research group has been deeply involved in the solution of this problem,[32] this aspect of glycopeptide synthesis will be the main thrust of this review.

5.1. The Lability of Glycosidic Linkages

The glycosidic bonds of the glycopeptides, being acetal-like bonds, are always more or less acid-sensitive. The most acid-stable are the *N*-glycosides of type **1** and the glycosyl derivatives of δ-hydroxylysine. Nevertheless, oligosaccharidic glycopeptides contain, besides these relatively stable connecting structures, *O*-glycoside bonds within the oligosaccharide portion, so that the sensitivity toward acids shown in the following examples applies also, in principle, to such glycopeptides.

Attempts to selectively remove the Z group from the glycosylserine derivative **22** by means of hydrobromic acid in glacial acetic acid brought about extensive cleavage of the glycoside bond[67] in addition to formation of the uncharacterized ammonium salt **31**. After *N*-terminal chain extension with Z-amino-acid *p*-nitrophenyl esters, the corresponding glycodipeptides were obtained in 12–34% yield based on **22**.

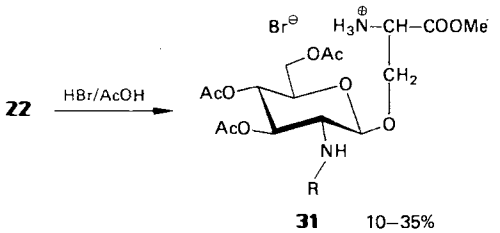

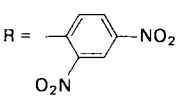

If only weak nucleophiles are present in the solution, the cleavage of the glycoside bond is suppressed; the danger of anomerization, however, is always present. We have observed this in the removal of the Boc group from **32**.[32,79] The *N*-terminal chain extension with Z-phenylalanine revealed that the amino-deblocked intermediate **33** was present as an anomeric mixture. The anomeric glycodipeptides **34a** and **34b**, which exhibit very similar chromatographic behavior, could be separated and their structures

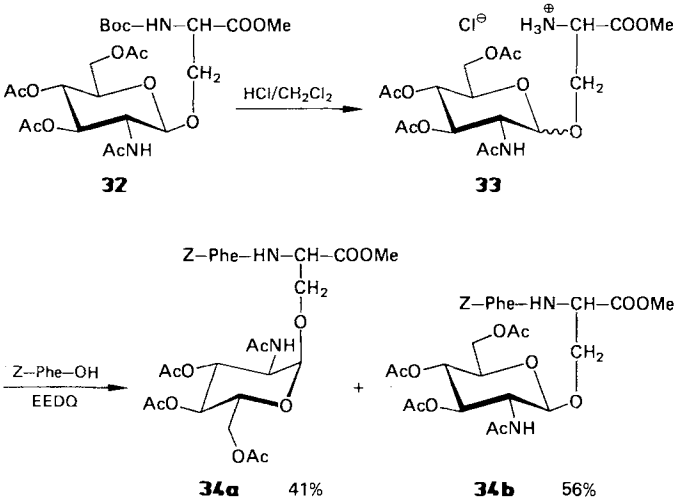

unequivocally characterized.[79] However, the Boc protective group has been used in a solid-phase glycopeptide synthesis in which the removal from the resin was even carried out with hydrofluoric acid in anisole,[80] the glycoside bond remaining intact. This is surprising since hydrofluoric acid normally attacks oligosaccharides and even 1-*O*-acyl monosaccharides very quickly.[62] Nevertheless, more recent work shows that the lability of the *O*-glycosidic bond appears to depend on the structure of the glycopeptide. *Sinaÿ* et al.[81] were able to remove the *tert*-butyl esters of *O*-glycopeptides selectively with trifluoroacetic acid without cleavage of the glycosidic bond. However, weakly nucleophilic trifluoroacetic acid can also cleave glycosidic linkages, e.g., in the chitobiosyl tripeptide **35**. Together with the desired **38**, which represents a partial structure of the human complement factor B, **36** and **37**, the products of cleavage, were obtained in a ratio of 2 : 9.[44,82] Analogues of **35** with acyl-protected carbohydrate portions were not attacked by trifluoroacetic acid at the glycosidic bond.[44] These different results show clearly that the acidolysis of protective groups in glycopeptide synthesis should be checked in each individual case.

The synthesis of glycopeptides of the glycosylserine or -threonine type (**2** or **3**) turns out to be more difficult, because of the characteristic base lability of the *O*-glycosyl-β-hydroxycarboxylic acid derivatives.[83] In fact, this reaction is used analytically to demonstrate the presence of the *O*-glycosylserine or -threonine linkage in glycoproteins.[84] For example, in sodium carbonate solution, the protected glycosylthreonine methyl ester **39** is cleaved quantitatively within seconds, before cleavage of the methyl ester occurs.[85]

The rate of the β-elimination to α-aminoacrylic acid derivatives, such as **40**, depends on the structure of the glycoconjugate and especially on the substituents on the amino

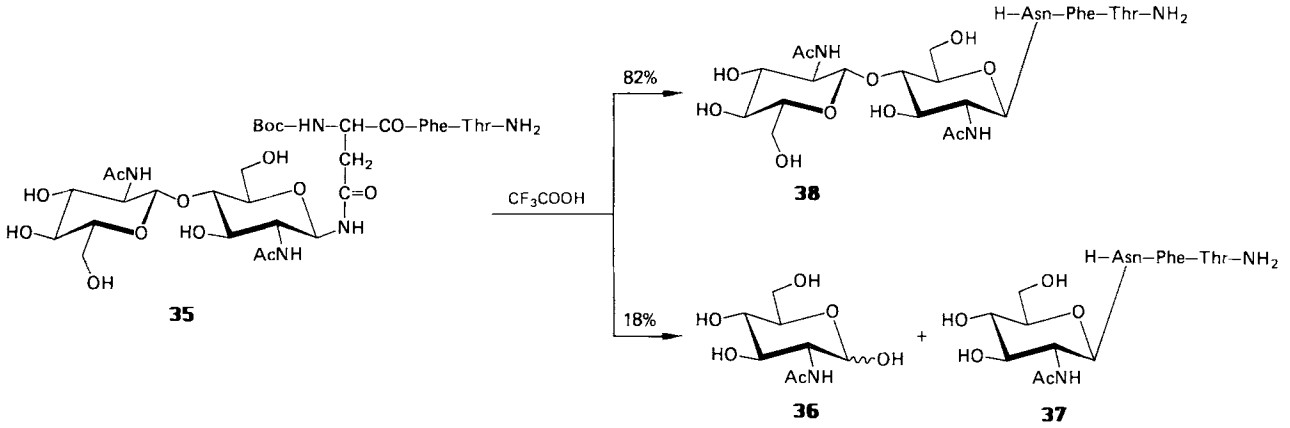

and carbonyl functions of the amino-acid portion. Esters and amides undergo elimination at room temperature already at pH 9.[85]

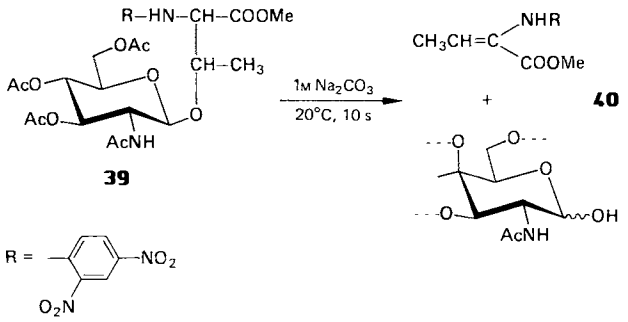

Since the benzyl- or *tert*-butyl-ether-protected serine and threonine derivatives commonly used in peptide synthesis are stable, the facile β-elimination of the glycan portion in compounds such as **39** appears, at first sight, to be surprising. It is understandable, however, when one takes into account the complexing ability of carbohydrates with respect to cations and amines. In the saponification of the unsymmetric benzylidenemalonic acid diester **41**, for example, this property explains the removal of only the secondary carbohydrate ester structure.[86]

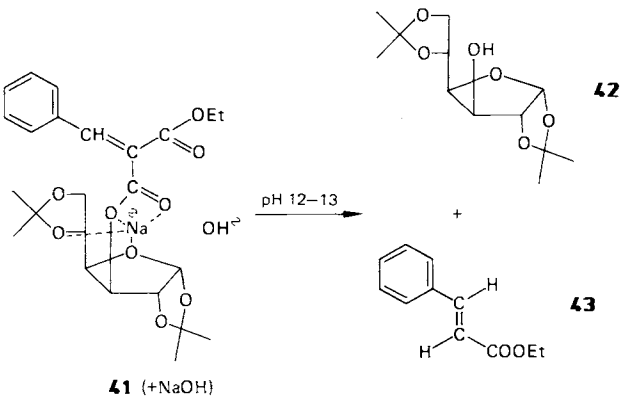

This ability to form complexes is also responsible for the active ester properties of the peptidylcarbohydrate esters that are biologically important in the peptidyl transfer step of protein biosynthesis, i.e., in the transfer of P-site-bound peptidyl-tRNA to the A-site-bound aminoacyl-tRNA.[87]

The base lability and the potential acid lability of the glycopeptides make it necessary, in the synthesis of these compounds, to use protective groups that can be removed under mild and, if possible, neutral conditions. In earlier work only the benzyl and the Z group fulfilled these demands.[30,31] Since they are removed simultaneously upon hydrogenolysis, however, they must be combined with other protective groups for selective deblocking, such as the methyl group, which themselves cannot be removed without destroying the glycoside bond (cf., for example, **39** → **40** and ref. [54, 67]). These problems could only be solved by the introduction of new, more suitable protective groups and the use of other known protective groups in glycopeptide synthesis.

5.2. The Phosphonioethoxycarbonyl (Peoc) Protective Group

Since the 2-triphenylphosphonioethoxycarbonyl (Peoc) protective group[88] can be removed from the amino group even under very mild basic conditions, we used it in our first glycopeptide syntheses.[89] It allowed the targeted synthesis of *N*-glycopeptides when combined with either the *C*-terminal benzyl or the *tert*-butyl group. Owing to the high stability of the Peoc group toward acids, the Peoc-amino acid chlorides,[90] which are stable at room temperature, can be used for chain extension.

The cleavage of the Peoc group with morpholine in dichloromethane is so mild that even the base-labile *O*-glycosylserine linkage remains completely intact, as, for example, in the deblocking of the glycopeptide **44**.[91] The ester groups and the *O*-glycoside bond, which is sensitive to elimination reactions, remain intact so that the peptide

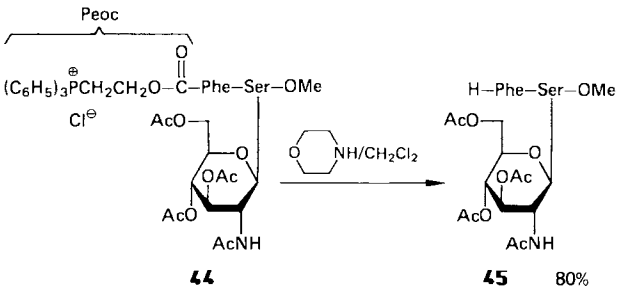

chain can be lengthened specifically at the deprotected amino group in **45**.[*]

In spite of the advantages of the Peoc group, which, in combination with the easily removable benzyl group, allowed, for the first time, a clean, selective deblocking of a glycopeptide,[89] there are some drawbacks to their general use in glycopeptide synthesis: (1) The Peoc group is a bulky residue which hinders the condensation reaction. (2) The high base-lability of the protective group, which is the basis for its easy removal, demands special care in performing the synthesis. (3) The Peoc protective group is a cationic substituent whose halogen counterion leads to problems in the glycosylation with silver or mercury reagents. Thus, it is necessary to use the Z group in the glycosylation step in the synthesis of the glycopeptide structure **44**.[91] To achieve its selective removal, however, a *C*-terminal methyl ester must be used, whose cleavage can no longer be carried out without breaking the glycoside bond by β-elimination[54,85] (see Section 5.1). From this it is clear that, for targeted glycopeptide synthesis, other alternatives to the benzyl group as a carboxy-protecting group had to be found.

5.3. The 2-Haloethyl Group as a Carboxy-Protecting Group

The use of the 2-bromoethyl group as a reversible carboxy-protecting group for peptide synthesis was first described by *Ugi* et al.,[92] who achieved its cleavage with a supernucleophilic cobalt(I) complex. In our investigations,[57] we had attempted to adopt the bromoethoxycarbonyl (Beoc) group, the precursor of the Peoc group,[93] to protect the carboxy group. We thereby found that the 2-chloro- and 2-bromoethyl esters of amino acids and peptides, after being converted into the iodoethyl ester, could be selectively cleaved with zinc in dimethylformamide (DMF). This neutral deblocking reaction provided the first opportunity to deblock the carboxy function on the base- and acid-labile glycosylserine derivative **13** in the presence of the Z group.[59]

Both the glycosylserine-2-iodoethyl ester **46** and the carboxyl-deblocked product **47** could be isolated and characterized. If the chain extension is performed with crude **46** and **47**, one obtains the glycotripeptide **48** in 71% yield based on **13**.[94] The gentle deblocking of the bromoethyl ester does not destroy either the ester-protecting groups in the carbohydrate part, the *N*-terminal Z protective group, or the *O*-glycoside bond, which easily undergoes elimination reactions.

The low yield in the deblocking step can be traced back to the fact that **47** is partly adsorbed on the zinc salts formed and, because of the acid and base lability of the *O*-glycosylserine linkage, cannot be isolated under the workup conditions. These disadvantages can be avoided if the cleavage of the 2-bromoethyl ester is carried out electrochemically.[95,96] The only disadvantage of this method lies in the apparatus required, which is not always readily available.

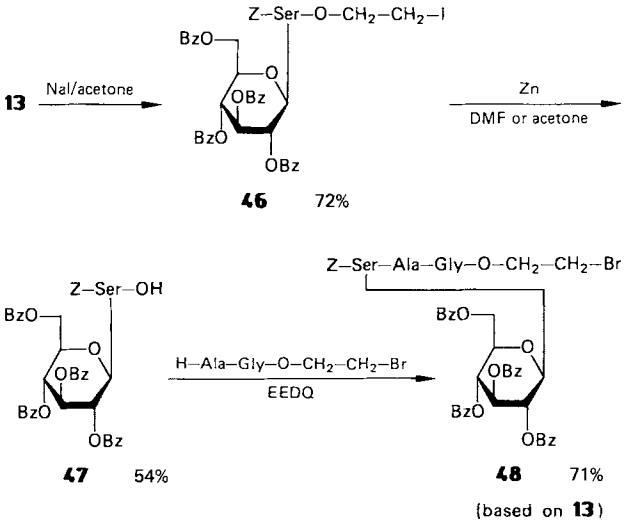

The bromoethyl ester[59,94,96] and the Peoc group,[89,91] together with the reversible protection provided by the Z or benzyl group, allowed, for the first time, effective and selective deblocking and chain extension even on the sensitive *O*-glycosylserine derivatives. The disadvantages mentioned above, however, still make it necessary to seek new methods. It appeared to be especially advantageous to find a protective group for glycopeptide synthesis that, like the Peoc residue, is easy to remove under similarly mild conditions but does not have the inherent disadvantage caused by the cationic structure in the glycosylation reaction. These demands are fulfilled by the (9-fluorenyl)methoxycarbonyl (Fmoc) protective group.[97]

5.4. The (9-Fluorenyl)methoxycarbonyl (Fmoc) Protective Group

The neutral Fmoc protective group[97] is somewhat less base-labile than the Peoc residue. However, we could show that the Fmoc group can be removed selectively, and practically quantitatively, from the protected *O*-glucosyl- and *O*-xylosylserine derivatives, **49** and **50**, respectively, which are sensitive to base-catalyzed β-elimination.[98] In contrast

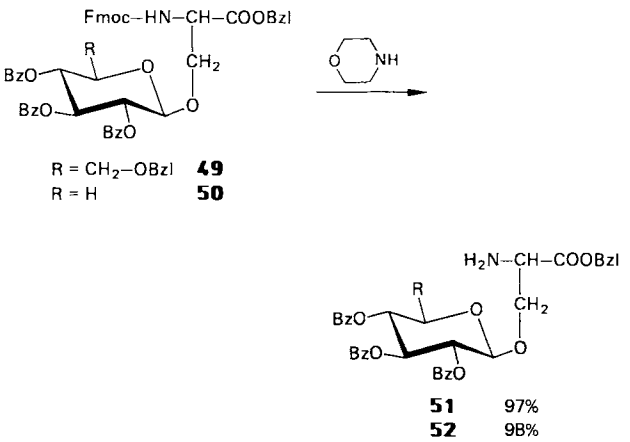

[*] In some cases, the carbohydrates are given as Haworth formulas, since these, in combination with the shorthand notation for the amino acids, are better suited to represent β-glycosides.

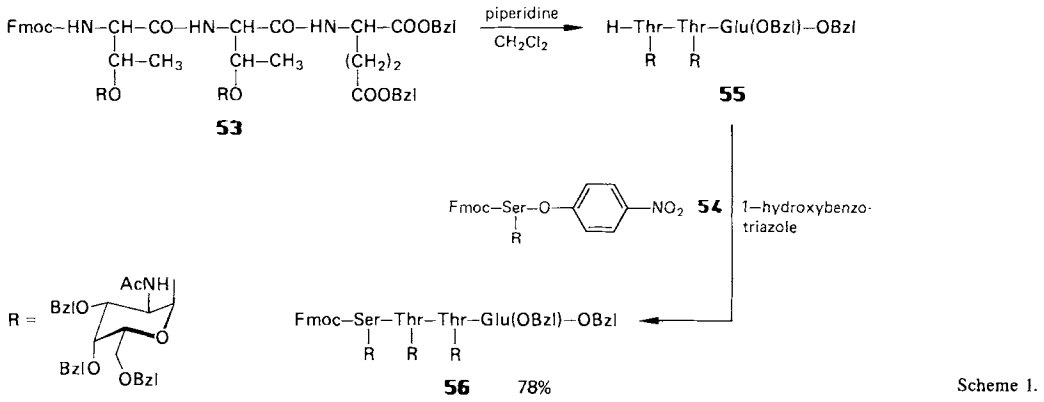

Scheme 1.

to the practice in peptide chemistry, and also to that of *Pavia* et al.,[78,99] who have also described the use of Fmoc, we do not use the relatively strongly basic piperidine ($pK_s \approx 11.1$) but the order of magnitude weaker morpholine ($pK_s \approx 8.3$) to remove the Fmoc group. In this way, we remain below the sensitivity limit above which the glycoside bond would be destroyed.

Once the problem of selective deblocking with retention of the numerous ester structures and the glycoside bond in products such as **51** and **52** has been solved, the subsequent chain extension presents no further problems. Morpholine can be used to remove the Fmoc group selectively and effectively from complex glycopeptides. This emphasizes the general usefulness of this method in the synthesis of glycopeptides.[98]

Ferrari and *Pavia*[100] applied the Fmoc group in combination with active esters, benzyl protective groups being used in the carbohydrate part of the molecule. They thereby synthesized the monosaccharidic T_N-antigen form of the *N*-terminal triglycopentapeptides of human glycophorin with M- and N-blood-group structures.[101] A typical example is presented in Scheme 1.

The only drawback to the combined use of Fmoc groups and benzyl esters shown in these examples is the insufficient stability of the Fmoc group during the hydrogenolysis of the benzyl ester.[102] Our own experiments have shown, however, that the Fmoc-*O*-xylosylserine benzyl ester **50** can be selectively cleaved at the *C*-terminus.[103] Thus, in the presence of the Fmoc group, selective *C*-terminal chain extension and the synthesis of larger glycopeptide units, for example, by means of the fragment-condensation technique,[14] is possible.

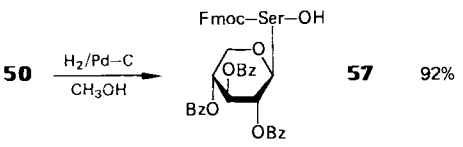

5.5. The *tert*-Butyl Ester Protective Group in Glycopeptide Synthesis

Despite the risks associated with acid treatment of glycopeptides (see Section 5.1), *Sinaÿ* and *Verez Bencomo*[81] have used the selective cleavage of the *tert*-butyl ester in the presence of the Z group for the construction of *N*-terminal triglycopentapeptides with the disaccharidic T-antigen structure,[104] which is important as a tumor-associated antigen structure.[8] In this way, the completely protected Z-glycosylthreonine *tert*-butyl ester **58** can be deblocked either *C*-terminally to give **59** or *N*-terminally to give **60**.[81]

Upon treatment with EEDQ, the two selectively deblocked compounds give the complex, completely protected, glycodipeptide **61**, which contains the same combination of protective groups as the starting material **58**. By means of this method, *Sinaÿ* and *Verez Bencomo*[104] were able to prepare the *N*-terminal T-antigen triglycopentapep-

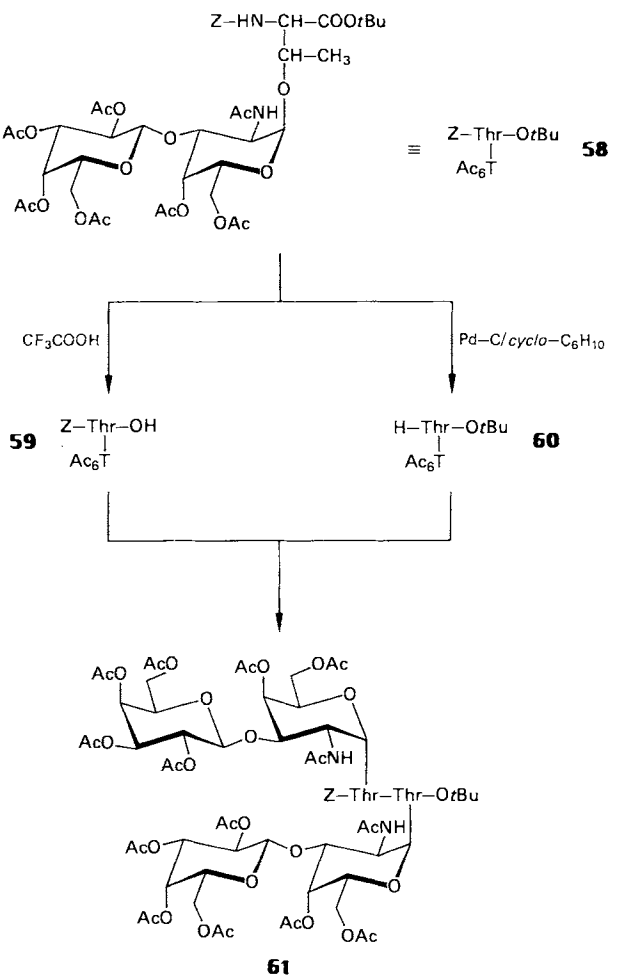

tides of glycophorin. The experimental details of this synthesis, however, have not yet been published.[81, 104]

By contrast, *Paulsen* et al.[74] have observed side reactions in the cleavage, with trifluoroacetic acid, of the *tert*-butyl esters of a compound very similar to **58**. They therefore used 98% formic acid for the deblocking. They mention, however, that two rotamers of the Z group are present in the quantitatively obtained product.

At this point, a brief comment should be made on the structure confirmation of complicated glycopeptides, which is only possible with high-field NMR spectroscopy. The structure confirmations of α-galactosaminylthreonine derivatives, such as **58** and **59**, have proved to be especially difficult since in their ^{13}C-NMR spectra the signals for the α- and β-anomeric carbon atoms are only slightly shifted relative to each other. *Pavia* et al.[77, 78, 100] have found the solution to this problem. They recognized that the ^{13}C-NMR signal for the γ-methyl group of threonine is a very sensitive probe for the anomeric configuration. For the α anomers it appears at $\delta = 18$–20, whereas in the spectra for the β anomers it is shifted about 2 ppm toward higher field.

Finally, a particular problem encountered in the use of *tert*-butyl esters[74, 78, 104] and the Boc group[80] in the syntheses of *O*-glycopeptides should be discussed. For the removal of the *tert*-butyl group, in peptide synthesis, nucleophilic trapping agents, such as 1,2-ethanedithiol,[106] must be added in order to avoid side reactions due to *tert*-butyl cations or *tert*-butyl trifluoroacetate.[107] The presence of these nucleophiles increases the risk of glycoside cleavage during the removal of protective groups under acidic conditions. The effects of powerful protonating agents on the sensitive compounds must be carefully checked in each case. This restriction applies even to the stable *N*-glycosylasparagine (**1**) and *O*-glycosyl-δ-hydroxylysine glycopeptides if oligosaccharide side chains are present. Monosaccharidic glycopeptides of this type have been successfully prepared, however, by means of *tert*-butyl[56] or Boc-protected amino acids, even in a solid-phase synthesis.[108] In the case of the solid-phase-synthesized somatostatin sequence, however, the structure could only be confirmed by mass spectrometry,[108] which usually gives no information about the stereochemistry.

If one wishes to eliminate the uncertainties associated with acid deblocking, one must make use of protective groups, such as Peoc and Fmoc (Sections 5.2–5.4), that are removable under mild conditions. Their disadvantage lies in their permanent sensitivity and, in part, in solubility problems inherent in their use in the synthesis of large glycopeptide units. To overcome these difficulties and to solve the competing requirements for stability of the protecting group during synthesis and lability during deblocking, we have turned our attention to the principle of the two-step protective group.[109]

5.6. The 2-Pyridylethoxycarbonyl (Pyoc) Protective Group

The 2-(2-pyridyl)ethoxycarbonyl (2-Pyoc)[110] and the 2-(4-pyridyl)ethoxycarbonyl (4-Pyoc)[111] protective groups are very stable toward acids and bases but can be removed under very mild conditions, after a simple modification, from the blocked amino function. The glycosylation of the 2-Pyoc-threonine benzyl ester **62** to give **63** with the benzoyl-protected glucopyranosyl bromide **12** by the silver triflate method[58] requires the addition of molar amounts of trifluoromethanesulfonic acid, since, without it, the corresponding ortho ester is formed exclusively.[112] The selective cleavage of the stable Pyoc group from the labile glycosylthreonine derivative **63** is achieved by first methylating the pyridine N atom. The α-methylene group is thereby made so acidic that quantitative cleavage occurs even with morpholine in dichloromethane to form **64**, which can undergo chain extension.[112]

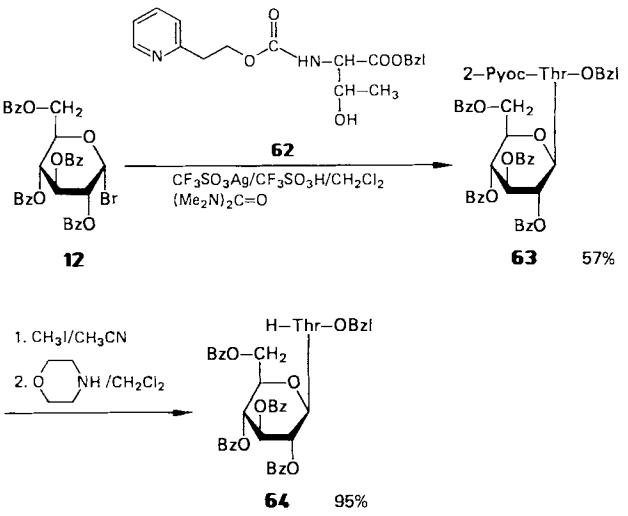

Because of the promotion of ortho ester formation by the Pyoc group, it is advantageous, to employ the Fmoc group in the glycosylation step; the advantages of stability and solubility due to the Pyoc group can then be exploited in the chain extension reactions. This combination method is shown in Scheme 2 for the synthesis of the completely protected, *N*-terminal diglycotripeptide **72** of the glycophorin with M specificity and of the disaccharidic T-antigen structure.[113] The selective removal of the Fmoc group with morpholine[98] also succeeded with the disaccharidic glycosylserine (**65**) and -threonine (**66**) derivatives without destroying the numerous ester groups and the sensitive *O*-glycoside bonds. The free amino compounds **67** and **68** tend to undergo base-catalyzed self-destruction. Therefore, they are immediately condensed with the 4-Pyoc-protected carboxyl components **69** or **71** to give **70** (51% based on **65**) or **72**, respectively. In the cleavage of the benzyl ester **70**, another advantage of the Pyoc group is evident: it is stable toward hydrogenolysis.

The stable 4-Pyoc group, after conversion to the pyridinium form, can then be removed, completely selectively under mild conditions, from the complex and sensitive glycopeptide **72**. In the base-sensitive product **73**, the free amino group is acetylated to give **74** (76% based on **72**).[113]

These and other glycopeptide syntheses[105, 112, 113] show the efficiency of the Pyoc method. The single restriction is that the alkylation of the stable protective group to give the labile form is not possible in the presence of amino acids that can undergo alkylation, e.g., cysteine.

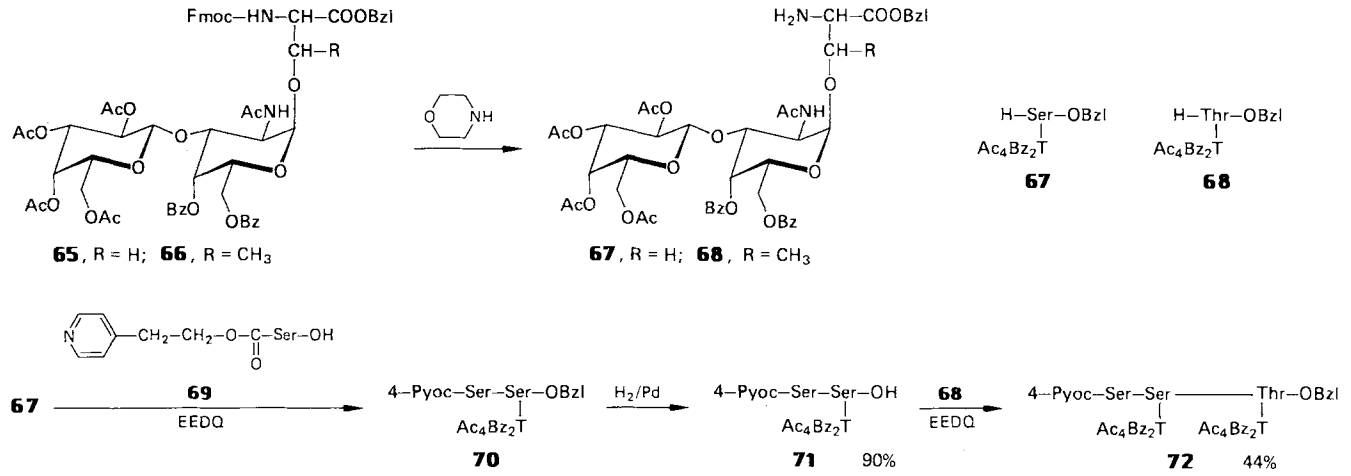

Scheme 2.

The ideal protective group for glycopeptide synthesis should have a stability similar to that of the Pyoc group but be removable under the mildest conditions, as is the pyridinium form of the Pyoc group, and require no preceding transformations. The allyl protective groups fulfill these requirements.[44,61,114,115]

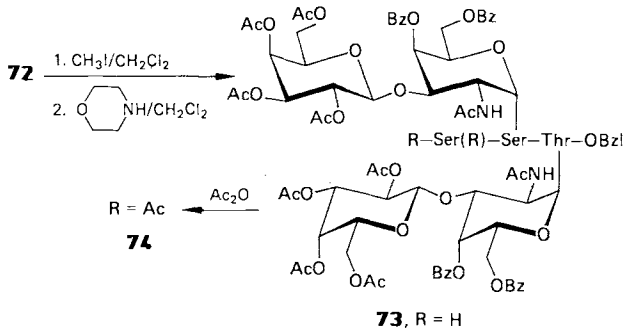

5.7. Allyl Esters and Allyloxycarbonyl (Aloc) Protective Groups

Allyl esters of amino acids are easy to prepare and are stable under a wide variety of glycosylation conditions.[44,61–63,115] In the less sensitive *N*-glycopeptides, such as **75**, the Boc group can be removed selectively in the presence of the allyl ester, either with hydrogen chloride in dichloromethane or with trifluoroacetic acid.[44] The quantitatively formed amino-deblocked product **76** can be *N*-terminally extended, e.g., to glycotripeptide **77**. In order to selectively cleave the allyl group from **77**,[115] the allyl ester is isomerized by means of a rhodium(I) catalyst[116] to a propenyl ester, which, under the reaction conditions, undergoes immediate hydrolysis. Under these neutral conditions, all the other bonds are retained. The practically quantitatively obtained product **78** can then be *C*-terminally extended, e.g., to the glycopentapeptide **79**, a partial structure of human orosomucoid (acidic α_1 glycoprotein).[117] The small allyl group has the advantage that it does not interfere in condensation reactions involving such large molecules, either sterically or by reducing their solubility. The yields are therefore always high.

For the selective allyl ester cleavage in the more sensitive *O*-glycosylserine or -threonine derivatives, which tend to undergo elimination reactions, we have found[61] an

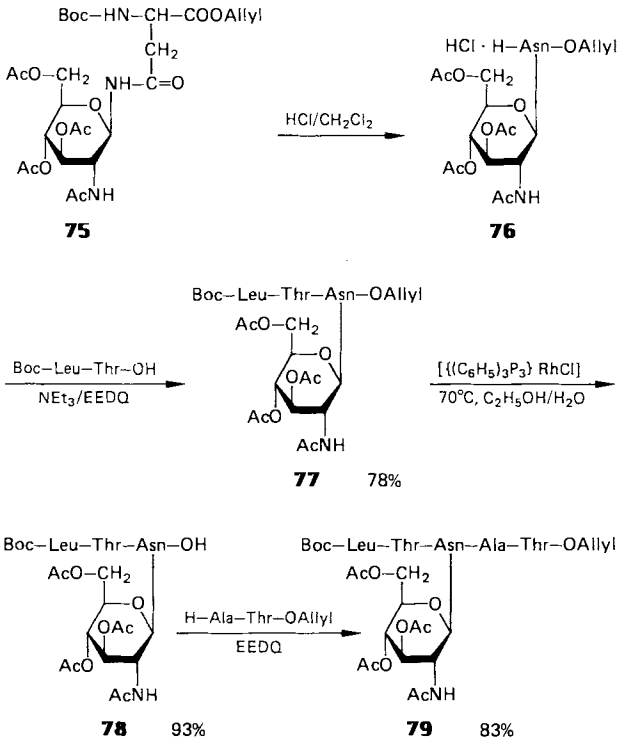

even milder method; namely, the allyl transfer to morpholine[118] as the accepting nucleophile. For example, the xylotripeptide **80** can be deblocked quantitatively and chemospecifically at the carboxy function in 30 min under almost neutral conditions in tetrahydrofuran (THF) to give **81**.[61]

In β-lactam antibiotic synthesis, unknown to us at that time, an allyl ester cleavage in the sense of a palladium(0)-catalyzed transesterification had already been used.[119] Even earlier the cleavage of allyl esters with palladium catalysts and ammonium formate had been described as a variant of hydrogenolysis.[120] However, it requires a tem-

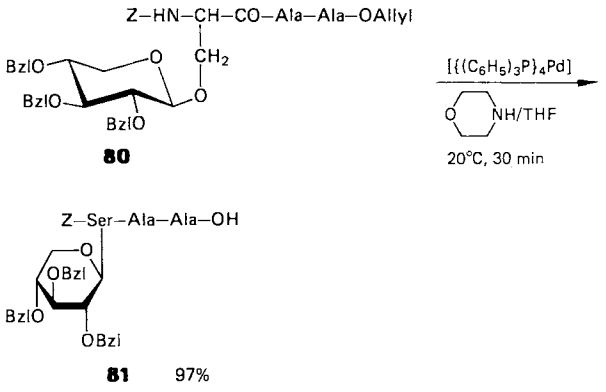

perature of 100 °C and is not usable in glycopeptide synthesis. Morpholine has the advantages that it is easily removed and does not attack the sensitive glycoside bond. The method is also successful with α-galactosaminylthreonine allyl ester **82**. The deblocked product **83** is coupled to the *N*-terminal N^4-glucosaminylasparagine allyl ester **76** to give diglycopeptide **84**, which contains both an α-*O*- and a β-*N*-glycosyl amino acid and embodies a particularly complex partial structure of human glycophorin.[96]

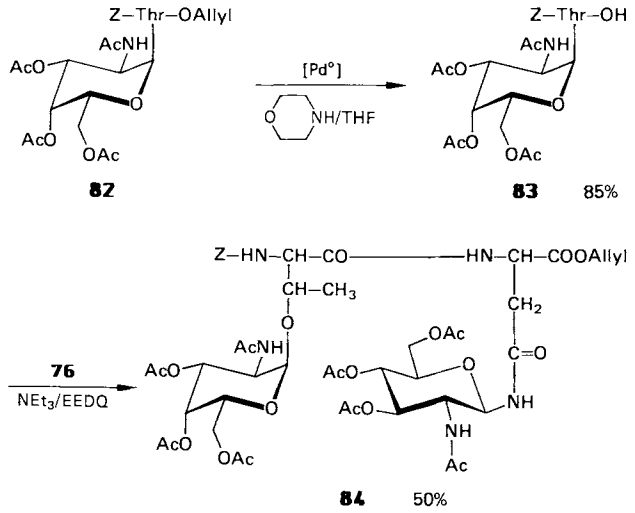

This extremely gentle cleavage of allyl esters under homogeneous conditions works equally well, both selectively and effectively, with the *N*-glycopeptides, such as chitobiosylasparagine **85**. The carboxyl-deblocked product **86**, obtained almost quantitatively, was converted by two chain extensions with dipeptide allyl esters into the chitobiosyl pentapeptide **87**, a partial structure of a transmembrane neuraminidase of an influenza virus.[44]

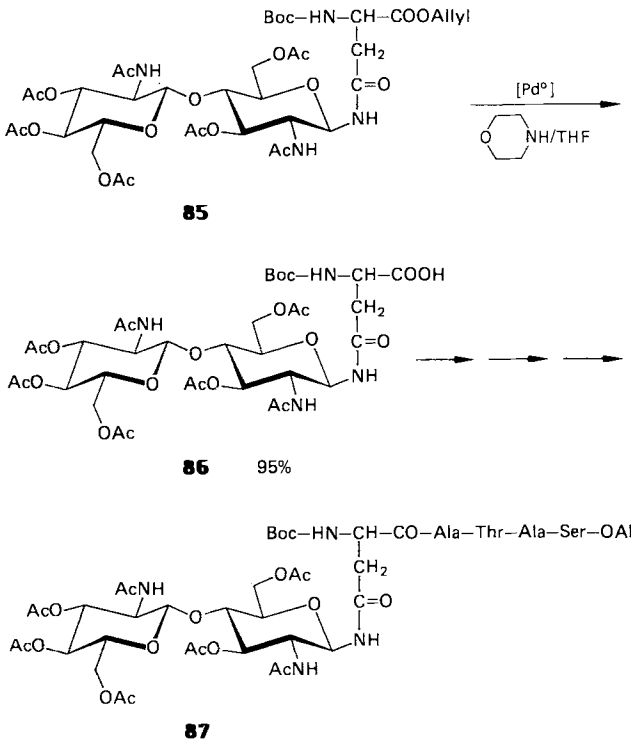

Palladium(0)-catalyzed allyl transfer to nucleophiles such as morpholine or dimedone (5,5-dimethyl-1,3-cyclohexanedione) can also be used to remove smoothly the allyloxycarbonyl (Aloc) group from peptides and glycopeptides.[114] This protective group, which had already been described,[121] was held to be unuseable, since even under

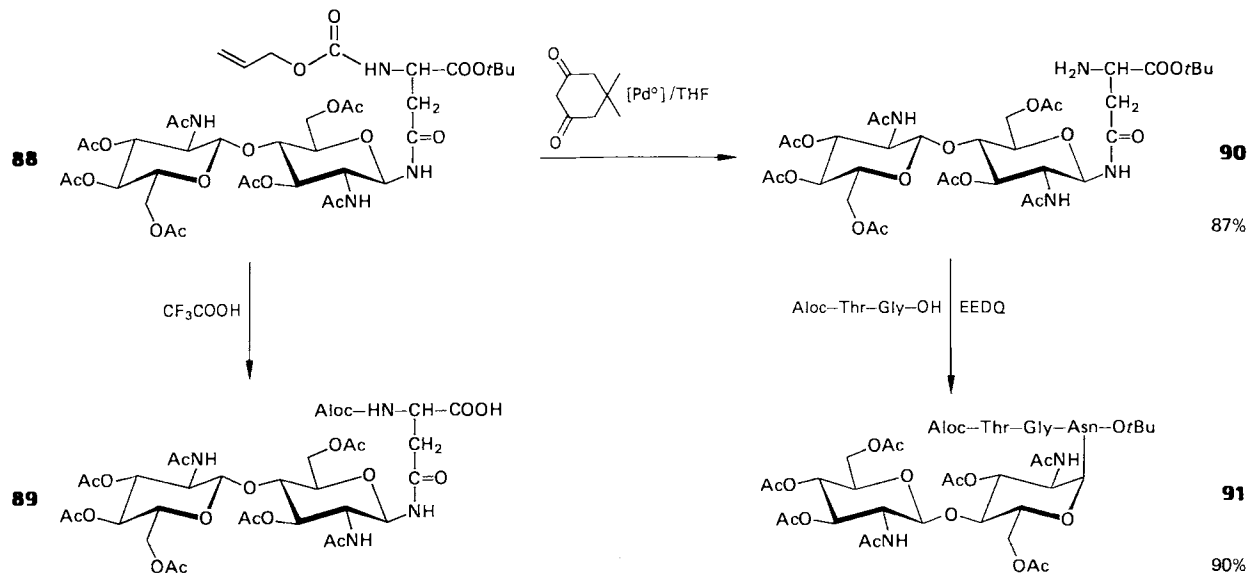

drastic conditions it was only incompletely removed.[122] However, an advantage of the Aloc group is its stability toward trifluoroacetic acid,[114] e.g., in the practically quantitative *tert*-butyl-ester cleavage of the chitobiosylasparagine derivative **88** to **89**.[47] The palladium(0)-catalyzed removal of the Aloc group is not affected by amino acids with nucleophilic groups (e.g., methionine).[114] Since an amino function is thereby deblocked, the CH acid dimedone is better suited than morpholine as the trapping reagent. This method has been employed to obtain compound **90** selectively and practically quantitatively from **88**. Compound **90** can be extended at the *N*-terminus, e.g., to chitobiosyl tripeptide **91**,[47] a partial sequence of the linkage region of a neuraminidase of another influenza virus.[123]

This synthesis is a further example of the use of these methods to construct immunologically interesting glycopeptides. The prerequisite for the immunological investigation of synthetic glycopeptides is, however, that they can be freed of the protective groups on the carbohydrate portion and that they can be bound to suitable carrier molecules.

6. The Removal of Protective Groups in the Carbohydrate Portion and the Attachment of Synthetic Glycopeptides to Proteins

The removal of the protective groups from the carbohydrate part of the molecule is problematic for two reasons: (1) There is the danger of β-elimination from glycosylserine and -threonine derivatives of type **2** and **3**. (2) The amino-acid residues can undergo racemization. Both processes occur under basic conditions when, for example, the ester protective group is cleaved with ammonia or triethylamine in methanol.[54,81] Such side reactions, especially racemization, were recently observed by *Paulsen* et al.[74] during the deblocking of a glycopeptide of the T-antigen type with various bases, e.g., amines. They described the removal of acyl protective groups in the saccharide part, without side reactions, by application of potassium cyanide in methanol/ethanol. With potassium cyanide in methanol, however, 20% racemization occurred in the threonine residue.

With base-sensitive glycosylserine derivatives, such as **92**, we were able to show that acetyl and benzoyl protective groups can be removed very safely and with no racemization by the use of hydrazine in methanol.[98] Excess hydrazine is removed by reaction with acetone.

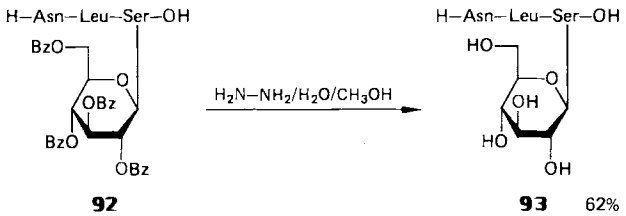

92 **93** 62%

Even *N*-glycopeptides, e.g., **95**, a partial sequence of fibroblast interferon, can be efficiently deblocked by use of the method.[124] In contrast, the hydrogenolytic cleavage of the γ-benzyl-ester group of glutamic acid in **94** did not work, so that the ester had to be removed simultaneously with the Boc group by means of hydrofluoric acid.[124] This demonstrates the limits of heterogeneous hydrogenation of the benzylic protective groups in complex molecules. On small units, the method is particularly suited for glycopeptide synthesis, because it proceeds under neutral conditions. The hydrogenation of benzyl ethers in the carbohydrate part of the glycopeptide was successfully used for deblocking by *Pavia* et al.[78,100]

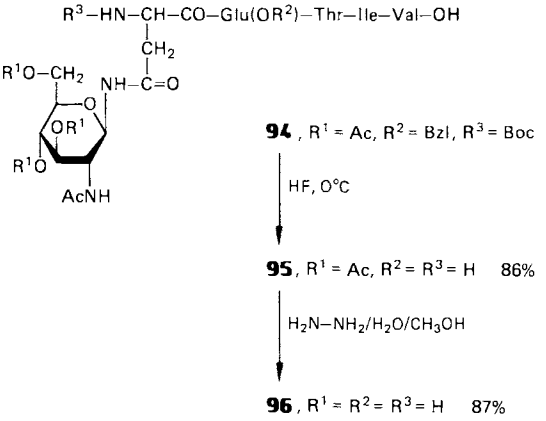

The cleavage of the numerous ester groups in the complex diglycopeptide **74** was achieved, after hydrogenolysis of the *C*-terminal benzyl ester to **97**, gently and smoothly with hydrazine in methanol.[113] The reaction yields the diglycotripeptide **98**, which, according to *Springer* et al.,[8] embodies the tumor-associated T-antigen structure in a pure state according to the high-field ^{13}C-NMR spectrum. With these selective techniques of synthesis as a starting point, we have been able to attach immunologically rele-

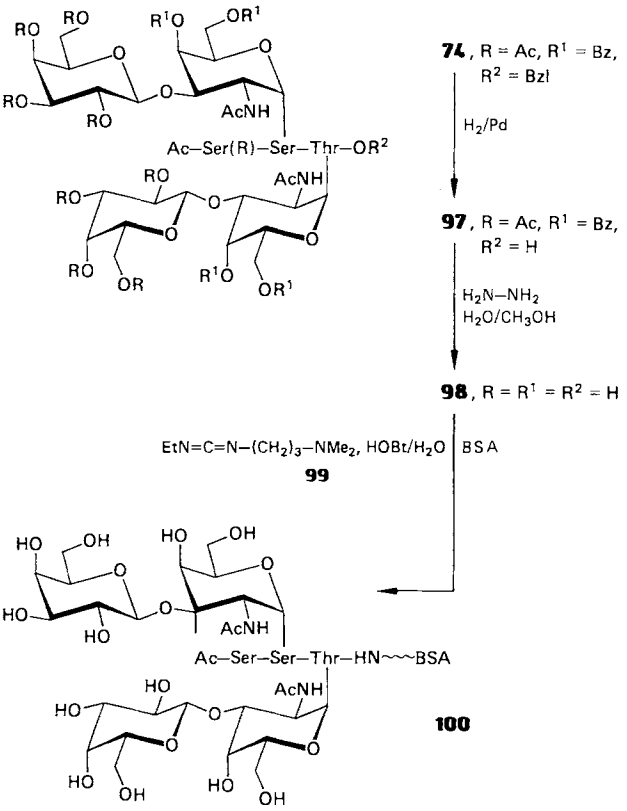

vant and clearly defined glycopeptides, such as **98**, to bovine serum albumin (BSA).[113] The free carboxy group of the synthetic glycopeptide **98** was bound, in water in the presence of 1-hydroxybenzotriazole (HOBt)[125] and with the aid of the water-soluble carbodiimide **99**,[126] to the carrier protein without the use of an artificial spacer, that is to say, in a more or less natural manner. The bonding sites in conjugate **100** are probably largely the ε-amino groups of the lysine residues. According to photometric carbohydrate analysis, 38 of the 60 free amino functions of the protein were connected with the synthetic glycopeptide antigen structure.[113]

7. Outlook

Advances in the methods of preparative chemistry in the last decade have made possible the synthesis of complex, structurally clearly defined glycopeptides corresponding to typical segments of glycoproteins, which themselves, in turn, are the defining factors in biological recognition and selectivity. These new possibilities have emerged, on the one hand, through recent developments in the field of oligosaccharide synthesis[36,37] and, on the other, by means of the solutions presented in this review to the problems that are raised by the targeted synthesis of peptides containing sensitive glycoconjugate structures. The synthetic glycopeptides do not have the disadvantage of microheterogeneity which is characteristic of the natural glycoconjugates. They are obtainable in preparative quantities and can be linked to complex biological carrier molecules. In this form they can be used in interdisciplinary research and applications; for example, for the induction of antibodies, for the simulation of recognition phenomena, and for the determination of the structures of sensitive glycoproteins. In addition, they open up perspectives in the development of tissue-specific drugs and proteolysis-stable peptide factors.

In view of the many side-chain functions on peptides, the further development of glycopeptide syntheses will clearly require additional new methods which extend the protective group techniques presented here for these sensitive molecules.

I would like to give my heartfelt thanks to my co-workers, who have pushed the development of glycopeptide synthesis ahead with commitment, courage, and a treasury of ideas. They are: Regina Barthels-Herweg, Stefan Birnbach, Michael Buchholz, Siglinde Friedrich-Bochnitschek, Wolfgang Günther, Albrecht Harreus, Hermann Kauth, Uwe Klinkhammer, Michael Kneip, Klaus-Jürgen Pees, Waldemar Pfrengle, Wilfried Sager, Marita Schilling, Petra Schultheiss-Reimann, Carlo Unverzagt, and Herbert Waldmann. I would like to thank the Deutsche Forschungsgemeinschaft and the Fonds der Chemischen Industrie for their support, without which this work would not have been possible.

Received: April 28, 1986;
revised: September 15, 1986 [A 614 IE]
German version: *Angew. Chem. 99* (1987) 297
Translated by Dr. *Douglas Maass*, Kronberg/Taunus

[1] A modern review of cell biology: B. Alberts, D. Bray, J. Lewis, M. Raff, K. Roberts, J. D. Watson: *The Molecular Biology of the Cell*, Garland, New York 1983; *Die Molekularbiologie der Zelle*, VCH Verlagsgesellschaft, Weinheim 1986.
[2] A review of glycoproteins: J. Montreuil in A. Neuberger, L. L. M. van Deenen (Eds.): *Comprehensive Biochemistry, Vol. 19B II*, Elsevier, Amsterdam 1982, p. 1.
[3] Review: G. Ashwell, A. G. Morell, *Adv. Enzymol. Relat. Areas Mol. Biol. 41* (1974) 99.
[4] T. Kawasaki, G. Ashwell, *J. Biol. Chem. 252* (1977) 6536.
[5] a) G. N. Sando, E. F. Neufeld, *Cell 12* (1977) 619; b) A. Kaplan, D. T. Achord, W. S. Sly, *Proc. Natl. Acad. Sci. USA 74* (1977) 2026; c) K. von Figura, A. Hasilik, *Trends Biochem. Sci. Pers. Ed. 9* (1984) 29.
[6] Reviews: a) R. T. Schwarz, R. Datema, *Adv. Carbohydr. Chem. Biochem. 40* (1982) 287; b) K. B. Olden, B. A. Bernard, M. J. Humphries, T. Yeo, K. Yeo, S. L. White, S. A. Newton, H. C. Bauer, J. B. Parent, *Trends Biochem. Sci. Pers. Ed. 10* (1985) 78.
[7] A recent review: M. Fukuda, *Biochim. Biophys. Acta 780* (1985) 119.
[8] See, e.g., G. F. Springer, P. R. Desai, M. S. Murthy, E. F. Scanlon, *ACS Symp. Ser. 80* (1978) 311.
[9] R. R. Race, R. Sanger: *Blood Groups in Man*, 6th ed., Blackwell Scientific, Oxford 1975.
[10] See, e.g., J. Ofek, E. H. Beachy, N. Sharon, *Trends Biochem. Sci. Pers. Ed. 3* (1978) 159.
[11] G. Gregoriadis, *Nature (London) 310* (1984) 186.
[12] Review: T. Feizi, *Nature (London) 314* (1985) 53.
[13] Review: K. Olden, J. B. Parent, S. L. White, *Biochim. Biophys. Acta 650* (1982) 209.
[14] a) A comprehensive discussion: E. Wünsch in *Houben-Weyl-Müller: Methoden der organischen Chemie, 4. Aufl., Band XV/1 und XV/2*, Thieme, Stuttgart 1974; b) A recent short review: H. D. Jakubke, H. Jeschkeit: *Aminosäuren, Peptide, Proteine*, Verlag Chemie, Weinheim 1982.
[15] P. G. Johansen, R. D. Marshall, A. Neuberger, *Biochem. J. 78* (1961) 518.
[16] Short review: a) A. J. Parodi, L. F. Leloir, *Trends Biochem. Sci. Pers. Ed. 1* (1976) 58; b) N. Sharon, *ibid. 9* (1984) 198.
[17] a) R. D. Marshall, *Biochem. Soc. Symp. 40* (1974) 17; b) E. Bause, G. Legler, *Biochem. J. 195* (1981) 639.
[18] F. Wieland, R. Heitzer, W. Schäfer, *Proc. Natl. Acad. Sci. USA 80* (1983) 5470.
[19] G. Paul, F. Lottspeich, F. Wieland, *J. Biol. Chem. 261* (1986) 1020.
[20] S. Shibata, H. Nakanishi, *Carbohydr. Res. 86* (1980) 316.
[21] T. Takeda, M. Sawaki, Y. Ogihara, S. Shibata, *Carbohydr. Res. 139* (1985) 133.
[22] H. Muir, *Biochem. J. 69* (1958) 195; review: L. Roden in [34], p. 267.
[23] T. Feizi, E. A. Kabat, G. Vicari, B. Anderson, W. L. Marsh, *J. Immunol. 106* (1971) 1578; K. O. Lloyd, E. A. Kabat, *Proc. Natl. Acad. Sci. USA 61* (1968) 13470.
[24] W. Dahr, K. Beyreuther, H. Steinbach, W. Gielen, J. Krüger, *Hoppe-Seyler's Z. Physiol. Chem. 361* (1980) 895, and references cited therein.
[25] D. H. van den Eijnden, N. A. Evans, J. F. Codington, V. Reinhold, C. Silber, R. W. Jeanloz, *J. Biol. Chem. 254* (1979) 12153.
[26] W. T. Butler, L. W. Cunningham, *J. Biol. Chem. 241* (1966) 3882; R. G. Spiro, *ibid. 242* (1967) 4813.
[27] M. A. Calcott, H.-J. Müller-Eberhard, *Biochemistry 11* (1972) 3443.
[28] E. Fischer, *Ber. Dtsch. Chem. Ges. 39* (1906) 530; *26* (1893) 2400.
[29] N. Sharon, H. Lis, *Chem. Eng. News 59* (1981), No 13, p. 21.
[30] Review: H. Garg, R. W. Jeanloz, *Adv. Carbohydr. Chem. Biochem. 43* (1985) 135.
[31] Review: R. Rocchi, V. Giormani in B. Weinstein (Ed.): *Chemistry and Biochemistry of Amino Acids, Peptides and Proteins, Vol. 7*, Dekker, New York 1983, p. 35.
[32] Short review: H. Kunz, *Nachr. Chem. Tech. Lab. 32* (1984) 11.
[33] A. Gottschalk: *Glycoproteins: Their Composition, Structure and Function*, Elsevier, Amsterdam 1972; R. C. Hughes: *Membrane Glycoproteins*, Butterworth, London 1976.
[34] W. J. Lennarz (Ed.): *The Biochemistry of Glycoproteins and Proteoglycans*, Plenum, New York 1980.
[35] H. Schachter, *Clin. Biochem. (Ottawa) 17* (1984) 3.
[36] a) H. Paulsen, *Angew. Chem. 94* (1982) 184; *Angew. Chem. Int. Ed. Engl. 21* (1982) 155; b) *Chem. Soc. Rev. 13* (1984) 15.
[37] R. R. Schmidt, *Angew. Chem. 98* (1986) 213; *Angew. Chem. Int. Ed. Engl. 25* (1986) 212.
[38] See e.g., a) H. G. Garg, R. W. Jeanloz, *J. Org. Chem. 41* (1976) 2480; b) M. A. E. Shaban, R. W. Jeanloz, *Bull. Chem. Soc. Jpn. 54* (1981) 3570, and references cited therein.
[39] a) G. S. Marks, R. D. Marshall, A. Neuberger, *Biochem. J. 87* (1963) 274; b) C. H. Bolton, R. W. Jeanloz, *J. Org. Chem. 28* (1963) 3228.
[40] D. Horton, M. L. Wolfrom, *J. Org. Chem. 27* (1962) 1794.
[41] F. Micheel, H. Wulff, *Chem. Ber. 89* (1956) 1521.
[42] A. Yamamoto, C. Miyashita, H. Tsukamoto, *Chem. Pharm. Bull. 13* (1965) 1041.

[43] M. Spinola, R. W. Jeanloz, *J. Biol. Chem. 242* (1970) 4158.
[44] H. Kunz, H. Waldmann, *Angew. Chem. 97* (1985) 885; *Angew. Chem. Int. Ed. Engl. 24* (1985) 883.
[45] C. H. Bolton, L. Hough, M. Y. Khan, *Biochem. J. 101* (1966) 184.
[46] H. Kunz, W. Pfrengle, M. Kneip, unpublished results; W. Pfrengle, *Diplomarbeit*, Universität Mainz 1985.
[47] H. Kunz, C. Unverzagt, unpublished results.
[48] H. G. Garg, R. W. Jeanloz, *Carbohydr. Res. 23* (1972) 437; *43* (1975) 371.
[49] B. Belleau, G. Malek, *J. Am. Chem. Soc. 90* (1968) 1651.
[50] H. Kunz, H. Waldmann, *Angew. Chem. 95* (1983) 47; *Angew. Chem. Int. Ed. Engl. 22* (1983) 62.
[51] H. Kunz, H. Waldmann, unpublished results.
[52] F. Micheel, H. Köchling, *Chem. Ber. 93* (1960) 2372.
[53] Siehe z. B. N. K. Kochetkov, V. A. Derevitskaya, A. Y. Khorlin, M. G. Vafina, A. F. Bochkov, *Izv. Akad. Nauk SSSR Ser. Khim. 1965*, 1698.
[54] B. Lindberg, B. G. Silvander, *Acta Chem. Scand. 19* (1965) 530.
[55] P. G. Garegg, B. Lindberg, T. Norberg, *Acta Chem. Scand. Ser. B 33* (1979) 449.
[56] H.-J. Koeners, C. Schattenkerk, J. Verhoven, J. H. van Boom, *Tetrahedron 37* (1981) 1763.
[57] H. Kunz, M. Buchholz, *Chem. Ber. 112* (1979) 2145.
[58] S. Hanessian, J. Banoub, *Carbohydr. Res. 53* (1977) C 13.
[59] H. Kunz, M. Buchholz, *Angew. Chem. 93* (1981) 917; *Angew. Chem. Int. Ed. Engl. 20* (1981) 894.
[60] R. R. Schmidt, J. Michel, *Angew. Chem. 92* (1980) 763; *Angew. Chem. Int. Ed. Engl. 19* (1980) 731.
[61] H. Kunz, H. Waldmann, *Angew. Chem. 96* (1984) 49; *Angew. Chem. Int. Ed. Engl. 23* (1984) 71.
[62] H. Kunz, W. Sager, *Helv. Chim. Acta 68* (1985) 283.
[63] H. Kunz, W. Pfrengle, *J. Chem. Soc. Chem. Commun. 1986*, 713.
[64] H. Kunz, A. Harreus, *Liebigs Ann. Chem. 1982*, 41.
[65] T. Ogawa, K. Beppu, S. Nakabayashi, *Carbohydr. Res. 93* (1981) C6.
[66] H. Kunz, U. Klinkhammer, unpublished results.
[67] H. G. Garg, R. W. Jeanloz, *Carbohydr. Res. 52* (1976) 246.
[68] H. Paulsen, C. Kolar, W. Stenzel, *Chem. Ber. 111* (1978) 2370.
[69] a) B. Ferrari, A. A. Pavia, *Carbohydr. Res. 79* (1980) C1; b) *Bioorg. Chem. 11* (1982) 85.
[70] R. U. Lemieux, M. M. Ratcliff, *Can. J. Chem. 57* (1979) 1224.
[71] H. Paulsen, J.-P. Hölck, *Carbohydr. Res. 109* (1982) 89.
[72] a) H. Paulsen, M. Paal, M. Schultz, *Tetrahedron Lett. 24* (1983) 1759; b) H. Paulsen, M. Paal, *Carbohydr. Res. 135* (1984) 53; c) K. Heyns, D. Feldmann, D. Hadamczyk, J. Schwentner, J. Thiem, *Chem. Ber. 114* (1981) 232.
[73] T. Adachi, Y. Yamada, J. Inone, *Synthesis 1977*, 45.
[74] H. Paulsen, M. Schultz, J.-D. Klamann, B. Waller, M. Paal, *Liebigs Ann. Chem. 1985*, 2028.
[75] S. Friedrich-Bochnitschek, *Dissertation*, Universität Mainz 1986; S. Birnbach, *Dissertation*, Universität Mainz 1985; H. Kunz, *Proc. München Shanghai Symp. Pept. Protein Chem. 1986*, 45.
[76] G. Grundler, R. R. Schmidt, *Liebigs Ann. Chem. 1984*, 1826.
[77] J. M. Lacombe, A. A. Pavia, J. M. Rocheville, *Can. J. Chem. 59* (1981) 573.
[78] A. A. Pavia, B. Ferrari, *Int. J. Pept. Protein Res. 22* (1983) 549, 539.
[79] M. Buchholz, *Dissertation*, Universität Mainz 1982.
[80] S. Lavielle, N. C. Ling, R. Saltman, R. C. Guillemin, *Carbohydr. Res. 89* (1981) 229.
[81] V. Verez Bencomo, P. Sinaÿ, *Carbohydr. Res. 116* (1983) C9.
[82] H. Waldmann, *Dissertation*, Universität Mainz 1985.
[83] R. Kuhn, I. Löw, *Ber. Dtsch. Chem. Ges. B 74* (1941) 219.
[84] Review: R. D. Marshall, A. Neuberger, *Adv. Carbohydr. Chem. Biochem. 25* (1970) 407.
[85] a) J. R. Vercellotti, R. Fernandez, C. J. Chang, *Carbohydr. Res. 5* (1967) 97; b) K. Wakabayashi, W. Pigman, *ibid. 35* (1974) 3.
[86] H. Kunz, K.-J. Pees, unpublished results.
[87] See pp. 206–208 and pp. 225–227 in the English and German versions, respectively, of [1].
[88] H. Kunz, *Chem. Ber. 109* (1976) 2670.
[89] a) H. Kunz, H. Kauth, *Angew. Chem. 93* (1981) 918; *Angew. Chem. Int. Ed. Engl. 20* (1981) 895; b) *Liebigs Ann. Chem. 1983*, 337.
[90] a) H.-H. Bechtolsheimer, H. Kunz, *Angew. Chem. 94* (1982) 637; *Angew. Chem. Int. Ed. Engl. 21* (1982) 630; b) *Liebigs Ann. Chem. 1982*, 2068.
[91] H. Kauth, H. Kunz, *Liebigs Ann. Chem. 1983*, 360.
[92] H. Eckert, J. Lagerlund, I. Ugi, *Tetrahedron 33* (1977) 2243.
[93] H. Kunz, *Justus Liebigs Ann. Chem. 1976*, 1674.
[94] M. Buchholz, H. Kunz, *Liebigs Ann. Chem. 1983*, 1859.
[95] L. Horner, H. Neumann, *Chem. Ber. 98* (1965) 3462.
[96] H. Kunz, S. Friedrich-Bochnitschek, unpublished results; S. Friedrich-Bochnitschek, *Diplomarbeit*, Universität Mainz 1982.
[97] L. A. Carpino, G. Y. Han, *J. Am. Chem. Soc. 92* (1970) 5748.
[98] P. Schultheiss-Reimann, H. Kunz, *Angew. Chem. 95* (1983) 64; *Angew. Chem. Int. Ed. Engl. 22* (1983) 62; *Angew. Chem. Suppl. 1983*, 39.
[99] J. M. Lacombe, A. A. Pavia, *J. Org. Chem. 48* (1983) 2557.
[100] B. Ferrari, A. A. Pavia, *Tetrahedron 41* (1985) 1939, and references cited therein.
[101] J. P. Carton in C. Salomon (Ed.): *Blood Groups and Other Red Cell Surface Markers in Health and Disease*, Masson, New York 1982, p. 39ff.
[102] J. Martinez, J. C. Tolle, M. Bodanszky, *J. Org. Chem. 44* (1979) 3596.
[103] H. Kunz, P. Schultheiss-Reimann, unpublished results; P. Schultheiß-Reimann, *Dissertation*, Universität Mainz 1984.
[104] V. Verez Bencomo, P. Sinaÿ, *Glycoconjugate J. 1* (1984) 1.
[105] S. Birnbach, *Dissertation*, Universität Mainz 1985.
[106] K. Inouye, Y. Sumitomo, M. Shin, *Bull. Chem. Soc. Jpn. 49* (1976) 3620.
[107] E. Wünsch, E. Jaeger, L. Kisfaludy, M. Löw, *Angew. Chem. 89* (1977) 330; *Angew. Chem. Int. Ed. Engl. 16* (1977) 317; B. F. Lundt, N. L. Johansen, A. Volund, G. Markussen, *Int. J. Pept. Protein Res. 12* (1978) 258.
[108] S. Lavielle, N. C. Ling, R. C. Guillemin, *Carbohydr. Res. 89* (1981) 221.
[109] P. Mamalis, H. N. Rydon, *J. Chem. Soc. 1955*, 1049; R. Barthels, H. Kunz, *Angew. Chem. 94* (1982) 302; *Angew. Chem. Int. Ed. Engl. 21* (1982) 292; *Angew. Chem. Suppl. 1982*, 702; *Chem. Ber. 115* (1982) 833, and references cited therein.
[110] H. Kunz, R. Barthels, *Angew. Chem. 95* (1983) 799; *Angew. Chem. Int. Ed. Engl. 22* (1983) 783.
[111] H. Kunz, S. Birnbach, *Tetrahedron Lett. 25* (1984) 3567.
[112] H. Kunz, A. Harreus, unpublished results; A. Harreus, *Dissertation*, Universität Mainz 1983.
[113] H. Kunz, S. Birnbach, *Angew. Chem. 98* (1986) 354; *Angew. Chem. Int. Ed. Engl. 25* (1986) 360.
[114] H. Kunz, C. Unverzagt, *Angew. Chem. 96* (1984) 426; *Angew. Chem. Int. Ed. Engl. 23* (1984) 436.
[115] H. Waldmann, H. Kunz, *Liebigs Ann. Chem. 1983*, 1712.
[116] E. J. Corey, J. W. Suggs, *J. Org. Chem. 38* (1973) 3234.
[117] L. Mester in K. Laki (Ed.): *Fibrinogen*, Dekker, New York 1980, p. 165.
[118] For *C*-allylation, see review: B. M. Trost, *Acc. Chem. Res. 13* (1980) 1.
[119] P. D. Jeffrey, S. W. McCombie, *J. Org. Chem. 47* (1982) 587.
[120] J. Tsuji, T. Yamakawa, *Tetrahedron Lett. 1979*, 613.
[121] C. M. Stevens, R. Watanabe, *J. Am. Chem. Soc. 72* (1950) 725.
[122] See [14a], Vol. 1, p. 96.
[123] S. Fields, G. Winter, *Nature (London) 290* (1981) 213.
[124] H. Kunz, H. Waldmann, *Helv. Chim. Acta 68* (1985) 618.
[125] W. König, R. Geiger, *Chem. Ber. 106* (1973) 3626.
[126] J. C. Sheehan, P. A. Cruickshank, G. L. Boshart, *J. Org. Chem. 26* (1961) 2525.

Emission of Microparticles from Automotive Sources—X-ray Photoelectron Spectroscopy in Environmental Analysis

By R. Schlögl*, G. Indlekofer, and P. Oelhafen

In the last fifteen years the necessity for efficient environmental protection has become generally accepted. However, before practical measures can be taken, a comprehensive assessment of the present environmental situation should be made, taking into consideration the risks involved in as well as the positive effects of any planned environmental changes—whether natural or man made. This clearly calls for close cooperation between the various scientific disciplines. For example, the treatment of exhaust fumes from motor vehicles has been of primary importance in measures taken to restrict the recent damage caused to woodland areas. The introduction of 3-Way-Catalyst technology has been regarded as a viable countermeasure. The following report is intended to describe a method for examining some side effects of catalyst usage. Accordingly, the chemical composition of microparticles emitted from combustion motors through the use of catalysts will be examined and some possible changes in the environment caused by such particles will be briefly considered. As in the area of research into catalysts for industrial synthesis a knowledge of the surface structure of such particles, i.e. the boundary layer between emission product and environment, is necessary in the investigation into their effects. Consequently, a surface sensitive technique from solid state physics, X-ray photoelectron spectroscopy (XPS or ESCA) has found novel use in the area of environmental analysis. In the following report emphasis will be placed on the description of measurement techniques and the interpretation of the results obtained. After a critical consideration of the experimental methods, examples from two different series of measurements on diesel and Otto motors equipped with soot filters or 3-way-catalysts respectively, will be given. Hopefully, this report will also stimulate establishment of the use of EPS in environmental research techniques.

1. Introduction

The catalytic cleaning of exhaust fumes from motors of all types is at present of considerable interest in the context of attempts being made to improve our environment.

The effects of such catalysts on the clearly harmful components of exhaust fumes has been thoroughly examined.[1, 2] The side effects of catalyst usage, such as the emission of metal microparticles—smaller than about 50 nm—and the alterations to emitted organic molecules are, however, less well known. This is due, on the one hand, to the fact that research conducted in this area about ten years ago in the USA concluded that such side effects were insignificant[2] and, on the other, to the fact that research methods have mainly concentrated on the analysis of gaseous emissions, while the investigation of sensitive techniques for the analysis of solid microparticles has been neglected.[3] This report describes the first results obtained in this area by means of the XPS technique—a technique that has long been known in analytical and surface physics,[4] but has, until now, been used only to a limited extent in environmental analysis in the USA.[5] A section outlining the possibilities and limitations of XPS in environmental analysis is followed by a section dealing with the experimental conditions. The experimental results then form the subject of the main section, where an attempt has been made to give a representative selection of available spectral data. This data was collected in investigations on the exhaust gases from a stationary diesel motor fitted with various soot filters and on the emissions from a motor vehicle with a 3-way-catalyst, also examined in a field test. The results are presented together in the order of the elements detected, with the main emphasis on gaining useful qualitative information. On the one hand because the quantification of the results is, in principle, methodologically difficult (this is alluded to in several places in the text) and, on the other because other techniques in surface physics (Auger electron spectroscopy or secondary ion mass spectrometry etc.) essentially afford more readily quantifiable results. Since the classical methods of environmental analysis lay emphasis in any case on the quantitative aspects, a further time-consuming and inaccurate *quantitative* method would seem superfluous. Nevertheless, a judicious combination of quantitative results obtained by conventional methods with the quantitative information about the chemical bonding obtained by XPS would greatly help in characterizing and assessing the effect of solid emissions.

The object of this study then is to illustrate the possibilities and limitations of XPS in environmental research in this context and a possible effect of the release of metal-containing microparticles into the environment will also be briefly discussed.

[*] Dr. R. Schlögl, [+] G. Indlekofer, Priv.-Doz. Dr. P. Oelhafen
Institut für Physik der Universität
Klingelbergstrasse 82, CH-4056 Basel (Switzerland)

[+] Present address:
Fritz Haber Institut der Max Planck Gesellschaft,
Faradayweg 4-6, D-1000 Berlin 33

 © VCH Verlagsgesellschaft mbH, D-6940 Weinheim, 1987 0570-0833/87/0404-0309 $ 02.50/0

2. The Method

2.1. The Photoemission Experiment

By photoemission is meant the release of electrons by interaction of photons with atoms. Depending upon the energy, one can distinguish between low energy photoemission from valence states (ultraviolet photoelectron spectroscopy, UPS, typical photon energy 10–50 eV) and from energetically low lying core orbitals (X-ray photoelectron spectroscopy, XPS, typical energy values 1200–1500 eV). The kinetic energy of a released electron can be related, to a first approximation, to the corresponding binding energy by setting the sum of kinetic energy and binding energy equal to the (monochromatic) excitation energy. This experimental electron binding energy, which, for core levels differs by about 5% from the quantum mechanically defined dissociation energy, contains information about the nuclear charge of the atom (elemental analysis), while superimposed fine structure yields information concerning the chemical environment of an atom (chemical shift; electron spectroscopy in chemical analysis, ESCA). UPS data can give information concerning the structure of the molecular orbitals or electron bands of a sample.

From a photoelectron spectrum, one can read off the number of electrons (Y-axis) of a particular binding energy (X-axis). The simplified picture of an incoming photon knocking an electron out of an orbital, which then, free of any interactive forces, leaves the atom within 10^{-5} seconds is only a very approximate interpretation of the real process. The spectra can be complicated, due to the many coupling and relaxation interactions involved. This manifests itself in the appearance of characteristic fine structure and in a large linewidth of up to five times the width of the excitation radiation (XPS) of about 1 eV.

The experimental setup is shown schematically in Figure 1. Since electrons have a very small escape depth from any material, experiments must be carried out in ultra-high vacuum. This also avoids any disturbances caused by adsorbed substances. Because of this small escape depth, the information contained in the spectra taken from solid samples refers only to a depth of a few atomic layers.

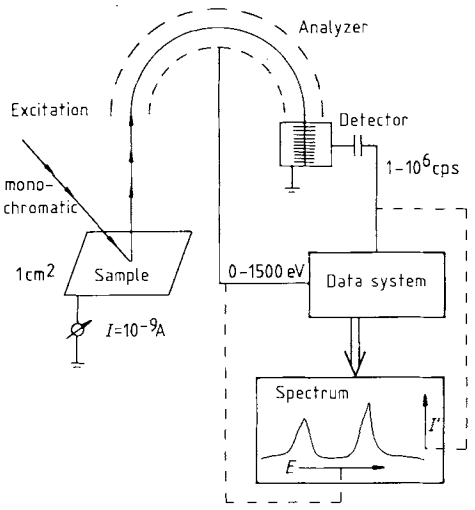

Fig. 1. Schematic representation of the photoemission experiment. For excitation the characteristic X-ray emission of a light element (Mg or Al) is generally used, as also here. In some cases monochromators are used to reduce the natural linewidth of the excitation of ca. 1 eV down to 0.25 eV. Recently, synchrotron radiation has become a valuable light source for photoemission experiments. The dashed lines in the diagram indicate the relations of abscissa and ordinate in the spectrum with the main components of the apparatus. Frequently, the kinetic energy of the electrons is also determined with a cylindrical mirror analyzer. cps = counts per second, I' = intensity.

In an XPS experiment an electrically conducting sample is irradiated with monochromatic X-rays of typically 250 W. The emitted electrons are then collected over a wide angle around the entry column of the normally hemispherical electrostatic analyzer. By application of a continuously changing potential to the hemispherical electrodes of the condensor, which make up the analyzer, only electrons of precisely one particular energy (proportional to the applied potential) will reach the detector. This is often a photomultiplier. Analyzer and detector functions of modern spectrometers are usually controlled by computers. This also enables the spectra to be accumulated, as well as allowing for easy mathematical processing of data by smoothing, background correction, integration, and deconvolution.

2.2. Practical Application

With XPS it is possible to investigate a solid surface for any chemical element, except hydrogen, to a depth of 1–2 nm, both qualitatively and quantitatively. Information concerning the chemical environment of an element (speciation) can also be obtained. Our study was carried out under conditions so chosen that no pretreatment of a sample was necessary. The sample to be investigated was introduced into an ultra-high vacuum chamber; hence, in the room-temperature measurements reported here only the non-volatile components of a surface were detected. The method may therefore be considered as complementary to the conventional methods of gas analysis, in which microparticles tend to disturb the analysis. If it is required that volatile components can be analyzed under these conditions, this may be achieved by cooling the sample to, for example, 78 K.

The detection limit lies between about 0.1% and 1.0% of the surface concentration for the various elements. One necessary condition for the use of this technique is that the sample be conducting; this could, in fact, be achieved with all the samples studied so far.

A particular advantage of XPS is its very high surface sensitivity; this allows for selective investigation of the boundary surface of an emitted particle and its environment and thus makes an estimation of its catalytic potential possible. It is known, for example,[6] that solid particles can play the role of carrier for toxic substances; dangerous substances can, in this manner, be brought into the environment on the surface of a harmless material. Other analytical methods such as the spectroscopic analysis of desorption of such toxic materials or elemental analysis must identify these substances in high dilution in a carrier,[7] while with the method described here, a monolayer coverage of a carrier particle can be easily detected and characterized.

In contrast to the good depth resolution, the lateral resolution on a surface is rather poor. The present measurements are summed over an area of about 5×10 mm^2. This

gives a good statistical analysis over many particles but does not provide any accurate information about the nature of individual particles.

In the case of metals, the XPS analysis of the chemical bonding of an element generally gives very clear-cut information, whereas in the case of organic substances only the type of bonding (e.g. aromatic, aliphatic, heterosubstituted etc.) can be determined. However, since the danger of chemical changes occurring in the sample during analysis is much smaller under XPS conditions than in classical high performance seperation methods[5,7] XPS can also be used to complement these techniques.

The depth of resolution of this technique warrants further mention. The information contained in the spectrum is taken from a depth of about 1–2 nm, i.e. a few atomic monolayers. Hence, the general understanding of the word 'surface' retains its literal meaning: with XPS only the topmost atomic layers are studied, i.e. layers which rarely can be made "visible" by other techniques.

The surface as seen under the microscope constitutes a much thicker layer of the solid; hence differences have often been reported to exist between the visible and the XPS-characterized surfaces. For example, a thin film of aromatic organic material (normally not visible) can, in this way, be seen on the surface of a soot particle. By repeated wearing down of the outer atomic layers, e.g. by bombarding with noble gas ions, the structure and composition of a particle layer can be followed from outside to inside (depth profile).[8]

Quantitative interpretations are rather difficult because of the irregular structure of the particles, but this difficulty may be partially overcome by studying the surface morphology with the electron microscope.[8]

An absolute quantification of the results (e.g. as emission in mg pro km) is, however, difficult. This is more easily achieved with conventional analytical methods;[3] such results can then be better interpreted with the help of bonding and depth distribution data obtained by XPS, and their importance with respect to the environment more easily estimated.[5,8]

Much more accurate are relative quantitative comparisons between different elements contained in the sample or comparisons between element concentrations following various treatments of the same sample (e.g. heating, ion-etching). It was shown that both the covering of the test plates with emitted materials as well as the internal structure of the particle itself are of a heterogeneous nature. It is therefore meaningless to extrapolate data acquired from a depth of a few monolayers to the entire bulk of the emission, as would be required for a quantitative description of the composition of a sample.

With the sampling technique used in the present investigation, only the very small microparticle portion of the emission[3b] was selected. Inspection under the scanning electron microscope revealed that, in general (except in the diesel soot samples), virtually no particles larger than 50 nm were present on the test plates examined. Such small particles are quantitatively characterizable, but only to a limited extent. Since however the emphasis in this study is laid on a qualitative description of the chemical nature of the emission products this was not seen as a serious drawback. It would, of course, be difficult to extrapolate quantitative data from the present measurements for an analysis of the total solid emission. On the other hand, because of the large surface to volume ratio such microparticles are of particular interest with regard to boundary effects such as in heterogeneous catalytic processes. The experiments were carried out as follows: the surface of a clean, conducting substrate (test plate) was exposed to the stream of exhaust gas to be analyzed. Some of the microparticles are deposited on the surface. After exposure for a prescribed length of time the test plate was analyzed in an XPS spectrometer (Leybold-Heraeus LHS 10, Mg excitation 240W). The energy scale was calibrated with the Au $4f_{7/2}$ line at 84.0 eV. In all diagrams the energy scale refers to the binding energy E_b in electron volts (eV). Gold, aluminum, and graphite test plates measuring 9 mm × 13 mm × 0.5 mm proved to be suitable for such experiments. Control experiments ensured that, after appropriate cleaning, only the element and its oxide were detectable. The plates were then exposed at an angle of 45 degrees to the exhaust fumes. In the experiments carried out with diesel motors soot filters and test plates were positioned about 1.5 m and 2.0 m, respectively, behind the exhaust manifold. In the experiments carried out with the automobile the plates were positioned about 10 cm before the end of the exhaust.

The various test plates showed differing capturing abilities for different types of particles: aluminum proved especially suitable for inorganic particles; the variety of inorganic particles adhering to graphite test plates was in contrast much smaller and many elements were found in much smaller concentrations than on aluminum. On the other hand, the spectra of the organic components deposited on graphite were better differentiated and the danger of subsequent reaction with the hot aluminum oxide could be ruled out. A gold test plate, to which the particles under investigation adhere far less easily, was used as a control substrate and was exposed together with an aluminum test plate for recording the platinum spectra, which are strongly affected by the Al-spectra (see Section 4.6).

It was found that there is an optimal exposure time for such experiments which ensures adequate coverage but precludes the deposition of too thick a layer. This avoids both the incidence of insufficient signal intensity and an electrostatic charging of the sample. Thus, for example, it was not possible to analyze a test plate from a longer test run of over 10000 km with an Otto motor.

The recording of the spectra necessitated long measurement times. After reaching ultra-high vacuum (10^{-9} mbar) in the analysis chamber of the spectrometer, 20 hours were needed to record a survey spectrum (all elements, low resolution). The spectra were collected on a data system. By comparison with stored data occasional deteriorations of the samples were recognized and the data therefrom were excluded from analysis. The data system was also used for smoothing and integration and for background subtraction. Since the line shapes of the spectra contained a considerable amount of information, the data was manipulated as little as possible and only raw data used for the final analysis (only a linear background correction was carried out).

For some spectra the satellite excitations from the Mg source were also subtracted from the raw data (Fig. 3, 15–17).

3. Samples

3.1. Diesel Motors with Various Soot Filters

The samples were taken from the exhaust system of a stationary (preignition) diesel motor fitted with a soot filter. The filter consisted of either a simple ceramic base (Al_2O_3–MgO–SiO_2) with activating metal additives or of a noble-metal-impregnated monolith. These filters (Corning) not only retain soot particles but also burn them to CO_2 and H_2O. The necessary activation energy is supplied by catalytic processes such as the dehydrogenation of aliphatic compounds (soot filter as catalyst). Samples of soot precipitate were taken from the walls of the exhaust system both in front of and behind the soot filter. Furthermore, in each case test plates of pure carbon (HOPG graphite) were placed in the exhaust area in front of and behind the filter as well as at the far end of the exhaust system and exposed for typically 16 hours to the exhaust gases.

3.2. Otto Motor with 3-Way-Catalyst

Detailed measurements were carried out on a production automobile equipped with a 3-way-catalyst. The performance of the catalyst was monitored on the basis of the CO emission during an approx. 7000 km test drive. Aluminum and/or graphite test plates were mounted in parallel at the input of the air filtering system and at the end of the exhaust system and examined after deposition of microparticles under various driving conditions (cold starts, city driving, mountain and motorway driving). Temperature measurements taken at intervals at test plates in the exhaust outlet showed values of about 620 °C at the test surfaces. Table 1 gives an overview of the test conditions.

Table 1. Origin of the samples referred to in the text.

Sample	Sampling Point	Testplate material	Motor	Operation
1	Filter support	Indium	Diesel	500 h
2	Before filter 1 [b]	Graphite	Diesel	16 h under load
3	After filter 1 [b]	Graphite	Diesel	16 h under load
4	Before filter 2 [c]	Graphite	Diesel	16 h under load
5	After filter 2 [c]	Graphite	Diesel	16 h under load
6	Exhaust	Aluminum	Otto	Motorway + city, 200 km
7	Exhaust	Aluminum	Otto	Cold start + warm run
8	Inlet manifold	Aluminum	Otto	Motorway, 550 km
9	Exhaust	Aluminum	Otto	Motorway, 550 km
10	Exhaust	Graphite	Otto	Motorway, 550 km
11	Exhaust	Aluminum	Otto	Motorway, 80 km
12	Exhaust	Aluminum	Otto	Motorway + city, 100 km
13	Exhaust	Aluminum	Otto	Mountain drive, 200 km

[a] Otto motor fitted with a 3-way-catalyst. [b] Without noble-metal impregnation. [c] With noble-metal impregnation.

4. Results

The results obtained for both exhaust cleaning systems will be compared systematically in the order of the elements analyzed. First of all, however, the qualitative survey spectra and the possibility of quantifying the results are discussed. This method of presentation has been chosen so as to correspond with the chronological order in which the results are obtained in the course of an analysis.

4.1. The Survey Spectra

For the qualitative analyses a series of survey spectra were recorded. Figure 2 shows portions of the survey spectra for a test plate positioned behind the impregnated diesel soot filter (sample 5) and for the soot precipitate on the metal lining of the exhaust pipe (sample 1). Table 2 gives a summary of the metals observed. The respective amounts measured are only semiquantitative since an exact calculation would entail physical assumptions about the photoemission which are completely unjustified in such a

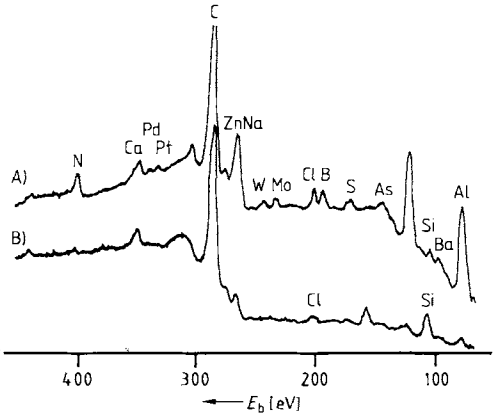

Fig. 2. Survey spectrum of diesel soot. A) Test plate exposed to the exhaust gas (sample 5). B) Sample of the soot deposited in the exhaust pipes (sample 1).

Table 2. Elements of the testplate of sample 6.

Element	Detected core levels [a]	Surface concentration [b]
O	1s	c
C	1s	c
Al	2s, 2p	c
Ca	2s, 2p	b
N	1s	b
Zn	2p, Auger	b
S	2s, 2p	b
Pd	3d	a
Pt	4p, 4d	a
W	3d, 4d	a
Mo	3d, 4p	a
Cl	2p, 2s	a
B	1s	a
Si	2s, 2p	a
Ba	3d, 4d	a
As	3p, Auger	a
Se	3p, 3d	a

[a] The core levels detected do not neccessarily correspond to the lines ideally suited for detection, but do so to those which could be unequivocally assigned. [b] Concentrations: a = between the limit of detection and 5%; b = between 5% and 20%; c = main component.

Table 3. Composition of the external surface of sample 6.

Binding energy [eV] [a]	Core level	Rel. concentration [atom %] [b]
1024	Zn 2p	0.2
937	Cu 2p	1.2
784	Co 2p	0.2
712	Fe 2p	1.0
644	Mn 2p	0.2
532	O 1s	10.2
439	Ca 2s	—
415	Cu, Auger	—
408	Cd 3d	0.7
400	N 1s	3.9
353, 349	Ca 2p	3.1
342, 337	Pd 3d	0.4
335, 317	Pt 4d	—
312, 307	Rh 3d	0.8
286	C 1s	25.6
271	Cl 2s	traces
265	Zn, Auger	traces
257	Ba 4s	traces
235	Mo 3d	2.4
227	S 2s	traces
201	Cl 2p	8.1
191	B 1s	1.3
182	Ba 4p, Zr 3d	traces
164, 171	S 2p	7.5
155	Si 2s	traces
145, 140	Pb 4f	1.9
132	P 2p	traces
104	Si 2p	5.9
103, 99	Hg 4f	0.5
94	Fe 3s	traces
71	Pt 4f	0.4
57	Fe 3p, Hg 5p	traces
48	Rh 4p	traces

[a] Where possible, weak Auger lines and overlapping peaks are not taken into consideration. Hence, not all the binding energies that were measured have been listed. [b] The difference to 100% is assigned to aluminium (Al 2p, ca. 74 eV).

complex system (see comments in Table 3). The following points should be noted:

a) Sample 5 contains many elements in a higher surface concentration than the carbon black (Sample 1). This is significant despite the differing layer thicknesses of the two preparations, since the emission intensities of both samples relative to the background intensity were about the same. The peak areas referred to the main carbon peak indicate that the soot is contaminated mainly with calcium silicate. In particular, very few heavy metals are present and the nitrogen content is strikingly low.

b) The main inorganic component detected on the test plates is aluminum in the form of aluminum oxide. In the case of nonmetals the high concentration of N_2 and S that cannot be explained by gaseous components such as SO_2 or NO_x in the samples is surprising, for neither evacuation to 10^{-9} mbar nor subsequent bombardment with $Ar^{\oplus}$ ions led to any change in the respective peaks.

c) Amongst the noble metals, Pd and Pt were observed to be present. The most intense bands of Pt (4f) and Pd (3d) are however obscured by signals from other elements.

d) The presence of the elements Zn, Ce, W, Mo and As was also evident from spectra obtained in regions outside of those shown in Figure 2.

Figure 3 shows a portion of the spectrum of the test plate with sample 6 (Otto motor).

This sample is a typical example of all the samples investigated and will therefore be discussed in detail. The high resolution spectrum indicates the presence of a large number of elements. The majority of these elements appear independently of the presence of an exhaust cleaning system and are also detectable in the emission products of a conventional automobile. This may be seen from the survey spectra of test plates that were installed simultaneously in the input to the air filter and at the exhaust output of an automobile equipped with a catalyst. After satellite subtraction the $Pt\,4f_{7/2}$ line is clearly visible at a binding energy of ca. 70 eV, which is a clear indication of the presence of a 3-way-catalyst. Pt was not observed in any sample taken from the inlet air of the motor. Noticeable in these analyses is the appearance of an intense Pb 4f doublet making up ca. 20% of the total intensity of the spectrum.

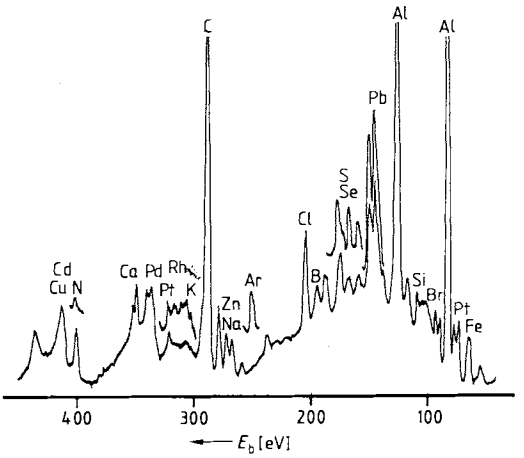

Fig. 3. Survey scans of a test plate from the Otto motor experiments (Sample 6). The complete assignment of the peaks is given in Table 3. The upper trace shows the alteration of the surface after bombardment with $Ar^{\oplus}$ ions.

The data in Table 3 show the quantitative analysis of this spectrum. Since an aluminum test plate was used, the aluminum concentration in these samples cannot be quantitatively determined—qualitative proof of the presence of aluminum was obtained from a simultaneously exposed graphite plate. The concentrations given for the noble metals were obtained from deconvolutions of the multiplets arising from superposition of the noble metal 3d and 4f subspectra with other metal core levels. The error in these estimations must be assumed to be about 25% and originates mainly from the uncertainty in the deconvolution. In order to calculate the concentration of the various elements a universal escape depth must be assumed for all elements. This does not take into account the influence of roughness and unevenness of the sample surface on the observed intensities.

Those regions of the spectrum that have obviously been changed by ion-etching with $Ar^{\oplus}$ ions (5 min, 5 kV, 10 mA, 4 $\mu A/cm^2$) are also shown in Figure 3. Under these conditions, ca. 6 nm would be removed from a smooth and uniform surface. The concentrations of carbon and nitrogen (enriched as organic compounds on the outer surface due to their volatility) are clearly decreased. The prominent Ar 2p peak indicates the presence of a soft, graphitic carbon, into which the Ar is implanted particulary well. Finally, S, Se, Br and Pb are present in an altered chemical state

(chemical shift) and larger quantities after ion-etching. Since the sensitivity of the chemical structure of many of these elements to ion-etching is well known, these alterations will not be discussed any further.

Table 4 shows which elements were detected by us in the above investigations and those which were also looked for with standard techniques under comparable emission conditions in catalyst-treated motor vehicle exhaust fumes.[9] In general, there is good agreement between the two sets of data. However, the core levels of the alkali metals could not be used for a quantitative determination (K and Na were qualitatively detected). The conventional methods, on the other hand, showed no noble metals to be present. We assume that the differing particle sizes in the experiments and the different sensitivities of the methods are responsible. A more accurate quantitative comparison should not be attempted, since the emission sources (US automobiles and European motor cars), the greases and fuels used, and the loading conditions are different.

Table 4. Comparison of particle analyses by conventional methods (Table G2 in [9] and XPS [a].

Element	Conventional methods	XPS
Cr	–	–
Pb	+	+
Mn	–	+
As	–	–
Hg	–	+
Br	+	+
P	+	+
Si	+	+
Cd	–	+ [b]
Al	+	+
S	+	+
Na	+	–
F	–	–
Mg	+	+
K	+	–
Cl	+	+
Pt	–	+
Zn	+	+
Cu	+	+
Ni	–	–

[a] Comparison on the basis of sample 6. [b] Possibly from tirewear.

4.2. The Carbon Spectra

Figure 4 shows the carbon 1s spectra of the test plate with sample 5 and of the soot deposit from behind the noble-metal-impregnated soot filter (sample 1); also shown is the corresponding spectrum of a test plate after exposure behind a non-impregnated diesel soot filter (sample 3). The spectra of samples 3 and 5 do not originate from the graphite test plate, to which the signal at 283.8 eV with ca. 100 times the intensity of the rest of the lines (reference lines in Fig. 4) belongs. When the test plate was examined under the scanning electron microscope the surface was seen to be thickly covered with particles. (Emissions with an average particle size of less than 100 nm from the Otto motor, on the other hand, were only rarely visible on the test plates.)

The spectra in Figure 4 may be interpreted in the following manner: The soot contains a significant proportion of non-graphitic carbon (intensity on the higher binding energy side relative to a graphite reference). If one compares the broad, asymmetric line shapes of the spectra (peak halfwidth 4.2 eV) with those of the spectra of some model aromatic organic compounds (Fig. 5), it follows that at least some aromatic organic components are present on the surface. The complex line shape, which is used as a 'fingerprint' for the class of arenes, is characterized by the high energy-loss feature (shake-up and shake-off) typifying this class of substances.[10] A mixture of such organic compounds yields, by combination of these characteristic structures, the observed wide asymmetric band in which the partial spectrum of the soot-like carbon is hidden (Fig. 4II).

In the analysis of the line shapes, one must also consider carbon-heteroatom structures such as C–N, C–O, C–S, and C–Cl, which, according to partial spectra of the heteroatoms (see Sections 4.3–4.5), are, in fact, present. These

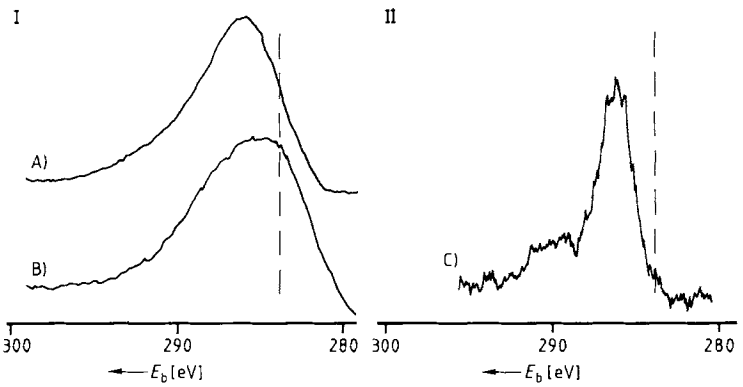

Fig. 4. C1s spectra of test plates exposed to diesel exhaust behind impregnated (I) and non-impregnated (II) soot filters. A) Sample 5; B) sample 1; C) sample 3. Note the influence of noble-metal impregnation (measured with pass energy 100 eV). The dotted line shows the C1s binding energy of graphite.

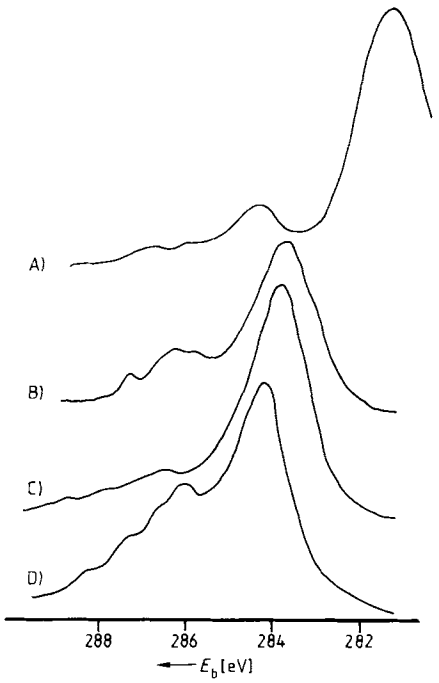

Fig. 5. C1s spectra of some aromatic reference compounds. All samples were measured as thin films sublimed on silver test plates (pass energy 50 eV). A) Coronene. B) Perylene. C) Tetracene. D) Naphthalene.

would not, however, alone explain the observed line shapes, since the chemical shift of the C1s signal in compounds of this nature is smaller than the observed linewidth. Furthermore, the intensities of the lines of the heteroatom partial spectra are so low that only a small portion of the entire C1s spectrum can be attributed to such structures.

Since the carbon on the test plates is not a regularly ordered graphite (also confirmed by X-ray diffraction), a large number of terminal carbon atoms must exist in the form of aromatic hydrocarbons or of their polymerization product—soot. These are normally saturated with either hydrogen or oxygen and thus a significant proportion of the C1s signal intensity at high binding energy may be explained by the presence of hydroxy and carbonyl groups.[11]

From a comparison of Figure 4 with earlier spectra measured by the authors[12] and with the O1s partial spectrum (Section 4.3, Fig. 10) it follows that the soot precipitated on the walls of the exhaust system of the diesel motor contains more aromatic hydrocarbon materials in its outer surface than the surface of the test plate, which exhibits a higher oxygen content and whose C1s binding energy is accordingly shifted to higher values.

Practically no aromatic hydrocarbons are found (narrow signal) on the test plate from behind the non-impregnated soot filter. A shoulder at higher binding energy typical of C-O bonds is clearly recognizable.[12]

The influence of the noble-metal-impregnated soot filter on the composition of the organic emission is shown in Figure 6. The C1s spectra of samples 4 and 5 are also shown. The two test plates were simultaneously exposed to the same exhaust stream at the same temperature. Instrumental broadening of the linewidth (by the analyzer and the doublet of the $Mg_{K\alpha}$ radiation) was corrected by deconvolution with an approximate function. The width at half height of these lines (at 2.2 eV) is still larger than for pure carbon.[12] The marked increase in the amount of arenes and heteroarenes due to the presence of the catalyst may be clearly seen from the additional intensities at high binding energy. It should be noted that the difference in the areas of the two spectra between 286 and 289 eV need not be proportional to the amount of aromatic hydrocarbons present, since according to Figure 5 the intensity measured in this energy range is heavily dependent on the structure of the arene. A comparison of the spectra shows, however, that the nature of the mixture of aromatic hydrocarbons is altered by the presence of a soot filter. This alteration was not detectable when a non-impregnated soot filter was employed. It may be concluded therefore that the dehydrogenating effect of noble-metal additives contributes to an increasing build up of aromatic hydrocarbons and to the incorporation of heteroatoms into the molecular structure.

A high resolution C1s spectrum of the test plate exposed to the exhaust gases of an Otto motor (sample 6) is shown in Figure 7. The line broadening (FWHM: 2.7 eV) due to the presence of arenes and heteroarenes is once again easily recognizable. The line shapes are altered during ion-etching (conditions as for Fig. 3) and the amount of C-O-structures decreases. This is indicative of a purer soot with higher carbon content in the center of the particle.

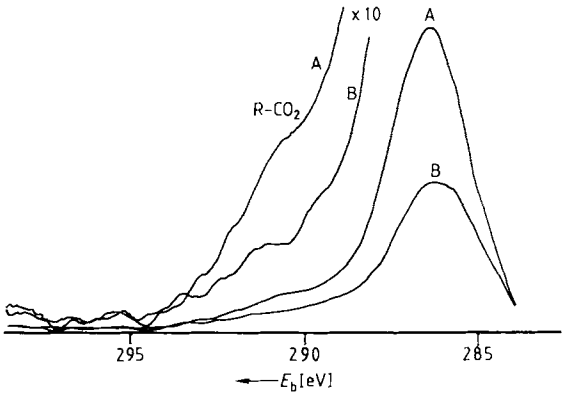

Fig. 7. C1s spectra of sample 6 A) before, B) after ion-etching. In the (normalized) amplified spectra the presence of carbon heteroatom bonds is recognizable. Ion etching removes these structures. These and all the following spectra were measured with an analyzer pass energy of 50 eV.

The heterogeneous composition of the particle from the Otto motor—at least in the cold-start stage—can be seen from the spectra in Figure 8 (sample 7). The outer surface

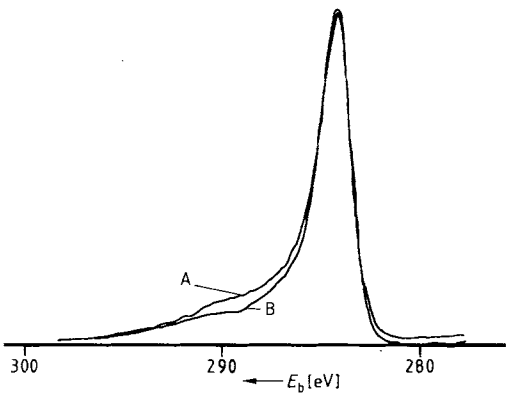

Fig. 6. Influence of noble-metal impregnation of the soot filter on the structure of the emitted carbon compounds. A) Sample 5 (behind the filter). B) Sample 4 (in front of the filter) (pass energy 25 eV).

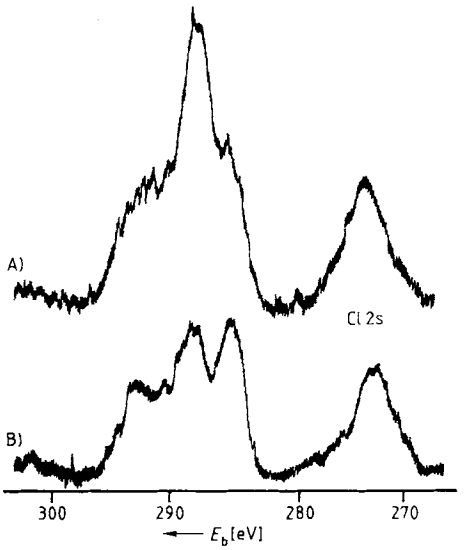

Fig. 8. C1s spectra of sample 7 A) particles emitted in the cold start phase of the Otto motor contained a high proportion of aliphatic compounds. B) These could easily be removed from the particle surface by ion etching.

contains a large proportion of aliphatic hydrocarbons. These can be removed quite easily and almost completely by a brief ion-etching treatment, while the graphitic, aromatic components (to the right of the main line) and the oxo- and chloro-organic compounds abundantly present in this sample (to the left of the main peak and Cl 2s peak) are hardly affected at all.

A quantitative comparison of the carbon emission from the Otto motor under various loading conditions is shown in Figure 9. The intensities of the signals were normalized to the intensity of the Al 2p signal assuming similar coverage. Particularly striking (spectrum B) is the high emission of aromatic hydrocarbons and soot after mixed city and motorway driving. After a drive of similar duration (at a speed of 120 k/h, spectrum A) on a motorway a spectrum of lower intensity signals and a noticeably higher ratio of heteroarenes to aliphatic and aromatic hydrocarbons was recorded. The effect of the higher temperature of the catalyst and test plate under more severe loads is clearly seen from the decrease in the total amount of detectable carbon. It cannot, however, be decided on the basis of these measurements whether the emission has actually been reduced or whether the higher temperature of the test plate has contributed to the loss of carbon (by combustion at the testplate) as a sampling artifact.

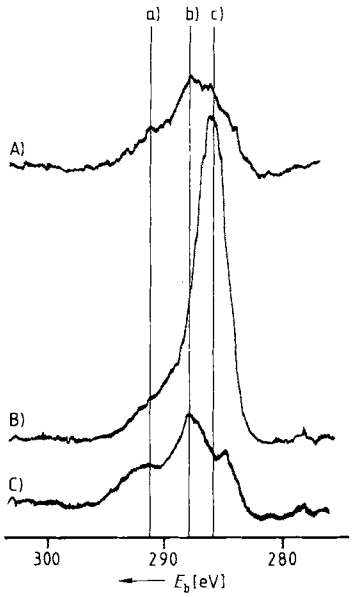

Fig. 9. Comparison of the C1s spectra of the surfaces of soot particles emitted from an Otto motor under various loading conditions. A) Sample 9. B) Sample 11. C) Sample 7 (identical to Fig. 8A). The spectra are normalized to the Al 2p signal intensity. a) Oxo- and halohydrocarbons, b) aliphatic hydrocarbons, and c) soot and graphite.

4.3. The Oxygen Spectra

The O1s spectra obtained in the present study are not very informative,[5,8] since the O1s binding energy for oxide oxygen (O^{2-}) depends relatively little on the chemical environment and the large variety of oxygen compounds in the sample determines the possible shapes of the spectrum. A characteristic spectrum of diesel motor exhaust gases is shown in Figure 10A. Quite a different spectrum (Fig. 10B) was obtained, however, from all diesel soot samples (e.g. sample 1). The lower intensity of the second spectrum is in keeping with the presumed enrichment of aromatic hydrocarbons on these samples (see Section 4.2). The shift of the O1s signal could indicate that acidic hydroxy groups and water dominate on the soots, and basic hydroxy groups and oxides on particles on the test plates.

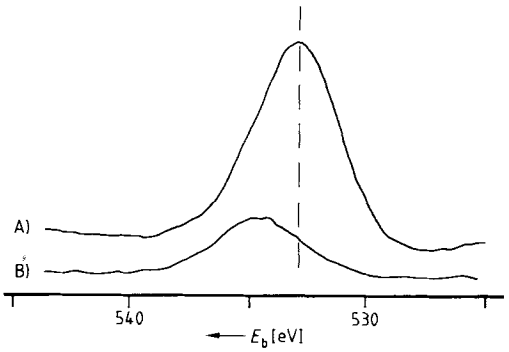

Fig. 10. O1s spectra of soot particles from a diesel motor. A) Sample 3. B) Sample 1 (see Fig. 4B). The reference line indicates an average value for metal oxides.

4.4. The Nitrogen Spectra

The N1s spectra of soot surfaces have already been compared with the cataloged N1s spectra of *N*-heteroarenes.[13] We have now established that in the diesel samples, nitrogen is mainly found on the test plates and rarely on the bulk soot close to the soot filter. A typical spectrum (sample 3) is shown in Figure 11; Figure 12 shows for comparison the N1s spectrum of an activated soot catalyst (Corax 3, not intended for use in motors, treated with HCN gas at 900°C). The binding energies of the nitrogen in the diesel soot and the low energy shoulder in the reference spectrum are typical for heterocyclic nitrogen and for amino groups. Nitro groups (from NO_x) would give rise to a peak at ca. 407.0 eV as in the reference spectrum.[12] Such nitro groups have not been observed in any of the samples from the diesel motor series which attests to the relatively high temperature sensitivity of these functional groups.

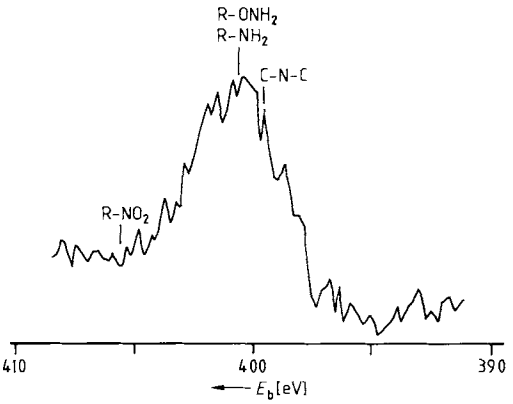

Fig. 11. N1s spectrum of a testplate exposed behind a non-impregnated soot filter (sample 3). The position of the N1s signal is clearly structure-dependent.

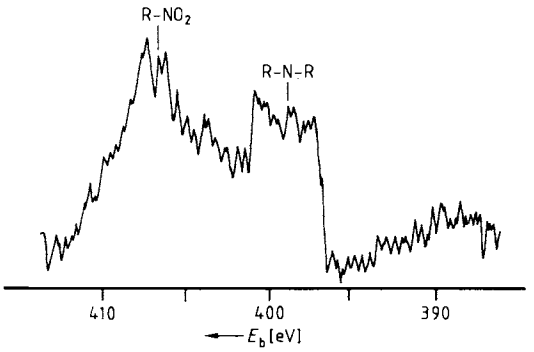

Fig. 12. N1s spectrum of a reference compound. A sample of activated carbon was treated with HCN gas. Note the high sensitivity of the N1s photoemission and the clear separation for various chemical species.

The influence of noble-metal catalysts on the qualitative composition of the types of organic compounds emitted is shown in Figure 13 (sample 5). The N1s binding energy for particles modified by the presence of noble metals is clearly lower than for the particles described in Figure 11. This is indicative of the presence of aromatic amines (signal structure at higher binding energy) and heterocyclics (main components). These types of organic compounds are not emitted in the absence of the catalyst (Fig. 13B).

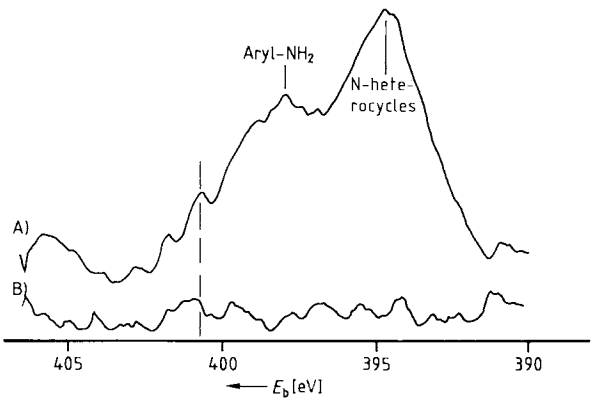

Fig. 13. Influence of a noble-metal impregnated soot filter on the formation of organonitrogen compounds. A) Sample 5. B) Sample 4. The dotted line shows the position of the N1s line of sample 3 (see Fig. 11).

Similar N1s spectra have been observed from emissions from the Otto motor. The spectrum of a test plate used in a test carried out on a motorway is especially interesting (sample 10, Fig. 14); in this sample, cyano compounds analogous to those found with KCN-treated carbon black are also observed as well as amines and nitrogen heteroarenes. Ion-etching experiments show the increased presence of aromatic cyano compounds in the interior of these particles (Fig. 14B); this is also reflected by the similarity to the changes observed in the C1s spectrum.

On one occasion during a test drive in a city center, the presence of chlorinated compounds in the air was established by an intense Cl 2p peak on the test plates taken from the inlet manifold. The presence of nitro groups in the nitrogen spectrum was observed only in this particular case (Fig. 14A). As was shown by repeated ion-etching, the nitro compounds were evenly distributed throughout the sample.

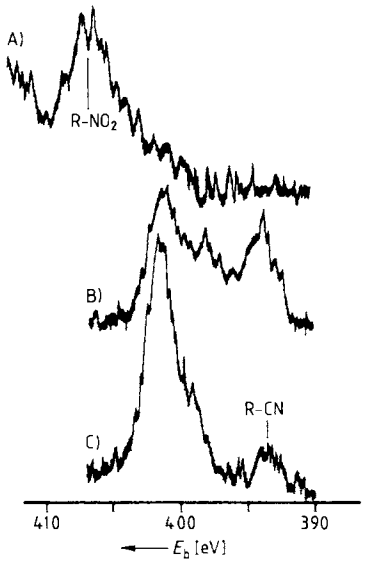

Fig. 14. N1s spectra of the emission products collected during a motorway test of an Otto motor. A) Sample 12. B) Sample 9 after ion etching. C) Sample 9 before ion-etching. Note the presence of cyano compounds in B and C. Only on one occasion (sample 12) were significant amounts of nitro compounds detected (see text).

4.5. The Sulfur Spectra

The sulfur components of emission products from various combustion plants had already been investigated by XP spectroscopy a number of years ago in the USA.[14] Samples taken from diesel motor exhausts contain sulfur with an S2p binding energy of ca. 168.5 eV. From a comparison with values in the literature[15] it may be seen that this value is neither related to sulfate (b.e. ca. 170 eV) nor sulfur, nor even to sulfide (b.e. ca. 160–162 eV). Sulfur in these states is formed in combustion plants.[14] In the present case, however, sulfur is present as part of an organic C–S- or C–O–S-group. These groups seem to be produced under the influence of the catalyst, since in the absence of noble-metal catalyst the exhaust gases contain sulfur only as sulfate or sulfite.

In the spectra obtained from the Otto motor test series under heavy loading conditions (motorway driving and driving in a mountainous terrain) a significant amount of sulfur was observed both in the form of sulfate and of sulfide (see shoulder in the S2p line of Fig. 3).

Since sulfur has a poisoning effect on the catalyst the emission may be seen as a kind of self-cleaning mechanism; the sulfate deposited in small amounts on the surface under normal operating conditions is largely removed at the higher catalyst temperatures caused by heavy loading of the motor.

4.6. The Platinum Spectra

Figure 15 shows the Pt 4f spectrum of a test plate (sample 5) taken from a diesel exhaust. Each of the chemically differently bound platinum atoms show two peaks in this spectrum ($4f_{5/2}$ and $4f_{7/2}$). The reference lines give the positions of some platinum compounds for comparison.[4] The greater amount of the noble metal is obviously present in the formal oxidation state of zero and its chemical envi-

ronment is similar to that of platinum in an industrial synthetic catalyst. (Pt-black is a very finely divided metal of an undefined, non-zero oxidation state and is used as an effective catalyst for hydrogenation in organic chemistry.)

A small portion of the platinum is present in an oxidation state of 4, very probably as the oxide. Its binding energy falls in the valley between the 5/2 and 7/2 components of the main component, giving the impression of a poorly resolved spectrum.

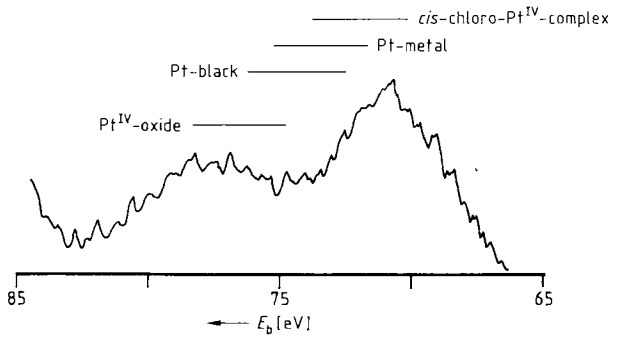

Fig. 15. Pt4f spectra of the emission from a noble-metal-impregnated diesel soot filter (sample 5). The bar lines indicate the positions of the $Pt4f_{7/2}$ peaks of some reference compounds. The length of the lines indicates the error bar mainly given by the uncertainties in the definition of a common energy scale.

Figure 16 shows the Pt4f region of the spectrum of sample 6 (Otto motor exhaust gases) after satellite subtraction and deconvolution. For comparison, the spectrum of a chemically oxidized Pt-foil is also shown (Fig. 13B). One can see how the $Pt4f_{5/2}$ peak is masked by the intense Al2p line and how the detection of Pt compounds in oxidation states of 2 and 4 is thus very difficult in such spectra. A quantitative estimation of the entire amount of Pt in

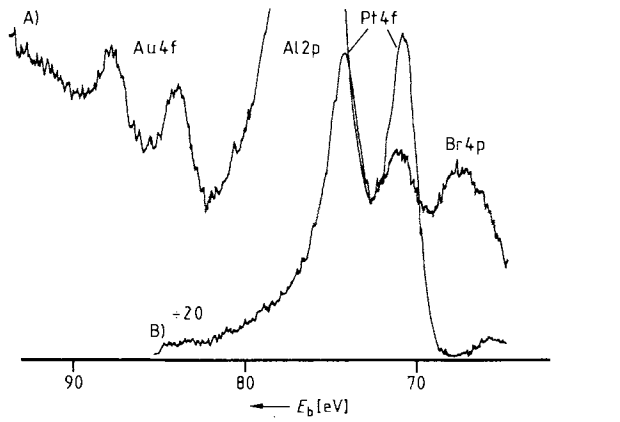

Fig. 16. Comparison of the Pt4f spectra of A) sample 6 and B) an oxidized platinum foil.

the exhaust samples is therefore not possible. According to these spectra the platinum may exist as a surface oxidized metal particle, which, as in the case of the working catalyst, can be attached to an oxide particle (Scheme 1).

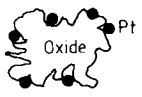

Scheme 1. Schematic representation of the possible deposition of noble-metal particles on larger emitted carrier particles.

The platinum emissions from the 3-way-catalyst under various loading conditions are compared in Figure 17. For this comparison a scaling procedure was used, similar to that described for the comparison of the C1s spectra in Section 4.2. Possible reasons for the shift of the $Pt4f_{7/2}$ lines of automobile emissions with respect to the positions of the lines of a platinum foil are the small particle size[16] and the incorporation of oxygen (without formal oxidation) into the metal lattice.[17] It is obvious that a detailed interpretation of the chemical shifts of such a heterogeneous system is critical, since the definition of a common scale for the binding energies of all microparticles of a macroscopic sample is difficult and since the concept of formal oxidation states for a metal in supported noble metal oxide systems is valid only to a first approximation.

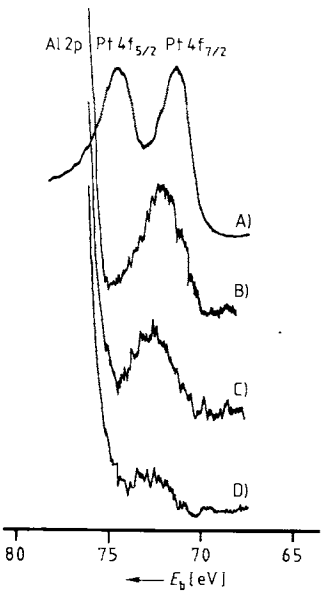

Fig. 17. Comparison of the Pt4f spectra of emissions from an Otto motor under various loading conditions with the spectrum of a platinum foil (A.) Only after subtraction of the intense satellites from the Al2p spectrum are the $Pt4f_{7/2}$ lines visible in full resolution. B) Sample 9. C) Sample 11. D) Sample 7.

5. Concluding Discussion

The first results of the X-ray photoelectron spectroscopic analysis of diesel emissions have shown that a large number of chemical elements, particulary heavy metals, are detectable in the portion of the exhaust emissions that is stable in ultra-high vacuum. On the other hand, the large particles precipitated in the exhaust system of a diesel motor seem to contain very few elements other than iron oxide and carbon particles covered with arenes. Noteworthy is the significant amount of selenium precipitated from the exhaust fumes near the open end of the exhaust system. It can be traced back to sulfur-analogous heterocyclic compounds contained in the diesel oil used.

In both types of motor, the noble metal catalyst seems to aid in the formation of carbon-heteroatom compounds in

the exhaust. From an analysis of the line shapes of the C1s peaks and a comparison with the concentration of the heteroelements it may be seen that the distribution of hydrocarbons on the carbon surface is shifted in favor of aromatic compounds.

The emitted microparticles of soot are composed, for the main part, not of graphite but rather of paracrystalline carbon,[18] which can act as activated carbon; i.e. it may tend not only to attach to a number of various chemical species, e.g. water and hydrophilic compounds (acids), but may also possess a catalytic activity of its own. Nitrogen-containing soot particles are of special importance from the chemical point of view because such systems are efficient catalysts for the oxidation of SO_2 to SO_3.[13]

The platinum emission of the 3-way-catalyst was more difficult to examine since on all test plates the Pt 4f line for higher oxidation states was overlapped by the Al 2p line (the aluminum originating from the catalyst carrier and the generally non-catalyst-specific emission). The observed binding energy of the emitted particles is very similar to that of a pure platinum surface oxidized in a stream of oxygen. As is known from the literature,[16] platinum surfaces and small platinum particles are oxidized by the oxygen present in the air even at room temperature, so that biologically relevant platinum(IV) is formed.[19]

These results at least do not rule out a hitherto only very schematically discussed[20,21] effect of particle emissions on the environment. For a better insight into such effects further studies must be carried out, for example, on the existence of emitted particles on living matter. This has, in fact, been successfully attempted with XPS.[22]

Fine dust particles emitted into the atmosphere can be distributed[23] over the entire environment and can be deposited and accumulated on the surfaces of living matter (e.g. on leaves). In this way a large number of inorganic compounds of catalytic importance are deposited on the surface of plants. Simple contact with polluted air carrying gases such as SO_2 can thus cause a localized build-up of poisons such as sulfuric acid. The inorganic deposits can also aid destructive processes such as halogenation or oxidation of the plant itself. This localized build-up of poisonous substances acts directly on the plants at volume concentrations far in excess of what might be expected from the global analyses of pollutants. Also the serious effects of the enrichment of pollutants in rain water collected by and falling from trees[20] are not difficult to envisage. Only very accurate bulk trace element analysis of plant sections[23] will reveal the extent of contamination of these surfaces. Using the method of surface analysis described here, some exploratory experiments have shown both needle and broad leaf surfaces to be covered with a mixture of inorganic substances. From these considerations we can draw the following important conclusions, which in our opinion, should contribute in no small way to an understanding of the phenomena of environmental pollution: The toxic agents formed by heterogeneous catalytic reactions might not be formed in the atmosphere nor at the site of emission (flue gas plumes, exhausts) but only at the site of action (i.e. site of deposition). Dilution effects would then be largely ineffective. Naturally, such metal oxide particles are conceivably present, not only in emissions from motor vehicles but also in all sources of fine dust particles.

Since the most effective catalysts are the smallest and thus the lightest particles, the statement that the total amount of all particles emitted into the environment has drastically decreased in the last 20 years is only of limited value if one wishes to estimate the influence of the emission of solids on the environment.

In conclusion, it should again be stressed that the analytical method employed here is one which complements conventional methods of gas analysis. It enables an analysis to be carried out on that portion of the emission which is otherwise difficult to examine. Alongside the advantages of high sensitivity for all environmentally relevant elements and the possibility of analysis of the emissions without sample preparations (important for the speciation of elements which are shown to be present in the environment by other methods), the disadvantages such as low selectivity for organic compounds and the rather complicated quantification of the results should also be mentioned.

The authors wish to acknowledge collaboration with the Oekozentrum Langenbruck (Switzerland) from where the samples of the diesel motor test series were obtained. We thank Prof. Dr. H. J. Güntherodt, Dr. K. Noack and Dr. W. Vetter for critical reading of the manuscript. One of us (R. S.) acknowledges financial support from the Swiss National Science Foundation during his stay at Basel University. We thank M. Skottke for the careful typing of the manuscript.

Received: May 9, 1986;
revised: September 17, 1986 [A 616 IE]
German version: *Angew. Chem. 99* (1987) 312
Translated by Dr. T. Twomey, Berlin

[1] F. C. Taylor in J. R. Anderson, M. Boudart (Eds.): *Catalysis, Science and Technology, Vol. 5*, p. 119, Springer Verlag 1984.
[2] E. Koberstein, *Chem. Unserer Zeit 18* (1984) 37.
[3] a) G. Rosner, R. F. Hertel, *Staub 46* (1986) 281; b) C. H. Murphy: *Handbook of Particle Sampling and Analysis Methods*, Verlag Chemie, Weinheim 1984.
[4] D. Briggs, M. P. Seah: *Practical Surface Analysis*, Wiley, New York 1983.
[5] T. Jack, C. J. Powell, *Environ. Sci. Technol. 18* (1984) 58; G. E. Canbaniss, R. W. Linton, *ibid. 18* (1984) 271.
[6] A. Bijorsetel, G. Lunde, A. Lindshog, *Atmos. Environ. 13* (1979) 45.
[7] R. C. Greaves, R. M. Barkley, R. E. Sievers, *Anal. Chem. 57* (1985) 2807.
[8] M. E. Farmer, R. W. Linton, *Environ. Sci. Technol. 18* (1984) B 19.
[9] C. Urban, *US Environ. Prot. Agency, Rep. EPA 1980*, 19-460/38-80-004.
[10] J. Riga, J. J. Pireaux, J. P. Boutique, R. Candano, J. J. Verbist, Y. Gobillion, *Synth. Met. 4* (1981) 99.
[11] H. P. Boehm, E. Diehl, W. Heck, R. Sappok, *Angew. Chem. 76* (1964) 742; *Angew. Chem. Int. Ed. Engl. 3* (1964) 669.
[12] R. Schlögl, H.-P. Boehm, *Carbon 21* (1983) 345.
[13] B. Teretzki, *Dissertation*, Universität München 1979.
[14] L. D. Hulett, T. A. Carlson, B. R. Fish, J. L. Durham, *Proc. Symp. Air Quality* (Los Angeles 1971) p. 765.
[15] B. J. Lindberg, *Int. J. Sulfur Chem. Part C 7* (1972) 33.
[16] M. Peuckert, H. P. Bonzel, *Surf. Sci. 145* (1984) 239.
[17] T. Wang, L. D. Schmidt, *J. Catal. 71* (1981) 411.
[18] B. E. Warren, *J. Chem. Phys. 2* (1934) 551.
[19] D. Henschler (Ed.): *Gesundheitsschädliche Arbeitsstoffe*, Verlag Chemie, Weinheim 1981.
[20] O. Schwarz (Ed.): *Säurehaltige Niederschläge, VDI Report*, VDI-Verlag, Düsseldorf 1983, p. 72ff.
[21] S. Jordan, R. Dlugi, *VDI Nachr. 5* (1980) 74.
[22] R. Schlögl et al., unpublished.
[23] K. T. Whitby, *Atmos. Environ. 12* (1978) 135.
[24] F. H. Evers, *Allg. ForstZ. 41* (1986) 6.

Allylamine Derivatives—a New Class of Active Substances in Antifungal Chemotherapy

By Anton Stütz*

Fungal infections (mycoses) are found throughout the world. Only a few structural classes of compounds currently satisfy the demands of modern chemotherapy in their treatment; hence, the quest for new types of active substances is of major scientific and therapeutic importance. The first representative of a new class of substances—the allylamine derivatives—namely naftifine ((*E*)-*N*-methyl-*N*-(1-naphthylmethyl)-3-phenylallylamine) was discovered by accident and has recently become commercially available as a topical antimycotic. The exploration of structure-activity relationships on the basis of naftifine and new synthetic strategies led to the discovery of the currently most active compound of this type, terbinafine, the first pharmaceutical agent to contain a (*E*)-1,3-enyne structural element. Terbinafine exhibits considerably higher activity than the original "lead" structure naftifine both *in vitro* and *in vivo*; it is also up to one order of magnitude more effective than standard preparations in various chemotherapeutic animal tests after topical or oral administration. According to clinical experience gained so far, terbinafine is well tolerated and shows promising activity against various types of mycoses. Allylamines act as potent, selective inhibitors of fungal squalene epoxidase via a novel mechanism, which, unlike in the case of other inhibitors of steroid biosynthesis, does not depend on cytochrome P450.

1. Introduction

Fungal diseases were until a few decades ago considered to be of minor importance, especially in relation to bacterial infections. This situation has changed. The incidence of observed mycoses has increased significantly in recent years whether this be due to a real increase in the number of infections, to improved methods of diagnosis or to a better awareness of hygiene. Nowadays, mycoses occupy an important position among the infectious diseases.[1-4]

The clinical pictures of mycoses vary widely and depend on the localization of the infection and the state of immunity of the affected individual. *Superficial* mycoses of the skin, mucous membranes, hair and nails may proceed harmlessly but may also involve highly inflammatory processes. They include epidemic diseases such as athlete's foot (Tinea pedis) or nail mycoses (onychomycosis). *Deep* mycoses are often life-threatening systemic infections which, even today, are extremely difficult or impossible to treat.

Human-pathogenic fungi constitute a morphologically and physiologically heterogeneous group of microorganisms. In the more recent literature they are classified into three main groups:

- *Dermatophytes*, pathogens causing dermatophytoses (trichophytosis, microsporosis, epidermophytosis)
- *Budding fungi* (yeasts) and *biphasic fungi*, pathogens causing candidoses, sporotrichosis, and infections that occur outside Europe such as coccidioidomycosis, histoplasmosis, and blastomycosis.
- *Molds* which, for instance, are responsible for aspergillosis and chromomycosis.

[*] Dr. Anton Stütz
SANDOZ Forschungsinstitut
Brunnerstr. 59, A-1235 Wien (Austria)

Fungi, unlike bacteria (prokaryotes), are eukaryotic microorganisms. They are more highly developed living organisms containing a true nucleus, i.e. they possess chromosomes that are enclosed by a nuclear membrane. The basic relationship with highly developed organisms accounts for the fact that it is difficult to treat fungal diseases efficiently and systemically without simultaneously harming the host.

A vast number of substances with antimycotic activity have been reported. Very few, however, satisfy the requirements of modern chemotherapy. Examples of the most important classes of substances are listed in Figure 1:

- Antibiotics
  a) polyenes: e.g. amphotericin B, nystatin
  b) griseofulvin
- Synthetic chemotherapeutic agents
  a) 5-fluorocytosine (flucytosin)
  b) thiocarbamates: e.g. tolnaftate
  c) azoles: e.g. clotrimazole, miconazole, ketoconazole

The latest and at present most intensely studied structural class is that of the azole antimycotics[5] which display a broad spectrum of activities. Azoles are potent inhibitors of ergosterol biosynthesis which is essential for the formation of intact fungal cell membranes. They block an important step in the sequence of reactions leading from lanosterol to ergosterol, namely the oxidative, cytochrome P450-dependent 14α-demethylation (cf. also Fig. 6).[6,7] Initially these compounds were only suitable for topical use but the discovery of ketoconazole a few years ago represented the breakthrough for systemic application.[8] Oral therapy, however, can provoke a number of side-effects[9] (liver toxicity, teratogenicity, interference with steroid hormone metabolism[10,11]) which are at least in part due to marked in-

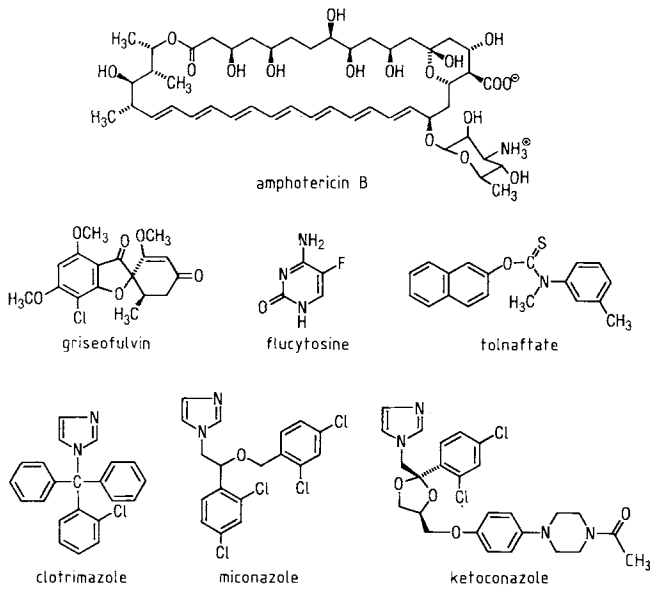

Fig. 1. Structures of representative antimycotics.

hibition of cytochrome P450-dependent enzyme reactions.[12-14] These effects have recently led to considerable restrictions being imposed on the use of ketoconazole.[15]

Research in the field of antimycotic chemotherapy is now being concentrated throughout the world on the investigation of the azoles and is documented by an exponentially growing flood of publications and patents.[5,16] It remains to be seen whether more effective, more selective and better tolerated compounds of this structural class can be developed.

In view of this restriction of attention to azoles, the search for new structural classes or the chemical investigation of new "leads" presents an alternative which may be of considerable scientific and therapeutic value.

2. Naftifine—an Accidental Discovery

In 1974 *Berney* was working in the Wander Laboratories, Bern (Switzerland), on spironaphthalenones with the aim of finding derivatives that acted on the central nervous system (CNS). After acid hydrolysis of one of these substances, he unexpectedly isolated a compound **1**, whose structure proved to be relatively simple but was previously unknown.[17]

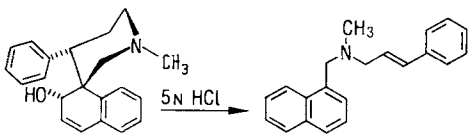

1

1 was subjected to tests in the Sandoz Forschungsinstitut in Wien (Austria) as part of a broadly based routine screening program. *Georgopoulos* et al. were able to show that the compound was highly effective against a number of human-pathogenic fungi. Results initially obtained with fungal cultures *(in vitro)*[18] were also confirmed in experiments on animals *(in vivo)*.[19] Activity was found to be at least as high as that of standard preparations after topical application in the guinea pig-trichophytosis model. Oral activity could only be demonstrated after administering a very high dose that was of no therapeutic relevance.[20]

After extensive investigation of its pharmacological and toxicological properties,[21,22] **1** (generic name: naftifine) was tested intensively for several years in hospitals.[23] Numerous studies have shown that naftifine is a highly effective topical antimycotic. Naftifine was compared with standard topical antimycotics or a placebo in open studies or under double blind conditions on patients with different dermatophytoses and candidoses. Naftifine proved to be equally as effective and in some cases superior to the standards. In many cases clinical symptoms were found to disappear more quickly[24] and an additional antiinflammatory effect was observed.[25]

Naftifine first became commercially available in various countries (the Federal Republic of Germany, Austria, Malaysia, and Singapore) in 1985 under the name Exoderil®.[26]

3. Allylamine Derivatives—a New Class of Antimycotic Agents

During the course of these developments, studies were begun on the mechanism of action[26-28] of naftifine and its chemical investigation to provide the answers to the following questions:

- Can naftifine be assigned to an already known structural class; is it a solitary compound or a representative of a new class of active substances?
- Do definable structure-activity relationships exist and which structural elements are essential for antifungal activity?
- Can this information be used to design new structures with higher activities and/or a broader spectrum of activity?
- Are there any compounds with therapeutically useful oral activities (when naftifine was discovered griseofulvin and 5-fluorocytosine were the only two known antimycotics with oral activity)?

It soon became evident that the antifungal activity of naftifine was specifically associated with defined structural elements which could not be related to any of the known classes of active substances.[29] A great many compounds with similar and, later on, with significantly higher activities were found. As all of the active compounds possessed a tertiary allylamine functionality they were termed the "allylamine derivatives".[30]

A concise and thus somewhat simplified account of the way in which terbinafine, the currently most active compound of this type, was discovered is given in the following section.

3.1. Basic Structure-Activity Relationships

In order to clarify basic structure-activity relationships the naftifine analogues **2**–**6** were synthesized.[29] They proved to be inactive in antimycotic tests *in vitro*. It was

therefore concluded that the nitrogen atom, the double bond and the 1-substituted naphthalene ring were of importance and also that the aromatic ring systems could not be interchanged.

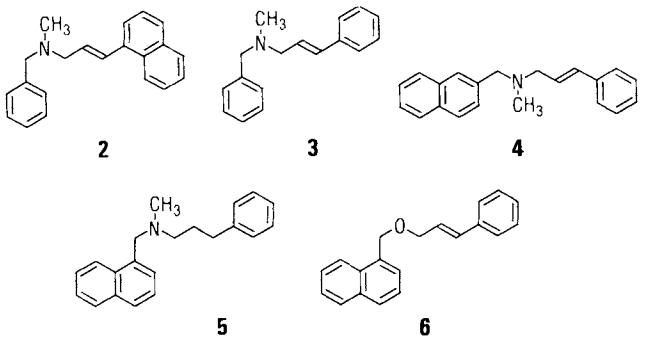

Compounds **7**–**11** were then studied to see whether the distances between the individual functional groups and between the aromatic systems could be decreased or increased without affecting the activity. These compounds were also either inactive or their activity was several orders of magnitude lower than that of **1**.[29] The altered parts of the molecules are indicated in the formulas by bold print.

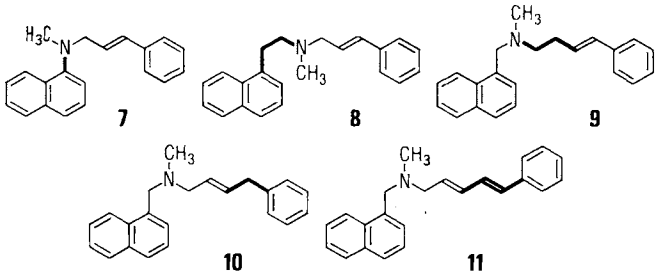

These studies demonstrate that the antifungal properties of **1** do indeed depend on specific structural requirements. Further detailed systematic variation of the individual structural elements confirmed and supplemented these preliminary structure-activity relationships.[29]

3.2. Semirigid Naftifine Analogues

The structure of **1** was subsequently assumed to be essential and its most active conformation was sought. Semirigid analogues were synthesized by incorporating the conformationally flexible structure of **1** in different ring systems; the effects of these changes on biological activity were investigated.[31] In an "all or nothing" effect, four of these compounds (**12**, **13**, **15**, and **16**) proved to be totally inactive while two (**14** and **17**) had activities that were within the same range as that of naftifine **1**.

As the piperidine compound **17** displayed an interesting spectrum of activity and also had a chiral center, it was resolved into its enantiomers. Animal experiments revealed that activity was restricted to the (*R*)-form (shown by X-ray structure analysis[32]). This compound was the first derivative[33,34] to exhibit significantly improved oral activity in the guinea pig-trichophytosis model and proved that the systemic activity of **1** could be increased.

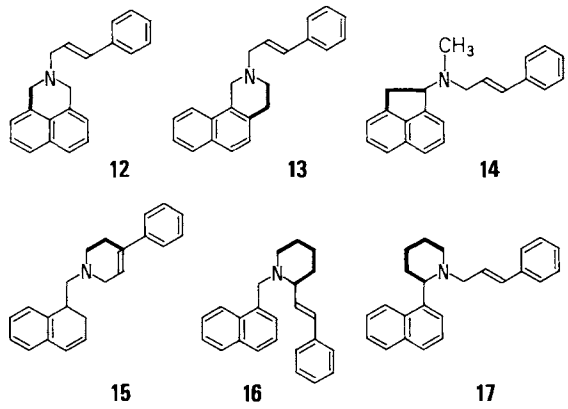

3.3. Systematic Variation of the *N*-Alkenyl Side Chain

In a systematic study the 3-phenylallyl (cinnamyl) group of **1** was replaced by C_{10}-alkyl chains with an increasing number of conjugated double bonds and these compounds (**18**–**22**) were then tested against various human-pathogenic microorganisms (Table 1). Biological activity reaches a clearly defined maximum when there are two conjugated double bonds (**20**). Analogues **21** and **19** with one double

Table 1. Effectiveness of allylamine derivatives in vitro. Top: Variation of the number of double bonds in the *N*-alk(en)yl side chains of the compounds **18**–**22**; Bottom: Variation of the alkyl groups in the *N*-(2,4-alkadienyl) side chains of the compounds **23**–**26** and **20** [a, b].

	R =	MIC [mg/L] *Trich. ment.*	*Epid. fl.*	*Micr. can.*	*Spor. sch.*	*Cand. par.*
18		100	100	100	100	>100
19		1.6	25	50	>100	>100
20		0.05	0.1	0.1	1.6	1.6
21		1.6	3.1	3.1	100	>100
22		50	50	25	>100	>100
23		1.6	50	25	100	>100
24		0.1	0.8	0.8	6.2	12.5
25		0.05	0.2	0.1	3.1	1.6
20		0.05	0.1	0.1	1.6	1.6
26		0.2	0.8	0.4	3.1	100

[a] MIC (minimum inhibitory concentration): lowest concentration of the substance that completely inhibits fungal growth. [b] *Trich. ment.: Trichophyton mentagrophytes; Epid. fl.: Epidermophyton floccosum; Micr. can.: Microsporum canis; Spor. sch.: Sporothrix schenckii; Cand. par: Candida parapsilosis.*

bond more and one double bond less, respectively, are considerably less effective. The derivatives without (**18**) or with four (**22**) conjugated double bonds are virtually inactive.[36]

Variation of the length of the 2,4-alkadienyl side chain has a similar although less pronounced effect, the highest activity being obtained with C_9 to C_{10} (compounds **20**, **25**). The effects of these modifications were also investigated in the guinea pig-trichophytosis model after topical and oral administration (Fig. 2). The activity *in vivo* was found to be even more dependent on the chain length. Topical application of a 2% solution of the derivatives completely cured the animals only in the case of compound **25**; homologue **20** proved to be the most effective compound after oral administration. Changes involving one to three methylene groups produced a decrease or total loss of activity.[36]

These results demonstrate that minor changes in the chemical structure can be critical not only for optimization but also for the possible discovery of a lead substance.

3.4. The (*E*)-1,3-Enyne Group—a New Structural Element in Pharmaceutical Agents

Table 2 reveals that the antifungal activity of compound **25**, which has an (*E,E*)-2,4-alkadienyl side chain (see also Table 1 and Fig. 2), is comparable to that of the lead structure naftifine **1** both *in vitro* and *in vivo*.

Substitution of the double bond between C4 and C5 by a triple bond (compound **27**, see also reduction with diisobutylaluminum hydride in Section 4.1) improves the activities *in vitro* and *in vivo*, especially after oral administration. In the latter case 75 mg/kg of **1** or **25**, for example, is ineffective in the guinea pig-trichophytosis model by mycological criteria, whereas the same dose of the (*E*)-1,3-enyne derivative **27** completely cures the animals. The *trans* configuration is essential for this effect: the corresponding *cis* isomer **30** is less active by several orders of magnitude, as are analogues with an inverted enyne group (**28**) or with two conjugated triple bonds (**29**).[37]

Bearing the results shown in Figure 2 in mind, the alkyl group adjacent to the triple bond in compound **27** was varied (Table 3). Increased branching finally improved the oral efficacy by one order of magnitude in the form of the *tert*-butyl compound **32** (terbinafine)![37,38] The *tert*-butyl

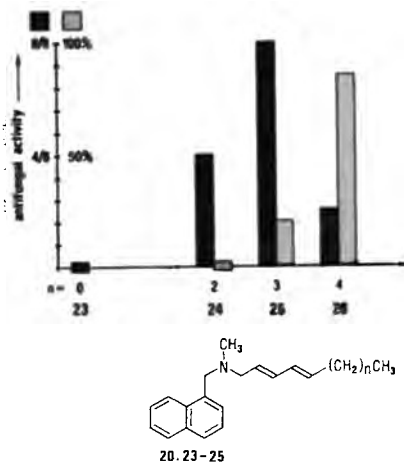

Fig. 2. In vivo activity of the *N*-2,4-alkadienyl derivatives **20** and **23**–**25** in the guinea pig trichophytosis model (cf. Table 1). Black: topical treatment: 2% polyethylene glycol (PEG) solution; mycologically cured animals after once-daily treatment over a period of 7 d.—Gray: oral treatment: mycologically cured animals after once-daily administration of 150 mg/kg over a period of 9 days.

Table 2. In vitro and in vivo activities (guinea pig-trichophytosis model) of the allylamine derivatives **1**, **25**, and **27**–**30**. Abbreviations, see Table 1.

		MIC [mg/L]				
R=		*Trich. ment.*	*Epid. fl.*	*Micr. can.*	*Spor. sch.*	*Cand. par.*
1	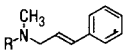	0.05	0.2	0.1	1.6	1.6
25	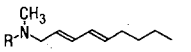	0.05	0.2	0.1	3.1	1.6
27	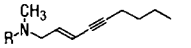	0.01	0.01	0.01	1.6	0.4
28	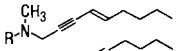	0.2	1.6	0.2	> 100	> 100
29	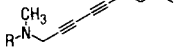	0.2	3.1	0.8	100	100
30	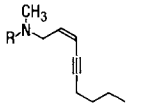	0.2	100	0.2	50	100

	In vivo [% myc. cured]				
	top. [a]			oral [b]	
	0.125%	0.5%	37.5	75	150
1	35	65	—	—	48
25	40	69	—	—	43
28	83	100	83	100	100

[a] PEG solution. [b] Daily dose [mg/kg].

Table 3. In vitro and in vivo activities (guinea pig-trichophytosis model) of the (*E*)-2-alken-4-ynyl derivatives **27**, **31**, and **32** [a].

		MIC [mg/L]							Oral [b] [% myc. cured]	
R=		*Trich. ment.*	*Epid. fl.*	*Micr. can.*	*Spor. sch.*	*Asp. fum.*	*Cand. alb.*	*Cand. par.*	5	10
27	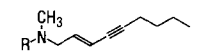	0.01	0.01	0.01	1.6	100	100	0.4	0	15
31	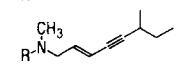	0.01	0.006	0.006	0.8	100	100	0.4	23	75
32	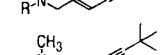	0.006	0.006	0.006	0.4	0.8	25	0.4	98	100

[a] Abbreviations, see Table 1; *Asp. fum.*: *Aspergillus fumigatus*; *Cand. alb.*: *Candida albicans*. [b] Daily dose [mg/kg].

group is, moreover, a prerequisite for activity *in vitro* against *Aspergillus fumigatus* and *Candida albicans*.

Attempts to replace the *tert*-butyl group in (*E*)-2-alken-4-ynylamines by other substituents are summarized in Table 4[39] and include compounds with substantial antifungal activities. The most active compounds in this group *in vivo* are the ether analogue **33** and the derivative **34**, in which the *tert*-butyl group is replaced by a trimethylsilyl residue and which, although its activity is relatively weak *in vitro*, is virtually as effective as terbinafine after oral administration! This is all the more surprising in view of the fact that the ≡C–Si bond is much less stable, both chemically and metabolically, than the corresponding ≡C–C bond.

The conjugated *trans*-enyne group has proved to be an important structural modification for improving the antimycotic activity of allylamines, particularly after oral administration, and as far as we are aware it represents a *novel structural element in pharmaceutical agents*[30,37,40]. Terbinafine (**32**) was shown to be by far the most suitable of this series of enynes for further development. Figure 3 shows a computer simulation of the spatial structure of terbinafine.

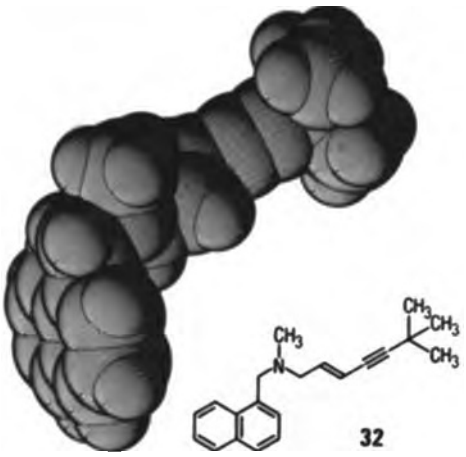

Fig. 3. Computer graphic representation of the 3D-structure of terbinafine **32** derived from the X-ray structure analysis of the hydrochloride [32].

Table 4. In vitro and in vivo activities (guinea pig-trichophytosis model) of (*E*)-2-alken-4-ynyl derivatives [a].

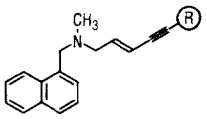

	R	MIC [mg/L] *Trich. ment.*	*Micr. can.*	*Spor. sch.*	*Asp. fum.*	*Cand. alb.*	*Cand. par.*	Oral [b] (myc. cured) 10 mg/kg
		0.01	0.02	1.6	>100	>100	3.1	
		0.8	1.6	>100	>100	>100	>100	
		3.1	3.1	>100	>100	>100	>100	
		0.2	0.4	>100	>100	>100	>100	
		0.006	0.01	1.6	6.2	100	3.1	
	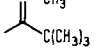	0.01	0.02	1.6	>100	25	0.8	
	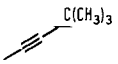	0.8	25	>100	>100	>100	>100	
		0.8	3.1	50	>100	>100	>100	
33		0.01	0.05	6.2	3.1	>100	12.5	95%
34		0.05	0.05	3.1	>100	25	1.6	100%
		6.25	1.6	25	3.1	100	6.2	

[a] Abbreviations, see Tables 1 and 3. [b] Daily dose [mg/kg].

4. Synthetic Aspects

4.1. A New Method of Synthesis for (*E*)-Allylamines

During attempts to develop widely applicable synthetic pathways for allylamine derivatives, a new method was found for the stereoselective *trans* reduction of tertiary

propargylamines with the aid of diisobutylaluminum hydride (DIBAH).[41,42] This reaction occurs under mild conditions (40 °C, toluene, 3 h) and gives high yields. Its trans-stereoselectivity, in contrast to the known *cis*-hydroalumination of disubstituted alkynes,[43,44] is attributable to a neighboring group effect of the α-amine. The reactivity and selectivity clearly differ from those of other reactions

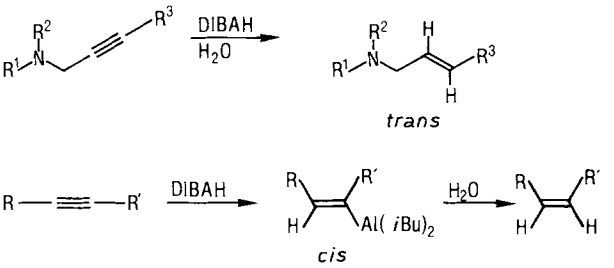

which also involve *trans*-hydroalumination such as the known $LiAlH_4$ reduction of α-hydroxyacetylenes to (*E*)-α-hydroxyalkenes.[45] 1,3-Diynes such as **35**, which contain both a propargylamine and a propargyl alcohol functionality are, for instance converted with DIBAH into **36** and with $LiAlH_4$ at the other triple bond into **37** (Scheme 1).[42]

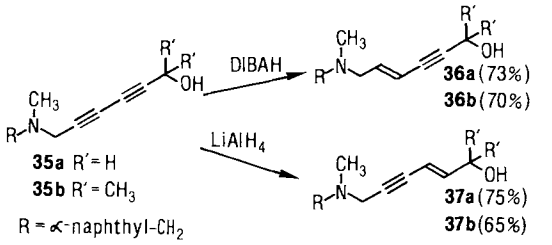

Scheme 1.

This raises the preparatively and mechanistically interesting question as to whether the reduction of a 2,4-alkadiynylamine with an excess of DIBAH proceeds *trans* at the triple bond between C-2 and C-3 (via a neighboring group effect of the nitrogen) and/or in the "normal" (*cis*) fashion at the other triple bond. Reaction of the diyne **29** (obtained by oxidative coupling) with DIBAH in the molar ratio 1:5 gives an approximately 1:1 mixture of the (*E*)-2-alken-4-ynylamine **27** and the (2*E*,4*Z*)-2,4-alkadienylamine **38** (Scheme 2). The direduction proceeds highly stereoselectively (*EZ*/*EE* = 98/2); this behavior has also been found in other examples.

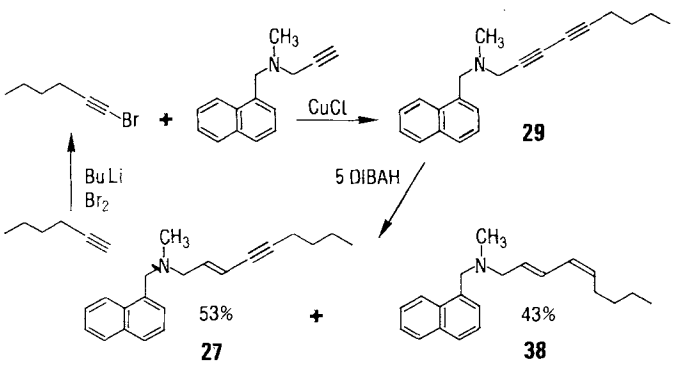

Scheme 2.

The (*E*)-enyne **27**, the product of monoreduction, represented the first breakthrough in efforts to discover highly effective allylamine derivatives with oral activity (see Section 3.4).

4.2. Synthesis of 2-Alken-4-ynylamines

The reaction sequence shown in Scheme 3 has proved to be extremely valuable for synthesizing a large number of differently substituted 2-alken-4-ynylamines: 1-alkynes are lithiated and allowed to react with acrolein in a 1,2-addition. The resulting secondary alcohols are then rearranged with concentrated aqueous HBr [route (a)] to give a stereoisomeric mixture of primary allylic bromides ($E/Z \approx 3:1$).

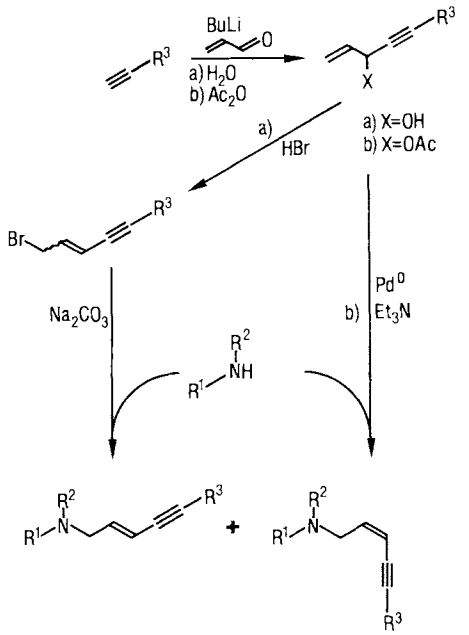

Scheme 3.

After reaction with a secondary amine the stereoisomeric products are separated either chromatographically or in the form of their hydrochlorides by selective crystallization of the *trans* isomers (as in the case of **32**).[37] Alternatively, the allylic rearrangement and *N*-alkylation can also be carried out [route (b)] via π-allylpalladium complexes with the aid of Pd(0) catalysts such as $[(Ph_3P)_4Pd]$ under particularly mild, neutral conditions.[46] Acetylenes with (acid-)sensitive functional groups give satisfactory yields via this route (Table 5). Furthermore, partial selectivity for the (*E*)- or (*Z*)-isomer has been achieved by modifying the experimental conditions or using a polymer-bound Pd catalyst.[47]

5. Mode of Action of Allylamine Derivatives

Accumulation of lipid-like vesicles was observed in electron microscopical studies on fungi treated with naftifine **1**.[48] The assumption that lipid metabolism was in some way affected was confirmed by biochemical investigations and the mode of action of the allylamines was subsequently elucidated.[26-28,49,50]

Table 5. Synthesis of 2-alken-4-ynylamines with the Pd^0-catalyst $[(Ph_3P)_4Pd]$ (5 mol-%) in tetrahydrofuran (15 h); cf. alternative b) in Scheme 3.

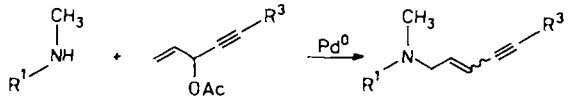

R^1	R^3	Yield [%] [a] *E*	*Z*
	$CH_2-S-C_2H_5$	29 (44)	22 (35)
	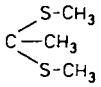	24 (34)	35 (52)
	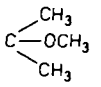	31 (45)	30 (45)
	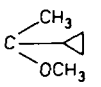	32	47
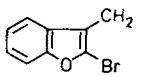	$Si(CH_3)_3$	31	24
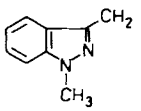	$C(CH_3)_3$	47	31

[a] Isolated material; values in parenthesis: yields according to HPLC analysis.

Naftifine, terbinafine and other allylamines interfere in the biosynthesis of ergosterol, an essential sterol in the cell membranes of fungi. They are very efficient inhibitors of squalene epoxidase from *Candida albicans* (terbinafine: $K_i = 3 \times 10^{-8}$ M; Fig. 5) and other fungi and cause intracellular accumulation of squalene (Fig. 4).[30,51,52] Squalene epoxidase is a key enzyme in sterol biosynthesis and is the first enzyme in this reaction pathway that requires molecular oxygen (Fig. 6). *Specific inhibition* of this enzyme was demonstrated *for the first time* with the *allylamines*.[53] At the present time no definite statements can be made about the molecular mechanism occurring at the enzyme.

Squalene epoxidation is an essential step in the biosynthesis not only of ergosterol in fungi but also of cholesterol in mammals. Comparative studies on squalene epoxidase from rat liver and fungi have shown, however, that terbinafine is highly selective for the fungal system. The relevant inhibition constants differ by more than three orders of

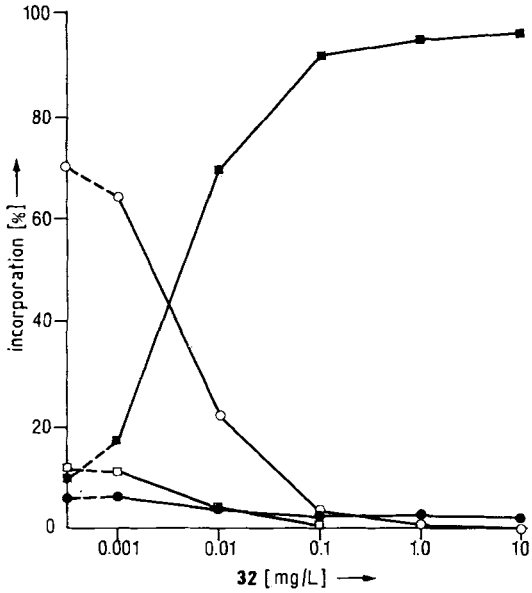

Fig. 4. Effect of terbinafine **32** on sterol biosynthesis in *Candida albicans* cells. Incorporation of ^{14}C-acetate into (○) ergosterol; (●) 4-monomethylsterols; (□) 4,4-dimethylsterols; (■) squalene (after *Ryder* [50]).

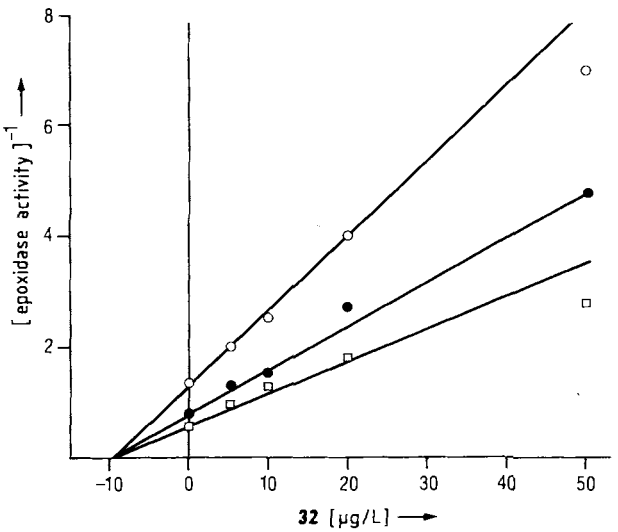

Fig. 5. Inhibition of squalene epoxidase from *Candida albicans* by terbinafine **32**. Dixon plots for three substrate concentrations (after *Ryder* et al. [30]). Substrate (squalene) concentration: ○ 12.8×10^{-6} M; ● 29.9×10^{-6} M; □ 116.2×10^{-6} M. $K_i = 9$ ng/mL (9 μg/L) ~ 3×10^{-8} M.

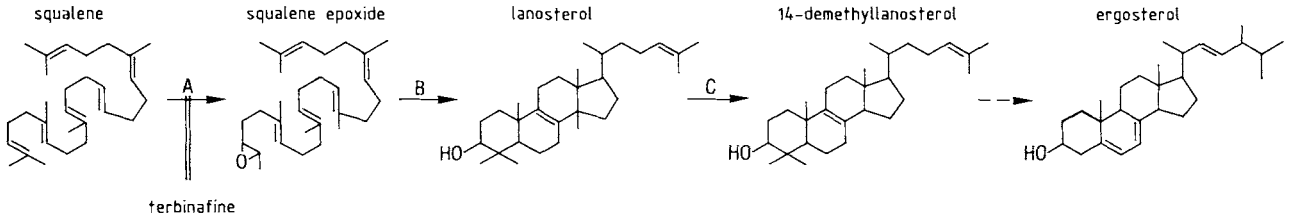

Fig. 6. Steps in the biosynthesis of ergosterol from squalene (after *Ryder* et al. [50]). Enzyme systems: A: squalene epoxidase (squalene monooxygenase, E.C. 1.14.99.7); B: squalene oxidocyclase (lanosterol synthase, E.C. 5.4.99.7); C: lanosterol-14α-demethylase complex, cytochrome P450-dependent; inhibited by azoles.

magnitude.[52] This finding is important as regards the use of terbinafine as a safe, systemically active chemotherapeutic agent without side-effects.

Squalene epoxidation, unlike the 14-α-demethylation of lanosterol, which is the main point of attack of the azole antimycotics, does not depend on cytochrome P 450 enzymes. Furthermore, allylamines do not exhibit an affinity for the cytochrome P 450 systems involved in steroid hormone synthesis in the adrenal glands, the placenta and the testes.[54] This is in agreement with the fact that none of the known side-effects of ketoconazole due to interaction with cytochrome P 450 have been observed in clinical trials carried out with terbinafine.

6. Terbinafine

In vitro terbinafine is effective against a wide range of human-pathogenic fungi (Table 6), but especially against dermatophytes such as *Trichophyton spp.*, *Microsporum canis* and *Epidermophyton flocc.* (MIC 0.0015–0.01 mg/L), *Aspergillus spp.* (MIC 0.02–1.56 mg/L and *Sporothrix schenckii* (MIC 0.1–0.4 mg/L). The sensitivities of yeasts vary more widely, displaying MIC values ranging from 0.1 to >100 mg/L. Terbinafine primarily acts fungicidally against dermatophytes and *Candida parapsilosis* and fungistatically against *Candida albicans*.[30,55–57]

Table 6. Spectrum and minimal inhibitory concentrations (MIC) of terbinafine[30,55] **32**.

Species	Number of strains tested	MIC [mg/L]	
		Range	$\bar{M}$
Trichophyton spp.	64	0.001–0.006	0.004
Epidermophyton flocc.	24	0.001–0.006	0.004
Microsporum canis	24	0.006–0.01	0.007
Aspergillus spp.	7	0.02 –1.56	0.63
Sporothrix schenckii	4	0.1 –0.4	0.2
Candida albicans	78	6.25 –100	29.3
Candida spp.	42	0.1 –>100	33.0

The oral effectiveness of terbinafine **32** is significantly greater than that of naftifine **1**. This was demonstrated by comparing the curative doses (dose at which 100% mycological cure rate is obtained) in the oral guinea pig-trichophytosis model:[35] in the case of naftifine it is 485 mg/kg,[20] and in the case of terbinafine it is 6 mg/kg.[30,58]

In the same model 60 and 80 mg/kg respectively of the clinical standards griseofulvin and ketoconazole were required to achieve a complete cure, these doses are one order of magnitude higher than that of terbinafine.[30,58]

Terbinafine was similarly shown to be more effective than the standards after topical application. Complete mycological cure of guinea pig trichophytosis and microsporosis was observed after treatment with 0.06 and 0.5% solutions of terbinafine respectively for 7 days. Under the same experimental conditions not even 2% solutions of the standards econazole or tolnaftate effected a complete or partial mycological cure. A guinea pig skin infection caused by *Candida albicans* was cured after topical application of a 1% terbinafine solution for 5 days.[30,58]

The pharmacokinetics, biotransformation and tolerance of terbinafine were extensively investigated in laboratory animals and later on in humans.[59–63] The remarkably low toxicity of terbinafine and its lack of teratogenic or embryotoxic effects in animal experiments are especially outstanding features. The plasma concentrations of the parent compound measured in humans and animals after oral administration far exceed its minimum inhibitory concentration despite considerable metabolism. The conditions for clinical application are therefore satisfied both as regards the required concentration of the active substance and drug safety.

Terbinafine is currently being tested world-wide in controlled clinical trials. The results so far obtained from, in some cases, incompleted studies are encouraging. Terbinafine was shown to be at least as effective as griseofulvin in the oral treatment of *Tinea corporis* although the daily terbinafine dose of 250 mg was only half that of the standard griseofulvin dose. In the topical treatment of *Tinea pedis* (athlete's foot) and *Tinea cruris*, terbinafine proved to be significantly more effective than clotrimazole even after only a few days.[64–66] As far as the topical treatment of skin candidiasis was concerned, terbinafine was comparable to clotrimazole.[67] It was also generally well-tolerated after both topical and oral administration.

In view of these studies it can be hoped that terbinafine will prove to be a valuable addition to the arsenal of drugs available for treating mycoses.

7. Conclusion

The allylamines constitute a new class of antifungal compounds with oral and topical activity.[68] This has been documentated not only in the case of naftifine and terbinafine but also with a multitude of derivatives, some of them highly active, which have been described in various patents.[33,69–80] The chemical and biological investigation of these compounds is by no means complete and further work is currently in progress.

The following aspects of these studies could be relevant to the concepts of drug-design and structure-activity relationships: 1) By a combination of systematic structural variation and development of new synthetic methods it was possible to increase the biological activity of a lead compound by several orders of magnitude. 2) In general, the rational approach to antimicrobial chemotherapy attempts to inhibit processes which occur in the pathogen but not in the host. However, as shown in the case of the allylamines, a biosynthetic process common to host and pathogen can be inhibited with a high degree of selectivity towards the microbe.

The work described in this report is the result of several years of intense, interdisciplinary collaboration. I would like to thank all my colleagues whose contributions are cited in the references. I am especially grateful to Dr. G. Petranyi and his co-worker I. Leitner for carrying out the mycological studies and to my own co-workers W. Granitzer, A. Pruckner

and S. Roth for performing the syntheses with skill and dedication. My thanks are also due to Dr. M. Grassberger, Dr. H. Mieth, Dr. N. S. Ryder, Dr. I. Schuster, Dr. P. Stütz and many other colleagues for their many critical discussions and suggestions.

Received: April 15, 1986 [A 613 IE]
German version: *Angew. Chem. 99* (1987) 323
Translated by Dr. *Gail Schulz*, Seeheim-Jugenheim (FRG)

[1] O. Male: *Medizinische Mykologie für die Praxis*, Thieme, Stuttgart 1981.
[2] B. Gedek: *Kompendium der medizinischen Mykologie*, Parey, Berlin 1980.
[3] J. W. Rippon: *Medical Mycology*, Saunders, Philadelphia 1982.
[4] H. Rieth, *Pharm. Unserer Zeit 1979*, 161; *1980*, 1; *1982*, 1.
[5] Reviews: R. A. Fromtling, *Med. Actual. 20* (1984) 325; *Chem. Abstr. 101* (1984) 143395; G. J. Ellames, *Top. Antibiot. Chem. 6*, Ellis Horwood, Chichester (1982) 22.
[6] H. Van den Bossche, G. Willemsens, W. Cools, W. F. Lauwers, L. Le Jeune, *Chem. Biol. Interact. 21* (1978) 59.
[7] H. Van den Bossche, G. Willemsens, W. Cools, F. Cornelisson, W. F. Lauwers, J. M. Van Cutsem, *Antimicrob. Agents Chemother. 17* (1980) 992.
[8] Reviews: H. B. Levine: *Ketoconazole in the Management of Fungal Diseases*, Adis Press, Sydney 1982; H. Koch, *Pharm. Int. 4* (1983) 151; R. C. Heel, R. N. Brogden, A. Carmine, P. A. Morley, T. M. Speight, G. S. Avery, *Drugs 23* (1982) 1.
[9] A. L. Hume, T. M. Kerkering, *Drug Intell. Clin. Pharm. 17* (1983) 169.
[10] D. S. Grosso, T. W. Boyden, R. W. Pameter, D. G. Johnson, D. A. Stevens, J. N. Calgiani, *Antimicrob. Agents Chemother. 23* (1983) 207.
[11] A. Pont, P. L. Williams, D. S. Loose, D. Feldman, R. E. Reitz, C. Bochra, D. A. Stevens, *Ann. Intern. Med. 97* (1982) 370.
[12] D. S. Loose, P. B. Kan, M. A. Hirst, R. A. Marcus, D. Feldman, *J. Clin. Invest. 71* (1983) 1495.
[13] J. J. Sheets, J. I. Mason, C. A. Wise, R. W. Estabrook, *Biochem. Pharmacol. 35* (1986) 487.
[14] J. I. Mason, B. A. Murray, M. Olcott, J. J. Sheets, *Biochem. Pharmacol. 34* (1985) 1087.
[15] *Scrip 1034* (1985) 26; *Pharm. J. 1985*, 291.
[16] L. Zirngibl, *Prog. Drug. Res. 27* (1983) 253.
[17] D. Berney, K. Schuh, *Helv. Chim. Acta 61* (1978) 1262.
[18] A. Georgopoulos, G. Petranyi, H. Mieth, J. Drews, *Antimicrob. Agents Chemother. 19* (1981) 386.
[19] G. Petranyi, A. Georgopoulos, H. Mieth, *Antimicrob. Agents Chemother. 19* (1981) 390.
[20] G. Petranyi, unpublished.
[21] F. Schatz, H. Haberl, F. Battig, D. Jobstmann, G. Schulz, M. Nefzger, R. Czok, A. Nikoforov, *Arzneim.-Forsch. 36* (1986) 248.
[22] R. C. Grimus, I. Schuster, *Xenobiotica 14* (1984) 287.
[23] Representative summary of preclinical and clinical results: Y. M. Clayton, W. Meinhof, H. Seeliger: *Topische Therapie der Dermatomykosen*, Grosse Verlag, Berlin 1985, p. 29–152 *(Mykosen 28, Suppl. 1)*.
[24] S. Nolting, G. Weidinger, *Mykosen 28* (1985) 69.
[25] H. C. Friederich, P. J. Haas, H. Tronnier, G. Weidinger, *Aktuelle Dermatologie 11* (1985) 77.
[26] F. Paltauf, G. Daum, G. Zuder, G. Högenauer, G. Schulz, G. Seidl, *Biochim. Biophys. Acta 712* (1982) 268.
[27] P. Periti, G. G. Grassi: *Current Chemotherapy and Immunotherapy, Vol. II*, American Society for Microbiology, Washington, DC 1982.
[28] N. S. Ryder, P. F. Troke in [27], p. 1016.
[29] A. Stütz, A. Georgopoulos, W. Granitzer, G. Petranyi, D. Berney, *J. Med. Chem. 29* (1986) 112.
[30] G. Petranyi, N. S. Ryder, A. Stütz, *Science 224* (1984) 1239.
[31] A. Stütz, G. Petranyi, unpublished.
[32] I would like to thank *H. P. Weber* and *A. Widmer*, Sandoz Basel, for the X-ray structure analysis and computer processing.
[33] G. Petranyi, A. Stütz, DOS 3020113; *Chem. Abstr. 94* (1981) 156765e.
[34] G. Petranyi, A. Stütz, *Curr. Chemother. Immunother., Proc. Int. Congr. Chemother., 12th, 1981*, Abstr. 933.
[35] G. Petranyi, I. Leitner, H. Mieth, *Sabouraudia 20* (1982) 101.
[36] A. Stütz, G. Petranyi in [27], p. 1021.
[37] A. Stütz, G. Petranyi, *J. Med. Chem. 27* (1984) 1539.
[38] A. Stütz, G. Petranyi, *Proc. Int. Congr. Chemother., 13th, 6* (1983) 116/1; *Chem. Abstr. 103* (1985) 153373u.
[39] A. Stütz, G. Petranyi, *Intersci. Conf. Antimicrob. Agents Chemother., 24th, 1984*, Abstr. 304.
[40] A. Stütz, G. Petranyi, *3rd Noordwijkerhout Symposium on Innovative Approaches in Drug Research*, Noordwijkerhout 1985, Abstr. p. 51.
[41] W. Granitzer, A. Stütz, *Tetrahedron Lett. 1979*, 3145.
[42] A. Stütz, W. Granitzer, S. Roth, *Tetrahedron 41* (1985) 5685.
[43] G. Wilke, H. Müller, *Justus Liebigs Ann. Chem. 618* (1958) 267.
[44] G. Wilke, H. Müller, *Justus Liebigs Ann. Chem. 629* (1960) 222.
[45] E. J. Corey, J. A. Katzenellenbogen, H. G. Posner, *J. Am. Chem. Soc. 89* (1967) 4245.
[46] A. Stütz, P. Fünfschilling, *Int. Conf. Organomet. Chem., 12th, 1985*, Abstr. 329.
[47] B. M. Trost, E. J. Keinan, *J. Am. Chem. Soc. 100* (1978) 7779.
[48] J. Meingassner, U. Sleytr, G. Petranyi, *J. Invest. Dermatol. 77* (1981) 444.
[49] N. S. Ryder, G. Seidl, P. F. Troke, *Antimicrob. Agents Chemother. 25* (1984) 483.
[50] N. S. Ryder in C. Nombela (Hrsg.): *Microbial Cell Wall Synthesis and Autolysis*, Elsevier, Amsterdam 1984, p. 313.
[51] N. S. Ryder, *Antimicrob. Agents Chemother. 27* (1985) 252.
[52] N. S. Ryder, M. C. Dupont, *Biochem. J. 230* (1985) 765.
[53] According to the most recent studies, tolnaftate also inhibits squalene epoxidase in fungi: T. Morita, Y. Nozawa, *J. Invest. Dermatol. 85* (1985) 434; N. S. Ryder, I. Frank, M. C. Dupont, *Antimicrob. Agents Chemother. 29* (1986) 858.
[54] I. Schuster, *Xenobiotica 15* (1985) 529.
[55] G. Petranyi, J. G. Meingassner, H. Mieth, *Proc. Int. Congr. Chemother., 13th, 6* (1983) 116/9; *Chem. Abstr. 103* (1985) 119765p.
[56] Y. M. Clayton, *Proc. Int. Congr. Chemother., 13th, 6* (1983) 116/13.
[57] S. Shadomy, A. Espinel-Ingroff, R. J. Gebhart, *Sabouraudia 23* (1985) 125.
[58] G. Petranyi, J. G. Meingassner, H. Mieth, *Proc. Int. Congr. Chemother., 13th, 6* (1983) 116/15.
[59] G. Petranyi, A. Stütz, U. Ganzinger, *Proc. Int. Congr. Chemother., 13th, 6* (1983) 20/21.
[60] F. Schatz, H. Haberl, R. Czok, *Proc. Int. Congr. Chemother., 13th, 6* (1983) 116/33; *Chem. Abstr. 104* (1986) 99e.
[61] F. Battig, M. Nefzger, R. Czok, *Proc. Int. Congr. Chemother., 13th, 6* (1983) 113/37; *Chem. Abstr. 104* (1986) 14440w.
[62] R. Grimus, I. Schuster, *Proc. Int. Congr. Chemother., 13th, 6* (1983) 116/47; *Chem. Abstr. 103* (1985) 205429p.
[63] U. Ganzinger, A. Stephen, G. Hitzenberger, R. Baumgartner, M. Madoerin, P. H. Mekler, B. P. Richardson, S. Brüggemann, W. Suter, R. Racine, P. Donatsch, F. Schatz, H. Haberl, *Proc. Int. Congr. Chemother., 13th, 6* (1983) 116/52; *Chem. Abstr. 104* (1986) 14539k.
[64] A. Stephen, U. Ganzinger, *Proc. Int. Congr. Chemother., 13th, 6* (1983) 116/59.
[65] U. Ganzinger, A. Stütz, G. Petranyi, A. Stephen, *Acta Derm.-Venereol., Suppl. 121* (1986) 155.
[66] A. Stephen, U. Ganzinger, R. Czok in J. Ishigami (Ed.): *Recent Advances in Chemotherapy*, University of Tokyo Press, Tokyo 1985, p. 1946.
[67] U. Ganzinger, N. Zaias, private communication.
[68] Parts of this review were also presented on May 28, 1984 at the 6th International Symposium on Future Trends in Chemotherapy in Pisa (Italy): A. Stütz, G. Petranyi, A. Georgopoulos, Abstr. 190.
[69] D. Berney, DOS 2716943; *Chem. Abstr. 88* (1978) 62215z.
[70] H. Hamberger, A. Stephen, A. Stütz, P. Stütz, Eur. Pat. Appl. 896 (1979).
[71] A. Stütz, Eur. Pat. Appl. 24587; *Chem. Abstr. 95* (1981) 169006d.
[72] M. Grassberger, G. Petranyi, Fr. Pat. Appl. 2496103; *Chem. Abstr. 97* (1982) 198114j.
[73] A. Stütz, Fr. Pat. Appl. 2498604; *Chem. Abstr. 98* (1983) 54196k.
[74] A. Stütz, DOS 3302814; *Chem. Abstr. 99* (1983) 212414g.
[75] A. Stütz, DOS 3316093; *Chem. Abstr. 100* (1984) 85436c.
[76] H. Hamberger, A. Stephen, A. Stütz, P. Stütz, DOS 3405332 (1985).
[77] M. Grassberger, A. Stütz, G. Petranyi, DOS 3405334 (1985).
[78] M. Grassberger, A. Stütz, DOS 3405333 (1985).
[79] A. Stütz, DOS 3405329 (1985).
[80] A. Stütz, DOS 3405330 (1985).

When submitting manuscripts, authors of articles intended for publication as "Communications" are requested to read the "Notice to Authors" reproduced in the January issue of the journal following the list of contents; upon request, a copy can be obtained from the editorial office.

Apparently Nonstereospecific Dihalocarbene Addition—an Explanation**

By *Eckehard V. Dehmlow** and *Thomas Stiehm*

The stereospecific addition of dihalocarbenes to alkenes has been observed in hundreds of cases and, in accordance with the Skell hypothesis, supports the singlet character of these transient species.[1] Only in the case of *trans*-cyclooctene has a nonstereospecific addition of dibromocarbene been observed.[2-4] Isomerization of the starting material occurred concurrently. Dichlorocarbene behaved "normally." We have now investigated the addition of CCl_2 and CBr_2 to the more highly strained *cis,trans*-1,5-cyclooctadiene **1**. In this case, dichlorocarbene also behaves anomalously if it is generated under the conditions of phase-transfer catalysis (PTC).

In agreement with earlier reports,[5] **1** reacted with $:CCl_2$ (generated from ethyl trichloroacetate and sodium methoxide) to give exclusively **3a**, which reacted further to give **5a**. When $:CCl_2$ was generated under PTC conditions, however, a 2:1 mixture of **5a** and **6a** was obtained.

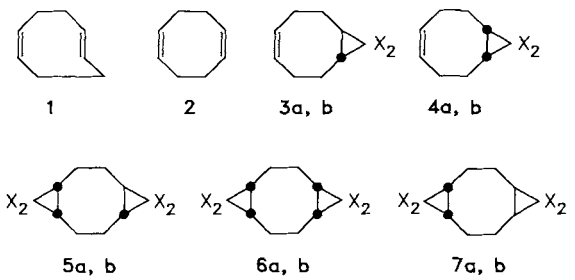

a, X = Cl; b, X = Br

Similar results were obtained for the reaction of **1** with $:CBr_2$. Reaction with potassium *tert*-butoxide/$CHBr_3$ gave only **5b**,[6] whereas with $CHBr_3$/50% aqueous sodium hydroxide/$(PhCH_2)Et_3NCl$ (TEBA) a mixture was once again obtained.[7] It consisted of a 2:1 ratio of **5b** and the *syn/anti* isomers **6b** and **7b**.[8]

The following observations are pertinent to explaining the mechanism of the reaction:

1. When the reaction with $:CCl_2$ was interrupted before completion, the recovered diene consisted of a mixture of **1** and *cis,cis*-1,5-cyclooctadiene **2**, and the monoadduct fraction (10% yield) contained a 2:1 mixture of **3a** and **4a**.[10] The bisadduct fraction (5% yield), on the other hand, consisted of pure **5a**. It is known that the *trans* double bond in **1** is the more reactive one. Apparently, **3a** undergoes further reaction more rapidly than **4a**.
2. Compound **1** did not isomerize to **2** either upon stirring for 24 hours in $CHCl_3$/petroleum ether or upon stirring for 24 hours in CH_2Cl_2/petroleum ether containing 50% aqueous sodium hydroxide and TEBA.
3. Compound **3a** was also stable toward 50% aqueous sodium hydroxide/TEBA.
4. Exposure of the reaction mixture to air did not affect the stereoselectivity. Therefore, radical and triplet-state processes can be excluded.
5. When **1** was allowed to stir for 17 hours in CH_2Cl_2/petroleum ether/50% aqueous sodium hydroxide/TEBA containing a small amount of ethanol (or acetylacetone), however, an 8:1 (or 5:1) mixture of **1** and **2** was isolated.[11] Products of nucleophilic addition to **1** or **2**[12] were not observed.

It is known from competition experiments that $:CCl_2$ generated under PTC conditions is a free singlet carbene.[13] In contrast to other methods of generation, however, this procedure results in a reversible equilibrium between $:CX_2$ and its precursor $CX_3^{\ominus}$.[14] The pK_a values of acetylacetone (9) and ethanol (19) encompass those of $CHBr_3$ (9[15]) and $CHCl_3$ (15[15]). Therefore, instead of the intermediate postulated initially by us, namely, a carbene–alkene complex,[3] it is necessary to assume a reversible nucleophilic addition to **1** accompanied by isomerization to **2**.

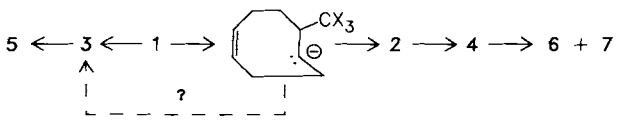

Experimental Procedure

1 (1 g, 9.3 mmol) in 40 mL of petroleum ether (30–40°C) and 30 mL of $CHCl_3$ was treated with TEBA (100 mg, 0.44 mmol) or an equivalent amount of Aliquat 336, Bu_4NHSO_4, or Ph_4AsCl. The mixture was then cooled in an ice bath and treated with 1 g of 50% aqueous sodium hydroxide, after which it was allowed to stir for 6 h at room temperature. Yield: 15–24%. M.p. of the preparatively nonseparable mixture of **5a** and **6a** = 115°C. Analysis by HPLC on an RP-18 column with methanol/H_2O = 2/1.

Received: July 11, 1986;
revised: January 21, 1987 [Z 1857 IE]
German version: *Angew. Chem. 99* (1987) 340

[*] Prof. Dr. E. V. Dehmlow, Dipl.-Chem. T. Stiehm
Fakultät für Chemie der Universität
D-4800 Bielefeld 1 (FRG)

[**] This work was supported by the Ministerium für Wissenschaft und Forschung Nordrhein-Westfalens (project No. IV B4-10302486).

[1] J. T. Sharp in D. Barton, W. D. Ollis (Ed.): *Comprehensive Organic Chemistry, Vol. 1*, Pergamon, Oxford 1979, p. 469.
[2] A. C. Cope, W. R. Moore, R. D. Bach, H. J. S. Winkler, *J. Am. Chem. Soc. 92* (1970) 1243.
[3] E. V. Dehmlow, R. Kramer, *Angew. Chem. 96* (1984) 700; *Angew. Chem. Int. Ed. Engl. 23* (1984) 706.
[4] The results of [3] were recently reproduced exactly: J. F. Hartwig, M. Jones, Jr., R. A. Moss, W. Ławrynowicz, *Tetrahedron Lett. 27* (1986) 5907.
[5] J. A. Deyrup, M. Betkouski, W. Szabo, M. Mathew, G. J. Palenik, *J. Am. Chem. Soc. 94* (1972) 2147; J. A. Deyrup, M. F. Betkouski, *J. Org. Chem. 40* (1975) 284.

[6] M.p. = 117°C; ^{1}H-NMR (300 MHz): δ = 0.75–0.9 (m, 1H), 1.02–1.2 (m, 2H), 1.2–1.45 (m, 3H), 1.5–1.65 (m, 2H), 2.2–2.5 (m, 4H).
[7] 30% yield, HPLC analysis with methanol/water = 3/1.
[8] Separation of the known compounds **6b** and **7b** [9] by HPLC was not possible; they were identified after fractional crystallization. On the other hand, **6a** was not accompanied by **7a**.
[9] E. V. Dehmlow, G. C. Ezimora, *Tetrahedron Lett. 1970*, 4047.
[10] Analytical separation by HPLC with acetonitrile/water = 1/1.
[11] We thank Prof. *J. Sauer*, Regensburg, for suggesting these experiments.
[12] Cf. R. D. Bach, C. L. Willis, *J. Organomet. Chem. 77* (1974) 31.
[13] Review: R. A. Moss in M. Jones, Jr., R. A. Moss (Eds.): *Carbenes, Vol. 1*, Wiley, New York 1973, p. 153–304.
[14] Review: E. V. Dehmlow, S. Dehmlow: *Phase Transfer Catalysis*, 2nd ed., Verlag Chemie, Weinheim 1983, p. 220–278.
[15] K. P. Butin, A. N. Kashin, I. P. Beletskaya, L. S. German, V. R. Polishchuk, *J. Organomet. Chem. 25* (1970) 11.

Titanium Hydride Formation through Hydrogen Transfer from 2-Methylpyridine to a Titanium Fulvene Compound; the First Structurally Characterized Terminal Titanium Hydride

By *Johannes W. Pattiasina, Fré van Bolhuis*, and *Jan H. Teuben**

In a study of the thermolysis of compounds of the type $[Cp^*_2TiR]$ ($Cp^* = \eta^5$-C_5Me_5; R = H or alkyl), we observed stepwise hydrogen abstraction from one of the Cp* ligands.[1]

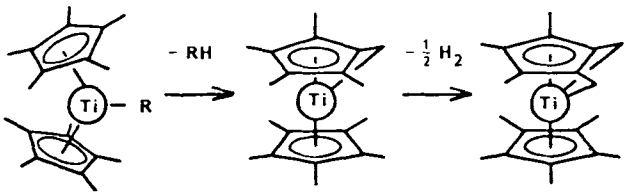

We are currently focusing our attention on the reactivity of these modified Cp* ligands. In **1** the tetramethylfulvene ligand may be coordinated either as a combined cyclopentadienyl-alkyl ligand, the "tucked-in" mode **A**,[2] or as a neutral conjugated triene **B**.[3]

In a series of exploratory studies with a variety of substrates with active protons, e.g., acids and alcohols, **1** reacted as a cyclopentadienyl-alkyl complex with transfer of hydrogen from the substrate to the fulvene ligand, thus restoring the original Cp* ligand.[4]

A completely different and unprecedented reaction took place when **1** was exposed to pyridine derivatives. At −80°C the dark purple **1** reacts quickly with 2-methylpyridine in Et_2O to give a dark green solution, which changes to an intense dark blue on warming to room temperature. Concentration and cooling of the solution to −30°C resulted in the formation of beautiful dark blue crystals of **2**.[5]

[*] Dr. J. H. Teuben, Dr. J. W. Pattiasina, F. van Bolhuis
Department of Chemistry, University of Groningen
Nijenborgh 16, NL-9747 AG Groningen (The Netherlands)

$$[Cp^*(C_5Me_4CH_2)Ti] + C_5H_4MeN \xrightarrow{Et_2O}$$

1

$$[Cp^*\{C_5Me_4CH_2(C_5H_3MeN)\}TiH]$$

2

The molecular structure of **2** (Fig. 1)[6] shows that hydrogen transfer from the 6-position of 2-methylpyridine to titanium, concurrent with C–C bond formation between pyridine and the methylene group of the fulvene ligand, has taken place. In this way a Cp* ligand is functionalized with a pyridine ligand to form a chelating ligand.

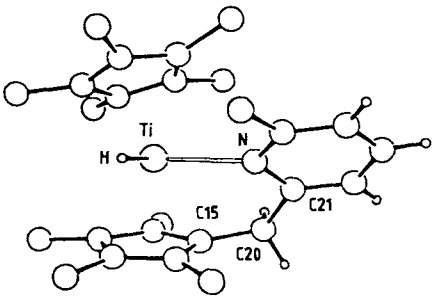

Fig. 1. Molecular crystal structure of $[Cp^*\{C_5Me_4CH_2(C_5H_3MeN)\}TiH]$ **2**.

Compound **2** is the first structurally characterized dicyclopentadienyltitanium hydride with a terminal Ti–H bond. The Ti–H distance (1.70(4) Å) is substantially longer than in other 3d-transition metal terminal hydrides, but comparable with hydrides of the early transition metals of the 4d and 5d series.[7] Until now only structure determinations of titanium hydrides with bridging hydrogen atoms, e.g., complexes containing a Ti–H–Ti, Ti–H–Al, or Ti–H–B structural element, have been published. In these complexes the Ti–H distances vary between 1.69(10) and 1.94(7) Å.[7]

The location of the pyridyl fragment with respect to the Ti atom and especially the Ti–N distance (2.340(3) Å) indicate that we are dealing with a dative Ti–N bond.[8] The angle formed between the Ti atom and the centroids of the substituted cyclopentadienyl rings is 142.7°; the distances between Ti and the centroids (2.086 and 2.064 Å) are close to those found in unsubstituted Cp^*_2Ti derivatives.[9]

The dihedral angle between the plane containing both ring centroids and Ti and the H–Ti–N plane is 91.6°; the H–Ti–N angle is 91(2)°. From this it is clear that **2** has all the characteristics of a regular $Cp^*_2M(L)X$ molecule. The C15–C20 bond deviates slightly from the ring plane (7.4°) toward the metal. The other C(ring)–C(methyl) bonds point away from the metal, thereby producing the normal "dish" shape of the Cp* ligands.[10] The C15–C20–C21 angle (111.5(3)°) shows that C20 is almost perfectly sp^3 hybridized.

The ^{1}H-NMR spectrum of **2**[5] affords assignments of the protons of the cyclopentadienyl ligands. Owing to the paramagnetism of **2**, the signals are broad and shifted strongly. The hydride resonance could not be located, a problem also encountered for the related compound $[Cp^*_2TiH]$.[3] In the IR spectrum, $\tilde{\nu}$(Ti–H) is found at 1475 cm^{-1}, slightly lower than for $[Cp^*_2TiH]$. The assignment was confirmed by the synthesis of the deuteride: $\tilde{\nu}$(Ti–D) was observed at 1065 cm^{-1} ($\tilde{\nu}$(Ti–H)/$\tilde{\nu}$(Ti–D) = 1.38). The ESR spectrum shows a well-resolved doublet, centered at

$g = 1.985$ ($a_H = 11.5$ G), and a clear hyperfine splitting due to interaction with titanium isotopes (^{47}Ti, I = 5/2, ^{49}Ti, I = 7/2, natural abundance 7.28% and 5.51%, respectively, $a_{Ti} = 9.3$ G).

Reaction of **2** with ethylene and DCl also confirmed the presence of a Ti–H functionality.

$$[Ti]H + CH_2{=}CH_2 \longrightarrow [Ti]Et \xrightarrow{D_2} [Ti]D + EtD$$
2 **3** [D]-**2**

$$[Ti]H + DCl \longrightarrow [Ti]Cl + HD$$
2 **4**

$[Ti] = Cp^*\{C_5Me_4CH_2(C_5H_3MeN)\}Ti$

In a Toepler pump controlled experiment, 1 mole of ethylene per mole of Ti was consumed. Compound **3** was isolated as a dark brown, analytically pure crystalline material; it reacts with D_2 to form EtD and [D]-**2** in a 1:1 molar ratio.[11]

The formation of a Ti–H bond through hydrogen transfer from 2-methylpyridine is completely different from what is regularly observed in reactions with compounds of early transition metals of the type $[Cp_2TiR]$[12] or $[Cp^*_2MR]$ (M = Sc,[13] Y,[14] Lu[15]). In the case of a "tucked-in" bonding mode, metalation of the pyridine with hydrogen transfer to the fulvene ligand and formation of $[Cp^*_2Ti(\eta^2\text{-}C_5H_3MeN)]$ is expected.

A further outstanding feature is the conversion of a fulvene ligand into a functionalized pentamethylcyclopentadienyl group. This reaction may be of considerable synthetic importance as an attractive route to bidentate Cp* ligands.

Experimental Procedure

2: **1** (0.574 g, 1.81 mmol) was dissolved in Et_2O (20 mL) and cooled to −196 °C. 2-Methylpyridine (0.168 g, 1.81 mmol) was added and the reaction mixture was warmed to −80 °C. Upon gradually warming the mixture to room temperature, the color of the solution changed from red-purple to dark green and finally dark blue. After stirring for 4 h, the solution was filtered, concentrated to 15 mL, and slowly cooled to −30 °C to give beautiful dark blue crystals. Yield: 0.335 g (0.82 mmol, 45%) of **2**. Correct elemental analysis.

Received: September 15, 1986;
revised: December 22, 1986 [Z 1931 IE]
German version: *Angew. Chem. 99* (1987) 342

CAS Registry numbers:
1, 53436-87-6; **2**, 107116-24-5; [D]-**2**, 107116-25-6; **3**, 107116-26-7; **4**, 107116-27-8; 2-methylpyridine, 109-06-8.

[1] J. W. Pattiasina, C. E. Hissink, J. L. de Boer, J. H. Teuben, A. Meetsma, A. L. Spek, *J. Am. Chem. Soc. 107* (1985) 7758.
[2] F. G. N. Cloke, J. C. Green, M. L. H. Green, C. P. Morley, *J. Chem. Soc. Chem. Commun. 1985*, 945.
[3] a) J. E. Bercaw, R. H. Marvich, L. G. Bell, H. H. Brintzinger, *J. Am. Chem. Soc. 94* (1972) 1219; b) C. McDade, J. C. Green, J. E. Bercaw, *Organometallics 1* (1982) 1629.
[4] J. H. Teuben in T. J. Marks, I. L. Fragalà (Eds.): *Fundamental and Technological Aspects of Organo-f-Element Chemistry*, Reidel, Dordrecht 1985, p. 195.
[5] ^{1}H-NMR (200.068 MHz, $[D_{10}]Et_2O$ at 0 °C; δ values relative to residual protons in the solvent at $\delta = 1.29$; multiplicity, intensity, width at half maximum height (Hz) in parentheses: $\delta = 25.0$ (s, 29 H, 280; $C_5Me_5(C_5Me_4CH_2)$),9.4 (m, 1 H, 280; C_5H_3MeN), 7.5 (m, 2 H, 170; C_5H_3MeN), 2.7 (s, 3 H, 50; C_5H_3MeN); IR (KBr/Nujol): $\tilde{\nu} = 2720$, 1596, 1565, 1475, 1450, 1415, 1370, 1310, 1265, 1225, 1210, 1195, 1160, 1102, 1055, 1015, 990, 925, 895, 835, 785, 728, 680, 610, 575, 437, 395 cm^{-1}.
[6] Cell data: $a = 10.045(4)$, $b = 19.333(5)$, $c = 11.504(4)$ Å, $\beta = 96.45(3)°$, $V = 2220.2$ Å^3, $\rho_{calcd} = 1.228$ g cm^{-3}, $\mu = 3.9$ cm^{-1}, $Z = 4$, $P2_1/n$, 4818 unique reflections, 2827 reflections with $I \geq 3\sigma(I)$, 398 parameters refined, $R = 0.052$, $R_w = 0.057$. Further details of the crystal structure investigation are available on request from the Fachinformationszentrum Energie, Physik, Mathematik GmbH, D-7514 Eggenstein-Leopoldshafen 2 (FRG), by quoting the depository number CSD-52363, the names of the authors, and the journal citation.
[7] a) R. G. Teller, R. Bau, *Struct. Bonding (Berlin) 44* (1981) 1; b) J. A. Jensen, G. S. Girolami, *J. Chem. Soc. Chem. Commun. 1986*, 1160.
[8] F. van Bolhuis, E. J. M. de Boer, J. H. Teuben, *J. Organomet. Chem. 170* (1979) 299.
[9] a) T. C. McKenzie, R. D. Sanner, J. E. Bercaw, *J. Organomet. Chem. 102* (1975) 475; b) S. A. Cohen, P. R. Auburn, J. E. Bercaw, *J. Am. Chem. Soc. 105* (1983) 1136; c) R. D. Sanner, D. M. Duggan, T. C. McKenzie, R. E. Marsh, J. E. Bercaw, *ibid. 98* (1976) 8358.
[10] K. H. den Haan, J. L. de Boer, J. H. Teuben, A. L. Spek, B. Kojić-Prodić, G. R. Hays, R. Huis, *Organometallics 5* (1986) 1726.
[11] J. H. Teuben et al., unpublished results.
[12] E. Klei, J. H. Teuben, *J. Organomet. Chem. 214* (1981) 53.
[13] M. E. Thompson, J. E. Bercaw, *Pure Appl. Chem. 56* (1984) 1.
[14] K. H. den Haan, Y. Wielstra, J. H. Teuben, *Organometallics*, in press.
[15] P. L. Watson, *J. Chem. Soc. Chem. Commun. 1983*, 276.

Sequential Configuration Analysis of Peptides**

By *Thomas Bolte, Dahai Yu, Hans-Thomas Stüwe,* and *Wilfried A. König**

Dedicated to Professor Ernst Bayer on the occasion of his 60th birthday

Stereochemical uniformity is an important criterion for the purity of synthetic peptides used as biologically active substances. Although partial racemization can be reliably detected and quantified by capillary gas chromatography on chiral stationary phases such as Chirasil-val®[1] or XE-60-L-valine-(*S*)-α-phenylethylamide,[2] only overall values for the individual amino acids are obtained.

For cases in which the same amino acid occurs repeatedly in the peptide sequence, it would be desirable to determine the degree of racemization as a function of position. Only then is it possible to modify the coupling and/or protecting group strategy in order to suppress racemization.

This problem can be solved by determining the enantiomeric purity of the phenylthiohydantoins (PTH derivatives) obtained by Edman degradation. *Davies* and *Mohammed*[3] used chiral isothiocyanates to show that the cleavage of thiocarbamoyl amino acids and their cyclization to the dihydrothiazolones does not occur without racemization, because an equilibrium is established with a quasi-aromatic, nonchiral tautomeric form. Although the use of chiral isocyanates[4] largely suppressed the racemization, the yields of diastereomeric hydantoins were unsatisfactory and their separation by HPLC incomplete.

Alkylcarbamoyl amino acid esters,[5] on the other hand, are easily separated by gas chromatography. We have used this approach to develop a procedure that allows the amino acids of a linear peptide to be sequentially removed from the *N*-terminus with retention of configuration (Scheme 1). The peptide **1** (0.5–1 mg) is first converted into the *tert*-butylcarbamoyl peptide **2** by reaction with *tert*-butyl isocyanate and pyridine (3:5, 30 °C, 45 min) and then treated with a solution of hydrogen chloride in isopropyl alcohol (1.0 N, 100 °C, 30 min). This results in cleav-

[*] Prof. Dr. W. A. König, T. Bolte, D. Yu, H.-T. Stüwe
Institut für Organische Chemie der Universität
Martin-Luther-King-Platz 6, D-2000 Hamburg 13 (FRG)

[**] This work was supported by the Deutsche Forschungsgemeinschaft and the Fonds der Chemischen Industrie.

age of the *N*-terminal amino acid as the *tert*-butylcarbamoyl amino acid isopropyl ester **3**. After extraction of **3** with chloroform, the enantiomer proportions can be determined very exactly by enantioselective gas chromatography (α values 1.07–1.11 on a 25-m glass capillary with XE-60-L-valine-(*S*)-α-phenylethylamide).

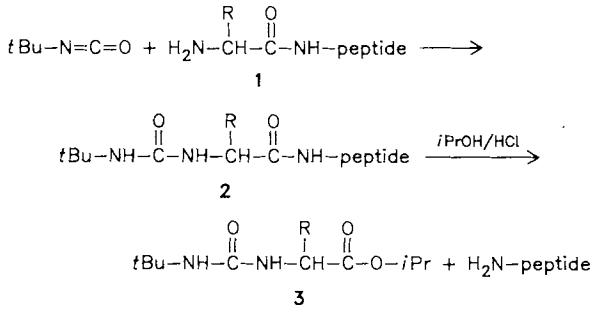

Scheme 1. For reaction conditions see text.

Under the given conditions, the use of isopropyl isocyanate and methanolic HCl results in the formation of *N*-isopropylhydantoins in addition to the isopropylcarbamoyl amino acid methyl esters. Although the former can also be separated by gas chromatography, they are not fully configurationally stable. In some cases, it proved to be advantageous to esterify the peptide with HCl/isopropyl alcohol (1.0 N) before the reaction with isocyanate, because the solubility in pyridine and the conversion to the carbamoyl derivative is often considerably improved.

Complete degradation of peptides containing 8–10 amino acids was achieved with 0.5–1 mg of starting material.

The method was used to investigate a synthetic octapeptide having the sequence H-Val-Ala-Leu-Ala-Lys-Lys-Ile-Leu-NH_2, for which gas chromatographic analysis to determine the degree of racemization after hydrolysis gave an unusually high value (8.7% D enantiomer) for Leu. Sequential degradation revealed a perfectly normal value (1.1%) for the D-isomer content of Leu[3] but a totally unexpected value (10.2%) for the D-isomer content of the *C*-terminal Leu. This finding is due to the synthesis of the peptide by the procedure of *Sheppard* et al.[6,7] using a polyacrylamide resin as solid support. In this procedure, the *C*-terminal Leu undergoes esterification with the polymer-bound anchor molecule 4-hydroxymethylbenzoic acid in a 4-dimethylaminopyridine-catalyzed reaction. The long reaction times required for complete esterification may be responsible for the unusually high degree of racemization.

Table 1. Proportion of D enantiomers in the synthetic octapeptide **1**. Gas chromatographic investigation of the *N*-trifluoroacetyl amino acid isopropyl esters after total hydrolysis and the *tert*-butylcarbamoyl amino acid isopropyl esters after sequential degradation.

1 2 3 4 5 6 7 8
H-Val-Ala-Leu-Ala-Lys-Lys-Ile-Leu-NH_2 **1**

Total hydrolysis D enantiomer [%]	Sequential degradation D enantiomer [%]
Σ Ala 3.6	Ala^2 0.8; Ala^4 1.2
Val 1.1	Val <0.3
Σ Leu 8.7	Leu^3 1.1; Leu^8 10.2
Ile 2.2	Ile 2.2
Σ Lys 3.8	[a]

[a] See text.

Comparison of the amounts of racemization after total hydrolysis and after sequential degradation (Table 1) reveals that the hydrolysis of the peptide in 6 N HCl also contributes to the racemization.

A further application of the procedure described here is provided by the investigation of peptide antibiotics, in which D- and L-amino acids are present in various positions.

For some amino acids (Lys, His, Arg, Trp), the carbamoyl derivatives are not sufficiently volatile for gas chromatographic investigation. In these cases, HPLC with chiral supports is a possible alternative. The first positive separation results were obtained with silica gel modified with covalently bound glucose derivatives.[8]

Received: December 22, 1986 [Z 2019 IE]
German version: *Angew. Chem. 99* (1987) 362

[1] H. Frank, G. J. Nicholson, E. Bayer, *Angew. Chem. 90* (1978) 396; *Angew. Chem. Int. Ed. Engl. 17* (1978) 363.
[2] W. A. König, I. Benecke, H. Bretting, *Angew. Chem. 93* (1981) 688; *Angew. Chem. Int. Ed. Engl. 20* (1981) 693.
[3] J. S. Davies, A. K. A. Mohammed, *J. Chem. Soc. Perkin Trans. 2 1984*, 1723.
[4] J. S. Davies, E. Hakeem, *Pept., Proc. Eur. Pept. Symp., 18th, 1984*, 137.
[5] W. A. König, I. Benecke, N. Lucht, E. Schmidt, J. Schulze, S. Sievers, *J. Chromatogr. 279* (1983) 555.
[6] E. Atherton, C. J. Logan, R. C. Sheppard, *J. Chem. Soc. Perkin Trans. 1 1981*, 538.
[7] E. Brown, R. C. Sheppard, B. J. Williams, *J. Chem. Soc. Perkin Trans. 1 1983*, 75.
[8] J. Schulze, W. A. König, *J. Chromatogr. 355* (1986) 165.

Benzene and Linearly Annelated Arenes as Dienophiles in Diels–Alder Reactions with Inverse Electron Demand

By *Gunther Seitz,* Reinhard Hoferichter,* and *Rolf Mohr*

As prototype aromatic 6π-electron systems, benzene and its simple derivatives show little tendency to react as dienes or dienophiles in [4+2] cycloadditions. Exceptions were observed in the case of extremely reactive dienophiles, such as dehydrobenzene derivatives, hexafluoro-2-butyne, dicyanoacetylene, and allenes, to which benzene adds inter- and intramolecularly as a *diene*.[1,2] Diels–Alder reactions in which benzene or simply substituted benzenes react as *dienophiles* have been rare so far.[3,4]

In bis(trifluoromethyl)tetrazine **1**, an extremely electron-poor diene, the s-*cis* diazabutadiene system exhibits the highest diene reactivity so far observed in Diels–Alder reactions with inverse electron demand.[5] We have now found that **1** can be used especially well to show that benzene and simply substituted benzenes can also exhibit *dienophilic properties*.

Whereas the [4+2] cycloaddition of benzene **2a** to **1** requires 24 h of heating at 140 °C in an autoclave, the donor-substituted benzenes **2b–e** react, in part, under somewhat milder conditions (Table 1).

[*] Prof. Dr. G. Seitz, Apotheker R. Hoferichter, Dr. R. Mohr
Pharmazeutisch-chemisches Institut der Universität
Marbacher Weg 6, D-3550 Marburg/Lahn (FRG)

[**] This work was supported by the Deutsche Forschungsgemeinschaft and the Fonds der Chemischen Industrie.

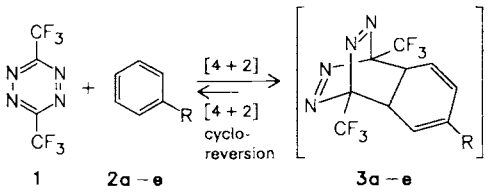

1 2a–e 3a–e

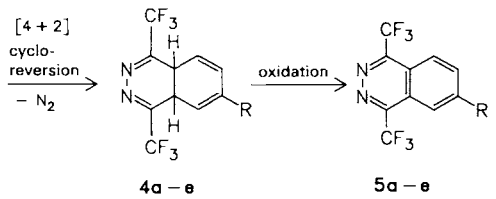

4a–e 5a–e

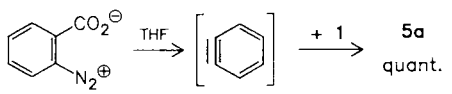

6 7 5a quant.

	a	b	c	d	e
R	H	CH_3	OCH_3	$N(CH_3)_2$	SCH_3

The Diels–Alder adduct **3a**, which is possibly formed in an equilibrium reaction, cannot be isolated. It undergoes further reaction, in the sense of a [4+2] cycloreversion[6] with elimination of nitrogen, to give **4a** irreversibly. Compound **4a** is sensitive to oxidation and is even oxidized by atmospheric oxygen or excess **1** to give a good yield of the phthalazine **5a**. The constitution of **5a** was confirmed by independent synthesis from **1** and dehydrobenzene **7** (generated from **6**, THF = tetrahydrofuran).[7]

Table 1. Characteristic data for the phthalazine derivatives **5a–e**, **9**, and **11**.

Compound	Reaction conditions	Yield [%]	M.p. [°C]	λ_{max} (lg ε) [nm] [a]	$\tilde{\nu}_{C=N}$ [cm^{-1}]
5a	24 h, 140°C	87	166	278 (3.53)	1580, 1570
5b	24 h, 140°C	40	146	280 (3.57)	1615
5c	12 h, 140°C	68	114	325 (3.32)	1605
5d	12 h, 110°C [b]	57	196	403 (3.70)	1600
5e	24 h, 140°C	56	150	358 (3.63)	1590
9	12 h, 140°C	59	170	360 (3.12)	1600
11	6 d, 110°C [b]	30	210	393 (3.79)	1610

[a] Solvent CH_2Cl_2; only the longest-wavelength maximum is given. [b] Temperature of boiling toluene.

The donor-substituted benzenes **2b–e** react similarly with **1**, resulting in preferential formation[8] of the 6-substituted phthalazines **5b–e** in preparative yields (Table 1).

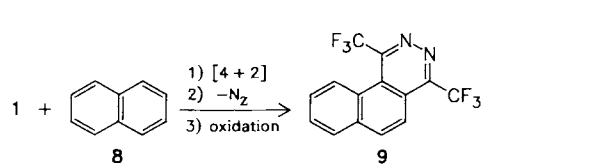

8 9

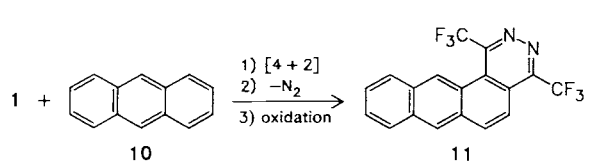

10 11

Their constitution can be derived unequivocally from the ^{1}H-NMR spectra (Table 2). The unusual reactivity is in accord with frontier orbital theory[9] and can be predicted on the basis of MNDO calculations.[10]

Linearly annelated arenes such as naphthalene **8** and anthracene **10** also exhibit pronounced dienophilicity, which has hardly been exploited so far in [4+2] cycloadditions.[1,11] Compound **1** reacts with **8** to give the benzophthalazine **9** and with **10** to give the naphthophthalazine **11**. The constitutions of the new compounds **5**, **9**, and **11** are in accord with the analytical and spectroscopic findings (^{1}H-NMR, ^{13}C-NMR, IR, UV, and mass spectra, see also Table 2).

Table 2. ^{1}H- and ^{13}C-NMR data for the phthalazine derivatives **5a–e**; in $CDCl_3$ with a 100-MHz NMR spectrometer if not given otherwise.

5a: ^{1}H-NMR: δ = 8.19 (mc, 2H; aryl H), 8.38 (mc, 2H; aryl H).—^{13}C-NMR: δ = 121.5 (q, $^1J_{CF}$ = 277 Hz; CF_3), 124.0 (m), 124.6 (dq, $^4J_{CF}$ = 3.2 Hz), 134.7 (dd), 150.0 (q, $^2J_{CF}$ = 34 Hz).

5b: ^{1}H-NMR: δ = 2.75 (s, 3H; CH_3), 8.00 (d, 1H, ^3J = 8.7 Hz; aryl H), 8.15 (br s, 1H; aryl H), 8.32 (br d, 1H, ^3J = 8.7 Hz; aryl H).—^{13}C-NMR: δ = 22.7 (q), 121.5 (q, $^1J_{CF}$ = 277 Hz), 122.3 (m), 123.4 (dm, $^4J_{CF}$ = 3 Hz), 124.3 (dm), 124.4 (m), 136.7 (dm), 146.3 (m), 149.5 (q, $^2J_{CF}$ = 34 Hz), 149.7 (q, $^2J_{CF}$ = 34 Hz)

5c: ^{1}H-NMR: δ = 4.08 (s, 3H; OCH_3), 7.55 (br s, 1H; aryl H), 7.66 (dd, 1H, ^3J = 9.4 Hz, ^4J = 2.4 Hz; aryl H), 8.31 (dq, 1H, ^3J = 9.4 Hz, $^5J_{FH}$ = 1.7 Hz; aryl H).—^{13}C-NMR: δ = 56.1 (q), 102.6 (dm, $^4J_{CF}$ = 3 Hz), 119.4 (m), 122.4 (q, $^1J_{CF}$ = 276 Hz), 122.5 (q, $^1J_{CF}$ = 276 Hz), 126.5 (m), 126.5 (dm, $^4J_{CF}$ = 3 Hz), 126.9 (dm), 139.1 (q, $^2J_{CF}$ = 33 Hz), 149.1 (q, $^2J_{CF}$ = 33 Hz), 163.7 (m)

5d: ^{1}H-NMR: δ = 3.24 (s, 6H; $N(CH_3)_2$), 7.11 (m, 1H; aryl H), 7.50 (dd, 1H, ^3J = 9.4 Hz, ^4J = 2.6 Hz; aryl H), 8.13 (dq, 1H, ^3J = 9.4 Hz, $^5J_{FH}$ = 1.7 Hz; aryl H).—^{13}C-NMR ([D$_6$]acetone): δ = 40.2 (q), 99.5 (dm, $^4J_{CF}$ = 3.3 Hz), 116.3 (m), 123.2 (q, $^1J_{CF}$ = 276 Hz), 123.3 (q, $^1J_{CF}$ = 276 Hz), 123.6 (dm), 126.2 (dm, $^4J_{CF}$ = 2.6 Hz), 127.1 (s), 148.4 (q, $^2J_{CF}$ = 33 Hz), 148.8 (q, $^2J_{CF}$ = 33 Hz), 154.3 (m)

5e: ^{1}H-NMR (400 MHz): δ = 2.69 (s, 3H; SCH_3), 7.91 (mc, 1H; aryl H), 7.93 (dd, 1H, ^3J = 9.0 Hz; ^4J = 1.8 Hz; aryl H), 8.22 (dm, 1H, ^3J = 9.0 Hz; aryl H).—^{13}C-NMR: δ = 14.5 (q), 116.4 (dm, $^4J_{CF}$ = 3 Hz), 121.2 (m), 121.5 (q, $^1J_{CF}$ = 275 Hz), 121.7 (q, $^1J_{CF}$ = 275 Hz), 124.0 (dm, $^4J_{CF}$ = 3 Hz), 124.5 (m), 132.9 (dm), 148.2 (q, $^2J_{CF}$ = 33 Hz), 148.4 (q, $^2J_{CF}$ = 33 Hz), 150.2 (m)

Received: September 29, 1986;
revised: January 7, 1987 [Z 1940 IE]
German version: *Angew. Chem. 99* (1987) 345

[1] Reviews: J. Sauer, *Angew. Chem. 78* (1966) 233; *Angew. Chem. Int. Ed. Engl. 5* (1966) 211; H. Wollweber: *Diels-Alder-Reaktion*, Thieme, Stuttgart 1972; T. Wagner-Jauregg, *Synthesis 1980*, 165; J. Sauer, R. Sustmann, *Angew. Chem. 92* (1980) 773; *Angew. Chem. Int. Ed. Engl. 19* (1980) 779; recent publications: A. F. Murad, J. Kleinschroth, H. Hopf, *Angew. Chem. 92* (1980) 388; *Angew. Chem. Int. Ed. Engl. 19* (1980) 389; J. Kleinschroth, H. Hopf, *Angew. Chem. 94* (1982) 485; *Angew. Chem. Int. Ed. Engl. 21* (1982) 469; K.-L. Noble, H. Hopf, L. Ernst, *Chem. Ber. 117* (1984) 474; K. Matsumoto, *Chem. Lett. 1985*, 1681.

[2] For the intramolecular Diels-Alder reaction of allenecarboxanilidene, see G. Himbert, L. Henn, *Angew. Chem. 94* (1982) 631; *Angew. Chem. Int. Ed. Engl. 21* (1982) 620; *Angew. Chem. Suppl. 1982*, 1473; L. Henn, G. Himbert, K. Diehl, M. Kaftory, *Chem. Ber. 119* (1986) 1953.

[3] Under an extremely high pressure of 10 kbar and at 220–240°C, benzene reacts twice as a dienophile with hexachlorocyclopentadiene: W. Jarre, D. Bieniek, F. Korte, *Angew. Chem. 87* (1975) 201; *Angew. Chem. Int. Ed. Engl. 14* (1975) 181.

[4] G. Seitz, T. Kämpchen, W. Overheu, U. Martin, *Chem. Ztg. 105* (1981) 342; K. Saito, Y. Omura, E. Maekawa, P. G. Gassman, *Tetrahedron Lett. 25* (1984) 2573.

[5] J. Sauer (Universität Regensburg), private communication.

[6] Cf. R. Huisgen, *Angew. Chem. 80* (1968) 329; *Angew. Chem. Int. Ed. Engl. 7* (1968) 321.

[7] Application of the reaction principle: J. Sauer, G. Heinrichs, *Tetrahedron Lett. 1966*, 4980; J. Sauer, A. Mielert, D. Lang, D. Peter, *Chem. Ber. 98* (1965) 1435.

[8] For example, reaction of **1** with **2c** affords, in addition to **5c**, a low yield (< 2%) of **5a**. Compound **5a** is presumably formed by [4+2] cycloaddition of **1** to the 1 and 2 positions of **2c** followed by elimination of ni-

trogen and methanol. In addition to **5a**, traces (< 1%) of *E*-1,2-bis[3,6-bis(trifluoromethyl)pyridazin-4-yl]ethene were also isolated (cf. [4]).
[9] Review: I. Fleming: *Frontier Orbitals and Organic Chemical Reactions*, Wiley, New York 1976, Chap. 4, p. 86ff; *Grenzorbitale und Reaktionen organischer Verbindungen*, Verlag Chemie, Weinheim 1979, Chap. 4, p. 133ff, and references cited therein.
[10] Dr. A. Heidenreich, Prof. Dr. A. Schweig (Universität Marburg), private communication.
[11] G. Seitz, R. Mohr, W. Overheu, R. Allmann, M. Nagel, *Angew. Chem. 96* (1984) 885; *Angew. Chem. Int. Ed. Engl. 23* (1984) 890.

Formation of Oxazolidinones and Oxazinanones by Reaction of Allylamines and of Homoallylamines with Carbon Dioxide and Iodine via Intramolecular Cyclization**

By *Takashi Toda** and *Yoshinori Kitagawa*

Recently, much attention has been focused on the utilization of carbon dioxide in organic synthesis.[1] However, almost all reactions of these types are carried out in the presence of biotin (or its analogues),[2] metal complexes,[3] large amounts of phosphorus compounds,[4] strong bases under high pressure,[5] or combinations of these methods.[6, 7] Furthermore, the reaction conditions are often rather severe.

We have been interested in carbon dioxide fixation via ammonium carbamates under mild conditions: without a catalyst, at atmospheric pressure, and, if possible, at ambient temperature. Since several aliphatic amines form stable carbamates **1** [Eq. (a)],[8] these salts were expected to

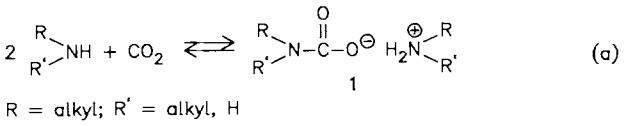

(a)

R = alkyl; R' = alkyl, H

offer certain advantages in carbon dioxide fixation. We have indeed reported several such reactions.[9] For example, intermolecular reactions between ammonium carbamates and oxiranes (or their synthons) give carbamate derivatives including cyclic carbamates [Eqs. (b)–(d)].

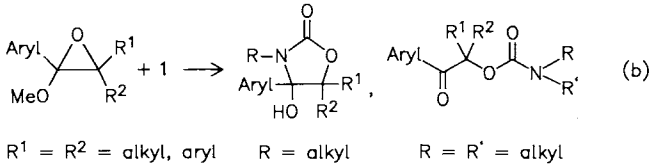

(b)

$R^1 = R^2$ = alkyl, aryl; R^1 = alkyl; R^2 = H — R = alkyl; R' = H — R = R' = alkyl

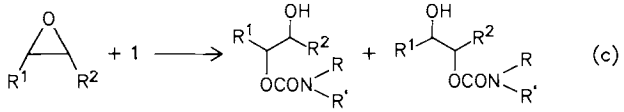

(c)

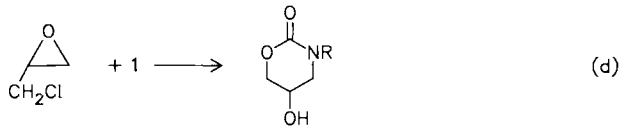

(d)

[*] Prof. Dr. T. Toda, Dr. Y. Kitagawa
Department of Industrial Chemistry,
Faculty of Engineering, Utsunomiya University
Utsunomiya 321 (Japan)

[**] Utilization of Carbon Dioxide in Organic Synthesis via Ammonium Carbamates, Part 8.

Herein we report on the synthesis of oxazolidinone and oxazinanone derivatives by reaction of allylamines and homoallylamines, respectively, with carbon dioxide and iodine via intramolecular cyclization under extremely mild conditions.[10]

Treatment of allyl- or homoallylamines with carbon dioxide in MeOH, followed by treatment with I_2 at ambient temperature for 20 h, gave iodoalkyloxazolidinones [Eq. (e)] or iodoalkyloxazinanones [Eq. (f)], respectively, in

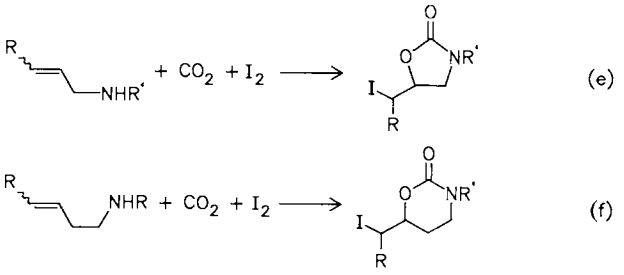

(e)

(f)

Table 1. Yields and some physical properties of the oxazolidinones and oxazinanones. The yields in parentheses are those obtained after prolonged reaction in the presence of Cs_2CO_3 (see text).

Reaction	Amine	Product	Yield [%]	M.p. [°C]	$\tilde{\nu}_{CO}$ (in KBr) [cm^{-1}]
1	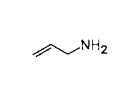	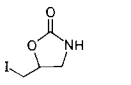	61 (70)	117–118.5	1730
2	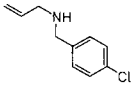	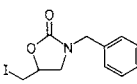	70 (90)	99–100.5	1735
3	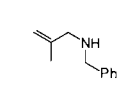	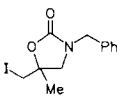	60 (90)	83–84	1730
4	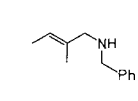	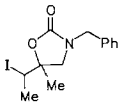	68 (80)	76.5–78	1735
5	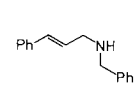	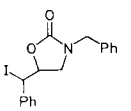	52 (80)	134.5–136 [a]	1735
6	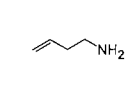	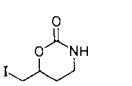	41 (60)	142.5–144 [a]	1680
7	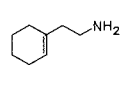	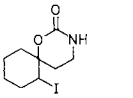	54 (70)	150–152 [a]	1690

[a] Decomposition.

fairly good yields (40–70%). The results and some physical properties of the products are summarized in Table 1. Pro-

longed reaction for a week in the presence of Cs_2CO_3 or Na_2CO_3 raised the yields to 70–90%. Since isolation of the intermediate ammonium carbamates is not necessary and the oxazolidinones and oxazinanones are the only isolable products, the reactions constitute one-pot procedures. Moreover, purification of the products is very easy. The structures of the products were deduced from their elemental analyses and from the IR or NMR spectra. As listed in Table 1, all the oxazolidinones exhibit their C=O absorption band near 1730 cm^{-1}, which is in agreement with a five-membered carbamate. The characteristic, strong C=O absorptions for the oxazinanones are observed around 1685 cm^{-1}. The scope and limitations of this reaction are now being studied.

Experimental Procedure

A solution of allylamine (4.0 mmol) in MeOH (4 mL) in an ice-cooled bath was saturated with CO_2. I_2 (2 mmol) was added to the solution, and CO_2 was admitted for an additional 5 min. The reaction mixture was then stirred for 20 h under CO_2 at room temperature. The excess iodine was removed by addition of aqueous $Na_2S_2O_3$, and the MeOH was removed in vacuo at 40°C. Extraction with ethyl acetate, drying over Na_2SO_4, and removal of the solvent gave 5-iodomethyl-2-oxazolidinone, which was purified by recrystallization from ethyl acetate. The reaction of the homoallylamines was carried out similarly. Reaction for one week in the presence of Cs_2CO_3 (2 mmol) raised the yields to the values shown in parentheses in Table 1.

Received: October 22, 1986;
revised: January 2, 1987 [Z 1961 IE]
German version: *Angew. Chem. 99* (1987) 366

CAS Registry numbers:
amine 1, 107-11-9; product 1, 107175-73-5; amine 2, 69957-80-8; product 2, 107175-74-6; amine 3, 52853-55-1; product 3, 107175-75-7; amine 4, 107175-79-1; product 4, 107175-76-8; amine 5, 107175-80-4; product 5, 107175-77-9; amine 6, 2524-49-4; product 6, 107175-78-0; amine 7, 3399-73-3; product 7, 107200-84-0; carbon dioxide, 124-38-9; iodine, 7553-56-2.

[1] Reviews: M. E. Vol'pin, I. S. Kolomnikov, *Organomet. React. 5* (1975) 313; S. Inoue, N. Yamazaki: *Organic and Bioorganic Chemistry of Carbon Dioxide*, Kodan-sha, Tokyo 1980, and references cited therein.

[2] N. Matsumura, T. Ohba, S. Yoneda, *Chem. Lett. 1981*, 317; T. Bodnar, S. J. LaCroce, A. R. Cutler, *J. Am. Chem. Soc. 102* (1980) 3928.

[3] H. Kisch, R. Millini, I.-J. Wang, *Chem. Ber. 119* (1986) 1090; P. Binger, H.-J. Weintz, *ibid. 117* (1984) 654; G. Burkhart, H. Hoberg, *Angew. Chem. 94* (1982) 75; *Angew. Chem. Int. Ed. Engl. 21* (1982) 76; *Angew. Chem. Suppl. 1982*, 147; D. J. Darensbourg, R. K. Hanckel, C. G. Banch, M. Pala, D. Simmons, J. N. White, *J. Am. Chem. Soc. 107* (1985) 7463; T. Aida, S. Inoue, *ibid. 105* (1983) 1304; T. Tsuda, Y. Chujo, T. Saegusa, *ibid. 102* (1980) 431; Y. Inoue, R. Ohashi, M. Toyofuku, H. Hashimoto, *Nippon Kagaku Kaishi 1985*, 533; T. Fujinami, T. Suzuki, M. Kamiya, S. Fukuzawa, S. Sakai, *Chem. Lett. 1985*, 199; B. Demerseman, R. Mahé, P. H. Dixneuf, *J. Chem. Soc. Chem. Commun. 1984*, 1394; F. Sato, S. Iijima, M. Sato, *ibid. 1981*, 180; A. Dohring, P. W. Jolly, *Tetrahedron Lett. 21* (1980) 3021; J.-E. Backvall, O. Karlsson, S. O. Ljunggren, *ibid. 21* (1980) 4985; H. Sugimoto, I. Kawata, H. Taniguchi, Y. Fujiwara, *J. Organomet. Chem. 266* (1984) C44.

[4] H. J. Bestmann, G. Schmid, *Tetrahedron Lett. 1977*, 3037; G. Ege, K. Gilbert, *ibid. 1979*, 4253.

[5] The Kolbe-Schmidt reaction is a typical one of this type; for a recent example, see L. A. Cate, *Synthesis 1983*, 385.

[6] Examples of carbonate ester formation from carbonate salts: G. Rokicki, W. Kuran, *Bull. Chem. Soc. Jpn. 57* (1984) 1662; J. A. Cella, S. W. Bacon, *J. Org. Chem. 49* (1984) 1122.

[7] Carbon dioxide fixation reactions by charge transfer or photochemical processes: S. W. Froelicher, B. S. Freiser, R. R. Squires, *J. Am. Chem. Soc. 106* (1984) 6863; K. Kitamura, S. Tazuke, *Chem. Lett. 1983*, 1109; S. Toki, S. Hida, S. Takamuku, H. H. Sakurai, *Nippon Kagaku Kaishi 1984*, 152.

[8] T. Hayashi, *Rikagaku Kenkyusho Iho 11* (1932) 133; H. B. Wright, M. B. Moor, *J. Am. Chem. Soc. 70* (1948) 3865; M. Kato, T. Ito, *Bull. Chem. Soc. Jpn. 59* (1986) 285.

[9] a) T. Toda, *Chem. Lett. 1977*, 957; *Nippon Kagaku Kaishi 1982*, 228; N. Saito, K. Hatakeda, S. Ito, T. Asano, T. Toda, *Bull. Chem. Soc. Jpn. 59* (1986) 1629; b) T. Asano, N. Saito, S. Ito, K. Hatakeda, T. Toda, *Chem. Lett. 1978*, 311; c) for analogous reactions, see: Y. Yoshida, S. Inoue, *ibid. 1977*, 1375; *J. Chem. Soc. Perkin Trans. 1 1979*, 3146; Y. Yoshida, S. Ishii, T. Yamashita, *Chem. Lett. 1984*, 1571.

[10] Very recently, *Cardillo* et al. reported similar reactions in which they used Amberlyst A 26 as a catalyst. However, their concept of utilizing carbon dioxide is different from ours: G. Cardillo, M. Orena, S. Sandri, *J. Org. Chem. 51* (1986) 713.

Synthesis and Properties of 1-Cycloheptatrienylidene-2-cyclopentadienylideneethylene Derivatives

By *Takashi Toda,* Norihiko Shimazaki,* and *Toshio Mukai*

Cycloheptatrienylidenecyclopentadienylideneethylene **1** is a novel system composed of fulvene and heptafulvene units connected by a cumulative double bond. Compound **1** may be considered as a push-pull-type cumulene because of the resonance contribution of the form **1'**. Since cumulenes have been intensively investigated,[1] this system is interesting from the viewpoint of the chemistry of both cumulenes and nonbenzenoid aromatic compounds.

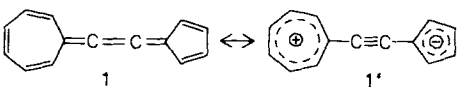

1 **1'**

Only a few examples of this type of compound have been reported in the literature.[2] As part of our investigation of compounds containing both cumulene and cycloheptatrienylidene units, we have already reported on cycloheptatrienylideneethylene derivatives **2**, which dimerized when prepared.[3]

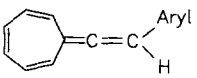

2

Aryl = C_6H_5, p-Br-C_6H_4

We have now synthesized derivatives of **1** (which may be viewed as higher homologues of **2**) and investigated their properties (IR, NMR, and electronic spectra).

Reaction of 2-cycloheptatrienylethynylmagnesium bromide[4] with the tetraarylcyclopentadienones **3a–c**[5] afforded the corresponding cycloheptatrienylcyclopentadienylacetylenes **4a–c** (Table 1). Treatment of these alkynols

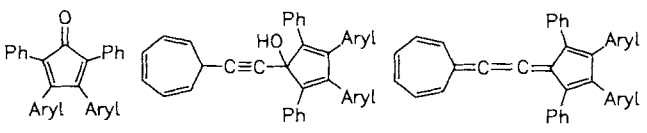

3a–c **4a–c** **1a–c**

a, Aryl = C_6H_5; **b**, Aryl = p-Cl-C_6H_4; **c**, Aryl = p-MeO-C_6H_4

with thionyl chloride in the presence of pyridine provided a mixture[6] of the corresponding chlorocyclopentadienyl-

[*] Prof. Dr. T. Toda [+], Dr. N. Shimazaki, Prof. Dr. T. Mukai
Department of Chemistry, Faculty of Science, Tohoku University
Sendai 980 (Japan)

[+] Present address:
Department of Industrial Chemistry, Faculty of Engineering,
Utsunomiya University
Utsunomiya 321 (Japan)

cycloheptatrienylacetylenes and the 1-chloro-1-cycloheptatrienyl-2-cyclopentadienylideneethylenes. Compounds **1a–c** (Table 1) were obtained by treatment of the mixture with excess triethylamine in ether. They are fairly stable in the solid state and give correct $M^{\oplus}$ peaks in their mass spectra. No dimer formation was observed and the compounds gradually decompose in solution.

Table 1. Yields and melting points of the products **1a–c** and **4a–c**.

Compound	Yield [%]	M.p. [°C]
1a	90	183–184 (dec.)
1b	61	198–199 (dec.)
1c	62	147–150 (dec.)
4a	57	182–184
4b	69	198–200
4c	68	121–123

The stretching vibrations due to the cumulene bonds (in KBr; $\tilde{\nu}$ [cm^{-1}] = 2036 m (**1a**), 2040 m (**1b**), 2028 m (**1c**)) resemble those of tri- and tetraarylbutatrienes, whose absorptions were reported[7] at about 2032 cm^{-1}. Compounds **1a–c** exhibit no absorptions in the acetylenic region, however. These values indicate that the small contribution of the resonance structure **1′** is influenced by the substituents on the aryl groups at the 3- and 4-positions of the cyclopentadienylidene ring: the −I effect of Cl in **1b** increases the contribution of the resonance structure corresponding to **1′**; the +M effect of OMe in **1c** decreases it.

The lowest-field ^{13}C-NMR signals of **1a–c** were observed around $\delta = 143$ (in $CDCl_3$). The high-field shift of **1a–c** compared with that of tetraphenylbutatriene ($\delta = 152$)[8] indicates a weak acetylenic character of the central bond of **1a–c**, corresponding to a small contribution of the resonance structure **1′**.

The electronic spectra of **1a–c** showed three different absorption bands: λ_{max} [nm] (ε): **1a**, 280 (27500, sh), 360 (4000, sh), and 538 (13200); **1b**, 287 (29500), 360 (5000), and 547 (37100); **1c**, 280 (25700), 360 (7250), and 545 (19900). The longest-wavelength bands are very broad.[9] An interesting feature of the cumulenes is their emission spectra. When **1a–c** were excited by 360-nm light, emission was observed around 450 nm. Since no emission was observed by excitation of the longest-wavelength absorption band at $\lambda = 530$–560 nm, the fluorescence spectra should be attributed to the emission from the S_2 state.[10]

Received: October 22, 1986;
revised: January 2, 1987 [Z 1962 IE]
German version: *Angew. Chem. 99* (1987) 367

[1] Reviews: H. Fischer in S. Patai (Ed.): *The Chemistry of Alkenes*, Wiley, New York 1964, Chap. 13; S. Patai (Ed.): *The Chemistry of Ketenes, Allenes, and Related Compounds*, Wiley, New York 1980, Part I and II.

[2] *Ried* reported the synthesis of tetrabenzo derivatives of this system. However, no properties were described: W. Ried, W. Schlegemilch, S. Piesch, *Chem. Ber. 96* (1963) 1221. *Iyoda* et al. and *Yoshida* reported the synthesis of the isoelectronic compounds containing the bisdehydro[13]annulene group as a terminal group. Also, *Gompper* reported the synthesis of butatrienes containing different push-pull functional groups: M. Iyoda, S. Tanake, K. Nishioka, M. Oda, *Tetrahedron Lett. 24* (1983) 2861; Z. Yoshida, *Pure Appl. Chem. 54* (1982) 1059; R. Gompper, U. Wolf, *Tetrahedron Lett. 1970*, 4263.

[3] T. Toda, N. Shimazaki, T. Mukai, *Chem. Lett. 1979*, 171; T. Toda, N. Shimazaki, T. Mukai, C. Kabuto, *Tetrahedron Lett. 21* (1980) 4001.

[4] R. M. Hoskinson, *Aust. J. Chem. 23* (1970) 399.

[5] The cyclopentadienones were prepared by *Johnson*'s method from dibenzylketone and the corresponding benzil: J. R. Johnson, O. Grummitt, *Org. Synth., Collect. Vol. 3* (1955) 805.

[6] All of the mixtures show weak stretching bands around $\tilde{\nu} = 2210$ and 1950 cm^{-1} in their IR spectra.

[7] R. Kuhn, H. Fischer, *Chem. Ber. 92* (1959) 1849.

[8] J. P. C. M. van Dongen, M. J. A. de Bie, R. Stern, *Tetrahedron Lett. 1973*, 1371.

[9] Redshift of the first absorption bands was observed when the electronic spectra of **1a–c** were measured in more polar solvents such as acetonitrile, acetone, anisole, indicating that the cumulenes **1a–c** are less polar in the ground state and more polar in the excited state.

[10] Emission from the S_2 state in solution is rather rare. For examples see: M. Beer, H. C. Longuet-Higgins, *J. Chem. Phys. 23* (1955) 1390; S. Murata, C. Iwanaga, T. Toda, H. Kokubun, *Ber. Bunsenges. Phys. Chem. 76* (1972) 1176. See also the following reviews: N. J. Turro: *Modern Molecular Photochemistry*, Benjamin/Cummings, Menlo Park, CA, USA 1978, p. 147–148, 184–185; N. J. Turro, V. Ramamurthy, W. Cherry, W. Franeth, *Chem. Rev. 78* (1978) 125.

Mycoloylpeptides and Other Lipopeptide Adjuvants from Higher Aldoketene Dimers**

By *Jörg Metzger* and *Günther Jung**

Dedicated to Professor Ernst Bayer on the occasion of his 60th birthday

During the development of carrier/adjuvant systems based on lipopeptides such as tripalmitoyl-*S*-glycerylcysteine,[1] we encountered an interesting side product, which was formed during the acylation of L-cystine bis(*tert*-butyl) ester with palmitoyl chloride (Pam-Cl) and which made the purification of larger batches of the symmetric cystine derivative[1b] more difficult: *N*-palmitoyl(α-palmitoyl)-*N′*-palmitoyl-L-cystine bis(*tert*-butyl) ester. The formation of the α-alkyl-β-ketoacyl moiety Pam(α-Pam) could be explained by the intermediary formation of a 4-alkylidene-3-alkyl-2-oxetanone, **1**, which was experimentally confirmed. Such diketenes, formed from higher fatty acid halides,[2] are known to react with amines **2** to give β-ketoamides **3**[3] (R = long-chain alkyl groups, R′ = alkyl, aryl).

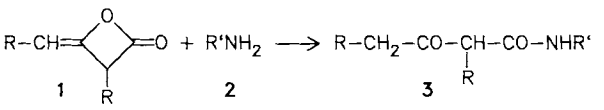

We have optimized this side reaction in order to develop a simple method for the preparation of lipopeptides, particularly mycolic acid derivatives (*N*-(α-alkyl-β-hydroxyacyl) amino-acid derivatives **6**), which are also valuable as adjuvants. Mycolic acids[4a] are found in naturally occurring lipids and, like the muramyldipeptide (MDP), are active components of *Freund's* adjuvant, a mixture of killed tubercle bacteria in paraffin oil that is used for the induction of antibodies.

An example is the toxic trehalose-6,6′-dimycolate ($C_{186}H_{366}O_{17}$, cord factor), isolated from Gram-positive mycobacteria.[4a] *O*-Acylated β-hydroxyacyl moieties are also present in lipid A, the toxic component of the endotoxin[4b] of Gram-negative bacteria. Finally, active analogues of MDP containing mycoloyl moieties are known.[4c] Previous syntheses of mycoloyl amino acids employed mycolic acids isolated from bacteria (semisyntheses).[5]

[*] Prof. Dr. G. Jung, Dipl.-Chem. J. Metzger
Institut für Organische Chemie der Universität
Auf der Morgenstelle 18, D-7400 Tübingen (FRG)

[**] *J. M.* thanks the Studienstiftung des Deutschen Volkes for a Promotionsstipendium. We thank Prof. Dr. *W. G. Bessler*, Institut für Immunbiologie der Universität Freiburg, for carrying out mitogenicity tests.

The aldoketene dimers **1** required for our synthesis are readily obtainable from fatty acid halides by reaction with tertiary amines[2] and are stable upon storage. They react with the free amino group of amino acid esters **4** in anhydrous pyridine in the presence of catalytic amounts of 4-dimethylaminopyridine (DMAP) within 2–4 h to give the α-alkyl-β-ketoacyl compounds **5**. In solvents such as dimethylformamide, CH_2Cl_2, or $CHCl_3$ and with bases such as triethylamine or *N*-methylmorpholine, however, mainly the simple acylation product, e.g., the *N*-palmitoyl derivative, is isolated, even when the reaction is carried out for long reaction times and at high temperatures.

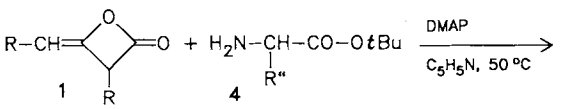

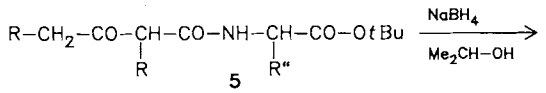

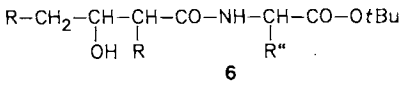

The reaction of aldoketene dimers **1** from higher fatty acids with amino acid esters **4** is thus a simple and economical route to novel lipoamino acids. The resulting α-alkyl-β-ketoacyl derivatives **5** (Table 1), after removal of the carboxyl protecting group, are mitogenic compounds (Fig. 1), which, for example, can be covalently linked to the free *N*-terminus of amino-acid or peptide sequences to give lipopeptides that are also biologically active (Fig. 1). Compounds **5** can be quickly reduced to give, in high yield, the mycoloyl compounds **6** (Table 2). For example, the dimeric tetradecylketene **1** (R = *n*-$C_{14}H_{29}$), obtained from Pam-Cl, reacts with alanine *tert*-butyl ester to give a product that can be reduced to a derivative of corynomycolic acid, a C_{32} fatty acid found in the lipids of *Corynebacterium diphtheriae*. The mixture of diastereomers formed in the reduction can, for example in the case of the alanine derivative, be separated on silica gel. However, it is also possible to use the mixture of diastereomers directly as a adjuvant or mitogen in animal experiments. Several of the *two-chain* mycoloyl compounds **6** can be transformed to *three-chain* derivatives by esterification of the OH group. The latter compounds are, in general, stronger mitogens than the non-*O*-acylated compounds **6**. *Four-chain* compounds are accessible via *N*-(α-alkyl-β-hydroxyacyl)-*S*-glycerylcysteine (Fig. 1) or N^{α},N^{ε}-bis[Pam(α-Pam)]lysine. Several of the prepared lipopeptides and amino acids are effective B-cell mitogens.

Table 1. *N*-(α-Hexadecyl-β-oxoicosanoyl) amino acid *tert*-butyl esters **5** (R = *n*-$C_{16}H_{33}$).

Amino acid ester **4**	Reaction time [h]	Yield [%]	M.p. [°C] [a]	R_F value [b] in $CHCl_3$	EA [c]
H-Gly-O*t*Bu·HCl	2	72	72	0.47	0.81
H-Ala-O*t*Bu·HCl	3	76	64	0.53	0.81
H-Ser(*t*Bu)-O*t*Bu	3	52	41	0.46	0.80
H-Lys(Boc)-O*t*Bu·HCl	2	63	60	0.14	0.80
(H-Cys-O*t*Bu)$_2$	3	50	76	0.41	0.83
H-Asp(*t*Bu)-O*t*Bu·HCl	3	62	48	0.44	0.79
H-Tyr(*t*Bu)-O*t*Bu·HCl	4	51	62	0.45	0.80
H-Phe-O*t*Bu·HCl	3	62	66	0.57	0.82

[a] Melting point of the mixture of diastereomers, uncorrected. [b] Silica gel plates 60 F_{254}, 10 × 20 cm (Merck), preequilibrated once in eluent; detection with iodine. The mixtures of diastereomers in Table 2 produce one or two long spots, the upper and lower edges of which are given. [c] EA = ethyl acetate.

Table 2. *N*-(α-Hexadecyl-β-hydroxyicosanoyl) amino acid *tert*-butyl esters **6** (R = *n*-$C_{16}H_{33}$).

Amino acid ester in **6**	Yield [%]	M.p. [°C] [a]	R_F value [b] in $CHCl_3$	EA [c]
Gly-O*t*Bu	92	91	0.19/0.28	0.82
Ala-O*t*Bu	92	84	0.17–0.24/0.29–0.35	0.81
Ser(*t*Bu)-O*t*Bu	72	55	0.21–0.26/0.29–0.35	0.81
Lys(Boc)-O*t*Bu	75	76	0.05/0.07	0.81
(Cys-O*t*Bu)$_2$	91	75	0.09–0.24	0.82–0.87
Asp(*t*Bu)-O*t*Bu	74	65	0.22–0.32	0.81
Tyr(*t*Bu)-O*t*Bu	92	78	0.20–0.27	0.82
Phe-O*t*Bu	77	75	0.33–0.40	0.81

[a–c] See Table 1.

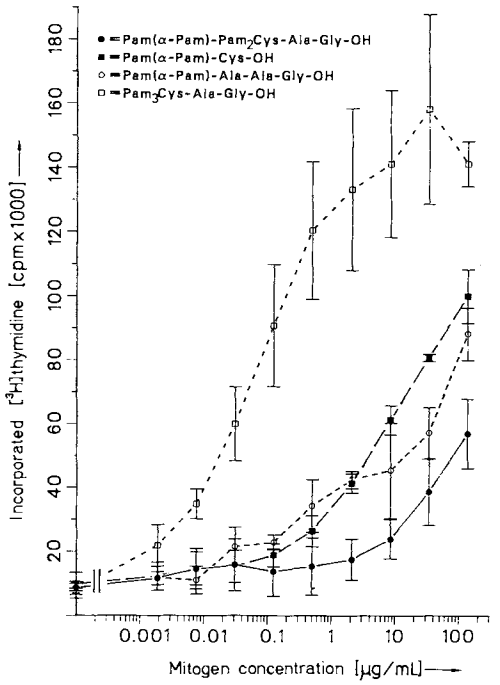

Fig. 1. Mitogenic effect of the two-chain lipids Pam(α-Pam)-L-Cys-OH and Pam(α-Pam)-L-Ala-L-Ala-Gly-OH, prepared from **5**, in comparison to the very potent, three-chain adjuvant *S*-[2,3-bis(palmitoyloxy)-(2*RS*)-propyl]-*N*-palmitoyl-(*R*)-cysteinyl-(*S*)-alanylglycine (Pam_3Cys-Ala-Gly-OH; J.-K. Wiesmüller et al., unpublished results) and the appreciably less active, four-chain derivative *S*-[2,3-bis(palmitoyloxy)-(2*RS*)-propyl]-*N*-palmitoyl(α-palmitoyl)-(*R*)-cysteinyl-(*S*)-alanylglycine (Pam(α-Pam)-Pam_2Cys-Ala-Gly-OH). The dose–response curves were obtained by incorporation of [^{3}H]thymidine in spleen cells of C3H/HeJ mice [6]. The three-chain *O*-acylated lipopeptides prepared from the mycoloyl amino acid esters **6** were also tested in vivo and in vitro [7]. cpm = counts per minute.

For the synthesis of immunogenic peptides and synthetic vaccines, it is important that the α-alkyl-β-ketoacyl moiety, like tripalmitoyl-*S*-glycerylcysteine,[1a] can be introduced at the end of a Merrifield synthesis (Fmoc/*t*Bu strategy). Since the lipid moiety is stable in trifluoroacetic acid, the resulting lipopeptide can be cleaved from the carrier with simultaneous removal of all protecting groups.

Experimental Procedure

N-(α-Alkyl-β-ketoacyl) amino acid *tert*-butyl ester **5**: The fatty acid diketene **1** (1 mmol) was added to a stirred solution of the amino acid ester **4** (1 mmol) in 3 mL of anhydrous pyridine. DMAP (0.1 mmol) was added at 50°C. During the reaction, the color of the solution turned from yellow to a cognaclike color and, after 2–4 h, thin-layer chromatography indicated the consumption of all the diketene. The pyridine was removed in vacuo and the crude product was precipitated from a small amount of chloroform by addition of methanol to the cooled solution. Impurities due to excess diketene could be precipitated from ethyl acetate or diisopropyl ether at 0°C, the usually still yellow or orange product remaining in solution. Final purification of **5** was achieved by flash chromatography on a silica gel column with chloroform.

Mycoloyl amino acid *tert*-butyl ester **6**: The *N*-(α-alkyl-β-ketoacyl) amino acid *tert*-butyl ester **5** (1 mmol) was dissolved in 15 mL of 2-propanol by heating and treated with solid sodium tetrahydridoborate (1 mmol). The reduction product slowly precipitated. After 3 h stirring, the precipitation was driven to completion by neutralization with 0.1 N HCl. The colorless mycoloyl compound **6** was filtered off, washed several times with water, and dried over P_2O_5.

Received: October 7, 1986;
revised: February 5, 1987 [Z 1950 IE]
German version: *Angew. Chem. 99* (1987) 343

[1] a) G. Jung, K.-H. Wiesmüller, G. Becker, H.-J. Bühring, W. G. Bessler, *Angew. Chem. 97* (1985) 883; *Angew. Chem. Int. Ed. Engl. 24* (1985) 872; b) K.-H. Wiesmüller, W. G. Bessler, G. Jung, *Hoppe-Seyler's Z. Physiol. Chem. 364* (1983) 593; c) G. Jung: *Synthesis and Perspectives of New Adjuvants and Carrier Systems for Potential Application for Synthetic Vaccines (Proc. Int. Symp. Synth. Antigens*, Siena, Italy October 29/30, 1984); *Ann. Sclavo 1984*, 191; d) W. G. Bessler, B. Suhr, H.-J. Bühring, C. P. Muller, K.-H. Wiesmüller, G. Becker, G. Jung, *Immunobiology (Stuttgart) 170* (1985) 239.

[2] a) J. C. Sauer, *J. Am. Chem. Soc. 69* (1947) 2444; b) E. S. Rothman, *J. Org. Chem. 32* (1967) 1683.

[3] a) S. Piekarski, *C. R. Hebd. Séances Acad. Sci. 38* (1954) 1241; b) *J. Rech. C. N. R. S. 40* (1957) 197.

[4] a) E. Lederer, *Angew. Chem. 72* (1960) 372; b) J. Y. Homma, S. Kanegasaki, O. Lüderitz, T. Shiba, O. Westphal (Eds.): *Bacterial Endotoxin. Chemical, Biological and Clinical Aspects*, Verlag Chemie, Weinheim 1984; c) T. Shiba, S. Kusomoto, M. Inage, S. Sawaki in E. Gross, J. Meienhofer (Eds.): *Peptides: Structure and Biological Function (Proc. 6th Am. Pept. Symp.)*, Pierce, Rockford, IL 1979, p. 425–430.

[5] a) Y. Yamamura, A. Tanaka, M. Kato, *J. Biochem. (Tokyo) 47* (1960) 505; b) A. Tanaka, K. Tanaka, T. Tsubone, Y. Kuroda, K. Sugiyama, *Int. Arch. Allergy Appl. Immunol. 28* (1965) 340.

[6] A. Lex, K.-H. Wiesmüller, G. Jung, W. G. Bessler, *J. Immunol. 137* (1986) 2676, and literature cited therein.

[7] G. Jung, J. Metzger, W. G. Bessler, unpublished results.

Arene Complexes with Weak Interactions: A Macrocyclic Tris(arene) Complex of Gallium(I) with η^{18} Coordination**

By *Hubert Schmidbaur,* Rudolf Hager, Brigitte Huber,* and *Gerhard Müller*

Main-group metals with an ns^2 configuration form centrically η^6-bonded complexes with aromatic hydrocarbons; however, the long contact distances between the metal and the ring center indicate relatively weak interactions.[1–3] In addition to 1:1 complexes (**A**), 1:2 complexes (**B**), in which the rings are bent toward each other, are known for gallium, indium, and thallium in the oxidation state +1. Owing to the entropy effect, considerable stabilization of this type of bonding is expected (in solution) when the arene ligands are linked.[1] Optimal conditions and thus the greatest tendency of formation and stability should exist, according to this concept, for doubly linked rings, such as those present in cyclophanes. However, all attempts to introduce Ga^+, In^+, or Tl^+ into the cavity between the benzene rings of [2.2]- and [3.3]paracyclophanes,[1,4] as well as between the arene rings of the related naphthalene derivatives,[5] have failed so far. The metal atoms in the resulting adducts are always coordinated to the benzene rings of the cyclophanes from the outside. Nevertheless, the centric η^6 coordination, present in **B**, is still found for the arene ligands, which are bent toward each other (e.g., in **C**).[4]

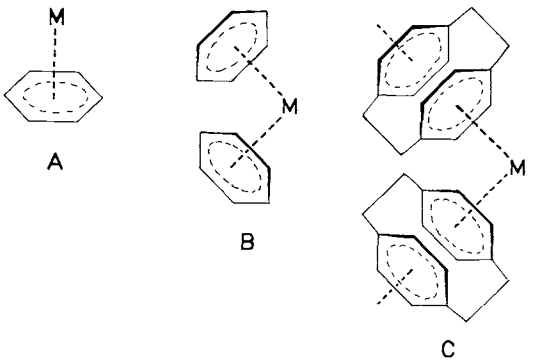

The knowledge of the preferred contact distances and modes of coordination has now been used by us to achieve centric coordination of the cation Ga^+ in the cavity of [2.2.2]paracyclophane. Indeed, it was surprisingly easy to achieve this novel coordination experimentally. Crystalline $Ga[GaBr_4]$, whose structure was recently elucidated,[6] dissolves in benzene as the dimeric tetraarene complex $[(C_6H_6)_2Ga \cdot GaBr_4]_2$.[7] Upon addition of the cyclophane, such solutions afford crystalline precipitates having the analytical composition of the 1:1 complex **1**.

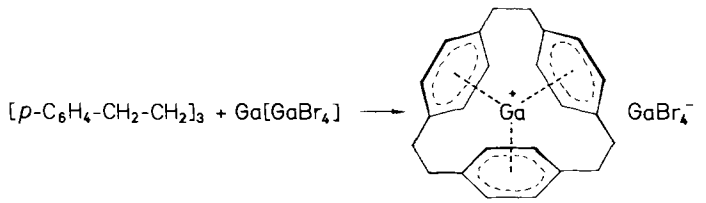

1

Complex **1** forms colorless, only slightly air-sensitive crystals, which are sparingly soluble in aromatic hydrocarbons and afford solutions exhibiting no electrical conductivity. The latter finding indicates that **1** has pronounced ion-pair character.

The X-ray crystal structure analysis revealed[8] that the metal atom in **1** is indeed located in the interior of the cyclophane macrocycle and is involved in identical centric (η^6) bonding to all three benzene rings (Fig. 1a). The gallium atom is thus equidistant, within narrow limits, from all 18 carbon atoms of the arenes. The distances correspond to values found earlier for similar bonds.[1] Instead of lying completely in the plane defined by the three ring centers (D1, D2, D3), however, the metal lies 0.43 Å above it. Taking into consideration the position of the anion, it becomes immediately clear that this displacement is due to the proximity of a bromine atom (Ga2–Br2 3.388(2) Å),

[*] Prof. Dr. H. Schmidbaur, R. Hager, Dipl.-Chem. B. Huber [+], Dr. G. Müller [+]
Anorganisch-chemisches Institut der Technischen Universität München
Lichtenbergstrasse 4, D-8046 Garching (FRG)

[+] X-ray structure analysis.

[**] This work was supported by the Deutsche Forschungsgemeinschaft (Leibniz program), the Fonds der Chemischen Industrie, Hoechst AG, Siemens AG, and Preussag AG. We thank *P. Kiprof* for preparing the SCHAKAL drawing on the cover.

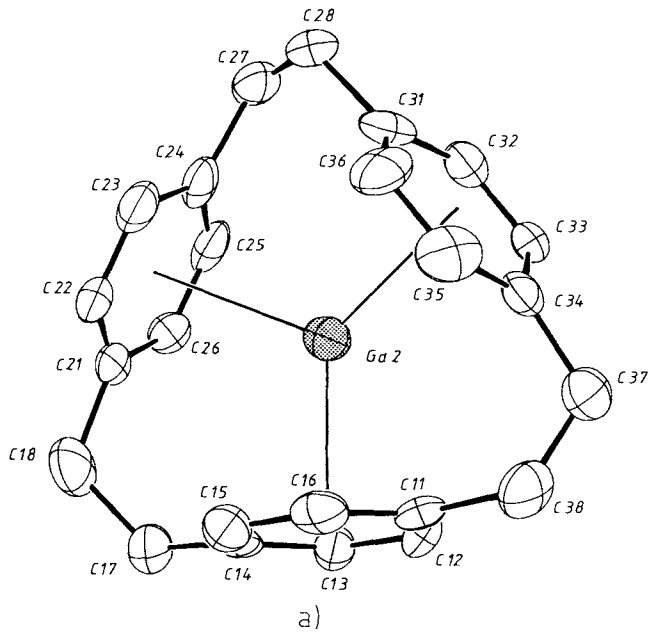

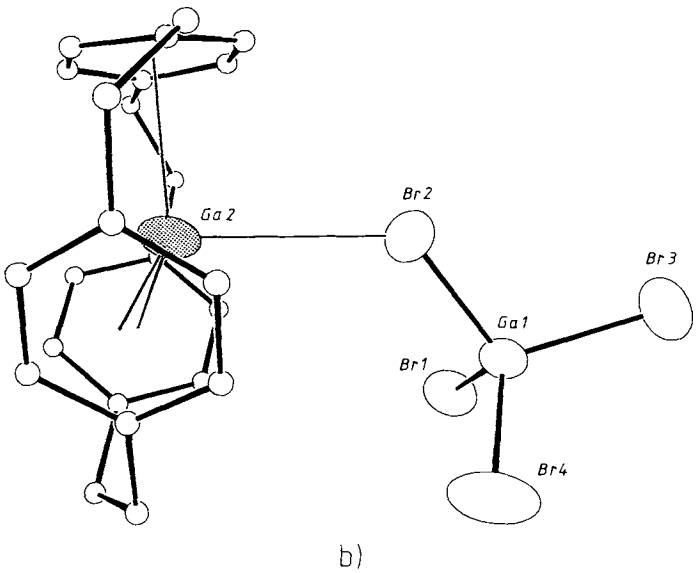

Fig. 1. a) Geometry of the cation of **1** (ORTEP, thermal ellipsoids at the 50% probability level, H atoms omitted). b) Side view of **1**. The Ga^1 atom, Ga2, is clearly displaced from the center of the cyclophane toward the bridging bromine atom, Br2. The three arene rings adjust to this displacement by a slight rotation, whereby, to a good approximation, the η^{18} coordination is retained. Important bond lengths [Å] of **1**: Ga2-C11 2.972(9), Ga2-C12 2.911(8), Ga2-C13 2.925(9), Ga2-C14 2.979(9), Ga2-C15 3.072(9), Ga2-C16 3.053(9), Ga2-C21 3.028(9), Ga2-C22 3.079(9), Ga2-C23 3.048(9), Ga2-C24 2.937(9), Ga2-C25 2.913(9), Ga2-C26 2.949(9), Ga2-C31 2.994(9), Ga2-C32 2.986(9), Ga2-C33 2.953(8), Ga2-C34 2.923(9), Ga2-C35 3.00(1), Ga2-C36 3.02(1), Ga2-D1 2.64, Ga2-D2 2.65, Ga2-D3 2.64, Ga1-Br1 2.333(1), Ga1-Br2 2.319(2), Ga1-Br3 2.313(2), Ga1-Br4 2.305(2), Ga2-Br2 3.388(2).—D1, D2, D3: centers of the three arene rings, C11–C16, C21–C26, and C31–C36.

which induces a distorted coordination geometry approaching that of a tetrahedron (Fig. 1b). Similar ion pairs are presumably present in solution (see above). A space-filling model of the cation clearly shows the perfect spatial fitting of the cyclophane ligand and the metal (Fig. 2).

Complex **1** is the first complex with three centrically coordinated, neutral arene ligands. The central atom contains no less than 19 atoms in its first coordination sphere.

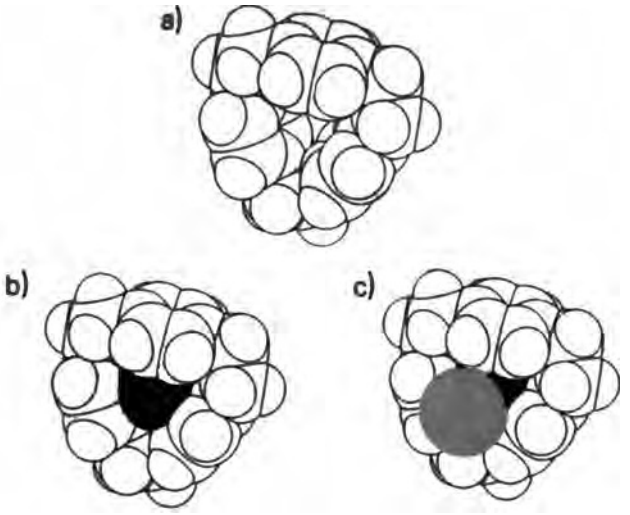

Fig. 2. Space-filling models for understanding the structure of **1**: a) space-filling model of [2.2.2]paracyclophane; b) with Ga^1 (black) in the interior; c) with bridging Br2 atom (grey).—It is readily apparent from a) to c) that the acentric coordination of Ga^1 in the cage is due to the dimensions of the cyclophane interior and the radii of Ga2 and Br2. An additional Br contact from the "backside" of the molecule is made difficult by the resulting reduction in the size of the cyclophane opening.

This high hapticity distinguishes the compound fundamentally from the analogous silver complex, $[C_6H_4CH_2CH_2]_3 \cdot AgClO_4$, in which the metal, instead of completely entering the ligand cavity, remains situated at the edge of the cavity, forming three η^2 bonds to the arene rings.[9] These differences are also found for the [2.2]- and [3.3]paracyclophane complexes of Ga^+, In^+, and Tl^+, on the one hand, and Cu^+ and Ag^+,[4, 10] on the other, as well as for simple arene adducts of these elements.[1, 2, 7] These findings may be regarded as confirmation of the fact that a simple classification of the organometallic compounds described here and in earlier reports cannot be made using simple solvation or van der Waals models, because the marked η^2/η^6 differentiation between d^{10} and $d^{10}s^2$ configurations cannot be explained in this way without additional assumptions. It is especially astounding that the arene coordination in **1** is so efficient that all eight Ga^+ contacts to bromine atoms observed in the crystal of $Ga[GaBr_4]$,[6] with the exception of one, are sacrificed. In all other structurally investigated cases, several anion contacts are retained.[1]

Experimental Procedure

Ga_2Br_4 (140 mg, 0.305 mmol) was dissolved in 10 mL of toluene and then allowed to react with a solution of [2.2.2]paracyclophane (100 mg, 0.323 mmol) [11] in 3 mL of toluene. Complex **1** spontaneously precipitated as a white, finely crystalline solid. Recrystallization from 25 mL of benzene afforded 0.19 g of pure product (81% based on Ga_2Br_4), m.p. = 176 °C. Very careful cooling of benzene solutions from 80 to 20 °C over 100 h afforded single crystals.—IR (Nujol): $\tilde{\nu}$ = 1515, 1435, 812, 802, 584, 465, 275 (νGaBr) cm^{-1}. Complex **1** exhibits no measureable electrical conductivity in benzene or toluene at 23 °C. Correct elemental analyses were obtained. The ^{1}H-NMR spectra show apparently equivalent CH_2 and CH protons for solutions in benzene or toluene, which were very dilute because of the sparing solubility of **1**. Presumably, the environments of the hydrogen atoms are identical on the NMR time scale owing to exchange processes. In polar solvents, desolvation or disproportionation occurs to give metallic gallium and gallium(III).

Received: January 29, 1987;
supplemented: February 23, 1987 [Z 2077 IE]
German version: *Angew. Chem.* *99* (1987) 354

[1] H. Schmidbaur, *Angew. Chem.* *95* (1983) 980; *Angew. Chem. Int. Ed. Engl.* *22* (1983) 907.

[2] S. H. Strauss, M. D. Noirot, O. P. Anderson, *Inorg. Chem. 25* (1986) 3850.
[3] A. Schier, J. M. Wallis, G. Müller, H. Schmidbaur, *Angew. Chem. 98* (1986) 742; *Angew. Chem. Int. Ed. Engl. 25* (1986) 757; W. Frank, J. Weber, E. Fuchs, *ibid. 99* (1987) 68 and *26* (1987) 74.
[4] H. Schmidbaur, W. Bublak, B. Huber, G. Müller, *Organometallics 5* (1986) 1647; *Helv. Chim. Acta 69* (1986) 1742.
[5] W. Bublak, *Dissertation*, Technische Universität München 1987.
[6] H. Schmidbaur, R. Nowak, W. Bublak, P. Burkert, B. Huber, G. Müller, *Z. Naturforsch. B42* (1987), in press; W. Hönle, A. Simon, G. Gerlach, *ibid. 42* (1987), in press.
[7] M. Uson-Finkenzeller, W. Bublak, B. Huber, G. Müller, H. Schmidbaur, *Z. Naturforsch. B41* (1986) 346.
[8] Crystal structure data: Enraf-Nonius CAD4, $Mo_{K\alpha}$ radiation, $\lambda = 0.71069$ Å, graphite monochromator, $T = 22°C$; monoclinic, space group $P2_1/c$, $a = 13.741(1)$, $b = 11.856(1)$, $c = 15.973(3)$ Å, $\beta = 90.24(1)°$, $V = 2602.2$ Å^3, $\rho_{calcd} = 1.969$ g cm^{-3}, $Z = 4$, $\mu(Mo_{K\alpha}) = 81.6$ cm^{-1}. 6162 measured intensities, of which 5650 were unique ($R_{int} = 0.02$) and 2168 "observed" with $I \geq 2.0\sigma(I)$ ($\theta - 2\theta$ scan, $\Delta\omega = 0.8 + 0.35 \tan\theta$, $(\sin\theta/\lambda)_{max} = 0.637$, +h, +k, ±l). Automated Patterson methods (SHELXS-86); $R = 0.045$, $R_w = 0.030$, $w = 1/\sigma^2(F_0)$, 271 parameters, $\Delta\rho(\max/\min) = +0.78/-0.68$ e/Å^3 (SHELX-76). Further details of the crystal structure investigation may be obtained from the Fachinformationszentrum Energie, Physik, Mathematik GmbH, D-7514 Eggenstein-Leopoldshafen 2 (FRG), on quoting the depository number CSD-52324, the names of the authors, and the journal citation.
[9] C. Cohen-Addad, P. Baret, P. Cheautemps, J.-L. Pierre, *Acta Crystallogr. Sect. C39* (1983) 1346. We thank Prof. *Baret* for advice and discussions (1986).
[10] H. Schmidbaur, W. Bublak, B. Huber, G. Reber, G. Müller, *Angew. Chem. 98* (1986) 1108; *Angew. Chem. Int. Ed. Engl. 25* (1986) 1089.
[11] I. Tabushi, H. Yamada, Z. Yoshida, R. Oda, *Tetrahedron 27* (1971) 4871.

The Fluorometric Determination of Thymine Glycol as Criterion of the Treatment of Foodstuffs (Biological Material) with Ionizing Radiation

By *Konrad Pfeilsticker** and *Jürgen Lucas*

The treatment of foodstuffs with ionizing radiation[1,2] for the purpose of sterilization and the inhibition of germination or ripening is currently forbidden in the Federal Republic of Germany. Detection of such a treatment is possible with limitations in the case of dried products, especially spices, by chemiluminescence and thermoluminescence.[3] A general method of detection, especially for water-containing biological material has so far been lacking. In the following communication we introduce a new method which, in principle, exploits the sensitivity of DNA to radiation.

In an aqueous DNA solution about 78% of the hydroxyl radicals formed radiolytically from the water react with the bases of DNA. The pyrimidine bases and especially thymine are the most sensitive.[4] A major product formed on radiolysis is 5,6-dihydroxy-5,6-dihydrothymine (thymine glycol),[5] which can now be determined fluorometrically and quantitatively as criterion of irradiation on the basis of the DNA determination method of *Roberts* and *Friedkin*:[6] hydroxyacetone (acetol) is cleaved under alkaline conditions from the radiolytic product thymine glycol bound in the DNA and allowed to react with *o*-aminobenzaldehyde (*o*-ABA) to give the fluorescent 3-hydroxyquinaldine. The oxidation of the thymine with bromine prescribed by *Roberts* and *Friedkin*[6] is hereby replaced by the irradiation.

For precipitation of the nucleic acids and proteins, 5 g of a food sample is dissolved in 25 mL of 6% trichloroacetic acid and the solution homogenized and centrifuged. The precipitate is then subjected to exactly the same homogenization and centrifugation procedure another two times. 10 mL of water is added to the final precipitate and the solution neutralized with 1 M KOH, diluted to 25 g with water, and finally re-homogenized. 400 mg of the homogenate is treated with 35 µL of a solution of 0.1 M ethylenediaminetetraacetic acid (EDTA) in 2.1 M NaOH and incubated for 90 min at 20°C.[7] The sample is then treated with 65 µL of an *o*-ABA solution (prepared according to the method described by *Roberts* and *Friedkin*[6]) and incubated for 20 min at 65°C. The reaction is terminated by addition of 4.5 mL of 0.1 M potassium phosphate buffer (pH 6.9).[6] Before carrying out any measurements the sample must be centrifuged to remove any suspended material. On excitation at $\lambda = 375$ nm the fluorescence at 444 nm is measured. The apparatus is previously calibrated with an aqueous solution of quinine sulfate in 0.1 N H_2SO_4 (0.1 mg/mL) ($IF = 100$) and with distilled water ($IF = 0$) at the same wavelengths (IF = fluorescence intensity).

Some components of the sample interfere and give rise to an increased fluorescence. We have found that this can be largely compensated for, if 400 mg of homogenate treated with 65 mL of an aqueous NH_3-solution (0.08 M) instead of *o*-ABA is used for the blank determination (see Tables 1 and 2, IF(N)). This important finding makes it possible to analyze a sample without recourse to an unirradiated authentic reference sample. The difference between the fluorescence intensities of the sample and the blank corresponds to the thymine glycol present in the sample. The conversion of the relative fluorescence values into absolute values for measuring the thymine glycol content was achieved by means of a calibration curve standardized according to the method described in ref. [6].

Table 1. Fluorescence intensity (IF) and thymine glycol contents in irradiated and unirradiated foodstuffs. TG = thymine glycol; IF(A) = fluorescence intensity with *o*-aminobenzaldehyde; IF(N) = fluorescence intensity with NH_4OH (blank); standard deviation $\sigma = \pm 1.9$ g TG/g sample.

a) Shrimps	Irradiation dose [kGy]	
	0	10
IF(A)	37	51
IF(N)	37	35
IF(A) − IF(N)	0	16
Thymine glycol content [µg TG/g sample]	0	16
Thymine glycol based on original thymine	0%	17%

b) Mock salmon	Irradiation dose [kGy]		
	0	5	10
IF(A)	11	19	28
IF(N)	8	8	10
IF(A) − IF(N)	3	11	18
Thymine glycol content [µg TG/g sample]	3.7	11.2	19.5
Thymine glycol based on original thymine	4%	12%	22%

c) Chicken breast	Irradiation dose [kGy]		
	0	5	10
IF(A)	27.5	43	43
IF(N)	26.0	31	29
IF(A) − IF(N)	1.5	12	14
Thymine glycol content [µg TG/g sample]	0.9	11.7	14.2
Thymine glycol based on original thymine	1%	13%	16%

The method was first tested on some irradiated (5 and 10 kGy, ^{60}Co) and unirradiated foodstuffs (shrimps, mock salmon, and chicken breasts, see Table 1). In each case a

[*] Prof. Dr. K. Pfeilsticker, Dipl.-Oecotroph. J. Lucas
Lehrstuhl für Lebensmittelwissenschaft
und Lebensmittelchemie der Universität
Endenicher Allee 11-13, D-5300 Bonn 1 (FRG)

significant increase in fluorescence intensity could be observed in the irradiated samples, so that the working principle looks very promising. Upon irradiation of the foodstuff samples with 10 kGy, 16–22% of the thymine is converted into thymine glycol (cf. Table 1), if one assumes that the sample material contains 1 g/kg DNA. It follows from Table 1 that it will be possible in this way to derive the applied irradiation dose, besides collecting qualitative information. This also follows from measurements on solutions of pure calf thymus DNA (see Table 2); these measurements also indicate the limits of detection of the method.

Table 2. Fluorescence intensity (*IF*) and thymine glycol content in irradiated and unirradiated calf thymus DNA in aqueous solution (0.5 mg/mL in 0.15 M NaCl). For abbreviations see Table 1.

	Irradiation dose [kGy]			
	0	0.05	5	10
IF(A)	2	3.5	120	143
IF(N)	0.5	0.5	17	27
IF(A) − *IF*(N)	1.5	3.0	103	116
Thymine glycol content [μg TG/mg DNA]	0.35	1.1	32	36
Thymine glycol based on original thymine	0.4%	1.2%	36%	40%

It is interesting in this connection that *Ames*' group[8] determine thymine glycol and thymidine glycol in human and rat urine analytically in order to demonstrate oxidative damage of DNA by mutagens and carcinogens.

Received: August 4, 1986;
revised: January 19, 1987 [Z 1887 IE]
German version: *Angew. Chem. 99* (1987) 341

CAS Registry number:
Thymine glycol, 2943-56-8.

[1] P. S. Zurer, *Chem. Eng. News 64* (1986) No. 18, p. 46.
[2] T. Grünewald, *Z. Lebensm.-Unters. Forsch. 180* (1985) 357.
[3] L. Heide, W. Bögl, *Z. Lebensm.-Unters. Forsch. 181* (1985) 283.
[4] A. P. Casarett: *Radiation Biology*, Prentice-Hall, Englewood Cliffs 1968, p. 57.
[5] P. V. Hariharan, J. F. Remsen, P. A. Cerutti in P. C. Hanawalt, R. B. Setlow (Eds.): *Molecular Mechanisms for the Repair of DNA*, Plenum Press, New York 1975, p. 51.
[6] D. Roberts, M. Friedkin, *J. Biol. Chem. 233* (1958) 483.
[7] P. V. Hariharan, *Radiat. Res. 81* (1980) 496.
[8] R. Cathcart, E. Schwiers, R. L. Saul, B. N. Ames, *Proc. Natl. Acad. Sci. USA 81* (1984) 5633.

Photoisomerization of Stilbazolium Chromophores with Potential Nonlinear Optical Applications**

By *George L. Gaines, Jr.**

There is currently much interest in the use of organic materials for nonlinear optical applications.[1] The largest values of β, the molecular second-order hyperpolarizability, have been reported for the related stilbazolium chromophores **1** and **2** (and their derivatives with an *n*-alkyl group instead of a methyl group on the pyridinium nitrogen atom).[2-3] Both the nonlinear response and the absorption wavelength (which governs the so-called "transparency-efficiency trade-off") are affected by the nature of the substituents in such chromophores.[4] A number of stilbazolium dyes with other substituents have been prepared, and most of them undergo facile *trans*→*cis* photoisomerization.[5] Protonated **1** (**1H**$^{\oplus}$) is also extensively

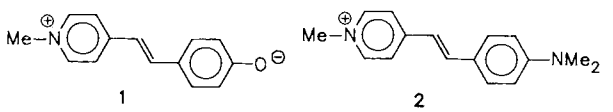

1 2

isomerized on irradiation, while **1** appears to be photostable.[6] In neutral solutions, the quantum yield of photoisomerization of **2** is also very low, and the photostationary state has a very small *cis* content.[7] I now report the preparation of some additional substituted methylstilbazolium iodides and observations on their susceptibility to photoisomerization which provide a rationale for the apparent photostability of **1** and **2**.

Table 1. Absorption and emission maxima and photoisomerization of stilbazolium chromophores.

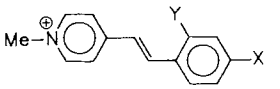

1 - 6

Compd	X	Y	λ_{max} [nm] (logε) H_2O	λ_{max} [nm] EtOH	λ_{fl} [a] [nm] H_2O	ΔA [b] [%]
1	$O^{\ominus}$	H	442 (4.49)	512	581 [c]	0
1H$^{\oplus}$	OH	H	372 (4.50)	395	515 [c]	49 [d]
2	NMe_2	H	448 (4.43)	478	610	0
2H$^{\oplus}$	$\overset{\oplus}{N}HMe_2$	H	328 (4.47)	—	408	43
3	Me	H	353 (4.52)	358	450	63
4	OMe	H	370 (4.56)	382	492	61
5	OMe	OMe	390 (4.55)	408	517	60
6	OMe	$O^{\ominus}$	462 (4.59)	528	603	4
6H$^{\oplus}$	OMe	OH	390 (4.62)	416	516	52

[a] Emission peak wavelength, uncorrected. [b] Decrease in absorbance of long-wavelength band after irradiation to photostationary state. [c] See [12]. [d] See [6].

The *N*-methyl compounds **1**–**6** (Table 1) were prepared by condensing *N*,4-dimethylpyridinium iodide with appropriately substituted benzaldehydes by the method of *Phillips*.[8] Those compounds capable of being protonated (**1**, **2**, and **6**) exhibit pH-dependent absorption spectra (Fig. 1); the pK_a values estimated from the spectra in aqueous buffers are 8.54 (**1H**$^{\oplus}$[6]), 3.53 (**2H**$^{\oplus}$), and 8.15 (**6H**$^{\oplus}$). The stronger the electron-donating ability of the substituent(s), the longer is the wavelength of the longest-wavelength absorption band (Table 1), and also the greater is the solvent sensitivity of this absorption. All of the compounds emit readily detectable fluorescence from solutions in water or ethanol at room temperature (Table 1). As had previously been noted for **1**,[6] protonation of **2** and **6** substantially increases the fluorescence efficiency. Qualitatively, the fluorescence intensities from solutions of **3**–**5**, as well as of

[*] Dr. G. L. Gaines, Jr.
General Electric Corporate Research and Development
Schenectady, NY 12301 (USA)

[**] This research was in part stimulated by a subcontract through the University of California, Davis, Department of Electrical and Computer Engineering, from the Air Force Weapons Laboratory, Kirkland AFB, under contract F29601-84-C-0084. I thank Mrs. *P. L. Karas* for technical assistance and one of the referees for helpful comments.

$2H^{\oplus}$ and $6H^{\oplus}$, are comparable to that from solutions of $1H^{\oplus}$, rather than its deprotonated form **1**.

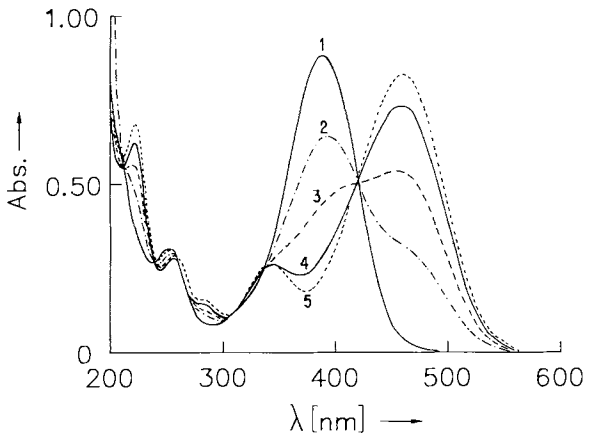

Fig. 1. Absorption spectra of **6** (2.1×10^{-5} M) in aqueous buffer solutions. 1, pH = 6.0; 2, pH = 7.9; 3, pH = 8.4; 4, pH = 9.1; 5, pH = 10.2.

Irradiation of solutions of most stilbazolium dyes in the long-wavelength band leads to isomerization, with a large decrease in the intensity of that band and a concomitant increase in the absorbance of the UV band.[5,6] The spectra of **1** and **2**, however, do not show such changes.[6,7] For example, no detectable spectral change was observed after 12 h of irradiation (in Pyrex, 10 cm from a 100-W medium-pressure Hg lamp) of neutral solutions of **2** in water or ethanol. After irradiation, on the other hand, solutions of $2H^{\oplus}$ exhibit spectroscopic changes exactly analogous to those of $1H^{\oplus}$ (Fig. 2); the photostationary state is attained within less than 15 min under these conditions. Solutions of **3**–**5**, and $6H^{\oplus}$, after irradiation, exhibit spectral changes analogous to solutions of $1H^{\oplus}$. In all cases, these absorption changes are accompanied by substantial decreases in fluorescent emission, as occurs on photoisomerization. Alkaline solutions of **6** are much less photolabile than acidic solutions, but small spectral changes do occur (approximately 4–7% decrease in absorbance at 461 nm after irradiation for 15–75 min.

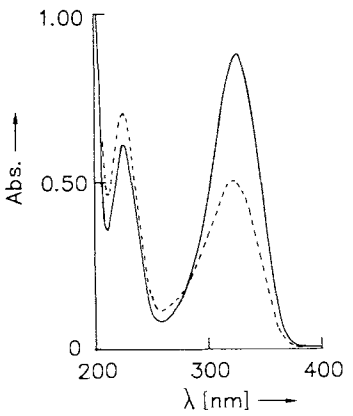

Fig. 2. Spectral change on irradiation of $2H^{\oplus}$ (3.0×10^{-5} M in 0.1 M HCl) to photostationary state (—— before irradiation; ---- after irradiation).

All of the spectral changes observed after irradiation are consistent with *trans*→*cis* photoisomerization. No quantification of the *cis*–*trans* ratio in the photostationary state has been attempted. However, the larger values of ΔA for **3**–**5**, compared with $1H^{\oplus}$, $2H^{\oplus}$, and $6H^{\oplus}$, may be due to excited-state deprotonation in the latter three cases competing with isomerization.[9]

In addition to the benzenoid structure of **1**, a quinonoid resonance structure, **1a**, is also possible; this structure is

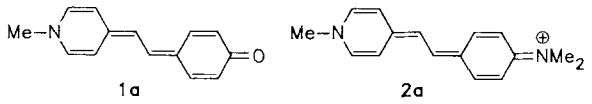

1a 2a

stabilized in nonpolar solvents, leading to a further red-shift of the lowest-energy absorption band.[10] Calculations[10b] suggest that the quinonoid form contributes significantly to the first excited state in all solvents; such an interpretation is also consistent with the fact that the dipole moment of the excited state is lower than that of the ground state.[11] In the quinonoid form, the barrier to rotation around the central bond is low, but the cisoid form is thermodynamically unstable by about 11 kcal/mol relative to the transoid form.[10c]

In the case of **2**, a similar resonance structure, **2a**, may be written. Since both **2** and **2a** bear a net charge, solvent polarity effects on the ground state are expected to be less pronounced. This is consistent with the decreased solvatochromism of **2** compared with **1**. Quinonoid resonance structures for **3**–**5** and the protonated compounds $1H^{\oplus}$, $2H^{\oplus}$, and $6H^{\oplus}$ will clearly be less stable than **1a** or **2a**; in the case of **6**, moreover, the *o*-quinone is expected to be of higher energy than the corresponding *p*-quinone. Hence, the accessibility of **1a** and **2a** in the excited state, together with the instability of their cisoid conformers, appear to impart photostability to these particular compounds.

Received: October 21, 1986;
revised: January 5, 1987 [Z 1960 IE]
German version: *Angew. Chem. 99* (1987) 346

CAS Registry numbers:
1, 23302-83-2; $1H^{\oplus}$, 67106-78-9; **2**, 68971-03-9; $2H^{\oplus}$, 107115-18-4; **3**, 29714-05-4; **4**, 95495-29-7; **5**, 107115-15-1; **6**, 107115-16-2; $6H^{\oplus}$, 107115-17-3.

[1] a) D. J. Williams: *Nonlinear Optical Properties of Organic and Polymeric Materials, ACS Symp. Ser. No. 233,* Washington, DC, USA, 1983; b) D. J. Williams, *Angew. Chem. 96* (1984) 637; *Angew. Chem. Int. Ed. Engl. 23* (1984) 690.
[2] a) A. Dulcic, C. Flytzanis, *Opt. Commun. 25* (1978) 402; b) I. R. Girling, N. A. Cade, P. V. Kolinsky, C. M. Montgomery, *Electron. Lett. 21* (1985) 169; c) I. R. Girling, P. V. Kolinsky, N. A. Cade, J. D. Earls, I. R. Peterson, *Opt. Commun. 55* (1985) 289.
[3] a) G. R. Meredith in [1a], p. 27; b) I. R. Girling, N. A. Cade, P. V. Kolinsky, J. D. Earls, G. H. Cross, I. R. Peterson, *Thin Solid Films 132* (1968) 101.
[4] R. J. Twieg, K. Jain in [1a], p. 57.
[5] H. Görner, A. Foytik, J. Wroblewski, L. J. Currell, *Z. Naturforsch. A 40* (1985) 525.
[6] U. Steiner, M. H. Abdel-Kader, P. Fischer, H. E. A. Kramer, *J. Am. Chem. Soc. 100* (1978) 3190.
[7] H. Görner, H. Gruen, *J. Photochem. 28* (1985) 329.
[8] A. P. Phillips, *J. Org. Chem. 14* (1949) 302.
[9] N. Ikeda, N. Mataga, U. Steiner, M. H. Abdel-Kader, *Chem. Phys. Lett. 95* (1983) 66.
[10] a) L. G. S. Brooker, G. H. Keyes, D. W. Heseltine, *J. Am. Chem. Soc. 73* (1951) 5350; b) A. Botrel, A. leBeuze, P. Jacques, H. Strub, *J. Chem. Soc. Faraday Trans. 2 80* (1984) 1235; c) P. Tavan, K. Schulten, *Chem. Phys. Lett. 110* (1984) 191.
[11] a) C. Varma, E. Groenen, *Recl. Trav. Chim. Pays-Bas 91* (1972) 296; b) F. J. Kampas, *Thesis,* Stanford University 1974.
[12] J. E. Kuder, D. Wychick, *Chem. Phys. Lett. 24* (1974) 69.

1,2-Diselenete and 1,2-Thiaselenete**

By *Frank Diehl* and *Armin Schweig**

The structure and properties of the valence isomeric 1,2-dithietes and dithiones have been rather satisfactorily documented;[1] in contrast nothing is known about their selenium counterparts, apart from a synthetic route for 3,4-bis(trifluoromethyl)-1,2-diselenete.[2] Mixed sulfur-selenium analogues were hitherto unknown. We report here on the first syntheses of 1,2-diselenete **2a** and 1,2-thiaselenete **2b**. The compounds are formed by gas-phase pyrolysis of 1,3-diselenol-2-one **1a** and 1,3-thiaselenol-2-one **1b**, respectively. The pyrolysis reaction is suitable for the synthesis of other substituted 1,2-diselenetes and 1,2-thiaselenetes too. This provides the first opportunity to systematically investigate the hitherto unknown chemical and physicochemical properties of these systems (e.g. valence isomerism, 6π-aromaticity, photochemistry, and electrical conductivity).

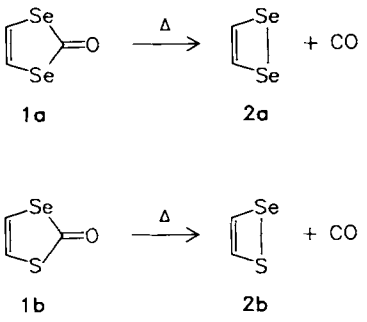

The reactants[3,4] were obtained according to procedures (**1b**) or modified procedures (**1a**) already described in the literature.[5,6] The pyrolyses were carried out in thermal reactors,[7] installed next to the ionization region of a UV-photoelectron spectrometer or as near as possible to the condensation region of a low-temperature cryostat. Optimization of the reactions with respect to the products **2a** and **2b** was achieved on the basis of photoelectron or IR spectra (in argon matrix). If the temperature falls short of the optimum temperature, increasing amounts of the starting materials are observed in the spectra; if however the temperature exceeds the optimum temperature, further reaction of **2a** and **2b** gains significance, as can be readily monitored by the increasing intensity of the acetylene bands in the spectra. At the optimum temperature, ca. 10% of the starting materials still remains in the gas mixtures. In the case of the photoelectron spectra, the product spectra were therefore refined by substraction of the spectra of the reactants (recorded under the same conditions).

The photoelectron spectra thus obtained are shown in Figure 1 together with the known photoelectron spectrum of 1,2-dithiete.[1] It can be seen that the spectra of the two new compounds **2a** and **2b** are very similar to the spectrum of 1,2-dithiete. From previous experience this is essentially true for analogous sulfur and selenium heterocycles[8] (because of the small difference in the electronega-

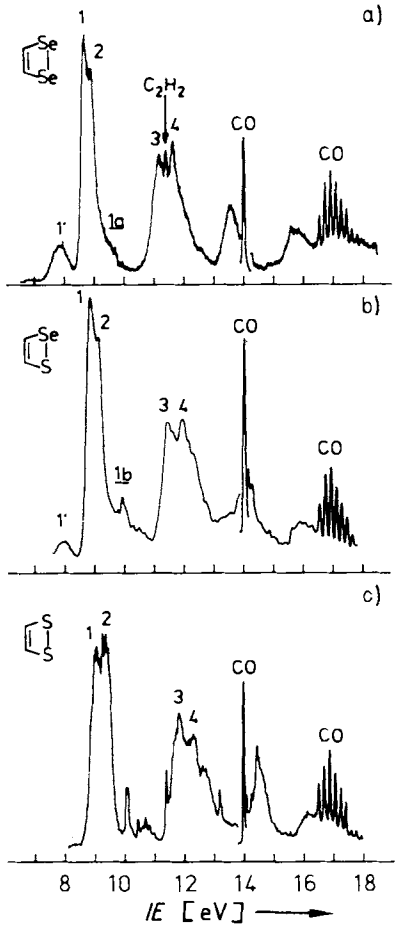

Fig. 1. He(I) photoelectron spectrum (*IE*/eV) of a) 1,2-diselenete **2a**: (1) 8.71, (2) 8.82, (3) 11.18, (4) 11.64, (1') 7.96 (presumably Se_5 [11]); b) 1,2-thiaselenete **2b**: (1) 8.87, (2) 9.13, (3) 11.46, (4) 11.97, (1') 8.04 (presumably Se_5 [11]); c) 1,2-dithiete [1]: (1) 9.05, $^2B_1(\pi)$; (2) 9.36, $^2A_2(\pi)$; (3) 11.83, $^2B_2(\sigma)$; (4) 12.31, $^1A_1(\sigma)$.

tivities of the two elements); thus, the photoelectron spectroscopic findings concomitantly provide unequivocal proof of the structure.

These results are confirmed by low-temperature IR spectra in an argon matrix. **2a** and **2b** show an intense absorption at 734 cm^{-1} (CH-δ_{oop} vibration), i.e. at practically the same wave number, namely 735 cm^{-1}, as 1,2-dithiete.[1] This is consistent with the general rule that the position of the IR absorption bands, in which the heteroatoms do not participate, remain almost unchanged on replacing sulfur by selenium.[9]

The thermal behavior of **1a** and **1b** has parallels in the electron impact-induced fragmentation of the compounds. The main fragmentation products (MS, 70 eV) are: Se_2^+ [*m/z* 160 (90%)], **2a**$^+$ or open form [*m/z* 186 (100%)], and SeS^+ [*m/z* 112 (50%)], **2b**$^+$ or open form [*m/z* 138 (100%)], respectively.[10]

Received: November 4, 1986;
supplemented: January 12, 1987 [Z 1978 IE]
German version: *Angew. Chem.* 99 (1987) 348

[*] Prof. Dr. A. Schweig, F. Diehl
Fachbereich Physikalische Chemie der Universität
Hans-Meerwein-Strasse, D-3550 Marburg (FRG)

[**] Theory and application of photoelectron spectroscopy, Part 110. This work was supported by the Deutsche Forschungsgemeinschaft and the Fonds der Chemischen Industrie.—Part 109: A. Heidenreich, N. Münzel, A. Schweig, *Z. Naturforsch. A 41* (1986) 1415.

[1] R. Schulz, A. Schweig, K. Hartke, J. Köster, *J. Am. Chem. Soc. 105* (1983) 4519.
[2] A. Davison, E. T. Shawl, *Inorg. Chem. 9* (1970) 1820.
[3] He(I) photoelectron spectra (IE/eV): **1a**: (1) 8.64, (2) 9.64, (3) 9.86, (4) 11.69; **1b** (1) 8.83, (2) 9.89, (3) 10.25, (4) 11.90. Both spectra are very similar to the known spectrum of 1,3-dithiol-2-one [1].

[4] H. Poleschner, R. Radeglia, H. Meyer, *Org. Magn. Reson. 22* (1984) 480.
[5] M. V. Lakshmikantham, M. P. Cava, *J. Org. Chem. 45* (1980) 2632.
[6] H. Poleschner, E. Fanghänel, *J. Prakt. Chem. 324* (1982) 691.
[7] In combination with a photoelectron spectrometer: stainless steel tube 200 × 4 mm, pressure ca. 10^{-2} mbar, optimum temperatures: 410°C (**1a**) and 600°C (**1b**); in combination with a low-temperature cryostat: quartz tube 50 × 4 mm, pressure 10^{-3} mbar, optimum temperatures: 530°C (**1a**) and 750°C (**1b**).
[8] Cf. e.g.: W. Schäfer, A. Schweig, S. Gronowitz, A. Taticchi, F. Fringuelli, *J. Chem. Soc. Chem. Commun. 1975*, 541; A. Schweig, N. Thon, E. M. Engler, *J. Electron Spectrosc. Relat. Phenom. 12* (1977) 335; J. Spanget-Larsen, R. Gleiter, M. Kobayashi, E. M. Engler, P. Shu, D. O. Cowan, *J. Am. Chem. Soc. 99* (1977) 2855.
[9] Cf. D. L. Klayman, W. H. H. Günther: *Organic Selenium Compounds: Their Chemistry and Biology*, Wiley-Interscience, New York 1973, p. 835f.
[10] The mass spectra were recorded in the Mass spectrometry Department of the University of Marburg (FRG).
[11] D. G. Streets, J. Berkowitz, *J. Electron Spectrosc. Relat. Phenom. 9* (1976) 269.

s-Tetrazine as Ligand for Monomeric and Bridged Macrocyclic Metal Complexes**

By *Uwe Keppeler, Sonja Deger, Armin Lange,* and *Michael Hanack**

Dedicated to Professor Ernst Bayer on the occasion of his 60th birthday

Macrocyclic transition metal compounds can be coupled by bidentate bridge ligands to axially bridged complexes (Scheme 1). In view of their interesting conductivities we have recently prepared and investigated a number of such polymeric complexes.[1]

Phthalocyanine (Pc), tetrabenzoporphyrin and, after development of an improved synthesis, also 2,3-naphthalocyanine (2,3-Nc) have been used as macrocycles, with transition metals such as Fe, Co, Rh and other metals as central metal atom. As coupling bidentate ligands we have not only used neutral ligands such as pyrazine (pyz), diisocyanobenzene and substituted diisocyanobenzenes but also anionic ligands such as cyanide or thiocyanate.[1] It was even possible to prepare a stable coordination compound, $[PcFe(tz)]_n$ **3**, with the unstable species *s*-tetrazine (tz).[2]

We now report on novel compounds bridged by *s*-tetrazine with phthalocyaninatoruthenium(II) (PcRu) and 2,3-naphthalocyaninatoiron(II) (2,3-NcFe) as metal macrocycles and compare the properties of the compounds **1** and **2** with those of **3** (Scheme 1).

1 and **2** were obtained upon heterogeneous reaction of the metal-macrocycles PcRu and 2,3-NcFe with a small excess of *s*-tetrazine[3] at 70°C and 50°C, respectively, in $CHCl_3$ for one to two days.

2 contained $CHCl_3$ as solvent of crystallization. In the reaction of *s*-tetrazine with PcRu a mixture of the monomer **4** and oligomers, which are soluble in $CHCl_3$, and **1**, which is insoluble in $CHCl_3$, is formed first. **1** was purified by extraction of the soluble fraction with $CHCl_3$. **1** and **2** are, respectively, violet and green, microcrystalline powders which are insoluble in organic solvents (Yield: **1**: 43%; **2**: 70–80%).

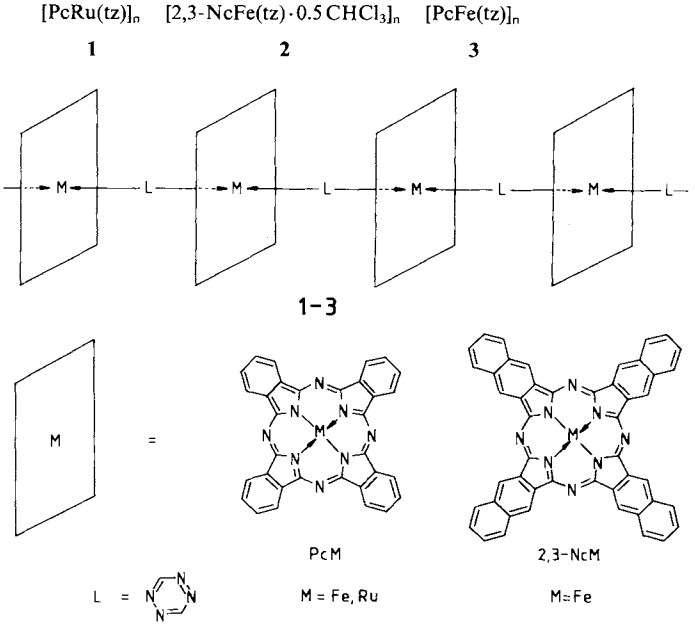

Scheme 1. Bridged compounds **1**–**3**.

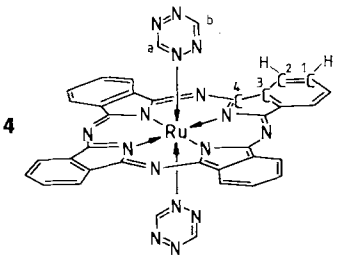

Only **4** could be obtained in pure form as a monomeric bisaxially coordinated complex; this was achieved by reaction of PcRu with *s*-tetrazine (molecular ratio 1:6) in $CHCl_3$ at 70°C. In order to separate unreacted PcRu, the deep blue solution was filtered off after 1 h and the solvent was removed under vacuum. **4** precipitated as a violet, microcrystalline powder. It still contained varying amounts of uncoordinated *s*-tetrazine, which was removed at 1.5 Pa (yield 40–45%). $[PcFe(tz)_2]$ **5** could not be separated from unreacted PcFe because of its sparing solubility. No monomeric complex was obtained with 2,3-NcFe.

The complexes **1**, **2**, and **4** were characterized by simultaneous TG/DTG/DTA measurements,[4] elemental analyses, and by their IR spectra.

The ^{57}Fe Mössbauer spectra of **2**, **3**, and **5**—with iron as central metal—were used for further characterization. In comparison to the square-planar environment of the iron atoms in PcFe[5] and 2,3-NcFe, a hexacoordinated arrangement of Fe^{II} can be concluded from the values for the isomeric shift δ and the quadrupole splitting ΔE_Q in the case of **2**, **3**, and **5** (Table 1). Pentacoordination can therefore be ruled out in the case of the bridged complexes **2** and **3**. Similar Mössbauer parameters had already been measured in the case of $[PcFe(pyz)_2]$ and $[PcFe(pyz)]_n$.[6] It follows from the ^{57}Fe-Mössbauer spectrum of **5** that unreacted PcFe is still present after the synthesis in ethanol.

X-ray powder diagrams show isomorphism between **3**

[*] Prof. Dr. M. Hanack, Dr. U. Keppeler, Dr. S. Deger, Dipl.-Chem. A. Lange
Institut für Organische Chemie,
Lehrstuhl für Organische Chemie II der Universität
Auf der Morgenstelle 18, D-7400 Tübingen (FRG)

[**] This work was supported by the Bundesministerium für Forschung und Technologie and by the Land Baden-Württemberg (Project 39—New Materials).

Table 1. ^{57}Fe Mössbauer data of some naphthalocyanine and phthalocyanine derivatives.

	Compound	T [K]	δ [mm/s]	ΔE_Q [mm/s]
	2,3-NcFe	293	0.36 [a]	2.21 [c]
2	$[2,3\text{-NcFe(tz)}\cdot 0.5\,CHCl_3]_n$	293	0.19 [a]	1.97 [d]
	PcFe	293	0.38 [a]	2.60 [c]
3	$[PcFe(tz)]_n$	293	0.13 [a]	2.23 [c]
		112	0.19 [a]	2.16 [c]
5	$[PcFe(tz)_2]$	293	0.15 [a]	1.79 [e]
	$[PcFe(pyz)_2]$ [6]	298	0.500 [b]	2.006
	$[PcFe(pyz)\cdot 0.5\,C_6H_6]_n$ [6]	298	0.500 [b]	2.009

[a] Referred to metalic iron. [b] Referred to sodium nitroprusside. [c] Fitted as simple quadrupole doublet. [d] Additional second weak doublet of low intensity. [e] Additional doublet for PcFe.

and **1**, the reflections in the case of **1** being shifted, as expected, to higher interplanar distances.

The solubility of **4** is satisfactory enough for a characterization by ^{1}H- and ^{13}C-NMR spectroscopy.[7] Noteworthy is the large upfield shift of the two *s*-tetrazine protons, caused by the ring current of PcRu and the unresolved *para* coupling in the free *s*-tetrazine, which is increased to 2.64 Hz by coordination to PcRu. This shows, once more, that phthalocyaninatometal complexes can serve as effective NMR-shift reagents.[8] Thus, both the ^{1}H-NMR as well as the ^{13}C-NMR spectra contribute to a clarification of the type of coordination of the *s*-tetrazine to the metal.[2] The appearance of two signals in each case for the two H and two C atoms of the coordinated *s*-tetrazine rules out an edge-on coordination via two nitrogen atoms.

In solution, complexes **4** tend to form oligomers. These give rise to additional signals (shifted upfield) due to the Pc protons. Such signals have already been observed in the spectra of complexes **4** with diisocyanotetramethylbenzene instead of *s*-tetrazine ($[PcRu(Me_4dib)_2]$).[1e]

The electric dark conductivities of **1**, **2**, **3**, and **4** were measured on pressed disks[9] (Table 2). The bridged compounds **1**, **2**, and **3** exhibit good semiconductor properties without additional doping, which otherwise are only achieved by oxidative doping of the coordination polymers. The conductivity of the monomer **4**, on the other hand, is about a factor of 10^9 lower.

Table 2. Powder conductivity at room temperature (σ_{RT}) and activation energies (E_a) [a] of the compounds **1**–**4**, measured in the dark.

	Compound	σ_{RT} [S/cm]	E_a [eV]
1	$[PcRu(tz)]_n$	0.01 [b]	0.1
2	$[2,3\text{-NcFe(tz)}]_n$	0.3 [b]	0.07
3	$[PcFe(tz)]_n$	0.02 [b]	0.1
4	$[PcRu(tz)_2]$	10^{-11} [c]	—

[a] $\sigma_T = \sigma_0 \cdot \exp\left(-\frac{E_a}{kT}\right)$; temperature range 80–350 K. [b] Four-probe method, 1×10^8 Pa. [c] Two-contact method 1×10^8 Pa.

Various theoretical considerations[10, 11] have indicated that the formation of the chain structure in bridged metal complexes such as **1**, **2**, and **3**, and, dependent thereof, their electrical behavior, is largely determined by the nature of the central metal and of the bridge ligand. The semiconductor behavior of compounds **1**, **2**, and **3** bridged by *s*-tetrazine can be explained in terms of a comparatively low-lying conduction band, whose formation is primarily due to the ligand *s*-tetrazine.

Received: November 4, 1986;
revised: December 18, 1986 [Z 1979 IE]
German version: *Angew. Chem. 99* (1987) 349

[1] a) M. Hanack, *Chimia 37* (1983) 238; b) M. Hanack, A. Datz, R. Fay, K. Fischer, U. Keppeler, J. Koch, J. Metz, M. Mezger, O. Schneider, H.-J. Schulze in T. Skotheim (Ed.): *Handbook of Conducting Polymers*, Marcel Dekker, New York 1986, p. 133; c) J. Metz, M. Hanack, *J. Am. Chem. Soc. 105* (1983) 828; d) S. Deger, M. Hanack, *Synth. Met. 13* (1986) 319; e) M. Hanack, U. Keppeler, *Chem. Ber. 119* (1986) 3363.
[2] O. Schneider, M. Hanack, *Angew. Chem. 95* (1983) 804; *Angew. Chem. Int. Ed. Engl. 22* (1983) 784.
[3] Synthesis of *s*-tetrazine: G. H. Spencer, P. Cross, K. B. Wiberg, *J. Chem. Phys. 35* (1961) 1939. *Before attempting to heat s-tetrazine with other solids in the absence of solvent one should take notice of the warning* given by T. Curtius, A. Darapsky, E. Müller, *Ber. Dtsch. Chem. Ges. 41* (1908) 3161.
[4] Thermoanalytically determined cleavage of the ligands, heating rate 2 K/min, N_2 25 mL/min: **1** TG 195–360°C, loss in weight 8.4% (calc. 11.8%), DTA exothermic (320°C). **2** a) TG 80–190°C, loss in weight 2.3% (calc. 2.7%), chloroform intercalated in the crystal lattice; b) 190–340°C, loss in weight 6.6% (calc. 9.4%), DTA exothermic (285°C).—**4** TG 90–500°C (without clear steps), loss in weight 20.2% (calc. 21.1%), DTA exothermic (220°C, 305°C).
[5] R. Taube, H. Drews, E. Fluck, P. Kuhn, K. F. Brauch, *Z. Anorg. Allg. Chem. 364* (1969) 297.
[6] B. N. Diel, T. Inabe, N. K. Jaggi, J. W. Lyding, O. Schneider, M. Hanack, C. R. Kannewurf, T. J. Marks, L. H. Schwartz, *J. Am. Chem. Soc. 106* (1984) 3207.
[7] **4**, ^{1}H-NMR (400 MHz, $CDCl_3$): $\delta = 8.04$ (m, 8H, H-1), 9.29 (m, 8H, H-2), 3.79 (d, 2H, H^a), 7.69 (d, 2H, $J_{ab} = 2.64$ Hz; H^b); ^{13}C-NMR (400 MHz, $CDCl_3$): $\delta = 143.96$ (C-4), 139.62 (C-3), 129.20 (C-1), 122.11 (C-2), 159.55, 156.19 (C^a, C^b).
[8] U. Keppeler, W. Kobel, H.-U. Siehl, M. Hanack, *Chem. Ber. 118* (1985) 2095.
[9] W. Kobel, *Dissertation*, Universität Tübingen 1983.
[10] E. Canadell, S. Alvarez, *Inorg. Chem. 23* (1984) 573.
[11] W. Koch, *Dissertation*, Universität Tübingen 1986.

First ENDOR Investigations of Biologically Relevant Organic Radicals in Reversed Micelles**

By *Norbert Bretz, Ingrid Mastalsky, Martin Elsner,* and *Harry Kurreck**

Reversed micelles ("water inside") are attracting increasing attention in biochemical research for several reasons:

a) Since enzymes preferentially function in an aqueous environment their stability toward the denaturing action of hydrophobic solvents can be enhanced by encapsulating them within the water pools of reversed micelles, and their catalytic activity can advantageously be used to enzymatically convert sparingly water-soluble substrates into the desired product in the nonaqueous phase.[1, 2]
b) Modified protein-free cofactors of enzymes, e.g. of flavoproteins, are rarely "good" model compounds since they exhibit undesirable properties that are not met with in intact native enzymes. Embedding of the flavin cofactors in reversed micelles could possibly suppress these properties, aggregate formation by stacking, light sensitivity, and—in the case of the semiquinoid states—radical disproportionation and radical dimerization.
c) For the spectroscopic investigation of free radicals by the magnetic resonance techniques EPR (electron paramagnetic resonance) and ENDOR (electron nuclear double resonance), water is known to be a particularly unsuit-

[*] Prof. Dr. H. Kurreck, Dipl.-Biochem. N. Bretz,
I. Mastalsky, Dipl.-Chem. M. Elsner
Institut für Organische Chemie der Freien Universität Berlin
Takustr. 3, D-1000 Berlin 33 (FRG)

[**] We thank Dr. *B. Kirste* for helpful discussions and assistance in the simulations of the spectra. *N. B.* thanks Professor Dr. *F. Müller*, University of Wageningen, for a stimulating Fellowship in his laboratory. This work was supported by the Deutsche Forschungsgemeinschaft and the Fonds der Chemischen Industrie.

able solvent because of its high microwave dielectric loss. On the other hand, investigations under physiological conditions usually require aqueous buffer solutions. If the paramagnetic species are generated within the water pools of reversed micellar solutions, such systems might enable one to study radicals in water compartments, thereby retaining the nonpolar hydrophobic character of the solution.

In studies on the nature of surfactant-solubilized water pools, interesting results, e.g. about the micellar microviscosities, have been obtained by taking advantage of the sensitivity of EPR measurements of spin probes to their environments[3] (*reporter group technique*[4]). However, evaluation of the important hyperfine data by means of EPR spectroscopy is often hampered by the limited resolution of this technique. In organic radical chemistry ENDOR spectroscopy has found wide application in attempts to overcome this drawback of EPR spectroscopy[5–7], and may therefore offer some prospect of success in the field of reversed micelles, too. The first ENDOR study of an *inorganic* radical ($ON(SO_3K)_2$) was performed in the dodecylammonium propionate (DAP)/toluene and sodium 1,2-bis(2-ethylhexyloxycarbonyl)-1-ethanesulfonate (AOT)/toluene system.[8] It could be shown by monitoring the temperature dependence of the intensity of the high-frequency ^{14}N-ENDOR signal that the micelle water is a more polar and viscous environment for the radical salt than is bulk water. Moreover, the influence of oxygen on the ENDOR response is less pronounced and aggregation of Fremy's salt at higher concentrations is suppressed. (This finding is comparable with the behavior of porphyrins in micelles, i.e., it was found that aggregation of porphyrins is suppressed, too, when they are embedded within micelles.[9, 10])

Here we report on the first successful ENDOR experiments on organic radicals in reversed micelles, with the flavin radical anions, specifically those of lumiflavin, riboflavin, FMN, and FAD as examples. Flavins are known to be ubiquitous redox cofactors in almost all biological redox chains and numerous reviews have been devoted to this field covering the chemical, biochemical and biological aspects of the flavin system (for example, cf. [11, 12]). Despite the fact that stable *aqueous solutions* of flavin radical anions have been obtained—as could be deduced from UV and EPR spectroscopy[13]—for reasons already mentioned it has so far been impossible to obtain ENDOR signals from these samples in fluid aqueous solution. However, radical anions of flavins generated electrochemically in the *nonaqueous solvents* CH_2Cl_2 or hexamethylphosphoric triamide (HMPT) using tetra-*n*-butylammonium tetrafluoroborate as supporting electrolyte could successfully be investigated by ENDOR spectroscopy in liquid solution.[14, 15] Cationic paramagnetic derivatives of flavin model compounds have also been studied by ENDOR spectroscopy in liquid *nonaqueous solvents*, e.g. mixtures of toluene/trifluoroacetic acid.[16] ENDOR investigations of radicals from flavoproteins are restricted to frozen aqueous solutions (for more detailed recent reports, see ref. [7, 16]).

We have been able to prepare remarkably stable solutions of flavin radical anions in hexane/hexanol using cetyltrimethylammonium bromide (CTAB) as surfactant. Figure 1 shows the ^1H- and ^2H-ENDOR spectra[17] of the radical anions of differently deuterated lumiflavins[18] in these reversed micelles (similar ENDOR spectra were obtained for the radical anions of riboflavin, FMN and FAD). The spectra obtained from the micellar solutions generally exhibit a good signal-to-noise ratio and resolution (linewidth ca. 150 kHz). This may be attributed to the fact that exchange processes (chemical and Heisenberg exchange) are essentially suppressed; this is likely under the assumption that each micelle contains, if at all, only *one* radical anion. Effective exchange processes of this kind are known to severely decrease the ENDOR response;[7] it is likely that these effects prevent the detection of ENDOR signals in liquid water.

Whereas the concentrations of *neutral* radicals of the flavins in fluid aqueous solutions are too low to allow ENDOR experiments (for studies of neutral flavin radicals

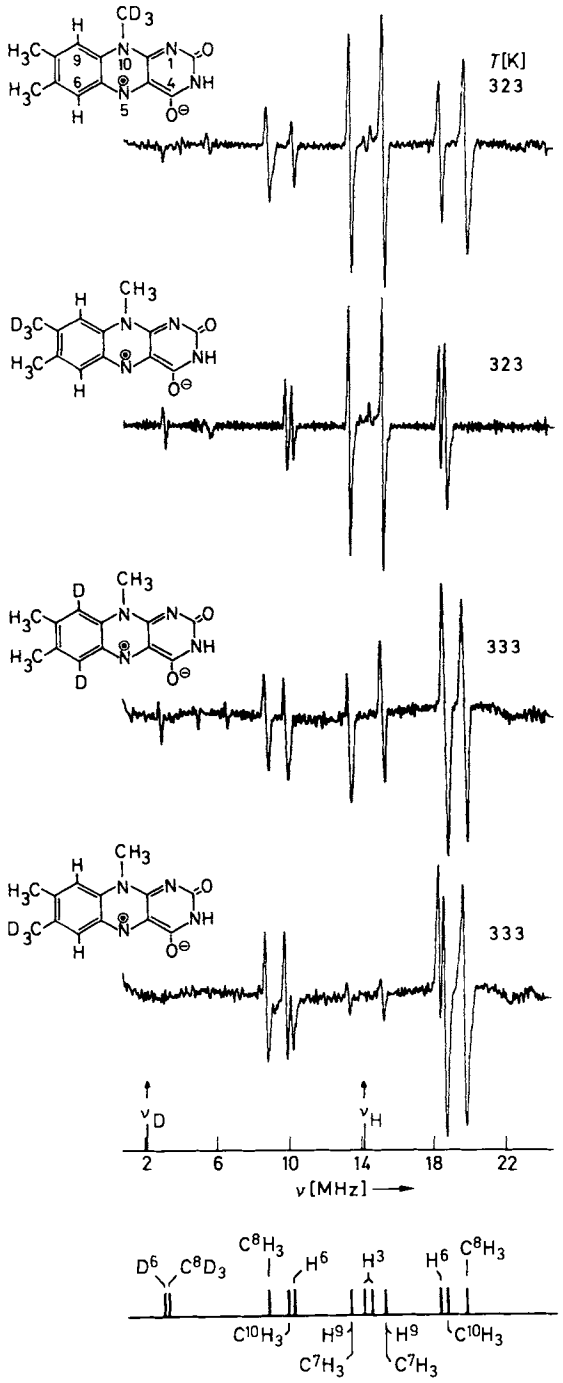

Fig. 1. ^1H- and ^2H-ENDOR spectra of radical anions of differently deuterated lumiflavins in reversed micelles. Assignment of the signals to molecular positions (see bottom) was deduced from the disappearance of ^1H-ENDOR signals on replacement of the respective protons by deuterons.

N5-alkylation is required[19]), higher concentrations of these species can be obtained in reversed micelles since effects such as dimerization and disproportionation are suppressed. Using AOT as surfactant in hexane, the ENDOR spectrum of the neutral radical of lumiflavin-3-acetate was successfully recorded.[20] Moreover, EPR spectra could be obtained from radical states of micellar solutions of flavoproteins, e.g., flavodoxins and glucose oxidase. However, attempts to detect ENDOR signals of these flavoproteins have so far failed. Further work in this interesting area is in progress.

Experimental

A 0.3 M solution of CTAB (recrystallized from ethanol and vacuum dried over silicagel) in hexane/hexanol (6:1) with a w_0-ratio [2d] of 15 ([H_2O]/[CTAB]) was prepared by adding the calculated volume of aqueous buffer solution, typically containing 25 mM of the flavin derivative, 75 mM of EDTA and 50 mM of Tris (pH 10) or pyrophosphate (pH 11) or NaOH (pH 12). The solution was vigorously shaken (1 min) and sonicated (2 × 25 s) to complete homogenization. The phase-stable solution was transferred to the EPR/ENDOR sample tube, degassed and sealed off on a high vacuum line. The radical anions were generated in the EPR cavity by illumination (halogen lamp, 250 W, 15 s intervals, 313 K) until optimum EPR signal intensity was achieved. For performing the ENDOR measurements the sample tube was transferred to an ENDOR cavity. (In situ radical generation was not possible with our ENDOR equipment.)

Received: November 5, 1986;
revised: December 30, 1986 [Z 1981 IE]
German version: *Angew. Chem. 99* (1987) 357

[1] H. H. Weetall, W. P. Vann, *Biotechnol. Bioeng. 18* (1976) 105; K. Martinek, A. V. Levashov, N. L. Klyachko, V. I. Pantin, I. V. Berezin, *Biochim. Biophys. Acta 657* (1981) 277; F. M. Menger, K. Yamada, *J. Am. Chem. Soc. 101* (1979) 6731; P. Lüthi, P. L. Luisi, *ibid. 106* (1984) 7285; C. Laane, R. Hilhorst, R. Spruijt, K. Dekker, C. Veeger in R. C. Bray, P. C. Engel, S. G. Mayhew (Eds.): *Flavins and Flavoproteins*, Walter de Gruyter, Berlin 1984.

[2] a) M. H. Hilhorst, *Ph. D. Dissertation*, Agricultural University, Wageningen, The Netherlands 1984; b) R. Hilhorst, C. Laane, C. Veeger, *Proc. Natl. Acad. Sci. 79* (1982) 3927; c) *FEBS Lett. 159* (1983) 225; d) P. L. Luisi, *Angew. Chem. 97* (1985) 449; *Angew. Chem. Int. Ed. Engl. 24* (1985) 439.

[3] Yau Yan Lim, J. H. Fendler, *J. Am. Chem. Soc. 100* (1978) 7490.

[4] L. J. Berliner (Ed.): *Spin Labeling. Theory and Applications, Vol. 1*, Academic Press, New York 1976.

[5] L. Kevan, L. D. Kispert: *Electron Spin Double Resonance Spectroscopy*, Wiley, New York 1976.

[6] H. Kurreck, B. Kirste, W. Lubitz, *Angew. Chem. 96* (1984) 171; *Angew. Chem. Int. Ed. Engl. 23* (1984) 173.

[7] H. Kurreck, B. Kirste, W. Lubitz in A. P. Marchand (Ed.): *Electron Nuclear Double Resonance Spectroscopy of Radicals in Solution*. A volume in the series *Methods in Stereochemical Analysis*, VCH Publishers, Deerfield Beach, FL, in press.

[8] E. G. Janzen, Y. Kotake, G. A. Coulter, U. M. Oehler, *Chem. Phys. Lett. 126* (1986) 205.

[9] J. H. Fuhrhop, M. Baccouche, *Justus Liebigs Ann. Chem. 1976*, 2058.

[10] J. H. Fuhrhop, T. Lehmann in G. Blauer, H. Sund (Eds.): *Optical Properties and Structure of Tetrapyrroles*, Walter de Gruyter, Berlin 1985, p. 19f.

[11] F. Müller, *Top. Curr. Chem. 108* (1983) 71.

[12] D. E. Edmondson, G. Tollin, *Top. Curr. Chem. 108* (1983) 109.

[13] A. Ehrenberg, F. Müller, P. Hemmerich, *Eur. J. Biochem. 2* (1967) 286.

[14] A more detailed comparison of the spin density distribution of differently protonated flavin radicals generated in solvents like toluene/trifluoroacetic acid, HMPT or CH_2Cl_2 with that obtained in reversed micelles will be published elsewhere: E. Weilbacher, N. Helle, R. D. Allendoerfer, H. Kurreck, unpublished.

[15] Dimethyl formamide has also been used for an ENDOR investigation of a lumiflavin radical anion, see L. E. G. Eriksson, J. S. Hyde, A. Ehrenberg, *Biochim. Biophys. Acta 192* (1969) 211.

[16] H. Kurreck, M. Bock, N. Bretz, M. Elsner, H. Kraus, W. Lubitz, F. Müller, J. Geissler, P. M. H. Kroneck, *J. Am. Chem. Soc. 106* (1984) 737.

[17] EPR and ENDOR spectra were recorded on a Bruker ER 220 D EPR spectrometer equipped with a Bruker cavity (ER 200 ENB) and laboratory-built NMR facilities described elsewhere [6, 7]. Microwave and radio frequency power levels of 130–160 mW and about 250 W (field strength of ca. 0.6 mT in the rotating frame), respectively, were applied.

[18] The synthesis of differently deuterated lumiflavins will be reported elsewhere: M. Elsner, H. Kurreck, manuscript in preparation; for a different synthetic route to deuterated flavins, see H. J. Grande, C. G. van Schagen, T. Jarbandhan, F. Müller, *Helv. Chim. Acta 60* (1977) 348.

[19] F. Müller, P. Hemmerich, A. Ehrenberg, G. Palmer, V. Massey, *Eur. J. Biochem. 14* (1970) 185.

[20] N. Bretz, H. Kurreck, unpublished results.

P_8iPr_4—the First Tricyclo[3.2.1.$0^{2,4}$]octaphosphane**

By *Marianne Baudler,* Bernhard Koll, Christoph Adamek,* and *Rolf Gleiter**

In contrast to cycloalkanes, cyclophosphanes are characterized by their pronounced tendency to form five-membered-ring structural elements.[1] Thus, the $P_8(4)$ unit **1** is an important group of Hittorf's phosphorus[2] and also constitutes the central partial framework of the organophosphanes $P_{10}iPr_4$ **2**[3] and $P_{12}iPr_4$ **3**.[4] Surprisingly, however, only relatively small amounts of the phosphorus hydride P_8H_4 could be identified by mass spectroscopy in the hydrolysis products of calcium phosphide.[5] Attempts to synthesize the corresponding organo derivatives[3,6] likewise showed that the isolated structural unit **1** does not exhibit a pronounced tendency of formation and is only moderately stable with respect to disproportionation reactions. Thus, the most readily accessible derivative, 2,4,6,8-tetraisopropyltricyclo[3.3.0.$0^{3,7}$]octaphosphane with a structure analogous to bisnoradamantane, could only be enriched initially to 15 mol-%,[3] and, more recently, up to 27 mol-%,[6] in a mixture together with other isopropylcyclophosphanes. Owing to the strain in **1**, which is revealed in **3**, for example, by a significant increase in the bond lengths of the two zero bridges,[4] stabilization of **1** is apparently only possible by incorporation into a larger P_n framework. We have now prepared the thermally very stable P_8iPr_4 isomer **4**, which represents a new P_8R_4 structure type having a constitution analogous to homonorbornene.

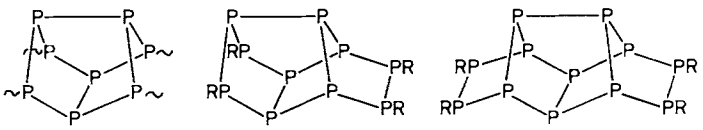

1 **2** **3**

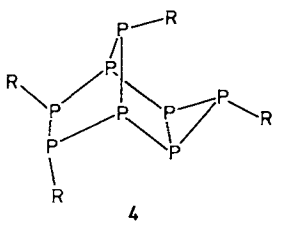

4

R = *i*Pr

[*] Prof. Dr. M. Baudler, Dr. B. Koll, Dr. C. Adamek
Institut für Anorganische Chemie der Universität
Greinstrasse 6, D-5000 Köln 41 (FRG)
Prof. Dr. R. Gleiter
Institut für Organische Chemie der Universität
Im Neuenheimer Feld 270, D-6900 Heidelberg (FRG)

[**] Contributions to the Chemistry of Phosphorus, Part 176. This work was supported by the Deutsche Forschungsgemeinschaft and the Fonds der Chemischen Industrie.—Part 175: M. Baudler, D. Düster, *Z. Naturforsch. B*, in press.

Compound **4** is formed to about 3 mol-% by thermolysis of the product mixture obtained in the reaction of iPrCl$_2$ and PCl$_3$ with magnesium, the main products being P$_7i$Pr$_5$, P$_9i$Pr$_5$, P$_7i$Pr$_3$, and P$_9i$Pr$_3$,[7] as shown by mass spectrometric investigations. In addition, P$_9i$Pr$_3$, P$_7i$Pr$_3$, (PiPr)$_4$, P$_7i$Pr$_5$, P$_6i$Pr$_4$, and small amounts of other isopropylcyclophosphanes are present. Stepwise separation of the thermolyzate (column chromatography, fractional sublimation) afforded **4** as a very pale yellow, oily, oxidation-sensitive liquid of about 95% purity.[8] The composition was established by elemental analysis and the mass spectrum, which revealed a characteristic peak corresponding to the fragment $[M-C_3H_7]^{\oplus}$.

That the framework **1** is not present in **4** is shown by the appearance of ^{31}P-NMR signals in the high-field region typical for phosphorus three-membered ring compounds.[1] The constitution and structure were derived from a complete analysis of the ^{31}P{^{1}H}-NMR spectrum; the order of magnitude and relative signs of the PP coupling constants were determined by "selective population transfer" (SPT) experiments.[9] As shown by the chemical shifts and the $^1J_{PP}$ coupling constants (Table 1), as well as by the splitting

Table 1. ^{31}P-NMR parameters [a] of **4** in [D$_6$]benzene at 25°C [b].

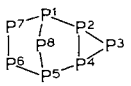

δ	^1J(PP)	^2J(PP)	^3J(PP)
+ 84.2 (P^1)	−301.3 (P^{1}P^2)	−11.5 (P^{1}P^3)	− 6.9 (P^{2}P^6)
−187.0 (P^2)	−233.9 (P^{2}P^3)	+ 8.1 (P^{1}P^4)	+ 6.5 (P^{3}P^6)
−103.8 (P^3)	−236.5 (P^{3}P^4)	+59.0 (P^{1}P^5)	−21.1 (P^{3}P^7)
−189.1 (P^4)	−327.3 (P^{4}P^5)	− 7.6 (P^{1}P^6)	−15.2 (P^{3}P^8)
+ 78.1 (P^5)	−330.6 (P^{5}P^6)	+14.5 (P^{2}P^5)	− 9.5 (P^{4}P^7)
+ 52.1 (P^6)	−269.7 (P^{6}P^7)	+62.1 (P^{2}P^7)	
+ 1.6 (P^7)	−333.3 (P^{1}P^7)	+27.3 (P^{2}P^8)	
+ 15.8 (P^8)	−276.1 (P^{1}P^8)	− 10.9 (P^{3}P^5)	
	−200.4 (P^{2}P^4)	+15.3 (P^{4}P^6)	
	−264.6 (P^{5}P^8)	+38.0 (P^{4}P^8)	
		− 2.0 (P^{5}P^7)	
		+29.3 (P^{6}P^8)	
		− 6.0 (P^{7}P^8)	

[a] J [Hz]; signs assuming negative ^1J(PP) couplings. [b] Root mean square (RMS) value of the spectrum calculation, 0.5; of 1196 transitions, 216, determined from SPT experiments, were assigned.

patterns of the individual signal groups, the framework of **4** consists of a norbornane-like P$_7$ group with an annelated three-membered ring. According to the nonequivalence of all the eight P atoms, the substituents on the two-atom bridge are arranged in a *trans* fashion. The *exo* positions of the iPr group on P^7 and the three-membered ring are inferred, on the basis of previous studies,[10] from the relation $\delta(P^6) \gg \delta(P^7)$ and from the large positive $^2J_{P^2P^7}$ coupling. The arrangement of the other substituents is derived from the $^2J_{PP}$ long-range couplings, which exhibit characteristic values depending on the orientation of the lone pairs of electrons relative to each other.[10, 11] Thus, **4** is a 3-*anti*-6-*endo*-7-*exo*-8-*syn*-tetraisopropyl-*exo*-tricyclo[3.2.1.0^{2,4}]octaphosphane (-octaphospha-*exo*-homonorbornene), which, as a result of the asymmetry of the molecule, is present as a pair of enantiomers. According to MNDO calculations[12] for P$_8$Me$_4$, the *exo*-homonorbornene isomer ($\Delta H_f^\circ = -120.1$ kcal/mol) is more stable than the bisnoradamantane isomer ($\Delta H_f^\circ = -115.8$ kcal/mol). The polycycloalkane C$_8$H$_{12}$ corresponding to **4** has already been known for some time.[13]

I II III IV

The P$_8$(4) framework I is derived from the P$_7$(5) and P$_6$(4) frameworks II[14] and III,[15] respectively, by condensation of a one-atom and a two-atom bridge, respectively, and from the P$_9$(3) skeleton IV[7] by removal of a one-atom bridge. These close structural relationships[1, 3] are probably decisive for the thermolytic formation of **4**.

Received: December 22, 1986 [Z 2025 IE]
German version: *Angew. Chem.* 99 (1987) 371

[1] M. Baudler, *Angew. Chem.* 94 (1982) 520; *Angew. Chem. Int. Ed. Engl.* 21 (1982) 492.
[2] H. Thurn, H. Krebs, *Angew. Chem.* 78 (1966) 1101; *Angew. Chem. Int. Ed. Engl.* 5 (1966) 1047; *Acta Crystallogr. B25* (1969) 125.
[3] M. Baudler, V. Arndt, *Z. Naturforsch. B39* (1984) 275.
[4] M. Baudler, Y. Aktalay, V. Arndt, K.-F. Tebbe, M. Fehér, *Angew. Chem.* 95 (1983) 1005; *Angew. Chem. Int. Ed. Engl.* 22 (1983) 1002.
[5] M. Baudler, H. Ständeke, M. Borgardt, H. Strabel, J. Dobbers, *Naturwissenschaften* 53 (1966) 106.
[6] M. Baudler, V. Arndt, B. Koll, unpublished results.
[7] M. Baudler, Y. Aktalay, K. Kazmierczak, J. Hahn, *Z. Naturforsch. B38* (1983) 428.
[8] *Experimental procedure:* 51.6 g of a stirred mixture of isopropylphosphanes (obtained by twice reacting iPrPCl$_2$ (123.2 g, 0.85 mol), PCl$_3$ (233.5 g, 1.70 mol), and magnesium (82.6 g, 3.40 mol) in 1200 mL of dry, refluxing tetrahydrofuran for 4 h) was thermolyzed for 7 h at 230°C under inert gas. The white phosphorus formed was condensed from the bright red oil (highly viscous at room temperature) at 10^{-2} torr by means of short-path distillation (bath temperature, 50°C; receiving flask, −196°C). The residue was dissolved in as little n-hexane as possible and chromatographed portionwise three times on Al$_2$O$_3$ with hexane (monitored by ^{31}P-NMR and mass spectroscopy). After combination of the fractions containing the largest amount of **4** and removal of the solvent, the crude product was subjected to high-vacuum fractional sublimation (Hg diffusion pump, cold finger at −196°C); at a bath temperature of 55–60°C and a rate of sublimation of approximately 13 mg/h, 0.22 g of **4** (purity >95% by ^{31}P-NMR) was obtained.
[9] K. G. R. Pachler, P. L. Wessels, *J. Chem. Soc. Chem. Commun. 1974*, 1038.
[10] See, for example: M. Baudler, J. Hahn, V. Arndt, B. Koll, K. Kazmierczak, E. Därr, *Z. Anorg. Allg. Chem. 538* (1986) 7; M. Baudler, E. Därr, G. Binsch, D. S. Stephenson, *Z. Naturforsch. B39* (1984) 1671.
[11] J. Hahn in J. G. Verkade, L. D. Quin (Eds.): *Phosphorus-31 NMR Spectroscopy in Stereochemical Analysis: Organic Compounds and Metal Complexes*, VCH Publishers, Deerfield Beach, FL, USA 1986, p. 331.
[12] M. J. S. Dewar, W. Thiel, *J. Am. Chem. Soc. 99* (1977) 4899, 4907.
[13] H. E. Simmons, R. D. Smith, *J. Am. Chem. Soc. 81* (1959) 4256; H. E. Simmons, E. P. Blanchard, R. D. Smith, *ibid. 86* (1964) 1347.
[14] M. Baudler, Y. Aktalay, J. Hahn, E. Därr, *Z. Anorg. Allg. Chem. 473* (1981) 20.
[15] M. Baudler, Y. Aktalay, K.-F. Tebbe, T. Heinlein, *Angew. Chem. 93* (1981) 1020; *Angew. Chem. Int. Ed. Engl. 20* (1981) 967.

P$_8t$Bu$_6$O$_6$—a Highly Oxidized Cyclophosphane with Intact P Framework**

By *Marianne Baudler** and *Joachim Germeshausen*

Compounds with a framework made up of trivalent P atoms are generally readily oxidizable and therefore frequently undergo spontaneous combustion.[1] In contrast,

[*] Prof. Dr. M. Baudler, Dr. J. Germeshausen
Institut für Anorganische Chemie der Universität
Greinstrasse 6, D-5000 Köln 41 (FRG)

[**] Contributions to the Chemistry of Phosphorus, Part 177. This work was supported by the Minister für Wissenschaft und Forschung des Landes Nordrhein-Westfalen and by the Fonds der Chemischen Industrie.—Part 176: M. Baudler, B. Koll, C. Adamek, R. Gleiter, *Angew. Chem. 99* (1987) 371; *Angew. Chem. Int. Ed. Engl. 26* (1987) 347.

hexa-*tert*-butyloctaphosphane **1** is stable for weeks upon exposure to air.[2] We recently synthesized the monooxides P_6tBu_4O and P_7tBu_5O, containing exocyclically bonded oxygen, by oxidation of P_6tBu_4 and P_7tBu_5, respectively, with air.[3] We have now been able to convert **1** into the hexaoxide **2** using other oxidation agents.

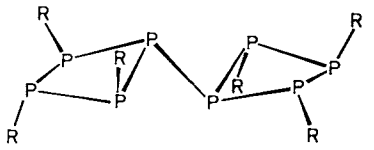

1

R = *t*Bu

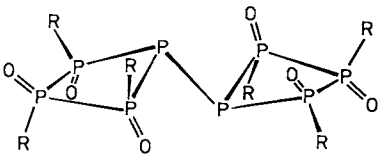

2

Compound **1** reacts with pure oxygen in solution only at higher temperatures and then with P–P bond cleavage and formation of mainly 1,2-di-*tert*-butyldiphosphane dioxide as a mixture of the two diastereomers.[4] With hydrogen peroxide, peracetic acid, and cumene hydroperoxide, on the other hand, reaction occurs already at room temperature to form the hexaoxide **2** with retention of the P_8 framework. Above 30°C, however, decomposition to P_2 units also takes place. The oxidation of **1** to **2** with cumene hydroperoxide **3** proceeds especially selectively.

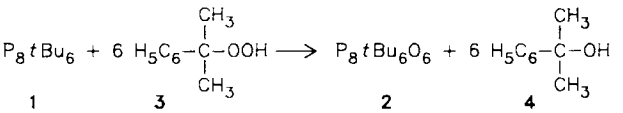

1 **3** **2** **4**

Compound **2** exhibits a pronounced tendency of formation and can be detected in addition to oxygen-poorer oxides by ^{31}P-NMR spectroscopy even at a reactant ratio of 1:1. For reactant ratios of 1:4 up to 1:90, **2** is the main product. By means of high-pressure liquid chromatography (HPLC), the by-product **4** can be separated and **2** can be isolated in analytically pure form.[5] The hexaoxide **2** is a colorless, finely crystalline solid (m.p. = 252–253°C, dec., sealed tube), which is air-stable. It is hardly soluble in organic solvents at room temperature; above about 50°C, it only dissolves with decomposition. In the mass spectrum (15 eV, 150°C), the fragment ion $[M-t\mathrm{Bu}]^{\oplus}$ is observed as the signal group with the highest mass numbers (*m/z* 629, 100%). The IR spectrum shows a band of medium intensity at 1260 cm^{-1} in the region of P=O stretching vibrations.

Proof of the constitution of **2** is provided by the $^{31}P\{^1H\}$-NMR spectrum (121.5 MHz), which, owing to the low solubility of the pure substance, was recorded for the crude product (80 P-% **2**, dissolved in toluene). It shows three multiplets of an $AA'B_2B_2'CC'$ spin system at $\delta = +117$, $+82$, and -57 (intensity ratio 1:2:1). The ^{1}H-coupled spectrum clearly reveals that the two low-field groups correspond to the six *tert*-butyl-substituted P atoms. The splitting patterns of the multiplets are an indication that oxygen is exclusively exocyclically bonded to **1**. Which of the P atoms are present as λ^5 phosphorus follows from the different low-field shifts of the signals of the individual P nuclei compared with the corresponding resonance positions in the starting compound ($\Delta\delta(P_A) = 155$; $\Delta\delta(P_B) = 129$; $\Delta\delta(P_C) = 45$ ppm). Only the organo-substituted P atoms show the strong deshielding expected for an oxidized phosphorus four-membered ring.[3] Accordingly, the product **2** is a 2,2',3,3',4,4'-hexa-*tert*-butyl-1,1'-bicyclotetraphosphane 2,2',3,3',4,4'-hexaoxide. The configuration and conformation should be analogous to those in **1** because of the method of formation.

The fact that **1** cannot be converted into the octaoxide, even with a large excess of **3**, is presumably a result of the relatively small bond angles at the exocyclic bridge (φ(P–P–P) = 96.6°[2]) and thus of the predominantly s character of the lone electron pairs at the "bridgehead" atoms.

Received: January 7, 1987 [Z 2039 IE]
German version: *Angew. Chem.* 99 (1987) 372

[1] Review: M. Baudler, *Angew. Chem.* 94 (1982) 520; *Angew. Chem. Int. Ed. Engl.* 21 (1982) 492.
[2] M. Baudler, J. Hellmann, P. Bachmann, K.-F. Tebbe, R. Fröhlich, M. Fehér, *Angew. Chem.* 93 (1981) 415; *Angew. Chem. Int. Ed. Engl.* 20 (1981) 406.
[3] M. Baudler, M. Michels, M. Pieroth, J. Hahn, *Angew. Chem.* 98 (1986) 465; *Angew. Chem. Int. Ed. Engl.* 25 (1986) 471.
[4] M. Baudler, H. Heumüller, *Z. Naturforsch. B*, in press.
[5] *Experimental Procedure:* 40 mL of a stirred, saturated solution of **1** in toluene (0.4 mmol) was allowed to react at room temperature with 0.52 g of an 80% solution of **3** in cumene (2.7 mmol peroxide, excess), the reaction mixture turning transiently yellow. After concentration of the colorless product solution to 1.6–2.0 mL, **2** was isolated by preparative HPLC (Nucleosil-5 C18 column, methanol, receiving flask at −78°C, rapid evaporation of the solvent at 0°C). The residue was washed three times with 2 mL of pentane, affording 28 mg of pure **2** (10% based on **1**).

Raman Spectrum of the Tetrasilatetrahedrane Anion Si_4^{4-}**

By *Gerhard Kliche, Martin Schwarz,* and *Hans-Georg von Schnering**

We recently reported the synthesis of the red, transparent metal silicides K_3LiSi_4 and $K_7Li(Si_4)_2$.[1] We have now also been able to prepare the long known silicide CsSi[2] as a pure compound in the form of red, transparent crystals,[3] thus making the first measurement of Raman spectra of the alkali-metal silicides possible. This is of special interest because of the tetrahedral structure of the Si_4^{4-} ions.

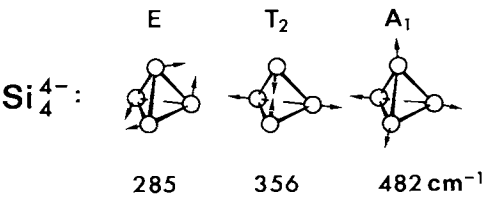

Si_4^{4-} is isostructural and isoelectronic with the P_4 molecule. Hence, with the symmetry $\bar{4}3m$-T_d one can expect to observe the three vibrations of the species A_1(R), E(R), and T_2(R,IR). However, one has to reckon with band splittings, which, on the one hand, can arise from the site symmetry, which generally deviates from the molecular symmetry, and, on the other, from the space groups and unit cells decisive for the mutual arrangement of the Si_4^{4-} anions. Finally, the anions Si_4^{4-} can only be regarded as iso-

[*] Prof. Dr. H. G. von Schnering, Dr. G. Kliche, Dr. M. Schwarz
Max-Planck-Institut für Festkörperforschung
Heisenbergstrasse 1, D-7000 Stuttgart 80 (FRG)

[**] This work was supported by the Fonds der Chemischen Industrie.

lated units to a limited extent: a) the cations M, as μ_3-ligands, extend the tetrahedrane structures to M_4Si_4 cubane structures (even if with weaker interactions); b) oligomers or polymers are formed via the M-ligands. CsSi crystallizes cubic ($P\bar{4}3n$) with eight isolated Si_4 (or Cs_4Si_4) in the unit cell. Of these, two Si_4 (Cs_4Si_4) possess tetrahedral symmetry $\bar{4}3m$-T_d, although the site symmetry in the space group is only 23-T.[4] The other six Si_4 (Cs_4Si_4) occupy sites of $\bar{4}$-S_4 symmetry. K_3LiSi_4 crystallizes orthorhombically (*Pnma*) with four Si_4 having m-C_s symmetry; these are coupled via two Li atoms to give a one-dimensional infinite chain $^1_\infty[Li_{2/2}Si_4]$. The structure of K_7LiSi_8 (cubic, $Pa\bar{3}$) contains four dimeric Si_4–Li–Si_4 dumbbells with $\bar{3}$-S_6 symmetry, whereby each Si_4 unit (or the pertinent cubane $[K_3LiSi_4]$) belongs to the symmetry $3m$-C_{3v}.

Figure 1 shows the Raman spectra of the three compounds. Almost independently of the completely different crystal structures, three intense bands with only small individual shifts and splittings are observed at about 290, 355, and 480 cm^{-1}. Numerous other bands lie separately therefrom at lower wave numbers. These should contain, besides external lattice vibrations, the librations of the Si_4^{4-} tetrahedra, whereas the three high-frequency bands can be unequivocally assigned to the internal vibrations of species E, T_2 and A_1 of the Si_4^{4-} ions. This convincingly justifies the treatment of the Si_4^{4-} ions as quasi-isolated units. *Bürger* and *Eujen*[5] had already observed two bands at 358 and 334 cm^{-1} in the IR spectrum of (black) CsSi and had assigned them to the T_2 vibration, split by site symmetry effects. Our IR spectra (cf. Fig. 2[6]) of the red, transparent samples of the compounds investigated show 2–3 modes in a region separated from the lattice vibrations (298 K: CsSi: 332, 352, 357 cm^{-1}; K_3LiSi_4: 340, 357 cm^{-1}; K_7LiSi_8: 339, 356 cm^{-1}; 10 K: CsSi: 335, 356, 362 cm^{-1}; K_3LiSi_4: 339, 345, 362 cm^{-1}; K_7LiSi_8: 344, 356, 362 cm^{-1}); the maxima of the higher wavenumbered modes are in good agreement with the maxima of the Raman bands. There are many factors which would suggest that the splitting observed in the IR spectra does not only arise from the different site symmetries of the Si_4^{4-} anions, but is also associated with a coupling of the μ_3 ligands (cations M). A quantitative interpretation however, will only be possible after detailed lattice dynamical calculations. In these calculations, the mode splittings found in the spectra of crystalline white phosphorus (α-P_4, β-P_4) can then also be taken into consideration.[6]

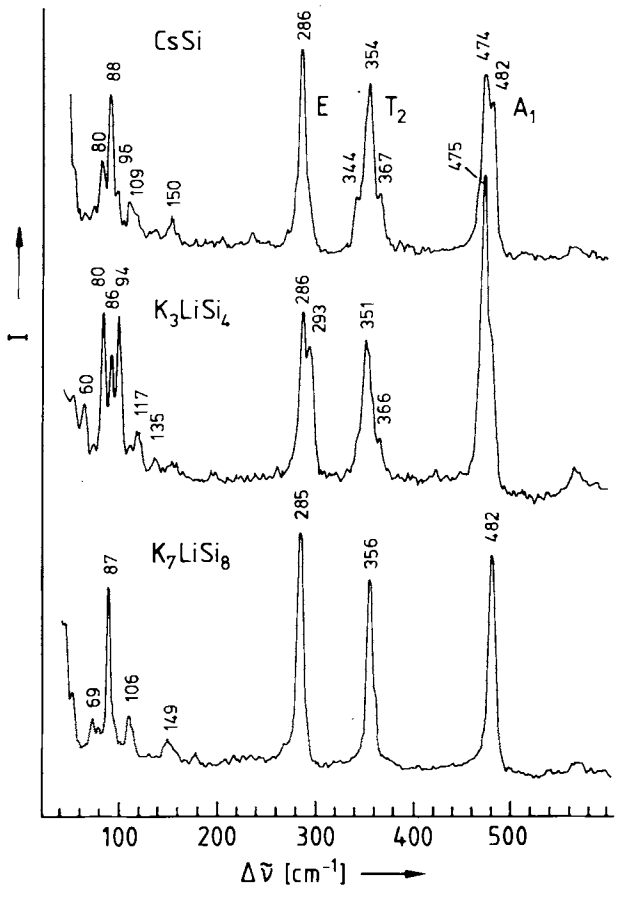

Fig. 1. Raman spectra of the silicides CsSi, K_3LiSi_4, K_7LiSi_8 (room temperature, krypton-ion laser, 676 nm (150 mW), resolution >4 cm^{-1}, back-scattering technique).

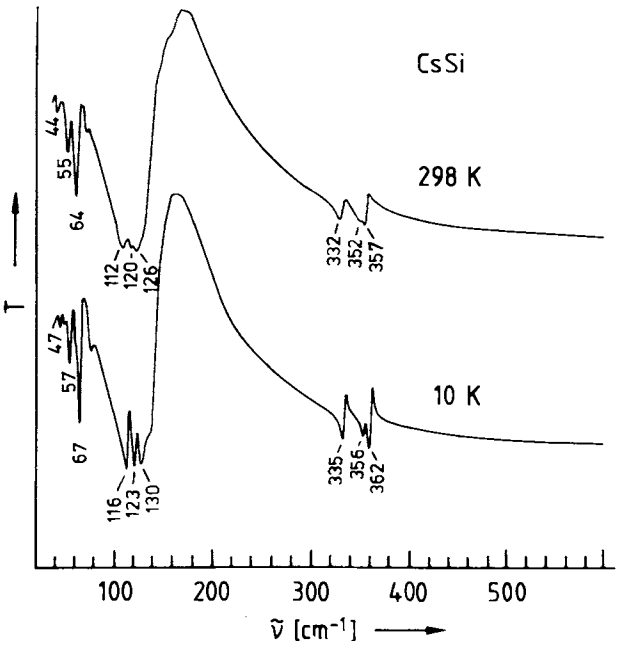

Fig. 2. IR spectra of CsSi at 298 and 10 K (PE pellet, Bruker IFS 113 v). Intense bands <200 cm^{-1}: lattice vibrations.

Table 1. Vibrational frequencies [cm^{-1}], ratio of vibrational frequencies $\tilde{\nu}$, force constants [mdyn $Å^{-1}$] mean distances [Å], bond order according to *Siebert* (N), and mean vibrational amplitudes (300 K) for the X–X distance [Å] for tetrahedral molecules.

X_4	A_1	T_2	E	$\tilde{\nu}(A_1)$	$\tilde{\nu}(T_2)$	$\tilde{\nu}(E)$	f_d	f'_{dd}	f_{dd}	$\bar{r}_{xx}$	N	u	Ref.
Si_4^{4-} [a]	482	356	285	1.69	1.25	1	1.13	0.08	−0.06	2.42	0.60	0.068	
P_4 [b]	606	464.5	363	1.67	1.28	1	2.07	0.10	−0.12	2.21	0.94	0.053	[11]
As_4 [c]	353	265.5	207.5	1.70	1.28	1	1.64	0.08	−0.09	2.44	0.87	0.054	[12]
Sb_4 [c]	241.5	178.5	137.1	1.76	1.30	1	1.20	0.05	−0.05		1.00 [d]	0.061	[13]
Bi_4 [e]	149.5	120.4	89.8	1.66	1.34	1	0.89	0	−0.05		0.84 [d]	0.069	[14]

[a] Data for K_7LiSi_8. [b] Gas-phase, calculation of force constants without anharmonicity correction. [c] Argon matrix. [d] Calculation using $\bar{r}_{xx} = r_{cov.}$ [e] Neon matrix.

In Table 1 the Raman spectrum of the anion Si_4^{4-} in K_7LiSi_8 (minimum mode splittings) is compared with the Raman spectra of P_4, As_4, Sb_4, and Bi_4. The force constants f_d, f'_{dd}, and f_{dd} of a general valence force field were calculated according to the method of *Pistorius*,[7] the bond order N according to the method of *Siebert*,[8] and the mean amplitude of vibration according to the method of *Cyvin*.[9] The analogy of the tetrahedral groups is immediately recognizable. Particularly striking is the large reduction of the vibrational frequencies of Si_4^{4-} compared to those of the (somewhat heavier) P_4 molecule. The force constant f_d(Si–Si) = 1.13 mdyn·Å^{-1} corresponds to the value derived from the IR spectrum (1.05 ± 0.1 mdyn·Å^{-1} [5]); the corresponding value for P_4 is 2.07 mdyn·Å^{-1}. The Si–Si bond in Si_4^{4-} is thus considerably weaker than both the P–P bond in P_4 as well as other Si–Si bonds;[5] this weakening is certainly associated with the negative partial charges of the Si atoms. This is also manifested in the bond order N = 0.60, calculated according to *Siebert*,[8] even if this value is not in very good agreement with the Pauling bond order,[10] PBO = 0.76, obtained alone from the distances d_1(Si–Si) = 235 pm and $\bar{d}_n$(Si–Si) = 242 pm. In any case, the additional ionic interactions with the cations will contribute decisively to the stability of the anions Si_4^{4-}.

Experimental

CsSi, K_3LiSi_4 and K_7LiSi_8 were prepared as described in ref. [1]. The Raman spectra were recorded on polycrystalline fragments of the silicides using a back-scattering technique at room temperature (krypton ion laser, 647 and 676 nm (150 mW); Jarrell-Ash double monochromator, RCA photomultiplier, resolution > 4 cm^{-1}). The IR spectra were recorded on PE pellets with an IFS 113v FT-IR spectrometer (Bruker), resolution 1 cm^{-1}.

Received: December 4, 1986;
supplemented: January 22, 1987 [Z 2000 IE]
German version: *Angew. Chem. 99* (1987) 350

[1] H. G. von Schnering, M. Schwarz, R. Nesper, *Angew. Chem. 98* (1986) 558; *Angew. Chem. Int. Ed. Engl. 25* (1986) 566.
[2] E. Hohmann, *Z. Anorg. Allg. Chem. 257* (1948) 113.
[3] M. Schwarz, *Dissertation*, Universität Stuttgart 1987.
[4] P. Engel, T. Matsumoto, G. Steinmann, H. Wondratschek, *The Non-characteristic Orbits of the Space Groups, Z. Kristallogr. Suppl. 1* (1984).
[5] H. Bürger, R. Eujen, *Z. Anorg. Allg. Chem. 394* (1972) 19.
[6] G. Kliche, M. Schwarz, H. G. von Schnering, unpublished.
[7] C. W. F. T. Pistorius, *J. Chem. Phys. 29* (1958) 1421.
[8] H. Siebert, *Z. Anorg. Allg. Chem. 273* (1953) 170.
[9] S. J. Cyvin, *Acta Chem. Scand. 13* (1959) 1397.
[10] L. Pauling, *J. Am. Chem. Soc. 69* (1947) 542.
[11] Y. M. Bosworth, R. J. H. Clark, D. M. Rippon, *J. Mol. Spectrosc. 46* (1973) 240.
[12] K. Manzel, W. Schulze, V. Wölfel, R. Minkwitz, *Z. Naturforsch. B37* (1982) 1127.
[13] H. Sontag, R. Weber, *Chem. Phys. 70* (1982) 23.
[14] V. E. Bondybey, J. H. English, *J. Chem. Phys. 73* (1980) 42.

Enantioselective Synthesis of α-Trialkylsilyl Ketones and Aldehydes**

By *Dieter Enders** and *Braj Bhushan Lohray*

Dedicated to Professor Gerhard Quinkert on the occasion of his 60th birthday

Silylenol ethers **B**[1] and their isomeric α-silyl ketones (β-ketosilanes) **A**[2] are interconvertable.[3] They belong to the synthetically most useful class of compounds in modern carbonyl chemistry. The *O*-silylated compounds **B** are readily accessible by silylation of the ketones (Z = O), whereas the synthesis of the *C*-silylated isomers **A** necessitates recourse to the corresponding azaenolates (Z = NR, NNR_2)[4a–d] or other coupling patterns (see retrosynthesis—Scheme 1).[4e–i]

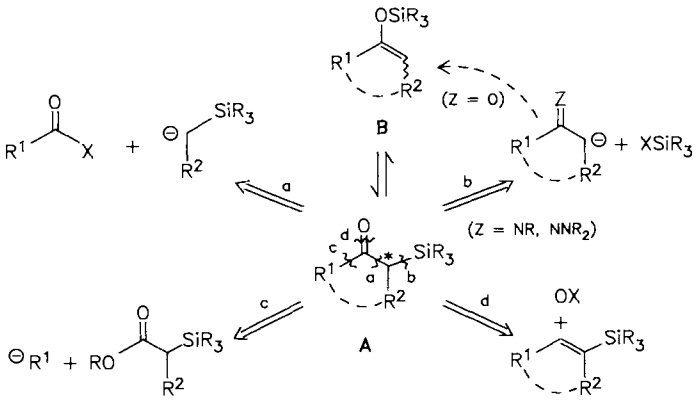

Scheme 1.

In continuation of our studies on metalated SAMP-/RAMP-hydrazones[5] we have now found that chiral α-silyl ketones and α-silylaldehydes **A** are accessible for the first time enantioselectively and highly enantiomerically pure via route b (Scheme 1). The ketones and aldehydes **1**, after conversion into the SAMP-hydrazones (*S*)-**2**, are metalated with lithium diisopropylamide and *C*-silylated with trialkylsilyl trifluoromethanesulfonates (triflates).[6] The silylhydrazones (*SR*)-**3** (*de* ≧ 96%) thus obtained are cleaved oxidatively and racemization-free with ozone, and afford, after chromatographic separation of (*S*)-**5** (recycling of the chiral auxiliary), the virtually enantiomerically pure (*ee* ≧ 96%) α-silylketones and α-silylaldehydes (*R*)-**4** in overall yields of 52–79% and 22–42%, respectively (Table 1).

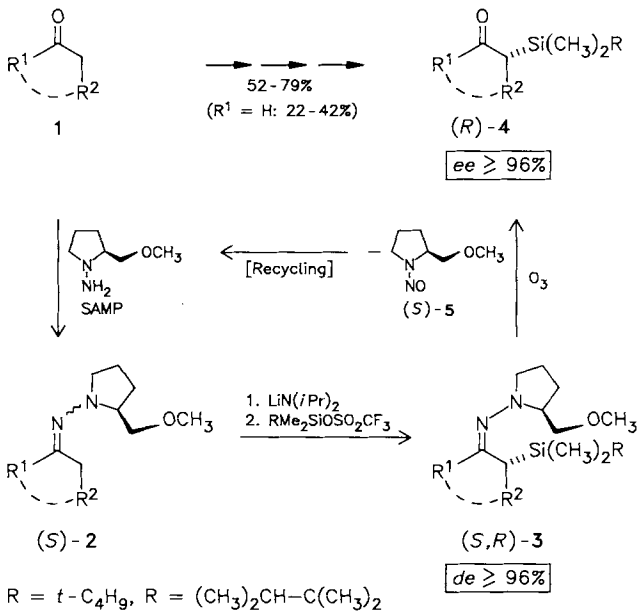

Scheme 2.

[*] Prof. Dr. D. Enders, Dr. B. Bhushan Lohray
Institut für Organische Chemie der Technischen Hochschule
Professor-Pirlet-Str. 1, D-5100 Aachen (FRG)

[**] This work was supported by the Fonds der Chemischen Industrie, by BASG AG, and by Degussa AG. We thank Dr. *H. Wetter*, Ciba-Geigy, Basel, for a gift of chlorodimethylthexylsilane.

Table 1. α-Silyl ketones and α-silylaldehydes **4** synthesized from aldehydes and ketones **1** by enantioselective silylation via SAMP-hydrazones. If not otherwise stated, R = *tert*-butyl.

4	R^1	R^2	Total yield [%]	$[\alpha]_D^{23}$ (c, C_6H_6) [°]	*ee* [%] [b]
(*R*)-**4a**	C_2H_5	CH_3	77	+188.2 (1.5)	≧96
(*S*)-**4a** [c]	C_2H_5	CH_3	74	−182.6 (1.5)	≧96
(*R*)-**4a** [d]	C_2H_5	CH_3	79	+152.0 (1.4)	≧96
(*R*)-**4b** [e]	$-(CH_2)_4-$		59	−173.7 (2.5)	≧96
(*R*)-**4c**	C_6H_5	CH_3	60	+48.4 (2.9)	≧96
(*R*)-**4c** [d]	C_6H_5	CH_3	68	+65.4 (1.1)	≧96
(*R*)-**4d**	2,4-dimethoxyphenyl	CH_3	78	−7.7 (0.6)	≧96
(*R*)-**4e**	2-naphthyl	CH_3	70	−51.4 (1.0)	≧96
(*R*)-**4f**	C_6H_5	C_6H_5	52	−4.8 (1.1)	≧96
(*R*)-**4g**	H	$C_6H_5CH_2$	42 [f]	+77.3 (1.6) [g]	≧96
(*R*)-**4h**	H	n-C_6H_{13}	22 [f]	+59.7 (1.0)	≧96

[a] Cyclopentanone and dibenzyl ketone could be silylated in 80% and 56% total yield, respectively, but with lower enantioselectivity (66 and 48% *ee*, resp.). [b] Determined ^{1}H-NMR spectroscopically with Eu(hfc)$_3$ by comparison with *rac*-**4a**–**h**; in each case the other enantiomer was not detectable. [c] RAMP was used as chiral auxiliary. [d] R = thexyl (1,1,2-trimethylpropyl). [e] (*S*)-(−)-1-amino-2-(1,1-dimethylmethoxymethyl)pyrrolidine was used as chiral auxiliary [7]. [f] The lower overall yields in the case of the aldehydes results from a partial *N*-silylation of (*S*)-**2** [8] or from a partial oxidation of (*S*,*R*)-**3** during the ozonolysis. [g] In diethyl ether.

The optical antipodes (*S*)-**4** can be obtained in the same way by simply replacing SAMP by the enantiomeric RAMP. The ^{13}C-NMR spectroscopically determined diastereomeric excesses of the product hydrazones **3** are in good agreement, within the limits of detection, with the enantiomeric excesses of the products **4** determined by ^{1}H-NMR shift experiments. In all cases, the racemic compounds *rac*-**4** were prepared via the dimethylhydrazones for comparison.[4b,c]

The (not yet confirmed) assignment of the absolute configurations is based on earlier investigations of the electrophilic substitutions via metalated SAMP-/RAMP-hydrazones. Preliminary studies involving the use of the α-silyl ketones **4** in asymmetric synthesis are very promising;[9,10] they are relatively insensitive to racemization.

Experimental

A solution of (*S*)-**2** (10 mmol) in ether (30 mL) was added dropwise to a stirred solution of lithium diisopropylamide (10.5 mmol) (prepared from 6.5 mL of 1.6 N *n*-butyllithium solution and 1.5 mL of diisopropylamine in 30 mL of ether at 0 °C). After 4 h the mixture was cooled to −78 °C and treated at once with 2.3 mL (10 mmol) of *tert*-butyldimethylsilyl triflate[6a] or 2.5 mL (10 mmol) of dimethylthexylsilyl triflate[6b]. After a further two hours' stirring the mixture was allowed to warm up to room temperature within ca. 10 h and was then worked up with ether. The extract was dried over magnesium sulfate and the solvent removed by evaporation. The crude product, (*SR*)-**3**, which was purified by flash-chromatography (silica gel, ether/*n*-pentane 1:4, R_f = 0.4) if necessary, was taken up in 50 mL of *n*-pentane and the solution cooled to −78 °C. Ozone was then passed through the solution until complete oxidative cleavage of the hydrazone (TLC monitoring). After removal of excess ozone by passage of argon, heating, and evaporation to dryness, (*R*)-**4** was separated from the nitrosamine (*S*)-**5** by flash chromatography (silica gel, ether/*n*-pentane 1:4, **5**: R_f = 0.3, **4**: R_f = 0.8).—For recycling of SAMP, (*S*)-**5** was reduced with $LiAlH_4$ in tetrahydrofuran.

Received: December 8, 1986 [Z 2001 IE]
German version: *Angew. Chem.* *99* (1987) 359

[1] P. Brownbridge, *Synthesis 1983*, 1, 85.
[2] Examples of synthetic applications: a) R. A. Ruden, B. L. Gaffney, *Synth. Commun.* *5* (1975) 15; b) I. Kuwajima, T. Inoue, T. Sato, *Tetrahedron Lett. 1978*, 4887; c) J. M. McNamara, Y. Kishi, *J. Am. Chem. Soc.* *104* (1982) 7371; d) I. Matsuda, H. Okada, S. Sato, Y. Izumi, *Tetrahedron Lett.* *25* (1984) 3879; e) M. Fiorenza, A. Mordini, S. Papaleo, S. Pastorelli, A. Ricci, *ibid.* *26* (1985) 787.
[3] a) E. J. Corey, C. Rücker, *Tetrahedron Lett.* *25* (1984) 4345; b) Y. Yamamoto, K. Ohdoi, M. Nakatani, K. Akiba, *Chem. Lett. 1984*, 1967; c) I. Matsuda, S. Sato, M. Hattori, Y. Izumi, *Tetrahedron Lett.* *26* (1985) 3215.
[4] a) E. J. Corey, D. Enders, *Chem. Ber.* *111* (1978) 1362; b) P. Weuster, *Dissertation*, Universität Giessen 1982; c) D. Enders in H. Nozaki (Ed.): *Perspectives in Organic Synthesis*, Special Report, *Kagaku, Zokan (Kyoto)* *99* (1983) 95; d) P. F. Hudrlik, A. K. Kulkarni, *J. Am. Chem. Soc.* *103* (1981) 6251; method a: e) C. R. Hauser, C. R. Hance, *ibid.* *74* (1952) 5091; f) M. Demuth, *Helv. Chim. Acta* *61* (1978) 3136; g) D. E. Seitz, A. Zapata, *Synthesis 1981*, 557; method c: h) G. L. Larson, I. Montes de López-Cepero, L. E. Torres, *Tetrahedron Lett.* *25* (1984) 1673; method d: i) M. Obayashi, K. Utimoto, H. Nozaki, *ibid.* *21* (1977) 1807; j) H. Beisswenger, M. Hanack, *ibid.* *23* (1982) 403; k) R. F. Cunico, *ibid.* *27* (1986) 4269; special methods: l) S. Sato, H. Okada, I. Matsuda, Y. Izumi, *ibid.* *25* (1984) 769.
[5] a) D. Enders in J. D. Morrison: *Asymmetric Synthesis, Vol. 3*, Academic Press, Orlando 1984, pp. 275–339; b) D. Enders, H. Eichenauer, U. Baus, H. Schubert, K. A. M. Kremer, *Tetrahedron* *40* (1984) 1345; most recent application: c) D. Enders, H. Schubert, C. Nübling, *Angew. Chem.* *98* (1986) 1118; *Angew. Chem. Int. Ed. Engl.* *25* (1986) 1109.
[6] a) E. J. Corey, H. Cho, C. Rücker, D. H. Hua, *Tetrahedron Lett.* *22* (1981) 3455; b) H. Wetter, K. Oertle, *ibid.* *26* (1985) 5511, 5515.
[7] H. Kipphardt, *Dissertation*, Technische Hochschule Aachen 1986.
[8] The silylation of 3-methylbutanal via SAMP hydrazone afforded 72% *N*-silylated product.
[9] Diastereo- and enantio-selective aldol reactions with (*R*)-**4** as chiral methylene component proceed with almost complete asymmetric induction. D. Enders, B. Bhushan Loray, unpublished results.
[10] All the new compounds gave correct elemental analyses and characteristic spectra.

"Two-Electron Reduction" of Phosphane-substituted Tricobalt Clusters—Evidence for a 17-Electron Intermediate in the Dissociative ETC Ligand Substitution**

By *Klaus Hinkelmann, Falko Mahlendorf, Jürgen Heinze,* Hans-Thomas Schacht, John S. Field,* and *Heinrich Vahrenkamp**

The reduction behavior of μ_3-alkylidyne tricobalt clusters has been the subject of several investigations.[1] In particular, their ability to engage in efficient ETC processes (ETC = *e*lectron-*t*ransfer *c*hain catalyzed) and thereby to exhibit catalytic activity has recently stimulated new investigations.[2] However, it has so far remained unclear whether these clusters, like other metal clusters,[3] can undergo reversible reduction in multistep redox processes. Although the radical anions of the clusters $[(\mu_3\text{-RC})Co_3(CO)_9]$ are known to exhibit prolonged stability, the dianions undergo irreversible decomposition with destruction of the metal framework.[1] In a new electrochemical investigation of phosphane-substituted derivatives of **1**, we have now observed, surprisingly, that these compounds can be reduced, in part, to give stable dianions via a formally two-electron process. A detailed analysis of the overall redox reaction revealed an unusual mechanism which has not been observed for clusters so far.

$[(\mu_3\text{-MeC})Co_3(CO)_9]$ **1**

$[(\mu_3\text{-MeC})Co_3(CO)_6(PR_2Ph)_3]$ **2a,b**

$[(\mu_3\text{-MeC})Co_3(CO)_8(PR_2Ph)]$ **3a,b**

[*] Priv.-Doz. Dr. J. Heinze, Dipl.-Chem. K. Hinkelmann, F. Mahlendorf
Institut für Physikalische Chemie der Universität
Albertstrasse 21, D-7800 Freiburg (FRG)
Prof. Dr. H. Vahrenkamp, Dipl.-Chem. H.-T. Schacht, Dr. J. S. Field
Institut für Anorganische und Analytische Chemie der Universität
Albertstrasse 21, D-7800 Freiburg (FRG)

[**] This work was supported by the Baden-Wurttemberg Research Program (Radicals and One-Electron Transfers, FR-NW 31) and by a Humboldt fellowship (to *J. S. F.*).

$[(\mu_3\text{-MeC})Co_3(CO)_6(PR_2Ph)_2]$ **4a,b**

a, R = Me; **b**, R = Et

Typical examples are the compounds **2a** and **2b**. Their striking voltammograms (e.g., of **2b**, Fig. 1a) reveal, in addition to an unusually high cathodic wave, the seldomly observed crossing effect as well as two distinct anodic

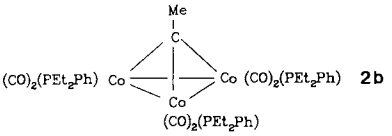

2b

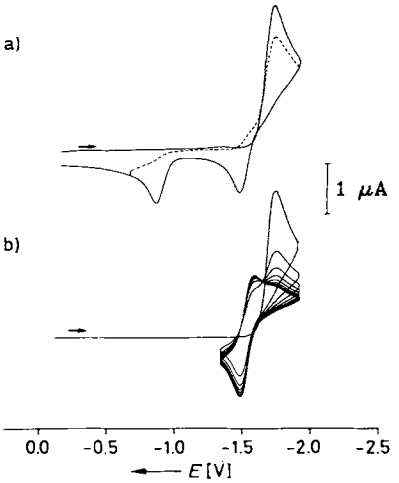

Fig. 1. a) Experimental cyclovoltammogram for the reduction of **2b** ($c = 8 \times 10^{-4}$ M), broken line = second cathodic scan, in CH_3CN/0.1 M Bu_4NPF_6, $T = 24$ °C, $v = 0.4$ V/s, Pt electrode, Ag/AgCl as reference electrode. b) Multisweep cyclovoltammogram (8 sweeps) for **2b**, recorded between −1.3 and −1.9 V; same conditions as in a).

waves in the reverse scan. Only two examples of this type of voltammogram have been reported so far: the 5,6-dihydrobenzo[*c*]quinoline system[4] and the phosphido-bridged rhodium complex $[\{Rh(\mu\text{-}t\text{Bu}_2P)(CO)_2\}_2]$.[5] After the first charge transfer, the former undergoes a conformational flattening, the latter an isomerization from a planar to a tetrahedral structure. Both processes energetically favor the second charge transfer. As a consequence of this, the corresponding voltammograms exhibit a two-electron transfer in the forward scan. In the reverse reaction, such redox systems proceed by two one-electron steps to the neutral state followed by the structural reorganization to the starting compounds. The overall process is thus reversible, but the forward and reverse reactions proceed, in part, via different intermediates.

It would appear reasonable to explain the behavior of **2** by a similar mechanism. The well-known chemical instability of the radical anions of phosphane-substituted tricobalt clusters,[2b] however, suggests another course of reaction (Scheme 1), in which a ligand is eliminated subsequent to formation of the radical anion $\mathbf{2}^{\odot\ominus}$. The resulting species, $\mathbf{4}^{\odot\ominus}$, owing to its higher redox potential, is immediately reduced to the dianion $\mathbf{4}^{2\ominus}$. The reoxidation would then take place in two distinct steps via the monoanion $\mathbf{4}^{\odot\ominus}$ to give the neutral species **4**, to which the stable cleaved ligand (which is still present in the diffusion layer) could be re-added.

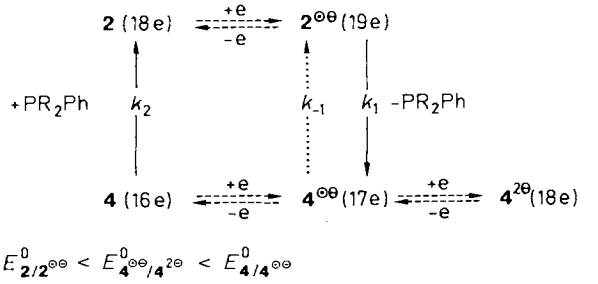

$$E^0_{2/2^{\odot\ominus}} < E^0_{4^{\odot\ominus}/4^{2\ominus}} < E^0_{4/4^{\odot\ominus}}$$

Scheme 1. Compound **2** is reduced to $\mathbf{4}^{2\odot}$ by an ECE mechanism; the reoxidation of $\mathbf{4}^{2\ominus}$ to **2** proceeds via an EEC mechanism (E = electrochemical, C = chemical).

That phosphane is, in fact, eliminated during the reduction of **2** can be shown by measurements carried out in the presence of **1**, since **1** reacts with free phosphane ligands, PR_3, via an ETC-catalyzed reaction, to form clusters of the general composition $[(\mu_3\text{-MeC})Co_3(CO)_8(PR_3)]$.[2] Indeed, voltammetric experiments with solutions containing both **1** and **2** demonstrate the formation of **3**. Because the forward potential scan results in the reduction of **1** and since the phosphane ligand is only released after reduction of **2** to the radical anion, the substitution product **3**, formed from **1**, can only be detected in the reverse scan as well as during the second cathodic sweep. In control experiments in which only **1** was present in solution, there was no evidence in the voltammograms for the formation of subsequent products. Further evidence for the mechanism shown in Scheme 1 is provided by voltammetric experiments with **2** in the presence of a large excess of the corresponding phosphane ligands. The cathodic scan remained unchanged; however, in the reverse, anodic scan, the wave corresponding to $\mathbf{4}^{\odot\ominus} \rightarrow \mathbf{4}$ disappeared and the wave corresponding to the normally stable redox pair $\mathbf{4}^{2\ominus}/\mathbf{4}^{\odot\ominus}$ became irreversible. This strongly implies that, after the reoxidation of $\mathbf{4}^{2\ominus}$ to $\mathbf{4}^{\odot\ominus}$, the phosphane ligand adds to the 17-electron species $\mathbf{4}^{\odot\ominus}$ with re-formation of $\mathbf{2}^{\odot\ominus}$. Thus, when the potential is scanned positively to $E^0_{2/2^{\odot\ominus}}$, $[E(t) > E^0_{2/2^{\odot\ominus}}]$, $\mathbf{2}^{\odot\ominus}$ is immediately transformed into **2**. The backward reaction becomes dominant, because, after the reoxidation of $\mathbf{4}^{2\ominus}$ to $\mathbf{4}^{\odot\ominus}$, the reaction sequence $\mathbf{2} \rightarrow \mathbf{2}^{\odot\ominus} \rightarrow \mathbf{4}^{\odot\ominus}$ can no longer occur owing to an electrode potential greater than $E^0_{2/2^{\odot\ominus}}$ (see Fig. 1a).

The voltammograms of **2** reveal no evidence of other reaction channels for **4**, e.g., addition of solvent or fragmentation of the metal framework. In fact, the second cathodic scan (Fig. 1a) reveals that, after the oxidation of $\mathbf{4}^{\odot\ominus}$ to **4**, only the regenerated starting system **2** and the still present $\mathbf{4}^{\odot\ominus}$ are reduced.

The neutral species **4** corresponds to the classical 16-electron intermediate involved in thermal dissociative CO substitution. A 17-electron intermediate is of analogous significance for the ETC reaction scheme, which has been carried out with much success on clusters.[2,6] The existence of such a species, formed by one-electron reduction and ligand elimination, could only be demonstrated up to now indirectly on the basis of kinetic data or product distributions, owing to its high lability.[2,7] Its detection in the form of $\mathbf{4}^{\odot\ominus}$ is presumably due to the presence of several phosphane ligands, which relieve the electron deficiency by their donor ability and help to shield the unsaturated species by their steric bulk.

Two further observations support this interpretation. The clearly visible crossing effect suggests a homogeneous disproportionation reaction, which, in accordance with

Equation (a), takes place in the diffusion layer in front of the electrode, in addition to the heterogeneous ECE process.[8]

$$4^{2\ominus} + 2 \rightleftharpoons 4^{\odot\ominus} + 2^{\odot\ominus} \qquad (a)$$

Although it is not thermodynamically favored ($E^0_{4^{\odot\ominus}/4^{2\ominus}} > E^0_{2/2^{\odot\ominus}}$), reaction (a) proceeds from left to right, since, owing to the elimination of phosphane, $2^{\odot\ominus}$ is transformed to $4^{\odot\ominus}$. Therefore, the product of the concentrations of $4^{\odot\ominus}$ and $2^{\odot\ominus}$ becomes smaller than that allowed by the thermodynamic equilibrium conditions. The radical anion $4^{\odot\ominus}$, which continues to be formed by disproportionation in the diffusion layer after potential reversal in the potential range $E < E^0_{4^{\odot\ominus}/4^{2\ominus}}$, can once again be reduced to the dianion $4^{2\ominus}$ at the electrode.

Furthermore, multisweep experiments (Fig. 1b) reveal the existence of an isopotential point, which can be interpreted in complete analogy to an isosbestic point. It shows that the transformation of $2^{\odot\ominus}$ into $4^{\odot\ominus}$ occurs without side reactions and quantitatively.[5,9] Thus, the only redox system remaining in this potential range is the pair $4^{\odot\ominus}/4^{2\ominus}$. Thereby, the existence of the intermediate (in this case, $4^{\odot\ominus}$) that is essential for the dissociative, ETC ligand exchange and its stability in solution for a finite length of time have been demonstrated.

Received: December 8, 1986 [Z 2002 IE]
German version: *Angew. Chem. 99* (1987) 373

CAS Registry numbers:
2a, 107246-46-8; **2b**, 68389-17-3.

[1] a) J. C. Kotz, J. V. Peterson, R. C. Reed, *J. Organomet. Chem. 120* (1976) 433; b) C. M. Kirk, B. M. Peake, B. H. Robinson, J. Simpson, *Aust. J. Chem. 36* (1983) 441, and references cited therein.
[2] a) G. J. Bezems, P. H. Rieger, S. Visco, *J. Chem. Soc. Chem. Commun. 1981*, 265; b) A. J. Downard, B. H. Robinson, J. Simpson, *Organometallics 5* (1986) 1122, 1132, 1140, and references cited therein.
[3] P. Lemoine, *Coord. Chem. Rev. 47* (1982) 55.
[4] M. Dietrich, J. Heinze, H. Fischer, F. A. Neugebauer, *Angew. Chem. 98* (1986) 999; *Angew. Chem. Int. Ed. Engl. 25* (1986) 1021.
[5] J. G. Gaudiello, T. C. Wright, R. A. Jones, A. J. Bard, *J. Am. Chem. Soc. 107* (1985) 888.
[6] a) M. I. Bruce, J. G. Matisons, B. K. Nicholson, *J. Organomet. Chem. 247* (1983) 321; b) A. Darchen, C. Mahe, H. Patin, *Nouv. J. Chim. 6* (1982) 539; c) H. H. Ohst, J. K. Kochi, *Inorg. Chem. 25* (1986) 2066.
[7] a) M. R. Richmond, J. K. Kochi, *Inorg. Chem. 25* (1986) 656; b) H. H. Ohst, J. K. Kochi, *J. Am. Chem. Soc. 108* (1986) 2897.
[8] C. Amatore, M. Gareil, J. M. Saveant, *J. Electroanal. Chem. Interfacial Electrochem. 147* (1983) 1, and references cited therein.
[9] D. F. Untereker, S. Brukenstein, *Anal. Chem. 44* (1972) 1009.

Thermolysis of NH_4HCO_3—A Simple Route to the Formation of Free Carbonic Acid (H_2CO_3) in the Gas Phase**

By *Johan K. Terlouw, Carlito B. Lebrilla,* and *Helmut Schwarz**

Dedicated to Professor Tilman J. De Boer

"Carbonic acid, $(HO)_2CO$, cannot exist in the free state."[1] A statement of this kind is warranted in so far as it has until now only been possible to prepare the ether adducts of carbonic acid $H_2CO_3 \cdot R_2O$ ($R = CH_3$, C_2H_5),[2] at temperatures below -30°C. In solution, the adducts decompose into H_2O, CO_2 and R_2O above 5°C. The hydration of CO_2 is one of the fundamental processes in many biological and ecological systems.[3] It is represented by equation (a), of which—at pH ~7—the first step is considered to be rate determining;[4] the formation of bicarbonate ions via step II is fast.[4,5]

$$CO_{2\,aq} + H_2O \overset{I}{\rightleftharpoons} H_2CO_{3\,aq} \overset{II}{\rightleftharpoons} HCO_3^{\ominus}{}_{aq} + H^{\oplus}_{aq} \qquad (a)$$

The reaction of CO_2 and H_2O in the gas phase [equation (b)] has been studied in detail by *ab initio*[6] and semiempirical (MNDO) MO calculations.[7] These predict that a sizeable activation energy (>40 kcal/mol) is involved in the formation and the dissociation of carbonic acid, **2**, and thus the *free* acid should exist as a stable molecule. The reaction pathway of minimum energy proceeds via **1**. This computational result provides a rationale in that this pathway is formally symmetry forbidden. In solution however, acid/base- and also solvent-catalysis occurs. This increases the rate of hydration of CO_2 and of the dissociation of carbonic acid to such an extent that **2** is inaccessible.

$$CO_2 + H_2O \rightleftharpoons \left[\; O{=}C\!\begin{array}{l}O\\ \diagup\\ \diagdown\\ O\end{array}\!H \;\right]^{\ddagger} \rightleftharpoons O{=}C\!\begin{array}{l}OH\\ \diagdown\\ \diagup\\ OH\end{array} \qquad (b)$$

1 **2**

We report here results of a simple experiment which unambiguously demonstrates that **2** and its radical cation $2^{\odot\oplus}$ can easily be generated as stable species in the gas phase.

Finely powdered NH_4HCO_3 decomposes upon heating, and its reaction products were analyzed using a vacuum generator (VG) analytical ZAB-2F mass spectrometer in the electron impact mode (70 eV ionizing electron energy, 50 μA emission current). The sample was introduced by the standard direct insertion probe and heated by the heat transfer of the ion source block ($T = 150$°C) to the quartz sample holder. Alternatively, the sample was put in an evacuated glass bulb—immersed in an oil bath at 120°C—which was connected to the ion source by a glass line of 30 cm. The mass spectra obtained from NH_4HCO_3 introduced by either method showed signals at *m/z* 17 ($NH_3^{\odot\oplus}$), *m/z* 18 ($H_2O^{\odot\oplus}$, $NH_4^{\odot\oplus}$) and also *m/z* 62. The signal to noise ratio for these *m/z* 62 ions was better than 100:1, although the peak is <1% of the base peak (*m/z* 44, $CO_2^{\odot\oplus}$), and irregular evaporation causes strong intensity fluctuations. An exact mass measurement was performed on the *m/z* 62 ions and the result, 62.00002 Daltons, is only compatible with the elemental composition CH_2O_3 (calculated 62.00039 Daltons); the next best combination, CH_4NO_2, has a calculated mass of 62.0241 Daltons. No signal was present at *m/z* 79 and a metastable transition for the reaction

$$m/z\ 79 \longrightarrow m/z\ 62 + NH_3$$

could not be detected. This strongly indicates that the $CH_2O_3^{\odot\oplus}$ ions must be generated by direct ionization of the

[*] Prof. Dr. H. Schwarz, Dr. C. B. Lebrilla
Institut für Organische Chemie der Technischen Universität Berlin
Strasse des 17. Juni 135, D-1000 Berlin 12
Dr. J. K. Terlouw
Analytical Chemistry Laboratory, University of Utrecht
Croesestraat 77A, NL-3522 AD Utrecht (The Netherlands)

[**] This work was supported by the Deutsche Forschungsgemeinschaft and the Fonds der Chemischen Industrie.

corresponding neutral molecule and not as fragment ions produced by loss of NH_3 from ionized NH_4HCO_3. As soon as the temperature used to evaporate the sample was lowered to ca. 100 °C the *m/z* 62 ions disappeared and the intensity of the other signals also became much lower.

Collision induced decomposition of the mass-selected *m/z* 62 ions (MS/MS experiments,[8]) yields the collisional activation[9] (CA) spectrum shown in Figure 1a. Both the pronounced loss of $OH^{\odot}$ by direct α-cleavage ($\rightarrow m/z$ 45) and the elimination of neutral H_2O ($\rightarrow m/z\ 44^{\odot\oplus}$) and CO_2 ($\rightarrow m/z\ 18^{\odot\oplus}$) are compatible with our proposal that the *m/z* 62 ions are carbonic acid radical cations, $\mathbf{2}^{\odot\oplus}$.

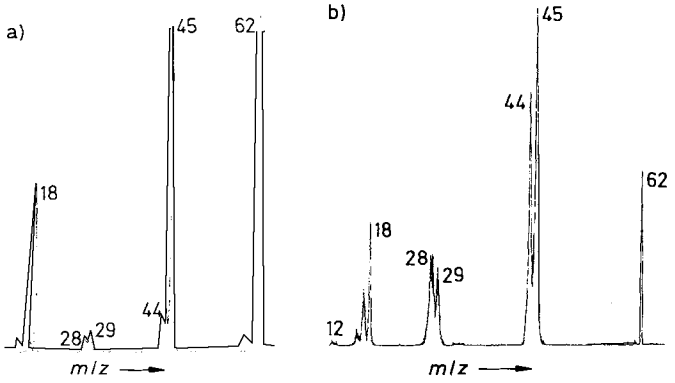

Fig. 1. a) CA mass spectrum (collision gas: He) of mass-selected $CH_2O_3^{\odot\oplus}$ ions (*m/z* 62) generated by electron impact ionization of NH_4HCO_3 followed by 70 eV ionization. b) NRMS spectrum of $CH_2O_3^{\odot\oplus}$ ions, using xenon for neutralization and oxygen for reionization.

Encouraged by our recent Neutralization-Reionization (NRMS[10]) experiments, which made it possible to generate exotic molecules like HC≡COH,[11a] HC≡CNH$_2$,[11b] and XC≡CY with X, Y = OH, NH$_2$[11c] by neutralizing the corresponding radical cations in the gas phase, we have also performed such an experiment with ions $\mathbf{2}^{\odot\oplus}$. The NRMS spectrum (Fig. 1b) leaves no doubt that a significant fraction of the *m/z* 62 $CH_2O_3^{\odot\oplus}$ ions remains intact upon neutralization followed by reionization.[12] We conclude that both $CH_2O_3^{\odot\oplus}$ *and* CH_2O_3 are stable species in the gas phase. It follows from the analysis of the potential energy surface of CH_2O_3[6] that the neutral *m/z* 62 molecule can only be the free carbonic acid, **2**.

Our MNDO calculations yield a value of −146.1 kcal/mol for the enthalpy of formation, ΔH_f^0, of **2** (*syn/anti* conformation of the OH groups). Use of *Benson*'s additivity scheme[13] yields the same value. The radical cation **2** is estimated to have a ΔH_f^0 of 110–115 kcal/mol using the Holmes/Lossing scheme[14] with an ionization energy of 10.8 eV[15] for $(CH_3O)_2C{=}O$.

Received: December 8, 1986;
revised: January 13, 1987 [Z 2003 IE]
German version: *Angew. Chem. 99* (1987) 352

[1] a) H. Beyer, W. Walter: *Lehrbuch für Organische Chemie*, 20th edit., Hirzel, Stuttgart 1984, p. 328; b) *Gmelin Handbuch der anorganischen Chemie: "Kohlenstoff", Part C3*, 8th edit., Verlag Chemie, Weinheim 1973, p. 117.

[2] a) A. G. Galinos, A. A. Carotti, *J. Am. Chem. Soc. 83* (1961) 752; b) G. Gattow, U. Gerwarth, *Angew. Chem. 77* (1965) 132; *Angew. Chem. Int. Ed. Engl. 4* (1965) 149.

[3] I. Zelitch, *Annu. Rev. Biochem. 44* (1975) 923, and references cited therein.

[4] a) D. M. Kern, *J. Chem. Educ. 37* (1960) 14; b) E. Magid, B. O. Turbeck, *Biochim. Biophys. Acta 165* (1968) 515; c) B. Jönsson, G. Karlström, H. Wennerström, B. Roos, *Chem. Phys. Lett. 41* (1976) 317.

[5] M. Eigen, G. G. Hammes, *Adv. Enzymol. Relat. Subj. Biochem. 25* (1964) 1.

[6] a) B. Jönsson, G. Karlström, H. Wennerström, S. Forsén, B. Roos, J. Almlöf, *J. Am. Chem. Soc. 99* (1977) 4628; b) J. O. Williams, C. v. Alsenoy, L. Schäfer, *J. Mol. Struct. (THEOCHEM) 76* (1981) 109; c) Y. Jean, F. Volatron, *Chem. Phys. 65* (1982) 107; d) C. McMichel Rohlfing, L. C. Allen, *J. Chem. Phys. 79* (1983) 4958; e) M. T. Nguyen, T.-K. Ha, *J. Am. Chem. Soc. 106* (1984) 599.

[7] C. B. Lebrilla, H. Schwarz, unpublished results.

[8] Review: F. W. McLafferty (Ed.): *Tandem Mass Spectrometry*, Wiley Interscience, New York 1983.

[9] Review: K. Levsen, H. Schwarz, *Mass Spectrom. Rev. 2* (1983) 77.

[10] For leading references see (a) C. Wesdemiotis, R. Feng, E. R. Williams, F. W. McLafferty, *Org. Mass Spectrom. 21* (1986) 689; b) J. L. Holmes, A. A. Mommers, J. K. Terlouw, C. E. C. A. Hop, *Int. J. Mass Spectrom. Ion Processes 68* (1986) 249.

[11] a) B. van Baar, T. Weiske, J. K. Terlouw, H. Schwarz, *Angew. Chem. 98* (1986) 275; *Angew. Chem. Int. Ed. Engl. 25* (1986) 282; b) B. van Baar, W. Koch, C. Lebrilla, J. K. Terlouw, T. Weiske, H. Schwarz, *Angew. Chem. 98* (1986) 834; *Angew. Chem. Int. Ed. Engl. 25* (1986) 827; c) J. K. Terlouw, P. C. Burgers, B. van Baar, T. Weiske, H. Schwarz, *Chimia 40* (1986) 357.

[12] A complete analysis of the spectra in Figures 1a and b is not given. Note, however, that the half height width of the *m/z* 44 signal in Figure 1b is considerably smaller than that of *m/z* 45. This implies that the larger part of the *m/z* 44 ions results from direct ionization of neutral CO_2. The intense broad peak at *m/z* 45, however, can only correspond with fragment ions, produced by the collision induced dissociations of *m/z* 62 *ions* (i.e. *m/z* 62 → *m/z* 45 + $OH^{\odot}$); see also Ref. [10b].

[13] S. W. Benson: *Thermochemical Kinetics*, 2. Ausgabe, Wiley, New York 1970.

[14] J. L. Holmes, F. P. Lossing, *Can. J. Chem. 60* (1982) 2365; *J. Am. Chem. Soc. 104* (1986) 2648.

[15] F. P. Lossing, unpublished results.

Azoalkane–Nitrene Cleavage on an Fe_3-Cluster**

By *Edward J. Wucherer* and *Heinrich Vahrenkamp**

It has already been demonstrated on several occasions that unsaturated substrates are capable of undergoing some very unusual reactions upon multicenter attachment to clusters.[1] Among the simplest of such reactions are the facile, in some cases even reversible, formation and cleavage of C≡C- and C≡N bonds in the ligand sphere.[2] In the context of our studies in this area we have so far been able to demonstrate the cleavage of a *formal* P=P bond and the oxidative decarbonation of an acetylide ligand.[3] In continuation of these studies we have now succeeded in cleaving the *formal* N=N bond of an azoalkane on a cluster without altering the overall composition of the complex.

The study of azoalkane-bridged triiron clusters such as **1** calls for a high-yield synthesis, which we found in the reaction of azoethane with the labile complex $[(CO)_3Fe(cyclo\text{-}C_8H_{14})_2]$.[4] The reactivity of **1** was immediately evident on investigating its thermal behavior: when a solution of **1** in ligroin was heated to 120 °C for 11 hours, ca. 5% of a decomposition product was obtained together with ca. 75% of **2** as the sole newly formed compound, which could be separated from unchanged **1** (ca. 20%) by chromatography on silica gel. During the transformation of **1** into **2** the six-electron azoalkane ligand R_2N_2 is converted into two four-electron nitrene ligands. Since the number of CO-ligands remains the same during this conversion, opening of a metal–metal bond must take place for compensation: the closed Fe_3-triangle in **1** becomes the angular open Fe_3-arrangement in **2**, which is typical

[*] Prof. Dr. H. Vahrenkamp, Dr. E. J. Wucherer
Institut für Anorganische und Analytische Chemie der Universität
Albertstraße 21, D-7800 Freiburg (FRG)

[**] This work was supported by the Fonds der Chemischen Industrie and by a NATO Postdoctoral Fellowship *(E. J. W.)*.

for $Fe_3(CO)_9$ complexes containing two four-electron μ_3-ligands.

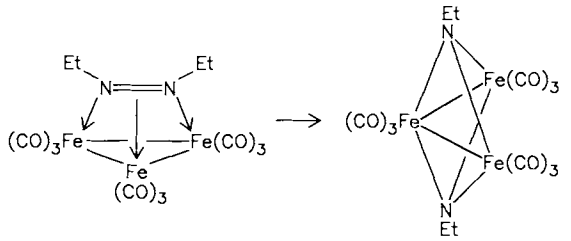

1 2

The green complex **1** and the red complex **2** were characterized by elemental analyses and by their EI-mass spectra. Representatives of both types of complex have already been prepared via other routes, and their molecular structures are known.[5] The IR data of **1** and **2** establish their relation to them; the NMR data, which reveal the diastereotopy of the CH_2 groups in **1** and the equivalence of the ethyl groups in **2** lend support to the assignment.[6]

The mechanism of the transformation of **1** into **2** can be explained in terms of the arguments presented by *Shapley* and *Hoffmann*[2] for the transformation of a μ_3-R_2C_2-ligand into two μ_3-RC-ligands.[7] Accordingly, the R_2N_2-ligand in **1** could slide to an edge of the metal triangle that is not parallel to the NN bond. The new Fe–N bonds would then be formed via a transition state such as **3** with synchronous opening of the Fe–Fe and N–N bonds. However, from our experience with the ready fragmentation of cluster frameworks[8] a mechanism involving reactive fragments also cannot be ruled out.

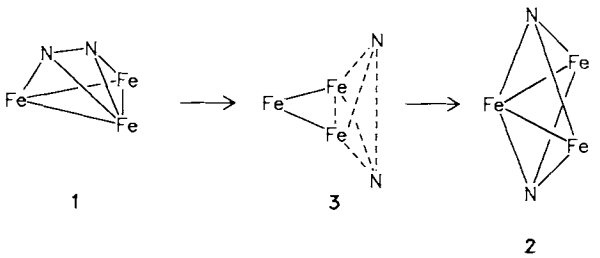

1 3 2

The cleavage of N=N bonds in, e.g. azides, azo compounds etc., in reactions with carbonylmetal compounds is not unusual and leads to numerous types of products.[9] Obviously, the transformation **1** → **2** can be seen as the elementary step in such reactions. Moreover, analogous cleavages with chemical reagents should correspond to the spontaneous thermal N–N cleavage in **1**. We therefore expect that, besides the chemistry developed by *Kisch*[10] for the organic molecular moiety of iron complexes of cyclic azoalkanes, also a new derivative chemistry at the nitrogen via complexes such as **1** and **2** and their dinuclear analogues can be elaborated.

Received: December 11, 1986;
revised: February 2, 1987 [Z 2006 IE]
German version: *Angew. Chem. 99* (1987) 353

[1] M. Moskovits: *Metal Clusters*, Wiley, New York 1986; B. C. Gates, L. Guczi, H. Knözinger: *Metal Clusters in Catalysis*, Elsevier, Amsterdam 1986.

[2] Cf. A. D. Clauss, J. R. Shapley, C. N. Wilker, R. Hoffmann, *Organometallics 3* (1984) 619; E. Boyar, A. J. Deeming, S. E. Kabir, *J. Chem. Soc. Chem. Commun. 1986*, 577; K. P. C. Vollhardt, M. Wolfgruber, *Angew. Chem. 98* (1986) 919; *Angew. Chem. Int. Ed. Engl. 25* (1986) 929; D. Nuel, R. Mathieu, *J. Organomet. Chem. 307* (1986) C5; and references cited therein.

[3] R. L. De, D. Wolters, H. Vahrenkamp, *Z. Naturforsch. B41* (1986) 283; W. Bernhardt, H. Vahrenkamp, *Organometallics 5* (1986) 2388.

[4] H. Fleckner, F. W. Grevels, D. Hess, *J. Am. Chem. Soc. 106* (1984) 2027.

[5] R. J. Doedens, *Inorg. Chem. 8* (1969) 570; H. Kisch, C. Krüger, A. Trautwein, *Z. Naturforsch. B36* (1981) 205; W. Clegg, G. M. Sheldrick, D. Stalke, S. Bhaduri, H. K. Khwaja, *Acta Crystallogr. Sect. C40* (1984) 2045.

[6] IR (hexane [cm^{-1}]): **1**: $\tilde{\nu}$ = 2079 w, 2033 vs, 1992 s, 1978 sh, 1970 w; **2**: $\tilde{\nu}$ = 2053 s, 2036 s, 1999 vs, 1970 w, 1962 vw.—^{1}H-NMR ($CDCl_3$, TMS int.): **1**: δ = 4.18 and 3.21 (J = 14.0, 7.0 Hz; CH_2), 1.60 (J = 7.0 Hz, CH_3); **2**: δ = 3.47 (J = 7.5 Hz; CH_2), 1.37 (J = 7.5 Hz; CH_3).

[7] For a modification of these arguments cf. B. Eaton, J. M. O'Connor, K. P. C. Vollhardt, *Organometallics 5* (1986) 394.

[8] H. Vahrenkamp, *Adv. Organomet. Chem. 22* (1983) 169.

[9] M. Dekker, G. Knox, *Chem. Commun. 1967*, 1243; M. M. Bagga, W. T. Flannigan, G. R. Knox, P. L. Pauson, *J. Chem. Soc. C1969*, 1534; E. W. Abel, T. Blackmore, R. J. Whitley, *Inorg. Nucl. Chem. Lett. 10* (1974) 941; P. Mastropasqua, A. Riemer, H. Kisch, C. Krüger, *J. Organomet. Chem. 148* (1978) C40; M. I. Bruce, M. G. Humphrey, O. B. Shawkataly, M. R. Snow, E. R. T. Tiekink, *ibid. 315* (1986) C51.

[10] R. Millini, H. Kisch, *Z. Naturforsch. B40* (1985) 187, and previous publications in this series.

Gas-Inclusion Crystals of Tetra-*tert*-butyltetrahedrane and Its Deformation Density**

By *Hermann Irngartinger,* Reiner Jahn, Günther Maier,* and *Rolf Emrich*

Having elucidated the structure of tetra-*tert*-butyltetrahedrane, **1**,[1] we decided to determine the deformation density in **1** by low-temperature X-ray diffraction at 103 K according to the X–X method.[2] We found thereby that the hexagonal crystals grown at 213 K had entrapped nitrogen

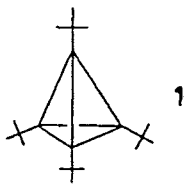

1

molecules at lattice sites. The solvent used for the crystallization had been purged with a stream of nitrogen beforehand in order to remove dissolved oxygen. The nitrogen molecules were found to be disordered at the centers of the threefold rotoinversion axes. To avoid disorder effects during the determination of the deformation density we grew argon-clathrates at 213 K.[3] These gas-inclusion crystals are held together exclusively by van-der-Waals forces. Such clathrates were previously only known in crystals with hydrogen bonds.[4] Two sorts of octahedral holes are present in the ratio 1:2 in the hexagonal closest packed structure of **1** (Fig. 1). The octahedral holes, each of which is surrounded by only one of the four *tert*-butyl groups per tetrahedrane molecule, entrap the gas molecules or atoms. The remaining holes are too small. In the packing diagram (Fig. 1) the positions of the argon atoms are marked by

[*] Prof. Dr. H. Irngartinger, Dr. R. Jahn
Organisch-chemisches Institut der Universität
Im Neuenheimer Feld 270, D-6900 Heidelberg 1 (FRG)
Prof. Dr. G. Maier, Dr. R. Emrich
Institut für Organische Chemie der Universität
Heinrich-Buff-Ring 58, D-6300 Giessen 1 (FRG)

[**] This work was supported by the Deutsche Forschungsgemeinschaft and the Fonds der Chemischen Industrie.

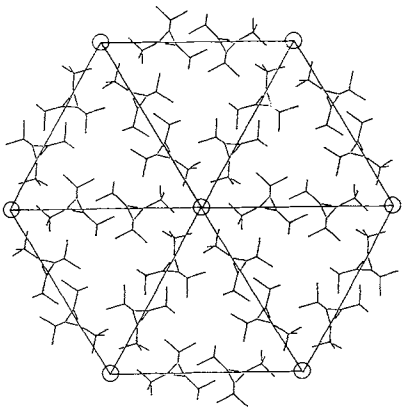

Fig. 1. Packing diagram of the argon inclusion crystal of **1** (projection along *c*); argon atoms marked by circles.

circles. The occupancy in the crystal used was 26%. On heating the crystals in the mother liquor to a temperature above 220 K under the microscope gas bubbles were observed escaping from the crystals and the solution. The crystals became cloudy; without the supporting gas-inclusions the lattice is destroyed. On the basis of low-temperature data, the two mirror-image torsional disorder sites of the *tert*-butyl groups, which extended into the holes occupied by argon atoms, could be refined separately. The torsional angle between the two disorder sites was found to be 26°. The thermal parameters yielded a torsional vibration of 9° for the *tert*-butyl groups, which can be explained in terms of dynamic libration or static disorder. In comparison to the measurement at 213 K[1] the bond lengths were essentially free of effects produced by the non-spherical electron density distribution in the bonds,[2] because of the refinement with reflections of high order.[3]

In all cases the deformation densities were calculated in sections (Fig. 2) along a tetrahedral bond and through the

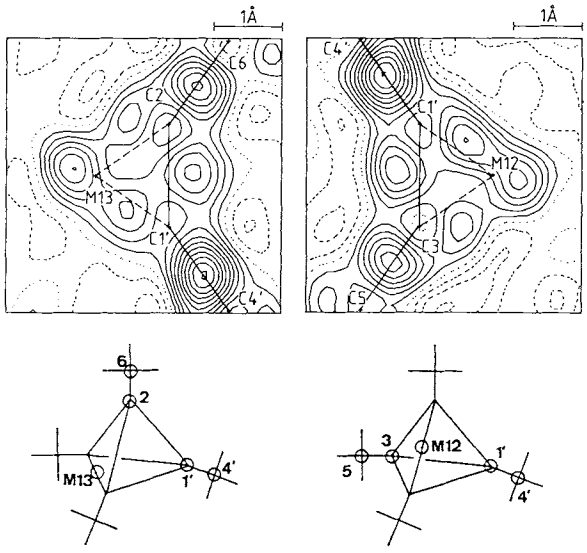

Fig. 2. Deformation densities of **1** [3]. All sections along a bond and perpendicular to the opposite bond of the tetrahedron. The atoms and midpoints of the bonds marked in the formulas with circles all lie in the plane of the section. Contour interval 0.05 e Å^{-3}.

midpoint of the opposite tetrahedral bond. Sections with maxima in special positions (mirror planes) have been ignored because of the high standard deviation ($\sigma(\rho)$ = 0.06 e Å^{-3} vs. 0.04 e Å^{-3} in general positions). The density maxima of the tetrahedral bonds are located 0.37 Å outwards from the bond axis. Therefore these bonds are bent by 26°. The tetrahedrane bond is thus one of the most strongly bent C–C bonds.[5] Theoretical calculations[6] give bends of the same order of magnitude. An arc over the density maximum between two tetrahedrane C-atoms is 1.7 Å long, whereas the distance between the atoms is 1.497 Å. The density maxima of the bonds between the tetrahedrane C-atoms and the quarternary C-atoms of the *tert*-butyl groups (Fig. 2) lie exactly on the connecting lines between the atoms. This is also the case for the C_{quart}–C_{methyl} bonds of the *tert*-butyl groups.

Received: December 15, 1986;
revised: January 22, 1987 [Z 2011 IE]
German version: *Angew. Chem.* 99 (1987) 356

[1] H. Irngartinger, A. Goldmann, R. Jahn, M. Nixdorf, H. Rodewald, G. Maier, K.-D. Malsch, R. Emrich, *Angew. Chem.* 96 (1984) 967; *Angew. Chem. Int. Ed. Engl.* 23 (1984) 993.

[2] P. Coppens, *Angew. Chem.* 89 (1977) 33; *Angew. Chem. Int. Ed. Engl.* 16 (1977) 32.

[3] Crystallographic data of the argon-clathrate of **1** at 103 K: crystal growth at 213 K from ethyl acetate, saturated with argon: $C_{20}H_{36}$ + 0.086 Ar; a = 15.732(2), c = 13.923(1) Å; hexagonal space group $P6_3/m$; Z = 6; ρ_{calc} = 0.94 × 10^6 g/m^3; three independent data sets with a total number of 12515 intensities (Enraf-Nonius CAD4 diffractometer, $Mo_{K\alpha}$ radiation, graphite monochromator): $\sin(\theta/\lambda)$ = 0–0.60 Å^{-1}; 1109 observed reflections ($I > 3\sigma(I)$) for calculation of the deformation densities; $\sin(\theta/\lambda)$ = 0.65–1.15 Å^{-1}: 637 observed reflections ($I > 2.5\sigma(I)$) for the refinement with reflections of high order (C anisotropic, full matrix); R = 0.06. The positional and the isotropic thermal parameters of the H atoms have been determined within the low-order refinement ($\sin\theta/\lambda \leq 0.65$ Å^{-1}; R = 0.04). Bond lengths (T = tetrahedron): C_T–C_T 1.497, C_T–C_{quart} 1.498, C_{quart}–C_{methyl} 1.529 Å; standard deviations: 0.003, 0.004, 0.006 Å. Further details of the crystal structure are available from the Fachinformationszentrum Energie, Physik, Mathematik GmbH, D-7514 Eggenstein-Leopoldshafen 2 (FRG), on quoting the depository number CSD-52295, the names of the authors, and the journal citation.

[4] J. L. Atwood, J. E. D. Davies, D. D. MacNicol: *Inclusion Compounds*, Academic Press, Bristol (England) 1984.

[5] H. Irngartinger, A. Goldmann, *Angew. Chem.* 94 (1982) 786; *Angew. Chem. Int. Ed. Engl.* 21 (1982) 769.

[6] a) T. Loerzer, R. Machinek, W. Lüttke, L. H. Franz, K.-D. Malsch, G. Maier, *Angew. Chem.* 95 (1983) 914; *Angew. Chem. Int. Ed. Engl.* 22 (1983) 878; b) K. Kovačević, Z. B. Maksić, *J. Org. Chem.* 39 (1974) 539.

Trimethylenemethane Complexes of Cr, Mo, and W by Novel Methylenation of Allenes with Carbene Complexes; Cyclopentanes by [3 + 2] Cycloaddition of Trimethylenemethane Complexes to Allenes**

By *Rudolf Aumann** and *Jürgen Uphoff*

The development of versatile C_3 building blocks for the synthesis of functionalized cyclopentanes by [3 + 2] cycloaddition continues to be a challenge for many synthetic chemists. In addition to ionic C_3 components,[1] organometallic C_3 building blocks exhibiting 1,3-dipolar behavior[2,3] have been used so far.

We recently described the synthesis of cyclopentanes by [3 + 1 + 1] cycloaddition of vinylcarbene[4] or arylcarbene complexes (as C_3 components) and two equivalents of methyl isocyanide (as C_1 components).[5]

[*] Prof. Dr. R. Aumann, Ing. (grad.) J. Uphoff
Organisch-chemisches Institut der Universität
Orléans-Ring 23, D-4400 Münster (FRG)

[**] Organic Syntheses with Transition-Metal Complexes, Part 22. This work was supported by the Fonds der Chemischen Industrie. — Part 21: [4].

In the course of our studies of metal-promoted cycloadditions, we have now found a novel type of methylenation of allenes **2** with carbene complexes **1**, leading to the diastereomeric trimethylenemethane complexes **4** and **5**. Previous syntheses of such complexes always started from C_4 building blocks in which the carbon framework of the ligand was preformed.[6] In contrast, we were able to construct the trimethylenemethane ligand from a C_1 and a C_3 building block. In this respect, there exists a parallel between this approach and the synthesis of such ligands by template-directed olefination of aldehydes with allenes, which involves the loss of an aldehyde oxygen as CO_2 by reduction with CO.[7]

The reaction sequence, described here for the first time, presumably proceeds via the metallacyclobutane **3**, whose regiochemistry is controlled by the steric demands of the tetracarbonyl metal fragment and by the charge distribution in **1** and **2**; **3** isomerizes to the complexes **4** and **5**. The reaction can be initiated thermally or photochemically. It was investigated for carbene complexes of Cr, Mo, and W (order of reactivity Mo > Cr > W) as well as of Fe.[8] The products **4** and **5** were isolated by chromatography and characterized spectroscopically (Table 1).

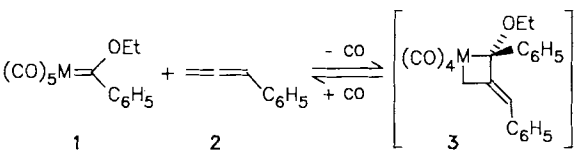

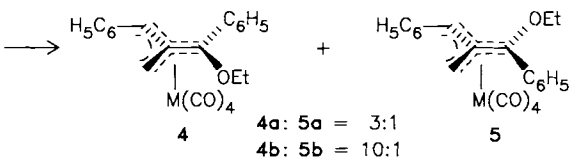

4a: **5a** = 3:1
4b: **5b** = 10:1
4c: **5c** = 10:1

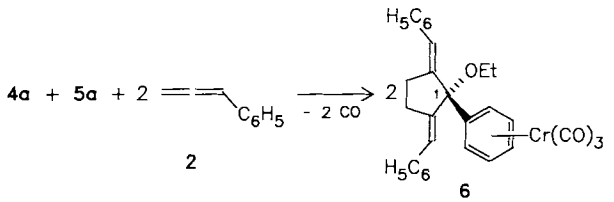

a: M = Cr, **b**: M = Mo, **c**: M = W

Table 1. Spectroscopic data for the complexes **4a–c**, **5a**, **6**, and **7**. The substituents and skeletal C atoms of **4** and **5** are numbered nonsystematically. The configurational assignment was based on the ^4J-"W" coupling and on the low-field shift of the resonance of the γ-H (in the *anti* position; cf. [7]).

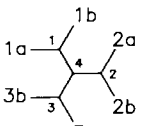

4a: ^{1}H-NMR (C_6D_6, 300 MHz): δ = 7.16 (10H, m, C_6H_5), 4.96 (1H, d, ^4J = 2 Hz, H-1b), 3.27 (2H, m, diastereotopic OCH_2), 2.26 (1H, ^2J = 1.5 Hz, H-3b), 1.60 (1H, ^4J = 2, ^2J = 1.5 Hz, H-3a), 0.87 (3H, t, CH_3). — ^{13}C-NMR (C_6D_6, 75 MHz): δ = 237.65 (4C, $Cr(CO)_4$), 138.34 and 134.76 (each 1C, *i*-C of C_6H_5), 132.86 (C-2), 130.72, 129.03, 128.52, and 128.33 (2:3:2:2, 4 *o*- and 4 *m*-C and 1 *p*-C), 126.60 (1 *p*-C), 90.41 (C-4), 71.99 (C-1), 67.48 (OCH_2), 46.38 (C-3), 14.81 (CH_3)

4b: ^{1}H-NMR (C_6D_6, 300 MHz): δ = 7.20 (10H, m, C_6H_5), 5.25 (1H, d, ^4J = 3.6 Hz, H-1b), 3.28 and 3.19 (each 1H, m, diastereotopic OCH_2), 2.27 (1H, ^2J = 3.6 Hz, H-3b), 1.61 (1H, ^4J = ^2J = 3.6 Hz, H-3a), 0.94 (3H, t, CH_3)

4c: ^{1}H-NMR (C_6D_6, 300 MHz): δ = 7.13 (10H, m, C_6H_5), 5.19 (1H, d, ^4J = 3.6 Hz, H-1b), 3.20 and 3.10 (each 1H, m, diastereotopic OCH_2), 2.17 (1H, ^2J = 3.6 Hz, H-3b), 1.66 (1H, ^4J = ^2J = 3.6 Hz, H-3a), 0.95 (3H, t, CH_3)

5a: ^{1}H-NMR (C_6D_6, 300 MHz): δ = 7.35 (2H, *o*-H of 2b-C_6H_5), 7.13 (5H, "s," 1a-C_6H_5), 7.00 (2H, "t," *m*-H of 2b-C_6H_5), 6.92 (1H, "t," *p*-H of 2b-C_6H_5), 3.57 (1H, d, ^4J = 2.3 Hz, H-1b), 3.22 (2H, m, diastereotopic OCH_2), 2.97 (1H, d, ^4J = 2.3 Hz, H-3a), 2.59 (1H, s, H-3b), 0.87 (3H, t, CH_3). — ^{13}C-NMR (C_6D_6, 75 MHz): δ = 237.47 (4C, $Cr(CO)_4$), 138.34 and 134.47 (each 1C, *i*-C), 132.86 (C-2), 130.72, 129.03, 128.33 and 128.33 (2:3:2:2, 4 *o*- and 4 *m*-C and 1 *p*-C), 126.67 (1 *p*-C), 90.80 (C-4), 69.49 (C-1), 67.48 (OCH_2), 48.33 (C-3), 14.81 (CH_3). — IR (hexane): $\tilde{\nu}$(C≡O) = 2033 cm^{-1} (30%), 1983 (20), 1949 (100), 1931 (30). — MS (70 eV): *m/z* 414 ($M^{\oplus}$, 0.5%), 386 (16), 358 (22), 330 (30), 302 (80, $M^{\oplus}$ − 4CO), 273 (60, 302 − C_2H_5), 258 (100, 302 − C_2H_4O)

6: ^{1}H-NMR (C_6D_6, 300 MHz): δ = 7.25 (4H, "d," *o*-H of 2 C_6H_5), 7.18 (4H, "t," *m*-H of 2 C_6H_5), 7.07 (2H, "t," *p*-H of 2 C_6H_5), 6.73 (2H, s, =CHPh), 5.27 (2H, "d," *o*-H of π-C_6H_5), 4.77 (1H, "t," *p*-H of π-C_6H_5), 4.50 (2H, "t," *m*-H of π-C_6H_5), 3.34 (2H, q(!), J = 7 Hz, of OCH_2, which is not diastereotopic owing to a mirror plane), 2.55 (4H, m, AA'BB' system, CH_2-CH_2), 1.26 (3H, t, CH_3). — ^{13}C-NMR (C_6D_6, 75 MHz): δ = 233.76 (s, 3C, $Cr(CO)_3$), 142.37 and 137.37 (each s, each 2C, 2 *i*-C of C_6H_5 and C-2, C-5), 129.32 and 128.66 (each d, each 4C, *o*-C and *m*-C of C_6H_5), 127.45 and 126.44 (each d, each 2C, 2 *p*-C of C_6H_5 and 2 =CHPh), 119.13 (s, *i*-C of π-C_6H_5), 94.05 (d, *p*-C of π-C_6H_5), 93.43 and 89.11 (each d, each 2C, *o*-C and *m*-C of π-C_6H_5), 88.02 (s, (C-1). 59.13 (t, OCH_2), 28.98 (t, 2C, C-3, C-4), 15.78 (q, CH_3). — IR (hexane): $\tilde{\nu}$(C≡O) = 1979 cm^{-1} (60%), 1906 (100). — MS (70 eV): *m/z* 502 ($M^{\oplus}$, 2%), 418 (10, $M^{\oplus}$ − 3CO), 374 (50, 418 − C_2H_4O), 366 (8, ligand), 322 (16, 374 − Cr), 321 (20, ligand C_2H_5O), 52 (100)

7: ^{1}H-NMR (C_6D_6, 300 MHz): δ = 7.35 (2H, "d," *o*-H), 7.24 (2H, "t," *m*-H), 7.16 (5H, s, C_6H_5), 7.08 (1H, "t," *p*-H), 6.46 (1H, s, =CHPh), 3.04 (2H, H-5), 1.98 (3H, s, CH_3). — ^{13}C-NMR ($CDCl_3$, 75 MHz): δ = 202.71 (C=O), 164.60 (s, C-3), 141.14, 137.08, 136.35 and 131.37 (each s, each 1C), 129.34, 129.04, 128.66, 128.11, 127.84, and 124.81 (each d, 2:2:2:2:1, 2 C_6H_5 and =CHPh), 39.56 (t, C-5), 12.99 (q, CH_3). — IR (KBr): $\tilde{\nu}$(C=O) = 1690 cm^{-1}. — MS (70 eV): *m/z* 260 ($M^{\oplus}$, 100%), 259 (16, $M^{\oplus}$ − H), 245 (16, $M^{\oplus}$ − CH_3), 231 (16, 259 − CO), 217 (60, $M^{\oplus}$ − C_2H_3O), 216 (30), 215 (44), 202 (40), 115 (70, 231 − $C_3H_3(C_6H_5)$)

Apparently, an η^4-trimethylenemethane complex is formed from the metallacyclobutane **3** of a transition metal only when a vacant coordination site on the metal is available. Otherwise, as in the case of titanacyclobutanes,[9] metathesis-like reactions may subsequently occur. Taking into consideration the prerequisites discussed above, we assume that our procedure opens up a general route from allenes to new trimethylenemethane complexes.

The diastereomeric trimethylenemethane complexes **4a** and **5a** slowly react with allene **2**, already at 25 °C, to give the carbocyclic five-membered ring compound **6**. In this reaction, which involves a [3 + 2] cycloaddition and the loss of CO, the carbonylchromium fragment migrates to the phenyl group of the original carbene ligand. The addition occurs regiospecifically and leads, with loss of three centers of chirality (!) of the ligands of **4a** and **5a**, to the same product **6**, which no longer has centers of chirality but possesses a mirror plane, as shown by the ^{1}H-NMR (300 MHz) and ^{13}C-NMR (75 MHz) spectra (Table 1).

In the reaction sequence **1a** → (**4a** + **5a**) → **6**, the $(CO)_5Cr$ fragment loses a total of two equivalents of CO. Interestingly, these are then used in a parallel reaction in which two equivalents of **2** and one equivalent of CO undergo a template-directed [2 + 2 + 1] cycloaddition to give the 4-methylenecyclopentenone **7**. The carbene complex

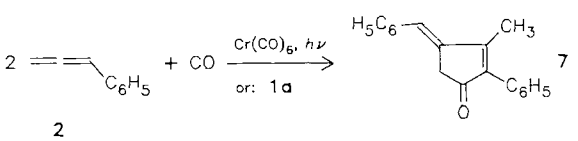

1a appears to catalyze this reaction *thermally*. However, the formation of **7** from **2** can also be induced *photochemically* with $Cr(CO)_6$.

Experimental Procedures

Syntheses of **4a**, **5a**, **6**, and **7**: **1a** (326 mg, 1.00 mmol) and **2** (348 mg, 3 mmol) in 5 mL of dry toluene were heated at 45 °C under an inert atmosphere in a screw-cap vessel for 2 h. After **1a** had been consumed (TLC), the solvent was removed, and the residue was dissolved in 2 mL of toluene and chromatographed on silica gel. Elution with petroleum ether/dichloromethane (10:1) afforded a pale yellow band ($R_f = 0.7$) containing **4a** and **5a** (250 mg, 60% based on **1a**, product ratio 3:1). Recrystallization from petroleum ether at −78 °C gave **5a** as yellow crystals, m.p. = 93.5 °C. Subsequent elution with petroleum ether/dichloromethane (4:1) gave a yellow band ($R_f = 0.5$) containing **6** (80 mg, 16% based on **1a**, m.p. = 174 °C, from petroleum ether at −78 °C). Prolonged reaction resulted in the formation of **6** at the expense of **4a** and **5a**. Finally, a colorless fraction ($R_f = 0.5$) containing **7** (200 mg, 77% based on **1a**, m.p. = 154.5 °C, from ether) was eluted with dichloromethane.

1b and **1c** were allowed to react analogously for 8 h at 20 °C and for 6 h at 80 °C, respectively. For spectroscopic data see Table 1.

Received: December 17, 1986;
revised: January 26, 1987 [Z 2014 IE]
German version: *Angew. Chem. 99* (1987) 361

[1] T. L. Gilchrist, R. C. Storr: *Organic Reactions and Orbital Symmetry*, 2nd ed., Cambridge University Press, London 1979; G. Boche, D. Martens, *Angew. Chem. 84* (1972) 768; *Angew. Chem. Int. Ed. Engl. 11* (1972) 724; T. Kauffmann, *Top. Curr. Chem. 92* (1980) 109; G. F. Luteri, W. T. Ford, *J. Am. Chem. Soc. 99* (1977) 5330; G. W. Klumpp, R. F. Schmitz, *Tetrahedron Lett. 1974*, 2911.

[2] P. Binger, M. Cetinkaya, M. J. Doyle, A. Germer, U. Schuchardt in M. Tsutsui, R. Ugo (Eds.): *Fundamental Research in Homogeneous Catalysis, Vol. 3*, Plenum Press, New York 1979, p. 271; P. Binger, H. M. Büch, *Top. Curr. Chem. 135* (1987) 77.

[3] B. M. Trost, *Angew. Chem. 98* (1986) 1; *Angew. Chem. Int. Ed. Engl. 25* (1986) 1, and references cited therein.

[4] R. Aumann, H. Heinen, *Chem. Ber. 120* (1987), in press.

[5] R. Aumann, H. Heinen, *Chem. Ber. 118* (1985) 4186; *119* (1986) 3801.

[6] Trimethylenemethane complexes with the following metals are known: iron (cf. review): A. Slawisch in *Gmelin Handbook of Inorganic Chemistry, Organoiron Compounds, Vol. 10*, Springer, Berlin 1986, p. 1–42), molybdenum (S. G. Barnes, M. Green, *J. Chem. Soc. Chem. Commun. 1980*, 267), ruthenium, osmium, iridium (M. D. Jones, R. D. W. Kemmitt, *ibid. 1985*, 811), palladium (B. M. Trost, D. M. T. Chan, *J. Am. Chem. Soc. 105* (1983) 2315, 2326), tantalum (J. M. Mayer, C. J. Curtis, J. E. Bercaw, *ibid. 105* (1983) 2651), chromium (J. S. Ward, R. Pettit, *Chem. Commun. 1970*, 1419; W. Henslee, R. E. Davies, *J. Organomet. Chem. 81* (1974) 389).

[7] R. Aumann, H.-D. Melchers, H.-J. Weidenhaupt, *Chem. Ber. 120* (1987) 17.

[8] R. Aumann, H.-D. Melchers, unpublished results.

[9] S. L. Buchwald, R. H. Grubbs, *J. Am. Chem. Soc. 105* (1983) 5490.

Glycosyl Isocyanide Dichlorides—Novel Synthetic Building Blocks in Sugar Chemistry**

By *Tillmann Hassel** and *Hanns Peter Müller*

Dedicated to Professor Ernst Bayer on the occasion of his 60th birthday

Owing to their universal reactivity,[1] organoisocyanide dichlorides are of special interest as intermediates in the synthesis of heterocycles. These compounds can be prepared by reaction of organoisothiocyanates with chlorine. We report here on the synthesis of the glycosyl isocyanide dichlorides **2a**–**c** by chlorination of the readily accessible[2,3] glycosyl isothiocyanates **1a**–**c**. By a series of different reaction examples we demonstrate that the synthetic potential[1] of the isocyanide dichlorides can be exploited in carbohydrate chemistry, too.

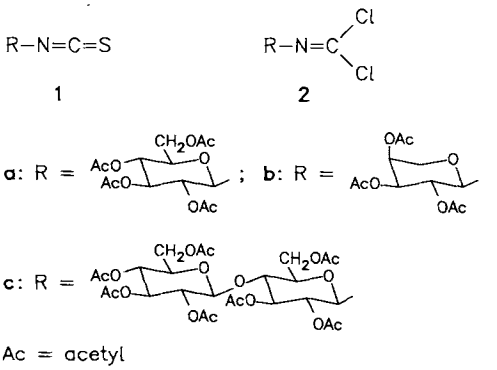

Reaction of the glucose derivative **1a**[3] with chlorine in chloroform[4] affords the isocyanide dichloride **2a** (m.p. 125 °C) in 92% yield. Glycosyl isothiocyanates of pentoses react analogously; the L-arabino-derivative **1b** furnishes **2b** as an oil in 78% yield. As example for a disaccharide we used cellobiose; the known isothiocyanate **1c**[2] is converted quantitatively into the isocyanide dichloride **2c** (m.p. 200 °C).

The compound **2a** undergoes reactions typical for isocyanide dichlorides[1] without aminolysis or acidolysis of the protecting groups. On heating 0.2 mol of **2a** with 0.2 mol of methanesulfonic acid[5] in 400 mL of chlorobenzene to 110 °C for 40 min the isocyanate **3**, m.p. 115 °C,[6] is obtained in 73% yield. Reaction of 0.1 mol of **2a** with 0.1 mol of cyclohexylamine in the presence of 0.2 mol of triethylamine in 200 mL of toluene at −20 °C to 0 °C leads quantitatively within 12 h to the carbodiimide **4**, m.p. 80 °C;[7] from a solution of 0.03 mol/L each of **2a**, dibutylamine, and triethylamine in toluene, the chloroformamidine **5** (m.p. 92 °C) can be isolated in 70% yield after 12 h.

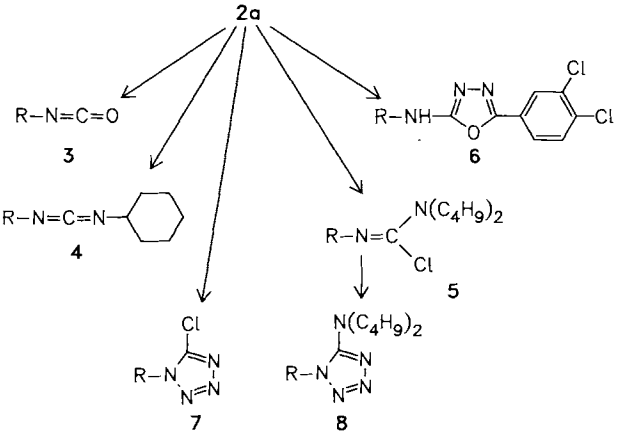

The synthesis of heterocycles is also possible with the glycosyl isocyanide dichlorides **2**. When a solution of 0.1 mol of 3,4-dichlorobenzoylhydrazine in 70 mL of dimethylformamide (DMF) is added dropwise to a solution of 0.1 mol of **2a** and 1.0 mol of triethylamine in 200 mL of DMF at 0 °C and the mixture then stirred for 15 min at room temperature, after work-up the oxadiazole **6** (m.p. 181 °C) can be isolated in 60% yield. Reaction of 0.05 mol

[*] Dr. T. Hassel, Dr. H. P. Müller
Bayer AG, Zentralbereich Zentrale Forschung,
ZF-FKH, Gebäude Q 18
D-5090 Leverkusen (FRG)

[**] This work was supported by the Bundesministerium für Forschung und Technologie (Project O3C 1439).

of **2a** with an equivalent amount of sodium azide in 150 mL of DMF at room temperature for 30 min affords the chlorotetrazole **7**, m.p. 172 °C, in 60% yield. The corresponding dibutylamino compound **8** can be prepared analogously from **2a** via **5** by reaction with sodium azide for 1 h. It melts at 87 °C and is isolated in 40% yield (based on **5**).

The structures of all the new compounds have been confirmed by elemental analysis and by IR, ^{1}H-NMR and ^{13}C-NMR spectroscopy.[8] The results reported here demonstrate that glycosyl isocyanide dichlorides are readily accessible, valuable intermediates for syntheses in carbohydrate chemistry.

Received: December 17, 1986;
revised: January 26, 1987 [Z 2015 IE]
German version: *Angew. Chem. 99* (1987) 368

[1] E. Kühle, B. Anders, G. Zumach, *Angew. Chem. 79* (1967) 663; *Angew. Chem. Int. Ed. Engl. 6* (1967) 649; E. Kühle, *ibid. 81* (1969) 18 and *8* (1969) 20.

[2] T. Hassel, H. P. Müller, DOS 3341018 (1985), Bayer AG; cf. *Chem. Abstr. 104* (1986) 51081a.

[3] M. J. Camarasa, P. Fernández-Resa, M. T. Garcia-Lopez, F. G. de las Heras, P. P. Mendez-Castrillón, A. San Felix, *Synthesis 1984*, 509.

[4] The isothiocyanate **1** is chlorinated in alcohol-free chloroform until disappearance of the IR band of the isothiocyanate group. Passage of chlorine is then continued for the same length of time again, the mixture heated to room temperature, and the solvent, excess chlorine, and dichlorosulfane removed in a cold trap. The residue consists of the product **2**, which can be purified by conventional methods.

[5] D. Arlt, DOS 1643975 (1967), Bayer AG; cf. *Chem. Abstr. 74* (1971) 87593.

[6] A. Piskala, F. Šorm, *Collect. Czech. Chem. Commun. 29* (1964) 2060.

[7] J. C. Jochims, *Angew. Chem. 77* (1965) 454; *Angew. Chem. Int. Ed. Engl. 4* (1965) 435.

[8] The isocyanide dichlorides **2a–c** show a characteristic IR band at 1660 cm^{-1}; in the ^{13}C-NMR spectra recorded in $CDCl_3$ the carbon signal of the functional group appears between $\delta = 131.4$ (**2b**) and 132.8 (**2a**).

The Influence of Substituents on Double-Bond Localization, e.g. in *s*-Indacene**

By *Edgar Heilbronner** and *Zhong-Zhi Yang*

For Gerhard Quinkert, on the occasion of his 60th birthday

There exists an extensive literature concerning the theory of double-bond localization, beginning with the work of *H. C. Longuet-Higgins* and *L. Salem*[1] up to the detailed investigations of *T. Nakajima* et al.[2,3] In connection with work on *s*-indacene **1A**, **1B**,[4] *Hafner* et al.[5] have dealt with an important extension of the problem, namely the direction and extent by which the tendency towards double-bond localization is influenced by substituents, or in other words, how substitution affects the difference $\Delta_{loc}^{deloc}H_m^{\ominus} = \Delta_f H_m^{\ominus}(\mathbf{1B}) - \Delta_f H_m^{\ominus}(\mathbf{1A})$ of the molar enthalpies of formation of **1B** and **1A**. Using the MINDO/3 procedure, they obtained the values given in Table 1.

Although many-electron treatments are required for the computation of reasonably reliable $\Delta_{loc}^{deloc}H_m^{\ominus}$-values, such models prove rather unsatisfactory for the derivation of heuristic rules of thumb which can be used qualitatively

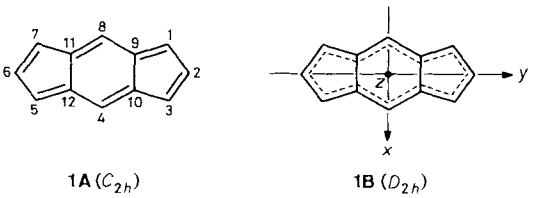

1A (C_{2h}) **1B** (D_{2h})

Table 1. Influence of substituents on double bond localization in *s*-indacene and *s*-indacene derivatives.

Substituents	$\Delta_{loc}^{deloc}H_m^{\ominus}$ [a] [kJ mol^{-1}]	λ_{max}	λ'_{max} [b]
1 (unsubstituted)	40	1.57	(1.57)
2 (1,3,5,7-tetraalkyl)	8	1.38 [c]	1.35
3 (2,4,6,8-tetraalkyl)	40	1.53 [c]	1.57
4 (4,8-diamino)	<0	1.03 [d]	
5 (2,6-dicyano)	25	1.44 [e]	

[a] From MINDO/3 calculations [5]. Note that the absolute values may be seriously in error; cf. D. F. V. Lewis, *Chem. Rev. 86* (1986) 1111. [b] According to equation (f) with $\delta h_\zeta = -0.3$ and taking multiple substitution into account. [c] For the inductive perturbation due to the alkyl groups, $\delta h_\zeta = -0.3$ has been used. [d] For the amino group: $\alpha_N = \alpha + \beta$, $\beta_{C-N} = \beta$. [e] For the nitrile group: $\alpha_N = \alpha + \beta$, $\beta_{C\equiv N} = 1.2\beta$, $\beta_{C-CN} = \beta/\sqrt{2}$.

when planning or rationalizing experiments. Taking *s*-indacene as an example, we wish to demonstrate how such rules may be obtained.

Some time ago an algorithm was presented[6] which allows one to answer the question of whether an unsubstituted π-system covering all n carbon centers of a hydrocarbon C_nH_m (e.g. $C_{12}H_8$ = *s*-indacene **1**) will prefer to localize its double bonds (e.g. **1A**) or not (e.g. **1B**). First one calculates the bond-bond-polarizability matrix $\boldsymbol{\pi} = (\pi_{\mu\nu,\rho\sigma})$ within the framework of a standard HMO treatment (i.e. all $\beta_{\mu\nu} = \beta$, all $\alpha_\mu = \alpha$, maximum symmetry) using, e.g., equation (a) for an even-centered, closed shell π system in

$$\pi_{\mu\nu,\rho\sigma} = 2\sum_{j=1}^{n/2}\sum_{k=\frac{n}{2}+1}^{n}\frac{(c_{\mu j}c_{\nu k} + c_{\mu k}c_{\nu j})(c_{\rho j}c_{\sigma k} + c_{\rho k}c_{\sigma j})}{x_j - x_k} \qquad (a)$$

its ground configuration ($c_{\mu j}$ is the coefficient of the p-orbital at the center μ in MO ψ_j; x_j is the jth eigenvalue of the Hückel matrix).[7] The second step consists in the computation of the eigenvalues λ_r and the eigenvectors $\mathbf{u}_r = (u_{\mu\nu,r})$ of matrix $\boldsymbol{\pi}$. If the largest eigenvalue, λ_{max}, exceeds a critical value λ_{crit}, then the π-system will localize its double bonds according to $\mathbf{u}_{max} = (u_{\mu\nu,max})$. The critical value λ_{crit} depends on the σ-force constant of the CC bonds, on the value β_0 of the resonance integral and on its derivative $\beta'_0 = (d\beta/dR)_0$ at distance R_0 between bonded centers. A rough estimate yields $\lambda_{crit} \approx 1.7$.[6] Application of the procedure to non-alternant π systems[8] yielded among other results: azulene, $\lambda_{max} = 1.3$; pentalene, $\lambda_{max} = 2.4$; *s*-indacene, $\lambda_{max} = 1.6$. It is known that azulene does not show double bond localization, in contrast to pentalene[9] which presents alternating single and double bonds (C_{2h} symmetry).

We limit our discussion to purely inductive perturbations by assuming that a substituent X in position ζ changes the local α-value by $\delta\alpha_\zeta = \beta \cdot \delta h_\zeta$. Under these conditions, the sign and absolute value of $\delta\lambda_{max}$ [Eq. (b)] yields the answers to the question if and how the substituent X will influence the tendency towards double bond localization of the π-system. Taking *s*-indacene as an ex-

[*] Prof. Dr. E. Heilbronner
Institut für Physikalische Chemie der Universität
Klingenbergstrasse 80, CH-4056 Basel (Switzerland)
Prof. Dr. Z.-Z. Yang
Institute of Theoretical Chemistry, Jilin University
Changchun (People's Republic of China)

[**] This work was supported by Ciba-Geigy AG, F. Hoffmann-La Roche & Co. AG, and Sandoz AG.

ample, and substituting symmetry equivalent positions $\zeta = 1, 3, 5, 7$ or $\zeta = 2, 6$ or $\zeta = 4, 8$ (thus conserving the D_{2h} symmetry of molecule **1B**) one finds:

$$\delta\lambda_{max} = \left(\frac{\partial\lambda_{max}}{\partial\alpha_\zeta}\right)\delta\alpha_\zeta = \left(\frac{\partial\lambda_{max}}{\partial h_\zeta}\right)\delta h_\zeta \qquad \text{(b)}$$

$$\begin{aligned} \zeta = 1, 3, 5, 7 \quad \left(\frac{\partial\lambda_{max}}{\partial h_\zeta}\right) &= 0.95 \\ = 2, 6 &= -0.50 \\ = 4, 8 &= 0.63 \end{aligned} \qquad \text{(c)}$$

For alkyl groups X the value $\delta\alpha_\zeta \approx 1$ eV may be used[10] i.e. $\delta h_\zeta \approx -0.3$ if $\beta \approx -3$ eV. Substitution of the values (c) into (b) leads to $\delta\lambda_{max} = -0.28$ for 1,3,5,7-tetraalkyl-*s*-indacene **2** and to $\delta\lambda_{max} = -0.04$ for 2,4,6,8-tetraalkyl-*s*-indacene **3** (cf. Table 1). It follows that with respect to **1**, our treatment predicts a smaller tendency towards double bond localization for **2** and no significant change for **3** in agreement with the MINDO/3 calculations.[5]

In view of an analysis of these results, it is of advantage to rewrite λ_{max} in the form of equation (d), from which one obtains (e), according to first order perturbation theory.

$$\lambda_{max} = \mathbf{u}^T_{max}\,\boldsymbol{\pi}\,\mathbf{u}_{max} \qquad \text{(d)}$$

$$\delta\lambda_{max} = \mathbf{u}^T_{max}\left(\frac{\partial\pi_{\mu\nu,p\sigma}}{\partial h_\zeta}\right)\mathbf{u}_{max} \qquad \text{(e)}$$

The expansion of the right-hand side of equation (e) reveals that the leading terms contributing towards $\delta\lambda_{max}$ are those with $j = n/2 = \text{HOMO}$ and $k = 1 + n/2 = \text{LUMO}$ [cf. eq. (a)]. These terms increase (decrease) in first order, if the difference $x_{HOMO} - x_{LUMO}$ decreases (increases) under the influence of the substituent. Note that in this approximation the $c_{\mu j}$ do not change. A purely inductive perturbation by a substituent X in position ζ leads to $x'_j = x_j + c^2_{\zeta j}\,\delta h_\zeta$, from which one obtains as a rough approximation for the λ'_{max} value of the perturbed system (cf. Table 1) the expression (f). Although this expression should be used with caution,[11] some qualitatively useful rules can be deduced from it:

$$\lambda'_{max} \approx \lambda_{max}\left(1 + \frac{(c^2_{\zeta,HOMO} - c^2_{\zeta,LUMO})\,\delta h_\zeta}{x_{HOMO} - x_{LUMO}}\right)^{-1} \qquad \text{(f)}$$

1) Substitution-induced changes in double bond localization tendency are expected to be *large* only for systems with a *small* $x_{HOMO} - x_{LUMO}$ gap.

2) If a substituent decreases (increases) the difference $x_{HOMO} - x_{LUMO}$, then the tendency towards double bond localization increases (decreases).

Remarks:

1) Because a small gap $x_{HOMO} - x_{LUMO}$ implies in general a high value of λ_{max} of the unperturbed system, one expects large changes $\delta\lambda_{max} = \lambda'_{max} - \lambda_{max}$ in the tendency of double bond localization only for such systems. Of special interest are systems with $\lambda_{max} \approx \lambda_{crit}$ (e.g. *s*-indacene, **1**), because substitution will then allow to switch them from a delocalized (**1B**) to a localized (**1A**) ground state, and vice versa, depending on the position(s) of the substituent(s). The discriminating quantity is $c^2_{\zeta,HOMO} - c^2_{\zeta,LUMO}$, the sign of which determines the direction, and the absolute value of the size of the change λ_{max}. In neutral, alternant closed shell π-systems one has $c^2_{\zeta,HOMO} = c^2_{\zeta,LUMO}$, and it follows from (f) that no (or very little) change in the tendency of double bond localization can be induced by substitution.

2) For a given δh_ζ, the sign and absolute value of $\delta(x_{HOMO} - x_{LUMO})$ can be read off orbital diagrams, e.g. those of *s*-indacene (Fig. 1), which is a particular case because of the presence of two accidentally degenerate HOMOs.[12]

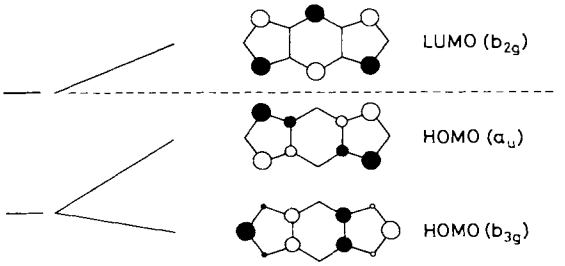

Fig. 1. HMO orbital diagram of the frontier orbitals of **1**.

Substituting, for example, the H atoms at centers 4 and 8 by alkylgroups ($\delta h_\zeta < 0$), leaves the HOMO energies unchanged, whereas the LUMO orbital will be raised. This increases the $x_{HOMO} - x_{LUMO}$ gap and consequently λ_{max} decreases, indicating a decreased tendency towards double bond localization. The above line of reasoning suggests the rule that inductive substituents which lead to a bathochromic (hypsochromic) shift of the LUMO←HOMO band in the UV/VIS spectrum of the molecule[13] will increase (decrease) the double bond localization tendency. In this connection the elegant treatment by *Nakajima* et al.[14] of double bond localization in terms of a pseudo Jahn-Teller effect should be mentioned. However, there are limitations to this attractive rule, which will be discussed elsewhere.[11]

3) The treatment outlined here can be extended to conjugative perturbations. Thus it is found that two amino groups in positions 4 and 8 of *s*-indacene lead to a completely delocalized molecule (**4** in Table) in agreement with the results of a MINDO/3 calculation[5] and the experimental findings.[15] Two nitrile groups in positions 2 and 6 should also reduce the double bond localization tendency in molecule **5**, however to a smaller extent than observed for **2**, as is also predicted by the MINDO/3 model.[5]

Received: December 22, 1986 [Z 2022 IE]
German version: *Angew. Chem. 99* (1987) 369

CAS Registry numbers:
1, 267-21-0; **4**, 107557-29-9; **5**, 107557-30-2.

[1] H. C. Longuet-Higgins, L. Salem, *Proc. R. Soc. London Ser. A 251* (1959) 172; *ibid. 257* (1960) 445.
[2] T. Nakajima, S. Katagiri, *Mol. Phys. 7* (1964) 149.
[3] A. Toyota, T. Nakajima, *J. Chem. Soc. Perkin Trans. 2* (1986) 1731; and references cited therein.
[4] K. Hafner, *Angew. Chem. 75* (1963) 1041; *Angew. Chem. Int. Ed. Engl. 3* (1964) 165; *Pure Appl. Chem. Suppl. 2* (1971) 1.
[5] K. Hafner, B. Stowasser, H.-P. Krimmer, S. Fischer, M. C. Böhm, H. J. Lindner, *Angew. Chem. 98* (1986) 646; *Angew. Chem. Int. Ed. Engl. 25* (1986) 630.
[6] G. Binsch, E. Heilbronner, J. N. Murrell, *Mol. Phys. 11* (1966) 305; G. Binsch, E. Heilbronner in A. Rich, N. Davidson (Eds.): *Structural Chemistry and Molecular Biology*, W. H. Freeman and Co., San Francisco 1968, p. 815.
[7] C. A. Coulson, H. C. Longuet-Higgins, *Proc. R. Soc. London Ser. A 181* (1947) 39; *ibid. A 193* (1948) 447; for a general definition of $\pi_{\mu\nu,p\sigma}$ see: E. Heilbronner, H. Bock: *Das HMO-Modell und seine Anwendung, Vol. 1*, 2nd Edit., Verlag Chemie, Weinheim 1978.
[8] G. Binsch, E. Heilbronner, *Tetrahedron 24* (1968) 1215.
[9] K. Hafner, H. U. Süss, *Angew. Chem. 85* (1973) 626; *Angew. Chem. Int.*

Ed. Engl. 12 (1973) 575; B. Kitschke, H. J. Lindner, *Tetrahedron Lett. 1977*, 2511.
[10] E. Heilbronner, J. P. Maier *(Some Aspects of Organic Photoelectron Spectroscopy)* in C. R. Brundle, A. D. Baker (Eds.): *Electron Spectroscopy: Theory, Techniques and Applications, Vol. 1*, Academic Press, London 1977.
[11] E. Heilbronner, Z.-Z. Yang, unpublished.
[12] According to a PPP-calculation the orbital a_u (= HOMO) lies above b_{3g} (= HOMO − 1).
[13] H. C. Longuet-Higgins, R. G. Sowden, *J. Chem. Soc. 1952*, 1404.
[14] T. Nakajima, A. Toyota, S. Fuji, *Bull. Chem. Soc. Jpn. 45* (1972) 1022.
[15] K. Hafner, *Pure Appl. Chem. 54* (1982) 939.

Total Synthesis of the Enantiomerically Pure Lichen Macrolide (+)-Aspicilin**

By *Gerhard Quinkert,* Nana Heim, Jürgen Glenneberg, Uta-Maria Billhardt, Volker Autze, Jan W. Bats,* and *Gerd Dürner*

After having established the absolute configuration of the title compound[1] and having opened up a new synthetic route to large ring sized lactones, we now report the total synthesis of the first isolated lichen macrolide.[2] The core of our total synthesis of (+)-aspicilin **8** is the photolactonization of the diastereomeric *o*-quinol acetates **1** and **3** (via the *seco*-isomeric diene ketene **2**[3]) to the diastereomeric macrolides **4** and **6** (69%, ratio 2.5 : 1;[4] see Scheme 1). The mixture of the photolactones **4** and **6** is converted, without the lactone ring ever being opened again, into the enantiomerically pure target compound **8** via the dienone lactone **5** and the dienol lactone **7a**.

Chemoselective azidolysis[6] of the enol acetate group of **4** and **6** and subsequent elimination of the benzenesulfinate anion, furnishes a 1 : 1 : 2 mixture of **5** and its (*E,E*)- and (*Z,E*)-stereoisomers. The (*E,Z*)-diastereomer **5** has been isolated in 72% overall yield (referred to the mixture of lactones **4** and **6**): 22% immediately after azidolytic elimination, the rest after photoisomerization of the (*E,E*)- and (*Z,E*)-stereoisomers of **5** with light of the wavelength region > 340 nm.[7]

Reduction of the keto group, at −90 °C in toluene, with *Yamamoto*'s reagent[8] converts the dienone lactone **5** with exceedingly high stereoselection almost exclusively into the dienol lactone **7a** (96%).[9] The relative and (as the (*S*)-chirality at C(17) is already known by use of **12**; see Scheme 2) absolute configuration of **7a** have been established by single-crystal X-ray analysis of *rac*-**7b**.[10] The center of chirality at C(17) already present prior to reduction, by the tendency of the CH_3 group to take up the pseudo equatorial position, determines the dominating conformation of the dienone lactone **5**. Due to the preferred approach of the reducing agent from the less occupied half space[11] C(17) finally controls the configuration of the dienol lactone **7a**.[12] Reaction of **7a** with OsO_4 in the presence of pyridine at room temperature in CH_2Cl_2 leads to formation of the target compound **8** in 40% yield. Table 1 lists some physical data of characteristic synthetic intermediates and substantiates, in particular, the identity of the macrolide isolated from *Aspicilia caesiocinerea* with the synthesized target compound **8**.

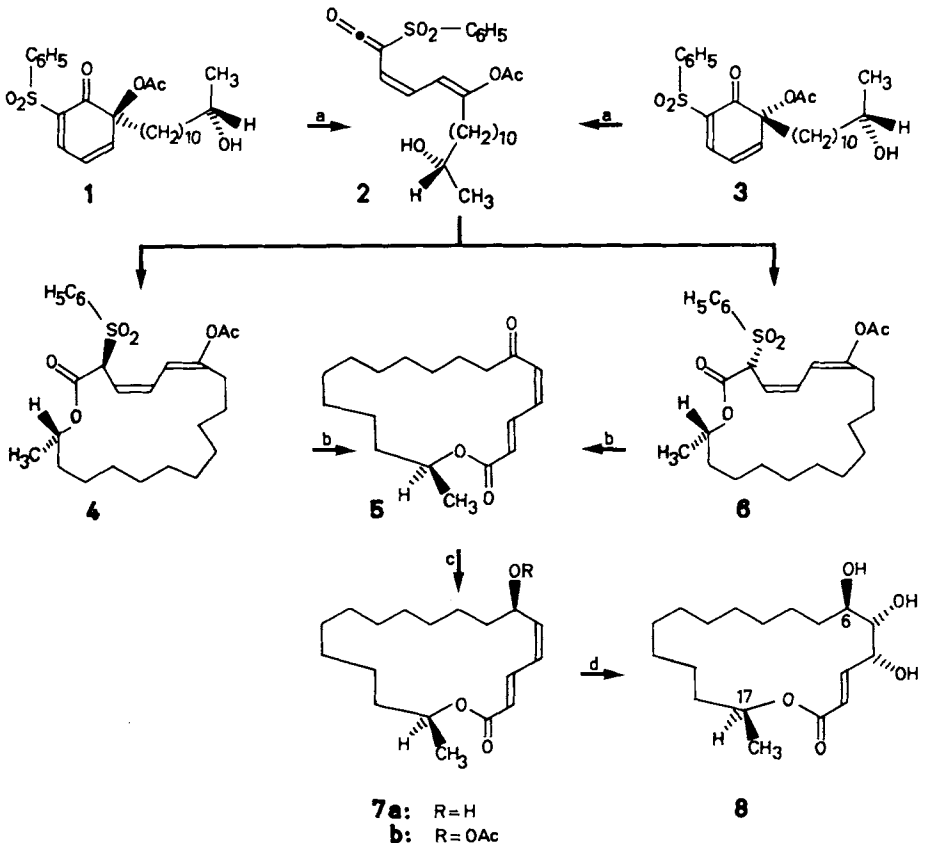

Scheme 1. a) *hv*, $\lambda > 340$ nm, *N*-methylimidazole (1.3 equiv.), CCl_4, 30 min; flash chromatography [5]. b) NaN_3 (11 equiv.), benzene/water (6 + 1), methyltrialkyl(C_8-C_{10})ammonium chloride (ADOGEN 464®, Janssen), RT, 120 h; separation of **5** by flash chromatography; *hv*, $\lambda > 340$ nm, hexane, 90 min; flash chromatography and threefold repetition of the irradiation-chromatography cycle [7]. c) Diisobutylaluminum hydride in toluene (14 equiv.), 2,6-di-*tert*-butyl-4-methylphenol (28 equiv.), 1 h, 0–4 °C; addition of **5** in toluene at −90 °C, 2 h at −90 °C, 2 h at −40 °C; 0.1 N HCl (aq.); Flash chromatography, crystallization. d) OsO_4 (1.25 equiv.) in CH_2Cl_2 at RT to **7a** (1 equiv.), pyridine (5 equiv.) in CH_2Cl_2, 30 min; methanol (15-fold amount), 15 min passage of H_2S, evaporation, dissolution of residue in ethyl acetate, filtration over Celite, semipreparative HPLC.

[*] Prof. Dr. G. Quinkert, Dipl.-Chem. N. Heim, Dr. J. Glenneberg, Dr. U.-M. Billhardt, Dipl.-Chem. V. Autze, Dr. J. W. Bats, Dr. G. Dürner
Institut für Organische Chemie der Universität
Niederurseler Hang, D-6000 Frankfurt am Main 50 (FRG)

[**] This work was supported by the Deutsche Forschungsgemeinschaft (Project Qu 15/22), by the Bundesministerium für Wirtschaft (Project AIF No. 5811), by the Fonds der Chemischen Industrie, and by Hoechst AG.

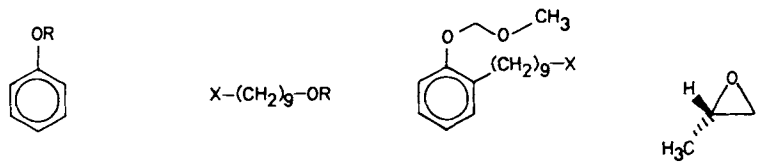

9a: R=H
b: R=CH_2-O-CH_3

10a: R=H; X=OH
b: R=H; X=Br
c: R=THP; X=Br

11a: X=OH; **b**: X=OTHP
c: X=OSO_2CH_3; **d**: X=Br

12

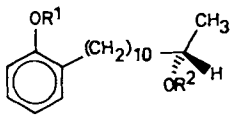

13a: $R^1=R^2=H$
b: $R^1=CH_2$-O-CH_3; $R^2=H$
c: $R^1=CH_2$-O-CH_3; R^2=THP

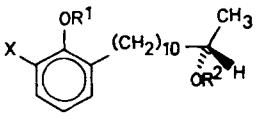

14a: $R^1=CH_2$-O-CH_3; R^2=THP; X=S-C_6H_5
b: $R^1=H$; $R^2=H$; X=S-C_6H_5
c: $R^1=R^2=H$; X=SO_2-C_6H_5

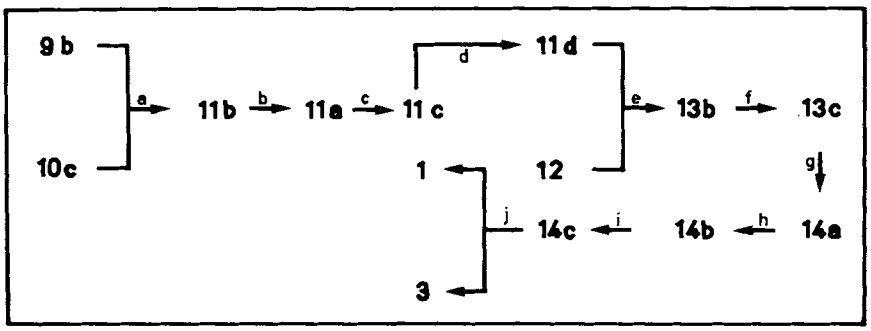

Scheme 2. a) BuLi (1.5 equiv.), tetramethylethylenediamine (TMEDA) (1.5 equiv.), tetrahydrofuran (THF); addition of **9b** (1.7 equiv.; from **9a** [14]) at 0°C; addition of **10c** (1 equiv.; from **10a** [15] via **10b**): 80%, THP = tetrahydropyranyl. b) Methanol, pyridinium *p*-toluenesulfonate (catalytic), 45 min reflux, filtration (SiO_2): 98%. c) Methanesulfonyl chloride (1.1 equiv.), triethylamine (1.3 equiv.), CH_2Cl_2, 0°C to RT, ca. 12 h; filtration (SiO_2): 98%. d) LiBr (4 equiv.), THF, RT, 3 d; distillation: 98%. e) THF, Mg (1.05 equiv.), **12** [16] (1.3 equiv.), CuCl-cyclooctadiene complex (0.1 equiv.), −4°C to RT; filtration (SiO_2): 80%. f) 3,4-Dihydro-2*H*-pyran (5 equiv.), pyridinium *p*-toluene sulfonate (catalytic), CH_2Cl_2, 0°C to RT, 15 h; filtration (SiO_2): 98%. g) BuLi (1.2 equiv.), TMEDA (1.25 equiv.), THF; diphenyl disulfide (1.4 equiv.), 0°C to RT, 14 h; preparative HPLC: 80%. h) *p*-Toluenesulfonic acid (catalytic), methanol, 3 h reflux; filtration (SiO_2): 99%. i) *m*-Chloroperbenzoic acid (2 equiv.), methanol, RT, 16 h; crystallization: 86%. j) $Pb(OAc)_4$ (1.5 equiv.), BF_3·ether (1.5 equiv.), ethyl acetate/methanol (4+1), 1.5 h, −10°C; 30 min RT; flash chromatography.

Scheme 2 shows how the *o*-quinol acetates **1** and **3** are smoothly synthesized from the conveniently accessible C_6-, C_9-, and C_3-building blocks phenol **9a**, 1,9-nonanediol **10a** (from azelaic acid), and (*S*)-(−)-methyloxirane **12** (from (*S*)-(−)-methyl lactate.[16]

It is well worth mentioning that the phenylsulfonyl

Table 1. Some physical data of the compounds **4**, **5**, **6**, **7a**, *rac*-**7b**, and **8** [13].

4: m.p. = 120.5°C (ether/pentane); UV (methanol): $\lambda_{max}(\varepsilon)$ = 221 (16300), 253 nm (21480); IR (KBr): $\tilde{\nu}$ = 3050 and 3030 (each w, C=CH), 1750 (s, enol acetate), 1725 (s, lactone), 1660 (m, C=C), 1310, 1145 cm^{-1} (m and s, $SO_2C_6H_5$); ^{1}H-NMR ($CDCl_3$): δ = 1.17–1.55 (m, 2 H-8 to 2 H-16), 1.27 (d, J = 6.2 Hz, CH_3), 2.13 (s, CH_3-CO), 2.24 (m, H-7), 2.56 (m, H'-7), 4.88 (dd, J = 10.4 Hz, H-2), 5.04 (m, H-17), 5.61 (t, J = 11 Hz, H-3), 5.84 (d, J = 12 Hz, H-5), 6.44 (t, J = 11.4 Hz, H-4), 7.55 (ψt, 2 *m*-H), 7.67 (m, *p*-H), 7.89 (ψd, 2 *o*-H); $[\alpha]_\lambda^{20}$ (c = 1.008 in dioxane) +20.3 (589), +20.9 (578), +23.4 (546), +39.7 (436), +71.6° (365 nm); $[\alpha]_{589}^{20}$ (c = 0.865 in chloroform) +43.2°

5: m.p. = 45.7°C (pentane); UV (methanol): $\lambda_{max}(\varepsilon)$ = 267 (20830); UV (*n*-hexane): $\lambda_{max}(\varepsilon)$ = 267 (20850), 341 nm (110); IR (film): $\tilde{\nu}$ = 3070, 3030 (each w, C=CH), 1710 (s, unsaturated lactone), 1685 (s, unsaturated ketone), 1625, 1575 (each m, C=C), 965 cm^{-1} (w, (*E*)-CH=CH–); ^{1}H-NMR ($CDCl_3$): δ = 1.15–1.85 (m, 2 H-8 to 2 H-16), 1.29 (d, J = 6.2 Hz, CH_3), 2.53 (m, 2 H-7), 4.98 (m, H-17), 6.05 (d, J = 15.6 Hz, H-2), 6.33 (d, J = 11.4 Hz, H-5), 6.46 (ψt, J = 11.3 Hz, H-4), 7.98 (dd, J = 11.4, 15.6 Hz, H-3); $[\alpha]_\lambda^{20}$ (c = 1.2460 in chloroform) +13.7 (589), +14.5 (578), +16.5 (546), +28.7° (436 nm)

6: m.p. = 130–132°C (above 126°C change of modification); UV (methanol): $\lambda_{max}(\varepsilon)$ = 221 (14740), 254 nm (22370); IR (KBr): $\tilde{\nu}$ = 3060, 3040, and 3020 (each w, C=CH), 1745 (s, enol acetate), 1730 (s, lactone), 1650 (m, C=C), 1320, 1145 cm^{-1} (m and s, $SO_2C_6H_5$); ^{1}H-NMR ($CDCl_3$): δ = 1.07–1.50 (m, 2 H-8 to 2 H-16), 1,14 (d, J = 6.2 Hz, CH_3), 2.16 (s, CH_3–CO), 2.33 (m, H-7), 2.55 (m, H'-7), 4.91 (d, J = 10.4 Hz, H-2), 5.01 (sext., J = 6.5 Hz, H-17), 5.39 (dt, J = 10.9, 0.7 Hz, H-3), 6.02 (d, J = 11.7 Hz, H-5), 6.48 (t, J = 11.2 Hz, H-4), 7.54 (ψt, 2 *m*-H), 7.66 (m, *p*-H), 7.90 (ψd, 2 *o*-H); $[\alpha]_\lambda^{20}$ (c = 1.5068 in dioxane) −128.8 (589), −135.5 (578), −158.5 (546), −321.6 (436), −655.1° (365 nm); $[\alpha]_{589}^{20}$ (c = 1.395 in chloroform) −142.0°

7a: m.p. = 84°C (ether/pentane); UV (methanol): $\lambda_{max}(\varepsilon)$ = 259 nm (22600); IR (KBr): $\tilde{\nu}$ = 3340 (m, broad, OH), 1700 (s, unsaturated lactone), 1640, 1600 (m and w, C=C), 965 cm^{-1} (w, (*E*)-CH=CH); ^{1}H-NMR ($CDCl_3$): δ = 1.00–1.85 (m, 2 H-7 to 2 H-16 and OH), 1.25 (d, J = 6.3 Hz, CH_3), 4.83 (m, H-6), 5.20 (m, H-17), 5.71 (ψt, J = 10 Hz, H-5), 5.93 (d, J = 15.2 Hz, H-2), 6.22 (ψt, J = 11 Hz, H-4), 7.57 (ddd, J = 11.6, 15.2, 1.0 Hz, H-3); $[\alpha]_\lambda^{20}$ (c = 0.9308 in chloroform) −99.2 (589), −104.0 (578), −121.5 (546), −242.9 (436), −479.6° (365 nm); $\theta(\lambda)$: −30880 (253 nm) (methanol)

rac-**7b**: m.p. = 55–57°C (ether/pentane); UV (methanol): $\lambda_{max}(\varepsilon)$ = 254 nm (23540); IR (KBr): $\tilde{\nu}$ = 3060, 2985 (w and m, C=CH), 1740 (s, acetate), 1710 (s, unsaturated lactone), 1640, 1610 (each m, C=C), 965 cm^{-1} (m, (*E*)-CH=CH); ^{1}H-NMR ($CDCl_3$): δ = 1.22–1.85 (m, 2 H-7 to 2 H-16), 1.25 (d, J = 6.3 Hz, CH_3–C17), 2.04 (s, CH_3–CO), 5.19 (m, H-17), 5.58–5.81 (m, H-2 and H-6), 5.93 (ψd, J = 15.3 Hz, H-5), 6.25 (ψt, J = 10.5 Hz, H-3), 7.67 (dd, J = 11, 1 Hz, H-4)

8 (total synthesis): m.p. = 155–157°C (ethyl acetate/hexane); UV (methanol): $\lambda_{max}(\varepsilon)$ = 210 nm (11500); IR (KBr): $\tilde{\nu}$ = 3450, 3380, 3280 (s, OH), 1720 (s, lactone), 1660 cm^{-1} (m, C=C); ^{1}H-NMR ($CDCl_3$): δ = 1.25 (d, J = 6.2 Hz, CH_3), 1.33–1.59 (m, 2 H-7 to 2 H-16), 2.41 (s, OH), 3.25 (s, OH), 3.50 (s, OH), 3.58 (s, H-5), 3.75–3.79 (m, H-6), 4.58 (m, H-4), 5.05 (m, H-17), 6.12 (dd, J = 15.8, 1.8 Hz, H-2), 6.91 (dd, J = 15.8, 5.0 Hz, H-3); $[\alpha]_\lambda^{20}$ (c = 0.734 in methanol) +42.6 (589), +44.8 (578), +53.3 (546), +86.4 (436), +133.6° (365 nm)

8 (isolated from *Aspicilia caesiocinerea*): m.p., UV- and IR spectra completely identical with the data of the synthetic product. With exception of the signals for H–O (exchangeable with D_2O, s at 2.60, m at 3.16–3.18 and m at 3.38–3.41) the ^{1}H-NMR spectra are also in complete agreement. $[\alpha]_\lambda^{20}$ (c = 1.000 in methanol) +42.9 (589), +45.6 (578), +51.5 (546), +86.6 (436), +133.5° (365 nm)

group in **14c** has been introduced for two reasons: firstly, for the later conversion of the photolactones **4** and **6** into the stereoisomeric dienone lactones and, secondly, to achieve regioselective Wessely acetoxylation. The oxidation of **14c** with $Pb(OAc)_4$, however, must then be catalyzed by Lewis acid: with BF_3·ether in a mixture of methanol and ethyl acetate[17] the *o*-quinol acetates **1** and **3** are isolated in 85% yield.

To sum up: the synthesis of **8** shows, for the first time, how useful photolactonization for the synthesis of macrolides really is and, once again, that in a cyclic system the information of a remote center of chirality can be transmitted to a high degree to a newly developing stereogenic center.

Received: December 22, 1986;
revised: January 26, 1987 [Z 2021 IE]
German version: *Angew. Chem. 99* (1987) 363

[1] G. Quinkert, N. Heim, J. W. Bats, H. Oschkinat, H. Kessler, *Angew. Chem. 97* (1985) 985; *Angew. Chem. Int. Ed. Engl. 24* (1985) 987.
[2] G. Quinkert, G. Fischer, U.-M. Billhardt, J. Glenneberg, U. Hertz, G. Dürner, E. F. Paulus, J. W. Bats, *Angew. Chem. 96* (1984) 430; *Angew. Chem. Int. Ed. Engl. 23* (1984) 440.
[3] Diene ketenes from *o*-quinol acetates: G. Quinkert, E. Kleiner, B.-J. Freitag, J. Glenneberg, U.-M. Billhardt, F. Cech, K. R. Schmieder, C. Schudok, H.-C. Steinmetzer, J. W. Bats, G. Zimmermann, G. Dürner, D. Rehm, E. F. Paulus, *Helv. Chim. Acta 69* (1986) 469.
[4] After the configuration of the lower homologues of **4** and **6** containing a 16-membered ring had been determined by single crystal X-ray structural analysis [5], it was possible to differentiate **4** and **6** NMR spectroscopically by analogy.
[5] G. Quinkert, U.-M. Billhardt, H. Jakob, G. Fischer, J. Glenneberg, P. Nagler, V. Autze, N. Heim, M. Wacker, T. Schwalbe, Y. Kurth, J. W. Bats, G. Dürner, G. Zimmermann, H. Kessler, *Helv. Chim. Acta*, in press.
[6] The azido anion is a better leaving group than the alkoxide anion of the lactone group and a poorer leaving group than the dienolate anion of the enol acetate group.
[7] After 90 min irradiation with light of the wavelength region >340 nm in hexane a stationary composition of (*E,E*)-, (*E,Z*)-, (*Z,E*)- and (*Z,Z*)-stereoisomers in the ratio 10:12:2:1 is established. The (*E,Z*)-stereoisomer **5** can be separated quantitatively by flash chromatography. After repeating the irradiation-chromatography cycle three times the total yield of **5** amounts to 72%.
[8] The reagent was prepared in situ from diisobutylaluminum hydride and 2,6-di-*tert*-butyl-4-methylphenol in toluene at 0°C; see S. Iguchi, N. Nakai, M. Hayashi, H. Yamamoto, M. Maruoka, *Bull. Chem. Soc. Jpn. 54* (1981) 3033.
[9] Besides **7** the C-6 epimer is also formed (ratio 250:1).
[10] X-ray structure analysis of *rac*-**7b**: $a=8.5357(8)$, $b=18.582(3)$, $c=12.715(1)$ Å; $\beta=91.605(8)°$, $V=2015.9(7)$ Å^3; monoclinic; $P2_1/c$; $Z=4$; $\rho=1.109$ g/cm^3; Enraf Nonius CAD4 diffractometer; $Cu_{K\alpha}$ radiation; quadrant to $2\theta=110°$, 2388 independent reflections with $I>\sigma(I)$; structure determination by direct methods. $R(F)=0.039$ $wR(F)=0.032$; SDP program system.—Further details of the crystal structure investigation are available on request from the Fachinformationszentrum Energie, Physik, Mathematik GmbH, D-7514 Eggenstein-Leopoldshafen 2 (FRG) on quoting the depository number CSD-52166, the names of the authors, and the journal citation.
[11] The more or less planar dienone lactone ring moiety subdivides three-dimensional space into two half spaces. The polymethylene ring moiety is in one half space; in the other half space reduction takes place by the bulky reagent.
[12] *W. C. Still* was the first to point out that in the case of medium and large ring systems, merely a methyl group at a center of chirality sufficed to control a newly formed stereogenic center by favoring a certain conformation; see W. C. Still, I. Galynker, *Tetrahedron 37* (1981) 3981.
[13] The compound *rac*-**7b** comes from the racemic series which was used for optimization; see N. Heim, Dissertation, Universität Frankfurt am Main (FRG) 1987.
[14] J. P. Yardley, H. Fletcher III, *Synthesis 1975*, 244.
[15] A. Butenandt, E. Hecker, M. Hopp, W. Koch, *Justus Liebigs Ann. Chem. 658* (1962) 39.
[16] B. Seuring, D. Seebach, *Helv. Chim. Acta 60* (1977) 1175.
[17] For oxidation with $Pb(OAc)_4$, catalyzed by BF_3·ether, see U.-M. Billhardt, Dissertation, Universität Frankfurt am Main (FRG) 1985.

Bond Stretch Isomerism in Bicyclo[1.1.0]tetrasilanes. Contrasts Between Strained Silicon and Carbon Ring Systems**

By *Paul von Ragué Schleyer,* Alexander F. Sax, Josef Kalcher,* and *Rudolf Janoschek*

Dedicated to Professor Tilman J. De Boer, Amsterdam

The strains in small ring silicon systems afford interesting contrasts with their carbon counterparts:[1] Three-membered silicon rings are more strained and four-membered silicon rings less strained than their carbocyclic analogs.[1,2] We now show how these differences may lead to *bond stretch isomerism*[3] in bicyclo[1.1.0]tetrasilanes. Although many such possibilities have been considered in carbon ring systems,[3,4] no example of isomers which differ principally in the length of a central bond has been demonstrated experimentally.

Masamune et al. have synthesized and determined the X-ray structure of a highly strained bicyclo[1.1.0]tetrasilane derivative, **1**.[5a,b] Although the ring inversion is extremely facile (barrier ca. 15 kcal/mol), the central bond length, 2.373(3) Å, is not very much longer than that found

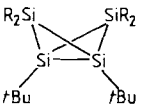

1 R=2,6-$Et_2C_6H_3$

for the other Si–Si bonds, which average 2.322 Å.[5c] In this respect, bicyclotetrasilane is similar to bicyclobutane **2** (where the two types of CC bonds have the same, nearly normal lengths),[6] rather than to 2,4-disilabicyclo[1.1.0]butane **3**, where both experiment and calculations find the central C–C bond to be exceptionally long (ca. 1.78 Å).[7] Since other heteroatom substituted bicyclobutanes have abnormally long central bonds,[6a] we have examined the nature of Si_4H_6, the parent compound of **1**, calculationally.

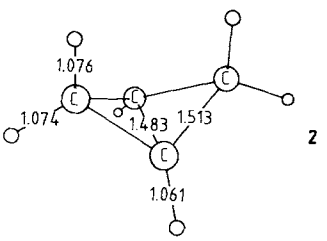

2

The results are quite surprising: At all levels of theory employed, two distinctly different minima were found: **4**[1a] corresponds closely to *Masamune*'s experimental structure, and **5**, *which is lower in energy*, to a geometry

[*] Prof. Dr. P. von R. Schleyer
Institut für Organische Chemie der Universität Erlangen-Nürnberg
Henkestrasse 42, D-8520 Erlangen (FRG)
Dr. A. F. Sax, Dr. J. Kalcher, Prof. Dr. R. Janoschek
Institut für Theoretische Chemie der Universität
Mozartgasse 14, A-8010 Graz (Austria)

[**] This work was supported by the Deutsche Forschungsgemeinschaft and the Fonds der Chemischen Industrie. We thank *Alexander Kos* and *Bernd Reindl*, Erlangen, for carrying out some of the calculations, and Prof. Dr. *W. W. Schoeller*, Bielefeld, for information prior to publication and an unknown referee for suggestions.

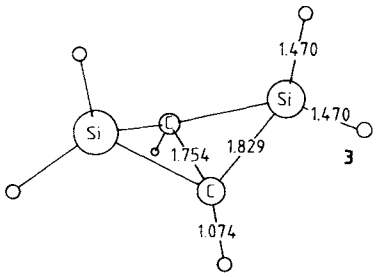

3

calculated recently for Si_4H_6 by *Dabisch* and *Schoeller*.[8] These are "bond stretch" isomers; the bridgehead Si–Si distance in **5** exceeds that in **4** by ca. 0.5 Å (Table 1).

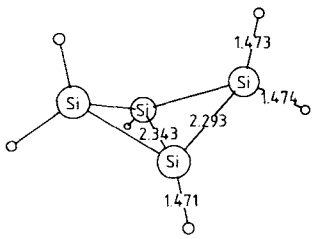

4

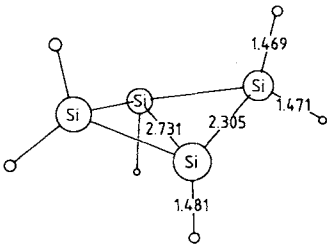

5

The Si_4H_6 structures were optimized at the all electron level with the 3-21G (split valence) and d-orbital augmented 3-21G* (polarized) basis sets[9] as well as with the pseudopotential multiconfiguration-self consistent field (MC-SCF) method, using a triply split but unpolarized valence basis set.[10, 11] Of the five configurations employed for the MC-SCF treatment, only two proved to be of major importance, namely $\Psi_b = \ldots(5a_1)^2$ and $\Psi_a = \ldots(3b_1)^2$; whereby $5a_1$ is the bonding MO of the Si–Si bridge, and $3b_1$ is the corresponding antibonding MO.

At all three levels two optimized structures, **4** and **5**, were found. Both have C_{2v} symmetry; the main differences are not only in the Si–Si distances mentioned above, but also in the interflap angles between the three-membered ring moieties (ca. 120° vs. 140°) and in the Si–Si–H angles at the bridgehead positions (ca. 140° vs. 90°). The key geometrical parameters of **4** and **5** are compared in Table 1, along with the corresponding experimental values for **1**.[5b] When one considers that the latter involves heavy substitution and that polarized basis sets are needed for the best results with second row molecules,[9] the agreement between the X-ray geometry and the 3-21G* data for **4** is quite satisfactory.

However, our data indicates structure **5** to be *lower* in energy than **4**. The difference depends on the theoretical level, but is 2.6 kcal/mol with the 6-31G* basis set (3-21G* geometries) and increases to 8.4 kcal/mol with inclusion of electron correlation via perturbation theory (MP2/6-31G*//3-21G*). The multiconfiguration treatment (MC-SCF), which should be better suited for this purpose, gave similar geometric parameters (Table 1) and an even greater energy difference, 17 kcal/mol, favoring **5** over **4**. While part of this further increase may be due to the lack of d-orbitals in the MC-SCF basis set, **5** should be considerably more stable than **4**. Furthermore, the energy barrier separating **4** from **5** is calculated to be quite small, 1 kcal/mol or less. Hence, **4** is not likely to be a viable isomer for Si_4H_6 itself. The MC-SCF lowering of the relative energy of **5** occurs due to considerable admixture of Ψ_a into the total wave function, $\Psi_{tot}(\mathbf{5}) = 0.95\,\Psi_b(\mathbf{5}) - 0.30\,\Psi_a(\mathbf{5})$, which reflects its diradicaloid character. In contrast, the wave function of structure **4** is well represented by $\Psi_b(\mathbf{4})$ only, $\Psi_{tot}(\mathbf{4}) = 0.98\,\Psi_b(\mathbf{4}) - 0.12\,\Psi_a(\mathbf{4})$. Additional consideration of singly and doubly substituted configurations (CI-SD) does not change these results. Thus, the electronic structure of **4** is similar to that of bicyclobutane (**2**).[6b, c] The central Si_1Si_3 bond of **4** has considerable π character (as in **2**) and Mulliken populations indicate the Si_1Si_3 interaction to be antibonding. The bond stretch isomer, **5**, has greater Si_1Si_3 antibonding character, and can be regarded to be a singlet diradical. The nature of this species has been discussed by *Schoeller* and *Dabisch*.[8] As in $SiH_3^{\oplus}$, the bond angles at the bridgehead positions in **5** are close to 90°. This results in a rather close approach of the bridgehead hydrogens. Although **5** is lower in energy than **4** for Si_4H_6, this order will be reversed if bulky substituents, instead of hydrogens, are present at the bridgeheads. We have shown this calculationally by replacing the two bridgehead H atoms in **4** and **5** by methyl groups (but otherwise retaining the Si_4H_6 geometries); this reverses the relative stabilities. The even larger *t*Bu-bridgehead substituents in **1** cannot be accommodated in a structure of type **5** at all; the **4**-like geometry of **1**, in which the *t*Bu groups are separated due to the large RSiSi angles (Table 1), results as a consequence.

$$Si_4H_6 + 5\,Si_2H_6 \longrightarrow 2\,i\text{-}Si_4H_{10} + 2\,Si_3H_8 \quad (a)$$

$$(SiH_2)_n + n\,Si_2H_6 \longrightarrow n\,Si_3H_8 \quad (b)$$

The strain energy of bicyclobutane (**2**) is 66.5 kcal/mol.[12, 13b] A somewhat higher value (70.6 kcal/mol, 3-21G*)[1a] is estimated theoretically for **4** by means of homodesmotic[13] equation (a). This reflects the generally higher strain energy of three-membered silicon over the

Table 1. Key geometrical parameters (bond lengths [Å] and angles [°]) of bicyclotetrasilane species, X-ray (**1**) and theoretical (**4** and **5**).

Data source	Species	Si1–Si3	Si1–Si2	Interflap angle	HSi1Si3	HSi2H
X-ray [a]	**1**	2.373(3)	2.322 [b]	121.0	146.9 [b]	108.8 [b]
HF/3-21G	**4**	2.452	2.375	116.4	143.3	113.2
HF/3-21G*	**4**	2.342	2.293	120.9	141.6	110.9
MC-SCF pseudopotential	**4**	2.485	2.317	123.2	144.0	112.2
HF/"STO-4/31G" [c]	**5**	2.850	2.338	142.6	94.5	109.6
HF/3-21G	**5**	2.972	2.406	141.9	88.0	112.5
HF/3-21G*	**5**	2.731	2.305	141.2	95.8	111.7
MC-SCF pseudopotential	**5**	2.974	2.352	140.5	90.7	111.3

[a] See ref. [5b]. Angles to substituents, instead of to H, are involved. [b] Averaged. [c] See ref. [8].

Table 2. Comparison of strain energies [kcal mol^{-1}] of carbon and silicon small ring systems [a].

Method	$(CH_2)_3$	$(SiH_2)_3$	$(CH_2)_4$, (D_{2d})	$(SiH_2)_4$, (D_{2d})	C_4H_6, **2**	Si_4H_6, **4** [b]
3-21G (sp basis)		43.0		19.2		78.4
3-21G* (spd basis)		40.3 [c]		18.4		70.6
Pseudopotential (sp basis)		40.6		18.1		69.7
Pseudopotential (spd)		39.2		16.6		
Experiment [d]	28.1	—	26.9	—	66.5	—

[a] Unless indicated otherwise, see [1] for the silicon and [12] for the carbon data. Based on equation (b). [b] This work. Based on equation (a). [c] Other values: 39.6 (6-31G*//6-31G*); 38.2 (MP2/6-31G*//6-31G*); see [1a]. [d] Ref. [12]. Theoretical calculations (6-31G* basis set) give nearly identical values; see K. B. Wiberg, *J. Comput. Chem. 5* (1984) 197.

corresponding carbon ring systems (Table 2).[1,14] However, cyclotetrasilane is less strained than cyclobutane.[1,3] Hence, the opening of bicyclobutane (**2**) to a hypothetical four-membered ring diradical bond stretch isomer would involve less strain relief than the corresponding change from **4** to **5**: roughly 40 kcal/mol for **2** vs. 52 kcal/mol for **4** (this assumes that the four membered ring diradicals have the same strain energy as *cyclo*-Si_4H_8 and *cyclo*-C_4H_8, respectively). A similar treatment has been used by *Wiberg* et al. to analyze ring opening processes in strained polycyclic ring systems.[15] This difference in ring-opening thermodynamic driving force and the inherently lower Si–Si bond dissociation energy (74 kcal/mol in H_3Si–SiH_3 vs. 88 kcal/mol in H_3C–CH_3)[16] are responsible for the preference of Si_4H_6 for the "bond-stretch" structure (**5**) in contrast to C_4H_6 which favors a geometry with normal bond lengths (**2**). These two factors also contribute to the smaller inversion barrier observed for the bicyclotetrasilane (**1**)[5b] than for bicyclobutane (**2**).[17,18]

We conclude that **1** only adopts a structure of type **4** due to the spacial requirements of the bulky bridgehead substituents. If these can be replaced experimentally by hydrogens or by a bridging ring, we predict that a geometry corresponding to the "bond-stretch" isomer **5** will result. Indeed, our preliminary calculations indicate pentasila[1.1.1]propellane to have only a single minimum with a large (ca. 2.9 Å) separation between the bridgehead atoms.

Received: July 21, 1986;
revised: January 2, 1987 [Z 1867 IE]
German version: *Angew. Chem. 99* (1987) 374

[1] a) P. von R. Schleyer, *NATO ASI Ser. C189* (1986) 69; b) A. F. Sax, *Chem. Phys. Lett. 127* (1986) 163; c) A. F. Sax, *ibid. 129* (1986) 66.

[2] W. Schoeller, T. Dabisch, *J. Chem. Soc. Chem. Commun. 1985*, 1706. The strain energies reported in this paper were not evaluated by means of homodesmotic equations (see ref. [13a]) and are too low; however, their subsequent use gives results in accord with those in ref. [1] and Table I (W. W. Schoeller, private communication).

[3] W. D. Stohrer, R. Hoffmann, *J. Am. Chem. Soc. 94* (1972) 779, 1661.

[4] M. N. Paddon-Row, L. Radom, A. R. Gregory, *J. Chem. Soc. Chem. Commun. 1976*, 477. A. R. Gregory, M. N. Paddon-Row, L. Radom, W.-D. Stohrer, *Aust. J. Chem. 30* (1977) 473.

[5] a) S. Masamune, Y. Kabe, S. Collins, D. J. Williams, R. Jones, *J. Am. Chem. Soc. 107* (1985) 5552; b) R. Jones, D. J. Williams, Y. Kabe, S. Masamune, *Angew. Chem. 98* (1986) 176; *Angew. Chem. Int. Ed. Engl. 25* (1986) 173; c) Si–Si bond lengths in unstrained organosilicon compounds normally are 2.34–2.35 Å, although steric effects can produce lengthening to 2.7 Å: N. Wiberg, H. Schuster, A. Simon, K. Peters, *Angew. Chem. 95* (1986) 100; *Angew. Chem. Int. Ed. Engl. 25* (1986) 79. For a discussion of Si···Si nonbonded distances, see M. J. Michalczyk, M. J. Fink, K. J. Haller, R. West, J. Michl, *Organometallics 5* (1986) 531.

[6] a) P. H. M. Budzelaar, E. Kraka, D. Cremer, P. von R. Schleyer, *J. Am. Chem. Soc. 108* (1986) 561, and references cited therein; b) M. D. Newton, J. M. Schulman, *J. Am. Chem. Soc. 94* (1972) 767; c) reviews: F. H. Allen, *Tetrahedron 38* (1982) 645; S. Hoz, *ibid.*, in press; and ref. [13b].

[7] a) G. Fritz, S. Wartanessian, E. Matern, W. Hönte, H. G. von Schnering, *Z. Anorg. Allg. Chem. 475* (1981) 87; b) the 3-21G(*) geometry of 2,4-disilabicyclobutane has r(CC) 1.754 Å, r(SiC) 1.829 Å, and an interflap angle of 125.8° (P. von R. Schleyer, unpublished calculations).

[8] T. Dabisch, W. W. Schoeller, *J. Chem. Soc. Chem. Commun. 1986*, 896.

[9] The Gaussian 82 program was used; see W. J. Hehre, L. Radom, P. von R. Schleyer, J. A. Pople: *Ab Initio Molecular Orbital Theory*, Wiley, New York 1986.

[10] R. Janoschek, A. Sax, E. A. Halevi, *Isr. J. Chem. 23* (1983) 58. A. F. Sax, *J. Comput. Chem. 6* (1985) 469.

[11] H.-J. Werner, W. Meyer, *J. Chem. Phys. 74* (1981) 5794; H.-J. Werner, E.-A. Reinsch, *ibid. 76* (1982) 3144.

[12] P. von R. Schleyer, J. E. Williams, K. R. Blanchard, *J. Am. Chem. Soc. 92* (1970) 2377.

[13] a) P. George, M. Trachtman, C. W. Bock, A. M. Brett, *Tetrahedron 32* (1976) 317; b) A. Greenberg, J. F. Liebman: *Strained Organic Molecules*, Academic Press, New York 1978.

[14] D. Cremer, J. Gauss, *J. Am. Chem. Soc. 108* (1986) 7467.

[15] K. B. Wiberg, F. H. Walker, *J. Am. Chem. Soc. 104* (1982) 5239.

[16] R. Walsh, *Acc. Chem. Res. 14* (1981) 246.

[17] a) R. B. Woodward, D. L. Dalrymple, *J. Am. Chem. Soc. 91* (1969) 4612; b) for a GVB-PRDDO calculation, see P. G. Gassman, M. L. Greenlee, D. A. Dixon, S. Richtsmeier, J. Z. Gougoutas, *ibid. 105* (1983) 5865.

[18] The transition structure for inversion of Si_4H_6 needs an MC-SCF Ansatz for the wave function [cf. 17b]; preliminary calculations indicate a transition structure of lower symmetry than D_{2h}. This is corroborated by the UHF optimized triplet state, which shows a non-planar silicon skeleton: P. von R. Schleyer and A. F. Sax, unpublished.

 © VCH Verlagsgesellschaft mbH, D-6940 Weinheim, 1987 0570-0833/87/0404-0366 $ 02.50/0

Methods in Enzymology. Vol. 114 and 115. Edited by *H. W. Wyckoff, C. H. W. Hirs,* and *S. N. Timasheff.* Academic Press, New York 1985. Vol. 114: **Diffraction Methods for Biological Macromolecules,** Part A, xxiv, 588 pp., hardcover, $ 64.00;—ISBN 0-12-182014-9. Vol. 115: Part B, xxii, 485 pp., hardcover, $ 55.00;—ISBN 0-12-182015-7

Despite the impressive developments in NMR spectroscopy in recent years, which now allow the secondary and tertiary structures of small polypeptides (< 10000 daltons) to be determined in solution, X-ray crystallography will probably remain the only method capable of providing detailed structural information (namely, three-dimensional atomic coordinates) on larger, globular proteins. Whereas application of NMR techniques to the determination of protein structure is limited by the requirements that the protein be available in large amounts, be sufficiently soluble, and exhibit good stability, the use of protein crystallography primarily depends on the ability to crystallize the macromolecule. Once suitable crystals of the protein have been obtained, the elucidation of its structure can be accomplished within a reasonable length of time, provided that its amino acid sequence is known.

New techniques for the collection of diffraction data (area detectors) and for the interpretation of electron density (high-resolution vector graphics) have not only decreased the time required for protein structure determination, but, even more importantly, have improved the accuracy of the structures obtained. Crystallographic refinement has progressed to a point where the methods available, while still requiring considerable patience, often afford atomic coordinates with error limits of only 0.1 to 0.2 Å. Such highly refined protein structures are, in turn, essential for modeling the interaction of these proteins with small molecules, such as substrates and inhibitors, or for planning site-directed mutagenesis experiments. These applications, in particular, have made protein crystallography an interesting and potentially important tool for the pharmaceutical industry.

The rapid development of this field makes periodic reviews of protein crystallographic methods all the more urgent, but these have been lacking so far. The standard textbook on protein crystallography by *Blundell* and *Johnson* is now ten years old and therefore no longer up to date, although it remains an essential source of information. Thus, there has been a crucial need for a current description of the new methods of high-resolution protein crystallography. This gap has now been filled by Volumes 114 and 115 of the renowned series "Methods in Enzymology." Well-known experts have contributed a total of 63 articles, which provide a more or less comprehensive account of protein crystallography. The individual contributions have been organized into sections dealing with the historical development of the field, crystallization, data collection, phase determination, model building, and presentation of the results. This arrangement, however, is not always optimal. For example, the clearly written article by *R. Sparks* on least-squares refinement is included, less than ideally, in the chapter on phase determination.

The volumes are a gold mine for the specialist if only because of the nearly 700 references to the scientific literature, which cover developments up to 1982 and even include articles published in 1984. It is questionable, however, whether the volumes achieve the goal explicitly stated in the introduction, namely, to provide biochemists with an introduction to macromolecular diffraction methods. This goal is a priori unrealistic for a work consisting of differently arranged contributions from a number of individuals. An exception is the collection of well-written articles on the crystallization of biological macromolecules, which should provide many biochemists with useful insights.

Some of the contributions are more technical in nature or describe specific computer programs; others are comparable to well-planned review articles. Even unpublished material is to be found: The method of "iterative single isomorphous replacement" of *B. C. Wang*, which is best described by the term "electron density modification" (although the author specifically disapproves of this term—I trust he will forgive me), is described here in detail for the first time. This method has been used for the past three years by many protein crystallographers with considerable success—an indication of the excellent communication within this scientific community.

Only a few topics are not covered by these volumes. For example, the important technique of phase combination is not mentioned at all. On the other hand, the section on the systematics of protein structures is remarkably encompassing (with very instructive pictures by *Jane Richardson, Arthur Lesk,* and *Karl Hardman*!). For this reason, Volume 115, in particular, is recommended to all those interested in protein structures, namely, spectroscopists, gene technologists, and theoreticians. Both volumes, however, belong on the book shelf of every protein crystallographer.

Rolf Hilgenfeld [NB 796 IE]
Hoechst AG, Frankfurt am Main (FRG)

Regulation of Secondary Metabolite Formation. Proceedings of the Sixteenth Workshop Conference, Hoechst, Gracht Castle, 12–16 May 1985. Edited by *H. Kleinkauf, H. von Döhren, H. Dornauer,* and *G. Nesemann.* VCH Verlagsgesellschaft, Weinheim 1986. xx, 402 pp., bound, DM 108.00.—ISBN 3-527-26475-2

The production of antibiotics using microorganisms is one of the standard tasks of biotechnology. Mutation and selection have been used to obtain strains giving the best production. This empirical procedure has been employed without knowing how the formation of secondary metabolites depends on the regulating processes. It is remarkable that, in spite of the great importance of antibiotics, the genetic instability of high performance strains is not yet understood, nor has an adequate bridge been established between our knowledge of the biosynthesis of antibiotics and that of the genetics of the organisms which produce them. The mutagenic mechanism for even such a technologically important group as the *Streptomycetes* is much less well understood than that for the classical model *Escherichia coli.*

It therefore seems very appropriate that the 16th Workshop conference arranged by Farbwerke Hoechst was on microbiology, being concerned with the topical theme of secondary metabolites. Twenty papers by acknowledged experts from throughout the world were presented.

Bu'Lock reported on genetic aspects of the production of mycotoxins. *Hopwood* reviewed his group's important and detailed studies on the genetics of the *Streptomycetes*. Problems concerning the genetics of eukaryotic cells were discussed by *Esser*. There were several papers dealing with the important topic of the production of penicillins and cephalosporins, e.g. *Demain* discussed the inhibition by ammonium salts of cephamycin formation in *Streptomyces clavuligerus*. There were contributions by *Luckner* and by *Keller* on alkaloid biosynthesis in molds. *Kleinkauf* and *von Döhren* discussed problems in the synthesis of peptide antibiotics using enzymatic systems. *Vining* reported on his group's researches on genetic and physiological control of chloramphenicol biosynthesis. *Gräfe* in his paper took a close look at the control of secondary metabolite formation in *Streptomyces* by the use of the A-factor (2-(6'-methylheptanoyl)-3-hydroxymethyl-4-butanolide) and its derivatives. *Behal* discussed the regulation of tetracycline biosynthesis, and, in a second paper, the control of formation and activity of secondary metabolic enzymes in general. Synthesis of these enzymes usually only begins after the readily available sources of carbon, nitrogen and phosphorus have been exhausted, and in some cases is inhibited by the end product. *Floss* reported on the biosyntheses of some polyketide antibiotics. *Omura* gave an interesting insight into tylosin biosynthesis and its control by ammonium salts and phosphates. There was also an opportunity to hear a representative of plant biochemistry, when *Grisebach* gave a contribution on the induction and regulation of phytoalexin synthesis in soya-beans. In a concluding discussion, summarized by *Hans von Döhren*, terms were defined and unresolved problems identified. A final summary by *Demain* led to a statement of the following desirable conditions to promote genetic studies aimed at resolving the puzzle of secondary metabolism: 1. that industry should develop genetic systems for technologically important organisms; 2. that there should be agreement in the academic world to use a suitable organism as a model; 3. that investigations on the control of secondary metabolism should be carried out on one particular organism, such as *Bacillus subtilis*, whose genetics are already well understood.

Those engaged in research on antibiotics or secondary metabolites will find this book stimulating. For others it makes interesting reading on an important interdisciplinary field of research, which is at the boundaries between biochemistry, organic chemistry, microbiology and genetics.

Franz Lingens [NB 782 IE]
Institut für Mikrobiologie
der Universität Hohenheim (FRG)

Methods of Enzymatic Analysis. Vol. 9. Proteins and Peptides. Edited by *H. U. Bergmeyer, J. Bergmeyer,* and *M. Grassl.* 3rd Edition. VCH Verlagsgesellschaft, Weinheim 1986. xxv, 571 pp., bound. Series price: DM 270.00; individual volume price: DM 310.00.—ISBN 3-527-26049-8

Volume 9 is an entirely new volume devoted to methods for the determination of biologically important proteins lacking enzymic activity, and of hormonal proteins, peptides, and amino acids. The volume is devoted almost entirely to enzyme-immunoassay (EIA) methods. It is divided into five parts, and summarizes methods for 37 compounds or classes of compounds and antibodies.

The first, introductory, part of volume 9 emphasizes current limitations of EIA methods with respect to validation and standardization, and notes the advantages of EIA once a suitable method has been devised. The four chapters in part one—introduction, enzyme immunoassay as an important methodology in biology and medicine, practical considerations in enzyme-immunoassays illustrated by a model system, and problems in the standardization of enzyme-immunoassay for antigens—provide a concise survey of the problems encountered in the development of an EIA method. Some comparisons with alternative methods give the newcomer to EIA some idea as to whether this methodology is worth pursuing further.

Parts 2 through 5 present assay methods for six transport proteins, four carcinoembryonic and pregnancy proteins, twelve structural and regulatory proteins, and fifteen hormones (proteins, peptides and the iodoamino acids triiodothyronine and tetraiodothyronine), respectively. The chapter on calmodulin presents a method based on activation of cAMP phosphodiesterase in the presence of calcium ions and calmodulin and is the only assay in this volume not based on EIA. Of the remaining assays, most are of the heterogeneous double-antibody sandwich-type as used in enzyme-linked immunosorbent assay (ELISA). The other assays represent a small selection of different or modified strategies for using EIA. Reading through the descriptions of the principles of these different assays provides those unfamiliar with EIA some idea of the varied ways in which EIA can be used for analysis.

In a number of chapters a second assay method is included in several different manners. The collagen chapter includes methods for the determination of collagen types as well as a method for the determination of collagen antibodies. The thyroglobulin chapter is of the same form with assays for antigen and antibody. The chapters for α_1- and β_2-microglobulins both contain two methods for use with different concentration ranges of antigen in the sample. The thyroid-stimulating hormone chapter includes a semi-automated assay intended for mass screenings of newborns. The tetraiodothyronine chapter contains assays for both total and free hormone.

A typical assay chapter is composed of seven sub-sections followed by references and is comparable in layout to the metabolite assays in volumes 6 to 8. A general section gives a brief discussion of the compound being assayed and indication of the major application of the assay whether in the clinical or research laboratory; substance properties assayed by alternative methods; and reference and standard methods if available. The assay is then described in detail in the remainder of the chapter, which includes a schematic representation of the assay, conditions for the assay, a listing of required equipment, a list of reagents and solutions, the procedure for carrying out the assay, a section on validation of the assay, and an appendix that typically includes comments on topics such as preparation of antibody and enzyme-antibody conjugates. While considerable detail is provided in these methods chapters, they are not as complete as enzyme-based assays from previous volumes with regard to detailed instructions on the determination of an experimental value. A typical requirement for a calibration curve and variability in the biologically-derived materials used in immunoassays precludes the formulation of an exact procedure.

This volume provides a uniform and detailed single-source reference for EIA methods of use in the clinic and laboratory. It will be most immediately useful to those already familiar with EIA and in need of methods for the

specific compounds covered in the volume. For those developing a new EIA method, this volume provides a variety of approaches to immunoassay and may be a suitable starting point for the development of a new assay. Workers unfamiliar with immunochemistry may find this volume difficult to read and should see chapter 2.7 of volume 1, if not a general textbook description of the science involved in order to be familiar with some of the terminology used.

The appendix to this volume contains lists of symbols, quantities, units and constants; abbreviations for chemical and biological compounds; and formulae useful in spectrophotometry. It is not as extensive as in previous volumes.

Anyone regularly using immunoassay methods in their work should have this book. Those needing to understand the nature and application of EIA and the practical aspects involved would do well to read part or all of volume 9.

Mark A. Findeis, George M. Whitesides [NB 787 IE]
Harvard University, Department of Chemistry
Cambridge, MA 02138 (USA)

Integral/Structural Polymer Foams. Technology, Properties and Applications. Edited by *G. Henrici-Olivé* and *S. Olivé*. Springer, Berlin 1986. xxii, 295 pp., bound, DM 198.00.—ISBN 3-540-15038-2

Integral polymer foams, or structural polymer foams (these being the names used in Europe and in the USA respectively), have a cellular structure, with the density increasing outwards from the core to a rigid skin, thus imitating the structure of wood or bone. Integral polymer foams are often used as a wood substitute.

F. A. Shutov and many other authors from Germany, the USA and elsewhere were involved in putting together this very carefully written book. It deals with the basic relationships between the morphology and properties on the one hand, and the formulating, the equipment and its setting up, and the manufacturing variables on the other. The applications are discussed, together with a summary of the molding of the materials and marketing problems. An economic analysis of commercial processes for marketable materials is also included.

The book deals with the starting materials, the technology of integral polymer foams, and applications using polyurethanes, polystyrenes, polyvinyl chloride, polyolefins, ABS copolymers, polyphenylene oxides, polycarbonates, polyamides, polyesters, polyacetals, polyimides, epoxides, phenyl resins, and other starting materials. It ends with a chapter on rigidity calculations, molding techniques, and considerations affecting manufacturers and users.

Useful features are the numerous figures illustrating equipment, the engineering drawings, flow diagrams and schematic diagrams, together with detailed indexes of manufacturers, processes, products, abbreviations, a contents list, and an excellent subject index.

The book is suitable both for those concerned with the production of these materials and for users, and also for students of the science, technology and applications of polymers.

Frank Wingler [NB 785 IE]
Central Research Laboratory,
Bayer AG, Leverkusen (FRG)

Radicals in Organic Synthesis: Formation of Carbon-Carbon Bonds. By *B. Giese*. Pergamon Press, Oxford 1986. XIII, 294 S., Paperback, $ 25.00.—ISBN 0-08-032494-0

During the last decade organic free-radical chemistry has undergone a remarkable metamorphosis from a rather prosaic area of limited utility for the construction of carbon-carbon bonds, except in polymers, to one of major synthetic importance with methods capable of providing chemo-, regio- and stereo-selectivity far beyond the most optimistic expectations of early workers in the field. Professor *Giese*, one of those who has played a significant role in bringing about these developments, now provides a timely account of the mechanistic basis and synthetic applications of free-radical methods, abundantly illustrated with examples from the recent literature.

The book opens with a short introduction in which well earned credit is rightfully accorded to those physical-organic chemists whose studies in this area laid that kinetic and mechanistic base upon which the present cornucopia of synthetically useful methods so firmly rests. The main substance of the book is contained in the following four long chapters, each of which deals with a major topic and is subdivided into a number of smaller sections.

In the first of these chapters (Basic Principles) the subsections cover general aspects of syntheses with radicals, elementary reaction steps between radicals and non-radicals, and the comparison of radicals and ions in synthesis. The Author wisely advises the reader to study this chapter carefully since an understanding of the factors which affect the relative reactivities of radicals is essential to the successful application of radical reactions in synthesis. This point is nicely exemplified by a thorough examination of the way in which a knowledge of the rate constants for the individual steps in the reaction of alkyl halides with activated olefins in the presence of trialkylstannane allows the choice of optimum experimental conditions. Another particularly useful topic in this chapter deals with the frontier-orbital approach to radical addition processes.

The next chapter provides a comprehensive account of the intermolecular formation of aliphatic carbon-carbon bonds. It is mainly devoted to addition processes subdivided according to the nature of the reagent (tin hydrides, mercury hydrides, etc.) which reacts with the adduct, but there is also a small section covering synthetic applications of radical-radical reactions. Pleasing features of this and following chapters are the diversity and number of illustrative examples, drawn for the most part from the very recent literature. Indeed dramatic evidence of the level of current activity in this area is provided by the fact that 55% of the 250 or so papers cited in this chapter have been published during the last six years.

The proportion of very recent papers cited is even higher in the next chapter which deals with intramolecular formation of aliphatic carbon-carbon bonds. The many examples in this chapter of the formation of bi- or tri-cyclic ring systems, often related to such important natural products as triquinanes, cephems, and pyrrolizidine alkaloids, clearly shows why this radical methodology is currently attracting so much interest. By comparison the formation of bonds to aromatic systems is somewhat neglected. However, chapter 5 which deals with this topic, indicates the potential synthetic utility of $S_{RN}1$ reactions, of additions involving aryl radicals, and of homolytic substitution in both aromatic and heteroaromatic systems.

The last chapter (Methods of Radical Formation) is quite different from those that precede it. It does not provide a full discussion of the ways in which radicals can be

generated; rather it is a summary index of all the various methods referred to in earlier chapters and as such provides a most useful way of rapidly finding illustrative examples of their use.

In summary, this is a splendid book. Inevitably it is stronger in some areas than in others; I personally would have welcomed a little more discussion of photochemical methods, of phenolic coupling, and of intramolecular aryl addition. But these are minor quibbles. Overall it gives not only a good account of the power and diversity of presently available methods, but also a feeling for the current state of intense activity in this area, and for the potential for new breakthroughs. Anyone who wishes to use the present methodology or to participate in the exciting developments that lie just around the corner should read this book from cover to cover.

A. L. J. Beckwith [NB 823 IE]
Research School of Chemistry
Australian National University, Canberra (Australia)

The Practice of Quantitative Gel Electrophoresis. By *A. Chrambach*. VCH Verlagsgesellschaft, Weinheim 1985. xv, 265 pp., bound, DM 110.00.—ISBN 3-527-26039-0

It must be said at the outset that this is an extremely useful book. Those who have previously used polyacrylamide gel electrophoresis (PAGE) only as an analytical technique will have found the texts by *Weber* and *Osborn*, by *Laemmli* and by *O'Farrell*, sufficient for obtaining reproducible one- or two-dimensional protein patterns, or for determining "apparent" molecular weights. The present book treats sodium dodecyl sulfate PAGE (SDS-PAGE) as just one of the possible forms of gel electrophoresis; everyone who casts gels knows that PAGE did not begin with *Maizel* or *Laemmli*, but a glance at current issues of biochemical journals might lead one to think that most other forms of analytical gel electrophoresis are now being forgotten.

A. Chrambach sees gel electrophoresis as an integrated whole. Consequently, as is stressed in the preface, polyacrylamide gel and agarose gel electrophoresis, isotachophoresis and electrofocussing are treated in unity. The objective is to isolate specific proteins or protein complexes by an appropriate combination of these various methods for passing a protein mixture through a gel. In this connection the native macromolecules themselves are chiefly of interest, as distinct from the dissociated individual proteins that are studied in SDS-PAGE. The concept of "quantitative" gel electrophoresis results from the methodology now available; suitable conditions for achieving a separation are determined using computer programs, taking into account results from theoretical physical chemistry and from statistics. (Some programs are listed in the appendix, while for others a source from which they can be obtained is given in the text.) Experimental arrangements for quantitative electrophoresis are described in detail. In the author's opinion no manufacturer yet offers a system which comes near to meeting all the requirements, e.g. precise temperature control and efficient heat conduction; hence the advice is to build one's own. Following a precise account of the properties of polyacrylamide and agarose gels, the many different available buffer systems for running these gels are described. This leads to a detailed plan for determining the "happiness conditions" which apply to the protein to be isolated, i.e. those conditions under which the protein will retain its native form during its passage through the system. From the determination of the optimal concentration, degree of cross-linking of the separating gel, and pH value, the computer program is used to define conditions for fractionation by PAGE, electrofocussing or isotachophoresis.

The book is arranged in a clear way, and is provided with a carefully compiled index and an extensive appendix. Information on a specific application can be found without difficulty by using the detailed contents list, and the many cross-references give rapid and precise access to important additional information. This book will probably be too complicated for someone wishing to carry out a gel electrophoresis for the first time. For all others, though, who daily encounter problems of protein separation, and are not regular readers of *Electrophoresis*, it will certainly provide useful ideas for new experiments, and open up the possibility of using an advanced technique.

Harald Herrmann [NB 783 IE]
Institut für Biochemie
der Universität Wien (Austria)

Corrigendum

The title of the communication by C. A. McAuliffe, B. Beagley, G. A. Gott, A. G. Mackie, P. P. MacRory, and R. G. Pritchard, *Angew. Chem. Int. Ed. Engl. 26* (1987) 264 should read "Structure of Triphenylarsanediiodine, $[Ph_3As \cdot I_2]$, a Compound Formed in the Thermal Decomposition of $[Mn(OAsPh_3)_3I_2(SO_2)_2]$."

Registered names, trademarks, etc. used in this journal, even when not marked as such, are not to be considered unprotected by law.

© VCH Verlagsgesellschaft mbH, D-6940 Weinheim, 1987. – Printed in the Federal Republic of Germany by Zechnersche Buchdruckerei, Speyer/Rhein.

All rights reserved (including those of translation into foreign languages). No part of this issue may be be reproduced in any form – by photoprint, microfilm, or any other means – nor transmitted or translated into a machine language without written permission from the publishers. Only single copies of contributions, or parts thereof, may be made for personal use.

Valid for users in the USA: The appearance of the code at tbe bottom of the first page of an article in this journal (serial) indicates the copyright owner's consent that copies of the article may be made for personal or internal use, or for the personal or internal use of specific clients. This consent is given on the condition, however, that the copier pay the stated per-copy fee through the Copyright Clearance Center, Inc., for copying beyond that permitted by Sections 107 or 108 of the U.S. Copyright Law. This consent does not extend to other kinds of copying, such as copying for general distribution, for advertising or promotional purposes, for creating new collective works, or for resale. For copying from back volumes of this journal see 'Permissions to Photo-Copy: Publisher's Fee List' of the CCC.

Editorial office: Pappelallee 3, D-6940 Weinheim, Federal Republic of Germany, Telephone (06201) 602315, Telex 465516 vchwh d, Telefax (06201) 602328.

Editor: *P. Gölitz.*

Associate editors: *D. I. Loewus, A. Stimson.* **Editorial assistant:** *E. Schweikart*

Publishers: VCH Verlagsgesellschaft mbH. (Managing Directors: *Prof. Dr. Helmut Grünewald* and *Hans Dirk Köhler*), Pappelallee 3, D-6940 Weinheim, Federal Republic of Germany. Correspondence concerning advertisements should be addressed to VCH Verlagsgesellschaft mbH. (Advertising Manager *R. J. Roth*), Boschstr. 12, P.O. Box 1260/1280, D-6940 Weinheim, Federal Republic of Germany, Telephone Weinheim (06201) 602-0, Telex 465516 vchwh d, Telefax (06201) 602328.

ANGEWANDTE CHEMIE
International Edition in English
Volume 26 · Number 5
May 1987
Pages 371–488

The Importance of Chemistry in the Development of High-Performance Ceramics

By Fritz Aldinger* and Hans-Jürgen Kalz

Dedicated to Professor Heinz Harnisch on the occasion of his 60th birthday

Due to their mechanical, thermal and chemical stability, high-performance ceramics have a range of properties which makes it possible in many fields to go beyond the limits of use of the various classes of materials nowadays available. In spite of this favorable starting situation, the worldwide endeavors to introduce this new group of materials have suffered some setbacks in both conventional applications and in new technologies. The ultimate reason is that these materials are very brittle. After the introduction of fracture mechanics, designers in many fields have learned how to handle brittle materials and how to exploit the potential of their properties in components subject to extreme loadings. Materials scientists have also been very successful in developing ceramics with high strength and fracture toughness characteristics. Nevertheless, the field of use has hitherto been restricted, since, in many cases, the reliability of the components is inadequate. Small and very small defects, such as micropores and cracks, as well as any other chemical and physical inhomogeneity in the structure can cause catastrophic failure of the components due to the high brittleness. Since, on the one hand, these defects are as a rule caused by inadequate control of the process sequences and, on the other, the production processes comprise a large number of chemical process steps, it is to be hoped that consistent application of the way of thinking and procedures of a chemist will make an important contribution in overcoming these difficulties.

1. Introduction

Ceramics are nonmetallic inorganic materials. Conventional ceramics have been used from prehistoric times and, for example in the form of fired clay, stoneware and porcelain, are some of the most important materials in industrial development. A group of materials based on certain specific oxides, nitrides, borides and carbides has only recently gained technological importance or is even still at the development stage with regard to future possible applications.[1,2] Some of the most important representatives of this group of materials, which are frequently called high-performance ceramics, are listed in Figure 1. They are attractive because of their unique combination of properties. They share mechanical strength, hardness and wear resistance coupled with high thermal and chemical stability and low density. Most of them are electrical and thermal insulators—but some combine a high electrical resistance with a high (Al_2O_3, Si_3N_4) and in some cases even a very high (AlN, SiC, BeO) thermal conductivity. Some are distinguished by semiconductor properties (SiC) or ion conductivity (ZrO_2), and others exhibit ferromagnetism (ferrite) or piezoelectricity ($PbZr_xTi_{1-x}O_3$) and advantageous dielectric properties ($BaTiO_3$) or are even optically translucent under certain conditions (Al_2O_3).

[*] Dr. F. Aldinger, Dr. H.-J. Kalz
Hoechst Aktiengesellschaft
Postfach 800320, D-6230 Frankfurt am Main 80 (FRG)

 © VCH Verlagsgesellschaft mbH, D-6940 Weinheim, 1987 0570-0833/87/0505-0371 $ 02.50/0

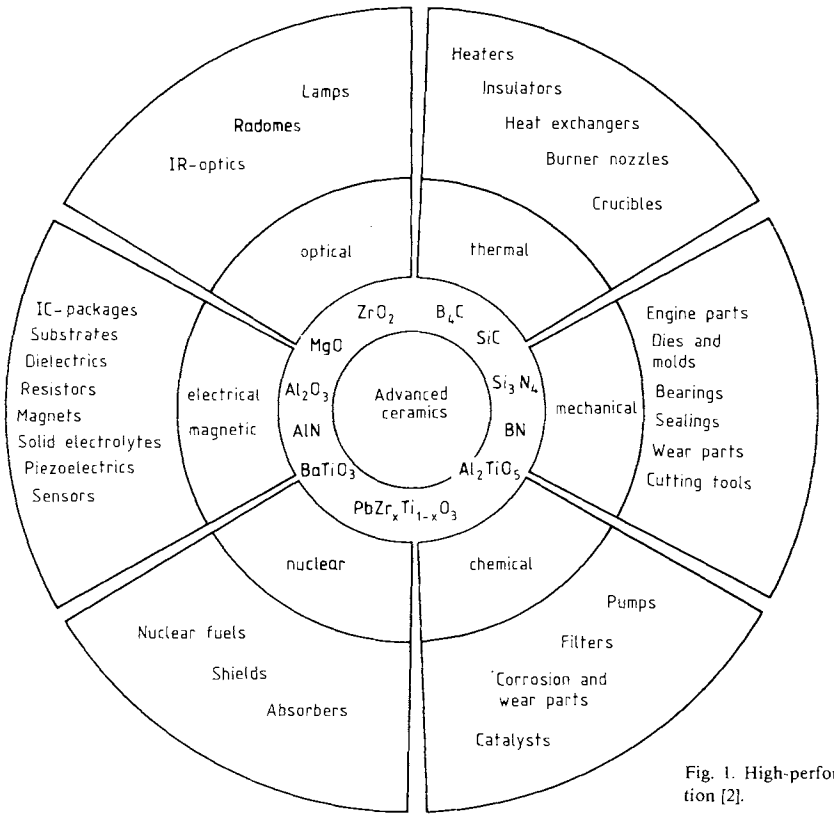

Fig. 1. High-performance (advanced) ceramics and some fields of application [2].

The possible applications, which are subdivided in Figure 1 according to various functions, are considerably diverse. The most important applications, apart from in a wide variety of electrical/magnetic components, are in the field of microelectronics as substrates for integrated circuits. A considerable increase in the use of these materials in engine and machine construction, in chemical process engineering, and in thermal engineering is expected in the future.

However, high-performance ceramics are not only novel with respect to their chemical composition and structure but, compared with conventional ceramics, impose completely new requirements in respect of absolute control of the preparation of the material. Only if starting powders of well defined composition and purity as well as controlled particle morphology are used, and only if all working steps for the preparation of parts (Fig. 2) are carried out under strictly controlled conditions is it possible to obtain the desired performance features in high-performance ceramics.

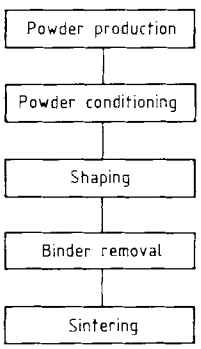

Fig. 2. Process diagram for the production of ceramics.

By contrast, imperfect production conditions lead as a rule to component faults and structural faults, i.e. to products of restricted quality and reliability.

Component faults such as, for example, unduly wide tolerances in the component dimensions, distortion, unevenness as well as surface defects and excessive roughness, cavities and scratches can be eliminated only by considerable subsequent effort or not at all. As a result, the use of such components is as a rule impossible or uneconomical.

Structural faults such as, for example, pores, microcracks, inclusions, i.e. any kind of chemical and physical inhomogeneities, can have adverse consequences when the component is subjected to mechanical stress.[3,4] Due to the extreme susceptibility of ceramics to brittle fracture, such faults lead as a rule to catastrophic failure by fracture even if they are very small (for example 20 to 50 μm) and even under low mechanical stresses. The reason is that stress intensities which are not degradable by plastic flow—as in the case of ductile materials—arise at the structural defects. Consequently, the fracture stress of the material can be reached locally, even if the total stress is far below the fracture strength of the undisturbed material. Since it is known that the stress intensities arising increase with the size of the structural defects, the largest defect present ultimately determines the strength. The strength of the ceramic component is therefore not a constant but a statistical parameter which depends on the type and population of defects (Fig. 3).

Reliable avoidance of defects in ceramics is no mean task in production. Table 1 shows the diversity of the defects which can arise during the most important process

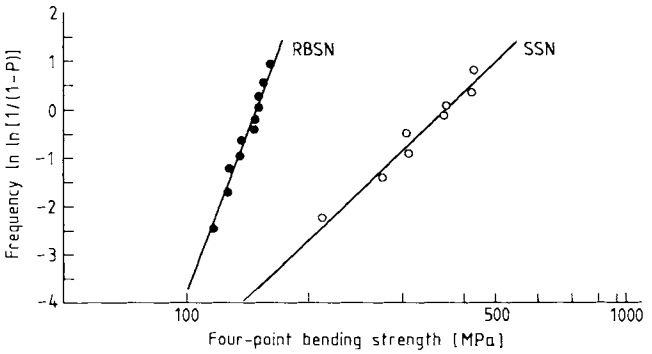

Fig. 3. Typical Weibull distribution of the flexural strength of reaction-sintered (RBSN) and normally sintered (SSN) silicon nitride [2]. P = population.

steps in ceramics production. Since many of the process steps are based on chemical process methods and procedures—as will be illustrated in detail below—avoidance of these defects and hence the economic production of ceramic components is highly dependent on the control of the chemical processes. Chemistry therefore plays a dominating role in solving the existing problems, i.e. its importance in implementing the possible applications of high-performance ceramics is substantially greater than, for example, in the case of the metallic materials which compete with ceramics.

Table 1. Defects in different stages of the processing of ceramics.

Powder	Conditioned powder	Green compact	Sintered parts
Unsuitable particle size distribution	Unsuitable agglomerate size distribution	Flows	Flows
Unsuitable mean particle size	Hard agglomerates	Void clusters	Voids
Nonuniform particle size	Hollow agglomerates	Cavities	Void clusters
Non-equiaxed particle shape	Regions of different density in agglomerates	Insufficient green density	Large voids
Deviations in the composition	Pores in agglomerates	Inhomogeneity in density	Cavities (cavity cracks)
Uncontrolled impurities	Unsuitable viscosity	Inhomogeneity in sintering additives	Circumferential cracks
Foreign particles	Insufficient inert phase suspension	Inhomogeneity in organic distribution	Unsuitable grain size distribution
Oversize particles	Inhomogeneity in additive distribution	Seggregations (inert phase, small particles etc)	Coarse grains
Hard agglomerates	Unstable suspension (sedimentation, flocculation)	Incomplete binder removal	Exaggerated grain growth
	Low inert phase content	Organic inclusions	Zones of different grain size
	Organic inclusions	Dirt	Unsuitable grain boundary phase distribution
		Texture due to particle shape	Second phases (free Si, free C, etc)
			Inclusions
			Surface roughness

Therefore, the chemical aspects in the individual process steps are analyzed below, and a few examples demonstrate the success which is expected or has already been achieved by the consistent application of chemical procedures.

2. Powder Preparation

The first step in the production of ceramics (Fig. 2) is the powder preparation. For ceramics, this is exclusively carried out by chemical processes. A well-known example is the Bayer process which converts bauxite to Al_2O_3. In the western world alone, about 25 million tonnes of Al_2O_3 is produced per year in this way, of which about 2% is processed further to give ceramic components (excluding refractory materials).[5]

2.1. Processes

The processes for the preparation of ceramic powders are very diverse. Depending on the type of starting components and on the requirements of the powders to be produced, different processes are used. Table 2 shows a few examples arranged according to the physical states of the starting compounds. More recent methods, for example powder preparation by the sol/gel process,[6] alkoxides,[7] organosilicon compounds[8] and hydrothermal synthesis[9] can also be included in this table. Supplementary process steps such as, for example, the calcination of intermediates or the processing of raw materials are not separately listed in the table.

Table 2. Preparation of ceramic powders.

Physical states [a] of the starting components	Example
Solid - Solid	Al_2TiO_5 from Al_2O_3 and TiO_2
Solid - Solid - Gaseous	AlN from Al_2O_3, C and N_2
Solid - Liquid	TiO_2 on Al_2O_3 from Al_2O_3 and $Ti(OR)_4$
Solid - Gaseous	Si_3N_4 from Si and N_2
Solid	MgO from $MgCO_3$
Liquid	Al_2O_3 by Bayer process
Gaseous	SiC from CH_3SiCl_3
Gaseous - Gaseous	SiC from SiH_4 and C_2H_4
Liquid - Liquid	Si_3N_4 from $SiCl_4$ and NH_3
Gaseous - Liquid	Si_3N_4 from $SiCl_4$ and NH_3

[a] Including multi-component systems, for example solutions.

The requirements to be met by the powders, and hence by the preparation processes, cannot be generalized. In each case, however, the process parameters of the diverse preparation processes must be controllable to the extent that powders of defined purity can be produced and specific requirements with regard to powder characteristics, for example particle shape and size distribution, can be met. In selecting the procedure, it is a fundamental condition that the economics, i.e. the acceptable cost of the manufacture of a product, must always be borne in mind. The procedure for the synthesis of specific powders therefore not only differs from one ceramic to another, but also from process to process. The chemist can, for example, control a process by way of the following parameters: by choice of starting components (anions of the metal salts, precipitants), of solvents, and of concentrations, and by the kinetics of hydrolyses, polymerizations (oligomerization) and crystallization.

As an example, the preparation of silicon nitride powders, which are intended especially for use in the engineering ceramics field, will be discussed. Such ceramics should exhibit very high strengths (for example 800 to 1200 MPa) at high temperatures (for example 1200 to 1400 °C). From experience gained so far this is best accomplished with powders which meet the following requirements:

mean particle size < 1 μm
narrow particle size distribution
equiaxed particles
95% α-modification
impurity contents for metals $< 0.1\%$, carbon $< 0.2\%$, oxygen $< 1.5\%$

In principle, four routes are presently available for the industrial production of silicon nitride powder:

Nitriding of silicon

$$3\,Si + 2\,N_2 \longrightarrow Si_3N_4 \quad (a)$$

Carbothermal nitriding

$$3\,SiO_2 + 6\,C + 2\,N_2 \longrightarrow Si_3N_4 + 6\,CO_2 \quad (b)$$

Gas phase reactions

$$3\,SiCl_4 + 4\,NH_3 \longrightarrow Si_3N_4 + 12\,HCl \quad (c)$$
$$3\,SiH_4 + 4\,NH_3 \longrightarrow Si_3N_4 + 12\,H_2 \quad (d)$$

Thermal decomposition of silicon diimide

$$3\,SiCl_4 + 6\,NH_3 \longrightarrow 3\,Si(NH)_2 + 12\,HCl$$
$$3\,Si(NH)_2 \longrightarrow Si_3N_4 + 2\,NH_3 \quad (e)$$

Each of these processes gives powders of special characteristics. The main impurities in each case are oxygen and carbon. In the direct nitriding of silicon [eq. (a)], the powders must be ground during the preparation. This could give rise to additional impurities. The same risk also exists in the carbothermal process [Eq. (b)]. Although the products obtained by the gas phase reaction [eqs. (c) and (d)] can exhibit high degrees of purity, there are problems with respect to the grain morphology. It is difficult to adjust the parameter profiles in the reaction zone—agglomerations, whisker formation and inhomogeneous particle size distributions are the consequences. Attempts have been made to overcome these problems, for example by decomposing the products in laser light.[10] The powders obtained in this way are very homogeneous and not agglomerated. However, production on a larger scale by this method has so far not been reported. In the synthesis according to equation (e), by-products are formed which can likewise lead to impurities (NH_4Cl).

2.2. Impurities

Aside from the overall purity, it is above all necessary in powder preparation that the impurities inherent in the preparation, namely oxygen, carbon, aluminum, calcium and iron, be generally controlled. Although a high oxygen content facilitates compaction on sintering, due to glass formation, an excessive glass content reduces the high-temperature strength of the sintered bodies. Moreover, a thick oxide layer on the particle surfaces reduces the sinter activity of a powder. Suitable powders have in general an oxygen content of $< 1.5\%$. Carbon makes compaction more difficult since, on sintering, it reduces the oxygen content or the content of sinter additives by the formation of CO. Residual carbon in a sintered sample increases the susceptibility of the latter to oxidation. For these reasons, the carbon content should be $< 0.2\%$. In the sintered structure, the metallic impurities are enriched in the grain boundary phase which is responsible, to a very large extent, for the mechanical properties. Total metal contents below 0.01% are nowadays reached in good commercial powders. Hitherto, there have been few investigations of the influence of non-metals on the sintering behavior and the properties of silicon nitride.

In the case of oxygen, apart from knowledge of the bulk analysis, it is of interest for the evaluation of the powders to have information on the location of the impurities in the powder particle and on their form of bonding. Figure 4

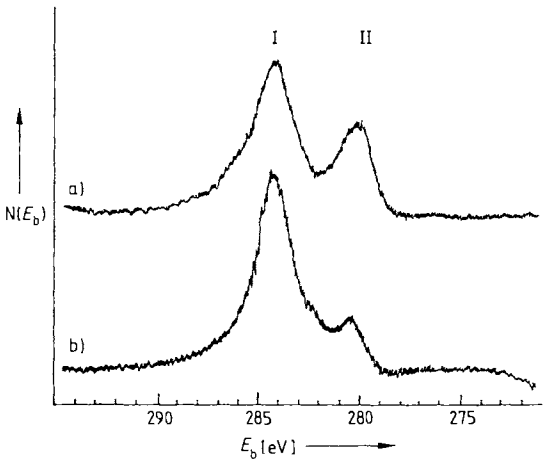

Fig. 4. C(1s)-XPS spectra of Si_3N_4 powders [11]. a) Anzon 1001. b) Ube E-10. I = graphitic carbon, II = carbidic carbon; E_b = binding energy.

shows the XPS signals of the 1s level of the carbon level in two silicon nitride powders.[11] The spectra clearly show that two different carbon species are present. One of these is graphitic carbon with a bond energy of 284–285 eV, and the other is carbide carbon (280–281 eV).

Graphitic carbon can be found on every surface exposed to the atmosphere. In general, it reacts with the residual

Table 3. Characterization of two commercial Si_3N_4 powders.

	LC 12 [a]	E 10 [b]
Elemental analysis [wt-%]		
N	38.6	39.1
Si	58.7	59.6
O	1.3	0.9
C	0.09	0.04
Fe	0.006	< 0.005
Al	0.041	< 0.01
Ca	0.012	< 0.005
Cl	–	< 0.01
Phase analysis α-Si_3N_4	≥ 95%	≥ 95%
Particle size d_{50} [μm] (Sedigraph)	0.5	0.7

[a] H. C. Starck Berlin. [b] Ube Industries, Tokyo.

oxygen in the sintering atmosphere to give volatile carbon monoxide. In contrast, carbide carbon is firmly bound. As a rule, it remains in the product and has a very pronounced influence on the properties.

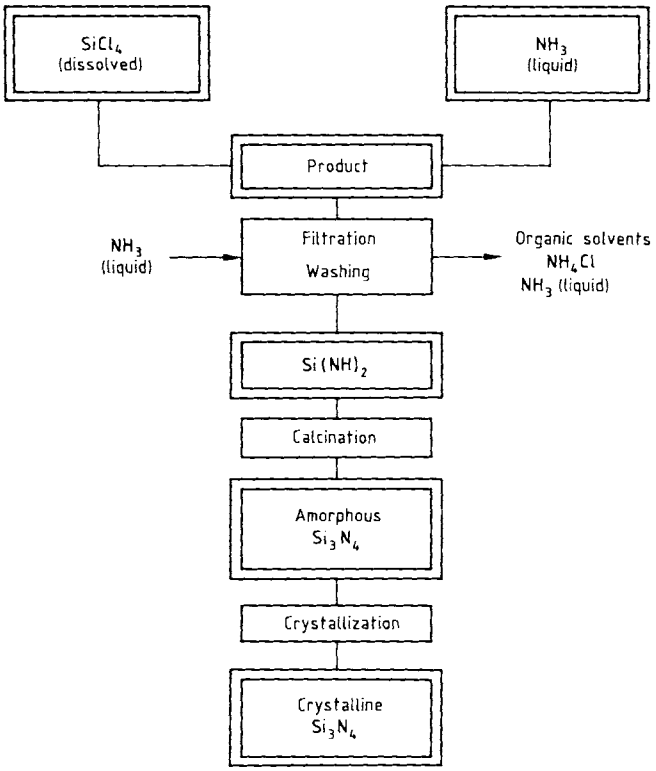

Fig. 5. Preparation of Si_3N_4 by decomposition of silicon diimide [12].

When comparing the qualities of the powders at present obtainable industrially, the impression gained is that powders prepared via direct nitriding and via the decomposition of the diimide (Fig. 5) best meet the aforementioned requirements. Table 3 shows the properties of commercially available powders which were prepared by these two processes. The particle characteristics are very homogeneous and, in particular, they are neither needle-shaped nor platelet-shaped particles, nor are there any extraneous particles visible (Fig. 6).

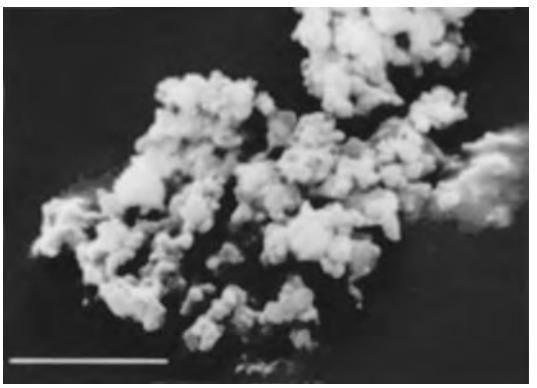

Fig. 6. Si_3N_4 powder (Ube E-10) of advantageous particle morphology. Scale mark = 2 μm.

Although, in the case of alumina ceramics, the sinter additives, frequently in the form of natural products such as kaolin, soapstone or wollastonite, can introduce impurities into the product, the alumina powder itself must also be carefully monitored, depending on the intended use. Impurities originating from the raw material or contaminations due to additives during production (for example calcining auxiliaries) can interfere with both the processing and the finished ceramics. The harmful effect of U and Th impurities is discussed in Section 3. Al_2O_3 ceramics are frequently used in the electronics sector. High insulation resistances and low dielectric constants then represent an essential part of the requirement profile. For example, sodium has an adverse effect on both these properties. In alumina ceramics of high Al_2O_3 content (>99%), impurities such as, for example, SiO_2, CaO, FeO and Na_2O, can reduce the quality of the material.

In the case of aluminum nitride, traces of oxygen (Fig. 7) and also magnesium, iron and silicon sharply reduce the high thermal conductivity of this material.[13]

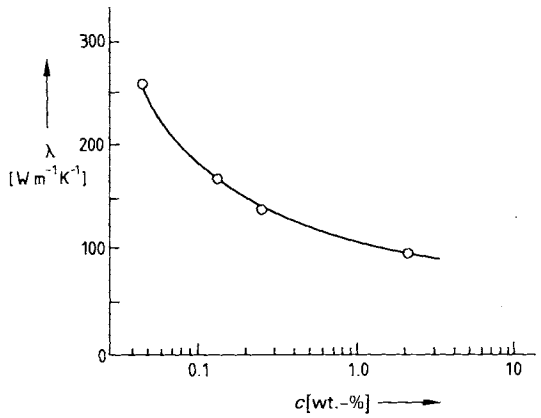

Fig. 7. Thermal conductivity λ of AlN ceramics as a function of the oxygen content c [13].

In the case of silicon carbide those impurities must above all be monitored, in addition to oxygen and carbon, which are introduced by the grinding processes during powder preparation (WC, CO, Ti, Fe). Free carbon has a deoxidizing action on the SiO_2 skins of the powder particles. Fairly large contents have a very disadvantageous effect on the high-temperature strength, particularly if they are present as lamellar graphite inclusions. Oxygen, water and oxides bind sinter additives (B, Al) and thus have an inhibiting effect on sintering. Alkali metal oxides and alkaline earth metal oxides (Na, K, Ca), which form low-melting silicates with SiO_2 and thus additionally impair the high-temperature strength, are particularly disadvantageous. Free silicon also has an inhibiting effect on sintering. Aluminum and iron, as impurities originating from the raw material, are not critical within certain limits. Iron has no substantial effect on sintering and on the strength properties. Aluminum has a getter action and is added as a sinter additive, in addition to boron. An excess of aluminum is disadvantageous, however, because it accelerates sub-critical crack growth at high temperatures.

2.3. Analysis

The composition of the powder is checked by chemical analysis. The analytical procedure for ceramic powders based on aluminum and silicon compounds will be briefly outlined.

The main constituents are analyzed as far as possible by classic wet-chemical methods. For silicon nitride and silicon carbide, the silicon is determined, for example gravimetrically,[14, 15] and aluminum in alumina is determined by complexometry (with *trans*-1,2-cyclohexylenediamine-*N*,*N*,*N'*,*N'*-tetraacetic acid (DCTE)[16]). Nitrogen is determined acidimetrically after a steam distillation, and the carbon and oxygen contents are determined by gas analysis using commercially available apparatus.[17, 18]

The accompanying metallic substances (for example B, Na, K, Mg, Ca, Al, Ti, Fe, Y, Zr) which are present in trace amounts or as secondary constituents are determined by optical methods such as, for example, atomic emission spectrometry with plasma excitation (ICP-AES) and atomic absorption spectrometry with flame excitation (FS-AAS). These methods enable the entire range of desired elements to be determined in a single sample solution. Acids or acid combinations matched as far as possible to the samples are used for digesting the samples in a bomb at elevated temperatures (250 to 320°C) under pressure and with stirring. Compared to alkalis or salts as the matrix for analysis solutions, acids always have the advantage of higher purity. This creates more favorable conditions for low determination limits, good reproducibility and a high degree of reliability of the measured data.

3. Powder Processing and Shaping

Even though powder processing and shaping are two separate working steps, they should be discussed together since they are closely interrelated. Ceramic parts are shaped by various processes (Fig. 8), depending on the form, size and required properties of the components. With a view to low manufacturing costs, the processes mainly of interest are those which involve the preparation of so-called green compacts. These are two-stage processes in which the powder is first compacted in the "cold" state, for example by tape-casting, slip-casting or dry pressing, to give a shape which is then sintered in a second step. In addition, there are processes, such as, for example, uniaxial hot-pressing or isostatic hot-pressing in capsules, where molding and sintering proceed simultaneously. However, these processes are economical only in certain cases. In particular, they appear to be inferior to the two-stage processes for the mass production of components of complicated shapes.

For every production process, the starting powders must be prepared in a suitable manner; in the narrower sense this involves the introduction of two types of additives. On the one hand, these are inorganic additives, i.e. so-called sinter additives, which promote sintering and/or are intended to vary the properties of the ceramic in a controlled manner. As a rule, these additives remain in the ceramic. In most cases they are likewise ceramic powders so that in principle the same conditions are applicable as for the matrix ceramic itself. On the other hand, substances are added which facilitate shaping or even make it possible. Aside from water, mainly organic substances are used which are highly volatile and/or combustible, so that they can be expelled again from the molding without leaving residues before the actual sintering.

3.1. Auxiliaries and Sinter Additives

The usual auxiliaries, as this group of additives is called, and their functions are listed in Table 4. The requirements

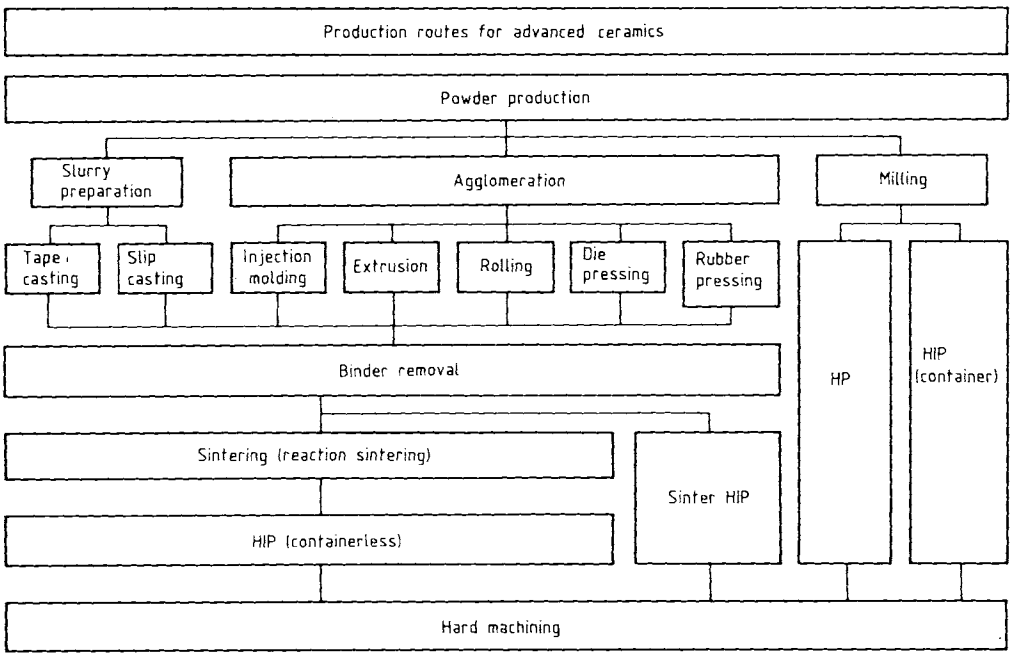

Fig. 8. Production routes for advanced (high-performance) ceramics [2].

to be met by the auxiliaries differ in the various molding processes. In dry pressing and isostatic pressing, they must essentially meet two requirements, firstly the formation of easily flowing and soft agglomerates which allow rapid and trouble-free filling of the press dies where they can be readily pressed, and secondly they must ensure good adhesion of the ceramic powder particles in the green compact, so that the strength of the latter suffices for trouble-free handling. In extrusion and injection-molding, the requirements to be met by the auxiliaries are very similar to those in dry pressing, except that substances to facilitate degassing are frequently also added in injection-molding, especially if the components are relatively large or have relatively thick walls. By contrast, slip-casting and tape-casting make completely different demands on the auxiliaries. For these molding processes, low-viscosity masses are required which dry rapidly after casting without the components distorting or cracking. In addition, easy separation from the tape carrier or the casting mold must be possible. In all cases, the green compacts should be easy to handle, i.e. they must have sufficient strength for further processing. This is in particular a major requirement whenever mechanical working of the green compacts is to be carried out, for example, by sawing, cutting, turning, milling or punching.

These general requirements to be met by the auxiliaries are very complex in individual cases, so that the demand for fault-free production presupposes a deep understanding of the interaction of the auxiliaries with one another, with the dispersed ceramic powders, and with the mold materials. Absolute control of molding and the production of perfect components is possible only with an exact knowledge of the composition of the molding masses and the influences of the processing parameters on their phase composition, structure, and rheological behavior.

These problems will be explained in more detail, taking tape-casting as an example. This forming process is nowadays used on a large scale throughout the world for the production of thin alumina plates as substrates for the mounting of electronic circuits (Fig. 9).

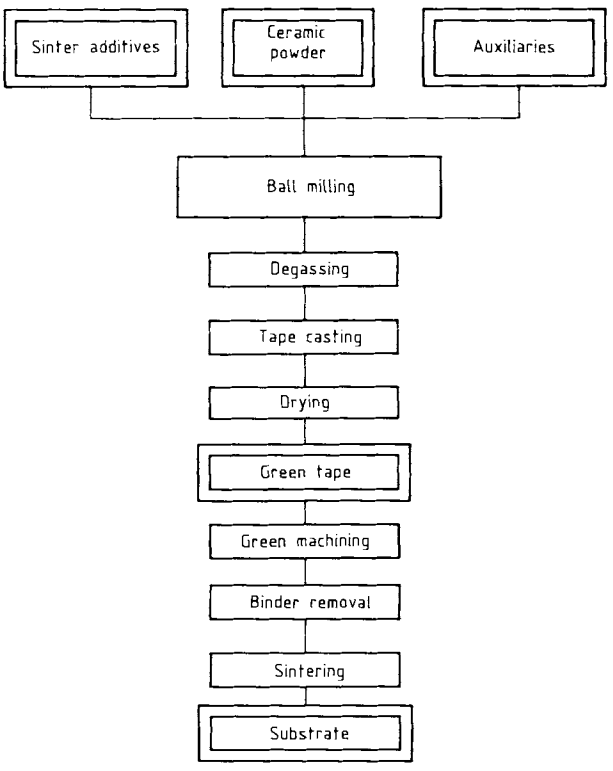

Fig. 9. Process diagram for the production of substrates for electronic circuits.

A low-viscosity casting mass (of about 5 to 20 Pa s) is prepared from the ceramic powders and the admixed sinter additives together with the auxiliaries; this can then be cast by the so-called doctor-blade process (Fig. 10) in which it is applied via the casting head to a tape carrier,

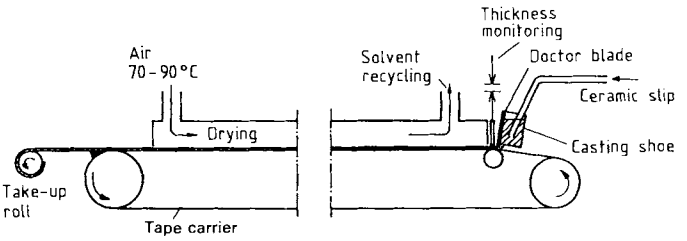

Fig. 10. Sketch of a production unit for ceramic green tapes.

i.e. an endless strip of steel or a polyester film. Between the casting head and the tape carrier, there is, in the direction of casting, a narrow gap (0.5 to 1 mm) which is adjustable by means of a blade (doctor blade) and by means of which the thickness of the tapes is controlled. After passing the doctor blade, the mass passes through a drying section where the solvent evaporates and a leathery sheet is formed. At the end of the drying section, the sheet is taken off the tape carrier and wound, for example on reels. The dimensions of such tape casting machines are about 20 to 25 m in length and about 1 m in width. Typical casting rates are about 0.5 to 2 cm s^{-1}.

The casting masses which can be processed by this method represent a very complex system. The starting point for a suitable formulation is in every case an alumina powder, with which the requirements to be met by the finished product can be fulfilled. In general, powder qualities of a mean particle size of 2 to 3 μm, a not unduly wide particle size distribution and a specific powder surface area of about 2 $m^2 g^{-1}$ are used. The purity is normally higher than 99.7%.

In spite of the high purity of the matrix powders, it is still usual to use natural products as the sinter additives. These are as a rule silicates such as kaolins, talcs, wollastonites and, for special applications, also zircon. Alternatives are carbonates and also basic carbonates. However, the natural substances have the disadvantage of impurities and of a composition which is not reliably constant from one charge supply to the next. Moreover, there are also problems with respect to the particle size properties as compared with the frequently very fine matrix powders.

The traces of uranium and thorium frequently present in kaolin, soapstone and zircon are very disadvantageous for applications in electronics. The α-radiation generated in the decay of these elements leads to the feared "soft er-

rors" in memory components.[19] A further problem in processing the natural layer silicates such as kaolin or talc is the loss of structural water in the temperature range from 600 to 900 °C. This is the range in which usually high rates of heating are used. There is therefore a fear of such effects damaging the microstructure of the ceramic components which are not very strong in this temperature range (at this point, there are no longer any "binding" organic constituents present), and this can later lead to defects in the ceramic product.

A sustained improvement can be achieved by using synthetic sinter additives such as oxides and silicates of calcium, magnesium, aluminum and zirconium. An advantage of the synthetic materials is that the release of water takes place at lower temperatures (<400 °C) than in the case of the natural sinter additives which contain structural water. Furthermore, with the synthetic additives a controlled surface treatment, e.g. a modification of the surface by means of auxiliary components such as dispersing groups is simpler. There are a number of classes of compounds which can be bonded, for example to silica surfaces, by chemical reactions, such as, for example, alcohols, esters, alkoxy compounds, and silanes.[20,21]

3.2. Examples of Auxiliaries and Their Uses

The conventional auxiliaries and their functions are listed in Table 4. Their nature and composition depends finally on the ceramic constituents. For casting masses for the production of a standardized material of 96% of alumina and further phases composed of SiO_2, MgO and CaO, the following composition has proved suitable (data in wt.-%):[22]

65% of ceramic substances
3% of binder (poly(vinyl butyral))
3% of plasticizer (dioctyl phthalate)
1% of dispersant (fish oil)
28% of dispersing agent (trichloroethylene/ethanol)

Table 4. Auxiliaries for the shaping of advanced ceramics.

Shaping	Auxiliaries	Function of the Auxiliaries
Dry pressing	Polyacrylates, huminates	Dispersants
	Polyvinyl alcohols, tylose, waxes	Binders
	Polyethylene glycols	Lubricants
Slip casting	Polyacrylates, fish oil	Dispersants
	Polyvinyl alcohols, mod. polysaccharids, polyvinyl butyrals	Binders
	Water, trichlorethylene, ethanol	Dispersing agents
Tape casting	Oleates, polyacrylates, phosphate esters	Dispersants
	Poly(vinyl butyrals), polyvinyl alkohols), polyacrylic resins, emulsions,	Binders
	Phthalates, polyethylene glycols, phosphate esters,	Plasticizers
	Toluene, trichlorethylene, methanol, methyl isobutyl ketone, water	Dispersing agents
Injection molding	Oleates, polyacrylates	Dispersants
	Polyethylene, polystyrene, waxes,	Binders (dispersing agents)
	Polyethylene glycols	Lubricants
	Caster oil	Baking aids
Extrusion	Polyacrylates	Dispersants
	Polyvinyl alcohols, tyloses	Binders
	Polyethylene glycols, glycerine	Lubricants

Initially, the ceramic constituents must be dispersed in a liquid phase. In the present example, an organic dispersing agent is chosen for this purpose. For absolute reproducibility of the processes, complete dispersing of the powders is absolutely necessary, and this is ensured by the use of dispersants, in addition to mechanical processing.

The choice of suitable *dispersants* is not easy and depends on both the nature of the powder surface and on the type of dispersing agent. There are particular problems when different powder species or sinter additives are used in a mass, where optimum dispersing of all the powders is not possible with a single dispersant. Should this be the case, and the use of several dispersants becomes necessary, there is a risk of mutual interaction of the dispersants, whereby the entire system may be destabilized. In this case, it is possible to use surface-modified powders (see Section 3.1) and thus to avoid these difficulties. Before choosing the dispersant, it is advisable to characterize the surfaces of the solids. In addition to the usual powder particle characteristics such as the BET surface area and the particle size distribution, a knowledge of the chemical properties of the powder surface is necessary.

Measurements of the potential in organic solvents are often difficult. Hence, microcalorimetric and potentiometric titrations in neutral solvents can provide supplementary information on the sign and quantity of charges on the powder surface. A further assessment of the ease with which, for example, surface-active substances carrying P=O, C=O, OH or NH groups (for selection of the dispersants) can be added to the powders can be obtained by measuring the band shift of those groups in FTIR spectra (measurement in diffuse reflection) as compared with the isolated substances.

Moreover, the effect of dispersants can also be evaluated via the sediment volumes by means of sedimentation tests on dispersions, which are easy to carry out. Rheological measurements of the dispersions give further indications. A dispersant which is very frequently used in the preparation of substrates is fish oil.[23]

The choice of *dispersing agent* depends above all on its dissolving capacity, on the binder, and on the temperature level in use. Other important aspects relate to safety, the environment, and the price.

A very frequently used dispersing agent is trichloroethylene in conjunction with ethanol. The addition of ethanol is necessary in order to raise the solubility of the organic binders used here. The mutual ratio of the two organic solvents is in the range of the azeotropic mixture (27% ethanol, 73% trichloroethylene, boiling point 72.9 °C).

Regarding the quality of the solvent, it goes without saying that the requirements in respect of purity are exacting.

In the case of ethanol, the composition (denaturant, water) must be carefully checked, since any change affects the rheology of the casting slurry and jeopardizes the reproducibility of the process. As a result of these requirements, for example, solvent recovery or solvent-reuse involve considerable difficulties.

Since, in addition, the solvents are either flammable and/or cause environmental problems, work is proceeding on the substitution of the organic solvents by water. Apart from the advantage of compatibility with the environment and the safety aspects, however, water has the disadvantage of lower volatility, so that drying takes longer. Of course, the use of water also involves different binder systems, which entails a large number of difficulties. For example, many of the available plastics dispersions have such a tendency to foam that complete removal of occluded air from the tape-casting mass raises problems. Cracks in the green tape are then the consequence. For these reasons, water-based systems for substrate preparation are not yet generally available.

To ensure adequate strength of the desired ceramic green tape—for example it must be workable by punching and notching steps—*binders* are added. Poly(vinyl butyral) has proven suitable for the preparation of ceramic Al_2O_3 substrates and IC packages. Poly(vinyl butyral) is produced from poly(vinyl alcohol) and butyraldehyde; the molecular weights of the products of interest are 30000—80000. Not all the OH groups of the poly(vinyl alcohol) are acetalized, and about 19% of the compound is in the form of poly(vinyl alcohol). Since these groups compete with other surface-active compounds (dispersants) and can undergo interactions with the ceramic particles, strict adherence to the chemical composition and molecular structure is here again necessary for reproducibility of the process. Small changes in the molecular structure can lead to changes in the density of the green tape, and these cause problems with the dimensional accuracy of the finished ceramic components.

The poly(vinyl butyrals) used have a glass transition temperature of 50°C. For this reason, *plasticizers* are added, which reduce the glass transition temperature down to the range of room temperature or even down to below 0°C. Easily workable tapes are obtained only in this way. Tape parameters such as, for example, the tear strength and extensibility can be controlled and adapted to the requirements of working the green product by means of an adroit combination of the quantities of binder and plasticizer and also the types of plasticizer. Usual plasticizers are dioctyl phthalate, dibutyl phthalate, benzyl butyl phthalate, and phosphate esters.

Other important parameters affecting the formulation of the casting mass are the drying and adhesion of the sheets to the tape carrier. Thus, for example, formation of a skin on the cast tape must be avoided, since it would impede the healing of casting defects and drying.[24] Sticking of the sheet to the tape carrier can be avoided by a suitable choice of the carrier material and/or by means of additives to the casting mass. Sticking to glass substrates can be reduced, for example, by the use of binders showing an acid reaction (after aging, the glass surface has an acid reaction).

Furthermore, apart from high flexibility, extensibility and tear strength, the sheet must have good storage stability, i.e. the structure of the binder phase should no longer change after drying. All these requirements make it clear that the tape-casting process gives products of constant quality only if detailed knowledge of the chemistry of casting masses has been exploited.

4. Finishing of Ceramics

The production of ceramics is concluded by a temperature treatment, in which essentially two processes take place. First, the auxiliaries added for molding must be "expelled" again from the green compact, i.e. they must be vaporized and/or burned. This process step—frequently called baking—takes place at moderately elevated temperatures and is in general complete at 600 to 700°C. In the second step, the so-called sintering which is carried out in the temperature range between 1200°C and 2300°C, the components are "fired". In this stage, the individual ceramic powder particles sinter together, and a more or less dense body having the known outstanding mechanical properties is formed.

4.1. Baking

The removal of the auxiliaries by *baking* must be carried out with great care, that is to say they must be removed quantitatively before the components undergo dense sintering, since even minute residues have as a rule a very detrimental effect on the mechanical properties of the materials. A forced procedure also involves the risk of an uncontrolled loss of mass or sudden melting of the binder phase causing irreparable damage (cracks) to the components, thus reducing the yield. If, on the other hand, baking is carried out too carefully, the process sometimes takes a long time, and this above all adversely affects the cost. The aim is therefore an optimized baking rate for obtaining components which are free of residues. This presupposes an exact knowledge of the reactions which occur during baking, and of their kinetics.

As explained in Section 3, the formulations for the individual forming processes involve a fair number of auxiliaries, some of which belong to very different classes of substances (Table 4). The reactions during baking and the time curve of the loss of mass as a function of temperature can be correspondingly complicated. Figure 11 shows the result of a thermogravimetric investigation, taking the example of a green tape composed of a mass system which is similar to that shown in Section 3.

The reaction starts at about 200°C and is complete at about 500°C. As can be seen from the diagram, the weight loss is not uniform at a given constant heating rate, but shows a maximum weight loss at about 220°C. In addition, the thermogravimetric investigation indicates the occurrence of several reactions.

The aim of every process development is uniform baking, i.e. a mass loss which is constant in time. There are two different possibilities for solving this problem. On the one hand, baking can be extended over a wider tempera-

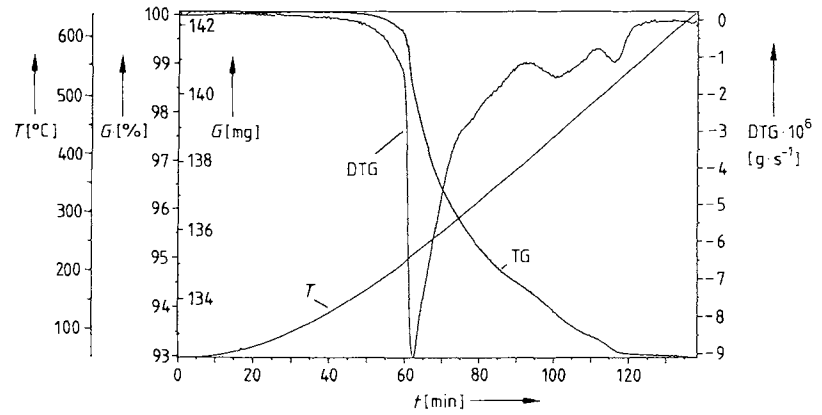

Fig. 11. Thermogravimetric (TG) investigation of an Al_2O_3 green sheet (heating rate 5 °C/minute in air). The result of the differential thermogravimetric analysis (DTG) is also shown. The absolute weight G of the sample and the weight relative to the initial weight are given.

ture range by means of a suitable blend of different types of binder and plasticizer. On the other hand, the temperature/time profile on heating up can be chosen such that the mass loss per unit time is constant over the entire reaction range. In general, this leads to temperature programs with widely fluctuating heating rates. In the case of highly exothermic reactions, temporary cooling phases may even be necessary.

Apart from the thermogravimetric and thermoanalytical investigations already mentioned, mass spectroscopic methods in particular are suitable for establishing optimized temperature programs for baking. Especially if carried out simultaneously, these investigations provide information on the reaction products and the type of reactions.

The ultimate technical and economic importance of knowledge of the processes during baking becomes clear from the example of the injection-molding of large and thick-walled components. For exhaust gas turbocharger wheels of, for example, silicon nitride, baking periods of several weeks or even months may become necessary because of high proportions of binder—particularly in the case of large wheels. The development of new mass systems with a chemical composition and reaction kinetics which allow rapid baking of the molded components without leaving any residues, is therefore of prime importance for ceramic high-performance materials. This problem can be solved only with the aid of a fundamental knowledge of the chemistry of these systems and their reaction kinetics.

4.2. Sintering

In the final high-temperature treatment—the actual sintering—the moldings are given their final properties. As already mentioned, the individual ceramic powder particles sinter together in this step. The driving force for this process is the reduction of the specific surface area of the compacted powder. The material transport occurring at this stage can proceed by very different mechanisms. In principle, these are diffusion processes, and the shares of surface diffusion, grain boundary diffusion and volume diffusion can differ widely for the individual types of ceramics. In addition, gas transport reactions may make an important contribution to the densification process. Since these are thermally activated transport processes in every case, the share of the individual mechanisms and hence the rate of densification are very highly dependent on the temperature.

The sinter additives, and especially those which form liquid, i.e. glassy phases, can be an important factor here. In many cases, sintering would be impossible without such additives. This is true, for example, in the case of silicon nitride, which has very low self-diffusion coefficients and the dissociation constant of which is relatively high. As a result, noticeable decomposition takes place before the temperatures are high enough for sufficient densification. This difficulty can be overcome only to a certain extent, even by working under high nitrogen pressures. The cause is the covalent structure of the silicon nitride, i.e. the strongly oriented bonds in conjunction with the extremely low self-diffusion coefficient make sintering more difficult. In general, only the simultaneous application of high mechanical pressures and temperatures, as in uniaxial or isostatic hot-pressing, is successful, that is to say processes which are economical only in exceptional cases. Information on sinter additives which noticeably reduce the diffusion coefficients is therefore indispensable.

So far, however, only additives are known with which a sufficiently fast densification takes place via the formation of glass phases. But, since the glass phases control the high-temperature resistance, i.e. greatly reduce the latter because of their limited viscosity, this approach is only sometimes successful with regard to high-temperature applications. It is not yet clear whether the current approaches to overcoming these difficulties represent a solution. For example, utilization of favorable phase equilibria is aimed at effecting dissolution of the glass phase in the matrix lattice or a devitrification, i.e. a transformation of the glass phase into crystalline phases.[25] Unfortunately, however, the results obtained so far represent only a partial success. The reason is the adverse change in the silicon nitride lattice, which accompanies the transformation of the glass phase, and/or adverse effects of the crystalline phases.

Hence the search for suitable additives which directly and significantly facilitate self-diffusion in silicon nitride still represents a major problem. For silicon carbide, boron and aluminum are known as additives which have this effect.[26] With a view to economical processes, however, the sintering temperatures of about 2300 °C are very high.

An interesting preparative variant for silicon carbide and in particular for silicon nitride is reaction-sintering. In the case of silicon nitride,[27] the starting material here is a molding of silicon powder which is nitrided at moderate temperatures (for example 1450°C) in a nitrogen atmosphere. However, the nitride being formed only partially fills the original pores so that, according to the present status, no dense samples can be prepared without additional process steps such as, for example, hot isostatic pressing.

For oxidic ceramics, which are predominantly of ionic character, sinter additives do not have this paramount importance. Here again, however, the choice of suitable sinter additives and especially their control is an important factor and, in many cases, they indirectly determine the quality of the product and the economics of the process.

5. Concluding Remarks

It is shown in this paper that, in the field of high-performance ceramics, the development of materials and the provision of reliable components crucially depend on the elucidation and control of the chemical relationships in the process steps including powder preparation. The great importance of these results is underlined by the fact that, for both the ceramic green compacts and for the fired products, no non-destructive test methods exist which would allow reliable detection of microscopically small but serious structural defects. It is therefore not always possible to pick out defective components and—if they are detected at all—these defects can be eliminated only in a limited number of cases. The emphasis of the measures to be taken is therefore on the prevention of defects, i.e. on a careful characterization of all precursors, intermediates, and finished products, combined with meticulously strict adherence to all working instructions and the particular production parameters.

A number of problems have here been discussed only briefly by reference to a few examples of selected ceramics. However, there are many fields in the high-performance ceramics sector, where a greater knowledge of chemistry is also highly desirable. Examples which may be mentioned here are questions relating to constitution and, in particular, compatibility. These are of great importance in connection with reinforcing mechanisms, i.e. the development of whisker-, fiber- or particle-reinforced ceramics. Many questions also remain with regard to the corrosion behavior in present and future applications of high-performance ceramics in engine construction and in chemical equipment manufacture. In the first place however, the raw material and process engineering aspects in the production of ceramic components are of predominant importance, and the feasibility of the numerous promising applications of high-performance ceramics crucially depends on the solution of these problems.

Received: January 29, 1987 [A 619 IE]
German version: *Angew. Chem. 99* (1987) 381

[1] H. K. Bowen, *Mater. Res. Soc. Symp. Proc. 24* (1984) 1.
[2] F. Aldinger in W. J. Huppmann, W. A. Kaysser, G. Petzow (Eds.): *Powder Metallurgy 1986/State-of-the-Art*, Schmid GmbH, Freiburg 1987, in press.
[3] R. W. Rice, *Treatise Mater. Sci. Technol. 11* (1977) 199.
[4] F. F. Lange, *J. Am. Ceram. Soc. 66* (1983) 396.
[5] G. Maczura, T. J. Carbone, *Am. Ceram. Soc. Bull. 65* (1986) 727.
[6] D. W. Johnson, *Am. Ceram. Soc. Bull. 64* (1985) 1597.
[7] H. Okamura, H. K. Bowen, *Ceram. Int. 12* (1986) 161.
[8] D. Seyferth, G. H. Wiseman in L. L. Hench, D. R. Ulrich (Eds.): *Science of Ceramic Processing*, Wiley, New York 1986, p. 354.
[9] E. Tani, M. Yoshimura, S. Somiya, *J. Am. Ceram. Soc. 64* (1981) C 181.
[10] W. R. Cannon, S. C. Danforth, J. H. Flint, J. S. Haggerty, R. A. Marra, *J. Am. Ceram. Soc. 65* (1982) 324.
[11] M. Peuckert, P. Greil, *J. Mater. Sci.*, in press.
[12] Y. Kohtoku, T. Yamada, H. Miyazaki, T. Iwai in H. Hausner, W. Bunk (Eds.): *Ceramic Materials and Components for Engines (Proc. Second Int. Symp. Lübeck-Travemünde 1986)*, Deutsche Keramische Gesellschaft, Bad Honnef 1986.
[13] N. Kuramoto, K. Nakajima, Tokuyama Soda Co. Ltd. (Tokyo), private communication.
[14] H. Biltz, W. Biltz: *Ausführung quantitativer Analysen*, Hirzel, Stuttgart 1953.
[15] J. Müseller, G. Staats, *Fresenius Z. Anal. Chem. 318* (1984) 317.
[16] R. Pribil: *Applied Complexometry*, Pergamon, Oxford 1982.
[17] R. Sulzberger, *Erzmetall 24* (1971) 123.
[18] G. Kraft, A. Kahles, *Fresenius Z. Anal. Chem. 281* (1976) 285.
[19] J. Rubin, J. Negrych: *Natural Raw Materials in Advanced Ceramics* (lecture at the annual conference of the Am. Ceram. Soc., Pittsburgh, PA, USA 1984).
[20] H. Ferch, *Chem. Ing. Tech. 48* (1976) 922.
[21] U. Deschler, P. Kleinschmit, P. Panster, *Angew. Chem. 98* (1986) 237; *Angew. Chem. Int. Ed. Engl. 25* (1986) 236.
[22] E. S. Tormey, R. L. Pober, H. K. Bowen, P. D. Calvert, *Adv. Ceram. 9* (1984) 140.
[23] P. D. Calvert, E. S. Tormey, R. L. Pober, *Am. Ceram. Soc. Bull. 65* (1986) 669.
[24] D. J. Shanefield, *Mater. Res. Soc. Symp. Proc. 40* (1985) 69.
[25] P. Greil, J. C. Bressiani, G. Petzow in S. Somiya, E. Kanai, K. Ando (Eds.): *Ceramic Components for Engines (Proc. First Int. Symp. Hakone, Japan 1983)*, KTK Scientific Publishers, Tokyo 1984, p. 228.
[26] K. A. Schwetz, A. Lipp, *Sci. Ceram. 10* (1980) 149.
[27] J. Heinrich, M. Böhmer, *Powder Metall. Int. 16* (1984) 233.

Genetic Engineering with Plants

By Peter Eckes, Günter Donn, and Friedrich Wengenmayer*

Dedicated to Professor Heinz Harnisch on the occasion of his 60th birthday

Today there are no longer any basic problems involved in isolating and characterizing plant genes. Our knowledge of the structure and function of the genes so far sequenced provides a beginning understanding of gene regulation in plants. In connection with the recently developed methods of gene transfer to plant cells, the most important application is the production of plants with new characteristics through genetic engineering. Since the genes can be transferred from any kind of plant—indeed even from any organism—completely new possibilities are opened up for plant breeding.

1. Introduction

Ten years ago molecular biologists succeeded in isolating the first structural gene of a plant enzyme.[1] Since then, developments in the field of plant molecular biology have opened up possibilities for practical applications that were previously inconceivable.

The first isolated gene, which is localized on the DNA of chloroplasts, encodes the large subunit of the enzyme ribulose-1,5-bisphosphate carboxylase (rubisco). This enzyme enables plants to bind CO_2 from the air. Indeed, the entire chloroplast DNA of tobacco has already been sequenced[2]—it consists of 155844 base pairs. Meanwhile, methods have become available for the stable transfer of foreign genes into plants; "transgenic plants" have already been obtained in numerous laboratories. In the USA, official approval has recently been given for the first field trials with plants that have been altered by genetic engineering.

The growing interest in the biochemistry and molecular biology of plants is also indicated by the increasing number of publications in this field. Industry, mainly in the United Kingdom, the United States, and Japan, has also begun to establish research groups in this area (Table 1).

Table 1. Number of companies involved in the application of biotechnology to agriculture (taken from [3]).

Country	Number
Italy	1
Federal Republic of Germany	2
France	5
Japan	12
United Kingdom	15
USA	73

Several factors are responsible for the recent successes and the growing interest in the biochemistry and molecular biology of plants. One of the most important is scientific interest in the gene structure and gene regulation of plants. Knowledge in this area lags far behind what is known about prokaryotic and animal cells.

[*] Dr. F. Wengenmayer, Dr. P. Eckes, Dr. G. Donn
Hoechst Aktiengesellschaft
Postfach 800320, D-6230 Frankfurt am Main 80 (FRG)

A further reason for the great interest in the molecular biology of plants is the close relationship between the basic knowledge obtained and its possible applications in agriculture. In principle, genes that are responsible for the expression of an important trait can be isolated from any plant or other organism and transferred into crop plants. In this way, characteristics that were not previously accessible to the classical methods of plant breeding become transferable to plants. Thus, for example, resistance genes could be isolated from exotic plants and transferred to domestic crops. Previously, genes and the corresponding characteristics could only be transferred naturally from parent plants that already possessed them. These limitations are now being overcome with the help of genetic engineering.

Scientists are also becoming more actively engaged in the molecular biology of plants because of the possibility that the knowledge obtained might help in an important way to solve the problem of worldwide famine. According to the most recent calculations of the U. S. Bureau of Statistics, the world population by the year 2000 will have risen from the present level of 4.9 billion to 6.2 billion.

The following factors have accounted for the impressive increase in food production over the last few decades:

—the introduction of new, high-yield varieties of plants
—the use of fertilizers and crop protection chemicals
—the increasing mechanization of agriculture

Crop yields will continue to increase in the future, but exponential increases such as occur in the world population will not appear. The large agricultural surpluses in the EEC and the USA at present do not represent a solution for the 80% of the world population that will be living outside Europe, the United States, and the Soviet Union in the year 2000. Especially in tropical and subtropical countries, plants with genetically engineered resistance toward pests, diseases, or stress conditions could acquire great importance.

A further consideration is that, after genetically engineered plants have been produced in the laboratory, they still have to be incorporated into cultivation programs and tested. This process takes several years, so that such plants will not be available to farmers in sufficient quantities un-

 © VCH Verlagsgesellschaft mbH, D-6940 Weinheim, 1987 0570-0833/87/0505-0382 $ 02.50/0

til the mid-1990s. Consequently, an evaluation of the possibilities of genetic engineering for agriculture must be based not on present food requirements but on the requirements anticipated for the year 2000. Of course, the problem of worldwide famine cannot be resolved solely by genetic engineering; political and sociological factors are also of decisive importance. However, genetic engineering could provide the basis for an adequate food supply in the form of high-yield and resistant plants.

2. Plant Cell Biology

The development of procedures in cell biology to regenerate plants from individual cells and to transfer genes to plant cells provided the prerequisite for the practical use of genetic engineering. Specific objectives of plant breeding could be achieved, in many cases, through the methods of genetic engineering as well as by suitable cell-biological selection procedures. Hence, this section will examine a few aspects of cell biology that are important for obtaining plants with new characteristics or for the application of genetic engineering. The techniques of plant cell cultivation that have been the focus of interest for the past decade have been described in several review articles and monographs.[4-7]

2.1. Vegetative Plant Reproduction

Plants are characterized by a large regenerative capacity. If plant shoots or segments of shoots are cultivated under suitable conditions (high humidity and absence of pathogens), these shoot segments develop roots. This asexual reproductive process, which is familiar in horticultural practice, can be carried out particularly efficiently on synthetic culture media under sterile conditions. The simplest of these culture media contain a balanced mixture of the salts and trace elements essential to plant nutrition, plus several required vitamins and suchrose.[8]

In a medium that is free of phytohormones, shoots or shoot meristems grow to complete plants. If the culture medium contains phytohormones, however, the reaction of the explant depends on the ratio of the auxin to the cytokinin concentration in the medium.[9] If both phytohormones are present in adequate concentrations, undifferentiated tissue, named callus, typically grows at the cut surface of the explant. This is true regardless of whether the explant is a leaf fragment, a piece of stem, or a root. If such a primary callus is transferred to fresh medium at regular intervals, it can be propagated for an indefinite time.

If cytokinin predominates in the medium, the formation of buds is favored, both on primary explants and on pre-

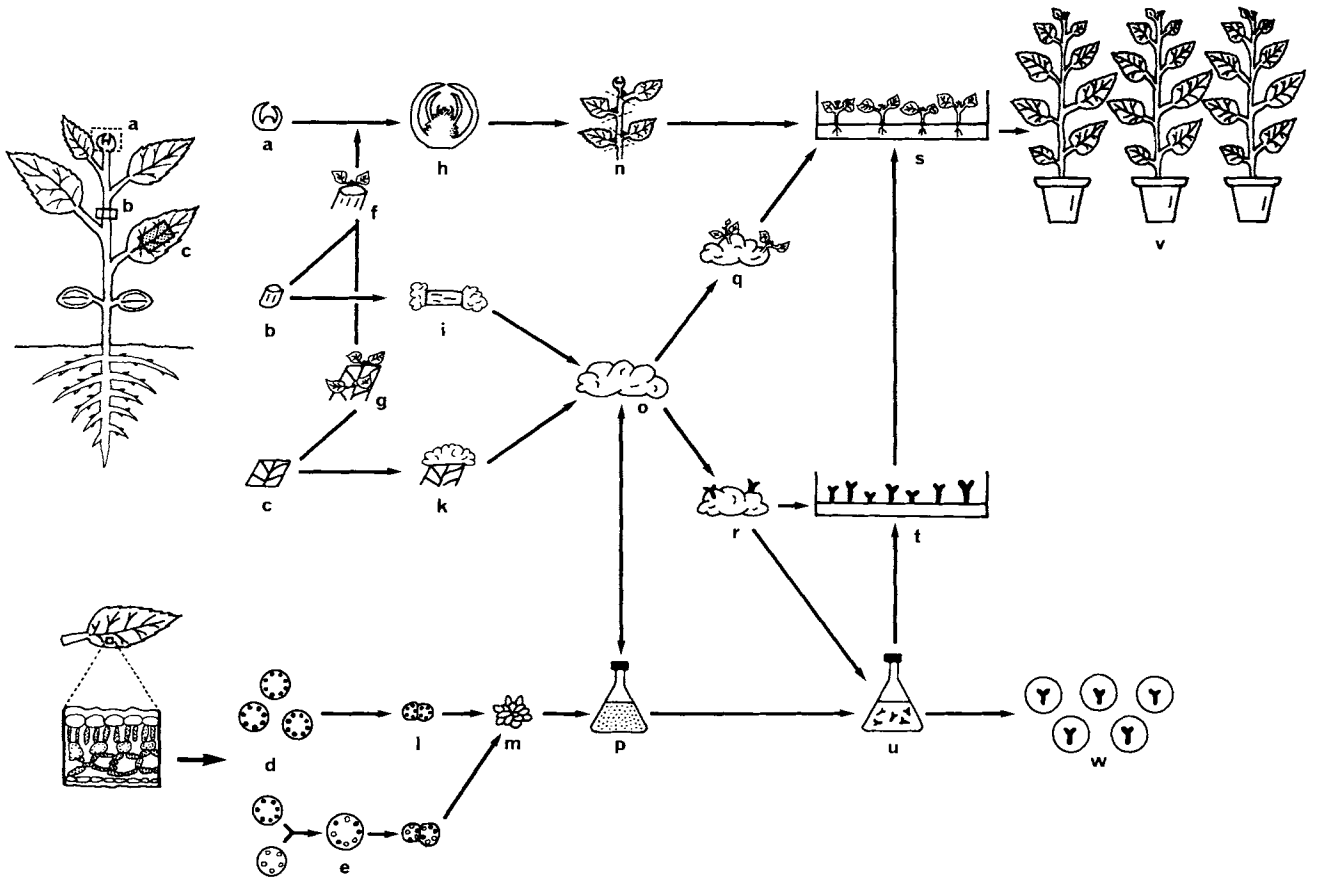

Fig. 1. Cell culture techniques used for mutant selection and production of transgenic plants. Shoot meristems (**a**), stem segments (**b**), leaf fragments (**c**), and mesophyll protoplasts (**d**) are used as explants both for the initiation of in vitro cultures and for gene-transfer methods. Through protoplast fusion, hybrid protoplasts (**e**) can be obtained. Plant regeneration may occur via shoot formation (**q**) either immediately at the explants (**f**-**h**) or at the callus stage (**i**, **k**, **o**). Alternatively, somatic embryos may develop (**r**). A cell wall is regenerated from protoplasts and cell division (**l**) begins, leading to cell clusters (microcalli) (**m**). They can be cultured as suspension cultures (**p**). In some species, the development of somatic embryos (**u**) can then be induced. On agar media, microcalli grow to form callus (**o**), which, as shown above, can undergo differentiation. If toxins, antibiotics, or herbicides are added to the media, resistant mutants or transformants can be selected preferentially at stages **f**-**p**. Shoot cultures (**n**), shoot-forming calli (**q**), and embryo cultures (**t**) are used for clonal propagation of genotypes (**s**, **v**). Under suitable conditions, somatic embryos may be converted into artificial seeds (**w**).

viously formed calli. However, the capability of a callus to differentiate depends strongly on its genotype. In some plant varieties (for example, tobacco) regeneration of a shoot, and hence of the plant, succeeds with practically every explant and even with callus that has already been cultivated for many years.[10] In other varieties (for example, soybeans), on the other hand, shoot regeneration from established callus cultures is not successful.

Regeneration from shoots is a prerequisite for the production of transgenic plants by the usual methods (Section 3). Alternative routes to shoot regeneration are shown in Figure 1. Shoots cultivated in vitro on culture media containing a cytokinin produce adventitious shoots, so that within a short time thousands of individuals of the same genotype can be produced from a single shoot. This method of vegetative propagation has so far proved economical for only a few types of plants (ornamental plants, potatoes[11]) because of the expensive manual labor required.

In a number of crop plants, including alfalfa,[12] soybean,[13] and rape,[14] the formation of somatic embryos can be induced in cell cultures. In contrast to the zygotic (sexual) embryos of seeds, somatic embryos arise from somatic cells (Figs. 1–3).

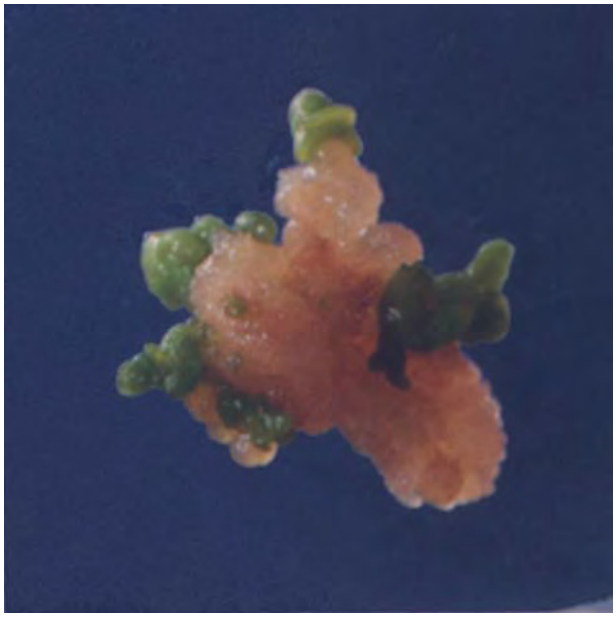

Fig. 2. Alfalfa callus (white) developing somatic embryos (green).

Somatic embryos can be cultivated in any desired number in synthetic media. On a laboratory scale it has already been shown that somatic embryos can be encapsulated together with a nutrient stock, stored for a short time, and then induced to germinate.[15] Such biotechnologically produced plant embryos that are enclosed in polymer capsules are called "artificial seeds." When this technology is further perfected it is conceivable that such artificial seeds could be sown like natural seed. This would make possible a productive and economical form of vegetative propagation of elite genotypes.

2.2. Protoplasts

Protoplasts are individual plant cells without cell walls which can be obtained from plant tissue by the digestion of the cell walls by hydrolytic enzymes (pectinases, hemicellulases, and cellulases). Several million mesophyll protoplasts can be obtained from 1 g of leaf tissue. In 1971, the first successful regeneration of plants[16] from mesophyll protoplasts was achieved with tobacco. Meanwhile, methods of plant regeneration have been worked out for a number of useful plants, including rape,[17] potatoes,[18] tomatoes,[19] alfalfa,[20] and rice.[21] Figure 3 shows the development of alfalfa protoplasts to complete plants. Protoplasts are especially interesting because they are able to take up macromolecules such as DNA[22] and even cell organelles[23] and chromosomes.[24] On the basis of these early observations, a method of direct DNA transfer to protoplasts has been developed in the last few years (see Section 3).

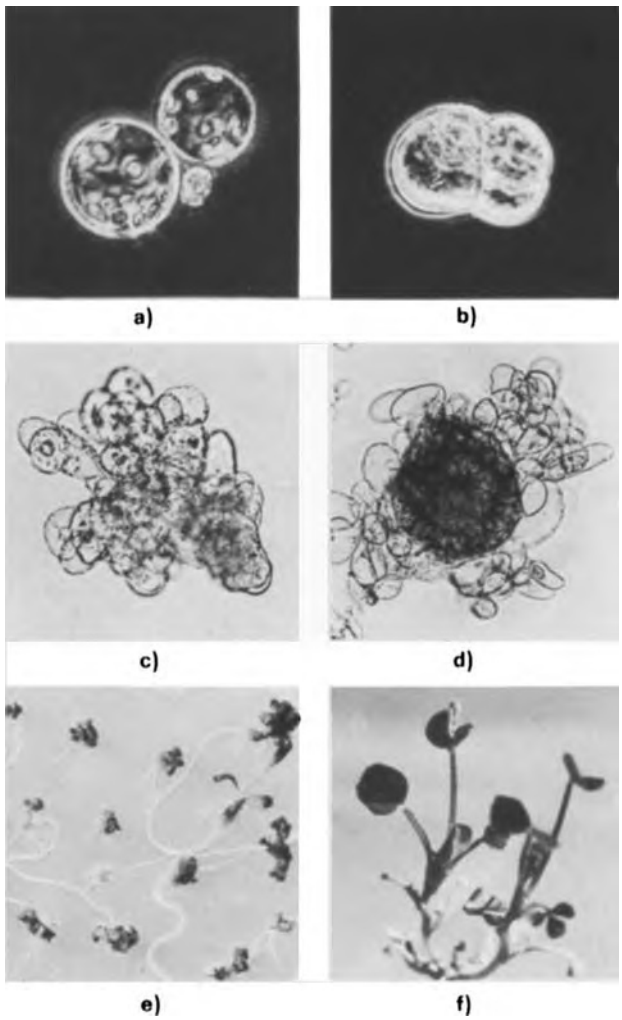

Fig. 3. Plant regeneration from protoplasts of alfalfa (*Medicago sativa*). a) Freshly isolated protoplasts (day 1); b) four-cell stage (day 4); c) microcallus (day 11); d) formation of embryogenic clusters (day 14); e) germinating somatic embryos (5 weeks after protoplast isolation); f) regenerated plant (8 weeks after protoplast isolation).

2.2.1. *Protoplast Fusion*

Plant protoplasts can fuse under various conditions, including the presence of Ca^{2+} ions at pH values over 9.5,[25] polyethylene glycol,[26] or dimethyl sulfoxide. Brief electric pulses[28] will also trigger protoplast fusion. The protoplasts of any plants can be fused, but, in general, the fusion products of protoplasts from different plant genera are difficult to regenerate. In only a few cases has it been possible so far to regenerate intergeneric hybrids, which, moreover, proved to be infertile.[29,30] A familiar example is the somatic hybrid from tomato and potato. This somatic hybrid is of theoretical importance, showing that, by means of protoplast fusion, hybrids can be produced that are not accessible via the sexual route. Fertile hybrid plants can be obtained by fusing the protoplasts of closely related plant species, even when these plants cannot be hybridized sexually.[31] If different selectable marker genes are present in the genomes of the two fusing protoplasts, the somatic hybrids can be sorted out easily in a selection medium. One method of protoplast fusion, which was already described in principle in 1980,[32] has excited much interest recently. Donor protoplasts whose genome has been fragmented by exposure to intense X-irradiation are fused with nonirradiated acceptor protoplasts. In some of the hybrid protoplasts, the fragments of the donor genome are integrated into the acceptor genome. If the donor genome contains genes that are responsible for the expression of resistances, it is possible to select out these recombinants. In this way, a chromosome fragment containing a gene for resistance against the antibiotic methotrexate could be transferred from carrots to tobacco protoplasts. The plants regenerated from these hybrid protoplasts resemble tobacco plants and, in addition to the transferred gene for methotrexate resistance, they possess some further carrot genes.[33] The plants are fertile (i.e., they produce seed) and transmit the methotrexate resistance to their progeny. This asymmetric protoplast fusion method could be a way of transferring several, even unknown, genes between species.

2.3. Mutant Selection in vitro

The isolation of protoplasts has enabled large populations of homogeneous, diploid, and totipotent cells to be obtained for many varieties of plants and to be regenerated to plants. Early in the development of protoplast techniques, attempts were made to use protoplast populations for mutant selection.[34] A single petri dish may contain 1–5 million protoplasts, all of which are potential plants. If mutations can be induced in this cell population and the mutants selected, it should be possible to regenerate plants with new characteristics.

Protoplasts are not a necessary condition for mutant selection, however; any readily regenerating plant cell culture may be used for this purpose. There are now a number of reports describing the successful selection of mutants from plant cell cultures, including pathogen-resistant (Table 2) and herbicide-resistant plants (cf. Table 5) as well as plants that overproduce specific amino acids. Most mutants and variants found in this way could already be selected and isolated at the cell level by means of a selection pressure—e.g., the addition to the culture medium of enzyme inhibitors, amino-acid analogues, pathogen toxins, or herbicides.[50] Strikingly, these variants were also found in experiments in which the mutation rate was not accelerated by chemical or physical mutagens.

Table 2. Pathogen-resistant crop plants obtained through tissue culture (taken in part from [35]).

Crop plant	Pathogen	Ref.
a) After in vitro selection for toxin resistance		
Tobacco	*Pseudomonas tabaci*	[34]
(Nicotiana tabacum)	*Alternaria solani*	[36]
Potato	*Phytophtora infestans*	[37]
(Solanum tuberosum)	*Fusarium oxysporum*	[38]
	Erwinia carotovora	[39]
Tomato	*Fusarium oxysporum*	[40]
(Lycopersicon esculentum)		
Rape	*Phoma lingam*	[41]
(Brassica napus)		
Alfalfa	*Fusarium oxysporum*	[42]
(Medicago sativa)	*Verticillium alboatrum*	[43]
Maize	*Helminthosporium maydis*	[44]
(Zea mays)		
b) Resistance observed without prior in vitro selection		
Potato	*Alternaria solani*	[45]
	Phytophtora infestans	[46]
	Potato Y virus	[47]
	Potato curling virus	[47]
Tobacco	Tobacco mosaic virus	[48]
Tomato	Tobacco mosaic virus	[49]

2.3.1. *Somaclonal Variation*

The high variability described above seems to arise spontaneously through the process of in vitro cultivation, especially when the cell cultures have been cultivated for a prolonged period as undifferentiated cells. Under such conditions, chromosome mutations can accumulate easily.[51] Only part of the observed variability, however, can be explained by the loss of individual chromosomes or by the presence of supernumerary chromosomes. The variability induced by cell cultivation is named "somaclonal variation."[52] An obvious application would be to use this source of variability for breeding programs.[53] Meanwhile, increasing evidence has appeared, indicating that, under the stress of in vitro cultivation, mechanisms are activated in plant cells that lead to reorganization of the genome.[54] In maize, for example, "jumping genes" can be activated by in vitro cultivation.[55]

2.4. Importance of Cell Biology for Genetic Engineering

The contribution of plant cell biology to genetic engineering consists in making competent (i.e., transformable) plant cells available, effecting DNA transfer, and regenerating plants from the transformed cells. These prerequisites have not been met to the required extent for important crop plants such as soybeans, cotton, and the cereals, with the exception of rice. The cell culture systems of species that are difficult to regenerate have to be improved further. It would be ideal to be able to regenerate proto-

plasts of these plants, too, since protoplasts are capable of taking up foreign DNA directly and integrating it into their genomes.

Hope that progress is also possible with the cereals has been inspired by the recent reports of three research groups that rice plants have been successfully regenerated from protoplasts.[21] This breakthrough was achieved by the use of embryogenic suspension cultures as starting material for the isolation of protoplasts.

3. Transfer of DNA

3.1. The *Agrobacterium tumefaciens* System

3.1.1. Tumor Formation

Until recently it was not possible to transfer foreign genes to plant cells. Although DNA could be isolated from plants and characterized, the function of certain DNA sequences was difficult to analyze because the possibility of transfer was lacking. Surprisingly, this dilemma was solved through studies of the formation of certain plant tumors, the so-called crown galls. These tumors are undifferentiated cell growths caused by the infection of a plant with gram-negative soil bacteria of the species *Agrobacterium tumefaciens* (Fig. 4). The formation of these tumors is caused by the introduction of bacterial DNA into plant cells.[56]

Agrobacterium tumefaciens is a soil bacterium that is capable of infecting a large number of dicotyledonous plants, such as tobacco, tomatoes, carrots, and potatoes, after an injury.[57] At the site of infection, strong undifferentiated cell growth begins, leading to the crown gall tumors. Once a tumor has formed, it can continue to grow even in the absence of agrobacteria.[58] Two properties of the tumor tissue should be especially emphasized: the tumor proliferates on sterile culture media of a defined composition without the addition of plant hormones (auxins and cytokinins), although these hormones are essential for the growth of normal cell tissue.[58] Furthermore, the tumor synthesizes specific metabolites, the so-called opines, that are not present in other plant tissues.[59] Opines are derivatives of amino acids and sugars; they can be used by agrobacteria but not by plants as sources of nitrogen and carbon.[59,60] The opines found in plants belong to four different classes: nopalines, octopines, agropines, and agrocinopines (Fig. 5).[61]

Fig. 4. Undifferentiated, growing tumor tissue (crown gall) on the stem of a tomato plant after infection of the wounded area with *Agrobacterium tumefaciens*.

A given strain of agrobacteria can, within certain limits, utilize only the class of opines whose synthesis it induces in the plant. Nopaline-inducing bacteria, for example, cannot metabolize octopine.[59] Corresponding to the opines, the agrobacteria have been divided into different classes,

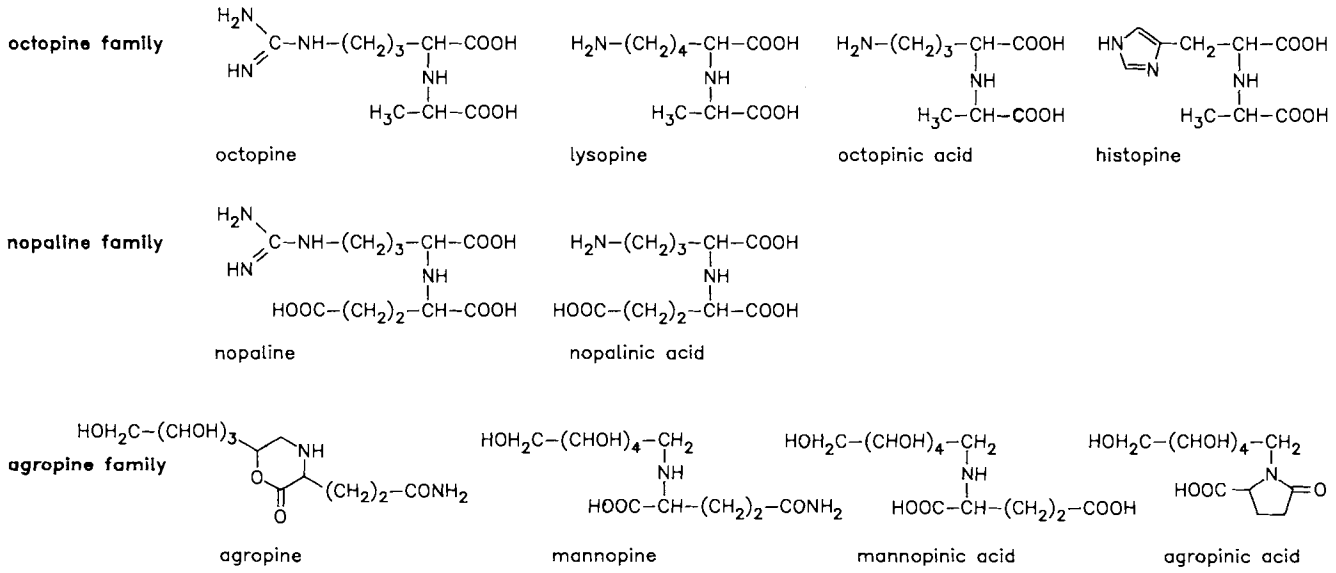

Fig. 5. Chemical structure of the opines (data from [61]). Agrocinopines are phosphorylated sugars of unknown structure.

of which the nopaline and octopine classes have been most thoroughly characterized.

3.1.2. The Ti Plasmid as the Tumor-inducing Principle

The hormone-independent growth of gall tumors in the absence of agrobacteria and the biosynthesis of opines led to the conclusion that agrobacteria must transmit a "tumor-inducing principle" to the plants.[62] Indeed, infectious bacteria were found to contain a megaplasmid, the Ti plasmid (Ti = tumor-inducing), which is approximately 200 kilobases (kb) long.[63] When the plasmid was removed from *Agrobacterium tumefaciens*, the bacterium lost its ability to induce plant tumors. Reintroduction of the plasmid restored the tumor-inducing capability. The plasmid was thus identified as the tumor-inducing principle being sought.[64] This Ti plasmid contains the genes that are responsible for hormone-independent growth of the tumor and those involved in opine formation and utilization (Fig. 6).[60,65-68]

Only a relatively small region of the overall Ti plasmid is integrated stably into the plant genome.[70-72] Hence, the transfer of DNA to plant cells is a natural process that has been practiced by *Agrobacterium tumefaciens* for ages. The integrated region of DNA, the so-called T-DNA, comprises about 20 kb. The genes responsible for opine biosynthesis and those causing tumor growth are localized on the T-DNA.[67,72,73]

Besides their striking similarities, the T-DNA regions of octopine and nopaline bacteria also exhibit several significant differences. Whereas nopaline T-DNA represents an approximately 23-kb-long DNA fragment on the Ti plasmid and is transmitted as such, octopine T-DNA is divided into two adjoining sections of about 14 kb (left T-DNA, TL) and about 7 kb (right T-DNA, TR).[74,75] TL and TR are integrated independently of each other into different sites on the plant genome.[75,76] TL-DNA and nopaline T-DNA possess a very homologous, approximately 9-kb-long nucleotide region, on which genes 5, 2, 1, 4, 6a, and 6b are localized (Fig. 6).[69] The functions of the known genes are compiled in Table 3. At least three of these genes (genes 1, 2, and 4) are responsible for tumor growth in infected plants. Since all three genes are active in wild-type agrobacteria, both auxins and cytokinins are formed, which leads to tumors with fully undifferentiated growth (cf. Fig. 4). Agrobacteria in which gene 4 is inactivated (much auxin, no cytokinin) induce root growth in the tumor, so that gene 4 (roi gene: root inhibition gene) prevents the differentiation of roots. Shoots are induced by inactivation of genes 1 and 2 (much cytokinin, no auxin). Thus, genes 1 and 2 (shi genes: shoot inhibition genes) prevent the formation of shoots.[83,85]

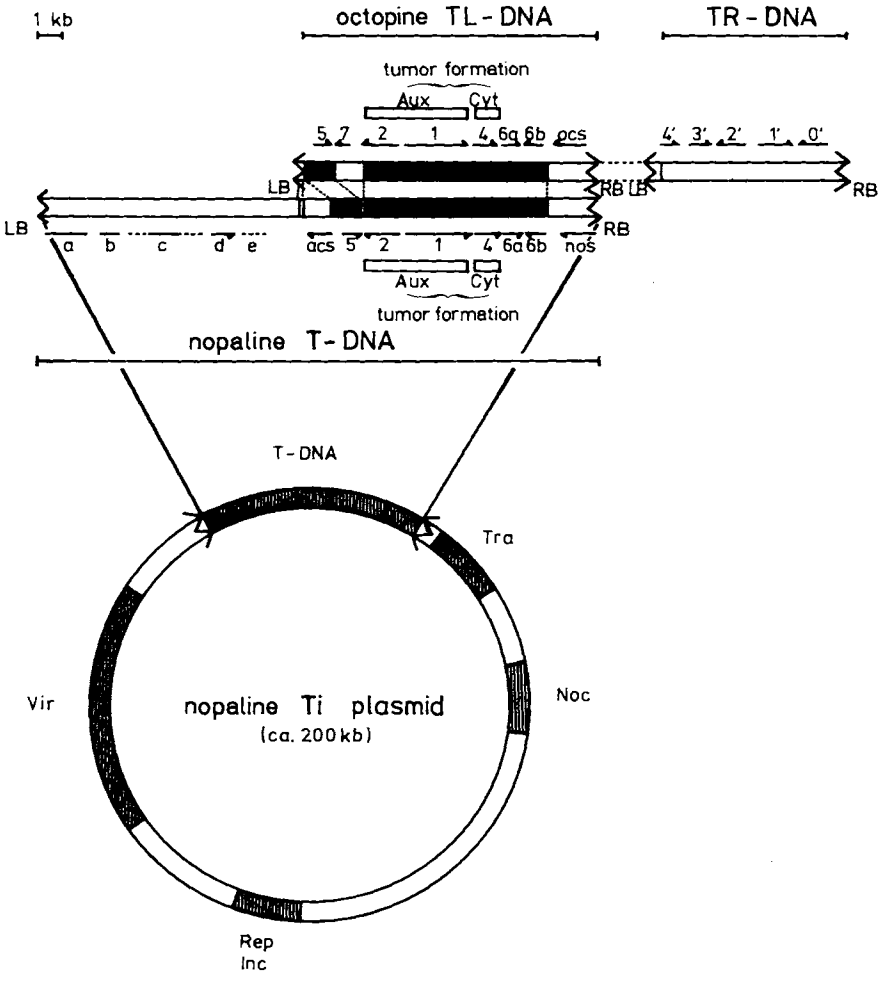

Fig. 6. Genetic organization of a Ti plasmid. Lower part: Functionally characterized regions of a nopaline Ti plasmid. Tra, functions for plasmid transfer between bacteria; Noc, nopaline catabolism; Rep, functions for plasmid replication in agrobacteria; Inc, functions that confer incompatibility of two different Ti plasmids in a single cell of *Agrobacterium tumefaciens* (i.e., nopaline and octopine Ti plasmids can't exist together in the same cell); Vir, virulence region; T-DNA, DNA region that becomes integrated in the plant genome. Upper part: Comparison of the T-DNAs of nopaline and octopine Ti plasmids. Polyadenylated transcripts are shown as either half-arrows or bars according to whether the direction of transcription is known or not. Nomenclature of transcripts is according to [69]. Black areas mark the regions of homology between the two T-DNAs. Nos, nopaline synthase gene; ocs, octopine synthase gene; acs, agrocinopine synthase gene; Aux, genes involved in auxin biosynthesis; Cyt, Gene involved in cytokinin biosynthesis; RB, right border sequence; LB, left border sequence.

Table 3. Functions of T-DNA genes. Functions of other genes included in Figure 6 are still unknown.

Gene	Function	Protein	Ref.
1	Auxin biosynthesis	Tryptophan 2-monooxygenase	[77]
2	Auxin biosynthesis	Indoleacetamide hydrolase	[78]
nos	Nopaline biosynthesis	Nopaline synthase	[79]
ocs	Octopine biosynthesis	Octopine synthase	[80]
4	Cytokinin biosynthesis	Isopentenyltransferase	[81]
5	Tumor growth		[78]
6a	Opine secretion		[82]
6b	Tumor growth		[83]
0′	Conversion of mannopine to agropine		[84]
1′	Mannopine biosynthesis		[84]
2′	Mannopine biosynthesis		[84]

Accordingly, T-DNA genes are responsible for tumor growth. They are not required, however, for the actual plant infection or for the integration of T-DNA into the plant genome.[86] Deletion of various regions of the Ti plasmid has shown that only two regions of the plasmid are essential for infection and integration. One of these is the virulence region ("vir") and the other the "border" regions of the T-DNA. These borders consist of two nearly identical nucleotide sequences,[87,88] which are 25 base pairs (bp) long and exhibit very strong conservation in all types of T-DNA (Fig. 7). Any DNA sequences up to 50 kb long that are inserted between these borders can be integrated into the plant genome.[6,89] The mechanism of this integration process has not yet been clarified. It has been shown, however, that during an infection the T-DNA is cut out of the Ti plasmid and circularized beyond these 25-bp-long border sequences to form unstable intermediate products.[90]

GCTGG	TGGCAGGATATATTG	TG	GTGTAAAC	AAATT	nopaline LB
GTGTT	TGACAGGATATATTG	GC	GGGTAAAC	CTAAG	nopaline RB
AGCGG	CGGCAGGATATATTC	AA	TTGTAAAT	GGCTT	octopine LB (TL-DNA)
CTGAC	TGGCAGGATATATAC	CG	TTGTAATT	TGAGC	octopine RB (TL-DNA)

Fig. 7. Comparison of the conserved border sequences of nopaline and octopine T-DNAs. Homologous areas are boxed. RB, right border sequences; LB, left border sequences.

The DNA of the approximately 40-kb-long virulence region is not itself integrated into the plant genome,[75] but the virulence genes are responsible for the infectiousness of the agrobacteria.[91] The vir region consists of at least six different complementation groups.[91,92] To determine a complementation group, a mutation that leads to avirulence was inserted into the vir region. An attempt was then made to restore virulence by introducing into the bacteria a second vir region with a mutation at a different site. If both mutations are in the same complementation group, the bacteria remain avirulent, but if they lie in different groups, the two groups complement each other and the bacteria become virulent again. Each complementation group corresponds to a single transcription unit. Two of these transcripts are expressed constitutively; the remaining four transcripts are induced only in the presence of plant cells.[92] The exact mechanism of virulence induction is not yet fully understood. Since in nature agrobacteria infect only injured plant cells, it was suspected that certain substances are synthesized by these plant cells to which the bacteria "react." Two of these compounds, acetosyringone **1** and α-hydroxyacetosyringone **2**, have so far been isolated (Fig. 8). These phenolic compounds interact with the

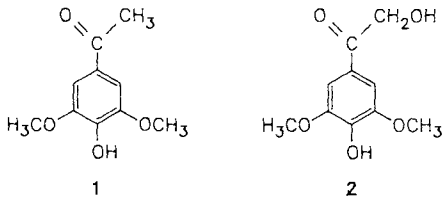

Fig. 8. The two compounds synthesized by wounded plant cells which activate the virulence region of *Agrobacterium tumefaciens*: acetosyringone **1** and α-hydroxyacetosyringone **2**.

products of the two constitutively expressed virulence genes and thus stimulate the activity of the other four vir loci.[93,94] In addition to the borders and the vir region of the Ti plasmid, agrobacteria contain at least two chromosomal loci that are responsible for the attachment of the bacteria to the plant cell walls.[95,96]

3.1.3. *Agrobacterium tumefaciens as a Gene Vector*

Knowledge of the basic processes involved in the infection of plant cells by *Agrobacterium tumefaciens* led to the development of two basically different methods of introducing foreign genetic material into a plant: the use of "integrative vectors" and the use of "binary vectors." In constructing the "integrative vectors," advantage is taken of the fact that the tumor-inducing genes are not required for the actual infection and that any DNA sequence that is inserted between the two borders will also be transmitted to the plant. In these integrative vectors, the tumor genes of T-DNA, for example, are replaced by sequences of the *E. coli* cloning vector pBR 322.[86] The foreign DNA that is to be integrated into the plant genome is simply cloned in a pBR vector in *E. coli* and then inserted by homologous recombination, via these pBR sequences, into the Ti plasmid (Fig. 9).

In the construction of the "binary vectors," the fact is utilized that the vir region and the "borders" can be localized on two separate plasmids without affecting the infectiousness of the agrobacteria.[97] Accordingly, the T-DNA borders are transferred to a plasmid that can be replicated in *E. coli* as well as in agrobacteria. These plasmids can be very much smaller than the Ti plasmid (about 10–20 kb),[98] and the different cloning steps can readily be carried out in *E. coli*. If the DNA to be transferred to plants has been cloned on such a plasmid, this plasmid is transferred to a strain of agrobacteria that already has a Ti plasmid, but which, although it still has a vir region, contains no further T-DNA. Agrobacteria with these two plasmids are also capable of stably integrating the DNA lying between the borders into the plant genome.

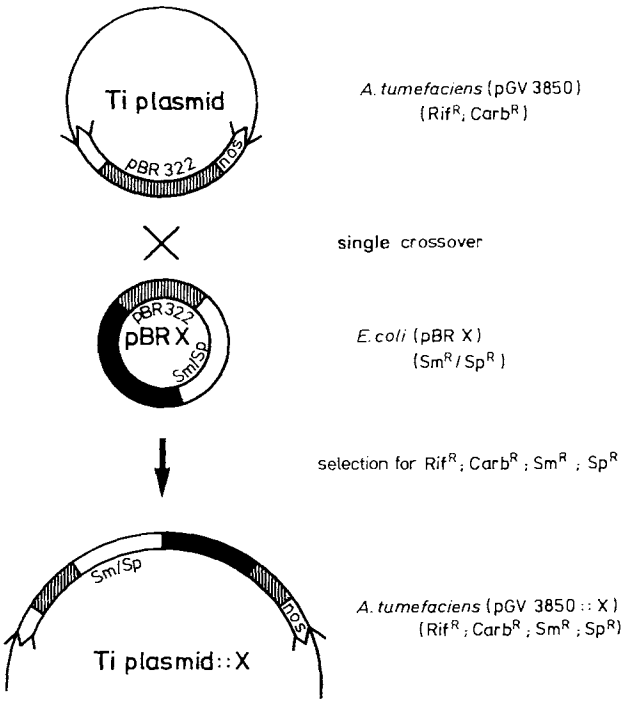

Fig. 9. Schematic drawing of the mobilization of a pBR vector of *E. coli* into a modified Ti plasmid of *Agrobacterium tumefaciens* (modified according to [86]). Antibiotics: Carb = carbenicillin; Rif = rifampicin; Sm = streptomycin; Sp = spectinomycin. ▥ = pBR322 sequences; ■ = transferred gene X; ≷ = border sequences.

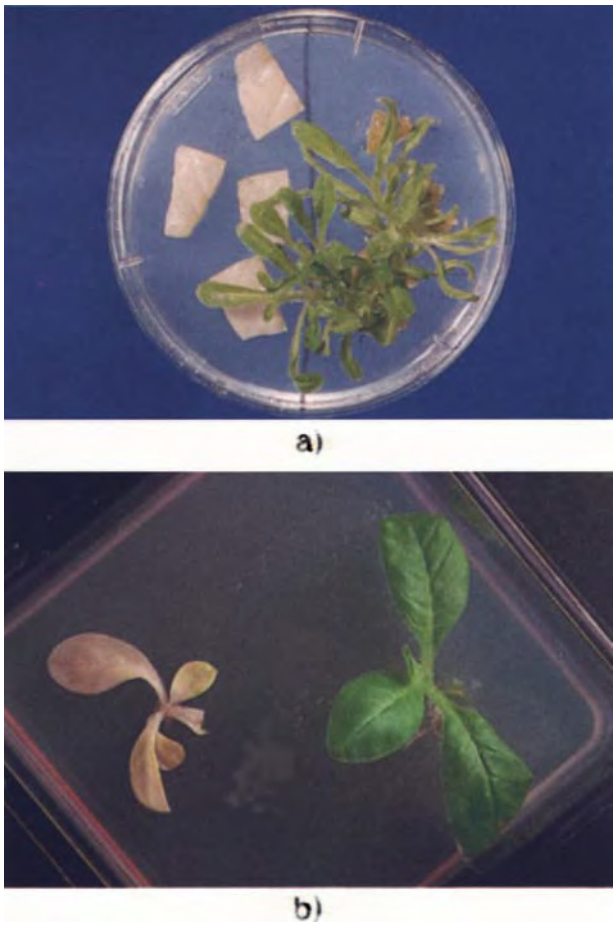

Fig. 10. Production of a transgenic plant by transferring a gene, imparting resistance against the phytotoxic antibiotic kanamycin. a) Leaf pieces after transformation with *Agrobacterium tumefaciens*. Transformed (right) and nontransformed leaf fragments (left) are cultivated on media containing kanamycin. Only the transformed leaf pieces form shoots. b) Transgenic tobacco plant regenerated from a shoot (right) and nontransformed tobacco plant (left) on media containing kanamycin. Only transformed plants survive.

3.1.4. Methods of Gene Transfer with Agrobacterium tumefaciens

The prerequisite for the transfer of DNA by *Agrobacterium tumefaciens* in plants is the infection of plant cells by the bacterium. The techniques for infecting plant tissue with *Agrobacterium tumefaciens* are relatively easy to perform. In the simplest case, plants are injured mechanically, e.g., with a scalpel, and a suspension of agrobacteria is applied to the site of the wound.

Better transformation efficiencies are achieved by incubating parts of the tissue with agrobacteria and then cultivating the tissue on synthetic culture media. Thus, with the "leaf disc" method, small parts of leaves are dipped into a bacterial suspension and then cultivated.[99] If a selectable marker gene such as the resistance gene to the phytotoxic antibiotic kanamycin (see Sections 3.3 and 4.1), is transferred by means of the agrobacteria, new plants can be regenerated only from transformed cells of the leaf parts on kanamycin-containing media (Fig. 10).

The incubation of plant protoplasts with agrobacteria and the subsequent regeneration of the treated protoplasts to plant tissue or intact plants, which is known as coculture, also leads to good transformation results.[100]

However, the advantages of the agrobacteria system, for example, the simple transformation technique and good transformation frequency, must be weighed against a large disadvantage, namely, the limited host range of the agrobacterium. A large number of dicotyledonous and also some monocotyledonous plants of the Liliaceae family, for example, *Asparagus officinalis* (asparagus)[101a] and *Chlorophytum capense* (spider plant),[101b] are susceptible to infection. With the exception of maize,[102] however, no susceptibility to infection by *Agrobacterium tumefaciens* has yet been observed for the economically important Gramineae to which all other cereal species belong.

3.2. Direct Transformation of Plant Cells with Isolated DNA

Owing to the limited host range of the agrobacteria, other methods were also sought at the same time for introducing genetic material into plants. The most successful method so far has proved to be the transformation of plant protoplasts with isolated DNA,[103, 104] as had already been carried out with bacteria[105] and animal cells.[106] In this approach, the transfer of the foreign DNA into the plant cells is carried out without using a natural plant-infectious system such as *Agrobacterium tumefaciens*. The cells to be transformed are simply incubated together with the DNA in a suitable solution and subjected to certain procedures which have already been used in microbiological research to transfer foreign genetic material. These procedures include, in particular, treatment with polyethylene glycol,

heat shocks, and electrical shocks (electroporation). In electroporation, short electrical pulses are used to produce small pores in the cell membrane through which the DNA is able to pass into the cell.[104, 107] Although this method may appear to be easy, the detailed procedure presents difficulties since the individual experimental parameters have to be optimized for each plant species.

Direct transformation has the undisputed advantage that it can be used with all plants from which protoplasts can be obtained. These include some of the Gramineae as well as many dicotyledonous plants. So far it has been possible to introduce foreign DNA into protoplasts from rice *(Oryza sativa)*,[108] maize *(Zea mays)*,[109] and wheat *(Triticum monococum)*,[110] among others.

One disadvantage of the direct transformation of protoplasts compared with transformation with *Agrobacterium tumefaciens* is the fact that the regeneration of intact plants from protoplasts takes much longer than regeneration from tissue parts. However, the greatest disadvantage of direct transformation is that so far, despite extremely intensive research with cereals, only rice protoplasts could be regenerated to intact plants.[21]

3.3. Other Methods of Gene Transfer

Since there has been only limited success in transforming and regenerating the most important crop plants by using either the direct transformation of protoplasts or by means of agrobacteria, other transformation methods have also been investigated, including the introduction of genetic material via phytopathogenic viruses. Although most plant viruses belong to the group of RNA viruses, experiments have mostly been carried out with DNA viruses, since work with RNA on the molecular biological level is vastly more difficult than with DNA. Only two classes of phytopathogenic DNA viruses that can be used as DNA vectors are currently known, namely, the gemini viruses and the caulimoviruses.[111] By far the best characterized DNA virus, namely, cauliflower mosaic virus (CaMV), which belongs to the class of caulimoviruses, has already been used for transferring genetic material into plants.[112] However, with CaMV, owing to the special genome structure of the virus, only very small pieces of DNA up to 500 nucleotides long can be integrated into the virus genome. In addition, the narrow host range of CaMV (only plants of the Brassicaceae family) and the fact that virus DNA is not integrated stably into the plant genome prevent cauliflower mosaic virus from being suitable as a universal transformation system.

In order to avoid the difficulties in regenerating intact plants from the protoplasts of many species, attempts have been made to transfer DNA directly into certain tissues. Several authors have described how, after incubation of pollen with foreign DNA and subsequent dusting of plants with this pollen, transformed progeny were obtained.[113, 114] However, it has not yet been possible to reproduce these experiments.[115]

Microinjection of DNA into cell nuclei using a very fine cannula is a proven method for the genetic manipulation of animal cells.[116] Microinjection has also been used for transforming plant cells.[117] Owing to the very large plant cell vacuole and the small cell nucleus into which the DNA has to be injected, this method requires special equipment and is not very efficient.

The injection of DNA into reproductive plant organs is also carried out. A breakthrough seems to have been achieved here with the injection of DNA into young inflorescences of rye plants.[118] After the injection of a gene for resistance to the phytotoxic antibiotic kanamycin, it was possible, for the first time, to regenerate resistant, transformed rye plants.

4. Gene Expression in Plants

4.1. Regulatory Regions of Plant Genes

The first successful attempts to introduce foreign DNA into plants by means of the Ti plasmid were carried out with bacterial genes for resistance to the antibiotics streptomycin and kanamycin.[119, 83] These genes were inserted into the T-DNA and introduced in this way into the plant genome. However, no transcription could be detected. The same result was obtained for an alcohol dehydrogenase gene obtained from yeast[120] and a β-globin gene from mammalian cells.[121] These genes were integrated into the genome but were not active in the plant. It was therefore assumed that certain transcription signals specific to plants are necessary in order to activate the genes. From the study of animal systems, the general structure of functional eukaryotic genes was already known.[122] In principle, plant genes show the same structure.[123] A typical plant gene is illustrated in Figure 11. The promoter is located in the nontranscribed 5′ region of eukaryotic genes. The enzyme RNA polymerase II, which catalyzes the synthesis of messenger RNA, binds to the promoter sequences, in particular to a region approximately 10 bp long which is rich in adenine and thymine, the so-called TATA box.[125] Promoter sequences are therefore responsible for the correct initiation of the transcription process. The transcription is terminated at DNA sequences in the 3′ region, namely at the end of the gene. These terminator sequences are involved, in a way that is not yet exactly clear, in the termination of transcription and the attachment of the poly-A sequences to the RNA chains produced (polyadenylation).[126] In order to express foreign genes in plants, attempts were therefore made to use promoter and terminator sequences of genes known to be actively expressed in all plant tissues. The best gene for this purpose was the nopaline synthase gene from *Agrobacterium tumefaciens*, which was first isolated at that time.[79] It possessed eukaryotic promoter and terminator sequences and, as was known from transformation experiments with wild-type agrobacteria, it was also expressed in callus and other plant tissues. The fusion of the promoter and terminator regions of this gene to the bacterial gene for chloramphenicol acetyltransferase (resistance to chloramphenicol) resulted in the first chimeric gene that could be expressed in plant cells.[127] Thus, certain regulatory regions are necessary to express genes in plants (Fig. 11).

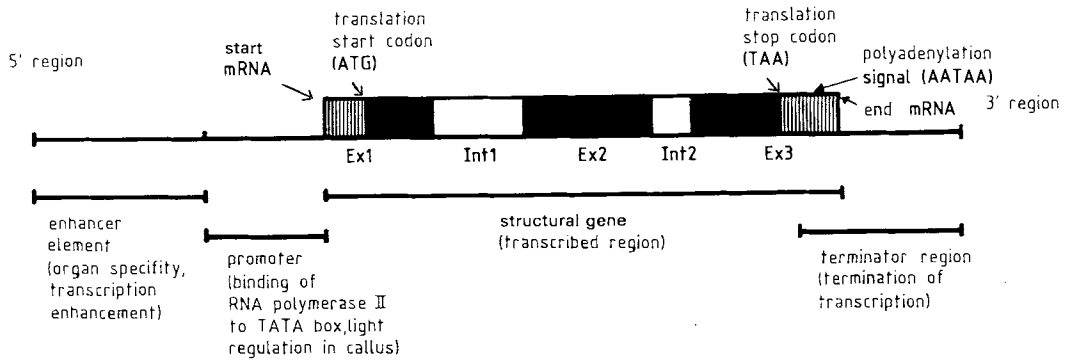

Fig. 11. General structure of a plant gene (ss-rubisco gene). Enhancer, promoter, and terminator elements regulate the expression of the structural gene. The whole structural gene is transcribed. After removal of introns (Int), the exons (Ex) are spliced to build up the mature m-RNA. ▥ = nontranslated regions of the m-RNA; ■ = translated regions of the m-RNA. Technical terms are explained in [124].

Most of the following research focused on achieving the expression of resistance genes to phytotoxic antibiotics in order to use these genes as selectable markers to differentiate transformed and nontransformed plant cells. Resistance to kanamycin **3**, hygromycin, and methotrexate could be expressed in plant cells.[128] Resistance to kanamycin, for example, is based on expression of the transferred gene for neomycin-kanamycin phosphotransferase, which catalyzes phosphorylation of the antibiotic and consequent inactivation.

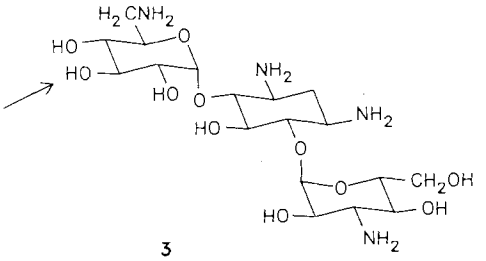

Fig. 12. Chemical structure of the phytotoxic antibiotic kanamycin **3** [129]. The hydroxyl group marked by an arrow is phosphorylated by the enzyme neomycin-kanamycin phosphotransferase, resulting in inactivation of the antibiotic.

4.2. Differential Gene Expression

Once evidence had been supplied that foreign genes can be introduced into the plant genome and expressed, more complex gene regulatory mechanisms in plants were investigated on the molecular level. The development of integrative and binary vector systems (see Section 3.1.3) was essential for this purpose. Using these systems it was possible for the first time to regenerate morphologically normal plants after the transformation.

Two phenomena of developmental biology are currently being investigated intensively, since their parameters can be defined quite easily: the light-specific and the organ-specific activation of certain genes.

The light-induced gene expression is being examined primarily in genes coding for the small subunit of ribulose-1,5-bisphosphate carboxylase (ss-rubisco) or for the chlorophyll a/b binding protein (CAB). Rubisco and CAB are key enzymes in CO_2 fixation and in plant photosynthesis.[130]

The organ-specific gene expression is also being investigated in the genes mentioned above, since, apart from their light-dependent expression, they are only activated in tissues containing chloroplasts (e.g., leaves and stems). Another important class of differentially expressed genes codes for the storage proteins, which are important from a nutritional and physiological point of view.[131] Thus, the zein genes of maize *(Zea mays)* or the legumin genes of pea *(Pisum sativum)*, for example, are active in seeds but not in other organs such as leaves or roots.

Below, we shall briefly describe a few attempts to elucidate gene regulatory mechanisms by the application of DNA transfer methods, as exemplified by ss-rubisco.

The enzyme ribulose-1,5-bisphosphate carboxylase is the most frequently occurring protein in the world, accounting for approximately 50% of all soluble plant protein. It is composed of eight identical large subunits (M_r 56000 daltons, LS-rubisco) and eight identical small subunits (M_r 14000 daltons, ss-rubisco). Whereas the gene of the large subunit is localized on the chloroplast genome, the small subunit is encoded by the nuclear DNA. The ss-rubisco subunits are formed in the cytosol and then transported to the stroma of the chloroplasts after proteolytic cleavage of a transit peptide of approximately 6000 daltons. Here, they combine with the LS-rubisco subunits formed in the chloroplasts to form the functional holoenzyme.

The enzyme rubisco can only be detected in the tissue of illuminated plants. In the dark, the synthesis of the enzyme stops after a short while.[132] Since no rubisco-specific mRNA can be detected once the plants have been put in the dark, the regulation of gene activity is effected on the level of transcription.[133] In order to transcribe a gene, RNA polymerase II has to bind to the corresponding promoter sequence. It was therefore assumed that a specific sequence exists in this promoter region which is somehow linked to light-dependent expression. Factors that enhance or inhibit polymerase binding to the DNA could bind to this sequence.[134] A possible way to investigate this hypothesis would be to isolate these DNA regions and fuse them with structural regions of suitable marker genes. The differential expression of these chimeric genes could then be investigated in transgenic plants. In order to achieve this, a region approximately 1000 nucleotides long that

was situated directly in front of the start site for transcription of an ss-rubisco gene was inserted into the corresponding position of the gene for the bacterial chloramphenicol acetyltransferase. This construction was light-regulated in transformed tobacco cells and therefore confirmed the above-mentioned hypothesis.[135] In the meantime, similar experiments showed that a 33-bp-long DNA region is sufficient for light-specific regulation of an ss-rubisco gene in callus tissue.[136] However, it was not possible to obtain strong expression of the gene with this region alone. A further "enhancer" (see Fig. 11) with a length of approximately 250 bp was discovered, which, independent of its orientation but dependent on light, enhanced the activity of an otherwise constitutively acting promoter.[130]

The plant-specific promoters that have been isolated to date can be divided into three categories: (1) the light-dependent promoters, (2) the tissue-specific regulated promoters, such as those from the seed storage protein genes in maize and wheat, and (3) the promoters of constitutively expressed genes. The degree of expression of transferred genes is usually lower in the transgenic (i.e., transformed) plants than in the plants from which the genes were isolated.[137] Therefore, promoters of highly expressed genes are of special interest. One of the strongest promoters so far used in plant transformation experiments is of viral origin. It is the constitutively acting promoter of the 35S transcripts of the phytopathogenic cauliflower mosaic virus and seems to be about 30 times as strong as the nopaline synthase promoter.[138] In the search for other inducible genes, gene sequences that are inducible by heat,[139] darkness,[140] and nitrate.[141] have been isolated.

Promoters of dicotyledonous plants appear to regulate the expression of genes in other dicotyledonous plants correctly. Thus, in addition to many other examples, an organ-specifically expressed seed-storage-protein gene from soybeans, after transfer into tobacco plants, was expressed in exactly the same time and tissue-specific pattern as in the soybean.[142]

There are contradictory reports, however, on the function of promoters of monocotyledonous plants in dicotyledonous species. For example, a CAB gene from wheat was correctly transcribed in tobacco plants,[143] whereas an ss-rubisco gene from wheat was not active in tobacco.[144]

In addition to the strength of a promoter, other factors play an important role in the level of expression of a transferred gene. Thus, often not just one gene copy is integrated into the plant genome when a gene is transferred. Indeed, more than five copies of a transferred gene have been detected in the genomes of transgenic plants.[137] But even when the different number of gene copies is taken into account, a large variability in expression is observed with different transgenic plants in a transformation experiment. This phenomenon is usually explained by what is called the position effect.[145] The integration loci of transferred DNA in the plant genome have so far shown no obvious similarities as regards the nucleotide sequence. The integration sites seem to be entirely coincidental.[146] Since the genes are presumably integrated into DNA regions that are transcribed to different extents, they are expressed to varying degrees. Owing to this variability in the degree of expression of a transferred gene, those plants that show the desired characteristics to the required extent have to be selected from a number of transgenic plants. However, once a gene is integrated in the plant genome, it will be stably maintained and transmitted to the progenies according to the Mendelian laws.[147]

5. Aims of Applied Genetic Engineering with Plants

Some of the most important aims of genetic engineering with plants are shown in Table 4. The aims mentioned only represent examples, which were selected to illustrate the many possibilities of genetic transfer to plants. This is therefore not a complete list.

Table 4. Genetic engineering with plants—some possible applications.

1. Generation of resistance to
herbicides
viral diseases
fungal diseases
pests
microorganisms
stress conditions
2. Changes in the compositions of plant substances
Modification of amino-acid composition
Modification in the composition of vegetable oils, carbohydrates, or plant metabolites
Modification in the content and activity of enzymes important for processing, transportation, or storage of agricultural products
3. Changes in physiological processes
Photosynthesis/photorespiration
4. Improvement of nitrogen fixation
5. Genetic engineering as an aid to plant breeding
Diagnosis of plant diseases
Restriction fragment length polymorphism (RFLP)

5.1. The Production of Resistant Plants

5.1.1. Resistance to Herbicides

The cultivation of plants that show resistance to herbicides has long been part of agricultural practice, "selective herbicides" being in widespread use. These herbicides are metabolically transformed in certain cultivated plants (e.g., by hydroxylation, conjugation with carbohydrates or glutathione, demethylation) in such a way that herbicidal action is lost. Examples are maize with resistance to atrazine,[148] wheat with resistance to diclofop-methyl,[149] sugar beet with resistance to phenmedipham,[150] and cereal species with resistance to chlorsulphuron. Thus, these plants have a physiologically based, natural herbicide resistance, which is exploited by the farmer.

Often, several different herbicides have to be used, because this is the only way that all weeds that occur can be controlled. By introducing a resistance to a nonselective herbicide, the use of several herbicides may no longer be necessary.

Plants with resistance to nonselective herbicides will be one of the first results of genetic engineering with plants to have an application in agriculture. The site of action of most modern herbicides is known and biochemically characterized. This knowledge is the prerequisite for the development of strategies for producing herbicide-resistant

plants with the aid of genetic engineering. This aim seems to be achievable in several cases by transferring only one or a few genes. Further reasons for intensive work on herbicide resistance are the advantages that resistant plants offer to the farmer.

The cultivation of resistant cultures makes the preventative use of herbicides superfluous. The farmer now has to use the herbicide only when it is needed, that is, only if the weeds exceed a tolerable level. This is contrary to usual practice today, where a preventative application of herbicides is commonly made.

Soil erosion can also be reduced by using herbicide-resistant plants, since the later application of herbicides makes it possible to avoid the occurrence of exposed areas. Herbicide-resistant cultures are also particularly well suited to the no-till (or "slot" planting) method.[151]

The possible use of herbicides according to the damage threshold concept and the replacement of several different herbicides by a single nonselective herbicide should result in decreased overall use of herbicides as herbicide-resistant cultures are introduced. In addition to simplified use, the economic advantage for the farmer is obvious.

The methods of classical cell biology (see Section 2.3) can also be used to obtain herbicide-resistant plants. The addition of a herbicide to the plant-cell culture medium enables the selection of resistant calli from which herbicide-resistant plants can later be obtained.[152, 153] The various possibilities for obtaining herbicide-resistant plants by means of cell biology and genetic engineering will be exemplified here for several newer herbicides (Table 5).

Relatively new herbicides have been obtained from the compound classes of sulfonylureas and dihydroimidazolones. These herbicides inhibit the enzyme acetolactate synthase, which is involved in the biosynthesis of the branched amino acids leucine, isoleucine, and valine in plants.[154, 155] With the sulfonylureas chlorsulfuron and sulfometuron-methyl, resistant plants were obtained by using selection against these herbicides.[156] The selection of plants resistant to dihydroimidazolones was also successful.[157] These plants show cross-resistance to sulfonylureas owing to the common site of action.

In both cases, the cause of the resistance seems to lie either in excess production of the enzyme or in a mutation of the gene. Both possibilities can easily be checked and reproduced with the aid of genetic engineering after isolation of the gene for acetolactate synthase.

Genetic engineering may be used to obtain herbicide-resistant plants via the following paths (the site of action refers to enzymes in these cases):

- —change in the site of action through mutation (e.g., glyphosate[158])
- —increase in the concentration of the site of action (e.g., glyphosate,[159] phosphinotricine[160])
- —introduction of metabolizing enzymes

In order to choose the most favorable strategy, exact knowledge of the site of action and the degradation pathway of the herbicide is necessary. Usually, several of the paths indicated are successful for producing herbicide resistance.

The herbicide glyphosate prevents the synthesis of aromatic amino acids in plant cells by inhibiting the enzyme 5-enolpyruvylshikimate 3-phosphate synthase (EPSP synthase).[161] Glyphosate is one of the most widespread nonselective herbicides. Resistant plant cell cultures were obtained by selection in the presence of glyphosate. The resistance was found to be due to an increase in the concentration of EPSP synthase, which, in turn, was caused by an increase in the number of genes (gene amplification).[159] For the production of tolerant plants by means of genetic engineering, a similar strategy was followed. The gene for EPSP synthase was first isolated from cell cultures of *Petunia hybrida*. Overproduction of the enzyme in plants was then achieved by exchanging the promoter of the EPSP synthase gene for the constitutively acting 35S promoter of the cauliflower mosaic virus (Section 4.2). After reintroducing this hybrid gene into petunia cells, a 40-fold increase in enzyme activity was detected in calli and is presumably responsible for the observed tolerance.[163] Tolerant plants were obtained from these calli.

Tolerant plants may also be obtained by means of mutants that have an altered site of action for the herbicide glyphosate. After mutagenesis of *Salmonella typhimurium*, a strain was obtained whose EPSP synthase was insensitive to glyphosate. The resistance was based on replacement of one of the 421 amino acids of the *Salmonella* enzyme.[158] The mutated structural gene was isolated, fused with regulatory elements that are recognized in plants, and then integrated into the genome of tobacco plants. With this bacterial resistance gene, it was thus possible to obtain plants that are tolerant to glyphosate.[164]

A final example is provided by the herbicide phosphinotricine,[162] which, by inhibiting the enzyme glutamine synthetase, prevents ammonium ions from being metabolized

Table 5. Examples of herbicide resistance in plants.

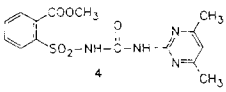

4

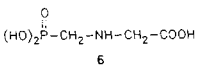

6

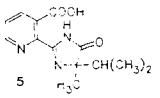

5

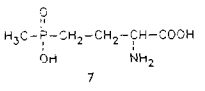

7

	Herbicide	Class	Mode of action	Ref.
4	Sulfometuron-methyl	Sulfonyl-urea	Inhibition of acetolactate synthase, thereby blocking biosynthesis of branched amino acids	[154, 156]
5	Imazapyr	Dihydro-imidazolone	Same as for 4	[155, 157]
6	Glyphosate	Amino-acid derivative	Inhibition of 5-enolpyruvylshikimate 3-phosphate synthase, thereby blocking biosynthesis of aromatic amino acids	[153, 159, 161]
7	Phosphinothricine (glufosinate)	Amino-acid derivative	Inhibition of glutamine synthetase, thereby increasing the intracellular concentration of ammonia and blocking biosynthesis of glutamine	[160, 162]

in plant cells. This enzyme catalyzes the following reaction:

$$\text{glutamate} + NH_4^{\oplus} + ATP \longrightarrow \text{glutamine} + H_2O + ADP + P_i$$

Resistant cell cultures were also obtained in this case. Gene amplification and a correspondingly increased concentration of the enzyme glutamine synthetase was determined as the cause of this resistance.[160] Owing to the increased number of copies of the glutamine synthetase gene, this cell line proved suitable for the isolation of the gene.[165]

Recently, the gene of a plant glutamine synthetase was expressed in an *E. coli* mutant that no longer had any glutamine synthetase of its own.[166]

5.1.2. Resistance to Viruses

In the production of virus-resistant plants by genetic engineering, considerable successes have recently been achieved. It was known for a long time, that, after an infection with a weakly pathogenic virus, plants do not develop any more symptoms when they are subsequently infected with a virulent strain. This property is used in the cultivation of tomatoes and potatoes. The molecular mechanism of this type of "cross resistance" has not yet been clarified. Different theories, some of them conflicting, are still waiting for experimental confirmation. Based on the consideration that cross-resistance could possibly be produced by the expression of specific genes of a virus, *Beachy* et al.[167] transferred the gene for the coat protein of the tobacco mosaic virus (TMV) by means of *Agrobacterium tumefaciens* to tobacco plants. Indeed, a high percentage of the transformed plants, which now form the coat protein of the virus, showed no symptoms after artificial infection with TMV. By contrast, a clear infection was observed in all the control plants after three to four days.

This very important success in producing virus-resistant plants enables specific investigations to be carried out into the phenomenon of cross-resistance, since only the expression of a single gene is required. This approach thus opens up the possibility of producing virus-resistant seed.

Induced resistance is possibly also linked to the formation of "pathogen-related proteins" (PR proteins). Several plants, after infection with viruses, viroids, bacteria, or fungi, form specific proteins whose occurrence can be correlated with resistance to further infections.[168] The concentration of PR proteins increases at the beginning of an infection to up to 100 times the initial value.[169, 170] They usually occur extracellularly and are frequently resistant to proteases. By crossing tobacco cultivars that form the same PR protein after induction with a pathogen, hybrids were obtained which form this PR protein constitutively and showed much greater resistance to virus infections.[171] Further investigations into the still unknown functions of these proteins promise to provide a better understanding of the resistance mechanism of plants.

Since gene sequences of some of these proteins have already been cloned,[170] the practical use of these resistance mechanisms may become possible in the foreseeable future. Investigation of the promoters of the PR protein genes may lead to numerous scientific and practical applications, since these genes are induced by infection and the genes for the PR proteins (about ten have been identified to date) may have different promoters. The overexpression of some of these proteins could activate specific protective mechanisms.

5.1.3. Resistance to Fungal Diseases and Microorganisms

In spite of the use of crop protection agents, damage caused by plant diseases continues to be very high. For 1976, worldwide crop losses due to disease, mainly of fungal origin, were estimated at 50 billion U.S. dollars.[172] Similarly to most of the previous examples mentioned, the genetic expression of resistances to diseases can be based on the utilization of natural resistance mechanisms, which are either intensified or transferred by genetic engineering between plants that were previously not capable of being crossed. As is the case with virus infections, an induced resistance also occurs in fungal and bacterial infections. It has not yet been possible, however, to explain its cause.[173] Plants possess a number of different defense mechanisms against infections:

- Increased lignin formation at the cell wall and thus greater protection against invaders
- Formation of hydrolases, whose function may be to degrade polysaccharides in the cell wall of invading fungi
- Formation of low-molecular-weight, secondary metabolites, which can have a toxic effect on infectious organisms
- Formation of "hydroxyproline-rich proteins" of unknown function, which occur in the cell wall of plants and whose concentration rises appreciably following an infection
- Formation of infection-specific proteins whose function has not yet been clarified, but which probably are an important factor in the defense against infections[174]

There are a number of possible approaches to producing resistance mechanisms against fungi or microorganisms by genetic engineering methods:

1. Clarification of the inducers and the mechanisms necessary for the expression of defense reactions in plants is necessary. Several triggers of defense mechanisms (elicitors) have already been identified. In addition, the genes of several important proteins whose expression rises sharply when infection occurs have been characterized.[175, 176]
2. Numerous plants contain the enzyme chitinase, whose activity increases considerably after fungal attack.[177] Chitin (poly-*N*-acetyl-D-glucosamine) is not found in plant cells, but is an important constituent of the cell wall of fungi. Therefore, the function of the chitinase formed during an infection is presumably to hydrolyze the fungal cell walls and thus defend the plant against fungal attack. Several chitinase genes have already been isolated.[178] The next step would be to use genetic engineering methods to achieve an increase in the formation of chitinase when fungal attack occurs.

3. Undomesticated relatives of our crops often possess important resistance genes. It has not in all cases been possible, however, to transfer these resistance genes to crops by means of crossing experiments. Here, genetic engineering could develop into an important tool for the breeder. One example is the occurrence of rust in soybeans *(Glycine max)*, which is caused by *Phakospora pachyrhizi* and can result in heavy crop losses. Although resistance genes have not been found in corresponding breeding plants, they are present in species of the genus *Glycine*. Their transfer to soybeans by genetic engineering methods would yield considerable economic benefits.[179]

4. Strains closely related to some plant-pathogenic organisms are often no longer able to cause infection in plants. Since it is often easier to carry out molecular biology studies in microorganisms than in plants, an attempt is frequently made to characterize the genes responsible for "recognizing" the susceptible host plants and for initiating the plant-pathogenic reaction.[180, 181] Once these mechanisms are understood, genetic engineering strategies can be devised to produce a resistance to these pathogens.

5.1.4. Resistance to Pests

As in the case of the examples discussed above, plants have presumably also developed defense mechanisms against insects. Fragments of the cell wall (oligosaccharides) are probably the inducing factors in some cases.[176, 182] One possible defense mechanism against animal pests is the formation of protease inhibitors as a reaction to plant lesions.[182] These are proteins that act as potent inhibitors of serine proteases, which are involved in the digestive process of insects.[183] The inhibitors can therefore act as feeding suppressants. Since the substances in question are proteins, genetic engineering should make it possible through overexpression of the corresponding genes to obtain increased formation of these inhibitors, perhaps specifically in leaves or fruits. The gene structure and sequence of an inhibitor of this type was published recently.[184]

The transfer of genes for proteins toxic to insects represents a further possibility for the creation of insect-resistant plants by genetic engineering methods. One example of such a protein is the toxin of *Bacillus thuringiensis*. The bacteria producing this toxin have already been used for decades in the biological control of certain species of caterpillars. However, because of their slow action compared with chemical crop protection agents, they have not been employed on a wide scale. Recently, the corresponding gene could be isolated and incorporated into tobacco plants.[185] Information is not yet available, however, on the insect resistance of a plant changed by this means. Another effective defense may consist in the formation of low-molecular-weight substances whose concentration rises considerably in the event of mechanical damage or insect attack and which at least suppress feeding.[175, 186, 187] These compounds can belong to a wide range of different chemical classes and are often secondary metabolites: phytoalexins, tannins, and even substances that function as hormones or signals (ecdysone, pheromones, and analogues of the juvenile hormone of insects). The utilization of this defense strategy for genetic engineering purposes appears problematic at present, since, on the one hand, numerous enzymes (and genes) are involved in the biosynthesis of the compounds mentioned, and on the other, these compounds frequently have unpleasant side effects on humans.

5.1.5. Stress Resistance

Many environmental factors produce stress conditions for plants: heat, aridness, excess moisture, high salt content of the soil, etc. As defense against these stress conditions, various counterreactions are initiated by the plant, the importance of which is not yet understood. In response to heat shock, for example, various proteins are synthesized whose precise function is not yet known. They are, however, certainly involved in a protective mechanism and are partly transported to the chloroplasts[188] and incorporated there.

Under other stress conditions, the formation of the same heat shock proteins frequently occurs, but on a smaller scale.[189] Stress-related fluctuations in the amino-acid content also occur; for example, a sharp increase in the proline content of plants is often observed.[190]

The genetic engineering approach to increasing stress resistance could lie in the identification and isolation of the most important genes involved in protection against stress conditions and the subsequent transfer of them from resistant to sensitive plants.

5.2. Changes in the Composition of Plant Substances

Several of the examples discussed in Section 5.1 in relation to the creation of resistance in plants already entailed the increased formation of specific plant substances. Further possibilities, which result in an "improvement" in the characteristics of a specific crop, will now be mentioned. This approach can be used, for instance, to influence both the production and processing of foodstuffs as well as plant raw materials used in industry.

Because of their high protein and amino-acid content, the seeds of cereals and vegetables constitute an important nutritional factor for humans and animals. However, the composition of the substances contained in this important food source does not always conform to requirements, since essential amino acids are often not present in the necessary amounts. Maize, for example, only has a low lysine and tryptophan content. For this reason, soybean flour is generally added when using maize as animal feed. Soya flour, however, is deficient in the amino acid methionine. A long-term goal of genetic engineering might be to change the amino-acid content of the storage proteins of important plants in such a way that a balanced composition is obtained. Using conventional breeding methods it has already been possible to develop maize varieties with a higher lysine content. However, this also resulted in undesirable features such as lower crop yields, lower protein content, and susceptibility to disease.[191] The genetic engineering approach to such a project is not simple, since large gene families are generally responsible for the forma-

tion of storage proteins. The increased expression of a single gene therefore does not appreciably affect the amino-acid content. Genetic engineering can be used, however, either to influence the metabolism in the seed in such a way that the content of a specific free amino acid is greatly increased or to introduce several, suitably altered genes. Other possibilities of improving the quality of plant seeds have been discussed.[192]

Apart from genetic changes in plant products used as food, the increased formation of substances of medicinal or industrial importance is doubtless also important.[193] An example is the genetic engineering of oil plants (e.g., soybean, rape, sunflower) with the aim of achieving a change in the oil composition. In principle, by transferring specific genes, it should be possible to obtain, within certain limits, uniform oil fractions which could be tailor-made for industrial application. For this purpose, however, much intensive basic research in the fields of biochemistry and molecular biology is still required. The new possibilities opened up for both agriculture and industry certainly appear to justify this kind of commitment.

5.3. Influencing Physiological Processes in Plants

Ribulose-1,5-bisphosphate carboxylase (rubisco) is a key enzyme in photosynthesis, since it is responsible for the fixation of carbon dioxide from the air (see Section 4.2). In addition to carbon dioxide, this enzyme also transfers oxygen to ribulose-1,5-bisphosphate and thus gives rise to the formation of undesirable side products. This reaction, known as photorespiration, diminishes the efficiency of photosynthesis.

Because of the fundamental importance of photosynthesis and photorespiration to all plants, there have been numerous attempts to use mutagenesis to create enzymes that exhibit a lower degree of photorespiration. Up to now, however, no commercially utilizable results have been obtained. The chances of reducing photorespiration have recently improved considerably, since the genes for the two subunits of rubisco have been isolated from photosynthetic bacteria and transferred to *E. coli*. An active enzyme was then formed in *E. coli*.[194] Furthermore, the three-dimensional structure of the enzymes from the photosynthetic bacteria *Rhodospirillum rubrum*[195a] and *Alcaligenes eutrophus*[195b] were recently published.

Moreover, gene transfer in *E. coli* has been used to create a hybrid, active enzyme of rubisco consisting of the large subunit from cyano bacteria and the small subunit from wheat.[196] It should now be possible, by means of site-directed mutagenesis with synthetic genes, to change almost any amino acid and subsequently study the effect on enzymatic activity. The great importance of an enzyme that, by means of an increased rate of fixation of carbon dioxide, gives rise to more efficient photosynthesis doubtless does not need to be emphasized.

5.4. Influencing Nitrogen Fixation

It should first be noted that nitrogen-fixing plants are unlikely to be produced before the turn of the millennium.

Table 6. Some applications of genetic engineering to nitrogen fixation.

a)	Fixation by free-living microorganisms
	Improvement of fixation reactions
b)	Fixation by symbiotic microorganisms
	Increase of efficiency (number of nodules, regulation)
	Host-range extension of rhizobia among leguminous plants
	Transfer of the capability to undergo symbiosis with other plants
c)	Nitrogen fixation in plants

However, this represents the "maximum requirement." A number of smaller steps could certainly be achieved in the next few years. Various possibilities for influencing nitrogen fixation are listed in Table 6. Numerous microorganisms in the soil, such as *Azotobacter*, *Azospirillum*, *Klebsiella*, and *Rhizobium*, are capable of fixing nitrogen from the air and forming ammonia. As a result of their metabolism, these bacteria contribute to nitrogen fertilization. The quantity of nitrogen bound by this biological fixation process is considerable. Worldwide, it amounts to many times the quantity of industrially produced ammonia.[179]

Nitrogen-fixing microorganisms can be divided into two large groups: free-living fixers and symbiontic fixers. Only in partnership with plants, frequently a leguminous crop, are the latter able to fix nitrogen. In this partnership, the microorganisms supply the product of their nitrogen fixation to the plant and in exchange receive from the plant assimilation products of photosynthesis. The proportion of symbiotically fixed nitrogen is far higher than the nitrogen combined by free-living microorganisms.

Structure and function of the genes involved in nitrogen fixation have up to now been investigated most thoroughly for *Klebsiella pneumoniae*, a free-living fixer, and *Rhizobium meliloti*, which forms a symbiosis with alfalfa.[198, 199]

In *K. pneumoniae*, the enzymes specifically involved in nitrogen fixation are coded by a block of 17 adjacent genes. The large number of genes involved in this process is one of the difficulties that has to be overcome for their transfer to plants. The control regions (promoters) of all these genes have to be changed and adapted to the conditions in the plant. Additional difficulties arise owing to the oxygen sensitivity of nitrogenase, the enzyme that reduces nitrogen, and the high energy requirement of the whole process of nitrogen fixation and assimilation.

When sufficient ammonium ions are present in the surrounding environment, the energy-consuming process of nitrogen fixation by free-living fixers is discontinued, since the requirement can now be met by uptake of ammonium ions. This regulation is achieved by specific genes, which, in the presence of ammonium ion, prevent the formation of the nitrogen-fixing enzymes. For agricultural application, strains in which this regulation is no longer operative can represent an important contribution toward improving the nitrogen supply.

The symbiotic nitrogen fixation of rhizobia takes place after formation of typical root nodules (Fig. 13). Development of a symbiosis depends on numerous complex steps: mutual recognition between microorganism and plant, infection of the root, formation of nodules, and finally the actual nitrogen fixation and exchange of molecules between plant and microorganism. About 40 genes of the plant are involved in the formation and functioning of the nodules.[200] In principle, each of the steps mentioned op-

Fig. 13. Symbiotic nodules on the roots of a broad bean plant as a consequence of infection with rhizobia. Fixation of nitrogen takes place in these nodules.

ens up a number of possibilities for influencing the overall process by means of genetic engineering. In the mutual recognition and formation of nodules, for instance, low-molecular-weight substances (flavones), which are excreted by the plant, are involved.[201] By influencing the type and quantity of the flavones that are biosynthesized and distributed, it may be possible to influence the number of nodules formed and thereby to achieve an increase in nitrogen fixation. The discovery of soybean plants that in comparison to the wild variety, possess a higher number of nodules, supports this possibility.[202]

The various symbiotic rhizobium strains exhibit a pronounced specificity for certain host plants. Marked differences arise in this regard in the growth behavior and fixation rates of the various bacterial strains. A realistic goal would be to widen the host spectrum of the rhizobia involved. This could result in a marked improvement in the supply of nitrogen to leguminous plants that up to now have only been capable of forming a symbiosis with slow-growing rhizobia.

Several of the plant gene products that are involved in the formation and functioning of nodules also occur in plants not able to form a symbiosis. It may be easier to use genetic engineering methods to enable these plants to form a symbiosis with bacteria than to transfer to them the ability to fix the nitrogen themselves.

5.5. Genetic Engineering as an Aid to Plant Breeding

Molecular biology methods can be used to supply precise information on the presence of specific genes in plants. The sensitivity of these techniques has been increased to the extent that they can be carried out with fewer than ten plant cells.[203] There are numerous possible applications of this technique in plant breeding: rapid examination of the progeny of crosses and of unknown genotypes for the presence of specific genes, characterization of certain varieties by identifying characteristic DNA restriction patterns (RFLP: restriction fragment length polymorphism),[204] information on the relationship between specific varieties, and tests for the presence of viruses in seed or breeding material. A comparison between such tests and the corresponding serological tests revealed that the results obtained by hybridization with DNA are more reliable and informative in determining the presence of viruses.[205]

6. Problems and Risks

The objectives of genetic engineering with plants, described in Section 5, are unlikely to cause any risk. Serious objections can hardly be raised against the development of resistant or high-yield varieties, since this has been the aim of conventional plant breeding methods for many decades. In the case of herbicide resistance, however, a discussion would appear to be useful in order to prevent misunderstandings. In addition to the hypothetical risks that might arise as a result of modifying plants by genetic engineering methods, herbicide resistance will also be discussed here.

6.1. Risks Resulting from Plants Modified by Genetic Engineering

Genetic engineering permits the isolation of genes from widely differing organisms and their incorporation in plants. With present methods it is only possible to transfer specific genes whose function is generally known. The following hypothetical sources of risk exist:

1. Development of rampant-growing plants with uncontrolled propagation (weeds);
2. Transmission of the transferred genes from crops to weeds by cross-fertilization;
3. Formation of toxic substances in plants modified by genetic engineering.

First, the release of plants modified by genetic engineering is far less problematic than the release of modified microorganisms or animals. Undesired plant growth can after all be controlled by various means (herbicides, mechanical weed control), which belong to the daily activities of the farmer.

Second, prior to a field experiment, plants modified by genetic engineering are first tested under laboratory conditions and in greenhouses. During this phase, any undesirable or harmful characteristics in a plant can be identified.

Third, plant breeders have for centuries achieved good results with widely differing crosses, including some that would never have come about without human assistance. In such experiments, tens of thousands of different genes are recombined. This has not up to now resulted in any serious problems. The methods of cell biology have also been used to create gene combinations in new plants,

which would never have resulted under natural conditions. Here one may call to mind the protoplast fusions between tomato and potato (cf. Section 2.2.1).[30] Even a critical examination gave no indication here of any possible risks. It is therefore inconceivable that the transfer of a few genes by genetic engineering methods might give rise to a dangerous situation.

Fourth, characteristics such as rapid, uncontrolled growth (weed formation) can be obtained only by means of a large number of genes which must be suitably adapted to one another. For this reason, it is also inconceivable that new weeds could be created unintentionally through genetic engineering with plants.

Fifth, characteristics unintentionally transferred to other plants (e.g., weeds) can only be preserved and dispersed if the necessary selection pressure is present. If the customary rules of good agricultural practice are observed (e.g., rotation of crops and herbicides), this is unlikely to occur when an unintentional transfer of individual genes takes place. Moreover, only in a few instances can crops cross with closely related weeds.

Sixth, in conventional breeding methods the possibility cannot be entirely ruled out that the concentrations of toxic substances peculiar to plants will be greater after a crossing experiment. One example of this is the development of varieties of potato possessing an unpleasant, burning taste due to an increased concentration of glycoalkaloids.[206] This was not a very surprising result, since many wild varieties of potato, which are frequently used in the development of new varieties, already contain high concentrations of these glycoalkaloids. Here, too, similar effects are unlikely to be obtained by selective transfer of a few genes. Moreover, toxic side effects can be easily identified by appropriate analyses and test methods.

In summary, it is difficult to recognize any specific or potential risk due to plants modified by genetic engineering.

6.2. Release of Plants Modified by Genetic Engineering

In the Federal Republic of Germany, organisms modified by genetic engineering may not be tested or released under field conditions. On request and after a hearing of the "Central Committee for Biological Safety," the Federal Health Department can, in agreement with the responsible federal biological institutes, allow exceptions.[207] As far as we know, no such experiments have hitherto been carried out.

It was recently reported in the press that in the USA two field experiments with tobacco plants modified by genetic engineering were approved by the responsible authorities. In one case, the plants contain an additional gene from yeast (the alcohol dehydrogenase gene) and, in the other case, they contain the toxin gene from *Bacillus thuringiensis*. The aim of the experiments now being conducted is to show that under field conditions an additional gene does not cause a change in growth behavior. In the latter case, resistance to caterpillars is also being tested under field conditions.

Within Europe, the preconditions and rules for carrying out field experiments on organisms modified by genetic engineering still vary considerably. From the viewpoint of both safety and competitiveness of the companies and research institutes involved, a uniform ruling, at least within Europe, would be extremely desirable.

6.3. Herbicide Resistance

The most important advantages resulting from the cultivation of herbicide-resistant crops are again summarized below:

- Use of herbicides only when required, and thus no further need for preventive application
- Increased economic efficiency for the farmer
- Increased use of ecologically favorable (more rapidly degradable) herbicides in place of older products
- Reduced soil erosion by preventing the appearance of exposed areas
- Replacement of herbicide mixtures by a single nonselective herbicide

These advantages are opposed by a number of potential disadvantages and apprehensions:

- Creation of ecological problems owing to increased use of herbicides when herbicide-resistant crops are grown
- Emergence of herbicide-resistant weeds
- Further decrease in the number of different varieties

The discussion on herbicide-resistant plants[208] should not overlook the fact that many years of experience have already been acquired in the use of selective herbicides in agriculture. The resistant crops possess metabolic pathways that render individual herbicides ineffective. A natural herbicide resistance thus exists, which applies only to the individual crop. The use of these selective herbicides on crops with natural resistance does not differ from the application of nonselective herbicides and the corresponding herbicide-resistant crops created by genetic engineering.

Because of the possibility of using herbicides only when required, i.e., not until weed infestation has gone beyond an acceptable level, and because of the replacement of several selective herbicides by a single nonselective one, the use of herbicide-resistant plants should result in less use of herbicides.

In the development of resistances to herbicides with long-lasting action, it cannot be ruled out that over a period of years the herbicide will accumulate in the soil and thus cause ecological problems. The trend observed at all research institutes toward the development of resistances only against ecologically favorable herbicides is therefore to be welcomed. This shows that the specific properties of the respective herbicide are the decisive factors in the discussion on herbicide resistance (degradation, environmental behavior, toxicity, possibility of accumulation, etc.). A separate discussion on each herbicide is therefore necessary.

The possible formation of herbicide-resistant weeds is probably not a major problem in the use of nonselective herbicides. For example, in spite of the fact that the herbi-

cide glyphosate has been used for over twelve years, no problems have yet arisen as a result of the development of resistances. In the event that herbicide-resistant weeds do indeed emerge, these can be controlled at any time by herbicides with other sites of action.

Herbicide resistance in a specific plant variety will probably be as important a characteristic, as, for example, resistance to disease, hardiness, or high yield. None of these characteristics alone, however, is a decisive factor in seriously eliminating other varieties of crops. Therefore, herbicide resistance is unlikely to reduce the existing number of varieties to a greater extent than the other breeding objectives mentioned. In this connection, it should also be emphasized that, as regards the modification of plants by genetic engineering, the preservation of as many different varieties as possible is of very considerable importance, since only in this way is a wide range of natural genes accessible.

Herbicide resistance is probably one of the most easily attainable objectives in genetic engineering with plants. The experience gained here can subsequently be utilized in solving more complex problems, such as the creation of resistances to virus infections, animal pests, or fungal diseases.

7. Summary and Prospects

A number of crop plants can be regenerated from single cells or protoplasts in any desired quantity by means of cell culture techniques. Such regenerating cell cultures are used both for selection of mutants and for DNA transformation experiments. DNA transfer by means of engineered Ti plasmids and *Agrobacterium tumefaciens* has become an established technique for a rapidly growing number of dicotyledonous plants.

Proof of general transformability by agrobacteria is still lacking in cereals. Alternative methods of DNA transfer are thus being developed. Direct gene transfer in protoplasts has proved to have universal applicability. Transformed cereal cell cultures are accessible from DNA-treated protoplasts by routine methods. The dogma that cereal protoplasts are incapable of being regenerated has been refuted by the successful plant regeneration from rice protoplasts.

Major efforts are being undertaken to render gene transfer independent of cell culture methods. For example, an attempt is being made to transfer foreign DNA into reproductive cells both by pollen transformation and by direct DNA injection into young inflorescences.

The number of isolated plant genes is rapidly increasing. By analysis of the regulation sequences of these genes, DNA segments are becoming accessible that are responsible for tissue-specific or environmentally stimulated expression of genes in plants.

The first genes that may be of economic importance to plant breeding and crop protection have already been transferred to plants. These include genes that impart to the transformants resistance against viruses, insects, or herbicides.

The further development of the biochemistry and molecular biology of plants will result in the elucidation of the molecular mechanisms of previously unexplained plant diseases, for example, fungal and viroid diseases. Although the complete sequence of the infectious RNA of a number of viroids has been determined,[209] there is still no explanation for the mechanism and causes of plant damage.

The efforts being made in the genetic engineering field will result in more resistant and productive plants. These plants will be available to the farmer in the 1990s. On the one hand, this will enable an important contribution to be made toward solving the problem of world famine; on the other hand, the production of tailor-made raw materials for industrial application will open up additional markets for agricultural products in industrialized countries. It may even be possible to use wild plants to create new types of crops with advantageous characteristics (e.g., salt tolerance, high biomass production, good protein quality in the harvested crop) by employing breeding and genetic engineering methods.[210]

Close cooperation between biochemists, cell biologists, molecular biologists, plant pathologists, and plant breeders is urgently necessary in order to obtain more productive crops with high adaptability and less susceptibility to disease.

Our thanks are due to H. Dräger for preparation of the light-optical micrographs. We wish to thank B. Diehls and R. Stehr for typing the manuscript and P. Spönemann for drawing the figures.

Received: January 26, 1987 [A 618 IE]
German version: *Angew. Chem. 99* (1987) 392

[1] D. M. Coen, J. R. Bedbrook, L. Bogorad, A. Rich, *Proc. Natl. Acad. Sci. USA 74* (1977) 5487.
[2] K. Shinozaki, M. Ohme, M. Tanaka, T. Wakasugi, N. Hayashida, T. Matsubayashi, N. Zaita, J. Chunwongse, T. Obohata, K. Yamaguchi-Shinozaki, C. Ohto, K. Torazawa, B. Y. Meng, M. Sugita, H. Deno, T. Kamogashira, K. Yamada, T. Kusuda, F. Takaiawa, A. Kato, N. Tohdoh, H. Schimada, M. Sugiura, *EMBO J. 5* (1986) 2043.
[3] M. D. Dibner, *Science 232* (1986) 1367.
[4] S. K. Sen, K. L. Giles (Eds.): *Plant Cell Culture in Crop Improvement*, Plenum, New York 1983.
[5] L. C. Fowke, F. Constabel (Eds.): *Plant Protoplasts*, CRC Press, Boca Raton 1985.
[6] I. K. Vasil (Ed.): *Cell Culture and Somatic Cell-genetics of Plants*, Academic Press, New York 1984.
[7] E. Thomas, P. J. King, I. Potrykus, *Z. Pflanzenzücht. 82* (1979) 1.
[8] T. Murashige, F. Skoog, *Physiol. Plant. 15* (1962) 473.
[9] F. Skoog, C. O. Miller, *Symp. Soc. Exp. Biol. 11* (1957) 118.
[10] M. D. Sacristan, G. Melchers, *MGG Mol. Gen. Genet. 105* (1969) 317.
[11] C. J. Sluis, K. A. Walker, *IAPTC Newslett. 47* (1985) 2.
[12] K. A. Walker, S. I. Sato, *Plant Cell Tissue Organ Cult. 1* (1981) 109.
[13] J. P. Ranch, L. Oglesby, A. C. Zielinski, *In Vitro 21* (1985) 653.
[14] E. Thomas, F. Hoffmann, I. Potrykus, G. Wenzel, *MGG Mol. Gen. Genet. 145* (1976) 245.
[15] K. Redenbaugh, I. Nichol, M. Kossler, B. Paasch, *In Vitro 20* (1984) 256.
[16] T. Nagata, I. Tabeke, *Planta 99* (1971) 12.
[17] K. K. Kartha, M. R. Michayluk, K. N. Kao, O. L. Gamborg, F. Constabel, *Plant Sci. Lett. 3* (1974) 265.
[18] J. F. Shepard, R. E. Totten, *Plant Physiol. 60* (1977) 313.
[19] F. J. Zapata, P. K. Evans, J. B. Power, E. C. Cocking, *Plant Sci. Lett. 8* (1977) 119.
[20] A. V. P. Dos Santos, D. E. Outka, E. C. Cocking, M. R. Davey, *Z. Pflanzenphysiol. 99* (1980) 261; K. N. Kao, M. R. Michayluk, *ibid. 96* (1980) 135.

[21] T. M. Fujimura, M. Sakurai, H. Akagi, T. Negishi, A. Hirose, *Plant Tissue Cult. Lett. 2* (1985) 74; J. A. Thompson, R. Abdullah, E. C. Cocking, *Plant Sci. 47* (1986) 123; Y. Yamada, Z. Q. Yang, D. T. Tang, *Plant Cell Rep. 5* (1986) 85.
[22] K. Ohyama, O. L. Gamborg, R. A. Miller, *Can. J. Bot. 50* (1972) 2077.
[23] I. Potrykus, *Z. Pflanzenphysiol. 70* (1973) 364.
[24] L. Szabados, G. Hadlaczky, D. Dudits, *Planta 151* (1981) 141.
[25] W. A. Keller, G. Melchers, *Z. Naturforsch. C28* (1973) 737.
[26] K. N. Kao, M. R. Michayluk, *Planta 115* (1974) 355.
[27] L. Menczel, K. Wolfe, *Plant Cell Rep. 3* (1983) 196.
[28] M. Senda, J. Takeda, S. Abe, T. Nakamura, *Plant Cell Physiol. 20* (1978) 1441.
[29] G. Melchers, M. D. Sacristan, A. A. Holder, *Carlsberg Res. Commun. 43* (1978) 203.
[30] Y. Y. Gleba, F. Hoffmann, *Planta 149* (1980) 112.
[31] O. Schieder, *MGG Mol. Gen. Genet. 162* (1978) 113.
[32] D. Dudits, O. Feijer, G. Hadlaczky, C. Koncz, G. B. Lazar, G. Horvath, *MGG Mol. Gen. Genet. 179* (1980) 283.
[33] D. Dudits, E. Maroy, T. Praznovszky, J. Györgyey, *Abstr. VIIth Int. Congr. Plant Tissue Cell Cult.*, University of Minnesota, Minneapolis 1986, p. 20.
[34] P. Carlson, *Science 180* (1973) 1366.
[35] G. Wenzel, *Annu. Rev. Phytopathol. 23* (1985) 149.
[36] P. Thanutong, J. Furusawa, M. Yamamoto, *Theor. Appl. Genet. 66* (1983) 209.
[37] M. Behnke, *Theor. Appl. Genet. 55* (1979) 69.
[38] M. Behnke, *Theor. Appl. Genet. 56* (1980) 151.
[39] E. Rehbein, *Dissertation*, Universität Bonn 1983, p. 64.
[40] E. A. Shahin, R. Spivey, *Theor. Appl. Genet. 73* (1986) 164.
[41] M. D. Sacristan, *Theor. Appl. Genet. 61* (1982) 193.
[42] C. L. Hartmann, T. Y. McCoy, T. R. Knons, *Plant Sci. Lett. 34* (1984) 183.
[43] A. O. Latunde-Duda, J. A. Lucas, *Plant Sci. Lett. 32* (1983) 205.
[44] B. G. Gengenbach, E. Green, C. M. Donovan, *Proc. Natl. Acad. Sci. USA 74* (1977) 5113.
[45] U. Matern, G. Strobel, J. Shepard, *Proc. Natl. Acad. Sci. USA 75* (1978) 4935.
[46] J. F. Shepard, D. Bidney, E. A. Shahin, *Annu. Rev. Phytopathol. 19* (1981) 145.
[47] G. J. Jellis, R. E. R. E. Gunn, R. E. Boulton, *EAPR Abstr. Conf. Pap. 1984*, 380.
[48] H. H. Murakishi, P. S. Carlson, *Plant Cell Rep. 1* (1982) 94.
[49] K. A. Barden, S. Schiller, H. H. Smith, H. H. Murakishi, *Plant Sci. 45* (1986) 209.
[50] F. Siegemund, *Biol. Zentralbl. 100* (1981) 155.
[51] F. D'Amato in J. Reinert, Y. P. S. Bajaj (Eds.): *Applied and Fundamental Aspects of Plant Cell, Tissue and Organ Culture*, Springer, Berlin 1977, p. 343.
[52] P. J. Larkin, W. R. Scowcroft, *Theor. Appl. Genet. 67* (1981) 443.
[53] D. A. Evans, W. R. Sharp, H. P. Medina-Filho, *Am. J. Bot. 71* (1984) 759.
[54] V. Walbot, C. A. Cullis, *Annu. Rev. Plant Physiol. 36* (1985) 367.
[55] V. M. Peschke, R. L. Phillips, B. G. Gengenbach, *Abstr. VIIth Int. Congr. Plant Tissue Cell Cult.*, University of Minnesota, Minneapolis 1986, p. 285.
[56] J. Schell in L. Ledoux (Ed.): *Genetic Manipulations with Plant Materials*, Plenum, New York 1975, p. 163.
[57] M. Cleene, J. De Ley, *Bot. Rev. 42* (1976) 389.
[58] A. C. Braun, P. R. White, *Phytopathology 33* (1943) 85.
[59] A. Petit, S. Delhaye, J. Tempé, G. Morel, *Physiol. Vég. 8* (1970) 205.
[60] G. Bomhoff, P. M. Klapwijk, H. C. M. Kester, R. A. Schilperoort, J. P. Hernalsteens, J. Schell, *MGG Mol. Gen. Genet. 145* (1976) 177.
[61] J. Tempé, A. Petit, S. K. Farrand in D. P. S. Verma, T. Hohn (Eds.): *Plant Gene Research: Genes Involved in Microbe-Plant Interactions*, Springer, Berlin 1984, p. 271.
[62] A. C. Braun, R. J. Mandle, *Growth 12* (1958) 255.
[63] I. Zaenen, N. van Larebeke, H. Teuchy, M. Van Montagu, J. Schell, *J. Mol. Biol. 86* (1974) 109.
[64] N. van Larebeke, G. Engler, M. Holsters, S. Van den Elsacker, J. Zaenen, R. A. Schilperoort, J. Schell, *Nature (London) 252* (1974) 169.
[65] A. Montoya, M.-D. Chilton, M. P. Gordon, D. Sciaky, E. W. Nester, *J. Bacteriol. 129* (1977) 101.
[66] J. Schell, M. Van Montagu, A. Depicker, D. De Waele, G. Engler, C. Genetello, J. P. Hernalsteens, M. Holsters, E. Messens, A. Silva, S. Van den Elsacker, N. van Larebeke, I. Zaenen in L. Bogorad, J. H. Weil (Eds.): *Nucleic Acids and Protein Synthesis in Plants*, Plenum, New York 1977, p. 329.
[67] J. Leemans, R. Deblaere, L. Willmitzer, H. De Greve, J. P. Hernalsteens, M. Van Montagu, J. Schell, *EMBO J. 1* (1982) 147.
[68] G. Schröder, S. Waffenschmidt, E. W. Weiler, J. Schröder, *Eur. J. Biochem. 138* (1984) 387.
[69] L. Willmitzer, P. Dhaese, P. Schreier, W. Schmalenbach, M. Van Montagu, J. Schell, *Cell (Cambridge, Mass.) 32* (1983) 1045.
[70] M. D. Chilton, M. H. Drummond, D. J. Merlo, D. Sciaky, A. L. Montoya, M. P. Gordon, E. W. Nester, *Cell (Cambridge, Mass.) 11* (1977) 263.
[71] M. D. Chilton, R. K. Saiki, N. Yadav, M. P. Gordon, F. Quetier, *Proc. Natl. Acad. Sci. USA 77* (1980) 4060.
[72] L. Willmitzer, M. De Beuckeleer, M. Lemmers, M. Van Montagu, J. Schell, *Nature (London) 287* (1980) 359.
[73] L. Willmitzer, G. Simons, J. Schell, *EMBO J. 1* (1982) 139.
[74] M. Lemmers, M. De Beuckeleer, M. Holsters, P. Zambryski, A. Depicker, J. P. Hernalsteens, M. Van Montagu, J. Schell, *J. Mol. Biol. 144* (1980) 353.
[75] M. F. Thomashow, R. Nutter, A. L. Montoya, M. P. Gordon, E. W. Nester, *Cell (Cambridge, Mass.) 19* (1980) 729.
[76] M. De Beuckeleer, M. Lemmers, G. De Vos, L. Willmitzer, M. Van Montagu, J. Schell, *MGG Mol. Gen. Genet. 183* (1981) 283.
[77] H. Van Onckelen, E. Prinsen, D. Inzé, P. Rüdelsheim, M. Van Lijsebettens, A. Follin, J. Schell, M. Van Montagu, J. De Greef, *FEBS Lett. 198* (1986) 357.
[78] L. S. Thomashow, S. Reeves, M. F. Thomashow, *Proc. Natl. Acad. Sci. USA 81* (1984) 5071.
[79] A. Depicker, S. Stachel, P. Dhaese, P. Zambryski, H. M. Goodman, *J. Mol. Appl. Genet. 1* (1982) 561.
[80] H. De Greeve, P. Dhaese, J. Seurinck, M. Lemmers, M. Van Montagu, J. Schell, *J. Mol. Appl. Genet. 2* (1983) 499.
[81] G. F. Barry, S. G. Rogers, R. I. Fraley, L. Brand, *Proc. Natl. Acad. Sci. USA 81* (1984) 4776.
[82] E. Messens, A. Lenaerts, M. Van Montagu, R. W. Hedges, *MGG Mol. Gen. Genet. 199* (1985) 344.
[83] D. J. Garfinkel, R. B. Simpson, L. W. Ream, F. F. White, M. P. Gordon, E. W. Nester, *Cell (Cambridge, Mass.) 27* (1981) 143.
[84] F. Salomon, R. Deblaere, J. Leemans, J. P. Hernalsteens, M. Van Montagu, J. Schell, *EMBO J. 3* (1984) 141.
[85] H. Joos, D. Inzé, A. Caplan, M. Sormann, M. Van Montagu, J. Schell, *Cell (Cambridge, Mass.) 32* (1983) 1057.
[86] P. Zambryski, H. Joos, C. Genetello, J. Leemans, M. Van Montagu, J. Schell, *EMBO J. 2* (1983) 2143.
[87] P. Zambryski, A. Depicker, K. Kruger, H. Goodman, *J. Mol. Appl. Genet. 1* (1982) 361.
[88] K. Wang, L. Herrera-Estrella, M. Van Montagu, P. Zambryski, *Cell (Cambridge, Mass.) 38* (1984) 455.
[89] J. Schell, M. Van Montagu, *Bio/Technology 1* (1983) 175.
[90] Z. Koukoliková-Nicola, R. D. Shillito, B. Hohn, K. Wang, M. Van Montagu, P. Zambryski, *Nature (London) 313* (1985) 191.
[91] H. J. Klee, F. F. White, V. N. Iyer, M. P. Gordon, E. W. Nester, *J. Bacteriol. 153* (1983) 878.
[92] S. E. Stachel, E. W. Nester, *EMBO J. 5* (1986) 1445.
[93] S. E. Stachel, E. Messens, M. Van Montagu, P. Zambryski, *Nature (London) 318* (1985) 624.
[94] S. E. Stachel, P. Zambryski, *Cell (Cambridge, Mass.) 46* (1986) 325.
[95] D. J. Garfinkel, E. W. Nester, *J. Bacteriol. 144* (1980) 732.
[96] C. J. Douglas, R. J. Staneloni, R. A. Rubin, E. W. Nester, *J. Bacteriol. 161* (1985) 850.
[97] A. Hoekema, P. R. Hirsch, P. J. J. Hoykaas, R. A. Schilperoort, *Nature (London) 303* (1983) 179.
[98] G. An, B. D. Watson, S. E. Stachel, M. P. Gordon, E. W. Nester, *EMBO J. 4* (1985) 277.
[99] R. B. Horsch, J. E. Fry, N. L. Hoffmann, D. Eichholtz, S. G. Rogers, R. T. Fraley, *Science 227* (1985) 1229.
[100] L. Marton, G. J. Wullems, L. Molendijk, R. A. Schilperoort, *Nature (London) 277* (1979) 129.
[101] a) J. P. Hernalsteens, L. Thia-Tong, J. Schell, M. Van Montagu, *EMBO J. 3* (1984) 3039; b) G. M. S. Hoykaas-Van Slogteren, P. J. J. Hoykaas, R. A. Schilperoort, *Nature (London) 311* (1984) 763.
[102] N. Grinsley, T. Hohn, J. W. Davies, B. Hohn, *Nature 325* (1987) 177.
[103] M. R. Davey, E. C. Cocking, J. Freeman, N. Pearce, J. Tudor, *Plant Sci. Lett. 18* (1980) 307.
[104] I. Potrykus, R. D. Shillito, M. W. Saul, J. Paszkowski, *Plant Mol. Biol. Rep. 3* (1985) 117.
[105] D. Hanahan, *J. Mol. Biol. 166* (1983) 557.
[106] H. Potter, L. Weir, P. Leder, *Proc. Natl. Acad. Sci. USA 81* (1984) 7161.

[107] R. D. Shillito, M. W. Saul, J. Paszkowski, M. Müller, I. Potrykus, *Bio/Technology 3* (1985) 1099.
[108] H. Uchimija, T. Fushimi, H. Hashimoto, H. Harada, K. Syono, Sugawara, *MGG Mol. Gen. Genet. 1987*, in press.
[109] M. E. Fromm, L. P. Taylor, V. Walbot, *Nature (London) 319* (1986) 791.
[110] H. Lörz, B. Baker, J. Schell, *MGG Mol. Gen. Genet. 199* (1985) 178.
[111] R. J. Shepard, R. H. Lawson in E. Kurstak (Ed.): *Handbook of Plant Virus Infections and Comparative Diagnosis*, Elsevier, Amsterdam 1981, p. 847.
[112] N. Brisson, J. Paszkowski, J. R. Penswick, B. Gronenborn, I. Potrykus, T. Hohn, *Nature (London) 310* (1984) 511.
[113] D. Hess, H. Lörz, E. M. Weissert, *Z. Pflanzenphysiol. 74* (1974) 52.
[114] Y. Ohta, *Proc. Natl. Acad. Sci. USA 83* (1986) 715.
[115] J. C. Sanford, K. A. Skubik, B. J. Reisch, *Theor. Appl. Genet. 69* (1985) 571.
[116] M. R. Capecchi, *Cell (Cambridge, Mass.) 22* (1980) 479.
[117] H. H. Steinbiß, P. Stabel, R. Toepfer, R. D. Hirtz, J. Schell in G. P. Chapman, S. H. Mantell, R. W. Daniels (Eds.): *The experimental manipulation of ovule tissue*, Longman, New York 1985, p. 64.
[118] A. de la Peña, H. Lörz, J. Schell, *Nature (London) 325* (1987) 274.
[119] J. P. Hernalsteens, F. Van Vliet, M. De Beuckeleer, A. Depicker, G. Engler, M. Lemmers, M. Holsters, M. Van Montagu, J. Schell, *Nature (London) 287* (1980) 654.
[120] K. A. Barton, A. N. Binns, A. J. M. Matzke, M.-D. Chilton, *Cell (Cambridge, Mass.) 32* (1983) 1033.
[121] C. H. Shaw, J. Leemans, C. H. Shaw, M. Van Montagu, J. Schell, *Gene 23* (1983) 315.
[122] R. Breathnach, P. Chambon, *Annu. Rev. Biochem. 50* (1981) 349.
[123] J. Messing, D. Geraghty, G. Heidecker, N. T. Hu, J. Kridl, J. Rubenstein in T. Kosuge, C. P. Meredith, A. Hollaender (Eds.): *Genetic Engineering of Plants, An Agricultural Perspective*, Plenum, New York 1983, p. 211.
[124] F. Wengenmayer, *Angew. Chem. 95* (1983) 874; *Angew. Chem. Int. Ed. Engl. 22* (1983) 842.
[125] F. Gannon, K. O'Hare, F. Perrin, J. P. Le Pennec, C. Benoist, M. Cochet, R. Breathnach, A. Royal, A. Garapin, B. Cami, P. Chambon, *Nature (London) 278* (1979) 428.
[126] M. Birnstiel, M. Busslinger, K. Strub, *Cell (Cambridge, Mass.) 41* (1985) 349.
[127] L. Herrera-Estrella, A. Depicker, M. Van Montagu, J. Schell, *Nature (London) 303* (1983) 209.
[128] L. Herrera-Estrella, M. De Block, E. Messens, J. P. Hernalsteens, M. Van Montagu, J. Schell, *EMBO J. 2* (1983) 987.
[129] J. Reden, W. Dürckheimer, *Top. Curr. Chem. 83* (1979) 105.
[130] R. Fluhr, C. Kuhlemeier, F. Nagy, N. H. Chua, *Science 232* (1986) 1106.
[131] T. J. V. Higgins, *Annu. Rev. Plant Physiol. 35* (1984) 191.
[132] E. M. Tobin, J. L. Suttie, *Plant Physiol. 65* (1980) 641.
[133] T. F. Gallagher, R. J. Ellis, *EMBO J. 1* (1982) 1493.
[134] M. P. Timko, A. P. Kausch, C. Castresana, J. Fassler, L. Herrera-Estrella, G. Van den Broeck, M. Van Montagu, J. Schell, A. R. Cashmore, *Nature (London) 318* (1985) 579.
[135] L. Herrera-Estrella, G. Van den Broeck, R. Maenhaut, M. Van Montagu, J. Schell, M. Timko, A. Cashmore, *Nature (London) 310* (1984) 115.
[136] G. Morelli, F. Nagy, R. T. Fraley, S. G. Rogers, N. H. Chua, *Nature (London) 315* (1985) 200.
[137] J. D. G. Jones, P. Dunsmuir, K. J. Bedbrook, *EMBO J. 4* (1985) 2411.
[138] P. R. Sanders, J. A. Winter, A. R. Barnason, S. G. Rogers, R. T. Fraley, *Nucl. Acids Res. 15* (1987) 1543.
[139] F. Schöffl, E. Raschke, R. T. Naguo, *EMBO J. 3* (1984) 2491.
[140] E. Mösinger, A. Batschauer, E. Schäfer, K. Apel, *Eur. J. Biochem. 147* (1985) 137.
[141] N. M. Crawford, W. H. Campbell, R. W. Davis, *Proc. Natl. Acad. Sci. USA 83* (1986) 8073.
[142] J. K. Okamuro, K. D. Jofuku, R. B. Goldberg, *Proc. Natl. Acad. Sci. USA 83* (1986) 8240.
[143] G. Lamppa, F. Nagy, N. H. Chua, *Nature (London) 316* (1985) 750.
[144] B. Keith, N. H. Chua, *EMBO J. 5* (1986) 2419.
[145] P. Eckes, S. Rosahl, J. Schell, L. Willmitzer, *MGG Mol. Gen. Genet. 205* (1986) 14.
[146] M. Holsters, R. Villarroel, J. Gielen, J. Seurinck, H. De Greeve, M. Van Montagu, J. Schell, *MGG Mol. Gen. Genet. 190* (1983) 35.
[147] M. De Block, L. Herrera-Estrella, M. Van Montagu, J. Schell, P. Zambryski, *EMBO J. 3* (1984) 1681.
[148] T. J. Mozer, D. C. Tiemeier, E. G. Jaworski, *Biochemistry 22* (1983) 1068.
[149] R. J. Shimabukuro, W. C. Walsh, R. A. Hoerauf, *J. Agric. Food Chem. 27* (1977) 615.
[150] H. Kassebeer, *Z. Pflanzenkrankh. Pflanzenschutz 78* (1971) 158.
[151] M. R. Gebhardt, T. C. Daniel, E. E. Schweizer, R. R. Allmaras, *Science 230* (1985) 625.
[152] R. S. Chaleff, *Science 219* (1983) 676.
[153] S. R. Singer, C. N. McDaniel, *Plant Physiol. 78* (1985) 411.
[154] D. Scheel, J. E. Casida, *Pestic. Biochem. Physiol. 23* (1985) 398.
[155] P. C. Anderson, K. A. Hibberd, *Weed Sci. 33* (1985) 479.
[156] R. S. Chaleff, T. B. Ray, *Science 223* (1984) 1148.
[157] D. Shaner, T. Malefyt, P. Anderson in C. G. Copping, P. Rodgers (Eds.): *Biotechnology and its Application to Agriculture*, BCPC Publications, Bracknell 1985, BCPC Monogr. No. 32, p. 45.
[158] D. M. Stalker, W. R. Hiatt, L. Comai, *J. Biol. Chem. 260* (1985) 4724.
[159] C. C. Smart, D. Johanning, G. Müller, N. Amrhein, *J. Biol. Chem. 260* (1985) 16338.
[160] G. Donn, E. Tischer, J. A. Smith, H. M. Goodman, *J. Mol. Appl. Genet. 2* (1984) 621.
[161] H. C. Steinrücken, N. Amrhein, *Biochem. Biophys. Res. Commun. 94* (1980) 1207.
[162] F. Schwerdtle, H. Bieringer, M. Finke, *Z. Pflanzenkrankh. Pflanzenschutz, Sonderheft IX* (1981) 431.
[163] D. M. Shah, R. B. Horsch, H. J. Klee, G. M. Kishore, J. A. Winter, N. E. Tumer, C. M. Hironaka, P. R. Sanders, C. S. Gasser, S. Aykent, N. R. Siegel, S. G. Rogers, R. T. Fraley, *Science 233* (1986) 478.
[164] L. Comai, D. Facciotti, W. R. Hiatt, G. Thompson, R. E. Rose, D. M. Stalker, *Nature (London) 317* (1985) 741.
[165] E. Tischer, S. Das Sarma, H. M. Goodman, *MGG Mol. Gen. Genet. 203* (1986) 221.
[166] S. Das Sarma, E. Tischer, H. M. Goodman, *Science 232* (1986) 1242.
[167] P. P. Abel, R. S. Nelson, B. De, N. Hoffmann, S. G. Rogers, R. T. Fraley, R. N. Beachy, *Science 232* (1986) 738.
[168] L. C. van Loon, *Plant Mol. Biol. 4* (1985) 111.
[169] R. A. M. Hooft van Huijsduijnen, B. J. C. Cornelissen, L. C. van Loon, J. H. van Boom, M. Tromp, J. F. Bol, *EMBO J. 4* (1985) 2167.
[170] R. A. M. Hooft van Huijsduijnen, L. C. van Loon, J. F. Bol, *EMBO J. 5* (1986) 2057.
[171] P. Ahl, S. Gianinazzi, *Plant Sci. Lett. 26* (1982) 173.
[172] C. James, *Seed Sci. Technol. 9* (1981) 679.
[173] R. A. Dean, J. Kuc, *Trends Biotechnol. 3* (1985) 125.
[174] R. C. Riggleman, B. Fristensky, L. A. Hadwiger, *Plant Mol. Biol. 4* (1985) 81.
[175] J. Chappell, K. Hahlbrock, *Nature (London) 311* (1984) 76; P. D. Bishop, D. J. Makus, G. Pearce, C. A. Ryan, *Proc. Natl. Acad. Sci. USA 78* (1981) 3536.
[176] K. R. Davis, A. G. Darvill, P. Albersheim, *Plant Mol. Biol. 6* (1986) 23.
[177] A. Schlumbaum, F. Mauch, U. Vögeli, T. Boller, *Nature (London) 324* (1986) 365.
[178] J. D. G. Jones, K. L. Grady, T. V. Suslow, J. R. Bedbrook, *EMBO J. 5* (1986) 467.
[179] J. J. Burdon, D. R. Marshall, *Plant Dis. 65* (1981) 44; W. J. Peacock, E. S. Dennis in S. Silver (Ed.): *Biotechnology: Potentials and Limitations*, Springer, Berlin 1986, p. 223.
[180] B. J. Staskawicz, D. Dahlbeck, N. T. Keen, *Proc. Natl. Acad. Sci. USA 81* (1984) 6024.
[181] C. Boucher, A. Martinel, P. Barberis, G. Alloing, C. Zischek, *MGG Mol. Gen. Genet. 205* (1986) 270.
[182] C. A. Ryan in P. K. Stumpf, E. E. Conn (Eds.): *The Biochemistry of Plants, Vol. 6*, Academic Press, New York 1981, p. 351.
[183] R. M. Broadway, S. S. Duffey, G. Pearce, C. A. Ryan, *Entomol. Exp. Appl. 41* (1986) 33.
[184] J. S. Lee, W. E. Brown, J. S. Graham, G. Pearce, E. A. Fox, T. W. Dreher, K. G. Ahren, G. D. Pearson, C. A. Ryan, *Proc. Natl. Acad. Sci. USA 83* (1986) 7277.
[185] H. M. J. De Greve, M. B. L. F. Salgado, M. C. E. Van Montagu, M. A. Vaeck, M. F. O. Zabeau, J. J. A. Leemans, H. F. P. Hofte, Eur. Pat.-Anm. 193259 (1986), Plant Genetic Systems.
[186] P. A. Hedin (Ed.): *Plant Resistance to Insects, ACS Symp. Ser. 208* (1983).
[187] A. G. Darvill, P. Albersheim, *Annu. Rev. Plant Pathol. 35* (1984) 243.
[188] E. Vierling, M. C. Mishkind, G. W. Schmidt, T. L. Key, *Proc. Natl. Acad. Sci. USA 83* (1986) 361.
[189] E. Czarnecka, L. Edelman, J. L. Key, *Plant Mol. Biol. 3* (1984) 45; E. Czarnecka, W. B. Gurey, R. T. Nagao, L. Mosquera, J. L. Key, *Proc. Natl. Acad. Sci. USA 82* (1985) 3726.

[190] G. R. Stewart, F. Larker in B. J. Miflin (Ed.): *Biochemistry of Plants, Vol. 5*, Academic Press, New York 1980, p. 609.
[191] W. D. Beversdorf, D. J. Hume in G. B. Collins, J. G. Petolino (Eds.): *Applications of Genetic Engineering to Crop Improvement*, Nijhoff, Dordrecht 1984, p. 189.
[192] J. C. Polacco in G. B. Collins, J. G. Petolino (Eds.): *Applications of Genetic Engineering to Crop Improvement*, Nijhoff, Dordrecht 1984, p. 255.
[193] M. F. Balandrin, J. A. Klocke, E. S. Wurtele, W. H. Bollinger, *Science 228* (1985) 1154.
[194] F. R. Tabita, C. L. Small, *Proc. Natl. Acad. Sci. USA 82* (1985) 6100; M. Gurevitz, C. R. Sommerville, C. McIntosh, *ibid. 82* (1985) 6546.
[195] a) G. Schneider, Y. Lindqvist, C. I. Bränden, G. Lorimer, *EMBO J. 5* (1986) 3409; b) A. Holzenburg, F. Mayer, G. Haranz, M. Van Heel, R. Tokuoka, T. Ishida, K. Harata, G. P. Pal, W. Saenger, *Nature (London) 325* (1987) 730.
[196] S. M. van der Vries, D. Bradley, A. A. Gatenby, *EMBO J. 5* (1986) 2439.
[197] D. Werner, *Angew. Bot. 54* (1980) 67.
[198] W. Klipp, A. Pühler in W. J. Broughton, A. Pühler (Eds.): *Nitrogen Fixation, Vol. 4: Molecular Biology*, Clarendon Press, Oxford 1986, p. 95; G. N. Gussin, C. W. Ronson, F. M. Ausubel, *Annu. Rev. Genet. 20* (1986) 567.
[199] A. L. M. Hodgson, G. Stacey, *CRC Crit. Rev. Biotechnol. 4* (1986) No. 1, p. 1; A. Kondorosi in W. J. Broughton, A. Pühler (Eds.): *Nitrogen Fixation, Vol. 4: Molecular Biology*, Clarendon Press, Oxford 1986, p. 245.
[200] D. P. S. Verma, M. G. Fortin, J. Stanley, V. P. Mauro, S. Purohit, N. Morrison, *Plant Mol. Biol. 7* (1986) 51; F. Govers, T. Gloudermans, M. Moermann, A. van Kammen, T. Bisseling, *EMBO J. 4* (1985) 861.
[201] J. W. Redmond, M. Batley, M. A. Djordevic, R. W. Innes, P. L. Knempel, B. G. Rolfe, *Nature (London) 323* (1986) 632; J. L. Firmin, K. E. Wilson, L. Rosien, A. W. B. Johnston, *ibid. 324* (1986) 90.
[202] B. J. Carrol, D. L. McNeil, P. M. Gresshoff, *Plant Physiol. 78* (1985) 34.
[203] A. Grossway, C. M. Houck, *Plant Mol. Biol. 5* (1985) 183.
[204] T. Helentjaris, G. King, M. Slocum, C. Siedenstrang, S. Wegman, *Plant Mol. Biol. 5* (1985) 109.
[205] R. Koenig, *Mitt. Biol. Bundesanst. Land- Forstwirtsch., Berlin-Dahlem 232* (1986) 90.
[206] S. L. Sinden, C. C. Sanford, R. E. Webb, *Am. Potato J. 61* (1984) 141.
[207] *Richtlinien zum Schutz vor Gefahren durch in vitro neukombinierte Nukleinsäure, 5.* - Revised version, Bundesminister für Forschung und Technologie (Ed.) (1986) Sections 19c (1) c and 19 (2).
[208] F. Herzfeld, D. Gorlitz, M. Kiper, *Naturwissenschaften 72* (1985) 582; M. Sun, *Science 231* (1985) 1360.
[209] M. Schnölzer, B. Haas, K. Ramm, H. Hofmann, H. L. Sänger, *EMBO J. 4* (1985) 2181.
[210] N. Vietmeyer, *Science 232* (1986) 1379.

Computer-Assisted Molecular Design (CAMD)—An Overview

By Horst Frühbeis,* Robert Klein, and Holger Wallmeier

Dedicated to Professor Heinz Harnisch on the occasion of his 60th birthday

A new instrument, long established as CAD in engineering, is beginning to make its presence felt in chemical research laboratories: Computer-Assisted Molecular Design (CAMD). The combined use of computer graphics and theoretical chemistry is opening up new perspectives in molecular research. Structures and properties of molecules such as spacefilling, charge distribution, or dynamic behavior can be determined and used for comparison. For research on complex systems like biomolecules (protein engineering), this new approach turns out to be indispensable.

1. Introduction

Computer-assisted molecular design is a new approach to molecular research using methods from theoretical chemistry. The essential feature is the use of models and their realization on a computer. This may be regarded as the continuation of an old tradition. Many important concepts of chemistry have been worked out using models.[1] As an example take *van't Hoff* and *Le Bel*'s tetrahedron model of the carbon atom, which gave rise to the terms valency and isomerism in organic chemistry. With his model of the benzene molecule, *Kékulé* likewise prepared the way for the concepts of delocalization, conjugation, and resonance. In developing the model of the DNA double helix, *Watson* and *Crick*[2] opened up a new dimension in the understanding of specificity.[3]

Concomitant with the increasing interest in large systems more and more detailed problems are being encountered, and there is a growing tendency to transfer molecular models from the chemist's desk to the computer. This offers the possibility of providing models with well-defined properties and boundary conditions, and thus obtaining quantitative information. The mathematical instruments of theoretical chemistry and many-particle physics can be used. Computer graphics as a tool for handling models has played a decisive role in this development.

The interest of industrial research in computer-assisted molecular design stems from the desire to make the search for new drugs and plant protection agents more efficient. Theoretical methods can help to keep research costs within limits and are therefore being used to an increasingly greater extent. At present, there are two complementary strategies. The one which is based on structure/activity relationships takes an indirect route by comparing known active compounds. For the large number of cases where site and mechanism of action are not known, comparative methods are indispensable. In contrast, the other strategy requires knowledge of the target of action. Active compound and receptor are both included in the model. The computer becomes the locus of an experiment.

From a large number of different applications it has become obvious that both strategies can be used for more than just drug design. In the present review, we therefore try to outline the spectrum of theoretical, molecular research by presenting a representative selection of the large variety of methods used and their possibilities. We regard computer-assisted molecular design as a new *additional* tool for research—combination with experiment still remains an essential precondition for successful molecular design.

2. Interactive Modeling

Computer-assisted molecular design (CAMD) was introduced into chemistry only a relatively short time ago, whereas computer-assisted design in engineering (CAD) has been well established for several years. One of the reasons for this is that interactive work with three-dimensional structures—a typical operation in molecular design—requires highly developed computer graphics systems, which have become available only in the last few years. They generally consist of a minicomputer, a graphics system, and very extensive software. Their development began with the MAC project at the Massachusetts Institute of Technology. Probably the first computer graphics system for molecular modeling was developed in the course of this project. *Cyrus Levinthal*, director of this project, also published the first papers on computer-assisted molecular graphics.[4] Since then a large number of modeling systems have been developed at universities and industrial research institutes,[5-7] but almost exclusively in the USA and Great Britain, only one important contribution coming from Germany.[8] For this reason, the major part of commercially available software now comes from the Anglo-Saxon countries.[9-13] This also applies to the hardware. A good review of the development of molecular graphics is given in Ref. [14]. Molecular graphics systems have now become a useful instrument in molecular research. They make it possible to employ substantially more complicated models than has been possible in the past. At the beginning, computer graphics was predominantly used in pro-

[*] Dr. H. Frühbeis, Dr. R. Klein, Dr. H. Wallmeier
Zentralforschung, Hoechst Aktiengesellschaft
Postfach 800320, D-6230 Frankfurt am Main 80 (FRG)

 © VCH Verlagsgesellschaft mbH, D-6940 Weinheim, 1987 0570-0833/87/0505-0403 $ 02.50/0

tein crystallography. As a consequence, the molecular modeling program, which is probably the one most widely used, was developed by a crystallographer.[8] Other areas followed, including drug and plant protection research.

The modeling systems mentioned above have more or less convenient user interfaces in their current versions and differ considerably in the number of features available. Some have been designed primarily for modeling large biopolymers,[11] while others are more suitable for medium-sized organic molecules.[10, 13] However, there are also program systems for handling any type of molecule.[6]

The important features of computer-assisted molecular design, to be found in most of the modeling systems, will be described in the following. To start modeling, chemical structures can be generated either by building them up from atoms and/or molecular fragments or by altering an existing structure, for example one taken from a data base.

Molecules can be displayed e.g. as vectors, which correspond to the bonds (Dreiding models), as overlapping spheres (space-filling CPK models), or as vectors together with a transparent space-filling representation, consisting of a dotted surface or a polygonal network (chicken wire model). The object displaced on the screen can be rotated, zoomed, and clipped (3D clipping). All operations work in real time. Furthermore, a number of techniques are available which give a three-dimensional impression of the object, for example by rotation and wagging, perspective representation, and depth cueing (the intensity of the vectors represented decreases with increasing distance between the object and the observer). The most elegant solution, however, is provided by the liquid crystal 3D viewer.[15] A detailed description of virtually all the techniques available is given in Ref. [16].

To visualize properties of three-dimensional structures, it is often helpful to superimpose them. Thus, for example, the space occupied, or atomic charge patterns can be compared (see Section 4.1). A typical problem in modeling is the analysis of the conformational space of a molecule. All the possible geometrical arrangements for a given structure at a specified level of energy have to be determined. This is performed interactively by connecting the relevant torsion angles to dials and rotating them, and monitoring the energy in real time. Such an analysis can also be carried out systematically by means of special algorithms (see Section 5). Conformation analysis was one of the first applications of computer modeling.[17]

The docking of substrate and inhibitor molecules into enzymes is used to determine whether or not a proposed structure will fit into the active site cavity of a particular enzyme. Some stages of such a docking manoeuvre are shown in Figure 1. One of the first programs for carrying out interactive docking was developed by a crystallography group.[18] Docking programs were generally designed so that enzyme and substrate can be subjected to rotations or translations, both together and separately. Moreover, any desired conformation of the substrate can be generated by rotation through the appropriate torsion angle. In the simplest case, it is possible to check by inspection whether or not an arrangement produced in this way is physically realizable. Overlap of van der Waals radii of the enzyme and inhibitor should be avoided. This can be checked easily with the above mentioned graphics facilities of a modern modeling system. In addition, the energy of the complex under consideration can be calculated. It has to be minimized in the course of the docking manoeuvre.

A more elegant tool for interactive docking is the display of 'hot spots' (Fig. 1b), which indicate sites of strong repulsion between enzyme and substrate. Such sites must be eliminated by means of the usual geometrical operations on the substrate. Interactive docking is very time-consuming and requires a lot of intuition; nowadays it should only be used for relatively rigid inhibitor or substrate molecules. For flexible molecules, automatic docking is the method of choice (see Section 5.5).

Apart from these basic functions of CAMD, the structure data banks at Cambridge (Cambridge Crystallographic Data File) and Brookhaven (Brookhaven Protein Data Bank) play a very important role. They provide a vast number of experimentally determined chemical structures which can be used for modeling directly, or in the form of

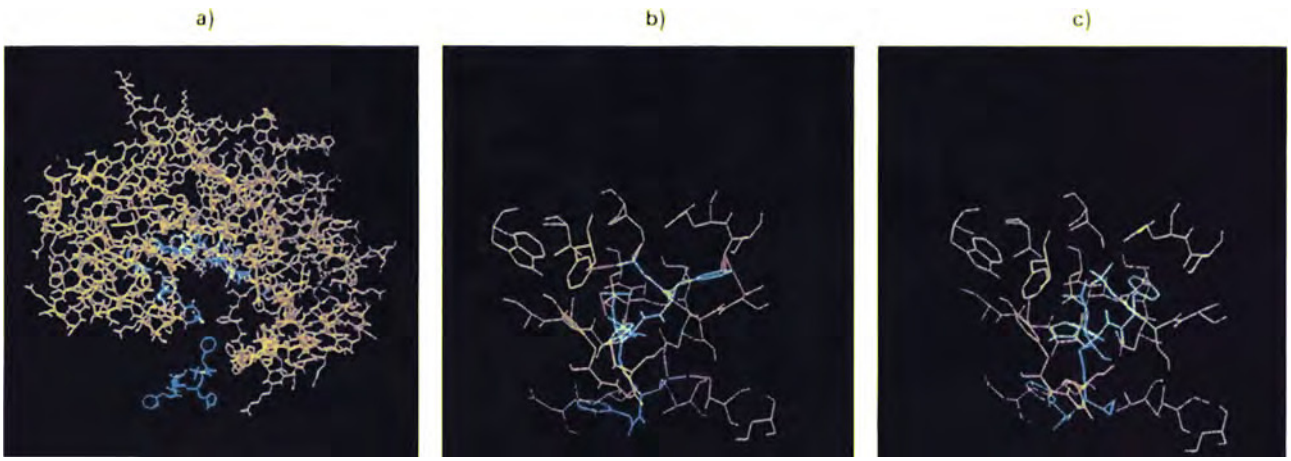

Fig. 1. a) Skeleton model of the enzyme renin (yellow) with a view into the active site (blue) and a model inhibitor (blue) in the lower part of the picture. b) Cavity of the active site (yellow) with poorly docked inhibitor (blue). The red vectors indicate 'hot spots'. The complex has an energy of 14220.53 kcal/mol. c) Optimally docked inhibitor. The energy is markedly less than in b) (180.61 kcal/mol).

templates. It is for this reason that virtually all CAMD program systems include interfaces to these data banks. A description how to exploit the Cambridge Data Bank in a skilful fashion is found in Ref. [19], for example, and in the literature cited therein.

3. Analytical Studies on Models—the Deductive Route

3.1. Basic Principles

To estimate the stability of molecules a number of quite different criteria are considered in chemistry. One may, for example, look at the lifetime of a molecule, i.e. the probability and conditions for decomposition or transformation. The behavior against various reagents is another aspect of stability. Frequently, molecular models are used to interpret the findings in terms of steric hindrance, ring strain, bond strengths, and polarities.[20] For computer models it is very useful that all those aspects of stability can be correlated with the total energies or energy changes of a system. Energy is thus the most important property of a computer model.

Quantum mechanics enables the calculation of the energy of atoms and molecules and therefore forms the basis of most computer models of chemical systems. The characteristic feature of a quantum mechanical model is the wave function, which, as a solution of the Schrödinger equation, contains all the information for a particular state of the system. An important simplification in calculating molecular wave functions is the Born-Oppenheimer approximation.[21] It allows the motions of nuclei and electrons to be considered separately. One obtains the electronic Schrödinger equation,[22] which describes the motion of electrons in the field of stationary nuclei. The electronic wave function is generally represented by orbitals, i.e. solutions for one-electron atoms. In the case of molecules, orbitals are combined according to their symmetry in the molecular orbital (MO) formalism, and according to the bonds between atoms in the valence bond (VB) formalism.[23]

Among the quantum mechanical methods used today, the ab initio methods are those which are closest to solving the electronic Schrödinger equation. The Hartree-Fock self-consistent field (SCF) method[24] is the most important method in practice, particularly in conjunction with basis set expansions, like the Roothaan SCF scheme.[26,27] It represents the lowest level at which the interaction between electrons can be described completely. The computational effort is proportional to the 4th power of the number of electrons, so that meaningful application is restricted to systems of, say 30 second-row atoms, even when supercomputers are used.

Approximations at a somewhat higher level are the method of configuration interaction (CI),[28] the multiconfiguration SCF (MCSCF),[29] and methods based on perturbation theory, such as the Møller-Plesset formalism (MP).[30] Usually they are based on the SCF scheme and provide an improved description of the electron interaction (electron correlation). When used correctly, these methods give substantially more reliable results than simple SCF calculations. Unfortunately, the computational effort for these methods increases with the 5th power of the number of electrons, so that possible applications are even further restricted.

An almost complete parametrization of electron interaction is the key feature of the so-called semiempirical methods.[31] As a consequence, the computational effort is at most proportional to the 3rd power of the number of electrons. The proper choice of parameters is crucial for the usefulness of the results. Hence, these methods can only be used to investigate phenomena, which the parameters chosen are able to describe. A considerable advantage, however, is that one can study quantum effects on systems which are not just trivial fragments of the systems one actually is interested in.

In the Born-Oppenheimer approximation, the energy E of the electronic Schrödinger equation is the potential for the motion of the N nuclei. The gradient of the energy hypersurface (energy as a function of the nuclear coordinates, $E=E(\vec{x}_1, \vec{x}_2, \ldots, \vec{x}_N)$) can be used to determine the forces which act on the nuclei. Minima in the hypersurface correspond to force-free arrangements of the atoms and are referred to as equilibrium geometries or conformations. For determining conformations, it is advantageous if the hypersurface is given as an analytical function (see Section 5.1). This can be achieved, at least locally, by approximation with suitably simple functions. One starts off from a representation in terms of interatomic distances, valence angles, and torsion angles, which correspond to the internal degrees of freedom of molecules.[32] Potential functions with adjustable parameters are used to represent the energy of the internal degrees of freedom.[33-35] In the harmonic approximation, harmonic oscillator potentials are used for bonds and valence angles, while trigonometric functions of proper periodicity are employed for the torsion angles (Fig. 2). In addition, long-range interactions

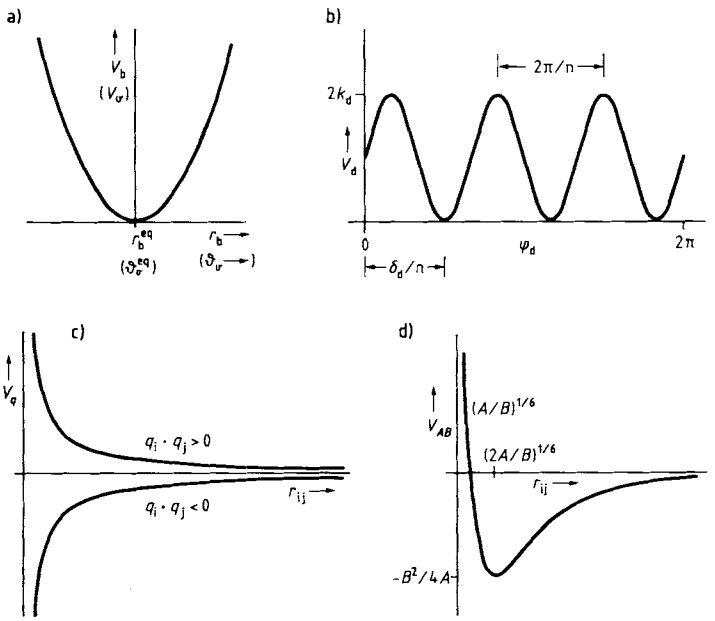

Fig. 2. Potential functions for valence force fields. a) Potential of the harmonic oscillator. b) Potential for torsion angle. c) Potential for Coulomb interaction. d) 12/6 Lennard-Jones Potential for van der Waals interaction.

are represented by Coulomb potentials for the effective charges and by Lennard-Jones potentials for the van der Waals interactions. In the valence force field, all coupling terms between the internal degrees of freedom are neglected, so that

$$
\begin{aligned}
E \approx V = & \sum_{b} k_b (r_b - r_b^{eq})^2 && \text{bond lengths} \\
& + \sum_{\nu} k_\nu (\vartheta_\nu - \vartheta_\nu^{eq})^2 && \text{valence angles} \\
& + \sum_{d} k_d (1 - \cos(n_d \varphi_d - \delta_d)) && \text{torsion angles} \\
& + \sum_{i,j} q_i \cdot q_j / (4\pi\varepsilon r_{ij}) && \text{effective charges} \\
& + \sum_{i,j} A_{ij}/r_{ij}^{12} - B_{ij}/r_{ij}^{6} && \text{van der Waals interactions}
\end{aligned} \qquad \text{(a)}
$$

'eq' denotes equilibrium values which fix the position of the particular potential minimum, and ε is the dielectric constant. The parameters k_b, k_ν, k_d, r_b^{eq}, ϑ_ν^{eq}, n_d, δ_d, q_i, A_{ij} and B_{ij} permit fitting to the energy hypersurface. In molecular models they serve to distinguish between different types of atoms and bonds, and thus determine the properties of the model. The term 'force field' usually refers to a set of such parameters in conjunction with the corresponding potential functions. The term is based on the relationship (b).

$$\vec{F} = -\text{grad}(V). \qquad \text{(b)}$$

The type of force field described above (valence force field) has been implemented in various program systems,[33,36,37] which are also used to study biomolecules. It constitutes the simplest form in which the most important interactions can be described and is also suitable as a basis for computer simulation (see Section 5). All contributions to the energy can be readily formulated in computer programs. The computational effort is proportional only to the square of the number of atoms.

Concerning the potential functions, a number of variants exist: for example, bonds are described by some authors in terms of anharmonic potentials;[38,39] linear combinations of trigonometric functions of different periodicities (Fourier expansions)[40] are used for torsion angles; and modified potentials for the van der Waals interaction are employed to describe hydrogen bonds.[37,40]

The extended valence force fields[39,41] contain a few of the coupling terms between the internal degrees of freedom, which is particularly advantageous for strained molecules[42] but makes calculation of the energy and determination of the parameters more complicated (see below). Models of large systems require force fields which are optimized with respect to the balance between computational effort and 'physical content'. This is most readily achieved with the valence force fields.

A common drawback of force fields is the treatment of Coulomb interaction in terms of effective charges. Due to the polarizability of the atoms, the charges have a mutual effect on one another and change with the conformation of the molecule. Distance-dependent as well as scaled dielectric constants have been used as a remedy.[40] The situation is critical because Coulomb interaction often accounts for the major part of the total energy of a conformation.

Given a set of potential functions, the number of force field parameters is determined by the number of atom types g to be distinguished. For example, in a valence force field of the form (a), $g(g+1)/2$ equilibrium distances and force constants are required for the bonds. For the valence angles, as many as $g^2(g+1)/2$ equilibrium angles and force constants are needed, and in principle $(g(g+1)/2)^2$ force constants, phase angles and periodicity factors are necessary to distinguish between all possible types of torsion angles. The nonbonding interactions can be described by g effective atomic charges and $g(g+1)/2$ Lennard-Jones coefficients. In order to keep their number as small as possible, atom types and parameters should be chosen such that there is maximum transferability. However, this imparts an artificial, internal symmetry to the force field, which becomes a property of the model, as well.

As indicated above, force field parameters can be determined by fitting the potential functions to quantum mechanical energy hypersurfaces. Furthermore, quantum mechanical calculations are the most important source of the effective charges of atoms (see Section 3.2).

In general, force field parameters are determined from experimental data.[35,42,43] A very widely used method is the so-called consistent force field procedure,[33] in which force field parameters are varied iteratively until given experimental data are reproduced. The most important sources of data are IR and Raman spectroscopy for force constants, and X-ray crystallography and microwave spectroscopy for equilibrium geometries. The parameters of the van der Waals interaction are frequently derived from thermodynamical data, such as heats of fusion and vaporization, as well as volume/temperature diagrams.

3.2. Calculation of Molecular Properties

Quantum mechanical models are necessary for the investigation of electronic properties. A population analysis, i.e. the summation of the moduli of orbital, atomic, or bond contributions to the wave function, permits the electron and charge distribution to be characterized in terms of effective charges and hybridizations.[44] The moments of the charge distribution (dipole moment, quadrupole moment, etc.)[26] and, using test charges, the entire electric field of the system can be determined.

Preferred positions for electrophilic or nucleophilic attack can be identified as regions of enhanced or reduced electron density.[45] The corresponding structuring of the electric field is very important for the initial phase (molecular recognition) of reactions.[3]

Optical properties of molecules are generally related to transitions between different states.[46] The chrominance, i.e. the ability to absorb light of certain wavelengths, is attributable to the energy difference between two states having a sufficiently high transition probability, the latter being a measure of intensity.[46]

Energy differences, regardless of whether they relate to conformational changes, rearrangements or reactions, can often be read off directly from the energy hypersurface as level differences. In some cases, however, structuring of the hypersurface is an indication of nonadiabatic phenomena, for which the Born-Oppenheimer approximation no longer holds.[47] This applies very frequently to transition states of reactions, if there is a competition between homolytic and ionic dissociation of a bond. In such critical cases, it is appropriate to use the more elaborate methods, such as CI or MCSCF, for determining both energy barriers and geometry.

Like the electric field, the geometry of a molecule is one of the important factors determining affinity and activity of molecules. Optimizing the geometry is equivalent to locating the deepest minimum of the energy hypersurface. If the initial geometry is not too far away from the minimum, it is sufficient to relax the structure, i.e. to vary the coordinates of the atoms so that the energy cannot be lowered further. Several methods[48,49] are available for carrying out optimizations of this type, which will not be discussed here in detail.

One aspect of the geometry is spacefilling, which brings into play the concept of molecular surface. From the quantum mechanical point of view, the surface of a molecule is a fractal, i.e. a geometric object with a dimensionality between two and three,[50] which can neither be readily represented nor easily handled. However, the concept of fractals makes it possible to quantify roughness and structuring, which is certain to become important with regard to the understanding of processes on solid surfaces and membranes.

A somewhat more pragmatic concept of spacefilling and surface can be derived from the van der Waals radii of the atoms. A molecule is taken as an arrangement of overlapping spheres (CPK spacefilling model). If the overlap of the spheres is taken into account, the volume and surface area of a molecule can be calculated[51-54] (also see Section 2).

Spacefilling by molecules is generally used to assess steric similarity of molecules (see Section 4). The surface area of a molecule provides information about the behavior towards solvents.[54,55] In addition to the effective charges of the atoms, the curvature of the surface is regarded as a measure for the ease of solvation, i.e. the accessibility of the particular atoms to solvent molecules. For this purpose, an imaginary sphere is allowed to roll on the surface of the spacefilling model, and the appropriate parameters are read from its path.

4. Comparative Methods

With the aid of so-called comparative methods, an attempt is made to extrapolate experimental data, i.e. to transfer the data which are available for a number of compounds to other molecules taking into account structural similarities and differences. In general, these data are reactivities or biological activities which, if they could be obtained prior to synthesis, would help to select the most promising compounds. A study of the relationships of structure and reactivity/activity is based on the experience that molecules which have similar structure also exhibit similar chemical and biological behavior.

Unlike the approaches described in Section 5 the comparative methods do not necessarily require experimental information about the site where the molecule finally acts or reacts. Thus, e.g. quantitative structure-activity relationships can be set up for a number of enzyme inhibitors without knowing anything about the enzyme itself.

4.1. Superposition Methods

In medicinal chemistry, activity of a low molecular weight substance is often equivalent to a specific receptor interaction. This correlation is attributed to a molecular recognition mechanism.[56] Consequently, all compounds which form a stable complex with the same receptor should exhibit a common structure-dependent feature which is referred to as a pharmacophore. In this context, a pharmacophore is not restricted to a certain substitution pattern as is generally done, since it has been found that a recognition pattern can, for example, also be realized by the charge distribution in a molecule.[57] The comparison of molecules by superposition with the aid of one of the methods discussed below is used to set up, confirm or discard a pharmacophore model for a particular biological action and to design new molecular structures which also carry the pharmacophoric pattern. A three-dimensional superposition is necessary because not only the presence of obvious common features like functional groups are responsible for the recognition by the receptor but the three-dimensional orientation of the pharmacophore as well.

In the simplest case of a structural comparison, the centers of functional groups in a set of structurally analogous molecules are considered. Using a least squares fit procedure, the sum of the distances between corresponding centers is minimized by displacing and rotating the rigid molecular skeletons. However, in general the initial conformations of the molecules under investigation do not correspond to those that allow a truly optimal fit. Therefore, it may also be necessary to perform rotations about single bonds or even to allow all atoms to move freely in space. In order to exclude unreasonable conformations or geometries the energy required for the geometry change or another suitable parameter (e.g. bump check) is calculated simultaneously. The remaining differences—possibly together with the energy required for the fit—provide qualitative information about the closeness of the fit of the basic pharmacophore model and the structural properties of the molecules investigated.

The van der Waals volumes too are suitable for testing steric correspondence.[51,52,58] For example, the degrees of freedom are varied so as to achieve a minimum of the united volume of all molecules. A pharmacophore model restricted to these space-filling properties is shown in Figure 3. The fungicides shown there inhibit the enzyme cytochrome P450 monooxidase which is vital to fungi.

The discovery of suitable evaluation functions for the matching of charge patterns by varying the degrees of freedom of the molecules is not a completely trivial matter.

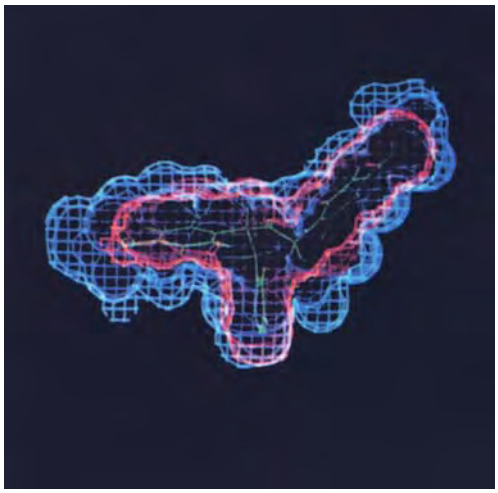

Fig. 3. Chickenwire representation of the van der Waals volumes of the natural substrate (blue) of cytochrome P450 and miconazole (red). The molecular skeleton of miconazole is shown in green.

Namasivayam and *Dean*[59] have described a statistical method for matching charge patterns on molecular surfaces. A least squares fit procedure can also be used to fit the electrostatic potentials of several molecules on an arbitrary surface which is resolved into grid points.[60] In Figure 4, the potential differences are projected on a section

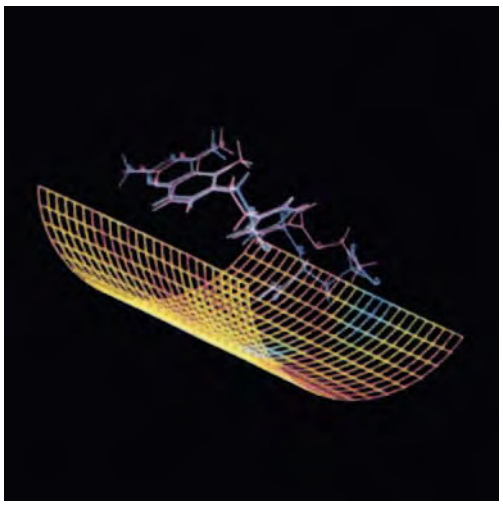

Fig. 4. Projection of the electrostatic potential difference of two quinazoline derivatives (dihydrofolate reductase (DHFR) inhibitors) onto a surface (red: small differences, blue: large differences).

of the curved surface of a cylinder which surrounds the molecules to be compared. By appropriately coloring the vectors between the grid points the differences in the charge patterns before and after the fit can conveniently be analyzed visually. *Broto* and *Moreau*[61] use a so-called intercorrelation function to superimpose structures with respect to the effective atomic charges (as well as other atomic properties). Here, they translated their concept of the autocorrelation function[62] for describing the "property distribution" within a molecule into the problem of making similarities in this distribution quantifiable. *G. Naray-Szabo*[63] uses an electrostatic lock-and-key model to investigate common features of trypsin inhibitors.

A very elegant method which makes it possible to confirm or reject a pharmacophore model is called the active analog approach developed by *Marshall* et al.[64] A pharmacophore hypothesis is first proposed by defining several functional groups or hetero atoms to be essential for activity. A systematic conformational search (torsion or rotatable bonds) in all molecules is supposed to give that three-dimensional arrangement of the pharmacophore which at least can be realized by all active compounds. If there is no such arrangement the initial hypothesis is rejected. If the search has been successful the three-dimensional pharmacophore found this way serves as an initial criterion for the classification of novel compounds. In a second step the volume provided by the receptor—the so-called excluded volume—is determined as the united volume of all active molecules in their active conformations. In spite of having the correctly oriented pharmacophore, inactive molecules should not be capable of being fitted into this volume. Otherwise, there will once again be a reason for doubting the correctness of the proposed pharmacophore.

The so-called distance geometry method developed by *Crippen*[65] for describing molecular geometry can also be applied to the problem of extracting common steric features from a set of molecules.[66,67] The flexibility of a molecule is represented by a minimum and a maximum distance matrix, i.e. by a range of validity of the interactomic distances. For the distance between two atoms (or representative points) of the pharmacophore, the only values allowed are those which lie within the range of validity for all active molecules. This considerably reduces the number of conformations which can be calculated from the distance matrices.

Frequently, the structure of the transition state of the natural substrate rather than a number of active compounds is used as a template for the design of novel drugs (transition state analogs)[68] (also see Section 3.2). Since the properties of transition states are in general difficult to determine experimentally, as a rule, extensive quantum-mechanical calculations (ab initio, MNDO, MINDO etc., also see Section 3.2) of the reaction path from the substrate to the product have to be carried out.

A pharmacophore model which has been derived by one or more of the methods described above provides, with certain restrictions, information about the structure and properties of the receptor. In the literature, the procedure for obtaining such a qualitative image of the receptor is often referred to as receptor (site) mapping.[58,67,69-71] Thereby, it is possible to design novel drugs which do not necessarily exhibit the same structural features as the active molecules compared or the lead compound, and yet to estimate the activity of the novel compound, even if purely qualitatively.

4.2. Qualitative Structure-Activity Relationships (SAR)

The methods described so far are suitable only for a relatively small number of compounds to be compared. Furthermore, they are based on the assumption that there is

essentially only one mechanism responsible for the biological activity, namely the formation of a receptor-ligand complex. The use of so-called pattern recognition (PR) methods[72] does not depend on any of these conditions. PR is based on structure-dependent molecular properties, so-called descriptors (e.g. number of oxygen atoms in the molecule, molecular diameter, etc.). Depending on the individual values of the descriptors each molecule has a particular descriptor pattern. Using artificial intelligence methods and mathematical procedures such as cluster analysis, principal component analysis and discriminant analysis these patterns serve to assign a compound to activity classes. PR is used in particular where a large number of structural inhomogeneous compounds is encountered, for example in studies on carcinogenicity and genotoxicity.[73]

In the approach of *Broto* et al.[62] a so-called autocorrelation vector is calculated for each molecule from atom-related parameters or properties (e.g. heteroatom/non-heteroatom, atomic log P increment etc.). These vectors can be considered to represent the property distribution within the molecules and are used to classify the compounds according to their activities.

The so-called CASE algorithm[74] (computer automated structure evaluation) breaks up the molecules under investigation into fragments and searches for those substructures which contribute to activity or those which lead to inactivity. Thus, this method immediately provides a pharmacophore model. A similar approach, which also permits the derivation of quantitative structure-activity relationships, has been reported by *Streich* and *Franke*.[75]

4.3. Quantitative Structure-Activity Relationships (QSAR)

In a study of quantitative structure-activity relationships an attempt is made to describe the activity or reactivity within a set of compounds by means of a mathematical formalism which incorporates structure-dependent parameters (descriptors).[76] Although the classical QSAR approaches were introduced purely empirically they can be derived in terms of an extrathermodynamic approximation[77] (additivity of substituent effects, separability of different effects etc.).

The first quantitative structure-activity relationship was developed as early as 1937 by *Hammett*.[78] He correlated the hydrolysis rate of *meta*-substituted and *para*-substituted benzoates with the so-called Hammett σ which is calculated from the dissociation constants of the corresponding benzoic acids. In order to obtain a relationship which could be applied to *ortho*-substitutions as well, *Taft*[79] added a steric parameter E_s to the Hammett equation.

In addition to electronic substituent effects, which were to be described by the Hammett σ, hydrophilic/hydrophobic properties were also considered responsible for biological activity. Therefore, *Hansch* et al.[80] introduced a further parameter, π, [eg. (c)] which is based on studies by *Meyer* et al.[81] and *Overton*[82] and is calculated from the octanol-water partition coefficient (log P value).

$$\log(1/C) = a \cdot \sigma + b \cdot \pi + c \qquad (c)$$

C is the (theoretical) activity; the coefficients a, b and c are determined by a least squares procedure so that equation (c) optimally reproduces the measured biological data of a selected set of molecules (regression analysis). Many systems, however, cannot adequately be described by this approach. *Hansch*[83] attributed these deficiencies to transport mechanisms which also manifested themselves in the in vivo activity data and therefore assumed a parabolic dependence of the activity on π [eq. (d)].

$$\log(1/C) = a \cdot \sigma + b \cdot \pi^2 + c \cdot \pi + d \qquad (d)$$

Probably the most frequently used form of the classical QSAR approach, based on a linear combination of descriptors, also takes into account steric effects with the aid of *Taft*'s E_s [eq. (e)].

$$\log(1/C) = a \cdot \sigma + b \cdot \pi^2 + c \cdot \pi + d \cdot E_s + e \qquad (e)$$

Extensive efforts are still being made to improve the substituent parameters, replace them by others or add new ones. *Hammett*[84] himself differentiated between σ_m for *meta*-substituents and σ_p for *para*-substituents. The knowledge that electronic effects comprise an inductive part and a resonant part led to a splitting of σ into σ_i and σ_r.[85]

In addition to the Hansch π, other substituent parameters which can be derived from measurable molecular properties, have been proposed for modeling hydrophobic interactions: the parachor which is related to the surface tension,[86] the Hildebrand-Scott solubility factor[87] and parameters obtained from chromatography.[88] An empirical hydrophobicity parameter can be calculated by the HIBIS method.[89] The classical QSAR approach employs only scalar descriptors. However, steric properties of substituents are based on three-dimensional orientation. It is therefore difficult to model steric effects by means of parameters such as *Taft*'s E_s or *Charton*'s U,[90] which is calculated from van der Waals radii. By separating the steric descriptor into components *Verloop* et al.[91,92] was nevertheless successful in introducing relative orientation into the so-called STERIMOL parameter. Further steric parameters, all of which are based on the superposition of molecular volumes, are the MSD,[93] MTD,[94] SIBIS,[70,95] and 3D-MSD[52,96] descriptors.

The typical PR descriptors and the components of autocorrelation vectors in *Broto*'s approach[97] are QSAR descriptors of a very special type. There have also been many attempts to correlate the biological activity with other computable parameters which describe the molecule or a substituent effect. For example, parameters derived from semi-empirical quantum mechanical calculations[98] and electron densities from Hückel and CNDO/2 calculations[99] have been used as QSAR descriptors.

Apart from (multiple) regression analysis[100] as the standard method, principal component analysis,[102] discriminant analysis[103] and cluster analysis[104] are also used for the statistical exploitation[101] of a Hansch or a similar QSAR approach. Several statistical parameters, such as the RMS deviation and the correlation coefficient, provide means to check the reliability of a regression analysis.[100]

The significance of a descriptor can be determined approximately by performing two QSAR procedures with and without the descriptor and by comparing the respective correlation coefficients. However, even satisfactory statistics cannot exclude random correlations.[105] The probability of chance correlations clearly grows when the number of descriptors becomes large compared with the number of structures used.[106]

In the QSAR approach by *Free* and *Wilson*,[107] structure-activity relationships are set up without physicochemical parameters. It is assumed that the substituents contribute additively to the activity. The activity value of a compound is taken to be the sum of a basic activity and the contributions of the substituents. The contribution of a substituent depends both on its type and its position in the molecule. If the equation is set up for all tested compounds a system of linear equations is obtained. By solving the equations using a least squares fit procedure the individual substituent contributions can be determined. The effect of substituents other than those present in the compounds tested cannot be calculated; only the effect of different combinations of substituents can be estimated by this approach.

It is possible to combine the Hansch and Free-Wilson methods.[76] In general however, they are used exclusively, since the application of the Hansch method is limited by the availability of physicochemical parameters whereas the Free-Wilson method needs large variations in the substitution pattern. Thus, the two approaches complement each other.

An approach similar to that of the Free-Wilson method has been described by *Crippen*,[108] who used the distance geometry algorithm to set up quantitative structure-activity relationships. This method too is based on substituent constants, which additively contribute to the activity and depend on the position within the receptor binding site. In general, receptor binding energies are used to quantify the activities. In contrast to the classical Free-Wilson method several (generally two) three-dimensional orientations of the pharmacophore are determined. The compounds investigated are assumed to bind to the receptor with different pharmacophore orientations. By taking these different "binding modes" into account the poor correlation between substituent contributions and activity when using only one orientation should be improved.

Some recent publications have been concerned with the combination of QSAR and superposition or receptor mapping methods in order to obtain a model of the receptor which also provides quantitative information.[92, 109, 110] A procedure,[111] which allows generation of a receptor model by means of pseudo atoms, will be described in Section 5.6. The method predicts activities without being based upon an extrathermodynamic approximation as are the classical QSAR approaches.

5. Inductive Modeling: Computer Simulation

The optimization of molecular geometries, as discussed in Section 3, generally gives only information about a single conformation. For molecules with many internal degrees of freedom, however, there may be a large number of minima in the energy hypersurface. Therefore, the most stable conformation can only be identified if all the minima are known. There are several methods of searching systematically for the most stable conformation. Unfortunately, these methods reach their limits very quickly. A molecule with only 50 atoms, for example an open-chain hydrocarbon with the formula $C_{16}H_{34}$, can already have several million local minima. Such a molecule does not remain in a single conformation but fluctuates between several conformations. In view of this, it seems more reasonable to depart from the concept of the most stable conformation and instead to model the dynamic properties of the molecule. All methods for this purpose, which are presented here, are based on force field energies.

5.1. Conformation Search

The systematic scanning of a conformation space in order to find the conformation with the lowest energy (global minimum of the hypersurface) is referred to as conformation search. Usually, advantage is taken of the fact that conformations can virtually always be distinguished by torsion angles. In principle, therefore, all conformations can be found by varying the torsion angles in all possible combinations. One selects a sufficiently large number of initial geometries[112] and relaxes them (see Section 3.2). The conformations thus determined are of course 'close' to the initial geometries. To become more independent of the critical choice of initial geometries, a grid can be placed over the space of torsion angles (grid search).[113]

The energy calculations necessary for the conformation search can be carried out using quantum mechanical methods, whenever high accuracy is required.[114] In general, however, force fields are used. The complexity of this type of conformation search increases exponentially with the number of bonds, so that it is reserved for small molecules.

In the case of large molecules, the search has to be simplified by means of additional restrictions. Frequently, it is possible to reduce the number of variable torsion angles by making use of local symmetry.[113, 115] The most favorable conformations of small subunits are determined and included as fixed blocks in the total molecule, or are used to define grid points for the global search. An important example is the prediction of secondary structure elements in polypeptides and proteins.[116] Introducing pleated sheets, turns, and helices constitutes a preselection of possible values for the main chain torsion angles.[117]

5.2. Molecular Dynamics

The huge number of internal degrees of freedom of biomolecules and polymers, and the coupling of degrees of freedom in cyclic molecules, suggest that use should be made of the dynamic properties of models in the conformation search. Conformation search is performed as a computer experiment in which the behavior of the model is observed, when subjected to external perturbations. This corresponds to the idea that a real molecule in thermal equilibrium finds its most favorable conformation in a se-

quence of reversible geometry changes. To transfer this to a mechanical model, one has to observe the time evolution of geometry ($\vec{x}=\vec{x}(t)$, trajectory). From the expansions for $t+\mathrm{d}t$ and $t-\mathrm{d}t$ one obtains equation (f).[118,119]

$$\vec{x}(t+\mathrm{d}t)=2\vec{x}(t)-\vec{x}(t-\mathrm{d}t)+\frac{\mathrm{d}^2\vec{x}}{\mathrm{d}t^2}(\mathrm{d}t)^2+0((\mathrm{d}t)^4) \quad \text{(f)}$$

According to *Newton*, for each atom i equation (g) holds and the force field [see Section 3.1, eq. (b)] provides the relationship (h).

$$\frac{\mathrm{d}^2\vec{x}_i}{\mathrm{d}t^2}=\vec{a}_i=\frac{\vec{F}_i}{m_i} \quad \text{(g)}$$

$$\vec{F}_i=-\mathrm{grad}_i(V) \quad \text{(h)}$$

Newtons equations of motion are solved by discrete integration over a very large number of finite time steps ($\mathrm{d}t\rightarrow\Delta t$). The size of the first change in geometry (perturbation of the system) defines the level of kinetic energy, which, according to statistical mechanics, corresponds to a temperature T [eq. (i)].

$$\frac{3}{2}NkT=\frac{1}{2}\sum_i^N m_i v_i^2. \quad \text{(i)}$$

The time evolution can also be formulated in terms of the velocities of the atoms [eq. (j)].

$$\vec{v}(t+\mathrm{d}t/2)=\vec{v}(t-\mathrm{d}t/2)+\frac{\mathrm{d}^2\vec{x}(t)}{\mathrm{d}t^2}(\mathrm{d}t)^2+0(\mathrm{d}t)^4 \quad \text{(j)}$$

whereby the model temperature can be kept constant by scaling the velocities. This corresponds to coupling the system to a heat bath.[119,120]

Molecular dynamics (MD) simulations can be carried out either with individual molecules or with entire ensembles of molecules. The molecules are arranged with the desired density in a cell of appropriate volume. In the case of liquids, a cube is generally used; for crystal structures, the form used corresponds to that of the unit cell. By means of so-called periodic boundary conditions, surface artefacts are eliminated and a quasi-infinite number of particles is generated by surrounding the cell with its own images in all directions of space[121] (Fig. 5). By scaling the cell volume, the pressure can be kept constant.[119,120]

The optimum time step Δt for the simulation of molecules with many internal degrees of freedom is 10^{-15} to 10^{-14} seconds. This roughly corresponds to the time scale of molecular vibrations. With supercomputers, it is possible to carry out simulations over 10^6 time steps[122] so that processes such as internal rotations and aggregations can be studied. The dynamics of molecules containing 500 atoms can be investigated very thoroughly, even including a few hundred solvent molecules. Rapid, periodic movements and slow, nonperiodic movements can be read off from the trajectory of the system. The latter are particularly interesting since they lead to conformational changes. In this way, the stability of a hypothetical conformation of a large molecule can be assessed directly. Transitions of the system to other conformations can be accelerated by means of high temperatures. However, the degree of aggregation may change, so that a completely different area of conformation space is entered. It is therefore possible to study phase transitions.

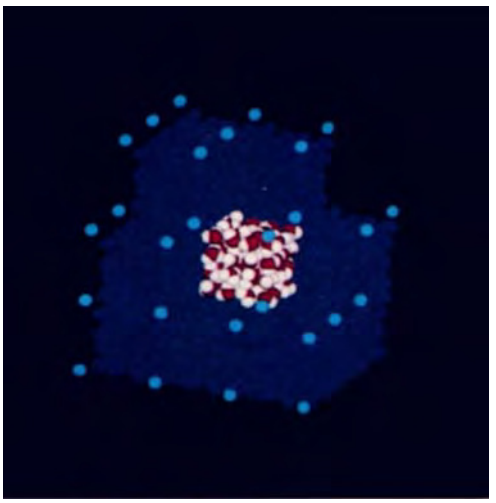

Fig. 5. Periodic boundary conditions for MD and Monte Carlo (MC) simulations (see text).

Correlation and averages play an important role in the evaluation of MD simulations. One considers correlations in time and in space which are represented by so-called correlation functions.[123,124] The different types of motions[125] (periodic, nonperiodic) and in particular coupling between different parts of the molecule can be read off from the time correlation functions. In the case of time-independent correlations, time averages are considered. Preferred local and global conformations can be identified, thereby. This procedure is often used to analyze the structure of solvation shells in the simulation of dissolved molecules to estimate hydrophilic or hydrophobic behavior.[126]

The above statements on the possibilities of MD simulations apply in principle to all types of systems, provided the necessary force field parameters are available. Most applications are found for fluid systems,[127] but solids and surfaces[128] as well as polymers[129] have also been simulated. Biomolecules such as nucleic acids,[130] peptides,[125,131,132] poteins[133] and membranes[134] have been studied. However, all types of systems are subject to the restriction that, with the computers available today,[122,135] it is impossible to consider any process which takes substantially longer than 10^{-9} seconds. Thus, for example, it is impossible to model the folding of proteins solely by means of MD simulation. The same applies to most biological transport processes. Nonetheless, the transport of ions through membrane channels [136] just constitutes the limit of meaningful investigations.

5.3. Monte Carlo Methods

Another type of computer experiments is based on statistical variations of the model. The Monte Carlo proce-

dure is a method for calculating properties of fluctuating systems as so-called ensemble averages.[123, 137] Integrals of the form (k) are made discrete in accordance with eq. (l).

$$\langle A \rangle = \frac{\int f(\vec{x}) \cdot A(\vec{x}) \cdot d\vec{x}_1 d\vec{x}_2 \ldots d\vec{x}_N}{\int f(\vec{x}) \cdot d\vec{x}_1 d\vec{x}_2 \ldots d\vec{x}_N} \quad (k)$$

$$\langle A \rangle \approx \frac{\sum_k^M f(\vec{x}^{(k)}) \cdot A(\vec{x}^{(k)})}{\sum_k^M f(\vec{x}^{(k)})} \quad (l)$$

Random numbers are used to generate M local variations of the system (displacement of an atom, change in a torsion angle), which lead to new states. If the energy of a new state is lower than that of the previous one, the new state is accepted, i.e. the next variation will start from this new state. On the other hand, if the energy is higher, the Boltzmann factor f [eq. (m)] is calculated, and compared

$$f = \exp(-E^{new} - E^{old})/kT \quad (m)$$

with another random number. If the random number is smaller than f, the new state is after all accepted; otherwise, the previous state is retained. f is thus the transition probability for a state of higher energy, and depends only on the directly preceding state. This type of random walk through the conformation space of the system is called a Markov chain.[138] In this way, the system is allowed to fluctuate (Fig. 6) according to a Boltzmann distribution for

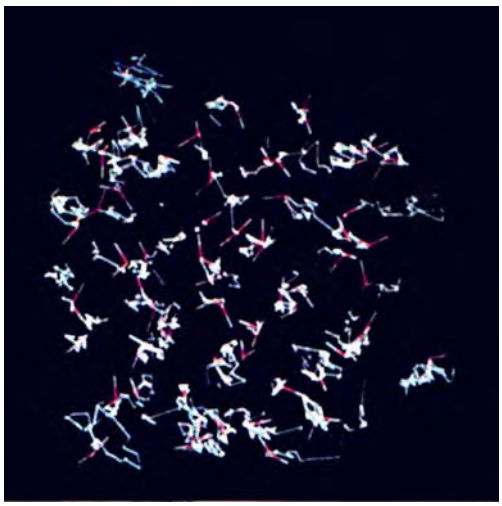

Fig. 6. Brownian motion of H_2O molecules simulated by a MC method.

temperature T. Using the Boltzmann factor as a transition probability is the essential feature of the metropolis sampling method.[139] As in molecular dynamics, it is customary to provide periodic boundary conditions for many-particle systems (see Fig. 5).

Calculation of averages is of course affected by statistical errors, showing up in the root mean square deviation of the values [eq. (n)]. Since s(A) is proportional to $1/\sqrt{M}$, the number of sample points M must be increased by a factor of a hundred to obtain a result which is more precise by one decimal place. In practice, M is of the order of magnitude of 10^6.

$$s(A) = \sqrt{\sum_k^M (A^{(k)} - \bar{A})^2 / M} \quad (n)$$

The Monte Carlo method (MC) too, has so far mainly been used for studying the properties of liquids.[137] The solvation of biomolecules has also been investigated by the MC method.[140] In addition, there are a number of studies on polymers which are primarily concerned with determining conformations.[141] Because of the statistical choice of variations, the MC method is very suitable for conformation search. A very important aspect of MC simulations is the calculation of thermodynamic entities, especially the entropy, which will be discussed in the next section.

5.4. Calculation of Entropy Contributions

The energy balance of a process is not determined solely by the differences in internal energies or enthalpies of the subsystems involved. The 'usable' free energy ΔG [eq. (o)]

$$\Delta G = \Delta H - T\Delta S \quad (o)$$

also has a contribution from the change in entropy, which is temperature-dependent. This may be taken as an indication that the dynamics of molecules play a role here. According to the third law of thermodynamics entropy is related to the probability of a state or a conformation of a system [eq. (p)]. This forms the basis for the calculation of entropy by means of computer models.

$$S = k \cdot \ln(W) \quad (p)$$

There are various contributions to the entropy. The external ones arise from the translational motion of particles, the rotational motion of particles, and the number of particles (solvation, aggregation), while the internal contributions are due to molecular vitrations and internal rotations.

The individual contributions can be calculated from the partition functions Z_{trans}, Z_{vib}, Z_{rot} of statistical mechanics [eq. (q)].[142]

$$S = Nk\left[T\frac{\partial \ln(Z)}{\partial T} + \ln(Z)\right] \quad (q)$$

Thus, in the approximation of the harmonic oscillator and the rigid rotator even quantum effects are taken into account. The contributions from the number of particles primarily manifest themselves as 'stoichiometric' factors but also have an indirect effect on the other contributions. They represent, for example, the main contribution to the entropic part of the hydrophobic interaction.[143]

For very large systems, the direct calculation of entropy via partition functions is too inexact owing to the approxi-

mations involved. Instead, MC[144] or MD simulations[145] can be used to calculate the entropy from the fluctuations of the internal coordinates. This is equivalent to determining the probability W. Unfortunately, only periodic motions can be taken into account. However, this is a viable method for determining the entropy contributions to the energy differences between different conformations of a molecule.

5.5. Docking

The interaction between a receptor molecule (R) and possible ligands decides whether a particular type of ligand is preferred, and can thus repress others. An example of this is the competitive inhibition of enzymes, the natural substrate (S) being displaced by an inhibitor (I). If entropy contributions are neglected, the relevant energy balances (r) apply.

$$\begin{aligned}\Delta E(\mathrm{S}) &= E(\mathrm{RS}) - E(\mathrm{R}) - E(\mathrm{S}) \\ \Delta E(\mathrm{I}) &= E(\mathrm{RI}) - E(\mathrm{R}) - E(\mathrm{I})\end{aligned} \qquad (\mathrm{r})$$

For a complex to be formed at all, ΔE must be negative. $|\Delta E(\mathrm{I})| > |\Delta E(\mathrm{S})|$ is then a necessary condition for I to have an inhibitory effect. In order to calculate ΔE, one has to know the optimum conformations of the R, S, and I molecules, and the conformations of the complexes RS and RI. For the free R molecule, the X-ray structure is generally used, while the methods described in Sections 3.1 and 5.1. can be employed for substrate and inhibitor molecules. Determining the conformations of the complexes, however, is a special problem since two molecules are involved. The search for the conformations of the complexes, generally referred to as docking, has three aspects:[146]

a) relative orientation of S/I with respect to R
b) optimum conformation of S/I in contact with R
c) optimum conformation of R in contact with S/I

In the docking of rigid ligands with rigid receptors, only (a) is important. In such cases, interactive docking (see Section 2) is the method of choice. However, if the ligands are not rigid, the problem of multiple minima is encountered immediately (b). Interactive docking can very easily give misleading results if the global minimum is not found. In such cases, a special form of MC simulation has proved useful.[147] This method uses an evolution algorithm[49] to search for several conformations simultaneously, and optimizes and accommodates them. Conformation changes in the receptor (c) can be taken into account by subsequent optimization of the entire receptor-ligand complex by MD or MC simulation, provided the changes in geometry of the receptor are small. At the same time, entropy contributions to complex formation can be determined.

5.6. Receptor Modeling

As already mentioned in Section 4 the comparative methods may also be used to produce receptor models.[58,67,69-71] Only when combined with classical QSAR methods (Free-Wilson or Hansch) do these models also provide quantitative information about the activity of analogs.[92,109,110]

The method described below makes direct use of the experimental activity data of a number of structurally analogous molecules in order to determine a receptor model[111]. But unlike classical QSAR methods it is not based on physicochemical parameters *(Hansch)* or empirically determined substituent contributions *(Free-Wilson)*. The method gives the active conformations of the active molecules and a model receptor, which makes it possible to calculate activities of untested compounds. Thus, receptor modeling provides information of both an active analog approach (see Section 4.1) and a QSAR procedure, but still is not a hybrid of the two methods. The essential feature is the calculation of the binding energy between each molecule investigated and a pseudomolecule, the model receptor. This pseudo-binding energy comprises the electrostatic and van der Waals interaction between a molecule and the model receptor and the conformational energy of the molecule. The energy terms used correspond exactly to the force field contributions described in Section 3 [eq. (a)]. The receptor consists of pseudoatoms which differ from "normal" atoms in that they are capable of varying their van der Waals radii and their effective charges during the calculation.

By an iterative procedure, the geometry of the molecules and of the model receptor and the effective charges and the van der Waals radii of the pseudoatoms are varied so as to achieve an optimal fit of the pseudo-binding energies and the experimentally determined enthalpies (calculated from the activity data). A further requirement is that the molecule/model receptor complexes are stable, i.e. are located in an energy minimum—as far as possible a global one. The method makes use of two approximations: a) the receptor is identical for all molecules and b) entropy and solvation effects are not taken into account explicitly. Figure 7 shows a model receptor which was calculated from six quinazoline derivatives which inhibit dihydrofolate reductase (DHFR) (also see Section 6.1).

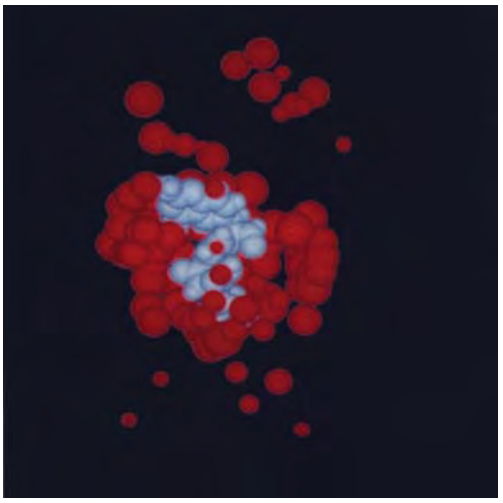

Fig. 7. Space-filling CPK representation of a model receptor (red) for DHFR inhibitors with a docked quinazoline derivative (blue).

In order to check the model receptor, further experimentally investigated molecules (so-called test molecules) are docked into the pseudomolecule. Comparison of the resulting pseudo-binding energies with the experimental binding energies of the test molecules gives information about the predictive power of the model receptor.

Novel untested compounds can now be docked into the model receptor. The calculated pseudo-binding energy allows the activity to be predicted, the reliability of which clearly depends on the predictive power of the model as determined by the test substances.

6. Applications

CAMD is already very widely used today. It will be quite impossible to list all areas of application here. We have therefore chosen three examples, which will illustrate the function and importance of this new instrument. So to speak for historic reasons, our first example is DHFR, which is both of great pharmacological interest and probably one of the enzymes which has been investigated the longest and the most thoroughly by computer-assisted methods. The same applies to renin. In the section on modeling for enzyme engineering, it is intended to demonstrate that this promising area is inconceivable without computer graphics.

6.1. Studies on Dihydrofolate Reductase

Interest in the structure and function of dihydrofolate reductase (DHFR) has grown very rapidly over the past few years and, consequently, so has the volume of relevant literature.

DHFR catalyzes the NADPH-dependent reduction of 7,8-dihydrofolate to 5,6,7,8-tetrahydrofolate and thus plays a key role in the metabolism of a large number of organisms. It is the target enzyme of the cytostatic methotrexate and the bactericide trimethoprim. Since the three-dimensional structures of DHFR from chicken liver,[148] *Lactobacillus casei*[149] and *Escherichia coli*[149] and the structure of a complex of methotrexate, cofactor and enzyme were available at about the same time as powerful molecular graphics, dihydrofolate reductase became a preferred research object for molecular design. A number of groups in industrial research[150] worked very intensively on the design of improved, more specifically acting analogs of the bactericide trimethoprim and on the development of new inhibitors with antimalarial activity.[151] At the universities, *Hansch* et al. and *Langridge* et al.[152] attempted to design more effective inhibitors for DHFR by combining QSAR and molecular modeling (also see Section 4.3), while *Höltje* et al. and *Richards* et al. tried to obtain better inhibitors using semiempirical[153] and ab initio quantum mechanical methods[154] (see Section 3). The work by *Cody*,[155] *North* et al.,[156] and *Ghose* and *Crippen*[109] on the modeling of DHFR inhibitors should also be mentioned. Extensive NMR studies of inhibitor-enzyme complexes were carried out as well.[157]

Recently, *Kraut*, *Matthews*[158] and co-workers succeeded in determining the structure of at least ten enzyme-inhibitor complexes of DHFR from chicken and *E. coli*. Analysis of these structures helped to explain why trimethoprim had a greater inhibitory effect on bacterial DHFR than on vertebrate DHFR. Those amino acids which are on opposite sides of the cavity of the active site are 1.5 to 2 Å further apart in chicken DHFR than in DHFR from *E. coli*, leading to different arrangements of the inhibitors in the enzyme-inhibitor complexes of the two enzymes and different levels of inhibition. These results give rise to the expectation that, after isolation and crystallographic analysis of a target protein, it may be possible in the future, to use the methods described in Section 5 to design selective inhibitors which do not intervene in the metabolism of the host organism. Drug development would thus become much more efficient.

6.2. Studies on Renin

Inhibitors of the enzyme renin are potential therapeutics against hypertension. No X-ray structure of the enzyme itself has so far been determined. However, some aspartyl proteinases, such as pepsin, *Rhizopus chinensis* pepsin, penicillopepsin and endothiapepsin are closely related to renin. Thus, when the high-resolution 3D-structures of these related enzymes[159-162] and the sequences of mouse renin[163-166] and subsequently also of human renin[164] became available, it was possible to develop three-dimensional models of mouse renin[165] and human renin[166, 167] with the aid of CAMD. On the basis of these computer models and the structures of the enzyme-substrate complexes of pepstatin in *Rhizopus chinensis* pepsin and penicillopepsin,[159, 160, 162] several research groups attempted to design renin inhibitors.[168] This was done in a number of steps:

1) The cavity in which the active site of the enzyme is located was investigated with regard to the available space and the possible sites of binding between the enzyme and the substrate or inhibitor molecule (structural elements which form hydrogen bonds, hydrophobic pockets, etc.).
2) Further important information was obtained from the arrangement of the inhibitor in the enzyme-inhibitor complex. Potential inhibitors should be capable of assuming the same geometry in certain parts of their structure and occupy the same enzyme-binding sites as the model inhibitor. The proposed structures were therefore subjected to special fitting algorithms (see Section 4).
3) Once a structure fulfilled these conditions at low conformation energy it was then introduced interactively into the cavity of the human renin model. If a subsequent relaxation procedure, carried out by means of a molecular mechanics calculation, led to an energetically favorable arrangement, a novel active structure had fortunately been designed. However, definitive information about the inhibitory activity which may have been achieved can only be obtained by experiment. More careful consideration of the transition state of the enzymatic reaction of renin led to novel, highly active compounds,[169] the so-called transition state analogs, and to a deeper understanding of the enzymatic mechanism.[160]

6.3. Protein Engineering

Protein engineering is a relatively new, promising field whose impact on other areas is difficult to assess. Protein engineering can be used to discover structure–activity relationships in enzymes and, based on this, to produce proteins with selectively altered, i.e. novel or improved, properties.[170, 171] These properties include thermal stability, substrate specificity and kinetic behavior of enzymes, as well as therapeutic properties of proteins. For example, the effect of disulfide bridges on the in vitro stability of T4 lysozyme derivatives has been very thoroughly investigated.[172] Extensive studies led among other things to the determination of the structure–activity relationships for subtilisin[171, 173] and for tyrosyl-tRNA synthetase.[174] This requires that one or more amino acids in a protein can be replaced selectively by a genetic engineering method (site-directed mutagenesis) and that the three-dimensional structures of the proteins are made available by crystallography or NMR. These structures are represented, modeled, and exploited by molecular modeling methods. In the simplest case, modeling is carried out interactively.[175] Starting from the structure of the wild type enzyme, the amino acids of interest are replaced. The backbone conformation of the original enzyme is retained and each of the side chains is oriented so that no forbidden steric interactions occur. This can be carried out completely visually, as described in Section 2, or by means of molecular dynamics calculations. The interaction between the protein and the substrate can be estimated by docking procedures (see Section 2). There are also sophisticated methods which include homologous substructures from the Brookhaven protein data bank.[176] To what extent replacement of certain amino acids is accompanied by a change in the tertiary structure of the protein cannot be readily predicted up to now.

Docking of the substrate into the active site of the mutated enzyme investigated can of course also be carried out using an automatic docking program (see Section 5.5). This will certainly give more objective results than interactive docking.

Other objects of interest in the field of enzyme engineering have been the peptide cleavage by thermolysin[177] and electrostatic effects in enzyme catalysis.[178]

7. Conclusions and Prospects

In this review, very different approaches have been described, all of which have a single goal: the design of molecular structures with very specific properties taking into account all available information. Consequently, CAMD is not restricted to one standard procedure; efficient molecular design, as described for the practical examples in Section 6, is based on the availability of several methods side by side and the awareness of the strengths and weaknesses of these methods.

CAMD has now become an indispensable tool in very different areas of molecular research. Apart from more "classic" applications, such as the drug design described in Section 6, CAMD is certain to be used extensively in protein research in the future. Thus, it may be speculated[179] whether, once the structures of the coat proteins of rhinovirus and poliovirus[180] have been solved, it will be possible to use computer-assisted methods to discover new drugs against these viruses.

In the industrial sector, the search for novel biologically active compounds is characterized by an increasing research expenditure. This trend may be reversed by reinforcing industrial research efforts in molecular biology and the use of computer-assisted molecular design to explain the biochemical mechanisms. CAMD will therefore be applied to an even greater extent to the development of new drugs and plant protection agents.

New perspectives are also expected to open up with regard to chemical reactions on solid surfaces (heterogeneous catalysis) and the elucidation of solid state properties.[181]

Further development of CAMD certainly depends on the extent to which supercomputers will be available in the future for calculations for molecular simulation, and on the progress made in the development of new methods and software, possibly involving artificial intelligence.

Received: December 29, 1986;
revised: January 19, 1987 [A 617 IE]
German version: *Angew. Chem. 99* (1987) 413

[1] C. Trindle, *Croat. Chem. Acta 57* (1984) 1231; H. Primas, U. Müller-Herold: *Elementare Quantenchemie*, Teubner, Stuttgart 1984.
[2] J. D. Watson, F. H. C. Crick, *Nature (London) 171* (1953) 737.
[3] J. Avery, *Int. J. Quantum Chem. 26* (1984) 843; P. Hobza, R. Zahradnik, J. Ladik, *ibid. 26* (1984) 857.
[4] C. Levinthal, *Sci. Am. 214* (1966) 42.
[5] R. Langridge, *Fed. Proc. Fed. Am. Soc. Exp. Biol. 33* (1974) 2332; R. J. Feldmann, *Annu. Rev. Biophys. Bioeng. 5* (1976) 477; C. Humblet, G. Marshall, *Drug Dev. Res. 1* (1981) 409; P. Gund, J. D. Andose, J. B. Rhodes, G. M. Smith, *Science (Washington DC) 208* (1980) 1425; R. Langridge, T. E. Ferrin, I. D. Kuntz, M. L. Conolly, *ibid. 211* (1981) 661; P. A. Bash, N. Pattabiraman, C. Huang, T. E. Ferrin, R. Langridge, *ibid. 222* (1983) 1325; R. Diamond, *Twelfth Int. Congr. Crystallogr. 1981*, Abstract 18 5-02; D. A. Pensak, *Ind. Res. Dev. 25* (1983) 74; J. G. Vinter, *Chem. Br. 21* (1985) 32; A. J. Hopfinger, *J. Med. Chem. 28* (1985) 1133.
[6] D. N. J. White, J. E. Pearson, *J. Mol. Graphics 4* (1986) 134.
[7] P. Kollman, *Acc. Chem. Res. 18* (1985) 105.
[8] T. A. Jones, *J. Appl. Crystallogr. 11* (1978) 268.
[9] Biograf, developed by *William Goddard* at the University of California, San Diego, CA.
[10] Chem-X, developed by *Keith Davies* at the University of Cambridge.
[11] Discover & Insight, developed by *Arnold Hagler* at the Agouron Institute, University of California, San Diego, CA; FRODO, orginally developed by *Alwyn Jones*, Max-Planck-Institut für Biochemie, Martinsried (FRG); HYDRA, developed at the University of York, England.
[12] Macromodel, developed by *Clark Still*, Columbia University, New York; MOGLI, developed by *A. Dearing* and Evans & Sutherland, Salt Lake City, UT.
[13] SYBYL, developed by *Garland Marshall*, Washington University, St. Louis, MO.
[14] A. J. Morffew, *J. Mol. Graphics 1* (1983) 83.
[15] For example, Leeds liquid crystal 3-D viewer, Millenium, Stevenage, Herfordshire SG1 4QX, England.
[16] W. M. Newman, D. F. Sproul: *Principles of Interactive Computer Graphics*, McGraw-Hill, New York 1979.
[17] N. C. Cohen, P. Colin, G. Lemoine, *Tetrahedron 37* (1981) 1711.
[18] B. Busetta, I. J. Tickle, T. L. Blundell, *J. Appl. Crystallogr. 16* (1983) 432.
[19] R. Taylor, *J. Mol. Graphics 4* (1986) 123, and references cited therein.
[20] L. Pauling: *The Nature of the Chemical Bond*, Cornell University Press, Ithaca, NY 1960.
[21] M. Born, R. Oppenheimer, *Ann. Phys. (Leipzig) 84* (1927) 457; H. Eyring, J. Walter, G. E. Kimball: *Quantum Chemistry*, Wiley, New York 1944.

[22] W. Kutzelnigg: *Einführung in die Theoretische Chemie, Band 1 und 2*, Verlag Chemie, Weinheim 1975.

[23] R. Daudel, R. Lefebvre, C. Moser: *Quantum Chemistry*, Wiley Interscience, New York 1965; R. McWeeny, B. T. Sutcliffe: *Methods of Molecular Quantum Mechanics*, Academic Press, London 1969.

[24] D. R. Hartree: *Calculation of Atomic Structure*, Wiley, New York 1957.

[25] C. C. J. Roothaan, *Rev. Mod. Phys. 23* (1951) 69, *32* (1960) 179.

[26] L. C. Snyder, H. Basch: *Molecular Wave Functions and Properties*, Wiley, New York 1972.

[27] H. F. Schaefer III: *The Electronic Structure of Atoms and Molecules*, Addison-Wesley, Reading, MA, USA 1972.

[28] I. Shavitt in H. F. Schaefer III (Ed.): *Methods of Electronic Structure Theory*, Plenum, New York 1977.

[29] A. C. Wahl, G. Das in H. F. Schaefer III (Ed.): *Methods of Electronic Structure Theory*, Plenum, New York 1977.

[30] J. S. Binkley, M. J. Frisch, D. J. De Frees, K. Raghavachari, R. A. Whiteside, H. B. Schlegel, E. M. Flunder, J. A. Pople, *Gaussian 82*, Carnegie-Mellon University, Pittsburgh, PA, USA 1983.

[31] G. A. Segal (Ed.): *Semiempirical Methods of Electronic Structure Calculations*, Plenum, New York 1977; M. Scholz, H. J. Köhler: *Quantenchemische Näherungsverfahren*, Hüthig, Heidelberg 1981.

[32] E. B. Wilson, J. C. Decius, P. C. Cross: *Molecular Vibrations*, McGraw-Hill, New York 1955.

[33] S. R. Niketic, K. Rasmussen, *Lecture Notes in Chemistry: The Consistent Force Field. Vol. 3*, Springer, Berlin 1977.

[34] O. Ermer: *Aspekte von Kraftfeldrechnungen*, Bauer, München 1981.

[35] U. Burkert, N. L. Allinger, *Molecular Mechanics* (*ACS Monogr. 177* (1982)).

[36] P. K. Weiner, P. A. Kollman, *J. Comput. Chem. 2* (1981) 287.

[37] B. R. Brooks, R. E. Bruccoleri, B. D. Olafson, D. J. States, S. Swaminathan, M. Karplus, *J. Comput. Chem. 4* (1983) 187.

[38] E. M. Engler, J. D. Andose, P. von R. Schleyer, *J. Am. Chem. Soc. 95* (1973) 8005; D. H. Wertz, N. L. Allinger, *Tetrahedron 30* (1974) 1579.

[39] A. T. Hagler, P. S. Starn, J. S. Ariel, *J. Am. Chem. Soc. 101* (1979) 813.

[40] S. J. Weiner, P. A. Kollman, D. A. Case, U. C. Singh, C. Ghio, G. Alagona, S. Profeta, P. Weiner, *J. Am. Chem. Soc. 106* (1984) 765.

[41] J. H. Schachtschneider, R. G. Snyder, *Spectrochim. Acta 19* (1963) 117.

[42] J. E. Williams, P. J. Stang, P. von R. Schleyer, *Annu. Rev. Phys. Chem. 19* (1968) 531.

[43] M. Levitt, *Annu. Rev. Biophys. Bioeng. 11* (1982) 251; A. Warshel in G. A. Segal (Ed.): *Semiempirical Methods of Electronic Structure Calculation*, Plenum, New York 1977.

[44] R. S. Mulliken, *J. Chem. Phys. 23* (1955) 1833; E. R. Davidson, *ibid. 46* (1967) 3320; K. R. Roby, *Mol. Phys. 27* (1974) 81; R. Heinzmann, R. Ahlrichs, *Theor. Chim. Acta 42* (1976) 33.

[45] M. J. S. Dewar: *The Molecular Orbital Theory of Organic Chemistry*, McGraw-Hill, New York 1969.

[46] J. Griffiths: *Colour and Constitution of Organic Molecules*, Academic Press, London 1976.

[47] H. C. Longuet-Higgins, *Adv. Spectrosc. 2* (1961) 49; E. E. Nikitin, *Adv. Quantum Chem. 5* (1970) 135.

[48] H. R. Schwarz, H. Rutishauser, E. Stiefel: *Numerik symmetrischer Matrizen*, 2nd ed., Teubner, Stuttgart 1972; R. Fletcher, M. J. D. Powell, *Comput. J. 6* (1963) 163; J. A. Nelder, R. Mead, *ibid. 7* (1965) 308; R. Fletcher, C. M. Reeves, *ibid. 7* (1964) 149; H. B. Curry, *Q. Appl. Math. 2* (1944) 258; A. S. Householder: *Principles of Numerical Analysis*, McGraw-Hill, New York 1953.

[49] H. P. Schwefel: *Numerical Optimization of Computer Models*, Wiley, New York 1981.

[50] B. Mandelbrot: *The Fractal Geometry of Nature*, Freeman, New York 1984.

[51] N. C. Cohen, *ACS Symp. Ser. 112* (1979) 371.

[52] I. Motoc, G. R. Marshall, R. A. Dammkoehler, J. Labanowski, *Z. Naturforsch. A40* (1985) 1108.

[53] B. Lee, F. M. Richards, *J. Mol. Biol. 55* (1971) 379; F. M. Richards, *Annu. Rev. Biophys. Bioeng. 6* (1977) 151.

[54] R. Lavery, A. Pullman, *Biophys. Chem. 19* (1984) 171.

[55] P. K. Ponnuswamy, P. Thiyagarajan, *Biopolymers 17* (1978) 2503; C. J. Alden, S.-H. Kim, *J. Mol. Biol. 132* (1979) 411.

[56] H. Weinstein, R. Osman, J. P. Green, *ACS Symp. Ser. 112* (1979) 161.

[57] D. Hadzi, M. Hodoscec, D. Kocjan, T. Solmajer, F. Avbelj, *Croat. Chem. Acta 57* (1984) 1065; P. M. Dean, *Pharmacochem. Libr. 6* (1983) 137.

[58] Z. Simon, A. Chiriac, I. Motoc, S. Holban, D. Ciubotariu, Z. Szabadai, *Stud. Biophys. 55* (1976) 217.

[59] S. Navasivayam, P. M. Dean, *J. Mol. Graphics 4* (1986) 46.

[60] R. Klein, unpublished.

[61] G. Moreau, P. Broto, *J. Mol. Graphics*, in press.

[62] P. Broto, G. Moreau, C. Vandycke, *Eur. J. Med. Chem. Chim. Ther. 19* (1984) 61.

[63] G. Naray-Szabo, *THEOCHEM 27* (1986) 401.

[64] G. R. Marshall, C. D. Barry, H. E. Bosshard, R. A. Dammkoehler, D. A. Dunn, *ACS Symp. Ser. 112* (1979) 205.

[65] G. J. Crippen, *J. Comput. Phys. 24* (1977) 96.

[66] G. J. Crippen, *J. Med. Chem. 23* (1980) 599.

[67] M. R. Linschoten, T. Bultsma, A. P. Ijzerman, H. Timmerman, *J. Med. Chem. 29* (1986) 278.

[68] P. R. Andrews, *ACS Symp. Ser. 112* (1979) 149.

[69] T. E. Klein, C. Huang, T. E. Ferrin, R. Langridge, C. Hansch, *ACS Symp. Ser. 306* (1986) 147.

[70] I. Motoc, G. R. Marshall, J. Labanowski, *Z. Naturforsch. A40* (1985) 1121.

[71] G. R. Marshall, *Pharmacochem. Libr. 6* (1983) 129.

[72] P. C. Jurs, J. T. Chou, M. Yuan, *ACS Symp. Ser. 112* (1979) 103; K. H. Ting, R. C. T. Lee, G. W. A. Milne, H. Shapiro, A. M. Gaurino, *Science (Washington DC) 180* (1973) 417; W. J. Dunn III, S. Wold, Y. C. Martin, *J. Med. Chem. 21* (1978) 922.

[73] T. R. Stouch, P. C. Jurs, *EHP Environ. Health Perspect. 61* (1985) 329; W. Sacco, W. P. Ashman, P. H. Broome, J. King, *DHEW Publ. FDA US 78-1046* (1978) 68; S. A. Leavitt, M. J. Mass, *Cancer Res. 45* (1985) 4741; S. L. Rose, P. C. Jurs, *J. Med. Chem. 25* (1982) 769.

[74] G. Klopman, *J. Am. Chem. Soc. 106* (1984) 7315.

[75] W. J. Streich, R. Franke, *Quant. Struct. Act. Relat. Pharmacol. Chem. Biol. 4* (1985) 13.

[76] R. Osman, H. Weinstein, J. P. Green, *ACS Symp. Ser. 112* (1979) 21.

[77] J. E. Leffler, E. Grunwald: *Rates of Equilibria of Organic Reactions*, Wiley, New York 1963.

[78] L. P. Hammett, *J. Am. Chem. Soc. 59* (1937) 96.

[79] R. W. Taft, *J. Am. Chem. Soc. 74* (1952) 3126, *75* (1953) 4538.

[80] C. Hansch, P. P. Malony, T. Fujita, R. Muir, *Nature (London) 194* (1962) 178.

[81] K. H. Meyer, H. Hemmi, *Biochem. Z. 277* (1935) 39.

[82] E. Overton: *Studium über die Narkose*, Fischer, Jena 1901.

[83] C. Hansch, *Acc. Chem. Res. 2* (1969) 232.

[84] L. P. Hammett: *Physical Organic Chemistry*, McGraw-Hill, New York 1940.

[85] H. H. Jaffé, *Chem. Rev. 53* (1953) 191; R. W. Taft, I. C. Lewis, *J. Am. Chem. Soc. 80* (1958) 2436; C. G. Swain, E. C. Lupton, *ibid. 90* (1968) 4328.

[86] O. R. Quayle, *Chem. Rev. 53* (1953) 484.

[87] J. H. Hildebrand, R. L. Scott: *The Solubility of Nonelectrolytes*, Reinhold, New York 1950.

[88] R. M. Carlson, R. E. Carlson, H. L. Kopperman, *J. Chromatogr. 107* (1975) 219; E. Tomlinson, *ibid. 113* (1975) 1.

[89] I. Motoc, O. Dragomir-Filimonescu, *MATCH 12* (1981) 127.

[90] M. Charton, *Prog. Phys. Org. Chem. 10* (1973) 81.

[91] A. Verloop, W. Hoogenstraaten, J. Tipker in E. J. Ariens (Ed.): *Drug Design, Vol. 7*, Academic Press, New York 1976.

[92] A. Verloop, *QSAR Strategies Des. Bioact. Compd. Proc. Eur. Symp. Quant. Struct. Act. Relat. 5th 1984* (1985) 98–104.

[93] Z. Simon: *Quantum Biochemistry and Specific Interactions*, Abacus Press, Kent, England 1976.

[94] A. T. Balaban, A. Chiriac, I. Motoc, Z. Simon, *Lecture Notes in Chemistry: Steric Fit in QSAR, Vol. 15*, Chapters 4, 5, 7, Springer, Berlin 1980.

[95] I. Motoc, O. Dragomir-Filimonescu, *MATCH 12* (1981) 117; Z. Simon, *ibid. 13* (1982) 357.

[96] I. Motoc, G. R. Marshall, *Z. Naturforsch. A40* (1985) 1114.

[97] P. Broto, G. Moreau, C. Vandycke, *Eur. J. Med. Chem. Chim. Ther. 19* (1984) 79.

[98] M. J. S. Dewar, P. J. Grisdale, *J. Am. Chem. Soc. 84* (1962) 3539.

[99] P. R. Andrews, *J. Med. Chem. 15* (1972) 1069.

[100] N. R. Draper, H. Smith: *Appl. Regression Analysis*, Wiley, New York 1966.

[101] P. P. Mager, *Med. Res. Rev. 2* (1982) 93.

[102] W. J. Streich, S. Dove, R. Franke, *J. Med. Chem. 23* (1980) 1452.

[103] S. Dove, R. Franke, O. L. Mndshojan, W. A. Schkuljiew, L. W. Chashakjan, *J. Med. Chem. 22* (1979) 90.

[104] C. Hansch, S. H. Unger, A. B. Forsythe, *J. Med. Chem. 16* (1973) 1217; W. J. Dunn III, W. J. Greenberg, S. S. Callejas, *ibid. 19* (1976) 1299.

[105] G. Klopman, A. N. Kalos, *J. Comput. Chem. 6* (1985) 492; Y. C. Martin: *Quantitative Drug Design*, Dekker, New York 1978.

[106] J. G. Topliss, R. P. Edwards, *ACS Symp. Ser. 112* (1979) 131.

[107] S. M. Free, Jr., J. W. Wilson, *J. Med. Chem. 7* (1964) 395.

[108] G. M. Crippen, *J. Med. Chem. 22* (1979) 988.

[109] A. K. Ghose, G. M. Crippen, *J. Med. Chem. 27* (1984) 901.

[110] C. Hansch, J. M. Blaney, *Proc. Rhone-Poulenc Round Table Conf. 3rd Meeting 1982* (1984) 185; M. Recanatini, T. Klein, C. Z. Yang, J. McClarin, R. Langridge, C. Hansch, *Mol. Pharmacol. 29* (1986) 436.

[111] R. Klein, unpublished.

[112] D. N. J. White, C. Morrow, *Comput. Chem. 3* (1979) 33.

[113] D. N. J. White, D. H. Kitson, *J. Mol. Graphics 4* (1986) 112.

[114] B. Pullman in B. Pullman (Ed.): *Quantum Mechanics of Molecular Conformations*, Wiley, New York 1976; L. Pedersen, *EHP Environ. Health Perspect. 61* (1985) 185.

[115] P. De Santis, A. M. Liquori, *Biopolymers 10* (1971) 699; G. Nemethy, H. A. Scheraga, *ibid. 3* (1965) 155; H. A. Scheraga, *ibid. 22* (1983) 1.

[116] P. Y. Chou, G. D. Fasman, *Adv. Enzymol. Relat. Areas Mol. Biol. 47* (1978) 45; G. D. Rose, L. M. Gierasch, J. A. Smith, *Adv. Protein Chem. 37* (1985) 1.

[117] G. N. Ramachandran, V. Sasisekharan, *Adv. Protein Chem. 23* (1968) 283.

[118] L. Verlet, *Phys. Rev. 159* (1967) 98; W. F. van Gunsteren, H. J. C. Berendsen, *Mol. Phys. 34* (1977) 1311.

[119] D. Fincham, D. M. Heyes, *Adv. Chem. Phys. 63* (1985) 493.

[120] H. J. C. Berendsen, J. P. M. Postma, W. F. van Gunsteren, A. DiNola, J. R. Haak, *J. Chem. Phys. 81* (1984) 3684.

[121] D. N. Theodorou, U. W. Suter, *J. Chem. Phys. 82* (1985) 955.

[122] W. van Gunsteren, H. Berendsen, J. Hollenberg, *Supercomputer 7* (1985) 26.

[123] F. Vesely: *Computerexperimente an Flüssigkeitsmodellen*, Physik Verlag, Weinheim 1978.

[124] T. Tsang, W. D. Jenkins, *Mol. Phys. 41* (1980) 797; J. G. Powles, *ibid. 48* (1983) 1083; G. S. Grest, S. R. Nagel, A. Rahman, T. A. Witten, *J. Chem. Phys. 74* (1981) 3532.

[125] P. J. Rossky, M. Karplus, A. Rahman, *Biopolymers 18* (1979) 825.

[126] K. Remerie, W. F. van Gunsteren, J. B. F. N. Engberts, *Mol. Phys. 56* (1985) 1393.

[127] J. L. Tallon, R. M. J. Cotterill, *Aust. J. Phys. 38* (1985) 209; W. M. Evans, G. J. Evans, *Adv. Chem. Phys. 63* (1985) 377; G. S. Pawley, M. A. Brass, T. M. Dove, K. Refson, *J. Chim. Phys. Phys. Chim. Biol. 82* (1985) 249.

[128] D. C. Wallace, *NATO ASI Ser. Ser. B121* (1985) 521; M. Kimura, F. Yonezawa, *Springer Ser. Solid State Sci. 46* (1983) 80; S. M. Levine, S. H. Garofalini, *Mater. Res. Soc. Symp. Proc. 61* (1986) 29.

[129] T. A. Weber, E. Helfand, *J. Chem. Phys. 71* (1979) 4760; E. Helfand, *Physica A (Amsterdam) 118* (1983) 123; D. Brown, J. H. R. Clarke, *J. Chem. Phys. 84* (1986) 2858.

[130] M. Levitt, *Cold Spring Harbor Symp. Quant. Biol. 47* (1983) 251; B. Tidor, K. K. Irikura, B. R. Brooks, M. Karplus, *J. Biomol. Struct. Dyn. 1* (1983) 231; S. Harvey, M. Prabhakaran, B. Mao, J. A. McCammon, *Science (Washington DC) 223* (1984) 1189.

[131] A. T. Hagler, P. Dauber, D. J. Osguthorpe, J. Hempel, *Science (Washington DC) 227* (1985) 1309.

[132] R. S. Struthers, J. Revier, A. T. Hagler, *Ann. NY Acad. Sci. 439* (1985) 81.

[133] J. A. McCammon, B. R. Gelin, M. Karplus, *Nature (London) 267* (1977) 585; M. Karplus, J. A. McCammon, *ibid. 277* (1979) 578; S. H. Northrup, M. R. Pear, J. A. McCammon, M. Karplus, T. Takano, *ibid. 287* (1980) 659; M. Levitt, *J. Mol. Biol. 168* (1983) 595; W. F. van Gunsteren, H. J. C. Berendsen, *ibid. 176* (1984) 559; W. F. van Gunsteren, M. Karplus, *Biochemistry 21* (1982) 2259; J. A. McCammon, M. Karplus, *Acc. Chem. Res. 16* (1983) 187; W. F. van Gunsteren, H. J. C. Berendsen, J. Hermans, W. G. J. Hol, J. P. M. Postma, *Proc. Natl. Acad. Sci. USA 80* (1983) 4315; P. Krüger, W. Strassburger, A. Wollmer, W. F. van Gunsteren, *Eur. Biophys. J. 13* (1985) 77.

[134] J. P. Ryckaert, A. Bellemans, *Faraday Discuss. Chem. Soc. 66* (1978) 95; P. van der Ploeg, H. J. C. Berendsen, *J. Chem. Phys. 76* (1982) 3271; *Mol. Phys. 49* (1982) 233; R. D. Mountain, R. M. Mazo, J. J. Volwerk, *Chem. Phys. Lipids 40* (1986) 35.

[135] N. S. Ostlund, R. A. Whiteside, *Ann. NY Acad. Sci. 439* (1985) 195.

[136] W. Fischer, J. Brickmann, P. Läuger, *Biophys. Chem. 13* (1981) 105; P. Läuger, H. J. Apell, *ibid. 16* (1982) 209; J. Brickmann, W. Fischer, *ibid. 17* (1983) 245; D. H. J. Mackay, P. H. Berens, K. R. Wilson, A. T. Hagler, *Biophys. J. 46* (1984) 229.

[137] K. Binder (Ed.): *Monte Carlo Methods in Statistical Physics*, Springer, Berlin 1979; B. J. Berne (Ed.): *Statistical Mechanics*, Plenum, New York 1977.

[138] G. G. Lowry (Ed.): *Markov Chains and Monte Carlo Calculations in Polymer Science*, Dekker, New York 1970.

[139] N. Metropolis, A. W. Rosenbluth, M. N. Rosenbluth, A. H. Teller, E. Teller, *J. Chem. Phys. 21* (1953) 1087.

[140] A. T. Hagler, J. Moult, *Nature (London) 272* (1978) 222; A. T. Hagler, D. J. Osguthorpe, B. Robson, *Science (Washington DC) 208* (1980) 601; G. Corongiu, E. Clementi, *Biopolymers 20* (1981) 551, *21* (1982) 763; V. Madison, D. J. Osguthorpe, P. Dauber, A. T. Hagler, *ibid. 22* (1983) 27.

[141] F. L. McCrackin, *J. Chem. Phys. 47* (1967) 1980; M. Lal, *Mol. Phys. 17* (1969) 57; M. Lal, D. Spencer, *ibid. 22* (1971) 649; R. De Santis, H. G. Zachmann, *Prog. Colloid Polym. Sci. 64* (1978) 281; R. Potenzone, D. C. Doherty, *Polym. Mater. Sci. Eng. 52* (1985) 264.

[142] B. J. McClelland: *Statistical Thermodynamics*, Chapman, London 1973; D. A. McQuarrie: *Statistical Mechanics*, Harper and Row, New York 1976.

[143] A. Ben-Naim: *Hydrophobic-Interactions*, Plenum, New York 1980.

[144] D. L. Beveridge, M. Mezei, G. Rhavishanker, B. Jayaram, *J. Biosci. 8* (1985) 167; M. Mezei, P. K. Mehrotra, D. L. Beveridge, *J. Am. Chem. Soc. 107* (1985) 2239.

[145] M. Karplus, J. Kushick, *Macromolecules 14* (1981) 325; R. M. Levy, M. Karplus, J. Kushick, D. Perahia, *ibid. 17* (1984) 1370.

[146] R. L. Humphries, *J. Theor. Biol. 91* (1981) 477.

[147] H. Wallmeier, unpublished.

[148] K. W. Volz, D. A. Matthews, R. A. Alden, S. T. Freer, C. Hansch, T. B. Kaufman, J. Kraut, *J. Biol. Chem. 257* (1982) 2528.

[149] J. T. Bolin, D. J. Filman, D. A. Matthews, R. C. Hamlin, J. Kraut, *J. Biol. Chem. 257* (1982) 13650; D. J. Filman, J. T. Bolin, D. A. Matthews, J. Kraut, *ibid.* 13663.

[150] L. F. Kuyper, B. Roth, D. B. Baccanari, R. Ferone, C. R. Beddell, J. N. Champness, D. K. Stammers, J. G. Dann, F. E. A. Norrington, *J. Med. Chem. 28* (1985) 303; A. Stuart, T. Paterson, B. Roth, E. Aig, *ibid. 26* (1983) 667; R. M. Hyde, R. A. Paterson, C. R. Beddell, J. N. Champness, D. K. Stammers, D. J. Baker, P. J. Goodford, L. F. Kuyper, R. Ferone in J. A. Blair (Ed.): *Chemistry and Biology of Pteridines*, de Gruyter, Berlin 1983, pp. 505–509; D. K. Stammers, J. N. Champness, J. G. Dann, C. R. Bedell, *ibid.*, pp. 567–571; D. J. Baker, C. R. Bedell, J. N. Champness, P. J. Goodford, F. E. Norrington, B. Roth, D. K. Stammers, *ibid.*, pp. 545–549; M. Mabilia, R. A. Pearlstein, A. J. Hopfinger, *Eur. J. Med. Chem. Chim. Ter. 20* (1985) 163; *QSAR Strategies Des. Bioact. Compd. Proc. Eur. Symp. Quant. Struct. Act. Relat. 5th 1984* (1985) 120; A. J. Hopfinger, *J. Med. Chem. 26* (1983) 990; L. F. Kuyper, B. Roth, D. B. Baccanari, R. Ferone, C. R. Beddell, J. N. Champness, D. K. Stammers, J. G. Dann, F. E. A. Norrington, D. J. Baker, P. J. Goodford, *ibid. 25* (1982) 1120; H. B. Schlegel, M. Poe, K. Hoogsteen, *Mol. Pharmacol. 20* (1981) 154.

[151] B. Birdsall, J. Feeney, C. Fascual, G. C. K. Roberts, I. Kompis, R. L. Then, K. Mueller, A. Kroehn, *J. Med. Chem. 27* (1984) 1672; H. Maag, R. Locher, J. J. Daly, I. Kompis, *Helv. Chim. Acta 69* (1986) 887; K. Mueller, *Actual. Chim. Ther. 11* (1984) 113.

[152] C. D. Selassie, Z. X. Fang, R. L. Li, C. Hansch, T. Klein, R. Langridge, T. B. Kaufman, *J. Med. Chem. 29* (1986) 621; C. Hansch, B. A. Hathaway, Z. Guo, C. D. Selassie, S. W. Dietrich, J. M. Blaney, R. Langridge, K. W. Volz, T. B. Kaufman, *ibid. 27* (1984) 129; C. Hansch, *Drug Intell. Clin. Pharm. 16* (1982) 391; R. Li, C. Hansch, D. Matthews, J. M. Blaney, R. Langridge, T. J. Delcamp, S. S. Susten, J. H. Freisheim, *Quant. Struct. Act. Relat. Pharmacol. Chem. Biol. 1* (1982) 1.

[153] H. D. Höltje, P. Zunker, *QSAR Strategies Des. Bioact. Compd. Proc. Eur. Symp. Quant. Struct. Act. Relat. 5th 1984* (1985) 127.

[154] A. F. Cuthbertson, W. G. Richards, *THEOCHEM 25* (1985) 167.

[155] V. Cody, *J. Mol. Graphics 4* (1986) 69; *Prog. Clin. Biol. Res. 172* (1985) 275.

[156] E. A. Potterson, A. J. Geddes, A. C. T. North in J. A. Blair (Ed.): *Chemistry and Biology of Pteridines*, de Gruyter, Berlin 1983, pp. 299–303.

[157] J. Feeney, *NATO ASI Ser. Ser. C164* (1986) 347.

[158] D. A. Matthews, J. T. Bolin, J. M. Burridge, D. J. Filman, D. J. Volz, J. Kraut, *J. Biol. Chem. 260* (1985) 392.

[159] M. N. G. James, A. R. Sielecki, *J. Mol. Biol. 163* (1983) 299.

[160] M. N. G. James, A. R. Sielecki, *Biochemistry 24* (1985) 3701.

[161] E. Subramanian, I. D. A. Swan, M. Liu, D. R. Davies, J. A. Jenkins, I. J. Tickle, T. L. Blundell, *Proc. Natl. Acad. Sci. USA 74* (1977) 556.

[162] R. Bott, E. Subramanian, D. R. Davies, *Biochemistry 21* (1982) 6956.
[163] K. S. Misono, J. J. Chang, T. Inagami, *Proc. Natl. Acad. Sci. USA 79* (1982) 4858; J.-J. Panthier, S. Foote, B. Chambreaud, A. D. Strosberg, P. Corvol, F. Rougeon, *Nature (London) 298* (1982) 90.
[164] F. Soubrier, J.-J. Panthier, P. Corvol, F. Rougon, *Nucleic Acids Res. 11* (1983) 7181; T. Imai, H. Miyazaki, S. Hirose, H. Hori, T. Hayashi, R. Kageyama, H. Ohkubo, S. Nakanishi, K. Murakami, *Proc. Natl. Acad. Sci. USA 80* (1983) 7405.
[165] T. Blundell, B. L. Sibanda, L. Pearl, *Nature (London) 304* (1983) 273.
[166] B. L. Sibanda, T. Blundell, P. M. Hobart, M. Fogliano, J. S. Bindra, B. W. Dominy, J. M. Chirgwin, *FEBS Lett. 174* (1984) 102; B. L. Sibanda, *Biochem. Soc. Trans. 12* (1984) 953; W. Carlson, E. Haber, R. Feldmann, M. Karplus, *Pept. Struct. Funct. Proc. Am. Pept. Symp. 8th 1983*, 821; W. Carlson, M. Handschumacher, M. Karplus, E. Haber, *J. Hypertens. 2 (Suppl. 3)* (1984) 281; K. Murakami, *ibid. 2 (Suppl. 3)* (1984) 285; W. Carlson, M. Karplus, E. Haber, *Hypertension (Dallas) 7* (1985) 13; K. Akahane, H. Umeyama, S. Nakagawa, I. Moriguchi, S. Hirose, K. Kinji, K. Murakami, *ibid. 7* (1985) 3.
[167] K. Murakami, N. Ueno, *Proc. Jpn. Acad. Ser. B 61* (1985) 257.
[168] B. L. Sibanda, A. M. Hemmings, T. Blundell, *Proc. FEBS Adv. Course 1984*, 339; de Gruyter, Berlin 1985. P. Raddatz, C. Schnittenhelm, G. Barnickel, *Kontakte 1985*, 3; J. Boger, *Spec. Publ. R. Soc. Chem. 55* (1986) 271; G. Breipohl, H. Frühbeis, J. Knolle, D. Ruppert, B. A. Schoelkens, *J. Hypertens. 3* (1985) 406.
[169] M. Szelke, B. J. Leckie, A. Hallett, D. M. Jones, J. Sueiras-Diaz, B. Atrash, A. F. Lever, *Nature (London) 299* (1982) 555.
[170] G. Winter, P. Carter, H. Bedouelle, D. Lowe, R. J. Leatherbarrow, A. R. Fersht, *Life Sci. Res. Rep. 35* (1986) 55; D. M. Blow, A. R. Fersht, G. Winter (Eds.): *Design, Construction and Properties of Novel Protein Molecules (Proceedings of a Royal Society Discussion Meeting held on June 5 and 6, 1985)*. The Royal Society, London 1986.
[171] D. A. Estell, J. V. Miller, T. P. Graycar, D. B. Powers, J. A. Wells, *World Biotech. Rep. 1984*, 181.
[172] L. J. Perry, H. L. Heyneker, R. Wetzel, *Gene 38* (1985) 259; L. J. Perry, R. Wetzel, *Science (Washington DC) 226* (1984) 555; *Biochemistry 25* (1986) 733.
[173] D. A. Estell, T. P. Graycar, J. V. Miller, D. B. Powers, J. P. Burnier, P. G. Ng, J. A. Wells, *Science (Washington DC) 233* (1986) 659; R. R. Bott, M. H. Ultsch, A. A. Kossiakoff, J. Burnier, J. A. Wells, D. B. Powers, B. A. Katz, B. C. Cunningham, S. S. Power, *World Biotech. Rep. 1985*, 611; J. A. Wells, D. B. Powers, *J. Biol. Chem. 261* (1986) 6564.
[174] A. R. Fersht, J.-P. Shi, A. J. Wilkinson, D. M. Blow, P. Carter, M. M. Y. Waye, G. P. Winter, *Angew. Chem. 96* (1984) 455; *Angew. Chem. Int. Ed. Engl. 23* (1984) 467; A. R. Fersht, R. J. Leatherbarrow, T. N. C. Wells, *Trends Biochem. Sci. 11* (1986) 321; T. N. C. Wells, C. K. Ho, A. R. Fersht, *Biochemistry 25* (1986) 6603; R. J. Leatherbarrow, A. R. Fersht, G. Winter, *Proc. Natl. Acad. Sci. USA 82* (1985) 7840; P. G. Thomas, A. J. Russell, A. R. Fersht, *Nature (London) 318* (1985) 375.
[175] R. R. Bott, *World Biotech. Rep. 1984*, 611.
[176] T. Blundell, M. J. E. Sternberg, *Trends Biotechnol. 3* (1985) 228.
[177] G. M. Smith, D. G. Hangauer, J. D. Andose, B. R. Bush, E. M. Fluder, P. Gund, E. F. McIntyre, *Drug. Inf. J. 18* (1984) 167.
[178] A. Warshel, F. Sussman, *Proc. Natl. Acad. Sci. USA 83* (1986) 3806.
[179] W. G. J. Hol, *Angew. Chem. 98* (1986) 765; *Angew. Chem. Int. Ed. Engl. 25* (1986) 767.
[180] M. G. Rossmann, E. Arnold, J. W. Erickson, E. A. Frankenberger, J. P. Griffith, H.-J. Hecht, J. E. Johnson, G. Kamer, M. Luo, A. G. Mosser, R. R. Rueckert, B. Sherry, G. Vriend, *Nature (London) 317* (1985) 145; J. M. Hogle, M. Chow, D. J. Filman, *Science (Washington DC) 229* (1985) 1358.
[181] C. R. A. Catlow, M. Doherty, G. D. Price, M. J. Sanders, S. C. Parker, *Mater. Sci. Forum 7* (1986) 163.

Polyphosphorus Compounds—New Results and Perspectives**

By Marianne Baudler*

Dedicated to Professor Heinz Harnisch on the occasion of his 60th birthday

In contrast to the numerous known and often technically important mono- and diphosphorus compounds with phosphorus in its maximum oxidation state, polyphosphorus compounds led only a shadowy existence up to about twenty years ago. One of the reasons for this was the properties of such compounds, which made their handling and structural characterization difficult. This problem was solved by the development of modern preparative techniques and, especially, by the further methodological development of nuclear magnetic resonance spectroscopy. Thus, a fascinating new branch of phosphorus chemistry has been opened up in recent years. The first comprehensive review on this subject was published five years ago. Since then, research on this "element-near" chemistry of phosphorus has produced further impressive advances with the result that a surprisingly large variety of compounds with skeletons consisting of chains or rings of phosphorus atoms is known today. However, the recent observation of the spontaneous formation of the "aromatic" pentaphosphacyclopentadienide ion, P_5^-, during the synthesis of phosphorus-richer polyphosphides from phosphorus-poorer compounds in solution and the discovery of the inversion of phosphorus in tetra- and pentacyclic organophosphanes demonstrate that this field is still capable of producing surprises.

1. Introduction

The chemistry of polyphosphorus compounds has undergone impressive developments in the past two decades. Whereas up to the 1970s compounds with a skeleton of directly linked phosphorus atoms were still considered as laboratory curiosities, phosphorus, after carbon, now appears to be the element with the most pronounced ability to form homonuclear element–element bonds. The fact that this "carbon-like" aspect of phosphorus chemistry was overlooked for so long is certainly related to the enormous technical importance of many "classical" phosphorus compounds of the oxidation state +5 and the resultant focus of interest on these classes of compounds. However, in recent years, the discovery of a surprising variety of "low-valent" phosphorus compounds with differing structural types has opened up a new chapter in the chemistry of this element, the extent and significance of which can hardly be estimated at the moment. This "element-near" chemistry covers a wide range, from small molecules through medium-sized ensembles of atoms up to high-molecular solids, and thus represents an important link between inorganic molecular chemistry and solid-state chemistry.

Developments in the field of polyphosphorus compounds up to 1982 have already been reviewed.[1] The present article is thus limited to recently obtained results. Research in the last few years has focused mainly on extension of the phenomenological basis in order to (1) obtain a comprehensive structural understanding and (2) explore the reaction behavior of chain- and ring-type polyphosphorus compounds.

2. Phosphorus Hydrides and Partially Organosubstituted Phosphanes

Compounds containing skeletons of trivalent phosphorus atoms may have open-chain or cyclic structures. They are derivatives of the corresponding phosphorus hydrides or phosphanes.

2.1. Existence, Properties, and Structural Elucidation

The number of known hydrides of phosphorus is only exceeded by that of carbon. The present state of knowledge is summarized in Table 1. In the last few years alone, 31 new phosphorus–hydrogen compounds with up to 22 phosphorus atoms in the molecule have been identified in the thermolyzates of diphosphane and other phosphorus-poorer hydrides by mass spectrometry. Thus, most of the gaps in an earlier systematic classification[1] have now been filled, and representatives of two further series of phosphanes with the compositions P_nH_{n-16} and P_nH_{n-18} have been discovered.

Without doubt, however, all possible types of compounds have not yet been verified experimentally. Thus, neither the hydride $P_{18}H_2$ nor the "triphosphirene" P_3H have yet been detected and, also, the maximum possible size of a phosphorus skeleton has by no means been attained. On the whole, however, the "scenary" has not changed in principle since the previous reviews:[2] with increasing number of phosphorus atoms, the stability of the open-chain phosphanes P_nH_{n+2} decreases significantly in favor of the formation of the monocyclic and polycyclic

[*] Prof. Dr. M. Baudler
Institut für Anorganische Chemie der Universität
Greinstrasse 6, D-5000 Köln 41 (FRG)

[**] Contributions to the Chemistry of Phosphorus, Part 178.—Part 177: [106].

 © VCH Verlagsgesellschaft mbH, D-6940 Weinheim, 1987 0570-0833/87/0505-0419 $ 02.50/0

Table 1. Phosphorus hydrides (phosphanes).

Phosphane series	Known compounds
P_nH_{n+2}	PH_3, P_2H_4, P_3H_5, P_4H_6, P_5H_7, P_6H_8, P_7H_9, P_8H_{10}, P_9H_{11}
P_nH_n	P_3H_3, P_4H_4, P_5H_5, P_6H_6, P_7H_7, P_8H_8, P_9H_9, $P_{10}H_{10}$
P_nH_{n-2}	P_4H_2, P_5H_3, P_6H_4, P_7H_5, P_8H_6, P_9H_7, $P_{10}H_8$, $P_{11}H_9$, $P_{12}H_{10}$
P_nH_{n-4}	P_5H, P_6H_2, P_7H_3, P_8H_4, P_9H_5, $P_{10}H_6$, $P_{11}H_7$, $P_{12}H_8$, $P_{13}H_9$
P_nH_{n-6}	P_7H, P_8H_2, P_9H_3, $P_{10}H_4$, $P_{11}H_5$, $P_{12}H_6$, $P_{13}H_7$, $P_{14}H_8$, $P_{15}H_9$
P_nH_{n-8}	$P_{10}H_2$, $P_{11}H_3$, $P_{12}H_4$, $P_{13}H_5$, $P_{14}H_6$, $P_{15}H_7$, $P_{16}H_8$, $P_{17}H_9$
P_nH_{n-10}	$P_{12}H_2$, $P_{13}H_3$, $P_{14}H_4$, $P_{15}H_5$, $P_{16}H_6$, $P_{17}H_7$, $P_{18}H_8$, $P_{19}H_9$, $P_{20}H_{10}$
P_nH_{n-12}	$P_{13}H$, $P_{14}H_2$, $P_{15}H_3$, $P_{16}H_4$, $P_{17}H_5$, $P_{18}H_6$, $P_{19}H_7$, $P_{20}H_8$
P_nH_{n-14}	$P_{15}H$, $P_{16}H_2$, $P_{17}H_3$, $P_{18}H_4$, $P_{19}H_5$, $P_{20}H_6$, $P_{21}H_7$
P_nH_{n-16}	$P_{17}H$, $P_{19}H_3$, $P_{20}H_4$, $P_{21}H_5$, $P_{22}H_6$
P_nH_{n-18}	$P_{19}H$, $P_{20}H_2$, $P_{21}H_3$, $P_{22}H_4$

phosphorus hydrides P_nH_n and P_nH_{n-2m} ($m = 1$-9), respectively.

In addition to the characterization of individual phosphanes by their mass spectra,[1] detailed information on the structures of a series of compounds has been obtained from their phosphorus nuclear magnetic resonance spectra (see Sections 2.2 to 2.5). The constitution, configuration, and conformation can be determined on the basis of the spin systems and the ^{31}P-NMR parameters, especially the coupling constants. However, for technical reasons, this method of structural determination can be applied at present only to liquid phosphanes and to solid phosphanes in solution. Since compounds with high phosphorus and low hydrogen contents are usually only very poorly soluble and, in addition, amorphous to X-rays, most of the polycyclic phosphorus hydrides are not as yet amenable to direct nuclear magnetic resonance spectroscopic or X-ray structural investigations.

1 P_7H_3 $(Me_3Si)_3P_7$ **2**

The only exception is the heptaphosphane(3) **1**,[4] which is obtainable by the mild methanolysis of the silyl compound **2**[3,4] in pure form.[4] The substance is amorphous to X-rays and insoluble in hydrocarbons, alcohols, ethers, chloroform, carbon disulfide, acetonitrile, cyclohexanone, dimethylformamide, dimethyl sulfoxide, hexamethylphosphoric triamide, diphosphane, and 1,2-di-*tert*-butyldiphosphane, as well as in molten white phosphorus. A solubility sufficient for nuclear magnetic resonance studies, however, can be achieved when **1** is prepared directly in benzene, 1-methylnaphthalene, or 1-methylnaphthalene/phenanthrene, which are particularly good solvents for higher phosphanes of the series P_nH_{n+2} and P_nH_n, and the nuclear magnetic resonance spectrum is recorded shortly thereafter.[5] The ^{31}P{^{1}H}-NMR spectrum of **1** (Fig. 1) shows nine complex signal groups, which, on the basis of their intensity ratios and splitting patterns, can be assigned to the two diastereomers **1a** and **1b** with symmetrically and unsymmetrically arranged hydrogen atoms, respectively. All the available data, in particular the results of a complete analysis of the partial spectrum of **1a** confirm that **1**, like the starting compound **2**, possesses a P_7 framework analogous to that of nortricyclene; however, in the case of **2**, only the symmetrical isomer could be detected by X-ray methods.[6]

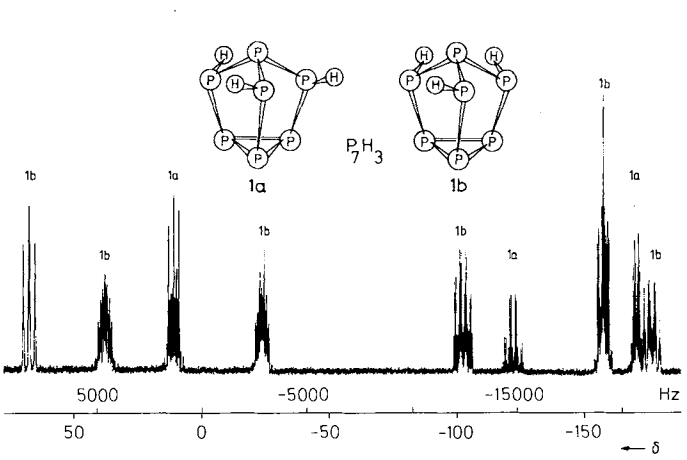

Fig. 1. ^{31}P{^{1}H}-NMR spectrum of P_7H_3, **1** (mixture of isomers), in 1-methylnaphthalene at 27 °C (121.497 MHz).

2.2. Open-Chain Triphosphanes

Open-chain phosphorus hydrides generally exhibit a pronounced tendency to undergo disproportionation, so that only the first members of the homologous series P_nH_{n+2} (up to $n = 3$) can be isolated in pure form. Triphosphane(5) **3** decomposes rapidly even at room temperature under diffuse daylight, thereby turning yellow.[1] In contrast, partially organosubstituted triphosphanes of the types **4** and **5** are more stable, especially when the phosphorus chain is protected toward intermolecular dispro-

$H_2P-P(H)-PH_2$

3

$H(R)P-P(R)-P(R)H$

4a: R=Ph [7]

4b: R=*t*Bu [8]

$R^1(Me_3Si)P-P(H)-P(SiMe_3)R^2$

5a: $R^1=R^2=SiMe_3$ [9]

5b: $R^1=SiMe_3$, $R^2=Me$ [9]

5c: $R^1=SiMe_3$, $R^2=tBu$ [9]

5d: $R^1=R^2=tBu$ [9]

5e: $R^1=Me$, $R^2=tBu$ [9]

portionation reactions by the presence of bulky substituents. Unlike **3**, these triphosphane derivatives—with the exception of **5a**—each contain phosphorus atoms as chiral centers, so that diastereomers exist.[7-9] Their populations depend on the respective molecular conformations, which, in turn, are governed by the tendency for *gauche* orientations of neighboring lone electron pairs[10] and by steric interactions of the substituents.

1,3-Diaminotriphosphane(5) **6**[11] is an "inorganic" derivative of **3** and, as such, a representative of the "mixed" non-metal hydrides. It is formed, together with $NaPH_2$,

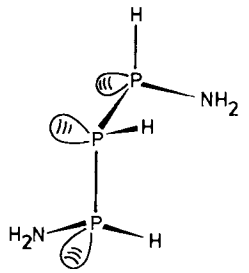

6

Na_2HP_7, and phosphorus-richer phosphides, in the reaction of white phosphorus with sodium in liquid ammonia (P : Na = 2 : 1 or 1.5 : 1). The composition and structure of **6**, which is only stable in liquid ammonia, were deduced from the phosphorus nuclear magnetic resonance spectrum. Of the three possible diastereomers, only the *erythro,erythro* isomer is formed and is probably stabilized energetically by hydrogen bonds between the central phosphorus atom and the transoid NH_2 groups.

2.3. Open-Chain Tetraphosphanes

Tetraphosphane(6) is always obtained as a mixture of the constitutional isomers *n*-P_4H_6 (*d,l* and *meso* forms) **7a** and iso-P_4H_6 **7b**.[1] According to the most recent ^{31}P-NMR

n-P_4H_6: $H_2P-PH-PH-PH_2$; iso-P_4H_6: $P(PH_2)_3$

7a **7b**

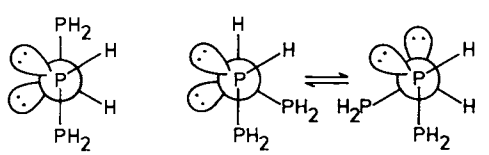

d,l-*n*-P_4H_6 *meso*-*n*-P_4H_6

spectroscopic results[12] on the *n*-P_4H_6 diastereomers, the AA'BB' spin system at higher field corresponds to the "bent" *meso* isomer and that at lower field to the "extended" *d,l* isomer.

The separation of *n*-P_4H_6 and iso-P_4H_6 has not yet been achieved owing to the hyperreactivity of these two compounds. However, tris(*tert*-butylphosphino)phosphane **8**, the first partially substituted derivative of iso-P_4H_6, has been prepared.[13]

The starting material for this synthesis is the three-membered ring compound **9**. Halogenative ring-opening of **9** with phosphorus(III) bromide initially produces the open-chain triphosphane **10**. The bromophosphanediyl (bromophosphinidene), formed as an intermediate, then inserts into the phosphorus chain with formation of the mixed substituted tetraphosphane **11**. As expected, the latter is unstable and rearranges spontaneously to furnish the constitutional isomer **12**.

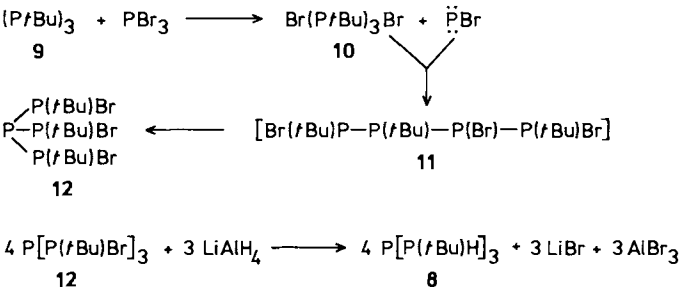

Compound **12**, which is stable at room temperature, can form two diastereomers; however, only the symmetrical isomer with (*R,R,R*) and (*S,S,S*) configuration can be detected by ^{31}P-NMR spectroscopy. On reaction with lithium aluminum hydride, smooth substitution of the bromine atoms by hydrogen atoms and formation of **8** occur.

Compound **8** is not stable at room temperature but can be isolated, below −30 °C, in the form of colorless crystals. Immediately after preparation, only the signals of the symmetrical isomer **8a** (A_3X spin system) can be observed in the $^{31}P\{^1H\}$-NMR spectrum, indicating that the hydrogenation of **12** proceeds stereoselectively. Subsequently, however, even at −78 °C, formation of the asymmetrical isomer **8b** (ABCX system) with (*R,R,S*) and (*S,S,R*) configuration proceeds until the statistical distribution of **8a** : **8b** = 1 : 3 is attained at equilibrium (the (*R,R,R*) enantiomer of **8a** and the (*R,R,S*) enantiomer of **8b** are shown). The rate of isomerization is strongly solvent-dependent; in *n*-pentane at −78 °C, equilibrium is attained after about 300 h.[13]

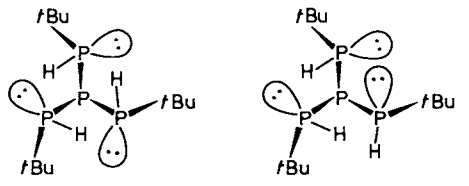

8a **8b**

Of the class of partially organosubstituted *n*-tetraphosphanes, only the compounds **13a** and **13b** are as yet known. They are prepared by the mild alcoholysis of the corresponding silyl compounds, which, in turn, are accessible from α,ω-dimetalated organophosphanes by reaction with chlorotrimethylsilane.[14,16] A particularly suitable method for the preparation of **13b** is the reaction of the dipotassium salt **14**[17] with *tert*-butyl chloride, which proceeds with elimination of isobutene.[15]

$H(R)P-(PR)_2-P(R)H$ **13a**: R = Ph[14]
13b: R = *t*Bu[15]

$K(t\mathrm{Bu})P-(Pt\mathrm{Bu})_2-P(t\mathrm{Bu})K + 2\,t\mathrm{BuCl} \longrightarrow$
14

13b + $2\,H_2C{=}CMe_2$ + 2 KCl

With increasing bulk of the substituents R, the configurations and conformations of the existing isomers are governed to an increasing extent by steric factors in addition to the tendency for *gauche* orientation of neighboring lone electron pairs. This is clearly seen in the case of **13b**; of the six possible configurational isomers, only the three diastereomeric forms *threo/d,l/threo, erythro/threo/threo,* and *erythro/d,l/erythro* are formed in solution in a ratio of 10:5:1, which deviates from statistical expectations.[15] Accordingly, only *d,l* and *threo* configurations, referred to the central P–P bond, occur in which both an all-*trans* arrangement of the *tert*-butyl substituents and a *gauche* orientation of the lone electron pairs of the phosphorus atoms of the middle bond are realized. This situation leads to a spiral-like structure of the P_4 chain, as exemplified for the dominating *threo/d,l/threo* isomer. The relative amounts of the observed isomers are governed by the orientations of the lone electron pairs on the outer P–P bonds (*gauche,gauche, trans,gauche,* or *trans,trans*).[15]

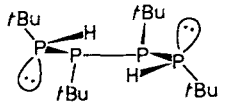

13b

threo/d,l/threo isomer

The three diastereomers of **13b** exist in a dynamic equilibrium at room temperature in solution,[15] whereas the triphosphane **4b** is configurationally stable under the same conditions.[8] As expected, the barriers to inversion of the phosphorus atoms decrease markedly with increasing length of the phosphorus chain.[18]

2.4. Phosphorus Hydrides P_nH_{n+2} with n > 4

To date, no methods are known for the synthesis of open-chain organophosphanes containing more than four phosphorus atoms. Thus, in order to obtain information on compounds with longer phosphorus chains, phosphorus hydride mixtures must be studied. These are obtained by the mild thermolysis of diphosphane[1] or as distillation residues from the purification of larger amounts of crude diphosphane[19] and, according to mass spectroscopic studies, contain varying amounts of the higher homologues. The unequivocal characterization of the individual species present in such mixtures is possible with the help of ^{31}P-NMR spectroscopy.

The procedure will be exemplified for the isomers of pentaphosphane(7) **15**.[1,20] Phosphane mixtures of the above-mentioned origin contain phosphorus-poorer members of the phosphane series P_nH_{n+2} with n = 2–4[1] as the major components. An enrichment of the higher homologues with n > 4 presents inherent difficulties as a result of the pronounced tendency of longer-chain compounds to undergo disproportionation. Thus, identification of the individual isomers of **15** by direct analysis of the appropriate ^{31}P spin systems is not possible since the corresponding partial spectra are partly masked by the intense signal groups of the P_4H_6 isomers and of P_3H_5. As can be seen from the $^{31}P\{^1H\}$-NMR spectra of such phosphane mixtures, however, the resonance signal of at least one phosphorus atom of each of the various isomers is clearly shifted to lower field into a signal-poorer region of the spectrum with increasing chain length. This opens up the possibility for a "spectroscopic separation" of the individual spin systems by application of double resonance experiments and, in particular, of homonuclear ^{31}P-selective population transfer (SPT) experiments.[21,22]

In SPT experiments, a selective pulse is applied to a specific line of a spin system, resulting in a change in the population difference of the corresponding energy levels and thus a change in the intensity of the lines associated with these levels. This is particularly clear after subtraction of the "unperturbed" spectrum from the SPT spectrum. Only the perturbed line and the progressively or regressively associated transitions (the latter being characterized by positive or negative line intensities, respectively) can be observed in the corresponding difference spectrum. In this way, masked or weak resonances of a spin system can be identified and, in combination with a simulation of the spectrum, questions of assignment can be answered unequivocally.

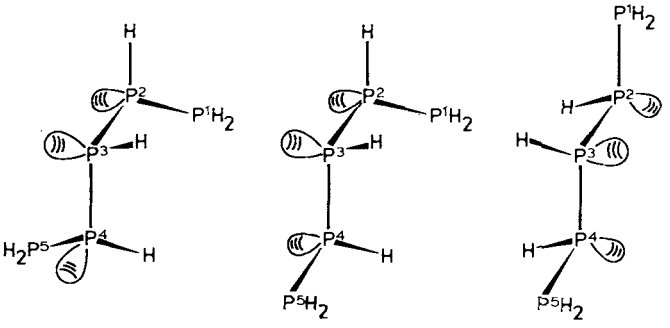

15a **15b** **15c**

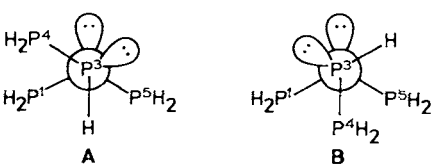

A **B**

15d

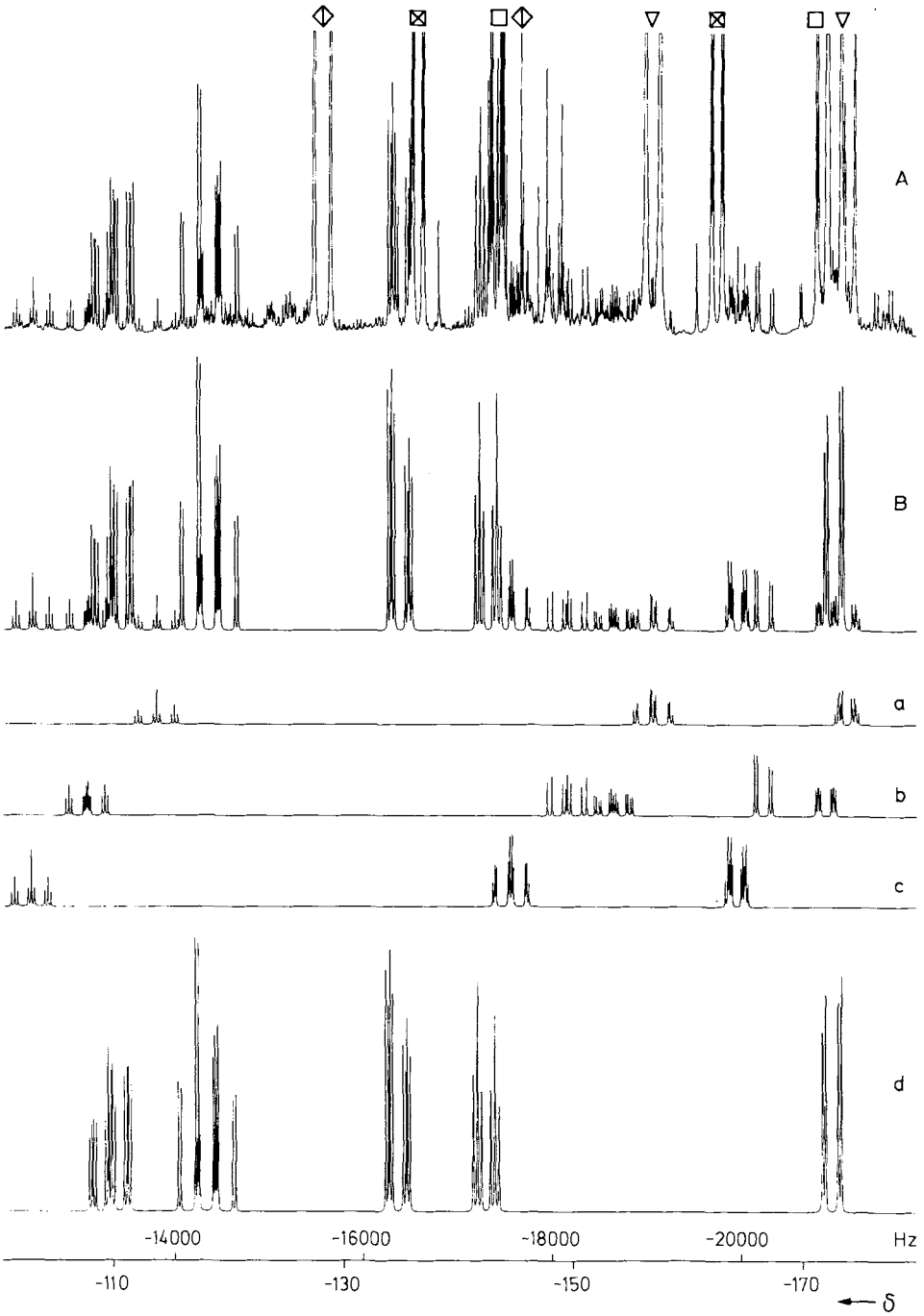

Fig. 2. Observed (A) and simulated (B) $^{31}P\{^1H\}$-NMR spectrum of pentaphosphane(7) in a phosphane mixture with 15 P-% P_5H_7 ($\nabla = P_3H_5$, $\square$ = *meso-n*-P_4H_6, $\boxtimes$ = *d,l-n*-P_4H_6, $\diamondsuit$ = iso-P_4H_6) at $-30°C$ (121.497 MHz); a, b, c, d: simulated spectra of the individual P_5H_7 isomers **15a**, **b**, **c**, **d**.

The sets of starting parameters obtained from a series of SPT experiments for the isomers of **15** were optimized by systematic variation of the values until an assignment of the calculated lines with the experimentally observed lines was possible. Since the NMR parameters are far overdetermined as a result of the large number of lines, it is sufficient to assign only those lines that are not influenced by neighboring signals. The final data sets are obtained by subsequent iteration. The superimposition of the individual simulated spectra reproduces the experimentally observed $^{31}P\{^1H\}$-NMR spectrum of **15** very satisfactorily (Fig. 2).

Accordingly, pentaphosphane(7) exists as a mixture of the three diastereomers of *n*-P_5H_7 (**15a**, *erythro,erythro*; **15b**, *erythro,threo*; **15c**, *threo,threo*) and the constitutionally isomeric 2-phosphinotetraphosphane (iso-P_5H_7) **15d**. The branched isomer is present in the largest relative abundance. From the determined ^{31}P-NMR parameters,[20] the three-dimensional structures of **15a–d** can be deduced directly. The isomer **15d** can occur in two conformations, **A** and **B**, of which **A** is probably favored for steric reasons.

With the complete sets of ^{31}P-NMR parameters for **15a–d**,[20] the general equations, formulated previously[1] on the basis of incomplete data for **15**, for the dependence of the chemical shifts δ and the coupling constants $^1J(PP)$ for open-chain phosphanes on the structural parameters (*a*, *b*,

c; number of phosphorus atoms in α, β, and γ positions) were optimized. The following equations were obtained for $t = -30\,^{\circ}C$:

$$\delta(^{31}P) = -214.9 + 21.7a + 31.8b - 7.3c\ (\pm 4.4)$$
$$^{1}J(PP) = -112.5 - 31.7a - 15.3b\ (\pm 4.7)\ Hz$$

The increasing low-field shift of the higher phosphanes in comparison with PH_3 is mainly a result of the increase in the bonding angles on replacement of a hydrogen atom by a more bulky PH_2, $P(H)PH_2$, or $P(PH_2)_2$ group (increase in the amount of p character in the hybrid orbital of the lone electron pair). Both equations are valuable tests in determining the constitutions of the phosphorus-richer homologues in the phosphane series P_nH_{n+2} with $n > 5$ by ^{31}P-NMR spectroscopy. The calculated $\delta(^{31}P)$ values, however, correspond only to the averaged positions of the resonances for the diastereomers, since their chemical shifts exhibit a "conformation effect" in the sense that molecules with extended P_n chains (such as **15c**) give rise to signals at lower field than those with bent structural elements (such as **15a** and **15b**; see Fig. 2). An analogous conformation dependence also exists for the $\delta(^{13}C)$ values of alkanes.[23]

In the case of hexaphosphane(8), **16**, because of the tendency to preferentially form branched compounds, only isomers with branched P_6 chains have so far been identified and their structures elucidated; none of the six diastereomers of *n*-P_6H_8 have been observed.[24] The isomers so far characterized are the two diastereomers of 2-phosphinopentaphosphane (**16a**, *erythro*; **16b**, *threo*), two of the three diastereomers of 3-phosphinopentaphosphane (**16c**, *erythro,erythro*; **16d**, *erythro,threo*), and the highly symmetrical 2,3-diphosphinotetraphosphane **16e**.

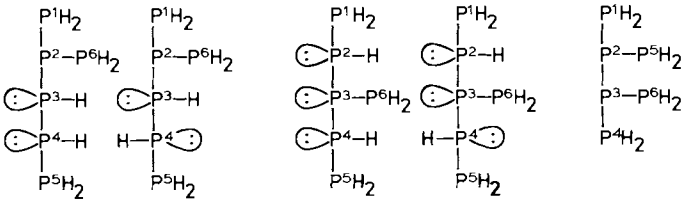

The trend for the formation of molecules with branched phosphorus skeletons is also continued by heptaphosphane(9) **17**. Of the six possible constitutional isomers, as yet only one of the two with maximum chain branching, namely, 2,3-diphosphinopentaphosphane, has been detected and its structure elucidated.[25] The diastereomers (**17a**, *erythro*; **17b**, *threo*) exist in comparable amounts, since the steric interactions between the phosphino groups in the two species are similar.

The pronounced tendency for the formation of tertiary phosphorus atoms in the synthesis of longer-chain phosphanes gives an insight into the route of formation of these compounds. The disproportionation of phosphorus-poorer homologues apparently proceeds preferentially by intermolecular elimination of PH_3 from a PH middle group and a PH_2 end group, thus resulting in chain branching.

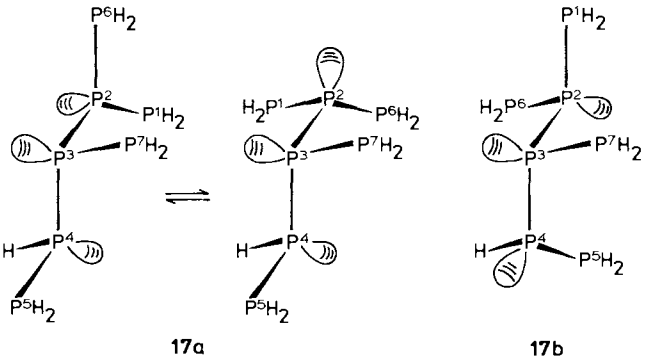

2.5. Monocyclic Phosphanes with Side Chains

Phosphanes with the compositions P_nH_n and $P_nR_{n-1}H$ where $n > 3$ do not necessarily consist of monocyclic skeletons of n phosphorus atoms, but may also be smaller monocycles with P_m side chains ($m = 1, 2$). Examples are the partially organosubstituted compounds **18**[26] and **19**[27] as well as the phosphorus hydride **20**.[28]

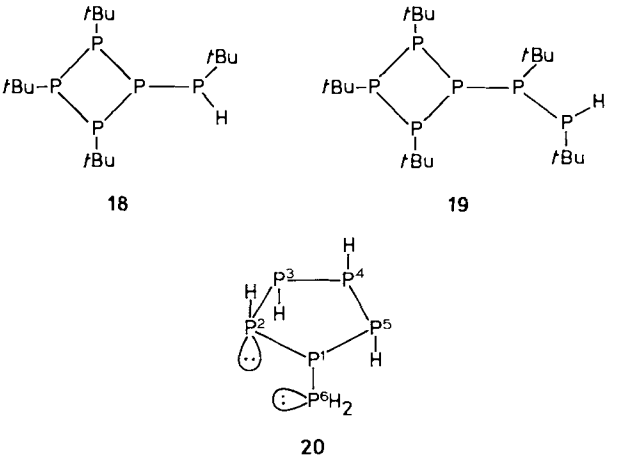

Compounds **18** and **19** are formed in the thermolysis of the diphosphane **21**[29] via the intermediacy of the triphosphane **4b**. After about 20 h at 170 °C, the proportion of **18** reaches a maximum and then decreases again on further thermolysis in favor of the formation of **19**. A further lengthening of the phosphorus side chain by reaction of **19** with **21** does not occur; instead, a retroreaction to give **18** and **4b** takes place at higher concentrations of **21**.

$$\underset{\mathbf{21}}{2\,H_2(PtBu)_2} \longrightarrow \underset{\mathbf{4b}}{H_2(PtBu)_3} + \underset{\mathbf{22}}{tBuPH_2}$$

$$\underset{\mathbf{4b}}{2\,H_2(PtBu)_3} \longrightarrow \underset{\mathbf{18}}{P_5tBu_4H} + \underset{\mathbf{22}}{tBuPH_2} + tBuH$$

$$\underset{\mathbf{18}}{P_5tBu_4H} + \underset{\mathbf{21}}{H_2(PtBu)_2} \longrightarrow \underset{\mathbf{19}}{P_6tBu_5H} + \underset{\mathbf{22}}{tBuPH_2}$$

$$\underset{\mathbf{18}}{P_5tBu_4H} + \underset{\mathbf{4b}}{H_2(PtBu)_3} \rightleftharpoons \underset{\mathbf{19}}{P_6tBu_5H} + \underset{\mathbf{21}}{H_2(PtBu)_2}$$

The four-membered ring structures for **18** and **19** have been confirmed by ^{31}P-NMR spectroscopy; accordingly, the compounds are 1-(*tert*-butylphosphino)- and 1-(1,2-di-*tert*-butyldiphosphino)-2,3,4-tri-*tert*-butylcyclotetraphosphane, respectively. Compound **18** is thus a constitutional isomer of 1,2,3,4-tetra-*tert*-butylcyclopentaphosphane,[30] which is formed on hydrolysis of $K(t\text{Bu})_4P_5$ and, like the starting material, possesses a five-membered ring of phosphorus atoms. Since the formation of four-membered ring structural elements is generally favored with *tert*-butyl-substituted cyclophosphanes,[1] compound **18**, as expected, possesses the higher thermodynamic stability of the two isomers.[30]

Hexaphosphane(6) **20** was detected by mass spectrometry among the thermolysis products of higher open-chain phosphanes already twenty years ago.[31] At temperatures up to +35 °C, pentaphosphane(5)[1] is the main product; in addition, small amounts of **20** (5–10 P-%) and other cyclic phosphorus hydrides are formed.

The structure elucidation of **20** was achieved only recently by complete analysis of the corresponding ^{31}P spin system on the basis of SPT experiments (see Section 2.4).[28] According to the data obtained, **20** has the constitution of a 1-phosphinocyclopentaphosphane in the configuration shown. Particularly informative in this respect is the large, positive, long-range coupling $^2J(P^2P^6)$ as an indication that the lone electron pairs of these phosphorus atoms are directed toward each other.[13, 15, 16, 32] The *cis* arrangement of the substituents at P^1 and P^5 was confirmed by the magnitude of the absolute value of the corresponding $^1J(PP)$ coupling. Evidence for the existence of the constitutional isomer with a six-membered ring of phosphorus atoms and an all-*trans* arrangement of the hydrogen atoms or lone electron pairs was not found.

The presently available results indicate that, on formation of the monocyclic phosphanes P_nH_n and $P_nR_{n-1}H$ under thermodynamically controlled conditions, the ring size (H, n = 5; *t*Bu, n = 4) is determined by the dominating substituent (H, R). Furthermore, in cases with sufficient kinetic stabilization, constitutional isomers with other ring sizes may be capable of existence and may be preparatively accessible by special synthetic routes.

3. Hydrogen Polyphosphides and Polyphosphides with Isolated Anions

In this section, only polyphosphides and hydrogen polyphosphides with isolated anions, P_n^{m-} and $H_xP_n^{(m-x)-}$, obtainable from solutions, and their reactions will be discussed.

3.1. New Hydrogen Polyphosphides by Metalation of Diphosphane

As reported previously,[1, 33] diphosphane **23** reacts with *n*-butyllithium or lithium dihydrogen phosphide in tetrahydrofuran (THF) or 1,2-dimethoxyethane with disproportionation, forming trilithium heptaphosphide **24** and phosphane.

$$9\,P_2H_4 + 3\,n\text{-}C_4H_9Li \xrightarrow[-20\,^\circ C]{THF} Li_3P_7 + 11\,PH_3 + 3\,n\text{-}C_4H_{10}$$

23 **24**

Recently, a series of new metal hydrogen polyphosphides (partially metalated higher phosphanes) were detected as intermediates in this metalation reaction and some of them were isolated in pure form at lower temperatures.[34–37] From the formation and degradation of the intermediates, the following detailed picture of the reaction of **23** with *n*-butyllithium has emerged.

The primary step is the formation of lithium trihydrogen diphosphide **25**, which, however, is not stable in the presence of diphosphane. In a rapid series of disproportionation and transmetalation reactions, **25** is initially converted into the highly reactive, monolithiated, phosphorus-richer, open-chain phosphanes $LiH_{n+1}P_n$ and then into cyclic compounds, until phosphides having insufficient nucleophilicity for attack on diphosphane are formed. Since the reaction temporarily comes to a standstill at this point, these phosphides are the first reaction products that can be identified.

$$P_2H_4 + n\text{-}C_4H_9Li \longrightarrow LiH_3P_2 + n\text{-}C_4H_{10}$$

23 **25**

When the metalation is performed at −78 °C, these products are mainly lithium tetrahydrogen heptaphosphide **26** and lithium pentahydrogen octaphosphide **27**, whereas at −25 °C two potential precursors of **26** additionally occur, namely, lithium octahydrogen heptaphosphide **33** and a not yet identified phosphide **34**. On the whole, a noticeable tendency for the formation of a $P_7(5)^-$ skeleton, which is analogous to that of norbornane and which apparently exhibits a relatively low nucleophilicity, is observed.

The reaction continues only after renewed addition of the metalating agent. At −78 °C, mainly further **26** is initially formed. This reacts further—as does **27**—to furnish the monocyclic lithium tetrahydrogen cyclopentaphosphide **28**, which, in turn, undergoes degradation to give the open-chain phosphides **29**, **25**, and **30**. The tricyclic heptaphosphide **24** is not formed at this temperature; however, above −30 °C, **28** does disproportionate to form dilithium hydrogen heptaphosphide **32**, PH_3, and P_2H_4, a reaction that is attributable to the particular stability of the $P_7(3)$ skeleton.

At −25 °C further **26** is initially formed from the precursors **33** and **34**. Whereas **26** remains unchanged until a **23** : *n*BuLi ratio of 8 : 1 has been reached, **27** is converted into the polycyclic compound **35**, which is insoluble in tetrahydrofuran and precipitates as an orange-red solid. Subsequently, **26** also reacts further to give lithium dihydrogen heptaphosphide **31**, which already exhibits the tricyclic $P_7(3)$ skeleton. Further metalation leads first to **32** and then to the final product **24**, which is also formed during the last step in the reaction by degradation of **35**. The differing courses of the reaction at −25 and −78 °C are attributed to the increasing solubility of PH_3 in tetrahydrofuran with decreasing temperature, so that, at −78 °C, PH_3 can also participate to an increasing extent in the reaction.

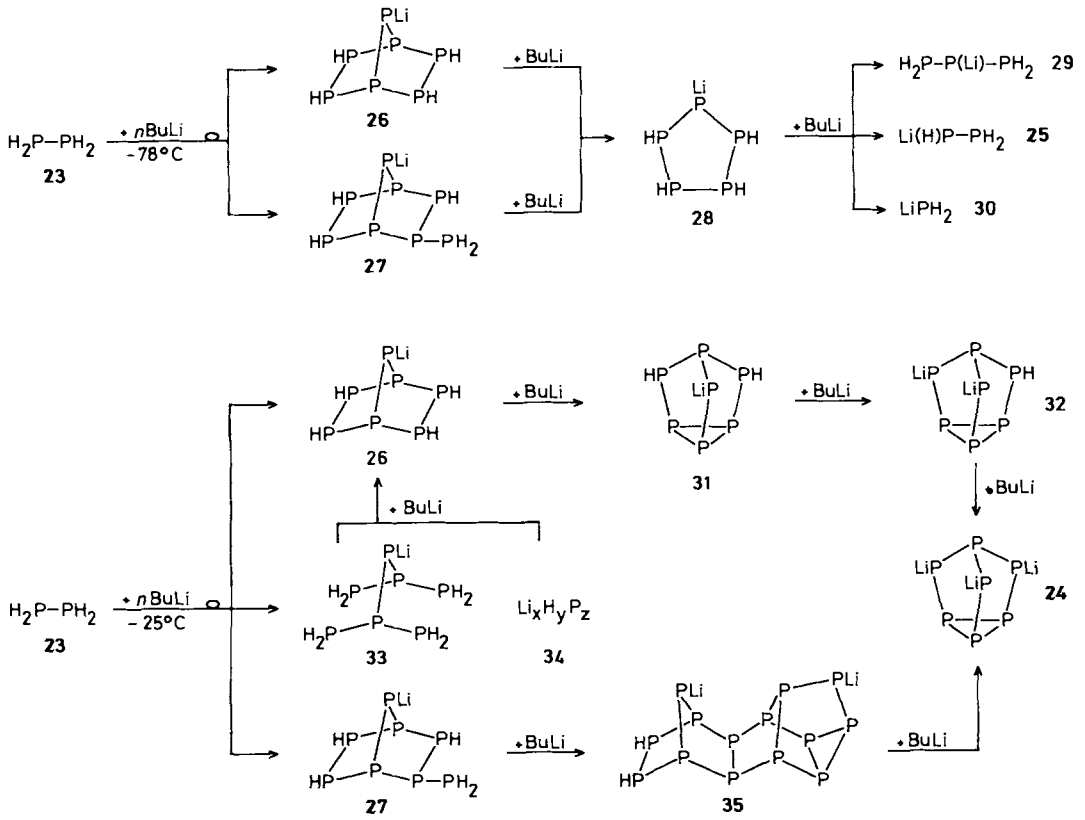

The compositions and structures of the new hydrogen polyphosphides were confirmed by complete analyses of their $^{31}P\{^1H\}$-NMR spectra or by their two-dimensional $^{31}P\{^1H\}$-NMR spectra. Of particular interest is the dilithium dihydrogen tetradecaphosphide **35**, whose polycyclic molecular skeleton is formed in the course of the transformation of a bicyclic P_7 skeleton with a side chain (**27**) to a tricyclic P_7 skeleton (**24**). The same compound is also accessible by a type of retroreaction starting from **24** and diphosphane **23** and is formed additionally in the reaction of **28** with diphosphane and on disproportionation of **26**.[36] Since difficultly separable by-products are formed in all cases, $Li_2H_2P_{14}\cdot 6THF$ can only be obtained in 80–90% purity. The $H_2P_{14}^{2-}$ ion is a typical conjuncto-phosphane, which is made up of a $P_7(5)$ partial structure analogous to that of norbornane and a $P_9(3)$ partial structure analogous to that of deltacyclane joined through a common two-atom bridge; thus, a $P_8(6)$ partial structure analogous to that of pentalane is formed.

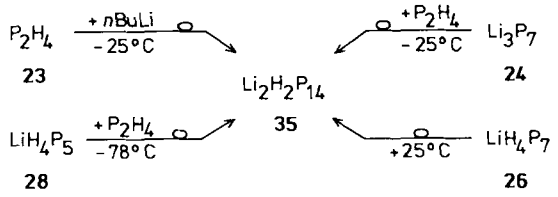

The dilithium hydrogen heptaphosphide **32**, a further intermediate, is also formed by the partial metalation of P_7H_3 **1** with $LiPH_2$ or **24** as well as by the partial protolysis of **24**. The best preparative route, however, is the reaction of **23** with **24**.[35]

$$9\,P_2H_4 + 2\,Li_3P_7 \xrightarrow[-25\,^\circ C]{THF} 3\,Li_2HP_7 + 11\,PH_3$$

23 **24** **32**

The special structural feature of the anion of **32** is—as in the case of **24**[1,33]—its fluxional behavior. As a result of its similarity to the hydrocarbon dihydrobullvalene,[38] the HP_7^{2-} ion is capable of a degenerate Cope rearrangement[39] and can be described at room temperature by two structurally equivalent valence tautomeric forms.[35] As can be seen, opening of the bond between P^2 and P^6 in the three-membered ring and formation of a bond between the

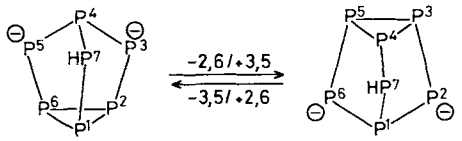

bridging atoms P^3 and P^5 with concomitant migration of the negative charges to the atoms P^2 and P^6 leaves the HP_7^{2-} ion unchanged. On the other hand, metal/hydrogen exchange in **32** occurs neither *intra-* nor *inter*molecularly.

3.2. Polyphosphides with Conjuncto-Phosphane Skeletons

Hydrogen-free polyphosphides with a larger number of phosphorus atoms generally possess conjuncto-phosphane skeletons, the partial structures of which are known from phosphorus-poorer phosphides or organophosphanes (see Section 4).

The hydrogen heptaphosphide **32** is not stable at room temperature but decomposes in a complex disproportionation reaction in which, among other products, dilithium hexadecaphosphide **36** is formed.[1,35,40] Compound **36** can be prepared more simply and in greater yield by the nucleophilic cleavage of white phosphorus with **30** in a molar ratio of 1.92 : 1.[41] The corresponding sodium salt **37** can be obtained in an analogous manner using sodium powder in the presence of [18]crown-6.[42] The formation of **36** was also observed by *Fritz* et al.[43] in the reaction of white phosphorus with $LiP(SiMe_3)_2$. In each case, **36** and **37** are formed as solvent adducts, which, on drying or warming, lose part of the bound solvent with a deepening of the color and a decrease in solubility. According to ^{31}P-NMR spectroscopic observations, isolated P_{16}^{2-} ions exist in solution in each case and have the same constitution as that found by *von Schnering* et al.[44,45] for solid $(Ph_4P)_2P_{16}$

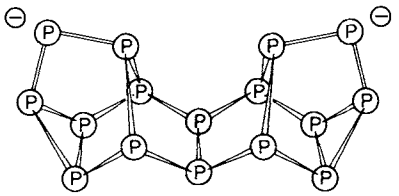

P_{16}^{2-}

by means of X-ray structural analysis. Thus, the $P_{16}(2)$ skeleton represents a conjuncto-phosphane made up of two $P_9(3)$ structural elements, analogous to that of deltacyclane, joined through a common two-atom bridge.

$$\underset{\mathbf{32}}{Li_2HP_7} \xrightarrow{-\Omega} \underset{\mathbf{36}}{Li_2P_{16}} + \cdots$$

$$23\,P_4 + 12\,LiPH_2 \longrightarrow \underset{\mathbf{36}}{6\,Li_2P_{16}} + 8\,PH_3$$
$$\mathbf{30}$$

Na_2P_{16} **37**

As a result of their reactive phosphidic phosphorus atoms, compounds **36** and **37** are suitable for the preparation of other compounds having $P_{16}(2)$ skeletons. However, it must be considered that covalent, higher phosphanes are readily attacked by nucleophiles with concomitant changes in the phosphorus skeleton upon alkylation according to the following equation:

$$\underset{\mathbf{36}}{Li_2P_{16}} + 2\,RBr \longrightarrow \underset{\mathbf{38}}{P_{16}R_2} + 2\,LiBr$$

a, R = Me; **b**, R = Et

If, by the choice of a suitable method for carrying out the reaction, the reaction of the basic phosphide with the already formed diorganohexadecaphosphane is suppressed, then **38a** and **38b** can be obtained in high yields and in pure form.[46] Their constitutions were confirmed by the similarity of their molecular vibration spectra with those of **36** and by the fragmentation patterns in their mass spectra.

39 $Na_3P_{21}\cdot 15\,THF$ $Li_4P_{26}\cdot 16\,THF$ **40**

Likewise, both the room temperature decomposition of **32** and the cleavage of white phosphorus with $LiPH_2$ or sodium under different stoichiometric conditions give rise to the henicosaphosphides $M_3^1P_{21}$ and the hexacosaphosphides $M_4^1P_{26}$ (M^1 = Li, Na, K). Of these products, the compounds **39** and **40** have been isolated in pure form.[47,48] According to ^{31}P-NMR spectroscopic investigations, they contain the isolated anions P_{21}^{3-} and P_{26}^{4-}, which

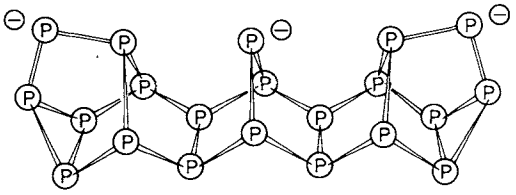

P_{21}^{3-}

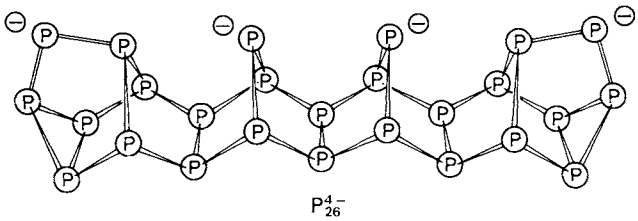

P_{26}^{4-}

are made up of two $P_9(3)$ terminal groups, analogous to that of deltacyclane, and one or two, respectively, $P_7(5)$ middle groups, analogous to that of norbornane. In K_4IP_{21}, synthesized by *von Schnering* et al.,[49] these P_{21}^{3-} groups are linked to form a polymeric $^2_\infty[P^-_7]$ structure by opening of their three-membered rings.

Noteworthy of the phosphorus-rich phosphides with conjuncto-phosphane skeletons is the preference for $P_9(3)$ terminal groups analogous to that of deltacyclane, whereas covalent, polycyclic organophosphanes P_nR_m ($m < n$) usually contain terminal, two-atom bridges with *trans*-oriented substituents (see Section 4). Apparently, two-atom bridges with negative charges on neighboring phosphorus atoms (in addition to the lone electron pairs) are energetically so unfavorable in phosphides that the system spontaneously stabilizes itself by closure of a zero bridge to form the three-membered ring of the partial structure analogous to deltacyclane. This explains why the corresponding polyphosphides with isolated P_n^{m-} ions do not exist for all covalent phosphanes P_nR_m (R = H, alkyl, aryl). In spite of intensive efforts, therefore, it was not possible to prepare nonaphosphides of the type $M_3^1P_9$ with constitutions analogous to that of deltacyclane.[50]

Investigations of the reaction behavior of **39** have shown[51] that, on treatment with alkyl halides or chloro(trimethyl)silane, smooth substitution occurs at the phos-

phidic phosphorus atoms of the $P_9(3)$ terminal groups but not at the phosphidic phosphorus atom of the $P_7(5)$ middle group for steric reasons. Partially substituted henicosaphosphides $NaP_{21}R_2$ **41a-d** with the substituents R on the

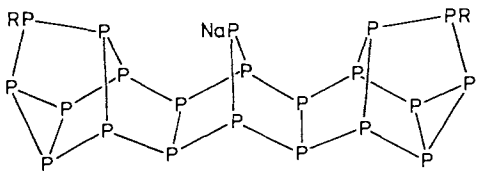

41a, R = Me; **41b**, R = Et; **41c**, R = *i*Pr; **41d**, R = $SiMe_3$

terminal groups in a *trans* arrangement are obtained in this way. Protonating agents such as acetylacetone, in contrast, attack primarily at the central phosphidic phosphorus atom, the site of greatest nucleophilicity, so that the hydrogen henicosaphosphide **42** is accessible in this man-

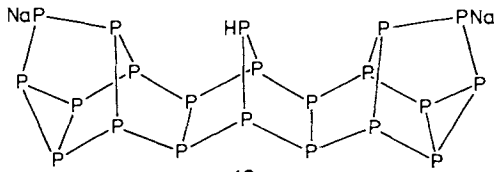

42

ner.[52] The basicity of the anion HP_{21}^{2-} toward acetylacetone or glacial acetic acid is not sufficient for the formation of $P_{21}H_3$. However, the partially organosubstituted henicosaphosphane(3) **43** can be obtained from **41a** and can, in turn, be quantitatively metalated by butyllithium to give $LiP_{21}Me_2$.[53]

$$\underset{\textbf{41a}}{NaP_{21}Me_2} \xrightarrow[-Na^+]{+H^+} \underset{\textbf{43}}{P_{21}HMe_2}$$

On alkylation, the hexacosaphosphide **40** gives the triorganohexacosaphosphides $LiP_{26}R_3$, **44a,b**, as the end products.[54] Primary attack here takes place also at the phosphidic phosphorus atoms of the $P_9(3)$ end groups, as confirmed by the ^{31}P-NMR identification and the structural

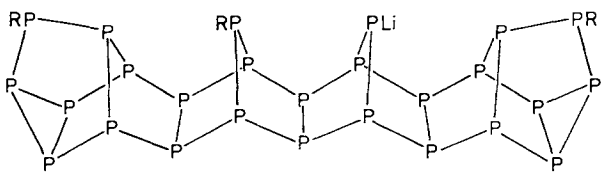

44a, R = Me; **44b**, R = Et

characterization of the intermediate products 45a,b. Since, compared with **39**, compound **40** contains an additional $P_7(5)$ middle group, the steric prerequisites for an alkylation in the middle part of the phosphorus skeleton are more favorable. By contrast, solely a rearrangement of the $P_{26}(4)$ skeleton takes place on reaction with protonating agents.[53]

45a $Li_2P_{26}Me_2$ $Li_2P_{26}Et_2$ **45b**

In addition to the already mentioned compounds, the nonadecaphosphides **46a-c** are also formed on nucleophilic cleavage of white phosphorus with $LiPH_2$ or an alkali metal.[55] They cannot be isolated in pure form and are only capable of existence in equilibrium with other polyphosphides up to a maximum of 16 P-% in the reaction mixture. Compound **46a** is also formed on degradation of the hexadecaphosphide **36** with $LiPH_2$ as well as in the reaction of the heptaphosphide **24** with white phosphorus or iodine or 1,2-dibromoethane.

Li_3P_{19} Na_3P_{19} K_3P_{19}
46a **46b** **46c**

As can be deduced from the two-dimensional ^{31}P-NMR spectrum and SPT experiments,[55] the P_{19}^{3-} ion has a conjuncto-phosphane skeleton with a five-membered ring middle group. The resultant, relatively "open" total structure is the reason for the high reactivity of this polyphosphide ion.

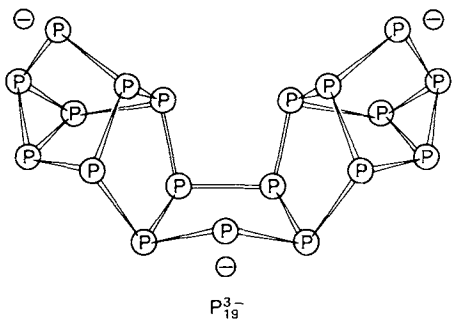

P_{19}^{3-}

The nonadecaphosphides **46** are further intermediates in the complex subsequent reactions of the nucleophilic cleavage of the P_4 molecule in which phosphorus-richer partial structures of Hittorf's phosphorus[56] are built up. Compounds **46a-c** are formed over a relatively wide range of reactant ratios $P_4 : M^IPH_2(M^I)$, which is limited on the phosphorus-poorer side by the stoichiometry required for the formation of $M_3^IP_7$[57] and which extends on the phosphorus-richer side beyond that necessary for the formation of $M_2^IP_{16}$.[41] As can also be seen from the other preparative routes (see above), the nonadecaphosphides represent important intermediates in the transformation of the heptaphosphides $M_3^IP_7$ to the hexadecaphosphides $M_2^IP_{16}$. As can be deduced from the compositions of known polyphosphides with conjuncto-phosphane skeletons (Table 2), the compounds **46** are direct "precursors" of the polyphosphides $M_4^IP_{26}$ and $M_3^IP_{21}$, whose $P_7(5)$ middle groups,

Table 2. Composition of polyphosphides of the general formula $M_m^IP_n$ with conjuncto-phosphane skeletons.

Compound type		Example	M^I : P ratio
$M_3^IP_7$	**24**	Li_3P_7	1 : 2.3
$M_3^IP_{19}$	**46a**	Li_3P_{19}	1 : 6.3
$M_4^IP_{26}$	**40**	$Li_4P_{26} \cdot 16THF$	1 : 6.5
$M_3^IP_{21}$	**39**	$Na_3P_{21} \cdot 15THF$	1 : 7.0
$M_2^IP_{16}$	**36**	Li_2P_{16}	1 : 8.0

analogous to that of norbornane, are apparently formed from the five-membered ring structural moiety of **46**. Furthermore, the synthesis of phosphorus-richer polyphosphides from phosphorus-poorer polyphosphides surprisingly does not proceed with a continuous increase in the size of the phosphorus skeleton. Instead, the conversion of $M_3^IP_{19}$ to $M_2^IP_{16}$ reveals that, in the case of the conjuncto-phosphanes, relatively large, "open," skeletal structures are first formed; the smaller and more "closed" phosphorus skeletons of the phosphorus-richer polyphosphides then take shape by successive elimination of the phosphidic middle groups (see Section 3.3).[55]

3.3. Polyphosphides with Phosphorus of Coordination Number 2

In the reaction of white phosphorus with sodium powder (P : Na = 3 : 1) in boiling diethylene glycol dimethyl ether (diglyme), small amounts of the compounds **47a**, **48**, and **49**[58] are formed in addition to those polyphosphides obtained when the reaction is performed in tetrahydrofuran or 1,2-dimethoxyethane.[55] These products are characterized by ^{31}P-NMR signals at low field in the region typical for diphosphenes[59-62] and phosphaalkenes.[63] With $LiPH_2$ in tetrahydrofuran, only **47b** is formed and, after separation of the other polyphosphides, it can be obtained as a pure solution in tetrahydrofuran.[58] The formation of **48** and **49** in the reaction with sodium is indicative of the participation of the solvent diglyme in the course of the reaction. Compounds **47**, **48**, and **49** are remarkably stable in solution; neither at room temperature nor after short-heating can the start of decomposition be detected by ^{31}P-NMR spectroscopy. In contrast, a partial conversion to phosphorus-richer polyphosphides, especially $M_2^IP_{16}$ and $M_3^IP_{21}$, takes place on complete removal of the solvent.

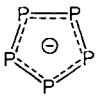

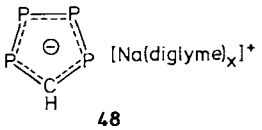

48

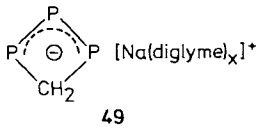

49

The compositions and structures of **47**–**49** were deduced from their ^{31}P-NMR spectra and, in the cases of **47a,b** also from the ^{23}Na- and ^{7}Li-NMR spectra, respectively. Compounds **47** each exhibit a sharp singlet in their ^{31}P-NMR spectra (**47a**, $\delta = +470.2$; **47b**, $\delta = +468.2$), which undergoes neither broadening nor splitting between -60 and $+30$ °C. A substitution at phosphorus by an organic group can thus be excluded with certainty. That the species responsible for the singlet exists as an anion can be deduced from the cation NMR spectra of **47a,b**. About two years ago, *von Schnering* et al.[64,65] observed, among other signals, a sharp singlet at $\delta = +473$ in the ^{31}P-NMR spectrum of the reaction mixture of K_4P_6 and Me_3SnCl in 1,2-dimethoxyethane and attributed it to the fluxional P_6^{4-} ion (10π-electron system). However, it seems difficult to correlate the strongly low-field position with a P_6 ring having four negative charges and only one PP double bond. Now that the same species has also been formed by the cleavage of white phosphorus (see above), the postulation of a P_6 ring structure is no longer imperative. Rather, the NMR spectroscopic data can be readily correlated with a resonance stabilized P_5^- ion, analogous to the cyclopentadienide ion (6π-electron system), in which the distribution of the negative charge over five phosphorus atoms somewhat reduces the strong deshielding effect of the sp^2 hybridization. Confirmation that the compounds **47** are actually salts with the pentaphosphacyclopentadienide ion is provided by the analytically determined Na : P ratio of 1 : 5 for solutions of **47a**.[58]

To date, the P_5^- species has only been observed in the negative ion mass spectrum of red phosphorus at 325 °C[66] and in the triple-decker complexes **50a,b** recently prepared by *Scherer* et al.[67] The formation of this ion in the

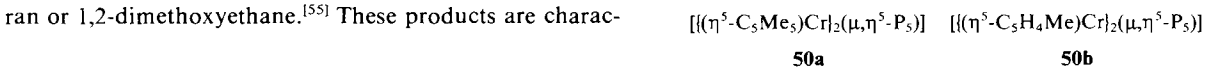

50a **50b**

subsequent reactions of the nucleophilic cleavage of white phosphorus under conditions that favor the formation of polyphosphides with conjuncto-phosphane skeletons is indicative of its direct participation in the complex reactions involved in the synthesis of phosphorus-richer from phosphorus-poorer polyphosphides (see Section 3.2). Its formation is apparently closely related with the transformation of $M_3^IP_{19}$ to $M_2^IP_{16}$ via successive elimination of small phosphidic middle groups from larger, "open," conjuncto-phosphane skeletons. The spontaneous formation and thermal stability of **47a,b** are in accord with the most recent MNDO calculations,[68] which predict a significant stability for the P_5^- ion. Studies on the reaction behavior of **47a,b** from various points of view are in progress.

The constitutional assignments for **48** and **49** are based on the analysis of the AA'BB' or AB_2 spin systems appearing at low field in the ^{31}P{^{1}H}-NMR spectra as well as on the splittings observed on ^{1}H-coupling.[58] Compound **48** is thus a salt with the tetraphosphacyclopentadienide ion, whereas **49** contains the triphosphacyclobutenide ion, for which no carbon analogue exists to date.

Common structural features of the ions P_5^-, P_4CH^-, and $P_3CH_2^-$ are resonance-stabilized rings of unsubstituted phosphorus atoms of coordination number 2. The existence of the "aromatic" anions P_5^- and P_4CH^- again documents the close relationship between phosphorus and carbon chemistry.[1] The phosphorus hydride P_5H,[1] first detected by mass spectroscopy several years ago, should thus have a structure analogous to that of cyclopentadiene and exhibit a high acidity. The latter has already been confirmed in preliminary experiments.[69]

4. Organopolycyclophosphanes

A branch of the chemistry of polyphosphorus compounds presently undergoing intensive further develop-

ment is that of the polycyclic organophosphanes. Since an unexpected variety of polycyclic phosphorus hydrides P_nH_m ($m < n$) had been detected earlier by mass spectrometry in the hydrolysis products of calcium phosphide and in the thermolyzates of diphosphane[1,2,3] (Table 1), particular interest has been placed on the structural elucidation of these compounds. As a result of their pronounced tendency to undergo disproportionation as well as their insolubility and lacking tendency to crystallize, polycyclic phosphorus hydrides are, in general, not amenable to nuclear magnetic resonance spectroscopic or X-ray structural investigations. Thus, a strategy involving the synthesis and structural elucidation of the corresponding *derivatives* is followed in which substitution of hydrogen atoms by alkyl groups is utilized to obtain structural information about the parent compounds.[1] *Organophosphanes* P_nR_m of this type generally have a higher kinetic stability toward disproportionation reactions and are considerably simpler to isolate on a preparative scale than the corresponding *phosphorus hydrides*. Since the initial preparation of a series of organopolycyclophosphanes (Table 3) and the elucidation

Table 3. Polycyclic organophosphanes with six to nine phosphorus atoms (structures of the phosphorus skeletons) [1].

P_nR_m / R	P_6R_4	P_7R_5	P_7R_3	P_8R_6	P_9R_5	P_9R_3
Me						
Et						
*i*Pr						
*t*Bu						

of their structures in the course of these investigations,[70] many further representatives of the various classes of compounds with 4–13 phosphorus atoms in the molecule have been prepared and their structures characterized unequivocally during the last few years. Furthermore, alkyl derivatives of all known phosphorus hydrides (Table 1) have been detected by mass spectroscopy in the crude reaction mixtures or in the thermolyzates of phosphorus-poorer organophosphanes. The organopolycyclophosphane with the largest phosphorus skeleton so far identified is the compound $P_{24}iPr_4$ of as yet unknown structure.

4.1. Synthetic Routes

As can be seen from Section 3.2, some of the polycyclic organophosphanes are accessible by direct alkylation of the corresponding polyphosphides. The tricycloheptaphosphanes P_7Me_3[71] and P_7iPr_3,[72] the octacyclohexadecaphosphanes $P_{16}R_2$, **38a,b**,[46] and the partially organosubstituted decacyclohenicosaphosphane $P_{21}HMe_2$, **43**,[53] have been obtained in this way. However, since polyphosphides with isolated P_n^{m-} ions corresponding to all covalent phosphanes P_nR_m ($R = H$, alkyl, aryl) (see Section 3.2) by no means exist, this route does not represent a generally applicable synthetic method.

The $P_n(m)$ skeleton of an organopolycyclophosphane, for which a saltlike starting material of analogous structure is not available, can sometimes be built up specifically from a phosphorus-poorer phosphide. Thus, starting from the tricyclic heptaphosphide **24**, the partially organosubstituted, tetracyclic nonaphosphide **52** was prepared by cyclocondensation with the diphosphane derivative **51**. The product can be isolated as the black-red, highly viscous solvent adduct $LiP_9tBu_2 \cdot 3$ monoglyme.[73,74] On reaction with protonating agents, **52** is converted into the partially substituted phosphorus hydride **53**; with alkyl halides, the mixed alkylated nonaphosphanes(3) **54a–c** are formed. According to their ^{31}P-NMR spectra, **53** and **54** are each present as mixtures of two configurational isomers, which differ in the spatial arrangements of the substituents at P^5 (see Section 4.4).

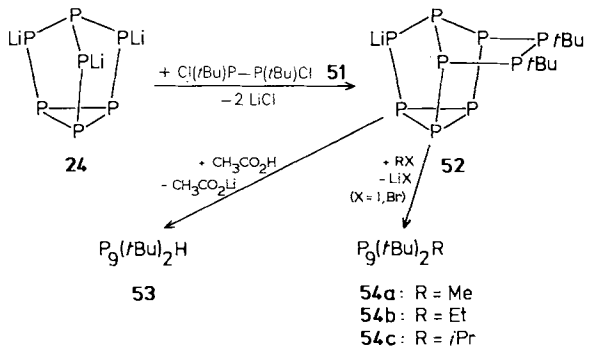

In some cases, *hetero*polycyclophosphanes in which the number of phosphorus atoms in the ring skeleton is equal to or larger than the number of heteroatoms can also be built up specifically by suitable reactions. Thus, 1,2-ethylenebisphosphane **55** reacts with dichloro(methyl)phosphane to give the bicyclic, disecondary phosphane **56**,[75] which, on treatment with $RPCl_2$, furnishes heterotricyclophosphanes of the type **57**.[76]

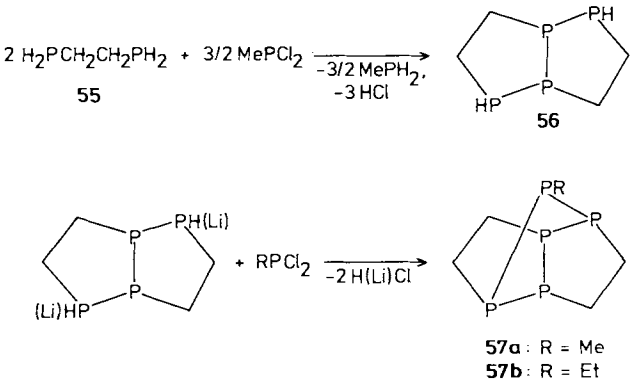

The successful preparation of the first organosubstituted bicyclotetraphosphane, **58**, reported very recently by *Fluck*

et al.,[77] represents a special case; previously, only the "inorganic"-substituted $P_4[N(SiMe_3)_2]_2$ was known.[78] Compound **58** is formed together with the diphosphene **59** by the reaction of 2,4,6-tri-*tert*-butylphenyllithium and 1-bromo-2,4,6-tri-*tert*-butylbenzene with white phosphorus; the reaction proceeds with elimination of lithium bromide.

$$4\,RLi + 4\,RBr + 3\,P_4 \longrightarrow \underset{\mathbf{58}}{2\,P_4R_2} + \underset{\mathbf{59}}{2\,P_2R_2} + 4\,LiBr$$

$R = 2,4,6\text{-}tBu_3C_6H_2$

According to the X-ray structural analysis (Fig. 3), the molecule exists as the sterically favorable *exo,exo* isomer with a folding angle of the P_4 bicyclic ring of 95.5°.[77]

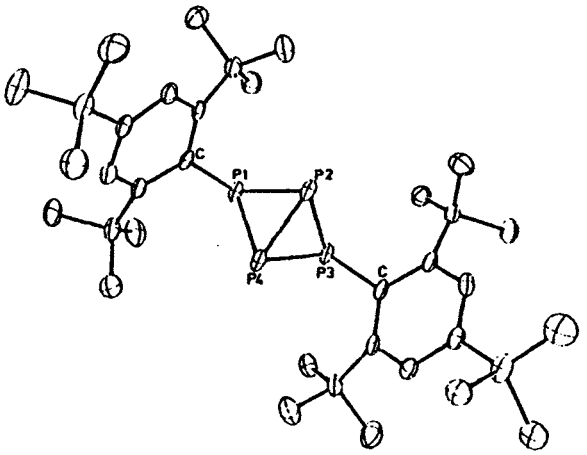

Fig. 3. Molecular structure of **58** in the crystal [77].

Whereas the synthetic routes described up to now have each been limited to only a few organopolycyclophosphanes, the synthetic methods described below have wide scopes of application. As has been repeatedly demonstrated by numerous results published in the last few years (see Section 4.2), substances of the general composition $P_{x+y}R_x$ (x, y = the number of organosubstituted or exclusively P-substituted phosphorus atoms, respectively) can generally be prepared by four different routes.[1,79-81] The first is the dehalogenation of a mixture of a dichloro(organo)phosphane and phosphorus(III) chloride. As can be seen from the following two synthetic sequences, the organosubstituted phosphorus atoms can also be introduced into the reaction in the form of the monocyclic compounds $(PR)_n$ and the unsubstituted phosphorus atoms in the form of white phosphorus. Other dehalogenating agents, such as

$$x\,RPCl_2 + y\,PCl_3 + \frac{2x+3y}{2}\,Mg \longrightarrow P_{x+y}R_x + \frac{2x+3y}{2}\,MgCl_2$$

$$\frac{x}{n}\,(PR)_n + y\,PCl_3 + \frac{3y}{2}\,Mg \longrightarrow P_{x+y}R_x + \frac{3y}{2}\,MgCl_2$$

$$x\,RPCl_2 + \frac{y}{4}\,P_4 + x\,Mg \longrightarrow P_{x+y}R_x + x\,MgCl_2$$

$$\frac{2x+3y}{2n}\,(PR)_n + y\,PCl_3 \longrightarrow P_{x+y}R_x + \frac{3y}{2}\,RPCl_2$$

alkali metals or lithium hydride, may also be used in place of magnesium. The last reaction route shown essentially represents a ring transformation of a monocyclic organophosphane by phosphorus(III) chloride in the absence of magnesium. In every case, the overall composition of the reaction product can be defined by the molar proportions of the two phosphorus-containing starting materials. However, since the P:R ratios of different organopolycyclophosphanes can be rather similar, a product mixture consisting of several compounds is always formed. Decisive for the product spectrum, furthermore, is whether the reaction is thermodynamically or kinetically controlled; this can be governed by the reaction conditions.

Thus, it is hardly possible to obtain compounds with more than nine phosphorus atoms by the first two synthetic routes, even with a large excess of phosphorus(III) chloride, when the reaction is performed rapidly in boiling tetrahydrofuran. The main products are always the organophosphanes P_nR_m with n = 5–9 and m = 3–5, in particular the thermodynamically favored compounds of the types P_9R_3 and P_7R_3. In contrast, the third synthetic method, based on white phosphorus, at moderate temperatures (10–35 °C) and high stationary concentrations of the reactants, favors the formation of phosphorus-rich compounds with up to 24 phosphorus atoms in the molecule. The degree of substitution is thereby influenced not only by the temperature but also by the steric bulk of the group R. On going from R = Me to R = *i*Pr, the proportion of phosphorus-rich, highly alkylated compounds increases markedly, as the corresponding $P_n(m)$ skeletons are increasingly stabilized kinetically. Thus, for each individual organopolycyclophosphane, the synthetic reaction must be optimized by changing the reaction conditions in order to maximize the proportion of the target molecule in the product mixture and thus to make its enrichment or isolation possible.

The same is true for another general method for the preparation of polycyclophosphanes: the thermolysis of the corresponding phosphorus-poorer compounds. As shown by systematic investigations,[81] open-chain and monocyclic phosphane derivatives always give only low yields of polycyclic compounds. Relatively high proportions of phosphorus-rich polycycles are obtained from bi- and tricyclic *methyl*phosphanes such as P_7Me_5, P_7Me_3, or P_9Me_5; however, the thermolyzates of the tricycles are generally insoluble and thus preparatively not useful.

Meanwhile, we have been able to perform the thermolysis reaction in such a way that it may be applied specifically for the preparative formation of phosphorus-rich polycyclic organophosphanes.[81] Generally, bicyclic heptaphosphanes, P_7R_5, are the most suitable starting materials since, with R = Me to R = *t*Bu, they give rise to soluble thermolyzates. The solubility increases with increasing number of carbon atoms in the substituents so that, with larger alkyl moieties, an admixture with higher cyclic—especially tricyclic—phosphane derivatives is possible. In the case of smaller alkyl groups, the solubility of the thermolyzate can be increased by addition of the monocyclic compound, $(PR)_5$, corresponding to the heptaphosphane(5) employed. The most suitable thermolysis temperature (within the range 180–230 °C) is dependent on the alkyl substituent. The duration of the thermolysis, which in-

creases with increasing size of the substituents and also with increasing amount of added monocycle $(PR)_n$, is in the range 7 to 150 h.

The thermolyzates contain as main products the compounds $(PR)_n$ (n = 4 or 5, depending on R) and P_9R_3, in addition to considerable proportions of P_7R_5, P_8R_6, P_9R_5, $P_{10}R_4$, $P_{11}R_5$, $P_{12}R_4$, and $P_{13}R_5$; furthermore, $(PR)_n$ (n = 3–6, depending on R) as well as preparatively interesting amounts of the polycyclophosphanes P_nR_{n-2} (n = 4–6, 9), P_nR_{n-4} (n = 6–8, 10, 12), P_nR_{n-6} (n = 8, 12), P_nR_{n-8} (n = 10, 11, 14–16), P_nR_{n-10} (n = 14–18), P_nR_{n-12} (n = 16, 18), and P_nR_{n-14} (n = 18) are also present. The quantitative product distribution depends on the substituent R and on the detailed thermolysis conditions. Generally, the proportion of lower alkylated compounds dominates so that the thermolysis provides a meaningful supplement to the previously described synthetic reactions.

The strategy of a combined application of fractional crystallization, column chromatography, high-pressure liquid chromatography, and sublimation has proved useful for the enrichment or isolation of the individual organopolycyclophosphanes.[81]

4.2. New Polycyclic Organophosphanes

As reported previously,[1,79] the dehalogenation of dichloro(organo)phosphanes or monocyclic organophosphanes in admixture with phosphorus(III) chloride leads, in the case of small alkyl groups, to the 2,3,5,6,7-pentaorganobicyclo[2.2.1]heptaphosphanes **60a–c**.

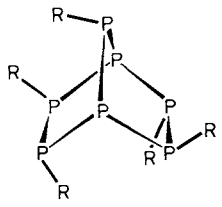

60a: R = Me
60b: R = Et
60c: R = *i*Pr

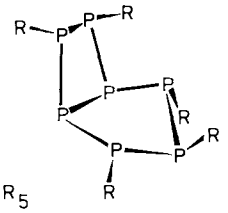

P_7R_5

61: R = *t*Bu

Surprisingly, the recently prepared P_7 *tert*-butyl compound **61** contains a completely different phosphorus skeleton, consisting of a five-membered ring and an annelated four-membered ring.[82] The structure of **61**, a 2,3,4,6,7-penta-*tert*-butylbicyclo[3.2.0]heptaphosphane, is apparently the result of a destabilization of the structural type **60** owing to increasing steric interactions with increasing steric bulk of the substituents at P^6 and P^7. Differing skeletal structures for R = Me, Et, *i*Pr, and R = *t*Bu have previously been found for the compound class P_8R_6[83,84] (see Table 3). In the case of **61**, a molecular, polycyclic phosphane has been forced, for steric reasons, to form an annelated four-membered ring as a structural element for the first time.

In the case of the hexaorganotricyclodecaphosphanes, the earlier reported assumption that the compounds $P_{10}R_6$ (R = *i*Pr, H), identified by mass spectroscopy, do not possess a phosphorus skeleton analogous to that of adamantane[11] has, in the meantime, been unequivocally confirmed. The compound **62b**, formed to 0.7 mol-% in the reaction of $EtPCl_2$, P_4, and magnesium, has now been enriched to 38% and definitely characterized as 3,4,5,8,9,10-hexaethyltricyclo[5.2.1.$0^{2,6}$]decaphosphane by ^{31}P-NMR spectroscopy.[81] Compound **62c** (present enrichment: 11%) has the same conjuncto-phosphane structure also assumed to be present in **62a** (as yet only identified by mass spectroscopy).

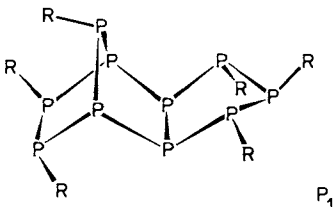

$P_{10}R_6$

62a: R = Me
62b: R = Et
62c: R = *i*Pr

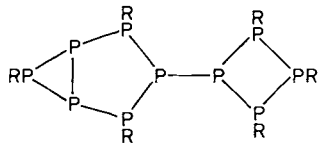

63: R = *t*Bu

On going to the *tert*-butyl compound (present enrichment: about 50%), a significant structural change occurs again: compound **63** is a 2,4,6-tri-*tert*-butyl-3-(2,3,4-tri-*tert*-butylcyclotetraphosphanyl)bicyclo[3.1.0]hexaphosphane.[85] The obvious close structural relationship with the bicyclic compounds P_6tBu_4[86] and P_8tBu_6[84] (see Table 3) helps to explain the unusual constitution. The spatial arrangement of the substituents of the two partial skeletons with respect to each other, however, remains to be clarified.

During the preparation of the low-temperature form of the tricyclooctaphosphanes P_8R_4 (see Section 4.3), small amounts of the corresponding tetracyclodecaphosphanes, of which **64c** has been enriched up to about 15%,[81] are always formed as well. The structure, a 4,5,9,10-tetraisopropyltetracyclo[5.2.1.$0^{2,6}$.$0^{3,8}$]decaphosphane, confirmed by ^{31}P-NMR spectroscopy, is derived from that of the P_8iPr_4 isomer, which is analogous to bisnoradamantane, by condensation of a two-atom bridge with formation of a new five-membered ring.

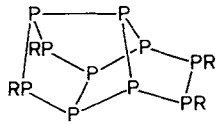

$P_{10}R_4$

64a: R = Me
64b: R = Et
64c: R = *i*Pr

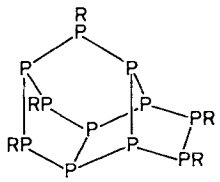

$P_{11}R_5$

65a: R = Me
65b: R = Et
65c: R = *i*Pr

An analogous state of affairs is valid for the tetracycloundecaphosphanes **65a–c** with respect to their structural relationship with the P_9R_5 isomers analogous to noradamantane (see Section 4.3), together with which they are usually formed. Thus, they are 3,4,7,9,11-pentaorganotetracyclo[6.2.1.$0^{2,6}$.$0^{5,10}$]undecaphosphanes. Compound **65b** has been isolated in 85% purity as an intense yellow,

highly viscous liquid.[81] According to the complex $^{31}P\{^1H\}$-NMR spectrum, several configurational isomers in comparable abundance and, possibly, an additional constitutional isomer with analogous structural elements are present.

Although the pentacyclic undecaphosphane **66** is built up exclusively of five-membered ring units and thus exhibits a relatively high thermodynamic stability, it is only formed to about 0.2 mol-% in the reaction of iPrPCl$_2$, P_4, and magnesium. Its abundance can be increased to about 1% by thermolysis of the crude product and, after stepwise separation, **66** can be isolated in pure form as intense yellow needles.[87] The $^{31}P\{^1H\}$-NMR spectrum shows twelve

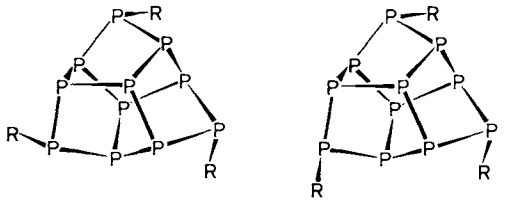

66a $P_{11}R_3$ **66b**

R = iPr

signal groups in the region from $\delta = +133$ to -38 (121.5 MHz), which, on the basis of their intensity ratios and splitting patterns, correspond to the two diastereomers **66a** and **66b** with symmetrically and unsymmetrically arranged isopropyl substituents in the statistical distribution of 1:3. According to an X-ray structural analysis,[88] the crystals consist solely of the unsymmetrical isomer, as had also been found for the only previously known "inorganic"-substituted species, $P_{11}(SiMe_3)_3$,[89] which has a phosphorus skeleton identical to that of **66**.

The phosphorus-richer pentacyclophosphanes **67** and **68** are also formed preferentially by the "thermolysis route"; of these, **67c** and **68c** have been isolated in pure form as pale yellow platelets or needles, respectively.[90]

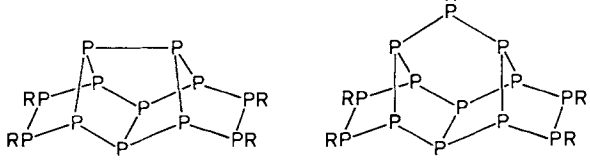

$P_{12}R_4$ $P_{13}R_5$

67a: R = Me
67b: R = Et
67c: R = iPr
67d: R = tBu

68a: R = Me
68b: R = Et
68c: R = iPr
68d: R = tBu

They are characterized by an exceptionally high thermal stability such that they can be heated up to 250°C without decomposition. According to the X-ray analysis of **67c** (Fig. 4), the P_{12} skeleton is made up of two P_7 moieties, which are analogous to that of norbornane and which are joined by a common two-atom bridge and a zero bridge. Compound **67c** is thus 3,4,9,10-tetraisopropylpentacyclo[6.4.0.0^{2,6}.0^{5,12}.0^{7,11}]dodecaphosphane. As can be seen

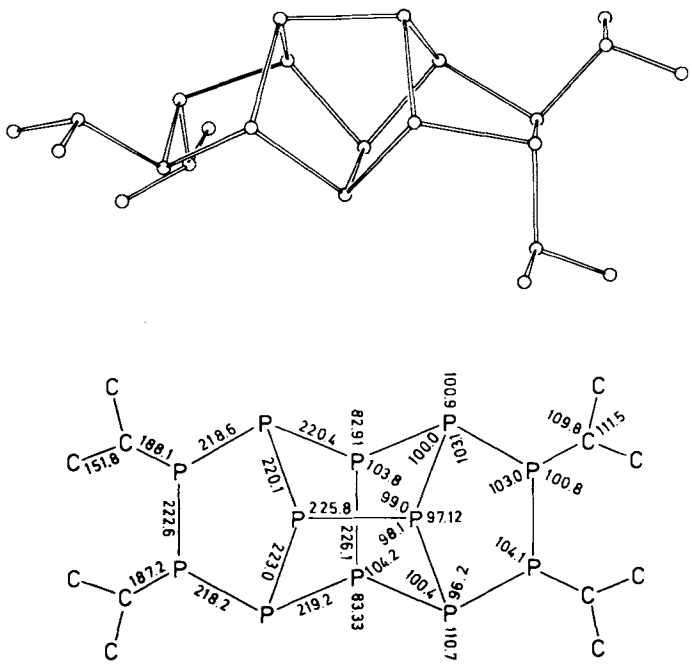

Fig. 4. Molecular structure of **67c** in the crystal. Above: ORTEP plot. Below: projection of the molecule parallel to the C_2 axis with averaged bond lengths in pm ($\sigma \leq 0.7$ pm) and selected, averaged bond angles in degrees ($\sigma \leq 0.6°$; exceptions: $110.7 \pm 1.2°$ and $96.2 \pm 1.4°$).

from a comparison of the P-P bond lengths, the zero bridges of the middle P_8 unit are markedly lengthened.

In the case of **68c**, the crystalline needles obtained so far have always been too thin for an X-ray structural determination. On the basis of the common route of formation of **68c** and of **67c** and **65c** as well as the analogy of the $^{31}P\{^1H\}$-NMR spectrum with those of **67c** and **65b**, however, **68c** should be a 3,4,7,10,11-pentaisopropylpentacyclo[7.4.0.0^{2,6}.0^{5,13}.0^{8,12}]tridecaphosphane. The P_{13} skeleton is again derived from the tetracyclic $P_{11}(5)$ partial skeleton by an additional two-atom bridge as part of a new five-membered ring.

The structures of the $P_{12}(4)$ and $P_{13}(5)$ skeletons are by no means unusual since both occur as important building units of Hittorf's phosphorus in which they are alternatingly joined through common two-atom bridges to form five-cornered tubes.[56] Thus, the existence of **67** and **68** shows that unchanged, phosphorus-rich partial structures of the element can exist as discrete molecules.

4.3. Constitutional Isomers of Organopolycyclophosphanes

The increasing information available on the polycyclic organophosphanes indicates that the formation of constitutional isomers is probably as common as it is with the polycycloalkanes. Whereas in Section 4.2 only those cases were discussed where the increasing steric demands of the substituents cause significant changes in the structural skeletons characteristic of the individual classes of compounds, the formation of different phosphorus skeletons for one and the same compound will be discussed in this section. "Actual" constitutional isomers in this sense apparently occur when several skeletons with comparable stabilities are possible for a single compound.

As reported previously,[1,79] on dehalogenation of a mixture of $RPCl_2$ or $(PR)_n$ and PCl_3 under suitable conditions, the tricyclononaphosphanes **69a-c**, with P_9 skeletons analogous to that of noradamantane (a-P_9R_5), are formed (see Table 3). In contrast, the synthesis with white phosphorus

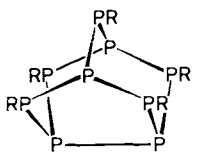

a-P_9R_5

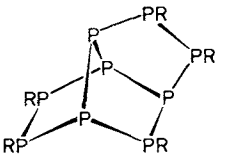

b-P_9R_5

69a: R = Me
69b: R = Et
69c: R = *i*Pr

70a: R = Me
70b: R = Et
70c: R = *i*Pr

gives rise to a mixture of **69** and a further constitutional isomer of lower relative abundance (b-P_9R_5), which, in the case of **70b**, has been isolated as a pale yellow, oily liquid and, in the cases of **70a** and **70c**, has been highly enriched.[81,91] As confirmed by a complete analysis of its $^{31}P\{^1H\}$-NMR spectrum, **70b** has a constitution analogous to that of the hydrocarbon brexane; thus **70a-c** are 2,4,5,8,9-pentaorganotricyclo[4.3.0.$0^{3,7}$]nonaphosphanes.
On the basis of an MNDO calculation of the ΔH_f° values of a-P_9H_5 and b-P_9H_5 (−54.5 and −58.7 kcal/mol, respectively) by *Gleiter* et al.,[92] the isomer with the structure analogous to that of brexane has the higher relative stability, in contrast to the carbocyclic analogues.[93] In accord with this, evidence for a rearrangement of **69b** to **70b** was found.[91] The isomers **69** and **70** are each formed as mixtures of several configurational isomers and this is the reason for the lacking tendency of the pure compounds to crystallize.

The tricyclic octaphosphanes **71** only show a low tendency for formation in the synthetic reactions given in Section 4.1, so that to date only **71c** has been enriched up to about 30 mol-%.[81,94] The constitution, a 2,4,6,8-tetraisopropyltricyclo[3.3.0.$0^{3,7}$]octaphosphane with a P_8 skeleton analogous to that of bisnoradamantane (a-P_8R_4), has been confirmed by ^{31}P-NMR spectroscopy.

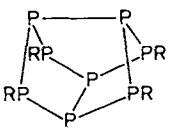

a-P_8R_4

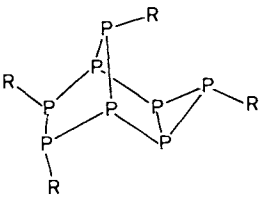

b-P_8R_4

71a: R = Me
71b: R = Et
71c: R = *i*Pr

72a: R = Me
72b: R = Et
72c: R = *i*Pr

In attempts to increase the proportion of **71c** by thermolysis of the crude product at 230 °C, an increase in the yield was indeed detected by mass spectroscopy. However, as was found already in the course of separation and again on complete analysis of the $^{31}P\{^1H\}$-NMR spectrum of the compound isolated in 95% purity, the constitutional isomer **72c** is formed by the "thermolysis route."[95] Compound **72c** contains a framework analogous to that of homonorbornene (b-P_8R_4) and is thus a 3,6,7,8-tetraisopropyltricyclo[3.2.1.$0^{2,4}$]octaphosphane. The compounds **72a** and **72b**, also identified by mass spectroscopy after thermolysis are assumed to have the same constitutions. According to a MNDO calculation, **72a** ($\Delta H_f^\circ = -120.1$ kcal/mol) is somewhat more stable than **71a** ($\Delta H_f^\circ = -115.8$ kcal/mol). Consequently, on slight warming, **71c** rearranges to **72c** with simultaneous partial disproportionation. By inclusion in larger P_n skeletons, like those of **64** and **67** or Hittorf's phosphorus,[56] the $P_8(4)$ unit of **71** apparently gains in stability.

Constitutional isomers of *conjuncto*-phosphanes can also vary by different linkage of the same partial skeletons. One example of this is the highly alkylated dodecaphosphane **74**, which is formed by thermolytic "dimerization" of the bicyclohexaphosphane **73**[86] (cf. Table 3) and can be isolated as colorless crystals.[96,97] It is produced as a mixture of the isomers **74a** and **74b** of comparable abundance, which can be separated by chromatography. According to

$$2\,P_6tBu_4 \xrightarrow{\Delta} P_{12}tBu_8$$

73 **74**

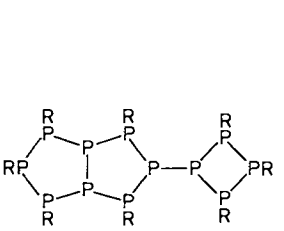

74a R = *t*Bu **74b**

the 2D $^{31}P\{^1H\}$-NMR spectrum, **74a** is 2,4,6,7,8-penta-*tert*-butyl-3-(2,3,4-tri-*tert*-butylcyclotetraphosphanyl)bicyclo-[3.3.0]octaphosphane and **74b** is the isomer with the large substituent in the 2 position. Both compounds have similar stabilities.

4.4. Inversion of Phosphorus in Organopolycyclophosphanes—First Examples

The tetracyclononaphosphanes **75** constitute a particularly interesting class of compounds on account of their exceptional thermal stability and pronounced tendency for formation. Following the initial preparation of **75b** in pure and **75c** in highly enriched form,[80] the preparation of **75a** and **75c** in pure form was also achieved recently.[98] Thus, the prerequisites for further intensive studies, especially of the most soluble compound, **75c**, are now provided.

P_9Et_3 **75a** P_9iPr_3 **75b** P_9tBu_3 **75c**

First, the deltacyclane-like constitution of the $P_9(3)$ skeleton, previously deduced from a qualitative interpretation

of the NMR spectra,[1,80] was confirmed by a complete analysis of the $^{31}P\{^1H\}$-NMR spectra of **75c** (Fig. 5) and **75a**. The results additionally show that, for each compound, two configurational isomers of varying abundance exist in solution and differ in the spatial arrangement of the substituents.

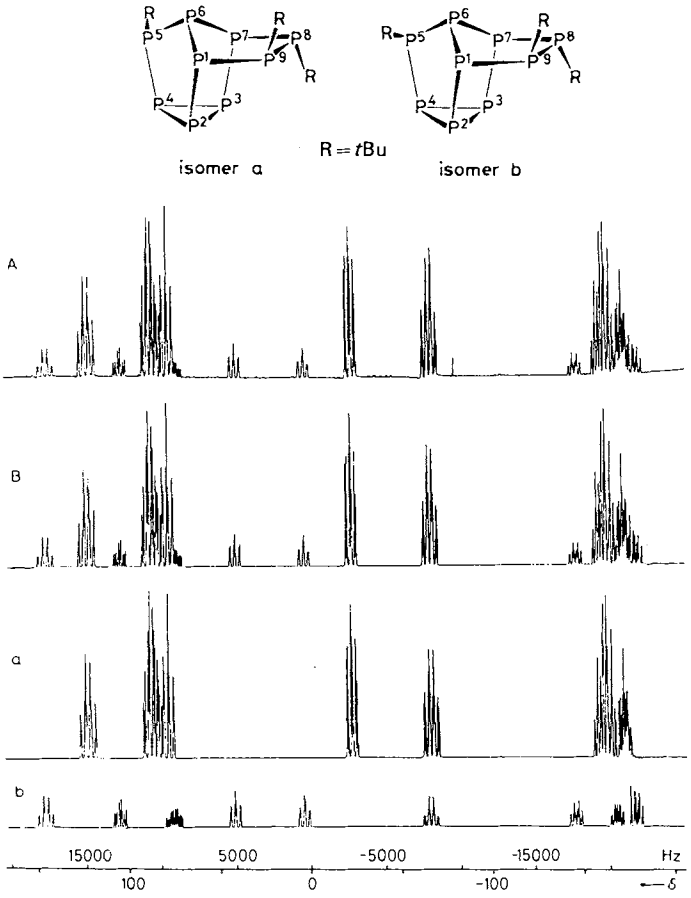

Fig. 5. Observed (A) and simulated (B) $^{31}P\{^1H\}$-NMR spectrum of P_9tBu_3 **75c** (mixture of isomers) in [D_6]benzene at 22°C (121.497 MHz); a, b: simulated spectra of the isomers a and b, respectively.

After completion of the nuclear magnetic resonance structural investigation, single crystals of **75c** suitable for an X-ray structural analysis were obtained.[98] As shown by the result (Fig. 6)[99] and confirmed for the whole solid substance by cold dissolution (−40°C) of a larger number of crystals under NMR spectroscopic control, the main isomer a separates out exclusively under suitable conditions.

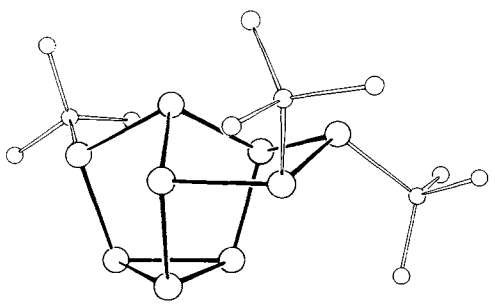

Fig. 6. Molecular structure of P_9tBu_3 **75c** (without hydrogen atoms) in the crystal [99].

After the solution of pure isomer a, prepared at −40°C, has been allowed to stand at 25°C for about 30 min, the isomer distribution characteristic of **75c** (a:b = 4:1, see Fig. 5) can be observed again in the $^{31}P\{^1H\}$-NMR spectrum.[98] This result is a clear indication that the transformation of isomer a into isomer b, which can only occur through inversion, takes place at a noticeable rate already at room temperature.

The inversion processes that must be taken into consideration for the transformations between the four different molecules of the enantiomer pairs a, a′ and b, b′ are summarized in Scheme I. The signal groups A–I (for the molecules a and a′) and a–i (for the molecules b and b′) corresponding to the phosphorus nuclei 1–9 are given below the individual configurational isomers.

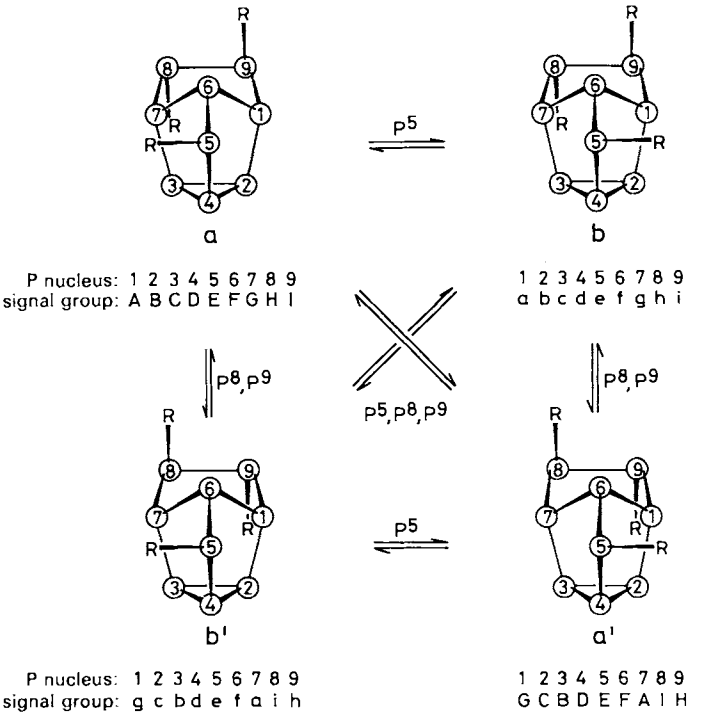

Scheme I. Possible inversion processes for the configurational isomers of P_9R_3 **75**.

As can be seen, the observed transformation of isomer a into isomer b can occur by inversion at P^5 or by simultaneous inversions at P^8 and P^9, whereby the molecules formed are mirror images of each other. Since enantiomers exhibit identical NMR spectra, a differentiation between these two possibilities can only be achieved with the help of dynamic NMR methods. This is also valid for a proof of the simultaneous inversion of all three organosubstituted phosphorus atoms (P^5, P^8, P^9), which transforms each of the molecules into its corresponding enantiomer. As can be seen from Scheme 1, the inversion at P^5 in isomer a causes a shift of the resonance of the nucleus P^1 from A to a. The associated magnetization transfer is visible in a two-dimensional exchange spectrum[100] as two cross peaks Aa between the respective groups. All possible inversion processes are given with the associated cross peaks in the upper part of Figure 7; the cross peaks emphasized by underlining are particularly characteristic of the respective process.

Inversion process	Cross-peaks
P^5	Aa, Bb, Cc, Dd, Ee, Ff, Gg, Hh, Ii
P^8, P^9	Ag, Bc, Cb, Dd, Ee, Ff, Ga, Hi, Ih
P^5, P^8, P^9	AG, BC, HI, ag, bc, hi

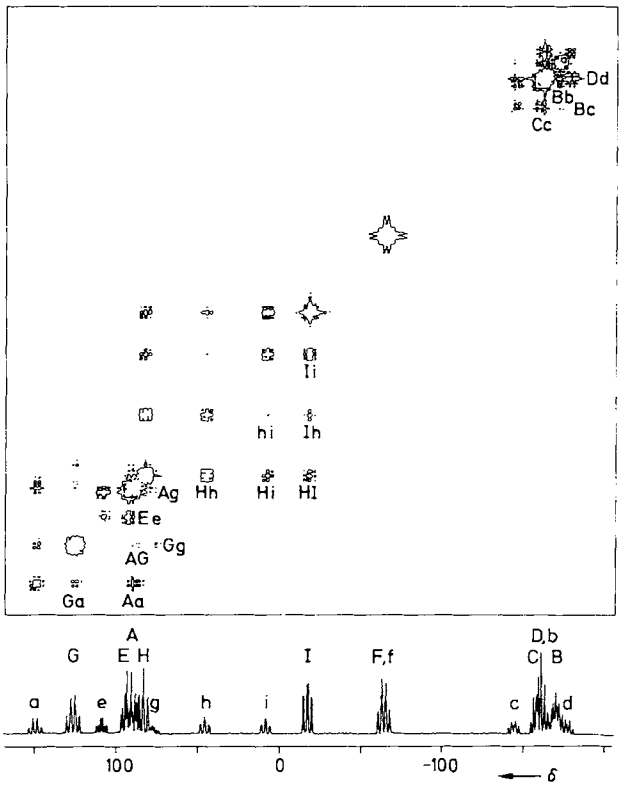

Fig. 7. Above: 2D exchange NMR spectrum of P_9tBu_3 **75c**; cross peaks for the possible inversion processes. Middle: 2D $^{31}P\{^1H\}$-NMR spectrum (pulse sequence: 90°, t_1, 90°, t_m, 90°, t_2), mixing time for magnetization transfer $t_m = 0.2\ s \pm 30\%$, measuring temperature 100°C, measuring frequency 121.497 MHz. Below: corresponding 1D $^{31}P\{^1H\}$-NMR spectrum.

The expected magnetization transfer is clearly observable in the two-dimensional nuclear magnetic resonance spectra recorded above 70°C.[98] As shown by the 2D $^{31}P\{^1H\}$ exchange spectrum recorded at 100°C (Fig. 7, middle), the cross peaks for the inversion process at P^5 have the highest relative intensity, so that this is, without doubt, the dominating process. In addition, however, configuration inversions take place at P^8 and P^9, and also possibly at P^5, P^8, and P^9, as can be seen from the occurrence of the corresponding cross peaks of lower intensity.[101] The activation parameters for the first two processes were determined by line-shape analysis of the ^1H-NMR spectra of **75c**; the third process could not be determined for methodological reasons.[102]

Inversion at P^5: $\Delta H^{\neq} = 18.5 \pm 2$ kcal/mol
$\Delta S^{\neq} = -9.3 \pm 0.5$ cal K^{-1} mol^{-1}
Inversion at P^8, P^9: $\Delta H^{\neq} = 30.1 \pm 2$ kcal/mol

As expected, the enthalpy of activation for the second process is considerably larger than that for the first, since steric interactions between the two *tert*-butyl groups inevitably occur during inversion at the two neighboring phosphorus atoms.[103] The value for the first process is about half as large as that for PH_3,[104] in confirmation of the analogous trends found for open-chain phosphanes (see Section 2.3).

The observation that the ethyl compound **75a**, independent of its method of preparation, always exhibits the same isomer distribution (a : b = 66 : 34) in solution at room temperature already indicates that, in this case also, a thermodynamic equilibrium exists between the two isomers. Indeed, the same inversion processes as for **75c** were demonstrated for **75a** by 1D and 2D NMR investigations. However, under the same conditions, the measured magnetization transfer is markedly lower than that for **75c**, in accord with the general rule that the presence of bulky substituents lowers the barrier to inversion.[18]

Very recently, it was shown that the configuration of the pentacycloundecaphosphane **66** also undergoes change in solution even under mild conditions.[87] After at most 2 h at room temperature, a solution of the pure, asymmetrical isomer **66b** (see Section 4.2), prepared by cold (−30°C) dissolution of its crystals, exhibits the statistical isomer distribution (**66a** : **66b** = 1 : 3). As can be seen from a comparison of the conditions for the isomerization of **66** and **75c**, the inversion barrier for **66** is markedly higher.

Before reliable statements on the mechanism of inversion of phosphorus in organopolycyclophosphanes can be made, further work is required.

4.5. Polycyclophosphane Oxides

Like all other compounds of trivalent phosphorus, organopolycyclophosphanes P_nR_m ($m < n$) readily undergo oxidative attack at the lone electron pairs on the phosphorus atoms. Although the resistance toward atmospheric oxygen increases with increasing phosphorus content and increasing bulk of the substituents, rapid oxidation generally takes place in solution. Until recently, nothing was known about the polycyclophosphane oxides thus formed. Of particular interest is whether oxygen reacts with insertion into the P_n skeleton, as in the formation of P_4O_6 from P_4, or by exocyclic addition to the intact polycyclophosphane. We have found conditions under which the latter reaction takes place exclusively.

The bicyclophosphanes P_6tBu_4 **73** and P_7tBu_5 **61** react with dry air in solution at room temperature to form the corresponding monoxides **76** and **77**, respectively, which can be isolated as pale yellow solids.[105] Both compounds are produced as a mixture of two constitutional isomers (abundance ratios **76a** : **76b** = 4.5 : 1; **77a** : **77b** ≈ 1 : 1). Their structures have been confirmed by complete analyses of their $^{31}P\{^1H\}$-NMR spectra. Accordingly, in each case, the oxygen atom is bonded exocyclically to the P_n skeleton of the parent compound. The product formation is apparently governed mainly by steric factors. Thus, for **76** the observed isomer distribution is an indication that the five-membered ring atom P^3 is more strongly shielded by the *tert*-butyl groups than the neighboring atoms P^2 and P^4 (statistical isomer abundance 2 : 1). In the case of **61**, the exocyclic bonding of oxygen to P^1 and P^7 is apparently

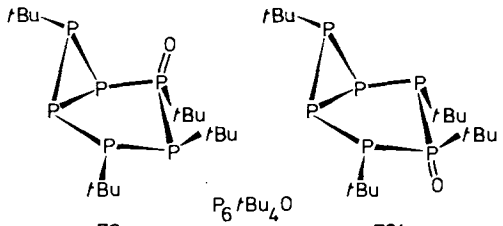

P_6tBu_4O

76a 76b

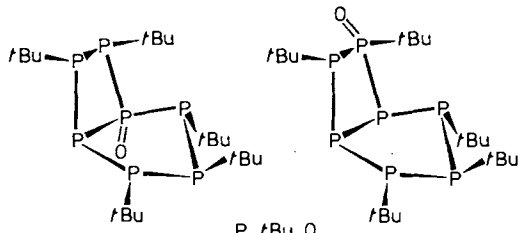

P_7tBu_5O

77a 77b

equally favorable, but at P^2 or P^4, in contrast, it is hindered by the *endo* position of the substituent at P^7. The fact that no isomers of **76** are formed with the oxygen bonded to the three-membered ring is presumably attributable to the predominant s character of the lone electron pairs on the corresponding phosphorus atoms of **73**.

The 1,1′-bicyclotetraphosphane **78**[84] (see Table 3) is more resistant to oxidation and only reacts in solution with pure oxygen at higher temperatures and then with cleavage of the P-P bonds and formation of 1,2-di-*tert*-butyldiphosphane dioxide. In contrast, it can be converted smoothly into the hexaoxide **79** with hydrogen peroxide, peracetic acid, or—particularly selectively—cumene hydroperoxide at room temperature,[106] whereas, above 30 °C, decomposi-

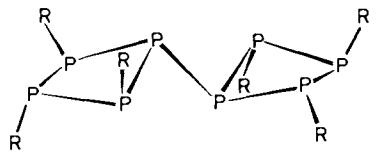

P_8tBu_6 **78**

R = *t*Bu

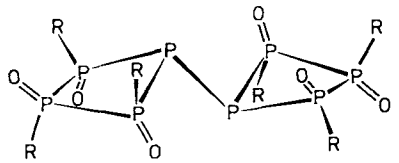

$P_8tBu_6O_6$ **79**

tion to P_2 units also takes place. Compound **79** is characterized by an exceptional tendency for formation and can be detected, along with oxygen-poorer oxides, by ^{31}P-NMR spectroscopy, even at a reactant ratio of 1 : 1. It can be isolated as a colorless, finely crystalline solid, which is hardly soluble in organic solvents and which, on warming, only dissolves with decomposition. The constitution was deduced from the $^{31}P\{^1H\}$-NMR spectrum, which shows three multiplets of an $AA'B_2B_2'CC'$ spin system with resonance positions, intensity ratios, and splitting patterns that are only compatible with an exocyclic bonding of oxygen to the organosubstituted phosphorus atoms. Compound **79** is thus 2,2′,3,3′,4,4′-hexa-*tert*-butyl-1,1′-bicyclotetraphosphane 2,2′,3,3′,4,4′-hexaoxide. The fact that **78** cannot be converted into an octaoxide even with a large excess of cumene hydroperoxide is presumably a result of the relatively small bonding angles at the exocyclic bridge ($\bar{\varphi}$(P-P-P) = 96.6°[84]) and the related, mainly s character of the lone electron pairs at the "bridgehead" atoms.

5. On the Structure of Polycyclic Phosphorus Hydrides and the Formation of Polycyclic P_n Skeletons

The new organopolycyclophosphanes mentioned in Section 4 open up possibilities for experimentally based statements concerning the structures of a series of polycyclic phosphorus hydrides. The structures of the compounds P_7H_5, P_7H_3, P_8H_6, P_9H_3,[1] and $P_{11}H_3$[107] have already been clarified. Since, in the individual classes of compounds P_nR_m, variation of the substituents within the range of relatively small alkyl groups (Me to *i*Pr) in no case is accompanied by a change in the phosphorus skeleton (see also Table 3), a structural change on replacement of these organic groups by hydrogen atoms can also be excluded with certainty. Thus, the molecular structures determined for the organopolycyclophosphanes are also representative of the corresponding phosphorus hydrides. The structures thus derived for a series of polycyclic phosphorus hydrides that have been identified by mass spectroscopy are shown in Scheme 2.

Tetraphosphane(2), P_4H_2, is bicyclo[1.1.0]tetraphosphane; octaphosphane(4), P_8H_4, exists as two constitutional isomers, namely, tricyclo[3.3.0.$0^{3,7}$]octaphosphane (a-P_8H_4) and tricyclo[3.2.1.$0^{2,4}$]octaphosphane (b-P_8H_4); nonaphosphane(5), P_9H_5, also occurs as two constitutionally isomeric forms, namely, tricyclo[3.3.1.$0^{3,7}$]nonaphosphane (a-P_9H_5)[1] and tricyclo[4.3.0.$0^{3,7}$]nonaphosphane (b-P_9H_5); decaphosphane(6), $P_{10}H_6$, is tricyclo[5.2.1.$0^{2,6}$]decaphosphane; decaphosphane(4), $P_{10}H_4$, is tetracyclo[5.2.1.$0^{2,6}$.$0^{3,8}$]decaphosphane; undecaphosphane(5), $P_{11}H_5$, is tetracyclo[6.2.1.$0^{2,6}$.$0^{5,10}$]undecaphosphane; dodecaphosphane(4), $P_{12}H_4$, is pentacyclo[6.4.0.$0^{2,6}$.$0^{5,12}$.$0^{7,11}$]dodecaphosphane; tridecaphosphane(5), $P_{13}H_5$, is pentacyclo[7.4.0.$0^{2,6}$.$0^{5,13}$.$0^{8,12}$]tridecaphosphane; hexadecaphosphane (2), $P_{16}H_2$, is octacyclo[7.7.0.$0^{2,6}$.$0^{3,8}$.$0^{5,7}$.$0^{10,14}$.$0^{11,16}$.$0^{13,15}$]-hexadecaphosphane.

The previously formulated[1] general structural principles for polycyclic phosphanes and their sterically unperturbed derivatives have proved their general validity in the course of the further expansion of this field. In particular, the outstanding significance of five-membered ring structural elements in the construction of mono- and polycyclic phosphane skeletons has been confirmed again and again in numerous examples. However, with the increasing annelation of five-membered rings in the formation of higher cyclic compounds, increasing strain energies are appar-

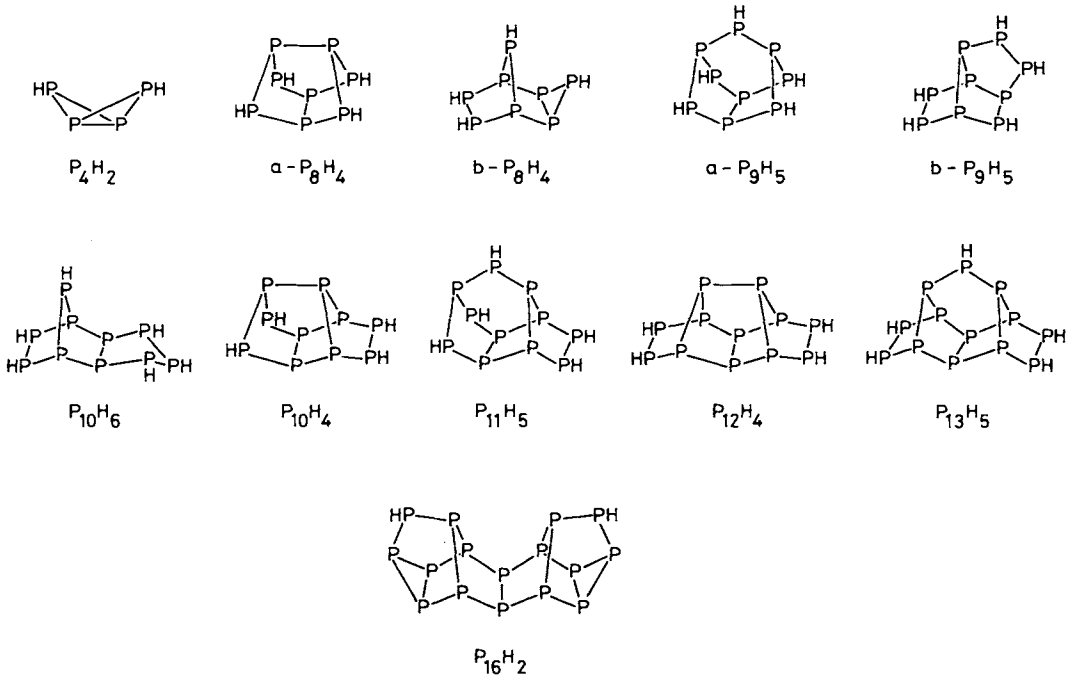

Scheme 2. Structures of polycyclic phosphorus hydrides.

ently built up, as can be seen, for example, in the stability order a-P_8Me_4 < b-P_8Me_4.[95]

Next to the five-membered ring units, three-membered ring units play a larger role than was initially assumed. This is now understandable since the strain energy of the P_3 ring as opposed to the nonstrained P_5 ring has been recently found to be 7.8 kcal/mol.[108] When this value is compared with *von Schleyer*'s[109] estimated value of 26.8 kcal/mol for the ring strain in cyclopropane compared with cyclohexane, it becomes clear that the deformations of the bonding angles at trivalent phosphorus result in considerably lower strain energies than do deformations of those at carbon. Accordingly, P_3 rings often occur as partial structures in polyphosphides and organopolycyclophosphanes.

On the other hand, according to *Ahlrichs*,[110] the fact that no sterically unperturbed $P_n(m)$ skeletons with four-membered ring partial structures exist is attributable to the general skeletal destabilization caused by parallel σ bonds at a separation corresponding to a single-bond distance. The first example in which a molecular polycyclic phosphane is forced to adopt an annelated four-membered ring as a structural element as the result of special steric relationships is the compound P_7tBu_5 **61**.

With increasing numbers of phosphorus atoms, the formation of conjuncto-phosphane structures in which lower-

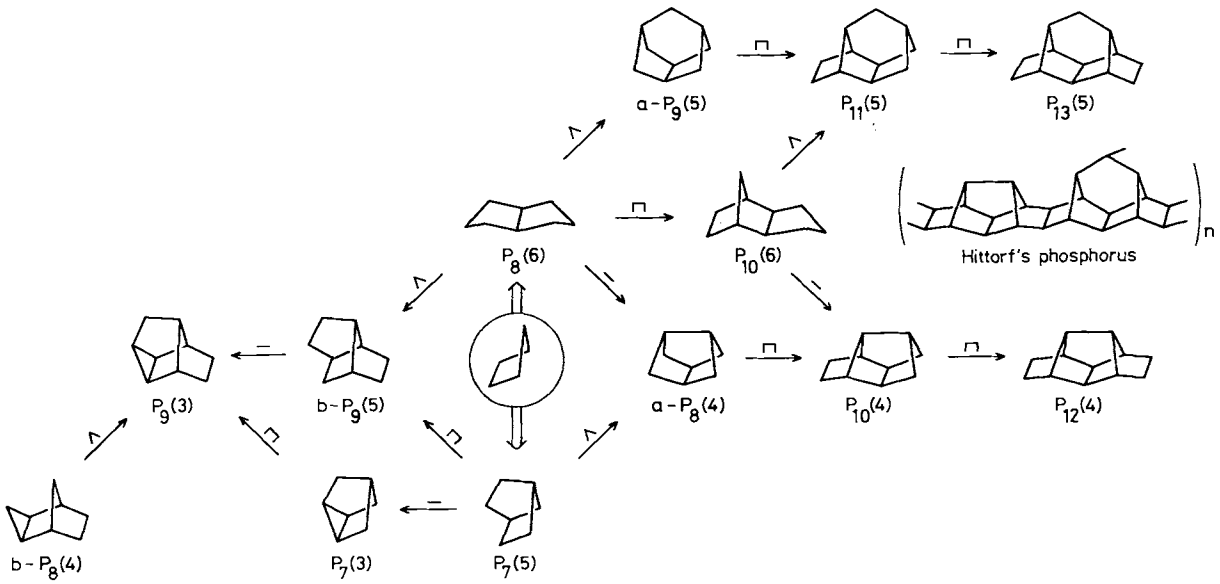

Scheme 3. Principles for the formation of sterically unperturbed, polycyclic phosphanes; the numbers in parentheses each represent the number of substituents at the positions in the phosphorus frameworks where only two bonds join together. ⊓ = two-atom bridge; ∧ = one-atom bridge; — = zero bridge.

cyclic partial skeletons are linked by single bonds or through two common phosphorus atoms dominates increasingly.

The polycyclic $P_n(m)$ skeletons show, on the whole, closely related features (Scheme 3). The dominating structural element is the five-membered ring. Either the $P_7(5)$ structural group analogous to that of norbornane or the $P_8(6)$ structural group analogous to that of pentalane is formed on condensation of two phosphorus five-membered rings. Both are major partial structures of the phosphorus-richer, polycyclic phosphanes. All sterically unperturbed polycyclophosphanes with up to thirteen phosphorus atoms can formally be interconverted, according to the construction principles shown in Scheme 3, by the use of three basic operations:

1. On condensation of a two-atom bridge to give a new five-membered ring, the next-higher cyclic and two-P-atom-richer phosphane is formed:[1]

$$P_n(m) \longrightarrow P_{n+2}(m)$$

2. On condensation of a one-atom bridge, the number of phosphorus atoms increases by one while the number of substituents is simultaneously reduced by one; this leads to a change from even- to odd-numbered phosphanes:

$$P_n(m) \longrightarrow P_{n+1}(m-1)$$

3. On intramolecular formation of a zero bridge, the next-higher cyclic phosphane with the same number of phosphorus atoms and a substituent number reduced by two is formed:

$$P_n(m) \longrightarrow P_n(m-2)$$

Furthermore, two identical or different phosphorus skeletons can be linked intermolecularly to form a bicyclo[3.3.0]octaphosphane structure; the resulting phosphorus-richer phosphane contains two five-membered rings with a common two-atom bridge,[1] e.g.,

$$2\,P_5(5) \longrightarrow P_8(6); \quad P_7(5) + P_5(5) \longrightarrow P_{10}(6)$$

On the whole, increasingly larger building units of Hittorf's phosphorus[56] whose free valencies are satisfied by hydrogen atoms or organic groups are formed with increasing numbers of phosphorus atoms.

Since the construction principles mentioned have retained their general validity up to now, they can be used to derive the most probable structural skeletons for phosphanes whose structures have not yet been clarified.

6. Perspectives

The investigations of the last five years have demonstrated that the field of open-chain and cyclic polyphosphorus compounds has undergone a remarkable development in this short time. A surprising variety of new compounds, some with unexpected structures, could be found and studied by application of generalizable synthetic routes and modern nuclear magnetic resonance spectroscopic methods. During this process, the close relationship between phosphorus and carbon chemistry[1] has become apparent to an extent that would hardly have been considered possible earlier. Who would have ever thought in their wildest chemical speculations that, in the course of the synthesis of phosphorus-richer from phosphorus-poorer polyphosphides, a resonance-stabilized pentaphosphacyclopentadienide ion with unsubstituted phosphorus atoms of coordination number 2 would form spontaneously? Just as surprising, however, is the "detour" that nature follows in this complex redox process: from relatively small, "compact" P_n^{m-} skeletons such as P_7^{3-}, relatively large, "open" structures such as P_{26}^{4-} are initially formed which then transform to medium-sized, more "closed" phosphorus skeletons of the phosphorus-richer polyphosphides, such as $M_2^I P_{16}$, with separation of individual building units. And finally, we were rather intrigued by the (not completely unexpected) inversion of phosphorus in the tetra- and pentacyclic organophosphanes P_9R_3 and $P_{11}R_3$.

What remains to be done? The structures of a considerable number of polycyclic phosphorus hydrides and the corresponding organopolycyclophosphanes remain to be elucidated. Although the most probable structures can be predicted with the help of the general principles given, the example of the constitutionally isomeric compounds P_8R_4 shows that surprises can still be expected and that the definitive elucidation of the skeletal structure of a compound can only be achieved by experimental methods. The syntheses of the corresponding molecules should, in principle, be only a question of the experimental effort and the chemist's patience. For structural studies on phosphorus-richer, higher-cyclic compounds, a major contribution may be expected from solid-state, multinuclear magnetic resonance spectroscopy.

All classes of compounds—the lower, homologous, open-chain phosphorus hydrides as well as the polyphosphides with isolated anions and also the organopolycyclophosphanes—promise a rich chemistry, on which research is just beginning. The expectations for the further development of *the chemistry* of polyphosphorus compounds can hardly be set high enough.

Ultimately, the perspectives reach beyond the limits of this topic. The question arises whether the heavier elements of the 5th main group also possess a comparable ability to form compounds with homonuclear molecular skeletons. On the basis of our present knowledge, the answer is, at least for arsenic, a definite yes. Table 4 lists the presently known polycyclic *tert*-butylarsanes.[111] These compounds have been identified unequivocally by spectroscopic methods, but most have not yet been prepared on a preparative scale or characterized structurally.

The question of the structures of these compounds is in no way trivial, even with knowledge of the corresponding phosphorus compounds. For example, As_8tBu_6 and P_8tBu_6[84] as well as the compound pair $As_{12}tBu_8$[112] and $P_{12}tBu_8$[96] have been found to have completely different skeletal structures. Thus, a further, extensive field of research is open for the future.

Table 4. Polycyclic *tert*-butylarsanes.

Arsanes	As_nR_{n-2}	As_nR_{n-4}	As_nR_{n-6}	As_nR_{n-8}	As_nR_{n-10}	As_nR_{n-12}	As_nR_{n-14}
Tetraarsanes	As_4R_2						
Pentaarsanes	As_5R_3						
Hexaarsanes	As_6R_4	As_6R_2					
Heptaarsanes	As_7R_5	As_7R_3					
Octaarsanes	As_8R_6	As_8R_4	As_8R_2				
Nonaarsanes	As_9R_7	As_9R_5	As_9R_3				
Decaarsanes		$As_{10}R_6$	$As_{10}R_4$	$As_{10}R_2$			
Undecaarsanes		$As_{11}R_7$	$As_{11}R_5$	$As_{11}R_3$			
Dodecaarsanes		$As_{12}R_8$	$As_{12}R_6$	$As_{12}R_4$	$As_{12}R_2$		
Tridecaarsanes		$As_{13}R_9$	$As_{13}R_7$	$As_{13}R_5$	$As_{13}R_3$		
Tetradecaarsanes			$As_{14}R_8$	$As_{14}R_6$		$As_{14}R_2$	
Pentadecaarsanes			$As_{15}R_9$				
Hexadecaarsanes			$As_{16}R_{10}$			$As_{16}R_4$	$As_{16}R_2$
Icosaarsanes				$As_{20}R_{12}$			

Special thanks are due to my co-workers, cited in our own contributions, for their dedicated and always personally pleasing collaboration, and to Dr. K. Glinka for drawing the structural formulas. The work of our research group was kindly supported by the Deutsche Forschungsgemeinschaft, the Minister für Wissenschaft und Forschung des Landes Nordrhein-Westfalen, the Fonds der Chemischen Industrie, and Hoechst AG, Frankfurt am Main.

Received: February 9, 1987 [A 620 IE]
German version: *Angew. Chem. 99* (1987) 429
Translated by Dr. *R. E. Dunmur*, Ditzingen

[1] Review: M. Baudler, *Angew. Chem. 94* (1982) 520; *Angew. Chem. Int. Ed. Engl. 21* (1982) 492.
[2] See also: a) M. Baudler, *Pure Appl. Chem. 52* (1980) 755; b) *ACS Symp. Ser. 171* (1981) 261; c) *Z. Chem. 24* (1984) 352.
[3] G. Fritz, W. Hölderich, *Naturwissenschaften 62* (1975) 573.
[4] M. Baudler, H. Ternberger, W. Faber, J. Hahn, *Z. Naturforsch. B34* (1979) 1690.
[5] M. Baudler, R. Riekehof-Böhmer, *Z. Naturforsch. B40* (1985) 1424.
[6] W. Hönle, H. G. von Schnering, *Z. Anorg. Allg. Chem. 440* (1978) 171.
[7] a) M. Baudler, D. Koch, B. Carlsohn, *Chem. Ber. 111* (1978) 1217; b) M. Baudler, G. Reuschenbach, *Phosphorus Sulfur 9* (1980) 81.
[8] M. Baudler, J. Hellmann, G. Reuschenbach, *Z. Anorg. Allg. Chem. 509* (1984) 38.
[9] G. Fritz, K. Stoll, *Z. Anorg. Allg. Chem. 538* (1986) 78.
[10] S. Wolfe, *Acc. Chem. Res. 5* (1972) 102.
[11] M. Baudler, D. Düster, *Z. Naturforsch. B42* (1987) 330.
[12] M. Baudler, R. Riekehof-Böhmer, U. M. Krause, *Z. Anorg. Allg. Chem. 543* (1986) 45.
[13] M. Baudler, J. Hellmann, T. Schmidt, *Z. Naturforsch. B38* (1983) 537.
[14] M. Baudler, G. Reuschenbach, J. Hahn, *Z. Anorg. Allg. Chem. 482* (1981) 27.
[15] M. Baudler, G. Reuschenbach, J. Hellmann, J. Hahn, *Z. Anorg. Allg. Chem. 499* (1983) 89.
[16] M. Baudler, G. Reuschenbach, J. Hahn, *Chem. Ber. 116* (1983) 847.
[17] K. Issleib, M. Hoffmann, *Chem. Ber. 99* (1966) 1320.
[18] a) A. Rauk, L. C. Allen, K. Mislow, *Angew. Chem. 82* (1970) 453; *Angew. Chem. Int. Ed. Engl. 9* (1970) 400; b) R. D. Baechler, K. Mislow, *J. Am. Chem. Soc. 93* (1971) 773.
[19] M. Baudler, H. Ständeke, M. Borgardt, H. Strabel, J. Dobbers, A. Schultes, D. Rackwitz in G. Brauer (Ed.): *Handbuch der Präparativen Anorganischen Chemie, Bd. 1*, 3rd ed., Enke-Verlag, Stuttgart 1975, p. 514.
[20] M. Baudler, U. M. Krause, J. Hahn, R. Riekehof-Böhmer, *Z. Anorg. Allg. Chem. 543* (1986) 35.
[21] K. G. R. Pachler, P. L. Wessels, *J. Chem. Soc. Chem. Commun. 1974*, 1038.
[22] J. Hahn in J. G. Verkade, L. D. Quin (Eds.): *Phosphorus-31 NMR Spectroscopy in Stereochemical Analysis: Organic Compounds and Metal Complexes*, VCH Publishers, Deerfield Beach 1986, p. 331.
[23] K. Seidman, G. E. Maciel, *J. Am. Chem. Soc. 99* (1977) 659.
[24] J. Hahn, R. Riekehof-Böhmer, M. Baudler, *Z. Anorg. Allg. Chem.*, in press.
[25] M. Baudler, R. Riekehof-Böhmer, J. Hahn, *Z. Anorg. Allg. Chem.*, in press.
[26] M. Baudler, H. Tschäbunin, *Z. Anorg. Allg. Chem. 511* (1984) 77.
[27] M. Baudler, H. Tschäbunin, *Z. Anorg. Allg. Chem. 516* (1984) 7.
[28] M. Baudler, R. Riekehof-Böhmer, J. Hahn, *Z. Anorg. Allg. Chem. 544* (1987) 81.
[29] M. Baudler, C. Gruner, H. Tschäbunin, J. Hahn, *Chem. Ber. 115* (1982) 1739.
[30] M. Baudler, B. Makowka, unpublished results.
[31] a) M. Baudler, H. Ständeke, M. Borgardt, H. Strabel, *Naturwissenschaften 52* (1965) 345; b) M. Baudler, H. Ständeke, M. Borgardt, H. Strabel, J. Dobbers, *ibid. 53* (1966) 106.
[32] M. Baudler, T. Pontzen, *Z. Naturforsch. B38* (1983) 955.
[33] M. Baudler, H. Ternberger, W. Faber, J. Hahn, *Z. Naturforsch. B34* (1979) 1690.
[34] M. Baudler, R. Heumüller, *Z. Naturforsch. B39* (1984) 1306.
[35] M. Baudler, R. Heumüller, K. Langerbeins, *Z. Anorg. Allg. Chem. 514* (1984) 7.
[36] M. Baudler, R. Heumüller, J. Germeshausen, J. Hahn, *Z. Anorg. Allg. Chem. 526* (1985) 7.
[37] M. Baudler, R. Heumüller, D. Düster, *Z. Anorg. Allg. Chem.*, in press.
[38] G. Schröder, *Chem. Ber. 97* (1964) 3140, 3150.
[39] W. J. le Noble: *Highlights of Organic Chemistry*, Marcel Dekker, New York 1974.
[40] M. Baudler, R. Heumüller, J. Hahn, *Z. Anorg. Allg. Chem. 529* (1985) 7.
[41] M. Baudler, O. Exner, *Chem. Ber. 116* (1983) 1268.
[42] M. Baudler, D. Düster, *Z. Naturforsch. B42* (1987) 335.
[43] G. Fritz, J. Härer, K. Stoll, T. Vaahs, *Phosphorus Sulfur 18* (1983) 65.
[44] H. G. von Schnering, *Angew. Chem. 93* (1981) 44; *Angew. Chem. Int. Ed. Engl. 20* (1981) 33.

[45] H. G. von Schnering, V. Manriquez, W. Hönle, *Angew. Chem. 93* (1981) 606; *Angew. Chem. Int. Ed. Engl. 20* (1981) 594.
[46] M. Baudler, R. Becher, *Z. Naturforsch. B 40* (1985) 1090.
[47] M. Baudler, D. Düster, K. Langerbeins, J. Germeshausen, *Angew. Chem. 96* (1984) 309; *Angew. Chem. Int. Ed. Engl. 23* (1984) 317.
[48] M. Baudler, R. Heumüller, D. Düster, J. Germeshausen, J. Hahn, *Z. Anorg. Allg. Chem. 518* (1984) 7.
[49] H. G. von Schnering in A. L. Rheingold (Ed.): *Homoatomic Rings, Chains and Macromolecules of Main-Group Elements*, Elsevier, Amsterdam 1977, p. 327.
[50] M. Baudler, O. Exner, D. Düster, unpublished results.
[51] M. Baudler, R. Becher, J. Germeshausen, *Chem. Ber. 119* (1986) 2510.
[52] M. Baudler, R. Becher, J. Germeshausen, *Z. Anorg. Allg. Chem.*, in press.
[53] M. Baudler, R. Becher, unpublished results.
[54] M. Baudler, R. Becher, J. Germeshausen, unpublished results.
[55] M. Baudler, D. Düster, J. Germeshausen, *Z. Anorg. Allg. Chem. 534* (1986) 19.
[56] H. Thurn, H. Krebs, *Angew. Chem. 78* (1966) 1101; *Angew. Chem. Int. Ed. Engl. 5* (1966) 1047; *Acta Crystallogr. B 25* (1969) 125.
[57] M. Baudler, W. Faber, *Chem. Ber. 113* (1980) 3394.
[58] M. Baudler, D. Düster, D. Ouzounis, *Z. Anorg. Allg. Chem. 544* (1987) 87.
[59] M. Yoshifuji, I. Shima, N. Inamoto, K. Hirotsu, T. Higuchi, *J. Am. Chem. Soc. 103* (1981) 4587; *104* (1982) 6167.
[60] A. H. Cowley, J. E. Kilduff, M. Pakulski, C. A. Stewart, *J. Am. Chem. Soc. 105* (1983) 1655.
[61] E. Niecke, M. Rüger, M. Lysek, S. Pohl, W. Schoeller, *Angew. Chem. 95* (1983) 495; *Angew. Chem. Int. Ed. Engl. 22* (1983) 486; *Angew. Chem. Suppl. 1983*, 639.
[62] A. H. Cowley, *Acc. Chem. Res. 17* (1984) 386.
[63] Review: R. Appel, F. Knoll, I. Ruppert, *Angew. Chem. 93* (1981) 771; *Angew. Chem. Int. Ed. Engl. 20* (1981) 731.
[64] H.-P. Abicht, W. Hönle, H. G. von Schnering, *Z. Anorg. Allg. Chem. 519* (1984) 7.
[65] H. G. von Schnering, *Nova Acta Leopold. N. F. Nr. 264; 59* (1985) 165.
[66] J. T. Snodgrass, J. V. Coe, C. B. Freidhoff, K. M. McHugh, K. H. Bowen, *Chem. Phys. Lett. 122* (1985) 352.
[67] O. J. Scherer, J. Schwalb, G. Wollmershäuser, W. Kaim, R. Groß, *Angew. Chem. 98* (1986) 349; *Angew. Chem. Int. Ed. Engl. 25* (1986) 363.
[68] N. C. Baird, *Can. J. Chem. 62* (1984) 341.
[69] M. Baudler, D. Ouzounis, unpublished results.
[70] For a review see [1], and references cited therein.
[71] M. Baudler, W. Faber, J. Hahn, *Z. Anorg. Allg. Chem. 469* (1980) 15.
[72] G. Fritz, K. D. Hoppe, W. Hönle, D. Weber, C. Mujica, V. Manriquez, H. G. von Schnering, *J. Organomet. Chem. 249* (1983) 63.
[73] M. Baudler, *Phosphorus Sulfur 18* (1983) 57.
[74] M. Baudler, W. Göldner, *Chem. Ber. 118* (1985) 3268.
[75] M. Baudler, M. Warnau, D. Koch, *Chem. Ber. 111* (1978) 3838.
[76] M. Baudler, S. Esat, *Chem. Ber. 116* (1983) 2711.
[77] R. Riedel, H.-D. Hausen, E. Fluck, *Angew. Chem. 97* (1985) 1050; *Angew. Chem. Int. Ed. Engl. 24* (1985) 1056.
[78] E. Niecke, R. Rüger, B. Krebs, *Angew. Chem. 94* (1982) 553; *Angew. Chem. Int. Ed. Engl. 21* (1982) 544.
[79] M. Baudler, Y. Aktalay, J. Hahn, E. Därr, *Z. Anorg. Allg. Chem. 473* (1981) 20.
[80] M. Baudler, Y. Aktalay, K. Kazmierczak, J. Hahn, *Z. Naturforsch. B 38* (1983) 428.
[81] M. Baudler, V. Arndt, *Z. Naturforsch. B 39* (1984) 275.
[82] M. Baudler, M. Michels, J. Hahn, M. Pieroth, *Angew. Chem. 97* (1985) 514; *Angew. Chem. Int. Ed. Engl. 24* (1985) 504.
[83] M. Baudler, Y. Aktalay, *Z. Anorg. Allg. Chem. 496* (1983) 29.
[84] M. Baudler, J. Hellmann, P. Bachmann, K.-F. Tebbe, R. Fröhlich, M. Fehér, *Angew. Chem. 93* (1981) 415; *Angew. Chem. Int. Ed. Engl. 20* (1981) 406.
[85] M. Baudler, C. Wiaterek, K. Kazmierczak, unpublished results.
[86] M. Baudler, Y. Aktalay, K.-F. Tebbe, T. Heinlein, *Angew. Chem. 93* (1981) 1020; *Angew. Chem. Int. Ed. Engl. 20* (1981) 967.
[87] M. Baudler, H. Jachow, J. Germeshausen, *Z. Anorg. Allg. Chem.*, in press.
[88] K.-F. Tebbe, Z. Anorg. Allg. Chem., in press.
[89] H. G. von Schnering, D. Fenske, W. Hönle, M. Binnewies, K. Peters, *Angew. Chem. 91* (1979) 755; *Angew. Chem. Int. Ed. Engl. 18* (1979) 679.
[90] M. Baudler, Y. Aktalay, V. Arndt, K.-F. Tebbe, M. Fehér, *Angew. Chem. 95* (1983) 1005; *Angew. Chem. Int. Ed. Engl. 22* (1983) 1002.
[91] M. Baudler, V. Arndt, unpublished results.
[92] R. Gleiter, G. Friedrich, unpublished results.
[93] P. von R. Schleyer, E. Wiskott, *Tetrahedron Lett. 1967*, 2845.
[94] M. Baudler, V. Arndt, B. Koll, unpublished results.
[95] M. Baudler, B. Koll, C. Adamek, R. Gleiter, *Angew. Chem. 99* (1987) 371; *Angew. Chem. Int. Ed. Engl. 26* (1987) 347.
[96] M. Baudler, *Phosphorus Sulfur*, in press.
[97] M. Baudler, M. Schnalke, unpublished results.
[98] M. Baudler, J. Hahn, V. Arndt, B. Koll, K. Kazmierczak, E. Därr, *Z. Anorg. Allg. Chem. 538* (1986) 7.
[99] K.-F. Tebbe, M. Fehér, *Acta Crystallogr. C*, in press.
[100] J. Jeener, B. H. Meier, P. Bachmann, R. R. Ernst, *J. Chem. Phys. 71* (1979) 4546.
[101] For a more detailed discussion, see [98].
[102] M. Baudler, C. Adamek, J. Hahn, unpublished results.
[103] The question of the mechanism of this process is still unanswered since the entropy of activation could not be determined reliably [102].
[104] A. Rauk, J. D. Andose, W. G. Frick, R. Tang, K. Mislow, *J. Am. Chem. Soc. 93* (1971) 6507.
[105] M. Baudler, M. Michels, M. Pieroth, J. Hahn, *Angew. Chem. 98* (1986) 465; *Angew. Chem. Int. Ed. Engl. 25* (1986) 471.
[106] M. Baudler, J. Germeshausen, *Angew. Chem. 99* (1987) 372; *Angew. Chem. Int. Ed. Engl. 26* (1987) 348.
[107] W. Wichelhaus, H. G. von Schnering, *Naturwissenschaften 60* (1973) 104.
[108] M. Baudler, J. Hahn, E. Clef, *Z. Naturforsch. B 39* (1984) 438.
[109] P. von R. Schleyer, J. E. Williams, K. R. Blanchard, *J. Am. Chem. Soc. 92* (1970) 2377.
[110] R. Ahlrichs, private communication (June 1986).
[111] M. Baudler, S. Wietfeldt-Haltenhoff, P. Bachmann, unpublished results.
[112] M. Baudler, S. Wietfeldt-Haltenhoff, *Angew. Chem. 97* (1985) 986; *Angew. Chem. Int. Ed. Engl. 24* (1985) 991.

When submitting manuscripts, authors of articles intended for publication as "Communications" are requested to read the "Notice to Authors" reproduced in the January issue of the journal following the list of contents; upon request, a copy can be obtained from the editorial office.

Stereoelectronic Effects and Chiral Recognition: A Natural System of Relationships between Chiral Compounds based on Selectivities in the Formation of Acetals

By *Christian R. Noe,* Max Knollmüller, Georg Göstl, Berndt Oberhauser,* and *Horst Völlenkle*

Stereoelectronic effects of the same type as the anomeric effect have been extensively investigated since the formulation of the latter by *R. U. Lemieux* et al.,[1] and their fundamental importance in carbohydrate chemistry is unquestionable.[2] In our studies using terpenoids of type **1** as models of carbohydrates, we have been especially concerned with the phenomenon of enantiomeric selectivity,[3,4] and, among other things, we have developed a rule that—based on this selectivity—allows a simple determination of the absolute configuration by means of the characteristic positions of the signals in the nuclear magnetic resonance spectra. The rule was derived, in particular, for secondary alcohols of type **2** (Scheme 1) having a bulky group (b) and a planar or linear group (pl), by analysis of numerous examples.[4–6] However, the rule is also generally applicable to compounds containing an amino or a thio group bonded to a secondary C atom.[4]

A compound has the absolute configuration *A* when, upon viewing the center of chirality in the direction of the heteroatom bound to this center—the exocyclic heteroatom in the case of lactol derivatives (acetals, thioacetals, aminals)—the groups b and pl and the H atom are arranged clockwise. Configuration *B* is present if they are arranged counterclockwise. Owing to enantiomeric selectivity, only a compound of the *A* type reacts preferentially with the lactol **1**, which was prepared from D-(+)-camphor. The designation *A* for the configuration of the isomer of **2** that reacts preferentially with **1** was chosen because the semiacetalic center of **1** exhibits the same configuration as α-D-glucose.[7]

By viewing the semiacetalic center of **1** in the direction of the OH group, it can be seen that this center also has a b ligand (CH_2), a pl ligand (O), and a hydrogen atom arranged in a clockwise sense. Thus, **1** is also a compound of type *A*. The enantiomer selectivity leading to preferential formation of the diastereomer **3** can therefore be formulated more generally: The reaction of two compounds of the same type is preferred over the reaction of a type-*A* compound with a type-*B* compound.

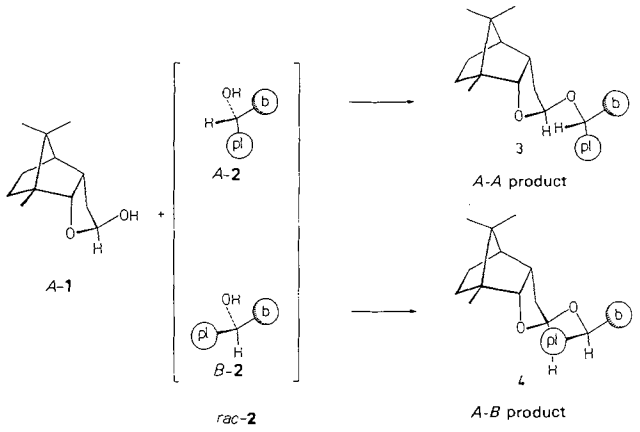

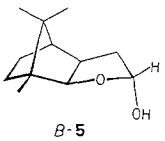

Scheme 1.

To test this assumption, the type-*A* lactol **1** was allowed to react with the type-*B* lactol **5**[9] in a 1 : 1 ratio under acid catalysis. Under these conditions, lactols generally condense to form acetals.[10] Indeed, the self-condensation products **6** (*A*-*A* type)[10] and **7** (*B*-*B* type)[9] were formed

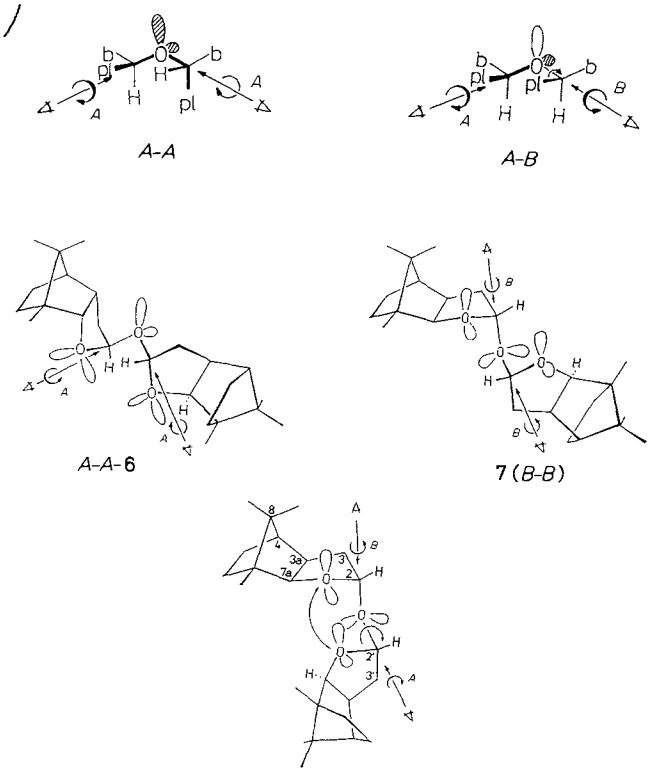

Scheme 2 [8].

[*] Univ.-Doz. Dr. C. R. Noe, Prof. Dr. M. Knollmüller, Dipl.-Ing. G. Göstl, Dr. B. Oberhauser
Institut für Organische Chemie der Technischen Universität
Getreidemarkt 9, A-1060 Wien (Austria)
Univ.-Doz. Dr. H. Völlenkle
Institut für Kristallographie und Mineralogie
der Technischen Universität
Getreidemarkt 9, A-1060 Wien (Austria)

 © VCH Verlagsgesellschaft mbH, D-6940 Weinheim, 1987 0570-0833/87/0505-0442 $ 02.50/0

preferentially (Scheme 2). The proportion of the mixed condensation product **8** (*A*-*B* type)[11] was only 15%.[12] Treatment of the condensation product **8**, isolated from the reaction mixture, with a catalytic amount of acid resulted in rapid equilibration. Compounds **6**, **7**, and **8** were thereby formed in the same ratio as obtained for the reaction of **1** with **5**. A similar result was obtained for the condensation of the racemic mixture of **1** and *ent*-**1**,[13] which is a 1 : 1 mixture of *A*-**1** and *B*-**1**. The main products were **6** (*A*-*A* reaction) and *ent*-**6** (*B*-*B* reaction) as a racemic mixture. The proportion of condensation products formed by reaction of *A*-**1** with *B*-**1** was only about 15% in this case. In a final experiment, *B*-**1** was synthesized from L-borneol,[14] and allowed to react with the type-*B* lactol **5**. In addition to the self-condensation products *B*-*B*-**6** and **7**, formed by *B*-*B* reaction, the mixed product **9**,[15] also formed by *B*-*B* reaction, was isolated as the main product (ratio of products according to ^{1}H-NMR: *B*-*B*-**6** : **7** : **9** ≈ 1 : 1 : 2).

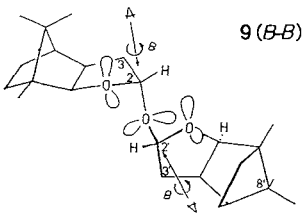

9 (*B*-*B*)

Although the b-pl-H rule appears to hold, at first glance, for geometric reasons, the type of chiral recognition described here is based, above all, on stereoelectronic anomeric effects. Only the preferentially formed diastereomer (*A*-*A* and *B*-*B* reaction) can assume a non-sterically hindered conformation in which one of the two lone electron pairs on the bridging oxygen atom can be involved in an *exo*-anomeric effect, while the second electron pair is oriented in an antiperiplanar fashion with respect to the pl ligand. In the diastereomer formed by the *A*-*B* reaction, such a conformation is strongly hindered sterically. The spectroscopic data that support the assumption of a preferred (in the *A*-*A* case) and a nonstabilized (in the *A*-*B* case) conformation are further supported by several X-ray structure analyses.[3,4,16]

The pl ligands investigated (CN, C≡C, aryl, O, CHO) are indeed substituents that—in the antiperiplanar position to a lone electron pair—can favor the stabilizing n-σ* interaction. In order to determine whether the relatively restricted spatial extension of the planar ligand (in comparison to the bulky ligand) is responsible for the conformation of the preferentially formed diastereomer in each case, the X-ray structure analysis of compound **10**[17] was performed (Fig. 1); in **10**, the bulky residue at C-2 (≙C12) is replaced by hydrogen.

Figure 1 shows that **10** indeed adopts a conformation in which one of the lone electron pairs on the exocyclic oxygen atom can be stabilized in an *exo*-anomeric fashion by interaction with the σ* orbital of the C-O bond in the ring. Moreover, the cyano group is arranged in such a way that a further anomeric stabilization is possible by n-σ* interaction of the second lone electron pair on the exocyclic oxygen atom with the σ* orbital of the C-CN bond. The conformational position of the cyano group is in excellent agreement with that of the pl ligand in the preferentially

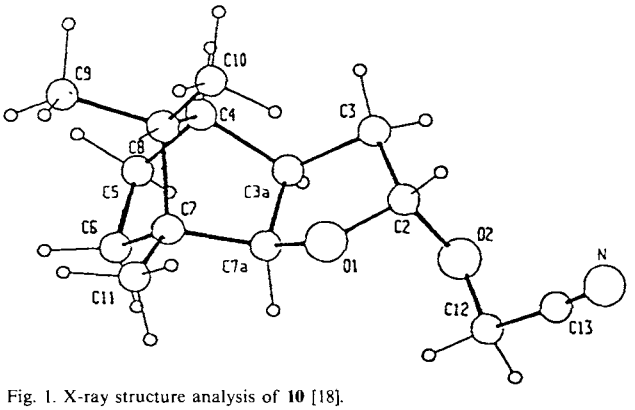

Fig. 1. X-ray structure analysis of **10** [18].

formed *A*-*A* and *B*-*B* products.[19] It can thus be assumed that, for b-pl-H compounds, the whole acetal group is stabilized by the interaction of three stereoelectronic effects (anomeric, *exo*-anomeric effect, n-σ* (C-pl) effect).

We believe that this type of chiral recognition, which we would like to refer to as family selectivity, is of fundamental importance in biological processes and that many chiral compounds that are naturally occurring in nature may be assigned to an *A* family or to a *B* family on the basis of the criteria mentioned here.

For instance, the reaction of racemic, benzyl-protected glyceronitrile with *A*-**1** (corresponding to α-D-glucose) results in preferential formation of the acetal **11**,[5,20] which corresponds to an α-glycoside of D-glyceronitrile—which, like D-glyceraldehyde, is a type-*A* compound. The observed enantiomeric selectivity could indicate that this mechanism played a prebiotic role in the spread of carbohydrate chirality[21] (type-*A* compound propagates type-*A* compound).

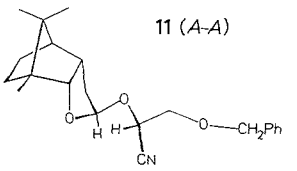

11 (*A*-*A*)

The small number of results that have been obtained so far for amines[4] indicate that this class of compounds behaves analogously. Since the natural α-amino acids (with the exception of glycine) are compounds containing b-pl-H ligands (L-amino acids are type-*B* compounds like β-D-glucose when viewed in the direction of the C-N bond, cf. *B*-*B* product **12** from an L-amino acid and β-D-glucose), it may be possible to develop an all-encompassing stereochemical picture of carbohydrates and amino acids.

We recommend the system of relationships described here above all on account of its simplicity and straightfor-

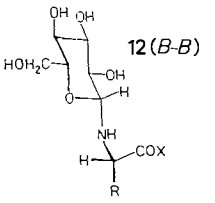

12 (*B*-*B*)

ward way of viewing glycosidic centers. For example, an analysis of the configuration of iridoid glucosides reveals that, in general, they contain a glycosidic center of the *B*-*B* type (*B* family). The b-pl-H rule can also explain the criteria established for this class of compounds for the configuration preferred by the glycosidic center,[22,23] as well as those worked out for the cyanogenic glycosides.[24]

Received: November 14, 1986;
revised: February 19, 1987 [Z 1984 IE]
German version: *Angew. Chem. 99* (1987) 467

[1] R. U. Lemieux, N. J. Chü, lecture delivered at the 133th Am. Chem. Soc. Meet. 1958, Abstract No. 31N; R. U. Lemieux in P. de Mayo (Ed.): *Molecular Rearrangements, Part 2*, Wiley Interscience, New York 1963.

[2] a) A. J. Kirby: *The Anomeric Effect and Related Stereoelectronic Effects at Oxygen*, Springer, Berlin 1983; b) P. Deslongchamps: *Stereoelectronic Effects in Organic Chemistry (Organic Chemistry Series, Vol. 1)*, Pergamon, Oxford 1983, and references cited therein.

[3] C. R. Noe, M. Knollmüller, E. Wagner, H. Völlenkle, *Chem. Ber. 118* (1985) 1733.

[4] C. R. Noe, *Chem. Ber. 115* (1982) 1591.

[5] C. R. Noe, M. Knollmüller, B. Oberhauser, G. Steinbauer, E. Wagner, *Chem. Ber. 119* (1986) 729.

[6] M. Knollmüller, C. R. Noe, B. Oberhauser, *Monatsh. Chem. 117* (1986) 407.

[7] The *B* form exhibits the same arrangement of the ligands as α-L-glucose. β-D-Glucose also exhibits this configuration and is therefore a type-*B* compound. It is necessary, however, to take into consideration the lack of anomeric stabilization of the equatorial lactolic hydroxyl group in these compounds.

[8] The conformations of the acetalic centers shown in the formulas are idealized (cf. [2a], p. 78f). The actual conformations, determined by nuclear magnetic resonance spectroscopy and X-ray crystallography, are very similar to those shown (only a slight outward rotation of the alkoxy residue in a clockwise sense; cf. [4, 5]) in the case of the stabilized *A*-*A*-type compounds. In the case of the *A*-*B*-type compounds **8**, a conformation is expected in which the alkoxy group is strongly rotated outward in the clockwise sense (cf. structure data in [3, 16]).

[9] Compound **5** was synthesized analogously by reduction of the corresponding lactone with diisobutyl aluminum hydride. Likewise, **7** and **6** were synthesized in an analogous fashion from **5** and **1**, respectively: C. R. Noe, M. Knollmüller, G. Steinbauer, unpublished results.

[10] C. R. Noe, *Chem. Ber. 115* (1982) 1576.

[11] [2*R*-[2α(2′*S**,3′a*R**,4′*R**,7′*R**,7′a*R**),3aα,4α,7α,7aα]]-2,2′-Oxybis[octahydro-7,8,8-trimethyl-4,7-methanobenzofuran] **8**: isolated from the reaction mixture by column chromatography (silica gel 0.04–0.063 mm, eluent: petroleum ether/ether = 100/1). Colorless oil; $[\alpha]_D^{20} = +10.4°$ ($c = 0.99$ in dichloromethane); ^{1}H-NMR ($CDCl_3$): $\delta = 5.43/5.41/5.38/5.36$ (dd) 1H; 2-H), 5.31–5.18 (m, 1H; 2′-H), 4.35/4.33/4.24/4.22 (dd, 1H; 7a-H), 3.94 (d, $J = 6.9$ Hz; 7′a-H), 3.03–2.51 (m, 1H; 3a-H), 2.38–0.98 (m, 15H; $H_{aliph.}$), 0.91, 0.90, 0.84, 0.80, and 0.72 (5s, 18H; 6 CH_3); ^{13}C-NMR ($CDCl_3$): $\delta = 106.1$ (d; C-2), 102.7 (d; C-2′), 91.6 (d; C-7′a), 89.9 (d; C-7a), 52.1 (s; C-7), 48.8 (s; C-8), 48.5 (d; C-4′), 47.6 (d; C-4), 47.6 (s; C-7′), 46.9 (s; C-8′), 45.7 (d; C-3′a), 40.0 (d; C-3a), 38.3 (t; C-3′), 32.4 (t; 2C, C-3, C-6′), 28.8 (t; C-5′), 26.5 (t; C-6), 22.8 and 20.5 (2q; 2 8′-CH_3), 20.8 and 18.7 (2q; 2 8-CH_3), 20.5 (t; C-5), 14.6 (q; 7-CH_3), 11.5 (q; 7′-CH_3).

[12] The configurations given for the acetalic centers of **8** were derived from the significant upfield shift of the signals for H-2 and H′-2 in the ^{1}H-NMR spectrum ($\Delta\delta = 0.16–0.21$ ppm) as well as from the downfield shift of the signals for C-2 ($\Delta\delta = 1.4–2.4$ ppm) and C-7a ($\Delta\delta = 0.3–0.6$ ppm) in the ^{13}C-NMR spectrum compared with the corresponding signals for **6**, **7**, and **9** (cf. [5]).

[13] Prepared from racemic camphor according to [10].

[14] The L-camphor obtained by oxidation of L-borneol (A. Vogel: *Vogel's Textbook of Practical Organic Chemistry*, Longman, London 1978, p. 427) was converted into *B*-**1** according to [10].

[15] [2*S*-[2α(2′*R**,3′a*S**,4′*S**,7′*S**,7′a*S**),3aα,4α,7α,7aα]]-2,2′-Oxybis[octahydro-7,8,8-trimethyl-4,7-methanobenzofuran] **9**: isolated from the reaction mixture by column chromatography (silica gel 0.04–0.063 mm, eluent: petroleum ether/ether = 100/1). Colorless crystals: m.p. = 125–127°C (methanol); $[\alpha]_D^{20} = -179.4°$ ($c = 0.77$ in dichloromethane); ^{1}H-NMR ($CDCl_3$): $\delta = 5.62/5.60/5.56/5.54$ (dd, 1H; 2-H), 5.46–5.36 (m, 1H; 2′-H), 4.28/4.27/4.18/4.17 (dd, 1H; 7a-H), 3.87 (d, $J = 6.8$ Hz, 1H; 7′aH), 3.09–2.70 (m, 1H; 3a-H), 2.38–1.06 (m, 15H; $H_{aliph.}$), 0.96, 0.95, 0.90, 0.86, and 0.78 (5s, 18H; 6 CH_3); ^{13}C-NMR ($CDCl_3$): $\delta = 104.0$ (d; C-2), 100.7 (d; C-2′), 91.0 (d; C-7′a), 89.3 (d; C-7a), 52.0 (s; C-7), 48.7 (s; C-8), 48.4 (d; C-4′), 47.5 (d; C-4), 47.5 (s; C-7′), 46.8 (s; C-8′), 45.9 (d; C-3′a), 40.2 (d; C-3a), 38.4 (t; C-3′), 32.3 (t; 2C: C-3, C-6′), 28.8 (t; C-5′), 26.4 (t; C-6), 22.8 and 20.3 (2q; 2 8′-CH_3), 20.8 and 18.7 (2q; 2 8-CH_3), 20.3 (t; C-5), 14.6 (q; 7-CH_3), 11.5 (q; 7′-CH_3).

[16] C. R. Noe, M. Knollmüller, G. Steinbauer, H. Völlenkle, *Chem. Ber. 118* (1985) 4453.

[17] [2*R*-(2α,3aα,4β,7β,7aα)]-[(Octahydro-7,8,8-trimethyl-4,7-methanobenzofuran-2-yl)oxy]acetonitrile **10**: prepared from **5** and glycolonitrile according to the general procedure in [4]; colorless crystals: m.p. = 64–66°C (*n*-hexane); $[\alpha]_D^{20} = -185.8°$ ($c = 1.244$ in trichlormethane); ^{1}H-NMR ($CDCl_3$): $\delta = 5.18$ (t, $J = 2.9$ Hz, 1H; 2-H), 4.27/4.16 (AB, $J = 16.5$, 2H; 12-H), 3.92 (d, $J = 7.1$ Hz, 1H; 7a-H), 2.44–1.01 (m, 8H; $H_{aliph.}$), 0.98, 0.93, and 0.80 (3s, 9H; 3 CH_3); ^{13}C-NMR ($CDCl_3$): $\delta = 116.2$ (s; CN), 104.6 (d; C-2), 91.7 (d; C-7a), 50.8 (t; C-12), 48.2 (d; C-4), 47.4 (s; C-7), 46.7 (s; C-8), 45.2 (d; C-3a), 38.3 (t; C-3), 32.0 (t; C-6), 28.6 (t; C-5), 22.6 and 20.1 (2q; 2 8-CH_3), 11.2 (q; 7-CH_3).

[18] Philips four-circle diffractometer PW-1100, $Mo_{K\alpha}$: orthorhombic unit cell $P2_12_12_1$, $Z = 4$, $a = 1901(1)$, $b = 965.8(4)$, $c = 732.7(3)$ pm; 1547 unique reflections, 679 observed with $I \geq 2\sigma(I)$, $R = 0.263$, $R_w = 0.109$, $w = 0.7465/\sigma^2(F)$. Further details of the crystal structure investigation may be obtained from the Fachinformationszentrum Energie, Physik, Mathematik GmbH, D-7514 Eggenstein-Leopoldshafen 2 (FRG), on quoting the depository number CSD-52202, the names of the authors, and the journal citation.

[19] Torsion angle C2-O2-C12-C13 = 72.6°; cf. torsion angle C2-O-C*-C(phenyl) = 73.5° in a compound related to **10** (O1 ⇒ S, $C^{12}H_2 \Rightarrow C^*H(CH_3)$, CN ⇒ C_6H_5): C. R. Noe, M. Knollmüller, E. Wagner, H. Völlenkle, *Chem. Ber. 118* (1985) 3299.

[20] K. J. Schönauer, P. Walter, C. R. Noe, *Monatsh. Chem. 117* (1986) 127.

[21] E. Wagner, *Dissertation*, Technische Universität Vienna, Austria 1985.

[22] L.-F. Tietze, U. Niemeyer, *Chem. Ber. 111* (1978) 2423.

[23] R. K. Chaudhuri, F. ü. Afifi-Yazar, O. Sticher, *Tetrahedron 36* (1980) 2317.

[24] W. Hübel, A. Nahrstedt, V. Wray, *Arch. Pharm. (Weinheim Ger.) 34* (1981) 609.

Formation of Diiridium(II) Complexes by Photoassisted Oxidative-Addition Reactions: Structure of a Stable Binuclear Iodo(iodomethyl)iridium(II) Complex**

By *Miguel A. Ciriano, Fernando Viguri, Luis A. Oro,* Antonio Tiripicchio,** and *Marisa Tiripicchio-Camellini*

Double oxidative-addition of dihaloalkanes to anionic[1] or neutral[2] binuclear complexes is only a restricted route to the syntheses of the unique and intensively studied class of alkylidene-bridged complexes.[3] In studies of the mechanism of this reaction, the highly reactive intermediate **1** which is involved in the formation of methylene-bridged digold(II) complexes,[2a] was recently isolated[4] and some pyrazolato-bridged halo(halomethyl)diiridium(II) complexes have been prepared.[2d, 5]

$[\{Au(CH_2)_2PPh_2\}_2(CH_2Cl)Br]$ **1**

Binuclear alkylmetal compounds, M-M-CH_2X, having a functional group X in the α position could be key reagents in organic synthesis, as are their mononuclear counterparts.[6] Some have been proposed as intermediates in reactions between coordinated ligands.[7] In addition, knowledge of their chemistry is basic to the understanding of some metal-promoted catalytic processes.[8]

[*] Prof. Dr. L. A. Oro, Dr. M. A. Ciriano, Dipl.-Chem. F. Viguri
Departamento de Química Inorgánica
Instituto de Ciencia de Materiales de Aragón
Universidad de Zaragoza, C. S. I. C.
E-50009 Zaragoza (Spain)
Prof. Dr. A. Tiripicchio, Prof. M. Tiripicchio-Camellini
Istituto di Chimica Generale ed Inorganica, Università di Parma
Centro di Studio per la Strutturistica Diffrattometrica del CNR
Via M. D'Azeglio 85, I-43100 Parma (Italy)

[**] This work was supported by C.A.I.C.Y.T. (Spain).

Herein we report the preparation, by photosensitive transannular oxidative-addition reactions, of a new family of binuclear iridium(II) complexes. In particular, the unusual complex **6**, which is stable toward a thermal intramolecular oxidative-addition (to give a methylene-bridged complex), has been fully characterized by X-ray methods and offers the possibility of studying its chemistry.

Reaction of lithium 2-pyridinethiolate with $[\{Ir(\mu\text{-}Cl)(cod)\}_2]$ (cod = 1,5-cyclooctadiene) in diethyl ether gives the complex **2** as a dark red air-stable crystalline solid in good yield. Carbon monoxide replaces the diolefin in **2** at atmospheric pressure in toluene to give a deep purple, very air-sensitive solution of **3**, from which **3** can be isolated as black-violet crystals having metallic luster. The IR and ^{1}H-NMR spectra of **3** (Table 1) are in accordance with a binuclear structure of C_2 symmetry in which the two carbonyl groups on each iridium are in *cis* positions and the two planes formed by the square-planar arrangement of the ligands are parallel.[6]

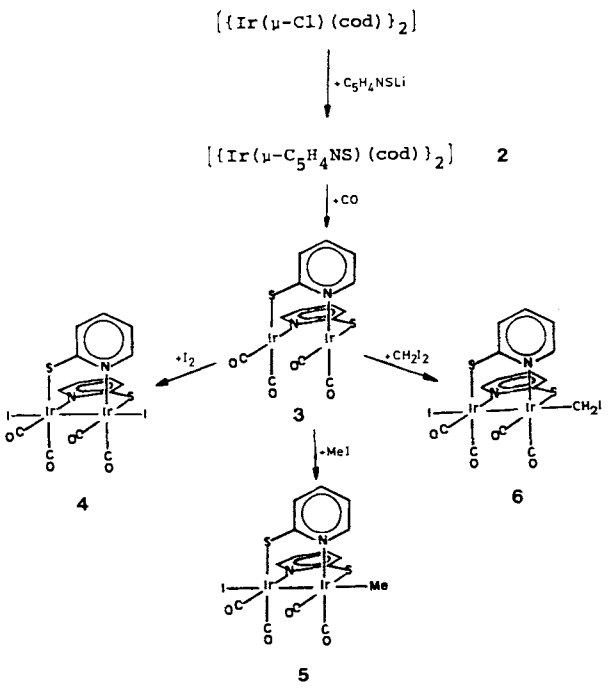

Complex **3**, prepared in situ in toluene, undergoes transannular oxidative-addition reactions, at room temperature upon exposure to direct sunlight or irradiation with a 150-W incandescent lamp, with an excess of iodine, methyl iodide, or diiodomethane to give the air-stable iridium(II) complexes **4** (red, 64% yield), **5** (orange-brown, 73%), and **6** (orange, 66%), respectively. These reactions are complete within a few minutes under these conditions but take about one day in the dark in accordance with the photoreductive properties of d^8–d^8 binuclear iridium(I) complexes.[5]

The structure of the complex **6**, determined by X-ray diffraction methods, is shown in the Figure 1.[9] It consists of two iridium atoms, at a distance of 2.695(2) Å, corresponding to a metal–metal bond, bridged by two 2-pyridinethiolate ligands through their N and S atoms and bonded to two terminal carbonyl groups. The Ir atoms are in different octahedral arrangements, Ir1 completing its coordination through two terminal carbonyls and one iodine atom, Ir2 through two terminal carbonyls and the CH_2I group. The Ir atoms have different environments, the sixth ligand being I in one case and CH_2I in the other.

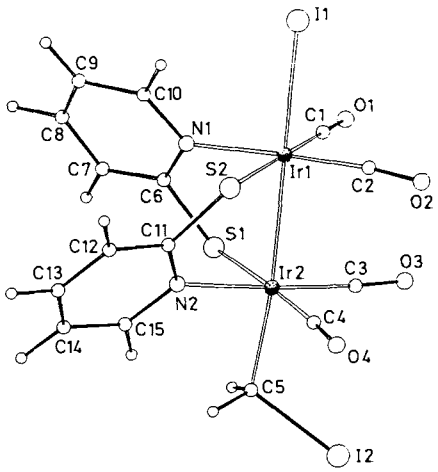

Fig. 1. Crystal structure of **6**. Selected bond lengths [Å] and angles [°]: Ir1-Ir2 2.695(2), Ir1-I1 2.833(2), Ir1-S2 2.360(4), Ir1-N1 2.112(12), Ir1-C1 1.878(17), Ir1-C2 1.826(17), Ir2-S1 2.361(4), Ir2-N2 2.109(11), Ir2-C3 1.874(14), Ir2-C4 1.906(13), Ir2-C5 2.173(15), I2-C5 2.133(15), S1-C6 1.761(12), S2-C11 1.742(16); Ir2-Ir1-I1 173.7(1), I1-Ir1-N1 96.8(3), I1-Ir1-S2 90.3(1), N1-Ir1-S2 88.0(3), Ir1-Ir2-C5 172.6(4), C5-Ir2-S1 88.4(4), C5-Ir2-N2 91.0(5), S1-Ir2-N2 87.3(3), Ir2-C5-I2 115.0(7).

Remarkably, no formation of the expected complex **7** occurs upon refluxing **6** in toluene, in contrast with previous observations.[4, 5a] Comparison of the structures of **1** and **6** shows a markedly different position of the halogen in the halomethyl group with respect to the nearest metal atom.

$[\{Ir(\mu\text{-}C_5H_4NS)I(CO)_2\}_2(\mu\text{-}CH_2)]$ **7**

The photosensitivity of the reactions of **3** described above and the their solvent dependence suggest that a radical mechanism might be involved.[11] On the other hand, if

Table 1. Selected spectroscopic data for the complexes **3**–**6**, **8**, and **9**. Numbering of the pyridine protons according to **A**; H(n) and H(n)′ indicate chemically but not magnetically equivalent protons of the two C_5H_4NS ligands [a].

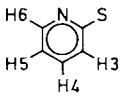

A

3: ^{1}H-NMR (C_6D_6): δ = 8.07 (d, 2H; Hh), 6.81 (d, 2H; H3), 6.09 (td, 2H; H4), 5.73 (td, 2H; H5); IR (cyclohexane): $\tilde{\nu}$(CO) = 2070 (s), 2045 (m), 2000 (s), 1990 (w) cm^{-1}

4: ^{1}H-NMR ($CDCl_3$): δ = 9.49 (dt, 1H; H6), 9.14 (dt, 1H; H6′), 7.46–7.40 (m, 2H; H4 and H4′), 7.22 (m, 2H; H3 and H3′), 6.87 (dt, 1H; H5), 6.75 (ddd, 1H; H5′); IR (CH_2Cl_2): $\tilde{\nu}$(CO) = 2110 (s), 2085 (s), 2065 (s), 2045 (s) cm^{-1}

5: ^{1}H-NMR ($CDCl_3$): δ = 9.74 (d, 1H; H6), 8.16 (d, 1H; H6′), 7.22–7.14 (overlapping m, 4H; H3, H4, H3′ and H4′), 6.71 (td, 2H; H5 and H5′), 1.24 (s, 3H; CH_3); IR (cyclohexane): $\tilde{\nu}$(CO) = 2110 (s), 2070 (m), 2050 (s), 2045 (s) cm^{-1}

6: ^{1}H-NMR ($CDCl_3$): δ = 9.69 (dt, 1H; H6), 8.10 (d, 1H; H6′), 7.24–7.14 (m, 4H; H3, H4, H3′ and H4′), 6.77 (td, 1H; H5), 6.73 (ddd, 1H; H5′), 3.06 and 2.90 (AB system, 2H, J(AB) = 6.9 Hz; CH_2); IR (CH_2Cl_2): $\tilde{\nu}$(CO) = 2110 (s), 2070 (m), 2055 (s), 2040 (m) cm^{-1}

8: ^{1}H-NMR ($CDCl_3$): δ = 9.67 (dt, 1H; H6), 7.98 (d, 1H; H6′), 7.20–7.10 (m, 4H; H3, H4, H3′ and H4′), 6.75–6.65 (m, 2H; H5 and H5V), 4.13 and 3.93 (AB system, 2H, J(AB) = 7.4 Hz; CH_2); IR (CH_2Cl_2): $\tilde{\nu}$(CO) = 2120 (s), 2090 (m), 2065 (s), 2050 (sh) cm^{-1}

9: ^{1}H-NMR ($CDCl_3$): δ = 9.73 (d, 1H; H6), 8.09 (d, 1H; H6′), 7.30–7.15 (m, 4H; H3, H4, H3′ and H4′), 6.80–6.65 (m, 2H; H5 and H5′), 3.82 and 3.63 (AB system, 2H, J(AB) = 6.9 Hz; CH_2)

[a] ^{1}H-NMR spectra at 200 MHz with TMS as internal standard.

the reaction of **3** with diiodomethane is carried out in the presence of a large amount of $[Bu_4N]Cl$ in dichloromethane, the main product is **8**. Moreover, complete replacement of the iodo ligand of **6** by chlorine takes place at room temperature or upon refluxing **6** and $[Bu_4N]Cl$ in dichloromethane for 1 h. If the reaction of diiodomethane with complex **3** is carried out in the presence of $[Bu_4N]Br$ in dichloromethane, a 20 : 10 : 70 mixture of **6**, **8**, and **9** (as analyzed by ^{1}H-NMR spectroscopy) is isolated. The formation of **8** shows that the chlorinated solvent can participate in the reaction.

$[\{Ir(\mu\text{-}C_5H_4NS)(CO)_2\}_2(CH_2I)Cl]$ **8**

$[\{Ir(\mu\text{-}C_5H_4NS)(CO)_2\}_2(CH_2I)Br]$ **9**

Satisfactory elemental analyses were obtained for all new compounds; selected spectroscopic data are collected in Table 1.

Received: November 18, 1986;
revised: February 24, 1987 [Z 1989 IE]
German version: *Angew. Chem. 99* (1987) 452

[1] C. E. Sumner, Jr., P. E. Riley, R. E. Davis, R. Pettit, *J. Am. Chem. Soc. 102* (1980) 1752; K. H. Theopold, R. R. Bergman, *ibid. 105* (1983) 464.
[2] A) P. Jandik, U. Schubert, H. Schmidbaur, *Angew. Chem. 94* (1982) 74; *Angew. Chem. Int. Ed. Engl. 21* (1982) 73; b) A. L. Blach, C. T. Hunt, C. L. Lee, M. M. Olmstead, J. P. Farr, *J. Am. Chem. Soc. 103* (1981) 3764; c) M. El-Amane, A. Maisonnat, F. Dahan, R. Prince, R. Poilblanc, *Organometallics 4* (1985) 773; d) D. G. Harrison, S. R. Rtobart, *J. Chem. Soc. Chem. Commun. 1986*, 285.
[3] W. A. Herrmann, *Adv. Organomet. Chem. 20* (1982) 159; J. E. Hahn, *Prog. Inorg. Chem. 31* (1984) 205.
[4] H. H. Murray, J. P. Fackler, Jr., D. A. Tocher, *J. Chem. Soc. Chem. Commun. 1985*, 1278.
[5] J. V. Caspar, H. B. Gray, *J. Am. Chem. Soc. 106* (1984) 3029.
[6] P. von R. Schleyer, T. Clark, A. J. Kos, G. W. Spitznagel, C. Rohde, D. Arad, K. N. Houk, N. G. Rondan, *J. Am. Chem. Soc. 106* (1984) 6467; E. K. Barefield, P. McCarten, M. C. Hillhouse, *Organometallics 4* (1985) 1682, and references cited therein.
[7] R. Zolk, H. Werner, *J. Organomet. Chem. 303* (1986) 233.
[8] W. A. Herrmann, *Angew. Chem. 94* (1982) 118; *Angew. Chem. Int. Ed. Engl. 21* (1982) 117.
[9] Siemens AED diffractometer ($Mo_{K\alpha}$): **6**: triclinic, $P\bar{1}$, $Z=2$, $a=10.714(6)$, $b=11.761(7)$, $c=9.046(4)$ Å, $\alpha=92.57(1)$, $\beta=71.95(2)$, $\gamma=97.48(1)°$, $V=1075(1)$ Å^3; $3\leq\theta\leq27°$, 4632 unique reflections, 3444 observed with $I\geq2\sigma(I)$, $R=0.0524$, $R_w=0.0570$. Further details of the crystal structure investigation may be obtained from the Fachinformationszentrum Energie, Physik, Mathematik GmbH, D-7514 Eggenstein-Leopoldshafen 2 (FRG), on quoting the depository number CSD-52319, the names of the authors, and the journal citation.
[10] J. A. Labinger, J. A. Osborn, N. J. Coville, *Inorg. Chem. 19* (1980) 3236.

Photo-CIDNP in the Vacuum-UV: Di-*tert*-butyl Ether and 2,2,5,5-Tetramethyltetrahydrofuran in Aqueous Solution**

By *Knut Hildenbrand, Heinz-Peter Schuchmann,* and *Clemens von Sonntag**

In the vacuum-UV photolysis of saturated ethers, homolytic cleavage processes are common (for a review see Ref. [1]). In particular, the 185-nm photolysis of the title compounds **1a** and **1b** has been studied in the neat liquid

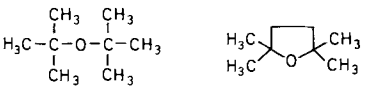

1a **1b**

state.[2,3] Alongside the homolytic cleavage processes leading to free-radical formation, molecular elimination reactions are thought to occur, which, however, cannot be distinguished from cage recombination reactions in these product studies. The photolysis of 1,4-dioxane[4,5] and dimethyl ether[6] has been studied also in aqueous solutions, with clear indications not only of cleavage to free radicals,[6] but also photoionization. So far, the UV photolysis of ditertiary ethers has not been studied in aqueous solutions; in this case, however, photoionization is expected to play an important part. Estimates indicate that the gas-phase ionization potential of di-*tert*-butyl ether lies below that of primary ethers by more than 0.5 eV.[7] In order to follow the photochemistry of aliphatic ethers by spectroscopic means, photo-CIDNP experiments (ArF excimer laser excitation, $\lambda=193$ nm) were carried out. Nonaqueous solutions (ether undiluted or dissolved in *cyclo*-C_6D_{12}), as well as aqueous solutions of primary, secondary, and monotertiary ethers, did not yield polarized NMR signals upon illumination. Only in solutions of di-*tert*-butyl ether, **1a**, and 2,2,5,5-tetramethyltetrahydrofuran, **1b**, in oxygen-free D_2O (concentration ≈0.01 M) was enhanced absorption observed ($\delta=0.23$) with a 1 : 1 : 1 triplet splitting of 1.9 Hz, which is assigned to CH_3D, and a singlet emission signal ($\delta=0.9$; C_2H_6) (Fig. 1).

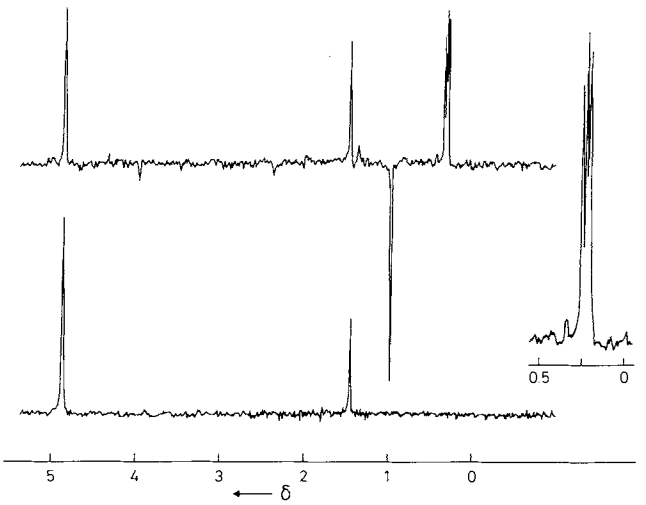

Fig. 1. Top: ^{1}H-NMR spectrum of a solution of di-*tert*-butyl ether, **1a**, in D_2O (0.01 M, deoxygenated) recorded directly after illumination with 20 laser pulses ($\lambda=193$ nm, frequency = 1 Hz). An expansion of the polarized CH_3D signal is shown on the right side. Bottom: ^{1}H-NMR spectrum of the same solution recorded 2 min after the end of the CIDNP experiment. In both experiments, five free induction decays were accumulated.

In the presence of H_2O a singlet at $\delta=0.25$ (CH_4) was superimposed on the triplet of CH_3D. The relative intensity of the signals of CH_4 and CH_3D was directly correlated to the ratio $H_2O:D_2O$, which supports the involvement of the aqueous environment in the photoreaction. These assignments were confirmed by the results of a product analysis.[8]

[*] Prof. Dr. C. von Sonntag, Dr. K. Hildenbrand, Dr. H.-P. Schuchmann
Max-Planck-Institut für Strahlenchemie
Stiftstrasse 34-36, D-4330 Mülheim a. d. Ruhr (FRG)

[**] We would like to thank Professor *H. Fischer* for helpful discussions, and Dr. *H. Görner* for his kind assistance with the laser experiments.

At first sight, the participation of water seems surprising because the concentration of the ethers is such that practically no light is absorbed by the solvent. Here, it is helpful to recall that in aqueous medium the ionization threshold of a solute is lowered by about 3 eV relative to its gas-phase ionization potential.[9] The title compounds are expected to have a gas-phase ionization potential below 9.2 eV,[7, 10] and photoionization with 193-nm light (~6.4 eV) appears likely in an aqueous medium.[11] With this assumption, the experimental observations can be explained by reactions (a)–(f).

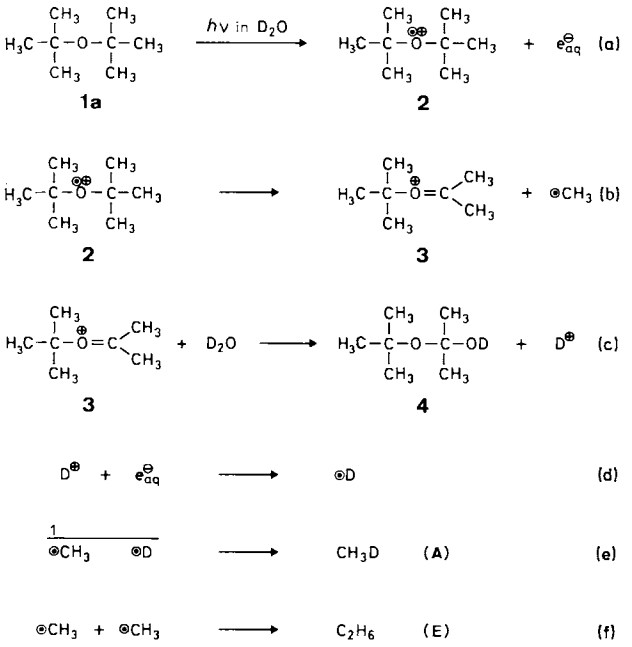

Upon photoionization, the ether **1a** gives rise to the radical cation **2** and a solvated electron [reaction (a)]. The radical cation **2** loses a methyl radical [reaction (b)]. The oxonium ion **3** thus formed reacts rapidly with water yielding the hemiacetal **4** and a deuteron [reaction (c)]. If this sequence of events is sufficiently fast, D atoms will be formed with a high probability from the solvated electron and the deuteron [reaction (d)]. The cage product would then be CH_3D [reaction (e)], the escape products ethane [reaction (f)] and D_2. The products CH_3D and C_2H_6 have been observed. D_2 is not detected by this ^{1}H-NMR experiment. (A) and (E) in reactions (e) and (f), respectively, mean enhanced absorption and emission.

Using Kaptein's rules[12] and $g(^{\odot}CH_3) = 2.0025$,[13] $g(^{\odot}D) = 2.00223$,[13] and $A(^{\odot}CH_3) = -23.04$ Gauss,[13] the signs of the polarizations can be explained by assuming that the $\overline{^{\odot}CH_3\ ^{\odot}D}$ radical pair is originally in a correlated singlet state before $S\text{-}T_0$ mixing and escape of $^{\odot}CH_3$ and $^{\odot}D$ radicals takes place.

Since photo-CIDNP studies carried out in the vacuum-UV have not been reported previously, the experimental requirements are reported here in somewhat more detail.

Experimental Procedure

The NMR experiments were performed with a Bruker WH 90 FT NMR spectrometer. The samples were irradiated in situ with an excimer laser (EMG 200, Lambda-Physik). The light entered the sample through a hole at the rear of the probe head. The insert consisted of a single-wall Suprasil cylinder. It is essential for the vacuum-UV experiment that the coil should not be densely wound and should only be fastened with glue at the side opposite the light beam. Wilmad 5-mm quartz tubes were used. A sequence of 20 laser pulses (100 mJ/pulse laser output; 20 mJ/pulse input into the sample, pulse frequency = 1 Hz) was applied and then the NMR experiment was started (rf pulse ≈ 25°, 8-K data memory). In order to improve the signal-to-noise ratio, the experiment was repeated five times with a delay in between of 2 min. For assignment of the polarized signals, the samples were saturated with CH_4 and C_2H_6 after the end of the CIDNP experiments. Chemical shifts were measured relative to sodium 3-trimethylsilylpropionate ($\delta = 0$).

Received: December 11, 1986;
revised: February 20, 1987 [Z 2005 IE]
German version: *Angew. Chem. 99* (1987) 453

CAS Registry numbers:
1a, 6163-66-2; **1b**, 15045-43-9.

[1] C. von Sonntag, H.-P. Schuchmann in S. Patai (Ed.): *The Chemistry of Functional Groups, Suppl. E*, Wiley, New York 1980, p. 903.
[2] H.-P. Schuchmann, C. von Sonntag, *Tetrahedron 29* (1973) 3351.
[3] N. Kizilkilic, H.-P. Schuchmann, C. von Sonntag, *Can. J. Chem. 58* (1980) 2819.
[4] H.-P. Schuchmann, H. Bandmann, C. von Sonntag, *Z. Naturforsch. B 34* (1979) 327.
[5] C. von Sonntag, H. Bandmann, *J. Phys. Chem. 78* (1974) 2181.
[6] H.-P. Schuchmann, C. von Sonntag, *J. Photochem. 16* (1981) 289.
[7] B. W. Levitt, L. S. Levitt, *Experientia 26* (1970) 1183.
[8] C. von Sonntag et al., unpublished results.
[9] A. Bernas, M. Gauthier, D. Grand, G. Parlant, *Chem. Phys. Lett. 17* (1972) 439; A. Bernas, J. Blais, M. Gauthier, D. Grand, *ibid. 30* (1975) 383.
[10] K. Watanabe, T. Nakayama, J. Mottl, *J. Quant. Spectrosc. Radiat. Transfer 2* (1962) 369.
[11] P. Ausloos, C. Lutz, F. Schwarz, S. G. Lias, *Radiat. Phys. Chem. 23* (1984) 97.
[12] R. Kaptein, *Chem. Commun. 1971*, 732.
[13] R. W. Fessenden, R. H. Schuler, *J. Phys. Chem. 39* (1963) 2147.

Shortened C–C Bonds and Antiplanar O=C–O–H Torsion Angles in 1,4-Cubanedicarboxylic Acid**

By *Otto Ermer** and *Johann Lex*

Whereas the structures of many molecules with considerably lengthened C–C single bonds have been determined (more than 50 cases with C–C distances > 1.60 Å), relatively little is known about shortened C–C bonds.[1] Generally, CC shortenings may be expected if the bond of interest is involved in bond angles widened beyond their normal values. This can be explained in terms of hybridization as well as by an analysis of the influence of stretch-bend cross terms or 1,3-repulsions in molecular force fields.[1, 2] On the other hand, CC bonds adjacent to compressed angles should be lengthened.[2] We report here on the crystal structure analysis of 1,4-cubanedicarboxylic acid **1**,[3]

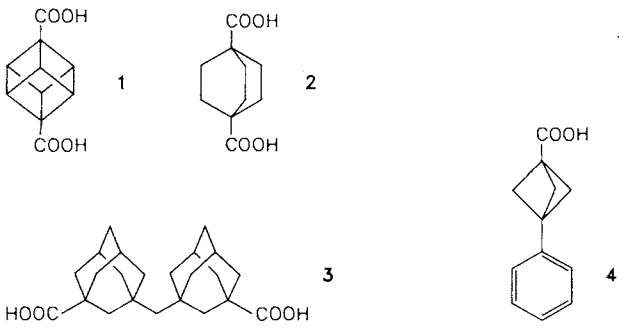

[*] Prof. Dr. O. Ermer, Dr. J. Lex
Institut für Organische Chemie der Universität
Greinstrasse 4, D-5000 Köln 41 (FRG)

[**] This work was supported by the Fonds der Chemischen Industrie.

which exhibits shortened $C(sp^3)$-$C(sp^2)$ bonds between the cubane and carboxyl C atoms, since the endocyclic C-C-C angles in the rigid cubane framework are compressed to about 90° and the exocyclic angles correspondingly widened to about 125°.

Important findings of the X-ray analysis are summarized in Figures 1 and 2.[4] The density of **1** is 1.643 g cm^{-3} and thus rather high, which may partly be due to the compression of the cubane C atoms ensuing from the small bond angles. Two conformationally different centrosymmetric molecules are present in the crystals of **1**. In both cases, the $C(sp^3)$-$C(sp^2)$ bond lengths are 1.480(1) Å (1.481 Å corrected for libration). For comparison, the corresponding C-C bonds of **2** and **3** that are not involved in widened bond angles have lengths of 1.513(4) and 1.523(4),[5] and 1.518(2) Å,[6] respectively. Thus, the $C(sp^3)$-$C(sp^2)$ bonds in **1** are shortened by about 0.04 Å. The angular deformations at the bridgehead C atoms of bicyclo[1.1.1]pentane are comparable to those in cubane.[7] Accordingly, the X-ray structure analysis of 3-phenylbicyclo[1.1.1]pentane-1-carboxylic acid **4** reveals similarly shortened $C(sp^3)$-$C(sp^2)$ bond lengths of 1.47(1) and 1.46(1) Å for the exocyclic bonds from the atoms C1 and C3, respectively.[8] The central C-C bond in 1,1'-binorbornyl is also slightly shortened (1.515(5) Å), which is ascribable to moderate widening of the exocyclic bond angles at the bridgehead C atoms.[9]

Model calculations on methylcubane, carried out with our consistent force field,[10a] gave a shortening of the exocyclic C-C bond approximately twice the amount observed in **1**. Similarly, this force field also overestimates bond lengthening due to bond angle compression.[10b] This originates from the relatively large stretch-bend cross terms of the potential, which are required for a good reproduction of vibrational frequencies. The MM2 force field[11] yields better bond length effects,[2b] since here these cross terms are smaller and since vibrational data are regarded as unimportant. The cubane C-C bonds of **1** are each involved in four compressed and two widened bond angles, resulting in an average lengthening to 1.566 Å (1.570 Å corrected for libration); for comparison, values of cubane are 1.575(1),[12a] 1.565(4),[12b] and 1.551(3) Å[12c] (1.566 Å corrected for libration).

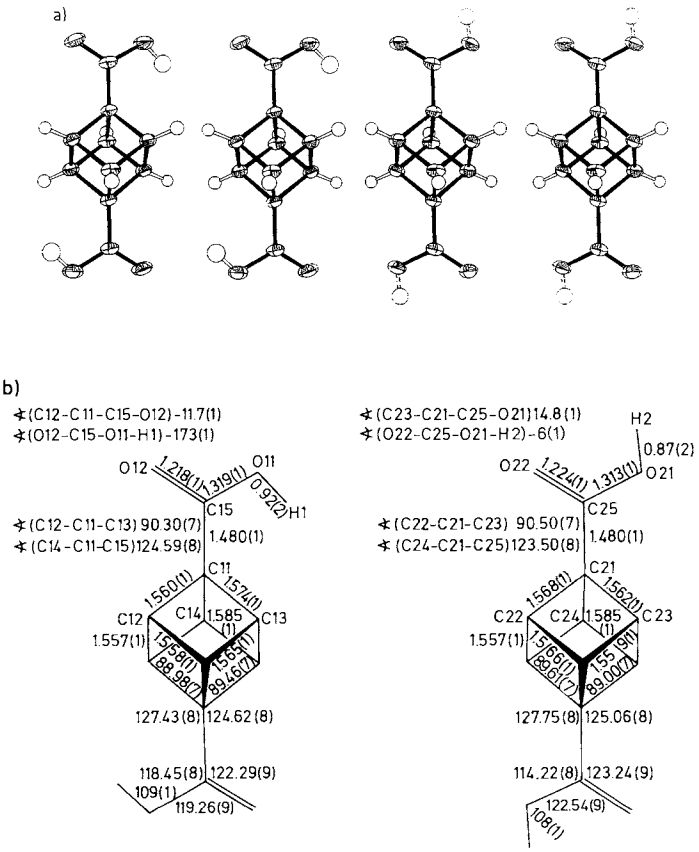

Fig. 1. a) Stereoview of the two conformers of **1** in the crystal with thermal ellipsoids (50% probability); temperature factors of the H atoms halved. b) Important bond lengths [Å], bond and torsion angles [°], and atomic numbering.

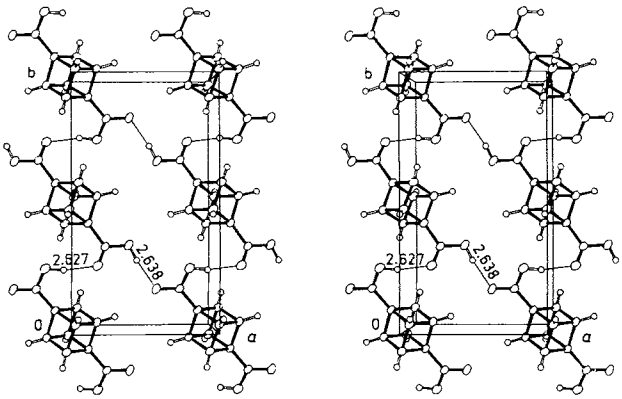

Fig. 2. Crystal structure of **1** with O···O distances of the hydrogen bonds ([Å], standard deviations 0.001 Å).

Two carboxyl conformations are observed in the crystals of 1,4-cubanedicarboxylic acid **1** (Figs. 1 and 2). The O=C-O-H torsion angle is synplanar for one-half of the molecules, yet antiplanar for the other half. This latter observation is very rare: Only one other crystal structure has been reported for a carboxylic acid without intramolecular hydrogen bonds that prefers an antiplanar O=C-O-H partial conformation.[13] Apparently, this unusual geometry is supported in **1** by the molecular packing, which also deviates from the usual pattern. Whereas dicarboxylic acids, e.g., **2**,[5] are normally linked in the crystal by hydrogen bonds to form chains,[14] the molecules of **1** join to set up layers (Fig. 2). Possibly, another crystal modification of **1** exists with an "ordinary" chain structure and exclusively synplanar O=C-O-H torsion angles; crystal force field calculations would be instructive.

The 14 strongest residual density maxima of a difference Fourier map of **1** may be assigned to electron densities in

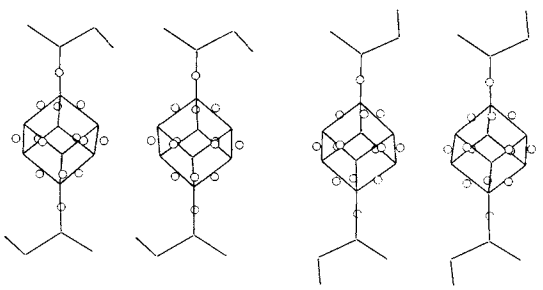

Fig. 3. Strongest 14 residual electron density maxima (empty spheres) from a difference Fourier synthesis of **1** (1213 reflection intensities with $\theta_{Mo} \leq 25°$; C and O atomic parameters from a refinement with 1423 reflections with $25° < \theta_{Mo} < 35°$; H parameters from a normal refinement [4]); residual electron density maxima between 0.22 and 0.34 eÅ^{-3}; stereoview as in Figure 1.

the 14 independent C–C bonds (Fig. 3). The cubane C–C bonds appear to be bent and the endocyclic interorbital angles at the C atoms amount to 105° on the average (maximum 112, minimum 96°); i.e., they are considerably larger than 90°.

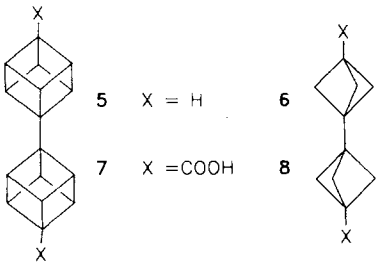

Extreme shortenings of up to 0.08 Å may be expected for the central C–C bonds of the hypothetical bicubyl **5** and 1,1′-bibicyclo[1.1.1]pentyl **6**, since they participate in six significantly widened C–C–C angles (compared with only three in the case of the $C(sp^3)$–$C(sp^2)$ bonds of **1**). Of interest are also the torsional barriers around these bonds in **5** and **6**, which presumably are unusually low. Preparative and structural work on **5**–**8** is in progress.

Received: December 15, 1986 [Z 2008 IE]
German version: *Angew. Chem. 99* (1987) 455

CAS Registry number:
1, 32846-66-5

[1] An exception is provided by three-membered ring compounds, in which endocyclic bonds can be shortened owing to special electronic effects. Shortened exocyclic CC bonds that are involved in widened CCC angles have also been observed at three-membered rings in some cases: F. H. Allen, *Acta Crystallogr. Sect. B36* (1980) 81, *Sect. B37* (1981) 890, *Sect. A37S* (1981) C198; K. Hagen, G. Hagen, M. Traetteberg, *Acta Chem. Scand. 26* (1972) 3649; M. Traetteberg, A. Simon, E.-M. Peters, A. de Meijere, *J. Mol. Struct. 118* (1984) 333; H. Irngartinger, A. Goldmann, R. Jahn, M. Nixdorf, H. Rodewald, G. Maier, K.-D. Malsch, R. Emrich, *Angew. Chem. 96* (1984) 967; *Angew. Chem. Int. Ed. Engl. 23* (1984) 993.

[2] a) O. Ermer, *Tetrahedron 30* (1974) 3103; b) N. L. Allinger, P. E. Eaton, *Tetrahedron Lett. 24* (1983) 3697.

[3] P. E. Eaton, T. W. Cole, *J. Am. Chem. Soc. 86* (1964) 962, 3157.

[4] Monoclinic crystals (from formic acid); m.p. = 226 °C (dec.); space group $P2_1/n$, $Z=4$, $a=7.2512(6)$, $b=12.9050(12)$, $c=8.3031(5)$ Å, $\beta=90.993(6)°$; $\rho_{calcd}=1.643$, $\rho_{exp}=1.64$ g cm^{-3}. Two independent centrosymmetric molecules with different O=C–O–H partial conformations; intensity measurements at room temperature on a four-circle diffractometer ($\lambda_{Mo}=0.71069$ Å, $\theta_{Mo}(max)=35°$); structure solution by direct methods; refinement (C,O anisotropic, H isotropic) using 2636 reflections with $F_0>3\sigma(F_0)$; $R=0.042$, $R_w=0.051$. We thank Prof. *P. E. Eaton*, Chicago, for a sample of **1**. Further details of the crystal structure investigation may be obtained from the Fachinformationszentrum Energie, Physik, Mathematik GmbH, D-7514 Eggenstein-Leopoldshafen 2 (FRG), on quoting the depository number CSD-52265, the names of the authors, and the journal citation.

[5] O. Ermer, J. D. Dunitz, *Helv. Chim. Acta 52* (1969) 1861.

[6] O. Ermer, C.-D. Bödecker, *Chem. Ber. 114* (1981) 652.

[7] A. Padwa, E. Shefter, E. Alexander, *J. Am. Chem. Soc. 90* (1968) 3717; J. F. Chiang, S. H. Bauer, *ibid. 92* (1970) 1614.

[8] T. L. Renken, *Ph. D. Thesis*, Urbana, IL, USA 1981; D. E. Applequist, T. L. Renken, J. W. Wheeler, *J. Org. Chem. 47* (1982) 4985. We thank Prof. *Applequist*, Urbana, for crystallographic data.

[9] R. A. Alden, J. Kraut, T. G. Traylor, *J. Am. Chem. Soc. 90* (1968) 74.

[10] a) O. Ermer, S. Lifson, *J. Am. Chem. Soc. 95* (1973) 4121; b) O. Ermer: *Aspekte von Kraftfeldrechnungen*, Wolfgang Baur Verlag, München 1981.

[11] N. L. Allinger, *J. Am. Chem. Soc. 99* (1977) 8127.

[12] a) Gas electron diffraction of cubane: A. Almenningen, T. Jonvik, H.-D. Martin, T. Urbanek, *J. Mol. Struct. 128* (1985) 239; b) rotational-vibrational spectrum (gas phase): A. S. Pine, A. G. Maki, A. G. Robiette, B. J. Krohn, J. K. G. Watson, T. Urbanek, *J. Am. Chem. Soc. 106* (1984) 891; c) crystal structure: E. B. Fleischer, *ibid. 86* (1964) 3889.

[13] M. Fujinaga, M. N. G. James, *Acta Crystallogr. Sect. B36* (1980) 3196; see also [14].

[14] L. Leiserowitz, *Acta Crystallogr. Sect. B32* (1976) 775; Z. Berkovitch-Yellin, L. Leiserowitz, *J. Am. Chem. Soc. 104* (1982) 4052.

1,2,3,5,8,8a-Hexahydronaphthalene from 1,2-Cyclohexadiene**

By *Manfred Christl** and *Michael Schreck*

Although the reactive intermediate 1,2-cyclohexadiene **1a** has been characterized very well both experimentally and theoretically,[1] applications of **1a** in synthesis have not yet been reported. Prompted by the rearrangement[2a] of the [2+2] cycloadduct of 1,3-butadiene with tricyclo[4.1.0.0^{2,7}]hepta-3,4-diene,[2b] which occurs under mild conditions, we have now studied the reactions of 1,3-butadiene and some of its methyl derivatives with **1a** and 1-methyl-1,2-cyclohexadiene **1b**,[3] as well as the rearrangement of the [2+2] cycloadducts **2** and **3** to the unknown 1,2,3,5,8,8a-hexahydronaphthalene **4a** and some of its methyl derivatives.

Bottini et al.[4] obtained 7-vinylbicyclo[4.2.0]oct-1(2)-enes of the type **2,3** by reaction of **1a** with *cis*-1,3-pentadiene, *trans,trans*-2,4-hexadiene and 2,3-dimethylbutadiene but they did not report the configurations of the products. We have now generated **1a** likewise by treatment of 6,6-dibromobicyclo[3.1.0]hexane with methyllithium,[5] and allowed it to react at −20 to −15 °C with 1,3-butadiene, *trans*-1,3-pentadiene, isoprene, and 2,3-dimethylbutadiene, each of which served as solvent, and obtained the [2+2] cycloadducts **2** and **3** and, in several cases, the [4+2] cycloadducts **4** (Scheme 1). Analogously, **1b**[3] reacted with 1,3-butadiene to afford the products **2f**, **4f**, and **5**.

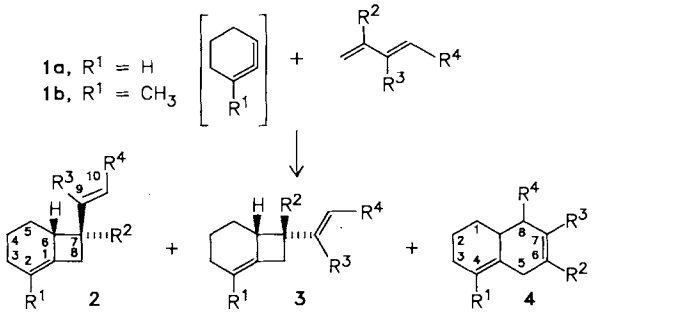

a, $R^1=R^2=R^3=R^4=H$; **b**, $R^1=R^3=R^4=H$, $R^2=CH_3$;
c, $R^1=R^2=R^4=H$, $R^3=CH_3$; **d**, $R^1=R^2=R^3=H$, $R^4=CH_3$;
e, $R^1=R^4=H$, $R^2=R^3=CH_3$; **f**, $R^1=CH_3$, $R^2=R^3=R^4=H$

Scheme 1 [6].

All the compounds **2**–**5** were purified by preparative gas chromatography (column: ethylene glycol adipate, ca. 100 °C). The yields are listed in Table 1. Table 2 contains selected NMR spectroscopic data.

We have investigated the reactions of **1a** with 1,3-butadiene and isoprene with special thoroughness. Compound

[*] Prof. Dr. M. Christl, Dr. M. Schreck
Institut für Organische Chemie der Universität
Am Hubland, D-8700 Würzburg (FRG)

[**] This work was supported by the Fonds der Chemischen Industrie.

Table 1. Yields [%] of **2**–**4** and **5** after purification by gas chromatography.

	a	b	c	d	e	f
2	31	27	5	17	42	29
3	4	5				
4	8	3	3			1 + **5** (2)

4a was found to be a primary adduct and not derived from **2** or **3** (see below). The same should be valid for the methyl derivatives of **4a**. The ratio (**2b** + **3b**) : **2c** = 6.4 shows that **1a** preferentially attacks the more highly substituted double bond of isoprene. By means of a competition experiment, we determined a value of 1.9 for the ratio of the rate constants for the reactions of 1,3-butadiene and 2,3-dimethylbutadiene with **1a**; thus, 1,3-butadiene is one of the more reactive trapping reagents for **1a**.[4]

Most probably, the mechanism of formation of **2** and **3** is a two-step process, similar to that proved for the addition of styrene to **1a**.[3, 7] Compound **1a** presumably reacts with 1,3-butadiene to give the diradical **6** having a *trans*-configurated allyl group in the side chain. Intermediate **6** then cyclizes to form **2a** or **3a**. The diradical 7 having a *cis*-configurated allyl group could be involved as an intermediate in the formation of the [4 + 2] cycloadduct **4a**, if 7 arose directly from **1a** and 1,3-butadiene.

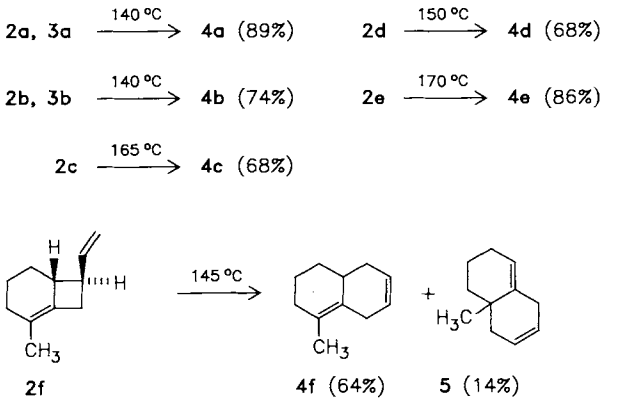

Scheme 2 [6].

Despite the formation of product mixtures, the addition of 1,3-butadienes to **1a** is of preparative interest, since the diastereomeric bicyclo[4.2.0]oct-1(2)-enes **2**, **3** undergo rearrangement to a single 1,2,3,5,8,8a-hexahydronaphthalene **4** upon thermolysis in C_6D_6. At 140 °C, the half-life of **2a** is about 2 h and that of **3a** about 18 min. These reactions and the yields isolated are summarized in Scheme 2. Thus, the previously unknown **4a** and some of its methyl derivatives are now readily accessible.

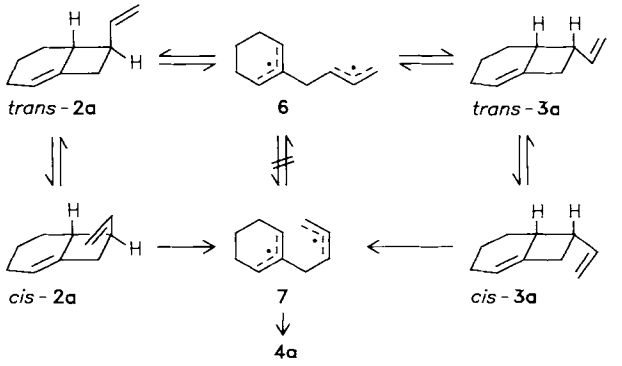

Scheme 3.

The formation of **4f** from **2f** rules out a Cope rearrangement in this case and makes one unlikely for the other ring expansions (**2**, **3** → **4**; **2f** → **5**). In analogy to the results obtained for the thermolysis of 3-vinylmethylenecyclobutane and some of its derivatives,[8] we propose the diradical 7 as a precursor of **4a**; the allyl group in the side chain of 7 has the *cis* configuration. Because of the rotation barrier of about 15 kcal/mol in the allyl radical,[9] 7 cannot arise directly from **6** but only from *cis*-**2a** and *cis*-**3a** (Scheme 3). A detailed study of the rearrangement of **2a** ($\Delta H^{\neq} \approx 33$ kcal mol^{-1}, $\Delta S^{\neq} = 1$ cal mol^{-1} K^{-1}) and **3a** showed that the isomerization **2a** ⇌ **3a** proceeds parallel to the ring expansion and that, starting from **2a**, the amount of **3a** was maximally 1%, whereas, starting from **3a**, that of **2a** was maximally 7%.

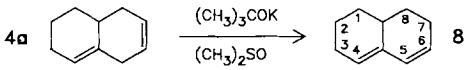

The base-induced isomerization of **4a** is also of preparative value. We isolated 1,2,3,7,8,8a-hexahydronaphthalene **8** in 49% yield, a compound that had been obtained previously, in a multistep synthesis, only as a mixture containing one other isomer.[10]

Table 2. ^{1}H- and ^{13}C-NMR data for **2a**, **3a**, **4a**, and **8** ($CDCl_3$, δ values, coupling constants in Hz).

2a: ^{1}H-NMR [a]: δ = 1.09 (5-H_{endo}), 1.38 (4-H_{exo}), 1.75 (4-H_{endo}), 1.91 (5-H_{exo}), 1.99 (3-H_{endo}), 2.08 (3-H_{exo}), 2.46 (7-H), 2.61 (6-H and 8-H_{exo}), 2.70 (8-H_{endo}), 4.89 (dt, J(7,10$_{trans}$) = J(10,10) = 1.3, J(9,10$_{trans}$) = 10.3; 10-H_{trans}), 4.95 (dt, J(7,10$_{cis}$) = 1.3, J(9,10$_{cis}$) = 17.3; 10-H_{cis}), 5.26 (2-H), 5.97 (ddd, J(7,9) = 6.5; 9-H). — ^{13}C-NMR [b]: δ = 21.54 (C-4), 25.01 (C-3), 27.71 (C-5), 37.88 (C-8), 45.19 (C-7), 48.70 (C-6), 112.96 (C-10), 113.18 (C-2), 138.55 (C-1), 141.71 (C-9)

3a: ^{1}H-NMR [a]: δ = 1.16 (5-H_{endo}), 1.41 (4-H_{exo}), 1.52 (5-H_{exo}), 1.74 (4-H_{endo}), 1.99 (3-H_{endo}), 2.04 (3-H_{exo}), 2.30 (8-H_{exo}), 3.00 (6-H, 7-H, and 8-H_{endo}), 4.98–5.04 (m; 10-H_{cis}, 10-H_{trans}), 5.31 (2-H), 5.90 (m, 9-H). — ^{13}C-NMR [b]: δ = 21.41 (C-4), 22.77 (C-5), 24.82 (C-3), 36.87 (C-8), 40.67 (C-7), 45.58 (C-6), 114.12 (C-10), 114.71 (C-2), 138.55 (C-9), 140.18 (C-1)

4a: ^{1}H-NMR: 1.37 (dddd, J = 13.0, 7.0, 4.8, 3.8) and 1.84 (dddd, J = 13.0, 9.8, 6.5, 3.5) (1-H_2), 1.48–1.63 (m; 2-H_2), 1.94 (m) and 2.12 (br dt, J = 17.2, 5.3) (8-H_2), 1.99 (m; 3-H_2), 2.29 (m; 8a-H), 2.58 (dt, J = 20.0, 3.7) and 2.86 (dm, J = 20.0) (5-H_2), 5.52 (tt, J = 3.5, 1.7; 4-H), 5.57–5.70 (m; 6-H, 7-H). — ^{13}C-NMR [b]: δ = 20.53 (C-2), 25.83 (C-3), 29.63 (C-1), 33.53 (C-8a), 34.18 and 34.44 (C-5, C-8), 120.00 (C-4), 126.50 (peak of double intensity; C-6, C-7), 137.16 (C-4a)

8: ^{1}H-NMR: δ = 1.00–2.30 (m, strong maxima at 1.82 and 2.14; 11H), 5.43 (m; 4-H), 5.65 (ddm, J = 9.9, 5.0; 6-H), 5.98 (dd, J = 9.9, 2.0; 5-H). — ^{13}C-NMR: δ = 22.68 (C-2), 25.89 and 26.09 (C-3, C-7), 30.50 and 30.73 (C-1, C-8), 35.70 (C-8a), 123.51 (C-4), 127.12 and 129.59 (C-5, C-6), 137.52 (C-4a)

[a] The coupling constants between the protons at the bicyclo[4.2.0]oct-1(2)-ene skeleton are as large as those in the 7-aryl derivatives [3]. [b] The assignment was assisted by the off-resonance decoupled or proton-coupled spectra as well as by the methyl substituent effects of the methyl derivatives.

Received: December 23, 1986;
revised: February 23, 1987 [Z 2026 IE]
German version: *Angew. Chem.* *99* (1987) 474

[1] Compare the references in the introduction of [3].
[2] a) M. Christl, *Angew. Chem.* *93* (1981) 515; *Angew. Chem. Int. Ed. Engl.* *20* (1981) 529; R. Lang, *Dissertation*, Universität Würzburg 1982; b) M. Christl, R. Lang, M. Lechner, *Liebigs Ann. Chem.* *1980*, 980.
[3] M. Christl, M. Schreck, *Chem. Ber.* *120* (1987), in press.
[4] A. T. Bottini, L. L. Hilton, J. Plott, *Tetrahedron* *31* (1975) 1997.
[5] W. R. Moore, W. R. Moser, *J. Org. Chem.* *35* (1970) 908.

[6] Correct C,H elemental analyses, mass spectra, and ^{1}H- and ^{13}C-NMR spectra were obtained for all compounds (see also Table 2).
[7] S. Harnos, S. Tivakornpannarai, E. E. Waali, *Tetrahedron Lett. 27* (1986) 3701.
[8] D. Hasselmann, *Tetrahedron Lett. 1972*, 3465; *1973*, 3739; J. A. Berson, J. M. Janusz, *J. Am. Chem. Soc. 96* (1974) 5939; W. R. Dolbier, Jr., G. J. Mancini, *Tetrahedron Lett. 1975*, 2141.
[9] R. Sustmann in H. G. Viehe, Z. Janousek, R. Merényi (Eds.): *Substituent Effects in Radical Chemistry*, Reidel, Dordrecht 1986, p. 143.
[10] H. Böhme, G. Peters, *Z. Naturforsch. B 12* (1957) 5.

The Pagodane Route to Dodecahedranes—Thermal, Reductive, and Oxidative Transformations of Pagodanes**

By *Wolf-Dieter Fessner, Bulusu A. R. C. Murty,* and *Horst Prinzbach**

"Pagodanes" are compounds having structures of type **I**, which we are synthesizing primarily as precursors of dodecahedranes **II**.[1] Variation of the X,Y bridges should allow diverse patterns of substitution and/or skeletal modifications in **II** as well as various methodologies for the transformation **I** → **II**.[2] The required cleavage of two cyclobutane bonds and the linking of opposing X positions are being attempted, depending on the nature of X, either catalytically (pathway A) or directly via a multistep sequence of reactions (**I** → **III** → **IV** → **V** → **II**, pathway B, or **I** → **VI** → **VII** → **V** → **II**, pathway C; Scheme 1).[3,4]

The prototypes of the series **I** and **II**, [1.1.1.1]pagodane **1** (**I**, X = CH_2)[1] and dodecahedrane **2** (**II**, X-Y-X = CH-CH),[5] are $C_{20}H_{20}$ isomers having high-symmetry (D_{2h} and I_h, respectively) undecacyclic skeletons, each containing twelve cyclopentane units. According to MM2 calculations,[6] the transformation **1** → **2** involves a considerable reduction in energy (enthalpy of formation difference: $\Delta\Delta H_f^\circ = -42.2$ kcal/mol; strain energy difference $\Delta E_{str} = -46.1$ kcal/mol).[7] Of primary interest was the possibility of specifically opening the four-membered ring of **1**, in particular a $2\sigma \rightarrow 2\pi$ cleavage with formation of the bissecododecahedradiene **6**[4] (Scheme 2). According to MM2 force-field calculations, the cleavage of the a bonds in **1** (to give **6** via **4**) is significantly favored both kinetically and thermodynamically over that of the b bonds (to give **5** via **3**). The findings reported here exemplify the thermal, reductive, and oxidative cyclobutane cleavage in **1**.

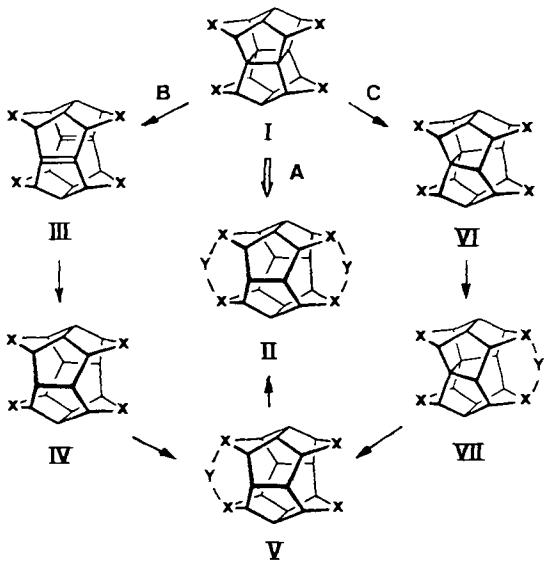

Scheme 1.

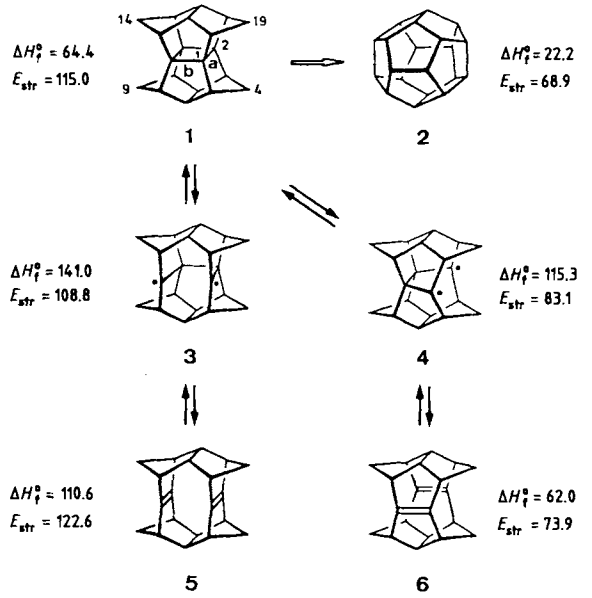

Scheme 2. ΔH_f° and E_{str} in kcal/mol.

Thermolysis of the "pagodane moiety" **8**,[8] which is accessible photochemically from **7**, provided a model for the thermal isomerization **1** → **6** (Scheme 3). According to recent measurements[9] and in good agreement with the results of force-field calculations, thermolysis of **8** above 400 °C results in selective cleavage of the a bonds with formation of the diene **9** ($\Delta H^\neq$ (430 °C) ca. 59 kcal/mol); the opening **8** ⇄ **9** is reversible.

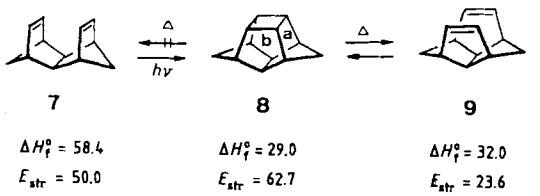

Scheme 3. ΔH_f° and E_{str} in kcal/mol.

Upon thermolysis in a vertical pyrolysis tube (in order to achieve longer contact times; benzene and ethanol solutions), **1** remained unchanged up to 500 °C; at 600–620 °C/700–720 °C/750 °C, the pyrolysates still contained at least 80%/< 10%/< 2% educt. The only product isolated (in yields of up to 60%) was naphthalene **12** (along with "polymeric" material)! Because of the rigidity of the molecular skeleton ("corset effect"), the backward reaction **4**(**6**) → **1** is apparently efficient, and product formation occurs via the kinetically and thermodynamically less favorable reaction channel **1** → **3** → **5**, from which the diene **5** can be removed by fragmentation. Consecutive [4 + 2] cycloreversions presumably lead to formation of the known $C_{10}H_{10}$ triene **10**,[10] which is transformed, probably via azulene **11**, to **12**. In control experiments at 650 °C (under the

[*] Prof. Dr. H. Prinzbach, Dr. W.-D. Fessner, Dr. Bulusu A. R. C. Murty
Chemisches Laboratorium der Universität,
Institut für Organische Chemie und Biochemie
Albertstrasse 21, D-7800 Freiburg (FRG)

[**] This work was supported by the Deutsche Forschungsgemeinschaft, the Fonds der Chemischen Industrie, and BASF AG. *B. A. R. C. M.* thanks the Alexander von Humboldt Foundation for a fellowship. We thank Dr. *H.-D. Beckhaus* for providing us with the MM2 force-field program parametrized for radicals.

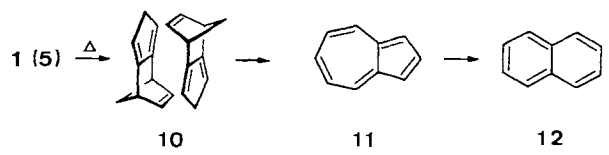

same conditions, the conversion of **1** was ca. 60%), **12** was formed nearly quantitatively from both **10** and **11**.

The cleavage of one of the two a bonds in **1** could be achieved, however, by hydrogenolysis. Heating of a 4% mixture of **1** on Pd/C (10%) in an autoclave under H_2 (10 atm H_2, 300°C, 14 h) resulted in nearly quantitative formation (95% isolated yield) of the high-melting (m.p. = 330 ± 5°C), C_{2v}-symmetric $C_{20}H_{22}$ decacycle **13a** (decacyclo[9.9.0.0^{1,8}.0^{2,15}.0^{3,7}.0^{5,12}.0^{6,10}.0^{11,18}.0^{13,17}.0^{16,20}]eicosane), the formal trapping product of the diradical **4**[11] (Scheme 4). Characteristic of the skeletal changes connected with the opening **1** → **13a** is, among other things, the increase in the vicinal H,H coupling constants in the ^{1}H-NMR spectrum (with decreasing torsional angle; **1**, H-C3-C7-H = 41.8°; **13a**, H-C2-C3-H = 27.8°, H-C3-C7-H = 20.9°; **2**, H-C-C-H = 0°). The low-field position of the 2(12) H signal (δ = 2.39, $CDCl_3$) reflects the trend, which culminates in δ = 3.38 for the perfect eclipsed orientation of the vicinal C–H bonds in **2**. The X-ray structure analysis of **13a**, also carried out as a control of the MM2 data, failed (as also was the case for the dibromide **13d**; cf., however, **13e**[12]) on account of crystallographic disorder. A structure simulating that of the diene **6** was obtained with oversized ellipsoids of thermal vibration for the "unsaturated" C atoms.[13] In agreement with the results of the force-field calculations, **13a** is remarkably stable. Even under drastic hydrogenolysis conditions, selective C–C bond cleavage, in particular of C1–C11 to give the saturated D_{2h} bissecododecahedrane,[4] could not be achieved. Drastic dehydrogenation conditions, moreover, did not result in (considerably endothermic) C–C bond formation between C4 and C14 to give the "isododecahedrane" **14** (cf. **VI** → **VII**, pathway C, Scheme 1), which it was hoped would occur because of the spatial proximity of the 4*syn*/14*syn* hydrogen atoms and the 4/14 carbon atoms (d = 1.926 and 3.1 Å, respectively) (Scheme 4).

2σ → 2π cleavages have been achieved in highly strained cyclobutane compounds under metal catalysis. That **1** remains unchanged up to 200°C in the presence of $AgClO_4$ and $[Rh_2(CO)_4Cl_2]$ is possibly explained by the weakly exothermic course of the opening **1** → **6** ($\Delta\Delta H_f^\circ = -2.4$ kcal/mol) and the steric shielding of the cyclobutane C–C bonds. In such situations, the symmetry-allowed cleavage via radical cations presents itself as a possibility.[14] Compound **1** reacted slowly with tris(*p*-bromophenyl)ammoniumyl hexachloroantimonate (ionization at 1.05 V versus the saturated calomel electrode) in chloroform at 20°C. A single product was obtained (only) if an equimolar amount of the radical cation salt was used; however, this product is not the diene **6** but the dichloride **13b** (Scheme 4). Heating of a $CHCl_3$ solution of **13b** in the presence of water or methanol results in formation of solely the crystalline diol **13c** (m.p. = 193°C, 86%) or the dimethoxy compound **13e**,[12] respectively. Compound **13b** is presumably formed via the (opened) radical cation of **1**,[15] which was detected by ESR spectroscopy and by electrochemical methods.

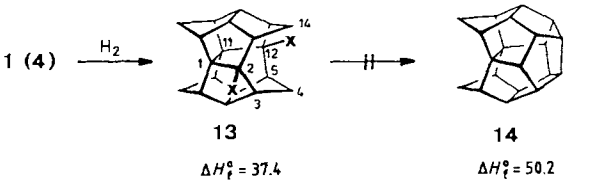

a, X = H; **b**, X = Cl; **c**, X = OH; **d**, X = Br; **e**, X = OCH_3

Scheme 4. ΔH_f° and E_{str} in kcal/mol.

Received: January 19, 1987 [Z 2052 IE]
German version: *Angew. Chem. 99* (1987) 482

[1] W.-D. Fessner, H. Prinzbach, G. Rihs, *Tetrahedron Lett. 24* (1983) 5857; W.-D. Fessner, *Dissertation*, Universität Freiburg 1986; W.-D. Fessner, P. R. Spurr, H. Prinzbach, *J. Am. Chem. Soc.*, in press.
[2] H. Prinzbach, W.-D. Fessner, *Pure Appl. Chem.*, in press.
[3] W.-D. Fessner, Bulusu A. R. C. Murty, J. Wörth, D. Hunkler, H. Fritz, H. Prinzbach, W. D. Roth, P. von R. Schleyer, A. B. McEwen, W. F. Maier, *Angew. Chem. 99* (1987) 484; *Angew. Chem. Int. Ed. Engl. 26* (1987) 452.
[4] P. R. Spurr, Bulusu A. R. C. Murty, W.-D. Fessner, H. Fritz, H. Prinzbach, *Angew. Chem. 99* (1987) 486; *Angew. Chem. Int. Ed. Engl. 26* (1987) 455.
[5] R. J. Ternansky, D. W. Balogh, L. A. Paquette, *J. Am. Chem. Soc. 104* (1982) 4503.
[6] N. L. Allinger, *J. Am. Chem. Soc. 99* (1977) 8127; E. Osawa, H. Musso, *Angew. Chem. 95* (1983) 1; *Angew. Chem. Int. Ed. Engl. 22* (1983) 1; A. Peyman, E. Hickl, H.-D. Beckhaus, *Chem. Ber.*, in press.
[7] Cf. E. M. Engler, J. D. Andose, P. von R. Schleyer, *J. Am. Chem. Soc. 95* (1973) 8005; J. Gasteiger, O. Dammer, *Tetrahedron 34* (1978) 2939; R. L. Disch, J. M. Schulman, M. L. Sabio, *J. Am. Chem. Soc. 107* (1985) 1904.
[8] T. Fukunaga, R. A. Clement, *J. Org. Chem. 42* (1977) 270.
[9] Bulusu A. R. C. Murty, P. R. Spurr, R. Pinkos, C. Grund, W.-D. Fessner, D. Hunkler, H. Fritz, W. R. Roth, H. Prinzbach, *Chimia 41* (1987) 32.
[10] K. Alder, F. H. Flock, P. Janssen, *Chem. Ber. 89* (1956) 2689; M. C. Böhm, R. V. C. Carr, R. Gleiter, L. A. Paquette, *J. Am. Chem. Soc. 102* (1980) 7218.
[11] All new compounds were characterized by their spectra (^{1}H-, ^{13}C-NMR, IR, MS) and elemental analyses.
[12] G. K. S. Prakash, V. V. Krishnamurthy, R. Herges, R. Bau, H. Yuan, G. A. Olah, W.-D. Fessner, H. Prinzbach, *J. Am. Chem. Soc. 108* (1986) 836.
[13] We thank *G. Rihs*, Ciba-Geigy AG, Basel, for the measurements.
[14] O. Hammerich, V. D. Parker, *Adv., Phys. Org. Chem. 20* (1984) 55, p. 115ff.
[15] H. Prinzbach, Bulusu A. R. C. Murty, W.-D. Fessner, J. Mortensen, J. Heinze, G. Gescheidt, F. Gerson, *Angew. Chem. 99* (1987) 488; *Angew. Chem. Int. Ed. Engl. 26* (1987) 457.

Dodecahedranes from [1.1.1.1]Pagodanes**

By *Wolf-Dieter Fessner, Bulusu A. R. C. Murty, Jürgen Wörth, Dieter Hunkler, Hans Fritz, Horst Prinzbach,* Wolfgang D. Roth, Paul von Ragué Schleyer,* Alan B. McEwen*, and *Wilhelm F. Maier**

For the conversion of [1.1.1.1]pagodane **3** into dodecahedrane **4**,[1,2] the catalytic, thermodynamically controlled

[*] Prof. Dr. H. Prinzbach, Dr. W.-D. Fessner, Dr. Bulusu A. R. C. Murty, Dr. J. Wörth, Dr. D. Hunkler, Prof. Dr. H. Fritz
Chemisches Laboratorium der Universität
Institut für Organische Chemie und Biochemie
Albertstrasse 21, D-7800 Freiburg (FRG)
Prof. Dr. P. von R. Schleyer, Dr. W. D. Roth
Institut für Organische Chemie der Universität Erlangen-Nürnberg
Henkestrasse 42, D-8520 Erlangen (FRG)
Prof. Dr. W. F. Maier, Dr. A. B. McEwen
Department of Chemistry, University of California
Berkeley, CA 94720 (USA)

[**] This work was supported by the Deutsche Forschungsgemeinschaft, the Fonds der Chemischen Industrie, the National Science Foundation (grant CHE 940093), BASF AG, and ARRADCOM, Dover, N. J. (USA). *B. A. R. C. M.* thanks the Alexander von Humboldt Foundation for a fellowship.

route A (see preceding communication[3]) seemed promising because a considerable reduction in energy should result.[3] With increasing spherical geometry, however, complications might result from the increasing difficulty in forming carbocationic[4] intermediates and the hyperstability and transannular reactivity of olefinic intermediates.[5]

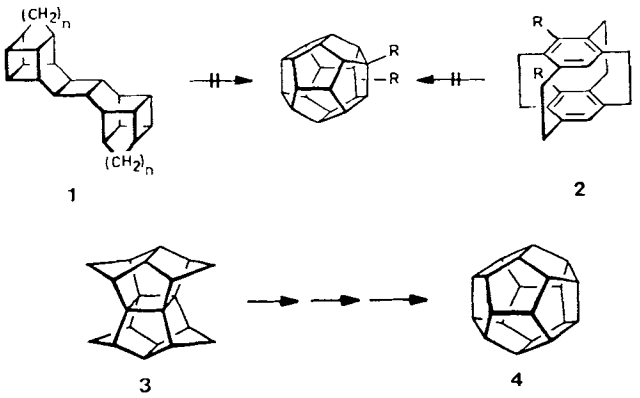

Encouraged by the preparation of adamantane and other cage hydrocarbons by isomerization,[6] there have been earlier attempts to obtain dodecahedrane **4** and its methylated derivatives from precursors like the basketene dimer **1** (n = 1) or homobasketene dimer **1** (n = 2)[7] or from cyclophanes like **2**.[8] However, no success was achieved under various isomerization conditions. Attempted acid-catalyzed isomerizations of **3** also failed. Treatment with CF_3SO_3H (CH_2Cl_2) led to rapid decomposition; this also occurred, but more slowly, with H_2SO_4.[9] Under *Olah*'s stable ion conditions (e.g., FSO_3H/SbF_5, SO_2ClF, −78°C), **3** was oxidized to a dication.[10] With diverse AlX_3 Lewis acids, **3** was converted slowly into undefined products.

In initial gas-phase isomerization experiments (flow apparatus;[11] $Pt/Re/Al_2O_3$, Pd/C, Rh/C, Pd/Al_2O_3 supported catalysts; 250–450°C), complicated mixtures of products (70–95%) were isolated and analyzed by GC/MS. Eventually after enrichment through crystallization, six main components could be separated in the following order by gas chromatography:[12] 4–12% $C_{20}H_{22}$ (unsymmetrical, 4 CH_2, 14 CH, 2 C); 19–47% $C_{20}H_{22}$ (**5**); 4–25% $C_{20}H_{24}$, (6 CH_2, 12 CH, 2 C(?)); 0.2–8% $C_{20}H_{24}$ (C_s, 6 CH_2, 12 CH, 2 C (?)), 1–5% $C_{20}H_{26}$ (unsymmetrical, 1 CH_3, 11 CH, 6 CH_2, 2 C), and 0.1–2.5% $C_{20}H_{20}$. This last product proved to be dodecahedrane **4**! Of the catalysts optimized for the conversion of cyclooctane to bicyclo[3.3.0]octane, Pd, Rh, and Ni on various supports, as well as modified Pd–Ti[13] and Pt–Ti catalysts, gave only very modest results, whereas Pt/Al_2O_3 brought about nearly quantitative conversion. By variation of the dispersion (D) of the platinum (Pt foil (0% D), 25% Pt/Al_2O_3 (2.7% D), 5% Pt/SiO_2 (40% D), 0.1% Pt/Al_2O_3 (80% D)), the reaction temperature, the flow rate, and the composition of the carrier gas (hydrogen–helium mixtures), the yield of **4** could be increased to 8% (0.1% Pt/Al_2O_3, reduced with H_2 at 360° for 1 h; reaction conditions: 315°C, H_2 flow rate 0.75 mL/min, He flow rate 2.25 mL/min, substrate temperature 250°C). Because of its long gas-chromatographic retention time and the remarkably downfield ^{1}H-NMR signal ($\delta = 3.38$, $CDCl_3$), dodecahedrane **4** can readily be identified even in mixtures. The ^{1}H-/^{13}C-NMR analysis of the other main components leads to the conclusion that the expected symmetrical [4]peristylanes **7/8**, which might have resulted from the hydrogenolysis of the longest C–C bond in **3**, or the secododecahedranes **9/10** were not formed. For the $C_{20}H_{24}$ compound with C_s symmetry, structure **6** seems likely, which could be helpful in the evaluation of route C.[3] Numerous experiments in condensed phases (treatment with Pd/C, 70 h, 300°C, ca. 1 atm H_2) only lead to 1–2% of **4** from **3**. Control reactions with the main product **5** gave a similarly complex product mixture, but no **4** could be detected in the gas-phase experiments and only 1–2% under solution conditions.

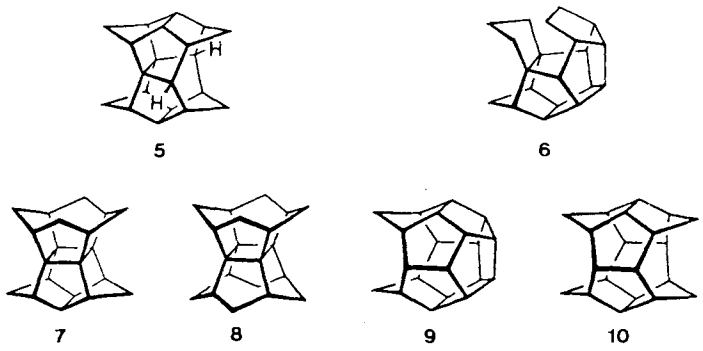

Schemes 1 and 2 summarize the first preliminary results from the B route.[3] The desired saturated bissecododecahedranes,[5] which could not be obtained through hydrogenation of the bisseco-dienes, became available by hydrogenolytic cleavage of appropriate cyclopropa derivatives, **11** (m.p. = 295–300°C) and **16** (m.p. > 340°C). These could be prepared by conventional reduction (Na/*t*BuOH, tetrahydrofuran (THF); 95–100°C) from their dichlorocyclopropa precursors.[5] Heating (150°C) a mixture of **11** with a tenfold quantity of Pd/C (10%) under 50 atm hydrogen pressure leads to complete conversion after 90 minutes. A mixture of 70–75% **12** and 5–10% each of **14** and **15** could be isolated and separated by gas chromatography (along with numerous minor components). Longer reaction times lead to the formation of more **14/15** at the ex-

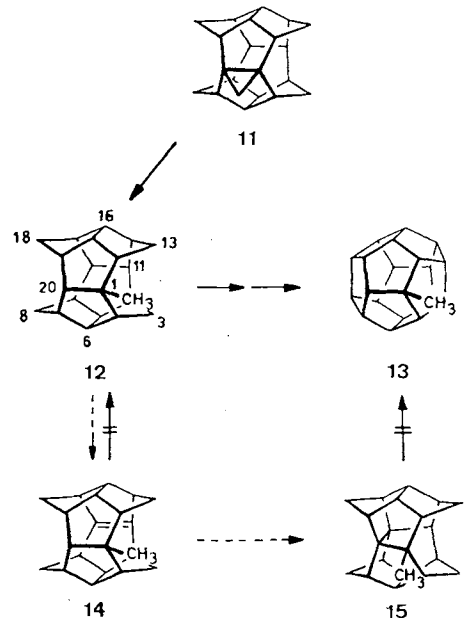

Scheme 1.

pense of **12**. Apparently, the dehydrogenation of **12** to give the "hyperstable" bisseco-olefin **14**, which isomerizes to **15**, is efficient even under hydrogenation conditions. Under similar conditions (20 mg **16**, 2 g Pd/C (10%), 150 °C, 20 atm H_2, total conversion in 6 h), **16** gives a 2:3 mixture (>90%) of the 1,10- and 1,11-dimethylbissecododecahedranes (C_{2h} and C_{2v} symmetry) **17** and **18**, respectively.

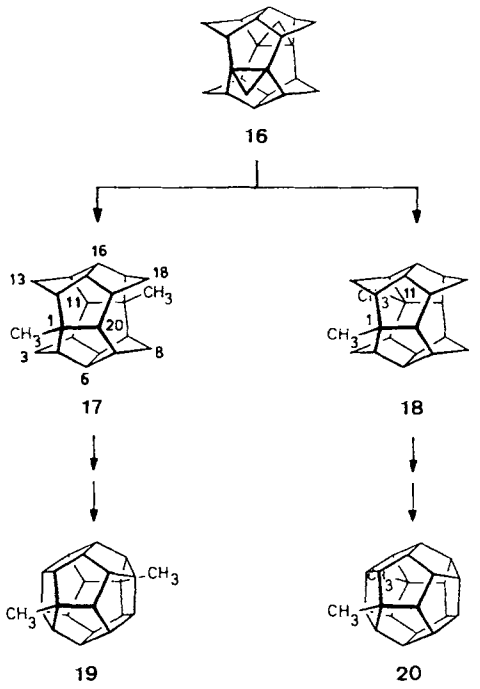

Scheme 2.

After careful drying and degassing, 40 mg of **11** and 4 g of Pd/C (ca. 1:10) were heated slowly (30 min) to 100 °C under 50 atm H_2 pressure and maintained at this temperature for ca. 2.5 h. The reaction mixture was cooled, the H_2 pressure was reduced to 5 atm, and the reaction mixture was then heated slowly to 250 °C and maintained for 5 h (3 h) at this temperature. After thorough extraction, an 80% isolated yield of a product mixture containing six components was obtained (GC/MS): $m/z = 276$ (21 (20)%), $m/z = 278$ (5 (3)%), $m/z = 278$ (9 (8)%), $m/z = 280$ (3 (0)%), $m/z = 274$ (31 (30)%), and $m/z = 260$ (9 (10)%). The last two products to be eluted could be obtained nearly pure by fractional sublimation (80 °C, 1 torr). Complete ^1H-/^{13}C-NMR data[14] permitted their definite identification as the dodecahedranes **4** and **13**.[15] Heating 40 mg of **16** with 4 g of Pd/C (10%) first under 20 atm H_2 pressure at 150 °C (5 h), then under 5 atm H_2 pressure at 300 °C (6 h) gave, after extraction and filtration over silica gel, 30–34 mg (75–85%) of a mixture with the following main components: $m/z = 276$ (29%), $m/z = 290$ (28%), $m/z = 288$ (29%), $m/z = 274$ (1%), and $m/z = 288$ (1%). Comparison of the spectra showed the first component to be **15**, the third and fifth to be the known dimethyldodecahedranes **19** and **20**,[13] and the fourth to be **13**. Under various conditions, **20** was formed in much lower yields than **19**. This suggests that dealkylation[13,16] (e.g., to **14** and **15**) is relatively rapid on the route from **18** to **20**.

The maximal 8% yield of dodecahedrane **4** in the gas-phase isomerization of **3** constitutes a remarkable improvement of the present situation in view of the availability of **3**. The limitation in the formation of **4** from **3** can be attributed to the irreversible formation of **5**, which effectively diverts the reaction from the desired course. By substitution of the presumed bisseco intermediates **2/3** (as described in the following communication[5]) in positions C-1,10,11,20, this competition, which is caused by transannular bond formation, can be hindered or precluded. The formation of ca. 25% of **13** (along with 8% of **4**) and ca. 25% of **19** (along with a little **4** and **20**) supports this assumption.

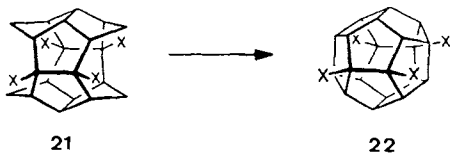

It is hoped that various saturated bisseco precursors **21** (X = OR, NHR, CO_2R, etc.), with modified catalysts and under milder conditions, will be dehydrogenated without loss of functional groups, to give **22**. Alternatively, C–C bond formation in the bisseco precursors might be achieved, e.g., via carbenoid intermediates or photochemical processes or by functionalization of all four methylene positions in the pagodane skeleton.

Received: January 19, 1987 [Z 2053 IE]
German version: *Angew. Chem. 99* (1987) 484

[1] J. C. Gallucci, C. W. Doecke, L. A. Paquette, *J. Am. Chem. Soc. 108* (1986) 1343, and references cited therein.
[2] P. E. Eaton, *Tetrahedron 35* (1979) 2189; E. Carceller, M. L. Garcia, A. Moyano, M. A. Pericas, F. Serratosa, *Tetrahedron 42* (1986) 1831, and references cited therein.
[3] W.-D. Fessner, Bulusu A. R. C. Murty, H. Prinzbach, *Angew. Chem. 99* (1987) 482; *Angew. Chem. Int. Ed. Engl. 26* (1987) 451.
[4] L. A. Paquette, D. W. Balogh, R. Usha, D. Kountz, G. G. Christoph, *Science 211* (1981) 575; L. A. Paquette, D. W. Balogh, *J. Am. Chem. Soc. 104* (1982) 774.
[5] P. R. Spurr, Bulusu A. R. C. Murty, W.-D. Fessner, H. Fritz, H. Prinzbach, *Angew. Chem. 99* (1987) 486; *Angew. Chem. Int. Ed. Engl. 26* (1987) 455.
[6] P. von R. Schleyer, *J. Am. Chem. Soc. 79* (1957) 3292; review: S. A. Godleski, P. von R. Schleyer, E. Osawa, W. T. Wipke, *Prog. Phys. Org. Chem. 13* (1981) 63.
[7] N. J. Jones, W. D. Deadman, E. LeGoff, *Tetrahedron Lett. 1973*, 2087; J. L. Fry, P. von R. Schleyer, unpublished results (Princeton University 1972/1973); P. Grubmüller, *Dissertation*, Universität Erlangen-Nürnberg 1979.
[8] K. Lammertsma, C. Brosz, I. Thies, J. Vieth, unpublished results (Universität Erlangen-Nürnberg 1978–1983).
[9] W.-D. Fessner, *Dissertation*, Universität Freiburg 1986.
[10] G. K. S. Prakash, V. V. Krishnamurthy, R. Herges, R. Bau, H. Yuan, G. A. Olah, W.-D. Fessner, H. Prinzbach, *J. Am. Chem. Soc. 108* (1986) 836; H. Prinzbach, Bulusu A. R. C. Murty, W.-D. Fessner, J. Mortensen, J. Heinze, G. Gescheidt, F. Gerson, *Angew. Chem. 99* (1987) 488; *Angew. Chem. Int. Ed. Engl. 26* (1987) 457.
[11] W. D. Roth, *Dissertation*, Universität Erlangen-Nürnberg 1984.
[12] The new compounds were characterized by their spectra (^1H-, ^{13}C-NMR, IR, MS) and elemental analyses.
[13] L. A. Paquette, Y. Miyahara, C. W. Doecke, *J. Am. Chem. Soc. 108* (1986) 1716.
[14] For example, **13**: ^1H-NMR (400 MHz, $CDCl_3$): $\delta = 3.43$ (3H), 3.35 (13H), 2.91 (3H), 1.13 (CH_3); ^{13}C-NMR ($CDCl_3$): $\delta = 75.6$ (1C), 74.7 (3C), 67.2, 67.1 (7C), 66.8 (6C), 66.4 (3C), 32.6 (CH_3).
[15] L. A. Paquette, R. J. Ternansky, D. W. Balogh, W. J. Taylor, *J. Am. Chem. Soc. 105* (1983) 5441.
[16] P. Grubmüller, W. F. Maier, P. von R. Schleyer, M. A. McKervey, J. J. Rooney, *Chem. Ber. 113* (1980) 1989.

Bissecododecahedraenes, Unusual Hyperstable Olefins**

By *Paul R. Spurr, Bulusu A. R. C. Murty, Wolf-Dieter Fessner, Hans Fritz*, and *Horst Prinzbach**

As an alternative to the catalytic procedure,[1] directed multistep pagodane→dodecahedrane transformations (routes A and/or B/C in Ref. [2]) are a current goal: for example, via the intermediates **2**–**5** (Fig. 1) in the case of the basic skeletons **1**/**6**. At intermediate **5**, this route converges with *Paquette*'s dodecahedrane synthesis, which was recently considerably improved for step **5**→**6**, which involves dehydrogenation and simultaneous C–C bond formation.[3] The calculated (MM2)[4] molecular structures (Fig. 1) clearly reveal how, with increasing expansion of the "waist" of **1** (1.55 Å) to 3.49 Å in **4**, the distance between the opposing methylene C atoms (which are eventually to undergo direct C–C bond formation) and their *syn* hydrogen atoms becomes increasingly small. The enthalpies of formation, ΔH_f°, decrease continuously on going from **1** to the "stabilomer"[5] **6**, while the strain energies, E_{str}, decrease discontinuously (Fig. 1). The increase of E_{str} in going from **2** via **3** to **4**, which is primarily a consequence of the increasing transannular and vicinal H/H interactions, necessarily implies considerably reduced "olefinic strain (*OS*)"[4,5] for **2**/**3** (*OS* = −11.4/−13.9 kcal/mol). The diene **2** is of further structural interest because the C=C bonds, held in an overall very rigid molecular skeleton, have an unusually small transannular distance, with ideal colinear orientation of the π orbitals;[6] the calculated value of 2.62 Å, however, is probably at least 0.1 Å too small.[7] The (transannular) strain inherent in **2** and **3** is manifested in a pyramidalization of the olefinic centers by about 10° and 5°, respectively. Comparable energetic and structural relationships were calculated for the reaction sequence starting from the diketone **7** and proceeding via the intermediates **10**–**12**.

After initial model studies,[8] a preparatively efficient entry into the reaction sequence **1**→**6** was made possible by the finding that [1.1.1.1]pagodane **1** reacts with bromine (in very large excess) regiospecifically and quantitatively to give the crystalline, moisture-sensitive dibromide **8** (m.p. = 240–241 °C (dec.)); the reaction occurs thermally within days and upon irradiation (300-W Osram Vitalux lamp, pyrex filter) within minutes. Under standard conditions (Zn, dimethylformamide, 160 °C, 3 h), **8** is converted in high yield (89%) into the crystalline bissecododecahedradiene **2** (m.p. = 260 °C (dec.)), which, especially in solution, is sensitive toward oxidation. Analogously, the pagodanedione **7** is transformed, via the dibromide **9** (m.p. = 294–295 °C (dec.), 100%), into the dienedione **10** (m.p. = 322–323 °C, 85%).[9] Heating or irradiation of the dibromides **8**/**9** results in loss of bromine with re-formation of **1**/**7**; this finding explains why a large excess of reagent is necessary in their preparation.

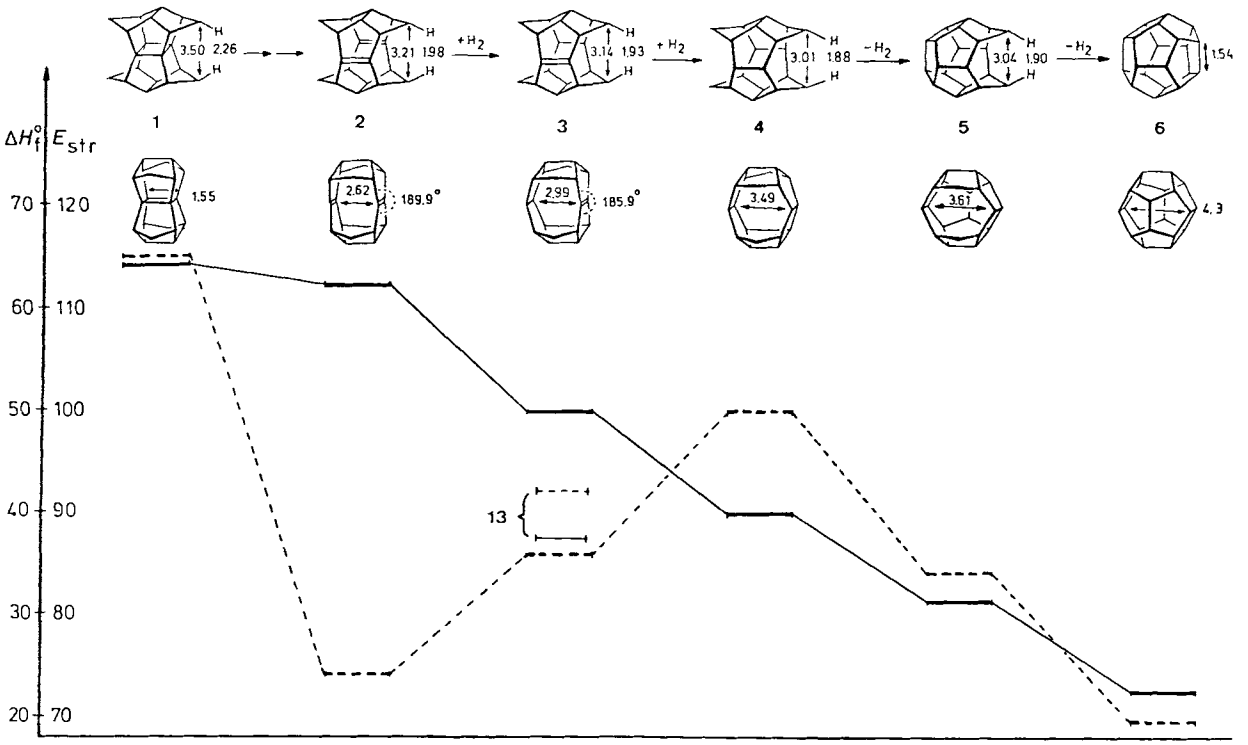

Fig. 1. Enthalpies of formation, ΔH_f° (——), and strain energies, E_{str} (----), of **1**–**6** in kcal/mol. Distances [Å].

[*] Prof. Dr. H. Prinzbach, Dr. P. R. Spurr, Dr. Bulusu A. R. C. Murty, Dr. W.-D. Fessner, Prof. Dr. H. Fritz
Chemisches Laboratorium der Universität,
Institut für Organische Chemie und Biochemie
Albertstrasse 21, D-7800 Freiburg (FRG)

[**] This work was supported by the Deutsche Forschungsgemeinschaft, the Fonds der Chemischen Industrie, and BASF AG. *P. R. S.* and *B. A. R. C. M.* thank the Alexander von Humboldt Foundation for a fellowship.

The unique orientation of the C–C double-bond π orbitals in the bissecododecahedradiene skeleton of **2** and **10** gives rise, according to PE spectroscopic analysis, to an unusually strong through-space π,π homoconjugation (ca. 2 eV),[10] which is presumably also responsible for the relatively long-wavelength UV absorption of **2** (isooctane, $\lambda = 270$ (sh, 180)), 250 nm (sh, $\varepsilon = 450$) and **10** (CH_3CN, $\lambda = 320$ nm (sh, $\varepsilon = 115$), 280 (sh, 170), 250 (190)). Acetone-

sensitized excitation of **2** and **10** results in rapid cycloaddition to give **1** and **7**, respectively.[11] Bromine adds regiospecifically to give **8** and **9**.

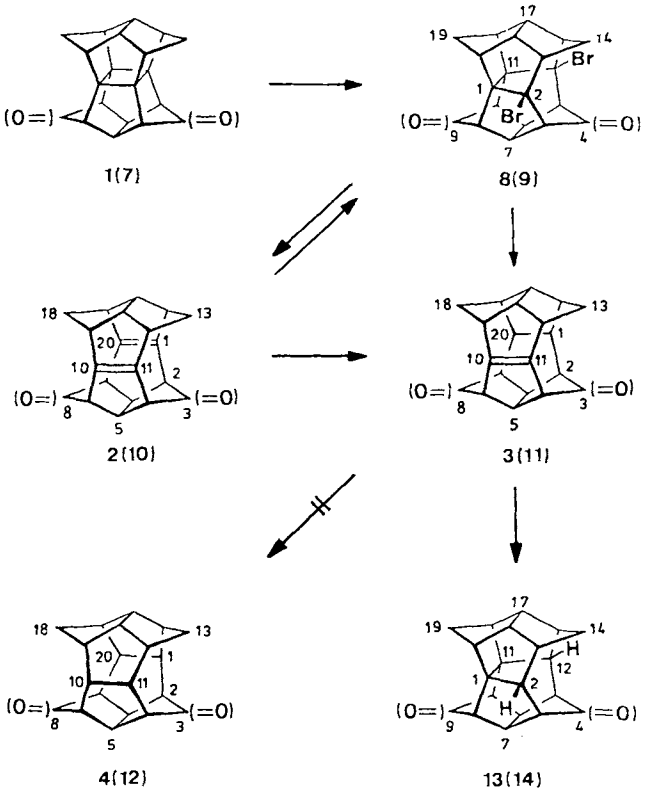

The predicted hyperstability of **2** and **3** has adverse consequences for our approach. Reaction of the dienes **2** and **10** with diimine, which has proved useful for the reduction of highly substituted olefins, only results in hydrogenation to the monoenes **3** and **11**, respectively; not even trace amounts (< 1%), even under forced conditions, of the tetrahydro derivatives can be detected. The greater reactivity of the dienes **2/10** compared with the enes **3/11** presumably reflects a partial compensation of the hyperstability by the destabilizing transannular π/π repulsion. Diverse noble metal catalysts (Pd, Pt, Rh) were also unable to effect the hydrogenations **3**→**4** and **11**→**12**; under the drastic conditions that are already necessary for steric reasons, varying amounts of **1** and **13**, in addition to **3**, are formed from **2**. Compounds **13** and **14**, respectively, are formed in nearly quantitative yields upon short heating of the enes **3** and **11** to 300 °C, which demonstrates the efficient transannular stabilization of the intermediate homoallyl radical (or cation) and an efficient competition with the catalytic route.[11]

As observed in similar cases, the hyperstability of the enes **3/11** can be overcome by the use of reagents having greater "driving force." They are oxidized quantitatively to the epoxides **15a/16a** with *m*-chloroperbenzoic acid ($CHCl_3$, NaOAc, 20 °C); under these conditions, the dienes **2/10** are oxidized to the epoxides **19a/20a** and the diepoxides **21a/22a**.[12] Under phase-transfer conditions, dichlorocarbene also adds to **3/11** (to give **15b/16b**) and to **2/10** (to give **19b/20b** and **21b/22b**). In these reactions, the second addition is usually so much slower that it is possible to obtain **19a,b** and **20a,b**, respectively, thereby allowing further functionalization of the molecular skeleton by reactions at the remaining C=C bond. For **15b/16b**, the quantitative C–H insertion of chlorocarbene (to give **17b/18b**), obtained with an excess of reagent, is so slow that **15b/16b** can be selectively prepared.

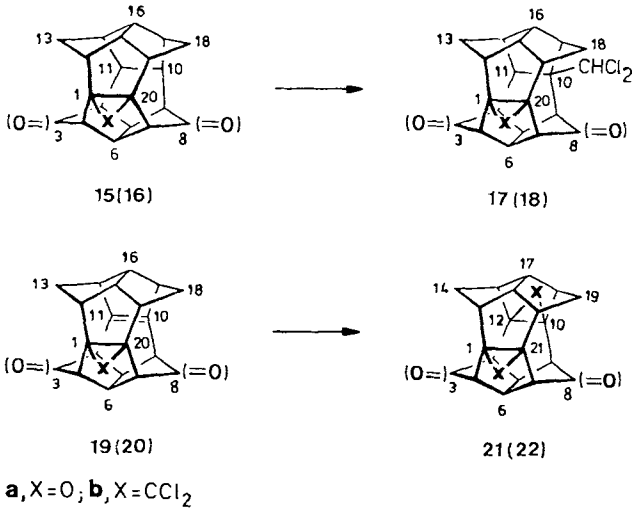

Received: January 19, 1987 [Z 2054 IE]
German version: *Angew. Chem. 99* (1987) 486

[1] W.-D. Fessner, Bulusu A. R. C. Murty, J. Wörth, D. Hunkler, H. Fritz, H. Prinzbach, W. D. Roth, P. von R. Schleyer, A. B. McEwen, W. F. Maier, *Angew. Chem. 99* (1987) 484; *Angew. Chem. Int. Ed. Engl. 26* (1987) 452.

[2] W.-D. Fessner, Bulusu A. R. C. Murty, H. Prinzbach, *Angew. Chem. 99* (1987) 482; *Angew. Chem. Int. Ed. Engl. 26* (1987) 451.

[3] L. A. Paquette, Y. Miyahara, C. W. Doecke, *J. Am. Chem. Soc. 108* (1986) 1716.

[4] W.-D. Fessner, *Dissertation*, Universität Freiburg 1986.

[5] W. F. Maier, P. von R. Schleyer, *J. Am. Chem. Soc. 103* (1981) 1891; A. B. McEwen, P. von R. Schleyer, *ibid. 108* (1986) 3951.

[6] Cf. K. B. Wiberg, M. G. Matturro, P. J. Okarma, M. E. Jason, *J. Am. Chem. Soc. 106* (1984) 2194.

[7] O. Ermer, C.-D. Bödecker, H. Preut, *Angew. Chem. 96* (1984) 57; *Angew. Chem. Int. Ed. Engl. 23* (1984) 55.

[8] G. Sedelmeier, W.-D. Fessner, R. Pinkos, C. Grund, Bulusu A. R. C. Murty, D. Hunkler, G. Rihs, H. Fritz, C. Krüger, H. Prinzbach, *Chem. Ber. 119* (1986) 3442.

[9] The new compounds were characterized by their spectra (^{1}H-NMR, ^{13}C-NMR, IR, MS) and by elemental analyses. For example, **2** (nonacyclo[12.6.0.0^{2,6}.0^{4,11}.0^{5,9}.0^{7,20}.0^{10,17}.0^{12,16}.0^{15,19}]eicosa-1(20),10-diene): ^{1}H-NMR (400 MHz, C_6D_6): δ = 3.22 (bs, 5-, 6-, 15-, 16-H), 3.12 (bs, 2-, 4-, 7-, 9-, 12-, 14-, 17-, 19-H), 2.83 (d, 3 *syn*-, 8 *syn*-, 13 *syn*-, 18 *syn*-H, J(3 *syn*/3 *anti*) = 13 Hz), 1.22 (dm, 3 *anti*-, 8 *anti*-, 13 *anti*-, 18 *anti*-H); ^{13}C-NMR (100.6 MHz, C_6D_6): δ = 155.4 (C-1, -10, -11, -20), 62.1 (C-5, -6, -15, -16), 47.0 (C-2, -4, -7, -9, -12, -14, -17, -19), 32.7 (C-3, -8, -13, -18). MS (EI): m/z = 260 ($M^{\oplus}$, 100%), 245 (5), 217 (5), 194 (8), 179 (8), 165 (6), 153 (5), 129 (6), 115 (10), 91 (5). UV (isooctane): λ_{max} = 250 nm (sh, ε = 460), 270 nm (ε = 180). — **10**: ^{1}H-NMR (400 MHz, $CDCl_3$): δ = 3.65 (m, 5-, 6-H), 3.47 (m, 15-, 16-H), 3.31 (m, 2-, 4-, 7-, 9-H), 3.26 (m, 12-, 14-, 17-, 19-H), 2.32 (d, 13 *syn*-, 18 *syn*-H, J = 14 Hz), 1.39 (dt, 13 *anti*-, 18 *anti*-H, J = 14 and 6 Hz); ^{13}C-NMR (100.6 MHz, $CDCl_3$): δ = 212.8 (C-3, -8), 161.2 (C-1, -10, -11, -20), 63.1 (C-15, -16), 56.2 (C-2, -4, -7, -9), 47.2 (C-5, -6), 45.4 (C-12, -14, -17, -19), 28.8 (C-13, -18). MS (EI, 70 eV): m/z = 288 ($M^{\oplus}$, 100), 232 (60), 167 (13), 166 (49), 165 (25), 115 (16). UV (CH_3CN): λ_{max} = 320 nm (ε = 115), 280 (170), 250 (190).

[10] IE_1^m = 7.12 eV, IE_2^m = 9.03 eV; K. Hassenrück, B. Mayer, H.-D. Martin, private communication.

[11] Bulusu A. R. C. Murty, P. R. Spurr, R. Pinkos, C. Grund, W.-D. Fessner, D. Hunkler, H. Fritz, W.-R. Roth, H. Prinzbach, *Chimia 41* (1987) 32.

[12] Transannular distances of 3.05 Å and 2.98 Å were obtained for C1-C12 and C3-C14, respectively, by X-ray structure analysis of the diepoxydiketone **22a** (*G. Rihs*, Ciba-Geigy, Basel).

One- and Two-Electron Oxidations of Pagodanes and Bissecododecahedradienes: Unusually Persistent Radical Cations**

By *Horst Prinzbach,* Bulusu A. R. C. Murty, Wolf-Dieter Fessner, John Mortensen, Jürgen Heinze,* Georg Gescheidt,* and *Fabian Gerson**

[1.1.1.1]Pagodane **1** (D_{2h}) and the valence-isomeric diene **3** (D_{2h}) undergo oxidation in super acid solution to give the same, novel 2π-aromatic dication **11** (D_{2h}). Its surprising stability is closely connected with its special structure; the dication **12**, generated from [2.2.1.1]pagodane **2**, is significantly less stable.[1] The preparatively important cleavage of the cyclobutane a bonds in **1** is made selectively possible by the use of radical cation salts.[2] Further insight into the course of this process should be provided by cyclovoltammetric and ESR spectroscopic measurements.[3]

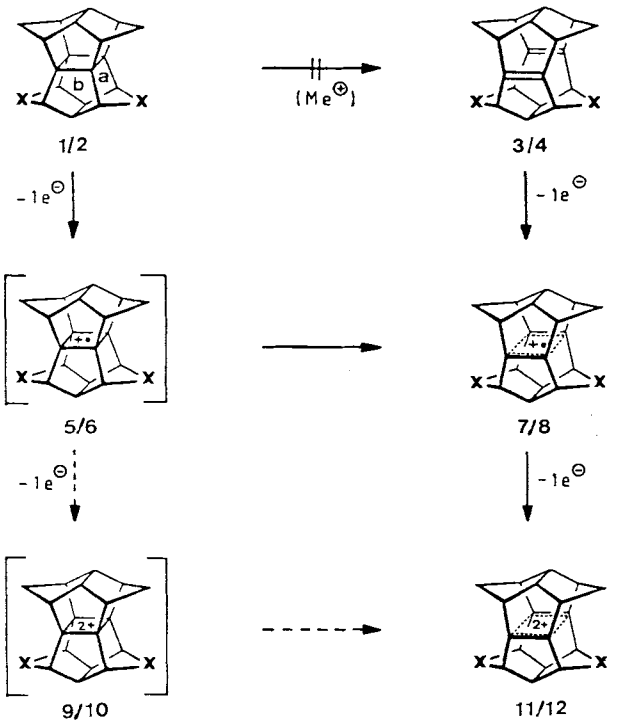

1,3,5,7,9,11, X=CH_2 ; **2,4,6,8,10,12**, X=$(CH_2)_2$

The oxidation of pagodane **1** and the diene **3** was investigated voltammetrically in CH_2Cl_2 and SO_2[4] in the presence of tetra-*n*-butylammonium hexafluorophosphate ($TBAPF_6$) as supporting electrolyte. Because of their low nucleophilicity, both solvents are ideal for the generation of reactive cations.[5] In the case of **1** (Fig. 1a), an irreversible wave is observed at +1.2 V vs. Ag/AgCl in both solvents, which indicates that a rapid chemical reaction (cycloreversion **5**→**7**) occurs following formation of the radical cation. The shape and height of this wave support the assumption that a further charge transfer (**7**→**11**) occurs subsequently to this chemical reaction and is possibly followed by another chemical step. An ECE process is further supported by the observation of a reversible wave at +0.65 V during the reverse scan, which is due to the reduction of the radical cation **7** to **3**. The presumed oxidation to a dication (**11**?) around +1.2 V cannot be confirmed under the experimental conditions owing to rapid reaction with nucleophilic partners (residual H_2O in SO_2; $Cl^\ominus$ in CH_2Cl_2). The diene **3** is reversibly oxidized to **7** in CH_2Cl_2 and SO_2 at +0.66 V vs. Ag/AgCl (Fig. 1b). The radical cation **7** is very stable in SO_2 but undergoes slow subsequent reactions in CH_2Cl_2. The oxidation to **11** occurs at +1.2 V. The dication **11** is appreciably less stable than the radical cation **7**; it reacts with $Cl^\ominus$ in CH_2Cl_2 and with residual H_2O in SO_2 so rapidly to give the known quenching products (cf. **13b,c** in Ref. [1, 2]) that its reduction can no longer be observed by cyclic voltammetry. From measurements with scan rates between 10 and 50 V/s it is possible to estimate a lifetime of ca. 0.05 s.

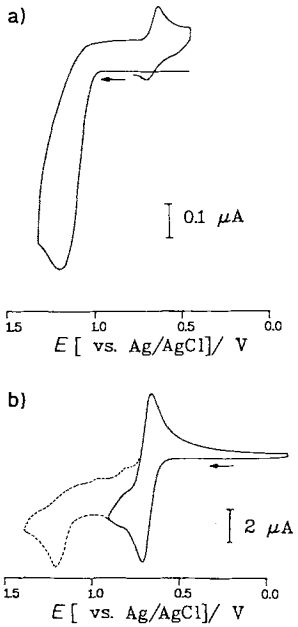

Fig. 1. a) Cyclic voltammogram of **1** (SO_2/0.1 M $TBAPF_6$, −20 °C, v = 100 mV/s); b) cyclic voltammogram of **3** (SO_2/0.1 M $TBAPF_6$, −20 °C, v = 50 mV/s).

For ESR studies, **1** was oxidized in CH_2Cl_2 both electrolytically on a helical Au anode[6] ($TBAClO_4$ as the supporting salt) and chemically with $AlCl_3$ or tris(*p*-bromophenyl)ammoniumyl hexachloroantimonate. The deeply colored radical cation ($\lambda_{max} \approx 610$ nm) thus generated is very persistent, having in vacuo a lifetime of ca. ten and two days at −70 and +20 °C, respectively. Its temperature-independent ESR spectrum ($g = 2.0031 \pm 0.0001$), shown in Figure 2, extends over 13 mT; the nine groups of lines, each group separated by 1.544 mT, are indicative of a hyperfine interaction with eight equivalent protons. The splittings within the groups arise from three sets of four equivalent protons each, with coupling constants of 0.117, 0.065, and 0.051 mT (±0.001 mT), as well as from a second-order interaction associated with the large coupling

[*] Prof. Dr. H. Prinzbach, Dr. Bulusu A. R. C. Murty, Dr. W.-D. Fessner
Chemisches Laboratorium der Universität,
Institut für Organische Chemie und Biochemie
Albertstrasse 21, D-7800 Freiburg (FRG)
Priv.-Doz. Dr. J. Heinze, Dr. J. Mortensen
Institut für Physikalische Chemie der Universität
Albertstrasse 21, D-7800 Freiburg (FRG)
Prof. Dr. F. Gerson, Dipl.-Chem. G. Gescheidt
Institut für Physikalische Chemie der Universität
Klingelbergstrasse 80, CH-4056 Basel (Switzerland)

[**] This work was supported by the Deutsche Forschungsgemeinschaft, the Fonds der Chemischen Industrie, BASF AG, and the Schweizerischer Nationalfonds zur Förderung der wissenschaftlichen Forschung. *B. A. R. C. M.* thanks the Alexander von Humboldt Foundation for a fellowship.

constant of 1.544 mT. By the use of the general TRIPLE resonance technique,[7] the values of 1.544 and 0.051 mT are found to have the same sign, which is opposite to that of 0.117 and 0.065 mT.

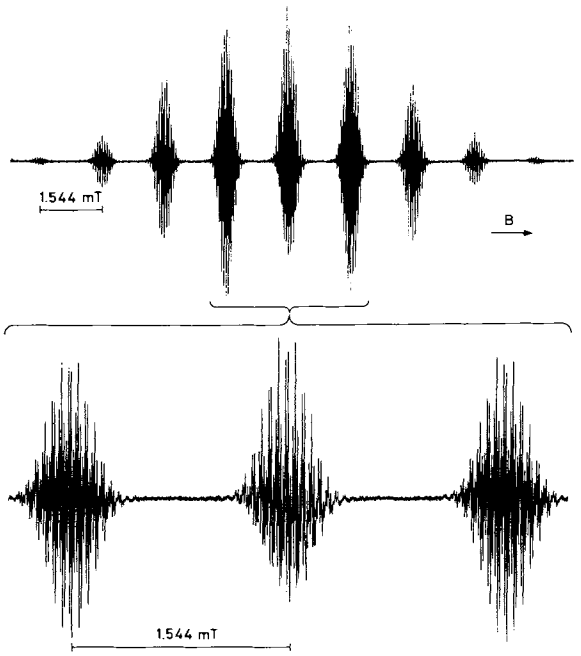

Fig. 2. ESR spectrum of the radical cation **7** generated from **1** or **3** (CH_2Cl_2, $-40°C$). Top: complete spectrum. Bottom: part of the spectrum including the three central groups of lines at an expanded magnetic field scale.

An identical ESR spectrum is observed for the diene **3** subjected to the same treatment; in line with the lower oxidation potential, the appearance voltage in the electrolysis is substantially lower than for **1**. The results of the ESR studies are thus fully consistent with the postulated cycloreversion **5**→**7**, so that the structure of the radical cation should be properly described by formula **7**.

Assignment of the large coupling constant (1.544 mT) to the eight equivalent β protons, i.e., to those that are separated by one C–C bond from the π system of **7**, is straightforward, considering the D_{2h} symmetry. The coupling constants, a_{H^β}, of β protons arise from hyperconjugation and obey the relationship[8] $a_{H^\beta} = \mathbf{B} \cdot \rho^\pi \cdot \cos^2\theta$, where ρ^π is the spin population at the adjacent π center and θ stands for the dihedral angle between the $2p_z$ axis at this center and the C–H^β bond. Since the total π-spin population in **7** is evenly distributed among the four π centers, ρ^π amounts to 0.25. Taking +6 mT as the proportionality factor B appropriate for radical cations and setting $\theta \approx 10°$ on the basis of structural data for **3**,[9] one obtains $a_{H^\beta} = +1.5$ mT. According to the evidence from TRIPLE, the positive sign thus predicted for 1.544 mT also holds for 0.051 mT, whence 0.117 and 0.065 mT must be negative. Assignments of the three last-mentioned coupling constants to the three sets of four equivalent γ protons in specific positions of **7** are hardly feasible without further information.

The colored radical cation ($\lambda_{max} \approx 610$ nm) generated under similar conditions from [2.2.1.1]pagodane **2** is also rather persistent; however, it decays faster than **7**. By analogy to **7**, its structure should be described by formula **8**. The ESR spectrum ($g = 2.0040 \pm 0.0001$) reflects the lower C_{2v} symmetry of **8** by exhibiting two large coupling constants, 1.76 ± 0.01 and 0.96 ± 0.01 mT, each due to a set of four equivalent β protons. The hyperfine splittings of the sixteen γ protons belonging to six different sets are not resolved in the ESR spectrum; they do not exceed 0.1 mT, as indicated by the ENDOR spectrum.[10]

The persistence of the radical cations **7/8** is closely connected with their polycyclic skeletons. Under a variety of oxidation conditions, it was not possible, by ESR spectroscopy, to detect radical cations generated from the "molecular moieties" of **1/3** (**8/9** in Ref. [2]). The opening of the four-membered ring, which occurs upon formation of the dications **11/12** from the pagodanes **1/2**, presumably also occurs in **5/6** (ECE) but not in **9/10** (EEC). Owing to the small exothermicity of the opening **1**→**3** ($\Delta\Delta H_f^\circ = -2.4$ kcal/mol),[11] and presumably also of **5**→**7**, and owing to the rigidity of the [1.1.1.1]pagodane **1**, there is a good chance that **5** might be identified directly at low temperature[12] and that **5** and **7** as well as **9** and **11** might be differentiated in the gas-phase oxidation ("charge stripping").[13]

Received: January 19, 1987 [Z 2055 IE]
German version: *Angew. Chem. 99* (1987) 488

[1] G. K. S. Prakash, V. V. Krishnamurthy, R. Herges, R. Bau, H. Yuan, G. A. Olah, W.-D. Fessner, H. Prinzbach, *J. Am. Chem. Soc. 108* (1986) 836.
[2] W.-D. Fessner, Bulusu A. R. C. Murty, H. Prinzbach, *Angew. Chem. 99* (1987) 482; *Angew. Chem. Int. Ed. Engl. 26* (1987) 451.
[3] The He(Iα) PE spectrum of **1** (recording temperature ca. 100°C) exhibits an initial, broad band with a maximum at $I_v^v \approx 8.2$ to 8.3 eV, followed by a band system with little structure. The point at which the first band emerges above the noise level is at 7.7 to 7.8 eV, which allows an upper limit for the adiabatic ionization energy I_v^a to be determined (E. Heilbronner, J. Lecoultre, private communication).
[4] J. Heinze, *Angew. Chem. 96* (1984) 823; *Angew. Chem. Int. Ed. Engl. 23* (1984) 831.
[5] M. Dietrich, J. Mortensen, J. Heinze, *Angew. Chem. 97* (1985) 502; *Angew. Chem. Int. Ed. Engl. 24* (1985) 508.
[6] H. Ohya-Nishiguchi, *Bull. Chem. Soc. Jpn. 52* (1979) 2064.
[7] Review: H. Kurreck, B. Kirste, W. Lubitz, *Angew. Chem. 96* (1984) 171; *Angew. Chem. Int. Ed. Engl. 23* (1984) 173.
[8] C. Heller, H. M. McConnell, *J. Chem. Phys. 32* (1960) 1535.
[9] W.-D. Fessner, H. Prinzbach, G. Rihs, *Tetrahedron Lett. 24* (1983) 5857.
[10] According to the relative intensities of the ENDOR signals, an appreciable part of the 16 γ protons must have a coupling constant close to 0.025 mT.
[11] P. R. Spurr, Bulusu A. R. C. Murty, W.-D. Fessner, H. Fritz, H. Prinzbach, *Angew. Chem. 99* (1987) 486; *Angew. Chem. Int. Ed. Engl. 26* (1987) 455.
[12] Cf. E. Haselbach, T. Bally, Z. Lanyiova, P. Baertschi, *Helv. Chim. Acta 62* (1979) 583; H. D. Roth, M. L. M. Schilling, T. Mukai, T. Miyashi, *Tetrahedron Lett. 24* (1983) 5815.
[13] W. Koch, F. Maquin, D. Stahl, H. Schwarz, *Chimia 39* (1985) 376.

Enzyme-Catalyzed Cyanohydrin Synthesis in Organic Solvents

By *Franz Effenberger,* Thomas Ziegler,* and *Siegfried Förster*

Pfeil et al. have described the enantioselective addition of hydrogen cyanide **2** to benzaldehyde and numerous other aldehydes **1** in the presence of the enzyme mandelonitrile lyase ("(*R*)-oxynitrilase") to give optically active (*R*)-cyanohydrins **3**.[1] However, in the aqueous and aqueous alcoholic systems exclusively used so far, the chemical reaction, leading to the formation of racemates, occurs in

[*] Prof. Dr. F. Effenberger, Dr. T. Ziegler, Dr. S. Förster
Institut für Organische Chemie der Universität
Pfaffenwaldring 55, D-7000 Stuttgart 80 (FRG)

addition to the enzyme-catalyzed reaction, so that only moderate optical yields are often obtained in this reaction.[1c]

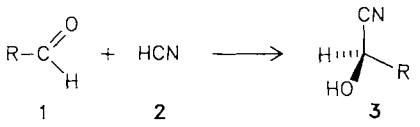

1 2 3

The ready accessibility[2] of mandelonitrile lyase (E.C. 4.1.2.10) from bitter almonds *(Prunus amygdalus)* and the great importance of optically active cyanohydrins for the preparation of optically active amino alcohols,[1c] α-hydroxy carboxylic acids, pyrethroid insecticides,[3a] imidazoles, and heterocycles,[3b] prompted us to investigate this reaction in more detail. Our goal was the preparative synthesis of cyanohydrins having the highest possible enantiomeric purity.

Variation of the reaction conditions (pH value, temperature, concentration) in water/ethanol led to no appreciable improvements.[1] The use of organic solvents that are not miscible with water but in which the enzyme-catalyzed reaction can take place,[4] however, resulted in suppression of the chemical reaction to a significant extent, whereas the enzymatic formation of cyanohydrin was only slightly slower (Fig. 1). The enantiomeric purity of the cyanohydrins is thereby considerably increased.

Of the organic solvents we tested, ethyl acetate proved to be the most suitable; the enantiomeric purity thereby achieved is higher than in H_2O/EtOH. The enzyme can be bound to a fixed support and consequently reisolated and used again. Of the supports tested, ECTEOLA cellulose, DEAE cellulose, glass beads, and cellulose, cellulose proved to be the best.

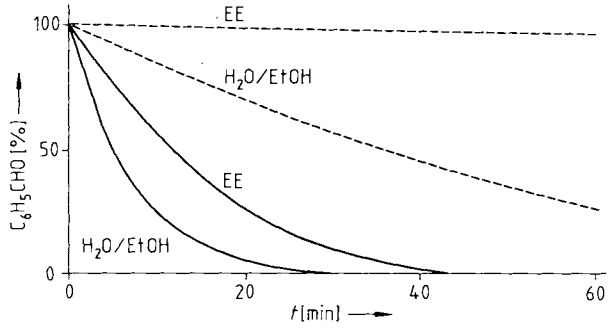

Fig. 1. Rate of the chemical (- - -) and enzymatic additions (——) of HCN to benzaldehyde (initial concentration 5×10^{-3} M) in H_2O/EtOH and in ethyl acetate (EE)/cellulose.

In the earlier investigations,[1] the optical yields were solely determined from the optical rotation of the products obtained. However, because only mandelonitrile was available in pure form, only the reaction of benzaldehyde with hydrogen cyanide allowed a statement to be made about the optical purity of the product; in general, precise statements as to the optical purity of a compound cannot be made from the optical rotation values. Furthermore, cyanohydrins undergo ready isomerization by means of the equilibrium reaction. We therefore converted the cyanohydrins so obtained into diastereomeric esters by reaction with (*R*)-α-methoxy-α-trifluoromethylphenylacetoyl chloride [*R*(+)-MTPA chloride][5] and determined their optical purity by gas chromatography. The results of the enzymatic cyanohydrin syntheses carried out by us, on the one hand, in H_2O/EtOH (according to Ref. [1]) and, on the other hand, in ethyl acetate, are compared in Table 1.

Table 1. Enzymatic formation of cyanohydrins **3** in H_2O/EtOH (see Experimental Procedure A) and in ethyl acetate (EE)/cellulose (see Experimental Procedure B).

Aldehyde **1**	**3** in H_2O/EtOH			**3** in EE/cellulose		
	Reaction time [h]	Yield [%]	*ee* [a] [%]	Reaction time [h]	Yield [%]	*ee* [a] [%]
Benzaldehyde	1	99	86	2.5	95	99
3-Phenoxybenzaldehyde	5	99	10.5	192	99	98
Furfural	2	86	69	4	88	98.5
Nicotinaldehyde	2.5	78	6.7	4.5	89	14
Crotonaldehyde	1.5	68	76	3	68	97
Phenylacetaldehyde	4	82	27	4.5	95	40
3-Methylthiopropionaldehyde	3	87	60	6.5	97	80
Pivalaldehyde	2.5	56	45	4.5	78	73
Butyraldehyde	2	75	69	4.5	75	96

[a] As (*R*)-(+)-MTPA derivatives.

The comparison shows that, although the synthesis in ethyl acetate requires longer reaction times, the enantiomeric purity is appreciably better than it is for the reaction in EtOH/H_2O.

More recent investigations into the preparation of *O*-acylated cyanohydrins by reaction of optically active cyanohydrins with dipeptide catalysts[6] or by enzymatic ester cleavage[7] were less satisfactory with respect to optical and preparative yields.

Experimental Procedure

A) Mandelonitrile lyase solution (150 μL, 700 Units/mL, A_{sp} = 65 Units/mg, in 0.02 M acetate buffer, pH 5.4) was added by pipette to 10 mL of 0.05 M acetate buffer (pH 5.4, 50% ethanol). The aldehyde **1** (5 mmol) and **2** (250 μL, 6.5 mmol) were then added. The mixture was shaken until a clear solution had formed, allowed to stand for the allotted length of time (Table 1), and extracted with chloroform. The extract was dried and the organic phase was removed in a rotary evaporator.

B) The support (2 g, AVICEL cellulose) was allowed to swell in 20 mL of 0.01 M acetate buffer (pH 5.4) for 1–2 h. The support was then filtered off, pressed, and transferred to a one-necked flask, and 150 μL of mandelonitrile lyase solution (see A) was added followed by 20 mL of ethyl acetate (saturated with 0.01 M acetate buffer, pH 5.4), 5.0 mmol of **1** and 250 μL (6.5 mmol) of **2**. The mixture was allowed to stand at room temperature for the allotted length of time (Table 1) and filtered. The filter cake was pressed and washed with ethyl acetate. The combined solutions were dried and the organic phase was removed in a rotary evaporator.

For example, 0.53 g of benzaldehyde **1**, R = Ph, gave, according to A in 1-h reaction time, 0.66 g (99%) of benzaldehydecyanohydrin **3**, R = Ph, $[\alpha]_D^{20} = +45°$ (c = 5, $CHCl_3$), *ee* = 86%. According to B in 2.5 h, 0.63 g (95%) of **3**, R = Ph, $[\alpha]_D^{20} = +49°$ (c = 5, $CHCl_3$), *ee* = 99.3%, was obtained.

Received: January 26, 1987;
supplemented: February 16, 1987 [Z 2068 IE]
German version: *Angew. Chem.* 99 (1987) 491

[1] a) W. Becker, U. Benthin, E. Eschenhof, E. Pfeil, *Biochem. Z. 337* (1963) 156; b) W. Becker, E. Pfeil, *ibid. 346* (1966) 301; c) W. Becker, H. Freund, E. Pfeil, *Angew. Chem. 77* (1965) 1139; *Angew. Chem. Int. Ed. Engl. 4* (1965) 1079; E. Pfeil, W. Becker, DBP 1300111 (1969); *Chem. Abstr. 72* (1970) P 3061t.

[2] E. Hochuli, *Helv. Chim. Acta 66* (1983) 489.

[3] a) T. Matsuo, T. Nishioka, M. Hirano, Y. Suzuki, K. Tsushima, N. Itaya, H. Yoshioka, *Pestic. Sci. 1980*, 202; b) D. G. Neilson, D. A. V. Peters, L. H. Roach, *J. Chem. Soc. 1962*, 2272.
[4] a) P. L. Luisi, *Angew. Chem. 97* (1985) 449; *Angew. Chem. Int. Ed. Engl. 24* (1985) 439; b) A. M. Klibanov, *CHEMTECH 1986*, 354.
[5] a) J. A. Dale, D. L. Dull, H. S. Mosher, *J. Org. Chem. 34* (1969) 2534; b) J. D. Elliot, V. M. F. Choi, W. S. Johnson, *ibid. 48* (1983) 2294.
[6] a) S. Asada, Y. Kobayashi, S. Inoue, *Makromol. Chem. 186* (1985) 1755; b) W. R. Jackson, Brit. Pat. 2143823 (1985), ICI Australian Ltd.; *Chem. Abstr. 104* (1986) 68624c.
[7] H. Hirohara, S. Mitsuda, E. Ando, R. Komaki, *Stud. Org. Chem. (Amsterdam) Vol. 22* (1985) p. 119; *Chem. Abstr. 104* (1986) 67464p.

Quino[7,8-*h*]quinoline, a New Type of "Proton Sponge"**

By *Michael A. Zirnstein* and *Heinz A. Staab**

So far, "proton sponges" have been defined as bis(dialkylamino)arenes whose dialkylamino groups are in close spatial proximity.[1] The unusual basicity of these compounds is ascribed to the destabilizing overlap of the lone electron pairs on the nitrogen atoms, to the formation of especially strong hydrogen bonds in the monoprotonated diamines, and to the hydrophobic shielding of these hydrogen bonds. In order to differentiate and assess the relative importance of these factors, we were interested in quino[7,8-*h*]quinoline **1**, whose nitrogen atoms exhibit a mutual orientation similar to that in 1,8-bis(dimethylamino)naphthalene **2** ("proton sponge"). In contrast to **2**, however, **1** lacks the hydrophobic shielding of the hydrogen bonds of its monoprotonated derivative. This shielding is considered to be responsible for the low rates of proton transfer, which make the "proton sponges" reported so far unsuitable as auxiliary bases in chemical reactions.

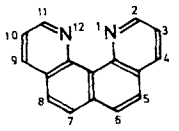

1

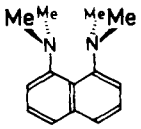

2

The synthesis and properties of **1** have been reported by several groups.[2] In all cases, however, these claims proved to be incorrect,[3] so that, to the best of our knowledge, **1** was unknown until now.

Our synthesis of **1** started from tetramethyl 2,2'-(1,8-naphthylenediimino)difumarate **3**, which was obtained, by a modified procedure of *Honda* et al.,[4] from 1,8-diaminonaphthalene and dimethyl acetylenedicarboxylate (molar ratio 1:2, methanol; m.p. = 142–143 °C; 71% yield).[5] Thermal cyclization of **3** (diphenyl ether, 240 °C) gave dimethyl 4,9-dioxo-1,4,9,12-tetrahydroquino[7,8-*h*]quinoline-2,11-dicarboxylate **4** (m.p. = 276–278 °C; 64% yield).[5,6]

Alkaline hydrolysis of **4** afforded the corresponding dicarboxylic acid **5** (m.p. = 314–315 °C, dec.; 93% yield),[5] which underwent decarboxylation at 335 to 370 °C/10^{-5} torr in a sublimation apparatus to give quino[7,8-*h*]quinoline-4,9-(1*H*,12*H*)-dione **6** (m.p. = 375–377 °C, dec.; 76% yield).[5] Short heating of **6** at reflux with phosphoryl chloride gave 4,9-dichloroquino[7,8-*h*]quinoline **7** (m.p. = 234–235 °C; 81% yield),[5] which was converted into **1** (m.p. = 196–197 °C, 39%)[5] by catalytic hydrogenation (Pd/C, glacial acetic acid, sodium acetate).

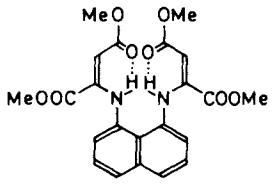

3

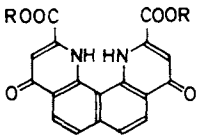

4: R = Me, 5: R = H

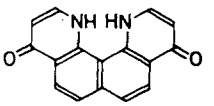

6

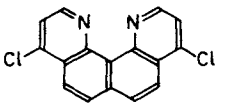

7

The compound thereby obtained gave the correct elemental analysis and spectroscopic data for the structure of **1**. In the mass spectrum, besides *m/z* 230 ($M^{\oplus}$, 100%), 229 (25%), and 115 ($M^{2\oplus}$, 13%), no other fragment ions with $I_{rel} > 5\%$ appear. Comparison of the ^{1}H-NMR spectrum ($CDCl_3$, 360 MHz) with that of quinoline leads to the following assignments: $\delta = 7.60$ (dd, $J = 4.3$ Hz, 8.1 Hz, 2H; 3,10-H), 7.98 ('s,' 4H; 5,8-H and 6,7-H), 8.32 (dd, $J = 1.9$ Hz, 8.1 Hz, 2H; 4,9-H), 9.43 (dd, $J = 1.9$ Hz, 4.5 Hz, 2H; 2,11-H).

Like other "proton sponges," **1** reacts with perchloric acid in excess to form only a *mono*perchlorate (colorless needles, m.p. = 282–285 °C).[5] The structure **8**, containing a very strong N···H···N hydrogen bond, was established from the ^{1}H-NMR spectrum,[7] which exhibits a broadened singlet at $\delta = 19.38$, the most strongly downfield-shifted proton resonance observed so far for an N···H···N hydrogen bond (in dimethyl sulfoxide (DMSO)). Analogously, the monoperchlorate **9** (m.p. = 317–318 °C, dec.)[5] is obtained from **7**. The hydrogen-bonded proton of **9** absorbs at $\delta = 19.34$.

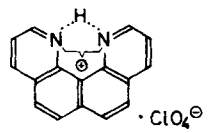

8

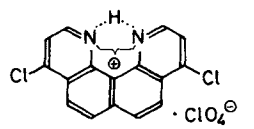

9

On the basis of transprotonation experiments of **1** with protonated **2** and of **2** with **8**, the pK_a value of **1** was estimated to be 12.8 by ^{1}H-NMR spectroscopy (500 MHz, [D$_6$]DMSO). Accordingly, the basicity of **1** compared with quinoline ($pK_a = 4.91$) is increased by nearly eight orders of magnitude, which roughly corresponds to the increase of basicity of **2** compared with *N,N*-dimethylaniline.[1] Whereas the hydrophobic shielding of the N···H···N hydrogen bond plays only a minor role in the basicity of "proton sponges," it has a great effect on the rate of proton transfer: the ^{1}H-NMR spectra of mixtures of **1** and **8** in [D$_6$]dimethyl sulfoxide at 30 °C exhibit coalesced signals

[*] Prof. Dr. H. A. Staab, Dipl.-Chem. M. A. Zirnstein
Abteilung Organische Chemie,
Max-Planck-Institut für medizinische Forschung
Jahnstrasse 29, D-6900 Heidelberg (FRG)

[**] New "Proton Sponges," Part 4.—Part 3: [1c].

for each of the various groups of protons at averaged δ values corresponding to the respective **1/8** ratio. Thus, in contrast to the "proton sponges" reported so far,[1] a rapid proton exchange obviously exists between **1** and **8**. Quantitative investigations of the equilibrium and the kinetics of proton transfer in the system **1/8** have been initiated. The preliminary results have already shown that not only strong, but also kinetically active bases are accessible according to the "proton sponge" concept.

Received: January 26, 1987 [Z 2070 IE]
German version: *Angew. Chem. 99* (1987) 460

[1] a) R. W. Alder, P. S. Bowman, W. R. S. Steele, D. R. Winterman, *Chem. Commun. 1968*, 723; b) H. A. Staab, T. Saupe, C. Krieger, *Angew. Chem. 95* (1983) 748; *Angew. Chem. Int. Ed. Engl. 22* (1983) 731; c) T. Saupe, C. Krieger, H. A. Staab, *ibid. 98* (1986) 460 and *25* (1986) 451, respectively, and references cited therein.

[2] a) I. Iwai, S. Hara, *Yakugaku Zasshi (J. Pharm. Soc. Japan) 70* (1950) 32; b) K. Shibata, *Bull. Chem. Soc. Jpn. 24* (1951) 187; c) M. Dufour, N. P. Buu-Hoï, P. Jaquignon, *J. Chem. Soc. C1967*, 1415.

[3] a) I. Iwai, S. Hara, S. Sayegi, *Yakugaku Zasshi (J. Pharm. Soc. Japan) 71* (1951) 1152; b) S. V. Nekrasov, A. V. El'tsov, *J. Org. Chem. USSR (Engl. Transl.) 7* (1971) 186; c) A. Edel, P. A. Marnot, J. P. Sauvage, *Tetrahedron Lett. 26* (1985) 727; I. Newsom, H. A. Staab, unpublished results.

[4] K. Honda, H. Nakanishi, A. Yabe, *Bull. Chem. Soc. Jpn. 56* (1983) 2338.

[5] The structures reported here are in agreement with the elemental analyses and spectroscopic data.

[6] There are considerable differences with respect to both the melting point and the ^{1}H-NMR spectrum between our results and the results reported in [4].

[7] ^{1}H-NMR ([D$_6$]DMSO, 360 MHz) of **8**: $\delta = 8.25$ (dd, $J = 5.1$ Hz, 8.1 Hz, 2H; 3,10-H), 8.52 and 8.57 ('AB,' $J = 8.8$ Hz, 4H; 5,8-H and 6,7-H), 9.20 (dd, $J \approx 1.5$ Hz, 8.0 Hz, 2H; 4,9-H), 9.52 (dd, $J \approx 1.2$ Hz, 4.7 Hz, 2H; 2,11-H), 19.38 (br. s, 1H; N···H···N).

Decarbonylation on Carbon-Supported Nickel Catalysts**

By *Hans Bock** and *Olaf Breuer*

Dedicated to Professor Heinz Harnisch on the occasion of his 60th birthday

Surface reactions of gases on[1a-c,f,g] and with[1d,e] solids can be detected and optimized most readily by PE-spectroscopic real-time analysis[2] of the gas mixture after it has flowed through the reaction zone (compare Fig. 1). As a model reaction for the heterogeneously catalyzed decarbonylation,[3a] we have investigated the cleavage of crotonaldehyde[3c] to CO and propene at 10 Pa on quartz wool, on metal powders, and on supported catalysts (Scheme 1). A carbon-supported nickel catalyst proved to be the most suitable,[4] lowering the decarbonylation temperature by more than 500 K relative to that for quartz wool.[5]

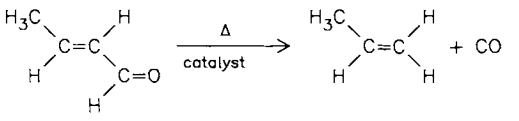

catalyst	[SiO$_2$]	[Cu]	[Ni]	[Ni/SiO$_2$]	[Rh/C]	[CO/C]	[Ni/C]
T[K]	870	770	670	570	520	470	360

Scheme 1.

The selective cleavage of CO from furfurylaldehyde at 400 K shows that the reaction is catalyzed by nickel clusters[4] that are presumably present in the pores of the carbon, which has a large surface area. The uncatalyzed decomposition of furfurylaldehyde requires a 700-K higher temperature, resulting mainly in the formation of propyne and CO (Fig. 1).[3b]

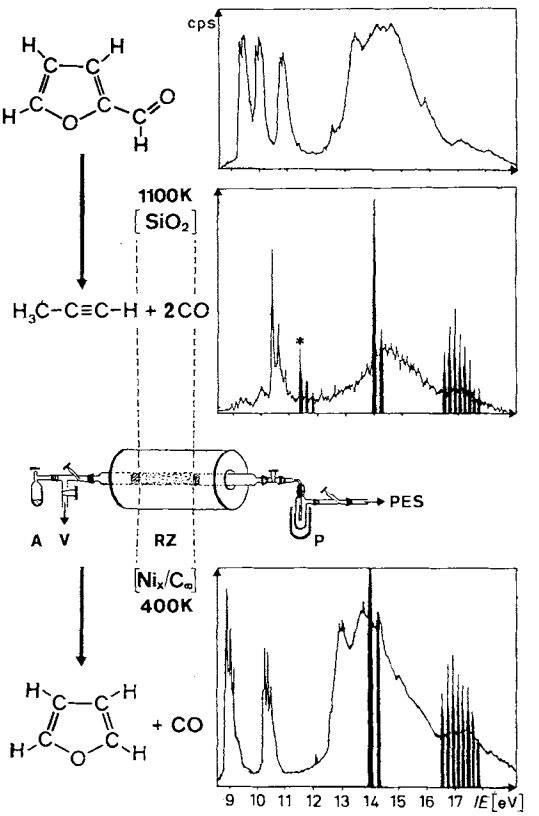

Fig. 1. Thermal decomposition of furfurylaldehyde on quartz wool (above) and selective decarbonylation on a carbon-supported nickel catalyst (below). He(I) PE spectra and experimental apparatus (A, starting material; V, vacuum-pump connection; RZ, heated reaction zone; P, product cold trap for GC analysis; PES, connection to PE spectrometer). In the uncatalyzed decomposition, a small amount of acetylene (*) was observed as a side product. The black bands in the middle and lower spectra are due to CO [9]. The PE spectrum of pure furan is known [9]. The absence of an acetylene band in the lower spectrum proves that no side products are formed in the Ni$_x$/C$_\infty$-catalyzed decarbonylation of furfurylaldehyde.

Numerous other organic compounds can be decarbonylated, on carbon-supported nickel catalysts[4] at low temperatures on a preparative scale and largely selectively (according to the gas chromatograms):[5] aldehydes, acid chlorides, and acyl cyanides (Scheme 2, R = CH_3, C_6H_5). The uncatalyzed reactions require temperatures that are up to 700 K higher.

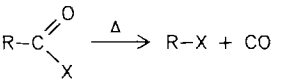

X	H	Cl	CN
T[K]	370-420	420-470	430-470

Scheme 2.

[*] Prof. Dr. H. Bock, Dipl.-Chem. O. Breuer
Institut für Anorganische Chemie der Universität
Niederurseler Hang, D-6000 Frankfurt am Main 50 (FRG)

[**] Surface Reactions, Part 8. This work was supported by Hoechst AG, the Fonds der Chemischen Industrie, and the Max-Buchner Stiftung.—Earlier Parts: cf. [1].

An unexpected course was observed for the reaction of alkyl isocyanates on carbon-supported nickel catalysts.[4] For example, isopropyl isocyanate undergoes noncatalyzed decomposition above 920 K with the formation of propene and HNCO; the reaction is suitable for the synthesis of pure isocyanic acid.[6] In contrast, reaction on Ni_x/C_∞ catalysts occurs at 500 K, yielding CO, methane, and acetonitrile as the main products (Fig. 2). Since CO cleavage already takes place above 400 K, presumably a chemisorbed isopropyl nitrene is involved as a surface-bound intermediate. It possibly stabilizes by eliminating CH_4 to a presumably π-bound[7] acetonitrile, which, under the reaction conditions, begins to desorb only after about one hour and at a 50-K higher temperature. The

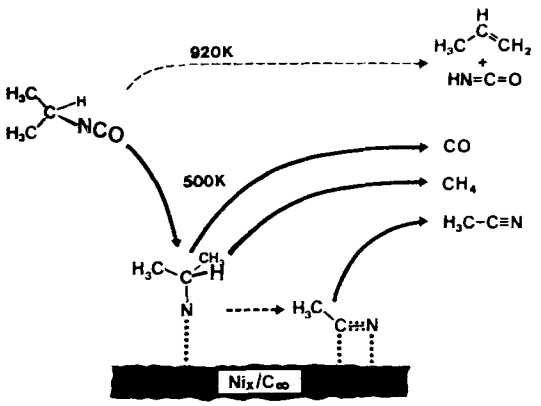

Fig. 2. Possible mechanism for the decomposition of isopropyl isocyanate.

uncatalyzed thermal decomposition of *tert*-butyl isocyanate requires a temperature of 900 K and affords HNCO and isobutene. In contrast, on the carbon-supported nickel catalyst, isobutene and CO already form at temperatures above 500 K, as well as NH_3 and N_2—possibly by disproportionation of NH species bound to the surface.[8]

Received: January 27, 1987;
supplemented: March 23, 1987 [Z 2071 IE]
German version: *Angew. Chem. 99* (1987) 492

[1] Cyanation of benzene on $[Cu_x/Al_2O_3]$: H. Bock, J. Wittmann, H.-J. Arpe, *Chem. Ber. 115* (1982) 2326; b) bromination of F_3CH on $[NiF_2/AlF_3]$: H. Bock, J. Wittmann, J. Mintzer, J. Russow, *ibid. 115* (1982) 2346; c) hydration and simultaneous dehydrogenation of olefins on $[SnO_2/P(MoO_x)_y]$: H. Bock, M. Haun, J. Mintzer, *8th Int. Congr. Catal. Proc. Vol. 5*, Verlag Chemie, Weinheim 1984, p. 691; d) decblorination of $XPCl_3$ on [Ag]: M. Binnewies, B. Solouki, M. Bock, R. Becherer, R. Ahlrichs, *Angew. Chem. 96* (1984) 704; *Angew. Chem. Int. Ed. Engl. 23* (1984) 731; e) $SiCl_2$ from Si_nCl_{2n+2} and [Si]: H. Bock, B. Solouki, G. Maier, *ibid. 97* (1985) 205 and *24* (1985) 205, respectively; f) reactions on Raney nickel: H. Bock, H. P. Wolf, *ibid. 97* (1985) 411 and *24* (1985) 418, respectively; g) carbene dimerization on Raney nickel: H. Bock, G. Tschmutowa, H. P. Wolf, *J. Chem. Soc. Chem. Commun. 1986*, 1069.

[2] H. Bock, B. Solouki, *Angew. Chem. 93* (1981) 425; *Angew. Chem. Int. Ed. Engl. 20* (1981) 427.

[3] a) In contrast to the extensive literature on homogeneously catalyzed carbonylation equilibria, e.g., in the oxo synthesis (cf. K. Weissermel, H. J. Arpe: *Industrielle Organische Chemie*, 2nd ed., Verlag Chemie, Weinheim 1978), there are only a few publications on heterogeneously catalyzed decarbonylations (cf., e.g., *Houben-Weyl: Methoden der Organischen Chemie, Band VII, Teil 1*, Thieme, Stuttgart (1954), p. 494f). b) For CO elimination from furfurylaldehyde on nickel or cobalt catalysts cf. A. P. Dunlop, W. J. McKillip, S. Winderl in *Ullmanns Encyklopädie der technischen Chemie, Bd. 12*, Verlag Chemie, Weinheim 1976, p. 15, especially p. 19, on $[Cr_2O_3/ZnO/Mn_2O_3]$ contact catalysts, for example, O. W. Can, *Ind. Eng. Chem. 40* (1948) 216 or S. A. Hiller, A. Y. Karmilchik, U. U. Stonkus, B. S. Kalayew, S. Shymanska in B. Delmon, P. A. Jacobs, G. Poncelet (Eds.): *Preparation of Catalysts*, Elsevier, Amsterdam 1976, p. 579f. c) For the decarbonylation of crotonaldehyde on nickel powder, cf. P. Sabatier, J. W. Senderens, *Ann. Chim. Paris 4* (1905) 433.

[4] Active carbon (20 g, Strem, 4021-s 06-005, particle size 2 mm, surface area 1000 m^2/g) was degassed to a final pressure of 1 Pa in a 250-mL round-bottom flask fitted with a dropping funnel and then subjected to ultrasonication in a solution containing $Ni(NO_3)_2 \cdot 6H_2O$ (40 g) in 50 mL of H_2O for approximately 1 h until gas evolution had ceased. After decantation of the liquid layer, the product was dried for 12 h at 370 K. In each experiment, 5 g of the catalyst was placed in the reaction tube (Fig. 1) between quartz-wool plugs; the tube was flushed for 15 min each with N_2 and H_2; reduction was then carried out in a stream of H_2 (10 L/h) for 30 min at 320 K, 1 h at 520 K, and 3 h at 720 K; finally, the water formed was removed at 1 Pa and 720 K. The carbon-supported nickel catalyst so formed contains 7% Ni; further characterization by means of the X-ray powder diagrams is being carried out in collaboration with Prof. *M. Trömel*, Universität Frankfurt. In general, the diameters of metal particles of supported catalysts prepared by adsorption of metal nitrates from solution, thermal decomposition, and subsequent reduction with H_2 are in the nm range (cf. J. R. Anderson: *Structure of Metallic Catalysts*, Academic Press, London 1975, Chapter 4 (Dispersed Metal Catalysts), p. 163ff).

[5] For decarbonylation of crotonaldehyde at 530 K and a flow rate LHSV $\approx$ 1/h, the conversion amounts to 80% and the propene selectivity amounts to 89%. Control experiments using undoped active carbon confirm that no CO cleavage is observed up to 750 K.

[6] Usually, HNCO is synthesized by depolymerization of cyanuric acid above 970 K with formation of CO_2, HCN, and H_2O as side products (*Gmelins Handbuch der Anorganischen Chemie, Bd. Kohlenstoff D1*, 8th ed., Verlag Chemie, Weinheim 1971, p. 327f). In contrast, the pyrolysis of isopropyl isocyanate for short contact times results solely in the formation of readily separated propene (b.p. (760 torr) = 226 K; HNCO, b.p. (760 torr) = 297 K); for the kinetics, cf. P. G. Blake, S. Ijadi-Maghsoodi, *Int. J. Chem. Kinet. 15* (1983) 609.

[7] The π coordination of alkyl cyanides on copper surfaces could be detected by, among other methods, IR spectroscopy (A. M. Bradshaw, Fritz-Haber-Institut, Berlin, private communication).

[8] For the detection of $NH_{(ads)}$ as intermediate in the synthesis of NH_3 on $Fe/K/Al_2O_3$ supported catalysts by physical methods of surface analysis, cf. G. Ertl, *Catal. Rev. 21* (1980) 201.

[9] K. Kimura, S. Katsumata, Y. Achiba, T. Yamasaki: *Handbook of He(I)-Photoelectron Spectra of Fundamental Organic Molecules*. Halsted Press, New York 1981.

Glycolate and Thioglycolate Complexes of Rhenium and Their Oxidative Elimination of Ethylene and of Glycol**

By *Wolfgang A. Herrmann,* Dieter Marz, Eberhardt Herdtweck, Adolf Schäfer, Werner Wagner,* and *Heinz-Josef Kneuper*

Dedicated to Professor Gerhard Quinkert on the occasion of his 60th birthday

Selenium dioxide and osmium tetroxide are effective reagents and catalysts for olefin oxidation, although, owing to their toxicity, reservations remain as to their applicability.[1] We are therefore seeking more easily handled metal oxides that are soluble in organic solvents and that are as effective as osmium tetroxide in carrying out stereospecific *cis* hydroxylation of olefins. The rhenium(VII) oxide **1**, which has meanwhile become readily accessible, is a favorable candidate.[2]

Complex **1** reacts with germanium dichloride (as the dioxane adduct) in a clean redox reaction, according to

[*] Prof. Dr. W. A. Herrmann, D. Marz, Dr. E. Herdtweck, Dr. A. Schäfer, W. Wagner, Dr. H.-J. Kneuper
Anorganisch-chemisches Institut der Technischen Universität München
Lichtenbergstrasse 4, D-8046 Garching (FRG)

[**] Multiple Bonds between Main-Group Elements and Transition Metals, Part 40. This work was supported by Hoechst AG, Degussa AG, the Fonds der Chemischen Industrie, and the Bundesministerium für Forschung und Technologie.—Part 39: W. A. Herrmann, B. Koumbouris, E. Herdtweck, M. L. Ziegler, T. Zahn, *Chem. Ber.*, in press.

Scheme 1, to give the oxo dichloride **2**,[3] which, upon treatment with glycolate or dithioglycolate solutions (sodium salts), is converted nearly quantitatively into the novel metallacycles **3a** or **3b**, respectively.[4]

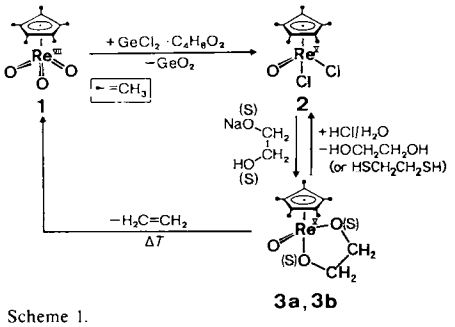

Scheme 1.

A single-crystal X-ray structure analysis of the parent glycolate complex **3a** (Fig. 1) gave the following results: In addition to an acentrically π-coordinated five-membered ring ligand and a double-bonded oxo group (Re-O3 169.6(2) pm), the molecule contains a puckered ReO_2C_2 five-membered ring (*twist* conformation) in which the interatomic distances correspond to those of single bonds. In the metallacycle, the planes defined by the atoms O1/Re/O2 and C1/Re/C2 form an angle of 23.6°.

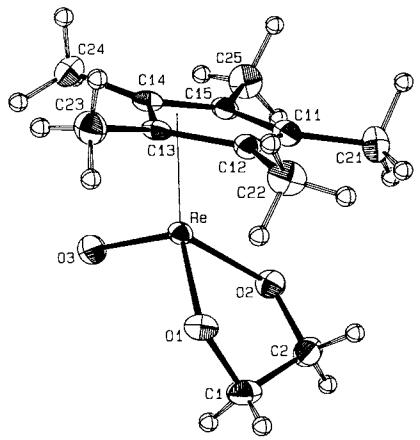

Fig. 1. ORTEP of the molecular crystal structure of the glycolate complex **3a**. The hydrogen atoms were localized by X-ray structure analysis. The ellipsoids of thermal vibration are drawn at the 50% probability level, except for the H atoms, where they are arbitrary.—**3a** forms orthorhombic crystals (*n*-hexane, −30°C) in the space group $P2_12_12_1$. $a=788.0(1)$, $b=1258.0(1)$, $c=1278.6(1)$ pm, $\alpha=\beta=\gamma=90°$, $Z=4$, $V=1267\times10^7$ pm^3, $\rho_{calcd}=2.083$ g cm^{-3}. 2496 measured reflections of which 2145 were unique, 221 parameters, $R=0.016$, $R_w=0.017$, GOF = 2.314. Selected distances [pm] and angles [°]: Re-O(1) 196.6(2), Re-O(2) 196.3(2), Re-O(3) 169.6(2), C(1)-C(2) 149.8(5), C(1)-O(1) 143.7(4), C(2)-O(2) 143.0(4); O(1)-Re-O(2) 80.2(1), O(1)-Re-O(3) 108.3(1), O(2)-Re-O(3) 110.9(1) [5].

Of particular interest is the thermal behavior of the glycolate complex **3a**: Heating of the solid at 150°C (15 min, vacuum) or refluxing of a toluene solution in the absence of oxygen results in *quantitative* elimination of ethylene with regeneration of the trioxorhenium(VII) educt **1** (Scheme 1). This special case of cycloreversion, which has not before been encountered in organometallic chemistry,[9] may be regarded as an oxidative elimination of type (a), since the oxidation state is formally changed from Re^V

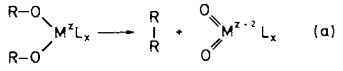

to Re^{VII}. This cleavage reaction can also be followed by NMR spectroscopy; when **3a** is heated in [D_8]toluene at 100°C with strict exclusion of O_2, the signals for **1** ($\delta=1.98$) and ethylene ($\delta=5.28$) are observed.

The dithioglycolate complex **3b** is thermally more stable than **3a**; however, heating of **3b** at 200°C over 30 min likewise results in quantitative loss of ethylene. The 2,3-butanediolato complex **3c** (synthesized from (2*R*,3*R*)-2,3-butanediol; red-violet crystals), corresponding to **3a**, eliminates *trans*-butene (100%) above 150°C to form **1** once again. The 1,3-propanediolate derivative **3d** (violet oil),

$[(\eta^5\text{-}C_5Me_5)(O)\overline{ReOCH_2CH_2CH_2O}]$ **3d**

which was synthesized analogously, behaves similarly; it eliminates propene already at room temperature (!) and can therefore be handled without decomposition only below 0°C.

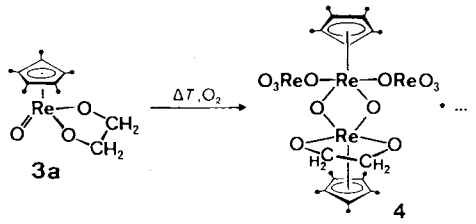

Scheme 2.

In the presence of air, **3a** is transformed, according to Scheme 2, into the more complex oxidation product **4**,[6] which, according to a single-crystal X-ray structure analysis, is related constitutionally to the known complex [(η^5-$C_5Me_5)_2Re_2O_4$][7] (Fig. 2). The two nonidentical Re(v) fragments are joined through oxo bridges; one fragment (Re1) still contains the bidentate glycolate ligand, whereas the

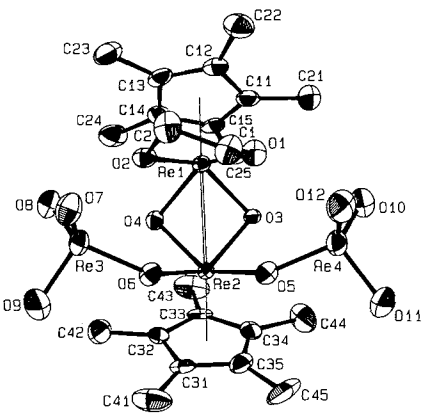

Fig. 2. ORTEP of the molecular crystal structure of the tetranuclear glycolate complex **4** (without hydrogen atoms).—**4** forms triclinic crystals (toluene), containing two molecules of the solvent, in the space group $P\bar{1}$. $a=938.2(1)$, $b=1452.3(1)$, $c=1543.7(1)$ pm, $\alpha=81.42(1)$, $\beta=82.60(1)$, $\gamma=72.88(1)°$, $Z=2$, $V=1980\times10^6$ pm^3, $\rho_{calcd}=2.381$ g cm^{-3}. 7005 measured reflections, of which 6008 were independent, 469 parameters, $R=0.028$, $R_w=0.031$, GOF = 3.934. Selected distances [pm] and angles [°]: Re(1)-Re(2) 260.2(<1), Re(1)-O(1) 199.6(3), Re(1)-O(2) 203.0(3), O(1)-C(1) 143.2(5), C(1)-C(2) 148.8(6), C(2)-O(2) 143.2(5), Re(1)-O(3) 193.4(2), Re(1)-O(4) 192.1(3), Re(2)-O(3) 192.7(2), Re(2)-O(4) 193.7(2), Re(2)-O(5) 208.1(3), Re(2)-O(6) 204.0(3); Re(1)-O(3)-Re(2) 84.7(1), Re(1)-O(4)-Re(2) 84.8(1), Re(2)-O(5)-Re(4) 139.7(2), Re(2)-O(6)-Re(3) 134.6(2), Re(1)-O(1)-C(1) 116.2(3), Re(1)-O(2)-C(2) 112.0(2) [5].

other (Re2) has two perrhenate groups (Re3/4). Thus, air oxygen effects both partial elimination of glycolate and oxidation of $[(C_5Me_5)Re^{V}O_x]$ fragments with loss of the ring ligand. The ReO_2C_2 metallacycle still present in **4** no longer decomposes with elimination of ethylene (monitored by GC), even at temperatures as high as 250 °C (vacuum).

The glycolate ligand in **3a** may also be split off intact, however. Thus, on the one hand, treatment of **3a** with dilute aqueous hydrochloric acid results in rapid formation of the oxo dichloride **2** (IR and MS detection) with quantitative formation of glycol (GC detection, Scheme 1); this reaction is the reversal of the route of formation leading to **3a**. On the other hand, treatment with HCl/ether results in formation of the complex $[(\eta^5\text{-}C_5Me_5)ReCl_4]$.[2] Furthermore, oxidative cleavage of the ReO bonds in **3a** may be achieved with hydrogen peroxide; in addition to glycol, the rhenium(VII) oxide **1** is cleanly formed under such conditions.

The mechanisms of decomposition of the oxidic glycolate complexes of rhenium presented here support, on the one hand, the supposition that structurally analogous intermediates are involved in the permanganate and osmium tetroxide systems (Criegee and Sharpless reactions) used in practice for the oxidation of olefins;[1,8] on the other hand, they suggest novel applications of the organometallic oxide **1**. However, the direct addition of **1** to CC double bonds must be accomplished in the next step of research.

Received: December 23, 1986 [Z 2027 IE]
German version: *Angew. Chem. 99* (1987) 462

[1] For the use of OsO_4 for olefin hydroxylation, see M. Schröder, *Chem. Rev. 80* (1980) 187.

[2] a) W. A. Herrmann, R. Serrano, H. Bock, *Angew. Chem. 96* (1984) 364; *Angew. Chem. Int. Ed. Engl. 23* (1984) 383. b) Recent reviews: W. A. Herrmann, *J. Organomet. Chem. 300* (1986) 111; W. A. Herrmann, E. Herdtweck, M. Flöel, J. Kulpe, U. Küsthardt, J. Okuda, *Polyhedron*, in press; W. A. Herrmann, J. Okuda, *J. Mol. Catal.*, in press.

[3] W. A. Herrmann, U. Küsthardt, M. Flöel, J. Kulpe, E. Herdtweck, E. Voss, *J. Organomet. Chem. 314* (1986) 151.

[4] *Experimental Procedure:* **2** (200 mg, 0.5 mmol) in 40 mL of tetrahydrofuran (THF) was treated at 25 °C with a 0.1 M solution (1.0 mL) of ethylene glycol monosodium salt in glycol. The solution immediately turned color from green to red-violet. After separation of the NaCl precipitate on cotton filter aid, the clear filterate was concentrated in vacuum. After extraction of the residue with *n*-hexane and recrystallization from *n*-hexane, 187 mg (94%) of analytically pure **3a** was obtained. Red-violet crystals, m.p. = 53 °C. — IR (cm^{-1}, KBr): 907 vs (νReO); 629 s, 511 s (νReOC). ^{1}H-NMR (270 MHz, $CDCl_3$, 28 °C): $\delta(CH_3) = 1.96$ (s, 15H), $\delta(CH_2) = 3.90$ (ddd, 2H), $\delta(CH_2) = 3.54$ (ddd, 2H); $^2J(H,H) = 15.6$ Hz; $^3J(H,H;trans) = 11.2$ Hz; $^3J(H,H;cis) = 6.8$ Hz. ^{13}C-NMR (67.80 MHz, $CDCl_3$, 28 °C): $\delta(C_5Me_5) = 108.25$, $\delta(CH_3) = 11.19$, $\delta(CH_2) = 80.63$. ^{17}O-NMR (36.634 MHz, CD_2Cl_2, 28 °C): $\delta(ReO) = 731.3$ (glycolate O not observed owing to lack of ^{17}O enrichment). EI-MS (70 eV; relative to ^{187}Re): *m/z* 398 ($M^{\oplus}$, 22%), 370 ($[M - C_2H_4]^{\oplus}$, 6%), 338 ($[M - C_2H_4O_2]^{\oplus}$, 12%), 134 ($[C_{10}H_{14}]^{\oplus}$, 100%), 28 ($[C_2H_4]^{\oplus}$, 10%; high resolution). Correct C,H,O,Re elemental analyses. — **3b** was prepared analogously; brown, metallic-lustrous prisms, m.p. = 115 °C. IR (cm^{-1}, KBr): 908 vs (νReO). ^{1}H-NMR (270 MHz, $CDCl_3$, 28 °C): $\delta(CH_3) = 2.00$ (s, 15H), $\delta(CH_2) = 2.53$ (ddd, 2H), 2.63 (ddd, 2H). ^{13}C-NMR (67.80 MHz, $CDCl_3$, 28 °C): $\delta(C_5Me_5) = 102.13$, $\delta(CH_3) = 12.38$, $\delta(CH_2) = 41.48$. ^{17}O-NMR (36.634 MHz, $CDCl_3$, 28 °C): $\delta(ReO) = 769$. EI-MS (70 eV; relative to ^{187}Re): *m/z* 430 ($M^{\oplus}$, 100%), 402 ($[M - C_2H_4]^{\oplus}$, 80%), 384 ($[C_5Me_5ReS_2]^{\oplus}$, 20%), 352 ($[C_5Me_5ReS]^{\oplus}$, 20%), 64 ($S_2^{\oplus}$, 18%), 28 ($[C_2H_4]^{\oplus}$); high resolution). Correct C,H,S elemental analyses.

[5] Further details of the crystal structure investigation may be obtained from the Fachinformationszentrum Energie, Physik, Mathematik GmbH, D-7514 Eggenstein-Leopoldshafen 2 (FRG), on quoting the depository number CSD-52337, the names of the authors, and the journal citation.

[6] Green crystals; no m.p. up to 250 °C. IR (cm^{-1}, KBr): 910 vs (νReO); 606 m (νReORe); 543 m, 518 m (νReOC). ^{1}H-NMR (270 MHz, $CDCl_3$, 28 °C): $\delta(CH_3) = 2.161$ (s, 15H), 2.147 (s, 15H); $\delta(CH_2) = 3.92$ (ddd, 2H), 4.40 (ddd, 2H). ^{17}O-NMR (36.50 MHz, $C_6D_5CD_3$, 28 °C): $\delta(ReO_3) = 701$, $\delta(ReO_2Re) = 657$; further ReO signals not observed owing to lack of ^{17}O label.

[7] E. Herdtweck, W. A. Herrmann, M. Flöel, unpublished results.

[8] Oxyamination and -diamination reactions at Os^{VIII} complexes also appear to follow this mechanism; cf. A. O. Chong, K. Oshima, K. B. Sharpless, *J. Am. Chem. Soc. 99* (1977) 3420; the corresponding reactions may also be possible for rhenium-containing systems in view of the availability of complexes such as $[(\eta^5\text{-}C_5Me_5)ReCl_2(=N-R)]$ [2b].

[9] One example in tungsten chemistry is known but requires the presence of a further reagent: R. R. Schrock, S. F. Petersen, M. R. Churchill, J. W. Ziller, *Organometallics 3* (1984) 1574.

Novel Rhenium(v) Carbonato and Sulfato Chelate Complexes: Synthesis and Investigation of Molecular Dynamics by ^{17}O-NMR Spectroscopy**

By *Wolfgang A. Herrmann,* Karin A. Jung, Adolf Schäfer,* and *Heinz-Josef Kneuper*

Dedicated to Professor Heinz Harnisch on the occasion of his 60th birthday

Oxidic rhenacycles with four-, five-, and six-membered rings have recently become accessible, either by substitution of halogen accompanied by cyclization in the rhenium(V) complex **1** or by (reductive) cycloaddition to the rhenium(VII) oxide **4**.[1] The pronounced stability of ReO bonds prompted us to investigate the tendency of carbonate and sulfate ions to react at Lewis-acidic d^2-configurated rhenium centers to give cyclic products.

The oxo dichloride **1** reacts with the anhydrous silver salts of mono- and polybasic oxo acids in organic solvents with precipitation of silver chloride. Thus, reaction with silver carbonate affords the carbonato complex **2** and reaction with silver sulfate gives the sulfato complex **3** (Scheme 1).[2]

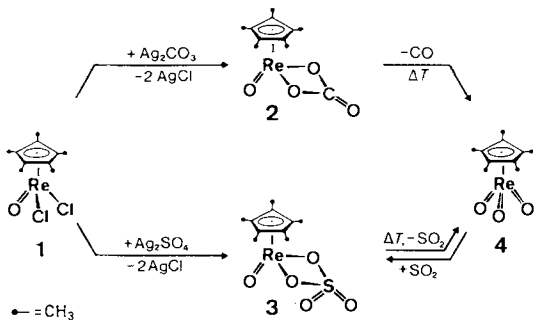

Scheme 1.

The two new metallacycles **2** and **3** are not only sensitive to moisture but also decompose upon heating with elimination of carbon monoxide and sulfur dioxide, respectively (GC and MS detection), as well as quantitative formation of the rhenium(VII) oxide **4**. Other cleavage products are not observed.[3] The sulfato complex **3** can also be prepared from the oxide **4** by treating it with dry SO_2 in hot toluene (80 °C) for several hours. The structures of **2** and **3** are presumably similar to that of the related complex $[(\eta^5\text{-}C_5Me_5)(O)Re(\mu\text{-}O)_2ReCl_2(\eta^5\text{-}C_5Me_5)]$,[4]

[*] Prof. Dr. W. A. Herrmann, K. A. Jung, Dr. A. Schäfer, Dr. H.-J. Kneuper
Anorganisch-chemisches Institut der Technischen Universität München
Lichtenbergstrasse 4, D-8046 Garching (FRG)

[**] Multiple Bonds between Main-Group Elements and Transition Metals, Part 41. — Part 40: [1d].

which is folded along the O···O vector at the central oxygen bridges.

During the ^{17}O-NMR spectroscopic characterization, we observed a previously unknown exchange phenomenon for the metallacycle **3**. In order to carry out this study, the starting complex **1** was $^{17}O/^{18}O$-labeled to about 10% and 40%, respectively, by subjecting the tetrachloride $[(\eta^5\text{-}C_5Me_5)ReCl_4]$ to partial hydrolysis with exactly one equivalent of $^{17}O/^{18}O$-labeled water[5] and then allowing the isotopomeric mixture [*O]-**1**, isolated as crystals, to react with *nonlabeled* silver sulfate according to Scheme 1. The ^{17}O-NMR spectrum of the product [*O]-**3**, shown in Figure 1,

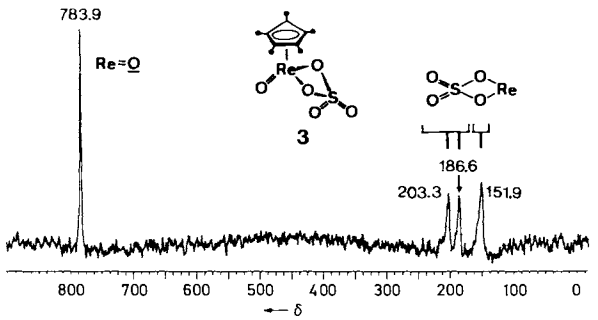

Fig. 1. ^{17}O-NMR spectrum of the complex [*O]-**3** (ca. 10% overall ^{17}O plus 40% ^{18}O enrichment; MS determination), prepared from $[(\eta^5\text{-}C_5Me_5)Re(*O)Cl_2]$ and *nonlabeled* Ag_2SO_4.—Recording parameters: 36.634 MHz, CD_2Cl_2, 27°C, 10000 scans, acquisition time 0.041 s, pulse delay 0.010 s, 90° pulse; δ values with respect to external H_2O ($\delta = 0.00$ ppm).

proves that, in agreement with the infrared[2] and mass spectra, the oxygen label is by no means found only in the ReO group (as was expected) but is *distributed statistically over all possible five positions* in the molecule. This means that an exchange of oxygen atoms bound to rhenium and sulfur occurs and must therefore be due to a dynamic process. Opening of the rhenium-oxygen bonds of the ReO_2S metallacycle alone is not sufficient, since this would only lead to exchange of the oxygen atoms bound to rhenium. The sulfur-oxygen bonds must also be involved in bond breaking and bond formation. The exchange mechanism proposed in Scheme 2 can explain these findings. Apparently, the Lewis acidity of d^2-configurated rhenium, which has already been demonstrated elsewhere, initiates this exchange process by allowing intramolecular coordination of either one of the two terminal SO groups to the metal atom. Comparable, although much more stable, adducts of this kind are formed upon reaction of the Lewis base trimethylphosphane with the pentavalent rhenium complexes $[(\eta^5\text{-}C_5Me_5)ReCl_4]$ and $[(\eta^5\text{-}C_5Me_5)ReCl_3Me]$;[6,7] $[(\eta^5\text{-}C_5Me_5)ReCl_4(PMe_3)]$ has been

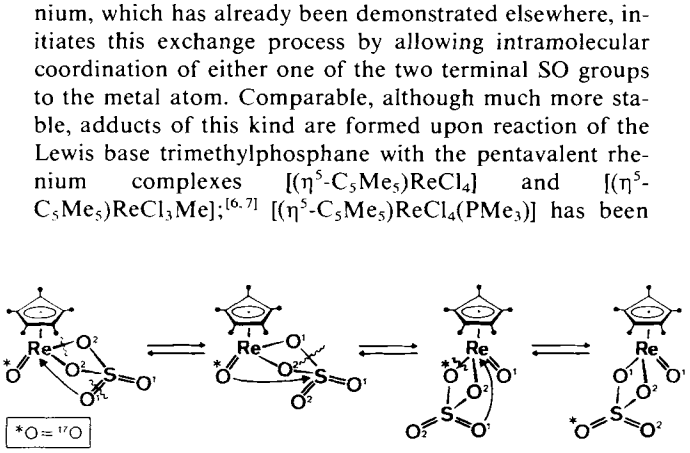

Scheme 2. Proposed mechanism for complete oxygen exchange in the rhenium(v) metallacycle **3**, assuming an intramolecular exchange process. The bond cleavages shown correspond, in each case, to the formation of the following isotopomer.

characterized by means of X-ray structure analysis (distorted octahedral coordination) and contains a phosphane group in the *trans* position to the π-bonded ring ligand.[6]

Increasing the temperature does not result in an appreciable change of the spectrum. The comparably short time scale of ^{17}O-NMR spectroscopy in this case, due to the large line separation, does not allow coalescence to be observed, within the realm of experimental possibility. A related exchange phenomenon at a η^2-sulfato ligand has previously been detected only by IR spectroscopy.[8]

We have thus been able to show that oxidic organorhenium complex fragments react with simple oxo anions to form stable chelate complexes, the surprising molecular dynamics of which are due to the Lewis acidity of the d^2-configurated Re^V centers. Furthermore, reactions of the type in Scheme 1 offer the possibility of constructing extended metal oxide structures by complexation of oxometallates (e.g., di- and polychromates) in which different metal atoms are linked to one another through oxo bridges.

Received: December 23, 1986 [Z 2028 IE]
German version: *Angew. Chem. 99* (1987) 464

[1] a) W. A. Herrmann, U. Küsthardt, M. L. Ziegler, T. Zahn, *Angew. Chem. 97* (1985) 857; *Angew. Chem. Int. Ed. Engl. 24* (1985) 860; b) U. Küsthardt, W. A. Herrmann, M. L. Ziegler, T. Zahn, B. Nuber, *J. Organomet. Chem. 311* (1986) 163; c) H. J. R. de Boer, B. J. J. van de Heisteeg, M. Flöel, W. A. Herrmann, O. S. Akkerman, F. Bickelhaupt, *Angew. Chem. 99* (1987) 88; *Angew. Chem. Int. Ed. Engl. 26* (1987) 73; d) W. A. Herrmann, D. Marz, E. Herdtweck, A. Schäfer, W. Wagner, H.-J. Kneuper, *Angew. Chem. 99* (1987) 462; *Angew. Chem. Int. Ed. Engl. 26* (1987) 462.

[2] *Experimental Procedure* for **3**: A suspension of **1** (100 mg, 0.25 mmol) and Ag_2SO_4 (156 mg, 0.50 mmol) in 20 mL of dry tetrahydrofuran (THF) was allowed to stir for 10 h at room temperature in the dark. After separation of the AgCl by filtration through degassed, dry celite (D3 frit), the brown solution was evaporated under vacuum. The residue was washed with 10 mL of toluene and 10 mL of diethyl ether and finally recrystallized from CH_2Cl_2/*n*-pentane. Yield 83 mg (78%) of brown, microcrystalline η^2-sulfato complex **3**. Dec. at 150°C with green coloration (in the air).—Complex **2** was synthesized analogously; rust-red powder; dec. at 190°C.—Spectroscopic data for the η^2-sulfato complex **3**: IR (KBr, cm^{-1}; ^{18}O satellites of the sample, enriched up to about 40%, in parentheses, cf. text): 1337 vs (1317), 1188 vs (1162), 1118 s (1100) (νSO); 974 s, 954 m, 914 m (νReO); 852 vs (844), 830 vs, 808 s (801), 679 vs (667), 623 s (611). ^1H-NMR (270 MHz, 30°C, $CDCl_3$): $\delta(CH_3) = 2.15$ (s). ^{13}C-NMR (67.80 MHz, 30°C, $CDCl_3$): $\delta(C_5Me_5) = 113.34$, $\delta(CH_3) = 12.11$. EI-MS (70 eV; relative to ^{187}Re): *m/z* 434 ($M^{\oplus}$, 8%), 370 ($[M-SO_2]^{\oplus}$, 8%), 354 ($[C_5Me_5ReO_2]^{\oplus}$, 80%), 64 ($[SO_2]^{\oplus}$, 33%). Correct C,H,O,Re elemental analyses.

[3] Thermolysis of **3** at 200°C, 1 torr, 15 min; Perkin-Elmer Sigma 3B, Porapak Q, 2.6 m·1/8", 80/100 mesh, $T = 100$°C, isothermal, WLD detector, 200°C; carrier gas helium; injector 125°C.

[4] The dihedral angle along the O···O vector is 127°, thereby allowing the two rhenium atoms to approach each other to within 269.1(0) pm. This compound should also exhibit a fluxional structure in solution; in this case, the fluxional process occurs faster than the ^{17}O-NMR time scale ($\delta(ReO_3) = 469$, sharp signal; CD_2Cl_2, 23°C; line broadening at −40°C): W. A. Herrmann, E. Herdtweck, M. Flöel, J. Kulpe, U. Küsthardt, J. Okuda, *Polyhedron*, in press; J. Kulpe, *Diplomarbeit*, Universität Frankfurt am Main 1986.

[5] Cf. H.-J. Kneuper, *Dissertation*, Technische Universität München 1986.—The labeled water was obtained from Amersham-Buchler Company (Braunschweig, FRG) and contained ca. 10% ^{17}O and ca. 40% ^{18}O.

[6] a) W. A. Herrmann, E. Voss, U. Küsthardt, E. Herdtweck, *J. Organomet. Chem. 294* (1985) C37; b) W. A. Herrmann, *ibid. 300* (1986) 111.

[7] W. A. Herrmann, J. K. Felixberger, E. Herdtweck, A. Schäfer, J. Okuda, *Angew. Chem. 99* (1987) 466; *Angew. Chem. Int. Ed. Engl. 26* (1987) 466.

[8] a) R. W. Horn, E. Weissberger, J. P. Collman, *Inorg. Chem. 9* (1970) 2367; b) J. Valentine, D. Valentine, Jr., J. P. Collman, *ibid. 10* (1971) 219; c) S. P. Mehandru, A. B. Anderson, *ibid. 24* (1985) 2570.

Concerning the Role of Organotin Compounds in Olefin Metathesis: Synthesis, Structure, and Lewis Acidity of $[(\eta^5\text{-}C_5Me_5)CH_3ReCl_3]$**

By *Wolfgang A. Herrmann,* Josef K. Felixberger, Eberhardt Herdtweck, Adolf Schäfer,* and *Jun Okuda*

Dedicated to Professor Heinz Harnisch on the occasion of his 60th birthday

Tetraorganotin compounds are the most effective cocatalysts for olefin metathesis. Rhenium, after molybdenum and tungsten, is the most active metal present in catalysts for this reaction.[1] A soluble reaction product formed from $ReCl_5$ and $Sn(n\text{-}C_4H_9)_4$ (molar ratio 2:3), which was not further characterized, was found in 1971 to be the first rhenium-containing system for olefin metathesis in homogeneous catalysis.[2] The related heterogeneous system $Re_2O_7/Al_2O_3/Sn(CH_3)_4$ even effects the metathesis of functionalized olefins.[3,4] Although the actual mechanism of metathesis[1] may be regarded as having been established at least for soluble catalysts (olefin cycloaddition to metal carbene species), this statement does not apply to the mode of activation of such catalysts by the tetraorganotin compounds (alkylation vs. reduction).[5] We have therefore attempted, by means of the readily accessible, simple organorhenium(v) complexes **1a,b**, to determine the elementary steps involved in the reaction of tin-containing cocatalysts with higher-valent, soluble rhenium compounds and report herein the synthesis, characterization, and reactivity of novel alkylrhenium complexes.

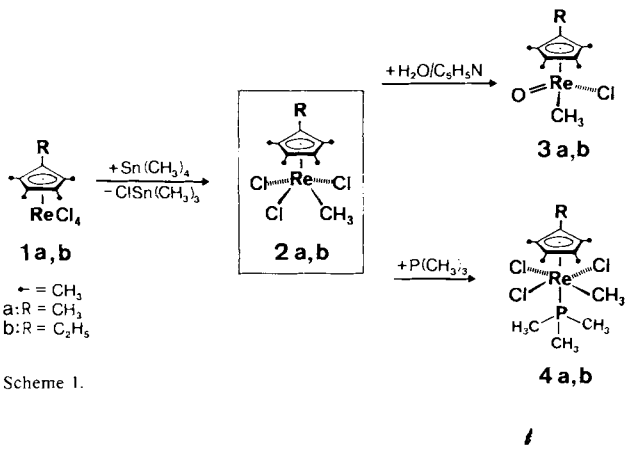

Scheme 1.

Treatment of a CH_2Cl_2 solution of **1a** at room temperature with 1.1 equivalents of tetramethylstannane results in smooth transmethylation, according to Scheme 1, to give, in addition to trimethyltin chloride (^{1}H-NMR detection), the new Re^V complex **2a** as brown, slightly air-sensitive, and strongly moisture-sensitive crystals. According to elemental analysis and the FD mass spectrum, this substance, which dissolves in polar organic solvents without undergoing decomposition, has the formula $[(C_5Me_5)CH_3ReCl_3]$. The IR spectrum exhibits, in addition to the band pattern for the $(C_5Me_5)Re$ fragment, characteristic bands for the ReCl and CH_3Re groups.[6] The complex $[(\eta^5\text{-}C_5Me_5)CD_3ReCl_3]$ ($[CD_3]$-**2a**, 99.5% labeling), which is obtained analogously from **1a** and $Sn(CD_3)_4$, allows the assignment of all CH and CD vibrations, respectively.[6] A single-crystal X-ray structure analysis of the better crystallizing derivative **2b** (Fig. 1), despite the disorder of a Cl atom with the CH_3 group, confirms the expected structure, namely, a half-sandwich complex with square-pyramidal coordination;[7] the analogously synthesized derivative $[(\eta^5\text{-}C_5Me_4Et)CH_3ReBr_3]$ has the same geometry in the crystal but exhibits no disorder.

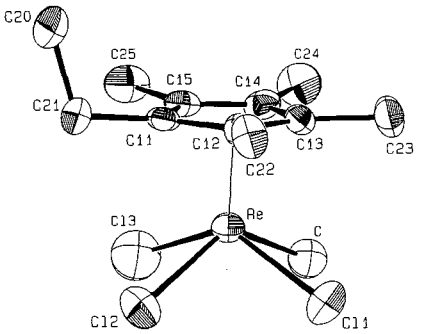

Fig. 1. Molecular crystal structure of **2b**. The complex forms orthorhombic crystals (dichloromethane/*n*-pentane, −30°C) in the space group *Pbca* (I.T. No. 61) [7]. The atoms Cl3 and C are disordered (75:25).—Selected distances [pm] and angles [°]: Re-Cl1 235.4(1), Re-Cl2 236.6(1), Re-Cl3 233.0(2), Re-C 229.7(3); Cl1,Re,Cl2 80.8(1).—Further details of the crystal structure investigation may be obtained from the Fachinformationszentrum Energie, Physik, Mathematik GmbH, D-7514 Eggenstein-Leopoldshafen 2 (FRG), on quoting the depository number CSD-52335, the names of the authors, and the journal citation.

In contrast to the oxidic d^2-Re^V complexes of the type $[(\eta^5\text{-}C_5Me_5)ReOX_2]$ (X = alkyl, halogen),[8] the aromatic π ligand of **2b** is nearly symmetrically bound to the metal. As shown by MO analysis of the d^2-complexes $[(\pi\text{-}C_5Me_5)ReX_4]$ (X = anionic ligand), these complexes can form singlet/triplet equilibria.[9] As a consequence, the metal-bound CH_3 group of **2a** exhibits a strongly temperature-dependent paramagnetic shift in the ^{1}H-NMR spectrum. Whereas the resonance absorption appears at $\delta = +36.5$ (!) at +50°C, it is shifted to higher field with decreasing temperature and appears at $\delta = +13.5$ at −50°C.

Because of the pronounced flattening of the $ReCl_3C$ pyramid in **2** (sum of angles of $ReCl_3C$ in **2b** 325°; Fig. 1), complexes of type **2** should allow an additional ligand to add at the *trans* position to the π-bonded ring system when the rhenium(v) centers act as Lewis acids. This is indeed the case (see Scheme 1): for example, **2a** reacts with water in the presence of two equivalents of pyridine to give the oxo derivative **3a** (*four* different ligands!),[10] and with trimethylphosphane to give the stable adducts **4a,b**,[11] which presumably have octahedral structures in analogy to the complex $[(\eta^5\text{-}C_5Me_5)ReCl_4(PMe_3)]$,[12] which has been characterized by X-ray structure analysis.

When higher alkyltin compounds are allowed to react with the tetrachloride **1a** under otherwise identical conditions, one obtains, in the case of $Sn(C_2H_5)_4$ and $Sn(n\text{-}C_4H_9)_4$, in addition to the corresponding trialkyltin chlorides, a rhenium(IV) complex, which does *not* contain the ethyl or *n*-butyl groups expected according to Scheme 1. Instead, the product, which is soluble in CH_2Cl_2, has the

[*] Prof. Dr. W. A. Herrmann, J. K. Felixberger, Dr. E. Herdtweck, Dr. A. Schäfer, Dr. J. Okuda
Anorganisch-chemisches Institut der Technischen Universität München
Lichtenbergstrasse 4, D-8046 Garching (FRG)

[**] Multiple Bonds between Main-Group Elements and Transition Metals, Part 42. This work was supported by Hoechst AG and the Bundesministerium für Forschung und Technologie.—Part 41: W. A. Herrmann, K. A. Jung, A. Schäfer, H.-J. Kneuper, *Angew. Chem.* 99 (1987) 464; *Angew. Chem. Int. Ed. Engl.* 26 (1987) 464.

$[\{(\eta^5\text{-}C_5Me_5)ReCl_3\}_2]$ **5a** $[(\eta^5\text{-}C_5Me_5)ReCl_3(PMe_3)]$ **6a**

formula **5a**.[13] Its binuclear constitution follows from the diamagnetism, which requires a direct metal-metal interaction, and from the reaction with trimethylphosphane leading to formation of the paramagnetic Re^{IV} complex **6a**.[14] Taking into consideration the liberation of ethylene/ethane and 1-butene/*n*-butane, respectively (detected by gas chromatography), the formation of **5a**, which involves reduction ($Re^V \rightarrow Re^{IV}$), may be explained by a β-hydride shift and its consequences (Scheme 2): the alkyl intermediate **A** rearranges to give the hydrido(olefin) isomer **B**, which then undergoes reductive decomposition with olefin elimination and intermolecular alkane formation; elemental hydrogen does *not* appear during the formation of **5a**. These findings show that alkyltin compounds of higher-valent metal halide systems, although alkylating initially in a redox-neutral reaction, can subsequently lead to reduction of the transition metal when, sterically and electronically (Lewis acids), the metal allows alkyl rearrangement processes such as the β-hydride shift to occur. It is interesting that even an excess of $Sn(CH_3)_4$ does not lead to multiple methylation of the tetrachloro complexes **1a,b**; the compound $[(\eta^5\text{-}C_5Me_5)Re(CH_3)_4]$ is obtainable, however, from **1a** via the Grignard route.[15]

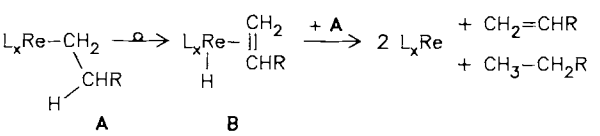

Scheme 2.

Experimental Procedure

2a: A suspension of **1** (463 mg, 1.00 mmol) in 20 mL of CH_2Cl_2 was treated at room temperature with $Sn(CH_3)_4$ (0.15 mL, 1.08 mmol) and then allowed to stir for 2 h (N_2 atmosphere). The violet suspension was thereby transformed into a red-brown solution. After removal of the solvent, the crude product was washed three times with 10 mL of *n*-pentane and finally recrystallized from CH_2Cl_2/*n*-pentane at −30°C. Yield 375 mg (85%) red-brown, analytically pure crystals; no m.p. up to 250°C.—**2b** was synthesized analogously; brown-red crystals; m.p. = 135°C (dec.).

3a: A suspension of **2a** (160 mg, 0.36 mmol) in 10 mL of toluene was allowed to react at 25°C with a solution of H_2O (6.5 μL, 0.36 mmol) and pyridine (58 μL, 0.72 mmol) in 1 mL of tetrahydrofuran (THF). After stirring for 2 h under N_2, the brown reaction solution was filtered to separate the precipitated pyridinium hydrochloride and then concentrated. Addition of a layer of *n*-pentane resulted in the precipitation at −30°C of 84 mg (60%) of black crystals; m.p. = 174°C.

Received: December 23, 1986 [Z 2029 IE]
German version: *Angew. Chem. 99* (1987) 466

[1] Reviews: R. H. Grubbs, *Prog. Inorg. Chem. 24* (1978) 1; T. J. Katz, *Adv. Organomet. Chem. 16* (1977) 283.
[2] J. A. Moulijn, C. Boelhouwer, *Chem. Commun. 1971*, 1170.
[3] E. Verkuijlen, F. Kapsteijn, J. C. Mol, C. Boelhouwer, *J. Chem. Soc. Chem. Commun. 1977*, 198; J. C. Mol, E. F. G. Woerlee, *ibid. 1979*, 330.
[4] J. C. Mol, *J. Mol. Catal. 15* (1982) 35.
[5] E. L. Muetterties, *Inorg. Chem. 14* (1975) 951.
[6] **2a**: IR (KBr, cm^{-1}; *: bands for CD_3 derivative): 1198 m ($\delta ReCH_3$), 745 m ($\gamma ReCH_3$); 3000 2-m/*2256, 2958 w-m/*2203, 2912 w-m/*2098 (νCH); 1482 s (δCH); 1378 vs, 1018 s (νCC); 330 vs ($\nu ReCl$). FD-MS (CH_2Cl_2; $^{187}Re/^{35}Cl$): *m/z* 442 ($M^{\oplus}$, 100%; correct isotope pattern). ^1H-NMR (270 MHz, $CDCl_3$, 20°C): $\delta(ReCH_3) = 27.98$ (s, 3H), $\delta(C_5(CH_3)_5) = 2.41$ (s, 15H); chemical shift of the rhenium-bound CH_3 group strongly temperature dependent (cf. text). $^{13}C\{^1H\}$-NMR (67.8 MHz, $CDCl_3$, 20°C): $\delta(C_5Me_5) = 143.8$, $\delta(C_5(CH_3)_5) = 16.0$, $\delta(ReCH_3)$ not unambiguously assignable. Correct C,H,Cl elemental analyses.
[7] Red-brown octahedra; space group *Pbca*; $a = 1247.0(3)$, $b = 836.6(1)$, $c = 2854.0(8)$ pm, $\alpha = \beta = \gamma = 90°$; $V = 2977 \times 10^6$ pm^3, $Z = 8$; $M = 456.9$; $T = 25°C$; $\rho_{calcd} = 2.038$ g cm^{-3}; $F_{000} = 1744$; CAD4 (Enraf-Nonius), graphite monochromator, $\lambda = 0.7107$ Å ($Mo_{K\alpha}$), measuring range: $1° \leq \theta \leq 25°$, $t(max) = 60$ s, $h(0/14)$, $k(0/9)$, $l(-33/33)$; 5844 measured reflections, of which 728 were not observed, 2591 unique reflections, 1816 unique reflections with $I > 3.0\sigma(I)$ used for refinement; structure solution by Patterson methods; all non-hydrogen atoms refined anisotropically, H atoms calculated at ideal positions and included in the calculation of structure factors; empirical absorption correction, $\mu = 87.93$ cm^{-1}; $R = \Sigma(||F_o| - |F_c||)/\Sigma|F_o| = 0.029$; $R_w = [\Sigma w(|F_o| - |F_c|)^2/\Sigma w F_o^2]^{1/2} = 0.028$; $GOF = [\Sigma w(|F_o| - |F_c|)^2/(NO - NV)]^{1/2} = 3.316$ ($w = 1/\sigma^2(F_o)$); $\Delta e_0/Å^3 = 1.32$.
[8] W. A. Herrmann, E. Herdtweck, M. Flöel, J. Kulpe, U. Küsthardt, J. Okuda, *Polyhedron*, in press.
[9] P. Kubáček, R. Hoffmann, Z. Havlas, *Organometallics 1* (1982) 180.
[10] **3a**: IR (KBr, cm^{-1}): 1203 m ($\delta ReCH_3$); 2978 m, 2955 m, 2915 m, 2893 m (νCH); 1460 m (sh) (δCH); 1389 m, 1378 s, 1040 s (sh) (νCC); 963 vs, 951 vs (νReO); 365 w, 343 s ($\nu ReCl$). ^1H-NMR (400 MHz, C_6D_6, 30°C): $\delta(ReCH_3) = 2.75$ (s, 3H), $\delta(C_5(CH_3)_5) = 1.54$ (s, 15H). $^{13}C\{^1H\}$-NMR (100.4 MHz, C_6D_6, 30°C): $\delta(C_5Me_5) = 103.65$, $\delta(C_5(CH_3)_5) = 10.79$, $\delta(ReCH_3) = -11.04$. EI-MS (70 eV; $^{187}Re/^{35}Cl$): *m/z* 388 ($M^{\oplus}$, 50%), 373 ($[M - CH_3]^{\oplus}$, 100%), 337 ($[M - CH_3 - HCl]^{\oplus}$, 90%). Correct C,H,Cl elemental analyses.
[11] **4a**: Dark brown crystals, m.p. = 138°C (dec.). IR (KBr, cm^{-1}): 3000 m, 2980 m, 2915 s (νCH); 1490 m, 1455 m, 1420 m (δCH); 1372 s, 1022 m (νCC); 1288 s, 970 vs (sh) (PMe_3); 305 m (sh) ($\nu ReCl$); 1005 m, 870 w, 730 m, 680 m, 370 w (without assignment). ^1H-NMR (270 MHz, C_6D_6, 20°C): $\delta(PCH_3) = 1.562$ (d, 9H; $^2J(H,P) = 11.7$ Hz); $\delta(ReCH_3) = 1.536$ (d, 3H; $^3J(H,P) = 14.7$ Hz); $\delta(C_5(CH_3)_5) = 1.491$ (s, 15H). $^{31}P\{^1H\}$-NMR (36.43 MHz, C_6D_6, 20°C; ext. H_3PO_4): $\delta = 6.70$ (s). $^{13}C\{^1H\}$-NMR (67.8 MHz, C_6D_6, 30°C): $\delta(C_5Me_5) = 108.03$, $\delta(ReCH_3) = 15.37$, $\delta(P(CH_3)_3) = 15.12$ (d; $^1J(P,C) = 39.9$ Hz), $\delta(C_5(CH_3)_5) = 10.63$. EI-MS (70 eV; $^{187}Re/^{35}Cl$): *m/z* 517 ($M^{\oplus} - H$; correct isotope pattern). Correct C,H,Cl,P elemental analyses.
[12] W. A. Herrmann, E. Voss, U. Küsthardt, E. Herdtweck, *J. Organomet. Chem. 294* (1985) C37.
[13] **5a**: Dark brown crystals; no melting point up to 250°C. IR (selected; KBr, cm^{-1}): 335 vs/305 s ($\nu ReCl$); 1485 s/1450 s (δCH); 1375 vs/1025 vs (sh) (νCC); 1078 m. ^1H-NMR (270 MHz, CD_2Cl_2, −50°C): $\delta(CH_3) = 1.85$ (s). EI-MS (70 eV, $^{187}Re/^{35}Cl$): *m/z* 427 ($[C_5Me_5ReCl_3]^{\oplus}$, 30%), 392 ($[C_5Me_5ReCl_2]^{\oplus}$, 5%), 355 ($[C_5Me_5ReCl_3 - 2HCl]^{\oplus}$, 100%), 36 ($[HCl]^{\oplus}$, 38%). Correct C,H,Cl elemental analyses.—The formulation of this compound as a dimeric species also results from the observation that it can be reduced to the structurally characterized Re^{III} complex of composition $[(\eta^5\text{-}C_5Me_5)Re(\mu\text{-}Cl)Cl]_2$: W. A. Herrmann, R. A. Fischer, E. Herdtweck, unpublished results.
[14] **6a**: Brown crystals, m.p. = 163°C (dec.). IR (selected, KBr, cm^{-1}): 275 s, 305 s, 320 vs ($\nu ReCl$); 950 vs, 965 vs, 1282 s, 1290 s, 1310 m (PMe_3). EI-MS (70 eV, $^{187}Re/^{35}Cl$): *m/z* 503 (molecular ion, 5%), 468 ($[M - Cl]$, 30%), 433 ($[M^{\oplus} - 2Cl]$, 15%), 356 ($[C_{10}H_{14}ReCl]^{\oplus}$, 100%). Correct C,H,Cl,P elemental analyses.
[15] M. Flöel, E. Herdtweck, P. Härter, J. Kulpe, W. A. Herrmann, *Angew. Chem. 99* (1987), *Angew. Chem. Int. Ed. Engl. 26* (1987), in press.

$[Ph_4P]_2[Sb_2I_8]$: Weak Interactions between Phenyl Groups of the Cation and Antimony Atoms of the Anion**

By *Siegfried Pohl,** *Wolfgang Saak*, and *Detlev Haase*

Arene-$SbCl_3$ adducts have already been well documented.[1,2] In the last few years numerous comparable complexes of gallium(I),[3] tin(II), and lead(II),[4] as well as of halides of trivalent elements of the fifth main group[5–7] with neutral arenes have also been synthesized or characterized for the first time. We report here on the complex

$[Ph_4P]_2[Sb_2I_8] \cdot 2CH_3CN$ **1**

in which we found similar interactions characteristically revealing that the phenyl groups of the cation function as

[*] Prof. Dr. S. Pohl, W. Saak, D. Haase
Fachbereich Chemie der Universität
Carl-von-Ossietzky-Strasse, D-2900 Oldenburg (FRG)

[**] This work was supported by the Fonds der Chemischen Industrie.

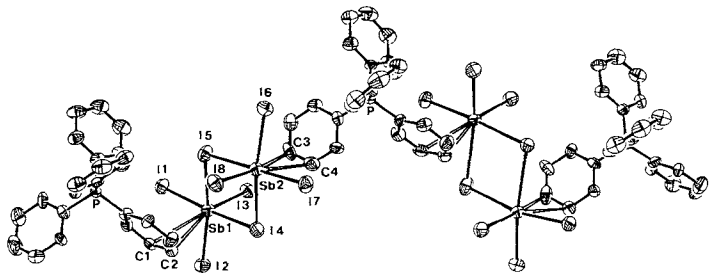

Fig. 1. Section of the structure of **1** [8]. The unit shown has crystallographic symmetry C_2. The fourth cation is not shown (see text). Selected bond lengths [pm]: Sb1-I1 286.4, Sb1-I2 288.3, Sb1-I3 277.3, Sb1-I4 324.7, Sb1-I5 328.8, Sb2-I4 335.3, Sb2-I5 318.7, Sb2-I6 287.3, Sb2-I7 287.2, Sb2-I8 276.7 (standard error 0.2 pm in each case); Sb1-C1 350, Sb1-C2 358, Sb2-C3 345, Sb2-C4 343 (standard error 2 pm in each case); angle between the normals to the planes through Sb1,C1,C2 and the phenyl ring: 114.7°; Sb2,C3,C4—phenyl ring: 115.3°.

donors towards the metal in the anion. The complex **1** is obtained in quantitative yield upon reaction of equimolar amounts of tetraphenylphosphonium iodide and antimony triiodide in acetonitrile at 81 °C; on evaporation of the solution to dryness, the compound crystallizes in the form of orange-red, prismatic crystals.

Figure 1 shows a section of the structure of **1** which was determined by an X-ray structure analysis.[8] The group shown is singly negatively charged per formula unit. The fourth, omitted tetraphenylphosphonium ion does not interact with the anion. The acetonitrile molecules are highly disorded. The antimony atoms in the $[Sb_2I_8]^{2\ominus}$ ions are square-pyramidally coordinated by iodine; $[As_2Cl_8]^{2\ominus}$, $[As_2Br_8]^{2\ominus}$, and $[Sb_2Br_8]^{2\ominus}$ ions have a comparable structure.[9] However, in these cases the non-bonding electron pairs each occupy the sixth coordination site, whereas in **1** η^2-bonded phenyl rings of the cations complement the coordination polyhedron around antimony(III). Hence, the non-bonding electron pair should, in this case, be largely stereochemically inactive.

Although a soft ligand such as iodine lowers the Lewis acidity of antimony on the one hand, on the other it probably favors the inert-pair effect and thus the observed phenyl–antimony interaction. As a result of the low acidity, the acceptor properties of Sb in $[Sb_2I_8]^{2\ominus}$ are not very pronounced. The Sb–C distances of between 343 and 358 pm, are somewhat larger than in $C_6H_6 \cdot 2SbCl_3$, where distances of 336 to 343 pm have been measured.[6] The bond lengths in the $[Sb_2I_8]^{2\ominus}$ ion correspond to those in other iodoantimonates.[10, 11] That the distances between antimony and the iodine atoms *trans* to the phenyl–antimony contacts are shortest indicates that the π-system of the phenyl group is here a weaker donor than iodine. The C–C distances are, within the limits of error, equal.

Received: December 10, 1986;
revised: February 23, 1987 [Z 2004 IE]
German version: *Angew. Chem. 99* (1987) 462

[1] W. Smith, G. W. Davies, *J. Chem. Soc. 41* (1882) 411; B. N. Menshutkin, *Zh. Russ. Fiz. Khim. 43* (1911) 1298, 1786.

[2] H. H. Perkampus: *Wechselwirkungen von π-Elektronensystemen mit Metallhalogeniden*, Springer, Berlin 1973, and references cited therein.

[3] H. Schmidbaur, *Angew. Chem. 97* (1985) 893; *Angew. Chem. Int. Ed. Engl. 24* (1985) 893.

[4] P. F. Rodesiler, T. Auel, E. L. Amma, *J. Am. Chem. Soc. 97* (1975) 7405; P. F. Rodesiler, E. L. Amma, *Inorg. Chem. 18* (1979) 751; A. G. Gash, P. F. Rodesiler, E. L. Amma, *ibid. 13* (1974) 2429.

[5] A. Schier, J. M. Wallis, G. Müller, H. Schmidbaur, *Angew. Chem. 98* (1986) 742; *Angew. Chem. Int. Ed. Engl. 25* (1986) 757.

[6] D. Mootz, V. Händler, *Z. Anorg. Allg. Chem. 533* (1986) 23, and references cited therein.

[7] R. Hulme, J. T. Szymanski, *Acta Crystallogr. B25* (1969) 753.

[8] Monoclinic, $C2/c$, $a = 4562.9(5)$, $b = 1408.6(2)$, $c = 1987.3(3)$ pm, $\beta = 105.97(1)°$, $V = 12290.4 \times 10^6$ pm^3, $Z = 8$; 8337 independent reflections were measured, 5146 thereof with $I > 2\sigma(I)$. Diffractometer: Siemens AED2; solution by Patterson methods, $R = 0.053$, $R_w = 0.052$ (SHELX-76).—Further details of the crystal structure investigation are available on request from the Fachinformationszentrum Energie, Physik, Mathematik GmbH, D-7514 Eggenstein-Leopoldshafen 2 (FRG), on quoting the depository number CSD-52390, the names of the authors, and the journal citation.

[9] J. Kaub, W. S. Sheldrick, *Z. Naturforsch. B39* (1984) 1252, 1257; A. T. Mohammed, U. Müller, *Z. Naturforsch. B40* (1985) 562; *Acta Crystallogr. C41* (1985) 329.

[10] A. F. Wells: *Structural Inorganic Chemistry*, 5th Edit., Clarendon Press, Oxford 1984, p. 888, and references cited therein.

[11] S. Pohl, W. Saak, P. Mayer, A. Schmidpeter, *Angew. Chem. 98* (1986) 813; *Angew. Chem. Int. Ed. Engl. 25* (1986) 825.

Preparation of β-Halothiophenes by Isomerization of α-Halothiophenes on Zeolite Catalysts

By *Udo Dettmeier, Klaus Eichler, Klaus Kühlein, Ernst Ingo Leupold,* and *Heinz Litterer**

Dedicated to Professor Heinz Harnisch on the occasion of his 60th birthday

Halothiophenes and their secondary products are intermediate compounds in the synthesis of drugs and plant protection agents. Whereas predominantly α-thienyl compounds were prepared in the past,[1] β-halo derivatives[2] are increasingly being resorted to nowadays for the synthesis of active substances. However, the tediousness of the methods so far available for access to these derivatives has been a drawback to their general use in such syntheses.

Thus, for example, 3-bromo and 3,4-dibromothiophenes are obtained by exhaustive bromination of thiophene to give 2,3,5-tribromo- and 2,3,4,5-tetrabromothiophene and subsequent treatment of these with Grignard reagents,[3] organolithium compounds[4] or zinc dust in acetic acid.[5] The synthesis of the β-chlorothiophene derivatives is likewise time-consuming. According to a current method by *Conde*[6] 3-chlorothiophene is obtained by reaction of 3-bromothiophene with CuCl. Treatment of 2,3,4,5-Tetrachlorotetrahydrothiophene with ethanolic potassium hydroxide[7] furnishes approximately equal amounts of 2,4- and 3,4-dichlorothiophene, whereas thermolysis of this chlorothiolane furnishes 2,3- and 2,4-dichlorothiophene.

We have now found that β-halothiophenes can be obtained in good yields in a simple way by isomerization of α-halothiophenes on silicon-rich zeolites.[8]

Zeolites of the pentasil type[9] have proven especially suitable for such syntheses. Depending on the reactivity of the α-halothiophenes, the proton-forms of these zeolites are used in the gas phase or the liquid phase. Thus, 2-chlorothiophene is converted with high selectivity into 3-chlorothiophene on an H-ZSM-5 fixed-bed catalyst at 300–450 °C and atmospheric pressure (Fig. 1). With increasing residence time, the equilibrium amount of 3-chlorothiophene of ca. 85 mol-% is established. The secondary reactions of thiophene and its derivatives normally observed with other acid catalysts, e.g. oligomerization and sulfur-elimination,[10] do not occur; the only by-product formed in any mentionable amount is thiophene.

An analogous selectivity is observed in the isomerizations of 2-bromo- and 2-iodothiophene at 150 and 100 °C, respectively, in the liquid phase.

[*] Dr. H. Litterer, Dr. U. Dettmeier, Dr. K. Eichler, Prof. Dr. K. Kühlein, Dr. E. I. Leupold
Hoechst Aktiengesellschaft
Postfach 800320, D-6230 Frankfurt am Main 80 (FRG)

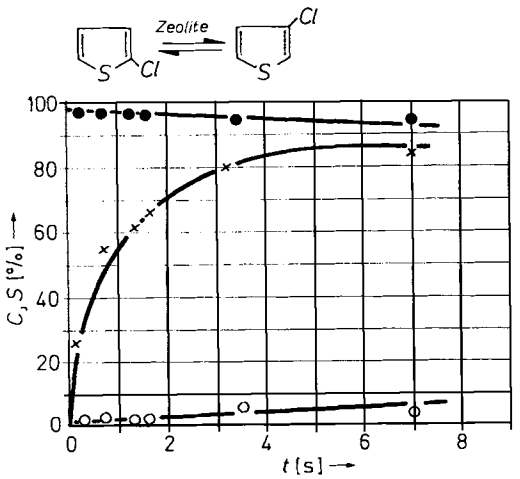

Fig. 1. Isomerization of 2-chlorothiophene with zeolites of the pentasil type [9]. C and S: conversion and selectivity. ×——×: conversion of 2-chlorothiophene; •——•: selectivity for 3-chlorothiophene; o——o: selectivity for thiophene. t = residence time. $T = 350°C$, $p_{tot} = 1$ atm.

Of special importance for carrying out such isomerizations is a well-balanced relationship between catalyst activity and catalyst life. As has been shown in exploratory experiments with a large number of ZSM-5 zeolites with varying aluminum content, ZSM-5 zeolites with ca. 0.5–0.9 wt-% Al are especially suitable for the isomerization of halothiophenes (Fig. 2).

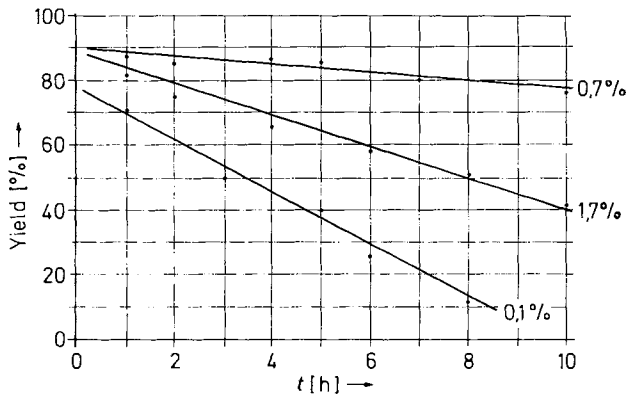

Fig. 2. Relationship of aluminum content and catalyst deactivation in the isomerization of 2- to 3-chlorothiophene. Catalyst: zeolite H-ZSM-5. The numerical data relate to the aluminum content (wt-%). t = duration of isomerization in hours.

By using these zeolites in combination with chlorination steps it has now been possible for the first time to obtain all the dichlorothiophene isomers in good yields via an industrially practicable route (Fig. 3).

A further interesting aspect of this new method is that mixed di- or trihalothiophenes can be isomerized selectively. Thus, the bromine atom in the α-position of 5-bromo-2-chlorothiophene migrates at 180–190°C in the liquid phase to the thermodynamically more favorable β-position with formation of 4-bromo-2-chlorothiophene. The migration of the less reactive chlorine is largely suppressed under these experimental conditions. In the gas phase above 300°C, however, the usual 3 mol-% of 4-bromo-3-chlorothiophene and 5-bromo-3-chlorothiophene increases to about 20 mol-% (Table 1).

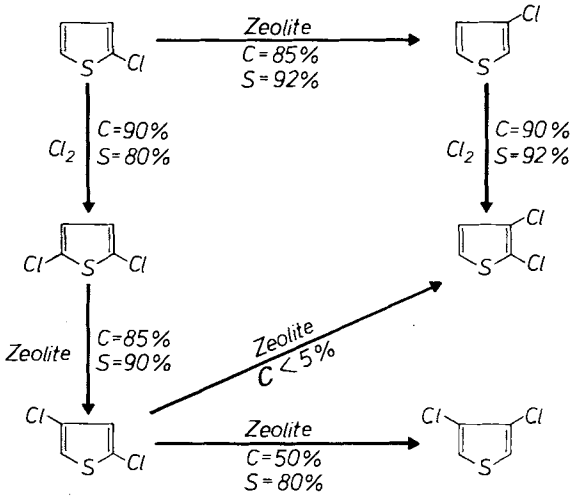

Fig. 3. New synthetic routes to 3-chlorothiophene and the dichlorothiophenes. C, S = conversion and selectivity, respectively.

Table 1. Distribution of the isomeric bromochlorothiophenes and influence of temperature on the conversion of 5-bromo-2-chlorothiophene in the presence of zeolite ZSM-5 containing 0.6 wt-% Al (see text).

T [°C]	5-Br, 2-Cl [%]	4-Br, 2-Cl [%]	4-Br, 3-Cl [%]	5-Br, 3-Cl [%]
190	15	82	2.5	0.5
300	10	70.5	17.3	2.2

The zeolite-catalyzed isomerization method provides a novel entry to a larger number of halothiophenes. The simplicity of the reaction is clearly evident from the following experimental procedure.

Experimental

1500 g of 5-bromo-2-chlorothiophene and 30 g of H-ZSM-5 zeolite powder are transferred to a 2 L four-necked flask fitted with a stirrer, reflux condenser and thermometer and the mixture heated under reflux for 7 h with vigorous stirring. The reaction mixture is then separated from the catalyst. On rectification with an efficient column, 880 g of 4-bromo-2-chlorothiophene (b.p. 192°C) and 590 g of a first fraction consisting of 4-bromo-2-chloro- and 5-bromo-2-chlorothiophene are obtained. The first fraction can be recycled for renewed isomerization.

Received: December 15, 1986;
revised: February 6, 1987 [Z 2007 IE]
German version: *Angew. Chem. 99* (1987) 470

CAS Registry numbers:
2-chlorothiophene, 96-43-5; 3-chlorothiophene, 17249-80-8; 2,5-dichlorothiophene, 3172-52-9; 2,3-dichlorothiophene, 17249-79-5; 2,4-dichlorothiophene, 17249-75-1; 3,4-dichlorothiophene, 17249-76-2; 5-bromo-2-chlorothiophene, 2873-18-9; 4-bromo-2-chlorothiophene, 32431-93-9; 4-bromo-3-chlorothiophene, 36155-88-1; 5-bromo-3-chlorothiophene, 32431-92-8.

[1] L. S. Fuller, J. W. Pratt, F. S. Yates, *Manuf. Chem. Aerosol News 49* (5) (1978) 67.
[2] J. Engel, *Chem.-Ztg. 103* (1979) 161; A. Carpita, R. Rossi, *Gaz. Chim. Ital. 115* (1985) 575; H. Kuchnis, DOS 3445356 (1985), Ciba-Geigy AG; *Eur. Chem. News*, December 2, 1985, p. 22.
[3] S. Gronowitz, *Ark. Kemi 7* (1954) 267.
[4] O. Lawesson, *Ark. Kemi 11* (1956) 373.
[5] S. Gronowitz, *Acta Chem. Scand. 13* (1959) 1045.
[6] S. Conde, *Synthesis 1976*, 412.
[7] H. L. Coonradt, D. Hartough, *J. Am. Chem. Soc. 70* (1948) 1158.
[8] K. Eichler, E. 1. Leupold, Eur. Pat.-Anm. 0166182 (1986), Hoechst AG.
[9] R. J. Argauer, G. R. Landolt, US-Pat. 3702866 (1972), Mobil Oil Corp.
[10] G. Collin, H. W. Kleffner in *Ullmanns Encyklopädie der Technischen Chemie*, 4th Edit., Vol. 23, Verlag Chemie, Weinheim 1983, p. 218.

Biphenylenes with Strongly Distorted Trapezoidal Four-Membered Ring**

By *Fritz Vögtle,* Klaus Saitmacher, Sigrid Peyerimhoff, Dorothee Hippe, Heinrich Puff,* and *Petra Büllesbach*

The skeleton of biphenylene **1** has hitherto only been described in terms of a four-membered rectangular ring with bond dimensions 151 pm (C4a-C4b) and 143 pm (C4a-C8b).[1] We have now examined how biphenylene might evade any additional strain[2] imposed by attachment of as short as possible a bracket at the 1,8-position.[3] The problem is that distortion becomes all the more extensive and consequential, and the synthesis all the more difficult the shorter the length of the bridge.

In exploratory experiments we therefore tried to attach a four-membered bridge, which, according to molecular models exhibited little strain,[3] to **1** to give the disulfide **2**, whose new ring ought to contract upon desulfurization.

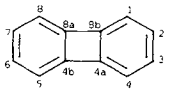

1

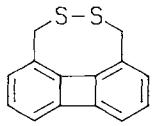

2

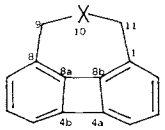

3 : X = S

4 : X = SO_2

5 : X = –

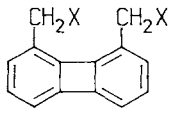

6 : X = Br

7 : X = SH

Reaction of the dibromo compound **6** with thiourea and subsequent oxidation of the dithiol **7** with H_2O_2 suffers from the low stability of **7**. In the mass spectrum of the crude product of the synthesis, however, we surprisingly observed signs of the existence of the monosulfide **3** with a shorter bridge. Studies on molecular models on the other hand, had indicated that **3** was so strained that its direct formation in a single step was not to be expected. Encouraged by the observed formation of **3** as by-product of **2**, we allowed the dibromo compound **6** (or more simply the mixture of 1,8- (**6**) and 1,5-isomer formed in its preparation[3]) to react with sodium sulfide in the presence of Cs_2CO_3 according to the dilution principle.[4] The strained sulfide **3** was obtained in 24% yield. Oxidation with H_2O_2 afforded the sulfone **4** in more than 90% yield.

At room temperature the 90-MHz ^{1}H-NMR spectra of **3** and **4** show a sharp singlet for the CH_2-protons ($\delta = 3.78$ and 4.56, respectively, in $CDCl_3$), which is considerably broadened in the 400-MHz ^{1}H-NMR spectrum of **4**. The CH_2 signals of both compounds split on lowering the temperature to give an AB system ($\Delta\nu = 31$ Hz, $J_{AB} = 17$ Hz and $\Delta\nu = 61$ Hz, $J_{AB} = 16$ Hz, respectively; coalescence temperatures $-34°$ and $-10°$C, respectively). The ring inversion barriers (flip-flopping of the C-S-C group from one side of the biphenylene system to the other; cf. Scheme 1) of **3** and **4** are thus calculated to be 49 and 53 kJ/mol, respectively.[5] The small difference in the barriers of sulfide **3** and sulfone **4** is remarkable considering a possible additional inversion of lone pairs on the sulfide sulfur, which is not possible in the case of sulfone sulfur.

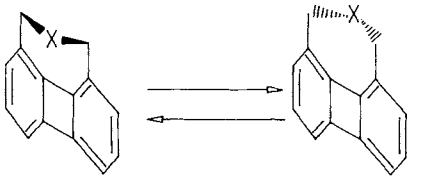

3a **3b** : X = S

4a **4b** : X = SO_2

Scheme 1.

The mass spectrum of the sulfone **4** shows, in addition to the $M^{\oplus}$ peak, a significant $[M^{\oplus} - SO_2]$ peak. This could be an indication of the existence of the extremely strained, hitherto unknown hydrocarbon **5**. We therefore tried to obtain it by photolysis of the sulfide **3** in triethyl phosphite at 230 nm, but neither this reaction nor the pyrolysis of the sulfone **4** at 650°C/10^{-3} torr in a quartz tube afforded the product **5**.

The result of an X-ray structure analysis[6] of the sulfide **3** is reproduced in Figure 1 (an X-ray structure analysis was also carried out on **4**): In both compounds the ring strain gives rise to very different bond lengths in the four-membered ring. In the trapezoidally distorted four-membered ring of **4**, similarly as in the case of **3**, the C8a-C8b bond (144.4 pm) is shortened and the C4a-C4b bond (154.6 pm) is stretched; this bond is thus longer than an isolated single bond. Remarkably, dispite this distortion the entire biphenylene framework remains practically planar. However, the bond angles in the two benzene rings are markedly altered by the bracketing: the ideal angle of 120° for C8b-C1-C2 is reduced to 114.5° in **4** (and even to 113.2° in **3**) and that for C4a-C8b-C1 is increased to 128°.

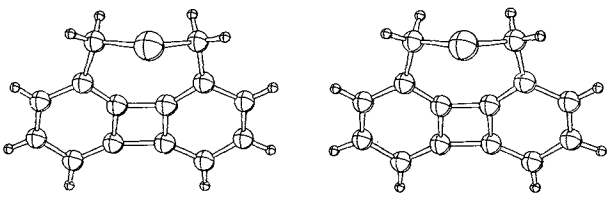

Fig. 1. Crystal structure of **3** (stereodiagram) [6].

The UV spectra of **3** ($\lambda_{max} = 359$, 258 nm; $\varepsilon = 2720$ and 28550, resp.) and **4** ($\lambda_{max} = 363$, 257 nm; $\varepsilon = 1780$ and 15390, resp.) show measurable red shifts and significant decreases in intensity of the long-wave bands (in ethanol)

[*] Prof. Dr. F. Vögtle, Dipl.-Chem. K. Saitmacher
Institut für Organische Chemie und Biochemie der Universität
Gerhard-Domagk-Strasse 1, D-5300 Bonn 1 (FRG)
Prof. Dr. S. Peyerimhoff, Dipl.-Chem. D. Hippe
Institut für Theoretische Chemie der Universität
Wegeler-Strasse 12, D-5300 Bonn 1 (FRG)
Prof. Dr. H. Puff, Dr. P. Büllesbach
Anorganisch-Chemisches Institut der Universität
Gerhard-Domagk-Strasse 1, D-5300 Bonn 1 (FRG)

[**] We thank Dr. *F. Knoch* for carrying out the X-ray structure analysis of **3**.—Thanks are also due to Prof. Dr. *W. Thiel* for supplying us with the computer program MNDOC (correlated semiempirical calculations with geometry optimization). The computations were carried out at the Regionales Hochschulrechenzentrum der Universität Bonn.

compared to biphenylene (λ_{max} = 278, 248 nm)[7] and dimethylbiphenylene (1,5-/1,8-mixture, λ_{max} = 357, 254 nm). This is an indication of perturbation of the π-electron system; analogous perturbations were observed in the transition from naphthalene to 1,8-methanonaphthalene.[8,9]

It has been shown by MNDO calculations[10] that the spatial structure of the molecule **3** is consistent with the results of the X-ray crystal structure analysis. To ensure reaching as near as possible the absolute energy minimum, the structure was optimized in three ways: a) simultaneous optimization of all bond lengths and angles, using approximate standard values for bond lengths and angles as starting values; b) simultaneous optimization of all bond lengths and angles using the structural data determined by an X-ray structure analysis as starting values; c) stepwise optimization, involving successive optimization of the carbon skeleton of the benzene ring, then the sulfur bridge, and then the H atoms, and repeating this procedure in the same succession after each individual optimization. In addition, optimization was begun with a U-shaped biphenylene skeleton, to make certain that the optimization led to a planar carbon skeleton. All three complete optimizations afforded the values listed in Table 1. Good agreement is found between experimental and calculated values.

Table 1. Calculated bond lengths [pm] and angles [°] of **3** and **5** and, for comparison, the values obtained by an X-ray structure analysis of **3** [a].

	3 (calc.)	**5** (calc.)	**3** (exp.)
C8b-C1	136	135	134.2-135.6
C1-C2	145	144	140.9-142.1
C2-C3	140	140	138.2-138.4
C3-C4	145	146	140.8-142.2
C4-C4a	137	138	135.5-136.4
C8b-C4a	146	145	140.9-141.1
C8b-C8a	146	142	145.9
C4a-C4b	150	154	154.9
C1-C11	150	153	150.1-150.2
C9-C11	—	161	—
C8b-C1-C2	112	107	113.2
C1-C2-C3	122	121	120.3-121.2
C2-C3-C4	124	126	123.6-124.4
C3-C4-C4a	116	116	115.2-115.4
C4a-C8b-C1	130	139	127.1-128.0
C4a-C8b-C8a	90.3	92.2	91.3- 92.3

[a] Deviations between the values calculated: 1 pm and 1-3°, resp.; mean deviations of the experimental values: 1-3 pm and 1-2°, resp.

The hypothetical hydrocarbon skeleton **5** was also calculated in this way (Table 1). A further shortening of the C8a-C8b bond and a further lengthening of the C4a-C4b bond are accompanied by an even greater distortion of the benzene ring (angles between 107 and 139°). According to calculations, the bond between the two "bracket" carbon atoms C9 and C11 is unusually long (161 pm).

If the enthalpy of formation ΔH_0 is used as a measure of the stability (or the ring strain), it follows from the calculated values ΔH_0 = 395 kJ/mol for biphenylene **1**[2] and 431 kJ/mol for **3** that **5** (with 586 kJ/mol) is a considerably less stable system. On the basis of these data it is easy to comprehend that all previous attempts to prepare **5** met without success.

From the calculated atomic charges of the molecules **1**, **3** and **5** it follows that the charge distribution does not essentially alter upon bracketing **1** to give **3**.

3 and **4** are the shortest bracketed biphenylene derivatives known so far. The comparatively slight additional ring strain introduced thereby results in a surprisingly large distortion of the four-membered ring. From the existence of **3** and **4** it can be safely predicted that further three-membered bridged biphenylenes such as **3** (X = O, NR, CR_2) with even higher ring strain and larger distortions could be synthesized.

Experimental

2-Thia[3](1,8)biphenylenophane **3**: A mixture of benzene (1.6 L), ethanol (1.2 L) and cesium carbonate (3.00 g, 9.20 mmol) [4] contained in a 4 L three-necked flask was heated to boiling and treated dropwise and synchronously under N_2 for 13 h with solutions of the 56:44 mixture (formed during the preparation [3]) of 1,8- and 1,5-bis(bromomethyl)biphenylene (2.88 g, 8.59 mmol) [corresponding to ca. 1.60 g (4.80 mmol of pure (**6**)] in benzene (250 mL) and $Na_2S \cdot 9H_2O$ (1.91 g, 8.60 mmol) in ethanol (250 mL). After cooling, the yellow solution was evaporated down and the insoluble cesium compounds removed by filtration through a frit. The crude product was separated by column chromatography (SiO_2, cyclohexane/chloroform). Aside from unchanged starting compound, a dimeric product ($C_{28}H_{20}S_2$) and the disulfide compound **2** could be detected mass spectrometrically. The desired monosulfide **3** (240 mg, 24%) was obtained as yellow crystals, m.p. 142-144°C (from *n*-hexane/chloroform 2:1). — 90-MHz ^{1}H-NMR ($CDCl_3$, TMS int.): δ = 3.78 (s, 4H, CH_2), 6.5-6.7 (m, 6H, aromatic H).

4: M.p. 233°C (from acetone/cyclohexane 1:1); M_r = 242.0402, high resolution MS: 242.0396.

Received: December 22, 1986;
revised: February 18, 1987 [Z 2020 IE]
German version: *Angew. Chem. 99* (1987) 459

[1] J. K. Fawcett, J. Trotter, *Acta Crystallogr. 20* (1966) 87; A. Yokozeki, C. F. Wilcox, Jr., S. H. Bauer, *J. Am. Chem. Soc. 96* (1975) 1026.
[2] For the ring strain of biphenylene see: M. Mulin, *Z. Naturforsch. B28* (1973) 478, where a value of 364 kJ/mol is quoted.
[3] A longer bridge with four C atoms does not lead to any significant changes in the bond lengths: cf. C. F. Wilcox, Jr., J. P. Uetrecht, G. D. Grantham, K. G. Grohmann, *J. Am. Chem. Soc. 97* (1975) 1914; C. F. Wilcox, Jr., D. A. Blain, J. Clardy, G. Van Duyne, R. Gleiter, M. Eckert-Makric, *ibid. 108* (1986) 7693.
[4] Cf. E. Hammerschmidt, W. Bieber, F. Vögtle, *Chem. Ber. 111* (1978) 2445. For further details of cesium-assistance cf. W. Kissener, F. Vögtle, *Angew. Chem. 97* (1985) 782; *Angew. Chem. Int. Ed. Engl. 24* (1985) 794.
[5] J. Sandström: *Dynamic NMR Spectroscopy*, Academic Press, New York 1982.
[6] Further details of the crystal structure investigation of **3** and **4** are available on request from the Fachinformationszentrum Energie, Physik, Mathematik GmbH, D-7514 Eggenstein-Leopoldshafen 2 (FRG) on quoting the depository number CSD-52236, the names of the authors, and the journal citation.
[7] UV-Atlas of Organic Compounds, Vol. 2, Verlag Chemie, Weinheim/Butterworths, London 1966.
[8] Cf. R. J. Bailey, H. Shechter, *J. Am. Chem. Soc. 96* (1974) 8116.
[9] The photoelectron spectrum of **3** can, as expected, be interpreted as a superposition of the biphenylene spectrum and a sulfide band. We thank Prof. Dr. *E. Heilbronner*, Basel (Switzerland), for collaboration.
[10] M. J. S. Dewar, W. Thiel, *J. Am. Chem. Soc. 99* (1977) 4899, 4907.

Dihydrocyclobutafuran**

By *Norbert Münzel* and *Armin Schweig**

The thermodynamics and kinetics of the equilibrium gas-phase reaction (a) of *o*-quinodimethane **1** and dihy-

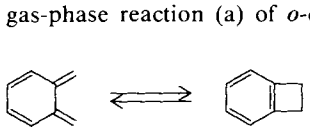

1 2 (a)

[*] Prof. Dr. A. Schweig, Dipl.-Chem. N. Münzel
Fachbereich Physikalische Chemie der Universität
Hans-Meerwein-Strasse, D-3550 Marburg (FRG)

[**] Theory and Application of Photoelectron Spectroscopy, Part 111. This work was supported by the Deutsche Forschungsgemeinschaft and the Fonds der Chemischen Industrie. — Part 110: F. Diehl, A. Schweig, *Angew. Chem. 99* (1987) 348; *Angew. Chem. Int. Ed. Engl. 26* (1987) 343.

drocyclobutabenzene **2** have already been the subject of detailed studies.[1,2] The measured data[3] suggest that **1** can be observed together with **2** either thermally at high temperatures in equilibrium [equilibrium constants $K_{581\,°C} = 20.8$ (measured[2,3]) and $K_{800\,°C} \approx 4$ (estimated[4])] or much more efficiently at low temperatures as intermediate after the decomposition of a suitable starting compound in a thermal flow reactor [rate constant (**1**→**2**) $k_{\rightarrow,225\,°C} \approx 3.3\ s^{-1}$; this corresponds to a half-life $t_{1/2}$ of ca. 0.2 s (estimated); reaction time t_R in the reactor, e.g. in combination with a UV photoelectron spectrometer, ca. 0.1 s[5]]. The latter strategy[6,7] made it possible for the first time to measure the photoelectron spectrum of **1**.[6]

In contrast, nothing is known about the analogous equilibrium reaction (b) between 2,3-dimethylene-2,3-dihydrofuran **3** and dihydrocyclobutafuran **4**, apart from the de-

(b)

3 **4**

tection of **3** by trapping reactions, and MS and NMR spectra;[8,9] **4**, in particular, has remained unknown.

According to MNDO calculations, the standard reaction enthalpy $\Delta_r H^{\ominus}$ of the reaction **1**→**2** is -82.8 kJ mol^{-1}, about 24.2 kJ mol^{-1} below the experimental value[3] (mainly a result of the overestimated stability of the closed form **2** compared to the open form **1** by the MNDO method). For the reaction **3**→**4** the MNDO method gives $\Delta_r H^{\ominus} = 75.3$ kJ mol^{-1} and, corrected by the same deviation as for **1**→**2** (-24.2 kJ mol^{-1}), ca. 99.5 kJ mol^{-1}. According to these results the reaction **3**→**4** is about twice as endothermic as the reaction **1**→**2** is exothermic. The standard reaction entropy $\Delta_r S^{\ominus}$ of the reaction **1**→**2** is negative[3] (ring closure unfavorable). Using the same value for the similar reaction **3**→**4** leads to an estimated value of ca. 10^{-13} at 200 °C to 10^{-7} at 800 °C for the equilibrium constant of this unknown gas-phase reaction. It thus follows from these data that it can hardly be possible to observe the thermodynamically "unfavorable" compound **4** in equilibrium with **3** at high temperatures in the same way as the thermodynamically "unfavorable" compound **1** in the equilibrium **1**⇄**2**.

1 could be generated thermally and observed as an adequately long-lived intermediate for the following gas-phase secondary reaction

suitable starting compound → **1** → **2**

after completion of the first step in a thermal flow reactor at low temperature. An analogous procedure for the generation of **4** is less likely to succeed, since the reaction **4**→**3** will probably be much more rapid than the reaction **1**→**2** (pre-exponential factor A presumably of the same order of magnitude as for the reaction **2**→**1**,[3] activation energy E_a presumably lower than for the reaction **1**→**2**[3]), the ratio of the rates of forward and reverse reaction for (b) is much more unfavorable than for (a) [$k_{4\rightarrow3}/k_{4\leftarrow3} \approx 10^{13}$ for (b) at 200 °C, $k_{1\rightarrow2}/k_{1\leftarrow2} \approx 10^{4}$ for (a) at a comparable temperature], and, not least, since a suitable starting compound, i.e. one which first reacts to give **4** and only then to give **3**, is not in the offing.

For these reasons, dihydrocyclobutafuran—other than dihydrocyclobutabenzene—can very probably not be generated thermally. This is consistent with the hitherto unsuccessful attempts[9,11] to obtain **4** thermally.

We have therefore explored a photochemical route [eq. (c)]. The first (thermal) reaction step, unlike in other methods already described in the literature,[8,9a] proceeds without formation of interfering by-products and is quantitative at pressures in the region of ca. 10^{-2} mbar.[13] The subsequent ring closure reaction **3**→**4** was then accomplished photochemically in the consensed phase (argon-matrix).

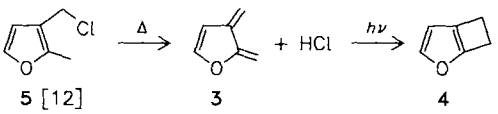

(c)

5 [12] **3** **4**

First of all, the reaction **5**→**3** was carried out in a thermal flow reactor,[13] which was installed as close as possible to the ionizing region of a UV photoelectron spectrometer. As a result of a product optimization under the conditions dictated by the photoelectron spectrometer, only **3** as well as HCl can be detected photoelectron spectroscopically, even at 550 °C (Fig. 1). The structure of **3** is substantiated by comparison with the photoelectron spectrum of **1**[6] and by comparison of the measured ionization energies with those calculated by the MNDO[10]-PERTCI,[14] CNDO/S[15]-PERTCI, LNDO/S[16]-PERTCI (Fig. 1b), and HAM/3[17] methods. Especially characteristic is the band system of reduced intensity in the region of 10–11.5 eV as a result of an unusually strong interaction of two Koopmans configurations via the HOMO-LUMO configuration (cf. Ref. [6]). The PE spectrum (Fig. 1a) remains unchanged, even at very high pyrolysis temperatures. Thus, in contrast to **1**, **3** proves to be a thermally very stable compound showing no tendency to undergo a thermally induced ring-closure reaction in the gas phase [according to the photoelectron spectra[18] of 2,3-dimethylfuran and 4,5,6,7-tetrahydrobenzofuran as well as the calculated ionization energies (Fig. 1c), the photoelectron spectrum of **4** should differ considerably from the photoelectron spectrum of **3**].

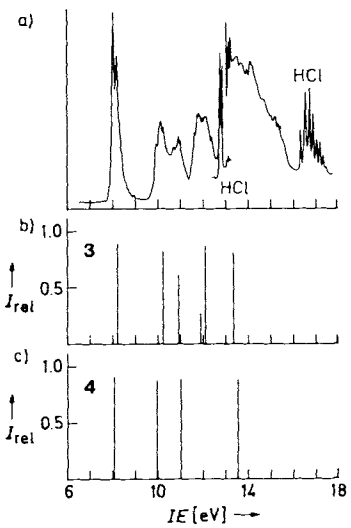

Fig. 1. a) HeI photoelectron spectrum (count rate vs ionization energy IE [eV]) of **3**; for the first three bands: assignment, measured vertical ionization energies [eV]: $^2A''(\pi)$, 8.00 (vibrational structure: $\Delta\tilde{\nu} = 1450 \pm 150$ cm^{-1}); $^2A''(\pi)$, 10.09, $^2A''(\pi)$, 10.93. b) LNDO/S-PERTCI ionization spectrum of **3** (relative intensity I_{rel} vs IE [eV]): for the first six ionizations: assignment, calculated vertical IE [eV] (I_{rel}): $^2A''(\pi)$, 8.21 (0.89); $^2A''(\pi)$, 10.23 (0.82); $^2A''(\pi)$, 10.92 (0.61); $^2A''(\pi)$, 11.89 (0.27); $^2A'(\sigma)$, 12.04 (0.87); $^2A'(\sigma)$, 13.35 (0.86). c) LNDO/S-PERTCI ionization spectrum of **4**; for the first four ionizations: $^2A(\pi)$, 8.07 (0.91); $^2A(\pi)$, 9.96 (0.88); $^2A(\sigma)$, 11.02 (0.89); $^2A(\sigma)$, 13.54 (0.89).

The reaction **5** → **3** was then carried out at the same temperature (optimized at the photoelectron spectrometer), but at a lower pressure (by about a power of ten as a result of the experimental set-up) in a reactor of the same construction,[13] which was installed as close as possible to the matrix carrier of a low-temperature cryostat. The gaseous reaction mixture was condensed together with a large excess of argon onto a NaCl-carrier at 16 K. Figure 2a shows the low-temperature IR spectrum of the reaction mixture in the solid solution (argon matrix) thus prepared, while Figure 2c shows the UV/VIS absorption spectrum of the same low-temperature matrix. From Figure 2a it can be seen that **5** does not react completely to give **3** under the reaction conditions. However, this is of no importance for the investigation described here. The UV/VIS spectrum (Fig. 2c) with a well-resolved vibrational structure of the long-wave band at $\lambda = 318$ nm is unequivocally shown, by its similarity with the UV/VIS absorption spectrum of **1**[19] and by the agreement with calculated CNDO/S-SECI,[15] LNDO/S-PERTCI and HAM/3 excitation energies (Fig. 2c) and oscillator strengths, to be the (previously unknown) spectrum of **3**.

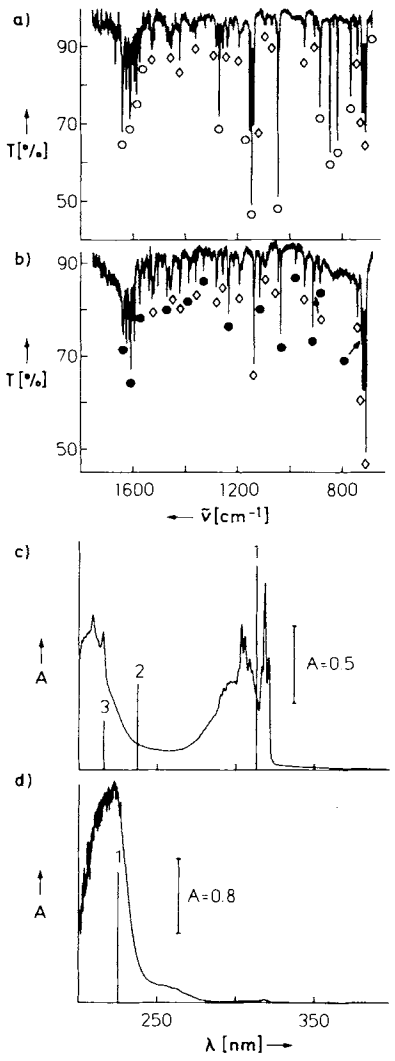

Fig. 2. a) IR spectrum (background subtracted) of the reaction mixture in argon matrix at 16 K after pyrolysis of 2-methyl-3-chloromethylfuran in a thermal reactor, T = transmission; bands of **5** and **3** are indicated by ◇ and ○, respectively; the five most intense absorptions ($\tilde{\nu}$ [cm^{-1}]) of **5**: 1421.6 (m), 1137.2 (s), 723.0 (vs), 717.4 (vs), 709.8 (vs); of **3**: 1639.6 (s), 1145.6 (vs), 1044.8 (vs), 845.6(s), 816.8 (s). b) IR spectrum (background subtracted) of the matrix of a) irradiated with UV-light of wavelength $\lambda = 300$ nm with the five most intense bands of **4** (indicated by ●): 1608.8 (s), 1234.2 (s), 1115.4 (m), 1034.6 (s), 912.4 (s). c) UV/VIS absorption spectrum (background subtracted) of the reaction mixture isolated as described in a) and HAM/3 electron excitation spectrum of **3**, A = absorbance; wavelength [nm] (oscillator strength): 1: 313.2 (0.661); 2: 237.4 (0.282); 3: 216.0 (0.163). d) UV/VIS absorption spectrum (background subtracted of the matrix of b) (i.e. after irradiation) and HAM/3 electron excitation spectrum of **4**: 1: 225.3 (0.357).

If the argon matrix containing **3** is irradiated with UV-light of wavelength $\lambda = 300$ nm for 13.5 h,[13] the absorption bands in the IR spectrum of **3** completely disappear (Fig. 2b), and the band system located at $\lambda = 318$ nm in the UV/VIS spectrum of **3** is likewise no longer observed (Fig. 2d). The new spectra unambiguously identify **4** as photoproduct: The IR spectrum (Fig. 2b) is in full agreement with the theoretical spectrum of **4** calculated according to the AM1 method,[20] both as far as the number of observed IR bands as well as their frequency and intensity are concerned. The new UV/VIS absorption band at $\lambda = 223$ nm (Fig. 2d) is best interpreted by the results of theoretical studies as a HOMO-LUMO($\pi \rightarrow \pi^*$) excitation of **4**. Moreover, the UV/VIS spectrum of **4** excellently agrees with the spectra of other 2,3-alkyl-substituted furans, whose longest wave $\pi \rightarrow \pi^*$ transition is observed at $\lambda \approx 220$ nm.[21]

The results impressively show how a thermodynamically unfavorable (because of restricted mobility, high ring strain, and lack of resonance stability) and thus thermally inaccessible compound can be generated photochemically from its thermodynamically more favorable isomeric form.

Received: December 22, 1986;
revised: January 26, 1987 [Z 2023/2024 IE]
German version: *Angew. Chem. 99* (1987) 471

CAS Registry numbers:
1, 32796-95-5; **2**, 694-87-1; **3**, 73567-98-3; **4**, 6681-01-2; **5**, 14497-33-7.

[1] W. R. Roth, M. Biermann, H. Dekker, R. Jochems, C. Mosselman, H. Hermann, *Chem. Ber. 111* (1978) 3892.
[2] W. R. Roth, B. P. Scholz, *Chem. Ber. 114* (1981) 3741.
[3] Standard enthalpies of formation $\Delta_f H^{\ominus}_{25\,°C}(\mathbf{1}) = 254.4$, $\Delta_f H^{\ominus}_{25\,°C}(\mathbf{2}) = 199.6$ kJ mol^{-1}; standard reaction enthalpies $\Delta_r H^{\ominus}_{25\,°C}(\mathbf{1} \rightarrow \mathbf{2}) = -54.8$, $\Delta_r H^{\ominus}_{500-600\,°C}(\mathbf{1} \rightarrow \mathbf{2}) = -58.6$ kJ mol^{-1}; standard reaction entropy $\Delta_r S^{\ominus}_{500-600\,°C}(\mathbf{1} \rightarrow \mathbf{2}) = -43.1$ J K^{-1} mol^{-1}; equilibrium constant $K_{509\,°C}(\mathbf{1} \rightarrow \mathbf{2}) = 45.5$, $K_{581\,°C}(\mathbf{1} \rightarrow \mathbf{2}) = 20.8$; activation energy $E_a(\mathbf{1} \rightarrow \mathbf{2}) = 112.6$, $E_a(\mathbf{1} \leftarrow \mathbf{2}) = 166.9$ kJ mol^{-1}; pre-exponential factor $A(\mathbf{1} \rightarrow \mathbf{2}) = 2.1 \times 10^{12}$, $A(\mathbf{1} \leftarrow \mathbf{2}) = 2.8 \times 10^{14}$ s^{-1}.
[4] The estimation is in agreement with the following experiment: After the thermolysis of **2** in a thermal flow reactor [corundum tube 180 × 3 mm in combination with a low-temperature cryostat, pressure $< 10^{-3}$ mbar, temperature (not optimized) 910 °C] and condensation of the reaction mixture with excess argon on an NaCl carrier at 16 K, one can distinctly recognize the most intense bands of **1** ($\tilde{\nu} = 869.2$, absorbance $A = 0.05$; 775.4 cm^{-1}, $A \approx 0.03$) together with the predominant bands of **2** ($\tilde{\nu} = 780.2$, $A = 0.679$, 715.4 cm^{-1}, $A = 0.493$) in the low-temperature IR spectrum after subtraction of background: N. Münzel, A. Schweig, unpublished.
[5] R. Schulz, A. Schweig, *J. Electron Spectrosc. Relat. Phenom. 28* (1982) 33.
[6] J. Kreile, N. Münzel, R. Schulz, A. Schweig, *Chem. Phys. Lett. 108* (1984) 609.
[7] For a further low-temperature method (using a plasma flow reactor) for the generation of **1** cf. [19].
[8] J. Julien, J. M. Pechine, F. Perez, J. J. Piade, *Tetrahedron Lett. 1979*, 3079.
[9] a) W. S. Trahanovsky, T. J. Cassady, T. L. Woods, *J. Am. Chem. Soc. 103* (1981) 6691; b) C. H. Chou, W. S. Trahanovsky, *ibid. 108* (1986) 4138; c) *J. Org. Chem. 51* (1986) 4208.
[10] M. J. S. Dewar, W. Thiel, *J. Am. Chem. Soc. 99* (1977) 4899.
[11] N. Münzel, A. Schweig, unpublished results.
[12] H. E. Winberg, F. S. Fawcett, W. E. Mochel, C. W. Theobald, *J. Am. Chem. Soc. 82* (1960) 1428.
[13] Thermal reactor: Stainless steel tube 200 × 4 mm; in combination with the photoelectron spectrometer: pressure ca. 10^{-2} mbar, optimum temperature 550 °C; in combination with the low-temperature cryostat:

pressure $< 10^{-3}$ mbar, temperature not optimized. Radiation source for the matrix irradiation: 450 W mercury high-pressure lamp, interference filter with 10 nm in bandwidth.
[14] H. L. Hase, G. Lauer, K.-W. Schulte, A. Schweig, *Theor. Chim. Acta 48* (1978) 47.
[15] K.-W. Schulte, A. Schweig, *Theor. Chim. Acta 33* (1974) 19, and references cited therein.
[16] G. Lauer, K.-W. Schulte, A. Schweig, *J. Am. Chem. Soc. 100* (1978) 4925.
[17] L. Åsbrink, C. Fridh, E. Lindholm, *Chem. Phys. Lett. 52* (1977) 63, 69, 72.
[18] N. Münzel, A. Schweig, unpublished results; data for the HeI-photoelectron spectra in the sequence: assignment, LNDO/S-PERTCI ionization energies [eV] (calculated relative intensities), measured vertical ionization energies [eV] a) for 2,3-dimethylfuran: $^2A(\pi)$, 8.36 (0.92), 8.22; $^2A(\pi)$, 9.87 (0.90), 9.70; $^2A(\sigma)$, 12.43 (0.89), 12.05; b) for 4,5,6,7-tetrahydrobenzofuran: $^2A(\pi)$, 8.55 (0.93), 8.15; $^2A(\pi)$, 10.16 (0.91), 9.65; $^2A(\sigma)$, 11.84 (0.91), 11.09.
[19] K. L. Tseng, J. Michl, *J. Am. Chem. Soc. 99* (1977) 4840.
[20] M. J. S. Dewar, E. G. Zoebisch, E. F. Healy, J. J. P. Stewart, *J. Am. Chem. Soc. 107* (1985) 3902.
[21] H. Monti, M. Bertrand, *Tetrahedron Lett. 1969*, 1235: $\lambda_{max} = 218.0$ nm in *n*-hexane for 2,3-dimethylfuran; N. Münzel, A. Schweig, unpublished results: $\lambda_{max} = 220.9$ nm in *n*-hexane for 4,5,6,7-tetrahydrobenzofuran.

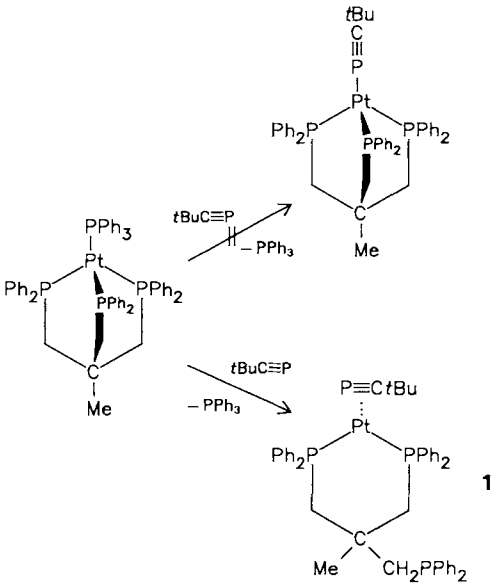

Scheme 1.

1

First Examples of Complexes Containing η^1-Bonded Phosphaalkynes—Synthesis and Crystal and Molecular Structure of *trans*-[Mo(AdC≡P)$_2$(Et$_2$PCH$_2$CH$_2$PEt$_2$)$_2$] (Ad = adamantyl)**

By *Peter B. Hitchcock, Mohd Jamil Maah, John F. Nixon,* Jalal A. Zora, G. Jeffery Leigh,* and *Mohamad Abu Bakar*

In a series of papers[1-2] we have described the wide variety of ligating behavior exhibited by phosphaalkynes RC≡P (R = *t*Bu or adamantyl (Ad)). UV photoelectron spectroscopic studies on RC≡P (R = H, F, Me, Ph, or *t*Bu) establish that the HOMO is of the π-type with the orbital of the lone pair on the P atom significantly lower in energy. It is therefore not surprising that only η^2-type coordination has hitherto been found for the coordination of phosphaalkynes to transition metals.[3] We had previously[2a] attempted to facilitate η^1-coordination of a phosphaalkyne to a metal by treating [Pt(triphos)(PPh$_3$)] (triphos = (Ph$_2$PCH$_2$)$_3$CMe) with *t*BuC≡P but obtained instead the η^2-phosphaalkyne complex **1** (Scheme 1).

We now report the synthesis of **2**–**7**, the first η^1-phosphaalkyne complexes (Scheme 2). They are readily obtained by displacement of dinitrogen from appropriate *trans*-[M(N$_2$)$_2$(R$'_2$PCH$_2$CH$_2$PR$'_2$)$_2$] (M = Mo or W) complexes[4,5] (Scheme 2).

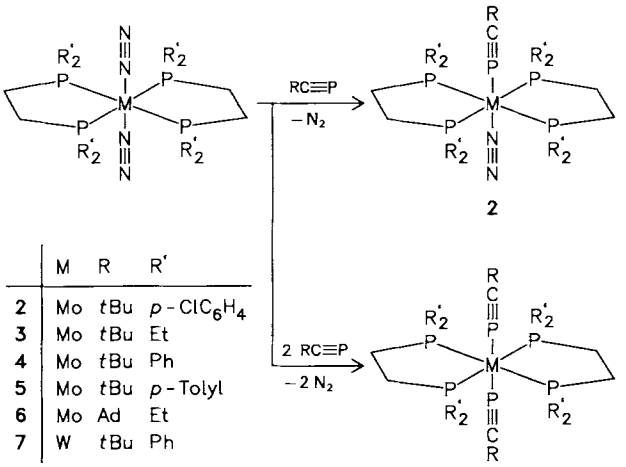

	M	R	R'
2	Mo	*t*Bu	*p*-ClC$_6$H$_4$
3	Mo	*t*Bu	Et
4	Mo	*t*Bu	Ph
5	Mo	*t*Bu	*p*-Tolyl
6	Mo	Ad	Et
7	W	*t*Bu	Ph

Scheme 2.

2

3-7

The formulation of complexes **2**–**7** is supported by their solution $^{31}P\{^1H\}$-NMR spectra which give typical patterns expected for [AA'BB'X] or [A$_4$X$_2$] spin systems,[6] and the magnitude of $^2J_{PMP'}$ is typical for this type of pseudooctahedral MP$_6$-complex (P = phosphorus ligand). Much smaller values of $^2J_{PMP'}$ would be expected for an η^2-bonded phosphaalkyne complex.

Confirmation of the proposed η^1-bonding mode comes from a single crystal X-ray diffraction study on **6**;[7] the molecular structure is shown in Figure 1. As expected, the complex contains the linear seven-atom CCPMoPCC framework involving the two *trans*-η^1-coordinated phosphaalkynes. Other features of interest in **6** are:

1) The short Mo–P$_{alkyne}$ distance (2.305(3) Å) compared with the Mo–P$_{phosphane}$ length (ca. 2.433(4) Å), reflecting the smaller sp radius of phosphorus (0.94 Å) compared with the sp^3 radius (1.07 Å).
2) The short P≡C bond distance (1.520(12) Å) compared with an average value of 1.540(4) Å observed in the free RC≡P ligands (R = H, F, Me, or *t*Bu)[8] and 1.672(17) Å in the η^2-complex [Pt(PPh$_3$)$_2$(*t*BuC≡P)].[2b]
3) The metal-phosphorus network exploited here is such that only ligands which are long and thin can approach the metal to bind in the axial position. Examples include N$_2$, CO, and MeNC. The network is also particularly robust, and consequently side-on coordination of AdC≡P is excluded on steric grounds.

Studies to investigate whether the P≡C bonds in **6** will undergo further η^2-interaction with other metals are underway.

[*] Prof. Dr. J. F. Nixon, Dr. P. B. Hitchcock, M. J. Maah, Dr. J. A. Zora
School of Chemistry and Molecular Sciences, University of Sussex
Brighton BN1 9QJ, Sussex (UK)
Prof. Dr. G. J. Leigh, Dr. M. A. Bakar
AFRC Unit of Nitrogen Fixation, University of Sussex
Brighton BN1 9RQ, Sussex (UK)

[**] This work was supported by the British Science and Engineering Research Council (SERC), the Malaysian Government (grants for *M. J. M.* and *M. A. B.*), and Basrah University (grant for *J. A. Z.*).

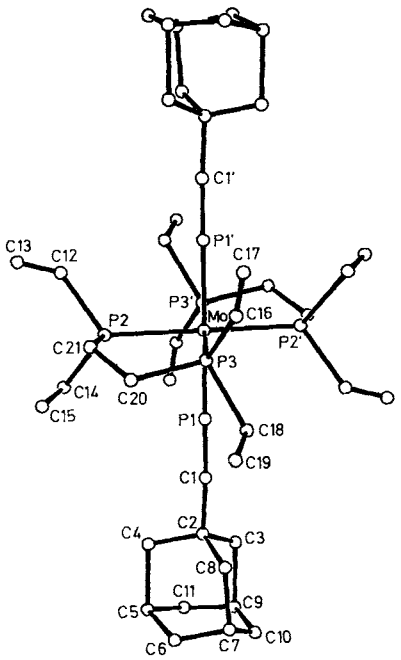

Fig. 1. The molecular structure of **6** [7]. Important bond lengths [Å] and angles [°]: Mo-P1 2.305(3), Mo-P2 2.431(4), Mo-P3 2.436(4), P1-C1 1.520(12), C1-C2 1.46(2); P1-Mo-P2 89.9(1), P1-Mo-P3 92.0(1), P2-Mo-P3 81.2(1), Mo-P1-C1 176.3(5), P1-C1-C2 177.9(8).

Experimental

An evacuated sealed tube containing a mixture of $[Mo(N_2)_2(Et_2PCH_2CH_2PEt_2)_2]$, (0.0436 g, 0.082 mmol), and AdC≡P, (0.0292 g, 0.164 mmol), in dry degassed toluene was slowly warmed from −196 °C to room temperature. After agitating the solution with ultrasound for 8 h the color changed from yellow to deep-red and on standing dark red crystals of **6** formed (yield 0.067 g, 94%; satisfactory elemental analysis).

Received: December 29, 1986;
revised: February 10, 1987 [Z 2030 IE]
German version: *Angew. Chem. 99* (1987) 497

[1] P. B. Hitchcock, M. J. Maah, J. F. Nixon, *J. Chem. Soc. Chem. Commun. 1986*, 737, and references cited therein.

[2] a) S. I. Al-Resayes, S. I. Klein, H. W. Kroto, M. F. Meidine, J. F. Nixon, *J. Chem. Soc. Chem. Commun. 1983*, 930; b) J. C. T. R. Burckett-St. Laurent, P. B. Hitchcock, H. W. Kroto, J. F. Nixon, *ibid. 1981*, 1141.

[3] For reviews on the problem see: O. J. Scherer, *Angew. Chem. 97* (1985) 905; *Angew. Chem. Int. Ed. Engl. 24* (1985) 924; E. A. Ishmaeva, I. I. Patsonovskii, *Russ. Chem. Rev. (Engl. Transl.) 54* (1985) 243.

[4] J. R. Dilworth, R. L. Richards, *Inorg. Synth. 20* (1980) 119.

[5] W. Hussain, G. J. Leigh, H. Mohd. Ali, C. J. Pickett, D. A. Rankin, *J. Chem. Soc. Dalton Trans. 1984*, 1703.

[6] **2**: $^{31}P\{^1H\}$-NMR (80 MHz, THF): $\delta(P^X)=7.2$ (q), $\delta(P^A)=65.8$ (t), $\delta(P^B)=63.0$ (t), $^2J(P^XP^B)=^2J(P^AP^X)=37.8$ Hz, $^2J(P^AP^B)=^2J(P^{A'}P^{B'})=91.1$ Hz; IR (THF): $\tilde{\nu}(N{\equiv}N)=1965\ cm^{-1}$ (s, br); −**3**: $^{31}P\{^1H\}$-NMR (THF): $\delta(P^X)=10.0$ (q), $\delta(P^A)=55.0$ (t), $^2J(P^AP^X)=40.3$ Hz; −**4**: $^{31}P\{^1H\}$-NMR (THF): $\delta(P^X)=0.1$ (q), $\delta(P^A)=67.8$ (t), $^2J(P^AP^X)=38.4$ Hz; −**5**: $^{31}P\{^1H\}$-NMR (THF): $\delta(P^X)=0.3$ (q), $\delta(P^A)=64.3$ (t), $^2J(P^AP^X)=37.8$ Hz; −**6**: $^{31}P\{^1H\}$-NMR ([D$_8$]toluene): $\delta(P^X)=7.7$ (q), $\delta(P^A)=51.4$ (t), $^2J(P^AP^X)=40.3$ Hz; −**7**: $^{31}P\{^1H\}$-NMR ([D$_8$]toluene): $\delta(P^X)=-16.9$ (q), $\delta(P^A)=39.9$ (t), $^2J(P^AP^X)=26.9$ Hz.

[7] Crystal data: $C_{42}H_{78}MoP_6$, $M=864.9$, triclinic, space group $P\bar{1}$, $a=10.458(3)$, $b=10.889(3)$, $c=11.247(3)$ Å, $\alpha=85.46(3)$, $\beta=68.37(3)$, $\gamma=80.66(3)°$, $V=1174.6$ Å^3, $Z=1$, $\rho_{calc}=1.23$ g cm^{-3}. The structure was solved by heavy atom methods and refined to $R=0.096$ ($R'=0.132$) using 2796 reflections with $|F^2|>\sigma(F^2)$ measured on an Enraf-Nonius CAD4 diffractometer. Further details of the crystal structure investigation are available on request from the Director of the Cambridge Crystallographic Data Centre, University Chemical Laboratory, Lensfield Road, Cambridge CB2 1EW, England, on quoting the names of the authors and the full citation of the journal.

[8] H. Oberhammer, G. Becker, G. Gresser, *J. Mol. Struct. 75* (1981) 283; J. Lavenge, A. Cabana, *Can. J. Phys. 60* (1982) 304; J. K. Tyler, *J. Chem. Phys. 40* (1964) 1170; H. W. Kroto, J. F. Nixon, N. P. C. Simmons, *J. Mol. Spectrosc. 82* (1980) 185; *ibid. 77* (1979) 270.

Photooxidation of 2,5-Dimethyl-2,3,4-hexatriene—Matrix Isolation of a Trisdioxetane**

By *Wolfram Sander** and *Andreas Patyk*

Photooxidations of reactive double bonds via singlet oxygen to give dioxetanes or ene-type products are well known,[1] but evidence for the direct photoreaction of olefins with triplet oxygen is still rare.[2] Although most unsaturated compounds are only slowly oxidized when exposed to air and light (autoxidation), some cumulenes are extremely reactive. For example 2,5-dimethyl-2,3,4-hexatriene (tetramethylbutatriene **1**) is reported to react rapidly to form an oxygen containing polymer if exposed to air.[3] We therefore used **1** as a model to study the photooxidation of reactive olefins. To investigate the primary reaction steps and to avoid radical chain and other intermolecular reactions, all operations were carried out at cryogenic temperatures (10–40 K) in oxygen/argon matrices.

1,[4] matrix-isolated in Ar at 10 K, showed two UV absorptions at $\lambda=256$ and 278 nm and no absorption in the visible part of the spectrum. Prolonged irradiation of the argon matrix with a mercury arc lamp and quartz optics ($\lambda>230$ nm) did not give any photoproducts observable in the UV/VIS or IR spectra.

In O_2-containing matrices (1–100% O_2), oxidation products were readily formed even on visible light irradiation (interference filter, $\lambda=543\pm10$ nm). The UV/VIS spectrum of **1** in solid O_2 showed a broad maximum at $\lambda\approx250$ nm with a long tail extending into the visible region. The photooxidation of **1** at $\lambda=543$ nm can be explained either by the excitation of a contact charge-transfer (CCT) complex $^3[\mathbf{1}^{\oplus}\cdots O_2^{\ominus}]$[2b] or by the direct excitation of a singlet-triplet transition of **1**.[5] These transitions are weakly allowed in O_2 matrices by the magnetic perturbation of triplet O_2.[5] Direct singlet-triplet transitions of organic compounds in solid O_2 have been spectroscopically observed at very high compound/O_2 ratios (>1/

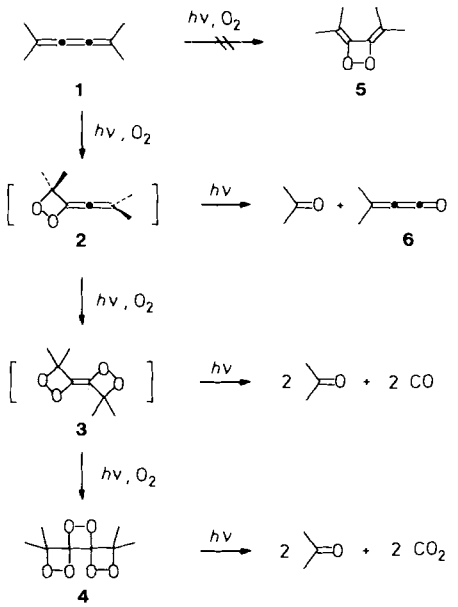

Scheme 1.

[*] Dr. W. Sander, A. Patyk
Organisch-chemisches Institut der Universität
Im Neuenheimer Feld 270, D-6900 Heidelberg (FRG)

[**] We thank Professor Dr. *R. Gleiter*, Heidelberg, for supporting this work and Professor Dr. *O. L. Chapman*, Los Angeles, for helpful discussions. This work was supported by the Deutsche Forschungsgemeinschaft.

10).[5] For matrix isolation, a ratio $< 1/500$ is necessary; thus it was not possible to observe these transitions spectroscopically. A similar photooxidation of an olefin (2,3-dimethyl-2-butene) by visible light irradiation in solid O_2 was reported recently and was explained by excitation of a CCT complex.[2b]

The products formed in the photooxidation of **1** depended on the O_2 content of the matrix and on the wavelength used for irradiation. At O_2 concentrations between 10% and 100%, 543-nm irradiation led to a single photoproduct **4** almost exclusively (Fig. 1). **4** was very labile and fragmented to acetone and CO_2 upon irradiation (slowly at $\lambda > 500$ nm and rapidly at $\lambda > 300$ nm) or by warming the matrix from 10 K to 45 K and evaporating the argon (see Scheme 1).

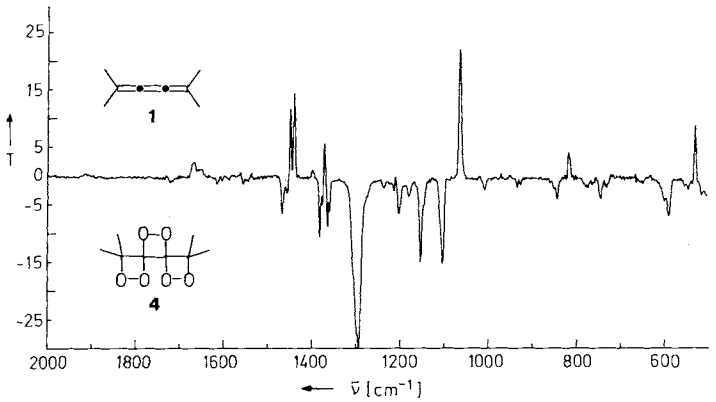

Fig. 1. Difference IR spectrum of the photooxidation of **1** in Ar/O_2 (20% O_2) at 10 K. The matrix was irradiated with the 543-nm Hg line (interference filter, Osram HBO 200W high-pressure mercury arc lamp). Top: IR-bands of **1** vanishing after irradiation. Bottom: newly occurring bands of the trisdioxetane **4**. T = transmission.

The most intense band in the IR spectrum of **4** (Fig. 1) was a broad band at $\tilde{\nu} = 1292\ cm^{-1}$.[6] This band showed an isotopic shift of approximately 2-5 cm^{-1} if the experiments were repeated in $^{18}O_2/Ar$ matrices.[7] The frequency of the band and the magnitude of the isotopic shift is typical for C-O stretching vibrations.[8] Other bands exhibiting pronounced isotopic shifts were found at $\tilde{\nu} = 1154\ cm^{-1}$ (20 cm^{-1} shift) and 1103 cm^{-1} (48 cm^{-1} shift). The latter band can be assigned to an O-C-O stretching vibration of the skeleton of **4**.[9] No bands were found in the carbonyl- (1650-1800 cm^{-1}) or cumulene- (1800-2200 cm^{-1}) regions of the spectrum.

On the basis of the observed fragmentation pattern and the IR data, we conclude that compound **4** has the structure of a trisdioxetane.[10] More evidence for this assignment came from the observation of the isotopic pattern in the CO_2 formed by the fragmentation of partially ^{18}O-labeled **4**. If a 1:1 mixture of $^{16}O_2$ and $^{18}O_2$ in argon was used to generate **4**, $C^{16}O_2$, $C^{16}O^{18}O$ and $C^{18}O_2$ were formed in a 1:2:1 ratio after short-wavelength irradiation ($\lambda > 300$ nm). This proves that the oxygen atoms in CO_2 come from two different O_2 molecules. Other possible products of the fragmentation of the trisdioxetane **4** such as peroxylactones[12] can be excluded by the IR data.

Attempts to observe chemiluminescence during the thermal fragmentation of **4** failed. In control experiments with various ketones, it was found that the high O_2 content (> 5%), required to generate **4** was sufficient to quench completely the phosphorescence of the ketones.

At lower O_2 concentrations (1-10%) a second photoproduct was formed on long-wavelength irradiation (slowly at $\lambda = 543$ nm and rapidly at $\lambda > 500$ nm). This photoproduct showed a very intense IR band at $\tilde{\nu} = 2100\ cm^{-1}$ and was identified as methyl-1,2-butadien-1-one (dimethylpropadienone **6**) by comparison with an authentic matrix-isolated sample.[13] The most likely precursor of **6** is dioxetane **2** (Scheme 1). This dioxetane, with a vinylidene side chain, is expected to show an allene band in the IR at $\tilde{\nu} \approx 1900\ cm^{-1}$ which was not observed under any conditions used in our experiments. Short-wavelength irradiation ($\lambda >$ 300 nm) of **6** gave CO, traces of carbon suboxide, and other, unidentified photooxidation products. Dimethylketene, the expected final product of the fragmentation of the isomeric dioxetane **5**, was not observed. From that we conclude that the first O_2 molecule attacks a terminal double bond in **1** to give **2** rather than the central double bond to give **5** (Scheme 1).

The second O_2 molecule can attack **2** either at the double bond adjacent to the dioxetane ring or at the terminal double bond. In the first case, a bisdioxetane is formed, which should fragment to acetone, CO_2, and to dimethylketene (which was not found). In the latter case bisdioxetane **3** is formed which should fragment to acetone and CO (Scheme 1). The only hint for the formation of **3** came from the observation of small amounts of CO upon short-wavelength irradiation ($\lambda > 300$ nm) under conditions (> 10% O_2) where only traces of **6** were formed. Although **3** is a likely source of CO, it was not possible to identify it spectroscopically in the presence of a large excess of **4**.

Interestingly, even prolonged irradiation ($\lambda > 500$ nm) in pure O_2 matrices did not lead to complete consumption of **1**. After a fast initial reaction step (ca. 30 min), the rate of photooxidation slowed down and finally stopped after several hours. Annealing the matrix at 40 K and cooling back to 10 K led to further photoreactivity. This shows that the formation of dioxetanes **2**, **3**, or **4** requires a well-defined orientation of O_2 molecules relative to **1**.

Received: January 5, 1987;
revised: February 24, 1987 [Z 2036 IE]
German version: *Angew. Chem.* 99 (1987) 495

[1] A. A. Frimer *(Singlet Oxygen in Peroxide Chemistry)* in: S. Patai (Ed.): *The Chemistry of Functional Groups, Peroxides*, Wiley, New York 1983.
[2] a) C. L. Pedersen, C. Lohse, *Tetrahedron Lett. 1978*, 3141; b) S. Hashimoto, A. Akimoto, *J. Phys. Chem. 90* (1986) 529.
[3] L. Skattebøl, *Tetrahedron 21* (1965) 1357.
[4] **1** was prepared by reaction of 2,5-dichloro-2,5-dimethyl-3-hexyne with Zn: H. Gotthardt, R. Jung, *Chem. Ber. 118* (1985) 3438.
[5] A. J. Rest, K. Salisbury, J. R. Sodeau, *J. Chem. Soc. Faraday Trans. 2* (1977) 265, 1396.
[6] Infrared spectra were recorded on an Perkin Elmer PE580 spectrometer. The resolution was generally 1.7 cm^{-1}. Some bands assigned to **4** showed matrix effects up to $\Delta\tilde{\nu} = 5\ cm^{-1}$ on changing from 5% to 100% O_2. On annealing the matrix at 40 K and recooling to 10 K, the broad band at 1293 cm^{-3} was split into two bands at 1304 and 1291 cm^{-1}. This can be explained best by a thermal reorientation of the matrix cage to give the thermodynamically most stable arrangement. **4**: IR (90% Ar, 10% O_2, 10 K): $\tilde{\nu}$ [cm^{-1}] = 2998 s, 1468 m, 1383 m, 1293 s, 1154 m, 1110 m, 1103 m, 746 w, 589 w, 547 w.
[7] [^{18}O]-**4**: IR (90% Ar, 10% $^{18}O_2$, 10 K): $\tilde{\nu}$ [cm^{-1}] = 2998 s, 1462 m, 1380 m, 1289 br s, 1134 m, 1055 m, 718 w, 580 w.
[8] S. Pinchas, I. Laulicht: *Infrared Spectra of Labelled Compounds*, Academic Press, New York 1971, p. 238 ff.
[9] The assignment of the band at $\tilde{\nu} = 1103\ cm^{-1}$ to an acetal group is based on the following considerations: The large isotopic shift of 48 cm^{-1} can only be explained if at least two ^{18}O atoms are involved in this vibration (maximum $\Delta\tilde{\nu}$ for a diatomic C-O oscillator at 1103 cm^{-1}: 27 cm^{-1}). Acetals show a series of strong absorptions in the region 1070-1190 cm^{-1}: E. D. Bergman, S. Pinchas, *Recl. Trav. Chim. Pays-Bas 71* (1952) 161.

[10] Three stereoisomers are possible for **4**: two enantiomers with C_2 symmetry and one isomer with C_s symmetry. Owing to nonbonding interactions of two methyl groups, the C_s isomer is calculated by the MNDO [11] method to be 8 kcal/mol less stable than the C_2 isomer.
[11] M. J. S. Dewar, W. Thiel, *J. Am. Chem. Soc. 99* (1977) 4899.
[12] W. Adam *(Four-membered Ring Peroxides)* in S. Patai (Ed.): *The chemistry of functional groups. Peroxides*, Wiley, New York 1983.
[13] For the authentic sample, **6** was generated by flash vacuum pyrolysis of 2-methyl-1-propene-1,1-dicarboxylic acid: R. F. C. Brown, F. W. Eastwood, K. J. Harrington, *Aust. J. Chem. 27* (1974) 2373.

The First Direct Evidence for a Cram Chelate**

By *Manfred T. Reetz,* Michael Hüllmann,* and *Thomas Seitz*

The reaction of alkyllithium and Grignard reagents with α-chiral α-alkoxyketones **1**, first investigated systematically by *Cram*, preferentially affords the "chelation controlled" diastereomer **3**.[1,2] Since the more reactive α-alkoxyaldehydes usually react unselectively,[2] other organometallic reagents were examined, of which Lewis acidic and/or chelate-forming titanium compounds such as CH_3TiCl_3 lead to excellent diastereoselectivities.[3] *Cram*'s postulate that short-lived chelates of type **2** are formed and react preferentially at the sterically less hindered side

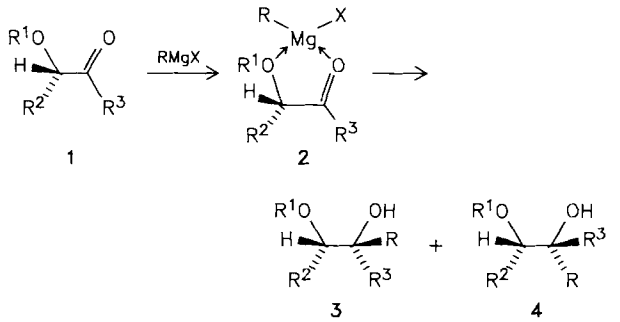

has been used as a model for 30 years.[3] However, it is based solely on the stereochemical outcome of the CC coupling.

We now report on the first direct evidence for an intermediate Cram chelate. When CH_3TiCl_3 or the more reactive reagents CH_3MgCl and CH_3Li are allowed to react with the ketone **5**, the sole product is the "chelation controlled" diastereomer **8**.[4] In the case of the monomeric organotitanium compound CH_3TiCl_3[5] we were able to monitor the reaction at −45 °C in CD_2Cl_2 by ^{13}C-NMR spectroscopy.

The spectrum recorded immediately after addition of CH_3TiCl_3 to the ketone **5** (Fig. 1) shows two signals in the carbonyl region at $\delta = 225.1$ and 225.9 in the ratio 60 : 40.[6] This means a downfield shift of about 11 ppm relative to the noncomplexed ketone **5** ($\delta = 214.2$) and corresponds to the change that is observed on complexation with $TiCl_4$ ($\delta = 227.4$).[7] A double set of signals is also observed in the other part of the ligand system (some signals overlap): $\delta = 7.5$ (slight splitting recognizable in the original spectrum; methyl group of the ethyl moiety), 15.0, 16.1, 32.4, 32.5, 75.1, 81.0, 82.4, 89.0 (arene signals appear in the δ-range 129–133). The complexation of the ether function

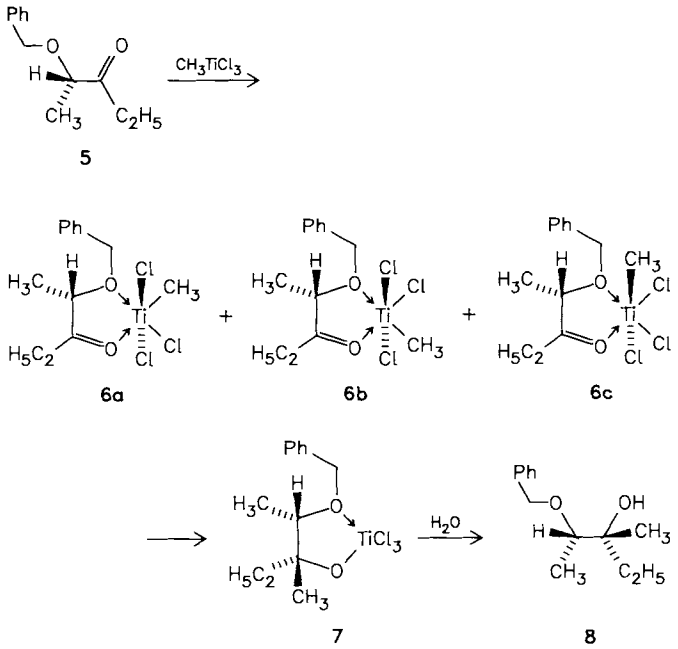

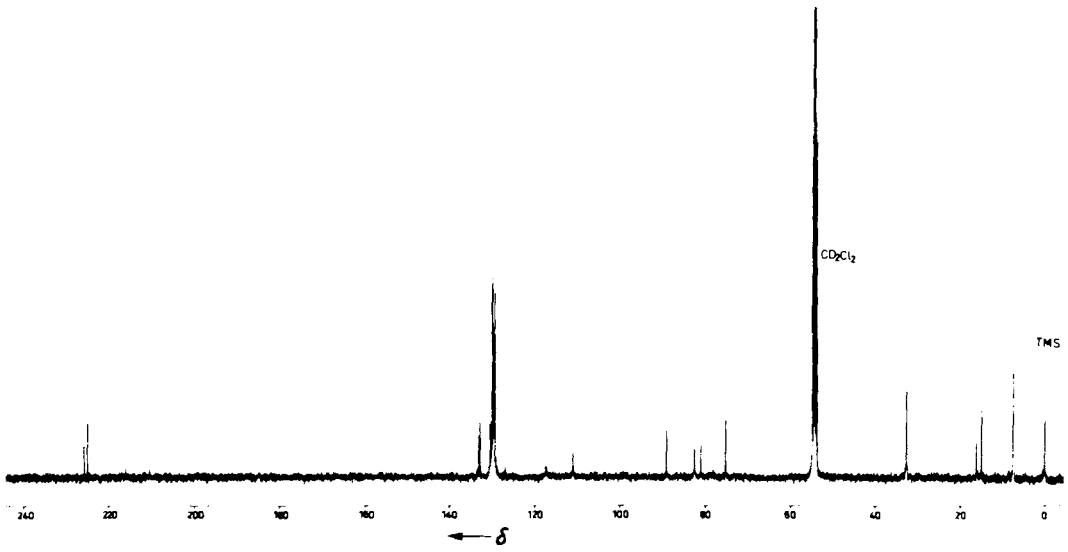

Fig. 1. ^{13}C-NMR spectrum of the freshly prepared reaction mixture CH_3TiCl_3/**5** (400 MHz instrument, −45 °C, CD_2Cl_2, after 30 min).

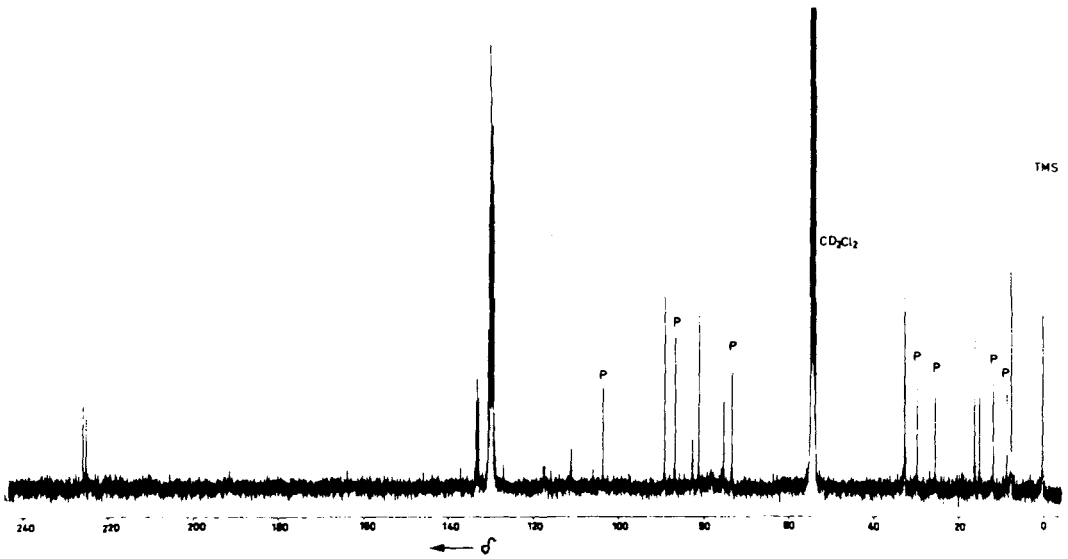

Fig. 2. ^{13}C-NMR spectrum of the reaction mixture CH_3TiCl_3/**5** after 1 h. Conditions: see Fig. 1.

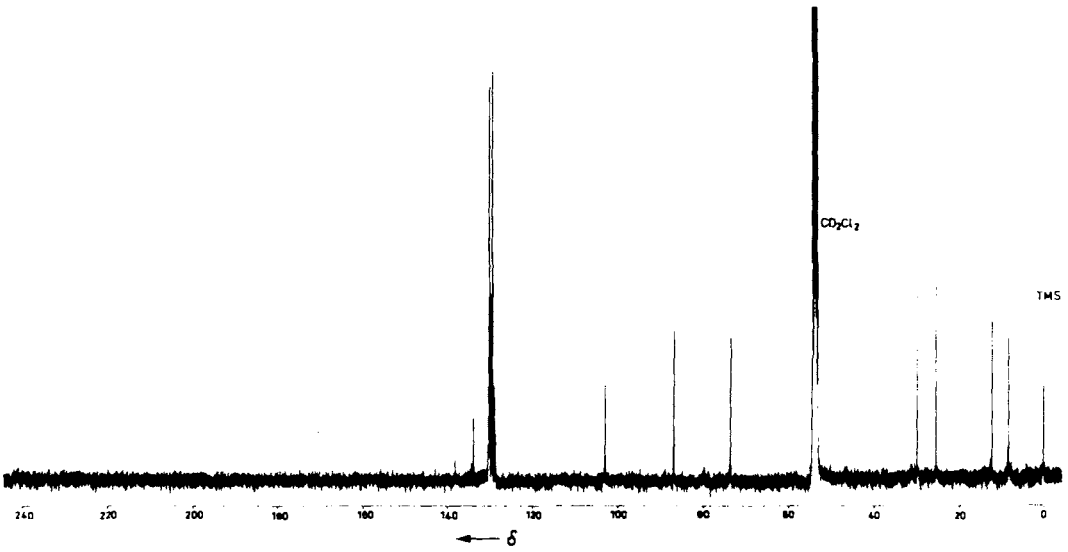

Fig. 3. ^{13}C-NMR spectrum of the reaction mixture CH_3TiCl_3/**5** after 4 h. Conditions: see Fig. 1.

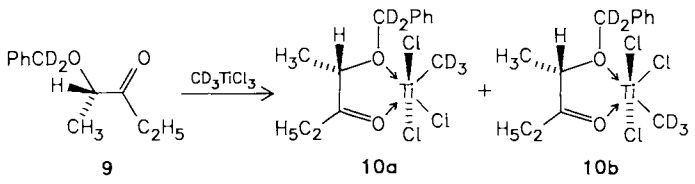

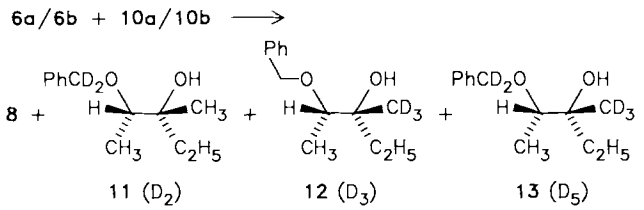

ligand exchange reactions between **6a/6b** and **10a/10b** are conceivable, which would simulate an intermolecular CC bond formation.

To check this ambiguity, kinetic experiments were performed. In the case of a purely intramolecular CC coupling step **6a/6b** → **7** a first order reaction with respect to the complex is expected, whereas in case of an intermolecular reaction, second order kinetics should pertain. Experimentally, we observed the latter ($k = 3.29 \times 10^{-3}$ L mol^{-1} s^{-1} at -15 °C). Hence an intramolecular methyl transfer can be ruled out.

Our investigations thus show[13] that *Cram*'s chelate model has a real basis and that a seemingly simple and stereochemically clean reaction can proceed in a complex manner (multistep).

Received: January 9, 1987;
revised: February 5, 1987 [Z 2043 IE]
German version: *Angew. Chem.* *99* (1987) 478

CAS Registry numbers:
5, 107798-64-1; $MeTiCl_3$, 4015-75-2.

[1] D. J. Cram, J. D. Knight, *J. Am. Chem. Soc.* *81* (1959) 2748.
[2] W. C. Still, J. H. McDonald, *Tetrahedron Lett.* *21* (1980) 1031.
[3] Review of chelation and non-chelation controlled additions to chiral alkoxy-ketones and -aldehydes: M. T. Reetz, *Angew. Chem.* *96* (1984) 542; *Angew. Chem. Int. Ed. Engl.* *23* (1984) 556.
[4] M. T. Reetz, M. Hüllmann, *J. Chem. Soc. Chem. Commun.* *1986*, 1600.
[5] Distilled CH_3TiCl_3 was used. Review of organotitanium reagents in organic synthesis: M. T. Reetz: *Organotitanium Reagents in Organic Synthesis*, Springer, Berlin 1986.
[6] Racemic **5** was used; only one enantiomer is shown.—When CH_3TiCl_3 is mixed with **5** at -78 °C virtually only the diastereomer with the carbonyl absorption at higher field is formed in a kinetically controlled reaction. On warming to -45 °C, isomerization to give a mixture of the diastereomers takes place first, followed by CC coupling.
[7] Chiral α- and β-alkoxycarbonyl compounds react with $TiCl_4$ to give characteristic 1 : 1 complexes, which have been investigated ^{1}H- and ^{13}C-NMR spectroscopically: M. T. Reetz, K. Kesseler, S. Schmidtberger, B. Wenderoth, R. Steinbach, *Angew. Chem.* *95* (1983) 1007; *Angew. Chem. Int. Ed. Engl.* *22* (1983) 989; *Angew. Chem. Suppl.* *1983*, 1511; G. E. Keck, S. Castellino, *J. Am. Chem. Soc.* *108* (1986) 3847; K. Kesseler, *Dissertation*, Universität Marburg 1986; see also [5].
[8] R. J. H. Clark, A. J. McAlees, *Inorg. Chem.* *11* (1972) 342.
[9] J. Dawoodi, M. L. H. Green, V. S. B. Mtetwa, K. Prout, *J. Chem. Soc. Chem. Commun.* *1982*, 1410.
[10] In contrast, the position of the benzyl groups (arrangement around the oxygen of the ether function) is unclear; NOE experiments do not allow any reliable conclusions to be drawn.
[11] Some additional but very weak signals are observed in the original spectrum; they probably arise from a product of ether cleavage. The titanium alkoxide **7** is likely to have the chelate structure shown, since the ^{13}C-NMR signals of the α,α'-C-atoms of the ether function are shifted markedly downfield compared to the absorptions of the titanium-free product (M. Hüllmann, *Dissertation*, Universität Marburg 1986). Normal titanium alkoxides of the type $ROTiCl_3$ are monomeric compounds which do not display any additional coordination: R. L. Martin, G. Winter, *J. Chem. Soc.* *1961*, 2947.
[12] After 2 h reaction time the ratio of the unreacted diastereomeric complexes is 27 : 73 in favor of the compound with the carbonyl signal at $\delta = 225.9$.
[13] We have also been able to monitor the reaction described here by ^{1}H-NMR spectroscopy: M. Hüllmann, *Dissertation*, Universität Marburg 1986.

Influence of H-Donor and Temperature on the Stereoselectivity of Radical Reactions**

By *Bernd Giese*,* *Juan Antonio González-Gómez*, *Stephen Lachhein*, and *Jürgen O. Metzger**

Radical reactions are finding increasing use in organic synthesis, whereby a knowledge of the reactivities and selectivities is of decisive importance. Stereoselectivity plays a crucial role, for it is dependent not so much on the product stability but rather on the shielding of the radical center because of the early transition states of rapid radical reactions. This is important in the case of H-abstraction reactions because the transfer of the small H-atoms from the less shielded side leads to the thermodynamically less stable product. Thus the addition of alkyl radicals to methylmaleic anhydride **1** and to phenylacetylene **3** in the subsequent H-abstraction step by cyclohexylmercury hydride preferentially affords the isomers (*Z*)-**2** and (*Z*)-**4**, respectively, whereby the selectivity increases with increasing size of the substituent R.[2]

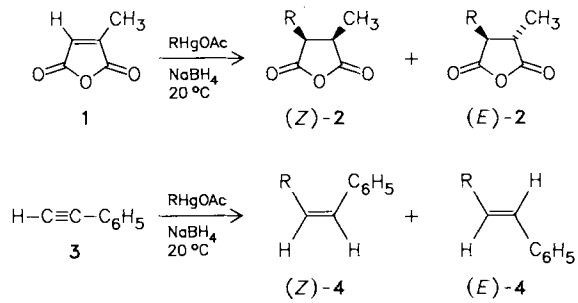

R	**a** *n*-C_6H_{13}	**b** *c*-C_6H_{11}	**c** *t*-C_4H_9
(*Z*)-**2** : (*E*)-**2**	62 : 38	89 : 11	94 : 6
(*Z*)-**4** : (*E*)-**4**		74 : 26	97 : 3

In the case of the π-vinyl radical **5b**,[3] formed by addition of cyclohexyl radicals to phenylacetylene, we have now observed that the (*Z*)/(*E*) ratio can also be influenced, and even reversed, by variation of the H-donor and the reaction temperature. Measurements between -20 °C and 260 °C show that (*Z*)-**4b** is formed with less activation enthalpy then (*E*)-**4b** (Table 1).

The approach of the H-donor from the *anti* side of the vinyl radical **5b** (away from the cyclohexyl group), for instance, requires less activation enthalpy than the attack from the *syn* side. The energy difference $\Delta H^{\neq}$((*E*)-**4b**) $-$ $\Delta H^{\neq}$((*Z*)-**4b**) thereby increases with decreasing

[*] Prof. Dr. B. Giese, Dr. J. A. González-Gómez, Dr. S. Lachhein
Institut für Organische Chemie und Biochemie
der Technischen Hochschule
Petersenstrasse 22, D-6100 Darmstadt (FRG)
Priv.-Doz. Dr. J. O. Metzger
Fachbereich Chemie der Universität
Carl-von-Ossietzky-Strasse 9-11, D-2900 Oldenburg (FRG)

[**] This work was supported by the Deutsche Forschungsgemeinschaft and the Fonds der Chemischen Industrie.

Table 1. Activation parameters for the stereoselectivity of H-transfer to the vinyl radical **5b**.

H-Donor	$\Delta H^{\neq}((E)\text{-}\mathbf{4b}) - \Delta H^{\neq}((Z)\text{-}\mathbf{4b})$ [kJ/mol]	$\Delta S^{\neq}((E)\text{-}\mathbf{4b}) - \Delta S^{\neq}((Z)\text{-}\mathbf{4b})$ [J mol^{-1} K^{-1}]	Temperature [°C]
c-C_6H_{11}HgH	2.5 ± 0.2	1.2 ± 0.5	−20–80
Bu_3SnH	4.6 ± 1.5	7 ± 5	0–84
c-C_6H_{12}	11.7 ± 1.0	28 ± 1.3	120–260

reactivity of the H-donor. It increases from 2.5 (cyclohexylmercury hydride) to 4.6 (tributyltin hydride) to 11.7 kJ/mol (cyclohexane). At the same time, the rate of H-transfer in this series decreases by about a factor of 10^7.[4]

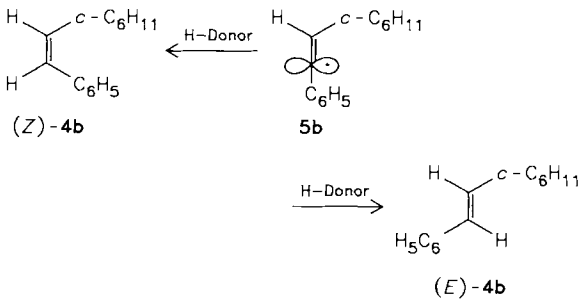

Apparently, the differences in the steric shielding have greater influence on the activation enthalpies the less reactive the H-donor is, because the distance between the reactants is smaller in the later transition states.[5] Since the difference in the activation entropies in the same series also increases from 1.2 to 7 to 28 J/mol^{-1} K^{-1}, the compensation of the activation enthalpies and activation entropies leads to an isoselective temperature,[6] which lies between 60 and 80°C (Fig. 1). In this temperature range the H-donors mentioned here react with the same selectivity. In the case of cyclohexane the entropy effects are so large that above 140°C the isomer (*E*)-**4b** is the major product. Thus, at 0°C the ratio (*Z*)-**4b**:(*E*)-**4b** is 78:22 with Bu_3SnH as donor, whereas at 260°C with cyclohexane as H-donor the selectivity (29:71) is reversed.[7]

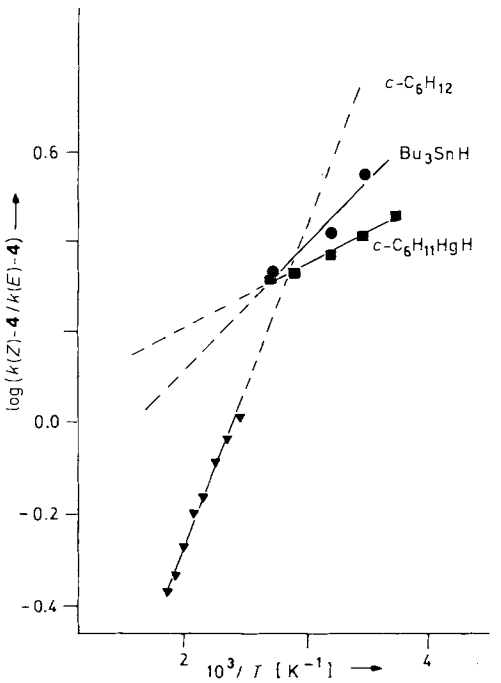

Fig. 1. Temperature dependence of the stereoselectivity for H-transfer to the vinyl radical **5b** by c-C_6H_{12}, Bu_3SnH, and c-$C_6H_{11}HgH$ as H-donors.

These investigations on the vinyl radical **5b** show how the stereoselectivities of radical reactions can be steered by varying the H-donors (radical trapping agents) and the reaction temperature.

Received: January 13, 1987 [Z 2045 IE]
German version: *Angew. Chem. 99* (1987) 475

[1] B. Giese, *Angew. Chem. 97* (1985) 555; *Angew. Chem. Int. Ed. Engl. 24* (1985) 553; *Radicals in Organic Synthesis*, Pergamon Press, Oxford 1986.
[2] B. Giese, S. Lachhein, *Angew. Chem. 94* (1982) 780; *Angew. Chem. Int. Ed. Engl. 21* (1982) 768; B. Giese, G. Kretzschmar, *Chem. Ber. 117* (1984) 3175.
[3] The phenyl substituent enforces sp hybridization at the radical center: R. M. Kochik, J. A. Kampmeier, *J. Am. Chem. Soc. 90* (1968) 6733; J. E. Bennett, J. A. Howard, *Chem. Phys. Lett. 9* (1971) 460; L. Bonazzola, S. Fenistein, R. Marx, *Mol. Phys. 22* (1971) 689.
[4] The rate coefficients for H-transfer to alkyl radicals for cyclohexylmercury hydride, tributyltin hydride, and cyclohexane have been reported to be about 10^7, 10^6 and 1 L mol^{-1} s^{-1}, respectively at 20°C: B. Giese, G. Kretzschmar, *Chem. Ber. 117* (1984) 3160; C. Chatgilialoglu, K. U. Ingold, J. C. Scaiano, *J. Am. Chem. Soc. 103* (1981) 7739; D. J. Boddy, E. W. R. Steacie, *Can. J. Chem. 39* (1961) 13.
[5] Later transition states are required by the Hammond postulate for slower reactions: G. S. Hammond, *J. Am. Chem. Soc. 77* (1955) 334.
[6] B. Giese, *Angew. Chem. 89* (1977) 162; *Angew. Chem. Int. Ed. Engl. 16* (1977) 125; *Acc. Chem. Res. 17* (1984) 438.
[7] For the experimental procedure with cyclohexane see J. Hartmanns, K. Klenke, J. O. Metzger, *Chem. Ber. 119* (1986) 488. Control experiments show that an isomerization (*Z*)-**4b** → (*E*)-**4b** is not apparent up to 260°C.

Asymmetric Synthesis of α-Amino-γ-nitrocarboxylic Esters by the Bislactim Ether Method**

By *Ulrich Schöllkopf,* Wulf Kühnle, Ernst Egert,** and *Michael Dyrbusch*

Dedicated to Professor Hans Paulsen on the occasion of his 65th birthday

Optically active γ-nitro-α-amino acids are attracting attention lately because of their potential biological activity and there usefulness as building blocks for modified oligopeptides. Moreover, they are suitable as starting compounds for the synthesis of further unusual amino acids, since the nitro group can be reduced to an amino group[1,2] or converted into a carbonyl group by the Nef reaction.[1,3] So far, however, no method for the asymmetric synthesis of this class of compounds has been reported in the literature. We now describe here an asymmetric synthesis for the methyl α-amino-γ-nitrocarboxylates **7** starting from the titanium derivative **3** of the (commercially available[4]) bislactim ether **1** of cyclo(-L-Val-Gly) and the nitroolefins **4**. Intermediates of the synthesis are the adducts **5**, which, in the case of the (*E*)-nitroolefins **4a–c**, are formed with high asymmetric induction with respect to the two stereocenters (C-2 and C-1') (Table 1). Surprising is not only the

[*] Prof. Dr. U. Schöllkopf, Dipl.-Chem. W. Kühnle
Institut für Organische Chemie der Universität
Tammannstrasse 2, D-3400 Göttingen (FRG)
Dr. E. Egert, M. Dyrbusch
Institut für Anorganische Chemie der Universität
Tammannstrasse 4, D-3400 Göttingen (FRG)

[**] Asymmetric Syntheses via Heterocyclic Intermediates, Part 34.—Part 33: U. Schöllkopf, J. Bardenhagen, *Liebigs Ann. Chem. 1987*, 393.

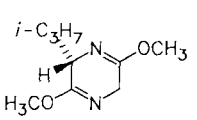

1

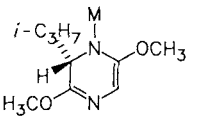

2, M = Li
3, M = $Ti[N(C_2H_5)_2]_3$

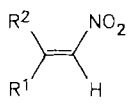

4

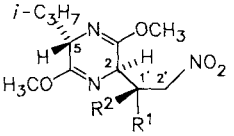

(2R,1'S)-5

Table 1. Synthesis of the diastereomeric compounds **5**.

5	R^1	R^2	B.p. [b] [°C/ 0.01 torr]	Yield [%]; diastereomers [a] with **3** [c]	with **2** [d]
a	CH_3	H	80	51; 97.4 : 0.8 : 1 : 0.8	81; 86 : — : 10 : 4
b	C_6H_5	H	140	57; 94 : 2.7 : 3.3 : —	78; 45 : 38 : 11 : 6
c	[e]	H	94–95 [f]	60; 99 : — : 1 : —	52; 49 : 41 : 6 : 4
d	CH_3	CH_3	80	—	80; 98 : 2 [g]

[a] The ratio (2*R*,1'*S*):(2*R*,1'*R*):(2*S*,1'*S*):(2*S*,1'*R*) is given; the 1'-configuration in the case of (2*S*)-isomers is arbitrary. A dash means no longer clearly recognizable. [b] (Kugelrohr). [c] GC Capillary. [d] Mean value of a capillary GC analysis and a ^{13}C-NMR analysis. [e] R^1 = 3,4-methylenedioxyphenyl. [f] M.p.: purified by low-pressure chromatography [silica gel, ether/petroleum ether (1 : 5)]. [g] (2*R*):(2*S*).

high stereoselectivity with which the two stereocenters are simultaneously formed, but also the finding that nitroolefins **4** react in satisfactory yields with the azaenolate **3** (or **2**). SET processes between the nitro group and the azaenolate were to be expected, because **3** affords a relatively stable "diazapentadienyl radical". The 2,2-dimethyl-substituted nitroolefin **4d** does not react with **3** however, but does so—and with high induction—with the lithium compound **2**.[5]

The C-2/C-5-*trans* configuration of the main components of **5** follows from the (in the bislactim ether system typical) *trans*-$^5J_{H\text{-}5/H\text{-}2}$-NMR coupling constants of ca. 4 Hz, and from the fact that 1'-aryl compounds show a high-field shift of the *cis*-H-5, which is attributed to the "aryl-inside" preferred conformation ("folded" conformation). The (1'*S*)-configuration was determined, by way of example on **5c**, by an X-ray structure analysis (Fig. 1), which concomitantly confirmed the NMR-spectroscopically identified "folded" conformation. The diastereomeric ratio (Table 1) was determined by capillary gas-chromatography[6] (with and without combined GC/MS) and/or by ^{1}H- and ^{13}C-NMR spectroscopy (Table 2).

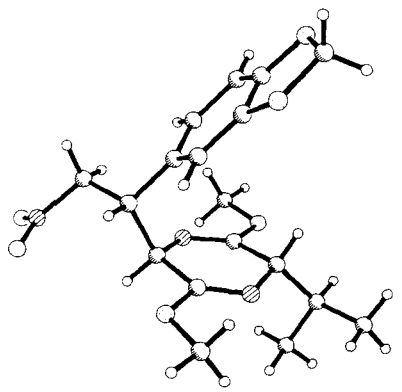

Fig. 1. Crystal structure of (5*S*,2*R*,1'*S*)-**5c** [11]. Remarkable is the "aryl-inside" conformation ("folded" conformation). O atoms dotted, N atoms hatched.

Hydrolysis of the adducts **5** to methyl L-valinate **6** and the methyl (2*R*,3*S*)-2-amino-4-nitrobutanoates **7** (Table 2), the target compounds, was accomplished under such mild conditions (0.1 N HCl, room temperature, tetrahydrofuran (THF) as cosolvent) that the nitro group remained intact. However, on attempting to hydrolyze the ester **7a** to the amino acid under acidic conditions (4 N HCl) a Nef reaction took place. An example has been described in the literature[2] for an alkaline ester hydrolysis (1 N NaOH) in which the nitro group remained intact. As shown by an ex-

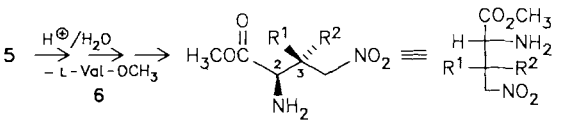

6 7

Table 2. Some physical data of **5** and **7**. ^{1}H- and ^{13}C-NMR: δ values ($CDCl_3$). B.p.: Kugelrohr; $[\alpha]_D^{20}$: *c* = 2.0; ethanol.

5a: ^{1}H-NMR: 0.70, 1.04 (2 d, *J* = 7 Hz; 6 H, $CH(CH_3)_2$), 1.13 (d, *J* = 7 Hz; 3 H, CH_3 on C-1'), 2.04–2.50 (dsp, J_1 = 3 Hz, J_2 = 7 Hz; 1 H, $CH(CH_3)_2$), 2.7–3.25 (m; 1 H, 1'-H), 3.68, 3.73 (2 s; 6 H, OCH_3), 3.98, 3.99 (2 dd, ^5J = 3.5 Hz, *J* = 3.5 Hz; 2 H, 2-H, 5-H), 4.13 (dd, J_{AB} = 11 Hz, J_{AX} = 8 Hz; A part of ABX, 1 H, 2'-H), 4.34 (dd, J_{BA} = 11 Hz, J_{AX} = 6 Hz; B part of ABX, 1 H, 2'-H).—^{13}C-NMR: 14.25 (CH_3 on C-1'), 16.59, 18.89 ($CH(CH_3)_2$), 31.88 ($CH(CH_3)_2$), 36.01 (C-1'), 52.48, 52.57 (OCH_3), 57.79, 60.84 (C-2, C-5), 78.51 (CH_2NO_2), 161.42, 164.81 (C-3, C-6)

5b: ^{1}H-NMR: 0.62, 0.94 (2 d, *J* = 7 Hz; 6 H, $CH(CH_3)_2$), 2.04–2.30 (dsp, J_1 = 3.5 Hz, J_2 = 7 Hz; 1 H, $CH(CH_3)_2$), 3.54 (dd, $^5J_1$ = 3.8 Hz, J_2 = 3.5 Hz; 1 H, 5-H), 3.73, 3.76 (2 s; 6 H, OCH_3), 4.16 (ddd, J_{AX} = 6 Hz, J_{BX} = 9 Hz, J_3 = 3.5 Hz; X part of ABX, 1 H, 1'-H), 4.30 (dd, $^5J_1$ = 3.8 Hz, J_2 = 3.5 Hz; 1 H, 2-H), 4.74 (dd, J_{AB} = 6 Hz; A part of ABX, 1 H, 2'-H), 4.85 (dd, J_{BA} = 12 Hz, J_{AX} = 9 Hz; B part of ABX, 1 H, 2'-H), 7.3–7.37 (m; 5 H, phenyl-H).—^{13}C-NMR: 16.22, 19.01 ($CH(CH_3)_2$), 31.53 ($CH(CH_3)_2$), 46.90 (C-1'), 52.72, 52.72 (OCH_3), 58.45, 60.57 (C-2, C-5), 78.33 (CH_2NO_2), 127.8, 128.23, 128.44, 128.54, 128.57, 137.23 (phenyl-C), 160.91, 165.28 (C-3, C-6)

5c: ^{1}H-NMR: 0.64, 0.99 (2 d, *J* = 7 Hz; 6 H, $CH(CH_3)_2$), 2.08–3.32 (dsp, *J* = 3.5 Hz, *J* = 7 Hz; 1 H, $CH(CH_3)_2$), 3.70 (dd, $^5J_1$ = 3.5 Hz, J_2 = 3.5 Hz; 1 H, 5-H), 3.76, 3.78 (2 s; 6 H, OCH_3), 4.10 (ddd, J_{AX} = 3.5 Hz, J_{BX} = 9.5 Hz, J_3 = 3.5 Hz; X part of ABX, 1 H, 1'-H), 4.26 (dd, $^5J_1$ = 3.5 Hz, J_2 = 3.5 Hz; 1 H, 2-H), 4.64 (dd, J_{AB} = 13 Hz, J_{AX} = 6 Hz; A part of ABX, 1 H, 2'-H), 4.73 (dd, J_{AB} = 13 Hz, J_{AX} = 9.5 Hz; B part of ABX, 1 H, 2'-H), 5.96 (s; 2 H, CH_2O_2), 6.6–6.95 (m; 3 H, aryl-H).—^{13}C-NMR: 16.48, 18.92 ($CH(CH_3)_2$), 31.60 ($CH(CH_3)_2$), 45.48 (C-1'), 52.76, 52.52 (OCH_3), 57.18, 60.34 (C-2, C-5), 77.14 (CH_2NO_2), 101.08 (CH_2O_2), 108.10, 108.88, 122.07, 128.93, 147.23, 147.49 (Aryl-C), 160.46, 165.00 (C-3, C-6)

5d: ^{1}H-NMR: 0.67, 1.08 (2 d, *J* = 6 Hz; 6 H, $CH(CH_3)_2$), 1.01, 1.20 (2 s; 6 H, CH_3 an C-1'), 2.1–2.5 (dsp, J_1 = 3 Hz, J_2 = 6 Hz; 1 H, $CH(CH_3)_2$), 3.69, 3.72 (2 s; 6 H, OCH_3), 3.90 (dd, J_1 = 3 Hz, J_2 = 3 Hz; 1 H, 5-H), 4.13 (d, *J* = 3 Hz; 1 H, 2-H), 4.40, 4.61 (2 d, J_{AB} = 11 Hz; AB spectrum, 2 H, 2'-H).—^{13}C-NMR: 16.37, 19.19 ($CH(CH_3)_2$), 21.39, 22.91 (CH_3 an C-1'), 31.06 ($CH(CH_3)_2$), 40.00 (C-1'), 52.34, 52.70 (OCH_3), 60.45, 61.10 (C-2, C-5), 84.03 (CH_2NO_2), 161.68, 164.75 (C-3, C-6)

7a: (2*R*,3*S*); yield 78%; B.p. = 60 °C/0.001 torr; $[\alpha]_D^{20}$ = −40.7°; ^{1}H-NMR: 1.06 (d, *J* = 6.5 Hz; 3 H, CH−CH_3), 2.66 (s, br; 2 H, NH_2), 2.4–3.1 (m; 1 H, 3-H), 3.42 (d, *J* = 6.5 Hz; 1 H, 2-H), 3.76 (s; 3 H, OCH_3), 4.31 (dd, J_{AB} = 12 Hz, J_{AX} = 8 Hz; A part of ABX, 1 H, 4-H), 4.64 (dd, J_{AB} = 12 Hz, J_{BX} = 6.5 Hz; B-Teil von ABX, 1 H, 4-H).—^{13}C-NMR: 14.59 (CH−CH_3), 36.63 (C-3), 52.25 (OCH_3), 57.02 (C-2), 78.25 (C-4), 174.54 (C-1)

7c: (2*R*,3*S*); yield 47%; not distilled; $[\alpha]_D^{20}$ = −8.0°; ^{1}H-NMR: 1.62 (s, br; 2 H, NH_2), 3.59 (s; 3 H, OCH_3), 3.63 (d, *J* = 7.5 Hz; 1 H, 2-H), 3.73 (ddd, J_{AX} = 8.5 Hz, J_{BX} = 5.5 Hz, J_{AB} = 7.5 Hz; X part of ABX, 1 H, 3-H), 4.70 (dd, J_{AB} = 10.3 Hz, J_{AX} = 8.5 Hz; A part of ABX, 1 H, 4-H), 5.05 (dd, J_{AB} = 10.3 Hz, J_{BX} = 5.5 Hz; B part of ABX, 1 H, 4-H), 5.93 (s; 2 H, CH_2O_2), 6.6–6.8 (m; 3 H, aryl).—^{13}C-NMR: 47.50 (C-3), 52.15 (OCH_3), 57.90 (C-2), 77.35 (C-4), 101.26 (CH_2O_2), 108.10, 108.54, 121.52, 130.07, 147.42, 148.01 (aryl-C), 173.98 (C-1)

7d: (2*R*); yield 41%; B.p. 65 °C/0.001 torr; $[\alpha]_D^{20}$ = −1.4°; ^{1}H-NMR: 1.08, 1.16 (2 s; 6 H, CH_3), 1.70 (s; br; 2 H, NH_2), 3.54 (s; 1 H, 2-H), 3.77 (s; 3 H, OCH_3), 4.33 (d, J_{AB} = 11 Hz; A of AB, 1 H, 4-H), 4.73 (d, J_{AB} = 11 Hz; B of AB, 1 H, 4-H)

ploratory hydrogenation experiment (Pd/C) with **7a**—here, as usual[1,2]—the nitro group of **7** can be reduced to an amino group. Hence, the bislactim ether method also affords access to optically active α,γ-diamino acids (NH_2 instead of NO_2 in compounds of type 7), which, as analogues of GABA, are of interest as potential enzyme inhibitors.[7]

Experimental

Compounds **5**: The bislactim ether **1** [4, 8] was lithiated to **2** [8] (1.1 equivalents of butyllithium, −78 °C, 10 min, 8 mL of THF per mmol of **1**).—Experiments with **2**: The solution of **2** was treated at −78 °C with the solution of one equivalent of **4** in THF (10 mL per mmol of **4**). After 12 hours' stirring the mixture was treated with 1.1 equivalents of acetic acid and allowed to warm to room temperature. Water (30 mL per mmol of **4**) was then added and the mixture extracted with ether. The ether extract (containing **5**) was dried over $MgSO_4$ and the ether removed under vacuum. **5** was isolated from the residue by Kugelrohr distillation (Table 1).—Experiments with **3** : **1** (0.42 g, 3.0 mmol) was lithiated to **2**. The solution of $ClTi[N(C_2H_5)_2]_3$ [9] (3.15 mmol) in hexane (ca. 3.5 mL) was then added to **2** and, after 45 min, the mixture was forced under pressure (with argon) into a solution of **4** (3.0 mmol) in THF (30 mL). After 12 hours' stirring the mixture was treated with 3.2 mmol of acetic acid and then worked-up as described above [10].

Compounds **7**: The solution of **5** (3.0 mmol) in THF (2 mL) was treated with 60 mL of 0.1 N HCl and the resulting suspension stirred at room temperature until complete dissolution (ca. 24–80 h). After saturation with NaCl and subsequent addition of 20 mL of ether, concentrated ammonia was added to the stirred mixture until a pH of 9 was reached. The phases were then separated; the aqueous phase was extracted with 4 × 20 mL of ether and, after drying the extract over $MgSO_4$ the solvent was removed under vacuum. Methyl L-valinate **6** was then removed by evaporation at 30 °C/0.01 torr in a Kugelrohr apparatus and **7** isolated from the resulting residue by Kugelrohr distillation (0.01 torr); **7c** was purified by low-pressure chromatography (silica gel, ether, $R_F = 0.16$). When prepared via **3** the crude compounds **7** were isomerically pure (^{13}C-NMR, CGC and CGC/MS; ^{1}H-NMR with Eu(hfc)$_3$ [10]).

Received: January 16, 1987 [Z 2048 IE]
German version: *Angew. Chem. 99* (1987) 480

[1] For examples of the diastereoselective reaction of lithium enolates with nitroolefins and for the hydrogenation and Nef reaction of nitro compounds see: G. Calderi, D. Seebach, *Helv. Chim. Acta 68* (1985) 1592, and references cited therein.

[2] For the synthesis and modification of methyl 2-amino-4-nitrobutanoate (the only compound of type 7 described hitherto) see Z. Prochazka, J. Smolikova, P. Malon, K. Jost, *Collect. Czech. Chem. Comm. 46* (1981) 2935.

[3] For a review of the Nef reaction cf. W. E. Noland, *Chem. Rev. 55* (1955) 137.

[4] Merck-Schuchardt, Frankfurter Str. 250, D-6100 Darmstadt (FRG), MS Info 85-14.

[5] As a rule, organolithium compounds are more reactive but less selective than organotitanium. Cf. M. T. Reetz: *Organotitanium Reagents in Organic Synthesis*, Springer, Berlin 1986.

[6] Carlo-Erba-Fractovap 2300, Chrompack-WCOT-CP-SIL-5CB column, 50 m, 0.22 mm diameter, hydrogen.

[7] See also [1].

[8] U. Schöllkopf, U. Groth, C. Deng, *Angew. Chem. 93* (1981) 793; *Angew. Chem. Int. Ed. Engl. 20* (1981) 798.

[9] M. T. Reetz, R. Urz, T. Schuster, *Synthesis 1983*, 540.

[10] All the compounds **5** and **7** gave satisfactory elemental analyses.

[11] **5c**: Space group $P2_12_12_1$, $a = 732.6(1)$, $b = 964.5(1)$, $c = 2712.5(2)$ pm, $V = 1.916$ nm^3, $Z = 4$, $\mu = 0.08$ mm^{-1} ($Mo_{K\alpha}$); crystal dimensions $0.5 \times 0.4 \times 0.3$ mm^3, 4538 measured intensities, $2\theta_{max} = 50°$, 2367 symmetry independent reflections with $|F| > 3\sigma_F$ used for the structure solution (direct methods) and refinement; C, N, and O atoms refined anisotropically, H atoms located by differential electron density determination and refined with a riding model, $R = 0.073$, $R_w = 0.062$, $w^{-1} = \sigma_f^2 + 0.0005F^2$). Further details of the crystal structure investigation are available on request from the Fachinformationszentrum Energie, Physik, Mathematik GmbH, D-7514 Eggenstein-Leopoldshafen 2 on quoting the depository number CSD-52299, the names of the authors, and the journal citation.

Synthesis of Valienamine**

By *Richard R. Schmidt** and *Arnim Köhn*

Valienamine **1** has interesting biological properties. Aside from its inhibitory action towards α-glucosides[1,2] it exhibits antibiotic activity.[2] Much more important, however, is its occurrence as central building block of several complex aminoglycoside antibiotics, such as, e.g., the validamycins,[3] and a series of pseudooligosaccharidic α-glucosidase inhibitors, including acarbose.[1,4]

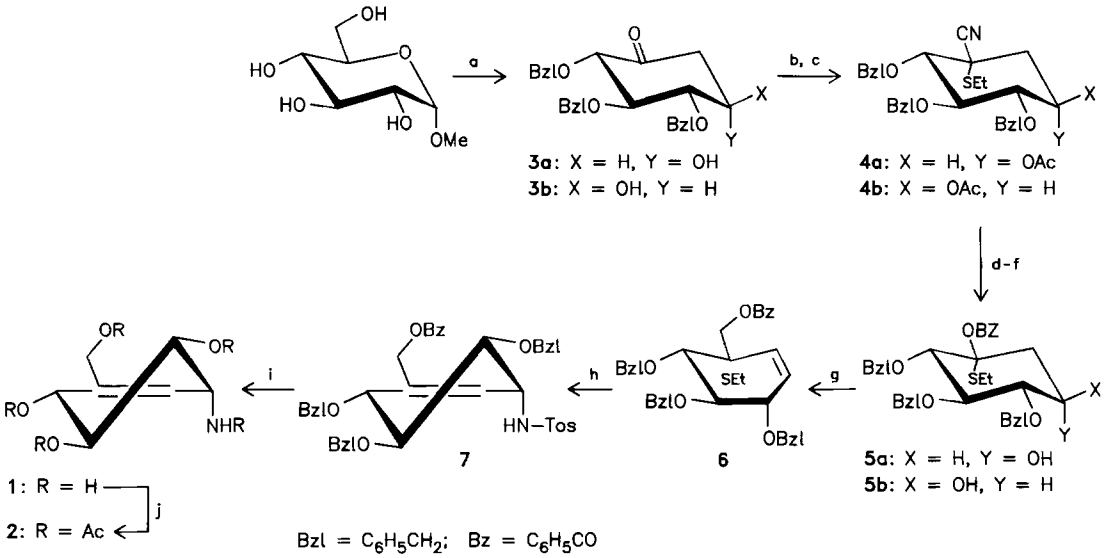

Scheme 1. Synthesis of valienamine, **1**, from methyl α-D-glucopyranoside. a) Six steps, see text and [10]; b) EtSH/MeOH, HCl; Ac_2O, pyridine (86%); c) Me_3Si–CN, $SnCl_4$, CH_2Cl_2, 0 °C (85%); d) DIBAH, CH_2Cl_2/petroleum ether, −70 °C to room temperature (RT) (78%); e) $LiAlH_4$, tetrahydrofuran, 0 °C to RT (85%); f) BzCN, CH_3CN/NEt_3, −15 °C (73%); g) PPh_3, DEAD, toluene, RT (79%); h) chloramine T, BTAC, CH_2Cl_2, RT (78%); i) NH_3(liq.), Na, −70 °C (58%); j) Ac_2O, pyridine (quantitative).

However, in its synthesis described by *Paulsen* and *Heiker* leads from (+)-quebrachitol via several steps to op-

[*] Prof. Dr. R. R. Schmidt, Dipl.-Chem. A. Köhn
Fakultät für Chemie der Universität
Postfach 5560, D-7750 Konstanz (FRG)

[**] α-Glucosidase Inhibitors, Part 4. This work was supported by the Deutsche Forschungsgemeinschaft and the Fonds der Chemischen Industrie.—Part 3: [4].

tically active valienamine.[5] Other syntheses described in the literature afford either the racemate[6] or (with **3a** as starting compound) a diastereoisomeric mixture.[7] For the decisive diastereospecific allylic amination of an alkoxy-substituted cyclohexene we chose the [2,3]-sigmatropic shift of a sulfimide group[8] as reaction step[9] (see Scheme 1). The starting compound is the cyclitol derivative **3a**, **b**, which can be obtained via Ferrier rearrangement as a 4:1 diastereomeric mixture in an overall yield of 40% in six simple steps from the commercially available methyl α-D-glucopyranoside.[7, 10] For introduction of the C_1 side-chain, and preparatory to the sigmatropic shift, the 4:1 diastereomeric mixture was converted (without separation) in an HCl-catalyzed reaction with ethanethiol into the thioketal derivative, which on reaction with trimethylsilyl cyanide and tin(IV) chloride as catalyst according to a method described by *Reetz* and *Müller-Starke*[11] afforded **4a**,**b** (4:1 diastereomeric mixture). Reduction of the nitrile group with diisobutylaluminum hydride (DIBAH) led directly to the corresponding aldehyde, which on further reduction with $LiAlH_4$ and selective benzoylation with benzoyl cyanide (BzCN)[5] furnished the cyclitol derivative **5a**,**b** (1:4 diastereomeric mixture) in good yield. This product mixture was regiospecifically dehydrated by treatment with triphenylphosphane/diethyl azodicarboxylate (DEAD) to compound **6**. Imination of the thioether group with chloramine T in a two-phase process with benzyltriethylammonium chloride (BTAC) in dichloromethane afforded directly and diastereospecifically the valienamine derivative **7** in good yields. The protecting groups on **7** were removed with sodium in liquid ammonia[12] to give valienamine, **1**, which was characterized by peracetylation to the known compound **2**.[6]

Received: January 21, 1987 [Z 2061 IE]
German version: *Angew. Chem.* *99* (1987) 490

CAS Registry numbers:
1, 38231-86-6; **2**, 38231-89-9; **3a**, 85716-45-6; **3b**, 87984-31-4; **4a**, 107960-16-7; **4b**, 108032-87-7; **5a**, 108032-89-9; **5a**, aldehyde precursor, 107960-17-8; **5a**, alcohol precursor, 107960-18-9; **5b**, 107960-19-0; **5b**, aldehyde precursor, 108032-88-8; **5b**, alcohol precursor, 104976-78-5; **6**, 107960-20-3; **7**, 107960-21-4.

[1] E. Truscheit, W. Frommer, B. Junge, D. D. Schmidt, W. Wingender, *Angew. Chem.* *93* (1981) 738; *Angew. Chem. Int. Ed. Engl.* *20* (1981) 744; B. Junge, H. Böshagen, J. Stoltefuss, L. Müller in U. Brodbeck (Ed.): *Enzyme Inhibitors*, Verlag Chemie, Weinheim 1980, p. 123, and references cited therein.
[2] Y. Kameda, N. Asano, M. Yoshikawa, K. Matsui, *J. Antibiot.* *33* (1980) 1575; T. Takehara, E. Newbrun, C. I. Hoover, *Caries Res.* *19* (1985) 266.
[3] T. Isawa, H. Yamamoto, M. Shibata, *J. Antibiot.* *23* (1970) 595.
[4] A. Köhn, R. R. Schmidt, *Liebigs Ann. Chem.* *1985*, 775, and references cited therein.
[5] H. Paulsen, F. R. Heiker, *Angew. Chem.* *92* (1980) 930; *Angew. Chem. Int. Ed. Engl.* *19* (1980) 904; *Liebigs Ann. Chem.* *1981*, 2180.
[6] S. Ogawa, T. Toyokuni, T. Suami, *Chem. Lett.* *1980*, 713; *1981*, 947; S. Ogawa, T. Toyokuni, M. Omata, N. Chida, T. Suami, *Bull. Chem. Soc. Jpn.* *53* (1980) 455; S. Ogawa, N. Chida, T. Suami, *J. Org. Chem.* *48* (1983) 1203; T. Toyokuni, S. Ogawa, T. Suami, *Bull. Chem. Soc. Jpn.* *56* (1983) 1161.
[7] N. Sakairi, H. Kuzuhara, *Tetrahedron Lett.* *23* (1982) 5327.
[8] W. Ando, *Acc. Chem. Res.* *10* (1977) 179; R. W. Hoffmann, *Angew. Chem.* *91* (1979) 625; *Angew. Chem. Int. Ed. Engl.* *18* (1979) 563.
[9] A. Köhn, *Dissertation*, Universität Konstanz 1987.
[10] D. Semeira, M. Phillippe, J.-M. Delaumeny, A.-M. Sepulchre, D. Gero, *Synthesis* *1983*, 710. This method has been improved: A. Köhn, unpublished results (1984) (see [9]); S. Mirza, L.-P. Molleyres, A. Vasella, *Helv. Chim. Acta* *68* (1985) 989.
[11] M. T. Reetz, H. Müller-Starke, *Tetrahedron Lett.* *25* (1984) 3301.
[12] E. J. Reist, V. J. Bartuska, L. Goodman, *J. Org. Chem.* *29* (1964) 3725; V. G. Nayah, R. C. Whistler, *ibid.* *34* (1969) 97.

IR Spectroscopic Determination of the Enzyme Content of Carrier-fixed Enzymes

By *Willi Herzog, Reinhold Keller,* Erhart Neukum,* and *Dieter Wullbrandt*

Dedicated to Professor Heinz Harnisch on the occasion of his 60th birthday

Enzymes are attracting increasing attention as catalysts for organic syntheses.[1] They are employed both in hydrolyses on an industrial scale as well as for the preparation of reagents for analyses and syntheses on a laboratory scale. Improvements in the preparation of the enzymes and in their stabilization and manipulation by immobilization continually make these catalysts all the more attractive.

In order to find optimal conditions for the immobilization of the enzymes it is necessary to determine not only the activity but also the enzyme content and then to calculate the specific activity. In this way one obtains activities based on the amounts of enzyme used, thus enabling a comparison of the catalysts. We now show with the enzyme α-chymotrypsin as example that the enzyme content can be determined by IR spectroscopy. α-Chymotrypsin is an endoprotease and catalyzes, inter alia, the enantiospecific ester cleavage of L-phenylalanine methyl ester.[2] α-Chymotrypsin is preferentially immobilized on inorganic substances such as silica gels. The support is first aminated on the surface and then coupled via glutaric dialdehyde with the enzyme (Fig. 1).

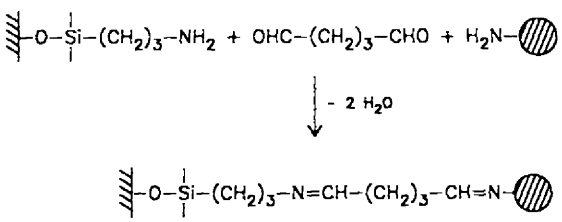

Fig. 1. Coupling of an aminated silicate support via glutaric dialdehyde with an enzyme (schematic).

The IR measurements were carried out with a Perkin-Elmer grating spectrometer 580B coupled to a computer (Perkin-Elmer PC-7300 with CDS-IR software). First of all, it was demonstrated by recording the IR spectra of self-supporting targets of ca. 10 mg weight (diameter: 13 mm, thickness < 0.1 mm), prepared from the carrier material, the carrier material treated with glutaric dialdehyde and carrier-fixed α-chymotrypsin (Fig. 2) with a pressure of 100 kN, that there is no band overlap.

The spectrum of the catalyst shows a broad band at $\tilde{\nu} = 3350\ cm^{-1}$, which is mainly due to the NH_2- and NH-groups of the enzyme. Besides the absorption bands of the CH_3- and CH_2-valence vibration in the region of 2970–2880 cm^{-1} and those of the lattice overtone vibrations of the carrier material at 2000–1850 cm^{-1}, the amide-I and amide-II bands of the enzyme are clearly observable at 1650 and 1540 cm^{-1}, respectively. The integral of these two amide bands is a valid measure of the enzyme content. After recording the IR spectrum the target was weighed and the spectrum normalized to 10 mg initial weight. Be-

[*] Dr. R. Keller, Dr. W. Herzog, E. Neukum, Dr. D. Wullbrandt
Hoechst Aktiengesellschaft, Zentralforschung
D-6230 Frankfurt am Main 80 (FRG)

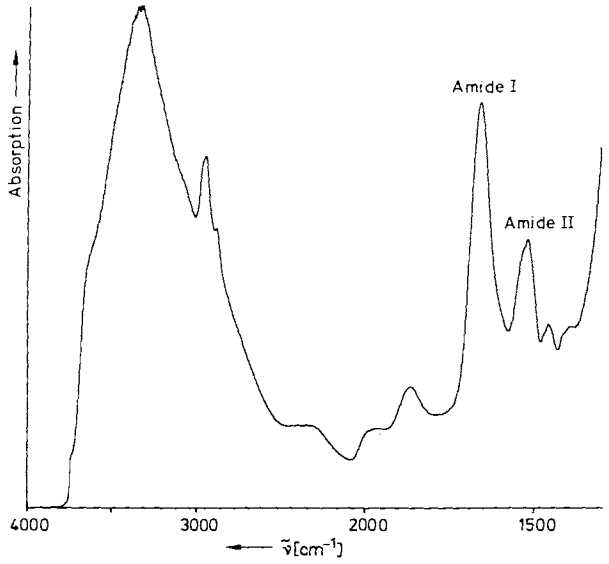

Fig. 2. IR spectrum of the fresh catalyst of propylamine-silica gel, glutaric dialdehyde and α-chymotrypsin (see text).

cause of the relatively strong absorption of water at 1650 cm^{-1} the sample had to be carefully dried before being pressed. This was carried out using a pump equipment with (forepump) backing pump and diffusion pump, first to a pressure of 1 mbar and then, after pulverization of the catalyst, to a pressure of less than 5×10^{-3} mbar.

For constructing the calibration curve a stock mixture of 880 mg propylamine-silica gel and 120 mg α-chymotrypsin was prepared; this was moistened to improve mixing, and finally dried. From this stock mixture, containing 12 wt-% α-chymotrypsin, further aliquoted mixtures ranging down to a content of 2 wt-% α-chymotrypsin were prepared by addition of propylamine-silica gel (Fig. 3). In order to determine the scatter, the spectra of four pressed disks from each mixture were recorded.

Finally an integration was carried out in the region of the amide bands from 1736 to 1426 cm^{-1}. The calibration curve was then plotted after subtraction of the background (absorption of the propylamine-silica gel in the same region (Fig. 4).

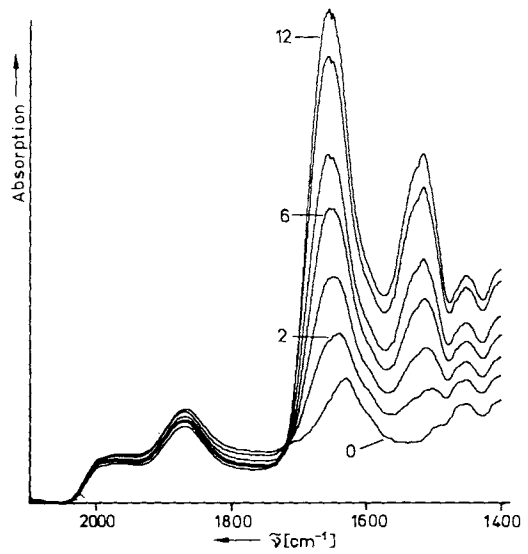

Fig. 3. IR spectra of fresh catalysts (cf. Fig. 2) as a function of the α-chymotrypsin content (data in wt-%).

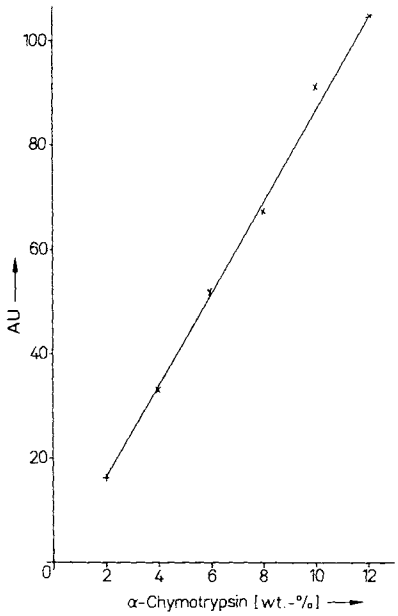

Fig. 4. Calibration curve for the IR spectroscopic determination of the α-chymotrypsin content of support catalysts (cf. Fig. 2). AU denotes arbitrary units.

On completion of the calibration curve, the α-chymotrypsin contents of five fresh contact catalysts containing varying amounts of enzyme were determined IR spectroscopically (lower limit of measurement ca. 1 wt-%, relative error 3%). As shown in Table 1, α-chymotrypsin is completely bound to the silica gel during the catalyst preparation.

Table 1. Comparison of enzyme loss to be expected after preparation of the catalyst with the IR spectroscopically determined enzyme content.

Enzyme content [wt-%] after catalyst prepn.	Enzyme content [wt-%] IR spectroscopic
1	1.3
5	4.8
8	7.7
10	9.9
15	14.5

Since the catalytic activity of freshly prepared catalysts increases during the reaction it was necessary to check whether this is due to loss of enzyme or deactivation of the enzyme. The enzyme contents of the fresh and the used contact catalysts determined from Figure 5 are listed together with other values in Table 2.

These results clearly show that a loss of enzyme occurs during the use of the catalyst. From measurements on used catalysts it follows that the catalytic activity decreases proportionally with the enzyme content; accordingly, the loss in activity must in the first place be attributed to a loss of enzyme and not to a deactivation. The catalyst was used in a continuously operating fixed bed reactor with flow rates of $SV \geq 400\ h^{-1}$. The large initial drop in activity is most

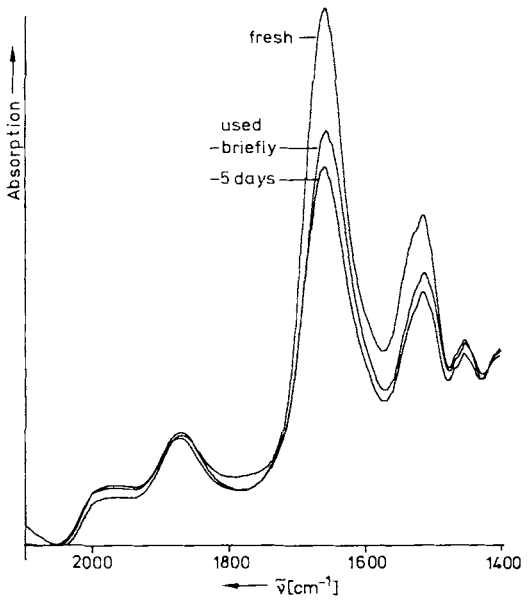

Fig. 5. Comparison of the IR spectra of fresh and used catalysts (cf. Fig. 2 and Table 2).

Table 2. Enzyme loss during the reaction (see Fig. 5 and text).

Catalyst	Time [h]	Enzyme content [wt-%]	Enzyme remaining [%] [a]
Fresh contact I	—	9.5	
Used	1	7.2	74.5
Used	120	7.0	72.1
Fresh contact II	—	10.3	
Used	120	6.8	66.1

[a] Referred to enzyme content of the fresh catalyst.

probably due to the fact that protein is released from the outer sheath of the carrier grain because of the high flow rates and associated shearing.

Received: January 30, 1987;
revised: March 5, 1987 [Z 2080 IE]
German version: *Angew. Chem. 99* (1987) 493

CAS Registry number:
α-chymotrypsin, 9004-07-3.

[1] G. M. Whitesides, C.-H. Wong, *Angew. Chem. 97* (1985) 617; *Angew. Chem. Int. Ed. Engl. 24* (1985) 617.
[2] J. B. Jones, C. J. Sih, D. Perlman: *Applications of Biochemical Systems in Organic Chemistry, Part I*, Wiley, New York 1976, p. 116.

Stabilization of the $[AlMe_2]^{\oplus}$ Cation by Crown Ethers**

By *Simon G. Bott, Abbas Alvanipour, S. David Morley, David A. Atwood, C. Mitchell Means, Anthony W. Coleman,* and *Jerry L. Atwood**

Although alkylaluminum compounds have played a commanding role in many areas of chemistry for more than 30 years, the simple species $[AlMe_2]^{\oplus}$ has not been structurally characterized in the presence of neutral donor ligands.[1] We now report that crown ethers stabilize this cation and show the interesting features of its coordination to [18]crown-6 and to [15]crown-5.

We have recently shown that the $[AlCl_2]^{\oplus}$ cation is generated in the reaction of $AlCl_3$,[2] $EtAlCl_2$,[3,4] and Et_2AlCl[5] with such crown ethers as [15]crown-5 and [18]crown-6.[6] Indeed, crown ethers are not necessary: the $[AlCl_2]^{\oplus}$ cation results from the reaction of $EtAlCl_2$ with two equivalents of dimethoxyethane,[7] or from the reaction of $AlCl_3$ with four equivalents of tetrahydrofuran in toluene.[8] The cationic species are of two structural types: those in which the chlorine atoms are *cis* and those in which they are *trans*. In $[AlCl_2 \cdot [18]crown\text{-}6]^{\oplus}$, the aluminum atom exists in an octahedral environment with *cis* chlorine ligands,[4] whereas in $[AlCl_2 \cdot [15]crown\text{-}5]^{\oplus}$ the aluminum atom is in a pentagonal bipyramidal array with *trans* chlorine ligands.

The $[AlMe_2]^{\oplus}$ cation has been seen often in our attempts to trap species related to Ziegler/Natta catalysis with crown ethers. In a typical experiment, one equivalent of Cp_2TiCl_2 is allowed to react with two equivalents of $AlMe_3$ in toluene in the presence of one equivalent of [18]crown-6.[9] Mass balance indicates the reaction as shown in equation (1).

$$Cp_2TiCl_2 + 2\,AlMe_3 + [18]crown\text{-}6 \xrightarrow{\text{toluene}} [AlMe_2 \cdot [18]crown\text{-}6]^{\oplus}[AlMe_2Cl_2]^{\ominus} + Cp_2TiMe_2 \quad (1)$$

$Cp = \eta^5\text{-}C_5H_5$

Related reactions may be written for Cp_2ZrCl_2 and $CpTiCl_3$, and $[AlMe_2 \cdot [18]crown\text{-}6]^{\oplus}$ has been obtained from each of these.[10] $[AlMe_2 \cdot [15]crown\text{-}5]^{\oplus}$ has also been isolated in accord with equation (1) with [15]crown-5 and from the reaction of $CoCl_2$ with $AlMe_3$ and [15]crown-5 (in toluene, molar ratio 1 : 4 : 1).[11]

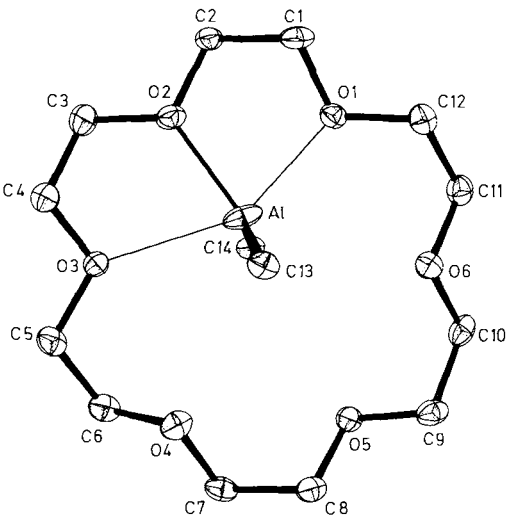

Fig. 1. Crystal structure of the cation of $[AlMe_2 \cdot [18]crown\text{-}6]^{\oplus}[AlMe_2Cl_2]^{\ominus}$ in the crystal [12, 13].

The structure of the $[AlMe_2 \cdot [18]crown\text{-}6]^{\oplus}$ cation is shown in Figure 1.[12,13] The visually most surprising feature is that the crown ether exhibits its full symmetry configuration. (The six oxygen atoms are planar to within 0.29 Å.) The aluminum atom is strongly coordinated to O(2) at a distance of 1.929(5) Å, but also interacts with O(1) at 2.181(5) Å, and with O(3) at 2.435(5) Å. The latter is

[*] Prof. Dr. J. L. Atwood, Dr. S. G. Bott, Dr. A. Alvanipour, S. D. Morley, D. A. Atwood, C. M. Means, Dr. A. W. Coleman
Department of Chemistry, University of Alabama
Tuscaloosa, AL 35487 (USA)

[**] This work was supported by the U. S. National Science Foundation.

the longest Al-O length to be referred to as a bond in the literature,[14] but the interaction is further substantiated by the Me-Al-Me angle of 140.6(3)°. Indeed, a comparison of van der Waals radii shows that even O(6) interacts to a small extent with the aluminum (Al···O = 3.093(5) Å). O(4) and O(5) are outside the contact distance with the aluminum atom (Al···O = 3.460(5) and 3.800(5) Å, respectively), and, significantly, the two methyl groups incline toward O(5). However, the aluminum atom should be regarded as 5-coordinate. The two Al-$C_{(methyl)}$ distances in the cation are short, Al-C(13) = 1.915(6) Å and Al-C(14) = 1.939(7) Å, compared to those in the anion of 2.005(7) and 2.053(6) Å.

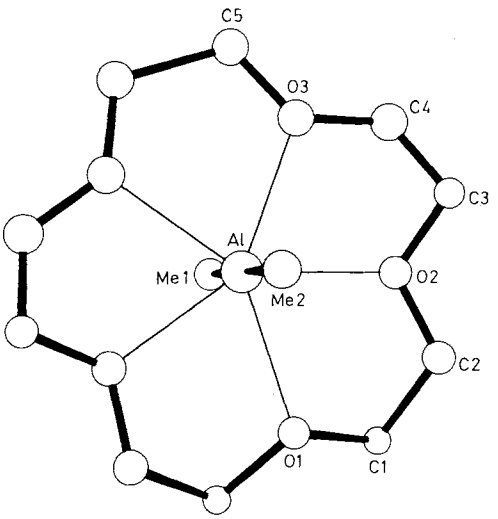

Fig. 2. Crystal structure of the cation of $[AlMe_2 \cdot [15]crown\text{-}5]^{\oplus}[AlMe_2Cl_2]^{\ominus}$. Al-O1 = 2.26(1), Al-O2 = 2.18(2), Al-O3 = 2.13(1) Å [13, 15].

The structure of $[AlMe_2 \cdot [15]crown\text{-}5]^{\oplus}$ is shown in Figure 2.[13, 15] It has a similar configuration to that found for the $[AlCl_2 \cdot [15]crown\text{-}5]^{\oplus}$ cation.[3] The Al-C distances are 1.99(1) and 2.01(1) Å, and the Me-Al-Me angle is 178(1)°.

These studies indicate that $[AlR_2]^{\oplus}$ species may be important in the reaction chemistry of Ziegler/Natta systems with donor ligands.

Received: January 2, 1987;
revised: February 2, 1987 [Z 2035 IE]
German version: *Angew. Chem. 99* (1987) 476

[1] $AlR_2^{\oplus}$ species have been implicated in solution studies. See for example: E. Bonitz, *Chem. Ber. 88* (1955) 742; H. Lehmkuhl, H. D. Kobs, *Tetrahedron Lett. 29* (1965) 2505; H. Lehmkuhl, *Liebigs Ann. Chem. 719* (1968) 40; R. Benn, A. Rufinsky, *Angew. Chem. 98* (1986) 851; *Angew. Chem. Int. Ed. Engl. 25* (1986) 861.
[2] S. G. Bott, *Dissertation*, University of Alabama 1986.
[3] S. G. Bott, H. Elgamal, J. L. Atwood, *J. Am. Chem. Soc. 107* (1985) 1796.
[4] J. L. Atwood, H. Elgamal, G. H. Robinson, S. G. Bott, J. A. Weeks, W. E. Hunter, *J. Inclusion Phenom. 2* (1984) 367.
[5] H. Elgamal, *Dissertation*, University of Alabama 1985.
[6] The formation of a two phase liquid system is indicative of the presence of ionic material. This is the liquid clathrate phenomenon: J. L. Atwood in J. L. Atwood, J. E. D. Davies, D. D. MacNicol (Eds.): *Inclusion Compounds*, Vol. 1, Academic Press, London 1984, pp. 375–405.
[7] S. G. Bott, H. Elgamal, A. W. Coleman, A. J. Baskar, C. M. Means, J. L. Atwood, *Inorg. Chem.*, submitted.
[8] N. C. Means, C. M. Means, S. G. Bott, J. L. Atwood, *Inorg. Chem.*, in press.
[9] In a typical experiment 2.50 g (0.01 mol) of $[Cp_2TiCl_2]$ and 2.65 g (0.01 mol) of [18]crown-6 were mixed together in toluene (ca. 50 ml). $AlMe_3$ (2.0 ml, 0.02 mol) was slowly added. The reaction began immediately and from the red solution ca. 2.64 g (62%) of colorless crystalline material was deposited. The latter was shown by an X-ray crystallographic analysis to be $[AlMe_2 \cdot [18]crown\text{-}6]^{\oplus}[AlMe_2Cl_2]^{\ominus}$.
[10] In each case signals due to M-Me (M = Ti, Zr) resonances have been recorded in the NMR. It is likely that the $[Cp_2M(Cl)Me]$ species is formed rather than $[Cp_2MMe_2]$. Other products which apparently contain M-crown linkages have been found in low yield. It is reasonable to assume that the $[AlMe_2 \cdot [18]crown\text{-}6]^{\oplus}$ species comes from the attack of $AlMe_2Cl$ on the crown after the $AlMe_3$ alkylates the transition metal. The formation of $AlMe_2Cl$ in the reaction of $AlMe_3$ with $[Cp_2TiCl_2]$ has been reported: K. Claus, H. Bestian, *Justus Liebigs Ann. Chem. 654* (1962) 8; F. N. Tebbe, G. W. Parshall, G. S. Reddy, *J. Am. Chem. Soc. 100* (1978) 3611.
[11] $CoCl_2$ (0.65 g, 0.005 mol) was slurried with [15]crown-5 (1.0 ml, 1.1 g, 0.005 mol) in toluene (ca. 50 ml). $AlMe_3$ (2.0 ml, 0.02 mol) was slowly added. A vigorous reaction ensued, and a black liquid clathrate was immediately noted. Colorless, air-sensitive crystals of $[AlMe_2 \cdot [15]crown\text{-}5][AlMe_2Cl_2]$ grew from the liquid clathrate.
[12] $P2_1/n$, $a = 11.397(4)$, $b = 12.670(4)$, $c = 17.075(6)$ Å, $\beta = 93.08(4)°$, $V = 2462$ Å^3, $Z = 4$. CAD-4 diffractometer, $Mo_{K\alpha}$, $2.0 \leq 2\theta \leq 46°$, 1326 measured reflections with $I \geq 3\sigma(I)$, MULTAN and difference Fourier methods, hydrogen atoms located and refined, all non-hydrogen atoms refined with anisotropic thermal parameters, $R = 0.044$.
[13] Further details of the crystal structure investigation may be obtained from the Director of the Cambridge Data Centre, Cambridge CB2 1EW, England, on quoting the names of the authors, and the journal citation.
[14] In $[AlCl_2 \cdot$ benzo[15]crown-5$][AlEtCl_3]$ [3], the five Al-O lengths range from 2.03(1) to 2.30(1) Å. The latter is the longest previously reported as a formal bond.
[15] *Pnma*, $a = 11.184(3)$, $b = 10.928(8)$, $c = 17.717(9)$ Å, $V = 215$ Å^3, $Z = 4$. CAD-4 diffractometer, $Mo_{K\alpha}$, $2 \leq 2\theta \leq 44°$, 1104 measured reflections with $I \geq 3\sigma(I)$. MULTAN and difference Fourier methods. The crown was badly disordered. This problem has been discussed: P. C. Stark, M. Huff, E. A. Babaian, L. M. Barden, D. C. Hrncir, S. G. Bott, J. L. Atwood, *J. Incl. Phenom. 5*, in press. $R = 0.152$.

BOOK REVIEWS

Ion Solvation. By *Y. Marcus*. John Wiley, Chichester 1985. viii, 306 pp., bound, £ 42.00.—ISBN 0-471-90756-1

Chemical reactions are usually carried out in solution, and often involve ions as reactants. A knowledge of the interactions between solvent molecules and dissolved ions is therefore of great importance for understanding and thereby influencing such reactions.

The better-known books on this topic are already rather outdated, and Prof. *Yizhak Marcus* of the Hebrew University of Jerusalem has therefore taken on the task of bringing the subject up to date, and treating some parts of it in a completely new way. It must be said at the outset that he appears to have succeeded very well. The nine chapters cover every important aspect of the solvation of ions in aqueous and nonaqueous media.

Following a brief introductory chapter (Significance and Phenomenology of Ion Solvation), the simple case of an interaction between a single ion and a single solvent mole-

cule in the gas phase is first discussed (Ion Solvation in the Gas Phase). This is followed by a treatment of the solvation of a single ion by many solvent molecules, as in a dilute solution, dealing with structural, spectrochemical, and kinetic aspects. Chapter 3 (Interaction Models for Ion Solvation) describes various theoretical models based on statistical thermodynamics considerations. Chapter 4 (Structural and Kinetic Aspects) deals with changes in the dynamic behavior of the solvent molecules caused by ion solvation. Concepts such as first and second solvation shells, primary and secondary solvation, and coordination and solvation numbers, are here put into an up-to-date context. Chapter 5 (Ion Hydration) deals with the special position occupied by water as a solvent for electrolytes, being concerned exclusively with the thermodynamic and structural aspects of the ion/water interaction. The growing importance of ions in nonaqueous organic solvents is recognised in the following chapter (Ion Solvation in Nonaqueous Solvents). Detailed tables listing relevant properties of nonaqueous solvents (including empirical parameters of solvent polarity), and of Gibbs transfer energies ΔG_t^0 (X, $H_2O \rightarrow S$)/kJ·mol^{-1}) for single ions, make this chapter one of the most useful in the book. Here the reader benefits from the knowledge which the author gathered in compiling (for IUPAC) critical tables of Gibbs transfer energies, enthalpies, and entropies for the transfer of single ions from water into nonaqueous solvents [Y. Marcus, *Pure & Appl. Chem. 55* (1983) 977; *ibid. 57* (1985) 1103]. Attempts at correlating such Gibbs transfer energies with intrinsic solvent properties using multiparameter equations are also described.

Chapter 7 is devoted to the selective solvation of ions in binary solvent mixtures. Chapter 8 deals with solvation of ion pairs, with particular attention to molten hydrated salts, perhaps as a result of the author's laboratory being near the Dead Sea (Dead Sea Water contains a 8.8 mol ions/liter!). In the final chapter (Some Applications of Ion Solvation) many different applications in the fields of electrochemistry, hydrometallurgy, solvent extraction, and organic synthesis are discussed.

The book excels in having a lucid, readable style, and the detailed author and subject indexes make it easy to use. Lists of references at the end of each chapter (more than 310 references altogether) enable the reader to gain easy access to original papers—although that should often be unnecessary, since the 64 tables and 36 figures provide a wealth of useful information. The book should be included in every library, and anyone who can afford to (at the price of DM 175.00!) should have the book on his desk—he will certainly get a lot of use from it.

Christian Reichardt [NB 813 IE]
Fachbereich Chemie
der Universität Marburg (FRG)

Molybdenum Enzymes. Edited by *T. G. Spiro*. Wiley, Chichester, England 1985. x, 611 pp., hardcover, $ 125.00.—ISBN 0-471-88542-8

This book collects some excellent reviews on the inorganic chemistry and biochemistry of molybdenum, molybdenum-containing enzymes, and the molybdenum-containing cofactors. As noted by *P. J. Stephens* in his chapter, the general area of molybdenum enzymes, especially as related to nitrogen fixation, has been extensively reviewed in comparison to research productivity. These reviews are, however, a significant new contribution because of the emphasis on the chemical aspects as opposed to the agricultural and genetic aspects. The authors are well chosen, critical, and careful to avoid oversimplification or overinterpretation. The literature is completely covered through 1983 with some references to 1984. The ten chapters overlap some in their scope; thus, there is some redundancy that would not occur in a monograph by a single author. However, to carry on the editor's analogy, although some of the same territory is being explored, it is being seen through different eyes and to different purposes.

Chapter 1, by *R. H. Holm* and *E. Simhon*, is a thorough survey of molybdenum- and tungsten-containing iron-sulfur clusters, their structure, physical properties, reactivity, especially with respect to substitution and electrochemistry, and synthesis. These results are then discussed by comparison to the properties of the iron-molybdenum cofactor from nitrogenase. The second chapter, by *E. Stiefel* and *S. Cramer*, concerns the isolation, composition, physical and chemical properties, assay, and biosynthesis of the iron-molybdenum cofactor. The same authors discuss the molybdenum cofactor (the molybdenum center of enzymes other than nitrogenase) in Chapter 8.

Chapter 3, by *P. J. Stephens*, reviews structures of the iron and iron-molybdenum proteins that compose the nitrogenase enzyme. This review is organized by presenting the "Dominant Hypothesis" concerning each protein, and then presenting the experimental data. Conflicts between the "Dominant Hypothesis" and the data are pointed out in a stimulating presentation. For example, there are problems with the hypotheses about the types and number of clusters in light of the cysteine analysis of the proteins.

The next two chapters concern the reactions of nitrogenase. *B. Burgess* presents a discussion of the varied substrates of nitrogenase and describes the steady-state kinetics results. Emphasis is put on the importance of considering electron flow through the enzyme, careful product analysis, and the problems of controlling the "inputs" to the enzyme (reducing equivalents, MgATP, substrate, medium). There is also some discussion of substrate interaction, the evidence for interacting sites on the enzyme, and the problem of the competition between hydrogen evolution and substrate reduction.

Chapter 5, by *R. Thorneley* and *D. Lowe*, is the most detailed discussion of the mechanism of nitrogenase. The authors attempt to fit a mechanism and individual rate constants particularly to the reactions of the *Klebsiella pneumoniae* proteins. The work especially involves the authors' pre-steady-state kinetics measurements, but also encompasses the steady-state measurements. This type of detailed analysis is necessary in order to get a real understanding of this complex system, and in order to avoid errors from too facile interpretation of individual experiments, but the details will appeal more to committed kineticists. The next chapter, by *M. Hidai*, reviews the diverse work on the inorganic and organometallic chemistry of complexes of dinitrogen and their reactivity. Unfortunately, there still remains little connection between these studies and advances in the understanding of nitrogenase.

The remaining four chapters concern molybdenum-containing proteins other than nitrogenase. Chapter 7 by *D. Garner* and *S. Bristow* presents the inorganic background through a discussion of oxomolybdenum chemistry. This long presentation also demonstrates the relevance of the measurements on the inorganic complexes to the study of the enzymes. Chapter 8 on the molybdenum cofactor is next, followed by a detailed discussion by *R. Hille* and *V. Massey* primarily on xanthine oxidase. Here the emphasis

is properly on the molybdenum chemistry, but the flavin chemistry is presented as necessary. A good discussion is presented of the problem of the oxidation-reduction potentials of the centers and whether they are in equilibrium with each other. The last chapter, by *M. Adams* and *L. Mortenson*, discusses nitrate reductase and formate dehydrogenase. Here, there is less physical information on the proteins and the sites and more discussion on physiology, purification, and characterization.

The book is well printed, with only a few errors in layout, such as misplaced figures in Chapter 2 and some missing compound numbers in Chapter 1. This is a solid addition to any library for those interested in the chemistry of molybdenum in biological systems and related inorganic chemistry.

Scot Wherland [NB 790 IE]
Washington State University
Pullman, WA (USA)

Organized Multienzyme Systems: Catalytic Properties. (Biotechnology and applied Biochemistry Series.) Edited by *G. R. Welch*. Academic Press, New York 1985. xiii, 458 pp., bound, $ 75.00.—ISBN 0-12-744040-2

This monograph summarizes, mainly from a biochemical and biological viewpoint, the extraordinary wealth of information which exists on organized multienzyme systems. In each of the nine chapters an expert in the relevant topic outlines its most important features, with examples. The topics discussed include the fundamentals of protein organisation in mitochondria, catalytic processes and energy transfer in membranes, dynamic compartmentalization of multienzyme complexes in the cytoplasm, questions concerning the flexibility and co-operativity of enzyme molecules in the kinetics and regulatory mechanism of allosteric enzymes, and reversible adsorption as a modulator of enzymatic activity. Mechanistic models for sequential enzymatic pathways are also proposed and discussed, and detailed analyses of the kinetics of multienzyme systems are given. The monograph concludes with a chapter on long-range energy continua, and their role in the transfer and conservation of chemical energy in multienzyme sequences, and thus in the regulation of metabolism.

Chapters on naturally occurring multienzyme sequences are especially appropriate to the aims of this monograph, in showing the mode of action and structural features of organized multienzyme systems and the role of the microenvironment, together with a critical discussion of current theoretical models. On the other hand, Chapter 7, on the kinetic analysis of multienzyme systems in homogeneous solutions, falls outside the proper scope of the book. Kinetic models for sequential reactions, some of which are already well-known, are laboriously presented here in a complicated and unconventional notation. The inclusion of a lengthy and not very useful 13-page digression into the use of the Laplace-Carson transformation to solve ordinary differential equations is quite incomprehensible. Apart from the availability of numerical computation methods nowadays, there is no obvious advantage in using such laborious integral transformations rather than conventional integration methods. Furthermore, the literature referred to is not always truly representative; for example the book by *Ayres* (1952) on the theory of differential equations is now hardly the most appropriate source on the trivial solution of the differential equations for a first-order reaction. However, readers who are engaged in theoretical work or interested in these aspects will be compensated by the discussion in Chapter 8 on the behaviour of immobilized multienzyme systems, particularly in membranes. Here we find a successful combined presentation of experimental studies of diffusion-limited enzymic reactions together with the relevant theoretical models, using mathematical techniques of a practical nature which are described in a comprehensible way. Especially noteworthy is the elegant theoretical modelling of the highly nonlinear diffusion-limited reaction effects in multienzyme systems with complex control mechanisms. A reading of this chapter will also be of value to all process-oriented biotechnologists. Elsewhere in the monograph, however, there are many places where, although it is assumed that the knowledge presented will be of interest to biotechnologists, no relevant cross-reference is included. Consequently those involved in the practice of biotechnology may have difficulty in making use of the abundant fundamental knowledge displayed. The one chapter whose title mentions practical applications (Chapter 6—Models of organized multienzyme systems: use in microenvironmental characterization and in practical application) is comparatively vague, and deals with the practical aspects in a mere five pages. The main emphasis is on coenzyme regeneration, but the discussion of coupled equilibria does not, unfortunately, include the latest developments which have been reported, e.g. for the enzyme membrane reactor.

The monograph thus demonstrates the importance and the difficulties of communication in interdisciplinary fields of knowledge. The book can be recommended to all who are concerned with setting up immobilized cells for bioconversions, as the results, concepts and theoretical models presented here are of considerable importance for them. Because of the comparatively high price, only highly specialized readers and those with theoretical interests will wish to buy it for their private libraries.

Maria-Regina Kula [NB 788 IE]
Institut für Enzymtechnologie
der Universität Düsseldorf
at KFA Jülich GmbH (FRG)

Registered names, trademarks, etc. used in this journal, even when not marked as such, are not to be considered unprotected by law.

© VCH Verlagsgesellschaft mbH, D-6940 Weinheim, 1987. - Printed in the Federal Republic of Germany by Zechnersche Buchdruckerei, Speyer/Rhein.

All rights reserved (including those of translation into foreign languages). No part of this issue may be be reproduced in any form – by photoprint, microfilm, or any other means – nor transmitted or translated into a machine language without written permission from the publishers. Only single copies of contributions, or parts thereof, may be made for personal use.

Valid for users in the USA: The appearance of the code at the bottom of the first page of an article in this journal (serial) indicates the copyright owner's consent that copies of the article may be made for personal or internal use, or for the personal or internal use of specific clients. This consent is given on the condition, however, that the copier pay the stated per-copy fee through the Copyright Clearance Center, Inc., for copying beyond that permitted by Sections 107 or 108 of the U.S. Copyright Law. This consent does not extend to other kinds of copying, such as copying for general distribution, for advertising or promotional purposes, for creating new collective works, or for resale. For copying from back volumes of this journal see 'Permissions to Photo-Copy: Publisher's Fee List' of the CCC.

Editorial office: Pappelallee 3, D-6940 Weinheim, Federal Republic of Germany, Telephone (06201) 602315, Telex 465516 vchwh d, Telefax (06201) 602328.

Editor: *P. Gölitz.*

Associate editors: *D. J. Loewus, A. Stimson.* **Editorial assistant:** *E. Schweikart*

Publishers: VCH Verlagsgesellschaft mbH. (Managing Directors: *Prof. Dr. Helmut Grünewald* and *Hans Dirk Köhler*), Pappelallee 3, D-6940 Weinheim, Federal Republic of Germany. Correspondence concerning advertisements should be addressed to VCH Verlagsgesellschaft mbH. (Advertising Manager *R. J. Roth*), Boschstr. 12, P.O. Box 1260/1280, D-6940 Weinheim, Federal Republic of Germany, Telephone Weinheim (06201) 602-0, Telex 465516 vchwh d, Telefax (06201) 602328.

ANGEWANDTE CHEMIE
International Edition in English
Volume 26 · Number 6
June 1987
Pages 489–594

Stereoselective Syntheses of Building Blocks with Three Consecutive Stereogenic Centers: Important Precursors of Polyketide Natural Products

New Synthetic Methods (68)

By Reinhard W. Hoffmann*

Sequences of directly adjacent stereogenic centers were first discovered for the monosaccharides, which therefore constituted the first focus of interest in stereoselective synthesis. The structures of many polyketide-derived natural products that have been elucidated in recent years often exhibit longer sequences of stereogenic centers in which hydroxy-substituted secondary carbon atoms alternate with tertiary carbon atoms. This finding inspired the development of methods allowing the specific construction of first two and then—more importantly—three neighboring stereogenic centers. The diverse methodologies that have thereby emerged reveal common principles and stress the variety of approaches possible in stereoselective synthesis.

1. Introduction

Each era of preparative organic chemistry has its own target molecules. Those of the 1980s include polyketide-derived natural products such as erythronolide and rifamycin (Scheme 1). The synthetic challenge thereby results from the large number of directly adjacent stereogenic centers (in this article, the term "stereogenic center" will be shortened to "stereocenter").

Although synthetic chemists have been interested in this class of compounds for a long time,[1] attempts at their syntheses were not practical as long as analytical methods were not available by which the many stereoisomers that could be formed during synthesis could be detected separately, characterized individually, and identified. These prerequisites were fulfilled at the end of the 1970s with the development of high-field ^{1}H- and ^{13}C-NMR spectroscopy and the new HPLC techniques. As a logical consequence, the first complicated polyketide natural products were then synthesized in impressive pioneering work.[2] Since then, many reports concerning the syntheses of polyketide-derived natural products have been published.[3] The increasing interest in this class of compounds soon led to the development of general principles for their elaboration. One limitation, however, was the state of development of methods for the specific construction of stereocenters in

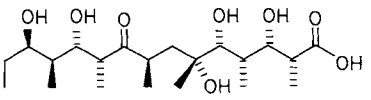

seco acid of erythronolide B

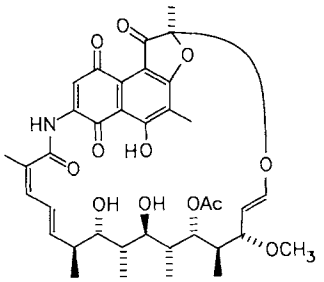

rifamycin S

Scheme 1.

[*] Prof. Dr. R. W. Hoffmann
Fachbereich Chemie der Universität
Hans-Meerwein-Strasse, D-3550 Marburg (FRG)

 © VCH Verlagsgesellschaft mbH, D-6940 Weinheim, 1987 0570-0833/87/0606-0489 $ 02.50/0

open-chain systems ("acyclic stereocontrol"). The renaissance of stereoselective synthesis has also led, therefore, to the rapid development of such methods during the last few years. Thus, it seems to me that the time has come for a review and critical evaluation of the achievements to date.

Long sequences of stereocenters have been most conveniently analyzed in terms of subunits of three stereocenters each. These, in turn, can be classified into four triads of stereogenic centers (for short, stereotriads) **A** to **D** (Scheme 2). Only the relative and not the absolute configu-

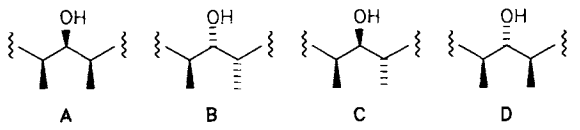

Scheme 2.

ration will be considered at first (i.e., if the end groups differ, an enantiomer exists for each of the triads). One of the strategies for the synthesis of polyketide-derived natural products consists in the preparation of individual building blocks containing the stereotriads **A**–**D** in order to incorporate them as units into the target molecule. Thus, for example, all four diastereomers of **1**[4] and **2**[5] as well as three of the four possible diastereomers of **3**[6] have been obtained in enantiomerically pure form from, for instance, D-glucose or D-mannitol (Scheme 3).

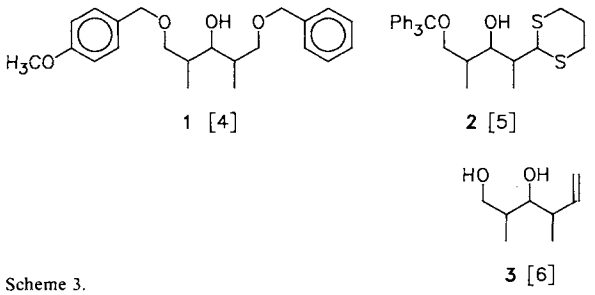

1 [4] 2 [5] 3 [6]

Scheme 3.

The Achilles' heel of this strategy becomes apparent, however, when the individual blocks have to be linked to form longer sequences of directly adjacent stereocenters. While the stereocenters in the linkage region must be constructed with the correct configurations, external stereocontrol of the C–C coupling step is no longer possible, since the chirality of *both* reaction partners is predetermined by the synthetic objective. Part of the synthesis of rifamycin S by *Kinoshita* et al.[7] exemplifies this problem (Scheme 4).

For this class of compounds, therefore, the useful principle of convergent synthesis meets with inherent difficulties for which no generally valid solutions are in sight. Thus, linear synthesis strategies must be employed instead. These include iterative chain lengthening in which each new stereotriad is constructed by adding two new stereocenters to an existing stereotriad (e.g., transformation of **4** to **5**, Scheme 5).

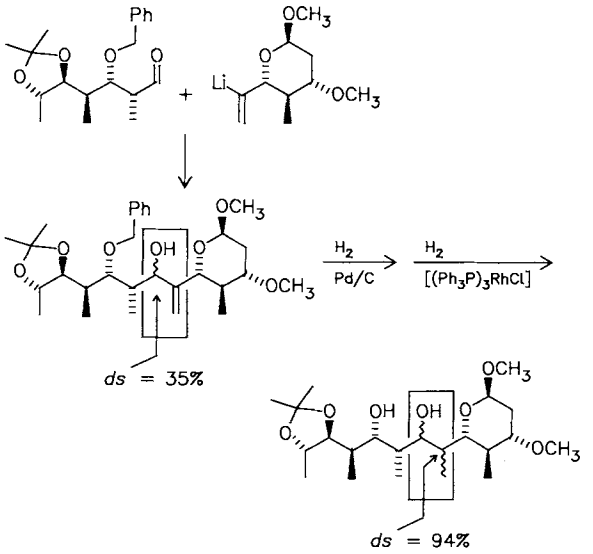

Scheme 4. Part of the synthesis of rifamycin S by *Kinoshita* et al. [7]. The linkage region is shown in the box.

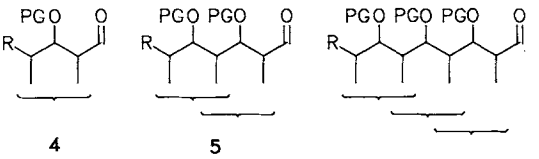

4 5

Scheme 5. PG = protecting group.

Once these transformations can be performed in a small number of steps, in high yields, and with high stereoselectivity, it becomes possible to construct all imaginable sequences of stereocenters with the desired flexibility. The importance of this approach is increased still further by the fact that the exact configurations of the stereocenters of many polyketide-derived natural products are not known with sufficient certainty or, as in the case of hygrolidin (Scheme 6),[8] for example, are only partially known. In such cases the only alternative at present is to synthesize all of the stereoisomers in order to determine the configuration of the natural product.[8]

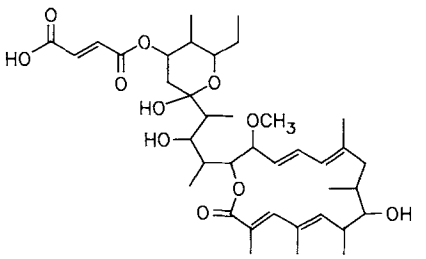

Scheme 6. Hygrolidin.

A further reason for this, at first surprising, preference for linear synthesis strategies is, in principle, the possibility of using an iterative procedure, which is amenable to automatization. Following on the development of automatic synthesizers for oligonucleotides and oligopeptides, the development of an automated, highly stereoselective syn-

thesis of polyketide-derived natural products no longer seems utopian. However, reliable procedures for the specific construction of the stereotriads **A** to **D** are first required. The present status of this development is the topic of this review.

The chain lengthening of **4** to **5** requires at least one C–C coupling step to build up the skeleton, resulting in the formation of two new stereocenters. At first, procedures in which both new stereocenters can be defined in one stroke appear most favorable. Those methods that involve simultaneous C–C coupling would be particularly efficient. Ideally, a one-step, repeatable chain lengthening could be achieved in this manner. In practice, any number of steps larger than one is the result of the as yet unavoidable refunctionalization steps.

2. C–C Coupling and Construction of Both Stereocenters in One Step

Aldol additions[9] and aldol-like C–C coupling reactions[10] already come close to the above-postulated, ideal process for an iterative chain lengthening (Scheme 7).

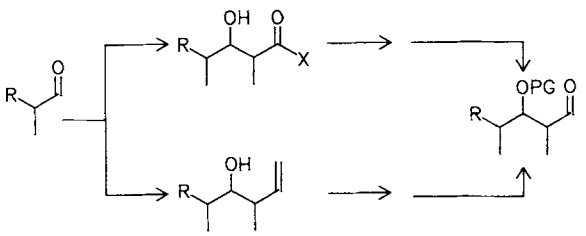

Scheme 7. X = H or a substituent that can be transformed into X = H.

Here, two stereochemical problems need to be solved. The first is the "simple" diastereoselectivity,[9, 10] which concerns the relative configuration at the two newly formed stereocenters (Scheme 8). The second is the 1,2-asymmetric

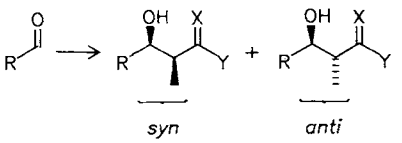

Scheme 8. Relative configuration at the newly formed stereocenters. X, Y = substituents that permit the ultimate generation of an aldehyde function.

induction, the Cram/anti-Cram selectivity, which concerns the configuration at the newly formed stereocenters relative to the resident stereocenter introduced with the aldehyde (Scheme 9).[11]

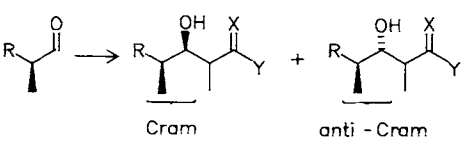

Scheme 9. Relative configuration at newly formed and previously present stereocenters. For X and Y see Scheme 8.

Whereas the problem of simple diastereoselectivity had already been more or less solved at the beginning of the 1980s, the solution of the Cram/anti-Cram problem required and continues to require greater efforts. Only the solution of both problems will open up specific routes to each of the desired stereotriads.

2.1. Aldol Additions

Enolates of acid derivatives, such as **6** (Scheme 10), are often employed in order to make the reaction sequence repetitive (cf. Scheme 5), since a new aldehyde function can be generated after the C–C coupling. Alternatively, enolates **7** of α-siloxy ketones can be used (Scheme 10). In this case, a new aldehyde function can be obtained after the C–C coupling by oxidative glycol cleavage.

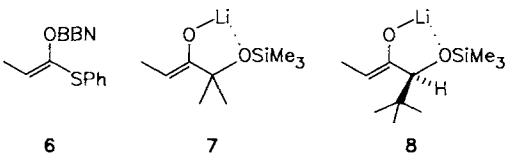

Scheme 10. BBN = 9-borabicyclo[3.3.1]nonan-9-yl.

These enolates are obtained with uniform "*Z*" configuration of the double bond by deprotonation of the corresponding carbonyl compounds. They undergo addition to aldehydes to give *syn*-aldols with very high simple diastereoselectivities. The Cram/anti-Cram selectivities of additions to chiral aldehydes, however, exhibit a wide range of values.[12, 13] Thus, an extensive study by *S. Masamune*[14] showed that, depending on the aldehyde **9** employed (steric demands of the group R, presence or absence of other functional groups, and centers of chirality in R which could eventually make chelation control[11] possible), the Cram-**10** : anti-Cram-**10** selectivity was scattered[14] over a range from 15 : 1[9] to 1 : 27 (Scheme 11).[15]

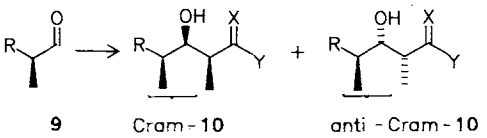

Scheme 11. For X and Y see Scheme 8.

The boron enolate **6** and the lithium enolate **7** did not differ principally in this respect. Hence, only in a few lucky cases is it possible to obtain a homogeneous diastereomer having the stereotriad **A** or **B** with high selectivity (Scheme 12).

The Mukaiyama variant of the aldol addition, the Lewis acid-catalyzed reaction of aldehydes with silyl enol ethers, also shows a good selectivity in favor of the Cram-diastereomer.[21] This is also valid, of course, when an alkoxy-substituted aldehyde exhibits a high diastereofacial differentiation as a result of chelation control (Scheme 13).[11, 19]

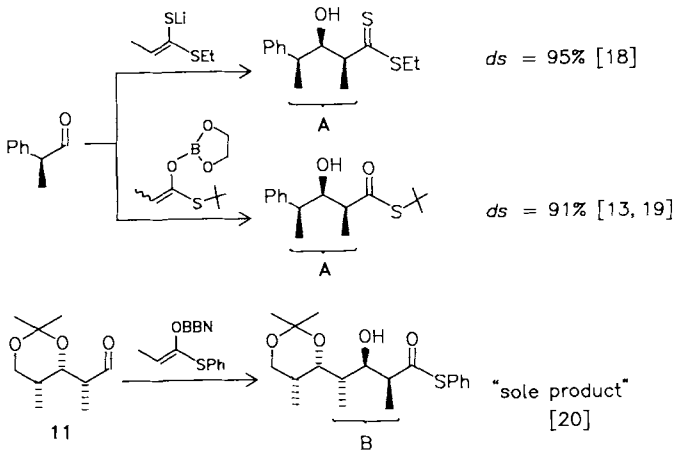

Scheme 12.

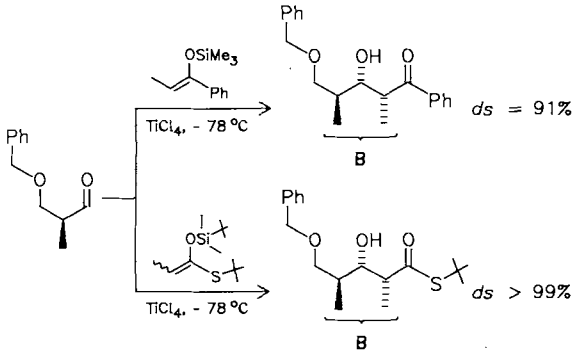

Scheme 13.

In view of the arbitrary factors governing the extent and direction of the diastereoselectivity in the aldol addition, reliable access to the stereotriad **A** or **B** (for **C** and **D**, see the last paragraph of this section) is not guaranteed. For this reason, chiral enolates (e.g., **8**, Scheme 10) were developed so that an insufficient asymmetric induction of the aldehyde can be increased by a reagent-controlled asymmetric induction (double stereodifferentiation).[22] The logical further development focused on chiral enolates with such high asymmetric inductions that they could override the asymmetric induction of the aldehyde. This effect is known as "reagent control of stereoselectivity."[23] This principle is clearly illustrated by the reaction shown in Scheme 14,[23] in which (*R*)- and (*S*)-**12** must be employed in order to obtain the stereotriads **A** and **B**, respectively.

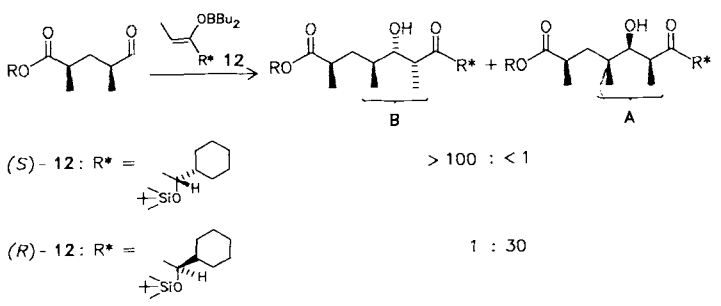

Scheme 14.

Alternatively, stereochemically complementary reagents (e.g., **13** and **14**, Scheme 15) can also be utilized.[24] Compounds **13** and **14** are particularly versatile reagents since the parent chiral compounds norephedrine and valine are readily accessible and the acyloxazolidinone group in the product can be converted very simply into an ester, a carboxylic acid, or a primary alcohol.

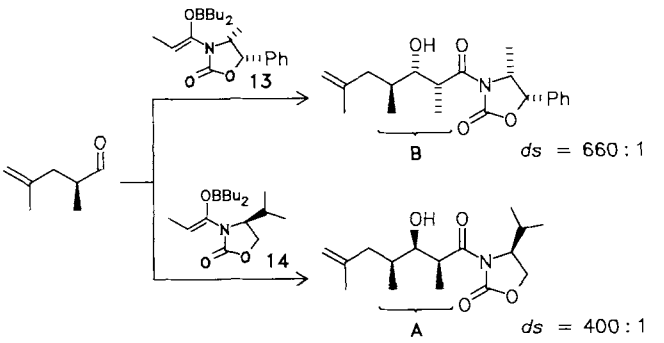

Scheme 15.

Higher asymmetric inductions were achieved with boron enolates such as **6** (or with zirconium[25] and tin enolates,[26]) than with lithium enolates. Presumably, the transition states are more compact[27] in the former cases so that the steric interactions mainly responsible for the asymmetric induction are more pronounced.

In order to override the inherent 1,2-induction of a chiral aldehyde, the diastereofacial selectivity of the reagent should be greater than 100 : 1. This is the case for the reagents **12**–**14**. A further important point, however, must be emphasized. Reagent control of stereoselectivity in the reaction of a chiral aldehyde can only be applied when this aldehyde is enantiomerically pure. Racemates cannot be utilized! Since the configurations of the new stereocenters are defined by the reagent, use of a racemic substrate would result in the formation of two diastereomers in a 1 : 1 ratio. Of course, recourse to reagent control of stereoselectivity will only then be taken when the reaction with achiral reagents is unsuccessful.

Whereas the problem of obtaining the stereotriads **A** and **B** can thus be considered as firmly solved in principle, the lack of general, *anti*-selective aldol additions necessitated for a long time the use of other routes or the acceptance of tedious refunctionalizations[28,29] in order to obtain the stereotriads **C** and **D**. However, even after the discovery of a series of *anti*-selective aldol additions,[30,31] it was found that, e.g., for the addition of the lithium enolate **15**, the Cram/anti-Cram selectivity is again dependent on the nature of the chiral aldehyde.[32] In a favorable case, such as that of the aldehyde **11**, which exhibits a high asymmetric induction, a single diastereomer could be obtained (Scheme 16)[33] (for further examples, see Refs. [19, 34]).

In this situation as well, only reagent control of stereoselectivity will help in the long term. New chiral, *anti*-selective enol derivatives such as **16**,[35] **17**,[36] **18**,[37] **19**,[38] and **20**[39] can be considered as promising starting points (Scheme 17).

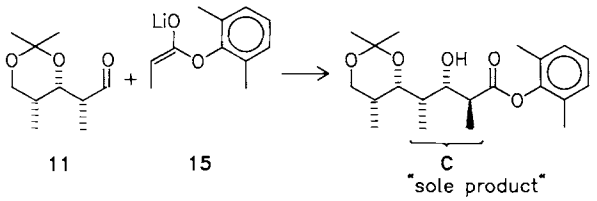

Scheme 16.

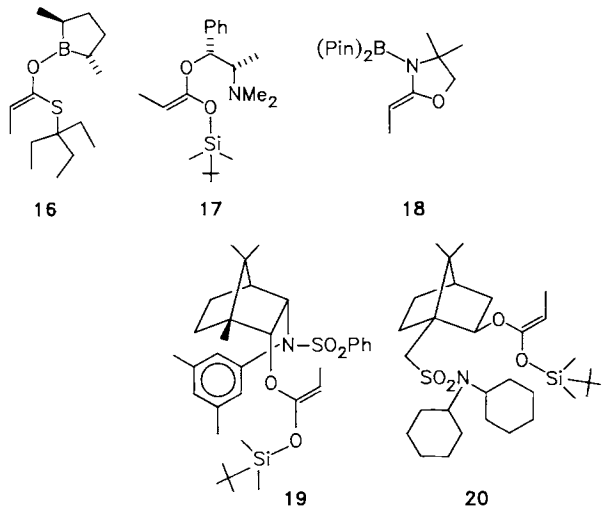

Scheme 17. New chiral, *anti*-selective enol derivatives. Pin = isopinocamphenyl.

As far as the final result is concerned, the cycloaddition of Danishefsky's diene to aldehydes corresponds to an aldol addition. Here, the Cram product **22** (Scheme 18) was formed with a normal diastereoselectivity of 4.3 : 1 and,

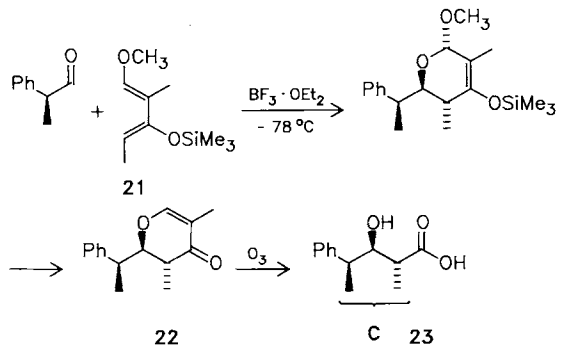

Scheme 18.

after refunctionalization, gave the carboxylic acid **23** (stereotriad **C**).[40] By changing the solvent, a structure with the stereotriad **A** could be obtained with a selectivity of up to 10 : 1.[41] It remains to be clarified whether or not high diastereoselectivities can be obtained generally with the reagent **21** on addition to chiral aldehydes.

2.2. Crotyl-Metal Compounds

The problem of simple diastereoselectivity can also be considered as solved for the additions of crotyl-metal compounds to aldehydes.[10] Again, the Cram/anti-Cram selectivity of the addition to chiral aldehydes remains a problem.

2.2.1. Crotyl-Tin Compounds

The additions of crotyltributylstannane to aldehydes, which proceed under Lewis acid catalysis and result in good *syn*-selectivities, will be mentioned first (Scheme 19). In many cases of additions to chiral aldehydes, high diastereoselectivities in favor of the formation of the triad **A** have been reported (Scheme 20).

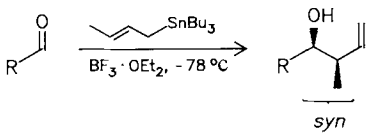

Scheme 19.

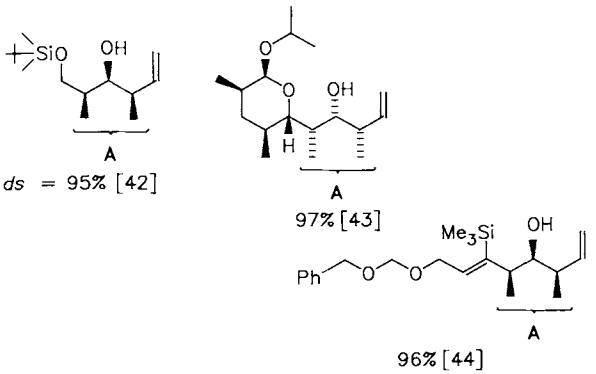

Scheme 20.

Furthermore, recent results[45] suggest that changing the Lewis acid and the reaction conditions could make other stereotriads accessible. In any case, however, it is the nature of the aldehyde that governs the extent of the diastereoselectivity.[46, 47] In cases in which it is possible to fix the aldehyde in a different conformation by chelation with a multidentate Lewis acid, products with the stereotriad **B** also become accessible (Scheme 21).

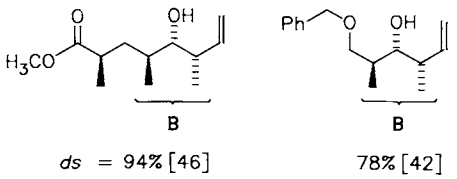

Scheme 21.

2.2.2. Crotyl-Chromium Compounds

There are many reports on the addition of crotyl-chromium compounds to aldehydes proceeding with high *anti*-selectivity (Scheme 22).

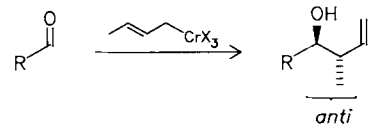

Scheme 22.

For reactions with α-chiral aldehydes, the reagent should be prepared from pure $CrCl_2$ instead of from $CrCl_3 + LiAlH_4$ in order to avoid an epimerization (racemization) of the aldehyde.[48] The Cram diastereomer (stereotriad **C**) predominates in the addition to α-chiral aldehydes.[49–51] Here again, the selectivity varies over a wide range: the examples in Scheme 23 represent exceptionally good selectivities.

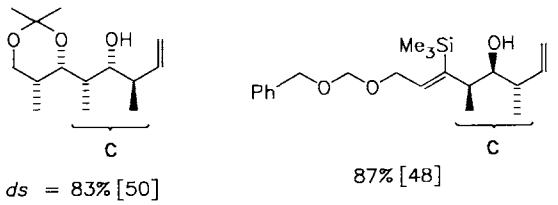

Scheme 23.

2.2.3. *Crotylboronate Esters*

In the case of crotylboronate esters, both the *Z* and the *E* isomers are accessible. They undergo addition to aldehydes with high simple diastereoselectivities (Scheme 24).[10, 52, 53] In additions to α-chiral aldehydes, *E*-crotylboronate esters gave a higher Cram selectivity in comparison to the reactions of allylboronate esters, whereas *Z*-crotylboronate esters generally led to preferential formation of the anti-Cram diastereomers, albeit often in only small excess.[54] Since boronate esters are monodentate Lewis acids, the aldehyde conformation is not fixed by chelation in any of the cases.

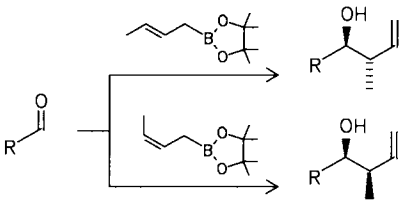

Scheme 24.

The results in Table 1 show unequivocally for the first time that, in the case of a given chiral aldehyde, not only the extent but also the *direction* of the asymmetric induction can be determined by the nature of the achiral reaction partner. This situation occurs when the steric interactions across the forming partial bond are energetically similar to the steric interactions responsible for the 1,2-asymmetric induction, owing to a late, compact transition state—such as that transversed in the addition of an allylboronate ester to an aldehyde. In principle, this signifies a reagent control of the stereoselectivity by *achiral* reagents! On the basis of these data, it was possible for the first time to probe experimentally the conformation of the aldehyde side chain responsible for the asymmetric induction in the transition state of the allylboronate ester addition.[54] The most favorable transition states are shown in Scheme 25.

Table 1. Cram/anti-Cram selectivities of additions of boronate esters to chiral aldehydes.

Aldehyde \ Boronate ester	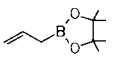	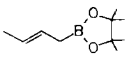	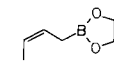
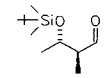	49 : 51	95 : 5	9 : 91
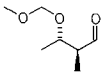	61 : 39	89 : 11	22 : 78
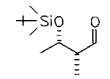	79 : 21	98 : 2	40 : 60
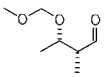	79 : 21	94 : 6	41 : 59
	62 : 38	83 : 17	30 : 70

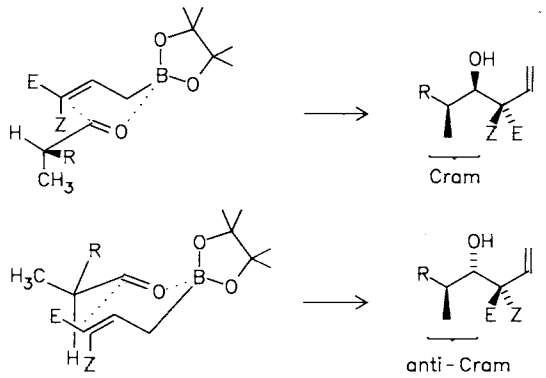

Scheme 25. E and Z indicate the positions of the substituents for a double bond having an E and Z configuration, respectively.

With respect to the synthesis of stereotriads, one can summarize that *E*-crotylboronate esters give frequently good to very good selectivities in favor of **24**. With *Z*-crotylboronate esters, however, usually only modest selectivities in favor of **25** result (Scheme 26).

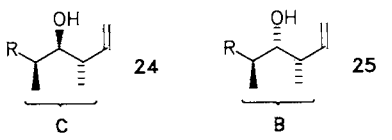

Scheme 26.

In order to obtain stereotriads other than the stereotriad **C** by this methodology, it is thus again necessary, as in the case of the aldol addition, to employ chiral reagents. Chiral, α-substituted crotylboronate esters, such as **26**, have been developed for this purpose.[55]

In this way, the principle of reagent-controlled stereoselectivity was demonstrated again, for example, in the case

of the aldehyde **27** (Scheme 27). However, the approximately 30:1 asymmetric induction originating from reagent **26** did not reach the desired range of >100:1. Thus, other α-chiral *E*-crotylboronate esters are at present being tested for their suitability.

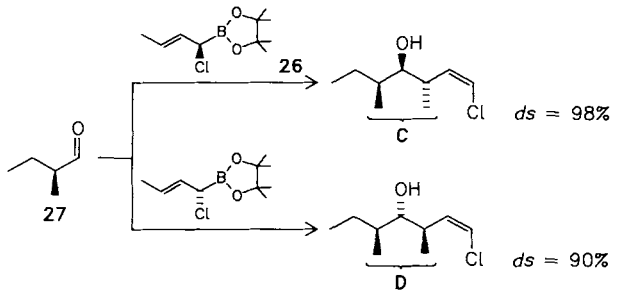

Scheme 27.

Further crotylboron compounds that have given encouraging results are the crotylboranes **28** and **29** reported by *H. C. Brown* et al.[56] and the chirally modified crotylboronate esters **30** and **31** reported by *W. R. Roush* et al.,[52,53] all of which are available in both enantiomeric forms (Scheme 28).

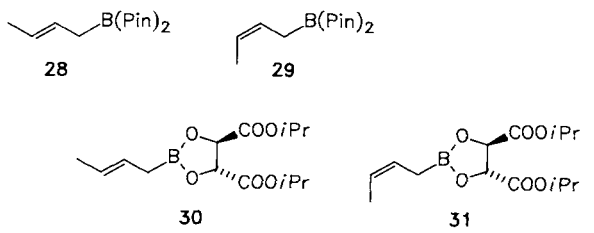

Scheme 28.

Here also, it remains to be seen how near these reagents approach the desired selectivity of >100:1. The utility of α-chiral crotyl-metal reagents has also been demonstrated for the tin compound **32**, which undergoes thermal addition at 130°C to benzaldehyde with formation of a homogeneous, *anti*-configurated product (Scheme 29).[57]

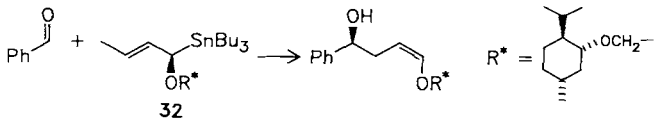

Scheme 29.

2.3. Pentenyl-Metal Compounds

Pentenyl-metal compounds of the type **33** (Scheme 30) already have a center of chirality at the α-position to the metal, which may be employed for control of the addition

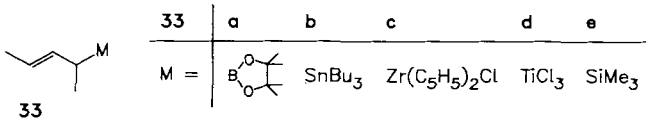

Scheme 30.

to aldehydes. This has also been realized in the case of the *Z*-pentenylboronate ester **34**, which, on addition to benzaldehyde, resulted in an asymmetric induction of 99% *ee* (Scheme 31).[58] Correspondingly, the aldehyde **35** was converted specifically into the compound with the stereotriad **B**. Experiments in the racemic series, however, indicated that the asymmetric induction of the *E*-pentenylboronate ester **33a**, corresponding to **34**, is low.

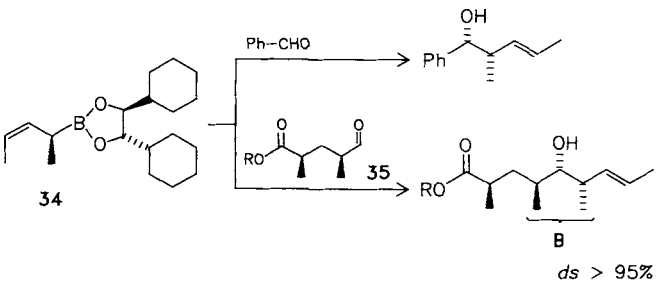

Scheme 31.

Moreover, the reactions of *rac*-**35** with racemic **33b-d** under Lewis acid catalysis exhibited a wide range of diastereoselectivity in favor of individual stereotriads (Scheme 32).[59] For the reaction of racemic **33e**, a high selectivity in favor of **36** (stereotriad **B**) has been reported.[60] The same reaction using the enantiomerically pure aldehyde **35** gave both stereoisomers **36** and **37** in a ratio of 1:1.[58]

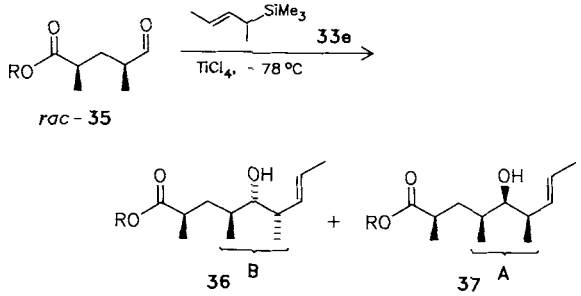

Scheme 32.

This shows that each enantiomer of **35** leads specifically to one of the products; the diastereoselectivity of the reaction is therefore subject to reagent control. This is not surprising in light of the reactions of other α-chiral crotylsilanes with aldehydes.[61]

3. Construction of the Skeleton and the Stereocenters in Separate Steps

Procedures will first be discussed in the first step of which the carbon skeleton is extended by chain lengthening introducing a prochiral C=C bond. In a subsequent step, the diastereotopic sides of the C=C bond are functionalized in such a way that only one of the desired stereotriads results. In principle, these procedures are also designed so that they can be performed repetitively (Scheme 33, **41** can be used again as educt **38**).

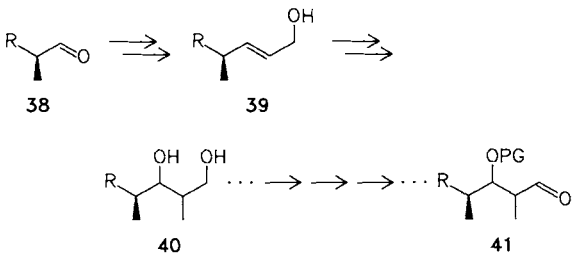

Scheme 33. The exclusive formation of an olefin having either a *Z* or an *E* configuration is decisive for this synthetic sequence.

However, since the chain lengthening and the construction of the stereocenters are now performed in two separate steps, longer reaction sequences than those described in Section 2 are inevitable. In the first, chain-lengthening step a double bond with uniform prochirality (i.e., homogeneous *E* or *Z* configuration) must be formed initially. Effective methods, such as the Wittig reaction or analogous procedures, are available for this.[62,63]

3.1. Epoxidation

The isomerically uniform olefins thus obtained (e.g., **39** from **38**) can be functionalized, e.g., epoxidized, utilizing the asymmetric induction from the resident center of chirality. The epoxide can then be opened regioselectively with inversion at C-2 by means of cuprates to give compounds **40**. A typical sequence[64] is shown in Scheme 34.

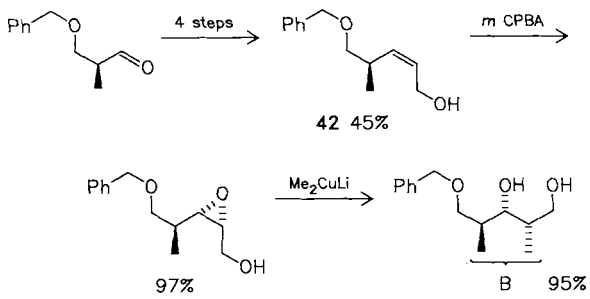

Scheme 34. *m*CPBA = *m*-chloroperbenzoic acid.

The key to the high diastereoselectivity observed in the epoxidation of the olefins lies in the *Z* conformation of the double bond. This practically allows only one configuration for **42**, namely, **42'** (Scheme 35), in which the benzyloxy group is fixed on one side of the double bond. Since *m*-chloroperbenzoic acid reacts by coordination with the benzyloxy group, the epoxidation of **42** occurs selectively from this side. When the *E*-allyl alcohol **43** is the starting material, the situation is less favorable since the position of the benzyloxy group relative to the double bond is not fixed by a preferred conformation. For this reason, the epoxidation of **43** proceeds unselectively.[64]

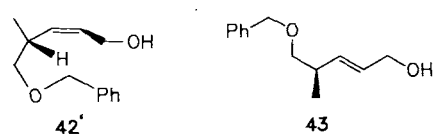

Scheme 35.

This situation can be corrected by temporary introduction of an auxiliary substituent (e.g., Me_3Si) into the *Z* position of the olefin. The epoxidation then takes place once again with high diastereoselectivity (Scheme 36).[65] However, the number of reaction steps is increased.

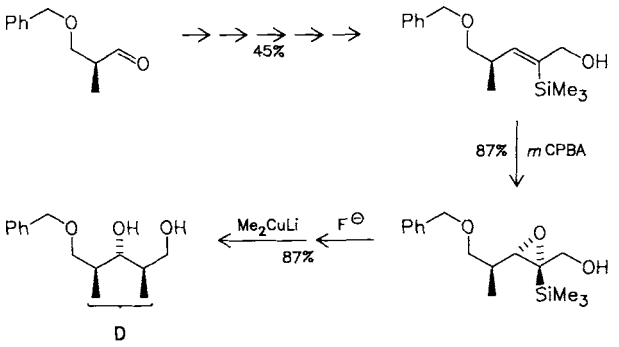

Scheme 36.

It might therefore be more favorable to epoxidize the double bond under reagent control of stereoselectivity, i.e., an asymmetric induction resulting from the reagent (e.g., Sharpless epoxidation[23]). In this way, three (**A**, **C**, and **D**) of the four stereotriads were obtained in yields of about 80% (Scheme 37).[66]

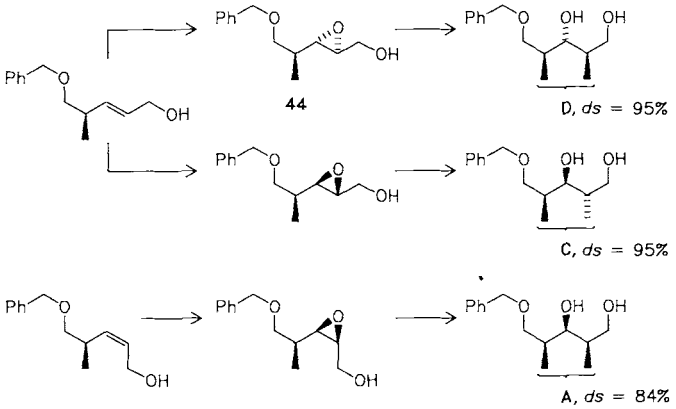

Scheme 37.

The fourth stereotriad (**B**) is accessible utilizing the asymmetric induction resulting from the educt (see Scheme 34). Furthermore, a method has been developed by which a compound of the type **44** has been converted into the stereotriad **B**. This has been realized by reductive conversion of the CH_2OH group into a methyl group followed by introduction, via cuprate, of the C_1 unit at the oxidation level of an aldehyde.

The repetitive chain lengthening of **38** to **41** allows access to all four stereotriads with high diastereoselectivities and thus is the most flexible strategy. However, it requires many steps.[68] This also arises from the fact that the OH groups on the primary and secondary carbon atoms in the intermediate products **40** must be differentiated. In a synthesis of avermectin, eight steps were required for the "simple" lengthening of **27** to **45**, which, nevertheless, was achieved in 40% yield (Scheme 38).[69]

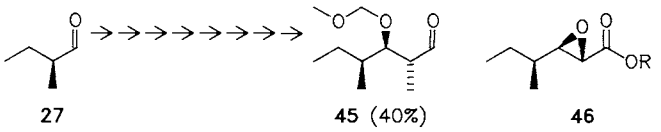

Scheme 38.

The differentiation of the hydroxyl groups would be easier if the epoxide opening were performed on the epoxycarboxylic acid or the epoxy ester **46** rather than on the epoxy alcohol.[70]

Instead of introducing the methyl group by means of dimethylcuprate (see Scheme 36), it can be introduced in the chain-lengthening step (Scheme 39).[65] Since a substituent

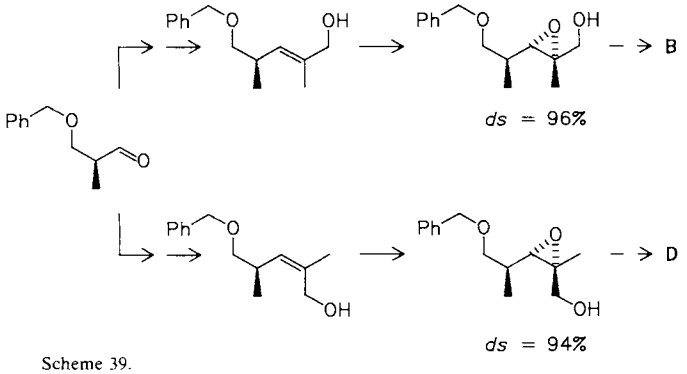

Scheme 39.

is now present at the double bond in the *Z* position with respect to the chiral moiety, the asymmetric induction from the resident center of chirality in the epoxidation step is high; once again, the benzyloxy group directs the peracid onto only one side of the double bond. If, instead of the benzyl group, a sterically more demanding protecting group (tBuMe$_2$Si) is used, this group shields this particular side of the double bond so that, with the same starting configuration and a different epoxidizing agent, the other side of the double bond can now be epoxidized (Scheme 40).[71]

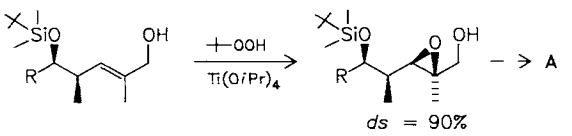

Scheme 40.

In order to obtain the stereotriads **A**, **B**, or **D** from the trisubstituted epoxides, the latter must be hydrogenolytically opened in a regioselective manner. Sodium hydridobis(2-methoxyethoxy)aluminate (REDAL) has proved useful for this purpose (for the use of AlH_3, see Ref. [72]). This sequence (Scheme 41) has been used, for example, in a synthesis of protomycinolide,[73] in which the regioselectivity of epoxide opening was 9 : 1.

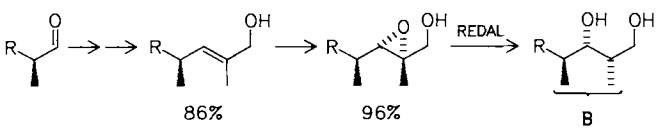

Scheme 41.

In summary, the routes involving epoxidation of prochiral olefins are reliable and versatile with respect to stereochemical control but require a large number of steps.

3.2. Hydroboration or Hydrosilylation

Epoxidation of a double bond followed by a REDAL reduction is, however, only one possibility for the regioselective addition of water to a double bond. The standard method for anti-Markownikoff addition is hydroboration. It was thus of interest to determine whether hydroboration of substrates of the type **47** (Scheme 42) could be achieved with sufficient asymmetric induction from the resident centers of chirality.

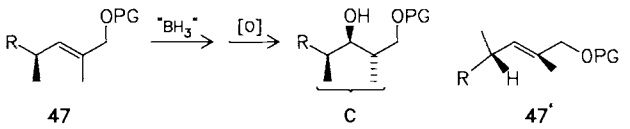

Scheme 42.

It is the difference in spatial requirements of the groups R and CH_3 (cf. **47'**) that governs the extent of the asymmetric induction, which varied from 3 : 1 to 8 : 1.[17,64,66,74] This reaction sequence was developed by *Kishi* et al. and then used in the synthesis of rifamycin S.[2] By changing the prochirality—*Z* configuration of the double bond—the stereotriad **A** could be obtained with a selectivity ranging from 2.5 : 1 to 12 : 1 (Scheme 43).[17,64]

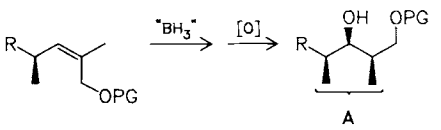

Scheme 43.

Generally, higher diastereoselectivities in the hydroboration would be desirable in most cases. It is therefore surprising that the possibility of double stereodifferentiation by means of chiral hydroborating agents[75] has not been utilized in these cases.

The diastereoselectivity can also be increased, however, by performing the hydroboration intramolecularly instead of intermolecularly (Scheme 44). In addition, since the hydroborating agent is linked to the group R, the other side of the double bond is now attacked.[76,77]

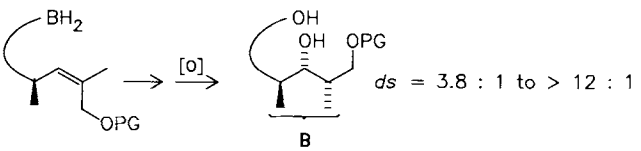

Scheme 44.

The same is true for the intramolecular hydrosilylation (Scheme 45). Depending on the prochirality of the double bond used, the stereotriad **D** or **B** is thereby accessible after oxidative cleavage of the C–Si bond.[78] Here, good to very good (20 : 1) selectivities have been achieved.

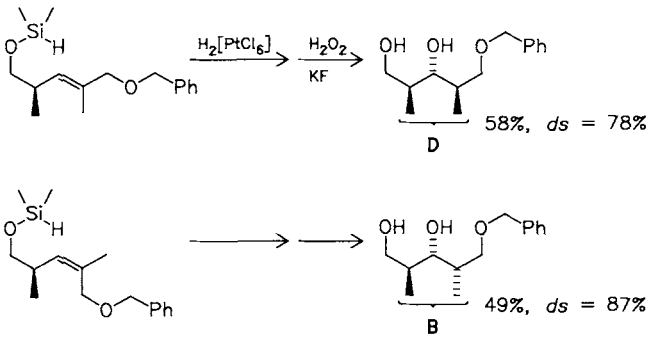

Scheme 45.

While hydrosilylation results in simultaneous introduction of the C–Si and C–H bonds, it is also possible to form these two bonds sequentially. The acceptable diastereoselectivities of the reaction sequence shown in Scheme 46[79] could serve as the basis for an iterative chain lengthening with formation of the stereotriad **A**. In this case, the ste-

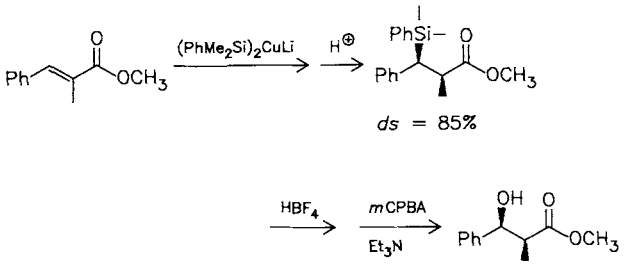

Scheme 46.

reocenters would be formed in a series of asymmetric induction steps, in the first of which the differences in size of the R and CH_3 groups in **48**, for a fixed conformation (cf. **47'** in Scheme 42), are again assumed to be responsible (Scheme 47).

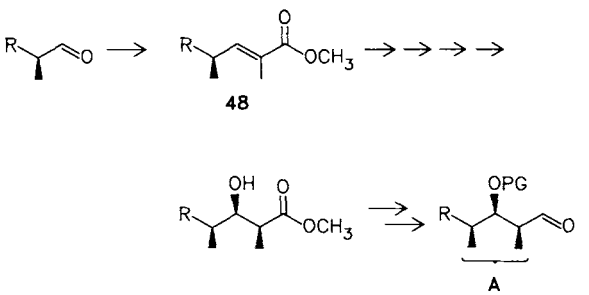

Scheme 47. The four steps required for addition of water to the C=C bond of **48** correspond to those of Scheme 46.

The procedures described in this section for the iterative construction of stereotriads require as well a large number of steps, because of the frequently necessary protecting group manipulations.

4. Stepwise Construction of Both New Stereocenters

The last example in Section 3.2 already demonstrated a stepwise construction of the two new stereocenters. Since the problem of asymmetric induction must be solved in each step, this approach appears at first to be inherently unfavorable. The following examples, however, demonstrate that this is not necessarily the case and that even relatively short reaction sequences for the iterative construction of stereotriads can be realized.

4.1. Vinylation/Hydrogenation

If this stepwise route is selected, it is logical to construct neighboring, not distal, stereocenters utilizing 1,2-asymmetric induction (Scheme 48). This route has already been realized several times using **49**[80] as an acrolein d^2 synthon (Scheme 49).[81]

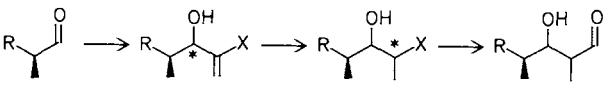

Scheme 48. X = a protected or latent aldehyde function.

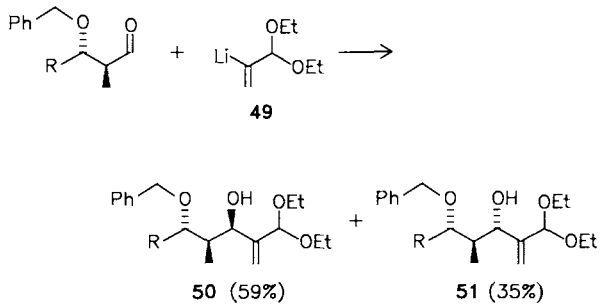

Scheme 49.

Unfortunately, the Cram selectivity in the first step is unsatisfactory. However, an extensive arsenal of acrolein and acrylate d^2 building blocks[82] is available, some of which should most certainly result in a high Cram/anti-Cram selectivity (see, e.g., Ref. [83]). This could also be achieved by the use of the corresponding ketene acetals, such as **52** (Scheme 50), under Mukaiyama conditions.[84] Since the above-mentioned synthons are all achiral, the stereoselectivity is solely dependent on the magnitude of the inherent asymmetric induction of the chiral aldehydes.[11]

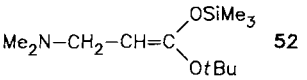

Scheme 50.

In the second step, the last stereocenter of the stereotriad must be constructed by hydrogenation of the double bond (e.g., of **50** or **51**). Here, it has been shown that in the case of the Cram diastereomer **50**, a rhodium-catalyzed hydrogenation takes place with very high *anti*-selectivity (Scheme 51),[81] whereas with the anti-Cram diastereomer **51** the stereoselectivity varied widely.[85] The rhodium-catalyzed hydrogenation of acrylates of the type **53** also generally proceeds with high *anti*-selectivity (Scheme 51). If necessary, the selectivity can be increased by employing chiral catalysts or by utilizing menthyl esters.[86] In cases with a high stereoselectivity in the first step, stereotriads of

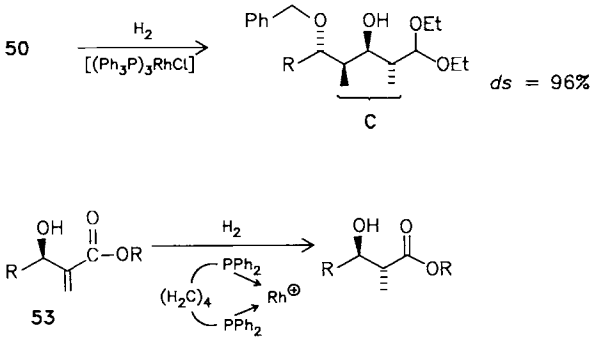

Scheme 51.

the type **C** are generally accessible in this manner. Of interest is the observation by *Scolastico* et al.[83] that addition of thiophenol to an acrylate of the type **54** followed by desulfurization gave just the other isomer (Scheme 52). In connection with the chain lengthening described in this section, this method should make possible the selective construction of the stereotriad **A**.

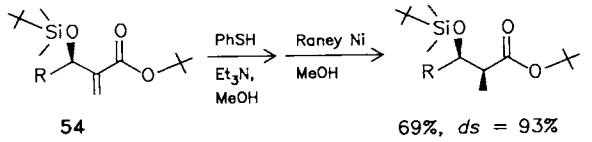

Scheme 52.

4.2. Vinylation/Hydroboration

A related reaction sequence consists in a diastereoselective propenylation[87] of the chiral aldehyde **38** to form **55** (Scheme 53); however, no direct information on the magnitude of the achievable diastereoselectivity is available. The second step, the hydroboration to give **56**[88] proceeds, in contrast, with very high diastereoselectivity to yield the stereotriad **C**.[89,90] Protection of the OH group in **55** reduces the diastereoselectivity.[72] All the other stereotriads have also been prepared, albeit in multistep sequences, from a starting compound of the type **55**.[5] This led to the recognition that the $ZnBH_4$ reduction of **57** to **58**[5] represents a further method to convert an α-chiral β-hydroxycarboxylic acid into intermediate products of the type **55** (Scheme 54).

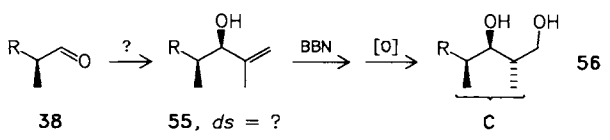

Scheme 53.

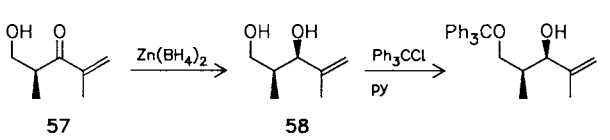

Scheme 54.

4.3. Vinylation/Cyclization

The reaction sequence in Scheme 55 represents a completely different approach which has not yet been employed for the iterative construction of the stereotriad **C**. In the first step, a Cram-selective vinylation[87,91] of the starting aldehyde to give **59** must be realized. The further transformation to **60** by radical cyclization proceeds with high (*ds* > 95%) *anti*-selectivity.[89,92] Subsequent refunctionalizations should result in the formation of the desired aldehyde **61** having the stereotriad **C**.

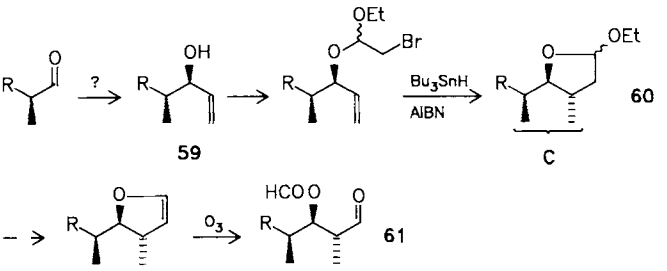

Scheme 55. AIBN = azobisisobutyronitrile.

4.4. Acetate-Enolate Addition/Frater Alkylation

In the procedure discussed in Section 4.3, the second step consisted in a stereoselective C–C coupling with formation of the main chain. A C–C coupling with introduction of the methyl group is just as feasible (Scheme 56).

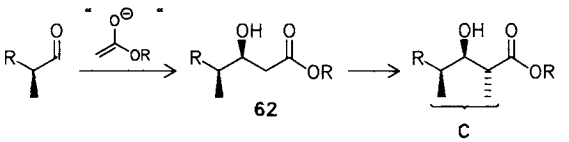

Scheme 56.

However, the first step in this case poses difficulties since easily controlled achiral[18] or chiral[93] acetate-enolate equivalents are rare. The first step must, if necessary, be achieved by other routes.[94,95] For example, a chelation-controlled allylation of β-alkoxyaldehydes is a possibility (Scheme 57)[45] (for non-chelation control, see Ref. [96]).

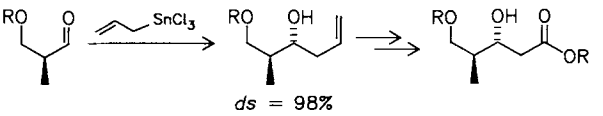

Scheme 57.

The second part of the reaction sequence, in contrast, is well substantiated. The methylation of the β-hydroxy ester **62**, after conversion to the dianion according to the method of *Frater* et al.,[94,97] is successful with good (*ds* ≥ 90%) *anti*-selectivity. *Oppolzer* et al.[95] have described an analogous sequence that is of interest here.

Although the procedures described in Sections 4.3 and 4.4 are mainly limited to the formation of the stereotriad **C**, they require only four to five steps for an iterative chain lengthening.

4.5. Acylation/Reduction

The reverse order for the stepwise construction of the stereocenters remains to be discussed (Scheme 58). In this case, the more distant stereocenter (* in **63**) is defined in the first step and the now central center (* in **64**) is constructed in the second step. This procedure at first seems to

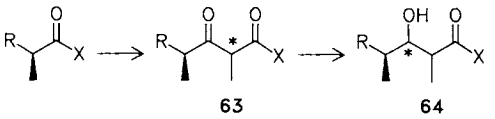

Scheme 58. For example, X = an oxazolidinane residue.

be of little value since a high 1,3-asymmetric induction from the stereocenter present in the starting material can hardly be expected. Just this fact, however, demands and allows the use of reagent control of the stereoselectivity, thereby making all four stereotriads possibly accessible. Furthermore, since the stereocenter marked with an asterisk in **63** is flanked by two carbonyl groups, a rapid epimerization appears unavoidable. Fortunately, groups X exist that are capable of hindering an enolization in **63** for stereoelectronic reasons. Finally, this sequence is also involved in the natural biogenesis of the polyketide-derived natural products, whereby the *S*-coenzyme A moiety serves as the group X. This iterative chain lengthening is short and, furthermore, takes place at the oxidation state of the acid derivative (not that of the aldehyde as in the preceding sections), thus bringing further advantages. In short, on closer consideration, the approach shown in Scheme 58 could be one of the more attractive routes to obtain the desired stereotriads simply and specifically.

What does the reality look like? The lithium enolates **66** are cleanly acylated by acid chlorides (**65**, X = Cl) to give the products **67** with an asymmetric induction of about 95% (Scheme 59).[99] Depending on the configuration of

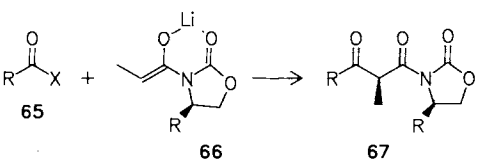

Scheme 59. For example, X = Cl.

the controlling oxazolidinone group in **66**, either configuration at the new stereocenter in **63** can be attained. The special β-dicarbonyl system withstands weakly basic and weakly acidic conditions without epimerization.[100] Application of this method to iterative chain lengthening requires acylating agents **65** that do not undergo epimerization of the α center of chirality during preparation, handling, and reaction. Perhaps, among other derivatives, the *N*-methoxyamides, **65** (X = $N(CH_3)OCH_3$), introduced by *Weinreb* et al.[101] could be suitable.[102]

The α-methyl-β-oxo carboxylic acid derivatives **63** thus obtained can be stereoselectively reduced with $Zn(BH_4)_2$ in the second step of the reaction sequence (Scheme 60).[103]

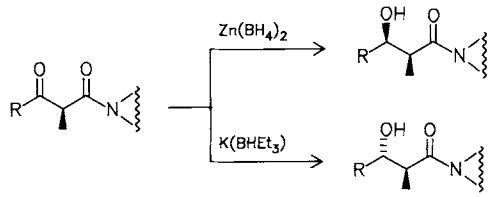

Scheme 60.

In this way, *syn*-configurated β-hydroxy-α-methylcarboxylic acid derivatives are obtained under chelation control. Starting from the intermediate products **63**, this leads to the stereotriads **A** and **B**, the ones which are also accessible by the aldol addition (see Section 2.1) under reagent control of stereoselectivity. In this respect, an *anti*-selective reduction of α-methyl-β-oxo esters would be much more valuable. This was recently realized by the use of potassium triethylhydridoborate.[104] Thus, the construction of the stereotriads **C** and **D** should also be possible by this method.

Another type of control is based on the observation that, in the reduction of β-hydroxy ketones, a 1,3-induction from the stereocenter bearing the hydroxyl group is possible. Thus, reduction with triacetoxyhydridoborate leads to *anti*-1,3-diols (Scheme 61).[105] A hydroxyl group in the δ-

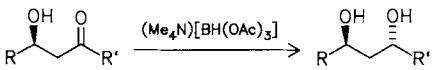

Scheme 61.

position of a β-dicarbonyl system can thus take over the stereochemical control in the reduction (Scheme 62).[105, 106]

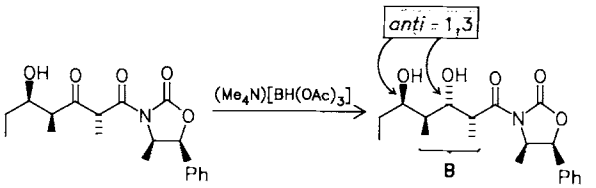

Scheme 62.

Use of $Zn(BH_4)_2$ or diisobutylaluminum hydride (DIBAH) to reduce β-hydroxy ketones,[107] in contrast, should lead to *syn*-1,3-diols. The example shown in Scheme 63[100]

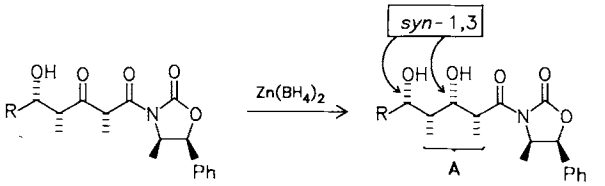

Scheme 63.

does not answer the question whether the control results from the β-hydroxy ketone moiety or from the methyl group of the β-dicarbonyl unit. The reduction of **68** with DIBAH (Scheme 64)[100] demonstrates that the former method of control dominates over the latter. Thus, not only the stereotriad **C** but probably also the stereotriad **D** should be accessible by exploiting the 1,3-induction from a hydroxyl group in the δ-position.

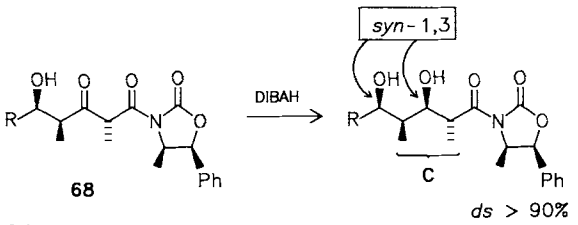

Scheme 64.

5. Interconversion of Stereotriads

The reduction of **68** with DIBAH opens up the possibility of converting, for example, compound **69** with the stereotriad **B**, accessible by direct aldol addition (see Section 2.1), into **70** by oxidation; **70** could then be converted into

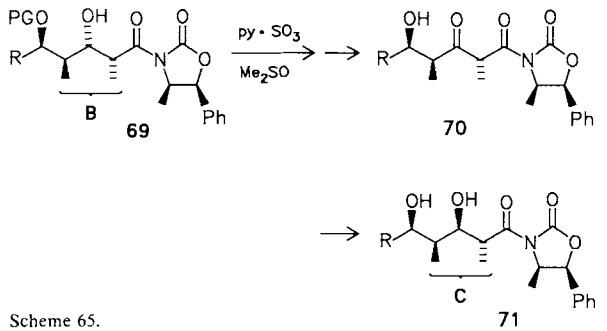

Scheme 65.

71 having the stereotriad **C** (Scheme 65). Indeed, oxidation of such (β-hydroxyacyl)oxazolidinones to the corresponding β-dicarbonyl compounds without epimerization of the central stereocenter is possible.[98]

In another case, the conversion of the stereotriad **C** to **B** or **A** to **D** has been realized by an oxidation-reduction sequence (Scheme 66).[44]

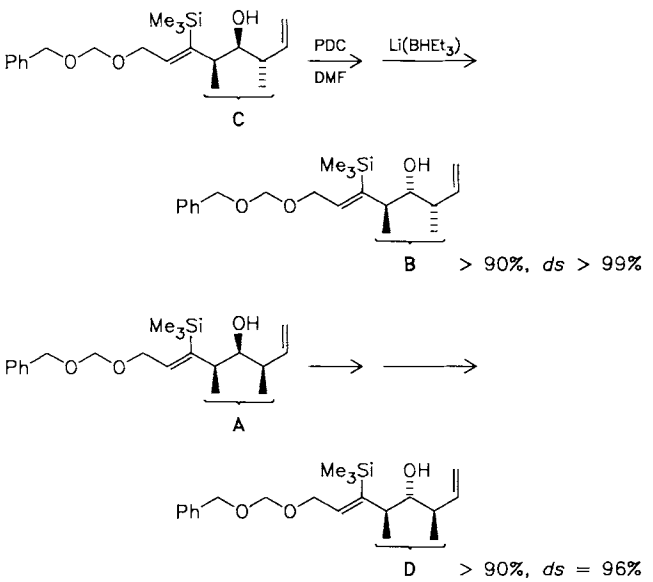

Scheme 66. PDC = pyridinium dichromate, DMF = dimethylformamide.

The presence of the bulky (but removable[48, 108]) Me_3Si group is most certainly favorable[109, 110] but not absolutely necessary[109] for the high diastereoselectivity in the reduction. Whereas the above-mentioned interconversions can be realized in only one direction, the Mitsunobu reaction[111] offers, in principle, bidirectional interconversions of the stereotriads **C** and **B** or **A** and **D**. However, to the best of my knowledge, this possibility has not yet been exploited. Application of this method may be necessary when, for example, an aldehyde with high asymmetric induction is employed in an aldol addition and where one would have to override this by reagent control of stereoselectivity. In this situation, the aldol addition will inevitably be very slow so that side reactions could dominate. In this case, it would be more favorable to build up another stereotriad, which is epimeric at the OH group, in a process that utilizes the high asymmetric induction of the aldehyde and then to invert the configuration of the carbon atom bearing the OH group in a second step.

6. Summary and Outlook

The extent of the results reported here clearly shows that this field of stereoselective synthesis has been widely developed in only a few years. Thus, a sufficient arsenal of methods is now available for the chemist interested in the synthesis of polyketide-derived natural products. The summary in Table 2 shows, however, that not all stereotriads are equally well accessible.

Table 2. Survey of methods for the preparation of the stereotriads **A**–**D**.

Methods	OH A	OH B	OH C	OH D
2.1	+	+	[a]	
2.2.1	+	[a]		
2.2.2			+	
2.2.3		[a]	+	[a]
2.3	[a]	+		
3.1	+	+	+	+
3.2	+	+ [b]	+	+ [b]
4.1	[a]		+	
4.2, 4.3, 4.4			+	
4.5	+	+	+	
5		+	[a]	[a]

[a] Few examples or frequently low diastereoselectivity. [b] Only with certain structural features in the substrate.

In this respect, it is important to know that, in the synthesis of polyketide-derived natural products by such repetitive procedures, the nature of the stereotriads to be constructed also depends on the direction of the synthesis (Scheme 67). Whereas the symmetrical stereotriads **A** and **D** are obtained irrespective of whether the chain is built up from left to right or from right to left, the stereotriads **B** and **C** are dependent on the direction of construction of the molecule.

The large number of methods available for the construction of the triad **C** could hence be of importance for choosing the direction of synthesis. The methods described here are not all equal. The most mature are the methods described in Section 2.1, for the preparation of the stereotriads **A** and **B** by means of aldol additions with chiral enolates. In other cases, the choice must be made between

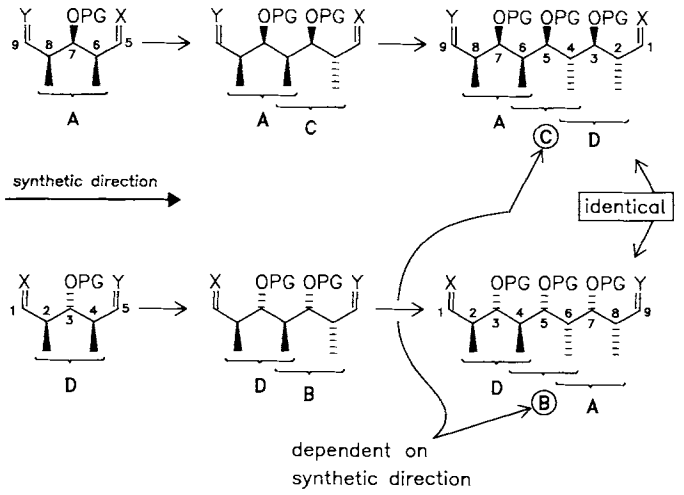

Scheme 67. C=X, C=Y = real or latent aldehyde functions.

high stereoselectivity and versatility but a large number of steps (epoxidation of prochiral olefins, Section 3.1), on the one hand, and moderate to good stereoselectivity with a lower number of steps, on the other hand.

Further development of methods for stereoselective syntheses is in full progress. Therefore, it can be safely predicted that the unsatisfactory results in Table 2 will eventually be improved and that the gaps will be filled. More important, however, is the elucidation of the principles by which the synthesis of molecules with long sequences of stereocenters can be approached. The emphasis on the stereotriads **A**–**D** is completely arbitrary. A review of the newly developed methods for the synthesis of the four diastereomers of the type **72**,[88, 112–114] **73**,[23, 115] or **74**[6, 11, 116] would be equally possible (Scheme 68).

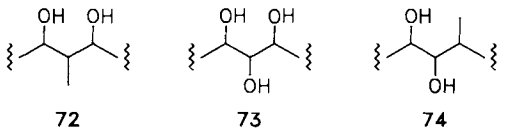

Scheme 68.

Even the limitation of this review to the synthesis of stereo*triads* as steps in the synthesis of larger molecules was only opportune initially; it is by no means binding. For example, the eight stereotetrads, e.g., with the structures **75** and **76** (Scheme 69), are still waiting for the development of specific methods for their synthesis. Impressive routes of access to specific representatives have already been developed.[117] Moreover, the direct approach to some of the sixteen stereopentads of type **77** (Scheme 69) has already begun.[100, 106, 117, 118] In this decade a new continent of stereoselective synthesis will be opened up to exploration.

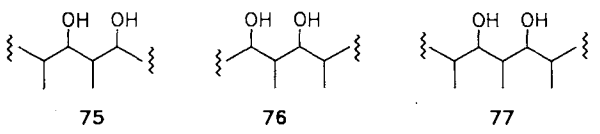

Scheme 69.

Received: December 19, 1986 [A 622 IE]
German version: *Angew. Chem. 99* (1987)
Translated by Dr. *Richard E. Dunmur*, Ditzingen

[1] R. B. Woodward in A. Todd (Ed.): *Perspectives of Organic Chemistry*, Wiley, New York 1956, p. 155.
[2] Methynolide: S. Masamune, H. Yamamoto, S. Kamata, A. Fukuzawa, *J. Am. Chem. Soc. 97* (1975) 3513; erythronolide B: E. J. Corey, S. Kim, S. Yoo, K. C. Nicolaou, L. S. Melvin, Jr., D. J. Brunelle, J. R. Falck, E. J. Trybulski, R. Lett, P. W. Sheldrake, *ibid. 100* (1978) 4620; erythromycin A: R. B. Woodward, E. Logusch, K. P. Nambiar, K. Sakan, D. E. Ward, B.-W. Au-Yeung, P. Balaram, L. J. Browne, P. J. Card, C. H. Chen, R. B. Chênevert, A. Fliri, K. Frobel, H.-J. Gais, D. G. Garratt, K. Hayakawa, W. Heggie, D. P. Hesson, D. Hoppe, I. Hoppe, J. A. Hyatt, D. Ikeda, P. A. Jacobi, K. S. Kim, Y. Kobuke, K. Kojima, K. Krowicki, V. J. Lee, T. Leutert, S. Malchenko, J. Martens, R. S. Matthews, B. S. Ong, J. B. Press, T. V. Rajan Babu, G. Rousseau, H. M. Sauter, M. Suzuki, K. Tatsuta, L. M. Tolbert, E. A. Truesdale, I. Uchida, Y. Ueda, T. Uyehara, A. T. Vasella, W. C. Vladuchick, P. A. Wade, R. M. Williams, H. N.-C. Wong, *ibid. 103* (1981) 3215; rifamycin S: Y. Kishi, *Pure Appl. Chem. 53* (1981) 1163.
[3] See, e.g., I. Paterson, M. M. Mansuri, *Tetrahedron 41* (1985) 3569.
[4] Y. Oikawa, T. Nishi, H. Itaya, O. Yonemitsu, *Tetrahedron Lett. 24* (1983) 1987.
[5] T. Nakata, M. Fukui, H. Ohtsuka, T. Oishi, *Tetrahedron 40* (1984) 2225.
[6] J. Mulzer, L. Authenrieth-Ansorge (Berlin), personal communication; J. Mulzer, lecture at the ORCHEM conference, Bad Nauheim (FRG) 1986.
[7] M. Nakata, H. Takao, Y. Ikeyama, T. Sakai, K. Tatsuta, M. Kinoshita, *Bull. Chem. Soc. Jpn. 54* (1981) 1749.
[8] H. Seto, H. Akao, K. Furihata, N. Otake, *Tetrahedron Lett. 23* (1982) 2667; cf. E. J. Corey, J. W. Ponder, *ibid. 25* (1984) 4325.
[9] C. H. Heathcock in J. Morrison (Ed.): *Asymmetric Synthesis, Vol. 3*, Academic Press, New York 1984, p. 111.
[10] R. W. Hoffmann, *Angew. Chem. 94* (1982) 569; *Angew. Chem. Int. Ed. Engl. 21* (1982) 555; Y. Yamamoto, K. Maruyama, *Heterocycles 18* (1982) 357.
[11] Cf. M. T. Reetz, *Angew. Chem. 96* (1984) 542; *Angew. Chem. Int. Ed. Engl. 23* (1984) 556.
[12] D. A. Evans, J. V. Nelsen, T. R. Taber, *Top. Stereochem. 13* (1982) 1.
[13] C. Gennari, A. Bernardi, S. Cardani, C. Scolastico, *Tetrahedron 40* (1984) 4059.
[14] For further examples, see [16, 17].
[15] S. Masamune in B. M. Trost, C. R. Hutchinson (Eds.): *Organic Synthesis, Today and Tomorrow*, Pergamon, Oxford 1981, p. 197.
[16] D. W. Brooks, R. P. Kellogg, *Tetrahedron Lett. 23* (1982) 4991.
[17] G. Schmid, T. Fukuyama, K. Akasaka, Y. Kishi, *J. Am. Chem. Soc. 101* (1979) 259.
[18] A. I. Meyers, R. D. Walkup, *Tetrahedron 41* (1985) 5089.
[19] C. Gennari, M. G. Beretta, A. Bernardi, G. Moro, C. Scolastico, R. Todeschini, *Tetrahedron 42* (1986) 893.
[20] D. V. Patel, F. VanMiddlesworth, J. Donaubauer, P. Gannett, C. J. Sih, *J. Am. Chem. Soc. 108* (1986) 4603.
[21] C. H. Heathcock, L. A. Flippin, *J. Am. Chem. Soc. 105* (1983) 1667.
[22] C. H. Heathcock, M. C. Pirrung, J. Lampe, C. T. Buse, S. D. Young, *J. Org. Chem. 46* (1981) 2290.
[23] S. Masamune, W. Choy, J. S. Petersen, L. R. Sita, *Angew. Chem. 97* (1985) 1; *Angew. Chem. Int. Ed. Engl. 24* (1985) 1.
[24] D. A. Evans, J. Bartroli, *Tetrahedron Lett. 23* (1982) 807.
[25] D. A. Evans, L. R. McGee, *J. Am. Chem. Soc. 103* (1981) 2876.
[26] Y. Nagao, T. Inoue, K. Hashimoto, Y. Hagiwara, M. Ochiai, E. Fujita, *J. Chem. Soc. Chem. Commun. 1985*, 1419.
[27] D. A. Evans, J. M. Takacs, L. R. McGee, M. D. Ennis, D. J. Mathre, J. Bartroli, *Pure Appl. Chem. 53* (1981) 1109.
[28] S. Masamune, T. Kaiho, D. S. Garvey, *J. Am. Chem. Soc. 104* (1982) 5521.
[29] D. A. Evans, *Aldrichimica Acta 15* (1982) 23; R. Baker, M. A. Brimble, *Tetrahedron Lett. 27* (1986) 3311.
[30] Y. Tamaru, Y. Amino, Y. Furukawa, M. Kagotani, Z. Yoshida, *J. Am. Chem. Soc. 104* (1982) 4018; S. G. Davies, I. M. Dordor-Hedgecock, P. Warner, *Tetrahedron Lett. 26* (1985) 2125; M. Hirama, S. Masamune, *ibid. 1979*, 2225; A. I. Meyers, P. J. Reider, *J. Am. Chem. Soc. 101* (1979) 2501.
[31] T. H. Chan, T. Aida, P. W. K. Lau, V. Gorys, D. N. Harpp, *Tetrahedron Lett. 1979*, 4029; C. Gennari, A. Bernardi, S. Cardani, C. Scolastico, *ibid. 26* (1985) 797.
[32] M. C. Pirrung, C. H. Heathcock, *J. Org. Chem. 45* (1980) 1727.
[33] T. Tschamber, N. Waespe-Sarcevic, C. Tamm, *Helv. Chim. Acta 69* (1986) 621; see also F. Sato, M. Kusakabe, T. Kato, Y. Kobayashi, *J. Chem. Soc. Chem. Commun. 1984*, 1331; Y. Kitano, M. Kusakabe, Y. Kobayashi, F. Sato, *Chem. Lett. 1986*, 523.
[34] Y. Kobayashi, H. Uchiyama, H. Kanbara, F. Sato, *J. Am. Chem. Soc. 107* (1985) 5541.
[35] S. Masamune, T. Sato, B. M. Kim, T. A. Wollmann, *J. Am. Chem. Soc. 108* (1986) 8279.

[36] C. Palazzi, L. Colombo, C. Gennari, *Tetrahedron Lett. 27* (1986) 1735.
[37] A. I. Meyers, Y. Yamamoto, *Tetrahedron 40* (1984) 2309.
[38] G. Helmchen, U. Leikauf, I. Taufer-Knöpfel, *Angew. Chem. 97* (1985) 874; *Angew. Chem. Int. Ed. Engl. 24* (1985) 874.
[39] W. Oppolzer, J. Marco-Contelles, *Helv. Chim. Acta 69* (1986) 1699.
[40] S. J. Danishefsky, E. Larson, D. Askin, N. Kato, *J. Am. Chem. Soc. 107* (1985) 1246.
[41] S. Danishefsky, N. Kato, D. Askin, J. F. Kerwin, Jr., *J. Am. Chem. Soc. 104* (1982) 360; S. Danishefsky, K.-H. Chao, G. Schulte, *J. Org. Chem. 50* (1985) 4650; cf. also S. J. Danishefsky, *Aldrichimica Acta 19* (1986) 59.
[42] G. E. Keck, D. E. Abbott, *Tetrahedron Lett. 25* (1984) 1883.
[43] N. Nakajima, T. Hamada, T. Tanaka, Y. Oikawa, O. Yonemitsu, *J. Am. Chem. Soc. 108* (1986) 4645.
[44] K. Suzuki, E. Katayama, K. Tomooka, T. Matsumoto, G. Tsuchihashi, *Tetrahedron Lett. 26* (1985) 3707.
[45] See [42] and G. E. Keck, D. E. Abbott, E. P. Boden, E. J. Enholm, *Tetrahedron Lett. 25* (1984) 3927.
[46] Y. Yamamoto, H. Yatagai, Y. Ishihara, N. Maeda, K. Maruyama, *Tetrahedron 40* (1984) 2239.
[47] J. M. Coxon, S. J. van Eyk, P. J. Steel, *Tetrahedron Lett. 26* (1985) 6121.
[48] K. Suzuki, K. Tomooka, E. Katayama, T. Matsumoto, G. Tsuchihashi, *J. Am. Chem. Soc. 108* (1986) 5221.
[49] T. Hiyama, Y. Okude, K. Kimura, H. Nozaki, *Bull. Chem. Soc. Jpn. 55* (1982) 561; C. T. Buse, C. H. Heathcock, *Tetrahedron Lett. 1978*, 1685; S. F. Martin, C. Gluchowski, C. L. Campbell, R. C. Chapman, *J. Org. Chem. 49* (1984) 2512.
[50] M. D. Lewis, Y. Kishi, *Tetrahedron Lett. 23* (1982) 2343.
[51] D. A. Evans, E. B. Sjogren, J. Bartroli, R. L. Dow, *Tetrahedron Lett. 27* (1986) 4957.
[52] W. R. Roush, R. Halterman, *J. Am. Chem. Soc. 108* (1986) 294; W. R. Roush, A. D. Palkowitz, *ibid. 109* (1987) 953; W. R. Roush, A. D. Palkowitz, M. A. J. Palmer, *J. Org. Chem. 52* (1987) 317.
[53] W. R. Roush, M. A. Adam, A. E. Walts, D. J. Harris, *J. Am. Chem. Soc. 108* (1986) 3422.
[54] R. W. Hoffmann, U. Weidmann, *Chem. Ber. 119* (1985) 3966.
[55] R. W. Hoffmann, S. Dresely, *Angew. Chem. 98* (1986) 186; *Angew. Chem. Int. Ed. Engl. 25* (1986) 189.
[56] H. C. Brown, K. S. Bhat, *J. Am. Chem. Soc. 108* (1986) 5919; cf. also H. C. Brown, K. S. Bhat, R. S. Randad, *J. Org. Chem. 52* (1987) 319.
[57] V. J. Jephcote, A. J. Pratt, E. J. Thomas, *J. Chem. Soc. Chem. Commun. 1984*, 800; cf. also D. Hoppe, T. Krämer, *Angew. Chem. 98* (1986) 171; *Angew. Chem. Int. Ed. Engl. 25* (1986) 160.
[58] K. Ditrich, T. Bube, R. Stürmer, R. W. Hoffmann, *Angew. Chem. 98* (1986) 1016; *Angew. Chem. Int. Ed. Engl. 25* (1986) 1028; K. Ditrich, T. Bube, R. W. Hoffmann, unpublished results.
[59] Y. Yamamoto, K. Taniguchi, K. Maruyama, *J. Chem. Soc. Chem. Commun. 1985*, 1429.
[60] C. Santelli-Rouvier, *Tetrahedron Lett. 25* (1984) 4371.
[61] T. Hayashi, M. Konishi, H. Ito, M. Kumada, *J. Am. Chem. Soc. 104* (1982) 4962.
[62] J. M. Takacs, M. A. Helle, F. L. Seely, *Tetrahedron Lett. 27* (1986) 1257; W. C. Still, C. Gennari, *ibid. 24* (1983) 4405.
[63] M. R. Johnson, Y. Kishi, *Tetrahedron Lett. 1979*, 4347.
[64] M. R. Johnson, T. Nakata, Y. Kishi, *Tetrahedron Lett. 1979*, 4343.
[65] I. Hasan, Y. Kishi, *Tetrahedron Lett. 21* (1980) 4229, see also H. Tomioka, T. Suzuki, K. Oshima, H. Nozaki, *ibid. 23* (1982) 3387.
[66] H. Nagaoka, Y. Kishi, *Tetrahedron 37* (1981) 3873.
[67] Cf., e.g., B. H. Lipshutz, H. Kotsuki, W. Lew, *Tetrahedron Lett. 27* (1986) 4825.
[68] D. Boschelli, T. Takemasa, Y. Nishitani, S. Masamune, *Tetrahedron Lett. 26* (1985) 5239.
[69] S. Hanessian, A. Ugolini, D. Dubé, P. J. Hodges, C. André, *J. Am. Chem. Soc. 108* (1986) 2776.
[70] Cf. J. M. Chong, K. B. Sharpless, *Tetrahedron Lett. 26* (1985) 4683; J. Mulzer, O. Lammer, *Chem. Ber. 119* (1986) 2178.
[71] M. Isobe, M. Kitamura, S. Mio, T. Goto, *Tetrahedron Lett. 23* (1982) 221.
[72] Y. Oikawa, T. Nishi, O. Yonemitsu, *J. Chem. Soc. Perkin Trans. 1 1985*, 7.
[73] M. Honda, T. Katsuki, M. Yamaguchi, *Tetrahedron Lett. 25* (1984) 3857.
[74] C. H. Heathcock, E. T. Jarvi, T. Rosen, *Tetrahedron Lett. 25* (1984) 243.
[75] H. C. Brown, P. K. Jadhav, A. K. Mandal, *J. Org. Chem. 47* (1982) 5074; S. Masamune, B. M. Kim, J. S. Petersen, T. Sato, S. J. Veenstra, *J. Am. Chem. Soc. 107* (1985) 4549.
[76] D. J. Morgans, Jr., *Tetrahedron Lett. 22* (1981) 3721.
[77] W. C. Still, K. R. Shaw, *Tetrahedron Lett. 22* (1981) 3725.
[78] K. Tamao, T. Nakajima, R. Sumiya, H. Arai, N. Higuchi, Y. Ito, *J. Am. Chem. Soc. 108* (1986) 6090.
[79] W. Bernhard, I. Fleming, D. Waterson, *J. Chem. Soc. Chem. Commun. 1984*, 28; I. Fleming, R. Henning, H. Plaut, *ibid. 1984*, 29; H.-F. Chow, I. Fleming, *Tetrahedron Lett. 26* (1985) 397.
[80] J. Ficini, J. C. Depezay, *Tetrahedron Lett. 1969*, 4797; J. P. Marino, J. S. Farina, *J. Org. Chem. 41* (1976) 3213.
[81] M. Nakata, K. Toshima, T. Kai, M. Kinoshita, *Bull. Chem. Soc. Jpn. 58* (1985) 3457 and earlier papers.
[82] See, e.g., H. M. R. Hoffmann, J. Rabe, *J. Org. Chem. 50* (1985) 3849, and references cited therein.
[83] A. Bernardi, M. G. Beretta, L. Colombo, C. Gennari, G. Poli, C. Scolastico, *J. Org. Chem. 50* (1985) 4442.
[84] C. Scolastico in Società di Chimica Italiana (Ed.): *Horizons in Selective Organic Synthesis* (abstract volume of the Ischia Advanced School of Organic Chemistry II), Ischia (Italy) 1986, p. 44.
[85] M. Nakata, H. Enari, M. Kinoshita, *Bull. Chem. Soc. Jpn. 55* (1982) 3283.
[86] J. M. Brown, I. Cutting, *J. Chem. Soc. Chem. Commun. 1985*, 578; J. M. Brown, I. Cutting, P. L. Evans, P. J. Maddox, *Tetrahedron Lett. 27* (1986) 3307; J. M. Brown, *Angew. Chem. 99* (1987) 169; *Angew. Chem. Int. Ed. Engl. 26* (1987) 190.
[87] Cf. also K. Mead, T. L. Macdonald, *J. Org. Chem. 50* (1985) 422; W. C. Still, J. A. Schneider, *Tetrahedron Lett. 21* (1980) 1035.
[88] W. C. Still, J. C. Barrish, *J. Am. Chem. Soc. 105* (1983) 2487.
[89] E. Nakai, E. Kitahara, N. Sayo, Y. Ueno, T. Nakai, *Chem. Lett. 1985*, 1725.
[90] D. J.-S. Tsai, M. M. Midland, *J. Am. Chem. Soc. 107* (1985) 3915.
[91] See, e.g. M. Tsukamoto, H. Iio, T. Tokoroyama, *Tetrahedron Lett. 26* (1985) 4471.
[92] G. Stork, R. Mook, Jr., S. A. Biller, S. D. Rychnovsky, *J. Am. Chem. Soc. 105* (1983) 3741; Y. Ueno, O. Moriya, K. Chino, M. Watanabe, M. Okawara, *J. Chem. Soc. Perkin Trans. 1 1986*, 1351, and references cited therein.
[93] M. Braun, *Angew. Chem. 99* (1987) 24; *Angew. Chem. Int. Ed. Engl. 26* (1987) 24; M. Braun, R. Devant, *Chem. Ber. 119* (1986) 2191; Y. Nagao, S. Yamada, T. Kumagai, M. Ochiai, E. Fujita, *J. Chem. Soc. Chem. Commun. 1985*, 1418; Y. Nagao, Y. Hagiwara, T. Kumagai, M. Ochiai, T. Inoue, K. Hashimoto, E. Fujita, *J. Org. Chem. 51* (1986) 2391.
[94] M. Hirama, T. Nakamine, S. Ito, *Tetrahedron Lett. 27* (1986) 5281.
[95] W. Oppolzer, R. J. Mills, W. Pachinger, T. Stevenson, *Helv. Chim. Acta 69* (1986) 1542.
[96] M. T. Reetz, K. Kesseler, *J. Chem. Soc. Chem. Commun. 1984*, 1079; Y. Yamamoto, K. Maruyama, *J. Am. Chem. Soc. 107* (1985) 6411.
[97] G. Frater, *Helv. Chim. Acta 62* (1979) 2825; G. Frater, U. Müller, W. Günther, *Tetrahedron 40* (1984) 1269.
[98] D. A. Evans, M. D. Ennis, T. Le, *J. Am. Chem. Soc. 106* (1984) 1155.
[99] Y. Ito, T. Katsuki, M. Yamaguchi, *Tetrahedron Lett. 25* (1984) 6015.
[100] D. A. Evans in Società di Chimica Italiana (Ed.): *Horizons in Selective Organic Synthesis* (abstract volume of the Ischia Advanced School of Organic Chemistry II), Ischia (Italy) 1986, p. 48.
[101] S. Nahm, S. M. Weinreb, *Tetrahedron Lett. 22* (1981) 3815.
[102] J. A. Turner, W. S. Jacks, *lecture at the 192nd Am. Chem. Soc. Meet. 1986*, Abstract No. ORGN 219.
[103] T. Nakata, T. Oishi, *Tetrahedron Lett. 21* (1980) 1641; Y. Ito, M. Yamaguchi, *ibid. 24* (1983) 5385; T. Oishi, T. Nakata, *Acc. Chem. Res. 17* (1984) 338.
[104] Y. Ito, T. Katsuki, M. Yamaguchi, *Tetrahedron Lett. 26* (1985) 4643; cf. M. Fujita, T. Hiyama, *J. Am. Chem. Soc. 107* (1985) 8294.
[105] D. A. Evans, K. T. Chapman, *Tetrahedron Lett. 27* (1986) 5939.
[106] D. A. Evans, M. DiMare, *J. Am. Chem. Soc. 108* (1986) 2476.
[107] S. Kiyooka, H. Kuroda, Y. Shimasaki, *Tetrahedron Lett. 27* (1986) 3009.
[108] F. Sato, Y. Tanaka, M. Sato, *J. Chem. Soc. Chem. Commun. 1983*, 165.
[109] K. Suzuki, E. Katayama, G. Tsuchihashi, *Tetrahedron Lett. 25* (1984) 2479.
[110] F. Sato, M. Kusakabe, Y. Kobayashi, *J. Chem. Soc. Chem. Commun. 1984*, 1130; F. Sato, M. Kusakabe, T. Kato, Y. Kobayashi, *J. Chem. Soc. Chem. Commun. 1984*, 1331; K. Suzuki, T. Ohkuma, G. Tsuchihashi, *Tetrahedron Lett. 26* (1985) 861.
[111] O. Mitsunobu, *Synthesis 1981*, 1.
[112] Cf. G. Stork, S. D. Rychnovsky, *Pure Appl. Chem. 58* (1986) 767.
[113] See, e.g. S. Thaisrivongs, D. Seebach, *J. Am. Chem. Soc. 105* (1983) 7407.
[114] D. B. Collum, W. C. Still, F. Mohamadi, *J. Am. Chem. Soc. 108* (1986) 2094.
[115] S. Okamoto, T. Shimazaki, Y. Kitano, Y. Kobayashi, F. Sato, *J. Chem. Soc. Chem. Commun. 1986*, 1352.
[116] G. E. Keck, E. P. Boden, *Tetrahedron Lett. 25* (1984) 1879.
[117] S. Danishefsky, D. F. Harvey, *J. Am. Chem. Soc. 107* (1985) 6647.
[118] S. J. Danishefsky, D. C. Myles, D. F. Harvey, *J. Am. Chem. Soc. 109* (1987) 862.

The Pyrolysis of Azides in the Gas Phase**

By Hans Bock* and Ralph Dammel

*In memoriam Wilhelm Klemm****

*Dedicated to Professor Friedrich Hund on the occasion of his 90th birthday****

The chemistry of the non-metallic elements has in recent years passed through a period of rapid development, often referred to as its "renaissance". To emphasize just one of the key facets: numerous short-lived molecules containing multiple bonds to elements of the third and higher periods have been discovered, often accompanied by the planned synthesis of derivatives which are sterically shielded by bulky groups and thus kinetically stabilized. Thus today molecules such as silabenzenes $H_6C_{6-n}Si_n$ and silaethenes $H_2Si{=}CH_2$ or $R_2Si{=}CR_2$, disilenes $R_2Si{=}SiR_2$ and diphosphenes $RP{=}PR$, silaphenylisonitrile $H_5C_6{-}N{\equiv}Si$, or methylidyne-phosphanes $R{-}C{\equiv}P$, are all well-known species. Sandwich compounds with P_6 rings or silicon centers demonstrate that there are now hardly any barriers to impede the imagination of the non-metal chemist. In sharp contrast is our lack of knowledge regarding the "microscopic" pathways of chemical reactions: thus apart from information provided for example by molecular beam experiments, or from exact numerical calculations involving species consisting of only a few atoms, it remains largely unknown from which directions medium-sized molecules must approach each other to successfully collide and form a "reaction complex", in which way their structures are changed in such a process or which role is played by molecular dynamics in the energy transfer.—The pyrolysis of azides $X{-}N_3$, i.e. compounds which tend to explode violently when ignited in the condensed phase but can be heated in low-pressure gas flow systems without much risk, illustrates that studies of reactive intermediates are of interest not only because novel molecules may be discovered and isolated, and thereby possibilities for synthesis expanded. Moreover, some aspects of the "microscopic" pathways of these azide pyrolyses can be described satisfactorily on the basis of calculated energy hypersurfaces, and the influence of molecular dynamics becomes experimentally visible in the "chemical activation" of intermediates which leads to their "thermal explosion".

"Despite all that is known about reaction behavior, understanding of it is rather shallow ..."

(George C. Pimentel[1])

1. Azides and Imines—Prototypes for Reactive Nitrogen Compounds

The pyrolysis of methyl azide[2] can be carried out to advantage by passing an undiluted stream of gas at a pressure of 10^{-2} mbar through an externally heated quartz tube filled with quartz wool and following the decomposition by PE-spectroscopic gas analysis[3] (Figs. 1 and 3). At red heat, the cleavage of molecular nitrogen begins and methanimine is formed.

The nitrogen compounds of interest here, i.e. covalent azides $X{-}N_3$, the molecule N_2 and the readily polymerizing alkanimines $R_2C{=}NH$ as well as their most important properties will be presented first by way of introduction:

Covalent azides $X{-}N_3$ have been known for more than 120 years;[4] nitrogen is one of the few elements which form polyatomic homonuclear, unsaturated and linear

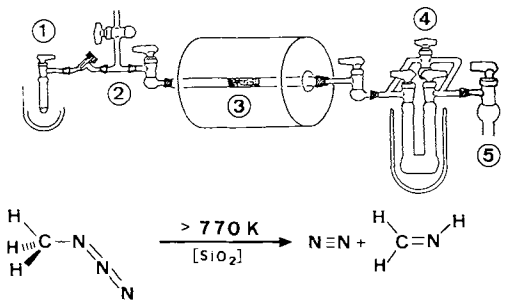

Fig. 1. The gas-phase pyrolysis of methyl azide: modular apparatus consisting of ① substance container, ② connector for evacuation, ③ reaction tube filled with quartz wool in a temperature-regulated oven, ④ cold trap with closable bypass and ⑤ connection to the PE-spectrometer.

[*] Prof. Dr. H. Bock, Dr. R. Dammel [+]
Institut für Anorganische Chemie der Universität
Niederurseler Hang, D-6000 Frankfurt/Main 50 (FRG)

[+] Present address: Hauptlaboratorium der Hoechst AG,
P.O. Box 800320, D-6230 Frankfurt/Main 80 (FRG)

[**] 15th essay on "Molecular Properties and Models".—14th essay: H. Bock "How Do Medium-Sized Molecules React?", Akademie der Wissenschaften und der Literatur Mainz, 1986/2, Verlag F. Steiner, Wiesbaden. Also Gas Phase Reactions, Part 66.—Part 65: R. Dammel, H. Bock, *Z. Naturforsch. B*, in press.

[***] A report on gas phase pyrolyses of methyl azide and vinyl azide and on the corresponding energy hypersurface calculations was given on the occasion of the First Hund/Klemm Lecture (November 14, 1983) at the Max-Planck-Institut für Festkörperforschung Stuttgart, in the presence of both honoured scientists.

substituent groups such as =N=N or –N=N=N. The structures of numerous azides have been determined using various methods (Scheme 1a. ND: neutron diffraction, UV: ultraviolet spectroscopy, MW: microwave spectroscopy, ED: electron diffraction; for further information see [4a, 5]). In general the NNN unit is linear; substituent effects may cause small deviations from linearity.[5]

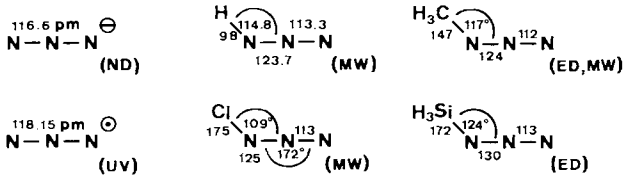

Scheme 1a.

Compounds containing a high proportion of azide nitrogen can be prepared;[4] Scheme 1b shows as examples P_3N_{21}, C_2N_{14} (with 89.1% one of the most nitrogen-rich organic molecules) and the salt $(CN_9)^{\oplus}X^{\ominus}$. It has been suggested that the empirical lower limit for explosivity of covalent azides corresponds to 25% by weight of azide nitrogen.[6]

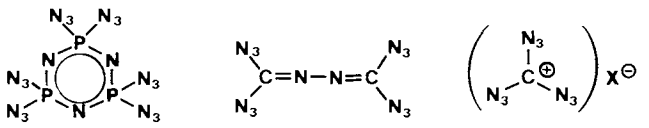

Scheme 1b.

In spite of the danger of explosion when they are improperly handled (cf. Section 2), the chemistry of covalent azides $X-N_3$ is attractive because of their multifarious reactivity: thus for the period 1967–1985 Chemical Abstracts has registered 10859 (!) publications dealing with them.[7] The subject areas listed range from the preparation of new azides via their preparative use, in particular in the synthesis of heterocycles, to the study of rearrangement and degradation reactions and their photochemical decomposition. Thermolyses of azides of small molecular size are, however, underrepresented,[8, 9] one particular difficulty being the detection of the unstable imines which are usually formed (see Section 3.10), since these require suitable real-time gas analysis procedures such as PE-spectroscopy.[2, 3]

The few alkyl azide pyrolyses in the gas phase which have so far been studied[8, 9] show first-order decay[9a] and yield complex product mixtures consisting of N_2, H_2, HN_3, NH_3, alkanes, alkenes and $H_2C=NH$ polymers such as urotropine.[9b] In mechanistic speculations, nitrene intermediates have often been postulated to be the primary products:[10] according to ESR studies[11] and quantum chemical calculations[12] alkyl nitrenes RN have a triplet ground state $\tilde{X}(^3A_2)$. However, in thermolysis or non-sensitized photolysis the alkyl nitrenes are formed in the excited singlet state $\tilde{A}(^1E)$ because of spin conservation; the singlet $\tilde{X}(^1\Sigma_g^+) \rightarrow$ triplet $\tilde{A}(^3\Sigma_u^+)$ excitation of the nitrogen molecule would require 590 kJ/mol (!)[13] (Scheme 2).

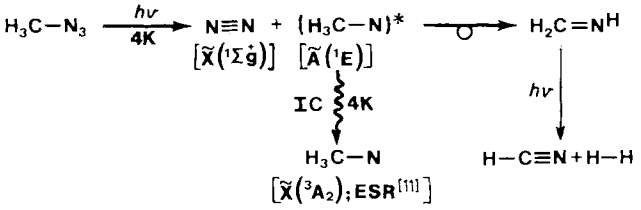

Scheme 2.

Excited singlet alkyl nitrenes (RN)* have only short lifetimes: thus an intersystem crossing (IC) to the ESR-active[11] triplet ground state ($\tilde{X}(^3A_2)$) occurs only under the extreme conditions of an inert gas matrix at 4 K.[10, 11] None of the typical intermolecular nitrene reactions such as insertion into σ-bonds or stereospecific addition to π-double bonds have been observed for the short-lived primary products (RN)*.[10] Instead, H- or R-migration to give open-chain imines or ring closure to N-heterocycles takes place. When our studies commenced, virtually no direct information on these unimolecular routes for stabilization of (RN)* was available, only indirect conclusions on the basis of the compounds formed on acid hydrolysis of the pyrolysis products.[9b, 10, 14] Direct detection of the rapidly polymerizing imine secondary products[14] had not been achieved at that time.

Dinitrogen N_2, the most stable modification of the element[15] is, because of its extremely high dissociation energy ($D_{298}^0 = 945.33 \pm 059$ kJ/mol[16]), one of the thermodynamically most favorable leaving groups.

Alkanimines, as simple and reactive nitrogen compounds,[17] probably play a part in the formation of bioorganic compounds in "primeval soup" experiments.[18] Radioastronomers have shown[19] that the simplest homologue methanimine $H_2C=NH$ is present in large quantities in hydrogen-rich nebulae such as Sagittarius B2. In contrast to the isoelectronic formaldehyde, which has been known since prehistoric times, it was first detected in a matrix experiment in 1961[13] and in the gas phase in 1965 by microwave spectroscopy of the reaction

$$H_3C-NH_2 + 2F^{\ominus} \rightarrow H_2C=NH + 2HF^{[20]}$$

There followed PE-spectroscopic detection in the mixtures formed by pyrolysis of methylamine[21] and as the main product of the thermal decomposition of methyl azide[2] (Figs. 1 and 4), and finally in 1982 its isolation as a pure substance.[22, 23]

The gaps in our knowledge of simple alkanimines are due entirely to their extreme reactivity under normal conditions (300 K, 1 bar, air): these cause immediate polymerization, oxidation or hydrolysis to occur. The azomethine[*] $(CH_3)CH=NCH_3$, the simplest alkanimine derivative, prepared in 1947 by condensation of acetaldehyde and methylamine, is a water-clear liquid, which, however, rapidly undergoes further reaction.[24] The smallest cyclic imine, the three-membered ring 2*H*-azirine, was first isolated in 1981 as the lowest-temperature decomposition product in the pyrolysis of vinyl azide[3, 25] (see Fig. 2). Even larger cyclic

[*] According to IUPAC rule C-185.3 only compounds of the type $>C=NH$ may be referred to as imines. Compounds of the type $R^1R^2C=NR^3$ form the class of compounds known as the azomethines.

imines such as 3,4-dihydro-2*H*-pyrrole or 2,3,4,5-tetrahydropyridine, which are important building blocks for alkaloid biosyntheses, could not until now be prepared in a pure form because of their tendency to trimerization.[26]

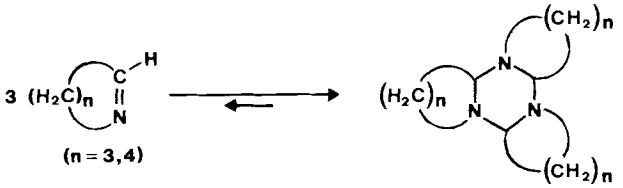

Even as monomers, cyclic azomethines are not always the thermodynamically most favorable constitutional isomers of the formula $C_nH_{2n-1}N$: thus 2*H*-azirine rearranges to acetonitrile on heating to 770 K.[3,25]

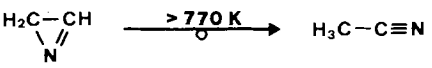

Imines can split off H_2 or hydrocarbons RH in order to form cyanides as thermodynamically favored end products; for example, the parent compound $H_2C{=}NH$ is dehydrogenated at yellow heat to $HC{\equiv}N$.[23]

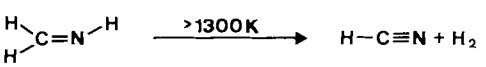

As this short survey illustrates, indeed, azides, imines, and simple azomethines are from "*a*ddition reactions to zero stability" prototypes for reactive nitrogen compounds. From the multitude of possible reactions we shall here select and report on their fascinating and largely unknown behavior in the gas phase, which is of preparative interest, and, moreover, offers some insight into the "no man's-land" of the reaction pathways of medium-sized molecules.

2. Synthesis and Handling of Covalent Azides

The preparation and properties of covalent azides $X{-}N_3$, including their pyrolysis in the gas phase, have been studied by us since 1980.[2,3] Because of the extreme care and meticulousness in handling this malicious class of compounds and the use of newly-developed measurement techniques,[3] we have so far experienced neither an explosion nor a case of poisoning.[27] The literature contains a number of explicit warnings in this respect; the following example is an excerpt from an original text reporting studies on bromine azide:[28]

> **Solid, liquid, and vapour are as sensitive to shock as iodoazoimide, the explosion (often apparently spontaneous) being accompanied by a flash of vivid blue light. Some idea of the instability of the compound, even at −200°, may be gathered from the fact that, of twenty-four attempts at freezing the compound and determining its melting point, only six were completed without explosion. Fortunately, in the majority of cases, the sphere of action was limited to a radius of about 3 feet. Within this radius, all glass apparatus was reduced to powder; beyond it, a reinforced glass screen proved a sufficient protection.**

The syntheses of the azides studied, which apart from $NC{-}N_3$[29] have all been isolated as pure compounds, follow standard literature procedures,[4b,29-39] though these were never used uncritically and wherever possible improved.[23] Starting from sodium azide (activated when necessary[29]), the azides **1** to **10** could be obtained in generally satisfactory yield and purity[23] from substitution reactions with dialkyl sulfates, alkyl tosylates and *C*- or *N*-halogen derivatives (Scheme 3a).

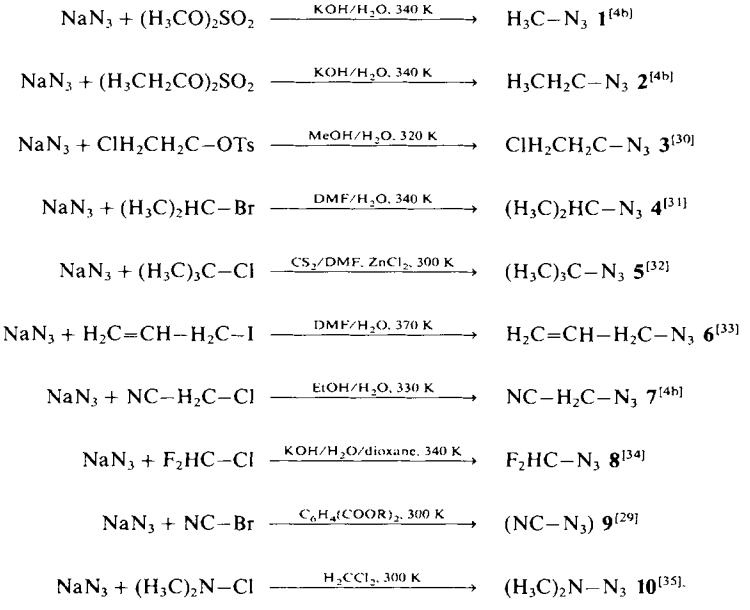

Scheme 3a.

Other azides are best prepared by special methods; e.g. trifluoromethyl azide **11**, vinyl azide **12**, or triazido(phenyl)silane **13** (Scheme 3b).

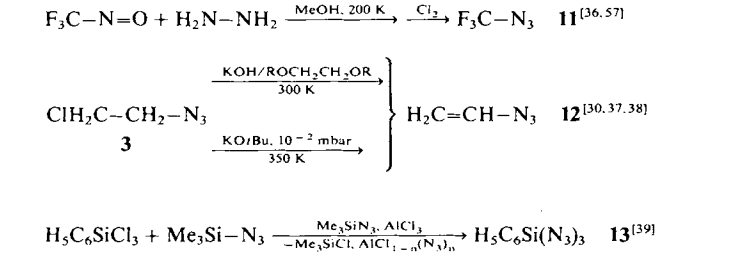

Scheme 3b.

The last-mentioned compound, triazido(phenyl)silane (**13**), can be distilled at a bath temperature of 600 K without decomposition and on ignition in a spatula burns quietly in air with formation of soot.[23] Nevertheless, the following warning should be heeded: the decomposition of covalent azides, accompanied by highly exothermal nitrogen formation, leads to a "heat explosion"[4a] due to reaction multiplication when the energy set free in a single step cannot be dissipated via an extended molecular skeleton with less than 25% by weight azide nitrogen[6] or via the surrounding solvent.[27] Since the extrusion of nitrogen

may be initiated not only thermally but also mechanically, photolytically or chemically,[27] even azides which have been handled several times without incident can detonate with considerable explosive power[8] for no apparent reason. Therefore, besides using the standard explosion protection methods (shatterproof glass shields, fencing masks, leather gloves), we have for example in all reactions of sodium azide with dialkyl sulfates (see Scheme 3a) always kept the pH above 10 in order to diminish the danger of HN_3 formation.[27] The metal azide-containing deposits precipitating during the syntheses of *tert*-butyl azide (**5**) or triazido(phenyl)silane (**13**) in the presence of metal halide Lewis acids were filtered off immediately and hydrolyzed in a fume cupboard using protic organic solvents. Only glass vessels with unscratched and unetched surfaces were used, in particular for distillation; if necessary, active centers can be deactivated by treatment with a refluxing mixture of R_3SiCl and R_2SiCl_2. All operations were carried out on a millimolar scale, and the covalent azides prepared were as far as possible only cooled within the range at which they remain liquid, since when for example solid samples of vinyl azide are allowed to thaw, an explosion can occur, probably due to a tribomechanical shock.[40]

The example of the particularly dangerous vinyl azide **12**[23,25,37,38,40] will be chosen to demonstrate the advantages of handling and decomposing explosive compounds such as S_4N_4[41] or $X-N_3$[2,3,23,25,34,42] under reduced pressure in the gas phase with the help of photoelectron-spectroscopic real-time analysis.[3] Thus the dehydrochlorination of β-chloroethyl azide **3** can advantageously be carried out as a heterogeneous gas phase reaction on solid potassium *tert*-butoxide,[37,38] avoiding the isolation of the explosive vinyl azide (Fig. 2).

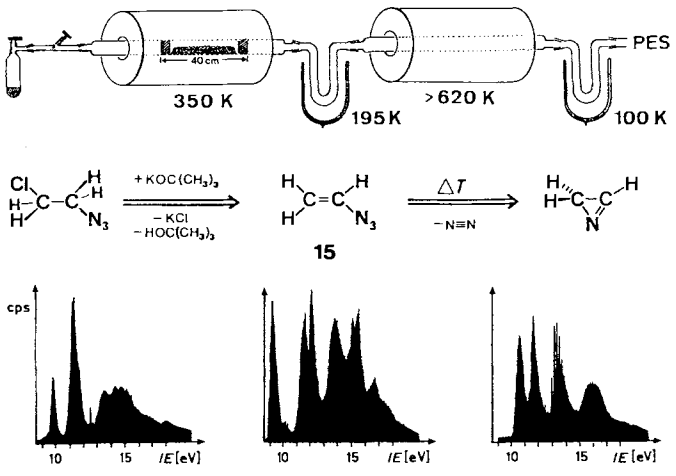

Fig. 2. The heterogeneous gas phase dehydrochlorination of β-chloroethyl azide on solid potassium *tert*-butoxide yielding vinyl azide **12**, and the subsequent thermal decomposition of the latter to 2*H*-azirine: double-oven apparatus with cold traps for the by-product *tert*-butyl alcohol and the end product 2*H*-azirine. The PE-spectroscopic ionization patterns of the pure compounds were used for optimization of the reaction conditions (see text).

The gaseous vinyl azide **12** formed is then pyrolyzed in a second oven to give 2*H*-azirine;[25] and at any one time only a few milligrams of the explosive **12** are present in the double-oven flow apparatus (Fig. 2). To collect the 2*H*-azirine on a preparative scale, cold traps are inserted between the second oven and the PE-spectrometer,[3] the vacuum pump system of which is used to sustain substance flow at a pressure of ca. 10^{-2} mbar. The PES real-time gas analysis has proved itself to be well-suited for the optimization of the reaction conditions, such as the length of the KOR zone necessary for the complete elimination of HCl, and the vinyl azide pyrolysis temperature:[3] with increasing conversion, the ionization "fingerprints" of the starting materials are increasingly replaced by those of the reaction products (Fig. 2).

The handling of covalent azides $X-N_3$ in a flow apparatus at reduced pressure, i.e. in most cases under virtually unimolecular conditions outside their explosion limits,[4a] was the indispensable precondition for their safe pyrolysis in the gas phase and for the identification of their decomposition products.

3. Gas Phase Pyrolysis of Covalent Azides

3.1. Experimental Procedure

Millimolar amounts of the azide $X-N_3$ are vaporized at ca. 10^{-2} mbar and are drawn by the vacuum pump system of the attached spectrometer through the heatable reaction tube (see Fig. 1) at the relatively high velocity of ~ 1 m/s, in the boundary region between laminar *(Newton)* and molecular *(Knudsen)* flow.[43] Depending on the volatility and thermolability of the starting material and in particular on the lifetime of the desired product, the decomposition can be performed either externally in a thermolysis tube, which is up to 40 cm long and if necessary is filled with quartz wool in order to increase the contact time (Figs. 1 and 2), or internally using a short-path pyrolysis oven built into the PE spectrometer. The molybdenum tube of the latter is heated both resistively and in addition by electron impact (Fig. 3: $U_{1,2}$), and the distance between the end of the oven zone and the PES ionization chamber amounts to only 3 cm (Fig. 3).[44] The use of the short-path pyrolysis technique permits the detection of decomposition products with lifetimes in the millisecond range.[45]

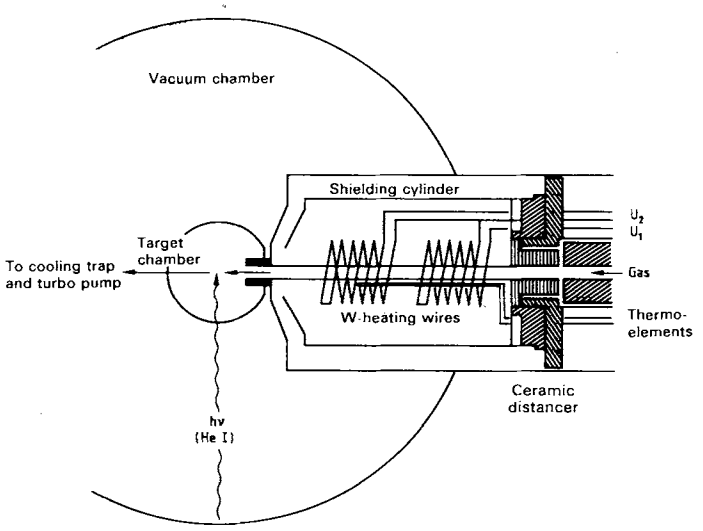

Fig. 3. Outline of the short-path pyrolysis apparatus integrated into the PE spectrometer (U_1 = resistive heating; U_2 = electron impact heating; for details see ref. [44]).

The temperature-dependence of the azide decomposition is monitored using the ionization pattern (see Fig. 4) continually recorded by the attached PE spectrometer.[3] Since there are no restrictive selection rules for the photoionization (in contrast e.g. to rotational and vibrational spectroscopy), all molecules leaving the heated zone in concentrations greater than ca. 5% may be identified from their unmistakable ionization "fingerprints".[52] In particular the "azide leaving group" N_2 is so clearly recognizable from the appearance of its needle-like bands above 15.5 eV (Fig. 4) that the decomposition temperature of the azide $X-N_3$ can be easily determined within the continuously heated flow system. Advantageously, the N_2 ionization pattern leaves blank a broad "observation window" in the low-energy range between 8 and 15.5 eV. On the other hand, covalent azides $X-N_3$ also generally exhibit a needle-like first band (at ca. 9.8 eV), corresponding to the ionization to the radical cation ground state $\tilde{X}(\pi^{*}_{N_3})$ (cf. Section 3.2); the disappearance of this band signals complete decomposition (Fig. 4: -----›).

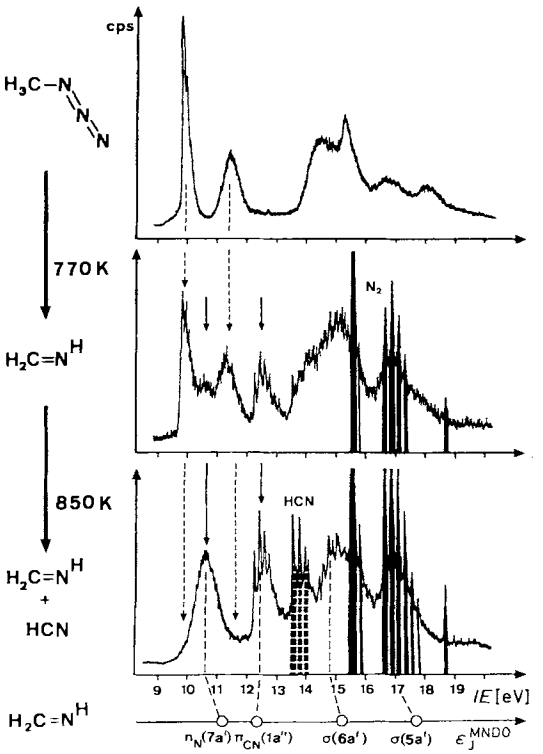

Fig. 4. He(I) PE spectra of methyl azide **1** and its decomposition products at 770 and 850 K. The start of the pyrolysis is recognized by the appearance of the unmistakable N_2 ionization needles (black) between 15.5 and 18.7 eV, and complete decomposition by the disappearance of the characteristic azide bands (-----›). At 770 K, the characteristic bands of $H_2C{=}NH$ (—›), here assigned by Koopmans-correlation [50] with MNDO calculations, are first observed. The second thermal reaction pathway to $H-C{\equiv}N$ (PE bands between 13.6 and 14.21 eV) and H_2 is populated at temperatures above 820 K (due to its low ionization cross-section, H_2 becomes visible only after PE spectrum subtraction [46, 47] or after freezing out the remaining products in a 77 K cold trap [47]).

When the azide pyrolysis is carried out at the optimal decomposition temperature as determined by PE spectroscopic gas analysis, a number of further measurements become possible: thus the externally heated reaction tube may also be attached to the inlet system of a mass spectrometer or, in the case of short-lived molecules, flanged directly onto its measurement chamber.[48] A 10 K argon matrix[49] or a cold finger incorporated between the heated zone and the PE spectrometer are suitable for the isolation of reactive decomposition products: in the latter case the cold condensate may for example be thawed to drop into a precooled NMR tube. After cocondensing $CDCl_3$ and sealing the tube, 2*H*-azirine from the pyrolysis of vinyl azide (Fig. 2) can thus be additionally characterized by its ^{1}H-NMR spectrum (Fig. 5).[23]

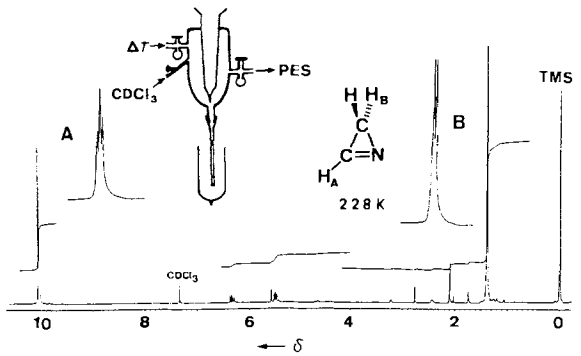

Fig. 5. Condensation apparatus for NMR sampling and 270-MHz ^{1}H-NMR spectrum ($CDCl_3$, 228 K) of 2*H*-azirine, which was obtained by vinyl azide pyrolysis.

3.2. Ionization Pattern of Azides $X-N_3$

When a He(I) photon of energy 21.21 eV hits a molecule M in its neutral ground state $\tilde{X}(M)$, an electron is ejected within 10^{-15} s, leaving behind a radical cation $M^{\oplus\ominus}$ in either its ground state $\tilde{X}(M^{\oplus\ominus})$ or in one of its singly excited states $\tilde{A}, \tilde{B}, \tilde{C}\ldots$ These rapid electron ejection processes IE_n^v are described as "vertical", since the vibrations in the molecular cation $M^{\oplus\ominus}$ only start after about 10^{-13} s and thus the coordinates of the neutral molecule initially remain "frozen". The vertical processes may be correlated with the SCF eigenvalues $-\varepsilon_j^{SCF}$ calculated for the neutral molecule in a generally satisfactory approximation[50] using *Koopmans*' theorem ($IE_n^v = -\varepsilon_j^{SCF}$). This forms the basis for other important advantages of PE-spectroscopic gas analysis: the ionization band patterns of unknown molecules can be precalculated to a degree of accuracy sufficient to facilitate the spectroscopic search for unknown and possibly short-lived compounds, which may be identified vice versa by the assignment of their PE spectra via Koopmans' correlation. Moreover, the comparison of equivalent radical cation states of chemically related compounds on the basis of perturbation arguments[51] provides the chemist with a multitude of information on the series of compounds which he is investigating.

The PE spectrum of methyl azide **1** in the He(I) measurement range (Fig. 4) shows, as expected,[52] seven ionization bands[2, 53] which can be correlated using *Koopmans*' theorem ($IE_n^v = -\varepsilon_j^{MNDO}$) with MNDO eigenvalues[2, 54, 55] (see Scheme 4, top). For a C_s conformation of the almost freely rotating[56] methyl group relative to the CNNN plane, the radical cation states may be subdivided into π- and σ-like ones, and their respective charge distributions

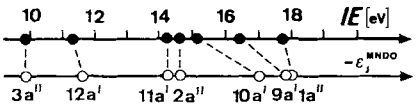

fifth band at 15.4 eV, which corresponds to the $D(^2A')$ state with a dominant σ_{CNNN} distribution.[2,54] When the three typical azide radical cation states, assigned via Koopmans' correlation with MNDO eigenvalues, are compared along

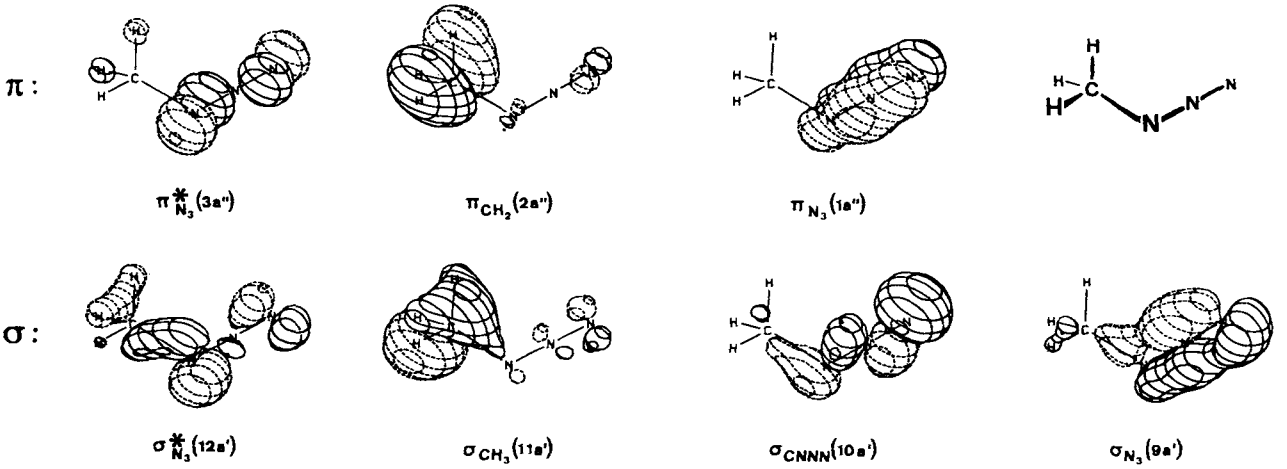

Scheme 4.

characterized qualitatively by the corresponding MNDO orbital diagrams (see Scheme 4, bottom).

Because of the nodes through the CNNN plane and the central nitrogen center, the radical cation ground state $\tilde{X}(^2A'')$ is often denoted in the short form $\pi^*_{N_3}$. The two other $\pi(a'')$ states of H_3C-N_3 at 14.7 and 18 eV with dominant H_2C- and NNN-contributions appear less prominently in the PE spectrum. More characteristic are the second band at 11.4 eV, which is assigned to the first excited radical cation state $\tilde{A}(^2A')$ and denoted as $\sigma^*_{N_3}$ because of its $\pi^*_{N_3}$-analogous node distribution rotated by 90°, and the the series of molecules $X-N_3$ (Fig. 6), a considerable amount of information on the effects of substituents X on the NNN unit becomes available.

The characteristic ionizations $\pi^*_{N_3}$, $\sigma^*_{N_3}$, and σ_{XN_3} of the azides $X-N_3$ studied (Fig. 6), in all of which the radical cation charge is predominantly localized in the NNN-unit[23], exhibit a marked dependence on the substituent X: the exchange of $C(CH_3)_3$ for CF_3 causes the ionization energies to fall by about 2 eV. This indicates that π- and σ-perturbations generally run parallel, so that acceptor or donor substituent effects may be defined relative to X = H

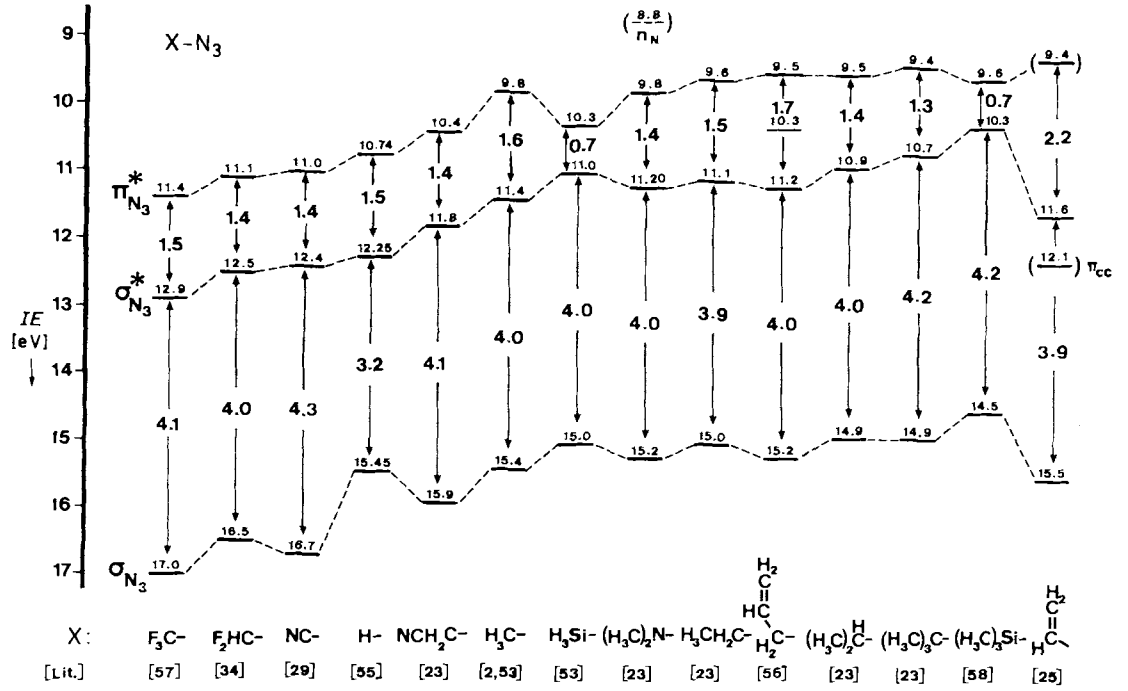

Fig. 6. Correlation diagram of the characteristic vertical ionization energies of azides $X-N_3$ (see text and Scheme 4).

or CH_3. The deviations in the cases of the parent compound, HN_3, of the silicon derivatives and of vinyl azide can be rationalized in a simplified manner as follows: the small difference of only 3.2 eV between $\sigma^*_{N_3}$ and σ_{XN_3} in HN_3[55] is due to the fact that inserted radical cation states with a large contribution in the substituent group X are lacking. In comparison with the alkyl substituents, the iso(valence)electronic R_3Si groups function as weaker π- and stronger σ-donors,[58] i.e. π-type states of $M^{\oplus\oplus}$ are less well stabilized than σ-type states, so that the ionization energies $\pi^*_{N_3}$ increase, whereas $\sigma^*_{N_3}$ and σ_{XN_3} decrease[53,58] (Fig. 6). In vinyl azide, strong $(\pi^*_{N_3}+\pi_{CC})$ conjugation and weak $\sigma^*_{N_3}$-stabilization by the $H_2C{=}CH$-group lead to an unusually large difference between the $\pi^*_{N_3}$ and $\sigma^*_{N_3}$ ionization energies.[25] In contrast, in allyl azide[56] the vinyl and azide groups are isolated from one another by the CH_2 bridge and all characteristic ionizations lie within the narrow regions typical for the alkyl azides from H_3C-N_3 to $(H_3C)_3C-N_3$. The donor effect of the $(H_3C)_2N$ substituent on the NNN unit is unexpectedly small,[59] and comparable to that of an ethyl group (Fig. 6). Finally one may note that the PE spectrum of $NC-N_3$[29] can be constructed from the ionization patterns of $NC-H$[60] and $H-N_3$[55] using a "molecules in a molecule" approximation with only small second order perturbations;[23] the π-interaction is thus considerably smaller than in vinyl azide (Fig. 6).

Naturally, neither the characteristic radical cation state patterns of azides $X-N_3$ nor the MO calculations for their assignments allow any conclusions regarding their thermal stabilities and the decomposition products formed after nitrogen extrusion. Since for example the thermal stability of many organosilyl azides (cf. Section 3.9) is repeatedly and erroneously attributed to $(p\rightarrow d)\pi$-bond contributions in the literature,[61] the considerably more complex nature of the nitrogen extrusion (cf. Section 4) will be emphasized here. On the other hand, comparison of radical cation states (Fig. 6) provide a valuable tool for assigning the PE-spectra and thus permit a critical check of the MO calculations, which for azides $X-N_3$ tend to somewhat larger deviations from *Koopmans'* theorem:[23,54] A correct assignment of the $X-N_3$ ionization patterns is an indispensable prerequisite for the use of PE spectroscopy to monitor azide pyrolyses (Fig. 4).

3.3. Pyrolysis of Methyl Azide

The thermal decomposition of methyl azide **1**[2,9b] (cf. Fig. 1) at 10^{-2} mbar begins at 720 K; concomitantly, the first PE bands of the decomposition and rearrangement product methanimine are clearly observed in the PE spectrum at 10.63 and 12.48 eV (Fig. 4: —). At the same time a further reaction channel is accessible in which HCN and H_2 are formed. At 850 K H_3C-N_3 is pyrolyzed completely: its characteristic ionization pattern has vanished (Fig. 4: - - -) and the two other bands of methanimine become visible at 15.1 and 17.0 eV, partially overlapped by the nitrogen ionization needles. The band between 13.6 and 14.21 eV (Fig. 4: dashed) exhibiting vibrational fine structure proves $H-CN$[60] to be an additional product.

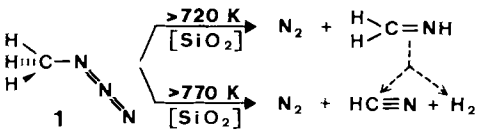

The formation of $H_2C{=}NH$ during the thermal decomposition of H_3C-N_3 can be confirmed as follows: On pyrolysis in a mass spectrometer, the H_3C-N_3 molecular ion parent peak at $m/z = 57$ vanishes at 870 K, while the intensity of the H_3CN peak at $m/z = 29$ has increased.[23] Methanimine can be prepared independently from *N*-chloromethylamine by elimination of HCl on solid KOR (Fig. 16) and isolated at a temperatures below 150 K.[22,62] The PE spectrum recorded on revaporization[62] contains no bands due to N_2 or HCN, and is identical with that recording during methyl azide pyrolysis at 850 K after electronic subtraction of the N_2 and HCN ionization bands.[21,62] Moreover, the $H_2C{=}NH$ ionization pattern and calculated SCF eigenvalues agree satisfactorily; energy hypersurface and gradient norm calculations for the reaction pathway of lowest energy (cf. Section 4.2) in the extrusion of N_2 from H_3C-N_3 also exclude the formation of other decomposition products.[23]

The temperature of 800 K[2] at which methyl azide splits off nitrogen under approximately unimolecular conditions is unexpectedly high, but agrees with the estimated energy (170 kJ/mol) for the dissociation of the H_3CN-N_2 bond.[10a,10e]

3.4. Pyrolysis of Higher Alkyl Azides

Ethyl azide **2** begins to split off nitrogen at 660 K; its thermolysis is complete above 770 K.[23] The main product is a mixture of *cis/trans* ethanimines. The by-products observed after condensation of the latter in an interposed 250 K cold trap are HCN, NH_3 and $HC{\equiv}CH$, all of which are probably formed from a "chemically activated" imine (see Section 4.3). When $H_3C-HC{=}NH$ is revaporized, crystals of the trimeric 2,4,6-trimethylhexahydro-*s*-triazine remain behind in the cold trap (Scheme 5).

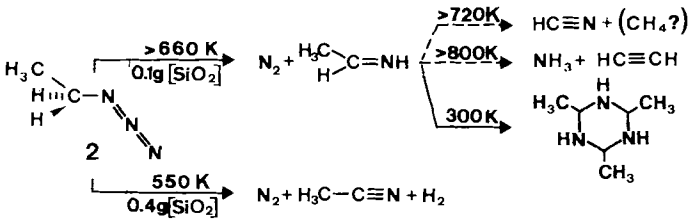

Scheme 5.

The increase in the contact time brought about by filling the tube more tightly with four times the original amount of quartz wool leads to abrupt decomposition of ethyl azide already at 550 K, yielding N_2, H_2 and acetonitrile; presumably under these conditions the explosion limit of $H_5C_2N_3$[9a] is reached.

Isopropyl azide **4** begins to decompose above 620 K, N_2 being completely cleaved off at 770 K.[23] The main prod-

uct is 2-propanimine, as can again be demonstrated by a PE-spectroscopic comparison with a sample prepared by dehydrochlorination of the respective *N*-chloroamine (Section 3.10).[62] Both H_3C-CN and H−CN are identified as by-products by their characteristic ionization needles (see Figs. 4 and 7 and Scheme 6).

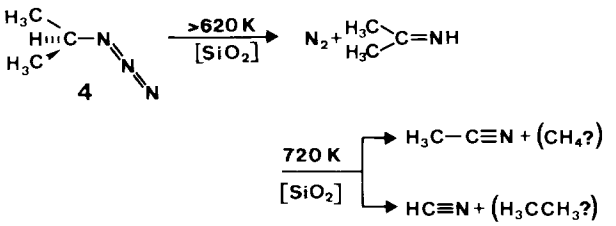

Scheme 6.

The stoichiometrically required decomposition products CH_4 and C_2H_6 from a "chemically activated" 2-propanimine cannot be identified with certainty due to their rather contourless PE spectra (see Fig. 7).

tert-Butyl azide **5** requires temperatures of at least 720 K before nitrogen is eliminated.[23] According to the PE spectra (Fig. 7), which are shown here as an example, acetonitrile and ethane are formed at 820 K as well as *N*-isopropylidenemethylamine (Scheme 7).

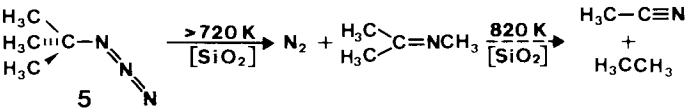

Scheme 7.

The PE spectroscopically determined temperatures for initial (Fig. 8: ●) and complete (Fig. 8: ▲) decomposition of alkyl azides $(H_3C)_nH_{3-n}C-N_3$ run parallel to one another.

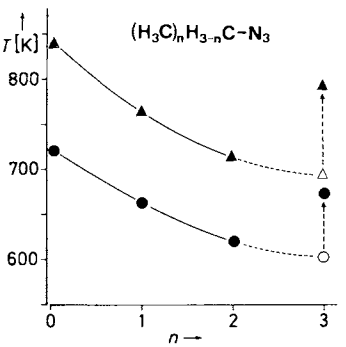

Fig. 8. Temperature dependence of initial (●) and complete (▲) decomposition in the pyrolysis of the alkyl azides $(H_3C)_nH_{3-n}C-N_3$.

Extrapolation of the parabolas for the 1,2-H shift (each defined by 3 points) to n = 3 for *tert*-butyl azide **5** results in temperatures (Fig. 8: ○, △) approximately 70 K below those measured, and thus confirms literature reports[9c, 10a, 10b] that 1,2-alkyl migrations require higher activation energies.

Allyl azide **6** is monomeric and planar in the gas phase.[23, 33, 56] Above 600 K it decomposes into N_2 and 1-azabutadiene ("acroleinimine"), which can be isolated by condensation in a cold trap (Fig. 1: ④).[62] At 760 K, a second reaction pathway to ethene and hydrogen cyanide opens up, presumably via "chemical activation" of 1-azabutadiene ("acroleinimine") (Scheme 8).

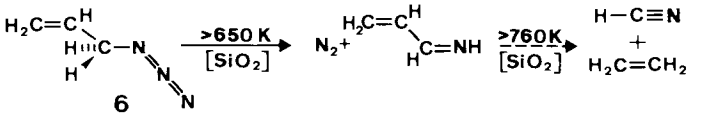

Scheme 8.

In summary, the alkyl azides $R-N_3$ with $R=CH_3$, $CH_{3-n}(CH_3)_n$ (n = 1-3) and $CH_2(HC=CH_2)$ exhibit rather similar thermolysis behavior: extrusion of nitrogen begins within a relatively narrow temperature range between 620 K for isopropyl azide **4** and 720 K for methyl azide **1** (Fig. 8). The primary products, alkanimines and azomethines formed via 1,2-H shifts or 1,2-CH_3 migration, are both detected by PE spectroscopy and isolated.[62] At temperatures 50 to 100 K higher or on prolonged contact time,[15] cleavage of H_2, alkanes or alkenes and formation of the cyanogen compounds HCN or H_3CCN takes place.

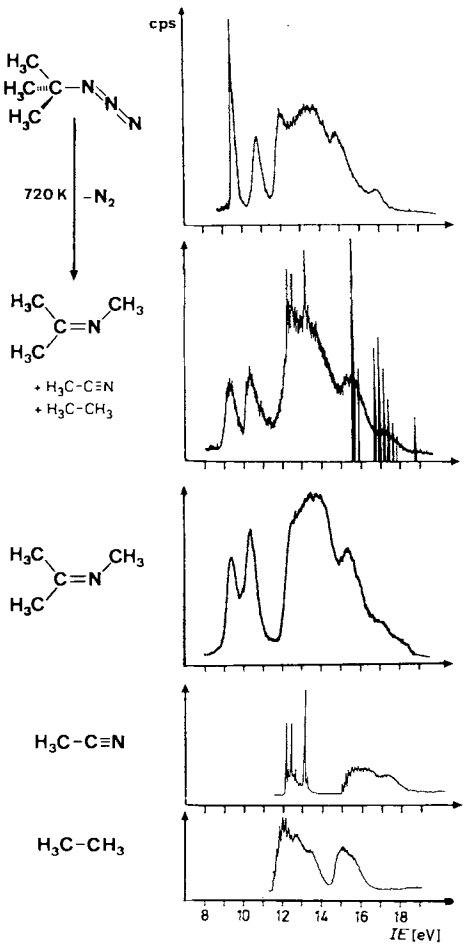

Fig. 7. He(I) PE spectra of *tert*-butyl azide **5** and the product mixture formed on its pyrolysis at 770 K (N_2 ionization needles are shown in black). For comparison, the PES band patterns of *N*-isopropylidenemethylamine (prepared by condensation of acetone with methylamine), of acetonitrile, and of ethane are shown.

3.5. Pyrolysis of Vinyl Azide

Substituted vinyl azides $R_2C=CR'-N_3$ (R, R'=alkyl, aryl or H), which contain two conjugated functional groups, are widely used in organic synthesis:[63] thermolysis and selective photolysis afford derivatives of 2*H*-azirine besides small amounts of substituted ketimines $R_2C=C=NR'$.[63]

The PE-spectroscopically monitored gas phase pyrolysis of the highly explosive parent compound vinyl azide **12**[3,25,37,38] (Figs. 2 and 9) already sets in above 620 K, i.e. 100 K lower than for H_3C-N_3 **1** (Fig. 4): the characteristic N_2 ionization needles (Fig. 9 (middle): black) appear, and at an oven temperature only 30 K higher the PE bands of **12** (Fig. 9: ----›) have disappeared. The main thermolysis product is 2*H*-azirine (Fig. 9 (middle): hatched), which can be isolated as a pure compound after the by-product acetonitrile (Fig. 9: dotted) has been frozen out in a U-tube cooled to 180 K (Fig. 2). The purity of the 2*H*-azirine so obtained may be checked either NMR-spectroscopically (Fig. 5) or from the PE spectrum assigned on the basis of $\Delta E^{SCF/CI}$ calculations (Fig. 9, bottom). When a stream of purified 2*H*-azirine is heated in a third oven to temperatures above 750 K, the unmistakable ionization pattern of H_3C-CN appears, and at 1000 K 2*H*-azirine rearranges quantitatively to acetonitrile.

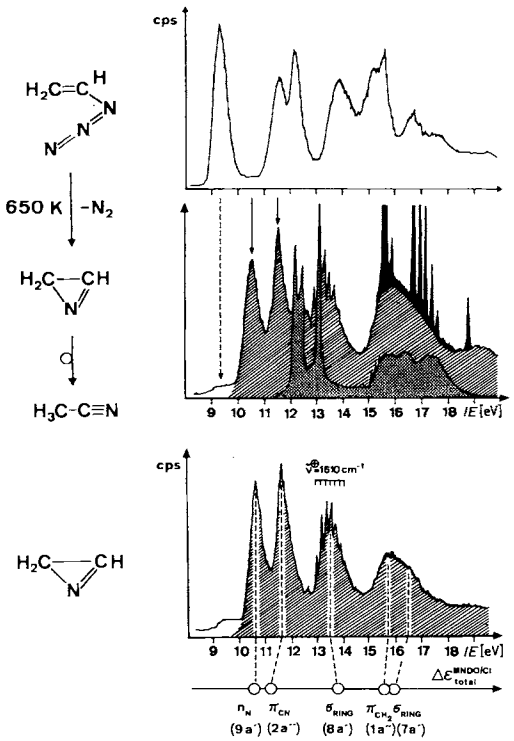

Fig. 9. He(I) PE spectra of vinyl azide **12** (for assignment see [25] and Fig. 6), of the mixture obtained from its thermolysis at 650 K (2*H*-azirine (hatched), acetonitrile (dotted, cf. Fig. 7) and nitrogen (black)) and of pure 2*H*-azirine with its $\Delta E^{SCF/CI}$ assignment (see text).

The PE spectroscopic pyrolysis studies have been extended to include the starting material for vinyl azide preparation, β-chloroethyl azide **3** (Fig. 2[37]), and the $C_2H_3N_3$ isomer 1*H*-1,2,3-triazole[25,64] (Scheme 9).

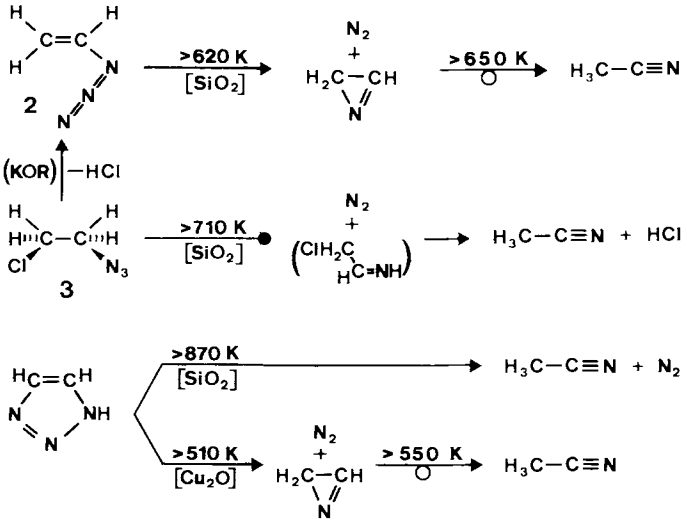

Scheme 9.

Above 710 K, β-chloroethyl azide **3** simultaneously splits off N_2 and HCl; its complete decomposition at 870 K yields acetonitrile and small amounts of HCN.[37] No unequivocal PE-spectroscopic evidence is obtained for the intermediate formation of 2-chloroethanimine or iminoethene ("ketenimine") $H_2C=C=NH$, another C_2H_3N isomer. Probably the excess energy from the azide pyrolysis initiates a rapid rearrangement to H_3C-CN, the most stable molecule in the C_2H_3N ensemble (see also Fig. 19). H_3C-CN is also formed as the sole product of nitrogen extrusion from 1*H*-1,2,3-triazole:[25] here the decomposition temperature of 870 K exceeds that at which 2*H*-azirine rearranges under similar conditions. When the pyrolysis of the electron-rich triazole is catalyzed by the "electron-poor" p-semiconductor copper(I) oxide, the decomposition temperature is reduced by 360 K (!) and the main product obtained is 2*H*-azirine. The amount of H_3C-CN in the thermolysis mixture, however, rises rapidly with increasing temperature.

The probable course of the pyrolysis of vinyl azide will be discussed in Section 4.2 on the basis of calculated energy hypersurfaces.[25,65]

3.6. Pyrolysis of Acceptor-substituted Methyl Azides

Alkyl azides R_3C-N_3 (R=H, CH_3) rearrange with thermal extrusion of nitrogen via 1,2-H shift or 1,2-CH_3 migration to methanimines or azomethines (cf. Sections 3.3 and 3.4). However, the pyrolysis of β-chloroethyl azide **3** proceeds with elimination not only of N_2 but also of HCl as another thermodynamically favorable leaving molecule, and H_3C-CN is formed. The PE spectra recorded at different temperatures provide no evidence for the intermediate formation of $ClH_2C-HC=NH$. The thermolysis of acceptor-substituted methyl azides such as F_2HC-N_3, F_3C-N_3 or $NC-H_2C-N_3$ should provide an answer to the question as to whether N_2-extrusion may also be accompanied by 1,2-X shifts (X=H, F, CN).

Difluoromethyl azide **8** starts to split off N_2 *and* HF above 720 K (Fig. 10); at 930 K complete reaction to F–CN can be demonstrated PE spectroscopically.[34]

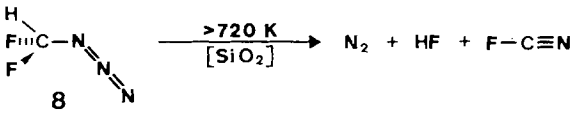

Difluoromethanimine $F_2C{=}NH$ is not observed as an intermediate.[34] An explanation of this unexpected result is that under unimolecular conditions the considerable activation energy for the decomposition of $F_2HC{-}N_3$ cannot be dissipated efficiently, so that the "chemically activated" (cf. Section 4.3) reaction complex apparently "bursts" to give the thermodynamically favored final products N_2, HF and F–CN. When carried out carefully,[68] the selective thermolysis may be suitable for the preparation of pure FCN,[23] the boiling point of which lies 60 K below that of the other product HF.

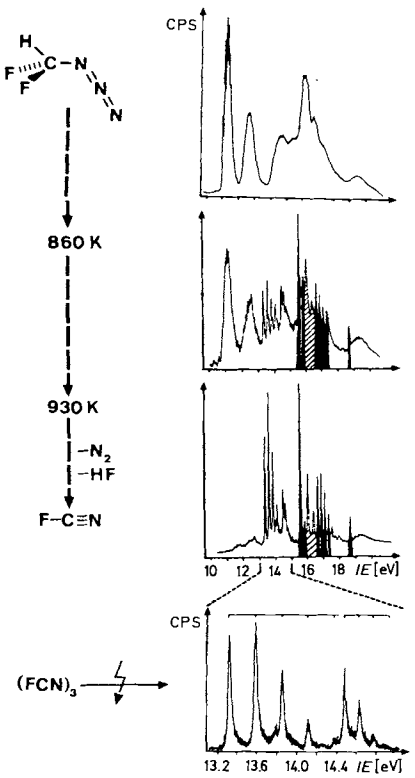

Fig. 10. He(I) PE spectra of difluoromethyl azide **8** at 300 K, 860 K and 930 K (N_2, black; HF [66], hatched) and of cyanogen fluoride [67], prepared from cyanuric fluoride by electrical discharge.

Trifluoromethyl azide **11** was studied because $F_2C{=}NF$, if produced on nitrogen extrusion,[69] could only react further via the thermodynamically unfavorable elimination of F_2 to give F–CN. The pyrolysis, which, because quartz is readily fluorinated by F_3CX compounds,[70] has been carried out in a molybdenum tube,[10] begins only above 1120 K, i.e. at a temperature 400 K higher than that observed for $F_2HC{-}N_3$ **8**, and proceeds quantitatively at 1270 K.[57]

The reaction partner for the fluorine molecule, which cannot be detected PE spectroscopically, is presumably the

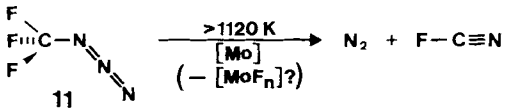

wall of the molybdenum tube. $F_2C{=}NF$, the PE spectrum of which was recorded for comparison,[57] is only produced in trace amounts, if at all. The formation of $F_3C{-}CF_3$ can also not be demonstrated with certainty. Hexafluoroazomethane, which decomposes completely at 870 K to N_2 and hexafluoroethane, can be excluded as a pyrolysis product of **11**.

Azidoacetonitrile **7** should afford one of the HCN dimers (Fig. 11)[71,72] on elimination of N_2. *Trans*- and *cis*-iminoacetonitrile NC–CH=NH have been predicted[71] to be the most stable isomers, followed by the linear dipole complex HCN···HCN and *N*-cyanomethanimine $H_2C{=}N{-}CN$.

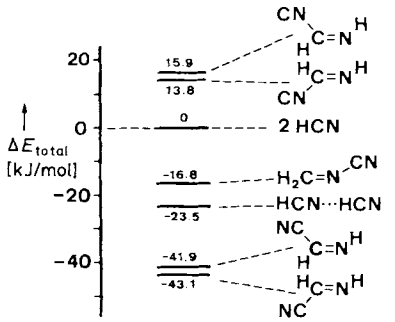

Fig. 11. Relative energies of $C_2H_2N_2$ isomers ("HCN dimers") [71].

Photolysis of $NC{-}H_2C{-}N_3$ **7** in a 12 K argon matrix yields via cleavage of N_2 and a 1,2-H shift the expected $NC{-}HC{=}NH$[73]; prolonged irradiation leads to HCN.[72] The HCN dimer NC–HC=NH has been suggested to be involved in the chemistry of the formation of life on earth as a precursor for HCN oligomers and polymers,[72] the hydrolysis of which can lead to the formation of amino acids and polypeptides.[74] Since a PE-spectroscopically optimized gas phase production of iminoacetonitrile is thus of interest, the pyrolysis of $NC{-}H_2C{-}N_3$ has been studied under various experimental conditions: when passed through a quartz tube of 1.5 cm internal diameter loosely filled with quartz wool (Fig. 1), the N_2 extrusion starts already at 750 K, but in the narrower and shorter molybdenum tube of the short-path pyrolysis apparatus (Fig. 3) a temperature of more than 900 K is needed.[23] In both experiments, the PE spectrum of a N_2/HCN mixture is recorded. On tenfold amplification of the region between 10 and 13.5 eV, however, weak band contours emerge out of the noise level; if these are due to one of the HCN dimers, its concentration in the pyrolysis mixture must be less than 1%.

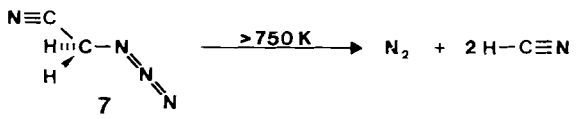

The gas phase pyrolyses of the acceptor-substituted methyl azides $X_nH_{3-n}C{-}N_3$ show the following parallels: in each case apart from N_2 a further "leaving molecule" HX or X_2 (F_2 as $[MoF_n]$) is eliminated under the experimental conditions chosen, and cyanogen compounds X–CN are formed as stable end products. The intermediate formation of methanimine derivatives $X_nH_{2-n}C{=}NH$ or $X_2C{=}NX$ cannot be detected by PE spectroscopy.[23]

3.7. Pyrolysis of Tetrazoles

In contrast to the thermally labile HCN dimer iminoacetonitrile NC–HC=NH, the isomeric *N*-cyanomethanimine $H_2C{=}N{-}CN$ is readily prepared by flash vacuum pyrolysis of trimethylenetetrazole, which opens above 550 K to its valence tautomeric azide (Scheme 10).[72,73]

N-Cyanomethanimine is also formed on heating dimethylcyanamide to 1270 K.[75] Since it contains two of the most frequently detected structural features in interstellar molecules, the cyano group and the methanimine skeleton,[76] it has been characterized by its microwave and millimeterwave spectra[72] for the purpose of facilitating radioastronomic search.

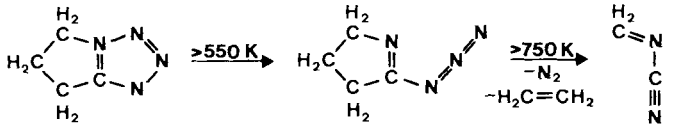

Scheme 10.

On heating trimethylenetetrazole in the short-path pyrolysis apparatus (Fig. 3), the N_2 ionization needles appear in the PE spectrum above 730 K; at 880 K the pyrolysis proceeds quantitatively.[77] The ionization pattern of *N*-cyanomethanimine can be obtained from the on-line PE spectra of the pyrolysis mixture by computer subtraction of the previously stored PE spectra of N_2 and ethene (Fig. 12).

The assignment of the seven radical cation states of $H_2C{=}N{-}CN$ observed in the He(I) range (Fig. 12), which leads to the expected sequence $n_N < \pi_{C=N} < n_{(C)N} < \pi_{C\equiv N}$,[60] is further corroborated by band shapes and by comparison with the ionization patterns of the isoelectronic molecules acrylonitrile $H_2C{=}CH{-}CN$[60] and nitrosyl cyanide $O{=}N{-}CN$.[78]

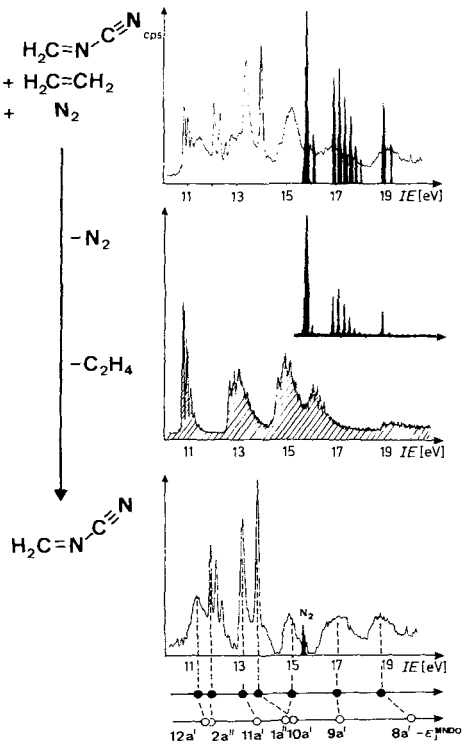

Fig. 12. He(I) PE spectra of the trimethylenetetrazole pyrolysis product mixture at 880 K, of N_2 (black) and of ethene (hatched) as well as the spectrum of $H_2C{=}N{-}CN$ obtained by computer subtraction, together with its Koopmans assignment based on MNDO eigenvalues (see text).

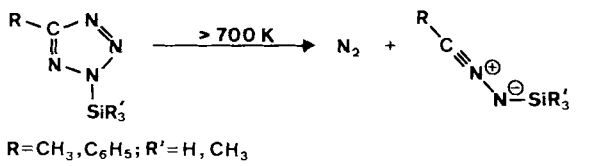

2,5-Disubstituted tetrazoles also cleave off nitrogen selectively during short-path pyrolysis at comparable temperatures. The products are gaseous nitrile imines,[77] which in solution are known as reactive intermediates in 1,3-dipolar cycloadditions.[79] In the low-energy range their PE spectra exhibit characteristic bands with ionization energies of ca. 8.0 (π_1), 8.6 (n_N), and 10.5 eV (π_2).

3.8. Pyrolysis of Cyanogen Azide and Azidodimethylamine

$NC{-}N_3$ **9** and $(CH_3)_2N{-}N_3$ **10**, whose typical ionization energies are found in the expected range and differ by ca. 1.3 eV (Fig. 6), in gas phase pyrolysis at reduced pressure lose nitrogen at relatively low temperatures; however, neither imines nor nitriles can be detected PE-spectroscopically as decomposition products.

Cyanogen azide, **9**, is a colorless, oily liquid which detonates when subjected to mechanical shock or on warming[29] and, therefore, should preferentially be handled as a dilute solution in an aprotic solvent.[29,80] The structurally[81] and spectroscopically[82] well-characterized molecule decomposes in a unimolecular manner on low pressure gas phase thermolysis or photolysis to linear cyanonitrile in its excited singlet state.[83]

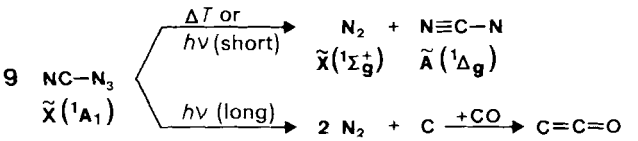

Prolonged irradiation of cyanogen azide **9** in a low-temperature matrix produces cyanonitrene in its triplet ground state[83] and then atomic carbon, which subsequently reacts, e.g., with co-condensed CO to give C_2O.[83] In contrast, pyrolysis at atmospheric pressure in a stream of nitrogen carrier gas at above 470 K proceeds via N_2 elimination and substantial deposition of a polymer to azodicarbonitrile.[84]

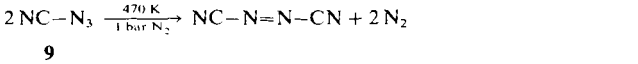

9

The orange-red $NC{-}N{=}N{-}CN$ is an explosive, volatile solid[84] with a melting point of 308 K. It reacts with stop-

cock grease as well as with a number of organic solvents;[84] its half-wave oxidation potential of +0.40 V (vs SCE) lies 0.25 V above that of tetracyanoethylene,[84] and its vertical first ionization energy amounts to 11.9 eV.[23]

We have examined the decomposition of NC–N_3 **9** and NC–N=N–CN in the gas phase under various conditions. Cyanogen azide[29] may be safely evaporated into the short-path pyrolysis apparatus from a ca. 3% solution in diethyl phthalate (b.p. 571 K) at 10^{-2} mbar. The evolution of N_2 begins at an oven temperature of 700 K, and at 860 K the complex ionization pattern of the pyrolysis mixture has changed: spectral comparison shows that neither NC–N=N–CN nor NC–CN are present. Other possible decomposition products such as NCN can however neither be completely excluded nor clearly identified.[23] Above 1000 K the PE spectrum consists only of the N_2 ionization needles (see, e.g., Fig. 12), and the deposition of carbon becomes visible if the decomposition is carried out in a quartz tube (Scheme 11, top). The intermediate formation of azodicarbonitrile may also be excluded by studying its pyrolysis, which starts at temperatures above 1280 K, i.e. 480 K above that for NC–N_3, and proceeds in a uniform manner yielding dicyanogen (Scheme 11, bottom).

$$\underset{\mathbf{9}}{NC-N_3} \xrightarrow[10^{-2}\ mbar]{>1000\ K} 2\,N_2 + (C)_\infty$$

$$NC-N=N-CN \xrightarrow[10^{-2}\ mbar]{>1280\ K} N_2 + NC-CN$$

Scheme 11.

The remarkable stability of NC–N=N–CN under unimolecular conditions is surprising, since in the condensed phase nitrogen is evolved even at room temperature. The PE spectra registered continuously during heating give no indication of a *trans→cis* isomerization of azodicarbonitrile in the gas phase even above 1000 K.[85]

Azidodimethylamine, **10**, the first 1,1-tetrazine,[35] might on elimination of nitrogen in the gas phase yield dimethylaminonitrene, which, according to the known reactions of this class of compounds in their singlet ground state,[86] could possibly stabilize itself as shown in Scheme 12.

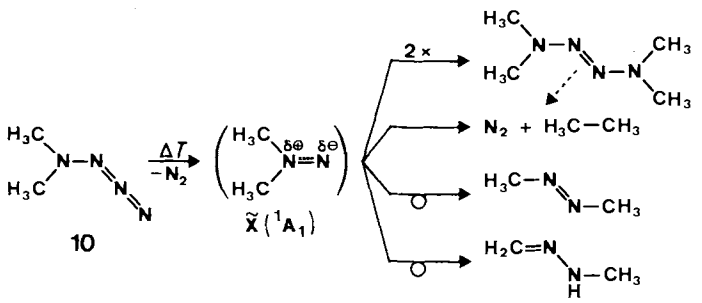

Scheme 12.

Sterically crowded dialkylaminonitrenes $(R_3C)_2NN$ can be handled in solution at 200 K,[87a] and it has even been possible to photolytically generate the blue parent compound H_2NN from carbamoyl azide $H_2N-CO-N_3$ in an 80 K matrix.[87b]

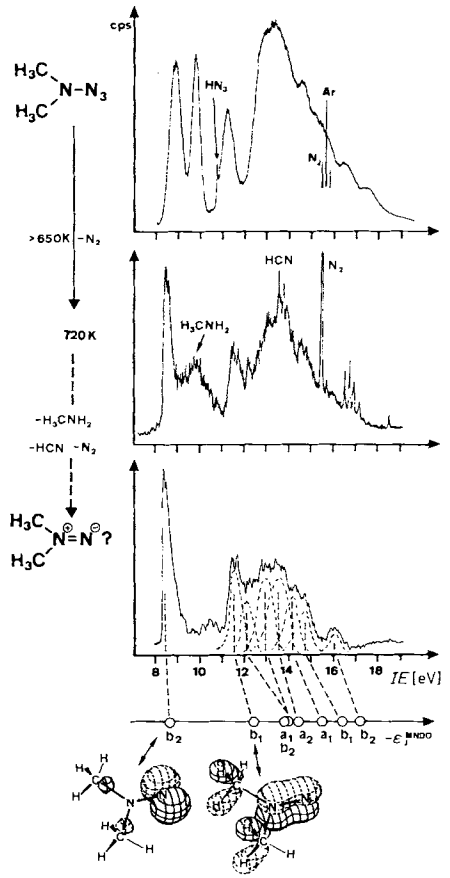

Fig. 13. He(I) PE spectra of $(H_3C)_2N-N_3$ **10** and its pyrolysis mixture at 720 K. The ionization pattern resulting from digital subtraction of H_3CNH_2, HCN and N_2, has tentatively been assigned to the nitrene $(H_3C)_2N-N$ on the basis of MNDO calculations (see text).

The decomposition of $(H_3C)_2N-N_3$ **10** begins at 620 K (loss of N_2) and is complete at 720 K. The PE spectrum of the pyrolysis mixture (Fig. 13) shows characteristic bands due to H_3CNH_2, HCN and N_2. Digital subtraction of their computer-stored PE spectra (see Fig. 12) leaves an ionization pattern which can be deconvoluted into eight partially overlapping bands (Fig. 13). For dimethylaminonitrene $(H_3C)_2N-N$, eight ionizations are expected in the He(I) range according to the reliable "electron counting" rule,[52] and Koopmans comparison with the calculated MNDO eigenvalue pattern (Fig. 13) would support such an assignment, allocating in particular the dominant sharp band at 8.22 eV to the radical cation ground state of the singlet dimethylaminonitrene with a preponderant contribution from the terminal nitrogen center. Moreover, from a comparison of the PE spectra the known R_2NN stabilization products (Scheme 12) can be ruled out:[86] thus tetramethyltetrazene decomposes only at temperatures above 700 K, forming *N*-methylenemethylamine and dimethylamine.[23]

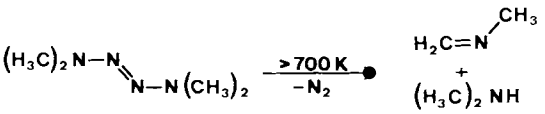

The ionization pattern of ethane only features bands above 12 eV, and $H_3C-N=N-CH_3$, which might result from $(H_3C)_2N-N$ via methyl migration (Scheme 12),

would show an ionization band at 9 eV.[88] The hydrazone $H_2C{=}N{-}NH{-}CH_3$ should have two characteristic bands at 8.9 and 10.2 eV.[23] Since no other likely nitrogen compound with about 20 valence electrons[52] has a first ionization energy of only 8.22 eV, we suggest that the decomposition of **10** proceeds as shown in Scheme 13. The validity of this suggestion must be checked by other experiments such as matrix isolation of dimethylaminonitrene produced in the gas phase. Both final products, hydrogen cyanide and methylamine, are detected PE-spectroscopically in the pyrolysis of **10** (Fig. 13).

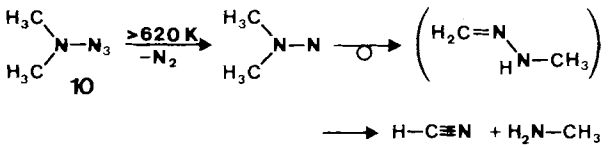

Scheme 13.

Altogether the results obtained thus indicate: in contrast to triplet alkyl nitrenes RN[10–12] but analogous to singlet phosphanitrenes $(R_2N)_2PN$,[4d] the singlet dialkylaminonitrenes R_2NN,[87a] known to be stable in solution at low temperatures, should also be observable in the gas phase.

3.9. Pyrolysis of Triazido(phenyl)silane

Almost 100 years after the preparation of $H_5C_6{-}N_3$, the first C-azide,[89] the unexpected formation of $(H_3C)_3Si{-}N_3$ in the pyrolysis of a silatetrazole[90] laid the foundation for the rather complex chemistry of the covalent silyl azides $R_{4-n}Si(N_3)_n$ (n = 1, 2, 3).[91] With only few exceptions,[92a] these exhibit higher thermal stability than their C-homologues,[92b] an experimental fact, which should by no means be explained in an oversimplifying way referring to fictitious (p→d)π-bond contributions $\geqslant Si{=}N_3$.[61,93] In fact, because of the lower effective nuclear charge at silicon, silyl substituents $R_{4-n}Si$- act predominantly as σ-donors with respect to the −NNN group (see Section 3.2) and thus increase the barrier for the kinetically important nitrogen extrusion $\geqslant SiN{-}N_2$. In addition, the Si substituent effect will reverse the relative thermodynamic stabilities of azides $R_3X{-}N_3$ and the corresponding imines or azomethines $R_2X{=}NR$, which for C azides are frequently the products of N_2 extrusion followed by 1,2-R migration.[4d,94] For analogous reasons, silyl azides may also decompose via a rearrangement to form isonitriles; the photolysis of $H_3Si{-}N_3$ in an argon matrix at 4 K yields the silaisocyanide $H{-}N{\equiv}Si$[95a] which, as confirmed by quantum chemical calculations,[95b,c] is stable with respect to a rearrangement to the isomeric hydrogen silacyanide $H{-}Si{\equiv}N$.

Triazido(phenyl)silane **13** can be prepared from trichloro(phenyl)silane by $AlCl_3$-catalyzed transazidation with trimethylsilyl azide (Scheme 3b) and, after careful decantation from the explosive $AlCl_x(N_3)_{3-x}$ flakes precipitated on the walls of the apparatus, it is purified by distillation. Its "controlled explosion" may be performed without risk if only small amounts are heated in the short-path pyrolysis apparatus (Fig. 3) using PE-spectroscopic real-time analysis (Fig. 14).[42]

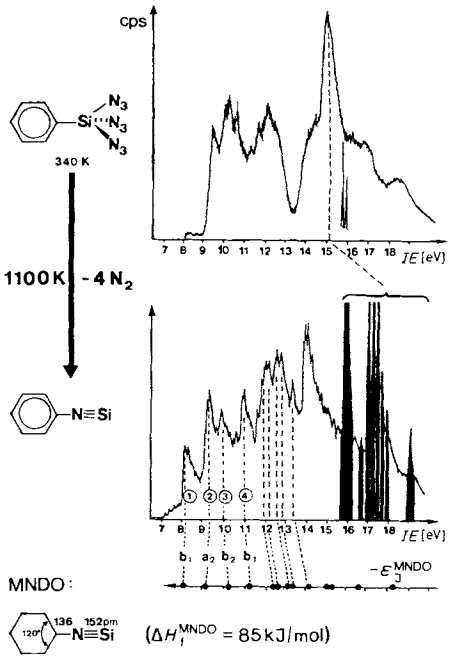

Fig. 14. He(I) PE spectra of triazido(phenyl)silane **13** at 340 K and of its pyrolysis products at 1100 K (N_2: black). The Koopmans' assignment of the ionization pattern of phenylsilaisocyanide is based on eigenvalues from a geometry-optimized MNDO calculation (see text).

According to the continuously recorded PE spectra **13** is completely decomposed at 1100 K: its strong (σ_{N_3})-band between 15 and 16 eV (cf. Fig. 6) has been replaced by the intense N_2 ionization needles. The ionization pattern consisting of 11 largely resolved bands between 8 and 14.5 eV is assigned on the basis of comprehensive calculations to the pyrolysis product phenylsilaisocyanide (Fig. 14). The calculations also predict $H_5C_6{-}N{\equiv}Si$ to be more stable than $H_5C_6Si{\equiv}N$ by ca. 400 kJ/mol, paralleling the behavior of the isomers HNSi,[95] and the optimized bond length $d^{MNDO}_{N-Si} = 152$ pm agrees well with the 154 pm determined IR-spectroscopically[95a] and from highly correlated calculations[95b] for $H{-}N{\equiv}Si$. As for the valence-isoelectronic phenylisocyanide,[96] a linear arrangement (C)−N≡Si with NSi triple bond character is calculated. In the meantime the PE-spectroscopic results[42] have been further supported by the matrix isolation of phenylsilaisocyanide.[97]

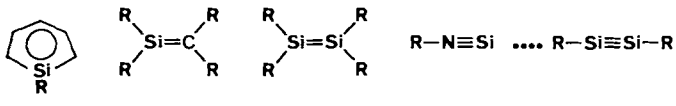

Scheme 14.

The pyrolysis of triazido(phenyl)silane **13**, driven by the energy-producing elimination of 4 molecules of N≡N (cf. Section 1), leads to the formation of a polar triple bond −N≡Si with a silicon atom of coordination number 1. In the series of organosilicon compounds with multiple bonds to silicon (Scheme 14), which since 1979 have either been identified in the gas phase by PE spectroscopy[98] or kinetically stabilized, and thus rendered isolable, by wrapping with bulky hydrocarbon residues, the present result represents a further step towards an as yet unknown mole-

cule with an Si≡Si triple bond.[98f] At present, we are trying to obtain such a species from the pyrolysis of tetraazidodisilanes $R(N_3)_2Si-Si(N_3)_2R$. However, quantum chemical calculations for the ensemble Si_2H_2 predict the energy minimum to correspond to the isomeric $Si(H_2)Si$.[99]

3.10. Preparation and Properties of Reactive Imines and Azomethines

Cyclic or acyclic imines RR'C=NH or azomethines RR'C=NR'' are detected PE-spectroscopically as intermediates in the gas phase pyrolyses of alkyl azides and of other organic compounds with unsaturated NNN groups such as 1,2,3-triazoles, tetrazenes or tetrazoles (Figs. 3, 5, 6 and 8). They can be isolated at low temperatures and characterized, for example, by their NMR spectra.

Imines of low molecular weight, which have been discovered in interstellar space[19,76] and some of which are considered to be of prebiotic importance,[18,72] are so short-lived in the condensed phase (see Section 1) that relatively little was known about these reactive substances at the beginning of our investigations.[2,3] Their handling in the gas phase and in particular the optimization of their syntheses and reactions is made easier by the fact that they exhibit characteristic n_N and π_{CN} ionization bands at relatively low energy (Figs. 4, 7, 9, 12 and 15), and thus can be detected in gas mixtures by means of PE-spectroscopic real-time analysis.[3]

The n_N and π_{CN} ionization energies of simple imines $X_2C=NX$ are greatly influenced by the substituents H, F, CF_3, CH_3, $(CH_2)_n$, and $CH=CH_2$ (Fig. 15: Δn_N up to 4 eV, $\Delta\pi_{CN}$ 3.4 eV). The normal sequence $n_N > \pi_{CN}$ may be reversed: perfluorosubstitution of $H_2C=NH$ expectedly changes π_{CN} only slightly,[102] but n_N is considerably shifted. CF_3 substitution at N lowers n_N more than π_{CN}, leading to an approximately equal energy; two CF_3 groups on carbon both lower n_N and π_{CN} relative to $H_2C=NH$ by 1.3 eV! Methyl substituents function as donors; the hyperconjugative interaction with π_{CN} is of comparable magnitude for both *C*- and *N*-substitution, while n_N is raised more by *N*-substitution. The n_N ionization energy of cyclopropanimine is comparable to that of $(H_3C)_2C=NH$.[23] In 2*H*-azirine only one CH_2 group exerts a hyperconjugative effect on π_{CN}, while the n_N ionization is comparable to that of $H_2C=NH$ (Fig. 11). Both n_N and π_{CN} increase with increasing ring size in the cyclic azomethinimines; vibrational fine structure analysis of the n_N band indicates that dihydroazete ("1-azetine") is distorted on ionization to the radical cation ground state.[101] The comparison between 1- and 2-azabutadienes again confirms the stronger π-interaction due to *N*-substitution. The comparison of the n_N and π_{CN} radical cation states outlined here for selected derivatives[100] leads in detail[23] to numerous correlations and thus to extensive information on the >C=N< bond system.[23]

PE-spectroscopic gas analysis makes possible not only the detection of reactive imines and azomethines as intermediates in azide pyrolysis but also the optimization of new procedures for their preparation: thus 2*H*-azirine is best prepared by elimination of HCl and N_2 from the stable β-chloroethyl azide[37,38] (Fig. 2). For other imines and azomethines, the method developed by *Denis* et al.[22,101,103] and optimized PE-spectroscopically by us[23,37,101,104] has proven suitable: it involves the successive chlorination of gaseous alkylamines on solid *N*-chlorosuccinimide and dehydrochlorination of the *N*-chloroamines so formed with solid potassium *tert*-butanolate or adamantolate (Scheme 15).[39] Imine syntheses in the gas phase are best carried out in a double-oven apparatus consisting of modules which are fitted together and varied as required (Fig. 16, see also Fig. 2), with the PE-spectroscopic optimization of the reaction parameters in two stages.[105]

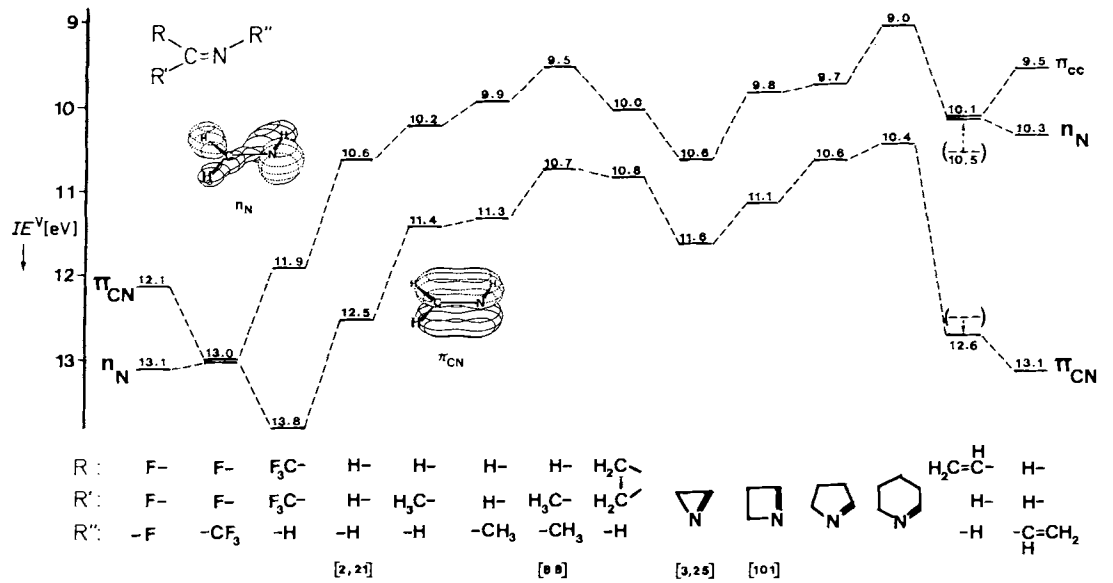

Fig. 15. Vertical n_N and π_{CN} ionization energies of selected [23, 100] imines and azomethines with various substituents and of cyclic azomethines with three- to six-membered rings (see text).

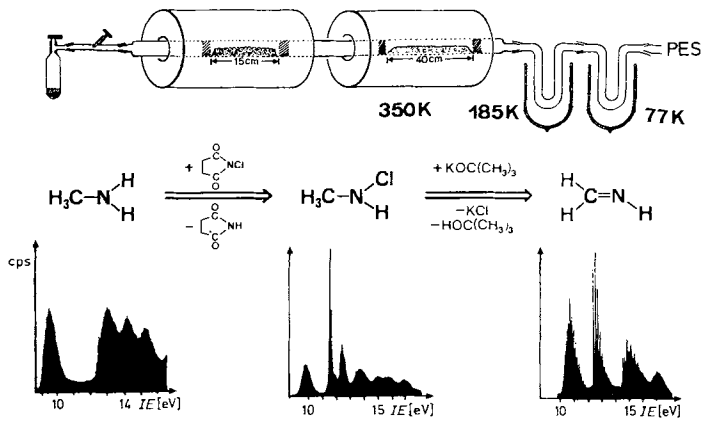

Fig. 16. Preparation of methanimine by successive chlorination of gaseous methylamine using solid *N*-chlorosuccinimide and dehydrochlorination of the *N*-chloromethylamine formed with potassium *tert*-butanolate (see Fig. 2). The PE-spectroscopic ionization patterns of the pure compounds used in the optimization of the reaction conditions are shown below (see text).

The imines and azomethines shown in Scheme 15 have been prepared (in some cases for the first time, see [103]) by consecutive chlorination of gaseous amines and dehydrochlorination of the resulting *N*-chloro derivatives.[39]

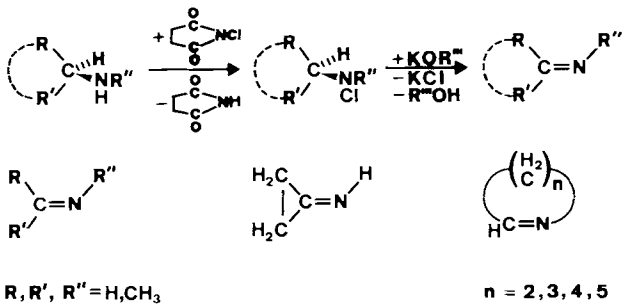

Scheme 15.

From N-chloroethylamine, the thermodynamically less stable[106] *E*-isomer is preferentially formed (70%).[103] During the chlorination of cyclopropylamine, the *N*-chlorosuccinimide layer atypically turns yellow while heat is evolved, and PE spectroscopy shows that among other products HCN is formed; pure cyclopropanimine is obtained only after the gas stream has passed through the KOR zone (Fig. 16). The cyclic imine 2*H*-azirine (Scheme 15: n = 1) cannot be prepared by HCl-elimination from *N*-chloroaziridine, since the three-membered ring opens under base catalysis to yield acetonitrile;[23] however, the two-step synthesis starting from β-chloroethyl azide offers convenient synthetic access[37,38] (Fig. 2). Imines with larger rings cannot pass through the 185 K cold trap (Fig. 16) because of their lower volatility and, therefore, potassium adamantanolate, the salt of a high-boiling alcohol, has to be used for the dehydrochlorination. 3,4-Dihydro-2*H*-pyrrole may also be prepared by thermal retro-trimerization of hexahydro-*s*-triazine[107] or by gas phase dehydrochlorination of *N*-chlorocyclobutylamine (Scheme 16).[23]

2-Azabutadiene is formed in quantitative yield in the gas phase pyrolysis of 2,3-dihydroazete (Scheme 17, top).[23, 103a] 1-Azabutadiene can be obtained either from gas phase pyrolysis of allyl azide or by thermal elimination of propene from diallylamine (Scheme 17, bottom).[56]

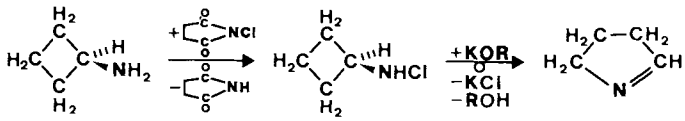

Scheme 16.

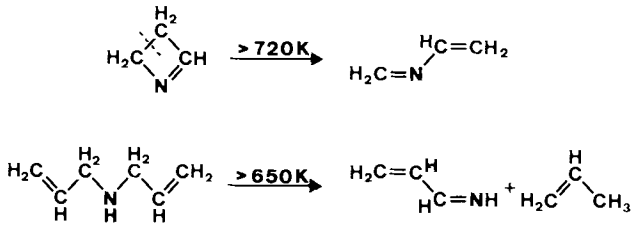

Scheme 17.

The synthetic methods discussed here, which have mainly been developed since 1980, provide a convenient access to simple methanimine derivatives $X_2C{=}NY$ with a variety of substituents X and Y such as H, CH_3, $(CH_2)_n$, $CH{=}CH_2$, F and CF_3.[2, 3, 23, 69, 103, 108] In spite of comparable structural data,[108] some of their molecular properties, are greatly influenced by the substituents. This is true not only for their ionization energies[100] (Fig. 15), IR stretching vibrations[103, 108] or ^{1}H-NMR signals[103, 108] (see Fig. 5), but in particular also for their tendency to polymerize. While acceptor-substituted imines such as $F_2C{=}NF$[69] or $Cl_2C{=}NCl$,[109] peralkylated[24] and F_3C-substituted[108] imines can be stored at least for a limited time at room temperature, others polymerize even in dilute solutions at temperatures below 273 K to give cyclic or linear[108] amines; this holds in particular for the NH-derivatives, but also for $H_2C{=}NCH_3$ and 2*H*-azirine (see Scheme 18: polymerization temperatures *T* (Polym.)).[23, 103]

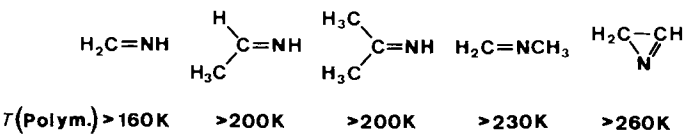

Scheme 18.

The parent compound $H_2C{=}NH$ is even converted in part into hexamethylenetetramine.[100] The behavior of many simple methanimine derivatives on heating in the gas phase emphasizes their nature as reactive intermediates. Thus $H_2C{=}NH$ eliminates hydrogen to form HCN under nearly unimolecular conditions[2] (cf. Fig. 4), 1-azetine opens to 2-azabutadiene (Scheme 17),[103a] and 2*H*-azirine rearranges to the thermodynamically stable end product acetonitrile[3, 25] (cf. Fig. 9). The PE-spectroscopic detection of the imine intermediates in the gas phase pyrolysis of alkyl azides provides the key information on the course of the N_2-extrusion.

4. Discussion of the Course of Azide Pyrolyses

4.1. Reaction Channels of Azides Involving N_2 Extrusion

A total of 16 covalent azides R_nE-N_3 with central elements E = C, N, and Si has been pyrolyzed under comparable and approximately unimolecular conditions in a gas flow system at a pressure of ca. 10^{-2} mbar.[23] Upon thermal elimination of N_2, the following reaction channels are accessible:

— formation of nitrenes or their dimerization products:

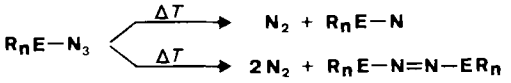

— elimination of further leaving molecules such as H_2, CH_4 or C_2H_6, $H_2C=CH_2$, HCl, HF, F_2, HCN, or N_2 to yield nitriles (E = C) or to rearrange to isocyanides (E = Si):

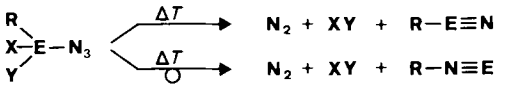

— rearrangement to methanimines (1,2-hydrogen shift) or azomethines (1,2-methyl migration) and ring closure to cyclic azomethines:

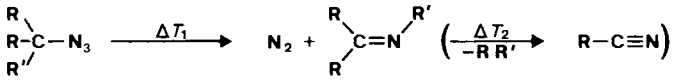

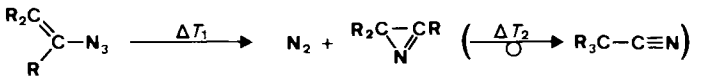

— at higher temperatures (ΔT_2), methanimine derivatives split off H_2[7, 14] or alkanes[16, 17] and form nitriles, while 2*H*-azirine rearranges with ring opening to acetonitrile.

The various reaction channels for azide pyrolysis may be commented on as follows: N_2 extrusion leading to stable singlet nitrenes is unusual (cf. Section 3.8); nitrene dimers are only observed at higher pressure. The elimination of additional leaving molecules may either occur simultaneously or be due to a "chemical activation" of the imines formed in the azide pyrolysis (cf. Section 4.3). In particular, no imine intermediates can be detected PE-spectroscopically during the decomposition of acceptor-substituted azides such as $ClH_2C-H_2C-N_3$ **3**, F_2HC-N_3 **8** or $NC-H_2C-N_3$ **7**. Corroborating evidence for "chemical activation" is provided by the fact that the imines and azomethines isolated in azide pyrolyses on revaporization are only converted into nitriles at considerably higher temperatures (see Section 4.3).

4.2. The N_2 Elimination: Substituent Effects and Energy Hypersurfaces

The temperatures of beginning nitrogen extrusion, which have been determined PE-spectroscopically under similar low-pressure conditions, range from 550 K for trimethylenetetrazole (Section 3.7) to 1100 K for trifluoromethyl azide (Section 3.6) and exhibit the following substituent effects:

— for methyl azide derivatives $(XYZ)C-N_3$, the decomposition point increases non-linearly with increasing acceptor perturbation by the substituents X, Y, Z (cf. Fig. 6): $(H_3C)_2HC-N_3$ shows the lowest nitrogen extrusion temperature of only 620 K, and F_3C-N_3 the highest with 1120 K. This observation parallels the sequence of their explosivity in the condensed phase;[4] trifluoromethyl azide cannot be caused to detonate even by heating to the softening point of the glassware used.[109]

— *tert*-butyl azide $(H_3C)_3C-N_3$ decomposes at a temperature 100 K higher than that of isopropyl azide $(H_3C)_2HC-N_3$ (Fig. 8) and thus confirms earlier observations[9c, 10a, 62] that barriers for 1,2-methyl migrations exceed those for 1,2-hydrogen shifts.

— the decomposition temperatures of silyl azides[91-95] ($(H_3C)_3Si-N_3$ 950 K, $(H_5C_6)_3Si-N_3$ 1170 K, cf. ref.[23]) are considerably higher than those of comparable carbon azides; based on the ionization energies (Fig. 6), this observation may be discussed as being due to a stronger σ-donor effect of the Si-substituent on the azide group (cf. Section 3.9).

— all azides, in which N_2 extrusion is assisted by neighboring groups, expectedly decompose at lower temperatures: notable examples are vinyl azide (620 K) and trimethylenetetrazole (550 K).

Altogether, the thermal N_2 elimination from the various azides is a complex process, which, even when the individual molecular dynamics (i.e. the vibratory and rotatory states of the molecules) are disregarded, raises numerous questions: Are short-lived nitrenes formed initially and if so, in their excited singlet or in their triplet ground states? Do nitrenes rearrange rapidly to the imines or azomethines isolated in a number of azide pyrolyses, or are the latter formed in an energetically favored synchronous process via a 1,2-substituent shift coupled to the N_2-extrusion? Are imines and azomethines actually intermediates even in cases where they cannot be detected by PE spectroscopy? For a discussion of the experimental results presented in Sections 3.2 to 3.9, extensive calculations[2, 3, 23, 25, 65] have been carried out using the semiempirical MNDO method[110] without explicit consideration of electron correlation.[111] As examples for the calculated MNDO energy hypersurfaces,[65] those of the simplest saturated and unsaturated organic azides, H_3C-N_3[2] and $H_2C=CH-N_3$,[3, 25] are presented.

For methyl azide, the N_2 extrusion temperature under approximately unimolecular conditions has been determined by PE spectroscopy to be 720 K, in agreement with the estimated H_3CN-N_2 dissociation energy of ca. 170 kJ/

mol.[10a,c] For the dissociation product methylnitrene, "double-zeta" SCF calculations[12] predict a triplet ground state $\tilde{X}(^3A_2)$, whereas the excited singlet state $\tilde{A}(^1E)$ should lie higher by 170 kJ/mol.[12, 13] However, the spin conservation principle would require that singlet methylene should be formed preferentially, because of the extremely large energy difference of 590 kJ/mol between the singlet ground state $\tilde{X}(^1\Sigma_g^+)$ of N_2 and its lowest excited triplet state $\tilde{A}(^3\Sigma_u^+)$ (Scheme 19).

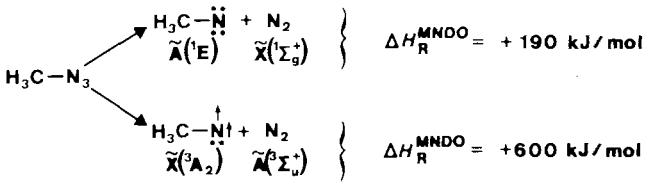

Scheme 19.

This, together with experimental observations (Sections 1 and 3),[112] suggests that both thermal formation and subsequent reactions of methylnitrene occur on singlet energy hypersurfaces. The asynchronous N_2-extrusion with formation of singlet methylnitrene can be described to a first approximation using a one-dimensional reaction coordinate (Fig. 17a) if, starting from the known structure of methyl azide,[113] the CH_3N-N_2 distance is increased in steps of 20 pm, and the remaining bond distances and angles are optimized by the MNDO procedure.[65, 111] The calculation[23] predicts an activation energy of ca. 220 kJ/mol and an elongated H_3CN-N_2 bond length of 202 pm in the product-like transition state.[114]

The subsequent 1,2-H shift starting from one of the Jahn-Teller minima of the methylnitrene singlet state $\tilde{A}(^1E)$ is predicted to be highly exothermic ($\Delta H_R^{MNDO} = -390$ kJ/mol).[23] This 1,2-H shift in the five-atom species H_3C-N, which possesses $3\times5-6=9$ degrees of freedom, can be visualized on a two-dimensional energy hypersurface projected out of the 9-dimensional hyperspace, if the bond angle $\sphericalangle HNC$ and the torsional angle $\omega(HNCH)$ are chosen as the reaction coordinates[65] and varied stepwise, optimizing the remaining structural parameters by MNDO calculations. Inspection of the resulting hypersurface (Fig.

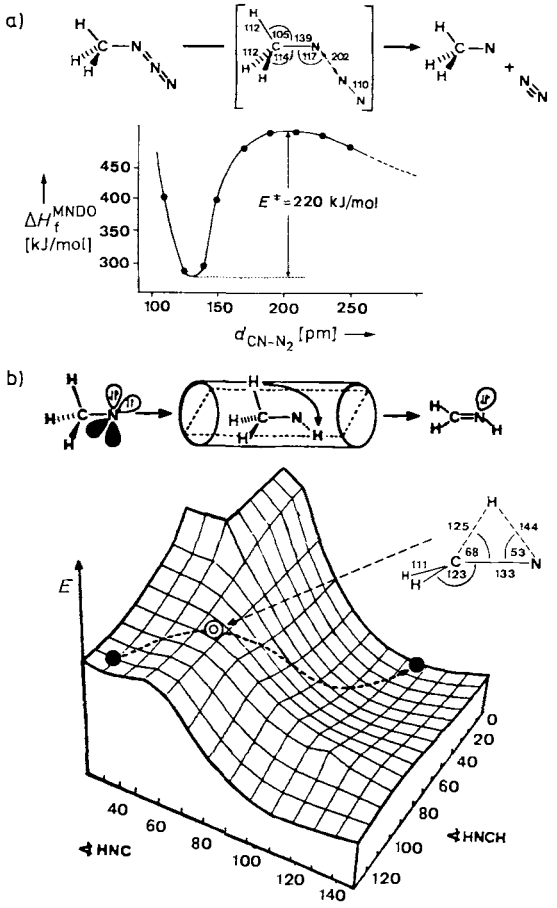

Fig. 17. MNDO energy hypersurfaces for asynchronous methyl azide decomposition: (a) barrier for the N_2 extrusion to singlet methylnitrene and (b) the rearrangement of the latter to methanimine (see text). Angles in degrees, bond lengths in pm.

17b) shows the potential well for singlet methylnitrene to be extremely flat; the barrier to the 1,2-H shift is estimated to be less than 20 kJ/mol, and the systematic search for a saddle point[115] leads to a three-membered ring transition state (Fig. 17b).

It is however more probable that the decomposition of methyl azide proceeds in a synchronous manner, since the different activation energies for the asynchronous partial

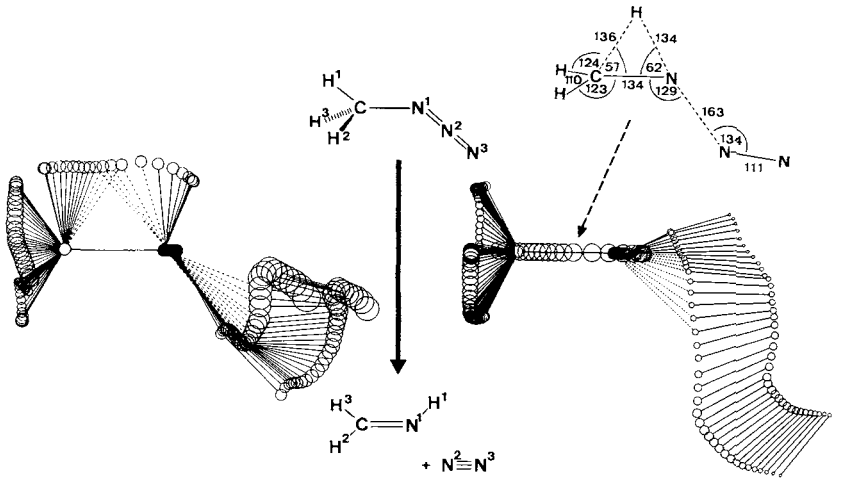

Fig. 18. Stroboscopic representation of geometry changes in synchronous methyl azide decomposition, as calculated by the MNDO method. Left: view onto the H^1CN^1 plane; right: view in the $^1HCN^1$ plane (---› position of H^1 at the saddle point; see text). Angles in degrees and bond lengths in pm.

steps lead one to expect a lower barrier for a concerted reaction. A stroboscopic representation of the calculated geometry changes along the reaction path (Fig. 18) shows a curved trajectory for the extruded N_2 molecule which appears to be coupled to the flattening and rotation of the H_2C fragment.

A further saddle point search[115] provides a structure for the transition state of the synchronous methyl azide decomposition, in which the H_3CN-N_3 distance is shorter by 40 pm (Fig. 18, top right) relative to that for asynchronous N_2-extrusion (Fig. 17a). A MNDO calculation of the barrier for simultaneous N_2-extrusion and 1,2-H shift predicts (within the error limits of the semiempirical approach with neglect of electron correlation and molecular dynamics) an activation energy which is comparable to that estimated for asynchronous methylnitrene formation. However, a synchronous process is supported by the temperature-dependence of the decomposition of alkyl azides $(H_3C)_nH_{3-n}C-N_3$ (Fig. 8): since the activation energies for the breaking of the $RN-N_2$ bond are largely substituent-independent[10c] and those for nitrene rearrangement negligibly small in comparison, the difference of more than 100 K in the decomposition temperatures indicates that the methyl azide pyrolysis occurs with coupled N_2-extrusion and 1,2-H shift.

Vinyl azide $H_2C=CH-N_3$ contains only one carbon atom more than the seven-atom molecule methyl azide; however, its different molecular topology requires consideration of the formation of several potential elimination products. MNDO calculations for the "normal" valence isomers of the ensemble C_2H_3N predict the enthalpies of formation shown in Figure 19.[25]

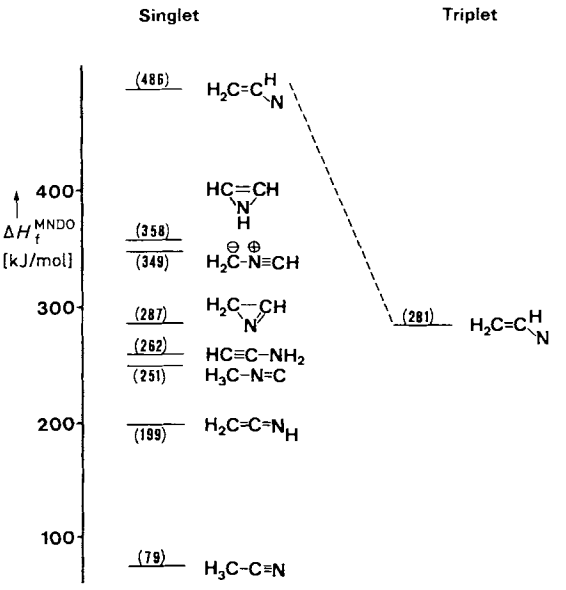

Fig. 19. MNDO calculated enthalpies of formation of low-energy C_2H_3N isomers.

Obviously, acetonitrile is by far the most stable isomer, followed by ketenimine, methyl isonitrile, aminoacetylene and 2*H*-azirine. Nitrile ylide and 1*H*-azirine are predicted to be relatively unstable, in agreement with chemical experience. The singlet ground state of vinylnitrene is estimated to lie ca. 205 kJ/mol above its triplet ground state.[25, 116] As for the decomposition of methyl azide, an energetically favored elimination of singlet N_2 should lead (with conservation of spin) to singlet vinylnitrene (Fig. 20).

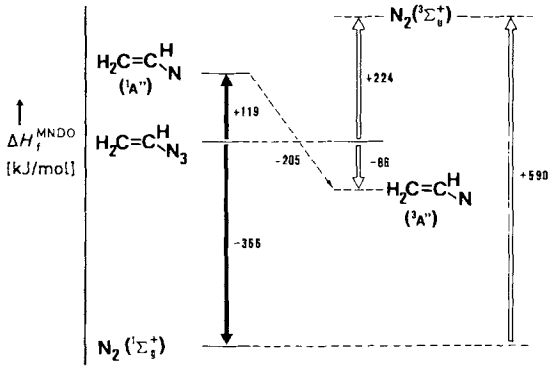

Fig. 20. Relative MNDO enthalpies of formation of vinyl azide and possible products of its thermal decomposition, N_2 and vinylnitrene, in their singlet and triplet ground states (see text).

Several of the C_2H_3N isomers (Fig. 19) can be formed from vinylnitrene only via multiple rearrangement steps. Thus two hydrogen atoms would have to migrate to produce $HC\equiv C-NH_2$, while for H_3C-NC even the molecular skeleton would have to be reorganized. Simpler processes such as ring closure or 1,2-H shift lead to 2*H*-azirine, acetonitrile or ketenimine. These three products can be projected onto favorable positions of a common singlet energy hypersurface, if the angles $\sphericalangle$HCN and $\sphericalangle$CCH are chosen from the possible $\binom{12}{2}=66$ pair combinations of the $(3\times 6-6)=12$ reaction coordinates (Fig. 21a).

The MNDO energy hypersurface for asynchronous vinyl azide decomposition shows that the resulting singlet vinylnitrene (Fig. 21a) would be located like H_3CN (Fig. 17b) in an extremely shallow potential minimum. The activation barrier for ring closure to 2*H*-azirine amounts to only a few kJ/mol, while that for the 1,2-H shift to acetonitrile is predicted to be ca. 40 kJ/mol. Ketenimine, which has been detected by microwave spectroscopy as a by-product of vinyl azide pyrolysis,[117] is separated by a hypersurface ridge over 70 kJ/mol high (Fig. 21a). The energy hypersurface for singlet vinylnitrene reproduces the observed decomposition products with the correct temperature dependence and relative concentrations. Additional MNDO calculations for the N_2 extrusion from $H_2C=CH-N_3$, however, predict, as for H_3C-N_3, an activation energy of ca. 240 kJ/mol.[23] This large barrier disagrees both with the observed decomposition temperature of vinyl azide in the gas phase, which is lower by 100 K, and with experimentally determined activation parameters in solution.[118] A refined energy hypersurface for synchronous N_2 extrusion and ring closure (Fig. 21b) can be calculated by choosing the torsional angle (HCCN) as the second reaction coordinate, thus allowing a twisting of the CH_2 group. This results in opening a trough through the activation barrier and in lowering the calculated enthalpy of activation by ca. 100 kJ/mol to 140 kJ/mol.

For substituted vinyl azides, the following decomposition routes have been discussed in the literature:[25, 63] the

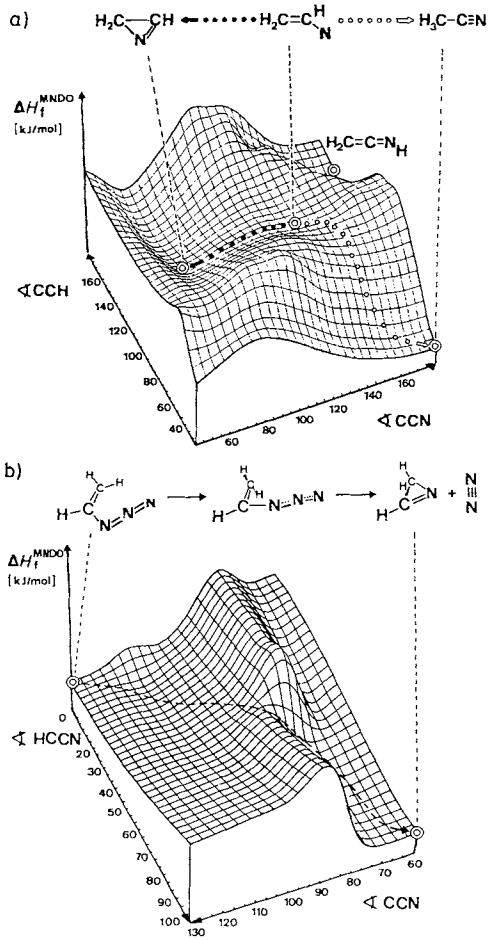

Fig. 21. MNDO singlet energy hypersurfaces for (a) vinylnitrene products accessible via ring closure (●●●●➡) or 1,2-H shift (○○○○⇨) in asynchronous vinyl azide decomposition and (b) synchronous N_2 extrusion and formation of the three-membered ring (see text).

asynchronous one via free vinylnitrene, the synchronous ring closure to 2*H*-azirine, and the intermediate formation of 4*H*-1,2,3-triazoles.[119] However, the parent molecule $H_2C=CH-N_3$ decomposes already at 620 K and thus ca. 100 K lower than methyl azide, while 1*H*-1,2,3-triazole does not decompose below 870 K. This is in agreement with the energy hypersurface calculations,[25, 116, 119] according to which N_2-extrusion and ring closure to the isolated 2*H*-azirine are the dominating mechanisms for vinyl azide decomposition.

4.3. "Chemical Activation" of Imine and Azomethine Intermediates

Imines or azomethines have been detected PE-spectroscopically as intermediates in the low-pressure gas phase pyrolyses of the following C-azides:

- alkyl azides $R_2R'C-N_3$, whose α-carbon carries a group R′ capable of undergoing a 1,2-shift, on N_2-elimination form derivatives $R_2C=N-R'$; R′=H migrates in the case of methyl, ethyl, isopropyl or allyl azide (formation of imines), while $R'=CH_3$ migrates in the case of *tert*-butyl azide (formation of an azomethine).
- trimethylenetetrazole (Scheme 10) simultaneously splits off both N_2 and its $-H_2CCH_2-$ bridge as ethene, forming the *N*-cyano derivative $H_2C=N-CN$.
- vinyl azide decomposes preferentially via ring closure to 2*H*-azirine.

In exothermic reactions in solution, the reaction enthalpy stored as vibrational, rotational and translational energy in the resulting molecules is generally quickly dissipated by frequent collisions. In the gas phase, however, the collision frequency is low, particularly at low pressures, and the heat of reaction contained in the products can induce further reactions; a phenomenon, called "chemical activation."[120, 121]

For the consecutive reactions of imines to nitriles considerable temperature differences are observed depending on whether the gas stream from azide pyrolysis is heated further or whether the "cold" imine isolated in a cooling trap is thermally decomposed after revaporation. The difference is particularly drastic for methanimine: for methanimine generated by pyrolysis of methyl azide a temperature of only 770 K is required for H_2-cleavage, while the isolated compound has to be heated to 1300 K (Scheme 20). The temperature difference amounts to over 500 K (!).[23] The rearrangement of 2*H*-azirine to acetonitrile also requires a temperature ca. 120 K higher than that necessary for its formation in the pyrolysis of vinyl azide[20].

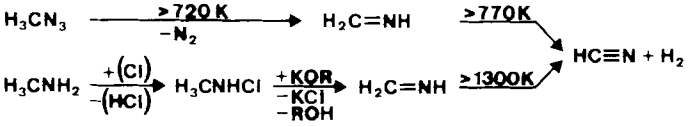

Scheme 20.

For the unimolecular thermal decomposition of methyl azide, it has been estimated from literature bond enthalpy data and from the activation energy for the N_2-extrusion[10a, d] that the methanimine molecule formed should be "chemically activated" by approximately 340 kJ/mol[23, 121] (Fig. 22).

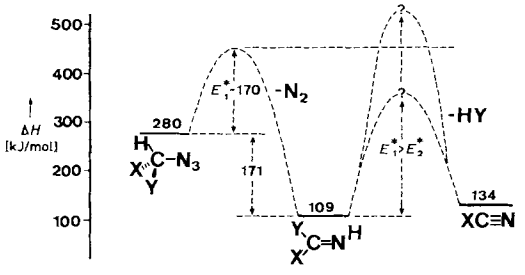

Fig. 22. Enthalpy diagram of methyl azide decomposition and methanimine dehydrogenation.

In satisfactory agreement, MNDO calculations predict for the N_2-extrusion from H_3C-N_3 an activation energy E_1^*(MNDO) of about 220 kJ/mol and for the strongly

exothermic formation of methanimine a reaction enthalpy ΔH_R^{MNDO} of about 170 kJ/mol. Since the "excess" energy stored in the molecule cannot be "dissipated" under the nearly unimolecular conditions in the gas stream,[12,1] a small increase in temperature leads to the additional elimination of H_2 and formation of HCN (Fig. 22: X, Y = H). In contrast, the thermal dehydrogenation of isolated methanimine requires that the full activation energy be supplied, i.e. a temperature higher by more than 500 K.

According to the PE-spectroscopic observations, the "chemically activated" imine and azomethine intermediates generated in alkyl azide pyrolyses can eliminate not only H_2 but also CH_4, H_3C-CH_3 or $H_2C=CH_2$, forming nitriles in an entropy-controlled reaction. Referring to the enthalpy diagram of Figure 22, all azides $(HYX)C-N_3$ for which the second activation barrier E_2^+ is relatively low should split off a further molecule fragment HY together with N_2. The experimental result that in gas phase pyrolyses of acceptor-substituted azides (cf. Section 3.6), the corresponding imines or azomethines are not observed PE-spectroscopically in spite of their demonstrated stability in some cases,[34,36] is thus readily explained: the N_2-extrusion from $ClH_2C-H_2C-N_3$, F_2HC-N_3 or $NC-H_2C-N_3$, which only commences at relatively high temperatures, leads to an "intramolecular explosion" of the "chemically activated" imine intermediate. The considerable reaction enthalpies which are stored in the molecular fragment remaining after N_2-extrusion also help to answer questions as to why for example tetramethylenetetrazole (Scheme 10) also eliminates $H_2C=CH_2$ with the formation of $H_2C=N-CN$, which under the reaction conditions is stable towards further decomposition to HCN, or why phenylsilyl triazide $H_5C_6Si(N_3)_3$ in its 1000 K gas-phase pyrolysis "suddenly" splits off four equivalents of N_2 and rearranges to the thermodynamically more stable isomer phenylsilaisocyanide $H_5C_6-N\equiv Si$ (Fig. 14).

5. "To What End Does One Study the Gas-phase Pyrolysis of Azides?"

An important precondition for our studies[23] has been the advantages offered by PE-spectroscopic real-time analysis[3] for gases flowing under reduced pressure (Sections 2 and 3.1). Using this technique we were able to safely pyrolyze azides and other nitrogen-rich substances and to determine their decomposition temperatures (Sections 3.2–3.9), to detect (in part for the first time) or to isolate imines and other short-lived intermediates, and to optimize synthetic routes to a number of nitrogen compounds which had previously either been unobtainable or obtainable only with difficulty (cf. Section 3.10). MNDO calculations have proven valuable in the assignment of unknown ionization patterns (Section 3.2) and thus in the identification of decomposition products (Section 3.10); calculated energy hypersurfaces (Section 4.2) agree with many experimental results and in addition permit some insight into the complex microscopic pathway of the apparently so simple azide decomposition, in which "chemically activated" intermediates (Section 4.3) have been detected.[23]

The decomposition of azides under unimolecular conditions, i.e. outside their explosion limits, requires unexpectedly high temperatures. Three substituent-dependent decomposition pathways to (singlet) nitrenes, to imines and to nitriles or isocyanides are observed. A comparison between experimental and calculated data suggests that in azide pyrolyses singlet nitrogen elimination and rearrangement to observed intermediates proceed in a synchronous manner. A number of imines have been detected as intermediates; their decomposition, studied in part using independently prepared samples, occurs only at high temperatures and provides evidence that they are formed "chemically activated" in azide pyrolyses. A series of new compounds such as phenylsilaisonitrile $H_5C_6N\equiv Si$ with a formally triply-bonded silicon atom of coordination number 1 (Section 3.9) extend the chemistry of the main group elements.

The title question may also be answered as follows: the gas-phase pyrolysis of azides—provided that necessary precautions are taken!—is not only a useful method for the preparation of compounds which are otherwise difficult to obtain as well as an illustration of the advantages of PE-spectroscopic gas analysis, but in addition is particularly suitable for studying the still largely unknown reaction paths of medium-size molecules with numerous degrees of freedom. The compounds discussed, which are often "malicious" in the condensed phase, and their demonstrated safe handling under reduced pressure in the gas phase, the thermodynamically favorable elimination of singlet N_2, or the proven formation of "chemically activated" intermediates should be of interest to other research groups with, for example, access to more time-resolved measurement techniques. We hope that in the future also the gas phase pyrolysis of azides, as a many-faceted model reaction, will contribute to improving our currently fragmentary knowledge of microscopic reaction pathways, a hope, which closes the circle to the quotation from *George C. Pimentel* at the beginning of this article.[1]

The "detours to the formation of elementary nitrogen" described here have been generously supported by the Deutsche Forschungsgemeinschaft within the special program "short-lived molecules", by the Fonds der Chemischen Industrie and by the Federal State of Hessen; R. D. thanks the Studienstiftung des Deutschen Volkes for a doctoral stipendium. Parts of this study were carried out in cooperation with Dr. J.-M. Denis (Rennes), Prof. Dr. W. A. Herrmann (München, formerly Frankfurt) and Prof. Dr. C. Wentrup (Brisbane (Australia), formerly Marburg); samples of other compounds were provided by Prof. Dr. H. Bürger (Wuppertal), Dr. K. O. Christie (Rocketdyne Corp., Canoga Park, California), Dr. D. Lentz (Berlin) and Prof. Dr. D. D. DesMarteau (Clemson, South Carolina).

Received: August 15, 1986 [A 615 IE]
German version: *Angew. Chem. 99* (1987) 518
Translated by Professor *T. N. Mitchell*, Dortmund (FRG)

[1] *Chem. Eng. News 58* (1980) No. 2, p. 7.
[2] H. Bock, R. Dammel, L. Horner, *Chem. Ber. 114* (1981) 220.
[3] Review: H. Bock, B. Solouki, *Angew. Chem. 93* (1981) 425; *Angew. Chem. Int. Ed. Engl. 20* (1981) 427.

[4] Cf., e.g., the following monographs and review articles: a) S. Patai (Ed.): *The Chemistry of the Azido Group*. Interscience, London 1971; b) C. Grundmann in *Houben-Weyl-Müller, Methoden der Organischen Chemie, Vol. X/3*, Thieme, Stuttgart 1965, p. 777; c) J. M. Boyer, F. C. Canter, *Chem. Rev. 54* (1954) 1; d) G. Bertrand, J.-P. Majoral, A. Baceiredo, *Acc. Chem. Res. 19* (1986) 17.

[5] U. Müller, *Struct. Bonding (Berlin) 14* (1973) 141, and references cited as well as [4a]; cf. also C. Glidewell, A. G. Robiette, *Chem. Phys. Lett. 28* (1974) 290; J. D. Murdoch, D. W. H. Rankin, *J. Chem. Soc. Chem. Commun. 1972*, 748.

[6] Cf., e.g., [4a], p. 782.

[7] We thank Prof. *D. Rehm*, Universität Frankfurt, for carrying out the CAS on-line literature search, which shows the bibliographic file CA to contain 10859 publications for AZIDE and AZIDO since 1967; 3010 of these include these terms in the title. At the last count (September 23, 1985) the databases of STN INTERNATIONAL/CAS ONLINE contained totals of 3936 and 23297 registry numbers for compounds with the fragments AZIDE and AZIDO, respectively.

[8] See also R. F. C. Brown: *Pyrolytic Methods in Organic Chemistry*. Academic Press, New York 1980 and the rather few literature references on alkyl azides.

[9] Examples studied include: a) the kinetics of the decomposition of ethyl, isopropyl, and *tert*-butyl azides: G. Geiseler, W. König, *Z. Phys. Chem. 227* (1964) 81; b) the flow pyrolysis of CH_3-N_3 at 1170 K: F. O. Rice, C. F. Grelicki, *J. Phys. Chem. 61* (1957) 830; c) the pyrolysis of higher alkyl azides: W. Pritzkow, D. Timm, *J. Prakt. Chem. 32* (1966) 178; d) the decomposition of ethyl azide at 870 K using microwave spectroscopy: R. D. Brown, P. D. Godfrey, D. A. Winkler, *Aust. J. Chem. 33* (1980) 1.

[10] a) For more recent discussions on nitrenes see: a) E. F. V. Scriven (Ed.): *Azides and Nitrenes*. Academic Press, New York 1984; b) W. M. Jones in P. de Mayo (Ed.): *Rearrangements of Ground and Excited States, Vol. 1*. Academic Press, New York 1980, p. 95ff. c) R. A. Abramovitch in S. P. M. McManus (Ed.): *Organic Reaction Intermediates*, Academic Press, New York 1973, p. 127ff; d) W. Lwowski (Ed.): *Nitrenes*, Interscience, New York 1970. e) C. Wentrup: *Reactive Molecules*, Wiley, New York 1984, p. 162ff.

[11] Generation of triplet nitrenes in low-temperature matrices by sensitized photolysis: E. Wassermann, G. Smolinski, W. A. Yager, *J. Am. Chem. Soc. 86* (1964) 3166. ESR detection of triplet methylnitrene: E. Wassermann, *Prog. Phys. Org. Chem. 8* (1971) 319, and references cited therein.

[12] Triplet methylnitrene is the lowest energy minimum of the triplet energy hypersurface, see H. F. Schaefer III, *Acc. Chem. Res. 12* (1979) 288, and references cited therein; J. Demuynck, D. J. Fox, H. F. Schaefer III, *J. Am. Chem. Soc. 102* (1980) 6204. See also [10a] and [10d].

[13] Cf. also: J. F. Milligan, *J. Chem. Phys. 35* (1961) 1491.

[14] For the products of the thermo- and photolysis of tertiary alkyl azides see also I. R. Dunkin, P. C. P. Thompson, *Tetrahedron Lett. 21* (1980) 3813; R. A. Abramovitch, E. P. Kyba, *J. Am. Chem. Soc. 96* (1974) 480.

[15] Attempts to prepare a nitrogen triazide $N(N_3)_3$ from NCl_3 and LiN_3 in tetrahydrofuran (THF) or with NaN_3 in diglyme (H. Bock, K. L. Kompa, *Z. Anorg. Allg. Chem. 332* (1964) 240) lead even at 200 K to the evolution of 5 molar equivalents of N_2.

[16] R. Weast (Ed.): *CRC Handbook of Chemistry and Physics*, 63rd Edit., CRC Press, West Palm Beach, FL, USA 1982, F-188.

[17] For accounts of imine chemistry see: Z. Rappoport (Ed.): *The Chemistry of the C=N Double Bond*, Interscience, London 1970; S. R. Sandler, W. Caro: *Organic Functional Group Preparations*, Academic Press, New York 1971, p. 246ff.

[18] Cf. also, e.g., R. D. Brown, *Chem. Br. 1979*, 570, and references cited therein; S. L. Miller, L. E. Orgel: *The Origins of Life on Earth*, Prentice-Hall, Englewood Cliffs, NJ, USA 1974.

[19] P. D. Godfrey, R. D. Brown, B. J. Robinson, M. Sinclair, *Astrophys. Lett. 13* (1973) 119; cf. also: E. Herbst, *Astrophys. J. 205* (1976) 94.

[20] D. R. Johnson, F. J. Lovas, *Chem. Phys. Lett. 15* (1972) 65; R. Pearson, Jr., F. J. Lovas, *J. Chem. Phys. 66* (1977) 4149.

[21] a) J. B. Peel, G. Willet, *J. Chem. Soc. Faraday Trans. 2 71* (1975) 1799; cf. also: D. C. Frost, S. T. Lee, C. A. MacDowell, N. P. C. Westwood, *J. Electron Spectrosc. Relat. Phenom. 12* (1977) 95; b) R. Schulz, A. Schweig, *ibid. 28* (1982) 33.

[22] B. Braillon, M. C. Lasne, J. L. Ripoll, J. M. Denis, *Nouv. J. Chim. 6* (1982) 121.

[23] H. Bock, R. Dammel, unpublished; R. Dammel, *Dissertation*, Universität Frankfurt 1986.

[24] R. Tiollais, *Bull. Soc. Chim. Fr. 14* (1947) 708.

[25] H. Bock, R. Dammel, S. Aygen, *J. Am. Chem. Soc. 105* (1983) 7681, and references cited therein.

[26] Cf., e.g.: a) K. Ogawa, Y. Nomura, Y. Takeuchi, S. Tomoda, *J. Chem. Soc. Perkin Trans. 1 1982*, 3031; b) C. Schöpf, A. Komcak, F. Braun, E. Jacobi, *Justus Liebigs Ann. Chem. 559* (1948) 559; *Chem. Ber. 65* (1952) 937, 945; *93* (1960) 2457; c) J. H. Boyer, F. C. Canter, *J. Am. Chem. Soc. 77* (1955) 3287.

[27] In their review article ("Toxic and Explosive Properties of Azides") in [4a], p. 61 et seq. *M. E. C. Biffin, J. Miller*, and *D. B. Paul* point out that HN_3 is particularly dangerous: it can be formed in various ways from salt-like and covalent azides. HN_3 boils at 310 K, is as poisonous as HCN, and is extremely explosive.

[28] D. A. Spencer, *J. Chem. Soc. 1925*, 216; the quotation reprinted here is to be found on p. 220.

[29] The preparation of $NC-N_3$ **9** in diethyl *o*-phthalate as solvent follows in the main the procedure of: B. Bak, P. Jansen, H. Stafast, *Chem. Phys. Lett. 35* (1975) 247. **9** was discovered by F. D. Marsh, M. E. Hermes, *J. Am. Chem. Soc. 86* (1964) 4506; cf. also F. D. Marsh, *J. Org. Chem. 37* (1972) 2966, and references cited therein.

[30] Cf. R. H. Wiley, J. Moffat, *J. Org. Chem. 22* (1957) 995, and references cited therein.

[31] Cf. G. A. Olah, D. J. Donovan, *J. Org. Chem. 43* (1978) 860.

[32] Cf. J. A. Miller, *Tetrahedron Lett. 1975*, 2959; R. A. Abramovitch, E. P. Kyba, *J. Am. Chem. Soc. 96* (1974) 480; P. Margaretha, S. Solar, O. E. Polansky, *Angew. Chem. 83* (1971) 410; *Angew. Chem. Int. Ed. Engl. 10* (1971) 412.

[33] M. O. Forster, H. E. Fierz, *J. Chem. Soc. 93* (1908) 1174. The structure of the dimer which slowly separates from stored allyl azide was determined: J. C. Pezzullo, J. Boyko, *J. Org. Chem. 38* (1973) 168.

[34] H. Bock, R. Dammel, *Inorg. Chem. 24* (1985) 4427, and literature cited therein; USSR-Pat. 375287, discoverers: V. L. Ginsburg, P. O. Gitel, I. M. Didina (cf. *Chem. Abs. 73* (1973) 41895f).

[35] H. Bock, K. L. Kompa, *Angew. Chem. 74* (1962) 327; the synthesis is described in detail in [15].

[36] H. Bock, R. Dammel, D. D. DesMarteau, *Z. Naturf. B42* (1987) 308. Cf. K. O. Christe, C. J. Schack, *Inorg. Chem. 20* (1981) 2566, and references cited therein.

[37] The PE-spectroscopic optimization of the gas phase dehydrochlorination of β-chloroethyl azide is described in detail in [23]; cf. H. Bock, R. Dammel, *Z. Naturforsch. B42* (1987) 301 as well as [25] and [38].

[38] J.-C. Guillemin, J.-M. Denis, M.-C. Lasne, J.-L. Ripoll, *J. Chem. Soc. Chem. Commun. 1983*, 238.

[39] W. Sundermeyer, *Chem. Ber. 96* (1983) 1293, and references cited therein.

[40] J.-M. Denis, private communication; cf. J.-C. Guillemin, *Dissertation*, University of Lille 1982.

[41] H. Bock, B. Solouki, H. W. Roesky, *Inorg. Chem. 24* (1985) 4425.

[42] H. Bock, R. Dammel, *Angew. Chem. 97* (1985) 128; *Angew. Chem. Int. Ed. Engl. 24* (1985) 111.

[43] R. Dammel, *Diplomarbeit*, Universität Mainz 1980. For the calculation of the substance flow cf., e.g., A. Roth: *Vacuum Technology*, North Holland, Amsterdam 1976, p. 106f; S. Dushman, J. M. Lafferty: *Foundation of Vacuum Techniques*, 2nd Edit., Wiley, New York 1962, p. 80f.

[44] B. Solouki, H. Bock, R. Appel, A. Westerhaus, G. Becker, G. Uhl, *Chem. Ber. 115* (1982) 3748.

[45] $H_2Si=CH_2$: P. Rosmus, H. Bock, B. Solouki, G. Maier, G. Mihm, *Angew. Chem. 93* (1981) 616; *Angew. Chem. Int. Ed. Engl. 20* (1981) 598.

[46] PE spectra can be digitally recorded on-line and stored in a computer. The so-called "spectrum stripping", in which the PE spectra of pure single components previously stored in a data bank are electronically subtracted, has often proved useful in PE-spectroscopic analysis. Cf. also, e.g., $SiCl_2$/naphthalene: H. Bock, B. Solouki, G. Maier, *Angew. Chem. 97* (1985) 205; *Angew. Chem. Int. Ed. Engl. 24* (1985) 205; or SPCl/PCl_3: M. Binnewies, B. Solouki, H. Bock, R. Becherer, R. Ahlrichs, *ibid. 96* (1984) 704 and *23* (1984) 731.

[47] It is advisable to first condense out less volatile decomposition products in a 77 K trap; cf., e.g., H. Bock, H. P. Wolf, *Angew. Chem. 97* (1985) 411; *Angew. Chem. Int. Ed. Engl. 24* (1985) 418.

[48] See, e.g., H. Bock, T. Hirabayashi, S. Mohmand, *Chem. Ber. 114* (1981) 2595, 2609; *115* (1982) 492.

[49] See, e.g., H. Bock, S. Mohmand, T. Hirabayashi, G. Maier, H. P. Reisenauer, *Chem. Ber. 116* (1983) 273.

[50] In particular, it is assumed that the electron relaxation energy stabilizing the radical cation and the correlation energy contribution of the expelled electron are comparable in magnitude and due to their opposing signs approximately cancel (cf. H. Bock, *Angew. Chem. 89* (1977) 631; *Angew. Chem. Int. Ed. Engl. 16* (1977) 613). Moreover the vibronic coupling between the various $M^{\oplus\oplus}$ states must be negligibly small (cf. H. Köppel, L. S. Cederbaum, W. Dancke, S. S. Shaik, *ibid. 95* (1983) 221 and *12* (1983) 210).

[51] Selected examples of molecular state comparisons for chemically related compounds according to topological considerations and pertur-

bational arguments are collected in H. Bock, *Angew. Chem. 89* (1977) 631; *Angew. Chem. Int. Ed. Engl. 16* (1977) 613 ("Molecular States and Molecular Orbitals").

[52] According to a useful rule of thumb (cf. H. Bock, B. G. Ramsey, *Angew. Chem. 85* (1973) 773; *Angew. Chem. Int. Ed. Engl. 12* (1973) 734) the ionizations of all $np_{element}$ and $1s_H$ electrons should be observable in the He(I) measurement range. Thus, taking into account the Pauli principle, we expect $(3+1\times2+3\times3)/2=7$ PES bands for methyl azide, with those at 14.4 and 14.8 eV overlapping considerably.

[53] S. Cradock, E. A. V. Ebsworth, J. D. Murdoch, *J. Chem. Soc. Faraday Trans. 67* (1971) 86.

[54] In particular, the higher-energy radical cation states of azides, in which the positive charge is mainly localized in the NNN group as for example in the $\tilde{D}$(10a) state of H_3C-N_3 [11], are generally reproduced only with considerable "Koopmans' defects" even by SCF calculations with large basis sets: the corresponding SCF eigenvalues differ by up to several eV from the experimental ionization energies, since electron reorganization and correlation effects no longer cancel [50]. Thus SCF calculations for the third ionization energy of HN_3 (Fig. 6: $IE_3^v=15.45$ eV [55]) deviate as follows: MNDO 16.80 eV [23], ab initio STO-3G 16.19 eV [55c], ab initio "double zeta" 18.51 eV (J. F. Wyatt, I. H. Hillier, V. R. Saunders, J. A. Connor, M. Barber, *J. Chem. Phys. 54* (1971) 5311).

[55] a) J. H. D. Eland, *Phil. Trans. R. Soc. London A 268* (1970) 87; b) T. H. Lee, R. J. Colton, J. W. Rabelais, *J. Am. Chem. Soc. 97* (1975) 4845; c) J. Bastide, J. P. Maier, *Chem. Phys. 12* (1976) 177; d) [53].

[56] W. A. Herrmann, G. W. Kriechbaum, R. Dammel, H. Bock, *J. Organomet. Chem. 254* (1984) 219. Alkyl azides $R-N_3$ with alkyl groups R of different size react with metal-metal triple bonds at different rates. For the preparation of acrolein imine by gas phase pyrolysis of diallylamine see B. Berkner, *Diplomarbeit*, Universität Frankfurt 1983 and [21h].

[57] H. Bock, R. Dammel, D. D. DesMarteau, *Z. Naturforsch. B 42* (1987) 308.

[58] H. Bock, B. Solouki, P. Rosmus, R. Dammel, P. Hänel, B. Hierholzer, U. Lechner-Knoblauch, H. P. Wolf in H. Sakurai (Ed.): *Organosilicon and Bioorganosilicon Chemistry*, Ellis Horwood, Chichester, England 1985, p. 45ff.

[59] Cf. H. Bock, P. Hänel, W. Kaim, U. Lechner-Knoblauch, *Tetrahedron Lett. 26* (1985) 5115, and references cited therein. Because of the antibonding n_N/n_{Cl} interactions, the n_N ionizations change but little on chlorine substitution of amines, e.g. H_3C-NH_2: 9.64, $H_3C-NHCl$: 9.75 eV; $(H_3C)_2-NH$: 9.5, $(H_3C)_2NCl$: 9.65 eV; aziridine 9.80, *N*-chloroaziridine 9.95 eV [23].

[60] Cf. H. Stafast, H. Bock (Photoelectron Spectra of Cyano Compounds) in S. Patai, Z. Rappoport (Eds.): *The Chemistry of Functional Groups, Supplement D*, Wiley, London 1983, p. 137ff., and references cited therein.

[61] Cf., e.g., W. T. Reichle, *Inorg. Chem. 3* (1964) 402; R. West, J. S. Thayer, *J. Am. Chem. Soc. 84* (1962) 1763; S. Cradock, E. A. V. Ebsworth, *J. Chem. Soc. A 1968*, 1420, and in each case references cited therein.

[62] H. Bock, R. Dammel, *Chem. Ber.*, in press.

[63] Reviews: G. L'abbé, *Angew. Chem. 87* (1975) 831; *Angew. Chem. Int. Ed. Engl. 14* (1975) 775; G. L'abbé, A. Hassner, *ibid. 83* (1971) 103 and *10* (1978) 98; F. W. Fowler, *Adv. Heterocycl. Chem. 13* (1973) 45.

[64] Cf. S. Cradock, R. H. Findley, M. H. Palmer, *Tetrahedron 29* (1973) 2173.

[65] Cf. H. Bock, R. Dammel, B. Roth in A. Cowley (Ed.): *Inorganic Rings and Clusters*, ACS Symp. Ser. 232, Am. Chem. Soc., Washington 1983, p. 139ff.

[66] Cf. K. Wittel, H. Bock (Photoelectron Spectra of Organic Halogen Compounds) in S. Patai, Z. Rappoport (Eds.): *The Chemistry of Functional Groups, Supplement D*. Wiley, London 1983, p. 1517, 1523, and references cited therein; G. Bieri, L. Asbrink, W. van Niessen, *J. Electron Spectrosc. Relat. Phenom. 23* (1981) 281.

[67] Cf. [60], p. 146, 153, and references cited therein; G. Bieri, *Chem. Phys. Lett. 46* (1977) 107.

[68] See also J. C. Bailar, Jr., H. J. Emeleus, R. Nyholm, R. F. Trotman-Dickenson (Eds.): *Comprehensive Inorganic Chemistry*, Pergamon Press, Oxford 1973, p. 1246. The polymerization of FCN in the presence of HF at room temperature can result in an explosion.

[69] We thank *D. D. DesMarteau* (cf. *J. Org. Chem. 46* (1981) 1277) for a sample of $F_2C=NF$. Cf. also D. Christen, H. Oberhammer, R. M. Hammaker, S. C. Chang, D. D. DesMarteau, *J. Am. Chem. Soc. 104* (1982) 6186.

[70] Cf. e.g. H. Bock, J. Wittmann, J. Mintzer, J. Russow, *Chem. Ber. 115* (1982) 2346.

[71] The relative thermodynamic stabilities given in Figure 11 were calculated by J. H. Clemmons, P. Jasien, C. E. Dystra, *Mol. Phys. 48* (1983) 631, using the SZEP method with (DZ+P) basis sets.

[72] For a review of studies on HCN dimers see: C. Wentrup in [10e], p. 402f.

[73] C. Wentrup, P. Lorenčak, unpublished; cf. P. Lorenčak, *Dissertation*, Universität Marburg 1985 and [72].

[74] C. N. Matthews, J. Nelson, P. Varma, R. Minard, *Science 198* (1977) 622; J. P. Ferris, E. H. Edelson, *J. Org. Chem. 31* (1978) 3989, and references cited therein.

[75] B. Bak, H. Svanholt, *Chem. Phys. Lett. 75* (1980) 528, and references cited therein.

[76] Cf., e.g., M. Winnewisser, *Chem. Unserer Zeit 18* (1984) 1, 54; R. D. Brown, *Chem. Br. 1979*, 570, and references cited therein. At present about 200 lines due to interstellar molecules have not been assigned: M. Winnewisser, G. Winnewisser, *Phys. Bl. 39* (1983) 9, 289.

[77] The PE-spectroscopic optimization of the gas-phase pyrolyses of trimethylenetetrazole and of 2,5-substituted tetrazoles was carried out in collaboration with *C. Wentrup, S. Fischer*, and *P. Lorenčak*; cf. [72, 73] and H. Bock, R. Dammel, S. Fischer, C. Wentrup, *Tetrahedron Lett. 28* (1987) 617.

[78] O. Walter, L. S. Cederbaum, B. Solouki, P. Rosmus, H. Bock, *J. Phys. Chem. 89* (1985) 1384, and references cited therein.

[79] R. Huisgen, M. Seidel, G. Wallbillich, H. Knupfer, *Tetrahedron 17* (1962) 3; W. Fliege, R. Grashey, R. Huisgen, *Chem. Ber. 117* (1984) 1194; P. Caramella, P. Grünanger in A. Padwa (Ed.): *1,3-Dipolar Cycloaddition Chemistry, Vol. 1*, Wiley, New York 1984, p. 291ff.

[80] For the formation of $NC-N=C(N_3)_2$ cf.: C. V. Hart, *J. Am. Chem. Soc. 50* (1928) 1922; M. G. Darzens, *C. R. Acad. Sci. 154* (1912) 1232.

[81] Cf. [29] and G. L. Blackman, K. Bolton, R. D. Brown, F. R. Burden, A. Mishra, *J. Mol. Spectrosc. 47* (1973) 457; C. C. Costain, H. Kroto, *Can. J. Phys. 50* (1972) 1543.

[82] a) PE spectroscopy: [60], and references cited therein; cf. also: D. C. Frost, H. Kroto, C. A. MacDowell, N. P. C. Westwood, *J. Electron Spectrosc. Relat. Phenom. 11* (1977) 147; b) IR spectroscopy: H. F. Shurvell, D. W. Hyslop, *J. Chem. Phys. 52* (1970) 881; B. Bak, O. Bang, F. Nicolaisen, O. Rump, *Spectrochim. Acta Part A 27* (1971) 1865; c) UV spectroscopy: [29].

[83] For a review on NCN see: O. D. Krough, C. H. Ward, J. M. Hollenbeck, *J. Phys. Chem. 86* (1982) 2892..

[84] F. D. Marsh, M. E. Hermes, *J. Am. Chem. Soc. 87* (1965) 1819; cf. also: M. G. K. Hutchins, D. Swern, *J. Org. Chem. 47* (1982) 4837. Structure: A. A. Almeningen, B. Bak, P. Jansen, T. G. Strand, *Acta Chem. Scand. 27* (1973) 1521.

[85] B. Bak, P. Jansen, *J. Mol. Struct. 12* (1972) 167; J. M. Howell, L. J. Kirschenbaum, *J. Am. Chem. Soc. 98* (1976) 877.

[86] See the reviews by *R. S. Atkinson* or *M. S. Platz* in [10a] and by *D. M. Lemal* in [10d].

[87] a) R_2NN: D. K. McIntyre, P. B. Dervan, *J. Am. Chem. Soc. 104* (1982) 6466, and references cited therein; b) H_2NN: A. P. Sylvester, P. B. Dervan, *ibid. 106* (1984) 4648.

[88] E. Haselbach, E. Heilbronner, *Helv. Chim. Acta 53* (1970) 684, and references cited therein.

[89] See the reviews in [4]. The first preparation of $H_5C_6-N_3$ was carried out by *P. Griess* in 1864 (*Justus Liebigs Ann. Chem. 137* (1866) 39, and references cited therein), that of H_3C-N_3 in 1905 by *O. Dimroth* and *W. Wislicenus* (*Ber. Dtsch. Chem. Ges. 38* (1905) 1573).

[90] L. Birkofer, A. Ritter, P. Richter, *Angew. Chem. 74* (1962) 293; *Chem. Ber. 96* (1963) 2750.

[91] See the reviews: R. M. Pike, N. Sobinski, P. J. McManus, *J. Organomet. Chem. 253* (1983) or those in [4d] and in the references cited therein.

[92] a) For example, $H_3CSi(N_3)_3$ explodes on attempted distillation (see [39] and W. T. Reichle, *Inorg. Chem. 3* (1964) 402); H_3SiN_3 decomposes below room temperature with the formation of SiH_4 (cf. W. R. Peterson Jr., *Rev. Silicon, Germanium, Tin, Lead Compd. 1* (1974) 206); see also [95a]. b) For closely related compounds the decomposition point determined under comparable conditions can differ by more than 200 K: thus N_2-extrusion from $(H_3C)_3SiN_3$ in the gas phase starts at 950 K [23], that from $(H_3C)_3CN_3$ at 720 K (Fig. 7).

[93] In spite of the relatively short SiN bond distance, which is 147 pm in $(H_3C)_3SiN_3$ (M. Dakkouri, H. Obernhammer, *Z. Naturforsch. A 27* (1972) 1331), the SiN stretch force constant of the SiN bond is not increased (H. Bürger, *Monatsh. Chem. 96* (1965) 1710). Furthermore, $(H_3C)_3SiN_3$ shows a bond angle $\sphericalangle$SiNN of 128° and, in contrast to H_3SiNCO, also H_3SiN_3 is non-linear (E. A. V. Ebsworth, M. J. Mays, *J. Chem. Soc. 1964*, 3450).

[94] Using the MNDO approximation, the following reaction enthalpies ΔH_{MNDO} (kJ/mol) for the reaction $R_3X-N_3 \rightarrow N_2+R_2X=NR$ [23] are estimated: R=H, X=C, −173; R=H, X=Si: +8; $R=CH_3$, X=C: −194; $R=CH_3$, X=Si: +91.

[95] a) *J. F. Ogilvie* and *S. Cradock* (*Chem. Commun. 1966*, 364) obtained the following structural data from IR spectroscopy $d_{NSi}=154$ pm, $d_{HN}=100$ pm and HNSi=180°. b) *J. N. Murrell, H. W. Kroto*, and *M. F. Guest* (*J. Chem. Soc. Chem. Commun. 1977*, 619; cf. also H. W. Kroto, J. N. Murrell, A. Al-Derzi, M. F. Guest, *Astrophys. J. 219* (1978) 886)

calculated HNSi to be 372 kJ/mol more stable than the isomer HSiN. c) On the basis of CI calculations, *R. Preuss, R. J. Buenker,* and *S. D. Peyerimhoff (J. Mol. Struct. 49* (1978) 171) predict the barrier for the rearrangement HSiN→HNSi to be only 55 kJ/mol.

[96] The CNC skeleton in the iso(valence) electronic phenyl isocyanide is linear according to microwave-spectroscopic studies (B. Bak, B. P. van Eijck, C. Kierkegaard, *J. Mol. Struct. 18* (1973) 429); the N=C bond length is only 114.2 pm.

[97] For the isolation of H_5C_6–N≡Si by *G. Gross* and *J. Michl* (University of Utah, Salt Lake City) cf. *Chem. Eng. News 63* (1985) No. 12, p. 31.

[98] a) H. Bock, R. A. Bowling, B. Solouki, T. J. Barton, G. T. Burns, *J. Am. Chem. Soc. 102* (1980) 429; b) B. Solouki, P. Rosmus, H. Bock, G. Maier, *Angew. Chem. 92* (1980) 56; *Angew. Chem. Int. Ed. Engl. 19* (1980) 51; G. Maier, G. Mihm, H. P. Reisenauer, *ibid. 92* (1980) 58 and *19* (1980) 52; c) G. Maier, G. Mihm, H. P. Reisenauer, *ibid. 93* (1981) 615 and *20* (1981) 597; P. Rosmus, H. Bock, B. Solouki, G. Maier, G. Mihm, *ibid. 93* (1981) 616 and *20* (1981) 598; d) A. G. Brook, S. C. Nyberg, F. Abdesaken, B. Gutekunst, G. Gutekunst, R. K. M. R. Kallury, Y. C. Poon, Y. Chang, W. Wong-Ny, *J. Am. Chem. Soc. 104* (1982) 5667; e) R. West, M. Fink, J. Michl, *Science 214* (1981) 1343; S. Masamune, Y. Hanazawa, S. Murakami, T. Bally, J. F. Blount, *J. Am. Chem. Soc. 104* (1982) 1150. f) For other attempts to prepare compounds containing a Si≡Si triple bond see: A. Sekiguchi, S. S. Zigler, R. West, *J. Am. Chem. Soc. 108* (1986) 4241.

[99] Cf. B. T. Luke, J. A. Pople, M. Krogh-Jespersen, Y. Apeloig, M. Karni, J. Chandrasekar, P. von R. Schleyer, *J. Am. Chem. Soc. 108* (1986) 277.

[100] Figure 11 contains the n_N and $\pi_{C=N}$ ionization energies of 14 of the 41 simple imines and azomethines which have been studied [23]; the literature references refer to PE spectra already published. F_2C=NF was provided by D. D. DesMarteau [69], F_2C=N–CF_3 by D. Lentz (Freie Universität Berlin). PE spectra of alkyl-substituted azabutadienes and higher alkylated "methanimines" are reported in Ph. D. theses by *M. Beez* and *H. Bergmann* (Universität Frankfurt 1971 and 1972).

[101] R. Dammel, H. Bock, J. M. Denis, *Chem. Phys. Lett. 102* (1983) 239.

[102] C. R. Brundle, M. B. Robin, N. A. Kuebler, H. Basch, *J. Am. Chem. Soc. 94* (1972) 1452.

[103] a) 2,3-Dihydroazete ("1-azetine"); J. C. Guillemin, J. M. Denis, A. Lablache-Combier, *J. Am. Chem. Soc. 103* (1981) 468; b) imines R_2C=NH: J. C. Guillemin, J. M. Denis, *Angew. Chem. 94* (1982) 715; *Angew. Chem. Int. Ed. Engl. 21* (1982) 690; *Angew. Chem. Suppl. 1982,* 1515; *Tetrahedron Lett. 27* (1986) 1147; *J. Chem. Soc. Chem. Commun. 1985,* 951, 1131; c) H_2C=NH: [22]; d) H_2C=C=NH: [38]; e) cf. also J. C. Guillemin, J. M. Denis, M. Bogey, J. L. Destombes, *Tetrahedron Lett. 27* (1986) 1147.

[104] Cf. H. Bock, B. Solouki, S. Aygen, G. Brähler, R. Dammel, J. Giordan, P. Hänel, H. Herrmann, B. Hierholzer, T. Hirabayashi, D. Jaculi, W. Kaim, U. Lechner-Knoblauch, S. Mohmand, H. Müller, P. Rittmeyer, B. Roth, U. Stein ("Kurzlebige Moleküle, Einelektronentransfer-Reaktionen und Ionenpaar-Wechselwirkungen"), *Nova Acta Leopoldina, Neue Folge 59* (1985) 102.

[105] The PE-spectroscopic optimisation of the gas phase synthesis of imines shall be exemplified here for the parent compound H_2C=NH; details are given in [23]: H_3CNH_2 is drawn at 10^{-2} mbar by the pump of the spectrometer into the horizontal reaction tube, the first part of which is half-filled with *N*-chlorosuccinimide (Fig. 16). The resulting H_3CNH_2/H_3CNCl_2 mixture is analyzed using the known ionization patterns (cf. E. Nagy-Felsobuki, J. B. Peel, *J. Chem. Soc. Faraday Trans. 2 74* (1978) 1927). After extensive optimization of the reaction parameters we obtained, at room temperature and with 18 cm length of *N*-chlorosuccinimide-filling, almost exclusively H_3CNHCl. This compound, which may explode on liquefaction, should therefore preferably not be isolated in a pure form. Next, the second part of the tube, which can be heated separately, is half-filled under argon with $KOC(CH_3)_3$. On starting the methylamine gas flow, the oven temperature is increased continuously until the band pattern of pure methanimine is recorded: optimal conditions are 350 K and a KOR zone 40 cm in length. After the removal of *tert*-butanol at 185 K, H_2C=NH may be frozen out in a 77 K cold trap; it contains PE-spectroscopically detectable traces of NH_3. Cf. also [62].

[106] I. Stolkin, T. K. Ha, H. H. Günthard, *Chem. Phys. 21* (1977) 327.

[107] For the production of imines by retro-trimerization of hexahydro-*s*-triazines and their PE-spectroscopic detection see D. C. Frost, B. McDonald, C. A. McDowell, N. P. C. Westwood, *J. Electron Spectrosc. Relat. Phenom. 14* (1978) 379. For H_2C=N–CH_3 cf. also: J. Demaison, J. Burie, J. M. Denis, B. P. van Eijck, *J. Mol. Spectrosc. 107* (1984) 250, [106] and references cited therein.

[108] D. Lentz, H. Oberhammer, *Inorg. Chem. 24* (1985) 4665, and references cited therein.

[109] K. O. Christe, C. J. Schack, *Inorg. Chem. 20* (1981) 2566; C. J. Schack, K. O. Christe, *ibid. 22* (1983) 33, and references cited therein.

[110] The MNDO calculation procedure and its parametrization is described by M. J. S. Dewar, W. Thiel, *J. Am. Chem. Soc. 99* (1977) 4899; we thank Prof. *Dewar* for providing us with the MNDO and MOPAC programme packages. SCF/CI calculations were performed using a MCI/MNDO method (B. Roth, *Dissertation,* Universität Frankfurt 1983). MNDO results for certain classes of molecules with the following elements a) H, C, N, O; M. J. S. Dewar, W. Thiel, *J. Am. Chem. Soc. 99* (1977) 4970; b) F; M. J. S. Dewar, H. S. Rzepa, *ibid. 100* (1978) 58; c) Si: M. J. S. Dewar, M. L. McKee, H. S. Rzepa, *ibid. 100* (1978) 3607 illustrate the scope and limitations of this method, which has proven especially valuable in the assignment of PE spectra [50, 55].

[111] Cf. W. Kutzelnigg: *Einführung in die Theoretischen Chemie, Vol. 1,* Verlag Chemie, Weinheim 1975, p. 213 f.

[112] Singlet methylnitrene rearranges rather rapidly even in a 4 K inert gas matrix [11, 13], and H_3CN-insertion into other bonds is neither observed during thermal nor during photolytic methyl azide decomposition [10a, d]. If the rearrangement H_3CN→H_2C=NH were to occur on a triplet energy hypersurface, singlet methylnitrene should have such a long lifetime because of the spin-forbidden transition $\tilde{A}(^1E)$→$\tilde{X}(^3A_2)$ that it ought to be chemically detectable. In addition, a triplet rearrangement would lead to triplet methanimine, the ground state of which lies above that of methylnitrene [12].

[113] W. F. Salathiel, R. F. Curt Jr., *J. Chem. Phys. 44* (1966) 1288.

[114] According to the Hammond criteria (H. S. Hammond, *J. Am. Chem. Soc. 77* (1955) 1288); cf. the transition states of exothermic reactions should be similar to the starting materials and those of endothermic reactions product-like.

[115] See also: K. M. Müller, *Angew. Chem. 92* (1980) 1; *Angew. Chem. Int. Ed. Engl. 19* (1980) 1. We thank Dr. Müller for his help in the preparation of the SPLOC programme developed in cooperation with Dr. *B. Roth* (*Dissertation,* Universität Frankfurt 1983) using his saddle point location algorithm.

[116] On the basis of our studies [25], *L. L. Lohr* and *K. Morokama* (*J. Am. Chem. Soc. 105* (1983) 5541) have carried out ab initio SCF calculations with a "double zeta + polarization functions" basis set; in the main their results confirm the conclusions from the MNDO energy hypersurfaces. In addition, they suggested H_3C–NC as a further intermediate, which, however, cannot be detected PE spectroscopically during the gas phase pyrolysis of vinyl azide [23, 25].

[117] R. G. Ford, *J. Am. Chem. Soc. 99* (1977) 2389.

[118] The following activation parameters have been measured for the decomposition of substituted vinyl azides in solution: $\Delta H^{\neq}$ = 100–200 kJ/mol and $\Delta S^{\neq}$ = −12 to −30 J mol^{-1} K^{-1} [63]. Higher values for $\Delta H^{\neq}$ (see, e.g., Fig. 19) and in particular positive entropies of activation are to be expected for reactions involving free nitrenes. The negative $\Delta S^{\neq}$-values observed are commensurable with a sterically demanding transition state involving synchronous N_2-elimination and 1,2-R migration.

[119] The formation of 4*H*-1,2,3-triazoles observed when substituted vinyl azides undergo base-catalyzed decomposition in solution (J. S. Meek, J. S. Fowler, *J. Org. Chem. 33* (1968) 985, cf. also [63] and L. A. Burke, G. Leroy, M. T. Nguyen, M. Sana, *J. Am. Chem. Soc. 100* (1978) 3668) is less probable for a gas-phase reaction: according to MNDO calculations [23], the bending of an NNN group requires a considerable amount of energy; in addition, 4*H*-1,2,3-triazole lacks the stabilization by cyclic 6-electron delocalization of the 1*H*-tautomer.

[120] Cf. e.g.: W. L. Hase ("Overview of Unimolecular Dynamics") in D. G. Truhlar (Ed.): *Potential Energy Surfaces and Dynamics Calculations,* Plenum Press, New York 1981, p. 1 f, and references cited therein.

[121] See for example the section on "Chemical Activation" in C. Wentrup: *Reactive Molecules,* Wiley, New York 1984, p. 225 ff, and references cited therein.

The Development of Bioglass Ceramics for Medical Applications

By Werner Vogel* and Wolfram Höland

The enormous progress made in the field of medicine over the past few decades has been partly due to the introduction of new instruments but also a result of the use of new materials. It is impossible to imagine modern medicine without metals, alloys, sintered corundum, organic high polymers (also as composite materials), glassy carbon, etc. Bioglass ceramics open up new possibilities for medical treatment and constitute a new area of research in the natural sciences and medicine. Owing to their widely variable combinations of properties, bioglass ceramics can be more easily adapted to suit medical requirements than can customary implants. Two properties of bioglass ceramics are of primary importance: their biocompatibility, i.e., acceptance of the material by the tissues of the human body without irritation, rejection reactions, or toxic effects; and their bioactivity, i.e., the ability to establish firm intergrowths with tissues of the human body. This property is not shared by any of the classical biomaterials. A wide range of applications is envisaged for the bioglass ceramics that have so far been developed; some are still undergoing animal tests while others are being clinically tested in humans. Possible applications are the replacement of vertebrae and use in the middle ear, throat, nose, and eye, in the entire head region, in the shoulder and leg, and in dental prosthetics, in particular the replacement of dental roots (a hard tissue substitute in the broadest sense of the word). The question as to the behavior of a bone/bioglass ceramic contact or bond on a long-term scale and on being exposed to varying mechanical stress has still not been satisfactorily answered, because interdisciplinary research in this field is still immature. All observations made so far indicate, however, that the materials do not cause any adverse effects.

1. Introduction

The development of new materials for bone implants and substitutes in man has gained major importance over the past five to ten years. In addition to metals, sintered corundum, and organic polymers, bioglasses and bioglass ceramics have come especially to the fore. These new implant materials are not only biocompatible, like the other customary materials, but are also bioactive. They are not regarded as foreign bodies and encapsulated by living bone tissue; instead, direct intergrowth takes place. The special combinations of properties required by medicine can be more easily adjusted and varied in bioglasses and bioglass ceramics than in metals, sintered corundum, or organic polymers. Moreover, bioglasses and bioglass ceramics can be more easily adapted to the natural composition of bone, which obviously adds greatly to their bioactivity and their compatibility with living human tissue. It should be mentioned at this point that some of the uses of these new materials in medicine extend considerably beyond mere bone replacement.

2. Conditions for Controlled Crystallization in Glass as the Basis for the Systematic Development of Glass Ceramics

A review article was published in this journal in 1965 concerning the "Structure and Crystallization Behavior of Glasses."[1] Subsequent studies, which considerably extended these earlier findings, have since been reviewed.[2, 3] They have provided a reliable basis for the development of a large number of new optical and technical glasses, for overcoming disturbances in glass production, and for the development of several families of new glass ceramics with widely differing properties and combinations of properties.

It can be demonstrated experimentally that most phase separations that occur when glass melts solidify to form a solid body produce a microheterogeneous structure. In the simplest case, a droplet-shaped microglass phase is incorporated in a matrix glass phase with a different composition. The resultant microglass phases are not the product of statistical variations in composition; they tend instead to assume a composition corresponding to that of defined, stable chemical compounds—the extent to which this is achieved depends on the degree of undercooling of the melt. Phase separation can be controlled in a multitude of ways and represents the key to the developments cited above. Figure 1a shows a typical example of a phase-separated glass with a microheterogeneous structure.

The reason for phase separation is presumably the presence of at least two different building groups with extremely different volume requirements. This phase separation entails considerable consequences for the crystallization behavior of a glass. (For a theoretical treatment of phase-separation phenomena in glasses, see Ref. [3].)

The theoretical basis for homogeneous nucleation is given by Volmer's equation [Eq. (1)], which states that the nucleation rate I depends primarily on the enthalpy of activation required to attain the critical nuclear size.

[*] Prof. Dr. W. Vogel, Dr. W. Höland
Otto-Schott-Institut der Sektion Chemie der Universität
Fraunhoferstrasse 6, 6900 Jena (GDR)

 © VCH Verlagsgesellschaft mbH, D-6940 Weinheim, 1987 0570-0833/87/0606-0527 $ 02.50/0

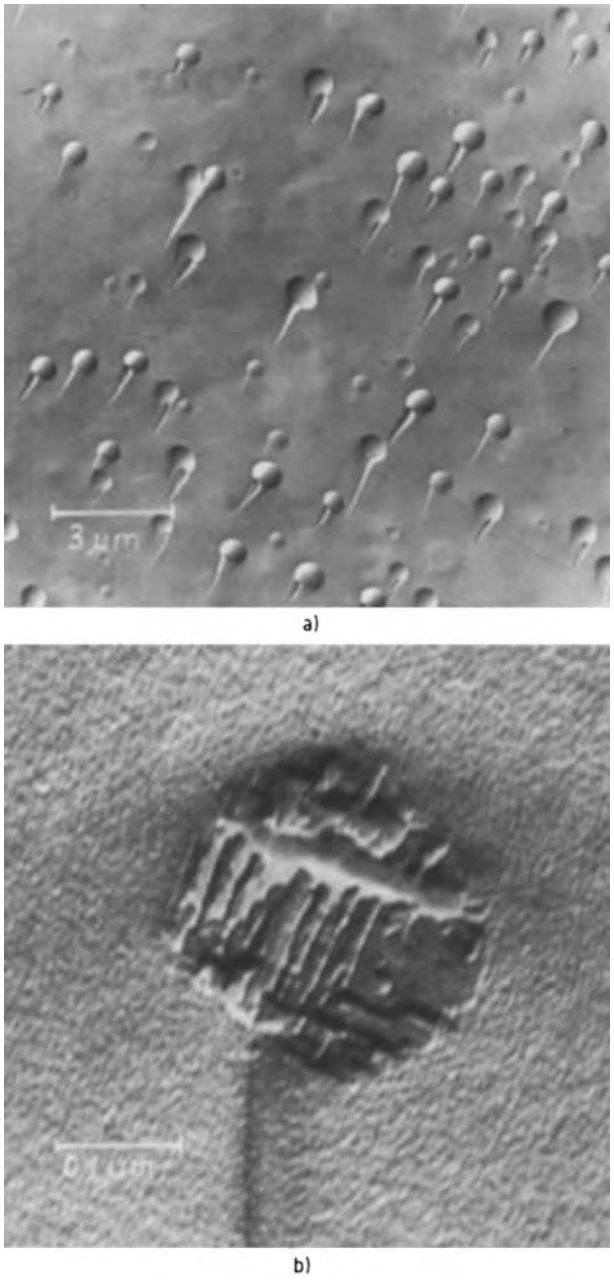

Fig. 1. a) Typical immiscibility phenomena in a silicate glass. Replica electron micrograph of a glass fracture surface prepared in a high vacuum. The droplets with their "fracture flags" are incorporated in a matrix glass phase of different composition. b) The start of nucleation within the droplet region (replica electron micrograph).

$$I = A \cdot e^{-\frac{(\Delta G^* + \Delta G_D)}{k \cdot T}} \quad (1)$$

A = constant
ΔG^* = enthalpy of activation for reaching the critical nuclear size
ΔG_D = enthalpy of diffusion
k = Boltzmann's constant
T = temperature

The enthalpy of activation consists of two terms ($\Delta G^* + \Delta G_D$). The total activation energy decreases by the amount ΔG_D if the building blocks of the nucleus are already present at the nucleation site. This is the case when phase-separated base glasses are induced to nucleate and crystallize (Fig. 1b). Since the composition of the droplet regions closely approaches that of defined, stable chemical compounds, nucleation begins simultaneously in all of the droplets. The number and size of the resulting crystals can accordingly be varied by controlling phase-separation phenomena in the glass. As is shown in Figure 1b, growth of the crystallite front is stopped when it reaches the droplet phase boundary; i.e., even if nucleation happens to be delayed in one or other of the droplets, the sizes of the crystals will be comparable because growth of the nuclei stops at the droplet boundary. The following main criteria must be satisfied for controlled crystallization in glass: the starting conditions for nucleation should be uniform at an infinite number of equally distributed sites within the total volume of glass and the final product should contain equal-sized crystallites with very small dimensions (usually only a few micrometers).

Heterogeneous nucleation (i.e., nucleation in the presence of a foreign nucleus) is described by Turnbull's relation [Eq. (2)]. Foreign nuclei can be produced in glass in a

$$I = A' \cdot e^{-\frac{(\Delta G^* \cdot f(\theta) + \Delta G_D)}{k \cdot T}} \quad (2)$$

variety of ways. If at least two of their lattice constants do not differ from those of the desired crystalline phase by more than $\pm 15\%$ (or a multiple of the lattice constants of the desired crystalline phase), epitaxial interactions can occur. In other words, the foreign nucleus that has become capable of growth can continue to grow with an unrelated substance, i.e., with the molecular building groups of the desired crystalline phase, which, for example, may be located in the droplets. This also accounts for the fact that it is often very difficult or even impossible to demonstrate and unequivocally identify the heteronuclei in cases of epitaxial interaction. Epitaxy further decreases the necessary critical enthalpy of activation for nucleation, ΔG^*, by a function of θ, $f(\theta)$. It is a function of the measurable contact angle θ between the foreign nucleus and the melt from which the main crystalline phase is to be formed. The contact angle reflects the strength of the epitaxial interaction. If deposition occurs, this function is always less than 1, which means that nucleation and crystallization proceed much more quickly than without a foreign nucleus. The action of foreign nuclei can to some extent be compared with that of initiators.

3. Development of Bioglass Ceramics—Present Status, Requirements, and Our Own Goals

Important advances have been made in the field of medicine as a result of developments generally involving the use of phosphosilicate glasses (which are closely related to the apatite-rich bone substance) to form coatings and thin films on implant materials such as metals and sintered corundum.[4–6] Thin glass films have also been employed which, in some cases, have been converted into crystalline apatite by tempering. These bone-related glasses and glassy crystalline films exhibit relatively good bioactivities and bonding with the bone tissue. As a rule, however, thin films ultimately dissolve and thus become useless. This behavior has been exploited for different purposes to de-

velop completely reabsorbable glasses and glass ceramics.[7-9] Another approach was to develop sintered ceramics as solid materials, usually sintered products consisting of crystalline apatite.[10] Powdered phosphate glasses in which crystalline apatite is formed by tempering have also been used as sintered products.[11, 12] The resulting properties were then further modified by sintering mixtures of a phosphate glass powder and a silicate glass powder in which crystalline silicates such as wollastonite or devitrite separate out.[13, 14] The products obtained are porous and of variable bioactivity, depending on their apatite content, and can be worked to a limited extent with tools made of hard metals. Their porosity and relatively poor mechanical strength, however, often prove to be serious disadvantages.

An important advance was made when glassy crystalline products were obtained by tempering solid glasses.

The first important step toward the formation of a solid bond between inorganic materials and bone was taken by *Hench* et al. with the preparation of glass films and partially crystalline glasses.[15, 16] Their base glass had the following composition [wt%]:

SiO_2	45	CaO	24.5
Na_2O	24.5	P_2O_5	6.0

In the 1970s, the development of the so-called ceravital material (which is based on the base glass system SiO_2-Na_2O-CaO-$Ca_3(PO_3)_2$-MgO-K_2O-CaF_2) led to a significant improvement in chemical stability and thus opened up the way for new applications.[17, 18] More recent developments, which are essentially all based on the above base glass system, have brought about further advances.[19-21] Extensive studies, especially on different possible applications, revealed that the bioactivity of these materials was good but that the bonding zone between the bone (or other tissue) and the glassy crystalline material broadened owing to the relatively high solubility of the latter; moreover, this process did not come to a standstill on prolonged contact of the material with the bone. This means that there is a risk that the implant will become loose if the bonding zone is subjected to mechanical stress. The bonding is adequate, however, for other types of applications. The main crystalline phases of the new materials cited are apatite ($Ca_5[F/(PO_4)_3]$), wollastonite ($Ca_3[Si_3O_9]$), and/or devitrite ($Na_2O \cdot 3\,CaO \cdot 6\,SiO_2$).

The authors' own aim has been to develop bioglass ceramics with novel properties by using available knowledge about the microprocesses occurring on solidification of a glass melt and during conversion of a glass to a glass ceramic by means of controlled crystallization. The requirements of our meanwhile large number of medical collaborators vary widely; it thus seems likely that a series of bioglass materials will be developed that is to a certain degree comparable with the range of stainless steels now available for various applications. The properties primarily required are:

- complete biocompatibility or
- maximum bioactivity with maximum mechanical strength,

a high degree of chemical resistance, especially against body fluids, and
good machinability, ideally carried out by the surgeon.

Good biocompatibility means, for example, that cell compatibility tests, both in vitro and in vivo, do not indicate the occurrence of defense reactions or toxic effects and that direct contact is established with the bone without the formation of connective tissue. Bioactivity is understood to be the ability of the implant to stimulate the tissue to form a true biochemical bond with it after a limited period of dissolution and ion exchange.

4. Development of Biocompatible, Machinable Glass Ceramics

4.1. Machinable Glass Ceramics from the System Na_2O-MgO-Al_2O_3-SiO_2-F with Flat, Flake-Shaped Mica Crystals[22]

A glass ceramic is defined as being machinable if it can be turned, milled, drilled, or threaded with metal-working tools (primarily those made of hard metals) without causing the workpiece to fracture as is the case with ordinary ceramics. The test devised to compare machinability involves measuring the time required for a hard-metal drill to penetrate to a specified depth under otherwise identical conditions.

The development made by *Beall* and *Grossmann* et al.[23-25] in the early 1970s entails the controlled separation of mica crystals in a given base glass. In order to ensure good machinability the crystals should be of optimal size, should be in mutual contact, and should account for about two-thirds of the total volume of the ceramic.[3]

Figure 2 shows a typical example of this type of material developed by our group. A standard base glass (15.5 mol%

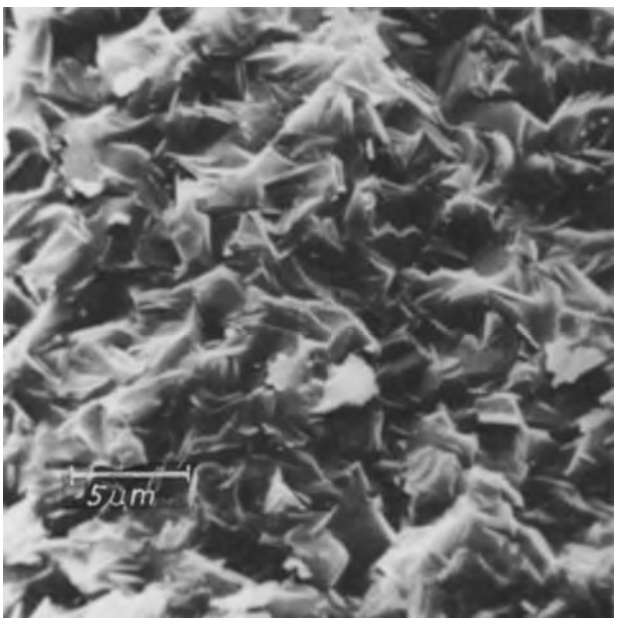

Fig. 2. Flat sodium phlogopite mica crystals arranged like a "card house" in a machinable glass ceramic (scanning electron micrograph).

MgO, 12.6 mol% Al_2O_3, and 71.9 mol% SiO_2) was used in which 11.2 mol% of the oxygen ions were replaced by fluoride ions and which was additionally doped with 5.2 mol% sodium oxide. By controlled phase separation of the base glass, sodium phlogopite crystals ($Na_{0.5-1}Mg_3[AlSi_3O_{10}F_2]$), a type of mica, were made to separate out in a specific fashion in accordance with the given requirements.[26,27]

The machinability is based on the fact that the microfractures produced by machining occur preferentially along the (001) plane of the mica crystals (see Fig. 3). Since the crystals are in mutual contact, the microfractures readily propagate to neighboring crystals. The material can thus be worked without shattering. The (001) plane of the mica crystal is the preferred direction of fracture owing to the presence of alkali ions (see Fig. 4), which loosely connect two triple-layer packets.

This ceramic, developed for special applications in scientific instruments and mechanical engineering, is also biocompatible and can be used in a variety of ways in medicine. Its physical properties are listed in Table 1.

Table 1. Properties of the machinable glass ceramic containing flat fluorophlogopite mica crystals. Composition [mol%]: Na_2O 3–15, MgO 7–23, Al_2O_3 10–30, SiO_2 45–70, F 3–6 [22].

Densitiy	2.5 g/cm³
Linear coefficient of thermal expansion (20–400 °C)	75×10^{-7} K^{-1}
Mechanical flex-cracking resistance	90 MPa
Modulus of elasticity	50 GPa
Pressure resistance	450 MPa
Shock resistance	2.0 kN/m
Hydrolytic class	1–2
Acid class	3
Alkali class	1–3
Roughness height after polishing	0.15 μm
Machinability	Very good

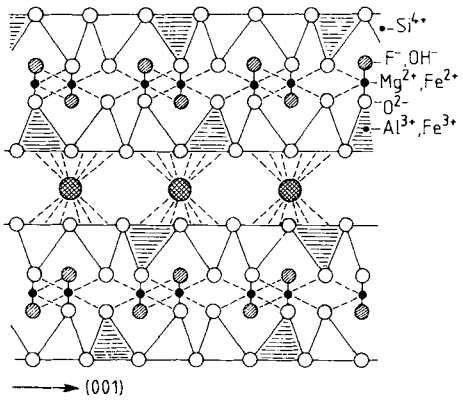

Fig. 3. Schematic representation of the structure of phlogopite. Triangles, $[SiO_4]$ tetrahedra; hatched triangles, $[AlO_4]$ tetrahedra; ⊗, K^+ or Na^+; ○, O^{2-}; ◎, F^-; ●, Mg^{2+}. F^- can be replaced by OH^-, Mg^{2+} by Fe^{2+}, Al^{3+} by Fe^{3+}, and K^+ by Na^+.

4.2. Glass Ceramic with Maximum Machinability from the System Na_2O/K_2O-MgO-Al_2O_3-SiO_2-F with Curved Mica Crystals[28,29]

A previously unknown mica phase could be induced to separate in a different standard base glass (21.2 mol% MgO, 19.5 mol% Al_2O_3, 59.3 mol% SiO_2) after doping with 11.2 mol% F^- and 6.4 mol% Na_2O/K_2O. Here, the mica crystals do not occur as flat flakes but as cabbagelike aggregations of curved "leaves" (see Fig. 4). Comparison of the Mg and Al peaks in the X-ray spectra obtained by energy-dispersive electron-beam microanalysis (EDAX)[30] (see Fig. 5) revealed that the Al concentration in the curved mica crystals is higher than that in the flat crystals. Increasing the total (Al_2O_3 + MgO) content of the glass relative to the SiO_2 content results in replacement of part of the Mg^{2+} ions by Al^{3+} ions (1.5 Mg^{2+} correspond to 1 Al^{3+}) in the new mica crystal. As a result, stresses develop

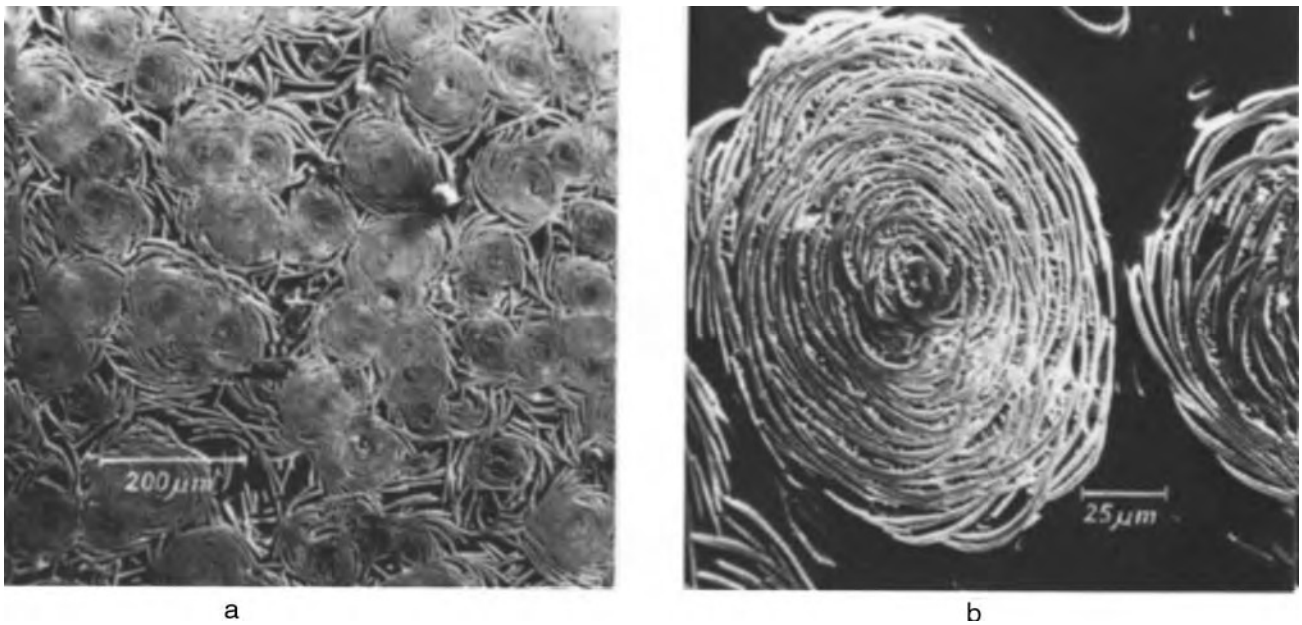

Fig. 4. a) Fluorophlogopite mica crystals in a new configuration. The mica flakes occur in the form of spherically arranged lamellae (cabbagelike). b) A single spherical aggregate (scanning electron micrograph).

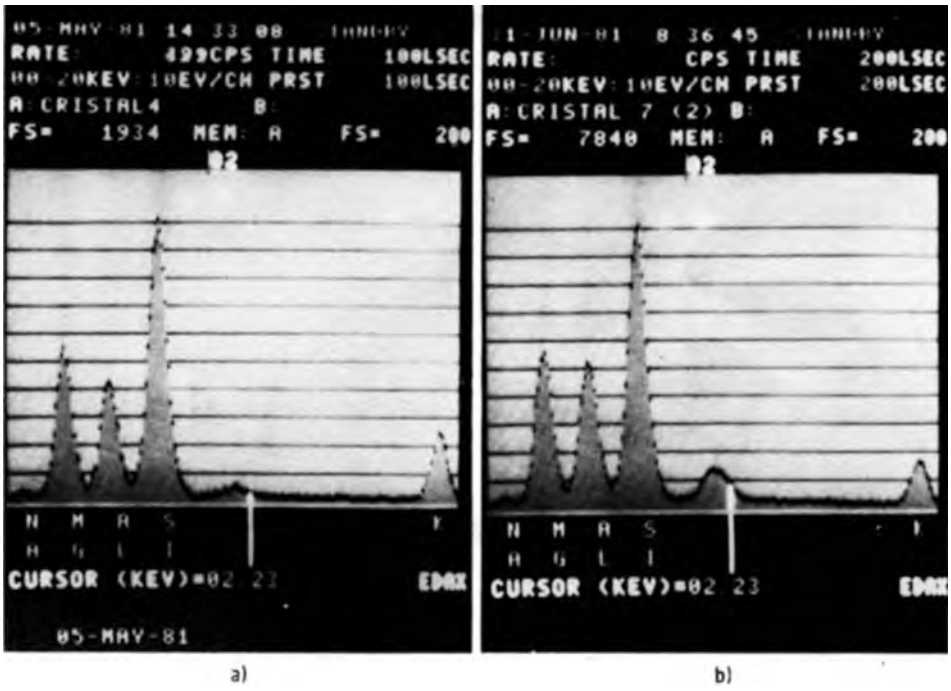

a) b)

Fig. 5. a) EDAX spectra of flat fluorophlogopite mica crystals. Mass ratio Al/Si = 0.43, Mg/Si = 0.71. b) EDAX spectra of curved fluorophlogopite mica crystals. Mass ratio Al/Si = 0.51, Mg/Si = 0.63.

in the octahedron layer of the mica structure, which cause the crystal to bend. This state is also reflected in the change of the dioctahedron–trioctahedron character of the crystals as shown by X-ray diffraction. If the $(MgO + Al_2O_3)$ concentration of the base glass were further increased, cordierite crystals ($Mg_2Al_3[AlSi_5O_{18}]$) would be formed. The $[AlO_{4/2}]$ groups of cordierite are stabilized by Mg^{2+} ions. The machinability of the glass ceramic containing curved mica crystals is four to five times better[28,29] than that of the glass ceramic with flat mica flakes described in Section 4.1.

This machinable glass ceramic is once again biocompatible and is suitable for many medical applications. Its main properties are compiled in Table 2.

Table 2. Properties of the best machinable glass ceramic containing curved fluorophlogopite mica crystals. Composition [mol%]: M_2O 5-12 (Na_2O 0-8, K_2O 0-6), MgO 8-17, Al_2O_3 21-36, SiO_2 34-60, F 1-7 [29].

Linear coefficient of thermal expansion (20-400 °C)	$50-75 \times 10^{-7}\ K^{-1}$
Mechanical flex-cracking resistance	Up to 110 MPa
Hydrolytic class	1-2
Alkali class	1-3
Machinability	Excellent

4.3. Machinable Glass Ceramic from the System Na_2O/K_2O-MgO-Al_2O_3-SiO_2-F with both Mica and Cordierite Crystals[31]

Machinable glass ceramics that only contain mica crystals have already been described. Glass ceramics containing solely cordierite crystals ($Mg_2Al_3[AlSi_5O_{18}]$) are also known.[26] The mechanical strength and fracture toughness of these materials are particularly high. Mica and cordierite crystals can be made to separate out simultaneously in specifically modified base glasses by means of controlled phase separation as described in Section 4.2. Glasses of the following composition were used [wt%]:

SiO_2	43-50	F^-	3.3-4.8
Al_2O_3	26-30	Cl^-	0.01-0.6
MgO	11-15	CaO	0.1-3
Na_2O/K_2O	7-10.5	P_2O_5	0.1-5

The glass ceramics thus obtained exhibited a combination of advantageous properties—good machinability, high mechanical strength, and high fracture toughess. This material is suitable for a wide range of uses in dentistry owing to these properties and because it is totally biocompatible, can readily be polished, has a very low roughness height, can be colored, etc.

Figure 6a shows a typical cordierite crystallite in a technical glass as a glass defect; cordierite-mica crystallization in the new glass ceramic described above is shown in Figure 6b for comparison. The close correlations (transition from the curved phlogopite crystal to the cordierite crystal) are clearly revealed in the figure.

The most outstanding properties of the biocompatible, machinable mica-cordierite glass ceramic are compiled in Table 3.

The three types of glass ceramics described above (see Tables 1-3) and other subtypes that satisfy special requirements can be used as biocompatible materials in science, technology, and medicine.

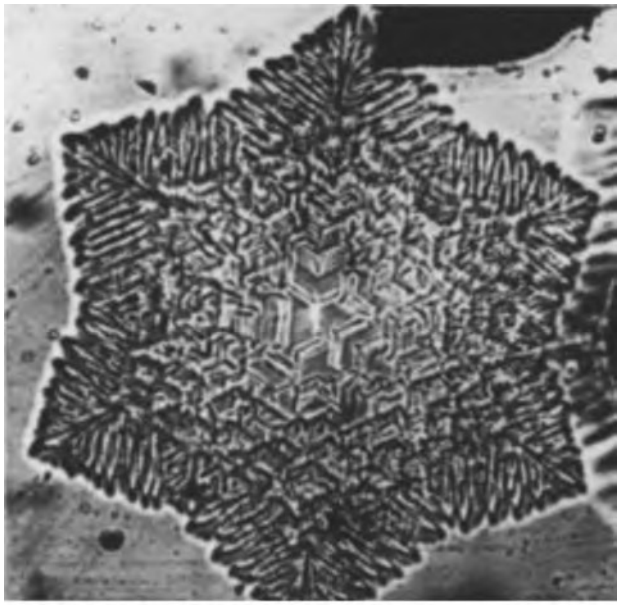

a

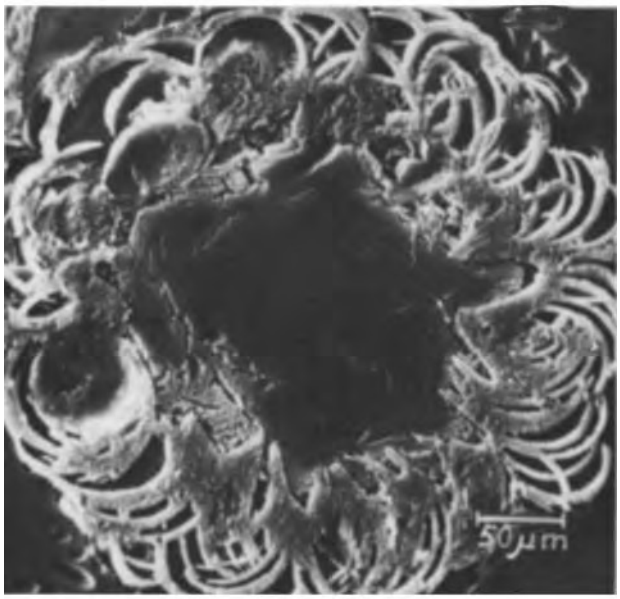

b

Fig. 6. a) Cordierite crystal as a defect in a technical glass (optical photomicrograph). b) Cordierite crystal in the new machinable glass ceramic that still has curved phlogopite mica crystals (scanning electron micrograph).

Table 3. Properties of the machinable mica (phlogopite)/cordierte glass ceramic.

Density	2.5 g/cm^3
Linear coefficient of thermal expansion (20-400°C)	75-125 × 10^{-7} K^{-1}
Mechanical flex-cracking resistance	90-140 MPa
Modulus of elasticity	70 GPa
Pressure resistance	450 MPa
Fracture toughness K_{Ic}	Up to 1.9 Pa·m$^{1/2}$
Vicker's hardness	Up to 8000 MPa
Hydrolytic class	1-2
Acid class	3
Alkali class	1
Roughness height after polishing	0.1 µm
Machinability	Good to very good

5. Development of Bioactive Glass Ceramics

5.1. Machinable, Bioactive Glass Ceramics and the Kinetic Processes Involved in Their Production[32,33]

The glass ceramics described in Section 4 have proved to be biocompatible and do not disturb living cells. An implant material is generally bioactive if it contains apatite crystals, i.e., the natural building substance of bone.[17,18,34] The next logical step, therefore, was to use controlled crystallization to simultaneously segregate both mica (phlogopite) and apatite crystals from a glass melt in variable proportions. In order to understand the procedures used, it should be remembered that controlled phase separation is both the basis of and a prerequisite for almost every controlled crystallization in glass. Phase separation occurs as a result of the formation of stable molecular structural groups and their enrichment in specific regions. As a rule, this considerably facilitates nucleation in the droplet phase since the full amount of the activation energy necessary for a base glass of homogeneous structure is not needed to attain the critical nuclear size. The phase-separation structure of the base glasses in the types of machinable glass ceramics already dealt with has been established. What subsequent steps are required for bioactivity?

5.1.1. CaO and P_2O_5 Doping of the Base Glass from which Fluorophlogopite Mica Crystals Separate Out

When the base glass from which phlogopite crystals separate out is doped with small proportions of CaO/P_2O_5, its phase-separation structure does not change. Figure 7a shows a silicate droplet phase in which Mg, Al, alkali metal, and fluoride ions along with silicic acid are enriched;

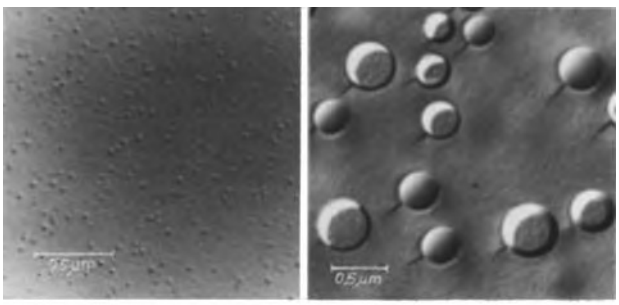

a) b)

Fig. 7. a) Phase-separation structure of the low CaO/P_2O_5-doped base glass after rapid undercooling. Small silicate droplets. b) Phase-separation structure of the high CaO/P_2O_5-doped base glass. Large phosphate droplets. The small silicate droplets have disappeared (replica electron micrograph).

the matrix phase, on the other hand, is very rich in SiO_2. Doping the same base glass with high proportions of CaO/P_2O_5 changes its phase separation behavior fundamentally. The silicate droplet phase disappears. Instead, relatively large droplet regions rich in P_2O_5 are formed in the silicate matrix phase (see Fig. 7b). If the two CaO/P_2O_5-doped base glasses are subjected to specific thermal treatment, only the familiar flat phlogopite crystal flakes and not apatite will separate out from the low CaO/P_2O_5-doped glass.

On the other hand, only apatite separates out from the high CaO/P_2O_5-doped glass; phlogopite crystals do not separate out simultaneously. This apparently negative result is due to the different phase-separation kinetics of the two doped base glasses (see Fig. 8).

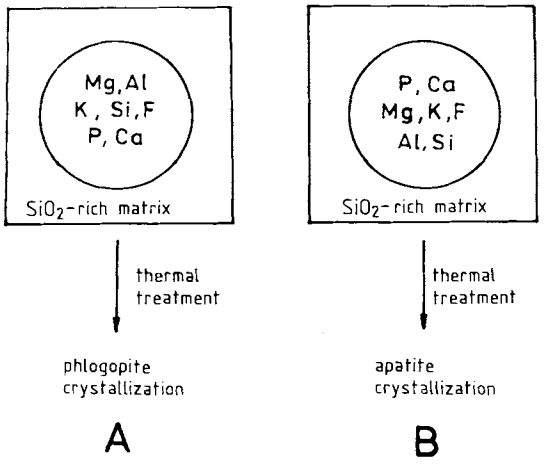

Fig. 8. Schematic representation of phase separation and crystallization kinetics in the glasses shown in Fig. 7.

In case A, most of the low CaO/P_2O_5 content is taken up homogeneously by the droplet phase without fundamental alteration of the familiar crystallization behavior. In case B, where CaO/P_2O_5 doping is high, a pure phosphate droplet phase enriched with Ca^{2+}, Mg^{2+}, Al^{3+}, K^+/Na^+, and F^- is formed in the solidified base glass. The P^{5+} ion has a higher field strength (z/a^2, where z is the valency and a is the distance between the anion and the cation) than the Si^{4+} ion (2.1 and 1.57, respectively); the P^{5+} ion therefore has a greater shielding tendency. A large proportion of the Mg^{2+}, Al^{3+}, and alkali-metal ions are consequently removed from the original silicatic droplet phase so that it disappears in favor of the phosphate droplet phase.

This process is promoted by increasing the fluorine content of the base glass because of a pronounced reduction of viscosity. If this base glass is tempered, only apatite crystallizes. The conditions required for simultaneous separation of phlogopite have been lost.

5.1.2. CaO (10–19 mol%) and P_2O_5 (2–9 mol%) Doping of the Base Glass from which Spherical, Lamellar Aggregates of Phlogopite Crystals Separate Out

Doping a base glass having a high Mg^{2+} and Al^{3+} ion content (see Section 4.2) with CaO and P_2O_5 primarily yields a three-phase glass (see Fig. 9a). Two droplet phases with different dimensions and compositions are embedded in a matrix glass phase that is very rich in SiO_2.

The large droplets constitute a phosphate phase that is enriched with MgO, Al_2O_3, K_2O/Na_2O, and F^-. The small droplets are also rich in MgO, Al_2O_3, Na_2O/K_2O, and F^- and represent the original silicate separation phase, which thus still coexists with the phosphate droplet phase.

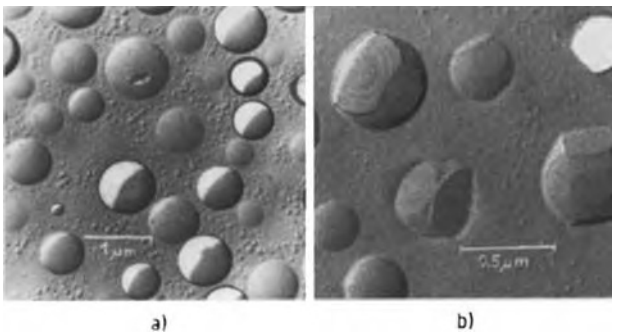

Fig. 9. a) Three-phase base glass. Large phosphate droplets and small silicate droplets coexist. b) The large phosphate droplets start to become transformed into apatite crystals (scanning electron micrograph).

In a standard base glass from which flat mica flakes separate out, the addition of phosphorus causes the formation of a new phosphate droplet phase and the distribution ratio for the Mg^{2+}, Al^{3+}, Ca^{2+}, fluoride, and alkali-metal ions is shifted considerably toward the phosphate phase. The silicate droplet phase disappears.

In the case of a base glass with a high MgO and Al_2O_3 content that separates out spherical, lamellar aggregates of phlogopite mica flakes, the basic aim of doping with CaO/P_2O_5 is to obtain the same change in the distribution of Mg^{2+}, Al^{3+}, fluoride, and alkali-metal ions as is found in the standard base glass. The ratio does not, however, favor the phosphate droplet phase so extremely. Owing to the high MgO and Al_2O_3 content of the base glass, sufficient Mg^{2+}, Al^{3+}, F^-, and alkali-metal ions remain in the original silicate droplet phase so that now both droplet phases can exist side by side (see Fig. 9a).

When this type of three-phase glass is tempered, fluoroapatite is formed in the large phosphate droplets. The small silicate droplets still contain enough Mg^{2+}, Al^{3+}, fluoride, and alkali-metal ions to permit formation of phlogopite mica crystals by reaction with the matrix phase. Since, however, the higher field strength of the P^{5+} ions compared with that of the Si^{4+} ions withdraws Mg^{2+}, Al^{3+}, fluoride, and alkali-metal ions from the silicate droplet phase, the mica crystals no longer separate out as lamellar spheres—they revert to the flat flake form. In Figure 9b, the large P_2O_5-rich droplets are beginning to be transformed into apatite crystals whose faces can already be discerned. Figure 10 shows apatite crystals together with fluorophlogopite crystals. The ratio of apatite to phlogopite crystals and the ratio between the residual glass phase and the crystalline phases can be varied. Although the machinability of the glass ceramic is reduced by the simultaneous formation of apatite crystals along with mica crystals, it is still adequate. A major part of the goal outlined at the outset has thus been successfully accomplished in the form of a base glass with the following composition [mol%]:

SiO_2	19–54	F^-	3–23
Al_2O_3	8–15	CaO	10–34
MgO	2–21	P_2O_5	2–10
Na_2O/K_2O	3–8		

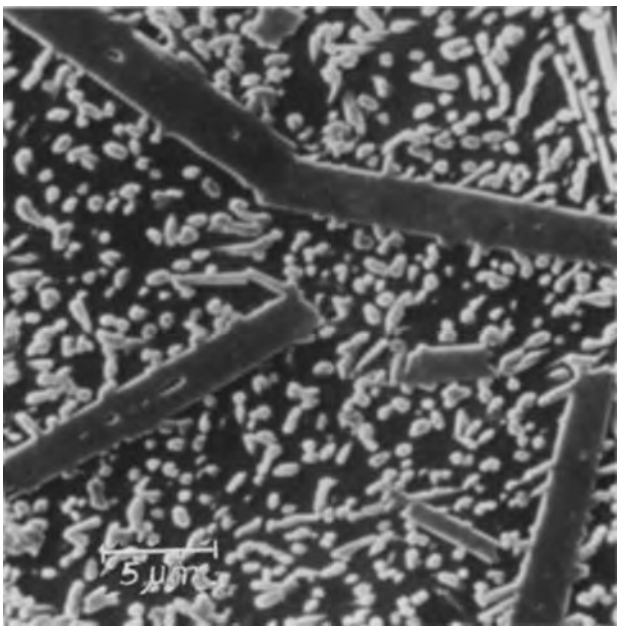

Fig. 10. Bioactive, machinable glass ceramic. Apatite and fluorophlogopite crystals occur side by side in a matrix glass phase (scanning electron micrograph).

5.1.3. Chemical and Mechanical Properties

The behavior of the surfaces of bioglass ceramics toward chemical agents is of particular interest with regard to their possible uses. In the standard water resistance test,[35] the bioglass ceramic optimized for medical applications was found to belong to the "hydrolytic class" 1–2. Machinable glass ceramics with a high apatite content belong to the "hydrolytic class" 2, whereas those with a high phosphate content and a low apatite content are classified in class 3. For comparison, the values for two internationally well-known bioglass ceramics (which are not machinable, however) belong to the "hydrolytic class" 5. The alkali class, determined by standard tests, is 1 and the acid class 3. These two properties are of little significance as far as medicine is concerned, however, because the test conditions are not comparable to those existing in the human body.

"Ringer's solution"[18] is a model liquid that resembles human physiological body fluid; it is an aqueous solution containing Na^+, Ca^{2+}, Cl^-, and CO_3^{2-} ions. Samples of the new machinable bioglass ceramic boiled in Ringer's solution for 40 h had a roughness height of only 0.5 µm. Tests to detect possible increases in the Na^+ and K^+ ion concentrations of the "Ringer solution" due to leaching proved to be negative.

Another highly informative method for determining the release of ions from an implant under quasi-physiological conditions consists in treating the powdered bioglass ceramic with "Tris" buffer solution (2-amino-2-hydroxymethyl-1,3-propanediol–HCl–H_2O mixture). The results of these tests are given in Table 4.

Further studies showed that the release of Na^+ and K^+ ions had almost stopped after 14 days and practically came to a standstill after 4 weeks. As has already been mentioned in Section 5.1.2, the properties of machinable glass ceramics containing apatite crystals can be varied within wide limits by changing the ratio of apatite to mica crystals. The machinability grades determined by a drilling test ranged from "machinable" to "excellently machinable." Mechanical flex-cracking resistance was measured using samples resting on three points; values ranged from 140 MPa for glass ceramics with a low apatite content to 220 MPa for samples with a high apatite content. In order to minimize scattering of the measured values, the surface of the sample under test was systematically damaged prior to measurement; this was done by exposing it to the action of SiC granules in a rotating drum. (For mechanical properties see Table 5.)

Table 4. Ion release in bioactive, machinable glass ceramics during treatment with Tris buffer solutions. Experimental conditions: pH of the buffer solution, 7.4; temperature, 37 °C; 3 g of glass ceramic powder with a particle size of 0.16–0.315 mm; 100 mL of solution; sample was agitated constantly. t = reaction time; the measured ion concentration is given.

Bioglass ceramic	t [h]	Ion concentration [mg/L]		
		Na^+	K^+	Al^{3+}
High apatite content	168	1.0	0.7	—
(apatite 40 vol. %,	336	1.1	0.7	—
phlogopite 20 vol. %)	672	1.8	0.7	—
High phlogopite content	168	1.8	2.1	—
(apatite 20 vol. %,	336	1.9	2.1	—
phlogopite 70 vol. %)	672	2.1	2.1	0.08

Table 5. Mechanical properties of the machinable, bioactive glass ceramic. For composition see Section 5.1.2.

Density	2.8 g/cm³
Linear coefficient of thermal expansion (20–300 °C)	$80–120 \times 10^{-7}\ K^{-1}$
Mechanical flex-cracking resistance	140–220 MPa
Modulus of elasticity	77–88 GPa
Pressure resistance	500 MPa
Fracture toughness K_{Ic}	0.5–1.0 MPa $m^{+1/2}$
Vicker's hardness	Up to 5000 MPa (500 H V 10)

5.1.4. Biocompatibility and Bioactivity

The results of laboratory tests commonly used in medicine such as the INT reduction test, the LDH release test, and, in particular, cell culture experiments were extremely favorable. In the latter case, the materials were added to the cell cultures in the form of a dust at a concentration of 0.4–3.2 mg/mL. Neither the glass ceramic nor the sintered corundum reference substance was found to have any effect on cell multiplication; the glass ceramic must thus be regarded as being completely biocompatible.

The animal experiments performed by *J. Gummel* and *K.-J. Schulze*[32] yielded further results of critical importance. Double implants of a glass ceramic and sintered corundum were made in each experiment; sintered corundum is known to be absolutely biocompatible.

To assess bioactivity, a series of implants were introduced into the tibial heads of guinea pigs. The animals were sacrificed 8, 12, or 16 weeks later or after up to two years, and the tibial heads were removed and subsequently subjected to special tests.

The shearing strength of the implant–bone boundary was determined by measuring the mechanical force necessary to push out the implant cubes. The values found for glass ceramic implants were on average eight times greater than those for the sintered corundum implants. The maximum values were 5 N/mm^2. Moreover, electron microscopic examination revealed that residues of bone adhered to the forcibly removed glass ceramic implants.

Optical and electron micrographs of the ceramic–bone bond provided further interesting insights. Figure 11 shows an optical photomicrograph revealing the direct bond between the bone and the glass ceramic. It can be seen that the alizarin-stained bone substance grows directly into the glass ceramic implant after only eight weeks. Furthermore, bone cells and a blood vessel are found in the immediate vicinity of the implant. Optimal bioactivity has thus been achieved.

Figure 12 shows an optical photomicrograph of the bone–sintered-corundum contact zone that has also been stained with alizarin for comparison. Even 16 weeks after implantation, no direct bonding with the bone is visible. A gap between the bone and the implant has become filled with a layer of connective tissue. The implant could consequently be pulled out like a cork from a bottle. Sintered corundum is therefore biocompatible but not bioactive.

Figure 13 shows a scanning electron micrograph of the boundary layer between the glass ceramic and the bone.

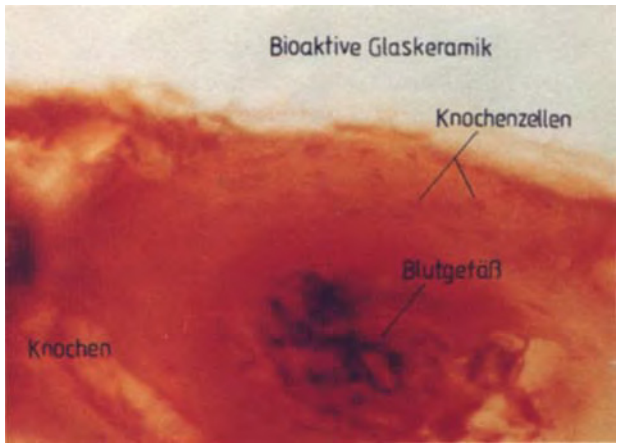

Fig. 11. Intergrowth between bone and glass ceramic eight weeks after implantation in an animal experiment. There is true intergrowth between the bioactive glass ceramic and the bone (optical photomicrograph taken by Dr. *J. Gummel* after alizarin staining [32]). Translation: Bioaktive Glaskeramik = bioactive glass ceramic; Knochen = bone; Knochenzellen = bone cells; Blutgefäß = blood vessel.

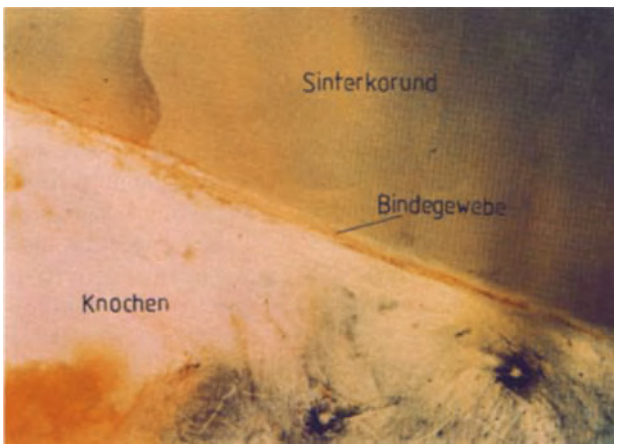

Fig. 12. Bone-sintered-corundum contact zone 16 weeks after implantation in an animal experiment. The implant is encapsulated by a layer of connective tissue (collagen). There is no intergrowth between the biocompatible implant and the bone (optical photomicrograph taken by Dr. *J. Gummel* after alizarin staining [32]). Translation: Sinterkorund = sintered corundum; Knochen = bone; Bindegewebe = connective tissue.

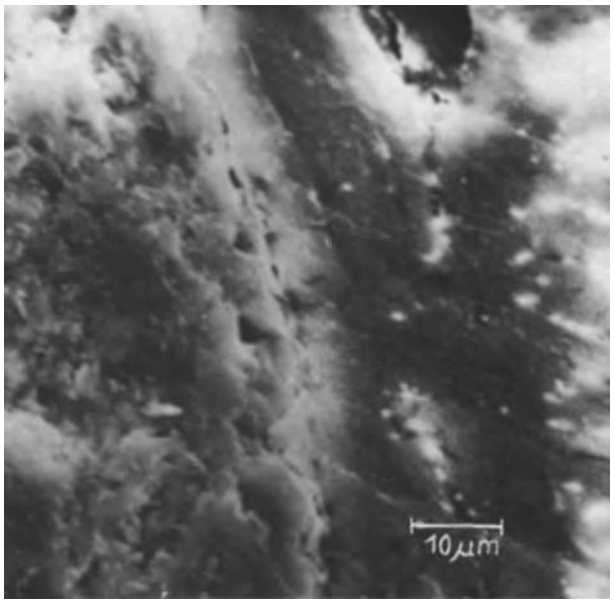

Fig. 13. Intergrowth zone between bioactive glass ceramic and bone in an animal experiment. The maximum thickness of the boundary layer is 5–10 µm (scanning electron micrograph).

Specific dissolution and ion diffusion processes must occur at the surface of the implant under the action of the cell fluid if a firm bond is to be formed between the bone and the implant and new crystals of apatite are to be produced. This dissolution must, however, be brought to a halt at not too great a depth, since the reaction zone will otherwise become too wide which may lead to loosening of the implant if it is subjected to continuous stress later on. Implantation experiments with the new machinable bioactive glass ceramic show that the reaction zone does not exceed 5–10 µm (see Fig. 13). In the case of other foreign bioactive implant materials, the corresponding zone was 100–150 µm and it was not even certain whether the reaction process had completely stopped at the time of examination.

Figure 14 shows an electron-beam microprobe analysis of the boundary layer between the bone and the implant. The X-ray intensity profiles for $Si_{K\alpha}$, $Ca_{K\alpha}$, $P_{K\alpha}$, and $K_{K\alpha}$ radiation suggest the following:

- There is slight leaching of the glass matrix from the surface of the glass ceramic; however, diffusion of SiO_2 into the bone does not occur.
- Leaching of potassium ions from the implant surface is almost quantitative up to a depth of 5 µm. This confirms the previous statement made concerning the width of the reaction zone.

The Ca and P content is higher in the reaction zone than in the glass ceramic. This indicates that new apatite is formed which results in a firm bond between the bioceramic and the bone. The possibility of further bone crystal growth using substances dissolved from the surface of the implant is not excluded.

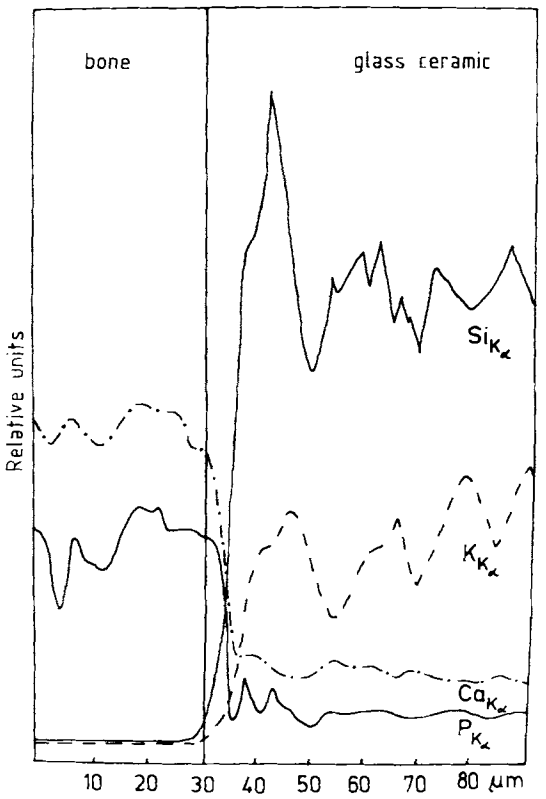

Fig. 14. Electron-beam microprobe investigation of the intergrowth zone shown in Fig. 13. X-ray intensity profiles for $Si_{K\alpha}$, $K_{K\alpha}$, $Ca_{K\alpha}$, and $P_{K\alpha}$ radiation in the boundary layer.

Figures 15a and b show the ceramic-bone bond after 54 and 71 weeks, respectively. The original zone of contact is hardly recognizable, particularly in Figure 15b.

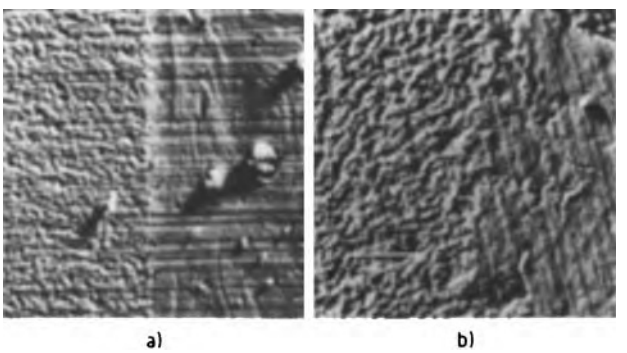

Fig. 15. Scanning electron micrograph of the glass ceramic-bone bond in an animal experiment: a) after 54 weeks; b) after 71 weeks. The contact zone does not broaden as a result of dissolution of the glass ceramic; instead, there is intimate intergrowth.

5.1.5. Interim Assessment and Evaluation of Results

Laboratory and animal experiments designed to test the suitability of the machinable, highly bioactive glass ceramic for bone implants and artificial bones have almost been completed. Experiments on several special applications are still in progress.

The first stage of clinical testing on humans has so far yielded solely positive results. The machinable, highly bioactive glass ceramics provide the surgeon with an implant material that can not only be subjected to the normal procedures used for machining metals but can also be fabricated into complex forms. The surgeon himself will be able to make special corrections and changes during an operation.

5.2. Bioactive, Piezoelectric Phosphate Glass Ceramic Devoid of Silicic Acid

5.2.1. Developmental Trends in Phosphate Glass Ceramics

The successful development of biocompatible and bioactive silicate bioglass ceramics and their medical uses have resulted in medical advances and new possibilities for medical treatment.

It is still not totally certain, however, whether prolonged contact of silicate compounds with the human body will produce undesirable reactions or negative interactions. It would thus be much better to replace bone with a pure biophosphate glass ceramic whose chemical composition corresponds more closely to that of bone than do those of all the bioglass ceramics so far developed. Preliminary efforts in this direction have been made.[38, 39]

The preparation of such a material has not yet been fully accomplished, however, because almost all phosphate glasses have a relatively homogeneous base glass structure and do not display the phase separation that is a prerequisite for controlled crystallization. Only "wild" crystallization is thus possible within or at the surface of the material and does not produce the distinctive properties of a "vitroceramic."

In some cases attempts have been made to overcome the natural structural barriers standing in the way of the development of phosphate glass ceramics by using the glass-powder sinter method.[11] This method consists in tempering, sintering, and crystallizing a phosphate glass powder of suitable composition whose particle sizes approximately correspond to the dimensions of the droplet-shaped immiscibility regions in silicate glasses. Crystallization starts mainly from the surfaces of the particles and proceeds inward toward the center of each glass granule. Uniform crystallization with equal-sized crystallites can thus be achieved in the sintered product by selecting a suitable particle size. The product is porous, however, and its mechanical resistance is lower than that of solid glass ceramics. These materials are therefore only of limited use for medicine; the same also holds for the sintered products of pure crystalline apatite.[10]

The main aim of our studies was to find a way of converting a pure phosphate glass into a glass ceramic by

means of controlled crystallization; one crystalline phase had to be composed of apatite, because existing evidence indicated that this material would be bioactive.

5.2.2. *Structure and Crystallization Behavior of Phosphate Glasses*

Silicate glasses are generally composed of a three-dimensional network of $[SiO_4]$ tetrahedra. The introduction of network-modifying oxides leads to the breaking of oxygen bridges in the $[SiO_4]$ tetrahedron network and results in the incorporation of the large network-modifying ions in the large network cavities consequently formed (see Fig. 16a).

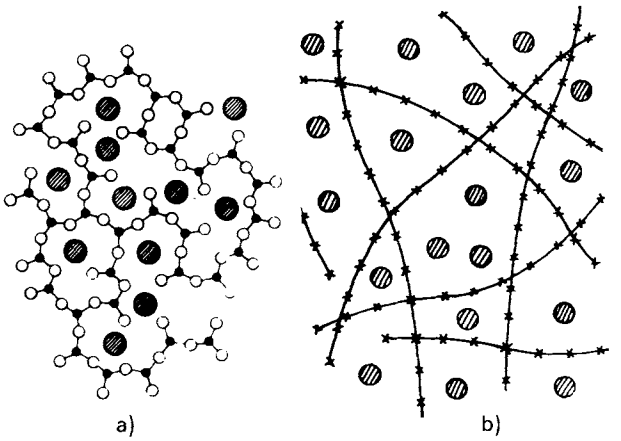

Fig. 16. Hypothetical models for the structure of a) a silicate glass having a network structure; ● = Si, O = O, ◎ = Na (according to *Zachariasen* and *Warren* [3]) and b) a basic phosphate glass having a chain structure; × — ×, PO_4–PO_4, ◎ = Na.

In many cases, however, the network-modifying ions are not distributed statistically within the three-dimensional network. Phase separation occurs owing to the different volume requirements of two different molecular building units, one of which tends to concentrate in one microphase and the other in another such phase.[3]

To some extent, the above phenomena can be compared, on the one hand, with mixed crystal formation in analogy with a homogeneous glass and, on the other hand, with a eutectic crystal mixture in analogy with a glass undergoing microphase separation. As has already been discussed in Section 2, however, microphase separation of a glass is of critical importance for controlled crystallization. The structure and thus the crystallization behavior of phosphate glasses differ from those of silicate glasses. Acidic phosphate glasses also consist of a network, but only three corners of each $[PO_4]$ tetrahedron are linked with neighboring tetrahedra. Basic phosphate glasses, especially those with a network-modifying oxide : P_2O_5 ratio > 1 have a chain structure[40–42] (see Fig. 16b). The cavities between tangled chains are so large, however, that they can easily accommodate a different molecular building block of the glass. A tendency to undergo phase separation is therefore not observed. It is thus impossible to use the customary approach to satisfy the criteria for controlled crystallization in these glasses. Other ways must be found.

5.2.3. *Development of Pure Biophosphate Glass Ceramics*[36, 37]

Glasses of the system CaO-Al_2O_3-P_2O_5: Melts of the ternary system CaO-Al_2O_3-P_2O_5[43] can solidify to form a glass within limited ranges of composition. The ^{31}P-NMR studies of *Haubenreisser* et al.[44], in particular, have clearly demonstrated the chain structure of these glasses. Tempering brings about surface or wild crystallization in which the $AlPO_4$, $Ca(PO_3)_2$, and $Ca_2P_2O_7$ crystalline phase is formed. Apatite does not separate out.

Glasses of the System Na_2O-CaO-Al_2O_3-P_2O_5 and Na_2O-CaO-Al_2O_3-P_2O_5-F: The chain structures of the system CaO-Al_2O_3-P_2O_5 can be specifically degraded by adding increasing amounts of Na_2O; this must improve the chances for the subsequent separation of apatite.

That all of these glasses are "invert glasses" with a P_2O_5 content of less than 50 mol% can be seen from the compositions of the melts [mol%]:

Na_2O	11.0–32.0	Al_2O_3	8.3–16.0
CaO	21.0–37.5	P_2O_5	29.9–42.0

The structural groups determined in the ^{31}P-NMR studies of *Haubenreisser* et al.[44] are solely mono- and diphosphate groups.

In 1959 *Trapp* and *Stevels* were the first to demonstrate the tendency of silicate melts with less than 50 mol% of SiO_2 to form glasses without a three-dimensional network, which they referred to as "invert glasses."[45] The results discussed here indicate that a similar situation may exist in phosphate glass melts. Hypothetical models for the structures of these glasses are presented in Figure 17.

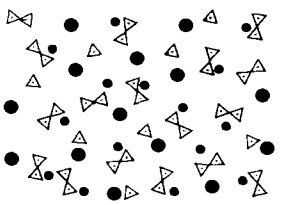

Fig. 17. Hypothetical model for the structure of a phosphate invert glass. Triangles, $[PO_4]$ tetrahedra; black circles, cations (Na^+, Ca^{2+}, Al^{3+}).

Invert glasses, i.e., glasses that are composed exclusively of very small molecular structural groups, tend to crystallize much more rapidly. It was hoped that this would perhaps provide a new way of achieving controlled crystallization in phosphate glasses.

After special thermal treatment, the following crystalline phases can be induced to separate from the above-mentioned glasses: the cristobalite-isotype $AlPO_4$ modification, the tridymite-isotype $AlPO_4$ modification, β-$Ca_2P_2O_7$, an unknown "complex phosphate," a diphosphate, and apatite. However, the crystallization is wild. Most important, a modified hydroxylapatite phase has been made to separate for the first time.

Considerable changes in the crystallization process are observed on addition of fluoride components to melts of the system Na_2O-CaO-Al_2O_3-P_2O_5 [mol%]:

Na_2O	24.1-26.1	P_2O_5	31.6-33.6
CaO	21.7-25.5	F	6.1-10.9
Al_2O_3	11.0-12.2		

Wild crystallization now produces the following crystalline phases: fluoroapatite, the lowquartz-isotype $AlPO_4$ ("berlinite"),[46] which displays piezoelectric properties, and the "complex phosphate phase." ^{27}Al-NMR studies conducted by *Haubenreisser* et al.[44] revealed that the ratio of fourfold- to sixfold-coordinated Al^{3+} was 3:1. This fact, together with the results of the ^{31}P-NMR studies and chemical analyses of the glasses, has been used to deduce a structural model for the "complex phosphate" (see Fig. 18). Such a structural model can indeed be constructed without any strain whatsoever. The precise structure still has to be determined, however. Although controlled crystallization has not yet been achieved in this base glass, attention should be drawn to the special importance of the fluoroapatite and piezoelectric berlinite crystalline phases that have been produced.

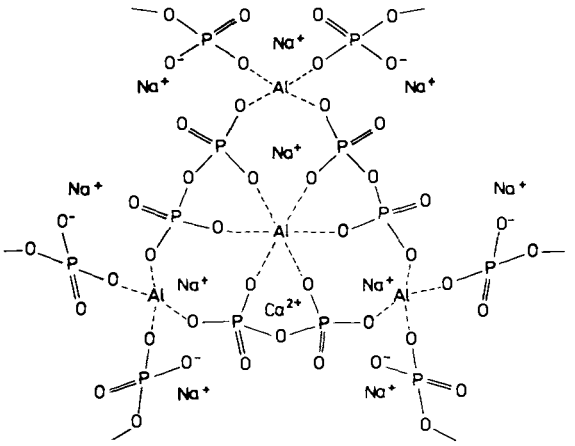

Fig. 18. Hypothetical structure of the crystalline "complex phosphate."

Glasses of the System Na_2O-CaO-Al_2O_3-P_2O_5-FeO/Fe_2O_3 and Na_2O-CaO-Al_2O_3-P_2O_5-F-FeO/Fe_2O_3: Controlled crystallization is not possible in glasses with phosphate chain structures. Phosphate glasses with an invert glass structure (i.e., which contain exclusively mono- or diphosphate structural groups) tend to undergo rapid nucleation and crystallization on tempering. In the corresponding melting diagram, they are located extremely close to the boundary of glass formation. Supersaturation of such melts belonging to the system Na_2O-CaO-Al_2O_3-P_2O_5 with FeO/Fe_2O_3 and cooling or subsequent tempering triggers an effect that resembles phase separation but has nothing at all to do with it.

The selected compositions of the base glasses are [mol%]:

Na_2O	24.1-25.7	P_2O_5	30.7-33.1
CaO	24.9-31.2	FeO/Fe_2O_3	1.2-6.2
Al_2O_3	9.9-14.5		

Figure 19a shows a replica electron micrograph of a selected glass belonging to the system Na_2O-CaO-Al_2O_3-

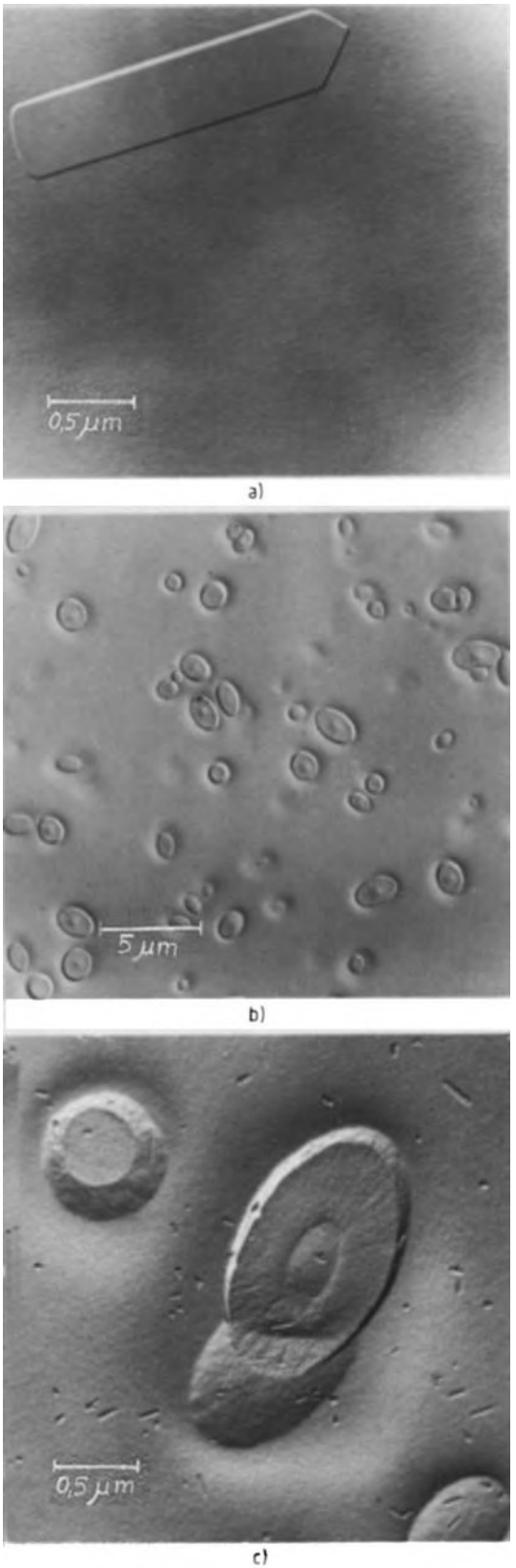

Fig. 19. Replica electron micrograph of a selected glass of the system Na_2O-CaO-Al_2O_3-P_2O_5-FeO/Fe_2O_3. a) After rapid undercooling, the glass displays a homogeneous structure. b) On tempering, supersaturation phenomena disappear; spontaneous nucleation and crystallization occur uniformly throughout the whole glass. c) A single crystallite; a primary iron phosphate nucleus apparently continues to grow by means of epitaxial interaction with the apatite building substance.

P_2O_5-FeO/Fe_2O_3. Comparison of the fractured surface with a MoO_3 crystal test plane clearly demonstrates the homogeneous structure of the glass.

Figure 19b shows a micrograph taken after subjecting the same glass to thermal treatment. Numerous, equal-sized, mostly ellipsoid structures can be seen throughout the glass and are of the kind produced by phase separation. Each ellipsoid region also contains a clearly defined nucleus (see particularly Fig. 19c). The textured structure in Figures 19b and c is a result of the termination of the supersaturation effects because of iron oxides in the base glass.

The nucleus of the ellipsoid region consists of crystalline iron phosphate which has not yet been fully identified. As soon as this primary nucleus has reached a critical size, it apparently continues to grow by means of epitaxial interaction with the hydroxylapatite building substance. Comparison of the lattice constants of apatite with those of various iron phosphates reveals that at least two constants of iron phosphate correspond with two constants of apatite or do not differ by more than ±15% (see Table 6). In principle, epitaxial interactions are therefore possible; the intermediary formation of iron apatites does not appear to be totally inconceivable either.

Table 6. Comparsion of the lattice parameters of some iron-containing phosphates with those of fluoro- and hydroxylapatite.

Crystalline phase	Lattice parameter [Å]	Difference with respect to apatite [%]
Fluoroapatite $Ca_5[F/(PO_4)_3]$	$a = 9.37$ $c = 6.88$	
Hydroxylapatite $Ca_5[OH/(PO_4)_3]$	$a = 9.43$ $c = 6.88$	
$Fe_3(PO_4)_2$	$a = 8.80$ $b = 11.50$ $c = 6.25$	-6.1 to -6.7 (1 × apatite a) -16.4 (2 × apatite c) -9.2 (1 × apatite c)
$NaFeP_2O_7$ I	$a = 7.11$ $b = 10.03$ $c = 8.09$	$+3.3$ (1 × apatite c) $+6.3$ bis 7.8 (1 × apatite a) -13.7 bis -14.3 (1 × apatite a)
$NaFeP_2O_7$ II	$a = 7.33$ $b = 7.90$ $c = 9.57$	$+6.5$ (1 × apatite c) $+14.8$ (1 × apatite c) $+1.5$ bis $+2.1$ (1 × apatite a)
$Ca_xFe_y(PO_4)_6O_z$ [a]	$a = 9.39$ $c = 6.90$	$+0.2$ bis -0.5 (1 × apatite a) $+0.3$ (1 × apatite c)

[a] $x \approx 9.5$, $y \approx 0.5$, $z \approx 1.25$.

An X-ray scanning micrograph taken using $Ca_{K\alpha}$ radiation demonstrates the enrichment of Ca in the ellipsoids (see Fig. 20). X-ray diffraction micrographs clearly indicate that the ellipsoids consist of crystalline hydroxylapatite. Further tempering of such glasses leads to the separation of the crystalline "complex phosphate phase" and the tridymite- or cristobalite-like $AlPO_4$ crystalline phase. Figure 21 shows the tridymite-like $AlPO_4$ crystalline phase; interestingly, this phase is extremely similar to the tridymite shape found in silicate glasses. It can also be seen, however, that as the temperature increases, the axes of the star-shaped crystals rearrange to give the cristobalite-like modification of $AlPO_4$ in which the axes intersect at right angles. Equally surprising are the identical appearances of the original cristobalite in silicate glasses and the cristobalite-like modification of $AlPO_4$.

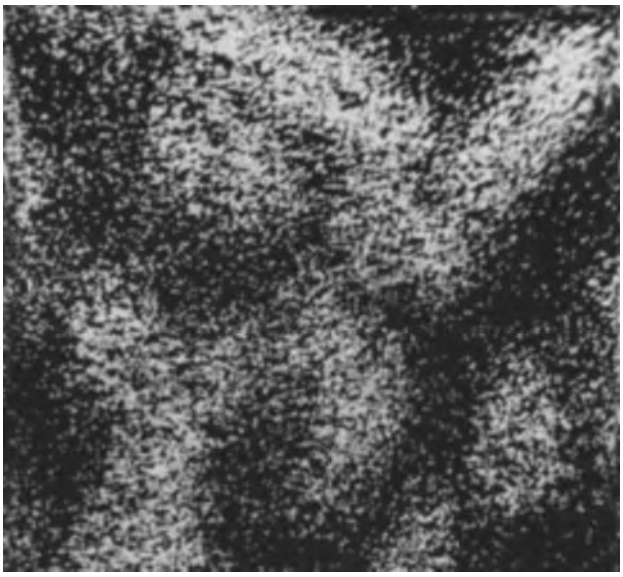

Fig. 20. $Ca_{K\alpha}$ X-ray scanning micrograph of the glass shown in Fig. 19b. Aggregation of Ca^{2+} ions (white dots) in the ellipsoid regions can clearly be seen.

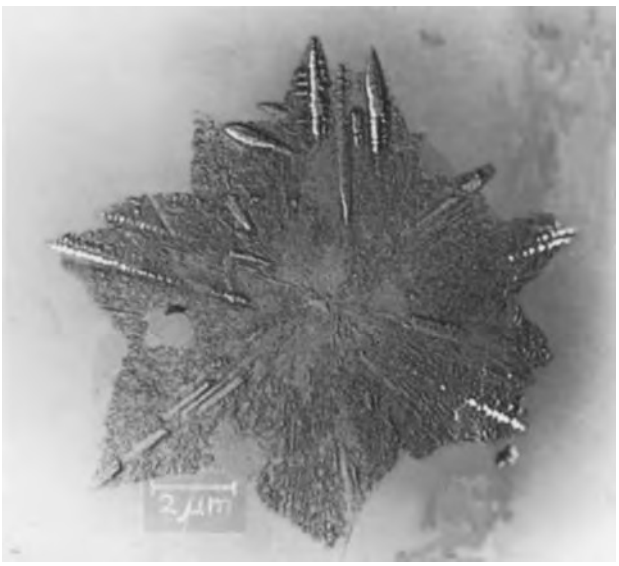

Fig. 21. Formation of the tridymite-like modification of the $AlPO_4$ crystal in the glass matrix obtained after further tempering of the glass shown in Fig. 19b. Transitions to the cristobalite-like $AlPO_4$ modification can be recognized at the ends of the main growth axes of the star-shaped crystal where the axes intersect at right angles (scanning electron micrograph).

A more important advance in attaining optimal bioactivity in phosphate glass ceramics would be achieved if, instead of the cristobalite- or tridymite-like modification of $AlPO_4$, the lowquartz-like $AlPO_4$ modification "berlinite," which exhibits piezoelectric properties,[46] would separate out. In modern medical practice, microcurrents are known to dramatically promote healing of bone fractures.[47,48] Crystallization of apatite and formation of a piezoelectric "berlinite" phase would complement each other very fa-

vorably as regards developing a bioactive pure phosphate glass ceramic.

Separation of "berlinite" can also occur, depending on the fluoride content, in the crystallization of melts belonging to the system Na_2O-CaO-Al_2O_3-P_2O_5-F. It thus seemed logical to add fluoride to melts of the system Na_2O-CaO-Al_2O_3-P_2O_5-FeO/Fe_2O_3 in order to produce the same effect. Separation of "berlinite" has indeed been obtained by adding 2.4–9.4 mol% of fluoride to base glasses of the system Na_2O-CaO-Al_2O_3-P_2O_5-FeO/Fe_2O_3.[36,37]

The complete crystallization sequence occurring during the tempering of certain glasses belonging to the system Na_2O-CaO-Al_2O_3-P_2O_5-F-FeO/Fe_2O_3 is shown in Figure 22. At low temperatures, an iron diphosphate phase and fluoroapatite are formed in addition to the tridymite-like

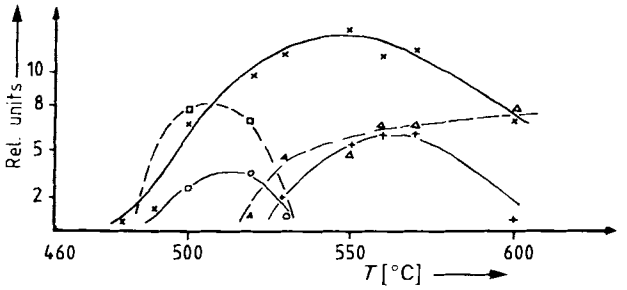

Fig. 22. The temperature dependence of the crystallization sequence of a glass from the system Na_2O-CaO-Al_2O_3-P_2O_5-F-FeO/Fe_2O_3. × — ×, apatite (211); ○—○, tridymite-like $AlPO_4$ ($10\bar{1}0$); +—+, berlinite (102), □—□, iron diphosphate phase; △—△, complex phosphate.

$AlPO_4$ modification; the latter decomposes at higher temperatures, however, to form "berlinite." At about 525°C, the crystalline "complex phosphate phase" is formed as well. Figure 22 also shows that an optimal apatite and berlinite content can be obtained at a temperature of approximately 560°C. Thus, a pure phosphate glass with an invert glass structure has been subjected to controlled crystallization (i.e., volume crystallization) by supersaturating it with iron oxides. Fluoroapatite and the piezoelectric lowquartz form of $AlPO_4$ particularly improve the bioactivity of the bioglass ceramic. It is not yet totally clear, however, whether the other crystalline phosphates also contribute to the increase in bioactivity.

5.2.4. Animal Experiments on the Bonding of Phosphate Glass Ceramics and Bone at the Medizinische Akademie Dresden

The first implantation experiments performed in the tibial heads of guinea pigs demonstrated that the bone substance grows into the phosphate glass ceramic without the formation of connective tissue (see Fig. 23). Moreover, microprobe investigations (see Fig. 24) reveal that the bonding zone is only about 10 μm wide and that the dissolution process, which is a prerequisite for intergrowth, stops after about 12 weeks (cf. Fig. 14). The width of the bonding zone in the glass ceramic was taken as being the distance

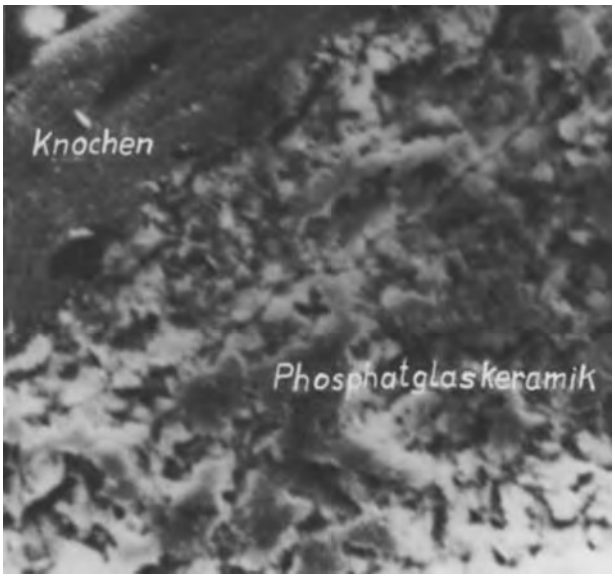

Fig. 23. Intergrowth of pure phosphate glass ceramic and bone in an animal experiment without the formation of connective tissue (scanning electron micrograph). Translation: Knochen = bone; Phosphatglaskeramik = phosphate glass ceramic.

between the point in Figure 24 where the $Ca_{K\alpha}$ intensity suddenly drops and the $Al_{K\alpha}$ intensity simultaneously increases and the point where the $Ca_{K\alpha}$ and $Al_{K\alpha}$ intensities again reach steady levels. If intergrowth is poor or a gap is formed between the glass ceramic and the bone tissue, a totally different microprobe profile is obtained.

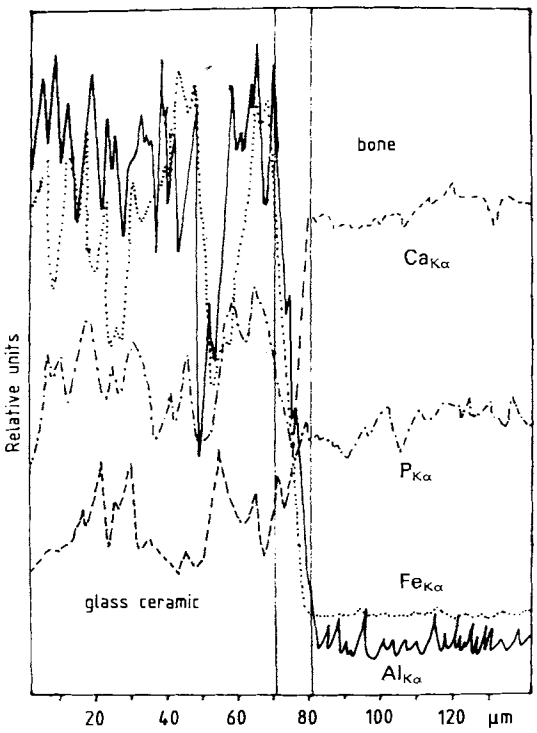

Fig. 24. Electron-beam microprobe profile of the bonding zone in Fig. 23. The zone is not significantly wider than that observed with silicate glass ceramics (cf. Fig. 14).

6. Development of an Inorganic-Organic Bonding Material as a Substitute for Hard Tissue

"Bone cement" is often required in medicine (e.g., to embed endoprostheses or for filling teeth) and usually consists of low-molecular-weight organic compounds that quickly polymerize and harden. Inorganic additives are often mixed with the organic components yielding composite materials. In keeping with more recent applications (e.g., for filling cavities in bones formed during operations), the term "bone cement" should be replaced by the more fitting term "moldable hard-tissue substitute."

If the organic compounds used (e.g., methyl methacrylates, polyurethanes, polyamides, epoxide resins) are applied to a fresh wound as monomers or oligomers, however, they may be removed by the blood during the initial phase prior to polymerization. They may then accumulate at other sites where they can have detrimental effects, including a pronounced drop in blood pressure, fat embolisms,[49] and blood clots.[50] Furthermore, non-reacted isocyanate groups or oligomers can react with body fluid, body tissues, blood corpuscles, or individual proteins, undergoing hydrolysis to give metabolites containing amino groups. Aromatic diamines, in particular, are potential carcinogens.[51]

In all cases, the biocompatible or bioactive glass ceramics or other inorganic materials added to the organic compounds were used exclusively as fillers. The optimal particle size for the inorganic filling materials is 40–60 μm. The reaction zone of many known bioactive glass ceramics reaches 150 μm or more during intergrowth; i.e., any bonding of bone to the mixture of filling material and bioceramic particles occurring in the initial phase is virtually cancelled out by complete dissolution of the particles.

A completely new solution to this problem has now been found.[52] A biocompatible, monomer-free, epoxidated, polymeric hydrocarbon is used which consists solely of C, H, and O. It has a mean molecular weight of 2000 to 6000 with 50 to 500 g of epoxide equivalents. After special surface treatment of the bioactive glass ceramic powders or other additives, they are mixed with the highly polymeric compound to form a chemically bonded substance. Since the surface reaction zones formed during intergrowth with the bone only become 5–12 μm wide (see Section 5.1.4), a sufficient amount of the 40–60-μm bioglass ceramic granule remains to allow firm intergrowth. It is possible to control hardening and the resulting properties of the product, which may vary from cartilage-like to bone-hard. There is no limit so far to the range of applications of these new composite materials.

7. Clinical Testing of the New Bioglass Ceramics in Man

A number of the bioglass ceramics described above have been successfully tested in animals by our medical collaborators. Other bioglass ceramics that are intended for more special applications (e.g., in the eye) are still undergoing tests in animals. Four clinics have been given the go-ahead to perform the first level of clinical tests in humans in special cases.

- At the Orthopädische Klinik (orthopedic clinic) of Charité der Humboldt-Universität Berlin, Prof. H. *Zippel*, in collaboration with Dr. *J. Gummel* and Dr. *H. Hähnel*, has supervised the replacement of single vertebrae in several tumor patients with a bioactive, machinable glass ceramic. Figures 25a–c show several views of a destroyed vertebra before the operation. Figures 25d and e show the substitute vertebra immediately after the operation; it is held in place with a Zielke bridge. The first patient was able to walk without pain after six months.
- At the Hals-, Nasen- und Ohrenklinik (throat, nose, and ear clinic) of the Friedrich-Schiller-Universität Jena, a large range of machinable, biocompatible, and bioactive glass ceramics have been successfully implanted in the middle ear, the nose, the jaw, and the entire skull region (operations performed by Dr. *E. Beleites* under the supervision of Prof. *K.-H. Gramowski*).

  The following operations have been performed as part of the first level of clinical tests:
  - collumellization in tympanoplasty
  - augmentation of the stapes

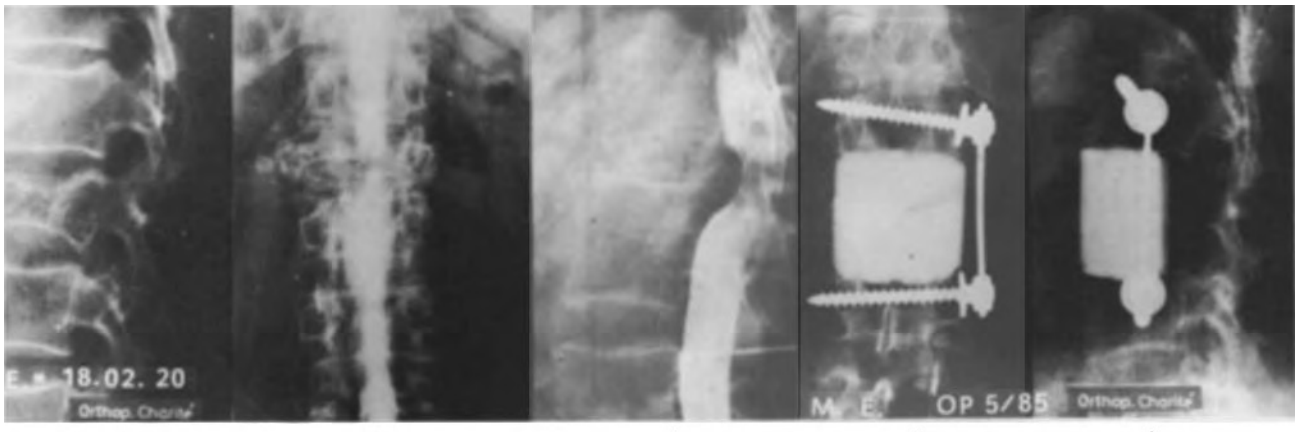

a) b) c) d) e)

Fig. 25. Replacement of a vertebra in a tumor patient with a machinable bioactive glass ceramic (Dr. *J. Gummel*, Charité der Humboldt-Universität Berlin). a)–c) Different views of the destroyed vertebra; d), e) The vertebral prosthesis (X-ray picture). See text.

- reconstruction of the posterior wall of the auditory canal
- reconstruction of the skull base
- maintenance of the base of the orbit
- construction of the anterior wall of the frontal sinus
- rhinoplasty

Figure 26 shows middle-ear implants made by the surgeon. They allowed the patient to hear normally. Animal experiments have demonstrated that intergrowth occurs without causing any adverse reactions and that the biocompatible implant is covered with epithelium. Intergrowth takes place as if the implant were part of the body (see Fig. 27).

Fig. 26. Middle-ear implants made of machinable biocompatible or bioactive glass that were shaped by the surgeon (Dr. *E. Beleites*, HNO-Klinik der Friedrich-Schiller-Universität Jena). Scale in cm.

Fig. 27. Intergrowth of an implant made of biocompatible, machinable glass ceramic in an animal experiment. Intergrowth proceeds without causing any irritation and the implant is covered with a layer of epithelium (optical photomicrograph, Dr. *E. Beleites*, HNO-Klinik der Friedrich-Schiller Universität Jena).

— At the Orthopädische Klinik (orthopedic clinic) of the Medizinische Akademie Dresden, machinable bioactive implants have been used for a wide range of applications. The following operations have been performed as part of the first level of clinical tests under the supervision of Prof. *K.-J. Schulze* in collaboration with Dr. *W. Purath* and Dr. *T. Schubert*:

- reconstruction of the root of the acetabulum in a dislocated hip at the dysplasic stage (pericapsular iliumosteotomy according to *Pemberton*)
- ligament fixation in capsule-ligament plastic surgery of the knee joint
- osteotomy of the tibial head and augmentation of the tibial plateau
- operation according to *Bandi*
- partial replacement of vertebrae in the dorsal part of the spine
- ventral spondylodesis in the cervical vertebra according to *Robinson*
- plastic surgery of the shoulder joint according to *Eden-Hybinette*
- distraction osteotomy for keeping of distance
- filling of large bone cysts (glass ceramic as filler)

— Figures 28 and 29 shows two examples for the broad application of machinable, bioactive glass ceramics at the Orthopädischen Klinik der Medizinischen Akademie Dresden.

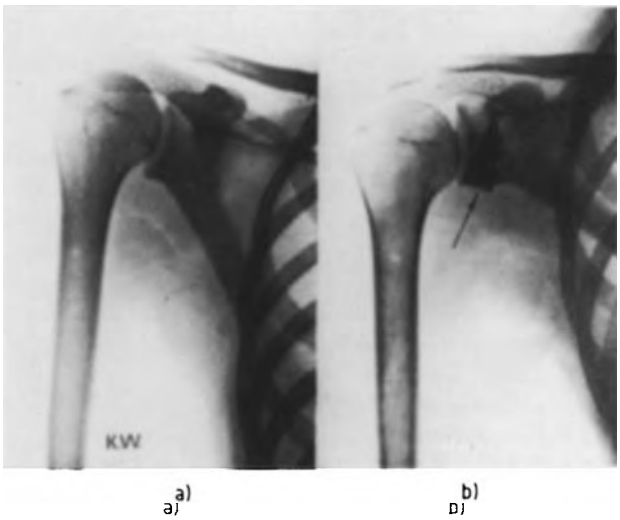

Fig. 28. Use of a wedge-shaped implant made of machinable, bioactive glass ceramic for treating recurrent dislocation of the shoulder by an *Eden-Hybinette* operation. a) Preoperative; b) eight months after the operation. Integration into the bone with good clinical results (Prof. *K.-J. Schulze*, Dr. *W. Purath*, Dr. *T. Schubert*, Medizinische Akademie Dresden).

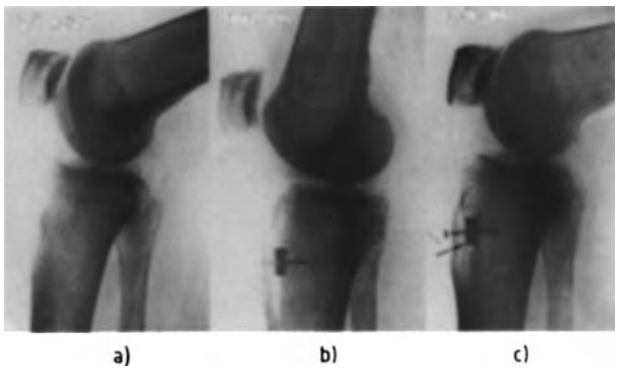

Fig. 29. Use of an oblique, cube-shaped implant made of machinable, bioactive glass ceramic with a central hole and a fixation pin for treating patellofemoral arthrosis by means of ventralization of the tubercle of the tibia according to *Bandi*. a) Preoperative; b) one week and c) eight months after the operation. Integration of the implant into the bone without loss due to correction (Prof. *K.-J. Schulze*, Dr. *W. Purath*, Dr. *T. Schubert*, Medizinische Akademie Dresden).

At the Klinik und Poliklinik für Kiefer-Gesichts-Chirurgie und Chirurgische Stomatologie (clinic and polyclinic for oral and facial surgery and surgical stomatology) of the Sektion Stomatologie of the Medizinische Akademie Dresden, dental roots have been replaced with machinable, highly bioactive glass ceramics following the successful completion of experiments on pigs performed by Doz. Dr. *R. Pinkert*. The preliminary results are extremely encouraging. Figure 30 shows some of these crude dental root implants; they are made from liquid glass by using a centrifugation technique and are later ceramicized. They were made from an impression of the original after preparing a ceramic mold by means of the centrifugation technique.

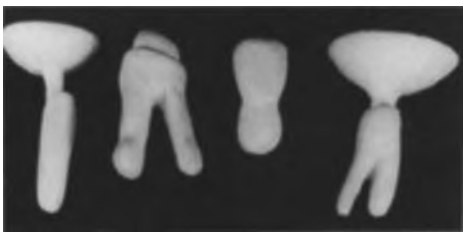

Fig. 30. Crude dental root implants made of machinable, highly bioactive glass ceramic. The implants were prepared by a centrifugation technique (Doz. Dr. *R. Pinkert*, Medizinische Akademie Dresden).

8. Summary and Outlook

Considerable progress has been made in this young, interdisciplinary area of science. Not just one but a whole spectrum of bioglass ceramics are now available for medical uses. The properties of these materials can be varied and adjusted within wide limits to suit special medical requirements and different types of applications. However, many questions have not yet been satisfactorily answered: What happens to a bioglass ceramic/bone contact and intergrowth on the long-term scale or when subjected to heavy, variable mechanical loads? How does the gum covering the jaw bone react to dental root implants? As far as prolonged contact is concerned, positive results have been obtained in animal tests extending over several years.

New, unpredictable problems sometimes arise during animal or clinical tests. It can be concluded, however, that the materials have not so far failed in any of their clinical applications. This has encouraged us to pursue further the current direction of development.

One of the advantages of the machinable bioglass ceramics in medicine that is repeatedly stressed is that an implant can be modified and fitted by the surgeon with his own instruments during the course of an operation. This is very important, for instance, in emergency surgery, oral surgery, and stomatology. One of our major aims is to increase the mechanical and shearing resistance of bioglass ceramics either directly or indirectly so that hip joint prostheses can be constructed. It is not yet possible to say whether this goal can be realized. It is evident, however, that the new opportunities for medical treatment that are offered by the development and utilization of new inorganic biomaterials in medicine are by no means exhausted.

The authors would finally like to thank their many coworkers and collaborators for their active and constructive cooperation. It is impossible to mention them all here but several at the Friedrich-Schiller-Universität Jena deserve special mention for their work on the development of biomaterials: Dr. K. Naumann, Dr. J. Vogel, Dr. G. Carl, Dipl.-Chem. P. Wange, Doz. Dr. habil. W. Götz (X-ray crystallography), Dr. G. Völksch and Ing. L. Horn (electron microscopy), Dr. sc. nat. Haubenreisser (nuclear magnetic resonance studies), Prof. Dr. habil. G. Heublein and Dipl.-Chem. M. Böse (organic polymer development). The numerous animal experiments and clinical tests performed by the following medical colleagues have made a decisive contribution to the present status of development: Dr. sc. med. J. Gummel (Humboldt-Universität Berlin), Dr. med. E. Beleites (Friedrich-Schiller-Universität Jena), Prof. Dr. sc. med. K.-J. Schulze (Medizinische Akademie Dresden), Dr. med. T. Schubert (Medizinische Akademie Dresden), Dr. med. W. Purath (Medizinische Akademie Dresden), Doz. Dr. Dr. sc. med. R. Pinkert (Medizinische Akademie Dresden). Our thanks also go to many other medical colleagues whose studies are still at the stage of laboratory and animal tests. Many of our own co-workers—research students, laboratory assistants, and technicians—have also made considerable contributions to the success of the work presented here.

Received: October 6, 1986 [A 621 IE]
German version: *Angew. Chem.* 99 (1987) 541
Translated by Dr. *Gail Schulz*, Seeheim-Jugenheim

[1] W. Vogel, *Angew. Chem.* 77 (1965) 109; *Angew. Chem. Int. Ed. Engl.* 4 (1965) 112.
[2] W. Vogel: *Struktur und Kristallisation der Gläser*, VEB Deutscher Verlag für Grundstoffindustrie, Leipzig 1965; 2nd ed. 1971; 3rd. ed., *Structure and Crystallization of Glass*, Edition Leipzig, Pergamon Press, Oxford 1971.
[3] W. Vogel: *Glaschemie*, VEB Deutscher Verlag für Grundstoffindustrie, Leipzig 1979; 2nd ed. 1982; 3rd. ed., *Chemistry of Glass*, American Ceramic Society, Columbus, OH (USA) 1985.
[4] C. G. Pantano, E. A. Clark, L. L. Hench, *J. Am. Ceram. Soc.* 57 (1974) 412.
[5] M. Ogino, F. Ohuchi, L. L. Hench, *J. Biomed. Mater. Res.* 14 (1980) 55.
[6] M. Ogino, L. L. Hench, *J. Non-Cryst. Solids 38/39* (1980) 673.
[7] S. Köhler, K. Retemeyer, G. Berger, R. Carow, R. Meyer, *Dtsch. Gesundheitswes. 35* (1980) 1343.
[8] R. L. Hentrich, G. A. Graves, H. G. Stein, *J. Biomed. Mater. Res.* 5 (1971) 25.
[9] K. Köster, H. Heide, *Z. Orthop. 115* (1977) 604.
[10] M. Akao, H. Aoki, K. Kato, *J. Mater. Sci. 16* (1981) 809.
[11] Zhu Peinan, Cheng Zongquion, Huang Jianong, Sim Quinlian, Feng Meizhen, Chien Pufan, Yang Quinghung, Cai Tidong, *J. Non-Cryst. Solids 52* (1982) 503.
[12] F. Pernot, J. Zarzycky, F. Bonnel, P. Rabischong, R. Baldet, *J. Mater. Sci. 14* (1979) 1694.
[13] T. Kokubo, M. Shigematsu, Y. Nagashima, *Bull. Inst. Chem. Res. Kyoto Univ. 60* (1982) 260.
[14] T. Kokubo, S. Ito, M. Shigematsu, T. Nakamura, T. Yamamuro, S. Higashi, *XIII. Int. Glaskongr.*, Hamburg 1983.
[15] L. L. Hench, *J. Non-Cryst. Solids 19* (1975) 27.
[16] L. L. Hench, H. A. Paschall, *J. Biomed. Mater. Symp. 4* (1973) 25.
[17] H. Käs, DAS 2349859 (1973).
[18] H. Brömer, H. Käs, E. Pfeil, DBP 2326100 (1973).
[19] F. Wihsmann, G. Berger, M. Kirsch, *Wiss. Z. Friedrich-Schiller-Univ. Jena Mat.-Naturwiss. Reihe 32* (1983) 553.
[20] V. Thieme, H. Hofmann, H. Heiner, G. Berger, *Z. Exp. Chir. 15* (1982) 310.

[21] S. Köhler, K. Retemeyer, G. Berger, R. Kunth, *Stomatol. DDR 34* (1984) 557.
[22] W. Vogel, E. Heidenreich, R. Ehrt, DDR-Wirtschafts-Pat. 113885 und DOS 2452076 (1973).
[23] G. H. Beall, M. R. Montierth, P. Smith, *Glas-Email-Keramo-Tech. 22* (1971) 409.
[24] D. G. Grossmann, DOS 2208236 (1972).
[25] G. K. Chyung, G. H. Beall, D. G. Grossmann, *Int. Congr. Glass (Pap.) 10th (Kyoto) 1974, Kongr. Bd. 14/33* (1974).
[26] W. Vogel, W. Höland, *Adv. Ceram. 4* (1982) 125.
[27] W. Vogel, W. Höland, *Z. Chem. 22* (1982) 429.
[28] W. Höland, K. Naumann, H.-G. Seyferth, W. Vogel, *Z. Chem. 21* (1981) 108.
[29] W. Vogel, W. Höland, K. Naumann, DDR-Wirtschafts-Pat. 0153108 (1980).
[30] W. Höland, W. Vogel, W. J. Mortier, P. H. Duvigneaud, G. Naessens, E. Plumat, *Glass Technol. 24* (1983) 318.
[31] G. Carl, K. Naumann, W. Höland, W. Vogel, DDR-Wirtschafts-Pat. 242216 (1985).
[32] W. Vogel, W. Höland, K. Naumann, J. Gummel, *J. Non-Cryst. Solids 80* (1986) 34.
[33] W. Höland, K. Naumann, W. Vogel, DDR-Wirtschafts-Pat. 237728 (1982).
[34] F. Trojer, P. G. O'Conner, H. Tannenberg, DOS 2606540 (1975).
[35] Technische Normen, Gütevorschriften und Lieferbedingungen (TGL) 14809 (DDR).
[36] J. Vogel, W. Höland, W. Vogel, DDR-Wirtschafts-Pat. 259561/1 (1984).
[37] W. Vogel, J. Vogel, W. Höland, P. Wange, 3rd Int. Otto-Schott-Kolloquium 1986.
[38] Y. Abe, A. Nagoya, DBP 3142813 (1981).
[39] Y. Abe, M. Hosoe, T. Kasuga, H. Ishikawa, N. Shiukai, Y. Suzuki, J. Nakayama, *J. Am. Ceram. Soc. 65* (1982) 189.
[40] J. R. Van Wazer, *J. Am. Chem. Soc. 72* (1950) 644.
[41] J. R. Van Wazer: *Phosphorus and its Compounds, Vol. 1*, Interscience, New York 1958.
[42] A. E. R. Westman, P. A. Gartaganis, *J. Am. Ceram. Soc. 40* (1957) 293.
[43] P. E. Stone, E. P. Egan, J. R. Lehr, *J. Am. Ceram. Soc. 39* (1956) 96.
[44] U. Haubenreisser, J. Vogel, W. Höland, W. Vogel, 3rd Int. Otto-Schott-Kolloquium 1986.
[45] H. J. L. Trapp, J. M. Stevels, *Glastech. Ber. 32* (1959) K, 32.
[46] *Landolt-Börnstein, Neue Serie Gruppe III, Band 2*, Springer, Berlin 1969.
[47] J. Nixon, *Brit. Med. J. 290* (1985) 490.
[48] T. Schubert, *Dissertation*, Medizinische Akademie Dresden 1981.
[49] P. Schultz, *Arch. Orthop. Unfall-Chir. 21* (1971) 301.
[50] M. Suzuki, *J. Biomed. Mater. Res. 15* (1981) 697.
[51] N. A. Mohamud: *Physiochemical Aspects of Polymer Surfaces, Vol. 2*, Plenum Press, New York 1983.
[52] W. Vogel, G. Heublein, W. Höland, M. Böse, K. Naumann, G. Carl, J. Vogel, P. Wange, J. Gummel, P. Zinner, E. Beleites, T. Schubert, DDR-Wirtschafts-Pat. 2776665 (1985).

When submitting manuscripts, authors of articles intended for publication as "Communications" are requested to read the "Notice to Authors" reproduced in the January issue of the journal following the list of contents; upon request, a copy can be obtained from the editorial office.

Amavadin, an Example for Selective Binding of Vanadium in Nature: Studies of Its Complexation Chemistry and a New Structural Proposal

By *Ernst Bayer,* Eckhard Koch,* and *Giorgio Anderegg*

The selective enrichment of metals in nature is of great interest.[1] For example, the concentration of vanadium in the blood of tunicates is a millionfold higher than in sea water.[2-4] Fly agaric *(Amanita muscaria)* also concentrates vanadium.[5,6] The structure of the vanadium compound of tunicates has not yet been elucidated.[7,8] However, a structure (**3**) has been proposed[9] for the vanadium compound of fly agaric, amavadin.[9-11] The structural elucidation and synthesis of the organic ligand **1b**[9b] allows, for the first time, the specificity of a naturally occurring vanadium ligand to be investigated. Amavadin can be prepared from $V^{IV}O$ salts and synthetic **1b**.[9b] Since the ligand **1b** was previously unknown and since all attempts to obtain crystals of amavadin suitable for an X-ray structure analysis failed, a detailed investigation of the complex formation of **1b** should also provide an answer to the question of the arrangement of the ligands around the central atom in amavadin.

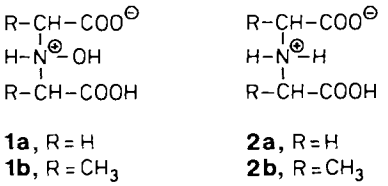

1a, R = H **2a**, R = H
1b, R = CH_3 **2b**, R = CH_3

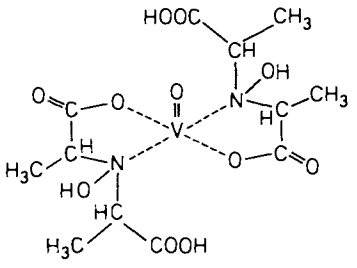

3

[*] Prof. Dr. E. Bayer, Dr. E. Koch
Institut für Organische Chemie der Universität
Auf der Morgenstelle 18, D-7400 Tübingen 1 (FRG)
Prof. Dr. G. Anderegg
Laboratorium für Anorganische Chemie
der Eidgenössischen Technischen Hochschule
Universitätsstrasse 6, CH-8092 Zürich (Switzerland)

The stability constants of the complexes of the amavadin ligand *N*-hydroxy-2,2′-iminodipropionic acid **1b** and the parent compound *N*-hydroxyiminodiacetic acid **1a** were determined for a variety of metals and are listed in Table 1 for the 1 : 1 (K_1) and 1 : 2 complexes (K_2). Most of the constants were determined potentiometrically by using the computer program of *Anderegg*.[12,13] The stability constants of the 1 : 1 copper complexes CuL were determined by ligand exchange with tris(β-aminoethyl)amine.[14] Potentiometric titration is not suitable, however, for measuring the stability of the vanadium(IV) complexes, since the formation of amavadin, namely, a 1 : 2 complex, is already complete before the start of the titration. For this reason, earlier attempts to determine the stability by means of potentiometric titration also led to false results.[15] Investigations by ESR and UV spectroscopy have also shown that, even for a less than stoichiometric amount of ligand, the 1 : 2 complex is formed so fast that no 1 : 1 complex can be detected. Monitoring of the dissociation of the complex at very low pH values by UV spectroscopy gave a value of $\lg\beta_2 = 23.0 \pm 1.0$ for the overall complex formation constant β_2. This value is eleven orders of magnitude larger than that for the copper complex and confirms the exceptional selectivity of the bonding of vanadium(IV) by the ligands of amavadin. This finding clearly reveals how nature selectively binds vanadium in fly agaric by providing a selective ligand.

Table 1. Logarithms of the stability constants K_n ($[ML_n]/([ML_{n-1}][L])$) for various metal ions. The threefold standard deviation in the last digit(s) is shown in parentheses. Measurements at 25°C (**1a**, **1b**, **2b**) and 20°C (**2a**) and ionic strength $I = 0.1$ (KNO_3).

Metal ion		Ligand **1a**	**1b**	**2a**	**2b**
$Ca^{2\oplus}$	$\lg K_1$	3.0(1)	2.7(1)	2.6 [a]	2.0(1)
$Ni^{2\oplus}$	$\lg K_1$	6.4(1)	5.7(1)	8.19 [a]	7.6(1)
	$\lg K_2$	4.65(10)	5.0(1)	6.11 [a]	5.9(1)
$Cu^{2\oplus}$	$\lg K_1$	8.45(10)	9.2(1)	10.63 [a]	10.6(2)
	$\lg K_2$	4.10(5)	3.45(10)	6.05 [a]	4.4(1)
$Zn^{2\oplus}$	$\lg K_1$	5.5(1)	5.05(10)	7.27 [a]	6.6(1)
	$\lg K_2$	3.96(1)	4.05(10)	5.33 [a]	4.5(1)
$VO^{2\oplus}$	$\lg K_1$	—	—	9.00 [b]	9.54 [b]
	$\lg\beta_2$ [c]	21.9 ± 1.0	23.0 ± 1.0		

[a] From [22]. [b] From [15], $T = 25$°C. [c] $\beta_2 = [VL_2^{2\oplus}]/[VO^{2\oplus}][L^{2\ominus}]^2$.

Comparison of the stability of complexes with *N*-hydroxyimino ligands **1a,b** with those with imino ligands **2a,b** is of particular interest. Whereas the *N*-hydroxy ligand **1b** was unknown prior to its discovery in amavadin, iminodiacetic acid **2a** and iminodipropionic acid **2b** belong to the same group of ligands as ethylenediaminetetraacetic acid (EDTA).

By slightly changing the structure of a ligand—namely, by insertion of an oxygen into the analogous imino compound—nature has achieved an effective selectivity for vanadium. The analogous imino compounds form only 1 : 1 complexes with $VO^{2\oplus}$, the stability of which is one to two orders of magnitude smaller than that of the corresponding copper complexes. With the exception of the vanadium complexes, all other metal complexes of the imino ligand **2** are more stable than those of the corresponding *N*-hydroxy compounds. This is expected because of the larger basicity of the NH group in comparison with the NOH group.

Why is such a dramatic increase in complex stability observed in the case of vanadium? This selectivity must be connected with the special arrangement of the ligands around the vanadium. However, the structure assumed so far, **3**, cannot provide an explanation.

Table 2. Complex formation constants K_n ($[ML_n]/[ML_{n-1}][L]$) for various amino and *N*-hydroxyamino acid metal complexes ($T = 25°C$, $I = 0.1$ (KNO_3)).

Ligand	$VO^{2\oplus}$			$Cu^{2\oplus}$	
	$\lg K_1$	$\lg K_2$	$\lg K_3$	$\lg K_1$	$\lg K_2$
$H_2N-O-CH_2-COOH$	$\bar{n}_{max} < 0.15$			5.02 [a]	
$H_2N-CH_2-CH_2-COOH$	< 7.5			7.10 [b]	5.40 [b]
$HO-NH-CH_2-COOH$	6.4	6.2	5.1	$Cu^{2\oplus}$ reduction	
H_2N-CH_2-COOH	< 6.6			8.46 [b]	6.83 [b]
$HO-N(CH_3)-CH_2-COOH$	6	5	4	$Cu^{2\oplus}$ reduction	
$H_3C-NH-CH_2-COOH$	< 7.5			7.94 [c]	6.65 [c]
$HOOC-CH_2-CH(NHOH)-COOH$	7.24	5.4		6.54	4.3
$HOOC-CH_2-CH(NH_2)-COOH$	9.2			8.57 [d]	6.78 [d]
$HON(CH_2CH_2COOH)_2$	5.8	4.2		7.3	

[a] From [23]. [b] From [24]. [c] From [25]. [d] From [26].

Synthesis of substances for comparison and investigation of their complex formation with $VO^{2\oplus}$ were used to establish which elements of structure are essential for the vanadium selectivity. These compounds, together with the stability constants for the $VO^{2\oplus}$ and $Cu^{2\oplus}$ complexes, are collected in Table 2. The complex stability of amavadin is not even approached with any of these ligands. We therefore conclude that, in addition to the NOH group, the two carboxyl groups are also necessary for the vanadium selectivity. On the basis of our results, we propose the new, symmetrical structure **4** as the true structure of amavadin. The absence of a VO group, as found in structure **3**, can be concluded from the following observations. The ESR spectra provide no evidence for the binding of additional ligands,[16] as is often observed to be the case for vanadyl complexes.[17] The IR band at 980 cm^{-1} exhibited by amavadin and assigned to the VO vibration is not observed for the vanadium(IV) complex of *N*-hydroxyiminodiacetic acid, even though this complex exhibits a stability similar to that of amavadin. Therefore, the band at 980 cm^{-1} cannot be assigned to the vanadyl group. Furthermore, recently performed large-angle X-ray scattering (LAXS) experiments show that the shortest metal-ligand distance is probably larger than 1.9 Å.[18] The V-O distance of a vanadyl group is 1.57–1.65 Å. The acidity of amavadin, $pK_a \approx 0$, moreover, does not support the presence of free carboxyl groups. A side-on binding of the anion of the NOH group, as postulated in structure **4**, has been observed for vanadium(V) hydroxylamine complexes.[19,20]

The vanadium compound of fly agaric, amavadin, represents the most stable vanadium(IV) complex known to date. Nitrogen-containing ligands in naturally occurring vanadium complexes are of growing interest because of the recent report of a vanadium nitrogenase.[21]

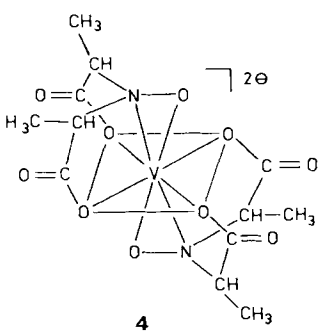

4

Received: December 18, 1986 [Z 2017 IE]
German version: *Angew. Chem. 99* (1987) 568

[1] E. Bayer, *Experientia 12* (1956) 365.
[2] H. J. Bielig, E. Bayer, L. Califano, L. Wirth, *Pubbl. Stn. Zool. Napoli 25* (1955) 26.
[3] M. Henze, *Hoppe-Seyler's Z. Physiol. Chem. 72* (1911) 494.
[4] E. D. Goldberg, W. McBlair, K. M. Taylor, *Biol. Bull. Woods Hole, Mass. 101* (1951) 84.
[5] H. Ter Meulen, *Recl. Trav. Chim. Pays-Bas 50* (1931) 491.
[6] D. Bertrand, *Bull. Am. Mus. Nat. Hist. 94* (1950) 409.
[7] K. Kustin, G. C. McLeod, T. R. Gilbert, L. B. R. Briggs, *Struct. Bonding Berlin 53* (1983) 139.
[8] H. J. Bielig, E. Bayer, H. D. Dell, G. Rohns, H. Möllinger, W. Rüdiger in H. Peeters: *Protides of the Biological Fluids*, Elsevier, Amsterdam 1967.
[9] a) H. Kneifel, E. Bayer, *Angew. Chem. 85* (1973) 542; *Angew. Chem. Int. Ed. Engl. 12* (1973) 508; b) *J. Am. Chem. Soc. 108* (1986) 3075.
[10] E. Koch, H. Kneifel, E. Bayer, *Z. Naturforsch. B 41* (1985) 359.
[11] E. Bayer, H. Kneifel, *Z. Naturforsch. B 27* (1972) 207.
[12] G. Anderegg, E. Koch, E. Bayer, *XXIV Int. Congr. Coord. Chem.*, Athens, August 1986; *Inorg. Chim. Acta*, in press.
[13] G. Anderegg, *Helv. Chim. Acta 44* (1961) 1673; *46* (1963) 2471.
[14] G. Schwarzenbach, E. Freitag, *Helv. Chim. Acta 34* (1951) 1147.
[15] J. Felcman, M. Candida, T. A. Vaz, J. J. R. Frausto da Silva, *Inorg. Chim. Acta 93* (1984) 101.
[16] P. Krauss, E. Bayer, H. Kneifel, *Z. Naturforsch. B 39* (1984) 829.
[17] C. M. Guzy, J. B. Raynor, M. C. R. Symons, *J. Chem. Soc. A 1969*, 2791.
[18] T. Vogt, E. Koch, G. Folkers, E. Bayer, unpublished results.
[19] L. Saussine, H. Mimoun, A. Mitschler, J. Fisher, *Nouv. J. Chim. 4* (1980) 235.
[20] K. Wieghardt, U. Quilitzsch, B. Nuber, J. Weiss, *Angew. Chem. 90* (1978) 381; *Angew. Chem. Int. Ed. Engl. 17* (1978) 351.
[21] R. L. Robson, R. R. Eady, T. H. Richardson, R. W. Miller, M. Hawkins, J. R. Postgate, *Nature 322* (1986) 388.
[22] L. G. Sillen, A. E. Martell *(Stability Constants of Metal-Ion Complexes) The Chemical Society, London, Special Publications 17* (1964); *25* (1971).
[23] Z. Warnke, C. Trojanoska, A. Liwo, *J. Coord. Chem. 14* (1985) 31.
[24] V. S. Sharma, H. B. Mathur, P. S. Kilharni, *Ind. J. Chem. 3* (1965) 146, 475.
[25] F. Basolo, Y. T. Chen, *J. Am. Chem. Soc. 76* (1954) 953.
[26] S. Chabarek, Jr., A. E. Martell, *J. Am. Chem. Soc. 74* (1952) 6021.

A Stable Stannaethene**

By *Harald Meyer, Gerhard Baum, Werner Massa, Stefan Berger,* and *Armin Berndt**

Silaethenes **1** have been completely characterized[1,2] and germaethenes **2** have been identified by trapping reactions;[3] 1,1-dimethylstannaethene **3a** has been generated in the gas phase.[4] Calculations have been carried out for the basic structures **1**–**3**.[5] We now describe the synthesis, spectroscopic characterization, and crystal structure of the stable stannaethene **3b**.

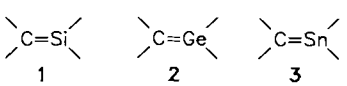

1 **2** **3**

The boranediylborirane **4**, which, according to calculations,[6] has the nonclassical structure shown in Scheme 1,

[*] Prof. Dr. A. Berndt, H. Meyer, G. Baum,
Priv.-Doz. Dr. W. Massa, Priv.-Doz. Dr. S. Berger
Fachbereich Chemie der Universität
Hans-Meerwein-Strasse, D-3550 Marburg (FRG)

[**] This work was supported by the Deutsche Forschungsgemeinschaft and the Fonds der Chemischen Industrie.

behaves toward suitable reagents as if it were the carbene **5**.[7,8] This observation prompted us to carry out the reaction of **4** with the stannanediyl **6**.[9] Reaction in pentane at room temperature led to formation of the stannaethene **3b** in quantitative yield as shown by ^{13}C-NMR spectroscopy.

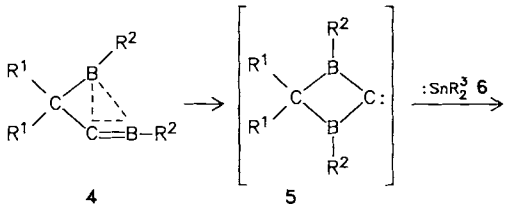

4 5

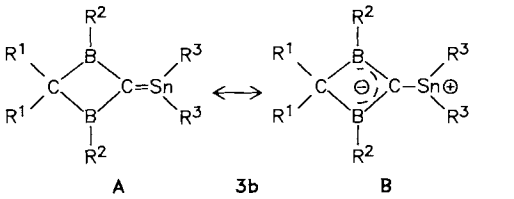

A 3b B

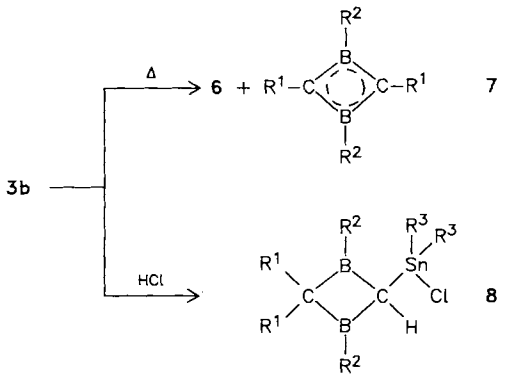

$R^1 = Si(CH_3)_3$; $R^2 = C(CH_3)_3$; $R^3 = CHR^1_2$

Scheme 1.

Compound **3b** crystallizes from pentane at −30 °C as Indian red cubes, which slowly lose their color (over 2 h) upon exposure to air. They melt at 133 °C, undergoing partial decomposition to give **6** and the 1,3-dihydro-1,3-diboretete **7**.[7] Compound **3b** reacts with HCl to give the colorless 1,3-diboretane **8** (m.p. = 178 °C) in quantitative yield according to ^{13}C-NMR spectroscopy.

The structures of **3b** and **8** were established from the ^{1}H-, ^{13}C-, ^{11}B-, and ^{119}Sn-NMR spectra (Table 1). Decisive proof for the presence of tricoordinated tin in **3b** is provided by the very high-frequency position of the ^{119}Sn-NMR signal at $\delta = 835$ (cf. $\delta = 75$ for **8**, both values relative to $\delta(Sn(CH_3)_4) = 0$). Chemical shifts of $\delta(^{119}Sn) = 427.3$[10] and 658.3[11] were found for the tricoordinated Sn atoms in **9** and **10**, respectively.

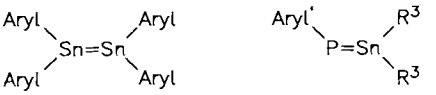

9 **10**

Aryl = 2, 4, 6-triisopropylphenyl

Aryl' = 2, 4, 6-tri-*tert*-butylphenyl

$R^3 = CH(Si(CH_3)_3)_2$

A typical chemical shift ($\delta(^{13}C) = 142$) for a tricoordinated C atom is observed for the C atom of the C=Sn bond. The shift of the ^{11}B-NMR signal of **3b** to lower frequencies ($\delta(^{11}B) = 64$) compared with the signals of **8** ($\delta(^{11}B) = 83$) reveals negative π charge on the B atoms and therefore a strong polarization of the C=Sn bond corresponding to the ylide form **B**.

An X-ray structure analysis[12] of **3b** gave a length of 2.025(4) Å for the bond between the Sn atom and the tricoordinated C2 atom and lengths of 2.152(5) and 2.172(4) Å for the bonds to the tetracoordinated C atoms C19 and C20 (Fig. 1). The torsion angles B1-C2-Sn-C19 and B3-C2-Sn-C20 (Fig. 2) are 40 and 82°, respectively;

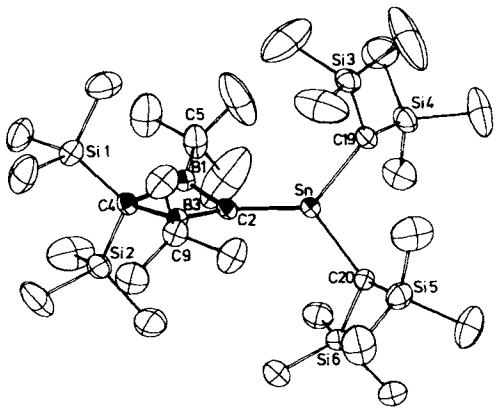

Fig. 1. ORTEP plot of a molecule of **3b** in the crystal (ellipsoids of thermal vibration at 30% probability level; view onto the plane C2,C19,C20; H atoms not shown). Important bond lengths [Å], bond angles and torsion angles [°]: Sn-C2 2.025(4), Sn-C19 2.152(5), Sn-C20 2.172(4), B1-C2 1.510(6), B1-C4 1.624(8), B1-C5 1.601(9), B3-C2 1.494(7), B3-C4 1.653(6), B3-C9 1.603(8), C4-Si1 1.868(4), C4-Si2 1.872(5), B1···B3 1.994(8), C3···C4 2.393(5); C2-Sn-C19 129.2(2), C2-Sn-C20 125.6(2), C19-Sn-C20 104.8(2), Sn-C2-B1 139.2(4), Sn-C2-B3 132.9(4), B1-C2-B3 83.2(4), C2-B1-C4 99.5, B1-C4-B3 75.0(3), C4-B3-C2 98.9(4), Si1-C4-Si2 113.3(3); B1-C2-Sn-C19 40.2(6), B1-C2-Sn-C20 −132.2(4), B3-C2-Sn-C19 −106.1(5), B3-C2-Sn-C20 81.5(5), Sn-C2-B1-C4 −170.5(4), Sn-C2-B3-C4 172.9(4).

the average twist angle around the C=Sn bond is therefore 61°. The angles between the line joining C2 and Sn and the planes C19,Sn,C20 and B1,C2,B3 are 5 and 16°, respectively; i.e., the Sn atom is slightly pyramidalized and the

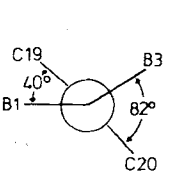

Fig. 2. Stereoprojection along the C2=Sn bond.

Table 1. NMR spectroscopic data for **3b** and **8** [a].

3b: ^{1}H-NMR: $\delta = 1.40$ (s, 2H; SnCH), 1.27 (s, 18H; $BC(CH_3)_3$), 0.20 (s, 18H; $BCSi(CH_3)_3$), 0.0 (s, 36H; $HCSi(CH_3)_3$); ^{13}C-NMR: $\delta = 142.0$ (br. s, 1C; C=Sn), 34.9 (d, 2C; SnCH), 32.4 (q, 6C; $BC(CH_3)_3$), 29.1 (br. s, 1C; BCSi), 24.2 (br. s, 2C; $BC(CH_3)_3$), 5.8 (q, 6C; $BCSi(CH_3)_3$), 4.5 (q, 12C; $SnCSi(CH_3)_3$); ^{11}B-NMR: $\delta = 64$; ^{119}Sn-NMR: $\delta = 835$

8: ^{1}H-NMR: $\delta = 1.36$ (s, 1H; BCHSn), 1.28 (s, 18H; $BC(CH_3)_3$, 0.51 (s, 2H; SnCHSi), 0.39 and 0.35 (s, each 18H; $SnCSi(CH_3)_3$), 0.29 and 0.21 (s, each 9H; $BCSi(CH_3)_3$); ^{13}C-NMR: $\delta = 56.7$ (br. s, 1C; BCSi), 53.1 (br. d, 1C; BCSn), 30.5 (q, 6C; $BC(CH_3)_3$), 27.5 (br. s, 2C; $BC(CH_3)_3$), 16.2 (d, $^1J(^{13}C^{119}Sn) = 183$ Hz, 2C; SnCSi), 7.1 and 5.6 (q, each 3C; $BCSi(CH_3)_3$), 5.2 and 5.1 (q, each 6C; $SnCSi(CH_3)_3$); ^{11}B-NMR: $\delta = 83$; ^{119}Sn-NMR: $\delta = 75$

[a] Solvent C_6D_6.

C2 atom is significantly pyramidalized. Despite these distortions, the C=Sn distance (2.025 Å) is in good agreement with that calculated for $H_2C{=}SnH_2$ (1.982 Å).[5] The short distances B1-C2 (1.510(6)) and B3-C2 (1.494(7) Å)—which are practically identical with the corresponding distances in the 1,3-dihydro-1,3-diborete (7 with $R^2 = N(CH_3)_2$) synthesized by *Siebert* et al.[13]—confirm the importance of the ylide resonance form **B**, which was concluded from the ^{11}B-NMR chemical shift data. This resonance form also helps to explain the extremely high-frequency ^{119}Sn-NMR signal.

Received: December 29, 1986;
supplemented: March 11, 1987 [Z 2032 IE]
German version: *Angew. Chem. 99* (1987) 559

CAS Registry numbers:
3b, 107940-89-6; **4**, 87556-27-2; **6**, 41823-72-7; **7**, 90028-93-6; **8**, 107940-90-9.

[1] A. G. Brook, S. C. Nyburg, F. Abdesaken, B. Gutekunst, G. Gutekunst, R. K. M. R. Kallury, Y. C. Poon, Y.-M. Chang, W. Wong-Ng, *J. Am. Chem. Soc. 104* (1982) 5667.
[2] N. Wiberg, G. Wagner, *Chem. Ber. 119* (1986) 1467, and references cited therein.
[3] J. Satgé, *Adv. Organomet. Chem. 21* (1982) 241; N. Wiberg, C.-K. Kim, *Chem. Ber. 119* (1986) 2966, 2980.
[4] W. J. Pietro, W. J. Hehre, *J. Am. Chem. Soc. 104* (1982) 4329.
[5] K. D. Dobbs, W. J. Hehre, *Organometallics 5* (1986) 2057, and references cited therein.
[6] a) P. H. M. Budzelaar, P. von R. Schleyer, K. Krogh-Jespersen, *Angew. Chem. 96* (1984) 809; *Angew. Chem. Int. Ed. Engl. 23* (1984) 825; b) G. Frenking, H. F. Schaefer III, *Chem. Phys. Lett. 109* (1984) 521.
[7] R. Wehrmann, H. Klusik, A. Berndt, *Angew. Chem. 96* (1984) 810; *Angew. Chem. Int. Ed. Engl. 23* (1984) 826.
[8] According to calculations performed on model systems for **4** and **5** (with SiH_3 instead of $Si(CH_3)_3$ and CH_3 instead of $C(CH_3)_3$, the carbene is only about 10.2 kcal/mol higher in energy than the nonclassical boranediylborirane [6a].
[9] R. J. Davidson, D. H. Harris, M. F. Lappert, *J. Chem. Soc. Dalton Trans. 1976*, 2268.
[10] S. Masamune, L. R. Sita, *J. Am. Chem. Soc. 107* (1985) 6390.
[11] C. Couret, J. Escudie, J. Satgé, *J. Am. Chem. Soc. 107* (1985) 8280.
[12] **3b**: space group $P\bar{1}$, $Z=2$, $a=10.123(1)$, $b=13.113(3)$, $c=17.689(3)$ Å, $\alpha=97.63(2)$, $\beta=91.87(1)$, $\gamma=107.65(1)°$. 4822 unique reflections with $F_0 > 3\sigma(F_0)$ measured at 294 K on a four-circle diffractometer (CAD4, Enraf-Nonius) with $Mo_{K\alpha}$ radiation. Refinement of the heavier atoms with anisotropic temperature factors; the boron atoms refined with isotropic temperature factors; H atoms localized by means of difference Fourier syntheses, but put on calculated positions (d(C-H) = 0.95 Å, riding model) with fixed isotropic temperature factors. $R_w = 0.036$ (weights $w = 1/\sigma^2(F_0)$), 392 parameters, goodness of fit S = 2.288. Further details of the crystal structure investigation may be obtained from the Fachinformationszentrum Energie, Physik, Mathematik GmbH, D-7514 Eggenstein-Leopoldshafen 2 (FRG), on quoting the depository number CSD-52451, the names of the authors, and the journal citation.
[13] M. Hildenbrand, H. Pritzkow, U. Zenneck, W. Siebert, *Angew. Chem. 96* (1984) 371; *Angew. Chem. Int. Ed. Engl. 23* (1984) 371.

A New Low-Temperature Synthesis of 1,2-Dihydro-1,2-diphosphetes

By *Louis Ricard, Nicole Maigrot, Claude Charrier,* and *François Mathey**

Among carbon-phosphorus heterocycles, 1,2-dihydro-1,2-diphosphetes **5** deserve special attention. In some instances, their chemistry can be controlled by their potentially aromatic π-electron sextet.[1,2] On the other hand, the cyclic strain within the ring varies widely according to the substitution pattern,[2,3] thus inducing significant differences in their chemical behavior. Finally, in some cases, compounds **5** may act as masked 1,4-diphosphabutadienes.[4] In spite of these interesting aspects, however, the chemistry of 1,2-dihydro-1,2-diphosphetes **5** is presently very poorly developed, undoubtedly because of the lack of a simple and general synthesis of this ring. The initial high-temperature route [$(RP)_n + R'C{\equiv}CR''$][2,3,5,6] yields complicated mixtures of products and can only provide an access to thermally stable 1,2-dihydro-1,2-diphosphetes **5**. The only other practical route [$RP(SiMe_3)_2 + ClCO{-}COCl$][4] has a limited generality since the two carbons of the ring necessarily bear Me_3SiO substituents.

Fortunately, the recent discovery in our laboratory of a new and simple access to tervalent phosphirenes[7] has allowed us to conceive a new and versatile synthesis of the title compounds. It relies on the formal insertion of a phosphanediyl into a phosphirene C-P bond.

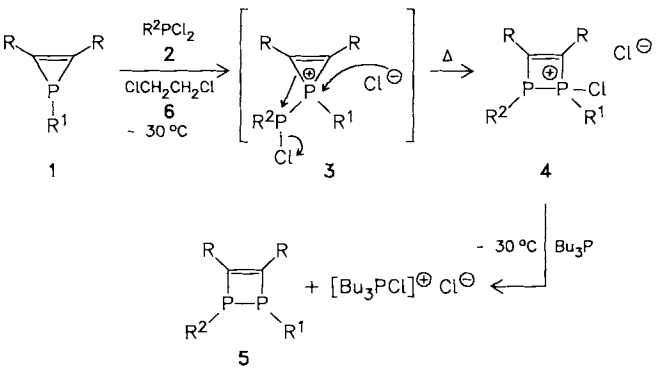

Table 1. Substituents of **1** and **3**–**5**; yields [%] of **5**.

	1		3–5			5
	R	R	R	R′	R″	Yield [%]
a	Ph	Ph	Ph	Ph	Ph	80
b	Ph	Me	Ph	Ph	Me	60
c	Ph	*t*Bu	Ph	Ph	*t*Bu	[a]
c′			Ph	*t*Bu	Ph	20
d	Et	Ph	Ph	Me	Me	15
e	Et	Me	Et	Ph	Ph	70
f	Et	*t*Bu	Et	Ph	Me	50
f′			Et	Me	Ph	15
g			Et	Ph	*t*Bu	[a]
g′			Et	*t*Bu	Ph	[a]
h			Et	*t*Bu	Me	30

[a] Unsatisfactory yields.

In the first step, a dichlorophosphane, **2**, is allowed to react with a phosphirene, **1**. The reaction probably proceeds through a transient phosphirenium salt, **3**. In the presence of $AlCl_3$, **3a** has been characterized by ^{31}P-NMR spectroscopy: AB system with $\delta(^{31}P) = -102.9$ ($P^{\oplus}$) and +67.6 ppm (PCl), $^1J(PP) = 503$ Hz. Without $AlCl_3$, **3** immediately rearranges to give a dihydrodiphosphetium salt, **4**, which is reduced in situ by Bu_3P to give **5** (for yields see Table 1).

The rearrangement to **4** probably involves the nucleophilic attack of $Cl^{\ominus}$ on $P^{\oplus}$ inducing the opening of the ring. The carbanion thus formed reacts with the P-Cl bond of the exocyclic phosphino group. Except for **5a** and **5e**,[3] all the 1,2-dihydro-1,2-diphosphetes **5** thus produced are new and have been fully characterized (Table 2). The ring expansion sometimes fails when bulky R^1 or R^2 groups are used (**5c**, **g**, **g′**).

[*] Prof. F. Mathey, Dr. L. Ricard, Dr. N. Maigrot, Dr. C. Charrier
Laboratoire de Chimie du Phosphore et des Métaux de Transition, DCPH, Ecole Polytechnique
F-91128 Palaiseau Cedex (France)

Table 2. Main spectroscopic data of **1e**, **f**, **5b–d**, **f**, **h** [a].

1e [b]: ^{31}P-NMR(**6**): $\delta = -192$

1f [b]: ^{31}P-NMR(**6**): $\delta = -146.1$

5b: ^{31}P-NMR: $\delta = -47.97$ and -40.94 ($^1J(PP) = 78.6$ Hz).—^{1}H-NMR: $\delta = 1.36$ (dd, $J(HP) = 4.2$, 12.7 Hz; Me–P).—^{13}C-NMR: $\delta = 10.22$ (dd, $J(CP) = 4.0$, 34.7 Hz; Me–P).—MS: m/z 332 ($M^{\oplus}$, 100%), 209 ($Ph_2C_2P^{\oplus}$, 25), 178 ($Ph_2C_2^{\oplus}$, 9)

5c: ^{31}P-NMR: $\delta = -62.06$ and $+6.20$ ($^1J(PP) = 92.8$ Hz).—^{1}H-NMR: $\delta = 1.04$ (dd, $J(HP) = 11.7$, 1.0 Hz; *t*BuP).—^{13}C-NMR: $\delta = 28.77$ (dd, $J(CP) = 12.2$, 7.3 Hz; Me). 32.80 (d, $^1J(CP) = 30.5$ Hz; CMe_3).—MS: m/z 374 ($M^{\oplus}$, 100%), 318 ($M^{\oplus} - C_4H_8$, 64), 209 ($Ph_2C_2P^{\oplus}$, 11), 178 ($Ph_2C_2^{\oplus}$, 3)

5d: ^{31}P-NMR: $\delta = -53.64$.—^{1}H-NMR: $\delta = 1.30$ (pseudo t; Me).—^{13}C-NMR: $\delta = 9.81$ (pseudo t; Me).—MS: m/z 318 ($M^{\oplus} + 3O$, 15%), 302 ($M^{\oplus} + 2O$, 100), 286 ($M^{\oplus} + O$, 54), 271 ($M^{\oplus} + H$, 26) (**5d**, like **5f** and **5h**, is very sensitive toward oxygen)

5f: ^{31}P-NMR (CD_2Cl_2): $\delta = -39.75$ and -34.44 ($^1J(PP) = 62$ Hz).—MS: m/z 284 ($M^{\oplus} + 3O$, 14%), 268 ($M^{\oplus} + 2O$, 40), 253 ($M^{\oplus} + OH$, 62), 237 ($M^{\oplus} + H$, 58), 113 (100)

5h: ^{31}P-NMR: $\delta = -63.68$ and $+1.15$ ($^1J(PP) = 74$ Hz).—^{1}H-NMR: $\delta = 1.22$ (dd, $J(HP) = 11.5$, 0.8 Hz; *t*BuP).—^{13}C-NMR: $\delta = 10.78$ (dd, $J(CP) = 30.5$, 6.1 Hz; MeP).—MS (70 eV): m/z 247 ($M^{\oplus} + 2OH$, 28%), 216 ($M^{\oplus}$, 4), 177 (100)

[a] NMR spectrum in $CDCl_3$ and 20-eV EI mass spectra unless noted otherwise. [b] Synthesized according to [7]; used in situ without further purification.

Experimental Procedure

Two typical experimental procedures are described. All reactions were carried out under argon. The synthesis of the dihydrodiphosphetes **5** relies on the insertion of a dichlorophosphane into the C–P bond of preformed phosphirenes **1**. Depending on the stability of **1**, they may or may not be isolated prior to conducting the insertion reaction [8].

5b: To **1** (2.86 g, 10 mmol) was added $MePCl_2$ (1.17 g, 10 mmol) in **6** at -30°C. After 10 min, the reaction mixture was added to a cold solution of Bu_3P (2.02 g, 10 mmol). The mixture was then concentrated and the residue extracted with hexane. The hexane extract was chromatographed as fast as possible on silica gel (70–230 mesh, Riedel de Haën) with hexane/toluene (80/20). Compound **5b** (2 g, 60%) was thereby obtained as a colorless oil.

5e: A phosphirenium adduct was formed from 3-hexyne (0.86 g, 10 mmol), $AlCl_3$ (1.7 g, 11.5 mmol), and $PhPCl_2$ (1.79 g, 10 mmol) at -30°C in **6** [9]. The reduction leading to **1d** was performed by pouring the adduct onto a solution of Bu_3P (2.02 g, 10 mmol) in 5 mL of **6** at -30°C. A stoichiometric amount of $PhPCl_2$ (as determined from ^{31}P-NMR spectroscopy, usually 70–80% of the initial amount of $PhPCl_2$) in 3 mL of **6** at -30°C. Reduction of **4e** to **5e** was carried out by pouring the solution onto a molar-equivalent solution of Bu_3P in 5 mL of **6** at -30°C. After addition of *N*-methylimidazole in excess, the reaction mixture was extracted with hexane. The extract was chromatographed on a well-degassed silica gel column with hexane. Yield: 2 g (70%) **5e**.

Received: January 29, 1987;
supplemented: March 6, 1987 [Z 2076 IE]
German version: *Angew. Chem. 99* (1987) 590

[1] C. Charrier, F. Mathey, F. Robert, Y. Jeannin, *J. Chem. Soc. Chem. Commun. 1984*, 1707.
[2] C. Charrier, N. Maigrot, F. Mathey, F. Robert, Y. Jeannin, *Organometallics 5* (1986) 623.
[3] C. Charrier, J. Guilhem, F. Mathey, *J. Org. Chem. 46* (1981) 3.
[4] R. Appel, V. Barth, *Tetrahedron Lett. 21* (1980) 1923.
[5] W. Mahler, *J. Am. Chem. Soc. 86* (1964) 2306.
[6] A. Ecker, U. Schmidt, *Chem. Ber. 106* (1973) 1453.
[7] S. Lochschmidt, F. Mathey, A. Schmidpeter, *Tetrahedron Lett. 27* (1986) 2635.
[8] Since only **1a** has been isolated by chromatography as a pure white crystalline solid, only derivatives **5a** and **5b** were obtained by the method described for **5b**. Compounds **5c–h** were formed from the non-purified phosphirene using the procedure described for **5e**. The method described for **5b** should be preferred as soon as purified phosphirenes **1** become available, since it greatly simplifies the final purification of the dihydrodiphosphetes **5**.
[9] K. S. Fongers, H. Hogeveen, R. F. Kingma, *Tetrahedron Lett. 24* (1983) 643.

$Cs_3Mo_5P_6O_{25}$: a Novel Molybdenum Phosphate Containing a Cubane-like Mo_4O_4 Cluster with Six Molybdenum–Molybdenum Bonds

By *Kwang-Hwa Lii*,* *Robert C. Haushalter*, and *Charles J. O'Connor*

Several different structure types have been discovered in the quaternary system M–Mo–P–O (M = metal cation) which contain molybdenum in oxidation states less than +6. For example, $K_4Mo_8P_{12}O_{52}$,[1] $TlMo_2P_3O_{12}$,[2] $Cs_4Mo_8P_{12}O_{52}$,[3] and $AgMo_5P_8O_{33}$[4] have tunnel structures with various pore sizes in which the metal cations M^+ reside. Interestingly, $Cs_2Mo_4P_6O_{26}$,[3] which has the same chemical composition as $Cs_4Mo_8P_{12}O_{52}$, adopts a layer structure. The formal oxidation state of the Mo atom in $TlMo_2P_3O_{12}$ is +4, and that in the other compounds is +5. In the Mo^V-containing compounds, the MoO_6 octahedra are "diluted" with either PO_4 or P_2O_7 groups, but corner-sharing MoO_6 octahedra exist in the Mo^{IV}-containing phosphate. As the formal oxidation state of the molybdenum atom is further reduced, one might expect the formation of metal–metal bonds. We report here a novel molybdenum phosphate, **1**, which contains tetrahedral Mo_4 clusters with six Mo–Mo bonds. Although tetrahedral Mo_4 cluster units have been found in $GaMo_4S_8$[5] and $Mo_4S_4Br_4$,[6] and in the organomolybdenum compounds containing cubane-like Mo_4S_4 units, e.g., $[\{(\eta^5\text{-}C_5H_5)Mo(\mu_3\text{-}S)\}_4]$,[7] the structure of **1** is unprecedented among metal phosphate systems.

$Cs_3Mo_5P_6O_{25}$ **1**

Black chunky crystals of **1** were obtained by heating an intimate mixture of Cs_2MoO_4, MoO_2, Mo, and P_2O_5 (mole ratio of 3:4:3:6) in a sealed quartz tube at 900°C for two days and its single crystal structure was determined.[8] Although the compound is pure by X-ray diffraction measurements, visual microscopic examination always showed the product was contaminated with a small amount of a pale green material.

The structure of **1**, viewed approximately parallel to the trigonal *c* axis, is shown in Figure 1 and contains tunnels where the Cs^+ ions are located. Figure 2a is a projection of the structure of **1** onto the (110) plane and shows the arrangement of the tetrahedral Mo_4 clusters and $Mo(2)O_6$ octahedra, which are connected by pyrophosphate groups, in the unit cell. The Mo_4 tetrahedra all point in the $+z$ direction with the apex atoms, Mo1, at the 2b special positions. The unique molybdenum atom, Mo2, is at the 2a special position and exhibits regular Mo2–O bond distances (2.067(6) Å (3×) and 2.090(5) Å (3×)), which excludes the possibilities of Mo^{6+} and Mo^{5+} for Mo2 (which would involve very asymmetrical configurations of Mo).

As shown in Figure 2b, which is a view approximately parallel to the threefold axis, each face of the Mo_4 tetrahe-

[*] Dr. K.-H. Lii [+], Dr. R. C. Haushalter
Corporate Research Laboratories
Exxon Research and Engineering Company
Route 22 East, Annandale, NJ 08801 (USA)
Professor C. J. O'Connor
Department of Chemistry
University of New Orleans
New Orleans, LA 70184 (USA)
[+] Present address:
Institute of Chemistry Academia Sinica
Nankang, Taipei (Taiwan)

 © VCH Verlagsgesellschaft mbH, D-6940 Weinheim, 1987 0570-0833/87/0606-0549 $ 02.50/0

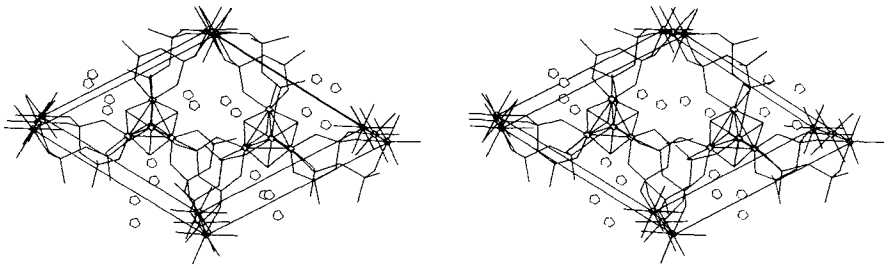

Fig. 1. A stereoscopic view of the crystal structure of **1** in a direction approximately parallel to the threefold axis. The Cs and Mo atoms are represented by large and small polygons, respectively. For clarity, the radii for P and O atoms are set equal to zero.

dron is capped with a μ_3-oxygen atom, three corners of the tetrahedron base are each coordinated by a bidentate P_2O_7 ligand, and the three slant edges (Mo1–Mo3) are each bridged by a P_2O_7 group. The four Mo atoms and four μ_3-O atoms form a distorted cube with edge lengths from 1.992 to 2.051 Å and angles from 95.2 to 102.7°. Each Mo atom of the cluster is coordinated by six oxygen atoms in a distorted octahedral geometry; the O–O distance is 2.84–3.15 Å for the $Mo(1)O_6$ unit and 2.68–3.15 Å for the $Mo(3)O_6$ unit. The cluster consists of four MoO_6 octahedra each sharing its three common edges such that each cluster unit is bound to 16 oxygen atoms. Alternatively, the Mo_4O_{16} cluster can be described as a cubic close-packed array of oxygen atoms with the molybdenum atoms at octahedral sites (AcBaC). The Mo_4 tetrahedron, which resides on a crystallographic site of 3 symmetry, is compressed along the threefold axis (Mo3–Mo3 2.697(1) Å, Mo1–Mo3 2.558(1) Å). Cluster **1** contains three P_2O_7 groups, each of which is coordinated to a corner of the Mo_4 tetrahedron as a bidentate ligand, bridges an edge of a neighboring Mo_4 cluster, and also forms a bridge between two neighboring Mo2 atoms. Both the configuration and the P1–O8–P2 bond angle of the pyrophosphate group in **1** are similar to those found in $Cs_4Mo_8P_{12}O_{52}$.[3] The Cs atom is surrounded by 11 oxygen atoms at distances ranging from 3.041 to 3.582 Å.

An assessment of the oxidation state of the Mo atoms using the bond-length bond-strength formula for the Mo–O bond $[s=(d_{Mo-O}/1.882)^{-6.0}]$[9] yields the following puzzling results: Mo1 +3.32, Mo2 +3.31, Mo3 +3.44 (2.69 e/Mo2, 10.36 e/Mo_4 cluster). However, the summation of the assessed oxidation states over the five Mo atoms of **1** is equal to 16.95, which is in excellent agreement with the value of 17 based on the stoichiometry.

The Mo_4 cluster in **1** has a pronounced distortion similar to that of the 10-electron cluster in $[Mo_4S_4(NCS)_{12}]^{6-}$,[10] which undergoes a Jahn–Teller distortion. However, the distortion in **1** could also be due to a geometric effect because the three Mo1–Mo3 bonds are bridged by P_2O_7 ligands. In order to determine the charge distribution between the Mo_4 cluster and the unique Mo2 atom in **1** magnetization data were obtained, using a SQUID magnetometer from 400 K to 2.3 K, on a crushed sample of manually selected crystals. Figure 3 displays the

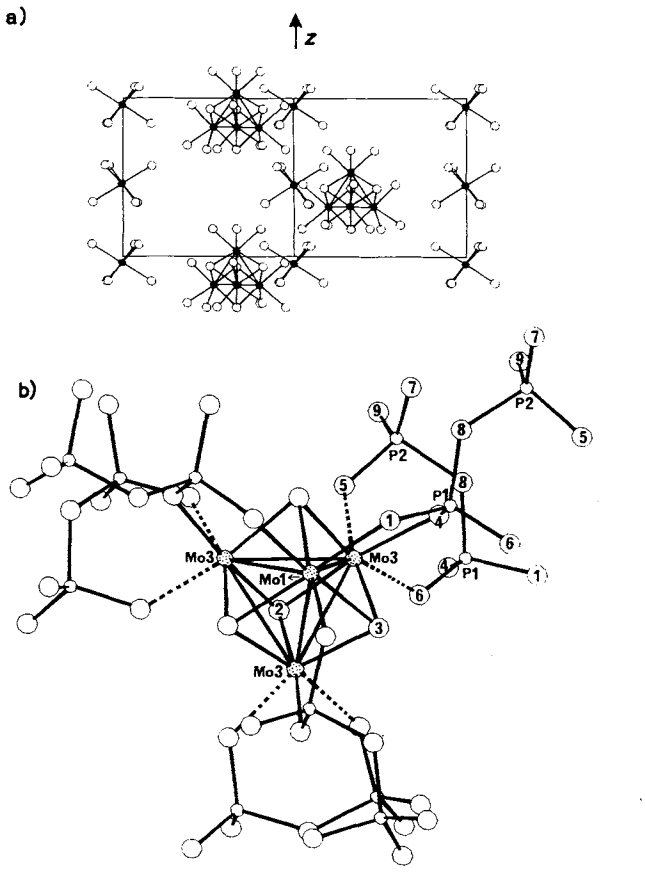

Fig. 2. a) A projection of the structure of **1** onto the (110) plane showing $Mo(2)O_6$ octahedra and Mo_4O_{16} clusters. The P, O8, and Cs atoms have been omitted for clarity. b) Ball-and-stick drawing of a Mo_4O_4 cluster with the pyrophosphate ligands.

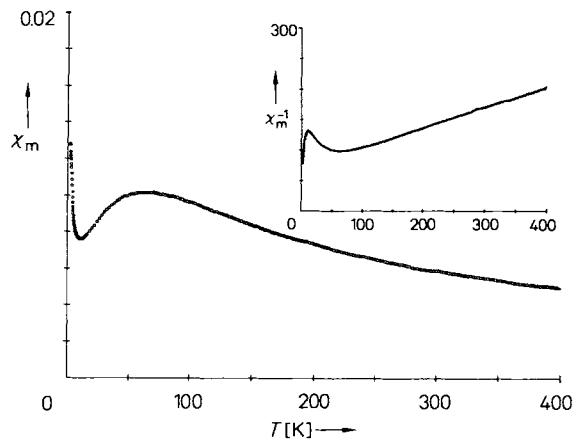

Fig. 3. Molar magnetic susceptibility (χ_m) of **1** vs. T and inverse molar magnetic susceptibility (χ_m^{-1}) vs. T (inset).

plots of molar magnetic susceptibility (χ_m) vs. T and inverse molar magnetic susceptibility vs. T (inset). A least-squares fit to the Curie–Weiss law ($\chi_m = C/(T-\theta)$) in the high-temperature interval gave $\chi_m = 2.91/(T+205)$. The effective magnetic moment (μ_{eff}) calculated from $\mu_{eff} = 2.828\sqrt{C}$, is 4.82 μ_B, which is in excellent agreement with the spin-only value (4.80 μ_B) for noninteracting S = 1

 © VCH Verlagsgesellschaft mbH, D-6940 Weinheim, 1987 0570-0833/87/0606-0550 $ 02.50/0

for the Mo_4 cluster and $S = 3/2$ for the unique Mo atom. The Curie tail below 10 K is due to the presence of a small amount ($< 1\%$) of magnetic impurity. However, the exact nature of the broad maximum around 60 K in the plot of χ_m vs. T is still not clear to us. The assumption of an unusual oxidation state ($+3$) for the unique Mo atom (Mo2) in **1** is supported by our recent discovery of $CsMoP_2O_7$,[11] which is isostructural with $KAlP_2O_7$[12] and contains isolated Mo^{3+} ions in the oxygen lattice.

Received: January 14, 1987 [Z 2046 IE]
German version: *Angew. Chem. 99* (1987) 574

[1] A. Leclaire, J. C. Monier, B. Raveau, *J. Solid State Chem. 48* (1983) 147.
[2] A. Leclaire, J. C. Monier, B. Raveau, *J. Solid State Chem. 59* (1985) 301.
[3] K.-H. Lii, R. C. Haushalter, *J. Solid State Chem.*, in press.
[4] K.-H. Lii, D. C. Johnston, D. P. Goshorn, R. C. Haushalter, unpublished results.
[5] J. M. Vandenberg, D. Rasen, *J. Solid State Chem. 14* (1975) 203.
[6] C. Perrin, R. Chevrel, M. Sergent, *C. R. Acad. Sci. Ser. 2 C281* (1975) 23.
[7] L. F. Dahl, presented at the VIth Int. Conf. Organomet. Chem., Amherst, MA, USA, August 1973.
[8] Crystallographic data for **1**: trigonal, space group $P31c$ (No. 159), $a = 11.868(4)$, $c = 9.352(2)$ Å, $V = 1141(1)$ Å^3, $Z = 2$, $\rho_{calcd} = 4.26$ g/cm^3, $\lambda(Mo_{K\alpha}) = 0.71069$ Å, $\mu(Mo_{K\alpha}) = 79.43$ cm^{-1}. Of the 2495 unique reflections measured at room temperature on an Enraf-Nonius CAD-4 diffractometer, 1199 reflections were unique and 1015 reflections were considered observed ($I > 3.0\sigma(I)$) after LP and empirical absorption corrections (transmission 0.70–1.00). The structure was solved by direct methods and refined by full-matrix least-squares refinement. All atoms were refined anisotropically. The absolute direction of the z axis was also determined. $R = 0.021$, $R_w = 0.027$, GOF = 0.88. Highest peak in final difference Fourier map: 1.04 e/Å^3. All calculations were performed on a VAX-based TEXRAY system. Further details of the crystal structure investigation may be obtained from the Fachinformationszentrum Energie, Physik, Mathematik GmbH, D-7514 Eggenstein-Leopoldshafen 2 (FRG), on quoting the depository number CSD-52355, the names of the authors, and the journal citation.
[9] I. D. Brown, K. K. Wu, *Acta Crystallogr. B32* (1976) 1957.
[10] F. A. Cotton, M. P. Diebod, Z. Dori, R. Llusar, W. Schwotzer, *J. Am. Chem. Soc. 107* (1985) 6735.
[11] K.-H. Lii, R. C. Haushalter, unpublished results.
[12] H. N. Ng, C. Calvo, *Can. J. Chem. 51* (1973) 2613.

Structural Dynamic of Collagen Fibers Cross-Linked with Isocyanates; Application of Synchrotron Radiation in Macromolecular Chemistry**

By *Erika Mosler, Hans Dieringer, Peter P. Fietzek, Waltraud Folkhard, Ernst Knörzer, Michel H. J. Koch,* and *Theobald Nemetschek**

Dedicated to Professor Klaus Kühn on the occasion of his 60th birthday

The reaction of collagen with mono- and dialdehydes[1] as well as with bifunctional reactive tannins[2] results in an increase in the thermal stability (shrinkage temperature T_m), the mechanical strength, and the enzymatic resistance of fibrillar-organized macromolecules, because of the additional cross-linking. However, so far it has been difficult to differentiate between intermolecular and interfibrillar cross-links by either chemical or structural analysis. In principle, structural analytical studies of modifications connected with cross-linking should be possible on the basis of dynamically induced intensity changes in the small-angle meridional X-ray diffraction spectra of fibers, since these changes are related to the sliding of parallel-aggregated collagen molecules relative to each other, a process that can be experimentally influenced.[3,4] However, such analyses proved difficult, because cross-linking with aldehydes already led to intensity changes in the spectra of the fibers.[5]

Diisocyanates,[6] such as hexamethylene diisocyanate (HMDI), can also be used to cross-link collagen.[7] The small-angle meridional X-ray diffraction spectra of HMDI cross-linked samples (Figures 1a and b) show reflections with intensities I and a periodicity identical to those observed for native fibers although the samples were otherwise comparable to fibers cross-linked with aldehydes. This initially unexpected finding can be ascribed to the practically identical electron density of HMDI and structure water of native fibers. The absent effect of HMDI on the small-angle meridional X-ray diffraction spectra of fibers thus provides, for the first time, an experimental way of quantifying the structural dynamics[9] of artificially cross-linked collagen fibers.[10]

The shrinkage temperature T_m shown in the box in Figure 2 reveals a time dependence of the cross-linking reaction; this finding leads to the expectation that the ability of parallel-aggregated collagen molecules to slide relative to

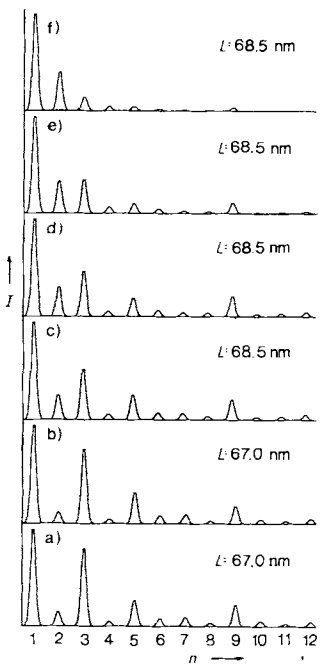

Fig. 1. Small-angle meridional X-ray diffraction spectra of unstretched (a, b) and stretched (c–f) collagen fibers (CF). "Molecular stretching" ΔL in c–f: 2.24%. a) Native CF, $\sigma = 0$; $I_2/I_3 = 0.2$. b) CF cross-linked for 60 min with HMDI, $\sigma = 0$; $I_2/I_3 = 0.15$. c) CF cross-linked for 60 min with HMDI, $\sigma > 0$; $I_2/I_3 = 0.48$. d) CF cross-linked for 30 min with HMDI, $\sigma > 0$; $I_2/I_3 = 0.65$. e) CF cross-linked for 15 min with HMDI, $\sigma > 0$; $I_2/I_3 = 0.95$. f) Native CF, $\sigma > 0$: $I_2/I_3 = 2.8$. The fibers (from rat tail tendon) were washed with Ringer's solution after cross-linking and the measurements were carried out in Ringer's solution. I = intensity; n = order; L = long period; σ = fiber tension; the first-order intensity is shown reduced by a factor of 10; measuring time, 3 s for each spectrum; fitting of the maxima and subtraction of the background by nonlinear regression analysis [8]; the intensity of the second- and third-order reflections (I_2 and I_3) should be noticed.

[*] Prof. Dr. T. Nemetschek, Dr. E. Mosler, Dr. W. Folkhard, Chem.-Ing. E. Knörzer
Pathologisches Institut der Universität
Abteilung für Ultrastrukturforschung
Im Neuenheimer Feld 326, D-6900 Heidelberg (FRG)
Dr. H. Dieringer, Prof. Dr. P. P. Fietzek
Carl Freudenberg GB Bioprodukte, D-6940 Weinheim
Dr. M. H. J. Koch
EMBL-Aussenstelle DESY, D-2000 Hamburg (FRG)

[**] Structural Dynamic, Part 6. This work was supported by the Deutsche Forschungsgemeinschaft and the Bundesministerium für Forschung und Technologie. — Part 5: [9].

each other is reduced. Indeed, a reduced sliding ability of the molecules, dependent on T_m, and thus an increase in *intermolecular* cross-linkage is demonstrated by the delayed increase in I_2/I_3 shown in Figure 2.

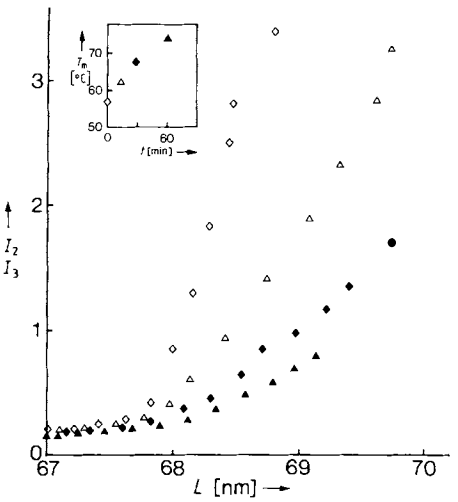

Fig. 2. Inset: Shrinkage temperature T_m of tendon fibers (from rat tail tendon) in Ringer's solution; native (◇) and as a function of the length of the cross-linking reaction t (△, 15 min; ◆, 30 min; ▲, 60 min). The figure shows stretching-induced changes in the ratio of the second- and third-order intensities (I_2/I_3) as a function of the long period L and the shrinkage temperature T_m as determined from the small-angle meridional X-ray diffraction spectra; for the meaning of ◇, △, ◆, and ▲, see above.

Comparison of the short-time diffraction spectra shown in Figure 1c–f reveals the possibility of carrying out, by measuring the I_2/I_3 value in comparison to ΔL, a differential analysis of the degree of cross-linkage as a function of the reaction time for the collagen fibers treated for varying times with HMDI.

These findings are important not only for collagen fibers but also for other fibrous biopolymers and high polymers that are accessible to analysis of the structural dynamic by X-ray diffraction.

Received: January 20, 1987 [Z 2058 IE]
German version: *Angew. Chem.* 99 (1987) 576

CAS Registry number:
HMDI, 822-06-0.

[1] K. H. Gustavson, *The Chemistry and Reactivity of Collagen*, Academic Press, New York 1956.
[2] H. Zahn, D. Wegerle, *Kolloid-Z. 172* (1960) 29.
[3] E. Mosler, W. Folkhard, E. Knörzer, H. Nemetschek-Gansler, T. Nemetschek, M. H. J. Koch, *J. Mol. Biol. 182* (1985) 589.
[4] Only the use of synchrotron radiation made possible the study of this molecular sliding process by diffraction analysis (on account of the reduction in the exposure time by a factor of 10^5), since relaxation of the fibers, which is equivalent to a return of the molecules to their original position, starts within seconds. This is indicated by a reflection at ca. 67 nm in the X-ray diffraction spectrum as well as its higher orders, which point to a dynamically modifiable axial long period due to a staggered parallel arrangement of the ca. 300-nm-long collagen molecules. Recording of the small-angle spectra was carried out with the EMBL camera X 33 in combination with a linear, position-sensitive detector [3].
[5] R. Jonak, H. Nemetschek-Gansler, T. Nemetschek, H. Riedl, J. Bordas, M. H. J. Koch, *J. Mol. Biol. 130* (1979) 511.
[6] O. Bayer, *Angew. Chem. 59* (1947) 257.
[7] K. Eitel, *Leder 4* (1953) 234.
[8] V. Schilling, R. Jonak, T. Nemetschek, H. Riedl, C. Pöppe, E. Schwander, *Z. Naturforsch. C36* (1981) 333.
[9] W. Folkhard, W. Geercken, E. Knörzer, M. H. J. Koch, E. Mosler, H. Nemetschek-Gansler, T. Nemetschek, *J. Mol. Biol. 193* (1987) 405.
[10] W. Folkhard, E. Mosler, W. Geercken, E. Knörzer, H. Nemetschek-Gansler, T. Nemetschek, M. H. J. Koch, *Int. J. Biol. Macromol. 9* (1987), in press.

2,5-Diazapentalenes**

By *Fritz Closs* and *Rudolf Gompper**

Pentalene is a thermally unstable compound belonging to the class of destabilized, antiaromatic π-systems.[1-3] Stabilization of the pentalene system can be achieved by steric shielding (e.g., by *tert*-butyl groups[4]) or by the introduction of donor groups in the 1(3,4,6) position and acceptor groups in the 2(5) position.[5-9]

According to MO calculations,[3,10] 2,5-diazapentalene (pyrrolo[3,4-*c*]pyrrole) (cf. **7** and **8**) is expected to be nonaromatic, whereas 2-azapentalene is expected to be antiaromatic, although less antiaromatic than pentalene. 2,5-Diazapentalene-1,4(2*H*,5*H*)-diones **1**,[11] which exhibit interesting pigment properties[12] and are readily accessible by reaction of esters of succinic acid with aryl cyanides, open up a new route to 2,5-diazapentalenes. We have found another simple synthesis of compounds of the type **1** as exemplified by **1b**, namely, the reaction of succindiamides with *N*,*N*-dimethylbenzamide diethyl acetal. Heating of the two components results in the formation of **1b** in 30% yield. The succinylbenzamidine **2** (35%,

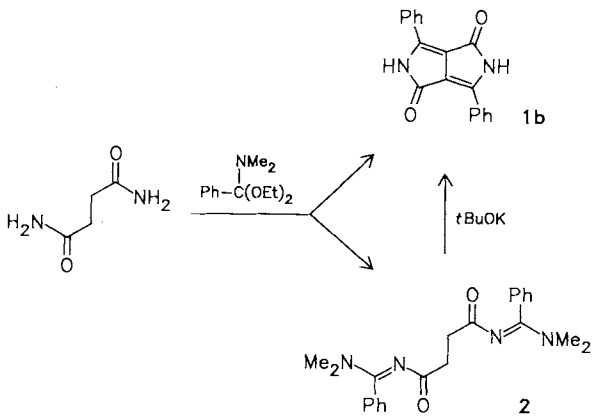

m.p. = 160–161 °C) can be isolated from the mother liquor and converted into **1b** in nearly quantitative yield by reaction with potassium *tert*-butoxide in tetrahydrofuran (THF) (overall yield ca. 60%; see Table 1 for UV/VIS data).

Treatment of the poorly soluble red diones **1** with tetraphosphorus decasulfide results in formation of the blue dithiones **3** (see Table 1). An alternative route to **3** consists in alkylation of **1** to give **4** (cf. Ref. [13]) followed by sulfurization of these more soluble compounds with Lawesson reagent to give the violet monothiones **5** (see Table 1) and the dithiones **6** (see Table 1). The preparation of **3** and **6** by reaction of compounds of the type **1** with sulfurization reagents has been independently described by a research group at Ciba-Geigy AG.[14] Debenzylation of **6be** with sodium in liquid ammonia also affords **3b**, although in varying yields (up to 35%).

The transformation of **1** and **3** into stable donor-acceptor-substituted 2,5-diazapentalenes **7** and **8** was achieved with chlorosilanes and with alkylation agents, respectively. 2,5-Diazapentalenes were previously unknown. Thus, reaction of the disodium salt of **1b** with *tert*-butyldimethylchlorosilane afforded the brown-red 1,4-bis(*tert*-butyldime-

[*] Prof. Dr. R. Gompper, Dipl.-Chem. F. Closs
Institut für Organische Chemie der Universität
Karlstrasse 23, D-8000 München 2 (FRG)

[**] This work was supported by the Deutsche Forschungsgemeinschaft and the Fonds der Chemischen Industrie.

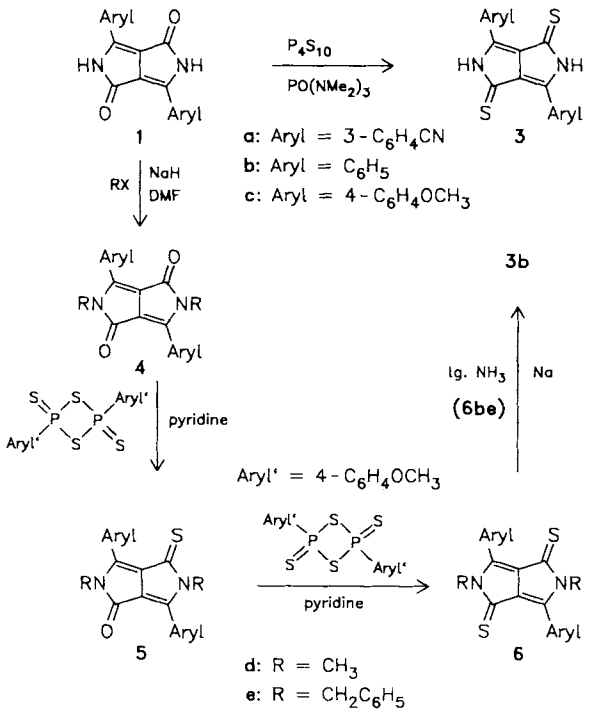

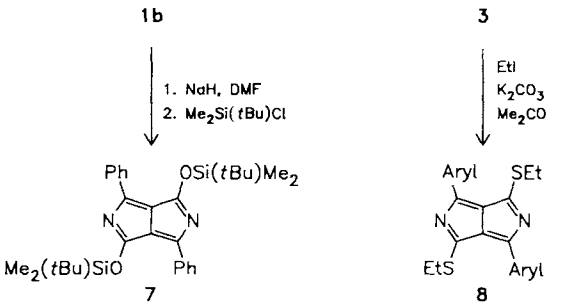

goes decomposition upon treatment with acids or upon heating in polar solvents, **8c** can be protonated with tetrafluoroboric acid–ether and ethylated with triethyloxonium tetrafluoroborate. The substituents in the aryl moiety of **8** have little effect on the absorption spectra.

Although, as esters of thioimidic acid, the diazapentalenes **8** undergo nucleophilic substitution, their reactivity is not very great. Reaction of **8b** with sodium malonodinitrile at room temperature affords the yellow monosubstitution product **9**. Heating of **8b** with malonodinitrile in acetonitrile only leads to formation of the orange adduct **10**. When **8b** is heated to ca. 50 °C with sodium malonodinitrile, partial ring opening occurs, leading to formation of the pyrrole derivative **11** (orange needles, m.p. = 338 °C).

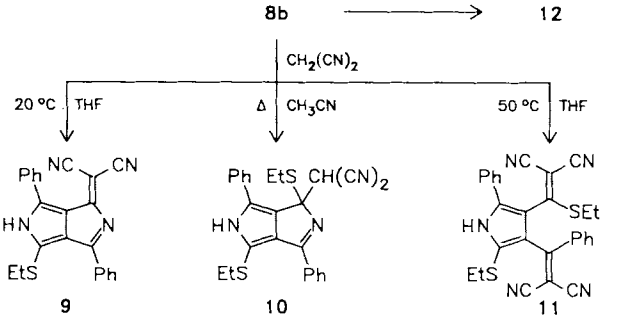

When **8b** is allowed to react in the melt with 2-aminobenzothiazole, the bright yellow compound **12** (see Table 1) is obtained, which exhibits yellow fluorescence in solution. This compound is presumably a pyrrolo[2′,3′:4,5]pyrimido[2,1-*b*]benzothiazole.

Ring opening, such as that observed in the formation of **11**, is also observed when **1b** is heated with a mixture of phosphorus oxychloride and phosphorus pentachloride in the presence of diethylaniline. Instead of the expected

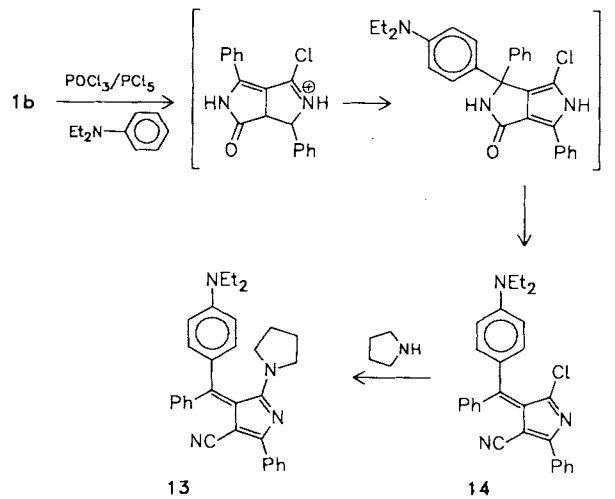

Table 1. Selected physical data for the compounds **1**, **3**, **5**–**9**, **12**–**14**. ^{1}H-NMR spectra: 80 MHz, $CDCl_3$. ^{13}C-NMR spectra: 20 MHz, $CDCl_3$. IR spectra: KBr; UV/VIS spectra: (a) dimethylformamide (DMF), (b) $CHCl_3$.

1a: UV/VIS (a): λ_{max} = 450 nm (sh), 477, 512

1b: UV/VIS (a): λ_{max} (log ε) = 443 nm (sh), 469 (4.21), 503 (4.33)

1c: UV/VIS (a): λ_{max} (log ε) = 450 nm (sh), 477 (4.07), 512 (4.25)

3a: UV/VIS (a): λ_{max} (log ε) = 596 nm (sh), 642 (3.66), 718 (3.77)

3b: UV/VIS (a): λ_{max} (log ε) = 360 nm (4.00), 582 (sh), 624 (4.44)

3c: UV/VIS (a): λ_{max} (log ε) = 580 nm (sh), 630 (3.94)

5bd: m.p. = 252–254 °C; UV/VIS (b): λ_{max} (log ε) = 290 nm (4.29), 534 (4.05)

6bd: m.p. = 224 °C; UV/VIS (b): λ_{max} (log ε) = 292 nm (4.32), 348 (3.92), 593 (4.04)

7: m.p. = 197–198 °C; ^{1}H-NMR: δ = 0.48 (s, 12H), 1.06 (s, 18H), 7.28–7.48 (m, 6H), 8.12–8.40 (m, 4H); ^{13}C-NMR: δ = −3.93, 18.06, 25.78, 121.01, 128.22, 129.67, 131.37, 133.58, 163.05, 168.14

8a: m.p. = 223 °C; UV/VIS (b): λ_{max} (log ε) = 307 nm (4.24), 390 (4.35), 515 (sh), 554 (4.48)

8b: m.p. = 212 °C; ^{1}H-NMR: δ = 1.50 (t, 6H), 3.45 (q, 4H), 7.35–7.46 (m, 6H), 8.03–8.17 (m, 4H); ^{13}C-NMR: δ = 14.90, 26.84, 128.36, 129.88, 131.58, 133.15, 134.88, 161.47, 168.74; IR: $\tilde{\nu}$ = 1595 cm^{-1}, 1538, 1478, 1287, 1247, 1122, 691; UV/VIS (b): λ_{max} (log ε) = 294 nm (4.59), 400 (4.78), 510 (sh), 543 (4.53)

8c: m.p. = 198 °C; UV/VIS (b): λ_{max} (log ε) = 294 nm (4.33), 403 (sh), 424 (4.77), 551 (4.62)

9: m.p. = 187 °C; UV/VIS (b): λ_{max} (log ε) = 288 nm (4.37), 384 (4.09)

12: m.p. = 355 °C; ^{1}H-NMR (CF_3COOH): δ = 7.55–7.75 (m, 6H), 7.78–8.27 (m, 7H), 8.76–8.92 (m, 1H); UV/VIS (b): λ_{max} (log ε) = 253 nm (4.53), 279 (4.55), 310 (sh), 380 (4.53)

13: m.p. = 188 °C; ^{1}H-NMR: δ = 1.20 (t, 6H), 1.57–1.82 (m, 4H), 2.77–3.15 (m, 4H), 3.39 (q, 4H), 6.44–6.68 (m, 2H), 6.90–7.45 (m, 10H), 8.02–8.25 (m, 2H); IR: $\tilde{\nu}$ = 2970 cm^{-1}, 2191, 1601, 1529; UV/VIS (b): λ_{max} (log ε) = 265 nm (4.31), 318 (4.29), 455 (4.28), 580 (4.11)

14: m.p. = 185 °C; ^{1}H-NMR: δ = 1.20 (t, 6H), 3.42 (q, 4H), 6.65 and 8.17 (AA′BB′, 4H), 7.17–7.62 (m, 10H); IR: $\tilde{\nu}$ = 2200 cm^{-1}, 1602, 1483; UV/VIS (CF_3COOH): λ_{max} (log ε) = 436 nm (sh), 515 (4.56); (hexane) 285 nm, 362, 538; (b) 305 nm (4.17), 383 (3.99), 506 (sh), 588 (4.58); (methanol) 300 nm (4.19), 372 (3.98), 486 (3.97), 603 (4.66)

thylsiloxy)-3,6-diphenylpyrrolo[3,4-*c*]pyrrole **7** (see Table 1) and reaction of **3** with ethyl iodide in potassium carbonate/acetone afforded the violet 1,4-diaryl-3,6-bis(ethylthio) derivative **8** (see Table 1). The stability of **8** is influenced by the substituents in the aryl moiety. Whereas **8a** under-

dichlorodiazapentalene, the violet azafulvene derivative **14** (see Table 1) is obtained, the formation of which can be formulated as shown. Nucleophilic substitution of the chlorine by pyrrolidine leads to formation of the green azafulvene **13** (85%).

Received: December 15, 1986;
revised: March 2, 1987 [Z 2010 IE]
German version: *Angew. Chem. 99* (1987) 564

CAS Registry numbers:
1a, 84632-50-8; **1b**, 54660-00-3; **1c**, 104616-31-1; **2**, 108472-45-3; **3a**, 108472-36-2; **3b**, 104616-26-4; **3c**, 104616-32-2; **4bd**, 96159-17-0; **5bd**, 108472-37-3; **6bd**, 104616-30-0; **6be**, 108412-46-4; **7**, 108472-38-4; **8a**, 108472-39-5; **8b**, 108472-40-8; **8c**, 108472-41-9; **9**, 108472-42-0; **10**, 108472-47-5; **11**, 108472-48-6; **13**, 108472-43-1; **14**, 108472-44-2; $H_2NCO(CH_2)_2CONH_2$, 110-14-5; $PhCNMe_2(OEt)_2$, 19429-87-9; $CH_2(CN)_2$, 109-77-3; Me_2NPh, 121-69-7; pyrrolidine, 123-75-1.

[1] M. Randic, *J. Am. Chem. Soc. 99* (1977) 444.
[2] PMO method: M. J. S. Dewar: *The Molecular Orbital Theory of Organic Chemistry*, McGraw-Hill, New York 1969, p. 221; M. J. S. Dewar, R. C. Dougherty: *The PMO Theory of Organic Chemistry*, Plenum Press, New York 1975, p. 94.
[3] REPE: I. Gutman, M. Milun, N. Trinajstic, *J. Am. Chem. Soc. 99* (1977) 1692.
[4] K. Hafner, H. U. Süss, *Angew. Chem. 85* (1973) 626; *Angew. Chem. Int. Ed. Engl. 12* (1973) 576; K. Hafner, *Nachr. Chem. Tech. Lab. 28* (1980) 222.
[5] B. M. Gimarc, *J. Am. Chem. Soc. 105* (1983) 1979.
[6] K. Hartke, R. Matusch, *Chem. Ber. 105* (1972) 2584.
[7] K. Hafner, K. F. Bangert, V. Orfanos, *Angew. Chem. 79* (1967) 414; *Angew. Chem. Int. Ed. Engl. 6* (1967) 451.
[8] K. Hafner, F. Schmidt, *Angew. Chem. 85* (1973) 450; *Angew. Chem. Int. Ed. Engl. 12* (1973) 418.
[9] H. J. Gais, K. Hafner, *Tetrahedron Lett. 1974*, 771.
[10] B. A. Hess, Jr., L. J. Schaad, C. W. Holyoke, Jr., *Tetrahedron 31* (1975) 295.
[11] D. G. Farnum, G. Mehta, G. I. Moore, F. P. Siegal, *Tetrahedron Lett. 1974*, 2549.
[12] L. Cassar, A. Iqbal, A. C. Rochat, Eur. Pat.-Anm. 98808 (1983), Ciba-Geigy.
[13] M. Jost, A. Iqbal, A. C. Rochat, Eur. Pat.-Anm. 133156 (1984), Ciba-Geigy.
[14] A. C. Rochat, A. Iqbal, R. Jeanneret, J. Mizuguchi, Eur. Pat.-Anm. 0187620 (1985), Ciba-Geigy.

Diasterane (Tricyclo[3.1.1.1^{2,4}]octane)**

By *Andreas Otterbach* and *Hans Musso**

Dedicated to Professor Gerhard Quinkert on the occasion of his 60th birthday

Diasterane **I**, the first member of the series of asteranes **I**, **II**,[1a] and **III**,[1b] has not been reported so far. In the asteranes, the axial hydrogen atoms at the bow and the stern of the boat-form cyclohexane structural moieties ("*endo*-1,4 H atoms") are in close proximity. Diasterane **I** should have a strain energy of 94 kcal/mol according to force-field calculations (MM 1).[2] The repulsion of ca. 5 kcal/mol of the *endo*-1,4 H atoms, forced by geometry to a distance of only 1.98 Å, is not sufficient to twist the molecule out of D_{2h} symmetry. The synthesis of **I** has been approached via various routes[3,4] in order to prove, among other things, that it is not formed upon hydrogenation of cubane **16**.[5] We have now succeeded in preparing diasterane **I** from tricyclo[4.2.1.1^{2,5}]decane **5** by two ring contractions.

I II III

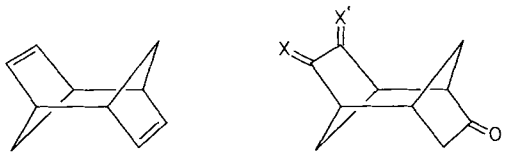

1

2a, X = O; X' = H, H
2b, X = H, H; X' = O

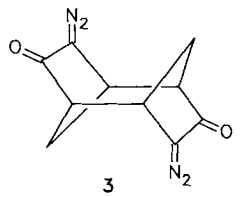

3

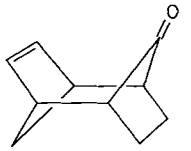

4

To do this twice in one step, the *anti*-diolefin **1**[6] was hydroborated. The two isomeric *exo*-3,7- and *exo*-3,8-diols were separated and oxidized with chromium trioxide in pyridine to the 3,7- and 3,8-diones **2**. However, the desired bis-diazoketone **3** could not be obtained. The deformylative diazo-group transfer reaction resulted only in the formation of a monodiazodiketone from **2** in poor yield. Other attempts to obtain the required bis-diazoketone **3** also failed. Furthermore, the diolefin **1** is not readily accessible in gram amounts by the method of *Grimme* et al.[6]

Therefore, the contraction of both rings was undertaken in two successive steps (Scheme 1). The tricyclic monoolefin **7** and the saturated hydrocarbon **5** were first synthesized by *Paquette* et al.[7] and *Ganter* et al.;[8] we have now prepared **5** by hydrogenation and Wolff-Kishner reduction of the unsaturated ketone **4**, obtained via the convenient route of *Zimmermann* and *Linder*.[9] The bromination of such hydrocarbons is unsatisfactory even under forced conditions.[7] However, the *exo*-bromide **6** could be obtained in 71% yield when **5** was photobrominated with deficient bromine in CCl_4 at 140°C and recycled. The direct Kornblum oxidation of **6** yielded at best 33% of ketone **9**. The main product was the olefin **7**, which could be obtained in better yield (87%) by elimination of HBr from **6** with 1,5-diazabicyclo[5.4.0]undec-5-ene (DBU) in dimethylformamide (DMF) at 150°C. Hydroboration of **7** to the *exo*-alcohol **8** (88%) and oxidation of **8** with dimethyl sulfoxide (DMSO) and oxalyl chloride provided ketone **9** in higher yield (97%). The conversion of **9** to the α-formyl derivative and subsequent reaction with tosyl azide yielded the diazoketone **10** (60%); photolysis and Wolff rearrangement at −150°C in methanol afforded the methyl ester of tricyclo[3.2.1.1^{2,4}]nonane-*endo*-3-carboxylic acid **11** in 51% yield, alkaline hydrolysis of which gave the *exo*-carboxylic acid **12** (90%). Decarboxylation of **12** to tricyclo[3.2.1.1^{2,4}]nonane **14**[10] was best achieved (82%) in one step by the method of *Barton* et al.[11] via free radical decarboxylation of the ester **13** in the presence of *t*BuSH as the source of hydrogen (82% yield, colorless crystals, m.p. = 109°C).

[*] Prof. Dr. H. Musso, Dr. A. Otterbach
Institut für Organische Chemie der Universität
Richard-Willstätter-Allee 2, D-7500 Karlsruhe (FRG)

[**] Asteranes, Part 18. This work was supported by the Deutsche Forschungsgemeinschaft and the Fonds der Chemischen Industrie. We thank *A. Kuiper*, *P. Lang*, *I. Maier*, *I. Rossnagel*, *I. Süss*, and *U. Tanger* for numerous spectra, gas chromatograms, and elemental analyses and *U. Kasten* for experimental work.—Part 17: G. Kaiser, H. Musso, *Chem. Ber. 118* (1985) 2266.

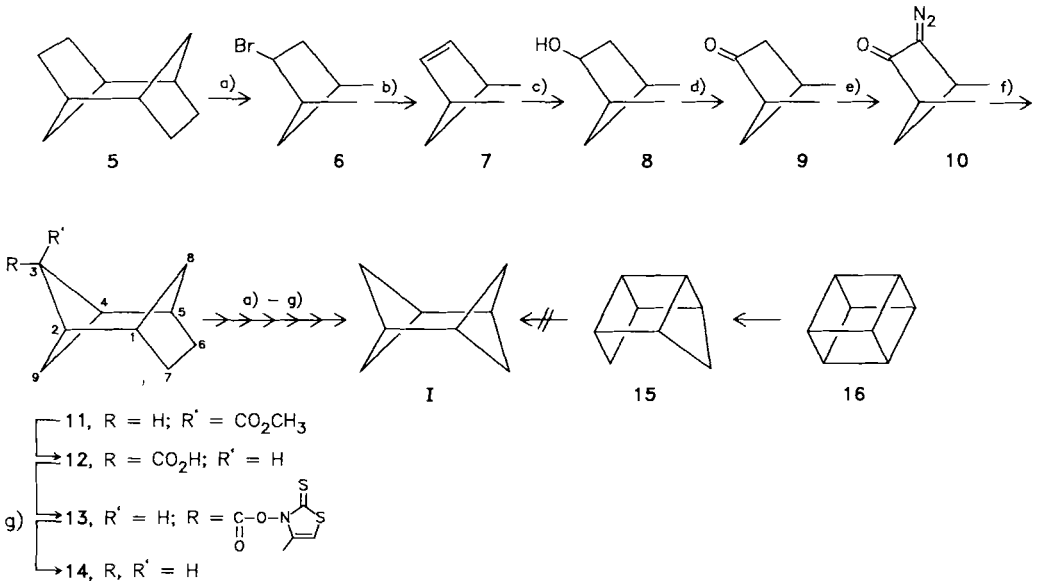

Scheme 1. a) Br_2 in CCl_4, irradiated in glass ampoules at 140°C for 1 h with a Philips HPK 125-W Hg lamp; 71% **6** after GC separation and recycling of the recovered **5**. b) DBU in DMF, 150°C, 16 h, 87% **7**; same physical data as reported in [7]. c) B_2H_6 in tetrahydrofuran (THF), 0°C, 1 h, room temperature, 12 h, then NaOH and 30% H_2O_2, 35–40°C, 4 h, 88% **8**, m.p. = 108°C. d) **8** was added to oxalyl chloride in DMSO at −50°C; triethylamine was then added and the reaction mixture was warmed to room temperature. 97% **9**, m.p. = 158°C. e) Sodium hydride in THF, then ethyl formate, 14 h, room temperature, formylketone in THF with tosyl azide and triethylamine, 24 h room temperature, 60% **10** after chromatography. Yellow crystals, m.p. = 58°C (dec.). f) **10** → **12**: irradiated in methanol at −50°C with a medium-pressure Hg lamp (HPK, 125 W) for 5 h, 51% *endo*-ester **11**; in ethanol, KOH, 12 h, 80°C, 90% *exo*-acid **12**, m.p. = 131°C; irradiation in dioxane/water (4:1) at 5°C gave 44% of the *endo*-acid **11** (R' = CO_2H), m.p. = 164°C. g) **12** → **14**: 3-hydroxy-4-methylthiazole-2(3*H*)thione, 4-dimethylaminopyridine and dicyclohexyl carbodiimide (DCC) in CH_2Cl_2, quant. *exo*-ester **13**, m.p. = 109–110°C; *endo*-ester **13** (R, R' reversed), m.p. = 101°C. Reaction of both esters with *t*BuSH in refluxing benzene for 7 h followed by flash chromatography and GC gave 82% of **14**, m.p. = 109°C.

This reaction sequence was repeated starting with **14**: bromide (78%), olefin (77%), alcohol (84%), ketone (84%), diazoketone (ca. 14%). The diazoketone was photolyzed in aqueous dioxane at 0°C. The *endo*-acid, thereby obtained in 45% yield, was degraded analogously to **12** via the corresponding thiohydroxamate. Diasterane **I** could be isolated by preparative gas chromatography: 23%, colorless, readily sublimable crystals (m.p. = 96–97°C, sealed capillary).[10]

The repulsive interaction of the *endo*-1,4 H atoms mentioned in the beginning is revealed in the ^{1}H-NMR signal at $\delta = 2.55$, which is shifted downfield beyond the signal of the bridgehead protons ($\delta = 2.45$). The corresponding signals of the hydrocarbons **5** ($\delta = 1.80$) and **14** ($\delta = 2.27$) exhibit significantly smaller downfield shifts. The long retention time upon gas-chromatographic separation is unexpected: $R_r = 1.065$ relative to cubane **16** ($R_r = 1.00$), whose hydrogenation products all come faster than seco cubane **15** ($R_r = 0.763$) on a 1G20 column at 40°C.

Received: January 26, 1987;
supplemented: March 6, 1987 [Z 2069 IE]
German version: *Angew. Chem. 98* (1987) 588

[1] a) V. Biethan, U. von Gyzycki, H. Musso, *Tetrahedron Lett. 1965*, 1477; b) H. M. Hutmacher, H.-G. Fritz, H. Musso, *Angew. Chem. 87* (1975) 174; *Angew. Chem. Int. Ed. Engl. 14* (1975) 180.
[2] E. Osawa, H. Musso, *Angew. Chem. 95* (1983) 1; *Angew. Chem. Int. Ed. Engl. 22* (1983) 1.
[3] W. Trautmann, H. Musso, *Chem. Ber. 114* (1981) 982.
[4] H. Rupp, W. Schwarz, H. Musso, *Chem. Ber. 116* (1983) 2554.
[5] R. Stober, H. Musso, E. Osawa, *Tetrahedron 42* (1986) 1757.
[6] W. Grimme, L. Schumachers, W. R. Roth, R. Breuckmann, *Chem. Ber. 114* (1981) 3197. W. Grimme, L. Schumachers, R. Gleiter, K. Gubernator, *Angew. Chem. 93* (1981) 98; *Angew. Chem. Int. Ed. Engl. 20* (1981) 113.
[7] C. W. Doeke, G. Klein, L. A. Paquette, *J. Am. Chem. Soc. 100* (1978) 1596; *101* (1979) 7599.
[8] B. Ernst, C. Ganter, *Helv. Chim. Acta 61* (1978) 1107.
[9] H. E. Zimmerman, L. W. Linder, *J. Org. Chem. 50* (1985) 1637.
[10] **14**: ^{1}H-NMR ($CDCl_3$, 250 MHz): $\delta = 0.79$ (m, 1H, *exo*-8-H, $J = 11.0$ Hz), 1.32 (m, 1H, *exo*-9-H, $J = 8.2$ and 3.8 Hz), 1.47–1.58 (m, 1H, *exo*-3-H, $J = 8.5$ Hz), 1.66 (pseudo s, 4H, 6,7-H), 1.67–1.86 (m, 2H, *endo*-3,9-H), 2.22–2.35 (m, 3H, 2,4-H and *endo*-8-H), 2.39 (br. s, 2H, 1,5-H). ^{13}C-NMR: $\delta = 27.44$ (*t*), 31.43 (*t*), 33.54 (*t*), 35.66 (*d*), 36.98 (*t*), 38.85 (*d*). — **1**: ^{1}H-NMR ($CDCl_3$, 250 MHz): $\delta = 1.66$ (br., pseudo s, 4H, *exo*-H), 2.42–2.48 (m, 4H at the bridgehead), 2.49–2.62 (m, 4H, *endo*-H). ^{13}C-NMR: $\delta = 35.81$ (d, bridgeheads), 37.35 (dd, CH_2). C_8H_{12} (108.2). MS: *m/z* 108 (0.5%, $M^{\oplus}$), 107 (2), 105 (1), 93 (18), 79 (56), 67 (68), 66 (50), 54 (100). The constitutions are in agreement with the other spectroscopic and analytical data; see A. Otterbach, *Dissertation*, Universität Karlsruhe 1986.
[11] D. H. R. Barton, D. Crich, W. B. Motherwell, *Tetrahedron 41* (1985) 3901.

β-Glycosylation in 2-Deoxysaccharides: Convergent Syntheses of the Oligosaccharides of Mithramycin**

By *Joachim Thiem** and *Bernhard Schöttmer*

Dedicated to Professor Hans Paulsen on the occasion of his 65th birthday

The cytostatic agent mithramycin **1**, which belongs to the class of aureolic acids and is highly glycosylated with oligosaccharides,[1] exhibits exclusively β-glycosidic bonds between the D-arabino and D-lyxo sugar components **A** and **B**, respectively, and between the sugars in the trisaccharide **E**–**D**–**C**, which have D-ribo, D-arabino, and D-ara-

[*] Prof. Dr. J. Thiem, Dipl.-Chem. B. Schöttmer
Organisch-Chemisches Institut der Universität
Wilhelm-Klemm-Strasse 4, D-4400 Münster (FRG)

[**] This work was supported by the Deutsche Forschungsgemeinschaft and the Fonds der Chemischen Industrie.

bino configurations, respectively, as well as between the sugar components and the aglycone.[2]

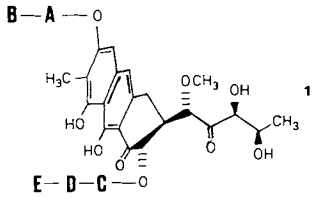

Whereas the α-glycosylated deoxyoligosaccharides are conveniently synthesized according to the *N*-iodosuccinimide (NIS) procedure,[3] and the problem of their synthesis may thus be regarded as having been solved,[4] this method has been applied with only moderate success to the β anomers.[5] In contrast, 2-bromo-2-deoxyglycosyl bromides, which are readily accessible according to the dibromomethyl methyl ether (DBE) procedure, can be favorably used for the β-glycosylation of even complex aglycones.[6]

The methyl rhamnoside **2**, which is accessible in only a few steps from mannose, can be oxidized to the 4-uloside with pyridinium dichromate (b, 62%). The product is stereospecifically reduced (c, 82%) and then benzoylated (d, 82%) to give the pure, crystalline D-talo compound **4**.[7] Reaction with dibromomethyl methyl ether and zinc bromide as catalyst (a, 70%) affords the highly reactive 2-bromo-2-deoxygalactosyl bromide **5**,[7] which can be selectively glycosylated to give the β-galactoside by reaction with benzyl alcohol in the presence of silver carbonate as catalyst at −20°C (e, 58%). Acid cleavage of the 3-formyloxy group (g, 80%) in the following step gives the alcohol component **7**.[7] Similarly, the benzoate **3** can be converted into the gluco-configurated bromide **6**[6c] by reaction with DBE (a, 89%), glycosylated (e, 72%), and selectively transformed into the partially esterified alcohol derivative **10**[6b] (g, 91%) (see Scheme 2).

Silver triflate can be used for the glycosylation of the gluco bromide **6** with the galacto alcohol **7** (f, 56%); mainly the (1→3) β-linked disaccharide **8**[7] is formed (β:α = 3:1). Reductive dehalogenation with tributyltin hydride (h, 76%) followed by alkaline treatment with sodium methoxide (i, 78%) results in formation of the **B**-**A** disaccharide fragment of **1** as the glycoside **9**.[7]

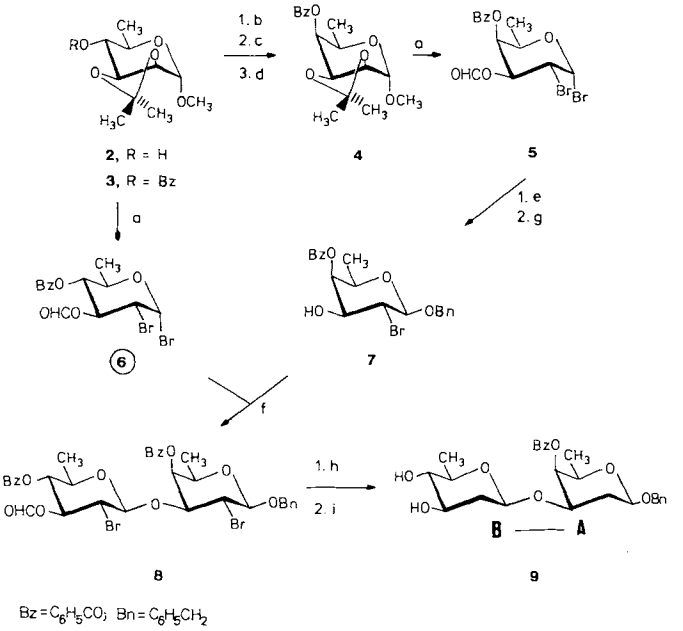

Bz = C_6H_5CO; Bn = $C_6H_5CH_2$

Scheme 1. a) $Br_2CHOCH_3/ZnBr_2$; b) $(C_5H_6N)_2Cr_2O_7/CH_3CO_2H/CH_2Cl_2$; c) $LiAlH_4$; d) C_6H_5COCl/C_5H_5N; e) $C_6H_5CH_2OH/Ag_2CO_3$; f) $AgOSO_2CF_3$; g) H_3COH/HCl; h) $(C_4H_9)_3SnH$; i) H_3CONa; j) $(C_6H_5)_3P{=}CH_2$; k) $(H_3C)_3SiCH_2MgCl$; l) *m*-Cl–C_6H_4–CO_3H.

A novel approach to the synthesis of the **E**-**D**-**C** trisaccharide with only (1→3) β-interglycosidic bonds was elaborated starting from the glycosyl bromide building block **6**. Condensation of **6** with the alcohol component **10** (f, 92%) gives a (1→3) β-linked disaccharide,[6c] which reacts, under acid catalysis (g, 90%) to give the crystalline derivative **17**.[8] Silver triflate-promoted glycosylation (f, 69%) with **6** then leads to the protected trisaccharide **18**[8] with a β:α ratio of 10:1. After selective deblocking (g, 80%) at the 3″ position, complete reductive debromination at the 2, 2′ and 2″ positions (h, 92%), and oxidation (b, 75%), the

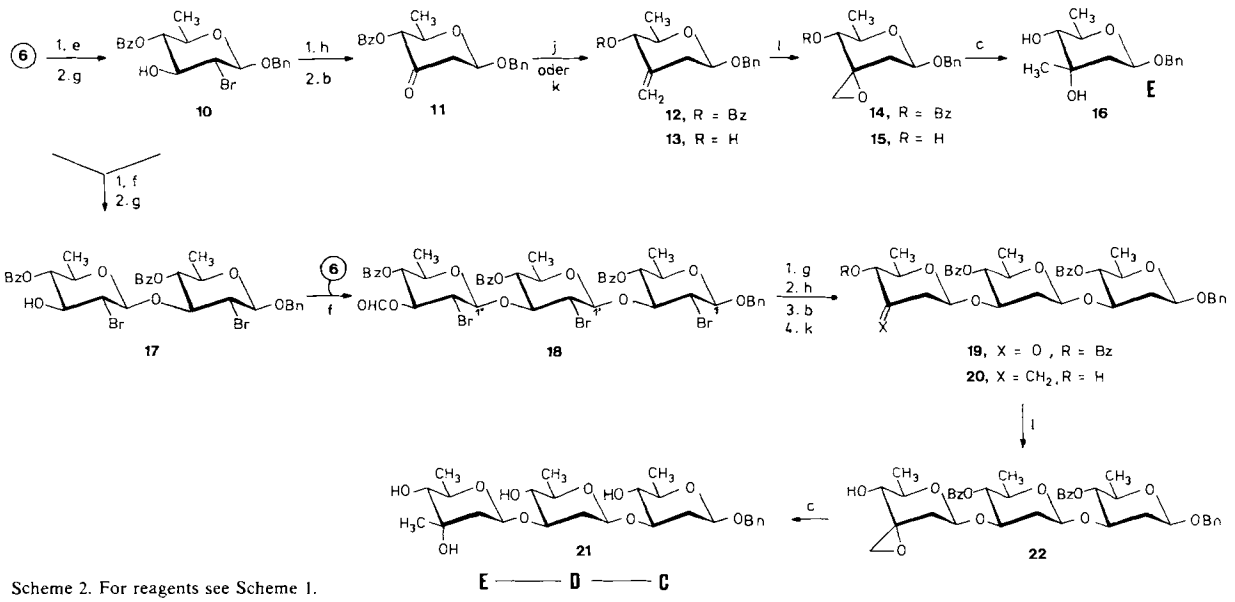

Scheme 2. For reagents see Scheme 1.

trisaccharide-3″-uloside **19**[8] is obtained, which, upon normal methyl branching reactions (MeLi, MeMgCl), gives the wrong, namely the D-arabino-configurated, terminal component (cf. [8]).

Thus, a controlled branching reaction was necessary, which was first worked out for the monosaccharide. Reductive debromination (h, 91%) of **10** and subsequent oxidation (b, 75%) affords the deoxygenated 3-uloside **11**.[8b] The methylene group can be introduced either by Wittig reaction (j, 64%) to give **12**[7] or by Peterson olefination (k, 46%) to give the derivative **13**.[7] All attempts to carry out a Sharpless epoxidation[9a] of the exocyclic allylic alcohol system of **13** were unsuccessful.[9b] Apparently, the chiral elements in the saccharide derivatives **12** and **13** already direct the epoxidation with *m*-chloroperbenzoic acid (l, 83%) completely stereospecifically to give the (3*R*)-configurated epoxides **14**[7] and **15**, respectively. Reductive opening of the epoxide results (c, 75%) in exclusive formation of the 3-*C*-methyl-branched and D-ribo-configurated glycoside **16**,[8] the *E* building block.

Whereas the Wittig olefination was unsuccessful in the case of the trisaccharide-uloside **19**, the Peterson reaction (k, 25%) gave a moderate yield of the exocyclic 3″ olefin **20**.[7] Reaction of **20** with peracid (l, 65%) leads to exclusive, stereospecific formation of the epoxide **22**,[7] which, after reductive opening (c, 68%), gives the **E**–**D**–**C** trisaccharide component **21**[7] of **1**. Comparison of the ^{1}H-NMR spectra of **21** and the trisaccharide having a terminal 3-*C*-methyl-branched D-arabino building block,[8] as well as NOE measurements, confirms the structure of **21**.

Received: January 30, 1987 [Z 2078 IE]
German version: *Angew. Chem. 99* (1987) 591

[1] W. A. Remers: *The Chemistry of Antitumor Antibiotics*, Wiley, New York 1979.

[2] a) J. Thiem, B. Meyer, *Tetrahedron 37* (1981) 551; b) J. Thiem, G. Schneider, *Angew. Chem. 95* (1983) 54; *Angew. Chem. Int. Ed. Engl. 22* (1983) 58; c) J. Thiem, G. Schneider, V. Sinnwell, *Liebigs Ann. Chem. 1986*, 814.

[3] J. Thiem, H. Karl, J. Schwentner, *Synthesis 1978*, 696.

[4] a) J. Thiem, *Nachr. Chem. Tech. Lab. 32* (1984) 6; b) *ACS Symp. Ser.*, in press; c) J. Thiem, M. Gerken, *J. Org. Chem. 50* (1985) 954.

[5] a) J. Thiem, P. Ossowski, U. Ellermann, *Liebigs Ann. Chem. 1981*, 2228; b) J. Thiem, P. Ossowski, *J. Carbohydr. Chem. 3* (1984) 287; c) J. Thiem, A. Prahst, I. Lundt, *Liebigs Ann. Chem. 1986*, 1044.

[6] a) K. Bock, C. Pedersen, J. Thiem, *Carbohydr. Res. 73* (1979) 85; b) J. Thiem, M. Gerken, *J. Carbohydr. Chem. 1* (1982/1983) 229; c) J. Thiem, M. Gerken, K. Bock, *Liebigs Ann. Chem. 1983*, 462; d) I. Lundt, J. Thiem, A. Prahst, *J. Org. Chem. 49* (1984) 3063.

[7] Selected analytical data ($[\alpha]_D^{20}$ for $c = 0.2$–1.3 in CH_2Cl_2; ^{1}H-NMR at 300 MHz in $CDCl_3$): **4**: $[\alpha] = +63.8°$; $\delta = 4.99$ (d, $J(1,2) = 1.2$ Hz; 1-H); m.p. = 132°C. — **5**: $[\alpha] = +297.6°$; $\delta = 6.59$ (d, $J(1,2) = 3.5$ Hz; 1-H). — **7**: $[\alpha] = +36.4°$; $\delta = 4.60$ (d, $J(1,2) = 8.4$ Hz; 1-H), 3.97 (ddd, $J(3,3\text{-OH}) = 3.8$ Hz; 3-H). — **8**: $[\alpha] = +38.5°$; $\delta(C_6D_6) = 4.49$ (d, $J(1,2) = 8.6$ Hz; 1-H), 4.69 (d, $J(1',2') = 8.6$ Hz; 1′-H). — **9**: $[\alpha] = -7.4°$; $\delta = 4.55$ (dd, $J(1,2a) = 9.2$ Hz; 1-H), 4.57 (dd, $J(1',2a') = 9.1$ Hz; 1′-H). — **12**: $[\alpha] = -70.6°$; $\delta = 4.62$ (dd, $J(1,2a) = 9.2$, $J(1,2e) = 2.6$ Hz; 1-H), 4.92, 5.28 (each m, each 1H; $H_2C=$). — **13**: $[\alpha] = -11.7°$; $\delta = 4.90$, 5.05 (each br. s, each 1H; $H_2C=$); m.p. = 96°C. — **14**: $[\alpha] = -33.7°$; $\delta = 2.61$, 2.72 (each d, each 1H; CH_2–O(epoxide)). — **20**: $[\alpha] = -53.7°$; $\delta = 4.79$, 4.94 (each br. d, each 1H; $H_2C=$), 3.45 (dd≈t, $J(4'',4''\text{-OH}) = 7.0$, $J(4'',5'') = 9.0$ Hz; 4″-H). — **21**: $[\alpha] = -58.3°$; $\delta = 4.83$ (dd, $J(1'',2a'') = 9.4$, $J(1'',2e'') = 2.2$ Hz; 1″-H), 3.69 (dq, $J(4'',5'') = 9.4$, $J(5'',6'') = 6.4$ Hz; 5″-H), 1.21 (s, 3H; 3″-CH_3). — **22**: $[\alpha] = -66.9°$; $\delta = 2.47$, 2.91 (each d, each 1H, $J(A,B) = 4.5$ Hz; CH_2–O(epoxide)).

[8] J. Thiem, M. Gerken, B. Schöttmer, J. Weigand, *Carbohydr. Res.*, in press.

[9] a) K. B. Sharpless, S. S. Woodard, M. G. Finn, *Pure Appl. Chem. 55* (1983) 1923; b) in accordance with the stereochemistry of the allylic alcohol fragment in **13**, the formation of the (3*R*) epoxide **15** was expected to occur via attack from the *Re* side with *tert*-butyl hydroperoxide, titanium isopropoxide, and (*R,R*) diethyl (+)-tartrate.

Diastereoselective Strecker Synthesis of α-Aminonitriles on Carbohydrate Templates**

By *Horst Kunz** and *Wilfried Sager*

Dedicated to Professor Hans Paulsen on the occasion of his 65th birthday

Chiral amino acids are of great biological and economic importance. This is also true of the nonproteogenic (*R*) enantiomers, which are found as components of many microbial products, in particular antibiotics. The diastereoselective syntheses of amino acids[1] are usually carried out via organometallic intermediates: for example, the approach via metalated bislactim ethers of cyclic dipeptides.[2] Besides the isolation from protein hydrolysates and the enzymatic reactions,[3] the Strecker synthesis is interesting from an economic viewpoint and has already been performed diastereoselectively with 1-phenylethylamine[4–6] and with (4*S*,5*S*)-5-amino-2,2-dimethyl-4-phenyl-1,3-dioxane.[7] Optical inductions of 50–75% were achieved.[5] The very high inductions (98% *de*) obtained in one case[8] proved to be a consequence of fractionations.[4] Highly enriched or even pure diastereomers are obtained only when one of the diastereomers precipitates out.[9, 10] This applies to the *N*-4-phenyl-1,3-dioxan-5-yl-substituted α-methyl-α-aminonitriles.[7]

Using the concept that the chirality of the carbohydrates can be exploited for diastereoselective reactions,[11] we have now developed a Strecker synthesis with glycosyl amines as chiral auxiliaries.[12] The 2,3,4,6-tetra-*O*-pivaloyl-β-D-galactopyranosylamine **3** proved to be especially effective. It can be obtained from penta-*O*-pivaloyl-β-D-galactopyranose **1** by reaction with trimethylsilyl azide/tin tetrachloride[13] to give the galactosyl azide **2** followed by its hydrogenation.[12, 14]

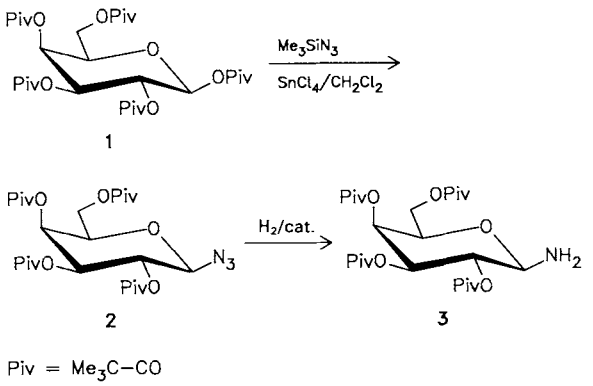

N-Glycosylaminonitriles are formed in high yields from aldehydes, sodium cyanide, and glacial acetic acid in 2-propanol, the (α*R*) diastereomers[15] being favored in a ratio of 5:1. However, reaction times of two weeks are necessary. This results in partial anomerization, presumably at the stage of the Schiff base intermediate, giving up to 20% of the α-configurated glycosylaminonitriles. The long reaction times can be avoided and the anomerization largely suppressed by first synthesizing the Schiff bases **4** from **3** and the respective aldehyde in 2-propanol or heptane in the presence of acetic acid. The aldimines **4**, formed in

[*] Prof. Dr. H. Kunz, Dipl.-Chem. W. Sager
Institut für Organische Chemie der Universität
J.-J.-Becher-Weg 18–20, D-6500 Mainz (FRG)

[**] This work was supported by the Fonds der Chemischen Industrie.

high yields, react with trimethylsilyl cyanide[5, 16, 17] in the presence of zinc chloride in 2-propanol or tin tetrachloride in tetrahydrofuran (THF) to give nearly quantitative yields of the corresponding *N*-glycosyl-α-aminonitriles **5** (Scheme 1).

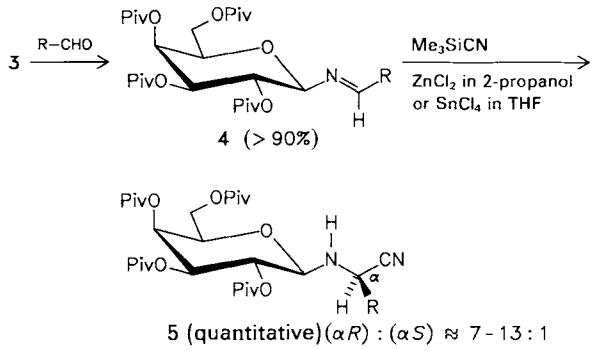

Scheme 1.

The reactions are complete after only a few minutes at room temperature and in the presence of equimolar amounts of Lewis acids as catalysts. At lower concentrations of catalyst (5 mol%), they require about 12 h. The (α*R*) diastereomers **5** are preferentially formed in a ratio of about 7 : 1. At lower temperatures and corresponding longer reaction times, the diastereoselectivity can be increased to more than 10 : 1. The ratios of diastereomers were determined by analytical HPLC (diode array detector 190–370 nm) and 400-MHz ^{1}H-NMR spectroscopy for the quantitatively produced mixture of products obtained by hydrolysis. The results of the two methods are in agreement. The HPLC chromatograms reveal that the α-anomeric α-aminonitriles are only formed in trace amounts or at most in amounts of up to 5%. The results of the diastereoselective Strecker synthesis are shown in Table 1. Recrystallizing once from heptane affords the (α*R*) diastereomers of the *N*-glycosyl-α-aminonitriles **5**, which are pure by elemental analysis and NMR spectroscopy, in yields of between 75 and 90%.

We ascribe the high selectivity of this Strecker reaction to steric and stereoelectronic effects arising from the carbohydrate. Charge transfer from the C=N π orbital into the σ* orbital of the ring C–O bond favors the conformation **A** for the Schiff base **4**. Conformation **A** is confirmed by a strong NOE in the ^{1}H-NMR spectrum between H-1 and the proton introduced by the aldehyde. Because of the large axial substituent at C-4, the Lewis acids presumably complex and attack the aldimines **4** in the conformation **A** from below. This is revealed in the ^{1}H-NMR spectrum of the complex by a pronounced broadening of the signals of the axial protons H-1, H-3, and H-5, which project below the ring. The cyanide generated from the silyl cyanide in the polar solution can then approach from the opposite, free side, i.e., from the side of the ring oxygen, resulting in preferential formation of the (α*R*) diastereomer. We conclude from this hypothesis that it should be possible, by suitably changing the reaction conditions, to reverse the sense of induction. Preliminary experiments substantiate this conclusion.[18]

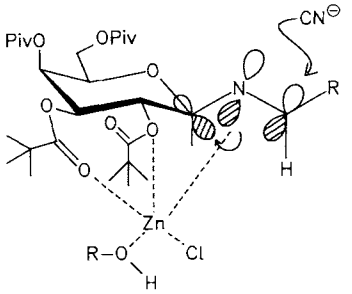

A

Interesting chiral products can be prepared from the (α*R*)-*N*-glycosyl-α-aminonitriles **5**, which are thereby selectively formed in high yields. For example, acid hydrolysis yields D-amino acids such as **6**. These do not contain the L enantiomers according to thin layer chromatography on "Chiral plate."[19] The measured optical rotations are also in agreement with reported values.[20] After hydrolysis, the pivaloylated galactose moieties can be recovered to a large extent (70–90%) by extraction with dichloromethane.

According to the procedure described here, enantiomerically pure D-amino acids and their derivatives are thus available by using inexpensive carbohydrate templates to

Table 1. Diastereoselective Strecker synthesis by reaction of the aldimines **4** with trimethylsilyl cyanide according to Scheme 1.

R	Solvent	Catalyst (mol %)	*T* [°C]	Reaction time [h]	Diastereoselectivity (α*R*)-**5** : (α*S*)-**5** [15]	α Anomer	Pure (α*R*)-**5** [15] (yield [%])
p-tolyl	2-propanol	$ZnCl_2$ (100)	0	1	6.5 : 1	traces	**5a** (78)
	THF	$SnCl_4$ (130)	−78 → −30	8	12 : 1	traces	**5a** (87)
p-NO_2-C_6H_4	2-propanol	$ZnCl_2$ (5)	20	48	7 : 1	5%	**5b** (80)
o-NO_2-C_6H_4	THF	$SnCl_4$ (130)	−30	8	only (*R*)	traces	**5c** (91)
p-F-C_6H_4	2-propanol	$ZnCl_2$ (5)	20	24	6.5 : 1	5%	**5d** (75)
	THF	$SnCl_4$ (130)	−78 → −30	8	10 : 1	traces	**5d** (84)
p-Cl-C_6H_4	THF	$SnCl_4$ (130)	−60 → −10	6	11 : 1	—	**5e** (84)
Me_2CH–	THF	$SnCl_4$ (130)	−78 → −10	5	8 : 1	traces	**5f** (74)
Me_3C–	THF	$SnCl_4$ (130)	−78 → −10	3	13 : 1	traces	**5g** (86)

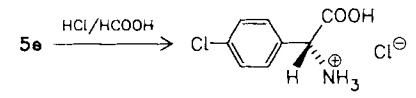

6 (94%)

direct the stereochemistry. The intermediacy of organometallic compounds, the exclusion of oxygen, and tedious separations and workup are thereby avoided.

Received: February 4, 1987;
supplemented: March 18, 1987 [Z 2090 IE]
German version: *Angew. Chem. 99* (1987) 595

[1] a) Review: J. Martens, *Top. Curr. Chem. 125* (1984) 165; b) D. A. Evans, A. E. Weber, *J. Am. Chem. Soc. 108* (1986) 6757.
[2] U. Schöllkopf, *Topl Curr. Chem. 109* (1983) 65.
[3] Review: A. Kleemann, W. Leuchtenberger, B. Hoppe, H. Tanner in: *Ullmann's Encyclopedia of Industrial Chemistry, Vol. A2*, VCH Verlagsgesellschaft, Weinheim 1985, p. 57.
[4] K. Harada, T. Okawara, *J. Org. Chem. 38* (1973) 707.
[5] J. Ojima, S. Inaba, *Chem. Lett. 1975*, 737.
[6] D. M. Stout, L. A. Black, W. L. Matier, *J. Org. Chem. 48* (1983) 3098.
[7] K. Weinges, H. Blackholm, *Chem. Ber. 113* (1980) 3098.
[8] M. S. Patel, M. Worsley, *Can. J. Chem. 48* (1970) 1881.
[9] K. Weinges, H. Brachmann, P. Stahnecker, H. Rodewald, M. Nixdorf, H. Irngartinger, *Liebigs Ann. Chem. 1985*, 566, see the two-step procedure discussed there.
[10] See also P. K. Subramanian, R. W. Woodard, *Synth. Commun. 16* (1986) 337; the product crystallizes from methanol; the optical induction is reported for the substance recrystallized a second time from methanol.
[11] H. Kunz, B. Müller, D. Schanzenbach, *Angew. Chem. 99* (1987) 297; *Angew. Chem. Int. Ed. Engl. 26* (1987) 294.
[12] H. Kunz, W. Sager, W. Pfrengle, M. Decker, unpublished results; German patent application P3624376.0 (18 July 1986).
[13] H. Paulsen, Z. Györgydeak, M. Friedmann, *Chem. Ber. 107* (1974) 1590.
[14] M. Decker, *Diplomarbeit*, Universität Mainz 1983.
[15] The *R/S* descriptor refers to the α-C atom of the aminonitrile moiety; the configuration of the carbohydrate moiety remains unchanged.
[16] W. Lidy, W. Sundermeyer, *Chem. Ber. 106* (1973) 587.
[17] D. A. Evans, L. K. Truesdale, G. L. Carroll, *J. Chem. Soc. Chem. Commun. 1973*, 55.
[18] H. Kunz, W. Sager, W. Pfrengle, unpublished results.
[19] K. Günther, J. Martens, M. Schickedanz, *Angew. Chem. 96* (1984) 514; *Angew. Chem. Int. Ed. Engl. 23* (1984) 506; see brochure "Chiral plate," Macherey & Nagel, Düren 1985/86.
[20] **6**: $[\alpha]_D^{22} = -135.1°$ ($c = 0.5$, 1 N HCl); according to [21] $[\alpha]_D = -138°$ ($c = 1$, 1 N HCl).
[21] K. Yokozeki, K. Mitsugi, C. Eguchi, H. Iwagami, DOS 285245 (December 14, 1978), Ajinomoto Inc., Tokyo.

Synthesis of Tricyclo[5.2.0.0^{1,3}]nona-4,6,8-triene, a Norcaradiene Structure Constrained by the Antiaromaticity of Cyclobutadiene

By *Takeshi Kawase, Masahiko Iyoda,* and *Masaji Oda**

Cycloheptatriene–norcaradiene tautomerism has long attracted the attention of organic chemists.[1] Although cycloheptatriene itself is thermodynamically more stable than norcaradiene by about 4 kcal mol^{-1},[2] the tautomeric equilibrium is sensitive to the steric and electronic effects of substituents. *Klärner* and co-workers have shown that the derivatives of 5*H*-cyclobutacycloheptene **1** exist exclusively in the norcaradiene form **2** owing to the strong antiaromaticity of cyclobutadiene.[3] However, no synthesis of the 3*H*-isomer **3** or its tautomer **4** has been described.

[*] Prof. Dr. M. Oda, Dr. M. Iyoda, Dr. T. Kawase
Department of Chemistry, Faculty of Science, Osaka University
Toyonaka, Osaka 560 (Japan)

We wish to report here the synthesis of tricyclo[5.2.0.0^{1,3}]nona-4,6,8-triene **4**, involving a novel thermal rearrangement of 1-chlorobicyclo[6.1.0]nona-2,4,6-triene **8**.

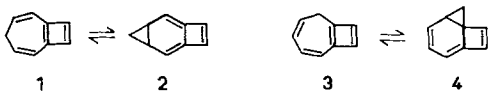

Photochemical chlorination of *cis*-bicyclo[6.1.0]nona-2,4,6-triene **5** with *tert*-butyl hypochlorite (1.5 equivalents) in rather concentrated CCl_4 solution (ca. 0.8 M) at −30 °C gave **8** in 50–70% yield after chromatographic purification (SiO_2, pentane, 0 °C). Although **8** (Table 1) is fairly stable below 0 °C, it underwent thermal rearrangement around and above room temperature in nonpolar solvents to give *cis*-7-chlorobicyclo[5.2.0]nona-2,4,8-triene **7** and indene **11** in an almost constant ratio of 7:3.[4] In a polar solvent (CH_3CN) or on adsorption to silica gel, **7** further rearranged to 1-[(*E*)-2-chlorovinyl]cycloheptatriene **9**.[5,6] Scheme 1 explains these rearrangements based on the results of trapping experiments and reported mechanistic pathways.[7,8] Notably, **7**, although its formation is symmetry allowed, is a new type of product that has not been previously observed in the extensively studied thermal rearrangement of bicyclo[6.1.0]nona-2,4,6-trienes.[8] The chlorine atom seems to play a role in changing the thermodynamics of these rearrangements.

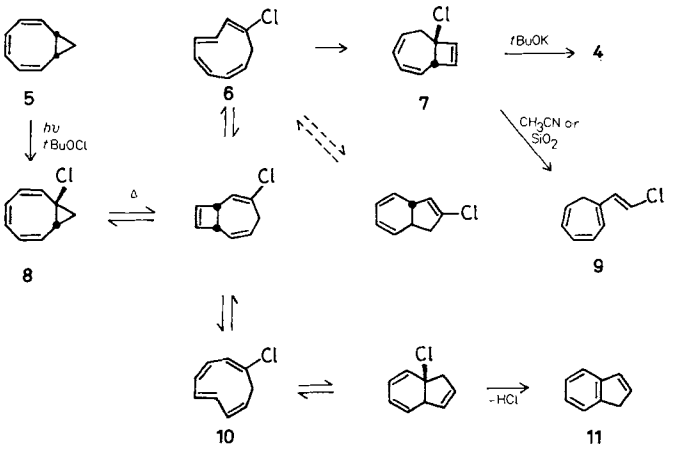

Scheme 1.

Having **7** in hand, we expected it to be a good precursor for **3** or **4**, even though the lability of **7** made its isolation in pure form difficult. Treatment of a mixture of **7** and **11** with *t*BuOK (1.5 equivalents) in tetrahydrofuran under air at room temperature gave **4** as sole hydrocarbon product in about 50% yield (from **8**). The presence of oxygen is advantageous for destroying indene through oxidation of the indenide ion. Compound **4** can be formed in principle either by direct 1,7-elimination of hydrogen chloride or by 1,2-elimination followed by valence isomerization; however, the former process seems more likely since the reluctant 1,2-elimination would result in the formation of a cyclobutadiene.[9]

The norcaradiene **4** tended to decompose giving oligomeric substances on removal of solvents. A fairly clean solution for NMR spectra could be obtained, however, by

column chromatography on silica gel at $-20°C$ (pentane elution) followed by careful replacement of the solvent with CCl_4 or C_6D_6. ^1H- and ^{13}C-NMR spectra (Table 1) of the solutions thus obtained are in accord with the norcaradiene structure of **4** without any indication of equilibration with the cycloheptatriene **3**.

Table 1. Physical data for the compounds **4**, **7**, **8**, **12**, and **13**. *J* in Hz.

4: ^1H-NMR (100 MHz, C_6D_6, 4°C): $\delta = 0.91$ (t, $J = 3.5$; H-2_{endo}), 1.32 (dd, $J = 8.5, 3.5$; H-2_{exo}), 1.82 (ddd, $J = 8.5, 4.0, 3.5$; H-3), 5.20 (d, $J = 5.5$; H-6), 5.53 (dd, $J = 9.5, 5.5$; H-5), 5.92 (dd, $J = 9.5, 4.0$; H-4), 6.21 (d, $J = 2.5$; H-9), 6.73 (d, $J = 2.5$; H-8); ^{13}C-NMR ($CDCl_3$): $\delta = 13.8$ (C-2), 21.6 (C-3), 42.8 (C-1), 104.5 (C-6), 121.7, 124.1 (C-4, 5), 132.6, 138.6 (C-8, 9), 152.6 (C-7)

7: ^1H-NMR ($CDCl_3$): $\delta = 2.60$ (2H, m), 3.67 (1H, m), 5.8–6.2 (6H, m); Diels–Alder adduct with 4-phenyl-1,2,4-triazole-3,5-dione: m.p. = 146°C; ^1H-NMR (C_6D_6): $\delta = 2.11$ (1H, dd, $J = 15.5, 3.3$), 2.62 (1H, dd, $J = 15.5, 3.9$), 3.09 (1H, d, $J = 4.5$), 4.52 (2H, m), 5.55 (2H, m), 5.72 (1H, dd, $J = 2.7, 1.0$), 5.81 (1H, dd, $J = 2.7, 1.0$), 6.9–7.3 (3H, m), 7.70 (2H, m)

8: ^1H-NMR ($CDCl_3$, $-30°C$): $\delta = 0.78$ (1H, dd, $J = 7.5, 5.5$), 1.45 (1H, dd, $J = 10.5, 5.5$), 2.09 (1H, br. dd, $J = 10.5, 7.5$), 5.73 (1H, dd, $J = 11.0, 1.5$), 5.8–6.4 (5H, m); MS: *m/z* 153, 151 ($M^{\oplus}$), 117 (46%), 115 (100%); UV (cyclohexane): $\lambda_{max} = 245$ nm ($\varepsilon = 3200$)

12: m.p. = 150°C (dec.); ^1H-NMR ($CDCl_3$): $\delta = 0.48$ (1H, dd, $J = 6.1, 2.2$), 0.84 (1H, dd, $J = 7.2, 6.1$), 2.40 (1H, ddd, $J = 7.2, 4.5, 2.2$), 5.14 (1H, ddd, $J = 6.0, 4.5, 1.0$), 6.00 (1H, dd, $J = 7.9, 6.0$), 6.38 (1H, dd, $J = 7.9, 1.0$), 6.68 (1H, d, $J = 2.4$), 6.86 (1H, d, $J = 2.4$), 7.1–7.5 (5H, m)

13: m.p. = 195°C; ^1H-NMR ($CDCl_3$): $\delta = 2.48$ (2H, d, $J = 5.5$), 3.37 (2H, m), 4.97 (1H, dt, $J = 10.0, 5.5$), 5.6–6.0 (3H, m), 7.0–7.8 (14H, m); UV (cyclohexane): $\lambda_{max} = 269$ nm ($\varepsilon = 4350$), 275 (4800), 298 (4000)

Reaction of **4** with 4-phenyl-1,2,4-triazole-3,5-dione gave the Diels–Alder adduct **12** (yield 60%),[10] whereas reaction with 1,3-diphenylisobenzofuran gave the adduct **13** (33%) (both at room temperature). The adduct **13** can be formed through either an addition–tautomerization or a tautomerization–addition (i.e., via **3**) process. Since no dimers of **3** were detected during decomposition of **4**, the addition–tautomerization process is more likely.

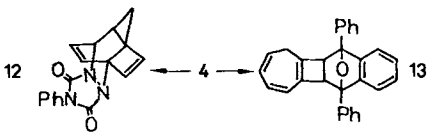

Thus, the large antiaromatic destabilization of cyclobutadiene forces **3**, like **1**,[3] to tautomerize to **4** despite the accompanying increase in strain.

Received: February 10, 1987 [Z 2100 IE]
German version: *Angew. Chem. 99* (1987) 572

[1] Reviews: a) G. Maier, *Angew. Chem. 79* (1967) 446; *Angew. Chem. Int. Ed. Engl. 6* (1967) 402; b) E. Vogel, *Pure Appl. Chem. 20* (1969) 237; c) K. Takeuchi, *Yuki Gosei Kagaku Kyokaishi (J. Synth. Org. Chem. Jpn.) 43* (1985) 40.

[2] M. B. Rubin, *J. Am. Chem. Soc. 103* (1981) 7791.

[3] a) F.-G. Klärner, E. K. G. Schmidt, M. A. Rahman, *Angew. Chem. 94* (1982) 136; *Angew. Chem. Int. Ed. Engl. 21* (1982) 138; b) F.-G. Klärner, E. K. G. Schmidt, M. A. Rahman, H. Kollmar, *ibid. 94* (1982) 137 and *21* (1982) 139.

[4] The decrease in the concentration of **8** (^1H-NMR in CCl_4) follows first-order kinetics: $\log k = (11.75 \pm 0.3) - (22300 \pm 500)/2.303\,RT$.

[5] Compound **9** was identified from its spectral data and by independent synthesis from 1,3,5-cycloheptatriene-1-carbaldehyde and chloromethylenetriphenylphosphorane.

[6] A similar rearrangement: R. Huisgen, W. E. Konz, *J. Am. Chem. Soc. 92* (1970) 4102.

[7] Intermediacy of the two isomeric chlorocyclononatetraenes **6** and **10** was confirmed by their trapping as Diels–Alder adducts with 1,3-diphenylisobenzofuran: m.p. = 180°C (dec.), yield 38% and m.p. = 240°C (dec.), 13%, respectively.

[8] A recent review: F.-G. Klärner, *Top. Stereochem. 15* (1984) 1.

[9] a) M. P. Cava, M. J. Mitchell: *Cyclobutadiene and Related Compounds*, Academic Press, New York 1967; b) R. Breslow, M. Oda, T. Sugimoto, *J. Am. Chem. Soc. 96* (1974) 1639.

[10] Eu(fod)$_3$-shifted ^1H-NMR spectra of **12** suggest the depicted stereochemistry, in agreement with the expectation based on steric effects for the cycloaddition.

Crystal Structure Analysis of the 1,2,4,7-*anti*-Tetramethyl-2-norbornyl Cation: an Unsymmetrically Bridged Carbocation**

By *Thomas Laube**

Since the discovery by *Meerwein* and *van Emster*[1] that carbocations can occur as intermediates in solvolysis reactions, these ions have been the subject of many investigations because of the numerous, usually very rapid rearrangements they undergo. The 2-norbornyl cation **1** has come to occupy a position of central importance in physical and organic chemistry; the question whether this ion, even at very low temperatures, exists as a pair of rapidly equilibrating, unsymmetrical ions, **1** and **1'** (both of which

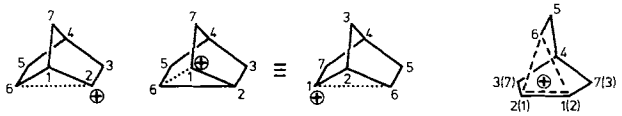

are unsymmetrically bridged according to the present state of knowledge; i.e., they exhibit weak C2–C6 and C1–C6 bonding, respectively) or as a symmetrically bridged ion **1''** having a plane of symmetry is extremely difficult to answer and has been approached by many methods[2] (NMR spectroscopy in liquid[2b] and solid[2c] phase, mass spectrometry,[2d] and ESCA,[2e] as well as solvolytic,[2f] thermochemical,[2g] and theoretical[2h] investigations). Of the more than 100 known substituted 2-norbornyl cations, the 1,2-dimethyl-substituted derivative **2** is particularly important[3] owing to its structural similarity to **1** and has been used as a model ("minimal perturbation introduced by the methyl groups"[4a]), even though **2** unquestionably exists as a pair of equilibrating, unsymmetrical ions.[4] Up to now, no crystal structure analysis of a 2-norbornyl cation or indeed of any bridged carbocation has been reported; there are only two reports providing evidence for the existence of crystalline 2-norbornyl salts.[2c,5] The reasons are the low thermal stability of many 2-norbornyl salts and their pronounced tendency to form plastic crystals.[6] After many unsuccessful attempts,[7] we have now succeeded in determining the crystal structure of the 1,2,4,7-*anti*-tetramethyl-2-norbornyl cation **3** (as the salt **3**-Sb_2F_{11}).

[*] Dr. T. Laube
Laboratorium für Organische Chemie der
Eidgenössischen Technischen Hochschule
ETH-Zentrum, Universitätstrasse 16, CH-8092 Zürich (Switzerland)

[**] I thank Prof. Dr. *D. Seebach* for financial support, Prof. Dr. *J. D. Dunitz* for providing me with measuring time, and Prof. Dr. *P. von R. Schleyer* (Universität Erlangen-Nürnberg) for numerous suggestions in the discussion of the results. I would like to especially thank *Thomas Blatter* for carrying out numerous syntheses and *Paul Seiler* for assistance in carrying out the measurements.

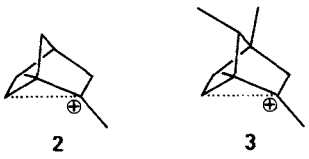

2 3

In order to synthesize this salt, isofenchone **4**[8] was converted into the fluoronorbornane **5**,[9] which, upon treatment with antimony pentafluoride,[10] underwent fluoride abstraction. The intention was to use a salt of the 1,2,5,5-tetramethyl-2-norbornyl cation **6**, which has a plane of symmetry in the transition state of the Wagner-Meerwein rearrangement, for the structure elucidation; the crystal structure analysis established,[11] however, that the crystalline compound was **3**-Sb_2F_{11}.[12]

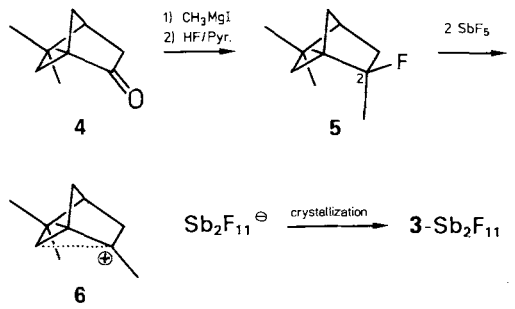

Figure 1 shows that the crystal consists of discrete cations and anions, neither of which exhibit symmetry. The shortest $C^{\delta+}\cdots F$ distances (C1···F15 3.28(1), C2···F15 3.27(1) Å) are probably longer than those in the trimethyladamantyl cation because of the (unsymmetrical) delocalization of the positive charge over C1 and C2 and because of several F···H van der Waals contacts.[13,14] A case of unsymmetrical σ-participation is evident in cation **3** (see Table 1). The formerly single bond C1-C6 is weakened by donating electron density to the electron-deficient center C2 and thereby lengthened to 1.74(2) Å. This increases the electron density in the bond C1-C2, which is thereby shortened to 1.44(2) Å. The angle C2-C1-C6 (81.6(8)°) and the distance C2-C6 (2.09(2) Å) also reflect the bridging between C2 and C6 (for comparison, in norbornane (see also Fig. 2) the distances C1-C6 and C1-C2 are 1.544 Å, the angle C2-C1-C6 is 108.2°, and the distance C2-C6 is 2.501 Å). The atom C2 exhibits nearly planar coordination, whereas C1 exhibits a pyramidalization of 0.23 Å (the partial bonds to C6 being ignored in each case); this finding is also in agreement with the assumption that the larger partial charge is on C2 and the smaller on C1 (the partial charge on C6 should be considerably smaller since a primary cationic center at C6 appears in the corresponding resonance formula). The Wagner-Meerwein rearrangement (analogous to **1** → **1'**) is thus indicated in the structure. The conformation of **3** is, at the same time, also stereoelectronically optimal for the two other rearrangements in 2-norbornyl cations, the 6,2-*endo*- and the 3,2-*exo*-hydride shift.[15] The bond of the *endo*-proton H62 to C6 forms a torsion angle of ca. +26° with the upward pointing part of the symmetry axis of the "empty" p orbital[16] at C2, and the bond of the *exo*-proton H31 to C3 forms a torsion angle of ca. +14° with the downward pointing part of the p symmetry axis at C2 (these torsion angles are only approximate values since they refer to calculated hydrogen positions).

The geometry of the skeleton of **3**, which significantly differs from the geometry of the norbornane skeleton (see

Table 1. The most important structure data of **3**-Sb_2F_{11} (distances in Å, angles and torsion angles in °; standard deviations (in parentheses) refer to the last decimal place given). The planes P*i* are formed by the following atoms: P*1*, C2,C7,C*11*; P2, C*1*,C3,C*21*; *P3*, C*1*,C2,C3,C7,C*11*,C*21*. pC*i* is a point on the direction vector of the p-like orbital on the threefold coordinated atom C*i* [16]; ′ means the symmetry operations 1−x, −0.5+y, 1.5−z.

C1-C2	1.44(2)	C1-C2-C6	55.4(6)	C4-C5	1.53(2)
C1-C6	1.74(2)	C1-C6-C2	43.0(5)	C5-C6	1.52(2)
C2-C6	2.09(2)	C2-C1-C6	81.6(8)	C1-C11	1.51(2)
				C2-C21	1.47(2)
P1-C1	−0.23	C6-C1-C7	98.8(8)	C4-C41	1.50(2)
		C6-C1-C11	113.2(9)	C7-C71	1.51(1)
P2-C2	+0.03	C6-C2-C3	95.8(7)		
		C6-C2-C21	116.6(9)	Sb1-F1-Sb2	163.0(7)
P3-C1	+0.20	C4-C5-C6	102.1(9)		
P3-C2	+0.06	C4-C7-C71	116.6(8)	pC1-C1-C6	15.2
P3-C3	−0.01	C1-C7-C71	115.8(8)	pC2-C2-C6	35.9
P3-C7	−0.10	C5-C6-C1	104.3(9)	pC1-C1-C2-pC2	− 4.0
P3-C11	−0.07	C5-C6-C2	97.2(8)	pC1-C1-C2-F15	+179.4
P3-C21	−0.07			pC2-C2-C1-F15	+176.6
		C1-C2-C3	108.0(9)	C1-C2-C3-C4	− 19.(1)
C2-C3	1.50(1)	C2-C3-C4	101.7(8)	C2-C3-C4-C7	+ 42.3(9)
C3-C4	1.55(1)	C3-C4-C7	100.0(8)	C3-C4-C7-C1	− 48.5(9)
C4-C7	1.53(1)	C4-C7-C1	98.4(8)	C4-C7-C1-C2	+ 38.(1)
C7-C1	1.52(1)	C7-C1-C2	106.7(9)	C7-C1-C2-C3	− 12.(1)
				C11-C1-C2-C3	−163.(1)
C1-F15	3.28(1)	pC1-C1-F15	173.5	C6-C1-C2-C3	+ 84.5(9)
C2-F15	3.27(1)	pC2-C2-F15	168.0	C7-C1-C2-C21	+164.(1)
C2-F21′	3.64(1)	pC2-C2-F21′	51.0	C11-C1-C2-C21	+ 13.(2)
				C6-C1-C2-C21	− 99.(1)

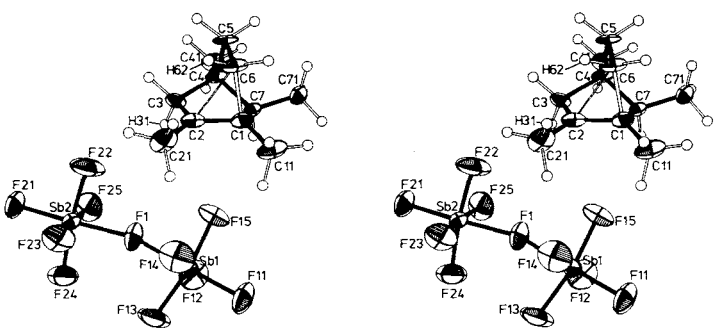

Fig. 1. Stereodrawing (ORTEP) of the crystal structure of 3-Sb_2F_{11}. The ellipsoids of thermal vibration are drawn at the 50% level. The ion pair shown forms the asymmetric unit.

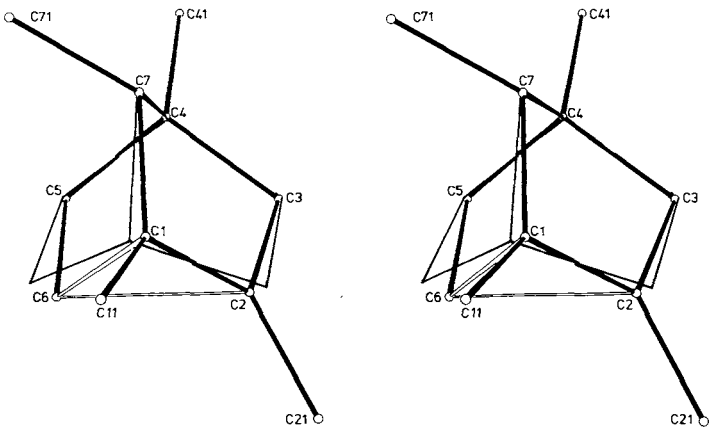

Fig. 2. Stereodrawing of superimposed skeletons of the cation **3** (atoms drawn as spheres; bonds drawn as thick lines) and norbornane [17] (bonds drawn as thin lines). The atoms C3, C4, C5, and C7 were fitted with a hundredfold weighting compared with C1, C2, and C6.

Fig. 2), is more similar to the geometry[18] calculated for the symmetrical 2-norbornyl cation **1''** (although significant differences still exist[19]). This is an unexpected finding, since a tertiary cation is transformed into a tertiary cation in the Wagner–Meerwein rearrangement of **3** (or **2**), both of which are much more stable than secondary cations and therefore should not exhibit the same tendency as the latter to engage in charge delocalization through bridging. Thus, the structural data establish that the skeleton of 2-norbornyl cations generally favors bridging.[20]

Overall, the results of the crystal structure analysis of **3** are in agreement with the results obtained earlier by other methods[4] for the rapidly equilibrating, partially σ-delocalized ion **2**.

Received: March 2, 1987;
supplemented: March 23, 1987 [Z 2122 IE]
German version: *Angew. Chem. 99* (1987) 578

[1] H. Meerwein, K. van Emster, *Ber. Dtsch. Chem. Ges. 55* (1922) 2500.

[2] Reviews: a) G. A. Olah, G. K. S. Prakash, J. Sommer: *Superacids*, Wiley, New York 1985, p. 132; H. C. Brown: *The Nonclassical Ion Problem*, Plenum Press, New York 1977, p. 83; P. Vogel: *Carbocation Chemistry*, Elsevier, Amsterdam 1985, p. 281.—Selected articles: b) G. A. Olah, G. K. S. Prakash, M. Arvanaghi, F. A. L. Anet, *J. Am. Chem. Soc. 104* (1982) 7105; c) C. S. Yannoni, V. Macho, P. C. Myhre, *ibid. 104* (1982) 907; d) R. Houriet, H. Schwarz, *Angew. Chem. 91* (1979) 1018; *Angew. Chem. Int. Ed. Engl. 18* (1979) 951; e) G. A. Olah, G. Liang, G. D. Mateescu, J. L. Riemenschneider, *J. Am. Chem. Soc. 95* (1973) 8698; f) H. C. Brown, M.-H. Rei, J. Chandrasekharan, V. Somayaji, *J. Org. Chem. 50* (1985) 5578; d) E. M. Arnett, C. Petro, *J. Am. Chem. Soc. 100* (1978) 5402, 5408; h) K. Raghavachari, R. C. Haddon, P. von R. Schleyer, H. F. Schaefer III, *ibid. 105* (1983) 5915; M. Yoshimine, A. D. McLean, B. Liu, D. J. DeFrees, J. S. Binkley, *ibid. 105* (1983) 6185.

[3] M. J. S. Dewar, K. M. Merz, Jr., *J. Am. Chem. Soc. 108* (1986) 5634.

[4] a) P. C. Myhre, K. L. McLaren, C. S. Yannoni, *J. Am. Chem. Soc. 107* (1985) 5924; b) G. A. Olah, G. Liang, *ibid. 96* (1974) 189, 195; G. A. Olah, J. R. DeMember, C. Y. Lui, R. D. Porter, *ibid. 93* (1971) 1442; P. von R. Schleyer, D. Lenoir, P. Mison, G. Liang, G. K. S. Prakash, G. A. Olah, *ibid. 102* (1980) 683; M. Saunders, M. R. Kates, *ibid. 102* (1980) 6867.

[5] G. A. Olah, *Aldrichim. Acta 12* (1979) 43. However, the crystal structure $1\lambda^4$,4-dithia-7-aza-1(7)-norbornenylium hexafluoroarsenate(v) was recently determined: N. Burford, J. P. Johnson, J. Passmore, M. S. Shriver, P. S. White, *J. Chem. Soc. Chem. Commun. 1986*, 966.

[6] J. N. Sherwood: *The Plastically Crystalline State (Orientationally-Disordered Crystals)*, Wiley, Chichester 1979; C. N. R. Rao in: *Studies in Physical and Theoretical Chemistry, Vol. 37: "Topics in Molecular Interactions,"* Elsevier, Amsterdam 1985, p. 181.

[7] The following salts were prepared, but they proved to be noncrystalline, microcrystalline, plastically crystalline, or twinned (nb = 2-norbornyl): nb-Sb_2F_{11}, 2-methyl-nb-Sb_2F_{11}, 2-methyl-nb-$SbCl_6$, 2-phenyl-nb-Sb_2F_{11}, 2-phenyl-nb-$SbCl_6$, 2-phenyl-nb-SbF_6, 1,2-dimethyl-nb-Sb_2F_{11}, 1-methyl-2-ethyl-nb-Sb_2F_{11}, 1-methyl-2-propyl-nb-Sb_2F_{11}, 1,2,4-trimethyl-nb-Sb_2F_{11}, 1,2,4-trimethyl-nb-SbF_6.

[8] Synthesized as a (−)-fenchone/(+)-isofenchone mixture (≈1:1; J. M. Coxon, P. J. Steel, *Aust. J. Chem. 32* (1979) 2441) from (+)-fenchol (FLUKA) by tosylation, formolysis, and oxidation and isolated as a ca. 1°-higher-boiling component of the mixture by using a Spaltrohr® column (Fischer Labor- und Verfahrenstechnik AG; reflux ratio 250:1 to 500:1, ca. 90 theoretical plates) (**4**, 56% *ee*; isolated fenchone, 71% *ee*). For reasons of simplicity, **4** is drawn as (−)-isofenchone; racemization begins at the very latest after the generation of **6**.

[9] Mixture of the C2 epimers. Synthesized from **4** by reaction twice with CH_3MgI (in order to drive the reaction to completion) followed by fluorination with HF/pyridine at 0°C (G. A. Olah, J. T. Welch, Y. D. Vankar, M. Nojima, I. Kerekes, J. A. Olah, *J. Org. Chem. 44* (1979) 3872). The thermally labile product **5** was isolated as a colorless oil after quick aqueous workup at 0°C and distillation under high vacuum at room temperature (cold trap to cold trap) and stored under argon on dry ice. The 300-MHz ^{1}H-NMR spectrum already indicates the presence of small amounts of isomers.

[10] In a Freon mixture at −80°C. After 30 min of reaction, the salt was separated from the yellow suspension by filtration and then dried under high vacuum at −60°C. In order to carry out the recrystallization, a solution of the crude product in CH_2Cl_2 was allowed to stand for ca. 24 h at −78°C. After removal of the mother liquor and washing, the yellow crystals were dried under high vacuum. Suitable crystals were selected under the microscope and mounted in glass capillaries, which, after sealing, were immediately mounted in the diffractometer. (At no point were the crystals warmer than −60°C.)

[11] Enraf-Nonius CAD4 diffractometer, $Mo_{K\alpha}$ radiation, graphite monochromator, measuring temperature −80°C; space group $P2_1/c$, $a = 11.369(9)$, $b = 10.662(9)$, $c = 15.023(7)$ Å, $\beta = 94.88(5)°$, $V = 1814.4$ Å^3, $\rho_{calcd} = 2.210$ g·cm^{-3}, $\mu = 30.9$ cm^{-1} (no absorption correction), $Z = 4$, 3940 measured reflections ($\theta < 27°$), 2419 of which with $I > 3\cdot\sigma(I)$. Because of difficulties in fixing the crystal in the glass capillaries, the orientation had to be checked with four control reflections after every 50 reflections; during the measurement, 20 reorientations were carried out. Position of the Sb atom determined with the Patterson option of SHELX84, all other atoms except for hydrogen by subsequent difference Fourier synthesis with SHELX76. After anisotropic refinement of the non-hydrogen atoms, some of the H atoms could be localized by difference Fourier synthesis; for further refinement, however, the H-atom positions were calculated and the H temperature factors were refined using a riding model. The non-hydrogen atoms were refined once again in the XRAY system, first with unit weights, and finally with $w = 1/\sigma(I)^2$: $R = 8.0\%$, $R_w = 9.4\%$. Further details of the crystal structure investigation are available on request from the director of the Cambridge Crystallographic Data Centre, University Chemical Laboratory, Lensfield Road, Cambridge CB2 1EW (England), on quoting the name of the author and the journal citation.

[12] The course of the isomerization **6** → **3** was not investigated in more detail. It is known, however, that the 2,5,5-trimethyl-2-norbornyl cation mainly undergoes rearrangement in superacid medium at −92°C to give an equilibrium mixture consisting of the 1,2,3-*endo*- and the 1,2,7-*anti*-trimethyl-2-norbornyl cation (a "Wagner–Meerwein pair"), which undergoes further rearrangement at −15°C to give the 1,2,4-trimethyl-2-norbornyl cation before it can react further at higher temperatures to give a substituted cyclohexenyl cation by ring opening (E. Huang, K. Ranganayakulu, T. S. Sorensen, *J. Am. Chem. Soc. 94* (1972) 1779). The formation of **3** from the 1,2,3,3- or the 1,2,7,7-tetramethyl-2-norbornyl cation is discussed in: L. Huang, K. Ranganayakulu, T. S. Sorensen, *ibid. 95* (1973) 1936. The shortest possible route of isomerization **6** → **3** was determined by means of a computer program and consists of five steps: 6,2-*endo*-H shift/3,2-*exo*-CH_3 shift/Wagner–Meerwein rearrangement/6,2-*endo*-H shift/3,2-*exo*-H shift. A similar program is described in: C. K. Johnson, C. J. Collins, *ibid. 96* (1974) 2514. (The ion **6** can racemize via a Wagner–Meerwein rearrangement, the ion **3** via the sequence Wagner–Meerwein rearrangement/3,2-*exo*-H shift/Wagner–Meerwein rearrangement.)

[13] T. Laube, *Angew. Chem. 98* (1986) 368; *Angew. Chem. Int. Ed. Engl. 25* (1986) 349.

[14] Noteworthy is the practically symmetrical orientation of F15 with respect to the partial double bond C1–C2. The next smallest distance $C^{\delta+}\cdots F$ ($C2\cdots F21'$; see Table 1) is 3.64(1) Å. The contacts from F15 to C1 and C2 and from F21' to C2 reflect the situation for an *exo* and an *endo* attack, respectively, of a nucleophile on a 2-norbornyl cation. Only *exo* attack is observed (see discussion in W. F. Erman: *Chemistry of the Monoterpenes, Vol. B*. Marcel Dekker, New York 1985, p. 1067, 1083); *endo* attack on **3** would be strongly hindered sterically and stereoelectronically.

[15] T. Laube et al., unpublished results.

[16] R. C. Haddon, *J. Am. Chem. Soc. 108* (1986) 2837.

[17] The structure of norbornane has not yet been determined by X-ray diffraction because of the formation of plastically crystalline phases. R. L. Jackson, J. H. Strange, *Acta Crystallogr. Sect. B 28* (1972) 1645). Electron diffraction in the gas phase in connection with other spectroscopic data does not afford all inner coordinates with sufficient precision (L. Doms, L. Van den Enden, H. J. Geise, C. Van Alsenoy, *J. Am. Chem. Soc. 105* (1983) 158). The coordinates of norbornane used here were determined by nonlinear optimization of a force-field-like function (maintaining the C_{2v} symmetry) from the average values of the inner coordinates of substituted norbornanes (L. Doms, D. Van Hemelrijk, W. Van de Mieroop, A. T. H. Lenstra, H. J. Geise, *Acta Crystallogr. Sect. B 41* (1985) 270).

[18] It is probably only a coincidence that the skeletal geometry of **3** in the crystal is practically identical with the skeletal geometry of the unsymmetrical 2-norbornyl cation **1** calculated by ab initio methods (calculation of **1** and **1''**: J. D. Goddard, Y. Osamura, H. F. Schaefer III, *J. Am. Chem. Soc. 104* (1982) 3258). Calculations reported later [2h], however, showed that **1** did not correspond to a minimum and therefore that the symmetrically bridged ion **1''** is the only minimum on the potential surface.

[19] Average and maximal deviations of the corresponding skeletal atoms upon adjustment with the same weights in each case: **3**/norbornane [17]: $\bar{d} = 0.13$ Å, $d_{max} = 0.25$ Å; **3**/**1''** [18]: $\bar{d} = 0.08$ Å, $d_{max} = 0.15$ Å.

[20] Other bicycloalkyl cations are less stable compared with the hydrocarbons than are 2-norbornyl cations compared with the corresponding norbornanes: N. E. Okazawa, T. S. Sorensen, *Can. J. Chem. 60* (1982) 2180.

Nitrogen Heterocycles from Carbene Complexes and Alkenyl Isocyanides**

By *Rudolf Aumann,* Eberhard Kuckert, Carl Krüger,* and *Klaus Angermund*

Ketenimine complexes are readily accessible in good yields by the addition of isocyanides to carbene complexes.[1] They may be used, after isolation or in situ, for further transformations. Their reactivity patterns are completely different from those of ketenimines free of metals. Herein we describe novel template syntheses of four-, five-, and six-membered N-heterocycles by means of such complexes.

Complex **1** reacts rapidly with alkenyl isocyanides **2** at 0°C in hexane to form the 1:1 adducts (3-aza-1,2,4-pentatriene complexes) **3**. These can be trapped as aminocarbene complexes with protic nucleophiles.[1] In the absence of a suitable reactant, **3** adds a second molecule of **2**. The 1-azafulvene complexes **4** and **4'** and the azetidin-2-ylidene complexes **5** are thereby formed competitively by [4+1] and [3+1] cycloaddition, respectively.

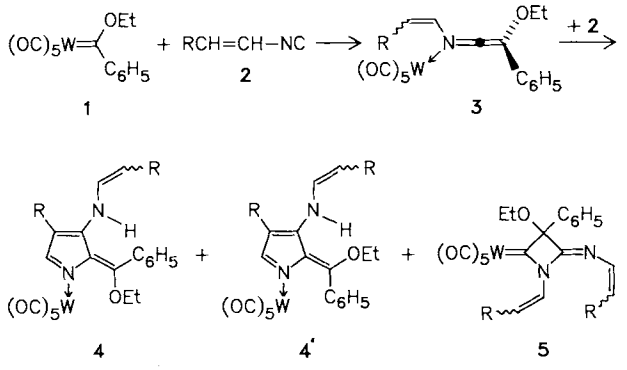

a, R = H; **b**, R = CH_3

4a : **4'a** : **5a** = 5 : 1 : 2 (80%); **4b** : **4'b** : **5b** = 5 : 1 : 3 (93%)

Complexes **4/4'** precipitate directly from the reaction mixture as red crystals. They are by far more stable than metal-free 1-azafulvenes.[2] However, **4/4'** cannot be separated, because they undergo interconversion in solution. The structures of the complexes were established on the basis of spectroscopic data (Table 1).

Upon hydrolysis in the presence of pyridine, **4b/4'b** afford 3-amino-2-benzoyl-4-methylpyrrole **6** in 90% yield and pentacarbonyl(pyridine)tungsten **7**.

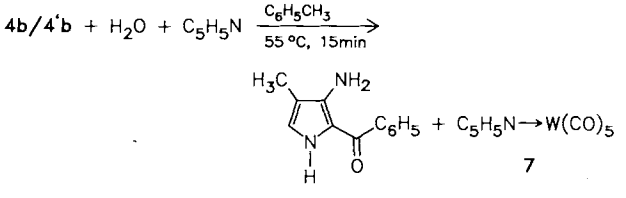

Thermolysis of **4a/4'a** gives the pyrrolo[3,2-*b*]pyridine complex **9** by a metal-promoted cyclization. The reaction presumably proceeds via **8** as an intermediate.

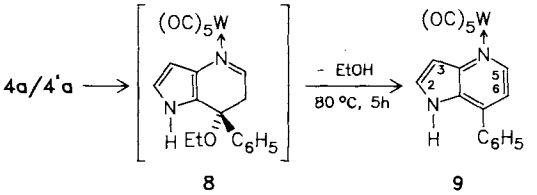

The formation of **4/4'** from **1** and **2** corresponds to the synthesis of indoles from carbene complexes and aromatic isocyanides.[1] The formation of azetidin-2-ylidene complexes **5**, on the other hand, must be regarded as a prototype of a novel [3+1] cycloaddition of a ketenimine ligand to an isocyanide. The reaction is favored by the migration of the $W(CO)_5$ group from the N atom to the central C atom of the C=C=N moiety, since this results in the formation of an especially stable aminocarbene structure.

Complexes **5** can be easily isolated by chromatography of the mother liquor after separation of the **4/4'** crystals. Complex **5b** was synthesized starting from a ca. 10:1 mixture of *cis*- and *trans*-**2b**.[3] A 15:1:1 mixture of three stereoisomers, which differ in the relative configurations of the C=C bonds, was obtained. As expected, the main product has a *cis* configuration at both C=C bonds [**5b**(*cis/cis*): R_f(petroleum ether) = 0.14, m.p. = 107°C; **5b**(*cis/trans*): R_f(petroleum ether) = 0.42, m.p. = 101°C; **5b**(*trans/cis*): R_f(petroleum ether/ether = 50/1) = 0.7, m.p. = 80°C].

The structure of the 3-methyl-3-ethoxyazetidin-2-ylidene-$W(CO)_5$ **5c**, which is analogous to **5a** (CH_3 instead of C_6H_5 in **5a**), was determined by an X-ray crystal structure analysis (Fig. 1).

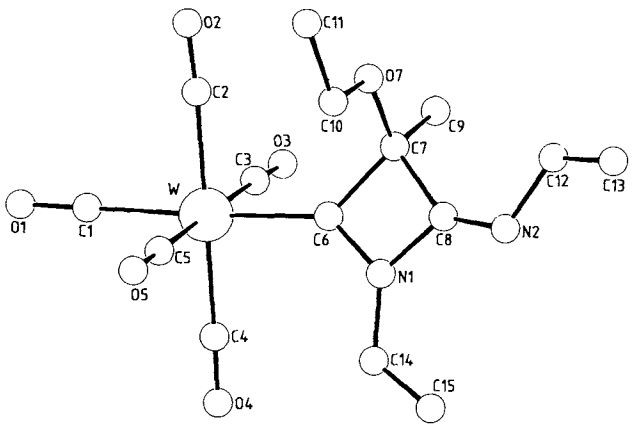

Fig. 1. Crystal structure of **5c** [4]. Important bond lengths [Å] and angles [°]: C1-W 2.044(6), W-C6 2.137(5), C6-C7 1.558(7), C6-N1 1.360(6), C7-C8 1.546(7), N1-C14 1.408(7), C14-C15 1.295(9), N1-C8 1.430(7), C8-N2 1.260(7), N2-C12 1.408(8), C12-C13 1.299(9); W-C6-C7 133.0(3), W-C6-N1 137.0(4), C7-C6-N1 89.9(4).

Oxidation of **5a** with pyridine *N*-oxide **10** in toluene leads to the β-lactam **11** in 88% yield.

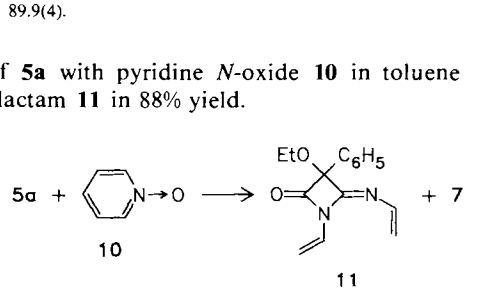

[*] Prof. Dr. R. Aumann, Dipl.-Chem. E. Kuckert
Organisch-chemisches Institut der Universität
Orléans-Ring 23, D-4400 Münster (FRG)
Prof. Dr. C. Krüger [+], Dr. K. Angermund [+]
Max-Planck-Institut für Kohlenforschung
Postfach 101353, D-4330 Mülheim/Ruhr 1 (FRG)

[+] X-ray structure analysis.

[**] Organic Syntheses with Transition-Metal Complexes, Part 24. This work was supported by the Deutsche Forschungsgemeinschaft and the Fonds der Chemischen Industrie.—Part 23: R. Aumann, H. Heinen, C. Krüger, *Chem. Ber.*, in press.

In contrast to **1**, $[(OC)_4Fe{=}C(OEt)C_6H_5]$ reacts with both aliphatic and aromatic isocyanides to give the $(OC)_4$Fe-azetidin-2-ylidene complexes corresponding to **5** as the only products. These are again readily oxidized to β-lactams.[5]

Table 1. Spectroscopic data for the compounds **4a**, **4'a**, **5a**, **6**, **9**, and **11** [a].

4a: ^{1}H-NMR: δ = 7.95 and 5.52 (each 1H, each d, AX system, ^3J = 1.9 Hz; H2 and H3), 7.73 and 7.49 (2H and 3H, each m; C_6H_5), 6.14 (1H, ddd, ^3J = 15.0, 11.0, and 8.2 Hz; NH–C*H*=CH$_2$), 4.69 (1H, br. d, ^3J = 11.0 Hz; NH, shifted to lower frequency owing to the anisotropy effect of C_6H_5), 4.03 (1H, d, ^3J = 8.2 Hz; NH–CH=C*H*$_{cis}$), 3.63 (1H, d, ^3J = 15.0 Hz; NH–CH=C*H*$_{trans}$), 4.08 and 1.48 (2H and 3H; C_2H_5).—^{13}C-NMR: δ = 199.76 and 203.00 (1:4; *cis* and *trans*-CO), 166.95 (d; C2), 162.03 (*C*–OEt), 153.40, 132.02, and 130.16 (C4, C5, and *i*-C of C_6H_5), 131.72 and 93.24 (N–CH=CH$_2$); 98.05 (d; C3), 131.94, 130.69, and 128.88 (1:2:2; C_6H_5), 67.65 and 15.23 (C_2H_5).—IR (hexane; ν(C≡O)): $\tilde{\nu}$ = 2060 (10), 1920 (100), 1898 (70) cm^{-1}.

4'a: ^{1}H-NMR: δ = 8.59 (1H, br. d, ^3J = 11.4 Hz; NH), 7.90 and 5.73 (each 1H, each d, AX system, ^3J = 1.9 Hz; H2 and H3), 7.6–7.4 (5H, m; C_6H_5), 6.64 (1H, ddd, ^3J = 15.2, 11.4, and 8.0 Hz; NH–C*H*=CH$_2$), 4.60 (1H, d, ^3J = 15.2 Hz; NH–CH=C*H*$_{trans}$), 4.45 (1H, d, ^3J = 8.0 Hz; NH–CH=C*H*$_{cis}$), 3.95 and 1.39 (2H and 3H; C_2H_5).

5a: ^{1}H-NMR: δ = 7.40 (5H, m; C_6H_5), 7.18, 6.66, and 5.65 (each 1H, dd with ^3J = 15.8 and 9.3 Hz, d with ^3J = 15.8 Hz, d with ^3J = 9.3 Hz; N$_{ring}$–CH=CH$_2$), 6.60, 5.40, and 5.00 (each 1H, dd with ^3J = 14.6 and 7.2 Hz, d with ^3J = 14.6, d with ^3J = 7.2 Hz; C=N–CH=CH$_2$), 3.66 and 3.45 (each 1H, each q of AB system; diastereotopic O–CH$_2$), 1.39 (3H; CH$_3$).—^{13}C-NMR: δ = 285.75 (d, ^1J(^{183}W-C) = 107.8 Hz; W=C), 203.52 and 195.29 (1:4; W(CO)$_5$), 160.09 (C=N), 136.01 and 116.34 (N$_{ring}$–CH=CH$_2$), 130.97 and 113.97 (=N–CH=CH$_2$), 134.87 (*i*-C of C_6H_5), 128.99, 128.93, and 125.40 (1:2:2; C_6H_5), 100.24 (*C*–OEt), 62.38 and 14.97 (OC_2H_5).—IR (hexane; ν(C≡O)): $\tilde{\nu}$ = 2070 (68), 1978 (45), 1944 (100), 1925 (90) cm^{-1}.—MS: *m/z* 564 ($M^{\oplus}$, 1.4%), 314 (3), 287 (3.5), 187 (60), 158 (20), 106 (18), 105 (100), 77 (36).

6: ^{1}H-NMR: δ = 7.83 (1H, br. d, ^3J = 3.2 Hz; NH), 7.67 and 7.48 (3H and 2H, each *m*; C_6H_5), 6.61 (1H, d, ^3J = 3.2 Hz, splitting vanishes upon addition of D_2O; H5), 5.00 (2H, br. s; NH$_2$), 1.97 (3H, s; CH$_3$).—IR (KBr): ν(NH): $\tilde{\nu}$ = 3451 (pyrrole), 3340 and 3310 cm^{-1} (NH$_2$); ν(CO) and δ(NH): $\tilde{\nu}$ = 1610, 1580, and 1550 cm^{-1}.—MS: *m/z* 200 ($M^{\oplus}$, 86%), 199 (100), 123 (40, $M^{\oplus}-C_6H_5$), 105 (20), 95 (28, $M^{\oplus}-C_6H_5CO$), 77 (55).

9: ^{1}H-NMR: δ = 8.76 (1H, br. d, ^3J = 2.2 Hz, signal vanishes upon addition of D_2O; NH), 7.64–7.54 (6H, m; C_6H_5 and H3), 8.81 and 7.06 (each 1H, AX system, ^3J = 5.6 Hz; H5 and H6), 7.03 (1H, dd, ^3J = 3.5 and 2.2 Hz, after coupling vanishes upon addition of D_2O; H2).—IR (hexane; ν(C≡O)): $\tilde{\nu}$ = 1933 (100), 1921 (57) cm^{-1}.—IR (KBr; ν(NH)): $\tilde{\nu}$ = 3420 cm^{-1}.—MS: *m/z* 490 ($M^{\oplus}$ – CO, 0.5%), 462 (3), 406 (6), 378 (7), 349 (4), 323 (4), 194 (100, ligand), 166 (20), 140 (28), 129 (23), 115 (14).

11: ^{1}H-NMR: δ = 7.46–7.36 (5H, m; C_6H_5), 6.62, 5.97, and 5.08 (each 1H, dd with ^3J = 16.2 and 9.3 Hz, d with ^3J = 16.2 Hz, d with ^3J = 9.3 Hz; N$_{ring}$–CH=CH$_2$), 6.91, 5.30, and 4.86 (each 1H, dd with ^3J = 14.9 and 7.5 Hz, d with ^3J = 14.9 Hz, d with ^3J = 7.5 Hz; C=N–CH=CH$_2$), 3.77 and 3.68 (each 1H, each q of AB system; diastereotopic O–CH$_2$), 1.34 (3H, t; CH$_3$).—^{13}C-NMR: δ = 168.01 (C=O), 155.72 (C=N), 132.91 (*i*-C of C_6H_5), 128.85, 125.71, and 123.00 (2:2:1; C_6H_5), 137.64 and 112.69 (N$_{ring}$–CH=CH$_2$), 129.29 and 106.80 (=N–CH=CH$_2$), 97.92 (*C*–OEt), 63.19 and 15.02 (OC_2H_5).—IR (KBr; ν(C=O)): $\tilde{\nu}$ = 1824 cm^{-1}.—MS: *m/z* 256 ($M^{\oplus}$, 1.2%), 228 (1.8), 187 (3.2), 162 (18), 134 (8), 105 (100), 77 (38).

[a] ^{1}H- and ^{13}C-NMR spectra in $CDCl_3$; 70-eV mass spectra.

Experimental Procedure

4a, **4'a**, and **5a** from **1** and **2a**: **2a** (106 mg, 2.00 mmol) was added to a stirred solution of **1** (458 mg, 1.00 mmol) in 20 mL of hexane at 0°C under inert gas. Dark red crystals of **4a/4'a** (338 mg, 60%, dec. above 66°C) precipitated at −15°C. Chromatography of the mother liquor (silica gel, 20 × 2 cm column, petroleum ether/ether = 50/1) afforded **5a** (113 mg, 20%), R_f = 0.7, m.p. = 97°C. **4** and **4'** are present in solution in a 5:1 equilibrium and were analyzed spectroscopically without attempting resolution.

6 by hydrolysis of **4b/4'b**: **4b/4'b** (300 mg, 0.51 mmol) were heated in 3 mL of toluene/pyridine/water (1/1/1) with stirring (15 min, 55°C). The pale red solution was then evaporated. The residue was dissolved in dichloromethane and chromatographed on silica gel (30 × 2 cm column, petroleum ether/ether = 1/1). After a yellow band containing **7** (170 mg, 83%), a pale yellow fraction containing **6** (92 mg, 90%, R_f = 0.15, m.p. = 135°C) was obtained.

9 by thermolysis of **4a/4'a**: **4a/4'a** was heated in toluene (5 h, 80°C); workup by chromatography on silica gel (ether/petroleum ether = 1/1), yellow crystals from petroleum ether/ether = 4/1, m.p. = 150°C (dec.).

11 by oxidative decomposition of **5a**: **5a** was heated with one equivalent of pyridine *N*-oxide in toluene (15 min, 80°C). Workup by chromatography afforded colorless crystals of **11**, m.p. = 37°C, in addition to yellow **7**.

Received: January 26, 1987;
revised: March 16, 1987 [Z 2067 IE]
German version: *Angew. Chem. 99* (1987) 587

[1] R. Aumann, H. Heinen, *Chem. Ber. 119* (1986) 2289.
[2] C. F. Candy, R. A. Jones, *J. Chem. Soc. B 1971*, 1405; R. A. Jones, G. P. Beans, *Org. Chem. (N. Y.) 34* (1977) 425.
[3] T. Saegusa, I. Murase, Y. Ito, *Tetrahedron 27* (1971) 3795.
[4] **5c**: $P\bar{1}$ (No. 2); a = 8.375(2), b = 9.167(4), c = 12.921(6) Å, α = 75.41(3), β = 80.05(2), γ = 71.93(2)°, Z = 2; $\mu_{K\alpha}$ = 65.25 cm^{-1}, (λ = 0.71069 Å), 5254 measured reflections ($\pm h$, $\pm k$, $+l$), of which 3919 were observed ($I \geq 2\sigma(I)$), 217 refined parameters; R = 0.032, R_w = 0.032 ($w = 1/\sigma^2(F_0)$), residual electron density ρ = 1.55 eÅ^{-3}, analytical absorption correction (min 1.180, max 1.717). Further details of the crystal structure investigation may be obtained from the Fachinformationszentrum Energie, Physik, Mathematik GmbH, D-7514 Eggenstein-Leopoldshafen 2 (FRG), on quoting the depository number CSD-52378, the names of the authors, and the journal citation.
[5] R. Aumann, H. Heinen, *Chem. Ber. 120* (1987), in press.

Mono- and Diarenium Ions from [2.2]Paracyclophanes**

By *Henning Hopf,** *Jung-Hyu Shin,** and *Heinrich Volz**

[2.2]Paracyclophanes **1a** contain two aromatic moieties, which, upon protonation, can be transformed into σ complexes. We reported earlier on the preparation of several new *dianions* of paracyclophane derivatives.[1] We have now studied the possibility of forming *dications* from **1a**. *Cram* and *Hefelfinger* have already reported on the observation of **2a**, a monoarenium ion of **1a**, but no mention was made of a second protonation.[2] The intermediate formation of σ complexes has been postulated for numerous substitution and rearrangement reactions[3,4] of phanes; however, few structural details of these unusual arenium ions are presently known. In investigations of the protonation of [2.2]cyclophanes with super acids (FSO_3H) and magic acid (FSO_3H–SbF_5), we have now been able to prepare both monoarenium ions and, for the first time, diarenium ions of these bridged hydrocarbons and to characterize them by NMR spectroscopy. The parent system **1a** was also reinvestigated since nuclear magnetic resonance spectroscopy has undergone dramatic advances in the meantime.

Owing to the angle deformations and the π–π repulsion between the two benzene rings, [2.2]paracyclophane **1a** has a strain energy of 31 kcal/mol.[5] Protonation of one of the benzene rings of **1a** leads to formation of the monoarenium ion **2a**, and the π–π repulsion is transformed into an

[*] Prof. Dr. H. Hopf
Institut für Organische Chemie der Universität
Hagenring 30, D-3300 Braunschweig (FRG)
Prof. Dr. J.-H. Shin
Department of Chemistry, College of Natural Sciences
Seoul National University, Seoul 151 (Korea)
Prof. Dr. H. Volz
Institut für Organische Chemie der Universität
Postfach 6380, D-7500 Karlsruhe (FRG)

[**] Stable Carbenium Ions, Part 32. This work was supported by the Deutsche Forschungsgemeinschaft and the Fonds der Chemischen Industrie. *J.-H. S.* thanks the DAAD for a fellowship.—Part 31: H. Volz, J.-H. Shin, H. Hettel, *Liebigs Ann. Chem. 1982*, 480.

energetically more favorable charge-transfer interaction. The reduction in energy should be at least as large as the bonding energy of 11 kcal/mol found for the cluster formed from protonated benzene and unprotonated benzene.[6] In contrast to methyl-substituted benzenes, which are always protonated at the unsubstituted position—see *p*-xylene, for example[7]—exclusive protonation of the *ipso* carbon atom occurs in the case of [2.2]paracyclophanes, resulting in a reduction in angle strain (Scheme 1).[2]

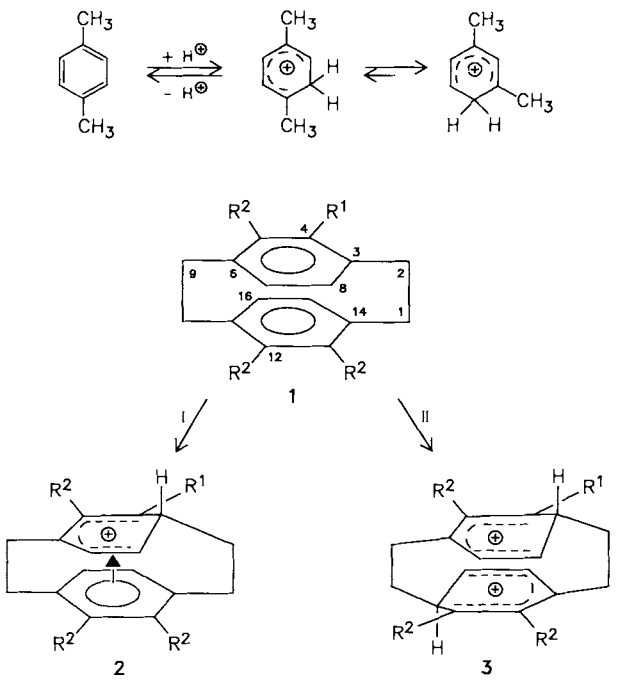

Scheme 1. Generation of the monocations **2** with FSO_3H-SO_2ClF (I) and the dications **3** with FSO_3H-SbF_5-SO_2ClF (II). **a**, $R^1=R^2=H$; **b**, $R^1=CH_3$, $R^2=H$; **c**, $R^1=R^2=CH_3$.

The monoarenium ions **2** are generated from the cyclophanes **1** in FSO_3H-SO_2ClF at $-80°C$ (**2a**,**2b**) and $-110°C$ (**2c**). All three cations exhibit a bright red color owing to the charge transfer from the unprotonated ring to the arenium ion. In the ^{1}H-NMR spectrum, the protons of the protonated ring absorb at higher field than the protons of similarly substituted methylbenzenium ions, and the protons of the unprotonated ring absorb at lower field than those of the parent compounds **1**. The cause is, on the one hand, the charge transfer and, on the other, the changed magnetic anisotropy effect of the ring system (Table 1).

Reaction of the [2.2]paracyclophane **1** with magic acid (FSO_3H-SbF_5-SO_2ClF) at $-100°C$ results in double protonation and formation of the pale yellow diarenium ions **3**. The angle strain in these species is further decreased compared with that in the monoarenium ions by protonation at two *ipso* carbon atoms. The spatial proximity of the two complexes should result in a certain degree of charge repulsion. For this reason, it is reasonable to assume that the positions of highest positive charge density in the diarenium ions **3** are separated as far as possible from one another. In the ^{1}H-NMR spectrum, the protons of the diarenium ions exhibit chemical shifts that are approximately the same as those found for the protons of similarly substituted monoarenium ions. Instead of the *ipso* protonation at C-3 and C-11 shown in the scheme, attack could in principle also occur at C-3 and C-14. The dications formed in this way, however, would be considerably more strained, according to molecular models, than the isomers **3** proposed by us. Protonation of the methyl-substituted ring of the unsymmetrical educt **1b** can lead to the formation of two isomeric monoarenium ions. However, there is no evidence in the nuclear magnetic resonance spectrum for the presence of isomers. If the cyclophane **1b** were also protonated in position 6, then, as shown by comparison of the spectra of the 4*H*-*o*-, the 4*H*-*m*-, and the 2*H*-*p*-xylenium ions,[7] the signals of the protons in the *ortho* and *meta* positions to the site of protonation (H-5,H-7 and H-8) should be found about 0.2 ppm downfield and the signal of the methyl protons about 0.3 ppm upfield compared with the corresponding signals of **2b**. No signals are observed in this region, however. The ions formulated as **2b** and **3b** are therefore the energetically more favorable alternatives.

Table 1. ^{1}H-NMR data for the monoarenium ions **2a**-**c** and the diarenium ions **3a**-**c** [a].

2a: $\delta=8.22$ (d, 2H, $J=8.3$; H-4, H-8), 7.59 (d, 2H, $J=8.3$; H-5, H-7), 7.19 (d, 2H, $J=7.6$; H-13, H-15), 6.86 (d, 2H, $J=7.6$; H-12, H-16), 4.07 (br. s, 1H; H-3), 3.63 (m, 4H; H-9, H-10), 3.48 (m, 2H; H-1), 2.88 (m, 2H; H-2)

3a: $\delta=9.32$ (d, 4H, $J=8.4$; H-4, H-8, H-12, H-16), 8.07 (d, 4H, $J=8.4$; H-5, H-7, H-13, H-15), 4.94 (br. s, 2H; H-3, H-11), 3.47 (m, 4H; H-1, H-9), 3.22 (br. s, 4H; H-2, H-10)

2b: $\delta=7.96$ (d, 1H, $J=8.6$; H-8), 7.44 (d, 1H, $J=8.6$; H-7), 7.2 (m, 3H; H-5, H-12, H-13), 6.98 (d, 1H, $J=7.5$; H-15), 6.89 (d, 1H, $J=7.5$; H-16), 3.82 (br. s; 1H, H-3), 2.72-3.64 (m, 8H; H-1, H-2, H-9, H-10), 2.64 (s; 3H, CH_3)

3b: $\delta=9.31$ (d, 2H, $J=8.4$; H-12, H-16), 8.94 (d, 1H, $J=8.5$; 8-H), 8.08 (t or dd, 2H, $J=8.4$; H-13, H-15), 7.78 (s, 1H; H-5), 7.75 (d, 1H, $J=8.5$; H-7), 5.06 (br. s, 1H; H-11), 4.66 (br. s, 1H; H-3), 3.54-3.05 (m, 8H; H-1, H-2, H-9, H-10), 3.02 (s, 3H; CH_3)

2c: $\delta=7.79$ (d, 1H, $J=8.9$; H-8), 7.41 (d, 1H, $J=8.9$; H-7), 6.98 (d, 1H, $J=7.8$; H-15), 6.51 (d, 1H, $J=7.8$; H-16), 3.78 (br. s, 1H; H-3), 3.48-3.18 (m, 8H; H-1, H-2, H-9, H-10), 2.5 (s, 3H; CH_3-4), 2.29 (s, 3H; CH_3-5), 2.25 (s, 3H; CH_3-13), 1.92 (s, 3H; CH_3-12)

3c: $\delta=8.79$ (dd, 2H, $J_1=8.9$, $J_2=1.8$; H-8, H-16), 7.47 (d, 2H, $J=8.9$; H-7, H-15), 4.67 (br. s, 2H; H-3, H-11), 3.6-3.0 (m, 8H; H-1, H-2, H-9, H-10), 2.95 (s, 6H; CH_3-4, CH_3-12), 2.42 (s, 6H; CH_3-5), CH_3-13)

[a] The chemical shifts were determined relative to dichloromethane and then recalculated relative to TMS as internal standard; coupling constant in Hz. The spectra were recorded on a Bruker Cryospec WM 250.

Received: February 4, 1987;
supplemented: March 18, 1987 [Z 2086 IE]
German version: *Angew. Chem. 99* (1987) 594

CAS Registry numbers:
3, 1633-22-3; **2**, 33936-87-7; **3**, 108122-79-8; **4**, 24262-07-5; **5**, 108122-77-6; **6**, 108122-80-1; **7**, 71779-89-0; **8**, 108122-78-1; **9**, 108122-81-2.

[1] R. Frim, F.-W. Raulfs, H. Hopf, M. Rabinovitz, *Angew. Chem. 98* (1986) 160; *Angew. Chem. Int. Ed. Engl. 25* (1986) 174.
[2] D. T. Hefelfinger, D. J. Cram, *J. Am. Chem. Soc. 93* (1971) 4754.
[3] J. Kleinschroth, S. El-Tamany, H. Hopf, J. Bruhin, *Tetrahedron Lett. 23* (1982) 3345.
[4] F. Vögtle, P. Neumann, *Synthesis 1973*, 85; cf. F. Vögtle, P. Neumann, *Top. Curr. Chem. 48* (1974) 67.
[5] R. H. Boyd, *Tetrahedron 22* (1966(119.
[6] M. Meot-Ner (Mautner), P. Hamlet, E. P. Hunter, F. H. Field, *J. Am. Chem. Soc. 100* (1978) 5466.
[7] D. M. Brouwer, E. L. Mackor, C. MacLean in G. A. Olah, P. von R. Schleyer (Eds.): *Carbonium Ions, Vol. 2*, Wiley-Interscience, New York 1970, p. 884.

Unusually Stable *cis,cis*-Trialkyltriaziridines by Azo/Nitrene Addition**

By *Otmar Klingler* and *Horst Prinzbach**

All attempts to obtain tetrazetidines **B** by azo/azo photocycloaddition (**A** → **B**) have so far been unsuccessful; only in the case of an azoxy/azo substrate was a tetrazetidine oxide a likely intermediate in the photochemical metathesis reaction.[1] As an alternative route to kinetically stabilized tetrazetidines **B**, we are investigating the ring expansion of ylides **D**, whose synthesis is being approached through nitrene addition to triaziridines **C**. Here we report on the preparation of *cis,cis*-trialkyltriaziridines.

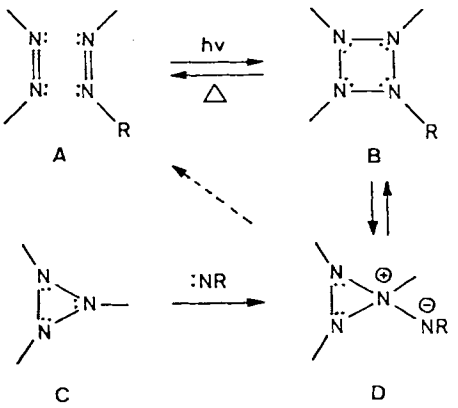

The thermally labile triaziridines described by *Dreiding* et al.,[2] as well as subsequent examples,[3] were obtained by photocyclization of acceptor-substituted azimines. Earlier attempts to achieve the intra- or intermolecular azo/nitrene addition resulted at best in the isolation of azimines.[2,4] In our approach,[5] the lability of the triaziridine ring, which is partly responsible for these earlier results, was counteracted by incorporation of the N_3 ring into a rigid molecular skeleton. This also guarantees a high degree of proximity of the azo/azide chromophore and the fixing of the potential nitrene in the N=N π plane.

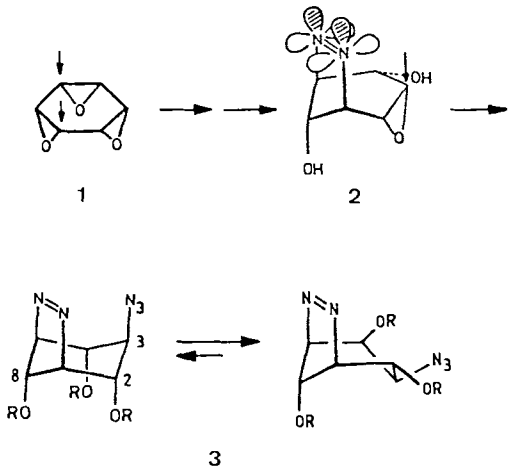

a, R = H; **b**, R = Ac

The azoepoxydiol **2** is accessible[6] starting from *cis*-benzene trioxide **1** via an intermediate of the streptamine synthesis.[7] The opening of the epoxide ring in **2** by $N_3^{\ominus}$ (NaN_3, Al_2O_3, CH_3OH/H_2O, room temperature) proceeds slowly, even under catalysis, but sufficiently selectively at C-4 to give the crystalline C_s-symmetric triol **3a** (50–60%, $J_{1,8}=5.3$, $J_{2,3}=8.8$ Hz), which, like the triacetate **3b** ($\lambda_{max}(CH_3CN)=346$ nm ($\varepsilon=150$); $J_{1,8}=5.3$, $J_{2,3}=7.0$ Hz), favors a flattened boat conformation with a quasi-equatorial azide group. Reaction of **3a** with trimethyl orthoformate gives the trioxaadamantane **4a** (m.p. = 174°C, 70%), with trimethyl orthoacetate the product **4b** (m.p. = 135°C, 66%), with $POCl_3$ the product **4c** (m.p. = 211°C (dec.), 60%), and with $P(OC_6H_5)_3$ the product **4d** (m.p. = 175°C (dec.), 70%).[8] The fixed axial position of the azide group in **4a–d**, and hence its spatial proximity to the azo group, is confirmed, inter alia, by the small $J_{1,11}$ and $J_{10,11}$ coupling constants (ca. 3 Hz) as well as by the relatively long-wavelength UV absorptions (e.g., **4a**: $\lambda_{max}(CH_3CN)=$ 361 nm ($\varepsilon=530$)).

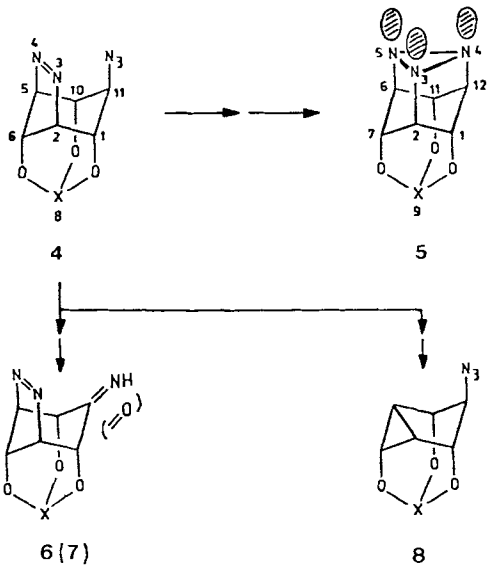

a, X = CH; **b**, X = CCH_3; **c**, X = PO; **d**, X = P

Direct irradiation of **4a** in a ca. 10^{-3} M degassed CH_3CN solution with monochromatic light (254 or 350 nm, Rayonet reactor, quartz photolysis vessel, room temperature), after 85–90% conversion, produces, in addition to a small amount of polymer, a mixture containing 45–50% or 50–65%, respectively, of triaziridine **5a** (m.p. = 233°C (dec.)), 15–20% or 10–20%, respectively, of azoimine **6a**, and 5–10% or < 2%, respectively, of azide **8a**. Compounds **5a** and **8a** can be isolated in pure form by chromatography; the imine **6a** is transformed, upon chromatography, into the ketone **7a**. Under the same conditions (350 nm), **4b** gives ca. 40% of **5b** (m.p. = 220°C (dec.)) and ca. 10% of **6b**; **4c** gives ca. 25% of **5c** (m.p. = 245°C (dec.)) and ca. 20% of **6c**, and **4d** gives ca. 20% of **5d** (m.p. = 230°C (dec.)) and ca. 20% of **6d**. The importance of the fixed proximity of the azo/azide chromophores in **4a–d** for the formation of the triaziridines **5a–d** is shown by control photolyses with **3b**. Under the same conditions (CH_3CN, 254 nm (350 nm), 85–90% conversion), along with a considerable (prevailing) amount of (mainly) polymeric material, ca. 35% (5%) of a 1:2 mixture

[*] Prof. Dr. H. Prinzbach, Dipl.-Chem. O. Klingler
Chemisches Laboratorium der Universität
Institut für Organische Chemie und Biochemie
Albertstrasse 21, D-7800 Freiburg (FRG)

[**] This work was supported by the Deutsche Forschungsgemeinschaft, the Fonds der Chemischen Industrie, and BASF AG.

of the epimeric bicyclic azides **10b/11b**, ca. 5% (5%) of aniline derivatives, and only ca. 5% (5%) of triaziridine **9b** ("triazatriaxane"; [3]triazaperistylane)[9] are formed.[10]

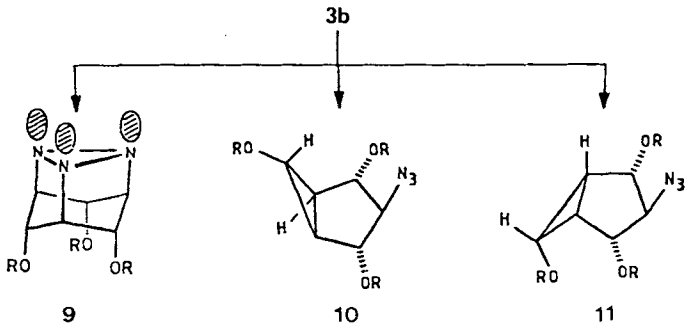

The C_{3v} symmetry of the triaziridines **5a-d** is revealed in the ^{1}H- and ^{13}C-NMR data. Characteristic for the triaziridine moiety are a short-wavelength UV absorption (**5a** (CH_3CN): $\varepsilon_{220}=250$), the ^{15}N-NMR shift (**5a** ([D$_6$]dimethyl sulfoxide): $\delta=180.6$), the photoelectron (PE) spectra,[11] and the expected weak basicity (**5a** is not protonated in CF_3CO_2H/CH_3CN). The kinetic stabilization of the triaziridine ring in **5a-d** by the trioxaadamantane "corset" is impressively manifested in the unusual thermal stability. For example, upon heating in a ca. 10^{-2} M degassed solution in CD_3CN at 200°C, **5a** remains unchanged over several hours. In the mass spectrum of **5a** (chemical ionization, isobutane), the $M^{\oplus}+1$ peak (*m/z* 182) is the base peak (100%). Accordingly, the triaziridines **5a-d** should be able to withstand the thermolysis temperatures (150-200°C) necessary for the generation of nitrenes from alkyl azides such as **4a-d**. Indeed, heating of **4a** at 200°C (in the melt or in degassed benzonitrile solution) results in the formation of **5a/6a** mixtures similar to those formed by photolysis. This result also supports the assumption that the photoreaction **4a** → **5a** occurs via a nitrene and not via a [4+2] azo/azide adduct (pentazoline). The question of energy transfer to the azide group, especially upon 350-nm excitation (N=N, n→π*), however, remains unanswered.

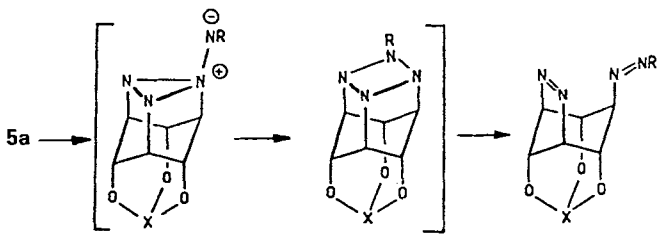

R = CO_2CH_3

In view of the project mentioned at the beginning, the following preliminary result is noteworthy: upon irradiation (254 nm) of a CH_2Cl_2 solution of **5a** (10^{-3} M, room temperature) and methyl azidoformate, the bisazo compound **14a** is formed selectively (via **12a/13a** ?).[6]

Received: February 4, 1987 [Z 2087 IE]
German version: *Angew. Chem. 99* (1987) 577

[1] H. Prinzbach, G. Fischer, G. Rihs, G. Sedelmeier, E. Heilbronner, Z.-z. Yang, *Tetrahedron Lett. 23* (1982) 1251.
[2] L. Hoesch, C. Leuenberger, H. Hilpert, A. S. Dreiding, *Helv. Chim. Acta 65* (1982) 2682; H. Hilpert, L. Hoesch, A. S. Dreiding, *ibid. 69* (1986) 2087, and references cited therein.
[3] G. Kaupp, O. Dengler, K. Burger, S. Rottegger, *Angew. Chem. 97* (1985) 329; *Angew. Chem. Int. Ed. Engl. 24* (1985) 341; G. Kaupp, J. A. Döhle, *Angew. Chem. 98* (1986) 814; *Angew. Chem. Int. Ed. Engl. 25* (1986) 828.
[4] J. Hancock, *Tetrahedron Lett. 1964*, 1585; W. Lwowski, T. W. Mattingly, Jr., T. J. Maricich, *ibid. 1964*, 1591; R. C. Kerber, P. J. Heffron, *J. Org. Chem. 37* (1972) 1592.
[5] G. Fischer, H. Fritz, H. Prinzbach, *Tetrahedron Lett. 27* (1986) 1269; P. Wilharm, *Diplomarbeit*, Universität Freiburg 1981.
[6] All new compounds were characterized by their elemental analyses and spectra (IR, ^{1}H- and ^{13}C-NMR, MS, UV): For example, 3,4,5-triaza-8,10,13-trioxahexacyclo[7.3.1.0^{2,7}.0^{3,5}.0^{4,12}.0^{6,11}]tridecane **5a**: ^{1}H-NMR ($CDCl_3$): $\delta=4.05$ (m, 2-, 6-, 12-H), 5.07 (m, 1-, 7-, 11-H), 5.68 (s, 9-H); ^{13}C-NMR ([D$_6$]DMSO): $\delta=100.3$ (C-9, $J_{C,H}=206.5$ Hz), 77.9 (C-1, -7, -11, $J_{C,H}=165.0$ Hz), 52.5 (C-2, -6, -12, $J_{C,H}=161.0$ Hz); MS (CI, isobutane): *m/z* 182 ($M^{\oplus}+1$, 100%). **14a**: ^{1}H-NMR ($CDCl_3$): $\delta=5.70$ (s, 8-H), 5.35 (dd, 2-, 5-H), 4.5-4.6 (m, 1-, 10-, 11-H), 4.21 (t, 6-H), 3.65 (s, CH_3), $J_{1,2(5,10)}=J_{2,6(5,6)}=5.3$ Hz.
[7] R. Schwesinger, W. Fritsche, H. Prinzbach, *Chem. Ber. 115* (1982) 946; W. Fritsche-Lang, P. Wilharm, E. Hädicke, H. Fritz, H. Prinzbach, *ibid. 118* (1985) 2044.
[8] Bicyclic phosphites such as **4d** are less nucleophilic and thus less reactive toward azides compared with acyclic phosphites: K. Taira, D. G. Gorenstein, *J. Am. Chem. Soc. 106* (1984) 7825, and references cited therein; cf. H. Stetter, K. H. Steinacker, *Chem. Ber. 85* (1952) 451.
[9] A. Nickon, G. D. Pandit, *Tetrahedron Lett. 1968*, 3663; P. J. Garratt, J. F. White, *J. Org. Chem. 42* (1977) 1733.
[10] Hydrolysis of **5a-d** offers a more efficient approach to **9a**. Because of the generally very demanding hydrolysis conditions required for 2,4,10-trioxaadamantanes, **5c/d** are primarily considered for this purpose: O. Bouah, G. Lamaty, C. Moreau, O. Pomares, P. Deslongchamps, L. Ruest, *Can. J. Chem. 58* (1980) 567; T. Fanni, K. Taira, D. G. Gorenstein, R. Vaidyanathaswamy, J. G. Verkade, *J. Am. Chem. Soc. 108* (1986) 6311.
[11] The PE spectroscopic analyses will be reported in collaboration with *R. Gleiter*. Cf. P_3, As_3, Sb_3 cage compounds: R. Gleiter, H. Köppel, P. Hofmann, H. R. Schmidt, J. Ellermann, *Inorg. Chem. 24* (1985) 4020, and references cited therein.

Organometallic Rhodium(III) Complexes as Catalysts for the Photoreduction of Protons to Hydrogen on Colloidal TiO_2**

By *Ulrich Kölle** and *Michael Grützel*

The reduction of protons to hydrogen by transition metal complexes functioning as electron relays is currently under active research by a number of laboratories throughout the world.[1-4] Apart from the development of an efficient sensitizer **S** which should be excitable by sunlight and may be a molecule or semiconductor particle, the transfer of the electrons from its excited state **S*** to the proton to be reduced is the key step of any light-driven hydrogen cycle. Recently developed relay systems **R** exhibit remarkable quantum yields for hydrogen production[2c] and also have enabled mechanistic studies of the relay function.[5] The essential steps of such a cycle are outlined in Scheme 1.

[*] Priv.-Doz. Dr. U. Kölle [+], Prof. Dr. M. Grätzel
Institut de Chimie Physique II, Ecole Polytechnique Fedérale
CH-1015 Lausanne (Switzerland)
[+] Permanent address:
Institut für Anorganische Chemie der Technischen Hochschule
Professor-Pirlet-Strasse 1, D-5100 Aachen (FRG)

[**] This work was supported by the Minister für Wissenschaft und Forschung des Landes Nordrhein-Westfalen (Project No. IVB4-10307185), the Fonds der Chemischen Industrie, and the Schweizerisches Amt für Energie.

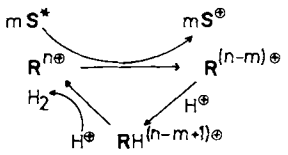

Scheme 1.

The relay $\mathbf{R}^{n\oplus}$ must be reducible by S* and the hydrogen atom in the protonated form $RH^{(n-m+1)\oplus}$ must be sufficiently hydridic in order to generate H_2 in, e.g., a subsequent proton-hydride reaction [see eq. (b)]. For m = 2, the initial form of the relay is regenerated directly. The redox potential of S* necessary for the generation of a sufficiently reducing species $\mathbf{R}^{(n-m)\oplus}$ is furnished for Co^{II}- and Rh^{III}-complexes as relays[1-3] by, e.g., $[Ru(bpy)_3]^{2\oplus *}$ (bpy = 2,2'-bipyridyl; $E_{1/2}([Ru(bpy)_3]^{2\oplus *}/[Ru(bpy)_3]^{3\oplus}) = -0.87$ V vs. NHE[6]) and — albeit only in strongly alkaline solution — by the conduction band (CB) of TiO_2 ($E_{1/2}(CB) = (-0.11 - 0.059\ pH)$ V vs. NHE[7]).

With the novel [Cp*Rh^{III}(ppy)] complexes, **1**, (Cp* = η^5-C_5Me_5; ppy = oligopyridine ligand) we have found a relay system capable of using the weakly reducing electrons of a TiO_2 colloid for hydrogen evolution without participation of colloidal Pt.

The complexes of constitution $[Cp^*Rh(ppy)L]^{n\oplus}$ (n = 1, 2; **1a**, ppy = 2,2'-bipyridyl; **1b**, ppy = [2,2'-bipyridyl]-4,4'-dicarboxylic acid; **1c**, ppy = 4,4'-diacetyl-2,2'-bipyridyl; **1d**, ppy = 1,10-phenanthroline; **1e**, ppy = 2,2'-bipyrazinyl; $L = H_2O$, $OH^\ominus$, $Cl^\ominus$, $I^\ominus$) are formed in 1–30 min at room temperature upon reacting a suspension of $[\{Cp^*RhCl(\mu\text{-}Cl)\}_2]$ in methanol with one equivalent of the oligopyridine ligand. They are stable in air and soluble in water. Their constitutions have been established by ^{1}H-NMR spectroscopy (Table 1) and by correct elemental analyses. Salts containing the cation $[Cp^*Rh(ppy)H_2O]^{2\oplus}$ crystallize from water or aqueous methanol, as has been confirmed for **1a** by a crystal structure analysis.[8] The neutral Rh^I-complexes [Cp*Rh(ppy)], **2**, can be obtained chemically by reduction of **1** with, e.g., Na-amalgam or $[Cp_2Co]$.[9]

Table 1. ^{1}H-NMR spectra of **1a**, **d**, **e** in $CDCl_3$, **1b** in D_2O and **1c** in $(CD_3)_2CO$ at 80 MHz. δ values in ppm.

1a (L = Cl): 1.68 (s, 15H; Cp*), 3.04 (s, 3H; CH_3OH), 8.85 (d, $J(3,4) = 4.7$ Hz, 2H; H^3, $H^{3'}$), 8.18 (ψt, $J(4,5) = 5.2$ Hz, 2H; H^4, $H^{4'}$), 7.81 (dd, $J(5,6) = 6.2$ Hz, 2H; H^5, $H^{5'}$), 8.93 (d, 2H; H^6, $H^{6'}$)

1b: 1.60 (s, 15H; Cp*), 8.87 (s, 2H; H^3, $H^{3'}$), 8.08 (d, 2H; H^5, $H^{5'}$), 9.02 (d, $J(5,6) = 4.7$ Hz, 2H; H^6, $H^{6'}$)

1c (L = Cl): 1.81 (s, Cp*), 2.97 (s, 6H; CH_3CO), 9.74 (d, $J(3,5) = 1.4$ Hz, 2H; H^3, $H^{3'}$), 8.30 (dd, $J(5,6) = 5.8$ Hz, 2H; H^5, $H^{5'}$), 9.31 (d, 2H; H^6, $H^{6'}$)

1d (L = Cl): 1.82 (s, 15H; Cp*), 8.06 (2H; H^5, H^6), 9.04 (d, 2H; H^2, H^9), 8.9 (dd, $J(3,4) = 7.6$ Hz, 2H; H^3, H^8), 8.72 (d, 2H; H^4, H^7)

1e (L = H_2O): 2.16 (s, 15H; Cp*), 9.52 (s, 4H; H^5, $H^{5'}$, H^6, $H^{6'}$), 10.21 (s, 2H; H^3, $H^{3'}$)

The reduction of Rh^{III} to Rh^I can be monitored electroanalytically in aqueous solution; this is especially easy in the case of the dicarboxylic acid **1b** where also the Rh^I-form is water soluble:

In alkaline solution, a single reduction wave is observed at $E_{1/2} = -0.75$ V (SCE); the cyclovoltammogram corresponds to an electrochemically irreversible (non-nernstian) but chemically reversible (peak current ratio = 1) two-electron reduction ($\Delta E_p = 40$ mV) $Rh^{III} \rightarrow Rh^I$. The observed half-wave potential is 0.2 V more positive than the redox potential of the pair $[Rh(bpy)_3]^{3\oplus}/[Rh(bpy)_3]^{2\oplus}$.[2b]

In acid solution (pH < 7.5) the reduction of Rh^{III} to Rh^I is also chemically irreversible (peak current ratio < 1). Polarograms recorded between pH 7.5 and pH 2 exhibit two waves changing in position ($E_{1/2}$) and height (i_g) with pH. In analogy with observations on related $Co\text{-}d^8/Co\text{-}d^6$ systems[5] we assign the more positive wave to the catalytic sequence [eqs. (a)–(c)], where only unprotonated Rh^{III} is reduced. The second wave, where also a protonated species, $(Rh^{III}H)^\oplus$, is reduced, could comprise the reactions (a), (b), and (d)–(f). (Here Rh^I, Rh^{II}, Rh^{III} designate complexes in their respective oxidation states.)

$$(Rh^{III}L)^{2\oplus} + 2e^\ominus \longrightarrow Rh^I + L \quad (a)$$
$$Rh^I + H^\oplus \longrightarrow (Rh^{III}H)^\oplus \quad (b)$$
$$(Rh^{III}H)^\oplus + H^\oplus + L \longrightarrow (Rh^{III}L)^{2\oplus} + H_2 \quad (c)$$
$$(Rh^{III}H)^\oplus + e^\ominus \longrightarrow Rh^{II}H \quad (d)$$
$$Rh^{II}H + H^\oplus \longrightarrow (Rh^{II})^\oplus + H_2 \quad (e)$$
$$(Rh^{II})^\oplus + e^\ominus \longrightarrow Rh^I \quad (f)$$

When complexes **1a**–**1e** (10^{-4} M) are irradiated in the presence of a TiO_2 colloid[10] at pH 10 (Suntest lamp, Hanau, or direct sunlight), the intense violet (**2a**) or green (**2d**) color of the respective Rh^I-complex develops.[11]

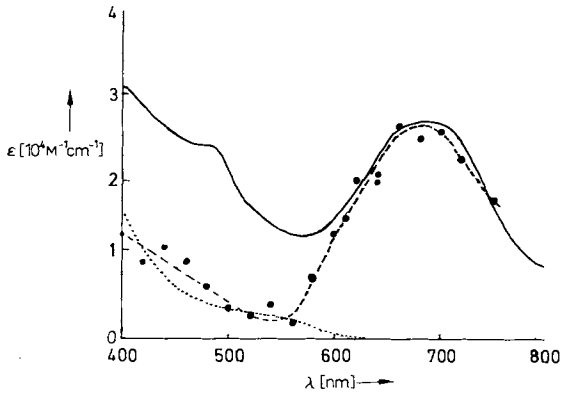

Fig. 1. Absorption spectra: **2d**, obtained by reduction of **1d** with Na/Hg in MeOH (——); transient spectrum 500 μs after triggering a laser flash at a solution of **1d** (2.8×10^{-4} M, 1 g/L TiO_2, pH 8.7 (---•---•-); **1d** (·····).

On laser-flash excitation[12] the absorption of **2** appears (transient spectrum after 500 μs, Fig. 1[13]) with a time constant of ca. 2×10^{-6} s^{-1} (Fig. 2a). The complex kinetics for the buildup of the Rh^I-absorption suggests a multistep reaction. Below pH 7.5, **2** becomes protonated, as evidenced from the absorption decay between 480 and 600 nm (Fig. 2b) followed by a further, much slower, proton-dependent reaction at acidic pH (< 2), assigned as the proton–hydride reaction [eq. (c), (Fig. 2c)]. Continuous irradiation at a pH < 7 does not change the color of the sample but causes hydrogen evolution. Thus, 20 mL of a solution containing 25 mg of TiO_2, 5 μmol of **1a** and 0.05% poly(vinyl alcohol), irradiated for three hours with direct sunlight yielded 0.5 mL H_2, corresponding to 4.5 turnovers.

The reduction and protonation steps via a Rh^{II} intermediate could be followed by means of pulse radiolysis.[14] The reduction of **1a** or **1b** with $e_{aq}^\ominus$ (G = 2.3) or $Me_2\dot{C}(OH)$ (G = 3.2 at pH 10) produces the absorption spectrum of the Rh^{II} complex shown in Figure 3 for **1b** in less than 1 μs.[13]

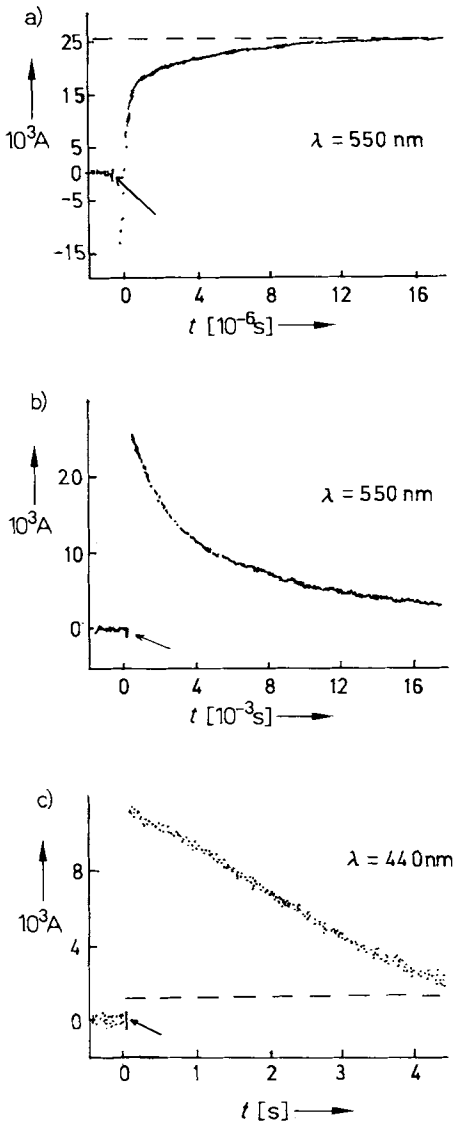

Fig. 2. Change in absorption of **2b** with time (2×10^{-4} M, 0.9 g/L TiO_2, pH 2.5, $\lambda_{exc} = 347$ nm): a) directly after the laser pulse, $\lambda_{obs} = 550$ nm, synthesis of the Rh^I species **2b**. b) $\lambda_{obs} = 550$ nm, decay of **2b** by protonation. c) $\lambda_{obs} = 440$ nm, back reaction of protonated **2b** ($+H^{\oplus}$) to give the starting complex **1b**. The arrow marks the time of triggering of the laser pulse.

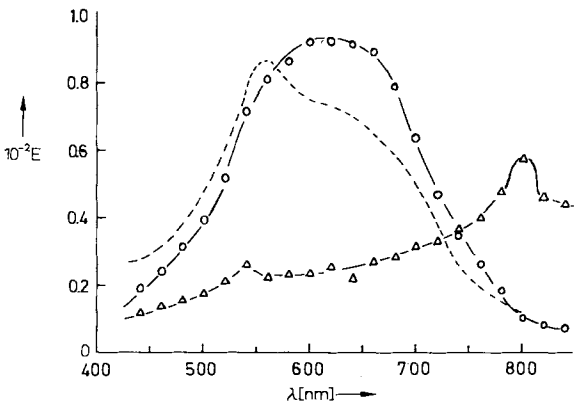

Fig. 3. Absorption spectra of the reduction products of **1b** (2×10^{-4} M, pH 10) obtained by pulse radiolysis: (Δ--Δ--Δ-) = Rh^{II}-complex, 2 μs after the pulse; (O--O--O-) = **2b**, 200 μs after the pulse; (------) spectrum of the reduced alkaline solution.

After ca. 200 μs, the spectrum of the Rh^I complex **2b**, identical to the one obtained by laser-flash excitation, is formed in a reaction between 1st and 2nd order, dependent on the pH and on L. Again, in acid solution the protonation of **2** (see rate constants in Scheme 2) and, at pH < 2, also the reaction of protonated **2** to reform the starting compound can be monitored. A reduction-protonation-oxidation cycle based on these results is depicted in Scheme 2.

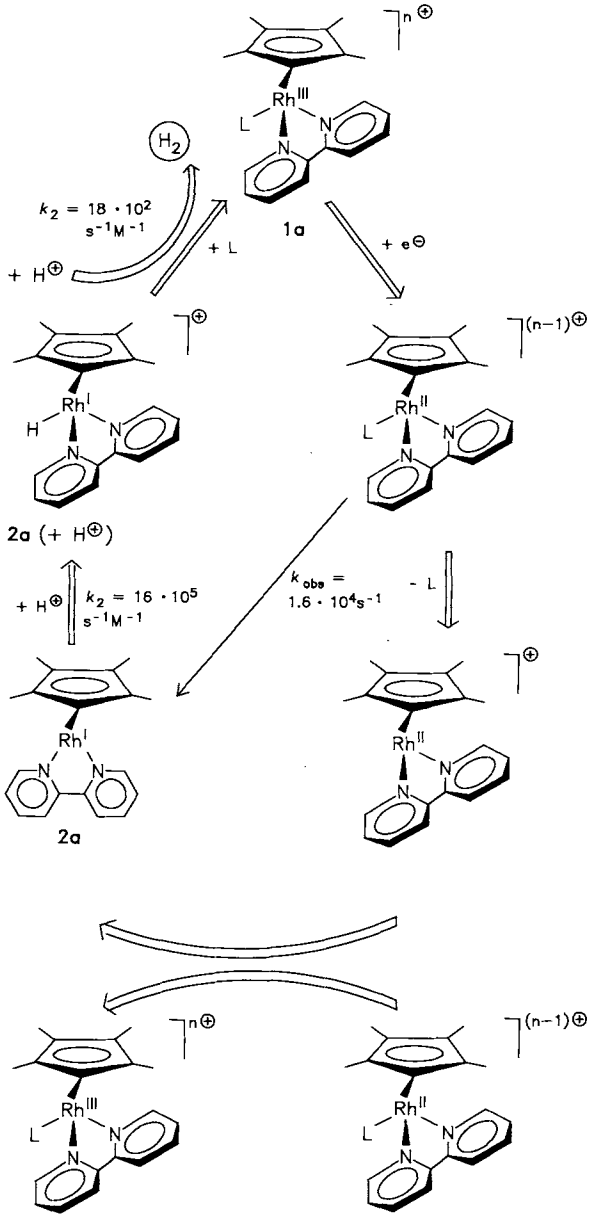

Scheme 2. Reduction-protonation-oxidation cycle for **1a** with rate constants measured by pulse radiolysis. k_{obs} for $L = OH^{\ominus}$; for $L = I^{\ominus}$ $k_{obs} = 1.6 \times 10^3$ s^{-1}.

In contrast to the complex $[Rh(bipy)_3]^{3\oplus}$, in the present case the conduction band potential of TiO_2 suffices for a reduction of Rh^{III} to Rh^I in *acid* solution. Also at variance with the $[Rh(bpy)_3]^{3\oplus}$ system, where the Rh^I species $[Rh(bpy)_2]^{\oplus}$ does not give hydrogen with protons,[15] complexes **2** react, as has been shown independently, with protonic acids (trifluoroacetic acid in tetrahydrofuran) with formation of hydrogen and regeneration of the starting complex. Intervening dimerization of the Rh^{II} and Rh^I intermediates is prevented in this case by the quasi fivefold

coordination of the metal. Moreover, concomitant with the change in oxidation state from Rh^{III} to Rh^{II} and Rh^{I} only one monodentate ligand L, in aqueous solution preferentially water, is lost, a fact that greatly facilitates the disproportionation of intermediary Rh^{II}. The combined effects now make the reactions with protons as shown in Scheme 2 rate determining in the overall cycle.

Experimental

A suspension of $[\{Cp^*RhCl(\mu\text{-}Cl)\}_2]$ (0.31 g = 0.5 mmol) in MeOH (10 mL) was treated with 1.2 mmol of the oligopyridine ligand and the mixture stirred for 10 min (in the case of the sparingly soluble ligand [2,2′-bipyridyl]-4,4′-dicarboxylic acid an ultrasonic bath was used). The resulting clear orange-yellow solution was evaporated to 2 mL and the complexes **1** were either precipitated by addition of ether or crystallized on diffusion of ether into the concentrated methanolic solution. The yields were almost quantitative.

Received: January 2,1987;
revised: January 30, 1987 [Z 2034 IE]
German version: *Angew. Chem. 99* (1987) 572

[1] K. Kalyanasundaram, *Nouv. J. Chim. 3* (1979) 511.
[2] a) C. Creutz, H. A. Schwarz, N. Sutin, *J. Am. Chem. Soc. 106* (1984) 3036; b) S. F. Chan, M. Chou, C. Creutz, T. Matsubara, N. Sutin, *ibid. 103* (1981) 369; c) C. V. Krishnan, B. S. Brunschwig, C. Creutz, N. Sutin, *ibid. 107* (1985) 2005.
[3] R. Ziessel, J. Hawecker, J.-M. Lehn, *Helv. Chim. Acta 69* (1986) 1065, and references cited therein..
[4] K. J. Brewer, W. R. Murphy, Jr., K. J. Moore, E. C. Eberle, J. D. Petersen, *Inorg. Chem. 25* (1986) 2470; b) S. Sakaki, G. Koga, K. Ohkubo, *ibid. 25* (1986) 2330; c) P. Connolly, J. H. Espenson, *ibid. 25* (1986) 2684.
[5] U. Kölle, S. Ohst, *Inorg. Chem. 25* (1986) 2689.
[6] V. Balzani, A. Juris, F. Barigelletti, P. Belser, A. von Zelewsky, *Sci. Pap. Inst. Phys. Chem. Res. (Jpn.) 78* (1984) 78.
[7] J. Moser, M. Grätzel, *J. Am. Chem. Soc. 105* (1983) 6547.
[8] The crystal structure analysis showed the presence of the cation **1a** ($L = H_2O$); no data can be deposited because of disorders in the anion region; we thank Dr. *E. Raabe* and Prof. Dr. *C. Krüger*, MPI für Kohlenforschung, Mülheim/Ruhr, for determining the structure.
[9] For example, **2a** by reduction of **1a** with $[Cp_2Co]$ in $[D_8]$tetrahydrofuran; ^{1}H-NMR: $\delta = 1.92$ (s, Cp*), 6.53 (t), 7.06 (t, 4H; H^4, $H^{4'}$, H^5, $H^{5'}$), 7.81 (d, 2H; H^3, $H^{3'}$), 8.94 (d, 2H, H^6, $H^{6'}$), $J(5,6) = 7.8$, $J(4,5) = 4.7$ Hz.
[10] 1–2.5 g/L = 1.8×10^{-8} to 6×10^{-7} mol particles/L, stabilized with 0.1% poly(vinyl alcohol), which simultaneously served as sacrificial electron donor.
[11] λ_{max} [nm] (ε_{max} M^{-1} cm^{-1}): **2a**: 512 (2.02×10^4); **2b**: 556 (1.3×10^4); **2c**: 636 (1.6×10^4); **2d**: 694 (1.77×10^4); **2e**: 544 (2.04×10^4).
[12] JK-2000 ruby laser, $\lambda = 347$ nm, pulse width 15 ns.
[13] The difference in the wavelength region <600 nm of the spectrum obtained by chemical reduction (——) and after laser flash excitation (—•—•) in Figure 1 can be explained by the bleaching of the Rh^{III} complex accompanying the formation of **2d**. The somewhat different spectrum of **2b** in Figure 3 is also obtained by laser flash excitation at pH 4. It is traced back to the carboxylate groups of the Rh^{I} complex being protonated under these conditions. (If pulse radiolysis is carried out at pH 10 in unbuffered solution, the pH value drops and the protonated dicarboxylic acid can be present.)
[14] Pulse radiolysis: Van-de-Graaf accelerator, electron energy 2.7 MeV, pulse width 500 ns. Solvent: water with 5% 2-propanol. $D = 7 \times 10^{-8}$ Gy.
[15] See [2b] and Q. G. Mulazzani, S. Emmi, M. Z. Hoffmann, M. Venturi, *J. Am. Chem. Soc. 103* (1981) 3362.

Diazo Coupling of Nortricyclene-(Tricyclo[2.2.1.$0^{2,6}$]heptane)-1-diazonium Ions

By *Georg Feldmann* and *Wolfgang Kirmse**

Cyclopropanediazonium ions react with azide ions[1,2] and with amines[1,3] by way of diazo coupling, but fail to couple with phenols (phenoxides). The "classical" diazo coupling reaction with phenoxides has now been achieved with nortricyclene-1-diazonium ions **4** to which the competitive pathways of ring opening[1,4] and inverting displacement[1,4] are not available.

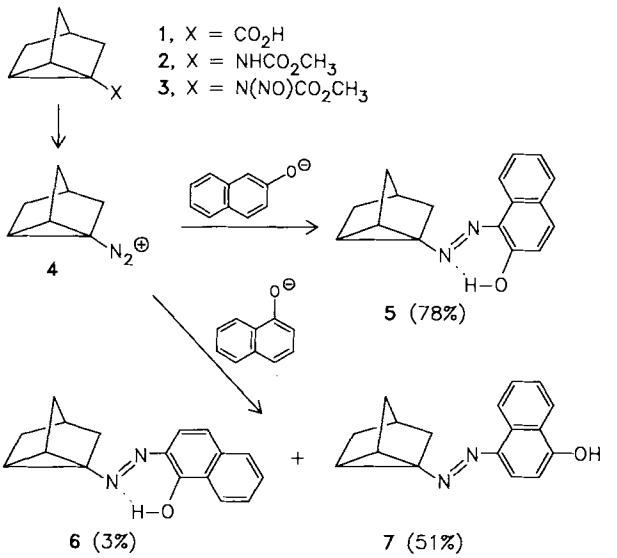

Curtius degradation of nortricyclene-1-carboxylic acid **1**[5] to give the carbamate **2** (61%) was followed by nitrosation, yielding the nitrosocarbamate **3** (90%). Deacylation of **3** with a mixture of potassium carbonate, 2-naphthol, and methanol afforded the azo compound **5** [m.p. 98 °C, intense yellow crystals from pentane]. The analogous reaction of **3** with 1-naphthol led to the azo compounds **6** and **7**. The isomers were separated by means of HPLC, but were not obtained crystalline. In contrast to **5** [δ(OH) = 13.7] and **6** [δ(OH) = 13.6], **7** [δ(OH) = 5.6] does not form an intramolecular hydrogen bond and deteriorates in the presence of air (see Table 1).

Table 1. Selected spectral data of the azo compounds **5**–**7**. ^{1}H-NMR spectra: 80 MHz, $CDCl_3$. UV/VIS spectra: *n*-heptane.

5: ^{1}H-NMR: $\delta = 1.45$–1.85 (m, 4H), 1.95 (d, 2H, $J = 1.4$ Hz, 7-H), 2.3 (m, 1H, 4-H), 2.37 (s, 2H, 2-H, 6-H), 7.1–8.05 (m, 5 aryl-H), 8.73 (d, 1H, $J = 8$ Hz, aryl-3-H), 13.7 (s, 1H, OH); UV/VIS: $\lambda_{max} = 250$ nm ($\varepsilon = 17600$), 335 (9700), 375 (10400)

6: ^{1}H-NMR: $\delta = 1.2$–1.65 (m, 4H), 1.85 (d, 2H, $J = 2$ Hz, 7-H), 2.25 (s, br, 3H, 2-H, 4-H, 6-H), 7.2–7.8 (m, 5 aryl-H), 8.3 (m, aryl-8-H), 13.6 (s, 1H, OH); UV/VIS: $\lambda_{max} = 285$ nm ($\varepsilon = 39800$), 315 (14550), 385 (9000)

7: ^{1}H-NMR: $\delta = 1.45$–1.75 (m, 4H), 1.90 (d, 2H, $J = 2$ Hz, 7-H), 2.26 (m, 1H, 4-H), 2.40 (s, br, 2H, 2-H, 6-H), 5.6 (s, br, 1H, OH), 6.79 (d, 1H, $J = 8$ Hz, aryl-2-H), 7.43 (d, 1H, $J = 8$ Hz, aryl-3-H), 7.5–7.7 (m, 2H, aryl-6-H, aryl-7-H), 8.19 (m, 1H, aryl-5-H), 8.78 (m, 1H, aryl-8-H); UV/VIS: $\lambda_{max} = 240$ nm ($\varepsilon = 17150$), 348 (10050)

The behavior of the diazonium ion **4** in alcohols is also remarkable. Instead of the expected ethers we obtained the hydrocarbon nortricyclene **8** (90%) by way of reductive deamination.[6] With isopropanol, an equivalent amount of acetone (88%) was formed, suggesting hydride abstraction from the α-position of the alcohol. Deuterium incorporation into nortricyclene from CH_3OD increased with increasing concentration of base (K_2CO_3/CH_3OD: 0.15 D/mol; 2 M $NaOCH_3/CH_3OD$: 0.54 D/mol). In the presence of sodium borohydride, similar results were obtained. The

[*] Prof. Dr. W. Kirmse, Dr. G. Feldmann
Fakultät für Chemie der Universität
Universitätsstr. 150, D-4630 Bochum 1 (FRG)

 © VCH Verlagsgesellschaft mbH, D-6940 Weinheim, 1987 0570-0833/87/0606-0570 $ 02.50/0

analogous behavior of arenediazonium ions[7,8] has been taken as evidence for a diazene (diimide) intermediate **11**. Regardless of the mechanism of diazene decomposition (*via* carbanions or free radicals),[9] the intervention of **11** will allow for (partial) exchange of hydrogen for deuterium. Hydride transfer at the carbocation stage cannot lead to incorporation of protons from the solvent.

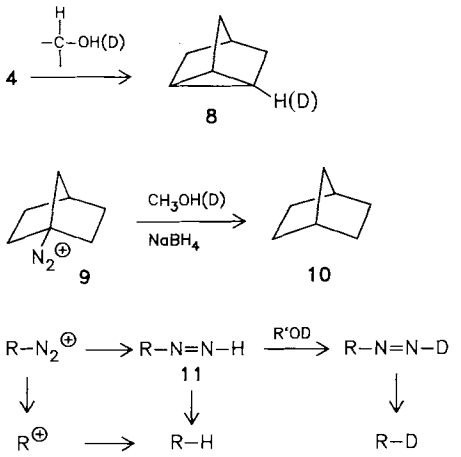

Under identical conditions, norbornane(bicyclo[2.1.1]heptane)-1-diazonium ions **9**[2] afforded undeuterated norbornane **10** exclusively. It appears that **9** is not sufficiently persistent to act as a hydride acceptor; accordingly, all attempted azo coupling reactions of **9** failed. The behavior of **9** is characteristic of aliphatic diazonium ions, whereas azo coupling and reductive deamination of **4** are reminiscent of arenediazonium ions. The comparison with **9** reveals that the arene-like reactivity of **4** is not due to the bridgehead position of the diazonium group but may be attributed to the special electron distribution (σ delocalization)[10] of the cyclopropane ring.

Experimental

A mixture of potassium carbonate (0.5 g, 3.6 mmol), 2-naphthol (1.50 g, 10.4 mmol) and anhydrous methanol (2 mL) was stirred for 15 min and then treated dropwise with a solution of **3** (208 mg, 1.06 mmol) in methanol (0.5 mL). After 1.5 h the mixture was diluted with 5 mL of methanol and extracted with pentane (2 × 5 mL). The combined pentane extracts were washed with water, dried over magnesium sulfate, evaporated down under vacuum, and chromatographed on Polygosil 60-5 (25 × 3 cm column, hexane/ether 9:1). 220 mg (78%) of **5** (m.p. 95 °C) could be separated from the excess 2-naphthol. **5** was recrystallized from pentane, m.p. 89 °C.

The reaction mixture consisting of **3** and 1-naphthol was worked up under nitrogen and the components eluted with pentane/ether (5:1) in the sequence **6** (10 mg), 1-naphthol, **7** (150 mg).

Received: January 9, 1987 [Z 2042 IE]
German version: *Angew. Chem. 99* (1987) 560

CAS Registry numbers:
1, 697-25-6; **2**, 100861-01-6; **3**, 107798-50-5; **3** (X = D), 38570-13-7; **5**, 107798-51-6; **6**, 107798-53-8; **7**, 107798-52-7; **8**, 279-19-6

[1] W. Kirmse, W. J. Baron, U. Seipp, *Angew. Chem. 85* (1973) 994; *Angew. Chem. Int. Ed. Engl. 12* (1973) 924.
[2] W. Kirmse, O. Schnurr, H. Jendralla, *Chem. Ber. 112* (1979) 2120.
[3] W. Kirmse, U. Seipp, *Chem. Ber. 107* (1974) 745.
[4] W. Kirmse, J. Rode, K. Rode, *Chem. Ber. 119* (1986) 3672.
[5] H. Hart, R. A. Martin, *J. Org. Chem. 24* (1959) 1267; K. Alder, H. Hartmann, W. Roth, *Chem. Ber. 83* (1960) 2271.
[6] D. S. Wulfman in S. Patai (Ed.): *The Chemistry of Diazonium and Diazo Groups*, Wiley, Chichester 1978, p. 286; H. Zollinger in S. Patai, Z. Rappoport (Eds.): *The Chemistry of Functional Groups, Supplement C, Part 1*, Wiley, New York 1983, p. 603; R. Tröndlin, C. Rüchardt, *Chem. Ber. 110* (1977) 2494.
[7] M. Bloch, H. Musso, U. I. Zahorsky, *Angew. Chem. 81* (1969) 392; *Angew. Chem. Int. Ed. Engl. 8* (1969) 370; E. König, H. Musso, U. I. Zahorsky, *ibid. 84* (1972) 33 and **11** (1972) 45.
[8] C. E. McKenna, T. G. Traylor, *J. Am. Chem. Soc. 93* (1971) 2313.
[9] E. M. Kosower, *Acc. Chem. Res. 4* (1971) 193.
[10] M. J. S. Dewar, *J. Am. Chem. Soc. 106* (1984) 669; D. Cremer, J. Gauss, *ibid. 108* (1986) 7467.

Nickel(0)-Catalyzed Production of a Functionalized Cyclopentanecarboxylic Acid from 1,3-Butadiene and CO_2

By *Heinz Hoberg,* Sabine Gross,* and *Armin Milchereit*

The C_1 building block CO_2 is gaining increasing significance in preparative chemistry.[1] Stoichiometric reactions of alkenes or alkadienes with CO_2 on Ni^0-,[2] W^0-, or Mo^0-complexes[3] can be regarded as model reactions for the catalytic production of carboxylic acids. The catalytic formation of linear carboxylic acids from 1,3-butadiene and CO_2 has already been achieved on Pd-compounds.[4] A knowledge of how various types of ligands L (mono- or multidentate ligands with various electronic and/or steric effects) influence CC coupling reactions to transition-metal complexes is of central importance in organometallic chemistry. We have investigated the influence of ligands and solvents on the reaction of 1,3-butadiene **1** with CO_2 **2** on a nickel(0) system[5] with the aim of obtaining carboxylic acids catalytically. A series of monodentate phosphanes were examined, since multidentate ligands (chelate formers) lead only to stoichiometric reactions.[6]

When a mixture of **1**, **2** and **3**, L = PPh_3 (molar ratio 3:3:1) in tetrahydrofuran (THF) is prepared in a steel autoclave at −20 °C and the stirred mixture is allowed to warm to 20 °C, subsequent hydrolysis of the reaction solution affords the two cyclopentanecarboxylic acids **7**[7] and **9** (molar ratio ca. 9:1). On heating the reaction mixture to 40 °C the molar ratio changes to 1:1. If, on the other hand, the reaction is not carried out in the presence of PPh_3, but in the presence of a less basic ligand, e.g. triisopropyl phosphite $P(OiPr)_3$, **7** is formed only in traces (detected gas-chromatically as methyl ester) whereas **9** is formed in ca. 95% yield (based on Ni^0). Since the carboxylic acid **9** is composed of two molecules of **1** and one molecule of CO_2, it was to be expected that it should also be preparable catalytically. This assumption could be realized when the following general conditions were maintained: 1) Use of polar solvent, e.g. dimethylformamide, dimethylacetamide, tetramethylurea and, though less effective, THF. 2) A reaction time of ca. 30 h at ca. 60 °C and a partial pressure P_{CO_2} of ca. 20 bar. 3) A concentration of ca. 0.3 mmol Ni^0/100 mL of solvent[8] at a molar ratio L:Ni^0 of ca. 3:1. Under these conditions the carboxylic acid **9** can be prepared in ca. 30 catalytic cycles per Ni atom.

We suggest the following reaction course for the catalytic formation of the carboxylic acid (Scheme 1). The catalysis is initiated by the well-known dimerization of 1,3-butadiene on the (L)Ni^0 system **3** to give **4**.[9] The CC coupling with CO_2 then takes place by insertion into an Ni-C σ-bond; because of the reactivity differential $Ni\text{-}C_{prim} < Ni\text{-}C_{sec}$ this step takes place in the case of **4a**, but not in

[*] Prof. Dr. H. Hoberg, Dipl.-Chem. S. Gross, A. Milchereit
Max-Planck-Institut für Kohlenforschung
Kaiser-Wilhelm-Platz 1, D-4330 Mülheim a. d. Ruhr (FRG)

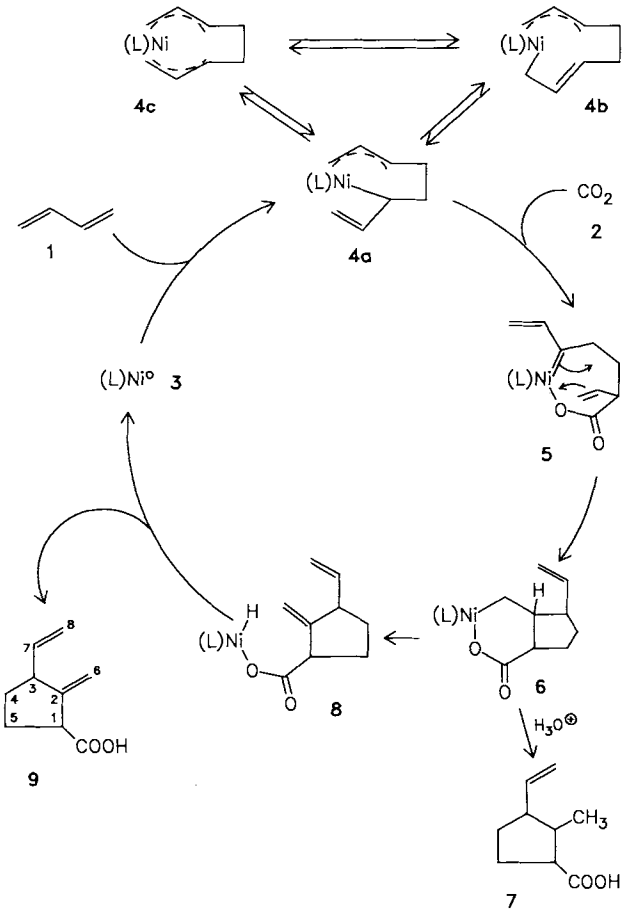

Scheme 1. L = PPh_3 or $P(OiPr)_3$.

the case of **4b**. The carboxylate **5** is formed, which likewise contains a reactive Ni–C_{sec} bond. The CC double bond of the allylcarboxylate moiety inserts intramolecularly into the latter. This novel CC coupling reaction is made possible by the formation of the carbocyclic five-membered ring in the bicyclic nickela-complex **6** (the hydrolysis of **6** affords **7**[10]). A subsequent β-H elimination now affords **8** initially, from which the carboxylic acid **9** is liberated by reductive elimination and the (L)Ni^0 starting complex **3** is regenerated.

Experimental

2-Methylene-3-vinylcyclopentanecarboxylic acid **9** (catalytic): A cold mixture of $[(cod)_2Ni]$ (0.055 g, 0.20 mmol), triisopropyl phosphite (0.14 g, 0.66 mmol), and 1,3-butadiene (9 g, 166 mmol) in 70 mL of dimethylformamide was transferred to a 200-mL steel autoclave cooled to −20 °C. CO_2 (ca. 20 bar) was then passed into the autoclave and the stirred mixture heated within ca. 3 h to 60 °C and kept at this temperature for approximately a further 20 h. The solvent was removed from the cold reaction solution by vacuum distillation. The residue was hydrolyzed with ca. 20 mL of 2 N H_2SO_4 and then extracted several times with diethyl ether. The organic phase was now extracted several times with 1 N NaOH solution. The aqueous phase was then rendered acidic with dilute H_2SO_4, re-extracted with diethyl ether and the etheral phase dried over $MgSO_4$. Removal of the ether by distillation furnished **9** as a colorless, viscous liquid. Yield: 0.89 g (5.86 mmol), which corresponds to 29.3 catalytic cycles per Ni atom.—IR (KBr): $\tilde{\nu}$ = 1705 (C=O), 1648 (C=C) cm^{-1}; δ = 910, 990 (C–H) cm^{-1}.—^{1}H-NMR ([D_8]THF, 20 °C, 200 MHz): δ = 5.67 (ddd, 1 H; 7-H), 5.24 (s, 1 H; 6 *E*-H), 5.03 (d, 1 H; 8 *E*-H), 5.00 (d, 1 H; 8 *Z*-H), 4.91 (s, 1 H; 6 *Z*-H), 3.35 (m, 1 H; 1-H), 3.01 (s, 1 H; 3-H), 1.7–2.1 (m, 4 H; 4-, 5-H).—^{13}C-NMR ([D_8]THF, 20 °C, 75.47 MHz): δ = 174.9 (s; CO_2H), 153.8 (s; C-2), 141.6 (d, J_{CH} = 153 ± 2 Hz; C-7), 115.1 (t, J_{CH} = 156 ± 1 Hz; C-8), 109.4 (t, J_{CH} = 158 ± 1 Hz; C-6), 50.8 and 49.2 (d; C-1,3), 33.2 (t, J_{CH} = 132 ± 1 Hz; C-4), 29.9 (t, J_{CH} = 133 ± 1 Hz; C-5).

Received: January 23, 1987;
revised: March 12, 1987 [Z 2066 IE]
German version: *Angew. Chem.* *99* (1987) 567

[1] T. Ito, A. Yamamoto in S. Inoue, N. Yamazaki (eds.): *Organic and Bioorganic Chemistry of Carbon Dioxide*, Kodansha, Tokio 1982; R. P. A. Sneeden in G. Wilkinson, F. G. A. Stone, E. W. Abel (Eds.): *Comprehensive Organometallic Chemistry, Vol. 8*, Pergamon Press, Oxford 1982, p. 225–283.
[2] H. Hoberg, D. Schaefer, B. W. Oster, *J. Organomet. Chem. 266* (1984) 313.
[3] R. Alvarez, E. Carmona, D. J. Cole-Hamilton, A. Galindo, E. Gutierrez-Puebla, A. Monge, M. L. Poveda, C. Ruiz, *J. Am. Chem. Soc. 107* (1985) 5529.
[4] U. M. Dzhemilev, R. V. Kunakova, V. V. Sidorova, *Bull. Acad. Sci. USSR Div. Chem. Sci. 34* (1985) 2102.
[5] Ni^0: [(cdt)Ni] (cdt = 1,5,9-cyclododecatriene) or $[(cod)_2Ni]$ (cod = 1,5-cyclooctadiene).
[6] H. Hoberg, Y. Peres, A. Milchereit, *J. Organomet. Chem. 307* (1986) C41, and references cited therein.
[7] If the reaction of **1** with **2** on the $[(PPh_3)Ni^0]$ system is not carried out in THF but in a nonpolar solvent, e.g. toluene, then only **7** is formed; cf. S. Stobbe, *Dissertation*, Universität Bochum 1979.
[8] When the Ni^0 concentration is increased tenfold, the number of catalytic cycles is halved.
[9] B. Büssemeier, P. W. Jolly, G. Wilke, *J. Am. Chem. Soc. 96* (1974) 4726.
[10] P. W. Jolly, S. Stobbe, G. Wilke, R. Goddard, C. Krüger, J. C. Sekutowski, Y.-H. Tsay, *Angew. Chem. 90* (1978) 144; *Angew. Chem. Int. Ed. Engl. 17* (1978) 124. These authors describe the preparation and structure of a tetrameric complex of **6** with tricyclohexylphosphane as ligand.

Isoelectronic Relationships in Cluster Chemistry: Nucleophilic Addition to a Vinylidene Ligand

By *Thomas Albiez* and *Heinrich Vahrenkamp**

The vinylidene group $=C=CH_2$ attracts interest in complex chemistry because it is one of the conceivable intermediates in the elementary processes for the production of petrochemical raw products. It is multifunctional, which means, e.g., that it can be bound to up to four metal atoms in complexes or on surfaces. Whereas this property is immediately apparent in the preparation of organometal-vinylidene complexes,[1] the associated consequences thereof, in the form of variable reactivity, have hitherto only been studied superficially.[1b,2] Thus, it is substantiated by experiment and theory that mononuclear vinylidene complexes are mostly electrophilic at the α-C atom;[3] this also seems to be true, to a limited extent, in the case of dinuclear complexes containing a bridging $=C=CH_2$ moiety.[1] Neutral trinuclear clusters containing a μ_3-vinylidene moiety have not as yet been studied theoretically with respect to their electron density distribution.[4] In the case of their cationic analogues such as **1**, however, which can be regarded as complex-stabilized carbenium ions,[5] it has long been known that they exhibit high electrophilicity at the β-C-atom.[6] It thus appears that their reactivity reverses with increasing number of the metal atoms bound to the vinylidene ligand.

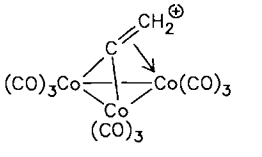

1

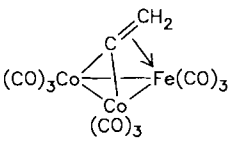

2

For the investigation of neutral vinylidene-trimetal complexes we chose the cluster **2**, for which we have devel-

[*] Prof. Dr. H. Vahrenkamp, Dipl.-Chem. T. Albiez
Institut für Anorganische und Analytische Chemie der Universität
Albertstr. 21, D-7800 Freiburg (FRG)

oped a convenient synthesis.[7] Although it is only moderately reactive towards nucleophiles and electrophiles, it undergoes reactions with basic phosphane ligands consistent with its isosteric relationship with **1**. Thus, **2** reacts with PMe_3 below 0°C practically quantitatively, undergoing addition to give the black, readily crystallizable cluster **4**, which is soluble only in polar solvents. **4** can be regarded as a zwitterion with positive charge on the phosphorus and negative charge on the iron. It is in turn isosteric with the cluster **3**,[8] which derives from **1**.

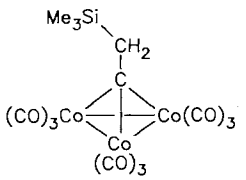

3

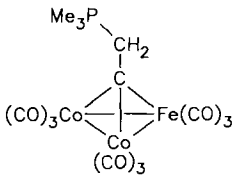

4

Spectroscopic characterization and structural analysis[9] confirm this isoelectronic relationship. The bond lengths in the $CFeCo_2$ nucleus of **4** (cf. Fig. 1) resemble very closely those in the $[(\mu_3\text{-}RC)Co_3(CO)_9]$-clusters;[6] the orientation of the vinylidene C–C axis at 82° to the $FeCo_2$-plane removes the outer C-atom of the $=C=CH_2$ unit from the bonding sphere of the metal atoms; the C–C distance of 153 pm is that of a single bond; and the phosphorus atom is surrounded by four P–C bonds of equal length (178.5 ± 1 pm). A further conceivable formulation even allows **4** to be considered as an ylide complex of the cluster $[CFeCo_2(CO)_9]$, drawing attention to its relationship with the "carbonyl complex" $[Fe_2Co(CO)_9(\mu_3\text{-}C\text{-}CO)]^{\ominus}$.[10]

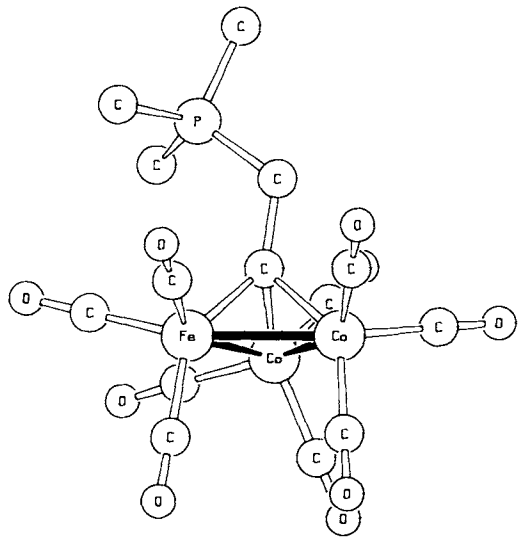

Fig. 1. Molecular structure of **4**. Central bond lengths [pm]: Fe-Co 250.9(1) and 251.7(1), Co-Co 248.4(1), Fe-C 188.0(7), Co-C 192.0(7) and 196.0(7).

The addition of the phosphane to the vinylidene ligands of **2** competes with CO-substitution at the Co atoms. The latter reaction predominates on increasing the temperature, and **4** is also converted into the substitution product **5** on heating. A decrease in the basicity or an increase in the bulkiness of the phosphane ligand has the same effect. Thus, with PMe_2Ph and $PMePh_2$ the increasingly more labile addition products are still obtainable, whereas with PPh_3 only the substitution product is formed. Finally, the ruthenium cluster **6** which is analogous to **2** reacts with phosphane ligands only with CO-substitution. A structure determination and comparison of the spectra have enabled an assignment of the constitution of **5**.[11]

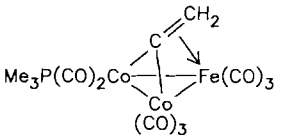

5

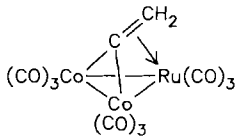

6

As a consequence of the formation and structure of the cluster **4** it could follow, to a limited extent, that an organic derivative chemistry of **2** analogous to that of **1** should be possible. It remains to be checked whether bonding of the vinylidene ligand to four metal atoms further increases the umpolung that is observed on going from a mono- to a multinuclear complex.

Received: January 28, 1987 [Z 2073 IE]
German version: *Angew. Chem. 99* (1987) 561

[1] a) J. Hilton, M. F. Lappert, R. Pearce, P. I. W. Yarrow, *Chem. Rev. 83* (1983) 135; b) M. I. Bruce, A. G. Swincer, *Adv. Organomet. Chem. 22* (1983) 59.
[2] Cf. A. Höhn, H. Werner, *Angew. Chem. 98* (1986) 745; *Angew. Chem. Int. Ed. Engl. 25* (1986) 759, and references cited therein.
[3] Cf. [1b]; regarding a departure from this behavior see: H. Werner, *Angew. Chem. 95* (1983) 932; *Angew. Chem. Int. Ed. Engl. 22* (1983) 927.
[4] Cf. J. Silvestre, R. Hoffmann, *Helv. Chim. Acta 68* (1985) 1461.
[5] B. E. R. Schilling, R. Hoffmann, *J. Am. Chem. Soc. 101* (1979) 3456; R. T. Edidin, J. R. Norton, K. Mislow, *Organometallics 1* (1982) 561.
[6] D. Seyferth, *Adv. Organomet. Chem. 14* (1976) 97.
[7] J. Ros, R. Mathieu, *Organometallics 2* (1983) 771; T. Albiez, W. Bernhardt, C. von Schnering, E. Roland, H. Bantel, H. Vahrenkamp, *Chem. Ber. 120* (1987) 141.
[8] D. Seyferth, J. E. Hallgren, R. J. Spohn, G. H. Williams, M. O. Nestle, P. L. H. Hung, *J. Organomet. Chem. 65* (1974) 99.
[9] ^{1}H-NMR (CD_2Cl_2, int. TMS): $\delta = 4.85$ (d, $J = 15.6$ Hz, 2H), 1.91 (d, $J = 14.0$ Hz, 9H). IR ($CHCl_3$, cm^{-1}): $\tilde{\nu} = 2065$ w, 2010 s, 1990 s, 1925 w, 1890 w. Crystallographic data: monoclinic, $P2_1$, $a = 994.4(2)$, $b = 1315.6(3)$, $c = 784.8(2)$ pm, $\beta = 106.06(2)°$, $Z = 2$, 3122 reflections, $R = 0.036$. Further details of the crystal structure investigation are available on request from the Fachinformationszentrum Energie, Physik, Mathematik GmbH, D-7514 Eggenstein-Leopoldshafen 2 (FRG), on quoting the depository number CSD-52269, the names of the authors, and the journal citation.
[10] J. W. Kolis, E. M. Holt, J. A. Hriljac, D. F. Shriver, *Organometallics 3* (1984) 496.
[11] W. Bernhardt, H. Vahrenkamp, unpublished.

A Test for Synergetic Captodative Radical Stabilization**

By *Hermann Birkhofer, Johannes Hädrich, Hans-Dieter Beckhaus*, and *Christoph Rüchardt**

Some years ago it was suggested that pairs of substituents of opposite polarity (captodative substitution) act synergetically in the stabilization of radicals, i.e. their sta-

[*] Prof. Dr. C. Rüchardt, Dr. H. Birkhofer, Dipl.-Chem. J. Hädrich, Dr. H. Beckhaus
Institut für Organische Chemie und Biochemie der Universität Albertstrasse 21, D-7800 Freiburg (FRG)

[**] This work was supported by the Deutsche Forschungsgemeinschaft, by the Land Baden-Württemberg, and by the Fonds der Chemischen Industrie.

bilizing effect is more than additive, while pairs of identical electron withdrawing (capto) or electron donating (dative) substituents act in a conflicting, i.e. less than additive, manner.[1, 2] This suggestion has been supported by qualitative arguments from synthetic work,[1a, b] by qualitative FMO theory,[3] by enhanced spin delocalization in ESR spectra of captodative substituted radicals,[4] by the influence of cd-substitution on rotational barriers of radicals,[5] and by kinetics.[1b, c, 6] It has been concluded, that the mutual interaction of cd-substituents causes enhanced delocalization of the unpaired spin by polarization[1] leading to an additional stabilization of the radical.

This simple model is based on the assumption that the stabilities of these radicals (relative to non-radical precursors) are predominantly determined by spin delocalization. However, it is well known that two geminal substituents at a *tetracoordinated* carbon may also interact and, accordingly, not contribute to the stability of molecules in an additive manner.[7] Any change of this mutual interaction of two groups by σ-type interaction in going from the radical to the parent saturated compound would cause the simple relationship between spin delocalization and thermodynamic stability of a radical to be misleading.

In the meantime, experiments have been performed which do not support a kinetic stabilization of cd-substituted radicals.[8, 9] Furthermore, an additive and not a synergetic effect of cd-substituents in the thermodynamic stabilization of CH_3O- and CN-substituted radicals was found. This was deduced from the rates of dissociation of several 2,3-dimethoxysuccinonitriles **1f**[9, 10, 11a] [Reaction

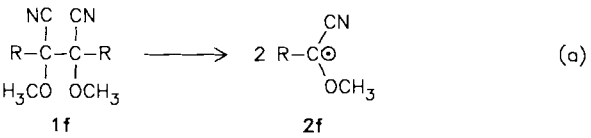

(a)

1f **2f**

R = C_6H_5[9], t-C_4H_9[11a], i-C_3H_7[11b]

(a)] and the known independent effects of α-cyano and α-methoxy substituents on the CC-bond strength in substituted ethanes.[10] These reactions are not susceptible to polar effects[12] and methods have been developed to account separately for steric effects in CC-cleavage reactions.[10] Furthermore, we could demonstrate that no measurable interaction of the geminal methoxy and cyano groups exists in ethanes **1f**, i.e. the group increments of ΔH_f° are additive.[9]

We have now exposed the claim stated in the first sentence of this note to an experimental test by comparing the activation parameters for the thermal cleavage reactions of the substituted ethanes **1d** and **1g**[13] with those of **1f** (see Table 1).[9, 11a] In all examples product analyses confirmed the homolytic cleavage [Reaction (b)] of the central CC-bond in the rate determining step.[10]

While the substitution of one OCH_3 group for a CH_3 group on each carbon of the ethane skeleton **1** (cf. **1c** vs. **1b**) results in a decrease of ΔH^+ by 4.4 kcal·mol^{-1}, the introduction of two further OCH_3 groups in **1d**[15]) (cf. **1c** vs. **1d**) leads to a 7.4 kcal·mol^{-1} *increase* in ΔH^+. This is a clear experimental proof that σ-type interactions of two geminal methoxy groups differ significantly between species with paired (**1**) and unpaired electrons (**2**). According to ab initio calculations by *Leroy* et al.,[16] **1d** is stabilized by the anomeric effect,[7, 17] but this stabilizing interaction of geminal methoxy groups is not present in **2d**. The thermal cleavage reactions of the series **1b**–**1d** are believed to be independent of steric effects, because the strain enthalpies of the three compounds are apparently comparable.[10]

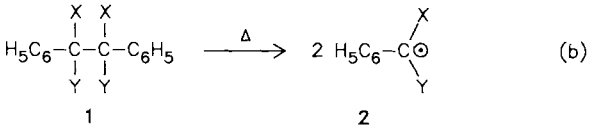

(b)

1 **2**

Table 1. Strain enthalpy of substituted ethanes **1** and free activation energy, activation enthalpy and entropy of their decomposition as well as ESR coupling constants of the radicals **2**.

Cpd.	X	Y	H_s [a] [kcal mol^{-1}]	ΔG^+ (300°C) [kcal mol^{-1}]	ΔH^+ [kcal mol^{-1}]	ΔS^+ [cal mol^{-1} K^{-1}]	a_H [b] [mT]
1a [10]	CH_3	CH_3	12.0	39.9	46.0	14.2	0.567 [19]
1b [10]	C_2H_5	CH_3 [c]	15.1	34.3	48.4	24.3	
1c [11b]	C_2H_5	OCH_3 [c]	15.6	34.5	44.0	16.6	0.625 [d]
1d	OCH_3	OCH_3	16 [e]	43.6	51.4	13.7	0.603
1e [14]	CN	CH_3 [c]	11.4	30.9	36.1	9.2	0.470
1f [9, 11a]	CN	OCH_3 [c]	12.8	27.9	36.6	15.1	0.409
1g [13]	CN	CN		18 [f]	26 [f]	14 [f]	0.503

[a] Strain enthalpy H_s as defined in [10]. [b] ESR hyperfine coupling constant of *p*-H of **2** in C_6H_5 from [4b]. [c] *meso*-Configuration. [d] For X = CH_3. [e] Preliminary value. [f] For 4-CH_3–C_6H_4 instead of C_6H_5 from [13].

From a comparison of ΔH^+ for the compounds **1a**, **1e**, **1f**, and **1g**, which again are similarly strained, one recognizes that introducing two cyano substituents for two methyls in **1** (cf. **1a** vs. **1e**) results in a decrease of ΔH^+ by almost 10 kcal·mol^{-1}. Exchanging the remaining methyl groups in **1e** by methoxy groups (cf. **1e** vs. **1f**) results in *no change* in ΔH^+ and causes only a 3 kcal·mol^{-1} decrease in ΔG^+.[18] On the other hand, by the substitution of cyano for methyl in **1e** (cf. **1e** vs. **1g**) a further decrease in ΔH^+ by approx. 10 kcal·mol^{-1} is observed.

We conclude that, in this series of compounds, pairs of captodative substituents stabilize a radical center in an additive way, in contrast to geminal dimethoxy substitution, which increases the C–C-bond strength of **1d** in comparison to monomethoxy substitution into **1b**, where the trend of monosubstitution (**1c**) is *reversed* by the introduction of a second methoxy group (**1d**). The fact that the first (**1a**/**1e**) and the second (**1e**/**1g**) substitution of methyl by cyano results in the same 10 kcal/mol^{-1} decrease in ΔH^+ is probably fortuitous. Neither the strain enthalpy of **1g**, H_s (**1g**), which is probably smaller than H_s (**1e**), is known nor is it possible to estimate the change of interaction energy between the geminal dicyano groups[16] on going from **1g** to the radical **2g**.

The *p*-H coupling constants a_H in the benzyl type radicals **2** are decreased in the series **2c** > **2d** ≫ **2g** > **2e** > **2f** (Table 1), indicating an increase of delocalization via the substituents X and Y in this order. It is clear that a_H responds to the substitution pattern X, Y in a different manner than the thermal stability of **1** does. It seems possible that a_H responds primarily to the SOMO and not to the total radical stability, expressed, for example, by $\Delta H_f^\circ(R^\odot)$.

Received: February 2, 1987 [Z 2083 IE]
German version: *Angew. Chem.* 99 (1987) 592

[1] a) H. G. Viehe, R. Merényi, L. Stella, Z. Janousek, *Angew. Chem.* 91 (1979) 982; *Angew. Chem. Int. Ed. Engl.* 18 (1979) 917; b) H. G. Viehe,

Z. Janousek, R. Merényi, *Acc. Chem. Res. 18* (1985) 148; c) R. Merényi, Z. Janousek, H. G. Viehe ("Substituent Effects in Radical Chemistry") *NATO ASI Ser. C. Vol. 189* (1986) 301.
[2] Similar suggestions have been published independently: M. J. S. Dewar, *J. Am. Chem. Soc. 74* (1952) 3353; A. T. Balaban, *Rev. Roum. Chim. 16* (1971) 725; R. W. Baldock, P. Hudson, A. R. Katritzky, F. J. Scott, *J. Chem. Soc. Perkin Trans. 1 1974*, 1422.
[3] D. Crans, T. Clark, P. von R. Schleyer, *Tetrahedron Lett. 21* (1980) 3681; E. M. Klessinger, *Angew. Chem. 92* (1980) 937; *Angew. Chem. Int. Ed. Engl. 19* (1980) 908.
[4] a) L. Stella, F. Pochat, R. Merényi, *Nouv. J. Chim. 5* (1981) 55; b) H.-G. Korth, P. Lommes, R. Sustmann, L. Sylvander, L. Stella in [1c], p. 167; c) D. R. Arnold, *ibid.*, p. 171 and references cited therein.
[5] R. Sustmann in [1c], p. 143; H.-G. Korth, P. Lommes, W. Sicking, R. Sustmann, *Chem. Ber. 118* (1985) 4627.
[6] a) R. Merényi, A. De Mesmaeker, H. G. Viehe, *Tetrahedron Lett. 24* (1983) 2765; b) L. Vertommen, M. Beaujean, R. Merényi, Z. Janousek, H. G. Viehe, in [1c], p. 329.
[7] A. G. Kirby, *The Anomeric Effect and Related Stereoelectronic Effects of Oxygen*, Springer, Berlin 1983.
[8] H.-G. Korth, R. Sustmann, R. Merényi, H. G. Viehe, *J. Chem. Soc. Perkin Trans. 2 1983*, 67.
[9] a) M. Zamkanei, J. H. Kaiser, H. Birkhofer, H.-D. Beckhaus, C. Rüchardt, *Chem. Ber. 116* (1983) 3216; b) H. Birkhofer, H.-D. Beckhaus, C. Rüchardt in [1c], p. 199.
[10] C. Rüchardt, H.-D. Beckhaus, *Top. Curr. Chem. 130* (1986) 1, and references cited therein.
[11] a) H. Birkhofer, Dissertation, Universität Freiburg 1986; b) H. Birkhofer, H.-D. Beckhaus, C. Rüchardt, *Tetrahedron Lett. 1983*, 185.
[12] a) C. Rüchardt, *Angew. Chem. 82* (1970) 845; *Angew. Chem. Int. Ed. Engl. 9* (1970) 830; b) C. Rüchardt, H.-D. Beckhaus, *Angew. Chem. 92* (1980) 417; *Angew. Chem. Int. Ed. Engl. 19* (1980) 429.
[13] H. A. P. de Jongh, C. R. H. I. de Jonge, H. J. M. Sinnige, W. J. de Klein, W. G. B. Huysmans, W. J. Mijs, W. J. van den Hoek, J. Smidt, *J. Org. Chem. 37* (1972) 1960.
[14] W. Barbe, H.-D. Beckhaus, C. Rüchardt, *Chem. Ber. 116* (1983) 1042.
[15] For the synthesis of **1d** see: R. Couture, B. Belleau, *Can. J. Chem. 50* (1972) 3424.
[16] a) G. Leroy, *Adv. Quantum Chem. 17* (1985) 1; b) G. Leroy, D. Peeters, M. Sana, C. Wilante in [1c], p. 1.
[17] P. von R. Schleyer, E. D. Jemmis, G. W. Spitznagel, *J. Am. Chem. Soc. 107* (1985) 6393.
[18] Due to the compensation effect [10] ΔG^{+} values have the advantage over ΔH^{+} values for comparison that they have no individual temperature functions.
[19] H. Sakurai, K. Mochida, M. Kira, *J. Organomet. Chem. 124* (1977) 235.

Crown Thioether Complexes of Ag^{I} and Cu^{I}: The Crystal Structures of $[\{Ag_3L_3\}\{AgL_2\}](ClO_4)_4$ and [LCuI] (L = 1,4,7-Trithiacyclononane)**

By *Heinz-Josef Küppers, Karl Wieghardt,* Yi-Hung Tsay, Carl Krüger, Bernhard Nuber,* and *Johannes Weiss*

The coordination chemistry of the macrocycle 1,4,7-trithiacyclononane (**L**), a crown thioether, is currently the subject of intensive investigations. It forms very stable 2 : 1 complexes with a variety of transition-metal ions (Fe^{II}, Fe^{III}, Co^{II}, Co^{III}, Ni^{II}, Pd^{II}, Pt^{II}, Cu^{II}, Ru^{II})[1] and can stabilize the metal centers in unusual oxidation states, e.g. Pd^{III} and Pt^{III} in $[PdL_2]^{3\oplus}$ and $[PtL_2]^{3\oplus}$, respectively.[2]

We report here on complexes of this ligand with Ag^{I} and Cu^{I}. Both metal centers, as soft Lewis acids, form stable coordination compounds with the soft S-atoms of the ligand. Of particular interest are the 1 : 1 complexes between the metal centers that preferentially coordinate tetrahedrally and the potentially tridentate ligand. The structure of such compounds $[ML]^{\oplus}$ ($M = Cu^{I}$, Ag^{I}) is dependent upon the hardness/softness of the anion used. In this work we show that when $X = I^{\ominus}$ (soft anion) a distorted tetrahedral structure is formed in which **L** functions as tridentate ligand and the fourth coordination site is occupied by $I^{\ominus}$. In contrast, with hard anions ($X = ClO_4^{\ominus}$, $NO_3^{\ominus}$), $[ML]_n^{n\oplus}$-oligomers are formed in which **L** is a bridging ligand, so that a distorted tetrahedral MS_4 coordination results.

Upon reaction of $AgNO_3$ in CH_3CN or CH_3OH with **L** in the ratio Ag : **L** = 1 : 1, a colorless solid of the composition $[AgL]NO_3$ is obtained. According to IR spectroscopic findings the anion $NO_3^{\ominus}$ is not bound coordinatively to the Ag^{I} ($\tilde{\nu}(N\text{-}O) = 1390\ cm^{-1}$). When $AgClO_4 \cdot H_2O$ is allowed to react with **L** in the ratio 1 : 3 or 1 : 1.7, colorless crystals of the composition $[AgL_2]ClO_4$ and $[Ag_4L_5](ClO_4)_4$ are formed. Also in this case the anion is not bound coordinatively, as shown by the crystal structure analysis.[3]

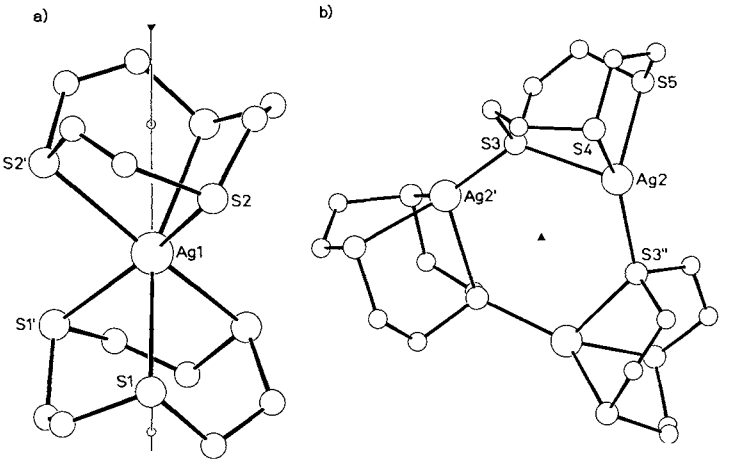

Fig. 1. a) Structure of the cation $[AgL_2]^{\oplus}$ in the crystal of $[\{Ag_3L_3\}\{AgL_2\}](ClO_4)_4$. Selected bond lengths [Å] and angles [°]: Ag1-S1 2.753(4), Ag1-S2 2.697(5); S2-Ag-S1 90.1(1), S2'-Ag1-S2 79.6(2), S2'-Ag1-S1 116.0(2), S1'-Ag1-S2 159.7(2), S1'-Ag1-S1 78.6(1). b) Structure of the trimeric cation $[Ag_3L_3]^{3\oplus}$ in the crystal of $[\{Ag_3L_3\}\{AgL_2\}](ClO_4)_4$. Selected bond lengths [Å] and angles [°]: Ag2-S3 2.724(2), Ag2-S4 2.595(4), Ag2-S5 2.613(4), Ag2'-S3 2.480(2); S3''-Ag2-S5 133.8(1), S3''-Ag2-S4 138.5(1), S3''-Ag2-S3 114.0(1), S5-Ag2-S4 84.9(1), S5-Ag2-S3 80.8(1), S4-Ag2-S3 81.7(1), Ag2'-S3-Ag2 126.0(1). ▲ denotes a crystallographic threefold axis.

Interestingly, the unit cell of $[Ag_4L_5](ClO_4)_4$ contains two different cations: the monomeric $[AgL_2]^{\oplus}$ (Fig. 1a) and a trimeric $[Ag_3L_3]^{3\oplus}$ (Fig. 1b), so that the salt can be formulated as $[\{Ag_3L_3\}\{AgL_2\}](ClO_4)_4$. Like the metal centers in other ML_2 complexes, the Ag^{I} center in the $[AgL_2]^{\oplus}$ ion is surrounded by a distorted octahedral array of six S atoms from two ligands **L**. In contrast, in the trimeric cation $[Ag_3L_3]^{3\oplus}$ the Ag^{I} ions are coordinated to a highly distorted tetrahedral array of four S atoms; one S atom of each nine-membered macrocycle is bound to two Ag^{I} centers. This is the first example of a bridging crown thioether. The Ag_3S_3 six-membered ring is, within the limit of error, planar.[8] We therefore assume that octahedral $[AgL_2]^{\oplus}$ ions are present in $[AgL_2]ClO_4$ and that $[AgL](NO_3)$ con-

[*] Prof. Dr. K. Wieghardt, Dipl.-Chem. H.-J. Küppers
Lehrstuhl für Anorganische Chemie I der Universität
Postfach 102148, D-4630 Bochum (FRG)
Dr. Y.-H. Tsay, Prof. Dr. C. Krüger
Max-Planck-Institut für Kohlenforschung
D-4330 Mülheim a.d. Ruhr (FRG)
Dr. B. Nuber, Prof. Dr. J. Weiss
Anorganisch-chemisches Institut der Universität
Im Neuenheimer Feld 270, D-6900 Heidelberg (FRG)

[**] This work was supported by the Fonds der Chemischen Industrie.

sists of oligomeric $[AgL]_n^{n\oplus}$ units with bridging thioether ligands and fourfold coordinated Ag^I ions. Possibly $n=3$ here also, but other values for n are conceivable.

To obtain information about the structures of these compounds in solution, the ^{1}H-NMR spectra of $[AgL]NO_3$, $[Ag_4L_5](ClO_4)_4$ and $[AgL_2]ClO_4$ in CD_3CN or [D$_6$]dimethyl sulfoxide were recorded. In all three cases only one broad singlet was observed. Therefore it could not be unequivocally established whether the structures of these salts in the solid state and in solution are identical.

The reaction of $[Cu(CH_3CN)_4](ClO_4)$ with **L** in CH_3CN in the ratio 1 : 1 under anaerobic conditions yields colorless crystals of $[CuL](ClO_4)$. In contrast to many coordinatively unsaturated Cu^I complexes, solutions of this salt in CH_3CN do not react with CO at $T=293$ K. The solid, on the other hand, is stable toward oxygen and water. We therefore assume that $[CuL]_n^{n\oplus}$-oligomers ($n\geq 3$) with bridging thioether ligands and Cu^IS_4 coordination polyhedra are likewise present in $[CuL](ClO_4)$.

Interesting in this context are the works of *Schröder* et al.[4] and *Cooper* et al.,[5] in which it is shown that the potentially hexadentate ligand hexathia[18]crown-6 $\mathbf{L}^1$ (1,4,7,10,13,16-hexathiacyclooctadecane) reacts with Cu^I to form the complexes $[CuL^1](BF_4)$ with distorted tetrahedral Cu^IS_4 polyhedra or the complexes $[Cu_2L^1(CH_3CN)_2](ClO_4)_2$ with two Cu^IS_3N polyhedra. That is, the coordination number six of Cu^I, other than in the case of Ag^I in the $[AgL_2]^{\oplus}$ cation described here, is not reached.

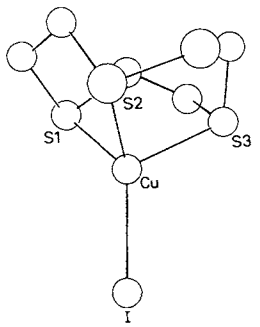

Fig. 2. Structure of [LCuI]. Selected bond lengths [Å] and angles [°]: Cu-I 2.490(1), Cu-S1 2.331(1), Cu-S2 2.343(1), Cu-S3 2.329(1); S1-Cu-I 128.6(1), S2-Cu-I 121.3(1), S3-Cu-I 118.7(1), S1-Cu-S2 92.6(1), S2-Cu-S3 93.9(1), S1-Cu-S3 93.1(1).

Upon reaction of a suspension of CuI in methanol with **L** in the ratio 1 : 1 we obtained the colorless solid [LCu^{I}I], which was recrystallized from CH_3CN. The crystal structure analysis of this compound,[6] was consistent with the monomeric neutral complex [LCuI] (Fig. 2). The Cu^I ion exhibits strongly distorted tetrahedral coordination; three S atoms of the macrocycle and a coordinatively bound $I^{\ominus}$ form the first coordination sphere. Unusual is the high stability of this complex toward oxygen in solution, as in the solid state.

Experimental

$[AgL](NO_3)$: A solution of **L** (0.1 g; 1 mmol) in CH_3CN (20 mL) was added to a solution of $AgNO_3$ (0.17 g, 1 mmol) in CH_3CN (10 mL) (298 K). After a few minutes a colorless precipitate formed, which was recrystallized from CH_3CN. Yield: 60-70%. IR spectrum (KBr): $\tilde{\nu}(NO_3)=1390$ cm^{-1} (s) and a weak band at $\tilde{\nu}=1760$ cm^{-1}. ^{1}H-NMR (80 MHz, CD_3CN, $T=298$ K): $\delta=2.94$ (broadened singlet).

$[\{Ag_3L_3\}\{AgL_2\}](ClO_4)_4$: A solution of $AgClO_4\cdot H_2O$ (0.13 g, 0.57 mmol) in CH_3OH (10 mL) was added to a solution of **L** (0.18 g, 1 mmol) in CH_3OH (30 mL). A colorless precipitate immediately separated; this was recrystallized from CH_3CN. Yield: 50-60%. ^{1}H-NMR (80 MHz, CD_3CN, $T=298$ K): $\delta=2.82$ (broadened signal).

$[AgL_2](ClO_4)$: A solution of $AgClO_4$ (0.10 g, 0.45 mmol) in CH_3OH (10 mL) was added to a solution of **L** (0.26 g, 1.4 mmol) in CH_3OH (30 mL). A colorless precipitate immediately separated out which, upon continued stirring (298 K) of the suspension, redissolved within 1 h. Upon concentration of the solution by evaporation, a colorless precipitate separated. Yield ca. 60%. ^{1}H-NMR (80 MHz, [D$_6$]dimethyl sulfoxide, $T=298$ K): $\delta=2.95$ (broadened singlet).

$[CuL](ClO_4)$: A solution of $[Cu(CH_3CN)_4](ClO_4)$ (0.33 g, 1 mmol) in oxygen-free CH_3CN (20 mL) was treated with 0.19 g (1.1 mmol) of **L** and the resulting mixture stirred for 3 h at 293 K. On evaporating down the solution, a colorless precipitate separated. Yield 30%.

[LCuI]: A suspension of CuI (0.13 g, 0.7 mmol) and **L** (0.12 g, 0.67 mmol) in CH_3OH (20 mL) was heated under reflux for 2 h. A colorless solid formed, which was insoluble in CH_3OH and H_2O but could be recrystallized from CH_3CN. Yield: 95%.

All the complexes gave correct analyses (C,H,S,I). The ligand 1,4,7-trithiacyclononane was prepared according to a procedure given in the literature [7].

Received: February 3, 1987;
revised: March 11, 1987 [Z 2085 IE]
German version: *Angew. Chem. 99* (1987) 583

CAS Registry numbers:
[AgL](NO$_3$), 108473-38-7; $[\{Ag_3L_3\}\{AgL_2\}](ClO_4)_4$, 108473-41-2; $[AgL_2](ClO_4)$, 108473-42-3; [CuL](ClO$_4$), 108473-44-5; LCuI, 108473-45-6.

[1] a) W. N. Setzer, C. A. Ogle, G. S. Wilson, R. S. Glass, *Inorg. Chem. 22* (1983) 266; b) K. Wieghardt, H.-J. Küppers, J. Weiss, *ibid. 24* (1985) 3067; c) K. Wieghardt, H.-J. Küppers, E. Raabe, C. Krüger, *Angew. Chem. 98* (1986) 1136; *Angew. Chem. Int. Ed. Engl. 25* (1986) 1030; d) A. J. Blake, A. J. Holder, T. I. Hyde, Y. V. Roberts, A. J. Lavery, M. Schröder, *J. Organomet. Chem. 323* (1987) 261; e) G. S. Wilson, D. D. Swanson, R. S. Glass, *Inorg. Chem. 25* (1986) 3827; f) J. R. Hartman, E. J. Hintsa, S. R. Cooper, *J. Chem. Soc. Chem. Commun. 1984*, 386; g) *J. Am. Chem. Soc. 108* (1986) 1208; h) M. N. Bell, A. J. Blake, H.-J. Küppers, M. Schröder, K. Wieghardt, *Angew. Chem. 99* (1987) 253; *Angew. Chem. Int. Ed. Engl. 26* (1987) 250.

[2] A. J. Blake, R. O. Gould, A. J. Holder, T. I. Hyde, A. J. Lavery, M. O. Odulate, M. Schröder, *J. Chem. Soc. Chem. Commun. 1987*, 118.

[3] Crystal data of $[\{Ag_3L_3\}\{AgL_2\}](ClO_4)_4$: hexagonal $P6_3$ (No. 173), $a=b=15.911(2)$, $c=13.459(2)$ Å, $V=2950.8$ Å^3, $Z=2$, $\rho_{calc}=1.95$ g cm^{-3}; $\mu(Mo_{K\alpha})=20.4$ cm^{-1}, 2329 independent reflections, 1915 observed with $I>2\sigma(I)$, 187 refined parameters, $R=0.049$. An analytical absorption correction was carried out, solution of the structure by heavy atom method, anisotropic temperature factors for all non-hydrogen atoms except the four oxygen atoms of a ClO_4 moiety [9].

[4] R. O. Gould, A. J. Lavery, M. Schröder, *J. Chem. Soc. Chem. Commun. 1985*, 1492.

[5] J. R. Hartman, S. R. Cooper, *J. Am. Chem. Soc. 108* (1986) 1202.

[6] Crystal data of [LCuI]: monoclinic, $C_{2h}^5(P2_1/c)$, $a=11.386(3)$, $b=7.956(3)$, $c=12.980(3)$ Å, $\beta=107.65(2)°$, $V=1120.5$ Å^3, $Z=4$, $\rho_{calc}=2.20$ g·cm^{-3}; $\mu=51.7$ cm^{-1}, 5005 independent reflections, 3288 observed with $I>2\sigma(I)$, $Mo_{K\alpha}$ radiation, 101 refined parameters, $R=0.03$, $R_w=0.029$. An empirical absorption correction was carried out; anisotropic temperature factors for all nonhydrogen atoms [9].

[7] D. Sellmann, L. Zapf, *Angew. Chem. 96* (1984) 799; *Angew. Chem. Int. Ed. Engl. 23* (1984) 807.

[8] Other such M_3S_3 six-membered rings: $[Cu_3(S_4)_3]^{3\ominus}$ (A. Müller, F. W. Baumann, H. Bögge, M. Römer, E. Krickemeyer, K. Schmitz, *Angew. Chem. 96* (1984) 607; *Angew. Chem. Int. Ed. Engl. 23* (1984) 632; $[Fe_3(SR)_3X_6]^{3\ominus}$ (M. A. Whitener, J. K. Bashkin, K. S. Hagen, J.-J. Girerd, E. Gamp, N. Edelstein, R. H. Holm, *J. Am. Chem. Soc. 108* (1986) 5607), $[Cu_3(SPh)_3(PPh_3)_4]$ (I. G. Dance, L. F. Fitzpatrick, M. L. Scudder, *J. Chem. Soc. Chem. Commun. 1983*, 546), $[Cu_3(Me_3PS)_3Cl_3]$ (J. A. Tiethof, J. K. Stalick, P. W. R. Corefield, D. W. Meek, *ibid. 1972*, 141).

[9] Further details of the crystal structure investigations are available on request from the Fachinformationszentrum Energie, Physik, Mathematik GmbH, D-7514 Eggenstein-Leopoldshafen 2, on quoting the depository numbers CSD-52362 (structure of the Cu complex) and CSD-52294 (structure of the Ag complex), the names of the authors, and the journal citation.

Dicyclopropa[*a,c*]naphthalene: a Compound Capable of Existence?**

By *Udo H. Brinker,* Hartmut Wüster,* and *Gerhard Maas*

Cycloproparenes have been the subject of intensive study for almost 25 years,[1] yet dicycloproparenes, which have *two* three-membered rings fused to the *same* aromatic ring, are thus far unknown. All cycloproparenes have a high strain energy; nevertheless, their kinetic stability strongly depends on their structure. *Linearly* coupled cycloproparenes such as **1**[2a-d] and **2**[2e] are generally more stable and also easier to prepare than, e.g., the *angular* species **3**[3] and **4**.[4] Thus, **3** explodes on melting,[3,4a] while solutions of **4** decompose on prolonged standing, even at −60 °C.

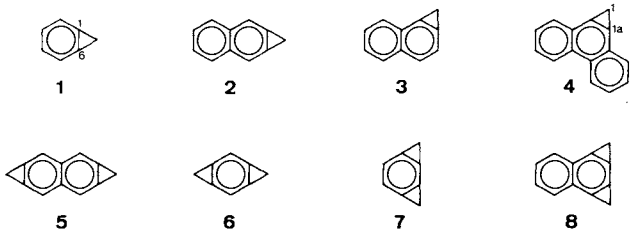

1 **2** **3** **4**

5 **6** **7** **8**

The dicyclopropa[*b,g*]naphthalene **5**[5] synthesized by *Vogel* et al. is the only dicycloproparene to have been isolated so far. Its strain energy has been determined as 166 kcal·mol^{-1} (lower limit);[6] it is sensitive to shock and explodes on melting.

Despite this there has been no lack of effort in attempting to prepare the more highly strained dicycloproparenes, in which *one* aromatic ring and *two* three-membered rings are annelated. Attempts to generate the parent compounds, the dicyclopropa[*a,d*]benzene **6**[7a] and dicyclopropa[*a,c*]benzene **7**,[7] have thus far failed. The species **8**, benzoannelated **7**, is expected to have a higher strain energy than **5**, in which the three-membered rings are located at the maximum distance from each other. We report here on the preliminary results of our attempts to generate and trap the species **8**.

An ideal starting compound for the generation of **8** is the benzoannelated *r*-1,*t*-2-dibromotricyclo[5.1.0.0^{2,4}]oct-5-ene **10**[8], which is obtained by 1,6-dehalogenation[8a] of the (±)-bisdibromocarbene adduct **9** with methyllithium at −78 °C (yield 60%). The dicycloproparene **8a** could be formed by twofold HBr-elimination from **10**, whereby the benzylic, tertiary protons (H-4 and H-7) should be attacked by a suitable base. Besides this there is the possibility of a competing 1,2-elimination taking place,[4] initiated by cleavage of one of the geminal cyclopropane ring protons. This process leads to an "exocyclic" double bond in the three-membered ring, which is not conjugatively bonded to the benzene ring (see **11**).

Upon reaction with potassium *tert*-butoxide (2.4 mol. equiv.) at 20 °C in THF/DMSO (1:1), **10** is already no longer detectable by gas chromatography after a few minutes. No significant signals could be observed in the temperature range from +20 to −70 °C during the ^{1}H-NMR and ^{13}C-NMR spectroscopic monitoring of the reaction of

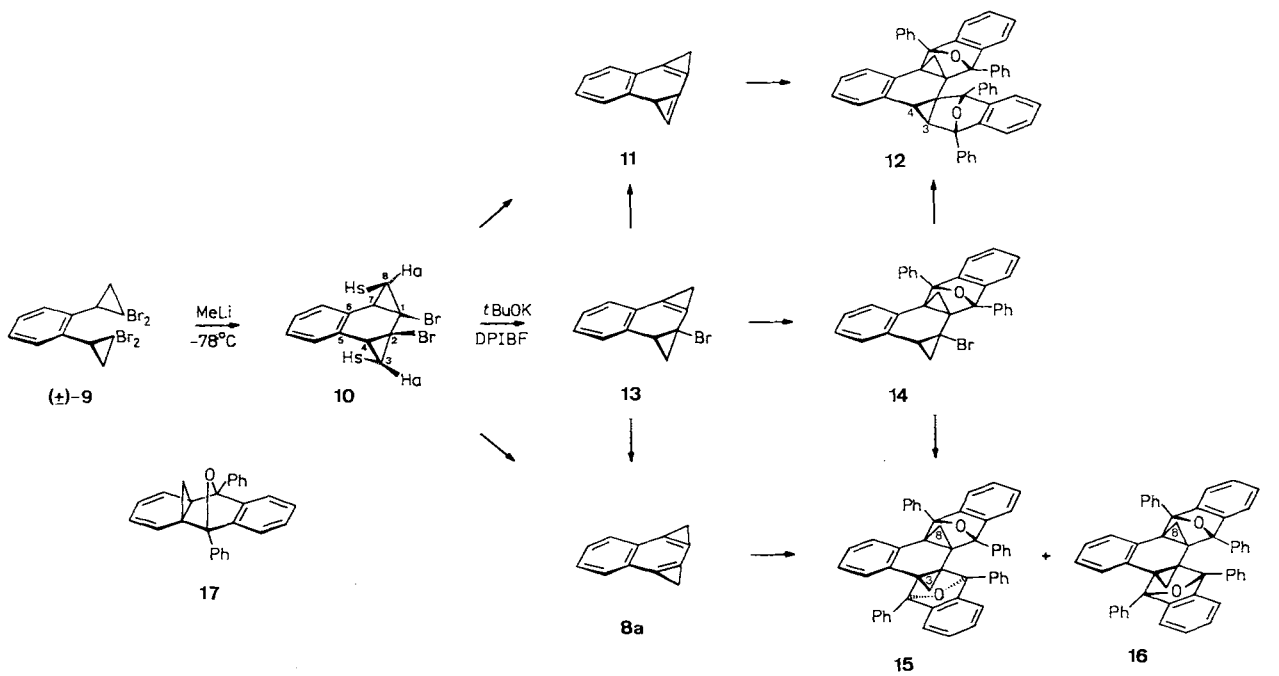

10 (2.4 mol. equiv. KO*t*Bu, 2.4 mol. equiv. 18-crown[6], [D$_8$]THF).

Of the two possible Kekulé forms of **8**, only **8a** can be formed directly from **10** by twofold 1,2-elimination. **8a** could be the energetically more stable form, since it contains an intact benzene ring and two cyclopropene units.[9] Attempts to trap the diene unit in **8a** with 4-phenyl-1,2,4-

[*] Prof. Dr. U. H. Brinker, Dipl.-Chem. H. Wüster
Fakultät für Chemie der Universität
Universitätsstr. 150, D-4630 Bochum-Querenburg (FRG)
Prof. Dr. G. Maas [+]
Fachbereich Chemie der Universität
Erwin-Schrödinger-Str., D-6750 Kaiserslautern (FRG)

[+] X-ray structure analyses.

[**] This work was supported by the Fonds der Chemischen Industrie and by Degussa AG. We thank Dr. *W. Dietrich* and Dipl.-Chem. *H. Kühne* for the NMR spectra of **12**, **15**, and **16** and Herr *K. Gomann* for assistance with the synthesis of **10**.

triazol-3,5-dione (PTAD) as dienophile met without success, since KO*t*Bu destroys the trapping agent.[10]

In view of the expected instability of **8** it was considered advisable from the very start to use the reactive 1,3-diphenylisobenzofuran (DPIBF) as diene.[11] Reaction of **10** with DPIBF in the molar ratio 1:9 (2.4 mol. equiv. KO*t*-Bu, THF:DMSO = 1:1, 20°C) led to the formation of three crystalline bisadducts (yield 81%), which could be separated by HPLC (silica gel Si 60-5, pentane: CH_2Cl_2 = 6:4). The bisadduct **12** (yield 28%) is formed via twofold Diels-Alder addition of DPIBF to **11** or one addition to **13** with formation of **14**, which after HBr-abstraction and creation of an "exocyclic" double bond (cf. **11**) is attacked again by DPIBF. The chemical shifts of H-3 and H-4 in **12** are in good agreement with those of the corresponding protons of the adduct of furan to C-1 and C-1a of **4**.[4, 12] The crystal structure analysis[13] can explain the observed high-field shift of two aromatic protons at $\delta = 5.25$ and 5.6.

Since the number of ^{13}C-resonance lines is only half as many as the maximum possible lines, the main product **15** (yield 44%) must be a symmetrical compound. The three-membered rings are oriented in the *anti*-position,[14] whereas the cyclopropane ring and O-atom of a five-membered ring are each *syn*-oriented. The signals of the protons on C-3 and C-8 ($\delta = -0.5$), which point towards the benzene ring, are shifted upfield. In contrast, the protons oriented in the direction of the oxygen atoms ($\delta = 2.75$) are shifted markedly downfield. The overall result is that **15** is formed by twofold *endo*-addition of the trapping agent.

In contrast, **16** (yield 9%) can be formed by an *endo*- and an *exo*-oriented [4+2]-cycloaddition. The characteristically large difference in the chemical shifts of the protons on C-8 observed in the case of **12** and **15** is not found in **16**. As indicated by the X-ray structure analysis,[13] *both* protons on C-8 are similarly shifted noticeably downfield by the O-atoms. Altogether, the Diels-Alder reactions of DPIBF with the double bonds generated from **10** or **13** and **14** with KO*t*Bu with formation of the bisadducts **12**, **15**, and **16** proceed with strongly preferred *endo*-attack (94%).

The crucial question is, whether dicyclopropa[*a,c*]naphthalene **8** is in fact formed as an intermediate in the reaction of **10** with KO*t*Bu, or whether or not two cyclopropene systems generated by consecutive 1,2-eliminations are each trapped directly by DPIBF as bisadducts **15** and **16**. A concerted twofold HBr-elimination in **10**, on the other hand, seems unlikely.

As evidenced by the formation of **12** in 28% yield, not only is a conjugated "endocyclic" double bond formed but also, to the extent of ca. 17% (based on all 1,2-eliminations), the strained "exocyclic" double bond of the cyclopropenes.[15] The fact that ca. 83% of the DPIBF adducts **12**, **15**, and **16** result from additions to the double bonds generated between C-1 and C-7 and/or between C-2 and C-4, proves the strongly preferred direction of elimination with cleavage of benzylic hydrogen atoms and formation of conjugated double bonds.[15] Under the standard conditions with 2.4 mol. equiv. of base, formation of the monoadduct **14**, as is expected in the addition of DPIBF to the monoelimination product **13**, could not be detected. When only 1.1 mol. equiv. of the base was used, 45% of the monoadduct **14** could be isolated along with 9% of the bisadducts **12**, **15**, and **16** (ratio ca. 1:2.5:1). In the reaction of **14** with 1.2 mol. equiv. of base and DPIBF under the conditions employed for the reaction of **10**, three bisadducts (24% of **12**, 48% of **15**, and 10% of **16**) were isolated (ratio 2.4:4.8:1). The comparable ratios of the bisadducts on starting from **10** and **14** suggests that the monoadduct **14** should also be formed as intermediate in the reaction of **10** with 2.4 mol. equiv. of base.

The annelation of a cyclopropane ring to the benzene nucleus effects a strain increment of ca. 14 kcal·mol^{-1} in excess of the sum of the E_s of the structural units benzene and cyclopropene [difference of the strain energies E_s of **1** (68 kcal·mol^{-1})[16] and of cyclopropene (53.7 kcal·mol^{-1})]. Accordingly, for dicyclopropa[*a,c*]naphthalene **8** an increase in strain is expected which exceeds the strain energies of the two cyclopropene units contained in **8** by at least 28 kcal·mol^{-1}. This large increase in strain energy obviously cannot be compensated by the gain in aromatization energy. When starting from **10** in the presence of KO*t*Bu, instead of the formation of **8a** or of the aromatic system **8**, stepwise 1,2-eliminations and additions of DPIBF apparently take place.

Received: January 28, 1987;
revised: March 13, 1987 [Z 2074 IE]
German version: *Angew. Chem. 99* (1987) 585

[1] a) B. Halton, *Ind. Eng. Chem. Prod. Res. Dev. 19* (1980) 349; b) W. E. Billups, *Acc. Chem. Res. 11* (1978) 245.

[2] a) E. Vogel, W. Grimme, S. Korte, *Tetrahedron Lett. 1965*, 3625; b) E. Vogel, S. Korte, W. Grimme, H. Günther, *Angew. Chem. 80* (1968) 279; *Angew. Chem. Int. Ed. Engl. 7* (1968) 289; c) B. Halton, P. J. Milsom, *Chem. Commun. 1971*, 814; d) W. E. Billups, A. J. Blakeney, W. Y. Chow, *ibid. 1971*, 1461; e) W. E. Billups, W. Y. Chow, *J. Am. Chem. Soc. 95* (1973) 4099.

[3] S. Tanimoto, R. Schäfer, J. Ippen, E. Vogel, *Angew. Chem. 88* (1976) 643; *Angew. Chem. Int. Ed. Engl. 15* (1976) 613.

[4] a) B. Halton, B. R. Dent, S. Böhm, D. L. Officer, H. Schmickler, F. Schophoff, E. Vogel, *J. Am. Chem. Soc. 107* (1985) 7175; b) P. Müller, H. C. Nguyen Thi, J. Pfyffer, *Helv. Chim. Acta 69* (1986) 855.

[5] J. Ippen, E. Vogel, *Angew. Chem. 86* (1974) 780; *Angew. Chem. Int. Ed. Engl. 13* (1974) 736.

[6] F. D. Rossini, W. E. Billups, unpublished, cited in W. E. Billups, *Acc. Chem. Res. 11* (1978) 245.

[7] a) M. G. Banwell, B. Halton, *Aust. J. Chem. 32* (1979) 849, 2689; b) E. Vogel, W. Püttmann, W. Duchatsch, T. Schieb, H. Schmickler, J. Lex, *Angew. Chem. 98* (1986) 727; *Angew. Chem. Int. Ed. Engl. 25* (1986) 720.

[8] a) U. H. Brinker, H. Wüster, G. Maas, *J. Chem. Soc. Chem. Commun. 1985*, 1812; b) J. Höhn, P. Weyerstahl, *Chem. Ber. 116* (1983) 808.

[9] Concerning bond fixation in cyclopropabenzene see: Y. Apeloig, D. Arad, *J. Am. Chem. Soc. 108* (1986) 3241.

[10] The addition of the dienophile PTAD to the diene moiety in **8a** should lead to a markedly nonplanar double bond between the three-membered rings.

[11] In order to check to what extent cycloproparenes actually undergo cycloadditions with DPIBF at 20°C and normal pressure we have used **1** as a model species. Whereas **1** does not react with the less reactive 1,4-diphenyl-1,3-butadiene under these conditions (B. Halton, unpublished results, cited in [1a]), with DPIBF it forms the *endo*-adduct **17**. The stereochemical assignment is based on the deshielding of the proton in the *anti*-position to the norcaradiene unit by the oxygen atom ($\delta = 3.15$). Accordingly a [2+4]- or [6+4]-cycloaddition to C-1 and C-6 in **1** could have taken place.

[12] T. T. Coburn, W. M. Jones, *J. Am. Chem. Soc. 96* (1974) 5218.

[13] The structures of **12** and **16** have been confirmed by X-ray structure analyses.

[14] On the basis of the spectroscopic data it cannot be completely ruled out that the cyclopropane rings in **15** are in the *syn*-position. The reaction of **13** with DPIBF to give **14** is an *endo*-addition. However, a second *endo*-addition of DPIBF—to the "conjugated" cyclopropene resulting from reaction of **14** with the base—requires a sterically unfavored transition state. This is not the case in the formation of **15** with *anti*-oriented three-membered rings.

[15] DPIBF-adducts, derived from a compound with *two* strained "exocyclic" double bonds, were not found.

[16] W. E. Billups, W. Y. Chow, K. H. Leavell, E. S. Lewis, J. L. Margrave, R. L. Sass, J. J. Shieh, P. G. Werness, J. L. Wood, *J. Am. Chem. Soc. 95* (1973) 7878.

Superconductivity—a Chemical Phenomenon?**

By *Arndt Simon**

The accepted theory of superconductivity by *Bardeen*, *Cooper*, and *Schrieffer*[1] is based on the assumption that electrons pair (Cooper pairs) via special interactions with the lattice. The Coulomb repulsion between electrons is overcome indirectly by electron-phonon coupling. The interaction of an ion in the crystal and a passing electron changes the vibrations of the ion. The interaction of the ion with a second electron finally leads to attraction between both electrons. In other terms, a virtual phonon is exchanged between both electrons. The superconducting ground state corresponds to pairs of electrons with opposite spin and wave vectors of equal length but opposite sign ($+k\uparrow$, $-k\downarrow$). All pairs have the same energy. An energy gap separates ground and excited states, so no continuous change in momentum can occur.

This abstract model, as also the nature of the "classical" superconductors—as a rule these are intermetallic phases—does not make it easy to correlate the phenomenon of superconductivity with the electronic properties of certain elements and the specific features of their chemical bonding. Moreover, it does not add to the descriptive value of the model that the electrons of a Cooper pair can be thousands of angstroms apart.

The discovery of high-temperature superconductivity in oxides[2,3] has not yet forseeable practical applications, but, to the chemist, in addition it opens up insights into the relationships between the phenomenon of superconductivity and such concepts as, e.g., oxidation number, change of coordination with oxidation state etc.

$BaPb_{1-x}Bi_xO_3$ ($x \approx 0.3$) **1** crystallizes in the simple (deformed) perowskite structure, i.e. $(Pb,Bi)O_6$ octahedra are linked via all apices. The compound is metallic and becomes superconducting at $T_c = 13$ K.[2] Bismuth has the unusual oxidation state +4 and exhibits the tendency to delocalize one electron in the conduction band ($Bi^{5+} + e^-$) or to localize one electron to form a lone pair (Bi^{3+}). Regular octahedra and tetragonal pyramids are common coordination polyhedra for Bi^{5+} and the lone-pair ion Bi^{3+}, respectively.

Lattice vibrations which lead to a deformation of the coordination octahedron around the Bi-atoms in **1** (longitudinal optical (LO) phonons in the direction of one of the main axes), "switch" the tendency to localize (off-center position with Bi^{3+}, lone pair with antiparallel spin) and delocalize (Bi^{5+} in the center of the octahedron, delocalized electron pair) electrons with the characteristic frequency of this vibration (cf. Fig. 1) and correlated for all atoms in the crystal. The coupling of electrons and phonons hereby corresponds to an oscillating change in the oxidation state of bismuth ("valence fluctuation") by *two*. The aforementioned characteristics of the Cooper pairs, e.g. antiparallel spin, $+k\uparrow$, $-k\downarrow$, same energy of all pairs, large correlation lengths, immediately follow from such a tendency of the conduction electrons to localize pairwise at the Bi atoms. Of course, the oxygen atoms are vitally important for this process. *Bilz* et al.[4,5] pointed out that O^{2-} exhibits a very unusual increase of its polarizability with increasing cation–anion separation, enhanced by anisotropy and covalency effects which make the strong coupling of the electronic states of the cation to the vibrations of the oxygen atoms (and vice versa) plausible.

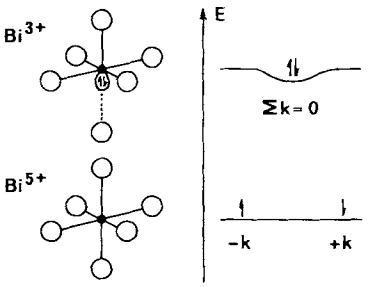

Fig. 1. Model of the pairing of electrons due to a change in the valence of the Bi atoms in **1**.

In $La_{1.8}Ba_{0.2}CuO_4$ **2** (K_2NiF_4 type), Cu has the oxidation state +2.2. The transition temperature of ca. 30 K[3] increases upon substitution of Ba by Sr to ca. 36 K.[6] Apparently, La, Ba and Sr merely determine the correct coordination dimensions and electron balance with Cu. Elongated CuO_6 octahedra (d^9, Jahn-Teller distorted, 4×190 and 2×240 pm) are linked according to $CuO_{4/2}O_2$ via the basal O atoms.[7] To a first approximation, networks of Cu-atoms square-planar coordinated to O-atoms are formed in layers (Fig. 2, top) and the indicated quadrupole mode

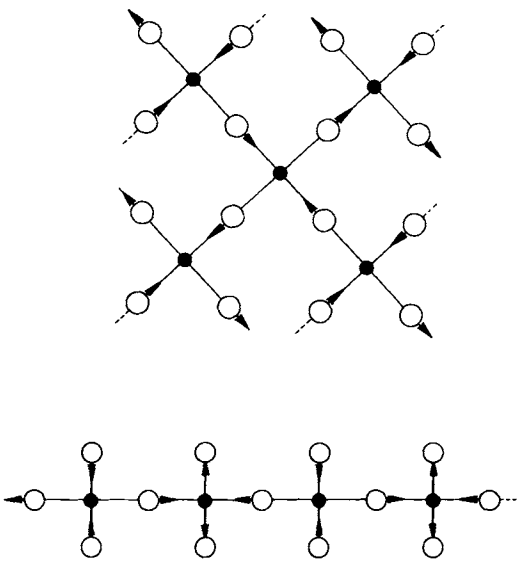

Fig. 2. Top: Cu atoms surrounded by a square-planar array of O-atoms. Bottom: CuO_2 units linked via bridging O-atoms.

leads to an oscillation between the coordination numbers 4 and 2 (+2). The deformation of the square-planar coordination, characteristic for Cu^{3+} (d^8, delocalized electron

[*] Prof. Dr. A. Simon
Max-Planck-Institut für Festkörperforschung
Heisenbergstrasse 1, D-7000 Stuttgart 80 (FRG)

[**] Discussed in part at the International Conference on Lanthanides and Actinides (IGLA), Lisbon (Portugal), April 5-10, 1987.

pair) could again result in a tendency to localize *two* electrons with antiparallel spin (Cu^+, d^{10}).[*]

The explanation given for the superconductivity in **2** is supported by the results of investigations with $YBa_2Cu_3O_{7-x}$ ($x \approx 0.1$) **3**, which contains Cu in a mixed valence state +2.27 and which exhibits the highest transition temperature, $T_c \approx 93$ K reported so far.[8] Neutron diffraction studies on powders revealed an orthorhombic structure[9, 10] containing Cu2 in slightly buckled layers $CuO_{4/2}$ (Fig. 2, top) which enclose the Y atoms. Superconductivity should not arise from this part of the structure as substitution of Y by magnetic 4f elements does not destroy the superconductivity. In contrast, the other Cu atoms (Cu1) form parallel ribbons $CuO_{2/2}O_2$ (Fig. 2, bottom), which can be described as linear CuO_2 units (d(Cu-O) = 183 pm) linked via bridging O-atoms (194 pm). The square-planar environment of the Cu atoms is strongly deformed in these ribbons and therefore the tendency to localize an electron pair (Cu^+, d^{10}) in the CuO_2 unit should be even more pronounced than in **2**.

This tendency can be switched on and off periodically for each atomic site via the indicated zone edge mode. Of course, such an ionic model is a crude approximation. The covalency of the Cu-O bonds and its dynamic variation is essential.

The explanation given for the pair-wise attraction of electrons at the Fermi level seems closely related to the model of the Peierls-instability and in particular the model of the "bipolaron".[13, 14] But the latter is distinctly different as it is based on electronic interactions without involving specific atomic properties. Unspecific local lattice distortions lead to a pairing of electrons in the bipolaron model. Here, it is intended to draw attention to the specific bonding of certain elements which might lead to the formation of "itinerant" electron pairs on the basis of the familiar chemistry of these elements.

Received: April 21, 1987 [Z 2216 IE]
German version: *Angew. Chem. 99* (1987) 602

[1] W. Buckel: *Supraleitung. Grundlagen und Anwendung*, Physik Verlag, Weinheim 1977.
[2] A. W. Sleight, J. L. Gilsson, P. E. Bierstedt, *Solid State Commun. 17* (1975) 27.
[3] J. G. Bednorz, K. A. Müller, *Z. Phys. B 64* (1986) 189.
[4] R. Migoni, H. Bilz, D. Bäuerle, *Phys. Rev. Lett. 37* (1976) 1155.
[5] A. Bussmann, H. Bilz, R. Roenspiess, K. Schwarz, *Ferroelectrics 25* (1980) 343.
[6] R. J. Cava, R. B. von Dover, B. Batlogg, E. A. Rietman, *Phys. Rev. Lett. 58* (1987) 408.
[7] J. B. Goodenough, G. Demazeau, M. Pouchard, P. Hagenmuller, *J. Solid State Chem. 8* (1973) 325.
[8] M. K. Wu, J. R. Ashburn, C. J. Torug, P. H. Hor, R. L. Meng, L. Gao, Z. J. Huang, Y. Q. Wang, C. W. Chu, *Phys. Rev. Lett. 58* (1987) 908.
[9] M. A. Beno, L. Soderholm, D. W. Capone II, D. G. Hinks, J. D. Jorgensen, I. K. Schuller, C. U. Segre, K. Zhang, J. D. Grace, *Appl. Phys. Lett.*, in press.
[10] J. E. Greedan, A. O'Reilly, C. V. Stager, *Phys. Rev. B 35*, in press.
[11] K. Hestermann, R. Hoppe, *Z. Anorg. Allg. Chem. 367* (1969) 249.
[12] C. L. Teske, Hk. Müller-Buschbaum, *Z. Anorg. Allg. Chem. 379* (1970) 113.
[13] B. K. Chakraverty, *J. Phys. (Paris) 42* (1981) 1351.
[14] T. M. Rice, L. Sneddon, *Phys. Rev. Lett. 47* (1981) 689.

[*] In this context the structures of $KCuO_2$ [11] and $SrCu_2O_2$ [12] are instructive. In $KCuO_2$ the Cu^{3+} ion has square coordination (4 × 184 pm). Other than in **3**, $CuO_{4/2}$ ribbons are formed by edge-sharing. In contrast, $SrCu_2O_2$ contains (interconnected) linear CuO_2 units (2 × 184 pm).

Regulation of the 6-s Equilibrium Conformation of Retinal in Bacteriorhodopsin by Substitution at C-5; 5-Methoxy- and 5-Ethylretinalbacteriorhodopsin**

By *Elisabeth Kölling,* Dieter Oesterhelt, Henning Hopf,* and *Norbert Krause*

Retinal proteins, which contain retinal as protonated Schiff base (**1** in Scheme 1), absorb visible light. This involves, on the one hand, the triggering of sensory processes, e.g., vision in vertebrates by the rhodopsins and photophobic/photoattractive reactions by membrane proteins of *Halobacterium halobium*. On the other hand, energy conversion takes place, which in bacteriorhodopsin[1] leads to proton translocation and in halorhodopsin[2] to chloride translocation. The absorption of the protonated Schiff base in solution is shifted bathochromically in these proteins. This is brought about by the charged environment in the protein and the specific conformation of the retinal formed by interaction with the protein. Contributing factors are: a) the distance between a negative charge in the protein and the positively charged nitrogen center of lysine 216[3] of the protonated Schiff base,[4] b) a further negative charge[5] or a dipole[6] above (below) the cyclohexene ring, and c) the planarization of ring and chain at the C-6–C-7 bond (6-s bond).[7–9] The steric and electronic interaction of the retinal with the protein part can be analyzed by use of retinal analogues and isosteric compounds as controls. Especially interesting in this respect are substitutions at the cyclohexene ring, which can influence the torsion angle C5-C6-C7-C8 of the 6-s bond ("6,7-torsion angle"). Therefore 5-methoxyretinal and 5-ethylretinal[10] were synthesized and their influence on the absorption of the corresponding bacteriorhodopsins was investigated.

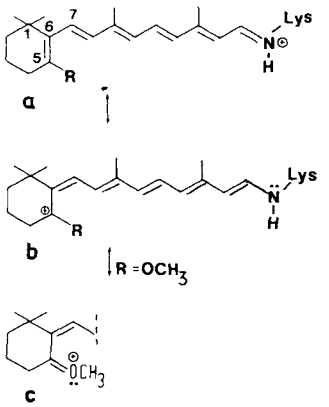

1, R = CH_3; **2**, R = CH_2CH_3; **3**, R = OCH_3

Scheme 1. The electron delocalization in the protonated Schiff base of retinal is illustrated by the resonance structures **a** and **b**. A methoxy group of C-5 additionally stabilizes the positive charge by a lone pair (resonance structure **c**).

[*] Dipl.-Chem. E. Kölling, Prof. Dr. D. Oesterhelt
Max-Planck-Institut für Biochemie
Am Klopferspitz, D-8033 Martinsried (FRG)
Prof. Dr. H. Hopf, Dr. N. Krause
Institut für Organische Chemie der Universität
Hagenring 40, D-3300 Braunschweig (FRG)

[**] Retinoids, Part 9.—Part 8: H. Hopf, N. Krause, *Tetrahedron Lett. 27* (1986) 6177.

For the synthesis of 5-methoxyretinal **9b** (Scheme 2), we used methyl 5,5-dimethyl-2-oxocyclohexanecarboxylate **4**[11] as key compound; the keto group is a masked enol ether function, and the ester group can serve for the coupling of the chain. The reaction of **4** with trimethyl orthoformate led exclusively to methyl 2-methoxy-5,5-dimethyl-2-cyclohexenecarboxylate **5a**. An isomerization to **5b**

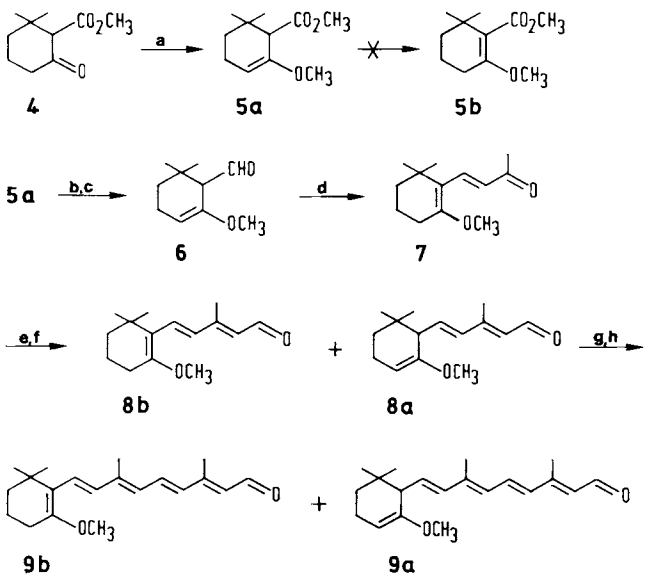

Scheme 2. Synthesis of 5-methoxyretinal **9b**. a) $HC(OCH_3)_3$, *p*-toluenesulfonic acid, reflux (83%). b) $LiAlH_4$, 0.2 equiv. ethanol, diethyl ether, reflux (95%). c) PDC/CH_2Cl_2 (35%). d) Acetone KO*t*Bu, toluene 12 h (17%). e) $PO(OEt)_2CH_2CN$, NaH, THF (36%). f) DIBAH, toluene (95%). g) $PO(OEt)_2CH_2C(CH_3)CHCN$, NaH, THF (36%). h) As for f) (70%).

could not be accomplished, even under basic conditions (sodium ethoxide, 24 h, room temperature). Reduction of **5a** with $LiAlH_4$ afforded the corresponding hydroxymethyl derivative, which was oxidized to 5-methoxy-α-cyclocitral **6**. This could be converted quantitatively into 5-methoxy-β-cyclocitral only on treatment with a base (aluminum oxide). The aldol condensation of **6** with acetone and potassium *tert*-butoxide in toluene afforded the ketone **7**, exclusively as the β-isomer. For further chain elongation Wittig–Horner reactions were carried out with phosphononitriles and subsequent reduction with diisobutylaluminum hydride (DIBAH). The Wittig-Horner reaction of **7** with diethylphosphonoacetonitrile led, according to ^{1}H-NMR-analysis, to the formation of 5-methoxy-C_{15}-nitrile, 66% of which as the all-*trans*-isomer and 33% as the 9-*cis*-isomer. Even after reduction to the 5-methoxy-C_{15}-aldehyde **8**, only the β-isomer **8b** was present. However, in the reaction leading to 5-methoxyretinic acid nitrile the α- and β-forms were formed in about an equimolar ratio. Upon reduction the amount of α-isomer **9a** was increased. The mixture of 5-methoxyretinal **9a** and **9b** was separated by HPLC, whereby the pure α-isomer and fractions containing β-isomer contaminated with α-isomer were obtained. The β-isomer proved to be labile under the conditions used for its isolation and also at low temperature under an inert gas.

Bacterio-opsin was isolated from the retinal-negative mutants JW5 of *H. halobium*.[12] Upon incubation with retinal or suitable analogues, bacteriorhodopsin (BR) and analogue-bacteriorhodopsins, respectively, are reconstituted. Figure 1a shows the absorption spectra of α-5-methoxyretinal-BR (Spectrum 1, $\lambda_{max} = 460$ nm, cf. α-retinal-BR; $\lambda_{max} = 482$ nm) and a mixture of α- and β-5-methoxyretinal-BR (Spectrum 2). The difference spectrum from the spectra of **1** and **2** with a weighting of Spectrum 2 by a factor of 0.4 (not shown) corresponds to the absorption spectrum of β-5-methoxyretinal-BR ($\lambda_{max} = 570$ nm, shoulder in the short wavelength region). Cell vesicles from JW 5, which were incubated with α/β-5-methoxyretinal, showed ca. 20% of the proton transport activity of the bacteriorhodopsin. 13-*cis*- and all-*trans*-5-ethylretinal[10] were incubated with bacterio-opsin and absorption spectra were recorded at intervals between 10 and 144 s after incubation (Fig. 1b). Already after 10 s an intermediate was formed with an absorption maximum at 420 nm; the subtle fine structure of this spectrum points to restricted conformational mobility[7] of the 5-ethylretinal.

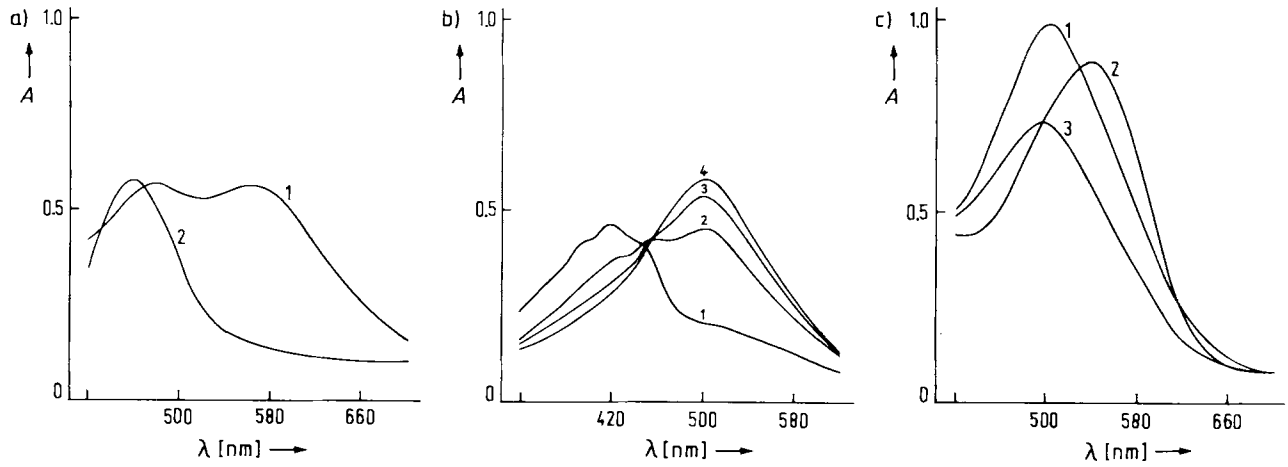

Fig. 1. a) Absorption spectra of bacterio-opsin in H_2O, incubated with α-5-methoxyretinal (Spectrum 1) and with a mixture of α- and β-methoxyretinal (Spectrum 2). b) Absorption spectra of bacterio-opsin in H_2O, incubated with all-*trans*-5-ethylretinal, after 10 s (Spectrum 1), 72 s (Spectrum 2), 108 s (spectrum 3), and 144 s (Spectrum 4); $\lambda_{max} = 504$ nm, $\varepsilon = 50000$. The time-dependent measurement at constant wavelength yields 3.2 mol/min for the rate of reconstitution of the chromophore with 13-*cis*-5-ethylretinal, 7 mmol/min with all-*trans*-5-ethylretinal, and 11 nmol/min with all-*trans*-retinal (not shown). c) Absorption spectra of 5-ethylretinal with bacterio-opsin in H_2O (Spectrum 1), with bacterio-opsin in 4M NaCl (Spectrum 2), and after dialysis against H_2O (Spectrum 3); cf. text.

The absorption spectra of 5-ethylretinal-BR in water ($\lambda_{max} = 505$ nm, Spectra 2–4 in Fig. 1b and Spectrum 1 in Fig. 1c) slope away unusually flatly at longer wavelengths for a retinal chromophore, thus indicating a mixture of chromophores. Indeed, addition of sodium chloride (final concentration 4 M) shifts the absorption maximum of the chromophore to $\lambda = 545$ nm (Fig. 1c, Spectrum 2). Removal of NaCl by dialysis again yielded the chromophore with a maximum at $\lambda = 504$ nm (Fig. 1c, Spectrum 3).

Table 1. Absorption maxima of retinal and 5- and 13-ethyl- and methoxyretinal and of the corresponding bacteriorhodopsins, and the proton transport activity measured on cell vesicles.

	λ_{max} [nm]		
	Retinal or analogue [a]	Bacterio-rhodopsin [b]	Proton transport activity [%]
Retinal	380	570	100
		(570) [e]	100
5-Ethylretinal	378	506	active
		(545) [e]	active
5-Methoxyretinal	385	570	active [c]
13-Ethylretinal [11]	379	559	70 [d]
13-Methoxyretinal [11]	360	550 [f]	active [d]

[a] In isopropyl alcohol. [b] In water. [c] In the mixture with α-5-methoxyretinal. [d] Corresponding to the amount of all-*trans*-isomer. [e] In 4 M NaCl. [f] From action spectrum for proton transport activity [14].

Both 5-ethylretinal-BR forms exhibit proton translocation activities; these are listed in Table 1 together with the absorption data and are compared with the data for the corresponding C-13 substituted compounds. To better understand the interpretation of the results it is important to remember the following facts.

Assumption of the planar conformation of the retinal in the bacteriorhodopsin with respect to the 6,7 single bond is based on the following findings: a) Retinol **10** contains the spectroscopic properties of retroretinol **11** at the binding

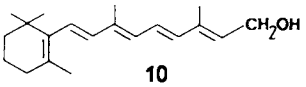

10

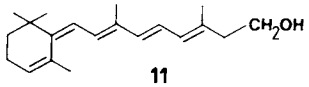

11

site of the bacterio-opsin and can be converted into retroretinal only photochemically in the binding site but not in free solution. Apart from retinol, only molecules which contain the cyclohexene ring bearing the side chain up to the C-13 atom of retinal exhibit this property.[7] b) In the reconstitution of the bacteriorhodopsin from bacterio-opsin and retinal an intermediate with an absorption shifted to the red region (BR_{400}) is formed in the first step without coupling of a covalent bond between retinal and protein.[13] This intermediate exhibits a fine structure in its absorption band.

Whether the planar conformation (6,7-torsion angle = 0°) is an s-*cis* or s-*trans*-conformation, is still uncertain. Analogous bacteriorhodopsins, in which these conformations are fixed by insertion of a second ring, which couples C-5 with C-8 and C-16 with C-8, respectively, have been studied.[8] In the case of the "*trans*-compound" the corresponding analogue-BR is formed more readily, is more active, and shows the absorption spectrum of bacteriorhodopsin; the *cis*-compound shows a strong red-shifted absorption maximum.[8] This effect is to be expected for *cis*-compounds but not for *trans*-compounds, and a very much smaller difference is predicted for open-chain, conjugated systems such as retinal itself.[7] There is no doubt, however, that a deviation of the 6,7-torsion angle from 0° must in each case effect a blue shift of the absorption maximum. On this basis the data in Table 1 can be interpreted in terms of different 6,7-torsion angles. The replacement of a methyl group at C-13 of retinal by an ethyl group gives rise to a blue shift of the absorption maximum of the corresponding bacteriorhodopsin of about 11 nm; neither large electronic nor steric effects are observed. The absorption maximum of all-*trans*-13-methoxyretinal-BR lies at about 550 nm,[14] i.e. even the methoxy group isosteric with ethyl does not have a very strong influence on the absorption maximum. In contrast, the introduction of the ethyl group in the 5-position causes a drastic blue shift of the absorption maximum from 570 nm to 506 nm. This cannot be determined by electronic effects; we assume that the 6,7-torsion angle is different, due to an alteration in steric interaction. NaCl obviously brings about a decrease in this angle, so that the absorption maximum is shifted to 545 nm and is once again similar to that exhibited by retinal-BR. This could be interpreted in terms of the forces which lead to a planarization of the cyclohexene ring of retinal in the binding site being overcompensated by steric hindrance of the ethyl group. Salt strengthens these forces, and thus reduces the 6,7-torsion angle again. Consistent with this, bacteriorhodopsin itself shows no dependence of its absorption maximum on the salt concentration. The absorption of the 5-methoxyretinal-BR (β-form) can also be understood on this basis. Due to the ethyl/methoxy isosteric relationship, the same steric repulsion was to be expected, but the stronger electronic interactions and the increased conjugation due to the donor property of the methoxy group (cf. the resonance structure **c** in Scheme 1) appear to lead to the planar conformation, and thus to the absorption maximum of the retinal remaining the same. For technical reasons the effect of salt on the absorption maximum could not be monitored. It is predicted that no change takes place on addition of salt.

The blue shift caused by an ethyl group in the C-13 position is smaller (11 nm) than that caused by such a group in the C-5 position (25 nm). Whether this is determined by electronic effects, different for both substitutions, or by incompletely compensated steric repulsion, cannot be established. With and without salt, 5-ethylretinal-BR shows proton translocation activity, even if reduced compared to BR, and hence substantiates that the position of the cyclohexene ring can reduce but not completely eliminate the activity.

Summarizing, it can be established that steric and electronic interactions of the cyclohexene ring with the protein environment determine the 6,7-torsional angle. It is 0° in retinal (6-*trans* or 6-*cis*), and, on suitable substitution, e.g. with an ethyl group in the C-5 position, it differs from 0°; however, it is then salt-dependent. These findings suggest a competition between electronic and steric interactions of the retinal with its environment. The 6,7-torsional angle has an influence on the activity of the proton pump, but only in quantitative form.

Received: February 5, 1987 [Z 2092 IE]
German version: *Angew. Chem.* 99 (1987) 598

[1] J. K. Lanyi in L. Ernster (Ed.): *New Comprehensive Biochemistry*, Elsevier/North Holland, Amsterdam 1984, p. 315.
[2] P. Hegemann, J. Tittor, A. Blanck, D. Oesterhelt in Y. Ovchinnikov (Ed.): *Retinal Proteins*, VNU Science Press, Utrecht, The Netherlands, in press.
[3] H. D. Lemke, D. Oesterhelt, *FEBS Lett. 128* (1981) 255.
[4] U. Fischer, D. Oesterhelt, *Biophysical J. 28* (1979) 211.
[5] K. Nakanishi, V. Balogh-Nair, M. Arnaboldi, T. Kazuo, B. Honig, *J. Am. Chem. Soc. 102* (1980) 7945.
[6] G. S. Harbison, S. O. Smith, J. A. Pardoen, J. L. M. Courtin, J. Lugtenburg, J. Herzfeld, R. A. Mathies, R. G. Griffin, *Biochemistry 24* (1985) 6955.
[7] T. Schreckenbach, B. Walckhoff, D. Oesterhelt, *Eur. J. Biochem. 76* (1977) 499.
[8] R. van der Steen, P. L. Biesheuvel, R. A. Mathies, J. Lugtenburg, *J. Am. Chem. Soc. 108* (1986) 6410.
[9] B. Honig, A. D. Greenberg, U. Dinur, T. Ebrey, *Biochemistry 15* (1976) 4593.
[10] Synthesis of 5-ethylretinal: N. Krause, *Dissertation*, Universität Braunschweig 1986.
[11] E. Kölling, *Diplomarbeit*, Universität Braunschweig 1982.
[12] D. Oesterhelt, W. Stoeckenius, *Methods Enzymol. 31* (1974) 667.
[13] T. Schreckenbach, D. Oesterhelt, *Fed. Proc. Fed. Am. Soc. Exp. Biol. 36* (1977) 1810.
[14] K. Fendler, W. Gärtner, D. Oesterhelt, E. Bamberg, unpublished.

Structure of a Crystalline Alkali-Metal Cyclopentadienide

By *Peter Jutzi,* Wilhelm Leffers, Bernd Hampel* (dec.), *Siegfried Pohl,** and *Wolfgang Saak*

Due to the rapid development of metallocene chemistry in the fifties, alkali metal salts of cyclopentadiene—already known since the turn of the century[1]—have become indispensable agents for the transfer of cyclopentadienyl groups. In spite of the obvious importance of these compounds there is still hardly any information available on their solid-state structure. Base-free alkali-metal cyclopentadienides are nearly insoluble in non-donating solvents; to our knowledge,[2] they hitherto have always been obtained as X-ray amorphous substances, and, accordingly, have not been further investigated.

We recently reported that the solubility of cyclopentadienyllithium compounds in nonpolar solvents can be increased significantly by incorporation of trimethylsilyl groups; thus, for example, tris(trimethylsilyl)cyclopentadienyllithium even dissolves in hexane.[3,4] Crystalline adducts of this compound with amines[3] and ethers[5] are likewise readily soluble and monomeric in the solid state, in solution, and in the gas phase. In systematic studies on silylated alkali-metal cyclopentadienides we now succeeded for the first time in preparing a base-free compound in crystalline form. Upon reaction of trimethylsilylcyclopentadiene with potassium or potassium hydride in toluene as solvent we obtained potassium trimethylsilylcyclopentadienide **1** as colorless, extremely air-sensitive platelets which can be shredded into very fine fibers.[6]

$$(Me_3Si)C_5H_5 \xrightarrow[-1/2H_2]{+K} (Me_3Si)C_5H_4K$$

1

A structure with parallel oriented one-dimensional infinite units, presumed for **1** alone on the basis of this property, is confirmed by an X-ray structure analysis[7] (see Fig. 1). Each of these units contains a "supersandwich complex," which is made up of a repeating sequence of potassium atoms and (on both sides) pentahapto bonded cyclopentadienyl rings. The trimethylsilyl groups attached to the cyclopentadienyl moieties are arranged "in gaps".

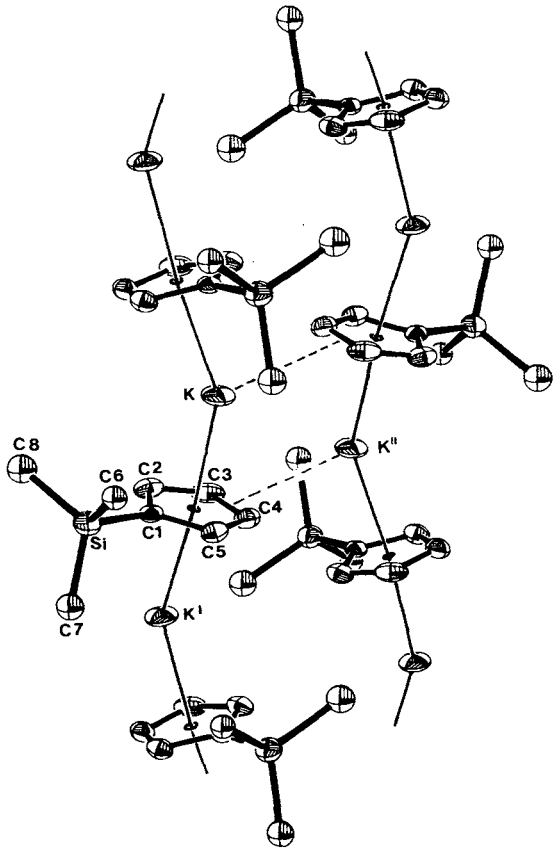

Fig. 1. Crystal structure of **1**; bond lengths [Å] and angles [°]: K-C1 3.006 (0.010), K-C2 2.988, K-C3 3.049, K-C4 3.079, K-C5 3.036, K'-C1 3.022, K'-C2 3.001, K'-C3 3.011, K'-C4 3.074, K'-C5 3.006, K''-C3 3.666, K''-C4 3.678, average CC distance in the C_5 ring 1.408, Si-C1 1.820; C5-C1-Si 126.3, Si-C1-C2 128.1.

The average distance between the potassium atoms and the carbon atoms of the cyclopentadienyl units is about 3.0 Å; this corresponds to a distance between potassium and ring center of about 2.78 Å. Considering the corresponding values for the tris(trimethylsilyl)cyclopentadienyllithium-quinuclidine adduct[3] (2.16 and 1.79 Å) and the increase in the ionic radius[8] of 0.73 Å on going from lithium to potassium, the distances found for **1** are exceptionally large, thus indicating an electrostatic interaction between anionic π-systems and potassium ions.[9]

Interestingly, an additional weak bonding relationship between potassium atoms and cyclopentadienyl units from neighboring strands (K–C distance about 3.7 Å) is observed in the structure of **1**. This interaction leads to a distortion of the geometry around each of the potassium atoms, resulting in a zig-zag chain structure for the polymeric potassium trimethylsilylcyclopentadienide **1**; the angle between the normals to the cyclopentadienyl rings (at

[*] Prof. Dr. P. Jutzi, W. Leffers, Dr. B. Hampel
Fakultät für Chemie der Universität
Universitätsstrasse, D-4800 Bielefeld (FRG)
Prof. Dr. S. Pohl, W. Saak
Anorganische Chemie der Universität
Carl-von-Ossietzky-Str. 9–11, D-2900 Oldenburg (FRG)

the potassium atom) is 150.7°. We presume that the weak interactions between the strands in **1** are responsible for the tendency to crystallize.[10]

Due to the sensitivity of **1**, molecular weight determinations in benzene solution are poorly reproducible; however, they clearly confirm the degradation of the polymer to low molecular units. According to mass spectrometric investigations, **1** becomes monomeric in the gas phase. Addition of tetrahydrofuran to a solution of **1** in toluene leads to the formation of $(Me_3Si)C_5H_4K \cdot THF$, a crystalline 1:1 adduct, whose structure has not yet been elucidated.

Received: February 6, 1987;
revised: March 5, 1987 [Z 2093 IE]
German version: *Angew. Chem. 99* (1987) 563

[1] J. Thiele, *Ber. Dtsch. Chem. Ges. 34* (1901) 68.
[2] An exception is the crystalline potassium dinitrotrichlorocyclopentadienide; the structure is determined by potassium-oxygen contacts and is thus atypical for a potassium cyclopentadienide: Y. Otaka, F. Marumo, Y. Saito, *Acta Crystallogr. Sect. B28* (1972) 1590.
[3] P. Jutzi, E. Schlüter, S. Pohl, W. Saak, *Chem. Ber. 118* (1985) 1959.
[4] At higher concentrations of tris(trimethylsilyl)cyclopentadienyllithium, a hexane solution solidifies to a gel.
[5] P. Jutzi, W. Leffers, unpublished.
[6] *Procedure*: Trimethylsilylcyclopentadiene (7.25 g, 52.4 mmol) was added dropwise to an ice-cooled suspension of potassium (2.00 g, 51.2 mmol) in toluene (150 mL). After the evolution of gas finished, the reaction mixture was filtered, concentrated, and cooled. Subsequent repeated recrystallization of the crude product afforded colorless needles of **1**; m.p. 203°C.—^{1}H-NMR (C_6D_6): $\delta(SiMe_3)=0.31$ (s, 9H), $\delta(C_5H_4)=5.85$ (AA'BB', 4H); ^{13}C-NMR (C_6D_6): $\delta(SiMe_3)=1.16$, $\delta(C_5H_4)=108.9$, 112.7, 110.1; ^{29}Si-NMR (C_6D_6): $\delta(SiMe_3)=-13.9$; MS (70 eV): *m/z* 176 ($M^{\oplus}$, 6%), 73 ($SiMe_3^{\oplus}$, 17%); 39 ($K^{\oplus}$, 100%).
[7] **1** crystallizes orthorhombically, space group *Pbca*, $a=7.967(1)$, $b=10.776(1)$, $c=24.661(1)$ Å, $V=2117.2$ Å^3, $Z=8$; 1261 symmetry independent reflections, 518 observed ($I>2\sigma(I)$); $R_w=0.057$ (measurements: Siemens AED 2; solution: SHELX 76). Further details of the crystal structure investigation are available on request from the Fachinformationszentrum Energie, Physik, Mathematik GmbH, D-7514 Eggenstein-Leopoldshafen 2, on quoting the depository number CSD-52381, the names of the authors, and the journal citation.
[8] Ionic radii for the coordination number 6 according to Pauling.
[9] Presumably lithium is also predominantly electrostatically bonded in tris(trimethylsilyl)cyclopentadienyllithium; it has not been possible so far to detect any covalent bonding. This also holds for other π-complexes of lithium (see: D. Seebach, R. Hässig, J. Gabriel, *Helv. Chim. Acta 66* (1983) 308).
[10] In potassium tris(trimethylsilyl)cyclopentadienide such an interaction is impossible for steric reasons. This explains why we could not obtain any crystals of this compound.

Synthesis and Characterization of Tetrakis[bis(trimethylsilyl)methyl]disilene**

By *Satoru Masamune,* Yuichi Eriyama,* and *Takeshi Kawase*

In recent years several ethene analogues **I** of elements of the fourth main group (E = Si, Ge, and Sn) have been synthesized.[1] Among the many unique physical and chemical properties that these compounds exhibit, the significant influence of the substituents R on the relative stability of **I** and **Ia** has attracted our attention. For instance, the digermene **1** and the distannene **2** dissociate in solution into the corresponding (monomeric) germanediyl **1a** and stannanediyl **2a**, respectively,[1j-m,2] whereas the tetraaryl compounds **3** and **4** retain their structural integrity both in solution and in the vapor phase.[1n-p] These facts naturally led to the query of how the stability of the hitherto unknown disilene **5** compares with that of **1** and **2** and with that of the known counterpart **6**.[1f]

$R_2E=ER_2$ **I** R_2E: **Ia**

1, 1a: E=Ge, R=$(Me_3Si)_2CH$
2, 2a: E=Sn, R=$(Me_3Si)_2CH$
3: E=Ge, R=2,6-diethylphenyl
4: E=Sn, R=2,4,6-triisopropylphenyl
5, 5a: E=Si, R=$(Me_3Si)_2CH$
6: E=Si, R=2,6-diethylphenyl

We describe here the synthesis of **5**, the first tetraalkyldisilene derivative isolated in pure, crystalline form, and present our answer to the above query.

$$SiH_2Cl_2 \xrightarrow{RLi} \underset{\mathbf{7}}{R_2SiH_2} \xrightarrow{I_2} \underset{\mathbf{8}}{R_2SiI_2} \xrightarrow{C_{10}H_8Li} \underset{\mathbf{5}}{R_2Si{=}SiR_2}$$

Scheme 1. R = $(Me_3Si)_2CH$.

The target compound **5** has defied many attempts at its synthesis both in our laboratory and in other laboratories, but a short and direct route has now turned out to be successful with the *proper* selection of intermediates (Scheme 1). Thus, reaction of dichlorosilane (3.4 M) in diethyl ether and pentane with 2.4 equivalents of $(Me_3Si)_2CHLi$[1j,3] (0.25 M) in ether (30 min at −78°C and then 5 h at 20°C) furnished **7** in 66% yield.[4] Subsequent reaction of **7** with 2.3 equivalents of iodine (2 h at 20°C and then 24 h at 100°C) afforded the corresponding diiodo compound **8**[4] (yield after recrystallization: 37%).

For the final step of reductive coupling the procedure used by *Weidenbruch* et al. for the synthesis of hexa-*tert*-butylcyclotrisilane was adopted,[5] but during the entire operation (including workup) contact of the product **5** with air and moisture had to be avoided. A 0.42 M solution of **7** in THF was added to a 0.5 M solution of lithium naphthalenide (2 equivalents) at −78°C; the mixture was stirred for 1 h at −78°C, for 2 h at −45°C, and finally for 1 h at 0°C. After dilution with hexane the mixture was filtered, the filtrate concentrated in vacuo, and naphthalene removed by sublimation at 10^{-4} torr. The resulting solid residue was dissolved in benzene and filtered in a glovebox. The residue remaining after evaporation of solvent from the filtrate was recrystallized from methylcyclohexane. Bright yellow crystals of **5** were obtained [yield: 40%, m.p. 224–226°C (decomp.)]. Occasionally **5** was contaminated with trace amounts of LiI, which was removed by washing with methanol (see below).

The physical and chemical properties of **5** are fully consistent with its formulation as the disilene structure:

1. Mass spectrum (EI, 70 eV), *m/z* calcd. for $C_{28}H_{76}Si_{10}$ 692.3698; found 692.36415; major fragments: *m/z* 692 ($M^{\oplus}$, 4.04%), 347 ($M^{\oplus}/2+1$, 100), 346 ($M^{\oplus}/2$, 38.87), 273 ($M^{\oplus}/2-Me_3Si$, 15.67). No fragment was registered with $m/z=1038$, which corresponds to the cyclotrimeric structure.[6]

[*] Prof. Dr. S. Masamune, Dr. Y. Eriyama, Dr. T. Kawase
Department of Chemistry, Massachusetts Institute of Technology
Cambridge, MA 02139 (USA)

[**] This work was supported by the National Science Foundation (USA) and Kao Corporation (Japan). The authors thank Professor *S. Collins*, University of Waterloo, Canada, for constructive discussions.

2. Electronic spectrum (methylcyclohexane, 20°C): $\lambda_{max}(\varepsilon)=393$ (12600), 357 (8600), 311 sh (2800), 224 nm (8300). The extinction coefficients remains constant with samples whose concentrations vary within the range 5×10^{-3} to 5×10^{-5} M. In comparison with the spectra reported for all known disilenes, the 393 nm absorption maximum and intensity of **5** is in the region expected for this disilene chromophore.[1a-i]

3. ^{1}H-NMR spectrum (250 MHz, C_6D_6, 20°C): $\delta=0.18$ (s, 2H; CH), 0.26 (s, 2H; CH), 0.37 (s, 36H; MeSi), 0.39 (s, 36H; MeSi). Although the chemical shifts of these signals are slightly temperature-dependent over the range -50 to 100°C, all spectra show only one set of signals, indicating that the sample solution contains a single species. While the appearance of more than one signal for the MeSi groups rules out the possibility of this species being (monomeric) $[(Me_3Si)_2CH]_2Si$ **5a**,[7] the presence of two signals for the CH groups and also for the MeSi groups in the spectra is consistent with the interpretation that **5** is undergoing rapid inversion between the two *trans*-bent conformers (S_2) via the planar conformer (C_{2h}) (Scheme 2)[8,9] or **5** might be frozen in the C_{2h} conformation.

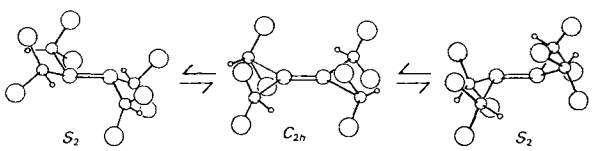

Scheme 2. The size of the circles symbolizes the different-sized groups/atoms $Me_3Si>Si>C>H$.

5 reacts with water (THF/H_2O 10:1) to give in 95% yield the corresponding hydrate **9** (half-life of **5** at 25°C, 18 h; at 80°C, 20 min).[10] In contrast, **5** is unexpectedly stable toward methanol and remains unchanged even when heated in a MeOH/THF solution for 24 h at 80°C. (Therefore LiI can be removed with MeOH.) However, photolysis (Hanovia medium pressure, Pyrex filter, MeOH/methylcyclohexane solution) immediately caused dissociation of **5** into **5a**, which subsequently reacted with MeOH to afford **10**[4] in 87% yield.[11] Bubbling O_2 through a methylcyclohexane solution of **5** produced in an estimated yield of 60–70% the epoxide **11**[4] as major product.[12]

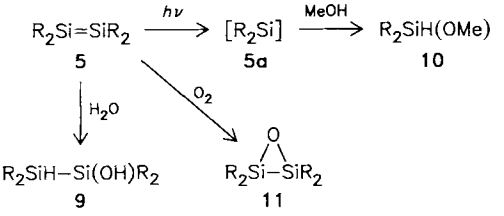

A preliminary characterization of **5** having been completed, a few comments and a brief summary are justified: 1. **5** is the first disilene derivative that has been prepared under reductive conditions. 2. The Si,Si double bond is well shielded by the substituents, as manifested in the inertness of **5** toward MeOH. 3. Unlike its Ge and Sn counterparts **1** and **2**, compound **5** shows no indication of dissociation into **5a** in solution to a detectable extent. This is obviously due to the expected high thermodynamic stability of the Si,Si double bond compared to the formal Ge,Ge and Sn,Sn double bonds.[13] This stability should also be reflected in the length of the Si=Si bond and in the size of the bent angle. For this reason, the crystal structure of **5** attracts special interest, and an X-ray analysis is currently under way.

Received: February 26, 1987 [Z 2117 IE]
German version: *Angew. Chem. 99* (1987) 601

[1] For the synthesis and X-ray analysis of disilenes, see: a) R. West, M. J. Fink, J. Michl, *Science (Washington DC) 214* (1981) 1343; b) M. J. Fink, M. J. Michalczyk, K. J. Haller, R. West, J. Michl, *Organometallics 3* (1984) 793; c) S. Masamune, Y. Hanzawa, S. Murakami, T. Bally, J. F. Blount, *J. Am. Chem. Soc. 104* (1982) 1150; d) S. Masamune, S. Murakami, H. Tobita, *Organometallics 2* (1983) 1464; e) S. Masamune, H. Tobita, S. Murakami, *J. Am. Chem. Soc. 105* (1983) 6524; f) S. Masamune, S. Murakami, J. T. Snow, H. Tobita, *Organometallics 3* (1984) 333; g) S. Murakami, S. Collins, S. Masamune, *Tetrahedron Lett. 25* (1984) 2131; h) H. Watanabe, T. Okawa, M. Kato, Y. Nagai, *J. Chem. Soc. Chem. Commun. 1983*, 781; i) H. Matsamoto, A. Sakamoto, Y. Nagai, *ibid. 1986*, 1768; digermenes: j) P. J. Davidson, D. H. Harris, M. F. Lappert, *J. Chem. Soc. Dalton Trans. 1976*, 2268; k) P. B. Hitchcock, M. F. Lappert, S. J. Miles, A. J. Thorne, *J. Chem. Soc. Chem. Commun. 1984*, 480; l) T. Fjeldberg, A. Haaland, B. E. R. Schilling, M. F. Lappert, A. J. Thorne, *J. Chem. Soc. Dalton Trans. 1986*, 1551; m) D. E. Goldberg, P. B. Hitchcock, M. F. Lappert, K. M. Thomas, T. Fjeldberg, A. Haaland, B. E. R. Schilling, *ibid. 1986*, 2387; n) S. Masamune, Y. Hanzawa, D. J. Williams, *J. Am. Chem. Soc. 104* (1982) 6136; o) J. T. Snow, S. Murakami, S. Masamune, D. J. Williams, *Tetrahedron Lett. 25* (1984) 4191; distannenes [j, l, m] and p) S. Masamune, L. R. Sita, *J. Am. Chem. Soc. 107* (1985) 6390.

[2] The ^{119}Sn{^{1}H}-NMR spectrum of **2** (149 MHz, [D$_{14}$]methylcyclohexane, Me_4Sn as reference) taken at -90.7°C shows the appearance of two signals, A and B, at $\delta_A=735$ and $\delta_B=750$, each with its own pair of ^{119}Sn-^{117}Sn coupling satellites. [$^1J_A(^{119}Sn-^{117}Sn)=3317$ Hz and $^1J_B(^{119}Sn-^{117}Sn)=1784$Hz]. The satellite intensities relative to the main resonances are roughly 3.5% for each satellite [1p]. These results suggest that **2** exists, at least partially, in a dimeric form in solution at cold temperatures (L. R. Sita, S. Masamune, unpublished results); cf. [1j-m].

[3] A. H. Cowley, R. A. Kemp, *Synth. React. Inorg. Met.-Org. Chem. 11* (1981) 591.

[4] Properties of the new compounds: **7**: MS: *m/z* 333 ($M^{\oplus}-15$, 100%), 259, 73; ^{1}H-NMR (C_6D_6): $\delta=4.23$ (t, $J=4.2$ Hz, 2H), 0.20 (s, 36H), -0.54 (t, $J=4.2$ Hz, 2H). **8**: m.p. 115–117°C; MS: *m/z* 584 ($M^{\oplus}-16$), 473 (100%), 385, 273, 129, 73; ^{1}H-NMR ([D$_8$]toluene): $\delta=1.07$ (s, 2H), 0.37 (br. s, 36H). **9**: m.p. 189–191°C (decomp.); MS: *m/z* 710 ($M^{\oplus}$), 679, 347 (100%); ^{1}H-NMR (C_6D_6): $\delta=4.53$ (br. s, 1H), 1.71 (s, 1H), 0.49 (s, 2H), 0.36 (s, 18H), 0.352 (s, 18H), 0.348 (s, 18H), 0.32 (s, 18H), -0.07 (br. s, 2H). **10**: MS: *m/z* 363 ($M^{\oplus}-16$), 73 (100%); ^{1}H-NMR (C_6D_6): $\delta=4.91$ (t, $J=3.5$ Hz, 1H), 3.35 (s, 3H), 0.23 (s, 18H), 0.20 (s, 18H), -0.35 (d, $J=3.5$ Hz, 2H). **11**: m.p. 294–302°C; MS: *m/z* 708 ($M^{\oplus}$), 565, 347, 73 (100%); ^{1}H-NMR (C_6D_6): $\delta=0.38$ (br. s, 72H), 0.13 (br. s, 2H), 0.06 (br. s, 2H).

[5] a) A. Schäfer, M. Weidenbruch, K. Peters, H.-G. von Schnering, *Angew. Chem. 96* (1984) 311; *Angew. Chem. Int. Ed. Engl. 23* (1984) 302; b) M. Weidenbruch, A. Schäfer, *J. Organomet. Chem. 269* (1984) 231.

[6] Cf. the reductive cyclization of dihalosilanes to form the corresponding cyclotrisilanes [1c, g–i, 5].

[7] **7**, **8**, and other compounds of the type $[(Me_3Si)_2CH]_2SiX_2$ show only one singlet for the MeSi groups.

[8] **1** and **2** have S_2 symmetry in the crystal.

[9] The energy difference between C_{2h}- and D_{2h}-disilene is small: 2.6 (HF/6-31G*), 0.3 (MP4SDTQ/6-31G*/HF/6-31G*) [(a) B. T. Luke, J. A. Pople, M.-B. K. Jespersen, Y. Apeloig, M. Karni, J. Chandrasekhar, P. von R. Schleyer, *J. Am. Chem. Soc. 108* (1986) 270], and 0.08 kcal/mol (HFR) [(b) K. Ohta, E. R. Davidson, K. Morokuma, *J. Am. Chem. Soc. 107* (1985) 3466].

[10] Cf. the behavior of **3** toward EtOH [1n]; see also S. Collins, S. Murakami, J. T. Snow, S. Masamune, *Tetrahedron Lett. 26* (1985) 1281.

[11] For the photolysis of other disilenes, see: S. Masamune, S. Murakami, H. Tobita, D. J. Williams, *J. Am. Chem. Soc. 105* (1983) 7776.

[12] Cf. M. J. Michaelczyk, R. West, J. Michl, *J. Chem. Soc. Chem. Commun. 1984*, 1525.

[13] The computed dissociation energy for the gas-phase process $H_2E=EH_2\rightarrow H_2E$ is ca. 30 kcal/mol for E=Ge, ca. 20 kcal/mol for E=Sn [1m], and 54 kcal/mol for E=Si [9b] and 62 kcal/mol for E=Si [B. T. Luke, J. A. Pople, M.-B. K. Jespersen, Y. Apeloig, J. Chandrasekhar, P. von R. Schleyer, *J. Am. Chem. Soc. 108* (1986) 260 and [9a].

 © VCH Verlagsgesellschaft mbH, D-6940 Weinheim, 1987 0570-0833/87/0606-0585 $ 02.50/0

The Chemistry of the Plasmodial Pigments of the Slime Mold *Fuligo septica* (Myxomycetes)**

By *Ingrid Casser, Bert Steffan,* and *Wolfgang Steglich**

The flowers of tan, *Fuligo septica* (L.) Wiggers, form yellow slime masses (plasmodia), which are often to be found in woods after damp weather. For reproduction, the plasmodium transforms into a sessile flat crust (aethalium) which contains the blackish spore mass. Light plays an important role in the complex life cycle of the slime mold.[2] Consequently, attempts have already been made on several occasions to isolate substances from the plasmodia, for they could be potential photoreceptors. Thus, it was assumed that the yellow pigments were flavins, flavones, polyenes, pteridines or phenolic compounds.[3] In the following communication it will be shown that the yellow color of the plasmodia of *Fuligo septica*[4] is due to the occurrence of tetramic acids with a polyene chromophore.

Extraction of the plasmodia or aethalia with methanol yields a yellow solution which turns orange on acidification with hydrochloric acid. Apparently a greater part of the pigments is present in the form of salts,[5] from which the free pigments are obtained on acidification. Evaporation of the methanolic solution to dryness and partition of the residue between ethyl acetate and water affords an organic phase, which after removal of the solvent and digestion with *n*-hexane, furnishes a red powder. According to the thin-layer chromatogram this consists in the main part of colorless components together with two main pigments and several minor pigments. The mixture can be separated by chromatography on Sephadex-LH-20 with methanol; the separation must be carried out in the absence of light using a cooled column. After re-chromatography on Sephadex-LH-20 (eluent: acetone/methanol 4/1) one of the two main pigments, fuligorubin A, is obtained in pure form.

It follows from the mass spectrum that fuligorubin A has the empirical formula $C_{20}H_{23}NO_5$, and that the fragments $C_{12}H_{12}O$, $C_{11}H_{13}$ and $C_9H_{10}NO_5$ indicate coupling of a polyene unit $C_{11}H_{13}CO$ with a nitrogen-containing residue $C_8H_{10}NO_4$. The UV spectrum (MeOH) shows absorption maxima at $\lambda = 243$ and 425 nm. On addition of sodium hydroxide the long wavelength absorption shifts hypsochromically to $\lambda = 377$ nm, and a color change from orange to lemon-yellow occurs.

In the ^{1}H-NMR spectrum ([D$_6$]acetone) signals for an all-*trans*-2,4,6,8,10-undecapentaene chain and a structural unit $-CH_2CH_2\underset{|}{C}HN(CH_3)-$ were observed, which could be assigned by a 2D-H-H-COSY (90°)-NMR experiment. Two further protons are observed at $\delta = 11.85$ and 14.10 at low temperature ($T = 180$ K).

The ^{13}C-NMR spectrum confirms the two partial structures; the five additional signals can be assigned to a carbonyl group ($\delta = 172.5$), an acid amide group ($\delta = 174.1$), and a $-C(OH)=C-CO-$ moiety, to which the polyene residue must be coupled via the carbonyl group. Taking into consideration the results of selective ^{1}H- decoupled ^{13}C-NMR spectra, fuligorubin A must have the structure **1**.[6] The spectroscopic data are in agreement with those of other tetramic acids, for which the hypsochromic shift of the long wavelength absorption on addition of NaOH is also characteristic.[7]

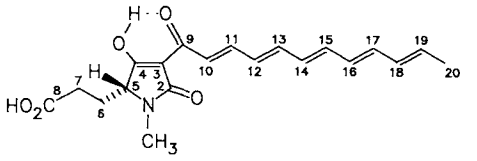

1

For determination of the absolute configuration, the chiroptic properties of decahydrofuligorubin A **2**[8] and the tetramic acid derivative **3**,[9] prepared from L-glutamic acid dimethyl ester and diketene, were compared. Since the CD curves are mirror-image-like, fuligorubin A must be 5*R*-configurated.

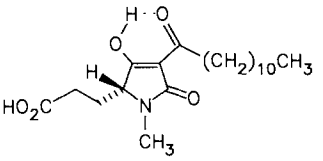

2

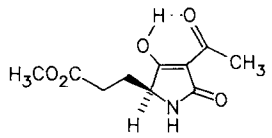

3

The isolation of a tetramic acid derivative from *Fuligo septica* is remarkable, since compounds of this type are known as mycotoxins, antibiotics and antitumor agents.[10] Whether the ability of **1** to form chelates with magnesium and calcium ions plays a role for the metabolism of *Fuligo* still has to be investigated.

Received: February 23, 1987 [Z 2110 IE]
German version: *Angew. Chem. 99* (1987) 597

[*] Prof. Dr. W. Steglich, Dr. I. Casser, Dr. B. Steffan
Institut für Organische Chemie und Biochemie der Universität
Gerhard-Domagk-Strasse 1, D-5300 Bonn (FRG)

[**] Fungal Pigments, Part 52. This work was supported by the Deutsche Forschungsgemeinschaft.—Part 51: [1].

[1] R. Marumoto, C. Kilpert, W. Steglich, *Z. Naturforsch. C41* (1986) 363.
[2] Cf. L. Rakoczy in H. Senger (Ed.): *The Blue Light Syndrome*, Springer, Berlin 1980, p. 570.
[3] Cf. review by L. Rakoczy, *Ber. Dtsch. Bot. Ges. 86* (1973) 141.
[4] Both plasmodia also as well as aethalia of *Fuligo septica* (L.) Wiggers var. *flava* Pers. were investigated; they were collected in October 1985 in the Kottenforst near Bonn (FRG) and identified by Dr. *H. Neubert* (Bühl/Baden). Voucher specimens are kept by Dr. *H. Neubert*.
[5] Since plasmodia and aethalia of *Fuligo septica* contain large amounts of calcium carbonate probably a calcium complex is involved.
[6] **1**: red microcrystals, m.p. 150°C (dec.); R_f: 0.50 (silica gel; eluent: benzene/ethyl formate/formic acid 10/5/3); CD (MeOH): $\Delta\varepsilon_{355} = 0.76$, $\Delta\varepsilon_{305} = 0$, $\Delta\varepsilon_{255} = 2.16$; UV (EtOH): λ_{max} (lgε) = 243 (4.16), 271 sh (4.11), 425 nm (4.43); after addition of one drop of NaOH $\lambda_{max} = 243$ and 377 nm; IR (KBr): $\tilde{\nu} = 3500$–2500 (br), 2930, 1705, 1615, 1445, 1405, 1260, 1010, 940, 820 cm^{-1}; ^{1}H-NMR ([D$_6$]acetone): $\delta = 1.80$ (d, $J = 7.0$ Hz; 3 20-H), 2.20 (m; 2 6-H), 2.31 (m; 2 7-H), 3.00 (s; N–CH$_3$), 3.90 (m; 5-H), 5.88 (dq, $J = 16$, 7 Hz; 19-H), 6.20 (dd, $J = 16$, 11 Hz; 18-H), 6.31 (dd, $J = 16$, 11 Hz; 16-H), 6.42 (dd, $J = 16$, 11 Hz; 17-H), 6.48 (dd, $J = 16$, 11 Hz; 14-H), 6.60 (m; 12-H, 15-H), 6.90 (dd, $J = 16$, 11 Hz; 13-H), 7.13 (d, $J = 16$ Hz; 10-H), 7.51 (dd, $J = 16$, 11 Hz; 11-H); ^{13}C-NMR ([D$_6$]acetone, capital letters: splitting by ^1J(CH)-couplings; small letters: splitting by C–H long-distance couplings): $\delta = 18.5$ (Qdd, $J = 125$, 8, 4 Hz; C-20), 24.4 (Tm, $J = 128$ Hz; C-6), 26.7 (Q, $J = 140$ Hz; N–CH$_3$), 28.3 (Ttd, $J = 128$, 9, 4 Hz; C-7), 66.1 (Dm, $J = 143$ Hz; C-5), 100.9 (br. s; C-3); polyene C: 121.0 (Dm, $J = 164$ Hz), 131.1 and 131.4 (each Dm, $J = 152$ Hz), 132.4 (Dm, $J = 156$ Hz), 132.8 and 133.2 (each Dm, $J = 152$ Hz), 137.6 (Dm, $J = 152$ Hz), 140.0 (Dm, $J = 154$ Hz), 144.5 (Dm, $J = 154$ Hz), 144.8 (Dm, $J = 154$ Hz); 172.5 (m; C-8), 174.0 (m; C-4), 174.1 (m; C-2), 194.5 (m; C-9); MS (DE, 180°C): *m/z* 357.1576 (54.5%, calc. 357.1576), 339 (6.5, $C_{20}H_{21}NO_4$), 212 (12.5, $C_9H_{10}NO_5$), 194 (47.3, $C_9H_8NO_4$), 172 (5.8, $C_{12}H_{12}O$), 145 (9.6, $C_{11}H_{13}$). According to the elemental analysis **1** contains two molecules of water of crystallization.
[7] Cf. R. J. Cole, R. H. Cox: *Handbook of Toxic Fungal Metabolites*, Academic Press, London 1981, p. 688.
[8] **2** By hydrogenation of **1** with H_2/Pd-C in methanol; colorless oil; $[\alpha]_D = 14°$ ($c = 0.05$, MeOH); CD (MeOH): $\Delta\varepsilon_{296} = 0.44$, $\Delta\varepsilon_{247} = 0.21$; ^{1}H-NMR (CD$_3$OD): $\delta = 0.94$ (t, $J = 7$ Hz; 3 20-H), 1.15–1.67 (m, 18 H), 2.23 (m, 4 H), 2.85 (br. t, $J = 7$ Hz; 2 10-H), 2.96 (s; N–CH$_3$), 3.79 (m; 5-H).

[9] **3**: Pale yellow crystals, m.p. 75–77°C; $[\alpha]_D = -65°$ ($c = 0.15$, MeOH); CD (MeOH): $\Delta\varepsilon_{285} = -1.33$, $\Delta\varepsilon_{242} = -0.91$; UV (MeOH): λ_{max} (lg ε) = 241 (3.67), 277 nm (3.87); ^{1}H-NMR ([D$_6$]acetone): $\delta = 1.89$ and 2.09 (each m; 2 6-H), 2.38 (s; 3 10-H), 2.46 (m; 2 7-H), 3.61 (s; OCH_3), 3.95 (m; 5-H), 7.80 (br. s; NH), 7.95 (br. s; OH).

[10] Cf. C. W. Holzapfel in P. S. Steyn (Ed.): *The Biosynthesis of Mycotoxins—A Study in Secondary Metabolism*, Academic Press, New York 1980, p. 327.

Tetrameric and Dodecameric *tert*-Butylethynyllithium; A Novel Aggregation Principle in Organolithium Compounds

By *Maren Geissler, Jürgen Kopf, Bernd Schubert, Erwin Weiss,* Wolfgang Neugebauer,* and *Paul von Ragué Schleyer*

Dedicated to Professor Hans-Ludwig Krauss on the occasion of his 60th birthday

Organolithium compounds almost always exist in the form of associates, e.g., as $[(MeLi)_4]$, $[(EtLi)_4]$, $[(C_6H_{11}Li)_6]$.[1] In the presence of donor ligands (amines, ethers) one also regularly finds associates, frequently as doubly or fourfold associated species. The structure can be decisively influenced by the nature of the solvent. For example, phenyllithium forms monomeric, dimeric, and tetrameric solvates.[2]

The structure of phenylethynyllithium also depends on the nature of the solvent molecule: with *N,N,N',N'*-tetramethyl-1,3-propanediamine (= TMPDA) the dimer $[\{PhC{\equiv}CLi(tmpda)\}_2]$ is present in the crystal,[3a] with the longer chain *N,N,N',N'*-tetramethyl-1,6-hexanediamine (= TMHDA) on the other hand, the polymer $[\{(PhC{\equiv}CLi)_4(tmhda)_2\}_n]$ with cubane-like Li_4C_4 structural units .[3b] Dimeric phenylethynyllithium has also been detected in tetrahydrofuran (THF) as solvent (low-temperature ^{13}C-NMR investigations[4a] and cryoscopic measurements[4b]).

In the case of *tert*-butylethynyllithium, which crystallizes from THF-containing solutions, we have now been able to demonstrate that both tetramers as well as dodecamers having the compositions $[(t\text{BuC}{\equiv}\text{CLi})_4(\text{thf})_4]$ **1** and $[(t\text{BuC}{\equiv}\text{CLi})_{12}(\text{thf})_4]$ **2**, respectively, can occur.[5]

Crystals of **1** were obtained from a hexane/THF solution at −78°C. An X-ray structure analysis revealed the structure depicted in Figure 1, with the cubane skeleton characteristic for tetrameric organolithium compounds. The THF molecules are bound as expected to the Li atoms. *Fraenkel* and *Pramanik*[6] had already deduced such a structure in THF solution from low-temperature ^{13}C-NMR measurements. According to cryoscopic investigations by *Bauer* and *Seebach*[4b] a dimer/tetramer equilibrium exists at −108°C.

With our equipment we were only able to carry out the X-ray structure analysis at room temperature, and observed a slow cleavage of the THF molecule. The structural data could not be significantly improved even after repeated sample preparation and additional measurements. Although an *R*-value of only 0.17 was finally achieved, acceptable bond lengths were nevertheless obtained for the Li-C skeleton, so that there can be no doubt of the fundamental "correctness" of the structure.

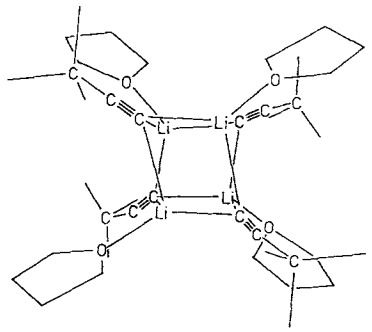

Fig. 1. Crystal structure of **1**. The center of the molecule lies on a twofold axis perpendicular to the plane of projection [7]. Important bond lengths [pm]: Li-C 219 (mean value; min. 217, max. 229); Li-O 192, 199; C≡C 120, 120; C-*t*Bu 145, 148; Li-Li 269 (mean value; min. 259, max. 278).

In further attempts to grow crystals under slightly modified conditions we unexpectedly obtained the dodecamer **2** with the structure shown in Figure 2. This indicates that the two structures are only slightly different energetically. Structure **2** results by linear coupling of three cubane-like subunits and can therefore only accomodate a total of four solvent molecules at the molecule terminals. Understandably, the crystals of **2** also effloresce very readily, and, consequently, the same problems are encountered as in the case of **1** in the X-ray structure analysis. Therefore, despite numerous repeated measurements, the structural data we present here are still inaccurate.

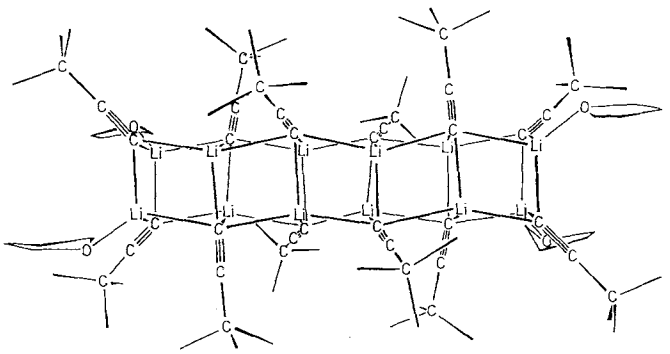

Fig. 2. Crystal structure of **2**. The center of the molecule lies on a twofold axis perpendicular to the plane of projection [10]. Some bond lengths [pm]: Li-C 222 (mean value; min. 207, max. 242); Li-O 206, 210; C≡C 115 (mean value; min. 111, max. 120); C-*t*Bu 146 (mean value; min. 140, max. 153); Li-Li 277 (mean value, min. 250, max. 302).

Disregarding polymeric compounds, **2** is the largest characterized associate of an organolithium compound reported so far. At the same time it represents a novel structural principle, according to which even still larger aggregates are conceivable, as well as smaller units such as decamers, octamers or hexamers: The cyclic, basic unit $[R_2Li_2]$ is stacked into aggregates $[(R_2Li_2)]_n$ (n = 1, 2, 3 ...). This structural principle is also taken into consideration in a theoretical study on the possible structures of LiH-oligomers.[11] Such structures are possibly also present in many solution equilibria of organolithium compounds.

[*] Prof. Dr. E. Weiss, Dipl.-Chem. M. Geissler, Doz. Dr. J. Kopf, Dr. B. Schubert
Institut für Anorganische und Angewandte Chemie
Martin-Luther-King-Platz 6, D-2000 Hamburg 13 (FRG)
Dr. W. Neugebauer, Prof. Dr. P. von R. Schleyer
Institut für Organische Chemie der Universität
Henkestr. 42, D-8520 Erlangen (FRG)

[**] Alkyl- and Arylmetal Compounds, Part 34. This work was supported by the Deutsche Forschungsgemeinschaft and the Fonds der Chemischen Industrie.—Part 33: [2].

For example, according to molecular weight determinations, allyllithium is associated to the extent of twelvefold in diethyl ether depending on the concentration of the solution,[12] the degree of association increasing with increasing concentration. Other structures are also conceivable, especially cyclic structures, as was recently demonstrated in the case of crystalline $[\{(PhCH_2)Na(tmeda)\}_4]$ (tmeda = *N,N,N',N'*-tetramethylethylenediamine).[13]

Experimental

Preparation of **1** and crystal growing: A solution of butyllithium (16.4 mmol) in hexane (10 mL) was treated at −78 °C firstly with THF (1.42 g, 19.7 mmol; 20% excess) and then with 3,3-dimethyl-1-butyne (1.39 g, 17.0 mmol). After 30 min at −78 °C the crystals that had formed were recovered by suction filtration and dried under vacuum until they no longer appeared moist. Yield ca. 1.8 g (70%). In order to avoid efflorescence, the crystals were treated with two drops of THF and prepared in a THF-saturated argon atmosphere.

Preparation of **2** and crystal growing: A solution of 3,3-dimethyl-1-butyne (1.7 g, 20.7 mmol) in cyclohexane (10 mL) was treated dropwise at room temperature with a 1.6 M solution of *n*-butyllithium in hexane until the initially precipitated *tert*-butylethynyllithium had re-dissolved (ca. 18 mL, 29 mmol). The solution was then evaporated down to 6 mL and treated with 1 mL of THF. After storage for several days at room temperature crystals of **2** separated out. Yield ca. 0.8 g (35%). To avoid cleavage of THF they were prepared in a THF-saturated argon atmosphere.

The THF content of **1** and **2** after hydrolytic decomposition was determined gas-chromatographically.

Received: October 23, 1987;
revised: February 23, 1987 [Z 1965 IE]
German version: *Angew. Chem. 99* (1987) 569

[1] a) J. L. Wardell in G. Wilkinson, F. G. A. Stone, E. W. Abel (Eds.): *Comprehensive Organometallic Chemistry, Vol. 1*, 1st edit., Pergamon, Oxford 1982, S. 64 ff; b) W. Setzer, P. von R. Schleyer, *Adv. Organomet. Chem. 24* (1985) 353.

[2] U. Schümann, J. Kopf, E. Weiss, *Angew. Chem. 97* (1985) 222; *Angew. Chem. Int. Ed. Engl. 24* (1985) 215.

[3] a) B. Schubert, E. Weiss, *Chem. Ber. 116* (1983) 3212; b) *Angew. Chem. 95* (1983) 499; *Angew. Chem. Int. Ed. Engl. 22* (1983) 496; *Angew. Chem. Suppl. 1983*, 703.

[4] a) R. Hässig, D. Seebach, *Helv. Chim. Acta 66* (1983) 2269; b) W. Bauer, D. Seebach, *ibid. 67* (1984) 1972.

[5] M. Geissler, J. Kopf, U. Schümann, E. Weiss, *Abstr. XIIth Int. Conf. Organomet. Chem.*, Wien 1985.

[6] G. Fraenkel, P. Pramanik, *J. Chem. Soc. Chem. Commun. 1983*, 1527.

[7] **1**: *P2/n*, $a = 1308.8(7)$, $b = 1184.6(14)$, $c = 1533.4(9)$ pm, $\beta = 97.63(4)°$, $\rho_{calc} = 0.903$ g cm^{-3}, $Z = 2$, $Mo_{K\alpha}$ radiation, structure determination by direct methods (SHELXS-84 [8]), refinement to $R = 0.167$ (unweighted) with 1235 reflections [$|F| > 4\sigma(F)$], measured to $\theta = 22.0°$. Anisotropic temperature factors for Li, O, and C, but C atoms of the *t*Bu groups and the THF molecules refined isotropically. No refinement of the H positions; these were placed at positions calculated from the C atoms. Number of refined parameters 156 [9].

[8] G. Sheldrick, SHELXS-84, Programs for Crystal Structure Solution, Göttingen 1984.

[9] Further details of the crystal structure investigations are available on request from the Fachinformationszentrum Energie, Physik, Mathematik GmbH, D-7514 Eggenstein-Leopoldshafen 2, on quoting the depository number CSD-52405, the names of the authors, and the journal citation.

[10] **2**: *C2/c*, $a = 2021.4(13)$, $b = 2302.6(11)$, $c = 2273.5(13)$ pm, $\beta = 98.10(5)°$, $\rho_{calc} = 0.8829$ g cm^{-3}, $Z = 4$, $Mo_{K\alpha}$ radiation, structure determination by direct methods (SHELXS-84 [8]), refinement to $R = 0.16$ (unweighted) with 1378 reflections [$|F| > 3\sigma(F)$], measured to $\theta = 20.0°$. Anisotropic temperature factors for Li, O, and C, but C atoms of the methyl groups and THF molecules isotropically refined; H-positions not refined, placed in calculated positions (analogous to **1** [7]). Number of refined parameters 394 [9].

[11] H. Kato, K. Hirao, K. Akagi, *Inorg. Chem. 20* (1981) 3659; cf. D. R. Armstrong, D. Barr, W. Clegg, R. E. Mulvey, D. Reed, R. Snaith, K. Wade, *J. Chem. Soc. Chem. Commun. 1986*, 869.

[12] G. R. Brubaker, P. Beak, *J. Organomet. Chem. 136* (1977) 147.

[13] C. Schade, P. von R. Schleyer, H. Dietrich, W. Mahdi, *J. Am. Chem. Soc. 108* (1986) 2485.

BOOK REVIEWS

Comprehensive Biotechnology. The Principles, Applications and Regulations of Biotechnology in Industry, Agriculture and Medicine. Editor-in-chief: *M. Moo-Young*. Pergamon Press, Oxford 1985. £695.00.

"Comprehensive Biotechnology" is yet another reference work, published in four volumes, on the subject of biotechnology. The executive editor claims that the publication of this work of reference has set a new standard in specialist literature on this multidisciplinary subject. The work is stated to be addressed to a broad readership including students, teachers, researchers, administrators and others in academia, industry and government. This ambitious claim imposes correspondingly high demands on the topicality, nature and scope of the contributions, and on facilitation of the use of the complete work.

A positive feature of the work worthy of first mention is that the four volumes comprising the set have been published simultaneously, lending to topicality of all the contributions. A guarantee of the quality of the contributions ought to be the choice of authors. The list of their names reads like an extract from Who's Who in Biotechnology. Regarding facilitation of the use of the reference work, it should however be mentioned, that only the last of the four volumes contains a cumulative subject index.

Volume 1. **The Principles of Biotechnology: Scientific Fundamentals.** Volume editors: *A. T. Bull* and *H. Dalton*. xxv, 688 pp., bound.—ISBN 0-08-032509-2

The first volume of the set attempts to outline the scientific fundamentals of biotechnology, a complex multidisciplinary field intersecting at some points with biological, chemical and engineering sciences.

The volume is organized in two main sections, viz. genetic and biological fundamentals (15 contributions), and chemical and biochemical fundamentals (16 contributions). The literature cited relates mainly to the period up to 1983, in some instances however up to 1985. The average length of the contributions is 20 pages.

The first section begins with an overview of the organisms of biotechnology, namely viruses, prokaryotes, eukaryotes represented by algae, protozoa and fungi, and animal and plant tissue cultures. In view of the wealth of the subject matter involved, it is understandable that only the most important distinguishing properties can be considered. For more detailed information, readers are referred to cited bibliography, in particular to certain handbooks. However, mention of the new edition of "*Bergey's Manual*", a standard work on microbiology, would have been desirable. The following contributions are devoted to the

isolation and preservation of microorganisms. The discussion of methods for genetic modification of microorganisms and in vitro recombination of DNA relates mainly to prokaryotes. Eukaryotic cloning systems for mammalian cells (SV 40), yeasts (ars system) and plants (Ti plasmid, cauliflower mosaic virus) are briefly mentioned. It is perhaps appropriate that very little space is devoted to the secretion of proteins at this juncture since this topic is discussed in detail in the second section of the volume in association with extracellular enzymes. Most of the first section is taken up by ten contributions on the subject of microbial growth. Aspects addressed include nutritional requirements of microorganisms, nutrient uptake, nutrient media, modes of growth of microorganisms, growth kinetics and mixed cultures, with special reference to prokaryotes. Animal and plant cell culture technologies are discussed and compared.

In the second section of Volume 1, particular emphasis is on the subject of microbial metabolism. Examples discussed include aerobic and anaerobic metabolism of glucose, and metabolism of C_1 compounds like methane, methanol and carbon dioxide. In the chapter that follows attention is drawn to the biotechnological importance of microorganisms that function as biocatalysts in methanogenesis.

A discussion of the different pathways involved in the microbial metabolism of aromatic compounds leads up to the question concerning microbial degradation of environmental chemicals. Readers wishing to have a comprehensive overview of this subject would have been still better served if the cited literature had included publications from a still wider circle of leading research workers.

The metabolism of polymeric substrates is illustrated by a description of the biosynthesis and degradation of fatty acids and lipids. Autotrophic metabolic pathways are treated by the presentation of a comparative description of patterns of microbial photosynthesis. Other pathways of electron transfer are also discussed, with bacterial respiratory chains and their regulation serving as an example. Principles of enzyme technology are explored in chapters on enzyme kinetics, mechanisms of enzyme catalysis, enzyme evolution and extracellular enzymes. In a contribution on the overproduction of microbial metabolites, the effects of nutrient limitation, pH and temperature are discussed. The final contribution presented in volume 1 is devoted to a description of the mechanisms of regulation relevant to metabolite synthesis, in particular prokaryotic biosynthesis of amino acids.

Olga Salcher
Bayer AG, Wuppertal (FRG)

Volume 2. **The Principles of Biotechnology: Engineering Considerations.** Volume editors: *C. L. Cooney* and *A. E. Humphrey*. xv, 632 pp., bound.—ISBN 0-08-032510-6

The material in Volume 2 addresses the state of technology in biochemical synthesis and processing. The division of the 37 chapters contributed by 44 authors into two sections (1. Bioreactor design, operation and control. 2. Upstream and downstream processing) is somewhat unusual in its organization. Whereas the fermenters, particularly the more recent developments in instrumentation and systems for fermentation process control, are dealt with in the first section, discussions on valves and pumps, gas compression, filtration systems, media sterilization, and problems associated with heat management are left until the second section.

The quality of individual chapters varies greatly. In Chapter 3, treatment of the very important areas of fermenter design and scale-up is completely inadequate. Criticism must be levelled at this particular contribution for its repetition of problems that have been described better elsewhere. The problem of asepsis is dismissed in eleven lines containing only two literature references in fact dating back to 1969 (!) and 1976 (!), and that of foam in as few as four lines including just one reference dated 1969 (!). By comparison, an excellent review of both the principles and practical applications of aqueous two-phase systems for liquid-liquid extraction of biopolymers is presented in chapter 28.

Bioreactor systems for plant and animal cells are addressed in two contributions but not discussed in any depth. There is not a single diagrammatic representation of a bioreactor shown fully equipped with valves, piping systems and sensors. On the other hand, a number of chapters describe the principles and state of the art of some downstream processing unit operations. But just as in the chapters on fermentation, the problems of asepsis are almost completely neglected in the discussions of the processing operations.

Each of the subjects addressed in the different chapters of this volume will now be reviewed briefly:

The first two chapters deal with the basics of transport phenomena in bioprocesses—oxygen transfer and heat transfer. Following an elaboration of the physical aspects, correlations with the oxygen consumption of the growing organisms are discussed. Purely biological problems like the critical oxygen concentration are examined, likewise questions relating to the structures of pellets and their supply with oxygen. As already indicated, it is considered that the chapter on fermenter design and scale-up is to all intents and purposes a nonentity. Fragments of this topic are discussed in other contributions.

Chapter 4 describes imperfectly mixed bioreactor systems, and examines the effects of micromixing and macromixing on bioprocesses. This is followed in Chapter 5 by a discussion of different types of nonmechanically agitated bioreactor systems some of which have been adopted for industrial applications; this chapter concludes with a comparison of the oxygen transfer efficiencies of different bioreactors. The next five chapters focus on dynamic modelling of fermentation systems, instrumentation for monitoring and controlling bioreactors, instrumentation for fermentation process control, use of computers for the control of fermentation processes, and computerized data analysis for on-line process applications. Here, too, accord among the authors would have been desirable to avoid duplication of material and to include instead more information on recent trends in measurement and control technologies.

The next three chapters (11 to 13) are devoted to techniques for immobilizing enzymes and cells. Based on comprehensive coverage of the latest literature data, these chapters not only describe the very large number of methods that have been developed but also explain why, in spite of the high potential of immobilized enzyme and cell technology, only relatively few of these elegant techniques have found industrial application.

The second section of Volume 2 begins with a chapter on transport and handling of bioprocess liquids and solids and on technologies for the mixing of these materials. Different types of pumps, valves (rather old data), piping systems and mixing equipment are discussed in detail. This is followed by two chapters on gas compression and filtra-

tion systems, including coverage of test procedures for air filtration. The next chapter discusses problems associated with media sterilization. The treatment of heat management in fermentation processes in the chapter that follows is considered to be inadequate.

The discussion of the unit operations of downstream processing begins with the disruption of microbial cells. It is considered that industrial use of disruption techniques could have been given greater coverage. The chapter on centrifugation reflects the state of technology in this area; it even addresses sterility and containment problems and puts forward suggestions for their solution.

Filtration processes are discussed in five chapters. Since crossflow filtration is the process generally used today, it is accorded considerable space. The discussion of membrane types and membrane methods is also vivified by examples of industrial applications. Ultrafiltration is dealt with in two large chapters in which the theory of the process, its economics and its biotechnological applications are discussed. The literature references on this fast growing technique are up to date.

Liquid-liquid extractions are discussed in two chapters. The first one in which examples relating to the production of antibiotics are given, is not of a particularly satisfactory standard because apart from the discussion of penicillin extraction processes, it does not present any recent data on extraction with organic solvents. The second of these two chapters reviews the latest developments in aqueous phase systems, contains a large number of tables giving examples of applications and listing methods, and discusses scale-up of the technology for the isolation of biopolymers.

The use of ion exchangers for the recovery of antibiotics and proteins is addressed in two relatively short chapters. The contributions on the unit operations of chromatography discuss methodologies and the constraints on their use at industrial level.

The section on upstream and downstream processing concludes with a discussion of the distillation system as a critical cost factor in the recovery of ethanol, a chapter on supercritical fluid extraction, and a contribution on the state of technology in electrodialysis.

It is considered that this volume, in its treatment of fermentation technology, fails to match the quality of comparable standard works. On the other hand, some of the unit operations addressed in the chapters on downstream processing are described in an excellent manner.

Wulf Crueger
Bayer AG, Wuppertal (FRG)

Volume 3. **The Practice of Biotechnology: Current Commodity Products.** Volume editors: *H. W. Blanch, S. Drew,* and *D. I. C. Wang.* xxv, 1136 pp., bound.—ISBN 0-08-032511-4

Following the discussion of the biological and engineering fundamentals of biotechnology in the first two volumes, Volume 3 provides a comprehensive overview of the products manufactured by biotechnological processes.

The book consists of fifty chapters organized in three sections. The first section describes the processes employed for manufacturing healthcare products. As one might expect, the largest amount of space in this section is devoted to processes for the production of antibiotics. Subjects addressed in other contributions include production and purification technologies for the development of anticancer agents; functions, production and uses of siderophores; bioconversions of steroids; microbial production of human proteins by recombinant DNA technology. The inclusion in this section of additional chapters on the production of vitamins, vaccines and immune globulins would have completed the spectrum of products in the healthcare sector.

In the second section of volume 3, processes are presented for the production of food and beverage products. The main emphasis is on descriptions of the classical technologies for the production of alcoholic beverages, cheese, fermented dairy products, bakers' yeast, and amino acids. Other topics addressed are biomass production and the processes employed in the Far East for the production of traditional fermented soybean foods.

The third and last section is devoted to those products which, in terms of quantity, play a key role as starting materials for the production of industrial chemicals (organic acids), biochemicals (hydrolytic enzymes) and fuels (ethanol).

Each of the three sections begins with a chapter dealing with the current market situation and the general problems of project selection and development in the particular product category. The following chapters furnish information on development and optimization of processes for the manufacture of individual products. Readers are provided, inter alia, with data on the biology and physiology of the microorganisms, on biosynthetic pathways, on production processes and product recovery (usually illustrated by diagrams), on production costs, and on the limitations of the different processes. These aspects are treated at varying depth by the respective authors. Notwithstanding, in its entirety the presented information provides a most useful overview of the state of research for anyone wishing to acquire a general insight into one of the areas covered. To obtain knowledge of much greater depth, readers are provided at the end of each chapter with a comprehensive bibliography generally containing references also to recent publications.

The authors of the third volume have succeeded convincingly in demonstrating how biological and engineering principles are translated into industrial processes so that this volume usefully complements the first two of the set. In view of the wealth of information it contains and the manner in which it is presented, it is considered that this volume compares most favorably with other standard works on industrial microbiology, and it can be recommended to anyone seeking a reference work on this field.

Wolfram Andersch
Bayer AG, Leverkusen (FRG)

Volume 4. **The Practice of Biotechnology: Speciality Products and Service Activities.** Volume editors: *C. W. Robinson* and *J. A. Howell.* xxix, 1308 pp., bound.—ISBN 0-08-032512-2

In contrast to the preceding volumes, the fourth volume of the set is very heterogeneous in its coverage of subject matter. Section 1 (Specialized Activities and Potential Applications) presents diverse new biotechnologies and bioprocesses considered to show promise of finding widespread applications in biomedicine, agriculture, process engineering and analysis. Section 2 addresses legal aspects of biotechnology, and Section 3 examines problems associated with waste management and pollution control.

The reviewer's curiosity was focussed first and foremostly on the contributions in Section 1 since some of the areas covered are witnessing such a rapid pace of new developments that the quality of a book devoted to these subjects obviously must be judged by the topicality of the information it contains and the manner in which it is presented. It is, however, generally concluded that the standard of these contributions by no means fully satisfies the claims formulated in the foreword. It is considered that this is mainly due, on the one hand, to the failure of most of the authors to relate their subject matter to the potentialities of technologies for product development, and, on the other hand, to the fact that the deadline set for receipt of most of the publications was 1982 yet they were not printed until three years later. Consequently, many of the biotechnological developments on which current interest is focussed, are not given adequate coverage.

The acknowledged authority *G. S. Eisenbarth*, in his contribution entitled "Monoclonal Antibodies", devotes only three sentences to the potential of monoclonal antibodies to replace conventional antibodies in assays. This fails to take consideration of the multiple development of new diagnostic agents; the use of monoclonal antibodies in downstream processing is not mentioned at all.

G. Gregoriadis discusses liposomes only in relation to their use as a drug delivery system, giving no regard to their use in bioprocess technology.

In the chapter by *K. Kano* on the rapidly developing field of Transplantation Immunology, the most recent literature reference cited by this author dates back to 1980!

In some of the articles, the literature references leave much to be desired not only in their up-to-dateness but also in balance of emphasis. *T. M. S. Chang* in his article on "Artificial Cells" gives more than 100 references to his own work (a few selected review articles would have sufficed), and the authors of the chapter "Surface Thermodynamics of Cellular and Protein Interactions" cite only their own work or that of their research group.

The relationship between biotechnology and agriculture is not adequately established. In fact, only one example is given to illustrate the potentialities of genetic engineering for the transfer of herbicide resistance.

The anthelmintic 22,23-dihydroavermectin B_{1a}, a biotechnological product for agriculture, which has a large sales volume, is not even mentioned.

However, Sections 2 and 3 of the fourth volume ("Governmental Regulations and Concerns" and "Waste Management and Pollution Control") both provide a good insight into the topics covered. Here too, though, it has to be pointed out that, especially in the discussion on risk-benefit assessment, information is wanting on the latest state of legislation and regulations.

Axel Kretschmer
Bayer AG, Wuppertal (FRG)

Summary

The detailed reviews of the four volumes indicate that the first three conform with the self-set high standards in both form and content. Conceptionally, these volumes constitute a logical unit although they can be recommended unreservedly for use as individual reference works. However, it is considered that the fourth volume is already in need of revision to update its contributions.

[NB 786 IE]

Interaction of Steroid Hormone Receptors with DNA. Edited by *M. Sluyser*. VCH Verlagsgesellschaft, Weinheim 1985. 242 pp., bound, DM 115.00.—ISBN 3-527-26221-0

The book is informative and extremely readable. The opening chapter provides an excellent overview of biochemical and histochemical studies in the steroid receptor field. It is thorough in both its historical perspective and its discussion of more recent findings concerning the intra- rather than extra-nuclear localization of unfilled receptors. The different views on receptor transformation are also well addressed and it is notable that opinions regarding activation not necessarily being associated with a change in sedimentation coefficient from 4 to 5S are discussed.

In the second chapter the philosophical question of why the steroid molecule should have been selected as the structure to control many diverse functions is raised. The role of nuclear ploidy and cell cycle on receptor binding is discussed. The significance of the similarities between receptor binding DNA regions and viral enhancer elements is also presented in this chapter as is the possibility of DNA helix destabilization resulting from interactions of the D ring of the steroid with specific DNA sequences.

The third chapter presents steroid-receptor interactions as they are viewed by an X-ray crystallographer. For example, the types of modification to the steroid molecule determine receptor binding potential and those modifications which determine function as an agonist or antagonist are discussed. It is argued that the conformation of the A-ring of the steroid determines the specificity of the receptor to which it binds and that the D-ring regulates its actual degree of activity.

Other chapters address the binding of activated estrogen receptor to specific DNA sequences and provide detailed specific discussions of the chick oviduct progesterone receptor and glucocorticoid receptor structure and function. The chapters on progesterone and glucocorticoid receptors essentially describe the state of the art (at publication date) regarding our understanding of steroid receptor structure and receptor mediated mechanisms. The chick oviduct system is an invaluable model for the study of progesterone receptor function since the egg white protein genes which are expressed in response to progesterone have been cloned and sequenced. The availability of antibodies to this receptor has also allowed careful studies to be made of the sub-unit structure of the receptor and its association with a non-steroid binding protein. This latter aspect is discussed in depth.

Studies with the glucocorticoid receptor are clearly presented and details are given of how, by the use of polyclonal and monoclonal antibodies the receptor can be divided into three functional domains. This chapter also provides a lucid summary of the use of the long terminal repeat (LTR) DNA sequences from the mouse mammary tumor virus to study the direct involvement of the receptor, which binds to these sequences, in determining glucocorticoid responsiveness. A brief description is also given of the significance of DNAse hypersensitive sites corresponding to the receptor binding region within the LTR.

Two chapters are devoted to the role of androgen receptors. One stresses the possible role of receptor-RNA binding which may modulate DNA binding, it also discusses the possible role of divalent cations on androgen-receptor interactions. The other chapter reviews the significance of receptor binding to the nuclear matrix and describes receptor binding to specific sequences adjacent to a prostatic binding protein (PBP) androgen induced gene in the pros-

tate. Associated with the nuclear matrix are specific DNA and RNA sequences involving actively transcribed genes, thus interactions of receptors with the matrix implies a role for their receptors on transcriptional events. The discussion of PBP gene receptor binding studies will be of particular interest to the reader because of the specific binding that has been observed within the first intron.

The final chapter provides an interesting discussion of the mechanism by which 20-hydroxyecdysone induces puffs in drosophila polytene chromosomes. The hypothesis is presented whereby the hormone-receptor complex is required to induce early puffing and that gene products of the early puffs lead to a removal of this complex and induce binding to late puff sites. The arguments supporting this hypothesis are well presented.

In summary, the topics are presented clearly, the book at time of printing is up to date, the choice of topics is good, and most commendably the book makes pleasurable reading because of its excellent balance in subject matter.

Roy G. Smith [NB 811 IE]
Baylor College of Medicine
Houston, Texas (USA)

Organotitanium Reagents in Organic Synthesis (Volume 24 in the series **Reactivity and Structure, Concepts in Organic Chemistry**). By *M. T. Reetz*. Springer, Berlin 1986. x, 236 pp., bound, DM 168.00.—ISBN 3-540-15784-0

In the first half of the 1980's the early transition metals, especially titanium, have taken on a markedly increased importance in organic synthesis. The appearance of a progress report which collects together information on the important and topical theme of the use of organotitanium reagents in organic synthesis, written by *M. T. Reetz*, a prominent investigator in this field, is therefore to be welcomed.

A short general introduction to the use of organotitanium compounds in organic chemistry is followed by two chapters describing the preparation and the chemical and physical properties of some simple organotitanium reagents. The enhancement of selectivity in reactions involving carbanions, primarily by the introduction of titanium, a dominant aspect, is explained in the third chapter, which deals with the chemical selectivity of organotitanium reagents. The considerable amount of information is presented clearly to the reader, with a convenient subdivision into topics.

The brief fourth chapter deals with investigations into reaction kinetics. As a focal point the fifth chapter deals with the stereoselectivity of the addition of organotitanium reagents to carbonyl compounds; topics discussed in detail include diastereofacial selectivity, both with and without chelate control effects, diastereoselectivity in the addition of prochiral titanium-containing anions, and enantioselective additions. A short sixth chapter on Michael addition reactions is followed by a more important seventh chapter on nucleophilic substitutions using organotitanium reagents. The book ends with a comparatively brief eighth chapter on methylenation of carbonyl groups.

Apart from the synthesis and stability of the reagents discussed, the main emphasis in this book is on the chapters that deal with the selectivity of the reactions of organotitanium reagents. This is to be welcomed, since organotitanium reagents have a particular advantage over others with respect to selectivity, which is especially important in the chemistry of natural products. This is made very clear here by the frequent comparisons with organolithium, organomagnesium and organocopper compounds. It is gratifying to find that the bewildering mass of information contained in the original papers is collected here in an orderly fashion and presented clearly and comprehensibly. In most cases reaction mechanisms are discussed, and the selectivity of product formation is explained on the basis of the transition states likely to be involved. The reader is also told how the stereochemical and electronic behavior is affected by the choice of organotitanium reagent.

The seventh chapter, on substitution reactions, describes another important application of organotitanium reagents, whereby the use of titanium enolates gives, for the first time, a general method for the α-alkylation of carbonyl compounds when the alkyl group is tertiary. A similar situation occurs in the use of alkyltitanium compounds for the alkylation of tertiary halides. The eight chapter, on methylenation of carbonyl groups, seems at first sight to be rather short; however, this reflects the state of research at the time when it was written. All the chapters have comprehensive lists of literature references (up to the beginning of 1985). I was, however, a little disturbed to find that sources such as diploma theses, which are not easily accessible, are also included.

The book provides a full, well arranged, and readable description of the present state of research in this field. It can be recommended both for the instruction of advanced students and for use by those engaged in research. The price will deter many from buying it privately, which makes the volume all the more indispensable for chemically orientated libraries.

Holger Butenschön [NB 800 IE]
Max-Planck-Institut für Kohlenforschung,
Mülheim a. d. Ruhr (FRG)

Chemistry of Organo-Zirconium and -Hafnium Compounds. By *D. J. Cardin, M. F. Lappert,* and *C. L. Raston*. Ellis Horwood, Chichester 1986. 451 pp., bound, £ 59.50.—ISBN 0-85312-475-2

The book "Organometallic Chemistry of Titanium, Zirconium, and Hafnium", by *P. C. Wailes, R. S. P. Coutts,* and *H. Weigold*, published twelve years ago, portrayed the quite rapidly growing interest at that time in the chemistry of the early transition metals. The further rapid developments in the organometallic chemistry of Group IV transition elements in particular have now made a new review of this topic desirable. *Cardin, Lappert,* and *Raston* have produced an excellent monograph surveying results for the two heavier elements. They have provided a very careful and virtually complete coverage of the literature published up to and including 1982, and have set out the material in twenty chapters dealing with different structural and chemical aspects. Each chapter is supplemented by an appendix detailing those papers from the period 1983/84 which the authors regard as most important.

An introductory chapter includes thermodynamic data and general information on bonding properties and stereochemistry, together with a section on "Developments and Perspectives". This is followed by a treatment of mono(cyclopentadienyl) complexes of zirconium and hafnium in which the metal is in the +4 or +3 oxidation states. The chapters on compounds of the bent metallocenes zirconocene and hafnocene take up considerable space, beginning with a general discussion of the structure and stereochemistry of Cp_2M compounds. These are followed by very ex-

tensive compilations on $[Cp_2ML_2]$ complexes containing ligands whose donor atoms are elements of main Groups V, VI and VII. Particular attention is given to the corresponding compounds containing metal-carbon σ bonds. Three separate chapters deal with the synthesis and reactions of σ-alkyl, σ-alkenyl and σ-alkynyl complexes of the type $[Cp_2MR_2]$. Many users of this book will find the richly illustrated chapter on the molecular structures of $[Cp_2M^{IV}R_2]$ compounds especially useful. The treatment of Cp_2M chemistry is continued with short chapters on metallocene-silyl, -germyl, and -stannyl compounds and on hydride complexes.

There is also much valuable information on metallocene(IV) compounds in the chapters which follow on Cp_2Zr^{III} and Cp_2Hf^{III} compounds and adducts of Cp_2M^{II} groups with neutral donor ligands. Cp_3M and Cp_4M compounds have a chapter to themselves, as also do complexes of zirconium and hafnium with anionic π ligands other than C_5H_5, and metal complexes with neutral π ligands. Two chapters on homoleptic and heteroleptic alkyl compounds complete the treatment of the inorganic chemistry and the special characteristics of the organometallic chemistry of zirconium and hafnium compounds.

The book ends with a chapter on organo-zirconium and organo-hafnium complexes in organic synthesis and catalysis, which unfortunately is too brief. Here, if not earlier in the book, it becomes apparent that restricting one's attention to the organometallic chemistry of the two heavier Group IV transition elements. leaving out titanium, is a marked disadvantage when comparisons with the corresponding titanium compounds need to be introduced for a better understanding of chemical properties.

The strength of the book lies in its wealth of well-presented factual information, which is mostly arranged in the form of clear tables, each with a list of literature references. It is definitely not a work of reference, if only because of its limited index (a subject index of eleven pages), but it is made for reading. The book is a must for libraries. For everyone actively concerned with the organometallic chemistry of zirconium or hafnium, it will be a welcome aid for many years to come. One only hopes that a similar review on the organometallic chemistry of titanium will soon be available.

Gerhard Erker [NB 802 IE]
Institut für Organische Chemie
der Universität Würzburg (FRG)

Three volumes in the series "Best Synthetic Methods": Hydrogenation Methods. By *P. N. Rylander*. Academic Press, New York 1985. xv, 193 pp., bound, $ 48.00.—ISBN 0-12-605365-0

Methods for the Oxidation of Organic Compounds. Alkanes, Alkenes, Alkynes, and Arenes. By *A. H. Haines*. Academic Press, New York 1985. xix, 388 pp., bound, $ 83.00.—ISBN 0-12-315501-0

Palladium Reagents in Organic Synthesis. By *R. F. Heck*. Academic Press, New York 1985. xx, 461 pp., bound, $ 99.00.—ISBN 0-12-336140-0

For some time now the original literature in organic chemistry has been producing a flood of new synthetic methods and reagents, most of which are implicitly claimed to be better than the established procedures. The synthetic chemist has the task of making a choice, and relies more on instinct than on rational evaluation. The series of books under review is designed to eliminate this unsatisfactory state of affairs by a direct assault, enabling the user to find, under such circumstances, not merely a suitable recipe, but quite simply the best one available. The claim of this series to provide a critical evaluation obviously goes beyond the information which has long been available from other highly regarded works such as "Organic Synthesis", "Organic Reactions", "Reagents for Organic Synthesis", or "Houben, Weyl and Müller". Consequently, one is keen to discover how successfully the "best" method for each case has been chosen from the hundreds of possibilities.

Rylander's "Hydrogenation Methods" seems to have an especially easy task in that respect, since the catalytic hydrogenation reaction discovered as long ago as 1899 is virtually an ideal example of a perfectly controlled method. The book begins with a general description of the variations of catalyst, solvent and apparatus, which is quite long (28 pp.) in relation to the book as a whole, but does not go beyond non-committal statements and well established knowledge. The second chapter (23 pp.) is devoted to hydrogenation of CC double bonds, and this again contains little that is new; the problem of double bond migrations is discussed in detail, but the much more troublesome one of racemization during the hydrogenation of α-chiral olefins is ignored. All stereochemical aspects are dismissed in a mere four pages. From the detailed chapter on acetylenes one concludes essentially that there is nothing better than the good old Lindlar catalyst, and the lengthy discussion on the hydrogenation of multiple bonds involving heteroelements (50 pp.) needs to be more selective in this age of complex hydrides. Arene hydrogenation reactions are of more significance in industrial practice than as laboratory methods. The three concluding chapters contain exhaustive treatments of the hydrogenolysis reactions of carbon-halogen bonds and of heteroatom single bonds in rings and in acyclic protecting groups (breaking of *O*-benzyl and *N*-benzyl bonds), and they offer much that is of interest to all readers. Altogether *Rylander*'s book contains much valuable and detailed information and many useful hints, but lacks a sufficiently clear and systematic organization of the material. One soon gets the impression that here is an expert who has dipped into his well-filled, but no longer completely up-to-date, card index, and has thereby produced only a few ideas which could help the reader over his immediate difficulty.

The book by *Haines*, in contrast, is very clearly set out, dealing in a lucid and exemplary way with the standard methods for oxidizing CH, C=C, and C≡C bonds. The many examples of reactions which are collected together in the form of tables, and the experimental details given (both of which are absent from *Rylander*'s book) make this a true laboratory handbook. Well-tried methods predominate on the whole, e.g. in the field of CH oxidations, those given prominence are dehydrogenation with DDQ and selenium, or allylic oxidations by the *Kharash-Sosnovski* method, and with selenium dioxide. Special techniques such as "remote functionalization" of the steroid ring system by the *Breslow* or *Barton* methods are, however, unduly stressed, whereas the equally important Vedejs reagent (MoO_5-pyridine-HMPT) for the α-hydroxylation of carbonyl compounds is not mentioned. The chapter on C=C oxidation without bond breakage describes the *syn*-glycolysis method with iodine/silver acetate, as given by *Woodward*, or with osmium tetraoxide, in all the possible variations. Detailed attention is also given to epoxidation using peracids, or using peroxides with transition metal cat-

alysts, and also to the Sharpless reaction; no reference is made, though, to the possibilities for diastereofacial control in the peracid epoxidation reaction. In the section on oxidative cleavage of C=C bonds, one finds a wealth of information on ozonolysis and the Lemieux variants. The chapter on alkynes confines its attention to the oxidation to 1,2-diketones, the scission of terminal acetylenic bonds to give carboxylic acids, and the Glaser coupling. In the final chapter the author gives a detailed discussion of such aspects of the oxidation of arenes as hydroxylation with peracids, peroxides or lead tetraacetate, the formation of quinones with cerium ammonium sulfate or thallium trifluoroacetate, oxidative ring cleavage by ozone, permanganate, peracetic acid or ruthenium tetraoxide, and oxidative phenol coupling with iron(III) salts. One quickly learns to find one's way around *Haine*'s book, helped considerably by the terse presentation, liberal use of structural formulas, and descriptive chapter titles.

The most up-to-date of the three volumes as regards content is undoubtedly *Heck*'s "*Palladium in Organic Synthesis*". Whereas in the two volumes already described, literature citations for the last ten years tend to be the exception, they are instead the rule in this one. A comparison with slightly older monographs on the same topic (e.g. Tsuji: *Organic Synthesis with Palladium Compounds*, Springer 1980) does, however, show that progress during the most recent years has not been quite so fast. The book starts with a brief summary of methods for preparing the most important of the catalytically active palladium complexes, and deals also with the recovery of this expensive noble metal. The subsequent chapters describe the areas of application of palladium catalysis. Thus, for example, Cope and Claisen rearrangements can be carried out under very mild conditions; acetate shifts or rearrangements of vinyl epoxides or of α,β-epoxyketones proceed readily even in neutral media. Again, many variations of the Wacker process have been developed. α-Olefins can be oxidized to give methyl ketones, and α,β-unsaturated esters to give β-keto-esters. The intramolecular version of the Wacker oxidation leads to tetrahydrofurans, or in the case of *o*-allylphenols to benzofurans, while the analogous *o*-allylanilines undergo cyclization to indoles. An extensive chapter (62 pp.) is devoted to substitutions which proceed via π-allylpalladium intermediates. These allow one to introduce dialkylamines and well-stabilized carbanions of the acetoacetic ester and malonic ester types into allyl esters and allyl ethers under mild conditions. An interesting variation of this type of reaction is the Diels-Alder-like [3+2] cycloaddition of trimethylenemethane complexes to electron-deficient olefins, as discovered by *Trost*. About half the book is concerned with variations on the theme of the palladium-catalyzed CC bond, which leads readily to biarylenes, 1,3-dienes or styrene derivatives. The carbonylation of unsaturated halogen derivatives gives a wide range of carboxylic acid derivatives, while the cyclopropanation of CC double bonds with diazomethane/palladium acetate gives a high yield only in the presence of electron-withdrawing substituents. Hydrogen transfer reactions using cyclohexene or sodium tetrahydroborate as the hydrogen donor, as described in the final chapter, offer a mild alternative in many cases to the classical method of catalytic hydrogenation. The usefulness of the *Heck* volume, like that of the *Haines*, benefits from the inclusion of many tables and working rules. In some places the author unfortunately gives way to his encyclopedic tendencies, where it would have been more useful to confine the discussion to the most advantageous applications of palladium catalysis.

Altogether "Best Synthetic Methods" is undoubtedly a very welcome work. Whether or not one really is given the best method is, however, debatable. To achieve that, the authors ought to have included many more critical comparisons with alternative methods. Some important volumes have yet to appear; one needs only to think of the possibilities of boron, silicon, titanium or selenium reagents. Whether it is worth buying the whole series is something that one must decide for oneself; the high prices of the individual volumes mean that one could quickly get into large figures. It is certainly worth having one or another single volume. Perhaps organic synthesis, influenced by practical monographs such as this, will become reorientated again towards practical realizability and good sense, which would be a desirable outcome. There have been many sins in this respect in the past, when one considers the tiny scale of the reactions described, the poor standard of reproducibility, and the exaggerated yield figures that are often given. Instead of setting oneself the task of preparing unduly complicated compounds, which are usually more easily made by microbiological methods, one should again concentrate attention more on that which is feasible and sensible. Only in this way will it be possible to mend the gulf between academic synthetic work and industrial practice which is now deplored on all sides.

Johann Mulzer [NB 797 IE]
Institut für Organische Chemie
der Freien Universität Berlin

Registered names, trademarks, etc. used in this journal, even when not marked as such, are not to be considered unprotected by law.

© VCH Verlagsgesellschaft mbH, D-6940 Weinheim, 1987. - Printed in the Federal Republic of Germany by Zechnersche Buchdruckerei, Speyer/Rhein.

All rights reserved (including those of translation into foreign languages). No part of this issue may be be reproduced in any form - by photoprint, microfilm, or any other means - nor transmitted or translated into a machine language without written permission from the publishers. Only single copies of contributions, or parts thereof, may be made for personal use.

Valid for users in the USA: The appearance of the code at the bottom of the first page of an article in this journal (serial) indicates the copyright owner's consent that copies of the article may be made for personal or internal use, or for the personal or internal use of specific clients. This consent is given on the condition, however, that the copier pay the stated per-copy fee through the Copyright Clearance Center, Inc., for copying beyond that permitted by Sections 107 or 108 of the U.S. Copyright Law. This consent does not extend to other kinds of copying, such as copying for general distribution, for advertising or promotional purposes, for creating new collective works, or for resale. For copying from back volumes of this journal see 'Permissions to Photo-Copy: Publisher's Fee List' of the CCC.

Editorial office: Pappelallee 3, D-6940 Weinheim, Federal Republic of Germany, Telephone (06201) 602315, Telex 465516 vchwh d, Telefax (06201) 602328.

Editor: *P. Gölitz.*

Associate editors: *D. I. Loewus, A. Stimson.* **Editorial assistant:** *E. Schweikart*

Publishers: VCH Verlagsgesellschaft mbH. (Managing Directors: *Prof. Dr. Helmut Grünewald* and *Hans Dirk Köhler*), Pappelallee 3, D-6940 Weinheim, Federal Republic of Germany. Correspondence concerning advertisements should be addressed to VCH Verlagsgesellschaft mbH. (Advertising Manager *R. J. Roth*), Boschstr. 12. P.O. Box 1260/1280, D-6940 Weinheim, Federal Republic of Germany, Telephone Weinheim (06201) 602-0, Telex 465516 vchwh d, Telefax (06201) 602328.

ANGEWANDTE CHEMIE
International Edition in English
Volume 26 · Number 7
July 1987
Pages 595–706

The Development of the Electron Microscope and of Electron Microscopy (Nobel Lecture)**

By Ernst Ruska*

1. Parents' House, Family

A month ago, the Nobel Foundation sent me its yearbook of 1985. From it I learnt that many Nobel lectures are downright scientific lectures, interspersed with curves, synoptic tables and quotations. I am somewhat reluctant to give here such a lecture on something that can be looked up in any modern schoolbook on physics. I will therefore not so much report here on physical and technical details and their connections but rather on human experiences—some joyful events and many disappointments which had not been spared me and my colleagues on our way to the final breakthrough. This is not meant to be a complaint though; I rather feel that such experiences of scientists in quest of new approaches are absolutely understandable, or even normal.

In such a representation I must, of course, consider the influence of my environment, in particular of my family. There have already been some scientists in my family: My father, *Julius Ruska*, was a historian of sciences in Heidelberg and Berlin; my uncle, *Max Wolf*, astronomer in Heidelberg; his assistant, a former pupil of my father and my godfather, *August Kopff*, Director of the Institute for astronomical calculation of the former Friedrich-Wilhelm University in Berlin. A cousin of my mother, *Alfred Hoche*, was Professor for Psychiatry in Freiburg/Breisgau; my grandfather from my mother's side, *Adalbert Merx*, theologian in Giessen and Heidelberg.

My parents lived in Heidelberg and had seven children. I was the fifth, my brother Helmut the sixth. To him I had particularly close and friendly relations as long as I can remember. Early, optical instruments made a strong impression on us. Several times uncle Max had shown us the telescopes at the observatory under his direction on the Königstuhl near Heidelberg. With the light microscope as well we soon had impressive, yet contradictory, relations. In the second floor of our house, my father had two study rooms connected by a broad sliding door which usually was open. One room he used for his scientific historical studies relating to classical philology, the other for his scientific interests, in particular mineralogy, botany and zoology. When our games with neighbours' kids in front of the house became too noisy, he would knock at the window panes. This usually only having a brief effect, he soon knocked a second time, this time considerably louder. At the third knock, Helmut and I had to come to his room and sit still on a low wooden stool, dos-à-dos, up to one hour at 2 meters distance from his desk. While doing so we would see on a table in the other room the pretty yellowish wooden box that housed my father's big Zeiss microscope, which we were strictly forbidden to touch. He sometimes demonstrated to us interesting objects under the microscope, it is true; for good reasons, however, he feared that childrens' hands would damage the objective or the specimen by clumsy manipulation of the coarse and fine drive.

[*] Prof. Dr. E. Ruska
Fritz-Haber-Institut der Max-Planck-Gesellschaft
Faradayweg 4–6, 1000 Berlin 33

[**] Copyright © The Nobel Foundation 1987.—We thank the Nobel Foundation, Stockholm, for permission to publish this article.

Thus, our first relation to the value of microscopy was not solely positive.

2. School, Vocational Choice

Much more positive was, several years later, the excellent biology instruction my brother had through his teacher *Adolf Leiber* and the very thorough physics teaching I received through my teacher *Karl Reinig*. To my great pleasure I recently read an impressive report on *Reinig*'s personality in the Memoirs of a two-years-older student at my school, the later theoretical physicist *Walter Elsasser*. Even today I remember the profound impression *Reinig*'s comments made upon me when he explained that the movement of electrons in an electrostatic field followed the same laws as the movement of inert mass in gravitational fields. He even tried to explain to us the limitation of microscopical resolution due to the wavelength of light. I certainly did not clearly understand all this then, because soon after that on one of our many walks through the woods around Heidelberg I had a long discussion on that subject with my brother Helmut, who already showed an inclination to medicine, and my classmate *Karl Deissler*, who later studied medicine as well.

In our college (Humanistisches Gymnasium), we had up to 17 hours of Latin, Greek and French per week. In contrast to my father, who was extremely gifted for languages, I produced only very poor results in this field. My father, at that time teacher at the same school, learnt daily about my minus efforts from his colleagues and blamed me for being too lazy—so I had some sorrowful school years. My Greek teacher, a fellow student of my father, had a more realistic view of things: He gave me for my confirmation the book "Hinter Pflug und Schraubstock" (Behind plow and vise) by the Swabian "poet" engineer *Max Eyth* (1836–1906). I had always been fascinated by technical progress; in particular, I was later interested in the development of aeronautics and the construction of airships and airplanes. The impressive book by *Max Eyth* definitely prompted me to study engineering. My father, having studied sciences at the universities of Strassbourg, Berlin and Heidelberg, obviously regarded study at a Technical High School as not being adequate and offered me one physics semester at a university. I had, however, the strong feeling that engineering was more to my liking and refused.

3. The Cathode-Ray Oscillograph and the Short Coil

After I had studied two years electrotechnical engineering in Munich, my father received a call to become head of a newly founded Institute for the History of Sciences in Berlin in 1927. Thus, after my pre-examination in Munich I came to Berlin for the second half of my studies. Here I specialized in high-voltage techniques and electrical plants and heard, among others, the lectures of Professor *Adolf Matthias*. At the end of the summer term in 1928 he told us about his plan of setting up a small group of people to develop from the Braun tube an efficient cathode-ray oscillograph for the measurement of very fast electrical processes in power stations and on open-air high-voltage transmission lines. Perhaps with the memory of my physics school lesson in the back of my head, I immediately volunteered for this task and became the youngest collaborator of the group, which was headed by Dr.-Ing. *Max Knoll*. My first attempts with experimental work had been made in the practical physics course at the Technical High school in Munich under Professor *Jonathan Zenneck*, and now in the group of *Max Knoll*. As a newcomer I was first entrusted with some vacuum-technical problems which were important to all of us. Through the personality of *Max Knoll*, there was a companionable relationship in the group, and at our communal afternoon coffee with him the scientific day-to-day problems of each member of the group were openly discussed. As I did not dislike calculations, and our common aim was the development of cathode-ray oscillographs for a desired measuring capability, I wanted to devise a suitable method of dimensioning such cathode-ray oscillographs in my "Studienarbeit"—a prerequisite for being allowed to proceed to the Diploma examination.

The most important parameters for accuracy of measurement and writing speed of cathode-ray oscillographs are the diameter of the writing spot and its energy density. To produce small and bright writing spots, the electron beams emerging divergently from the cathode had to be concentrated in a small writing spot on the fluorescent screen of the cathode-ray oscillograph. For this, already *Rankin* in 1905[1] used a short dc-fed coil, as had been used by earlier experimentalists with electron beams (formerly called "glow" or "cathode rays"). Even before that, *Hittorf* (1869) and *Birkeland* (1896) used the rotationally symmetric field lying in front of a cylindrical magnet pole for focussing cathode rays. A more precise idea of the effect of the axially symmetric, i.e. inhomogeneous magnet field of such poles or coils on the electron bundle alongside of their axes had long been unclear.

Therefore, *Hans Busch*[3] at Jena calculated the electron trajectories in such an electron ray bundle and found that the magnetic field of the short coil has the same effect on the electron bundle as has the convex glass lens with a defined focal length on a light bundle. The focal length of this "magnetic electron lens" can be changed continuously by means of the coil current. *Busch* wanted to check experimentally his theory, but for reasons of time he could not carry out new experiments. He made use of the experimental results he had already obtained sixteen years previously in Göttingen. These were, however, in extremely unsatisfactory agreement with the theory. Perhaps this was the reason that *Busch* did not draw at least the practical conclusion from his lens theory to image some object with such a coil.

In order to account more precisely for the properties of the writing spot of a cathode-ray oscillograph produced by the short coil, I checked *Busch*'s lens theory with a simple experimental arrangement under better, yet sill inadequate, experimental conditions (Fig. 1) and thereby found a better but still not entirely satisfactory agreement of the imaging scale with *Busch*'s theoretical expectations. The main

reason was that I had used a coil of the dimensions of *Busch*'s coil whose field distribution along the axis was much too wide. My Studienarbeit,[4] submitted to the Faculty for Electrotechnical Engineering in 1929, contained numerous sharp images with different magnifications of an electron-irradiated anode aperture of 0.3 mm diameter which had been taken by means of the short coil ("magnetic electron lens")—i.e. the first recorded electron-optical images.

Busch's equation for the focal length of the magnetic field of a short coil implied that a desired focal length could be produced by the fewer Ampere turns the more the coil field was limited to a short region alongside the axis,

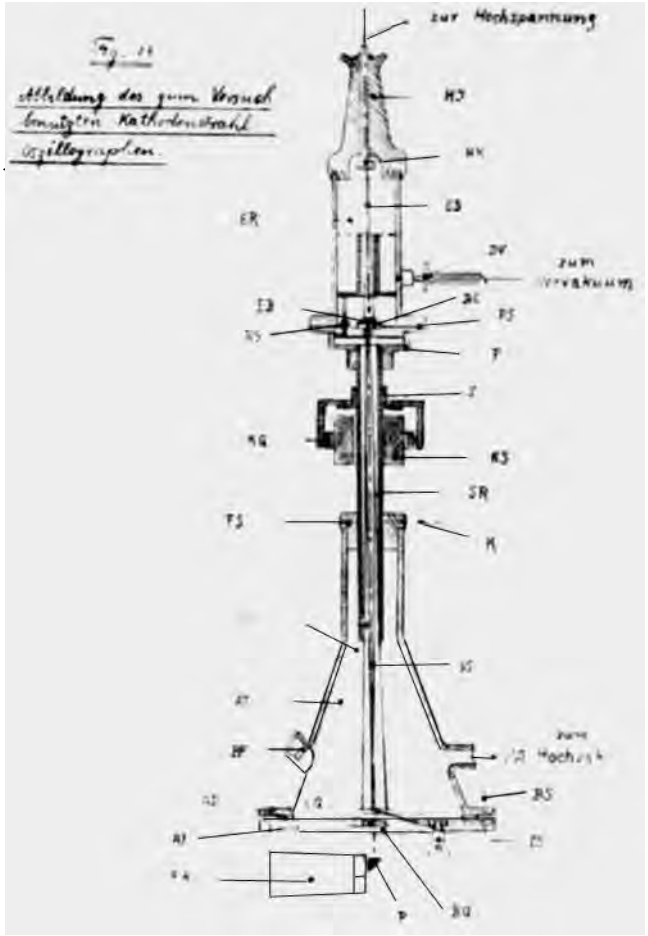

Fig. 1. Sketch by the author (1929) of the cathode ray tube for testing the imaging properties of the non-uniform magnetic field of a short coil [4, 5].

because in that case the field maximum is increased. It was therefore logical for me as a prospective electrotechnical engineer to suitably envelop the coil with an iron coating, with a ring-shaped gap in the inner tube. Measurements at such a coil immediately showed that the same focal length had been reached with markedly fewer Ampere turns.[4, 5] Vice versa, in this manner a shorter focal length can, of course, also be obtained by an equal number of Ampere turns.

4. Why I Pursued the Magnetic Electron Lens for the Electron Microscope

In my Diploma Thesis (1930) I was to search for an electrostatic replacement for the magnetic concentration of the divergent electron ray bundle, which would probably be easier and cheaper. To this end, *Knoll* suggested experimental investigation of an arrangement of hole electrodes with different electrical potential for which he had taken out a patent a year before.[6] We discussed the shape of the electric field between these electrodes, and I suggested that because of the mirror-like symmetry of the electrostatic field of the electrodes on either side of the lens center, a concentrating effect of the curved equipotential planes in the hole area could not take place. I only had the field geometry in mind then. But this conclusion was wrong. I overlooked that as a consequence of the considerably varying electron velocity on passage through such a field arrangement, a concentration of the divergent electron bundle must, in fact, occur. *Knoll* did not notice this error either. Therefore I pursued another approach in my Diploma Thesis.[7] I made the electron bundle pass through a bored-out spherical condenser with fine-meshed spherically shaped grids fixed over each end of the bore. With this arrangement I obtained laterally inverted images in the correct imaging scale. Somewhat later I found a solution which was unfortunately only theoretically correct. In analogy to the refraction of light rays at the surfaces ("Grenzflächen") on passage through optical lenses, I wanted to use, for the electrical lens, the potential steps at corresponding surfaces, which are shaped like glass lenses[8]. Thus, the energy of the electron beams is temporarily changed - just like light beams on passage through optical lenses. For the realization of this idea, on each side of the lens two closely neighbored fine-meshed grids of the shape of optical lenses are required which must be kept at electrical potentials different from each other. First attempts confirmed the rightness of this idea, but at the same time also the practical inaptness of such grid lenses because of the too-strong an absorption of the electron beam at the four grids and due to the field distribution by the wires. As a consequence of my false reasoning and the experimental disappointment I decided to continue with the magnetic lens. I only report this in so much detail to show that occasionally it can be more a matter of luck than of superior intellectual vigor to find a better—or perhaps the only acceptable way. The approach of the transmission electron microscope with electron lenses of electrostatic hole electrodes was later pursued by outstanding experimentalists in other places and led to considerable initial success. It had to be abandoned, however, because the electrostatic lens was, for physical reasons, inferior to the magnetic electron lens.

5. The Invention of the Electron Microscope

After obtaining my Degree (early 1931), the economic situation had become very difficult in Germany and it seemed impossible to find a satisfactory position at a University or in industry. Therefore I was glad that I could at

least continue my unpaid position as doctorand in the high-voltage institute. After having shown in my Studienarbeit of 1929 that sharp and magnified images of electron-irradiated hole apertures could be obtained with the short coil, I was now interested in finding out if such images—as in light optics—could be further magnified by arranging a second imaging stage behind the first stage. Such an apparatus with two short coils was easily put together (Fig. 2) and in April 1931 I obtained the definite proof that it was possible (Fig. 3). This apparatus is justifiably regarded today as the first electron microscope, even though its total magnification of about $3.6 \times 4.8 = 17.4$ was extremely modest.

The first proof had thus been given that—apart from light and glass lenses—images of irradiated specimens could be obtained also by electron beams and magnetic fields, and this in even more than one imaging stage. But what was the use of such images if even grids of platinum or molybdenum were burnt to cinders at the irradiation level needed for a magnification of only $17\times$? Not wishing to be accused of showmanship, *Max Knoll* and I agreed to avoid the term electron microscope in the lecture *Knoll* gave in June 1931 on the progress in the construction of cathode-ray oscillographs where he also, for the first time, described in detail my electron-optical investigations.[9, 10] But, of course, our thoughts were circling around a more efficient microscopy. The resolution limit of the light microscope due to the length of the light wave which had been recognized 50 years before by *Ernst Abbe* and others could not be important at such magnifications, since light was not used. *Knoll* and I simply hoped for extremely low dimensions for the electrons. As engineers we did not yet know about the thesis on the "material wave" by the French physicist de Broglie[11] that had been put forward several years earlier (1925). Even physicists only reluctantly accepted this new thesis. When I first heard of it in summer 1931, I was very much disappointed that the resolution should now be limited again by a wavelength (of the "Materiestrahlung") even in the case of the electron microscope. I was immediately heartened, though, when with the aid of the de Broglie equation I became satisfied that these waves must be around five orders of magnitude shorter in length than light waves. Thus, there was no reason to abandon the aim of electron microscopy surpassing the resolution of light microscopy.

In 1932 *Knoll* and I dared to make a prognosis of the resolution limit of the electron microscope.[12] Assuming that the equation for the resolution limit of the light microscope is valid also for the material wave of the electrons, we replaced the wavelength of the light by the wavelength of electrons at an accelerating voltage of 75 kV and inserted into the Abbe relation the imaging aperture of 2×10^{-2} rad which is what we had used previously. This imaging aperture is still used today. Thereby, even at that early date we came up with a resolution limit of $2.2\ \text{Å} = 2.2 \times 10^{-10}$ m, a value that was in fact obtained experimentally 40 years later.

Of course, at that time our approach was not taken seriously by most of the experts. They rather regarded it as a pipe-dream. I myself felt that it would be very hard to overcome the efforts still needed—mainly for solving the problem of specimen heating. In April 1932, *M. Knoll* had taken up a position with Telefunken (Berlin) involving developmental work in the field of television.

In contrast to many biologists and medical scientists, my brother Helmut, who had almost completed his medical

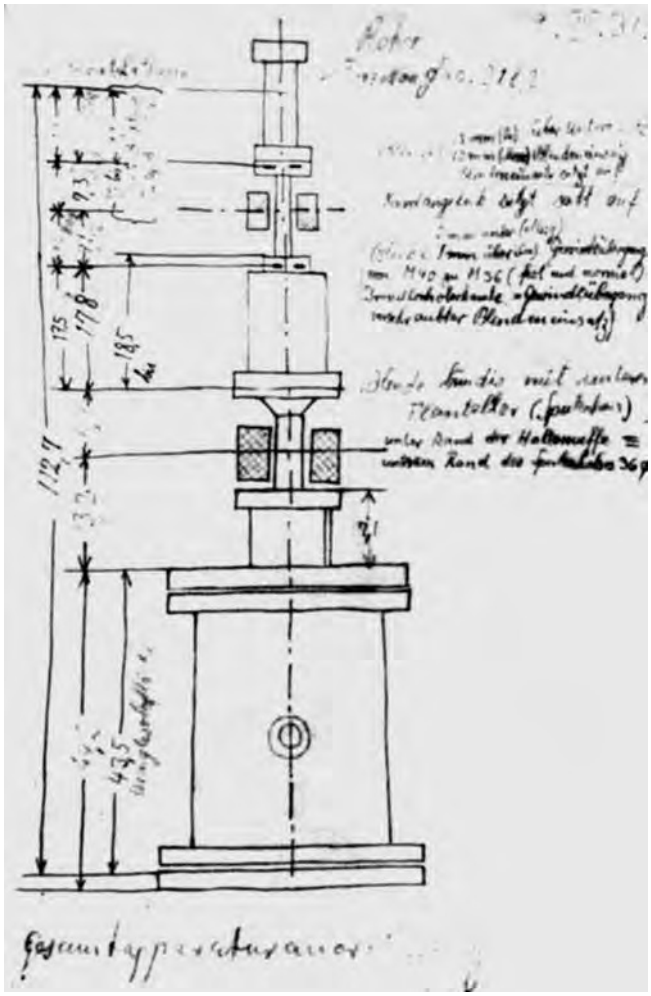

Fig. 2. Sketch by the author (March 9, 1931) of the cathode-ray tube for testing one-stage and two-stage electron-optical imaging by means of two magnetic electron lenses (electron microscope) [8].

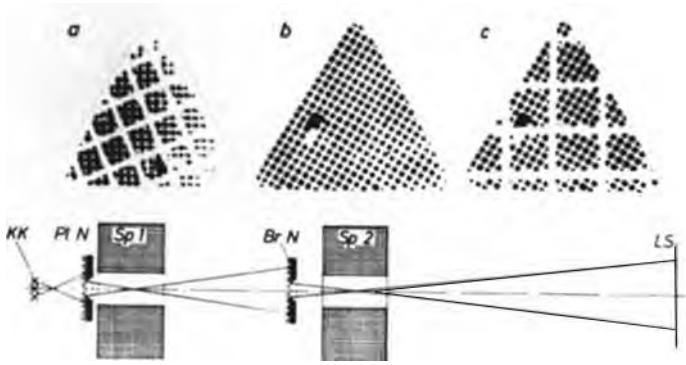

Fig. 3. First experimental proof (April 7, 1931) that specimens (aperture grids) irradiated by electrons can be imaged in magnified form not only in one but also in more than one stage by means of (magnetic) electron lenses ($U = 50$ kV) [8]. a) One-stage image of the platinum grid in front of coil 1 by coil 1; $M_{el} = 13:1$. b) One-stage image of the bronze grid in front of coil 2 by coil 2; $M_{el} = 4.8:1$. c) Two-stage image of the platinum grid in front of coil 1 and coil 2; $M_{el} = 17.4:1$ together with the one-stage image of the bronze grid in front of coil 2; $M_{el} = 4.8:1$; kk: cold cathode; Pt N: platinum grid; Sp. 1: coil 1; Br N: bronze grid; Sp 2: coil 2; LS: fluorescent screen.

studies, foresaw considerable progress in these disciplines should we be successful. With his confidence in a successful outcome he encouraged me to overcome the expected difficulties. In a next step I had to show that it was possible to obtain sufficiently high magnifications to prove a better-than-light-microscope resolution. To this effect a coil shape had to be developed whose magnetic field was compressed to a length that small in relation to the coil axis so as to allow short focal lengths as are needed for highly magnified images at not too great a distance behind the coil. The technical solution for this I had already given in my Studienarbeit of 1929 with the iron-clad coil. In 1932 I applied—together with my friend and co-doctorand *Bodo von Borries*—for a patent on the optimization of this solution,[13] the "Polschuhlinse", which is used in all magnetic electron microscopes today. Its realization and the measuring of the focal lengths which could be verified with it were the subject of my thesis.[14] It was completed in August 1933, and in my measurements I obtained focal lengths of 3 mm for electron rays of 75 kV acceleration (Fig. 4).

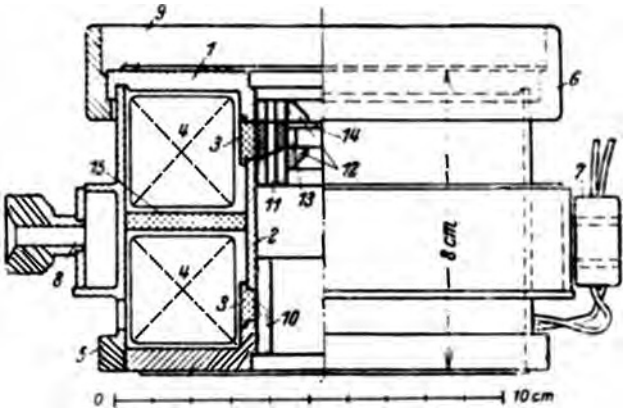

Fig. 4. Cross-section of the first polepiece lens [14, 15].

Of course, with these lenses I now immediately wanted to design a second electron microscope with much higher resolving power. To carry out this task I obtained, through the good offices of *Max von Laue*, a stipend of 100 Reichsmarks per month for the second half year of 1933 from the Notgemeinschaft der Deutschen Wissenschaft to defray running costs and personal expenses. Since I had completed the new instrument by the end of November (Fig. 5), I felt I ought to return my payment for December. To my great joy, however, I was allowed to keep the money "as an exception". Nevertheless, this certainly was the cheapest electron microscope ever paid for by a German Organization for the Promotion of Science.

For the reasons given at the beginning of the next chapter, I accepted a position in industry on December 1, 1933. Therefore I could only make a few images with this instrument which magnified 12000 × [15], but I noticed a decisive fact which gave me hope for the future: Even very thin specimens yielded sufficient contrast, yet no longer by absorption but solely by diffraction of the electrons, whereby—as is known—the specimens are heated up considerably less.

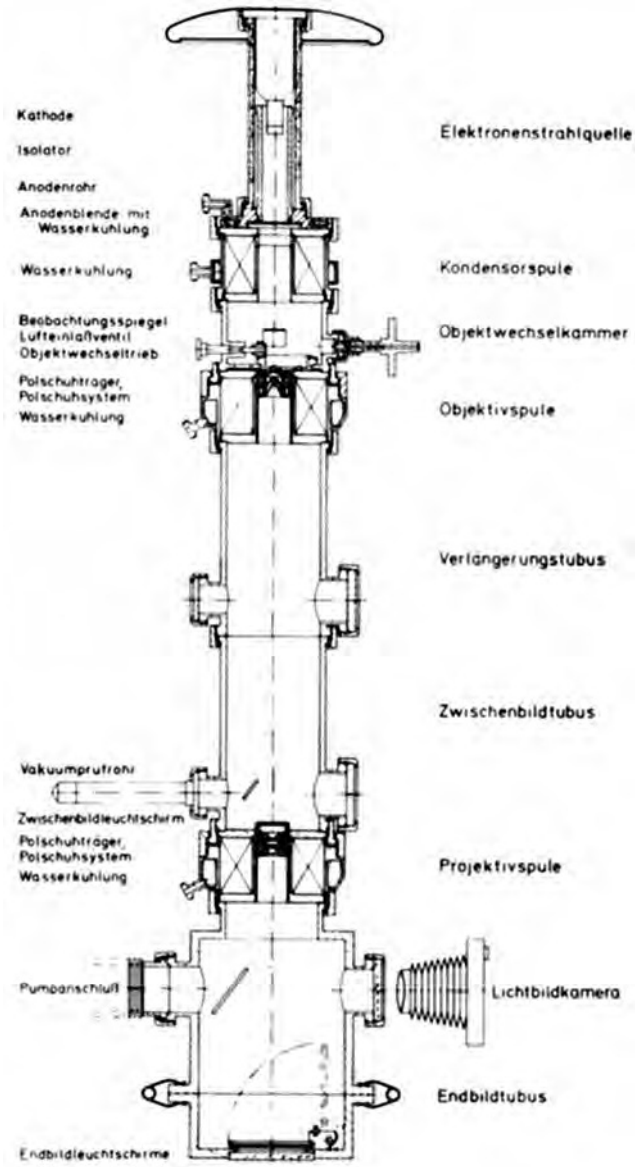

Fig. 5. First (two-stage) electron microscope magnifying higher than the light microscope. Cross-section of the microscope column [15] (redrawn 1976).

6. How the Industrial Production of Electron Microscopes Materialized

I also realized, however, that the further development of a practically useful instrument with better resolution would require a longer period of time and enormous costs. In view of the results achieved there was little hope of obtaining financial support from any side for the time being. I was prepared for a longer dry spell and decided to approach the goal of a commercial instrument later, together with *Bodo von Borries* and my brother Helmut. Therefore, I accepted a position with the Fernseh AG in Berlin-Zehlendorf where I was engaged in the development of Braun tubes for image pick-up and display tubes. In order to better coordinate our efforts to obtain financial support for the production of commercial electron microscopes, I con-

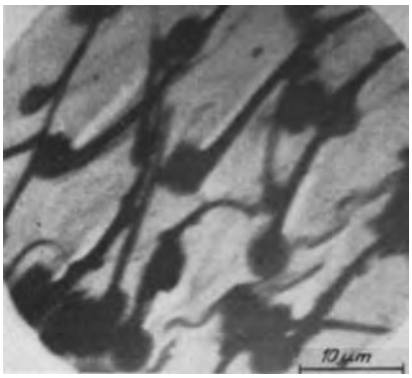

Fig. 6. Wing surface of the house fly. (First internal photography, $U = 60$ kV, $M_{el} = 2200\times$) (E. Driest, H. O. Müller: *Z. Wiss. Mikrosk. Mikrosk. Tech. 52* (1936) 53–57).

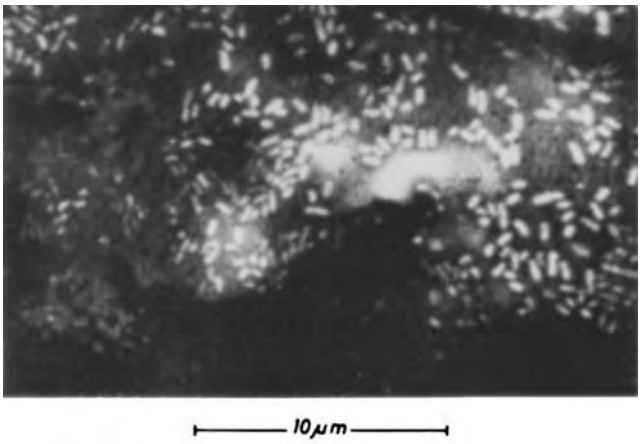

Fig. 8. Bacteria (culture infusion), fixed with formalin and embedded in a supporting film stained with a heavy metal salt ($U = 73.5$ kV, $M_{el} = 2000\times$) (F. Krause: *Naturwissenschaften 25* (1937) 817–825).

Fig. 7. Diatoms *Amphipleura pellucida* ($U = 53$ kV, $M_{el} = 3500\times$, $\delta'' = 130$ nm) (F. Krause in H. Busch and E. Brüche (Eds.): *Beiträge zur Elektronenoptik*, Johann Ambrosius Barth, Leipzig 1937, p. 55–61.

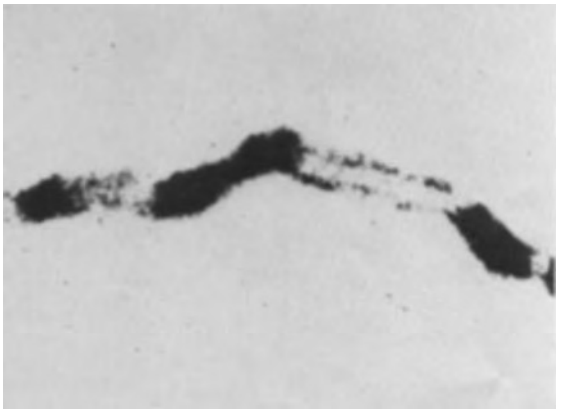

Fig. 9. Iron whisker ($U = 79$ kV, $M_{el} = 3100\times$) (D. Beischer, F. Krause: *Naturwissenschaften 25* (1937) 825–829).

vinced *Bodo von Borries* to give up his position at the Rheinisch-Westfälische Elektrizitätswerke at Essen and return to Berlin. Here, he found a position at Siemens-Schuckert in 1934. We approached many governmental and industrial research facilities for financial help.[16]

During this period, electron micrographs of biological specimens first appeared. *Heinz Otto Müller* (student in electrotechnical engineering) and *Friedrich Krause* (medical student) worked at the instrument I had built in 1933, and they published increasingly better results (Figs. 6 to 9). Unfortunately these two very gifted young scientists did not survive World War II.

At the University of Brussels *Ladislaus Marton* had built his first horizontal microscope and obtained relatively low magnifications of biological specimens.[17] In 1936 he built a second instrument, this time with a vertical column.[18]

In spite of these more recent publications, it took us three years to be successful in our quest for financial support through the professional assessment of *Helmut Ruska*'s former "clinical" teacher, Professor Dr. *Richard Siebeck*, Director of the I. Medical Clinic of the Berlin Charité. I quote two paragraphs of his assessment of October 2, 1936:[19]

"If these things were to be realized it hardly needs to be emphasised that the advances in the field of research into the causes of disease would be of immediate practical interest to the doctor. It would deeply affect real problems concerned to a large extent with diseases of growing clinical significance and thus of great importance for public health.

Should the possibilities of microscopical resolution exceed the assumed values by a factor of a hundred, the scientific consequences would be incalculable. What seems attainable now, I consider to be so important, and success seems to me so close that I am ready and willing to advise on medical research work and to collaborate by making available the resources of my Institute."

This expertise impressed Siemens in Berlin and Carl Zeiss in Jena, and they were both ready to further the development of industrial electron microscopes. We suggested the setting up of a common development facility in order to make use of the electrotechnical expertise of

Siemens and the know-how in precision engineering of Zeiss, but unfortunately the suggestion was refused and so we decided in favor of Siemens. As first collaborators we secured *Heinz Otto Müller* for the practical development and *Walter Glaser* from Prague as theorist. We started in 1937, and in 1938 we had completed two prototypes with condenser and polepieces for objective and projective as well as airlocks for specimens and photoplates. The maximum magnification was 30000×.[20] One of these instruments was immediately used for first biological investigations by *Helmut Ruska* and several medical collaborators. (*H. Ruska* was released from Professor *Siebeck* for our work at Siemens.) Unfortunately, for reasons of time I cannot give here a survey of this fruitful publication period.

In 1940, upon our proposal Siemens set up a guest laboratory, headed by *Helmut Ruska*, with four electron microscopes for visiting scientists. *Helmut Ruska* was able to show the first images of bacteriophages in 1940. An image taken somewhat later (Fig. 10) clearly shows the shape of these tiny hostile bacteria. This laboratory was destroyed during an air raid in the autumn of 1944.

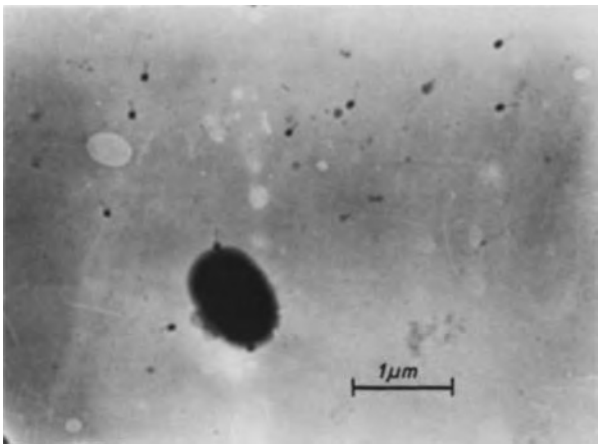

Fig. 10. Bacteriophages (M_{el} = 10000×) (H. Ruska: *Naturwissenschaften 29* (1941) 367-368 and *Arch. Ges. Virusforschung 2* (1942) 345-387).

Very gradually, interest in electron microscopy was now growing. A first sales success for Siemens was achieved in 1938 when the chemical industry which was represented largely by IG Farbenindustrie placed orders for an instrument in each of their works in Hoechst, Leverkusen Bitterfeld, and Wolfen. The instrument, however, was still only at the planning stage at the time, and not yet built or even tested. By the end of 1939 the first serially produced Siemens instrument[21] had been delivered to Hoechst (Fig. 11). The instrument No. 26 was, by the way, delivered to Professor *Arne Tiselius* in Uppsala in autumn 1943. By February 1945 more than 30 electron microscopes had been built in Berlin and delivered. Thus, now also independent representatives of various medical and biological disciplines could form their own opinions about the future prospects of electron microscopy. The choice of specimens was still limited though, since sufficiently thin sections were not yet available. The end of the war terminated the close cooperation with my brother and *Bodo von Borries*.

Fig. 11. The first serially produced electron microscope (Siemens). General view [21].

7. Development of Electron Microscopy after 1945

Our laboratory had to be reconstructed completely. I could start working with mainly new co-workers as early as June 1945. In spite of difficult conditions in Berlin and Germany, newly developed electron microscopes[22] could be delivered by the end of 1949. In 1954 Siemens had regained its former leading position with the "Elmiskop"[23] (Fig. 12). This instrument had, for the first time, two condenser lenses allowing thermal protection of the specimen by irradiating only the small region that is required for the desired final magnification. Since now, for a final magnification of 100000×, a specimen field of only 1 µm must be irradiated for an image of 10 cm diameter (in contrast to earlier irradiation areas of about 1 mm diameter), the power of the electron beam converted into heat in the object can be reduced down to the millionth part. The specimens are heated up just to the extent that the heat power produced can be radiated into the entire region around the object. If the heat power is low, a lower temperature rise with respect to the environment results.

The new instrument was, however, a big disappointment at first when we realized that at this "small region radiation" the image of the specimen field, which was now no longer hot, became so dark within seconds that all initially visible details disappeared. Investigations then showed that minor residual gases in the evacuated instrument, par-

ticularly hydrocarbons, condensed on the cold inner surfaces of the instrument, i.e. they now even condensed on the specimen itself. The image of the resulting carbon layer in the irradiated specimen field becomes darker with increasing thickness of the layer. Happily, also this hurdle could, after some time, be surmounted by relatively simple means: The entire environment of the specimen was cooled by liquid air so that the specimen was still markedly warmer than its environment, even without being heated by the beam. Thus, the residual gases of hydrocarbons condensed on the low-cooled surfaces and no longer on the specimen.

Along with the successful solution of this problem, another difficulty, that of specimen thickness, had also surprisingly been overcome by newly developed "ultramicrotomes". Instead of the ground steel knives whose blades were not sufficiently smooth due to crystallization, glass fracture edges were used which had no crystalline unevenness. The usual mechanical translation of the material perpendicular to the knife is—because of mechanical backlash or even oil layers—not sufficiently precise for the desired very small displacements of ca. 10^{-5} mm. Smallest displacements free of flaws were obtained by thermal extension of a rod at whose ends the specimen to be cut was fastened. In order to keep the extremely thin sections smooth, they were dropped into an alcoholic solution immediately after being cut so that they remained entirely flat. Moreover, more suitable fixing agents had been found for the new cutting techniques. The development of these new ultramicrotomes considerably reduced the limitation in the choice of specimens for electron microscopy. For 25 years now, almost all disciplines furthered by light microscopy have also been able to benefit from electron microscopy.

During the last decades, electron microscopy has been advanced in many countries by numerous leading scientists and engineers through new ideas and procedures. I can here only give a few examples: Figure 13 shows a cross-section through an electron microscope with single-field condenser objective, the specimen being in the field maximum of a magnetic polepiece lens.[24] Thereby, the region of increasing magnetic field in front of the specimen behaves like a condenser of short focal length and the decreasing field region behind the specimen as an objective of equal focal length. With this arrangement both lenses have a particularly small spherical aberration. Figure 14 gives an overall view of the same instrument. Figure 15

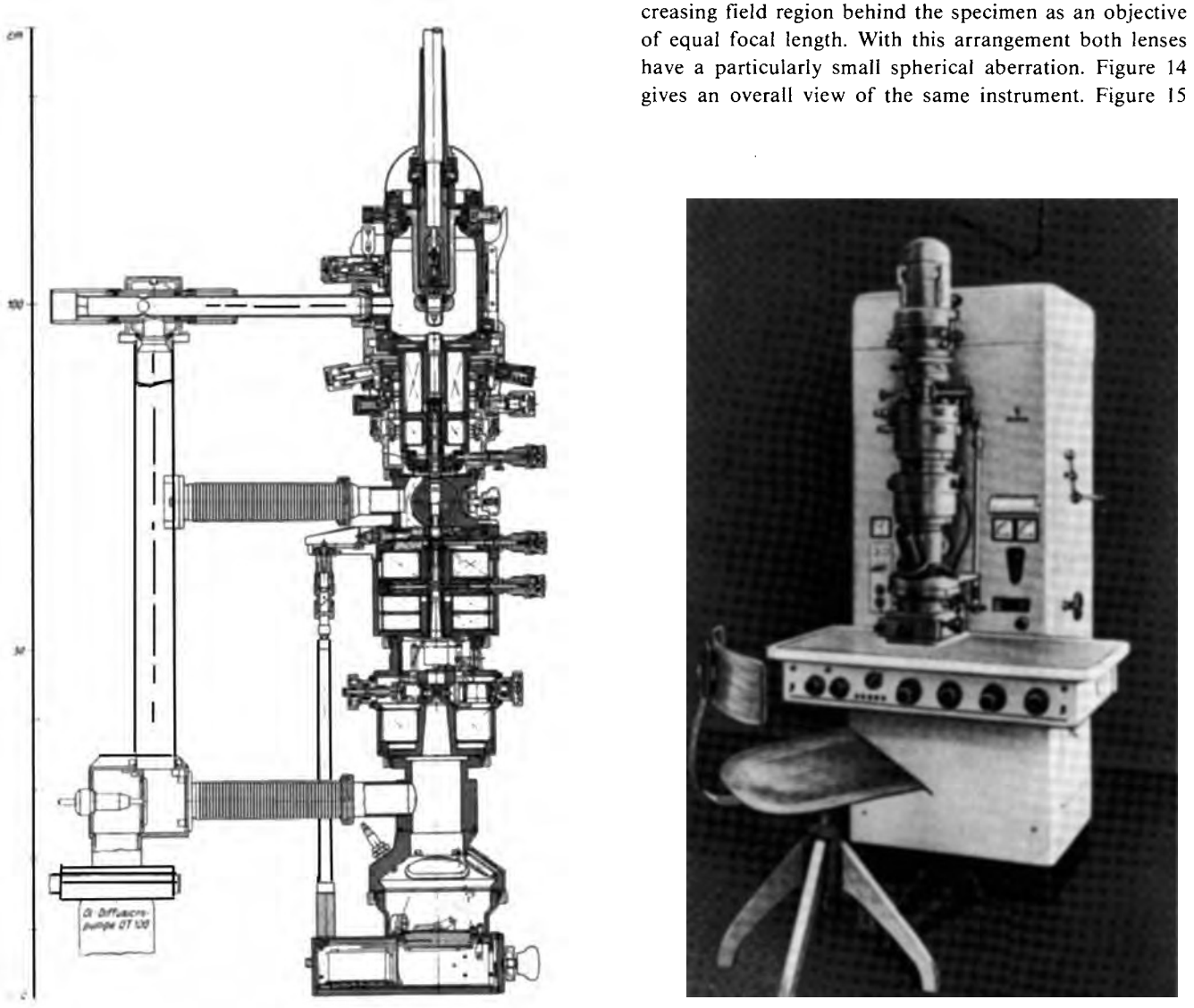

Fig. 12. The first serially produced 100 kV-Electron microscope with two condenser lenses for "small region radiation" (Siemens). Left: cross-section; right: general view [23].

shows an image obtained with this instrument of a platelet of a gold crystal. One can clearly see lattice planes separated by a distance of 1.4 Å. Two such instruments have

ments, whose development was mainly promoted by Gaston Dupouy (1900–1985), apart from extremely high costs, special problems occur in the stabilization of the accelera-

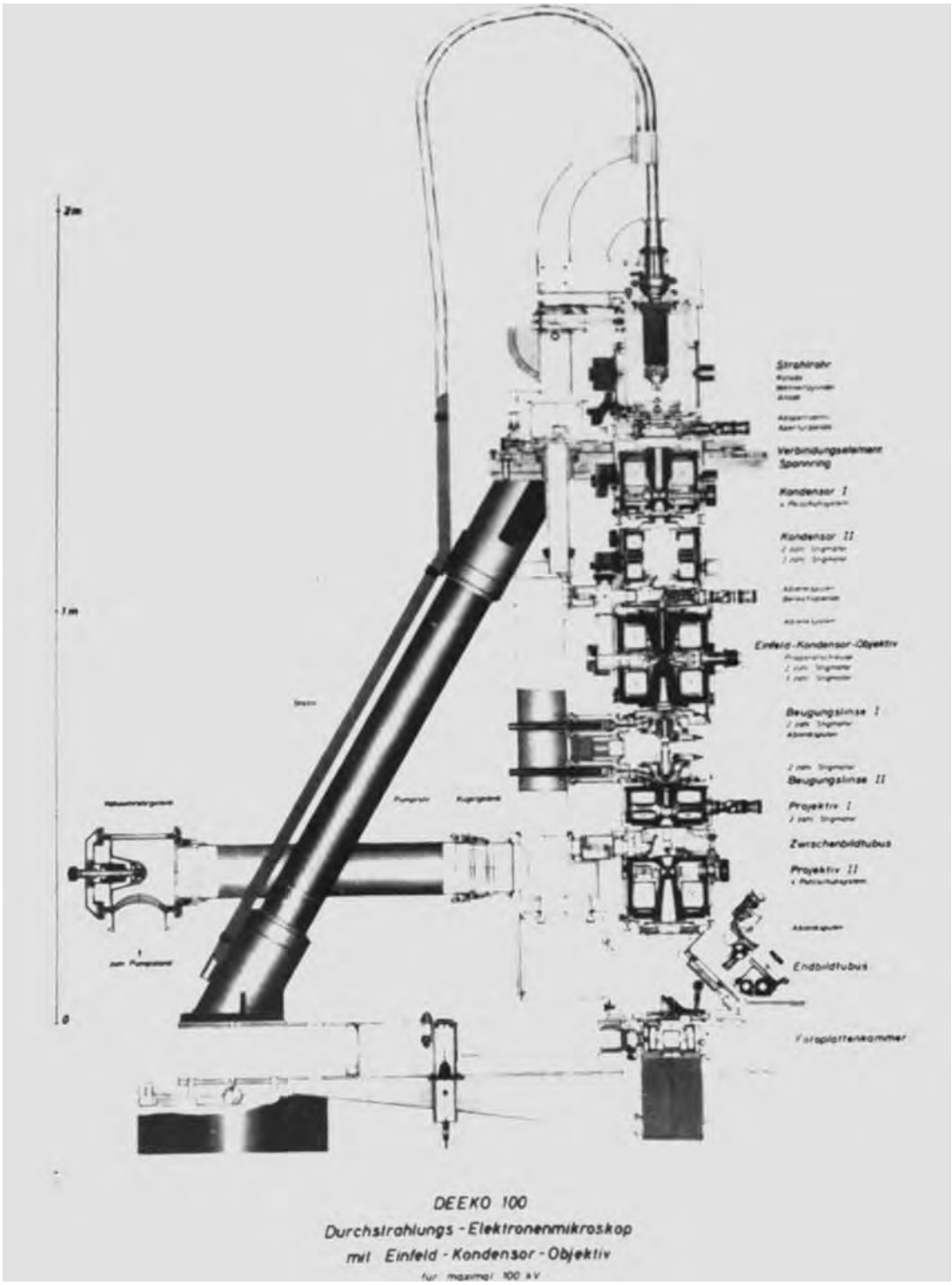

Fig. 13. 100 kV-Electron microscope with single-field condenser objective (cross-section) [24].

been further developed in the Institute for Electron Microscopy, which had been set up for me in 1957 by the Max-Planck-Gesellschaft after I had left Siemens. Figure 16 shows a 1 MV high-voltage instrument developed by Japan Electron Optics Laboratory Co. Ltd. With such instru-

tion voltage and with the protection of the operators against X-rays. The aim of the development of these instruments was the investigation of thicker specimens, but now that the problem of stabilizing the high voltages has been overcome, also the resolution has been improved by

Fig. 14. General view of the instrument shown in cross-section in Figure 13 [24].

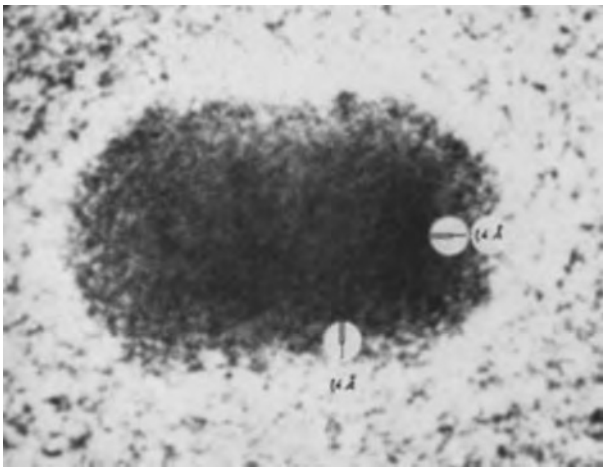

Fig. 15. Plate-like gold crystal, lattice planes with a separation of 0.14 nm, taken with axial illumination ($U = 100$ kV, $M_{el} = 800000\times$); taken in 1976 by *K. Weiss* and *F. Zemlin* with the 100-kV transmission electron microscope with single-field condenser objective at the Fritz-Haber-Institut of the Max-Planck-Gesellschaft.

the shorter material wavelength of particularly highly accelerated electrons, so that thinner specimens can also be investigated. For quite some time now, the cryotechnique—put forward mainly by *Fernandez-Moran* in the USA—has been of increasing importance. With this technique specimens cooled down to very low temperatures can be studied, because they are more resistant to higher electron doses, i.e. the mobility inside the specimen is very much reduced compared to that at room temperature. Thus, even after unavoidable ionization, the molecules keep their structure for a longer time. In the last few years it has been possible to image very beam-sensitive crystals with a resolution of 2.5 Å in a cryomicroscope[25,26] (Fig.

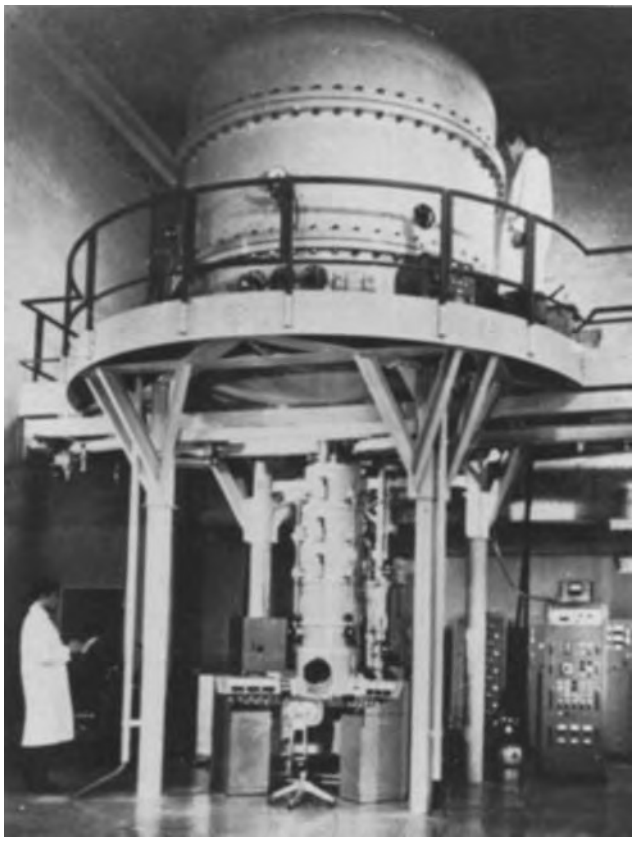

Fig. 16. 1 MV Electron Microscope (Japan Electron Optics Laboratory Co. Ltd.).

17).[27] The specimens were cooled down to a temperature of -269 °C. Direct imaging with sufficient contrast is not possible because the specimen is destroyed at the beam dose needed for normal exposure. Therefore, many very low-dose images are recorded and averaged. Such a single

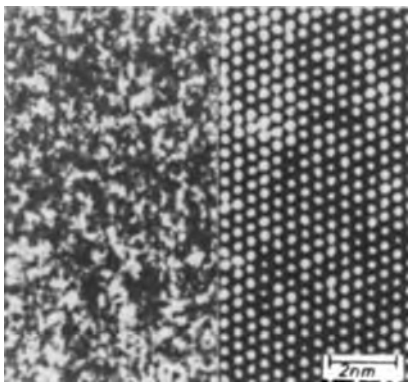

Fig. 17. Paraffin crystal (left: image taken with minimum dose, right: superposition of 400 sub-regions of the left image by means of the computer [25].

image is very noisy but still contains sufficient periodical information. The evaluation procedure is as follows: First, the micrograph is digitized using the densitometer so that each image point is given a number which describes the optical density. The underexposed image of the whole crystal is divided like a checker-board by the computer and then a large number—in our case 400—of these

image sub-regions is cross-correlated and summed up by the computer. The resulting image corresponds to a sufficiently exposed micrograph. On the left in Figure 17 the initial noisy image of a paraffin crystal is seen; the right side shows the averaged image. Each white point is the image of a paraffin molecule. The long paraffin molecules $C_{44}H_{90}$ are vertical to the image plane. With this procedure electron micrographical images can be processed by the computer. It is even possible to image three-dimensional protein crystals with very high resolution. The computer is a powerful tool in modern electron microscopy.

I cannot go into detail concerning the transmission electron microscopes with electrostatic lenses, the scanning electron microscopes which are widely used mainly for the study of surfaces as well as transparent specimens, the great importance of various image processing methods carried out partly by the computer, the field-electron microscope and the ion microscope.

The development of the electron microscopes of today was mainly a battle against the undesired consequences of the same properties of electron rays which paved the way for sub-light-microscopical resolution. Thus, for instance, the short material wavelength—prerequisite for good resolution—is coupled with the undesired high electron energy which causes specimen damage. The deflectability in the magnetic field, a precondition for lens imaging, can also limit the resolution if the alternating magnetic fields in the environment of the microscope are not sufficiently shielded by the electron microscope. We should not, therefore, blame those scientists today who did not believe in electron microscopy at its beginning. It is a miracle that by now the difficulties have been solved to such an extent that so many scientific disciplines today can reap its benefits.

Received: March 5, 1987 [A 626 IE]
German version: *Angew. Chem. 99* (1987) 611

[1] R. Rankin: The cathode ray oscillograph. *Elec. Club J. 2* (1905) 620-631.

[2] W. Hittorf: Über die Elektrizitätsleitung der Gase, I. und II. (On the electrical conductivity of gases.) *Ann. Phys. Chem. 16* (1869) 1-31 and 197-234 (Münster, October 9, 1868).

[3] H. Busch: Über die Wirkungsweise der Konzentrierungsspule bei der Braunschen Röhre. (On the mode of action of the concentrating coil in the Braun tube.) *Arch. Elektrotech. 18* (1927) 583-594 (Jena, Physikalisches Institut, March 1927).

[4] E. Ruska: Über eine Berechnungsmethode des Kathodenstrahloszillographen auf Grund der experimentell gefundenen Abhängigkeit des Schreibfleckdurchmessers von der Stellung der Konzentrierspule. (A method for designing a cathode ray oscillograph on the basis of the experimentally found dependence of the writing spot diameter on the position of the concentrating coil.) Carried out from November 1, 1928 in the High-Voltage Laboratory of the Technische Hochschule Berlin (Director Prof. *A. Matthias*). Student Project Thesis (117 pp.; submitted May 10, 1929).

[5] E. Ruska, M. Knoll: Die magnetische Sammelspule für schnelle Elektronenstrahlen. (The magnetic concentrating coil for fast electron beams.) *Z. Tech. Phys. 12* (1931) 389-400 and 448 (submitted April 18, 1931).

[6] M. Knoll: Vorrichtung zur Konzentrierung des Elektronenstrahls eines Kathodenstrahloszillographen. (Device for concentrating the electron beam of a cathode-ray oscillograph.) German Patent No. 690809, patented on November 10, 1929, granted on April 11, 1940.

[7] E. Ruska: Untersuchung elektrostatischer Sammelvorrichtungen als Ersatz der magnetischen Konzentrierspulen bei Kathodenstrahl-Oszillographen. (Investigation of electrostatic concentrating devices as a substitute for the magnetic concentrating coils in cathode-ray oscillographs.) Begun on July 18, 1930 in the High Voltage Laboratory of the Technological University of Berlin (Direktor Prof. Dr. *A. Matthias*) and submitted on December 23, 1930 as a Diploma Project (pp. 1-90).

[8] M. Knoll, E. Ruska: Beitrag zur geometrischen Elektronenoptik I und II. (Contribution to geometrical electron optics) *Ann Phys. 12* (1932) 607-640 and 641-661, submitted September 10, 1931.

[9] M. Knoll: Berechnungsgrundlagen und neuere Ausführungsformen des Kathodenstrahloszillographen. (The basic principles of design and new forms of construction of the cathode-ray oscillograph.) Manuscript of a lecture in the Cranz-Colloquium at the Technological University of Berlin on June 4, 1931, pp. 1-26.

[10] E. Ruska: *The Early Development of Electron Lenses and Electron Microscopy*, S. Hirzel Verlag, Stuttgart 1980, see pp. 113-116.

[11] L. de Broglie: Recherches sur la théorie des quanta. (Researches on the theory of quanta.) Dissertation. Masson & Cie, Paris 1924. *Ann. Phys. 3* (1925) 22-128.

[12] M. Knoll, E. Ruska: Das Elektronenmikroskop. (The electron microscope.) *Z. Phys. 78* (1932) 318-339 (submitted June 16, 1932).

[13] B. von Borries, E. Ruska: Magnetische Sammellinse kurzer Feldlänge. (Magnetic converging lens of short field length.) German Patent No. 680284, patented on March 17, 1932; Patent granted on August 3, 1939.

[14] E. Ruska: Über ein magnetisches Objektiv für das Elektronenmikroskop. (On a magnetic objective lens for the electron microscope.) Dissertation, Technological University of Berlin, submitted August 31, 1933. *Z. Phys. 89* (1934) 90-128 (submitted March 5, 1934).

[15] E. Ruska: Über Fortschritte im Bau und in der Leistung des magnetischen Elektronenmikroskops. (On progress in the construction and performance of the magnetic electron microscope.) *Z. Phys. 87* (1934) 580-602 (submitted December 12, 1933).

[16] See [10], pp. 120-122.

[17] L. Marton: La microscope électronique des objects biologiques. (Electron microscopy of biological objects.) *Acad. R. Belg. Bull. Cl. Sci., Ser. 5, 20* (1934) 439-446 (Université libre de Bruxells, May 1934).

[18] L. Marton: Le microscope électronique. (The electron microscope.) *Rev. Microbiol. Appl. Agric. Hyg. Ind. 2* (1936) 117-124.

[19] See [10], pp. 123-124.

[20] B. von Borries, E. Ruska: Vorläufige Mitteilung über Fortschritte im Bau und in der Leistung des Übermikroskops. (Preliminary communication on advances in the construction and performance of the ultramicroscope.) *Wiss. Veröff. Siemens-Werken 17* (1938) 99-106 (submitted February 29, 1938).

[21] B. von Borries, E. Ruska: Ein Übermikroskop für Forschungsinstitute. (An ultramicroscope for industrial research.) *Naturwissenschaften 27* (1939) 577-582 (submitted June 24, 1939).

[22] E. Ruska: Über neue magnetische Durchstrahlungs-Elektronenmikroskope im Strahlspannungsbereich von 40...220 kV, Teil I. (On new magnetic transmission-electron microscopes for beam voltages between 40 and 220 kV.) *Kolloid-Z. 116* (1950) 103-120 (submitted December 15, 1949).

[23] E. Ruska, O. Wolff: Ein hochauflösendes 100-kV-Elektronenmikroskop mit Kleinfelddurchstrahlung (A high-resolution transmission electron microscope (100 kV) with small-area illumination.) *Z. Wiss. Mikrosk. mikrosk. Tech. 62* (1956) 466-509 (submitted July 19, 1955).

[24] W. D. Riecke, E. Ruska: A 100 kV transmission electron microscope with single-field condenser objective. *VI. Int. Congr. Electron Microsc.*, Kyoto, Japan, Abstracts Vol. I (1966) pp. 19-20.

[25] F. Zemlin, E. Reuber, B. Beckmann, E. Zeitler, D. L. Dorset: Molecular Resolution Electron Micrographs of Monolamellar Paraffin Crystals. *Science 229* (1985) 461-462.

[26] I. Dietrich, F. Fox, E. Knapek, G. Lefranc, K. Nachtrieb, R. Weyl, H. Zerbst: Improvements in electron microscopy by application of superconductivity, *Ultramicroscopy 2* (1971) 241-249.

[27] R. Henderson, P. N. T. Unwin: Three-dimensional model of purple membrane obtained by electron microscopy, *Nature 257* (1975) 28-32.

Scanning Tunneling Microscopy—from Birth to Adolescence (Nobel Lecture)**

By Gerd Binnig* and Heinrich Rohrer*

We present here the historic development of scanning tunneling microscopy (STM); the physical and technical aspects have already been covered in a few recent reviews and two conference proceedings[1] and many others are expected to follow in the near future. A technical summary is given by the sequence of figures which stands alone. Our narrative is by no means a recommendation of how research should be done; it simply reflects what we thought, how we acted, and what we felt. However, it would certainly be gratifying if it encouraged a more relaxed attitude towards doing science.

Perhaps we were fortunate in having common training in superconductivity, a field which radiates beauty and elegance. For scanning tunneling microscopy, we brought along some experience in tunneling[2] and angstroms,[3] but none in microscopy or surface science. This probably gave us the courage and light-heartedness to start something which should "not have worked in principle" as we were so often told.

"After having worked a couple of years in the area of phase transitions and critical phenomena, and many, many years with magnetic fields, I [*H.R.*] was ready for a change. Tunneling, in one form or another, had intrigued me for quite some time. Years back, I had become interested in an idea of *John Slonczewski* to read magnetic bubbles with tunneling; on another occasion, I had been involved for a short time with tunneling between very small metallic grains in bistable resistors, and later I watched my colleagues struggle with tolerance problems in the fabrication of Josephson junctions. So the local study of growth and electrical properties of thin insulating layers appeared to me an interesting problem, and I was given the opportunity to hire a new research staff member, *Gerd Binnig*, who found it interesting, too, and accepted the offer. Incidentally, *Gerd* and I would have missed each other, had it not been for *K. Alex Müller*, then head of Physics, who made the first contacts."[1a]

The original idea then was not to build a microscope but rather to perform spectroscopy locally on an area less than 100 Å in diameter.

"On a house-hunting expedition, three months before my [*G. B.*] actual start at IBM, *Heini Rohrer* discussed with me in more detail his thoughts on inhomogeneities on surfaces, especially those of thin oxide layers grown on metal surfaces. Our discussion revolved around the idea of how to study these films locally, but we realized that an appropriate tool was lacking. We were also puzzling over whether arranging tunneling contacts in a specific manner would give more insight on the subject. As a result of that discussion, and quite out of the blue at the LT15 Conference in Grenoble—still some weeks before I actually started at IBM—an old dream of mine stirred at the back of my mind, namely, that of vacuum tunneling. I did not learn until several years later that I had shared this dream with many other scientists, who, like myself, were working on tunneling spectroscopy. Strangely enough, none of us had ever talked about it, although the idea was old in principle." Actually, it was 20 years old, dating back to the very beginning of tunneling spectroscopy.[4] Apparently, it had mostly remained an idea and only shortly after we had started, did *Seymour Keller*, then a member of the IBM Research Division's Technical Review Board and an early advocate of tunneling as a new research area in our laboratory, draw our attention to *W. A. Thompson*'s attempting vacuum tunneling with a positionable tip.[5]

We became very excited about this experimental challenge and the opening up of new possibilities. Astonishingly, it took us a couple of weeks to realize that not only would we have a local spectroscopic probe, but that scanning would deliver spectroscopic and even topographic images, i.e., a new type of microscope. The operating mode mostly resembled that of stylus profilometry,[6] but instead of scanning a tip in mechanical contact over a surface, a small gap of a few angstroms between tip and sample is maintained and controlled by the tunnel current flowing between them. Roughly two years later and shortly before getting our first images, we learned about a paper by *R. Young* et al.[7] where they described a type of field-emission microscope they called a "topografiner." It had much in common with our basic principle of operating the scanning tunneling microscope (STM), except that the tip had to be rather far away from the surface, thus, on high voltage, producing a field-emission current rather than a tunneling current and resulting in a lateral resolution roughly that of an optical microscope. They suggested to improve the resolution by using sharper field-emission tips, even attempted vacuum tunneling, and discussed some of its exciting prospects in spectroscopy. Had they, even if only in their minds, combined vacuum tunneling with scanning, and estimated *that* resolution, they would probably have ended up with the new concept, scanning tunneling microscopy. They came closer than anyone else.

In mid-January 1979, we submitted our first patent disclosure on the STM. *Eric Courtens*, then deputy manager of physics at the IBM Rüschlikon Laboratory, pushed the disclosure to a patent application with "thousands of future STM's." He was the first believer in our cause. Shortly afterwards, following an in-house seminar on our STM ideas, *Hans-Jörg Scheel* became the third.

[*] Dr. G. Binnig, Dr. H. Rohrer
IBM Research Division
Zurich Research Laboratory
Säumerstrasse 4, CH-8803 Rüschlikon (Switzerland)

[**] Copyright © The Nobel Foundation 1987.—We thank the Nobel Foundation, Stockholm, for permission to print this article.

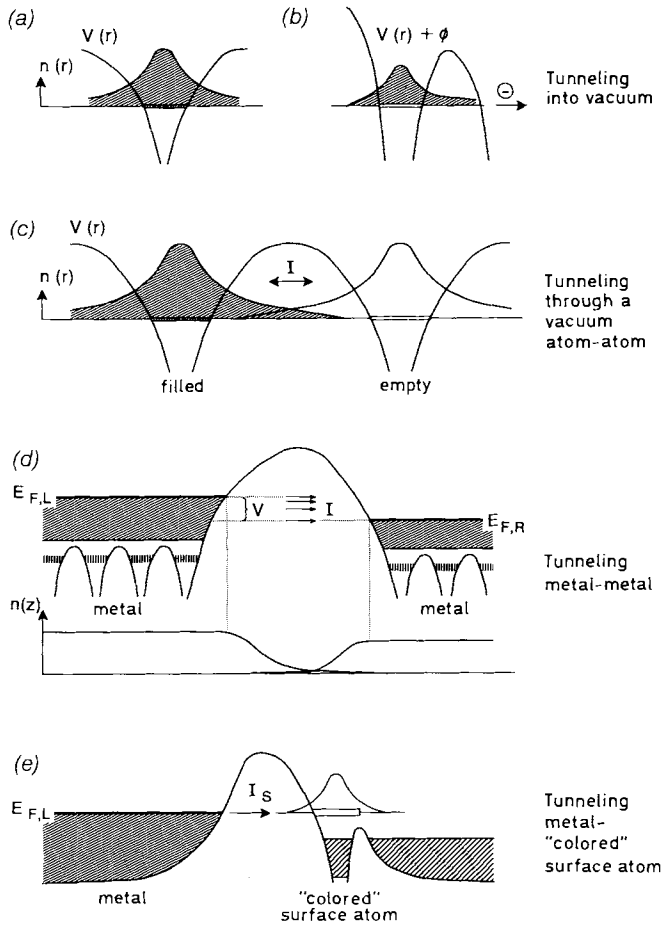

Fig. 1. Tunneling. (a) The wave function of a valence electron in the Coulomb potential well of the atom core plus other valence electrons extends into the vacuum; it "tunnels" into the vacuum. (b) Exposed to an electric field, the electron can tunnel through the potential barrier and leaves the atom. (c) If two atoms come sufficiently close, then an electron can tunnel back and forth through the vacuum or potential barrier between them. (d) In a metal, the potential barriers between the atoms in the interior are quenched and electrons move freely in energy bands, the conduction bands. At the surface, however, the potential rises on the vacuum side forming the tunnel barrier through which an electron can tunnel to the surface atom of another metal close by. The voltage V applied between the two metals produces a difference between the Fermi levels $E_{F,L}$ and $E_{F,R}$, thus providing empty states on the right for the electrons tunneling from the left side. The resulting tunnel current is roughly of the form $I = f(V) \cdot \exp(-\sqrt{\phi} \cdot s)$. $f(V)$ contains a weighted joint local density of states of tip and object; the exponential gives the transmittivity with ϕ the averaged tunnel barrier height in eV and s the separation of the two metals in Å. $f(V)$ and $\sqrt{\phi}$ are material properties obtained by measuring $d \ln I / d V$ and $d \ln I / d s$. (e) A simple case of local spectroscopy. A characteristic state, the "color," of a surface species is observed by the onset of the tunnel-current contribution I_s [see N. D. Lang, *Phys. Rev. Lett.* *58* (1987) 45, and references cited therein].

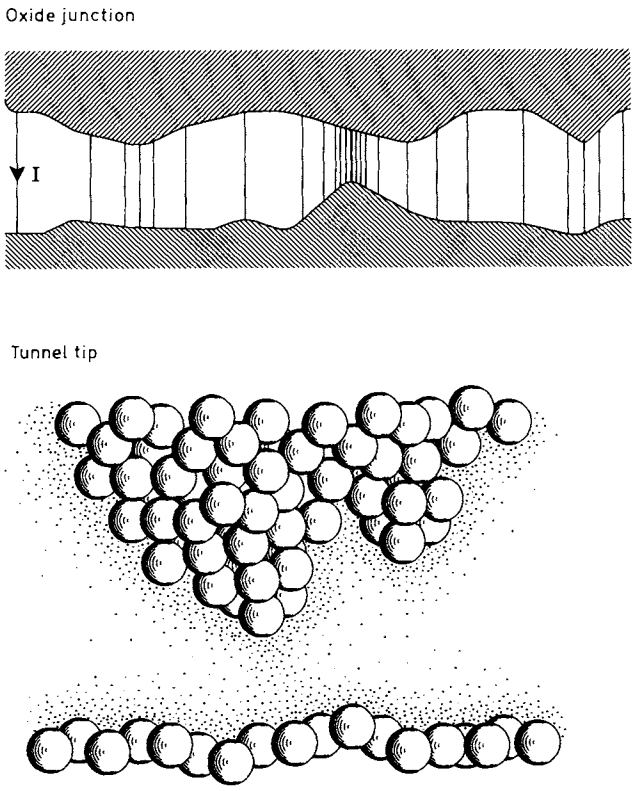

Fig. 2. The principle. The tunneling transmittivity decreases exponentially with the tunneling distance, in vacuum about a factor 10 for every Å. In an oxide tunnel junction, most of the current flows through narrow channels of small electrode separation. With one electrode shaped into a tip, the current flows practically only from the front atoms of the tip, in the best case from a specific orbital of the apex atom. This gives a tunnel current filament width and thus a lateral resolution of atomic dimensions. The second tip shown is recessed by about two atoms and carries about a million times less current.

For the technical realization of our project, we were fortunate in securing the craftsmanship of *Christoph Gerber*. "Since his joining IBM in 1966, *Christoph* had worked with me [*H. R.*] on pulsed high-magnetic fields, on phase diagrams, and on critical phenomena. By the end of 1978, we were quite excited about our first experimental results on the random-field problem, but when asked to participate in the new venture, *Christoph* did not hesitate an instant. He always liked things which were out of the ordinary, and, incidentally, was the second believer. This left me and the random-field problem without his diligent technical support. About a year later, *Edi Weibel* was the next one to join in, which left another project without technical support. Finally, I completed the team, leaving the random-field problem to others."

During the first few months of our work on the STM, we concentrated on the main instrumental problems and their solutions.[8] How to avoid mechanical vibrations that move tip and sample against each other? Protection against vibrations and acoustical noise by soft suspension of the microscope within a vacuum chamber. How strong are the forces between tip and sample? This seemed to be no problem in most cases. How to move a tip on such a fine scale? With piezoelectric material, the link between electronics and mechanics, avoiding friction. The continuous deformation of piezomaterial in the angstrom and subangstrom range was established only later by the tunneling experiments themselves. How to move the sample on a fine scale over long distances from the position of surface treatment to within reach of the tip? The "louse." How to avoid strong thermally excited length fluctuations of the sample and especially the tip? Avoid whiskers with small spring constants. This led to a more general question, and the most important one: What should be the shape of the tip and how to achieve it? At the very beginning, we viewed the tip as a kind of continuous matter with some radius of curvature. However, we very soon realized that a tip is never smooth, because of the finite size of atoms and be-

cause tips are quite rough unless treated in a special way. This roughness implies the existence of minitips as we called them, and the extreme sensitivity of the tunnel current on tip-sample separation then selects the minitip reaching closest to the sample.

Immediately after having obtained the first stable STM images showing remarkably sharp monoatomic steps, we focused our attention onto atomic resolution. Our hopes of achieving this goal were raised by the fact that vacuum tunneling itself provides a new tool for fabricating extremely sharp tips: The very local, high fields obtainable with vacuum tunneling at only a few volts can be used to shape the tip by field migration or by field evaporation. Gently touching the surface is another possibility. All this is not such a controlled procedure as tip sharpening in field-ion microscopy, but it appeared to us to be too complicated to combine STM with field-ion microscopy at this stage. We hardly knew what field-ion microscopy was, to say nothing of working with it. We had no means of controlling exactly the detailed shape of the tip. We repeated

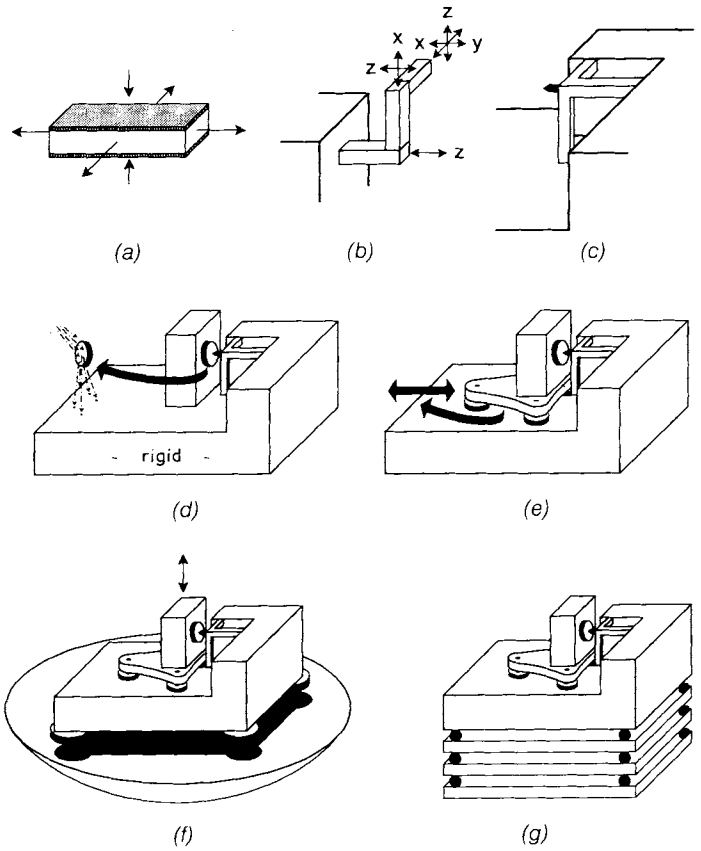

Fig. 3. The instrument. (a) A voltage applied to two electrodes contracts or expands the piezoelectric material in between. The practical total excursion of a piezo is usually in the region of micrometers. (b) A frictionless x-y-z piezodrive, which is quite vibration sensitive. (c) A rigid tripod is at present the piezodrive most used apart from the single-tube scanner. (d) Tripod and sample holder are installed on a rigid frame. The sample has to be cleared from the tip for preparation and sample transfer. (e) Positioning of the sample to within reach of the piezodrive was originally achieved with a piezoelectric "louse" with electrostatically clampable feet. Magnetic-driven positioners and differential screws are also now in use. (f) In the first vibration-isolation system, the tunnel unit with permanent magnets levitated on a superconducting lead bowl. (g) The simple and presently widely used vibration protection with a stack of metal plates separated by viton—a UHV-compatible rubber spacer.

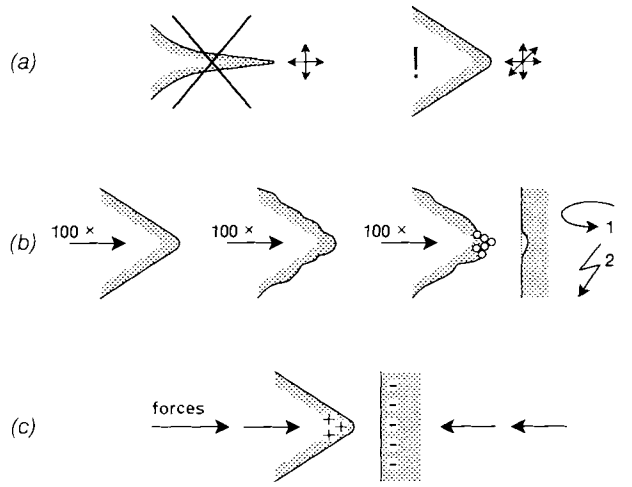

Fig. 4. Tips. (a) Long and narrow tips, or whiskers, are vibration-sensitive and thermally excited. (b) A mechanically ground or etched tip shows sharp minitips, only one of which usually carries the tunnel current. Further sharpening was initially achieved with gentle contact (1), later with field evaporation (2). (c) Electrostatic and interatomic forces between tip and sample do not deform a blunt tip, or a rigid sample, but they make the tunnel gap mechanically unstable when the tip carries a whisker. The response of soft sample materials like graphite or organic matter to such forces, however, can be appreciable and has to be taken into account.

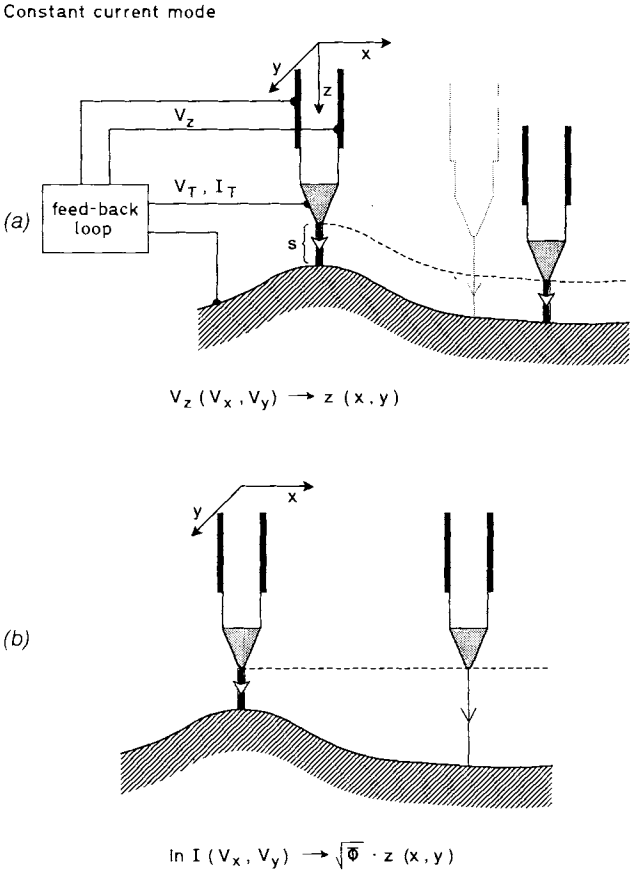

Fig. 5. Imaging. (a) In the constant current mode, the tip is scanned across the surface at constant tunnel current, maintained at a preset value by continuously adjusting the vertical tip position with the feedback voltage V_z. In the case of an electronically homogeneous surface, constant current essentially means constant s. (b) On surface portions with denivellations less than a few Å—corresponding to the dynamic range of the current measurement—the tip can be rapidly scanned at constant average z-position. Such "current images" allow much faster scanning than in (a) but require a separate determination of $\sqrt{\varphi}$ to calibrate z. In both cases, the tunnel voltage and/or the z-position can be modulated to obtain in addition, $d \ln I/dV$ and/or $d \ln I/ds$, respectively.

our trial and error procedures until the structures we observed became sharper and sharper. Sometimes it worked, other times it did not.

But first we had to demonstrate vacuum tunneling. In this endeavor, apart from the occurrence of whiskers, the most severe problem was building vibrations. To protect the STM unit also against acoustical noise, we installed the vibration-isolation system within the vacuum chamber. Our first set-up was designed to work at low temperatures and in ultrahigh vacuum (UHV). Low temperatures guaranteed low thermal drifts and low thermal length fluctuations, but we had opted for them mainly because our thoughts were fixed on spectroscopy. And tunneling spectroscopy was a low-temperature domain for both of us with a Ph.D. education in superconductivity. The UHV would allow preparation and retention of well-defined surfaces. The instrument was beautifully designed with sample and tip accessible for surface treatments and superconducting levitation of the tunneling unit for vibration isolation. Construction and first low-temperature and UHV tests took a year, but the instrument was so complicated, we never used it. We had been too ambitious, and it was only seven years later that the principal problems of a low-temperature and UHV instrument were solved.[9] Instead, we used an exsiccator as vacuum chamber, lots of Scotch tape, and a primitive version of superconducting levitation wasting about 20 L of liquid helium per hour. *Emil Haupt*, our expert glassblower, helped with lots of glassware and, in his enthusiasm, even made the lead bowl for the levitation. Measuring at night and hardly daring to breathe from excitement, but mainly to avoid vibrations, we obtained our first clear-cut exponential dependence of the tunnel current I on tip-sample separation s characteristic for tunneling. It was the portentous night of March 16, 1981.

So, 27 months after its conception the scanning tunneling microscope was born. During this development period, we created and were granted the necessary elbowroom to dream, to explore, and to make and correct mistakes. We did not require extra manpower or funding, and our side activities produced acceptable and publishable results. The first document on STM was the March/April 1981 in-house Activity Report.

A logarithmic dependence of the tunnel current I on tip–sample separation s alone was not yet proof of vacuum tunneling. The slope of $\ln I$ versus s should correspond to a tunnel-barrier height of $\phi \approx 5$ eV, characteristic of the average work functions of tip and sample. We hardly arrived at 1 eV, indicating tunneling through some insulating material rather than through vacuum. Fortunately, the calibration of the piezosensitivity for small and fast voltage changes gave values only half of those quoted by the manufacturers. This yielded a tunnel-barrier height of more than 4 eV and thus established vacuum tunneling. This reduced piezosensitivity was later confirmed by careful calibration with *H. R. Ott* from the ETH Zurich, and by *S. Vieira* of the Universidad Autónoma, Madrid.[10]

U. Poppe had reported vacuum tunneling some months earlier,[11] but his interest was tunneling spectroscopy on exotic superconductors. He was quite successful at that but did not measure $I(s)$. Eighteen months later, we were informed that *E. C. Teague*, in his Ph.D. thesis, had already observed similar $I(s)$ curves which at that time were not commonly available in the open literature.[12]

Our excitement after that March night was quite considerable. *Hirsh Cohen*, then Deputy Director of our laboratory, immediately asked us "What do you need?", a simple and obvious question people only rarely dare to ask. "*Gerd* immediately wanted to submit a post-deadline contribution[13] to the LT16 Conference to be held in Los Angeles in September. He was going there anyway with his superconducting strontium titanate, and I [*H. R.*] was sure we would have some topographic STM images by then. And indeed we had. I arranged an extended colloquium tour through the USA for *Gerd*, but about three weeks before his departure, a friend warned him, that once the news became public, hundreds of scientists would immediately jump onto the STM bandwagon. They did—a couple of years later. After two extended discussions on a weekend hike, he nevertheless became convinced that it was time for the STM to make its public appearance."[13] Our first attempt to publish a letter failed. "That's a good sign," *Nico Garcia*, a Visiting Professor from the Universidad Autónoma de Madrid, consoled us.

After this first important step with a complete STM set-up, it took us only three months, partly spent waiting for the high-voltage power supplies for the piezos, to obtain the first images of monosteps[14] on a $CaIrSn_4$ single crystal grown by *R. Gambino*. Here, the main problem was getting rid of the whiskers we continually created by bumping the tip into the surface. Now we were ready to turn to surface science, first to resolve surface reconstructions. We built a UHV-compatible STM (no longer with Scotch tape!) and, as a quick trial, operated it in vacuum suspended from a rubber band. The results indicated that superconducting levitation might be unnecessary.

That was the state of the art for the publicity tour through the USA in September 1981. Most reactions were benevolent, some enthusiastic, and two even anticipated the Nobel prize, but the STM was apparently still too exotic for any active outside engagement.

Next, we protected the STM from vibrations by a double-stage spring system with eddy-current damping,[8] and incorporated it in a UHV chamber not in use at that moment. We added sputtering and annealing for sample treatment, but no other surface tool to characterize and monitor the state of the sample or tip could yet be combined with that STM. Although the superconducting levitation served for three months only, it was cited for years. It would appear that something complicated is much easier to remember!

A most intriguing and challenging surface-science problem existed, namely, the 7×7 reconstruction of the Si(111) surface. A class of fashionable models contained rather rough features which should be resolvable by the STM. So we started to chase after the 7×7 structure, and succumbed to its magic. At first, with no success. The STM would function well, sometimes with resolutions clearly around 5 Å, but not our surface preparation. We occasionally found quite nice patterns with monolayer step lines[8] but usually the surface always looked rough and disordered on an atomic scale. One image even foreshadowed the 7×7 by a regular pattern of depressions, the precursors of the characteristic corner holes. However, a single event

is too risky to make a case for a new structure obtained with a new method. But it boosted our confidence.

By spring 1982, STM was already a subject talked about. Supposedly, an image of a vicinal surface expertly prepared with a regular step sequence would have eased the somewhat reserved attitude of the surface-science community. We, however, thought that the mono-, double-, and triple-steps of the $CaIrSn_4$ with atomically flat terraces[14] and the step lines of Si(111)[8] were convincing and promising enough. And instead of wasting further time on uninteresting step lines, we preferred to attack surface reconstructions with known periodicities and with a reasonable chance of learning and contributing something new.

For easier sample preparation and because the demand on resolution was only 8 Å, we changed to a gold single crystal, namely, the (110) surface known to produce a 1×2 reconstruction. This seemed to be well within reach of the STM resolution from what we had learned from the silicon step lines. Although some time earlier, we had returned to *Karl-Heinz Rieder*, the Laboratory's surface-science expert, his Si single crystal in a kind of droplet form, it did not deter him from proposing this gold experiment which meant lending us his Au crystal, and some weeks later we added another droplet to his collection! But in between, with his advice on surface preparation, we succeeded in resolving the 1×2 structure.[15] Contrary to expectations, we also had to struggle with resolution, because Au transferred from the surface even if we only touched it gently with our tip. The mobility of Au at room temperature is so high that rough surfaces smooth out after a while, i.e., really sharp Au-coated tips cease to exist. We should like to mention here that later, for measurements on Au(100), we formed sharp Au tips by field evaporation of Au atoms from sample to tip, and could stabilize them by a relatively high field resulting from a 0.8-V tunnel voltage.

In the case of the Au(110) surface, the atomic resolution was rather a matter of good luck and perseverance. It jumped from high to low in an unpredictable manner, which was probably caused by migrating adatoms on the tip finding a stable position at the apex for a while. We also observed an appreciable disorder leading to long but narrow ribbons of the 1×2 reconstruction mixed with ribbons of 1×3 and 1×4 reconstructions and step lines. Nevertheless, these experiments were the first STM images showing atomic rows with atomic resolution perpendicular to the rows. The disorder, intrinsic on this surface, but in its extent criticized from the surface-science point of view, demonstrated very nicely the power of STM as a local method and about a year later played an important role in testing the first microscopic theories of scanning tunneling microscopy.

With gold, we also performed the first spectroscopy experiment with an STM. We wanted to test a prediction regarding the rectifying I-V characteristic of a sample-tip tunnel junction induced by the geometric asymmetry.[16] Unfortunately, the sample surface became unstable at around 5 V, the sample being positive, and the small asymmetry observed in this voltage range could also have been due to other reasons. But with reversed polarity, the voltage could be swept up to 20 V, producing a whole series of marked resonant surface states.[8] We consider the gold exercise during spring and early summer of 1982 a most important step in the development of the method, and the STM had already exceeded our initial expectations. We had also won our first believers outside the Laboratory, *Cal Quate* from Stanford University[17] and *Paul Hansma* from the University of California at Santa Barbara.[18] We gave numerous talks on the Au work, and it attracted some attention, but, all in all, there was little action. We did not even take the time to write a paper—the 7×7 was waiting!

Meanwhile, we had also made the first attempts at chemical imaging: small Au islands on silicon. The islands were visible as smooth, flat hills on a rough surface in the topography, but they were also clearly recognizable as regions with enhanced tunnel-barrier height.[8] Thus, the Au islands were imaged thanks to their different surface electronic properties. It would certainly have been interesting to pursue this line, but we knew that, in principle, it worked—and the 7×7 was still waiting!

We started the second 7×7 attempt in autumn 1982 taking into consideration the advice of *Franz Himpsel* not to sputter the surface. This immediately worked and we observed the 7×7 wherever the surface was flat. We were absolutely enchanted by the beauty of the pattern.

"I [*G.B.*] could not stop looking at the images. It was like entering a new world. This appeared to me as the unsurpassable highlight of my scientific career and therefore in a way its end. *Heini* realized my mood and whisked me away for some days to St. Antönien, a charming village high up in the Swiss mountains, where we wrote the paper on the 7×7."

We returned convinced that this would attract the attention of our colleagues, even of those not involved with surface science. We helped by presenting both an unprocessed relief model assembled from the original recorder traces with scissors, Plexiglass, and nails, and a processed top view; the former for credibility, the latter for analysis and discussion.[19] It certainly did help, with the result that we practically stopped doing research for a while. We were inundated with requests for talks, and innumerable visitors to our Laboratory were curious to know how to build an STM. However, the number of groups that seriously got started remained small. It seemed there was still a conflict between the very appealing, conceptual easiness of displaying individual atoms in three-dimensional real space direct by recorder traces, and the intuitive reservation that, after all, it just could not be that simple.

Our result excluded all the numerous models that existed and, strangely enough, also some that followed. Only one came very close: The adatom model by *W. Harrison*[20] with just the number of adatoms not quite right. Nowadays, a variation of the adatom model where deeper layers are also reconstructed besides the characteristic 7×7 adatom pattern[21] is generally accepted and compatible with most results obtained by various experimental methods like ion channeling,[22] transmission electron diffraction,[23] and more detailed STM results from other groups.[24]

The 7×7 experiments also accelerated the first theoretical efforts of STM on a microscopic level. *Tersoff* and *Hamman* as well as *Baratoff*[25] applied *Bardeen*'s transfer Hamiltonian formalism to the small geometries of tip and

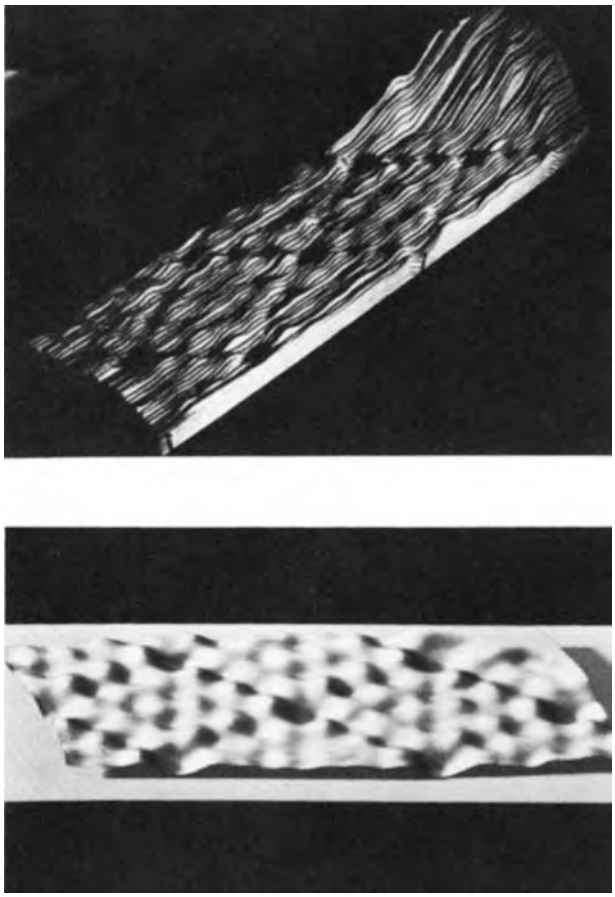

Fig. 6. 7 × 7 reconstruction of Si(111). (a) Relief assembled from the original recorder traces (from Ref. [19], © 1983 The American Physical Society) and (b) processed image of the 7 × 7 reconstruction of Si(111). Characteristic of the rhombohedral surface unit cell are the corner hole and the 12 maxima, the adatoms. In the processed image, the six adatoms in the right half of the rhombi appear higher. This is an electronic inequivalence on the surface owing to a structural left-right inequivalence in the underlying layers. The reconstruction extends undisturbed to the immediate vicinity of the large "atom hill" on the right.

an atomically corrugated surface. *Garcia, Ocal,* and *Flores* as well as *Stoll, Baratoff, Selloni,* and *Carnevali* worked out a scattering approach.[26] The two approaches converged; they consoled us by roughly confirming our intuitive view on tunneling in small geometries by simply scaling down planar tunneling, and they certainly improved the acceptance of STM in physics circles. The theoretical treatments concentrated on the nonplanar aspect of tunneling of free electrons, and the STM results on Au(110), still unpublished, served as a testing ground. They remained unpublished for quite some time, since the flashy images of the 7 × 7 silicon surface somehow overshadowed the earlier Au(110) experiments. One reaction to the first attempt to publish them was: "... The paper is virtually devoid of conceptual discussion let alone conceptual novelty ... I am interested in the behaviour of the surface structure of gold and the other metals in the paper. Why should I be excited about the results in this paper? ..." It was certainly bad publication management on our part, but we were not sufficiently familiar with a type of refereeing which searches for weak points, innocently ignoring the essence.

The gold and silicon experiments showed that STM in surface science would benefit greatly from additional, in-situ surface characterization, in particular low-energy electron diffraction (LEED). We had already learned that surfaces, even elaborately prepared, were frequently not as uniform and flat as generally assumed. The in-situ combination of LEED with STM proved extremely helpful, avoiding searching when there was nothing to be searched, and it gave us the opportunity to learn about and work with LEED and Auger electron spectroscopy (AES). The combination of STM with other established surface-science techniques also settled a concern frequently mentioned: How much did our STM images really have in common with surfaces characterized otherwise? We did not share this concern to such a degree, as we had also learned that reconstructions extended unchanged to the immediate vicinity of defect areas, and because we could detect most contaminants or defects individually. Thus, for us, the combined instrumentation was more a practical than a scientific issue.

After a short but interesting excursion with the new STM/LEED/AES combination into resolving and understanding the (100) surface of Au,[27] we proceeded into the realms of chemistry. Together with *A. Baró*, a Visiting Professor from Universidad Autónoma de Madrid, who also wanted to familiarize himself with the technique, we observed the oxygen-induced 2 × 1 reconstruction of Ni(110),[28] interpreting the pronounced and regularly arranged protrusions we saw as individual oxygen atoms. We had seen atomic-scale features before, which could be interpreted as adsorbates or adsorbate clusters, but they were more a nuisance than a matter of interest. The oxygen on Ni experiments demonstrated that the oxygen overlayer was not irreversibly changed by the imaging tunnel tip. This was a most significant result in regard to observing, studying, and performing surface chemistry with an STM tip. About a year later, when studying the oxygen-induced 2 × 2 reconstructed Ni(100) surface, we observed characteristic current spikes, which we could attribute to oxygen diffusing along the surface underneath the tip.[29] We noted that the same type of spikes had already been present in our earlier images of oxygen-covered Ni(110), but had been discarded at that time. Not only could diffusing atoms be observed individually, but their migration could be correlated to specific surface features like step lines or bound oxygen atoms, imaged simultaneously. Towards the end of 1983, we also started to probe the possibilities of STM in biology together with *H. Gross* from the ETH Zurich. We could follow DNA chains lying on a carbon film deposited on a Ag-coated Si wafer.[30]

That year ended with a most pleasant surprise: On Friday, December 9, we received a telegram from the secretary of the King Faisal Foundation, followed on Monday by a phone call from the secretary of the European Physical Society announcing the King Faisal Prize of Science and the Hewlett Packard Europhysics Prize, respectively. "The day the telegram arrived, *Gerd* was in Berlin delivering the Otto Klung Prize lecture. It was also my twentieth anniversary with IBM." This was an encouraging sign that scanning tunneling microscopy was going to make it. It also brought a new flood of requests.

In the summer of 1984, we were finally ready to assume what we had set out to do in autumn 1978, before the notion of microscopy had ever evolved, namely, performing local spectroscopy. Together with *H. Fuchs* and *F. Salvan*, we investigated the clean 7×7[1,31] and the $\sqrt{3}\times\sqrt{3}$ Au reconstructions on Si(111),[31] and—right back to the heart of the matter—a thin oxide film on Ni.[1,32] We could see that surfaces are electronically structured, as known, for example, from photoemission experiments, and that we could resolve these electronic structures in space on an atomic scale. We called this (and still do) the color of the atoms. Indeed, the oxide layers were inhomogeneous and most clearly visible in scanning tunneling spectroscopy (STS) images. On the 7×7, we could see by STS down to the second layer and observe individual dangling bonds between the adatoms.[1] At that time, *C. Quate* and his group already had an STM running, and they had performed local spectroscopy, not yet with atomic resolution but at low temperature.[33] They had measured the energy gap of a superconductor and later even plotted its spatial dependence. Spectroscopic imaging was not really surprising, yet it was an important development. We now had the tools to fully characterize a surface in terms of topographic and electronic structure. Although it is usually quite an involved problem to separate the property of interest from a set of STM and STS measurements, our vision of the scanning tunneling microscope had become true. But nevertheless, we heard that this view was not generally shared. Rumors reached us that scientists would bet cases of champagne that our results were mere computer simulations! The bets were probably based on the fact the STM was already three years old, and atomic resolution was still our exclusive property. This was also our concern, but in another way. In late summer 1983, *Herb Budd*, promoter of the IBM Europe Institute and an enthusiastic STM supporter, had asked us to run an STM Seminar in summer 1984 within the framework of the Institute. This meant one week with 23 lectures in front of a selected audience of the European academia. At that time, there was no way whatsoever of filling 23 hours, let alone of committing 23 speakers. A year later, we agreed, full of optimism for summer 1985. In December 1984, on *Cal Quate*'s initiative, nine representatives of the most advanced STM groups came together for a miniworkshop in a hotel room in Cancun. It was a most refreshing exchange of ideas, but there was still no other atomic resolution, and thus not a sufficient number of lectures in sight for the Seminar.

In the following few months, the situation changed drastically. *R. Feenstra* and co-workers came up first with cleaved GaAs,[34] *C. F. Quate*'s group with the 1×1 structure on Pt(100),[35] and *J. Behm*, *W. Hoesler*, and *E. Ritter* with the hexagonal phase on Pt(100).[36] At the American Physical Society March Meeting in 1985, *P. Hansma* presented STM images of graphite structures of atomic dimensions,[37] and when *J. Golovchenko* unveiled the beautiful results on the various reconstructions of Ge films deposited on Si(111),[38] one could have heard a pin drop in the audience. The atomic resolution was official and scanning tunneling microscopy accepted. The IBM Europe Institute Seminar in July turned into an exclusive workshop for STM'ers, and comprised some 35 original contributions, not all of them on atomic resolution, but already more than in March.[39] "A watershed of ideas" as *Cal Quate* expressed it.

Our story so far has dealt mainly with the striving for structural and electronic imaging in a surface-science environment with atomic resolution. Individual atoms had been seen before with field-ion microscopy and dealt with individually by the atom-probe technique.[40] The beauty of these techniques is relativized by the restriction to distinct atom sites on fine tips made from a rather limited selection of materials. Similarly, electron microscopy, the main source of present-day knowledge on submicron structures in practically all areas of science, technology, and industry, has advanced to the atomic level. Imaging of individual atoms or atomic structures, however, is still reserved for specific problems, expertise, and extraordinary equipment. The appeal and the impact of STM lie not only in the observation of surfaces atom by atom, but also in its widespread applicability, its conceptual and instrumental simplicity, and its affordability, all of which have resulted in a relaxed and almost casual perception of atoms and atomic structures.

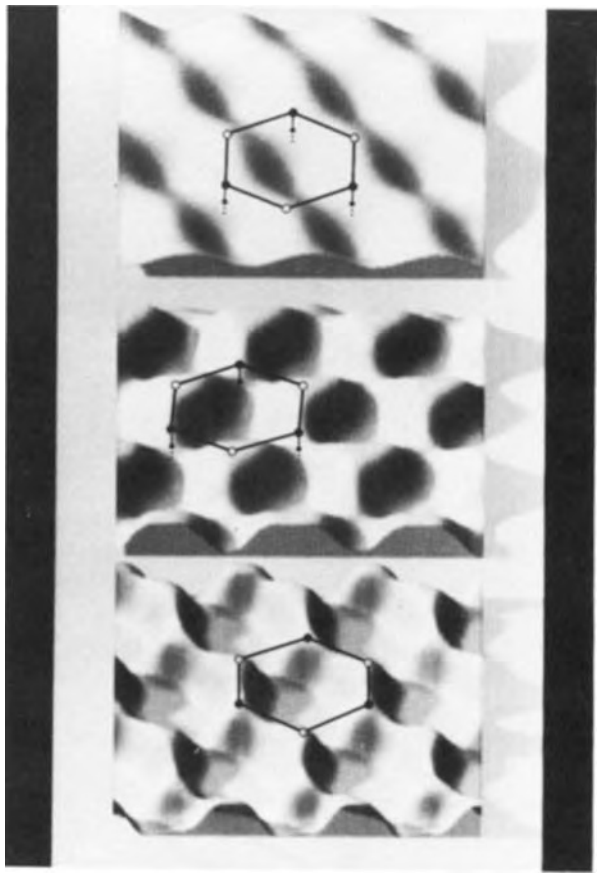

Fig. 7. STM image of cleaved graphite. The top image was taken at a constant tunnel current of 1 nA and at 50 mV. The corrugation traced by the tip reflects the local density of states (LDOS) at the Fermi level and *not* the positions of atoms, which form a flat honeycomb lattice as indicated. The LDOS at the atoms bound to the neighbors in the second layer (open circles) is lower than at the "free" atoms. The image is thus rather a spectroscopic than a topographic one. The middle image is a "current image" showing essentially the same pattern. In the bottom current image, taken closer to the surface, the two inequivalent atoms appear practically identical. This peculiar behavior is compatible with a different local elastic response of the two types of carbon atoms to the interatomic force exerted by the tip compensating for their different LDOS. A local perturbation of the electronic structure might also be important.

But there are many other aspects, maybe less spectacular but nonetheless significant, which have made STM an accepted and viable method now pursued in many areas of science and technology.

The instruments themselves have become simpler and smaller. Their greatly reduced size allows easy incorporation into other systems, for instance into a scanning electron microscope.[41] One type of instrument retains accurate sample positioning but is sufficiently rigid for in-situ sample and tip exchange. Other instruments are so rigid they are even insensitive to vibrations when immersed in liquid nitrogen[42] and even small enough to fit through the neck of a liquid-helium storage vessel.[43] These hummingbirds of STM, some concepts of which reach back to the squeezable tunnel junctions,[18] can also operate at television speed on relatively flat surfaces using single-tube scanners.[43, 44] Also, tip preparation has advanced to a level where well-defined pyramidal tips ending with one[45] or more[46] atoms can be fabricated in a UHV environment. Such tips are particularly important for investigations of nonperiodic structures, disordered systems, and rough surfaces. They are also interesting in their own right, for example, as low-energy electron and ion point sources.

Outside the physics and surface-science communities, the various imaging environments and imaging capabilities seem as appealing as atomic resolution. Images obtained at ambient-air pressure were first reported in 1984,[47] followed by imaging in cryogenic liquids,[42] under distilled water,[48] in saline solutions,[48] and in electrolytes.[49] Scanning tunneling potentiometry appears to have become an interesting technique to study the potential distribution on an atomic scale of current-carrying microstructures.[50] More recent advances include interatomic-force imaging with the atomic-force microscope,[51] with which the structure and elastic properties of conductors and insulators are obtained, and combined imaging of electronic and elastic properties of soft materials.[52] Also, the use of spin-polarized electron tunneling to resolve magnetic surface structures is being explored.

Finally, we revert to the point where the STM originated: The performance of a local experiment, at a preselected position and on a very small spatial scale down to atomic dimensions. Besides imaging, it opens, quite generally, new possibilities for experimenting, whether to study nondestructively or to modify locally: Local high electric fields, extreme current densities, local deformations, measurements of small forces down to those between individual atoms, just to name a few, ultimately to handle atoms[53] and to modify individual molecules, in short, to use the STM as a Feynman Machine.[54] This area has not yet reached adolescence.

The STM's "Years of Apprenticeship" have come to an end, the fundamentals have been laid, and the "Years of Travel" begin. We should not like to speculate where it will finally lead, but we sincerely trust that the beauty of atomic structures might be an inducement to apply the technique to those problems where it will be of greatest service solely to the benefit of mankind. *Alfred Nobel*'s hope, our hope, everybody's hope.

Fig. 8. Artist's conception of spheres. Art and Science are both products of the creativity of Man, and the beauty of nature is reflected in both. *Ruedi Rempfler*, the sculptor, found his interpretation in the deformation of a surface. It was the tension of the sphere in its environment which fascinated him, more than the mere portrayal of its shape. An independent creation, its visual and conceptual similarity with Fig. 6 is astounding. Original sculpture by *Ruedi Rempfler*, photograph courtesy of *Thomas P. Frey*.

We should like to thank all those who have supported us in one way or another and those who have contributed to the development of scanning tunneling microscopy, and express our appreciation of the pleasant and collegial atmosphere existing in the STM community. Thanks are also due to Dilys Brüllmann for her diligent handling of our manuscripts from the start and for her careful reading of this manuscript, and to Erich Stoll for processing Figures 6 and 7 using ideas of R. Voss.

Received: May 4, 1987 [A 627 IE]
German version: *Angew. Chem. 99* (1987) 622

[1] Reviews: a) G. Binnig, H. Rohrer, *IBM J. Res. Dev. 30* (1986) 355; b) J. A. Golovchenko, *Science (Washington) 232* (1986) 48; R. J. Behm, W. Hoesler: *Physics and Chemistry of Solid Surfaces, Vol VI*. Springer, Berlin 1986, p. 361. P. K. Hansma, J. Tersoff, *J. Appl. Phys. 61* (1987) R1; *Proceedings of the STM Workshop in Oberlech, Austria 1985* (*IBM J. Res. Dev. 30* (1986) Nos. 4 and 5); *Proceedings of STM '86 in Santiago de Compostela, Spain 1986* (*Surf. Sci. 181* (1987), Nos. 1 and 2; c) An article combining technical and biographical details is presented in R. L. Dordick, *IBM Res. Mag. 24* (1986) 2.
[2] G. K. Binnig, H. E. Hoenig, *Z. Phys. B32* (1978) 23.
[3] H. Rohrer, *Helv. Phys. Acta 33* (1960) 675.
[4] I. Giaever, *Rev. Mod. Phys. 46* (1974) 245.
[5] W. A. Thompson, S. F. Hanrahan, *Rev. Sci. Instrum. 47* (1976) 1303.
[6] B. P. Williamson, *Proc. Inst. Mech. Eng. 182* (1967) 21; K. H. Guenther, P. G. Wierer, J. M. Bennett, *Appl. Opt. 23* (1984) 3820.
[7] R. Young, J. Ward, F. Scire, *Rev. Sci. Instrum. 43* (1972) 999.
[8] Technical details: G. Binnig, H. Rohrer, *Helv. Phys. Acta 55* (1982) 726; *Surf. Sci. 126* (1983) 236; *Sci. Am. 253* (1985), No. 8, p. 40; *Spektrum. Wiss. 1985*, No. 10, p. 62.

[9] O. Marti, *Ph. D. Thesis*, Eidgenössische Technische Hochschule Zürich 1986; O. Marti, G. Binnig, H. Rohrer, H. Salemink, *Surf. Sci. 181* (1987) 230.
[10] H. R. Ott, H. Rohrer, unpublished; S. Vieira, *IBM J. Res. Dev. 30* (1986) 553.
[11] U. Poppe, *Verhandl. DPG (VI) 16* (1981) 476.
[12] E. C. Teague, *Dissertation*, North Texas State University, TA, USA 1978 (University Microfilms International, Ann Arbor, MI, USA, p. 141); *Bull. Am. Phys. Soc. 23* (1978) 290; *J. Res. Natl. Bur. Stand. (US) 91* (1986) 171.
[13] G. Binnig, H. Rohrer, C. Gerber, E. Weibel, *Physica B (Amsterdam) 109/110* (1982) 2075.
[14] G. Binnig, H. Rohrer, C. Gerber, E. Weibel, *Phys. Rev. Lett. 49* (1982) 57.
[15] G. Binnig, H. Rohrer, C. Gerber, E. Weibel, *Surf. Sci. 131* (1983) L379.
[16] N. M. Miskowsky, P. H. Cutler, T. E. Feuchtwang, S. J. Shepherd, A. A. Lucas, T. E. Sullivan, *Appl. Phys. Lett. 37* (1980) 189.
[17] C. F. Quate, *Phys. Today 39* (1986), No. 8, p. 26.
[18] J. Moreland, S. Alexander, M. Cox, R. Sonnenfeld, P. K. Hansma, *Appl. Phys. Lett. 43* (1983) 387; Actually, *Paul Hansma* was indisposed and could not attend the first seminar given on STM in the USA. However, his students attended, and with them *Paul* built the squeezable tunnel junction.
[19] G. Binnig, H. Rohrer, C. Gerber, E. Weibel, *Phys. Rev. Lett. 50* (1983) 120.
[20] W. A. Harrison, *Surf. Sci. 55* (1976) 1.
[21] K. Takayanagi, Y. Tanishiro, M. Takahashi, S. Takahashi, *J. Vac. Sci. Technol. A 3* (1985) 1502.
[22] R. M. Tromp, E. J. van Loenen, *Surf. Sci. 155* (1985) 441.
[23] R. M. Tromp, *Surf. Sci. 155* (1985) 432, and references cited therein.
[24] R. S. Becker, J. A. Golovchenko, E. G. McRae, B. S. Swartzentruber, *Phys. Rev. Lett. 55* (1985) 2028; R. J. Hamers, R. M. Tromp, J. E. Demuth, *ibid. 56* (1986) 1972.
[25] J. Tersoff, D. R. Hamann, *Phys. Rev. Lett. 50* (1983) 1998; A. Baratoff, *Physica B (Amsterdam) 127* (1984) 143.
[26] N. Garcia, C. Ocal, F. Flores, *Phys. Rev. Lett. 50* (1983) 2002; E. Stoll, A. Baratoff, A. Selloni, P. Carnevali, *J. Phys. C 17* (1984) 3073.
[27] G. Binnig, H. Rohrer, C. Gerber, E. Stoll, *Surf. Sci. 144* (1984) 321.
[28] A. M. Baró, G. Binnig, H. Rohrer, C. Gerber, E. Stoll, A. Baratoff, F. Salvan, *Phys. Rev. Lett. 52* (1984) 1304.
[29] G. Binnig, H. Fuchs, E. Stoll, *Surf. Sci. 169* (1986) L295.
[30] G. Binnig, H. Rohrer in J. Janta, J. Pantoflicek (Eds.): *Trends in Physics, Vol. 1*, European Physical Society 1984, 38.
[31] A. Baratoff, G. Binnig, H. Fuchs, F. Salvan, E. Stoll, *Surf. Sci. 168* (1986) 734.
[32] G. Binnig, K. H. Frank, H. Fuchs, N. Garcia, B. Reihl, H. Rohrer, F. Salvan, A. R. Williams, *Phys. Rev. Lett. 55* (1985) 991; R. Garcia, J. J. Saenz, N. Garcia, *Phys. Rev. B 33* (1986) 4439.
[33] A. L. de Lozanne, S. A. Elrod, C. F. Quate, *Phys. Rev. Lett. 54* (1985) 2433.
[34] R. M. Feenstra, A. P. Fein, *Phys. Rev. B 32* (1985) 1394.
[35] S. A. Elrod, A. Bryant, A. L. de Lozanne, S. Park, D. Smith, C. F. Quate, *IBM J. Res. Dev. 30* (1986) 387.
[36] R. J. Behm, W. Hoesler, E. Ritter, G. Binnig, *Phys. Rev. Lett. 56* (1986) 228.
[37] P. K. Hansma, *Bull. Am. Phys. Soc. 30* (1985) 251.
[38] R. S. Becker, J. A. Golovchenko, B. S. Swartzentruber, *Phys. Rev. Lett. 54* (1985) 2678.
[39] Proceedings: *IBM J. Res. Dev. 30* (1986) Nos. 4 and 5.
[40] Review: N. Ernst, G. Ehrlich, *Top. Curr. Phys. 40* (1986) 75.
[41] C. Gerber, G. Binnig, H. Fuchs, O. Marti, H. Rohrer, *Rev. Sci. Instrum. 57* (1986) 221.
[42] R. V. Coleman, B. Drake, P. K. Hansma, G. Slough, *Phys. Rev. Lett. 55* (1985) 394.
[43] D. P. E. Smith, G. Binnig, *Rev. Sci. Instrum. 57* (1986) 2630.
[44] A. Bryant, D. P. E. Smith, C. F. Quate, *Appl. Phys. Lett. 48* (1986) 832.
[45] H.-W. Fink, *IBM J. Res. Dev. 30* (1986) 460.
[46] Y. Kuk, P. J. Silverman, *Appl. Phys. Lett. 48* (1986) 1597.
[47] A. M. Baró, R. Miranda, J. Alaman, N. Garcia, G. Binnig, H. Rohrer, C. Gerber, J. L. Carrascosa, *Nature (London) 315* (1985) 253.
[48] R. Sonnenfeld, P. K. Hansma, *Science (Washington) 232* (1986) 211.
[49] R. Sonnenfled, B. C. Schardt, *Appl. Phys. Lett. 49* (1986) 1172.
[50] P. Muralt, D. W. Pohl, *Appl. Phys. Lett. 48* (1986) 514.
[51] G. Binnig, C. F. Quate, C. Gerber, *Phys. Rev. Lett. 56* (1986) 930.
[52] J. M. Soler, A. M. Baró, N. Garcia, H. Rohrer, *Phys. Rev. Lett. 57* (1986) 444; U. Dürig, J. K. Gimzewski, D. W. Pohl, *ibid. 57* (1986) 2403.
[53] R. S. Becker, J. A. Golovchenko, B. S. Swartzentruber, *Nature (London) 325* (1987) 419.
[54] R. P. Feynman, *Eng. Sci. 22* (1960) No. 2; S. Hameroff, C. Schneiker, A. Scott, P. Jablonka, T. Hensen, D. Sarid, S. Bell, unpublished.

New Cisplatin Analogues— On the Way to Better Antitumor Agents

By Alessandro Pasini* and Franco Zunino*

The clinical success of cisplatin (*cis*-diamminedichloroplatinum(II)) in antitumor chemotherapy has encouraged an all-out search for analogues with lower toxicity, improved therapeutic index and increased activity. Literally thousands of analogues, obtained by replacement of the ammine- and chloro-ligands by other amines and anionic ligands, respectively, have been systematically screened for activity in experimental tumor models. Some of these analogues have been selected for clinical evaluation, but only very few of them appear to be promising antitumor agents. More recently, cisplatin analogues have been designed and synthesized on the basis of, inter alia, the following considerations: 1) platinum complexes with carrier molecules as ligands should prove useful for achieving increasing drug concentration in tumor tissues; 2) platinum complexes with chemotherapeutic agents as ligands could afford polyfunctional drugs with synergistic action; 3) complexes containing more than one platinum atom might be more effective than complexes containing only one platinum atom; 4) platinum complexes could be used as sensitizers in radiation therapy. In this paper, we shall give a brief account of the "traditional" analogues, and then critically discuss what we believe could be the new trends in the design of cisplatin analogues.

1. Introduction

Although some established antitumor agents (e.g. bleomycins) are expected to react as metal complexes with their biological targets,[1] and although a variety of compounds designed to interact with transition metals (e.g. thiosemicarbazones[2]), have been proposed as potential antitumor agents, the only metal complex currently used in the chemotherapy of neoplastic diseases is *cis*-diamminedichloroplatinum(II) ("cisplatin"), **1**.[3] This complex, of a non-essential heavy metal, exhibits a remarkable antitumor effectiveness and a broad spectrum of activity.[4]

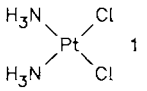

1

Cisplatin has proven very successful in the treatment of a variety of human solid tumors such as genito-urinary and gynecologic tumors as well as head, neck, and lung tumors, and it is currently one of the most important compounds used in the treatment of solid tumors.[5]

The increasing therapeutic interest in this drug, after its introduction into clinical trials in 1972,[6] and the early recognition of its limited use because of severe toxic effects, have stimulated a widespread effort to: a) optimize cisplatin treatment regimens and alleviate toxic side effects (particularly nephro- and gastrointestinal toxicities) and b) find alternative platinum complexes having more favorable properties.

[*] Prof. Dr. A. Pasini
Dipartimento di Chimica Inorganica e Metallorganica
Università degli Studi
Via G. Venezian 21, I-20133 Milano (Italy)
Dr. F. Zunino
Divisione di Oncologia Sperimentale B
Istituto Nationale per lo Studio e la Cura dei Tumori
Via G. Venezian 1, I-20133 Milano (Italy)

The dose-response curve for the treatment of sensitive human cancers with cisplatin is rather steep,[7] therefore high efficacy of the drug can be expected only by aggressive regimens, mainly in the treatment of advanced cancer. Several useful protective measures, such as hydration and the use of hypertonic saline, have successfully been adopted in the clinics to improve the therapeutic index of cisplatin,[8] but the use of high doses remains limited by other dose-related toxicities, especially myelosuppression and oto- and neurotoxicity.[9] Improved efficacy could however derive from the development of less toxic cisplatin analogues possessing the same or even higher antitumor activity. The goals in the search for new analogues include: a) decreased organ-specific and/or systemic toxicity, b) increased effectiveness against tumors characterized by natural or acquired resistance to cisplatin (lack of cross-resistance to cisplatin), c) more favorable physico-chemical properties such as solubility (cisplatin is only sparingly soluble) and stability in aqueous solution.

This paper is devoted to a critical discussion on present and possible future cisplatin analogues. For sake of simplicity we have deliberately avoided any reference to complexes of other metals, although some of them (those of tin, gallium, copper, gold, titanium, etc.) appear rather promising.[10]

2. The Design of a Cisplatin Analogue

2.1. A Brief Account of the Mechanism of Action of Cisplatin

A rational development of a more effective analogue of a drug requires a detailed knowledge of the drugs mechanism of action at the cellular level.

Chromosomal DNA has been proposed as the primary target of platinum antitumor agents,[11,12] but evidence that

this is the only site of attack is still a matter of debate.[13-15] For instance, if this hypothesis is correct, it remains to be explained why cisplatin, which reacts in a nonselective way with critical macromolecules of both tumor and normal cells, is so effective against some human neoplastic diseases. It is known that cisplatin reacts with a wide variety of cellular constituents, including (but not only) DNA. For example recent studies reported selective inhibitory effects of cisplatin on the amino acid transport system, thus indicating a drug-membrane interaction.[16] It is possible that these events may contribute to (selective?) lethal effects of the drug, since membranes play a critical role in the control of cell physiology.

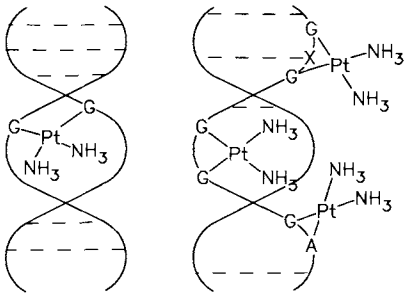

2

3

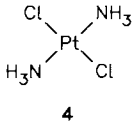

4

According to the generally accepted mechanism, cisplatin binds preferentially, but not exclusively, at the N(7) position of the guanine of DNA,[17] replacing the two Cl ligands, usually called leaving groups, and thereby forming inter- (**2**)[18] and intrastrand (**3**)[19] cross-links, the latter probably being the critical lesion.[19] Recent results suggest that the cisplatin-DNA adduct can be accomodated in the double helix, causing only such a small localized disruption of the helix that cannot be recognized by any repair enzymes.[20] In contrast, the disruptions caused by the inactive (see Section 2.2) *trans*-isomer **4** are more profound, and are easily recognized and repaired.[20]

The reaction with DNA may involve an intermediate aquation step,[21] especially when **1** enters the cell with its low chloride concentration; aqua or—in neutral solution—aqua-hydroxo compounds are formed, which can give rise to, most likely highly toxic,[23] μ-hydroxo oligomers.[22]

$$\underset{\mathbf{1}}{cis\text{-}[PtCl_2(NH_3)_2]} \longrightarrow cis\text{-}[PtCl(NH_3)_2(H_2O)]^{\oplus} \longrightarrow$$

$$cis\text{-}[Pt(NH_3)_2(H_2O)_2]^{2\oplus} \longrightarrow cis\text{-}[Pt(NH_3)_2(OH)(H_2O)]^{\oplus} \longrightarrow$$

$$\longrightarrow \text{polymeric } \mu\text{-OH species.}$$

2.2. Structure-Activity Relationships

A cisplatin analogue can be described in terms of structure **5**, where X is a leaving group and A is an amine or other firmly bound ligand (for cisplatin X = Cl and A = NH_3). It must be remembered that no ligand is completely inert to substitution; thus, examples of the replacement of ammonia in cisplatin during its reaction with nucleobases have been reported.[24] The terms "leaving" and "non-leaving groups", therefore, refer only to relative reactivity.

At a very early stage it was found that the *trans*- isomer **4** is inactive;[11,25] therefore, the following discussion will be based solely upon variations of the basic structure **5** with *cis*-configuration.

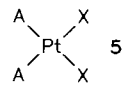

5

Several studies on structure–activity relationships for this basic structure have been reported, but simple relationships have seldom been found. Most of these studies have been carried out on different experimental models (murine L1210 and P388 ascitic leukemias, S180 sarcoma and ADJ/PC6 A plasmocytoma, etc.) using different treatment schedules, so a comparison of the relative efficacy is not easy. A further problem is presented by the structure-activity inconsistencies when the effects of the same compound are compared in different tumor systems. These observations underscore the importance of using a broad range of experimental models for preclinical evaluations, because of the predictive uncertainties of transplantable tumor systems.[26] The use of human tumors (e.g. ovarian adenocarcinoma) transplanted and grown in nude mice has recently been proposed as a useful strategy for acquiring models that overcome these drawbacks.[27]

2.2.1. *The Role of the Leaving Groups X*

The solubility of cisplatin in water is rather low (the Merck index quotes 0.253 g/100 g). To overcome this problem, other leaving groups, mainly carboxylates, were originally proposed. However, when A is kept unchanged, the nature of X determines the rate of its substitution, and thus also the antitumor effectiveness of an analogue.[28,29] Useful antitumor properties are generally associated with intermediate lability of the Pt-X bonds. Complexes with highly labile groups are very toxic and cannot be used as antitumor agents, because the compound can react with almost any nucleophile in the body. On the other hand, strongly bound ligands give rise to kinetically inert complexes. An exception to this generalization is found in the bidentate dicarboxylate ligands. It has been suggested that complexes with these leaving groups most likely require metabolic activation in order to exert their cytotoxic effects.[30]

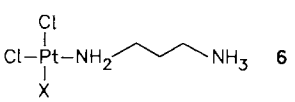

6

The lability of a particular leaving group X depends, inter alia, on the nature of the ligand *trans* to it ("*trans* effect"). For example, the cytotoxicity of compounds of the type **6** (which contain monoprotonated diamines to ensure charge neutralization, see Section 2.2.4) is determined by the nature of X (Cl, NO_2, SCN, etc.)[31]

Some typical leaving groups are listed in Table 1.[28,32-39]

Table 1. Some typical leaving groups X for *cis*-[PtA_2X_2] **5** [28, 32-39].

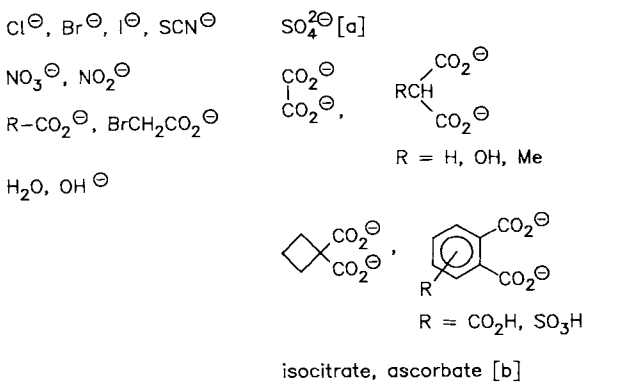

[a] The sulfate ion has been found to be monodentate both in the solid state [35] and in aqueous solution [36]. In these cases the other ligand is water. [b] A Pt-C bond has been reported in the case of a diaminocyclohexane complex [39].

2.2.2. *The Role of the Non-leaving Groups A*

A number of non-leaving groups have been proposed, mainly amines, from the simplest one, ammonia, to linear, branched, or cyclic aliphatic amines, bidentate chelating amines (including diamino acids), and diaminocycloalkanes; in fact almost any ligand is possible (see Table 2[28,32-34,40-43]).

The role of these ligands is less clear, but since they are relatively difficult to replace (see Section 2.2), it is assumed that they accompany the platinum atom to the target macromolecules inside the cell, thus representing a major factor in governing the pharmacokinetic behavior, penetration into the cells, and interaction with DNA. In conclusion, therefore, these groups should modulate cytotoxicity and antitumor effects.[29]

Ligands with polar substituents reduce the activity of an analogue.[28] Ammonia and primary amines give rise to the more active compounds, while complexes with tertiary amines are inactive.[28] It has been suggested that hydrogen bonds between the amine and polar groups of DNA may play a role in the interaction with this macromolecule.[44] Recent molecular mechanics calculations are in agreement with this hypothesis.[45]

Complexes with the chelating 1,2-diaminocyclohexane **8**[46] (cf. Table 3) and 1,3-diaminopropane, substituted in position 2[47] (cf. Tables 2 and 3), are of special interest since these ligands are responsible for lack of cross-resistance to cisplatin, at least in experimental models. The complex with 1,2-diaminocyclohexane **9** appears to be particularly active when the (*R,R*)- rather than the (*S,S*)- or the *meso*-stereoisomer is used.[48] However, we were not able to detect any significant difference in the activity against murine tumors, of cisplatin analogues with diastereoisomeric diamines as ligands.[49] Furthermore, these complexes were found to lack any chiral recognition in the

Table 2. Some typical non-leaving groups A for *cis*-[PtA_2X_2] **5** [25, 29-34].

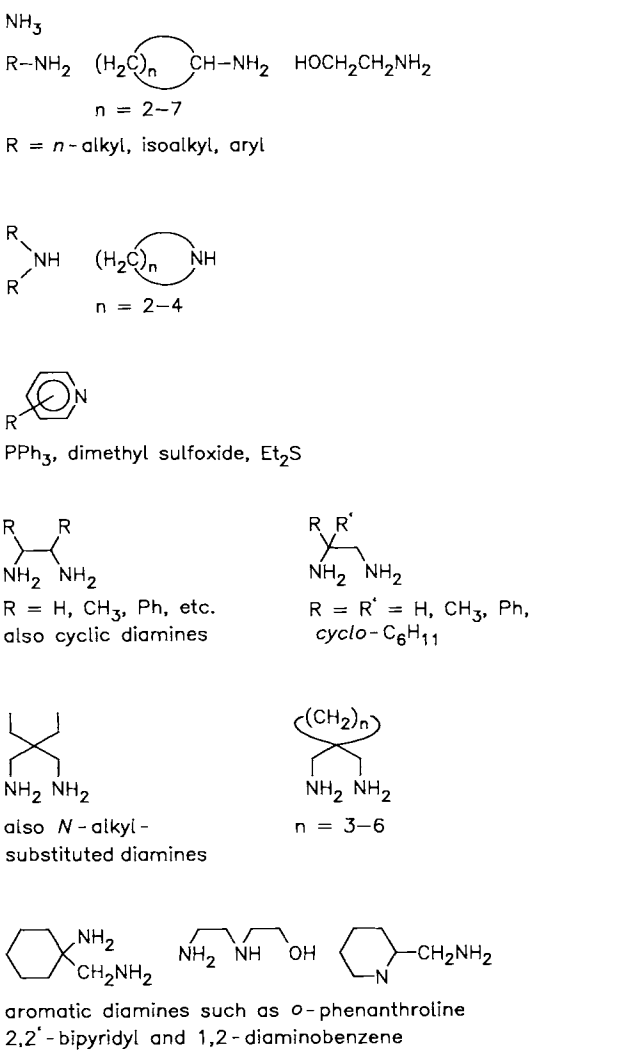

reaction with DNA,[50,51] but not so upon reaction with a dinucleotide.[52] We believe this matter is rather important and should be investigated in more detail.

2.2.3. *The Role of the Oxidation State of Platinum*

Studies have also been extended to platinum(IV) complexes.[28] These compounds are usually less potent than the corresponding platinum(II) complexes: They are most likely reduced in vivo, probably by cysteine,[53] to active Pt^{II} derivatives, since they neither form radical species[54] nor interfere with DNA in the absence of reducing agents.[55] Their utility resides mainly in their high solubility in water.

The so called "platinum blues" may be cited in this context. These are paramagnetic oligomers in which mixed-valence platinum is coordinated to nucleobases such as uracil.[56] Although some derivatives have been found to be rather active they are no longer used, mainly because of their toxicity and poor chemical characterization.[57]

2.2.4. The Role of the Charge of the Complex

Neutrality is generally regarded as a prerequisite for antitumor activity,[28] presumably on the grounds that neutral complexes can cross the cell membrane more easily. However, both cationic (e.g. *cis*-$[Pt(NH_3)_2(guanosine)_2]^{2\oplus}$[58]) and anionic complexes (e.g. $[PtCl_3A]^{\ominus}$; $A = NH_3$,[29] *tert*-butylamine[59]), show some low but significant activity. Clearly too little is known about the mechanism by which these molecules enter the cells. For cisplatin itself, an active transport has been proposed which is probably mediated by an amino acid transport system;[60] but different mechanisms could be operative for different analogues. Moreover, compounds of the type $[PtCl_3A]^{\ominus}$ can interact with endogenous low molecular weight amines and form neutral complexes.

3. Cisplatin Analogues in Clinical Trials

Most of the clinical studies with cisplatin analogues are still only at an exploratory stage, so only some general aspects of the clinical evaluation of new platinum complexes can be dealt with here.

Table 3 lists some cisplatin analogues which have recently been introduced into clinical trials in rapid succession.[61-66] As with other classes of antitumor agents, improvement in tumor selectivity remains the greatest challenge in the development of new analogues. The design of selective drugs is at present a difficult task, mainly because we ignore the factors determining the selectivity, if any, of the parent compound.

The criteria for selecting promising cisplatin analogues to be evaluated in clinical trials are favorable physicochemical properties (solubility and stability) and possible therapeutic advantages, as inferred from preclinical studies (high efficacy, favorable spectrum of activity, high therapeutic index and low toxicity). There are great expectations for derivatives which could prove to be effective against human cancers refractory to cisplatin; for instance, complexes with 1,2-diaminocyclohexane **8** reflect this expectation, since they lack cross-resistance to cisplatin.[34] This property is also shared by the derivatives of 1,1-bis(aminomethyl)cyclohexane **10** such as TNO6.[34] The clinical development of this compound has, however, been discouraged because it is inferior to cisplatin and exhibits unpredictable severe toxicity.[35,62,67] Other analogues have substantially inert leaving groups, e.g. **7** in JM8 and malonate in JM40, which could contribute to a reduced nephrotoxicity.

With few exceptions (e.g. JM8) insufficient experience has been gained with any of the analogues to be confident that they will have established therapeutic utility.

In general the pattern of toxicity predicted by preclinical evaluations has been confirmed. These analogues (with few exceptions) do not exhibit any nephrotoxic activity, but myelosuppression remains a general toxic property.

The widely divergent properties exhibited by some of these compounds were expected to lead to specific clinical indications not necessarily replacing those of cisplatin. Their therapeutic potential and clinical advantages over the parent drug remain, however, to be documented.

Table 3. Some cisplatin analogues *cis*-$[PtA_2X_2]$ **5** in clinical trials [51-56].

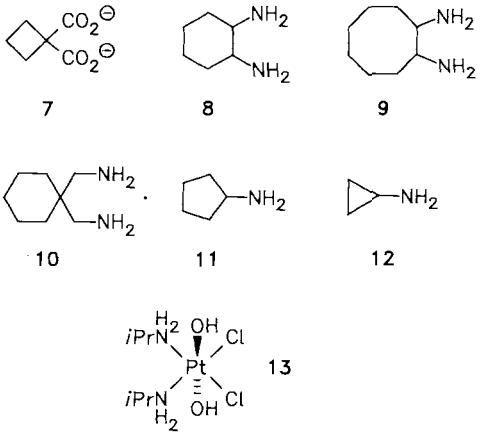

Non-leaving groups A	Leaving groups X	Name
$2NH_3$	2 Cl	cisplatin
$2NH_3$	**7**	JM8, CBDCA, carboplatin
$NH_2CH_2CH_2NH_2$	malonate	JM40
rac-**8**	malonate	JM74
rac-**8**	$SO_4^{2\ominus}$, H_2O [a]	JM20, SHP
(−)-**8**	$SO_4^{2\ominus}$, H_2O [a]	neoSHP
rac-**8**	$2BrCH_2CO_2^{\ominus}$	MBA
rac-**8**	isocitrate	PHIC
rac-**8**	4-carboxyphthalate	JM82
(−)-**8**	oxalate	L-OHP
rac-**8**	pyruvate	
9	$2BrCH_2CO_2^{\ominus}$	BOP
10	$SO_4^{2\ominus}$, H_2O [a]	TNO6
2 **11**	2 Cl	JM11
2 **12**	2 Cl	CP
13		JM9, CHIP

[a] See Footnote [a] in Table 1.

4. New Concepts in the Development of Cisplatin Analogues

A close look at Tables 1-3 reveals that most of the compounds derive from a somewhat empirical rationale: a change in the *cis*-$[PtA_2X_2]$ scheme with different A- and X-ligands, in the hope of finding superior analogues, the only guidelines being the results of structure-activity studies (see the cases of 1,2-diaminocyclohexane and of the lability of the Pt-X bond). However approaches based on different rationales have been attempted and realized. In this section we shall critically review some of the results obtained in these studies.

The antitumor activities of some selected compounds and platinum complexes are listed in Table 4. Since some variability is common in dealing with experimental tumor models in vivo, caution is required in comparing the antitumor activity data reported by different authors. Whenever possible the data of Table 4 contain a schematic description of the experiment and the activity of cisplatin itself, as a reference compound, when reported in the same paper and determined under the same conditions. The data of Table 4 must be examined taking into account that the evaluation parameters depend critically on tumor model, tumor burden, and treatment schedule. The compounds so far tested are discussed in the following sections.

Table 4. Antitumor activities of some representative cisplatin analogues. (for discussion see Sections 4.1 to 4.3).

Compound	Model	Schedule [a]	T/C% [b]	Dose	Ref.
1	P388	s.d.	246	8 mg/kg	[59]
22, R = H	10^6 cells	s.d.	155	80 mg/kg	
1	P388	s.d.	240	8 mg/kg	[69]
16	10^6 cells	s.d.	155	270 mg/kg	
1	Walker 256	s.d.	510 [c]	8 mg/kg	[74]
20, aa = Gly		qd × 3	520 [c]	80 mg/kg × 3	
1	L5522	qd × 3	207	3.5 mg/kg × 3	[77]
23	10^6 cells	qd × 3	257	20 mg/kg × 3	
1	ascites	s.d.	180 [c]	7 mg/kg	[83]
Adduct of **1** and **26**	sarcoma	s.d.	208 [c]	10 mg/kg	
1	P388,	s.d.	246	23 μmol/kg	[84]
26	10^6 cells	s.d.	300	26 μmol/kg	
27		s.d.	388	26 μmol/kg	
1	L1210/DDP [d],	s.d.	100	23 μmol/kg	[84]
26	10^5 cells	s.d.	159	26 μmol/kg	
27		s.d.	145	24 μmol/kg	
1	L1210/DDP [d]	q4d × 4	< 120	—	[102]
32		q4d × 4	213	20 mg/kg	
$[PtCl_3(caffeine)]^{\ominus}$	P388	—	150	36 mg/kg	[103]
Bis(selenoguanine)platinum(II)	L1210,	q4d × 2	177.8	0.56 mmol × 2	[108]
Selenoguanine	10^4 cells		140	1.62 mmol × 2	
Selenoguanine			190	0.65 mmol × 2	
33, R = arabinofuranosyl	L1210, 10^4 cells	q4d × 2	181	100 mg/kg × 2	[110]
cis-Bis(3'-amino-3'-deoxythymidine) dichloroplatinum(II)	L1210, 10^5 cells	q12h × 6	175	320 mg/kg (total)	[112]
1	S180,	s.d.	237	8 mg/kg	[115]
$[PtCl_2$(diaminoglucose)]	10^6 cells	s.d.	411	50 mg/kg	
36	P388	—	130	—	[121]
1	L1210	s.d.	205	27 μmol/kg	[29]
4		s.d.	116	133 μmol/kg	
$[PtCl_3NH_3]^{\ominus}$		s.d.	146	70 μmol/kg	
$[PtCl_2(en)]$ [e]		s.d.	132	18 μmol/kg	
$[PtCl_2$(*rac*-**8**)]		s.d.	177	10.5 μmol/kg	
$[Pt(ox)(NH_3)_2]$ [e]		s.d.	158	47 μmol/kg	
[Pt(mal)(*rac*-**8**)] [e]		s.d.	190	122 μmol/kg	

[a] Treatment was started on day one after tumor transplantation. s.d., single dose; for other schedules, for instance q4d × 3 means three administrations every four days. [b] T/C%: ratio between the median survival time of treated and untreated (control) animals × 100. Activity is considered to be significant for T/C% > 125. [c] Evaluted from the data reported by the authors. [d] L1210/DDP, L1210 leukemia resistant to cisplatin. [e] en = ethylenediamine; ox = oxalate; mal = malonate.

4.1. Low Molecular Weight Carriers as Ligands

Known anticancer drugs are substances which are cytotoxic to any cell. Their antitumor activity and selectivity, if any, is mainly due to a kinetic factor, i.e. they preferentially kill rapidly growing cancer tissues, but of course normal proliferating tissues may also be affected. An ideal antitumor agent should therefore be a compound which is selectively accumulated in the cancer tissues, thus displaying its action only towards cancer cells. This can be achieved by binding the antitumor agent to carrier molecules. Some attempts have already been made at designing drugs of this sort and we shall briefly discuss this point with regard to cisplatin analogues.

4.1.1. Sulfadiazine

Sulfadiazine, **14**, accumulates in some cancer tissues, and sulfadiazine-substituted alkylating agents (e.g. **15**) have been proposed.[68] Compound **15**, however, exhibits a pharmacokinetic behavior different from that of **14** and accumulates preferentially in the liver.[68] We have synthesized some sulfadiazine-platinum complexes and one of

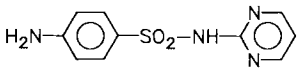

14

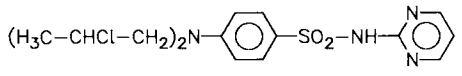

15

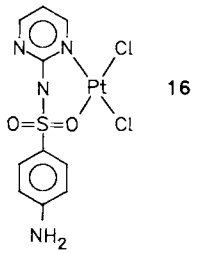

16

them, **16**, was found to be more active in vivo against some murine tumor models than expected on the grounds of its in vitro cytotoxicity.[69]

4.1.2. Nutrients and Metabolic Precursors

Rapidly growing tumor tissues have a high requirement for nutrients and metabolic precursors that are needed for cell proliferation. These substances (for instance amino acids) can be used as low molecular weight carriers. Incidentally, this observation has been exploited to produce cytotoxic effects in certain tumor tissues by depriving cells of a supply of amino acids, for instance by the use of depleting enzymes[70] like L-asparaginase, a well established antileukemic agent. Amino acid derivatives of alkylating agents such as **17** have been reported, and some of them possess significant activity.[71] Compound **18** (phenylalanine mustard, melphalan) is particularly active and routinely used in the clinics. Note that **18**, quite unlike **17**, still has the essential structural features of an amino acid. In fact **18** is likely to be actively transported into L1210 leukemia cells by an amino acid transport system.[72]

Some cisplatin analogues like **19**–**21** contain amino acids or peptides (aa-aaOEt = *N*-coordinated dipeptide ethyl ester). Some marginal activity against L1210 leukemia in mice[73] (but not against sarcoma 180[28]) is displayed by **19** (R = H, CH_2OH) and by **20** (aa-aa = glycylglycine), for which a preferential accumulation in cancer tissues has been demonstrated.[74] **21** is inactive.[40]

We have synthesized compound **22** in which *tert*-butylamine was chosen to increase liposolubility, whereas the *N*-coordinated amino acid moiety should act as a carrier. The glycine, serine and alanine derivatives did show some activity against murine leukemias, but they proved to be far less effective than cisplatin.[59] Such a low activity could

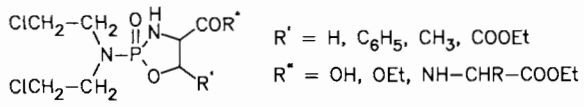

17

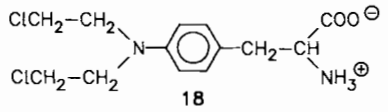

18

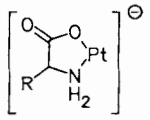

19

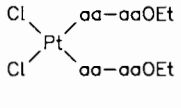

20

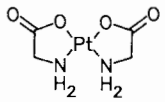

21

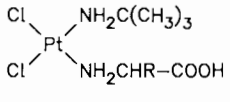

22

be due, inter alia, to some steric hindrance in the reaction with DNA.[75] Interestingly, however, we have found that the in vitro cytotoxicity of **22** against cisplatin-resistant L1210 cells is of the same order of magnitude as that for cisplatin-sensitive cells.[76] The reason for such a lack of cross-resistance is currently under investigation.

4.1.3. Non-Protein Hormones

The *cis*-PtX_2 moiety has been bound to estrogen-receptor binding molecules as in some derivatives of **23** with substituents in the ring. Thus, e.g., **23**, R = 4-OH, is an effective estrogen; since the hormone effect is retained upon complexation with platinum, it can be used as a carrier in the treatment of hormone-dependent mammary carcinomas.[77]

A similar recognizing moiety has also been bound to the leaving group as in **24**, where the leaving group malonic acid bears, as a substituent, ethylmethylstilbene, a compound with an estrogen-like activity.[78] The diammineplatinum derivative of **24** is active, but it has been shown that it does not bind to uterine estrogen receptors of the rat.[78] A *cis*-PtA_2 group (A = triphenylphosphane) has been bound via an *o*-catecholate to hormonally active steroids

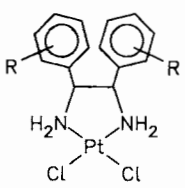

23

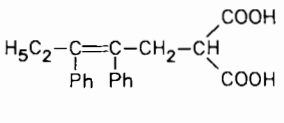

24

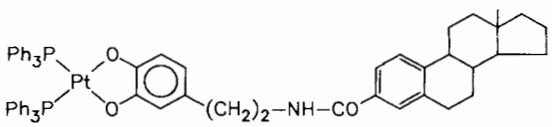

25

(e.g. compound **25**). The cytotoxicity in vitro is acceptable,[79] but the selectivity must still be documented.

In conclusion the above discussed examples stress the general difficulty of using low molecular weight carriers, since small variations in their structure may lead to substantial changes in their biological properties, e.g. their interaction with receptors.

4.2. Multifunctional Drugs

The success of combination chemotherapy is attributed to the fact that the development of resistant cell lines is prevented and that synergistic interactions between cytotoxic agents with different mechanisms of action occur.[80] Observations of this kind led to the idea of binding two different cytotoxic moieties within the same molecule.[81] Since synergism between cisplatin and other cytotoxic agents is well documented,[82] this approach would seem very promising.

4.2.1. Cytotoxic Drugs as Ligands

Some platinum complexes of the antitumor agent doxorubicin **26** have been described in the literature, however their activities are not higher than those of **1** or **26**.[83,84] The complex **27**, in which doxorubicin is coordinated to platinum via the amino group, is active against cisplatin- and doxorubicin-resistant murine tumors.[84] Doxorubicin probably owes its antitumor activity to intercalation in DNA[85] (although the base-sequence specificity is still a matter of debate[86]). Simple intercalating platinum complexes with no leaving groups (e.g. the complex **28**, which intercalates in the G-C regions[87]), are inactive, as expected, whereas it has been shown that compound **29** causes additive effects on the unwinding of superhelical DNA, i.e. through covalent binding of platinum and intercalation.[88] Moreover, the intercalating moiety of **29** influences the regioselectivity of the binding of platinum to DNA.[89] **29** has been reported to be active against cisplatin-resistant tumors.[90]

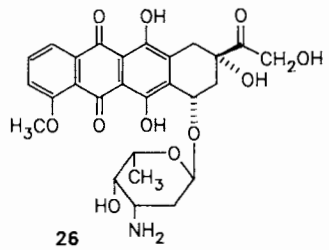

26
("doxo")

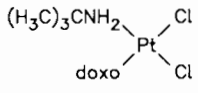

27

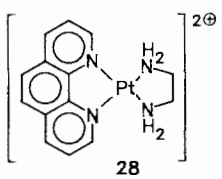

28

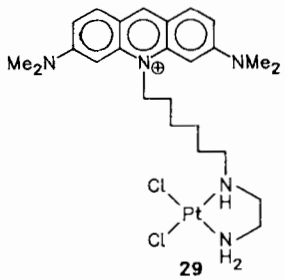

29

Further examples of complexes in which intercalating groups are bound to *cis*-$PtCl_2$, are $[PtCl_2(NH_3)$(acridine orange)] and the interesting $[\{PtCl_2(NH_3)\}_2$(proflavine)] (with two Pt atoms bound to proflavine). These complexes are less toxic than the parent ligands and are cytotoxic against L1210 cells.[91]

The antitumor activity of mitoxantrone, **30**, is also ascribed to DNA intercalation[92]—probably in the G-C rich regions[93]—and a patent has been registered claiming a very high activity of some platinum complexes of **30**.[94] These compounds were, however, poorly characterized.

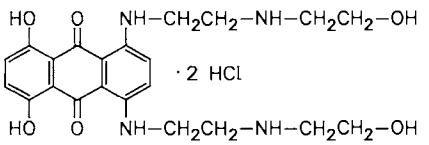

30

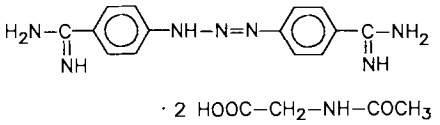

31

· 2 $HOOC–CH_2–NH–COCH_3$

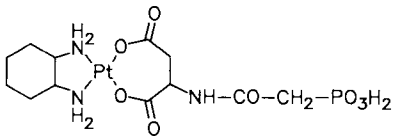

32

Other examples of these multifunctional compounds are some complexes of triazenes (alkylating agents)[95] and complexes of mitomycin, which, however, are less active than mitomycin itself.[96]

A platinum complex of berenil, **31** (a trypanocide drug), has been prepared[97] on the grounds that there are certain parallels in the pharmacological activity of antitumor agents and drugs active against *Trypanosoma Rhodosiense* (the agent that causes sleeping sickness in man).[98,99] It has, in fact, been shown that cisplatin itself is active against this microbial agent.[97,99]

Here again the alternative approach is to use the pharmacologically active molecule, or some derivative of it, as the leaving group(s). One example is the use of melphalan, **18**, as the leaving group.[100] In the complex **32** the leaving group is *N*-(phosphonoacetyl)-L-aspartate (PALA), which is an antitumor agent in clinical evaluation.[101] This complex is rather active toward a number of experimental murine tumors, and is not cross-resistant to cisplatin.[102]

4.2.2. Repair Inhibitors

Trichloro(caffeine)platinate(1−) has been reported to possess some low, but significant, antitumor activity.[103] This complex has been synthesized because caffeine is an inhibitor of DNA repair and should enhance the lethal effect on cancer cells by the $PtCl_2$ moiety.

4.2.3. Polar Solvents

Some polar solvents, such as dimethyl sulfoxide (DMSO) and methylformamide induce differentiation of malignant cells and have been proposed as a class of antineoplastic agents.[104] DMSO has been bound to platinum both as non-leaving[28] and leaving group. In this case active compounds, less toxic than cisplatin, have been obtained.[99,105] Note that DMSO exercises a strong *trans* effect; hence, complexes of type **5** (X = DMSO) are less stable if A is a monodentate amine. To avoid extensive solvolysis, complexes of the type $[Pt(en)(DMSO)_2]^{2\oplus}$ (en = ethylenediamine) must be used.[106]

4.2.4. Antimetabolites

Antimetabolites are another important class of antitumor drugs. The rationale is that these agents should compete with normal metabolites, with increased cytotoxic action against rapidly growing cells. Long before the original paper by *Rosenberg* et al.,[3] which describes the antitumor properties of cisplatin, *Kirschner* et al. reported that platinum(IV) complexes of the antimetabolite 6-mercaptopurine were effective against murine tumors.[107] Similar results were obtained in the USSR.[33] More recently thio- and selenoguanine-platinum complexes have been reported.[108] However, with the probable exception of the selenoguanine–platinum complex, the antitumor activity of these complexes seems to be due to a slow release of the ligands, rather than to the action of the complexes as such.[109]

In the case of the complexes **33** and **34** the activity is again due to the *cis*-$PtCl_2$ moiety.[110] Compound **34** is interesting because the $PtCl_2$ group is part of a purine-like structure and could itself behave as an antimetabolite. In contrast, in **33** the platinum is bound to the antimetabolite. Some complexes of the type **33** and **34** (R = deoxyribosyl,

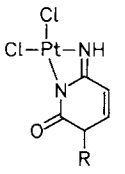

33

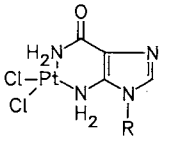

34

ribofuranosyl, or arabinofuranosyl) are active against murine L1210 leukemia, cause inhibition of DNA synthesis, and are not nephrotoxic in mice.[110] $PtCl_2$-complexes of 6-(aminoethyl)aminopurine[111] and 3′,5′-diaminodeoxythymidine[112] have also been reported. Relevant to this approach is the well known synergistic interaction between cisplatin and purine- and pyrimidine-analogues in the treatment of experimental and human tumors.[113]

The tumor growth inhibition by glucosamine may arise, inter alia, from an alteration of multiple metabolic pathways.[114] Complexes of amino sugars have been reported as being active against some experimental model tumors.[115]

4.3. Dimeric and Polymeric Derivatives

One way of increasing the effectiveness of an antitumor agent is to incorporate it in a molecule able to modify the pharmacokinetics in a favorable way. The complex **35** is probably an example of this approach.[116,117] It may be that these types of compounds act as depot systems releasing *cis*-PtA_2Y_2 species (Y = H_2O, OH). Another example may be the aforementioned proflavine–Pt_2 compound (see Section 4.2.1).[91]

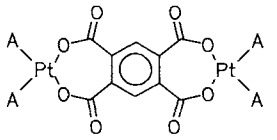

35

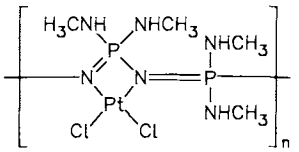

36

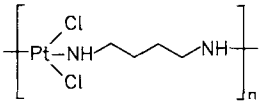

37

The idea of binding antineoplastic drugs to polymers is not new.[118,119] There are many reasons for doing so. Some tumor cells display a preferential uptake of macromolecules;[120] in addition, certain natural and synthetic macromolecules display intrinsic antitumor activity.[118–120] The antitumor activities of polymeric cisplatin analogues **36** and **37** have been reported.[119,121] We have prepared some *cis*-$PtCl_2$(poly-L-lysine) derivatives which were more cytotoxic than the polymer itself; however, the toxicity of the latter precluded in vivo experiments. Finally, an adduct of polylactic acid and cisplatin slowly releases the drug. The life-span of tumor-bearing mice, has been reported to be prolonged to a greater extent by this adduct than by cisplatin.[122]

Other polymer derivatives of platinum have been reviewed.[123]

4.4. Natural Polymers as Carriers

There are a series of natural macromolecules which, at least on paper, should be the carriers of choice because of their specificity: namely, the antibodies. Binding of antitumor agents to these macromolecules should in fact yield highly selective drugs, providing such a binding does not occur at the recognition sites of the protein. Indeed, platinum complexes with tumor-directed immunoglobulins specifically inhibit DNA synthesis in tumor cells.[124] More recently, the activity of diaminoplatinum complexes with malonate or succinate ions bound to monoclonal antibodies has been reported.[125]

This area is rather exciting, but problems are encountered regarding the identity of the active moiety and how it can leave the protein and enter the cell; moreover, it is not known how many protein-bound platinum atoms are needed to kill a cell (i.e. whether the number of antibody proteins which can bind to a tumor cell multiplied by the number of platinum atoms bound to the antibody suffices to kill a cell).

4.5. Platinum Complexes as Radiation Sensitizers

Cisplatin and its congeners enhance the effect of radiation therapy, the enhancement being more than additive.[126] Analogues characterized by low toxicity also have this property.[127] This is interesting since a high local concentration of the sensitizer is needed, and compounds with low toxicity are therefore desirable. Many complexes have been proposed and some of them were designed specifically for this purpose; as examples we might mention the platinum complexes of nitroimidazole, which is itself a radiation sensitizer.[128,129] These compounds sensitize hypoxic tumor cells (i.e. cells receiving insufficient oxygen) which are not sensitive to radiation. The overall mechanism must be different from that of the cytotoxicity of cisplatin, since *trans* isomers also share this property.[127]

5. Conclusions

Extensive structure-activity studies have played a key role in attempts at optimizing the structure of cisplatin analogues. These studies have led to some important guidelines for the design of new complexes. In particular they have stressed the possibility of dissociating antitumor activity from some organ-specific toxic manifestations.[130] Thus, a number of analogues no longer appear to be nephrotoxic. However, since the toxicity toward rapidly proliferating cells (e.g. myelosuppression) becomes dose limiting in second generation cisplatin analogues, it is likely that changes in the therapeutic index of these drugs are associated with a reduction in the systemic toxicity, rather than due to an unexpected biochemical selectivity for tumor cells.[131]

Therapy with cisplatin is limited not only by its toxicity for a variety of normal tissues, but also by a resistance, which may be present initially in the treatment of less sensitive tumors, or which may emerge during the therapy of sensitive tumors. It is now generally agreed that future progress in the therapy of human cancer will be improved by the development of analogues with a wider spectrum of activity. In this respect promising derivatives are the platinum complexes with 1,2-diaminocyclohexane **8** because of their peculiar biological properties.[46]

New strategies have recently been developed. In our opinion the more interesting analogues will be compounds in which some biologically relevant molecules are complexed to platinum either as the inert or the leaving group. The biologically relevant molecules proposed are nutrients, recognizing entities such as steroids, and specific proteins (carrier approach), and substances with an intrinsic pharmacological activity, such as antimetabolites or other anticancer drugs (multifunctional approach). Other recent strategies included the preparation of "polyplatinum drugs" and of complexes which are suitable as sensitizers in radiation therapy.

Although it is difficult to predict whether these new types of complexes could be selective towards tumor cells, or possess therapeutic advantages over the second generation analogues, they are structural novelties worthy of biological evaluation.

In the authors' opinion, a rational development of new analogues requires a detailed knowledge of the mechanism of action of cisplatin itself. For instance very little is known on how cisplatin reaches certain organs, how it enters the cells, and why it ultimately reaches the chromosomal DNA, despite the fact that thousands of potential ligand groups, with high affinity for platinum, can be encountered before the medicament reaches its primary target. Thus, for example, it has been proposed that cisplatin enters the cells through an active membrane transport system.[60] Alteration of this system may be the cellular basis of natural and acquired resistance to a drug[132] and there are indications that this may be the case also for cisplatin,[76] although other mechanisms may also be involved.[133] The question therefore arises whether such a transport system can be characterized and eventually exploited to increase intracellular drug accumulation thus improving drug effectiveness, and to design analogues which use different cell membrane transport mechanisms to overcome the problems of resistance to cisplatin.

The discovery that cisplatin is an effective anticancer drug was, however, a fortuitous one.[3] Although at times we wonder whether only mere chance will bring us a really advanced cisplatin analogue, we believe that at the present stage more basic research is needed in order to elucidate many aspects of the cisplatin mode of action before new analogues with a really improved effectiveness can be designed.

We thank the CNR (Rome) and the Italian Ministry of Education for support of this work.

Received: May 5, 1986;
revised: September 25, 1986 [A 623 IE]
German version: *Angew. Chem. 99* (1987) 632

[1] a) S. Neidle, M. J. Waring (Eds.): *Molecular Aspects of Anticancer Drug Action*. McMillan, London 1983; b) L. F. Povirk in [1a], p. 157.
[2] a) H. Siegel (Ed.): *Metal Ions in Biological Systems, Vol. 11*. Dekker, New York 1980; b) D. H. Petering in [2a], p. 197.
[3] B. Rosenberg, L. Van Camp, J. E. Trosko, V. H. Mansour, *Nature (London) 222* (1969) 385.
[4] a) M. P. Hacker, E. B. Douple, I. H. Krakoff (Eds.): *Platinum Coordination Complexes in Cancer Chemotherapy*. Nijhoff, Boston 1984; b) S. K. Carter in [4a], p. 359.
[5] A. W. Prestayko, J. C. D'Aoust, B. F. Issel, S. T. Crooke, *Cancer Treat. Rev. 6* (1979) 17; M. Rozencweig, D. D. Von Hoff, R. Abele, F. M. Muggia, in H. M. Pinedo, B. A. Chabner, (Eds.): *Cancer Chemotherapy Annual, Vol 1*. Elsevier, Amsterdam 1979, p. 107.
[6] A. J. Lippman, C. Helson, L. Helson, I. H. Krakoff, *Cancer Chemother. Rep. Part 1 57* (1973) 191; J. A. Gottlieb, B. Drewinko, *ibid. Part 1 59* (1975) 621.
[7] J. Abrams, *Eur. J. Cancer Clin. Oncol. 22* (1986) 9.
[8] B. J. Corden, R. L. Fine, R. F. Ozols, J. M. Collins, *Cancer Chemother. Pharmacol. 14* (1985) 38.
[9] R. F. Ozols, R. C. Young, *Semin. Oncol. 12* (1985) 21.
[10] See, e.g., M. J. Cleare, P. C. Hydes in [2a], p. 1; Pd: D. S. Gill in [4a], p. 267; Ti, V, Nb, Mo: P. Köpf-Maier, H. Köpf in [4a], p. 279; Cu, Ag, Au: P. J. Sadler, M. Nasr, V. L. Narayanan in [4a], p. 290; Sn: A. J. Crowe, P. J. Smith, G. Atassi, *Inorg. Chim. Acta 93* (1984) 178.
[11] B. Rosenberg, *Cancer Chemother. Rep. Part 1 59* (1975) 589.
[12] J. J. Roberts, M. F. Pera, Jr., *Platinum, Gold, and other Metal Chemotherapeutic Agents (ACS Symp. Ser. 209* (1983) 3); A. L. Pinto, S. J. Lippard, *Biochim. Biophys. Acta 780* (1985) 167.
[13] J. J. Roberts, M. F. Pera, Jr. in [1a], p. 183.
[14] J. P. Macquet, J. L. Butour, N. P. Johnson, H. Razaka, B. Salles, C. Vieussens, M. Wright in [4a], p. 27.
[15] K. J. Scanlon, R. L. Safirstein, H. Thies, R. B. Gross, S. Waxmann, J. B. Guttenplan, *Cancer Res. 43* (1983) 4211.
[16] J. A. Hickman, K. J. Scanlon, T. R. Tritton, S. Shionoya, Y. Lu, *Cancer Res. 46* (1986) 3445.
[17] D. E. Hathway, G. F. Kolar, *Chem. Soc. Rev. 9* (1980) 241; R. M. Wing, P. Pjura, H. R. Drew, R. E. Dickerson, *EMBO J. 3* (1984) 1201; N. P. Johnson, A. M. Mazard, J. Escalier, J. P. Macquet, *J. Am. Chem. Soc. 107* (1985) 6376.
[18] K. W. Kohn in A. C. Sartorelli, J. S. Lazo, J. R. Bertino (Eds.): *Molecular Action and Targets for Cancer Chemotherapeutic Agents*, Academic Press, New York 1981, p. 3; A. Eastman, *Biochemistry 24* (1985) 5027.
[19] A. M. J. Fichtinger-Schepman, P. H. M. Lohman, J. Reedijk, *Nucl. Acids Res. 10* (1982) 5345; J. P. Caradonna, S. J. Lippard in [4a], p. 14.
[20] R. B. Ciccarelli, M. J. Solomon, A. Varshavsky, S. J. Lippard, *Biochemistry 24* (1985) 7533; S. E. Sherman, D. Gibson, A. H.-J. Wang, S. J. Lippard, *Science (Washington DC) 230* (1985) 412.
[21] A. F. Le Roy, *Cancer Treat. Rep. 63* (1979) 231.
[22] See, e.g., C. A. Bignozzi, C. Bartocci, C. Chiorboli, V. Carassiti, *Inorg. Chim. Acta 70* (1983) 87, and references cited therein.
[23] J. A. Broomhead, D. P. Fairlie, M. W. Whitehouse, *Chem.-Biol. Interact. 31* (1980) 113.
[24] B. Lippert, H. Schoellhorn, U. Thewalt, *Inorg. Chem. 25* (1986) 407, and references cited therein.
[25] J. J. Roberts, A. J. Thompson, *Prog. Nucleic Acid Res. Mol. Biol. 22* (1979) 71.
[26] M. J. Staquet, D. P. Byar, S. B. Green, M. Rozencweig, *Cancer Treat. Rep. 67* (1983) 753.
[27] E. Bowen, M. M. Nauta, H. M. M. Schluper, F. Elferink, W. J. F. Van der Vijgh, H. M. Pinedo, *Eur. J. Cancer Clin. Oncol. 21* (1985) 1253.
[28] M. J. Cleare, J. D. Hoeschele, *Bioinorg. Chem. 2* (1973) 187; M. J. Cleare, *Coord. Chem. Rev. 12* (1974) 349.
[29] J. P. Macquet, J. L. Butour, *J. Nat. Cancer Inst. (USA) 70* (1983) 899.
[30] J. Drobnik, *Cancer Chemother. Pharmacol. 10* (1983) 145.
[31] D. B. Brown, A. R. Khokhar, M. P. Hacker, L. Lokys, J. H. Burchenal, R. A. Newman, J. J. McCormack, D. Frost, *J. Med. Chem. 25* (1982) 952; S. L. Doran, A. R. Khokhar, M. P. Hacker, *Inorg. Chim. Acta 108* (1985) 113.
[32] J. H. Burchenal, K. Kalaher, K. Dew, L. Lokys, *Cancer Treat. Rep. 63* (1979) 1493; L. M. Hall, R. J. Speer, H. J. Ridgway, S. J. Norton, *J. Inorg. Biochem. 11* (1979) 139.
[33] A. I. Stetsenko, M. A. Presnov, A. L. Konovalova, *Russ. Chem. Rev. (Engl. Transl.) 50* (1981) 353.
[34] W. C. Rose, J. E. Schurig, J. B. Huftalen, W. T. Bradner, *Cancer Treat. Rep. 66* (1982) 135.
[35] H. A. Meinema, F. Verbeek, J. W. Marsman, E. J. Bulten, J. C. Dabrowiak, B. S. Krishnan, A. L. Spek, *Inorg. Chim. Acta 114* (1986) 127.
[36] T. G. Appleton, R. D. Berry, C. A. Davis, J. R. Hall, H. A. Kimlin, *Inorg. Chem. 23* (1984) 3514.
[37] J. P. Macquet, S. Cros, J. P. Armand, *Cancer Res. 44* (1984) 3736.
[38] M. P. Hacker, D. B. Brown, A. R. Khokhar, J. J. McCormack, *Proc. Am. Assoc. Cancer Res. 23* (1982) 160.
[39] L. S. Hollis, A. R. Amundsen, E. W. Stern, *J. Am. Chem. Soc. 107* (1985) 274.
[40] R. J. Speer, H. Ridgway, L. M. Hall, D. P. Stewart, K. E. Howe, D. Z. Liebermann, A. D. Newmann, J. M. Hill, *Cancer Chemother. Rep. Part 1 59* (1975) 629.
[41] S. J. Meischen, G. R. Gale, L. M. Lake, C. J. Frangakis, M. G. Rosenblum, E. M. Walker, Jr., L. M. Atkins, A. B. Smith, *J. Natl. Cancer Inst. 57* (1976) 841.
[42] B. K. Chakraborthy, N. Biswas, K. Chondhury, R. K. Neogy, B. Das Sarma, *Chemotherapy (Basel) 31* (1985) 55.
[43] K. Inagaki, K. Tajima, Y. Kidani, T. Tashiro, S. Tsugagoshi, *Inorg. Chim. Acta 37* (1979) L457.
[44] M. Gullotti, G. Pacchioni, A. Pasini, R. Ugo, *Inorg. Chem. 21* (1982) 2006, and references cited therein; A. T. M. Marcelis, C. Erkelens, J. Reedijk, *Inorg. Chim. Acta 91* (1984) 129.
[45] J. Kozelka, G. A. Petsko, S. J. Lippard, *J. Am. Chem. Soc. 107* (1985) 4079; J. Kozelka, G. A. Petsko, G. J. Quigley, S. J. Lippard, *Inorg. Chem. 25* (1986) 1077.
[46] T. A. Connors, M. Jones, W. C. Rose, P. D. Braddock, A. R. Khokhar, M. L. Tobe, *Chem.-Biol. Interact. 5* (1972) 415; J. H. Burchenal, K. Kalaher, T. O'Toole, J. Chisholm, *Cancer Res. 37* (1977) 3455.
[47] J. B. Vermorken, W. W. ten Bokkel Huinink, J. G. McVie, W. J. F. van der Vijgh, H. M. Pinedo in [4a], p. 330.
[48] R. J. Speer, L. M. Hall, D. P. Stewart, H. J. Ridgway, J. M. Hill, Y. Kidani, K. Inagaki, M. Noji, S. Tsugagoshi, *J. Clin. Hematol. Oncol. 8* (1978) 44.
[49] M. Gullotti, A. Pasini, R. Ugo, S. Filippeschi, L. Marmonti, F. Spreafico, *Inorg. Chim. Acta 91* (1984) 223.
[50] A. Pasini, A. Velcich, A. Mariani, *Chem.-Biol. Interact. 42* (1982) 311.
[51] K. Inagaki, Y. Kidani, *Inorg. Chim. Acta 46* (1980) 35; W. R. Leopold, R. P. Batzinger, E. C. Miller, J. A. Miller, R. H. Earhart, *Cancer Res. 41* (1981) 4368; B. Wappes, M. Jennerwein, E. von Angerer, J. Engel, H. Schoenenberger, H. Brunner, M. Schmidt, M. Berger, D. Schmaehl, S. Seeber, *J. Cancer Res. Clin. Oncol. 107* (1984) 15.
[52] K. Inagaki, Y. Kidani, *Inorg. Chem. 25* (1986) 1.

[53] M. Laverick, A. H. W. Nias, I. M. Ismail, P. J. Sadler, *Br. J. Cancer 43* (1981) 732.
[54] R. J. Brandon, J. C. Dabrowiak, *J. Med. Chem. 27* (1984) 861.
[55] E. E. Blatter, J. F. Vollano, B. S. Krishnanan, J. C. Dabrowiak, *Biochemistry 23* (1984) 4817.
[56] S. J. Lippard, *Science (Washington, D.C.) 218* (1982) 1075.
[57] J. M. Hill, E. Loeb, A. McLellan, N. O. Hill, A. Khan, J. J. King, *Cancer Chemother. Rep. Part 1 59* (1975) 647.
[58] R. E. Cramer, P. L. Dahlstrom, M. J. T. Seu, T. Norton, M. Kashiwagi, *Inorg. Chem. 19* (1980) 148.
[59] E. Bersanetti, A. Pasini, G. Pezzoni, G. Pratesi, G. Savi, R. Supino, F. Zunino, *Inorg. Chim. Acta 93* (1984) 167.
[60] J. E. Byfield, P. M. Calabro-Jones, *Nature (London) 294* (1981) 281.
[61] J. M. Hill, R. J. Speer, *Anticancer Res. 2* (1982) 173.
[62] K. R. Harrap in F. M. Muggia (Ed.): *Cancer Chemotherapy*, Nijhoff, den Haag 1983, p. 171; *Platinum Met. Rev. 28* (1984) 14.
[63] F. H. Lee, R. Canetta, B. F. Issell, L. Lenaz, *Cancer Treat. Rev. 10* (1983) 39.
[64] A. Khan, J. Tseng, R. Young, *J. Clin. Hematol. Oncol. 14* (1984) 35.
[65] S. E. Owens, N. Thatcher, H. Sharma, N. Adam, R. Harrison, A. Smith, A. Zaki, J. C. Baer, C. A. McAuliffe, D. Crowther, B. W. Fox, *Cancer Chemother. Pharmacol. 14* (1985) 253.
[66] G. Mathe, Y. Kidani, M. Noji, R. Maral, C. Bourut, E. Chenu, *Cancer Lett. (Shannon, Ireland) 27* (1985) 135; P. Ribaud, J. Gouveia, J. L. Misset, G. Mathe, *Oncology 43* (1986) 78.
[67] N. Colombo, E. Sartori, F. Landoni, G. Favalli, L. Vassena, L. Zotti, E. Materman, C. R. Franks, S. Pecorelli, C. Mangiani, *Cancer Treat. Rep. 70* (1986) 793.
[68] C. Abel, T. A. Connors, W. C. Ross, N. H. Nam, H. Hoellinger, L. Pichot, *Eur. J. Cancer 9* (1973) 49.
[69] A. Pasini, E. Bersanetti, F. Zunino, G. Savi, *Inorg. Chim. Acta 80* (1983) 99.
[70] L. J. Hanka, *Cancer Treat. Rep. 63* (1979) 1009.
[71] M. Szekerke, *Cancer Treat. Rep. 60* (1976) 347.
[72] D. T. Vistica, *Biochim. Biophys. Acta 550* (1979) 390; *Blood 56* (1980) 427.
[73] A. J. Charlson, W. A. Shorland, *Inorg. Chim. Acta 93* (1984) L67.
[74] W. A. Beck in A. Müller, E. Diemann (Eds.): *Transition Metal Chemistry*, Verlag Chemie, Weinheim 1981, p. 3, and references cited therein.
[75] A. Pasini, E. Bersanetti, *Inorg. Chim. Acta 107* (1985) 259.
[76] A. Colombo, R. Di Gioia, A. Pasini, T. Dasdia, F. Zunino, *Inorg. Chim. Acta 125* (1986) L1.
[77] E. von Angerer, G. Egginger, G. Kranzfelder, H. Bernhauer, H. Schoenenberger, *J. Med. Chem. 25* (1982) 832; B. Wappes, M. Jennerwein, E. von Angerer, H. Schoenenberger, J. Engel, M. Berger, K.-H. Wrobel, *ibid. 27* (1984) 1280; H. Schoenenberger, B. Wappes, M. Jennerwein, M. Berger, *Cancer Treat. Rep. 11* (1984) 125.
[78] R. C. Richmond, T. J. Curphey, J. A. Katzenellenbogen in [4a], p. 262.
[79] O. Gandolfi, J. Blum, *Inorg. Chim. Acta 80* (1983) 103; O. Gandolfi, J. Blum, F. Mandelbaum-Shavit, *ibid. 91* (1984) 257.
[80] V. T. De Vita, Jr. in V. T. De Vita, Jr., S. Hellman, S. A. Rosenberg (Eds.): *Cancer*, Lippincott, Philadelphia 1985, p. 257.
[81] M. A. Khaled, R. D. Morin, F. Benington, J. P. Daugherty, *Cancer Chemother. Pharmacol. 13* (1984) 73.
[82] See, e.g., B. Rosenberg, *Cancer (Amsterdam) 55* (1985) 2303.
[83] a) R. C. Manaka, W. Wolf in R. P. Spencer (Ed.): *Radiopharmaceuticals: Structure Activity Relationships*, Grune and Stratton, New York 1981, p. 183; b) S. Yolles, R. M. Roat, M. F. Sartori, C. L. Washburne, *Biological Activities of Polymers (ACS Symp. Ser.) 186* (1982) 233.
[84] F. Zunino, G. Savi, A. Pasini, *Cancer Chemother. Pharmacol. 18* (1986) 180.
[85] F. Zunino, R. Gambetta, A. Di Marco, A. Velcich, A. Zaccara, F. Quadrifoglio, V. Crescenzi, *Biochim. Biophys. Acta 476* (1977) 38.
[86] J. B. Chairs, N. Dattagupta, D. M. Crothers, *Biochemistry 21* (1982) 3933; J. B. Chairs, *ibid. 22* (1983) 4204.
[87] M. Howe-Grant, S. J. Lippard, *Biochemistry 18* (1979) 5762; W. D. McFayden, L. P. G. Wakelin, I. A. G. Roos, V. A. Leopold, *J. Med. Chem. 28* (1985) 1113.
[88] B. E. Bowler, L. S. Hollis, S. J. Lippard, *J. Am. Chem. Soc. 106* (1984) 6102.
[89] R. E. Bowler, S. J. Lippard, *Biochemistry 25* (1986) 3031.
[90] S. J. Lippard, B. E. Bowler, Eur. Pat. 163316A (1984).
[91] N. P. Farrell, M. P. Hacker, J. J. McCornack, *Proc. Am. Assoc. Cancer Res. 27* (1986) 288.
[92] J. Feigon, W. A. Denny, W. Leupin, D. R. Kearns, *J. Med. Chem. 27* (1984) 450.
[93] J. W. Lown, A. R. Morgan, S. F. Yen, Y. H. Wang, W. D. Wilson, *Biochemistry 24* (1985) 4028.
[94] S. A. Lang, Jr., K. C. Murdock, Eur. Pat. 37486 B1 (1984).
[95] M. Julliard, G. Vernin, J. Metzger, T. Garcia-Lopez, *Synthesis 1982*, 49.
[96] B. S. Iyengar, T. Takahashi, W. A. Remers, W. T. Bradner, *J. Med. Chem. 29* (1986) 144.
[97] N. P. Farrell, J. Williamson in [4a], p. 261.
[98] See e.g., E. A. Steck, D. S. Rane, *Antimicrob. Agents Chemother. 15* (1979) 157.
[99] N. Farrell, *Platinum, Gold and other Metal Chemotherapeutic Agents (ACS Symp. Ser. 209* (1983) 279).
[100] D. Cracinescu, R. Maral, G. Mathe, A. Doadrio in [4a], p. 256.
[101] H. N. Jayaram, D. A. Cooney, *Cancer Treat. Rep. 63* (1979) 1095.
[102] S. J. Meischen, G. R. Gale, M. B. Naff, *J. Clin. Hematol. Oncol. 12* (1982) 67.
[103] R. E. Cramer, D. M. Ho, W. Van Doorne, J. A. Ibers, T. Norton, M. Kashiwagi, *Inorg. Chem. 20* (1981) 2457.
[104] E. N. Spremulli, D. L. Dexter, *J. Clin. Oncol. 2* (1984) 227.
[105] N. Farrell, *J. Chem. Soc. Chem. Commun. 1982*, 331.
[106] S. J. S. Kerrison, P. J. Sadler, *J. Chem. Soc. Chem. Commun. 1977*, 861; *Inorg. Chim. Acta 104* (1985) 197.
[107] S. Kirschner, Y. K. Wei, D. Francis, J. G. Bergman, *J. Med. Chem. 9* (1966) 369.
[108] M. Maeda, N. Abiko, T. Sasaki, *J. Med. Chem. 24* (1981) 167; *J. Pharm. Dyn. 5* (1982) 81.
[109] F. Kanzawa, M. Maeda, T. Sasaki, H. Hoshi, K. Kuretani, *J. Natl. Cancer Inst. (USA) 68* (1982) 287.
[110] M. Maeda, N. Abiko, H. Uchida, T. Sasaki, *J. Med. Chem. 27* (1984) 444.
[111] J. Baranowska-Kortylewicz, E. J. Pavlik, W. T. Smith, Jr., R. C. Flanigan, J. R. van Nagell, Jr., D. Ross, D. E. Kenady, *Inorg. Chim. Acta 108* (1985) 91.
[112] T. Lin, R. X. Zhou, K. J. Scanlon, W. F. Brubaker, Jr., J. J. Shim Lee, K. Woods, C. Humphreys, W. H. Prusoff, *J. Med. Chem. 29* (1986) 681.
[113] B. Drewinko, M. A. Dipasquale, L. Y. Yang, B. Barlogie, J. M. Trujillo, *Chem.-Biol. Interact. 55* (1985) 1.
[114] See e.g., F. Gonzalez, H. Amos, *J. Natl. Cancer Inst. (USA) 58* (1977) 1519; E. Krug, A. Zweibaum, C. Schulz-Holstege, D. Keppler, *Biochem. J. 217* (1984) 701.
[115] W. Beck, G. Thiel, DBP 3108842 (1982); T. Tsubomura, S. Yano, K. Kobayashi, T. Sakurai, S. Yoshikawa, *J. Chem. Soc. Chem. Commun. 1986*, 459.
[116] F. D. Rochon, P. C. Kong, *J. Clin. Hematol. Oncol. 12* (1982) 39.
[117] P. J. Andrulis, Jr., P. Schwartz, G. R. Gale in [4a], p. 259.
[118] L. Gros, H. Ringsdorf, H. Schupp, *Angew. Chem. 93* (1981) 311; *Angew. Chem. Int. Ed. Engl. 20* (1981) 305.
[119] C. G. Gebelein, *Biological Activities of Polymers (ACS Symp. Ser.) 186* (1982) 193.
[120] D. S. Zaharko, M. Przybylski, V. T. Oliverio, *Methods Cancer Res. 16* (1979) 347.
[121] H. R. Allcock, R. W. Allen, J. P. O'Brien, *J. Chem. Soc. Chem. Commun. 1976*, 717.
[122] S. Yolles, J. F. Morton, B. Rosenberg, *Acta Pharm. Suvec. 15* (1978) 382.
[123] C. E. Carraher, Jr., D. J. Giron, I. Lopez, D. R. Cerutis, W. J. Scott, *Org. Coat. Plast. Chem. 44* (1981) 120.
[124] E. Hurwitz, R. Kashi, M. Wilchek, *J. Natl. Cancer Inst. (USA) 69* (1982) 47.
[125] J. G. Hefferman, M. J. Cleave, D. H. Picker, Eur. Pat. 169645A (1985).
[126] E. B. Douple, R. C. Richmond, *Int. J. Radiat. Oncol. Biol. Phys. 5* (1979) 1369.
[127] J. J. Roberts, W. J. F. van der Vijgh, J. B. Vermorken, E. B. Douple, *Cancer Chemother. Ann. 6* (1984) 118,and references cited therein.
[128] J. R. Bales, P. J. Sadler, C. J. Coulson, M. Laverick, A. H. W. Nias, *Br. J. Cancer 46* (1982) 701.
[129] K. A. Skov, N. P. Farrell, T. G. de Carneiro, F. W. B. Einstein, T. Jones in [4a], p. 260.
[130] W. C. Rose, J. E. Schurig, *Cancer Treat. Rev. 12* (1985) 1.
[131] M. J. Cleare, P. C. Hydes, B. W. Malerbi, D. M. Watkins, *Biochimie 60* (1978) 835.
[132] F. M. Sirotnak, P. L. Chello, R. W. Brockman, *Methods Cancer Res. 16* (1979) 381.
[133] R. B. Gross, K. J. Scanlon, *Chemioterapia 5* (1986) 37.

Direct Identification of the Carbon Skeleton of Organic Compounds using Double Quantum Coherence ^{13}C-NMR Spectroscopy. The INADEQUATE Pulse Sequence

New Analytical Methods (32)

By Joachim Buddrus* and Hans Bauer

NMR spectroscopy plays an important part in the determination of the structures of organic compounds. The parameters of importance here are the chemical shifts of the ^{1}H and ^{13}C nuclei and the spin-spin interactions both between ^{1}H nuclei and between ^{1}H and ^{13}C nuclei. Couplings between ^{13}C nuclei were almost completely neglected until a few years ago, since they were extremely difficult to observe because of the low natural abundance of ^{13}C. However, it is these couplings which afford information directly on the carbon–carbon connectivities in the molecule. It is now possible to use a special NMR pulse sequence to make these couplings more readily visible: the result of using this sequence is a ^{13}C-NMR spectrum from which the carbon skeleton concerned can be directly read off. Two-dimensional spectra in particular are very easy to evaluate. The pulse sequence involved, which bears the somewhat puzzling name INADEQUATE, produces double-quantum coherences from which the NMR signals of the coupled carbon nuclei can be obtained. In this article the principle of double-quantum coherence is described and a number of examples for the application of the INADEQUATE pulse sequences to problems in synthetic organic chemistry, biosynthesis and natural products chemistry are presented; in addition, the possibility of applying the INADEQUATE method to other nuclei is considered.

1. Introduction

It is not uncommon to come across carbon compounds which do not reveal the secret of their structure or of a detail of that structure: examples are provided by polycyclic hydrocarbons, compounds with several neighboring non-hydrogen-bearing carbon atoms or polyhalogen compounds. In such cases ^{1}H-, ^{13}C and if possible ^{15}N-NMR spectra have already been obtained, but to no avail. X-ray structural analysis, the last possibility, is not feasible, either because the compound of interest does not crystallize or because the crystals obtained exhibit unfavorable properties. If enough of the substance is available ($\geqslant$200 mg for a molecular weight of ca. 300), the technique of ^{13}C-NMR spectroscopy should again be applied; however, in this case spectra must be accumulated until molecules containing two neighboring ^{13}C nuclei can be observed (only one molecule in 10000 contains two such directly bonded nuclei). This can be done either using conventional techniques or, much more readily, using the INADEQUATE pulse sequence, since the latter eliminates the unwanted signals of isolated ^{13}C nuclei by subtraction. A comparison of the ^{13}C,^{13}C spin-spin coupling constants shows which molecular fragments (CH_3, CH_2, CH, C, CX, C=O etc.) are bonded together, and thus the exact nature of the carbon skeleton present.

[*] Priv.-Doz. Dr. J. Buddrus, Dr. H. Bauer
Institut für Spektrochemie und angewandte Spektroskopie
Bunsen-Kirchhoff-Str. 11
D-4600 Dortmund 1 (FRG)

2. Isotopomeric Carbon Compounds

The element carbon contains 98.9% of the isotope ^{12}C (spin quantum number I = 0) and 1.1% of the isotope ^{13}C (I = 1/2). Almost all carbon compounds thus consist of a number of isotopomers. Thus for example even the simple three-carbon molecule 1-propanol exists as a mixture of the following eight isotopomers (when hydrogen and oxygen are considered to be isotopically pure):

$H_3C-CH_2-CH_2-OH$ 96.73%	$H_3{}^{13}C-{}^{13}CH_2-CH_2-OH$ 0.01%
$H_3{}^{13}C-CH_2-CH_2-OH$ 1.08%	$H_3{}^{13}C-CH_2-{}^{13}CH_2-OH$ 0.01%
$H_3C-{}^{13}CH_2-CH_2-OH$ 1.08%	$H_3C-{}^{13}CH_2-{}^{13}CH_2-OH$ 0.01%
$H_3C-CH_2-{}^{13}CH_2-OH$ 1.08%	$H_3{}^{13}C-{}^{13}CH_2-{}^{13}CH_2-OH$ 0.0001%

The proportion of an isotopomer with a ^{13}C atom in a certain position is $0.011^{1} \times 0.989^{n-1}$ (n is the number of carbon atoms in the molecule), that of an isotopomer with two ^{13}C atoms in defined positions (whether these are directly neighboring or not) is $0.011^{2} \times 0.989^{n-2}$, and so on. This means that only one single molecule in 10000 has two neighboring ^{13}C atoms in a certain position.

Broad-band decoupling of the attached protons converts isotopomers with only a single ^{13}C nucleus to spin systems of type A, so that singlet signals are observed (this is the conventional ^{13}C-NMR spectrum). Isotopomers with two ^{13}C nuclei behave just like those with only a single ^{13}C

Table 1. $^1J(C,C)$ coupling constants as a function of carbon hybridization and of the substituent X in the fragment ^{13}C-^{13}C-X (substituent effects in brackets [a]).

Compound	Hybridization	X = H	X = CH_3	X = Cl	X = O-Alkyl
H_3C-CH_2-X	sp^3-C, sp^3-C	34.6	34.6 (0)	36.1 (1.5)	38.9 (4.3)
$H_2C=CH-CH_2X$	sp^2-C, sp^3-C	41.9	41.8 (0)	45.2 (3.3)	46.7 (4.3)
$H_2C=CX-CH_3$	sp^2-C, sp^3-C	41.9	41.9 (0)	48.5 (6.6)	51.8 (9.9)
H_5C_6-X	sp^2-C, sp^2-C	56.0 [b]	57.1 (1.1) [b]	65.2 (9.2) [b]	67.0 (11.0) [b]
$H_2C=CH-X$	sp^2-C, sp^2-C	67.6	70.0 (2.4)	77.6 (10.0)	78.1 (10.5)
$HC\equiv C-X$	sp-C, sp-C	171.5	175.0 (3.5)	207 [c] (35.5)	216.5 (45.0) [5]
$H_3C-CO-X$	sp^3-C, sp^2-C	39.7	40.1 (0.7)	56.1 (16.7)	58.8 (19.4)
$HCO-CH_2X$	sp^3-C, sp^2-C	39.7	38.3 (−1.4)		

[a] Values taken in part from Ref. [1] and in part determined by us. [b] $^1J(C_1,C_2)$. [c] Calculated [5].

nucleus if the ^{13}C nuclei are separated by several bonds. If however the ^{13}C nuclei are separated by only a few bonds (generally one to three), they couple and thus, unless they are isochronous, they form AB or AX spin systems whose spectra consist of two doublets. $^1J_{C,C}$, the coupling constant over one bond, depends on the hybridization of the carbon orbitals and on the substituent X in the fragment $^{13}C,^{13}C$-X and varies between ca. 35 and 220 Hz (Table 1).[1-4] Coupling constants over 2 or 3 bonds are much smaller, typically between 0 and 5 Hz. Isotopomers with three (and more) ^{13}C nuclei are present in vanishingly small amounts and cannot be detected by NMR spectroscopy at the present time unless their ^{13}C content is artificially increased.[6,7]

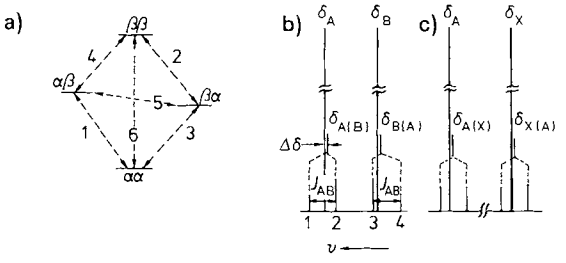

Fig. 1. Term scheme and NMR spectrum of a ^{13}C-^{13}C fragment. (a) Term scheme: 1, 2, 3, and 4 are allowed single-quantum transitions, 5 and 6 forbidden zero- and double-quantum transitions respectively. (b) and (c): NMR spectra of an AB and an AX spin system. The chemical shifts of the coupled ^{13}C nuclei are shifted to higher field by between 0 and 0.03 ppm (isotope effect on the chemical shift).

In ^{13}C-NMR spectra with a sufficient signal-to-noise ratio (> 500 : 1) the weak signals of the coupled nuclei can be seen on either side of the strong singlet signals of the isolated ^{13}C nuclei (see Fig. 1). The intensity ratio of the singlet signal to one of the four signals of the coupled nuclei is ca. 200 : 1. If the various coupling constants have different values, a comparison of the coupling constants of all ^{13}C nuclei in a molecule shows which atom is bonded to which and thus the exact structure of the carbon skeleton present.

3. Conventional ^{13}C-NMR Spectroscopy

The conventional ^{13}C-NMR procedure, by which we mean the sequence pulse-data acquisition, has been used several times to determine the coupling constants between two neighboring ^{13}C nuclei.[8-10] The coupling constants were used in part for an unequivocal assignment of ^{13}C-NMR signals and in part for the determination of biosynthetic pathways (starting from ^{13}C-labeled compounds).

We observed that the $^1J_{C,C}$ values in a conventional spectrum can also be used to determine the constitution of unknown compounds; this will be demonstrated below.

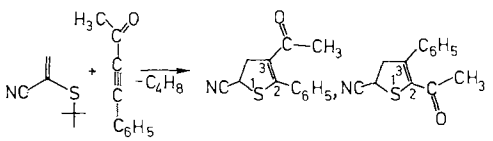

1 2 3 4

When the unsaturated compounds **1** and **2** are heated, isobutene is split off to give the dihydrothiophene **3** or its isomer **4**.[11] The use of conventional spectroscopic techniques to distinguish between these two possibilities is problematic, one reason being that in **2** the reacting carbon atoms bear no hydrogens. The distinction is however simple when $^{13}C,^{13}C$ spin-spin couplings are used (Fig. 2); the singlet at 154 ppm, which because of its position must be assigned to the olefinic carbon atom β to the carbonyl group, has only two pairs of satellites in the ratio 1 : 1. It can thus only be the C-2 signal in **3**. Further C,C couplings, which for reasons of clarity are not shown in Figure 2, confirm the suggested constitution.[12]

This example shows that the evaluation of the satellite signals of just one single ^{13}C signal can suffice to distinguish between alternative constitutions. However, in the case of completely unknown constitutions it is necessary to take into account the satellites of a large number of signals. Such a process is often difficult, since a) spinning side bands or signals due to impurities can be incorrectly identified as satellite signals or b) satellite signals can be hidden (by other satellite signals or by signals due to isolated ^{13}C nuclei).

Many of these difficulties can be avoided when instead of the conventional recording technique the pulse sequence INADEQUATE (*I*ncredible *N*atural *A*bundance *D*oubl*E* *QUA*ntum *T*ransfer *E*xperiment) is used; this sequence was first suggested by *Freeman* et al.[13] The basis for this particular pulse sequence is the technique of multi-

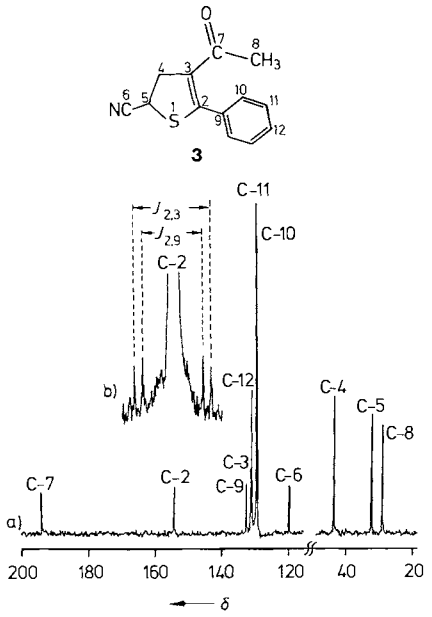

Fig. 2. 25-MHz $^{13}C\{^1H\}$-NMR spectrum of **3** (0.5 g) + [Cr(acac)$_3$] (acac = acetylacetonate) (ca. 10 mg) in $CDCl_3$ (1.5 mL). Digital resolution: 0.5 Hz/data point. a) Single transient. b) 60000 transients, repetition interval 4 s (partial spectrum). $J_{2,3} = 72.9$, $J_{2,9} = 57.7$ Hz.

quantum NMR spectroscopy developed by *Ernst* et al.[14, 15] (for reviews see Refs. [16, 17]).

Three methods are used to describe the influence of high-frequency pulses on spin systems: the vector model method, density matrix formalism, or product operator formalism. Vector models are simple to understand, but cannot generally be used to describe systems other than those containing only isolated nuclei. The density matrix formalism reproduces the behavior of isolated spins or of coupled spins correctly, but becomes cumbersome for systems containing a number of coupled nuclei. The latter systems are most conveniently described by the product operator formalism,[18] which is based on density matrix formalism. We shall use density matrix formalism (for details see Appendix), which is still easy to follow for two-spin systems; the results of the calculations will be represented by vector diagrams.

4. One-Dimensional INADEQUATE ^{13}C-NMR Spectroscopy

The INADEQUATE method consists of a pulse sequence which in the simplest version is executed twice (the "two-step cycle"), whereby the direction (phase) of the last 90° pulse and of the detector (data acquisition system) differ in the two steps. Two FIDs are thus obtained, and the co-addition of these leads to the elimination of the strong signals due to the isolated ^{13}C nuclei.

$90^\circ_x - \tau - 180^\circ_y - \tau - 90^\circ_x - \Delta - 90^\circ_x$ - data acquisition (x) step 1
$90^\circ_x - \tau - 180^\circ_y - \tau - 90^\circ_x - \Delta - 90^\circ_y$ - data acquisition $(-y)$ step 2

The effect on a C_2 fragment is shown in Figure 3. The first part of the INADEQUATE pulse sequence ($90^\circ_x - \tau - 180^\circ_y - \tau$) is identical to a homonuclear spin-echo experiment (for a review of modern pulse sequences and their

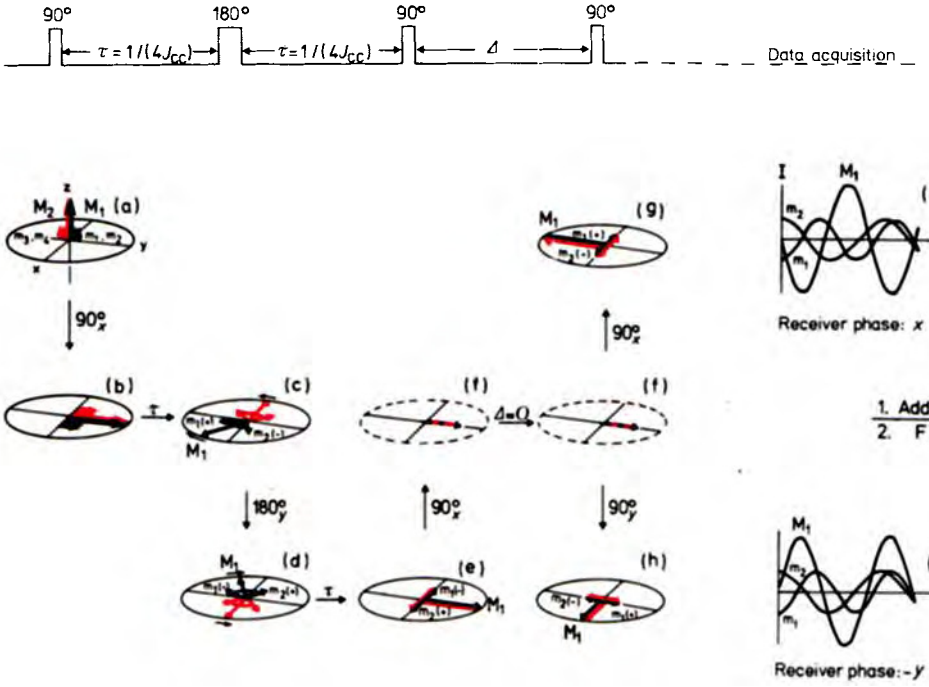

Fig. 3. The INADEQUATE pulse sequence and its effect on a C_2 fragment. M_1, M_2 and m_1 to m_4 are the magnetizations of the isotopomeric fragments ^{13}C-^{12}C, ^{12}C-^{13}C and ^{13}C-^{13}C. The delay time τ and the switching time Δ (ca. 10 μs) are not shown to scale. M_1, $m_1(+)$, $m_2(-)$: the Larmor frequency of m_1 is larger, that of m_2 smaller than that of M_1. The coordinate systems for single- and double-quantum transitions are denoted by full and dotted perimeters respectively. For clarity there have been omitted: the notations M_2, m_3 and m_4 in (b)–(e) and (h), and their Fourier components in (i) and (j). For the same reason the magnetizations M_1 and M_2 after the third and before the fourth pulse are not shown, since this would require a separate coordinate system (for single-quantum coherence). It can however readily be seen that M_1 and M_2 are transferred by the third and fourth pulses into the $-y$-direction ($90^\circ_x + 90^\circ_x$) and x-direction ($90^\circ_x + 90^\circ_y$) respectively, as shown in (g) and (h).

effects see [19]); when the total time $2\tau = 1/(2J_{C,C})$, the magnetization of the isolated ^{13}C nuclei (M_1 and M_2) is separated from that of the coupled nuclei (m_1 to m_4) so that the magnetizations lie on orthogonal axes of the rotating coordinate system (rotating frame) (Fig. 3e). The subsequent $90°_x$ pulse shifts the magnetizations M_1 and M_2 from the y-direction to the $-z$-direction, while the magnetizations m_1 to m_4 are transferred from the $\pm x$-direction into the so-called double-quantum coherence and directed along the y-axis of the rotating double-quantum coordinate system (Fig. 3f). In contrast to the single-quantum coherence (M_1, M_2), the double-quantum coherence does not represent observable magnetization. Thus it cannot be accommodated in the coordinate system for rotating single-quantum coherences and requires a separate rotating frame (Fig. 3f). The rotation of M_1 and M_2 is of the classical type. The conversion of m_1 to m_4 into double-quantum coherence and the phase direction of the latter follows from the density matrix formalism (see Appendix).

The last pulse (the "read pulse") is in the x-direction in the first step and in the y-direction in the second. It converts the double-quantum coherence into single-quantum coherence, whereby M_1 and M_2, and m_1 to m_4, are directed as shown in Figures 3g and 3 h respectively. The phase of the detectors is then switched in such a way that it follows only the magnetizations m_1 to m_4 of interest: in the first step in the x-direction and in the second in the $-y$-direction. Two free-induction decays are recorded; these contain the Fourier components of the magnetizations M_1, M_2 and m_1 to m_4 shown in Figures 3i and 3j. Addition of the FIDs leads to addition of m_1–m_4 and, if the high-frequency pulses are perfect, to the simultaneous *elimination of M_1 and M_2*. Finally, Fourier transformation affords the frequency spectrum (Fig. 3k), which only contains the two doublets (in antiphase in each case) of the AX spin system.

A one-dimensional INADEQUATE ^{13}C-NMR spectrum consists in theory only of signals from coupled nuclei: the unwanted signals due to isolated ^{13}C nuclei (whether from the main component or from impurities) as well as the spinning sidebands from these signals are not present.

The power of the one-dimensional INADEQUATE method is demonstrated by the following example: Dieckmann condensation of the diester **5** affords a compound which according to its 300-MHz ^1H-NMR spectrum is either **6** or **7**.[20]

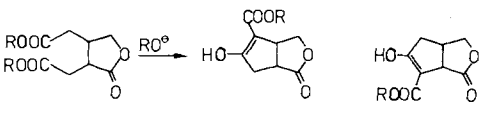

5 **6** **7**

A decision as to which compound is present is made possible by the $^{13}C,^{13}C$ couplings (Fig. 4). The connectivity $O{=}C{-}CH{-}CH_2$ is demonstrated by the observed couplings, so that the structure must be **6**; further connectivities support this structure.[12] A distinction on the basis of the satellite signals in a normal ^{13}C-NMR spectrum would be difficult: **6** contains an impurity, the NMR signals of which overlap the all-important satellites of the signal of

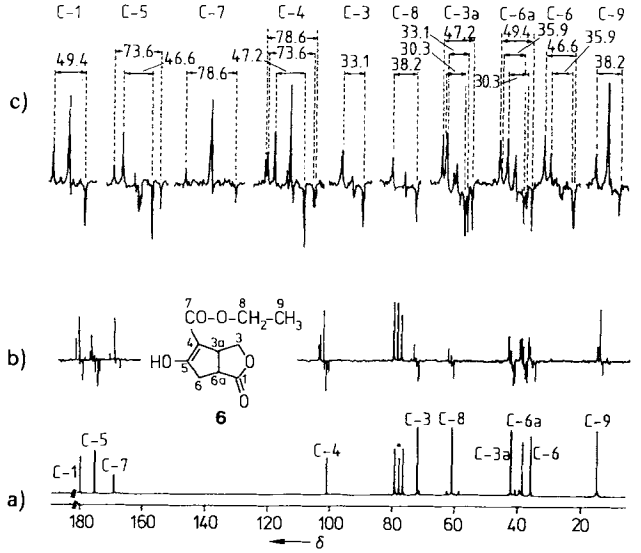

Fig. 4. 25-MHz ^{13}C-NMR spectrum of **6** (1.2 g) + [Cr(acac)$_3$] (20 mg) in $CDCl_3$ (1.0 mL). a) Conventional spectrum, 1000 transients. b) One-dimensional INADEQUATE spectrum; $\tau = 1/(4J)$ ($J = 50$ Hz); 122000 transients, repetition interval 4 s (total measuring time 135 h); digital resolution 0.5 Hz/data point. c) Expanded INADEQUATE spectrum. * Solvent signals.

C-6a. In general, the presence of up to 20% of impurities can be tolerated when structures are to be determined by the INADEQUATE method.

The determination of the carbon skeleton from $^{13}C,^{13}C$ coupling constants can also be carried out using a computer program. The frequencies of the satellite signals are first read off (automatization of this process is prevented by signal overlap) and stored: the program then searches for coupling constant values which appear twice.[21]

5. Two-Dimensional INADEQUATE ^{13}C-NMR Spectroscopy

If the $^{13}C,^{13}C$ coupling constants differ only slightly from one another, overlap of satellite signals (for AX spectra) or ambiguities in recognizing the coupling partner may occur. Difficulties of this type can be avoided when the INADEQUATE sequence is made two-dimensional.

The pulse sequence for the two-dimensional experiment is almost exactly the same as that in one dimension: the change is that the short switching time Δ in Figure 3 is replaced by the time t_1, which is incremented stepwise.

When $t_1 = 0$, the non-observable double-quantum coherence is directed along the y'-axis of the double-quantum coordinate system (Fig. 5a). It then rotates at the double-quantum frequency ν_{DQ} in the x', y'-plane of this coordinate system; after the evolution times $t_1 = n/(4\nu_{DQ})$,

$\nu_{DQ} = \nu_A + \nu_X - 2\nu_0$

ν_A, ν_X: resonance frequency of the nuclei A and X;
ν_0: exciting frequency

$n = 1$–4 in the directions shown in Figure 5. Conversion to single-quantum coherence by means of the 90° read pulse, followed by Fourier transformation, gives the satellite signals, the intensity of which is now modulated by ν_{DQ}.

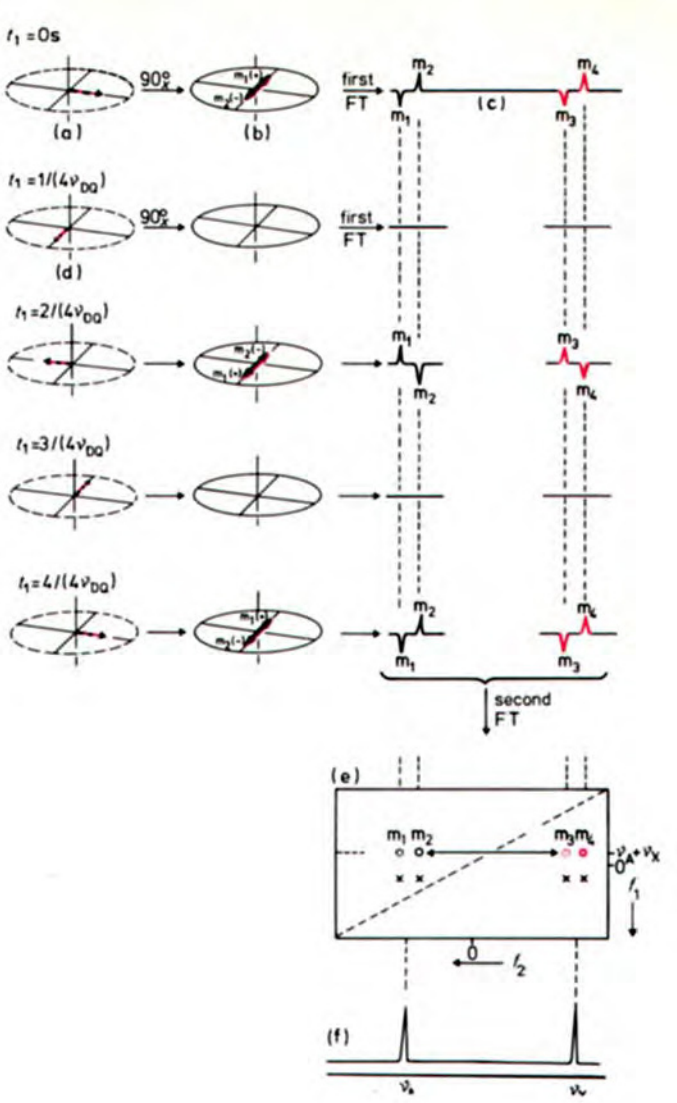

Fig. 5. Influence of the evolution time t_1 (which replaces Δ in Fig. 3) on the magnetization of a C_2 fragment. For clarity only the effect of the read pulse 90°$_x$ (step 1 in Section 4) on the magnetizations m_1 to m_4 is shown and the notations m_3 and m_4 are omitted. One should note the general agreement between (a), (b), and (c) and 3f, 3g and 3k. (e) shows the contours (full and dotted circles: above and below the plane of the paper respectively) of the four signals m_1 to m_4 of an AX spin system. The mid-points of those contours which belong together lie on the frequency diagonal $f_1 = 2f_2$ (f_1, f_2: double- and single-quantum frequencies respectively). The positions marked by an "×" are those of the mirror frequencies (see Section 7.3). (f) = conventional ^{13}C-NMR spectrum of the C_2 fragment.

A second Fourier transformation—in this case applied on the intensity variation of the satellite signals—gives the double-quantum frequency ν_{DQ} of the AX spin system. Since this frequency is equal for all four signals of an AX spin system, the satellite signals appear in the same row (f_1 = constant) of the two-dimensional spectrum, though with differing phase. The situation is analogous for each further AX spin system.

The projection of the contours of a two-dimensional INADEQUATE spectrum onto the x-axis of a coordinate system (f_2) gives the chemical shifts of the satellite signals, that onto the y-axis the double-quantum frequencies of the different AX spin systems. The advantage over a one-dimensional spectrum is that no overlap can occur, even when $^1J_{C,C}$ values are equal, since the double doublets of each of the different AX spin systems occur in different rows.[22]

An application of the two-dimensional INADEQUATE method is shown in the following example: the acid-catalyzed elimination of water from the bicyclic lactone **8** gives a tricyclic ketone of the formula $C_{12}H_{18}O$, the constitution of which could not be established using the standard spectroscopic techniques.

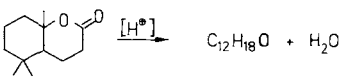

8

Figure 6b shows the two-dimensional INADEQUATE spectrum, which to obtain better digital resolution in f_2 was recorded only for the aliphatic carbons. In order to identify the carbon skeleton, the signals are numbered from left to right, the corresponding numbers are joined up as in **9a**, and finally the numbers are replaced by the corresponding CH_n fragments (which have previously been obtained from another experiment, e.g. via off-resonance decoupling). The result is **9b**; after the keto group (δ = 229.5 ppm) has been added, the final structure **10** is obtained.[23]

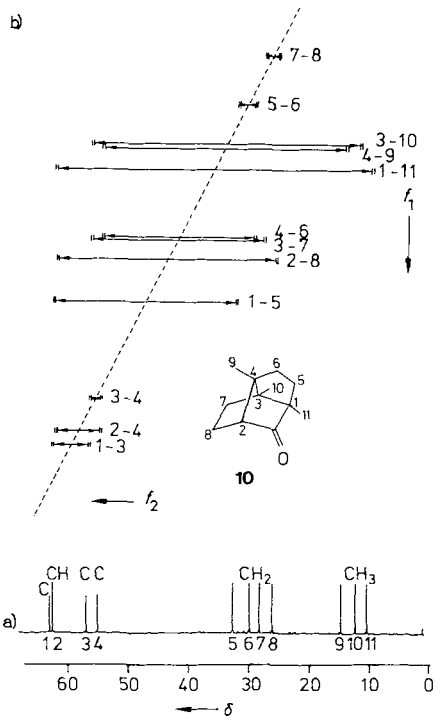

Fig. 6. 100-MHz ^{13}C-NMR spectrum (aliphatic part) of **10** (1.2 g) + [Cr(acac)$_3$] (10 mg) in $CDCl_3$ (1.5 mL). a) Conventional spectrum. b) Two-dimensional INADEQUATE spectrum, $\tau = 1/(4J)$ (J = 35 Hz). f_2 = 8771 Hz (8 K data points), f_1 = 8771 Hz/(512 data points). 113 rows were recorded, each with 128 transients; repetition interval 4 s; measuring time 16 h. The data matrix was zero-filled to 16 K · 512 and Fourier transformed after Gaussian multiplication in f_1 and f_2.

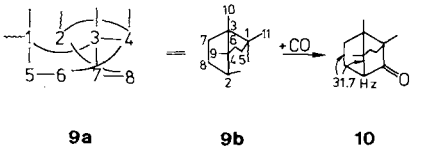

9a **9b** **10**

A conventional or one-dimensional INADEQUATE ^{13}C-NMR spectrum would not have provided the answer here, since several coupling constants are equal or very similar. Thus the coupling constant of 31.7 Hz would have suggested the connectivities C-7–C-2 and C-8–C-4 as well as the correct ones C-4–C-2 and C-7–C-8.

If all the contours in a 2D-INADEQUATE spectrum are visible, its interpretation requires little time and can be carried out without any particular spectroscopic or chemical experience.

6. Other NMR Methods for the Determination of the Carbon Skeleton

The carbon skeleton of an organic molecule can also be determined by using the method of zero-quantum coherence. The pulse sequence used is as follows:

$90°_{\phi_1}$-τ-$180°_{\phi_2}$-τ-$45°_{\phi_3}$-t_1-$90°_{\phi_4}$-data acquisition (ϕ_5)

For details of the phases ϕ_1–ϕ_5 see Ref. [24a]. The y-axis of the two-dimensional spectrum now contains the zero-quantum frequencies $\nu_{DQ}=\nu_A-\nu_B-2\nu_0$, the x-axis the chemical shifts of satellite signals. The signal intensities in the zero-quantum NMR spectrum are however reduced by a half compared with those in the INADEQUATE NMR spectra.[24b]

Apart from the direct methods of determining the carbon skeleton via coupling between ^{13}C nuclei, there are also indirect methods which use the coupling between ^{1}H nuclei or between ^{1}H and ^{13}C nuclei (Table 2). H,H-COSY (*CO*rrelation *S*pectroscop*Y*),[14] the most sensitive technique, detects relationships between hydrogen atoms, while an H,C-COSY experiment[25] (which uses polarization transfer) shows which H-atom is bonded to which C-atom. In suitable cases, an H-relayed H,C-COSY experiment[26] permits the construction of a connection pattern involving CH_n or CH_n–XH_m groups. An H,C-correlation via small coupling constants ($^3J_{C,H}$, $^2J_{C,H}$) using the pulse sequence H,C-COLOC (*CO*rrelation spectroscopy via *LO*ng-range *C*oupling)[27] permits relationships to quaternary carbon atoms to be established. The number of bonds between the coupling nuclei cannot however be extracted from spectra of this type. Unambiguous conclusions regarding connections between quaternary carbon atoms and CH_n-groups can be obtained with the help of a C-relayed H,C-COSY experiment,[28] in which the information on the chemical shift of the hydrogen atom is transferred via $^1J_{C,H}$ and $^1J_{C,C}$ to the quaternary C-atom. The latter method has been used to distinguish between regioisomers.[28]

As can be seen from Table 2, the INADEQUATE method is the least sensitive of those mentioned. Because of the resulting long measurement time, this method should be used only when the others are unsuccessful.

7. Practical INADEQUATE NMR Spectroscopy

7.1. The Intensity of the Residual Signal

In practice, the two-step cycle described above affords only an incomplete elimination of the signals of isolated ^{13}C nuclei. The reasons for this are firstly the non-ideal spectrometer conditions such as pulse angle errors and phase errors, and secondly differences between the two recording channels (receiver systems), each of which has its own analog-digital converter and amplifier. However, the residual signals can be reduced further by using extended phase cycles (Table 3).

The double-quantum coherence produced by the pulse sequence $90°_x$-τ-$180°_y$-τ-$90°_x$ can be read by a $90°_{-x}$ or $90°_{-y}$ pulse as well as by a $90°_x$ or $90°_y$ pulse. This 4-step cycle[13] compensates for the inequality of the recording channels with respect to the satellite signals, but not with respect to the main signals, since the subtraction of the latter still requires the use of both recording channels. A phase cycle for the excitation of the double-quantum coherence (i.e. equal phase changes for *all* pulses and of the receiver) leads to a 16-step cycle in which the inequality of the recording channels now also has no influence on the

Table 2. Two-dimensional NMR techniques for the direct and indirect determination of carbon skeletons.

Puls sequence	Skeleton	Correlation	Relevant couplings	Sensitivity with respect to INADEQUATE pulse sequence
INADEQUATE	C^1-C^2	δ(C-1) with δ(C-2)	^1J(C,C)	1
C-relayed H,C-COSY	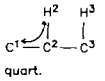	e.g. δ(C-1) with δ(H-2)	^1J(C-1,C-2), ^1J(C-2,H-2)	2 for CH–$C_{quart.}$
H-relayed H,C-COSY	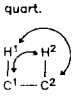	e.g. δ(C-1) with δ(H-2)	^1J(C-1,H-1), ^3J(H-1,H-2)	20–200, according to J(H,H)
H,C-COLOC		e.g. δ(C-2) with δ(H-1)	^nJ(C-2,H-1) ($n \geq 2$)	20–200
H,C-COSY		e.g. δ(C-1) with δ(H-1)	^1J(C-1,H-1)	~200
H,H-COSY		e.g. δ(H-1) with δ(H-2)	^nJ(H,H)	1000–10000

Table 3. Phase cycles in INADEQUATE NMR measurements with the pulse sequence $90°_x - \tau - 180°_y - \tau - 90°_\varphi - \Delta - 90°_\varphi$, data acquisition (*e*).

Step [a]	*a*	*b*	*c*	*d*	*e*
1	x	y	x	x	x
2	x	y	x	y	$-y$
3	x	y	x	$-x$	$-x$
4	x	y	x	$-y$	y
5	y	$-x$	y	y	y
6	y	$-x$	y	$-x$	x
7	y	$-x$	y	$-y$	$-y$
8	y	$-x$	y	x	$-x$
9	$-x$	$-y$	$-x$	$-x$	$-x$
10	$-x$	$-y$	$-x$	$-y$	y
11	$-x$	$-y$	$-x$	x	x
12	$-x$	$-y$	$-x$	y	$-y$
13	$-y$	x	$-y$	$-y$	$-y$
14	$-y$	x	$-y$	x	$-x$
15	$-y$	x	$-y$	y	y
16	$-y$	x	$-y$	$-x$	x

[a] Steps 1–2: 2-step cycle; Steps 1–4: 4-step cycle; Steps 1–16: 16-step cycle.

main signals. This cycle is the smallest which should be used in practice. The influence of pulse angle and pulse phase errors on the height of the residual signal can be reduced by further *separate* phase cycles for the various pulses. The 180° pulse has the largest effect on the height of the residual signal. Inversion of this pulse leads to a 32-step cycle, which in most cases affords good signal suppression; this phase cycle is contained in the software provided by most instrument manufacturers for INADEQUATE measurements. The residual signal can be reduced to practically zero by variation of the phase of the 180° pulse in all 4 possible directions (64-step cycle), inversion of the phase of the first pulse (128-step cycle)[29] and inversion of the phase of the third pulse (256-step cycle). Elimination of the residual signal however is possible only with sufficiently large repetition intervals (establishment of equilibrium of the longitudinal magnetization). This must be taken into account in particular when determining $^{13}C,^{13}C$ long-distance couplings.

7.2. The Intensity of the Satellite Signals

The only magnetizations observable after the application of an INADEQUATE pulse sequence are those resulting from a double quantum coherence. Thus the intensity of the satellite signals is determined by the effectiveness of the generation of double-quantum coherence.

The *delay time* has the greatest effect. Optimum generation of double-quantum coherence only occurs when τ and the coupling constant $^1J_{C,C}$ are related by Equation (a).

$$\tau = \frac{2n+1}{4 \times {}^1J_{C,C}} \quad (n = 0, 1, 2, 3, \ldots) \qquad (a)$$

The value to be used for the order n depends on the spin system.[30] In the AX case ($\delta/J > 3$), n has no influence on the intensity, and in practice $n = 0$ is used because of the influence of the transverse relaxation (time constant T_2^*); in the AB-case ($\delta/J < 3$), $n = 1$ or 2 is better (Fig. 7). In some cases only the conventional NMR method affords

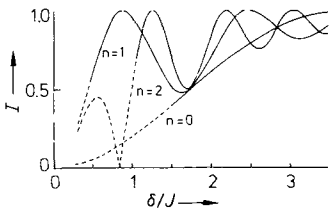

Fig. 7. Calculated total intensity of the four signals of a $^{13}C,^{13}C$ fragment as a function of the coupling strength δ/J. $\tau = 1/(4J)$ is an optimum for weak coupling, while for strong coupling ($\delta/J < 2.8$) $\tau = 3/(4J)$ or $5/(4J)$ is better. The dotted lines show the areas in which only low satellite intensities are observed in spite of an optimally chosen τ-value [30].

the satellite signals. The two techniques are compared in Figure 8 using example **11**[12]. The INADEQUATE experiment gives no satellite signals for C-1–C-5, since the order $n = 0$ set without knowledge of the δ/J ratio is unfavorable for C-1, C-5 coupling (the signals would have become visible with $n = 2$). In the conventional ^{13}C-NMR spectrum,

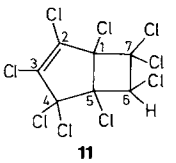

11

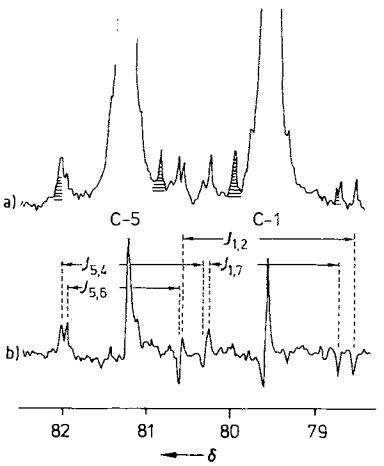

Fig. 8. 25-MHz ^{13}C-NMR spectrum (part only) of **11** in $CDCl_3$. a) Conventional spectrum. The shaded signals are due to $^1J_{1,5}$. b) One-dimensional INADEQUATE spectrum. $^1J_{5,4} = 42.4$, $^1J_{5,6} = 33.8$, $^1J_{1,2} = 51.2$, $^1J_{1,7} = 38.1$, $^1J_{1,5} = 30.4$ Hz.

the signals (shaded) are readily apparent. It is generally the case that only the conventional technique affords the maximum intensity for the satellite signals (for the calculation of strongly coupled AB spin systems ($\delta/J < 1$) from the inner lines see Ref. [8a]).

If the actual coupling constant (J_a) differs from the value J used in Equation (a), the intensity I will be decreased in the AX case according to Equation (b), since

$$I = I_{max} \sin(2\pi J_a \tau) \qquad (b)$$

the magnetization is no longer directed exactly along the $\pm$-axis (Fig. 3e). However, the results of this deviation

from ideality are not serious: 50% or more of the maximum intensity I_{max} is still observed when

$1/3J \leqslant J_a \leqslant 5/3J$ [for n = 0, Eq. (a)]

Thus, the satellite signals due to the coupling C-1–C-6a (49.4 Hz) in **6** have a greater intensity than those due to the coupling C-4–C-7 (78.6 Hz) if, as was the case, the NMR experiment is set up for $J = 50$ Hz (Fig. 4). (For the intensity decrease observed in the AB case see [30].)

Pulse imperfections, such as inhomogeneity of the high-frequency field within the measuring volume (pulse angles not constant) or "off-resonance" effects (when the effective high-frequency field is not constant across the chemical shift range), will also reduce the intensity of the satellite signals. Off-resonance effects can become particularly important at very high magnetic field and can lead to inversion of the phase of the satellite signals or even to a disappearance of the latter. The imperfections mentioned cannot be avoided by the use of a phase cycle, but may be removed by the use of composite pulses.[31-33]

The *linewidth* of the satellite signals in a 1D-INADEQUATE NMR spectrum is the same as that in a conventional spectrum. However, the linewidth of 2D-INADEQUATE spectra on the double-quantum frequency axis is increased on instrumental grounds by a factor of two.[29b]

All the factors discussed so far cause the signal-to-noise ratio (S/N) of the satellite signals to decrease as follows (assuming equal measurement time for all methods):

$$S/N_{normal} > S/N_{1D\text{-}INADEQUATE} > S/N_{2D\text{-}INADEQUATE}$$

In a conventional ^{13}C-NMR spectrum the two satellite pairs of an AX spin system have different intensities, since they are subject to differing influences such as the NOE (Nuclear Overhauser Effect) and T_1 (the longitudinal relaxation time). In the INADEQUATE experiment the magnetizations are distributed via the double-quantum coherence between the two nuclei, and equal intensities are observed for the satellite signals even in extreme cases such as $C_{quat.}$–CH_3.

When a carbon atom couples with several other C-atoms, the satellite pairs for this atom also have different intensities if the T_1-values for the coupling partners differ. Coupling between quaternary C-atoms is often only observed when either a long repetition interval is used (the optimal repetition interval for 90° observation pulses is $1.3\,T_1$[34]) or when relaxation reagents such as [Cr(acac)$_3$] are added to reduce the measurement time.

7.3. Modification of the INADEQUATE Pulse Sequence

The INADEQUATE pulse sequence has undergone a number of modifications which increase the information content of the spectra; both the one- and the two-dimensional versions have been varied.

In the one-dimensional version, signal cancellation can occur if two satellite signals lie very close together and are in antiphase. Such cancellations can be avoided by incorporating a delay time $\tau = 1/(2J_{C,C})$, which causes a refocussing of the phase directions of the satellite signals.[13] (For intensity distortions in AB spin systems see Ref. [35].) During the refocussing time, the methods applied in conventional ^{13}C-NMR spectroscopy for spectral editing according to the CH multiplicity can also be incorporated.[36,37] A further technique for the determination of multiplicities, SEMINA (*S*ubspectral *E*diting using a *M*ultiple quantum trap for *INA*DEQUATE) divides the spectra according to the sum of the H-atoms in the CH_n–CH_m-fragment: all satellite signals for C_2-fragments with this sum even (e.g. $C_{quat.}$–CH_2 or CH–CH) appear in one spectrum, while those for which the sum is odd appear in a second spectrum.[38]

One-dimensional INADEQUATE spectra can also be simplified by variation of the time period Δ in the INADEQUATE pulse sequence. If the signals of a certain AX spin system are to be eliminated, Δ is set to the corresponding double-quantum coherence according to $\Delta = 1/(4\nu_{DQ})$[39] (see Fig. 5d). If on the contrary only the signals of a particular AX spin system are to be recorded, the transmitter frequency is set at exactly the mid-point between the single frequencies ν_A and ν_B, and Δ is varied in a random manner. This method, known as DOUBTFUL (*DOUB*le quantum *T*ransition for *F*inding *U*nresolved *L*ines)[40-42] eliminates all signals which have a non-zero double-quantum frequency.

As shown by Figure 5, the 90° read pulse in the two-dimensional version results in an *amplitude* modulation: the Fourier transformation of the FIDs gives not only the required signals (echos) with double-quantum frequency ν_{DQ}, but also the unrequired reflected signals (antiechos) whose frequency is ν_{-DQ} (marked in Fig. 5e by crosses). The latter can be eliminated by a *phase* modulation, which is realized by adding to the two-step cycle ($\Delta = t_1$) the following sequence:[43]

$90°_x$ - τ - $180°_y$ - τ - $90°_x$ - $45°_{\bar{z}}$ - t_1 - $90°_x$ - acquisition (y)
$90°_x$ - τ - $180°_y$ - t - $90°_x$ - $45°_{\bar{z}}$ - t_1 - $90°_y$ - acquisition (x)

The $45°_{\bar{z}}$ pulse, which is in practice replaced by the combination $90°_{-x}$ - $45°_{-y}$ - $90°_x$, rotates the double-quantum coherence by 90°; its imaginary part is then converted by the read pulse into observable magnetization. Phase shifting the receiver by 90° allows these magnetizations to be added as imaginary parts to the real parts obtained from the pulse sequence without the $45°_{\bar{z}}$ pulse, which have already been stored. In this way quadrature detection with respect to the f_1-axis is also achieved.

A partial phase modulation can also be achieved by setting the read pulse angle to 135°:[44]

$90°_x$ - τ - $180°_y$ - τ - $90°_x$ - t_1 - $135°_x$ - data acquisition (x)
$90°_x$ - τ - $180°_y$ - t - $90°_x$ - t_1 - $135°_y$ - data acquisition ($-y$)

The result is a good suppression of the antiecho and at the same time an increase in the intensity of the echo. The ratio of echo to antiecho is now ca. 6 : 1 (instead of 1 : 1 for a read pulse angle of 90°). A further improvement (to 9 : 1) is obtained by setting the third and fourth pulses of the INADEQUATE pulse sequence to 120°.[45]

When the read pulse occurs in the middle of the evolution time t_1 as follows[46]

$$90^\circ_x - \tau - 180^\circ_y - \tau - 90^\circ_x - \frac{t_1}{2} - 135^\circ - \frac{t_1}{2} - \text{data acquisition}$$

the intensities of the satellite signals are modulated by half the frequency of the coupling partner, $(\nu+J/2)/2$, instead of by the double-quantum frequency.[47] The resulting two-dimensional spectrum resembles a COSY spectrum and can thus also be symmetrized. There is disagreement as to whether this variation leads to a worthwhile improvement in the signal-to-noise ratio.[47,48]

The relative insensitivity of the INADEQUATE method has been mentioned several times (Table 2). An increase in the sensitivity can be achieved by using the combined pulse sequences INEPT-INADEQUATE (INEPT: *IN*sensitive *E*nhancement by *P*olarization *T*ransfer)[49] and DEPT-INADEQUATE (DEPT: *D*istortionless *E*nhancement by *P*olarization *T*ransfer).[50] In these cases, the intensity of the satellite signals can be increased by polarization transfer from protons to carbon-13 (by a factor $\geq 4/3$); in addition the repetition interval can be decreased (as long as the relaxation times T_1 of the protons are shorter than those of the ^{13}C nuclei). A sensitivity increase is also provided by the sequence INSIPID (*IN*ADEQUATE *S*ensitivity *I*mprovement by *P*roton *I*ndirect *D*etection).[51a] The INSIPID sequence transfers ^{13}C coherence modulated by $^1J_{C,C}$ to proton coherence and thus takes advantage of the higher sensitivity of ^1H- relative to ^{13}C-NMR spectroscopy. The theoretical gain in sensitivity of $(\gamma_H/\gamma_C)^3 = 64$ is however not reached because of the inverse polarization transfer (from C to H) and because of signal splitting due to $^nJ_{H,H}$ and $^2J_{C,H}$. The authors estimate a tenfold gain in sensitivity to be more realistic. However, INSIPID experiments are not easy to carry out, since spectrometer modifications are necessary (pulses on the ^{13}C nuclei via the decoupler channel; recording of the ^1H-magnetization via the decoupler channel). (For the problem of suppressing the ca. 10^4-fold more intense H signals in the H-^{12}C-^{12}C fragments see Ref. [51b].)

7.4. Problems Due to Overlapping Signals from Isolated ^{13}C Nuclei

When the ^{13}C-NMR signals from two (or more) CH_2, CH or $C_{quat.}$ fragments lie on top of one another, the determination of the constitution of the molecule by means of INADEQUATE is not possible. Thus when the signals from two CH_2 groups overlap there are three possible connectivities, and one cannot establish which are correct. The situation is not quite so hopeless if the signals of a CH_n fragment and a quaternary carbon are superimposed: the addition of a delay time $t = 1/(2J_{C,H})$ to the INADEQUATE pulse sequence, during which the proton decoupler is switched off, causes the satellite signals of all protonated carbon atoms to be removed while those of the quaternary carbons remain (see **26** in Table 4).[36]

If two ^{13}C signals do not lie on top of each other but only very close together, another problem is encountered. The two-dimensional experiment now requires a very high digital resolution in f_2, which is often not compatible with the limited computer memory available. The one-dimensional experiment can fail when the $^1J_{C,C}$ values are similar. Two selective experiments which are not subject to these limitations will be described below. The first one is not an INADEQUATE experiment.

Selective irradiation at the resonance frequency of a certain ^{13}C nucleus using a field strength B_2, where $\gamma \cdot B_2/2\pi = 0.5\,{}^1J_{C,C}$, followed by a non-selective observing pulse leads to the observation of satellite signals only for those ^{13}C nuclei which are connected to that which is irradiated.[52a] It is necessary for the selective and unselective pulses to differ in phase by 90°.

$135^\circ_{x,\text{selective}} - 90^\circ_y$ - data acquisition (x)	step 1
$135^\circ_{x,\text{selective}} - 90^\circ_{-y}$ - data acquisition (x)	step 2

An application of this technique is shown in the following example. When compound **12** is reduced, one of the products is a compound of molecular formula $C_{13}H_{20}O$; the investigation of this molecule using INADEQUATE affords the fragments **13** and **14** but not the manner in which they are linked, since the signals of C-4 and C-8a which can provide the necessary information lie very close together.

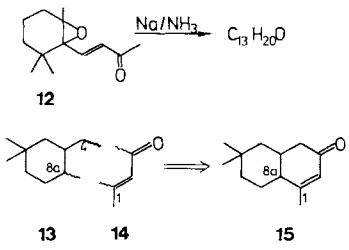

Selective excitation at the frequency of C-1 gives a satellite pair (Fig. 9) which must be assigned to the signal C-8a; its assignment to C-4 would imply an unrealistically large isotope effect of -0.08 ppm on the chemical shift (see also Fig. 1): isotopic effects of $^{13}C/^{12}C$ on ^{13}C are between 0 and -0.03 ppm.[52b] Thus the compound has structure **15**.[53]

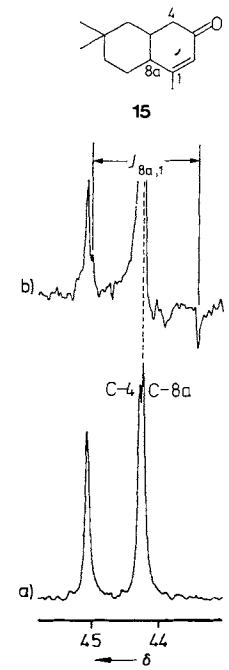

Fig. 9. 25-MHz ^{13}C-NMR spectrum of **15** (part only). Sample concentration: 1.9 g in 0.8 mL of $CDCl_3$. a) Conventional spectrum. b) Spectrum obtained using the pulse sequence described in Ref. [52a] with selective irradiation of C-1, power (corresponding to $0.5J_{C,C} = 20$ Hz) and phase adjusted using a "spin-lock" unit. 14000 transients with 6s repetition interval (total measuring time 23 h). Digital resolution: 0.4 Hz/data point. $J_{8a,1} = 40.5$ Hz.

The satellite spectrum is also simplified when the one-dimensional INADEQUATE experiment is carried out with selective ^{13}C saturation. In contrast to the experiment described above, all satellite signals in which the selectively saturated ^{13}C nucleus is involved are now removed.[54]

7.5. Hints on Carrying Out INADEQUATE NMR Measurements

The following points should be taken into account when INADEQUATE measurements are carried out:

1) The solution should be so concentrated that a single 90° pulse affords a ^{13}C-NMR spectrum with $S/N \geq 25$ (for a definition of S/N see Ref. [55]). 40000 scans then give an INADEQUATE NMR spectrum with a similar S/N ratio (neglecting saturation effects).
2) The T_1-values for the isolated ^{13}C nuclei should be determined prior to the INADEQUATE measurement and if necessary reduced with the help of relaxation reagents so that the longest T_1-values are only 2–3 s (pulse repetition time $1.3\,T_1$).
3) The 90° and 180° pulses should be determined using the solution to be investigated.
4) The delay time τ should be set to ca. 5.5 ms for molecules containing aliphatic and olefinic carbon atoms; from Equation (a) this corresponds to a J-value of about 45 Hz (cf. Table 1).
5) In a two-dimensional INADEQUATE experiment, the S/N ratio for each row should be at least 5, and the number of time increments (and thus rows) should be so chosen that all double-quantum frequencies are sufficiently separated. In practice, resolutions of 50–200 Hz per data point have proven adequate.

8. Applications

$^{13}C,^{13}C$ spin-spin coupling constants can be used for the determination of the constitution of the following types of carbon compound, the structures of which can either not be determined or can be determined only with difficulty using other NMR methods (including two-dimensional techniques):

- Hydrocarbons or hydrocarbon-like compounds (referred to below as "hydrogen-rich carbon compounds"): their ^1H-NMR spectra are complex, while normal ^{13}C-NMR spectra do not afford much information.
- Compounds in which those carbon atoms which are important for determining their constitution carry further carbon atoms or heteroatoms and few if any hydrogens. These will be referred to below as "hydrogen-poor carbon compounds", even when they contain groups such as methyl or phenyl at their periphery. In such cases ^1H-NMR is unsuccessful because of the lack of hydrogen atoms, while normal ^{13}C spectra can often not be interpreted with certainty.
- Compounds with particular symmetry properties, independent of whether they are hydrogen-rich or hydrogen-poor in the sense discussed above.

8.1. Hydrogen-Rich Carbon Compounds

Polycyclic hydrocarbons with but a few functional groups provide a challenge to the structural chemist. Thus the structures of several tricyclic triquinanes could not be determined;[56–58] only X-ray structural analysis of derivatives of some others provided the required structural information.[59,60] As the examples **15**–**20**, **21a**–**c**, **25**, **26** (Table 4) and further triterpenes[61] show, the determination of the carbon skeletons of hydrogen-rich compounds is readily possible, even when some (often redundant) connectivities are missing in their INADEQUATE spectra. In the case of ketones, the satellite signals due to coupling between the carbonyl carbon and the two α-carbon atoms are often not visible because only the aliphatic carbon range is measured; in such cases it is possible to determine the coupling between these two α-carbons over *two* bonds (**10**, **19**, **20**, **22b**). The aggregation state of the hydrocarbon is unimportant: non-polar, oily terpenes can also be studied. Because of the similar $^1J_{C,C}$-values observed for hydrocarbons, the two-dimensional INADEQUATE technique is required.

8.2. Hydrogen-Poor Carbon Compounds

The structural analysis of hydrogen-poor compounds using INADEQUATE will be demonstrated below for two types of compound, namely for certain types of cycloaddition products and for highly chlorinated hydrocarbons.

Products of cycloaddition reactions normally carry sufficient hydrogen atoms to make the determination of their structures by ^1H-NMR spectroscopy unproblematic. However, when hydrogen atoms are not present on the carbons which contain the necessary information, INADEQUATE ^{13}C-NMR spectroscopy can be successfully used. In this way it was possible to determine the structures of the products **27**, **28** and **30** of [3+2]-cycloadditions and of the product **11** of a [2+2]-cycloaddition directly (i.e. without using data from reference compounds). In the case of **29** the structure was also unambiguous, even though the one-dimensional experiment carried out afforded only three connectivities, since these were the decisive ones (the other signals were overlapped). INADEQUATE ^{13}C-NMR spectroscopy is the method of choice when the regiochemistry of cycloadditions is to be determined: the wavy lines in formulas **11** and **26**–**30** indicate the starting materials used and thus make clear the regiochemical problem.

The chemistry of highly-chlorinated hydrocarbons went through a period of vigorous development in the 1950s and 1960s, although not all the structures of the compounds formed were determined.[77] The determination of the constitution of such compounds is readily carried out using INADEQUATE ^{13}C-NMR spectroscopy, as is demonstrated for the examples of the compounds **31**,[75b] **32**–**34**,[76] and **11**[12] (Table 4).

Table 4. Compounds whose structures have been determined by means of INADEQUATE-^{13}C-NMR spectroscopy (boldlines: measured C,C connectivities)

Structure	Notes on INADEQUATE-NMR-measurement (1D, 2D = one- and two-dimensional)
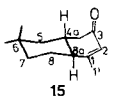 **15** 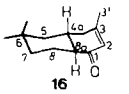 **16**	25 MHz, 2D [53] Aliphatic carbon range, ca. 1.5 g substance Crotyl fragments detected from conventional spectra Connectivity C-1–C-8a in **15** obtained from selective irradiation (Fig. 9) Configuration from H,H-coupling
17	Aliphatic carbon range [62]
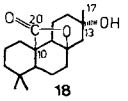 **18**	100 MHz, 1D und 2D [63] Aliphatic carbon range; 470 mg substance C-10–C-20 not detected, since, a) ^1J larger than the value set according to Eq. (a), b) T_1-values relatively large, c) off-resonance effects (140 ppm) are present Configuration at C-13 from δ-value for C-17
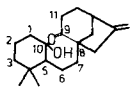 **19** Velloziolone	100 MHz, 1D and 2D [64] 850 mg substance $T > 60$ °C to shorten T_1 C-11–C-9–C-8 from $^2J_{11,8} \approx 9.3$ Hz Configuration from δ-values
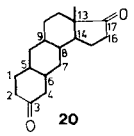 **20**	100 MHz, 1D and 2D [65] Aliphatic carbon range, 1.2 g substance C-2–C-3–C-4 from $^2J_{2,4} = 11.3$ Hz C-13–C-17–C-16 from $^2J_{13,16} = 15.2$ Hz Configuration from δ-values
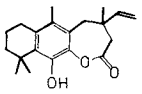 **21** Velloziolide	100 MHz, 1D [66] 500 mg substance $T = 95$ °C (for solubility reasons) Some CC-connectivities not detected because of presence of large ^1J(C,C)-values or strongly coupled AB spin systems.
22a	50 MHz, 2D [67] 30% solution in $CDCl_3$
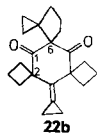 **22b**	100 MHz, 2D [68] 360 mg substance in 2.5 mL $CDCl_3$ C-2–C-1–C-6 from $^2J_{2,6} = 9.7$ Hz Compound has mirror plane.
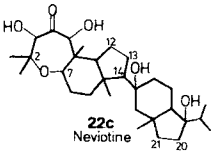 **22c** Neviotine	90 MHz, 2D [69] 2.5 g substance Two spectra recorded ($\delta = 12$–217 and $\delta = 12$–89) C-12–C-13 and C-20–C-21 not detected (strongly coupled AB-spin systems) C-12–C-13 follows from correlations 12-H–C-14, C-20–C-21 from a relay experiment C-2–O–C-7 follows from correlations 7-H–C-2 Crystals not suitable for X-ray structural analysis
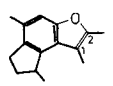 **22d** Marmelerin	75 MHz, 2D [70] 250 mg substance and a few mg [Cr(acac)$_3$] in 1 mL $CDCl_3$ Sample prepared in 10 mm NMR tube; vortex plug used. C-1–C-2 not detected
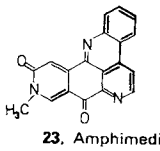 **23**, Amphimedine	75 MHz, 2D [71] 300 mg substance Reason for non-detection of certain correlations: long T_1's of non-protonated C-atoms
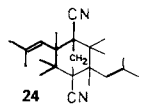 **24**	50 MHz, 1D [72] Configuration determined using NOESY
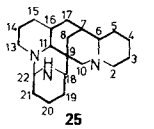 **25** Panamine	50 MHz, 2D [73] 950 mg substance C-3–C-4 and C-15–C-16 not detected, since strongly coupled AB spin systems present($\Delta\delta = 0.33$ and 0.17 ppm respectively) Crystal structure determined previously
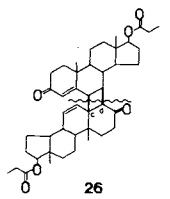 **26**	50 MHz, 2D [36] 840 mg substance Other C,C bonds apart from those emphasized were detected. In order to make the bonding partners of C-c better visible, the satellite signals of the proton-carrying C-atom d, which was fortuitously isochronous with C-c, were eliminated by incorporation of an additional delay time $\tau = 1/(2J(C,H))$ and appropriate switching of the decoupler X-ray structural analysis was not possible.
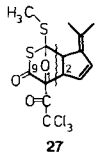 **27**	25 MHz, 1D [74] 900 mg substance plus 10 mg [Cr(acac)$_3$] in 1.5 mL $CDCl_3$ Two experiments with τ corresponding to 38 and 76 Hz ($J\tau = 1/4$) were carried out in order to obtain all connectivities The *endo*-configuration was assigned on the basis of ^3J(C-9, 2-H) = 5.9 Hz
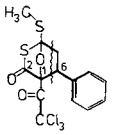 **28**	25 MHz, 1D [74] 900 mg substance plus 10 mg [Cr(acac)$_3$] in 1.5 mL $CDCl_3$ Not all connectivities in benzene ring determined because of the presence of strongly coupled AB spin systems The *endo*-configuration was assigned on the basis of ^3J(C-2,6-H) = 7.9 Hz
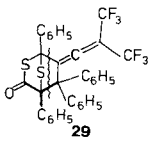 **29**	25 MHz, 1D [75a] 1 g substance plus 10 mg [Cr(acac)$_3$] in 1.5 mL $CDCl_3$ Further connectivities could not be determined because of signal overlap and long-range fluorine coupling
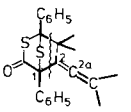 **30**	25 MHz, 1D and 2D [75b] 1 g substance plus 10 mg [Cr(acac)$_3$] in 1.5 mL $CDCl_3$ The coupling in the "broken" bond was only observed for one C-atom C-2–C-2a not observed, since coupling about twice as large as $J = 45$ Hz used for Equation (a) (n = o)
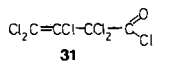 **31** 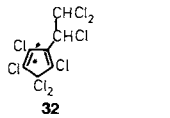 **32** 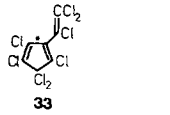 **33**	25 MHz, 1D and/or 2D [12, 75b, 76] 0.5–2 g substance, in each case with ca. 10 mg [Cr(acac)$_3$] and 1.5 mL $CDCl_3$ * = Connectivities determined from the inner signals of the strongly coupled AB spin systems
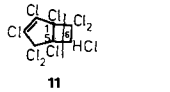 **11**	**11**: C-1–C-5 ($\Delta\delta = 1.7$ ppm) determined from conventional ^{13}C NMR spectroscopy (Fig. 8) Configuration at C-6: determined from ^3J(C,C) and ^3J(C,H)
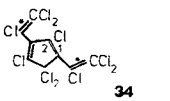 **34**	**34**: C-1–C-2 not visible, since $\Delta\delta = 0.8$ ppm

8.3. Symmetrically Substituted Carbocyclic Compounds

Symmetrically substituted carbocycles are often not easily distinguished from one another. Molecules with a center of symmetry can be recognized fairly easily because of the different band positions in their IR and Raman spectra (the "exclusion rule"; see however Ref. [78]). When the molecule contains sufficient hydrogens at the informative positions the structure can be determined by simulation of the ^{1}H-NMR spectrum,[79] though the results so obtained are not always unambiguous.[80] We shall demonstrate below that certain symmetry properties can be read off directly from the intensity ratios of the ^{13}C,^{13}C satellite signals.[12]

When a ^{13}C atom is bonded to a second which has the same chemical shift, no satellite signals are observed; if it is bonded to two others which both have the same chemical shift, satellite signals of double intensity occur. Figure 10 shows how structures can be distinguished on the basis of such intensity ratios. The method will be demonstrated for two cyclobutanes, one planar and the other non-planar; no information is presently available on larger rings.

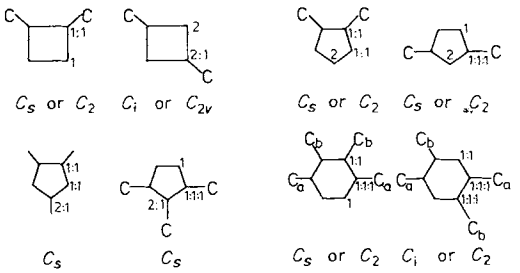

Fig. 10. Derivation of the constitution of symmetrically substituted hydrocarbons from the relative intensities of the ^{13}C,^{13}C-satellite signals.

The photochemical dimerization of **35** leads to a product which according to its normal ^{13}C-NMR spectrum can be either **36** (head-to-tail adduct) or **37** (head-to-head adduct).[81]

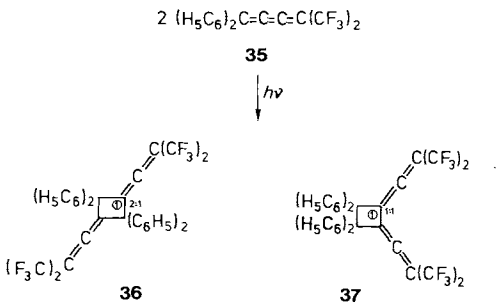

These two structures can be distinguished on the basis of an evaluation of the ^{13}C,^{13}C satellite signals (Fig. 11). The signal at $\delta = 123.7$, which because of the lack of long-range couplings to H or F is assigned to C-1, exhibits two pairs of satellites in the ratio 2 : 1. Thus the correct structure is **36**, since for **37** the ratio would be 1 : 1. The satellite signals for the C-2 signal at $\delta = 68$ should afford the same result, but these are not visible due to broadening caused by long-range proton coupling. The Raman and IR spectra also agree with the suggested structure **36**.[12]

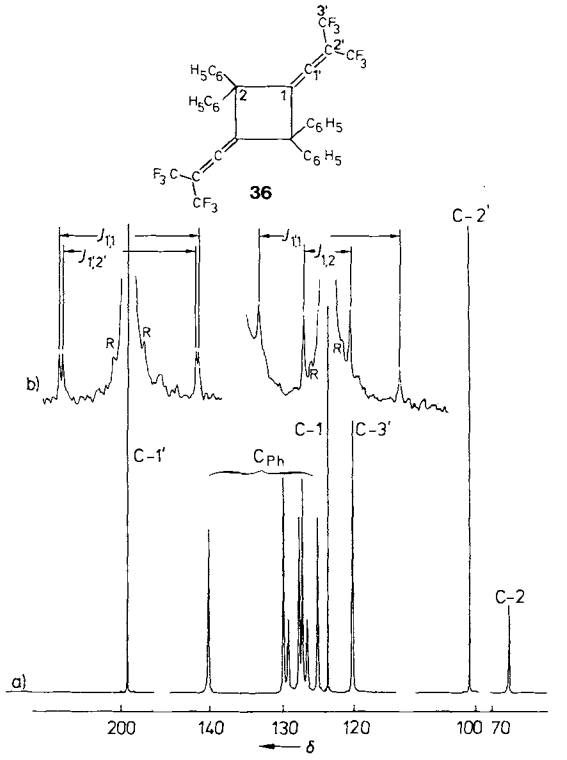

Fig. 11. a) Proton-coupled 62.5-MHz ^{13}C{^{19}F}-NMR spectrum of **36** (0.6 g) + [Cr(acac)$_3$] (10 mg) in $CDCl_3$ (1.5 mL). 35200 transients. Repetition interval 1.6 s. Digital resolution 0.6 Hz/data point. b) Expansion of the signals due to C-1 and C-1'. $J_{1,2} = 38.2$, $J_{1,1'} \approx 116.0$, $J_{1',2'} = 111.1$ Hz. R = spinning side bands.

The photochemical dimerization of methylmaleic anhydride gives a product whose structure could initially not be determined; the same is true for the ester derived from the product (one of the structures **38a–d**).[82]

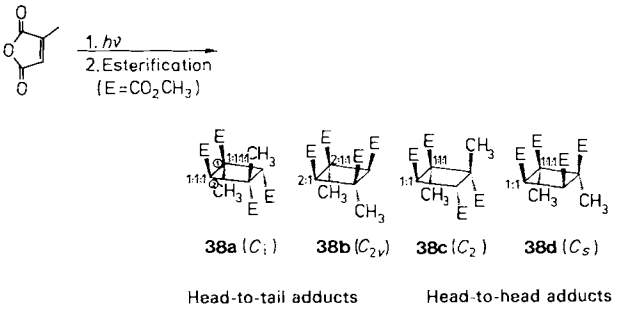

The C-2 signal of the ester shows three pairs of satellites in the ratio 1 : 1 : 1. Thus the product is the *anti* head-to-tail adduct **38a**. The pairs of satellites at C-1 are less informative because of partial overlapping. For confirmation the ^{1}H-NMR spectrum was recorded using the optically active shift reagent Eu(hfbc)$_3$. The splitting of each of the two methoxy signals into doublets proves them to be enantiotopic, as is expected for **38a** (in **38b** the methoxy groups are pairwise homotopic). This result agrees with that of the X-ray structure determination.[83,84]

These two examples show that it is possible to distinguish between head-to-head and head-to-tail products with

the help of $^{13}C,^{13}C$ satellite signals, independent of the substituents which are attached to the cyclobutane ring. When satellite signals are overlapped by signals of isolated ^{13}C nuclei the INADEQUATE method is recommended. However, deviations from the postulated intensity ratios can occur by incorrectly chosen τ-values or off-resonance effects (Section 7.2).

8.4. Assignment of ^{13}C-NMR Signals

Assignments of the ^{13}C-NMR signals of known compounds are of considerable importance for the determination of the structures of unknown compounds. When the chemical shifts of the carbon atoms of a parent substance are known, changes carried out on it can readily be localized.[85] In addition, correctly assigned signals are an important precondition for certain biosynthesic studies.[86]

Assignments on the basis of chemical shifts and CH-couplings are not free of uncertainties, particularly for complex structures. Evaluation of the $^{13}C,^{13}C$-couplings can remove such uncertainties, the two-dimensional INADEQUATE pulse sequence giving the most unambiguous results. In this manner the ^{13}C-NMR signals of several compounds were either assigned for the first time[87-92] or reassigned with the correction of previous errors.[86,93-96]

8.5. Electron Distribution in Carbon Compounds

$^{13}C,^{13}C$ coupling constants are often determined in order to obtain an insight into the bonding situation in a molecule. A detailed discussion of this topic is not possible in the present article, so that only the most important results will be presented. As mentioned initially, the $^1J_{C,C}$ values increase a) with increasing s-character of the carbon orbitals involved in the C–C bond,[97] b) with increasing electronegativity of the substituents at the two carbon atoms[98,99] (see Table 1), and c) with increasing π-bond order in aromatic compounds[100,101] (cf. however Ref. [102]). Multipath coupling can occur in cyclic compounds, which thus often exhibit large ^nJ-values.[103,104] The isotopic perturbation method for distinguishing between classical and non-classical electron arrangements can be used not only for deuterated compounds, but also for compounds which are not isotopically enriched: it then involves the comparison of the chemical shifts for isotopomers with one and two ^{13}C nuclei.[105]

8.6. Biosynthetic Studies

^{13}C-labeled precursors have long been used in the determination of biosynthetic pathways.[106] One important precursor is sodium acetate, which is labeled either in the 1- or the 2-position or in both. Its addition to nutrient solutions for bacterial or fungal cultures or its introduction into the transport channels of plants results in the formation of polyketides which ideally exhibit the ^{13}C distribution shown in Figure 12. If it is assumed that no dilution with unlabeled acetate occurs, singly labeled acetate gives a polyketide in which the ^{13}C nuclei are geminal to one another (Fig. 12a, b). When a 1 : 1 mixture of 1- and 2-^{13}C-acetate is used, the result (assuming no dilution) is an isotopomer mixture in which the ^{13}C nuclei are either neighboring (Fig. 12d), geminal (Fig. 12c, e) or vicinal (Fig. 12f). Doubly labeled acetate gives a polyketide whose carbon skeleton (again assuming no dilution) consists only of ^{13}C atoms (Fig. 12h); if it is diluted with unlabeled acetate the result is an isotopomer mixture containing fragments with two neighboring ^{13}C atoms (Fig. 12j, k).

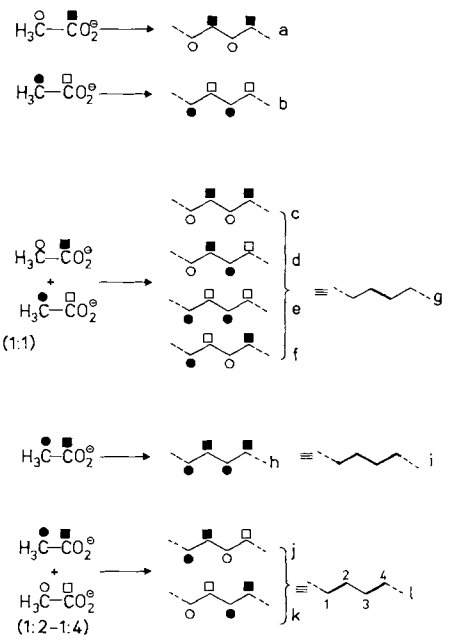

Fig. 12. Distribution of ^{13}C nuclei in polyketide chains: sections of chain after the incorporation of differently labeled acetates. For explanation see text. ^{12}C is denoted by O or □, ^{13}C by ● or ■.

Isotopomers which contain neighboring ^{13}C nuclei in increased abundance are also indicated by bold lines at the appropriate positions (Fig. 12g, i, l). The structure fragment shown in Figure 12l indicates that double labeling occurs at C-1 and C-2 *or* C-3 and C-4: thus $^{13}C,^{13}C$ satellite signals of increased intensity are observed due to the couplings between C-1 and C-2 and between C-3 and C-4, but not between C-2 and C-3.

Double labeling with [1,2-$^{13}C_2$] acetate gives information on how polyketide chains are folded prior to cyclization and on whether rearrangements occur. The following two examples should make this clear. The conventional ^{13}C spectrum of labeled **39** contains corresponding satellite pairs: it thus follows that the C_{20}-precursor is folded as shown in **A** and not as in **B**.[107]

The conventional ^{13}C spectrum of labeled **41** shows satellite signals of increased intensity only for the seven C_2

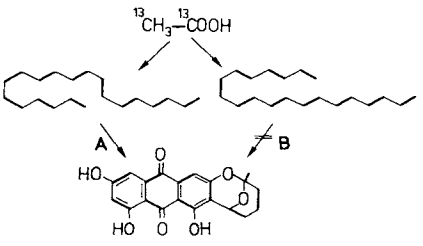

39

fragments.[108] It follows that the cyclization of **40** occurs with 1,2-rearrangement in which ^{13}C-9 and ^{13}C-10 are separated and subsequently each bonded to a ^{12}C nucleus.

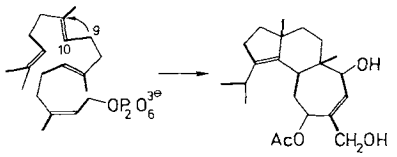

40 **41**

Not only biosynthetic pathways have been determined using ^{13}C-labeled acetate, but also the constitution of natural products. Because of the artificially increased ^{13}C-content, relatively small amounts of substance (ca. 50 mg) are sufficient. However, two feeding steps must be carried out, as shown by the elegant studies of *Seto* et al.[109] A mixture of doubly labeled and unlabeled acetate is used in the first feeding step. The conventional ^{13}C-NMR spectrum of the natural product so formed gives the C–C connectivities *within* the C_2 building blocks (see Fig. 12l). The second step consists of feeding with a 1:1 mixture of the two singly labeled acetates. The NMR analysis now affords C–C connectivities *between* the C_2 building blocks (see Fig. 12g). In this manner the complete carbon skeleton of the pigment **42**, as far as it is built up from acetate, has been determined[110] (see also Ref. [111]).

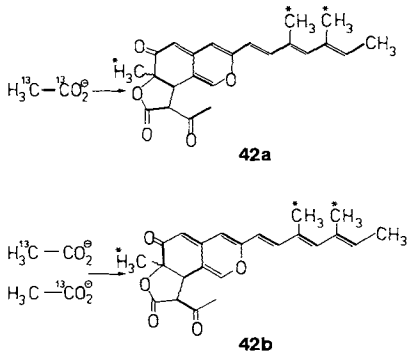

Fig. 13. Elucidation of the structure of **42**. The CH_3 groups marked with an * are formed from methionine. The connectivities indicated by wavy lines were obtained using other spectroscopic techniques.

The investigations described above were carried out in the 1970's with the help of conventional ^{13}C-NMR spectroscopy. Difficulties of the type described initially had to be accepted. Since the beginning of the 1980's the INADEQUATE pulse sequence[4] has been used increasingly for solving such problems. Its one- or two-dimensional versions have been used to study the biosynthesis of the following compounds (^{13}C-labeled precursor in brackets): mevinoline ([1,2-$^{13}C_2$]acetate),[112] lignin ($^{13}CO_2$),[113] the antibiotic ICI 139603 ([1,2-$^{13}C_2$]acetate),[114] cationomycin ([1,2-$^{13}C_2$]acetate),[115] 24-methylsterine ([1,2-$^{13}C_2$]acetate),[116] various compounds in the cells of *E. coli* (U-^{13}C glucose),[117] riboflavin (U-^{13}C glucose, [2,3-$^{13}C_2$]succinate),[118] ravidomycin ([1,2-$^{13}C_2$]acetate),[119a] brevitoxin B (*inter alia* [1,2-$^{13}C_2$]acetate).[119b] The study of the latter compound was performed using only 1.5 mg, although its molecular formula is $C_{50}H_{70}O_{14}$.

9. INADEQUATE-NMR Spectroscopy of Other Nuclei

The INADEQUATE pulse sequence can also be used to investigate inorganic compounds containing elements with a spin-1/2 isotope of *low natural abundance* (< 15%): examples are provided by the elements silicon (4.7% ^{29}Si), tin (7.6% ^{117}Sn, 8.6% ^{119}Sn) and tungsten (14.3% ^{183}W). The INADEQUATE-NMR spectra contain only signals due to AX spin systems, so that atomic frameworks can easily be recognized. Thus the two-dimensional ^{183}W-INADEQUATE-NMR spectra of polytungstates, obtained by using a delay time set for $^2J(^{183}W\text{-}O\text{-}^{183}W)$, permit not only an unambiguous assignment of the ^{183}W-NMR signals (in compounds whose structures are known) but also the recognition of the way in which the W-O-W-O building blocks are linked together.[120, 121]

When an element consists mainly or entirely of only one spin-1/2 isotope (the latter is the case for H, P and F) several double-quantum transitions are generally possible (for a survey see Ref. [17]). The term scheme of an AMX spin system (Fig. 14) contains a total of six double-quantum coherences:

$$\nu_{DQ} = \nu_A + \nu_M \pm (J_{AX} + J_{MX})/2 - 2\nu_0$$
$$\nu_{DQ} = \nu_A + \nu_X \pm (J_{AM} + J_{MX})/2 - 2\nu_0$$
$$\nu_{DQ} = \nu_M + \nu_X \pm (J_{AM} + J_{AX})/2 - 2\nu_0$$

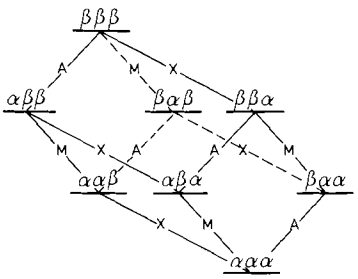

Fig. 14. Term scheme for an AMX spin system with six zero-quantum transitions (two each for AM, MX and AX), twelve single-quantum transitions (four each for A, M and X), six double-quantum transitions (two each for AM, AX and MX) and a triple-quantum transition AMX).

The two-dimensional INADEQUATE-NMR spectrum thus consists of six rows, each row containing all the twelve signals of the AMX spin system. Eight of the twelve signals are arranged symmetrically about a frequency diagonal: these signals are due to the "active spins", i.e. spins which determine the double-quantum frequency (e.g. AM). The remaining four signals are due to the "passive spin" (e.g. X). A simplification is achieved when a 135° read pulse is used instead of a 90° pulse. Each row then contains basically only eight signals; these are arranged symmetrically about a diagonal, so that the interpretation is made easier. Figure 15 shows two-dimensional proton INADEQUATE-NMR spectra of 2,3-dibromopropionic acid, recorded with read pulse angles of 90° and 135° respectively.[122]

Several proton spin systems have been studied using INADEQUATE as a tool for spectral assignment. The advantages and disadvantages with respect to COSY have been

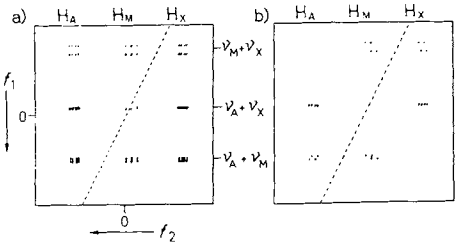

Fig. 15. Two-dimensional INADEQUATE ^{1}H-NMR spectrum of 2,3-dibromopropionic acid $BrH_MH_XC-CH_ABr-COOH$ (OH-signal not shown; quadrature detection in f_1). Read pulse angle 90°. (b) Read pulse angle 135°. Comparison of the two spectra shows that no appreciable coherence transfer to the passive spins has occurred [122].

discussed.[123, 124] Two-dimensional proton INADEQUATE-NMR spectroscopy has also been used to determine the constitution of a natural product.[125]

10. Summary and Outlook

The determination of $^{13}C,^{13}C$ coupling constants makes possible the direct determination of the carbon skeleton of organic compounds. The interpretation of the spectra, particularly of those from two-dimensional experiments, is simple. The use of reference compounds, which is of paramount importance in conventional spectroscopic structural analysis, is not necessary. The reliability of the method is due to the fact that $^{13}C,^{13}C$ coupling constants larger than 35 Hz are virtually always due to neighboring carbon atoms: exceptions are provided by certain substituted cyclobutanone derivatives (e.g. **43**), in which incorrect C,C-connectivities are suggested by extremely large geminal couplings.[126]

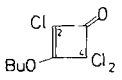

43 $^2J_{2,4}=64.1$ Hz

If strongly coupled AB systems are present one must reckon with a loss in intensity of the satellite signals due to poorly chosen delay times. Ambiguities with regard to connectivities occur if NMR signals due to isolated ^{13}C nuclei overlap.[127] In both cases the limits of the method have been reached.

If heteroatoms are present in the form of structural fragments C–X–C (X = O, S, N), gaps occur in the carbon skeleton: sometimes these can be "closed" by taking the chemical shifts of the ^{13}C nuclei into account.

The determination of *configurations* with the help of the Karplus equation is only possible in exceptional cases.[128a] However, when the *constitution* is known and the proton NMR signals can be correctly assigned (via a C,H-correlation), the configuration can generally also be determined by using trusted methods such as proton–proton coupling and nuclear Overhauser effects.

The low sensitivity of INADEQUATE ^{13}C-NMR spectroscopy at present limits its broad application: several hundred milligrams of substance (for a molecular weight of ca. 300) and measurement times of between 10 and 50 h (according to the field strength of the magnet) are required. In the case of natural products formed from ^{13}C-labeled precursors, however, the amount of compound needed for an NMR investigation is drastically reduced: at an incorporation rate of 1%, only a few milligrams are needed to permit the detection of selected C,C-connectivities.[109, 119b, 128b] Combined pulse sequences for increasing signal intensity (such as INEPT- and DEPT-INADEQUATE, C-relayed H,C-COSY or INSIPID) require the presence of sufficient hydrogens on the carbons concerned, and have in some cases not as yet proved themselves in practical structural analysis. In addition, a number of the compounds listed in Table 4 contain several *hydrogen-free* carbon atoms in a chain. It remains to be seen what sort of improvement in the S/N ratio results from the mathematical treatment of the NMR signals of two-dimensional spectra. A decrease in the noise signals of 2D-INADEQUATE NMR spectra, which improves the S/N ratio by a factor of three to four, was recently reported.[51b] A better S/N ratio for a given measuring time was obtained in each case when the measurements were carried out in the presence of relaxation reagents.

If $^{13}C,^{13}C$ couplings are to be used for the structure determination, a conventional ^{13}C-NMR spectrum should first be recorded using only a *single* transient: if all the ^{13}C signals are visible, the necessary precondition for the use of $^{13}C,^{13}C$ coupling constants for the structure determination is fulfilled. If the NMR signals are well-separated and free from unwanted signals (impurities), the conventional ^{13}C-NMR technique should be used, as it is the most sensitive and because in addition all the $^{13}C,^{13}C$ satellite signals are of optimum intensity (see Figs. 2 and 11). If the latter preconditions are not fulfilled, the INADEQUATE pulse sequence should be used. The two-dimensional version of INADEQUATE represents a great achievement in the use of spectroscopic techniques for determining the constitution of carbon compounds: the conclusions it provides can hardly be surpassed for simplicity and logic.

Appendix: Density Matrix Formalism

Modern multipulse NMR experiments can be described quantitatively with the help of the density matrix formalism.[14, 29c, 129] The basis of this formalism and its application to the INADEQUATE pulse sequence have been described.[29c]

A homonuclear AX spin system can be described with the help of a complex 4×4 matrix σ. For thermal equilibrium this matrix is as given by (A1).

$$\sigma=\frac{p}{4}\begin{pmatrix}1&0&0&0\\0&0&0&0\\0&0&0&0\\0&0&0&-1\end{pmatrix} \qquad (A1)$$

The diagonal elements correspond to the populations of the four energy levels of the spin system (with p equal to the excess population of the niveau of lowest energy), while the off-diagonal elements describe the interactions between the niveaus, the so-called "coherences". If the value of a matrix element is zero, the corresponding coher-

ence is not excited. The four elements σ_{12}, σ_{13}, σ_{24} and σ_{34} represent the observable magnetizations (single-quantum coherence; $\Delta m = 1$), the elements σ_{23} and σ_{14} the non-observable zero- and double-quantum coherences ($\Delta m = 0$ and 2 respectively). The intensity of a coherence is described by a complex number, the real part of which corresponds to the component in the x-direction and the imaginary part to that in the y-direction of the rotating frame. The observation of an NMR experiment is carried out in the coordinate system of the single-quantum coherence; separate coordinate systems exist for the zero- and double-quantum coherences.[130] The temporal change of a coherence and the effect of non-selective pulses on the spin system can be described with the help of two simple mathematical rules.

The temporal variation of a coherence (e.g. the rotation of a magnetization during a delay time) corresponds to the multiplication of the matrix elements by a time-dependent function [Eq. (A2)].

$$\sigma_{kl}(t) = e^{i\omega_{kl}t} \cdot \sigma_{kl} \quad (t=0)$$
$$e^{i\omega_{kl}t} = \cos\omega_{kl}t + i\sin\omega_{kl}t \tag{A2}$$

The angle velocity ω_{kl} is given by the difference of the two energy niveaus E_k and E_l. Relaxation effects are not taken into account. The absolute values of the matrix elements are not changed by the multiplication (which corresponds to a rotation in an orthogonal coordinate system).

The effect of a non-selective pulse (of angle α) on the spin system is obtained by multiplication of the matrix by the rotation matrix R and its inverse matrix R^{-1} [Eq. (A3)].

$$\sigma(\alpha) = R^{-1}(\alpha) \cdot \sigma \cdot R(\alpha) \tag{A3}$$

For a 90° pulse in the four directions of the rotating coordinate system (x, y, $-x$, $-y$) these rotation matrices are as follows:

$$R_x^{-1} = R_{-x} = \frac{1}{2}\begin{pmatrix} 1 & -i & -i & -1 \\ -i & 1 & -1 & -i \\ -i & -1 & 1 & -i \\ -1 & -i & -i & 1 \end{pmatrix}$$

$$R_x = R_{-x}^{-1} = \frac{1}{2}\begin{pmatrix} 1 & i & i & -1 \\ i & 1 & -1 & i \\ i & -1 & 1 & i \\ -1 & i & i & 1 \end{pmatrix}$$

$$R_y^{-1} = R_{-y} = \frac{1}{2}\begin{pmatrix} 1 & 1 & 1 & 1 \\ -1 & 1 & -1 & 1 \\ -1 & -1 & 1 & 1 \\ 1 & -1 & -1 & 1 \end{pmatrix} \tag{A4}$$

$$R_y = R_{-y}^{-1} = \frac{1}{2}\begin{pmatrix} 1 & -1 & -1 & 1 \\ 1 & 1 & -1 & -1 \\ 1 & -1 & 1 & -1 \\ 1 & 1 & 1 & 1 \end{pmatrix}$$

The corresponding matrices for a $180°_{-y}$ pulse ($= R_y(90) \cdot R_y(90)$) are as follows:

$$R_y^{-1} = R_y = \frac{1}{2}\begin{pmatrix} 0 & 0 & 0 & 1 \\ 0 & 0 & -1 & 0 \\ 0 & -1 & 0 & 0 \\ 1 & 0 & 0 & 0 \end{pmatrix} \tag{A5}$$

The variation of the density matrix during the INADEQUATE pulse sequence can be followed with the help of these two mathematical rules (time dependence, effect of pulse).

The first part of the sequence ($90°_x - \tau - 180°_y - \tau$; see Figs. 3a–e) corresponds to a spin-echo experiment. When the delay time $\tau = 1/(4J)$, the following density matrix results at the end of this sequence:

$$\sigma = \frac{1}{2}\begin{pmatrix} 0 & 1 & 1 & 0 \\ 1 & 0 & 0 & -1 \\ 1 & 0 & 0 & -1 \\ 0 & -1 & -1 & 0 \end{pmatrix} \tag{A6}$$

Only those matrix elements which correspond to the single-quantum coherences are now non-zero (e.g. nucleus A: $\sigma_{12} = 1$, $\sigma_{34} = -1$) and their values show that these coherences are, as shown in Figure 3e with the help of the vector model, oriented along the $\pm x$-axis of the rotating frame; they show a phase difference of 180°. A 90° pulse in the x-direction then gives:

$$\sigma = \frac{1}{2}\begin{pmatrix} 0 & 0 & 0 & i \\ 0 & 0 & 0 & 0 \\ 0 & 0 & 0 & 0 \\ -i & 0 & 0 & 0 \end{pmatrix} \tag{A7}$$

All observable magnetizations are now no longer present ($\sigma_{12} = \sigma_{13} = \sigma_{24} = \sigma_{34} = 0$), as they have been transferred into the double-quantum coherence (σ_{14}). The numerical value of the matrix element σ_{14} shows that the corresponding vector is oriented along the y-axis of the double-quantum coordinate system (Fig. 3f). During a delay time t_1 in Fig. 3, $t_1 = \Delta = 0$) the density matrix changes to:

$$\sigma = \frac{1}{2}\begin{pmatrix} 0 & 0 & 0 & ia \\ 0 & 0 & 0 & 0 \\ 0 & 0 & 0 & 0 \\ ia^* & 0 & 0 & 0 \end{pmatrix} \tag{A8}$$

with $a = e^{i\omega_{14}t_1}$; $a^* = e^{i\omega_{41}t_1} = e^{-i\omega_{14}t_1}$

There now follows the 90° "read pulse": the resultant density matrices are dependent on the direction of this pulse and are given in Table 5. The orientations of the observable magnetizations can be derived from these matrices. The single-quantum coherences which result from the double-quantum coherence are always oriented along the axis in which the read pulse is applied. If the phase of this pulse is changed by a certain amount, the phase of the resulting single-quantum coherences is changed by double this amount. (It should be noted that the phases of $m_2(-)$ in Figures 3g and 3h are opposite with respect to the direction of the read pulse.) This description is equivalent to the statement that a phase change in the single-quantum coordinate system corresponds to double this phase change in the double-quantum coordinate system.

When the detector phase is switched in such a way that it follows the phase of the magnetization resulting from the double-quantum coherence, these coherences are added,

Table 5. Density matrices with orientation of the single-quantum coherences subsequent to read pulses of different phase.

Phase of read pulse	Density matrix σ after the variable time t_1 and the 90° read pulse		Orientation of the magnetization at $t_1=0$ according to the coherences	
	t_1 [a]	$t_1=0$	σ_{24}, σ_{34}	σ_{12}, σ_{13}
x	$\frac{1}{2}\begin{pmatrix} s & -c & -c & -s \\ -c & -s & -s & c \\ -c & -s & -s & c \\ -s & c & c & s \end{pmatrix}$	$\frac{1}{2}\begin{pmatrix} 0 & -1 & -1 & 0 \\ -1 & 0 & 0 & 1 \\ -1 & 0 & 0 & 1 \\ 0 & 1 & 1 & 0 \end{pmatrix}$	x	$-x$
y	$\frac{1}{2}\begin{pmatrix} -s & ic & ic & -s \\ -ic & s & s & -ic \\ -ic & s & s & -ic \\ -s & ic & ic & -s \end{pmatrix}$	$\frac{1}{2}\begin{pmatrix} 0 & i & i & 0 \\ -i & 0 & 0 & -i \\ -i & 0 & 0 & -i \\ 0 & i & i & 0 \end{pmatrix}$	$-y$	y
$-x$	$\frac{1}{2}\begin{pmatrix} s & c & c & -s \\ c & -s & -s & -c \\ c & -s & -s & -c \\ -s & -c & -c & s \end{pmatrix}$	$\frac{1}{2}\begin{pmatrix} 0 & 1 & 1 & 0 \\ 0 & 0 & 0 & -1 \\ 1 & 0 & 0 & -1 \\ 1 & -1 & -1 & 0 \end{pmatrix}$	$-x$	x
$-y$	$\frac{1}{2}\begin{pmatrix} -s & -ic & -ic & -s \\ ic & s & s & ic \\ ic & s & s & ic \\ -s & -ic & -ic & -s \end{pmatrix}$	$\frac{1}{2}\begin{pmatrix} 0 & -i & -i & 0 \\ i & 0 & 0 & i \\ i & 0 & 0 & i \\ 0 & -i & -i & 0 \end{pmatrix}$	y	$-y$

[a] $c=\cos\omega_{14}t_1$; $s=\sin\omega_{14}t_1$.

while the single-quantum coherences resulting from the isolated nuclei are eliminated even after only two steps (the "two-step cycle") since in the second step the phases of the detector and the read pulse differ by 180°.

We thank Prof. Dr. G. Bodenhausen (Lausanne), Dr. W. E. Hull (Heidelberg), Prof. Dr. H. Kessler (Frankfurt), Dr. T. Kämpchen (Marburg), Dr. J. Lambert (Dortmund), and Priv.-Doz. Dr. H. Uzar (Siegen) for valuable comments.

Received: June 3, 1986;
revised: December 10, 1986 [A 624 IE]
German version: *Angew. Chem. 99* (1987) 642
Translated by Professor *T. N. Mitchell*, Dortmund (FRG)

[1] H. O. Kalinowski, S. Berger, S. Braun: *^{13}C-NMR-Spektroskopie*, Thieme, Stuttgart 1984, S. 493.
[2] V. Wray, *Prog. Nucl. Magn. Reson. Spectrosc. 13* (1979) 177.
[3] Summary of C,C-spin-spin-coupling constants, determined by biogenetic studies: P. E. Hansen, *Annu. Rep. NMR Spectrosc. 11* (1981) 65; V. Wray, P. E. Hansen, *ibid. 11* (1981) 99.
[4] R. M. Horak, P. S. Steyn, R. Vleggaar, *Magn. Reson. Chem. 23* (1985) 995.
[5] K. Kamienska-Trela, R. Machinek (Göttingen), private communication; cf. also K. Kamienska-Trela, Z. Biedrzycka, R. Machinek, B. Knierim, W. Lüttke, *Org. Magn. Reson. 22* (1984) 317.
[6] S. J. Gould, *J. Am. Chem. Soc. 104* (1982) 343.
[7] T. Loerzer, R. Machinek, W. Lüttke, L. H. Franz, K.-D. Malsch, G. Maier, *Angew. Chem. 95* (1983) 914; *Angew. Chem. Int. Ed. Engl. 22* (1983) 878.
[8] a) A. Neszmelyi, G. Lukacs, *J. Am. Chem. Soc. 104* (1982) 5342; b) *J. Chem. Soc. Chem. Commun. 1981*, 1275.
[9] F. Wehrli, T. Wirthlin: *Interpretation of Carbon-13-NMR-Spectra*, Heyden, London 1976, p. 121.
[10] Determination of ^1J(C,C) values by CW-NMR spectroscopy: F. Weigert, J. D. Roberts, *J. Am. Chem. Soc. 94* (1972) 6021.
[11] D. Döpp, H. Libera (Duisburg), private communication.
[12] J. Buddrus, H. Bauer, unpublished.
[13] A. Bax, R. Freeman, S. P. Kempsell, *J. Am. Chem. Soc. 102* (1980) 4849; A. Bax, R. Freeman, T. A. Frenkiel, *ibid. 103* (1981) 2102.
[14] W. P. Aue, E. Bartholdi, R. R. Ernst, *J. Chem. Phys. 64* (1976) 2229.
[15] A. Wokaun, R. R. Ernst, *Chem. Phys. Lett. 52* (1977) 407.
[16] G. Bodenhausen, *Prog. Nucl. Magn. Reson. Spectrosc. 14* (1981) 137.
[17] L. Braunschweiler, G. Bodenhausen, R. R. Ernst, *Mol. Phys. 48* (1983) 535.
[18] O. W. Sørensen, G. W. Eich, M. H. Levitt, G. Bodenhausen, R. R. Ernst, *Prog. Nucl. Magn. Reson. Spectrosc. 16* (1983) 163.
[19] R. Benn, H. Günther, *Angew. Chem. 95* (1983) 381; *Angew. Chem. Int. Ed. Engl. 22* (1983) 350.
[20] H. J. Gais, K. L. Lukas, *Angew. Chem. 96* (1984) 140; *Angew. Chem. Int. Ed. Engl. 23* (1984) 142.
[21] W. Amman, R. Richards, T. Wirthlin, *J. Magn. Reson. 45* (1981) 270.
[22] K. Roth, R. Richarz, *Nachr. Chem. Tech. Lab. 30* (1982) 1015.
[23] V. Jäger, W. Kühn, J. Buddrus, *Tetrahedron Lett. 27* (1986) 2587.
[24] a) L. Müller, *J. Magn. Reson. 59* (1984) 326. b) L. Müller, A. Pardi, *J. Am. Chem. Soc. 107* (1985) 3484.
[25] A. A. Maudsley, R. R. Ernst, *Chem. Phys. Lett. 50* (1977) 368.
[26] G. Eich, G. Bodenhausen, R. R. Ernst, *J. Am. Chem. Soc. 104* (1982) 3731; P. H. Bolton, G. Bodenhausen, *Chem. Phys. Lett. 89* (1982) 139; H. Kessler, M. Berndt, H. Kogler, J. Zarbock, O. W. Sørensen, G. Bodenhausen, R. R. Ernst, *J. Am. Chem. Soc. 105* (1983) 6944.
[27] H. Kessler, C. Griesinger, J. Zarbock, H. R. Loosli, *J. Magn. Reson. 57* (1984) 331; H. Kessler, C. Griesinger, J. Lautz, *Angew. Chem. 96* (1984) 434; *Angew. Chem. Int. Ed. Engl. 23* (1984) 444.
[28] H. Kessler, W. Bermel, C. Griesinger, *J. Magn. Reson. 62* (1985) 573; H. Kessler, W. Bermel, C. Griesinger, P. Hertl, E. Streich, A. Rieker, *J. Org. Chem. 51* (1986) 596.
[29] A. Bax: *Two-Dimensional Nuclear Magnetic Resonance in Liquids*, Reidel, Dordrecht 1982 a) p. 159, b) p. 140, c) Appendix 1 (some signs have been changed).
[30] A. Bax, R. Freeman, *J. Magn. Reson. 41* (1980) 507.
[31] M. H. Levitt, R. R. Ernst, *Mol. Phys. 50* (1983) 1109.
[32] M. H. Levitt, *Prog. Nucl. Magn. Reson. Spectrosc. 18* (1986) 61.
[33] K. V. Schenker, W. von Philipsborn, *J. Magn. Reson. 66* (1986) 219.
[34] R. R. Ernst, R. E. Morgan, *Mol. Phys. 26* (1973) 49.
[35] H. Kluge, *Dissertation*, Universität Braunschweig 1984.
[36] R. Freeman, T. A. Frenkiel, M. B. Rubin, *J. Am. Chem. Soc. 104* (1982) 5545.
[37] R. Benn, *J. Magn. Reson. 55* (1983) 460.
[38] O. W. Sørensen, U. B. Sørensen, H. J. Jakobsen, *J. Magn. Reson. 59* (1984) 332; U. B. Sørensen, H. J. Jakobsen, O. W. Sørensen, *ibid. 61* (1985) 382; P. E. Hansen, A. Lyčka, *Magn. Reson. Chem. 24* (1986) 772.
[39] P. Schmitt, H. Günther, *J. Magn. Reson. 52* (1983) 497.
[40] P. J. Hore, E. R. P. Zuiderweg, K. Nicolay, K. Dijkstra, R. Kaptein, *J. Am. Chem. Soc. 104* (1982) 4286.
[41] A. D. Bain, D. W. Hughes, J. M. Loddington, R. A. Bell, *J. Magn. Reson. 58* (1984) 490.
[42] S. R. Johns, R. I. Willing, *Magn. Reson. Chem. 23* (1985) 16.
[43] A. Bax, R. Freeman, T. A. Frenkiel, M. H. Levitt, *J. Magn. Reson. 43* (1981) 478.
[44] T. H. Mareci, R. Freeman, *J. Magn. Reson. 48* (1982) 158.
[45] D. Piveteau, M. A. Delsuc, E. Guittet, J. Y. Lallemand, *Magn. Reson. Chem. 23* (1985) 127.
[46] D. L. Turner, *Mol. Phys. 44* (1982) 1051; *J. Magn. Reson. 49* (1982) 175; *ibid. 53* (1983) 259.
[47] A. Bax, T. H. Mareci, *J. Magn. Reson. 53* (1983) 360.
[48] D. L. Turner, *J. Magn. Reson. 58* (1984) 500.

[49] O. W. Sørensen, R. Freeman, T. A. Frenkiel, T. H. Mareci, R. Schuck, *J. Magn. Reson. 46* (1982) 180.
[50] S. W. Sparks, P. D. Ellis, *J. Magn. Reson. 62* (1985) 1.
[51] a) P. J. Keller, K. E. Vogele, *J. Magn. Reson. 68* (1986) 389; b) P. H. Bolton, *J. Magn. Reson. 68* (1986) 180.
[52] a) D. M. Doddrell, W. Brooks, J. Field, *J. Magn. Reson. 55* (1983) 481; b) P. E. Hansen, *Annu. Rep. NMR Spectrosc. 14* (1983) 181.
[53] W. Kreiser, V. Rüschenbaum, H. Bauer, J. Buddrus, *Helv. Chim. Acta 67* (1984) 2231.
[54] C. J. Unkefer, W. L. Earl, *J. Magn. Reson. 61* (1985) 343.
[55] M. L. Martin, G. J. Martin, J. J. Delpuech: *Practical NMR Spectroscopy*. Heyden, London 1980.
[56] F. Bohlmann, C. Zdero, *Phytochemistry 18* (1979) 1747.
[57] L. A. Paquette, R. A. Galemmo, J. P. Springer, *J. Am. Chem. Soc. 105* (1983) 6976.
[58] T. Tsunoda, Y. Kabasawa, S. Ito, *Tetrahedron Lett. 25* (1984) 773.
[59] L. H. Zalkow, R. N. Harris III, D. Van Derveer, J. A. Bertrand, *J. Chem. Soc. Chem. Commun. 1977*, 456; L. H. Zalkow, R. N. Harris III, D. J. Van Derveer, *ibid. 1978*, 420.
[60] F. Bohlmann, N. Le Van, J. Pickardt, *Chem. Ber. 110* (1977) 3777.
[61] R. A. Komoroski, E. C. Gregg, J. P. Shockcor, J. M. Geckle, *Magn. Reson. Chem. 24* (1986) 534.
[62] A. J. Ragauskas, J. B. Stothers, *Can. J. Chem. 63* (1985) 1250.
[63] A. C. Pinto, W. S. Garcez, W. E. Hull, A. Neszmelyi, G. Lukacs, *J. Chem. Soc. Chem. Commun. 1983*, 464.
[64] A. C. Pinto, S. K. Do Prado, R. B. Filho, W. E. Hull, A. Neszmelyi, G. Lukacs, *Tetrahedron Lett. 23* (1982) 5267.
[65] R. Jacquesy, C. Narbonne, W. E. Hull, A. Neszmelyi, G. Lukacs, *J. Chem. Soc. Chem. Commun. 1982*, 409.
[66] A. C. Pinto, M. L. A. Gonçalves, R. B. Filho, A. Neszmelyi, G. Lukacs, *J. Chem. Soc. Chem. Commun. 1982*, 293.
[67] V. V. Krishnamurthy, J. G. Shih, G. A. Olah, *J. Org. Chem. 50* (1985) 3005.
[68] L. Fitjer, D. Wehle, H. Bauer, J. Buddrus, unpublished.
[69] S. Carmely, Y. Kashman, *J. Org. Chem. 51* (1986) 784.
[70] J. D. McChesney, E. R. Silveira, A. A. Craveico, J. N. Shoolery, *J. Org. Chem. 49* (1984) 5154.
[71] F. J. Schmitz, S. K. Agarwal, S. P. Gunasekera, P. G. Schmidt, J. N. Shoolery, *J. Am. Chem. Soc. 105* (1983) 4835.
[72] E. Guittet, S. A. Julia, G. Linstrumelle, R. Lorne, *Tetrahedron 40* (1984) 4267.
[73] N. S. Bhacca, M. F. Balandrin, A. D. Kinghorn, T. A. Frenkiel, R. Freeman, G. A. Morris, *J. Am. Chem. Soc. 105* (1983) 2538.
[74] H. Gotthardt, H. G. Kinzelmann, J. Buddrus, *Chem. Ber. 119* (1986) 2317.
[75] a) H. Gotthardt, R. Jung, *Chem. Ber. 118* (1985) 3438; b) J. Buddrus, H. Bauer, H. Gotthardt, R. Jung, *Angew. Chem. 95* (1983) 565; *Angew. Chem. Int. Ed. Engl. 22* (1983) 548.
[76] H. Bauer, J. Buddrus, W. Auf der Heyde, W. Kimpenhaus, *Chem. Ber. 119* (1986) 1890.
[77] G. E. Hawkes, R. A. Smith, J. D. Roberts, *J. Org. Chem. 39* (1974) 1276.
[78] H. Ziffer, I. W. Levin, *J. Org. Chem. 34* (1969) 4056.
[79] W. Metzner, D. Wendisch, *Justus Liebigs Ann. Chem. 730* (1969) 111.
[80] H. Ulrich, D. V. Rao, F. A. Stuber, A. A. R. Sayigh, *J. Org. Chem. 35* (1970) 1121.
[81] H. Gotthardt, R. Jung (Wuppertal), private communication.
[82] G. O. Schenck, W. Hartmann, S.-P. Mannsfeld, W. Metzner, C. H. Krauch, *Chem. Ber. 95* (1962) 1642.
[83] D. Rabinovich, G. M. J. Schmidt, *J. Chem. Soc. B 1967*, 144.
[84] H. Ziffer, J. R. Williams, *J. Org. Chem. 33* (1968) 920.
[85] S. L. Platt, F. Sauriol, A. S. Perlin, *Carbohydr. Res. 107* (1982) C1.
[86] S. Rajan, H. Tsou, P. C. Mowery, M. W. Bullock, G. W. Stockton, *J. Antibiot. 37* (1984) 1495.
[87] P. Joseph-Nathan, R. L. Santillan, P. Schmitt, H. Günther, *Org. Magn. Reson. 22* (1984) 450.
[88] T. Kikuchi, S. Kadota, S. Matsuda, H. Suehara, *Tetrahedron Lett. 25* (1984) 2565.
[89] G. Buchbauer, A. Fischlmayr, E. Haslinger, W. Robin, H. Völlenkle, C. Wessmann, *Monatsh. Chem. 115* (1984) 739.
[90] M. J. Musmar, M. R. Willcott, G. E. Martin, R. T. Gampe, M. Iwao, M. L. Lee, R. E. Hurd, LeRoy F. Johnson, R. N. Castle, *J. Heterocycl. Chem. 20* (1983) 1661.
[91] J. A. Robinson, D. L. Turner, *J. Chem. Soc. Chem. Commun. 1982*, 148.
[92] A. Neszemelyi, G. Lukacs, *J. Chem. Soc. Chem. Commun. 1981*, 999.
[93] A. Neszemelyi, W. E. Hull, G. Lukacs, *Tetrahedron Lett. 23* (1982) 5071.
[94] W. Ammann, R. Richarz, T. Wirthlin, D. Wendisch, *Org. Magn. Reson. 20* (1982) 260.
[95] C. Kruk, A. W. H. Jans, J. Lugtenburg, *Magn. Reson. Chem. 23* (1985) 267.
[96] D. H. Welti, *Magn. Reson. Chem. 23* (1985) 872.
[97] K. Frei, H. J. Bernstein, *J. Chem. Phys. 38* (1963) 1216.
[98] V. V. Krishnamurthy, P. S. Iyer, G. A. Olah, *J. Org. Chem. 48* (1983) 3373.
[99] M. Stöcker, *Monatsh. Chem. 113* (1982) 1415.
[100] P. E. Hansen, U. K. Poulsen, A. Berg, *Org. Magn. Reson. 12* (1979) 43.
[101] S. Berger, *Org. Magn. Reson. 22* (1984) 47.
[102] S. Berger, K. Zeller, *J. Org. Chem. 49* (1984) 3725.
[103] J. L. Marshall, L. G. Faehl, R. Kattner, *Org. Magn. Reson. 12* (1979) 163.
[104] M. Klessinger, H. von Megen, K. Wilhelm, *Chem. Ber. 115* (1982) 50.
[105] V. V. Krishnamurthy, G. K. Surya Prakash, P. S. Iyer, G. A. Olah, *J. Am. Chem. Soc. 107* (1985) 5015.
[106] Review: A. G. McInnes, J. L. C. Wright, *Acc. Chem. Res. 8* (1975) 313.
[107] C. P. Gorst-Allman, K. G. R. Pachler, P. S. Steyn, P. L. Wessel, B. De Scott, *J. Chem. Soc. Perkin Trans 1 1977*, 2181.
[108] W. A. Ayer, S. P. Lee, T. T. Nakashima, *Can. J. Chem. 57* (1979) 3338.
[109] H. Seto, T. Sato, H. Yomehara, *J. Am. Chem. Soc. 95* (1973) 8461.
[110] H. Seto, M. Tanabe, *Tetrahedron Lett. 1974*, 651.
[111] S. Omura, A. Nakagawa, Y. Tanaka, *J. Org. Chem. 47* (1982) 5413.
[112] R. N. Moore, G. Bigam, J. K. Chan, A. M. Hogg, T. T. Nakashima, J. C. Vederas, *J. Am. Chem. Soc. 107* (1985) 3694.
[113] E. Guittet, J. Y. Lallemand, *Tetrahedron Lett. 26* (1985) 2671.
[114] J. M. Bulsing, E. D. Laue, F. J. Leeper, J. Staunton, D. H. Davies, G. A. J. Ritchie, A. Davies, A. B. Davies, R. P. Mabelis, *J. Chem. Soc. Chem. Commun. 1984*, 1301.
[115] M. Ubukata, J. Uzawa, K. Isono, *J. Am. Chem. Soc. 106* (1984) 2213.
[116] S. Seo, A. Uomori, Y. Yoshimura, K. Takeda, *J. Chem. Soc. Chem. Commun. 1984*, 1174.
[117] E. Mackenzie, R. L. Baxter, A. I. Scott, P. E. Fagerness, *J. Chem. Soc. Chem. Commun. 1982*, 145.
[118] P. J. Keller, Q. Le Van, A. Bacher, *Tetrahedron 39* (1983) 3471.
[119] a) G. T. Carter, A. A. Fantini, J. C. James, D. B. Borders, R. J. White, *Tetrahedron Lett. 25* (1984) 255; b) M. S. Lee, D. J. Repeta, K. Nakanishi, M. G. Zagorski, *J. Am. Chem. Soc. 108* (1986) 7855.
[120] C. Brevard, R. Schimpf, G. Tourne, C. M. Tourne, *J. Am. Chem. Soc. 105* (1983) 7059.
[121] P. J. Domaille, *J. Am. Chem. Soc. 106* (1984) 7677.
[122] T. H. Mareci, R. Freeman, *J. Magn. Reson. 51* (1983) 531.
[123] R. Rösch, K. H. Gross, *Z. Naturforsch. C 39* (1984) 738.
[124] S. W. Fesik, T. J. Perun, A. M. Thomas, *Magn. Reson. Chem. 23* (1985) 645.
[125] G. M. Martin, R. Sanduja, M. Alam, *J. Org. Chem. 50* (1985) 2383.
[126] H. Bauer, J. Buddrus, W. Auf der Heyde, W. Kimpenhaus, *Angew. Chem. 97* (1985) 860; *Angew. Chem. Int. Ed. Engl. 24* (1985) 854.
[127] T. Nishida, C. R. Enzell, G. A. Morris, *Magn. Reson. Chem. 24* (1986) 179.
[128] a) J. Marshall: *Carbon-Carbon and Carbon-Proton NMR Couplings: Applications to Organic Stereochemistry and Conformational Analysis (Methods in Stereochemical Analysis Vol. 2)*, Verlag Chemie Int., Deerfield Beach 1982. b) G. Müller, J. Schmiedl, E. Schneider, G. Wörner, A. I. Scott, H. J. Williams, P. J. Santander, N. J. Stolowich, P. E. Fagerness, N. E. Mackenzie, *J. Am. Chem. Soc. 108* (1986) 7875.
[129] S. Schäublin, A. Höhener, R. R. Ernst, *J. Magn. Reson. 13* (1974) 196.
[130] R. M. Lynden-Bell, J. M. Bulsing, D. M. Doddrell, *J. Magn. Reson. 55* (1983) 128.

Biological Exploitation of Solar Energy by Photosynthetic Water Splitting

By Gernot Renger*

The cleavage of water by solar radiation into dioxygen and metabolically bound hydrogen during photosynthesis is of central importance for the existence of higher forms of life on earth. The realization of this process in biological organisms made possible the use of the earth's huge water reservoir for the exploitation of solar energy and, at the same time, led to the creation of an aerobic atmosphere. The dioxygen thereby formed is a powerful oxidant which permits an energetically highly efficient nutrient turnover. In recent years considerable progress has been made in understanding the functional and structural organization of photosynthetic water splitting. This article attempts to give a review of our current state of knowledge with special emphasis on the oxidation of water to O_2 in biological systems.

1. Introduction

The relevance of solar energy as the prerequisite for the existence of the biosphere was already recognized in 1845 by *R. J. Maier* and was interpreted and formulated correctly by *L. Boltzmann* in thermodynamic terms in 1886:[1]

> The common fight for life is therefore neither a struggle for the basic elements nor for energy, present in every body in the form of heat—plentiful yet unfortunately nontransformable—but a fight for the entropy that becomes disposable during the transfer from the hot sun to the cold earth. Using this transfer to the utmost, plants spread the immense area of their leaves and, in still unexplained ways, force the energy of the sun, before it is reduced to the temperature level of the earth's surface, to perform chemical syntheses which are still unknown to our laboratories.

The second part of *Boltzmann*'s statement can now be considerably modified because remarkable progress has been made during the last 100 years in understanding the principles of biological solar energy exploitation.

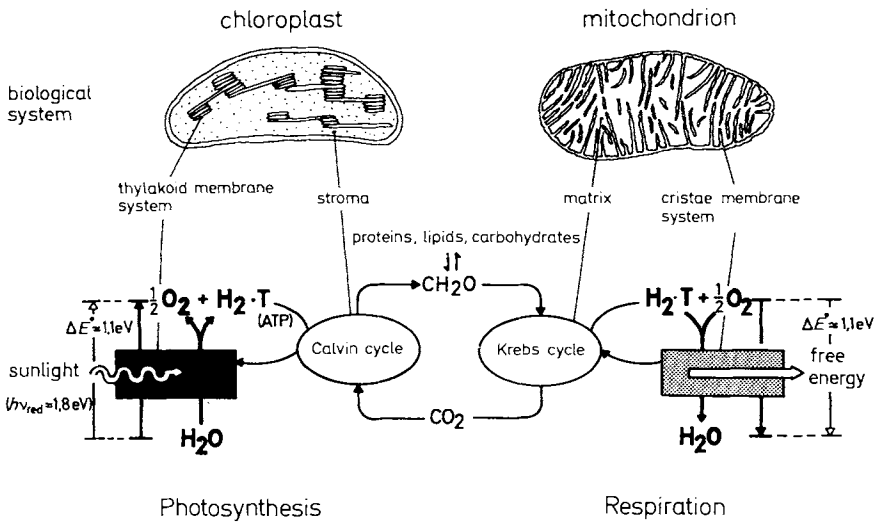

Fig. 1. Overall organization scheme of bioenergetics in higher organisms (for the sake of simplicity the energy differences are shown arbitrarily scaled). Bioenergetically important processes are symbolized as black (primary processes of photosynthesis) or grey (respiration chain) boxes. The complex anabolic and catabolic processes, which are responsible for the metabolism of the great variety of biological materials (proteins, lipids, carbohydrates), are only shown by arrows, since they do not possess the same bioenergetic importance as the primary processes of photosynthesis and respiration (for a review see Ref. [4]). Abbreviations: T = metabolite with chemically bound hydrogen; in the case of chloroplasts, T is NADP® (nicotinamide adenine dinucleotide phosphate); in the case of mitochondria, $H_2 \cdot T$ represents various kinds of bound hydrogen (e.g., NADH, succinate). CH_2O symbolizes a carbohydrate unit.

[*] Prof. Dr. G. Renger
Max-Volmer-Institut für Biophysikalische und Physikalische Chemie der Technischen Universität Berlin
Strasse des 17. Juni 135, D-1000 Berlin 12

The basic principle of the functional and structural organization of the bioenergetic processes in all higher organisms is illustrated in Figure 1. The crucial phylogenetic

step in the biological exploitation of solar energy was the "invention" of photolytic water splitting, which took place two to three billion years ago on the level of cyanobacteria. This made the huge water reservoir of the earth's surface available as a raw material for the complex chemistry of metabolically bound hydrogen and simultaneously led to O_2 enrichment of the previously anaerobic atmosphere of the earth.[2] The availability of O_2 resulted in a tenfold increase in the exploitation of the free energy content of nutrients, thereby satisfying the bioenergetic prerequisite for the development of higher-organized heterotrophic organisms (for a review see Ref. [3]). From a bioenergetic point of view (based on a unit of bound hydrogen), the complex variety of enzyme-catalyzed reaction sequences, leading to the diverse forms of biological organization, is much less important than the light-driven water cleavage and its reversal (water production) in the dark in heterotrophic organisms. The differentiation of cells in higher organisms permitted a spatial separation of all reaction sequences by compartmentation, special organelles being developed for specific functions. The bioenergetically crucial processes take place in highly organized membrane systems:

1. The photosynthetic water splitting caused by visible light occurs in the thylakoid membrane of chloroplasts (Fig. 1);
2. The oxidative reaction of bound hydrogen ($H_2 \cdot T$) with O_2 takes place in the inner membrane of mitochondria (Fig. 1), the free energy thereby released being stored in the form of ATP.

Figure 1 shows that the initial and the terminal stage of the global chemical processes in all higher organisms are reactions of the redox chain $H_2 \cdot T/H_2O/O_2$, whereby the "management" of the redox system H_2O/O_2 is of crucial importance for the realization of the entire reaction. The four-step redox reaction sequence leading directly from two H_2O molecules to O_2 [Eq. (1)] involves intermediates that could lead to rapid destruction of biological material.

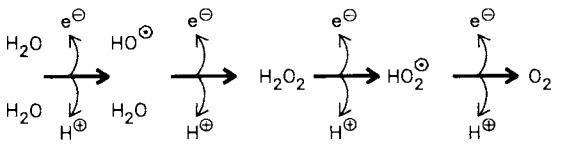

(1)

Therefore, nature had to evolve special catalysts (enzymes) which assure a "safe" course of reaction. Water cleavage requires a suitable source of free energy, whereas the reverse reaction produces free energy. Hence, different catalysts were evolved by nature. The oxidation of water with sufficiently strong oxidizing redox equivalents generated by a light reaction with consumption of free energy is catalyzed by the water-oxidizing enzyme system, whereas the reverse reaction takes place in a complex called cytochrome oxidase. For clarity it should be noted that "water splitting" refers to the overall process by which water is decomposed by light in photosynthesis. This reaction produces O_2 and bound hydrogen. "Water oxidation" refers to one step in the water splitting process, namely, the transformation of $2\,H_2O$ into O_2, $4\,H^{\oplus}$, and $4\,e^{\ominus}$.

In a time of intensive research activities directed at solving the energy crisis caused by our civilization, it is certainly worthwhile to analyze the mechanistic principles selected by nature, during a long evolutionary process, for efficient solar energy exploitation. Accordingly, in this review article only those reactions will be discussed that permit the storage of solar energy through water cleavage.

2. Organization Scheme of Photosynthetic Water Splitting

Water cleavage takes place via a sequence of redox steps coupled with protolytic reactions and is energetically driven by two light reactions. The redox groups participating in this process are anisotropically arranged in the thylakoid membrane (for a review see Ref. [4]). The essential steps of water cleavage take place in photosystem II (PS II) and can be summarized by Equation (2), whereby PQ stands for a plastoquinone and PQH_2 for a plastohydroquinone.

$$2\,PQ + 2\,H_2O \xrightarrow{4\,h\nu\,(II)} 2\,PQH_2 + O_2 \qquad (2)$$

In the subsequent light reaction of photosystem I (PS I), the hydrogen is formally transferred from PQH_2 to oxidized nicotinamide adenine dinucleotide phosphate ($NADP^{\oplus}$) and thereby reaches almost the same reduction potential (to within 0.1 V) as free H_2.[4] The reaction sequence of photosystem I can be summarized by Equation (3).

$$2\,PQH_2 + 2\,NADP^{\oplus} \xrightarrow{4\,h\nu\,(I)} 2\,PQ + 2\,NADP^{\oplus} \cdot H_2 \qquad (3)$$

Because of the central relevance of the reaction sequence summarized in Equation (2) for the overall bioenergetics, the discussion in this article is restricted to the realization of this sequence in algae and higher plants. Owing to limited space, other processes are not discussed (see Ref. [4]).

Photosynthetic water cleavage takes place via light-induced redox reactions, whereby PQ reduction and H_2O oxidation are spatially separated processes. Correspondingly, three functionally distinguishable types of reactions are involved in the overall process [Eqs. (4)–(6)]:

1. The transformation of an electronically excited state (generated by absorption of light) into an electron–hole pair with sufficient stability and redox power (P and A stand for a photochemically active pigment and an electron acceptor, respectively; see Fig. 2):

$$PA \xrightarrow{h\nu} P^*A \longrightarrow P^{\oplus}A^{\ominus} \qquad (4)$$

2. The cooperative reaction of four holes ($\oplus$) with H_2O:

$$4\oplus + 2\,H_2O \longrightarrow O_2 + 4\,H^{\oplus} \qquad (5)$$

3. The cooperative reaction of two electrons with PQ and H_2O:

$$2e^{\ominus} + PQ + 2H_2O \longrightarrow PQH_2 + 2OH^{\ominus} \quad (6)$$

Because of the anisotropic arrangement of the redox groups, the overall process consists of vectorial subprocesses. Accordingly, the protolytic reactions, which are coupled to the redox processes, lead to the formation of a transmembrane electrochemical potential difference for protons, which is utilized for ATP synthesis (for a discussion of the latter process, see, e.g., Refs. [3, 4]).

The mechanism of chemical reactions is not only determined by the participating functional groups but also by their environment. Biological systems have a unique tool for the regulation of reactions by the environment, namely, proteins. Their great variability enables them to adapt to the circumstances, so that practically every degree of specificity, efficiency, and regulatory control can be achieved that is required for carrying out specific biological functions. In order to understand the process of water cleavage it is therefore necessary to analyze the reactive properties of the redox components in situ and to view the prosthetic groups together with their protein matrices as operational units. Thus, the cooperation of three functional units is required for the process of water cleavage: (1) a photogenerator for light-induced charge separation, (2) the water-oxidizing enzyme system, and (3) the plastoquinone-reducing enzyme. Figure 2 shows the overall organization scheme of photosystem II, which is based on a stoichiometry of one H_2O molecule.

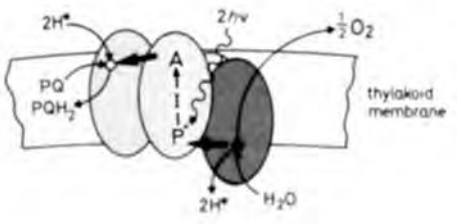

Fig. 2. Basic organization scheme of photosynthetic water cleavage in the thylakoid membrane. The functional units, described more fully in the text, are characterized as follows: reaction center (dotted), water-oxidizing enzyme system (dark grey), and plastoquinone-reducing enzyme (light grey). Thick arrows symbolize the electron-transfer route of photosystem II; white and black circles characterize the catalytic sites for PQ reduction [see Eq. (6)] and H_2O oxidation [see Eq. (5)], respectively. The excitation energy transfer from antenna pigment proteins to the reaction center is not shown (see Fig. 3). Abbreviations: P* = photochemically active pigment in the electronically excited singlet state [P = P680, see text and Eq. (4)]; I = intermediary redox component(s) (I contains Pheo, see text); A = electron acceptor responsible for the "stable" charge separation (primary plastoquinone acceptor Q_A, see text).

The functional principles of the reaction center and of the plastoquinone-reducing enzyme were already evolved at early stages of evolution, i.e., at the level of photosynthetic bacteria, which use easily oxidizable compounds as substrates (for a review see Ref. [5]). Therefore, two steps were of crucial importance for the realization of biological solar energy exploitation through water cleavage: (1) an appropriate modification of the reaction center in order to permit the generation of sufficiently strong oxidizing redox equivalents and (2) the "invention" of a water-oxidizing enzyme system. Accordingly, the focus of this review article is the mechanism of water oxidation and especially the "manageability" of the redox couple H_2O/O_2 in photosynthesis; the formation of bound hydrogen (in the form of PQH_2) is only briefly outlined.

3. The Reaction Center Complex of Photosystem II

In all photosynthetic organisms, the transformation of light into electrochemical free energy takes place in special pigment protein complexes, which are referred to as reaction center complexes. Only the reaction center complex of photosystem II is essential for water cleavage (this operational unit will be abbreviated as RC II in the following discussion).

For optimal adaptation to different light conditions, the reaction centers are coupled with pigment protein complexes that act as antennas, thereby increasing the optical cross section of the photoactive chromophore P [Eq. (4)] by more than two orders of magnitude (for a review see Refs. [6, 7]). In addition, the incorporation of carotinoids, which act as triplet quenchers, largely eliminates the probability of photodynamic destruction by O_2 at high light intensities.[8, 9]

3.1. Organization Scheme of Reaction Center Complexes of Photosystem II

According to Equation (4), each photogenerator has to include at least two functional groups: (1) a chromophore P, which forms the electronically excited state P*, which, in turn, gives rise to the photochemical reaction, and (2) an acceptor system A, which readily accepts the electron ejected from P* in a photoredox process and simultaneously permits a sufficient stabilization of the charge separation.

The functional scheme of RC II is shown in Figure 3. The photoactive pigment P in RC II is a specially bound chlorophyll a molecule,[10] which, in accordance with its red absorption band at around 680 nm, is referred to as pigment 680 (P680). It is still not yet clarified whether P680 is a monomeric chlorophyll a (Chl) or a special dimer complex, but comparison with other reaction centers (see below) makes a dimer structure more likely.[11, 12] P680 becomes photooxidized from its first singlet state ^{1}P680* in ≤ 1 ps (as estimated indirectly by fluorescence measurements, see Ref. [13]). A pheophytin a molecule (Pheo) is probably the primary electron acceptor I.[14] The initially formed $P680^{\oplus}Pheo^{\ominus}$ radical-ion pair is very unstable.[15, 16] A sufficient stabilization of the primary charge separation, which can be used for water oxidation,[17] can only be achieved if the electron from $I^{\ominus}$ (i.e., presumably $Pheo^{\ominus}$) is transferred to a specially bound plastoquinone molecule, symbolized as Q_A. Whether the intermediate electron car-

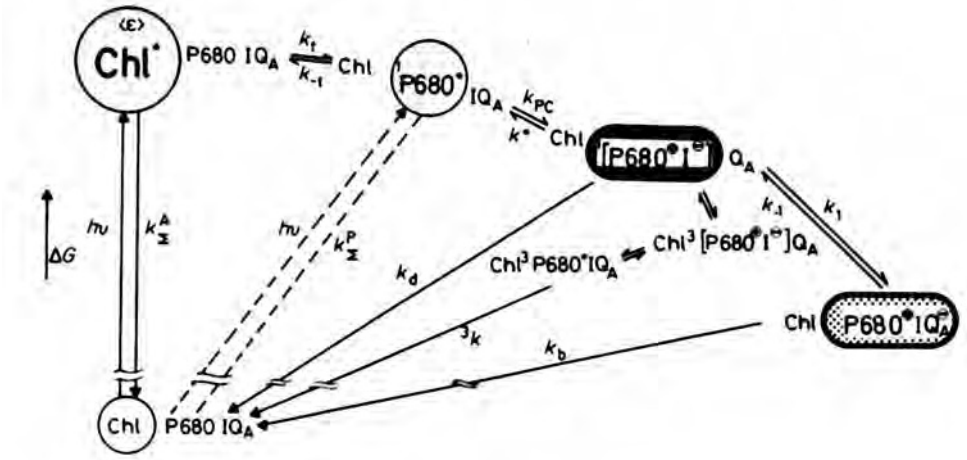

Fig. 3. Functional scheme of the light-induced charge separation of photosystem II. After light absorption, a singlet exciton (ε) is formed in chlorophyll a (Chl), an antenna pigment (the grey circle symbolizes an electronically excited antenna). This electronically excited state transfers its energy to the reaction center (see Refs. [6, 7]), thereby generating the first excited singlet of the photoredox active pigment P680, a specially bound chlorophyll a (dotted circle). Oxidation of ^{1}P680* leads to formation of the primary radical-ion pair ^{1}[P680$^\oplus$I$^\ominus$] (black oval), which is converted into the "stable" radical-ion pair P680$^\oplus$IQ$_A^\ominus$ (dotted oval) by electron transfer from the intermediary component I$^\ominus$ to the plastoquinone acceptor Q_A (component A of Fig. 2). Q_A is a specially bound plastoquinone. The rate constants describe the following processes: excitation energy transfer to the reaction center (k_1) and back to the antenna (k_{-1}), electron-transfer processes (k_{PC}, k^*, k_t, k_{-t}), radiationless decay processes of excited states within the antenna (k_Σ^A) or in P680* (k_Σ^P), dissipative recombination reactions (k_b, k_d), and decay of the triplet state of ^{3}P680* (^3k), which is created by a radical-ion pair mechanism (the rate constants of these processes are not explicitly given). The energy scale is interrupted because the energy difference between Chl* and Chl is much larger (1.83 eV) than that between Chl* and P680$^\oplus$IQ$_A^\ominus$ (0.5–0.6 eV).

rier(s), symbolized as I in Figure 3, is (are) identical with Pheo or whether further redox groups participate in the electron transfer between P680 and Q_A[18–20] is still a matter of debate. Q_A is complexed with $Fe^{2\oplus}$ (high spin)[21,22] and can only act as a one-electron acceptor[23] (the chemically interesting possibility of stabilizing semiquinones will be discussed in more detail in Sections 4 and 5). The functional role of $Fe^{2\oplus}$ is not yet understood, but investigations of the reaction centers of purple bacteria (removal of $Fe^{2\oplus}$ and replacement by $Zn^{2\oplus}$ or other bivalent cations) indicate that the electrostatic charge of $Fe^{2\oplus}$ and not its special 3d-electron configuration is important for the stabilization of the primary charge separation by Q_A.[24]

According to our current state of knowledge, only π electrons participate in the redox reactions of RC II. An analogous functional principle was already realized in the phylogenetically more ancient reaction centers of purple bacteria.[25] In this case, the photoactive pigment is a bacteriochlorophyll dimer, which transfers its electron from the excited singlet state via bacteriopheophytin to ubiquinone *(Rhodopseudomonas sphaeroides)* or menaquinone *(Rhodopseudomonas viridis)*, which is also complexed with $Fe^{2\oplus}$ (high spin).

The essential functional difference between the two types of "π-electron" reaction centers in RC II and purple bacteria is the oxidizing power of the holes generated at the photoactive pigment. In contrast to P680$^\oplus$, the bacteriochlorophyll radical cation is incapable of water oxidation for thermodynamic reasons. Therefore, the "invention" of P680 was the indispensable prerequisite for the development of O_2-evolving photosynthetic organisms. It could be speculated that this problem was simply solved by exchanging chlorophyll a (Chl) for the bacteriochlorophyll dimer, because the first excited singlet state of Chl is energetically higher by about 0.4 eV than that of bacteriochlorophyll (BChl) and because there is no large difference between the redox potential for the reduction of bacteriopheophytin (BPheo) and pheophytin (Pheo).[25] However, the utilization of Chl a was a necessary but not a sufficient condition, as is shown by the example of Chl a (P700) in reaction centers of photosystem I. The P700$^\oplus$ radical cation cannot support water oxidation because the redox potential of P700/P700$^\oplus$ is around +0.5 V (for a review see Ref. [25]). Therefore, the nature of the protein matrix is of central functional relevance for the redox potential of P680$^\oplus$/P680. The large influence of the apoprotein is clearly exemplified by the cytochromes. The redox potentials of their functional heme groups span a range of nearly 800 mV.[26,27] Based on model calculations, the effect of the protein matrix in cytochromes mainly consists in the establishment of an environment with a low dielectric constant around the heme group.[28]

Besides its thermodynamic role in controlling the redox potential of P680$^\oplus$/P680, the protein matrix possesses another essential function. It determines the rate constants of the elementary processes, which take place via vibronically coupled electron tunneling.[29,30] This "fine tuning" of the rate constants of the individual elementary electron-transfer processes in the reaction center is crucial for ensuring a high quantum yield for the entire reaction sequence;[31] the quantum yield is almost 1 for RC II.[32] Thus, the matrix protein has to be regarded as an apoenzyme of RC II, which determines the π-electron redox chemistry of this operational unit.[32] Therefore, the nature of this matrix is of great mechanistic importance and a topic of current research activities (see Section 3.2). How the individual reactions are regulated in detail by the protein matrix is still an open question.

3.2. Structural Arrangement of Reaction Center Complexes of Photosystem II

The decisive breakthrough in understanding the structure of the reaction centers of photosynthetic organisms was achieved by *Michel* and *Deisenhofer* et al. with the crystallization and X-ray analysis of this operational unit from *Rhodopseudomonas viridis* (for a review see Ref. [34]). Both the arrangement of the prosthetic groups and the essential details of the structure of the apoprotein were thereby unraveled. The apoprotein consists of two polypeptides, which are designated as the L and M subunits, each containing five transmembrane helices.[34] The basic arrangement of these bacterial reaction centers is shown schematically in Figure 4. Purple bacteria are not able to oxidize H_2O to O_2. This raises the crucial question whether further phylogenetic evolution of the L and M subunits of purple bacteria and replacement of bacteriochlorophylls (or bacteriopheophytins) by chlorophyll a (or pheophytin a) were sufficient to create the PS II reaction center complex coupled with a water-oxidizing enzyme system or whether new polypeptides had to be evolved.[35] There are striking analogies between purple bacteria and PS II in the organization scheme of reaction-center electron transport from the photochemically active pigment to the quinone acceptors.[36] Moreover, the photosystem II of water-splitting photosynthetic organisms contains two polypeptides with relative molecular masses of 32–34 kDa (designated D-1 and D-2), which show striking sequence homologies with the L and M subunits of bacterial reaction centers.[37] Both D-1 and the L subunit are essential for binding hydroquinones; both polypeptides also possess specific binding sites for herbicides.[38,39] Furthermore, the hydrophobic properties of the protein sequences indicate that[40] D-1 and D-2 contain five transmembrane helices similar to those of the L and M subunits.[34,41] These striking analogies led to the conclusion that D-1 and D-2 constitute the RC II apoprotein. If this is true, then these polypeptides ohould also bind chlorophyll a. Recently, we succeeded in the identification of two Chl-containing polypeptides in the range of 30–34 kDa from PS II preparations from spinach,[42] but it is still a matter of question whether these are really identical with D-1 and D-2.

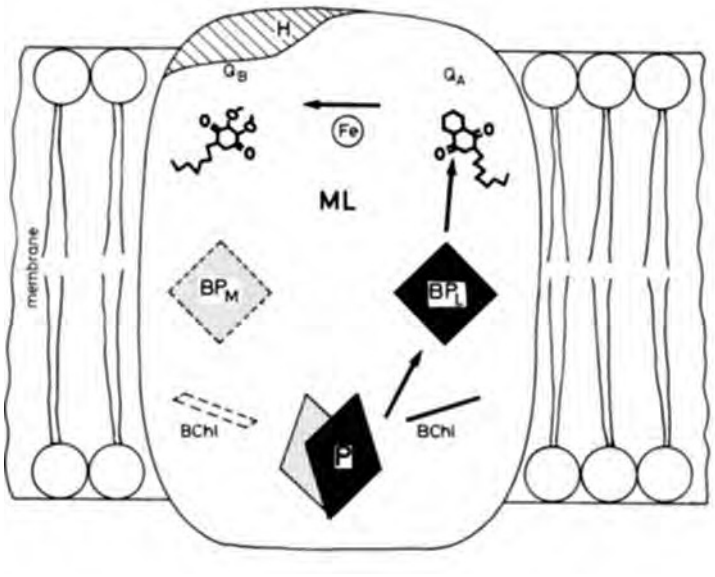

Fig. 4. Structural organization scheme of the reaction center complexes (RC) in photosynthetic purple bacteria *(Rhodopseudomonas viridis)* according to *Michel* and *Deisenhofer* et al. (see Ref. [34]). The bacteriochlorophylls of the photoactive dimer P and bacteriopheophytin (BP) are shown as parallelepipeds and squares, respectively; the monomeric bacteriochlorophylls (BChl) are symbolized as a small parallelepiped and a bar. The two functional quinones of the reaction center are menaquinone (Q_A) and ubiquinone (Q_B). A high-spin $Fe^{2\oplus}$ is located between these two quinones. The apoprotein, which consists of L and M subunits, is not shown; the regulatory H subunit is shown as a stripe pattern and the structures of the quinones are indicated.

The results mentioned above support the hypothesis that the structure of the PS II reaction centers of O_2-evolving organisms is basically similar to that of purple bacteria.[34,41] In all PS II RC preparations, however, a Chl-containing, 47-kDa polypeptide (CP47) exists, which is closely associated with D-1 and D-2. This raises the question of the functional role of CP47. Originally, CP47 itself was thought to be the RC II apoprotein.[43–45] According to the D-1/D-2 hypothesis, on the other hand, CP47 is assumed to be merely a special antenna for P680.[34,41] In an alternative model, the possibility is discussed that D-1, D-2, and CP47 act as subunits of the RC II apoprotein.[35] Recently, Chl-containing complexes were isolated which did not include either CP47 or polypeptides in the range of 30–34 kDa.[46a] Functional studies with these preparations have not yet led to definite conclusions.

The most recent studies, however, showed that a complex containing only D-1, D-2, cytochrome b 559, Chl, and Pheo (as well as β-carotene) exhibits the characteristic features (light-induced changes in absorption) for the formation of radical-ion pairs ($P680^{\oplus}Phe^{\ominus}$).[46b–c] These findings support the D-1/D-2 reaction center model of PS II.

In the next few years the structural elucidation of the PS II reaction center will be an important goal of basic photosynthesis research.

The reaction center complex RC II is anisotropically incorporated into the thylakoid membrane, whereby P680 is located on the inner side (lumen) and Q_A on the outer side (stroma) (see Fig. 2). Light-induced electron transfer from P680 to Q_A thus leads to the formation of an electrical potential difference across the thylakoid membrane[47] (the other reaction center complexes are also anisotropically integrated within the membrane, see Fig. 4).

4. The Water-Oxidizing Enzyme System

4.1. Organization Scheme of Photosynthetic Water Oxidation

A milestone for understanding the functional organization of photosynthetic water oxidation was the fundamental work of *Joliot* and *Kok* and their co-workers.[48–50] They found that the O_2 evolution after illumination of dark-adapted algae and chloroplasts with a sequence of short flashes shows a characteristic oscillation pattern, which has a periodicity of four. A typical trace is shown in Figure 5. The results clearly show that practically each reaction center is functionally connected with only one water-oxidizing enzyme system (for a review see Ref. [51]). The wa-

ter oxidation therefore occurs via a sequence of one-electron redox reactions, which can be described by the

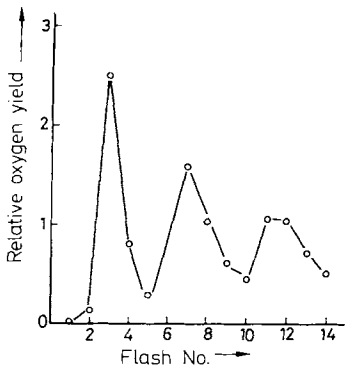

Fig. 5. Relative oxygen yield of dark-adapted chloroplasts as a function of the flash number in a sequence of short (10-μs) saturating flashes. The values are taken from the Thesis of *G. Dohnt* (Technische Universität Berlin 1984).

scheme depicted in Figure 6. Here, S_i (i = 0–4) symbolizes the redox state of the water-oxidizing enzyme system (i = 0 corresponds to the redox state of water, i = 4 to that of molecular oxygen). The coupling between P680 of RC II and the water-oxidizing enzyme system Y is symbolized by the dotted ovals in Figure 6. The nature of this coupling will be described in the following section.

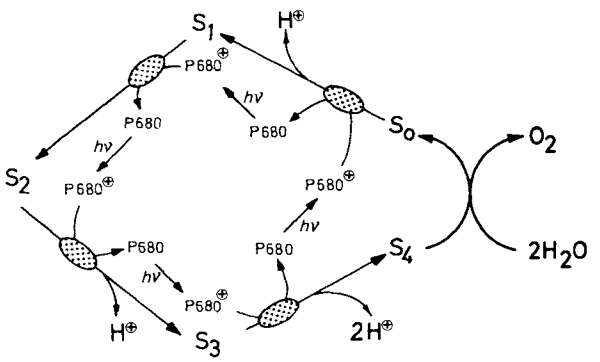

Fig. 6. Functional organization scheme of photosynthetic water oxidation as a sequence of a four one-electron redox reactions. S_i (i = 0–4) symbolizes the redox states of the catalytic site of the water-oxidizing enzyme system; P680 represents the photoactive chlorophyll a component of the reaction center (see Figs. 2, 3); the acceptor components are not shown. The functional coupling of the reaction center to the water-oxidizing enzyme system is symbolized by dotted ovals.

4.2. The Coupling between the Reaction Center and the Water-Oxidizing Enzyme System

Since $P680^{\oplus}$ reduction is much faster (ns to μs range[52–55]) than the redox transitions within the water-oxidizing enzyme system Y,[56,57] the functional connection to RC II presumably involves at least one redox component,[51] which is usually referred to as Z. This raises questions about the nature of Z and the possible participation of further redox components. Z was first detected by EPR spectroscopy.[58] An EPR signal at $g = 2.0046$ (called signal II_{vf}[*]) was observed after excitation of dark-adapted chloroplasts with a series of short flashes. The relaxation kinetics of signal II_{vf} depend on the redox state S_i of the water-oxidizing enzyme system.[59] Signal II_{vf} is ascribed to the oxidized form Z^{ox}. Destruction of system Y changes the kinetics of the EPR signal[60] significantly (this signal is thus called II_f[*]) as well as its microwave-power saturation.[61] Concomitantly, the $P680^{\oplus}$ reduction slows down. In this case, the kinetics of signal II_f formation and of $P680^{\oplus}$ reduction coincide. Both processes exhibit a characteristic pH dependence and have half-lives in the range of 2–40 μs.[62–64] If only Z^{ox} is present, $P680^{\oplus}$ is reduced via a back reaction with $Q_A^{\ominus}$ characterized by a half-life of 100–200 μs.[65,66]

A detailed analysis of the EPR spectrum of signal II_f and a comparison of this spectrum with those of corresponding in vitro model systems led to the conclusion that the redox-active group in the oxidized form Z^{ox} is a plastosemiquinone radical cation, whose ring plane is perpendicularly oriented with respect to the membrane.[67,68] Spectroscopic investigations in the UV/VIS range do not contradict this assumption.[69–72] Figure 7 shows the UV difference spectra of Z^{ox}/Z, which were obtained from analyses of flash-induced absorption changes.[69] The measurements were carried out with PS II membrane fragments (the contamination with photosystem I was ≤5%), where the water-oxidizing enzyme system Y was functionally intact in one case and totally destroyed in the other.

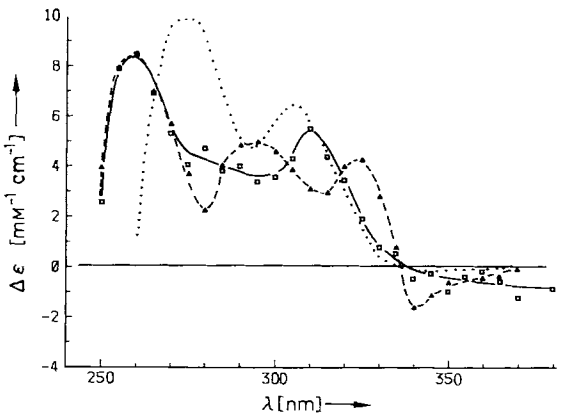

Fig. 7. Difference spectra of the redox components Z^{ox} and Z in PS II membrane fragments with intact (dashed curve) and inactivated (full curve) water-oxidizing enzyme system (for experimental details, see Ref. [69]) and of $PQH_2^{\oplus}/PQH_2$ in 9 M H_2SO_4 and 1 M CH_3OH (see Ref. [73]) (dotted curve).

A comparison with the system durosemiquinone/durohydroquinone in 9 M H_2SO_4 and 1 M methanol[73] shows that in the UV range the difference spectra of the durosemiquinone radical cation in solution and of Z^{ox} in photosystem II are similar. The hypsochromic shift of the 275-nm band to 260 nm and the slight bathochromic shift of the 305-nm band (to 310 nm) can be explained by the binding of the plastohydroquinone to the protein matrix. It should be emphasized, however, that an unambiguous identification of the prosthetic group of Z as PQH_2 has not

[*] The indices "vf" (very fast) and "f" (fast) are related to the different rates of relaxation.

yet been achieved, so that alternative assignments cannot be totally excluded (e.g., flavins, see Ref. [74], or tyrosine residues). Confirmation of the plastohydroquinone model for Z would have two interesting mechanistic consequences:

1. In solution, semiquinone radical cations can only exist in a strong acidic medium because of their negative pK values.[75] Therefore, the formation of a relatively stable plastosemiquinone radical cation in biomembranes requires its integration into a special protein matrix that prevents its rapid deprotonation[69,72] and thus plays an essential functional role. An experimental indication for the very strong isolation of the functional group of Z is the failure to observe deuterium exchange with the microenvironment of the prosthetic group when PS II membrane fragments are incubated in D_2O.[76a] Recent labeling experiments with ^{125}I suggest that the binding site of the functional group of Z is located in D-1 or in close proximity to this polypeptide.[76b,c]
2. Since the primary acceptor is a specially bound plastoquinone molecule associated with $Fe^{2\oplus}$ (high spin) (see Section 3), the generation of the [$P680^{\oplus}Pheo^{\ominus}$] radical-ion pair by the primary light reaction would eventually lead to the formation of a radical-ion pair consisting of spatially separated and fixed semiquinones,[77] which contain at least 60% of the free energy of the first excited singlet state of P680*. This implies that, for the intermediary storage (in the μs range) of solar energy, a system was evolved that maintains a relatively high electrochemical potential difference of approximately 1 V by using the same prosthetic groups (plastosemiquinones) and by controlling their microenvironments in order to achieve dramatic differences in the degree of protonation.

In addition, it is mechanistically interesting that, in contrast to the usual two-electron redox chemistry of quinoid systems, both prosthetic plastoquinone (or hydroquinone) groups act only as one-electron redox systems.[*] The oxidation of the functional plastohydroquinone in Z to the quinone stage is probably prevented by an efficient protonation (the formation of a doubly protonated quinone requires a very high oxidation potential, see Ref. [75]). The redox properties of the plastoquinone on the acceptor side are probably regulated by interaction with the $Fe^{2\oplus}$ center, but this process is mechanistically still unclear (see Section 5).

There are distinct differences between the difference spectra (Fig. 7) of Z^{ox}/Z for PS II membrane fragments whose water-oxidizing enzyme system Y is functionally intact and for those whose enzyme system Y is inactivated by selective treatments. These differences are typical for shifts caused by electrochromic effects. Therefore, the additional electrochromic band shifts might be caused by the electrostatic interaction between charged groups in the water-oxidizing enzyme system Y and the reaction center of photosystem II.[69] To what extent these interactions also affect the EPR spectra of the signals II_{vf} and II_f remains to be clarified.

Kinetic analyses of $P680^{\oplus}$ reduction led indirectly to the conclusion that two redox components participate in the functional coupling between RC II and the water-oxidizing enzyme system.[79,80] Since the kinetics of the signal II_{vf} relaxation[59] is in good agreement with that of the redox transitions $S_i \rightarrow S_{i-1}$,[56,57] Z is presumably associated directly with the water-oxidizing enzyme system. Therefore, if a further redox component D_x does exist, it should be located between Z and P680. Direct experimental evidence for the existence of D_x is still lacking (for a detailed discussion see Ref. [69]).

An interesting question with respect to the coupling mechanism between RC II and system Y is if and to what extent the redox state S_i in system Y influences the kinetics of $P680^{\oplus}$ reduction. If there is no interdependence between the two functional units, the electron-transport kinetics should be characterized only by the electronic and vibronic coupling between P680 and Z and therefore would be independent of S_i. Based on measurements of absorption changes at 690 nm, which reflect the turnover of P680, the kinetics of $P680^{\oplus}$ reduction was found to depend on the redox state of the water-oxidizing enzyme system.[79] Recent measurements with markedly higher time-resolution have confirmed this conclusion.[80] The regulation of the kinetics of electron transfer between $P680^{\oplus}$ and Z was attributed entirely to simple electrostatic interactions between the functional groups.[80] The possible influence of changes in the protein structure due to redox transitions of the prosthetic group was ignored. Such effects are well known for redox enzymes; e.g., the structure of the apoprotein of cytochrome c is significantly changed during oxidation of the functional heme group.[26] Recently, it was also shown for plastocyanin that the oxidation of the functional cation $Cu^{\oplus}$ to $Cu^{2\oplus}$ induces conformational changes, which are probably responsible for fine tuning of the electron transfer.[81] Therefore, it remains to be clarified whether or not the observed dependence of the kinetics of $P680^{\oplus}$ reduction on the redox state S_i of the water-oxidizing enzyme system is primarily caused by effects of the polypeptide structure on the electron transfer.

4.3. Functional Mechanism and Structural Composition of the Water-Oxidizing Enzyme System

A consideration of the formal sequence of one-electron reactions leading from two H_2O molecules to O_2 and $4H^{\oplus}$ (Fig. 8) readily reveals that the central problem of water oxidation in biological membrane systems is the mechanistic stabilization of the intermediary redox states.[82] The free energies of the oxidation products formed by a stepwise abstraction of electrons from water molecules ($HO^{\odot}$, H_2O_2, $HO_2^{\odot}$) immediately reveal that these intermediates cannot be involved as free species in photosynthetic water oxidation.[83,84] Furthermore, owing to the reactive properties of these compounds, a rapid oxidative degradation of sensitive biomolecules would occur. Accordingly, appropriate functional groups have to participate directly in the redox reaction sequence of photosynthetic water oxidation. The overall reaction consists in the cleavage of the

[*] Under nonphysiological experimental conditions in the presence of $Na_2S_2O_4$, reduction of Q_A to the hydroquinone stage [78] can be achieved.

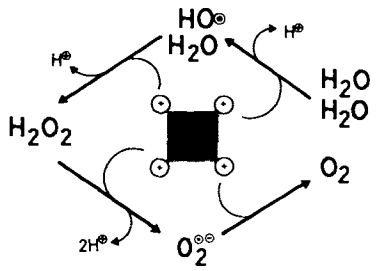

Fig. 8. Reaction scheme for the oxidation of two H_2O molecules to O_2 and $4H^{\oplus}$ by a sequence of four one-electron redox reactions. The grey area symbolizes a source of holes, which is not characterized in detail. With respect to the coupled protolytic reactions, it is assumed that the reaction takes place at a pH that is large compared with the pK value of HO_2.

bonds between the O and H atoms and the formation of σ and π bonds between two O atoms. Therefore, presumably systems with π orbitals and/or transition metals with incompletely filled d orbitals are especially suitable as functional groups. Investigations of O_2 enzymology[85] indicate that such systems (flavins, quinones; Fe, Cu, Mn, Mo) play an essential role as functional groups. Manganese is well known as an indispensable cofactor in photosynthetic water cleavage (for reviews see Refs. [51, 86–88]). Therefore, it seems plausible and logical to view the water-oxidizing enzyme system as a manganese protein, where the metal centers with their specific ligand shells act as the redox-active functional groups of the enzyme.[89, 90] From this basic postulate and from a comparison with the reaction schemes depicted in Figures 6 and 8, several important questions emerge regarding the mechanism of photosynthetic water oxidation:

1. What is the structure of the active site where the formation of O_2 from two H_2O molecules takes place?
2. What are the electronic structure and the nuclear configuration of the prosthetic groups that constitute the redox states S_i (see Fig. 6)?
3. Why does the water-oxidizing enzyme system almost completely attain the redox state S_1 after sufficient dark-adaptation?[51, 91]
4. What deprotonation reactions are coupled with the redox transitions $S_i \rightarrow S_{i+1}$?
5. How is the apoenzyme structurally arranged and how does it functionally influence the redox transitions?
6. What regulatory subunits are additionally involved in the function of the water-oxidizing enzyme system?

4.4. The Catalytic Site and the Functional Role of Manganese

The mechanistically crucial step for the formation of O_2 from two water molecules is the formation of an oxygen–oxygen bond. This requires a suitable geometric arrangement of the reactants, which can be achieved if the catalytic active site contains at least two centers. Moreover, the formation of a peroxidic precursor is thereby made possible. If the essential redox transitions are assumed to take place at these centers, then they constitute, together with their associated ligand shells, the prosthetic group of the water-oxidizing enzyme system. Redox-active groups that are required only for the electronic coupling with RC II (via component Z, see Section 4.2), or molecules and amino-acid residues that participate exclusively in deprotonation reactions (e.g., by the formation of hydrogen bonds) that are not directly involved in the reactive center, should not be considered as a part of the prosthetic group itself.

Based on these considerations, the prosthetic group of the water-oxidizing enzyme system Y is postulated to be a binuclear manganese complex. Stoichiometric analyses show that there are four Mn per system Y.[92, 93] These four Mn are assumed, however, to serve different functions. Indeed, even a structurally symmetric tetranuclear manganese complex can act as a functional binuclear group if it is incorporated into an asymmetric protein matrix (for a detailed discussion see Ref. [94]). Several reports suggest that the four Mn in system Y are not equivalent. They are distinguishable by (1) the magnetic interaction with Z^{ox},[61] (2) the interaction with $Cl^{\ominus}$,[95] (3) the binding strength after dissociation of the regulatory 33-kDa subunit (see Section 4.6.2),[96] and (4) the mechanism of the photoactivation of system Y.[97] After partial depletion of Mn, moreover, a reactivation of O_2 evolution without addition of Mn seems to be possible.[98] Furthermore, there are indications that two of the four manganese ions are replaceable by other bivalent metal cations.[99]

A binuclear manganese complex as the prosthetic group involved in water oxidation was already proposed in earlier models.[100, 101] This assumption is supported by the fact that, although enzyme systems catalyzing the reduction of O_2 to H_2O (cytochrome oxidase, laccase, etc.; for a review see Ref. [85]) also contain four metal centers, only two of them constitute the catalytic active site. Inorganic complexes containing binuclear metal centers have also been found to catalyze the oxidation of water.[102, 103]

If one assumes that the prosthetic group of the water-oxidizing enzyme system is a binuclear manganese complex, three questions arise: (1) What are the valence states of the two manganese centers in the redox states S_i? (2) How are the manganese centers coordinatively arranged in the protein and in what state of protonation will the substrate (H_2O) be bound? (3) Are further redox-active components (e.g., in the ligand sphere) involved in the electron-transfer processes of the catalytic center?

A variety of spectroscopic methods are available in order to characterize the electronic states of functional groups containing transition metals as redox-active species: NMR, EPR, UV/VIS, IR, EXAFS,[*] and XAES[*] spectroscopy. However, investigations of complex biological systems are confronted, in principle, with two difficulties. First, the difference spectra may overlap with those of components that do not participate in the reaction sequence in question. Secondly, even if good separation of the difference spectra can be achieved, tremendous problems arise for the interpretation of the data if neither the structure nor the chemical nature of the ligand shell is known. Both problems complicate the analysis of the reaction sequence in the water-oxidizing enzyme system so

[*] EXAFS = extended X-ray absorption fine structure; XAES = X-ray absorption edge structure.

strongly that a satisfactory answer to the above questions has not yet been possible. Therefore, we can only describe pieces of the puzzle formed by today's fragmentary state of information; these findings were obtained by the use of several spectroscopic methods. An attempt is then made to put together the pieces of the puzzle in order to draw a tentative picture of the whole mechanism. Since the isolation of the water-oxidizing enzyme system in a functionally intact state has not yet been achieved, the experiments have to be carried out with systems in which at least the processes occurring in RC II and the electron transfer to exogenous acceptors concomitantly take place. Therefore, the assignment of measured spectral properties to specific redox states S_i in the water-oxidizing enzyme system is based on the use of the characteristic oscillation pattern (see Fig. 5) as a "label" of the S_i states and their redox transitions $S_i \rightarrow S_{i+1}$.

4.4.1. NMR Spectroscopic Investigations

Strongly relaxing paramagnetic metal centers with suitable electron configuration (singlet orbital states with a low static zero-field splitting) influence the relaxation kinetics of water protons.[104] A change in the valence state of the manganese centers at the catalytic active site should therefore result in a change in the spin-lattice or spin-spin relaxation kinetics, which, in turn, should permit conclusions to be drawn about the redox states of the individual S_i states of the water-oxidizing enzyme system. Illumination of dark-adapted chloroplasts with a series of short flashes results in an oscillation pattern in the relaxation kinetics, which can be used to identify the S_i states.[105] This method requires the selection of suitable experimental conditions in order to exclude secondary effects caused by nonfunctional centers (for a review see Ref. [106]). Recent measurements unambiguously show that changes in the relaxation kinetics are associated with redox changes in the S_i states.[107] The results led to the preliminary conclusion that the transition $S_1 \rightarrow S_2$ is probably associated with an oxidation of Mn^{III} to Mn^{IV}, whereas the reaction $S_2 \rightarrow S_3$ might not involve a valence change in the manganese centers. The oxidation of S_0 to S_1 could be a $Mn^{II} \rightarrow Mn^{III}$ transition.[108] However the NMR results reported so far do not allow an unambiguous conclusion to be drawn about the redox state of manganese in the catalytic site.

4.4.2. EPR Spectroscopic Investigations

The bound manganese in photosystem II is EPR-inactive at room temperature (for a review see Refs. [87, 88]). Inactivation of the water-oxidizing enzyme system results in the appearance of a typical hyperfine EPR signal for $[Mn(H_2O)_6]^{2\oplus}$. Therefore, an attempt was made to release the manganese by sufficiently fast destruction of the enzyme system after occupation of specific S_i states and then to draw conclusions about the valence state of manganese from the amplitude of the measured EPR signal.[109] The results obtained by this indirect method suggested that the manganese is present as Mn^{II} and Mn^{III} during the redox cycle, whereby Mn^{IV} is also formed as an intermediate (during the transition $S_1 \rightarrow S_2 \rightarrow S_3$).[109]

Crucial for the applicability of EPR methods for analyses of the catalytic site of water oxidation was the discovery of a low-temperature EPR signal, which appears upon formation of the S_2 state.[110] The spectral simulation of the characteristic hyperfine structure led to the conclusion that the S_2 multiline signal is due to the mixed valence state of a bi- or tetranuclear manganese complex, whereby either a Mn^{II}–Mn^{III} or a Mn^{III}–Mn^{IV} configuration is possible.[110–116] Investigations on model complexes do not exclude the existence of a peroxo-bridged $[Mn^{II} \cdots O_2 \cdots Mn^{III}]$ state.[117] The influence of $H_2{}^{17}O$ on the hyperfine lines led to the conclusion that H_2O is associated directly with the catalytic manganese during the formation of S_2.[118] The S_2 multiline signal disappears when the water-oxidizing enzyme system is destroyed, as shown in Figure 9.[119] Besides the multiline signal, a further EPR

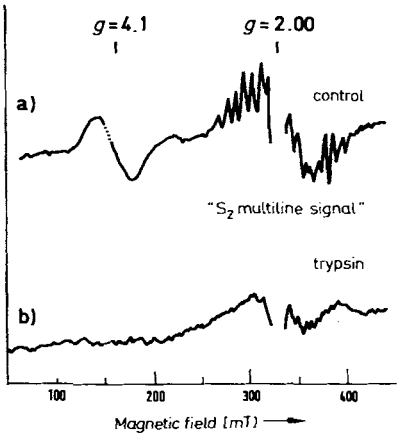

Fig. 9. Light-induced EPR signals of a) untreated and b) trypsin-treated PS II membrane fragments at pH = 7.5. The characteristic S_2 multiline signal (see text) is clearly resolved for untreated chloroplasts (the narrow range around $g = 2.0$ is not shown because of the superposition of very intense signals due to other radicals) (for experimental details see Ref. [119]).

signal exists at $g = 4.1$,[115, 120] which also belongs to S_2.[121, 122] The properties of these EPR signals suggest that the $g = 4.1$ signal arises from S_2 in the ground spin state ($S = 3/2$), and that the S_2 multiline signal is due to the excited spin state ($S = 1/2$) of an antiferromagnetic exchange-coupled binuclear Mn^n–Mn^{n+1} group, which is ferromagnetically coupled with a second ($S = 1$) center (possibly the second Mn dimer of a distorted Mn tetramer).[116, 121] In a recent model, a distorted cubane-like Mn_4O_4 structure is discussed.[122a] However, direct experimental evidence is still lacking. The analysis of the spin states alone does not permit a definite interpretation of the Mn valence state n. At present a value of $n = 3$ is most likely, [115, 116] whereby in the "cubane" model a Mn^{III}–Mn_3^{IV} configuration is assumed for S_2.[122a]

Structural information about the ligand sphere of the functional manganese centers, especially the distribution of the electron density, has not yet been obtained. In this connection a general problem of low-temperature EPR spectroscopy should be discussed. Measurements with manganese model complexes containing redox-active ligands[123, 124] do not exclude the possibility that the distribution of the electron density between ligands and central atoms depends on the temperature. If this phenomenon

also occurs in the water-oxidizing enzyme system, then low-temperature EPR measurements cannot provide any information, in principle, about the electronic configuration and hence the actual redox state of the manganese centers at the catalytic site at room temperature.

4.4.3. UV/VIS Spectroscopic Investigations

In principle, it should be possible to determine the UV/VIS difference spectra for the redox transitions $S_i \rightarrow S_{i+1}$ from flash-induced absorption changes because of the characteristic oscillation pattern (cf. Fig. 5). However, serious difficulties arise because of the superposition with binary oscillations, which are due to PQ reduction (see Section 5) (for a discussion see Refs. [94, 125]). By means of a proper modification of the apoprotein (mild trypsin treatment at $pH \leq 6.5$), it was possible to suppress PQH_2 production in thylakoids; simultaneously, $Q_A^{\ominus}$ becomes easily oxidizable with $K_3[Fe(CN)_6]$.[126-128] Illumination of dark-adapted trypsin-treated thylakoids with a sequence of short flashes in the presence of $K_3[Fe(CN)_6]$ gives rise to the absorption changes at 320 nm shown in Figure 10.[129]

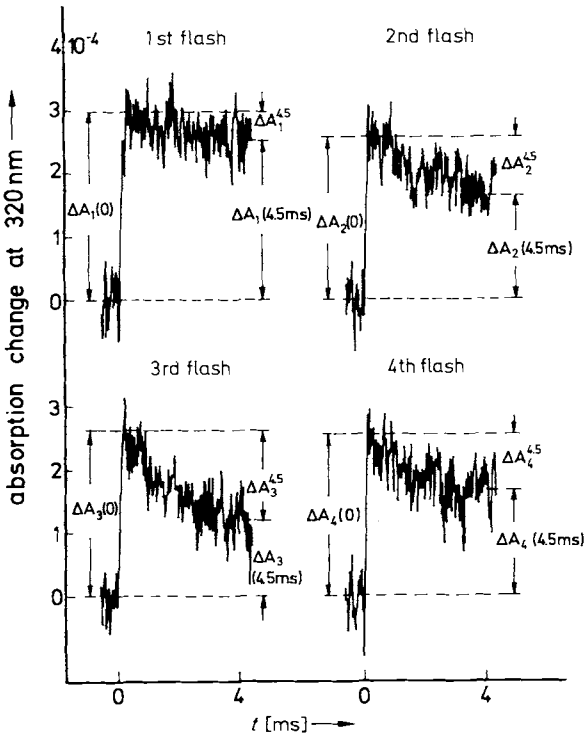

Fig. 10. Absorption changes at 320 nm as a function of the flash number in a sequence of short (10-μs) saturating flashes in dark-adapted and trypsin-treated thylakoids. $\Delta A_n(0)$ describes the initial amplitude of the n-th flash, ΔA_n (4.5 ms) represents the corresponding amplitude 4.5 ms after the excitation flash, and $\Delta A_n = \Delta A_n(0) - \Delta A_n(4.5\ ms)$ is the difference between the two values, which is a measure for the relative contribution of the 1-ms relaxation to the total relaxation (for experimental details see Ref. [129]).

Clearly revealed is a 1-ms relaxation, whose amplitude oscillates characteristically depending on the number of the flash. The half-life of about 1 ms corresponds to the time required for the rate-limiting step of O_2 production as derived from polarographic measurements.[130] Figure 11 shows that the amplitude of the 1-ms relaxation and the O_2 yield per flash of dark-adapted thylakoids exhibit practically the same oscillation pattern. Based on kinetic considerations, the amplitude of the 1-ms relaxation in trypsin-treated thylakoids corresponds to the following reaction:[53]

$$Z^{ox}S_3 + 2\,H_2O \longrightarrow ZS_0 + O_2 + 2\,H^{\oplus}$$

Thus, the difference spectrum of this reaction (Fig. 11, inset) can be obtained. A separation of the difference spectra for each individual redox transition $S_i \rightarrow S_{i+1}$ could not be achieved because of the poor optical properties of the thylakoid suspensions.

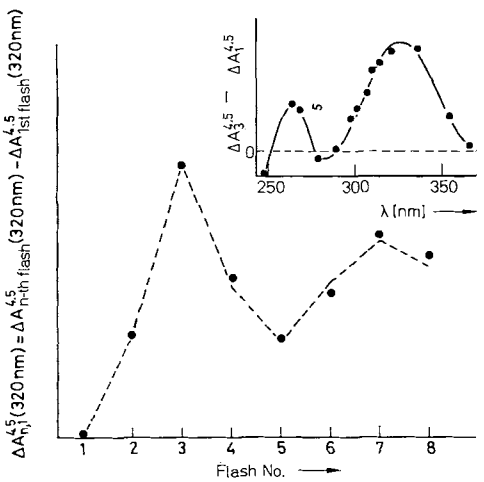

Fig. 11. Amplitude difference (●) of the 1-ms relaxation between the n-th and the first flash ($\Delta A_{n,1}^{4.5}$) and relative oxygen yield (----) as a function of the flash number in a sequence of short (10-μs) saturating flashes in dark-adapted trypsin-treated thylakoids. The inset shows the amplitude difference (●) of the 1-ms relaxation between the third and first flash as a function of wavelength (for further details see Ref. [53]).

Significant progress in all spectroscopic investigations of photosystem II was achieved by the development of preparative methods for the isolation of membrane fragments that contain almost no photosystem I, exhibit full O_2-evolving activity, and have convenient optical properties (low dispersion, small particle size).[131, 132] Measurements of flash-induced absorption changes with PS II particles and analyses of the results on the basis of the Kok scheme (see Section 4.2) were performed by several groups.[125, 133, 134] Different conclusions were drawn from these studies, the details of which will not be discussed here. However, it has to be emphasized that even the basic question is still open whether each redox transition $S_i \rightarrow S_{i+1}$ leads practically to the same difference spectrum for $i = 0$, 1, and 2[133] or whether significant differences appear.[125, 134] The most recent theoretical considerations reveal that, even in the ideal case of the absence of any interferring processes, the absorption changes per se do not permit an unambiguous deconvolution into the difference spectra $\Delta\varepsilon_{i+1,i}(\lambda)$.[135]

An attempt was also made to use the difference spectra obtained in these investigations to derive information about the nature of the participating redox groups. A comparison with the spectra of manganese gluconate complexes led to the conclusion that each $S_i \rightarrow S_{i+1}$ transition

for i = 0, 1, and 2 corresponds to an oxidation from Mn^{III} to Mn^{IV}.[133] This assignment remains equivocal, however, because, regardless of possible differences between various redox transitions,[125,134] the difference spectra by themselves do not permit a definite interpretation of the electron configuration of the manganese centers in the S_i states; the UV spectra of manganese complexes are primarily determined by the structure of the ligands[136a] rather than by the manganese centers. Recent investigations[136b] confirm these conclusions.

4.4.4. *IR Spectroscopic Investigations*

After illumination of dark-adapted PS II membrane fragments with a series of laser flashes, absorption changes were observed with a maximum at 820 nm ($\Delta\varepsilon$ on the order of 100 M^{-1} cm^{-1}), which reveal a characteristic dependence on the flash number.[137] The absorption changes show typical properties of an intervalence transition in binuclear manganese complexes. It was concluded that in the transition $S_1 \rightarrow S_2$ a Mn^{III}-Mn^{IV} configuration is formed, which disappears in the $S_3 \rightarrow (S_4) \rightarrow S_0$ transition. This assignment implies that the redox transitions $S_0 \rightarrow S_1$ and $S_2 \rightarrow S_3$ probably do not involve a valence change of the manganese centers at the catalytic site.

4.4.5. *EXAFS and XAES Spectroscopic Investigations*

The first attempts to measure the K edge of manganese (XAES measurements) in thylakoids led to the conclusion that S_1 is a mixed-valence $Mn^{II,III}$ state.[138] Later investigations with PS II membrane fragments showed that dramatic changes occur in the edge properties of the sample (a shift of 2.5 eV as well as a broadening of the main absorption peak) during the transition $S_1 \rightarrow S_2$.[139] In contrast, only marginal changes in the transition $S_2 \rightarrow S_3$ were observed. From these results it was inferred that manganese in the binuclear catalytic center exists only in the states Mn^{II}-Mn^{III} and Mn^{III}-Mn^{IV} and that the $S_1 \rightarrow S_2$ transition is a two electron transition with respect to the redox states of the manganese; moreover, a further redox-active component was assumed to be involved in this process.[139] EXAFS analyses revealed that a binuclear manganese complex with a Mn–Mn distance of 270 pm exists in S_1 and S_2.[140] Recent EXAFS investigations confirm this value. They also show that the manganese in the binuclear cluster is located in a special noncentrosymmetric environment, where each Mn has 3 ± 1 terminal ligands (N or O atoms) at a distance of 198 pm and 2 ± 1 bridge ligands (also N or O atoms) at a distance of 175 pm. Possibly, a μ-oxo-bridge structure is involved. An additional binuclear Mn cluster or a monomeric Mn atom is probably also present in the environment.[141]

4.5. Proposed Models for the Molecular Mechanism of Photosynthetic Water Oxidation

The results discussed in Section 4 permit two initial conclusions to be drawn. First, a mixed-valence configuration $Mn^n \cdots Mn^{n+1}$ probably exists in the state S_2. Second, water is directly bound in the first coordination sphere of the functional manganese.

Furthermore, no significant valence change appears to take place at the manganese centers of the catalytic site during the redox transition $S_2 \rightarrow S_3$, i.e., in this redox step the oxidation presumably occurs within the ligand sphere or at an additional redox component. Additionally, thermodynamic considerations led to the conclusion that a redox-active component (symbolized by M) with a relatively low redox potential participates in the redox transition $S_0 \rightarrow S_1$.[100,101] Whether M is a redox-active ligand[53] or a special redox state of the manganese itself[142] still remains to be clarified. A proposed mechanism, which takes these findings into account, is presented schematically in Figure 12.[142]

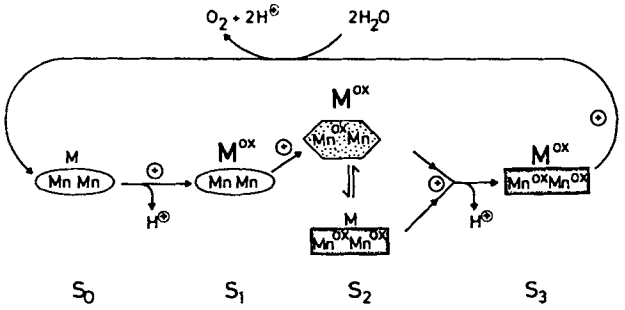

Fig. 12. Reaction scheme for the oxidation of two H_2O molecules to O_2 and $4H^{\oplus}$ at a binuclear manganese center containing an additional redox-active component M (see text). ⊕ symbolizes a hole.

The symbols MnMn, $Mn^{ox}Mn$, and $Mn^{ox}Mn^{ox}$ in Figure 12 represent the functional binuclear manganese center in different oxidation states, whereby the different symbols refer to conformational changes possibly taking place in the apoenzyme during the redox transitions. The existence of two fundamentally different conformations (S_0 and S_1 are markedly different from S_2 and S_3) was recently inferred on the basis of $Cl^{\ominus}$ affinity measurements (see Section 4.6.1).[143a] This conclusion is further supported by measurements of the temperature dependence of the individual redox transitions $S_i \rightarrow S_{i+1}$ ($i = 1, 2, 3$),[143a] which provided information about the activation enthalpies and entropies.[143b] It remains to be shown whether or not these structural differences also influence the kinetics of $P680^{\oplus}$ reduction (see Section 4.2).

The distribution of electron density between the central atoms and the ligand sphere is not explicitly taken into consideration in Figure 12 (see following discussion).

In Figure 12, the "upper" reaction route corresponds to our previously proposed scheme,[100,101] while the "lower" reaction path better describes results obtained more recently.[108,125,139] It still remains to be confirmed whether the postulated S_2 equilibrium exists in the form shown. The existence of this equilibrium would imply the possibility of a shift of the equilibrium constant, so that the measured difference spectra for the redox transitions $S_1 \rightarrow S_2$ and $S_2 \rightarrow S_3$ might depend on experimental conditions.[142]

Until now, we have excluded the possible participation of water as a reactant in the different redox transitions

$S_i \rightarrow S_{i+1}$. Water can undergo protolytic as well as redox reactions. Of central mechanistic relevance for the O_2 production is the following question: At which redox stage S_i is the O–O bond formed? Based on possible analogies with the mechanism of the reverse reaction (namely, the reduction of O_2 to H_2O) in biological systems (for a review see Ref. [85]), it was concluded that the O–O bond is formed at the level of a binuclearly bridged peroxide at the redox stage S_3.[100, 101] Taking into consideration the equilibrium for S_2 formulated in Figure 12, peroxide formation is already possible in S_2. This is also true if $M \rightarrow M^{ox} + e^{\ominus}$ is a special valence-state transition at the catalytic Mn itself. Generally, O–O bond formation at the redox stage of a peroxide can be described by an equilibrium reaction of the type shown in Equation (7).

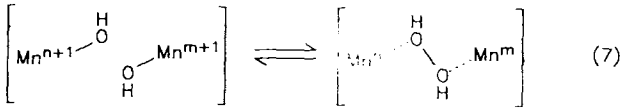

(7)

In this context it is interesting to note that in cytochrome oxidase the cleavage of the O–O bond takes place at the level of a three-electron reduction of the binuclearly complexed oxygen. This reaction is highly entropy-driven.[144] Analogously, O–O bond formation could occur at the redox stage of two or three holes (S_2 or S_3) in the water-oxidizing enzyme system. This raises the following question: Which redox state S_i satisfies the enthalpic and entropic prerequisites for a significant population of an electronic and nuclear configuration corresponding to the peroxidic form described in Equation (7)? This problem is still unsolved. There are experimental results that support the existence of a μ-peroxo bridge in S_2.[117, 118] Furthermore, the increase in the light-induced production of H_2O_2 after depletion of the regulatory subunits of the water-oxidizing enzyme system (see Section 4.6.2) could be ascribed to a destabilization of peroxide-like intermediary states in S_2 and/or S_3.[145]

In contrast, mass spectroscopic analyses of flash-induced O_2 production after incubation with $H_2{}^{18}O$ were interpreted to exclude the possible formation of peroxidic intermediates at the level of S_3 (or S_2).[146] For kinetic reasons, however, the interpretation of these data is not unequivocal (for a detailed discussion see Ref. [94, 125]). Furthermore, it was recently shown that a very stable S_3 state exists, whose O atoms do not undergo exchange.[147] Unequivocal results as to the possible existence of peroxidic intermediary stages can only be expected if either the time resolution of mass spectroscopic methods can be improved considerably or other spectroscopic methods (IR vibrational spectroscopy, Raman spectroscopy) become available for a selective detection of OH and O–O vibrations in the water-oxidizing enzyme system for the redox states S_i. The electronic configuration of the catalytic site in the different redox states is determined by the actual distribution of the electron density between the binuclear manganese center, the postulated component M, and the substrate ligand. In model systems many examples are known for an electron-density distribution between ligand and central atoms after binding of O_2 to transition-metal centers with only partly occupied d orbitals. The actual distribution can vary between that of O_2 and that of a peroxidic configuration depending on the nature of the entire ligand sphere.[148–152]

Analogous phenomena can appear in enzymatic systems. In a plant cytochrome oxidase, for example, a partial distribution of the charge density of the following form was found ($\delta_1 + \delta_2 \approx 1$, $\delta_1 > 0.5$, and $\delta_2 < 0.5$):[153]

$$Cu_B^{(1+\delta_1)} \cdots O^{\ominus(\delta_1+\delta_2)} O^{\ominus} \cdots Fe^{(2+\delta_2)} Cyt\, a_3$$

The formation of hydrogen bonds could play an essential role in determining the actual charge distribution, as shown by quantum-mechanical model calculations for a Zn–Cu superoxide dismutase.[154]

The possible role of a charge delocalization between ligands and the central atom for the stabilization of the intermediary redox stages of the water oxidation was discussed in detail in earlier proposed models.[100, 101] These considerations led to the conclusion that, in photosynthetic water oxidation, the redox transitions $S_1 \rightarrow S_2$, $S_2 \rightarrow S_3$, and $S_3 \rightarrow S_0$ have almost the same redox potential difference ($\Delta E \approx 1$ V), whereas the transition $S_0 \rightarrow S_1$ has a significantly lower redox potential difference (see Fig. 13).

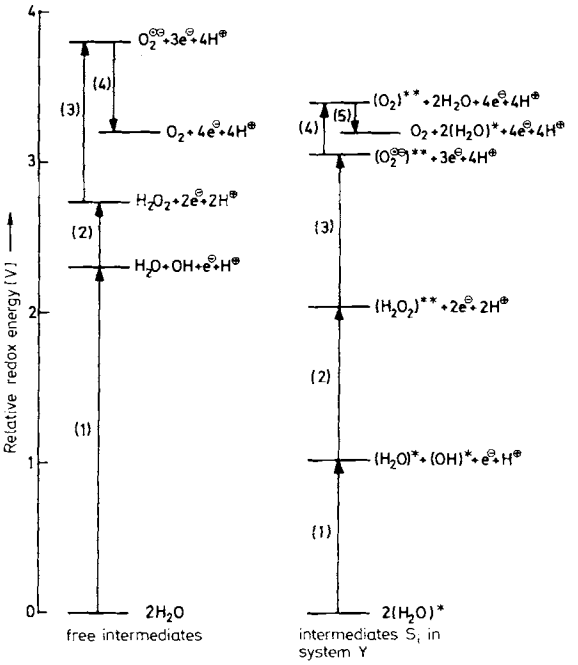

Fig. 13. Redox energy scheme for the oxidation of two H_2O molecules to O_2 and $4H^{\oplus}$ by a sequence of four one-electron redox reactions in vitro (left side) and in the water-oxidizing enzyme system (right side). For the sake of simplicity, the energy of the H_2O molecules in vitro and their energy in the catalytic center of the water-oxidizing enzyme system are shown at the same level, although the absolute values are considerably different. $(OH)^*$, $(H_2O_2)^{**}$, and $(O_2^{\ominus\ominus})^{**}$ represent the formal intermediates of photosynthetic water oxidation relative to the same zero level. These species describe the state of the entire catalytic site. The transitions (1), (2), (3), and (4) (right side) correspond to the transitions $S_1 \rightarrow S_2$, $S_2 \rightarrow S_3$, $S_3 \rightarrow S_4$, and $S_0 \rightarrow S_1$, respectively. The formal analogy does not correspond to the real reaction sequence. The comparison only serves to indicate that the oxidation state S_1 (M^{ox}) acts as an oxidant in the last step of the sequence: $(S_1) \cdot S_0' \rightarrow (S_0) \cdot S_4$. Theoretically, M^{ox} can also enter the redox sequence at S_3 or even at S_2 (see Eq. (12)). It is still unclear at what stage the formation of the O–O bond actually occurs (see text). In this scheme, the possibility is not explicitly considered that a μ-peroxo bridge may already be formed in S_2 [see Fig. 12 and Eq. (7)] (for further details see Refs. [94, 101]).

Similar values were estimated from the results of delayed fluorescence measurements.[155] Measurements of thermoluminescence confirm that the transitions $S_1 \rightarrow S_2$ and $S_2 \rightarrow S_3$ require practically the same redox energy.[156] This implies that, for a significant occupation of state $M(Mn^{ox}Mn^{ox})$ in S_2, the redox potential of the M/M^{ox} couple is strongly shifted for the transition $S_2 \rightarrow S_3$ compared with the reaction $S_0 \rightarrow S_1$. This can be plausibly explained by strong electrostatic interactions. Additionally, it is mechanistically interesting that the life-time of S_2 and S_3 is dramatically shortened by so-called ADRY substances,[157-159][*] while S_1 remains unaffected. Furthermore, thermodynamic considerations led to the conclusion that, at the catalytic center, the educt–product exchange

$$2\,H_2O + (O_2)\cdot X \longrightarrow O_2 + 2(H_2O)\cdot X$$

(X symbolizes a product (O_2) or educt (H_2O) that is coordinated to Mn) is an exergonic process.[100, 101] Hydrogen bonds could play a crucial function in this reaction, because they were shown to be decisive in determining the strength of O_2 bonding in hemoglobins and model systems where considerable changes can occur in the binding geometry of O_2 to the metal center.[160]

The use of highly sensitive glass electrodes or suitable pH indicators to study the protolytic reactions coupled with H_2O oxidation have shown that $H^{\oplus}$ release is not synchronous with O_2 production.[161-163] A deprotonation pattern of 1, 0, 1, 2 $H^{\oplus}$ per PS II appears to be linked with the redox transitions $S_i \rightarrow S_{i+1}$ ($i = 0$–3).[162-168] However, it has to be emphasized that this pattern does not necessarily indicate the actual deprotonation reactions of the water molecules bound to the manganese centers (or of other redox states of the substrate), because pK_a shifts of groups in the protein matrix that can undergo deprotonation also result in a release of protons. Therefore, the intrinsic deprotonation pattern of the ligand sphere of the catalytic manganese must be distinguished from the measured proton-release pattern.[101] This consideration also implies the possibility of an apparent stoichiometry with nonintegral values for the $H^{\oplus}$ release coupled with redox transitions $S_i \rightarrow S_{i+1}$ in the water-oxidizing enzyme system. In this case, a pH dependence for the $H^{\oplus}$ release pattern should be expected. This was not observed in measurements between pH = 6.0 and 8.0 using different preparations.[166-168] At pH < 6.0, the extrinsic proton release pattern seems to shift toward a 1:1:1:1 stoichiometry.[167b] So far, no method has been found to measure directly the intrinsic deprotonation pattern (for a detailed discussion see Ref. [94]).

4.6. Polypeptide Structure and Additional Cofactors in the Water-Oxidizing Enzyme System

The discussion so far has been limited to the nature of the redox-active manganese centers (including the postulated component M) and the bound water. In redox enzymes, however, one can hardly overemphasize the functional role of the surrounding protein matrix and of additional cofactors, which influence the redox processes and, in particular, the thermodynamics of the individual $S_i \rightarrow S_{i+1}$ transitions. The mechanism of this "fine tuning" of the four-step oxidation reaction sequence leading from H_2O to O_2 is still not understood. Therefore, only a short summary of some experimental results will be given.

4.6.1. The Role of $Cl^{\ominus}$ and $Ca^{2\oplus}$ as Cofactors

$Cl^{\ominus}$ has long been known to play an important role in photosynthetic H_2O oxidation (for reviews see Refs. [169–171]). In contrast to the absolute specificity for manganese, $Cl^{\ominus}$ can be replaced by other anions (e.g., $Br^{\ominus}$, $I^{\ominus}$). ^{35}Cl-NMR measurements indicate that reversible $Cl^{\ominus}$ binding occurs with an average exchange rate of $> 3 \times 10^4\ s^{-1}$ (25 °C).[172] The affinity for $Cl^{\ominus}$ depends on the redox state of the water-oxidizing enzyme system; it is low in S_0 and S_1, but high in S_2 and S_3.[174] Binding studies with the radioisotope $^{36}Cl^{\ominus}$ led to the conclusion that four $Cl^{\ominus}$ per PS II are required for the reactivation of the O_2 production of $Cl^{\ominus}$-"free" thylakoids.[173] Two specific binding sites exist for $Cl^{\ominus}$,[175, 176] the affinities of which differ from each other by approximately one order of magnitude.[176] In $Cl^{\ominus}$-depleted PS II membrane fragments, certain $S_i \rightarrow S_{i+1}$ transitions are blocked.[177-180] In the case of $Cl^{\ominus}$ deficiency, a light-induced S_2^* state with unusual properties is formed.[181] This S_2^* state does not exhibit a multiline EPR signal but rather the signal at $g = 4.1$. After addition of $Cl^{\ominus}$ in the dark, S_2^* is converted into S_2 with a normal multiline signal.

$Cl^{\ominus}$ probably plays a functional role in charge compensation during redox transitions in the water-oxidizing enzyme system and may be involved in protonation/deprotonation reactions coupled with H_2O oxidation.[170, 182, 183] In addition, reversible $Cl^{\ominus}$ binding to the redox states S_i possibly influences their thermodynamic properties.[181, 184] EXAFS measurements practically exclude the participation of $Cl^{\ominus}$ as a bridging ligand between the manganese centers[183, 185]—a function similar to that involved in inner-sphere electron-transfer processes between complexed transition-metal ions in solution (for a review see Ref. [186]). The EXAFS data show that the distance between bound $Cl^{\ominus}$ and Mn is at least 3–4 Å.[141] Furthermore, the superhyperfine splitting of the multiline EPR signal indicates that $Cl^{\ominus}$ is not very likely to be directly associated with the Mn of the functional group.[187]

The first evidence for a possible function of $Ca^{2\oplus}$ came from measurements of O_2 production in cyanobacteria.[188, 189] After depletion of regulatory subunits (see Section 4.6.2) from PS II membrane fragments of higher plants (e.g., by salt treatment, see Refs. [190, 191]), a restoration of the O_2-evolving activity can be achieved solely by the addition of $CaCl_2$.[192, 193] It was concluded that the lack of $Ca^{2\oplus}$ blocks the following reaction:[194]

$$Z^{ox}S_3 + 2\,H_2O \longrightarrow ZS_0 + O_2 + 2\,H^{\oplus}$$

Recently, a partial restoration of the ns-kinetics of $P680^{\oplus}$ reduction, which is specific for $Ca^{2\oplus}$, was found for

[*] Examples of ADRY substances: derivatives of carbonylcyanida and α-acyl-α-cyanocarbonylphenylhydrazones, of 2-anilino-3,5-dinitrothiophenes [158b] and of dipicryle-mine [158c].

PS II membrane fragments that had been modified by mild proteolysis.[195] Thus, $Ca^{2\oplus}$ appears to be essential for the functional coupling of the catalytic site with the reaction center.[195, 196] Depletion of $Ca^{2\oplus}$ from its native binding site probably leads to a total blockage of the water-oxidizing enzyme system.[197] $Ca^{2\oplus}$ is bound to an intrinsic membrane protein, whose conformation is influenced by an extrinsically bound 24-kDa protein (see Section 4.6.2).[198] The nature of the $Ca^{2\oplus}$-binding protein and the function of $Ca^{2\oplus}$ are still unclear. Probably structural effects in the environment of the catalytic active site are essential.[195]

4.6.2. *Polypeptide Structure of the Water-Oxidizing Enzyme System*

Generally, the processes at the catalytic center of an enzyme are directly affected by the nature of the apoprotein. Additional polypeptides, which are not functional parts of the catalytic site, can act as regulatory subunits to influence indirectly the reaction sequence via structural changes. This was clearly demonstrated for the cytochrome oxidase enzyme system, which catalyzes the reverse reaction, i.e., the reduction of O_2 to H_2O (for reviews see Refs. [199, 200]). Interestingly the nature of the polypeptides constituting the catalytic center of cytochrome oxidase (Cu_B, $Cyt\,a_3$) has changed comparatively little during the course of phylogenetic evolution, while the number of regulatory subunits has increased markedly.[201] Therefore, it was thought that an analogous phenomenon might have also occurred for the water-oxidizing enzyme system.[51] These considerations led to questions about the nature of both the polypeptides (or polypeptide) that contain(s) the catalytic, binuclear manganese center and the proteins that act as regulatory subunits.

The apoprotein of the functional manganese group has not yet been identified. Possible candidates include CP47[196, 202] and an integral 34-kDa polypeptide,[203] which could be D-1[204] (or D-2) (see Section 3.2).

The stability of the manganese binding is enhanced by a lysine-rich extrinsic 33-kDa protein, which is attached to the membrane surface and is not related to the integral 34-kDa protein (the 34-kDa protein is encoded in the plastid DNA, the 33-kDa protein in the nuclear DNA[205]). Several lines of evidence indicate that the 33-kDa polypeptide does not directly participate in manganese binding: (1) Mn incorporation into the catalytic site during photoactivation takes place even in the absence of this polypeptide.[206] (2) The polypeptide does not contain histidine,[207] which plays an important role in the complexation of metal centers.[208] (3) Selective depletion of the 33-kDa protein leads to a marked decrease in the O_2-evolving activity but not to loss of manganese;[96] however, Mn binding does become destabilized.

Surface enhanced Raman-scattering spectroscopy (SERS) measurements led to the conclusion that the binuclear Mn group of the catalytic center is arranged at the surface of the binding protein that is in contact with the associated 33-kDa polypeptide. The measured Raman frequency of 225 cm^{-1} can be assigned to either a Mn–O or a Mn–N as well as to a Mn–Cl vibration.[209] Investigations with NH_2OH and NH_2NH_2 led to the conclusion that the H_2O binding site at the functional group has a dimension of $4 \times 2.5 \times 1.5$ Å.[210] However, recent investigations show that cooperative binding of two NH_2NH_2 molecules takes place at or near the catalytic center.[211, 212] This means that either the H_2O binding site is flexible in dimension or the above-mentioned calculation has to be modified.

The 33-kDa polypeptide is an essential regulatory subunit, which appears in all O_2-evolving, photosynthetic organisms so far analyzed. The close relationship of this subunit between different species is shown by immunological cross-reactions with appropriate antibodies[213] and by reconstitution experiments.[214] Besides this universal regulatory subunit of the water-oxidizing enzyme system, there are additional polypeptides possessing regulatory functions. Like the corresponding subunits of cytochrome oxidase,[201] these polypeptide subunits have undergone marked variation during the course of phylogenetic development. This appears to be a general phenomenon of enzyme systems that can make the redox system H_2O/O_2 biologically "available" for the processes of photosynthesis and respiration. In higher plants a 17-kDa and a 24-kDa polypeptide, which do not appear in cyanobacteria,[215] are well characterized.[216] The 24-kDa polypeptide influences the effect of $Ca^{2\oplus}$[198] and simultaneously increases the effective concentration of $Cl^{\ominus}$.[217] After depletion of the 24-kDa polypeptide (by NaCl treatment), part of the water-oxidizing enzyme system is functionally disconnected from the reaction center; rebinding of the polypeptide leads to restoration of the ability to produce O_2.[218, 219] To what extent this effect correlates with a change in $Ca^{2\oplus}$ affinity has yet to be shown quantitatively. The 17-kDa polypeptide binds specifically to the 24-kDa subunit[220] and also leads to an increase in the effective $Cl^{\ominus}$ concentration in the water-oxidizing enzyme system. Recently, several other polypeptides were discovered in the range of 4–6 kDa[221] whose functions in photosystem II are still unclear.

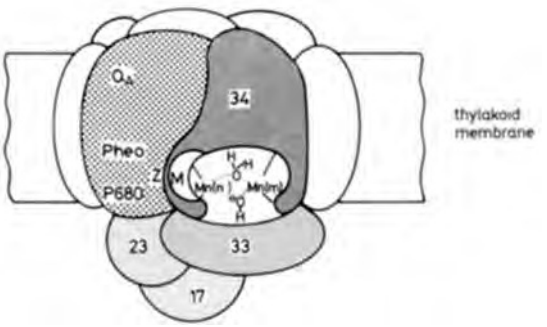

Fig. 14. Scheme of the structural organization of the water-oxidizing enzyme systems in higher plants. In contrast to Fig. 2, the catalytic active site of the water oxidation (black circle in Fig. 2) is specified and the three well-characterized regulatory polypeptides (17, 23, and 33 kDa) are explicitly shown. Further polypeptides with unknown functions are not shown; $Ca^{2\oplus}$ and $Cl^{\ominus}$ are also omitted, because only little is known about their binding sites (see text). The components P, I, and A of Fig. 2 are shown in their identified form (P680, Pheo, Q_A). The different shading of the polypeptide complexes in the membrane only corresponds to their function (reaction center, dotted; water-oxidizing enzyme system, dark grey; PQ-reducing enzyme, white). These differences do not stringently imply different polypeptides (e.g., the whole 34-kDa polypeptide may participate in binding of reaction center components and the catalytic active site of water oxidation; see Sections 3.2 and 4.6.2).

Summarizing the results outlined above leads to the highly simplified scheme for the structural organization of the water-oxidizing enzyme system shown in Figure 14. Only the binuclear Mn center where the water oxidation takes place is shown. The other two manganese atoms, which are also of importance for the H_2O oxidation,[94] are not shown because their role and exact structural arrangement have not yet been fully determined. Analogously to laccase[222] or cytochrome oxidase,[85] both of these Mn centers could participate in the electron transport from the catalytic site to the reaction center[51] or constitute the component M[125] or contribute to the stabilization of the geometry at the catalytic site via hydrogen bonding of H_2O molecules of the coordination sphere.[223] For the sake of simplicity in Figure 14, only the well-characterized 17-, 24-, and 33-kDa polypeptides are shown as regulatory subunits.

4.6.3. Possible Function of Lipids in the Water-Oxidizing Enzyme System

A comparison of the structural and functional organization of the water-oxidizing enzyme system with that of cytochrome oxidase leads directly to a further general question: What role do lipids play as essential and specific components for the function of these enzyme complexes? The negatively charged lipid cardiolipin is associated via a comparatively strong noncovalent bond with cytochrome oxidase and is crucial for its catalytic activity.[224,225] An analogous effect may also exist for the water-oxidizing enzyme system, because the negatively charged lipid sulfoquinovosyldiacylglycerol is relatively tightly bound to PS II protein complexes.[226] The O_2-evolving rate of PS II membrane fragments whose lipid content was decreased by detergent treatment during the preparation was stimulated up to 80% by the addition of lipids.[227] Therefore, lipids may also be of functional significance for the activity of the water-oxidizing enzyme system. Interestingly, in contrast to most of the lipids of the thylakoid membrane, sulfoquinovosyldiacylglycerol contains a high percentage of saturated fatty acids. This could suggest that the acidic lipid is bound to protein. However, the possible functional role of lipids in enzyme systems and especially in the water-oxidizing enzyme system is still totally unknown. Therefore, lipids were not included in Figure 14.

5. The PQ-Reducing Enzyme

The reductive formation of plastohydroquinone (PQH_2) from plastoquinone (PQ) requires the cooperation of two electrons. Analogously to water oxidation, the reduction of PQ to PQH_2 takes place via a sequence of one-electron redox steps.[228,229] In this process, one PQ molecule of the pool is statistically associated with a special binding site. After accepting one electron from $Q_A^{\ominus}$ of the reaction center (see Section 3.1), the newly formed semiquinone, which is designated $Q_B^{\ominus}$, is highly stabilized at the binding site.[*] A second electron transfer from $Q_A^{\ominus}$ leads to the formation of the redox state of a plastohydroquinone. The plastohydroquinone, formed by protonation, is bound relatively weakly and is replaced by another oxidized PQ molecule of the pool (for a review see Ref. [230]). The binding site of Q_B is located within a 32-kDa polypeptide, called D-1 (see Section 3.2). A high-spin $Fe^{2\oplus}$, which is probably coordinatively bound to four histidine residues of the polypeptides D-1 and D-2, is located between Q_A and Q_B (for a review see Ref. [231]). It has been proposed that this $Fe^{2\oplus}$ undergoes transient valence change to $Fe^{3\oplus}$ via a so-called "push-pull" mechanism, thereby participating directly in the electron transport from $Q_A^{\ominus}$ to Q_B (or $Q_B^{\ominus}$).[232] Recent investigations of the isolated reaction centers of photosynthetic purple bacteria have shown, however, that the kinetics of electron transfer are practically unaffected by depletion of $Fe^{2\oplus}$.[233] Interestingly, after depletion of $Fe^{2\oplus}$, the photochemical quantum yield of $Q_A^{\ominus}$ formation in the reaction center decreases significantly. This effect is caused by a 20–50-fold retardation of the electron transfer from bacteriopheophytin to $Q_A^{\ominus}$.[24] The incorporation of other bivalent cations ($Mn^{2\oplus}$, $Co^{2\oplus}$, $Ni^{2\oplus}$, $Cu^{2\oplus}$, $Zn^{2\oplus}$, but not $Mg^{2\oplus}$ or $Ca^{2\oplus}$) into the $Fe^{2\oplus}$ binding site leads to the restoration of the electron transport rate and the high quantum yield.[233] The results show that neither $Fe^{2\oplus}$ itself nor another bivalent cation is required for the fast electron transfer from $Q_A^{\ominus}$ to Q_B (or $Q_B^{\ominus}$). Instead, the $Fe^{2\oplus}$ is necessary in situ in order to establish the special functional properties of Q_A.

Recently, it was shown that the properties of the PQ-reducing enzyme are changed after detergent treatment.[234–236] This could suggest that the interaction with specific lipids is of functional significance for this polypeptide.

6. Reaction Scheme of the Photosynthetic Water Splitting

A summary of the results and models discussed in this review article for the mechanism of photosynthetic water splitting is given by the reaction sequence depicted in Figure 15.

7. Future Aspects

This short review has attempted to show what functional and structural principles are used by biological systems in order to exploit solar energy by water cleavage, leading to the formation of a biological "hydrogen-oxygen chain" involving bound hydrogen. The intensive research activities of the last two decades have led to important insights into the organization pattern of the entire process. However, essential mechanistic aspects are still not understood. Moreover, the significance of protein dynamics for the regulation of the individual reaction steps and for their coupling to the entire process is still unclear. Hopefully, new knowledge, especially in the field of protein physics and the fast developing area of molecular dynamics, will lead to a deeper mechanistic understanding of photosynthetic water

[*] In Figure 4, Q_A and Q_B refer to two different quinones.

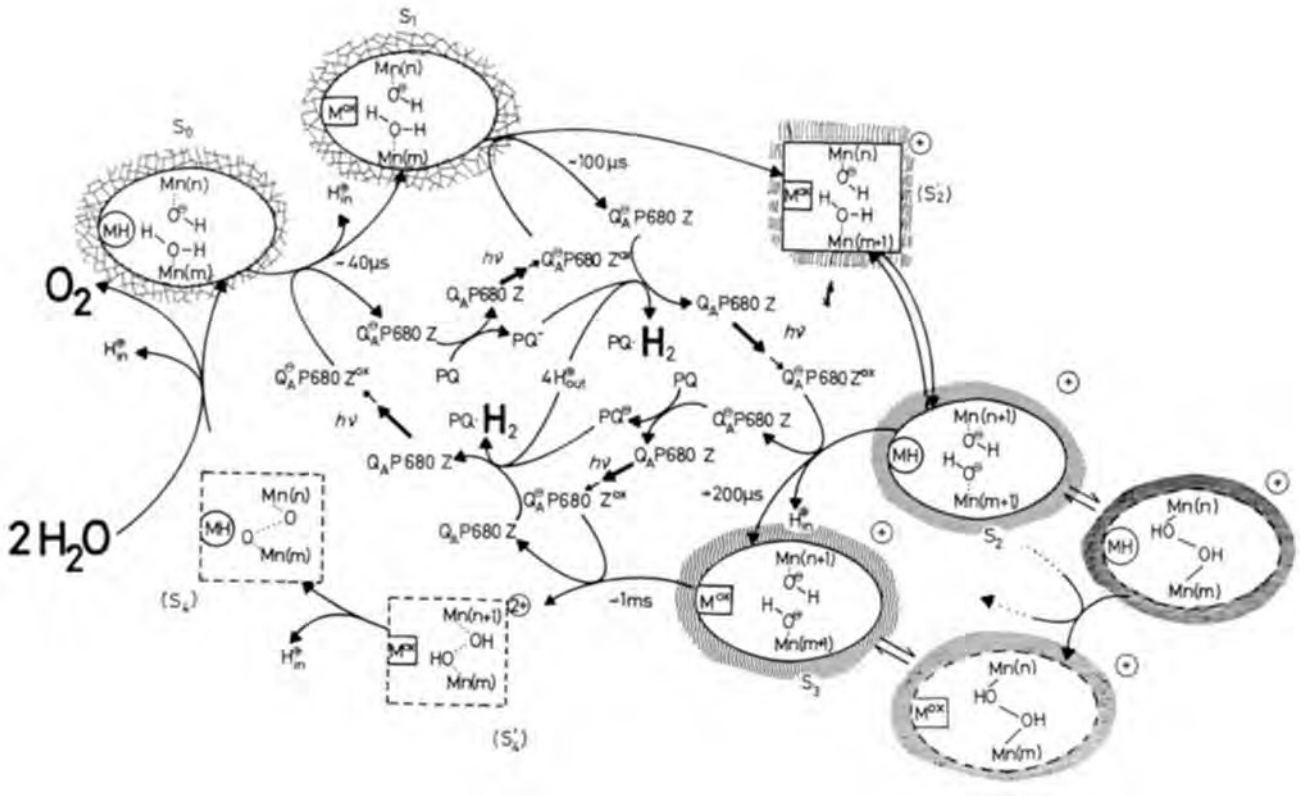

Fig. 15. Reaction scheme of photosynthetic water cleavage in photosystem II. The reaction sequences of the functional units are indicated by different shades of grey: (1) The grey circle in the middle symbolizes the reaction sequence in the reaction center, but the oxidation of Z by $P680^{\oplus}$ is not explicitly shown. (2) The outer circle represents the reaction sequence in the catalytic site of the water-oxidizing enzyme system and the inner white area shows the reaction sequence of the PQ-reducing enzyme. The catalytic site of the water oxidation is only symbolically shown because neither the ligand sphere nor the nature of M is known; n and m characterize the valence state of manganese (see text). The protein environment is indicated by hatched areas. For different conformational states in S_0, S_1 and S_2, S_3, different symbols are used (see Section 4.5 and Ref. [143]). The other symbols are described in the text. Supposedly, S_2 and S_3 are positively charged (in contrast to the other redox states), but it has so far been impossible to localize these charges. With respect to the deprotonation pattern, m and n are assumed to be different, so that deprotonation takes place at higher valence states of manganese ($n > m$) during $O_2/2H_2O$ ligand exchange. If the oxidation $M \rightarrow M^{ox}$ only corresponds to a special redox transition at the catalytic manganese with a small redox potential difference (see Section 4.5), then n should be equal to m and, in S_0, the binuclear manganese site would attain the redox state n and $n-1$. The possibility of a charge transfer from the substrate ligands to the central atoms accompanied by the formation of a µ-peroxo bridge [see Eq. (7)] is considered in the scheme. In accordance with the extrinsic deprotonation pattern, M presumably releases one $H^{\oplus}$ during oxidation.

cleavage as the central process of biological solar energy exploitation.

I would like to thank all my collaborators for their enormous efforts, their enthusiasm, and their excellent teamwork. Without their engagement, much of the work reported in the cited papers would have been impossible. I am very grateful to my colleagues from abroad for international collaboration, especially to the members of the solar energy group headed by Dr. Inoue (RIKEN, Japan) and to Dr. A. W. Rutherford (Saclay, France). For their special contributions, critical reading of the manuscript, and useful hints, I would like to thank H. J. Eckert, P. Gräber, B. Hanssum, K.-D. Irrgang, and M. Völker. I also thank A. Bowe-Gräber for drawing the figures. The financial support of our research by the Deutsche Forschungsgemeinschaft (Einzelprojekte und Sfb 312), the Fonds der Chemischen Industrie, the Bundesministerium für Forschung und Technologie, and the EPR-Sondervermögen is gratefully acknowledged.

Received: August 12, 1986;
revised: January 8, 1987 [A 625 IE]
German version: *Angew. Chem. 99* (1987) 660
Translated by *K. Patzelt*, Berlin

[1] L. Boltzmann: *Der zweite Hauptsatz der Wärmetheorie.* In: *Populäre Schriften.* J. A. Barth, Leipzig 1904.

[2] E. A. Berghorn, *Sci. Am. 224* (1971), No. 1, p. 30.

[3] a) W. Hoppe, W. Lohmann, H. Markl, H. Ziegler (Eds.): *Biophysics*, Springer, Berlin 1983; b) G. Renger in [3a], p. 515–542.

[4] G. Renger in [3a], p. 347–371.

[5] a) Govindjee (Ed.): *Photosynthesis, Energy Conservation by Plants and Bacteria, Vol. 1*, Academic Press, New York 1982; b) M. Y. Okamura, G. Feher, N. Nelson in [5a], p. 195–272.

[6] a) Govindjee (Ed.): *Bioenergetics of Photosynthesis*, Academic Press, New York 1975; b) R. p. Knox in [6a], p. 183–221.

[7] A. C. Ley, D. Mauzerall, *Biochim. Biophys. Acta 680* (1982) 95.

[8] C. Wolff, H. T. Witt, *Z. Naturforsch. B 24* (1969) 1031.

[9] G. Renger, C. Wolff, *Biochim. Biophys. Acta 460* (1977) 57.

[10] G. Döring, G. Renger, J. Vater, H. T. Witt, *Z. Naturforsch. B 24* (1969) 1139.

[11] M. p. Davis, A. Forman, J. Fajer, *Proc. Natl. Acad. Sci. USA 76* (1979) 4170.

[12] a) H. J. den Blanken, A. J. Hoff, A. P. J. M. Jongenelis, B. A. Diner, *FEBS-Lett. 157* (1983) 21; b) M. E. Michel-Beyerle (Ed.): *Antennas and Reaction Centers of Photosynthetic Bacteria*. Springer, Berlin 1985; c) A. J. Hoff in [12b], p. 150–163.

[13] W. L. Butler, D. Magde, S. S. Berens, *Proc. Natl. Acad. Sci. USA 80* (1984) 7510.

[14] V. V. Klimov, A. V. Klevanik, V. A. Shuvalov, A. A. Krasnovsky, *FEBS-Lett. 82* (1977) 183.

[15] a) J. Biggins (Ed.): *Progress in Photosynthetic Research*, Nijhoff, Dordrecht 1987; b) A. R. Holzwarth, H. Brock, G. H. Schatz in [14a], *Vol. 1*, p. 61–65.

[16] H. J. Eckert, G. Renger, J. Bernarding, P. Faust, H. J. Eichler, J. Salk, *Biochim. Biophys. Acta* (1987), in press.

[17] H. J. Eckert, G. Renger, *Photochem. Photobiol. 31* (1980) 501.

[18] G. Renger, Y. Koike, M. Yuasa, Y. Inoue, *FEBS-Lett. 163* (1983) 89.

[19] M. C. W. Evans, Y. E. Atkinson, R. C. Ford, *Biochim. Biophys. Acta 806* (1985) 247.
[20] A. J. Hoff, I. I. Proskuryakov, *Biochim. Biophys. Acta 808* (1985) 343.
[21] J. H. A. Nugent, B. A. Diner, M. C. W. Evans, *FEBS-Lett. 154* (1981) 328.
[22] A. W. Rutherford, P. Mathis, *FEBS-Lett. 154* (1983) 328.
[23] K. Witt, *FEBS-Lett. 38* (1973) 116.
[24] C. Kirmeier, D. Holton, R. J. Debus, G. Feher, M. Y. Okamura, *Proc. Natl. Acad. Sci. USA 83* (1986) 6407.
[25] W. W. Parson, B. Ke in [5a], p. 331-385.
[26] R. P. J. Williams, G. R. Moore, P. E. Wright in A. W. Addison, W. R. Cullen, D. Dolphin, B. R. James (Eds.): *Biological Aspects of Inorganic Chemistry*, Wiley, New York 1977, p. 369-401.
[27] A. V. Xavier, J. J. G. Moura, I. Moura, *Struct. Bonding (Berlin) 43* (1981) 187.
[28] A. K. Churg, A. Warshel, *Biochemistry 25* (1986) 1675.
[29] D. De Vault, *Q. Rev. Biophys. 13* (1980) 387.
[30] R. A. Marcus, N. Sutin, *Biochim. Biophys. Acta 811* (1985) 265.
[31] R. T. Ross, R. J. Anderson, T. L. Hsia, *Photochem. Photobiol. 24* (1976) 267.
[32] A. S. K. Sun, K. Sauer, *Biochim. Biophys. Acta 234* (1971) 399.
[33] G. Renger, H. J. Eckert, *Bioelectrochem. Bioenerg. 7* (1980) 101.
[34] J. Deisenhofer, O. Epp, K. Miki, H. Michel, R. Huber, *Nature (London) 318* (1985) 618.
[35] G. Renger, *Physiol. Veg. 24* (1986) 509.
[36] A. W. Rutherford, *Biochem. Soc. Trans. 14* (1985) 12.
[37] J. D. Rochaix, M. Dron, M. Rahire, P. Malnoe, *Plant Mol. Biol. 3* (1984) 363.
[38] D. J. Kyle, *Photochem. Photobiol. 41* (1985) 107.
[39] A. A. Brown, C. W. Gilbert, R. Guy, C. J. Arntzen, *Proc. Natl. Acad. Sci. USA 81* (1984) 6310.
[40] J. Kyte, R. F. Doolittle, *J. Mol. Biol. 157* (1982) 105.
[41] A. Trebst, B. Depka in [13a], p. 216-224.
[42] K.-D. Irrgang, G. Renger, J. Vater, *FEBS-Lett. 204* (1986) 67.
[43] a) Y. Inoue, A. R. Crofts, Govindjee, N. Murata, G. Renger, K. Satoh (Eds.): *The Oxygen Evolving System in Photosynthesis*, Academic Press, (Japan) 1983; b) A. Yamagishi, p. Katoh in [43a], p. 39-48.
[44] H. Y. Nakatani in [43a], p. 49-54.
[45] C. de Vitry, F. A. Wollmann, P. Delepelaire, *Biochim. Biophys. Acta 767* (1984) 415.
[46] a) K. D. Irrgang, H. J. Eckert, G. Renger, J. Vater, unpublished results; b) O. Nanba, K. Satoh, *Proc. Natl. Acad. Sci. USA 84* (1987) 109; c) R. V. Danielius, K. Satoh, P. J. M. van Kan, J. J. Plijter, A. M. Nuijs, H. van Gorkum, *FEBS-Lett. 213* (1987) 241; d) J. B. Marder, D. J. Chapman, A. Telfer, P. J. Nixon, J. Barber, *Plant. Mol. Biol.* (1987), in press.
[47] W. Junge, H. T. Witt, *Z. Naturforsch. B23* (1968) 244.
[48] P. Joliot, G. Barbieri, R. Chabaud, *Photochem. Photobiol. 10* (1969) 302.
[49] B. Kok, B. Forbush, M. P. McGloin, *Photochem. Photobiol. 11* (1970) 457.
[50] P. Joliot, B. Kok in [6a], p. 387-412.
[51] G. Renger, Govindjee, *Photosynth. Res. 6* (1985) 33.
[52] J. A. van Best, P. Mathis, *Biochim. Biophys. Acta 503* (1978) 178.
[53] G. Renger, H. J. Eckert, W. Weiss in [43a], p. 73-82.
[54] K. Brettel, H. T. Witt, *Photobiochem. Photobiophys. 6* (1983) 253.
[55] H. J. Eckert, G. Renger, H. T. Witt, *FEBS-Lett. 167* (1984) 316.
[56] J. P. Dekker, J. J. Plijter, L. Ouwehand, H. J. van Gorkom, *Biochim. Biophys. Acta 767* (1984) 176.
[57] G. Renger, W. Weiss, *Biochem. Soc. Trans. 14* (1985) 17.
[58] G. T. Babcock, K. Sauer, *Biochim. Biophys. Acta 376* (1975) 315.
[59] G. T. Babcock, R. E. Blankenship, K. Sauer, *FEBS-Lett. 61* (1976) 286.
[60] J. T. Warden, R. E. Blankenship, K. Sauer, *Biochim. Biophys. Acta 432* (1976) 462.
[61] C. F. Yocum, C. T. Yerkes, R. E. Blankenship, R. R. Sharp, G. T. Babcock, *Proc. Natl. Acad. Sci. USA 78* (1981) 7507.
[62] H. Conjeaud, P. Mathis, *Biochim. Biophys. Acta 590* (1980) 353.
[63] M. Boska, K. Sauer, W. Buttner, G. T. Babcock, *Biochim. Biophys. Acta 722* (1983) 327.
[64] G. Renger, M. Völker, W. Weiss, *Biochim. Biophys. Acta 766* (1984) 582.
[65] G. Renger, C. Wolff, *Biochim. Biophys. Acta 423* (1976) 610.
[66] G. Havemann, P. Mathis, *Biochim. Biophys. Acta 440* (1976) 346.
[67] P. J. O'Malley, G. T. Babcock, R. C. Prince, *Biochim. Biophys. Acta 766* (1984) 283.
[68] M. Brok, F. C. Ebskamp, A. J. Hoff, *Biochim. Biophys. Acta 809* (1985) 421.
[69] W. Weiss, G. Renger, *Biochim. Biophys. Acta 850* (1986) 173.
[70] B. A. Diner, C. de Vitry, *Adv. Photosynth. Res. Proc. Int. Congr. Photosynth. 6th 1983 1* (1984) 407.
[71] J. P. Dekker, M. Brok, H. G. van Gorkom, *Adv. Photosynth. Res. Proc. Int. Congr. Photosynth. 6th 1983 1* (1984) 171.
[72] W. Weiss, G. Renger, *FEBS-Lett. 169* (1984) 219.
[73] E. J. Land, in [71].
[74] E. K. Pistorius, A. E. Gau, *FEBS-Lett. 206* (1986) 243.
[75] P. Rich, *Photosynth. Res. 6* (1985) 335.
[76] a) W. C. Rodriguez, T. K. Chandrasheker, G. T. Babcock in [14a]. *Vol. 1*, p. 471; b) Y. Takahashi, M. Takahashi, K. Satoh, *FEBS-Lett. 208* (1986) 347; c) M. Ikeuchi, Y. Inoue, *ibid. 210* (1987) 71.
[77] G. Renger, W. Weiss, *Adv. Photosynth. Res. Proc. Int. Congr. Photosynth. 6th 1983 1* (1984) 253.
[78] J. Fajer, M. S. Davis, A. Forman, V. K. Klimov, E. Dolan, B. Ke, *J. Am. Chem. Soc. 102* (1980) 7143.
[79] M. Gläser, C. Wolff, G. Renger, *Z. Naturforsch. C31* (1976) 712.
[80] K. Brettel, E. Schlodder, H. T. Witt, *Biochim. Biophys. Acta 766* (1984) 403.
[81] G. P. Anderson, J. E. Draheim, E. L. Gross, *Biochim. Biophys. Acta 810* (1985) 123.
[82] G. Renger, *Top. Curr. Chem. 69* (1977) 39.
[83] P. George in T. E. King, H. S. Mason, M. Morrison (Eds.): *Oxidases and Related Redox Systems, Vol. 1*, Wiley, New York 1965, p. 3-36.
[84] L. T. Krishtalik, *Biochim. Biophys. Acta 849* (1986) 162.
[85] B. G. Malmström, *Annu. Rev. Biochem. 51* (1982) 21.
[86] R. Radmer, G. Cheniae in J. Barber (Ed.): *Primary Processes of Photosynthesis*, Elsevier/North Holland, Amsterdam 1977.
[87] T. Wydrzynski in [5a], p. 469-506.
[88] J. Amesz, *Biochim. Biophys. Acta 726* (1983) 1.
[89] J. M. Olson, *Science 168* (1970) 438.
[90] a) G. Renger, *Z. Naturforsch. C25* (1970) 966; b) G. Renger, *Eur. J. Biochem. 27* (1972) 259.
[91] W. J. F. Vermaas, G. Renger, G. Dohnt, *Biochim. Biophys. Acta 704* (1984) 194.
[92] G. M. Cheniae, I. F. Martin, *Biochim. Biophys. Acta 197* (1971) 219.
[93] N. Tamura, G. M. Cheniae, *Biochim. Biophys. Acta 809* (1985) 245.
[94] G. Renger, *Photosynthetica 21* (1987), in press.
[95] G. Mavankal, D. C. McCain, T. M. Bricker, *FEBS-Lett. 202* (1986) 235.
[96] T. Ono, Y. Inoue, *FEBS-Lett. 168* (1984) 281.
[97] T. Ono, H. Kajikawa, Y. Inoue, *Plant Physiol. 80* (1986) 85.
[98] J. Barber, H. Y. Nakatani, R. Mansfield, *Isr. J. Chem. 21* (1981) 243.
[99] S. T. Allakhverdief, M. A. Shafiev, V. V. Klimov, *Photobiochem. Photobiophys. 12* (1986) 61.
[100] G. Renger, *FEBS-Lett. 81* (1977) 223.
[101] G. Renger in H. Metzner (Ed.): *Photosynthetic Water Oxidation*, Academic Press, London 1978, p. 229-248.
[102] J. A. Gilbert, D. S. Eggleston, W. R. Murphy, Jr., D. A. Geselowitz, D. J. Hodgson, T. J. Meyer, *J. Am. Chem. Soc. 107* (1985) 3855.
[103] R. Ramaraj, A. Kira, M. Kaneko, *Angew. Chem. 98* (1986) 1012; *Angew. Chem. Int. Ed. Engl. 25* (1986) 1009.
[104] W. B. Lewis, L. O. Morgan in R. L. Carloer (Ed.): *Paramagnetic Relaxation in Solutions in Transitional Metal Chemistry, Vol. 4*, Marcel Dekker, New York 1986, p. 33-112.
[105] T. Wydrzynski, N. Zumbulyadis, P. G. Schmidt, Govindjee, *Biochim. Biophys. Acta 408* (1975) 349.
[106] T. Wydrzynski, G. Renger, *Biochim. Biophys. Acta 851* (1986) 65.
[107] A. N. Srinivasan, R. R. Sharp, *Biochim. Biophys. Acta 850* (1986) 211.
[108] A. N. Srinivasan, R. R. Sharp, *Biochim. Biophys. Acta 851* (1986) 369.
[109] T. Wydrzynski, K. Sauer, *Biochim. Biophys. Acta 589* (1980) 56.
[110] G. C. Dismukes, Y. Siderer, *Proc. Natl. Acad. Sci. USA 78* (1981) 274.
[111] G. C. Dismukes, Y. Siderer, *FEBS-Lett. 121* (1980) 78.
[112] Ö. Hansson, L.-E. Andreasson, *Biochim. Biophys. Acta 679* (1982) 261.
[113] L.-E. Andreasson, Ö. Hansson, T. Vänngard, *Chim. Scr. 21* (1983) 71.
[114] G. W. Brudvig, J. L. Casey, K. Sauer, *Biochim. Biophys. Acta 723* (1983) 366.
[115] J.-L. Zimmermann, A. W. Rutherford, *Biochim. Biophys. Acta 767* (1984) 160.
[116] J. C. de Paula, G. W. Brudvig, *J. Am. Chem. Soc. 107* (1985) 2643.
[117] B. Mabad, J. P. Tuchagues, Y. T. Hwang, D. N. Hendrickson, *J. Am. Chem. Soc. 107* (1985) 2801.
[118] Ö. Hansson, L.-E. Andreasson, T. Vänngard, *FEBS-Lett. 195* (1986) 151.
[119] M. Völker, G. Renger, A. W. Rutherford, *Biochim. Biophys. Acta 851* (1986) 424.
[120] J. L. Casey, K. Sauer, *Biochim. Biophys. Acta 767* (1984) 21.
[121] J. L. Zimmermann, A. W. Rutherford, *Biochemistry 25* (1986) 4609.
[122] a) J. C. de Paula, W. F. Beck, G. W. Brudvig, *J. Am. Chem. Soc. 108* (1986) 4002; b) J. Cole, V. K. Yachandra, R. D. Guiles, A. E. McDermott, R. D. Britt, S. L. Dexheimer, K. Sauer, M. P. Klein, *Biochim. Biophys. Acta 890* (1987) 395.
[123] M. W. Lynch, D. N. Hendrickson, B. Y. Fitzgerald, C. G. Pierport, *J. Am. Chem. Soc. 106* (1984) 2041.
[124] M. W. Lynch, D. N. Hendrickson, B. J. Fitzgerald, C. G. Pierport, *J. Am. Chem. Soc. 103* (1981) 3961.
[125] G. Renger, W. Weiss, *Biochim. Biophys. Acta 850* (1986) 184.
[126] G. Renger, *Biochim. Biophys. Acta 440* (1976) 287.
[127] G. Renger, *FEBS-Lett. 137* (1976) 217.

[128] G. Renger, W. Weiss, *FEBS-Lett. 137* (1982) 217.
[129] G. Renger, W. Weiss, *Biochim. Biophys. Acta 722* (1983) 1.
[130] P. Joliot, M. Hoffnung, R. Chabaud, *J. Chim. Phys. 63* (1966) 1423.
[131] D. A. Berthold, G. T. Babcock, C. F. Yocum, *FEBS-Lett. 134* (1981) 231.
[132] R. Kuwabara, N. Murata, *Plant Cell Physiol. 23* (1982) 583.
[133] J. P. Dekker, H. J. van Gorkom, J. Wessink, L. Ouwehand, *Biochim. Biophys. Acta 767* (1984) 1.
[134] a) J. Lavergne, *Photochem. Photobiol. 43* (1986) 311; b) Ö. Saygin, H. T. Witt in [15a], *Vol. 1*, p. 537.
[135] G. Renger, B. Hanssum, U. Wacker, *Chim. Scr.* (1987), in press.
[136] a) L. J. Boucher, C. G. Coe, *Inorg. Chem. 14* (1975) 1289; b) J. B. Vincent, G. Christou, *FEBS-Lett. 207* (1986) 250.
[137] G. C. Dismukes, P. Mathis, *FEBS-Lett. 178* (1984) 51.
[138] J. A. Kirby, D. B. Goodin, T. J. Wydrzynski, A. S. Robertson, M. P. Klein, *J. Am. Chem. Soc. 103* (1981) 5537.
[139] D. B. Goodin, V. K. Yachandra, R. D. Britt, K. Sauer, M. Klein, *Biochim. Biophys. Acta 767* (1984) 209.
[140] J. A. Kirby, A. S. Robertson, J. P. Smith, A. C. Thompson, R. S. Cooper, M. P. Klein, *J. Am. Chem. Soc. 103* (1981) 5529.
[141] V. K. Yachandra, R. D. Guiles, A. McDermott, R. D. Britt, S. L. Dexheimer, K. Sauer, M. P. Klein, *Biochim. Biophys. Acta 850* (1986) 324.
[142] G. Renger, B. Hanssum, W. Weiss in [15a], *Vol. 1*, p. 541-544.
[143] a) C. Preston, R. J. Pace, *Biophys. J. 49* (1986) 25a; b) H. Koike, B. Hanssum, Y. Inoue, G. Renger, *Biochim. Biophys. Acta* (1987), in press.
[144] D. F. Blair, S. N. Witt, S. I. Chan, *J. Am. Chem. Soc. 107* (1985) 1389.
[145] W. P. Schröder, H. E. Akerlund, *Biochim. Biophys. Acta 848* (1986) 359.
[146] R. Radmer, O. Ollinger, *FEBS-Lett. 195* (1986) 285.
[147] K. P. Bader, P. Thibault, G. H. Schmidt in [15a], *Vol. 1*, p. 549-552.
[148] B. M. Hoffmann, T. Szymanski, T. G. Brown, F. Basolo, *J. Am. Chem. Soc. 100* (1978) 7253.
[149] A. B. P. Lever, J. P. Wilshire, S. K. Onan, *J. Am. Chem. Soc. 101* (1979) 3368.
[150] T. G. Taylor, D. K. White, D. H. Campbell, A. P. Berzinis, *J. Am. Chem. Soc. 103* (1981) 4932.
[151] D. E. Hamilton, R. S. Drago, J. Telser, *J. Am. Chem. Soc. 106* (1984) 5353.
[152] K. D. Karlin, R. W. Cruse, Y. Gultneh, J. C. Hayes, J. Zubieta, *J. Am. Chem. Soc. 106* (1984) 3372.
[153] M. Denis, G. M. Clore, *Plant Physiol. 68* (1981) 229.
[154] R. Osman, H. Basch, *J. Am. Chem. Soc. 106* (1984) 5710.
[155] B. Bouges-Bocquet, *Biochim. Biophys. Acta 594* (1980) 85.
[156] A. W. Rutherford, G. Renger, H. Koike, Y. Inoue, *Biochim. Biophys. Acta 767* (1984) 548.
[157] G. Renger, *Biochim. Biophys. Acta 256* (1972) 428.
[158] a) G. Renger, B. Bouges-Bocquet, R. Delosme, *Biochim. Biophys. Acta 292* (1973) 796; b) G. Renger, B. Bouges-Boequet, K. H. Büchel, *J. Bioenerg. 4* (1973) 491; c) W. Oettmeier, G. Renger, *Biochim. Biophys. Acta 593* (1980) 113.
[159] B. Hanssum, G. Dohnt, G. Renger, *Biochim. Biophys. Acta 806* (1985) 210.
[160] G. F. Jameson, R. S. Drago, *J. Am. Chem. Soc. 107* (1985) 3017.
[161] W. Junge, G. Renger, W. Ausländer, *FEBS-Lett. 79* (1977) 155.
[162] S. Saphon, A. R. Crofts, *Z. Naturforsch. C32* (1977) 617.
[163] C. F. Fowler, *Biochim. Biophys. Acta 462* (1977) 414.
[164] B. R. Velthuys, *FEBS-Lett. 115* (1980) 167.
[165] B. Wille, J. Lavergne, *Photobiochem. Photobiophys. 4* (1982) 131.
[166] W. Förster, W. Junge, *Photochem. Photobiol. 41* (1985) 183.
[167] a) G. Renger, U. Wacker, M. Völker, *Photosynth. Res.* (1987), in press; b) U. Wacker, G. Renger, unpublished results.
[168] R. Dietrich-Glaubitz, M. Völker, G. Renger, P. Gräber in [15a], *Vol. 1*, p. 519-522.
[169] S. Izawa, A. Muallen, N. K. Ramaswamy in [43a], p. 293-302.
[170] Govindjee, *Adv. Photosynth. Res. Proc. Int. Congr. Photosynth. 6th 1983 1* (1984) 227.
[171] C. Critchley, *Biochim. Biophys. Acta 811* (1985) 33.
[172] I. C. Bainu, C. Critchley, Govindjee, H. S. Gutowsky, *Proc. Natl. Acad. Sci. USA 81* (1984) 3713.
[173] S. M. Theg, P. H. Homann, *Biochim. Biophys. Acta 679* (1982) 22.
[174] C. Preston, R. J. Pace, *Biochim. Biophys. Acta 810* (1985) 388.
[175] J. Sinclair, *Biochim. Biophys. Acta 764* (1984) 247.
[176] P. O. Sandusky, C. F. Yocum, *Biochim. Biophys. Acta 766* (1984) 603.
[177] S. M. Theg, P. A. Jursinic, P. H. Homann, *Biochim. Biophys. Acta 766* (1984) 636.
[178] S. Itoh, C. T. Yerkes, H. Koike, H. H. Robinson, A. R. Crofts, *Biochim. Biophys. Acta 766* (1984) 612.
[179] T. Ono, Y. Inoue, *Biochim. Biophys. Acta 806* (1985) 331.
[180] P. H. Homann, H. Gleiter, T. Ono, Y. Inoue, *Biochim. Biophys. Acta 850* (1986) 10.
[181] T. Ono, J. L. Zimmermann, Y. Inoue, A. W. Rutherford, *Biochim. Biophys. Acta 851* (1986) 193.
[182] R. Damoder, V. V. Klimov, G. C. Dismukes, *Biochim. Biophys. Acta 848* (1986) 378.
[183] P. H. Homann, *Biochim. Biophys. Acta 809* (1985) 311.
[184] a) G. C. Dismukes, *Photochem. Photobiol. 43* (1986) 99; b) T. Ono, H. Nakayama, H. Gleiter, Y. Inoue, A. Kawamori, *Arch. Biochem. Biophys.* (1987), in press.
[185] P. O. Sandusky, C. F. Yocum, *FEBS-Lett. 162* (1983) 339.
[186] H. Taube, *Angew. Chem. 96* (1984) 315; *Angew. Chem. Int. Ed. Engl. 23* (1984) 329.
[187] V. K. Yachandra, R. D. Guiles, K. Sauer, H. M. Klein, *Biochim. Biophys. Acta 850* (1986) 333.
[188] R. Piccioni, D. Mauzerall, *Biochim. Biophys. Acta 504* (1978) 384.
[189] J. J. Brand, P. Mohanty, D. C. Fork, *FEBS-Lett. 155* (1983) 120.
[190] H. E. Akerlund in [43a], p. 201-208.
[191] N. Murata, M. Miyao, T. Kubawara in [43a], p. 213-222.
[192] T. Ono, Y. Inoue, *FEBS-Lett. 166* (1983) 381.
[193] D. F. Ghanotakis, G. T. Babcock, C. F. Yocum, *FEBS-Lett. 167* (1984) 127.
[194] A. Boussac, B. Maison-Peteri, C. Vernotte, A. L. Etienne, *Biochim. Biophys. Acta 808* (1985) 225.
[195] M. Völker, H. J. Eckert, G. Renger, *Biochim. Biophys. Acta 890* (1987) 66.
[196] M. Völker, H. J. Eckert, G. Renger in [15a], *Vol. 1*, p. 545-548.
[197] T. Ono, Y. Inoue, *Biochim. Biophys. Acta 850* (1986) 380.
[198] M. Miyao, N. Murata, *Photosynth. Res. 10* (1986) 489.
[199] B. G. Malmström, *Biochim. Biophys. Acta 549* (1979) 281.
[200] L. Powers, B. Chauce, Y. Cling, P. Angiohillo, *Biophys. J. 39* (1981) 465.
[201] J. J. Jarausch, B. Kadenbach, *Eur. J. Biochem. 146* (1985) 211.
[202] M. Miyao, N. Murata, *FEBS-Lett. 170* (1984) 350.
[203] N. I. Bishop, *Adv. Photosynth. Res. Proc. Int. Congr. Photosynth. 6th 1983 1* (1984) 321.
[204] J. G. Metz, H. B. Pakrasi, M. Seibert, C. J. Arntzen, *FEBS-Lett. 205* (1986) 269.
[205] T. M. Bricker, J. G. Metz, D. Miles, L. A. Sherman, *Biochim. Biophys. Acta 724* (1983) 447.
[206] N. Tamura, G. M. Cheniae, *FEBS-Lett. 200* (1986) 231.
[207] H. Oh-Oka, S. Tanaka, K. Wada, T. Kuwabara, N. Murata, *FEBS-Lett. 197* (1986) 63.
[208] R. J. Sundberg, R. B. Martin, *Chem. Rev. 74* (1974) 471.
[209] M. Seibert, T. M. Cotton, *FEBS-Lett. 182* (1985) 34.
[210] R. Radmer in [43a], p. 135-144.
[211] B. Hanssum, G. Renger, *Biochim. Biophys. Acta 810* (1985) 234.
[212] V. Förster, W. Junge, *Photosynth. Res. 9* (1986) 197.
[213] K. L. Greer, F. G. Plumley, G. W. Schmidt, *Plant. Physiol. 82* (1986) 114.
[214] H. Koike, Y. Inoue, *Biochim. Biophys. Acta 807* (1985) 64.
[215] B. Andersson in L. A. Staehelin, C. J. Arntzen (Eds.): *Encyclopedia of Plant Physiology, New Series, Vol. 19*, Springer, Berlin 1986, p. 447-456.
[216] A. C. Stewart, M. Siczkowski, U. Ljungberg, *FEBS-Lett. 193* (1985) 175.
[217] D. F. Ghanotakis, G. T. Babcock, C. F. Yocum, *FEBS-Lett. 192* (1985) 1.
[218] G. Renger, H. E. Akerlund in [43a], p. 209-212.
[219] H. E. Akerlund, G. Renger, W. Weiss, R. Hagemann, *Biochim. Biophys. Acta 765* (1984) 1.
[220] T. Kuwabara, T. Murata, M. Miyao, N. Murata, *Biochim. Biophys. Acta 850* (1986) 146.
[221] U. Ljungberg, T. Henrysson, C. P. Rochester, H. E. Akerlund, B. Andersson, *Biochim. Biophys. Acta 849* (1986) 112.
[222] J. Cline, B. Reinhammer, P. Jensen, R. Venters, B. M. Hoffmann, *J. Biol. Chem. 258* (1983) 5124.
[223] S. Padhye, T. Kambara, D. N. Hendrickson, Govindjee, *Photosynth. Res. 9* (1986) 103.
[224] N. C. Robinson, F. Strey, L. Talbert, *Biochemistry 19* (1980) 3656.
[225] N. C. Robinson, *Biochemistry 21* (1982) 184.
[226] K. Gounaris, J. Barber, *FEBS-Lett. 188* (1985) 68.
[227] K. Gounaris, D. Whitford, J. Barber, *FEBS-Lett. 163* (1983) 230.
[228] B. Bouges-Bocquet, *Biochim. Biophys. Acta 314* (1973) 250.
[229] B. Velthuys, J. Amesz, *Biochim. Biophys. Acta 333* (1974) 85.
[230] A. R. Crofts, C. A. Wraight, *Biochim. Biophys. Acta 726* (1983) 149.
[231] A. Trebst, *Z. Naturforsch. C41* (1986) 240.
[232] V. Petrouleas, B. A. Diner, *Biochim. Biophys. Acta 849* (1986) 193.
[233] R. J. Debus, G. Feher, M. Y. Okamura, *Biochemistry 25* (1986) 2276.
[234] G. Renger, R. Hagemann, R. Fromme, *FEBS-Lett. 203* (1986) 210.
[235] N. Adir, I. Ohad, *Biochim. Biophys. Acta 850* (1986) 264.
[236] R. Fromme, R. Hagemann, G. Renger in [15a], *Vol. 3*, p. 783-786.

When submitting manuscripts, authors of articles intended for publication as "Communications" are requested to read the "Notice to Authors" reproduced in the January issue of the journal following the list of contents; upon request, a copy can be obtained from the editorial office.

Molecular Structure of a [3]-Catenate: Curling Up of the Interlocked System by Interaction between the Two Copper Complex Subunits**

By *Christiane O. Dietrich-Buchecker, Jean Guilhem, Abdel Kader Khemiss, Jean-Pierre Kintzinger, Claudine Pascard,* and *Jean-Pierre Sauvage**

Interlocked macrocyclic systems have appeared as fascinating molecules for many years.[1, 2] The templating properties of transition metals have recently been taken advantage of for interlocking coordinating acyclic molecules,[3] leading to catenands after demetalation of the corresponding catenates. [3]-Catenanes, consisting of three interlocked rings, have been synthesized by *Schill* et al.[4] [3]-Catenates have been prepared very recently[5] by using a surprisingly efficient synthetic procedure based on the oxidative coupling of terminal diynes.[5b] We now report both the crystallographic study and an NMR solution study of $1^{2\oplus}$. Both methods demonstrate that $1^{2\oplus}$ has a geometry dramatically different from that implied by Figure 1.

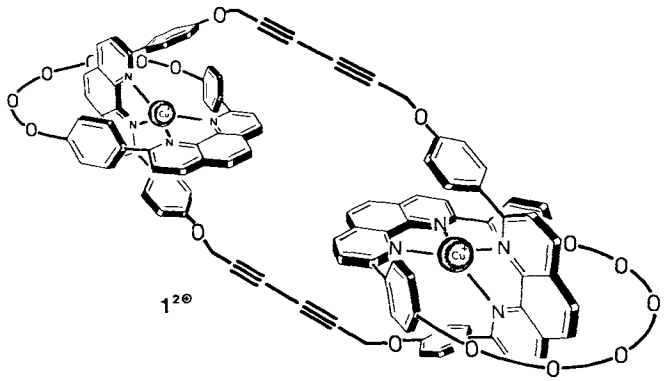

Fig. 1. Formula of the [3]-catenate $1^{2\oplus}$. The curved linkages joining the oxygen atoms correspond to CH_2CH_2 units.

[*] Dr. J.-P. Sauvage, Dr. C. O. Dietrich-Buchecker, Dr. A. K. Khemiss
Laboratoire de Chimie Organo-Minérale,
Institut de Chimie, Université Louis Pasteur
F-67000 Strasbourg (France)
Dr. J. Guilhem, Dr. C. Pascard
Laboratoire de Cristallochimie,
Institut de Chimie des Substances Naturelles, CNRS
F-91190 Gif-sur-Yvette (France)
Dr. J.-P. Kintzinger
Laboratoire de Chimie Organique Physique,
Institut Le Bel, Université Louis Pasteur
F-67000 Strasbourg (France)

[**] This work was supported by the Centre National de la Recherche Scientifique (CNRS). We would like to thank *P. Maltese* for his contribution to the NMR study.

The dicopper(I) complex $1^{2\oplus}$ contains two peripheral 30-membered rings separately interlocked with a central 44-membered ring. The molecular structure of $1^{2\oplus}$, as determined by X-ray diffraction, is shown in Figure 2. Owing to the large size of $1^{2\oplus}$, a tight packing is not possible; channels are formed, parallel to the *b* axis, in which solvent molecules and anions can be located. A clearly distinguishable CH_2Cl_2 molecule was localized halfway between the 1,10-phenanthroline (phen) nuclei B and B′ of the large ring.

Previous crystallographic studies of a [2]-catenate and its corresponding [2]-catenand clearly showed that the molecular shapes are dramatically different for both systems, a complete conformational change of the molecule taking place upon complexation.[6] The molecular structure of $1^{2\oplus}$ is strikingly different from the structure shown in Figure 1, which was drawn before any conformation or crystallographic study. The globular shape of $1^{2\oplus}$ is obvious from the view given on the cover of this issue. Figure 2 represents another view of $1^{2\oplus}$. The bottom half of Figure 2 clearly shows the folding up of the large central ring B, whose phen subunits are almost parallel (dihedral angle 7°) and 7.7 Å apart. The diacetylenic chains are also parallel to one another and located 10.5 Å apart. The four oxygen atoms of the 44-membered ring B form a 10.5-Å × 8.0-Å rectangle and the phenyl rings consist of two pairs of nearly parallel nuclei (dihedral angles φ1B, φ1B′ 6° and φ2B, φ2B′ 14°).

The 30-membered rings A and C are placed as bracelets in an approximately parallel fashion, their respective phen nuclei being similarly tilted with respect to the two corresponding phen subunits of the central ring (dihedral angle phen A, phen B 57°8 and phen C, phen B′ 58°2). The copper(I) centers are only 8.0 Å apart.

Some important structural features are collected in Table 1. Each aromatic ring is in close contact with another

Table 1. Some important distances between nuclei [Å] and angles [°] between aromatic rings [a] and the interatomic distances between the oxygen atoms of a 2,9-diphenyl-1,10-phenanthroline (dpp) fragment. The standard deviations values are 0.1 Å and 1°, respectively.

Aromatic nuclei		Distance			Dihedral angle
phen B	φ1A	N1B	C16A	3.30	20
		C12B	C17A	3.44	
phen B	φ2A	C11B	C38A	3.31	21
		N10B	C39A	3.16	
φ2A	φ2B	C41A	C26B	3.24	18
		C40A	C25B	3.50	
phen C	φ2B′	N1C	C25B′	3.29	9
phen B′	φ1C	N10B′	C15C	3.37	14
		C12B′	C16C	3.44	
		C12B′	C17C	3.34	
phen B′	φ2C	N1B′	C41C	3.16	24
φ2A	φ2C	C39A	C41C	3.47	35
φ1B	φ2C	C20B	C37C	3.41	15
phenA	φ2B′	H8A	H29B′	2.30	24

dpp Fragment	O···O Distance	Deviation from theoretical value [b]
A	9.2	−1.4
C	9.2	−1.4
B	10.4	−0.2
B′	10.5	−0.1

[a] The distances considered are only the shortest ones (<3.5 Å) between atoms belonging to different aromatic rings. [b] The theoretical value calculated taking normal bond lengths and angles (60°) is 10.6 Å.

 © VCH Verlagsgesellschaft mbH, D-6940 Weinheim, 1987 0570-0833/87/0707-0661 $ 02.50/0

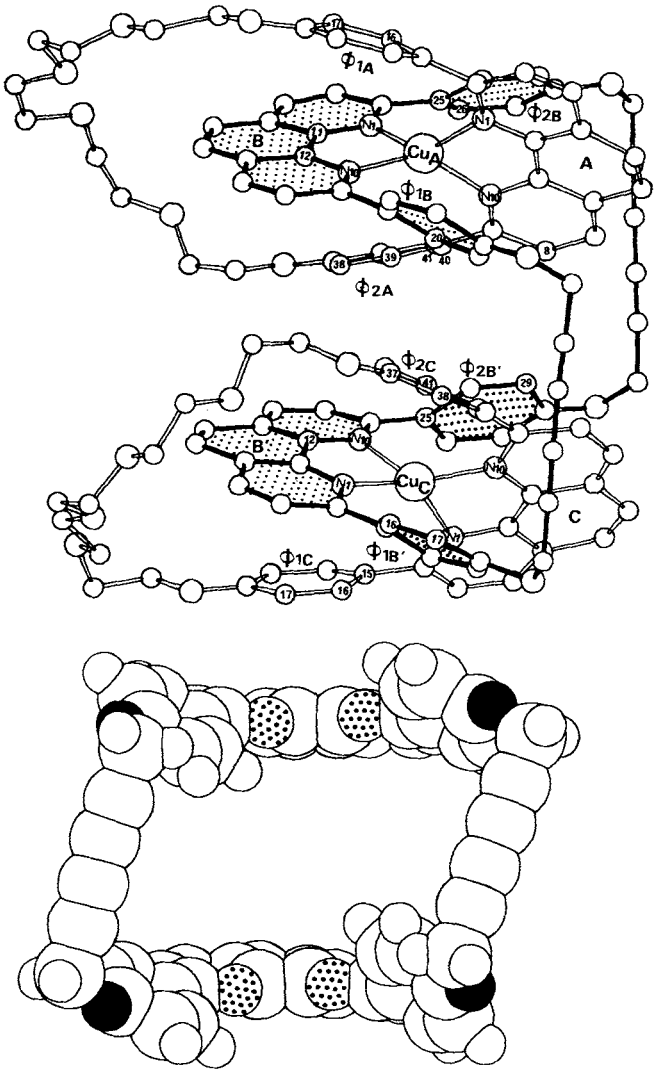

Fig. 2. Top: Computer drawing of the crystal structure of $1^{2\oplus}$. The carbon atoms of the 44-membered ring are yellow, those of the two 30-membered rings are green and light brown. The copper (I) centers are purple; the nitrogen and oxygen atoms are blue and dark red, respectively. Middle: Crystal structure of $1^{2\oplus}$. Bottom: Conformation of the central ring B of $1^{2\oplus}$ in the solid state showing the folding up of B and its boatlike shape. N atoms, dotted; O atoms, black.

one (distance less than 3.5 Å), a rough parallelism being observed (dihedral angles range between 9° and 35°; average value 20°). All the phenyl rings are rotated around their link to their respective phen nucleus, the average torsion angle being 43° (35° to 51°).

The geometry of the 2,9-diphenyl-1,10-phenanthroline (dpp) subunits is different for both types of rings. In B, no distortion is observed, whereas in the peripheral rings A and C, the phen nucleus is nonplanar and the dpp fragment undergoes a noticeable pinching. The closure of the angle between the phenoxy moieties (from 60° to 50°) is evidenced by the shortening of the oxygen–oxygen distance, the latter being normal in the large ring B.

As shown by the data collected in Table 2, the coordination polyhedra around the copper atoms are not equivalent: around Cu_A, the two phen nuclei are symmetrically disposed, but around Cu_C, phen C slides so that one of its N atoms lies in the phen B′/Cu_C plane, leading to a geometry similar to that of the copper(I) [2]-catenate previously studied.[6]

Table 2. Structure details of the coordination polyhedra around the Cu centers.

Around Cu_A		Around Cu_C	
Angles [°]			
N1A Cu N10A	80.4	N1C Cu N10C	80.2
N1B Cu N10B	81.2	N1B′ Cu N10B′	81.9
N1A Cu N1B	113.7	N1C Cu N1B′	133.9
N1A Cu N10B	138.6	N1C Cu N10B′	99.2
N10A Cu N1B	139.4	N10C Cu N1B′	132.9
N10A Cu N10B	114.0	N10C Cu N10B′	130.8
Distances [Å]			
Cu N1A	2.01	Cu N1C	2.13
Cu N10A	2.00	Cu N10C	1.93
Cu N1B	2.04	Cu N1B′	2.05
Cu N10B	2.03	Cu N10B′	2.05

The curling up of $1^{2\oplus}$ and the close proximity of the two copper(I) complex subunits could be detected, independently of the crystallographic study, by ^{1}H-NMR solution measurements. The ^{1}H-NMR spectrum of $1^{2\oplus}$ and an NOE difference spectrum are presented in Figure 3. The ^{1}H-NMR spectrum and the ^{13}C-NMR spectrum[8] are as expected for a molecule containing (1) two dpp fragments entwined around a copper(I) center, (2) a $CH_2(CH_2OCH_2)_4CH_2$ link, and (3) a propargylic group. The assignment of all the hydrogen atoms was obtained by a dipolar correlation 2D NMR[9] experiment, allowing the unambiguous distinction between the signals corresponding to the 30-membered rings A and C (starting from $OCH_{2\alpha}$) and those of the central ring B (starting from the propargylic CH_2 group).

The signals of all the hydrogen atoms belonging to the dpp moiety of $1^{2\oplus}$ are shifted upfield compared with the corresponding signals of the same fragment in the [2]-catenate consisting of two 30-membered rings.[1, 10] This shielding indicates that the phenyl–phenyl and phenyl–phen stackings between the two complex subunits are retained in solution. The analogy between the molecular shapes in the solid state and in solution is also confirmed by the observation of a nuclear Overhauser effect (NOE) between H_{m} of the 44-membered ring and $H_{3,8}$ of the pe-

ripheral rings (Fig. 3, top). Indeed, such an NOE would be very difficult to explain without a curled-up conformation of the central ring. In fact, a particularly short distance is found in the solid state (Table 1): H8A and H29B′ (corresponding respectively to an $H_{3,8}$ of ring A and an H_m of ring B) are 2.30 Å apart.

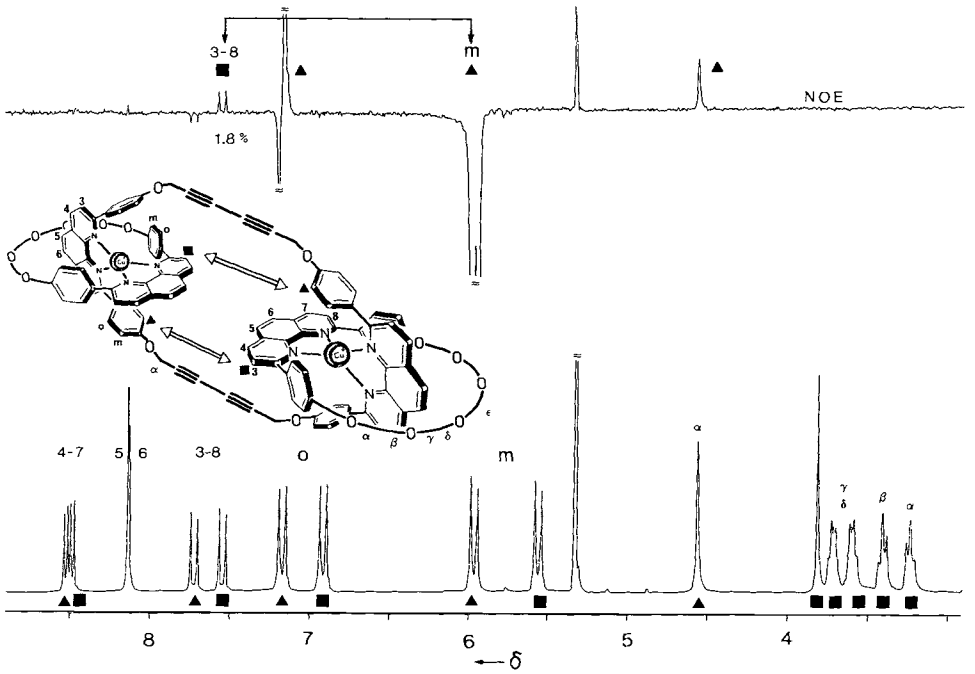

Fig. 3. ^{1}H-NMR spectrum of $\mathbf{1}^{2\oplus}$ (200 MHz) in CD_2Cl_2 (top). The signals indicated by a solid square belong to rings A and C whereas those marked by a solid triangle correspond to the large ring B. The difference spectrum (bottom) obtained by partial saturation of H_m (ring B) shows a clear Overhauser effect [7] on the propargylic OCH_2, a multiplet effect on H_o, a slight and negative three-spin effect on $H_{3,8}$ (ring B) and an effect amounting to 1.8% on $H_{3,8}$ (rings A and C). The H_m (ring B)-$H_{3,8}$ (ring A and C) interaction is indicated by a double arrow. In the solid state the interfragment contacts between H_m (ring B) and $H_{3,8}$ (rings A and C) are clear (see Table 1 and Fig. 2).

The folding up of the 44-membered ring and the subsequent globular shape of the molecule might be explained by a stabilizing π–π interaction between the aromatic rings belonging to the two copper complex subunits. It is noteworthy that the "ternary structure" of $\mathbf{1}^{2\oplus}$ (by analogy to proteins) is stable enough to be maintained in solution. The curled-up geometry of $\mathbf{1}^{2\oplus}$ and the internal stacking observed are reminiscent of recently reported systems consisting of a cationic noble-metal complex linked to a large macrocyclic polyether (second-sphere coordination) which has to fold up in order to adjust its geometry to the shape of the bound transition-metal complex.[11]

Experimental Procedure

Crystallographic study: Crystals of $\mathbf{1}^{2\oplus}[BF_4]_2$ (0.5 mm × 0.3 mm × 0.1 mm) were grown from CH_2Cl_2/C_6H_6 and sealed in a capillary tube. Intensity data collected at 1.1-Å resolution ($\theta_{max} = 45°$) with an automatic Philips PW 1100 diffractometer. Wavelength 1.5418 Å; graphite monochromator. From 10472 measured reflexions, 5561 ($I < 3\sigma(I)$) were used in the computations. Final R value: 14% for 181 identified atoms in the asymmetric unit. $[C_{128}H_{104}N_8O_{16}Cu_2][BF_4]_2$: $M_r = 2309$; monoclinic, $P2_1/a$; $a = 28.355(16)$, $b = 31.262(18)$, $c = 15.115(10)$ Å, $\beta = 103.9(2)°$, $V = 12980$ Å^3, $Z = 4$, $\rho_{calcd} = 1.18$ (12% solvent, CH_2Cl_2 and benzene). Further details of the crystal structure investigation are available on request from the director of the Cambridge Crystallographic Data Centre, University Chemical Laboratory, Lensfield Road, Cambridge CB2 1EW (England), on quoting the name of the author and the journal citation.

NMR study: Spectra were run either on a Bruker WP 200 SY or on a Bruker AN 400 spectrometer with standard software. They were obtained from a degassed and sealed 5-mm sample tube containing about 2.5 mg of $\mathbf{1}^{2\oplus}$ in 0.5 mL of CD_2Cl_2.

Received: February 4, 1987 [Z 2088 IE]
German version: *Angew. Chem. 99* (1987) 711

[1] E. Wasserman, *J. Am. Chem. Soc. 82* (1960) 4433.
[2] G. Schill: *Catenanes, Rotaxanes and Knots*, Academic Press, New York 1971, and references cited therein.
[3] C. O. Dietrich-Buchecker, J. P. Sauvage, J. P. Kintzinger, *Tetrahedron Lett. 24* (1983) 5095; C. O. Dietrich-Buchecker, J. P. Sauvage, J. M. Kern, *J. Am. Chem. Soc. 106* (1984) 3043.
[4] G. Schill, K. Rissler, H. Fritz, W. Vetter, *Angew. Chem. 93* (1981) 197; *Angew. Chem. Int. Ed. Engl. 20* (1981) 187, and references cited therein.
[5] a) J. P. Sauvage, J. Weiss, *J. Am. Chem. Soc. 107* (1985) 6108; b) C. O. Dietrich-Buchecker, A. Khemiss, J. P. Sauvage, *J. Chem. Soc. Chem. Commun. 1986*, 1376.
[6] M. Cesario, C. O. Dietrich-Buchecker, J. Guilhem, C. Pascard, J. P. Sauvage, *J. Chem. Soc. Chem. Commun. 1985*, 244.
[7] J. H. Noggle, R. E. Schirmer: *The Nuclear Overhauser Effect, Chemical Applications*, Academic Press, New York 1971.
[8] ^{13}C-NMR spectrum (100 MHz, CD_2Cl_2, TMS, δ values (CD_2Cl_2: $\delta = 54.2$)): dpp fragments: 159.45, 158.0, 156.85, 155.9, 143.95, 143.6, 138.5, 137.7, 132.4, 132.4, 130.1, 129.8, 128.8, 128.5, 127.85, 127.0, 124.6, 124.2, 113.5, 113.15; $CH_2(CH_2OCH_2)_4CH_2$ chain: 71.85, 71.55, 71.4, 69.4, 67.6; propargylic CH_2 groups: 56.05; acetylenic C atoms: 75.65, 71.35.
[9] Phase-sensitive NOESY NMR experiment at 400 MHz. We thank Dr. *A. Pagelot* (Sadis Bruker) for this spectrum.
[10] ^{1}H-NMR chemical shifts of signals corresponding to the central ring B and the peripheral rings ($CHDCl_2$, TMS, δ values ($CDHCl_2$: $\delta = 5.32$). For comparison, the values corresponding to a [2]-catenate containing two interlocked 30-membered rings [3] are indicated in parentheses; $H_{4,7}$: 8.51, 8.49 (8.66); $H_{5,6}$: 8.13, 8.14 (8.28); $H_{3,8}$: 7.72, 7.54 (7.87); H_o: 7.16, 6.90 (7.37); H_m: 5.96; 5.54 (6.02); CH_2 (α,β,γ,δ): —, 3.2–3.8 (3.4–3.7); CH_2(ε): —, 3.80 (3.82); propargylic CH_2 groups: 4.55, — (—).
[11] H. M. Colquhoun, J. F. Stoddart, D. J. Williams, *Angew. Chem. 98* (1986) 483; *Angew. Chem. Int. Ed. Engl. 25* (1986) 487, and references cited therein.

New Lead Structures by Diels-Alder Reactions of Streptazolin with Naphthoquinones**

By *Susanne Grabley, Heinz Kluge*, and *Hans-Ullrich Hoppe**

Dedicated to Professor Heinz Harnisch on the occasion of his 60th birthday

An important current goal of screening natural products[1] is the discovery of novel lead structures, which, possibly after derivatization, exhibit interesting pharmacological properties. Diels-Alder reactions of naphthoquinones **2** with streptazolin **1**,[2,3] which was reported for the first time in 1981 and has been isolated from various strains of *Streptomyces luteogriseus* in our natural-products screening program, have enabled us to attain this goal.

The metabolite **1** can be obtained in yields of more than 300 mg/mL from culture filtrates by centrifugation, extraction with ethyl acetate, and subsequent chromatography on silica gel, thereby affording adequate amounts of this chiral diene. In contrast to streptazolin **1**, the new compounds **3**, **4**, and **5** have striking antibiotic and cytotoxic properties.

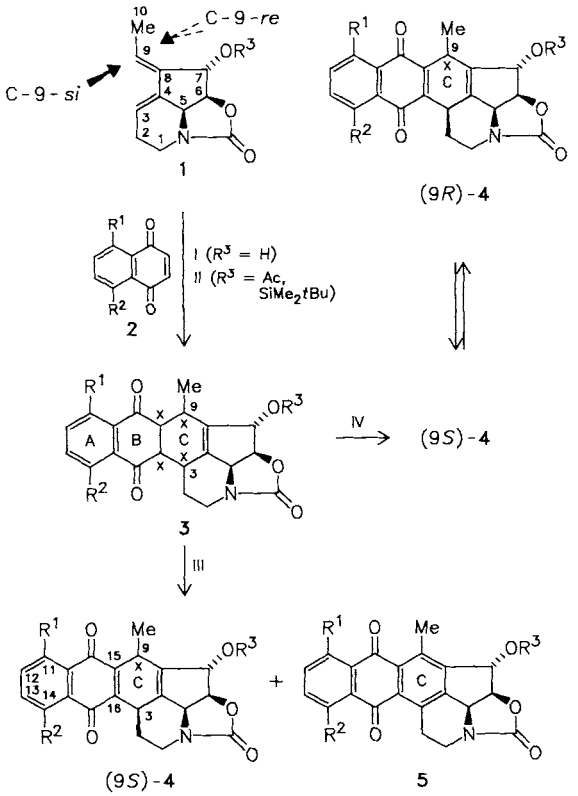

Scheme 1. Diels-Alder reactions: I: toluene, 100°C, 4 h. II: $AlCl_3$ or $TiCl_4$, −20 to 0°C, 30 min. Oxidation: III: aqueous sodium hydroxide, air, room temperature, 15 min. IV: pyridine, oxygen, water-free, room temperature, 4 h. **a**, $R^1=R^2=H$; **b**, $R^1=R^2=OH$; **c**, $R^1=R^2=OAc$; **d**, $R^1=OH$, $R^2=H$; $R^3=H$, Ac, $SiMe_2tBu$. In addition, the reactions of derivatives with R^1, $R^2=OMe$, OCH_2Ph, $R^3=SiMe_3$, Glu, Glu-Ac_4 were investigated. x designates the newly formed center of chirality. The (unsystematic) numbering is intended for assignment of the NMR signals.

[*] Dr. H.-U. Hoppe, Dr. S. Grabley, Dr. H. Kluge
Hoechst Aktiengesellschaft
Postfach 800320, D-6230 Frankfurt am Main 80

[**] This work was supported by the Bundesministerium für Forschung und Technologie. We thank Dr. *Kraemer* (Behringwerke), Dr. *Raether*, and Prof. *Siebert* (Hoechst) for carrying out the tests for cytotoxicity as well as antibiotic and other effects, Dr. *Voelskow* (Hoechst) for the microbiological work, and Professor *Laatsch* (Universität Göttingen) for helpful discussions.

The thermal cycloaddition of **1** to **2** can be carried out either at elevated temperatures (I in Scheme 1) or, if the hydroxyl groups are protected as acetates or silyl ethers, under Lewis acid catalysis (II). The yields by either route are over 90%. Mixtures of Diels-Alder adducts **3** are obtained, which can be only partly separated on silica gel but can be completely separated by analytical HPLC on RP18. Assuming a concerted mechanism for the Diels-Alder reaction, the symmetrical dienophiles **2a**-**2c** could yield, in principle, four stereoisomers (Scheme 2), whereas the unsymmetrical juglone **2d** could yield eight isomers owing to the possible regioisomers.[4]

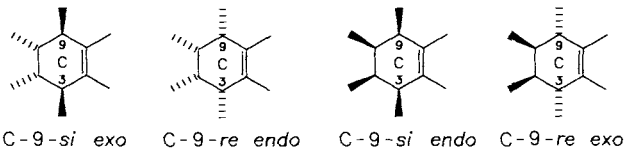

Scheme 2. The four possible configurations of the ring C of **3** assuming a concerted Diels-Alder reaction.

The reactions of **2a**, **2b**, and **2d** with **1** do not exhibit pronounced *endo/exo* or diastereofacial selectivity. Three Diels-Alder adducts (five in the case of **2d**) are obtained, one of which predominates in each case depending on the dienophile used, as shown by the ^{1}H-NMR spectra of the reaction mixtures.[5]

This variety of products is welcome in terms of our search for new lead structures. However, despite the practically identical electronic substitution of the diene, the cycloaddition can also be carried out in a more controlled fashion. In the case of **2c**, the π-facial or *endo/exo* selectivity is significantly higher, the amounts of the two side products being reduced to less than 10%. Since we were able to determine the configuration at C-3 of **4b** (the oxidation product of **3c** after deacetylation) by ^{1}H-NOE measurements, we think that the main component of **3c** has the *endo* configuration as a result of attack of the dienophile from the C-9 *si* side of **1** (C-9 *si endo* in Scheme 2).

The oxidation of compounds **3** leads to both the more highly oxidized anthraquinones **5** and the 1,4-dihydroanthraquinones **4**, which can be differentiated unequivocably by NMR spectroscopy (Table 1) and can be separated on silica gel. Since, under the same conditions, **4** cannot be oxidized further to give **5**, compound **5** is not a subsequent product of **4**, but rather **4** and **5** are formed from different adducts.

Procedure III (Scheme 1) has been used to oxidize quantitatively all compounds **3** investigated so far; the ratio **4** : **5** varies depending on the pattern of substitution. In addition, epimerization at C-9 may be induced by control of the pH value. The two epimers (9*S*)-**4** and (9*R*)-**4** can be differentiated by ^{1}H-NMR spectroscopy and separated on silica gel. Comparison of the configurations of the 1,4-dihydroquinones **4** (see above for **4b**) with the theoretically possible configurations of the ring C (Scheme 2) leads us to conclude that compounds of type **4** are formed only from those isomers of **3** that arise by attack of the dienophiles from the C-9 *si* side of **1**. Procedure IV was developed for the oxidation of compounds **3** containing hydrolysis-sensitive substituents (R^1, R^2, R^3=OAc) and has so far afforded—although not quantitatively—exclusively 1,4-dihydroanthraquinones **4**.

Table 1. ^{1}H-NMR data for the compounds **3a**, **4b**, and **5a** (400 MHz, $CDCl_3$/TMS, dilute solutions, $T = 300$ K); (*) = assignment questionable.

3a, R^1 = H: $\delta = 1.160$ (d, 3H, $J(9,10) = 7.1$ Hz; H-10), 1.358 (tdd, 1H, $J(1a,2a) = 12$, $J(1b,2a) = 4.5$, $J(2a,2b) = -13$ Hz; H-2a), 1.957 (d, 1H, $J(15,16) = 7.0$ Hz; H-15), 2.03 (br., m, 1H, $J(1b,2b) = 1.5$ Hz; H-2b), 2.78 (br., 1H; 7-OH), 3.06 (m, 1H, $J(1a,1b) = -14.5$ Hz; H-1a), 3.06 (m, 1H, $J(3,16) = 4.5$ Hz; H-3), 3.09 (dd, 1H; H-16), 3.17 (br., 1H; H-9), 3.895 (ddd, 1H; H-1b), 4.419 (br. d, 1H, $J(5,6) = 6.0$ Hz; H-5), 4.708 (d, 1H; H-6), 4.74 (br., 1H; H-7), 7.771 (m, 1H, $J(11,12) = 8.0$, $J(12,13) = 7.4$, $J(12,14) = 1.5$ Hz; H-12 (*)), 7.779 (m, 1H, $J(11,13) = 1.1$, $J(13,14) = 7.6$ Hz; H-13 (*)), 8.014 (m, 1H, $J(11,14) = -0.6$ Hz; H-14 (*)), 8.091 (m, 1H; H-11)

4b, R^1 = H: $\delta = 1.307$ (tdd, 1H, $J(1a,2a) = 12.8$, $J(2a,2b) = -12.6$, $J(2a,3) = 11.2$, $J(1b,2a) = 4.5$ Hz; H-2a), 1.353 (d, 3H, $J(9,10) = 7.0$ Hz; H-10), 2.09 (br., 1H; 7-OH), 2.532 (dddd, 1H, $J(2b,3) = 4.4$, $J(1a,2b) = 2.9$, $J(1b,2b) = 1.7$ Hz; H-2b), 3.356 (ddd, 1H, $J(1a,1b) = -14.5$ Hz; H-1b), 3.780 (dtd, 1H, $J(3,9) = 4.5$, $J(3,5) = 0.9$ Hz; H-3), 3.918 (qdd, 1H, $J(5,9) = 2.2$ Hz; H-9), 4.015 (ddd, 1H; H-1a), 4.669 (ddt, 1H, $J(5,6) = 6.0$, $J(5,7) = 1.0$ Hz; H-5), 4.834 (d, 1H; H-6), 4.930 (br., 1H; H-7), 7.240 (d, 1H, $J(12,13) = 9.5$ Hz; H-12 (*)), 7.248 (d, 1H; H-13 (*)), 12.556 (s, 1H; OH), 12.640 (s, 1H; OH). The absolute configuration at C-9 is currently being determined by X-ray crystallography.

5a, R^1 = H: $\delta = 2.60$ (br., 1H; 7-OH), 2.845 (d, 3H, $J(2a,10) = 0.6$ Hz; H-10), 2.934 (dddd, 1H, $J(2a,2b) = -16.4$, $J(1a,2a) = 11.8$, $J(1b,2a) = 8.5$ Hz; H-2a), 3.370 (td, 1H, $J(1a,1b) = -12.1$, $J(1a,2b) = 6.2$ Hz; H-1a), 3.750 (ddt, 1H, $J(1b,2b) = 1.0$, $J(1b,5) = 0.8$ Hz; H-1b), 4.479 (ddd, 1H; H-2b), 4.960 (br. d, 1H, $J(5,6) = 6.1$ Hz; H-5), 5.108 (d, 1H; H-6), 5.436 (br., 1H; H-7), 7.771 (m, 1H, $J(11,13) = 1.3$, $J(12,13) = 7.4$, $J(13,14) = 7.8$ Hz; H-13 (*)), 7.781 (m, 1Hk $J(11,12) = 7.8$, $J(12,14) = 1.3$ Hz; H-12 (*)), 8.171 (m, 1Z, $J(11,14) = 0.6$ Hz; H-14 (*)), 8.191 (m, 1H; H-11)

Nearly all compounds **3**, **4**, and **5** are active against Gram-positive bacteria and yeast and some are even active against protozoa. Cytotoxicity was tested in vitro on leukemia cells of the type L 1210. Many compounds proved to be as effective as the standard compound adriamycin and were comparably less acutely toxic to mice. In those cases that afforded mixtures of stereo- and regioisomers in the syntheses, the mixtures themselves were initially tested. Only in very promising cases was subsequent separation carried out by HPLC on RP18 in methanol/water.

Received: January 30, 1987;
revised: April 6, 1987 [Z 2079 IE]
German version: *Angew. Chem. 99* (1987) 692

[1] Chemical screening methods: a) W. A. König, H. Drautz, H. Zähner, *Liebigs Ann. Chem. 1980*, 1384; b) M. Noltemeyer, G. M. Sheldrick, H.-U. Hoppe, A. Zeeck, *J. Antibiot. 35* (1982) 549.

[2] Isolation and structure elucidation: a) H. Drautz, H. Zähner, E. Kupfer, W. Keller-Schierlein, *Helv. Chim. Acta 64* (1981) 1752; b) A. Karrer, M. Dobler, *ibid. 65* (1982) 1432.

[3] Syntheses: a) A. P. Kozikowski, P. Park, *J. Org. Chem. 49* (1984) 1674; b) *J. Am. Chem. Soc. 107* (1985) 1763.

[4] W. Oppolzer, *Angew. Chem. 96* (1984) 840; *Angew. Chem. Int. Ed. Engl. 23* (1984) 876.

[5] The different Diels-Alder adducts **3** can be differentiated on the basis of the resonances of the methyl group at C-9 or the hydroxyl groups in the dienophile portion; e.g., for **3b**: $\delta(\text{C9-CH}_3) = 0.85$, 1.1, 1.16 (each d, $J = 7.1$ Hz); $\delta(\text{OH}) = 11.4$–12.2 (6 × s); intensities of each ca. 1 : 2 : 1.

The First Synthesis of a Benzoborole**

By *Wolfgang Schacht* and *Dieter Kaufmann**

Since the calculation of the geometries and resonance energies of boron-containing small-ring systems by *P. von R. Schleyer* et al.,[1] this field has also proven to be experimentally productive. So far, however, only highly substituted, sterically[2] or electronically[3] stabilized derivatives of antiaromatic boroles have been reported. Benzocyclobutadiene[4] **6**, which is related to the benzoborole **3**, has only been isolated at low temperatures. Since flash vacuum pyrolysis has already been used successfully for the generation of benzoannulated boracycloalkenes,[5] we have attempted to open up the first approach to benzoboroles via the pyrolysis of boraindanes. Matrix isolation appeared to offer a suitable way of isolating the borole derivatives, which, since they were substituted on only one side, were expected to exhibit very high reactivity.

1-Chloro-1-boraindane **2**[6] could be obtained in good yields (81%) by flash vacuum pyrolysis of dichloro(2-ethylphenyl)borane **1** at 700 °C/10^{-3} torr, without the formation of side products.[7] Dehydrogenation occurred at a pyrolysis temperature of 900 °C. At 77 K, the pyrolysate was intense yellow. The color largely disappeared upon warming to room temperature. Workup of the pyrolysate afforded colorless crystals of a dimer of **3** in a yield of 56%. According to ^{1}H-, ^{13}C-, and ^{11}B-NMR and mass spectroscopic data, this product is *cis*-11,12-dichloro-4b,11,11a,12-tetrahydro-11,12-diboradibenzo[*a*,*f*]azulene **4**.

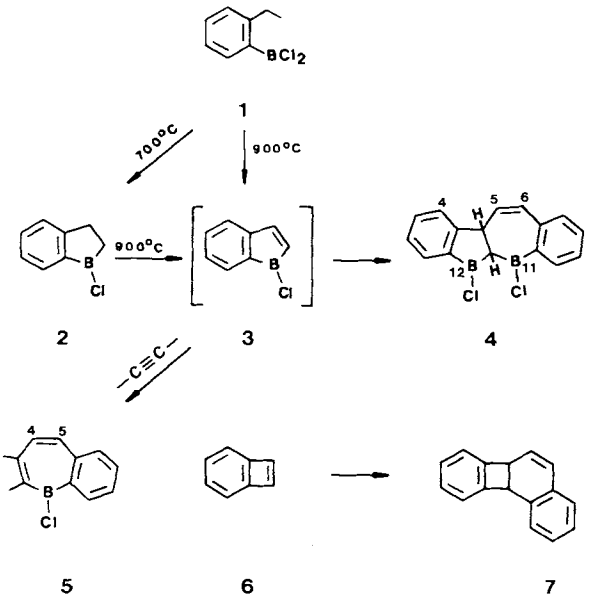

The exclusive formation of the dimer **4** is also interesting in view of the similar reactivities of the benzoborole **3** and the related benzocyclobutadiene **6**, since, depending on the reaction conditions, **6** can react to give two different kinds of dimers, namely, the [2 + 2]cycloadduct dibenzotricyclooctadiene[8] and the product of a formal insertion reaction, the dibenzobicyclo[4.2.0]octatriene **7**.[9] Compound **7** corresponds structurally to the benzoborole dimer **4**, whose formation can be explained in terms of a regiospecific *syn*-vinylboration of a borole double bond with the B–C_{vinyl} bond of a second molecule of **3** upon warming of the matrix.

The yellow color of the cooled pyrolysate of **2** was a further indication for the initial formation of **3** since the crystals of *B*-chlorodibenzoborole are also yellow.[3a] ^{1}H-NMR spectroscopic identification of the monomer could not even be achieved at −90 °C. Apparently, **3** is very reactive, since, even at this temperature, it undergoes complete dimerization to **4**.

[*] Priv.-Doz. Dr. D. Kaufmann, Dipl.-Chem. W. Schacht
Institut für Organische Chemie der Universität
Martin-Luther-King-Platz 6, D-2000 Hamburg 13 (FRG)

[**] This work was supported by the Deutsche Forschungsgemeinschaft.

Photoelectron spectroscopy (PES) allows the characterization of reactive molecules in high vacuum. Upon pyrolytic dehydrogenation (925 °C) of the boraindane **2** in the photoelectron spectrometer (He(I)), a new absorption band at lower ionization energy (8.53 eV) was observed, which can be assigned to the π ionization of a benzoborole.[10] Complete assignment of all the bands has not yet been possible, however, since, even at this temperature, the conversion is too low to separate all the bands of **2** and **3**.

Trapping reactions in the matrix further establish the formation of **3**. Whereas **3** could not be trapped with alkenes such as *Z*-butene or cyclopentadiene (dimerization is more rapid), it reacts smoothly with 2-butyne to give 1-chloro-2,3-dimethyl-1-benzoborepin **5**. This reaction opens up the first approach to the 10π-aromatic 1-benzoborepins; 3-benzoborepins are known.[11]

Reaction with electrophilic reagents such as DCl led to exclusive B–C_{vinyl} bond cleavage and formation of a 1:1 mixture of the *Z*- and *E*-[2-(β-deuteriovinyl)phenyl]boranes **8** and **9**, respectively. Their formation can be explained in terms of initial addition of $D^{\oplus}$ to the 2,3 double bond of **3**, followed by addition of the chloride ion to the boron atom and opening of the B–C2 bond.

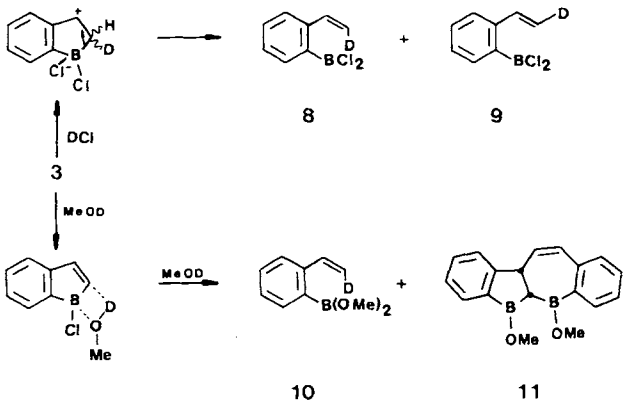

Table 1. Physical data for the compounds **4**, **5**, **8**–**10**, and **11**. NMR spectra: δ values, J in Hz, ^{1}H-NMR at 270 MHz.

4: yield 56%, colorless crystals, m.p. (sealed tube) = 78 °C. — ^{1}H-NMR (C_6D_6): 3.60 (d, $^3J_{4b,11a}$ = 5.6, 1 H, 11a-H), 3.66 (dd, $^3J_{4b,5}$ = 8.4, 1 H, 4b-H), 6.03 (dd, $^3J_{5,6}$ = 11.6, 1 H, 5-H), 6.31 (d, 1 H, 6-H), 6.64 (m, 2 H), 6.78 (m, 2 H), 7.06 (t, 1 H), 7.14 (d, 1 H), 7.52 (d, 1 H), 7.61 (d, 1 H). — ^{13}C-NMR (C_6D_6): 47.6, 68.5 (br.), 124.7, 126.5, 126.7, 129.4, 131.1, 132.0, 133.6, 134.3, 134.7, 135.0, 138.4 (br.), 140.6, 140.9 (br.), 166.5. — ^{11}B-NMR (toluene): 67.4. — MS (70 eV): *m/z* (%): 296 ($M^{\oplus}$, 92), 260 (100), 214 (96), 148 (38), 71 (27)

5: yield 10%, colorless liquid, redistilled at 70 °C/0.005 torr. — ^{1}H-NMR ($CDCl_3$): 1.95 (q, $^5J_{10,11}$ = 0.7, 3 H, CH_3), 2.36 (q, $^5J_{10,11}$ = 0.7, 3 H, CH_3), 6.25 (d, $^3J_{4,5}$ = 12.8, 1 H, 5-H), 6.98 (d, $^3J_{4,5}$ = 12.8, 1 H, 4-H), 7.32 (m, 2 H), 7.40 (d, 1 H), 9.02 (d, 1 H). — ^{11}B-NMR (C_6H_6): 53.6. — MS (70 eV): *m/z* (%): 202 ($M^{\oplus}$, 100), 187 (47), 156 (35), 142 (75), 141 (61), 115 (33)

8 and **9**: yield 50%, colorless, very sensitive liquid, which could not be purified by distillation. — ^{1}H-NMR (C_6D_6): 5.09 (–CH=C*H*$D_{(trans)}$, $^3J_{trans}$ = 17.4, 1 H), 5.34 (–CH=C*H*$D_{(cis)}$, $^3J_{cis}$ = 10.9, 1 H) and 7.15 (–C*H*=CHD, 2 H, AB systems), 6.79 (t, 2 H), 7.70 (d, 2 H), 8.02 (d, 2 H), 8.10 (t, 2 H). — ^{11}B-NMR (C_6H_6): 49.8

10: yield 35%, colorless liquid. — ^{1}H-NMR (C_6D_6): 5.10 (–CH=C*H*$D_{(cis)}$) and 6.85 (–C*H*=CHD, AB system, 2 H), 7.10 (t, 1 H), 7.15 (t, 1 H), 7.28 (d, 1 H), 7.88 (d, 1 H)

11: yield 15%, colorless crystals, m.p. (sealed tube) = 55 °C. — ^{1}H-NMR (C_6D_6): 2.82 (d, 1 H, 11a-H), 3.64 and 3.73 (br. s, each 3 H, OCH_3), 3.85 (dd, 1 H, 4b-H), 6.37 (dd, 1 H, 5-H), 6.57 (d, 1 H, 6-H), 6.75–6.95 (m, 4 H), 7.10 (t, 1 H), 7.33 (m, 2 H), 7.48 (d, 1 H). — ^{11}B-NMR (*n*-hexane): 49.3. — MS (70 eV): *m/z* (%): 288 ($M^{\oplus}$, 88), 273 (54), 245 (25), 213 (78), 144 (44), 73 (100)

Cocondensation with the significantly more weakly acidic [D_1]methanol at 77 K, on the other hand, led, after warming of the matrix, to a mixture of the *Z*-[2-(β-deuteriovinyl)phenyl]borane **10** (73%) and the doubly methoxylated dimer **11** (27%). The stereospecific formation of **10** can be explained in terms of the cleavage of the B–C2 bond of **3**. Compound **11**, which was obtained independently by methanolysis of **4** at 0 °C, is presumably formed this way in the matrix as well, since no *E*-[2-(β-deuteriovinyl)phenyl]dimethoxyborane could be detected. Physical data for the new compounds are collected in Table 1.

The pyrolytic dehydrogenation of 2-chloro-2-boraindane[7] to the corresponding 2-benzoborole, on the other hand, was unsuccessful.

Received: March 9, 1987;
revised: April 10, 1987 [Z 2129 IE]
German version: *Angew. Chem. 99* (1987) 682

[1] K. Krogh-Jespersen, D. Cremer, J. D. Dill, J. A. Pople, P. von R. Schleyer, *J. Am. Chem. Soc. 103* (1981) 2589.
[2] a) L. Killian, B. Wrackmeyer, *J. Organomet. Chem. 148* (1978) 137; b) G. E. Herberich, B. Buller, B. Hessner, W. Oschmann, *ibid. 195* (1980) 253; c) J. J. Eisch, J. E. Galle, S. Kozima, *J. Am. Chem. Soc. 108* (1986) 379.
[3] a) R. A. Köster, M. A. Grassberger, *Justus Liebigs Ann. Chem. 719* (1968) 169; b) K. Narula, H. Nöth, *J. Organomet. Chem. 281* (1985) 131; c) G. E. Herberich, H. Ohst, *Chem. Ber. 118* (1985) 4303.
[4] O. L. Chapman, C. C. Chang, N. R. Rosenquist, *J. Am. Chem. Soc. 98* (1976) 261.
[5] W. Schacht, D. Kaufmann, *J. Organomet. Chem.* (1987), in press.
[6] The synthesis of **2** was mentioned, but the properties of the borane were not described: [3a].
[7] W. Schacht, D. Kaufmann, *Chem. Ber. 120* (1987), in press.
[8] M. Avram, D. Dinu, G. Matescu, C. D. Nenitzescu, *Chem. Ber. 93* (1960) 1789.
[9] M. P. Cava, D. R. Napier, *J. Am. Chem. Soc. 79* (1957) 1701.
[10] We thank Dr. *S. Elbel*, Universität Hamburg, for the PES measurements.
[11] a) A. J. Leusink, W. Drenth, J. G. Noltes, G. J. M. van der Kerk, *Tetrahedron Lett. 1967*, 1263; b) G. Axelrad, D. Halpern, *J. Chem. Soc. D1971*, 291.

Vanadium Carbene Complexes by Reaction of (Diene)metallocenes with [CpV(CO)$_4$]**

By *Gerhard Erker,* Rainer Lecht, Rüger Schlund, Klaus Angermund,* and *Carl Krüger*

A large number of carbene complexes of nearly all the d elements have become accessible[1] by varying the reaction sequence developed by *E. O. Fischer* et al.[2] for the transformation of a carbonyl complex into a carbene complex. There are only a few transition metals that are not well represented with examples of this important class of ligand. One such transition metal is vanadium. To the best of our knowledge, only two special routes to simple Fischer-type vanadium carbene complexes have been described so far and supported by examples (Scheme 1).[3]

Carbene complexes may play an important role in vanadium-catalyzed olefin metathesis and polymerization reactions. Their availability could open up new routes to the

[*] Prof. Dr. G. Erker, Dipl.-Chem. R. Lecht, Dipl.-Chem. R. Schlund
Institut für Organische Chemie der Universität
Am Hubland, D-8700 Würzburg (FRG)
Dr. K. Angermund, Prof. Dr. C. Krüger
Max-Planck-Institut für Kohlenforschung
Kaiser-Wilhelm-Platz 1, D-4330 Mülheim a. d. Ruhr (FRG)

[**] This work was supported by the Stiftung Volkswagenwerk, the Fonds der Chemischen Industrie, and the Alfried-Krupp-von-Bohlen-und-Halbach-Stiftung.

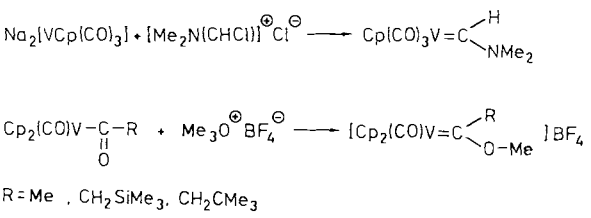

Scheme 1. Reported vanadium carbene complexes, Cp = η^5-C_5H_5.

preparation of proposed intermediates in vanadium-promoted oxidations.[4] The development of simple syntheses of vanadium carbene complexes is therefore of interest.

We recently described a new approach to the formation of heteroatom-stabilized carbene complexes from carbonyl complexes. In the key step, a metallacyclic oxycarbene complex is formed by C–C bond formation between an olefinic C atom of a reactive (η^2-olefin)metallocene complex and the C atom of an M–CO group.[5] Suitable reagents for this reaction are (*s-trans*-η^4-butadiene)zirconocene and -hafnocene.

The readily accessible equilibrium mixture of the *s-cis* and *s-trans* isomers **2a** and **1a**, respectively (**2a** : **1a** = 55 : 45)[6] reacts rapidly with $[CpV(CO)_4]$ **3** in toluene at room temperature, resulting in C–C bond formation between the zirconium-bound diene ligand and a V–CO unit (Scheme 2). The red oxycarbene complex **4a** precipitates from the reaction solution at room temperature.[7a]

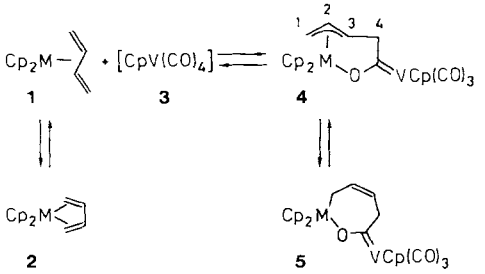

a, M = Zr; **b**, M = Hf

Scheme 2. The (unsystematic) numbering of **4** is intended for the assignment of the NMR signals.

The X-ray structure analysis of **4a**[7b] reveals a binuclear Zr–V complex having the arrangement of ligands (Fig. 1) expected for a bent metallocene and a $CpVL_4$ group. Three of the C atoms derived from the butadiene ligand are bound to the zirconium center as a distorted π-allyl moiety.[8] The fourth C atom is coupled to a CO ligand which is bound to the vanadium center. Noteworthy features of the structure of **4a** are the short C1–O1 bond[5] (for comparison, see Ref. [2]) and the significantly lengthened V–C1 bond (compared with the other V–CO bonds).[9]

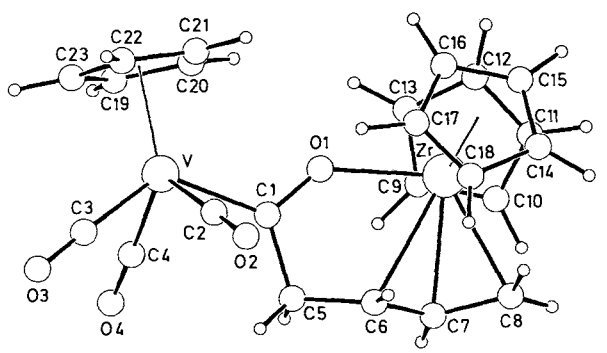

Fig. 1. Crystal structure of **4a**. Selected bond lengths [Å] and bond angles [°]: V-C1 2.102(3), V-C2 1.889(4), V-C3 1.899(4), V-C4 1.921(4), V-C19 2.302(4), V-C20 2.293(4), V-C21 2.268(4), V-C22 2.261(5), V-C23 2.286(4), C1-O1 1.270(4), C1-C5 1.545(5), C5-C6 1.505(5), O1-Zr 2.188(2), C6-Zr 2.653(4), C7-Zr 2.514(4), C8-Zr 2.443(4); V-C1-O1 120.7(2), O1-C1-C5 112.4(3).

The formation of the carbene complex is reversible in solution. When crystalline **4a** is dissolved in $[D_8]$toluene at room temperature, the educts **1a** and **3**, in addition to **4a** (ca. 1 : 1 : 1), can be detected almost immediately by ^{1}H-NMR spectroscopy. A subsequent equilibrium is then established between **1a** and the isomer **2a**. In order to use the carbene complex synthesis shown in Scheme 2, it is important that the position of the **1** + **3** ⇌ **4** equilibrium be easily controlled to give preferentially the vanadium carbene complex. Thus, reaction of **3** and the (η^4-butadiene)hafnocene system **1b**/**2b** gives the complex **4b** [65%, m.p. = 140 °C (dec.)],[10] which is not in equilibrium with the educts in solution at room temperature but rather with the seven-membered-ring σ-allyl isomer **5b** (which does not affect the preparative use of the carbene moiety).[10]

Experimental procedure

4a: (η^4-butadiene)zirconocene (0.82 g, 3 mmol), as an equilibrium mixture of **1a** and **2a**, and **3** (0.68 g, 3 mmol) were dissolved in 100 mL of toluene at 0 °C. The reaction mixture was allowed to warm to room temperature and then stirred for 4 h; the carbene complex **4a** thereby precipitated as an orange-red solid. After filtration and washing with petroleum ether, 1.06 g (71%) of **4a** was obtained. Suitable crystals for X-ray structure analysis were obtained by recrystallization from benzene. M.p. = 132 °C (dec.), correct elemental analysis (C,H).

Received: February 13, 1987;
supplemented: April 13, 1987 [Z 2101 IE]
German version: *Angew. Chem. 99* (1987) 708

[1] U. Schubert, H. Fischer, P. Hofmann, K. Weiss, K. H. Dötz, F. R. Kreissl: *Transition Metal Carbene Complexes*. Verlag Chemie, Weinheim 1983.

[2] E. O. Fischer, A. Maasböl, *Angew. Chem. 76* (1964) 645; *Angew. Chem. Int. Ed. Engl. 3* (1964) 580; *Chem. Ber. 100* (1967) 2445.

[3] a) A. J. Hartshorn, M. F. Lappert, K. Turner, *J. Chem. Soc. Dalton Trans. 1978*, 348; J. Martin, C. Moise, J. Tirouflet, *C. R. Hebd. Séances Acad. Sci. Ser. 2, 292* (1981) 1143; b) polynuclear complex: U. Behrens, F. G. A. Stone, *J. Chem. Soc. Dalton Trans. 1984*, 1605; c) EHMO calculation: O. V. Gritsenko, M. I. Mitkov, A. A. Bagatur'yants, V. B. Kazanskii, *Zh. Fiz. Khim. 58* (1984) 1041 (*Chem. Abstr. 101* (1984) 130819p); see also N. Aristov, P. B. Armentrout, *J. Am. Chem. Soc. 108* (1986) 1806.

[4] a) K. J. Ivin: *Olefin-Metathesis*, Academic Press, London 1983, and references cited therein; b) G. Natta, I. Pasquon, A. Zambelli, *J. Am. Chem. Soc. 84* (1962) 1488; cf. H. W. Turner, R. R. Schrock, J. D. Fellmann, S. J. Holmes, *ibid. 105* (1983) 4942; c) E. J. Lyons, *Tetrahedron Lett. 1974*, 2903; H. Mimoun, M. Mignard, P. Brechot, L. Saussine, *J. Am. Chem. Soc. 108* (1986) 3711; S. G. Davies: *Organotransition Metal Chemistry: Applications to Organic Syntheses*, Pergamon, Oxford 1982, Chap. 8, and references cited therein.

[5] a) G. Erker, U. Dorf, R. Benn, R.-D. Reinhardt, J. L. Petersen, *J. Am. Chem. Soc. 106* (1984) 7649; b) G. Erker, U. Dorf, R. Mynott, Y.-H. Tsay, C. Krüger, *Angew. Chem. 97* (1985) 572; *Angew. Chem. Int. Ed. Engl. 24* (1985) 584; c) G. Erker, T. Mühlenberndt, R. Benn, A. Rufinska, *Organometallics 5* (1986) 402; d) G. Erker, R. Lecht, *J. Organomet. Chem. 311* (1986) 45; e) G. Erker, U. Dorf, C. Krüger, Y.-H. Tsay, *Organometallics 6* (1987) 680; G. Erker, R. Lecht, J. L. Petersen, H. Bönnemann, *ibid.*, in press; G. Erker, R. Lecht, C. Krüger, Y.-H. Tsay, H. Bönnemann, *J. Organomet. Chem.*, in press; f) see also K. Mashima, K. Jyodoi, A. Ohyoshi, H. Takaya, *J. Chem. Soc. Chem. Commun. 1986*, 1145.

[6] G. Erker, J. Wicher, K. Engel, C. Krüger, *Chem. Ber. 115* (1982) 3300; G. Erker, C. Krüger, G. Müller, *Adv. Organomet. Chem. 24* (1985) 1.

[7] a) Spectroscopic data: ^{1}H-NMR (C_6D_6, 400 MHz): δ = 5.34, 5.22 (each s, each 5H; Cp_2Zr), 4.94 (s, 5H; CpV), 1.52, 1.53 (m, 2H; 2H1), 2.78 (m, 1H; H4), 4.23 (dd, 1H; H4'), 4.67 (m, 1H; H3), H2 overlapped (data for comparison, see [5]).—IR (KBr): $\tilde{\nu}$(CO) = 1925 (m), 1840 (s), 1820 (vs) cm^{-1} [cf. **3**: $\tilde{\nu}$(CO) = 2016, 1916 cm^{-1} (Nujol) (H. P. Fritz, E. F. Paulus, *Z. Naturforsch. B18* (1963) 435); $[CpV(CO)_3(CS)]$: $\tilde{\nu}$(CO) = 2005, 1885,

1835 cm^{-1} (Nujol) (S. Rajan, *Indian J. Chem. Sect. A 15* (1977) 920)]; b) X-ray structure analysis: space group $P\bar{1}$ with $a = 8.189(1)$, $b = 10.327(2)$, $c = 14.783(1)$ Å, $\alpha = 93.88(1)$, $\beta = 103.29(1)$, $\gamma = 99.52(1)°$, $V = 1192.8$ Å^3, $\rho_{calcd} = 1.62$ g cm^{-3} ($\mu(Mo_{K\alpha}) = 8.42$ cm^{-1}, 6871 unique reflections, 5750 observed ($I > 2\sigma(I)$), $R = 0.041$, $R_w = 0.062$), a disordered molecule of solvent in the asymmetric unit of the unit cell. Further details of the crystal structure investigation may be obtained from the Fachinformationszentrum Energie, Physik, Mathematik GmbH, D-7514 Eggenstein-Leopoldshafen 2 (FRG), on quoting the depository number CSD-52307 the names of the authors, and the journal citation.

[8] a) G. Erker, K. Engel, U. Dorf, J. L. Atwood, W. E. Hunter, *Angew. Chem. 94* (1982) 915; *Angew. Chem. Int. Ed. Engl. 21* (1982) 913; *Angew. Chem. Suppl. 1982*, 1974; b) D. J. Brauer, C. Krüger, *Organometallics 1* (1982) 204, 207; c) W. J. Highcock, R. M. Mills, J. L. Spencer, P. Woodward, *J. Chem. Soc. Chem. Commun. 1982*, 128; d) Y. Kai, N. Kanehisa, K. Miki, N. Kasai, K. Mashima, K. Nagasuna, H. Yasuda, A. Nakamura, *Chem. Lett. 1982*, 1979; e) G. Erker, K. Engel, J. L. Atwood, W. E. Hunter, *Angew. Chem. 95* (1983) 506; *Angew. Chem. Int. Ed. Engl. 22* (1983) 494; *Angew. Chem. Suppl. 1983*, 678; f) G. Erker, K. Berg, C. Krüger, G. Müller, K. Angermund, R. Benn, G. Schroth, *ibid. 96* (1984) 445 and *23* (1984) 455; see also [5a].

[9] J. B. Wilford, A. Whitla, H. M. Powell, *J. Organomet. Chem. 8* (1967) 495; C. E. Holloway, M. Melnik, *ibid. 304* (1986) 41, and references cited therein.

[10] Spectroscopic data: **4b**: IR (KBr): $\tilde{\nu}$(CO) = 1925, 1840, 1820 cm^{-1}.—^{1}H-NMR (C_6D_6, 400 MHz): $\delta = 5.30$, 5.20 (Cp_2Hf), 4.90 (CpV), 1.35 (2H1), 4.65 (H3), 4.2 and 2.8 (H4 and H4'), H2 overlapped; **5b**: ^{1}H-NMR (C_6D_6, 400 MHz, room temperature): $\delta = 5.53$ (Cp_2Hf), 4.93 (CpV), 5.9, 4.8 (pseudo q, −CH=CH−), CH_2 groups not localized (for the dynamic behavior of similar oxametallacycloheptene compounds, see [8e]).

broad-band filter permitted selective excitation of the N=N π electrons ($\lambda_{max} \approx 350$ nm) without excitation of the aromatic π electrons of **1**, **3**, or **4**.

The formation of **3** and **4** is best explained by assuming the occurrence of the short-lived diradical intermediate **2**[2] after the photoinduced expulsion of a nitrogen molecule. Depending on its conformation, this diradical may undergo either ring-closure to give **3** or hydrogen transfer to give **4** (Scheme 1).

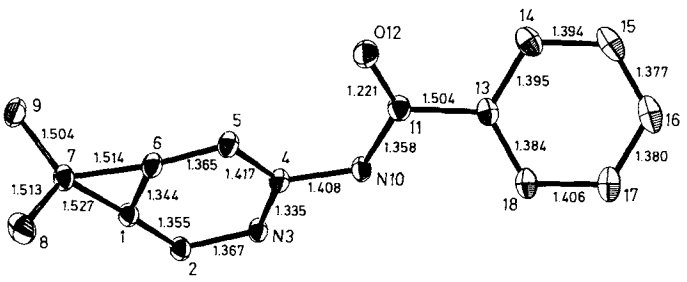

Fig. 1. Crystal structure of **3**. Bond lengths in Å; angles of the cyclopropene moiety [°]: C1-C7-C6 52, C1-C6-C7 64, C6-C1-C7 63.

Synthesis and Structure of a Cyclopropapyridine**

By *Ramesh Bambal, Hans Fritz, Grety Rihs, Théophile Tschamber,* and *Jacques Streith**

Dedicated to Professor Gerhard Quinkert on the occasion of his 60th birthday

Ultraviolet photolysis (CH_2Cl_2/pentane, 10°C, MTO-A365b broad-band filter, medium-pressure mercury vapor lamp) of the known pyrazolopyridine **1**[1] led to the formation of the corresponding cyclopropapyridine **3** and the isomeric isopropenylpyridine **4** in moderate yields. The

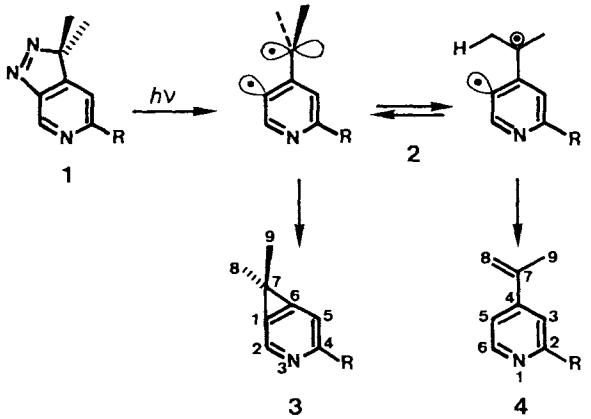

Scheme 1. R = NH−COPh.

An X-ray structure analysis of **3** (Fig. 1) showed that the geometric parameters of the cyclopropene moiety and of its immediate surroundings were very similar to those that had been measured previously for a cyclopropabenzene derivative[3] and for a cyclopropanaphthalene.[4] The pyridine ring of **3** appears to have a normal geometry, an observation that is reminiscent of the structural similarity between benzene and cyclopropabenzene, or between naphthalene and cyclopropanaphthalene. It is worthy of note, however, that there is a lengthening of the C2–N3 bond (1.367 Å, instead of the normal bondlength of 1.335 Å for the C4–N3 bond), a result that is most likely the consequence of the shortening of the C1–C6 bond (1.344 Å).[5]

Compound **3** is the first cyclopropapyridine to have been synthesized.[6]

Experimental Procedure

In a typical experiment, a stirred solution of **1** (100 mg, 0.38 mmol) in CH_2Cl_2 (20 mL) and pentane (135 mL), which was kept under argon atmosphere at 10°C, was irradiated with a Philips HPK125 lamp for 5 h. The photolysis was stopped before consumption of **1** was complete. The reaction products were separated at 5°C by preparative thin-layer chromatography (TLC) (ethyl acetate/cyclohexane 1/9; Merck type E alumina). The following products were isolated in the order given (decreasing R_f values): **3** (24 mg, 27%), **4** (23 mg, 26%), and **1** (16 mg, 16%). As expected, **3** is sensitive toward acids and could not be purified by TLC on silica gel. In its crystalline state, it is quite stable when kept under argon at room temperature.

3 (from ether/pentane): m.p. = 114–116°C with partial decomposition (determined on a Kofler bank). Correct C,H,N analysis.—UV (MeCN): λ_{max} [nm] (ε) = 264 (12600), 226 (10200).—^{1}H-NMR (400 MHz, $CDCl_3$, $T = 263$ K): $\delta = 8.27$ (d, $J = 2$ Hz; H-5), 7.86 (d, $J = 2$ Hz; H-2), 9.66 (s; N−H), 7.96 (m, 2H; *o*-phenyl H), 7.48 (m, 2H; *m*-phenyl H), 7.56 (m; *p*-phenyl H), 1.67 (s, 6H; Me-8, Me-9).—^{13}C-NMR (100.6 MHz, $CDCl_3$, $T = 263$ K): $\delta = 149.82$ (C-4), 101.39 ($^1J = 180$ Hz; C-5), 154.49 (C-6), 130.12 (C-1), 130.75 ($^1J = 189$ Hz; C-2), 39.68 (C-7), 27.94 ($^1J = 128$ Hz; Me-8, Me-9), 166.22 (CO), 134.20 (*i*-C of Ph), 127.34 ($^1J = 160$ Hz; *o*-C of Ph), 128.71 ($^1J = 162$ Hz; *m*-C of Ph); 132.18 ($^1J = 161$ Hz; *p*-C of PH). $^1J(^{13}C,^{13}C) = 42.9$ Hz for the Me–C-7 coupling.

4: m.p. = 105°C; correct C,H,N analysis.—UV (EtOH): λ_{max} [nm] (ε) = 299 (18700), 273 (18900), 230 (13700).—^{1}H-NMR (400 MHz, $CDCl_3$, $T = 263$ K): $\delta = 9.69$ (s; NH), 7.97 (d, $J = 5.5$ Hz, 1H; H-6), 7.70 (dd, $J = 5.5$, 1.5 Hz, 1H; H-5), 8.56 (d, $J = 1.5$ Hz, 1H; H-3), 5.66 and 5.31 (2H; H-8), 2.19 (3H; Me), 7.96 (m, 2H; *o*-phenyl H), 7.58 (m, 1H; *p*-phenyl H), 7.49 (m, 2H; *m*-phenyl H).—^{13}C-NMR (100.6 MHz, $CDCl_3$, $T = 263$ K): $\delta = 166.33$ (CO), 152.09 (C-2), 150.95 (C-7), 147.41 (C-6), 140.88 (C-4), 116.57 (C-8), 116.56 (C-5), 110.79

[*] Prof. Dr. J. Streith, Dr. R. Bambal, Dr. T. Tschamber
École Nationale Supérieure de Chimie,
Université de Haute-Alsace, rue Alfred Werner,
F-68093 Mulhouse-Cédex (France)
Prof. Dr. H. Fritz, G. Rihs
Physikalische Abteilung, Ciba Geigy AG
CH-4002 Basel (Switzerland)

[**] We thank the Centre National de la Recherche Scientifique for its continuous support and the Fondation pour l'Ecole de Chimie de Mulhouse for a postdoctoral grant to *R. B.* We also thank *F. Klinger* (Mulhouse) for an independent synthesis of **4**.

(C-3), 134.20 (*p*-C of Ph), 132.23 (*i*-C of Ph); 128.75 (*m*-C of Ph), 127.34 (*o*-C of Ph).

Received: February 13, 1987;
revised: March 23, 1987 [Z 2104 IE]
German version: *Angew. Chem. 99* (1987) 710

[1] P. Gesche, F. Klinger, H. Strub, J. Streith, *Tetrahedron Lett. 21* (1980) 1223.
[2] B. Halton, *Chem. Rev. 73* (1973) 113; *Ind. Eng. Chem. Prod. Res. Dev. 19* (1980) 349; W. E. Billups, *Acc. Chem. Res. 11* (1978) 245.
[3] E. Carstensen-Oeser, B. Müller, H. Dürr, *Angew. Chem. 84* (1972) 434; *Angew. Chem. Int. Ed. Engl. 11* (1972) 422.
[4] W. E. Billups, W. Y. Chow, K. H. Leavell, E. S. Lewis, J. L. Margrave, R. L. Sass, J. J. Shieh, P. G. Werness, J. L. Word, *J. Am. Chem. Soc. 95* (1973) 7878.
[5] **3**: triclinic crystals; space group $P\bar{1}$ (No. 2, centrosymmetric); $a=8.687$, $b=10.345$, $c=16.557$ Å, $\alpha=72.79$, $\beta=103.50$, $\gamma=116.33°$; $V=1265$ Å^3, $\rho_{calcd}=1.251$ g cm^{-3}, $Z=4$. $\lambda(Mo_{K\alpha})=0.70926$ Å. 6356 reflections were measured ($\theta-2\theta$ scan mode) of which 4574 with $I>2\sigma(I)$ were used for the solution by direct methods (MULTAN 78). Further details are available on request from the Director of the Cambridge Crystallographic Data Centre, University Chemical Laboratory, Lensfield Road, Cambridge CB2 1EW (England) by quoting the full literature citation.
[6] S. J. Buckland, B. Halton, B. Stanovnik, *Tetrahedron Lett. 27* (1986) 1309.

Synthesis and Structure of [(OC)$_4$Fe=Si(O*t*Bu)$_2$·HMPT], a Donor-Stabilized Silanediyl ("Silylene") Complex**

By *Christian Zybill** and *Gerhard Müller*

The existence of stable, monomeric silanediyl ("silylene") complexes was long in question.[1] A coordination of free silanediyls[2] to transition metals was previously assumed to occur only for reactive intermediates (for example, in platinum-catalyzed Si–Si coupling reactions[3]) or was observed in the gas phase by means of molecular beam experiments.[4] In contrast, the chemistry of the heavier homologues[5] of the carbene complexes is well established; particularly in the case of Sn, both donor-stabilized[6] and donor-free stannanediyl ("stannylene") complexes have been prepared.[7] We have now found that silylene complexes can be stabilized, both thermodynamically and kinetically, by bulky heteroatom substituents.

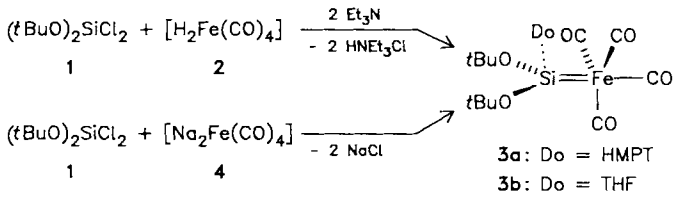

Starting from di(*tert*-butoxy)dichlorosilane **1**, the silylene complexes **3a**,**b** (THF = tetrahydrofuran) are accessible in two ways, each of which involves the use of the tetracarbonylferrate ion as the key reagent.[8,9] The colorless compounds **3a**,**b**, which sublime in high vacuum, are monomeric both in the solid state and in solution. In each case, the iron atom exhibits rigid trigonal-bipyramidal (tbp) coordination. According to the ^{13}C-NMR data, the FeSi bond undergoes unhindered rotation down to -30°C. Investigations at lower temperatures are difficult owing to the low solubility of **3a**,**b**.[10]

The X-ray structure analysis of **3a**[11] (Fig. 1) confirms this structural assignment. The silylene ligand occupies an apical position of the tbp-coordinated Fe fragment, which is a direct indication of its strong σ-donor properties.[12] The HMPT O atom is coordinated to the "unsaturated" Si atom and completes its distorted tetrahedral coordination sphere. The Si–O3 distance (1.730(3) Å) is significantly longer than the Si–O1 and Si–O2 distances (1.610(3) and 1.636(4) Å, respectively). The Fe–Si distance is 2.289(2) Å. A comparison with normal Fe–Si single bonds is difficult owing to the absence of reference compounds in which the Fe atom has a similar coordination number and oxidation state.[13]

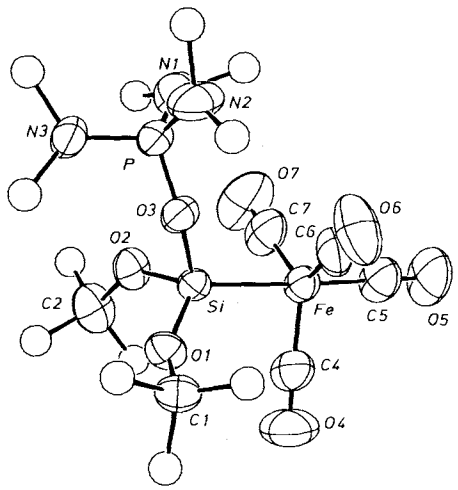

Fig. 1. Crystal structure of **3a** (ORTEP, thermal ellipsoids at the 50% probability level, methyl C atoms with arbitrary radii, without H atoms). Important distances [Å] and angles [°]: Fe-Si 2.289(2), Si-O1 1.610(3), Si-O2 1.636(4), Si-O3 1.730(3), P-O3 1.524(3), Fe-C4 1.754(7), Fe-C5 1.758(6), Fe-C6 1.769(7), Fe-C7 1.761(7); Fe-Si-O1 120.5(1), Fe-Si-O2 117.6(1), O1-Si-O2 104.0(2), O3-Si-Fe 112.1(1), O3-Si-O1 101.8(2), O3-Si-O2 97.5(2).

The deviations of the Si bond angles from the tetrahedral standard exhibit remarkable parallels to those of the donor adducts of silaethenes and silaketimines, which also form long bonds to the donor atoms.[14] As in those cases, the donor stabilization of **3a** presumably leads to a significantly lengthened Si–Fe bond in comparison with a "free" silylene complex. In **3a**, furthermore, the *t*BuO substituents also are expected to contribute to a lengthening of the Fe–Si bond.

Our results are in agreement with theoretical studies: According to ab initio SCF MO calculations, increased acceptor ability is predicted for nucleophilic attack on the Si atom of [(OC)$_5$Cr=SiH(OH)] in comparison with the carbene complex.[1] This explains the greater stability of the adducts **3a** and **3b**, which are presumably formed by nucleophilic attack on the donor-free system **3**.

Received: March 10, 1987;
revised: April 2, 1987 [Z 2130 IE]
German version: *Angew. Chem. 99* (1987) 683

[*] Dr. C. Zybill, Dr. G. Müller
Anorganisch-chemisches Institut der Technischen Universität München
Lichtenbergstrasse 4, D-8046 Garching (FRG)

[**] HMPT = hexamethyl phosphoric triamide.

[1] H. Nakatsuji, J. Ushio, T. Yonezawa, *J. Organomet. Chem. 258* (1983) C1; G. Schmid, E. Welz, *Z. Naturforsch. B 34* (1979) 929; H. Sakurai, Y. Kamiyama, Y. Nakadaira, *Angew. Chem. 90* (1978) 676; *Angew. Chem. Int. Ed. Engl. 17* (1978) 674.
[2] P. P. Gaspar in M. Jones, Jr., R. A. Moss (Eds.): *Reactive Intermediates, Vol. 2*, Wiley, New York 1981, p. 335; R. S. Grev, H. F. Schaefer III, *J.*

Am. Chem. Soc. 108 (1986) 5804; G. Raabe, H. Vančik, R. West, J. Michl, *ibid. 108* (1986) 671.
[3] K. A. Brown-Wenseley, *XIXth Organosilicon Symposium 1985*, Louisiana State University, Baton Rouge, LA, USA.
[4] H. Kang, D. B. Jacobson, S. K. Shin, J. L. Beauchamp, M. T. Bowers, *J. Am. Chem. Soc. 108* (1986) 5668.
[5] P. Jutzi, B. Hampel, K. Stroppel, C. Krüger, K. Angermund, P. Hofmann, *Chem. Ber. 118* (1985) 2789; W. A. Herrmann, *Angew. Chem. 98* (1986) 57; *Angew. Chem. Int. Ed. Engl. 25* (1986) 56.
[6] T. J. Marks, A. R. Newman, *J. Am. Chem. Soc. 95* (1973) 769; D. Uhlig, H. Behrens, E. Lindner, *Z. Anorg. Allg. Chem. 401* (1973) 233; M. D. Brice, F. A. Cotton, *J. Am. Chem. Soc. 95* (1973) 4529.
[7] D. H. Harris, M. F. Lappert, *J. Chem. Soc. Chem. Commun. 1974*, 859; P. J. Davidson, D. H. Harris, M. F. Lappert, *J. Chem. Soc. Dalton Trans. 1976*, 2268.
[8] K. Farmery, M. Kilner, *J. Chem. Soc. A 1970*, 634.
[9] *Experimental procedure:* A solution of **2** (5.0 g, 14.8 mmol) in 80 mL of THF was treated simultaneously with **1** (3.6 g, 14.8 mmol) in 20 mL of THF and Et_3N (1.1 g, 14.8 mmol) in 10 mL of THF. After filtration at low temperature, the crude product was purified by column chromatography on a silica gel column cooled to $-10°C$ (diameter 2.5 cm, height of silica gel 45 cm). Elution was carried out with THF, the quickly eluting, colorless zone being collected. After removal of the volatile products in vacuum, **3b** was obtained as a colorless powder. Yield 0.76 g (12%); m.p. = 153 °C. Addition of 0.5 mL of HMPT to the THF solution of **3b** resulted in crystallization of **3a**. Yield 0.96 g (12%), m.p. = 163 °C.—Compounds **3a,b** could also be synthesized by treatment of a suspension of 1.7 g (5.0 mmol) of **4** · 0.5 dioxane in 50 mL of THF at $-40°C$ with 1.2 g (5.0 mmol) of **1**. The workup was the same as that described above. Yield 12%.
[10] **3a**: ^{1}H-NMR (60 MHz, C_6D_6): $\delta = 1.6$ (s, 18H), 2.2 (d, 18H, $^3J(^{31}P^1H) = 10.4$ Hz); ^{13}C-NMR (36.0 MHz, C_7D_8): $\delta = 31.9$ (s, $(H_3C)_3C$), 36.1 (d, $^2J(^{31}P^{13}C) = 5.9$ Hz, $(H_3C)_2N$), 72.5 (s, $(H_3C)_3C$), 224.0 (s, CO_{eq}), 228.9 (s, CO_{ap}); ^{29}Si-NMR (53.54 MHz, C_6D_6): $\delta = 7.1$ (d, $^2J(^{31}P^{29}Si) = 26.4$ Hz); IR (KBr, cm^{-1}) 2005 (w), 1920 (vs, br), 1883 (vs, br) (νCO), 1000 (s) (νPO), 633 (s) (νPN). Correct elemental analyses (C, H, N, Si, Fe).—**3b**: ^{1}H-NMR (60 MHz, C_6D_6): $\delta = 1.6$ (s, 18H), 1.8 (m, 4H), 3.6 (m, 4H); ^{13}C-NMR (36.0 MHz, C_7D_8): $\delta = 32.0$ (s, $(H_3C)_3C$), 71.9 (s, $H_3C)_3C$), 223.5 (s, CO_{eq}), 229.1 (s, CO_{ap}), 25.1, 68.5 (s, THF); ^{29}Si-NMR (53.54 MHz, C_6D_6): $\delta = -9.4$; MS (70 eV): *m/z* 414 ($M^{\oplus}$, 7.3%). Correct elemental analyses (C, H, N, Si, Fe).
[11] Crystal structure data: Enraf-Nonius CAD4 diffractometer, $Mo_{K\alpha}$ radiation, $\lambda = 0.71069$ Å, graphite monochromator, $T = 23°C$. monoclinic, $P2_1/n$, $a = 10.069(1)$, $b = 16.950(1)$, $c = 15.986(1)$ Å, $\beta = 94.17(1)°$, $V = 2721.1$ Å^3, $\rho_{calcd} = 1.273$ g cm^{-3}, $Z = 4$, $\mu(Mo_{K\alpha}) = 6.9$ cm^{-1}. 4761 unique reflections, 2812 with $I \geq 2.0\sigma(I)$ "observed" ($\vartheta - 2\vartheta$ scan, $\Delta\omega = 0.8 + 0.35 \tan\vartheta$, *hkl*: +11, +20, ±18, $(\sin\vartheta/\lambda)_{max} = 0.593$). Lp, isotropic decay and empirical absorption correction; solution by direct methods (SHELXS-86), $R = 0.054$, $R_w = 0.044$, $w = 1/\sigma^2(F_o)$ for 280 refined parameters (anisotropic, H constant, SHELXS-76); $\Delta\rho_{fin}$(max./min.) = +0.50/−0.37 eÅ^{-3}. Further details of the crystal structure investigation may be obtained from the Fachinformationszentrum Energie, Physik, Mathematik GmbH, D-7514 Eggenstein-Leopoldshafen 2 (FRG), on quoting the depository number CSD-52415, the names of the authors, and the journal citation.
[12] A. R. Rossi, R. Hoffmann, *Inorg. Chem. 14* (1975) 365.
[13] *Sixfold*-coordinated Fe^{II} silyl compounds exhibit typical Fe–Si bond lengths of 2.22–2.45 Å, the shortest bonds being those to halosilyl ligands: M. Knorr, J. Müller, U. Schubert, *Chem. Ber. 120* (1987) 879; L. Vancea, M. J. Bennett, C. E. Jones, R. A. Smith, W. A. Graham, *Inorg. Chem. 16* (1977) 897, and references cited therein.
[14] N. Wiberg, G. Wagner, G. Reber, J. Riede, G. Müller, *Organometallics 6* (1987) 35; N. Wiberg, K. Schurz, G. Reber, G. Müller, *J. Chem. Soc. Chem. Commun. 1986*, 591; G. Müller, *Nachr. Chem. Tech. Lab. 34* (1986) 778.

Proton-Controlled Equilibration between [4$^+$ + 2] and [4 + 2$^+$] Cycloadducts: A Characteristic Example for the Aberrant Diels–Alder Reactions between Two 1,3-Dienes**

By *Karin Beck* and *Siegfried Hünig**

The cleavage of *endo*-dicyclopentadiene to cyclopentadiene at ca. 200 °C is often cited as an example for the thermal reversibility of Diels–Alder reactions.[1] In just this case, however, *Woodward* and *Katz*[2] already showed unequivocally in 1959 that a degenerate Cope rearrangement occurs at 140 °C before the cycloreversion. Since *endo*-type [4 + 2] cycloadducts formed from two 1,3-dienes necessarily contain two double bonds in ideal positions for [3.3] rearrangements, this finding is of fundamental importance: An endo cycloadduct formed from two identical or different (hetero)-1,3-dienes can be formed either by a Diels–Alder reaction (**A**) or by a Diels–Alder reaction followed by a Cope rearrangement (**B**).[3]

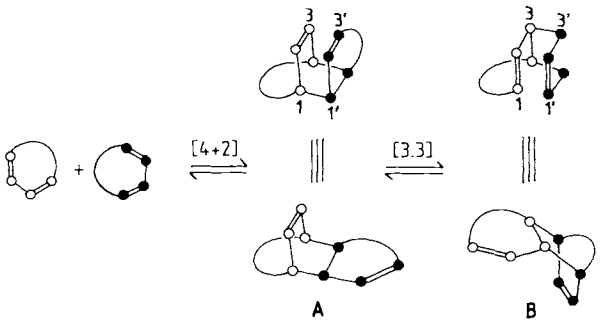

To the best of our knowledge, this obvious conclusion has not been explicitly stated previously. Furthermore, the isomerization of a series of cycloadducts has been described as a Cope rearrangement, even though the intramolecular course of the reaction has been established in only a few cases.[4] We present here a novel example in which the problem discussed above becomes readily apparent owing to the high mobility of the system.

In the presence of traces of acids, cyclic five- and six-membered azines, acting as electron-deficient 2,3-diaza-1,3-dienes, undergo addition to olefins in a Diels–Alder reaction with inverse electron demand to give polycycles containing azo bridges.[5] Cyclopentadiene (**2**) proved to be a particularly reactive dienophile in these [4 + 2] cycloadditions. For example, **2** adds to protonated 4,4-dimethyl-4*H*-pyrazole **1**-H$^{\oplus}$—generated in situ from the trimer $\mathbf{1}_{tr}$—to form the azo compound **3** (Scheme 1).[5c] Under optimized conditions,[6] reaction between $\mathbf{1}_{tr}$ and **2** in the presence of trifluoroacetic acid (TFA) (molar ratio 0.33 : 1.1 : 0.1) in chloroform is complete after 2 h (76% **3**, isolated). The ^{1}H-NMR spectrum of the reaction solution reveals, besides **3**, traces of a second product, which was identified as the dihydropyrazole **4**-H$^{\oplus}$.[7] The species **4**-H$^{\oplus}$ is formed immediately and quantitatively upon treatment of a solution of **3** with three equivalents of TFA. Neutralization of the reaction mixture containing **4**-H$^{\oplus}$ with an aqueous solution of sodium hydroxide at room temperature followed by the conventional workup, however, affords not the expected **4** but rather **3** in 70% yield! The free pyrazole derivative **4** can only be obtained by the slow addition of an acidic solution of **4**-H$^{\oplus}$ to an ice-cold, aqueous, saturated solution of potassium carbonate (Scheme 1).[8]

The rapid rearrangement of **4** to **3** is easily confirmed. Upon heating (70 °C, 3 h) or, appreciably faster, under acid catalysis (0.1 equivalents of TFA, $CDCl_3$, room temperature, 20 min), **4** undergoes a quantitative rearrangement to **3**. Thus, this system represents an unusual case of a proton-controlled equilibrium between **3** and **4** having high mobility. In acidic medium, the higher basicity of **4** is apparently decisive, whereas, as a free base, **3** is thermodynamically more stable.[9]

[*] Prof. Dr. S. Hünig, Dr. K. Beck
Institut für Organische Chemie der Universität
Am Hubland, D-8700 Würzburg (FRG)

[**] This work was supported by the Fonds der Chemischen Industrie and BASF AG, Ludwigshafen.

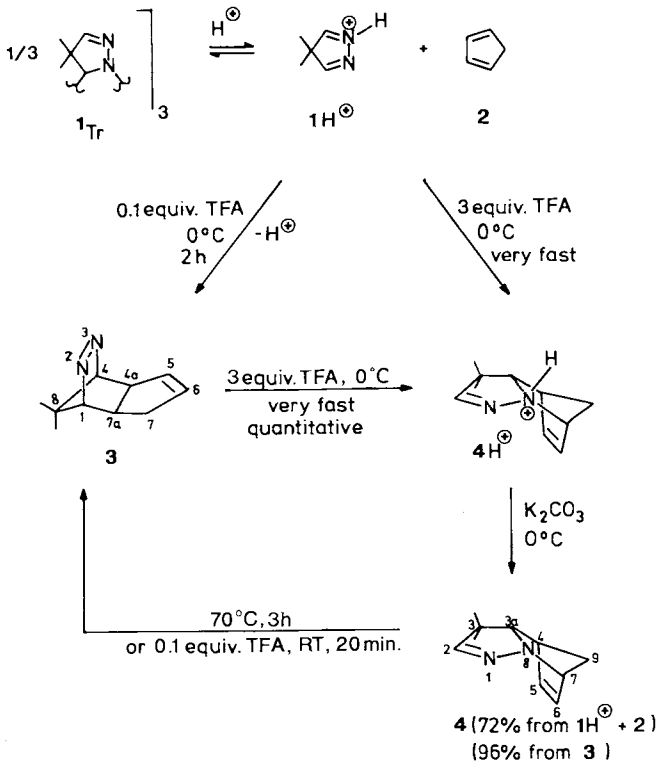

Scheme 1.

In light of these findings, it is not surprising that reaction of $\mathbf{1}_{tr}$ and **2** in the presence of 3 equivalents of TFA in chloroform at 0°C immediately yields **4**-H$^{\oplus}$ as the sole product, from which **4** can be isolated in 72% yield.

Interpretation of these confusing results requires the consideration of the following three hypotheses:

I. The isomers **3**-H$^{\oplus}$ and **4**-H$^{\oplus}$ are formed by competing [4$^+$ + 2] and [4 + 2$^+$] cycloaddition (Diels–Alder reaction with inverse electron demand[10]). The transformation of **3**-H$^{\oplus}$ to **4**-H$^{\oplus}$ takes place via cycloreversion (Scheme 2, pathway A and B).

II. The species **3**-H$^{\oplus}$ and **4**-H$^{\oplus}$ are formed as formulated under I. However, their interconversion involves a [3.3] rearrangement (Scheme 2, pathway C appreciably faster that the back reactions A and B).

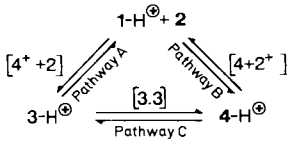

Scheme 2.

III. The formation of both **3**-H$^{\oplus}$ and **4**-H$^{\oplus}$ and their interconversion occur via a common intermediate, **5**-H$^{\oplus}$, which undergoes either further reaction to give the cycloadducts **3**-H$^{\oplus}$ and **4**-H$^{\oplus}$ or reverse cleavage to give the educts **1**-H$^{\oplus}$ and **2** (Scheme 3).

These mechanistic possibilities can be in part differentiated by experiment:

1. A 1:2 mixture of **4** and maleic anhydride (MA) was allowed to react with 0.1 equivalents of TFA in $CDCl_3$ at 0°C. Within 60 min, the ^{1}H-NMR signals of **4** had disappeared and those of **3** had appeared, with only traces of the cycloadduct between **2** and MA being detected. The latter was formed as the main product after 2 weeks.
2. Compounds **3** and **4** were replaced by the derivatives [D$_6$]-**3** and [D$_6$]-**4**, deuterated in the five-membered ring.[11] The rearrangement of [D$_6$]-**4** in $CDCl_3$ in the presence of five equivalents of undeuterated **2** was initiated by the addition of 0.05 equivalents of TFA.[12] After 2 h, [D$_6$]-**4** had undergone rearrangement to [D$_6$]-**3**, without the apparent formation of undeuterated **3**. This occurred only after 1–2 d upon addition of a further 0.25 equivalents of TFA.

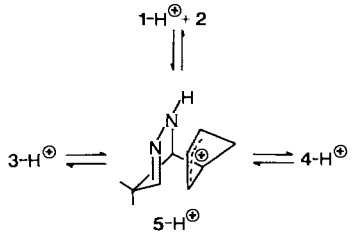

Scheme 3.

According to these experiments, the rapid rearrangement of **4**-H$^{\oplus}$ to **3**-H$^{\oplus}$ occurs *intramolecularly* as a [3.3] rearrangement, with the retro Diels–Alder reaction proceeding much more slowly. The same is true for the thermal rearrangement **4** → **3**, since the reaction [D$_6$]-**4** → [D$_6$]-**3** in the presence of undeuterated **2** (5 equivalents) proceeds without incorporation of the latter. Hypothesis I is thus ruled out. It is not possible, however, to distinguish between hypotheses II and III. Although Diels–Alder reactions and Cope rearrangements normally proceed in a concerted fashion,[13] the reaction can occur via an intermediate under certain conditions.[4a, 14–16] A large difference in the π-MO energies of the reactants can lead to a strong reduction in the HOMO–LUMO interaction, so that there is no longer a compensation for the large negative entropy of the concerted transition states.

This situation could readily apply to the very different dienes **1**-H$^{\oplus}$ and **2**. Thus, in accordance with hypothesis III, an intermediate of the type **5**-H$^{\oplus}$[17] could be involved as the key species connecting the Diels–Alder and Cope products (see Scheme 3).

The rearrangement **3**-H$^{\oplus}$ → **4**-H$^{\oplus}$ is the first example of a Cope rearrangement involving a nonstabilized azo group without loss of nitrogen. This rearrangement can be extended to other systems.[18]

Received: March 2, 1987 [Z 2118 IE]
German version: *Angew. Chem. 99* (1987) 694

[1] Cf. S. N. Ege: *Organic Chemistry*, D. C. Heath, Lexington, MA, USA 1984, p. 531; G. M. Loudon: *Organic Chemistry*, Addison-Wesley, Reading, MA, USA 1984, p. 521; A. Streitwieser Jr., C. H. Heathcock: *Organische Chemie*, Verlag Chemie, Weinheim 1980, p. 764.

[2] R. B. Woodward, T. J. Katz, *Tetrahedron Lett. 1959*, No. 19, p. 5; *Tetrahedron 5* (1959) 70.

[3] The same statement is also valid for the cycloadducts obtained from open-chain 1,3-dienes, insofar as they have the "*endo*" configuration. Cf. [18].

[4] Cf. following reviews: Diels–Alder reactions: J. Sauer, R. Sustmann, *Angew. Chem. 92* (1980) 772; *Angew. Chem. Int. Ed. Engl. 19* (1980) 779; b) catalyzed Cope and Claisen rearrangements: R. P. Lutz, *Chem. Rev. 84* (1984) 205.

[5] a) W. Berning, S. Hünig, *Angew. Chem. 89* (1977) 825; *Angew. Chem. Int. Ed. Engl. 16* (1977) 777; b) W. Berning, S. Hünig, F. Prokschy, *Chem. Ber. 117* (1984) 1455; c) K. Beck, A. Höhn, S. Hünig, F. Prokschy, *ibid.*

117 (1984) 517; d) S. Hünig, F. Prokschy, *ibid. 117* (1984) 534; e) K. Beck, S. Hünig, *ibid. 120* (1987) 477.
[6] See K. Beck, *Dissertation*, Universität Würzburg 1986.
[7] Species **4**-H$^{\oplus}$ should be described as *endo*-**4**-H$^{\oplus}$, which is completely transformed within 28 d to *exo*-**4**-H$^{\oplus}$. In contrast to *endo*-**4**, *exo*-**4** does not rearrange to **3** under the same conditions.
[8] **3**: ^{1}H-NMR (400 MHz, $CDCl_3$) cf. [4c]. ^{13}C-NMR (100 MHz, $CDCl_3$): $\delta = 18.28$, 19.46 (each q, CH_3), 31.29 (t, C-7), 38.24 (d, C-7a), 49.92 (d, C-4a), 51.55 (s, C-8), 85.92, 87.13 (each d, C-1,4), 127.8, 132.2 (each d, C-5,6).—**4**: ^{1}H-NMR (400 MHz, $CDCl_3$): $\delta = 0.85$ (s, 3H, CH_3), 0.99 (s, 3H, CH_3), 1.41, 1.60 (each d, 9-H_2, $J_{9,9'} = 8.5$ Hz), 2.80 (bs, 1H, 4-H), 3.39 (d, 1H, 3a-H), $J_{3a,4} = 1.5$ Hz), 4.34 (bs, 1H, 7-H), 5.69 (m, 1H, 6-H), 6.02 (m, 1H, 5-H), 6.29 (s, 1H, 2-H). ^{13}C-NMR (100 MHz, $CDCl_3$): $\delta = 20.37$ (q, CH_3), 29.12 (q, CH_3), 44.88 (s, C-3), 45.76 (d, C-4), 49.92 (t, C-9), 66.44 (d, C-3a), 75.72 (d, C-7), 131.5, 133.8 (each d, C-5,6), 155.9 (d, C-2).
[9] Differential thermal analysis gave $\Delta H = 4.5$ kcal/mol (72.1°C) for **3**→**4** (Dr. *H. D. Beckhaus*, Universität Freiburg). Enthalpies of formation determined from force-field calculations (SCRIPT: N. C. Cohen, *Tetrahedron 37* (1981) 1711): **3**, 58.1 kcal/mol; **4**, 62.1 kcal/mol (Dr. *H. Burghard*, Pharmasynthese, Hoechst AG). We thank the authors for these data.
[10] Reviews on cycloaddition with iminium salts: a) M. Lora-Tamayo, R. Madronero in J. Hamer (Ed.): *1,4-Cycloaddition Reactions*, Academic Press, New York 1967, p. 129f; b) S. M. Weinreb, J. I. Levin, *Heterocycles 12* (1979) 949; c) S. M. Weinreb, R. R. Staib, *Tetrahedron 38* (1982) 3087. See also: d) B. Schmied, *Dissertation*, Universität Regensburg 1980; e) S. D. Larsen, P. A. Grieco, *J. Am. Chem. Soc. 107* (1985) 1768.
[11] The deuterated cycloadducts [D_6]-**3** and [D_6]-**4** were synthesized from **1** and [D_6]-**2** according to the same method used for the undeuterated products.
[12] The rearrangement was followed by observing the NMR signals for 1-H and 4-H (**3**) and 3a-H (**4**).
[13] See the detailed discussion in M. S. Dewar, S. Olivella, J. J. P. Stewart, *J. Am. Chem. Soc. 108* (1986) 5771.
[14] F.-G. Klärner, B. M. J. Dogan, O. Ermer, W. von E. Doering, M. P. Cohen, *Angew. Chem. 98* (1986) 109; *Angew. Chem. Int. Ed. Engl. 25* (1986) 108.
[15] R. Huisgen in A. Padwa (Ed.): *1,3-Dipolar Cycloaddition Chemistry*, Wiley-Interscience, New York 1984, p. 48.
[16] R. Sustmann, *Pure Appl. Chem. 40* (1974) 569. See also K. N. Houk in A. P. Marchand, R. E. Lehr (Eds.): *Pericyclic Reactions*, Academic Press, New York 1977, p. 181f.
[17] The species **5**-H$^{\oplus}$ is an intramolecular charge-transfer complex. After transfer of an electron, it could also be present as a diradical monocation.
[18] K. Beck, H. Burghard, G. Fischer, S. Hünig, P. Reinold, *Angew. Chem. 99* (1987) 695; *Angew. Chem. Int. Ed. Engl. 26* (1987) 672.

Azo Cope Rearrangements of Nonstabilized Azo Compounds**

By *Karin Beck, Harald Burghard, Gabriele Fischer, Siegfried Hünig,** and *Petra Reinold*

The numerous hetero-1,5-dienes for which Cope rearrangements are known include 3,4-diaza- and 2,5-diaza derivatives. In the first case, the N–N bond is broken during the rearrangement; in the second case, the azomethine function is merely shifted.[1] To the best of our knowledge, only one 2,3-diaza Cope rearrangement is known, namely, **1**→**2**. This rearrangement, which is expected to form an azo compound, leads to loss of nitrogen and the formation of 1-butene **3**.[2] Recently, the system **4**, which is stabilized by an aryl group, was shown to undergo an azo Cope rearrangement, resulting in the formation of the expected hydrazone **5**.[3]

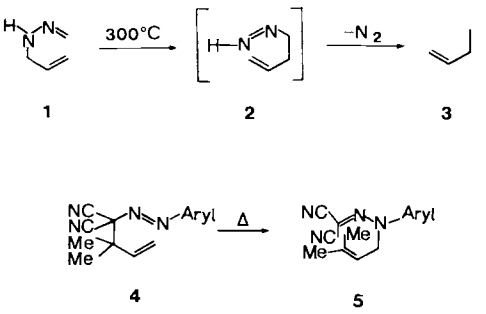

We now report the first azo Cope rearrangement of the type **4**⇆**5** that, despite the absence of an aryl-group-stabilized azo group, proceeds without loss of nitrogen and, depending on the pattern of substitution, affords either the azo or the hydrazone isomer (partially reversible). In this reaction, the known charge acceleration of the rearrangement[1] is exploited by protonation of the N atom. The starting point of this reaction sequence is the cycloaddition of the isopyrazole **6a** to the cyclopentadiene **7d**, which, depending on the acid concentration, leads to a mobile equilibrium between the azo compound **8ad** and the hydrazone **9ad** (as **9ad**-H$^{\oplus}$). It was established that the transformation **8ad**-H$^{\oplus}$→**9ad**-H$^{\oplus}$ proceeds via an intramolecular [3.3] Cope-type rearrangement and not via the appreciably slower retro Diels–Alder reaction.[4] A series of further cycloadducts **8** and **9** that were also capable of undergoing isomerization were correspondingly obtained according to Scheme 1.[5] The structural dependence of the rearrangement was determined for five examples (Scheme 2).[6]

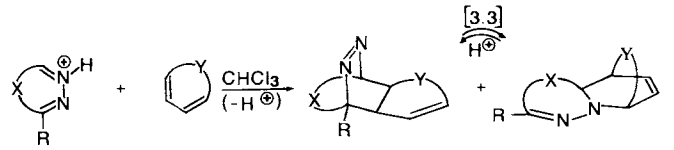

6	R	X
a	H	$C(CH_3)_2$
b	CH_3	$C(CH_3)_2$
c	H	$(CH_2)_2$

7	Y
d	CH_2
e	$(CH_2)_2$

8	9
ad	ad
bd	bd
ae	ae
cd	cd

Scheme 1.

As shown in Scheme 2, the reversibility of the rearrangement **8ad**⇆**9ad** is completely maintained upon introduction of a methyl group (**8bd**⇆**9bd**), although the reaction rate is markedly decreased. The cycloadducts obtained from isopyrazole **6a** and 1,3-cyclohexadiene **7e** or isoprene **7f**, namely, **8ae** or **8af**, respectively, undergo only irreversible isomerization to the dihydropyrazoles **9ae** and **9af**. In the case of the cycloadducts obtained from dihydropyridazine **6c** and cyclopentadiene **7d**, only rearrangement of **9cd** to the azo compound **8cd** occurs!

Calculations performed using the SCRIPT force-field program[7] revealed that, for the systems U1 and U4, the azo compounds are 3.0 kcal/mol and 6.8 kcal/mol, respectively, more stable, whereas, for U2 and U3, the hydrazones are 2.4 kcal/mol and 21.4 kcal/mol, respectively, lower in energy (Scheme 2). Indeed, treatment with 0.1

[*] Prof. Dr. S. Hünig, Dr. K. Beck, Dipl.-Chem. P. Reinold
Institut für Organische Chemie der Universität
Am Hubland, D-8700 Würzburg (FRG)
Dr. H. Burghard [+], Dipl.-Ing. G. Fischer [+]
Hoechst AG, Pharmasynthese
Postfach 800320, D-6230 Frankfurt am Main 80 (FRG)
[+] Force-field calculations
[**] This work was supported by the Fonds der Chemischen Industrie and BASF AG, Ludwigshafen.

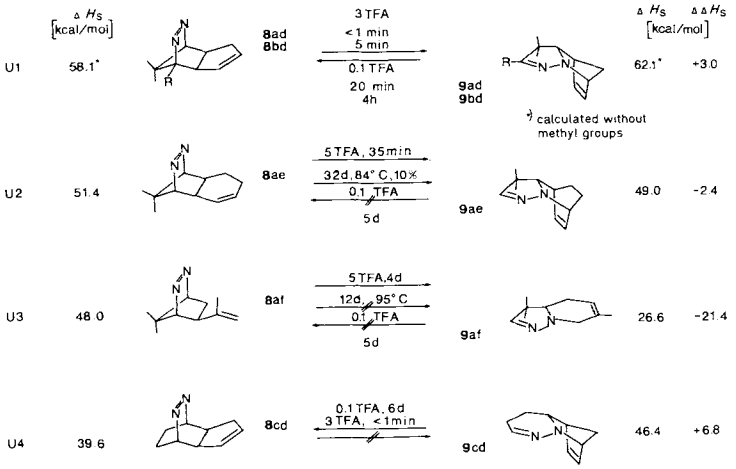

Scheme 2. Acid-catalyzed diaza Cope rearrangements in $CDCl_3$, at room temperature if not stated otherwise (the hydrazones **9** are protonated if an excess of acid is present).

equivalent of TFA results in the smooth isomerization of **9ad**, **9bd**, and **9cd** into the isomeric azo compounds; however, despite the larger difference in energy, **9cd** rearranges significantly more slowly. The influence of structure on the energy barrier for the isomerization is so large in the case of U2 and U3 that the calculated differences in energy can no longer be confirmed. The rearrangements carried out in the presence of a large excess of acid proceed in the appropriate direction but are not conclusive owing to the appreciably stronger basicity of the hydrazone form. With 0.1 equivalent of TFA, the conversion of **8ae** to **9ae** asymptotically approaches the limiting value of 10% after 32 d at 84°C, because **9ae**-$H^{\oplus}$ is such a poor protonating agent. An isomerization of **8af** to **9af** with 0.1 equivalent of TFA cannot be detected even after 12 d at 95°C. The reaction of **6a** with isoprene **7f** establishes that the regioselective rearrangement driven by an excess of TFA proceeds intramolecularly. In three competing reactions (monitored by GC), **8af**, **9af**, and the isomer **9'af** are simultaneously formed. Therefore, **9af**, which is formed exclusively according to U3, is not formed by cycloreversion, since **9'af** is absent. Accordingly, all isomerizations presumably involve a one- or two-step, intramolecular [3.3] rearrangement.[4]

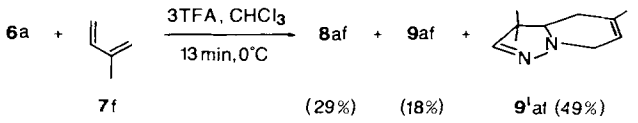

Received: March 2, 1987 [Z 2119 IE]
German version: *Angew. Chem. 99* (1987) 695

[1] Review: R. P. Lutz, *Chem. Rev. 84* (1984) 206; H. Heimgartner, H.-J. Hansen, H. Schmid in H. Böhme, H. Viehe (Eds.): *Iminium Salts in Organic Chemistry, Part II*, Wiley, New York 1979, p. 655.

[2] R. V. Stevens, E. E. McEntire, W. E. Barnett, E. Wenkert, *J. Chem. Soc. Chem. Commun. 1973*, 662.

[3] T. Mitsuhashi, *J. Am. Chem. Soc. 108* (1986) 2400.

[4] K. Beck, S. Hünig, *Angew. Chem. 99* (1987) 694; *Angew. Chem. Int. Ed. Engl. 26* (1987) 670.

[5] Cf. K. Beck, *Dissertation* and P. Reinold, *Diplomarbeit*, Universität Würzburg 1986.

[6] All new compounds were characterized by elemental analyses, UV spectra (hexane), ^{1}H- and ^{13}C-NMR spectra (400 and 90 MHz, respectively, $CDCl_3$), and IR and mass spectra. Typical signals: UV: **8**: $\lambda_{max} \approx 380$ nm, $\lg\varepsilon \approx 2.1$; **9**: $\lambda_{max} \approx 245$ nm, $\lg\varepsilon \approx 3.7$. ^{1}H-NMR: **8**: $\delta = 4.8$–5.2 (bridgehead protons); **9**: $\delta = 6.6$–6.8 (azomethine protons).

[7] SCRIPT: N. C. Cohen, *Tetrahedron 37* (1981) 1711. For the scope of application of force-field calculations as well as the effect of methyl groups, see E. Osawa, H. Musso, *Angew. Chem. 95* (1983) 1; *Angew. Chem. Int. Ed. Engl. 22* (1983) 1.

Redox Disproportionation of Ge^{II} Compounds: Synthesis and Structure of $[(Me_3Si)C(PMe_2)_2]_2GeCl_2$ and $[\mu\text{-}\{(Me_3Si)C(PMe_2)_2\}]_2Ge_2$**

By *Hans H. Karsch,* Brigitte Deubelly, Jürgen Riede,* and *Gerhard Müller*

Low-valent, monomeric germanium compounds are known; to the best of our knowledge, however, there are no reports concerning spontaneous redox reactions of germanium(II) compounds under normal conditions. We have already shown that the stabilization of phosphane complexes of main-group elements can be extended to low-valent elements (e.g., Ge^{II}, Sn^{II}, Pb^{II})[1] if *anionic* phosphane ligands, such as phosphinomethanides **1**, are employed.

$[R_2P\text{–}CXY]^{\ominus}$ **1**, X, Y = H, PMe_2, $SiMe_3$; R = alkyl, aryl

We show here, by way of germanium as example, that such ligands can also be used to initiate redox reactions of low-valent element-phosphane complexes, leading to the formation of novel products having element-element bonds.

$SnCl_2$ smoothly reacts with $Li[(Me_2P)_2CX]$ (**1a**, X = PMe_2; **1b**, X = $SiMe_3$) to give Sn^{II}-phosphane complexes having pseudo trigonal-bipyramidal configurations.[2] An analogous reaction can also be carried out with $GeCl_2 \cdot$dioxane [Eq. (a)]; the germanium complexes **2**, corresponding to the tin complexes, are formed. The colorless crystals[3] of **2a**,**b** are stable indefinitely at room temperature. However, when the phosphinomethanide **1b** is used in less than the required stoichiometric amount, a redox process occurs, which presumably proceeds via the intermediate $[(Me_3Si)C(PMe_2)_2]GeCl$. For optimized stoichiometry, the reaction can be formulated as Equation (b).[4]

$$GeCl_2 \cdot \text{dioxane} + 2\,Li[(PMe_2)_2CX] \xrightarrow{-2\,LiCl} Ge[(PMe_2)_2CX]_2 \quad \text{(a)}$$
1a, b **2a, b**

$$3\,Ge^{II}Cl_2 \cdot \text{dioxane} + 4\,\mathbf{1b} \xrightarrow{-4\,LiCl} \begin{matrix}[(Me_3Si)C(PMe_2)_2]_2Ge^{IV}Cl_2\ \mathbf{3b} \\ + \\ [(Me_3Si)C(PMe_2)_2]_2Ge_2^{I}\ \mathbf{4b}\end{matrix} \quad \text{(b)}$$

The *oxidation* product **3b** can also be synthesized from $GeCl_4$ and **1b** [Eq. (c)], which confirms its formulation as a

$$GeCl_4 + 2\,\mathbf{1b} \xrightarrow{-2\,LiCl} \mathbf{3b} \quad \text{(c)}$$

Ge^{IV} complex.[5] Complex **3b** is the first example of a *trans*-octahedral structure (Fig. 1)[6] having 4 P and 2 Cl donors at a germanium center.[7]

[*] Priv.-Doz. Dr. H. H. Karsch, Dipl.-Chem. B. Deubelly, J. Riede, Dr. G. Müller
Anorganisch-chemisches Institut der Technischen Universität München
Lichtenbergstrasse 4, D-8046 Garching (FRG)

[**] Complexes with Phosphinomethane and -methanide Ligands, Part 12.—Part 11: H. H. Karsch, A. Appelt, B. Deubelly, G. Müller, *J. Chem. Soc. Chem. Commun.*, in press.

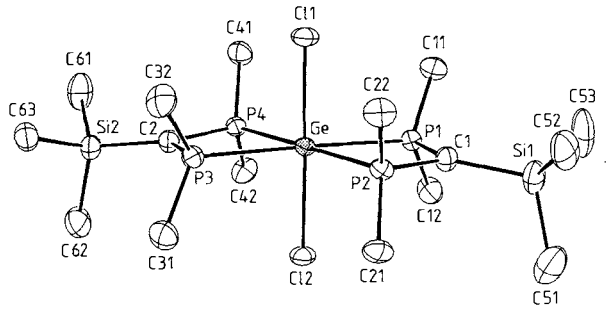

Fig. 1. Molecular structure of **3b** (ORTEP, thermal ellipsoids at the 50% probability level, without H atoms). Important bond lengths [Å] and angles [°]: Ge-Cl1 2.386(1), Ge-Cl2 2.434(1), Ge-P1 2.410(1), Ge-P2 2.412(1), Ge-P3 2.415(1), Ge-P4 2.411(1), C1-P1 1.727(5), C1-P2 1.725(4), C1-Si1 1.838(5), C2-P3 1.722(4), C2-P4 1.734(4), C2-Si2 1.829(4); Cl1-Ge-Cl2 178.7(1), P1-Ge-P2 69.9(1), P3-Ge-P4 69.8(1), P1-Ge-P4 109.5(1), P2-Ge-P3 110.7(1).

Searching for the *reduction* product, we investigated more closely the second fraction of crystals, likewise yellow, obtained according to Equation (b). The shift of their ^{31}P-NMR resonances to lower frequencies compared with those of **3a,b** indicates the presence of a reduced species.[5] Under reductive conditions, **4b** is obtained nearly quantitatively in pure form according to Equation (d)

$$GeCl_2\cdot\text{dioxane} + \mathbf{1b} \xrightarrow[THF]{Mg\ (excess)} \mathbf{4b} \qquad (d)$$

(THF = tetrahydrofuran). The X-ray structure analysis[6] of crystals obtained from pentane reveals a doubly phosphinomethanide-bridged $[Ge^{I}\text{-}Ge^{I}]^{2\oplus}$ structural unit (Fig. 2). The Ge atoms are each surrounded in a pseudo-tetrahedral fashion by one electron pair, two P atoms, and a Ge atom; this results in a nonplanar eight-membered ring perimeter having approximate $C_2(2)$ symmetry. The Ge-P distances, which are significantly shorter than, for example, those in $(Ph_3P)GeCl_2$ (2.51(1) Å[8]) and the nearly planar environment of the carbanionoid C atoms of the ligands are in agreement with the findings for **3b** (Fig. 1). The central Ge-Ge bond (2.540(1) Å), is ca. 0.1 Å *longer* than those in polygermanes.[9] This also means that the "bisgermanediyl" **4b** clearly differs from the digermenes having formal Ge-Ge double bonds, which are obtained by dimerization of germanediyls.[10]

Complex **4b** thus represents a new class of low-valent main-group-element compounds with element-element bonds. Its high stability (dec. at $T > 190$ °C) and formation tendency are supported by the novel redox reaction of Equation (b) and are undoubtedly based in part on the bridging function of the diphosphinomethanide ligands, which has not yet been observed for main-group elements. The phosphane donors should effect activation of the lone pairs at the germanium centers, which, together with the reactive Ge-Ge bond, should lead to interesting reactivity.

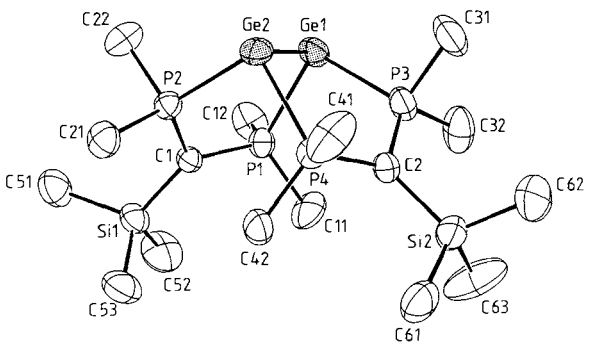

Fig. 2. Molecular structure of **4b**. Important bond lengths [Å] and angles [°]: Ge1-Ge2 2.540(1), Ge1-P1 2.420(1), Ge1-P3 2.370(1), Ge2-P2 2.368(1), Ge2-P4 2.420(1), C1-P1 1.734(3), C1-P2 1.741(3), C1-Si1 1.840(4), C2-P3 1.740(4), C2-P4 1.731(4), C2-Si2 1.845(4); Ge2-Ge1-P1 95.1(1), Ge2-Ge1-P3 86.7(1), P1-Ge1-P3 96.9(1), Ge1-Ge2-P2 87.6(1), Ge1-Ge2-P4 95.0(1), P2-Ge2-P4 96.1(1).

Received: March 10, 1987 [Z 2131 IE]
German version: *Angew. Chem. 99* (1987) 703

[1] H. H. Karsch, A. Appelt, G. Hanika, *J. Organomet. Chem. 312* (1986) C 1, and references cited therein.
[2] H. H. Karsch, A. Appelt, G. Müller, *Organometallics 5* (1986) 1664.
[3] Formation, properties, structure, and solution dynamics of **2a,b**: H. H. Karsch, B. Deubelly, G. Hanika, J. Riede, G. Müller, unpublished results.
[4] *Experimental procedure:* Reaction (b) $GeCl_2\cdot$dioxane (926 mg, 4 mmol) and $Li[(Me_2P)_2C(SiMe_3)]$ (1285 mg, 6 mmol) were suspended in 40 mL of ether at −78 °C. The stirred solution was allowed to warm to room temperature. The solvent was removed under vacuum and the yellow solution was filtered. Slow cooling afforded several yellow crystalline fractions. Complex **3b** crystallized first, followed, after further cooling and (if necessary) concentration of the mother liquor, by **4b**. (Yields are strongly dependent on the crystallization conditions; pure products were obtained quantitatively from the reactions (c) and (d), which were carried out analogously).
[5] $^{31}P\{^{1}H\}$-NMR (C_6D_6, 25 °C): **3b**: $\delta = 76.4$ (s); **4b**: $\delta = 18.0$ (s).
[6] Crystal structure determinations: **3b**: Syntex $P2_1$ diffractometer, $Mo_{K\alpha}$ radiation, $\lambda = 0.71069$ Å, graphite monochromator, $T = -40$ °C; monoclinic, $P2_1/c$, $a = 10.578(1)$, $b = 11.723(1)$, $c = 23.721(3)$ Å, $\beta = 94.97(1)$°, $V = 2930.5$ Å^3, $\rho_{calcd} = 1.265$ g cm^{-3}, $Z = 4$, $\mu(Mo_{K\alpha}) = 15.1$ cm^{-1}. 4542 unique reflections, 3732 with $I \geq 2.0\,\sigma(I)$ "observed" (ω scan, $\Delta\omega = 0.9$°, $+h$, $+k$, $\pm l$, $(\sin\vartheta/\lambda)_{max} = 0.572$). Lp and empirical absorption correction, solution by Patterson methods, $R = 0.040$, $R_w = 0.046$, $w = 1/\sigma^2(F_0)$ for 268 refined parameters (anisotropic, CH_3 as rigid groups, SHELX-76), $\Delta\rho_{fin} = 0.42/-0.48$ eÅ^{-3}.—**4b**: Enraf-Nonius CAD4, $T = 23$ °C; monoclinic, $P2_1/c$, $a = 16.531(2)$, $b = 11.352(1)$, $c = 16.838(1)$ Å, $\beta = 117.41(1)$°, $V = 2805.1$ Å^3, $\rho_{calcd} = 1.325$ g cm^{-3}, $Z = 4$, $\mu(Mo_{K\alpha}) = 24.2$ cm^{-1}. 5473 unique reflections, 3567 "observed" ($\vartheta - 2\vartheta$ scan, $\Delta\omega = 0.8 + 0.35\tan\vartheta$, $(\sin\vartheta/\lambda)_{max} = 0.617$). Direct methods, $R = 0.033$, $R_w = 0.028$, $w = 1/\sigma^2(F_0)$ for 259 refined parameters, $\Delta\rho_{fin} = 0.33/-0.39$ eÅ^{-3}. Further details of the crystal structure investigations may be obtained from the Fachinformationszentrum Energie, Physik, Mathematik GmbH, D-7514 Eggenstein-Leopoldshafen 2 (FRG), on quoting the depository number CSD-52418, the names of the authors, and the journal citation.
[7] Vibrational-spectroscopic investigations revealed a *trans*-octahedral structure for $(Me_3P)_2GeCl_4$: I. R. Beattie, G. A. Ozin, *J. Chem. Soc. A 1970*, 370.
[8] N. G. Bokii, Yu. T. Struchkov, S. P. Kolesnikov, I. S. Rogozhin, O. M. Nefedov, *Izv. Akad. Nauk SSSR Ser. Khim. 1975*, 812.
[9] M. Dräger, L. Ross, *Z. Anorg. Allg. Chem. 476* (1981) 95, and references cited therein.
[10] a) S. Masamune, Y. Hanzawa, *J. Am. Chem. Soc. 104* (1982) 6136; b) D. E. Goldberg, P. B. Hitchcock, M. F. Lappert, K. M. Thomas, A. J. Thorne, T. Fjeldberg, A. Haaland, B. E. R. Schilling, *J. Chem. Soc. Dalton Trans. 1986*, 2387.

[{μ-[(Me$_3$Si)C(PMe$_2$)$_2$]}$_2$Ge$_2$]$_2$GeCl$_2$, a Germanediyl-Donor Germanediyl-Acceptor Complex Containing a Mixed-Valent Ge$_5$ Chain**

By *Hans H. Karsch,* Brigitte Deubelly, Jürgen Riede,* and *Gerhard Müller**

The carbene-like compounds of divalent elements of the fourth main group having electron sextets can act as either

[*] Priv.-Doz. Dr. H. H. Karsch, Dipl.-Chem. B. Deubelly, J. Riede, Dr. G. Müller
Anorganisch-chemisches Institut der Technischen Universität München
Lichtenbergstrasse 4, D-8046 Garching (FRG)

[**] Complexes with Phosphinomethane and -methanide Ligands, Part 13.—Part 12: [4].

Lewis acids or Lewis bases. As Lewis acids, they react with bases to form adducts ("ylides") which, as strong donors for transition metals, lead to the formation of interesting complexes.[1] However, the reactivity of the lone pair toward main-group acceptors appears to be low.[2] Structurally confirmed examples are limited to only a few donor-stabilized stannanediyl complexes.[3] Compounds of elements of the fourth main group acting as mutual donor and acceptor and thus being capable of forming complexes with homonuclear element-element bonds were unknown until now.

According to X-ray structure analyses, the "germanediyls" **1** and "bisgermanediyls" **2** (**a**, $X=PMe_2$; **b**, $X=SiMe_3$),[4,5] recently prepared by us, contain stereochemically active lone pairs. We have now attempted to

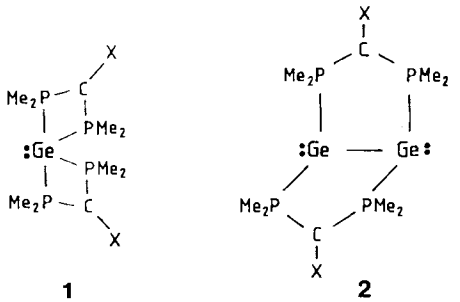

1 **2**

exploit the strongly increased donor ability of **1** and **2**, caused by the (anionic) phosphane ligands, to synthesize homonuclear complexes with $GeCl_2$ as acceptor. The complexes **1b** and $GeCl_2$·dioxane **3** do not form such donor–acceptor complexes. In contrast, **2b** reacts with **3** to give the 2:1 adduct **4b** [Eq. (a)]. This adduct can also be obtained by means of an "in situ" reaction [Eq. (b)] (cf. Ref. [4]).

$$2\,\mathbf{2b} + \underset{\mathbf{3}}{GeCl_2\cdot\text{dioxane}} \longrightarrow \underset{\mathbf{4b}}{[\{\mu\text{-}[(Me_3Si)C(PMe_2)_2]\}_2Ge_2]_2GeCl_2} \quad (a)$$

$$7\,\mathbf{3} + 8\,Li[(Me_3Si)C(PMe_2)_2] \xrightarrow[-8\,LiCl]{} \mathbf{4b} + 2[(Me_3Si)C(PMe_2)_2]_2GeCl_2 \quad (b)$$

Complex **4b**, obtained as pale yellow crystals from ether/pentane, is apparently the first homonuclear adduct of a divalent donor/acceptor pair of elements of the fourth main group. In solution, however, **4b** undergoes nearly complete dissociation: the $\delta(^{31}P)$ value of **4b** in solution at room temperature is identical with that of **2b**.[4] At $-100\,^{\circ}C$, on the other hand, the signals of an incompletely resolved ABCD spin system (four nonequivalent phosphorus atoms) are observed, as is expected for undissociated **4b**.

The X-ray structure analysis[6] (Fig. 1) confirms the presence of a mixed-valent donor–acceptor complex containing two equatorial bisgermanediyl ligands **2b** bound to a nearly linear $GeCl_2$. This results in a pseudo trigonal-bipyramidal environment for the central Ge3 atom (with the lone pair in the third equatorial position). To the best of our knowledge, the coordinative bonds Ge3-Ge2 (2.554(1) Å) and Ge3-Ge4 (2.562(1) Å) are the longest Ge–Ge bonds reported yet[7] and indicate weak coordination of the bisgermanediyl moieties; the Ge–Ge bonds of the bisgermanediyl ligands (2.485(1) and 2.492(1) Å), on the other hand, are noticeably shorter (by ca. 0.07 Å). Interestingly, they are also significantly shorter than those in uncomplexed **2b** (2.540(1) Å).[4] The P–Ge–P angles at Ge2/Ge4 (101.5(1)/99.7(1)°), whose electron pairs function as donors to Ge3, are significantly larger than those at Ge1/Ge5 (95.3(1)/96.3(1)°). The latter are in good agreement with those in **2b**.[4] The bond shortening and angle expansion thus appear to be analogous to those observed upon complexation of phosphanes R_3P. Equally revealing is a comparison of **4b** with the coordination polymer $GeCl_2$·dioxane **3**, which contains linear $C_4H_8O_2$–Ge–$C_4H_8O_2$ chains.[8] The angle Cl-Ge-Cl in **3** is about as small as the angle Ge2-Ge3-Ge4 in **4b**. In agreement with expectations, therefore, the more electronegative donor atoms (**3**, O; **4b**, Cl) in both complexes occupy the axial positions of the pseudo trigonal bipyramid and the Ge–Cl bonds in **3** are correspondingly shorter than in **4b**.

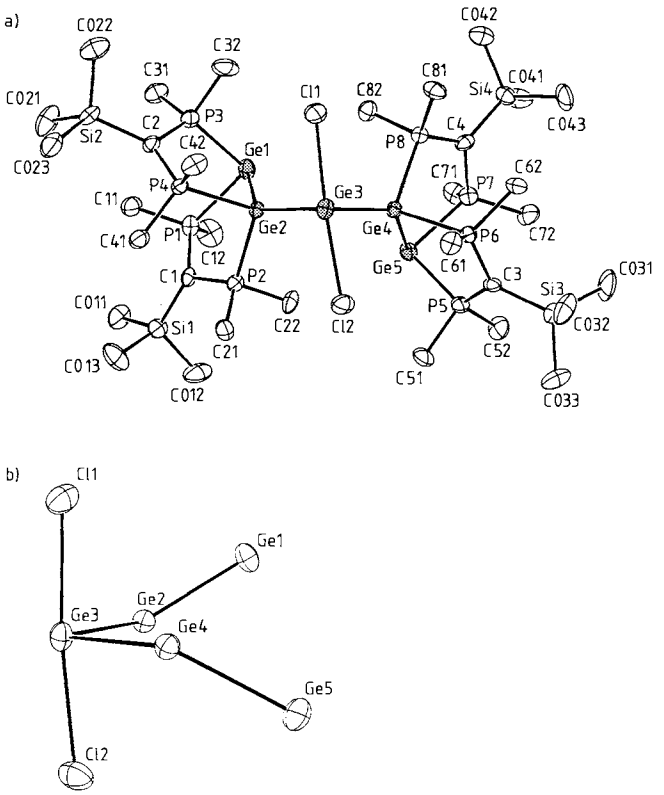

Fig. 1. a) Crystal structure of **4b**. b) $GeCl_2(Ge_2)_2$ partial structure in **4b** (ORTEP, thermal ellipsoids at the 50% probability level; H atoms omitted). Important bond lengths [Å] and angles [°]: Ge3-Cl1 2.596(2), Ge3-Cl2 2.644(2), Ge3-Ge2 2.554(1), Ge3-Ge4 2.562(1), Ge1-Ge2 2.492(1), Ge4-Ge5 2.485(1), Ge1-P1 2.433(2), Ge1-P3 2.378(2), Ge5-P5 2.389(2), Ge5-P7 2.435(2), Ge2-P2 2.351(2), Ge2-P4 2.391(2), Ge4-P6 2.401(2), Ge4-P8 2.367(2); Cl1-Ge3-Cl2 172.3(1), Ge2-Ge3-Ge4 94.8(1), Ge1-Ge2-Ge3 133.7(1), Ge3-Ge4-Ge5 136.3(1).

Overall, the structure of **4b** is characterized by a bent Ge_5 chain; taking into consideration the (formal) oxidation states, it may thus be viewed as a mixed-valent compound (Ge^{I}-Ge^{I}-Ge^{II}-Ge^{I}-Ge^{I}). A "chain lengthening" to form a coordination polymer with Ge–Ge chains appears favorable, since the terminal Ge atoms of the bisgermanediyl ligands should in principle also be able to act as donor atoms to $GeCl_2$.

Received: March 10, 1987 [Z 2132 IE]
German version: *Angew. Chem.* 99 (1987) 705

[1] W. Petz, *Chem. Rev. 86* (1986) 1019.
[2] J. J. Zuckerman, *XIth Int. Conf. Organomet. Chem. 1983* (Callaway Gardens, GA, USA), Abstr. p. 167.
[3] a) M. Veith, W. Frank, *Angew. Chem. 97* (1985) 213; *Angew. Chem. Int. Ed. Engl. 24* (1985) 223; b) S. J. Archer, K. R. Koch, S. Schmidt, *Inorg. Chim. Acta 126* (1987) 209, and references cited therein.
[4] H. H. Karsch, B. Deubelly, J. Riede, G. Müller, *Angew. Chem. 99* (1987) 703; *Angew. Chem. Int. Ed. Engl. 26* (1987) 673.
[5] H. H. Karsch, B. Deubelly, G. Hanika, J. Riede, G. Müller, unpublished results.
[6] Crystal structure determination: Syntex $P2_1$ diffractometer, $Mo_{K\alpha}$ radiation, $\lambda = 0.71069$ Å, graphite monochromator, $T = -40°C$; monoclinic, $P2_1/n$, $a = 21.886(3)$, $b = 11.977(1)$, $c = 22.339(3)$ Å, $\beta = 96.47(1)°$, $V = 5818.4$ Å^3, $\rho_{calcd} = 1.442$ g cm^{-3}, $Z = 4$, $\mu(Mo_{K\alpha}) = 29.3$ cm^{-1}. 8058 unique reflections, 6222 with $I \geq 2.0\sigma(I)$ "observed" (ω-scan, $\Delta\omega = 0.8°$, $+h, +k, \pm l$, $(\sin\vartheta/\lambda)_{max} = 0.549$). Solution by automated Patterson methods (SHELXS-86), $R = 0.044$, $R_w = 0.045$, $w = 1/\sigma^2(F_0)$ for 460 refined parameters (anisotropic, H constant, GFMLX). $\Delta\rho_{fin} = 0.60$ e Å^{-3}. Further details of the crystal structure investigation may be obtained from the Fachinformationszentrum Energie, Physik, Mathematik GmbH, D-7514 Eggenstein-Leopoldshafen 2 (FRG), on quoting the depository number CSD-52416, the names of the authors, and the journal citation.
[7] Cf., e.g., d(Ge-Ge) = 2.541 Å in $[\{C_6H_3(CH_3)_2\}_2Ge]_3$: S. Masamune, Y. Hanzawa, *J. Am. Chem. Soc. 104* (1982) 6136.
[8] V. I. Kulishov, N. G. Bokii, Yu. T. Struchkov, O. M. Nefedov, S. P. Kolesnikov, B. L. Perl'mutter, *Zh. Strukt. Khim. 11* (1970) 71.

The Morphology and Microstructure of Colloidal Silver and Gold**

By *D. G. Duff, A. C. Curtis, Peter P. Edwards,* D. A. Jefferson, Brian F. G. Johnson, A. I. Kirkland,* and *D. E. Logan*

The brilliant colors characteristic of colloidal gold and silver have been known for over a millennium.[1-3] Although the technique of electron microscopy has been applied previously to study the nucleation, growth, and topology of colloidal particles,[3,4] it is only recently that the resolution of the microscopes has been improved to such an extent[5,6] as to yield reliable images which may reflect the atomic microstructure of these divided metals.[2-7] Here we demonstrate how direct structural imaging by high-resolution electron microscopy (HREM), coupled with appropriate *chemical* routes to ultrafine particles, can indeed yield important information on the morphology and atomic structure of individual colloidal metal particles. Thus, the atomic imaging of a 35-Å-diameter silver particle by HREM enables a direct observation of the packing of individual silver atoms around a dodecahedral core. This observation is supported by computer-simulated images for an entire particle; the silver particle exhibits a perfect pentagonal symmetry in its atomic arrangement around the central C_5 axis.

All HREM examinations were carried out in a modified JEOL-200CX operating at 200 kV, with a new type of side-entry specimen stage utilizing an objective lens with characteristics $C_s = 0.6$ mm, $C_c = 1.05$ mm, and focal length $(f) = 1.6$ mm. Full details of this modification are given elsewhere.[8] The interpretable point resolution of the modified instrument at optimum defocus, as defined by the first zero of the phase-contrast transfer function[9] was 2.03 Å, as compared with 2.41 Å for the standard instrument. For gold, therefore, both {111} and {200} diffracted beams (corresponding to spacings of 2.35 and 2.04 Å, respectively) could be recombined into the image with the same relative phase shift at optimum defocus, and the atoms appeared as black dots in images viewed down the {110} directions. With silver, however, the most useful images were recorded at a defocus setting considerably greater than optimum with the atoms being resolved as white dots.

Owing to the extremely small size of the colloidal metal particles, no attempt was made to orient them with respect to the electron beam and particles were examined by systematic screening of the grid. Micrographs were recorded at ca. 490 000 ×, a series of pictures for each group of particles being taken, with a variation of objective lens defocus of ca. 300 Å between successive exposures. Astigmatism was corrected by observing the granularity of the amorphous support film, and diffraction patterns were obtained when required by means of optical diffraction from the recorded images.

The gold particles could be classified into two categories:

1. The first type includes multiply twinned particles (MTPs) similar to those previously described for gold samples prepared by evaporation of the bulk metal.[10,11] These particles gave very similar HREM images and varied in size from ca. 100 to 400 Å in diameter. A typical example of a decahedral particle being illustrated in Figure 1a. Strong diffraction contrast at the twin boundaries between the individual regions within these MTPs suggested that either considerable strain or defects were present at the boundaries. In all cases, however, the individual sub-

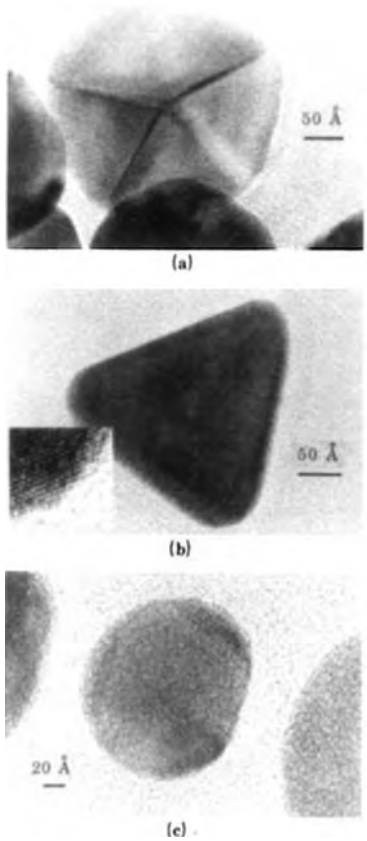

Fig. 1. a) Typical decahedral particle in colloidal gold, with strong contrast observable at the boundaries. b) Pseudo-trigonal particle of colloidal gold. The inset shows the atomic detail at the truncated corners. c) Small, apparently flat single-crystal gold particle, believed to be a precursor of the larger flat particles.

[*] Dr. P. P. Edwards, D. G. Duff, A. C. Curtis, D. A. Jefferson, Dr. B. F. G. Johnson, A. I. Kirkland
University Chemical Laboratory
Lensfield Road, Cambridge CB2 1EW (England)
D. E. Logan
Physical Chemistry Laboratory, University of Oxford
South Parks Road, Oxford OX1 3QZ (England)

[**] We thank the SERC, Johnson Matthey, and ICI for support. *P. P. E.* also thanks the Nuffield Foundation for the award of a One Year Research Fellowship.

units within the MTPs examined were of roughly equal size.

2. The second type of gold particle is shown in Figure 1b. Tilting experiments on a lower-resolution instrument confirmed the flat nature of these particles. Although some were of irregular outline, most were clearly triangular, generally with truncated corners (Fig. 1b). Surface steps were visible at the corners, as shown in the inset. The lateral dimensions of these particles showed a wide variation, but were rarely less than 200 Å and frequently extended to greater than 1000 Å. Smaller particles without twinning were observed (Fig. 1c). Although not of triangular outline, they were definitely *not* of the icosahedral or decahedral type, and were possibly representative of the first stages of triangular particle formation, before the characteristic shape had developed.

Colloidal silver was prepared by the reduction of a solution of silver nitrate in acetonitrile by poly(ethylene imine) $(-H_2CCH_2NH-)_n$ (PEI). The use of PEI as a protecting agent for stabilizing gold sols against particle aggregation was first investigated by *Thiele* and *von Levern*.[12] Later work by *Thiele* ahd *Kowallik*[13] demonstrated that PEI could be used as a reducing agent in the preparation of colloidal gold from chloroauric acid, this method producing stabilized sols of extremely small particle size. In these reactions the polymer has the twin function of reducing and protecting agent.

In the present study we adapted this method for the production of colloidal silver in acetonitrile. This reaction mixture was treated in two ways. Immediate preparation of a sample for electron microscopy (involving dessication of the polymer–metal ion adduct onto a carbon film) produced a myriad of particles of diameter less than 50 Å. Allowing the mixture to stand in daylight caused the development, over the course of several weeks, of a rather unstable silver sol and the appearance of larger particles (ca. 100–500 Å diameter), as determined by transmission electron microscopy (TEM). If the sol was kept in the dark, this nucleation process was slowed down considerably. A partially reacted sol yielded a bimodal size distribution of particles on the electron microscope grid; the number of smaller particles decreased and the number of larger particles increased as the reaction proceeded. The samples under examination here were exposed to daylight for three days; this procedure yielded a good number of large and small particles for examination.

For the silver samples, no flat plates were observed, but again the particles could be classified into two categories:

1. MTPs were the predominant type, generally of lateral dimensions less than 500 Å and, by contrast with those observed in the gold samples, typically showed an arrangement of individual subunits that was far from perfect. A typical particle is shown in Figure 2a, where, although at first sight the particle appears to be of the decahedral type, closer examination reveals the existence of six component units. At least one of the boundaries within this particle is not along a crystallographic direction, and this may possibly be the method by which the metal adapts the bulk face-centered cubic structure to the developed morphology of the MTP. Also in contrast to the gold samples, no major strain contrast was observed at the boundaries within the MTPs, indicating that the manner in which the lattice adapts to strain might differ between these two colloidal samples.

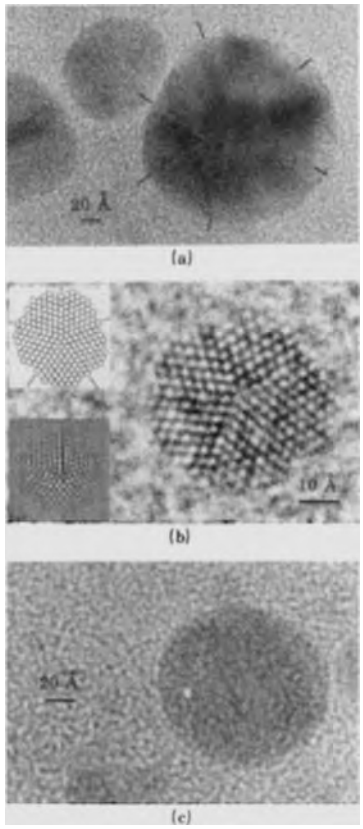

Fig. 2. a) Typical MTP in colloidal silver, viewed down {110}. The positions of the boundaries are indicated. b) Almost perfect decahedral particle of silver, with no visible strain at the boundaries. The inset shows the structural model deduced from the image and the simulated image at an objective lens defocus of ca. 650 Å. c) Agglomerate-like particle of silver, with no clear indication of distinct subunits or boundaries between them. The detail of the amorphous support film suggests that the objective lens defocus of this image is similar to that of Figure 2b.

When the particle dimensions become very small (<40 Å), they appeared to adopt only the decahedral form (Fig. 2b). Although faceting leading to truncation of the edges of the particles was noted, the atomic arrangement appeared to be a perfect decahedral one, and no strain contrast or zigzagging of boundaries was noted. Computer-simulated images of the particle of Figure 2b were calculated using the multislice method[14] as previously applied to image calculations of very small particles by *Gai* et al.,[15] although in the present investigation a simplified version was adopted; i.e., no account was taken of the atomic structure of the amorphous carbon background. This simplification is appropriate since the particles studied here are much larger, and the corresponding percentage contrast is much greater, than those in the studies carried out by *Gai* et al.[15]

The structural model employed and a simulated image are shown in the inset in Figure 2b. The model used contained 1427 silver atoms and, if a homogeneous strain[16, 17] was employed, necessitated a maximum expansion of 2.75% in the metal–metal bond length parallel to the edges of the decahedron. At the position where the notches at the boundaries occurred, the metal–metal distance in this direction was allowed to relax back to its ideal position, and this appeared to correspond to the actual arrangement within the particle. Given the small size of particle, it was found to be impossible to incorporate any type of dislocation to eliminate this strain without it being immediately visible in the simulated image; this would have not been in agreement with the experimental image (Fig. 2b). In addition, the image simulation indicated that the particle was elongated parallel to the fivefold symmetry axis, this again being as predicted by the theory of *Marks*.[18] Consequently, the homogeneous strain appeared to be most appro-

priate in these very small particles and their real structure did not therefore correspond exactly to the bulk face-centered-cubic structure.

2. The second type of silver particle (Fig. 2c) observed was much more enigmatic. These particles were approximately spherical, and initially were assumed to consist of small icosahedral units. However, the number of distinct individuals was in many cases much too large for a single icosahedral MTP; it is possible, however, that these particles are "polyparticles" as observed by *Smith* and *Marks* for evaporated samples. These particles varied considerably in size, although most were less than 100 Å. When they were of very small dimensions (<25 Å), they gave every indication of being quasiamorphous, in that no lattice rows were discernable, and it was often quite difficult to distinguish them from the background of the amorphous support film. Although it is tempting to consider such poorly structured particles as a type of large cluster, the number of atoms contained is still relatively high (from density calculations, 479 atoms in a 25-Å sphere) and little can be said about their structure until further image simulations are performed. It is possible, however, to consider that this second type of particle may actually form at a later stage than the MTPs, possibly in the final stages of evaporation of the sol. Although this would in turn imply that they were an essentially nonequilibrium phenomena, continued annealing in the electron beam did not appear to produce atomic rearrangement, unlike the case of gold particles on a silicon support, as observed recently.[6]

In this work we hope to have demonstrated that, in conjunction with appropriate chemical synthetic routes, direct imaging by HREM provides much detailed information about the atomic structure of colloidal metal particles on a nanometer scale. Perhaps the most striking results are the observations that certain small particles of colloidal silver exhibit a fivefold symmetry axis (Fig. 2b) and that metal particles grown from colloidal solutions show marked similarities to those produced by evaporation methods. The relative ease of experimental control on both the particle dimensions and morphology is considerably more straightforward in the case of colloidal preparations.

Experimental Procedure

Stringent conditions of experimental cleanliness were followed throughout for both the gold and silver preparations—glassware was washed variously with aqua regia, nitric acid, or chromic acid and then rinsed copiously with water, the last few times with doubly distilled water. The sols were initially characterized by low-resolution TEM (JEOL 200-CX) with scanning electron microscope facility. Optical spectra were obtained using a Pye-Unicam SP8800 UV-VIS spectrophotometer, the samples being contained in quartz cells.

Colloidal gold was prepared by citric acid reduction of chloroauric acid using the method of *Turkevich* et al. [4]: 5 mL of a 1% aqueous solution of citric acid (AR grade, monohydrated salt) was added to 95 mL of a refluxing 0.01% aqueous solution of chloroauric acid (49.42% Au) with stirring and the mixture was boiled for one hour (all water was doubly distilled before use).

Silver sol: The silver nitrate used was in the form of analytical reagent grade crystals (99.99% pure). Acetonitrile (HPLC grade) was distilled over calcium hydride before use. PEI was used as received as a very viscous liquid ($M = 1800$ g/mol). The concentrations of reagents used were so as to yield a sol containing 10^{-3} M silver nitrate. The starting mixture consisted of a 5.4 : 1 molar ratio of imine residues to silver ions: 0.120 g of PEI was dissolved in 100 mL of freshly distilled acetonitrile. A 20 mL aliquot of this solution was added to a further 70 mL of acetonitrile and then 10 mL of a 0.01 M solution of silver nitrate in acetonitrile was added with stirring. For subsequent procedure, see text.

Received: December 4, 1986;
revised: March 24, 1987 [Z 1999 IE]
German version: *Angew. Chem. 99* (1987) 688

[1] See, for example, M. Kerker, *J. Colloid Interface Sci. 105* (1985) 297.
[2] M. Faraday, *Philos. Trans. R. Soc. London 147* (1857) 145.
[3] M. Kerker: *The Scattering of Light and other Electromagnetic Radiation*, Academic Press, New York 1969.
[4] B. von Borries, G. A. Kausche, *Kolloid-Z. 90* (1940) 132; J. S. Turkevich, P. S. Stevenson, J. Hillier, *Discuss. Faraday Soc. 11* (1951) 55; W. O. Milligan, R. H. Morriss, *J. Am. Chem. Soc. 86* (1964) 3461; N. Uyeda, M. Nishino, E. Suito, *J. Colloid Interface Sci. 43* (1973) 264.
[5] J.-O. Bovin, L. R. Wallenberg, D. J. Smith, *Nature (London) 317* (1985) 47; D. J. Smith, A. K. Petford-Long, L. R. Wallenberg, J.-O. Bovin, *Science (Washington) 233* (1986) 872.
[6] S. Iijima, T. Ichihashi, *Phys. Rev. Lett. 56* (1986) 616.
[7] P. P. Edwards in C. N. R. Rao (Ed.): *Advances in Solid State Chemistry (Proc. INSA Gold Jubilee Symposium*, New Delhi 1984), Indian National Science Academy, New Delhi 1986, p. 265.
[8] D. A. Jefferson, J. M. Thomas, G. R. Millward, K. Tsuno, A. Harriman, R. D. Brydson, *Nature (London) 323* (1986) 428.
[9] H. P. Erickson, A. Clug, *Philos. Trans. R. Soc. London Sect. B 261* (1971) 105.
[10] L. D. Marks, A. Howie, *Nature (London) 282* (1979) 196; L. D. Marks, A. Howie, D. J. Smith, *Conf. Ser. Inst. Phys. (Bristol) 52* (1980) 397.
[11] L. D. Marks, D. J. Smith, *J. Cryst. Growth 54* (1981) 425; *J. Microsc. (Oxford) 130* (1983) 249.
[12] H. Thiele, H. Schröder von Levern, *J. Colloid Sci. 20* (1965) 679.
[13] H. Thiele, J. Kowallik, *Kolloid-Z. Z. Polym. 234* (1969) 1017.
[14] J. M. Cowley, A. F. Moodie, *Acta Crystallogr. 10* (1957) 609; P. Goodman, A. F. Moodie, *ibid. Sect. A 30* (1974) 280.
[15] P. L. Gai, M. J. Goringe, J. C. Barry, *J. Microsc. (Oxford) 142* (1986) 9.
[16] S. Ino, *J. Phys. Soc. Jpn. 27* (1969) 941.
[17] K. Heinemann, C. Y. Yang, M. J. Yacaman, H. Poppa, *Thin Solid Films 58* (1979) 163.
[18] L. D. Marks, *Philos. Mag. Part A 49* (1984) 81.

The Synthesis of 1,3- and 1,4-Phenylene-Linked Bisquinone-Substituted Porphyrin Dimers**

By *Jonathan L. Sessler** and *Martin R. Johnson*

A key feature of photosynthesis in both green plants and bacteria is light-induced electron transfer from a "special pair" dimeric chlorophyll (or bacteriochlorophyll) donor (P), via a series of intermediate prosthetic groups, to a quinone acceptor (Q). Recent X-ray structural studies of the bacterial photosynthetic reaction center (RC) from *Rhodopseudomonas viridis* have revealed a well-defined orientation of six tetrapyrrolic macrocycles at the active site: The dimeric bacteriochlorophyll special pair (P) is flanked on two sides, at a distance of 13 Å and interplane angle of 70°, by two monomeric bacteriochlorophylls (Bchls), each of which is in turn in contact with a bacteriopheophytin (Bph). The Bchl and Bph are separated by an interplane angle of 65° and a center-to-center distance of 11 Å.[1] These structural results suggest that both donor–acceptor distances and intermacrocycle orientations play a crucial role in mediating the photosynthetic charge separation process. In recent years a number of photosynthetic model systems have been synthesized and studied in an effort to understand the first of these factors.[2] Intermacrocycle orientation effects, however, have not been thoroughly addressed in model systems.[3] We report here the synthesis of the quinone-substituted 1,3-phenylene-linked "gable"-type[4] porphyrin dimer **1** and its more open 1,4-phenylene-bridged analogue **2**. System **1** was specifically designed so as to constrain the two porphyrin subunits to a

[*] Prof. J. L. Sessler, M. R. Johnson
Department of Chemistry, University of Texas
Austin, TX 78712 (USA)

[**] This work was supported by the Robert A. Welch Foundation, by the Camille and Henry Dreyfus Foundation (Distinguished New Faculty Grant 1984), and by a National Science Foundation (USA) Presidential Young Investigator Award.

configuration that approximates the skewed geometry existing between Bchl and Bph in the RC of *R. viridis*.[1]

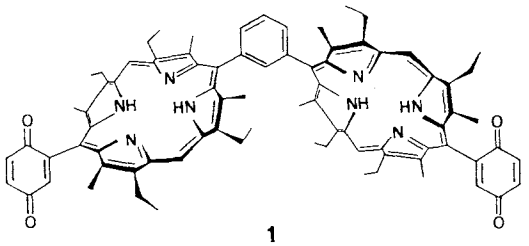

1

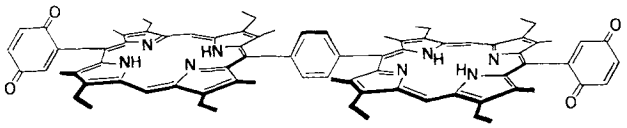

2

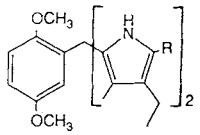

5: R = H
6: R = CHO

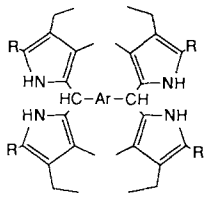

7: Ar = A, R = CO_2Et
8: Ar = A, R = H
9: Ar = B, R = CO_2Et
10: Ar = B, R = H

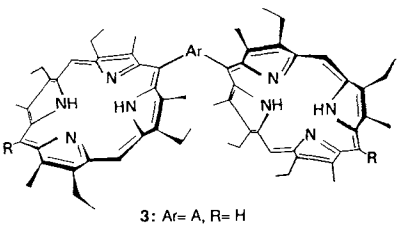

3: Ar = A, R = H
4: Ar = B, R = H
11: Ar = A, R = hqe
12: Ar = A, R = hq
13: Ar = B, R = hqe
14: Ar = B, R = hq

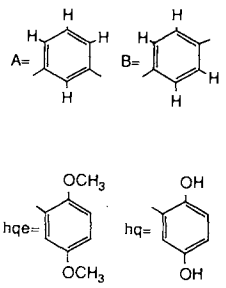

The porphyrin precursors, **11** and **13**, of the quinone-substituted dimers **1** and **2** were prepared by the coupling of dipyrrylmethanes[5] using a procedure similar to that employed earlier to synthesize the "gable"-type porphyrin **3**.[6] The key dipyrrolic intermediate **6** was prepared in two steps. An acid-catalyzed condensation of dimethoxybenzaldehyde with ethyl 3-ethyl-4-methyl-2-pyrrolecarboxylate[7] in warm ethanol was followed directly by saponification and decarboxylation in boiling basic ethylene glycol to give **5** as a yellow powder (m.p. = 128–130 °C, 97% yield).[8] Vilsmeier formylation[9] then gave **6** in 68% yield as off-white crystals (m.p. = 208–209 °C). The *para*-phenylene-linked α-unsubstituted bis(dipyrrylmethane) **10** (m.p. = 162–163 °C, 90% yield) was prepared, via **9** (m.p. = 237 °C), from terephthalaldehyde and ethyl 3-ethyl-4-methyl-2-pyrrolecarboxylate[7] by the procedure used to produce **8** (via **7**).[6] Acid-catalyzed condensation of a 2 : 1 molar ratio of **6** and **8**, or **6** and **10**, for 12 h at room temperature in degassed methanol containing 1% $HClO_4$, followed by basification with triethylamine and oxidation with *o*-chloranil, gave **11** and **13** along with polymeric by-products. Chromatographic purification of the copper complexes[5d] (silica gel, $CHCl_3/CCl_4$ 1 : 1) followed by demetalation and recrystallization from $CHCl_3$/hexane gave **11** ($\lambda_{max}(CHCl_3) = 419$, 512, 545, 579, 630 nm) and **13** ($\lambda_{max}(CHCl_3) = 418$, 510, 543, 576, 626 nm) in 8% and 12% yields, respectively.[8] Compound **10** was also coupled with bis(4-ethyl-5-formyl-3-methyl-2-pyrryl)methane,[8] in a straightforward manner,[6] to give the unsubstituted, *para*-phenylene-linked reference dimer **4** (12%, $\lambda_{max}(CHCl_3) = 410$, 507, 540, 576, 627 nm).[3c,8]

Treating **11** with an excess of BBr_3 in dry CH_2Cl_2 and neutralizing the reaction solution with aqueous sodium bicarbonate gave **12** ($\lambda_{max}(CHCl_3) = 415$, 511, 545, 578, 628 nm) in 67% yield following chromatography on silica gel (1% MeOH in $CHCl_3$) and recrystallization from $CHCl_3$/EtOH.[8] The bishydroquinone **12** was oxidized to **1** in $CHCl_3$/MeOH (10 : 1) by treatment with a slight excess of 2,3-dichloro-5,6-dicyano-1,4-benzoquinone (DDQ). Following chromatographic purification (silica gel, 0.1% triethylamine in $CHCl_3$) and recrystallization from $CHCl_3$/hexane, **1** was obtained in 93% yield as blue-violet crystals ($\lambda_{max}(CHCl_3) = 417$, 510, 543, 578, 628 nm).[8] An insoluble precipitate, assumed to have structure **14**,[8] was obtained when **13** was reacted with BBr_3. Following treatment with DDQ (as a slurry in $CHCl_3$/MeOH/pyridine 3 : 1 : 1), chromatographic purification (silica gel, 0.1% triethylamine in $CHCl_3$), and recrystallization from $CHCl_3$/hexane, the bisquinone **2** was isolated as blue-violet crystals in 72% yield based on **13** ($\lambda_{max}(CHCl_3) = 416$, 508, 541, 575, 626 nm).[8] The ^{13}C-NMR spectra of compounds **1** and **2** shows, in addition to the expected peaks in the alkyl and aromatic regions, a pair of signals at $\delta = 187.0$, 188.8 and 187.3, 188.9, respectively, corresponding to carbons 1 and 4 of the quinone ring.

Evidence for the dimeric nature of the porphyrins **1**, **2**, **11**, **12**, and **13** came from fast-atom-bombardment mass spectrometry (FAB, glycerol/oxalic acid matrix, 8-keV accelerating voltage). Only peaks corresponding to the expected $M^{\oplus} + nH$ (n = 1–5) ions were observed. Further support for the assigned dimeric structures came from ^1H-NMR spectroscopy. As expected for a porphyrin substituted in the 5 and 15 positions, the spectra of compounds **1**, **2**, **11**, **12**, and **13** in $CDCl_3$ show only one peak at $\delta \approx 10$, integrating for four protons and assignable to the *meso* protons. Signals, integrating for six and four protons, respectively, and assignable to both the hydroquinone/quinone and bridging phenylene rings were also resolved in the 360-MHz ^1H-NMR spectrum. For the *m*-phenylene-linked dimers **1**, **11**, and **12**, three signals are observed for the aromatic spacer. In the case of the *p*-phenylene-linked dimers **2** and **13**, the corresponding set of peaks appears as a doublet of doublets centered at $\delta \approx 8.6$. This splitting may indicate that even in the *para*-substituted series the two porphyrin macrocycles are not entirely coplanar.

The *p*-phenylene- and *m*-phenylene-linked free-base porphyrin dimers all show absorbance bands that are broadened and redshifted with respect to the reference monomer 2,8,13,17-tetraethyl-3,7,12,18-tetramethyl-5-phenylporphine ($\lambda_{max} = 402$, 501, 534, 559, 626 nm),[10] with the degree of broadening (but not shift) being greater in the *meta* series. Not surprisingly, the substituted dimers **1**, **2**, **10**, **11**, and **13** all showed larger bathochromic shifts than the unsubstituted dimers **3** and **4**; similar observations had been made earlier in the case of simple quinone-substituted monomeric porphyrins.[11] Dramatic differences

between the two isomeric sets of phenylene-linked dimers are seen in the case of the bis-zinc(II) complexes. The bis-zinc complexes of the *p*-phenylene-linked compounds **2**, **13**, and **14** all display one strong Soret band at ca. 420–425 nm with only a faint shoulder appearing at higher energy. The bis-zinc(II) complexes of the "gable"-type porphyrins **1**, **11**, and **12**, on the other hand, all display a Soret band that is split into two peaks of nearly equal intensity (at ca. 412 and 428 nm). This splitting of the Soret band, arising by virtue of dipole–dipole coupling, is indicative of interaction between the two porphyrin chromophores.[4] The observation of fluorescence quantum yields for the *meta*-linked dimers **3** and **11** that are both lower by ca. 25% than those of the corresponding *p*-phenylene-linked analogues (**4** and **13**) further confirms that a greater level of excitonic interaction pertains in the "gable" series of dimers.

As was expected on the basis of earlier work with quinone-substituted monomeric porphyrins,[11] neither **1** nor **2**, as ca. 10^{-6} M solutions in toluene, showed detectable fluorescence when irradiated at $\lambda = 418$ nm ($\Phi_f < 10^{-5}$). This suggests that rapid photoinduced intermolecular electron transfer is occurring from the porphyrins to the quinone acceptors. Compounds **1** and **2** thus appear to be suitable systems with which to model the primary events of photosynthetic charge separation.

Received: January 22, 1987 [Z 2063 IE]
German version: *Angew. Chem. 99* (1987) 679

[1] J. Deisenhofer, O. Epp, K. Miki, R. Huber, H. Michel, *J. Mol. Biol. 180* (1984) 385.

[2] J. Weiser, H. A. Staab, *Angew. Chem. 96* (1984) 602; *Angew. Chem. Int. Ed. Engl. 23* (1984) 623; B. Morgan, D. Dolphin, *ibid. 97* (1985) 1000 and *24* (1985) 1004, and references cited therein; P. Leighton, J. K. M. Sanders, *J. Chem. Soc. Chem. Commun. 1985*, 24; J. R. Bolton, T.-F. Ho, S. Liauw, A. Siemiarczuk, C. S. K. Wan, A. C. Weedon, *ibid. 1985*, 559; M. R. Wasielewski, M. P. Niemczyk, W. A. Svec, E. B. Pewitt, *J. Am. Chem. Soc. 107* (1985) 1080, 5562; J. A. Schmidt, A. Siemiarczuk, A. C. Geedon, J. R. Bolton, *ibid. 107* (1985) 6112; B. A. Leland, A. D. Joran, P. M. Felker, J. J. Hopfield, A. H. Zewail, P. B. Dervan, *J. Phys. Chem. 89* (1985) 5571; C. Krieger, J. Weiser, H. A. Staab, *Tetrahedron Lett. 26* (1985) 6055; J. Weiser, H. A. Staab, *ibid. 1985*, 6059; A. Osuka, H. Furuta, K. Maruyama, *Chem. Lett. 1986*, 479; D. N. Beratan, *J. Am. Chem. Soc. 108* (1986) 4321; D. Gust, T. A. Moore, L. R. Makings, P. A. Liddell, G. A. Nemeth, A. L. Moore, *ibid. 108* (1986) 8028.

[3] a) Only one report of a quinone-substituted porphyrin dimer has appeared: Y. Sakata, S. Nishitani, N. Nishimizu, S. Misumi, A. R. McIntosh, J. R. Bolton, Y. Kanda, A. Karen, T. Okada, N. Mataga, *Tetrahedron Lett. 26* (1985) 5207; b) for examples of photosynthetic models containing two or more porphyrin-like macrocycles (but no quinones) see: S. G. Boxer, *Biochim. Biophys. Acta 726* (1983) 265, and references cited therein; M. R. Wasielewski, M. P. Niemczyk, W. A. Svec, *Tetrahedron Lett. 23* (1982) 3215; J. C. Mialocq, C. Giannotti, P. Maillard, M. Momenteau, *Chem. Phys. Lett. 112* (1984) 87; G. M. Dubowchik, A. D. Hamilton, *J. Chem. Soc. Chem. Commun. 1986*, 665, 1391; R. L. Brookfield, H. Ellul, A. Harriman, G. Porter, *J. Chem. Soc. Faraday Trans. 2 1986*, 219. c) The synthesis of an analogue of the unsubstituted photosynthetic model compound **4** was reported subsequent to the submission of this work: D. Heiler, G. McLendon, P. Rogalskyj, *J. Am. Chem. Soc. 109* (1987) 604.

[4] I. Tabushi, T. Sasaki, *Tetrahedron Lett. 23* (1982) 1913; I. Tabushi, S.-I. Kugimiya, M. G. Kinnaird, T. Sasaki, *J. Am. Chem. Soc. 107* (1985) 4192.

[5] a) G. P. Arsenault, E. Bullock, S. F. MacDonald, *J. Am. Chem. Soc. 82* (1960) 4384; b) C. K. Chang, I. Abdalmuhdi, *Angew. Chem. 96* (1984) 154; *Angew. Chem. Int. Ed. Engl. 23* (1984) 164; c) I. Abdalmuhdi, C. K. Chang, *J. Org. Chem. 50* (1985) 411; d) S. S. Eaton, G. R. Eaton, C. K. Chang, *J. Am. Chem. Soc. 107* (1985) 3177.

[6] J. L. Sessler, J. Hugdahl, M. R. Johnson, *J. Org. Chem. 51* (1986) 2838.

[7] J. L. Archibald, D. M. Walker, K. B. Shaw, A. Markovac, S. F. MacDonald, *Can. J. Chem. 44* (1966) 345; D. H. R. Barton, S. Z. Zard, *J. Chem. Soc. Chem. Commun. 1985*, 1098.

[8] With the exceptions of **14**, which proved too insoluble to purify, and **12**, which was only characterized spectroscopically, all new porphyrin compounds gave satisfactory spectroscopic, analytical, and mass spectral data; dipyrrolic intermediates were characterized by ^{1}H-NMR and high-resolution mass spectrometry.

[9] R. Chong, P. S. Clezy, A. J. Liepa, A. W. Nichol, *Austr. J. Chem. 22* (1969) 229.

[10] C. K. Chang, I. Abdalmuhdi, *J. Org. Chem. 48* (1983) 5388.

[11] J. Dalton, L. R. Milgrom, *J. Chem. Soc. Chem. Commun. 1979*, 609; A. Harriman, R. J. Hosie, *J. Chem. Soc. Faraday Trans. 2 1981*, 1695; M. A. Bergkamp, J. Dalton, T. L. Netzel, *J. Am. Chem. Soc. 104* (1982) 253; A. C. Chan, J. Dalton, L. R. Milgrom, *J. Chem. Soc. Perkin Trans. 2 1982*, 707.

Highly Polarizing Co^{2+} Ions from $[Co_2(CO)_8]$ and Pyridine in Hydrocarbons: Synthesis and Structure of $[\{Co_3(CO)_{10}\}_2\{Co(py)_4\}]$ and $[(CO)_4CoCo(py)_3][Co(CO)_4]$**

By *Giuseppe Fachinetti,* Giovanni Fochi, Tiziana Funaioli,* and *Pier Francesco Zanazzi**

Large excesses of Lewis bases promote metal carbonyl disproportionation,[1] with base-encapsulated cations and carbonylmetalate anions being formed. However, when relatively weak bases or only moderate amounts of strong bases in solvents having low dielectric constants are used, the disproportionation of neutral metal carbonyls yields complex cations and carbonylmetalate anions associated in homonuclear ion pairs (HNIP).[2] The reactivity of the anions is affected by ion pairing with acidic countercations;[3] therefore, HNIP phenomena are likely to yield a better understanding of metal carbonyl chemistry. Firm evidence for such behavior was obtained in the case of $[V(CO)_6]$ **1** and $[Fe(CO)_5]$ **2**. The reaction of **1** with tetrahydrofuran (THF) gave the structurally characterized complex $[(OC)_5VCOV(thf)_4OCV(CO)_5]$;[5] similarly, **2** reacts with pyridine (py) to yield the tetranuclear HNIP $[(py)_2FeFe(CO)_4]_2$.[6] The molecular structure shows cation–anion association through direct metal–metal interactions. Upon addition of moderate amounts of py to $[Co_2(CO)_8]$ **3** in THF solution, we obtained spectroscopic evidence for a $Co^{2+}/[Co(CO)_4]^-$ HNIP,[7] which led to the formation of both isocarbonyl compounds and species showing direct metal–metal interactions. We now report that, in hydrocarbon solutions containing moderate amounts of py with respect to the cobalt, HNIP formation from **3** occurs; two compounds of this class have been isolated and their molecular structures solved.

The addition of an equimolar amount of py to **3** in *n*-hexane results in gas evolution and the formation of a carmine solid in 60% yield analyzing as $[Co_7(CO)_{20}(py)_4]$ **4**.[8] The IR spectrum (Nujol mull) in the CO stretching region (2078 (w), 2016 (vs), 1995 (sh), 1980 (m), 1964 (m), 1520 (m) cm^{-1}) resembles the pattern for the $[Co_3(CO)_{10}]^-$ cluster in ether solvents.[4] Crystals suitable for X-ray diffraction grew from the mother liquor.[9]

Complex **4** (Fig. 1) contains an approximately octahedrally coordinated Co^{2+} ion bound to four py nitrogen atoms in the equatorial plane; the axial positions are occupied by the carbonyl oxygen atoms of the μ_3-CO groups

[*] Prof. G. Fachinetti, Dr. G. Fochi, Dr. T. Funaioli
Dipartimento di Chimica e Chimica Industriale
dell'Università degli Studi di Pisa
Via Risorgimento 35, I-56100 Pisa (Italy)
Prof. P. F. Zanazzi
Dipartimento di Scienze della Terra
dell'Università degli Studi di Perugia
Piazza dell'Università, I-06100 Perugia (Italy)

[**] This work was supported by the Ministero della Pubblica Istruzione (Rome). We thank Prof. *Fausto Calderazzo* for helpful discussions.

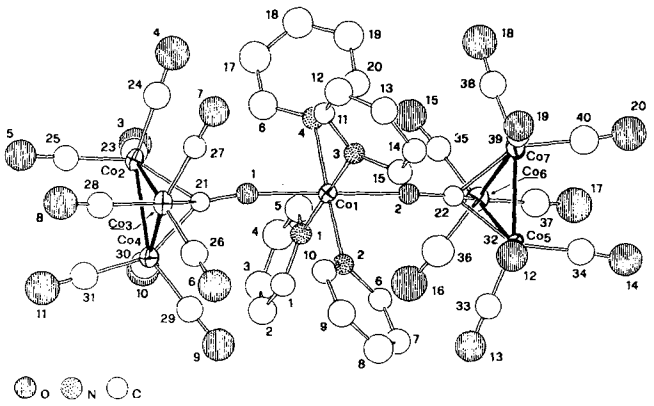

Fig. 1. Molecular crystal structure of $[\{Co_3(CO)_{10}\}_2\{Co(py)_4\}]$ **4**. Important distances [Å] and angles [°]: Co-Co (in the $[Co_3(CO)_{10}]^-$ units) 2.502 (average); C-O (terminal) 1.16 (average); C21-O1 1.233(12), C22-O2 1.239(13), Co1-O1 2.154(7), Co1-O2 2.146(7), Co1-N 2.144; C21-O1-Co1 168.7(6), C22-O2-Co1 173.0(6) (average).

belonging to two $[Co_3(CO)_{10}]^-$ units. The interatomic distances and angles in the two $[Co_3(CO)_{10}]^-$ clusters are comparable to those reported for other oxymethylidyne $Co_3(CO)_9$ clusters.[4]

Complex **4** is indefinitely stable in the solid state but decomposes quickly in THF or toluene, dark green solutions being obtained. In both these solvents, the IR spectra show the complex pattern already observed[2] for THF solutions of **3** containing moderate amounts of py, thus indicating the formation of other types of $Co^{2+}/[Co(CO)_4]^-$ HNIPs from **4**. Slow diffusion of *n*-hexane vapor into a toluene solution of **4** resulted in the formation of large black-green crystals having the composition $[Co_3(CO)_8(py)_3]$ **5** in low yield.[10] The IR spectrum of **5** (Nujol mull) shows absorptions at 2050 (m), 1992 (m), 1947 (s), 1933 (s), 1887 (m), and 1867 (s) cm^{-1}. Complex **5** can be obtained in 90% yield directly from **3** and py in toluene/*n*-hexane mixtures.[11] The X-ray crystal structure analysis of **5** showed that it consists of nearly regular tetrahedral $[Co(CO)_4]^-$ anions and dinuclear $[(OC)_4CoCo(py)_3]^+$ cations (Fig. 2). The geometry around the cobalt carrying the carbonyl groups is a distorted trigonal bipyramid, while that around the cobalt carrying the py groups is a distorted tetrahedron. The Co-Co distance is short (2.490(2) Å) compared with that in **3** (2.52 Å). The isolation of **5** from solutions containing both **3** and py suggests that electron transfer in disproportionation and

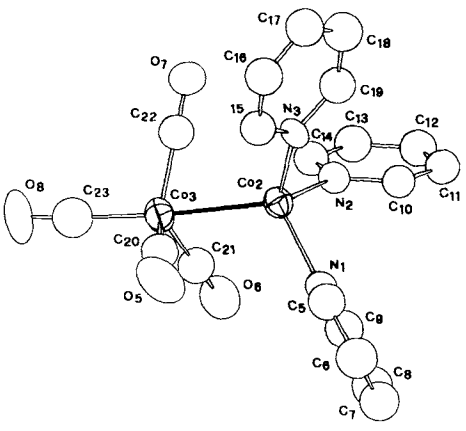

Fig. 2. Molecular crystal structure of $[(OC)_4CoCo(py)_3]^+$. Important distances [Å] and angles [°]: Co2-Co3 2.490(2), C-O 1.14 (average), Co3-C23 1.816(13), Co3-C_{eq} 1.74 (average), Co2-N 2.035 (average); Co2-Co3-C23 175.7(4), Co2-Co3-C_{eq} 77.9 (average), Co3-Co2-N 112.8 (average), Co3-C_{eq}-O 176.7 (average).

synproportionation of metal carbonyls can occur with[12] or without the intermediacy of isocarbonyl compounds.

These findings show that, through a base-promoted disproportionation reaction, $[Co_2(CO)_8]$ **3** can be the source of highly polarizing Co^{2+} ions when only moderate amounts of bases are employed.

Received: February 2, 1987 [Z 2081 IE]
German version: *Angew. Chem.* 99 (1987) 681

[1] W. Hieber, *Adv. Organomet. Chem.* 8 (1970) 1.
[2] G. Fachinetti, F. Del Cima, G. Sbrana, T. Funaioli, *J. Organomet. Chem.* 287 (1985) C 23.
[3] M. Y. Darensbourg, *Prog. Inorg. Chem.* 33 (1985) 221.
[4] C. P. Horwitz, D. F. Shriver, *Adv. Organomet. Chem.* 23 (1984) 219, and references cited therein.
[5] M. Schneider, E. Weiss, *J. Organomet. Chem.* 121 (1976) 365.
[6] G. Fachinetti, G. Fochi, T. Funaioli, P. F. Zanazzi, *J. Chem. Soc. Chem. Commun.* 1987, 89.
[7] G. Fachinetti, G. Fochi, T. Funaioli, *J. Organomet. Chem.* 301 (1986) 91.
[8] Pyridine (1.5 mL, 18.6 mmol) in 100 mL of *n*-hexane was added dropwise to a stirred solution of **3** (6.6 g, 19.3 mmol) in 500 mL of *n*-hexane. Simultaneously with gas evolution, **4** starts to precipitate immediately as a carmine microcrystalline solid. At the end of the addition, the solid was collected and washed with 25 mL of *n*-hexane. Yield: 4.25 g (60%).
[9] **4**: triclinic crystals, $P\bar{1}$, $a=16.910(3)$, $b=13.171(3)$, $c=12.125(3)$ Å, $\alpha=104.80(2)$, $\beta=97.45(2)$, $\gamma=108.95(2)°$, $V=2401.7$ Å^3, $Z=2$. The structure was solved by direct methods using the SIR package (G. Cascarano, C. Giacovazzo, M. C. Burla, A. Nunzi, G. Polidori, M. Camalli, R. Spagna, D. Viterbo, IXth European Crystallographic Meeting, Torino 1985, Abstracts 1-046) and refined by the full-matrix least-squares method with the SHELX-76 program. To avoid a too high number of parameters, the pyridine rings were constrained to perfect hexagons with an edge of 1.395 Å and refined as rigid groups. The hydrogen atoms were included at the calculated positions (C-H = 1.08 Å, $U=0.16$ Å^2). Anisotropic thermal parameters were assigned to the Co atoms only. $R=0.059$, $R_w=(\Sigma w(|F_o|-|F_c|)^2/\Sigma w|F_o|^2)^{1/2}=0.064$ ($1/w=\sigma^2(F_o)+0.0039F_o^2$) for 2837 unique reflections ($I\geq 3\sigma(I)$); Philips PW1100 single-crystal diffractometer, $Mo_{K\alpha}$ radiation, graphite monochromator).
[10] **5**: monoclinic crystals, $P2_1/n$, $a=22.699(3)$, $b=13.340(3)$, $c=9.050(3)$ Å, $\beta=98.79(2)°$, $V=2708.2$ Å^3, $Z=4$). The structure was solved and refined with the procedure described in [9]. The contribution of H atoms at the calculated positions was included, with an overall isotropic thermal parameter (U) that refined to 0.15 Å^2. Anisotropic thermal parameters were refined only for Co, O, and N atoms. $R=0.048$; $R_w=(\Sigma w(|F_o|-|F_c|)^2/\Sigma w|F_o|^2)^{1/2}=0.051$ ($1/w=\sigma^2(F_o)+0.0003F_o^2$) for 2172 unique reflections ($I\geq 3\sigma(I)$). Further details of the crystal structure investigation are available on request from the Fachinformationszentrum Energie, Physik, Mathematik GmbH, D-7514 Eggenstein-Leopoldshafen 2 (FRG), on quoting the depository number CSD-52384, the names of the authors, and the journal citation.
[11] To 3.8 g (11.1 mmol) of **3** dissolved in 100 mL of a mixture of toluene and *n*-hexane, 1.85 mL (22.9 mmol) of py was added. The solution was kept under reduced pressure and stirred for 4 hours. Complex **5** was obtained as an emerald-green microcrystalline solid. Yield: 4.1 g (87%).
[12] T. G. Richmond, Q. Shi, W. C. Trogler, F. Basolo, *J. Am. Chem. Soc.* 106 (1984) 76.

Alkylaluminum Cations: Synthesis and Structure of $[Al[2\text{-}C(SiMe_3)_2C_5H_4N)_2][AlCl_4]$**

By *Lutz M. Engelhardt, Ulrich Kynast, Colin L. Raston,** and *Allan H. White*

Alkylaluminum compounds, $[(AlR_3)_2]$, and alkylaluminum chlorides, $[(AlR_2Cl)_2]$, are negligibly ionized in so-

[*] Dr. C. L. Raston, Dr. L. M. Engelhardt, Dr. U. Kynast, Dr. A. H. White
Department of Physical and Inorganic Chemistry,
University of Western Australia
Nedlands, 6009 (Australia)

[**] We thank the Australian Research Grants Scheme for supporting this work.

[***] Note added by the editorial staff: A crown-ether-stabilized $[AlMe_2]^{\oplus}$ ion was reported in the May issue of *Angew. Chem.* (cf., however, dates of receipt): S. G. Bott, A. Alvanipour, S. D. Morley, D. A. Atwood, C. M. Means, A. W. Coleman, J. L. Atwood, *Angew. Chem.* 99 (1987) 476; *Angew. Chem. Int. Ed. Engl.* 26 (1987) 485.

 © VCH Verlagsgesellschaft mbH, D-6940 Weinheim, 1987 0570-0833/87/0707-0681 $ 02.50/0

lution, having low electrical conductivities.[1] In the presence of neutral donor ligands such as pyridine and 2,2'-bipyridyl, however, their conductivities increase dramatically, presumably as a consequence of autoionization to $[AlR_2L_2]^{\oplus}$ and $[AlR_4]^{\ominus}$ or $[AlR_2Cl_2]^{\ominus}$ (L = Lewis base).[2] While anionic aluminate species are well known from other studies, there are no authenticated alkylaluminum cations.[***] Such cationic species for the heavier congeners of the Group III elements, in contrast, have been substantiated.[3] As part of a systematic study of the coordination chemistry of the bulky *N*-functionalized alkyl ligand **1**, we have prepared and structurally characterized a complex containing an alkylaluminum cation.

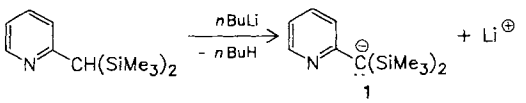

1

Solutions of $[(Li\,\mathbf{1})_2]$[4,5] in Et_2O/hexane react with $AlCl_3$ in Et_2O to yield $[Al\,\mathbf{1}_2Cl]$, **2**, in modest yield.[6] The corresponding gallium complex has a five-coordinate metal center, the alkyl ligands generating four-membered chelate rings,[7] as in the corresponding Mg, Zn, and Cd (but not Hg) complexes.[8] Complex **2** is also likely to have a five-coordinate metal center, a novelty for alkylaluminum sys-

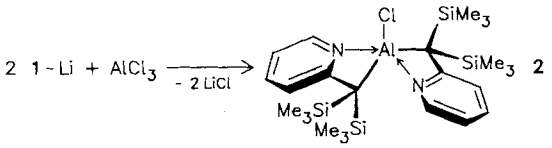

tems devoid of multicenter bonding. The nonequivalence of the $SiMe_3$ groups on the ^{1}H-NMR time scale is in agreement with this structure in solution.

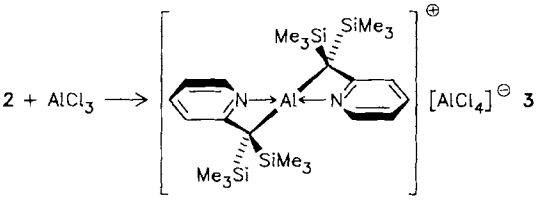

Compound **2** rapidly underwent metal-halogen cleavage with $AlCl_3$ in benzene yielding $[Al\,\mathbf{1}_2][AlCl_4]$, **3**,[9] which was isolated initially as a liquid clathrate of composition $\mathbf{3}\cdot(C_6H_6)_{14}$ (^{1}H-NMR). Despite the nonequivalence of the $SiMe_3$ groups in the cation as shown by an X-ray crystal structure determination,[10] the dynamic equivalence of these groups was evident in benzene on the ^{1}H-NMR time scale. Compound **3** was also isolated as a minor product in the above synthesis of **2**.

Overall, the environment about the metal in the cation of **3** is a distorted tetrahedron, which relates to the small "bite" of the bidentate ligand. The Al-C distances (mean 1.99 Å) are typical of terminal Al-C bonds; e.g., 1.995(8) Å in $[Al(2,4,6\text{-}Me_3C_6H_2)_3]$[11] and 1.982(6)-1.997(6) Å in $[Al(CH_2C_6H_4)_3]$.[12] The Al-N distances (mean 1.92 Å) are well below those for other N-centered Lewis base adducts of organoaluminum complexes. These distances are, however, for sp^3 rather than sp^2 nitrogen donors (e.g., Al-N is 2.02 Å in $[AlIMe_2(NMe_3)]$[13]) and therefore reflect a large polarization of the N electron cloud by electropositive aluminum in $[Al\,\mathbf{1}_2]^{\oplus}$. The geometry of the anion $[AlCl_4]^{\ominus}$ is unexceptional.

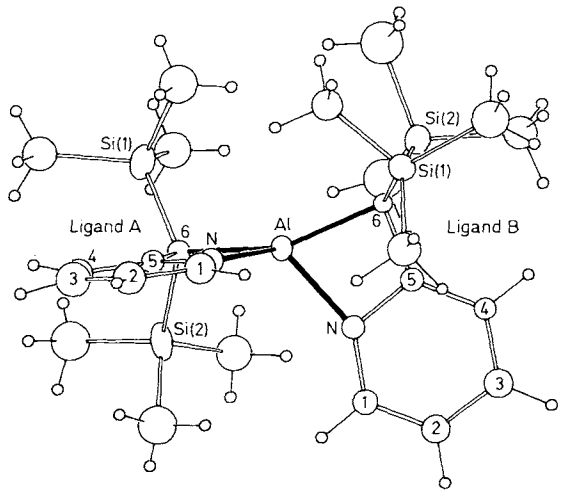

Fig. 1. Crystal structure of the cation in **3** (thermal ellipsoids at the 20% probability level). The hydrogen atoms have arbitrary radii of 0.1 Å. Selected bond distances [Å] and angles [°]: Al-N(A) 1.91(2), Al-C(A6) 1.98(2), Al-N(B) 1.93(2), Al-C(B6) 2.01(2), N(A)-Al-C(A6) 72.7(9), N(A)-Al-N(B) 114.6(10), C(A6)-Al-N(B) 123.9(6), N(A)-Al-C(B6) 123.2(8), C(A6)-Al-C(B6) 152.2(10), N(B)-Al-C(B6) 73.2(7).

Experimental Procedure

The syntheses were carried out with exclusion of air and water. To 20 mL of *n*BuLi in hexane (1.71 M, 34.2 mmol) was added 20 mL of Et_2O, then 7.3 g (30.0 mmol) of **1**-H. After stirring the resulting orange solution for 1 h, 2.0 g (14.7 mmol) of freshly sublimed $AlCl_3$ in 40 mL of Et_2O was added over 1 h. The mixture was stirred at room temperature overnight, then filtered and cooled to −30 °C, affording **2**. Complex **2** was recrystallized from benzene as colorless needles (4.3 g, 54%).

3: To **2** (0.81 g, 1.40 mmol) in 10 mL of benzene was added 0.25 g (1.87 mmol) of $AlCl_3$. Two liquid phases immediately separated. The solvent was then removed in vacuo and the product, **3**, recrystallized as colorless plates from 5 mL of tetrahydrofuran (0.74 g, 83%).

Received: December 30, 1986;
revised: March 23, 1987 [Z 2038 IE]
German version: *Angew. Chem. 99* (1987) 702

[1] E. Bonitz, *Chem. Ber. 88* (1955) 742; *Angew. Chem. 67* (1955) 525; *Z. Anal. Chem. 186* (1962) 206.
[2] H. Lehmkuhl, H.-D. Kobs, *Justus Liebigs Ann. Chem. 719* (1968) 11.
[3] D. G. Tuck, H. Kurosawa in G. Wilkinson, F. G. A. Stone, E. W. Abel (Eds.): *Comprehensive Organometallic Chemistry, Vol. 1*. Pergamon, Oxford 1982, pp. 712 and 732ff.
[4] D. Colgan, R. I. Papasergio, C. L. Raston, A. H. White, *J. Chem. Soc. Chem. Commun. 1984*, 1708.
[5] R. I. Papasergio, C. L. Raston, A. H. White, *J. Chem. Soc. Chem. Commun. 1983*, 1419.
[6] **2**: ^{1}H-NMR (C_6H_6, rel. TMS): $\delta = -0.27$, -0.67 (2s, 36H; $SiMe_3$), 5.9 (m, 2H), 6.6 (m, 4H), 7.5 (m, 2H).—^{13}C-NMR: $\delta = 3.2$, 4.3 (s), 31.6 (m), 118.9, 125.1, 139.3, 143.9, 173.3 (s).—MS (EI): *m/z* 534 ($M^{\oplus}$, 20%), 222 (100). IR (Nujol): $\tilde{\nu}$(Al-Cl) = 441 cm^{-1} (s).
[7] U. Kynast, C. L. Raston, B. W. Skelton, A. H. White, unpublished results.
[8] M. J. Henderson, R. I. Papasergio, C. L. Raston, A. H. White, M. F. Lappert, *J. Chem. Soc. Chem. Commun. 1986*, 672.
[9] **3**: ^{1}H-NMR (C_6H_6): $\delta = -0.37$ (s, 36H; $SiMe_3$), 6.6 (m, 4H), 7.2 (m, 4H).—IR (Nujol): $\tilde{\nu}$(Al-Cl) = 480 cm^{-1} (s).
[10] Crystal structure determination of **3**: monoclinic, $P2_1/c$, $a = 15.638(9)$, $b = 15.714(8)$, $c = 18.02(1)$ Å, $\beta = 122.94(4)°$, $V = 3717(4)$ Å^3, $Z = 4$, $\rho_{calcd} = 1.20$ g cm^{-3}, $F(000) = 1408$, $\mu = 5.1$ cm^{-1}, no absorption correction, $2\theta_{max} = 40°$, 3133 reflections (1153 with $I > 2\sigma(I)$) (data very weak and limited in scope), $R = 0.081$, $R_w = 0.072$. Full matrix refinement; anisotropic thermal parameters for Al, Si, Cl only. [Syntex $P\bar{1}$ diffractometer, monochromatic $Mo_{K\alpha}$ radiation, $\lambda = 0.7106$ Å.] Further details of the crystal structure investigation may be obtained from the Fachinformationszentrum Energie, Physik, Mathematik GmbH, D-7514 Eggenstein-Leopoldshafen 2 (FRG), on quoting the depository number CSD-52368, the names of the authors, and the journal citation.
[11] J. J. Jerius, J. M. Hahn, A. F. M. M. Rahman, O. Mols, W. H. Ilsley, J. P. Oliver, *Organometallics 5* (1986) 1812.
[12] A. F. M. M. Rahman, K. F. Siddiqui, J. P. Oliver, *Organometallics 1* (1982) 881.
[13] J. L. Atwood, P. A. Milton, *J. Organomet. Chem. 52* (1973) 275.

Optically Active α-Arylglycine Esters by Friedel-Crafts Alkylation with the Chiral Cation of the Bislactim Ether of *cyclo*-(L-Val-Gly)**

By *Ulrich Schöllkopf,** *Sabine Grüttner, Ralf Anderskewitz, Ernst Egert,** and *Michael Dyrbusch*

During the past few years, we have developed an asymmetric synthesis of nonproteinogenic amino acids, which makes use of metalated (anionic) bislactim ethers of 2,5-piperazinediones and has come to be called the bislactim ether method.[1] Its scope of application would be increased if it were possible to generate the bislactim ether cation **3**—a chiral, nonracemic glycine-cation equivalent[2]—and to allow this cation to react with olefins or arenes in a Friedel-Crafts (FC) reaction. Reaction with arenes would afford optically active α-arylglycines, which are of pharmacological interest on account of their potential biological activity and as components of drugs.[3] Although asymmetric syntheses of α-arylglycines according to the Strecker method have already been described,[4] there has been no report of their syntheses by asymmetric FC reactions.

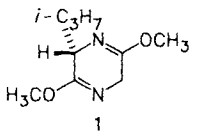

1

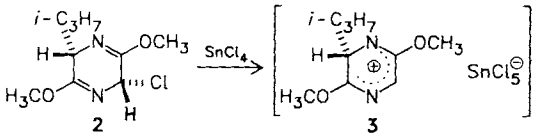

2 **3**

We report here on the asymmetric synthesis of alkoxy-substituted α-arylglycine methyl esters of the type **9**. This synthesis starts from the chloride **2**[5] of the bislactim ether **1**;[6] compound **2** is allowed to react with alkoxy-substituted arenes **4** or **5** in the presence of tin tetrachloride as Lewis acid. The ion pair **3**, which is formed as an intermediate, reacts with **4** or **5** in an FC reaction[7] to give the compounds **6** or **7**, respectively (Table 1). In addition, small amounts of the pyrazine derivatives **8a** or **8b** are formed. Reaction with anisole **4c** is plagued—as is the case for other FC alkylations—by the problem of regioselectivity. However, the regioisomers **6c** and **6d** could be separated by gas chromatography.[8]

The *trans* arrangement of the substituents at C2 and C5 in **6** and **7** was confirmed (1) by the $^5J_{H\text{-}5/H\text{-}2}$ values of ca. 4 Hz, which are typical for the *trans* configuration in the bislactim ether system, (2) by the X-ray structure analysis of an FC adduct (**6c** with OiC_3H_7 instead of OCH_3, Fig. 1),[10] and (3) by hydrolysis of **9c** (cf. below) to (*R*)-(−)-*p*-anisylglycine.

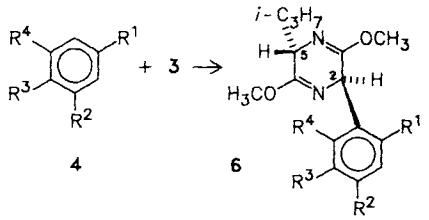

4 **6**

4,6: **a**, $R^1 = R^3 = OC_2H_5$, $R^2 = R^4 = H$
b, $R^1 = R^2 = R^4 = OCH_3$, $R^3 = H$
c, $R^1 = R^3 = R^4 = H$, $R^2 = OCH_3$
6d, $R^1 = OCH_3$, $R^2 = R^3 = R^4 = H$

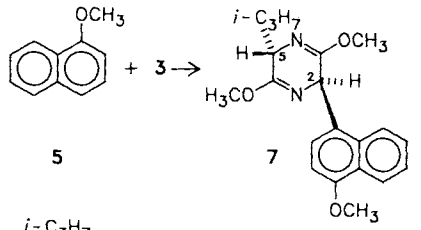

5 **7**

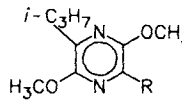

8a, R = H
8b, R = Aryl

Table 1. FC adducts **6a–d**, **7**.

	6a	**6b**	**6c**	**6d**	**7**
Yield [%]	65	67	62 (11.5 : 1) [a]		71
(2*R*,5*S*) : (2*S*,5*S*) [b]	93.5 : 6.5 [c]	65 : 35 [d]	95 [a] : 5 [a]	97 : 3 [a]	94.5 : 5.5 [e]
M.p. [°C]	66–67 [c]	172–174 [d]	42–43 [f]		96–97 [e]

[a] Separated by GC [8]; only the (2*R*,5*S*) isomer was isolated in the case of **6d**. [b] Determined by capillary GC [9] of the crude products. [c] The main diastereomer crystallizes from cyclohexane. [d] The main diastereomer crystallizes from cyclohexane/dichloromethane at 4°C. [e] The main diastereomer crystallizes from pentane. [f] The main diastereomer crystallizes upon standing.

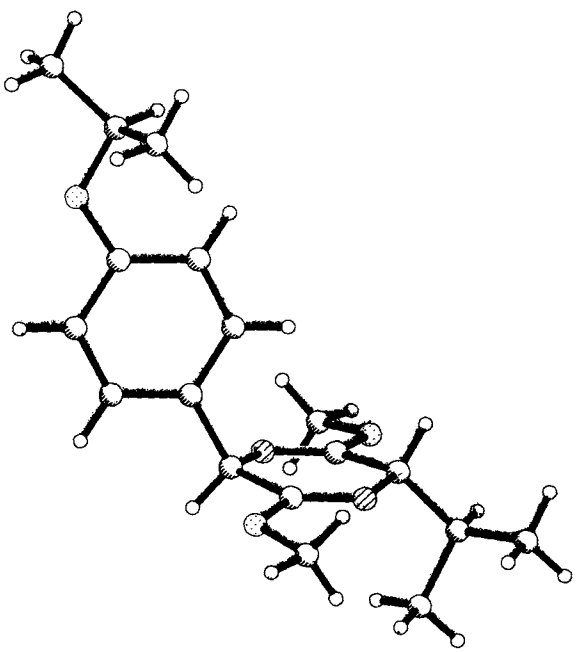

Fig. 1. Crystal structure of an FC adduct (**6c** with OiC_3H_7 instead of OCH_3); ⊗ = O, ⊘ = N. Noteworthy is the orthogonality of the aryl ring and the heterocycle [11].

[*] Prof. Dr. U. Schöllkopf, Dipl.-Chem. S. Grüttner, Dr. R. Anderskewitz
Institut für Organische Chemie der Universität
Tammannstrasse 2, D-3400 Göttingen (FRG)
Dr. E. Egert, M. Dyrbusch
Institut für Anorganische Chemie der Universität
Tammannstrasse 4, D-3400 Göttingen (FRG)

[**] Asymmetric Syntheses via Heterocyclic Intermediates, Part 35.—Part 34: U. Schöllkopf, W. Kühnle, E. Egert, M. Dyrbusch, *Angew. Chem. 99* (1987) 480; *Angew. Chem. Int. Ed. Engl. 26* (1987) 480.

Because of the danger of epimerization or racemization, the FC adducts **6a–c** have to be hydrolyzed, under the mildest conditions possible (0.1 N HCl, 2 equivalents, room temperature), to the previously unknown (*R*)-α-arylglycine methyl esters **9a–c** and L-valine methyl ester **10**.[11] As for **6c**, even under these conditions, 5–10% epimerization/racemization took place. The L-valine methyl ester that is formed along with the desired compound **9** could be removed under vacuum. Since the configuration of *p*-anisylglycine is known,[12] we hydrolyzed **9c** with 6 N HCl

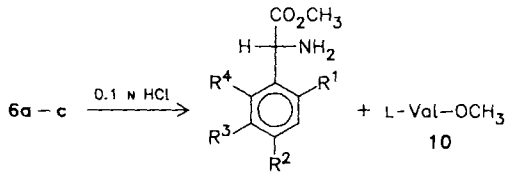

9a – c

a, $R^1 = R^3 = OC_2H_5$, $R^2 = R^4 = H$
b, $R^1 = R^2 = R^4 = OCH_3$, $R^3 = H$
c, $R^1 = R^3 = R^4 = H$, $R^2 = OCH_3$

and obtained (*R*)-(−)-*p*-anisylglycine even though partial racemization occurred under the relatively drastic reaction conditions.

Experimental Procedure

Correct elemental analyses of all compounds. $[\alpha]_D^{20}$ values for $c \approx 1.3$ g/100 mL ethanol; 100-MHz ^{1}H-NMR spectra in $CDCl_3$.

6a: To the solution of **4a** (3.32 g, 20.0 mmol) in 40 mL of dichloromethane, $SnCl_4$ (1.30 g, 5.0 mmol) was injected at −78°C, the resulting solution was stirred for a short period, and the chloride **2** (as a solution in dichloromethane [5]), prepared from 0.92 g (5.0 mmol) of **1** according to [5], was then injected. After 6 h at −78°C, 50 mL of phosphate buffer (pH = 7) and 20 mL of dichloromethane were added, the phases were separated, and the aqueous phase was extracted three times with 30 mL of chloroform [13]. After drying of the organic phase with $MgSO_4$ and removal of the solvent under reduced pressure (12 torr), a residue was obtained which contained excess **4a**, **6a**, and a small amount of **8a**; the latter was removed at 25°C/10^{-3} torr. Distillation of the residue at 10^{-2} torr in a kugelrohr apparatus gave **4a** as forerun. Yield of **6a**: 1.14 g (65%), b.p. = 150°C/10^{-2} torr. Addition of a small amount of cyclohexane eventually resulted in the crystallization of (2*R*,5*S*)-**6a** (m.p. = 66–67°C).

6b: Synthesized analogously to **6a** from **4b** (0.84 g, 5.0 mmol), $SnCl_4$ (1.04 g, 4.0 mmol), and **1** (0.74 g, 4.0 mmol). Excess **4b** was removed from the final residue at 60°C/10^{-4} torr. Yield of **6b**: 0.94 g (67%), mixture of diastereomers. Crystallization from cyclohexane/dichloromethane at 4°C gave (2*R*,5*S*)-**6b**, m.p. ≈ 172–174°C.

6c/d: Synthesized analogously to **6a** from **4c** (0.43 g, 4.0 mmol), $SnCl_4$ (0.52 g, 2.0 mmol), and **1** (0.37 g, 2.0 mmol). Excess **4c** was removed from the residue at 20°C/10^{-3} torr. Yield of **6c/d**: 0.36 g (62%), contaminated with a small amount of **8a,b** [14]. **6c** and **6d** had to be separated by gas chromatography [8].

7: Synthesized analogously to **6a** from **5** (0.55 g, 3.5 mmol), $SnCl_4$ (0.78 g, 3.0 mmol), and **1** (0.55 g, 3.0 mmol). Most of the excess **5** was removed from the residue at 20°C/10^{-4} torr. Crude yield of **7**: 0.32 g (71%). Recrystallization from pentane gave (2*R*,5*S*)-**7**, m.p. = 96–97°C.

9a: **6a** (0.32 g, 1.0 mmol) was allowed to stir for 12 h at room temperature with 20 mL (2.0 mmol) of 0.1 N HCl and ca. 5 mL of tetrahydrofuran. The reaction mixture was extracted with ca. 20 mL of ether (which was discarded) and then saturated with NaCl. Approximately 15 mL of ether was added followed by conc. NH_3 (with vigorous stirring) until the pH was 9–10. The ether phase was separated and the aqueous phase was extracted three times with 15 mL of ether. The combined ether extracts were dried with $MgSO_4$. Removal of the ether under vacuum and of **10** at 50°C/10^{-3} torr (kugelrohr) gave 0.26 g (89%) of **9a**, *ee* > 95% [15], $[\alpha]_D^{20} = -94.4°$. Partial racemization of **9a** occurred upon distillation (100°C/10^{-2} torr). ^{1}H-NMR: $\delta = 1.34$ (t, $J = 7$ Hz, 6H; OCH_2CH_3), 1.97 (s, 2H; NH_2), 3.68 (s, 3H; CO_2CH_3), 3.96 (q, $J = 7$ Hz, 4H; OCH_2CH_3), 4.64 (s, 1H; CH–CO–), 6.65–6.90 (3H; aryl-H).

9b: Synthesized analogously to **9a** from (2*R*,5*S*)-**6b** (0.35 g, 1.0 mmol); **9b** (0.135 g, 60%), *ee* > 95% [15], $[\alpha]_D^{20} = -77.6°$, m.p. ≈ 75–77°C. ^{1}H-NMR: $\delta = 1.93$ (br. s, 2H; NH_2), 3.66 (s, 3H; CO_2CH_3), 3.80 (s, 6H; *o*-OCH_3), 3.81 (s, 3H; *p*-OCH_3), 4.93 (s, 1H; CH–CO–), 6.13 (2H; aryl-H).

9c: Synthesized analogously to **9a** from (2*R*,5*S*)-**6c** (0.43 g, 1.5 mmol) (*de* ≈ 89%, separated from **6d** by GC [8]), 2 h hydrolysis; **9c** (0.20 g, 69%), *ee* ≈ 84% [15], $[\alpha]_D^{20} = -117.3°$, m.p. = 64–65°C. ^{1}H-NMR: $\delta = 1.90$ (s, 2H; NH_2), 3.66 (s, 3H; *p*-OCH_3), 3.77 (s, 3H; CO_2CH_3), 4.52 (s, 1H; CH–CO–), 6.81–7.22 (4H; aryl-H).

Received: February 13, 1987;
revised: March 24, 1987 [Z 2103 IE]
German version: *Angew. Chem. 99* (1987) 717

[1] Reviews: U. Schöllkopf, *Pure Appl. Chem. 55* (1983) 1799; *Chem. Scr. 25* (1985) 105; in H. Prinzbach, G. Schill, K. Streith (Ed.): *Organic Synthesis: An Interdisciplinary Challenge*, Blackwell, Oxford 1985, p. 101ff.
[2] For achiral glycine-cation equivalents, see D. Ben-Ishai, S. Hirsch, *Tetrahedron Lett. 24* (1983) 955 and other publications of this group, T. Shono, *Tetrahedron 40* (1984) 811; R. Kober, W. Hammes, W. Steglich, W. D. Bennet, M. J. O'Donell, R. L. Polt, *Tetrahedron Lett. 26* (1985) 695; Y. Ozaki, T. Iwasaki, H. Harikawa, M. Miyoshi, K. Madzumoto, *J. Org. Chem. 44* (1979) 391; for chiral glycine-cation equivalents, see R. Kober, K. Papadopoulos, W. Miltz, D. Enders, W. Steglich, H. Reuter, H. Puff, *Tetrahedron 41* (1985) 1693; P. J. Sinclair, D. Zhai, J. Reibenspies, R. M. Williams, *J. Am. Chem. Soc. 108* (1986) 1103.
[3] For example, D-phenylglycine or D-*p*-hydroxyphenylglycine as side chains in the semisynthetic penicillins, ampicillins, or amoxycillins.
[4] a) K. Weinges, H. Brachmann, P. Stahnecker, H. Rodewald, M. Nixdorf, H. Irngartinger, *Liebigs Ann. Chem. 1985*, 566; b) K. Weinges, G. Brune, H. Droste, *ibid. 1980*, 212; c) S. Yamada, S. Hashimoto, *Chem. Lett. 1976*, 921.
[5] U. Schöllkopf, H.-J. Neubauer, M. Hauptreif, *Angew. Chem. 97* (1985) 1065; *Angew. Chem. Int. Ed. Engl. 24* (1985) 1066. The procedure is carried out initially as described starting from **1** (0.92 g, 5.0 mmol). After reaction with hexachloroethane, the tetrahydrofuran is removed under vacuum, **2** is extracted with ca. 40 mL of petroleum ether, the LiCl is filtered off, the petroleum ether is removed under vacuum, and **2** (5.0 mmol) is dissolved in 10 mL of dichloromethane.
[6] U. Schöllkopf, U. Groth, C. Deng, *Angew. Chem. 93* (1981) 791; *Angew. Chem. Int. Ed. Engl. 20* (1981) 798; **1** is commercially available: Merck-Schuchardt, D-6100 Darmstadt (FRG), MS-Info 85-14.
[7] Nonactivated arenes do not react.
[8] Preparative GC: Varian 220, 2.2-m glass column, OV-220 on Chromosorb-W (AW-DMCS, 60/80 mesh), $p = 14$–17 N·cm^{-2} ($T = 160$°C, H_2 as carrier gas. Relative retention times: *trans*-**6c** : *cis*-**6c** : **6d** = 1 : 1.64 : 1.74.
[9] Varian 3700, Durabond-1; 30 m, H_2 as carrier gas.
[10] Space group $P2_1$, $a = 1376.7(1)$, $b = 1026.4(1)$, $c = 1435.6(1)$ pm, $\beta = 114.66(1)°$, $V = 1.844$ nm^3, $Z = 4$, $\mu = 0.07$ nm^{-1} ($Mo_{K\alpha}$); crystal dimension: $0.7 \times 0.6 \times 0.5$ mm^3; 3961 measured intensities, $2\omega_{max} = 50°$, 3448 unique reflections with $|F| > 3\sigma(F)$ used for the structure solution (direct methods) and refinement; C, N, and O atoms refined anisotropically, H atoms localized by difference electron density determinations and refined with a "riding" model. $R = 0.037$ ($R_w = 0.040$, $w^{-1} = \sigma(F^2) + 0.0006 \cdot F^2$). Further details of the crystal structure investigation may be obtained from the Fachinformationszentrum Energie, Physik, Mathematik GmbH, D-7514 Eggenstein-Leopoldshafen 2 (FRG), on quoting the depository number CSD-52388, the names of the authors, and the journal citation.
[11] It is surprising that the compounds **6a–c**, which contain an aryl ring at C2 capable of undergoing conjugation, do not rapidly tautomerize in acidic medium to enamines and thus undergo epimerization at C2. As shown by the X-ray structure analysis (Fig. 1), the aryl ring is orthogonal to the heterocycle. This conformation is presumably strongly fixed by the *o*-substituted aryl rings (**6a,b**, 7). Thus, no π conjugation is possible between the aryl ring and the potential enamine double bond.
[12] R. F. Eizemberger, A. S. Ammons, *Org. Prep. Proced. Int. 8* (1976) 149.
[13] The use of chloroform instead of dichloromethane results in better separation of the phases upon extraction.
[14] If necessary, **8a** can be separated by low-pressure chromatography (silica gel, ether/petroleum ether = 1/3). However, **6c/d** thereby epimerize to a small extent.
[15] Determined with 40-mol% Eu(tfc)$_3$ at the ^{1}H-NMR signal of the ester OCH_3 group ($CDCl_3$); >95% was assumed when the signals were shifted but no splitting occurred.

A Mixed-Metal Cluster with Two Quadruply-Bridging Carbonyl Ligands**

By *Richard D. Adams,* James E. Babin,* and *Miklos Tasi*

Although complexes containing quadruply bridging (μ_4) carbonyl ligands have been known for over ten years,[1] the number of examples of these bonding modes is still very small.[2,3] Sideways coordination and CO bond order reduction[3,4] are believed to be prerequisites for the C–O bond cleavage reactions that occur on metal surfaces.[5] We now wish to report the first example of a transition metal cluster compound that contains two quadruply bridging carbonyl ligands.

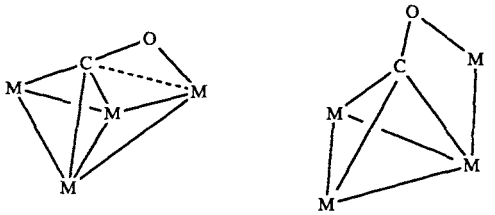

A B

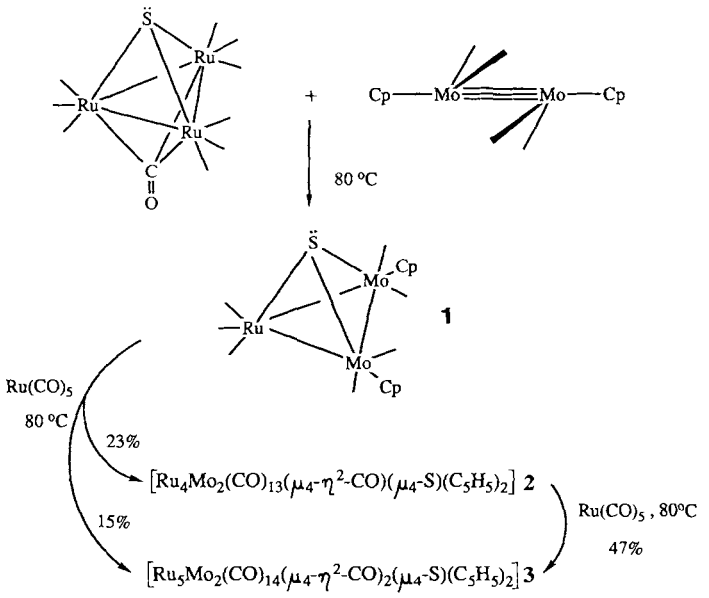

Scheme 1. The lines from the metal atoms represent CO-ligands.

The products **1** (49%),[6] **2** (3%), and **3** (9%) were isolated by thin-layer chromatography from the reaction of $[Ru_3(CO)_9(\mu_3\text{-}CO)(\mu_3\text{-}S)]$ with $[CpMo(CO)_2]_2$ in benzene at 80 °C (Scheme 1). All three compounds were characterized by IR and ^{1}H-NMR spectroscopy and X-ray crystallographic analyses.[7,8] The molecular structures of **2** and **3** are shown in Figure 1. Both compounds contain square-pyramidal Ru_3Mo_2-clusters. The molybdenum atoms occupy the apical and one basal position of the pyramid. The base is bridged by a μ_4-sulfido ligand. Compound **3** contains two μ_4-carbonyl ligands and has a crystallographically imposed plane of symmetry that passes through the two molybdenum atoms, Ru1 and the sulfur atom. In **2**, one Ru–Ru basal edge is bridged by a $Ru(CO)_3$ group, while in **3** both Ru–Ru basal edges are bridged by $Ru(CO)_3$ groups. Both compounds contain π-bonded μ_4-carbonyl groups arranged such that the carbon atoms bridge Ru_2Mo triangular faces of the cluster and the oxygen atoms are bonded to the bridging $Ru(CO)_3$ groups. The C–O distances in these ligands are large; they are 1.262(8) Å in **2** and 1.25(1) Å in **3**, and indicate a significant reduction in the CO bond order. This is further supported by the IR spectra, which show very low frequencies for the C–O stretching vibrations in **2** (1457 cm^{-1}) and **3** (1453 and 1419 cm^{-1}).[2] The observation of two IR absorptions for the μ_4-CO ligands in **3** indicates that vibrational coupling is important even for quadruply bridging carbonyl ligands. Compounds **2** and **3** can also be obtained from the reaction of **1** with $[Ru(CO)_5]$ at 80 °C (Scheme 1).

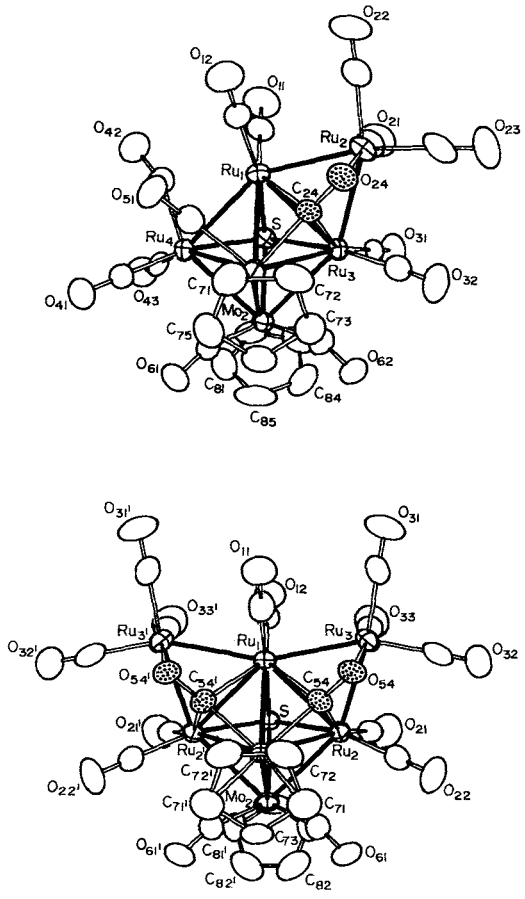

Fig. 1. Top: Crystal structure of **2**. Selected bond distances [Å] and angles [°]: Ru1-Ru3 2.864(1), Ru1-Ru4 2.841(1), Mo1-Ru1 3.022(1), Mo1-Ru3 2.887(1), Mo1-Ru4 2.937(1), Mo1-Mo2 3.117(1), Mo1-C24 1.940(8), Ru1-C24 2.315(7), Ru3-C24 2.259(8), Ru2-O24 2.136(5), C24-O24 1.262(8), Mo1-C24-O24 149.1(6).—Bottom: Crystal structure of **3**. Selected bond distances [Å] and angles [°]: Ru1-Ru2 2.867(1), Mo1-Ru1 2.918(2), Mo1-Ru2 2.897(1), Mo1-Mo2 3.049(2), Mo2-Ru2 2.887(1), Mo1-C54 1.98(1), Ru1-C54 2.36(1), Ru2-C54 2.18(1), Ru3-O54 2.125(7), C54-O54 1.25(1), Mo1-C54-O54 148.0(8).

A flurry of interest has greeted the growing study of mixed metal compounds.[9] An understanding of the heterosite-coordination and -reactivity[10] that occurs in

[*] Prof. R. D. Adams, J. E. Babin, Dr. M. Tasi
Department of Chemistry
University of South Carolina
Columbia, SC 29208 (USA)

[**] This work was supported by the National Science Foundation (USA).

these compounds could contribute to an understanding of catalysis by metal alloys.[11]

Received: February 16, 1987;
supplemented: April 27, 1987 [Z 2105 IE]
German version: *Angew. Chem. 99* (1987) 691

[1] M. Manassero, M. Sansoni, G. Longoni, *J. Chem. Soc. Chem. Commun. 1976*, 919.
[2] C. P. Horwitz, D. F. Shriver, *Adv. Organomet. Chem. 23* (1984) 219.
[3] P. Brun, G. M. Dawkins, M. Green, A. D. Miles, A. G. Orpen, F. G. A. Stone, *J. Chem. Soc. Chem. Commun. 1982*, 926.
[4] E. L. Muetterties, *Bull. Soc. Chim. Belg. 85* (1976) 451.
[5] a) E. L. Muetterties, J. Stein, *Chem. Rev. 79* (1979) 479; b) V. Ponec, *Catal. Rev.-Sci. Eng. 18* (1978) 151; c) K. Kishi, M. W. Roberts, *J. Chem. Soc. Faraday Trans. 71* (1975) 1715; d) A. Jones, B. D. McNicol, *J. Catal. 47* (1977) 384; e) P. Biloen, J. N. Helle, W. H. Sachtler, *J. Catal. 58* (1979) 95; f) H. H. Nijs, P. A. Jacobs, *ibid. 66* (1980) 401; g) J. A. Rabo, A. P. Risch, M. L. Poutsma, *ibid. 53* (1978) 295.
[6] F. Richter, E. Roland, H. Vahrenkamp, *Chem. Ber. 117* (1984) 2429.
[7] ^{1}H-NMR ($CDCl_3$, 298 K)—**1**: IR (hexane, cm^{-1}): $\nu = 2065$ vs, 2007 vs, 1989 m, 1977 w, 1890 w (CO); ^{1}H-NMR: $\delta = 5.28$ (s, 10H).—**2**: IR (CH_2Cl_2, cm^{-1}): $\nu = 2082$ vs, 2049 s, 2017 vs, 2002 s, sh, 1956 m, 1841 m, 1802 w, 1457 w; ^{1}H-NMR: $\delta = 5.67$ (s, 5H), 5.03 (s, 5H).—**3**: IR (CD_2Cl_2, cm^{-1}): $\nu = 2090$ s, 2073 vs, 2020 vs, 2004 s, sh, 1993 m, 1958 m, 1847 w, 1801 vw, 1453 vw, 1419 vw; ^{1}H-NMR: $\delta = 5.72$ (s, 5H), 5.23 (s, 5H).
[8] **2**: $Ru_4Mo_2SO_{14}C_{24}H_{10}$, monoclinic, $P2_1/c$, $a = 16.094(1)$, $b = 11.559(2)$, $c = 17.420(3)$ Å, $\beta = 113.67(1)°$, $Z = 4$, $V = 2968(1)$ Å^3, 3202 reflections ($I > 3\sigma(I)$), $R = 0.029$, $2\theta_{max} = 48°$, $T = 296$ K, $Mo_{K\alpha}$. Structure solution by direct methods (MITHRIL).—**3**: $Ru_5Mo_2SO_{16}C_{26}H_{10} \cdot 0.5\,C_6H_6$, monoclinic, $P2_1/m$, $a = 13.045(3)$, $b = 15.308(4)$, $c = 10.055(1)$ Å, $\beta = 111.79(1)°$, $Z = 2$, $V = 1864(1)$ Å^3, 2161 reflections ($I > 3\sigma(I)$), $R = 0.040$, $2\theta_{max} = 48°$, $T = 296$ K, $Mo_{K\alpha}$. Structure solution by direct methods (MITHRIL). Further details of the crystal structure investigation may be obtained from the Fachinformationszentrum Energie, Physik, Mathematik GmbH, D-7514 Eggenstein-Leopoldshafen 2 (FRG), on quoting the depository number CSD-52314, the names of the authors, and the journal citation.
[9] a) M. I. Bruce, *J. Organomet. Chem. 257* (1983) 417. b) M. I. Bruce, *ibid. 242* (1982) 147. c) D. A. Roberts, G. L. Geoffroy in G. Wilkinson, F. G. A. Stone, E. Abel (Eds.): *Comprehensive Organometallic Chemistry, Vol. 6*, Pergamon, Oxford 1982, Chap. 40.
[10] a) H. Vahrenkamp, *Adv. Organomet. Chem. 22* (1983) 169; b) H. Vahrenkamp, *Phil. Trans. R. Soc. London A 308* (1982) 17; c) C. von Schnering, T. Albiez, W. Bernhardt, H. Vahrenkamp, *Angew. Chem. 98* (1986) 474; *Angew. Chem. Int. Ed. Engl. 25* (1986) 479.
[11] V. Ponec, *Adv. Catal. 32* (1983) 149.

Hydride Abstraction From $[C_6H_6Os(CO)(CH_3)_2]$: Does a Metal-bound Methyl Group Migrate Preferentially to a CO or to a CH_2 Ligand?**

By *Karin Roder* and *Helmut Werner**

Dedicated to Dr. Reinhard Schliebs on the occasion of his 60th birthday

The concepts regarding the mechanism of the Fischer–Tropsch process include the assumption that primary C–C bond formation on the surface of the catalyst occurs by combination of a CH_3 with a CO group or with a CH_2 group formed in a hydrogenation step.[1] Model examples for both of these processes are known using both mono- and dinuclear metal complexes as starting materials.[2,3] However, a remaining question is whether the C–C bond forming step (a) or (b) of Scheme 1 is preferred, i.e., which of the competing ligands CH_2 or CO couples with the CH_3 group.

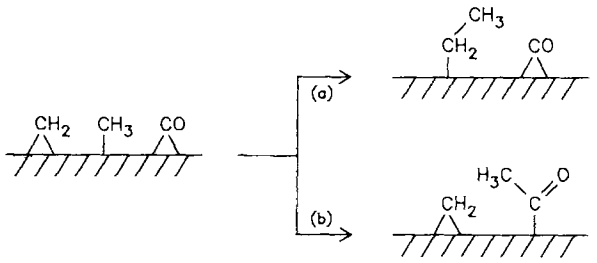

Scheme 1.

To answer this question, we have prepared compound **3** from **1** and studied its reaction with Ph_3CPF_6. Besides $CHPh_3$ (detected by ^{1}H-NMR and MS), only the ethylene hydrido complex **5a** is formed. In accord with the results of previous investigations,[4] we propose that the trityl cation abstracts a hydride ion from one of the CH_3 groups. The intermediate **4** can then rearrange by CH_3 migration (probably not by CH_2 insertion![3e]) to give the corresponding ethylmetal compound, from which complex **5a** is formed by β-hydride elimination. There is no evidence that radical species (which have been observed during the formation of $[(C_5H_5)_2WH(C_2H_4)]^+$ from $[(C_5H_5)_2W(CH_3)_2]$ and Ph_3CPF_6[5]) are involved in this process.

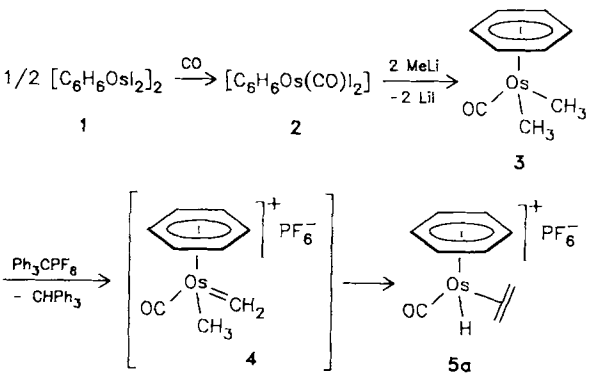

The properties (color, thermal stability, conductivity) and spectroscopic data of **5a**[6] are similar to those of the analogous complex $[C_6H_6OsH(C_2H_4)PMe_3][PF_6]$,[7] which has recently been prepared by a completely different route. For neither $OsH(C_2H_4)$ complex has an equilibrium with the corresponding alkyl isomer been detected by NMR spectroscopy.

Deprotonation of the cation of **5a** with NaH in tetrahydrofuran (THF) leads to the formation of **6**, which is the first example of a half-sandwich type complex $[C_6H_6OsLL']$ which contains *two monodentate* π-acceptor ligands. Although the electron density at the metal atom in **6** is lower than that in the analogous complexes **7**[7] and **8**,[8] compound **6** can be protonated by strong acids. With HBF_4 (in ether) **5b** is obtained; however, NH_4PF_6 does not react with **6** to give **5a**. Therefore, complex **6**, like **7**, **8** and the compounds $[C_6H_6OsL_2]$ ($L = PPh_3$, $P(OMe)_3$)[8] behaves as a *metal base*. The metal basicity of compound **6** is comparable to that of $[C_6H_6Ru(C_2H_4)PMe_3]$ and $[C_6Me_6Ru(CO)PMe_3]$.[9]

5a $\xrightarrow[-NaPF_6,\ -H_2]{NaH}$ $[C_6H_6Os(C_2H_4)CO]$ (**6**) $\xrightarrow{HBF_4}$ $[C_6H_6OsH(C_2H_4)CO][BF_4]$ (**5b**)

$[C_6H_6Os(C_2H_4)PMe_3]$ (**7**) $[C_6H_6Os(CO)PMe_3]$ (**8**)

[*] Prof. Dr. H. Werner, Dipl.-Chem. K. Roder
Institut für anorganische Chemie der Universität
Am Hubland, D-8700 Würzburg (FRG)

[**] This work was supported by the Deutsche Forschungsgemeinschaft, the Fonds der Chemischen Industrie and Degussa AG. We highly appreciate the active collaboration of Miss *I. Keupp* in this project.

Using the bis(ethylene) complexes $[C_5H_5M(C_2H_4)_2]$ (M = Rh, Ir) as starting materials, *Perutz* and *Haddleton* et al.[10] have recently generated in low-temperature matrices the compounds $[C_5H_5M(C_2H_4)CO]$, which are structurally similar to **6**. These $[C_5H_5M(C_2H_4)CO]$ complexes activate C–H bonds (including methane!). Since $[C_6H_6Os(C_2H_4)_2]$ is as yet unknown, compound **6** is not accessible via this route. Furthermore, it has not been possible to prepare **6** by the same method which leads to **7**, **8** and the complexes $[C_6H_6OsL_2]$[7,8] (reduction of the corresponding haloosmium(II) cation with $NaC_{10}H_8$). The transformation of **3** into **6** by stepwise abstraction of a hydride ion and a proton represents a valuable alternative to previous synthetic routes and promises further possible applications. The observation made in this study, that a CH_3 group prefers to migrate to a CH_2 instead of a CO group, can also be regarded as indirectly supporting the "polymerization of methylene groups" mechanism first proposed by *Fischer* and *Tropsch* as long ago as 1926.[11]

Experimental

2: A suspension of **1** (1.00 g, 0.96 mmol) in CH_2Cl_2 (60 mL) was saturated with CO in a Schlenk tube fitted with N_2 inlet. After stirring for 20 h at room temperature under a CO atmosphere, the solution was concentrated to ca. 5 mL and the product precipitated with hexane. The precipitate was separated from the solution, repeatedly washed with hexane, and finally dried in vacuo; m.p. 197 °C (decomp.); yield quantitative.

3: A suspension of **2** (276 mg, 0.50 mmol) in benzene (5 mL) was treated slowly at room temperature with 3.3 mL of a 0.6 N solution of methyllithium in ether (2.0 mmol). An orange-brown solution immediately formed which was stirred for 10 min and then evaporated to dryness in vacuo. The residue was treated with a few mL of benzene/hexane (1 : 1), and excess of methyllithium was destroyed by careful addition of deactivated Al_2O_3 (activity grade V). After chromatography of the benzene/hexane solution on Al_2O_3 (activity grade III), a yellow fraction containing **3** was eluted with benzene/hexane (1 : 1). Removal of the solvent furnished **3** as a yellow microcrystalline powder; m.p. 130 °C (decomp.); yield 63%.

5a: A solution of **3** (75 mg, 0.23 mmol) in ether (3 mL) was treated dropwise at −78 °C with a solution of Ph_3CPF_6 (89 mg, 0.23 mmol) in CH_2Cl_2 (3 mL). After slow warming, the reaction mixture was stirred for 1 h at room temperature. The precipitation of a light-brown solid was completed by addition of 15 mL of ether. The precipitate was separated from the solution, washed with ether and hexane, and dried in vacuo; yield 91%.

6: A suspension of **5a** (107 mg, 0.23 mmol) in THF (3 mL) was treated at −78 °C with NaH (ca. tenfold excess). After warming to room temperature, the solution was stirred for 30 min (evolution of gas occurs), and the golden-brown suspension was then reduced to dryness. The residue was extracted in small portions with 20 mL of benzene/hexane (1 : 1), the solution filtered, and the solvent removed in vacuo. A yellow microcrystalline powder was obtained; m.p. 98 °C (dec.); yield 77%. The protonation of **6** with HBF_4 in ether to give **5b** proceeds quantitatively.

Received: February 17, 1987 [Z 2108 IE]
German version: *Angew. Chem.* *99* (1987) 719

[1] a) C. K. Rofer-DePoorter, *Chem. Rev.* *81* (1981) 447; b) W. A. Herrmann, *Angew. Chem.* *94* (1982) 118; *Angew. Chem. Int. Ed. Engl.* *21* (1982) 117; c) G. Henrici-Olivé, S. Olivé in F. R. Hartley, S. Patai (Eds.): *The Chemistry of the Metal-Carbon Bond, Vol. 3*, Wiley, New York 1985, Chapter 9.

[2] CO + CH_3: a) A. Wojcicki, *Adv. Organomet. Chem.* *11* (1973) 87; b) F. Calderazzo, *Angew. Chem.* *89* (1977) 305; *Angew. Chem. Int. Ed. Engl.* *16* (1977) 299; c) E. J. Kuhlmann, J. J. Alexander, *Coord. Chem. Rev.* *33* (1980) 195; d) T. C. Flood, *Top. Stereochem.* *12* (1981) 37; e) J. J. Alexander in F. R. Hartley, S. Patai (Eds.): *The Chemistry of the Metal-Carbon Bond. Vol. 2*, Wiley, New York 1985, Chapter 5.

[3] CH_2 + CH_3: a) R. C. Brady III, R. Pettit, *J. Am. Chem. Soc.* *102* (1980) 6181; b) K. Isobe, D. G. Andrews, B. E. Mann, P. M. Maitlis, *J. Chem. Soc. Chem. Commun.* *1981*, 809; I. M. Saez, N. J. Meanwell, A. Nutton, K. Isobe, A. Vazquez de Miguel, D. W. Bruce, S. Okeya, D. G. Andrews, P. R. Ashton, I. R. Johnstone, P. M. Maitlis, *J. Chem. Soc. Dalton Trans.* *1986*, 1565; c) D. L. Thorn, T. H. Tulip, *J. Am. Chem. Soc.* *103* (1981) 5984; D. L. Thorn, *Organometallics* *4* (1985) 192; *5* (1986) 1897; d) J. C. Hayes, G. D. N. Pearson, N. J. Cooper, *J. Am. Chem. Soc.* *103* (1981) 4648; e) Theoretical Work: H. Berke, R. Hoffmann, *ibid.* *100* (1978) 7224.

[4] a) H. Kletzin, H. Werner, O. Serhadli, M. L. Ziegler, *Angew. Chem.* *95* (1983) 49; *Angew. Chem. Int. Ed. Engl.* *22* (1983) 46; b) H. Werner, H. Kletzin, A. Höhn, W. Paul, W. Knaup, M. L. Ziegler, O. Serhadli, *J. Organomet. Chem.* *306* (1986) 227.

[5] J. C. Hayes, N. J. Cooper, *J. Am. Chem. Soc.* *104* (1982) 5570.

[6] **2**: M_r = 552 (MS); IR (KBr): ν(CO) = 1992 cm^{-1}; ^{1}H-NMR ([D$_6$]dimethyl sulfoxide): δ = 6.43 (s).—**3**: M_r = 328 (MS); IR (KBr): ν(CO) = 1925 cm^{-1}; ^{1}H-NMR (C_6H_6): δ = 4.64 (s, C_6H_6), 1.07 (s, CH_3).—**5a**: IR (KBr): ν(CO) = 2020 cm^{-1}; ^{1}H-NMR (CD_3NO_2): δ = 6.87 (s, C_6H_6), 3.31 (δ_A) and 2.63 (δ_B, AA'BB' spin system, N = 8.0 Hz) (C_2H_4), −11.97 (s, OsH); ^{13}C-NMR (CD_3NO_2): δ = 172.94 (s, CO), 99.61 (s, C_6H_6), 27.22 (s, C_2H_4).—**6**: M_r = 326 (MS); IR (KBr): ν(CO) = 1878 cm^{-1}; ^{1}H-NMR (C_6H_6): δ = 4.80 (s, C_6H_6), 2.05 (m, probably AA'BB' system of higher order, C_2H_4).

[7] R. Werner, H. Werner, *Chem. Ber.* *116* (1983) 2074.

[8] R. Werner, H. Werner, *Chem. Ber.* *115* (1982) 3781.

[9] Review: H. Werner, *Angew. Chem.* *95* (1983) 932; *Angew. Chem. Int. Ed. Engl.* *22* (1983) 927.

[10] a) D. M. Haddleton, R. N. Perutz, S. A. Jackson, R. K. Upmacis, M. Poliakoff, *J. Organomet. Chem.* *311* (1986) C15; b) D. M. Haddleton, *ibid.* *311* (1986) C21; c) D. M. Haddleton, R. N. Perutz, *J. Chem. Soc. Chem. Commun.* *1986*, 1734.

[11] F. Fischer, H. Tropsch, *Brennst.-Chem.* *7* (1926) 97; see also Ref. [1].

Square Hg_4 Clusters in the Compound CsHg

By *Hans-Jörg Deiseroth** and *Axel Strunck*

It is astounding that all the studies reported thus far on the phase diagrams and magnetic properties of such apparently uncomplicated substances as the binary rubidium- and cesium-amalgams were carried out exclusively in the first half of the century.[1–3] And, with the exception of $RbHg_{11}$,[4] nothing has hitherto been reported about the structures of these experimentally problematical compounds, which are of special interest in view of the possibility of weak bonding interactions between the electronically saturated mercury atoms. Extremely air-sensitive, lustrous single crystals and microcrystalline samples of the compounds $RbHg_2$, $CsHg_2$, RbHg[5] and CsHg[6] have now been prepared and structurally characterized for the first time.[7] Only CsHg will be reported upon in this communication.

The peritectically melting CsHg, probably the most mercury-deficient compound in the cesium-mercury system, is characterized by isolated, square-planar Hg_4 clusters with metallic Hg-Hg contacts ($d_{Hg\text{-}Hg} \approx 300$ pm) corresponding to a formulation Cs_4Hg_4 (Fig. 1). CsHg is thus the second example of a structure type which was previously only found in the isotypic KHg investigated in an older and lesser known work.[8] Cs_4Hg_4 and K_4Hg_4, however, differ in a remarkable way: whereas the distances between the square Hg-clusters in K_4Hg_4 (336 pm) resemble those between the nearest neighbors in α-Hg (300–340 pm), in Cs_4Hg_4 they are so large (419 pm) that there can be no direct Hg-interaction between neighboring clusters.

The crystal structure of CsHg depicted in Figure 1a clearly reveals a columnar stacking of the Hg_4 clusters, which are surrounded by larger rectangular stacks of Cs atoms. The plane of the Hg_4 square is so strongly inclined to the stacking axis [001] that there would appear to be the possibility of there being shorter Hg–Hg distances within the stacks. These distances are, however, considerably longer than the shortest Hg–Hg distances between neighboring stacks.

[*] Prof. Dr. H.-J. Deiseroth, Dipl.-Chem. A. Strunck
Fachbereich 8—Anorganische Chemie der
Universität-Gesamthochschule
Postfach 1012 40, D-5900 Siegen (FRG)

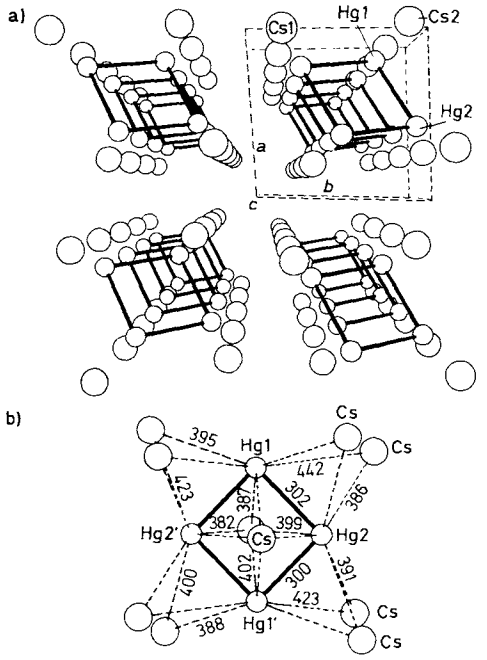

Fig. 1. a) Central perspective projection of the crystal structure of CsHg along [001]. b) Section from the crystal structure of CsHg with a Hg_4-cluster in the plane of the projection (all distances in pm, standard deviations smaller than 1 pm, distances not quoted can be completed by way of the symmetry center (midpoint of the Hg_4 square). The direction of viewing roughtly corresponds to the [111] direction of the triclinic unit cell. Angles [°]: Hg2-Hg1-Hg2' 88.2, Hg1-Hg2-Hg1 91.8.

The special role of the almost exactly square-planar Hg_4 units also follows from Figure 1b: the Hg atoms together with the Cs atoms in the immediate neighborhood form a characteristically distorted, almost cubic-face-centered unit with the Hg atoms located at four opposite face centers, but drastically shifted in the direction of the center of the cube. This immediately gives the impression of a bonding interaction between the Hg atoms.

So far, the only example of a compound containing similarly isolated square-planar Hg_4 clusters was the alkali-metal rich compound Na_3Hg_2 ($= Na_6Hg_4$).[9, 10] The structural data of the Hg_4 units in the three compounds Cs_4Hg_4, K_4Hg_4, and Na_6Hg_4 are almost identical. A square-planar Hg_4-unit as part of a Mn_4Hg_4 eight-membered ring is also present in the compound $[(\eta^5\text{-}CH_3C_5H_4)Mn(CO)_2Hg]_4$.[11]

The chemical bonding in Cs_4Hg_4 could correspond to a state between the two extremes $(Cs^{\oplus})_4(Hg_4)^{4\ominus}$ (mercuride, saltlike) and $(Cs^{\oplus})_4(Hg_4)^0 4e^{\ominus}$ (metallic with four free electrons). Measurements of the temperature-dependence of the electrical resistivity[12] clearly show that Cs_4Hg_4 and the other amalgams newly prepared by us are metals. The formulation $(Cs^{\oplus})_4(Hg_4)^0 4e^{\ominus}$ must therefore be regarded as being the more appropriate. Our assumption of isolated $(Hg_4)^0$ in Cs_4Hg_4 is also supported by the results of a relativistic MO calculation for free $(Hg_4)^0$.[13] Accordingly, the Hg-Hg bonds in $(Hg_4)^0$ have a bond order of 0.5, so that the cluster can be expected to be stable—even if only slightly so.

Photoionization spectroscopic studies of Hg_n clusters in the gas phase[14] do indeed confirm the presence of Hg_4 units, but do not permit any conclusions to be drawn about their structure and abundance.

Received: February 24, 1987;
revised: April 3, 1987 [Z 2112 IE]
German version: *Angew. Chem. 99* (1987) 701

[1] N. S. Kurnakov, G. J. Zukowsky, *Z. Anorg. Chem. 52* (1907) 416.
[2] W. Biltz, F. Weibke, H. Eggers, *Z. Anorg. Allg. Chem. 219* (1983) 119.
[3] W. Klemm, H. Hauschulz, *Z. Elektrochem. 45* (1939) 346.
[4] N. C. Baenziger, E. J. Duwell, *Acta Crystallogr. 7* (1954) 635.
[5] Part of the Dissertation by *A. Strunck*, Universität-Gesamthochschule Siegen 1987.
[6] *Sample preparation:* Extremely air-sensitive, gold-bronze colored microcrystalline CsHg (m.p. 96°C) was obtained by careful, dropwise addition (capillary dropping pipet) of an equimolar amount of mercury to doubly-distilled cesium. Single crystals of CsHg crystallized from a sample of Cs_3Hg prepared in a corresponding way after allowing the sample to stand for one week at room temperature.
[7] Crystallographic data for CsHg: space group $P\bar{1}$, $Z=4$, $a=715.4$, $b=747.0$, $c=763.5$ pm, $\alpha=107.82$, $\beta=103.34$, $\gamma=90.95°$; CAD4 single crystal diffractometer, $Mo_{K\alpha}$, room temperature, 1195 independent reflections with $I>3\sigma(I)$. Refinement factors: $R_{anisotr.}=0.074$, $R'=0.078$, experimental absorption correction (ψ-scan). Further details of the crystal structure investigation are available on request from the Fachinformationszentrum Energie, Physik, Mathematik GmbH, D-7514 Eggenstein-Leopoldshafen 2, on quoting the depository number CSD-52491, the names of the authors, and the journal citation.
[8] E. J. Duwell, N. C. Baenziger, *Acta Crystallogr. 8* (1955) 705.
[9] J. W. Nielsen, N. C. Baenziger, *Acta Crystallogr. 7* (1954) 277.
[10] J. D. Corbett, *Inorg. Nucl. Chem. Lett. 5* (1969) 81.
[11] W. Gäde, E. Weiss, *Angew. Chem. 93* (1981) 796; *Angew. Chem. Int. Ed. Engl. 20* (1981) 803.
[12] Measurements of the DC conductivity in the temperature range $T=1.4$ K to 290 K on powder pellets (method according to *van der Pauw*); Cs_4Hg_4: $\rho=208$ μΩ cm ($T=290$ K); $\rho=10$ μΩ cm ($T=1.4$ K); we thank Herr Dr. *Bauhofer* and Herr *Diem* (Max-Planck-Institut für Festkörperforschung, Stuttgart) for carrying out the measurements.
[13] W. H. E. Schwarz, H.-J. Deiseroth, unpublished; calculations with the relativistic Extended-Hückel Program ITEREX-85 (P. Pyykko, S. Larsson (Helsinki) 1985; $(Hg_4)^0$: D_{4h} symmetry, $d(Hg\text{-}Hg)=300$ pm.
[14] C. Brechignac, P. Cahuzac in S. Träger, G. zu Putlitz (Eds.): *Metal Clusters*, Springer, Berlin 1986, p. 21.

FCu[AuF_4], an Unusual Copper(II) Fluoroaurate(III)**

By *Bernd G. Müller**

Complex fluorides containing Cu^{2+} and Au^{3+} are of special interest because of their unusual structural chemistry: on the one hand, copper(II) fluorides with $3d^9$ configurated Cu^{2+} exhibit a structural behavior (Jahn-Teller effect) different from that of formally analogous compounds (such as those of the neighboring elements Ni, Zn), and, on the other, Au^{3+} is the only transition metal ion which exhibits exclusively coordination number four with square-planar arrangement toward fluorine. Furthermore, in the system CuF_2/AuF_3 the expected compound with the composition $Cu[AuF_4]_2$ (comparable to $M^{II}[AuF_4]_2$, $M^{II}=Mg$, Ni, Pd etc., up to Ba[1]) does not occur, instead (formally) only one F^- in CuF_2 is replaced by $[AuF_4]^-$.

The crystal structure of FCu[AuF_4] is remarkably simple:[2] in the center of the (triclinic) unit cell, linear $^1_\infty[-F(1)-Cu-F(1)-]$ chains (bond angle 180.0°) run parallel to [001]; four uncoupled $[AuF_4]^-$ groups are so arranged around each Cu^{2+} that the coordination number for Cu^{2+} is increased to C.N. = 6 (2+2+2). The structure of FCu[AuF_4] is reproduced in Figure 1: $[AuF_4]^-$ anions are stacked one above the other parallel to [001], each being so shifted (as a result of $\beta=98.7°$) that F(3) of one lies above Au^{3+} of the next $[AuF_4]^-$ unit at a distance $d_{Au-F(3)}=286.8$ pm. The $[AuF_4]^-$ group deviates only slightly from D_{4h} symmetry (all the F-Au-F angles are ap-

[*] Dr. B. G. Müller
Institut für Anorganische und Analytische Chemie der Universität
Heinrich-Buff-Ring 58, D-6300 Giessen (FRG)

[**] This work was supported by the Deutsche Forschungsgemeinschaft.

proximately 90° or 180°; only the distances (cf. Table 1) d_{Au-F} are slightly different), while the octahedral array around Cu^{2+} is noticeably distorted, especially with re-

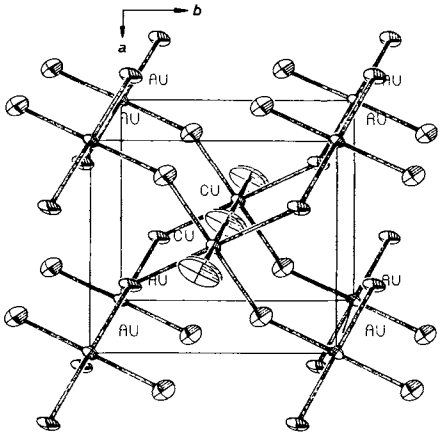

Fig. 1. Crystal structure of $FCu[AuF_4]$, view along [001].

spect to the distances d_{Cu-F} (cf. Table 1, the F(2)-Cu-F(3) angles are 87° (93°), all other angles are 180°). The interatomic distances are listed in Table 1, together with the motifs of mutual adjunction,[3] which provide information about the coupling and coordination sphere of the individual ions.

Table 1. Motifs of mutual adjunction, interatomic distances [pm], and coordination numbers.

	F(1)	F(2)	F(3)	C.N.
Cu^{2+}	2/2	2/1	2/1	6
d(Cu-F)	2×185.4(0)	2×221.6(1)	2×202.1(1)	(2+2+2)
Au^{3+}	—	2/1	2/1	4
d(Au-F)		2×193.0(1)	2×190.7(1)	
C.N. (F^-)	2	2	2	

As shown by the interatomic distances, $FCu[AuF_4]$ is an example of a structure with a d^9-configurated cation, in which this shows neither the "usual" environment with C.N. = 4+2 (elongated octahedron) nor the rarily observed C.N. = 2+4 (compressed octahedron), but assumes a special position with C.N. $[Cu^{2+}] = 2+2+2$. This is comparable with the situation found in $Ag_3Hf_2F_4$, in which isoelectronic Ag^{2+} ions with the coordination numbers C.N. = 4+2 as well as C.N. = 4+4 (more exactly: 4+2+2) are present.[4]

Magnetic measurements on $FCu[AuF_4]$ (μ_{eff}(251 K) = 1.32 B.M., μ_{eff}(13 K) = 0.32 B.M.) point to strong antiferromagnetic interaction along the linear [Cu-F(1)-Cu]-chains, which are shielded by diamagnetic $[AuF_4]^-$ groups. The ordering temperature, at which the (one-dimensional) antiferromagnetic coupling along these chains occurs, is $T_N \approx 85$ K.

Experimental

A mixture of equimolar amounts of CuO (Merck AR) and Au powder (prepared from 99.999% Au sheet (Degussa) by dissolution in HNO_3/HCl, repeated fuming-off with HCl and precipitation with SO_2) was treated with an F_2/N_2 mixture ($\approx 1:10$) at $T \leq 320$°C (AuF_3 sublimes from the reaction mixture at $T > 350$°C) ($t \approx 3$ d). The bright-yellow, microcrystalline samples were transferred under inert gas (dry Ar) to an annealed gold tube, which was then seal-welded and annealed at $T = 580$°C for ca. 4–5 weeks. The bright-yellow, transparent, irregular crystals could be selected and isolated under anhydrous petroleum (Na wire).

Received: February 26, 1987 [Z 2113 IE]
German version: *Angew. Chem.* 99 (1987) 685

[1] B. G. Müller in *Chemie-Dozententagung 1985* (Aachen, March 25-29, 1985), VCH Verlagsgesellschaft, Weinheim 1985, p. 105.
[2] $P\bar{1}$; $a = 553.6$, $b = 497.9$, $c = 370.7$ pm; $\alpha = 107.6$, $\beta = 98.77$, $\gamma = 89.63$°; Philips PW1100 four-circle diffractometer, $Ag_{K\alpha}$; 770 reflections; $R = 0.080$, $R_w = 0.068$. Further details of the crystal structure investigation are available on request from the Fachinformationszentrum Energie, Physik, Mathematik GmbH, D-7514 Eggenstein-Leopoldshafen 2 (FRG), on quoting the depository number CSD-52382, the name of the author, and the journal citation.
[3] R. Hoppe, *Angew. Chem.* 92 (1980) 106; *Angew. Chem. Int. Ed. Engl.* 19 (1980) 110.
[4] B. G. Müller, *J. Fluorine Chem.* 29 (1985) 69.

$Ag[MF_6]_2$ (M = Nb, Ta), Ternary fluorides of Divalent Silber**

By *Bernd G. Müller**

Ternary silver(II) fluorides are compounds of general interest, yet very little is known about their structures and properties. Thus, the structures of complex fluorides of divalent silver (just like the structure of AgF_2 itself) differ noticeably from those of formally analogous compounds of other elements—so far as they exist—due to the $4d^9$-configuration of Ag^{2+} (Jahn-Teller effect). Because of different ionic radii this also holds for corresponding fluorides containing isoelectronic $Cu^{2+}(3d^9)$. Furthermore, as a result of the frequently changing coordination numbers (C.N.) of Ag^{2+} toward F^- (e.g. $BaAgF_4$, C.N. = 4;[1] $CsAgFeF_6$, C.N. = 2+4;[2] $NaAgZr_2F_{11}$, C.N. = 2+2+2;[3] $Ag_3Hf_2F_{14}$, C.N. = 4+2 as well as 4+4[4]) predictions of the type and extent of Jahn-Teller deformation to be expected is not possible, particularly in the case of silver(II) compounds; detailed single-crystal investigations are therefore necessary in each of these cases. In addition, due to the high redox potential of Ag^{2+}, the number of compounds of simple composition (i.e. those compounds without additional stabilization by organic ligands such as py, bpy etc.) remains limited to fluorides and a few oxides (cf. e.g. ref. [5]), and, moreover, these are relatively difficultly accessible and readily decomposable.

The synthesis of $Ag[MF_6]_2$ (M = Nb, Ta), especially in the form of single crystals, is not simple because of the volatility of MF_5 and the thermal instability of $Ag[MF_6]_2$ (decomposition to $AgMF_6$, MF_5, F_2 as well as AgF and MF_5); the brilliant bright-blue samples are extremely sensitive to hydrolysis and attack the walls of the glass ampules on prolonged storage. The synthesis must therefore be carried out in autoclaves ($p_{F_2} \approx 3$ kbar) and the samples are usually inhomogeneous as a result of partial decomposition. Remarkably, in such experiments (360°C < $T \leq 400$°C) the needle-like, frequently clustered and twinned crystals separate out on the upper (colder) part of the autoclave (m.p. $(AgF_2) > 620$°C!).

[*] Dr. B. G. Müller
Institut für Anorganische und Analytische Chemie der Universität
Heinrich-Buff-Ring 58, D-6300 Giessen (FRG)

[**] This work was supported by the Deutsche Forschungsgemeinschaft.

Table 1. Motifs of mutual adjunction, interatomic distances [pm], and coordination numbers (C.N.).

	F(1)	F(2)	F(3)	F(4)	F(5)	F(6)	C.N.
Ag^{2+}	—	—	—	2/1	2/1	2/1	4+2
d(Ag-F)	—	—	—	2×236.7(7)	2×206.7(7)	2×203.0(6)	
Ta^{5+}	1/1	1/1	1/1	1/1	1/1	1/1	6
d(Ta-F)	181.7(7)	186.5(7)	183.4(6)	191.0(7)	197.6(6)	200.0(6)	
C.N.(F^-)	1	1	1	2	2	2	

The structure of $Ag[TaF_6]_2$ is best described in terms of a layer structure (Fig. 1):[6] Three $[AgF_6]$-octahedra are each coupled alternately "above and below" the (100) plane by three *cis* F^- forming a triangular face of a markedly distorted $[TaF_6]$-octahedron; cf. motifs of mutual adjunction[7] in Table 1.

No further coupling via cations takes place between these (two-dimensional) "layer packets".

$$[Ag(\overset{4}{F}_{1/2})_2\,(\overset{5}{F}_{1/2})_2\,(\overset{6}{F}_{1/2})_2]\,[\overset{4}{F}_{1/2}\,\overset{5}{F}_{1/2}\,\overset{6}{F}_{1/2}\,Ta\,\overset{1}{F}_{1/1}\,\overset{2}{F}_{1/1}\,\overset{3}{F}_{1/1}]_{6/3}$$

As follows from the interatomic distances (Table 1), Ag^{2+} in this type of compound shows the expected and favored elongated octahedral coordination for d^9-configurated cations. This, as mentioned at the outset, is certainly not the rule but rather an exception in the case of divalent silver. According to the crystal data ($a=906.1$, $b=560.7$, $c=520.7$ pm, $\alpha=118.7$, $\beta=91.61$, $\gamma=102.3°$) (four-circle diffractomer measurement) $Ag[NbF_6]_2$ is isotypic.

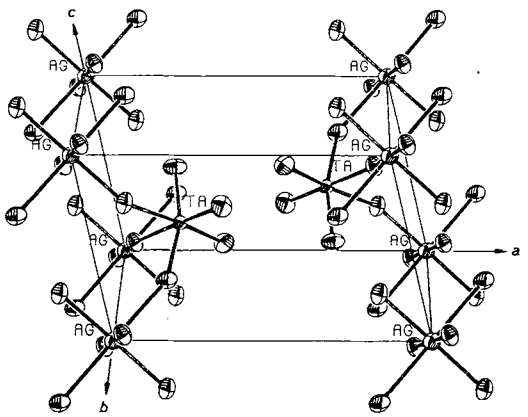

Fig. 1. Crystal structure of $Ag[TaF_6]_2$.

$Ag[TaF_6]_2$ is paramagnetic, the Curie or Curie-Weiss law is obeyed down to ca. 13 K ($\mu_{eff}(251\,K)=1.95$ B.M.; $\mu_{eff}(13\,K)=1.90$ B.M., $\theta_{calc}=3.1$ (± 1.1) K). This finding is understandable, because the AgF_6 octahedra are isolated from each other and consequently a magnetic interaction via F^- bridges is not possible.

Experimental

About 200–300 mg of an equimolar amount of Ag_2O (Merck p.a.) and M_2O_5 (pure, Merck) was transferred to an open Monel cylinder and inserted into a stainless-steel autoclave furnished with a Monel inlet. The autoclave (total volume: ca. 6 mL) was then cooled (with $(N_2)_{liq}$) to $-196°C$ and filled with ca. 4.5 mL $(F_2)_{liq}$ (the fluorine was taken from a steel bomb (Kali Chemie), passed over NaF to remove HF, condensed into a calibrated cold finger (Duran glass), and finally distilled into the autoclave). The (still) cold autoclave was placed in a furnace preheated to ca. 300°C; the furnace was then brought to 380–400°C ($p_{F_2}=3.4$ kbar) and kept at this temperature for 5–6 weeks (formation of single crystals). After slow cooling to room temperature the F_2/O_2 mixture still remaining was removed by distillation at $-196°C$ and the autoclave (again at room temperature and still under residual fluorine) finally opened. The samples were transferred into carefully baked out glass vessels under dry argon and worked up or stored at $-20°C$ in a refrigerator.

Received: February 26, 1987 [Z 2114 IE]
German version: *Angew. Chem.* 99 (1987) 685

[1] R.-M. Odenthal, R. Hoppe, *Z. Anorg. Allg. Chem.* 385 (1971) 92.
[2] B. G. Müller, *J. Fluorine Chem.* 17 (1981) 317/329.
[3] B. G. Müller, *Z. Anorg. Allg. Chem.*, in press.
[4] B. G. Müller, *J. Fluorine Chem.* 29 (1985) 22.
[5] B. Standke, M. Jansen, *Angew. Chem.* 97 (1985) 114; *Angew. Chem. Int. Ed. Engl.* 24 (1985) 118.
[6] $P\bar{1}$; $a=904.4(4)$, $b=559.6(2)$, $c=519.8(2)$ pm; $\alpha=118.76(2)$, $\beta=91.53(3)$, $\gamma=102.42(3)°$. Siemens AED2 four-circle diffractometer; $Mo_{K\alpha}$; 1260 independent reflections; $R=0.073$, $R_w=0.038$. Further details of the crystal structure investigation are available from the Fachinformationszentrum Energie, Physik, Chemie GmbH, D-7514 Eggenstein-Leopoldshafen 2 (FRG), on quoting the depository number CSD-52382, the name of the author, and the journal citation.
[7] R. Hoppe, *Angew. Chem.* 92 (1980) 106; *Angew. Chem. Int. Ed. Engl.* 19 (1980) 110.

Generation and Interception of 1-Oxa-3,4-cyclohexadiene**

By *Michael Schreck* and *Manfred Christl**

The short-lived 1,2-cyclohexadiene **1**, the most highly strained of the previously known monocyclic allenes, is regarded as well characterized.[1] Very little is known, however, about hetero derivatives of this reactive intermediate; we therefore searched for an access to the title compound **2**. Allene **1** is best generated by treatment of 6,6-dibromobicyclo[3.1.0]hexane with methyllithium.[2] Hence, 6,6-dichloro- **3a**[3] and 6,6-dibromo-3-oxabicyclo[3.1.0]hexane **3b**[3a,4] are potential precursors for **2**. The reactions of **3a**[5] and **3b**[4] with *n*-butyllithium have already been investigated, but products derived from **2** were neither sought for nor found.[6] Utilizing well-established reaction partners[7] of **1** as solvents, we have now repeated such experiments at -40 to $-20°C$ and obtained trapping products of **2**.

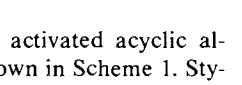

The results of the reactions with activated acyclic alkenes and the yields obtained are shown in Scheme 1. Styrene yielded a 10 : 1 mixture of the *exo*- and *endo*-8-phenyl-

[*] Prof. Dr. M. Christl, Dr. M. Schreck
Institut für Organische Chemie der Universität
Am Hubland, D-8700 Würzburg (FRG)

[**] This work was supported by the Fonds der Chemischen Industrie.

3-oxabicyclo[4.2.0]oct-5-enes **4**. 1,3-Butadiene gave rise to the [2+2]-cycloadduct **5** and the [4+2]-cycloadduct **6**. Isoprene afforded a 10:1 mixture of the diastereomeric [2+2]-cycloadducts **8** and a small amount of the [4+2]-cycloadduct **9**, while 2,3-dimethyl-1,3-butadiene furnished only the [2+2]-cycloadduct **7** (for selected physical data see Table 1).

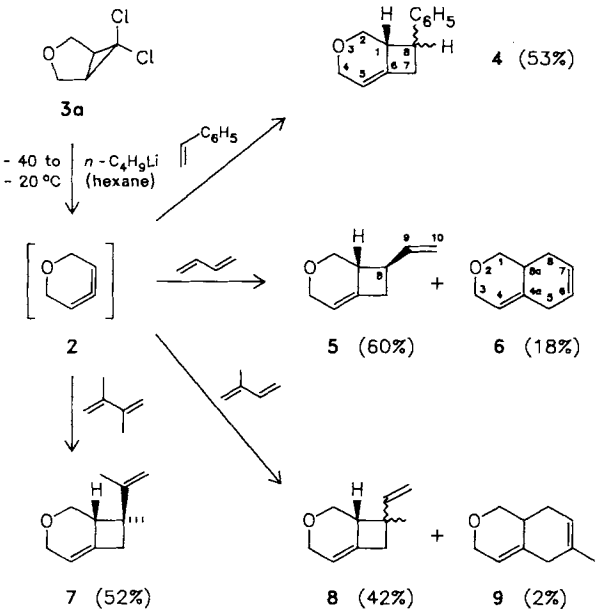

Scheme 1. [8]

As shown in Scheme 2, the 8-vinyl-3-oxabicyclo[4.2.0]-oct-5-enes **5**, **7**, and **8** could be converted into the 3,5,8,8a-tetrahydro-1*H*-2-benzopyrans **6**, **10**, and **9**, respectively, in good yields by heating at 160–165°C. With regard to the mechanisms of all these processes, the same concepts may be applied which have been outlined for the formation of the corresponding adducts of **1**[7,9] and their rearrangement.[7c]

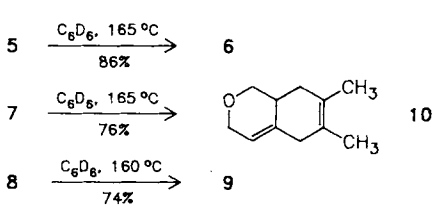

Scheme 2. [8]

The reaction of *n*-butyllithium with **3a** in furan, which counts among the less reactive trapping agents for **1**,[7b] did not produce an adduct of the heteroarene but gave the butylpentadienol **11**[8] in 49% yield[6] (Scheme 3). We also obtained **11** when using petroleum ether as solvent. *n*-Butyllithium probably attacks the central C-atom of the allene moiety of **2** and initiates ring-opening in an S_N2' reaction, in which the oxygen atom, possibly complexed by a lithium ion, serves as leaving group. Since furan is obviously not reactive enough to compete with *n*-butyllithium for **2** we generated **2** from **3b**[3] in furan by the less nucleophilic

Table 1. Selected physical data of **4**–**6**, **11**, **12**, and **14**; IR (CCl_4; cm^{-1}), NMR ($CDCl_3$; δ values, coupling constants in Hz).

exo-**4**: ^{1}H-NMR: 3.02 and 3.08 (each br. dd, $J_{7,7}=13.0$, $J_{7,8}=7.8$; 7-H_2), 3.17 (q, $J_{1,8}=7.8$; 8-H), 3.19 (t, $J_{1,2endo}=J_{2,2}=9.5$; 2-H_{endo}), 3.24 (m; 1-H), 4.13 and 4.26 (each br. d, $J_{4,4}=16.2$; 4-H_2), 4.17 (dd, $J_{1,2exo}=5.5$; 2-H_{exo}), 5.38 (m; 5-H), 7.14–7.32 (m; C_6H_5).—^{13}C-NMR: 40.05 (t, C-7), 43.46 (d, C-8), 48.56 (d, C-1), 65.37 (t, C-4), 67.97 (t, C-2), 112.44 (d, C-5), 126.27 (d, *p*-C), 126.39 (d, *o*-C), 128.39 (d; *m*-C), 135.49 (s, C-6), 143.46 (s, *ipso*-C)

5: ^{1}H-NMR: 2.61 (≈br. quint, $J_{1,8}=J_{7endo,8}=J_{7exo,8}=7.8$, $J_{8,9}=6.5$; 8-H), 2.75 and 2.84 (each br. dd, $J_{7,7}=12.5$; 7-H_2), 2.99 (m; 1-H), 3.09 (t, $J_{1,2endo}=J_{2,2}=9.6$; 2-H_{endo}), 4.08 (dd, $J_{1,2exo}=6.4$; 2-H_{exo}), 4.10 and 4.23 (each br. d, $J_{4,4}=16.2$; 4-H_2), 4.98 (br. d, $J_{9,10trans}=10.3$; 10-H_{trans}), 5.02 (br. d, $J_{9,10cis}=16.7$; 10-H_{cis}), 5.32 (br. s; 5-H), 5.95 (ddd; 9-H).—^{13}C-NMR: 38.67 (t, C-7), 42.07 (d; C-8), 47.16 (d, C-1), 65.36 (t, C-4), 67.58 (t, C-2), 112.04 (d, C-5), 113.74 (t, C-10), 136.00 (s, C-6), 140.59 (d, C-9)

6: ^{1}H-NMR: 2.05 (ddm, $J_{8,8a}=17.0$, $J_{8,8a}=11.0$) and 2.14 (br. dt, $J_{7,8}=J_{8,8a}=5.2$) (8-H_2), 2.36 (m; 8a-H), 2.63 (dt, $J_{5,5}=19.4$, $J=2.9$) and 2.88 (dm) (5-H_2), 3.49 and 3.91 (each dd, $J_{1,1}=11.4$, $J_{1,8a}=4.9$; 1-H_2), 4.08 and 4.12 (each dq, $J_{3,3}=15.6$, $J\approx2.8$; 3-H_2), 5.53 (quint, $J=2.5$; 4-H), 5.64 and 5.69 (each dm, $J_{6,7}\approx10.0$; 6-H, 7-H).—^{13}C-NMR: 30.21 (t, C-8), 33.03 (t, C-5), 33.63 (d, C-8a), 65.97 (t, C-3), 69.70 (t, C-1), 118.50 (d, C-4), 125.95 (double intensity, d, C-6, C-7), 135.09 (s, C-4a)

11: IR: 3620, 3480 (broad), 3400 (broad) (OH).—^{1}H-NMR: 0.92 (t, $J_{3',4'}=7.2$; 4'-H_3), 1.33 (m; 3'-H_2), 1.45 (m; 2'-H_2), 1.89 (br. s; OH), 2.21 (br. t, $J_{1',2'}=7.6$; 1'-H_2), 4.29 (d, $J_{1,2}=7.0$; 1-H_2), 5.17 (dt, $J_{2,5trans}=J_{5,5}=1.4$, $J_{4,5trans}=11.0$; 5-H_{trans}), 5.30 (br. d, $J_{4,5cis}=17.5$; 5-H_{cis}), 5.56 (br. t; 2-H), 6.61 (ddd, $J_{2,4}=0.7$; 4-H).—^{13}C-NMR: 13.85 (q, C-4'), 22.56 (t, C-3'), 30.77 (t, C-2'), 32.90 (t, C-1'), 58.47 (t, C-1), 115.16 (t, C-5), 127.74 (d, C-2), 132.27 (d, C-4), 139.69 (s, C-3)

12: B.p. 60–80°C (bath)/0.2 torr.—^{1}H-NMR: 2.34 (t, $J_{1,1}=J_{1endo,8a}=10.0$; 1-$H_{endo}$), 2.64 (≈dtq, $J_{1exo,8a}=4.8$, $J_{8,8a}=4.3$, $J_{4,8a}=3.1$; 8a-H), 3.94 (dt, $J_{3,3}=16.5$, $J_{3,4}=J_{3,8a}=3.1$) and 4.28 (dt, $J_{3,4}=J_{3,8a}=2.1$) (3-H_2), 4.18 (dd; 1-H_{exo}), 5.06 (dm; 8-H), 5.18 (m; 5-H), 5.62 (m; 4-H), 6.02 and 6.38 (each dd, $J_{6,7}=5.7$, $J_{5,6}=J_{7,8}=1.7$; 6-H, 7-H).—^{13}C-NMR: 39.43 (d, C-8a), 64.60 (t, C-3), 67.57 (t, C-1), 79.50 and 79.70 (each d, C-5, C-8), 115.77 (d, C-4), 128.82 (d, C-7), 136.01 (d, C-6), 137.16 (s, C-4a)

14: IR: 3600, 3400 (broad) (OH).—^{1}H-NMR: 3.49 (br. s; OH), 4.26 (dd, $J_{1,2}=6.5$, $J_{1,3}=1.6$; 1-H_2), 5.76 (dtd, $J_{2,3}=11.2$, $J_{2,4}=1.1$; 2-H), 6.23 (tt, $J_{3,4}=11.3$; 3-H), 6.71 (dd; 4-H).—^{13}C-NMR: 58.96 (t, C-1), 123.90, 124.14, and 132.97 (each d, C-2, C-3, C-4), 124.89 (s, C-5)

methyllithium and isolated the [4+2]-cycloadduct **12**[8] in 21% yield (Scheme 3).

Because of the smaller covalent radius of the oxygen atom, the oxa derivative **2** should have a more bent allene moiety in comparison to 1,2-cyclohexadiene **1** and, as a

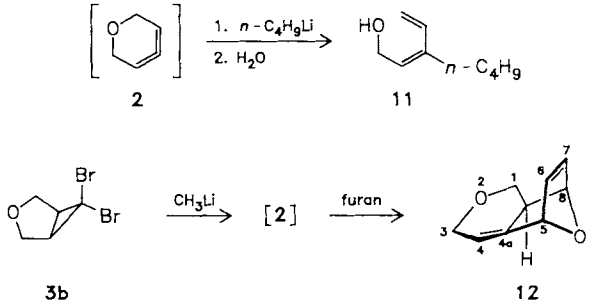

Scheme 3.

consequence, should exhibit a higher strain energy. Despite this, **2** can be generated in an analogous way as **1**, and cycloaddition products with activated alkenes are formed in similar yields as in the case of **1**. A specific feature of **2** is the addition of the nucleophile *n*-butyllithium to give **11**.

The majority of the above reactions of **3a** were not carried out with the pure substance but in the presence of the insertion product **13** of dichlorocarbene and 2,5-dihydrofuran which is also formed in the synthesis of **3a**.[3] *n*-Bu-

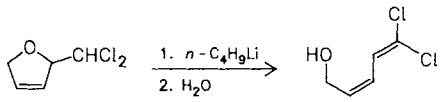

13 14

tyllithium converts **13** by ring-opening β-elimination into (*Z*)-5,5-dichlorpenta-2,4-dienol **14**,[10] which could, however, be readily separated from the cycloadducts.

Received: February 26, 1987 [Z 2115 IE]
German version: *Angew. Chem. 99* (1987) 720

[1] R. P. Johnson in J. F. Liebman, A. Greenberg (Eds.): *Molecular Structure and Energetics, Vol. 3*, p. 85, VCH Publishers, Deerfield Beach, FL, USA 1986.
[2] W. R. Moore, W. R. Moser, *J. Am. Chem. Soc. 92* (1970) 5469.
[3] a) J. C. Anderson, D. G. Lindsay, C. B. Reese, *J. Chem. Soc. 1964*, 4874; b) E. V. Dehmlow, K. Franke, *Liebigs Ann. Chem. 1979*, 1456.
[4] H. Maskill, *J. Chem. Soc. Perkin Trans. 2 1975*, 197.
[5] K. G. Taylor, W. E. Hobbs, M. Saquet, *J. Org. Chem. 36* (1971) 369.
[6] In ref. [5], "butyl-containing products" are mentioned without any further information. Presumably the product in question was **11**.
[7] a) Styrene: W. R. Moore, W. R. Moser, *J. Org. Chem. 35* (1970) 908; b) 2,3-dimethyl-1,3-butadiene: A. T. Bottini, L. L. Hilton, J. Plott, *Tetrahedron 31* (1975) 1997; c) 1,3-butadiene and isoprene: M. Christl, M. Schreck, *Angew. Chem. 99* (1987) 474; *Angew. Chem. Int. Ed. Engl. 26* (1987) 449.
[8] The products of Schemes 1 and 2 and the compounds **11** and **14** were isolated by preparative gas chromatography (1.5m-column, 20% EGA on Chromosorb, 110–150°C), the diastereomeric pairs **4** and **8** as mixtures. Compound **12** was purified by distillation. All the compounds gave correct elemental analyses (except **12**) and were characterized by ^{1}H-NMR, ^{13}C-NMR and mass spectra.
[9] a) S. Harnos, S. Tivakornpannarai, E. E. Waali, *Tetrahedron Lett. 27* (1986) 3701; b) M. Christl, M. Schreck, *Chem. Ber. 120* (1987) 915.
[10] A compound of the structure **14** is described, but the data do not allow any conclusions to be drawn about the configuration: M. Julia, J. Bouchaudon, *C. R. Acad. Sci. 253* (1961) 1111.

Second Sphere Coordination of Tetraammineplatinum(II) by a Macropolycyclic Crown Ether Bisamide Receptor**

By *David R. Alston, Alexandra M. Z. Slawin, J. Fraser Stoddart,* David J. Williams,* and *Ryszard Zarzycki*

In our quest to find a molecular receptor more highly designed than [18]crown-6 (18C6)[1] for the antitumour drug cisplatin, [*cis*-$Pt(NH_3)_2Cl_2$], we decided to modify chemically those macrobicyclic polyethers with the demonstrated ability[2] to form adducts with cationic *cis*-diamminerhodium complexes. Since preliminary experiments indicated that **1** does not form adducts in a variety of organic solvents with cisplatin, it was decided, in view of our observation[1] of the inter-adduct hydrogen bonding interactions (a) between ammine and chlorine ligands and (b) between ammine ligands and solvating dimethylacetamide (dma) molecules in [{*cis*-$[Pt(NH_3)_2Cl_2]\cdot dma\}_2$-18C6], to incorporate between the two trisubstituted benzene rings a fourth chain containing two amide linkages as potential hydrogen bonding donors to the chlorine ligands. Here, we describe the preparation[3] in eight steps (→**2**→**3**→**4**→**5**→**6**→**7**→**8**→**9**) of the macropolycyclic bisamide **9** starting from 4-bromo-2,6-dimethylphenol and the X-ray crystal structures[4] of both the free receptor and its 2:1 adduct with $[Pt(NH_3)_4][PF_6]_2$.

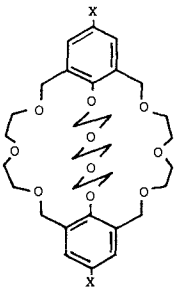

1, X = H
4, X = Br
5, X = CN
6, X = $CONH_2$
7, X = CO_2H
8, X = COCl

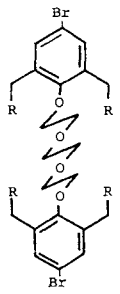

2, R = H
3, R = Br

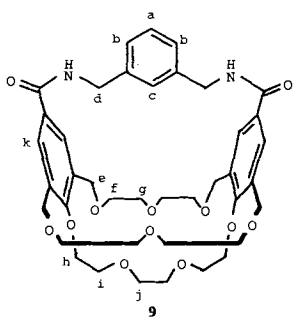

9

The structure (Fig. 1, top) of **9**, when viewed from **A**[5] shows (Fig. 1, bottom) the existence of a shallow elongated cavity bounded at the bottom by the bisamide bridge, at the top by the three adjacently-located polyether chains and, on either side, by the two slightly inclined (33° between their mean planes) tetrasubstituted benzene rings (centroid-centroid distance, 4.9 Å). Of particular note is the directing of the two amide N–H bonds towards mouth **A** of the receptor cleft.

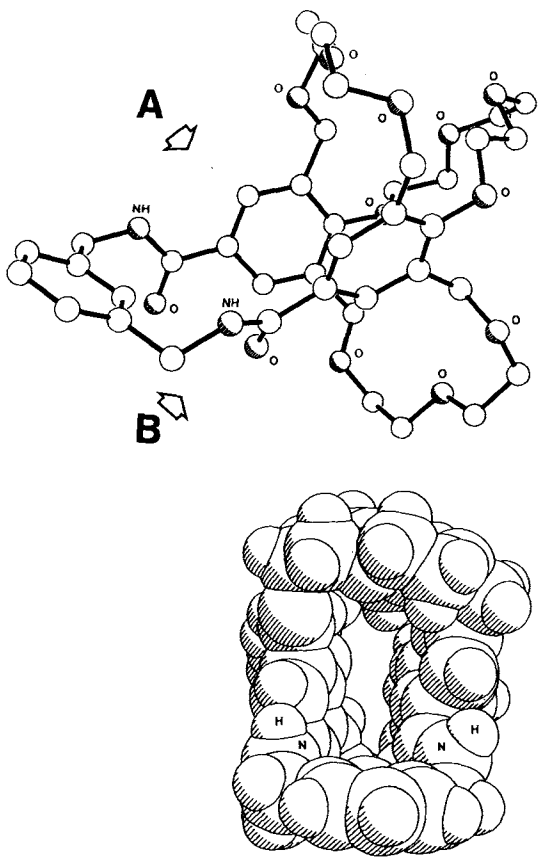

Fig. 1. Top: Structure of **9** in the crystal with the **A** and **B** mouths indicated. Bottom: Space-filling representation of the structure of **9** viewed from the **A** mouth.

[*] Dr. J. F. Stoddart, Dr. D. R. Alston, R. Zarzycki
Department of Chemistry, The University
Sheffield S3 7HF (UK)
Dr. D. J. Williams, A. M. Z. Slawin
Chemical Crystallography Laboratory
Department of Chemistry, Imperial College
London SW7 2AY (UK)

[**] This work was supported by the Johnson Matthey Technology Centre and the Science and Engineering Research Council in the United Kingdom. We thank the Leverhulme Trust for the award of a Research Fellowship (*J. F. S.*).

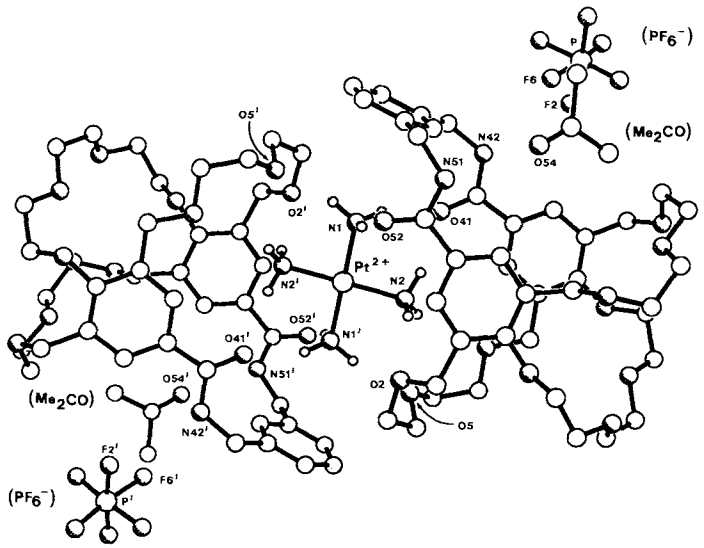

Fig. 2. Structure of $[Pt(NH_3)_4 \cdot (\mathbf{9})_2][PF_6]_2[Me_2CO]_2$ in the crystal. Distances for N1 to O5′, O41, and O52: 3.01, 2.90, and 2.90 Å, respectively. Those for N2 to O2, O5, and O41: 3.14, 3.08, and 3.18 Å, respectively. Contacts to $PF_6^{\ominus}$ and Me_2CO: N42···F2 3.20, N42···F6 3.29, N51···O54 2.83 Å.

Despite these favorable features, cisplatin is not solubilized[6] in halocarbon solvents containing **9**. On the other hand, $[Pt(NH_3)_4][PF_6]_2$ dissolves in $CH_2Cl_2/Me_2CO/MeOH$ (1 : 1 : 1, v/v) in the presence of 1 molar equivalent of **9**. However, a 2 : 1 crystalline adduct with m.p. 216–218 °C is formed[7] (see Fig. 2 for X-ray structure) as an acetone solvate[4] upon covering this solution with *n*-pentane. The reason for the formation of a 2 : 1 adduct can be rationalized by $[Pt(NH_3)_4]^{2\oplus}$ seeking a hydrogen bonding acceptor surface such as that provided by the two amide carbonyl oxygen atoms (O41 and O52) and two ethereal oxygen atoms (O2 and O5) which dominate the surface of the **B**-face. We surmise that this prevents[6] insertion of the tetraammine into the receptor cleft of **9** and so results in the approach of a second symmetry related receptor molecule. The **B** mouth is more open than in free **9**, the two tetrasubstituted benzene rings being nearly parallel (3° between their mean planes) with their centroid-centroid distance increased to 5.2 Å. The two N–H amide bonds emanating from N42 and N51 at the **A** mouth provide hydrogen bond donor sites for $PF_6^{\ominus}$ and Me_2CO, respectively.

Although we still have to improve[8] the design of **9** to induce it to form a 1 : 1 adduct with cisplatin, two novel features have emerged from this investigation: (i) the formation of a discrete adduct in which *two* receptor molecules serve simultaneously as outer sphere ligands for a transition metal complex, and (ii) the involvement of amide linkages in molecular receptors as hydrogen bond acceptors, pointing to a role for cyclic peptides as alternative second sphere coordinators to crown ethers.

Received: March 13, 1987 [Z 2142 IE]
German version: *Angew. Chem.* 99 (1987) 697

[1] D. R. Alston, J. F. Stoddart, D. J. Williams, *J. Chem. Soc. Chem. Commun. 1985*, 532.

[2] D. R. Alston, A. M. Z. Slawin, J. F. Stoddart, D. J. Williams, *Angew. Chem.* 96 (1984) 804; *Angew. Chem. Int. Ed. Engl.* 23 (1984) 821.

[3] *Experimental:* Reaction (NaH, THF) of 4-bromo-2,6-dimethylphenol with triethylene glycol bistosylate afforded the acyclic polyether **2** (78%, m.p. 74.5–75.5 °C). Photochemical bromination (NBS, CCl_4) gave the hexabromide **3** (20%, m.p. 143.5–144.5 °C). Reaction (NaH, THF, high dil.) of **3** with diethylene glycol in the molar ratio 1 : 2 afforded **4** (20%, m.p. 126–127 °C). Treatment (CuCN, DMF) of **4** generated the dinitrile **5** (72%, m.p. 160–161 °C). Reaction (H_2O_2, KOH, EtOH, H_2O) of the dinitrile **5** yielded the diamide **6** (77%, m.p. 230–232 °C). Hydrolysis (KOH, EtOH, H_2O) of the amide functions in **6** produced the dicarboxylic acid **7** (99%, m.p. 213–214 °C). Reaction ($SOCl_2$, CH_2Cl_2) of **7** generated the diacid chloride **8**, which was allowed to react (Na_2CO_3, CH_2Cl_2, high dil.) *in situ* with *m*-xylylenediamine to afford the polycycle **9** [73%, m.p. 249–250 °C, single crystals suitable for an X-ray structure analysis from EtOH; ^{1}H-NMR (CD_2Cl_2): δ = 3.55–3.69 (8 H^f + 8 H^g, m), 3.70 (4 H^j, s), 3.78 (4 H^i, t), 4.06 (4 H^h, t), 4.25 and 4.66 (8 H^c, AB system), 4.54 (4 H^d, d), 6.57 (2 H, t, N*H*), 7.18–7.33 (H^a + 2 H^b + H^e, m), 7.57 (4 H^k, s)]. All new compounds gave satisfactory elemental analyses and spectroscopic data.

[4] Crystal data for **9**: monoclinic, a = 15.136(5), b = 16.032(5), c = 16.839(6) Å, β = 111.50(3)°, V = 3802 Å^3, space group, $P2_1/n$, Z = 4, ρ_{calc} = 1.31 g cm^{-3}, $\mu(Cu_{K\alpha})$ = 7.6 cm^{-1}, 3285 independent observed reflections with [$|F_0| > 3\sigma(|F_0|)$, $\theta \leq 50°$], R = 0.090, R_w = 0.103. The high R factor is a consequence of severe disorder in one of the bridging polyether chains and in other portions of the molecule.—Crystal data for $[Pt(NH_3)_4 \cdot (\mathbf{9})_2][PF_6]_2[Me_2CO]_2$: triclinic, a = 12.218(2), b = 13.989(2), c = 16.133(3) Å, α = 69.82(1), β = 71.55(1), γ = 79.00(1)°, V = 2445 Å^3, space group $P\bar{1}$, Z = 1, ρ_{calc} = 1.47 g cm^{-3}, $\mu(Cu_{K\alpha})$ = 39 cm^{-1}, 5017 independent observed reflections with [$|F_0| > 3\sigma(|F_0|)$, $\theta \leq 50°$], R = 0.033, R_w = 0.038. The NH_3 hydrogen atoms were obtained from a ΔF map and these groups were refined as rigid bodies. The $PF_6^{\ominus}$ ions are disordered. Data were measured on a Nicolet R3m diffractometer using the ω-scan routine with graphite-monochromated $Cu_{K\alpha}$ radiation. In the case of the free receptor **9** no absorption correction was applied. However, a numerical absorption correction for a face-indexed crystal was applied in the case of the adduct. The structure of the adduct was solved by the heavy atom method and that of the free receptor by direct methods. Both structures were refined anisotropically. Further details of the crystal structure investigations can be obtained from the Cambridge Crystallographic Data Centre, University Chemical Laboratory, Lensfield Road, Cambridge CB2 1EW (England). Any request should be accompanied by the full literature citation for this communication.

[5] Although there is the possibility of the existence of a similar cleft when **9** is viewed from **B** (Fig. 1, top), the inclination of the two tetrasubstituted benzene rings and their coplanar carbonyl substituents, together with the relative spatial disposition of the *meta*-disubstituted benzene ring within the bisamide chain, effectively bars the approach by substrates from this direction. The amide nitrogen atoms both form intermolecular hydrogen bonds, one (2.88 Å) to an amide carbonyl oxygen atom and the other (2.87 Å) to an ether oxygen atom.

[6] Although $[Rh(cod)(NH_3)_2][PF_6]$ (cod = 1,5-cyclooctadiene) dissolves in CD_2Cl_2 in the presence of equimolar amounts of **9**, the fact that there are no significant changes in the ^{1}H-NMR chemical shifts of the resonances for the complex or receptor protons indicates that the rhodium complex does not enter the receptor cleft: however, steric factors could be responsible for this observation. Addition of an equimolar amount of $[Pt(NH_3)_4][PF_6]_2$ to **9** dissolved in either CD_2Cl_2 or CD_3COCD_3 gives rise to only small (i.e. $< +0.1$ ppm) ^{1}H-NMR chemical shift changes to higher frequencies of the resonances for the aromatic protons (H^a/H^b/H^c/H^k). These results are in contrast with the considerably larger ^{1}H-NMR chemical shift changes (+0.23 and +0.26 ppm) observed (D. R. Alston, A. M. Z. Slawin, J. F. Stoddart, D. J. Williams, R. Zarzycki, *Angew. Chem.* 99 (1987) 698; *Angew. Chem. Int. Ed. Engl.* 26 (1987) 693) on addition of an equimolar amount of $[Pt(NH_3)_4][PF_6]_2$ to a solution of **1** in CD_3COCD_3.

[7] There is a crystallographic center of symmetry at the center of the 2 : 1 adduct which is coincident with the platinum atom of $[Pt(NH_3)_4]^{2\oplus}$.

[8] To date, all attempts to reduce the two –CONH– groups in **9** to $-CH_2NH-$ units have been unsuccessful.

Macrobicyclic Polyethers as Second Sphere Ligands for Tetraammineplatinum(II)**

By *David R. Alston, Alexandra M. Z. Slawin, J. Fraser Stoddart,* David J. Williams,* and *Ryszard Zarzycki*

Two macropolycyclic crown ether bisamide receptor molecules of a compound derived from **1** enter into sec-

[*] Dr. J. F. Stoddart, Dr. D. R. Alston, R. Zarzycki
Department of Chemistry, The University
Sheffield S3 7HF (UK)
Dr. D. J. Williams, A. M. Z. Slawin
Chemical Crystallography Laboratory
Department of Chemistry, Imperial College
London SW7 2AY (UK)

[**] This work was supported by the Johnson Matthey Technology Centre and the Science and Engineering Research Council in the United Kingdom. We thank the Leverhulme Trust for the award of a Research Fellowship (*J. F. S.*).

ond sphere coordination with $[Pt(NH_3)_4]^{2\oplus}$, mainly on account of the hydrogen bonding of its ammine ligands to the carbonyl oxygen atoms of the two pairs of amide linkages that characterize the entrance to the receptor cavity of each molecule.[1] Since we suspect that these interactions, rather than any structural property of the dication, prevent its total encapsulation, we decided to investigate adduct formation of $[Pt(NH_3)_4]^{2\oplus}$, both with **1** and with its pinacol analogue **2**.[1-3]

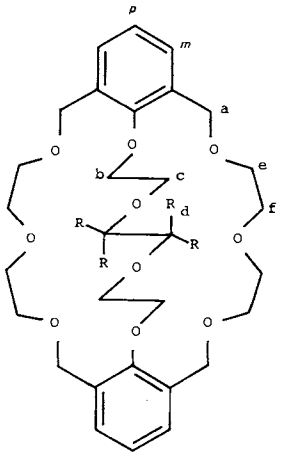

1, R = H
2, R = Me

The X-ray crystal structure[4] of $[Pt(NH_3)_4 \cdot \mathbf{1}][PF_6]_2$[5] (Fig. 1) reveals the presence of two crystallographically independent 1:1 adducts. The gross conformations of both receptor molecules are very similar[6] to that observed[2] in the 1:1 adduct of **1** and $[Rh(cod)(NH_3)_2]^{\oplus}$ (cod = 1,5-cyclooctadiene), there being an approximate C_2 symmetry axis passing through the middle of the C-C bond of the central polyether chain, the Pt atom, and bisecting two pairs of Pt-NH_3 bonds. In contrast to the encapsulation of $[Pt(NH_3)_4]^{2\oplus}$ by two macropolycyclic crown ether bisamide receptor molecules, here the dication is nearly totally enveloped in both instances by a single receptor molecule **1**. It is notable that, in the absence of a bulky organic ligand such as is present[6] in $[Rh(cod)(NH_3)_2]^{\oplus}$, $[Pt(NH_3)_4]^{2\oplus}$ inserts itself (Fig. 1) still further into the receptor cavity. As a consequence, all four ammine ligands are involved in hydrogen bonding interactions with all three polyether chains participating. All ten oxygen atoms of **1** lie within 3.3 Å of a nitrogen atom of the tetraammine. Another key

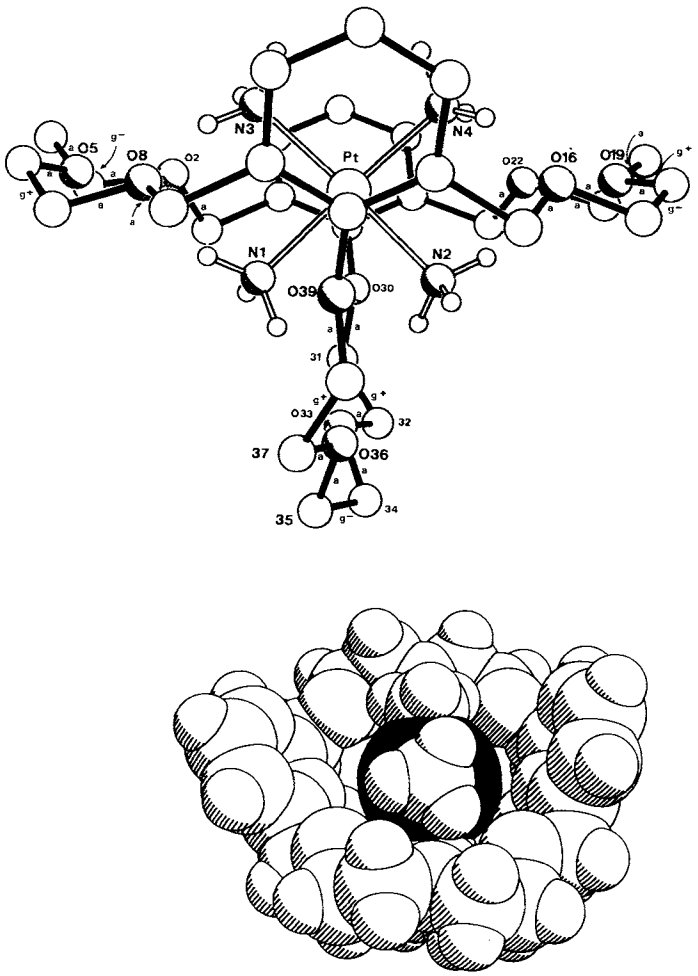

Fig. 1. Top: Structure of one of the $[Pt(NH_3)_4 \cdot \mathbf{1}]^{2\oplus}$ dications in the crystal. Distances for N1 to O8, O30, O33, O36, and O39: 3.22, 3.25, 3.15, 3.21, and 3.07 Å, respectively. Those for N2 to O16, O19, O30, and O33: 3.27, 3.30, 3.03, and 3.18 Å, respectively. Those for N3 to O2, O5, and O8: 3.13, 3.08, and 3.13 Å, respectively. Those for N4 to O16, O19, and O22: 3.12, 3.04, and 3.27 Å, respectively. Atoms N1 and N2 are displaced 1.62 and 1.63 Å respectively, and atoms N3 and N4 both 1.18 Å on opposite sides of the mean plane described by the six peripheral oxygen atoms. Cleft angle between the mean planes of the aromatic rings is 62°. The conformations of the three polyether chains are indicated in terms of their *gauche* (*g*) or *anti* (*a*) geometries. — Bottom: Space-filling representation of the second $[Pt(NH_3)_4 \cdot \mathbf{1}]^{2\oplus}$ dication in the crystal looking into the receptor cavity. The Pt atom is blackened.

feature of this structure is the involvement of the middle two oxygen atoms (O33 and O36) of the central polyether chain in hydrogen bonding interactions to N1 and N2.

Table 1 records ^{1}H-NMR spectroscopic data which sug-

Table 1. ^{1}H-NMR chemical shift data [δ values ($\Delta\delta$ values) in CD_3COCD_3] [a].

	m	*p*	a_A	a_B	b	c	d(H)	d(Me)
1	7.25	6.96		4.53[b]	4.09	3.91	3.76	—
$[Pt(NH_3)_4 \cdot \mathbf{1}][PF_6]_2$	7.48	7.22		ca. 4.6 [c]	4.27	4.04	3.95	—
	(+0.23)	(+0.26)			(+0.18)	(+0.13)	(+0.19)	
2	7.25	6.95	4.79	4.26	3.99	3.99	—	1.31
$[Pt(NH_3)_4 \cdot \mathbf{2}][PF_6]_2$	7.46	7.19	4.91	4.33	4.22	4.01	—	1.39
	(+0.21)	(+0.24)	(+0.12)	(+0.07)	(+0.23)	(+0.02)		(+0.08)

[a] The spectra were recorded at ambient temperature on a Bruker AM250 spectrometer using the signal of CD_2HCOCD_2H in the CD_3COCD_3 as reference. The $\Delta\delta$ values in brackets indicate the shifts with respect to the appropriate receptors **1** and **2**. [b] The rate constant ($k_c = 322\ s^{-1}$) at the coalescence temperature ($T_c = -52$°C) of this AB system ($\Delta\nu_{AB} = 42.5$ Hz, $J_{AB} = 10.4$ Hz) corresponds to a $\Delta G_c^{\ddagger}$ value of 10.3 kcal mol^{-1} for the conformational inversion [2] of the free receptor **1**. [c] In the presence of 1 equivalent of $[Pt(NH_3)_4][PF_6]_2$, the coalescence temperature ($T_c = +18$°C) of the AB system ($\Delta\nu_{AB} = 136$ Hz, $J_{AB} = 10$ Hz) is considerably higher for a very similar rate constant ($k_c = 307\ s^{-1}$), reflecting a substantial increase in $\Delta G_c^{\ddagger}$ to 13.7 kcal mol^{-1}. This observation provides further evidence for the existence of the $[Pt(NH_3)_4 \cdot \mathbf{1}]^{2\oplus}$ dication in CD_3COCD_3 solution.

gest that the gross structural features of $[Pt(NH_3)_4 \cdot \mathbf{1}][PF_6]_2$ are retained in [D$_6$]acetone solution. Significant downfield shifts are observed for the methylene protons in the polyether chains as well as for the aromatic protons. Further evidence for 1 : 1 adduct formation was obtained in the ^{1}H-NMR spectrum, recorded at $-80\,^\circ$C, of a [D$_6$]acetone solution of **1** and $[Pt(NH_3)_4][PF_6]_2$ in a 2 : 1 molar ratio. Multiplets for the aromatic protons centered at $\delta = 7.50$, 7.25, and 7.00 with relative intensities of 2, 3, and 1, respectively, indicate the presence of equal amounts of the 1 : 1 adduct and the free receptor **1** undergoing equilibration on the ^{1}H-NMR time scale (cf. Table 1).

Although the ^{1}H-NMR spectrum of $[Pt(NH_3)_4 \cdot (\mathbf{2})_2][PF_6]_2$ run at $-80\,^\circ$C also shows that a 1 : 1 adduct exists in equilibrium with **2** in [D$_6$]acetone solution, the X-ray structure analysis[4] (Fig. 2, top) of the crystalline adduct of **2** and $[Pt(NH_3)_4][PF_6]_2$ reveals a 2 : 1 stoichiometry in the crystal. The dication is engulfed by the two symmetry-related molecules of **2** (Fig. 2, bottom). There are no fewer

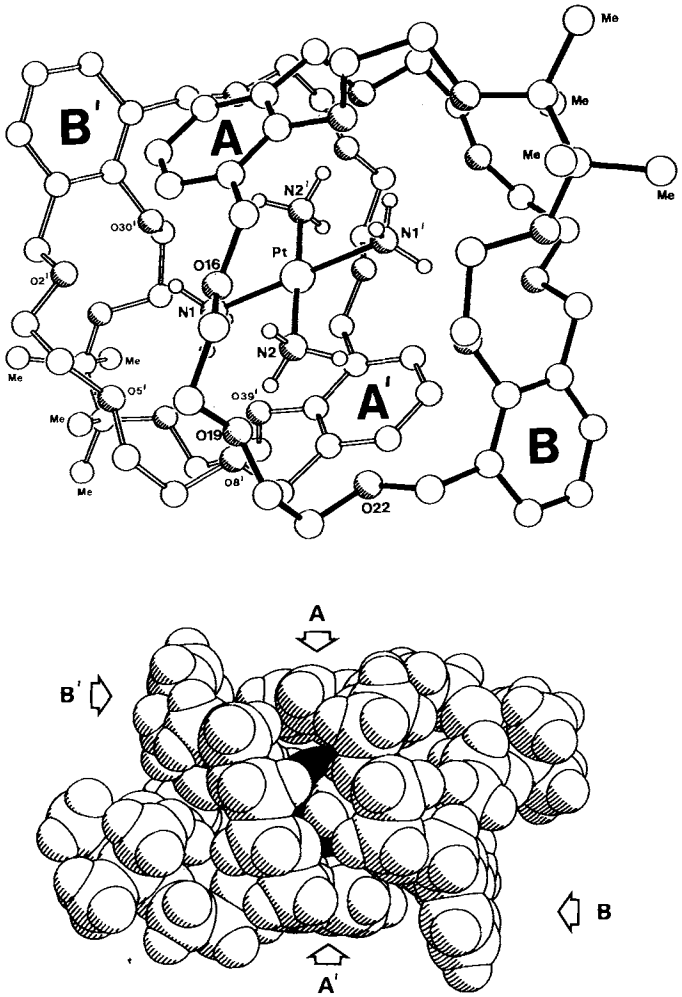

Fig. 2. Top: Skeletal illustration of the $[Pt(NH_3)_4 \cdot (\mathbf{2})_2]^{2\oplus}$ dication in the crystal. One receptor molecule is shown with open bonds. Distances for N1 to O2′, O5′, O8′, O30′, and O39′: 3.21, 3.00, 3.21, 3.25, and 3.26 Å, respectively. Those for N2 to O8′, O16, O19, and O22: 3.00, 3.06, 3.05, and 3.26 Å, respectively. Equivalent distances exist for the symmetry related N1′ and N2′. Cleft angle between the mean planes of the aromatic rings **A** and **B** is 102°. Angle between the mean planes of ring **A** and PtN1N1′N2N2′ is 8° and the Pt atom lies 3.53 Å from the **A** ring plane. The dihedral angle between the mean planes of the aromatic rings **A** and **B**′ is 78° and the distance between their centroids is 4.92 Å. The centroid-centroid vector is inclined 10° to the normal to ring **B**′.—Bottom: Space-filling representation of the 2 : 1 adduct with the Pt atom blackened.

than 18 contacts of < 3.30 Å between the four ammine ligands and ether oxygen atoms in the two receptors. In addition to these cohesive noncovalent binding forces, there are pronounced attractive edge-to-face electrostatic interactions between the aromatic rings **A** and **B**′, and **A**′ and **B** (Fig. 2, top). This T-shaped geometry is characteristic of that associated with the global potential energy minimum for two interacting aromatic rings.[7–9] In turn the $[Pt(NH_3)_4]^{2\oplus}$ dication is sandwiched between aromatic rings **A** and **A**′ in a mutually near parallel arrangement with interplanar separations of ca. 3.5 Å.

Comparison of Figures 3 and 1 (top) demonstrates the principal differences in the conformations of the polyether chains in the $[Pt(NH_3)_4 \cdot \mathbf{1}]^{2\oplus}$ and $[Pt(NH_3)_4 \cdot (\mathbf{2})_2]^{2\oplus}$ dica-

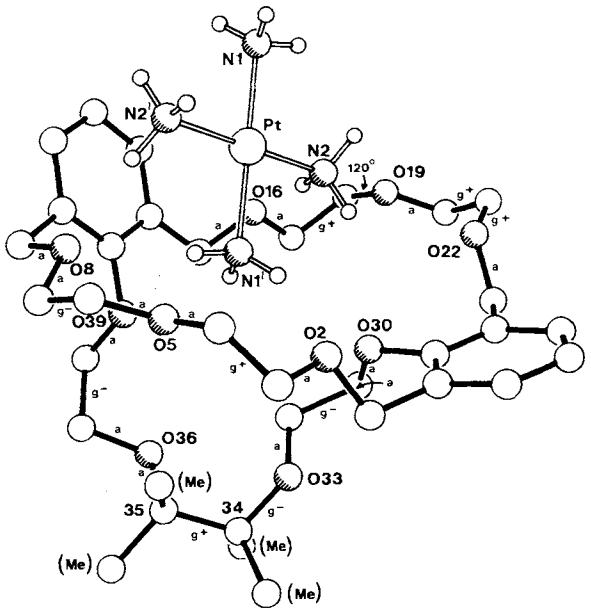

Fig. 3. Perspective view of a portion of the 2 : 1 adduct $[Pt(NH_3)_4 \cdot (\mathbf{2})_2]^{2\oplus}$: a polyether receptor has been removed from the structure shown in Figure 2 (top). The conformations of the three polyether chains are indicated in terms of their *gauche* (*g*) or *anti* (*a*) geometries.

tions. The major desymmetrizations take place in the C20 to O22 and C31 to O33 regions of **2**. This results in an opening of the receptor cleft and a filling-in by the methylene group at C32 of the bottom of the cavity.[10] Clearly, the nature of the second sphere coordination of transition metal complexes can change between solution and solid states.

Received: March 13, 1987 [Z 2143 IE]
German version: *Angew. Chem.* *99* (1987) 698

[1] D. R. Alston, A. M. Z. Slawin, J. F. Stoddart, D. J. Williams, R. Zarzycki, *Angew. Chem.* *99* (1987) 697; *Angew. Chem. Int. Ed. Engl.* *26* (1987) 692.

[2] D. R. Alston, A. M. Z. Slawin, J. F. Stoddart, D. J. Williams, *Angew. Chem.* *96* (1984) 804; *Angew. Chem. Int. Ed. Engl.* *23* (1984) 821.

[3] We chose to examine the macrobicyclic polyethers **1** and **2** as potential second sphere ligands for $[Pt(NH_3)_4]^{2\oplus}$ because they provide examples of conformationally-mobile and conformationally-constrained receptors, respectively; see also ref. [2].

[4] Crystal data for $[Pt(NH_3)_4 \cdot \mathbf{1}][PF_6]_2 \cdot 0.25\,EtOH$: triclinic, $a = 10.401(4)$, $b = 21.552(7)$, $c = 22.165(7)$ Å, $\alpha = 75.00(3)$, $\beta = 79.94(3)$, $\gamma = 76.35(3)^\circ$, $V = 4629$ Å^3, space group $P\bar{1}$, $Z = 4$ (2 independent complexes), $\rho_{calc} = 1.62$ g cm^{-3}, $\mu = 73$ cm^{-1}, 7790 independent observed reflections [$|F_o| \geq 3\sigma(|F_o|)$, $\theta \leq 50^\circ$], $R = 0.064$, $R_w = 0.069$.—Crystal data for $[Pt(NH_3)_4 \cdot (\mathbf{2})_2][PF_6]_2$: monoclinic, $a = 10.825(3)$, $b = 16.318(8)$, $c = 23.744(9)$ Å, $\beta = 101.58(3)^\circ$, $V = 4109$ Å^3, space group $P2_1/c$, $Z = 2$

(the adduct possesses a center of symmetry) $\rho_{calc} = 1.45$ g cm^{-3}, $\mu = 41$ cm^{-1}, 3620 independent observed reflections [$|F_o| \geq 3\sigma(|F_o|)$, $\theta \leq 50°$], $R = 0.031$, $R_w = 0.032$. All hydrogen atoms were obtained from a ΔF map and these groups refined as rigid bodies. The $PF_6^{\ominus}$ ions in $[Pt(NH_3)_4 \cdot (\mathbf{2})_2][PF_6]_2$ are disordered and were refined as two distinct orientations of occupancies 0.65 and 0.35. Data were measured on a Nicolet R3m diffractometer using the ω-scan routine with graphite monochromated $Cu_{K\alpha}$ radiation. In both cases, the structures were solved by the heavy atom method and empirical absorption corrections were applied. Both structures were refined anisotropically. Further details of the crystal structure investigation can be obtained from the Cambridge Crystallographic Data Centre, University Chemical Laboratory, Lensfield Road, Cambridge CB2 1EW (England). Any request should be accompanied by the full literature citation for this communication.

[5] *Experimental:* $[Pt(NH_3)_4 \cdot \mathbf{1}][PF_6]_2$: A solution of **1** (7.3 mg, 0.013 mmol) and $[Pt(NH_3)_4][PF_6]_2$ (7.2 mg, 0.013 mmol) in Me_2CO/EtOH (1 ml) was filtered and Et_2O was layered on top until a faint permanent precipitate was observed. After 24 h, colorless crystals, suitable for X-ray investigation, were obtained of the 1 : 1 adduct [6.1 mg, 42%, m.p. 238–242 °C with decomposition, *m/z* (positive-ion FABMS), 970 for $[M - PF_6^{\ominus}]^{\oplus}$.— $[Pt(NH_3)_4 \cdot (\mathbf{2})_2][PF_6]_2$: A solution of **2** (6.2 mg, 0.01 mmol) and $[Pt(NH_3)_4][PF_6]_2$ (5.6 mg, 0.01 mmol) in CH_2Cl_2/Me_2CO (1 ml) was filtered and Et_2O was layered on top until a faint permanent precipitate was observed. After 24 h, colorless crystals, suitable for X-ray investigation, were obtained of the 2 : 1 adduct [m.p. 238–242 °C with decomposition].

[6] In both independent complexes, the polyether components of the macrorings display the *a ag*$^-$ *a ag*$^+$ *a a* conformation from C1 to C9 and from C15 to C23 observed [2] in $[Rh(cod)(NH_3)_2 \cdot \mathbf{1}]^{\oplus}$. The only major differences in the receptor conformations of the two independent complexes are in the torsional geometries of the central polyether chains from C32 to O39. In $[Pt(NH_3)_4 \cdot \mathbf{1}]^{2\oplus}$, there is an *ag*$^+$*a aga*$^-$*a ag*$^+$*a* conformation from O30 to O39 whereas the analogous polyether chain in $[Rh(cod)(NH_3)_2 \cdot \mathbf{1}]^{\oplus}$ reads *ag*$^-$*a ag*$^+$*a ag*$^-$*a*.

[7] R. O. Gould, A. M. Gray, P. Taylor, M. D. Walkinshaw, *J. Am. Chem. Soc. 107* (1985) 5921.

[8] S. K. Burley, G. A. Petsko, *Science 229* (1985) 23; *J. Am. Chem. Soc. 108* (1986) 7995.

[9] A. M. Z. Slawin, N. Spencer, J. F. Stoddart, D. J. Williams, *J. Chem. Soc. Chem. Commun. 1987*, in press.

[10] Recalling the fact that 2,2,3,3,11,11,12,12-octamethyl-1,4,7,10,13,16-hexaoxacyclooctadecane adopts an all-*gauche* conformation when it forms a 1 : 2 adduct with 2 equivalents of BH_3NH_3 (D. R. Alston, J. F. Stoddart, J. B. Wolstenholme, B. L. Allwood, D. J. Williams, *Tetrahedron 41* (1985) 2923), there is no apparent reason why the central polyether chain in the $[Pt(NH_3)_4 \cdot (\mathbf{2})_2]^{2\oplus}$ dication (Fig. 3) should exist in a different conformation from that observed (Fig. 1) for the $[Pt(NH_3)_4 \cdot \mathbf{1}]^{2\oplus}$ dication. Interestingly, in CD_3COCD_3 solution at low temperatures ($T_c = -70$ °C), the singlet observed in the ^{1}H-NMR spectrum for the methyl protons in $[Pt(NH_3)_4 \cdot \mathbf{2}][PF_6]_2$ separates ($\Delta\nu = 30$ Hz) into two equal intensity signals. The rate constant of 67 s^{-1} calculated at the coalescence temperature (T_c) corresponds to a $\Delta G_c^{\neq}$ value of 10.0 kcal mol^{-1}. We have ascribed this temperature-dependent behavior tentatively to hindered rotation about the C34–C35 bond of the pinacol unit in an otherwise conformationally-symmetrical polyether chain.

Crystal Structure of the η^1-Allyl-Grignard Compound Bis(allylmagnesium chloride-TMEDA)**

By *Michael Marsch, Klaus Harms, Werner Massa,* and *Gernot Boche**

Although allyl-transition-metal complexes[1] and, more recently, also allyllithium compounds[2–4] have been studied in the solid state, the determination of the crystal structure of an allyl-Grignard compound has thus far not been reported. Herein we report on the crystal structure of bis(allylmagnesium chloride-TMEDA) **1** (TMEDA = tetramethylethylenediamine).

[*] Prof. Dr. G. Boche, M. Marsch, Dr. K. Harms,
Priv.-Doz. Dr. W. Massa
Fachbereich Chemie der Universität
Hans-Meerwein-Strasse, D-3550 Marburg (FRG)

[**] This work was supported by the Fonds der Chemischen Industrie and the Deutsche Forschungsgemeinschaft (SFB 260).

The allylmagnesium chloride-TMEDA complex formed on treatment of allylmagnesium chloride in tetrahydrofuran (THF) with TMEDA crystallizes as the dimer **1**.[5,6] The two allylmagnesium chloride-TMEDA units are coupled via a Mg–Cl–Mg–Cl four-membered ring in which the Mg–Cl and Mg–Cl′ distances are markedly different (240.0(1) pm and 269.4(1) pm, respectively).

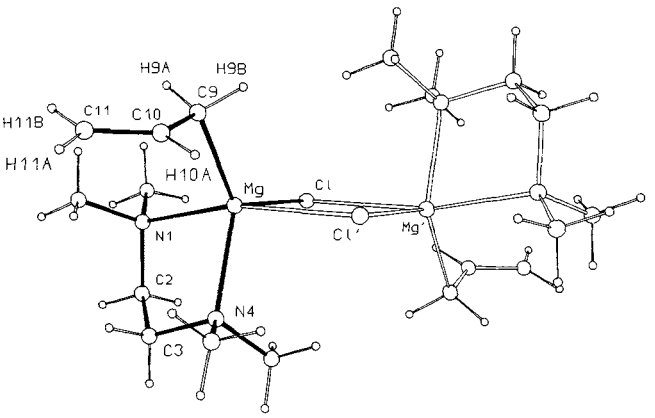

Fig. 1. Crystal structure of **1**. The atoms are represented by spheres with arbitrary radii. Selected bond lengths [pm] and angles [°]: Mg-Cl 240.0(1), Mg-Cl′ 269.4(1), C9-Mg 217.9(3), C10-Mg 300.5(3), Mg-N1 228.5(2), Mg-N4 221.1(2), C9-C10 144.2(4), C10-C11 133.5(4); Mg-C9-C10 110.5(2), C9-C10-C11 130.2(3), H9A-C9-H9B 109(2), H11A-C11-H11B 119(2), C9-C10-H10A 114(1), C11-C10-H10A 115.5(1.5), C10-C11-H11A 123.6(1.6), C10-C11-H11B 117.3(1.6), Cl-Mg-Cl′ 84.69(3), Mg-Cl-Mg′ 95.32(3), Cl-Mg-C9 125.29(7), N1-Mg-C9 99.26(8), N1-Mg-N4 80.28(7), Cl-Mg-N4 107.18(6), Cl′-Mg-N4 87.84(5); torsion angle [°]: C11-C10-C9-Mg −109.2(3), C11-C10-C9-H9A 14(1), C11-C10-C9-H9B 138(1).

The characteristic feature of **1** is the η^1-allyl-magnesium bond. The C9–Mg distance is 217.9(3) pm and thus lies in the range of C–Mg distances in alkyl-Grignard compounds.[7] There should be no bonding between C10 and Mg (300.5(3) pm). From the size of the C10-C9-Mg angle (110.5(2)°) and of the torsional angle C11-C10-C9-Mg (−109.2(3)°) it follows that the Mg atom juts out significantly from the allyl-CCC moiety. As a consequence H9A and H9B are twisted "inwards".

In contrast to the Grignard compound **1**, in many allyl-transition-metal complexes,[1] and in (1,3-diphenylallyllithium-diethyl ether)$_n$ **2**,[3] one finds η^3-structures; allyllithium-pentamethyldiethylenetriamine **3** contains at least a markedly unsymmetric η^3-(if not an η^2-)allyl-lithium bond.[4] Comensurate with the η^1-structure of **1** the C-C distances in the allyl moiety are different: C10-C11 133.5(4) pm and C9-C10 144.2(4) pm. The C9-C10-C11 angle is noticeably widened (130.2(3)°) and reaches almost the size of the CCC angles in the allyllithium compounds **2** (131(1)°)[3] and **3** (131.5(3)°).[4] The bond angles at C9 correspond to tetrahedral geometry and those at C11 to trigonal geometry (see caption to Fig. 1). The hydrogen atoms H10A, H11A, and H11B lie in the C9-C10-C11 plane.

An η^1-structure in allyl-Grignard compounds in *solution* had been concluded earlier by *Roberts* et al. from their classical NMR investigations.[8] The proof for such a structure was furnished by *Schlosser* and *Stähle* by means of the isotope-perturbation method.[10] *Benn* and *Rufińska* et al. confirmed the η^1-structure with ^{25}Mg-NMR data[11] and

$^1J(^{13}C,^{13}C)$ coupling constants.[11h] Ab initio calculations on ("*gaseous*") allylmagnesium hydride also favor an η^1-structure.[12] Marked deviations from the solid-state structure of **1** are found in the C9-C10 bond length, which is 149.9 instead of 144.2(4) pm, and in the location of the Mg atom, which according to the calculations assumes a position representing "a compromise between a "classical" geometry and a bridged structure."[12]

Summary: The structure of **1** in the solid state should serve as a good model for the structure of allyl-Grignard compounds in solution and as a criterion for further calculations.

Received: April 13, 1987 [Z 2203 IE]
German version: *Angew. Chem. 99* (1987) 706

CAS Registry numbers:
1, 109013-41-4; TMEDA, 110-18-9; allylmagnesium chloride, 2622-05-1.

[1] Important works: a) G. Wilke, B. Bogdanović, P. Hardt, P. Heimbach, W. Keim, M. Kröner, W. Oberkirch, K. Tanaka, E. Steinrücke, D. Walter, H. Zimmermann, *Angew. Chem. 78* (1966) 157; *Angew. Chem. Int. Ed. Engl. 5* (1966) 151; b) R. Uttech, H. Dietrich, *Z. Kristallogr. 122* (1965) 60; c) U. Franke, E. Weiss, *J. Organomet. Chem. 139* (1977) 305; d) J. A. Kaduk, A. T. Poulos, J. A. Ibers, *ibid. 127* (1977) 245 (in this work the structures of many allyl-transition metal complexes are discussed); e) T. H. Tulip, J. A. Ibers, *J. Am. Chem. Soc. 101* (1979) 4201; f) D. M. P. Mingos in G. Wilkinson, F. G. A. Stone, E. W. Abel (Eds.): *Comprehensive Organometallic Chemistry, Vol. 3*, Pergamon, Oxford 1982, p. 1; g) T. H. Cymbaluk, R. D. Ernst, V. W. Day, *Organometallics 2* (1983) 963; h) R. Benn, A. Rufińska, *ibid. 4* (1985) 209, and references cited therein; i) R. Goddard, C. Krüger, F. Mark, R. Stansfield, X. Zhang, *ibid. 4* (1985) 285, and references cited therein; j) P. W. Jolly, *Angew. Chem. 97* (1985) 279; *Angew. Chem. Int. Ed. Engl. 24* (1985) 283.

[2] H. Köster, E. Weiss, *Chem. Ber. 115* (1982) 3422.

[3] G. Boche, H. Etzrodt, M. Marsch, W. Massa, G. Baum, H. Dietrich, W. Mahdi, *Angew. Chem. 98* (1986) 84; *Angew. Chem. Int. Ed. Engl. 25* (1986) 104.

[4] U. Schümann, E. Weiss, H. Dietrich, W. Mahdi, *J. Organomet. Chem. 322* (1987) 299.

[5] Preparation: 2 mL of a 2.0 M solution of allylmagnesium chloride in THF (Aldrich) was treated with 2 mL of TMEDA (13.3 mmol) at 20°C. The colorless crystals of **1** can be isolated after 12 h (yield 100%).

[6] X-ray structure analysis: 150 K, colorless crystals ca. $0.5\times0.4\times0.6$ mm^3, $P2_1/n$, $a=844.5(1)$, $b=1102.0(1)$, $c=1350.4(1)$ pm, $\beta=92.58(1)°$, $Z=4$, $\rho_{calcd}=1.148$ g cm^{-3}. 3254 reflections measured (Enraf-Nonius CAD4 four-circle diffractometer, $Mo_{K\alpha}$ radiation), 1353 of which, with $F_o>3\sigma(F_o)$ after Lp correction and averaging of equivalent reflections, were used for the calculations. Solution by direct methods, anisotropic refinement of all non-hydrogen atoms. The H-atoms on TMEDA were refined to calculated positions (C-H 96 pm) according to a riding model with common temperature factors for the CH_2- and CH_3-hydrogen atoms, the H-atoms at C9, C10, and C11 calculated first, then isotropically refined with fixed C-H distances (96 pm). $R=0.035$, $R_w=0.037$ with $w^{-1}=\sigma^2(F)+0.0005F^2$, 152 parameters. Further details of the crystal structure investigation are available on request from the Fachinformationszentrum Energie, Physik, Mathematik GmbH, D-7514 Eggenstein-Leopoldshafen 2 (FRG), on quoting the depository number CSD-52424, the names of the authors, and the journal citation.

[7] Examples: a) ethylmagnesium bromide·2diethyl ether, C-Mg 215(2) pm; L. J. Guggenberger, R. E. Rundle, *J. Am. Chem. Soc. 90* (1968) 5375; b) bis(ethylmagnesium bromide-triethylamine)$_2$, C-Mg 218 pm; J. Toney, G. D. Stucky, *Chem. Commun. 1967*, 1168.

[8] a) J. E. Nordlander, J. D. Roberts, *J. Am. Chem. Soc. 81* (1959) 1769; b) G. M. Whitesides, J. E. Nordlander, J. D. Roberts, *Discuss. Faraday Soc. 34* (1962) 185; c) *J. Am. Chem. Soc. 84* (1962) 2010; d) diallylmagnesium: H. E. Zieger, J. D. Roberts, *J. Org. Chem. 34* (1969) 1976; e) D. Leibfritz, B. O. Wagner, J. D. Roberts, *Justus Liebigs Ann. Chem. 763* (1972) 173 [9].

[9] See also: D. A. Hutchison, K. R. Beck, R. A. Benkeser, J. B. Grutzner, *J. Am. Chem. Soc. 95* (1973) 7075.

[10] a) M. Schlosser, M. Stähle, *Angew. Chem. 92* (1980) 497; *Angew. Chem. Int. Ed. Engl. 19* (1980) 487; b) M. Stähle, M. Schlosser, *J. Organomet. Chem. 220* (1981) 277.

[11] R. Benn, H. Lehmkuhl, K. Mehler, A. Rufińska, *Angew. Chem. 96* (1984) 521; *Angew. Chem. Int. Ed. Engl. 23* (1984) 534.

[12] T. Clark, C. Rohde, P. von R. Schleyer, *Organometallics 2* (1983) 1344.

Dinuclear Fulvalene Complexes of Tri- and Tetravalent Zirconium**

By *Wolfgang A. Herrmann,* Tomás Cuenca, Babil Menjón*, and *Eberhardt Herdtweck*

The high reactivity of organozirconium(III) compounds, which also includes extreme sensitivity to air, has hitherto precluded a systematic development of this class of compounds comparable to that of organotitanium(III) compounds, whose chemistry is very well documented.[1,2] In view of the importance of low-valent organozirconium species in catalytic processes[1,3] we have directed our attention to the synthesis of polynuclear systems of this type exploiting the fulvalene bracketing effect and have recently reported on the zirconium(III) derivative **1**, a complex which is readily accessible by reductive CC-coupling of zirconocene dichloride with sodium.[4] We have now also succeeded in carrying out the directed methylation and oxidation of this derivative, thus opening up the possibility of further functionalization.

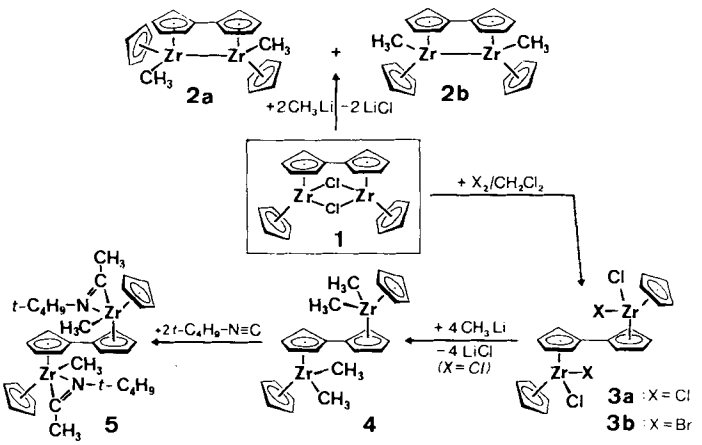

Reaction of 2.1 molar equivalents of methyllithium with **1** in the complete absence of air, moisture and light leads to formation of the chlorine-free methylation product **2**, a red solid, in 65% yield; NMR spectroscopic data (^1H, ^{13}C) show that **2** is formed as a *cis/trans*-mixture **2a** + **2b**.[5]

2 is one of the few unequivocally characterized alkyl compounds of *tri*valent zirconium;[1,2] it can be stored without decomposition for prolonged periods of time only in the absence of light and oxygen at temperatures below −20°C. The directed solid-state thermolysis of pure **2** (200°C/15 min/vacuum) yields chiefly methane as gaseous cleavage product (94%) together with small amounts of ethane, propane, propene and *cis*-2-butene. This finding can be explained in terms of initial formation of an unstable $ZrCH_2Zr$ species, which continuously decomposes like other μ-methylene complexes.[6]

Moreover, owing to its ready oxidizability, **1** can for example be converted in good yields (80–90%) into the CC-

[*] Prof. Dr. W. A. Herrmann, Dr. T. Cuenca, Dr. B. Menjón, Dr. E. Herdtweck
Anorganisch-chemisches Institut der Technischen Universität München
Lichtenbergstrasse 4, D-8046 Garching (FRG)

[**] Chemistry of Oxophilic Transition Metals, Part 3. This work was supported by the Alexander-von-Humboldt-Stiftung (*T. C.* and *B. M.*) and by Hoechst Aktiengesellschaft.—Part 2: [4c].

coupled greenish-yellow zirconocene dihalide complexes **3a** and **3b**. Even upon further reaction of **3** the fulvalene bracket between the two zirconium atoms remains intact. Thus, exhaustive methylation with methyllithium or methylmagnesium bromide in the molar ratio 1:4.2 leads to the tetramethyl derivative **4**,[7] a crystalline, yellow substance, whose methyl groups are capable of undergoing CC-coupling: treatment of **4** with **2** molar equivalents of isocyanide (e.g. *tert*-butyl isocyanide) at room temperature leads, via insertion of the NC function into Zr–CH_3 bonds, to smooth formation of the yellow azazirconiacyclopropene complex ("iminoacyl" complex) **5**; the η^2-fixation of the NC ligand is confirmed by the IR and ^{13}C-NMR spectra ($\tilde{\nu}$(CN) = 1637 cm^{-1}; δ(CN) = 234 ppm [C_6D_6]).[8,9]

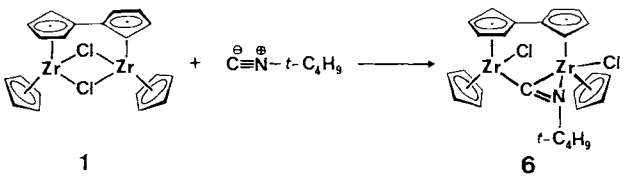

1 **6**

Both chloro-bridges in the extremely reactive zirconium(III) complex **1** are opened upon reaction with isocyanide; with *tert*-butyl isocyanide, the derivative **6** is formed.[10]

The optimal orientation for the $\eta^1:\eta^2$-bridge coordination of the NC ligand is achieved by a twisting of the two zirconocene moieties through 22.6° about the C11–C21 bond joining them (Figure 1). The isocyanide ligand is puckered [$\sphericalangle$(C-N-C1) = 130.5(1)°], while the sequence of atoms Zr1-C-N, on the other hand, is almost linear

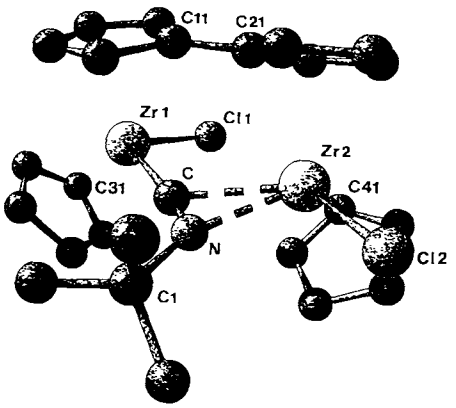

Fig. 1. Crystal structure of the fulvalene-bridged isocyanide complex **6** (SCHAKAL-representation, without hydrogen atoms). Selected bond lengths [pm] and angles [°]: Zr1-C 218.0(2), C-N 124.9(2), N-C1 151.7(2), Zr2-C 236.5(1), Zr2-N 221.2(1), Zr1-Cl1 250.5(1), Zr2-Cl2 258.3(1), C11-C21 140.9(2), Zr1-C11...15 250.0 (mean value), Zr1-C31...35 250.8 (mean value), Zr2-C21...25 254.8 (mean value), Zr2-C41...45 251.6 (mean value); Zr1-C-N 168.0(1), C-N-C1 130.5(1), Zr1-C-Zr2 122.1(1), Zr2-N-C1 148.2(1), C-N-Zr2 81.0(1).

[168.0(1)°].[11] As expected, the Zr1–C bond, with a length of 218.0(2) pm, is considerably shorter than a Zr–methyl bond (230–236 pm[1]), and the NC bond (124.9(2) pm) is somewhat shorter than a normal N=C bond.[1] The atoms Zr1, Zr2, Cl1, C, N, and C1 lie almost in a plane. The two zirconium atoms are so far apart (398 pm) that a bonding interaction between them can be disregarded. The electronic differences caused by the side-on complexation of the isocyanide ligand allows for the bonds from Zr-2 being longer than the corresponding bonds from Zr1. Diazoalkanes yield complexes structurally analogous to **6** (*N,N*-coordination).[12]

It is thus demonstrated that zirconium(III) complexes of the fulvalene series are functionalizable with retention of the oxidation state as well as with oxidation of the metal center, and no degradation or bond formation reactions to give mono- or oligomeric species are likely to occur because of the stable fulvalene bracket.

Experimental

2a/2b: A solution of **1** (1.02 g, 2 mmol) in toluene was treated at −78 °C with a 1.6 M solution of methyllithium in hexane (2.6 mL, 4.2 mmol) and the stirred mixture heated within ca. 2 h to −20 °C. The resulting reddish-brown solution was filtered off from insoluble material at −78 °C and evaporated to dryness under vacuum. **2a/2b** was washed with cold *n*-hexane and diethyl ether and dried under vacuum. Yield: 620 mg (65%).

3a/3b: A solution of **1** [4a] (5.11 g, 10 mmol) in toluene was treated with a stoichiometric amount of Cl_2 or Br_2, respectively, dissolved in CH_2Cl_2. The oxidation product **3a** or **3b**, respectively, immediately precipitated as a yellow solid. After 2 h, the product was evaporated down in a vacuum and the residue washed with tetrahydrofuran, *n*-hexane, and acetone. Yield: 5.30 g (90%) of **3a** or 5.40 g (80%) of **3b**, respectively.

4: A suspension of **3a** (582 mg, 1 mmol) in toluene (20 mL) was treated at −78 °C with a 1.6 M solution of CH_3Li in hexane (2.6 mL, 4.2 mmol). After warming to room temperature the yellow solution was separated from the sediment on dry celite, evaporated to dryness, and the resulting residue washed with diethyl ether and *n*-hexane; yellow crystals from toluene/hexane; yield 461 mg (92%).

5: A solution of **4** (501 mg, 1 mmol) in toluene was treated at room temperature with *t*-C_4H_9NC (0.25 mL, 2.2 mmol). After 15 h the mixture was filtered and the filtrate evaporated to dryness. Recrystallization of the residue from toluene/*n*-hexane furnished yellow crystals of **5**; yield 400 mg (60%).

6: A solution of **1** (500 mg, 0.98 mmol) in toluene (70 mL) was treated at room temperature with *t*-C_4H_9NC (110 µL, 0.98 mmol); the dark-violet solution immediately turned red. After filtration the solution was evaporated to dryness and the residue washed with *n*-hexane and diethyl ether. Yield: 490 mg (85%); m.p. 216 °C (decomp.).

Received: January 16, 1987 [Z 2047 IE]
German version: *Angew. Chem. 99* (1987) 687

[1] Recent monograph: D. J. Cardin, M. F. Lappert, C. L. Raston: *Chemistry of Organo-zirconium and -hafnium Compounds*, Horwood/Wiley, Chichester/New York 1986.

[2] Recent examples: a) J. H. Wengrovius, R. R. Schrock, C. S. Day, *Inorg. Chem. 20* (1981) 1844; b) J. Blenkers, P. Bruin, J. H. Teuben, *J. Organomet. Chem. 297* (1985) 61.

[3] R. Choukronn, M. Basso-Bert, D. Gervais, *J. Chem. Soc. Chem. Commun. 1986*, 1317.

[4] a) T. V. Ashworth, T. Cienca, E. Gerdtweck, W. A. Herrmann, *Angew. Chem. 98* (1986) 278; *Angew. Chem. Int. Ed. Engl. 25* (1986) 289; b) W. A. Herrmann, T. Cuenca, U. Küsthardt, *J. Organomet. Chem. 309* (1986) C 15; c) T. Cuenca, W. A. Herrmann, T. V. Ashworth, *Organometallics 5* (1986) 2514; d) X-ray structure of **1**: S. Gambarotta, M. Y. Chiang, *ibid. 6* (1987) 897.

[5] Data for **2a/b**: ^{1}H-NMR (270 MHz, C_6D_6, 28 °C): $\delta(CH_3) = -0.30/0.01$ [s, 6H]; $\delta(C_5H_5) = 5.74/5.70$ [s, 10H]; $\delta(C_{10}H_8) = 6.44/6.33$, 5.88/5.51, 5.44/5.18, 5.02/4.98 [4m, 8H].—^{13}C-NMR (67.8 MHz, C_6D_6, 28 °C): $\delta(CH_3) = 22.61/22.72$; $\delta(C_5H_5) = 109.53/108.71$; $\delta(C_{10}H_8) = 125.62$, 124.51, 120.39, 113.58, 110.20, 108.51, 107.68, 105.48, 100.00, 95.00.—EI-MS (70 eV): *m/z* 468 ($M^{\oplus}$ für $C_{22}H_{24}Zr_2$).—Correct C,H,Zr analysis.

[6] a) A. Schäfer, W. A. Herrmann, *J. Organomet. Chem. 297* (1985) 229; b) A. Schäfer, *Dissertation*, Technische Universität München 1987.

[7] Data for **4**: ^{1}H-NMR (270 MHz, C_6D_6, 28 °C): $\delta(CH_3) = -0.10$ [s, 12H]; $\delta(C_5H_5) = 5.74$ [s, 10H]; $\delta(C_{10}H_8) = 5.91$, 5.99 [2t, A_2B_2 system, $J = 2.60$ Hz, 8H].—^{13}C-NMR (67.8 MHz, C_6D_6, 28 °C): $\delta(CH_3) = 31.57$; $\delta(C_5H_5) = 110.85$; $\delta(C_{10}H_8) = 107.56$, 110.08, 120.60.—EI-MS (70 eV): *m/z* 498 ($M^{\oplus}$ für $C_{24}H_{30}Zr_2$).—Correct C,H,Zr analysis.

[8] Data for **5**: ^{1}H-NMR 270 MHz, $C_6H_5CD_3$, −25 °C): $\delta(ZrCH_3) = 0.25$ [s, 6H]; $\delta(CCH_3) = 2.16$ [s, 12H]; $\delta(t\text{-}C_4H_9) = 1.03$ [s, 18H]; $\delta(C_5H_5) = 5.38$ [s, 10H]; $\delta(C_{10}H_8) = 5.2$–5.6 [m, 8H].—IR (cm^{-1}, KBr): $\tilde{\nu}$(CN) = 1637.—EI-MS (70 eV): *m/z* 568 ($M^{\oplus}$ für $C_{34}H_{48}N_2Zr_2$).—Correct C,H,N analysis.

[9] Other "η^2-iminoacyl" complexes: a) R. D. Adams, D. F. Chodosh, *Inorg. Chem. 17* (1978) 41; b) P. T. Wolczanski, J. E. Bercaw, *J. Am. Chem. Soc. 101* (1979) 6450; c) M. F. Lappert, N. T. Luong-Thi, C. R. C. Milne, *J. Organomet. Chem. 174* (1979) C35.

[10] Data for **6**: ^{1}H-NMR (270 MHz, [D$_8$]THF, 28 °C): $\delta(CH_3)=1.49$ [s, 9 H]; $\delta(C_5H_5)=6.21$ and 5.81 [2s, 2 × 5 H]; $\delta(C_{10}H_8)=6.47$, 6.34, 6.21, 6.01, 5.69, 5.54, 5.06, 4.88 [8m, 8 × 1 H].—^{13}C-NMR (67.80 MHz, [D$_8$]THF, 30 °C): $\delta(C_5H_5)=110.89$ and 110.34; $\delta(CH_3)=29.93$; $\delta(C(CH_3)_3)=30.82$; $\delta(NC)=218.12$; $\delta(C_{10}H_8)=94.54$, 100.37, 102.91, 103.32, 103.37, 104.75, 112.43, 114.83, 118.22, 125.67.—IR (cm^{-1}, KBr): $\tilde{\nu}(CN)=1652/1648$.—EI-MS (70 eV): m/z 538 ([$M-C(CH_3)_3$]$^{\oplus}$).—Correct C,H,N analysis.

[11] X-ray structure analysis of **6**: orthorhombic (from toluene/*n*-hexane, 25 °C), space group $P2_12_12_1$ (IT-No. 19); $a=823.3(1)$, $b=1689.1(2)$, $c=1731.2(2)$ pm; $\alpha=\beta=\gamma=90°$; $V=2407\times10^6$ pm^3; $Z=4$; $\rho_{calcd}=1.641$ g cm^{-3}; empirical absorption correction: $\mu=10.9$ cm^{-1}; $\lambda=71.073$ pm ($Mo_{K\alpha}$ radiation); $T=23+1$ °C; Enraf-Nonius-CAD-4; measuring range $2.0\leq\theta\leq25.0°$; 4517 measured reflections, 4029 independent reflections with $I>1\sigma(I)$; $R=\Sigma\|F_0|-|F_c\|\Sigma|F_0|=0.017$; $R_w=[\Sigma w(|F_0|-|F_c|)^2/\Sigma w|F_0|^2]^{1/2}=0.018$ with $w=1/\sigma^2(F_0)$; structure solved by Patterson methods. A difference Fourier synthesis with heavy metal atom positions only, revealed almost all hydrogen positions which were calculated for ideal geometry (d(C-H)=95 pm). The hydrogen atoms and their temperature factors were included in the calculation of the structure factors but not refined. The temperature factors are the same for all hydrogen atoms. Anomolous dispersion was taken into account. The asymmetric unit contains 30 "heavy" atoms (anisotropic temperature factors), 27 H atoms; 271 parameters were "full-matrix" refined.—Shift/error <0.00 in the last refinement cycle; residual electron density: +0.39 e/Å^3. Further details of the crystal structure investigation are available on request from the Fachinformationszentrum Energie, Physik, Mathematik GmbH, D-7514 Eggenstein-Leopoldshafen 2 (FRG), on quoting the depository number CSD-52358, the names of the authors, and the journal citation.

[12] W. A. Herrmann, B. Menjón, E. Herdtweck, unpublished.

Precipitates with β-Pleated Sheet Structure by Mixing Aqueous Solutions of Helical Poly(D-lysine) and Poly(L-lysine)**

By *Jürgen-Hinrich Fuhrhop,* Matthias Krull,* and *Georg Büldt*

Alkaline solutions of poly(D-lysine) ($c=3\times10^{-2}$ monomol/L, pH = 11; mean chain length n = 373, Sigma) and poly(L-lysine) ($c=3\times10^{-2}$ monomol/L, pH = 11; n = 430, Sigma) are stable and remain clear for weeks on storage under nitrogen at room temperature. The solution of poly(L-lysine) contains *P*- or right-handed helices, which are characterized by their molar ellipticities $[\theta]_\lambda$ per amino acid residue in CD spectra.[1,2] The $[\theta]$-values immediately after preparation of the solution and those after a week differ only slightly: $[\theta]_{219}=-31000$ and -27000, resp.; $[\theta]_{206}=-30000$ and -28000, resp.; $[\theta]_{189}=74000$ and 70000 grad cm^2/dmol, resp. The same holds for the *M*-helix of poly(D-lysine): $[\theta]_{219}=31000$ and 34000, resp.; $[\theta]_{206}=31000$ and 33000, resp.; $[\theta]_{189}=-73000$ and -71000 grad cm^2/d mol, resp. In D_2O, both solutions also show IR bands at 1636 cm^{-1}, which are typical for α-helices.[3]

When equal volumes of the clear solutions are mixed, a colorless precipitate is formed within a few minutes. The racemic mixture precipitates almost quantitatively, the association constant K is greater than 9×10^8 monomol lysine/L. To our knowledge, a similar phenomenon has previously only been observed in the case of the methyl esters of the *M*- and *P*-helical polyglutamates in organic solvents.[4] We explain the precipitation of the racemate in terms of an irreversible union of the disordered terminals of the *P*- and *M*-helices (= α-structures) and accompanying formation of insoluble pleated structures (= β-structures). The β-structures then grow at the cost of the α-structures. An intermediary coiling of the whole polypeptide does not occur.

We propose an antiparallel pleated sheet as the most likely structure for the racemic aggregate, i.e. a structure corresponding to the "polar pleated sheet" described by *Pauling* and *Corey*.[5] The impairment of aggregation, by the side chains, would in this case be minimal, so that pleating and curling of the individual sheets to fibers[6] should be less pronounced. The lengths of the hydrogen bonds linking the skeletal framework are also minimal in this structure (Fig. 1). The steric hindrance in the racemic β-structure is less than in the pure enantiomer.

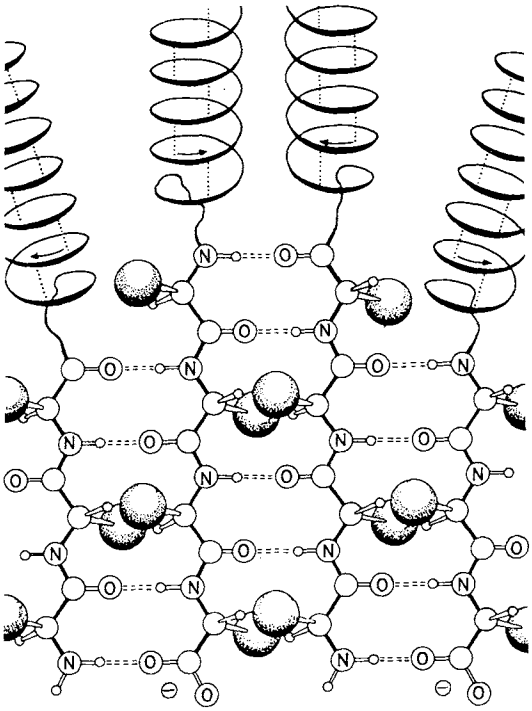

Fig. 1. Model for the aggregation of right-handed (*P*-) helices of poly(L-lysine) and left-handed (*M*-)helices of poly(D-lysine) and for the formation of a racemic pleated structure. The large spheres symbolize the $NH_2-(CH_2)_4$-residue.

The assumption of a β-structure for the racemic precipitate is based on the following: 1) The visual and electron microscopic images of the precipitate point to a pleated structure (Fig. 2a). 2) The X-ray reflections of the precipitate are consistent with a pleated structure, but not with helices.[7,8] X-ray powder photographs of the precipitate (Fig. 2b) show rings at 0.46 (chain interval), 0.74, and 1.46 nm (pleat interval),[7,8] whereas the characteristic reflections at 0.54 and 0.15 nm for a helix are missing. The rings between 2.0 and 4.9 nm point to superstructures, which are also visible in electron micrographs (Fig. 2a). 3) The strong amide-I band at $\tilde{\nu}=1688$ cm^{-1} in the IR spectrum is typical for pleated structures.[3] 4) The marked increase in the fluorescence of the pigment 6-(toluidino)-2-

[*] Prof. Dr. J.-H. Fuhrhop, Dipl.-Chem. M. Krull
Institut für Organische Chemie der Freien Universität
Takustrasse 3, D-1000 Berlin 33
Prof. Dr. G. Büldt
Institut für Physik der Freien Universität
Arnimallee 14, D-1000 Berlin 33

[**] This work was supported by the Deutsche Forschungsgemeinschaft (SFB 312) and the Förderungs-Kommission der Freien Universität.

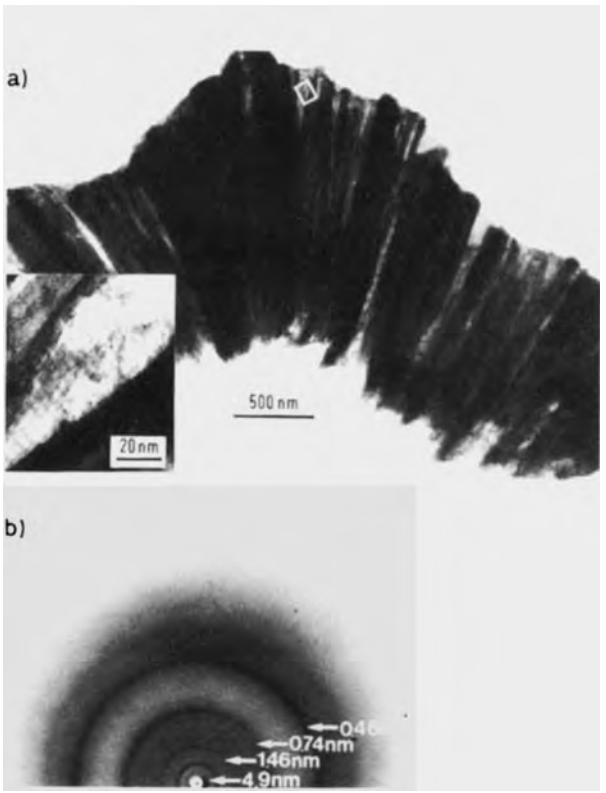

Fig. 2. a) Electron micrographs of the racemic precipitate with a magnified section showing 5-nm threads. b) X-ray powder diagram of the same sample (see text).

naphthalenesulfonic acid suggests an insertion of the pigment into the hydrophobic region of the micellular pleated structure during the precipitation.[9] No films could be prepared from the solutions of the pure enantiomers which would give well-defined electron microscopic images.[10]

The spontaneous structural transformation upon mixing the enantiomeric helices is a further example for the chiral bilayer effect postulated by us[11] for aggregates with a hydrophobic bilayer. This effect is the reason for the helical fibers of chiral amphiphiles aggregating and precipitating only slowly and the racemic hydrophobic bilayers rapidly forming insoluble crystal platelets on union of the two enantiomeric helices. The effect has been demonstrated previously with helical aggregates of chiral fatty acids in organogels[12] and with *N*-alkylgluconamides in aqueous gels.[11] Its validity demonstrated here also for polymers may be regarded as an indication of the relevance of the effect for biological organisates in which polymer fibers play a dominating role (e.g. collagen in muscles).[13] In these cases it can be predicted that racemic crystals precipitate on addition of the enantiomeric polymer-fiber. If the hydrophobic effect dominates in the stabilization of the chiral fiber,[11] pleated structures should form in the racemate. In the case of chiral fibers in non-aqueous media[4] or membranes, dipole interactions should dominate and the helices should remain intact during the precipitation.[12] In both cases the chirality of the fibers appears to be a necessary prerequisite for the longevity of metastable organisates.

Received: February 9, 1987;
revised version: March 30, 1987 [Z 2096 IE]
German version: *Angew. Chem. 99* (1987) 707

[1] U. Greenfield, G. D. Fasman, *Biochemistry 10* (1969) 4108.
[2] R. Townend, F. Kumosinski, S. N. Timasheff, G. D. Fasman, B. Davidson, *Biochem. Biophys. Res. Commun. 23* (1966) 163.
[3] T. Miyazawa, E. R. Blout, *J. Am. Chem. Soc. 83* (1961) 712.
[4] T. Yoshida, S. Sakurai, T. Okuda, Y. Takagi, *J. Am. Chem. Soc. 84* (1962) 3590.
[5] L. Pauling, R. B. Corey, *Proc. Natl. Acad. Sci. USA 37* (1951) 729.
[6] K.-C. Chou, M. Pottle, G. Némethy, Y. Ueda, H. A. Scheraga, *J. Mol. Biol. 162* (1982) 89.
[7] M. Goodman, A. S. Verdini, M. S. Choi, Y. Masuda, *Top. Stereochem. 5* (1970) 69.
[8] F. J. Padden, H. D. Keith, G. Giannoni, *Biopolymers 7* (1969) 793.
[9] J. Lynn, G. D. Fasman, *Biochem. Biophys. Res. Commun. 33* (1968) 327.
[10] G. Harauz, D. W. Andrews, F. D. Ottensmeyer, *Ultramicroscopy 12* (1983) 59.
[11] J.-H. Fuhrhop, P. Schnieder, J. Rosenberg, E. Boekema, *J. Am. Chem. Soc. 109* (1987) 3387.
[12] T. Tachibana, T. Yoshizuma, K. Hori, *Bull. Chem. Soc. Jpn. 52* (1979) 34.
[13] B. Alberts, D. Bray, J. Lewis, M. Raf, K. Roberts, J. D. Watson: *Molekularbiologie der Zelle*, VCH Verlagsgesellschaft, Weinheim 1986, pp. 773, 297.

Electron Delocalization in Diruthenium Complexes of Polycyclic Arenes**

By *Klaus-Dieter Plitzko* and *V. Boekelheide**

Related to the discovery of the Creutz-Taube ion,[1] a tremendous amount of work has been done with respect to both experimental examples[2] and the theory[3] of intramolecular one-electron-transfer in mixed-valence ions. Much less is known about intramolecular multi-electron-transfers. Only recently, we reported on **1**, the first example of a discrete mixed-valence molecular ion (class II), showing a

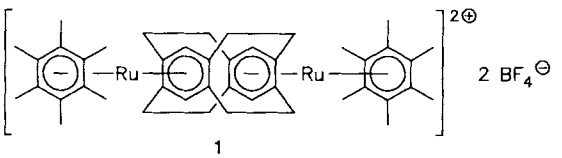

1

net, two-electron transfer.[4] Almost simultaneously, the first, quantitative, theoretical analysis of an intramolecular two-electron transfer, using the vibronic coupling model (PKS), has appeared.[5] As an outgrowth of our studies on diruthenium complexes of [2$_n$]cyclophanes, we have been interested in various types of hydrocarbon ligands. Prior work by *Hendrickson* et al.[6] indicated that diiron complexes of polycyclic arenes show mixed-valence properties involving one-electron transfer. It was important, therefore, to study some examples of diruthenium complexes of polycyclic arenes in order to compare their properties, as mixed-valence ions involving net two-electron transfers, with those of **1**.

We now report on the preparation and properties of the bis(η^6-hexamethylbenzene)diruthenium complexes of phenanthrene, **3**, and 9,10-dihydrophenanthrene, **6**. The cation of **3** is a typical class II, mixed-valence ion, quite similar to the cation of **1**, but having a much larger thermal energy barrier for electron transfer. Quite surprisingly,

[*] Prof. Dr. V. Boekelheide, Dr. K.-D. Plitzko
Department of Chemistry, University of Oregon
Eugene, Oregon 97403 (USA)

[**] This work was supported by the National Science Foundation (Grant CHE-8210282). *K.-D. P.* thanks the Studienstiftung des Deutschen Volkes for a Dissertation Stipend (1985-1987).

though, **6** shows electron delocalization throughout the temperature range experimentally accessible. At present it is not certain whether **6** is an average-valence ion with complete electron delocalization, or whether it is a class II ion with a very low thermal energy barrier to electron transfer. In either case, the cation of **6** is a highly unusual ion involving the lower oxidation states of ruthenium.

son of the ^{1}H-NMR spectrum of **3** with the ^{1}H-NMR spectra of the model compounds, (η^6-hexamethylbenzene)(η^6-phenanthrene)ruthenium(II) and (η^6-hexamethylbenzene)(η^4-phenanthrene)ruthenium(0), clearly shows that the two different ruthenium environments present in **3** correspond to a Ru^{II} site and a Ru^0 site.[7] This is further supported by a comparison of the corresponding ^{13}C-

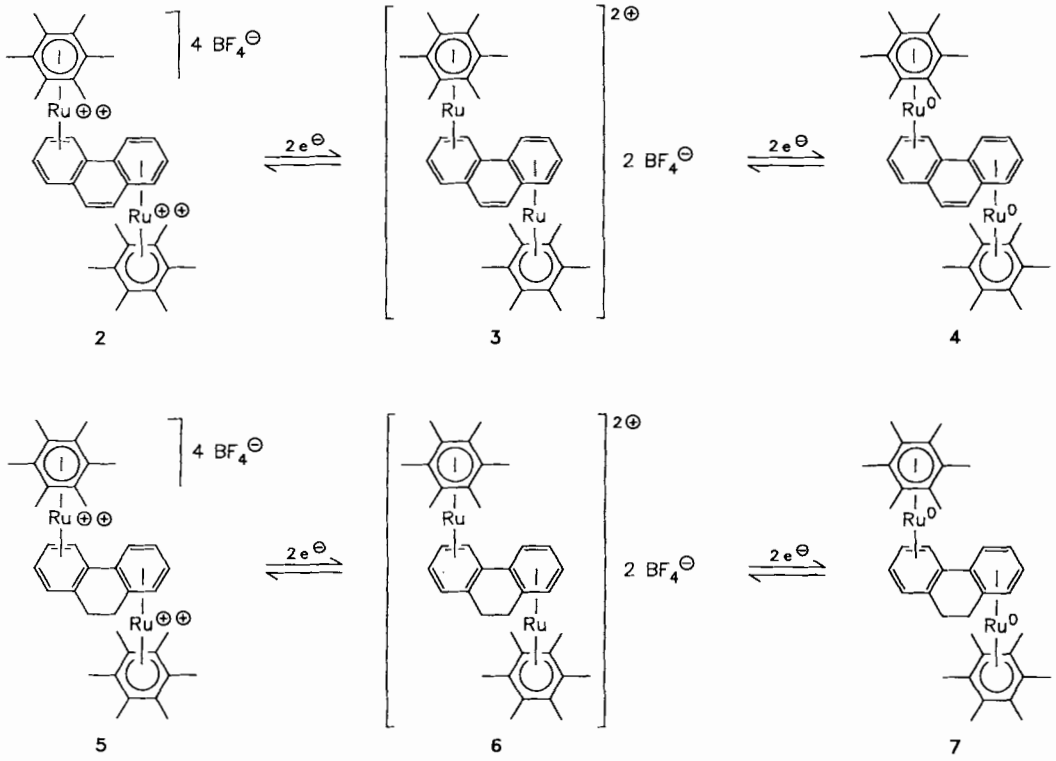

The preparation of the complexes **2** and **5** proceeded readily in high yield by the reaction of phenanthrene and 9,10-dihydrophenanthrene, respectively, with the solvate of (η^6-hexamethylbenzene)ruthenium(II) bis(tetrafluoroborate) following the usual procedure,[4] but using propylene carbonate as solvent.[7] Cyclic voltammetry and coulometry measurements of **2** showed two, reversible, two-electron reduction waves corresponding to the formation of **3** and **4**; $E^{I}_{1/2}$ (vs. SCE) $= -0.185 \pm 0.005$ V and $E^{II}_{1/2} = -0.677 \pm 0.005$ V. From the difference (492 mV) between the two redox potentials, the comproportionation constant (K_c) for the equilibrium, $\mathbf{2} + \mathbf{4} \rightleftharpoons 2\,\mathbf{3}$, is calculated to be 4.4×10^{16}. Similarly, cyclic voltammetry and coulometry measurements of **5** showed two, reversible two-electron reduction waves corresponding to the formation of **6** and **7**; $E^{I}_{1/2}$ (vs. SCE) $= -0.195 \pm 0.005$ V and $E^{II}_{1/2} = -1.77 \pm 0.010$ V. The difference in redox potentials in the case of the 9,10-dihydrophenanthrene derivatives is 982 mV, indicating the comproportionation constant (K_c) for the equilibrium, $\mathbf{5} + \mathbf{7} \rightleftharpoons 2\,\mathbf{6}$, to be 1.6×10^{33} and suggesting a strong electron delocalization for **6**. Separate chemical reductions of **2** and **5**, respectively, using bis(hexamethylbenzene)ruthenium(0) as a reducing agent,[4] made possible the isolation of both **3** and **6** as dark red crystals in quantity and in high yield.[7]

From the ^{1}H-NMR spectra of **3** and **6**, given in Table 1, it is apparent that **3** has two different sets of aromatic protons and two different types of methyl protons. Compari-

Table 1. ^{1}H-NMR data for **3** and **6**. hmb = hexamethylbenzene.

3: ^{1}H-NMR (CD_2Cl_2, 360 MHz): $\delta = 7.63$–7.61 (m, 2H, 7,8-H), 7.43–7.39 (m, 1H, 6-H), 7.15–7.12 (m, 1H, 5-H), 6.36 (tt, $J_1 = 5.76$, $J_2 = 1.08$ Hz, 1H, 2-H), 6.29 (dd, $J_1 = 5.76$, $J_2 = 1.08$ Hz, 1H, 9-H), 5.98 (tt, $J_1 = 5.76$, $J_2 = 1.08$ Hz, 1H, 3-H), 4.15 (dd, $J_1 = 5.76$, $J_2 = 1.08$ Hz, 1H, 10-H), 3.68–3.66 (m, 1H, 1-H), 3.22 (dd, $J_1 = 5.76$, $J_2 = 1.08$ Hz, 1H, 4-H), 2.04 (s, 18H, hmb-CH_3-Ru^{II}), 1.90 (s, 18H, hmb-CH_3-Ru^0)

6: ^{1}H-NMR (CD_2Cl_2, 360 MHz): $\delta = 5.84$ (tt, $J_1 = 5.04$, $J_2 = 1.08$ Hz, 2H, 2,7-H), 4.85 (tt, $J_1 = 6.84$, $J_2 = 1.08$ Hz, 2H, 3,6-H), 4.71 (dd, $J_1 = 5.04$, $J_2 = 1.08$ Hz, 2H, 1,8-H), 4.12 (dd, $J_1 = 6.84$, $J_2 = 1.08$ Hz, 2H, 4,5-H), 2.13 (s, 36H, hmb-CH_3), 2.03 (d, $J = 9.6$ Hz, 2H, 9,10-H), 1.52 (d, $J = 9.6$ Hz, 2H, 9,10-H)

NMR spectra.[7] Thus, on the NMR time scale at room temperature the mixed-valence ion **3** has a frozen conformation corresponding to **3a** or **3b** as shown below. The thermal energy barrier for this postulated equilibrium must

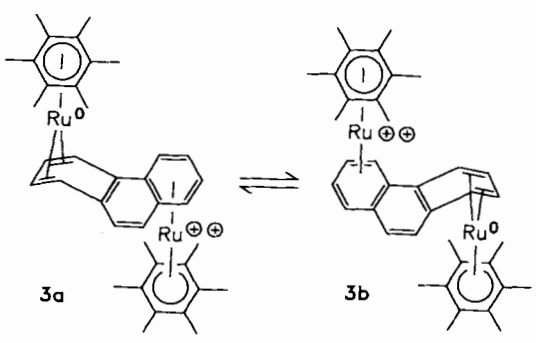

 © VCH Verlagsgesellschaft mbH, D-6940 Weinheim, 1987 0570-0833/87/0707-0701 $ 02.50/0

be quite large, though, since the ^{1}H-NMR spectrum of **3** in [D$_6$]ethylene glycol is unchanged over the temperature range of 25 to 170°C.

In sharp contrast to the data for **3**, the ^{1}H-NMR spectrum of **6** is completely symmetrical, showing a singlet for the methyl protons, two doublets for the bridging methylene protons, and signals for four aromatic protons. The ^{13}C-NMR spectrum of **6** is likewise completely symmetrical.[7] Furthermore, a solution of **6** in $CD_2Cl_2/CHClF_2$ showed no NMR-spectroscopic change over the temperature range of 25 to −135°C. Thus, **6** must be a delocalized average-valence ion or, if class II, the thermal energy barrier for intervalence electron transfer must be very low. A decision between these two possibilities is not easily made and will require further study.[8] The sharp contrast in the properties of **3** and **6** illustrates the remarkable difference a double bond can make. Also, fast electron transfer in diruthenium complexes of polycyclic arenes can apparently rival, or exceed, that present in diruthenium complexes of [2$_n$]cyclophanes.

Received: March 12, 1987 [Z 2154 IE]
German version: *Angew. Chem. 99* (1987) 715

[1] C. Creutz, H. Taube, *J. Am. Chem. Soc. 91* (1969) 3988; *ibid. 95* (1973) 1086.
[2] D. E. Richardson, H. Taube, *Coord. Chem. Rev. 60* (1984) 107.
[3] G. C. Allen, N. S. Hush, *Prog. Inorg. Chem. 8* (1967) 357.
[4] R. H. Voegeli, H. C. Kang, R. G. Finke, V. Boekelheide, *J. Am. Chem. Soc. 108* (1986) 7010.
[5] K. Prassides, P. N. Schatz, K. Y. Wong, P. Day, *J. Phys. Chem. 90* (1986) 5588.
[6] W. H. Morrison, Jr., E. Y. Ho, D. N. Hendrickson, *Inorg. Chem. 14* (1975) 500.
[7] K.-D. Plitzko, *Dissertation*, University of Oregon, Eugene, OR, USA, March 1987. The physical and spectral properties of all the new compounds referred to in this communication are in full accord with their assigned structures.
[8] For example, the classification of the Creutz-Taube ion is still controversial (see U. Fürholz, H.-B. Bürgi, F. E. Wagner, A. Stebler, J. H. Ammeter, E. Krausz, R. J. H. Clark, M. J. Head, A. Ludi, *J. Am. Chem. Soc. 106* (1984) 121).

Macrocyclic Dienes by Metathetic Dimerization of Cycloheptene and Cyclooctene on Re_2O_7/Al_2O_3**

By *Siegfried Warwel,* Hans Kätker,* and *Claudia Rauenbusch*

Dedicated to Professor Friedrich Asinger on the occasion of his 80th birthday

The present syntheses of cyclic hydrocarbons are limited at the C_{12}-ring; 1,5,9-cyclododecatriene is also prepared on an industrial scale by butadiene-cyclotrimerization.[1] We report here on a simple one-step synthesis of the C_{14}-ring and of the C_{16}-ring starting from technically accessible cycloheptene and cyclooctene, respectively, using olefin metathesis[2] as reaction principle.

The metathesis of cycloolefins normally leads to unsaturated, mainly linear polymers, the "polyalkenamers", as major products and to cyclooligomers as byproducts. This bimodal product composition can be explained in terms of the carbene mechanism, the generally accepted mechanism for olefin metathesis:[3]

- linear polymers are formed via metallacyclobutanes as central intermediates by intermolecular reactions of the cycloolefins with the carbenemetal complexes (active catalytic species) formed from homogeneous or heterogeneous metathesis catalysts (Scheme 1).

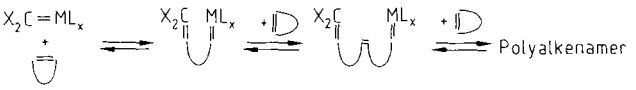

Scheme 1.

- cyclic oligomers are formed by intramolecular reactions of the carbenemetal center of a growing polymer chain with C=C double bonds of the same molecule; Scheme 2 shows possible reaction routes for dimer and trimer formation.

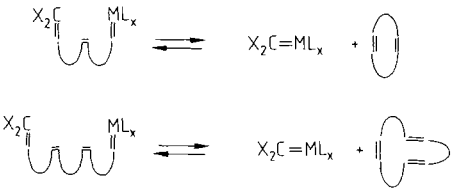

Scheme 2.

The amount of oligomers can of course be increased significantly by using the Ziegler-Ruggli dilution principle in the case of cyclooctene,[4] but the preparative exploitation of the reaction, e.g. for the synthesis of macrocyclic dienes, has so far never been resorted to because of the low yields.[5]

With Re_2O_7/Al_2O_3 as catalyst and by carrying out the reaction in a Soxhlet-like cycling apparatus, in which only small amounts of cycloolefin are continuously fed through the catalyst as fix bed by a low-boiling solvent (pentane, hexane), we have now been able to smoothly convert cycloheptene **1a** into 1,8-cyclotetradecadiene **2a** and cyclooctene **1b** into 1,9-cyclohexadecadiene **2b** and larger macrocycles. The activity of the catalyst could be increased even further by addition of $Sn(CH_3)_4$ to Re_2O_7/Al_2O_3 (see also ref. [6]).

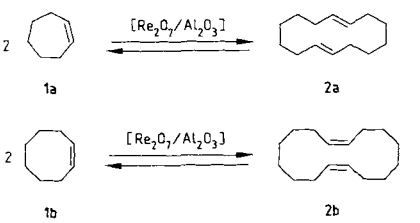

A characteristic feature of our method, besides the low reactant concentration on the catalyst, is a short contact residence time and thus the rapid removal of the metathesis product, whereby secondary reactions to higher oligomers and polymers are impaired. Surprisingly, **1a** and **1b** behave quite differently in the metathesis reaction (Table 1). The reaction of cyclooctene **1b** leads to an homologous series of cyclic oligomers, including the desired 1,9-cyclohexadecadiene **2b**, but also containing the higher polyenes in larger concentrations. In contrast the reaction of cyclo-

[*] Prof. Dr. S. Warwel, Dipl.-Chem. H. Kätker, C. Rauenbusch
Institut für Technische Chemie und Petrolchemie der Technischen Hochschule
Worringer Weg 1, D-5100 Aachen (FRG)

[**] Olefin Metathesis, Part 14. This work was supported by the Fonds der Chemischen Industrie.—Part 13: S. Warwel, W. Winkelmüller, *J. Mol. Catal. 28* (1985) 247.

heptene **1a** leads preferentially to 1,8-cyclotetradecadiene **2a** with a selectivity of 80%.

Table 1. Metathetic dimerization of cycloheptene **1a** and cyclooctene **1b** on Re_2O_7/Al_2O_3 activated by $Sn(CH_3)_4$.

	Cycloheptene **1a**	Cyclooctene **1b**
Conversion [%]	85	90
Selectivity to **2** [%]	80	34
Yield of **2** [%] [a]	68 (**2a**)	30 (**2b**)
Product composition [wt.-%] [b]		
Dimer	80 (**2a**)	34 (**2b**)
Trimer	8	26
Tetramer	1	12
Pentamer	trace	7
Higher oligomers and polymers	11	21

[a] Isolated diene, yield referred to **1**. Yields in the absence of $Sn(CH_3)_4$: for **2a** 60%, for **2b** 25%. [b] Determined by GC: 50 m × 0.25 mm ID, fused silica, OV1. Temperature program: 50–280 °C, 5 min isotherm, 8 °C/min (1.0 bar N_2) and gel permeation chromatography (GPC): polystyrene-gel cross-linked with 2% divinylbenzene, tetrahydrofuran (THF) as eluent [11].

With both cyclic dienes the thermodynamic equilibrium mixture of the configurational isomers is formed (Table 2). In the case of **2a** this consists of 90% of the *trans,trans*-isomer, whereas in the case of **2b** an almost statistical mixture of the three possible stereoisomers is formed.

Table 2. Proportion of configurational isomers of **2a** and **2b** [%] [a]; equilibrium values according to [7] in brackets.

Isomer	**2a**	**2b**
trans-trans	87.8 (90.2)	16.2 (17.7)
cis-trans	8.7 (7.5)	57.5 (59.2)
cis-cis	3.5 (2.3)	26.3 (23.1)

[a] Determined by GC, cf. Table 1.

We attribute the preferred formation of the C_{14} ring in the metathesis of cycloheptene to the exceptional conformational stability of *trans,trans*-1,8-cyclotetradecadiene.[8]

Experimental[10]

2a: A mixture of **1a** (11.6 g, 0.12 mol) and *n*-pentane (45 mL) was heated to boiling in a 250 mL three-necked flask. The vapor phase was fed through a heated tube and condensed in a high-efficiency condenser. The condensate was then passed through a heated spiral cooler, where it was brought to 35 °C and transferred dropwise onto a fixed bed of 6.7 g Re_2O_7/Al_2O_3 (3.5 wt.-% Re_2O_7 on γ-Al_2O_3, Akzo CK 300 Al_2O_3; for preparation of catalyst: cf. ref. [9]), previously saturated with 5.8 mL of a 0.25 M solution of $Sn(CH_3)$ in *n*-hexane. After passage through the catalyst the reaction mixture was fed back into the flask, where the products of metathesis were enriched, while unchanged **1a** was again fed to the catalyst by the low-boiling solvent. After 24 h the solvent and unchanged **1a** were distilled off. Sublimation of the residue at 60 °C/10^{-3} torr afforded 7.9 g (68%) of **2a**. M.p. 64 °C, correct elemental analysis. MS (70 eV): *m/z* 192 ($M^{\oplus}$, 12%), IR (KBr): 3045 (=C–H); 2975, 2940, 2875 (ν-CH_2–); 1650 (C=C); 1475, 1445 (δ-CH_2–); 980 (γ=C–H); 722 (γ=C–H) cm^{-1}. ^{1}H-NMR (90 MHz, TMS): δ = 1.33 (s, 12H); 2.02 (s, 8H); 5.20 (m, 4H).—As expected, the metathesis of **2a** with ethene in an autoclave (50 bar, 90 °C), using the same catalyst, afforded exclusively 1,8-nonadiene. Hydrogenation of **2a** on Pd/C led quantitatively to cyclotetradecane.

2b: Catalyst and reactants: 11.2 g of Re_2O_7/Al_2O_3 saturated with 9.7 mL of a 0.25 M solution of $Sn(CH_3)_4$ in *n*-hexane; 22.7 g (0.21 mol) of cyclooctene, 140 mL of *n*-hexane. Procedure as above, but catalyst temperature 50 °C, reaction time 72 h, and isolation of **2b** by rectification. Yield of **2b**: 6.3 g (30%). B.p. 115 °C/10^{-3} torr. Correct elemental analysis. MS (70 eV): *m/z* 220 ($M^{\oplus}$, 21%). IR (KBr): 3005 (=C–H); 2980, 2920, 2850 (ν–CH_2–); 1650 (C=C); 1460, 1440 (δ–CH_2–); 970 (γ=C–H); 725 (γ=CH) cm^{-1}. ^{1}H-NMR (90 MHz, TMS): δ = 1.31 (s, 16H); 2.03 (s, 8H); 5.40 (m, 4H).—As expected the metathesis of **2b** with ethene in an autoclave (50 bar, 90 °C) using the same catalyst afforded exclusively 1,9-decadiene. Hydrogenation of **2b** on Pd/C led quantitatively to cyclohexadecane.

Received: March 12, 1987 [Z 2138 IE]
German version: *Angew. Chem. 99* (1987) 714

[1] G. Wilke, *Angew. Chem. 69* (1957) 397; *75* (1963) 10; *Angew. Chem. Int. Ed. Engl. 2* (1963) 105; K. Kosswig in: *Ullmanns Encyklopädie der technischen Chemie, 4th Edit. Vol. 9*, Verlag Chemie, Weinheim 1975, p. 676.
[2] Reviews: J. Ivin: *Olefin Metathesis*, Academic Press, London 1983; V. Dragutan, A. T. Balaban, M. Dimonie: *Olefin Metathesis and Ring-Opening Polymerization of Cyclo-Olefins*, Wiley, Chichester/Editura Academiei, Bucharest 1985.
[3] J. L. Hérisson, Y. Chauvin, *Makromol. Chem. 141* (1970) 161.
[4] H. Höcker, R. Musch, *Makromol. Chem. 157* (1972) 201.
[5] L. Turner, C. P. C. Bradshaw, Br. Pat. 1105565 (March 6, 1968), British Petroleum Co.; L. G. Wideman, *J. Org. Chem. 33* (1968) 4541; E. Wasserman, D. A. Ben-Efraim, R. Wolovsky, *J. Am. Chem. Soc. 95* (1968) 3286; H. J. Alkema, R. Van Helden, Br. Pat. 1118517 (July 3, 1968), Shell Internationale Research Maatschappij N.V.
[6] H.-J. Eberle, F.-H. Kreuzer, N. Zeitler, DOS 3524977 (May 22, 1986), Consortium für elektrochemische Industrie GmbH.
[7] J. Dale, C. Moussebois, *J. Chem. Soc. C1966*, 264.
[8] C. Moussebois, J. Dale, *J. Chem. Soc. C1966*, 260.
[9] S. Warwel, H. Ridder, G. Hachen, *Chem.-Ztg. 107* (1983) 115.
[10] Cf. also H. Kätker, *Dissertation*, Technische Hochschule Aachen 1987.
[11] We thank Dr. *H. Keul*, Aachen, for carrying out the GPC analyses.

Correspondence

Questions of Assignment

In a communication[1] published at the end of 1986 in *Angewandte Chemie*, *Adam* et al. included the following statement in footnote[1] regarding our article[2] on cycloadditions to homodienes: "... the assignment of the ^{1}H-NMR spectrum of their product **3** formed from TCNE and **1** is questionable." The assignments of the *endo* and *exo* cyclopropyl protons of compound **3** are in fact reversed. This is one of the rare cases where the signal of the *exo* proton appears at lower field than that of the *endo* proton. Evidence for the correct assignment is provided by the larger coupling constants for the coupling between the *exo* proton and the *cis* proton of the three-membered ring.

Dr. R. Herges, Prof. Dr. I. Ugi
Organisch-chemisches Institut
der Technischen Universität München
Lichtenbergstrasse 4, D-8046 Garching (FRG)

[1] W. Adam, A. Griesbeck, F.-G. Klärner, D. Schröer, *Angew. Chem. 98* (1986) 1006; *Angew. Chem. Int. Ed. Engl. 25* (1986) 989.
[2] R. Herges, I. Ugi, *Chem. Ber. 119* (1986) 829.

An Introduction to Organometallic Chemistry

Despite the strong tradition of organometallic chemistry that exists in the German-speaking world, there has for several decades been a lack of secondary literature in that language which combines the qualities of competent expertise, balanced content, a modern style, and convenient presentation. *Christoph Elschenbroich* and *Albrecht Salzer* are therefore to be applauded on having now written a textbook based on their obviously excellent course of lectures on the subject, namely:

Organometallchemie. By *Ch. Elschenbroich* and *A. Salzer*. Teubner, Stuttgart 1986. 472 pp., paperback, DM 42.00.—ISBN 3-510-03501-4.

The response of this reviewer to the authors' commendably self-critical reflections in their preface is that no-one else has ever achieved so much as they have done here! Furthermore, I predict that this will be a unanimous verdict on the book.

The authors, in a very clever and instructive presentation based on examples, have managed to extract, from the cornucopia of organometallic reactions, compound classes and structures, all the important concepts which have become firmly established in this interdisciplinary and complex branch of modern chemistry. The contents are arranged in a conventional way according to groups of elements ("Main-group organometallics, pp. 23–196), types of ligands ("Transition metal complexes", pp. 218–384), extent of aggregation ("Metal-metal compounds and transition metal atom cluster compounds", pp. 385–410), and applications ("Organometallic homogeneous catalysts", pp. 412–441). Nevertheless, the danger of merely producing a list of compounds and reactions has been recognized and avoided, and the contents of the chapters are well balanced one with another. The authors' boldness in simplifying the subject matter works to the reader's advantage by stimulating him to reflect further on principles of reactivity and structure, and helps him to recognize the broad features which are common to the organic chemistry of main-group and sub-group elements. Thus, from the unavoidably large mass of chemical data, there emerges again and again the underlying plan of this student text, which is based on showing the resemblances and differences in behaviour between the elements. At points where a deeper understanding of relationships of a more far-reaching and general nature becomes necessary, the authors include "digressions" into fundamental aspects of spectroscopy and bonding theory. This type of presentation will be much appreciated, especially by advanced chemistry students such as graduates working for higher degrees. However, these are by no means the only groups of readers who will find the book useful. An industrial chemist too could save himself much time by reading up on modern catalytic processes in *Elschenbroich* and *Salzer*; he would, moreover, obtain an economically priced source of instruction in this subject, and a review of new developments which are at present mainly of academic interest, such as multiple bonds between atoms of silicon or transition metals, or methods for synthesizing cluster compounds. At the price of DM 42 this 470-page book is within everyone's means. University and technical institute lecturers too will not only thumb twice through this book, once from front to back, then in reverse, and not just for mere curiosity—and will then reward the authors with gratitude and admiration. We will all learn from the book, will discard our old lectures and insert new material, will refer back to other monographs cited therein—in short, we will work from this book!

Compared with other books in the field of organometallic and organo-heteroelement chemistry, including those in English, "Elschenbroich and Salzer" is a unique achievement, which one hopes will have a stimulating effect on future standards in the secondary chemical literature. In view of this high recommendation, it would seem churlish to search for printing errors in this first edition.

Wolfgang A. Herrmann [NB 822 IE]
Anorganisch-chemisches Institut
der Technischen Universität München, Garching (FRG)

Syntheses of Fluoroorganic Compounds. By *I. L. Knunyants* and *G. G. Yakobson*. Springer, Berlin 1985. vii, 299 pp., bound, DM 218.00.—ISBN 3-540-15077-3

Despite having been shortened to one volume, this English language version of the two-volume Russian work with the same title still contains more than 300 synthetic methods for organofluorine compounds. Apart from a few descriptions of preparative methods for intermediates, the methods nearly all originate from the relevant laboratories of the Soviet Academy of Sciences. They have previously been published in Russian language scientific journals, but English translations exist in only a few cases. This book therefore provides specialist readers with details, not readily accessible elsewhere, of experimental work in Russian centers of research in organofluorine chemistry. It is probably the first such publication on this specialist topic in the English-speaking world.

Some of the method of presentation in this book is undoubtedly borrowed from the well-known "Organic Syntheses" series. A single self-contained chapter is devoted to each compound, the same formal sequence of presentation being maintained for each substance. After the chemical name, the structural and molecular formulae, molecular weight, and physical data (so far as these are known), a list of the most important published methods of preparation is given, followed by the experimental details of the method itself. In some cases the chapter concludes with a list of other compounds having similar structures which can be prepared by the same method. Evidence of revision of the previous edition is seen in the inclusion of comments on critical features of the preparative method described.

The book is divided into three sections, each having a systematic structure. Each section begins with methods for preparing fluorinated hydrocarbons, then deals with derivatives containing other halogens as substituents, and then, so to speak following the conventional structure of an organic chemistry textbook, treats compounds which contain the various functional groups. Each section concludes with a list of the numerous literature references cited in the text. Subject and formula indexes at the end of the book facilitate searching for particular compounds.

The first section deals with "Fluoroaliphatic Compounds", and has been compiled by a team of authors at the Moscow laboratory of the Soviet Academy of Sciences. The main emphasis is on the chemistry of fluoro-olefins

and their derivatives, in particular the highly toxic compound octafluoro-isobutene ($LC_{50}=0.5$ ppm!).

The main subject of the second section, entitled "Fluoroaromatic Compounds", are the perfluoro-arenes, on the basis of which the Novosibirsk research group led by *G. G. Yakobson* has developed an extensive area of chemistry, here described in a very expert fashion.

L. M. Yagupolski et al., of the Kiev laboratory of the Soviet Academy of Sciences, have produced the third section on "Aromatic Compounds with Fluorinated Side Chains". The main type of fluorinated side chain dealt with is the trifluoromethyl group. As one would expect, the conversion of carboxyl groups into CF_3 substituents using SF_4 assumes an important role here, whereas only a few examples of fluorine-chlorine exchange in the corresponding chlorinated starting materials using SbF_3 are given, and that using hydrogen fluoride is not mentioned at all.

This compilation of synthetic methods for organofluorine compounds is not only of interest to organofluorine chemists in academic or industrial laboratories. It is also of value to the preparative organic chemist, as the methods have generally been chosen such that no special equipment is needed to put them into practice; information is also given in an introductory chapter concerning the toxicities of the most important fluorinating agents and reactive fluorine-containing products, together with advice on handling them.

The positive impression gained from the book as a whole is somewhat diminished by an abnormally large number of printing errors in the text and structural formulae, leaving the user with a feeling that, for whatever reason, careful correction of the proofs has been omitted.

Günter Siegemund [NB 817 IE]
Hoechst AG, Frankfurt am Main (FRG)

High-Performance Liquid Chromatography in Biochemistry. Edited by *A. Henschen, K.-P. Hupe, F. Lottspeich,* and *W. Voelter.* VCH Verlagsgesellschaft, Weinheim 1985. xiii, 638 pp., bound, DM 198.00.—ISBN 3-527-26057-9

Practice of High-Performance Liquid Chromatography. Edited by *H. Engelhardt.* Springer, Berlin 1986. xii, 461 pp., bound, DM 198.00.—ISBN 3-540-12589-2

Biochemical research is scarcely imaginable without the use of chromatographic methods for analytical and preparative work, and the latest high performance versions have vastly improved the precision and speed of separations and the accuracy of quantitative analysis. The first of these two books, which includes contributions from authors in the German-speaking world, is of great interest to all who work in this field, since, following the appearance of a number of symposium volumes and one less successful attempt at the topic (Hancock and Sparrows: HPLC Analysis of Biological Compounds), we now have for the first time a complete summary of the basic principles and scope of applications to all the relevant classes of substances.

The book has as its introduction three chapters which deal with the fundamentals of chromatography, the column as the heart of the chromatographic set-up, and the remaining experimental requirements for analytical and preparative work. The presentation of this material is relatively condensed, but is essentially adequate as a basis for beginners. However, the instrumentation section really does no more than list components, without discussing the advantages and disadvantages of different arrangements.

A further group of articles deals with individual classes of substances: amino acids, peptides and proteins, peptide hormones, biogenic amines, lipids, carbohydrates, nucleic bases, nucleosides and nucleotides, porphyrins, steroidal hormones, vitamins, organic acids, and substances present in plant tissues. These articles contain many illustrations and typical examples of separations, and details of columns and mobile phases that can be used, usually summarized in the form of tables with a more detailed discussion in the text. Information is also given on detection problems and the optimized pre-treatment of the sample, which in biological materials often includes an extraction step. Unfortunately the details of the methods are not always collected together in a form which stands out clearly from the text, in the way that they are set out in the example given for the section on porphyrins.

The subject index and bibliography are very comprehensive, though the literature cited extends only up to 1981 in some cases, and in no case later than 1982. Thus, as often occurs in books of this kind, topicality has been sacrificed in favor of keeping to a pristine appearance of the text, a policy which one must sometimes feel to be a disadvantage in such a fast changing field. This can be seen in the case of proteins, where it has not been possible to take account of the very extensive knowledge gained recently on retention mechanisms for biological macromolecules and on the mechanisms and kinetics of denaturation in contact with the carrier. The latter point is, in fact, of considerable importance, since it has now led to a shift of emphasis away from reversed phases towards biocompatible systems (ion exchange chromatography, hydrophobicity chromatography, and affinity chromatography).

However, despite the above shortcoming this is a book which will deservedly become a standard work on the subject, and its purchase can be well recommended, even for inclusion in one's personal collection. Against the general tendency to deal with ever narrower specialized topics, this book brings together theoretical fundamentals and practical applications in a form which is suitable even for newcomers, and at the same time affords a look out beyond one's own "backyard fence".

The title of the second book could easily lead to misunderstanding. This work, written through the collaboration of an international team of authors, is definitely not intended as a general source of advice on HPLC laboratory practice; instead it deals with a few selected aspects, mainly of a practical nature, burdened with only a little theory. Separation mechanisms are discussed in detail only in two of the chapters, on liquid-liquid chromatography and on ion pair liquid chromatography. Other sections which treat questions of general importance are those on quantitative analysis, special requirements for high resolution preparative work, and sample preparation together with methods for automating it. The chapter on column switching techniques also includes discussions on pre-concentration from complex mixtures, and on the removal of interfering substances before analysis. This group of topics is introduced by a descriptive list of the various components available for HPLC systems, which is impressive in its wide scope and completeness, including even automatic control equipment and data recording (although columns are not included!). The various ideas are not simply listed, but are discussed.

The second half of the book is devoted to applications, which include a wide variety of fields such as forensic chemistry, the separation of lipids, analysis of natural and synthetic drugs, analysis of psychotropic substances in body fluids, HPLC of amino acids and proteins, the separation of nucleic acid metabolites present in physiological

fluids, and lastly the chromatography of coal and oil products. Careful editorial attention is apparent in this part of the book too; for example, one feature deserving special praise is that important steps in sample preparation and preliminary separation into different types of substances are always clearly emphasized, rather than being buried in the rest of the text.

All the chapters are quite well balanced with regard to length, although it is true that this can sometimes give grounds for criticism. Thus, for example, three pages on "HPLC of proteins" simply does not do justice to the wide range of applications that exists in this field of work. It would have been more sensible here to limit the length of the chapter by confining the discussion to amino acids.

Because of the rather arbitrary collection of topics which it brings together, it is difficult to recommend this very well produced book to a specific group of readers. Many will at first be interested only in individual chapters, and beginners in the field will regret the absence of chromatographic fundamentals. Consequently few readers will consider it for their own bookshelves, but it certainly ought not to be omitted from any library.

Gerhard Seipke [NB 798 IE]
Hoechst AG, Frankfurt am Main (FRG)

Science of Ceramic Chemical Processing. Edited by *L. L. Hench* and *D. R. Ulrich*. John Wiley, New York 1986. 594 pp., bound, $ 90.30.—ISBN 0-471-82645-6

With the growing interest during recent years in new materials, especially in advanced ceramics, and the high expectations that are associated with them, their chemistry has attracted an increasing amount of attention. This trend is catered for by a series of international symposia entitled "Ultrastructure Processing of Ceramics, Glasses and Composites", held at two-yearly intervals since 1983. The papers of the second of these meetings (1985) are published in this book, edited by *Hench* and *Ulrich*.

The title "Science of Ceramic Chemical Processing" could easily mislead German-speaking readers, as the term "ceramics" is used here in its broader sense to include also glasses, a usage which differs from that of the German "Keramik". In fact fewer than half of the sixty papers are concerned with technical ceramics in the narrower sense. The majority deals instead with glasses, general colloid chemistry, and organic polymers, some of those in the last category having only a tenuous connection with ceramics.

It would be best to regard the papers presented here as having the common theme of "Ultrastructure (chemical) processing". Ultrastructures, also referred to by some authors as "nanostructures", can be taken to mean ordering phenomena in solids with a scale of distances intermediate between the Angström dimensions of molecular structures and the micron dimensions typical for particulate structures. Essentially three main routes for the production of such materials are discussed, namely the sol-gel technique, the processing of colloidal particles with a well-defined size distribution, and the conversion of covalent polymers, e.g. polysilanes, polycarbosilanes and polysilazanes. The sol-gel technique received especially detailed coverage at this meeting; the 35 papers on this topic dealt with both the scientific basis of the technique and with its applications, but nevertheless one got the impression that the high hopes that are held for this process have not yet been realized in practice. On p. 121 *J. D. Mackenzie* quite rightly says that "The science of sol-gel processing is still in its infancy at present". The same is also true of the two other routes mentioned above.

With regard to the book as a whole, the comments that generally apply to books of conference proceedings are, of course, also true here. The quality of the papers, and the amount of care put into writing them, varies greatly from author to author. A number of the articles have already been published elsewhere, and there are many instances of overlapping and repetition. Articles on highly specialized topics are sometimes grouped together in an unrelated fashion. The editors have succeeded in imposing a certain amount of structure by dividing the book into six chapters: Sol-gel science, Applications of sol-gel processing, Materials from organometallic precursors, Ultrastructure in macromolecular materials, Micromorphology science, and Quantum chemistry. The presentation, the printing and the quality of the illustrations are all good. The detailed subject index provided at the end of the book is also a welcome feature.

Despite the limitations mentioned, this book, in common with the preceding symposium volume (published in 1984), can be recommended to all those readers seeking a review of the latest developments in this topical interdisciplinary field between chemistry, chemical engineering and materials science.

M. Peuckert [NB 821 IE]
Keramikforschung,
Hoechst AG, Frankfurt am Main (FRG)

Registered names, trademarks, etc. used in this journal, even when not marked as such, are not to be considered unprotected by law.

© VCH Verlagsgesellschaft mbH, D-6940 Weinheim, 1987. - Printed in the Federal Republic of Germany by Zechnersche Buchdruckerei, Speyer/Rhein.

All rights reserved (including those of translation into foreign languages). No part of this issue may be be reproduced in any form - by photoprint, microfilm, or any other means - nor transmitted or translated into a machine language without written permission from the publishers. Only single copies of contributions, or parts thereof, may be made for personal use.

Valid for users in the USA: The appearance of the code at the bottom of the first page of an article in this journal (serial) indicates the copyright owner's consent that copies of the article may be made for personal or internal use, or for the personal or internal use of specific clients. This consent is given on the condition, however, that the copier pay the stated per-copy fee through the Copyright Clearance Center, Inc., for copying beyond that permitted by Sections 107 or 108 of the U.S. Copyright Law. This consent does not extend to other kinds of copying, such as copying for general distribution, for advertising or promotional purposes, for creating new collective works, or for resale. For copying from back volumes of this journal see 'Permissions to Photo-Copy: Publisher's Fee List' of the CCC.

Editorial office: Pappelallee 3, D-6940 Weinheim, Federal Republic of Germany, Telephone (06201) 602315, Telex 465516 vchwh d, Telefax (06201) 602328.

Editor: *P. Gölitz.*

Associate editors: *D. I. Loewus, A. Stimson.* **Editorial assistant:** *E. Schweikart*

Publishers: VCH Verlagsgesellschaft mbH. (Managing Directors: *Prof. Dr. Helmut Grünewald* and *Hans Dirk Köhler*), Pappelallee 3, D-6940 Weinheim, Federal Republic of Germany. Correspondence concerning advertisements should be addressed to VCH Verlagsgesellschaft mbH. (Advertising Manager *R. J. Roth*), Boschstr. 12. P.O. Box 1260/1280, D-6940 Weinheim, Federal Republic of Germany, Telephone Weinheim (06201) 602-0, Telex 465516 vchwh d, Telefax (06201) 602328.

ANGEWANDTE CHEMIE
International Edition in English
Volume 26 · Number 8
August 1987
Pages 707–804

The Nerve Growth Factor: 35 Years Later (Nobel Lecture)**

By Rita Levi-Montalcini*

1. Neurogenesis and Its Early Experimental Approach

"Embryogenesis is in some way a model system. It has always been distinguished by the exactitude even punctilio, of its anatomical descriptions. An experiment by one of the great masters of embryology could be made the text of a discourse on scientific method. But something is wrong, or has been wrong. There is no *theory* of development in the sense in which Mendelism is a theory that accounts for the results of breeding experiments. There has therefore been little sense of progression or timeliness about embryological research. Of many papers delivered at embryological meetings, however good they may be in themselves ... one too often feels that they might have been delivered five years beforehand without making anyone much the wiser, or deferred for five years without making anyone conscious of a great loss".[1]

This feeling of frustration so incisively conveyed by these considerations by *Peter Medawar*, pervaded, in the forties, the field of experimental embryology, which had been enthusiastically acclaimed in the mid-thirties, when the upper lip of the amphibian blastopore brought this area of research to the forefront of the biological stage. The side branch of experimental neuroembryology, which had stemmed out from the common tree and was entirely devoted to the study of the trophic interrelations between neuronal cell populations and between these and the innervated organs and tissues was then in its initial vigorous growth phase. It in turn suffered from a sharp decrease in the enthusiasm that had inflamed the pioneers in this field ever since *R. G. Harrison* delivered his celebrated lecture on this topic at the Royal Society in London in 1935.[2] Although alternate 'wax and wane' cycles are the rule rather than the exception in all fields of human endeavor, in the biological sciences the 'wane' is all too often indicative of a justified loss of faith in the rational and methodical approach that had at first raised so much hope.

A brief account of the state-of-the-art of experimental neuroembryology in the forties, when interest in this approach to the study of the developing nervous system was waning, is a prerequisite for understanding the sudden unforeseeable turn of events which resulted in the discovery of the Nerve Growth Factor (NGF).

2. Experimental Neuroembryology in the Early Forties

The replacement, in 1934 by *Viktor Hamburger*, of the chick embryo with that of the amphibian larva as object of choice for the analysis of the effects of limb bud extirpation on spinal motor neurons and sensory nerve cells innervating the limbs,[3] signed the beginning of a long series of investigations centered on the analysis of this and related experimental systems in avian embryos. Here I shall

[*] Prof. Dr. Rita Levi-Montalcini
Istituto di Biologica Cellulare
Consiglio Nazionale delle Ricerche
Via G. Romagnosi 18A, I-00196 Rome (Italy)

[**] Copyright © The Nobel Foundation 1987.—We thank the Nobel Foundation, Stockholm, for permission to publish this lecture.

only list the major advantages offered by the chick embryo over amphibian larvae as object of neurological investigations.

The avian nervous system is built according to a more elaborate design than that of amphibians, and it lends itself to a more rigorous analysis of its nerve centers than that of lower vertebrates. Extensive fundamental studies on the nervous system of the chick embryo, with use of the invaluable silver specific techniques by *Ramon y Cajal* and co-workers, extended recently by myself and other investigators,[4, 5] provided a very accurate blueprint of most nerve centers and their developmental history during neurogenesis. This allowed the detection of even small infractions to normal developmental rules in experimentally manipulated embryos. At variance with ontogenetic processes in amphibians, in chick embryos the same processes unfold according to a rigidly scheduled time sequence which never departs from the anticipated. It is therefore possible to compare the central and peripheral nerve centers of experimental and control specimens in embryos incubated under the same temperature and other environmental conditions. The analysis in amphibian larvae was extended to the brain, spinal cord, and peripheral nervous system and various experimental situations. In the chick embryo it was mainly confined to the study of the effects called forth by extirpation of limb primordia or implantation of additional wing or leg buds on their innervating motor and sensory nerve centers. In 1934, *Viktor Hamburger* published an article[3] on the effects of wing bud extirpation on the development of the brachial spinal motor segment and sensory dorsal root ganglia innervating the wing. He came to the conclusion that the hypoplasia of motor nerve cells of the ventral horn, and of other nerve cells of the same hemisection of the spinal cord, resulted from lack of stimuli centripetally transmitted by nerve fibers of the first differentiated neurons. These normally exert a regulatory effect on proliferation and differentiation of neighboring nerve cells. A reinvestigation of the effects produced by limb bud extirpation, prospected a different control mechanism of the developing nerve centers by peripheral tissues. Through serial studies of silver stained embryos, the conclusion was reached that the severe hypoplasia of nerve centers deprived of their fields of innervation, resulted from death of differentiated neurons and not from failure of recruitment of neurons from a pool of still uncommitted nerve cell precursors.[6, 7] In 1947, *Hamburger* invited me to join him for the purpose of reinvestigating together this problem. This invitation marked the beginning of a thirty year period that I spent at Washington University, and of my life-long friendship with *Viktor*. Our 1949 article[7] confirmed the hypothesis previously submitted by *G. Levi* and myself. The satisfaction of this confirmation of an important theoretical issue, and the successful analysis of other neuroembryological problems[8, 9] was, however, perturbed by the realization of the low resolution power of the techniques in our possession for in-depth exploration of the tremendously complex neurogenetic processes. The temptation to abandon the experimental analysis of the developing nervous system and move into the phage field, in full blossom in the nineteen-forties, did, however, not take hold thanks to unpredictable and most fortunate events which occurred at the same time and opened a new era in developmental neurobiology.

3. The Unexpected Break: A Gift from Malignant Tissues

In a 1948 article, a former student of *Viktor Hamburger*, *Elmer Bueker*, reported the results of a bold and imaginative experiment consisting in the graft of fragments of mouse sarcoma 180 into the body wall of three-day chick embryos. The histological study of the embryos fixed 3–5 days later, showed that sensory nerve fibers emerging from adjacent dorsal root ganglia had gained access into the neoplastic tissue while no motor nerve fibers entered into the tumor.[10] The author concluded that histochemical properties of the fast growing mouse sarcoma offered a favorable field for growth of sensory fibers. This condition, in turn, resulted in a slight but consistent volume increase of these ganglia as compared to that of homologous ganglia innervating the wing of the contralateral side. *Viktor* and I reinvestigated this remarkable phenomenon adopting the method I had developed during my first neuroembryological studies, i.e., that of a daily inspection of control and experimental embryos serially sectioned and impregnated with a specific silver technique. Our results confirmed those reported by *Bueker*, but at the same time uncovered other effects elicited by grafts of the mouse tumor which hardly fit in with the hypothesis that they were in the same range and of the same nature as those called forth by transplants of normal embryonic tissues. They differed from the latter in the following, most significant, respects: sympathetic and not only sensory fibers gained access into the neoplastic tissues, where they built a network of extraordinarily high density; nerve fibers branched at random between tumoral cells without, however, establishing synaptic connections with them; sensory and sympathetic ganglia innervating the tumor underwent a progressive increase in volume, attaining, in the case of sympathetic ganglia, a size about six times larger than that of the corresponding control ganglia.[11]

Subsequent experiments uncovered another astonishing deviation from the norm in embryos bearing transplants of mouse sarcoma 180 or of another tumor of identical origin, known as sarcoma 37. It was found that embryonic viscera which in normal specimens are devoid of innervation, such as the mesonephroi, or which become scarcely innervated only in late developmental stages, such as the sex glands, the thyroid, the parathyroid, and the spleen, were loaded with sympathetic nerve fibers at early embryonic stages.[12] A patent infraction of all developmental rules came to light with the finding of thick sympathetic fiber bundles inside the veins of the host, where they protruded in the form of large neuromas obstructing blood circulation (Fig. 1). All sympathetic chain ganglia, and not only ganglia adjacent to or in direct connection with neoplastic tissues, were enormously enlarged. The hypothesis that these anomalous effects could result from the release by neoplastic cells of a soluble, diffusible agent which altered the differentiative and growth properties of its target cells, received full confirmation from experiments transplanting one or

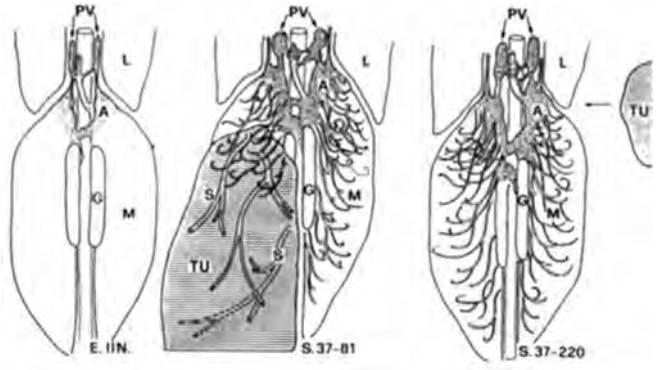

Fig. 1. Semi-diagrammatic reconstruction of a normal 11-day chick embryo (E. 11N), of an 11-day embryo carrying an intra-embryonic transplant of mouse sarcoma (S. 37-81), and of an 11-day embryo with transplant of sarcoma 37 on the chorio-allantoic membrane (S. 37-220). Note the hyperplastic growth of the prevertebral chain ganglia in embryos carrying tumor transplants. Visceral nerve fibers from these ganglia invade the nearby mesonephroi. A, adrenal; G, gonad; L, lung; M, mesonephros; PV, prevertebral ganglia; S, sensory nerves; TU, tumor (from Ref. [12]).

the other mouse sarcoma onto the chorio-allantoic membrane of 4-6 day chick embryos in such a position as to prevent a direct contact between embryonic and neoplastic tissues (Fig. 2). Embryonic and tumoral tissues were, however, in reciprocal connection through the circulatory system. The finding that these extra-embryonic transplants elicited the same effects as intraembryonic grafts gave definite evidence for the diffusible nature of the tumoral nerve growth promoting factor.[12, 13]

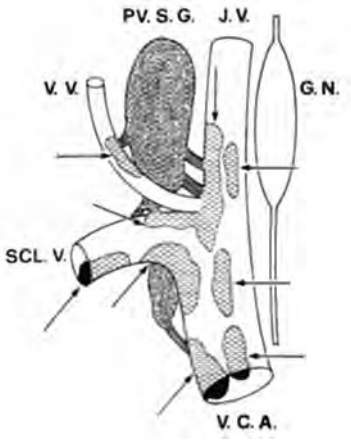

Fig. 2. Sixteen-day chick embryo with intra-embryonic tumor (sarcoma 180). Ingrowth of sympathetic nerve fibers into the Jugular, Vertebral, Subclavian, Anterior Caval Veins. G.N., Ganglium Nodosum; J.V., Jugular Vein; PV. S.G. Paravertebral Sympathetic Ganglion; SCL.V., Subclavian Vein; V.C.A., Anterior Caval Vein; V.V., Vertebral Vein. Arrows point to nerve agglomerations (from Ref. [12]).

Attempts to replicate these effects by implanting dried tumor pellets or by injecting extract of either sarcoma were unsuccessful. I then thought of resorting to the tissue culture technique, which I had practiced with *G. Levi* at the University of Turin. Lack of facilities in this field in the Department of Zoology at Washington University, prompted me to ask Professor *Carlos Chagas*, Director of the Biophysics Institute of the University of Brazil in Rio de Janeiro, whether he would approve of me joining him as a scientific guest at his institute. There, a friend of mine, *Hertha Meyer*, had built and was director of a most efficient tissue culture unit. Upon approval and invitation by Professor *Chagas*, I boarded a plane for Rio de Janeiro, carrying in my handbag two mice bearing transplants of mouse sarcomas 180 and 37.

4. The Nerve Growth Factor at Its Early in-vitro and in-vivo Debut

"The tumor had given a first hint of its existence in St. Louis but it was in Rio de Janeiro that it revealed itself, and it did so in a theatrical and grand way, as if spurred by the bright atmosphere of that explosive and exhuberant manifestation of life that is the Carnival in Rio".[14]

The discovery of the growth response elicited by a soluble tumoral agent revealed the receptivity of developing nerve cells to hitherto unknown humoral factors, and in this way opened a new area of investigation. The in-vitro bioassay also offered a practical and invaluable tool for uncovering the identity card of this factor and paving the way for the study of its mechanism of action. Ink drawings which I enclosed in several letters mailed from Rio to *Viktor*, give an eloquent account of the spectacular way in which this still unknown agent revealed itself. Sensory and sympathetic ganglia explanted from 8-day chick embryos in a semi-solid medium in proximity to but not in contact with fragments of mouse sarcoma 180 or 37, produced, in a 24 hour period, a halo of nerve fibers of maximal density on the side facing the tumor[15] (Fig. 3). The euphoric state

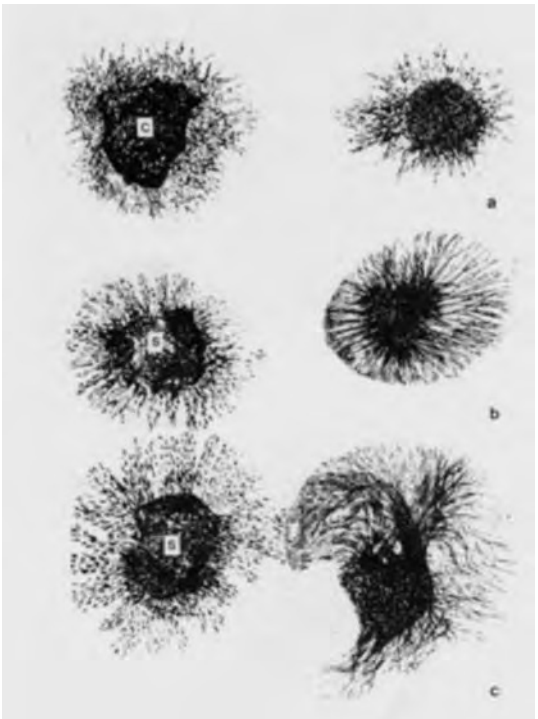

Fig. 3. Drawings illustrating the in-vitro "halo" effect on 8-day chick embryo sensory ganglia cultured in the presence of fragments of mouse sarcoma 180 for 24 hours (b) or 48 hours (c). In (a), the ganglion, which faces a fragment of chick embryonic tissue, shows fibroblasts but few nerve fibers. In (b) and (c), the ganglia, facing fragments of sarcoma 180, show the typical "halo" effect elicited by the growth factor released from the sarcoma. Note in (c) the first evidence of a neurotropic effect of the growth factor.

elicited by this discovery was, however, dampened shortly after by the discovery that normal mouse tissues, at variance with those of chick embryos, induce a milder (Figs. 3a), but not substantially different effect from that of mouse sarcomas. In retrospect, this should have alerted us to a novel and even more significative aspect of these in-vitro experiments; namely, the widespread presence of the factor endowed with nerve growth promoting activity in normal and neoplastic tissues. The failure to realize the significance of this 'mouse effect' was beneficial rather than detrimental, since for the next two years our attention was entirely focussed on the study of the chemical nature of the factor released by the two mouse sarcomas, in much larger quantities than from normal mouse tissues.

A young biochemist, *Stanley Cohen*, who joined our Group shortly before my return from Rio, isolated from the two tumors a nucleoprotein fraction endowed with the in-vitro nerve growth promoting activity.[16] Chance, rather than calculated search, signed a new, most fortunate turn of events. In order to degrade the nucleic acids present in this active fraction, *Stan* made use of snake venom which contains, among other enzymes, also the nucleic acid degrading enzyme, phosphodiesterase. Its addition in minute amounts to the nucleoprotein tumor fraction was expected to suppress the formation of the fibrillar halo if nucleic acids rather than the protein were responsible for the nerve growth promoting effect elicited by this fraction. The startling result was a marked increase in the density of the fibrillar halo around the ganglia incubated in the presence of the tumoral fraction treated with snake venom. Since a dense fibrillar halo was produced also around ganglia cultured in the presence of minute amounts of snake venom alone, it became apparent that the venom itself was a most potent source of nerve growth promoting activity. On the basis of biochemical studies, *Cohen* was in fact able to show that equivalent growth stimulation effects were obtained by 15000 μg of a sarcoma 180 homogenate and 6 μg of the moccasin snake venom. From the latter, after several purification steps, he isolated a non-dialyzable, heat-labile particle endowed with nerve growth promoting activity, identified in a protein molecule of molecular weight of the order of 20000.[17, 18] Microgram quantities of the purified snake venom fraction endowed with nerve growth promoting property, when injected daily into the yolk of 6–8 day chick embryos for a 3–5 day period, resulted in the overgrowth of sensory and sympathetic ganglia and excessive production of their fibers. Sympathetic nerve bundles branched profusely into the viscera and protruded into the cavity of the veins, mimicking in all details the effects elicited by grafts of mouse sarcomas.[19]

If chance brought to our attention the unforeseeable presence of two nerve growth promoting sources in mouse sarcomas and in snake venom, the subsequent finding that mouse submandibular salivary gland extract added in a minute quantity to the culture medium elicits an even denser and more compact fibrillar halo, was the result of a calculated search. These glands, as the homologues of the snake venom glands, were chosen by *Stanley Cohen*[20] as more likely than other organs screened with the in-vitro bioassay, to store the nerve growth factor (NGF). These results were soon followed by purification and identification by *Cohen* of the salivary factor in a protein molecule of evaluated molecular weight of 44000.[20] Its availability in larger quantities than the venom NGF, and its moderate toxicity when injected in a highly purified form, made possible the exploration of its biological activity in neonatal, young, and adult mammals.[21] The results of these investigations signaled the beginning of an ever more extensive and systematic in-vivo and in-vitro analysis of the salivary NGF, of its chemical structure, mechanism, and spectrum of action. Only the most significant findings reported from several laboratories in original and review articles will be considered in the following pages.

5. The Vital Role of NGF in the Life of Its Target Cells

In spite of, or perhaps because of its most unusual and almost extravagant deeds in living organisms and in-vitro systems, NGF did not at first find enthusiastic reception by the scientific community, as also indicated by the reluctance of other investigators to engage in this line of research. The finding that a protein molecule from such diverse and unrelated sources as mouse sarcomas, snake venom, and mouse salivary glands, elicited such a potent and disrupting action on normal neurogenetic processes, did not fit into any conceptual pre-existing schemes, nor seem to bear any relationship to normal control mechanisms at work during ontogenesis. It was in this skeptical atmosphere that NGF asserted, in a most forceful way, its vital role in the life of its target cells. Previous in-vitro experiments had shown that incubation of snake venom with its antiserum inhibited the fiber outgrowth induced by the venom NGF. A specific antiserum to salivary NGF likewise abolished the formation of the in-vitro fibrillar halo. These results suggested testing the effect of daily injections of small amounts of this antiserum (AS-NGF) in neonatal rodents. Inspection of treated mice under stereo and optical microscopes at the end of the first month revealed the near total disappearance of sympathetic para- and prevertebral chain ganglia.[22–24] This dramatic effect, which deprives newborn rodents and other neonatal mammals injected with antiserum to salivary NGF of the sympathetic system, without interfering with their normal development and vitality, became known as immunosympathectomy.[25, 26] The same treatment produces much less damaging effects in young and adult animals.

Two alternative hypotheses were submitted to explain the mechanism underlying the destructive effects of the antiserum: 1) a complement-mediated cytotoxic effect, or 2) the inactivation of NGF or of an NGF-like protein essential for differentiation and survival of sympathetic nerve cells. Although the first hypothesis was favored in early articles, the second progressively gained support and is now generally accepted on the basis of this and an in-vitro experimental approach which provided additional, unequivocal evidence of the essential role NGF plays in the early differentiation stages of its target cells. The in-vitro experiments consisted of the dissociation of sensory and sympathetic nerve cells from ganglia of 8–11 day chick embryos and their incubation in minimum essential media. Nerve

cells failed to survive unless nanogram quantities of NGF were added daily to the culture medium.[27] The in-vitro evidence for the role of NGF in the early phases of development of sensory nerve cells received confirmation from subsequent experiments, which proved that administration of NGF antiserum to rodent fetuses[28,29] and autoimmunization of pregnant rodents against endogenous NGF result in failure of sensory ganglia to undergo normal development.[30]

6. NGF as a Retrograde Trophic Messenger and Tropic Factor

The evidence in favor of the hypothesis that immunosympathectomy results from removal, by AS-NGF,[31] of circulating endogenous NGF, posed the questions of how NGF reached its target cells and what were its sources of production. Subsequent experimental pharmacological and surgical approaches provided satisfactory answers to both questions, and, in view of the interest in these problems, the techniques and main findings will be briefly reported.

Administration to neonatal rodents of drugs such as 6-hydroxydopamine, which destroys adrenergic nerve endings,[32] or of vinblastine, which blocks axonal transport,[33] results in death of the large majority of sympathetic nerve cells in their most active phase of differentiation and growth. The degenerative effects produced by these pharmacological components compare in magnitude to those produced by administration of AS-NGF and result in the destruction of para- and prevertebral sympathetic ganglia through a process which became known as chemical sympathectomy.[32,33] A third experimental manipulation, consisting of the surgical transectomy of postganglionic axons of superior cervical ganglion performed in neonatal rodents, results in the death of about 90% of immature sympathetic cells in this ganglion.[34] The experimental evidence that in all instances nerve cell death is prevented by supply of exogenous NGF,[30,35-37] demonstrates the vital role played by this molecule in the life and differentiation of these cells. The subsequent demonstration that labeled NGF is taken up by nerve endings of sympathetic[38] or sensory fibers[39] and is retrogradely transported to the cell perikarya, lent strong support to the concept of NGF as a trophic messenger, conveyed through nerve fibers from peripheral cells to the innervating neurons. Disconnection of the partners by chemical or surgical axotomy results in the death of differentiating nerve cells deprived of this essential molecule.

At the same time as the vital role of NGF in developing sympathetic and sensory nerve cells was assessed and its retrograde transport from peripheral tissues was well documented, another important property of NGF—its ability to direct growing or regenerating axons of sensory and sympathetic fibers along its concentration gradient (neurotropism)—was definitely established through different in-vivo and in-vitro experimental approaches.[40-45]

The first strong evidence for an NGF neurotropic effect was obtained from experiments of daily micro-injections of NGF into the floor of the fourth ventricle. A 7-day treatment resulted in the penetration of fiber bundles originating from sympathetic ganglia into the neural tube and in their ending at the level of experimentally produced NGF pools[40-41] (Fig. 4). In-vitro experimental approaches gave more rigorous proof that neurites of NGF target cells grow along an NGF concentration gradient and change their route according to the changed position of the NGF releasing pipette.[42] While these studies unequivocally establish the NGF neurotropic effect as independent from its trophic action, they leave unanswered the question of whether this effect is exerted through a local control of growth cone motility,[43] altered adhesion of this locomotor organelle to the substratum,[44-45] or via other mechanism(s).[46-47]

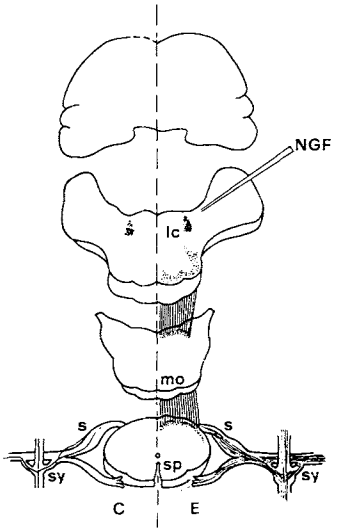

Fig. 4. Diagrammatic representation of sympathetic fiber bundles which enter the spinal cord and medulla oblongata from adjacent sympathetic ganglia in intracerebrally NGF injected neonatal rats. Left half: control (C). Right half: experimental (E) case. NGF, site of injection of NGF into the floor of the fourth ventricle; lc, locus coeruleus; mo, medulla oblongata; sp, spinal cord; s, sensory ganglia; sy, sympathetic ganglia. Sympathetic fibers run across the sensory ganglion and enter into the neural tube with the dorsal roots (from Ref. [40]).

7. Neuronal and Non-Neuronal Target Cells

As indicated in Table 1, targets of NGF action that have been well characterized up to now, can be classified under three main categories: 1) neural-crest derivatives; 2) central nervous system (CNS) neurons; and 3) cells of non-neuronal origin. For a thorough analysis of the many and diversified effects exerted by NGF on each one of these cells, the reader is referred to review articles on this specific matter.[47-52] I wish to make in this context only some general considerations.

A generally valid rule is that all cells are maximally responsive to NGF action during their early differentiation; the response undergoes progressive restriction in the adult, without, however, being totally effaced. Long sympathetic neurons and sensory neurons, with particular reference to those of the dorso-medial quadrant of spinal ganglia in chick embryo,[12] provided a most valuable system for demonstrating the three main activities of NGF, i.e., 1) its

vital trophic role during the early developmental stages, 2) its ability to enhance differentiative processes such as neurite outgrowth, and 3) its ability to guide the growth or regeneration of neurites along its own concentration gradient.[43-44] These same cells offered an in-vivo model system to study the introduction of enzymes involved in neurotransmitter synthesis[53] and were also instrumental in providing the first demonstration of NGF retrograde transport[54] and its role as a trophic messenger.[55] While sensory and sympathetic cells played a key role in revealing these properties of NGF, chromaffin cells and their neoplastic counterpart, the clonal cell line PC12, became the models of choice for studying the capacity of NGF to modulate phenotypic expression and the molecular mechanism subserving this process.[56] The phenotypic shift induced by NGF both in chromaffin[57-58] and PC12 cells,[56,59] resulting in their neuronal differentiation accompanied by a plethora of chemical, ultrastructural, and morphological changes characteristic of the neuronal rather than glandular phenotype, is too well known to warrant a detailed description.[50] These cells, moreover, uncovered the startling capacity of NGF to act as both a mitogenic[60] or antimitotic agent,[56] even within the context of the same clonal cell line PC12 and of a mutated version of it.[61] This, in turn, clearly pointed to the 'versatility' of NGF receptors and of their transduction machinery, whose message is evidently read and interpreted in different ways according to the cell type and previous cell history. The 'priming model' prospected to give a molecular account for the very fast and very slow onset of neurite outgrowth occurring, respectively, in sensory and sympathetic cells[24] on the one hand and PC12 cells on the other,[50] is an excellent example of the contribution of these latter cells to studies on the mode of action of NGF.

Other examples of the wide and at the same time diversified NGF effects are illustrated by other sympathoadrenal derivatives such as paraganglia, small intensely fluorescent cells (SIF), and carotid body cells.[62-64] The capacity of NGF to modulate phenotypic expression is impressively evidenced by the SIF cells, which have been hypothesized as immediate precursors of both sympathetic and chromaffin cells. When these cells are cultured under appropriate conditions, they can be channeled towards the first or the second phenotype in media supplied with NGF or with dexamethasone.[63,64] Such an interplay, even in fully differentiated cells, between NGF and steroid hormones, is also indirectly suggested by in-vivo studies on the short adrenergic neurons which innervate, in both sexes, the genito-urinary systems.[65]

In more recent years, two new populations came to the forefront of studies on NGF target cells: CNS neurons and cells originating from the hematopoietic system.

Small and large neuronal populations located in different brain areas have been shown to exhibit all properties and responses typical of sensory and sympathetic cells, such as: 1) the presence of specific receptors,[66] 2) retrograde transport of NGF,[67] 3) increased neurotransmitter synthesis with special reference to acetylcholine,[68-70] and 4) trophic response manifested as protection by exogenous NGF administration to selective noxious treatments or surgical transections otherwise leading to cell death.[71,72] A role for NGF in the development of as yet unidentified hypothalamic brain centers has been suggested by the finding that injections of affinity purified polyclonal antibodies against NGF in rat fetuses induce a severe postnatal neuroendocrine syndrome.[29] The loop of an unquestionable NGF role in brain is completed by the demonstration that other nerve cells, especially those located in the hippocampus and cortical areas, manufacture large quantities of NGF mRNA and of NGF protein, thus closing the functional link between NGF-producing and NGF-responding cells.[73-75] As indicated in the last section of this article, although the range of NGF action in the CNS is qualitatively comparable to that previously observed in peripheral neurons, the actual extent of the NGF role in brain is far from foreseeable due to the vast repertoire of possible responses from nerve cells in the CNS.

An analogous general consideration holds for the effect exerted by NGF on mast cells and possibly on other cells of the immune system. The increased in-vivo and in-vitro number of mast cells following NGF treatment,[76,77] as well as the effect of this growth factor on histamine release,[78-80] point to an unquestionable role in the physiology of these cells. It is not yet clear, however, whether such an effect is exerted through a generalized action on all mast cell precursors or through a sort of clonal selection mechanism. The more recent report of an NGF effect on other spleen cells such as mononuclear cells[81] and the existence of NGF receptors on thymocytes,[82] clearly suggests that the NGF action extends also to cells belonging to a network of enormous functional significance. The role played by histamine as an immunomodulator and the obvious involvement of spleen cells in the immune response of the organism would indicate new scenarios in which NGF may gain access, not through a back door, but through the main entrance.

Table 1. Targets of NGF action.

Neural crest Derivatives	Sympathoadrenal cells	Long sympathetic neurons
		Short sympathetic neurons
		Cells of paraganglia (carotid & abdominal paraganglia)
		SIF (small intensely fluorescent) cells
		Chromaffine cells: normal, neoplastic (PC12)
	Sensory neurons	
Central nervous system	Cholinergic neurons	Corpus striatum, basal forebrain, septum, nucleus diagonal band of Broca
	Adrenergic, indoleaminergic & peptidergic neurons	Xenopus laevis tadpoles
Non neuronal origin	Mast cells	

8. The I.D. Card of NGF

The sequencing of mouse submandibular gland NGF, achieved in 1971,[83] not only provided invaluable information on its primary structure but was recently instrumental in the preparation of synthetic oligonucleotides which resulted in the identification of NGF cDNA.[84] The cloning, which followed in rapid succession, of mouse,[84] human,[85] bovine[86] and chick[87] genes, demonstrated their high degree of homology. The NGF gene, located in the human species on the proximal short arm of chromosome 1,[88] codes for a large polypeptide of 307 amino acid residues, which, upon cleavage, yields a mature NGF subunit protein with 118 amino acids and, possibly, other peptides of unknown function and with no sequence homology with presently identified proteins.[84] NGF is a dimer made up of two identical subunits held together by non-covalent bonds. The dimer can be isolated as such,[89] or in the form of a complex consisting also of two other proteins, one with an esteropeptidase activity, probably involved in processing an NGF precursor, and the other with an as yet unknown function.[90-92] While it remains to be established whether each NGF subunit is biologically active, it has been demonstrated that a covalently cross-linked form of the dimer maintains full activity.[91,92] Between the two well-identified molecular entities of NGF and of its coding gene, which can be visualized as the summit and the base of an iceberg, there are several other possible intermediate forms of unknown nature and biological properties. Their identification would answer important questions such as: Are other biologically active peptides coded for by the NGF gene? What is the significance of different splicing in different cells of NGF mRNA?[93] Is the processing of pre-pro-NGF identical in all neuronal and non-neuronal cells or, as in other peptides,[94] do alternate processing pathways result in the production of peptides endowed with different biological functions? Since the same peptides may undergo post-transcriptional or post-translational modification, the submerged areas of the NGF iceberg loom very large.

Studies on the immunological and biological relatedness of NGFs purified from different species strongly support the hypothesis that the site(s) of interaction with their receptors has (have) remained structurally more constant than is the case for other epitopes, which are probably free to mutate in view of their less fundamental biological functions.[95]

9. NGF, Growth Factors and Oncogenes

The discovery of NGF and, soon thereafter, of EGF led to the biological identification of an ever-growing list of polypeptide growth factors.[48] In the seventies, another apparently unrelated area of biology came to the forefront of research with the discovery of single gene products (oncogenes) causing transformation. PGF and oncogene research, pursued at first independently from each other, converged when homology between some oncogenes and growth factors or their receptors was shown by sequence analysis. Evidence is steadily increasing that excessive synthesis or an altered version of PGFs or of their receptors may result in transformation of recipient cells.[95-98] More recently, the demonstration that the opposite is also true, namely that certain oncogene products may induce differentiation of recipient cells, called attention to another facet of this intricate interplay between differentiative and transforming processes. Examples are H-*ras* and V-*src*, whose expression into PC12 cells[99,100] results in mitotic arrest and neuronal differentiation comparable to that elicited by NGF; further examples will certainly follow. The obvious conclusion is that a given polypeptide growth factor, or intracellular proteins playing essential roles in the cell cycle or in the differentiation of some cells, may exert markedly different actions in distinct cell types. In the case of NGF, one wonders if and how other actions are elicited by this versatile molecule. For instance, is an altered version of NGF or of its receptors capable of causing transformation of some recipient cells, as has been shown for other PGFs? If this is the case, could NGF in a modified version or its receptors be implicated in neoplasia in the central and peripheral nervous systems?

10. NGF in Exocrine Glands: a Fortuitous Presence or a Biological Function?

The early discovery that mouse submandibular glands synthesize and release into the saliva large quantities of NGF, that the synthesis of this protein molecule is under the control of testosterone and of thyroxine,[101,102] and that the NGF protein content is about tenfold higher in male than in female mice, remained puzzling and unexplained findings for about three decades. The conflicting but altogether negative attempts to reveal the presence of this molecule in the circulating blood,[49,51] and the lack of any adverse effects on sympathetic and sensory cells by removal of these glands, which deprived these rodents of such a large NGF source, militated against the hypothesis that salivary NGF gains access to their target cells. An alternative biological function for salivary NGF was first hypothesized by our group,[103] and recently proved by us[104] and another investigator.[105] We demonstrated that intraspecific fighting, experimentally induced in adult male mice by 6–8 weeks of social isolation, results in massive NGF release into the blood stream, an event prevented by previous sialoadenectomy. Since injections of NGF induce weight and size increase of the adrenal glands[105] and stimulate the synthesis of the catecholamine key enzyme, TH,[106] we suggested that such a massive discharge into the blood circulation of endogenous salivary NGF may be instrumental in defense and/or offense mechanisms of vital significance for male mice that engage in intraspecific fighting among individuals of the same sex. In favor of this hypothesis is a recent report that aggressive behavior results in the release into the blood of another biologically active protein, renin, synthesized in the same tubular portions of these glands.[107] The mechanism triggering this NGF release is not yet understood, nor whether other stations are activated and play a role in this specific stress syndrome.

As for the presence of large NGF sources in snake venom[18] and male genital organs,[108, 109] they may be conceived as instances of bizarre evolutionary gene expression. Alternatively, in these cases NGF may subserve other functions which may somehow be linked with the poisonous action of snake venom, or the reproductive activity of the genital apparatus. In the case of snake venom, one can envisage the possibility that a highly specific neurotropic molecule such as NGF is utilized by reptiles as a carrier of other neurotoxins devoid of specific receptors in the central and peripheral nervous systems. For instance, enzymes such as phospholipases, phosphodiesterases, and proteases of various nature, which by themselves may lack specific recognition sites in target cells, may exploit NGF as a carrier to gain access inside cells wherever there are specific NGF receptors. The widespread distribution of these specific molecules also in several non-neuronal cells could offer some toxins or enzymes a better access to their target organs.

In the reproductive tract, NGF could participate in fertilization mechanisms by cytoskeletal mediated activation of spermatozoa locomotion much in the same way as in neurite outgrowth, or by favoring egg implantation, via inhibition of rejection through the immune system. This latter hypothesis is presently under investigation (*Geraci, Cocchiara,* and *Calissano*) by assessing the effect of NGF on uterine mast cells which, through histamine release, are postulated to prevent the local immune reaction.[110]

11. Foreseeable Approaches and Predictions of the Unpredictable

The most obvious among the foreseeable approaches is the search for other NGF target cells, using the ever more sophisticated in-vivo and in-vitro techniques which became available during the past few decades from the molecular to the supercellular levels. It was this multimodal approach which in recent years led to the discovery of NGF target cells in the CNS of lower and higher vertebrates and in cell lineages playing a role in the immune system. This list is likely to increase, as the search extends to other neuronal and non-neuronal cell populations. Furthermore, one should take into account the fact that some of these populations are receptive to NGF mainly during developmental stages in prenatal life. This was already demonstrated in sensory cells of avian and mammalian species,[49, 51, 52] and in cells lining the third ventricle in amphibian tadpoles[111] and prenatal and neonatal rodents (*Aloe* and *Levi-Montalcini*, unpublished observations). Likewise, the systematic screening of neuroendocrine and hematopoietic cell lines in in-vitro and in-vivo systems may reveal other as yet uncovered roles of this growth factor.

Another foreseeable approach, now in progress in many laboratories, is the search and characterization of NGF-like factors active on other neuronal populations. These factors may be subdivided into two major classes: 1) those coded by the NGF gene itself but processed through alternate post-transcriptional or post-translational pathways leading to PGFs with a somewhat different structure and function; 2) other proteins or peptides having the trophic, chemotactic and/or differentiative activity of NGF, but coded by other genes.

The search and identification of factors belonging to the first group will take advantage of the techniques of molecular biology and immunology. These should provide valuable information on some of the still unexplored, submerged areas of the NGF iceberg, dealing with the processes of the NGF gene transcription or translation. Of particular importance would be the identification of the NGF sequence responsible for its binding to receptors which may presumably trigger a given cellular response.[47] As previously surmised,[95] this portion has possibly been better conserved than other parts of the molecule. Once identified, it will be feasible to introduce, in its synthetic counterpart, amino acid substitutions and/or chemical modifications and explore the biological potency of the newly manufactured peptide. This approach should not only provide invaluable information on the nature and properties of the NGF active center, but, hopefully, will result in the synthesis of peptides endowed with an activity even higher than that of NGF itself, so brilliantly achieved in the field of other biologically active peptides.[112, 113]

Within this category of studies on NGF and its coding gene, one can conceive a strategy aimed at exploiting the property of non-neuronal cells in peripheral tissues and of neurons and satellites in the CNS to manufacture and release NGF by resorting to pharmacological agents that modify NGF gene expression or processing. The well-established finding that NGF synthesis is increased following transection of nerve fibers connecting NGF receptive nerve cells to their targets[114] or via hormonal action,[101, 102] is an additional indication of the remarkable plasticity of the mechanisms controlling NGF gene expression. It is conceivable that this property might be modulated by pharmacological agents acting on the same path as those involved in the regulation of the synthesis and release of NGF.

The search for neurotrophic factors coded by genes other than the NGF gene could take advantage, at least in its main strategy, of the classical approach so successfully applied in the isolation and identification of NGF. Two main causes may explain why extensive work invested in this attempt has not been so successful in providing evidence for the existence of other PGFs activating different neuronal cell lines: 1) the lack of fast and reliable bioassays such as those developed for NGF, and 2) the failure to detect large sources of these factors comparable to those fortuitously discovered in early NGF studies. The realization of rapid, highly reliable bioassays can, however, now be achieved by resorting to the use of most stringent, chemically defined media, permitting survival and differentiation of only given cell types, upon addition to the medium of putative growth factors extracted from different sources and screened with the in-vitro bioassay for their potential specific growth enhancing activity. The problem of finding by sheer chance large sources of NGF-like peptides, such as those which played a key role in the discovery of NGF, can be solved by resorting to techniques of protein chemistry and recombinant DNA technology. Only a few micrograms of purified protein suffice in order to decipher the sequence, prepare the corresponding cDNAs,

identify the gene of the PGF in question, and express it in bacteria, thus replacing a search once guided by unpredictable strikes of luck by a rational and systematic strategy.

Predictions of the unpredictable are encouraged by the same history of NGF which may be defined as a long sequence of unanticipated events, which each time resulted in a new turn in the NGF unchartered route and opened new vistas on an ever-changing panorama. This trend, which became manifest from the very beginning and in fact alerted me to the existence of NGF, is perhaps the most attractive, even though elusive, trait of this thirty-five year long adventure. One can at present only predict where future developments are most likely to occur. The main causes of unpredictability of the findings reside in the intricacy of the new surroundings where NGF is moving—the CNS and the immune system—rather than in NGF itself. The enormous complexity of these two networks, which on the basis of recent findings are closely interrelated and influence each other through bidirectional signals,[115, 116] opens endless possibilities for NGF activation of distinct repertoires of cells belonging to one or the other system. How many indirect effects can be elicited by direct NGF action on cholinergic, adrenergic, and peptidergic neurons interlinked via fiber pathways and humoral channels or through short-distance diffusion? Likewise, how many effects could follow the simple histamine release by NGF-activated mast cells, considering the well-established role of this amine as an immunomodulator or an immunosuppressor? These considerations hold also for the potential utilization of NGF in brain and immunosystem disorders. For instance, whenever cell death or specific neuronal populations may be linked to a decreased local availability of neurotrophic factors, such as NGF, its exogenous supply or stimulation of its endogenous production via pharmacological agents may offer a promising approach to presently incurable diseases.

I shall end this account of the unfolding of the NGF story with a remark made more than a decade ago by *Viktor Hamburger*: "... the fact that this discovery, which grew out of a seemingly peripheral problem (peripheral in every sense of the word), has blazed so many new trails is its greatest contribution to neuroembryology"[117] Studies in this last decade have not only provided new strong evidence of the most important contributions of NGF in the field of neuroembryology, but also have brought to the fore its significance in the more general field of neuroscience and its prospective role in the immune system.

I dedicate this article to Viktor Hamburger, who promoted and took part in this search, and to whom I am forever indebted for invaluable suggestions and generosity. Without him, the Nerve Growth Factor would never have come to our attention. To my dear friends, Pietro Calissano and Luigi Aloe, I wish to express my deepest gratitude for their fundamental contributions. In this thirty-five year long investigation, a large number of colleagues, research associates and graduate students took part in this scientific adventure. I am particularly indebted to and very gratefully acknowledge the most important work performed by two of them: Drs. Piero Angeletti and Vincenzo Bocchini. To Professor Carlos Chagas, for his generous hospitality in the Biophysics Institute of the University of Brazil, and to Dr. Hertha Meyer who helped me in devising the tissue culture bioassay of NGF, my warmest thanks.

Received: March 5, 1987 [A 631 IE]
German version: *Angew. Chem. 99* (1987) 727

[1] P. B. Medawar: *The Art of the Soluble*, Methuen, New York 1967, pp. 106-107.
[2] R. G. Harrison, *Proc. R. Soc. London Ser. B 118* (1935) 155-196.
[3] V. Hamburger, *J. Exp. Zool.* 1934, 449-494.
[4] J. F. Tello, *Trab. Lab. Invest. Biol. Univ. Madrid 21* (1922) 1-93.
[5] R. Levi-Montalcini, *Prog. Brain Res. 4* (1964) 1-29.
[6] R. Levi-Montalcini, G. Levi, *Arch. Biol. Liège 54* (1943) 183-206.
[7] V. Hamburger, R. Levi-Montalcini, *J. Exp. Zool. 111* (1949) 457-502.
[8] R. Levi-Montalcini, *J. Comp. Neurol. 91* (1949) 209-242.
[9] R. Levi-Montalcini, *J. Morphol. 86* (1950) 256-283.
[10] E. D. Bueker, *Anat. Rec. 102* (1948) 369-390.
[11] R. Levi-Montalcini, V. Hamburger, *J. Exp. Zool. 116* (1951) 321-362.
[12] R. Levi-Montalcini, *Ann. N. Y. Acad. Sci. 55* (1952) 330-343.
[13] R. Levi-Montalcini, V. Hamburger, *J. Exp. Zool. 123* (1953) 233-288.
[14] R. Levi-Montalcini in F. G. Worden, J. P. Swayzey, G. Adelman (Hrsg.): *The Neurosciences: Paths of Discovery*, MIT Press, Cambridge, MA, USA 1975, pp. 245-265.
[15] R. Levi-Montalcini, H. Meyer, V. Hamburger, *Cancer Res. 14* (1954) 49-57.
[16] S. Cohen, R. Levi-Montalcini, V. Hamburger, *Proc. Natl. Acad. Sci. USA 40* (1954) 1014-1018.
[17] S. Cohen, R. Levi-Montalcini, *Proc. Natl. Acad. Sci. USA 42* (1956) 571-574.
[18] S. Cohen, *J. Biol. Chem. 234* (1959) 1129-1137.
[19] R. Levi-Montalcini, S. Cohen, *Proc. Natl. Acad. Sci. USA 42* (1956) 695-699.
[20] S. Cohen, *Proc. Natl. Acad. Sci. USA 46* (1960) 302-311.
[21] R. Levi-Montalcini, B. Booker, *Proc. Natl. Acad. Sci. USA 46* (1960) 373-384.
[22] R. Levi-Montalcini, B. Booker, *Proc. Natl. Acad. Sci. USA 46* (1960) 384-391.
[23] R. Levi-Montalcini, *Science 143* (1964) 105-110.
[24] R. Levi-Montalcini, *Harvey Lect. 60* (1966) 217-219.
[25] R. Levi-Montalcini, P. U. Angeletti, *Pharmacol. Rev. 18* (1966) 819-828.
[26] G. Steiner, E. Schönbaum, *Immunosympathectomy*, Elsevier, Amsterdam 1972.
[27] R. Levi-Montalcini, P. U. Angeletti, *Dev. Biol. 7* (1963) 653-659.
[28] R. Levi-Montalcini, L. Aloe, P. Calissano, C. Cozzari, *Abstr. 1st Meet. Int. Soc. Dev. Neurosci., Vol. 1*, p. 5, Strasbourg 1980.
[29] L. Aloe, C. Cozzari, P. Calissano, R. Levi-Montalcini, *Nature London 291* (1981) 413-415.
[30] E. M. Johnson, P. D. Gorin, L. D. Brandeis, J. Pearson, *Science 210* (1980) 916-918.
[31] M. Goedert, U. Otten, T. Schaefer, M. Schwab, H. Thoenen, *Brain Res. 201* (1980) 399-409.
[32] P. U. Angeletti, R. Levi-Montalcini, *Proc. Natl. Acad. Sci. USA 65* (1970) 114-121.
[33] P. Calissano, G. Monaco, Menesini-Chen, J. S. Chen, R. Levi-Montalcini in S. W. Perry, A. Margret, R. S. Adelstein (Eds.): *Contractile Systems in Non-Muscle Tissue*, Elsevier, Amsterdam 1976, pp. 201-211.
[34] I. A. Hendry, *Brain Res. 90* (1975) 235-244.
[35] R. Levi-Montalcini, L. Aloe, E. Mugnaini, F. Oesch, H. Thoenen, *Proc. Natl. Acad. Sci. USA 72* (1975) 595-599.
[36] I. A. Hendry, *Brain Res. 94* (1975) 87-97.
[37] L. Aloe, E. Mugnaini, R. Levi-Montalcini, *Arch. Ital. Biol. 113* (1975) 326-353.
[38] K. Stöckel, U. Paravicini, H. Thoenen, *Brain Res. 76* (1974) 413-421.
[39] V. Hamburger, V. J. K. Brunso-Bechtold, J. W. Yip, *J. Neurosci. 1* (1981) 60-71.
[40] R. Levi-Montalcini, *Prog. Brain Res. 45* (1976) 235-258.
[41] Menesini-Chen, J. S. Chen, R. Levi-Montalcini, *Arch. Ital. Biol. 116* (1978) 53-84.
[42] R. W. Gundersen, J. N. Barrett, *Science 206* (1979) 1079-1080.
[43] R. W. Gundersen, J. N. Barrett, *J. Cell Biol. 87* (1980) 546-554.
[44] R. B. Campenot, *Dev. Biol. 93* (1982) 1-12.
[45] R. B. Campenot, *Dev. Biol. 93* (1982) 13-41.
[46] K. H. Pfenninger, M. P. Johnson, *Proc. Natl. Acad. Sci. USA 78* (1981) 7797-7800.
[47] P. Calissano, A. Cattaneo, L. Aloe, R. Levi-Montalcini in C. H. Li (Ed.): *Hormonal Proteins and Peptides, Vol. XII*, Academic Press, New York 1984, pp. 1-56.

[48] R. A. Bradshaw, *Annu. Rev. Biochem. 47* (1978) 191-216.
[49] H. Thoenen, Y. A. Barde, *Physiol. Rev. 60* (1980) 1284-1335.
[50] L. A. Greene, E. M. Shooter, *Annu. Rev. Neurosci. 3* (1980) 353-402.
[51] P. Calissano, A. Cattaneo, S. Biocca, L. Aloe, D. Mercanti, R. Levi-Montalcini, *Exp. Cell Res. 154* (1984) 1-9.
[52] R. Levi-Montalcini, P. Calissano, *Trends NeuroSci. Pers. Ed. 9* (1986) 473-476.
[53] H. Thoenen, P. U. Angeletti, R. Levi-Montalcini, R. Kettler, *Proc. Natl. Acad. Sci. USA 68* (1971) 1598-1602.
[54] U. Paravicini, K. Stöckel, H. Tmoenen, *Brain Res. 84* (1975) 279-291.
[55] E. M. Johnson, H. K. Yip, *Nature 314* (1985) 751-753.
[56] L. A. Greene, A. S. Tischler, *Proc. Natl. Acad. Sci. USA 73* (1976) 2424-2428.
[57] K. Unsicker, B. Krisch, U. Otten, H. Thoenen, *Proc. Natl. Acad. Sci. USA 75* (1978) 3498-3502.
[58] L. Aloe, R. Levi-Montalcini, *Proc. Natl. Acad. Sci. USA 76* (1979) 1246-1250.
[59] L. A. Greene, R. K. H. Liem, M. L. Shelanski, *J. Cell Biol. 96* (1983) 76-83.
[60] L. E. Lillien, P. Claude, *Nature London 317* (1985) 632-634.
[61] D. E. Burnstein, L. A. Greene, *Dev. Biol. 94* (1982) 477-482.
[62] R. Levi-Montalcini, L. Aloe, *Adv. Biochem. Psychopharmacol. 25* (1980) 3-16.
[63] A. J. Doupe, P. H. Patterson, S. C. Landis, *J. Neurosci. 5* (1985) 2143-2160.
[64] A. J. Doupe, S. C. Landis, P. H. Patterson, *J. Neurosci. 5* (1985) 2119-2142.
[65] C. Owman, N. O. Sjoberg in V. H. T. James (Ed.): *Proc. 5th Int. Congr. Endocrinol., Vol. I*, Excerpta Medica, Amsterdam 1977, p. 205-209.
[66] A. Szutowicz, W. A. Frazier, R. A. Bradshaw, *J. Biol. Chem. 251* (1976) 1516-1523.
[67] M. Seiler, M. Schwab, *Brain Res. 30* (1984) 33-39.
[68] H. Gnahn, F. Hefti, R. Heumann, M. E. Schwab, H. Thoenen, *Dev. Brain Res. 9* (1983) 45-52.
[69] F. Hefti, A. Dravid, J. Hartikka, *Brain Res. 293* (1984) 305-311.
[70] W. C. Mobley, J. L. Rutkowski, G. I. Tennekoon, K. Buchanan, M. V. Johnston, *Science 229* (1985) 284-287.
[71] L. R. Williams, S. Varon, G. M. Peterson, K. Wictorin, W. Fischer, A. Bjorklund, F. H. Gage, *Proc. Natl. Acad. Sci. USA 83* (1986) 9231-9235.
[72] L. F. Kromer, *Science 235* (1987) 214-216.
[73] S. Korsching, G. Auburger, R. Heumann, J. Scott, H. Thoenen, *EMBO J. 4* (1985) 1389-1393.
[74] D. L. Shelton, L. F. Reichardt, *Proc. Natl. Acad. Sci. USA 83* (1986) 2714-2718.
[75] S. R. Whittemore, T. Ebendal, L. Lärkfors, L. Olson, A. Seiger, I. Strömberg, H. Persson, *Proc. Natl. Acad. Sci. USA 83* (1986) 817-821.
[76] L. Aloe, R. Levi-Montalcini, *Brain Res. 133* (1977) 358-366.
[77] A. Böhm, L. Aloe, *Accad. Naz. Lincei 80* (1986) 1-6.
[78] A. Bruni, E. Bigon, E. Boarato, A. Leon, G. Toffano, *FEBS Lett. 138* (1982) 190-192.
[79] K. Sugiyama, Y. Suzuki, H. Furata, *Arch. Oral Biol. 30* (1985) 93-95.
[80] N. Mazurek, G. Weskamp, P. Erne, U. Otten, *FEBS Lett. 198* (1986) 315-320.
[81] L. W. Thorpe, K. Werrbach-Perez, J. R. Perez-Polo, *Abstr. 2nd Workshop Neuroimmunomodul.*, Dubrovnik 1986, p. 151.
[82] A. Cattaneo, D. S. Secher, *Exp. Cell Res.*, in press.
[83] R. Hogue-Angeletti, R. A. Bradshaw, *Proc. Natl. Acad. Sci. USA 68* (1971) 2417-2420.
[84] J. Scott, M. Selby, M. Urdea, M. Quiroga, G. Bell, W. J. Rutter, *Nature London 302* (1983) 538-540.
[85] A. Ullrich, A. Gray, C. Berman, T. J. Dull, *Nature London 303* (1983) 821-823.
[86] R. Meier, M. Becker-Andre, R. Gotz, R. Heumann, A. Shaw, H. Thoenen, *EMBO J. 5* (1986) 1489-1493.
[87] T. Ebendal, D. Larhammar, H. Persson, *EMBO J. 5* (1986) 1483-1487.
[88] V. Francke, B. De Martinville, L. Coussens, A. Ullrich, *Science 222* (1983) 1248-1250.
[89] V. Bocchini, P. U. Angeletti, *Proc. Natl. Acad. Sci. USA 64* (1969) 787-792.
[90] S. Varon, J. Nomura, E. M. Shooter, *Biochemistry 6* (1967) 2202-2210.
[91] S. Varon, J. Nomura, E. M. Shooter, *Biochemistry 7* (1968) 1296-1303.
[92] R. W. Stach, E. M. Shooter, *J. Biol. Chem. 249* (1974) 6668-6674.
[93] R. H. Edwards, M. J. Selby, W. J. Rutter, *Nature London 319* (1986) 784-787.
[94] B. A. Eipper, R. E. Mains, E. Herbert, *Trends Neurosci. 100* (1986) 463-467.
[95] R. Doolittle, M. W. Hunkapiller, L. E. Hood, S. G. DeVare, K. L. Robbins, S. A. Aaronson, H. N. Antoniades, *Science 221* (1983) 275-276.
[96] J. Downward, Y. Yraden, E. Mayes, G. Scrace, N. Totty, P. Stockwell, A. Ullrich, J. Schlessinger, M. D. Waterfield, *Nature 307* (1984) 521-527.
[97] C. J. Sherr, C. W. Rettenmier, R. Sacca, M. F. Roussel, T. A. Look, E. R. Stanley, *Cell 41* (1985) 665-676.
[98] C. Weinberger, S. M. Hollenberg, M. G. Rosenfeld, R. M. Evans, *Nature London 318* (1985) 670-673.
[99] D. Bar-Sagi, J. R. Feramisco, *Cell 42* (1985) 841-848.
[100] S. Alemà, P. Casalbore, E. Agostini, F. Tatò, *Nature London 316* (1985) 557-559.
[101] R. Levi-Montalcini, P. U. Angeletti in L. M. Sreebny, J. Meyer (Eds.): *Salivary Glands and their Secretions*, Pergamon, Oxford 1964, pp. 129-141.
[102] L. Aloe, R. Levi-Montalcini, *Exp. Cell Res. 125* (1980) 15-22.
[103] L. Aloe, C. Cozzari, R. Levi-Montalcini, *Brain Res. 332* (1985) 259-265.
[104] L. Aloe, E. Alleva, A. Böhm, R. Levi-Montalcini, *Proc. Natl. Acad. Sci. USA 83* (1986) 6184-6187.
[105] J. Lakshmanan, *Am. J. Physiol. 250* (1986) E386-391.
[106] U. Otten, M. Schwab, C. Gagnon, H. Thoenen, *Brain Res. 133* (1977) 291-303.
[107] J. Bing, K. Poulsen, E. Hackenthal, E. Rix, R. Taugner, *J. Histochem. Cytochem. 28* (1980) 874-880.
[108] G. P. Harper, Y. A. Barde, G. Burnstock, J. R. Carstairs, M. E. Dennison, K. Suda, C. A. Vernon, *Nature London 279* (1979) 160-162.
[109] G. P. Harper, H. Thoenen, *J. Neurochem. 34* (1980) 893-903.
[110] D. J. Beer, S. M. Matloff, R. E. Rocklin, *Adv. Immunol. 35* (1984) 209-215.
[111] R. Levi-Montalcini, L. Aloe, *Proc. Natl. Acad. Sci. USA 82* (1985) 7111-7115.
[112] E. T. Kaiser, D. S. Lawrence, *Science 226* (1984) 505-511.
[113] B. Rajashekhar, E. T. Kaiser, *J. Biol. Chem. 261* (1986) 13617-13623.
[114] T. Ebendal, L. Olson, A. Seiger, K. O. Hedlund, *Nature London 286* (1980) 25-28.
[115] T. L. Roszman, J. C. Jackson, R. J. Cross, M. J. Titus, W. R. Markesberry, W. H. Brooks, *J. Immunol. 135* (1985) 769-772.
[116] N. R. Hall, J. P. McGillis, B. L. Spangelo, A. L. Goldstein, *J. Immunol. 135* (1985) 806-811.
[117] V. Hamburger, *Perspect. Biol. Med. 18* (1975) 162-178.

Epidermal Growth Factor (Nobel Lecture)**

By Stanley Cohen

1. Introduction

Upon the foundations provided by experimental embryology, endocrinology, cell biology, biochemistry, and molecular biology, the intricacies of the regulatory processes that occur during embryonic development are slowly coming to light. While the importance of "classical" hormones in the control of growth and development has long been recognized, we now know that many more intercellular signals are involved in these highly complex processes. The recent advances in this area have, somewhat unexpectedly, also provided mechanisms that may lead to a more detailed understanding of important biomedical questions, such as the growth behavior of malignant cells.

My own efforts in this area of research over the past thirty years have been directed toward the understanding, on a biochemical level, of two biological observations, both initially made in the Department of Zoology, directed by Dr. *Viktor Hamburger*, at Washington University.

The first observation was that of Dr. *Rita Levi-Montalcini* who noted that certain mouse tumors, when implanted into chick embryos, released a factor that stimulated the growth of specific embryonic neurons. The second biological observation was made during my study of the nerve growth factor detected in male mouse submaxillary glands. It was noted[1] that when crude submaxillary gland preparations were injected into newborn mice, unexpected "side effects" not related to the activities of nerve growth factor, were produced. These effects included precocious eyelid opening (6–7 days, compared with 12–14 days for controls) and precocious tooth eruption (5–6 days, compared with 8–10 days for controls).

After I transferred to the Biochemistry Department at Vanderbilt University in 1959, these "side effects" were to become the focus of my research. From my training in embryology, I felt that any substance that altered the timing of specific developmental processes would be of biological significance. I, of course, did not foresee that the biochemical mechanism by which these extracts induced precocious eyelid opening would be related to those involved in oncogenic transformation by one class of retroviruses. This lecture summarizes briefly some of the thoughts and key experiments that have led to our present understanding of epidermal growth factor (EGF).

2. The First Decade

By employing precocious eyelid opening as an assay, the factor, a small protein, responsible for these effects was isolated from murine submaxillary glands in the early 1960s.[2] Histological examination (see Fig. 1) of control and EGF-treated newborn animals (mouse, rat, rabbit) revealed that the observed precocious eyelid separation was the consequence of a more generalized biological effect, namely, an enhancement of epidermal growth and keratinization.[3] The apparent precocious incisor eruption induced by EGF was, in reality, caused by an enhanced differentiation of the lips of the treated animals.

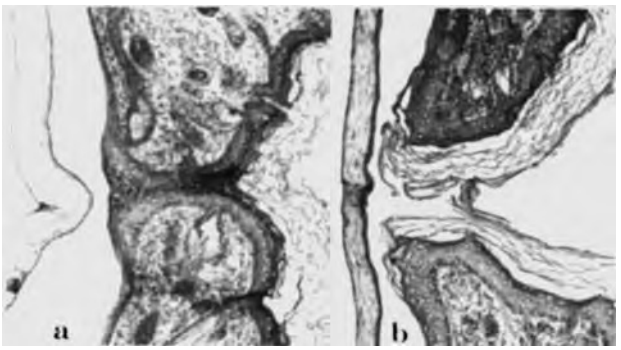

Fig. 1. Cross sections of the eyelid area from control (a) and experimental (b) eight-day-old rats. The experimental animal had received daily injections (1 μg per g body weight) of the active protein. × 100. (Reprinted from *J. Invest. Dermatol. 40* (1963) 1–5.)

Since these were whole animal experiments, we were faced with the problem of whether the factor operated directly on epidermal cells or whether growth was induced indirectly, possibly by the increased production of a more "classical" hormone.

The techniques of tissue and organ culture seemed ideally suited for resolving this problem. A preliminary organ culture study was carried out during a sabbatical at the Instituto Superiore di Sanità in Rome in collaboration with Drs. *Rita Levi-Montalcini* and *Domenica Attardi*, and the study subsequently was continued at Vanderbilt University. The name epidermal growth factor was first used in the initial reports of these studies.[4] The results demonstrated that EGF directly stimulated the proliferation of epidermal cells in organ cultures of chick embryo skin; this mitogenic action of EGF, therefore, did not necessarily depend on other systemic or hormonal influences. During these experiments, the range of responsive animals was widened to include birds as well as mammals, suggesting that knowledge of the evolutionary origins of EGF would contribute to our understanding.

By 1970 we had accumulated a spectrum of information regarding many aspects of the physiology of EGF:

1. We described a series of metabolic alterations (enhancement of polysome formation, induction of ornithine decarboxylase, etc.) that accompany the growth-stimulating effects of EGF on epidermal cells. Many of these

[*] Prof. S. Cohen
Department of Biochemistry, Vanderbilt University
School of Medicine
Nashville, TN 37232 (USA)

[**] Copyright © The Nobel Foundation 1987.—We thank the Nobel Foundation, Stockholm, for permission to print this article.

changes are now known to take place in a variety of cells when a growth stimulus is applied.

2. We identified the tubular cells of the submaxillary gland, which in the mouse exhibit sexual dimorphism, as the major site of synthesis of EGF in this species and noted, with the aid of a radioimmunoassay, that the synthesis of EGF, especially in female mice, was markedly enhanced by the administration of testosterone.
3. We demonstrated that, in crude homogenates of the mouse submaxillary gland, EGF existed as a high-molecular-weight noncovalent complex (≈ 75000 Da) consisting of two molecules of EGF and two molecules of an EGF-binding protein that possessed arginyl esterase activity.
4. On a more practical level, we and others found that the topical application of EGF accelerated corneal re-epithelialization in rabbits with wounded corneas.

The reader is referred to a number of early review articles wherein this information is detailed and references are provided.[6,7] By the end of the first decade, I was convinced that EGF plays a normal physiological role in many species, either during embryonic development or in homeostasis; what this role was at the whole animal level and how EGF interacted with cells at the molecular level were problems for the future.

3. The Second Decade

The development of a rapid, essentially two-step procedure for isolation of milligram quantities of EGF from murine submaxillary glands in the early 1970s[7] permitted the purification of sufficient quantities of mouse-derived EGF (mEGF) for a thorough characterization. This single technical advance opened the door to the application of many biochemical methodologies and insights. Amino-acid analysis revealed that mEGF is a 53-residue polypeptide, entirely devoid of alanyl, phenylalanyl, or lysyl residues.[8] The primary sequence of mEGF[9] and the position of the three internal disulfide bonds[10] were determined and are depicted in Figure 2. Though mEGF has yet to be crystallized and subjected to X-ray diffraction analysis, considerable spectroscopic data has been accumulated suggesting that the hormone has little periodic secondary structure; the presence of β-sheet structures has been detected (reviewed in Ref. [11]).

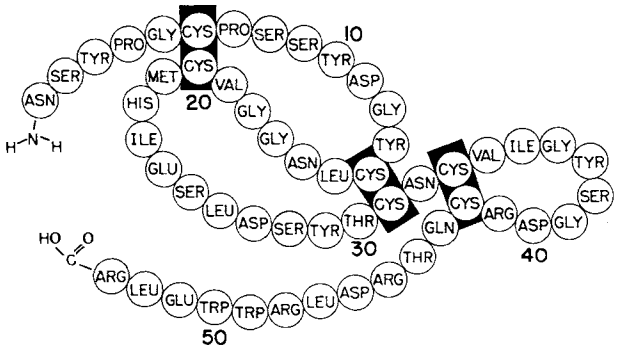

Fig. 2. The amino-acid sequence of EGF with placement of disulfide bonds. (Reprinted from *J. Biol. Chem. 248* (1973) 7669–7672.)

At about this time (1973) a new facet of the biology of EGF was uncovered. *Armelin*[12] and *Hollenberg* and *Cuatrecasas*[13] were the first to report that fibroblasts in culture responded to EGF with enhanced DNA synthesis. These findings were corroborated in our laboratory with human fibroblasts.[14,15]

The finding that mouse-derived EGF was a potent mitogen for human cells indicated that receptors for EGF were present on human cells and, therefore, a polypeptide similar to EGF might be found in human tissue. We took two approaches in an attempt to isolate EGF-like molecules from human urine. First, an immuno-affinity column procedure (using anti-mouse EGF antibodies) was used to partially purify a substance from human urine that was similar to the mouse hormone in its biological activity.[16] In another approach, we developed a sensitive and specific radioreceptor competitive-binding assay for EGF-related polypeptides, using cultured human fibroblasts and ^{125}I-labeled mouse EGF, that permitted the isolation of microgram quantities of pure growth factor from protein concentrates of human urine.[17] The biological effects of the purified human polypeptide were qualitatively identical to those previously described for the mouse growth factor. These included the stimulation of the proliferation in vitro of fibroblasts and corneal epithelial cells, as well as the induction of precocious eyelid opening in the newborn mouse, which still remains the most specific biological assay for EGF. The amino-acid compositions of the human and mouse polypeptides differed, but clear similarities were noted. Both polypeptides apparently competed for the same site on the cell membrane and antibodies to the mouse polypeptide cross-reacted with the human hormone. We concluded that we had isolated the human counterpart of murine EGF.

As is usual in science, an unexpected and completely new aspect of the biology of EGF emerged with the report by *Gregory*[18] that urogastrone, a gastric antisecretory hormone isolated from human urine, appeared to be identical to human EGF and closely related to murine EGF. Human EGF (urogastrone) and murine EGF are now believed to invoke identical response in all target cells. The relationship between human EGF and urogastrone could only have been detected from a structural comparison of these molecules; even today, no rationale is available to connect inhibition of acid secretion and stimulation of cell growth.

Given a cell culture system (human fibroblasts) in which EGF acted as a "growth factor," we were faced in 1975 with a rather formidable task: how does EGF stimulate cell growth? Although neuronal uptake and retrograde transport of nerve growth factor had been demonstrated in 1974,[19] almost all endocrinologists were of the opinion that peptide hormones, after binding to their receptors on the plasma membrane, were released into the extracellular environment.

Our initial experiments[20] utilizing ^{125}I-EGF and human fibroblasts confirmed the presence of plasma membrane receptors for EGF. Two additional and significant observations were made. First, the binding of ^{125}I-EGF to the

cell surface of intact fibroblasts was rapidly followed by proteolytic degradation of the growth factor by a cell-mediated process. Secondly, it was noted that NRK cells lost their ability to bind ^{125}I-EGF following transformation by the Kirsten virus. The former observation directed us to an examination of the possibility that cell-bound EGF was internalized prior to degradation.[21] The latter observation was later generalized to include a variety of cells transformed by retroviruses[22] and eventually led *George Todaro* and others to isolate the EGF-related polypeptide, α-transforming growth factor (α-TGF), and to propose the autocrine hypothesis.[22]

As a step in defining the biochemical events that occur during and subsequent to the interaction of EGF with the cell surface, we examined the metabolic fate of the bound hormone. We came to the conclusion[21] that subsequent to the initial binding of ^{125}I-EGF to specific plasma membrane receptors, the EGF-receptor complex is internalized and the hormone is ultimately degraded in lysosomes. These conclusions, drawn from studies of the interaction of ^{125}I-EGF with human fibroblasts, were based on the following series of observations:

1. Cell-bound ^{125}I-EGF was rapidly degraded to [^{125}I]monoiodotyrosine at 37°. At 0°, however, cell-bound ^{125}I-EGF was not degraded, but slowly dissociated from the cell surface.
2. When the binding of ^{125}I-EGF was first carried out at 37° and the cells then incubated at 0°, almost no release of cell-bound radioactivity was detected.
3. Degradation of ^{125}I-EGF, but not binding, required metabolic energy.
4. The degradation was blocked by drugs that inhibit lysosomal function, such as chloroquine and ammonium chloride.
5. When ^{125}I-EGF was bound to cells at 0°, the hormone was readily accessible to surface-reactive agents, such as trypsin and antibodies to EGF. However, when the hormone was bound to cells at 37° it was much less accessible to either of these reagents.
7. Exposure of fibroblasts to EGF resulted in an apparent loss of plasma membrane receptors for EGF.

Taken together, these observations, which have subsequently been extended by others to a number of polypeptide hormones, provided quantitative biochemical evidence for a complex mechanism through which cells interact with extracellular regulatory signals.

The challenge of direct visualization of the internalization of EGF was approached using three general procedures: the preparation and tracing of fluorescent derivatives of EGF,[23,24] the tracing of ^{125}I-EGF by electron microscopic autoradiography,[25] and the preparation and tracing of EGF-ferritin conjugates by electron microscopy.[26,27]

Although all three morphological approaches confirmed the original biochemical studies with ^{125}I-EGF,[21] the use of the biologically active EGF-ferritin conjugate provided the clearest and most direct picture of the metabolic fate of EGF. At 4° the EGF-ferritin conjugate specifically bound to the plasma membrane of cells and appeared to be randomly distributed on specific receptor sites. When the cells were warmed to 37°, the EGF-ferritin redistributed on the surface of the plasma membrane within one minute to form many small clusters. The clusters of receptor-bound EGF-ferritin molecules were then rapidly internalized into endocytic vesicles. Within 30 min approximately 84% of the ferritin was seen in multivesicular bodies that were considered to be lysosome-related. These data also provided morphological evidence for the hypothesis that "down-regulation" of surface receptors for EGF involves internalization of intact hormone-receptor complexes. A diagram that illustrates our conclusions is presented in Figure 3. It was subsequently demonstrated, by metabolic labeling and immunoprecipitation with anti-receptor antibodies, that EGF-mediated internalization of the EGF-receptor complex is associated not only with the degradation of EGF but also with enhanced degradation of the receptor.[28]

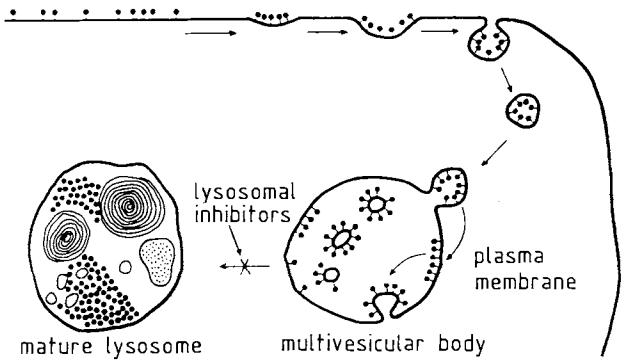

Fig. 3. Diagram of ferritin-EGF (F-EGF) interaction with A-431 cells. F-EGF-receptor complexes, identified by the characteristic spatial relationship of particles and membrane (4- to 6-nm separation), are apparent at initial binding and are preserved through the processes of clustering, pinocytosis, and incorporation into multivesicular bodies. Further incubation at 37°C allows disruption of the F-EGF-receptor complex (attested by pools of free ferritin), a process blocked by the presence of amines. (Reprinted from *Proc. Nat. Acad. Sci. USA 76* (1979) 5689–5693.)

A critical question in this area of hormone research is whether the intracellular processing of hormones and their receptors is related to, or necessary for, the generation of biological responses to the hormone. My opinion is that no clear experimental evidence exists to answer this very important question.

In view of our inability to define the relevance of receptor-mediated internalization to the growth factor's biological activity and our belief that cellular alterations induced by EGF result from the amplification and propagation of a series of "signals" generated during the binding and internalization of the hormone, we sought, in the late 1970s, to obtain a cell-free system that responded in vitro to the addition of EGF. Since the A-431 human epidermoid carcinoma cell line had been shown to have an extraordinarily high concentration of EGF receptors ($2-3 \times 10^6$ receptors/cell),[29,24] we utilized a membrane preparation from these cells to look for an EGF-dependent alteration of membrane structure and/or function. Like the technical turning point that the rapid purification of milligram quantities of EGF provided (see above), the identification of the A-431

cell line as an enriched source of EGF receptors has been instrumental for both biochemical and molecular biological studies of the mechanism of action of EGF.

As expected, membranes from these cells were able to specifically bind relatively large quantities of ^{125}I-EGF. Since phosphorylation and dephosphorylation reactions participate in the control of many metabolic pathways and membranes contain endogenous protein kinases and phosphatases, a study[30] was initiated to assess the possible role of EGF as a modulator of these regulatory processes. Aliquots of the A-431 membrane preparation were examined for their ability to phosphorylate endogenous membrane components and to determine whether the binding of EGF resulted in a perturbation of this biochemical system. The incubation of A-431 membranes at 0° with [γ-^{32}P]ATP in the presence of Mg^{2+} or Mn^{2+}, resulted in the incorporation of radioactivity into trichloroacetic acid-insoluble material. Of key importance was the discovery that the prior addition of EGF to the reaction mixture resulted in a threefold enhancement of the phosphorylation of endogenous membrane-associated proteins (Fig. 4).

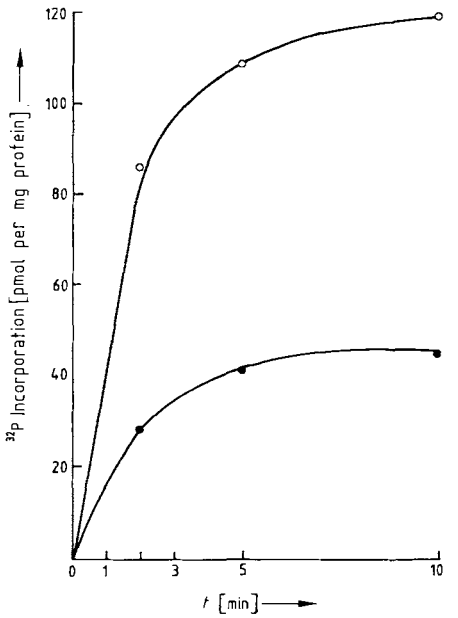

Fig. 4. Stimulation by EGF of the incorporation of ^{32}P-phosphate from [γ-^{32}P]ATP into cell membranes. The reaction mixtures contained A-431 membrane (27 μg protein), HEPES buffer (20 mM, pH 7.4), $MnCl_2$ (1 mM), [γ-^{32}P]ATP (15 μM, 8×10^5 cpm), EGF (40 ng), and bovine serum albumin (7.5 μg) in a final volume of 60 μL. The reaction tubes were placed on ice and preincubated for 10 min in the presence (○) or absence (●) of EGF. The reaction was initiated by the addition of labeled ATP, and incubation at 0°C was continued for the indicated times. The reaction was terminated by pipetting 50-μL aliquots onto squares (4 cm^2) of Whatman 3 MM filter paper and immediately dropping the paper into a beaker of cold 10% trichloroacetic acid (TCA) containing 0.01 M sodium pyrophosphate. The filter papers were washed extensively with pyrophosphate-containing 10% TCA at room temperature, extracted with alcohol and ether, and dried, and the radioactivity was measured in a Nuclear Chicago gas-flow counter. (Reprinted from *Nature 276* (1978) 409-410.)

The enhanced incorporation of ^{32}P into the membrane preparations was specific for EGF; the major phosphorylated membrane components detected were proteins having molecular weights of ≈170000 Da and 150000 Da. The addition of EGF to A-431 membrane preparations stimulated the phosphorylation of not only endogenous membrane proteins, but also a number of exogenously added protein substrates.

It was suggested at that time (1978) that the phosphorylation of membrane or membrane-associated components might be an initial event in the generation of intracellular signals that regulate cell growth. The reader is referred to a review[31] that summarized our knowledge as of 1979.

By the end of this second decade, I was encouraged and excited by the prospect that we had made a significant inroad into the understanding of the mechanism of action of EGF at the cellular and biochemical level.

4. The Third Decade

The detection of a direct effect of EGF on a chemical reaction in a cell-free system led to a more detailed biochemical characterization of the reaction in A-431 membranes and to its extension to membrane preparations from normal human placenta and cultured human fibroblasts.[32-34] The EGF-stimulated kinase activity of A-431 membranes was not removed by extraction of the membranes with a variety of solutions, such as high salt or urea, suggesting that the kinase, receptor, and substrates were integral membrane proteins. We, at this time, were aware of reports from several laboratories[35-37] that the molecular weight of the putative receptor for EGF, as detected by cross-linking with ^{125}I-EGF, was in the range of our major phosphorylated membrane glycoproteins, i.e., 150-170 kDa.

Our studies provided the following data concerning the mechanism by which EGF regulated protein phosphorylation in the cell-free A-431 membrane system:

1. Activation of the membrane-associated kinase activity by EGF was a rapid process, even at 0°.
2. Dephosphorylation reactions in the membrane also occurred with great rapidity, but were not affected by the presence of EGF.
3. EGF does not cause the release from the membrane of either a soluble protein kinase or a modulator of the kinase.
4. The EGF-induced activation of the membrane kinase could be reversed by removal of the hormone from the membrane by anti-EGF IgG, indicating that proteolytic activation was not involved.

We originally assumed, on the basis of data that clearly indicated different heat sensitivities of the receptor and the kinase,[32] that at least two separate entities were involved. However, the possibility that the receptor and the kinase activities were present in the same molecule was raised by two unexpected observations. First, A-431 membranes could be solubilized by detergents with retention of EGF-enhanced phosphorylation activity as well as ^{125}I-EGF binding activity. Second, the EGF-receptor and the EGF-dependent kinase activity, as well as the substrate, were copurified by EGF affinity chromatography as a major 150-kDa protein.

We originally had reported[32] that the EGF-stimulated protein kinase phosphorylated mainly threonine residues, and in this and other regards it resembled the kinase activity of the transforming protein of Rous sarcoma virus (RSV). Soon thereafter, however, it was reported that the RSV-associated protein kinase and other tumor virus-associated protein kinases[38,39] actually phosphorylated tyrosine residues, originally mistakenly identified as threonine due to co-migration of the two phosphorylated amino acids in the electrophoretic system employed. Since we had employed a similar electrophoretic system, we reinvestigated the nature of the EGF-stimulated protein-kinase reaction and discovered that the affinity-purified EGF-activated receptor-kinase also phosphorylated tyrosine residues.[40]

To determine whether the EGF-receptor-associated kinase activity might be due to trace contamination with $pp60^{src}$, we looked for an interaction of the EGF receptor-kinase preparations with $pp60^{src}$ antisera. Although the receptor kinase was able to specifically phosphorylate these anti-src antibodies, the receptor-kinase was not precipitated by such antisera.[41,42] We interpreted these results to mean that while the EGF receptor-kinase might be related to $pp60^{src}$, the two kinases were not identical.

We then attempted to further purify the EGF receptor.[43] When the previous affinity purification procedure[34] was applied to A-431 membrane vesicles in the absence of Ca^{2+}, the receptor-kinase was isolated as a 170-kDa protein. The 150-kDa receptor protein initially observed in preparations from scraped membranes has been shown to be a proteolytic fragment of the 170-kDa native species, produced by the action of a Ca^{2+}-dependent neutral protease.[44,45]

The receptor properties of both the 170-kDa and 150-kDa preparations were demonstrated not only by their capacities to bind ^{125}I-EGF, but also by covalent cross-linking to ^{125}I-EGF. The major functional difference between the 170- and 150-kDa preparations appeared to be the ability of the former to "autophosphorylate" at a rate five to ten times greater than the latter. This observation is now understandable since it is now known that the major autophosphorylated tyrosine residues are located near the carboxy-terminus of the 170-kDa receptor and are not present in the 150-kDa proteolytic fragment.

We addressed the question whether the three domains present in our receptor preparation (binding, kinase, and substrate) reside in one or more than one molecule by applying more stringent purification procedures. The three domains remained associated not only following EGF affinity chromatography but also lentil lectin-Sepharose chromatography, indicating that both the receptor and the kinase are associated with lectin-reactive carbohydrate groups. More importantly, the three detectable domains remain associated following electrophoresis in nondenaturing gels and immunoprecipitation using antisera to the purified receptor. Although these results were not considered definitive, they encouraged speculation that all of the domains were present in the same molecule.

The question was resolved by a series of experiments designed to identify the EGF-stimulated kinase by affinity labeling.[46,47] When A-431 membrane vesicles were treated with 5′-(*p*-fluorosulfonylbenzyl)adenosine (5′-*p*-FSO_2BzAdo), a reagent previously shown to affinity label ATP or ADP binding sites in a variety of enzymes, the EGF-stimulated kinase was irreversibly inhibited. When A-431 membrane vesicles were labeled with 5′-*p*-FSO_2Bz[^{14}C]Ado and then subjected to sodium dodecylsulfate (SDS)-polyacrylamide gel electrophoresis and autoradiography, most of the covalently attached affinity label migrated with the 170-kDa receptor and its 150-kDa proteolytic fragment. The labeling observed was at an ATP binding site, since it was inhibited by adenosine 5′-iminodiphosphate (AMP-PNP), a hydrolysis-resistant ATP analogue, but not by adenosine, AMP, ADP, GTP, or NAD. Furthermore, after labeling A-431 vesicles or scraped membranes with 5′-*p*-FSO_2Bz[^{14}C]Ado, the receptor was affinity-purified under conditions previously shown to copurify the receptor and the kinase. The receptor was the only component of the purified preparation that contained detectable affinity label. Thus, we concluded that the receptor and the kinase are two domains of the same polypeptide. Lastly, if the EGF-sensitive kinase activity was inactivated, by mild heating or exposure to *N*-ethylmaleimide, the 150-kDa and 170-kDa receptor species could not be labeled with the ATP affinity reagent. The mechanism by which binding of EGF to the external domain of the receptor activates the cytoplasmic catalytic domain is not yet known.[11,48]

That the EGF receptor is a glycoprotein was first suggested by observations that a variety of lectins inhibit the binding of ^{125}I-EGF to cultured human fibroblasts[49] or to human placental membranes[50] and that the receptor may be purified by lectin chromatography.[51] The biosynthesis and glycosylation of the receptor in A-431 cells have recently been addressed in several studies in which cells have been metabolically labeled and the receptor species identified by immunoprecipitation.[48,52]

It is not possible to consider here the thousands of reports regarding EGF and its receptor in biology and medicine. The reader is referred to several recent reviews that summarize various aspects of this ever-burgeoning area.[11,48,53,54]

I now, very briefly, indicate some of the major advances made in other laboratories throughout the world that I believe will lead to a more complete understanding of the role of EGF and its receptor-kinase in growth regulation.

1. The elucidation of the amino-acid sequence of the EGF receptor, deduced from the nucleotide sequence of cDNA clones, and the discovery that the *erb*-B transforming gene of avian erythroblastosis virus probably is derived from the avian EGF receptor.[55]
2. The elucidation of the nucleotide sequence of the cDNA for prepro-EGF, which predicts a protein precursor with a molecular weight of 128000 Da.[56,57] The EGF precursor may be a membrane-spanning protein, conceivably a receptor for an as yet unknown ligand. Of great interest in this regard has been the detection of prepro-EGF in the kidney,[58] the detection of two EGF-related loci (in *Drosophila* and in *Caenorhabditis*) that regulate development,[59,60] and the detection of an EGF-related sequence in the genome of the vaccinia vi-

rus.[61] These findings suggest that EGF is of ancient origin and may have been used for a variety of functional roles.

3. The discovery that both fetal and malignant cells produce an EGF-related protein (α-TGF) that appears to interact with the EGF receptor and mimics the biological activity of EGF.[62]
4. The discovery that the receptors for insulin as well as a number of other growth factors are ligand-activated tyrosine kinases.[48,54]

Although our current working hypothesis is that the initial functional signal transmitted by EGF is related to the tyrosine kinase activity of its receptor, the exact pathway of growth activation, especially between the receptor and cell nucleus, remains elusive. This is true not only for EGF, but also for the other growth factors whose receptors are tyrosine kinases as well as those oncogenes whose products are tyrosine kinases.

5. Where Do We Go from Here?

Do we look for specific cellular proteins whose functions are altered by tyrosine phosphorylation? Is the intracellular translocation of tyrosine kinases of physiological significance? Is it possible that autophosphorylated receptors or related oncogene proteins serve some still unidentified regulatory role? What are the mechanisms for sending stimulatory or inhibitory signals to the nucleus? What is the normal physiological role of EGF during development and homeostasis? The answers to these and a host of other questions must be found before we can fully comprehend this important regulatory system.

To the many colleagues, students, and technical assistants who have contributed to these investigations, I am most grateful. I also wish to acknowledge, with gratitude, the support of the National Institutes of Health and the American Cancer Society.

Received: March 5, 1987 [A 630 IE]
German version: *Angew. Chem. 99* (1987) 738

[1] S. Cohen, *Proc. Natl. Acad. Sci. USA 46* (1960) 302-311.
[2] S. Cohen, *J. Biol. Chem. 237* (1962) 1555-1562.
[3] S. Cohen, G. A. Elliott, *J. Invest. Dermatol. 40* (1963) 1-5.
[4] S. Cohen, *Dev. Biol. 12* (1965) 394-407.
[5] S. Cohen, J. M. Taylor, *Recent Prog. Horm. Res. 30* (1974) 533-550.
[6] S. Cohen, C. R. Savage, Jr., *Recent Prog. Horm. Res. 30* (1974) 551-574.
[7] C. R. Savage, Jr., S. Cohen, *J. Biol. Chem. 247* (1972) 7609-7611.
[8] J. M. Taylor, W. M. Mitchell, S. Cohen, *J. Biol. Chem. 247* (1972) 5928-5934.
[9] C. R. Savage, Jr., T. Inagami, S. Cohen, *J. Biol. Chem. 247* (1972) 7612-7621.
[10] C. R. Savage, Jr., J. H. Hash, S. Cohen, *J. Biol. Chem. 248* (1973) 7669-7672.
[11] J. V. Staros, S. Cohen, M. W. Russo in S. Cohen, Houslay (Eds.): *Molecular Mechanisms of Membrane Signalling*, p. 253-277, Elsevier, Amsterdam 1985.
[12] H. Armelin, *Proc. Natl. Acad. Sci. USA 70* (1973) 2702-2706.
[13] M. D. Hollenberg, P. Cuatrecasas, *Proc. Natl. Acad. Sci. USA 70* (1973) 2964-2968.
[14] S. Cohen, G. Carpenter, K. J. Lembach, *Adv. Metab. Disord. 8* (1975) 265-284.
[15] G. Carpenter, S. Cohen, *J. Cell Physiol. 88* (1976) 227-237.
[16] R. H. Starkey, S. Cohen, D. N. Orth, *Science 189* (1975) 800-802.
[17] S. Cohen, G. Carpenter, *Proc. Natl. Acad. Sci. USA 72* (1975) 1317-1321.
[18] H. Gregory, *Nature London 257* (1975) 325-327.
[19] I. A. Hendry, K. Stoeckel, H. Thoenen, L. L. Iverson, *Brain Res. 68* (1974) 103-121.
[20] G. Carpenter, K. J. Lembach, M. M. Morrison, S. Cohen, *J. Biol. Chem. 250* (1975) 4297-4304.
[21] G. Carpenter, S. Cohen, *J. Cell Biol. 71* (1976) 159-171.
[22] G. J. Todaro, J. E. DeLarco, S. Cohen, *Nature London 264* (1976) 26-31.
[23] J. Schlessinger, Y. Shecter, M. C. Willingham, I. Pastan, *Proc. Natl. Acad. Sci. USA 75* (1978) 2659-2663.
[24] H. T. Haigler, J. F. Ash, S. J. Singer, S. Cohen, *Proc. Natl. Acad. Sci. USA 75* (1978) 3317-3321.
[25] P. Gordon, J.-L. Carpentier, S. Cohen, L. Orci, *Proc. Natl. Acad. Sci. USA 75* (1978) 5025-5029.
[26] H. T. Haigler, J. A. McKanna, S. Cohen, *J. Cell Biol. 81* (1979) 382-395.
[27] J. A. McKanna, H. T. Haigler, S. Cohen, *Proc. Natl. Acad. Sci. USA 76* (1979) 5689-5693.
[28] C. M. Stoscheck, G. Carpenter, *J. Cell Biol. 98* (1984) 1048-1053.
[29] R. N. Fabricant, J. E. DeLarco, G. J. Todaro, *Proc. Natl. Acad. Sci. USA 74* (1977) 565-569.
[30] G. Carpenter, L. King, Jr., S. Cohen, *Nature London 276* (1978) 408-410.
[31] G. Carpenter, S. Cohen, *Annu. Rev. Biochem. 48* (1979) 193-216.
[32] G. Carpenter, L. King, Jr., S. Cohen, *J. Biol. Chem. 254* (1979) 4884-4891.
[33] L. King, Jr., G. Carpenter, S. Cohen, *Biochemistry 19* (1980) 1524-1528.
[34] S. Cohen, G. Carpenter, L. King, Jr., *J. Biol. Chem. 255* (1980) 4834-4842.
[35] M. Das, T. Miyakawa, C. F. Fox, R. M. Pruss, A. Aharonov, H. R. Herschman, *Proc. Natl. Acad. Sci. USA 74* (1977) 2790-2794.
[36] M. M. Wrann, C. F. Fox, *J. Biol. Chem. 254* (1979) 8083-8086.
[37] R. A. Hock, E. Nexo, M. D. Hollenberg, *Nature London 277* (1979) 403-405.
[38] T. Hunter, B. M. Sefton, *Proc. Natl. Acad. Sci. USA 77* (1980) 1311-1315.
[39] O. N. Witte, A. Dasgupta, D. Baltimore, *Nature London 283* (1980) 826-831.
[40] H. Ushiro, S. Cohen, *J. Biol. Chem. 255* (1980) 8363-8365.
[41] M. Chinkers, S. Cohen, *Nature London 290* (1981) 516-519.
[42] J. E. Kudlow, J. E. Buss, G. N. Gill, *Nature London 290* (1981) 519-521.
[43] S. Cohen, H. Ushiro, C. M. Stoscheck, M. Chinkers, *J. Biol. Chem. 257* (1982) 1523-1531.
[44] R. E. Gates, L. E. King, Jr., *Mol. Cell. Endocrinol. 27* (1982) 263-276.
[45] D. Cassel, L. Glaser, *J. Biol. Chem. 257* (1982) 9845-9848.
[46] S. A. Buhrow, S. Cohen, J. V. Staros, *J. Biol. Chem. 257* (1982) 4019-4022.
[47] S. A. Buhrow, S. Cohen, D. L. Garbers, J. V. Staros, *J. Biol. Chem. 258* (1983) 7824-7827.
[48] G. Carpenter, *Annu. Rev. Biochem. 56* (1987), in press.
[49] G. Carpenter, S. Cohen, *Biochem. Biophys. Res. Commun. 79* (1977) 545-552.
[50] R. A. Hock, E. Nexo, M. D. Hollenberg, *Nature London 277* (1979) 403-405.
[51] S. Cohen, R. A. Fava, S. T. Sawyer, *Proc. Natl. Acad. Sci. USA 79* (1982) 6237-6241.
[52] A. M. Soderquist, G. Carpenter, *J. Membr. Biol. 90* (1986) 97-105.
[53] G. Carpenter, J. G. Zendegui, *Exp. Cell. Res. 164* (1986) 1-10.
[54] T. Hunter, J. A. Cooper, *Annu. Rev. Biochem. 54* (1985) 897-930.
[55] A. Ullrich, L. Coussens, J. S. Hayflick, T. J. Dull, A. Gray, A. W. Tam, J. Lee, Y. Yarden, T. A. Liberman, J. Schlessinger, J. Downward, E. L. V. Mayes, N. Whittle, M. D. Waterfield, P. H. Seeburg, *Nature London 309* (1984) 418-425.
[56] J. Scott, M. Urdea, M. Quiroga, R. Sanchez-Pescador, N. Fong, M. Shelby, W. J. Rutter, G. I. Bell, *Science 221* (1983) 236-240.
[57] A. Gray, T. J. Dull, A. Ullrich, *Nature London 303* (1983) 722-725.
[58] L. B. Rall, J. Scott, G. I. Bell, R. J. Crawford, J. D. Penschow, H. D. Niall, J. P. Coghlaw, *Nature London 313* (1985) 228-231.
[59] K. A. Wharton, K. M. Johansen, T. Xu, S. Artavanis-Tsakonas, *Cell 43* (1985) 567-581.
[60] D. Greenwald, *Cell 43* (1985) 583-590.
[61] D. R. Twardzik, J. P. Brown, J. E. Rauchalis, G. J. Todaro, B. Moss, *Proc. Natl. Acad. Sci. USA 82* (1985) 5300-5304.
[62] M. B. Sporn, A. B. Roberts, *Nature London 313* (1985) 745-747.

Diene, Alkyne, Alkene, and Alkyl Complexes of Early Transition Metals: Structures and Synthetic Applications in Organic and Polymer Chemistry

By Hajime Yasuda* and Akira Nakamura*

An unprecedented series of highly reactive alkene- and diene-complexes of the early transition metals (Groups 3A–5A of the periodic system) have been isolated recently. Diene complexes of this sort (M = Ti, Zr, Hf, Nb, Ta) prefer, besides the (η^4-s-*cis*-diene)metal structure, either a novel bent η^4-metallacyclo-3-pentene structure or the unique (η^4-s-*trans*-diene)metal structure. In bis(diene)metal complexes of Nb and Ta the η^4-s-*cis*-dienes assume an unusual *exo-endo* (*supine-prone*) geometry. The M–C bonds in these diene-metal complexes generally exhibit highly polarized σ-bonding along with π-bonding character. The complexes therefore undergo a variety of regio- and stereoselective carbometalations with substrates containing C–C, C–O, or C–N multiple bonds. Examples of the products that can be obtained include ketones, vinyl ketones, unsaturated primary, secondary, and tertiary alcohols, as well as diols and unsaturated acids. Mechanistic studies on the stoichiometric and catalytic conversions of unsaturated hydrocarbons provides, inter alia, some insights into the course of polymerization reactions.

1. Introduction

Organic compounds of the early transition metals (groups 3A–5A of the periodic system) are currently attracting considerable attention because of their fascinating structural features, their mode of M–C bonding, and their unusually high selectivity in carbometalations; all these features distinguish them from the conventional middle and late transition metal complexes. The recent accelerated development of alkene–metal chemistry in this area is largely a consequence of the successful isolation of highly reactive novel species with suitable auxiliary ligands, especially cyclopentadienyl (Cp) and pentamethylcyclopentadienyl (Cp*) ligands. The first part of this article is concerned with new aspects of the structural chemistry of diene-, alkene-, and alkyne- as well as allyl- and pentadienyl-metal complexes of the early transition metals, while the second part deals with the unusual C–C coupling reactions that have been accomplished with these complexes. For an overview of the organometallic chemistry of the early transition metals in its entirety, the reader should consult some of the excellent monographs[1] and reviews on alkylmetal compounds,[2] carbene-complexes,[3] and metallacycles[4] that are available.

2. Remarkable Structural Features of Diene, Alkene, and Alkyne Complexes of the Early Transition Metals

2.1. Structures of η^4-Metallacyclo-3-pentene- and η^4-s-*trans*-Diene-Metal Complexes

Conjugated dienes, typified by 1,3-butadiene, may coordinate to a metal in several ways. The relative contribution of each of the limiting structures **1**–**6** would appear to depend upon the ligands of the metal and the substituents of the diene. The vast majority of middle and late transition metal-diene complexes assume the conventional (η^4-s-*cis*-1,3-diene) structure **1** or the ($1,2$-η^2-s-*trans*-1,3-diene) structure **6**, where the diene interacts with Fe, Ru, Rh, Mo, Mn etc. via alkene π-orbitals.[5] It is now apparent from

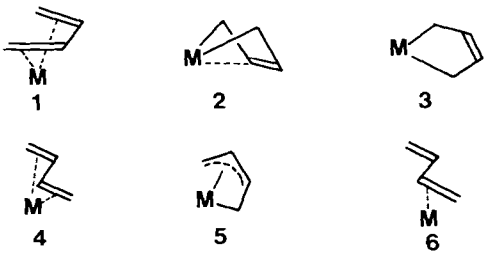

X-ray and NMR data that the diene complexes of early transition metals of groups 4A (Ti,[6] Zr,[7–9] Hf[10]) and 5A (Nb,[11] Ta[12]), like those of group 3A (U,[13] Th[13,14]), prefer the bent (σ^2,π-bonded)η^4-metallacyclo-3-pentene structure **2**, the planar (σ^2-bonded)η^2-metallacyclo-3-pentene structure **3** or the novel (η^4-s-*trans*-diene)metal structure **4**. Unequivocal evidence for the structure of type **5** is still lacking. Differentiation of the η^2-structure **6** from its σ-bonded counterpart (2-vinylmetallacyclopropane) seems improbable on the basis of the prediction made by *Dewar* et al.,[15] although the latter geometry is well known in 2-vinylphosphiranes.[16] Typical synthetic routes to these diene complexes involve the use of dienemagnesium reagents[7] or of pentadienyl anions,[17] the chemical or photochemical reduction of the corresponding precursor complex in the presence of the diene,[8,9] metal atom vapor techniques,[18] rearrangements of transitory divinyl complexes,[19] or β-hydride elimination from allylmetal compounds or metallacycles.[20] As typical example of such a

[*] Prof. Dr. H. Yasuda, Prof. Dr. A. Nakamura
Department of Macromolecular Science, Faculty of Science
Osaka University, Toyonaka, Osaka 560 (Japan)

 © VCH Verlagsgesellschaft mbH, D-6940 Weinheim, 1987 0570-0833/87/0808-0723 $ 02.50/0

synthesis, a route leading to the isoprenezirconium complex **7b** in high yields from dienemagnesium adducts[21] is outlined. This type of reaction finds universal application in preparative chemistry.

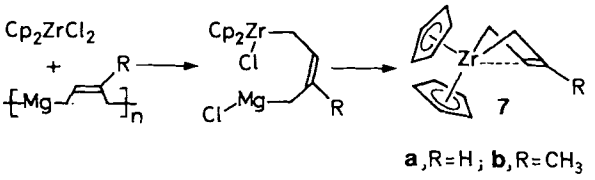

a, R=H; **b**, R=CH$_3$

The complexes **7** kinetically favor the η^4-s-*trans*-coordination **4** but thermodynamically they favor the s-*cis* metallacyclic structure **2**. Thus, the η^4-s-*trans*-butadiene complex of zirconocene can be converted by heating in solution, into the s-*cis*-complex, which, in turn, can be converted by irradiation with UV light into the η^4-s-*trans*-isomer.[9b] Alkyl or aryl substitution of the butadiene ligand in position 2 or positions 2 and 3 always leads to zirconacyclo-3-pentene complexes such as **7**. The strong steric repulsion between the C_5H_5 ligands (Cp) and the substituents (see, e.g., R) should be the crucial factor forcing this type of coordination instead of the η^4-s-*trans*-coordination. Substitution at C-1 or C-1 and C-4, on the other hand, induces preferential formation of the η^4-s-*trans*-diene complexes by conjugation or hyperconjugation.[22]

This situation changes drastically upon replacing Zr by Ti, Ta or Nb. The relative ratios of the s-*cis* and s-*trans* isomers of the complexes are listed in Table 1. Typical examples for the molecular structures of the s-*cis* (type **2**) and s-*trans*-diene complexes (type **4**) are shown in Figures 1[6a] and 2,[7d] respectively.

Table 1. Proportion of s-*cis*-isomers of type **2** in

[$ML_2(R^1CH{=}CR^2{-}CR^3{=}CHR^4)$], M = Ti, Zr, Hf, and
[$ML(R^1CH{=}CR^2{-}CR^3{=}CHR^4)_2$], M = Nb, Ta.

Cp = C_5H_5, Cp* = $C_5(CH_3)_5$.

M	L	R^1	R^2	R^3	R^4	s-*cis* [%] [a]
Zr	Cp	H	H	H	H	0–100 [b]
		CH_3	H	H	CH_3	36
		CH_3	H	H	H	39
		Ph	H	H	Ph	2
		H	CH_3	H	H	100
		H	CH_3	CH_3	H	100
		CH_3	CH_3	H	H	100
Zr	Cp*	H	H	H	H	0
		H	CH_3	H	H	100
Hf	Cp	H	H	H	H	0–100 [b]
		H	CH_3	H	H	100
Ti	Cp* }	H	H	H	H	100
	Cl, Br, I } [c]	H	CH_3	H	H	100
		Ph	H	H	Ph	100
Nb	Cp*	H	H	H	H	100
		H	CH_3	H	H	100
Nb	Cp	H	CH_3	CH_3	H	100
Ta	Cp	H	H	H	H	100
	Cp*	H	H	H	H	100

[a] The other component is the s-*trans*-isomer (Type **4**). [b] The proportion of s-*cis*-isomer varies, depending upon the method of preparation and the temperature of measurement. [c] Formulas of the Ti compounds: [$TiCp^*Cl(R^1CH{=}CR^2{-}CR^3{=}CHR^4)$] and bromo and iodo analogues.

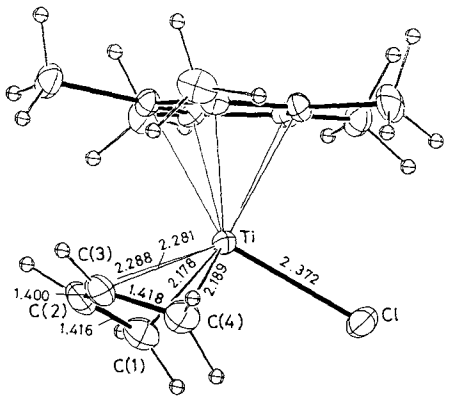

Fig. 1. Molecular structure of a typical s-*cis*-diene complex of type **2**, [$TiCp^*Cl$(butadiene)] (cf. **11b**).

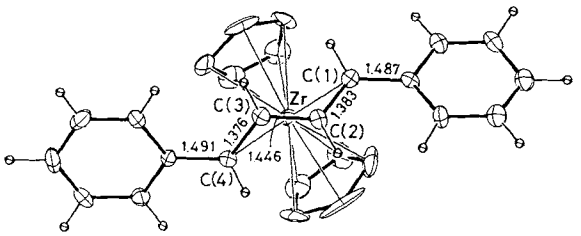

Fig. 2. Molecular structure of a typical s-*trans*-diene complex of type **4**, [$ZrCp_2$(1,4-diphenylbutadiene)].

The η^4-metallacyclo-3-pentene complexes **2** of elements of groups 3A–5A generally exhibit fluxional behavior, which may be attributed, on the basis of variable temperature ^{1}H-NMR studies, to rapid ring inversion (flipping) via a transitory planar metallacyclopentene species **3**. From

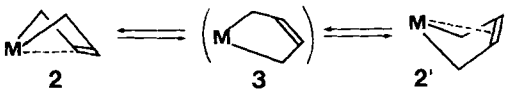

the shape of the signal pattern, a simple rotational mechanism can be ruled out. More exact direct evidence for ring inversion has recently been provided by a sterochemical labeling experiment with a [CoCp(1,3-diene)] complex whose 1,3-diene ligand was deuteriated in positions 1 and 4.[23] The typical free energy of activation, ΔG^+ (at the coalescence temperature), for the ring inversion in zirconacyclo-3-pentenes such as **7** varies in the range 6.5–17 kcal/mol.[9]

Very unusual is the large value (>25 kcal/mol) for [MCl_2Cp^*(s-*cis*-butadiene)], M = Ta, Nb; Cp* = C_5Me_5.[24] Such a fluxional behavior could arise from the strong σ-bonding character of the M–C bonds at the diene termini. The ^{13}C-^{1}H coupling constant clearly confirms the enhanced sp^3 character of C-1 and C-4.[25] The value of n for sp^n hybridization of the carbon is in the range 2.0–2.2 in the case of conventional diene complexes of the late transition metals (Fe, Rh, etc.), but it reaches 2.7–3.0 in the case of [MCp_2(2,3-dimethylbutadiene)], M = Zr, Hf, and [$ZrCp_2^*$(isoprene)], which remain fluxional even at −90 °C.

The fluxional structure is also apparent in crystallographic data and it is reflected in the dihedral angle (θ) subtended by the C1–M–C4 and C1–C2–C3–C4 planes and the difference in the M–C bond distances (Δd), defined by

$$\Delta d = [d(\text{M–C1}) + d(\text{M–C4})]/2 - [d(\text{M–C2}) + d(\text{M–C3})]/2$$

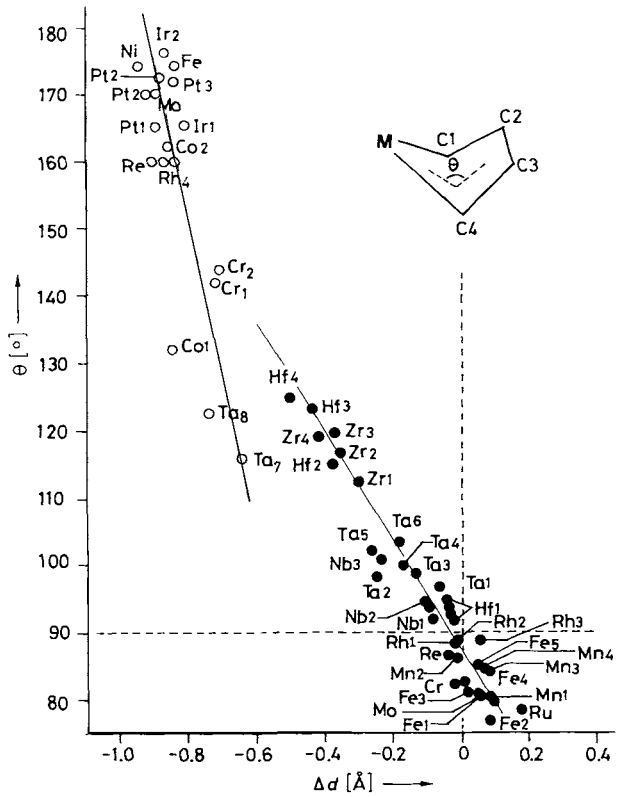

Fig. 3. Correlation plots between dihedral angle (θ) and difference in metal-carbon distances (Δd) in dienemetal complexes of type **1** or **2** (●) and metallacyclopentanes of type **8** (○). Data are selected from Cambridge Crystallographic Database (see ref. [26] for the structural details). The numbers next to the element symbols identify the complexes used.

As shown in the correlation plots (Fig. 3), the dihedral angles for s-*cis*-diene complexes (type **1**) of the late transition metals fall in the narrow range of 75–90°, and Δd lies between −0.1 and 0.1 Å, i.e. the M–C1 and M–C4 bonds are nearly equal or slightly longer than the M–C2 or M–C3 bond.[12,26] On the other hand, the corresponding dihedral angles for the complexes of the early transition metals always exceed 90°, with a corresponding change in Δd of −0.4 to 0 Å. Thus, the dihedral angles increase with decreasing Δd. The dihedral angle of the metallacyclopentanes (type **8**), where no interaction takes place between the metal and the inner carbon atoms, is in the range 140–175° for late transition metals, since the four carbon atoms are not coplanar, as in **8b** (the angle given refers to "best planes").[26] In the case of tantala- or cobaltacyclopentanes

8a **8b**

(type **8a**), θ lies in the range 115–130°; this is nearly the same range as for [MCp_2(s-*cis*-butadiene)], M = Zr, Hf. We can conclude, therefore, that the diene complexes of metals of group 4A exhibit rather weak interaction between the metal atom and the inner carbon atoms, consistent with their high fluxional properties, whereas the diene complexes of metals of group 5A exhibit a rigid structure because of the strong π-interaction between the inner carbon atoms and the metal atom. There is also an approximate linear correlation between the dihedral angle (θ) and the difference in the C–C bond lengths (Δl), defined by

$$\Delta l = [l(\text{C1–C2}) + l(\text{C3–C4})]/2 - l(\text{C2–C3})$$

In the case of diene complexes of the late transition metals, Δl lies between −0.1 and 0.0 Å, while in those of the early transition metals it falls in the range 0.0–0.2 Å. Thus, the dihedral angle increases with increasing Δl.[12,26] A fairly good linear correlation is also observed between the values of n for sp^n hybridization of the diene terminal carbons and Δd and Δl.

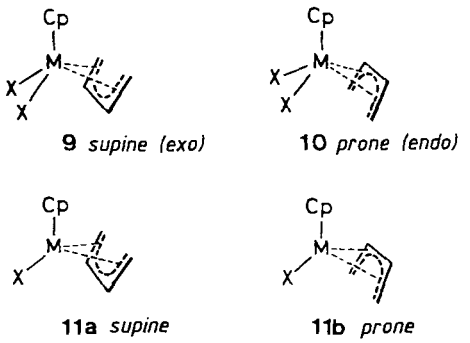

9 *supine (exo)* **10** *prone (endo)*

11a *supine* **11b** *prone*

The diene complexes of metals of group 5A always have the metallacyclo-3-pentene structure **2**. Two orientations are possible for [MCl_2Cp(diene)], M = Ta, Nb: *supine* and *prone* (we propose this nomenclature because the classical *exo* and *endo* nomenclature does not adequately characterize this type of conformation). A comparison of the total energy of [$TaCl_2$Cp(butadiene)] for the *supine* (*exo*)-type **9** and *prone* (*endo*)-type **10** on the basis of an EHMO calculation revealed that the former is more stable than the latter by 15.7 kcal/mol due to the large overlap integrals S(2a″-π_3^*) of **9a** and S(1a′-π_3^*) of **9b** respectively.[12]

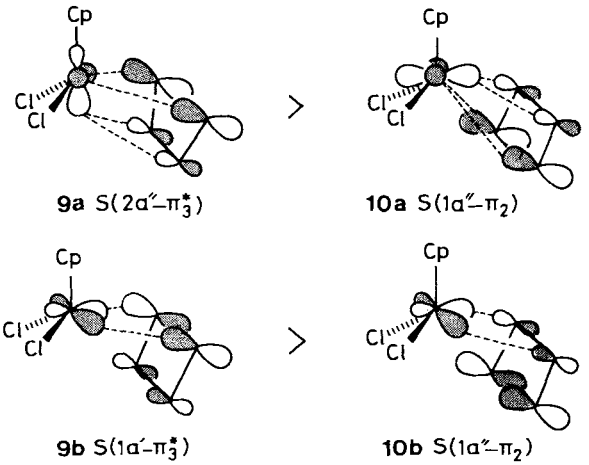

9a S(2a″–π_3^*) **10a** S(1a″–π_2)

9b S(1a′–π_3^*) **10b** S(1a″–π_2)

The dimeric niobium complex $[NbClCp^*(butadiene)]_2$,[11] $[TiClCp^*(diene)]$, diene = isoprene, 2,3-dimethylbutadiene,[6a] as well as $[HfClCp^*(2,3\text{-dimethylbutadiene})]$,[6b] and the molybdenum complex $[MoCp(CO)_2(butadiene, 1,4\text{-diphenylbutadiene})$ exhibit a unique *prone* to $[TaCl_2Cp(C_4H_6)]$[12] as a result of steric repulsion between Cp* or Cp and the methyl groups of the diene ligands, while $[TiClCp^*(diene)]$ complexes (diene = butadiene, 1,4-diphenylbutadiene) exhibit a unique *prone* (*endo*) orientation **11b** (cf Fig. 4).

When a metal complex contains more than one diene, there are many possibilities for its coordination geometry. Thus, the complexes $[LM(diene)_2]$ may assume square-pyramidal or trigonal-bipyramidal structures if the diene ligand is assumed to occupy two coordination sites via its terminal carbon atoms. The bis(diene)metal complexes reported so far all prefer the square-pyramidal structure: the two diene ligands orient themselves in a parallel *supine-supine*(or *exo-exo*) fashion (**12**) with nearly C_{2v} symmetry, while L occupies the apical position. The novel *supine-prone* (*exo-endo*) orientation (**13**), observed for the first time in $[Ta(C_5R_5)(diene)_2]$ (R = H, Me; diene = butadiene, isoprene, 2,3-dimethylbutadiene),[12] has recently also been found in the analogous niobium complexes.[11] A similar *supine-prone* orientation is also found in the mixed-ligand zirconiumcomplex$[ZrCp^*(\eta^4\text{-butadiene})(\eta^3\text{-allyl})]$.[9f]

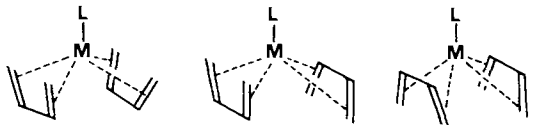

$[Hf(diene)_2(dmpe)]$, an unusual complex with the formula $[L_2M(diene)_2]$, prefers octahedral geometry[8] (dmpe = 1,2-bis(dimethylphosphino)ethane is a bidentate ligand). Bis(diene)metal complexes with a *prone-prone* (*endo-endo*) orientation (**14**) or a trigonal-bipyramidal conformation are still unknown. The relative stabilities of the conformations estimated from EHMO calculations for $[TaCp(butadiene)_2]$ indicate that the *supine-prone* conformation is more stable than the *prone-prone* or *supine-supine* conformation by 23.3 and 28.2 kcal/mol, respectively, whereas for $[RhCl(butadiene)_2]$, the *supine-supine* conformation is more stable than the *prone-prone* or *prone-supine* conformation by 25.8 and 27.2 kcal/mol, respectively.[7c] The calculated overlap population indicates that $[TaCp(butadiene)_2]$ favors the bent η^4-metallacyclo-3-pentene structure of type **2**, while $[RhCl(butadiene)_2]$ prefers the conventional η^4-s-*cis*-diene coordination of type **1**, in agreement with the crystallographic data. An unusual mixed diene complex, $[TaCp^*(butadiene)(2,3\text{-dimethylbutadiene})]$, also assumes the *prone-supine* structure, as shown in Figure 4.[28]

The s-*trans*-diene coordination to mononuclear species (type **4**), first found in complexes of the early transition metals in the case of $[ZrCp_2(1,4\text{-diphenyl-1,3-butadiene})]$[7d] and $[ZrCp_2(butadiene)]$,[9b] has recently also been found in $[HfCp_2(butadiene)]$[29] and $[MoCp(NO)(2,4\text{-dimethyl-2,4-hexadiene})]$;[30] a bridging s-*trans*-diene coordination, on the other hand, had already been reported for several binuclear and trinuclear metal complexes. $[Mn_2Cp_2(CO)_4(butadiene)]$[31] and $[(Pt_2Cl_6)_2(butadiene)]^{2\ominus}$[32] are typical examples for complexes of type **15**, while $[Mn_2(CO)_8(butadiene)]$[33] and $[Os_3(CO)_{10}(butadiene)]$[34] represent complexes of the type **16**. (The third Os atom does not participate in the coordination.) The s-*trans*-diene molecule coordinated to $ZrCp_2$ or MoCp(NO) has a non-

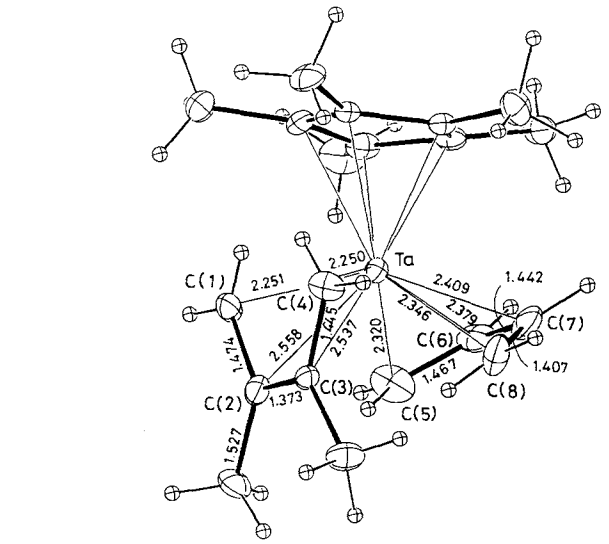

Fig. 4. Molecular Structure of a bis(diene) complex of type **13**, [TaCp*(butadiene)(2,3-dimethylbutadiene)].

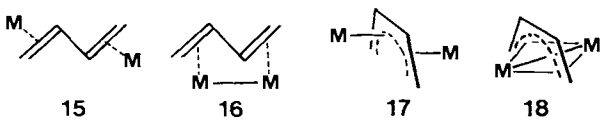

planar arrangement with torsional angles of ca. 124–126° (cf. Fig. 2). As a consequence, the bond lengths of M–C1 and M–C4 are very similar to those of M–C2 and M–C3. In sharp contrast to the behavior of the $[ZrCp_2(diene)]$ complexes, [MoCp(NO)(diene)] thermodynamically favors the s-*trans* coordination rather than s-*cis* coordination (in agreement with Fenske-Hall MO calculations).[30a] The HOMO energy of the former is ca. 0.9 eV lower than that of the latter. The asymmetry of the *trans*-diene ligand enables stabilization of the high-lying occupied orbitals of the MoCp(NO) fragment. The discovery of s-*trans*-diene coordination to mononuclear complexes of the early transition metals is of special importance, since it provides a new aspect of the reaction mechanism of the titanium- or zirconium-assisted oligomerization and polymerization of dienes (see Sections 5.3 and 6.1).

A novel type of binuclear metal complex containing a *cis*-coordinated diene (**17**), $[Rh_2(i\text{Pr}_2\text{PCH}_2\text{CH}_2\text{CH}_2\text{P}i\text{Pr}_2)_2(butadiene)]$, has appeared recently.[35] The butadiene unit is sandwiched between the two rhodium centers; the metal atoms interact with the twisted s-*cis*-butadiene (torsion angle of 45.0°) in an η^3-fashion. Coordination of a bridging s-*cis*-diene to M–M bonded binuclear complexes (**18**), e.g. $[Co_2Cp_2(CO)(butadiene)]$,[36] has also been reported.

The collection of structural details on s-*cis*- and s-*trans*-diene complexes and mononuclear and dinuclear metal species has thus only recently been completed. This information is indispensable for gaining an insight into the reaction mechanism of the oligomerization, polymerization and carbometalation of dienes by early transition metals.

2.2. Characteristic Properties of the M–C Bonding of Alkenemetal- and Alkynemetal-Complexes, and Related Complexes

Several reactive alkene complexes of the early transition metals (M = Ti,[37,38] Ta,[39] Nb[40,41]) have become available in recent years, while a number of alkene complexes of the late transition metals, represented by Zeise's salt, are already well documented. Table 2 lists the structural data for selected ethylene complexes together with the values for the chemical shift in the ^{1}H-NMR spectrum; α is the angle between the normals of the H–C–H planes shown in **19**. It is clear from the data in Table 2 that electron-rich

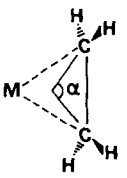

19

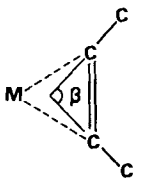

20

Table 2. C-C bond distances, dihedral angle α (see **19**) and ^{1}H-NMR data (δ-values) for ethylene-transition metal complexes.

	C-C [Å]	α [°]	δ
$CH_2=CH_2$	1.337	0	123
$[Ni(dmpe)_2PPh_3(C_2H_4)]$ [a]	1.320	3.3	—
$[IrCl(PPh_3)_2(C_2H_4)]$	1.376	24.2	—
$[RuCl_2(CO)(PMe_2Ph)_2(C_2H_4)]$	1.376	24.2	58.6
$[Mo(PMe_3)_3(CO)(C_2H_4)]$	1.403	59.07	—
$[NbCpC_2H_5(C_2H_4)]$	1.407	52.5	29.4
$[TiCp^*_2(C_2H_4)]$ **43**	1.408	70	105.1
$[TaCp^*(CHCMe_3)(PMe_3)(C_2H_4)]$	1.477	68.5	—
Cyclopropane	1.510	—	−3.5

[a] dmpe = 1,3-bis(dimethylphosphino)propane.

ethylenemetal complexes exhibit relatively large α values and significant lengthening of the ethylene C–C bond; this confirms the enhanced sp^3 character of the carbon atoms. In general, the α value increases with increasing C–C bond length. The δ values—apart from in the case of the Ti complex **43**—are also consistent with the structural data. (In **43** the downfield shift could be explained in terms of the deshielding effect of the Cp* ring.) The enhanced carbon sp^3 hybridization must arise from substantial electron back-donation from the metal.

Alkynemetal complexes show a similar trend with respect to the metal–carbon bonding. In the case of the electron-rich metal complexes there is usually a considerable lengthening of the acetylenic C–C bonds; however, the bite angle β (angle between the two C–C bonds in **20**) is hardly influenced by the metal and ligands.[26,42]

Let us now turn to the allylmetal complexes! For allylmetal complexes, primarily two limiting structures, **21** and **22**, are possible (see also Ref. [43a] for classification of the

21

22

allylmetal complexes). The mode of M–C bonding varies depending upon the valence state of the metal and the hapticity of the ligand. Formally, the Zr^{IV} complexes $[ZrCp_2(CH_2CH{=}CHCH_3)_2]$ and $[ZrCp_2Cl(CH_2CH{=}CHCH_3)]$ exist in a σ-2-butenylmetal form (**21**) at low temperatures.[43b,c] However, low valent allylmetal species, for example $[TiCp_2\{CH_2C(CH_3){=}CHCH_3\}]$, exist in a η^3-*syn* form (**22**).[44] In general, in the compounds of the early transition metals and some nickel compounds,[45] the bond distances between metal and η^3-allyl terminal carbons are nearly equal to or a little shorter than that between the metal and the central carbon atom, while this trend is reversed in the compounds of the electrophilic late transition metals.[26]

When the conjugation is extended further to pentadienyl systems, the ligand should be capable of binding to a metal in σ-, η^3-, and η^5 modes. The structural preference depends on the valence state of the metal and the π-acceptor properties of the ligands. Thus, the ligand in $[ZrCp_2(2,4\text{-pentadienyl})_2]$ and its alkyl-substituted derivatives always prefer the terminally σ-bonded zigzag-like (*E*)-geometry (**23**),[17] while $[M(2,4\text{-dimethylpentadienyl})_2]$, M = V, Cr, Fe, Ti, and $[M(PR_3)(2,4\text{-dimethylpentadienyl})]$, M = Zr, Nb, prefer the U-shaped (**25**) or S-shaped (**26**) η^5-bonded structure, because this type of coordination is effective in stabilizing

23

24

25

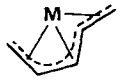

26

the naked or highly coordinatively unsaturated metal species.[46] Note that $[Ti(\eta^5\text{-pentadienyl})_2]$ derivatives are isolable, while $[Ti(\eta^5\text{-cyclopentadienyl})_2]$ is thermally unstable. Transition metal complexes of type **24**, which contain *syn*- or *anti*-η^3-pentadienyl ligands, include $[Fe(PMe_3)_2(C_5H_7)_2]$,[47] $[Co(PMe_3)_3(C_7H_{11})]$,[48] $[Co(CO)_2(PPh_3)(C_5H_7)]$,[49] and $[Mn(CO)_3(PMe_3)(C_5H_7)]$.[50] The manganese complex is converted into the η^5-coordinated isomer upon heating in solution, while the thermodynamic stability is reversed in the case of the cobalt complex. The corresponding change in hapticity for Cp ligands has not yet been well established, except for $[(\eta^3\text{-Cp})(\eta^5\text{-Cp})W(CO)_2]$,[51a] $[MCp_4]$, M = Ti, Zr, Hf,[51b] and some indenyl complexes.[51c-d]

3. Selective Carbometalation of Organic Substrates Containing C–O and C–N Multiple Bonds with Organic Compounds of the Early Transition Metals

3.1. Regio- and Stereoselective Addition of Diene Complexes to Carbonyl Compounds, Nitriles, and Oxiranes

Carbometalation with organic compounds of metals of groups 3A–5A is one of the more important strategies in modern organic synthesis. The metal–carbon bond in these compounds is generally polarized as $M^{\oplus}$–$C^{\ominus}$ and hence renders the carbon site susceptible to electrophilic attack. Dienezirconium complexes, especially those with an unsymmetrical diene, e.g. isoprene, may serve as models for demonstrating the unique chemical behavior of complexes of the early transition metals, for they can readily rearrange into various geometrical isomers (see **1**–**6**) depending on the reaction conditions, and can afford a variety of products upon reaction with numerous unsaturated organic and inorganic molecules. As typical examples of such reactions, the carbometalation of oxygen-containing compounds with [$ZrCp_2$(isoprene)] **7b** and related reactions are illustrated in Scheme 1.[7a] The most striking feature is the exceptionally high regioselectivity (>95%) in the reactions with saturated and unsaturated aldehydes, ketones, and nitriles. The yields exceed 90% in all reactions. The reaction proceeds irreversibly at the sterically more congested 1-position of the isoprene rather than at the sterically favorable 4-position. Subsequent acid cleavage of the product of aldehyde or ketone insertion furnishes 3-methyl-4-penten-1-ol derivatives selectively (>90%), while base-catalyzed cleavage with secondary amines (e.g. pyrrolidine, piperidine) leads to 3-methyl-3-penten-1-ol derivatives.[52a] Esters and nitriles also react at C-1 of the isoprene and afford acylated compounds upon hydrolysis of the adduct.[52b] The mode of this reaction markedly differs from that of the well documented Grignard reaction or the reaction of [$ZrCp_2$(2-butenyl)$_2$] with

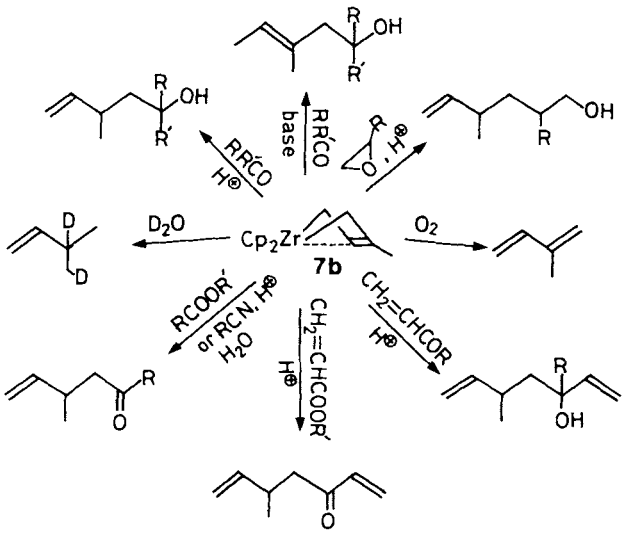

Scheme 1. Nucleophilic addition of [$ZrCp_2$(isoprene)] **7b** to oxygenated or nitrogenated unsaturated compounds.

esters, which leads to tertiary alcohols by double allylation. Some of the alkyllanthanoids react analogously with esters, with monoalkylation to give products which can be hydrolyzed to acylates.[53] Especially noteworthy is the highly selective 1,2-addition (>95%) observed in the reaction of dienezirconium complexes with α,β-unsaturated ketones and esters. The regiochemical selectivity may be ascribed to the high ionicity of the Zr–C bond and the high oxophilicity of the zirconium metal together with the rigid tetrahedral geometry of the complexes, since simple [$RTiCl_3$][54] and alkyllanthanoids[55] are also able to promote the selective 1,2-addition to enones. The carbometalation of oxiranes (R = aryl or vinyl) with the isoprenezirconium complex **7b** leads, with 99% regioselectivity, to C–C bond formation between C-1 of the isoprene and C-2 of the oxirane.[56] Thus, the subtle electronic and steric difference existing between C-1 and C-4 of isoprene could be clearly enhanced by complexation to zirconium. Analogous diene complexes, for example [TiCp*Cl(diene)], [$HfCp_2$(diene)], [$TaCl_2Cp$(diene)], [TaCp(diene)$_2$], and [$NbCp$(diene)$_2$], also promote the selective carbometalation, although diene complexes of metals of group 5A generally show relatively low reactivity toward these electrophiles.[57] The selective carbometalation with [$M(OR)_2$(diene)], M = Ti, Zr, generated in situ from $M(OR)_4$ or $M(OR)_2Cl_2$ and dienemagnesium, could be useful for large-scale organic syntheses.

Two reaction pathways seem conceivable: insertion into the *cis*-dienemetal species (Type **2**), and insertion into the s-*trans*-isomer (type **4**). In order to obtain information on the reaction pathways, the reactions of the analogues of **7**, [$ZrCp^*_2$(isoprene)] (100% *cis*) and [$ZrCp^*_2$(butadiene)] (100% s-*trans*), with 2,4-dimethyl-3-pentanone were examined.[25] Both diene complexes are thermally stable even at 90 °C but readily react with the ketone at 30 °C. If the reactions proceed straightforwardly with retention of configuration, each of the stereoisomers might give rise to (*Z*)- and (*E*)-oxazirconacycloheptenes, **27** and **28** respectively. The X-ray analyses of the above two insertion products clearly confirm that both compounds have essentially the same configuration at the double bond, namely a (*Z*)-configuration as in **27** (Fig. 5). Hence, the s-*trans*-diene complex undergoes reaction with change of configuration, while the *cis* isomer retains its geometry. A similar (*Z*)-oxazirconacycloheptene structure is also found in a diphenyl ketone adduct of [$ZrCp_2$(butadiene)] **7a**.[58] However, we cannot immediately conclude that the (*Z*)-form of the isoprene adduct is a direct consequence of the *cis*-structure of the precursor, since an isomerization via **27b** is probable (*vide infra*).

In sharp contrast to the thermally induced reactions, a photoinduced reaction occurs preferentially (78%) at the sterically less crowded 4-position at −70 °C. At this temperature the thermal reaction is completely suppressed.[59] The s-*trans* isomer of the isoprene complex (generated photochemically) also furnishes predominantly the same regioisomer **32b**, even in the absence of light. Thus, the geometry of the coordinated dienes is the crucial factor in determining the regiochemistry. A [2+2]-type oxidative coupling process has been proposed for both the photochemically- and the thermally-induced addition of the s-

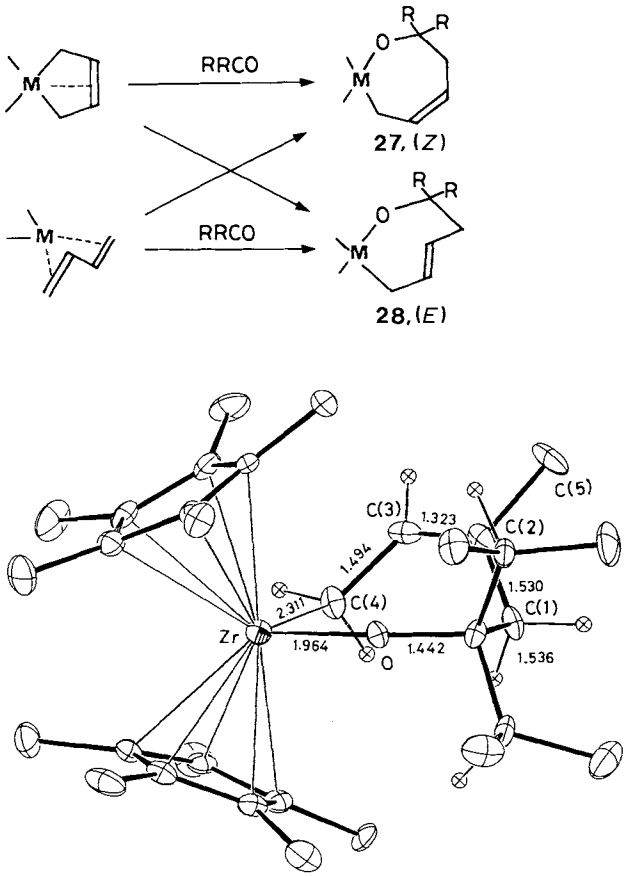

Fig. 5. Molecular structure of a (*Z*)-configurated complex of type **27**, $[Cp_2^*ZrOC(iPr)_2CH_2C(CH_3)=CHCH_2]$. The complex is formed by ketone insertion.

trans-diene complexes, since the regiochemistry is consistent with that found in the addition of the diene complex to unsaturated hydrocarbons (see Section 4). The insertion should proceed via **31**. A competition experiment with a mixture of s-*trans*- and *cis*-butadiene complexes confirmed the higher reactivity of the s-*trans* isomer.[58] On the basis of these findings, a four-centered insertion mechanism or a dipolar mechanism has been proposed for the thermally induced addition reaction of the *cis*-diene complexes. The coupling of a planar zirconacyclo-3-pentene species of type **3** with a carbonyl group via the four-centered transition state **29a** and further reaction via **29b** seems most likely. The C–C bond formation occurs at C-1 with cyclization to give **30**, since substantial negative charge accumulates on the C-1 atom rather than the C-4 atom by the inductive effect of the methyl group. Since the LUMO of [Cp_2Zr(s-*cis*-butadiene)] **7a** has a similar shape as $1a_1$ of the "Cp_2Zr" fragment,[60] the carbonyl group can approach the metal only in the C1–Zr–C4 plane, as shown in **29a**. Actually, such a planar arrangement of the three M–X bonds is commonly seen in pentacoordinated zirconocene derivatives.[61] The attack of allylic carbon atoms (C-2 or C-3) via the usual nonplanar six-membered transition state is forbidden because of this orbital symmetry requirement.

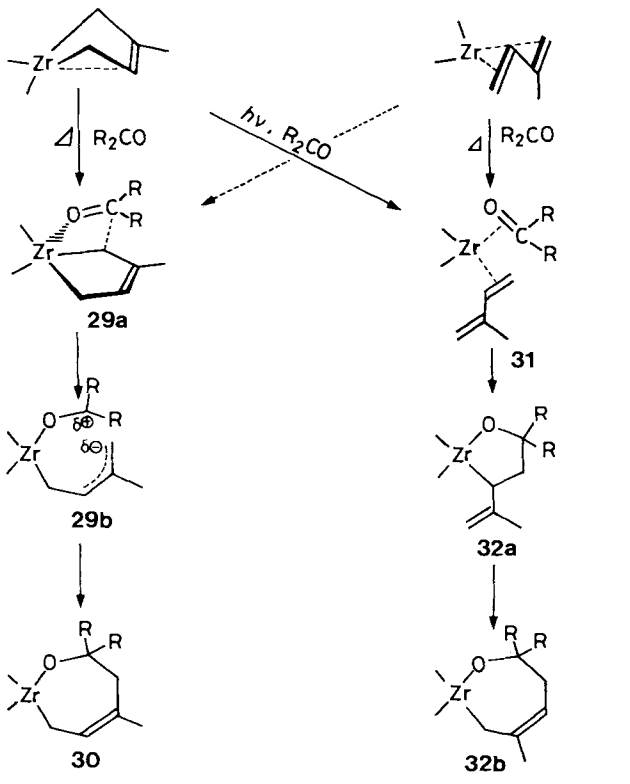

The result of the carbometalation of *cis*- and *trans*-2-methyl-3-phenyloxirane with the isoprene complex **7b** may support the above dipolar insertion mechanism.[56h] The insertion to give **33b** occurs with excellent regioselectivity (100%), but the configuration at C-2 and C-3 of the oxirane is destroyed during the reaction. To explain the free rotation around the oxirane C–C bond prior to the coupling, which leads to a mixture of the diastereoisomers (1 : 2 ratio), a transition state **33a** has been proposed.

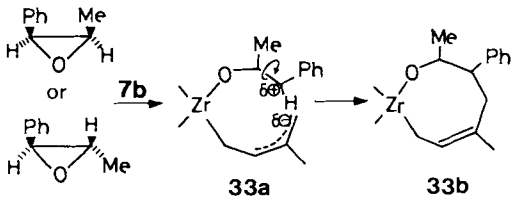

Isoprene-, 2,3-dimethylbutadiene-, and 3-methyl-1,3-pentadienezirconium complexes (with s-*cis* geometry) undergo only the 1 : 1 addition reaction of carbonyl compounds, even when the reaction is carried out at higher temperatures (≈ 100 °C) in the presence of excess carbonyl compound, whereas s-*cis*-butadiene-, pentadiene-, and 2,4-hexadiene-complexes (ca. 1 : 1 mixture of the s-*cis* and s-*trans* isomers) readily add two equivalents of butanal or 3-pentanone in high yields (95%) at lower temperature (30 °C).[17] Especially noteworthy is that the s-*cis*-butadiene complex predominantly forms an (*E*)-dioxazirconacyclo-4-nonene (**35**) as a result of double insertion; upon hydrolysis, **35** selectively affords (*E*)-3-hexene-1,6-diol derivatives. If the second incoming carbonyl compound directly attacks the (*Z*)-oxazirconacycloheptene **27a**, the (*Z*)-analogue of **35** ought to be formed. This controversy can be resolved by assuming an insertion process via a six-membered transition state in a chair form (**34**). The mode of this reaction is, in principle, the same as that postulated for the *threo*-selective incorporation of aldehydes and ketones into zirconium-[43b,62a] or titaniumallyl compounds[62b–c]

such as $[ZrCp_2(2\text{-butenyl})_2]$, $[ZrCp_2Cl(2\text{-butenyl})]$, and $[TiCp_2(2\text{-butenyl})]$. In the case of ketone or aldehyde adducts of isoprene- and 2,3-dimethylbutadiene-complexes, the equilibrium between **27a** and **27b** may be shifted to the

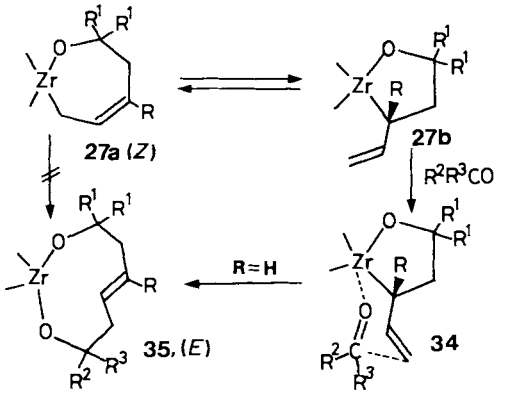

thermodynamically more favored species **27a**, because the steric repulsion between Cp and tertiary α-carbon interferes with the generation of 3-vinyl-1,2-oxazirconacyclopentanes (**27b**, R = Me). In fact, five- and six-membered 1,2-oxazirconacycloalkenes, $Cp_2\overline{ZrO(CH_2)_n}$ (n = 3, 4, 5) without vinyl component,[63] are completely inert to carbonyl compounds under normal reaction conditions. Despite the presence of a methyl group at C-2, s-*cis*-2-methyl- and s-*cis*-2,4-dimethyl-1,3-pentadienezirconium complexes can promote double insertion, since the carbonyl compound is first attacked predominantly at C-4, affording an intermediate with a conformation similar to **34** (R = H).[64] As an extension of this reaction, the successive insertion of two kinds of electrophiles, e.g., isobutanal/3-pentanone, ethyl acetate/isobutanal, and 3-pentanone/acetonitrile, into both ends of the butadiene molecule to give **35** has been realized by treating $[ZrCp_2$(s-*cis*-butadiene)] with a carbonyl compound at 0°C in hexane and then with the other electrophile in THF at 60°C. However, attempts to carry out addition of the electrophiles in the reverse order, e.g. isobutanal/ethyl acetate or acetonitrile/3-pentanone, met without success.[64]

3.2. Addition of Diene Complexes to CO_2 and Heterocumulenes

Alkenyl- and aryltitanium compounds readily react with CO_2, thus reflecting their high oxophilicity, while alkylzirconium derivatives are not reactive enough for practical purposes.[65] Dienezirconium complexes undergo a variety of reactions, resulting in 1 : 1, 1 : 2 or 2 : 1 addition depending on the bulkiness of the Cp ligand, the geometry of the coordinated diene, and the nature of the alkyl substituents on the diene. $[ZrCp^*_2$(butadiene)] (**36**), containing a bulky pentamethylcyclopentadienyl group together with an s-*trans*-diene ligand, undergoes the 1 : 1 addition reaction, even when excess CO_2 is introduced at elevated temperatures. The reaction should proceed via **37** by oxidative [2 + 2]-coupling or directly with generation of a 3-vinyl-1,2-oxazirconacyclopentan-5-one (**38a**), which immediately

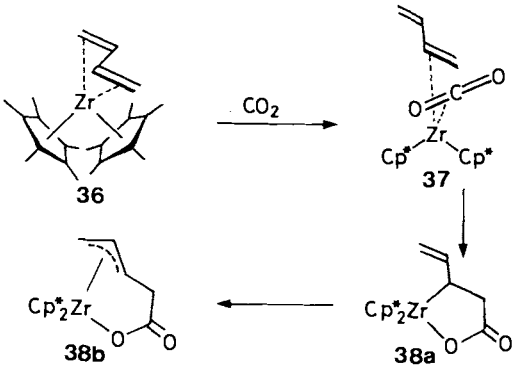

rearranges into the more stable complex **38b**. The C=O group in **38b** is bent away from the metal, as confirmed by the X-ray structure analysis (Fig. 6).[66] A similar metal-

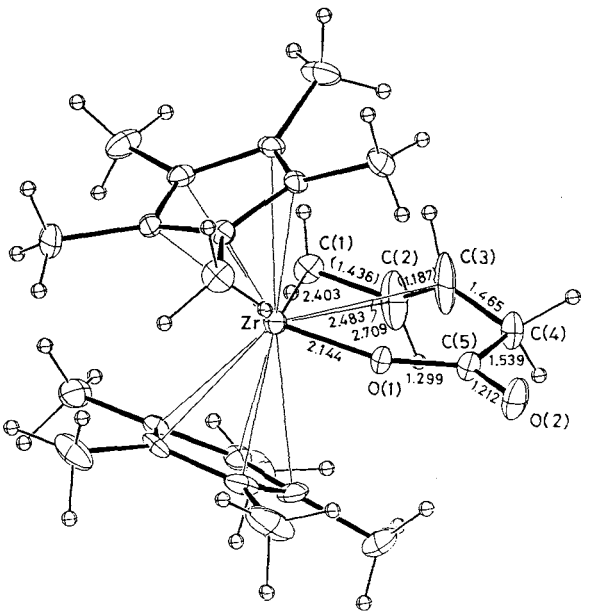

Fig. 6. Molecular structure of the complex $[Cp^*_2\overline{ZrOCOCH_2CH{=}CH{=}CH_2}]$ **38** formed by CO_2 insertion.

carbon linkage is also found in the product of the stoichiometric reaction between $[MCp_2$(butadiene)], M = Zr,[67] Th,[14] and $[M(CO)_6]$, M = Cr, Mo, W. In sharp contrast to the above reaction, a double insertion of CO_2 yielding **40** occurs at the diene termini when $[ZrCp^*_2$(s-*cis*-isoprene)] or $[ZrCp^*_2$(s-*cis*-2,3-dimethylbutadiene)] is used. This drastic difference may be attributed to the conformational instability of the transient 1 : 1 adduct **39** (i.e. the steric repulsion between the methyl group at the α-carbon atom and the Cp* ligand cannot stabilize the conformation **39** and hence forces a further reaction.[68]

When the Cp* ligand is replaced by a less bulky Cp li-

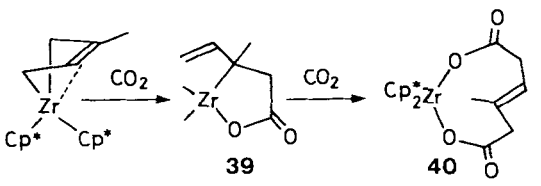

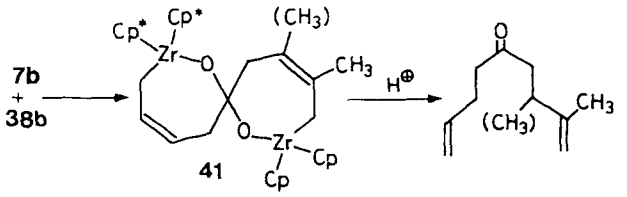

gand, all the [$ZrCp_2$(s-*cis*-diene)] complexes examined undergo the 2:1 addition reaction leading to dioxadizirconaspiroalkadienes. An example is complex **41**. A reaction pathway for this insertion has been proposed which is based on the stoichiometric reaction between **38b** and **7b**. This sequence affords the expected spiro compound **41**, which yields a mixture of butenyl 2-methylbutenyl ketone and butenyl 3-methylbutenyl ketone in ca. 5:3 ratio on hydrolysis. Thus, a delicate balance of the electronic and steric effects determine the reaction course.

A heterocumulene, RN=C=O (R = Me, *t*Bu, Ph), readily reacts with both [$ZrCp_2$(s-*cis*-butadiene)] **7a** and [$ZrCp^*_2$(s-*trans*-butadiene)] **36** to give *syn*-allyl compounds of type **42b**, while reaction of [ZrL_2(isoprene)], L = Cp, Cp*, with *t*BuNCO gives oxazirconacycles **42a** with (*Z*)-geometry. When **7a**, **7b**, **36**, or **42b** was treated with an excess of reactive PhNCO the 1:2 adduct **42c**, R = Ph, with (*E*)-geometry was obtained in high yield. These results indicate that the conformational stability of the adducts, and not the configuration of the precursor dienemetal complexes, is the crucial factor in determining the geometry [(*E*) or (*Z*)] of the products.[69] The direct transformation of **42a** into **42c** seems very unlikely on steric grounds.

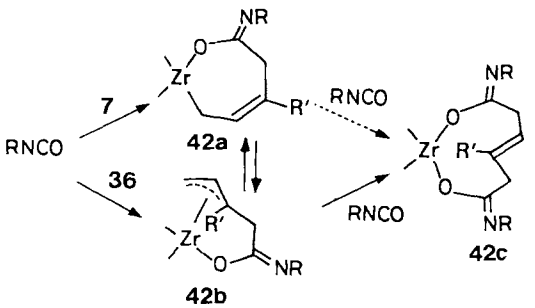

R' = H, Me.

3.3. Regiochemistry of the Reactions of Allylmetal Compounds

The chemistry of the allylzirconium and -titanium compounds is of fundamental importance for demonstrating the characteristic properties of the complexes of group 4A metals and for unfolding the origin of the fascinating regiochemistry observed in reactions with dienezirconium complexes, since the metal-carbon linkage of metallacyclo-3-pentenes can be regarded as representing a special case of the bis(2-butenyl)metal complexes. [$ZrCp_2CH_3$(3-methyl-2-butenyl)], [$ZrCp_2CH_3$(2-methyl-2-butenyl)], and [$ZrCp_2$(2-butenyl)$_2$], containing σ-bonded allyl groups, react, like the corresponding η^3-2-butenyltitanium(III) compounds, with acetone or ethanal exclusively at C-3 of the 2-butenyl group. High regio- and *threo*-selectivity (85–100%) are observed in reactions with aldehydes.[43b,62] A six-membered chair-like transition state has been proposed for these reactions. The corresponding allylic compounds of main group metals likewise react at C-3, but show almost no *threo*-selectivity.[70] Nine-membered metallacycles, [$ZrCp_2(C_{10}H_{16})$] and [$ZrCp_2(C_8H_{12})$], containing a 4–4 bonded dimeric isoprene or a 1–1 bonded dimeric butadiene unit (see Section 4.2), however, react with isobutanal or 3-pentanone at the 3-position of these ligands, and not at the terminal carbon atoms. Thus, the five-membered ring is crucial for the selective insertion at the terminals of the diene. The 1:1 magnesium–isoprene adduct, (polymeric 2-methyl-2-butenediylmagnesium) exhibits a completely different chemical behavior, as shown in Scheme 2. All of the electrophiles react selectively at C-3 (γ-position), presumably via a conventional six-membered transition state; the transmetalation with trimethylsilyl chloride occurs exclusively at C-4, thus lending support to the reaction pathway leading to **7** (Section 2.1). σ-Pentadienylzirconium compounds of type **23**, higher homologues of allylzirconium compounds, behave similarly, and add aldehydes and ketones selectively at C-3 (γ-position).[17a]

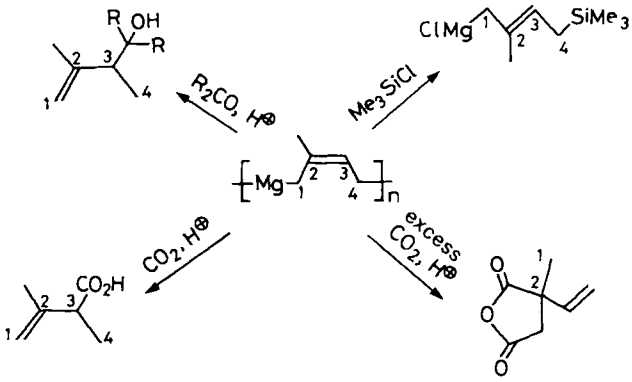

Scheme 2. Mode of reaction between magnesium isoprene (1:1) adduct with electrophiles.

3.4. Nucleophilic Addition of Alkenemetal and Alkynemetal Complexes

Alkene complexes of group 4A metals readily react with electrophiles in essentially the same manner as described for the diene complexes of these metals, whereas the coordinated olefin in the compounds [MCpH(CH_2=CHR)], M = Ta, Nb, is completely inert. The ethylene complex [$TiCp^*_2(C_2H_4)$] (**43**), undergoes a variety of nucleophilic

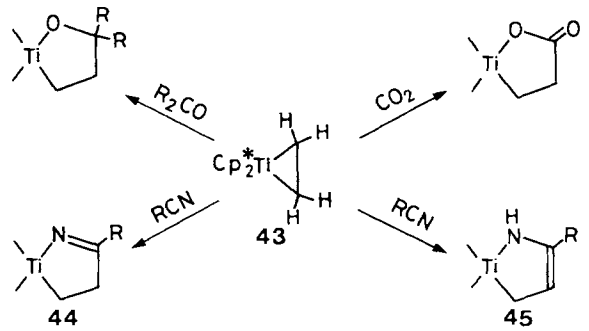

Scheme 3. Addition reaction of [$TiCp^*_2(C_2H_4)$] **43** to electrophiles.

additions, affording oxa- or azametallacycles (Scheme 3).[71] Reactions with ketones and esters are rather complex. *tert*-Butyl and *p*-tolyl cyanide (RCN with bulky R group) undergo direct addition to give **44**, whereas alkyl cyanides with less bulky groups (CH_3, C_2H_5) favor formation of the metallacycloenamine tautomer **45**.

The chemical reactivity of alkyne complexes of Ti and Zr toward electrophiles resembles that of the alkene complexes.[72] The addition of acetone or CO_2 to the 1,2-diphenylacetylene complex **46** led to oxametallacycles. Such a

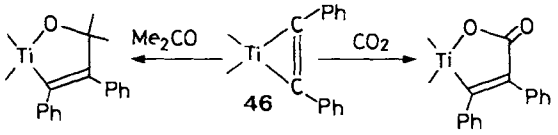

nucleophilicity has never been demonstrated for the corresponding alkyne complexes of group 5A metals (Ta, Nb) or late transition metals.

With regard to the alkene complexes, there exist four-membered metallacyclobutanes of type **48** containing W,[73] Ta[74] or Ti[75] which function as alkene-metathesis catalysts or active species for the polymerization or oligomerization of olefins. Stoichiometric reactions of these compounds with electrophiles should provide valuable information about the characteristic properties of their M-C bond, since the complexes are in equilibrium with a methylenemetal-ethylene species. We can observe the enhanced carbene-complex property of **48**, $>M=Cp_2^*Ti$, in the reaction with carbonyl compounds, which is essentially a condensation reaction of the Wittig type (cf. **47**).[75b] Wittig-type reactions are also known for $>M=Cp^*Cl_2Ta$,[74b] 1,3-dititanacyclobutane derivatives[76] and $[Cp_2TiCHR\cdot AlMe_2Cl]$ species.[77] However, such a

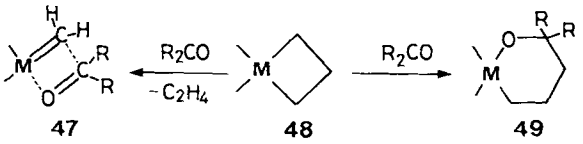

metal-carbene character is virtually lacking in the case of $>M=Cp_2Hf$, i.e., this complex undergoes only normal carbometalation, leading to an oxahafnacyclohexane derivative of type **49**.[78] A related carbenezirconium complex, $[Cp_2Zr=CHCH_2R]$, has recently been isolated by stabilizing it with a trialkylphosphane.[79] Metallacyclopentanes with M = Ti, Zr, Hf (cf. **8**) are less reactive than metallacyclobutanes toward electrophiles and behave similarly to dialkylmetal compounds.

3.5. Metal-Assisted Selective Three-Component Addition

A stepwise three-component addition reaction has been realized by taking advantage of the highly regioselective reaction between dienezirconium complexes and alkenes,

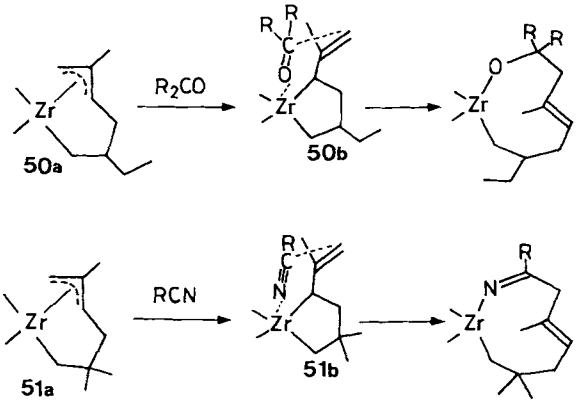

dienes or alkynes (see Sections 4.1 and 4.2). The allylic moiety of the resulting complexes **50a** and **51a** selectively inserts a variety of aldehydes, ketones, esters, and nitriles.[74a] Thus successive diene-alkene-aldehyde, diene-alkene-ketone or diene-alkene-nitrile additions take place in the reaction sphere of $ZrCp_2$ species with excellent regioselectivity (>95%) in ca. 90% yield. Similarly, successive three-component addition of diene-alkyne-aldehyde and diene-alkyne-nitrile has been achieved via the isoprenezirconium complex **52a** with inserted 2-butyne. These processes should have potential utility in organic synthesis, since a variety of combinations can be chosen. It

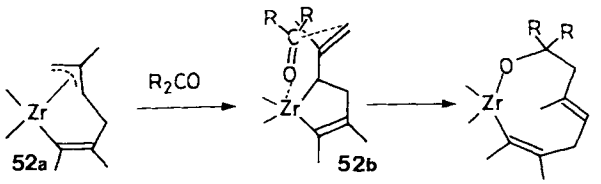

should be noted that these compounds react in a completely different fashion to the conventional allylzirconium compounds. In **50a**, **51a**, and **52a** the C-C bond formation occurs at the α-position, thus suggesting involvement of the intermediates **50b**, **51b**, and **52b**. In the case of normal allylmetal compounds bond formation takes place at the sterically more crowded γ-position (see, e.g., Scheme 2).

3.6. Oxidation of Complexes of the Early Transition Metals with Hydrogen Peroxide or Air

Generally, oxidation of organozirconium complexes is effected by the addition of aqueous H_2O_2 (30%), *t*BuOOH, *m*-$ClC_6H_4CO_3H$ or even air in some cases. Transformation of an alkylzirconium complex into a zirconium alkoxide, e.g. $[ZrCp_2Me_2]$ into $[ZrCp_2(OMe)_2]$, has already been achieved with these oxidizing agents.[80] However, such protic oxidizing agents are not suitable for the oxidation of allylzirconium, allyltitanium, or dienezirconium complexes, because a protonolysis takes place prior to the oxidation. Therefore, only the alkylmetal part of σ,η³-allyl compounds (**50a**, **51a**) is oxidized with aqueous H_2O_2, whereby monoalcohols are formed in good yield.[81] Oxazirconacycles **30** are however readily oxidized by aqueous

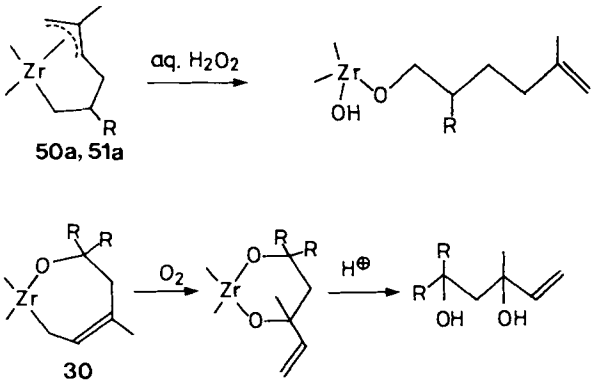

H_2O_2 or by air, whereupon 1,3-diols are formed in high yield (80%) with high selectivity (96%). The diene ligands in $[ZrCp_2(diene)]$, $[TaCl_2Cp(diene)]$, and $[NbCp(diene)_2]$ are readily removed quantitatively in solution by passage of air.

4. Oxidative Coupling of 1,3-Dienes and Alkenes with Unsaturated Hydrocarbons in the "MCp_2" Sphere

4.1. Regioselective Addition of Dienemetal Complexes to Alkenes

Most of the simple alkenes (ethylene, 1-butene, 2-butene, isobutene etc.) rapidly react with both $ZrCp_2$(s-*cis*-diene)] and $[ZrCp_2$(s-*trans*-diene)] complexes (diene = butadiene, isoprene) at ambient temperatures with formation of 1:1 adducts of the type **50a** and **51a**.[82] In the case of the s-*cis*-isoprene complex, the C–C bond formation takes

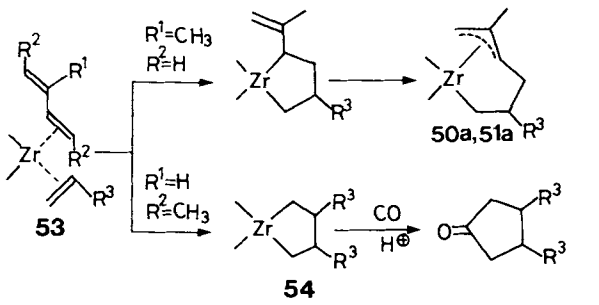

place quantitatively at the sterically less crowded C-4 atom of the isoprene with >98% regioselectivity. The regiochemistry contrasts sharply with that of the additions to compounds with C–O and C–N multiple bonds. In the case of s-*cis*- and s-*trans*-butadiene complexes the C–C bond formation presumably takes place via the same transition state **53**, $R^1 = R^2 = H$, since the products have the same structure in both cases. Alkenes with internal double bonds (e.g. 2-pentene, 2-hexene) undergo migratory insertion into the isoprene complex **7b** at elevated temperature (>60°C) to give the same compounds as are obtained from alkenes with terminal double bonds (e.g. 1-pentene, 1-hexene). $[Cp_2Zr$(1,4-diphenylbutadiene)], however, is completely inert to these alkenes because of its strong M–C bonding.

As confirmed by ligand exchange experiments, the relative strength of the diene–zirconium bond is found to decrease in the following order:[83]

1,4-diphenylbutadiene > 2,3-dimethylbutadiene > butadiene > isoprene > 1,3-pentadiene > 1,3-hexadiene > 2,4-hexadiene

The order approximately parallels the π-acidity of the dienes. 2,4-Hexadiene counts among the most weakly bound ligands, so it is very easily displaced by 1-butene or 1-hexene.[17] At the same time, 3,4-dialkylzirconacyclopentanes (**54**) are generated by oxidative coupling between the two 1-alkene molecules in the $ZrCp_2$ sphere. Direct reduction of $[ZrCl_2Cp_2]$ with $NaC_{10}H_8$ or RMgX in the presence of 1-alkenes provides a more convenient route to the compounds **54**.[84] The subsequent carbonylation with CO under atmospheric pressure affords an enolate, which upon hydrolysis furnishes a 3,4-dialkylcyclopentanone in 70–80% yield. The synthesis of cyclopentanones by carbonylation of metallacycles is already well known.[85] The 1,4-diphenylbutadiene and 2,3-dimethylbutadiene ligands are bound to the metal very tightly, and hence they are completely inert toward almost all alkenes. Thus, zirconium complexes of butadiene and isoprene (dienes with a moderate π-acidity) can promote the stoichiometric carbometalation of alkenes.

4.2. Diene–Diene Coupling in the "$ZrCp_2$" Sphere

Conjugated dienes show fairly good reactivity toward $[ZrCp_2$(diene)] complexes. Depending upon the π-acidity of the dienes, either a ligand exchange reaction or a 1:1 coupling reaction takes place.[86] Addition of one equivalent of (*E,E*)-1,4-diphenyl-1,3-butadiene to butadiene-, isoprene-, and hexadienezirconium complexes results in the quantitative displacement of the coordinated dienes, with concomitant formation of $[ZrCp_2$(s-*trans*-1,4-diphenylbutadiene)]. Addition of one equivalent of isoprene to the isoprene complex **7b** at 20°C, on the other hand, promotes 1:1 coupling with formation of the equilibrium mixture **55** ⇌ **56**, (4–4 bonded) together with **75** (3,4-bonded, cf.

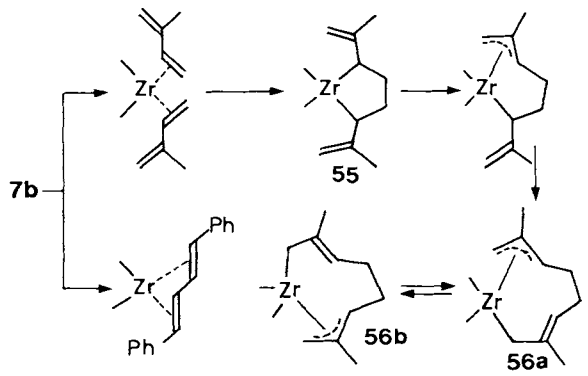

Section 5.3) in a 76:24 ratio. According to the NMR spectrum, the 4–4 bonded compound assumes the thermodynamically more favored structure **56**. The complex **56** could be prepared in a high state of purity by treating $[ZrCl_2Cp_2]$ with a 4–4 bonded isoprene–dimer/Mg adduct,

$[MgC_{10}H_{16}]_n$, at $-20°C$. The corresponding butadiene-dimer complex, $[ZrCp_2(C_8H_{12})]$, is accessible by 1:1 reaction of $[ZrCp_2(butadiene)]$ with butadiene or by reaction of $[ZrCl_2Cp_2]$ with $[MgC_8H_{12}]_n$. The resulting 18e complexes have a fluctional structure: σ-π rearrangement occurs rapidly between **56a** and **56b** even at $-70°C$. The bis(η^3-allyl) structure is favored when these ligands are bound to coordinatively unsaturated species such as Zr(cyclooctatetraene),[87] CpV,[88] etc.

Group 5A metal–diene complexes of the type $[MCl_2(C_5R_5)(diene)]$ and $[M(C_5R_5)(diene)_2]$ (M = Ta, Nb; R = H, Me), are, with exception of $[NbClCp(butadiene)]_2$, generally inert to alkenes and dienes.[89] This is due to the enhanced stabilization of the M–C bonding by strong π-electron donation from internal carbon atoms to vacant metal d-orbitals together with back donation from filled metal orbitals to π* orbitals of the diene C–C bonds. The very strong M–C bonding in these complexes may be the major reason why organic compounds of group 5A metals generally do not catalyze diene oligomerization and polymerization.

4.3. Selective Coupling of Dienes with Alkynes

A series of alkynes readily react with zirconium-diene complexes by way of either a 1:1 addition reaction or a ligand exchange reaction, depending upon the nature of the alkynes.[82,90] Most 1- or 2-alkynes bearing one or more alkyl groups (e.g., 1-butyne, 2-hexyne etc.) react with $[ZrCp_2(s\text{-}cis\text{-isoprene})]$ irreversibly at ambient temperature to give 1:1 addition compounds, where the alkyne binds selectively to the C-4 atom of isoprene. The whole geometry of the resulting σ,η^3-*syn*-allyl compounds **58** (cf. **52a**) is very similar to that of the compounds **50a** and **51a** with inserted alkene. The molecular structure of the complex with inserted 2-butyne is representative of this type of

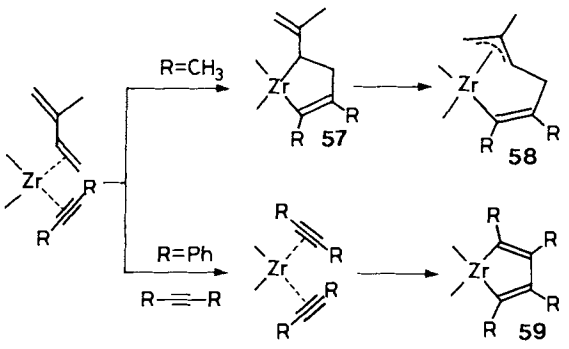

complexation (Fig. 7). Alkynes with aromatic substituents, however, favor the ligand exchange reaction. A typical example is seen in the stoichiometric reaction between $[ZrCp_2(isoprene)]$ and diphenylacetylene leading to 2,3,4,5-tetraphenylzirconacyclo-2,4-pentadiene (**59**). Analogous zircona- or titanacyclo-2,4-pentadiene derivatives are also accessible by reduction of $[MCl_2Cp_2]$ in the presence of alkynes.[91] Recently, the isolation of alkynezirconium and alkyneytterbium complexes has been reported.

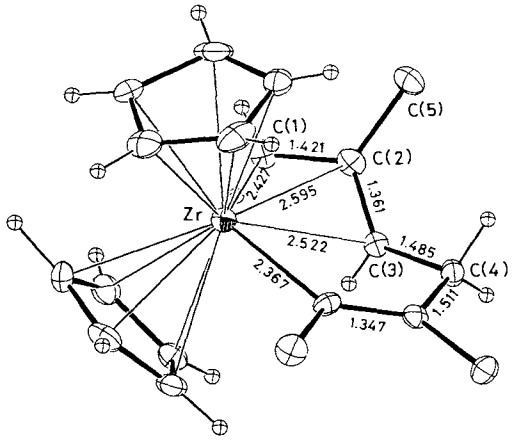

Fig. 7. Molecular structure of a 2-butyne inserted complex of type **58**, $[Cp_2ZrC(CH_3)=C(CH_3)CH_2CH=C(CH_3)=CH_2]$.

From competition experiments, it can be concluded that the relative reactivity of aliphatic substrates toward $[ZrCp_2(diene)]$ decreases in the following order:

aldehydes > ketones ≈ nitriles ≈ isocyanates > CO_2 > oxiranes ≈ esters ≈ alkynes > dienes > alkenes

4.4. Reactions of Alkenemetal Complexes with Unsaturated Hydrocarbons

$[TiCp^*_2(CH_2=CH_2)]$ (**43**) is a typical alkene complex of an early transition metal which undergoes facile reactions with a variety of unsaturated hydrocarbons.[71] Ethylene reacts reversibly with **43** to yield an equilibrium mixture containing a titanacyclopentane; higher alkenes (propene, butene, etc.), however, are generally inert to **43**, presumably because of the unfavorable steric interaction between the bulky Cp* ligand and the alkyl substituents. Alkynes are more reactive toward **43**; their modes of reaction can be classified into three types (Scheme 4). Alkynes with internal double bonds, whose π-acceptor property is less pronounced, are incorporated into the Ti–C bond to give metallacyclo-2-pentene derivatives, while alkynes which are good π-acceptor ligands exclusively undergo ligand exchange to give, for example, a diphenylacetylene complex, preventing the formation of 2,3-diphenyltitanacyclo-2-pen-

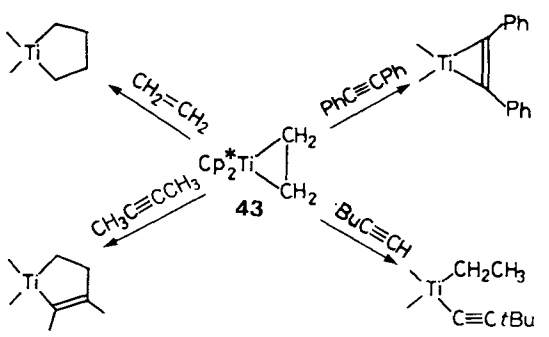

Scheme 4. Coupling reaction between $[TiCp^*_2(C_2H_4)]$ **43** and unsaturated hydrocarbons.

tene. Terminal alkynes, typically *t*BuC≡CH, react with **43** to yield alkynyl(ethyl)titanium compounds. Alkene complexes of Ta and Nb, e.g. $[TaCp_2H(RCH{=}CH_2)]$ and $[NbCp_2H(RCH{=}CH_2)]$, generally do not form metallacycles like the corresponding titanium complexes, but they can undergo ligand exchange reactions with other alkenes and alkynes.[92c]

5. New Aspects of the Catalytic Conversion of Hydrocarbons

5.1. Regioselective Dimerization of 1-Alkenes

The metal-assisted selective linear or cyclic oligomerization of 1-alkenes has recently become a subject of intensive study.[93] Although various homogeneous catalyst systems involving low-valent organonickel[94] and organopalladium species[95] are known to effect the linear dimerization of 1-alkenes, highly regioselective dimerization leading to an isomerically pure head-to-head, head-to-tail or tail-to-tail dimer has been achieved in only a few cases.[96] Recently, selective coupling of propylene has been achieved with $[TaCp^*Cl_2(propylene)]$;[97] the catalytic dimerization leads, with high regioselectivity (95%), to formation of 2,3-dimethyl-1-butene (head-to-head dimer).

A reaction path via a metallacyclization to give a 3,4-dimethyltantalacyclopentane (**60**) followed by β-hydride elimination has been proposed for the tantalum mediated dimerization.[98] This type of β-elimination has already been confirmed by thermal degradation of titana-[99] and

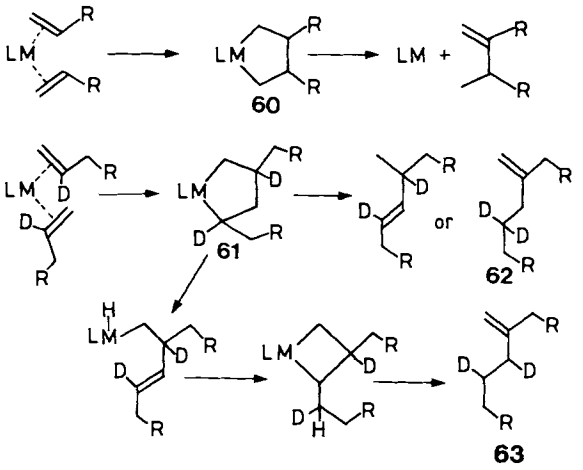

zirconacyclopentanes[100] bearing two Cp ligands. In the case of dimethyl substituted titanacyclopentanes, the formation of 2,4-dimethyltitanacyclopentane is electronically more favorable than that of the 3,4- and 2,5-isomers; according to MO calculations, however, 3,4-dimethyltitanacyclopentane is sterically the more stable.[101] As found in the dimerization of 3,3-dimethyl-1-butene or 1-hexene, when bulky 1-alkenes are employed in the tantalum-mediated dimerization, head-to-tail dimerization predominates over head-to-head dimerization.[98] A novel reaction pathway has been proposed for this reaction based on a labeling experiment using [2-D]-1-hexene. If the head-to-tail dimerization were to arise directly from the β-elimination of the resulting 2,4-dialkylmetallacyclopentane **61**, it should lead to a 4,4-dideuterated 1-alkene derivative (**62**); in practice, however, the two deuterium atoms in **63** are found exclusively at the 3- and 4-positions, thus indicating that the reaction proceeds via a ring closure. A similar ring closure is reported for metallacyclopentanes containing Pt,[102a] Rh,[102b] and Re[102c] atoms. However, an alternative mechanism via an intermolecular ring opening process must be taken into consideration, as has been reported recently for platinacyclopentanes.[102d]

5.2. Selective Migration of the Double Bond of 1-Alkenes

Transition-metal-catalyzed isomerization of 1-alkenes has been extensively studied with soluble metal hydrides[103] or carbonyl metal compounds[104a] and, more frequently, with heterogeneous catalysts.[104b-d] These catalysts generally require a relatively high temperature (>70°C) for initiation of the reaction, and consequently a mixture of isomeric alkenes is formed as a result of the thermodynamic equilibrium. It therefore appears necessary to conduct the catalytic reaction at lower temperatures in order to freeze out the equilibrium. Recently, a catalytic system prepared by reduction of $[TiCl_2Cp_2^*]$ with $NaC_{10}H_8$, *i*PrMgBr, BuLi or $LiAlH_4$ was found to effect a highly stereoselective isomerization of 1-alkenes **64** to (*E*)-2-alkenes

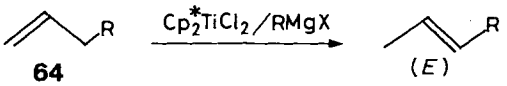

(R=CH_3, C_2H_5, C_6H_5, NEt_2, etc.).[105] The reaction proceeds quantitatively and with extremely high selectivity (>98%) within a few minutes. The maximized turnover is ca. 130 mol/(mol·min) in the case of 1-hexene. 1,5-Hexadiene and 1,7-octadiene are similarly converted into (*E,E*)-2,4-hexadiene and (*E,E*)-2,6-octadiene, respectively, with 99% selectivity. However, this catalyst proved to be inert in attempts to isomerize 2-methyl- and 3-methyl-1-alkenes. Exploiting this property, 2-methyl- and 3-methyl-1,5-hexadiene could be isomerized successfully to pure (*E*)-2- and (*E*)-3-methyl-1,4-hexadiene, respectively, in quantitative

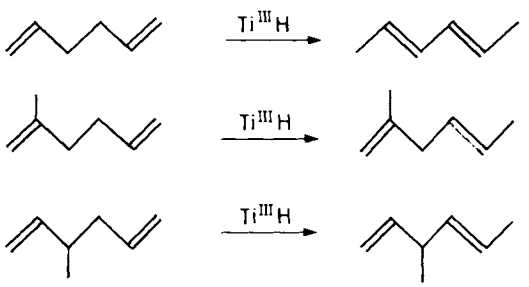

yields. The $[TiCl_2Cp_2]$/*i*PrMgBr and $[TiCl_2Cp_2]/NaC_{10}H_8$ systems containing less bulky auxiliary ligands exhibit similar or higher activity, but the stereoselectivity is much

lower (50–75%).[105, 106] The $[ZrCl_2Cp_2]/i$PrMgBr system also promotes selective isomerization (95–99%), but the rate of reaction is less than 1/10 of that observed for the $[TiCl_2Cp^*_2]/i$PrMgBr system.

Two major mechanisms have been proposed for the double bond migration: addition-elimination[103, 107] and 1,3-hydrogen shift.[108a] These two mechanisms are usually differentiated by a deuterium labeling experiment. Since a hydrogen/deuterium scrambling occurs in the closely related reaction between $[TiCp^*_2(CH_2{=}CH_2)]$ (**43**) and a mixture of $CH_3CH{=}CH_2$ and $CD_3CD{=}CD_2$, which presumably proceeds via a hydride species, $[Cp^*(C_5Me_4\text{-}\mu\text{-}CH_2)TiH(CH_2{=}CH_2)]$,[71] the addition-elimination mechanism seems the most likely one for these isomerizations

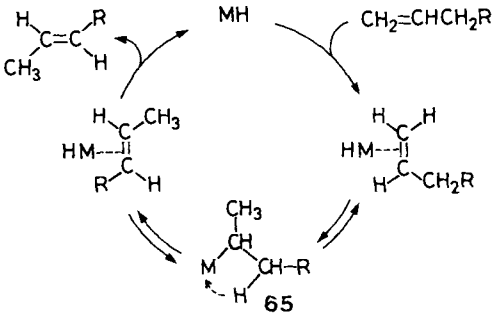

Scheme 5. Proposed mechanism for the selective isomerization of 1-alkenes to (*E*)-2-alkenes.

(Scheme 5). A metal hydride reacts reversibly with a 1-alkene to give an alkylmetal derivative (**65**), and then the alkyl group undergoes β-hydride elimination to give either the original 1-alkene or a 2-alkene. The factor which determines the configuration is almost certainly the conformation of the complex **65**, M = Cp^*_2, Ti, with inserted 1-alkene. Informative is the view along the C2–C3 bond. The preferential formation of the (*E*)-isomer will arise from steric re-

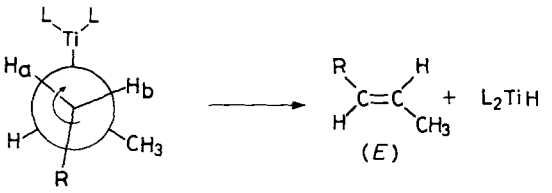

pulsion between R and Cp* or TiCp* as well as between CH_3 and R groups. The RCH_2 group should rotate clockwise for steric reasons to place the Ti and H_a in elipsed position. The subsequent *cis*-elimination yields an (*E*)-2-alkene. For the isomerization of allyl ethers and allylamines, Ir[108b] and Rh[108c] organometallic catalysts were recently found to be more effective than catalysts containing group 3A–5A metals.

5.3. Regioselective Dimerization of Conjugated Dienes

$[ZrCp_2(s\text{-}cis\text{-isoprene})]$ (**7b**) has been found to be a relatively good catalyst for the dimerization of isoprene to 4–4

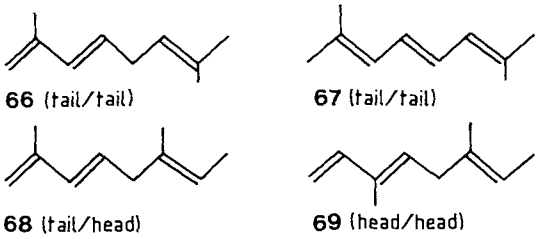

bonded (*E*)-2,7-dimethyl-1,3,6-octatriene (**66**) at 30 °C and (*E*)-2,7-dimethyl-2,4,6-octatriene (**67**) at 60 °C. An excellent regioselectivity (99%) and ca. 70% conversion was achieved when five equivalents of isoprene were added to the catalyst.[82] A catalytic cycle (Scheme 6) involving a single or double β-elimination sequence has been proposed on the basis of the following findings: 1) The stoichiometric reaction between $[ZrCp_2(s\text{-}cis\text{-isoprene})]$ and isoprene at 10 °C affords **56** (see Section 4.2) or **70** in equilibrium with **56**. 2) The complex **70** is immediately isomerized via **71** to **72a** and **72b** upon warming in benzene to 40 °C without further addition of isoprene. This transformation is confirmed by a chemical trapping experiment with mo-

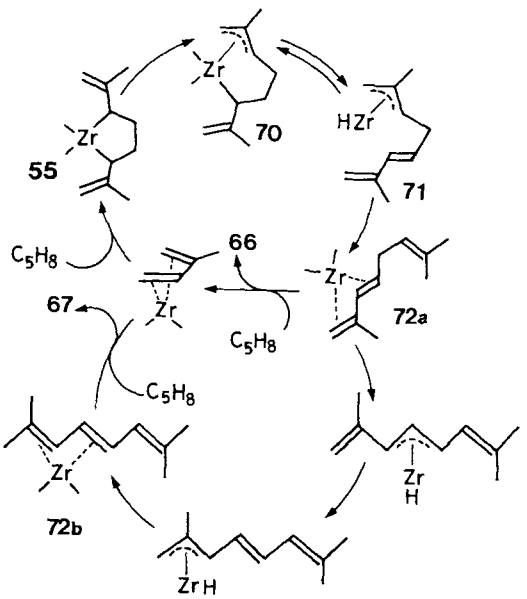

Scheme 6. Proposed mechanism for the selective dimerization of isoprene.

lecular oxygen: a 3 : 2 mixture of **66** and **67** is obtained at the initial stage, but the ratio is reversed (2 : 5) when the solution is kept at 30 °C for prolonged periods of time before treatment with O_2. 3) Addition of 1,4-diphenylbutadiene to **56** leads to a ligand exchange reaction. The 1,4-diphenylbutadiene complex is formed, and **66** and **67** (2 : 5) are liberated. $[HfCp_2(isoprene)]$ also catalyzes the corresponding dimerization at elevated temperatures (80 °C), but the catalytic activity is much lower than that of $[ZrCp_2(isoprene)]$, presumably due to the predominant formation of catalytically inactive metal species of the type **75**.

The mode of reaction changes drastically when diene-titanium complexes are used as catalysts. The complexes are generated in situ by treating [$TiCl_3Cp$], [$TiCl_2Cp$] or [$TiCl_2Cp_2$] with isoprene-Mg adducts or RMgX in the presence of isoprene. These catalysts effect the tail-to-head (**68**) and/or sterically unfavorable head-to-head (**69**) dimerization of isoprene in ca. 3 : 2 ratio, with complete suppression of the tail-to-tail dimerization.[86] The use of bulky auxiliary ligands is highly effective for improving the selectivity. Thus, the sole isomer with tail-to-head bonding was prepared for the first time using [$TiCl_3Cp^*$]/BuMgBr as catalyst. It seems reasonable to postulate that the active species is the isoprene complex of Ti^{III}, not of Ti^{IV}, as can be concluded from the following observations: 1) A Ti^{III} species was detected by EPR spectroscopy. 2) Ti^{IV} compounds are generally easily reduced to Ti^{III} species by treating them with RMgX, Mg etc., while the reduction of Zr^{IV} to Zr^{III} species is quite difficult. 3) The shape and the orientation of the vacant d-orbitals of "$TiCp_2$", as well as the whole geometry, are quite similar to those for "$ZrCp_2$", as predicted from EHMO calculations. This indicates that Ti^{IV} species should, contrary to the observations, produce a tail-to-tail dimer. 4) Isolated [TiClCp*(diene)] complexes of Ti^{IV} (diene = butadiene, isoprene, 2,3-dimethylbutadiene) exhibit very weak or practically no catalytic activity, but the reduction of these complexes with RMgX or Mg leads to excellent catalysis with tail-to-head dimerization.[6]

On the basis of these findings, we can postulate the coordination geometry of the transient bis(diene) complexes. According to molecular models the coordination of two isoprene molecules with geometries **73** and **74** are sterically most favorable for the zirconocene species. The

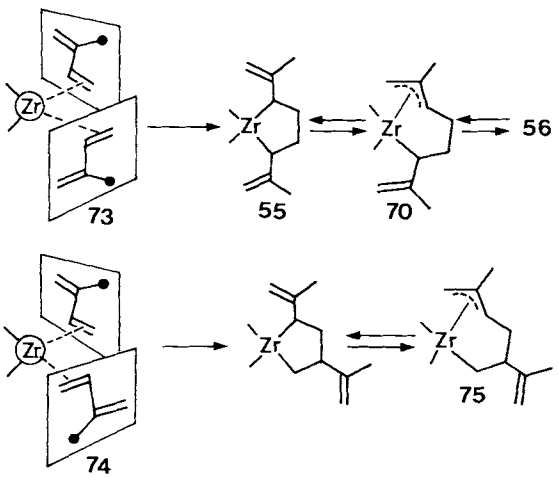

4-4 bonding of isoprene should occur via **73**; subsequent β-elimination from **70** then leads to **72a**. Scheme 6 shows this further reaction to **66** and **67**. If the β-hydrogen elimination proceeds at the metallacycle **55** and the subsequent hydrometalation occurs at the γ-position (referred to **71**), then 1,3,7-octatriene derivatives should be formed instead of the 1,3,6-octatriene derivative **66**. Actually, such a catalytic reaction to produce 1,3,7-octatriene derivatives via an intermediate of type **55** takes place in the Pd-mediated dimerization of 1,3-conjugated dienes.[109a,b] The molecular structure of platinacycles of the type **55** has indeed been confirmed crystallographically.[109c] Unlike **73**, the intermediate **74** will lead to a catalytically inactive complex **75**. The complexes **50a**-**52a**, which are related to **75**, also exhibit no catalytic activity in the dimerization. These results indicate that the methyne group at the β-position is highly resistant to hydrogen elimination. The reaction pathway discussed here is essentially the same as that predicted for the metallacyclization starting from [Cp_2Ti(ethylene)$_2$].[60, 110]

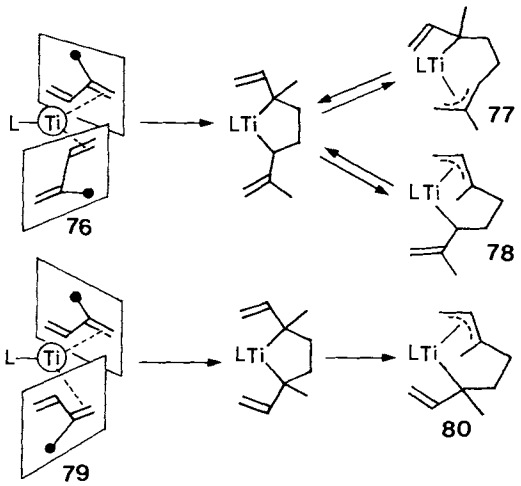

From experimental results, two types of intermediates (**76**, **79**) are conceivable for the titanium-catalyzed dimerization. In the species **76**, two isoprene molecules coordinate in the anti-parallel orientation to avoid the steric repulsion between the two methyl groups. The resulting coordinatively unsaturated 2,5-disubstituted titanacyclopentane should be rapidly transformed into either **77** or **78**. β-Hydrogen elimination from **78** dominates over the elimination from **77**, since the latter has a sterically less favorable conformation. $Zr(OR)_4/AlR_3$ catalysts also promote tail-to-head dimerization.[109d,e] The head-to-head coupling of isoprene most likely proceeds via the intermediate **80**. The coordinatively unsaturated Ti^{III} species has an enhanced σ-acceptor capability and free space around the metal; hence, when the acceptor orbital is suitably positioned, an isoprene molecule can coordinate to a metal at the C1-C2 bond, rather than the C3-C4 bond. This reflects the higher electron density of the Ti^{III} species.

5.4. Highly Selective Cyclotrimerization of Conjugated 1,3-Dienes

Regio- and stereo-controlled catalytic cyclotrimerization of monoalkyl substituted dienes has not yet been accomplished despite concerted efforts by many workers, although several nickel, titanium, and chromium catalyst systems are already known to promote the cyclotrimerization of isoprene and pentadiene, albeit with insufficient regioselectivity.[26, 109f,g] Recently, a novel catalyst system, [$TiCl_3Cp$]/[$AlClEt_2$]/H_2O, was found to be capable of converting isoprene into a single isomer, (*Z*,*E*,*E*)-1,5,10-trimethyl-1,5,9-cyclododecatriene (**81**), with exceptionally high

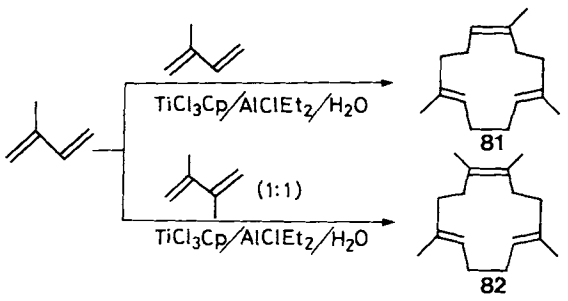

selectivity (86%).[84] The contaminating product in this system is exclusively 2,4-dimethyl-4-vinylcyclohexene (14%), a compound easily separable by flash distillation. The addition of water is crucial to promote the cyclic trimerization; in the absence of water the reaction furnishes only 2,4-dimethyl-4-vinylcyclohexene in low yield. Both yield and selectivity can be optimized by addition of $[TiCl_3Cp]/[AlClEt_2]/H_2O$ in the ratio 1:3:1. A catalyst prepared by addition of water to a 1:3 mixture of $[TiCl_3Cp]/[AlClEt_2]$ at 20°C exhibits almost the same catalytic activity as that prepared from the product of the reaction of $AlClEt_2$-H_2O (3:1) and $[TiCl_3Cp]$ at 20°C. The addition of products from $AlEt_3$-H_2O and $AliBu_3$-H_2O (3:1) also leads to good catalytic activity but insufficient regioselectivity. Use of alcohols (BuOH etc.) or secondary amines (Bu_2NH etc.) instead of water led to inactivation of the catalysts.

The addition of one to two equivalents of electron donors (NEt_3, pyridine, PBu_3) to the $[TiCl_3Cp]/[AlClEt_2]/H_2O$ system causes a drastic change in the distribution of the products, i.e., a mixture of tail-to-head and head-to-head linear isoprene dimers (cf. **68** and **69**, respectively) was obtained in place of **81**. The association of the EtClAl-O-AlClEt and Ti[11] species is apparently disrupted by the coordination of donor ligands. This behavior would indicate that the diene ligands in the intermediate of the cyclic trimerization have the same coordination geometry as in the intermediate of the linear dimerization. If this assumption is correct, the principle of the catalytic cycle may be represented as in Scheme 7. The present catalytic system is also effective for cyclic homo- and cotrimerization of other dienes. Butadiene is converted with 87% selectivity (90% yield) into (*E,E,E*)-1,5,9-cyclododecatriene, while a 1:1 mixture of isoprene and 2,3-dimethylbutadiene is converted with 85% selectivity into (*E,E,Z*)-1,6,9,10-tetramethyl-1,5,9-cyclododecatriene (**82**) (30% conversion). The polymerization of ethylene and propylene catalyzed by $[MCl_2Cp_2]/AlMe_3/H_2O$ (M = Ti, Zr) is also accelerated by addition of water.[111] These systems, however, require a large excess of $AlMe_3/H_2O$ (1:0.9) component (see Section 6.2).

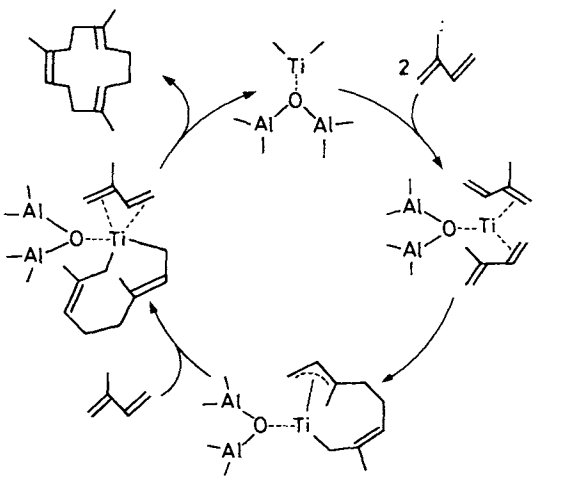

Scheme 7. Proposed mechanism for the selective cyclotrimerization of isoprene.

5.5. Regioselective Linear Dimerization of 1-Alkynes

Three different structures are conceivable for the linear dimers of 1-alkynes when steric interference is taken into consideration. A dimer of the type **83** has been prepared in good yield with $[RuH_2(CO)(PPh_3)_3]$[112] and a dimer of the type **84** with $[RhCl(PPh_3)_3]$[113] or $[Cr(OtBu)_4]/ZnEt_2$.[114] The $[TiCl_2Cp^*_2]/[AlEt_2Cl]$ (1:3) system exhibits an excellent catalytic activity and effects the highly regioselective (>99%) dimerization of RC≡CH to 1-buten-3-yne derivatives **85**, R = C_2H_5, C_3H_7, C_6H_{11}, C_6H_5, Me_3Si, Me_3SiCH_2, etc., in quantitative yield.[115] The use of a bulky ligand

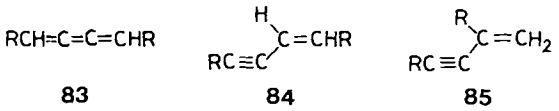

83 **84** **85**

such as Cp* is essential for achieving this type of selective dimerization. When Cp* is replaced by the less bulky Cp ligand only a mixture of cyclic trimers, i.e. 1,3,5- and 1,2,4-trisubstituted benzene is obtained. By exploiting the excellent catalytic activity of $[TiCl_2Cp^*_2]/[AlClEt_2]$, highly selective codimerization of two alkynes has been realized for the first time. A combination of acidic 1-alkynes and less

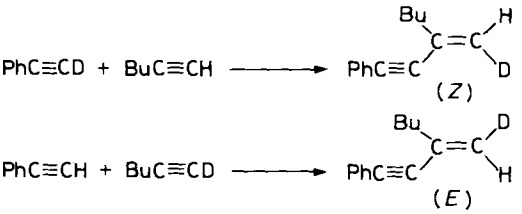

acidic 1-alkynes provides the best result concerning both selectivity and yield. For example, highly stereo- and regioselective codimerization occurred in quantitative yield when a 1:1 mixture of PhC≡CD (acidic alkyne) and BuC≡CH (less acidic alkyne) or of PhC≡CH and BuC≡CD was used. The (*Z*)- and (*E*)-dimers, respectively, were formed in 98% yield. The reaction completely suppresses the homodimerization of each alkyne. A proposed mechanism for the formation of the (*Z*)-isomer is illus-

trated in Scheme 8. The active species should be the complex [$Cp^*_2TiC{\equiv}CPh$], generated by reaction of [$Cp^*_2Ti^{III}R$] or [$Cp^*Ti^{III}H$] with PhC≡CD, isolation of which is quite difficult.[116] The thermally more stable [$Cp_2M(C{\equiv}CPh)_2$]

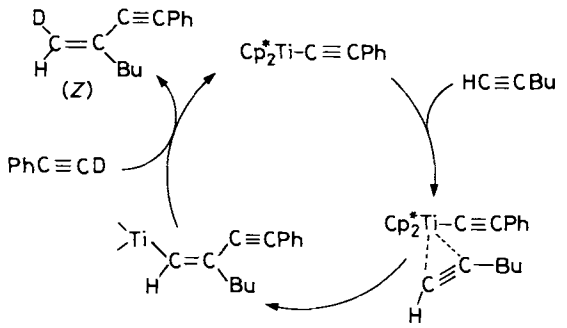

Scheme 8. Proposed mechanism for the selective linear codimerization of 1-alkynes.

species, $M = Ti^{IV}$, Zr^{IV}, are almost catalytically inactive. Insertion of BuC≡CH into the TiC≡CPh bond followed by Ti–C bond cleavage by PhC≡CD leads to regeneration of the [$Cp^*_2TiC{\equiv}CPh$] species.

5.6. Cyclic Trimerization of Alkynes

The selective cyclization of 1-alkynes is of special interest, since the products are of potential commercial utility. Various transition-metal complexes in both high and low oxidation states are known to catalyze the cyclotrimerization of 1-alkynes; however, an efficient regiocontrol has not yet been achieved.[117] $TaCl_5$ and $NbCl_5$ exhibit rela-

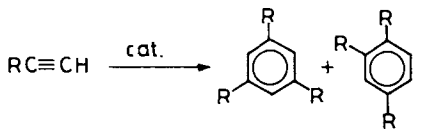

tively high selectivity (ca. 90%) in the conversion of 1-butyne into 1,2,4-triethylbenzene, while the closely related compounds [$TaCl_4Cp$], [$NbCl_4Cp$], [$TiCl_3Cp$], and [$TiCl_4$] are practically inactive. A binuclear low valent niobium complex, [NbClCp(butadiene)]$_2$, and the [$NbCl_4Cp$]/[$AlClEt_2$] system show a similar selectivity in the cyclization of 1-butyne to 1,2,4-triethylbenzene.[117d] Several mechanisms have been proposed for the alkyne cyclization, but the issue is still controversial. The most commonly accepted mechanism involves a metallacyclopentadiene with low valent metal as intermediate which can undergo reductive elimination by the attack of a third alkyne molecule.[118a,b] However, the π-complex multicenter mechanism, in which alkyne molecules are assembled into a ring on one or more metals cannot, as yet, be ruled out.[118c]

6. Stereocontrolled Polymerization of Dienes, Alkenes, and Alkynes

6.1. Stereoselective Polymerization of Conjugated Dienes

Several mechanisms have been proposed for the stereoselective polymerization of conjugated dienes. The η^4-s-*cis*-coordination (type **1**) of dienes to the metal was postulated to be the determining factor for formation of the *cis*-1,4-polymer[119] and the η^2-s-*trans* coordination (type **6**) for formation of the *trans*-1,4-polymer.[120] In the meantime it has been shown (see Section 2.1) that early transition metals (Zr, Hf, Mo) occasionally prefer the η^4-s-*trans*-(type **4**) rather than the η^2-s-*trans*- (type **6**) or η^4-s-*cis*-butadiene coordination (type **1**). In agreement with this trend, butadiene forms a *trans*-1,4-polymer with $TiCl_4$/$AlEt_3$,[121a] $TiCl_3$/$AlEt_3$,[121b] and VCl_3/$AlEt_3$ catalyst systems.[122] EHMO calculations on the s-*cis*- and s-*trans*-butadiene complexes of $[ZrCl_4]^{n-}$ (n = 0, 1, 2) with C_{2v} symmetry have revealed that the total energy for the s-*trans* complex is similar to or slightly smaller (1.0–2.0 kcal/mol) than that for the s-*cis* complex but significantly smaller than that for the η^2-s-*trans*-butadiene complex [1.8 for Zr^{IV} (n = 0), 9.9 for Zr^{III} (n = 1), and 18.4 kcal/mol for Zr^{II} (n = 2)].[7c] Therefore, the η^4-s-*trans*-diene coordination of type **4**, as in **86**, is regarded as an important factor in the

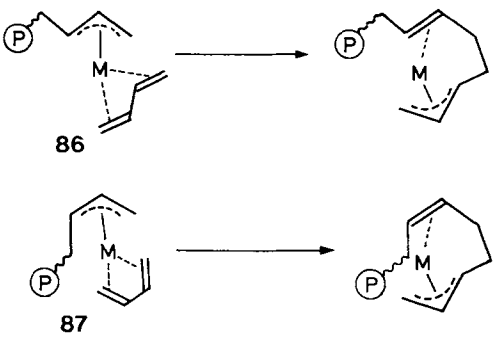

trans-polymerization of butadiene (Ⓟ signifies polymer). The s-*trans*-diene ligand is smoothly transformed into a *syn*-η^3-allyl complex by insertion into the polymer end. Very high thermal instability and chemical reactivity preclude isolation of the active species. For the *cis*-1,4-polymerization, the reaction pathway via **87** has been proposed. [ZrCp(η^3-butenyl)(s-*cis*-butadiene)], a Zr^{IV} species, has a structure very similar to that of the intermediate **87**,[9f,123] but shows no catalytic activity in the polymerization. A more electron-deficient low-valent allyl(diene)metal species should, on the other hand, be catalytically active.

A terminally disubstituted butadiene, e.g. (*E,E*)-2,4-hexadiene, has been polymerized to a stereoregular polymer with an *erythro-trans*-1,4-diisotactic structure by catalysis with [Ti(acac)$_3$]/[$AlEt_2Cl$] or [Co(acac)$_2$]/[$AlEt_2Cl$].[124] 2,4-Hexadiene, however, favors the s-*trans* coordination to $ZrCp_2$ species.[17] Furthermore, it is reported that the (*E,E*)-isomer of $ZrCp_2$(2,4-hexadiene) is thermally more stable than the (*E,Z*)- or (*Z,Z*)-isomer.[125] The good corre-

lation between the preferred geometry of the complex and the s-*trans* structure of the polymer suggests that the titanium-catalyzed 2,4-hexadiene polymerization may proceed via an intermediate of type **86**. The diene should be coordinated to the metal in an η^4-s-*trans*-(*E*,*E*)-fashion and

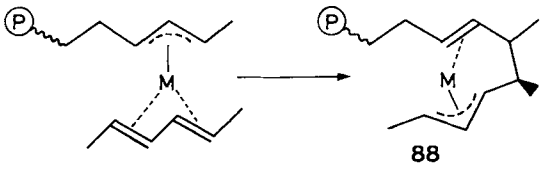

88

eventually transformed into the *syn*-allyl species **88** during the insertion into the polymer end. The *trans*-1,4-polymerization of 1,3-pentadiene catalyzed by $VCl_3/AlEt_3$[126] or $[VO(acac)_2]/[AlEt_2Cl]$[127] may be rationalized in essentially the same way as the alternating copolymerization of butadiene and propylene.[128]

6.2. Novel Catalytic Systems for Alkene- and Alkyne-Polymerization

Notable topics in this area involve the discovery of highly reactive systems for homogeneous catalysis (Kaminsky catalysts) having the composition $[MCp_2R_2]/AlMe_3$–H_2O (M = Ti, Zr; R = CH_3, Cl)[111] and a novel reaction mechanism proposed for the polymerization of alkenes[102b, 129a] or alkynes[130] via metallacyclic species. The Kaminsky catalyst is prepared from a large excess of aluminoxane and a metallocene compound (Al : M = 1000 : 1). Its activity in ethylene polymerization is 1000 times higher per Ti atom than that of a typical Ziegler catalyst system, $TiCl_4/AlEt_3$. Isotactic propylene polymerization in homogeneous solution has been realized for the first time with this system, but the exact reaction mechanism still a matter for debate.

In place of the well known Cossee's mechanism, an alternative mechanism via metallacycles has been proposed for the transition-metal-catalyzed alkene polymerization.[131] The reaction pathway via titanacyclobutane species well accounts for the kinetic studies on ring opening polymerization of norbornene and cyclopentene,[129a] but is untenable for the polymerization of linear alkenes.[129b, c] A similar metallacycle-mechanism via tungstenacyclo-1,3-butadiene has also been proposed for the alkyne polymerization with olefin metathesis catalysts.[102b, 130]

7. Conclusion

The chemistry of complexes of the early transition metals is now in a state of rapid development. A variety of highly regio- and stereoselective stoichiometric as well as catalytic reactions has already been realized using specifically designed complexes of the type mentioned in this article. Continued efforts in the preparation and characterization of coordinatively more unsaturated organometallics (e.g., with Ti^{III}, Zr^{III}, Ta^{IV}, Ta^{III}) surely promises further development in this field.

We are indebted to many coworkers whose names are listed in the references. Thanks are also due to Prof. N. Kasai and Prof. Y. Kai of Osaka University for their cooperation in the X-ray diffraction studies and to Prof. P. Legzdins of the University of British Columbia for valuable discussions.

Received: August 22, 1986;
revised: January 29, 1987 [A 629 IE]
German version: *Angew. Chem. 99* (1987) 745

[1] a) D. J. Cardin, M. F. L. Lappert, C. C. Raston: *Chemistry of Organozirconium and -hafnium Compounds*, Ellis Horwood, Chichester 1986; b) M. T. Reetz: *Organotitanium Reagents in Organic Synthesis*, Springer, Berlin 1986; c) R. P. Quirk (Ed.): *Transition Metal Catalyzed Polymerizations, Alkenes and Dienes*, Harwood Academic Publishers, London 1983.

[2] a) B. Weidmann, D. Seebach, *Angew. Chem. 95* (1983) 12; *Angew. Chem. Int. Ed. Engl. 22* (1983) 31; b) H. Schumann, *ibid. 96* (1984) 475 and *23* (1984) 474; c) H. B. Kagan in K. A. Gschneider, Jr., L. Eyring (Eds.): *Handbook on the Physics and Chemistry of Rare Earths*, Elsevier, Amsterdam 1984, p. 525; d) G. P. Pez, J. N. Armour, *Adv. Organomet. Chem. 19* (1981) 2; e) D. J. Sikora, D. W. Macomber, M. D. Rausch, *ibid. 25* (1986) 318; f) W. J. Evans, *ibid. 24* (1985) 131; g) R. S. P. Coutts, P. C. Wailes, *ibid. 9* (1970) 126; h) M. E. Thompson, J. E. Bercaw, *Pure Appl. Chem. 56* (1984) 1.

[3] a) R. R. Schrock, *Acc. Chem. Res. 12* (1979) 98; b) R. R. Schrock in P. S. Braterman (Ed.): *Reaction of Coordinated Ligands*, Plenum Press, New York 1983; c) R. R. Schrock, G. W. Parshall, *Chem. Rev. 76* (1976) 243; d) K. H. Dötz, *Angew. Chem. 96* (1984) 573; *Angew. Chem. Int. Ed. Engl. 23* (1984) 587.

[4] R. H. Grubbs, A. Miyashita in M. Tsutsui (Ed.): *Fundamental Research in Homogeneous Catalysis. Vol. 3.* Plenum Press, New York 1979, p. 151.

[5] a) E. A. Koerner von Gustorf, F.-W. Grevels, I. Fischler: *The Organic Chemistry of Iron. Vol. 1.* Academic Press, New York 1978; b) G. Wilkinson, F. G. A. Stone, E. W. Abel (Eds.): *Comprehensive Organometallic Chemistry, Vol. 4*, Chap. 31.1 and 32.3; *Vol. 5*, Chap. 35, Pergamon Press, Oxford 1982.

[6] a) J. Chen, Y. Kai, N. Kasai, H. Yamamoto, H. Yasuda, A. Nakamura, *Chem. Lett. 1987*, in press; b) J. Blenkers, B. Hessen, F. VanBolhuis, A. J. Wagner, J. H. Teuben, *Organometallics 6* (1987) 459.

[7] a) H. Yasuda, K. Tatsumi, A. Nakamura, *Acc. Chem. Res. 18* (1985) 120; b) H. Yasuda, Y. Kajihara, K. Mashima, K. Nagasuna, K. Lee, A. Nakamura, *Organometallics 1* (1982) 388; *2* (1983) 478; c) A. Nakamura, K. Tatsumi, H. Yasuda in I. Bernal (Ed.): *Stereochemistry of Organometallic and Inorganic Compounds, Vol. 1*, Elsevier, New York 1986, p. 1; d) Y. Kai, N. Kanehisa, K. Miki, N. Kasai, K. Mashima, K. Nagasuna, H. Yasuda, A. Nakamura, *J. Chem. Soc. Chem. Commun. 1982*, 191; e) H. Yasuda, K. Mashima, M. Akita, A. Nakamura in H. Yaozeng, A. Yamamoto, B. Teo (Eds.): *New Frontiers in Organometallic and Organic Chemistry*, Science Press, Beijing 1984.

[8] a) S. Datta, S. S. Wreford, R. P. Beatty, T. J. McNeese, *J. Am. Chem. Soc. 101* (1979) 1053; b) S. Datta, M. B. Fischer, S. S. Wreford, *J. Organomet. Chem. 188* (1980) 353; c) R. P. Beatty, S. Datta, S. S. Wreford, *Inorg. Chem. 18* (1979) 3139.

[9] a) G. Erker, C. Krüger, G. Müller, *Adv. Organomet. Chem. 24* (1985) 1; b) G. Erker, J. Wicher, K. Engel, F. Rosenfeldt, W. Dietrich, C. Krüger, *J. Am. Chem. Soc. 102* (1980) 6346; c) G. Erker, T. Mühlenbernd, R. Benn, A. Rufińska, Y.-H. Tsay, C. Krüger, *Angew. Chem. 97* (1985) 336; *Angew. Chem. Int. Ed. Engl. 24* (1985) 321; d) G. Erker, K. Engel, C. Krüger, A. P. Chiang, *Chem. Ber. 115* (1982) 3311; e) G. Erker, K. Engel, P. Vogel, *Angew. Chem. 94* (1982) 791; *Angew. Chem. Int. Ed. Engl. 21* (1982) 776; *Angew. Chem. Suppl. 1982*, 1746; f) G. Erker, K. Berg, C. Krüger, *Angew. Chem. 96* (1984) 445; *Angew. Chem. Int. Ed. Engl. 23* (1984) 455; g) U. Dorf, K. Engel, G. Erker, *Organometallics 2* (1983) 462.

[10] a) H. Yasuda, Y. Kajihara, K. Mashima, K. Lee, A. Nakamura, *Chem. Lett. 1981*, 519; b) C. Krüger, G. Müller, G. Erker, U. Dorf, K. Engel, *Organometallics 4* (1985) 215.

[11] Y. Kai, N. Kanehisa, N. Kasai, T. Okamoto, H. Yasuda, A. Nakamura, *52th Annu. Meet. Chem. Soc. Jpn. 1986*, Abstr. 1E36, 1K39.

[12] H. Yasuda, K. Tatsumi, T. Okamoto, K. Mashima, K. Lee, A. Nakamura, Y. Kai, N. Kanehisa, N. Kasai, *J. Am. Chem. Soc. 107* (1985) 2410.

[13] G. M. Smith, H. Suzuki, D. C. Sonnenberger, V. W. Day, T. J. Marks, *Organometallics 5* (1986) 540.

[14] G. Erker, T. Mühlenbernd, R. Benn, A. Rufińska, *Organometallics 5* (1986) 402.

[15] M. J. S. Dewar, G. P. Ford, *J. Am. Chem. Soc. 101* (1979) 783.

[16] W. J. Richter, *Chem. Ber. 116* (1983) 3293.
[17] a) H. Yasuda, K. Nagasuna, M. Akita, K. Lee, A. Nakamura, *Organometallics 3* (1984) 1470; b) A. Nakamura, H. Yasuda, K. Tatsumi, K. Mashima, M. Akita, K. Nagasuna in B. L. Shapiro (Ed.): *Organometallic Compounds. Synthesis. Structure and Theory. Vol. 1*, p. 29, Texas A & M University Press, Austin, TX 1983.
[18] P. S. Skell, M. J. McGlinchey, *Angew. Chem. 87* (1975) 215; *Angew. Chem. Int. Ed. Engl. 14* (1975) 195.
[19] a) R. Bechhais, K.-H. Thiele, *J. Organomet. Chem. 268* (1984) C7; b) P. Czisch, G. Erker, H.-G. Korth, R. Sustmann, *Organometallics 3* (1984) 945.
[20] a) J. D. Fellman, G. A. Rupprecht, R. R. Schrock, *J. Am. Chem. Soc. 101* (1979) 5099; b) J. M. Mayer, J. E. Bercaw, *ibid. 104* (1982) 2157; c) J. Blenkers, H. J. D. Meijer, J. H. Teuben, *J. Organomet. Chem. 218* (1981) 383.
[21] a) H. Yasuda, Y. Nakano, K. Natsukawa, H. Tani, *Macromolecules 11* (1978) 586; b) K. Fujita, Y. Ohnuma, H. Yasuda, H. Tani, *J. Organomet. Chem. 113* (1976) 210; c) Y. Kai, N. Kanehisa, N. Kasai, K. Mashima, H. Yasuda, A. Nakamura, *Chem. Lett. 1982*, 1277; d) H. Yasuda, K. Tatsumi, A. Nakamura in T. E. Hogen-Esh, J. Smid (Eds.): *Recent Advances in Anionic Polymerization*, Elsevier, New York 1987, p. 59; e) The procedure reported in the patent literature (H. E. Ramsden, U. S. Pat. 3388279, 1968) is unsuitable for preparation of the diene-metal complexes, since the product comprises mainly 1:2 magnesium-diene adduct accompanied by 1:1 and 1:3 adducts.
[22] K. Tatsumi, H. Yasuda, A. Nakamura, *Isr. J. Chem. 23* (1983) 455.
[23] B. Eaton, J. A. King, Jr., K. P. C. Vollhardt, *J. Am. Chem. Soc. 108* (1986) 1357.
[24] T. Okamoto, H. Yasuda, A. Nakamura, unpublished.
[25] Y. Kai, N. Kanehisa, K. Miki, N. Kasai, M. Akita, H. Yasuda, A. Nakamura, *Bull. Chem. Soc. Jpn. 56* (1983) 3735.
[26] H. Yasuda, A. Nakamura, Y. Kai, N. Kasai *Topics in Physical Organometallic Chemistry. Vol. 2*, Freund Publishing House, 1987.
[27] J. W. Faller, A. M. Rosan, *J. Am. Chem. Soc. 99* (1977) 4858.
[28] H. Yasuda, T. Okamoto, A. Nakamura, Y. Kai, N. Kanehisa, N. Kasai, unpublished.
[29] a) R. Benn, G. Schroth, *J. Organomet. Chem. 228* (1982) 71; b) W. H. Hersh, F. J. Hollander, R. G. Bergman, *J. Am. Chem. Soc. 105* (1983) 5834.
[30] a) A. D. Hunter, P. Legzdins, C. R. Nurse, F. W. B. Einstein, A. C. Willis, *J. Am. Chem. Soc. 107* (1985) 1791; b) A. D. Hunter, P. Legzdins, F. W. B. Einstein, A. C. Willis, B. E. Bursten, M. G. Gatter, *ibid. 108* (1986) 3843.
[31] M. L. Ziegler, *Z. Anorg. Allg. Chem. 392* (1972) 173.
[32] V. C. Adam, J. A. T. Jarvis, B. T. Kilbourn, P. G. Owston, *Chem. Commun. 1971*, 467.
[33] H. Sasse, M. L. Ziegler, *Z. Anorg. Allg. Chem. 392* (1972) 167.
[34] C. G. Pierpont, *Inorg. Chem. 17* (1978) 1976.
[35] M. D. Fryzuk, W. E. Piers, S. J. Rettig, *J. Am. Chem. Soc. 107* (1985) 8259.
[36] J. A. King, K. P. C. Vollhardt, *Organometallics 2* (1983) 684.
[37] a) H. G. Alt, H. E. Engelhardt, M. D. Rausch, L. B. Kool, *J. Am. Chem. Soc. 107* (1985) 3717; b) B. H. Edwards, R. D. Rogers, D. J. Sikora, J. L. Atwood, M. D. Rausch, *ibid. 105* (1983) 416.
[38] S. A. Cohen, P. R. Auburn, J. E. Bercaw, *J. Am. Chem. Soc. 105* (1983) 1136.
[39] a) A. H. Klazinga, J. H. Teuben, *J. Organomet. Chem. 157* (1978) 413; *165* (1979) 31; b) S. M. Rocklage, R. R. Schrock, *J. Am. Chem. Soc. 104* (1982) 3077.
[40] A. H. Klazinga, J. H. Teuben, *J. Organomet. Chem. 194* (1980) 309.
[41] N. M. Doherty, J. E. Bercaw, *J. Am. Chem. Soc. 107* (1985) 2670.
[42] a) S. Otsuka, A. Nakamura, *Adv. Organomet. Chem. 14* (1976) 245; b) S. D. Ittel, J. A. Ibers, *ibid. 14* (1976) 33.
[43] a) G. Wilke, *Pure Appl. Chem. 50* (1978) 677, and references cited therein; b) K. Mashima, H. Yasuda, K. Asami, A. Nakamura, *Chem. Lett. 1983*, 219; c) H. Yasuda, A. Nakamura, *J. Organomet. Chem. 285* (1985) 15.
[44] R. B. Helmholdt, F. Jellinek, H. A. Martin, A. Vos, *Recl. Trav. Chim. Pays-Bas 86* (1967) 1263.
[45] B. Henc, P. W. Jolly, R. Salz, S. Stobbe, G. Wilke, R. Benn, R. Mynott, K. Seevogel, R. Goddard, C. Krüger, *J. Organomet. Chem. 191* (1980) 449.
[46] a) R. D. Ernst, *Acc. Chem. Res. 18* (1985) 56; b) *Struct. Bonding (Berlin) 57* (1984) 1.
[47] J. R. Bleeke, M. K. Hyo, *Organometallics 3* (1984) 506.
[48] a) J. R. Bleeke, W.-J. Peng, *Organometallics 3* (1984) 1422; b) P. V. Rinze, U. Müller, *Chem. Ber. 112* (1979) 1973.
[49] G.-H. Lee, S.-M. Peng, M.-Y. Liao, R.-S. Liu, *J. Organomet. Chem.*, unpublished.
[50] M. A. Paz-Sandoval, P. Powell, M. G. B. Drew, R. N. Perutz, *Organometallics 3* (1984) 1026.
[51] a) J. W. Faller, R. H. Crabtree, A. Habib, *Organometallics 4* (1985) 929; b) R. D. Rogers, R. V. Bynum, J. L. Atwood, *J. Am. Chem. Soc. 100* (1978) 5238; c) R. M. Kowalesky, A. L. Rheingold, W. C. Trogler, F. Basolo, *ibid. 108* (1986) 2460; d) C. P. Casey, J. M. O'Connor, *Organometallics 4* (1985) 384.
[52] a) H. Yasuda, Y. Kajihara, K. Mashima, K. Nagasuma, A. Nakamura, *Chem. Lett. 1981*, 671; b) M. Akita, H. Yasuda, A. Nakamura, *ibid. 1983*, 217.
[53] T. Fukagawa, Y. Fujiwara, H. Taniguchi, *Chem. Lett. 1981*, 771.
[54] a) E. C. Ashby, *Pure Appl. Chem. 52* (1980) 545; b) M. T. Reetz, S. H. Kyung, J. Westermann, *Organometallics 3* (1984) 1716; c) G. J. Erskine, B. K. Hunter, J. D. McCowan, *Tetrahedron Lett. 26* (1985) 1371.
[55] a) K. Yokoo, Y. Yamanaka, T. Fukagawa, H. Taniguchi, Y. Fujiwara, *Chem. Lett. 1983*, 1301; b) H. Schumann, W. Genthe, E. Hahn, J. Pickardt, H. Schwarz, K. Eckart, *J. Organomet. Chem. 306* (1986) 215.
[56] a) M. Akita, *Dissertation*, Osaka University 1984; b) M. Akita, K. Matsuoka, K. Asami, H. Yasuda, A. Nakamura, *J. Organomet. Chem.*, in press.
[57] a) T. Okamoto, H. Yasuda, A. Nakamura, *31st Symp. Organomet. Chem. Jpn.*, Abstr. A208 (1984); b) M. Akita, K. Matsuoka, K. Asami, H. Yasuda, A. Nakamura, *J. Organomet. Chem. 327* (1987) 193.
[58] G. Erker, K. Engel, J. L. Atwood, W. E. Hunter, *Angew. Chem. 95* (1983) 506; *Angew. Chem. Int. Ed. Engl. 22* (1983) 494; *Angew. Chem. Suppl. 1983*, 678.
[59] G. Erker, U. Dorf, *Angew. Chem. 95* (1983) 800; *Angew. Chem. Int. Ed. Engl. 22* (1983) 777; *Angew. Chem. Suppl. 1983*, 1120.
[60] J. W. Lauher, R. Hoffmann, *J. Am. Chem. Soc. 98* (1976) 1729.
[61] a) J. A. Marsella, J. C. Huffman, K. G. Caulton, B. Langato, J. R. Norton, *J. Am. Chem. Soc. 104* (1982) 6360; b) S. Gambarotta, M. Basso-Bert, C. Floriani, C. Gaustini, *J. Chem. Soc. Chem. Commun. 1982*, 374; c) G. S. Bristow, P. B. Hitchcock, M. F. Lappert, *ibid. 1982*, 462.
[62] a) Y. Yamamoto, K. Maruyama, *Tetrahedron Lett. 21* (1980) 4607; b) F. Sato, S. Iijima, M. Sato, *ibid. 22* (1981) 243; c) Y. Kobayashi, K. Ueyama, F. Sato, *J. Chem. Soc. Chem. Commun. 1984*, 621.
[63] a) H. Takaya, M. Yamakawa, K. Mashima, *J. Chem. Soc. Chem. Commun. 1983*, 1283; b) K. Mashima, H. Takaya, *Organometallics 4* (1985) 1464.
[64] H. Yasuda, K. Matsuoka, A. Nakamura, unpublished.
[65] a) D. J. Darensbourg, R. A. Kadaroski, *Adv. Organomet. Chem. 22* (1983) 129; b) R. P. A. Sneeden in G. Wilkinson, F. G. A. Stone, E. W. Abel (Eds.): *Comprehensive Organometallic Chemistry, Vol. 8*, Chap. 50.4, Pergamon Press, Oxford 1982.
[66] H. Yasuda, K. Matsuoka, T. Okamoto, A. Nakamura, Y. Kai, N. Kasai, *52nd Annu. Meet. Chem. Soc. Jpn. 1986*. Abstr. 1K37.
[67] G. Erker, U. Dorf, R. Benn, R.-D. Reinhardt, *J. Am. Chem. Soc. 106* (1984) 7649.
[68] H. Yasuda, Y. Matsuoka, A. Nakamura, *Proceedings of the 5th International Symposium on Homogeneous Catalysis*, B-3, Kobe 1985.
[69] T. Okamoto, H. Yasuda, A. Nakamura, unpublished.
[70] a) R. W. Hoffmann, *Angew. Chem. 94* (1982) 569; *Angew. Chem. Int. Ed. Engl. 21* (1982) 555; b) Y. Yamamoto, K. Maruyama, *J. Organomet. Chem. 284* (1985) C45.
[71] S. A. Cohen, P. R. Auburn, J. E. Bercaw, *J. Am. Chem. Soc. 105* (1983) 1136.
[72] a) B. Demerseman, R. Mahé, P. H. Dixneuf, *J. Chem. Soc. Chem. Commun. 1984*, 1394; b) V. B. Shur, V. V. Burlakov, A. I. Yanovsky, P. V. Petrovsky, Y. T. Struchkov, M. E. Volpin, *J. Organomet. Chem. 297* (1985) 51.
[73] a) L. G. McCullough, M. L. Listemann, R. R. Schrock, M. R. Churchill, J. W. Ziller, *J. Am. Chem. Soc. 105* (1983) 6729; b) M. E. Ephritikhine, M. L. H. Green, *J. Chem. Soc. Chem. Commun. 1976*, 929.
[74] a) H. W. Turner, R. R. Schrock, J. D. Fellmann, S. J. Holmes, *J. Am. Chem. Soc. 105* (1983) 4942; b) M. M. Francl, W. J. Pietro, R. F. Hout, Jr., W. J. Hehre, *Organometallics 2* (1983) 281.
[75] a) S. L. Buchwald, R. H. Grubbs, *J. Am. Chem. Soc. 105* (1983) 5490; b) S. L. Buchwald, E. V. Anslyn, R. H. Grubbs, *ibid. 107* (1985) 1766; c) T. Ikariya, S. C. H. Ho, R. H. Grubbs, *Organometallics 4* (1985) 199.
[76] a) F. W. Hartner, Jr., J. Schwartz, S. M. Clift, *J. Am. Chem. Soc. 105* (1983) 640; b) B. J. J. van de Heisteeg, G. Schat, O. S. Akerman, F. Bickelhaupt, *Organometallics 4* (1984) 1141.
[77] a) F. W. Hartner, Jr., J. Schwartz, *J. Am. Chem. Soc. 103* (1981) 4979; b) J. R. Stille, R. H. Grubbs, *ibid. 105* (1983) 1664; c) K. C. Ott, E. J. M. deBoer, R. H. Grubbs, *Organometallics 3* (1984) 223; d) F. N. Tebbe, R. L. Harlow, *J. Am. Chem. Soc. 102* (1980) 6149.
[78] G. Erker, P. Czisch, C. Krüger, J. M. Wallis, *Organometallics 4* (1985) 2059.
[79] S. M. Clift, J. Schwartz, *J. Am. Chem. Soc. 106* (1984) 8380.
[80] T. F. Backburn, J. A. Labinger, J. Schwartz, *Tetrahedron Lett. 1975*, 3401.
[81] H. Yasuda, K. Nagasuna, K. Asami, A. Nakamura, *Chem. Lett. 1983*, 955.
[82] a) H. Yasuda, Y. Kajihara, K. Nagasuna, K. Mashima, A. Nakamura, *Chem. Lett. 1981*, 719; b) G. Erker, K. Engel, U. Dorf, J. L. Atwood, W. Hunter, *Angew. Chem. 94* (1982) 915; *Angew. Chem. Int. Ed. Engl. 21* (1982) 914; *Angew. Chem. Suppl. 1982*, 1974.

[83] H. Yasuda, K. Matsuoka, K. Nagasuna, A. Nakamura, unpublished.
[84] H. Yasuda, M. Akita, A. Nakamura, unpublished.
[85] a) C. McDade, J. E. Bercaw, *J. Organomet. Chem. 279* (1985) 281; b) G. Erker, *Acc. Chem. Res. 17* (1984) 103; c) J. X. McDermott, G. M. Whitesides, *J. Am. Chem. Soc. 96* (1974) 947; d) E. Negishi, S. J. Holmes, J. M. Tour, J. A. Miller, *ibid. 107* (1985) 2568.
[86] H. Yasuda, T. Okamoto, H. Yamamoto, A. Nakamura, *Shokubai 28* (1986) 97.
[87] D. J. Brauer, C. Krüger, *Organometallics 1* (1982) 207.
[88] K. Jonas, V. Wiscamp, *Z. Naturforsch. B38* (1983) 1113.
[89] T. Okamoto, H. Yasuda, T. Arai, A. Nakamura, *52nd Annu. Meet. Chem. Soc. Jpn. 1986*. Abstr. 1K38.
[90] a) Y. Kai, N. Kanehisa, K. Miki, N. Kasai, K. Mashima, K. Nagasuna, H. Yasuda, A. Nakamura, *Chem. Lett. 1982*, 1979; b) V. Skibbe, G. Erker, *J. Organomet. Chem. 241* (1983) 15.
[91] a) S. B. Jones, J. L. Petersen, *J. Am. Chem. Soc. 105* (1983) 5503; b) B. H. Edwards, R. D. Rogers, D. J. Sikora, J. L. Atwood, M. D. Rausch, *ibid. 105* (1983) 416; c) H. G. Alt, H. E. Engelhardt, M. D. Rausch, L. B. Kool, *ibid. 107* (1985) 3717.
[92] a) T. Takahashi, D. R. Swanson, E. Negishi, *Chem. Lett. 1987*, 623; b) C. J. Burns, R. A. Andersen, *J. Am. Chem. Soc. 109* (1987) 941; c) A. H. Klazinga, J. H. Teuben, *J. Organomet. Chem. 165* (1979) 31.
[93] H. Yasuda, A. Nakamura, *Rev. Chem. Intermed. 6* (1986) 365.
[94] P. W. Jolly, G. Wilke: *The Organic Chemistry of Nickel*, Academic Press, New York 1975.
[95] a) G. Henrici-Olivé, S. Olivé, *Angew. Chem. 87* (1975) 110; *Angew. Chem. Int. Ed. Engl. 14* (1975) 104; b) M. G. Barlow, M. J. Bryant, R. N. Haszeldine, A. G. Mackie, *J. Organomet. Chem. 21* (1970) 215.
[96] a) G. Wilke in M. Tsutsui (Ed.): *Fundamental Research in Homogeneous Catalysis, Vol. 3*, Plenum Press, New York 1979; b) B. Bogdanović, *Adv. Organomet. Chem. 17* (1979) 105.
[97] R. R. Schrock, S. McLain, J. Sancho, *Pure Appl. Chem. 52* (1980) 729.
[98] S. J. McLain, R. R. Schrock, *J. Am. Chem. Soc. 100* (1978) 315.
[99] G. M. Whitesides, J. McDermott, *J. Am. Chem. Soc. 96* (1974) 6462.
[100] J. M. Manriquez, D. R. McAlister, R. D. Sanner, J. E. Bercaw, *J. Am. Chem. Soc. 100* (1978) 2716.
[101] R. J. McKinney, *J. Chem. Soc. Chem. Commun. 1980*, 490.
[102] a) P. S. Braterman, *J. Chem. Soc. Chem. Commun. 1979*, 70; b) K. J. Ivin, J. J. Rooney, C. D. Stewart, M. L. H. Green, L. Mahtab, *ibid. 1978*, 604; c) G. K. Yang, R. G. Bergman, *J. Am. Chem. Soc. 105* (1981) 6500; d) G. M. Whitesides, M. Hackett, R. L. Brainard, J.-P. P. M. Lavalleye, A. F. Sowinski, A. N. Izumi, S. S. Moore, D. W. Brown, E. M. Staudt, *Organometallics 4* (1985) 1819.
[103] a) C. A. Tolman, *J. Am. Chem. Soc. 94* (1972) 2994; b) W. Hendrix, J. L. van Rosenberg, *ibid. 98* (1976) 4850.
[104] a) A. J. Pearson in G. Wilkinson, F. G. A. Stone, E. W. Abel (Eds.): *Comprehensive Organometallic Chemistry, Vol. 8*, Chap. 58, Pergamon Press, Oxford 1982; b) D. C. Bailey, S. H. Langer, *Chem. Rev. 81* (1981) 109; c) L. L. Murrell in J. J. Burtonand, R. L. Garten (Eds.): *Materials in Catalysis*, Academic Press, New York 1977; d) F. R. Hartley, P. N. Vezey, *Adv. Organomet. Chem. 15* (1977) 189.
[105] M. Akita, H. Yasuda, K. Nagasuna, A. Nakamura, *Bull. Chem. Soc. Jpn. 56* (1983) 554.
[106] a) D. E. Bergbreiter, G. L. Parsons, *J. Organomet. Chem. 208* (1981) 47; b) K. Mach, F. Trecek, H. Andropiusova, V. Hanus, *Synthesis 1982*, 53.
[107] D. Bingham, D. E. Webster, P. B. Wells, *J. Chem. Soc. Dalton Trans. 1974*, 1514, 1519.
[108] a) D. Bingham, B. Hudson, D. Webster, P. B. Wells, *J. Chem. Soc. Dalton Trans. 1974*, 1521; b) D. Baudry, M. Ephritikhine, H. Felkin, *J. Chem. Soc. Chem. Commun. 1978*, 694; c) K. Tani, T. Yamagata, S. Otsuka, S. Akutagawa, H. Kumobayashi, T. Taketomi, H. Takaya, A. Miyashita, R. Noyori, *ibid. 1982*, 600.
[109] a) M. Anteunis, A. DeSmet, *Synthesis 1974*, 800; b) A. Musco, *J. Mol. Catal. 1* (1976) 443; c) G. K. Barker, M. Green, J. A. K. Howard, J. L. Spencer, F. G. A. Stone, *J. Chem. Soc. Dalton Trans. 1978*, 1839; d) A. Misono, Y. Uchida, K. Furuhata, S. Yoshida, *Bull. Chem. Soc. Jpn. 42* (1969) 2303; e) Y. Uchida, K. Furuhata, S. Yoshida, *ibid. 44* (1969) 1966; f) H. Morikawa, S. Kitazume, *Ind. Eng. Chem. Prod. Res. Dev. 18* (1979) 254; g) Mitsubishi Petrochem. Co., Jap. Pat. 7812481 (1978).
[110] J. X. McDermott, M. E. Wilson, G. M. Whitesides, *J. Am. Chem. Soc. 98* (1976) 6529.
[111] a) H. Sinn, W. Kaminsky, *Adv. Organomet. Chem. 18* (1980) 299; b) W. Kaminsky, K. Külper, H. H. Brintzinger, F. R. W. P. Wild, *Angew. Chem. 97* (1985) 507; *Angew. Chem. Int. Ed. Engl. 24* (1985) 507; c) J. A. Ewen, *J. Am. Chem. Soc. 106* (1984) 6355.
[112] H. Yamazaki, *J. Chem. Soc. Chem. Commun. 1976*, 841.
[113] a) L. Carlton, G. Reed, *J. Chem. Soc. Perkin Trans. 1978*, 1631; b) S. Yoshikawa, T. Kiji, J. Furukawa, *Makromol. Chem. 178* (1977) 1077.
[114] N. Hagihara, M. Tamura, H. Yamazaki, M. Fujiwara, *Bull. Chem. Soc. Jpn. 34* (1961) 892.
[115] M. Akita, H. Yasuda, A. Nakamura, *Bull. Chem. Soc. Jpn. 57* (1984) 480.
[116] D. G. Sekutowski, G. D. Stucky, *J. Am. Chem. Soc. 98* (1976) 1376.
[117] a) T. Masuda, T. Mori, T. Higashimura, *Bull. Chem. Soc. Jpn. 53* (1980) 1152; b) A. F. Donda, G. Morreti, *J. Org. Chem. 31* (1966) 985; c) T. Masuda, Y.-X. Deng, T. Higashimura, *Bull. Chem. Soc. Jpn. 56* (1983) 2798; d) H. Yasuda, T. Okamoto, H. Yamamoto, A. Nakamura, *Shokubai 28* (1986) 97.
[118] a) G. W. Parshall: *Homogeneous Catalysis*, Wiley, New York 1980, p. 165; b) K. P. C. Vollhardt, *Acc. Chem. Res. 10* (1977) 1; c) G. N. Schrauzer, *Adv. Organomet. Chem. 2* (1964) 1.
[119] J. P. Durand, F. Dawans, P. Teyssie, *J. Polym. Sci. A 8* (1970) 979.
[120] a) G. Natta, L. Porri: *Polymer Chemistry of Synthetic Elastomer*, Interscience, New York 1968; b) J. Furukawa: *Transition Metal Catalyzed Polymerization* (in Japanese), Kagaku Dojin, Kyoto 1972.
[121] a) G. Natta, L. Porri, A. Mazzei, D. Morero, *Chim. Ind. (Milan) 41* (1959) 398; b) G. Natta, L. Porri, L. Fiore, *Gazz. Chim. Ital. 89* (1959) 761.
[122] G. Natta, L. Porri, P. Corradini, D. Morero, *Chim. Ind. (Milan) 40* (1958) 362.
[123] a) G. Erker, K. Berg, R. Benn, G. Schroth, *Chem. Ber. 118* (1985) 1383; b) A series of [ZrCp(allyl)(diene)] complexes are also available by reaction of [ZrCpCl(diene)] with allylmagnesium halides; see ref. [56].
[124] M. Kamachi, N. Wakabayashi, S. Murahashi, *Macromolecules 7* (1974) 744.
[125] G. Erker, K. Engel, V. Korek, P. Czisch, H. Berke, P. Caubère, R. Vanderesse, *Organometallics 4* (1985) 1531.
[126] a) B. A. Dolgoplosk, E. I. Tinyakova, I. S. H. Guzman, L. L. Afinogenova, *J. Polym. Sci. Polym. Chem. Ed. 22* (1984) 1535; b) G. Natta, L. Porri, P. Corradini, G. Zanini, F. Ciampelli, *J. Polymer Sci. 51* (1961) 463.
[127] a) L. Porri, P. Pini, *Chim. Ind. (Milan) 55* (1973) 156; b) L. Porri, M. Aglietta, *Makromol. Chem. 177* (1976) 465.
[128] J. Furukawa, R. Hirai, M. Nakamura, *J. Polym. Sci. B 7* (1965) 671.
[129] a) L. R. Gilliom, R. H. Grubbs, *J. Am. Chem. Soc. 108* (1986) 733; b) L. Clawson, J. Soto, S. L. Buchwald, M. L. Steigerwald, R. H. Grubbs, *ibid. 107* (1985) 3377; c) J. Soto, M. L. Steigerwald, R. H. Grubbs, *ibid. 104* (1982) 4479.
[130] a) T. J. Katz, S. J. Lee, *J. Am. Chem. Soc. 102* (1980) 422; b) T. J. Katz, T. M. Sivavec, *ibid. 107* (1985) 737; c) T. J. Katz, S. M. Hecker, *ibid. 107* (1985) 2182.
[131] M. L. H. Green, *Pure Appl. Chem. 50* (1978) 27.

RP-Bridged Metal Carbonyl Clusters: Synthesis, Properties, and Reactions

By Gottfried Huttner* and Konrad Knoll

Dedicated to Professor Larry F. Dahl

Metal carbonyl clusters possess a complicated chemistry that is only beginning to be understood. One of the main current goals in this area is thus an understanding of their reactivity. This article describes the syntheses and reactions of clusters that contain metal carbonyl fragments bridged by a main-group element. But what is the sense of making such clusters still more complicated by the incorporation of main-group elements? The example of μ_3-bridged carbonyl clusters will serve to show that the main-group element plays an important role in the study of reaction paths; it holds the metal carbonyl fragments together even when the bonds between them are broken in the course of a reaction. Trinuclear μ_3-bridged clusters prove to be small enough to allow the analysis of typical cluster reactions (such as the reversible breaking of metal-metal bonds) in terms of single reaction steps. They are also large enough to provide surprises by their multifaceted reactivity. It will be shown that a detailed study of trinuclear RX-bridged metal carbonyl clusters (X = N, P, As, Sb, Bi)—a very small part of carbonyl cluster chemistry—can lead to a better understanding of the general reaction principles involved.

1. Introduction

Low-nuclearity transition-metal carbonyl clusters are regarded[1] as model systems whose study can provide insights into the complicated reaction processes at catalytically active metal surfaces.[2] This fact, together with the hope of employing the clusters themselves in catalytic processes,[3b,4] has led to a considerable research potential in this area. An astonishing variety of cluster frameworks have been synthesized and structurally characterized.[5,6] However, only a few reactions have been analyzed in detail.[7,8] This fact is surprising in view of the large number of known clusters; why is it that we know so much about the structure of clusters and so little about their reactivity? The most important reasons are as follows:

- Large clusters have an aesthetic appeal; the synthesis of even larger and more attractive clusters is so entertaining that researchers easily forget to investigate reactivity.
- Clusters are polyfunctional molecules; all metal-metal and metal-ligand bonds[9] are potential sites of reaction. Selective reactions are unlikely to be achieved without the use of protecting groups.
  Clusters can fragment; metal-metal bonds may break in the course of a reaction at a metal cluster. Therefore, the question often arises whether the reaction has taken place at the cluster itself or at one of its mononuclear fragments.

The goal of understanding the reactions of clusters thus requires that several restrictions be imposed:

- The chemist must abstain from the pleasures of large, attractive clusters and concentrate instead on the satisfaction gained on achieving an insight into their reactivity. Reactions are attractive too!
- The systems to be studied must be restricted to "simple" clusters with the fewest possible reactive sites.
- The variety of potential reactions must be restricted, even for "simple" systems, by the use of suitable protecting groups.

It was with this goal in mind that the reactions of RP-bridged trinuclear clusters, which form the basis of this review, have been studied.

Clusters such as those shown in Figure 1 fulfill the requirement of "simplicity," since their triangles of metal atoms represent the simplest possible case of a metal surface. The μ_3 ligand functions as a "protecting group" that can hold the metal atoms together even when the metal-metal bonds break in the course of a reaction.

1.1. The Scope of this Review[10]

Although the species R-El (El = element of the third to the sixth main group) and also the elements El themselves can in principle function as μ_3-bridging ligands Z in trinuclear clusters, most cluster-specific reactions have been carried out using RP-bridged carbonyl clusters. It is this aspect of cluster chemistry that is reviewed here for the first time. Reactions at clusters with bridging elements of the sixth main group are included here only when they contribute directly to the understanding of the reactivity of the fifth-main-group analogues. Reactions of the well-

[*] Prof. Dr. G. Huttner [+], Dipl.-Chem. K. Knoll
Lehrstuhl für Synthetische Anorganische Chemie,
Fakultät für Chemie der Universität
Postfach 5560, D-7750 Konstanz (FRG)

[+] Present address:
Anorganisch-chemisches Institut der Universität
Im Neuenheimer Feld 270, D-6900 Heidelberg (FRG)

 © VCH Verlagsgesellschaft mbH, D-6940 Weinheim, 1987 0570-0833/87/0808-0743 $ 02.50/0

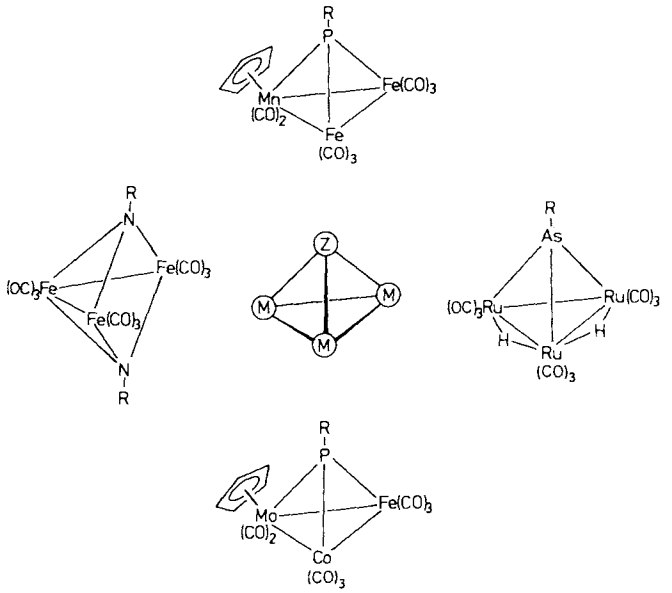

Fig. 1. Examples of μ_3-bridged clusters $[(\mu_3\text{-Z})M_3]$.

studied system $[(\mu_3\text{-RC})Co_3(CO)_9]$ are not discussed, since they have been reviewed already[11] and are generally not cluster-specific insofar as they mostly involve reactions at the organic group R. The μ_2-RX-bridged complexes (X = P, As, Sb, Bi) are not clusters; they are unsaturated systems by virtue of their trigonal-planar coordination at X and their chemistry has also been reviewed.[12, 13]

This review concerns itself not only with the reactivity of RX-bridged clusters (X = N, P, As, Sb, Bi; X always stands for an element of the fifth main group), but also with their synthesis, since this subtopic, too, has not yet been reviewed (except for X = N[14]).

2. Synthesis of Clusters with μ_3-RX Bridges

The first compound with a μ_3-RP group, $[(\mu_3\text{-}C_6F_5P)_2Fe_3(CO)_9]$, was synthesized in 1971 by the reaction of the corresponding oligocyclophosphane with iron carbonyls.[15] Although oligocyclophosphanes are established sources of RP fragments,[16] they have not been further used in the synthesis of μ_3-RP-bridged clusters. However, numerous unusual compounds with RX oligomers (X = P, As) as ligands have been prepared.[17] Another preparative method that immediately suggests itself is the reaction of metal carbonyls with RXH_2; this method was also employed very early.[18] Reactions between neutral or anionic metal carbonyls and $RXHal_2$ form another well-documented synthetic approach.[19]

2.1. Syntheses from RXH_2

The reaction of $[M_3(CO)_{12}]$ (M = Fe,[20] Ru,[21, 22] Os[22, 23]) with RPH_2 has proved a reliable method of obtaining μ_3-RP-bridged clusters; it leads smoothly and by an easily understood route to the compounds $[(\mu_3\text{-RP})M_3(CO)_9(H)_2]$. Although the reaction with $[Fe_3(CO)_{12}]$ leads, without a detectable intermediate, to good yields of the final product,[20] the reaction steps can be analyzed in detail if the kinetically and thermodynamically more stable $[Os_3(CO)_{12}]$ **1** is used as the carbonyl component (Scheme 1).[22, 23] The

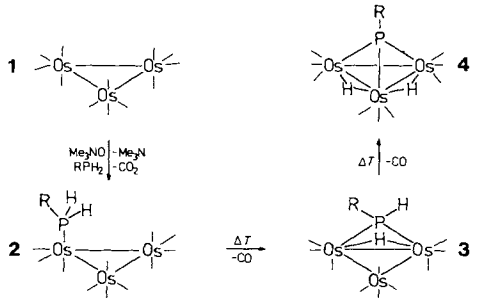

Scheme 1. Stepwise formation of μ_3-RP bridges from RPH_2 [*].

first step is the substitution of an axial carbonyl group by the RPH_2 ligand, which is made possible by oxidation of the carbonyl group to CO_2 by Me_3NO.[24] The intermediate **2** can be thermally decarbonylated; the electron deficit that arises is compensated by the formation of a new Os–P bond and the migration of a hydrogen from phosphorus to a μ_2-bridging position, forming **3**. Intermediate **3** can then undergo thermal decarbonylation, migration of a further hydrogen from phosphorus to a metal–metal edge, and formation of a third Os–P bond to give the final μ_3-RP-bridged cluster **4**.[22, 23]

The same reaction pattern has also been demonstrated for the reaction of $[Ru_3(CO)_{12}]$ with RPH_2.[21] The individual steps that have been discussed here in detail are also likely to occur in other reactions where μ_3-RX bridges are formed from polynuclear metal carbonyls and RPH_2[20] or $RAsH_2$,[23] even when the intermediate stages cannot be proved. One such example is the thermolysis of $[(OC)_4Fe(AsMeH_2)]$ to the cubane structure **5**.[25]

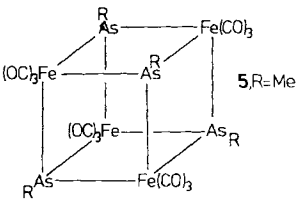

Reactions in which RX groups are formed from RXH_2 precursors can be modified to allow the synthesis of heterometallic RX-bridged clusters: complexed phosphanes or arsanes $[L_nM(RXH_2)]$ react with $[Fe_3(CO)_{12}]$ with the formation of heterometallic μ_3-RX-bridged clusters. In such reactions, the organometallic fragment L_nM is incorporated into the cluster together with the RX group and occupies one position of the triangular base of the μ_3-RX-bridged cluster. An example is the synthesis of **6**.[26] Complexes of primary phosphanes or arsanes react smoothly in this way with $[M_3(CO)_{12}]$ (M = Ru, Os).[26]

Binuclear phosphide complexes (e.g., **7**) with a P–H bond can be used instead of complexes of terminally

[*] Here and elsewhere in the text, a short line extending from a metal atom signifies a CO group.

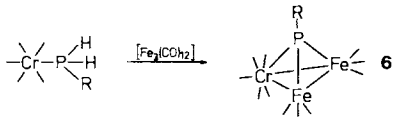

bonded primary phosphanes; their reactions with reactive metal carbonyls lead to μ_3-RP-bridged clusters such as **8**.[27] Although these reactions often give good yields,

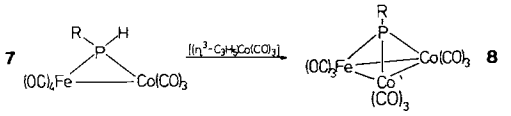

nothing appears to be known about the mechanism. The first step cannot be a simple substitution, because the starting materials $[L_nM(RXH_2)]$ cannot act as donors. The stoichiometry of the reactions show that the bond between M and X is preserved during the reaction. The deciding factor might well be the relative weakness of the P–H or As–H bond, and it seems plausible that radical reactions are involved. Radical insertions into P–H bonds have been thoroughly studied.[28] Furthermore, the radicals $[L_nM(RXH)]^{\odot}$ are expected to be electronically stabilized.[29]

2.2. Syntheses Starting from $RXHal_2$

The reactions of metal carbonyls or carbonylmetalates with halides of the heavier main-group elements have been described in the classical studies of *W. Hieber* et al.[30] Early systematic studies of the system $XHal_3/[Co(CO)_4]^{\ominus}$ by *L. Markó* et al.[32,35,36] led to a detailed knowledge of the element-bridged clusters $[(\mu_3\text{-}X)Co_3(CO)_9]$.[31–36] The early structure analyses in this field were almost all performed by *L. F. Dahl* et al.;[34,35] they also recognized the suitability of such reactions for the formation of unusual ligands such as complex-stabilized As_2 in $[Co_2(CO)_6(\mu_2\text{-}\eta^2\text{-}As_2)]$.[35] This synthetic route was not applied to the preparation of μ_3-RX-bridged clusters until fairly recently.[37–39] Scheme 2 shows the detailed course of such reactions for a well-studied example.[40]

Dihalophosphanes react with $[Fe_2(CO)_9]$ to give the $Fe(CO)_4$ derivatives **9**.[40] Further $[Fe_2(CO)_9]$ then reacts to give the binuclear, $(\mu_2\text{-Cl})(\mu_2\text{-RPCl})$-bridged clusters **10**;[40] the first step in their formation can be regarded as the insertion of a carbene-analogous[41] $Fe(CO)_4$ unit into a P–Cl bond. A subsequent decarbonylation, with the formation of a metal–metal bond and the incorporation of a previously terminal chlorine into a bridging position, would then explain the formation of **10**. The reductive dehalogenation of **10** presumably leads to the unsaturated 2π-system **11**, the existence of which is indicated by trapping reactions. Reaction with $[Fe_2(CO)_9]$, which acts as a source of $Fe(CO)_4$, gives the μ_3-RP-bridged cluster **12**.[40] Alkynes stabilize **11** by trapping it as the adduct **13**.[42] In the absence of trapping reagents, **11** undergoes dimerization and decarbonylation to give the doubly μ_4-RP-bridged cluster **14**,[40] which is also accessible by another synthetic route[43] (see Section 9). The products **12**–**14** are all formed in good yields.

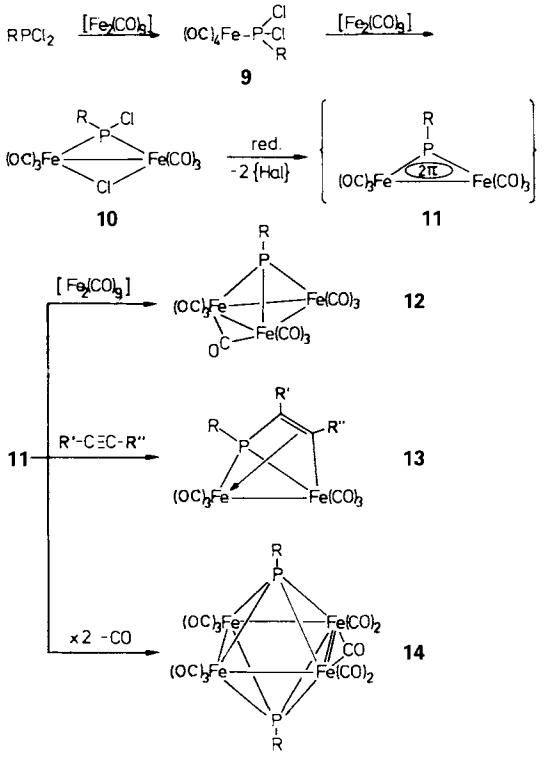

Scheme 2. Stepwise formation of μ_3-RP bridges from $RPCl_2$.

Only in isolated cases can the intermediate stages of the reductive dehalogenation of $RXHal_2$ to μ-RX groups be demonstrated in detail. The reaction of $[Ni_3(CO)_6]_2^{2\ominus}$ with $PhPCl_2$ forms the cluster **15** as the only identifiable product;[44] it consists of a cube of eight Ni(CO) units bridged on all six faces by μ_4-Ph groups.[45]

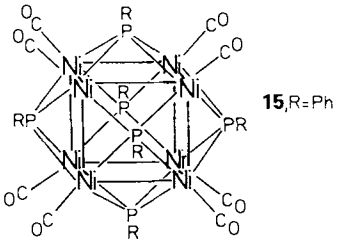

15, R = Ph

As discussed in Section 2.1 for RXH_2, syntheses based on $RXHal_2$ can also be modified to give heterometallic μ_3-RX-bridged clusters. The first example of such a synthesis is the reaction of $[Cp(OC)_2Mn(PhPCl_2)]$ ($Cp = \eta^5\text{-}C_5H_5$) with $[Fe_2(CO)_9]$ to give **16**.[46] Further applications of this synthetic principle are known.[47–50]

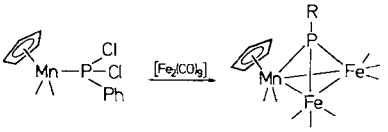

16a, R = Ph

The use of binuclear heterometallic μ_2-phosphido complexes with suitable functional groups on the phosphorus atom provides a simple way of synthesizing μ_3-RP-bridged

clusters with three different metal atoms; one example is the formation of **18** from **17**.[51] It is not always possible,

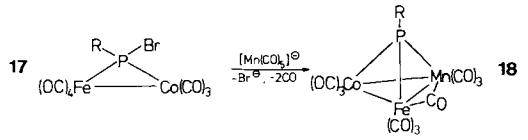

however, to introduce RX and L_nM simultaneously into the cluster. The reaction of $[MeC_5H_4)(OC)_2Mn(PPhBr_2)]$ with $Na[Co(CO)_4]$, for example,[52] leads to the well-known cluster **19**, which is more easily prepared by a different

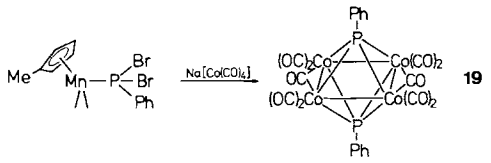

method.[53] The μ_4-RP-bridged cluster **20** arises in a similar manner in the reaction of $[Cp(OC)_2Mn(PhPCl_2)]$ with $[Ru_3(CO)_{12}]$.[54]

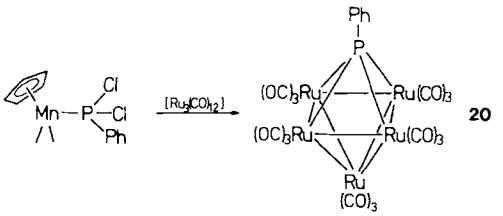

The chemistry of trinuclear μ_3-bridged clusters is connected in several respects with that of binuclear phosphinidene, arsinidene, stibinidene and bismuthinidine complexes $[(L_nM)_2XR]$ (L_nM = 16-electron fragment such as $Cp(OC)_2Mn$, $(OC)_5Cr$):[12, 13]

- The binuclear complexes, in which the main-group element X displays trigonal-planar coordination, are sometimes prepared by similar methods[12, 13] to those used for the μ_3-bridged clusters.
- Trinuclear μ_3-RX-bridged clusters can be regarded as π complexes of such "inidene" complexes[46] (see Section 9).
- Binuclear "inidene" complexes[12, 13, 55] such as **21** can be used to prepare μ_3-RP-bridged clusters (**22**).[56]

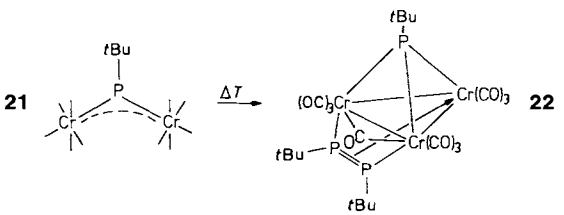

- The stibinidene complexes **23** are in equilibrium (via a valence tautomerism) with metallacyclic stibanes **24**;[12, 13] these can, as Lewis bases, be trapped with 16-electron fragments, forming μ_3-RSb-bridged complexes (**25**).[57]

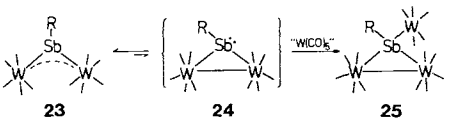

2.3. Synthesis by Cleavage of P–C or P–O Bonds

In connection with the use of phosphanes and phosphites as supporting ligands in catalytically active systems,[58] it is interesting to note that R_3P-substituted clusters are converted into μ_3-RP-functionalized complexes on heating.[59] Monodentate phosphanes or phosphites, as well as bidentate phosphane ligands, can fragment to form μ_3-RP groups. For example, the thermolysis of $[Os_3(CO)_{11}(P(OMe)_3)]$ leads to a complex analogous to **20** (POMe instead of PPh, Os instead of Ru).[60] The thermolysis of $[Os_3(CO)_{11}(PPh_3)]$ **26** leads to the cluster **27**, in which the osmium triangle has been opened on one edge and is bridged on one side by a μ_3-PhP group and on the other by an unusually bonded aryne moiety.[61]

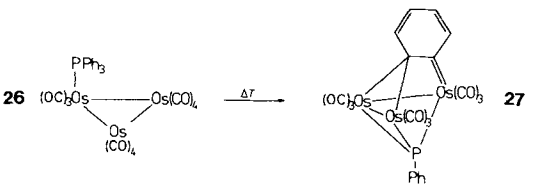

The formation of μ_3-RP groups from R_3P ligands clearly takes place in a stepwise manner. The conversion of **28** to **29**[62] shows that R_2P-bridged complexes can play a role here. The phosphido complex **28**, R = Ph, the first example of η^2-coordination of an aryl group bonded to phosphorus (see also Section 8.2), undergoes hydrogenolysis with elimination of benzene to form the μ_3-PhP-bridged complex **29**. (The synthesis of the analogous osmium complex **4** has been described in Section 2.1.).

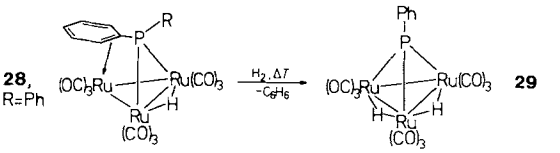

Bis(phosphino)methane ligands can also fragment in the presence of metal carbonyls to form μ_3-RP groups. The first example of a reaction of this type is the synthesis of **31** from **30**.[63]

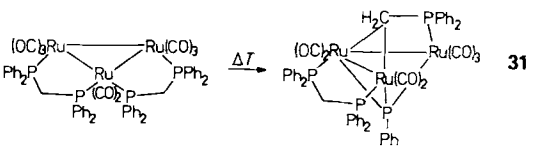

The extension of this principle to the reaction of iron carbonyls with chelating ligands $RHPCH_2PHR$ leads to a wide variety of compounds with μ_3- or μ_4-RP groups; these generally contain further fragments of the ligands, which exhibit widely differing types of coordination.[64]

3. Synthesis of Clusters with μ_3-RN Bridges

The synthetic routes to μ_3-RX clusters (X = higher homologues of group five) described in Section 2 are in general not applicable for μ_3-RN-bridged clusters. The energy required to break the stable N–H bonds is usually not compensated by the energy released upon conversion of an amine to a μ_3-bonded nitrene RN. Only for complexes of the heavier transition elements, which tend to form stronger bonds, are such transformations possible. The use of $RNHal_2$ as a starting material (analogously to the method described in Section 2.2) is impossible because of its strongly oxidizing nature. On the other hand, there are many synthetic equivalents for RN (NO,[65,66] RNO_2,[67] RN_3,[68] RCN,[69,70] $(RN)_2S$,[67,71] etc.) that may be used to form μ_3-RN groups and for which there generally are no stable analogues in the chemistry of the heavier homologues. The great variety of synthetic approaches that have been developed along these lines have been reviewed several times,[14] and therefore only selected examples will be presented here.

H. D. Kaesz et al. have carried out an elegant study of the reaction steps involved in the conversion of cluster-bonded nitrile (**32**) to a μ_3-RN ligand (**35**);[69] the most important intermediates are **33** and **34**.[72]

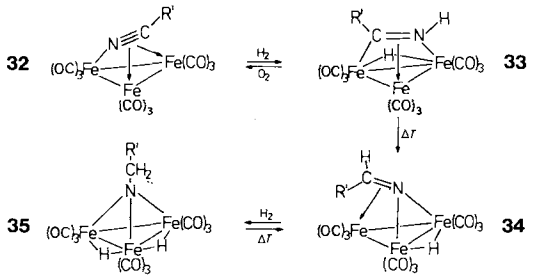

A further well-studied example is the conversion of NO groups to RN moieties.[66] The μ_2-NO group of the anionic complex **36** undergoes electrophilic addition to give the μ_3-RON ligand system of **37**. The μ_3-HON system **37** is

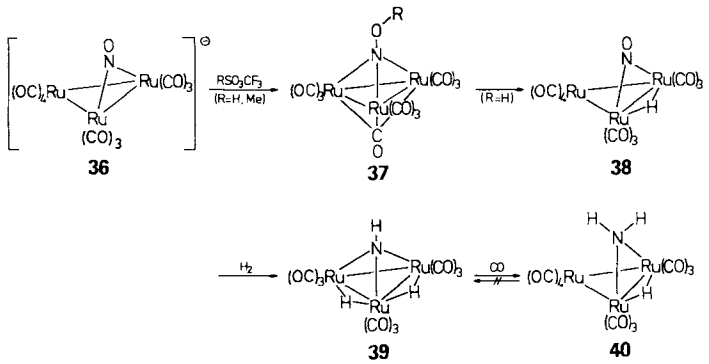

Scheme 3. Stepwise conversion of NO to RN groups.

converted into the tautomeric **38** under base catalysis (e.g., by treatment with $F_3CCOO^{\ominus}$); **38** is apparently more stable thermodynamically than **37** in this case. Cluster **38** reacts with H_2 to give the μ_3-HN-bridged complex **39**. The individual steps of this reaction have not been elucidated, but it is certain that the last step in the formation of the μ_3-NH group does not involve the conversion of μ_2-H_2N to μ_3-HN: Cluster **39** reacts with CO to give the μ_2-H_2N-bridged complex **40**, which, in contrast to its phosphorus analogue **3** (Section 2.1), does not undergo decarbonylation and H migration to form a μ_3-bridged complex (**39**).

Similarly, the thermolysis of **41** ($T = 170$ °C) produces only the μ_2-H_2N-bridged complex **42** (by a single H migration),[74] whereas the μ_2-RHP-bridged complexes analogous to **42** are transformed under relatively mild conditions to the μ_3-RP-bridged complexes (by a further H migration).[22,23] It is however possible for μ_2-RHN groups to

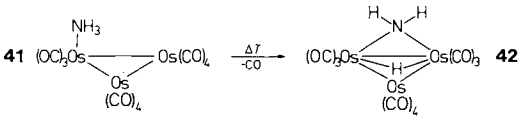

be converted into μ_3-RN groups by thermal activation, as is shown by the decarbonylation of $[(\mu_2\text{-MeHN})(\mu_2\text{-H})Os_3(CO)_{10}]$ to $[\mu_3\text{-MeN})(\mu_2\text{-H})Os_3(CO)_9]$ at $T = 150$ °C.[67] These reactivity differences can be understood in terms of the relative stabilities of the bonds: N–H bonds are more stable than P–H bonds, and M–P bonds (M = Os or Ru) are more stable than M–N bonds.

4. Properties of Trinuclear μ_3-Bridged Carbonyl Complexes

4.1. Bonding

Trinuclear complexes in which metal carbonyl fragments are held together by a μ_3-bridging ligand (as in Fig. 1) are generally diamagnetic and obey the 18-electron rule, which implies a localized bond model. The bridging ligands RX are isolobal analogues of the bridging elements Y (Y = O, S, Se, Te) and formally contribute four electrons to the cluster (see Section 9). Chalcogen bridging elements Y possess a lone pair of electrons which points away from the cluster and can be utilized in the synthesis of larger clusters.[75–77] The μ_3-X ligands (X = N, P, As, Sb) similarly possess a lone pair of electrons with donor properties;[32,52,55,78,79] they contribute three electrons to the cluster. μ_3-RY ligands participate in cluster bonding to the extent of five electrons.

These simple rules for counting electrons are consistent with the assertion that a cluster component containing three valence orbitals and the electrons therein contributes as a unit to cluster bonding.[80] Delocalized bonding models for cage molecules make use of this concept;[80] the counting method employed is therefore adequate for both the 18-electron model and for the newer theories. Both models lead to the same result for the compounds in Fig. 1; for larger clusters (e.g., **14**) the delocalized model is more appropriate (see also Section 9).

Many of the properties of trinuclear μ_3-bridged carbonyl complexes can be derived under the assumption that their HOMO and LUMO are largely metal-centered;[81] the HOMO has M–M-bonding character, the LUMO M–M-antibonding character.[81] Quantum-mechanical calculations support this simple picture.[82,83]

4.2. Analytical Findings

IR spectra: IR spectra in the carbonyl absorption region are very useful for the identification of the compounds discussed here and for following the course of their reactions. As in the case of mononuclear carbonyl complexes, they also provide information about the electron density at the metal atoms, which pass their excess electron density on to the carbonyl groups; the carbonyl absorption frequencies, as expected, become lower with increasing charge density at the metal and higher with increasing positive charge.[84] IR spectra in the longer-wavelength region or Raman spectra, which could provide information about the metal–metal bonding,[85] are unknown for the clusters discussed here.

Electronic spectra: Trinuclear metal carbonyl clusters are colored. The bands in the visible region are associated with electronic transitions between orbitals that are essentially metal-centered. The absorptions are therefore shifted to shorter wavelength as the metal–metal bonding becomes stronger (cf. $[(\mu_3\text{-RP})(\mu_2\text{-H})_2M_3(CO)_9]$: M = Fe, brown; M = Ru, orange; M = Os, pale yellow).

ESR spectra: The absence of a coupling to phosphorus in the ESR signal of the paramagnetic compound $[(\mu_3\text{-RP})Co_3(CO)_9]^{\odot}$,[36] which contains one more electron than expected for a stable compound, led to the conclusion that the singly occupied molecular orbital is exclusively metal-centered.[86] A detailed ESR study of oriented single crystals of $[(\mu_3\text{-S})Co_3(CO)_9]^{\odot}$ came to the same conclusion.[81] The ESR spectrum of the heterometallic cluster anion $[(\mu_3\text{-S})Co_2Fe(CO)_9]^{\odot\ominus}$ indicates a nonuniform distribution of the unpaired electron over the metal atoms.[87,88]

NMR spectra: The ^{31}P-NMR signals of μ_3- or μ_4-RP groups are generally shifted downfield with respect to those of organophosphorus compounds. There is a qualitative correlation between the chemical shift and the color of the compounds; the longer the wavelength of the UV/VIS absorption, the greater is the chemical shift. The ^{31}P-NMR shifts for the series $[(\mu_3\text{-PhP})(\mu_2\text{-H})_2M_3(CO)_9]$ are: M = Os (pale yellow), $\delta = 119$;[23] M = Ru (orange), $\delta = 279$;[26] M = Fe (brown), $\delta = 380$.[20] This observation would imply that the phosphorus chemical shift is determined by the small HOMO–LUMO separation. The extreme chemical shift in binuclear phosphinidene complexes (e.g., $[(\mu_2\text{-}t\text{BuP})(Cr(CO)_5)_2]$, $\delta = 1362$[89]) is rationalized by this model in a straightforward way.

^{13}C-NMR spectra are useful here, as they are generally in metal carbonyl chemistry, for studying CO-scrambling processes.[91]

Mössbauer spectra: Although many μ_3- and μ_4-RP-bridged clusters with iron carbonyl groups are known, Mössbauer spectroscopy has not been used to any significant extent for the analysis of bonding.[92]

Electrochemistry: Since the HOMO in a cluster exhibits metal–metal bonding character and the LUMO metal–metal antibonding character, redox reactions primarily affect the metal–metal bonding system. Metal–metal bonds are relatively weak (at least for 3d metals); therefore, no great expenditure of energy is necessary for one-electron oxidations or reductions. In other words, clusters should be easy to reduce or oxidize electrochemically. The pioneering work of *L. F. Dahl* et al. in this area (on the cluster $[Cp_3Co_3S_2]$) confirms this assertion;[93] it also shows that the total number of electrons in a cluster influences above all the bonding between the metal centers.[94] The μ_3-bridged metal carbonyl clusters do not display such a marked redox activity as the notoriously redox-active sulfur–cubane systems.[95] Single-electron redox processes are found, for example, for $[(\mu_3\text{-RP})Co_3(CO)_9]^{\odot}$[86] and for the corresponding heterometallic clusters in which one or two $Co(CO)_3$ fragments are replaced by other organometallic moieties.[86–88] More often, however, the one-electron reductions of the μ_3-bridged metal carbonyl clusters with noble-gas configurations are irreversible; the occupation of the metal–metal antibonding LUMO weakens the metal–metal bonds and renders the complexes labile to substitution (see Section 4.1). Cyclovoltammograms that appear irreversible in the coordinating solvent CH_3CN are therefore often reversible in the non-coordinating solvent CH_2Cl_2.

The one-electron oxidation of trinuclear metal carbonyl clusters having noble-gas configuration is almost always irreversible; the metal–metal bonds are weakened by removal of an electron from the bonding HOMO and, additionally, the bonding to the carbonyl groups becomes more labile owing to the positive charge. If some of the carbonyl groups are replaced by donor ligands,[96] however, one-electron oxidations can become reversible.[97]

Mass spectra: Most μ_3-bridged trinuclear metal carbonyl clusters give readily interpretable mass spectra, showing the molecular ion and fragments derived from it by successive decarbonylation, even under electron-impact (EI) conditions. A decarbonylation series of doubly positively charged cluster ions is also sometimes observed.

The energetically low-lying LUMO makes the clusters accessible to investigation by negative-ion mass spectrometry;[98] the relative yields of negative ions formed under EI conditions are at least as high as those attained with the standard examples of negative-ion mass spectrometry (e.g., $C_6H_3Cl_2NO_2$[99]). However, whereas these organic compounds almost exclusively give rise to chemically uninformative anion fragments such as $Cl^{\ominus}$ or $NO_2^{\ominus}$,[99] the μ_3-RP-bridged metal carbonyl clusters bear the negative charge themselves.[100] $M^{\odot\ominus}$ is not observed, the strongest signal usually being that of $M^{\odot\ominus} - CO$.[98,100] The lability of the metal–ligand bonds of cluster radical anions[88,101] is thus evident also in the gas phase.

5. Substitution Reactions

5.1. Substitution as an Addition–Elimination Sequence

Substitution reactions at mononuclear carbonyl complexes are usually initiated dissociatively; i.e., the first step is the breaking of an M–CO bond.[102] The activation can be induced thermally, photochemically, by one-electron redox processes, or by other chemical means.[102] For clusters, the same activation processes lead to substitution products. A side reaction, especially for 3d clusters with their weak metal–metal bonding, is the disintegration of

the cluster framework and consequent formation of mononuclear compounds;[103, 104] this can in some cases become the main reaction. Kinetic studies are made more difficult by these side reactions; although the partial fragmentation of the clusters must be seen as a clear indication of the reactivity of metal–metal bonds, the substitution of cluster-bound carbonyl groups is generally considered (by extrapolation from the chemistry of mononuclear complexes) to be based on an M–CO dissociative mechanism.[104] For $[Ir_4(CO)_{12}]$, on the other hand, it had been demonstrated already in an early investigation[105] that such reactions may be initiated associatively. Proof that CO substitution at clusters is mediated by the reactivity of the metal–metal bonds was provided by μ_3-RP-bridged clusters: Heterometallic clusters of the type **16** react with two-electron donors L (L = CO, R_3P, etc.) forming the adducts **43**, in which the ligand L has added to an iron atom with concomitant breaking of a manganese–iron bond.[106] The second manganese–iron bond of **43** reacts similarly, so that the clusters **43** can be converted into the adducts **44** by the action of further L; two metal–metal bonds of **16** are broken in going to **44**. Both reactions are strictly reversible; the stepwise elimination of L from **44** converts it into **43** and then to the closed tetrahedral starting material **16**.[106, 107] This reaction sequence shows for the first time that metal–metal bonds in trinuclear clusters can be opened by the addition of donor ligands and reformed by their elimination.

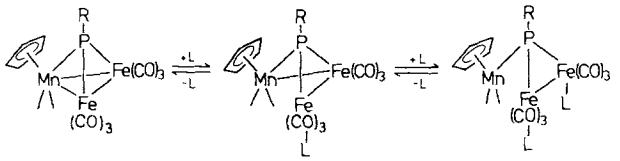

16 **43** **44**

This reactivity pattern was demonstrated some time ago for metal–metal bonds in binuclear complexes[108] and more recently in other trinuclear and in higher-nuclearity clusters;[109] the most striking example is the stepwise "unfolding" of the trigonal bipyramidal cluster $[Os_5(CO)_{16}]$ and its derivatives[110] with the eventual formation of a structure with two vertex-bridging triangles.

5.2. Clusters as Valence-Tautomeric Systems

The mechanism of the reversible opening of a metal–metal bond was investigated by kinetic methods for the system **16/43** in a detailed study.[111] The bond-opening process seems at first sight to follow a second-order rate law (first order in both L and **16**); a large excess of ligand, however, inhibits the reaction, which indicates the existence of a preequilibrium species. The activation parameters for the formation of the species **16**$^+$ involved in this equilibrium (necessarily independent of the nature of L) are $\Delta H^+ = 93$ kJ mol^{-1} and $\Delta S^+ = 34$ J mol^{-1} K^{-1} for **16a**$^+$ (R = Ph). Both values are consistent with the proposed intermediate **16**$^+$ derived from the starting cluster **16** by the breaking of an Fe–Mn bond;[111] the bond enthalpies of 3d metals in clusters are usually ca. 100 kJ mol^{-1},[112] and the activation entropy should be positive

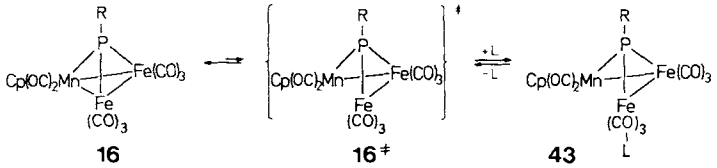

16 **16**‡ **43**

because of the release of strain on forming the edge-opened intermediate. The opening of a metal–metal bond by a two-electron donor L therefore corresponds to the trapping of a bond-opened form that is in valence-tautomeric equilibrium with the closed cluster. The reconversion of **43** to **16** is first order with respect to **43**; the activation parameters for this process suggest that it is initiated by dissociation of L.[111]

The essential result of these studies is that the metal–metal bonds are not broken by the nucleophile L in an S_N2-type reaction, but that an unsaturated form of the cluster with one bond opened (a form in valence-tautomeric equilibrium with the normal cluster) is trapped by the nucleophile.[111]

5.3. Clusters as Sterically Protected Systems

Stereochemical considerations suggest that a direct reaction between a ligand L and a metal–metal bond should barely be possible; metal–metal bonds in saturated carbonyl clusters are so effectively shielded that even a sterically undemanding ligand cannot approach them closely enough to initiate a direct interaction. This is confirmed by kinetic studies of the deprotonation of the cluster **45a** to form **46a** (Table 1).[113]

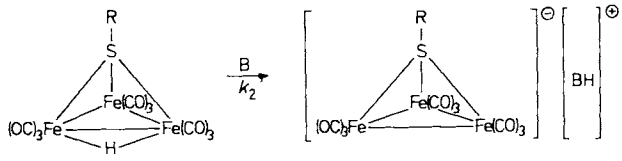

45 **46**

a, R = *t*Bu

Table 1. Kinetic parameters for the deprotonation of **45a** [a].

Base B	nBuNH$_2$	nBu$_2$NH	nBu$_3$N	[b]
k_2 [L mol^{-1} s^{-1}]	2.8	4.3×10^{-2}	1.5×10^{-3}	6×10^{-4}
k_H/k_D	13	3.6	1.6	1.1

[a] $T = 303$ K; solvent, toluene. [b] 2,2,6,6-tetramethylpiperidine.

The deprotonation in toluene with various amines as the base B is first order both in **45a** and B. The rate constants k_2 decrease with increasing size of B, as do the isotope effects k_H/k_D. The interpretation of these observations is obvious from examination of Figure 2. The space-filling model shows that even as small a base as methylamine can scarcely reach the hydrogen atom that bridges a metal–metal edge. The larger the base, the more activation energy must be expended to deform the cluster sufficiently to allow the base to reach the hydrogen and remove it as a proton. The isotope effects show that the proton transfer step in each case plays a role in determining the reaction rate.

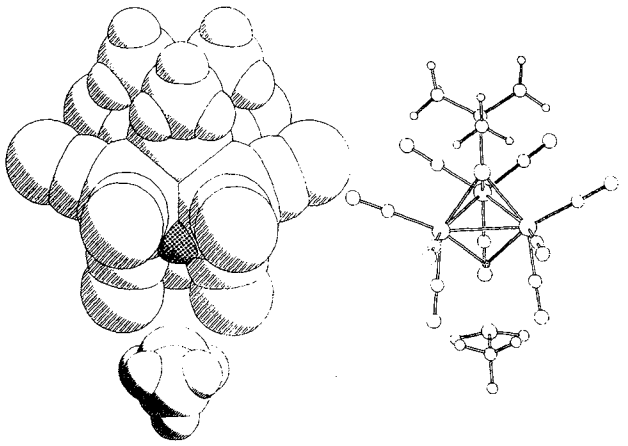

Fig. 2. Steric hindrance in clusters: space-filling model and ball-and-stick model of **45a** and of the base $MeNH_2$. The bridging hydrogen atom is dotted.

The unusually large isotope effect $k_H/k_D = 13$ observed for the small base nBuNH$_2$ may be ascribed to proton tunneling through a narrow energy barrier.[114]

These studies[113] support the view that a μ_2-H ligand in a tetrahedral carbonyl cluster is very strongly shielded. If a bridging hydrogen above the edge of a metal cluster is so well shielded, the metal-metal bond itself must be even less accessible to direct attack by a nucleophile. Therefore, the metal-metal bonds in carbonyl clusters cannot react directly, but must first be broken.

5.4. Substitution at Saturated Clusters

The photochemical cleavage of metal-metal bonds has been thoroughly investigated.[115, 116] It is therefore not surprising that the formation of the adducts **43** from **16** and L can be markedly accelerated by irradiation;[107] the reactive intermediate is presumably a bond-opened form similar to the species **16**$^+$ invoked for the thermal activation. The selectivity of the reverse thermal reaction **43** → **16** (elimination of L only) is not observed for the photochemical process; CO is eliminated also, leading to the substituted derivatives **16**′.[107] The conversion **16** → **16**′ via the adduct **43** demonstrates one possible mechanism of photochemical substitution at clusters.

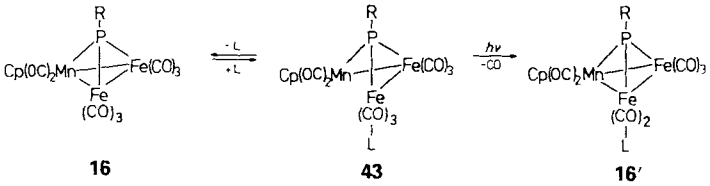

16 **43** **16′**

The investigation of the reaction of $[(\mu_3\text{-RP})Fe_3(CO)_{10}]$ **12** with the two-electron ligand $P(OMe)_3$ shows that substitution at clusters can occur by addition-elimination reactions even in the case of thermal activation (Scheme 4).[117] All compounds in Scheme 4 that are not in brackets have been isolated, and all processes indicated by arrows have been studied in detail.[117, 118]

It is probable, from the results discussed here, that substitution reactions of clusters always occur by addition-elimination sequences involving the breaking of metal-metal bonds, as long as the energy required to break a metal-metal bond is no greater than that required to dissociate a peripheral ligand. Such a mechanism is particularly likely for clusters of 3d elements.

For photochemically induced substitutions, the breaking of a metal-metal bond and the associated addition-elimination mechanism is the most probable process irrespective of the relative strengths of the metal-metal and metal-carbonyl bonds (cf. Sections 4.1 and 4.2). Similarly, it can be assumed that the first step of reduction-catalyzed substitution is the breaking of a metal-metal bond (the LUMO is M-M antibonding) (however, see Section 8), and that here, too, addition and elimination are the natural steps of the substitution process.

5.5. Addition and Elimination in Unsaturated Clusters

The addition-elimination mechanism is the natural and experimentally well-substantiated route of substitution for unsaturated clusters, i.e., those that possess two electrons

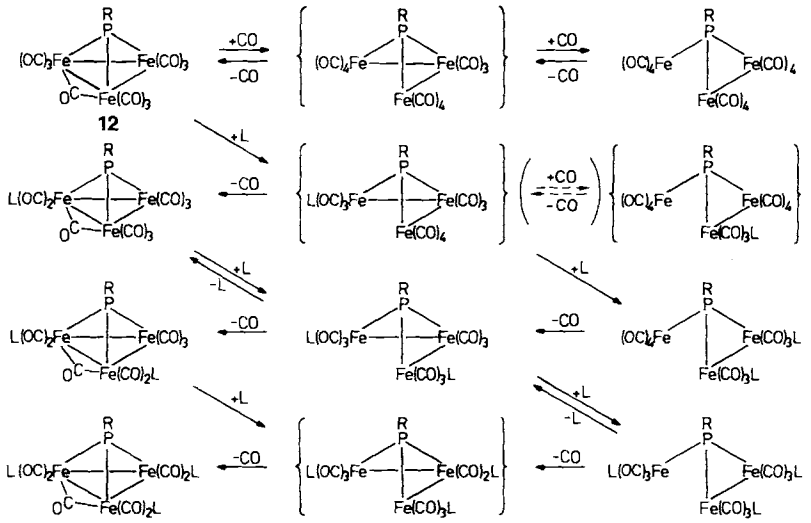

Scheme 4. Addition-elimination sequences for the system **12**/L (L = P(OMe)$_3$).

too few according to the noble-gas rule and thus can accommodate a donor ligand electronically and, usually, also sterically.[119] The cluster geometry is altered comparatively little by the addition of a donor ligand; a formal metal-metal double bond is transformed to a somewhat longer single bond. Unsaturated RP-bridged clusters also display this type of reactivity, as has been shown for the tetranuclear iron compound **14**.[120] The doubly μ_4-RP-bridged **14** is unsaturated according to the noble-gas rule; it possesses two electrons fewer than the rule would predict. Although

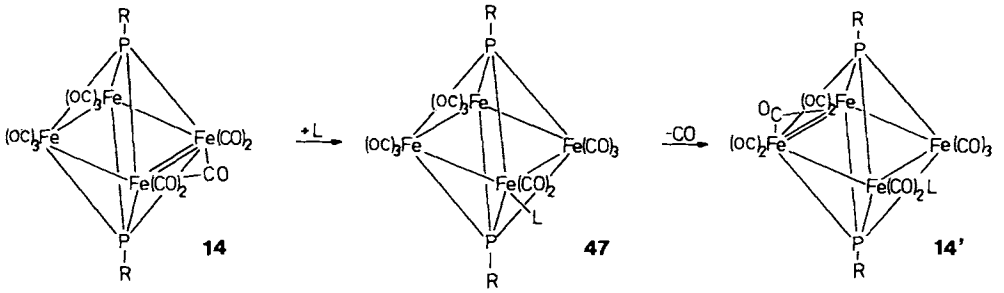

the bond lengths of the cluster do not reveal the localized unsaturation implied by the metal-metal double bond of formula **14**, its ability readily to add two-electron ligands can best be understood in terms of this formula. For L = CO, the reaction sequence **14** ⇄ **47** ⇄ **14** leads, via the adduct **47**, back to the starting complex. If L is a different two-electron ligand, the same reaction sequence corresponds to a substitution reaction that leads to **14'** via an intermediate addition product.[121]

6. Oxidative Addition and Reductive Elimination

6.1. Oxidative Breaking of Metal-Metal Bonds

The formal counterpart of the opening of metal-metal bonds by nucleophiles (see Section 5) is their opening by electrophiles. This reaction type has been observed for μ_3-RP-bridged clusters.[122] However, since the structure of the addition products has not been firmly established,[122] a well-established example from the chemistry of μ_3-RS-bridged clusters will be presented instead. Reaction of the anionic cluster **46** with inorganic electrophiles EHal results in breaking of one iron-iron bond and formation of

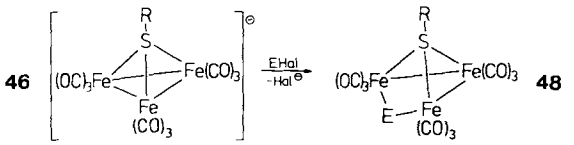

48;[123] the electrophilic groups E are thereby inserted into a metal-metal bond, and the negative charge of the starting cluster **46** is transferred to the halogen. The overall process, as an oxidative addition, corresponds to a standard reaction type observed for mononuclear organometallic compounds,[84] which is also established for some polynuclear compounds.[7]

The cluster **46a** reacts with divalent electrophiles such as $RPCl_2$ or $SOCl_2$ with elimination of *t*BuCl and $Cl^{\ominus}$ to form the doubly μ_3-bridged clusters $[(\mu_3\text{-S})(\mu_3\text{-RP})Fe_3(CO)_9]$ and $[(\mu_3\text{-S})(\mu_3\text{-SO})Fe_3(CO)_9]$, respectively.[124]

6.2. Reductive Elimination

The groups E of the clusters **48** (prepared by oxidative addition) are generally so firmly bound as three-electron bridging ligands that the reverse reaction, the reductive elimination of $E^{\oplus}$, is generally not realizable. The reduction of **48**, E = I, to **46** by reducing agents such as iodide[125] furnishes an exception to this statement and thus shows that such reactions are in principle possible. The re-

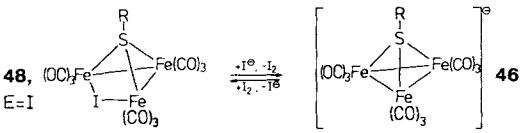

ductive elimination and oxidative addition in this system are in equilibrium, so that either **48**, E = I, or **46** may be present in the reaction solution depending on the $I_2/I^{\ominus}$ content.[125, 126]

6.3. CO/H_2 Exchange: Hydride Metal Clusters[127]

The bridging carbonyl group in the compounds $[(\mu_3\text{-RX})M_3(CO)_{10}]$ (M = Fe, Ru, Os) can usually be replaced easily by two bridging hydrogen atoms, forming $[(\mu_3\text{-RX})(\mu_2\text{-H})_2M_3(CO)_9]$. The photochemically initiated conversion of **49** to **35a** is an example of such a reaction.[128]

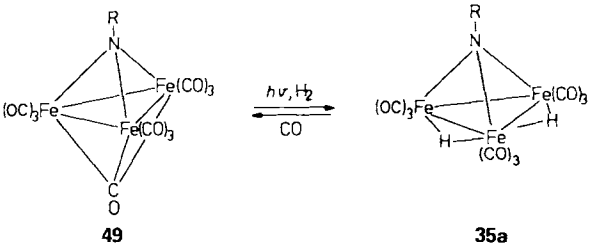

The available evidence would seem to indicate that the photochemical or thermal replacement of CO by H_2 is easier for those clusters $[(\mu_3\text{-RX})(\mu\text{-CO})M_3(CO)_9]$ that contain

a μ_3-bridging CO. Compounds with a μ_2-CO group, such as $[(\mu_3\text{-RP})(\mu_2\text{-CO})Fe_3(CO)_9]$ **12**, do not give selective reactions with this method.[129] Their conversion to the μ_2-H-bridged clusters **50** must therefore be achieved by indirect routes.[130, 131] The reconversion of the μ_2-H-bridged complexes to the carbonyl-bridged clusters with carbon dioxide is often possible by thermal activation. Chemical methods of activation are also available (e.g., **50** → **12'**).[132]

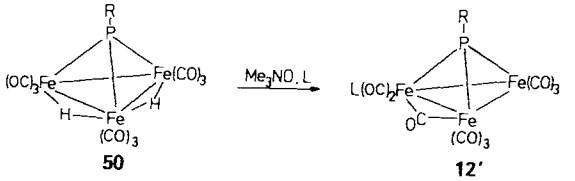

The mechanism of CO/H_2 exchange (in either direction) is unknown. From Section 5 it seems plausible that the thermally or photochemically induced reactions of $[(\mu_3\text{-RX})M_3(CO)_{10}]$ proceed via breaking of metal–metal bonds. For the symmetrical μ_3-CO-bridged complexes such bond breaking should be homolytic, whereas the results presented in Section 5 suggest that heterolytic bond cleavage should occur for the μ_2-CO-bridged species. The differing reactivities of the two structural variants of $[(\mu_3\text{-RX})M_3(CO)_{10}]$ with respect to CO/H_2 exchange could be explained in this way.

RX-bridged hydride metal clusters such as the ruthenium cluster **29** and the iron cluster **50**, like other clusters with hydride bridges, react with bases, $H^{\oplus}$ being abstracted.[130, 131, 133] The triiron compounds are the strongest acids of the cluster type $[(\mu_3\text{-RP})(\mu_2\text{-H})_2M_3(CO)_9]$.[130, 134] The ruthenium and osmium homologues of **50** are less acidic than **50** itself;[133] this is consistent with the general observation that all metal ligand bonds become stronger when a transition metal in a given complex is replaced by a heavier homologue. Cluster **50** is such a strong acid (for its first dissociation) that it is in equilibrium with its conjugate base even in tetrahydrofuran.[131] The second deprotonation of **50** is, as would be expected, appreciably more difficult, but is possible with strong bases such as $NaNH_2$.[131] The fact that metal cluster hydrides are sterically hindered acids was discussed above (Section 5.3).

The μ_3-RX-bridged cluster anions undergo a variety of reactions with electrophiles; the synthesis of higher-nuclearity clusters (**51** → **52**)[133] and the introduction of further μ_3-bridging ligands (**53** → **54**)[124] are two examples.

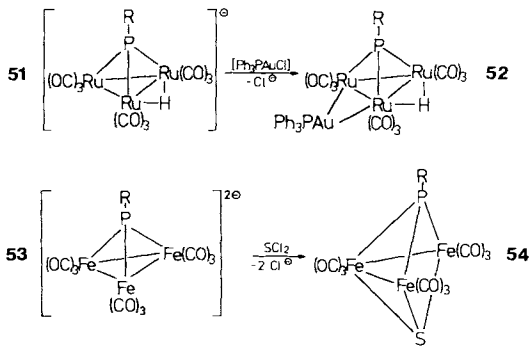

7. Metal-Exchange Reactions

The metal carbonyl fragments $M(CO)_n$ that form part of the base of the clusters $[(\mu_3\text{-Z})(M(CO)_n)_3]$ can be replaced by other organometallic moieties. The cobalt clusters (M = Co) are particularly reactive in this respect; metal exchange occurs for the diamagnetic complexes (Z = RC[136–138]) and for the more labile paramagnetic complexes (Z = RP, S[139]).

The replacement of $Co(CO)_3$ units by the isoelectronic complex fragment $CpM(CO)_2$ (M = Cr, Mo, W) follows a particularly clear course; the metal-substituted arsane $[Cp(OC)_3M(AsMe_2)]$[140] first replaces a carbonyl group at the base of the cluster **8**, forming **8'**. Thermal activation of **8'** leads to the elimination of $[Co(CO)_3(AsMe_2)]_x$, whereby the $Cp(OC)_2M$ group, previously indirectly bound to the cluster, takes the place of the $Co(CO)_3$ unit. This elegant method made possible, for the first time, the synthesis of clusters such as **55**; these are chiral because of the three different metals in the base of the tetrahedron.[141, 142]

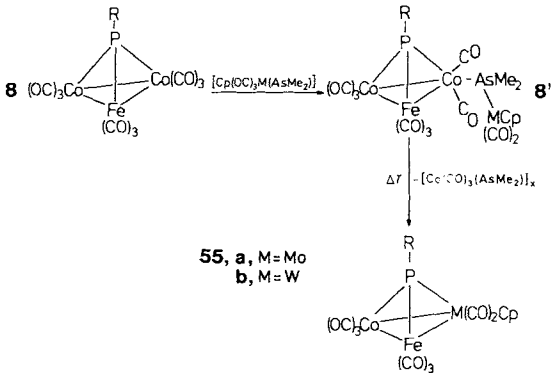

Less systematic, but often productive, methods of exchanging metal atoms in the base of a cluster include metathesis with compounds such as $[(CpNiCO)_2]$, $[Co_4(CO)_{12}]$, and $[Fe_2(CO)_9]$.[137, 138, 143–145]

The reaction sequence **56** → **8** → **55a** can be regarded as an example of a redox-catalyzed exchange of metals in the base of a cluster.[139] The replacement of $Co(CO)_3$ by

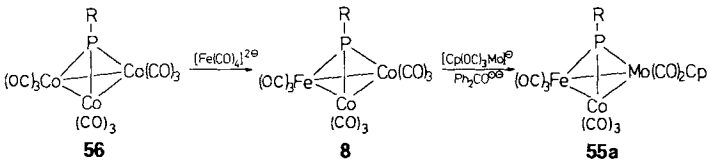

$Fe(CO)_3$ using $[Fe(CO)_4]^{2\ominus}$ necessarily involves intermediate redox stages. The first stage of this reaction could be the breaking of a metal–metal bond and/or carbonyl substitution with $[Fe(CO)_4]^{2\ominus}$ acting as a Lewis base, without any primary electron transfer. The second step, like the conversion of **8** into **55a** mediated by $Ph_2CO^{\odot\ominus}$,[146] is doubtless a redox-catalyzed reaction (cf. Sections 4 and 8.1) in which the bonding in the metal triangle is weakened by the uptake of an electron into the M–M antibonding LUMO.

8. Reactions Involving Participation of the RX Bridge

The examples presented in Sections 5 and 6 have shown that the metal-metal bonds are the reactive sites in μ_3-RX-bridged clusters and that reactions at μ_3-RX-bridged clusters are susceptible to detailed analysis because the metal-X bonds hold the metal carbonyl fragments together. The metal-metal exchange reactions described in Section 7, however, showed that metal-X bonds as well as metal-metal bonds can be broken in the course of a reaction.[147]

8.1. The Cleavage of M-X Bonds[148]

The bond types involved in a reaction (whether only the metal-metal bonds or, in rarer cases, only the metal-X bonds, or both) clearly depend on the nature of the reagents just as much as they depend on the type of activation or the nature of the cluster. The principles determining the particular mechanism are poorly understood. An important factor determining the reaction path is the relative stability of the metal-metal and metal-X bonds on the one hand and the metal-substrate and X-substrate bonds on the other. The conversion of the μ_3-HN group of **39** to the μ_2-H_2N group of **40** (Scheme 3) is an example of the selective breaking of a metal-X bond by the addition of a two-electron ligand to a μ_3-bridged cluster. The selective opening of the osmium-sulfur bond in **57**[149a] is an even more direct counterpart of the opening of metal-metal bonds by two-electron ligands (Section 5). The osmium-sulfur bond is obviously less stable than the osmium-osmium bond.

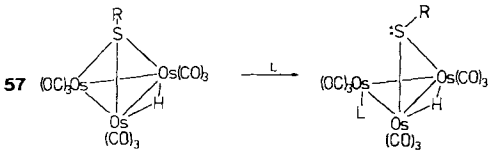

The ability of trinuclear osmium carbonyl compounds to form unsaturated metallacycles (cf. $[Os_3(CO)_{10}(H)_2]$) could also favor the observed reaction path. A similar mechanism has been discussed for the reaction of $[(\mu_3\text{-RP})(\mu_2\text{-H})_2Os_3(CO)_9]$ **4** (which is isoelectronic to **57**) with carbonyl metal fragments.[149b]

An example of the breaking of a metal-phosphorus bond by two-electron ligands is the reaction of the unsaturated ruthenium cluster **58** (homologous with **14**) with CO.[150] Whereas the tetranuclear iron cluster **14** adds CO reversibly to the multiple bond,[120] its ruthenium homologue **58** incorporates two CO groups, one metal-metal and one metal-phosphorus bond being broken.[150] The product **59** can be regarded as a derivative of a complex of

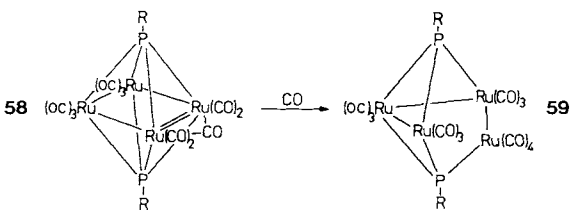

the type $[(\mu_3\text{-RP})_2M_3(CO)_9]$ in which a carbene-analogous $Ru(CO)_4$ group has been inserted into a Ru-P bond. In this case, both metal-metal and metal-phosphorus bonds are involved. An example where only the metal-phosphorus bond is broken is the photochemically initiated addition of diphenylacetylene to **60** to give **61**.[151] Photochemically excited **60** apparently reacts as a diradical with the

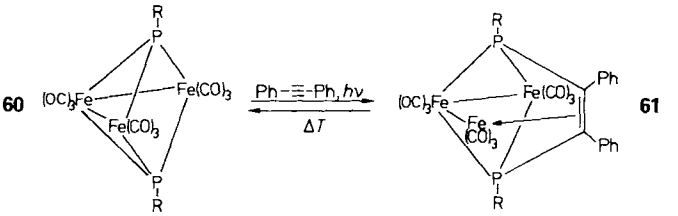

radical centers at phosphorus. Two iron-phosphorus bonds are replaced by two carbon-phosphorus bonds. The reaction is thermally reversible.

Electrocatalytic CO substitution in **60** apparently proceeds similarly.[152] The ESR spectrum of the one-electron reduction product of **60** shows that a species with two different coordinated RP bridges is involved as intermediate. The most probable structure of this intermediate is therefore **60**$^{\odot\ominus}$.[152] Electrochemical activation of μ_4-RP-bridged clusters appears to involve similar steps.[153]

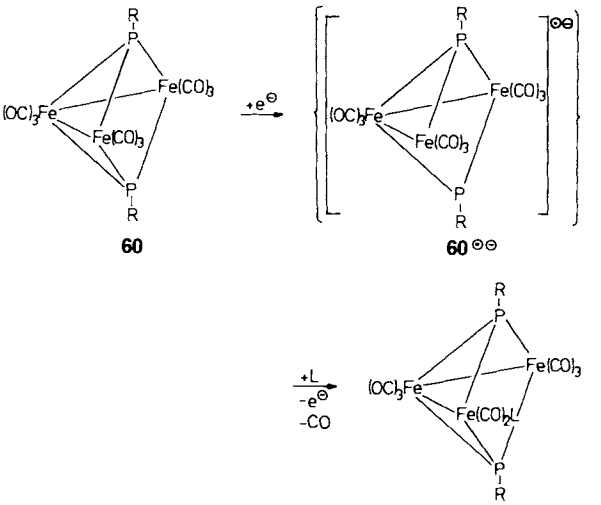

8.2. Addition of Carbenes to μ_3-RP Groups

The pyrophoric dianions **53**[130, 131] react as nucleophiles with CH_2I_2, the CH_2 group adding to a Fe-P bond.[130, 131] The adduct, the complex **62**, can be regarded as a cluster-

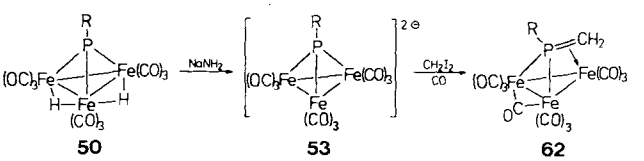

stabilized phosphaalkene.[130, 131, 154, 155] Even if the formation of a phosphaalkene ligand does not necessarily imply the existence of an intermediate with a complex-bound CH_2 group, this still seems probable in view of the fact that **53** reacts with Ph_2SnCl_2 to give **63**, in which the carbene analogue Ph_2Sn bridges one metal edge.[156] The reaction

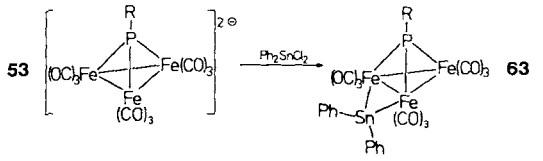

stops at the stage **63** because a further reaction to form a molecule analogous to **62** would involve the formation of an unstable phosphastannaalkene.[157]

Proof of the migration of a metal-bonded carbene to a μ_3-bridging phosphorus is provided by the conversion of the acylato complex **64** (obtained from $[(\mu_3\text{-PhP})_2Fe_3(CO)_9]$[158]) to the phosphaalkene complex **65** by

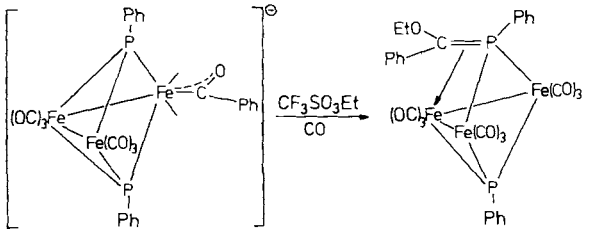

treatment with ethyl trifluorosulfonate.[158] The generation of a Fischer-type carbene complex as intermediate is implied by the isolation of such complexes (**66**) from analogous reactions with $[(\mu_3\text{-PhN})_2Fe_3(CO)_9]$.[158] The carbene complex **66** reacts with CO with the elimination of the corresponding imidoester **68** and the generation of **67**.[158]

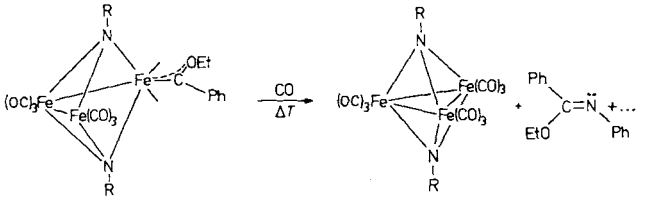

Cluster-bound phosphaalkenes can be derived from methylenephosphoranes $R_3P{=}CH_2$ by the formal replacement of two R–P bonds by metal–P bonds. However, whereas methylenephosphoranes are carbon nucleophiles,[160] phosphaalkenes possess an electrophilic center at carbon.[130, 131] Thus **62** reacts with complex hydrides as the nucleophilic reagents at the methylene carbon,[130, 131] its

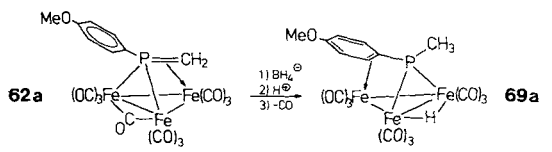

phosphaalkene group $RPCH_2$ being converted into a μ_2-RPMe phosphido bridge. If R is an aryl group (e.g., *p*-MeO–C_6H_4 in **62a**), the acid workup of the anionic phosphido complexes affords products in which one of the formal double bonds of the aromatic system coordinates to the third (non-phosphido-bridged) metal atom (**69a**, the iron homologue of the ruthenium complex **28**). This coordination mode of an aryl group of a cluster-bound phosphido ligand is also known from other studies[62] (cf. Section 2.3). It is certainly energetically unfavorable from enthalpy considerations alone (the 6π system becomes partially localized); the driving force is entropy, i.e., the chelate effect. Accordingly, the η^2-coordinated aryl group in **28** and **69** is reversibly removed from the coordination sphere by two-electron ligands L, forming **70** and **71**, respectively.[62, 131]

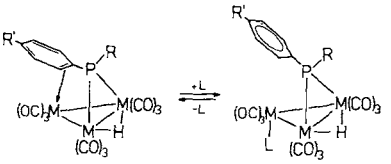

69 M = Fe, R' = OMe **70**
28 M = Ru, R' = H **71**

8.3. Reactions with Alkynes

The reactions of polynuclear metal carbonyls are among those cluster reactions that were the subject of early and detailed studies by *W. Reppe*.[161] The basic principles of alkyne bonding in clusters were expounded first by *W. Hübel* and co-workers.[162, 163]

Main-group elements as bridges introduce a new variant into this coordination chemistry; the reactions of **12** with alkynes R'C≡CR'' show that the latter can insert into either Fe–Fe or P–Fe bonds. Depending on the phosphorus substituents R and on the type of activation, compounds **72** are formed by insertion of the alkyne into the Fe–Fe bond and subsequent decarbonylation, and compounds **73** by insertion of the alkyne into the P–Fe

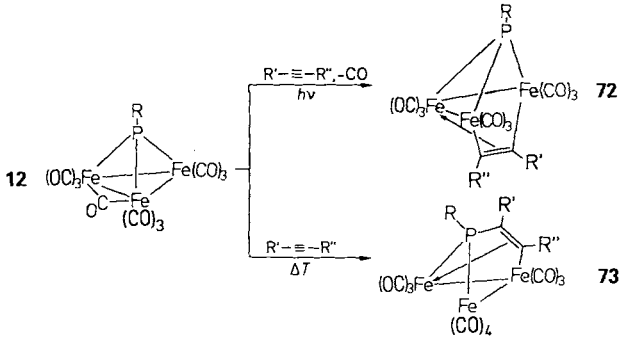

bond.[164] Under suitable conditions, two further isomers of **72**, the compounds **74** and **75**, can be selectively prepared.[165, 166]

Thermal decarbonylation of **76** in the presence of diphenylacetylene leads to the tetranuclear cluster **77**.[167] The C_2 unit links two metal centers that were not directly joined in the starting complex. The reaction is formally similar to the reaction of **60** with diphenylacetylene. How-

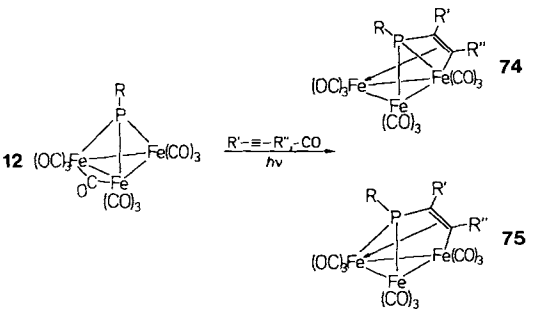

ever, the activation steps are different (cf. Section 8.1); the initiating step in the conversion of **76** to **77** could well be the dissociation of CO, which thereby provides a free coordination site. There are too few kinetic analyses available for the individual steps of such reactions to allow an experimentally sound and unified mechanistic model to be postulated. Clusters of type **61** are also formed, for instance, when the tetranuclear clusters **14** are treated with alkynes.[168]

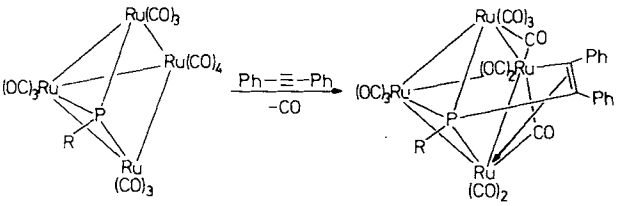

76 **77**

The structures of these alkyne adducts, which appear complicated at first sight, as well as their reactions, can be easily understood using a simple model (see Section 9).

9. Cluster Fragments as π Ligands

According to a concept developed by *K. Wade*,[80] the structure of a cage compound can be derived from the number of electron pairs that are available for bonding in the cluster. The number of electrons that each cluster unit contributes to the total electron balance can be calculated quite simply; each cluster unit is involved in cage bonding via its three highest-lying valence orbitals and the electrons present in them. A main-group element has four (s and p), a transition element nine (s, p, and d) valence orbitals. The number of electrons in the three highest-lying orbitals of a cluster constituent can then be easily counted.

Two examples: (1) The boron in an RB group has an outer shell of four electrons (one from the covalently bound group R and three from itself). It therefore has four electrons fewer than the maximum number it could accommodate (eight electrons in four orbitals) and has just two electrons in its highest three orbitals. (2) An iron atom has eight valence electrons, and the three carbonyl groups in an $Fe(CO)_3$ fragment contribute a further two each; the iron thus acquires a total of 14 valence electrons. Just as for the boron case, the iron has four electrons fewer than the maximum 18 that it could accommodate in nine valence orbitals; i.e., the highest three valence orbitals contain, like the boron of the RB group, a total of two electrons. Groups with equal numbers of electrons in the highest three orbitals can be substituted for each other in a cluster without changing its overall geometry.

The analogy thus demonstrated for RB and $Fe(CO)_3$ was refined by *R. Hoffmann*, who showed that the symmetry properties of the three frontier orbitals of RB and $Fe(CO)_3$ are congruous.[41] This extended isoelectronic relationship (identical symmetry properties of frontier orbitals and identical number of electrons in frontier orbitals) was termed isolobality.[41, 169] Some of the many relationships that can be drawn up in this way are presented in Scheme 5.

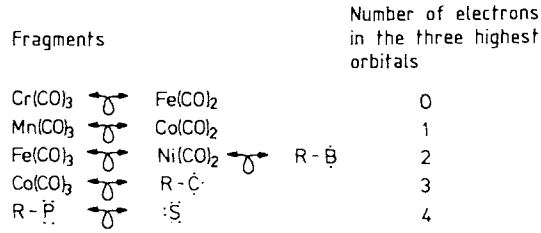

Scheme 5. Isolobal fragments.

Wade's concept states further[80] that if n electron pairs are available for cluster bonding, then the triangular polyhedron with n − 1 vertices will be the stablest form of the cluster. If the number of cluster units is less than n − 1, the cluster geometry can still be described as a polyhedron with n − 1 vertices, only some of which are occupied by cluster constituents. Clusters with all vertices occupied are termed *closo*, those with one missing vertex *nido*, and those with two missing vertices *arachno*. According to this terminology, half-sandwich complexes such as **78** are *nido* type and triple-decker complexes[170, 171] such as **79**[172] are *closo* type.

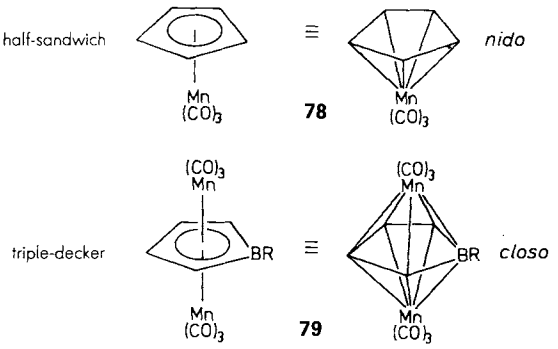

It is a reversal of this concept that can be developed into an analysis of clusters that is (at least heuristically) useful: Cluster fragments may be regarded as π ligands that—similarly to organic[170] or organoboron[171] π systems—form π complexes or triple-decker compounds.[173] Early examples of such an analysis are the description of the complex **80** as a triple-decker complex of the 2π-electron system $[Ni_3(CO)_6]^{2\ominus}$ by *L. F. Dahl* et al.[174] and the description of a tetrahedral manganese-iron cluster with one bond broken, **43a** (**43**, L = CO), as a π complex of the phosphini-

dene complex $[(\mu_2\text{-RP})\{Fe(CO)_4\}\{Mn(CO)_2Cp\}]$ (a homologue of the allyl anion) and $Fe(CO)_3$.[46]

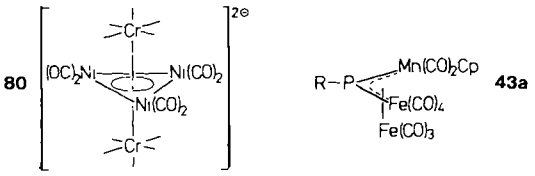

80 **43a**

This model implies a partial localization of the bonds in the cluster; each of the three $Ni(CO)_2$ fragments of **80** possesses two electrons in the highest three valence orbitals, and these are used to form the σ bonds in the Ni_3 triangle. The three remaining valence orbitals of the $Ni(CO)_2$ units, the symmetry of which is suitable for π interactions between them, then acquire two electrons corresponding to the negative charge of the complex.[174] Similar considerations apply to the phosphinidene complex $[(\mu_2\text{-RP})\{Fe(CO)_4\}\{Mn(CO)_2Cp\}]$ as an allylic-anion-analogous 4π system that functions in **43a** as an η^3 ligand.[46]

Any formal dissection of a molecule into units is artificial and can only be justified by the success with which it can be used to classify known facts into a uniform system and with which it can be used to predict previously unforeseen possibilities. Scheme 6 presents a series of complexes (**13**, **60**, and **81**–**83**) that can be regarded as $Fe(CO)_3$ ad-

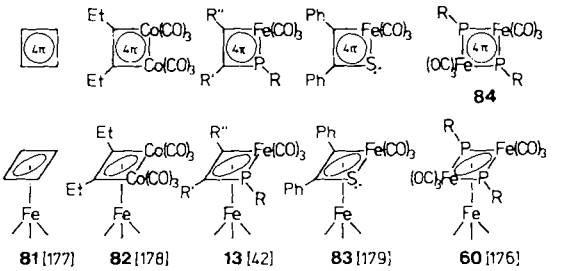

84

81 [177] **82** [178] **13** [42] **83** [179] **60** [176]

Scheme 6. Cyclobutadiene and analogous four-membered metallacycles as 4π-electron ligands.

ducts of η^4-coordinated cyclic 4π-electron ligands on the basis of the model discussed here.[180] All these 4π-electron ligands are unstable in the free state.[181] Their $Fe(CO)_3$ complexes, however, are stable. The bond lengths in the "π systems," together with the fact that the substituents at carbon and phosphorus lie almost in the ring plane, show that the model used here provides a suitable description of the structural characteristics of the complexes in Scheme 6.

Scheme 7 shows a selection of five-membered rings as 4π-electron ligands together with some of their half-sandwich and triple-decker complexes. In the stable $Fe(CO)_3$ complexes **85**, **86**, and **72**, each containing η^5-coordinated π ligands, the bond lengths in the π ligand, together with the fact that the bonds to C, P, and B lie almost in the ring plane, demonstrate once again the usefulness of this model for the interpretation of the structures.

Half-sandwich-type complexes can be "stacked" to form triple-decker complexes. The compounds **87**, first described by *W. Hübel* et al.[182], must be regarded as the first

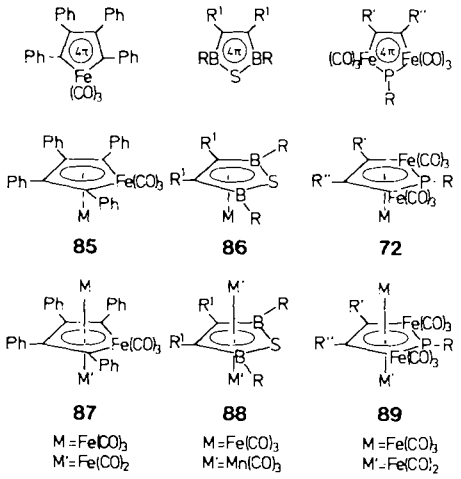

85 **86** **72**

87 **88** **89**

M = $Fe(CO)_3$, M' = $Fe(CO)_2$ | M = $Fe(CO)_3$, M' = $Mn(CO)_3$ | M = $Fe(CO)_3$, M' = $Fe(CO)_2$

Scheme 7. Five-membered metallacycles as 4π-electron ligands.

examples of triple-decker complexes. The compounds **88**[183] and **89**[166] are other variations on this theme; they are consistent with the electron-counting rules for triple-decker complexes, as proposed by *R. Hoffmann* et al.[173] and of course also with *Wade*'s rules. This shows that the partial localization of electrons in fragments that are regarded as π ligands (the model used here) does not lead to inconsistencies; a fully localized description (along the lines of the 18-electron rule) would, in contrast, picture all these triple-decker complexes as unsaturated.[184–186]

Since **72** had been described as a half-sandwich complex of a metallacyclic π ligand (in the sense of Scheme 7) and its analogy to **86** had been discussed,[164] it seemed worthwhile to test the suitability of **72** for stacking into a triple-decker complex (such as **88**). The reaction of **72** with $[Fe_2(CO)_9]$, as a source of "$Fe(CO)_2$," led, as ex-

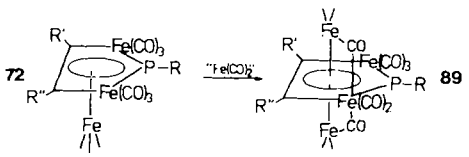

72 **89**

pected, to formation of the triple-decker complex **89**.[187] The pronounced stability of the triple-decker structure of **89** is shown, for instance, by the thermal decarbonylation of the compound **77** to a structural homologue of **89**.[167] Sulfur can assume the role of the RP unit in these complexes; this is shown by the formation of an osmium complex structurally homologous to **89** from $[(\mu_3\text{-S})Os_4(CO)_{13}]$ (structurally equivalent to **76**) and alkynes.[188] The formation of an iron-sulfur analogue of **89** from **83** and $[Fe_2(CO)_9]$ is a further example.[189]

Several cluster-forming processes can be understood using the concept of cluster fragments as π ligands. The reaction of **60** with $[Fe_2(CO)_9]$ leads to the interesting cluster **14**, which is unsaturated according to the noble-gas rule.[43] Cluster **60** may also be regarded, however, as a half-sandwich compound that "stacks" with "$Fe(CO)_2$" to form the triple-decker complex **14**.

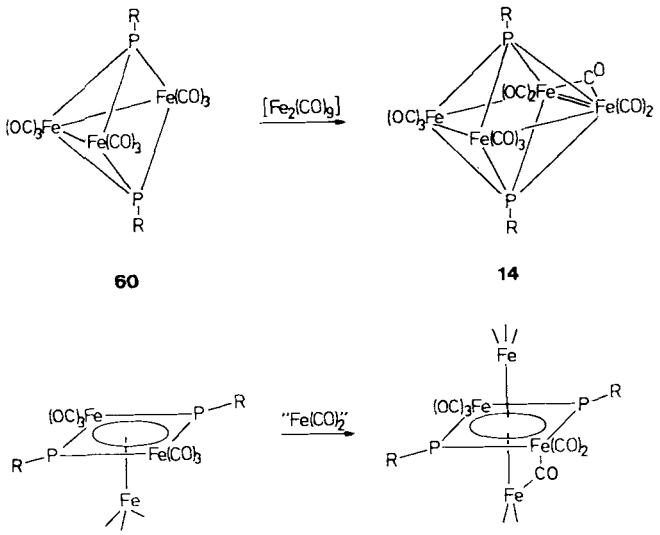

The model developed here is useful in that it provides a new and unconventional view of clusters and thus suggests new experiments.

10. Skeletal Rearrangement Processes

Carboranes provide the classic example of skeletal rearrangements of cage compounds.[190] Since *Wade*'s rules regard carboranes and metal clusters as different manifestations of the same bonding concepts,[80] both classes of compounds can be expected to display similar rearrangement processes. The interconversion of different skeletal topologies, however, requires that the bond energies between the units of the cage molecule be similar. The system $[(\mu_3\text{-RP})Fe_3(CO)_{10}]$ **12**/R'C≡CR'' appears to fulfill this requirement for Fe–P, P–C, and Fe–C bonds; all the transformations depicted in Scheme 9 can thus be preparatively realized.[164–166, 187] This scheme, in which the reactions and rearrangements of an organometallic cluster system are presented in the graph of the dodecahedral $B_8H_8^{2\ominus}$ cage,[191] brings together two "different" areas of chemistry in a manner that is more than mere symbolism.

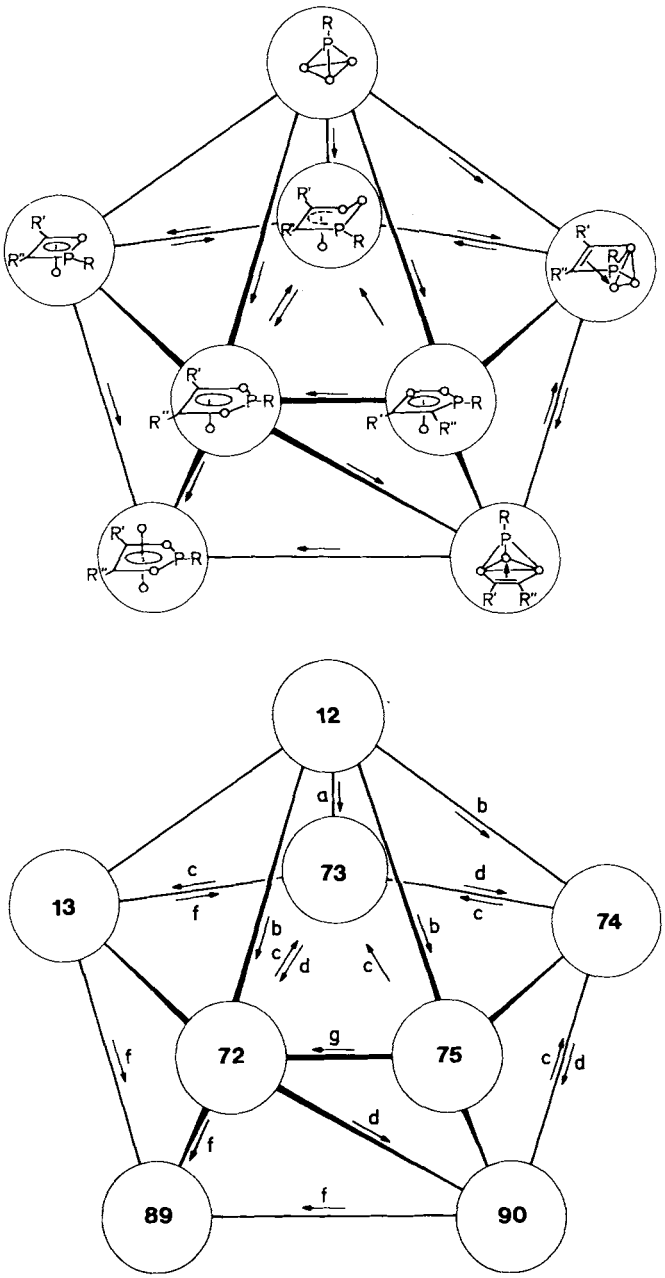

Scheme 9. Skeletal rearrangements in the system **12**/R'C≡CR''. a) R'C≡CR''. b) R'C≡CR'', *hν*. c) CO. d) −CO. e) *hν*, −CO. f) $[Fe_2(CO)_9]$. g) ΔT. **90** = $[(\mu_3\text{-RP})(\mu_3\text{-}\eta^2\text{-R'CCR''})Fe_3(CO)_8]$ [165]. The circles symbolize $Fe(CO)_n$ centers.

11. Summary

Trinuclear, μ_3-RX-bridged metal carbonyl clusters (X = N, P, As, Sb, Bi) represent only a small part of the much wider field of cluster chemistry. Among the many known clusters, they present two advantages; they are "small" (a cluster should contain at least three metal atoms) and they possess a bridging ligand RX that holds the metal atoms together even when metal–metal bonds are broken. This makes possible the kinetic-mechanistic investigation of their reactivity. For such clusters it can be shown that those with weaker metal–metal bonds enter into reactions in a valence-tautomeric form that has one metal–metal bond broken. Substitution of ligands occurs as an addition–elimination sequence with opening and closing of metal–metal bonds. The possibility of analyzing the individual reaction steps depends on the main-group bridging ligand, which is not directly involved in the reaction but instead fulfills the role of a clamp. Under some circumstances, this clamp can be broken, as is shown by the exchange of μ_3-RX-bridged metal carbonyl units by other metal–ligand fragments. Chiral clusters, in which the chirality arises from the framework of the cluster itself, were first made accessible in this way.

The reaction of μ_3-RP-bridged clusters with alkynes shows that both metal–metal and metal–phosphorus bonds can be reactive; the variety of cluster frameworks obtained in such reactions can be described in an integrated manner if fragments of such clusters are regarded as π ligands that can form half-sandwich and/or triple-decker complexes. The diverse rearrangement reactions of the cluster frameworks of the alkyne adducts illuminate perfectly the rela-

tionship with the chemistry of boranes and carboranes and show that the P–C, M–C, and M–P bonds in clusters are very similar in energy to each other.

Our thanks for enthusiastic and stimulating contributions to our own research in this field are due to Dr. B. Sigwarth, Dr. U. Weber, Dr. J. Borm, Dr. L. Zsolnai, Dr. G. Mohr, Dr. J. von Seyerl, Dr. J. Schneider, Dr. B. Pritzlaff, Dr. A. Winter, Dr. O. Scheidsteger, Dr. I. Jibril, Dr. H. Lang, Dipl.-Chem. L.-R. Frank, T. Fässler, and Dipl.-Chem. D. Buchholz. We thank Dr. H. Berke and Dipl.-Chem. K. Evertz for many productive discussions. We are grateful to the Deutsche Forschungsgemeinschaft and the Fonds der Chemischen Industrie for financial support.

Received: April 1, 1986;
revised: August 11, 1986 [A 628 IE]
German version: *Angew. Chem. 99* (1987) 765

[1] Review: J. Evans, *Chem. Soc. Rev. 12* (1983) 159; E. L. Muetterties, *Angew. Chem. 90* (1978) 577; *Angew. Chem. Int. Ed. Engl. 17* (1978) 545.

[2] Review: G. Ertl, *Nachr. Chem. Tech. Lab. 31* (1983) 178; *CRC Crit. Rev. Solid State Mater. Sci. 10* (1982) 349; G. A. Somorjai, *Chem. Soc. Rev. 13* (1984) 321.

[3] a) B. F. G. Johnson (Ed.): *Transition Metal Clusters*, Wiley, New York 1980; b) R. Whyman in [3a], p. 545.

[4] Review: E. L. Muetterties, M. J. Krause, *Angew. Chem. 95* (1983) 135; *Angew. Chem. Int. Ed. Engl. 22* (1983) 135; R. D. Adams, *Acc. Chem. Res. 16* (1983) 67; R. M. Laine, *J. Mol. Catal. 14* (1982) 137; P. C. Ford, *Acc. Chem. Res. 14* (1981) 31.

[5] For example, G. Wilkinson, F. G. A. Stone, E. W. Abel (Ed.): *Comprehensive Organometallic Chemistry*, Pergamon, Oxford 1982.

[6] For the structural relationships between the chemistry of clusters and solid-state chemistry, see, for example, H. G. von Schnering, *Angew. Chem. 93* (1981) 44; *Angew. Chem. Int. Ed. Engl. 20* (1981) 33.

[7] Osmium clusters are an exception; for a review see A. J. Deeming in [3a], p. 391.

[8] Review: H. Vahrenkamp, *Adv. Organomet. Chem. 22* (1983) 169.

[9] The word "bond" is used here even when the "observed" bond is not a localized two-center two-electron bond. It indicates more a geometrical relation between two centers; if they are as close as would be predicted from the sum of the covalent radii, they form a "bond"; if the bond is broken, this geometrical condition is no longer fulfilled.

[10] "Daran merkt man, daß wir nicht nur blöd, sondern auch gebildet sind.", Karl Valentin, Liesl Karlstadt; all titles available from Piper, Munich; recordings available from Ariola Eurodisc GmbH.

[11] Review: D. Seyferth, *Adv. Organomet. Chem. 14* (1976) 97; B. R. Penfold, B. H. Robinson, *Acc. Chem. Res. 6* (1973) 73; G. Pályi, F. Piacenti, L. Markó, *Inorg. Chim. Acta Rev. 4* (1970) 109.

[12] For complexes such as $[\{Cp(OC)_2Mn\}_2(XR)]$ (X = P, As, Sb, Bi) the terms phosphinidene, arsinidene, stibinidene, and bismuthinidene complex, respectively, are accepted internationally. We have therefore used these terms, instead of the rarely used IUPAC recommendations: phosphanediyl, arsanediyl, ... complex.

[13] Review: G. Huttner, K. Evertz, *Acc. Chem. Res. 19* (1986) 406; G. Huttner, *Pure Appl. Chem. 58* (1986) 585.

[14] Review: W. A. Nugent, B. L. Haymore, *Coord. Chem. Rev. 31* (1980) 123; S. Cenini, G. La Monica, *Inorg. Chim. Acta 18* (1976) 279.

[15] P. S. Elmes, P. Leverett, B. O. West, *J. Chem. Soc. Chem. Commun. 1971*, 747.

[16] Review: U. Schmidt, *Angew. Chem. 87* (1975) 535; *Angew. Chem. Int. Ed. Engl. 14* (1975) 523.

[17] See B. O. West in A. L. Rheingold (Ed.): *Homoatomic Rings, Chains and Macromolecules of Main-Group Elements*, Elsevier, Amsterdam 1977; A. L. Rheingold, M. J. Foley, P. J. Sullivan, *J. Am. Chem. Soc. 104* (1982) 4727.

[18] P. M. Treichel, W. K. Dean, W. M. Douglas, *Inorg. Chem. 11* (1972) 1609.

[19] The reactions of $RX(SiMe_3)_2$ with metal halides, which can lead to interesting RX-bridged carbonyl-free clusters, are not discussed here: D. Fenske, R. Basoglu, J. Hachgenei, F. Rogel, *Angew. Chem. 96* (1984) 160; *Angew. Chem. Int. Ed. Engl. 23* (1984) 160; D. Fenske, J. Hachgenei, F. Rogel, *ibid. 96* (1984) 959 and *23* (1984) 982.

[20] G. Huttner, J. Schneider, G. Mohr, J. von Seyerl, *J. Organomet. Chem. 191* (1980) 161.

[21] K. Natarajan, O. Scheidsteger, G. Huttner, *J. Organomet. Chem. 221* (1981) 301.

[22] F. Iwasaki, M. J. Mays, P. R. Raithby, P. L. Taylor, P. J. Wheatley, *J. Organomet. Chem. 213* (1981) 185.

[23] K. Natarajan, L. Zsolnai, G. Huttner, *J. Organomet. Chem. 220* (1981) 365.

[24] Y. Shvo, E. Hazum, *J. Chem. Soc. Chem. Commun. 1974*, 336; Review: T.-Y. Luh, *Coord. Chem. Rev. 60* (1984) 255.

[25] E. Röttinger, H. Vahrenkamp, *Angew. Chem. 90* (1978) 294; *Angew. Chem. Int. Ed. Engl. 17* (1978) 273.

[26] J. Schneider, L. Zsolnai, G. Huttner, *Chem. Ber. 115* (1982) 989.

[27] M. Müller, H. Vahrenkamp, *Chem. Ber. 116* (1983) 2311.

[28] G. Huttner, H.-D. Müller, P. Friedrich, U. Kölle, *Chem. Ber. 110* (1977) 1254. Further examples: *Organophosphorus Chem. 15* (1985), A Specialist Periodical Report, The Royal Society of Chemistry.

[29] Compare the radicals $[L_nM'(XR_m)]$ (X = N, P, S): P. M. Treichel, D. C. Molzahn, K. P. Wagner, *J. Organomet. Chem. 174* (1979) 191; D. Sellmann, J. Müller, P. Hofmann, *Angew. Chem. 94* (1982) 708; *Angew. Chem. Int. Ed. Engl. 21* (1982) 691; A. H. Cowley, R. A. Kemp, J. C. Wilburn, *J. Am. Chem. Soc. 104* (1982) 331; A. Winter, G. Huttner, L. Zsolnai, P. Kroneck, M. Gottlieb, *Angew. Chem. 96* (1984) 986; *Angew. Chem. Int. Ed. Engl. 23* (1984) 975; D. Sellmann, J. Müller, *J. Organomet. Chem. 281* (1985) 249.

[30] W. Hieber, O. Geisenberger, *Z. Anorg. Chem. 262* (1950) 15; W. Hieber, J. Gruber, *Z. Anorg. Allg. Chem. 296* (1958) 91.

[31] Review: G. Schmid, *Angew. Chem. 90* (1978) 417; *Angew. Chem. Int. Ed. Engl. 17* (1978) 392.

[32] A. Vizi-Orosz, V. Galamb, G. Pályi, L. Markó, G. Bor, G. Natile, *J. Organomet. Chem. 107* (1976) 235; A. Vizi-Orosz, V. Galamb, I. Ötvös, G. Pályi, L. Markó, *Transition Met. Chem. (Weinheim Ger.) 4* (1979) 294; A. Vizi-Orosz, V. Galamb, G. Pályi, L. Markó, *J. Organomet. Chem. 216* (1981) 105.

[33] G. Etzrodt, R. Boese, G. Schmid, *Chem. Ber. 112* (1979) 2574.

[34] C. H. Wei, L. F. Dahl, *Inorg. Chem. 6* (1967) 1229.

[35] A. S. Foust, M. S. Foster, L. F. Dahl, *J. Am. Chem. Soc. 91* (1969) 5633; A. S. Foust, C. F. Campana, J. D. Sinclair, L. F. Dahl, *Inorg. Chem. 18* (1979) 3047; C. F. Campana, A. Vizi-Orosz, G. Pályi, L. Markó, L. F. Dahl, *ibid. 18* (1979) 3054.

[36] A. Vizi-Orosz, G. Pályi, L. Markó, *J. Organomet. Chem. 60* (1973) C25; L. Markó, *Inorg. Chim. Acta 14* (1975) L39.

[37] J.-P. Lampin, F. Mathey, *C. R. Hebd. Séances Acad. Sci. Ser. C282* (1976) 979.

[38] G. Huttner, A. Frank, G. Mohr, *Z. Naturforsch. B31* (1976) 1161.

[39] G. Huttner, G. Mohr, A. Frank, U. Schubert, *J. Organomet. Chem. 118* (1976) C73.

[40] H. Lang, L. Zsolnai, G. Huttner, *J. Organomet. Chem. 282* (1985) 23.

[41] R. Hoffmann, *Angew. Chem. 94* (1982) 725; *Angew. Chem. Int. Ed. Engl. 21* (1982) 711.

[42] H. Lang, L. Zsolnai, G. Huttner, *Chem. Ber. 118* (1985) 4426.

[43] H. Vahrenkamp, D. Wolters, *J. Organomet. Chem. 224* (1982) C17.

[44] L. D. Lower, L. F. Dahl, *J. Am. Chem. Soc. 98* (1976) 5046.

[45] Similar cage structures: [19]; D. F. Rieck, R. A. Montag, T. S. McKechnie, L. F. Dahl, *J. Am. Chem. Soc. 108* (1986) 1330, and references cited therein.

[46] G. Huttner, G. Mohr, A. Frank, *Angew. Chem. 88* (1976) 719; *Angew. Chem. Int. Ed. Engl. 15* (1976) 682.

[47] G. Huttner, G. Mohr, P. Friedrich, H.-G. Schmid, *J. Organomet. Chem. 160* (1978) 59.

[48] G. Huttner, G. Mohr, P. Friedrich, *Z. Naturforsch. B33* (1978) 1254.

[49] R. L. De, J. von Seyerl, G. Huttner, *J. Organomet. Chem. 178* (1979) 319.

[50] J. Borm, K. Knoll, L. Zsolnai, G. Huttner, *Z. Naturforsch. B41* (1986) 532.

[51] M. Müller, H. Vahrenkamp, *Chem. Ber. 116* (1983) 2322.

[52] H. Lang, G. Huttner, B. Sigwarth, I. Jibril, L. Zsolnai, O. Orama, *J. Organomet. Chem. 304* (1986) 137.

[53] R. C. Ryan, L. F. Dahl, *J. Am. Chem. Soc. 97* (1975) 6904.

[54] K. Natarajan, L. Zsolnai, G. Huttner, *J. Organomet. Chem. 209* (1981) 85; K. Natarajan, G. Huttner, *Proc. Indian Acad. Sci. Chem. Sci. 91* (1982) 507.

[55] H. Lang, G. Huttner, L. Zsolnai, G. Mohr, B. Sigwarth, U. Weber, O. Orama, I. Jibril, *J. Organomet. Chem. 304* (1986) 157.

[56] J. Borm, G. Huttner, L. Zsolnai, *Angew. Chem. 97* (1985) 1069; *Angew. Chem. Int. Ed. Engl. 24* (1985) 1069.

[57] U. Weber, G. Huttner, O. Scheidsteger, L. Zsolnai, *J. Organomet. Chem. 289* (1985) 357.

[58] Catalytic activity of RX-bridged clusters: R. C. Ryan, C. U. Pittman, Jr., J. P. O'Connor, *J. Am. Chem. Soc. 99* (1977) 1986; C. U. Pittman, Jr., G. M. Wilemon, W. D. Wilson, R. C. Ryan, *Angew. Chem. 92* (1980) 494; *Angew. Chem. Int. Ed. Engl. 19* (1980) 478; C. U. Pittman, Jr., M. G. Richmond, M. Absi-Halabi, H. Beurich, F. Richter, H. Vahrenkamp, *ibid. 94* (1982) 805 and *21* (1982) 780; Y.-P. Wang, S.-M. Zhang, N. Wu, *J. Organomet. Chem. 307* (1986) 65.

[59] Review: P. E. Garrou, *Chem. Rev. 85* (1985) 171.
[60] J. M. Fernandez, B. F. G. Johnson, J. Lewis, P. R. Raithby, *J. Chem. Soc. Chem. Commun. 1978*, 1015; *Acta Crystallogr. Sect. B 35* (1979) 1711.
[61] S. C. Brown, J. Evans, *J. Chem. Soc. Chem. Commun. 1980*, 1021.
[62] S. A. MacLaughlin, A. J. Carty, N. J. Taylor, *Can. J. Chem. 60* (1982) 87.
[63] G. Lavigne, J.-J. Bonnet, *Inorg. Chem. 20* (1981) 2713; C. Bergounhou, J.-J. Bonnet, P. Fompeyrine, G. Lavigne, N. Lugan, F. Mansilla, *Organometallics 5* (1986) 60.
[64] O. Stelzer, S. Hietkamp, H. Sommer, *Phosphorus Sulfur 18* (1983) 279; D. J. Brauer, S. Hietkamp, H. Sommer, O. Stelzer, *J. Organomet. Chem. 281* (1985) 187; D. J. Brauer, S. Hietkamp, H. Sommer, O. Stelzer, G. Müller, C. Krüger, *ibid. 288* (1985) 35; D. J. Brauer, G. Hasselkuß, S. Hietkamp, H. Sommer, O. Stelzer, *Z. Naturforsch. B40* (1985) 961.
[65] See, for example, D. E. Fjare, W. L. Gladfelter, *J. Am. Chem. Soc. 103* (1981) 1572; D. E. Fjare, D. G. Keyes, W. L. Gladfelter, *J. Organomet. Chem. 250* (1983) 383; B. F. G. Johnson, J. Lewis, J. M. Mace, *J. Chem. Soc. Chem. Commun. 1984*, 186; J. A. Smieja, W. L. Gladfelter, *J. Organomet. Chem. 297* (1985) 349; M. L. Blohm, D. E. Fjare, W. L. Gladfelter, *J. Am. Chem. Soc. 108* (1986) 2301.
[66] Review: W. L. Gladfelter, *Adv. Organomet. Chem. 24* (1985) 41.
[67] E. Sappa, L. Milone, *J. Organomet. Chem. 61* (1973) 383, and references cited therein.
[68] E. Koerner von Gustorf, R. Wagner, *Angew. Chem. 83* (1971) 968; *Angew. Chem. Int. Ed. Engl. 10* (1971) 910; K. Burgess, B. F. G. Johnson, J. Lewis, P. R. Raithby, *J. Organomet. Chem. 224* (1982) C 40.
[69] M. A. Andrews, H. D. Kaesz, *J. Am. Chem. Soc. 101* (1979) 7238, 7255. The results obtained here for iron carbonyl clusters also apply to osmium and ruthenium clusters; see [70].
[70] J. Banford, Z. Dawoodi, K. Henrick, M. J. Mays, *J. Chem. Soc. Chem. Commun. 1982*, 554; Z. Dawoodi, M. J. Mays, K. Henrick, *J. Chem. Soc. Dalton Trans. 1984*, 433; W. Bernhardt, H. Vahrenkamp, *Angew. Chem. 96* (1984) 362; *Angew. Chem. Int. Ed. Engl. 23* (1984) 381; W. Bernhardt, C. von Schnering, H. Vahrenkamp, *ibid. 98* (1986) 285 and *25* (1986) 279.
[71] G. Süss-Fink, U. Thewalt, H.-P. Klein, *J. Organomet. Chem. 224* (1982) 59.
[72] Whether the RCP complexes prepared by *D. Seyferth* et al. [73] can similarly be converted into μ_3-RP-clusters has not been investigated.
[73] D. Seyferth, J. S. Merola, R. S. Henderson, *Organometallics 1* (1982) 859.
[74] G. Süss-Fink, *Z. Naturforsch. B35* (1980) 454.
[75] F. Richter, H. Vahrenkamp, *Angew. Chem. 90* (1978) 474; *Angew. Chem. Int. Ed. Engl. 17* (1978) 444.
[76] A. Winter, I. Jibril, G. Huttner, *J. Organomet. Chem. 247* (1983) 259.
[77] R. D. Adams, I. T. Horváth, S. Wang, *Inorg. Chem. 24* (1985) 1728.
[78] A. Vizi-Orosz, *J. Organomet. Chem. 111* (1976) 61; R. L. De, H. Vahrenkamp, *Z. Naturforsch. B40* (1985) 1250.
[79] W. Malisch, P. Panster, *Angew. Chem. 88* (1976) 680; *Angew. Chem. Int. Ed. Engl. 15* (1976) 618.
[80] K. Wade, *Adv. Inorg. Chem. Radiochem. 18* (1976) 1.
[81] C. E. Strouse, L. F. Dahl, *Discuss. Faraday Soc. 47* (1969) 93.
[82] B. E. R. Schilling, R. Hoffmann, *J. Am. Chem. Soc. 101* (1979) 3456.
[83] P. T. Chesky, M. B. Hall, *Inorg. Chem. 20* (1981) 4419.
[84] F. A. Cotton, G. Wilkinson: *Advanced Inorganic Chemistry*, Wiley, New York 1980; *Anorganische Chemie*, 4th ed 1st reprint, VCH Verlagsgesellschaft, Weinheim 1985; P. S. Braterman: *Metal Carbonyl Spectra*, Academic Press, London 1975.
[85] R. J. H. Clark, T. J. Dines, *Angew. Chem. 98* (1986) 131; *Angew. Chem. Int. Ed. Engl. 25* (1986) 131.
[86] H. Beurich, T. Madach, F. Richter, H. Vahrenkamp, *Angew. Chem. 91* (1979) 751; *Angew. Chem. Int. Ed. Engl. 18* (1979) 690.
[87] B. M. Peake, P. H. Rieger, B. H. Robinson, J. Simpson, *Inorg. Chem. 20* (1981) 2540.
[88] For further ESR spectroscopic studies, B. H. Robinson, J. Simpson, D. J. Watson, *Inorg. Chem. 16* (1977) 405; P. A. Dawson, B. M. Peake, B. H. Robinson, J. Simpson, *ibid. 19* (1980) 465; P. J. Krusic, J. San Filippo, Jr., B. Hutchinson, R. L. Hance, L. M. Daniels, *J. Am. Chem. Soc. 103* (1981) 2129; P. N. Lindsay, B. M. Peake, B. H. Robinson, J. Simpson, U. Honrath, H. Vahrenkamp, A. M. Bond, *Organometallics 3* (1984) 413.
[89] G. Huttner, J. Borm, L. Zsolnai, *J. Organomet. Chem. 263* (1984) C 33.
[90] G. Huttner, *J. Organomet. Chem. 308* (1986) C 11.
[91] B. F. G. Johnson, R. E. Benfield in [3a], p. 471.
[92] H. Schäfer-Stahl, J. Schneider, G. Huttner, *Z. Naturforsch. B37* (1982) 610.
[93] P. D. Frisch, L. F. Dahl, *J. Am. Chem. Soc. 94* (1972) 5082.
[94] Review: H. Vahrenkamp, *Angew. Chem. 87* (1975) 363; *Angew. Chem. Int. Ed. Engl. 14* (1975) 322.
[95] Trinh-Toan, B. K. Teo, J. A. Ferguson, T. J. Meyer, L. F. Dahl, *J. Am. Chem. Soc. 99* (1977) 408; C. D. Garner in [3a], p. 265.
[96] The one-electron oxidation of $[(\mu_3\text{-}t\text{BuP})Fe_3(CO)_7\{P(OMe)_3\}]$ [117] is fully reversible in CH_2Cl_2, in contrast to the behavior of the parent compound: T. Fässler, K. Knoll, G. Huttner, unpublished results.
[97] Review of the electrochemistry of transition-metal clusters: P. Lemoine, *Coord. Chem. Rev. 47* (1982) 55.
[98] Only reported example so far $[(\mu_3\text{-}Y)_2Fe_3(CO)_9]$ (Y = S, Se, Te): R. P. Ferrari, G. A. Vaglio, M. Valle, *J. Chem. Soc. Dalton Trans. 1978*, 1164.
[99] See, for example, R. T. Aplin, H. Budzikiewicz, C. Djerassi, *J. Am. Chem. Soc. 87* (1965) 3180; M. von Ardenne, K. Steinfelder, R. Tümmler: *Elektronenanlagerungs-Massenspektrographie organischer Substanzen*, Springer, Berlin 1971.
[100] The negativ-ion EI and CI mass spectra of numerous compounds containing the $(RP)Fe_3(CO)_9$ fragment: K. Knoll, G. Huttner, *J. Organomet. Chem.*, in press.
[101] Review of radical-induced ligand exchange in organometallic chemistry: J. K. Kochi, *J. Organomet. Chem. 300* (1986) 139.
[102] Review: D. J. Darensbourg, *Adv. Organomet. Chem. 21* (1982) 113.
[103] A. F. Clifford, A. K. Mukherjee, *Inorg. Chem. 2* (1963) 151; S. M. Grant, A. R. Manning, *Inorg. Chim. Acta 31* (1978) 41.
[104] J. D. Atwood: *Inorganic and Organometallic Reaction Mechanisms*, Brooks/Cole, Monterey, CA, USA 1985.
[105] K. J. Karel, J. R. Norton, *J. Am. Chem. Soc. 96* (1974) 6812.
[106] G. Huttner, J. Schneider, H.-D. Müller, G. Mohr, J. von Seyerl, L. Wohlfahrt, *Angew. Chem. 91* (1979) 82; *Angew. Chem. Int. Ed. Engl. 18* (1979) 76.
[107] J. Schneider, G. Huttner, *Chem. Ber. 116* (1983) 917.
[108] A. Mayr, W. Ehrl, H. Vahrenkamp, *Chem. Ber. 107* (1974) 3860.
[109] Relevant articles are referred to in [111] under references 3-26. A nice example of the rediscovery of this principle is given by B. F. G. Johnson, *Inorg. Chim. Acta 115* (1986) L39; a review of edge-opened clusters is provided by M. O. Albers, D. J. Robinson, N. J. Coville, *Coord. Chem. Rev. 69* (1986) 127.
[110] G. R. John, B. F. G. Johnson, J. Lewis, W. J. Nelson, M. McPartlin, *J. Organomet. Chem. 171* (1979) C 14; D. H. Farrar, B. F. G. Johnson, J. Lewis, P. R. Raithby, M. J. Rosales, *J. Chem. Soc. Dalton Trans. 1982*, 2051; R. J. Goudsmit, B. F. G. Johnson, J. Lewis, P. R. Raithby, K. H. Whitmire, *J. Chem. Soc. Chem. Commun. 1982*, 640.
[111] J. Schneider, M. Minelli, G. Huttner, *J. Organomet. Chem. 294* (1985) 75.
[112] J. A. Connor in [3a], p. 345.
[113] L.-R. Frank, *Diplomarbeit*, Universität Konstanz 1984; L.-R. Frank, A. Winter, G. Huttner, *J. Organomet. Chem.*, in press.
[114] A. V. Willi: *Isotopeneffekte bei chemischen Reaktionen*, Thieme, Stuttgart 1983.
[115] M. S. Wrighton, J. L. Graff, J. C. Luong, C. L. Reichel, J. L. Robbins, *ACS Symp. Ser. 155* (1981) 85; M. S. Wrighton (Ed.): *Inorganic and Organometallic Photochemistry* (*Adv. Chem. Ser. 168* (1978)).
[116] Further reviews: T. J. Meyer, J. V. Caspar, *Chem. Rev. 85* (1985) 187; A. E. Stiegman, D. R. Tyler, *Acc. Chem. Res. 17* (1984) 61.
[117] K. Knoll, G. Huttner, L. Zsolnai, I. Jibril, M. Wasiucionek, *J. Organomet. Chem. 294* (1985) 91.
[118] The kinetics of adduct formation corresponds to the pattern discussed for the conversion **16** → **43**: D. Buchholz, *Diplomarbeit*, Universität Konstanz 1986; G. Huttner, D. Buchholz, unpublished results.
[119] See Ref. 22 in [117].
[120] H. Vahrenkamp, D. Wolters, *Organometallics 1* (1982) 874.
[121] T. Jaeger, S. Aime, H. Vahrenkamp, *Organometallics 5* (1986) 245.
[122] J. A. Iggo, M. J. Mays, P. L. Taylor, *Philos. Trans. R. Soc. London A 308* (1982) 27.
[123] A. Winter, L. Zsolnai, G. Huttner, *J. Organomet. Chem. 250* (1983) 409.
[124] A. Winter, L. Zsolnai, G. Huttner, *J. Organomet. Chem. 234* (1982) 337.
[125] A. Winter, L. Zsolnai, G. Huttner, *J. Organomet. Chem. 232* (1982) 47.
[126] A similar reaction sequence has been demonstrated for non-bridged osmium carbonyl clusters: D. H. Farrar, P. G. Jackson, B. F. G. Johnson, J. Lewis, W. J. H. Nelson, M. D. Vargas, M. McPartlin, *J. Chem. Soc. Chem. Commun. 1981*, 1009.
[127] Review: R. Bau (Ed.): *Transition Metal Hydrides*, (*Adv. Chem. Ser. 167* (1978)).
[128] I. Fischler, R. Wagner, E. A. Koerner von Gustorf, *J. Organomet. Chem. 112* (1976) 155.
[129] B. Pritzlaff, *Dissertation*, Universität Konstanz 1985.
[130] K. Knoll, G. Huttner, M. Wasiucionek, L. Zsolnai, *Angew. Chem. 96* (1984) 708; *Angew. Chem. Int. Ed. Engl. 23* (1984) 739.
[131] K. Knoll, G. Huttner, L. Zsolnai, O. Orama, M. Wasiucionek, *J. Organomet. Chem. 310* (1986) 225.
[132] K. Knoll, G. Huttner, unpublished results.
[133] M. J. Mays, P. R. Raithby, P. L. Taylor, K. Henrick, *J. Chem. Soc. Dalton Trans. 1984*, 959.
[134] J. Schneider, *Dissertation*, Universität Konstanz 1982.

[135] Review: H. Vahrenkamp, *Comments Inorg. Chem. 4* (1985) 253.
[136] R. A. Epstein, H. W. Withers, G. L. Geoffroy, *Inorg. Chem. 18* (1979) 942.
[137] H. Beurich, H. Vahrenkamp, *Angew. Chem. 93* (1981) 128; *Angew. Chem. Int. Ed. Engl. 20* (1981) 98.
[138] H. Beurich, R. Blumhofer, H. Vahrenkamp, *Chem. Ber. 115* (1982) 2409.
[139] U. Honrath, H. Vahrenkamp, *Z. Naturforsch. B39* (1984) 559.
[140] W. Malisch, M. Kuhn, *Angew. Chem. 86* (1974) 51; *Angew. Chem. Int. Ed. Engl. 13* (1974) 84.
[141] F. Richter, H. Beurich, H. Vahrenkamp, *J. Organomet. Chem. 166* (1979) C5.
[142] The first chiral clusters had a μ_3-S-bridge: F. Richter, H. Vahrenkamp, *Angew. Chem. 90* (1978) 916; *Angew. Chem. Int. Ed. Engl. 17* (1978) 864; for chiral RP-bridged clusters, see M. Müller, H. Vahrenkamp, *Chem. Ber. 116* (1983) 2748.
[143] P. Gusbeth, H. Vahrenkamp, *Chem. Ber. 118* (1985) 1770.
[144] M. Müller, H. Vahrenkamp, *Chem. Ber. 116* (1983) 2765.
[145] F. Richter, E. Roland, H. Vahrenkamp, *Chem. Ber. 117* (1984) 2429.
[146] M. I. Bruce, D. C. Kehoe, J. G. Matisons, B. K. Nicholson, P. H. Rieger, M. L. Williams, *J. Chem. Soc. Chem. Commun. 1982,* 442.
[147] The thermal decomposition of μ_3-RP-bridged clusters breaks both metal–metal and metal–phosphorus bonds. Nearly all clusters of the type $[(\mu_3\text{-RP})Fe_2(CO)_6(ML_n)]$ give the complex $[(\mu_3\text{-RP})_2Fe_3(CO)_9]$ **60** as the end product of thermal decomposition. The thermolysis of $[(\mu_2\text{-}Ph_2P)(\mu_2\text{-H})Ru_3(CO)_9]$ to $[(\mu_3\text{-PhP})Ru_4(CO)_{13}]$ shows that clusters of higher nuclearity can be formed on heating [62].
[148] Reactions in which only the substituents at phosphorus are modified or exchanged (e.g., the conversion of $[(\mu_3\text{-}R_2NP)Fe_3(CO)_{10}]$ to $[\mu_3\text{-}ClP)_2Fe_3(CO)_{10}]$ by HCl [123], are not discussed here, since they do not involve the cluster itself.
[149] a) B. F. G. Johnson, J. Lewis, D. Pippard, P. R. Raithby, *J. Chem. Soc. Chem. Commun. 1978,* 551; b) S. B. Colbran, B. F. G. Johnson, J. Lewis, R. M. Sorrell, *ibid. 1986,* 525.
[150] J. S. Field, R. J. Haines, D. N. Smit, K. Natarajan, O. Scheidsteger, G. Huttner, *J. Organomet. Chem. 240* (1982) C23.
[151] K. Knoll, G. Huttner, L. Zsolnai, *J. Organomet. Chem. 307* (1986) 237.
[152] H. H. Ohst, J. K. Kochi, *J. Chem. Soc. Chem. Commun. 1986,* 121; *J. Am. Chem. Soc. 108* (1986) 2897.
[153] M. G. Richmond, J. K. Kochi, *Inorg. Chem. 25* (1986) 656, 1334.
[154] The μ_3-η^2 coordination of a phosphaalkene-analogous RP=NR ligand was reported by O. J. Scherer, R. Walter, W. S. Sheldrick, *Angew. Chem. 97* (1985) 132; *Angew. Chem. Int. Ed. Engl. 24* (1985) 115; review: O. J. Scherer, *ibid. 97* (1985) 905 and *24* (1985) 924; R. Appel, F. Knoll, J. Ruppert, *ibid. 93* (1981) 771 and *20* (1981) 731.
[155] The adducts between Cp(OC)Rh fragments at the Ru–P bonds of μ_3-RP-bridged ruthenium clusters (D. Mani, H. Vahrenkamp, *Angew. Chem. 97* (1985) 428; *Angew. Chem. Int. Ed. Engl. 24* (1985) 422) are isolobal analogues of phosphaalkene complexes.
[156] K. Knoll, G. Huttner, unpublished results; H. Vahrenkamp (Freiburg), private communication.
[157] A phosphagermaalkene was recently reported: J. Escudie, C. Couret, J. Satge, M. Andrianarison, J.-D. Andriamizaka, *J. Am. Chem. Soc. 107* (1985) 3378.
[158] G. D. Williams, G. L. Geoffroy, R. R. Whittle, *J. Am. Chem. Soc. 107* (1985) 729.
[159] U. Schubert, H. Fischer, P. Hofmann, K. Weiss, K. H. Dötz, F. R. Kreissl: *Transition Metal Carbene Complexes,* Verlag Chemie, Weinheim 1983.
[160] H.-J. Bestmann, R. Zimmermann in *Houben-Weyl-Müller: Methoden der Organischen Chemie, Band E1, Organische Phosphorverbindungen I,* Thieme, Stuttgart 1982.
[161] W. Reppe, *Chimia 3* (1949) 233, 257; *Chem. Ing. Tech. 22* (1950) 273, 361, 437, 527.
[162] W. Hübel, E. H. Braye, *J. Inorg. Nucl. Chem. 10* (1959) 250.
[163] W. Hübel in I. Wender, P. Pino (Eds.): *Organic Syntheses via Metal Carbonyls,* Interscience, New York 1968.
[164] K. Knoll, O. Orama, G. Huttner, *Angew. Chem. 96* (1984) 989; *Angew. Chem. Int. Ed. Engl. 23* (1984) 976.
[165] K. Knoll, G. Huttner, L. Zsolnai, O. Orama, *Angew. Chem. 98* (1986) 1099; *Angew. Chem. Int. Ed. Engl. 25* (1986) 1119.
[166] K. Knoll, G. Huttner, L. Zsolnai, *J. Organomet. Chem.*, in press.
[167] J. Lunniss, S. A. MacLaughlin, N. J. Taylor, A. J. Carty, E. Sappa, *Organometallics 4* (1985) 2066.
[168] T. Jaeger, H. Vahrenkamp, *Z. Naturforsch. B41* (1986) 789; the spectroscopic properties indicate that compound **3** in this article is a compound of type **61**.
[169] M. Elian, M. L. Chen, D. M. P. Mingos, R. Hoffmann, *Inorg. Chem. 15* (1976) 1148.
[170] H. Werner, A. Salzer, *Synth. Inorg. Met. Org. Chem. 2* (1972) 239; A. Salzer, H. Werner, *ibid. 2* (1972) 249; *Angew. Chem. 84* (1972) 949; *Angew. Chem. Int. Ed. Engl. 11* (1972) 930.
[171] Review: W. Siebert, *Adv. Organomet. Chem. 18* (1980) 301.
[172] G. E. Herberich, J. Hengesbach, U. Kölle, G. Huttner, A. Frank, *Angew. Chem. 88* (1976) 450; *Angew. Chem. Int. Ed. Engl. 15* (1976) 433.
[173] J. W. Lauher, M. Elian, R. H. Summerville, R. Hoffmann, *J. Am. Chem. Soc. 98* (1976) 3219.
[174] J. K. Ruff, R. P. White, Jr., L. F. Dahl, *J. Am. Chem. Soc. 93* (1971) 2159.
[175] G. Huttner, H.-G. Schmid, *Angew. Chem. 87* (1975) 454; *Angew. Chem. Int. Ed. Engl. 14* (1975) 433; G. Huttner, J. von Seyerl, M. Marsili, H.-G. Schmid, *ibid. 87* (1975) 455 and *14* (1975) 434.
[176] S. L. Cook, J. Evans, L. R. Gray, M. Webster, *J. Organomet. Chem. 236* (1982) 367.
[177] J. D. Fitzpatrick, L. Watts, G. F. Emerson, R. Pettit, *J. Am. Chem. Soc. 87* (1965) 3254; R. P. Dodge, V. Schomaker, *Acta Crystallogr. 18* (1965) 614.
[178] S. Aime, L. Milone, D. Osella, A. Tiripicchio, A. M. Manotti Lanfredi, *Inorg. Chem. 21* (1982) 501.
[179] G. N. Schrauzer, H. N. Rabinowitz, J. A. K. Frank, I. C. Paul, *J. Am. Chem. Soc. 92* (1970) 212.
[180] Application of this model to alkyne complexes: D. M. Hoffmann, R. Hoffmann, *J. Chem. Soc. Dalton Trans. 1982,* 1471; further preparative applications: J. C. Jeffery, K. A. Mead, H. Razay, F. G. A. Stone, M. J. Went, P. Woodward, *ibid. 1984,* 1383; review: F. G. A. Stone, *Angew. Chem. 96* (1984) 85; *Angew. Chem. Int. Ed. Engl. 23* (1984) 89.
[181] A derivative of the 4π-electron system **84** containing bulky substituents is known: K. M. Flynn, R. A. Bartlett, M. M. Olmstead, P. P. Power, *Organometallics 5* (1986) 813; the tetrahedrane-type isomer is more stable for small substituents R: H. Vahrenkamp, D. Wolters, *Angew. Chem. 95* (1983) 152; *Angew. Chem. Int. Ed. Engl. 22* (1983) 154.
[182] Structure: R. P. Dodge, V. Schomaker, *J. Organomet. Chem. 3* (1965) 274; A. A. Hock, O. S. Mills, *Acta Crystallogr. 14* (1961) 139; cf. R. D. Adams, *J. Am. Chem. Soc. 102* (1980) 7476.
[183] W. Siebert, K. Kinberger, *Angew. Chem. 88* (1976) 451; *Angew. Chem. Int. Ed. Engl. 15* (1976) 434.
[184] The MO analysis of clusters that consist of organometallic fragments and main-group units generally involves the study of interactions between the main-group ligands (e. g., RP [185] or acetylene [186]) and the transition-metal cluster fragment. This method corresponds to the view that "building blocks" with similar orbital energies should be grouped together. The fragment analysis suggested here (which has not yet been substantiated by MO studies) does not follow this method. This can be justified by the view that the interactions between "soft" ligands such as RP, S, or acetylene and transition metals are certainly strongly influenced by overlap, so that the difference in orbital energies between main-group centers and transition-metal centers is no longer so important. We thank Dr. *H. Berke* (Konstanz) for this comment.
[185] J.-F. Halet, R. Hoffmann, J.-Y. Saillard, *Inorg. Chem. 24* (1985) 1695.
[186] J.-F. Halet, J.-Y. Saillard, R. Lissilour, M. J. McGlinchey, G. Jaouen, *Inorg. Chem. 24* (1985) 218.
[187] K. Knoll, G. Huttner, unpublished results.
[188] R. D. Adams, unpublished results, presented at the International Workshop *Fundamental Pathways at Dinuclear and Polynuclear Transition Metal Centers,* Königstein/Taunus, September 1985.
[189] T. Fässler, G. Huttner, unpublished results.
[190] R. N. Grimes, *Adv. Inorg. Chem. Radiochem. 26* (1983) 55.
[191] F. Klanberg, D. R. Eaton, L. J. Guggenberger, E. L. Muetterties, *Inorg. Chem. 6* (1967) 1273; L. J. Guggenberger, *ibid. 8* (1969) 2771.

When submitting manuscripts, authors of articles intended for publication as "Communications" are requested to read the "Notice to Authors" reproduced in the January issue of the journal following the list of contents; upon request, a copy can be obtained from the editorial office.

Four-Center Two-Electron Bonding in a Tetrahedral Topology. Experimental Realization of Three-Dimensional Homoaromaticity in the 1,3-Dehydro-5,7-adamantanediyl Dication**

By *Matthias Bremer, Paul von Ragué Schleyer,* Karl Schötz, Michael Kausch,* and *Michael Schindler*

Dedicated to Professor George A. Olah on the occasion of his 60th birthday

Four orbitals placed at the bridgeheads of adamantane extend towards the center of the cage. Of the four possible combinations of phases, only the nondegenerate one, **I**, is

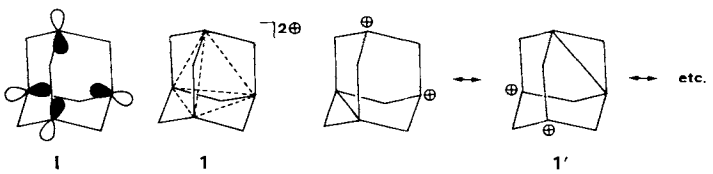

I 1 1′

bonding. The occupation of this molecular orbital by two electrons (Fig. 1)—e.g., as in the dication **1/1′**—should result in considerable stability, provided the overlap is sufficient.

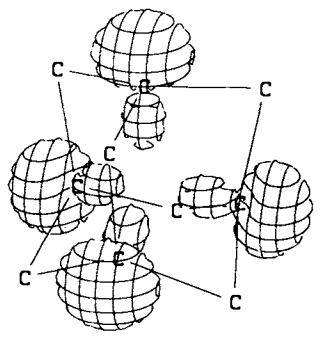

Fig. 1. Jorgensen plot of the highest occupied molecular orbital of **1**. (The STO-3G basis set employed underestimates the overlap of the bridgehead orbitals. The Jorgensen program cannot deal with higher basis sets.)

[*] Prof. Dr. P. von R. Schleyer, Dipl.-Chem. M. Bremer, Dr. K. Schötz, Dr. M. Kausch
Institut für Organische Chemie der Universität Erlangen-Nürnberg
Henkestrasse 42, D-8520 Erlangen (FRG)
Dr. M. Schindler
Lehrstuhl für Theoretische Chemie der Universität
Postfach 102148, D-4630 Bochum 1 (FRG)

[**] We thank the Deutsche Forschungsgemeinschaft, the Fonds der Chemischen Industrie, ARDEC, Dover, NJ, and the CONVEX Corporation (the most recent calculations were carried out on a CONVEX C1 computer) for support, Dr. *Alan Reed* (Erlangen) for discussions, and Dr. *W. Bauer* (Erlangen) for the NMR spectra.

Attractive ideas based on *qualitative* molecular orbital considerations often have not survived or have given disappointing results when subjected to experimental test. Homoaromaticity in neutral and carbanionic systems is a case in point.[1] Hence, such ideas are best tested calculationally at an adequate level of quantitative theory before investing the much greater effort needed for an experimental investigation.

When this project was begun a decade ago,[2,3] MINDO/3[4] was employed to evaluate the energies of the isodesmic reactions (a) and (b). The former predicts the

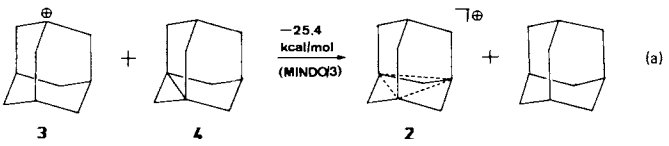

3 4 2

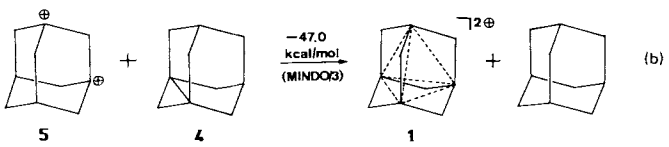

5 4 1

trishomoaromatic 1,3-dehydro-5-adamantyl cation **2**, an intermediate which has been implicated in solvolysis reactions,[5] to be stabilized by about 25 kcal/mol relative to the 1-adamantyl cation **3** and 1,3-dehydroadamantane **4**. Equation (b) indicates that the extension of the two-electron delocalization from three centers (as in **2**) to all four bridgeheads nearly doubles the stabilization. While **1** is tetratrishomoaromatic, this large resonance energy, along with the delocalized electronic structure, qualifies it for the designation "aromatic," as well. While *Olah* et al. have not succeeded in preparing the 1,3-adamantanediyl dication **5**,[6] nor, indeed, any other 1,3-carbodication in solution,[3] the high degree of stabilization indicated for **1** by Equation (b) encouraged us to seek experimental verification.

The problem of obtaining a suitable precursor for dication **1** was complicated by the known instability of 1,3-dehydroadamantane derivatives, e.g., towards reaction with oxygen and polymerization.[5] After a large number of preliminary experiments,[2] a simple route was found. When reacted with mercury(II) fluoride, 1,3,5,7-tetraiodoadamantane[7] gives a trisubstituted product, 1,3,5-trifluoro-7-iodoadamantane **6**, almost exclusively. This obviates the need for tedious chromatographic separations of polyhaloadamantane mixtures. With butyllithium in ether/pentane solution at −80°C, **6** gave (presumably via I–Li exchange and LiF elimination) 1,3-dehydro-5,7-difluoroadamantane **7** directly. As **7** only is stable at room temperature in solution (the solid polymerizes with near explosive exothermicity above 0°C), workup had to be carried out below −30°C. After crystallization from pentane at −70°C, **7** shows ^{13}C- and ^{1}H-NMR spectra typical of dehydroadamantanes.[5,17] Chemical characterization was achieved by reaction of **7** with iodine in hexane; 1,3-difluoro-5,7-diiodoadamantane **8** is formed in over 80% yield.[17]

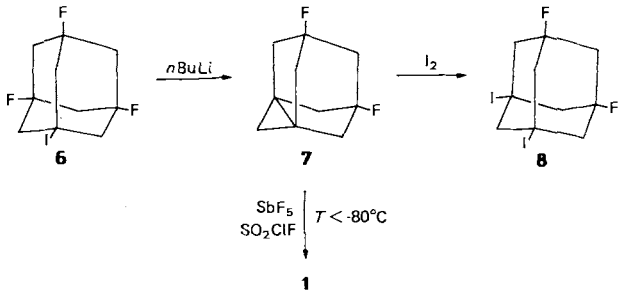

Kept cold, solid **7** was added to a solution of SbF_5 in SO_2ClF (ca. 5 M) at temperatures below $-80\,^{\circ}C$ in order to prepare the NMR sample. The resulting dication **1** appears to be rather stable in superacid media, as spectra could be taken successfully at temperatures up to $0\,^{\circ}C$. The NMR parameters of **1** are remarkable, and constitute a proof of the nonclassical structure. The ^{13}C-NMR chemical shift of the bridgehead carbons, which share the positive charge at least in a formal sense, comes *upfield* ($\delta = 6.6$ at $-71\,^{\circ}C$, with internal [D_6]acetone/TMS capillary) of the methylene carbon resonances ($\delta = 35.6$), despite the presence of the two positive charges. *Shielded* values are characteristic of hypercoordinate carbocation centers. A good analogy is provided by the trishomocyclopropenyl cation **9**, which exhibits similar NMR parameters: $\delta = 4.9$ (CH) and 17.6 (CH_2).[8]

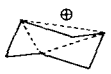

9

The triplet splitting of the CH_2 group in **1**, $J_{(C,H)} = 165$ Hz, in line with the trend found for adamantane (125 Hz)[9] and the 1-adamantyl cation **3** (148 Hz),[6] confirms not only the formation of dication **1** but also the strong deformation of the C-CH_2-C angles predicted by the calculations. Figure 2 gives the 3-21G ab initio geometry. The $J_{(C,H)}$ value, 168.4 Hz, for **9** is similar.[8] The single, sharp ^1H chemical shift of **1**, $\delta = 3.8$, also is unusual in comparison with $\delta = 4.2$[6] for the α-CH_2 groups of the 1-adamantyl cation, and $\delta = 1.74$[9] for the adamantane methylenes.

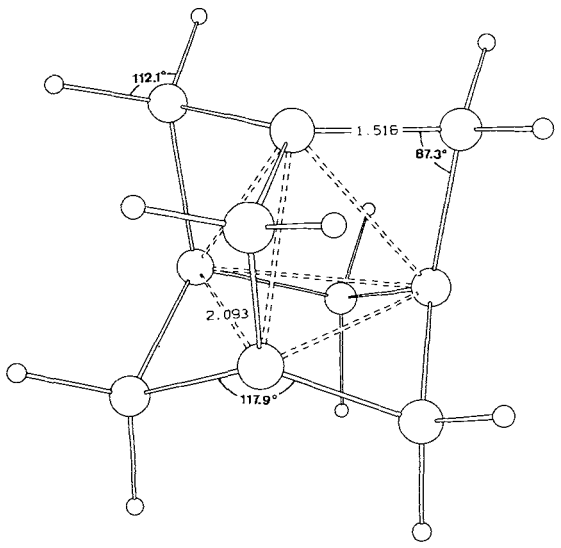

Fig. 2. The 3-21G-optimized structure of the dehydroadamantanediyl dication **1** (distances in Å). The 6-31G*-optimized data are similar: C-C = 1.504, 2.052 Å, C-C-C = 86.0, 118.2°, H-C-H = 114.2°.

These chemical shifts can be analyzed in several ways. If **1** were a classical, rapidly equilibrating dication (an unlikely possibility!), the bridgehead carbon chemical shift should be an average of the values found for the carbocation center in the 1-adamantyl cation **3** ($\delta = 300$)[6] and a cyclopropane bridgehead in 1,3-dehydroadamantane **4** ($\delta = 37.3$).[5] The chemical shift ($\delta = 169$), predicted for the bridgehead carbons by the classical model on this basis, deviates from the experimental value by over 160 ppm! Alternatively, the sums of all the ^{13}C chemical shifts for **1** (240 ppm) and for 1,3-dehydroadamantane **4** (454 ppm) may be used as a classical-nonclassical classification criterion.[10] For typical classical carbodications, the dication-neutral difference is on the order of +800 ppm (i.e., about twice that found on the same basis for monocarbocations). For **1**, the difference is *negative*, −214 ppm! Such negative values (but not as large) are found, e.g., for the related trishomocyclopropenyl cation **9** (−48 ppm),[10] and for the 7-norbornadienyl cation (−96 ppm).[10]

Clearly, the ^{13}C-NMR data for **1** cannot be reconciled with a classical, rapidly equilibrating model. But how well do the experimental shifts compare with those predicted by a nonclassical model? The IGLO (individual gauge for localized molecular orbitals) method has been demonstrated to give good to excellent agreement between calculated and experimental chemical shifts for both classical and nonclassical carbocations.[11] For example, the IGLO (DZ basis set) and experimental (in parentheses) ^{13}C-NMR chemical shifts for the 1-adamantyl cation **3** are: $\delta = 337.7$ (300.0), 57.7 (66.6), 67.8 (87.6), and 37.2 (34.6). When applied to **1** (without prior knowledge of the experimental results), bridgehead ($\delta = 7$) and methylene carbon ($\delta = 33$) chemical shifts were calculated (DZ basis on the 3-21G geometry). The remarkable agreement with the experimental values ($\delta = 6.6$ and 35.6) speaks for itself. The calculated proton chemical shift, $\delta = 3.0$, is lower than experiment ($\delta = 3.8$), but the latter, measured from an internal standard, depends on the magnetic anisotropy of the medium and is somewhat uncertain.

As indicated by population analysis at various theoretical levels (MNDO, MINDO/3, STO-3G, 3-21G), the bonding and charge distribution in **1** are revealing. The positive charge resides not only on the bridgehead carbons but also on the 12 hydrogens; the methylene carbons are neutral or even negatively charged. The overlap among the bridgehead carbons at 3-21G//3-21G (0.38 vs. about 0.7 for a normal C-C single bond),[16] is significant, consistent with the dotted-line representation. Each bridgehead carbon is involved with one electron, and each has a total bond order of 0.5. Charge delocalization in a nearly spherical topology, as well as partial bridging among the bridgehead positions, is responsible for the stability of **1**.

The dehydroadamantanediyl dication **1** now takes its place along with pyramidal cations,[12–14] e.g., those based on $(CH)_5^{\oplus}$ and $(CH)_6^{2\oplus}$, as purely "organic" examples of *three-dimensional aromaticity*[15] which exhibit large resonance energies. *Hückel's* $4n+2$ rule, involving *interstitial* instead of π electrons, can easily be extended to such systems.[15]

Received: February 27, 1987 [Z 2116 IE]
Publication delayed at the authors' request
German version: *Angew. Chem. 99* (1987) 795

[1] For recent references, see P. von R. Schleyer, E. Kaufmann, A. J. Kos, H. Mayr, J. Chandrasekhar, *J. Chem. Soc. Chem. Commun. 1986*, 1583; A. McEwen, P. von R. Schleyer, *J. Org. Chem. 51* (1986) 4357. A recent claim to have demonstrated 4.5 kcal/mol of "homoaromaticity" in triquinacene (J. F. Liebman, L. A. Paquette, J. R. Peterson, D. W. Rogers,

J. Am. Chem. Soc. 108 (1986) 8267), is not "unequivocal" as no attempt was made to dissect electronic from strain effects. "Homoconjugation" may be a better term to describe stabilizations of such small magnitude, if present.

[2] We thank *Michael Waeber, Herbert Gareis,* and *Roland Hacker,* Erlangen, for preliminary experimental investigations, and *E. M. Engler* for early STO-3G calculations. Further work is described in the Diplomarbeit of *M. B.*, Universität Erlangen-Nürnberg 1986.

[3] See a review on stable carbodications: G. K. Surya Prakash, T. N. Rowdah, G. A. Olah, *Angew. Chem. 95* (1983) 356; *Angew. Chem. Int. Ed. Engl. 22* (1983) 390. Also see: G. K. Surya Prakash, M. Formia, S. Keyonian, G. A. Olah, H. J. Kuhn, K. Schaffner, *J. Am. Chem. Soc. 109* (1987) 911.

[4] a) R. C. Bingham, M. J. S. Dewar, D. H. Lo, *J. Am. Chem. Soc. 97* (1975) 1285; b) for reviews, see T. Clark: *A Handbook of Computational Chemistry*, Wiley, New York 1986; c) D. F. V. Lewis, *Chem. Revs. 86* (1986) 1111.

[5] a) R. E. Pincock, J. Schmidt, W. B. Scott, E. J. Torupka, *Can. J. Chem. 50* (1972) 3958; b) C. S. Gibbons, J. Trotter, *ibid. 51* (1973) 87; c) R. E. Pincock, F.-N. Fung, *Tetrahedron Lett. 21* (1980) 19; d) W. B. Scott, R. E. Pincock, *J. Am. Chem. Soc. 95* (1973) 2040; e) R. E. Pincock, E. J. Torupka, *ibid. 91* (1969) 4593.

[6] G. A. Olah, G. K. Surya Prakash, J. G. Shih, V. V. Krishnamurthy, G. D. Mateescu, G. Liang, G. Sipos, V. Buss, T. M. Gund, P. von R. Schleyer, *J. Am. Chem. Soc. 107* (1985) 2764. The pagodane dication is of interest in this context: G. K. S. Prakash, V. V. Krishnamurthy, R. Herges, R. Bau, H. Yuan, G. A. Olah, W.-D. Fessner, H. Prinzbach, *J. Am. Chem. Soc. 108* (1986) 836.

[7] G. P. Sollott, E. E. Gilbert, *J. Org. Chem. 45* (1980) 5405, and references cited therein. A modified procedure using CS_2 and AlI_3, prepared in situ, was employed here.

[8] a) S. Masamune, M. Sahai, A. V. K. Jones, T. Nakashima, *Can. J. Chem. 52* (1974) 855; b) G. A. Olah, G. K. Surya Prakash, D. Whittaker, J. C. Rees, *J. Am. Chem. Soc. 101* (1979) 3935; c) G. K. Surya Prakash, M. Arvanaghi, G. A. Olah, *ibid. 107* (1985) 6017; d) also compare the pentacyclononyl cation reported by R. M. Coates, E. R. Fretz, *J. Am. Chem. Soc. 97* (1975) 2538.

[9] R. C. Fort, P. von R. Schleyer, *J. Org. Chem. 30* (1965) 789.

[10] P. von R. Schleyer, D. Lenoir, P. Mison, G. Liang, G. K. Surya Prakash, G. A. Olah, *J. Am. Chem. Soc. 102* (1980) 683.

[11] M. Schindler, *J. Am. Chem. Soc. 109* (1987) 1020.

[12] Reviews on pyramidal carbocations: H. Schwartz, *Angew. Chem. 93* (1981) 1046; *Angew. Chem. Int. Ed. Engl. 20* (1981) 991; P. Vogel: *Carbocation Chemistry*, Elsevier, Amsterdam 1985.

[13] S. Masamune, M. Sahai, H. Ona, A. J. Jones, *J. Am. Chem. Soc. 94* (1972) 8956; A. V. Kemp-Jones, N. Nakamura, S. Masamune, *J. Chem. Soc. Chem. Commun. 1974*, 109, and references cited therein.

[14] H. Hogeveen, P. W. Kwant, *Acc. Chem. Res. 8* (1975) 413.

[15] E. D. Jemmis, P. von R. Schleyer, *J. Am. Chem. Soc. 104* (1982) 4781, and earlier papers in the same series. E. D. Jemmis, *ibid. 104* (1982) 7017; J. Chandrasekhar, E. D. Jemmis, P. von R. Schleyer, in preparation.

[16] Natural population analysis (A. E. Reed, R. B. Weinstock, F. Weinhold, *J. Chem. Phys. 83* (1985) 735) based on natural localized molecular orbitals (A. E. Reed, F. Weinhold, *ibid. 83* (1985) 1736) and the STO-3G//STO-3G and the 3-21G//3-21G wave functions (W. J. Hehre, L. Radom, P. von R. Schleyer, J. A. Pople: *Ab Initio Molecular Orbital Theory*, Wiley, New York 1986) were employed.

[17] Spectroscopic data of **6**, **7**, and **8**. (The multiplicities of the NMR signals are taken from ^{1}H-decoupled ^{13}C-NMR spectra; $^1J_{(C,H)}$ coupling constants from "gated" spectra): **6**, m.p. = 72–73 °C; ^{1}H-NMR (400 MHz, $CDCl_3$): δ = 2.10, 2.19 (2 mc, 6H, CF–CH_2–CF), 2.50 (s, 6H, CF–CH_2–Cl); ^{13}C-NMR (100 MHz, $CDCl_3$): δ = 25.5 (q, $^3J_{(C,F)}$ = 14 Hz, *Cl*), 45.7 (t, $^2J_{(C,F)}$ = 20 Hz, CF–CH_2–CF, $^1J_{(C,H)}$ = 134 Hz), 53.6 (d, $^2J_{(C,F)}$ = 20 Hz, CF–CH_2–Cl, $^1J_{(C,H)}$ = 136 Hz), 90.2 (dt, $^1J_{(C,F)}$ = 195 Hz, $^3J_{(C,F)}$ = 15 Hz, *CF*); IR (KBr): $\tilde{\nu}$ = 2920, 2810, 1440, 1430, 1310, 1295, 1230, 1205, 1130, 1025, 1005, 970, 940, 885, 860, 780, 700 cm^{-1}. — **7**, ^{1}H-NMR (400 MHz, [D$_8$]tetrahydrofuran): δ = 1.36 (d, 4H, $^2J_{(H,H)}$ = 10 Hz, CF–CH_2–C), 1.64 (d, 2H, $^5J_{(F,H)}$ = 8 Hz, C–CH_2–C), 2.01 (d, 4H, $^2J_{(H,H)}$ = 10 Hz, CF–CH_2–C), 2.22 (t, 2H, $^3J_{(F,H)}$ = 4 Hz, CF–CH_2–CF); ^{13}C-NMR (100 MHz, [D$_8$]tetrahydrofuran): δ = 18.9 (t, $^3J_{(C,F)}$ = 9 Hz, CH_2–*C*–CH_2), 37.2 (t, $^4J_{(C,F)}$ = 4 Hz, C–*C*H$_2$–C, $^1J_{(C,H)}$ = 159 Hz), 45.3 (dd, $^2J_{(C,F)}$ = 15 Hz, $^4J_{(C,F)}$ = 3 Hz, CF–*C*H$_2$–C, $^1J_{(C,H)}$ = 136 Hz), 46.0 (t, $^2J_{(C,F)}$ = 18 Hz, CF–*C*H$_2$–CF, $^1J_{(C,H)}$ = 132 Hz), 98.4 (dd, $^1J_{(C,F)}$ = 226 Hz, $^3J_{(C,F)}$ = 5 Hz, *CF*). — **8**, m.p. = 132–134 °C; ^{1}H-NMR (400 MHz, $CDCl_3$): δ = 2.18 (t, 2H, $^3J_{(F,H)}$ = 5 Hz, CF–CH_2–CF), 2.52 (d, 4H, $^2J_{(H,H)}$ = 11 Hz, CF–CH_2–Cl), 2.62 (d, 4H, $^2J_{(H,H)}$ = 11 Hz, CF–CH_2–Cl), 2.91 (s, 2H, Cl–CH_2–Cl); ^{13}C-NMR (100 MHz, $CDCl_3$): δ = 28.8 (t, $^3J_{(C,F)}$ = 12 Hz, *Cl*), 45.3 (t, $^2J_{(C,F)}$ = 20 Hz, CF–CH_2–CF, $^1J_{(C,H)}$ = 136 Hz), 53.1 (dd, $^2J_{(C,F)}$ = 18 Hz, $^4J_{(C,F)}$ = 3 Hz, CF–CH_2–Cl, $^1J_{(C,H)}$ = 135 Hz), 60.2 (s, Cl–CH_2–Cl, $^1J_{(C,H)}$ = 136 Hz), 89.7 (dd, $^1J_{(C,F)}$ = 198 Hz, $^3J_{(C,F)}$ = 14 Hz, *CF*); IR (KBr): $\tilde{\nu}$ = 2910, 2820, 1430, 1310, 1290, 1250, 1215, 1205, 1095, 1015, 995, 960, 945, 930, 870, 815, 725, 675 cm^{-1}.

Dimerization of 1,6-Dithiacyclodeca-3,8-diyne in the Presence of Cobalt Complexes. A Simple Synthesis of a [2.2](2,5)Thiophenophane Derivative**

By *Rolf Gleiter,* Michael Karcher, Bernhard Nuber,* and *Manfred L. Ziegler*

Dedicated to Professor Hermann Schildknecht on the occasion of his 65th birthday

Recently, we showed that cyclodeca-1,6-diyne **1** undergoes dimerization in the presence of $[CpCo(CO)_2]$ or $[CpCo(C_8H_{12})]$ ($Cp = \eta^5$-C_5H_5) to give a superphane of cyclobutadiene, **3**, doubly capped by CpCo units.[1]

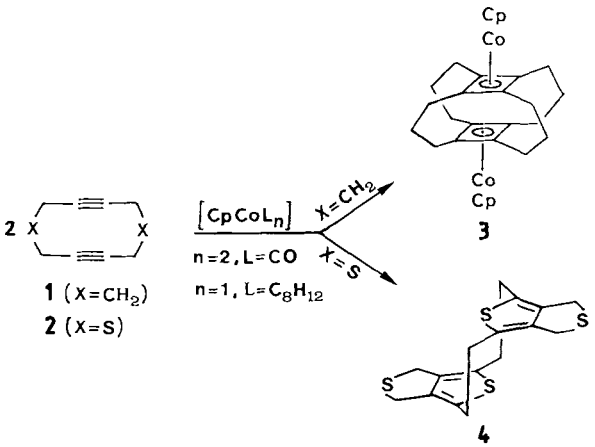

To test the scope and limitations of this new reaction, we have investigated the reaction of 1,6-dithiacyclodeca-3,8-diyne **2**[2] with $[CpCo(CO)_2]$ and $[CpCo(C_8H_{12})]$. Heating **2** (1.0 g, 5.95 mmol) with $[CpCo(CO)_2]$ (1.07 g, 5.95 mmol) in *n*-octane yielded a colorless product (120 mg) which contained no CpCo unit. The analytical data of the product (see Table 1) showed a molecular weight of 336, and the IR, UV,[3] and NMR data indicated the presence of thiophene units and two nonequivalent CH_2 bridges. When **2** was heated with less than the equimolar amount (10%) of the Co complexes, we obtained the same product. Three structural possibilities, the *anti* and *syn* isomers **4** and **5**, respectively, and the cage compound **6**, are compatible with the spectroscopic data.

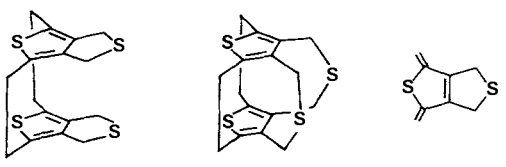

From the observation that the most intense peak in the mass spectrum of the product is at *m/z* 168 ($M^{\oplus}$/2), we favored **4** and **5** over **6**.

[*] Prof. Dr. R. Gleiter, Dipl.-Chem. M. Karcher
Institut für Organische Chemie der Universität
Im Neuenheimer Feld 270, D-6900 Heidelberg (FRG)
Prof. Dr. M. L. Ziegler, Dr. B. Nuber
Institut für Anorganische Chemie der Universität
Im Neuenheimer Feld 234, D-6900 Heidelberg (FRG)

[**] This work was supported by the Deutsche Forschungsgemeinschaft, the Fonds der Chemischen Industrie, BASF AG, and Degussa AG.

Table 1. Most relevant physical data of **4**.

IR (KBr): $\tilde{\nu}$ = 2950 (w), 2940 (m), 2920 (m), 2840 (w), 1440 (m), 1430 (m), 1365 (m), 1315 (m), 1170 (m), 1045 (w) cm^{-1}

UV (CH_2Cl_2): λ_{max} (lgε) = 253 (3.91), 288 nm (3.83)

^{1}H-NMR ($CDCl_3$, 300 MHz, TMS): δ = 2.73-2.84, 2.97-3.07 (AA'BB'), 3.94, 3.78 (AB, J_{AB} = 12.8 Hz)

^{13}C-NMR ($CDCl_3$, 75.46 MHz): δ = 146.2 (s), 138.8 (s), 30.3 (t), 27.8 (t)

MS (70 eV): m/z = 336 (2.9%, $M^{\oplus}$), 168 (100%, $M^{\oplus}/2$)

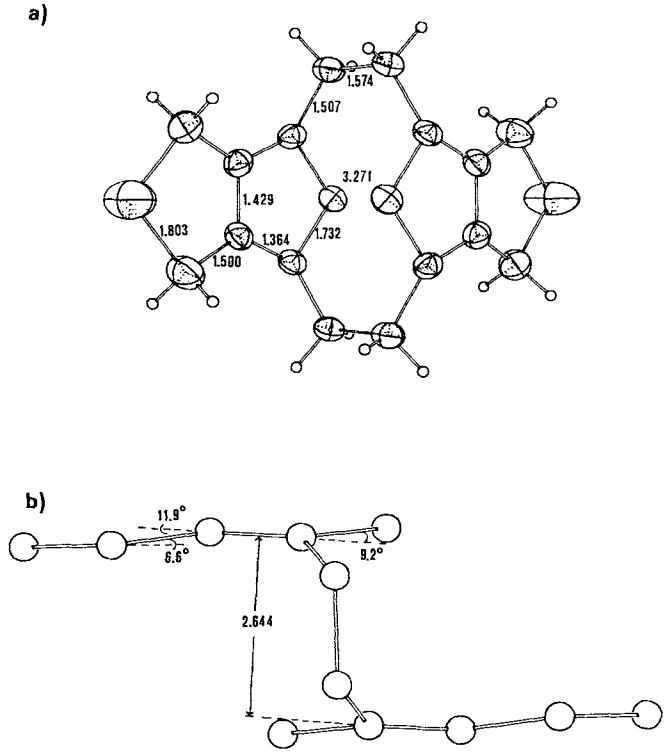

Fig. 1. Crystal structure of **4** with important distances [Å] and angles. a) View from above; b) side-on view.

To solve this structural problem and to obtain further details of the molecular structure, we carried out an X-ray investigation.[4] The results show that **4** is present in the crystal (Fig. 1). The thiophene rings are envelope shaped; the plane C2-S-C5 forms an angle of 9.2° with the plane of the sp^2 carbon atoms. The planes of the latter are separated by 2.644 Å. Similar geometric parameters were found for the parent system [2.2](2,5)thiophenophane.[5]

Concerning the mechanism of the reaction, we assume as intermediate a cobaltacyclopentadiene[6] in which one sulfur center is associated with the metal. Such a complex may yield the exomethylene derivative **7**, which dimerizes to give **4**.

Received: March 2, 1987 [Z 2121 IE]
Publication delayed at the authors' request
German version: *Angew. Chem. 99* (1987) 805

[1] R. Gleiter, M. Karcher, M. L. Ziegler, B. Nuber, *Tetrahedron Lett. 28* (1987) 195.
[2] G. Eglington, I. A. Cardy, R. A. Raphael, G. A. Sim, *J. Chem. Soc. 1964*, 1154.
[3] H. E. Winberg, F. S. Fawcett, W. E. Mochel, C. W. Theobald, *J. Am. Chem. Soc. 82* (1960) 1428.
[4] **4**: a = 7.528(2), b = 8.646(3), c = 11.742(3) Å, β = 98.44(2)°, V = 756.0 Å^3, Z = 2. Space group $P2_1/c$ (No. 14). Data were collected on a Siemens Stoe diffractometer using a crystal of dimension 0.11 × 0.22 × 0.42 mm^3 (obtained from CH_2Cl_2); ω scan (3° < 2θ < 60°), $Mo_{K\alpha}$ radiation (λ = 0.7106(9) Å); 1492 reflections, of which 1453 were judged to be observed ($I > 2.5\sigma(I)$). All crystallographic calculations employed the SHELXTL program package 5.1 (December 1985). Empirical absorption correction (5 refletions, 2θ range 9-36°, ω scan). Relative range of transmission factors: 0.89-1.00 (μ = 5.9 cm^{-1}). Least-squares refinement with $\Sigma w|F_o| - xF_c|)^2$ ($w = 1/\sigma^2(F)$). The structure was solved by direct methods (SOLVE, SHELXTL). The hydrogen atoms were located from a difference Fourier map and subjected to isotropic refinement; R = 0.046, R_w = 0.041. A final difference Fourier map revealed no peaks greater than 0.55 e/Å^3. Further details of the crystal structure investigation are available on request from the Fachinformationszentrum Energie, Physik, Mathematik GmbH, D-7514 Eggenstein-Leopoldshafen 2 (FRG), on quoting the depository number CSD-52317, the names of the authors, and the journal citation.

[5] N. B. Pahor, M. Calligaris, L. Randaccio, *J. Chem. Soc. Perkin Trans. 2 1978*, 42.
[6] H. Yamazaki, N. Hagihara, *J. Organomet. Chem. 7* (1967) 22; R. B. King, I. Haiduc, *J. Am. Chem. Soc. 94* (1972) 4044.

Bis(η^5-cyclopentadienyl)-1,3-diphosphabicyclo[1.1.0]butane-2,4-diylzirconium: A Simple Synthesis of an Unusual Molecule**

By *Paul Binger,* Bruno Biedenbach, Carl Krüger,* and *Manfred Regitz*

Recently, both we[1] and an English group[2] succeeded independently in preparing η^4-1,3-diphosphacyclobutadiene metal complexes **1** (M = Co, Rh; R = *tert*-butyl) starting from λ^3-phosphaalkynes. The 2-metalla-1,4-diphosphacyclopentadienes **2**, which are analogues of the intermediates involved in the numerous reported syntheses of η^4-cyclobutadiene metal complexes,[3] can be postulated as being involved in this cyclodimerization. However,

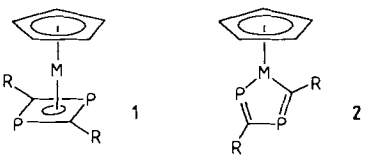

compounds of the type **2** have never been detected or isolated. We therefore attempted to synthesize analogous compounds of zirconium by reaction of λ^3-phosphaalkynes with [Cp_2Zr] (Cp = η^5-C_5H_5) generated in situ. These coordinatively unsaturated Zr^{II} species react with a variety of alkynes to give zirconacyclopentadiene derivatives.[4-8]

Reaction of [Cp_2ZrCl_2] with magnesium and 2,2-dimethylpropylidynephosphane **3** in the presence of $HgCl_2$[4] afforded orange-red crystals having the stoichiometry [$Cp_2Zr\{P_2C_2(C(CH_3)_3)_2\}$] (53% yield, correct elemental analysis, molecular weight (MS) = 420), to which structure **4** has been assigned. Complex **4** can also be obtained from [Cp_2ZrCl_2], butyllithium, and **3**[7] (yield 26%) or from [Cp_2Zr(butadiene)] and **3**[8] (58%).

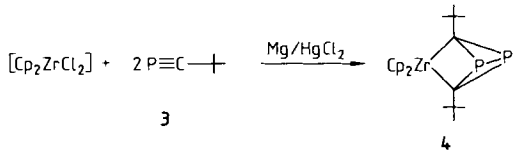

3 4

[*] Priv.-Doz. Dr. P. Binger, Dipl.-Chem. B. Biedenbach, Prof. Dr. C. Krüger
Max-Planck-Institut für Kohlenforschung
Kaiser-Wilhelm-Platz 1, D-4330 Mülheim a. d. Ruhr (FRG)
Prof. Dr. M. Regitz
Fachbereich Chemie der Universität
Erwin-Schrödinger-Strasse, D-6750 Kaiserslautern (FRG)

[**] This work was supported by the Stiftung Volkswagenwerk.

The ^{31}P-NMR spectrum of **4** (singlet at $\delta = -247$) shows that the new compound cannot be a zirconium complex of the type **1** or **2**. Since the structure of **4** could not be established unequivocally from its ^{1}H- and ^{13}C-NMR spectra,[9] an X-ray crystal structure analysis was performed, the result of which is presented in Figure 1.[10] The X-ray

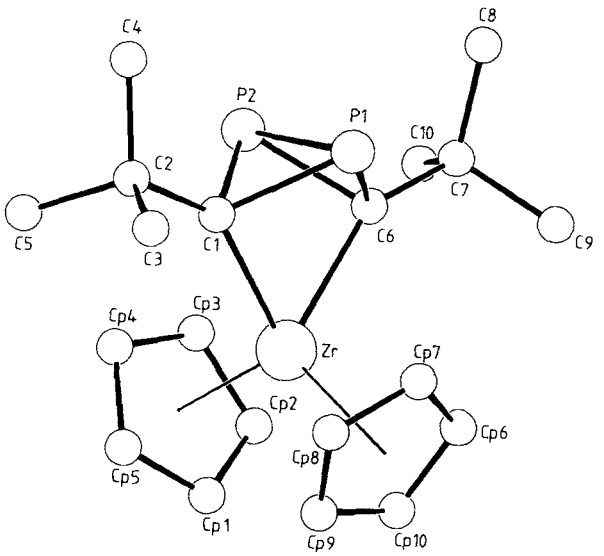

Fig. 1. Crystal structure of **4**. Important bond lengths [Å]: Zr-C1 2.213(3), Zr-C6 2.210(3), C1-P1 1.900(3), C1-P2 1.891(3), C6-P1 1.912(3), C6-P2 1.886(3), P1-P2 2.147(1).

structure reveals that **3** has undergone dimerization to form a folded 1,3-diphosphabicyclo[1.1.0]butane, which is bonded to the metal through two Zr–C σ bonds. These bonds are approximately 0.04 Å shorter than Zr–C_{sp^3} bonds (2.25–2.27 Å).[11] The distance between the bonded phosphorus atoms is only 2.147(1) Å. By contrast, in planar or slightly bent $1\lambda^3,3\lambda^3$-diphosphetanes[12] or $1\lambda^5,3\lambda^5$-diphosphetes,[13] this distance is 2.68–2.75 Å; we measured earlier a P–P distance of 2.73 Å for **1** (M = Co).[1] No bond is evident between Zr and the P1–P2 bridge (Zr-P1, 2.906 Å; Zr-P2, 2.909 Å).

The interplanar angle (123.8°) of the staggered Cp rings bonded to the tetrahedrally coordinated Zr atom is normal for Cp_2Zr systems.[11] The ring puckering characteristic of bicyclobutanes (110–128°)[14] is 100° for **4** (between the planes C1-C6-P1 and C1-C6-P2) and 70° (between the planes P1-P2-C1 and P1-P2-C6). Molecular models[15] reveal that this leads to steric interactions between the Cp rings and the *tert*-butyl groups; for this reason, the *tert*-butyl groups deviate slightly from an eclipsed arrangement along the C1–C6 axis.

Accordingly, complex **4** is derived from a new λ^3-phosphaalkyne dimer. At present, we can only speculate as to how it is formed. Presumably, an initially formed η^4-1,3-diphosphabicyclobutadienezirconium complex **1** (M = ZrCp, R = *tert*-butyl) undergoes transformation to **4**. This suggestion is supported by the observation that the fragments $[CpCoP_2]^{\oplus}$ and $[CpCo(RC{\equiv}CR)]^{\oplus}$ are preferentially formed in the mass spectrum of **1** (M = Co).[1] Furthermore, SCF calculations have shown that diphosphatetrahedrane is significantly more stable than 1,3-diphosphacyclobutadiene.[16]

Experimental Procedure

Compound **3** (2.20 g, 22.0 mmol) [17] was added over 1 h to a suspension of $[Cp_2ZrCl_2]$ (1.67 g, 5.71 mmol), magnesium powder (0.7 g, 28.8 mmol), and $HgCl_2$ (1.55 g, 5.71 mmol) in 40 mL of tetrahydrofuran (THF) at 0°C. The orange-red suspension was then allowed to warm to room temperature, stirred for approximately 15 h, and filtered through Celite, and the THF was removed at approximately 20°C/12 torr. The residue was dissolved in 20 mL of diethyl ether and the resulting solution was filtered once again through Celite and then cooled to −78°C. After approximately 12 h, the orange-red crystals of **4** were filtered off and dried at 10^{-3} torr: 1.27 g (53%), m.p. > 300°C.

Received: March 6, 1987 [Z 2128 IE]
German version: *Angew. Chem. 99* (1987) 798

[1] B. Binger, R. Milczarek, R. Mynott, M. Regitz, W. Rösch, *Angew. Chem. 98* (1986) 645; *Angew. Chem. Int. Ed. Engl. 25* (1986) 644.
[2] P. B. Hitchcock, M. J. Maah, J. F. Nixon, *J. Chem. Soc. Chem. Commun. 1986*, 737.
[3] E. Lindner, *Adv. Heterocycl. Chem. 39* (1986) 237, and references cited therein.
[4] S. Thandar, M. F. Farona, *J. Organomet. Chem. 235* (1982) 65.
[5] K. I. Gell, J. Schwartz, *J. Am. Chem. Soc. 103* (1981) 2687.
[6] M. Yoshifuji, K. I. Gell, J. Schwartz, *J. Organomet. Chem. 153* (1978) C15.
[7] E. Negishi, F. E. Coderbaum, T. Takashi, *Tetrahedron Lett. 27* (1986) 2829.
[8] V. Skibbe, G. Erker, *J. Organomet. Chem. 241* (1983) 15.
[9] Spectroscopic data of **4**: MS (70 eV): *m/z* (%) 420 (4, $M^{\oplus}$), 282 (29, $Cp_2ZrP_2^{\oplus}$), 220 (100, $Cp_2Zr^{\oplus}$).—^{1}H-NMR (200 MHz, [D_8]toluene): $\delta = 5.61$ (s, 10H; C_5H_5), 1.23 (s, 18H; $C(CH_3)_3$).-^{13}C-NMR (75.5 MHz, [D_8]toluene): $\delta = 34.54$ ($J(H,C) = 125$ Hz, $J(C,P) = 6.1$ Hz; $C(CH_3)_3$), 38.74 ($J(C,P) = 3.8$ Hz; $C(CH_3)_3$), 104.14 ($J(H,C) = 171$ Hz, $J(C,P) = 2.6$ Hz; C_5H_5), 131.04 ($J(C,P) = 69.7$ Hz; CP).
[10] X-ray structure analysis of **4**: space group $P2_1/c$, $a = 12.720(3)$, $b = 8.835(1)$, $c = 18.166(2)$ Å, $\beta = 100.81(1)°$, $V = 2005.2$ Å^3, $\rho_{calcd} = 1.40$ g cm^{-3}, $\mu(Mo_{K\alpha}) = 6.94$ cm^{-1}, 4502 unique reflections, 3574 observed ($I > 2\sigma(I)$), $R = 0.031$, $R_w = 0.035$. Further details of the crystal structure investigation may be obtained from the Fachinformationszentrum Energie, Physik, Mathematik GmbH, D-7514 Eggenstein-Leopoldshafen 2 (FRG), on quoting the depository number CSD-52580, the names of the authors, and the journal citation.
[11] G. Erker, C. Krüger, G. Müller, *Adv. Organomet. Chem. 24* (1985) 1.
[12] a) G. Becker, W. Massa, O. Mundt, R. Schmidt, *Z. Anorg. Allg. Chem. 485* (1982) 23; b) G. Becker, W. Massa, R. E. Schmidt, G. Uhl, *ibid. 517* (1984) 75.
[13] J. Weiss, B. Nuber, *Z. Anorg. Allg. Chem. 473* (1981) 101.
[14] a) I. Haller, R. Srinivasan, *J. Chem. Phys. 41* (1964) 2745; b) M. Eisenstein, F. L. Hirshfeld, *Acta Crystallogr. Sect. B 39* (1983) 61.
[15] MOGLI program, Graphisches System PS 300, Evans & Sutherland 1986.
[16] G. Olbrich (Max-Planck-Institut für Strahlenchemie, Mülheim a. d. Ruhr), in preparation.
[17] G. Becker, G. Gresser, W. Uhl, *Z. Naturforsch. B 36* (1981) 16.

The Role of Debye Screening Length in Ordered Arrays of Cylindrical Nickel Dimethylglyoxime Particles**

By *Tsuneo Okubo**

There are many systems of biological interest in which long cylindrical particles of macromolecular dimensions form three-dimensional, hexagonal arrays with an interparticle center-to-center distance that may be several times the diameter of the cylinders.[1,2] *Bernal* and *Fankuchen*[1] carried out detailed X-ray analyses of cylindrical tobacco mosaic virus (length 300 nm, diameter 17 nm) and found

[*] Prof. Dr. T. Okubo
Department of Polymer Chemistry
Kyoto University, Kyoto 606 (Japan)

[**] This work was supported by the Kurata Foundation and the Ministry of Education, Science, and Culture (Japan).

that a distinct ordered phase of the particles formed in solution. The ordering has been clarified experimentally and theoretically and has been ascribed to the interplay between electrostatic interparticle repulsion and attractive van der Waals forces. However, the balancing of these forces in the formation of the ordered hexagonal arrays remains an open question.[3,4] Recently, this author described in detail the lattice structures of heavy spheres (specific gravity 1.05–19.3) in sedimentation equilibrium.[5–7] From these experiments it was concluded that the ordered structure of the spheres is caused by electrostatic intersphere repulsions and elongated Debye screening lengths around the spheres, which are counterbalanced by the force due to the gravitational field.

Monodisperse, cylindrical particles of nickel dimethylglyoxime (length 9.6 μm, diameter 0.12 μm) have now been used to form hexagonal arrays in sedimentation equilibrium. The interparticle distances at different initial concentrations were determined and then used to obtain the Young's modulus of the lattice structures.

The particles were obtained by the reaction of nickel acetate with dimethylglyoxime: 0.5 g of dimethylglyoxime (biacetyldioxime) in 50 mL of ethanol and 0.4 g of nickel acetate in 40 mL of water were added to 200 mL of an aqueous solution (1.75 wt%) of nonionic surfactant OP-30 (polyoxyethylene(30)octylphenyl ether, Nikko Chemicals Co., Tokyo (Japan)). The mixture was stirred and 400 mL of water was added. The scarlet-red sols thus obtained were purified by dialysis against deionized pure water for more than three weeks. The size of the cylindrical (rodlike) particles was determined using an electron microscope. The length and the diameter were 9.6 ± 1.4 μm and 0.12 ± 0.03 μm, respectively. The monodispersity in their sizes was rather high. The zeta potential of the sols was -44.4 ± 1.4 mV in pure water (Lazer Zee meter, model 501, Pen Kem, Inc., Bedford Hills, NY (USA)). The water used for the purification and for solution preparation was deionized by using cation- and anion-exchange resins (Amberlite IR-120B and IRA-400) and further purified by a Milli-Q reagent-grade water system (Millipore Co., Bedford, MA (USA)).

Photographing of the particles of nickel dimethylglyoxime was carried out with a reversed-type metallurgical microscope (Axiomat IAC, Carl-Zeiss, D-7082 Oberkochen (FRG)). The suspension cell was made from a glass tube (height 7 cm, diameter 2 cm), which had an object glass at one end. The ordered structure was observed within several hours after 10 mL of the suspension was introduced into the cell, and reliable data on the interparticle distance could be obtained after 24 h. The height of the sedimentation layer of the cylindrical particles was less than 1 mm in sedimentation equilibrium.

Microscopic observation was made through the object glass at the bottom of the cell. A typical picture is shown in Figure 1. The cylindrical particles are hexagonally arranged in the salt-free suspension. The microscopic observation revealed that the particles behaved like enlarged cylinders according to the Debye screening length (D_1), and the effective sizes of the cylinders including D_1 decreased as the ionic strength of the solvent increased ([NaCl] = 10^{-6}–10^{-3} M). It should be mentioned here that the ordered distribution was observed throughout the whole range of the object glass, although the grain boundaries were often observed. The Debye screening length (D_1) is calculated from Equation (1):

$$D_1 = (4\pi B n)^{-1/2} \quad (1)$$

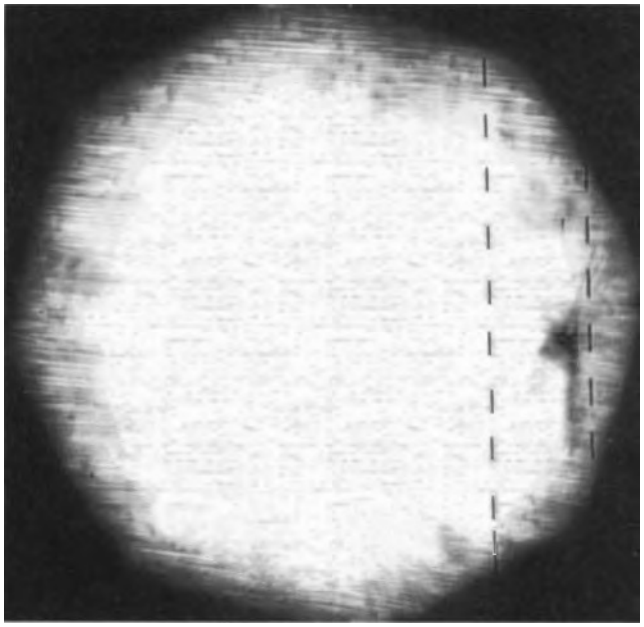

Fig. 1. A typical picture showing the ordered arrays of cylindrical particles of nickel dimethylglyoxime in sedimentation equilibrium. $\phi^* = 0.0816$ vol% in salt-free aqueous suspension. The distance between the dashed parallel lines is 10 μm. The cylindrical particles move around the equilibrium points and are distributed regularly along the object glass.

Here, B is the Bjerrum length given by $e^2/\varepsilon k T$, where e is the electronic charge, ε the dielectric constant of the solvent, and n is the concentration of "free" cations and anions in solution. In the absence of foreign salts, n is the sum of the concentration of diffusible counterions and concentrations of hydrogen and hydroxide ions from the dissociation of water. We have no information on the stoichiometric charge number on the surface of the particle. Furthermore, the fraction of free-state counterions of spherical particles has been reported to be smaller than 0.1.[8,9] In this experiment, the concentration of the free-state counterions could be negligible, or at most does not exceed the concentrations of the hydrogen and hydroxide ions. We estimated the effective ionic concentration of the water used to be ca. 1×10^{-6} M. D_1 was evaluated as 0.43 μm. This calculated value is very close to the experimental value, $D_1 = 0.42$ μm, determined from the extrapolated value of the interparticle distance at the top layer of the sedimentation suspension, $2D_{\mathrm{exp,u}}$ ($= 0.95$ μm). It is clear that the observed value of $2D_{\mathrm{exp,u}}$ is explained satisfactorily by the Debye screening length, although the more reliable repulsive potential of electrical double layers must be taken into account for a quantitative comparison.

It is interesting that the observed interparticle distance at the bottom of the sedimented layer, $2D_{\mathrm{exp}}$, decreased continuously as the initial concentration of the particles increased. This means that the shells of Debye screening length around the cylinders are soft and elastic and can be compressed rather easily by the cylinders of the upper layers owing to the earth's gravity. According to *Crandall* and *Williams*[10] and this author,[5] Young's modulus of the sedimented suspension layer, E, can be estimated from Equation (2):

$$2D_{\mathrm{exp}} = 2D_{\mathrm{exp,u}} - (\rho_{\mathrm{eff}} g l 2 D_{\mathrm{exp,u}} \phi^*)/(100 E) \quad (2)$$

Here, ϕ^* is the initial concentration of nickel dimethylglyoxime sols, g the gravitational constant, ρ_{eff} the effective density, given by the specific gravity of cylinders minus

that of solvent, and l the height of the liquid layer in the observation cell. Figure 2 shows plots of $2D_{exp}$ vs. ϕ^* for the cylindrical particles in the deionized state. The linearity was satisfactory in the region of $\phi^* < 0.05$ vol%, and the values of $2D_{exp,u}$ and E were estimated from the intercept and slope as 0.95 μm and 0.47 Pa, respectively. It is interesting to note that this value of E is similar to those of ordered structures of spherical particles reported hitherto[5-7,9-11] (i.e., between 0.01 to 100 Pa).

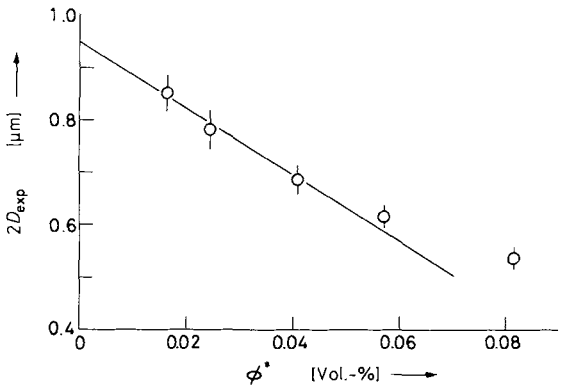

Fig. 2. $2D_{exp}$ vs. ϕ^* plots for cylindrical particles of nickel dimethylglyoxime in salt-free aqueous suspension. $2D_{exp,u} = 0.95$ μm.

These experiments show that the Debye screening length plays an important role in the ordering of the cylinders. Although a quantitative discussion still remains, the ordering of the cylinders can be attributed to the effective hard-sphere model for spheres, where the Debye length is added to the real size of spheres. This model is consistent with the Derjaguin–Landau–Verwey–Overbeek theory (DLVO theory) on colloidal stability.[12]

Received: March 6, 1987;
revised: May 4, 1987 [Z 2127 IE]
German version: *Angew. Chem. 99* (1987) 803

CAS Registry numbers:
Ni dimethylglyoxi,me, 13478-93-8; Ni acetate, 373-02-4; dimethylglyoxi,me, 95-45-4.

[1] J. D. Bernal, J. Fankuchen, *J. Gen. Physiol. 25* (1941) 111.
[2] D. P. Riley, G. Oster, *Discuss. Faraday Soc. 11* (1951) 107; E. Rome, *J. Mol. Biol. 27* (1967) 591; R. J. Goldacre, *Nature (London) 174* (1954) 732.
[3] L. Onsager, *Ann. N. Y. Acad. Sci. 51* (1949) 624; R. Zwanzig, *J. Chem. Phys. 39* (1963) 1714; V. A. Parsegian, *Annu. Rev. Biophys. Bioeng. 2* (1973) 221; S. L. Brenner, D. A. McQuarrie, *Biophys. J. 13* (1973) 301; S. L. Brenner, V. A. Parsegian, *ibid. 14* (1974) 327.
[4] V. A. Parsegian, S. L. Brenner, *Nature (London) 259* (1976) 632.
[5] T. Okubo, *J. Chem. Phys. 86* (1987) 2394.
[6] T. Okubo, *J. Chem. Phys. 86* (1987) 5182.
[7] T. Okubo, *Colloid Polym. Sci.*, in press.
[8] W. Vanderhoff, H. J. van de Hul, R. J. M. Tausk, J. Th. G. Overbeek in G. Goldfinger (Ed.): *Clean Surfaces: Their Preparation and Characterization for Interfacial Studies*, Dekker, New York 1970; K. Ito, N. Ise, T. Okubo, *J. Chem. Phys. 82* (1985) 5732; S. Alexander, P. M. Chaikin, P. Grant, G. J. Morales, P. Pincus, D. Hone, *ibid. 80* (1984) 5776.
[9] T. Okubo, *Polym. Prepr. Jpn. 36* (1987) 1120; *Ber. Bunsenges. Phys. Chem.*, in press.
[10] R. S. Crandall, R. Williams, *Science (Washington, DC) 198* (1977) 293.
[11] S. Mitaku, T. Otsuki, K. Enari, A. Kishimoto, K. Okano, *Jpn. J. Appl. Phys. 17* (1978) 305; T. Otsuki, S. Mitaku, K. Okano, *ibid. 17* (1978) 627; S. Mitaku, T. Otsuki, K. Okano, *ibid. 19* (1980) 439; T. Otsuki, A. Kishimoto, S. Mitaku, K. Okano, *ibid. 20* (1981) 509; H. M. Joanicot, M. Jorand, P. Pieranski, F. Rothen, *J. Phys. (Orsay, Fr.) 45* (1984) 1413; H. M. Lindsay, P. M. Chaikin, *J. Chem. Phys. 76* (1982) 3774; T. Okubo, *J. Colloid Interface Sci. 117* (1987) 165.
[12] E. J. W. Verwey, J. Th. G. Overbeek: *The Theory of the Stability of Lyophobic Colloids*, Elsevier, Amsterdam 1948.

Metathesis of CS_2-Like Heteroallenes on 1,1-Dithio Complexes of Rhodium(III)

By *Claudio Bianchini,* Andrea Meli,* and *Franco Vizza*

A reaction of both technological and scientific relevance is the metal-assisted metathesis of unsaturated molecules such as alkenes,[1] alkynes,[2] and nitriles.[3] It is now generally recognized that the rupture and formation of chemical bonds within metallocyclic intermediates are important mechanistic steps of these reactions. Here we report on a new type of metal-promoted metathesis reaction which involves as unsaturated substrates CS_2-like heteroallene molecules (Scheme 1).

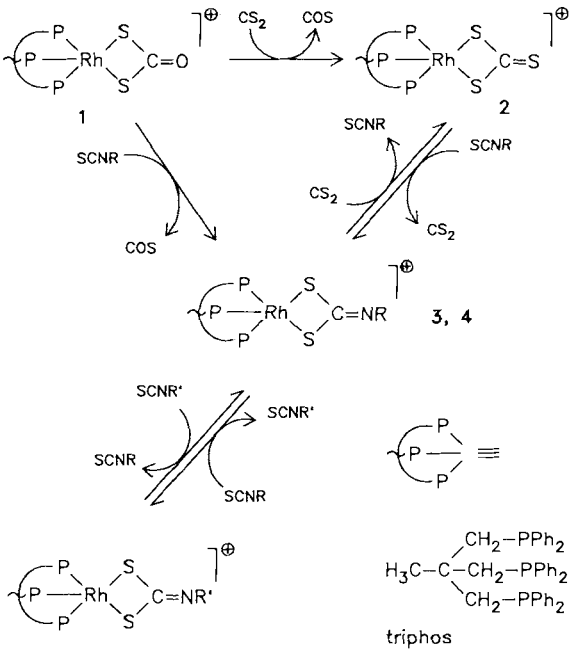

Scheme 1. The anions BPh_3^- are omitted. **3**, R = Ph; **4**, R = Et.

The dithiocarbonate complex **1**[4] reacts immediately in CH_2Cl_2 at room temperature with an equimolar amount of CS_2 to give, in quantitative yield, trithiocarbonate **2**[5] (red crystals) and COS. By treatment of **2** with a twofold excess of SCNR (R = Ph, Et), the dithiocarboimidic acid derivatives **3**, R = Ph,[6] and **4**, R = Et,[7] are precipitated as deep violet crystals, and CS_2 is evolved. The latter reactions are reversible; i.e., the addition of a twofold excess of CS_2 to **3** or **4** leads to quantitative formation of **2** and liberates the organoisothiocyanate. Alternatively, **3** and **4** can be directly obtained by reacting **1** with equimolar amounts of SCNPh or SCNEt, respectively. These isothiocyanates are also metathesized by the rhodium system, the only reaction condition being a twofold excess of the appropriate isothiocyanate.

Compound **1** and the related derivatives **2**, **3**, and **4** are coordinatively and electronically unsaturated complexes. The two sulfur atoms, although capable of transferring electron density to rhodium via π interaction, do not adequately satisfy the electron requirement of the metal,

[*] Dr. C. Bianchini, Dr. A. Meli, Dr. F. Vizza
Istituto per lo Studio della Stereochimica ed Energetica
dei Composti di Coordinazione del C.N.R.,
Via J. Nardi 39, I-50 132 Firenze (Italy)

which therefore still remains an electrophilic center.[8] Indeed, all of these compounds contain polarized Rh–S linkages which can promote the heterolytic activation of H_2.[8] In addition, **1** tends to eliminate CO or COS either photochemically[9] or thermally.[10] When COS is eliminated, the [(triphos)RhS]$^{\oplus}$ fragment dimerizes to give [(triphos)Rh(μ-S)$_2$Rh(triphos)]$^{2\oplus}$.[9, 11] Although to a lesser extent, **2**, **3**, and **4** exhibit the same tendency to chelotropically eliminate heteroallene moieties from the RhSC(X)S rings (X = S, NR).[10]

In view of these results and considerations, a reasonable mechanistic interpretation of the reactions in Scheme 1 is shown in Scheme 2. This mechanism involves the formation of intermediary metallocycles of type **A** via [2+2] cycloadditions.[12] The extrusion of one of the two heteroallene moieties of the intermediates **A** completes the reactions. These can be monitored by ^{31}P-NMR spectroscopy.[13]

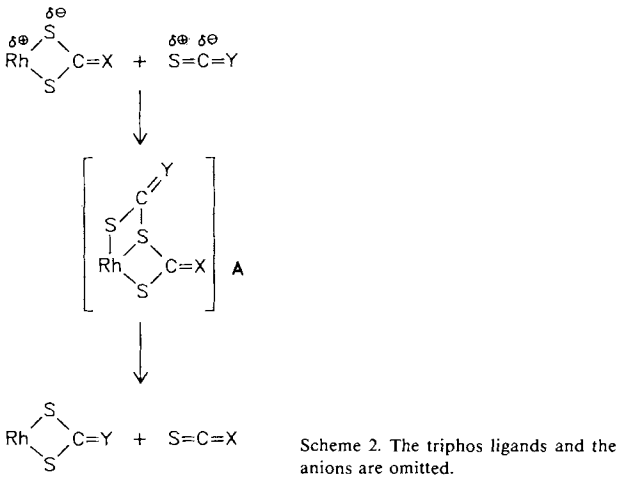

Scheme 2. The triphos ligands and the anions are omitted.

The replacement of the COS fragment in **1** by CS_2 or SCNR appears as the most favored reaction pathway, being quantitatively achieved by equimolar amounts of the latter coreactants. By contrast, **2** and **3** (or **4**) seem to have comparable thermodynamic stabilities. Their quantitative interconversion occurs only when large excesses of CS_2 or SCNR are used, whereas stoichiometric reactions give equimolar mixtures of **2** and **3** (or **4**). In nice agreement with the apparent, minor stability of the dithiocarbonate complex **1**, complexes **2** and **3** (or **4**) are not converted into **1** even when treated with a large excess of COS.

Experimental Procedure

2: Neat CS_2 (0.06 mL, 1 mmol) was added to a solution of **1** (1.14 g, 1 mmol) in 30 mL of CH_2Cl_2. There was an immediate color change from red brown to brilliant red and, simultaneously, COS evolution. Addition of ethanol (40 mL) gave red crystals of **2**, which were collected by filtration and washed with ethanol and petroleum ether; yield 95%.

3, **4**: Dark violet crystals of **3** and **4** were obtained in excellent yields (ca. 95%) following the same procedure as above but replacing CS_2 with SCNR (R = Ph, Et). Alternatively, **2** was treated in CH_2Cl_2 with a twofold excess of SCNR and worked up as above. The interconversion between **3** and **4** was simply achieved by adding an excess of SCNEt or SCNPh to a CH_2Cl_2 solution of **3** or **4**, respectively.

The formation of COS, CS_2, and SCNR in the course of the reactions was determined by GC. Correct elemental analyses were found for all of the products here described.

Received: March 27, 1987;
revised: May 4, 1987 [Z 2166 IE]
German version: *Angew. Chem.* 99 (1987) 821

[1] Recent reviews on the metathesis reaction: a) N. Calderon, J. P. Lawrence, E. A. Ofstead, *Adv. Organomet. Chem. 17* (1979) 449; b) R. H. Grubbs, *Prog. Inorg. Chem. 24* (1978) 1; c) T. J. Katz, *Adv. Organomet. Chem. 16* (1977) 28.

[2] T. J. Katz, J. McGinnis, *J. Am. Chem. Soc. 92* (1975) 1592.

[3] R. H. A. Bosma, G. C. N. Van Den Aardweg, J. C. Mol, *J. Organomet. Chem. 280* (1985) 115.

[4] C. Bianchini, C. Mealli, A. Meli, M. Sabat, *J. Chem. Soc. Chem. Commun. 1985*, 1024. **1**: Λ_M(nitroethane) = 43 ohm^{-1} cm^2 mol^{-1}.

[5] **2**: IR (Nujol): $\tilde{\nu}$ = 995 cm^{-1} (C=S); ^{31}P{^{1}H}-NMR (DMF, 298 K): δ = 9.92 (d, J(R–Rh) = 101 Hz); Λ_M(nitroethane) = 43 ohm^{-1} cm^2 mol^{-1}.

[6] **3**: IR (Nujol): $\tilde{\nu}$ = 1570 (C–N), 1590 cm^{-1} (N–Ph); ^{31}P{^{1}H}-NMR (CH_2Cl_2, 298 K): δ = 34.19 (d, J(P–Rh) = 98 Hz); Λ_M(nitroethane) = 42 ohm^{-1} cm^2 mol^{-1}.

[7] **4**: IR (Nujol): $\tilde{\nu}$ = 1570 cm^{-1} (C–N); ^{31}P{^{1}H}-NMR (CH_2Cl_2, 298 K): δ = 33.70 (d, J(P–Rh) = 98 Hz); ^{1}H-NMR: δ = 4.40 (q, NCH_2CH_3), 1.35 (t, NCH_2CH_3); Λ_M(nitroethane) = 42 ohm^{-1} cm^2 mol^{-1}.

[8] C. Bianchini, A. Meli, unpublished.

[9] C. Bianchini, A. Meli, *Inorg. Chem. 26* (1987) 1345.

[10] C. Bianchini, A. Meli, unpublished.

[11] C. Bianchini, C. Mealli, A. Meli, M. Sabat, *Inorg. Chem. 25* (1986) 4617.

[12] C. Bianchini, C. Mealli, A. Meli, M. Sabat, J. Silvestre, R. Hoffmann, *Organometallics 5* (1986) 1733.

[13] Because of the rapid intramolecular exchange of the three phosphorus atoms of triphos around the metal, the ^{31}P{^{1}H}-NMR spectra of **1**–**4** consist of a doublet (A_3X spin system) ([5–7]).

Reactions of $[Pd_2(\mu\text{-dppm})_2Cl_2]$ with Electrophilic Complexes of Copper and Gold. Synthesis of the Pd_4 Cluster $[Pd_4(\mu\text{-Cl})_2(\mu\text{-dppm})_4](PF_6)_2 \cdot 2(CH_3)_2CO$**

By *Pierre Braunstein,* Michael A. Luke, Antonio Tiripicchio,* and *Marisa Tiripicchio Camellini*

The rich chemistry of the binuclear complexes $[M_2(\mu\text{-dppm})_2X_2]$ (M = Pd and/or Pt; X = Cl, Br, or I; dppm = *P,P'*-methylenebis(diphenylphosphane) has been widely studied.[1] However, most of the investigations have been concerned with the formation of A-frame complexes via insertion of small molecules, e.g., CO, SO_2, or RCN, into the M–M bond or with their reactivity toward nucleophilic metal reagents, e.g., carbonylmetalates.[2] Two recent publications have described the reactions of such diplatinum complexes, as exemplified by $[Pt_2(\mu\text{-dppm})_2Cl_2]$, toward electrophilic metal reagents.[3] In both cases, the expected complexes of the A-frame type were obtained. This prompted us to present some new results involving the reaction of the analogous dipalladium complex **1** with copper and gold complexes. In the reactions with copper complexes, we unexpectedly isolated the novel, tetranuclear palladium cluster complexes **2a** and **2b**. The X-ray crystal structure of **2a** revealed a 10-membered ring structure, unprecedented in this class of compounds.

When the solution resulting from the reaction of $[(PPh_3)CuBr]_4$ and $TlPF_6$ in tetrahydrofuran (THF) was added to a suspension of **1** in THF (Cu : **1** = 1 : 1), the solu-

[*] Dr. P. Braunstein, Dr. M. A. Luke
Laboratoire de Chimie de Coordination,
UA 416 CNRS, Université Louis Pasteur
4 rue Blaise Pascal, F-67070 Strasbourg Cédex (France)
Prof. A. Tiripicchio, Prof. M. Tiripicchio Camellini
Istituto di Chimica Generale ed Inorganica dell'Università
Centro di Studio per la Strutturistica Diffrattometrica del C.N.R.
Viale delle Scienze, I-43100 Parma (Italy)

[**] The Royal Society is thanked for the award of a European Exchange Fellowship (*M. A. L.*). Financial support from the CNRS (Paris), Atochem, CNR (Rome), and NATO (Grant 257/83 to *P. B.* and *A. T.*) is gratefully acknowledged.

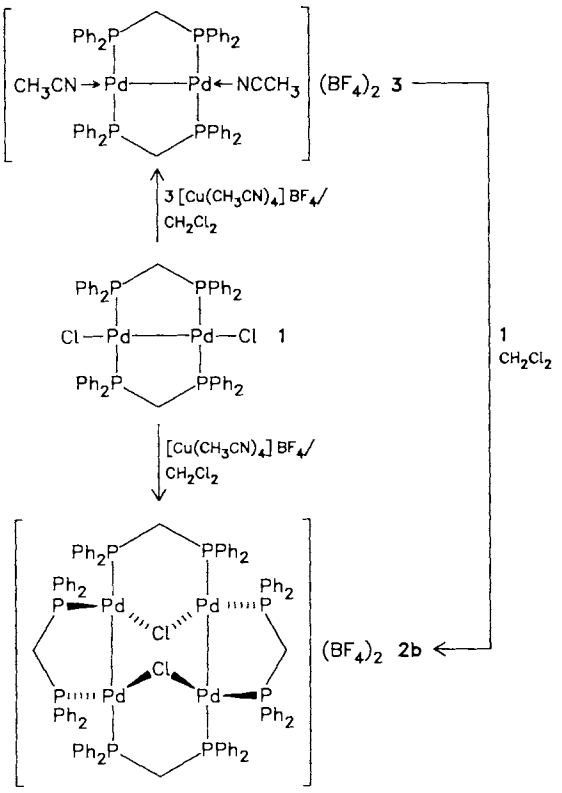

$$1 \xrightarrow[\text{THF}]{[(PPh_3)CuBr]_4/TlPF_6} [Pd_4(\mu\text{-}Cl)_2(\mu\text{-}dppm)_4](PF_6)_2 \quad \textbf{2a}$$

tion rapidly turned red accompanied by the formation of a small amount of white precipitate (CuCl). After filtration and removal of the solvent, a red powder was obtained. Layering an acetone solution of this mixture with pentane yielded red crystals of **2a** in ca. 40% yield. The identity and structure of **2a** was established by an X-ray diffraction study.[4] Complex **2a** crystallizes as an acetone solvate; the cations are centrosymmetrical (crystallographically imposed symmetry). Figure 1 shows a rectangular array for the four Pd atoms with the two shorter Pd–Pd distances (2.594(2) Å) being consistent with a metal–metal bond. Each Pd atom is in a distorted square-planar environment determined by two P atoms from dppm ligands, one Cl atom, and one other Pd atom. All four sides of the Pd_4 rectangle are bridged by dppm ligands. It is noteworthy that the Pd–P bonds have different lengths. The dppm ligands bridging the longer sides form much longer bonds (2.350(6) and 2.353(7) Å) than those bridging the shorter sides (2.220(5) and 2.229(6) Å). This difference is possibly due to both steric and electronic factors arising from the *trans* influence of the Pd–Pd bond and the bulk of the phenyl substituents. The longer sides of the metal array (3.742(3) Å) are also bridged by two chlorine atoms in an almost symmetrical fashion. The spectroscopic data[6] of **2a** are consistent with its solid-state structure.

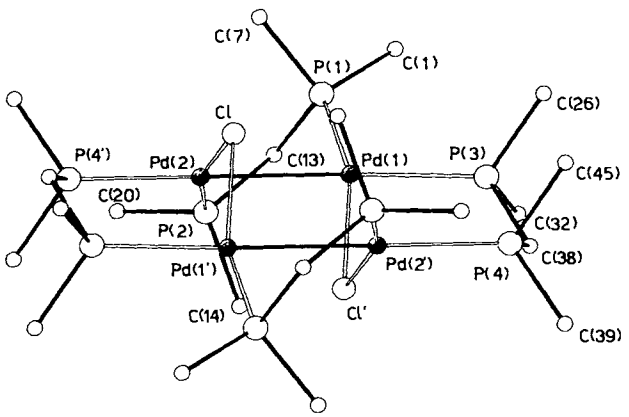

Fig. 1. Molecular structure of the cation of **2a**. Important bond distances [Å] and angles [°]: Pd1-Pd2 2.594(2), Pd1-Pd2' 3.742(3), Pd2-Cl 2.391(5), Pd1-Cl' 2.422(4), Pd1-P1 2.220(5), Pd2-P2 2.229(6), Pd1-P3 2.350(6), Pd2'-P4 2.353(7); Pd2-Cl-Pd1' 102.1(2), P1-Pd1-P3 104.0(2), P3-Pd1-Cl' 91.0(2), P1-Pd1-Cl' 158.0(2), Pd2-Pd1-P3 174.1(2), Cl'-Pd1-Pd2 84.3(2), P1-Pd1-Pd2 81.5(2), Pd1-Pd2-Cl 80.7(2), Cl-Pd2-P4' 91.2(2), P4'-Pd2-P2 105.2(3), P2-Pd2-Pd1 83.0(2), P2-Pd2-Cl 163.5(2), Pd1-Pd2-P4' 171.4(2). The 16 phenyl groups are each represented by their *ipso* carbon atom.

We found that the $BF_4^{\ominus}$ salt **2b** could be readily synthesized from **1** and $[Cu(CH_3CN)_4]BF_4$ (1 : 1). The choice of solvent appears to play a crucial role in determining the rate and selectivity of the reaction; in particular, the use of CH_2Cl_2 gave **2b** in virtually quantitative yield. The stoichiometry of the reagents is also of vital importance, since a slight excess of the copper reagent results in the formation of another complex, **3**. Indeed, the use of a threefold excess of $[Cu(CH_3CN)_4]BF_4$ resulted in the quantitative formation of **3**. Complex **3** is also formed from the reaction of **1** with two equivalents of $AgBF_4$ in CH_3CN.

Reaction of **1** with $[(PPh_3)AuCl]$ and $TlPF_6$, instead of with $[(PPh_3)CuBr]_4$ and $TlPF_6$, resulted in an extremely oily mixture of phosphane-containing cluster compounds ($^{31}P\{^1H\}$-NMR evidence). Despite extensive efforts, no solid material could be isolated. Since no precipitate was formed, the gold must be complexed in some form or other. The $^{31}P\{^1H\}$-NMR data of the product obtained from the reaction of **1** with $[(C_2H_5)_2SAuCl]$ reveal that all four phosphane atoms of the dppm ligands are now chemically and magnetically nonequivalent. Presumably, the Au atom has inserted into a Pd–P bond.[7] This reaction emphasizes the greater lability of the Pd–P compared with the Pt–P bond, since with the diplatinum precursor an A-frame structure was observed in which AuCl bridges the Pt–Pt bond.[3b]

Our results illustrate that the main driving force in the reactions of **1** with copper reagents is the precipitation of CuCl, thus leaving a vacant site on the palladium center. If no other suitable ligands are present in the reaction medium, this unit then dimerizes to give the tetranuclear palladium cluster. This is supported by the observation that the reaction of **1** with **3** leads to the formation of **2b** (1 : 1 molar ratio, CH_2Cl_2, 25°C, 2 h, 90% yield based on $^{31}P\{^1H\}$-NMR). These results also illustrate that in certain systems the isolobal analogy between group 11 metal complexes does not always guarantee similar reactivity.

Received: March 30, 1987 [Z 2167 IE]
German version: *Angew. Chem.* 99 (1987) 802

[1] A. L. Balch in L. H. Pignolet (Ed.): *Homogeneous Catalysis with Metal Phosphine Complexes*, Plenum, New York 1983, p. 167; R. J. Puddephatt, *Chem. Soc. Rev. 12* (1983) 99, and references cited therein.

[2] a) P. Braunstein, J.-M. Jud, Y. Dusausoy, J. Fischer, *Organometallics 2* (1983) 180; b) P. Braunstein, J.-M. Jud, J. Fischer, *J. Chem. Soc. Chem. Commun. 1983*, 5; c) M. C. Grossel, R. P. Moulding, K. R. Seddon, *J. Organomet. Chem. 253* (1983) C 50; d) P. Braunstein, C. de Meric de Bellefon, M. Ries, *ibid. 262* (1984) C 14; e) P. Braunstein, J. Kervennal, J.-L. Richert, *Angew. Chem. 97* (1985) 762; *Angew. Chem. Int. Ed. Engl. 24* (1985) 768.

[3] a) P. R. Sharp, *Inorg. Chem. 25* (1986) 4185; b) G. J. Arsenault, L. Manojlovic-Muir, K. W. Muir, R. J. Puddephatt, I. Treurnicht, *Angew. Chem. 99* (1987) 79; *Angew. Chem. Int. Ed. Engl. 26* (1987) 86.

[4] **2a**·$(CH_3)_2CO$: triclinic, space group $P\bar{1}$, $a=14.826(7)$, $b=16.440(7)$, $c=12.598(5)$ Å, $\alpha=68.15(3)$, $\beta=84.63(2)$, $\gamma=67.76(2)°$, $V=2634(2)$ Å^3, $Z=1$, $\rho_{calcd}=1.538$ g cm^{-3}, $F(000)=1228$, $\lambda=0.7107$ Å, $\mu(Mo_{K\alpha})=9.31$ cm^{-1}. 6651 independent reflections (Siemens AED diffractometer, θ in the range 3–23°, $\theta/2\theta$ scan technique and Nb-filtered radiation. The structure was solved by direct and Fourier methods and refined by full-matrix least-squares analysis on the basis of 3278 observed reflections [$I \geq 2\sigma(I)$] with anisotropic thermal parameters for the Pd, Cl, and P atoms (SHELX programs [5]). The phenyl rings were treated as rigid groups in the last cycles of the refinement. The hydrogen atoms were placed at their geometrically calculated positions. $R=0.076$, $R_w=0.080$. Further details of the crystal structure investigation can be obtained from the Fachinformationszentrum Energie, Physik, Mathematik GmbH, D-7514 Eggenstein-Leopoldshafen 2 (FRG), by quoting the depository number CSD-52428, the names of the authors, and the journal citation.

[5] G. M. Sheldrick: SHELX, *System of Computing Programs*, University of Cambridge 1976.

[6] **2a**: ^{1}H-NMR ([D$_6$]acetone): $\delta=4.70$ (t, 4H, ^2J(P–H) = 11.5 Hz, P–CH_2–P), $\delta_A=3.5$, $\delta_B=3.1$ (each unresolved multiplet, each 2H). ^{31}P{^{1}H}-NMR (CH_2Cl_2/D_2O ext.): AA'A''A'''BB'B''B''' spin system observed as an AB pattern with unresolved splittings, $\delta_A=-6.36$, $\delta_B=-14.96$. IR (KBr): $\tilde{\nu}=845$ s, br ($PF_6^\ominus$) cm^{-1}.— **2b**: ^{1}H-NMR (CD_2Cl_2): $\delta=4.33$ (t, 4H, ^2J(P–H) = 11.5 Hz, P–CH_2–P), $\delta_A=3.22$, $\delta_B=3.0$ (each unresolved multiplet, each 2H). ^{13}P{^{1}H}-NMR (CH_2Cl_2/D_2O ext.): as for **2a**, couplings were not resolved, $\delta_A=-6.16$, $\delta_B=-15.2$. IR (KBr): $\tilde{\nu}=1075$ s, br ($BF_4^\ominus$) cm^{-1}.— **3**: ^{1}H-NMR ($CDCl_3$): $\delta=4.34$ (virtual quintet, 4H, $J_{app}=4.5$ Hz, P–CH_2–P), 1.48 (s, 6H, CH_3CN ligand). ^{31}P{^{1}H}-NMR (CH_2Cl_2/D_2O ext.): $\delta=-5.25$ (s). IR (Nujol): $\tilde{\nu}=2285$ w (C≡N), 1075 s, br ($BF_4^\ominus$) cm^{-1}. Satisfactory elemental analyses were obtained for all complexes.

[7] The ^{1}H- and ^{31}P{^{1}H}-NMR data are consistent with a *triangulo* $Pd_2Au(\mu\text{-dppm})_2$ structure in which the dppm ligands span Pd–Au and Pd–Pd bonds, giving rise to patterns previously encountered in related heterometallic clusters synthesized in this laboratory [2a, d].

The Effect of Solvent on the Stability of mero-Substituted Alkyl Radicals**

By *Hans-Dieter Beckhaus* and *Christoph Rüchardt**

In analogy to the stabilization of carbenium ions by electron-donating substituents (donors) and of carbanions by electron-withdrawing substituents (acceptors), a particularly strong stabilization of radicals by pairs of substituents having opposite polarity ("captodative"- or "mero"-substituted) has been postulated to occur.[1] The experimental testing of this concept[2] on several examples did not lead to evidence for more than an additive effect of the substituents on lowering the enthalpy of formation of radicals of this type, e.g. **1a**, **b**.[3] Moreover, theoretical studies[4] do not allow conclusions to be drawn concerning a particularly strong stabilization of captodative-substituted radicals. Indeed, ab initio calculations showed that the effect of the substituents on tetracoordinated carbon atoms can give rise to changes in energy that are similar to those observed for radicals. This was also established experimentally by determining the strengths of C–C bonds.[5] The interaction of two geminal substituents with the σ-electron framework is about as strong as that with the unpaired electron (π system) of the radical.

Accordingly, a discussion of the effect of substituents on radicals cannot be restricted to only electron resonance phenomena. Nonetheless, a dramatic increase in "mero stabilization" by polar solvents was recently suggested on the basis of the resonance between substituents having opposite polarities at a radical center, which formally leads to charge-separated structures.[6] Calculations by an INDO-UHF-SCRF method indicated a reduction in energy of the radical **1c** by approximately 30 kcal/mol on going from a nonpolar (dielectric constant $\varepsilon=1$) to a polar ($\varepsilon=80$) medium.[6] The suggestion of such an enormous solvent effect motivated us to test this postulate experimentally.

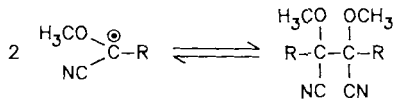

1 **2**

a, R = C_6H_5; **b**, R = t-C_4H_9; **c**, R = H

We therefore studied the effect of solvent on the homolysis of the symmetrically hexasubstituted ethanes **2a** and **2b** to give the radicals **1a** and **1b**, respectively. Using the ESR method described earlier,[3] we determined the position of the equilibrium between **2a** and **1a** as well as the reaction enthalpy and entropy of dissociation (ΔH_r and ΔS_r, respectively) from its temperature dependence between 140 and 200°C. A stabilization of the radicals by amounts of the order calculated for **1c** should reduce the reaction enthalpy in polar solvents ($\varepsilon=80$) by up to 60 kcal/mol. However, the results of the measurements revealed no significant effect of the solvent on the dissociation (Table 1). The formation of the radicals is no more favored in ethylene glycol [$\varepsilon(100°C)=25.6$][7] and in succinic anhydride [$\varepsilon(60°C)=50$][7] than in the less polar diphenyl ether ($\varepsilon\approx3$). The agreement of the reaction enthalpy ΔH_r with the enthalpy of activation $\Delta H^{\neq}$[3] measured earlier in mesitylene supports the reliability of the results. This is unequivocal evidence in disfavor of the postulated increase in the "mero stabilization" by polar solvents, even when one takes into account that the polarity of the solvent at the temperatures of measurement is somewhat lower. The use of solvents of still higher polarity was not possible owing to technical problems in the ESR measurements. In order to also include a highly polar solvent in the investigation, we determined the activation parameters $\Delta H^{\neq}$ and $\Delta S^{\neq}$ of the thermal dissociation of **2b** by ki-

Table 1. Thermodynamic reaction and activation parameters for the formation of α-cyano-α-methoxyalkyl radicals **1** by homolytic dissociation of the dimers **2** in different solvents (with standard deviation; for the method of measurement, see [3] and [8]).

Compound	Solvent	Method	ΔH_r [kcal mol^{-1}]	$\Delta H^{\neq}$ [kcal mol^{-1}]	ΔS_r [cal mol^{-1} K^{-1}]	$\Delta S^{\neq}$ [cal mol^{-1} K^{-1}]
meso-**2a** [3]	mesitylene[a]	NMR	—	36.6 ± 0.4	—	15.1 ± 0.8
D,L-**2a** [3]	mesitylene[a]	NMR	—	36.0 ± 0.2	—	13.2 ± 0.6
2a [b][3]	diphenyl ether	ESR	35.0 ± 1.8	—	31.8 ± 3.8	—
2a [b]	ethylene glycol	ESR	35.3 ± 0.6	—	29.8 ± 1.3	—
2a [c]	succinic anhydride	ESR	37.2 ± 0.7	—	33.6 ± 1.6	—
meso-**2b** [3]	mesitylene[a]	DSC	—	34.8 ± 0.5	—	10.9 ± 1.3
meso-**2b**	*N*-methylacetamide[a]	DSC	—	34.8 ± 0.4	—	10.9 ± 1.0
D,L-**2b** [3]	mesitylene[a]	DSC	—	34.8 ± 0.3	—	12.6 ± 0.8
D,L-**2b**	*N*-methylacetamide[a]	DSC	—	34.2 ± 0.7	—	11.0 ± 1.8
2b [c][3]	diphenyl ether	ESR	34.3 ± 0.5	—	41.2 ± 1.2	—

[a] 20% thiophenol as radical trap. [b] Diastereomeric equilibrium (^{1}H-NMR) *meso*-**2a** : D,L-**2a** = 0.8, at 110–150°C in diphenyl ether, mesitylene, and *N*-methylacetamide. [c] Diastereomeric equilibrium (^{1}H-NMR) *meso*-**2b** : D,L-**2b** = 2.4, at 100–150°C in mesitylene.

[*] Prof. Dr. C. Rüchardt, Dr. H.-D. Beckhaus
Institut für Organische Chemie und Biochemie der Universität
Albertstrasse 21, D-7800 Freiburg (FRG)

[**] This work was supported by the Deutsche Forschungsgemeinschaft, the State Baden-Württemberg, and the Fonds der Chemischen Industrie.

netic differential scanning calorimetry (DSC) measurement[8] at 100–150 °C in *N*-methylacetamide [ε = 70 (150 °C), 110 (100 °C)].[9] In order to suppress the back reaction, we added the usual[3] 20% of thiophenol as radical trap. The activation data determined were in excellent agreement with those obtained in the nonpolar medium (mesitylene/thiophenol 8 : 2) (Table 1).

These results unequivocally rule out a "mero stabilization" of α-cyano-α-methoxyalkyl and -benzyl radicals by polar solvents. The findings show that semiempirical calculations or simple resonance rules do not allow general conclusions to be drawn concerning the relationship between the structure and stability of radicals. An experimental test is also required.

Received: April 2, 1987 [Z 2177 IE]
German version: *Angew. Chem. 99* (1987) 807

[1] M. J. S. Dewar, *J. Am. Chem. Soc. 74* (1952) 3353; A. T. Balaban, *Rev. Roum. Chim. 16* (1971) 725; R. W. Baldock, P. Hudson, A. R. Katritzky, F. J. Scott, *J. Chem. Soc. Perkin Trans. 1 1974*, 1422; H. G. Viehe, R. Merényi, L. Stella, Z. Janousek, *Angew. Chem. 91* (1979) 982; *Angew. Chem. Int. Ed. Engl. 18* (1979) 917; H. G. Viehe, Z. Janousek, R. Merényi, *Acc. Chem. Res. 18* (1985) 148.

[2] a) H. G. Viehe, Z. Janousek, R. Merényi (Eds.): *Substituents Effects in Radical Chemistry (NATO ASI Series C, Vol. 189* (1986)), Reidel, Dordrecht 1986; b) R. Merényi, Z. Janousek, H. G. Viehe in [2a], p. 301.

[3] M. Zamkanei, J. H. Kaiser, H. Birkhofer, H.-D. Beckhaus, C. Rüchardt, *Chem. Ber. 116* (1983) 3216; H. Birkhofer, H.-D. Beckhaus, C. Rüchardt in [2a], p. 199.

[4] G. Leroy, *Adv. Quantum Chem. 17* (1985) 1; G. Leroy, D. Peeters, M. Sana, C. Wilante in [2a], p. 1.

[5] H. Birkhofer, J. Hädrich, H.-D. Beckhaus, C. Rüchardt, *Angew. Chem. 99* (1987) 592; *Angew. Chem. Int. Ed. Engl. 26* (1987) 573.

[6] A. R. Katritzky, M. C. Zerner, M. M. Karelson, *J. Am. Chem. Soc. 108* (1986) 7213.

[7] K. H. Hellwege, A. M. Hellwege (Eds.): *Landolt-Börnstein, Zahlenwerte und Funktionen aus Physik, Chemie, Astronomie, Geophysik und Technik, 6. Aufl., Bd. II, Teil 6*, Springer, Heidelberg 1959, p. 618, 669.

[8] A. Peyman, E. Hickl, H.-D. Beckhaus, *Chem. Ber. 120* (1987) 713.

[9] R. J. Lemire, P. G. Sears, *Top. Curr. Chem. 74* (1978) 45.

A 1-Oxa-2-nickela-5-cyclopentanone from Ethene and Carbon Dioxide: Preparation, Structure, and Reactivity

By *Heinz Hoberg,* Yolande Peres, Carl Krüger,* and *Yi-Hung Tsay*

Heterocycles containing metal atoms in the ring are of increasing importance.[1] Metallacycles have been prepared from CO_2 and compounds containing C–X multiple bonds (X = C, O, NR) in the presence of transition-metal complexes.[2] The ligands so far used have been chelating ligands, which promote the 1 : 1 couplings at nickel(0) complexes but largely suppress subsequent reactions.[3] 1,8-Diazabicyclo[5.4.0]undec-7-ene (DBU) has been employed to carry out C–C bond formation between CO_2 and ethene as well as styrene at Ni^0 complexes with the formation of unsaturated carboxylic acids.[4] However, it has not been possible so far to isolate intermediates involved in these reactions, which are important for catalytic processes. We have now succeeded in isolating in 70% yield a 1 : 1 coupling product, the metallacycle **5**, formed from ethene **1** and CO_2 **2** at a Ni^0 complex **3** in the presence of DBU **4** (Scheme 1)[5] and in determining its structure. In addition, we have investigated the subsequent reactions of **5** with systems containing CC double bonds (Scheme 2). The results have provided insights into the course of the reactions of alkenes with CO_2 at nickel complexes.[4]

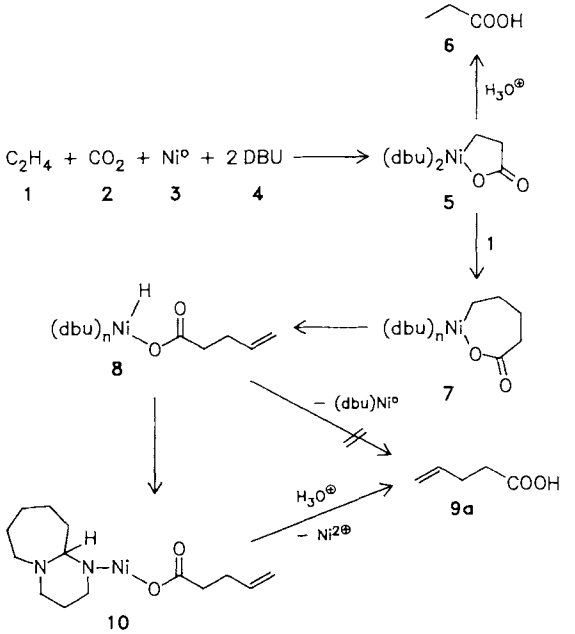

Scheme 1. Ni^0 = [Ni(cod)$_2$], cod = 1,5-cyclooctadiene.

It was not possible from the IR spectrum of **5** to determine which N atoms of the two DBU ligands are bonded to the Ni atom; i.e., the question whether **5** is a 16-, 18-, or 20-electron complex could not be answered. An X-ray crystal structure analysis of **5**[6] (Fig. 1), however, revealed that it is a 16-electron complex with square-planar coordination of the Ni atom, in which two N atoms of the DBU ligands occupy neighboring coordination positions and the carboxylate moiety is bound to the metal through both a Ni–O bond and a relatively short Ni–C(sp^3) bond.[7] A strong *trans* effect of the Ni–C23 bond is revealed by a large Ni–N distance to one of the two DBU ligands. Because of the planarity of the metallacycle (torsion angle O1-C21-C22-C23: 2.8°), nonbonding interactions between the Ni atom and the H atoms at C22 (Ni–H 3.6 Å) and C23 (Ni–H 2.4 Å) are not possible.

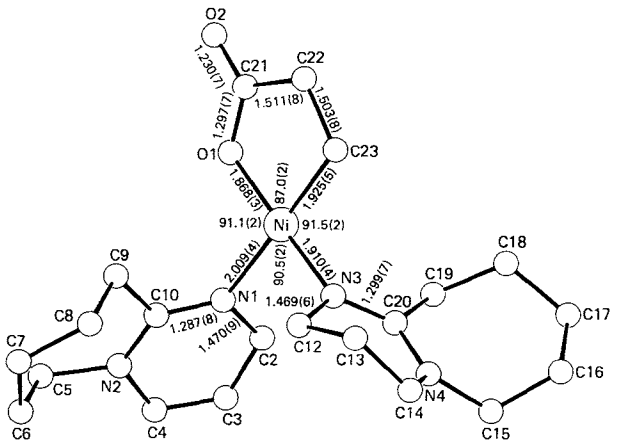

Fig. 1. Crystal structure of **5** with the most important bond lengths [Å] and angles [°] [6].

[*] Prof. Dr. H. Hoberg, Dr. Y. Peres, Prof. Dr. C. Krüger [+], Dr. Y.-H. Tsay [+]
Max-Planck-Institut für Kohlenforschung
Kaiser-Wilhelm-Platz 1, D-4330 Mülheim a. d. Ruhr 1 (FRG)

[+] X-ray crystal structure analysis.

Complex **5** exhibits properties characteristic for an organometallic compound. Thus, hydrolysis yields, as expected, propionic acid **6** (85%, identified as the methyl ester, see Scheme 1). The Ni-C bond is available for insertion reactions with systems containing CC double bonds; the products obtained after acid hydrolysis are shown in Scheme 2.[8]

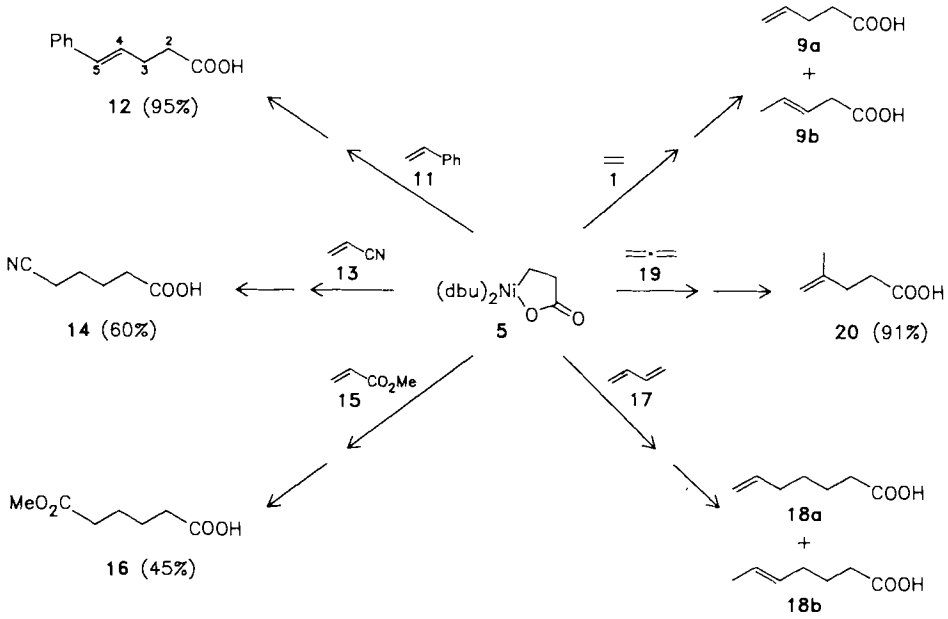

Scheme 2. Products, after acid hydrolysis, of the reactions of **5** with systems containing C=C bonds. Yields based on **5**.

For example, **5** reacts with ethene **1** with formation of the linear, unsaturated carboxylic acids **9** (together 79%, **9a** : **9b** = 1 : 2; (*E*)-**9a** : (*Z*)-**9a** = 3 : 2), with styrene **11** with regioselective C-C bond formation to give **12**, with acrylonitrile **13** to give **14**, with methyl acrylate **15** to give **16**, with 1,3-butadiene **17** to give a mixture of the acids **18** (together 10%, **18a** : **18b** = 2 : 1), and with allene **19** to give the branched carboxylic acid **20**. It is noteworthy that **5** reacts with both **1** and **11** to give products in which the double bond of the starting material is still present. For this reason, **5** can be regarded as a model complex for a possible intermediate involved in catalysis.

The formation of *n*-pentenoic acid **9a** from **1** and **2** presumably occurs by the mechanism shown in Scheme 1. Following C-C coupling of **1** with **2** to give **5**, a second molecule of **1** is inserted, with ring expansion, to give **7**; subsequent β-H elimination results in the formation of the NiH species **8**. The reductive elimination to give the carboxylic acid **9a** accompanied by regeneration of the starting Ni^0 complex, which is important for a catalytic course of the reaction, is not possible; instead, Ni-H addition to the DBU CN double bond occurs with formation of the catalytically inactive complex **10**. Acid hydrolysis results in cleavage of the Ni carboxylate **10** to the *n*-pentenoic acid **9a**.

The synthesis of **5** represents the first isolation of an intermediate involved in the reaction of CO_2 with alkenes and has allowed its subsequent reactions to be investigated. That these C-C couplings have so far only taken place stoichiometrically and not catalytically is due to the DBU ligand. With other ligands, it should be possible to carry out the catalytic reaction of alkenes with CO_2 to give unsaturated carboxylic acids.

Received: March 30, 1987 [Z 2168 IE]
German version: *Angew. Chem. 99* (1987) 799

[1] E. Lindner, *Adv. Heterocycl. Chem. 39* (1986) 237.
[2] H. Hoberg, K. Jenni, C. Krüger, E. Raabe, *Angew. Chem. 98* (1986) 819; *Angew. Chem. Int. Ed. Engl. 25* (1986) 810, and references cited therein.
[3] H. Hoberg, B. W. Oster, *J. Organomet. Chem. 266* (1984) 321, and references cited therein.
[4] H. Hoberg, Y. Peres, A. Milchereit, *J. Organomet. Chem. 307* (1986) C38, C41.
[5] *Experimental procedure* for **5**: **4** (6 mL, 39 mmol) was added to [Ni(cod)$_2$] [9] (3.54 g, 12.9 mmol) in 100 mL of tetrahydrofuran (THF) at −78°C in a 200-mL steel autoclave. CO_2 (ca. 15 bar) and ethene (ca. 30 bar) were then admitted. The stirred reaction mixture was gradually warmed to 40°C and kept at this temperature for ca. 90 h. Approximately 50 mL of THF was distilled under vacuum from the cooled solution and replaced with ca. 60 mL of diethyl ether. The resulting precipitate was filtered, washed with ether, and dried in vacuum. Yield: 3.64 g (60%) **5**. After cooling the filtrate to 0°C, additional **5** crystallized in the form of well-shaped crystals (0.425 g, 7%).—IR (KBr): 1560—1650 cm^{-1} (C=O overlapped by C=N bands), correct elemental analysis, m.p. = 92°C (dec.).
[6] **5** crystallizes in the space group $P2_1/n$, $a = 10.958(1)$, $b = 12.198(2)$, $c = 18.101(2)$ Å, $\beta = 90.81°$, $V = 2419$ Å^3, $Z = 4$, $\mu(Mo_{K\alpha}) = 8.3$ cm^{-1}, $\rho_{calcd} = 1.29$ g cm^{-3}, 5889 measured reflections ($\pm h$, $+k$, $+l$), 5458 unique reflections, 2900 observed ($I > 2\sigma(I)$), 258 refined parameters, $R = 0.059$, $R_w = 0.062$. Two molecules of THF in the unit cell, disordered around a center of inversion. Further details of the crystal structure investigation may be obtained from the Fachinformationszentrum Energie, Physik, Mathematik GmbH, D-7514 Eggenstein-Leopoldshafen 2 (FRG), on quoting the depository number CSD-52379, the names of the authors, and the journal citation.
[7] Compound **5** does not react (via the Ni-C bond) with typical electrophiles such as aldehydes, ketones, and imines to give insertion products.
[8] *Experimental procedure* for **12**: Styrene **11** (5 mL, 40 mmol) was added to **5** (1.76 g, 4.04 mmol) in 100 mL of THF and the reaction mixture was then warmed to 60°C for ca. 30 h. The THF was then distilled off and the residue was hydrolyzed with ca. 20 mL of 2 N H_2SO_4 and extracted with ether. The ether phase was shaken several times with 1 N NaOH, the aqueous phase was acidified again with 2 N H_2SO_4, and the carboxylic acid was extracted with ether. The ether phase was dried over $MgSO_4$ and the ether was distilled off. The residue is analytically pure **12**. Yield: 0.404 g (95%).—m.p. = 80°C, MS: *m/z* 176 ($M^{\oplus}$). ^{1}H-NMR (200 MHz, $CDCl_3$, TMS, 20°C): $\delta = 7.30$ (d, 5H, Ph-H), 6.45 (d, 1H, 5-H), 6.22 (m,

1 H, 4-H), 2.55 (m, 4 H, 2,3-H; $J(2,3)=15.8$ Hz).—The other reactions of **5** shown in Scheme 2 were carried out analogously (no optimization). In each case, the reaction products were converted into the methyl esters with CH_3OH/HCl. The characterization and quantification of the ester was carried out by GC or by GC-MS (reference compounds).

[9] B. Bogdanović, M. Kröner, G. Wilke, *Justus Liebigs Ann. Chem. 699* (1966) 1.

Inversion of the Configuration of Secondary Alcohols via Isourea Ethers Prepared in situ

By *Johannes Kaulen**

Procedures for the inversion of the configuration of secondary alcohols,[1] e.g., the Mitsunobu procedure for "inverting esterification,"[1a,b] are of considerable preparative interest. Such methods can be employed to establish the correct stereochemistry of secondary alcohols in those cases where the direct synthesis only leads to the undesired, "false" stereoisomer. In connection with the resolution of racemates, inversion procedures are also of interest as a way of utilizing the undesired enantiomer, thereby making chiral synthesis more economical. We have now found that the esterification of secondary alcohols via isourea ethers,[2] which has been known in principle for many years, offers a new, simple procedure for the inversion of the configuration of alcohols.[3]

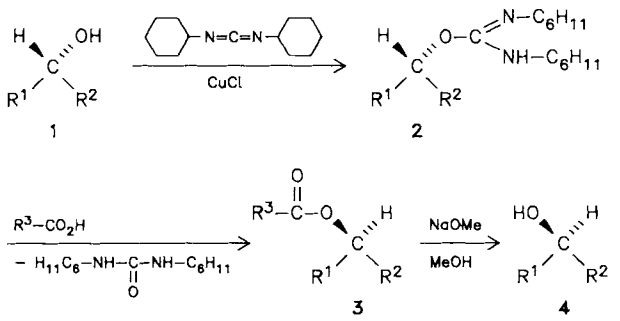

The secondary alcohol **1** (as the pure enantiomer or diastereomer) is converted in situ into the isourea ether **2** by addition to dicyclohexylcarbodiimide. When **2**, without isolation, is allowed to react further with carboxylic acids in a one-pot procedure, the esters **3** are obtained in a smooth reaction; the dicyclohexylurea that is formed simultaneously can be removed by filtration.

We have been able to show, for the first time, that the esterification proceeds with practically complete inversion of the configuration, so that the ester **3** has the opposite configuration of the alcohol **1** ("inverting esterification"). Saponification of the ester **3** leads to ready formation of the inverted alcohol **4**.

The new procedure can be applied to a variety of secondary alcohols, high enantiomeric excesses and good yields[4] being obtained in every case (Table 1). Small amounts of the corresponding olefins are sometimes formed as by-products.

Of the carboxylic acids used to carry out the "inverting esterification," formic acid proved to be particularly useful, but other carboxylic acids can be employed as well.

[*] Dr. J. Kaulen
Bayer AG
Zentrale Forschung ZF-FGF
D-5090 Leverkusen (FRG)

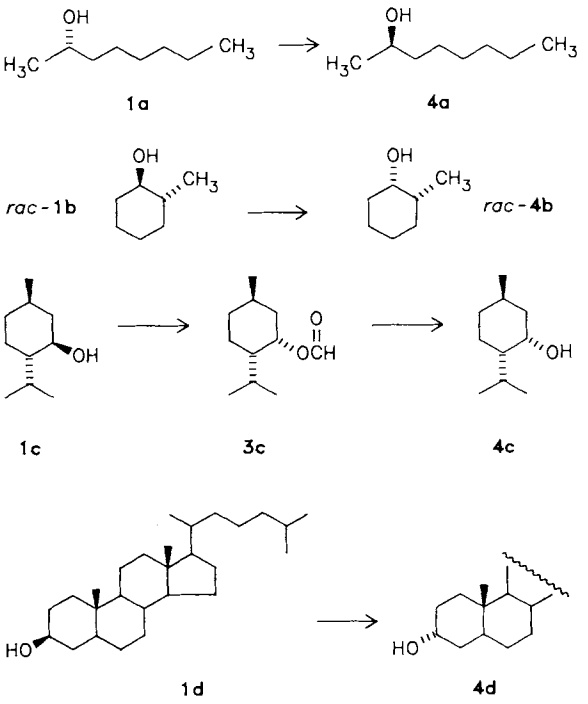

Table 1. "Inverting esterification" of secondary alcohols. All inverted esters **3** and alcohols **4** were formed with >99% *ee* (or, if applicable, >99% *de*).

Alcohol **1**	Conditions **2**→**3** [a]	Invert. ester **3** R^3 [b]	Yield **1**→**3** [%]	Invert. alcohol **4** [b]	Yield **3**→**4** [%]
1a	A	CH_3	66	**4a**	90
1a	A	H	83		
1b	B	H	50	**4b**	91
1c	B	H	80	**4c**	90
1c	B	$CH{=}CH_2$	51		
1c	B	$C(CH_3){=}CH_2$	64		
1d	C	H	75	**4d**	90

[a] A: dioxane, 100°C, 20 h; B: toluene, 110°C, 20 h; C: dioxane, 110°C, 20 h. [b] The structures were established by IR and ^{1}H-NMR spectroscopy. The chemical purity was checked by capillary gas chromatography. The determination of the enantiomeric purity was carried out by measuring the optical rotations or, in cases in which other centers of asymmetry are present in the molecule, by capillary gas chromatographic separation of the diastereomers.

When acrylic acid or methacrylic acid is used, the inverted acrylates and methacrylates, respectively, are obtained directly and can be polymerized to yield optically active polymers.

Dioxane and especially toluene are particularly advantageous as solvents for the esterification; chlorinated solvents are unsuitable, since mainly exchange of the hydroxyl group for chlorine occurs in such solvents.

Owing to the mild reaction conditions, the simple workup, and the relatively inexpensive reagents, the "inverting esterification" via isourea ethers promises to be an interesting alternative to the known inversion procedures.

General Experimental Procedure

2 [2]: **1** (0.5 mol) was allowed to stir with dicyclohexylcarbodiimide (0.6 mol) and copper(I) chloride (50 mg) for 3 d in the absence of moisture at room temperature [5]. Solid, high-melting alcohols were allowed to stir in a small amount of anhydrous dioxane for 3 d at 40–50°C.

3: Crude **2** (0.5 mol) was dissolved in 200 mL of dry solvent (preferably toluene) and the carboxylic acid (0.6 mol, preferably formic acid) was added to the stirred solution at room temperature. The resulting mixture was heated at

reflux for 20 h and allowed to cool, and the nearly quantitatively precipitated dicyclohexylurea was filtered off and washed with a small amount of dichloromethane. The combined organic phases were concentrated in vacuum and the residue was dissolved in ether. The ether solution was washed with $NaHCO_3$ solution to a final pH of 7 and then dried over Na_2SO_4 and concentrated once again. The crude **3** was purified by distillation (or by column chromatography).

4: **3** (0.5 mol) was allowed to stir in 250 mL of methanol with 5 mL of 30% $NaOCH_3$ for 12 h. After concentration in vacuum, the residue was distilled without further workup.

Example: Neomenthyl formate **3c**: The isourea ether **2c** obtained from (−)-menthol **1c** (156 g, 1.0 mol) and dicyclohexylcarbodiimide (248 g, 1.2 mol) was allowed to stir with 45 mL (1.2 mol) of formic acid in 400 mL of dry toluene for 20 h at 110 °C. The reaction mixture was then worked up according to the general procedure described above. After distillation, 147 g (80%) of **3c** was obtained, b.p. = 52–60 °C/0.25 mbar, $[\alpha]_D^{20} = +51.9°$ (neat) ($[\alpha]_D^{20} = +51°$ [6]).

Received: April 13, 1987 [Z 2199 IE]
German version: *Angew. Chem. 99* (1987) 800

[1] a) O. Mitsunobu, *Synthesis 1981*, 1; b) O. Mitsunobu, M. Eguchi, *Bull. Chem. Soc. Jpn. 44* (1971) 3427; c) B. Radüchel, *Synthesis 1980*, 292; d) G. Cainelli, F. Manescalchi, G. Martelli, M. Panunzio, L. Plersi, *Tetrahedron Lett. 26* (1985) 3369; e) W. H. Kruizinga, B. Strijtveen, R. M. Kellogg, *J. Org. Chem. 46* (1981) 4321; f) Y. Torisawa, H. Okabe, S. Ikegami, *Chem. Lett. 1984*, 1555; g) E. J. Corey, K. C. Nicolaou, M. Shibasaki, Y. Machida, C. S. Shiner, *Tetrahedron Lett. 1975*, 3183; h) J. S. Filippo, C.-I. Chern J. S. Valentine, *J. Org. Chem. 40* (1975) 1678; i) D. M. Floyd, G. A. Crosby, N. M. Weinshenker, *Tetrahedron Lett. 1972*, 3265, 3269; j) A. K. Bose, B. Lal, W. A. Hoffmann, M. S. Manhas, *ibid. 1973*, 1619; k) H. Vorbrüggen, *Justus Liebigs Ann. Chem. 1974*, 821.

[2] E. Däbritz, *Angew. Chem. 78* (1966) 483; *Angew. Chem. Int. Ed. Engl. 5* (1966) 470; E. Vowinkel, *Chem. Ber. 100* (1967) 16; L. J. Mathias, *Synthesis 1979*, 561.

[3] For the synthesis of iodides from alcohols (with inversion) via carbodiimidium salts, see R. Scheffold, E. Saladin, *Angew. Chem. 84* (1972) 158; *Angew. Chem. Int. Ed. Engl. 11* (1972) 229.

[4] Yields for the "inverting esterification" of (*S*)-2-octanol **1a**: 20% [1a, b], 75% [1h], 86% [1e]; many procedures [1] fail for sterically hindered alcohols such as (−)-menthol **1c** or afford large amounts of olefins as by-products.

[5] The reaction times were not optimized; at higher temperatures and with reaction control (IR or GC), shorter reaction times are possible.

[6] *Beilsteins Handbuch der Organischen Chemie, Bd. 6, 4. Ergänzungsband*, Springer, Berlin 1978, p. 153.

Structure Elucidation of a New Icosapeptide from Human Semen**

By *Klaus Schneider, Josef Reiner,* and *Gerhard Spiteller**

The Edman degradation as modified by *Chang* and *Wittmann-Liebold* has proved extremely useful in the structure elucidation of peptides.[1] The only disadvantage of this method is the uncertainty in determining the *C* terminus, since, once the peptide has been degraded to two or three residues, the extraction of the hydantoin can result in partial loss of the remaining peptide. Therefore, at the very least, an amino-acid determination is necessary.

This determination may no longer be necessary when the exact molecular weight of the peptide is known; the molecular weight, in turn, can be determined by "soft ionization methods."[2] However, the amount of sample required increases greatly with increasing molecular weight (by a factor of approximately 10 in going from mass 1500 to mass 2500). In our experience, the amounts of small, unknown peptides thus required are hardly obtainable.

In order to investigate peptides having molecular weights between 2000 and 3000 dalton, which we isolate from biological material, we employ the following strategy: We carry out tryptic and chymotryptic cleavage of the peptide, separate the fragments by HPLC (since the highest degree of purity possible is necessary for subsequent sequencing by MS), and then determine the molecular weights of these fragments by LSIMS.[***] Only in optimal cases—usually when the peptide has a molecular weight of < 1000 dalton—is a direct and unequivocal structure derivation of the fragments appearing in the LSIMS spectrum possible. Only a very small amount of the sample used for the LSIMS measurement (ca. 1 μg) is consumed. So far, the remainder of the sample had been discarded. We have now found, however, that the remainder of the sample can be eluted unchanged from the target and separated from the matrix substance (glycerol) by HPLC. Part of the remaining sample is then treated with a drop of CH_3OH/2 N HCl. After 12 h standing, all COOH and all $CONH_2$ groups have been converted into $COOCH_3$ groups. An LSIMS determination of this sample gives the number of COOH and $CONH_2$ groups originally present. The greater part of the remaining sample is subject to sequencing by double Edman degradation according to the modified procedure of *Chang* and *Wittmann-Liebold* et al.[3] Each cleaved amino-acid fragment is subjected to both thin-layer chromatography and HPLC (to be certain of the results). The recovered sample can, if necessary, be used for determination of the *N* terminus by dansylation. Either an LSIMS analysis of the whole peptide[4] or hydrolytic cleavage of the peptide followed by determination of the derivatized *N*-terminal amino acids by HPLC is possible.

The application of the procedure outlined above is exemplified by the sequencing of a new 20-amino-acid peptide that we isolated in 300-μg amounts from human semen. Determination of the molecular weight of the whole peptide by LSIMS was not successful. The amount of sample used for the measurement was approximately 20 μg.

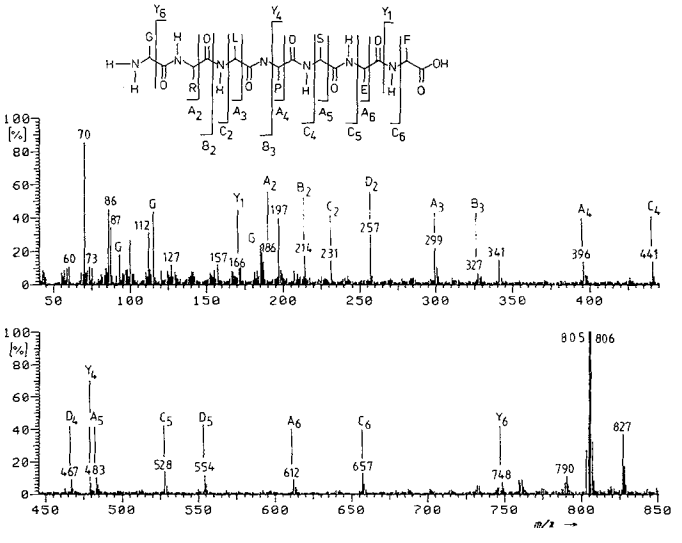

Fig. 1. LSI mass spectrum of positive ions of the fragment C1: Gly-Arg-Leu-Pro-Ser-Glu-Phe; in the one-letter code, G-R-L-P-S-E-F, m/z 805 = $MH^{\oplus}$. The signals marked with "G" are due to the matrix material (glycerol). The peptide fragment ions (A_n ... Z_n) are denoted according to the system of *Roepstorff* et al. [7]. In the scheme above the spectrum, the one-letter code applies only to the side chains of the amino acids.

[*] Prof. Dr. G. Spiteller, Dr. K. Schneider, J. Reiner
Lehrstuhl für Organische Chemie I der Universität
Postfach 101251, D-8580 Bayreuth (FRG)

[**] This work was supported by the Deutsche Forschungsgemeinschaft.

[***] LSIMS = liquid secondary ion mass spectrometry. In this method, charged molecules are ejected from a liquid matrix by bombardment with Cs^+, thereby making mass spectrometry possible. FAB mass spectrometry functions similarly, Xe atoms, instead of Cs^+, being used.

In order to analyze the peptide mass spectrometrically, we therefore cleaved it with trypsin and chymotrypsin. (Carboxamidomethylation[5] and reaction with cyanogen bromide[6] in order to modify the SH groups and to cleave the peptide chain on the carboxyl side of a methionine residue were unsuccessful). After tryptic digestion, separation by RP-HPLC yielded three fragments (T1, T2, and T3), whereas the chymotryptic digestion gave only two fragments (C1 and C2).

The LSI mass spectrum of C1 (Fig. 1) showed, in addition to the pronounced $MH^{\oplus}$ ion of mass m/z 805, intense fragments that made it possible to derive the sequence up to the *N*-terminal dipeptide of mass 231. There are only two possibilities for this remaining peptide in terms of amino-acid sequence: namely, (1) Asn-Val or Val-Asn or (2) Gly-Arg or Arg-Gly.

In order to distinguish between the four possibilities, the peptide fragment C1 was treated, as described above, with a drop of CH_3OH/2 N HCl. An LSIMS analysis of the reaction product (Fig. 2) gave the number of COOH and $CONH_2$ groups originally present from the shift of the molecular weight from mass 805 to mass 833. This demonstrates the presence of two ester groups.

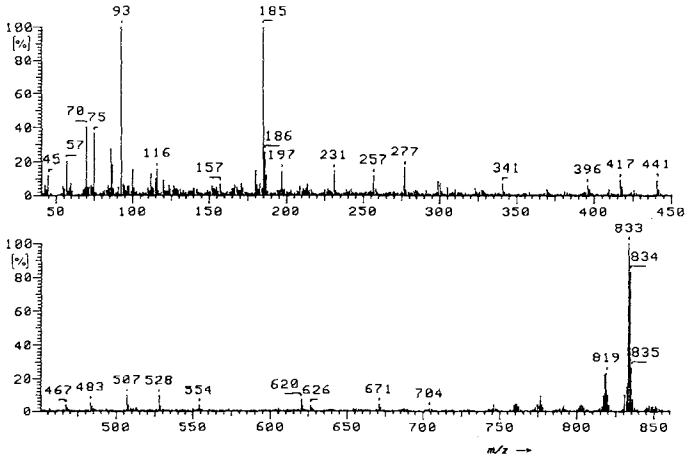

Fig. 2. LSI mass spectrum of positive ions of the fragment C1, treated with MeOH/2 N HCl; m/z 833 = $MH^{\oplus}$. The ions m/z 93 and m/z 185 are due to the matrix material (glycerol).

This finding rules out the end groups Asn-Val and Val-Asn. In order to distinguish between Gly-Arg and Arg-Gly, the end group was determined with dansyl chloride (Dns-Cl)[8] and the resulting Dns derivative determined by HPLC. Reaction of the hydrolysate with Dns-Cl made it possible to distinguish between the two possible amino acids of equal molecular weight, leucine and isoleucine (by HPLC). Therefore, the sequence for C1 was determined to be Gly-Arg-Leu-Pro-Ser-Glu-Phe.

Although the LSI mass spectrum of the fragment C2 showed a molecular ion of mass m/z 1412, a sequence analysis from the spectrum was not possible owing to the lack of sufficient sequence-specific ions.

Also in the case of the tryptic fragments T1 and T2 it was only possible with LSIMS to determine the molecular weights (Figs. 3 and 4). The fragment T3, no molecular ion of which could be obtained by LSIMS, yielded two secondary fragments upon chymotryptic digestion: CT1 is identical with C1; for CT2, having the mass 927, the LSI mass spectrum (Fig. 5) revealed several sequence-specific ions, but their intensities were too small for a structure der-

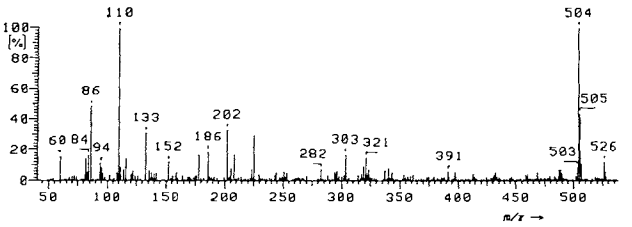

Fig. 3. LSI mass spectrum of positive ions of the fragment T1: Gly-Gln-His-Tyr; m/z 504 = $MH^{\oplus}$, m/z 526 = $MNa^{\oplus}$; glycerol background subtracted.

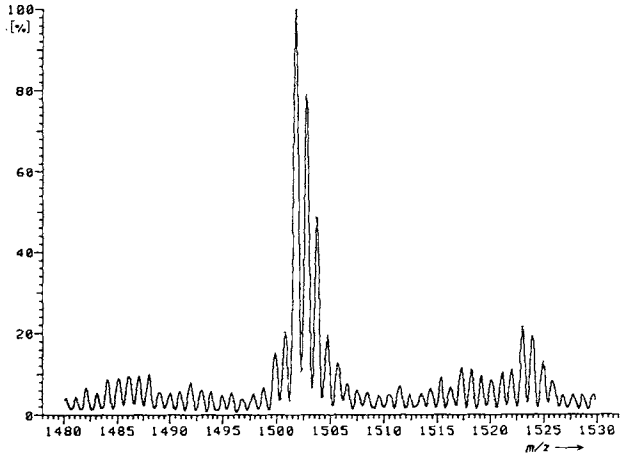

Fig. 4. LSI mass spectrum of the molecular ion region of the fragment T3: m/z 1501 = $MH^{\oplus}$: Leu-Pro-Ser-Glu-Phe-Ser-Gln-Phe-Pro-His-Gly-Ala-Gly-Lys. The amount of sample used in the measurement was approximately 5 μg.

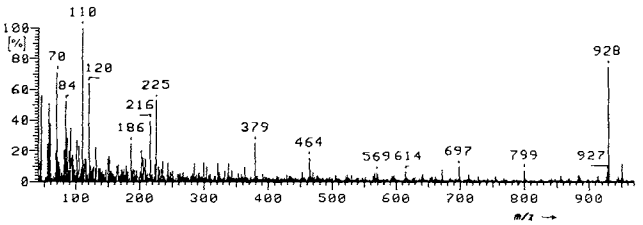

Fig. 5. LSI mass spectrum of positive ions of the fragment CT2: Ser-Glu-Phe-Pro-His-Gly-Ala-Gly-Lys; m/z 928 = $MH^{\oplus}$; glycerol background subtracted.

ivation. The sequence of the peptide CT2 was therefore determined by means of the manual microsequencing method of *Chang*[9] to be Ser-Gln-Phe-Pro-His-Gly-Ala-Gly-Lys and that of the partial fragment T1 to be Gly-Gln-His-Tyr.

The chymotryptic digestion of T2 yielded a fragment of mass m/z 591 (CT3) and the already known fragment CT2 of mass m/z 927.

CT3 has the sequence Leu-Pro-Ser-Glu-Phe and thus, except for the absence of the *N*-terminal dipeptide Gly-Arg, the same sequence as C1 and CT1. Therefore, the fragment T3 is only an incompletely tryptic-digested peptide.

If the molecular weights of the chymotryptic fragments C1 (mass 804) and C2 (mass 1412) are added, one obtains, after subtraction of 18 amu (= mass of H_2O) a molecular

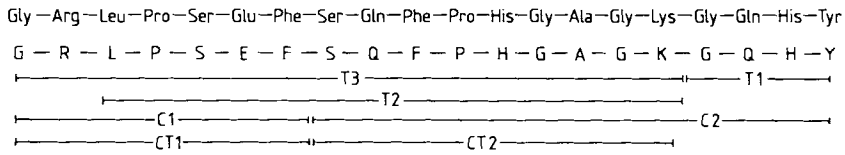

Scheme 1. Structure of the new icosapeptide. For fragments, see text. Second line: one-letter code.

weight of 2198 for the peptide. The same mass is obtained from the fragments of the tryptic digestion T3 = CT1 (*M* 804) + CT2 (*M* 927) and T1 (*M* 503) after subtraction of 2 × 18. The structure shown in Scheme 1 is thereby obtained for the peptide. Analogous structures are unknown.

Received: February 23, 1987 [Z 2109 IE]
German version: *Angew. Chem. 99* (1987) 814

[1] C. Y. Yang, E. Pauly, H. Kratzin, N. Hilschmann, *Hoppe-Seyler's Z. Physiol. Chem. 348* (1981) 1077; B. Peeters, W. Rombauts, J. Mous, W. Heyns, *Eur. J. Biochem. 115* (1981) 115.
[2] M. Barber, R. S. Bordoli, G. V. Garner, D. B. Gordon, R. D. Sedgwick, W. Tetler, A. N. Tyler, *Org. Mass Spectrom. 16* (1981) 256.
[3] J.-Y. Chang, D. Brauer, B. Wittmann-Liebold, *FEBS Lett. 93* (1978) 205; J.-Y. Chang, *Biochim. Biophys. Acta 578* (1979) 188; J.-Y. Chang, *Biochem. J. 199* (1981) 557.
[4] D. Renner, G. Spiteller, *Angew. Chem. 97* (1985) 408; *Angew. Chem. Int. Ed. Engl. 24* (1985) 408.
[5] F. R. Gurd, *Methods Enzymol. 11* (1967) 532.
[6] E. Gras, B. Wittkop, *J. Biol. Chem. 237* (1962) 1856.
[7] P. Roepstorff, J. Fohlmann, *Biomed. Mass Spectrom. 11* (1984) 604.
[8] W. R. Gray, *Methods Enzymol. 25* (1972) 121.
[9] J.-Y. Chang, *Methods Enzymol. 91* (1983) 455.

Phosphasilirenes, Three-Membered Rings Containing PC Double Bonds**

By *Annemarie Schäfer, Manfred Weidenbruch,* Wolfgang Saak,* and *Siegfried Pohl*

The photolysis of cyclotrisilanes **1** leads to cleavage of two Si–Si bonds to give a mixture of silanediyls (silylenes) **2** and disilenes **3**, which, for appropriate patterns of substitution, is completely transformed to **3**.[1,2] In the case of

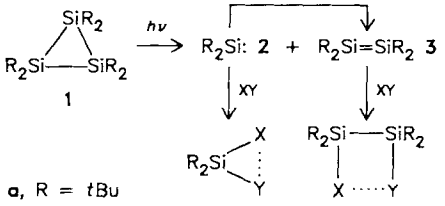

compounds **3** that are thermally less stable, compounds **2** and **3** can be simultaneously or individually trapped by means of a variety of insertion and addition reactions.[3]

For example, di-*tert*-butylsilanediyl **2a**, obtained by irradiation of hexa-*tert*-butylcyclotrisilane **1a**,[4] undergoes [2 + 1] addition to the triple bond of nitriles (XY = RC≡N) to give azasilirenes, which, presumably owing to high ring

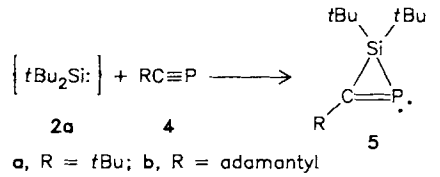

strain, undergo spontaneous dimerization to give 1,4- or 1,3-diaza-2,5-disila-1(6),3-cyclohexadienes.[5] Because the C=P bond is significantly longer than the C=N bond, addition of **2a** to phospha-alkynes[6] should lead to less strained and therefore more stable three-membered rings.

Irradiation of **1a** and the phospha-alkynes **4a**[7] and **4b**[8] in a molar ratio of 1 : 2 (in order, if possible, to trap the disilene **3a** in addition to **2a**) gives, in a surprisingly straightforward fashion, the phosphasilirenes **5a** and **5b**,[9] the first three-membered ring compounds containing a PC double bond.

The three-membered ring compounds **5** differ significantly from the formally similar "side-on"- bonded complexes of **4a** and platinum(0).[10] The differing bonding is reflected in the ^{31}P-NMR spectra: The signals for **5a** ($\delta = 274.0$) and **5b** (272.6) appear in the region characteristic of phospha-alkenes, whereas the "phosphaplatinacyclopropenes" give rise to values ($\delta \approx -55$[11]) typical of phospha-alkynes.[6]

Reaction of **5b** with [W(CO)$_5$(thf)] results in replacement of tetrahydrofuran (THF) and formation of the crystalline complex **6**.[12] The X-ray structure analysis of **6**[13] (Fig. 1) confirms the three-membered ring structure. The PC dis-

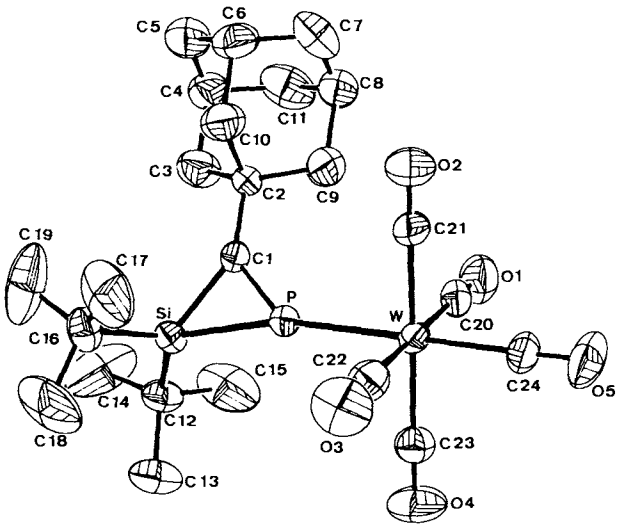

Fig. 1. Crystal structure of **6** (H atoms omitted). Selected bond lengths [pm] and angles [°] (standard deviations): P-C1 168.6(6), P-Si 219.6(2), C1-Si 184.2(6), P-W 247.5(2), W-C24 199.2(7), W-C$_{av}$ 203.6($\bar{d}$), C1-C2 150.0(9), Si-C12 189.5(8), Si-C16 190.7(8); Si-P-C1 54.8(2), P-C1-Si 76.9(3), C1-Si-P 48.4(2), Si-P-W 165.1(11), C1-P-W 139.9(2). Dihedral angles [°]: W-P-Si-C1 171.1, W-P-C1-Si 176.4.

[*] Prof. Dr. M. Weidenbruch, Dr. A. Schäfer, Dipl.-Chem. W. Saak, Prof. Dr. S. Pohl
Fachbereich Chemie der Universität
Carl-von-Ossietzky-Strasse 9-11, D-2900 Oldenburg (FRG)

[**] Silicon Compounds with Strong Intramolecular Steric Interactions, Part 30. This work was supported by the Deutsche Forschungsgemeinschaft, the Fonds der Chemischen Industrie, and Bayer AG.—Part 29: M. Weidenbruch, K.-L. Thom, S. Pohl, W. Saak, *Monatsh. Chem.*, in press.

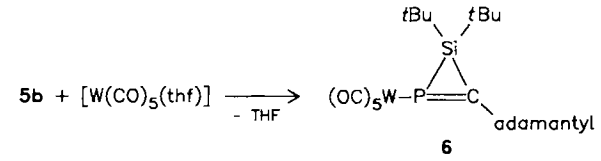

6

tance (168.6 pm) is typical of phospha-alkenes.[6] Within the three-membered ring, the smallest bond angle is at silicon, the largest at carbon. Together with the remarkably short C1–Si distance, the values found here establish the great similarity between the phosphasilirenes and the silirenes (silacyclopropenes), for which similar structural parameters have been measured.[14] The formation and structure of **5** thus provide a further example of the analogy between the reaction behavior of phospha-alkynes and that of acetylenes.[10]

Experimental Procedures

5a: Irradiation of **4a** (0.23 g, 2.3 mmol) and **1a** (0.50 g, 1.17 mmol) in 80 mL of *n*-hexane with a high-pressure mercury lamp (Heraeus TQ 150) led, within 1.5 h, to quantitative conversion. After distillation of the *n*-hexane, **5a** could be isolated as a bright yellow, unstable oil by HPLC (RP 18, acetonitrile as eluent).

5b: Analogously, irradiation of **4b** (0.65 g, 3.65 mmol) and **1a** (0.75 g, 1.76 mmol) in 80 mL of *n*-hexane for 3 h gave a product mixture, from which **5b** could be separated nearly quantitatively (based on **2a**) by HPLC (Polygosil 60, *n*-hexane) or column chromatography (silica gel 60, petroleum ether, 40–60 °C).

6: $W(CO)_6$ (2.4 g, 6.9 mmol) in 80 mL of THF was irradiated until approximately 80% of the amount of CO necessary to form $[W(CO)_5(thf)]$ had evolved and was removed. Compound **5b**, prepared from **4b** (0.97 g, 5.4 mmol) and **1a** (1.10 g, 2.6 mmol) in 80 mL of *n*-hexane, was then added to this solution and the resulting mixture was stirred for 30 min at room temperature. The solvent was removed under vacuum, petroleum ether 40–60 °C was added, and $W(CO)_6$ was filtered off. Yellow crystals of **6** formed from the reddish brown solution at −18 °C. These were recrystallized twice from pentane. Yield: 0.91 g (55% based on **2a**), dec. > 140 °C.

Received: March 31, 1987 [Z 2175 IE]
German version: *Angew. Chem. 99* (1987) 806

[1] S. Masamune, Y. Hanzawa, S. Murakami, T. Bally, J. F. Blount, *J. Am. Chem. Soc. 104* (1982) 1150.
[2] S. Murakami, S. Collins, S. Masamune, *Tetrahedron Lett. 25* (1984) 2131.
[3] Review: M. Weidenbruch, *Comments Inorg. Chem. 5* (1986) 247.
[4] A. Schäfer, M. Weidenbruch, K. Peters, H. G. von Schnering, *Angew. Chem. 96* (1984) 311; *Angew. Chem. Int. Ed. Engl. 23* (1984) 302.
[5] M. Weidenbruch, A. Schäfer, K. Peters, H. G. von Schnering, *J. Organomet. Chem. 314* (1986) 25.
[6] Review: R. Appel, F. Knoll, I. Ruppert, *Angew. Chem. 93* (1981) 771; *Angew. Chem. Int. Ed. Engl. 20* (1981) 731.
[7] G. Becker, G. Gresser, W. Uhl, *Z. Naturforsch. B36* (1981) 16.
[8] T. Allspach, M. Regitz, G. Becker, W. Becker, *Synthesis 1986*, 31.
[9] **5a**: ^{1}H-NMR (C_6D_6): $\delta = 1.01$ (s, 18H), 1.33 (d, 9H, $^4J(PH) < 1$ Hz). ^{31}P-NMR (C_6D_6): $\delta = 274.0$. MS (CI): m/z 243 ($M^{\oplus}+1$, 100%). **5b**: ^{1}H-NMR (C_6D_6): $\delta = 1.03$ (s, 18H), 1.6–2.1 (m, 15H). ^{13}C-NMR ([D$_8$]THF): $\delta = 129.3$ (d, PC), $^1J(PC) = 58$ Hz. ^{31}P-NMR (C_6D_6): $\delta = 272.6$. MS (70 eV): m/z 320 ($M^{\oplus}$, 47), 263 ($M^{\oplus} - 57$, 100).
[10] Review: G. Becker, *Nova Acta Leopold. 264* (1985) 59, p. 55.
[11] J. C. T. R. Burckett-St. Laurent, P. B. Hitchcock, H. W. Kroto, J. F. Nixon, *J. Chem. Soc. Chem. Commun. 1981*, 1141; S. I. Al-Resayes, P. B. Hitchcock, M. F. Meidine, J. F. Nixon, *ibid. 1984*, 1080.
[12] **6**: ^{1}H-NMR (C_6D_6): $\delta = 0.95$ (d, 18H, $^4J(PH) < 1$ Hz), 1.55–2.1 (m, 15H). ^{31}P-NMR (C_6D_6): $\delta = 193.0$ ($^1J(^{31}P^{183}W) = 186$ Hz). IR (Nujol): 2085 sh, 2080 m, 1995 m, 1975 s, 1960 s (ν(CO)). MS (70 eV): m/z 644 ($M^{\oplus}$, 55), 560 ($M^{\oplus} - 3 \times CO$, 55), 532 ($M^{\oplus} - 4 \times CO$, 8).
[13] Triclinic, space group $P\bar{1}$ (No. 2). $a = 839.1(1)$, $b = 1059.7(2)$, $c = 1623.9(3)$ pm, $\alpha = 99.71(1)$, $\beta = 93.39(2)$, $\gamma = 104.36(2)°$, $V = 1372.4 \cdot 10^6$ pm^3; $Z = 2$, $\rho_{calcd} = 1.56$ g cm^{-3}, 4365 unique reflections, 4131 observed ($I > 2\sigma(I)$), number of variables 298, empirical absorption correction, $R = 0.0412$, $R_w = 0.0407$. Further details of the crystal structure investigation may be obtained from the Fachinformationszentrum Energie, Physik, Mathematik GmbH, D-7514 Eggenstein-Leopoldsharen 2 (FRG), on quoting the depository number CSD-52472, the names of the authors, and the journal citation.
[14] K. Hirotsu, T. Higuchi, M. Ishikawa, H. Sugisawa, M. Kumada, *J. Chem. Soc. Chem. Commun. 1982*, 726; O. M. Nefedov, M. P. Egorov, S. P. Kolesnikov, A. M. Gal'minas, Yu. T. Struchkov, J. V. Sereda, *Izv. Akad. Nauk SSSR, Ser. Khim. 1986*, 1693.

Synthesis and Chirality of Sixfold-Bridged Triple-Decker Phanes**

By *Norbert Sendhoff, Karl-Heinz Weissbarth,* and *Fritz Vögtle**

The few triple-decker phanes described so far were constructed either via several steps or from preformed cyclic partial structures.[1,2a] We describe here the first one-step synthesis, starting from open-chain educts, of the first sixfold bridged[2b] triple-decker cyclophanes **4**.

The recently achieved one-step multiple bridging[3] made it reasonable to attempt the synthesis of such triple-decker compounds from the partial structures constituting the three layers. Our earlier experiences[4] with steric factors indicated that the synthesis of the phane **3**, augmented with *meta*-phenylene rings, should be most promising. Moreover, the readily available and readily soluble *meta*-functionalized educts **1** and **2** could be employed in this synthesis.

The first reactions of **1** and **2a** carried out according to the dilution principle and "one-pot" procedures or the corresponding reactions of the components **5** and **6**, which do not contain spacers, in dimethylformamide (determined earlier to be the best solvent[3]), however, did not afford detectable amounts of the triple-decker compounds **3** and **4** or **7**, respectively. In preliminary experiments, therefore, the model reaction **2a** + **2b** → **8**[5] and the corresponding cyclization leading to the *meta*-/*para*-substituted double-decker phane **9** were optimized so that, in addition to a simple procedure, a relatively high yield was obtained [37% **8**, m.p. > 300 °C, $R_F = 0.6$ (CH_2Cl_2/CCl_4 1:1); 11% **9**, m.p. > 300 °C, $R_F = 0.5$ (CH_2Cl_2/cyclohexane 7:3)]. Decisive factors proved to be choosing the solvent mixture benzene/ethanol (2:1) and working at a not too high dilution.[6] These findings indicate that such multiple bond formations require exactly tailor-made reaction conditions in each case.

The first attempted application of the one-pot procedures worked out for the double-decker phanes to the sixfold bridge formation starting from **1**[3] and **2a** gave two chromatographically readily separable crystalline substances in a molar ratio of 1:2, together in 6% yield. The expected isomer **4**[7] having C_2 symmetry (a C_2 axis), m.p. > 300 °C, correlates with the following ^{1}H-NMR data: (CD_2Cl_2, 400 MHz): $\delta = 2.9$–3.7 (8 d, $J = 14.5$ Hz, 16H, CH_2; 2 dd, $J = 14.5$ and 5.6 Hz, 8H, CH_2), 6.05–7.8 (8 s,

[*] Prof. Dr. F. Vögtle, Dipl.-Chem. N. Sendhoff,
Dipl.-Chem. K.-H. Weissbarth
Institut für Organische Chemie und Biochemie der Universität
Gerhard-Domagk-Strasse 1, D-5300 Bonn 1 (FRG)

[**] This work was supported by the Fonds der Chemischen Industrie and by Degussa (supply of palladium dichloride). We thank Dr. *J. Peter-Katalinic*, Institut für Physiologische Chemie der Universität Bonn, Dr. *C. Wünsche*, Bayer AG, Wuppertal, and Prof. Dr. *H. Schwarz*, Technische Universität Berlin, for the mass spectra.

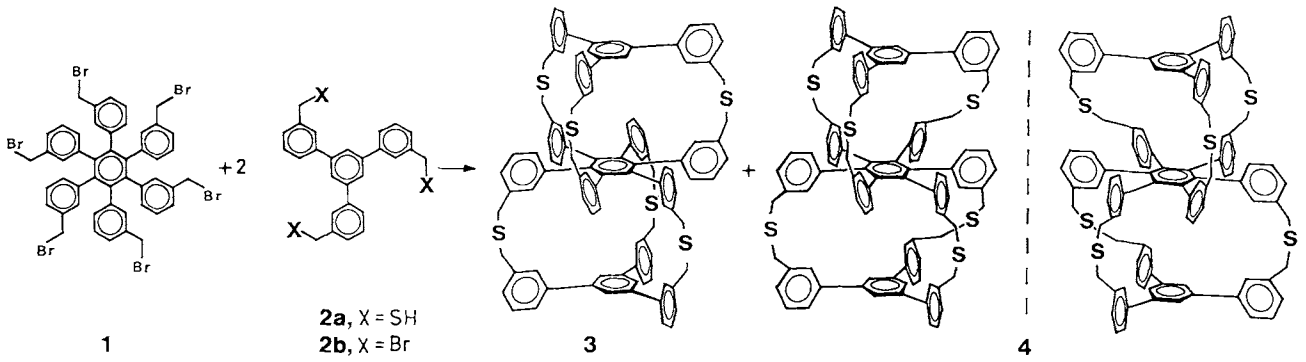

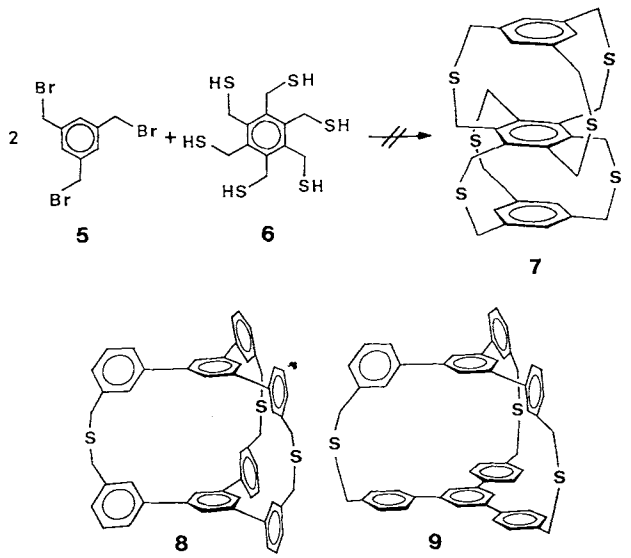

12 d, $J=8$ Hz, 6 t, $J=8$ Hz, 54 H, aromat. H).[8] FAB mass spectrometry gave a correct $[M\mathrm{H}]^{\oplus}$ ion peak for **4** ($m/z=1496$).[9]

Analysis of models reveals that the triple-decker **4**—despite the absence of chiral centers and in contrast to **3**—is helically chiral. Indeed, attempted chromatographic separations (HPLC) on Okamoto column material[10] were successful (eluent: *n*-hexane/methanol/2-propanol 3:1:0.6): the (−)-enantiomer is bound less strongly to the (+)-PTrMA column material than the (+)-enantiomer. Figure 1 shows the circular dichroism spectra of the enriched enantiomers of **4** obtained in this way (Cotton effect at $\lambda=252$ nm).[11]

The following optical rotations were obtained for the enriched enantiomers: $M^{22}_{436}=+271.97$, $[\alpha]^{22}_{436}=+18.18$ (in $CHCl_3$, $c=0.27$) and $M^{22}_{436}=-84.43$, $[\alpha]^{22}_{436}=-2.09$ (in $CHCl_3$, $c=0.48$).[11]

This study shows that "multilayered" molecules of this size and number of bridges may be easily prepared, characterized, and manipulated, when the steric requirements are already taken into consideration in designing the structure. Compounds **3** and **4** provide the largest molecular cavities in triple-decker cyclophanes so far. The simple synthesis opens up the possibility of preparing new cavities for the inclusion of guests in neighboring compartments and of synthesizing even higher oligo deckers.

Experimental Procedure

3[8] and **4**: **1** (2.00 g, 1.80 mmol) [3a], **2a** (1.63 g, 3.60 mmol) [3a], and Cs_2CO_3 (3.70 g, 11.3 mmol) were heated at reflux in 400 mL of benzene and 200 mL of ethanol in a 1-L flask (without dilution apparatus!) for 8 h. The reaction mixture was then evaporated to dryness and the residue was dissolved in dichloromethane. The resulting solution was refluxed for 3 h and then filtered while still hot. Column chromatographic separation of the nearly colorless, powdery mixture on silica gel (0.063–0.1 mm) with dichloromethane/cyclohexane 7:3 gave the two isomers **3** ($R_F=0.6$) [8] and **4** ($R_F=0.23$) in 2 and 4% yield, respectively. Compound **3** was further purified by repeated chromatography on a silica gel column with dichloromethane/cyclohexane 1:1 ($R_F=0.26$). **4**: MS: $[M\mathrm{H}]^{\oplus}=1496$.

Received: April 13, 1987 [Z 2202 IE]
German version: *Angew. Chem. 99* (1987) 794

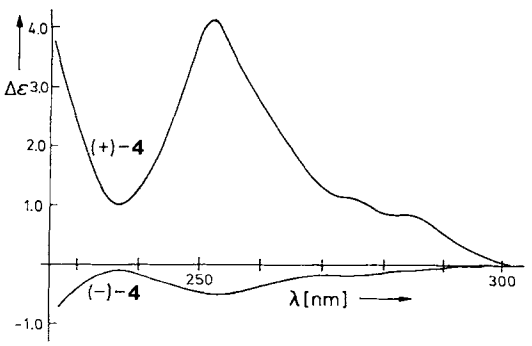

Fig. 1. Circular dichroism diagram of the enriched enantiomers of **4** (in CH_2Cl_2).

[1] a) Review: S. Misumi, T. Otsubo, *Acc. Chem. Res. 11* (1978) 751; b) P. M. Keehn, S. M. Rosenfeld: *Cyclophanes II*, Academic Press, New York 1983; c) cf. J. Weiser, H. A. Staab, *Angew. Chem. 96* (1984) 602; *Angew. Chem. Int. Ed. Engl. 23* (1984) 623; d) cf. D. M. Dubowchik, A. D. Hamilton, *J. Chem. Soc. Chem. Commun. 1986*, 665.

[2] An earlier described pyridinophane contains only four bridges and the layers do not lie in parallel planes: I. D. Reingold, W. Schmidt, V. Boekelheide, *J. Am. Chem. Soc. 101* (1979) 2121; b) see also A. J. Hubert, *J. Chem. Soc. C 1967*, 13.

[3] a) W. Kissener, F. Vögtle, *Angew. Chem. 97* (1985) 782; *Angew. Chem. Int. Ed. Engl. 25* (1985) 794; b) D. Heyer, J.-M. Lehn, *Tetrahedron Lett. 27* (1986) 5869.

[4] B. Klieser, F. Vögtle, *Angew. Chem. 94* (1982) 632; *Angew. Chem. Int. Ed. Engl. 21* (1982) 618; *Angew. Chem. Suppl. 1982*, 1392.

[5] X-ray structure analysis of **8**: S. Franken, H. Puff, N. Sendhoff, F. Vögtle, manuscript in preparation.

[6] J. Fastrez, *Tetrahedron Lett. 27* (1987) 419.

[7] The formation of isomers was expected since earlier attempts had led to isomeric double-decker structures by means of fourfold bridging [4].

[8] We tentatively [9] assign the other cyclization product, m.p. > 300 °C, on the basis of the ^{1}H-NMR spectrum [(CD_2Cl_2, 400 MHz): $\delta = 3.6$ (m, br., CH_2), 3.7 (m, CH_2), 7.0 (s, aromat. H), 7.3–7.5 (m, aromat. H)] to the constitution **3** having D_{3h} symmetry. The ^{1}H-NMR spectra of **3**, but not of **4**, show a broad and a sharp CH_2 absorption at 20 °C, which we ascribe to a slow CH_2–S–CH_2 rotation.

[9] Despite repeated attempts, no $M^{\oplus}$ peak for **3** could be obtained.

[10] a) Y. Okamoto, H. Urakawa, K. Ohta, H. Yuki, *Macromolecules 11* (1978) 719; b) Y. Okamoto, S. Henda, I. Okamoto, H. Yuki, S. Murata, R. Noyori, H. Takaya, *J. Am. Chem. Soc. 103* (1981) 6971; c) K. Meurer, A. Aigner, F. Vögtle, *J. Inclusion Phenom. 3* (1985) 51; d) F. Vögtle, J. Struck, H. Puff, P. Woller, H. Reuter, *J. Chem. Soc. Chem. Commun. 1986*, 1248.

[11] Since the separation on a preparative column was not successful, it had to be repeated several times on an analytical column (over three months). The (+) enantiomer was purified several times and can be regarded as highly enriched.

1,4-Diphospha-1,3-butadienes**

By *Rolf Appel,** *Johannes Hünerbein,* and *Nikolaos Siabalis*

Phosphacarbadienes are of interest because, owing to the similar behavior of the PC and the CC double bond, they can undergo a variety of pericyclic reactions such as the Cope rearrangement and cycloadditions.[1] Of the four possible diphospha-1,3-butadienes, derivatives of the 1,3- and 2,3-diphospha-1,3-butadienes are known at present.[2–4] Earlier attempts to obtain a missing member of this

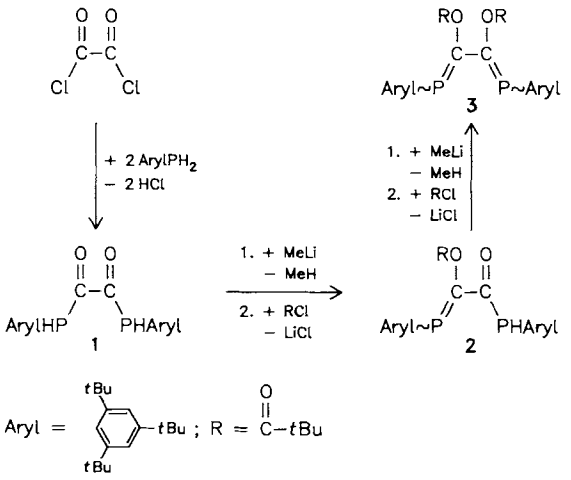

series, the open-chain 1,4-diphospha-1,3-butadiene, by reaction of oxalyl chloride with disilylphosphanes led only to 1,2-dihydro-1,2-phosphete derivatives (diphosphacyclobutenes)[2] as a result of intramolecular [2+2] cycloaddition. These are also formed in the high-temperature reaction of cyclophosphanes with alkynes[5–7] and upon reaction of dichlorophosphanes with phosphirenes.[8] We have now found that the cycloaddition that occurs when the oxalyl chloride method is used can be suppressed by the introduction of 2,4,6-tri-*tert*-butyl moieties at the P atoms.

The reaction, carried out at −60 °C in *n*-pentane with the reactants in a 1:2 molar ratio, leads initially to the oxalic acid diphosphide **1** as a violet powder. It can be converted into its lithium enolate by reaction with methyllithium in tetrahydrofuran (THF) at −60 °C. The enolate, in turn, reacts with pivaloyl chloride to give the 1,4-diphospha-1-butene. Repetition of this sequence of reactions at room temperature leads to the 1,4-diphospha-1,3-butadiene derivative **3**. It is precipitated by addition of acetonitrile and recrystallized from toluene/acetonitrile (1:2). The structure of **3** (correct elemental analysis) is supported by the NMR, MS, and IR spectroscopic data.[9]

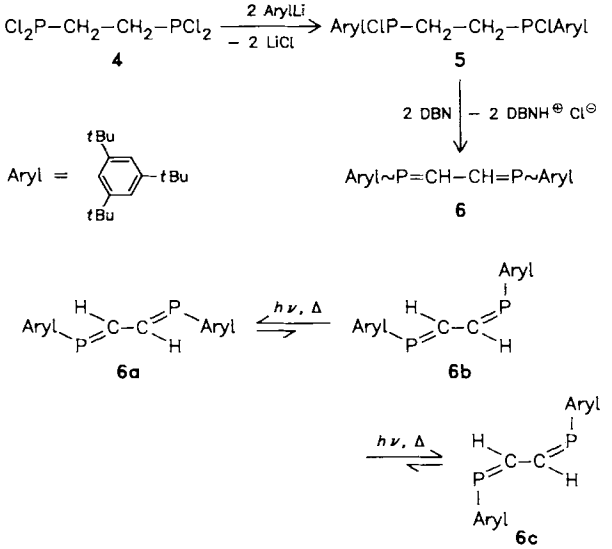

We prepared the *C*-unsubstituted 1,4-diphospha-1,3-butadiene **6** by reaction of ethylenebis(dichlorophosphane) **4** with 2,4,6-tri-*tert*-butylphenyllithium in a molar ratio of 1:2 at −80 °C in THF. The compound **5** thereby obtained can be dehydrochlorinated at −40 °C with 1,5-diazabicyclo[4.3.0]non-5-ene (DBN). Compound **6** is obtained as a mixture of the stereoisomers **6a** (*E,E*) and **6b** (*E,Z*), which can be separated by fractional crystallization from toluene. The isomer **6c** (*Z,Z*) is exclusively formed from **6b** upon irradiation ($\lambda = 254$ nm) or warming in benzene (60 °C). The assignment of the three isomers (which gave appropriate IR and MS data as well as correct elemental analyses) to the proposed structures is based on the NMR spectroscopic data,[14] taking into consideration the information available for similarly substituted phosphaalkenes.[10–13] The ^{1}H-NMR spectrum of **6b** shows the typical pattern of an ABXY system, which, upon phosphorus decoupling, is reduced to a doublet of doublets with 14.4 Hz for the $^3J_{HH}$ coupling constant. The other coupling constants, which could not be determined from the experimental spectra, were determined by simulation.[14]

The 1,4-diphospha-1,3-butadienes are suitable as ligands for σ-coordinated complexes with transition metals.[15] Attempts to carry out pericyclic reactions with maleic anhydride, acetylene dicarboxylate esters, dimethylbutadiene, or cyclopentadiene were unsuccessful.[15]

Received: March 25, 1987 [Z 2160 IE]
German version: *Angew. Chem. 99* (1987) 810

[*] Prof. Dr. R. Appel, J. Hünerbein, N. Siabalis
Anorganisch-chemisches Institut der Universität
Gerhard-Domagk-Strasse 1, D-5300 Bonn 1 (FRG)

[**] Low-Coordinate Phosphorus Compounds, Part 61.—Part 60: R. Appel, C. Behnke, *Z. Anorg. Allgem. Chem.*, in press.

[1] a) R. Appel, V. Barth, W. Paulen, F. Knoch, *Phosphorus Sulfur 26* (1986) 1; b) R. Appel, V. Winkhaus, F. Knoch, *Chem. Ber. 120* (1987) 125; c) R. Appel, C. Casser, *ibid. 118* (1985) 3419; d) R. Appel, J. Menzel, F. Knoch, *ibid. 118* (1985) 4068.

[2] a) R. Appel, V. Barth, F. Knoch, *Chem. Ber. 116* (1983) 938; b) G. Märkl, H. Sejpka, *Tetrahedron Lett. 27* (1986) 171.
[3] R. Appel, U. Kündgen, F. Knoch, *Chem. Ber. 118* (1985) 1352.
[4] R. Appel, P. Fölling, W. Schuhn, F. Knoch, *Tetrahedron Lett. 27* (1986) 1661.
[5] W. K. Mahler, *J. Am. Chem. Soc. 86* (1964) 2306.
[6] A. Ecker, U. Schmidt, *Chem. Ber. 106* (1973) 1453.
[7] C. Charrier, J. Guilhem, F. Mathey, *J. Org. Chem. 46* (1985) 3.
[8] L. Ricard, N. Maigrot, C. Charrier, F. Mathey, *Angew. Chem. 99* (1987) 590; *Angew. Chem. Int. Ed. Engl. 26* (1987) 548.
[9] **3**: bright yellow crystals, dec. above 210°C; ^{13}C-NMR (20 MHz, $CDCl_3$, δ values, selected): 177.7 (dd, $J_{CP}=19.6$ Hz, $^2J_{CCP}=16$ Hz, P=C); ^{31}P-NMR (32.4 MHz, $CDCl_3$, H_3PO_4 ext.): $\delta=188.7$ (s).
[10] G. Becker, O. Mundt, *Z. Anorg. Allg. Chem. 462* (1980) 130.
[11] G. Becker, M. Rössler, W. Uhl, *Z. Anorg. Allg. Chem. 473* (1981) 7.
[12] M. Yoshifuji, K. Toyota, N. Inamoto, *Tetrahedron Lett. 26* (1985) 1727.
[13] R. Appel, J. Menzel, *Z. Anorg. Allg. Chem. 534* (1986) 100.
[14] **6a**: yellow crystals, dec. above 260°C, yield 29%; ^{1}H-NMR (60 MHz, $CDCl_3$, δ values, selected): 8.3 (dd, $J_{HH}=0$ Hz, $^2J_{PH}=4.7$ Hz, $^3J_{PH}=1.1$ Hz, 2H, P=C–H); ^{13}C-NMR (20 MHz, $CDCl_3$, δ values, selected): 176.3 (pseudo t, $J=10.25$ Hz, P=C); ^{31}P-NMR (32.4 MHz, $CDCl_3$, H_3PO_4 ext.): $\delta=269.5$ (s).—**6b**: yellow crystals, dec. above 150°C, yield 39%; ^{1}H-NMR (60 MHz, $CDCl_3$, δ values, selected, ABXY system): $\delta_A=8.25$, $\delta_B=6.52$, P=C–H, $J_{AB}=14.4$ Hz, $J_{AX}=22.2$ Hz, $J_{AY}=10.7$ Hz, $J_{BY}=39.4$ Hz, $J_{BX}=17$ Hz, $J_{XY}=188$ Hz; ^{13}C-NMR (20 MHz, $CDCl_3$, δ values, selected): 167.5 (dd, $J_{CP}=46.5$ Hz, $^2J_{CCP}=17.1$ Hz, P=C), 171 (dd, $J_{CP}=36.3$ Hz, $^2J_{CCP}=28.8$ Hz, P=C); ^{31}P-NMR (32.4 MHz, $CDCl_3$, H_3PO_4 ext., AB system): $\delta_A=243.1$, $\delta_B=284.5$, $J_{AB}=188$ Hz.—**6c**: yellow solid, no elemental analysis; ^{1}H-NMR (60 MHz, $CDCl_3$, δ value, selected): 6.85 (dd, $J_{HH}=0$ Hz, $^2J_{PH}=30$ Hz, $^3J_{PH}=26$ Hz, P=C–H); ^{13}C-NMR (20 MHz, $CDCl_3$, δ value, selected): 161 (pseudo t, $J=38$ Hz, P=C); ^{31}P-NMR (32.4 MHz, $CDCl_3$, H_3PO_4 ext.): $\delta=246$ (s).
[15] R. Appel et al., unpublished.

Synthesis and Structure of a Stable Iodoselenide**

By *Wolf-Walther du Mont,* Silvia Kubiniok, Karl Peters,* and *Hans-Georg von Schnering*

Stable binary compounds between selenium and iodine, elements having very similar electronegativities, have not been characterized so far; the system selenium–iodine is only characterized by a eutectic.[1,2] Diorganosulfides and -selenides react with iodine to give only charge-transfer adducts. The formation of iodo(phenyl)selenide as a reactive intermediate has been suggested to occur during C–C bond formation and accompanying cyclization of 1,5-dienes using the recommended Toshimitsu reagent, diphenyldiselane/iodine,[3] but it has not been possible to isolate this species.[4]

Similar behavior is found in the system tellurium–phosphorus, for which we were able to shift telluration/detelluration and dismutation equilibria in favor of the formation of compounds containing Te–P bonds and to slow down the attainment of the equilibria by the introduction of bulky substituents.[5] It thus appeared promising to exploit steric factors to activate a compound containing Se–Se bonds in such a way that reaction with iodine should lead to the formation of products containing Se–I bonds.

[*] Prof. Dr. W.-W. du Mont, Dipl.-Chem. S. Kubiniok
Fachbereich Chemie der Universität
Carl-von-Ossietzky-Strasse 9-11, D-2900 Oldenburg (FRG)
Prof. Dr. H.-G. von Schnering, Dr. K. Peters
Max-Planck-Institut für Festkörperforschung
Heisenbergstrasse 1, D-7000 Stuttgart 80 (FRG)

[**] This work was supported by the Deutsche Forschungsgemeinschaft and the Fonds der Chemischen Industrie.

The bulkiest compound containing a Se–Se bond, which, in addition, exhibits the highest barrier to rotation around the Se–Se bond, is bis(2,4,6-tri-*tert*-butylphenyl)diselane **1**,[6,7] which is obtained by oxidation of lithium 2,4,6-tri-*tert*-butylphenylselenide with oxygen.[8] Whereas the diselane is quite stable upon exposure to air, it is rapidly attacked by iodine with the formation of 2,4,6-tri-*tert*-butylphenyl(iodo)selenide **2**. The formation of **2** is practically quantitative if an excess of iodine is used. Compound **2** is obtained in pure form as anthracite-black crystals by recrystallization, m.p. = 156°C (dec.).[9]

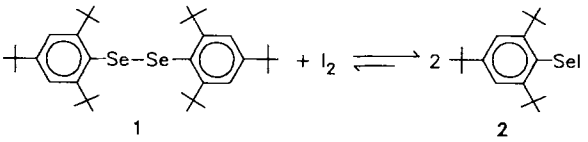

1 2

In the solid state, the iodoselenide **2** is present as a monomer with a bent C–Se–I structural unit (97.5°) (Fig. 1). Significant intermolecular Se···I, Se···Se, or I···I contacts do not exist.[10] The arylseleno moiety of **2** exhibits deviations from planarity—which are characteristic of

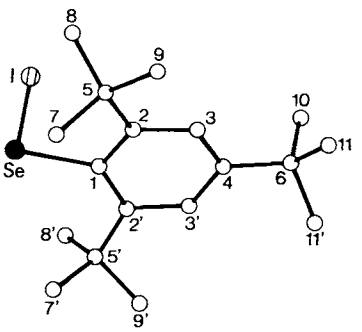

Fig. 1. Crystal structure of **2** (hydrogen atoms omitted). The compound forms orthorhombic crystals, space group *Pnma*, $a=1160.9(3)$, $b=1541.3(4)$, $c=1078.8(3)$ pm; $Z=4$, $\rho_{calcd}=1.553$ g cm^{-3}, 1808 *hkl* with $F>3\sigma(F)$, $R=0.027$. Further details of the crystal structure investigation may be obtained from the Fachinformationszentrum Energie, Physik, Mathematik GmbH, D-7514 Eggenstein-Leopoldshafen 2 (FRG), on quoting the depository number CSD-52420, the names of the authors, and the journal citation.

2,4,6-tri-*tert*-butylphenyl-substituted systems.[11] The Se–I distance (252.9 pm) is in good agreement with the value expected for a Se–I single bond[12] and is slightly longer than the bond in *Passmore*'s cationic species containing iodine of coordination number 1.[1,2b]

When crystals of **2** are dissolved in benzene or in aliphatic hydrocarbons, re-dismutation occurs to a small extent, which is confirmed by the ^{1}H-NMR spectra (integrals of the signals of **1** approximately 10–15% those of **2**; the equilibrium is established within only a few minutes after dissolving the crystals in benzene), ^{13}C-NMR spectra,[9] ^{77}Se-NMR spectra,[9] and UV/VIS spectra (in cyclopentane: weak absorption at 538 nm, I_2). The equilibrium constants for the dismutation of diselane **1** with iodine to give the iodoselenide **2** can thereby be estimated to be approximately 10^2 mol^2 L^{-2}. The attainment of the dismutation equilibrium is slow compared with the time scales of ^{1}H-, ^{13}C-, and ^{77}Se-NMR measurement.[9] The attainment of the

dismutation equilibrium between diphenyldiselane/iodine and iodo(phenyl)selenide, on the other hand, is rapid at room temperature on the 80-MHz ^{1}H-NMR and 75-MHz ^{13}C-NMR time scales.[13] This clearly explains why it is easy to overlook iodoselenide in equilibria when following, by NMR spectroscopy, the reactions of diselanes with iodine.

The ability to control, by means of the substituents, the dismutation of compounds containing Se–Se bonds with those containing I–I bonds and the surprising stability of **2**, the first base-free iodoselenide to be isolated in pure form, should also make it possible, in the future, to better characterize mechanistically the reactions in the system chalcogen/iodine.

Received: March 18, 1987;
supplemented: May 29, 1987 [Z 2145 IE]
German version: *Angew. Chem. 99* (1987) 820

[1] a) W. Behrendt, U. W. Gerwarth, S. Jäger, I. Kreuzbichler, K. Seppelt in: *Gmelin Handbook of Organic Chemistry, 8th Ed., Selenium Supplement Vol. B2*, Springer, Berlin 1984, p. 272; b) N. N. Greenwood, A. Earnshaw: *Chemistry of the Elements*, Pergamon Press, Oxford 1984, p. 817–819 and 901–904.

[2] a) J. Passmore, P. Taylor, T. K. Whidden, P. White, *J. Chem. Soc. Chem. Commun. 1976*, 689; b) W. A. S. Nandana, J. Passmore, P. S. White, C.-M. Wong, *ibid. 1982*, 1098.

[3] A. Toshimitsu, S. Uemura, M. Okano, *J. Chem. Soc. Chem. Commun. 1982*, 87.

[4] In contrast, iodosulfides have been prepared—by Cl/I exchange performed on chlorosulfides, among other methods—and have been characterized at low temperatures. These metastable iodosulfides decompose under normal conditions to give disulfanes and iodine: R. Minkwitz, U. Nass, H. Preut, *Z. Anorg. Allg. Chem. 538* (1986) 143, and references cited therein. Cl/I exchange at chloro(phenyl)selenide: S. Tomoda, Y. Takeuchi, Y. Nomura, *Synthesis 1985*, 212.

[5] W.-W. du Mont, T. Severengiz, B. Meyer, *Angew. Chem. 95* (1983) 69; *Angew. Chem. Int. Ed. Engl. 23* (1983) 61; W.-W. du Mont, S. Kubiniok, T. Severengiz, *Z. Anorg. Allg. Chem. 531* (1985) 21.

[6] W. Rundel, *Chem. Ber. 101* (1968) 2956.

[7] H. Kessler, W. Rundel, *Chem. Ber. 101* (1968) 3350.

[8] L. Lange, *Dissertation*, Universität Oldenburg 1987; see also: L. Lange, W.-W. du Mont, *J. Organomet. Chem. 286* (1985) C 1.

[9] *Experimental procedure* for **2**: A solution of iodine (0.55 g, 2.17 mmol) in 8 mL of toluene was added at room temperature to a solution of **1** (1.4 g, 2.17 mmol) [8] in 20 mL of toluene. After stirring for 1 h, the solution was concentrated under reduced pressure. Recrystallization of the crude product from petroleum ether 40/60 gave 1.5 g (77%) of **2** in the form of black crystals (m.p. = 156 °C). Compound **2** is readily soluble in benzene and toluene and moderately soluble in aliphatic hydrocarbons. Correct elemental analyses. MS (EI, 70 eV, 100 °C): *m/z* 648 (0.1%, $M^{\oplus}$ of **1**), 452 (12, $M^{\oplus}$ of **2**), 326 (2, tBu$_3$C$_6$H$_2$SeH$^{\oplus}$), 311 (1, C$_{17}$H$_{27}$Se$^{\oplus}$), 269 (10, tBu$_2$C$_6$H$_3$Se$^{\oplus}$), 255 (4, C$_{13}$H$_{19}$Se$^{\oplus}$), 213 (41, tBuC$_6$H$_4$Se$^{\oplus}$), 57 (100, C$_4$H$_9^{\oplus}$). ^{1}H-NMR (80 MHz, C$_6$D$_6$): **2**: δ = 1.2 (s, 9H), 1.7 (s, 18H), 7.5 (s, 2H). In the presence of an excess of iodine, only these three signals are observed; when crystals of **2** are dissolved in benzene, the signals of **1** are still visible with 10–15% of the integral of **2**. **1**: δ = 1.3 (s, 18H), 1.45 (s, 36H), 7.4 (s, 4H). ^{13}C-NMR (20 MHz, C$_6$D$_6$) **2** (in the presence of excess iodine): δ = 31.1 (*p*-CC$_3$), 33.4 (*o*-CC$_3$), 35.3 (*p*-CC$_3$), 39.9 (*o*-CC$_3$), 123.7 (*m*-C), 153.5 (*p*-C), 157.7 (*o*-C). **1**: δ = 31.4 (*p*-CC$_3$), 33.4 (*o*-CC$_3$), 39.3 (*o*-CC$_3$), 122.6 (*m*-C), 150.5 (*p*-C), 156.5 (*o*-C); these shifts are in agreement with those of pure **1** [8]. ^{77}Se-NMR (57.24 MHz, C$_6$D$_6$, Me$_2$Se standard): **1**, δ = 515.8; **2**, δ = 516.0; we thank *M. Dettlaff* and Prof. Dr. *H. Schumann*, Berlin, for the ^{13}C- and ^{77}Se-NMR measurements.

[10] Important bond lengths and angles of **2**: I-Se 252.9(1), Se-C1 194.1(3), C-C (ring) 138.3 to 140.9, C2-C5 155.4(4), C4-C6 154.7(5). I-Se-C1 97.5(1), Se-C1-C2 118.8(2), Se-C1-C2′ 118.8(2), angle in the ring 116.6–122.8, C1-C2-C5 125.2(2).

[11] M. Yoshifuji, I. Shima, N. Inamoto, K. Hirotsu, T. Higuchi, *Angew. Chem. 92* (1980) 405; *Angew. Chem. Int. Ed. Engl. 19* (1980) 399.

[12] A. F. Wells: *Structural Inorganic Chemistry, 5th Ed.*, Clarendon Press, Oxford 1984, p. 289.

[13] ^{13}C-chemical shifts (20 °C, CDCl$_3$): PhSeSePh 127.7, 129.2, 131.5; PhSeSePh/I$_2$ (2:1) 128.2, 129.2, 132.4 (br.); PhSeSePh/I$_2$ (1:1) 128.8, 129.3, 133.1 (75.47 MHz for all ^{13}C-NMR spectra).

Synthesis and Structure of a 2,5-Dihydro-1*H*-1,2,5-phosphadiborole Derivative**

By *Matthias Driess, Hans Pritzkow*, and *Walter Siebert**

Dedicated to Professor Reinhard Schliebs on the occasion of his 60th birthday

2,5-Dihydro-1*H*-1,2,5-phosphadiboroles such as **2** are of interest because of possible boron–phosphorus interactions. Attempts to synthesize them by substitution of the sulfur in a 2,5-dihydro-1,2,5-thiadiborole derivative[1] or by insertion of phenylphosphanediyl into the B–B bond of the 1,2-dihydro-1,2-diborete[2] (HC)$_2$(*i*Pr$_2$NB)$_2$, however, have been unsuccessful,[3] as was the reaction of 1,2-bis(dichloroboryl)ethene with tris(trimethylsilyl)phosphane.[4] We have now succeeded in synthesizing the first 2,5-dihydro-1*H*-1,2,5-phosphadiboroles. Reaction of (*Z*)-1,2-bis[chloro(diisopropylamino)boryl]ethene **1a** (R = *i*Pr) with dilithium phenylphosphide leads to **2a**.[5] Similarly, the corresponding derivatives of **2a** are prepared starting from **1b** (R = Et) and **1c** (R = Me).

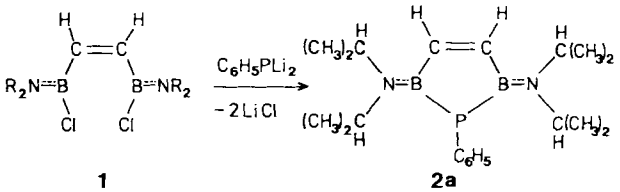

1 **2a**

Compound **2a** is a colorless, crystalline substance with an extremely unpleasant smell. It undergoes only slow decomposition in air. In solution, it reacts with oxygen, exchanging C_6H_5P for O to give the corresponding 2,5-dihydro-1*H*-1,2,5-oxadiborole derivative. The ^{1}H- and ^{13}C-NMR data of **2a** are characterized by long-range PH and PC couplings, respectively,[6] which was confirmed by ^{1}H/^{1}H double resonance and ^{13}C DEPT NMR experiments. As in the case of phosphinoboranes,[7] the different $^4J_{PH}$ and $^3J_{PC}$ coupling constants between phosphorus and the methine hydrogens and methine carbon atoms, respectively, of the diisopropylamino groups can be interpreted in terms of the *Z*/*E* arrangement with respect to the BN π bond. Assuming that the relation $J_E > J_Z$ is valid for alkenes, the signal at lower field (δ = 4.09) can be assigned to the "*E* methine proton" of the diisopropylamino group.[7]

Compound **2a** exhibits temperature-dependent ^{1}H-NMR spectra. At 283 K in [D$_8$]toluene, a doublet at δ = 0.86 as well as a broad signal at δ = 0.65 are observed for the methyl protons. Lowering the temperature results in the appearance of four doublets at 223 K (two doublets for the methyl protons of both the (*E*) and the (*Z*) isopropyl groups). We ascribe these dynamic effects to a lowered barrier of inversion at the pyramidal phosphorus atom. At still lower temperature, the rigid configuration of the phosphorus gives rise to diastereotopism of all four methyl groups of a diisopropylamino group. At raised temperature (up to 400 K), on the other hand, only two anisochronous sets of methyl groups are present owing to rapid

[*] Prof. Dr. W. Siebert, M. Driess, Dr. H. Pritzkow
Anorganisch-chemisches Institut der Universität
Im Neuenheimer Feld 270, D-6900 Heidelberg (FRG)

[**] This work was supported by the Deutsche Forschungsgemeinschaft, the Fonds der Chemischen Industrie, and BASF AG.

inversion at phosphorus. An estimation of the free energy of activation for the inversion at phosphorus from the coalescence temperature, according to the doublet analysis method,[8] gives, as in the case of phosphole,[9] 10–15 kcal mol^{-1}. The observation of two multiplets for the methine protons of the diisopropylamino groups up to 380 K shows that the rotation around the BN bond is hindered. The broad ^{11}B-NMR signal is found at $\delta = 47.7$ (halfwidth $w_{1/2} = 320$ Hz). In the $^{31}P\{^1H\}$-NMR spectrum, a singlet is observed at $\delta = -124.6$ ($w_{1/2} = 120$ Hz). The chemical shift indicates a significant s character of the lone pair of electrons at phosphorus and provides further spectroscopic evidence for its nonplanar coordination, which is confirmed by the X-ray structure analysis (Fig. 1).[10]

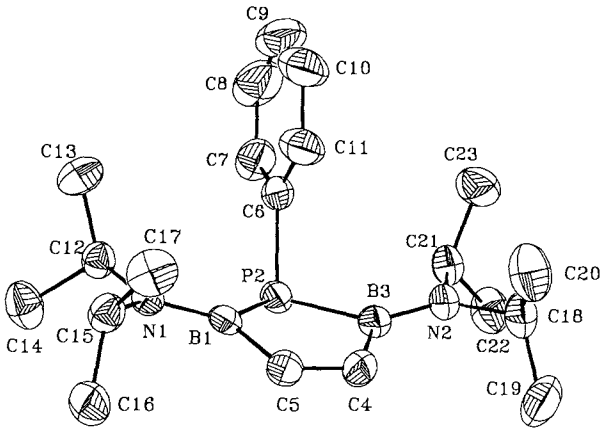

Fig. 1. Crystal structure of **2a** (thermal ellipsoids at 40% probability). Important distances [Å] and angles [°]: P-B 1.949(2), B-C 1.557(2), C-C 1.344(2), B-N 1.391(2), P-C 1.840(1); B-P-B 88.8(1), C-P-B 103.5(1), P-B-C 107.5(1), B-C-C 116.3(1).

The molecule has an approximate plane of symmetry through the phosphorus atom and the phenyl ring perpendicular to the five-membered ring, which is nonplanar. The angle between the planes B1-P2-B3 and B1-B3-C4-C5 is 17°. The phosphorus atom is located 0.4 Å above the plane B1-B3-C4-C5 and is pyramidally coordinated (sum of angles 295.9°).

Received: March 24, 1987;
supplemented: April 27, 1987 [Z 2158 IE]
German version: *Angew. Chem. 99* (1987) 789

CAS Registry numbers:
1a (R = *i*Pr), 109530-92-9; **1b** (R = Et), 109530-93-0; **1c** (R = Me), 109530-94-1; **2a** (R = *i*Pr), 109530-95-2; **2b** (R = Et), 109530-96-3; **2c** (R = Me), 109530-97-4; $C_6H_5PLi_2$, 13595-56-7.

[1] W. Rothermel, *Diplomarbeit*, Universität Marburg 1976.
[2] M. Hildenbrand, H. Pritzkow, W. Siebert, *Angew. Chem. 97* (1985) 769; *Angew. Chem. Int. Ed. Engl. 24* (1985) 759.
[3] M. Driess, *Diplomarbeit*, Universität Heidelberg 1985.
[4] W. Haubold, A. Gemmler, *Chem. Ber. 113* (1980) 3352.
[5] *Experimental Procedure:* **2a**: **1a** [3] (500 mg, 1.6 mmol) in 20 mL of toluene was added to $C_6H_5PLi_2$ (190 mg, 1.6 mmol) in 10 mL of toluene. The reaction mixture was then refluxed for 2 h. The resulting precipitate (LiCl) was filtered off and the bright yellow solution was allowed to form crystals at −30°C. After sublimation of the isolated crude product (96°C/10^{-3} torr), **2a** was recrystallized from CH_2Cl_2 at −78°C. Yield: 470 mg (84%), m.p. = 133–134°C; correct elemental analysis (C,H,P).
[6] ^{1}H-NMR (200 MHz, C_6D_6, 300 K): $\delta = 0.65$ (br. s, 12H), 1.21 (d, 12H, $J_{HH} = 7$ Hz), 2.9 (d, sept., 2H, $^4J_{PH} = 2.1$ Hz), 4.09 (d, sept., 2H, $^4J_{PH} = 4$ Hz), 6.99 (m, 2H), 7.05 (m, 1H), 7.54 (m, 2H), 7.71 (d, 2H, $^3J_{PH} = 6.2$ Hz); ^{13}C-NMR (C_6D_6): $\delta = 21.17$ (s, 4C, CH_3), 25.83 (s, 4C, CH_3), 45.7 (d, 2C, NCH, $^3J_{PC} = 3$ Hz), 56.56 (d, 2C, NCH, $^3J_{PC} = 13$ Hz), 128.35 (d, CH_{Ph}, $J_{PC} = 15$ Hz), 138.05 (d, CH_{Ph}, $J_{PC} = 13$ Hz), 140.38 (d, CH_{Ph}, $J_{PC} = 13.5$ Hz), 160.0 (br, BCH); MS: *m/z* 356 ($M^{\oplus}$, 23%); 313 ($M^{\oplus} - i$Pr, 56%), 249 ($M^{\oplus} - C_6H_4P$, 36%), 44 ($C_3H_8^{\oplus}$, 100%).
[7] G. Fritz, W. Hölderich, *Z. Anorg. Allg. Chem. 431* (1977) 61.
[8] H. Shanan-Atidi, R. H. Bar-Eli, *J. Phys. Chem. 74* (1970) 961.
[9] W. Egan, R. Tang, G. Zon, K. Mislow, *J. Am. Chem. Soc. 93* (1971) 6205.
[10] **2a** forms monoclinic crystals, space group $P2_1/n$, $a = 18.584(10)$, $b = 16.265(10)$, $c = 7.599(5)$ Å, $\beta = 95.83(5)°$, $V = 2285.1$ Å^3, $Z = 4$; $R = 0.050$ for 3353 unique reflections (Stoe two-circle diffractometer, $Mo_{K\alpha}$). Further details of the crystal structure investigation may be obtained from the Fachinformationszentrum Energie, Physik, Mathematik GmbH, D-7514 Eggenstein-Leopoldshafen 2 (FRG), on quoting the depository number CSD-52395, the names of the authors, and the journal citation.

Concerning the Structure of Benzene**

By *Otto Ermer**

The structure of benzene constituted one of the central problems of early organic chemistry which eventually culminated in the question whether its equilibrium geometry corresponds to a planar regular hexagon of symmetry D_{6h} or to a likewise planar D_{3h} (Kekulé) structure with localized alternating CC double and single bonds. It is claimed in many text books of organic chemistry that experimental proof for the equilateral D_{6h} structure of benzene derives from X-ray crystallography.[1] We deem it appropriate to point out in this communication that this is *not* true.

The atomic positions originating from the X-ray (and neutron) diffraction analysis of crystalline benzene are *averaged* over space and time and are compatible not only with a crystallographically ordered D_{6h} model of benzene, but also with a disordered D_{3h} model corresponding to a superposition of benzene molecules rotated with respect to each other by 60° around the three-fold axis (Fig. 1). The disorder may either be static or dynamic: In the first case, we would deal with a statistical distribution of both molecular orientations disregarding the crystallographic symmetry requirements, in the second instance with a rapid inter-

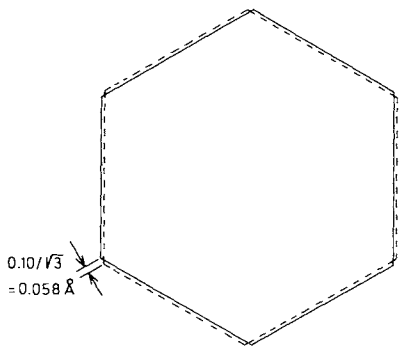

Fig. 1. Disorder model of benzene with localized single and double bonds. Both D_{3h} Kekulé structures are rotated with respect to each other by 60° around the threefold axis; C–C and C=C bond lengths of 1.45 and 1.35 Å, respectively, assumed.

[*] Prof. Dr. O. Ermer
Institut für Organische Chemie der Universität
Greinstrasse 4, D-5000 Köln 41 (FRG)

[**] This work was supported by the Fonds der Chemischen Industrie.

conversion (relative to the measuring time of usually many hours) of D_{3h} forms *via* the D_{6h} form corresponding to a symmetric double minimum potential. Dynamic disorder could also be due to a hindered rotation of the benzene molecules around the three-fold axis. Benzene crystallizes in the space group *Pbca* with four molecules in the unit cell;[2] it is pointed out that the ensuing molecular centrosymmetry is again merely an *averaged* structural property. D_{6h} symmetry is present in the crystal not exactly, yet to a very good degree of approximation.

Assuming a difference of 0.10 Å between the C–C and C=C bond lengths in the D_{3h} model, it is evident from Figure 1 that the superimposed carbon atoms are only $0.05/\sin 60° = 0.058$ Å apart. This small separation is far below the resolving power of an X-ray diffraction measurement. By cooling, it is sometimes possible to induce an ordering process in crystals which are disordered at higher temperatures. However, this may by no means always be achieved. Yet even in this case, there remains a possibility to uncover a disorder through an analysis of the temperature dependence of the crystallographic temperature factors. To this end, however, the disorder contribution to the temperature factors must be large enough. The CC bond length difference of the present example of 0.10 Å corresponds to a disorder contribution of only $(0.025/\sin 60°)^2 = 0.0008$ Å^2, much too small to allow safe conclusions with respect to a possible disorder even at very low temperatures. The consideration of the hydrogen atoms within a neutron diffraction experiment, for example, would not help much to improve the situation. In addition, the well-known experimental difficulties complicating the derivation of reliable temperature motion parameters from diffraction measurements are entirely neglected in this discussion! The quantitative analysis of the size and orientation of the anisotropic temperature factor tensors, e.g. in terms of rigid-body motions, may also provide insight into disorder phenomena of the present kind.[3] Nonetheless, in the extreme case of benzene such methods, too, are not capable of proving the absence of disorder.

Our experimental knowledge about the symmetry of the benzene molecule derives from the vibrational spectroscopic measurements (short-time spectroscopy) of *C. K. Ingold* et al. of more than 50 years ago.[4] The decision in favor of the D_{6h} structure is largely based on the analysis of selection rules: For example, no violations of the mutual exclusion rule are perceptible when comparing the infrared and Raman spectra of gaseous benzene. This indicates the presence of a molecular center of symmetry incompatible with the D_{3h} model. The D_{6h} equilibrium structure is also supported by the following simple consideration: A frequency of 1309 cm^{-1} is commonly assigned to the CC stretching vibration corresponding to the transition $D_{6h} \rightarrow D_{3h}$ (B_{2u} species).[5] Assuming a double minimum potential with D_{3h} minima, such a large B_{2u} frequency would require an unacceptably high D_{6h} barrier in order to achieve a correspondingly high curvature of the potential at the minima. Since at most a *very shallow* double minimum could be reasonably envisaged, it follows that in actual fact a relatively steep single minimum potential with D_{6h} minimum geometry must be present. On the whole, it may be stated that although the vibrational spectroscopic data of benzene (and deuteriated species)[4,5] provide strong indications in favor of the D_{6h} equilibrium geometry, they may not be regarded an irrefutable *proof* for this structure.

We have seen that although the X-ray and neutron diffraction results of crystalline benzene (and of many benzene derivatives) are compatible with the D_{6h} model, they do not allow one to discard the D_{3h} model. The analysis of the electron diffraction data of gaseous benzene confronts us with a similar dilemma since the resolving power of this method is in principle not better than about 0.1 Å; for interatomic distances differing by less than 0.1 Å only a weighted average can be measured.[6,7] This is due to zero-point vibrations which are responsible for the relatively broad maxima in the one-dimensional distance distributions. The presence of a shallow double minimum would also lead to analytical difficulties.[6] Finally, the structural information on benzene remains which may be extracted from rotational spectra. It turns out, however, that the D_{6h} and D_{3h} models cannot be distinguished by this method either.[8] Therefore, for the derivation of a quantitative structural model of benzene, i.e. in particular the CC bond length, by means of crystal X-ray and neutron diffraction, gas-electron diffraction, and gas-rotational spectroscopy (moments of inertia), D_{6h} symmetry has to be *assumed*. We are therefore faced with the rather remarkable situation that the experimental values of one of the most important structural quantities of organic chemistry originate from experimental techniques incapable of resolving the D_{6h}/D_{3h} symmetry problem of benzene. Under the (substantiated) *assumption* of D_{6h} symmetry the following selected values for the CC bond length of benzene have been determined: Crystal X-ray diffraction at 270 K, 1.377(10) Å (average value of three crystallographically independent distances; corrected for libration, 1.392 Å);[2a] crystal neutron diffraction at 138 K, 1.393(7) Å (average value; corrected for libration, 1.398 Å);[2b] gas-electron diffraction, $r_\alpha^0 = 1.3959(19)$, $r_g = 1.3992(8)$ Å;[9] gas-rotational spectroscopy (with vibrational coupling), $r_0 = 1.3964(2)$,[10] $r_z = 1.3967(9)$ Å.[9-11] An experimental r_e structure (vibrationless equilibrium structure of minimal potential energy) of benzene has as yet not been reported.

A few years ago, doppler-free electronic spectra of benzene with completely resolved rotational lines were recorded for the first time; this could not be accomplished previously, either by Raman or infrared spectroscopy.[12] In principle, it should be possible to decide between D_{6h} and D_{3h} symmetry with the help of the intensities of the rotational lines which depend on nuclear spin statistical factors. Although it is conceivable that the statistical intensity effects are indistinguishably similar for both cases, this is unlikely. The statistical weights of the D_{6h} model are in good accord with the observed line intensities; however, the statistical analysis for the D_{3h} model has not as yet been performed.[13a] Photoelectron spectra are of rather little value as regards the present benzene problem. For example, no conclusions may be drawn from the PE band locations since it can be shown that the π ionization energies of the D_{6h} and D_{3h} models, respectively, are practically the same.[13b] NMR data are of no help either; room temperature ^{1}H-NMR measurements of benzene molecules oriented in liquid crystals give sharp lines without *ortho* H–H couplings being observable.[14] This merely allows one to conclude that the average lifetime of an eventual D_{3h} minimum structure is at most 10^{-4} s, corresponding to $\Delta G^{\neq}_{max} \approx 12$ kcal mol^{-1}.[13c]

In view of the fact that the D_{6h}/D_{3h} structural problem of benzene is not strictly solved, enhanced significance is to be assigned to theoretical calculations on a reliable quantum-mechanical basis. Such calculations yield the optimal D_{6h} structure of benzene energetically more favorable than sensible D_{3h} structures and reproduce well the (positive) force constant and frequency of the B_{2u} CC

stretching vibration, in accord with a one-minimum potential.[15]

The present discussion is relevant not only in the context of the geometrical structure of benzene, it has even more general implications in connection with questions as to the CC bond length alternation and double bond localization (and the related aromaticity problems), respectively, in annulenes of arbitrary ring size, bridged annulenes, and polycyclic π systems with condensed rings. In particular, this holds for analyses of such problems by means of routine X-ray diffraction studies: *Caution is obviously called for!*[3, 16]

Received: January 21, 1987;
revised: March 30, 1987 [Z 2060 IE]
German version: *Angew. Chem. 99* (1987) 791

CAS Registry number:
C_6H_6, 71-43-2.

[1] Cf. e.g. the two widely distributed text-books: R. T. Morrison, R. N. Boyd: *Organic Chemistry*, Allyn and Bacon, Boston, MA 1983, p. 579; A. Streitweiser, C. H. Heathcock: *Introduction to Organic Chemistry*, Macmillan, New York 1980, p. 569.

[2] a) X-ray diffraction of benzene at 270 K: E. G. Cox, D. W. J. Cruickshank, J. A. S. Smith, *Proc. R. Soc. (London) A 247* (1958) 1; b) neutron diffraction of benzene at 138 and 218 K: G. E. Bacon, N. A. Curry, S. A. Wilson, *Proc. R. Soc. (London) A 279* (1964) 98.

[3] E. F. Maverick, J. D. Dunitz, unpublished. I thank Prof. J. D. Dunitz, Zürich, for preprints. See also: R. E. Rosenfield, K. N. Trueblood, J. D. Dunitz, *Acta Crystallogr. A 34* (1978) 828.

[4] Series of 21 publications; in particular see: W. R. Angus, C. R. Bailey, J. B. Hale, C. K. Ingold, A. H. Leckie, C. G. Raisin, J. W. Thompson, C. L. Wilson, *J. Chem. Soc. 1936*, 966, 971; C. R. Bailey, C. K. Ingold, H. G. Poole, C. L. Wilson, *ibid. 1946*, 222; N. Herzfeld, C. K. Ingold, H. G. Poole, *ibid. 1946*, 316; cf. [5].

[5] R. B. Mair, D. F. Hornig, *J. Chem. Phys. 17* (1949) 1236; S. Brodersen, A. Langseth, *Mat. Fys. Skr. Dan. Vidensk. Selsk. 1* (1956) No. 1; S. Brodersen, J. Christoffersen, B. Bak, J. T. Nielsen, *Spectrochim. Acta 21* (1965) 2077; J. C. Duinker, I. M. Mills, *Spectrochim. Acta A 24* (1968) 417; P. C. Painter, J. L. Koenig, *ibid. 33* (1977) 1003, 1019. Note that *Ingold* et al. originally assigned a frequency of 1648 cm^{-1} to the B_{2u} CC stretching vibration of benzene (last citation of [4]), considerably higher than the frequency of 1309 cm^{-1} nowadays commonly adopted.

[6] K. Kuchitsu, S. J. Cyvin in S. J. Cyvin (Ed.): *Molecular Structures and Vibrations*, Elsevier, Amsterdam 1972, p. 206. Regarding the D_{6h}/D_{3h} resolution problem of benzene, cf. also: I. L. Karle, *J. Chem. Phys. 20* (1952) 65.

[7] The one-dimensional distance distributions resulting from electron diffraction analyses may be compared to one-dimensional Patterson functions. From single crystal X-ray and neutron diffraction measurements one obtains three-dimensional Patterson functions (vector density distributions), such that in the absence of disorder and the usually sufficiently high reflection orders no resolution problems are encountered.

[8] B. P. Stoicheff, *Can. J. Phys. 32* (1954) 339; J. H. Callomon, T. M. Dunn, I. M. Mills, *Phil. Trans. R. Soc. London A 259* (1966) 499.

[9] K. Tamagawa, T. Iijima, M. Kimura, *J. Mol. Struct. 30* (1976) 243.

[10] A. Cabana, J. Bachand, J. Giguère, *Can. J. Phys. 52* (1974) 1949.

[11] For structural measurements of liquid benzene see: E. Bartsch, H. Bertagnolli, G. Schulz, P. Chieux, *Ber. Bunsenges. Phys. Chem. 89* (1985) 147; A. H. Narten, *J. Chem. Phys. 48* (1968) 1630.

[12] E. Riedle, H. J. Neusser, E. W. Schlag, *J. Chem. Phys. 75* (1981) 4231.

[13] Personal communications of a) H. J. Neusser, b) E. Heilbronner, c) P. Diehl. I thank the gentlemen mentioned for these pieces of information and an unknown referee for respective advice.

[14] P. Diehl, H. Bösiger, H. Zimmermann, *J. Magn. Reson. 33* (1979) 113.

[15] J. Paldus, M. Takahashi, *Int. J. Quantum Chem. 25* (1984) 423; R. C. Haddon, K. Raghavachari, *J. Am. Chem. Soc. 107* (1985) 289. A collection of benzene calculations which almost always *presuppose* D_{6h} symmetry, may be found with R. S. Mulliken, W. C. Ermler: *Polyatomic Molecules (Results of ab initio Calculations)*, Academic Press, New York 1981, p. 331. Theoretical interpretations of the benzene structure have recently sparked off controversy which is of some interest in the present context: N. C. Baird, *J. Org. Chem. 51* (1986) 3907; P. C. Hiberty, S. S. Shaik, G. Ohanessian, J.-M. Lefour, *ibid. 51* (1986) 3908; S. S. Shaik, P. C. Hiberty, J.-M. Lefour, G. Ohanessian, *J. Am. Chem. Soc. 109* (1987) 363. Finally some very recent quantum-mechanical calculations are pointed out which throw new light on the electronic structure of benzene: D. L. Cooper, J. Gerratt, M. Raimondi, *Nature London 323* (1986) 699; however, a critical reply has already appeared: W. H. E. Schwarz, *Nachr. Chem. Tech. Lab. 35* (1987) 178; see also P. A. Schultz, R. P. Messmer, *Phys. Rev. Lett. 58* (1987) 2416.—For demonstration purposes, a geometry optimization of benzene on a good quantum-mechanical basis would be desirable which starts out from a D_{3h} geometry with markedly different, alternating C–C and C=C bond lengths, and which shows smooth convergence towards the D_{6h} minimum. Newton-Raphson procedures should be applied for this optimization and the minimum nature of the optimal D_{6h} structure should be clearly assessed by diagonalization of the second-derivative matrix of the potential energy. At least for didactical purposes, such a calculation which is not documented in the literature, would be useful.

[16] O. Ermer, E. Heilbronner, *Angew. Chem. 95* (1983) 414; *Angew. Chem. Int. Ed. Engl. 22* (1983) 402; H. Irngartinger, M. Nixdorf, *Angew. Chem. 95* (1983) 415; *Angew. Chem. Int. Ed. Engl. 22* (1983) 403; R. Destro, T. Pilati, M. Simonetta, *Tetrahedron 36* (1980) 3301; O. Ermer, E. Vogel, unpublished.

The Absolute Configuration of the Ant Alarm Pheromone Manicone**

By *Hans Jürgen Bestmann,* Athula B. Attygalle, Jürgen Glasbrenner, Roland Riemer,* and *Otto Vostrowsky*

Manicone, (4*E*)-4,6-dimethyl-4-octen-3-one **1**, had been identified 15 years ago as an active pheromone constituent of the mandibular glands in two North American species of ants *Manica mutica* and *M. bradleyi* (Hymenoptera: Formicidae).[2] However, the absolute configuration of this chiral natural product was not determined. We have also been able to identify **1** as the main pheromone (2–3 μg/insect) in the mandibular gland secretion of the only known Euroasiatic Manica species, *Manica rubida* Latr.[3, 4] Assignment of the configuration of the chiral ketone **1** has now been accomplished, in an indirect way, by means of complexation gas chromatography[5] on a chiral phase. In total, only ten insects were required in order to elucidate the stereochemistry of **1**. The method employed is outlined below.

Hydrogenation of the double bond of synthetic, racemic manicone, *rac*-**1**, with Pd/activated carbon led to the formation of a new chiral center; as a result two diastereomeric pairs of dihydromanicone, *rac*-**2**, were produced. These four isomers could be separated by complexation gas chromatography[5] on nickel(II) bis[3-heptafluorobutyryl-(1*R*)-camphorate] (Fig. 1A).[6] *rac*-**1** could not be separated.

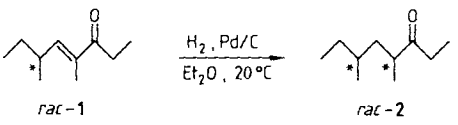

The same reaction was carried out with natural manicone **1**. The constituents of two heads of *M. rubida* female workers were hydrogenated by reaction gas chromatography (solid sample injector,[1] H_2 as carrier gas, 1% Pd catalyst in the GC injection block) and the dihydromanicone **2** thus formed was isolated, after GC separation, in cooled

[*] Prof. Dr. H. J. Bestmann, Dr. A. B. Attygalle, Dipl.-Chem. J. Glasbrenner, Dipl.-Chem. R. Riemer, Dr. O. Vostrowsky
Institut für Organische Chemie der Universität Erlangen-Nürnberg
Henkestrasse 42, D-8520 Erlangen (FRG)

[**] Pheromones, Part 61. This work was supported by the Deutsche Forschungsgemeinschaft. *A. B. A.* thanks the Alexander-von-Humboldt Stiftung for a grant.—Part 60: [1].

glass capillaries.[9] The condensate was subsequently rechromatographed on an optically active Ni^{II}-phase. Only two diastereomeric hydrogenation products **2** appeared in the gas chromatogram (Fig. 1B); these corresponded to the isomers 1 and 4 in Figure 1A.

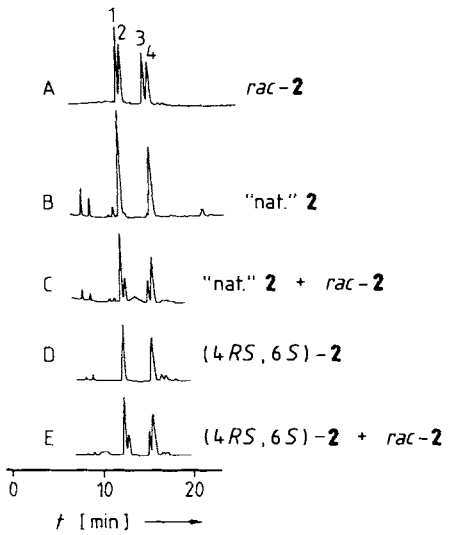

Fig. 1. Gas chromatographic separation of A) synthetic racemic dihydromanicone *rac*-**2**, B) "natural" **2**, obtained from the heads of *M. rubida* by hydrogenation, C) co-injected "natural" **2** and *rac*-**2**, D) synthetic (4*RS*,6*S*)-**2**, E) co-injected synthetic (4*RS*,6*S*)-**2** and *rac*-**2**.—Optically active GC phase: nickel(II) bis[3-heptafluorobutyryl-(1*R*)-camphorate] [5, 6]. The signals 1 and 4 correspond to the pair of diastereomers (4*RS*,6*S*)-**2**, the signals 2 and 3 correspond to (4*RS*,6*R*)-**2**.

The pair of diastereomers of dihydromanicone **2**, having (*S*)-configuration on C-6 (Fig. 1D), could be synthesized, as shown in Scheme 1, starting from commercially available (*S*)-(−)-2-methylbutanol **3**, via (*S*)-(+)-2-methylbutyl iodide **4**, (2*RS*,4*S*)-(+)-2,4-dimethylhexanoic acid **5** and its chloride **6** (for analytical data and spectra of **2** and **5**,

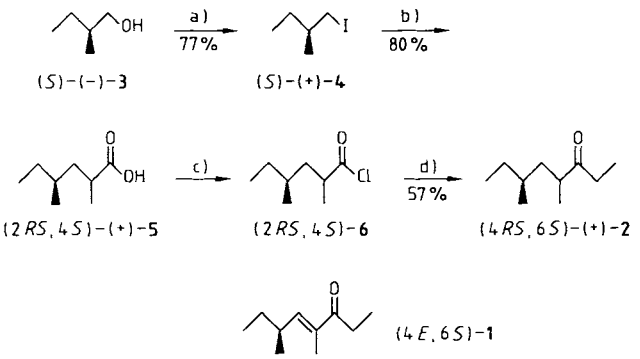

Scheme 1. a) I_2, $P(OPh)_3$, CH_2Cl_2, 0°C, 2 h; b) CH_3–CHLi–COOLi, tetrahydrofuran/hexamethylphosphoric triamide, −15°C, 2 h; c) $SOCl_2$, $CHCl_3$, 70°C, 2 h; d) $LiCuEt_2$, ether, −78°C, 45 min.

see Table 1). This (4*RS*,6*S*)-(+)-**2** corresponded to the isomers 1 and 4 of the racemic dihydromanicone **2**, as could be demonstrated by a co-injection of the two samples into the gas chromatograph (Fig. 1E; cf. Fig. 1C). The GC-mass spectra of the synthetic diastereomeric dihydromanicones (4*RS*,6*S*)-(+)-**2** were identical to those of the hydrogenation products of racemic manicone *rac*-**1** as well as to those of the diastereomeric reduction products of natural manicone, **1**, obtained from the insect heads (Table 1).

Table 1. Physical data of (4*RS*,6*S*)-**2** and (2*RS*,4*S*)-**5** [a].

2: IR (film): $\tilde{\nu}$ = 1735 cm^{-1} (s); ^{1}H-NMR ($CDCl_3$): δ = 0.60–2.00 (m, 17H), 2.10–2.85 (m, 3H); MS (70 eV): *m/z* 156 ($M^{\oplus}$, 0.3%), 127 (2), 99 (5), 86 (52), 71 (2), 69 (4), 57 (100), 43 (12), 41 (15); $[\alpha]_D^{25}$ = +10.3° (*c* = 4.90 in pentane); b.p. 76–78°C/18 torr (Kugelrohr)

5: IR (film): $\tilde{\nu}$ = 1710 cm^{-1} (s); ^{1}H-NMR ($CDCl_3$): δ = 0.80–2.10 (m, 14H), 2.20–2.90 (m, 1H), 12.25 (s, 1H); MS (70 eV): *m/z* 144 ($M^{\oplus}$, 2), 129 (2), 126 (4), 115 (23), 101 (24), 71 (98), 74 (100); $[\alpha]_D^{25}$ = +13.3° (*c* = 6.00 in CH_3OH); b.p. 81–83°C/0.5 torr (Kugelrohr)

[a] Correct elemental analyses.

Therefore it can be concluded that manicone **1** from *M. rubida* has (*S*)-configuration at C-6 and thus is present as (4*E*,6*S*)-4,6-dimethyl-4-octen-3-one.

Received: February 17, 1987 [Z 2107 IE]
German version: *Angew. Chem. 99* (1987) 784

[1] H. J. Bestmann, A. B. Attygalle, J. Schwarz, O. Vostrowsky, W. Knauf, *J. Chem. Ecol. 13* (1987), in press.
[2] H. M. Fales, M. S. Blum, R. M. Crewe, J. M. Brand, *J. Insect Physiol. 18* (1972) 1077.
[3] A. B. Attygalle, O. Vostrowsky, H. J. Bestmann, E. D. Morgan, M. C. Cammaerts in H. Rembold, J. Eder (Eds.): *Chemistry and Biology of Social Insects*. Johann Peperny, München, 1987.
[4] H. J. Bestmann, A. B. Attygalle, J. Glasbrenner, R. Riemer, O. Vostrowsky, M. G. Constantino, unpublished.
[5] V. Schurig, *Chromatographia 13* (1980) 263.
[6] Packard United Technologies 438A, 25 m × 0.2 mm FSCC OV101 with 0.1% nickel(II) bis[3-heptafluorobutyryl-(1*R*)-camphorate], 80°C isotherm, carrier gas N_2. Retention times of the four isomers of *rac*-**2**: 12.2, 12.47, 14.75, and 15.21 min. We thank Prof. Dr. *V. Schurig* (Tübingen) for lending us the GC column.
[7] A. B. Attygalle, M. Herrig, O. Vostrowsky, H. J. Bestmann, *J. Chem. Ecol. 13* (1987) 1299.
[8] E. D. Morgan, L. J. Wadhams, *J. Chromatogr. Sci. 10* (1972) 528.
[9] A. B. Attygalle, E. D. Morgan, *Anal. Chem. 55* (1983) 321.

Reduction of 2-Enoates and Alkanoates with Carbon Monoxide or Formate, Viologens, and *Clostridium thermoaceticum* to Saturated Acids and Unsaturated and Saturated Alcohols**

By *Helmut Simon,** *Hiltrud White, Herbert Lebertz,* and *Iordanes Thanos*

All the hitherto reported biological reductions of carboxylates to aldehydes proceed via an activation of the carboxy group. The carboxylate/aldehyde pair (with $E_0' \approx -550$ mV) has a large negative redox potential. The cosubstrates or prosthetic groups usually used by reductases have redox potentials of $E_0' = -320$ mV (pyridine nucleo-

[*] Prof. Dr. H. Simon, Dr. H. White, Dr. H. Lebertz, Dr. I. Thanos
Lehrstuhl für Organische Chemie und Biochemie
der Technischen Universität München
Lichtenbergstr. 4, D-8046 Garching (FRG)

[**] This work was supported by the Deutsche Forschungsgemeinschaft (SFB145) and the Fonds der Chemischen Industrie. We thank Herr *H. Leichmann* for excellent assistance and Dr. *P. Rauschenbach* and *F. Wendling* for carrying out the HPLC analyses.

tides) or up to $E_0' = -400$ mV (some flavoenzymes or iron-sulfur clusters). The activation usually consists in the formation of a thioester, which, as a rule, requires an ATP. These thioesters are reducible with NADH. We have now found a system that reduces carboxylates to alcohols and might also be preparatively useful. Due to the pH-dependence of the reduction, the undissociated acids could also be the substrates. The acids or carboxylates are apparently not activated. In this reduction the aldehyde must be an intermediate. The transition from aldehyde to alcohol is presumably catalyzed by another enzyme. Since a redox potential of -560 mV has been quoted for the carbon monoxide dehydrogenase occurring in *Clostridium thermoaceticum* which catalyzes the reaction[1]

$$CO + H_2O \longrightarrow CO_2 + 2H^{\oplus} + 2e^{\ominus}$$

we have incubated resting cells of this organism with unsaturated compounds in a CO-atmosphere. Hardly any reaction could be observed. However, if 1 mM methyl viologen is added to such a system[2] carbon monoxide is consumed and saturated and unsaturated carboxylates of diverse structures are reduced to alcohols. If no carboxylate or any other acceptor is added, then methanol is formed from the carbon monoxide (see Ref. [4]). In the case of 2-enoates the CC double bond and/or the carboxylate group can be reduced.

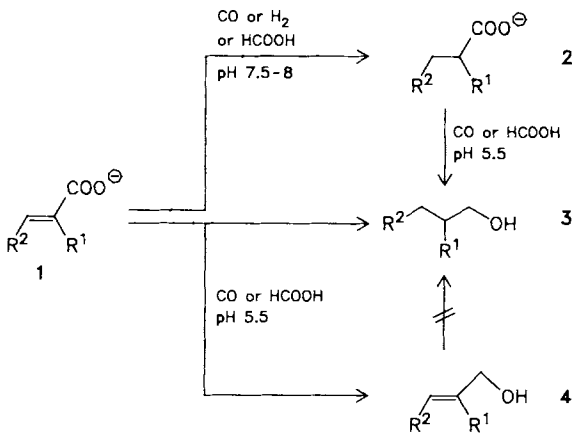

a, $R^1 = R^2 = CH_3$; b, $R^1 = CH_3$, $R^2 = C_6H_5$;
c, $R^1 = H$, $R^2 = CH_3-CH=CH$

Table 1 shows the large variety of substrates for the reduction of carboxylates. Both mono- as well as dicarboxylates are reduced and even such monocarboxylates as, e.g., 2-phenylbutyrate, the 2-position of which is occupied by very bulky groups. The relative rates in Table 1 should be regarded as approximate values, since not all reductions in a series were carried out in parallel experiments. The rate 100 signifies that about 30 μmol 1-propanol is formed per hour from propionate at 40°C under the given conditions.[2] At 50°C about 40 μmol per hour are formed. With *C. thermoaceticum*, reductions are also possible with hydrogen gas or formate as electron donors. Figure 1 and Table 2 show that the carboxylate group of **1a** is not attacked by any of the three reducing agents (CO, H_2, HCOOH) at pH 8.0. Due to the differing pH-dependence of the alkanoate- and enoate-reduction it is possible, e.g., to reduce an enoate at pH 7.5–8.0 with carbon monoxide first to the alkanoate **2**. After adjustment of the pH to 5.5, the saturated alcohol **3** can be obtained from **2** with formate or carbon monoxide. In this way (*R*)-2-methyl-3-phenyl-1-propanol **3b** and (*R*)-2-methyl-1-butanol **3a** can be obtained with *ee* values >95%.[5]

When an enoate **1** is reduced at pH 5.5 with CO a branching reaction ensues and a saturated alcohol **3** and

Fig. 1. pH-Dependence of the reduction of (*E*)-2-methyl-2-butenoate **1a** (30 μmol) with carbon monoxide at 40°C in the presence of 1 mM methyl viologen. **2a**, **3a**, and **4a** formed after 20 min: **2a** O—O, **3a** ●—●, **4a** ■—■.

Table 1. Substrates and their reduction products obtained under the given conditions at pH 5.5 with carbon monoxide. v_{rel} = relative rate.

Substrates	Products	v_{rel} [a]
Acetate	Ethanol	55
Propionate	1-Propanol	100
Butyrate	1-Butanol	65
(*E*)-2-Methyl-2-butenoate **1a**	2-Methyl-2-buten-1-ol **4a** and 2-Methyl-1-butanol **3a** [b]	60 110
(*R*)-2-Methylbutyrate **2a**	(*R*)-2-Methyl-1-butanol **3a**	—
(*R*)-2-Methyl-3-phenylpropionate **2b**	(*R*)-2-Methyl-3-phenyl-1-propanol **3b** [c]	—
(*R*)-Lactate	1,2-Propanediol [d]	10
(*S*)-Lactate	1,2-Propanediol [d]	7
Succinate	1,4-Butanediol	85
Glutarate	1,5-Pentanediol	106
Adipate	1,6-Hexanediol	175
Benzoate	Benzyl alcohol	115
(*R,S*)-2-Phenylbutyrate	(*S*)-2-Phenyl-1-butanol [e]	30
(*R,S*)-3-Phenylbutyrate	3-Phenyl-1-butanol [f]	20
3-Butenoate	3-Buten-1-ol	15
Sorbinate **1c**	Sorbinol **4c** and (*E*)-4-Hexen-1-ol	—

[a] For better comparison, the relative rates per electron pair are given. The formation of ethanol requires two, that of 2-methyl-1-butanol from (*E*)-2-methylbutenoate three, and that of 1,4-butanediol from succinate four electron pairs. [b] The saturated alcohol can also be obtained quantitatively (see next example). [c] **3b** was obtained with the same cells from **1b** and H_2 at pH 7; >95% *ee*, since stepwise reduction **1b**→**2b**→**3b**. [d] Enantiomeric excess not determined. [e] 62% *ee*. [f] The enantiomers were formed in the ratio 65:35.

Table 2. Reduction products [μmol] obtained after 20 min at 40°C from (*E*)-2-methyl-2-butenoate **1a** (100 μmol) as a function of the reducing agents hydrogen gas or formate at pH 5.0 or 8.0 in the presence of 80 mg (dry weight) of *C. thermoaceticum*. Total volume 3.0 mL; 0.3 M buffer.

Products		**2a**		**4a**		**3a**	
pH		5.0	8.0	5.0	8.0	5.0	8.0
Reducing agent:	H_2	1.5	1.5	0.3	0.1	0.05	0.1
	Formate	7.0	1.7	7.0	0.1	4.0	0.05

an allyl alcohol derivative which is not reduced further are formed. Sorbinate **1c** could be reduced under the given conditions[2] to more than 80% to sorbic alcohol **4c**, thus demonstrating the high chemoselectivity of the reduction of enoates **1**.

The rates of reduction of (*R,S*)-**2a** and (*S*)-**2a** in a CO atmosphere are in the ratio 1.6 : 1.0. In the case of the (*R*)- and (*S*)-lactate the ratio is 1.4 : 1.0.

This means that the reduction of enoates **1** with CO, which so far has not even been described in the literature, shows a high degree of product enantioselectivity for the formation of the alkanoates **2**. The reduction of a racemic alkanoate of type **2a** or **2b** to the alcohol **3**, on the other hand, is not highly stereoselective.

The special importance of the reduction under discussion lies in the fact that neither chemical nor biocatalyzed reactions have hitherto been described by which reductions of carboxylates occur in aqueous solution. In the case of the previously described examples[6–9] it is known that either the carboxylates are activated in an intermediary step or that activation is very likely under the conditions employed.

That the carboxylates are not activated in the usual way prior to the reduction can be concluded from the following findings: 1) the reaction even takes place in phosphate-free buffers with washed, resting cells, whereby 80 mg of cells (dry weight) reduce more than 430 μmol propionate to 1-propanol. The reaction presumably ceases because the pH value, despite the buffer, drops to 4.2 due to concomitant formation of formic acid. If in the meantime the pH value of 5.5 is reestablished, up to 1520 μmol of 1-propanol can be obtained. If the activation were to be brought about by degradation of endogenous material, the cells would have to consist by more than a half of carbohydrates for the formation of 430 μmol of 1-propanol, and there would be corresponding amounts of acetate to be expected. Such an experiment however gave less than 5% of the acetate expected. In addition the enzymes necessary for the activation were not found. 2) When an ultrafiltrated crude extract is employed, from which more than 95% of all compounds with a molecular weight smaller than 5000 are removed, then almost the same rate of reduction is obtained. Furthermore, lipid membranes are not necessary since the carboxylate group is still reduced after two column chromatographic separations of the crude extract. Consequently, a reduction of acyl-CoA as in the formation of 1-butanol from butyrate, e.g. by *Clostridium acetobutylicum*,[6–8] is not involved. The substrate specificity of the acyl-CoA reductase involved is also very limited.[6] The recently observed increase in butanol formation from butyrate by *C. acetobutylicum* in the presence of CO can be rationalized by the inhibitory effect of CO on the hydrogenase. Therefore, since the reduction equivalents cannot be released in the form of H_2 they are instead consumed for the reduction of acyl-CoA.[8] Carbon monoxide reductase purified by us exhibits no alkanoate and enoate reductase activity. Consequently, the reduction of carboxylates of very different structures appears to be an hitherto unknown enzyme reaction. The reduction described by *Howe* et al.[9] of 2-(4-chlorophenyl)thiazol-4-ylacetic acid to the corresponding alcohol by different microorganisms is carried out with growing cells. The authors postulate a mechanism corresponding to that of the formation of cinnamyl alcohol, i.e. by the sequence cinnamate → cinnamoyl-CoA → cinnamaldehyde → cinnamyl alcohol. In addition, the reductions described by *Howe* et al.[9] proceed with about 1% of the rate with which, e.g., 2-phenyl-1-butanol is formed from 2-phenylbutyrate by resting cells of *C. thermoaceticum* without the supply of energy yielding substrates.

Received: March 2, 1987;
supplemented: April 1, 1987 [Z 2120 IE]
German version: *Angew. Chem. 99* (1987) 785

[1] G. Diekert, G. Fuchs, R. K. Thauer, *Spec. Publ. Soc. Gen. Microbiol. 14* (1985) 115, and references cited therein.

[2] A Warburg flask under CO atmosphere, which was shaken at 40°C, contained in a total volume of 3.0 mL 0.3 M buffer (pH 5.5), 80 mg (dry weight) *Clostridium thermoaceticum* [3], 10–500 mM substrate, and 1 mM methyl viologen. When using formate as reducing agent the reaction was carried out under N_2.

[3] The cultivation of the cells was carried out on a 200 L scale according to the method of L. G. Ljungdahl, J. R. Andresen, *Methods Enzymol. 53* (1978) 360.—4 h and 0.5 h prior to harvesting, 5 mM glucose, 5 mM formic acid, 26 mM $NaHCO_3$, and 0.03 mM ferrous ammonium sulfate were again added to the mixture.

[4] H. White, H. Lebertz, I. Thanos, H. Simon, *FEMS Microbiol. Lett.*, in press.

[5] **3a** and **3b** were prepared on a 10 mmol and 1.5 mmol scale; finally, the values of optical rotation were measured. The enantiomeric excess of (*R*)-**3b** was also determined on a Chiral I column (Machery and Nagel). These columns separate both enantiomers very well.

[6] J. B. Jewell, J. B. Coutinho, A. M. Kropinski, *Curr. Microbiol. 13* (1986) 215.

[7] M. G. N. Hartmanis, T. Klason, S. Gatenbeck, *Appl. Microbiol. Biotechnol. 20* (1984) 66.

[8] C. L. Meyer, J. W. Roos, E. T. Papoutsakis, *Appl. Microbiol. Biotechnol. 24* (1986) 159.

[9] R. Howe, R. H. Moore, B. S. Rao, A. H. Wood, *J. Med. Chem. 15* (1972) 1040.

$[(\eta^5\text{-}C_5Me_5)Re(CH_3)_4]$, the First Organorhenium(V) Compound without Heteroatom Ligands**

By *Martina Flöel, Eberhardt Herdtweck, Werner Wagner, Jürgen Kulpe, Peter Härter*, and *Wolfgang A. Herrmann**

Despite a plethora of oxidation states encountered with the element rhenium, the explosive hexamethylrhenium, $Re(CH_3)_6$, has thus far remained the only homoleptic alkyl derivative of this metal.[1] The paramagnetic compound (d^1 configuration) is formed, according to *Wilkinson* et al., on reaction of trimethylaluminum with tetramethyl(oxo)rhenium and can be converted with methyllithium into the presumably square-antiprismatic Re^{V1}-dianion $[Re(CH_3)_8]^{2\ominus}$ (ESR and PE data);[2,3] however, the only species whose structure has been established unequivocally is the Re^{III}-dianion $[Re_2(CH_3)_8]^{2\ominus}$.[4] Interestingly, pentamethylrhenium is unknown, and even the so-called "trimethylrhenium" postulated by *Druce* in 1934[5a] could not be reproduced by *Gilman* et al.[5b] We have now succeeded in synthesizing **3a**, the first organorhenium(V) compound containing no heteroatom ligands.

The title compound **3a** is formed in 40–50% yield when the tetrachloro complex **2**—accessible from the trioxide **1**—is allowed to react with exactly 4.0 molar equivalents of methylmagnesium chloride in tetrahydrofuran (THF) at

[*] Prof. Dr. W. A. Herrmann, M. Flöel, Dr. E. Herdtweck, W. Wagner, J. Kulpe, Dr. P. Härter
Anorganisch-chemisches Institut der Technischen Universität München
Lichtenbergstrasse 4, D-8046 Garching (FRG)

[**] Part 66 in the series "Transition Metal Methylene Complexes." This work was supported by the Deutsche Forschungsgemeinschaft (Leibniz Program), the Fonds der Chemischen Industrie, and the Bundesministerium für Forschung und Technologie.—Part 65: W. E. Geiger, T. Gennett, W. K. McVicar, W. A. Herrmann, *Inorg. Chem.*, in press.

$-78\,^{\circ}C$ under scrupulous exclusion of light, air, and moisture. After purification of the crude product by column chromatography at $-30\,^{\circ}C$, low-temperature crystallization furnishes brilliant-red platelets which can be stored for some time, but only at the temperature of dry ice.

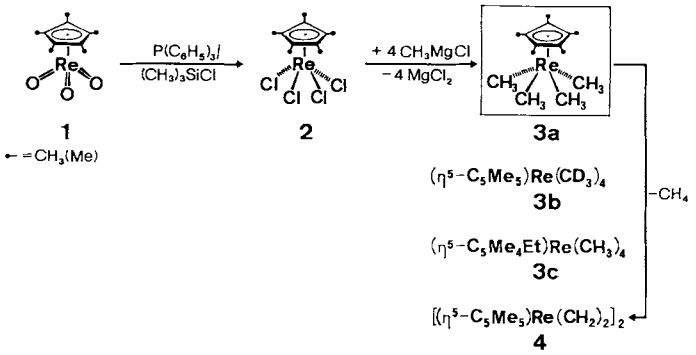

3a decomposes slowly at room temperature and very rapidly at 68 °C. The thermal decomposition is, according to a GC/MS study, determined by stepwise selective eliminations of methane; up to the decomposition point, exactly 2.0 molar equivalents of CH_4 are liberated.[6] Thereby, the mass-spectroscopically characterized dinuclear tetramethylene complex **4** is formed as coupling product of the formal monomeric precursor fragment of composition $\{(\eta^5\text{-}C_5Me_5)Re(CH_2)_2\}$.[7] At ca. 160 °C, another 0.5 equivalents of CH_4 are cleaved off. Other hydrocarbons are at most formed in only trace amounts in these thermolyses (C_2H_6 0.5%). Consequently, **3a** can be sublimed at room temperature under high vacuum only with drastic losses.

Methane is also eliminated from **3a** in solution, as confirmed by the ^{1}H-NMR signal appearing at $\delta = 0.17$ above ca. 0 °C ([D$_8$]toluene). UV irradiation of *n*-pentane solutions leads to comparable results.

Elemental analysis and the EI mass spectrum[7] confirm the empirical molecular formula $C_{14}H_{27}Re$ of **3a**. Because of the thermal sensitivity of **3a**, NMR spectra can be obtained only at low temperatures. The ^{1}H-NMR spectra show only a single, somewhat broadened signal ($\delta = 15.2$; [D$_8$]toluene, $-40\,^{\circ}C$), whose position is temperature-dependent. It could be established by control measurements that the signal is due to the ring CH_3 groups: the [D$_{12}$]-derivative **3b** synthesized in an analogous way from **2** and [D$_3$]methylmagnesium iodide (>99% D) furnished, in principle, the same ^{1}H-NMR spectrum ($\delta(CCH_3) = 17.2$, singlet; [D$_8$]toluene, $-40\,^{\circ}C$), whereas the complex **3c** afforded a correspondingly modified signal pattern.[8] The methyl groups on the metals are not traceable in the shift region $-200 \cdots +200$ ppm in any of the complexes **3**. This is true also in the case of the ^{13}C-NMR spectra, in which none of the carbon atoms bound directly to the metal atom are visible (**3a**: $\delta(CCH_3) = 56.16$; **3c**: $\delta(CCH_3) = 62.00$ and 54.00, $\delta(C_2H_5) = 41.98$ and 40.84, [D$_8$]toluene, $-80\,^{\circ}C$). Taking into consideration earlier observations on organorhenium(v) complexes[9] we rationalize these findings with the paramagnetic effects of a triplet state of the d^2 configuration of the pentavalent rhenium. In the ^{1}H-NMR spectra of the related Re^V-complex $[(\eta^5\text{-}C_5Me_5)ReCl_3CH_3]$ the CH_3 groups bound to the metal can, on the contrary, be observed; but once again the signal is strongly temperature-dependent ($\delta = 13.5$ at $-50\,^{\circ}C$ and 36.5 at $+50\,^{\circ}C$ in $CDCl_3$).[10]

With respect to the molecular structure, no reliable bond distances and angles can be given because of disorder problems, but, according to a low-temperature X-ray structure analysis (Fig. 1), crystalline **3a** has a square-pyramidal structure like $[(\eta^5\text{-}C_5Me_5)ReCl_3CH_3]$.[10] The Re–C(1...4) distances, which on average are 217(3) pm, and the CH_3,Re,CH_3 angles ($4 \times 82(1)^{\circ}$; $2 \times 136(1)^{\circ}$) correspond to those found in the dianion $[Re_2(CH_3)_8]^{2\ominus}$.[4]

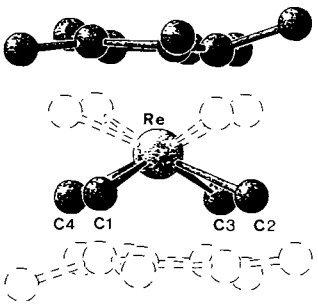

Fig. 1. Molecular structure (SCHAKAL drawing) of **3a** in the crystal (hydrogen atoms omitted; view parallel to the twofold axis [0, y, 1/4]; the same molecule rotated through 180° about Re is shown in dotted lines [11].—Further details of the crystal structure investigation are available on request from the Fachinformationszentrum Energie, Physik, Mathematik GmbH, D-7514 Eggenstein-Leopoldshafen 2 (FRG) on quoting the depository number CSD-52581, the names of the authors, and the journal citation.

Experimental

3a: A solution of methylmagnesium chloride (3.48 mmol) in THF (50 mL) was treated at $-78\,^{\circ}C$ with 400 mg (0.87 mmol) of **2**. Within a few minutes, the solution turned red. After warming to $-15\,^{\circ}C$ (ice/sodium chloride) the solvent was removed at this temperature under vacuum. The residue was purified by column chromatography (silanized silica gel, 0.063–0.200 mm, Merck 77719; $-30\,^{\circ}C$), **3a** separating as a brilliant red zone on elution with *n*-pentane. Crystallization of the eluate residue (*n*-pentane) afforded analytically pure **3a** as red crystals; these decomposed spontaneously at 68 °C under inert gas in a sealed capillary; typical yields: 130–165 mg (40–50%).

Received: March 23, 1987;
supplemented: May 11, 1987 [Z 2153 IE]
German version: *Angew. Chem. 99* (1987) 787

[1] N. M. Boag, H. D. Kaesz in G. Wilkinson, F. G. A. Stone, E. W. Abel (Eds.): *Comprehensive Organometallic Chemistry, Vol. 4*, Pergamon Press, Oxford 1982, p. 161 ff.

[2] K. Mertis, G. Wilkinson, *J. Chem. Soc. Dalton Trans. 1975*, 607; *1976*, 1488.

[3] a) J. F. Gibson, G. M. Lack, K. Mertis, G. Wilkinson, *J. Chem. Soc. Dalton Trans. 1976*, 1492; b) J. C. Green, D. R. Lloyd, L. Galyer, K. Mertis, G. Wilkinson, *ibid. 1978*, 1403.

[4] F. A. Cotton, L. D. Gage, K. Mertis, L. W. Shive, G. Wilkinson, *J. Am. Chem. Soc. 98* (1976) 6922.

[5] a) J. F. Druce, *J. Chem. Soc. 1934*, 1129; b) H. Gilman, R. G. Jones, F. W. Moore, M. Y. Kobezan, *J. Am. Chem. Soc. 63* (1941) 2525.—The compound concerned is presumably a polymer having the formula $[Re_3(CH_3)_9]_\infty$; cf. [1].

[6] Hewlett-Packard 5890 gas chromatograph with MSD 5970 mass-selecting detector.—Fused silica capillary column, Al_2O_3/KCl; internal diameter 0.32 mm, length 50 m; temperature program: 5 min at 50 °C, 10 °C/min, T_i 180 °C.

[7] EI-MS (70 eV; ^{187}Re): **3a**: *m/z* 382 ($M^{\oplus}$), 367 ($[M-CH_3]^{\oplus}$), 342 ($[M-2CH_3]^{\oplus}$), 337 ($[M-3CH_3]^{\oplus}$).—**4**: *m/z* 698 ($M^{\oplus}$) with correct isotopic pattern.—The mass lines of the molecular ion of **4** do not appear in the mass spectrum of **3a** at low inlet temperature ($T_i = 10\,^{\circ}C$), but gains in intensity on increasing the temperature of the source.—The synthesis of pure **4** by directed thermolysis has so far not been achieved, presumably because of the sensitivity of **4** towards conventional chromatographic carrier materials. The thermal degradation of the CD_3-derivative **3b** shows, however, that almost exclusively the CH_3 and CD_3 groups bound directly to the metal are cleaved; when **3b** is heated between 30 and 68 °C for 1 h, the vapor space contains 90% CD_4(!) and only 10% CD_3H; cf. Ref. [6].

[8] **3c**, ^{1}H-NMR ([D$_8$]toluene, −80°C): δ(CH$_3$) (ring) = 10.95 and 10.11 [2 × 6 H], δ(CH$_2$) = 2.29 [2 H], δ(CH$_3$) (C$_5$H$_5$) = 4.30 [3 H]; all signals are broadened, so ^2J(H,H)-couplings do not appear.

[9] Summaries: a) W. A. Herrmann, *J. Organomet. Chem. 300* (1986) 111; b) W. A. Herrmann, E. Herdtweck, M. Flöel, J. Kulpe, U. Küsthardt, J. Okuda, *Polyhedron 6* (1987) 1165; c) J. Okuda, W. A. Herrmann, *J. Mol. Catal. 41* (1987) 109.

[10] W. A. Herrmann, J. K. Felixberger, E. Herdtweck, A. Schäfer, J. Okuda, *Angew. Chem. 99* (1987) 466; *Angew. Chem. Int. Ed. Engl. 26* (1987) 466.

[11] **3a**: Red platelets from *n*-hexane at −78°C; orthorhombic, space group $P222_1$ (No. 17), $Z = 2$, $a = 674(1)$, $b = 773(1)$, $c = 1401(1)$ pm; $V = 730 \times 10^6$ pm^3; $T = 173$ K; $\rho_{calc} = 1.74$ g·cm^{-3}. Re occupies the special position 2c, giving rotational symmetric positions for the methyl groups and the C$_5$Me$_5$ ligand. Superstructure reflections and doubling of an axis were not observed. 586 measured reflections, 482 independent reflections with $I > 1\sigma(I)$; Enraf-Nonius CAD4, graphite monochromator, ω-scan, $2° < \theta < 18°$; $h \pm 5$, $k + 6$, $l + 12$; $F_{000} = 372$. Solution and refinement by Patterson and difference Fourier methods, anisotropic temperature factor for Re, common isotropic temperature factors for C(1...4) and C(11...15), individual isotropic temperature factors for methyl carbons C(21...25) at the ring ligands, anomalous dispersion taken into consideration, empirical absorption correction $\mu = 84.2$ cm^{-1}; $R = \Sigma||F_o| - |F_c||/\Sigma|F_o|$: 0.040; $R_w = [\Sigma w(|F_o| - |F_c|)^2/\Sigma w|F_o|^2]^{1/2}$: 0.046. Number of parameters: 55.—Shift/error: < 0.00 in the last cycle of refinement; residual electron density: + 1.52 e/Å^3. Hydrogen atoms were not considered.

Pentabenzylcyclopentadienylthallium(I): Synthesis and Structure of a "Dimeric" Organothallium Compound with Tl–Tl Interaction**

By *Herbert Schumann,* Christoph Janiak, Joachim Pickardt,* and *Ute Börner*

Cyclopentadienylthallium is valued as a mild reagent for the synthesis of difficultly isolable cyclopentadienyl derivatives of main group elements, transition metals, and lanthanoids.[1,2] In fact, some organometallic compounds with substituted cyclopentadienyl ligands can only be obtained from the corresponding cyclopentadienylthallium(I) reagents.[3] The preparative potential of these reagents is, however, limited, owing to their very different stabilities and solubilities, which depend on the ring substituents and are, in turn, also influenced by the molecular and crystal structures of the compounds. So far, however, X-ray structure analyses have been carried out only on C_5H_5Tl[4] and $(C_5Me_5)Tl$;[5] both compounds have a polymeric structure of zig-zag chains.

We have now been able for the first time to obtain a cyclopentadienylthallium(I) compound in dimeric form in the solid state, namely pentabenzylcyclopentadienylthallium(I) (**1**). Compound **1** is formed in two, reversibly interconvertible, air- and light-stable modifications upon addition of thallium ethoxide to pentabenzylcyclopentadiene in hexane[6] [Eq. (a)].

$$(C_6H_5CH_2)_5C_5H + TlOC_2H_5 \xrightarrow{-C_2H_5OH} \underset{\mathbf{1}}{[\{\eta^5\text{-}(C_6H_5CH_2)_5C_5\}Tl]} \quad (a)$$

The rapidly crystallizing needles exhibit a chain structure,[8] whereas the slowly crystallizing, thermodynamically more stable parallelepipeds exhibit a new type of structure (Fig. 1). According to an X-ray structure analysis[9] the two halves of the quasi-dimeric molecule are coupled to each other via a symmetry center between the two Tl atoms. The distance between the two Tl atoms is 3.632 Å, which is far too large for a conventional bonding. However, as in $[In_6(C_5Me_5)_6]$,[10] a bonding interaction is also essential in **1** in order to counteract an electronic repulsion of the $[(C_6H_5CH_2)_5C_5]Tl$ dipole terminals. A comparison with the interactions in d^{10}–d^{10} transition metal complexes such as Cu^I–Cu^I [11] and Au^I–Au^I complexes,[12] which had been interpreted theoretically in terms of an $s + p_z + d_{z^2}$ "mixing",[13] was called for.

The angle of 131.8° at the thallium (ring center-Tl1-Tl1*) is somewhat smaller than the Cp-Tl-Cp angle (Cp = C_5H_5 or C_5Me_5) in the polymeric compounds $(C_5H_5)Tl$ (137°)[4] and $(C_5Me_5)Tl$ (145°, mean value).[5] The C-Tl distances in **1** (Tl1-ring center 2.490 Å) are smaller than the distances in $(C_5H_5)Tl$ (3.19 Å) and $(C_5Me_5)Tl$ (2.71 Å), indicating an increased covalent character of the Cp–Tl bond in **1**. Remarkably, three of the five benzyl groups of a cyclopentadienyl ring in **1** are oriented toward the thallium atoms. The extrapolated surfaces of the total of six phenyl groups in a "dimeric" unit form a parallelepiped which envelops the two thallium atoms (Fig. 1, bottom). The smallest phenyl carbon–thallium distances are

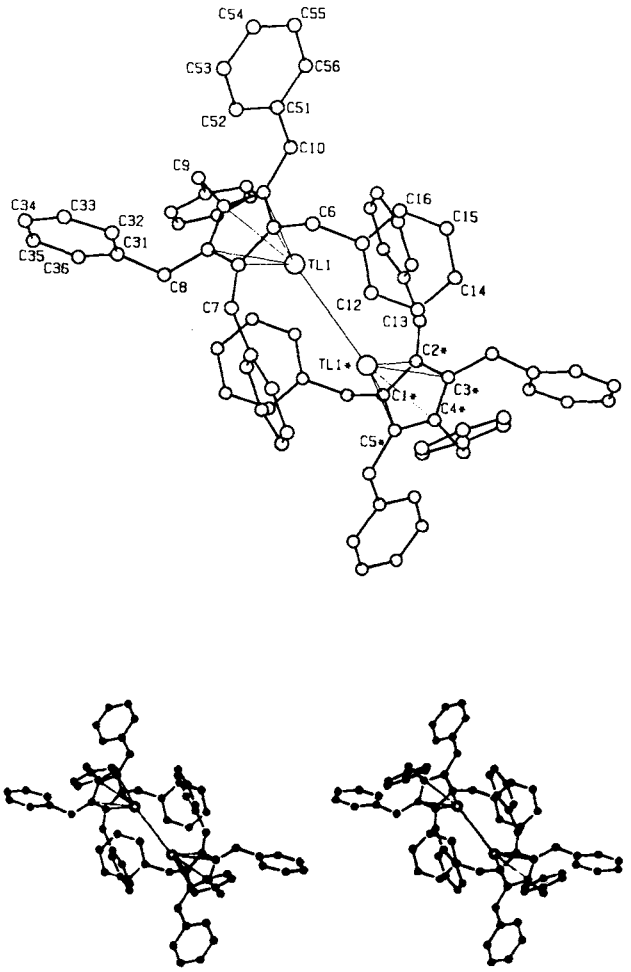

Fig. 1. Top: crystal structure of **1**. Selected bond lengths [Å] and angles [°]: Tl1-C1 2.753(6), Tl1-C2 2.808(7), Tl1-C3 2.816(6), Tl1-C4 2.749(7), Tl1-C5 2.704(6), Tl1-ring center 2.490, Tl1-Tl1* 3.632, ring center-Tl1-Tl1* 131.82.—Bottom: Stereodiagram of the structure of **1**.

[*] Prof. Dr. H. Schumann, Dr. C. Janiak, Prof. Dr. J. Pickardt, U. Börner
Institut für Anorganische und Analytische Chemie
der Technischen Universität Berlin
Strasse des 17. Juni 135, D-1000 Berlin 12

[**] This work was supported by the Fonds der Chemischen Industrie and the Deutsche Forschungsgemeinschaft.

those of the *meta*-C atoms to the other thallium of the quasi-dimeric unit (Tl1* -C13 3.495 Å; Tl1* C23 3.410 Å). A comparable protective shield arrangement of the benzyl groups was also found by us in the air-stable complexes decabenzyl-germanocene, -stannocene, and -plumbocene.[14]

Received: May 23, 1987 [Z 2155 IE]
German version: *Angew. Chem. 99* (1987) 788

CAS Registry numbers:
1, 109531-29-5; $(C_6H_5CH_2)_5C_5H$, 67209-29-4; $TlOC_2H_5$, 20398-06-5; Tl, 7440-28-0.

[1] A. G. Lee, *Organomet. React. 5* (1975) 1.
[2] G. B. Deacon, A. J. Koplick, T. D. Tuong, *Aust. J. Chem. 37* (1984) 517.
[3] D. G. Gassman, C. H. Winter, *J. Am. Chem. Soc. 108* (1986) 4228.
[4] E. Frasson, F. Menegus, C. Panattoni, *Nature London 199* (1963) 1087; J. F. Berar, G. Calvarin, C. Pommier, D. Weigel, *J. Appl. Crystallogr. 8* (1975) 386.
[5] H. Werner, H. Otto, H. J. Kraus, *J. Organomet. Chem. 315* (1986) C 57.
[6] Procedure: A solution of thallium ethoxide (0.68 g, 2.70 mmol) in hexane (1 mL) was added dropwise within 15 min at room temperature to a stirred solution of pentabenzylcyclopentadiene [7] (1.40 g, 2.70 mmol) in hexane (40 mL). The solution turned yellow and a fine precipitate separated out. After a further 10 minutes' stirring the solution was allowed to stand before decanting off the clear yellow solution. After careful evaporation of the solution and cooling with ice, 0.95 g (49%) of needle-like crystals separated out. After careful evaporation of the mother liquor and subsequent storage, 0.51 g (26%) of large, yellow, parallelepipedal crystals separated out. These are also obtainable on slow recrystallization of the needles from toluene/hexane. Both modifications darken at 60°C, and soften at 80°C; the needles melt at 133–136°C, the parallelepipeds at 137–140°C. Characterization by complete elemental analysis, IR, Raman, and mass spectra. ^{1}H-NMR (C_6D_6, 25°C): $\delta = 3.93$ (d, 10 H, CH_2, $^3J(TlH) = 10.7$ Hz), 7.19 (m, 25 H, C_6H_5).
[7] S. S. Hirsch, W. J. Bailey, *J. Org. Chem. 43* (1978) 4090.
[8] H. Schumann, C. Janiak, M. Khan, J. J. Zuckerman, unpublished.
[9] **1**: monoclinic, $P2_1/c$, $a = 10.288(3)$, $b = 15.858(4)$, $c = 18.890(6)$ Å, $\beta = 91.23(3)°$, $V = 3081.1$ Å^3, $Z = 4$, $Mo_{K\alpha}$ radiation, $\omega/2\theta$ scans, data reduction with Lorentz and polarization corrections, no absorption correction. The structure was solved by Patterson methods. 7415 independent reflections, 4473 with intensities $I \geq 2\sigma(I)$ used for the structure determination. $R = 0.0386$, $R_w = 0.0350$. Further details of the structure determination are available on request from the Fachinformationszentrum Energie, Physik, Mathematik GmbH, D-7514 Eggenstein-Leopoldshafen 2 (FRG), on quoting the depository number CSD-52453, the names of the authors, and the journal citation.
[10] O. T. Beachley, M. R. Churchill, J. C. Fettinger, J. C. Pazik, L. Victoriano, *J. Am. Chem. Soc. 108* (1986) 4666.
[11] A. Camus, N. Marsich, G. Nardin, L. Randaccio, *Inorg. Chim. Acta 23* (1977) 131; J. P. Fackler, *Prog. Inorg. Chem. 21* (1976) 55.
[12] H. Schmidbaur, T. Pollock, R. Herr, F. E. Wagner, R. Bau, J. Riede, G. Müller, *Organometallics 5* (1986) 566.
[13] P. K. Mehrotra, R. Hoffmann, *Inorg. Chem. 17* (1978) 2187; Y. Jiang, S. Alvarez, R. Hoffmann, *ibid. 24* (1985) 749.
[14] H. Schumann, C. Janiak, E. Hahn, J. Loebel, J. J. Zuckerman, *Angew. Chem. 97* (1985) 765; *Angew. Chem. Int. Ed. Engl. 24* (1985) 773; H. Schumann, C. Janiak, E. Hahn, C. Kolax, J. Loebel, M. D. Rausch, J. J. Zuckerman, *Chem. Ber. 119* (1986) 2656.

Substituted α-Pyrones as Starting Compounds for the Synthesis of 4,4-Disubstituted 1,4-Dihydropyridines

By *Vratislav Kvita** and *Hans-Peter Sauter*

Following the discovery that some 4-aryl-1,4-dihydropyridines are highly effective calcium antagonists,[1] numerous papers reporting the synthesis of derivatives of this class of substances appeared in the literature over a relatively short period of time. However, the derivatizations were for a long time restricted to the phenyl group and to C-2 and C-3 of the 1,4-dihydropyridine ring. 4,4-Disubstituted 1,4-dihydropyridines were not obtainable via the methods being used at the time.

The first synthetic method affording access to 4,4-disubstituted 1,4-dihydropyridines was that reported by *Goldmann*,[2] but even this method is not generally applicable; for instance, compounds with the mostly desired 2- or 3-nitrophenyl groups on C-4 cannot by synthesized by this method.

Starting from the α-pyrone derivative we have now obtained, via a new synthetic strategy, a 4-methyl-4-(3-nitrophenyl)-1,4-dihydropyridine which combines all the structural moieties which have previously proven to be advantageous.

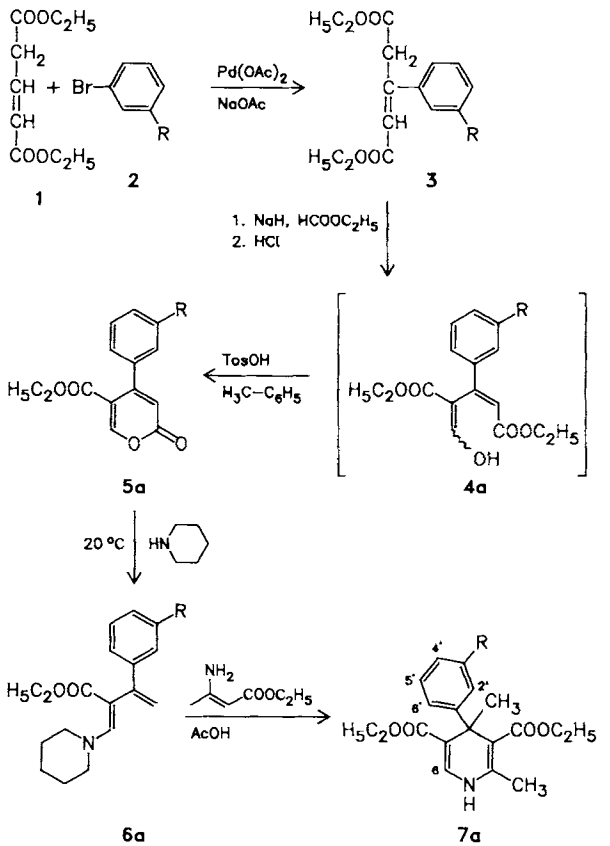

a, R = NO_2; b, R = $COCH_3$; c, R = $COOC_2H_5$

The diethyl 3-(3-nitrophenyl)-2-pentenedicarboxylate **3a** was prepared from diethyl glutaconate **1** and 1-bromo-3-nitrobenzene **2a** by a Heck reaction.[3] It was then formylated to **4a** and cyclized in toluene in the presence of a catalytic amount of toluenesulfonic acid to give the diethyl 4-(3-nitrophenyl)-1,4-dihydropyridine-3,5-dicarboxylate **5a**, which was allowed to react with piperidine at room temperature to furnish, via cleavage of CO_2, ethyl 3-(3-nitrophenyl)-2-piperidinomethylene-3-butenoate **6a**.[4] This was then cyclized with ethyl 3-aminocrotonate to diethyl 2,4-dimethyl-4-(3-nitrophenyl)-1,4-dihydropyridine-3,5-dicarboxylate **7a**. Also 3-Bromoacetophenone **2b** and ethyl 3-bromobenzoate **2c** react similarly to 1-bromo-3-nitrobenzene **2a**.

[*] Dr. V. Kvita, H.-P. Sauter
Zentrale Forschungslaboratorien und
Zentrale Funktion Forschung Physik der Ciba-Geigy AG
Rosental, CH-4002 Basel (Switzerland)

Experimental

3a: A solution of **2a** (45.25 g, 0.224 mol) in dimethylformamide (DMF) (90 mL) was added dropwise within 2 h to a stirred mixture of **1** (50.22 g, 0.27 mol), palladium(II) acetate (5.03 g, 0.0224 mol), sodium acetate (20.26 g, 0.247 mol), and DMF (54 mL) at 115°C. After heating for a further 8 h at 130°C, the mixture was evaporated to dryness under vacuum and the residue taken up in CH_2Cl_2 and water. The resulting solution was filtered over Hyflo Supercel (Fluka); the CH_2Cl_2 phase was separated off, washed with water, dried over Na_2SO_4, and evaporated to dryness. Unchanged **1** was removed by distillation at 100–110°C/10^{-2} torr, and the residue then chromatographed on a column (3000 g silica gel 60, Merck; eluent CH_2Cl_2). After evaporation under vacuum there remained **3a** as a yellow oil, which soon completely crystallized. Yield 34.5 g (50%), m.p. 47°C, b.p. 170°C/10^{-2} torr (Kugelrohrofen). Correct elemental analysis. IR (CH_2Cl_2): $\tilde{\nu}$ = 1735 (s), 1715 (s), 1640 (m), 1530 (s), 1350 (s), 1180 (s). ^{1}H-NMR ($CDCl_3$): δ = 8.30 (t, 1H), 8.22 (dd, 1H), 7.76 (dd, 1H), 7.58 (t, 1H), 6.30 (s, 1H), 4.22 (q, 2H), 4.18 (s, 2H), 4.13 (q, 2H), 1.28 (t, 3H), 1.18 (t, 3H).

3b and **3c** are obtained analogously to **3a** from **1** and **2b** or **2c**: **3b**: yield 57%, viscous oil, b.p. 154°C/10^{-2} torr (Kugelrohrofen). Correct elemental analysis. IR (CH_2Cl_2): $\tilde{\nu}$ = 1730 (s), 1710 (s), 1680 (s), 1630 (m). ^{1}H-NMR ($CDCl_3$): δ = 7.99 (t, 1H), 7.90 (dd, 1H), 7.60 (dd, 1H), 7.44 (t, 1H), 6.28 (s, 1H), 4.18 (q, 2H), 4.16 (s, 2H), 4.08 (q, 2H), 2.58 (s, 3H), 1.26 (t, 3H), 1.14 (t, 3H).—**3c**: Yield 32%, viscous oil, b.p. 160°C/10^{-2} torr (Kugelrohrofen). Correct elemental analysis. IR (CH_2Cl_2): $\tilde{\nu}$ = 1720 (s), 1710 (s), 1630 (m). ^{1}H-NMR ($CDCl_3$): δ = 8.08 (t, 1H), 7.98 (dd, 1H), 7.58 (dd, 1H), 7.39 (t, 1H), 6.26 (s, 1H), 4.32 (q, 2H), 4.15 (q, 2H), 4.14 (s, 2H), 4.07 (q, 2H), 1.34 (t, 3H), 1.25 (t, 3H), 1.14 (t, 3H).

5a: A suspension of 11.7 g (0.39 mol) of NaH (80% in oil), in ether (200 mL) was treated with 55.5 g (0.75 mmol) of ethyl formate. After 2 hours' stirring a solution of **3a** (46.1 g, 0.15 mol) in ether (150 mL) was added dropwise within 2 h. After H_2-evolution had subsided (1–2 h), the reaction mixture was poured onto 300 g of ice in 60 mL of conc. HCl. The ether layer was separated off and the aqueous phase was extracted with CH_2Cl_2. The combined extracts were finally washed with water and, after drying over Na_2SO_4, evaporated to dryness. The residue was chromatographed on a column (1700 g silica gel 60, Merck; eluent CH_2Cl_2). The product **4a** was dissolved without purification in 130 mL of toluene, treated with 0.2 g of TosOH, and the solvent slowly distilled off. The solution of the residue in $CHCl_3$ was washed with 2% aqueous $NaHCO_3$, dried over $MgSO_4$, and evaporated to dryness. The (initially) oily **5a** crystallized out and was washed with Et_2O. Yield 13 g (30%), m.p. 155°C, correct elemental analysis. IR ($CHCl_3$): $\tilde{\nu}$ = 1750 (s), 1730 (s), 1630 (m), 1530 (s), 1350 (s). ^{1}H-NMR ($CDCl_3$): δ = 8.35 (s, 1H), 8.28 (m, 1H), 8.15 (m, 1H), 7.63 (m, 1H), 7.58 (m, 1H), 6.25 (s, 1H), 4.15 (q, 2H), 1.13 (t, 3H).

7a: A suspension of **5a** (1.445 g, 0.005 mol) in acetonitrile (8 mL) was treated with 0.43 g (0.005 mol) of piperidine and the mixture stirred at room temperature for 17 h. Evolution of CO_2 was accompanied by formation of **6a**, which was evaporated down at 40°C, treated with a solution of diethyl aminocrotonate (1.94 g, 0.015 mol) in acetic acid (0.3 g, 0.005 mol) and heated to 130°C for 8 h. After removal of the acetic acid under vacuum the residue was chromatographed on a column (200 g of silica gel 60 Merck; eluent acetic acid-ethyl acetate/hexane, 1:2). Yield 0.48 g (26%) of oily product that crystallized on addition of Et_2O; m.p. 153°C, yellow fluorescence at 366 nm. Correct elemental analysis. IR ($CHCl_3$): $\tilde{\nu}$ = 3400 (w), 1675 (s), 1620 (m), 1530 (s), 1350 (s). ^{1}H-NMR ($CDCl_3$): δ = 8.37 (t, H-2'), 8.14 (dt) and 7.92 (dt, H-4', H-6'), 7.53 (t, H-5'), 7.89 (s, H-6), 5.00 (s, NH), 4.21 (q, CH_2), 4.00 (m, CH_2), 2.39 (s, CH_3), 2.03 (s, CH_3), 1.35 (t, CH_3), 1.15 (t, CH_3). Due to the chirality center C-4, the protons in the two $-OCH_2-$ groups are diastereotopic. The anisochronism possible as a result of this was, however, only observed for the protons of one of the two groups ($\Delta\delta$ = 0.04 ppm) (cf. Ref. [5]).

Received: April 2, 1987;
revised: May 11, 1987 [Z 2176 IE]
German version: *Angew. Chem. 99* (1987) 816

[1] A. Fleckenstein, *Med. Klin. (Munich) 70* (1975) 1665; F. Bossert, H. Meyer, E. Wehinger, *Angew. Chem. 93* (1981) 755; *Angew. Chem. Int. Ed. Engl. 20* (1981) 762; W. G. Nayler, *Eur. Heart J. 1* (1980) 225; R. A. Janis, D. J. Triggle, *J. Med. Chem. 26* (1983) 775.

[2] S. Goldmann, *Angew. Chem. 93* (1981) 798; *Angew. Chem. Int. Ed. Engl. 20* (1981) 779.

[3] R. F. Heck, *Org. React. 27* (1982) 345; A. Spencer, *J. Organomet. Chem. 258* (1983) 101; P. G. Ciattini, G. Ortar, *Synthesis 1986*, 70.

[4] For the reaction of α-pyrones with amines see V. Kvita, H. Sauter, G. Rihs, *Helv. Chim. Acta 66* (1983) 2769, 68 (1985) 1569; V. Kvita, *Synthesis 1986*, 786.

[5] K. Mislow, M. Raban, *Top. Stereochem. 1* (1967) 1.

The Spin Distribution in Ion Pairs of 1-Aminoanthraquinone Radical Anion and Alkali-Metal Cations**

By *Hans Bock,* Bernhard Hierholzer,* and *Petra Schmalz*

The two-step reversible reduction of *p*-quinones in aprotic solution is greatly influenced by added metal salts;[1–3] in particular the second electron is transferred irreversibly at considerably lower potentials. This observation can be rationalized assuming complexation of metal cations $M^{\oplus}$ by the solvated semiquinone radical anion $[Q^{\odot\ominus}]_{solv}$ with formation of contact ion pair radicals $[Q^{\odot\ominus}M^{\oplus}]^{\odot}_{solv}$ and triple ion-radical cations $[M^{\oplus}Q^{\odot\ominus}M^{\oplus}]^{\odot\oplus}_{solv}$ demonstrated ESR spectroscopically, e.g. with $M^{\oplus}$ = $Li^{\oplus}$[3] (cf. Scheme 1). The total positive charge of the triple ion-radical cation $[M_2Q]^{\odot\oplus}$, in which the final reduction product, a salt of a hydroquinone dianion, is already preformed, explains both the substantial lowering of the second reduction potential as well as the irreversibility of the electron transfer.[3]

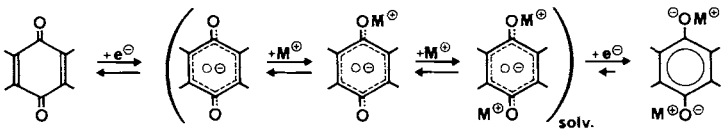

Scheme 1.

1-Aminoanthraquinone is a suitable model compound for ENDOR experiments[4] aimed to elucidate the spin distribution in the intermediary contact ion pair radicals $[Q^{\odot\ominus}M^{\oplus}]^{\odot}_{solv}$.[5,6] In dimethylformamide (DMF) with tetra-*n*-butylammonium perchlorate (TBAP) as supporting electrolyte it shows two reversible or quasi-reversible half-wave reduction potentials at −0.91 and −1.57 V (ΔE = 65 and 100 mV, resp.). Addition of, e.g., $LiClO_4$ or $Ba(ClO_4)_2$ influences the first half-wave potential only slightly ($\Delta\varepsilon^{1}_{1/2} \leq 0.05$ V); whereas the noticeable drop in the second half-wave potential of about 0.37 or 0.48 V to −1.20 and 1.09 V, respectively (ΔE = 120 and 130 mV, resp.) points to ion-pair formation (see Scheme 1).[2–5] The O···N distance in the peri-chelate claw of 1-aminoanthraquinone amounts to only ca. 250 pm, so that the O- and N-electron pairs interpenetrate in the preferred complex conformation in which the angle between the HNH-bisector and the six-membered ring plane (Fig. 1) will be close to 0°. In its radical anion, the electron density at the oxygen atom is increased by π-delocalization of the excess negative charge in the direction of the polarizing effective cationic charge ($M^{\oplus}$). The ESR signals of the 1-aminoanthrasemiquinone ion-pair radicals can be saturated, allowing to record highly resolved ENDOR spectra (Fig. 1)[7] and to determine the signs of the individual couplings a_H and $a_{M^{\oplus}}$ by TRIPLE experiments.[4]

[*] Prof. Dr. H. Bock, Dipl.-Chem. B. Hierholzer, Dipl.-Chem. P. Schmalz
Institut für Anorganische Chemie der Universität
Niederurseler Hang, D-6000 Frankfurt am Main 50 (FRG)

[**] Electron Transfer and Ion Pair Formation, Part 4. This work was supported by the Land Hessen, the Deutsche Forschungsgemeinschaft, the Fonds der Chemischen Industrie, and the A.-Messer Stiftung.—Parts 1-3: [1]-[3].

The ENDOR spectra (Fig. 1) of the contact ion pair radicals generated by stoichiometric alkali-metal reduction of 1-aminoanthraquinone and additionally stabilized by THF solvation, show significant differences e.g. for $X = Li^{\oplus}$ and $Cs^{\ominus}$, whose ionic radii of 60 and 170 pm, re-

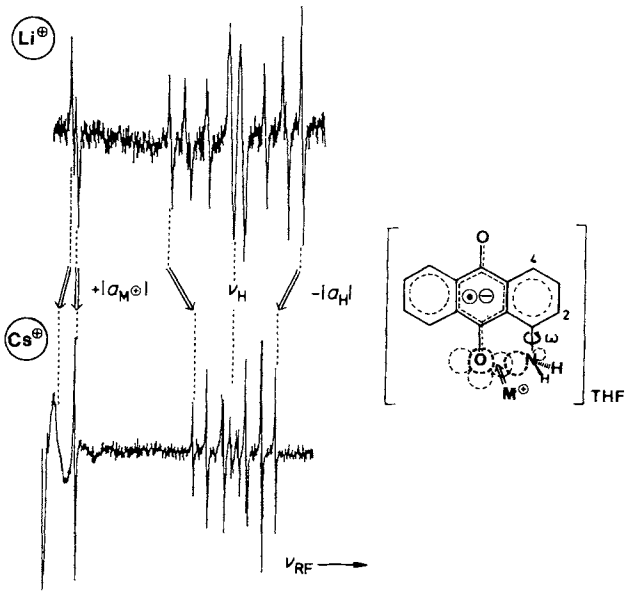

Fig. 1. ENDOR spectra of 1-aminoanthrasemiquinone ion-pair radicals with $Li^{\ominus}$ and $Cs^{\oplus}$ in tetrahydrofuran (THF) at 200 K [5].

spectively, differ the most: The spread of the ^{1}H-signal pairs about the frequency ν_H decreases, while the metal cation couplings $a_{M^{\ominus}}$ increase. Triple experiments prove[4] different signs for the couplings a_X: for all ring protons (X = H) they are, as expected, negative due to π/σ spin polarization, but positive for all added alkali-metal cations with ample hyperfine splitting constants ($X = Li^{\oplus}$, $Na^{\oplus}$, $Rb^{\oplus}$, $Cs^{\oplus}$) (cf. Ref. [4]).

The measured data yield the following information on the structure of the 1-aminoanthraquinone radical anion chelates in THF: A nitrogen coupling ($a^{14}_N = 0.06$ mT) is only observed with the nBu$_4$N$^{\oplus}$ countercation shielded by alkyl groups and, therefore, largely interaction-free,[7] i.e. when a considerable rotation of the NH_2 group favored by hydrogen bonding (Fig. 1: ω almost 90°) permits a substantial n_N/π delocalization. The positive $M^{\oplus}$ couplings suggest that the countercation is located outside the π-nodal plane and that, therefore, the N-electron pair is not rotated completely in the direction of the semiquinone oxygen atom (Fig. 1 = $0° < \omega < 90°$). This is consistent with the expectation that "docking" of the alkali cations should be energetically favored at the site of presumed highest electron density in the O,N-chelate claw, i.e. near to the semiquinone oxygen atom, but outside of the O···N axis in the π-nodal plane. All contact ion pairs investigated here should have comparable structures, as follows, e.g., from the observation that in all cases the ENDOR signals are temperature-independent.[2]

Expectedly, the ring proton couplings in the 1-aminoanthrasemiquinone radical anion chelates $[Q^{\odot\ominus}M^{\oplus}]^{\odot}_{THF}$ increase[1,4] with effective cationic charge $1/r_{M^{\oplus}}$ (Fig. 2; top). This result further supports the literature model,[4] that the charge increase on the semiquinone O-atoms due to $>C{=}O^{\delta\ominus}\cdots M^{\oplus}$ Coulomb interactions suppresses their π spin population in favor of that on the ring carbon atoms.

The dependence of the $>C{=}O^{\delta\ominus}\cdots M^{\oplus}$ Coulomb interaction on the alkali-metal cations can be demonstrated by correlation of their s spin densities $\rho_{M^{\oplus}}$ with their volumes $r^3_{M^{\oplus}}$ (Fig. 2, bottom). Based on the assumptions that the structures of all radical anion chelates dissolved in THF are comparable, and that the spin densities $\rho_{M^{\oplus}}$ of the almost spherically symmetrical chelate cations can be estimated from the McConnell analogous relationship[8a] $\rho_{M^{\oplus}} = a_{M^{\oplus}}|Q_M|^{-1}$ by inserting the ENDOR coupling constants $a_{M^{\oplus}}$ (Fig. 1) and the hyperfine splittings $|Q_M|$ of alkali metals as determined by atomic beam experiments.[8b] The resulting linear regression $\rho_{M^{\oplus}} = 0.157 + 0.0293 r^3_{M^{\oplus}}$

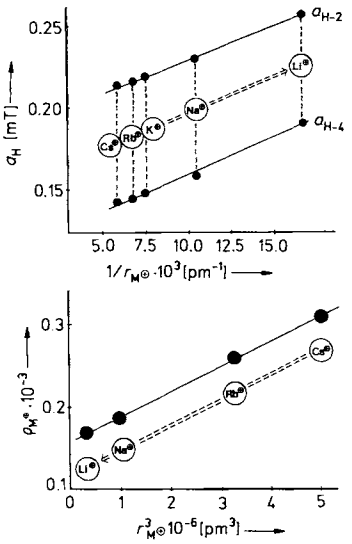

Fig. 2. Correlations of ENDOR data of the ion pairs of alkali-metal cations and 1-aminoanthraquinone radical anion. Top: ^{1}H-coupling constants of the ring protons a_{H-2} and a_{H-4} versus the effective $M^{\oplus}$ ionic charges $1/r_{M^{\oplus}}$. Bottom: $M^{\oplus}$-Spin densities $\rho_{M^{\oplus}}$ versus the cation volumes $r^3_{M^{\oplus}}$ (cf. text).

with a correlation coefficient $r = 0.999$ (Fig. 2, bottom) confirms that the transferred positive π-spin density $\rho_{M^{\oplus}}$ increases with the cation volume $r^3_{M^{\oplus}}$. According to the Coulomb interaction model $>C{=}O^{\delta\ominus}\cdots M^{\oplus}$, the spin density of the O-"docking" sites decreasing with increasing effective cationic charge from $Cs^{\oplus}$ to $Li^{\oplus}$ is the major contributing factor to this transfer.[2] Concomitantly the π-spin population of the ring carbon atoms increases, as can be demonstrated by the larger ring proton coupling constants (Fig. 1 and Fig. 2, top).

Received: March 23, 1987 [Z 2164 IE]
German version: *Angew. Chem.* 99 (1987) 811

[1] H. Bock, B. Hierholzer, F. Vögtle, G. Hollmann, *Angew. Chem.* 96 (1984) 74; *Angew. Chem. Int. Ed. Engl.* 23 (1984) 57.
[2] H. Bock, D. Jaculi, *Angew. Chem.* 96 (1984) 298; *Angew. Chem. Int. Ed. Engl.* 23 (1984) 305; D. Jaculi, *Diplomarbeit*, Universität Frankfurt 1983.
[3] H. Bock, B. Solouki, P. Rosmus, R. Dammel, P. Hänel, B. Hierholzer, U. Lechner-Knoblauch, H. P. Wolf in H. Sakurai (Eds.): *Organosilicon and Bioorganosilicon Chemistry*, Ellis Horwood, Chichester 1985, p. 45 ff (see expecially pp. 59–69). Cf. also H. Bock, B. Solouki, S. Aygen, G. Brähler, R. Dammel, J. Giordan, P. Hänel, H. F. Herrmann, B. Hierholzer, T. Hirabayashi, D. Jaculi, W. Kaim, U. Lechner-Knoblauch, S. Mohmand, H. Müller, P. Rittmeyer, B. Roth, U. Stein, *Nova Acta Leopoldina, N. F. 59* (1985) 92; H. Bock, *Abh. Math.-Naturwiss. Kl. Akad. Wiss. Lit. Mainz 1986*, No. 2, p. 1–35.

[4] Cf., e.g.: W. Lubitz, M. Plato, K. Möbius, D. Biehl, *J. Phys. Chem. 83* (1979) 3401; H. Kurreck, B. Kirste, W. Lubitz, *Angew. Chem. 96* (1984) 171; *Angew. Chem. Int. Ed. Engl. 23* (1984) 173, and references cited therein. ESR investigations of semiquinone ion pairs have been reported, for example, by E. A. C. Lucken, *J. Chem. Soc. 1964*, 4234; N. Hirota in E. T. Kaiser, L. Kevan (Eds.): *Radical Ions*, Wiley-Interscience, New York 1968, p. 35f; T. E. Gough, P. R. Hindle, *Can. J. Chem. 47* (1969) 1698, 3393.

[5] For summaries of investigations on ion pairs from various view points see, e.g. a) J. M. Masnovi, J. Kochi, *J. Am. Chem. Soc. 107* (1985) 7881; b) E. S. Gould, *Acc. Chem. Res. 18* (1985) 22; c) W. Kaim, *ibid. 18* (1985) 160; d) A. Streitwieser, Jr., *ibid. 17* (1984); e) J. M. Lehn, *Pure Appl. Chem. 52* (1980) 2303; f) A. Kaifer, D. A. Gustowski, L. Echegoyen, V. J. Gatto, R. A. Schultz, T. P. Cleary, C. R. Mor, D. M. Goli, A. M. Rios, G. W. Gokel, *J. Am. Chem. Soc. 107* (1985) 1958, and references cited therein. Cf. also [4].

[6] Reducible chelate molecules with O- or N-docking sites have already been used repeatedly for ESR/ENDOR investigations on radical ion pairs. Examples are a) crown ethers with reducible π systems such as quinones (cf. [1]); b) *ortho*-quinones (cf. e.g.: J. A. Pedersen, *CRC Handbook of EPR Spectra from Quinols*, CRC Press, Boca Raton, FL, USA 1985 or [2]); c) semidiones (cf. e.g.: G. A. Russell, C. E. Osuch, *J. Am. Chem. Soc. 100* (1984) 5979 or [4]); d) N-heterocycles such as α,α'-bipyridyl (cf. e.g.: W. Kaim, *J. Am. Chem. Soc. 104* (1982) 3833, and references cited therein).

[7] 1-Aminosemianthraquinone radical anion with $n\mathrm{Bu_4N^{\oplus}}$ as, largely interaction-free, countercation can be generated electrochemically in THF/TBAP solution. THF is chosen as solvent for the ESR investigations because it favors the formation of contact ion pairs relative to more polar solvents such as DMF (cf. e.g.: K. A. M. Greber, K. S. Chen, J. K. S. Wan, *Rev. Chem. Intermed. 5* (1984) 37; E. Lesniewska-Lada, M. K. Kalinowski, *Electrochim. Acta 28* (1983) 1415, and references cited therein). The radical ion pairs $[\mathrm{M^{\oplus}Q^{\ominus\ominus}}]^{\ominus}$ are prepared in THF by reduction of 1-aminoanthraquinone on the respective alkali metal mirrors; for the preparation of Rb- and Cs-mirrors, the thermal decomposition of their azides in the presence of fine-grained iron powder proved to be advantageous. The ENDOR measurements were carried out with a Bruker 220 D spectrometer; with magnetic fields of about 3.4 kG, the frequencies $\tilde{\nu}_X$ of the individual isotopes are (rel. abundance): ^{1}H 14.46 MHz (99.98%), ^{7}Li 5.62 MHz (92.6%), ^{23}Na 3.82 MHz (100%), ^{87}Rb 4.73 MHz (27%), and ^{133}Cs 1.90 MHz (100%).

[8] a) H. McConnell, *J. Chem. Phys. 24* (1956) 632; b) cf. e.g.: J. Bolton, J. Wertz, *Electron Spin Resonance—Elementary Theory and Applications*, McGraw-Hill, New York 1972.

Lactosylceramides with Unsaturated Fatty Acids—Synthesis and Use in the Generation of Bilayer Membranes**

By *Richard R. Schmidt,* Thomas Bär,* and *Hans-Juergen Apell*

Dedicated to Professor Wolfgang Pfleiderer on the occasion of his 60th birthday

Glycosphingolipids are membrane building blocks, which, with their lipid moiety, the *N*-acylated sphingosine (= ceramide), participate in the formation of the outer plasma membrane bilayer. The hydrophilic carbohydrate moiety is located on the outer membrane surface, and thus can determine the specificity of interactions with cells and various biofactors.[1] C_{18}-sphingosine is the most important sphingosine base in the majority of mammalian tissues, while considerable amounts of the C_{20} homologues are found in the gangliosides of the brain. Unsubstituted and α-hydroxy fatty acids are met as *N*-acyl groups which can contain double bonds.[2]

Bilayer membranes could not be obtained with the glycosphingolipids thus far available, which are mostly chemically heterogeneous. Recently, we developed a synthetic method with which pure glycosphinolipids can be prepared in good yields.[3] Since the fatty acid is coupled with the amino group of the sphingosine moiety in the last reaction step, this synthetic method is also suitable for systems with sensitive acids. We have now used it for the synthesis of lactosyl sphingolipids containing unsaturated fatty acids which promote membrane formation and membrane fluidity.[4] Reaction of *O*-acetylated *O*-(α-lactosyl) trichloroacetimidate[5] as donor and 3-*O*-benzoylated azidosphingosine[6] as acceptor with BF_3–OEt_2 as catalyst afforded the glycoside **1**[7] (yield 85%). Competing formation of *ortho* ester could be completely suppressed by successive addition of 0.05 equivalents of catalyst. Deacylation with sodium methoxide/methanol furnished **2** in quantitative yield, and reduction of the azide group with H_2S/pyridine afforded the lactopsychosine **3**, which has already been prepared via another route.[3] The acid chlorides, which were generated with oxalyl chloride, proved to be the best for the coupling of oleic, linolic, linolenic, and arachidonic acids. Their reaction with **3** in the presence of sodium acetate in tetrahydrofuran (THF)/water led in good yields (65–74%) to the lactosylceramides **4**–**7**.[7] These can be obtained pure by peracetylation and subsequent deacetylation with Florisil[8] (**4**, **5**), or directly by reversed phase chromatography (**6**, **7**; RP_{18},[8] *n*-butanol/methanol/water, 50 : 32 : 18).[7]

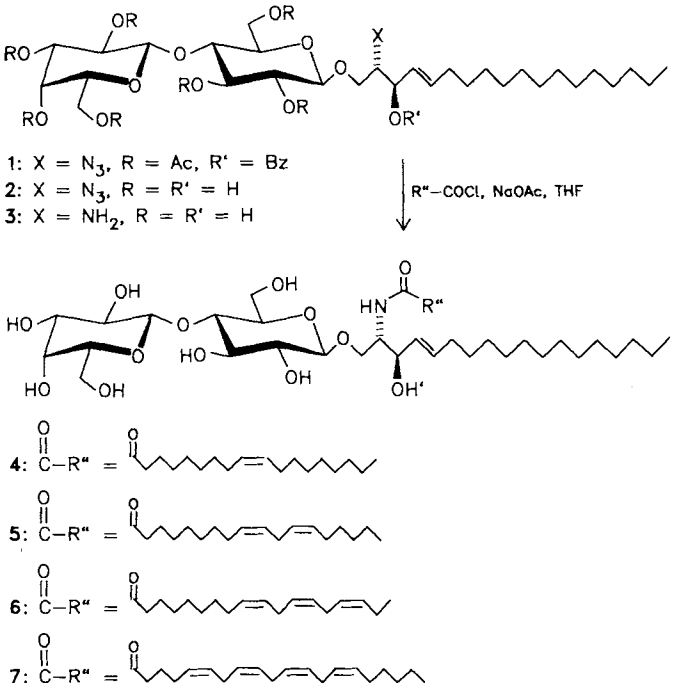

To gain insights into the complexity of the cell membranes it is essential first of all to investigate the properties and modes of reaction of the individual membrane components in simple models.[9] We have therefore generated bilayer membranes with the glycosphingolipids **4**–**7** using the bilayer technique of *Müller* et al.[9, 10] and have deter-

[*] Prof. Dr. R. R. Schmidt, Dipl.-Chem. T. Bär
Fakultät für Chemie der Universität
Postfach 5560, D-7750 Konstanz (FRG)
Dr. H.-J. Apell
Fakultät für Biologie der Universität
Postfach 5560, D-7750 Konstanz (FRG)

[**] Glycosyl Imidates, Part 30. This work was supported by the Deutsche Forschungsgemeinschaft and the Fonds der Chemischen Industrie. We thank Prof. Dr. *P. Läuger*, Konstanz, for valuable discussions.—Part 29: R. R. Schmidt, G. Effenberger, *Liebigs Ann. Chem.*, in press.

mined the thickness of the membranes from measurements of the electrical capacity on "black films" (black bilayer membranes BLM).[11, 12] Bilayer membranes with remarkable longevity (up to several hours) and stability toward higher potentials (measurements up to 300 mV) could be obtained (surface areas 0.15 mm^2) from 3–4% solutions of **4**–**7** in *n*-decane/*n*-butanol (100:1). The specific membrane capacities measured at potentials of 10–300 mV (Table 1) lie about a factor of 1.5 above those of phosphatidylcholine membranes.[12] This can be due to the altered dielectric properties of the hydrophilic head groups in the case of the lactosylceramides, or to the bilayer being thinner due to tighter coiling and kinking of the lipid moiety. The specific membrane capacities increase with the increasing number of *cis* double bonds in the C_{18}-acid derivatives **4**–**6**, whereas, conversely, the estimated layer thickness for the lipid moiety, presumably determined by the kinking, decreases. The specific membrane capacity of the arachidonic acid derivative **7** is of the same order of magnitude as that of the oleic acid derivative **4**, i.e. the chain lengthening by two C-atoms is balanced out by about three additional *cis* double bonds.

Table 1. Specific membrane capacity (C_m) and thickness (d) of the hydrocarbon region of the bilayer membranes of lactosylceramides **4**–**7** [a].

Compound	C_m [$\mu F/cm^2$] [b]	d [nm] [c]
4	0.563 ± 0.072	3.30 ± 0.26
5	0.755 ± 0.073	2.46 ± 0.25
6	0.818 ± 0.092	2.27 ± 0.20
7	0.570 ± 0.038	3.26 ± 0.49

[a] For details of the measurements see Refs. [9–12] and literature cited therein. [b] Mean value of ten measurements. [c] For calculation see Ref. [11].

Received: April 6, 1987 [Z 2180 IE]
German version: *Angew. Chem. 99* (1987) 813

[1] R. R. Schmidt, *Angew. Chem. 98* (1986) 213; *Angew. Chem. Int. Ed. Engl. 25* (1986) 212; R. R. Schmidt in W. Bartmann, K. B. Sharpless (Hrsg.): *Stereochemistry of Organic and Bioorganic Transformations*, VCH Verlagsgesellschaft, Weinheim 1987, p. 169, and references cited therein.
[2] N. K. Kochetkov, G. P. Smirnova, *Adv. Carbohydr. Chem. Biochem. 44* (1986) 387, and references cited therein.
[3] R. R. Schmidt, P. Zimmermann, *Angew. Chem. 98* (1986) 722; *Angew. Chem. Int. Ed. Engl. 25* (1986) 725.
[4] A. K. Akimoto, L. Dorn, H. Gros, H. Ringsdorf, H. Schupp, *Angew. Chem. 93* (1981) 108; *Angew. Chem. Int. Ed. Engl. 20* (1981) 90.
[5] R. R. Schmidt, J. Michel, M. Roos, *Liebigs Ann. Chem. 1984*, 1343; J. Michel, *Dissertation*, Universität Konstanz 1983.
[6] R. R. Schmidt, P. Zimmermann, *Tetrahedron Lett. 27* (1986) 481.
[7] ^{1}H-NMR: **1** (250 MHz, $CDCl_3$, TMS): δ = 7.42–8.06 (m, 5H, Bz), 5.85–5.96 (m, 1H, $CH_2-CH=$), 5.48–5.65 (m, 2H, $=CH-CH-OBz$), 5.35 (d, 1H, H-4', J = 2.7 Hz), 5.07–5.23 (m, 2H), 4.89–4.98 (m, 2H), 4.45–4.53 (m, 3H), 4.02–4.12 (m, 3H), 3.79–3.97 (m, 4H), 3.54–3.65 (m, 2H), 1.96–2.20 (m, 23H, 7Ac, $=CH-CH_2$), 1.24–1.37 (m, 22H, $11CH_2$), 0.88 (t, 3H, CH_3).—**4** (250 MHz, [D_6]Dimethyl sulfoxide, TMS): δ = 7.54 (d, 1H, NH, J = 8.8 Hz), 5.49–5.57 (m, 1H, $=CH-CH_2$), 5.30–5.39 (m, 3H, $=CH-CHOH$, $CH=CH$), 5.16 (d, 1H, OH, J = 3.7 Hz), 5.12 (d, 1H, OH, J = 3.3 Hz), 4.90 (d, 1H, OH, J = 5.5 Hz), 4.84 (d, 1H, OH, J = 3.1 Hz), 4.68 (very broad, 2H, 2OH), 4.58 (m, 2H, 2OH), 3.29–4.22 (m, 17H), 3.02–3.09 (m, 1H), 1.96–2.06 (m, 8H, $COCH_2$, 3 $=CH-CH_2$), 1.23–1.48 (m, 44H, $22CH_2$), 0.83–0.91 (2t, 6H, $2CH_3$). The compounds **5**–**7** also gave correct ^{1}H-NMR data.—The UV spectroscopically determined amounts of fatty acid esters with conjugated double bonds are: < 1% for 6 and < 3% for 7.
[8] Florisil (magnesium silicate), 16–30 mesh, Fluka AG; RP_{18}, Merck.
[9] P. Läuger, *Angew. Chem. 97* (1985) 939; *Angew. Chem. Int. Ed. Engl. 24* (1985) 905.
[10] P. Müller, D. O. Rudin, H. T. Tien, W. C. Wescott, *Nature London 194* (1962) 979.
[11] P. Läuger, W. Lesslauer, E. Marti, J. Richter, *Biochim. Biophys. Acta 135* (1967) 20.
[12] R. Benz, O. Fröhlich, P. Läuger, M. Montal, *Biochim. Biophys. Acta 394* (1975) 323; R. Benz, K. Janko, *ibid. 455* (1976) 721. Specific membrane capacities of various phospholipids are presented in this publication.

Deep-Colored, Through-Conjugated Multitriphenylmethylium Ions**

By *Dieter Hellwinkel,* Heinz Stahl,* and *Heinrich Georg Gaa*

Monocationic "conventional" triphenylmethylium dyes of the crystal violet type **1** and the tricationic "inverse" analogues **2** derivable from them by exchanging the functionalities show almost the same longest-wavelength absorptions in the electronic spectrum and have virtually the same green color.[1]

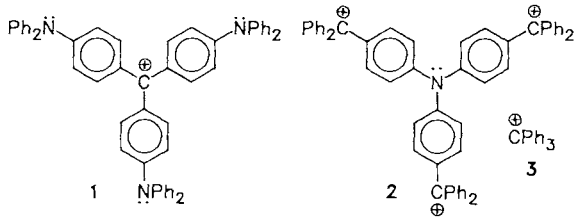

λ_{max} [nm] (lg ε):	627 (4.95)	641 (5.26)
	409 (3.27)	426 (4.35)
	(in CH_3CO_2H + 5% CF_3CO_2H)	(in CF_3CO_2H)

This can be readily explained with the aid of the characteristic HMO frontier orbital scheme for the alternating structural types shown above. The scheme is characterized by two non-bonding (n) orbitals and the weakly bonding and antibonding molecular orbitals b, a, respectively, of opposite but equal energies (Fig. 1).

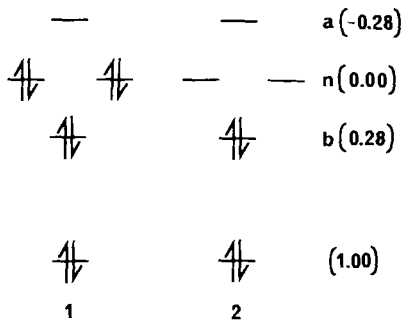

Fig. 1. Frontier orbital occupancy scheme for conventional triphenylmethylium ions **1** and their tricationic "inverse" analogues **2** in the Hückel approximation (energies in β-units).

[*] Prof. Dr. D. Hellwinkel, Dipl.-Chem. H. Stahl, Dipl.-Chem. H. G. Gaa
Organisch-chemisches Institut der Universität
Im Neuenheimer Feld 270, D-6900 Heidelberg 1 (FRG)

[**] This work was supported by the Deutsche Forschungsgemeinschaft, the Fonds der Chemischen Industrie, and by BASF AG.

From the different occupancies of the frontier orbital region of the dyes of type **1** and **2** it follows that at the level of the Hückel approximation even identical longest-wavelength electron excitations are to be expected.

If the two electrons in the weakly bonding molecular orbital b are also removed, a new chromophore-type emerges, which—corresponding to a frontier excitation $1.00\beta \rightarrow b(0.28\beta)$—should absorb in the UV/VIS spectrum at a shorter wavelength than **2** [$b(0.28\beta) \rightarrow n$, $\lambda_{max} = 641$ nm], yet at a still longer wavelength than the yellow triphenylmethylium ion **3** [$1.00\beta \rightarrow n$, $\lambda_{max} = 432$ nm].[2]

We have now transformed this idea into reality by replacing also the last N donor function in **2** by a carbenium center. Thus, we allowed the key reagent **4**,[3] accessible from benzophenone by reaction with 4-bromophenyllithium, to react, after bromine-lithium exchange to give **5**, with methyl chloroformate to give the trisether of the tetraalcohol **6**, which yielded the tetrakis(ethyl ether) **7** with ethanol.

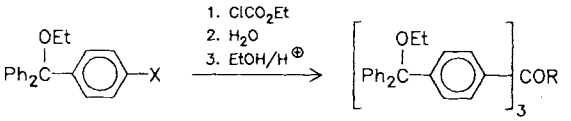

4, X = Br; **5**, X = Li

6, R = H; **7**, R = Et

Reaction of **7** with trifluoroacetic acid afforded exclusively the yellow trication **8**, which is none other than a spacer-coupled, and thus conjugatively separated, triple tritylium system.[4] Only stronger acids such as sulfuric acid or trifluoromethanesulfonic acid can liberate from **7** or **8** the novel reddish-violet tris[4-(diphenylmethyliumyl)phenyl]methylium ion **9**, which upon dilution with trifluoroacetic acid resolvolyzes to the yellow trication **8**.

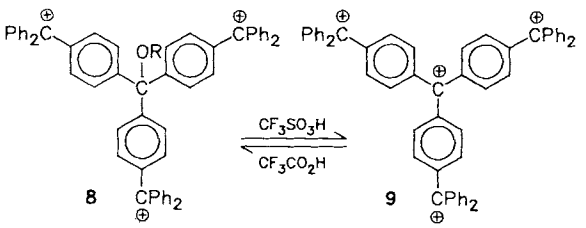

λ_{max} [nm] (lg ε): 437 (5.45) 517 (5.45)

R = Et or acid residue

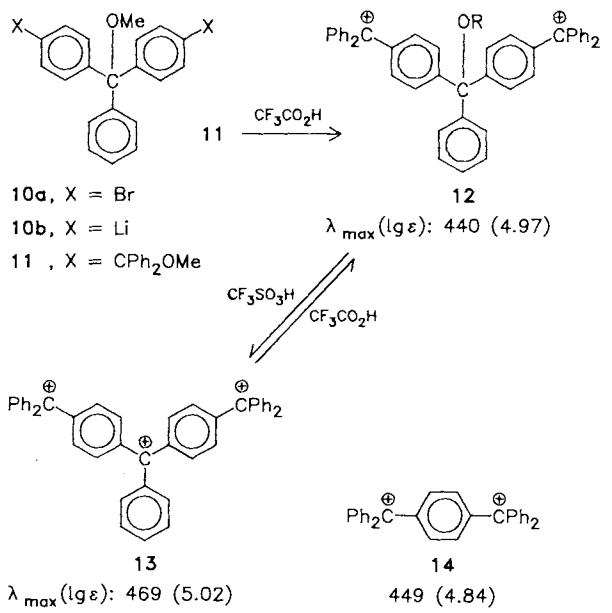

Table 1. ^{1}H-NMR data of the triphenylmethylium ions **2**, **3**, **8**, **9**, **13**, and **14** (room temperature, δ values rel. TMS), prepared from the corresponding ethers [a] with the given acids quoted under "solvent". Numbering scheme:

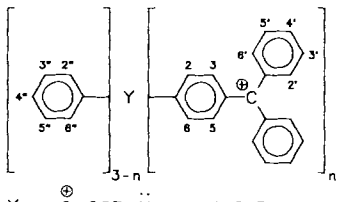

Y = ⊕C, COR, N; n = 1, 2, 3

Ion	Solvent	Charge	2′,6′ (2″,6″)	3′,5′ (3″,5″)	4′ (4″)	2,6 —	3,5 —
3	CF_3CO_2H/CD_2Cl_2 (1/1) [b]	⊕	7.77	7.95	8.34	—	—
14	$CF_3CO_2H/CF_3SO_3H/CD_2Cl_2$ (1/0.5/4) [b]	2⊕	7.92	8.07	8.50	8.03	8.03
2	CF_3CO_2D	3⊕	7.80	7.95	8.31	8.00	7.97
13	CF_3SO_3H [c]	3⊕	8.04 (8.32)	8.17 (8.35)	8.61 (**8.84**)	8.30	8.22
8	CF_3CO_2D	3⊕	7.80	7.94	8.36	7.98	8.25
9	CF_3SO_3H [c]	4⊕	8.14	8.22	**8.68**	8.57	8.38

[a] All precursors afforded correct analytical values and ^{1}H-NMR spectra. [b] Referred via $\delta(CH_2Cl_2) = 5.288$ to TMS. [c] Relative to $CDCl_2$/TMS extern.

Aside from the electronic spectrum, the 500-MHz ^{1}H-NMR spectrum[5] is especially informative regarding the structure of the tetracation **9**. For the *p*-protons of the outer phenyl groups it shows, with $\delta = 8.68$, a chemical shift value which lies well above the values hitherto observed for such protons in tritylium ions[1,6,7] (Table 1).

In a comparable way, a through-conjugated trication, the red bis[4-(diphenylmethyliumyl)phenyl]phenylmethylium ion **13** could be synthesized and characterized via the reaction of the difunctional key reagent **10b** analogous to **5** with benzophenone to give the trisether **11** and its dissolution in acids. Like **9**, the ion **13** is stable only in trifluoromethanesulfonic acid and is resolvolyzed with trifluoroacetic acid to give the yellow dication **12**. In **13** it is the *p*-proton of the phenyl group coupled to the central carbenium function which shows a record deshielding value of $\delta = 8.84$ in the ^{1}H-NMR spectrum (Table 1).

The tri- and tetra-cations **13** and **9**, respectively, are the first members of a series of novel, conjugated multitritylium systems of which we are presently synthesizing some representative examples. Hitherto, only one conjugated dication of this type, the yellow 1,4-phenylenebis(diphenylmethylium) **14**, was known.[8]

Received: April 13, 1987 [Z 2195 IE]
German version: *Angew. Chem.* 99 (1987) 822

[1] D. Hellwinkel, H. Stahl, H. G. Gaa, R. Gottfried, *Phosphorus Sulfur 18* (1983) 121; D. Hellwinkel, H. G. Gaa, R. Gottfried, *Z. Naturforsch. B 41* (1986) 1045.

[2] G. Olah, C. U. Pittman, Jr., M. C. R. Symons in G. A. Olah, P. von R. Schleyer (Eds.): *Carbonium Ions, Vol. I*, Interscience, New York 1968, p. 153.
[3] H. Stahl, *Diplomarbeit*, Universität Heidelberg 1981.
[4] Cf. also: H. Volz, *Tetrahedron Lett. 1977*, 4683.
[5] We thank Dr. *Grosskurth*, Max-Planck-Institut für Medizinische Forschung, Heidelberg, for recording the ^{1}H-NMR spectrum.
[6] Cf. also: D. Hellwinkel, G. Aulmich, M. Melan, *Chem. Ber. 114* (1981) 86.
[7] It has so far been impossible to obtain reproducible ^{13}C-NMR spectra.
[8] G. A. Olah, J. L. Grant, R. J. Spear, J. M. Bollinger, A. Serianz, G. Sipos, *J. Am. Chem. Soc. 98* (1976) 2501; H. Hart, T. Sulzberg, R. R. Rafos, *ibid. 85* (1963) 1800; H. Volz, M. J. Volz de Lecea, *Tetrahedron Lett. 1964*, 1871.

A Psoralen-Substituted Dioxetane as DNA Intercalator for Photogenotoxic Studies**

By *Waldemar Adam,* Axel Beinhauer, Roland Fischer,* and *Hermann Hauer*

The phototherapeutic action of psoralen **1**, a linearly fused furocoumarin composed of benzofuran and coumar-

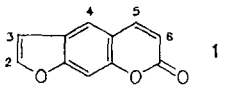

1

in, in psoriasis rests on its photochemical [2+2] cycloaddition to DNA under UVA irradiation (300–400 nm).[1] These polycyclic heteroaromatic molecules intercalate into the DNA ladder and on excitation by UV radiation they cycloadd at the α-pyrone and/or furan double bonds to proximate pyrimidine bases (preferably thymine) with formation of four-membered rings. Recently we were able to show[2] that 1,2-dioxetanes (chemical sources for electronically excited states[3]) cause photochemical damage to DNA. While in isolated DNA dioxetanes induce photochemical cycloaddition, in cellular DNA their photogenotoxic action mainly derives from radical-type damage, e.g. strand breaks.[2]

The aim of this study was to bind dioxetanes chemically to psoralen, with the intention that the intercalative ability of such furocoumarins would help to transport the psoralen-bound dioxetane to the DNA. Subsequent thermal decomposition of the dioxetane would then lead to electronically excited psoralen, which should cycloadd to the DNA.

We report here on the successful synthesis, by carbonate linking,[4] of the first psoralen-substituted dioxetanes **3a–c** and on their activation parameters and excitation yields (see Table 1).

The benzofuran- and the coumarin-substituted dioxetanes **3a** and **3b**, respectively, served as model substances in the synthesis of the psoralen-substituted dioxetane **3c**. These three dioxetanes will be used as model compounds in future photobiological experiments. The corresponding phenols were prepared in 43–58% yields from the methoxy derivatives by demethylation with Me_3SiI. Reaction of the phenols with the dioxetane-substituted chloroformate **2** in the presence of stoichiometric amounts of triethylamine in

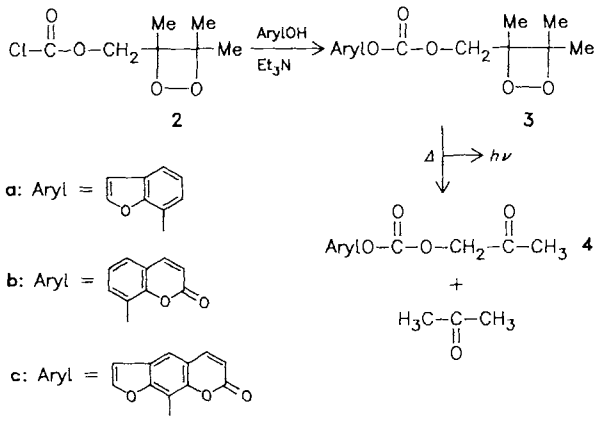

Table 1. Activation parameters and excitation yields for the thermal decomposition of dioxetanes **3a–c** and **5**.

	3a	**3b**	**3c**	**5** [a]
$\Delta H^{\neq}$ [kcal/mol]	24.5±0.4	23.5±0.3	23.7±0.4	23.7±0.3
$\Delta S^{\neq}$ [cal mol^{-1}K^{-1}]	−3.6±1.3	−6.5±0.7	−5.8±1.2	−5.3±0.9
$\Delta G^{\neq}$ [kcal/mol] [b]	25.6±0.40	25.5±0.3	25.5±0.4	25.3±0.3
$10^4\,\Phi^S$ [E/mol]	0.9±0.1	7±3	6±2	11±5
$10^2\,\Phi^T$ [E/mol]	15±3	14±2	4±1	14±3

[a] Data taken from Ref. [2]. [b] Calculated from $\Delta H^{\neq}$ and $\Delta S^{\neq}$ at 310 K.

dichloromethane at 0°C led to the dioxetanes **3a–c**. These were purified by chromatography on silica gel at low temperature (−30°C). Thermolysis (ca. 75°C) of **3a–c** afforded quantitatively the ketocarbonates **4a–c** with chemiluminescence. All the new compounds **3** and **4** were completely characterized (see Table 2[5]).

The activation parameters of the dioxetanes **3a–c** (Table 1) were determined photometrically by monitoring the chemiluminescence emission under isothermal conditions.[6] Within the limits of error, the dioxetanes **3** exhibit almost the same thermal stability, which hardly differs from that of dioxetane **2** and its precursor, the hydroxymethyl(trimethyl)-1,2-dioxetane **5**.[2a, 7]

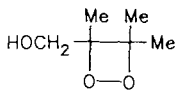

5

The excitation yields of the dioxetanes **3a–c** (Table 1) were determined photometrically using Stern-Volmer kinetics (9,10-diphenylanthracene for singlet yields and 9,10-dibromoanthracene for triplet yields).[8] In the case of **3a–c**, as in the case of **5**, the triplet excited carbonyl products predominate by a factor of 100. While **3a**, **b** furnish approximately the same triplet yields as **5**, that of the psoral-

[*] Prof. Dr. W. Adam, Dipl.-Chem. A. Beinhauer, R. Fischer, Dr. H. Hauer
Institut für Organische Chemie der Universität
Am Hubland, D-8700 Würzburg (FRG)

[**] This work was supported by the Deutsche Forschungsgemeinschaft (Sonderforschungsbereich 172: "Molekulare Mechanismen Kanzerogener Primärveränderungen"), the Fritz-Thyssen-Stiftung, and the Fonds der Chemischen Industrie.

Table 2. Some physical data of the dioxetanes **3** and carbonates **4**. ^{1}H-NMR: 200 MHz, in $CDCl_3$. ^{13}C-NMR: 50 MHz, in $CDCl_3$ (exception **3b**: 100 MHz). For the numbering of **3c** and **4c** see 1.

3a: 64%, yellow oil.—^{1}H-NMR (0°C): δ = 1.49 (s; 3H, CH_3), 1.56 (s; 3H, CH_3), 1.71 (s; 3H, CH_3), 4.73 (d, J = 11.1 Hz; 1H, CH_2), 4.86 (d, J = 11.1 Hz; 1H, CH_2), 6.84 (d, J = 2.1 Hz; 1H, 3-H), 7.12–7.28 (m; 2H, 4-H, 5-H 7.52 (dd, J = 7.6 Hz, 1.3 Hz, 1H, 6-H), 7.65 (d, J = 2.1 Hz; 1H, 2-H).—^{13}C-NMR (0°C): δ = 17.97 (q; CH_3), 22.25 (q; CH_3), 23.96 (q; CH_3), 70.14 (t; CH_2), 88.65 (s; C-OO), 89.23 (s; C-OO), 107.08 (d; C-3), 116.62 (d; C-4), 119.51 (d; C-6), 123.23 (d; C-5), 130.14 (s; C-3a), 135.53 (s; C-7), 145.42 (s; C-7a), 145.61 (d; C-2), 152.73 (s; *C*-carbonate)

3b: 26%, colorless oil.—^{1}H-NMR (0°C): δ = 1.51 (s; 3H, CH_3), 1.58 (s; 3H, CH_3), 1.70 (s; 3H, CH_3), 4.68 (d, J = 11.2 Hz; 1H, CH_2), 4.91 (d, J = 11.2 Hz; 1H, CH_2), 6.44 (d, J = 9.6 Hz; 1H, 3-H), 7.23–7.47 (m; 3H, aryl-H), 7.72 (d, J = 9.6 Hz; 1H, 4-H).—^{13}C-NMR (0°C): δ = 17.98 (q; CH_3), 22.30 (q; CH_3), 23.98 (q; CH_3), 70.34 (t; CH_2), 88.72 (s; C-OO), 89.30 (s; C-OO), 117.35 (d; C-3), 120.20 (s; C-4a), 124.34 (d), 124.85 (d), 125.92 (d), 137.65 (s; C-8a), 143.16 (d; C-4), 145.60 (s), 152.60 (s; C-carbonate), 159.15 (s; C-2)

3c: 35%, colorless needles, m.p. 129–131°C (decomp.) (ether/petroleum ether (30–50°C)).—^{1}H-NMR (0°C): δ = 1.54 (s; 3H, CH_3), 1.62 (s; 3H, CH_3), 1.75 (s; 3H, CH_3), 4.76 (d, J = 11.1 Hz; 1H, CH_2), 4.97 (d, J = 11.1 Hz; 1H, CH_2), 6.41 (d, J = 9.7 Hz; 1H, 6-H), 6.89 (d, J = 2.2 Hz; 1H, 3-H), 7.63 (s; 1H, 4-H), 7.73 (d, J = 2.2 Hz; 1H, 2-H), 7.83 (d, J = 9.7 Hz; 1H, 5-H).—^{13}C-NMR (0°C): δ = 18.02 (q; CH_3), 22.33 (q; CH_3), 23.98 (q; CH_3), 70.66 (t; CH_2), 72.07 (s), 88.68 (s, C-OO), 89.39 (s; C-OO), 106.93 (d; C-3), 115.00 (d; C-4), 116.17 (s), 117.54 (d; C-6), 123.06 (s), 125.96 (s), 143.48 (s), 143.97 (d; C-5), 147.44 (d; C-2), 147.84 (s), 152.02 (s; C-carbonate), 159.59 (s; C-7)

4a: 62%, colorless oil.—^{1}H-NMR: δ = 2.24 (s; 3H, CH_3), 4.81 (s; 2H, CH_2), 6.81 (d; J = 2.2 Hz; 1H, 3-H), 7.23 (m; 2H, 4-H and 5-H), 7.50 (dd, J = 6.8 Hz, 2.0 Hz; 1H, 6-H), 7.65 (d, J = 2.2 Hz; 1H, 2-H).—^{13}C-NMR: δ = 25.99 (q; CH_3), 7165 (t; CH_2), 107.04 (dd; C-3), 116.76 (d; C-4), 119.48 (d; C-6), 123.26 (d; C-5), 130.29 (s; C-3a), 135.48 (s; C-7), 145.69 (dd; C-2), 152.73 (s; C-carbonate), 200.69 (s; C-carbonyl)

4b: 25%, colorless rhombs, m.p. 134–135°C (ether/petroleum ether (30–50°C)).—^{1}H-NMR: δ = 2.27 (s; 3H, CH_3), 4.82 (s; 2H, CH_2), 6.45 (d, J = 9.6 Hz; 1H, 3-H), 7.24–7.47 (m; 3H, Aryl-H), 7.74 (d, J = 9.6 Hz; 1H, 4-H).—^{13}C-NMR: δ = 26.07 (q; CH_3), 71.92 (t; CH_2), 117.43 (d; C-3), 120.31 (s; C-4a), 124.28 (d), 124.79 (d), 125.86 (d), 137.89 (s; C-8a), 143.02 (d; C-4), 145.78 (s), 152.48 (s; C-carbonate), 158.97 (s; C-2), 200.81 (s; C-carbonyl)

4c: 35%, colorless needles, m.p. 145–147°C (ether).—^{1}H-NMR: δ = 2.31 (s; 3H, CH_3), 4.85 (s; 2H, CH_2), 6.38 (d, J = 9.7 Hz; 1H, 6-H), 6.87 (d, J = 2.2 Hz; 1H, 3-H), 7.60 (s; 1H, 4-H), 7.73 (d, J = 2.2 Hz; 1H, 2-H), 7.79 (d, J = 9.7 Hz; 1H, 5-H).—^{13}C-NMR: δ = 26.15 (q; CH_3), 72.18 (t; CH_2), 106.90 (d; C-3), 115.11 (d; C-4), 116.30 (s), 117.52 (d; C-6), 126.07 (s), 143.65 (s), 143.83 (d; C-5), 147.57 (d; C-2), 148.00 (s), 152.02 (s; C-carbonate), 159.37 (s; C-7), 200.93 (s; C-carbonyl)

en-substituted dioxetane **3c** is significantly lower. The lower triplet yield (ca. 4%) of **3c** should, however, still suffice for a photogenotoxic activity.

Received: April 6, 1987;
revised: May 13, 1987 [Z 2181 IE]
German version: *Angew. Chem.* 99 (1987) 817

[1] G. Rodighiero, F. Dall'Aqua, M. A. Pathak in K. C. Smith (Ed.): *Topics in Photomedicine*. Plenum Press, New York 1984.

[2] a) W. Adam, A. Beinhauer, B. Epe, R. Fuchs, A. Griesbeck, H. Hauer, P. Mützel, L. Nassi, D. Schiffmann, D. Wild in T. Friedberg, F. Oesch (Eds.): *Primary Changes and Control Factors in Carcinogenesis*, Deutscher Fachschriften-Verlag, Wiesbaden 1986, p. 64–67; b) L. Nassi, D. Schiffmann, W. Adam, R. Fuchs, A. Favre, *Mutation Res.*, in press.

[3] W. Adam, G. Cilento, *Angew. Chem.* 95 (1983) 525; *Angew. Chem. Int. Ed. Engl.* 22 (1983) 529.

[4] a) W. Adam, V. Bhushan, T. Dirnberger, R. Fuchs, *Synthesis 1986*, 330; b) W. Adam, V. Bhushan, R. Fuchs, U. Kirchgässner, *J. Org. Chem.*, in press.

[5] The compounds were characterized by the ^{1}H- and ^{13}C-NMR data given in Table 2 as well as by elemental analyses (C, H ± 0.3) and by IR and MS spectral data.

[6] W. Adam, K. Zinner in W. Adam, G. Cilento (Eds.): *Chemical and Biological Generation of Excited States*, Academic Press, New York 1982, Chapter 5.

[7] A. Beinhauer, unpublished.

[8] Chapter 4 in Ref. [6].

Cerium(IV)-Catalyzed Single Electron Transfer (SET) on Acenaphthene and 1,4-Dihydronaphtho-[1,8-*d,e*][1,2]diazepine: Chemical Evidence for Distinct Radical Cations**

By *Waldemar Adam,* Alicia Casado,* and *Miguel A. Miranda*

That the radical cation of acenaphthene (**1**) is naphthalenic-like (structure $\mathbf{1}^{\odot\oplus}$) rather than benzylic-like (structure $\mathbf{2}^{\odot\oplus}$) has been convincingly demonstrated by ESR and electronic spectra.[1] However, the question still is open, whether these structures rapidly interconvert and thus exhibit common chemistry, or whether a sufficiently large energy barrier separates them so that they manifest distinct chemical fates. Since a σ-π crossing obtains in the $\mathbf{1}^{\odot\oplus} \rightleftarrows \mathbf{2}^{\odot\oplus}$ interconversion, the latter behavior is anticipated. Indeed, we provide herewith experimental proof that the independently generated radical cations $\mathbf{1}^{\odot\oplus}$ and $\mathbf{2}^{\odot\oplus}$ are discrete species which undergo characteristic reactions.

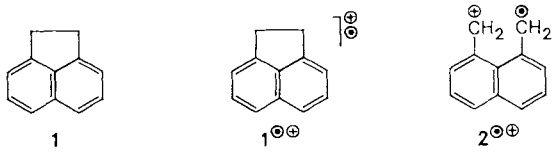

1 $1^{\odot\oplus}$ $2^{\odot\oplus}$

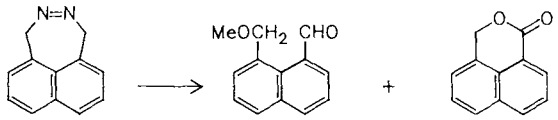

2 3 4

The azoalkane **2**[2] was oxidized with ceric ammonium nitrate in oxygen-saturated 80% aqueous methanol at 20°C, a potent single electron transfer (SET) oxidant that proved effective for the denitrogenation of azoalkanes[3] and the cleavage of carbon–carbon bonds in 1,2-diarylethanes[4] via the corresponding radical cations. Within 5 min complete nitrogen loss ensued and upon silica gel column chromatography the previously unknown methoxy aldehyde **3**[5] could be isolated in 25% yield and the lactone **4**[6] in 18% yield. Significant is that only traces of acenaphthene-derived products were observed. Furthermore, the triphenylpyrylium tetrafluoroborate(TPT)-sensitized photolysis of azoalkane **2**, which proved successful for the denitrogenation of cyclic azoalkanes via radical cations,[7] led exclusively to the tautomeric hydrazone.

To account for the products **3** and **4**, it is postulated that the benzylic-type radical cation $\mathbf{2}^{\odot\oplus}$ intervenes, which after trapping by methanol and molecular oxygen leads to

[*] Prof. Dr. W. Adam, A. Casado
Institut für Organische Chemie der Universität
Am Hubland, D-8700 Würzburg (FRG)
Prof. Dr. M. A. Miranda
Department of Organic Chemistry,
Faculty of Pharmacy
University of Valencia, E-46010 Valencia (Spain)

[**] This work was supported by the Alexander-von-Humboldt Foundation (*M. A. M.*), by the Deutschen Akademischen Austauschdienst (*A. C.*), as well as by the Deutsche Forschungsgemeinschaft and the Fonds der Chemischen Industrie.

the methoxy aldehyde **3**. Trapping of the radical cation $2^{\odot\oplus}$ with water and oxygenation affords first the corresponding hydroxy aldehyde, which is further oxidized to the lactone **4** via the hemiacetal. Related chemistry was reported for the Ce(IV)-catalyzed[4] and 1,4-dicyanonaphthalene-photosensitized[8] oxidation of 1,2-diarylethanes, except that the intervening radical cation had suffered rupture of the ethane bond since trapping products of the resulting benzyl cations and radicals were observed.

Oxidation of acenaphthene (**1**) with ceric ammonium nitrate in oxygen-saturated 80% aqueous methanol furnished methyl ether **5** (14%), alcohol **6** (12%), and ketone **7** (59%), all identified by comparison of TLC retention times and spectral data with those of the authentic materials. Clearly, these products are derived from the naphthalenic-type rad-

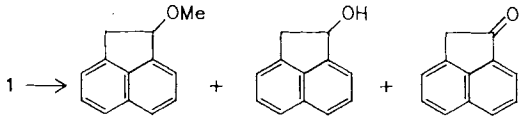

ical cation $1^{\odot\oplus}$,[1] which deprotonates to the acenaphthyl radical. Subsequent oxygenation with molecular oxygen affords eventually ketone **7**. Alternatively, further oxidation affords the acenaphthyl cation which is nucleophilically trapped by methanol or water to generate **5** and **6**, respectively. Significant is that only traces of ring-cleavage products such as the methoxy aldehyde **3** and lactone **4** were observed.

This dichotomy in chemical behavior in the Ce(IV)-catalyzed SET-oxidation of acenaphthene (**1**) and the azoalkane **2** is indicative of the structurally distinct radical cations $1^{\odot\oplus}$ and $2^{\odot\oplus}$, respectively of the naphthalenic and

$$\mathbf{1} \xrightarrow{\text{cerium(IV)}} \mathbf{1}^{\odot\oplus} \underset{}{\overset{\text{slow}}{\rightleftharpoons}} \mathbf{2}^{\odot\oplus} \xleftarrow{\text{cerium(IV)}} \mathbf{2}$$

benzylic type. An appreciable activation barrier ($E_a \geqq 20$ kcal/mol) must separate these two species for characteristic chemistry to become observable. At first sight this seems surprising since efficient carbon–carbon bond cleavage of radical cations derived from diarylethanes,[4] and more recently benzhydryl derivatives,[9] is well documented. However, in these flexible acyclic radical cations the σ-bond to be cleaved can align itself with the aromatic moiety to generate resonance-stabilized π-type benzyl or benzhydryl radicals and cations. In the rigid naphthalenic radical cation $1^{\odot\oplus}$ the σ-bond is fixed in the plane of the aromatic system, so that overlap of the orbitals of the incipient benzylic sites with the aromatic system to form the benzylic radical cation $2^{\odot\oplus}$ is only feasible after extensive σ-bond rupture. We propose that such σ-π crossing[10] is responsible for the slow $1^{\odot\oplus} \rightleftarrows 2^{\odot\oplus}$ valence isomerization on the chemical time scale. Related cases have been extensively investigated concerning photochemical transformations under matrix isolation.[11]

Received: April 8, 1987;
revised: May 13, 1987 [Z 2187 IE]
German version: *Angew. Chem. 99* (1987) 818

[1] A. C. Buchanan III, R. Livingston, A. S. Dworkin, G. P. Smith, *J. Phys. Chem. 84* (1980) 423; T. Shida, S. Iwata, *J. Am. Chem. Soc. 95* (1973) 3473; L. Andrews, R. S. Friedman, B. J. Kelsall, *J. Phys. Chem. 89* (1985) 4550.

[2] M. Gisin, J. Wirz, *Helv. Chim. Acta 59* (1976) 2273.

[3] J. Martelli, R. Grée, *J. Chem. Soc. Chem. Commun. 1980*, 355; H. Abdallah, R. Grée, R. Carrié, *Can. J. Chem. 63* (1985) 3031; A. K. M. M. Hoque, A. C. Kovelesky, W.-K. Lee, H. J. Shine, *Tetrahedron Lett. 26* (1985) 5655.

[4] W. S. Trahanovsky, D. W. Brixius, *J. Am. Chem. Soc. 95* (1973) 6778; I. P. Beletskaya, D. I. Makhon'kov, *Russ. Chem. Rev. 50* (1981) 534.

[5] **3**, colorless oil.—^{1}H-NMR ($CDCl_3$; 200 MHz): $\delta = 10.4$ (s; 1H), 8.10–7.20 (m; 6H), 4.73 (s; 2H), 3.37 (s; 3H).—^{13}C-NMR ($CDCl_3$; 50 MHz): $\delta = 192.1$ (d), 143.5 (s), 135.0 (s), 134.6 (s), 131.4 (d), 130.9 (s), 128.3 (d), 128.0 (d), 123.9 (d), 121.4 (d), 121.0 (d), 70.9 (t), 55.5 (q).

[6] J. Cason, D. M. Lynch, A. Weiss, *J. Org. Chem. 38* (1973) 1944.

[7] a) W. Adam, M. Dörr, *J. Am. Chem. Soc. 109* (1987) 1570; b) S. C. Blackstock, J. K. Kochi, *ibid. 109* (1987) 2484.

[8] L. W. Reichel, G. W. Griffin, A. J. Müller, P. K. Das, S. N. Ege, *Can. J. Chem. 62* (1984) 424.

[9] A. Okamoto, M. S. Snow, D. R. Arnold, *Tetrahedron 42* (1986) 6175.

[10] W. G. Dauben, L. Salem, N. J. Turro, *Acc. Chem. Res. 8* (1975) 41; E. M. Evleth, P. M. Horowitz, T. S. Lee, *J. Am. Chem. Soc. 95* (1973) 7948.

[11] T. Shida, E. Haselbach, T. Bally, *Acc. Chem. Res. 17* (1984) 180.

Stable Germaethenes**

By *Harald Meyer, Gerhard Baum, Werner Massa,* and *Armin Berndt**

The existence of short lived germaethenes has been demonstrated by trapping reactions.[1,2] We have now prepared stable germaethenes and characterized them spectroscopically, in one case also by a crystal structure analysis. Reaction of the electrophilic cryptocarbene **1** (**2**)[3] with the germanediylenes **3a**[4] and **3b**[5] in pentane at room temperature afforded the germaethenes **4a** and **4b**, respectively, as sole products. The lemon-yellow and pale yellow crystals of **4a** and **4b** very slowly decolorize on ex-

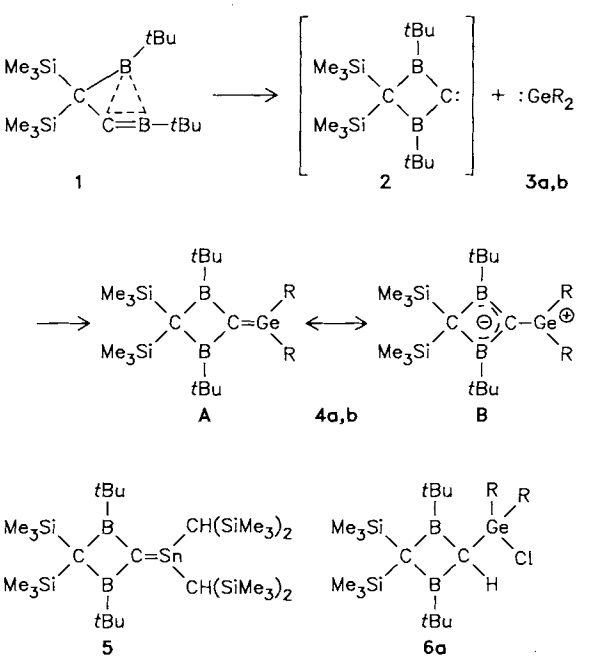

a, R = $N(SiMe_3)_2$; **b**, R, R = $NtBu(Si(CH_3)_2)NtBu$

[*] Prof. Dr. A. Berndt, H. Meyer, G. Baum, Priv.-Doz. Dr. W. Massa
Fachbereich Chemie der Universität
Hans-Meerwein-Strasse, D-3550 Marburg (FRG)

[**] This work was supported by the Deutsche Forschungsgemeinschaft and the Fonds der Chemischen Industrie.

posure to air (**4a** within 3d) and melt without decomposition at 167 and 183 °C, respectively. The recently described stannaethene **5**[3] decolorizes within 2 h under the same conditions and already decomposes at 133 °C. **4a** adds HCl with quantitative formation of the colorless, crystalline 1,3-diboretane **6a**.

The structures of **4a**, **4b**, and **6a** follow from their ^{1}H-, ^{13}C-, and ^{11}B-NMR spectra.[6] The tricoordinated C atoms of **4a** and **4b**, with $\delta(^{13}C) = 115$ and 93 respectively, are noticeably shielded compared to the corresponding atom in **5** ($\delta = 142$), whereas the B atoms, with $\delta(^{11}B) = 66$ and 65 respectively, exhibit almost the same chemical shift as in **5** ($\delta = 64$). They are more strongly shielded than the B atoms of the 1,3-diboretane **6a** ($\delta = 82$), thus indicating a relatively large amount of negative π charge on the B atoms and a similar ylide character (resonance formula **B**) of the CGe double bonds in **4a** and **4b** as in **5**.

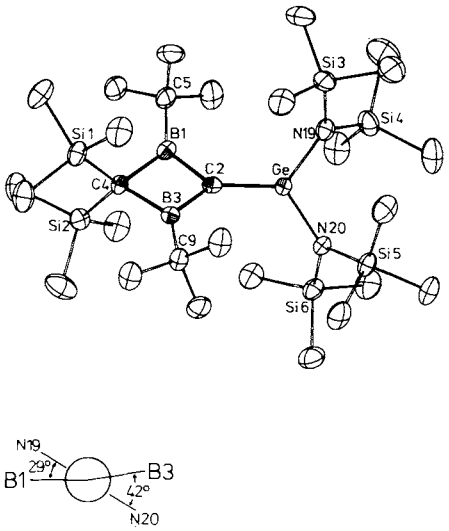

Fig. 1. Top: ORTEP drawing of the crystal structure of **4a**. The vibration ellipsoids are given at the 30% probability level. Projection onto the C2,N19,N20 plane; H atoms not shown. Important bond lengths [Å] and angles [°]: Ge-C2 1.827(4), Ge-N19 1.818(4), Ge-N20 1.835(4), B1-C2 1.534(7), B1-C4 1.626(6), B1-C5 1.586(8), B3-C2 1.523(6), B3-C4 1.628(6), B3-C9 1.604(7), C4-Si1 1.889(4), C4-Si2 1.887(5), B1···B3 2.070(7), C2···C4 2.374(5); C2-Ge-N19 125.3(2), C2-Ge-N20 124.1(2), N19-Ge-N20 110.5(2), Ge-C2-B1 138.6(4), Ge-C2-B3 135.8(4), B1-C2-B3 85.3(4), C2-B1-C4 97.4(4), B1-C4-B3 79.0(3), C4-B3-C2 97.8(4), Si1-C4-Si2 112.6(3). Torsion angle: B1-C2-Ge-N19 29.4(6), B1-C2-Ge-N20 −148.3(4), B3-C2-Ge-N19 −140.3(4), B3-C2-Ge-N20 42.0(5), Ge-C2-B1-C4 −178.9(4), Ge-C2-B3-C4 179.3(4).— Bottom: Newman projection along the C2-Ge bond.

An X-ray structure analysis[7] of **4a** (Fig. 1 top) confirmed the significance of the ylide resonance formula **B** with short distances C2-B1 (1.534(7) Å) and C2-B3 (1.523(6) Å). The distance from the germanium atom to the tricoordinated C2-atom (1.827(4) Å) is 3% longer than that calculated for $H_2C{=}GeH_2$ (1.773 Å).[8] The GeC single bond in $Ge(CH_3)_4$ (1.98 Å)[9] is 8.4% longer than in **4a**. The torsion angles B1-C2-Ge-N19 and B3-C2-Ge-N20 (Fig. 1, bottom) are 29.4(6) and 42.0(5)°, respectively, the average twist angle at the C=Ge bond is therefore 36°. The angles between the line through C2-Ge and the N19,Ge,N20 and B1,C2,B3 planes are 1.7 and 4.8°, respectively, i.e. the Ge atom is practically planar coordinated, the C2 atom slightly pyramidalized. The stannaethene **5** exhibits an average twist angle of 61° and dihedral angles of 5° and 16° respectively at the Sn and C2 atoms. Thus the germaethene **4a** is considerably less twisted than the stannaethene **5** and markedly less puckered, especially at the C atom.

Experimental:

4a: A solution of **3a** (1.42 g, 3.6 mmol) in pentane (10 mL) was treated with **1** (1.11 g, 3.6 mmol) at room temperature. After 2 d only **4a** is detectable by ^{13}C-NMR spectroscopy. It precipitates in the form of lemon-yellow crystals (m.p. 167 °C) on cooling the pentane solution to −25 °C.

Received: March 25, 1987 [Z 2162 IE]
German version: *Angew. Chem. 99* (1987) 790

CAS Registry numbers:
1, 87556-27-2; **3a**, 59863-12-6; **3b**, 84806-15-5; **4a**, 109531-23-9; **4b**, 109552-48-9; **6a**, 109531-24-0.

[1] J. Satgé, *Adv. Organomet. Chem. 21* (1982) 241.
[2] N. Wiberg, C.-K. Kim, *Chem. Ber. 119* (1986) 2966, 2980.
[3] H. Meyer, G. Baum, W. Massa, S. Berger, A. Berndt, *Angew. Chem. 99* (1987) 559; *Angew. Chem. Int. Ed. Engl. 26* (1987) 546.
[4] M. J. S. Gynane, D. H. Harris, M. F. Lappert, P. P. Power, P. Rivière, M. Rivière-Baudet, *J. Chem. Soc. Dalton Trans. 1977*, 2004.
[5] M. Veith, M. Grosser, *Z. Naturforsch. B37* (1982) 1375.
[6] Spectra recorded in C_6D_6, [D_{10}]dimethoxyethane (^{13}C-NMR of **4a**, **b** at −35 °C), and $CDCl_3$ (**6a**). **4a** (yield: ^{13}C-NMR-spectroscopically quantitative): ^{1}H-NMR: $\delta = 1.2$ (s, 18 H, *t*Bu), 0.3 (s, 18 H, $SiMe_3$), 0.25 (s, 36 H, $SiMe_3$); ^{13}C-NMR: $\delta = 115.0$ (br. s, 1 C, C=Ge), 31.8 (q, 6 C, *t*Bu), 26.3 (br. s, 2 C, CMe_3), 26.1 (br. s, 1 C, Si_2C), 6.5 (q, 6 C, $SiMe_3$), 5.9 (br. q, 12 C, $SiMe_3$), the signal at $\delta = 5.9$ is sharp at room temperature, ^{11}B-NMR: $\delta = 66$.—**4b** (yield: ^{13}C-NMR-spectroscopically quantitative): ^{1}H-NMR: $\delta = 1.3$, 1.2 (s, each 18 H, *t*Bu), 0.4 (s, 18 H, $SiMe_3$), 0.2 (s, 6 H, $SiMe_2$); ^{13}C-NMR: $\delta = 93.2$ (br. s, 1 C, C=Ge), 54.4 (s, 2 C, NC), 34.6 (q, 6 C, N*t*Bu), 31.2 (q, 6 C, B*t*Bu), 25.0 (br. s, 2 C, BC), 24.1 (br. s, 1 C, B_2C), 5.3 (q, 6 C, $SiMe_3$), 4.5 (q, 2 C, $SiMe_2$); ^{11}B-NMR: $\delta = 65$.—**6a**: colorless crystals, m.p. 195 °C (decomp.), yield: ^{13}C-NMR-spectroscopically quantitative; ^{1}H-NMR: $\delta = 1.57$ (s, 1 H, B_2CH), 1.26 (s, 18 H, *t*Bu), 0.37, 0.30 (s, each 18 H, $SiMe_3$); ^{13}C-NMR: $\delta = 59.3$ (br. d, $J(^{13}C\text{-}H) = 99$ Hz, 1 C, B_2CH), 52.5 (br. s, 1 C, CSi_2), 31.2 (q, 6 C, *t*Bu), 28.3 (br. s, 2 C, CMe_3), 7.8 (br. q, 12 C, $SiMe_3$), 7.2, 5.8 (q, each 3 C, $SiMe_3$); ^{11}B-NMR: $\delta = 82$.
[7] Space group $P2_1/c$, $Z = 4$, $a = 18.727(2)$, $b = 9.154(1)$, $c = 25.627(2)$ Å, $\beta = 105.01(1)°$, 4109 independent reflections $> 3\sigma(F_0)$, measured at 294 K on a four-circle diffractometer (CAD4, Enraf-Nonius) with $Mo_{K\alpha}$ radiation. Refinement of the heavier atoms with anisotropic temperature factors, H atoms riding at idealized positions (d(C-H) = 0.95 Å) and with isotropic temperature factors. $R_w = 0.036$ (weighting $w = 1/\sigma^2(F_0)$), 426 parameters, $S = 1.914$. Further details of the crystal structure investigation are available on request from the Fachinformationszentrum Energie, Physik, Mathematik GmbH, D-7514 Eggenstein-Leopoldshafen 2 (FRG), on quoting the depository number CSD-52600, the names of the authors, and the journal citation.
[8] K. D. Dobbs, W. J. Hehre, *Organometallics 5* (1986) 2057, and references cited therein.
[9] E. G. Rochow, E. W. Abel: *The Chemistry of Germanium, Tin and Lead*, Pergamon, Oxford 1975.

Preparation of $F_4S{=}CH{-}COF$ by Isomerization of $F_5S{-}CH{=}C{=}O$**

By *Thomas Krügerke, Jürgen Buschmann, Gert Kleemann, Peter Luger,* and *Konrad Seppelt**

The alkylidene sulfur tetrafluorides $R_2C{=}SF_4$ are of special interest because of their stable, essentially nonpolar C=S double bond and their unique structure. The first compound of this type, $CH_2{=}SF_4$, was prepared in several steps from pentafluoro-λ^6-sulfanylacetic acid **1**.[1] We have

[*] Prof. Dr. K. Seppelt, Dipl.-Chem. T. Krügerke, Dr. J. Buschmann, Dr. G. Kleemann, Prof. Dr. P. Luger
Institut für Anorganische und Analytische Chemie und
Institut für Kristallographie der Freien Universität
Fabeckstrasse 34-36 and Takustrasse 6, respectively, D-1000 Berlin 33

[**] This work was supported by the Deutsche Forschungsgemeinschaft and the Fonds der Chemischen Industrie.

now synthesized two new compounds from **1** by simple reactions, namely the ketene **2** and the compound **4**, the first alkylidenesulfur tetrafluoride with a functional group.

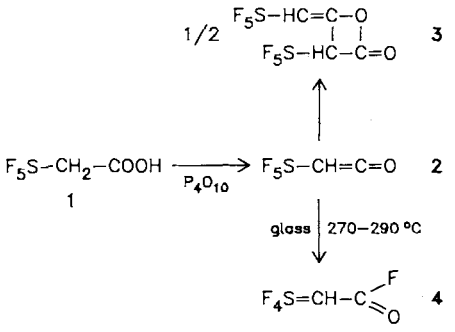

The interesting pentafluoro-λ^6-sulfanylketene **2** is first obtained from **1** by removal of water with P_4O_{10}. **2** is stable for long periods of time at room temperature. On heating, it dimerizes to **3**, and in the presence of active fluoride, such as KF, CsF, it polymerizes to a rubbery solid. Aside from this, **2** undergoes typical double bond addition reactions for ketenes (HCl, H_2O, EtOH, Br_2). Unexpectedly, we observed **2** to thermally isomerize to fluorocarbonylmethylidenesulfur tetrafluoride (tetrafluoro-λ^6-sulfanylideneacetyl fluoride) **4** at reduced pressure in the presence of glass (not quartz).

This 1,3-fluoride migration is surprising, because a C=C double bond is given up in favor of a C=S double bond. Due to the necessity of a weakly basic catalyst (glass powder) we assume that this isomerization proceeds intermolecularly. The driving force behind the isomerization is, of course, the gain in energy on replacement of cumulation by conjugation.

That conjugation is in fact present, follows from the low-temperature crystal structure analysis (−168 °C) of this compound, which is liquid at room temperature (Fig. 1). The molecular skeleton of **4** is planar, except for the

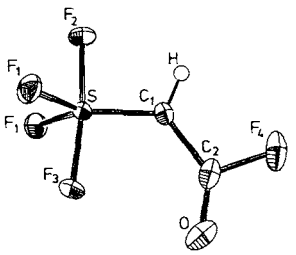

Fig. 1. Structure of F_4S=CH–COF **4** in the crystal [9] at −168 °C, ORTEP, 50% probability level. Bond lengths [pm] and selected angles [°]: S-F1 154.0(1), S-F2 158.3(2), S-F3 156.9(2), S-C1 160.2(2), C1-H 0.93(5), C1-C2 145.3(3), C2-O 117.8(4), C2-F4 136.6(4); F1-S-F1 101.72(7), F2-S-F3 172.19(9), S-C1-C2 126.2(2), O-C2-F4 119.0(2). All atoms except F1 are located on the crystallographic mirror plane.

two equatorial fluorine atoms F1 on the sulfur. Since H and COF lie in the same plane as the axial fluorine atoms F2 and F3, the structure type of the alkylidenesulfur tetrafluorides is confirmed.[1-3] The two heteroatomic double bonds are cisoid! The same structure as that found at −168 °C was also found at −40 °C. The C=S double bond in **4** (160.2 pm) is slightly longer than that in H_2C=SF_4 (155.4 pm),[3,4] as would be expected if conjugation is present. On the other hand, the central C–C bond (145.3 pm) is even shorter than the central C–C bond in butadiene (146.5 pm).[5] The CO bond is marginally shorter (117.8 pm), the CF bond somewhat longer (136.6 pm) than in H_3C–COF (118.5 and 136.2 pm).[6] For comparison: butadiene has its energetic ground state in the transoid form, whereas at −161 °C acryloyl fluoride (H_2C=CH–COF) exists 76% in the transoid form and 24% in the cisoid form.[7] Possibly, the cisoid form is favored for steric reasons: In the transoid conformation F3 and F4 would only be 187 pm apart.

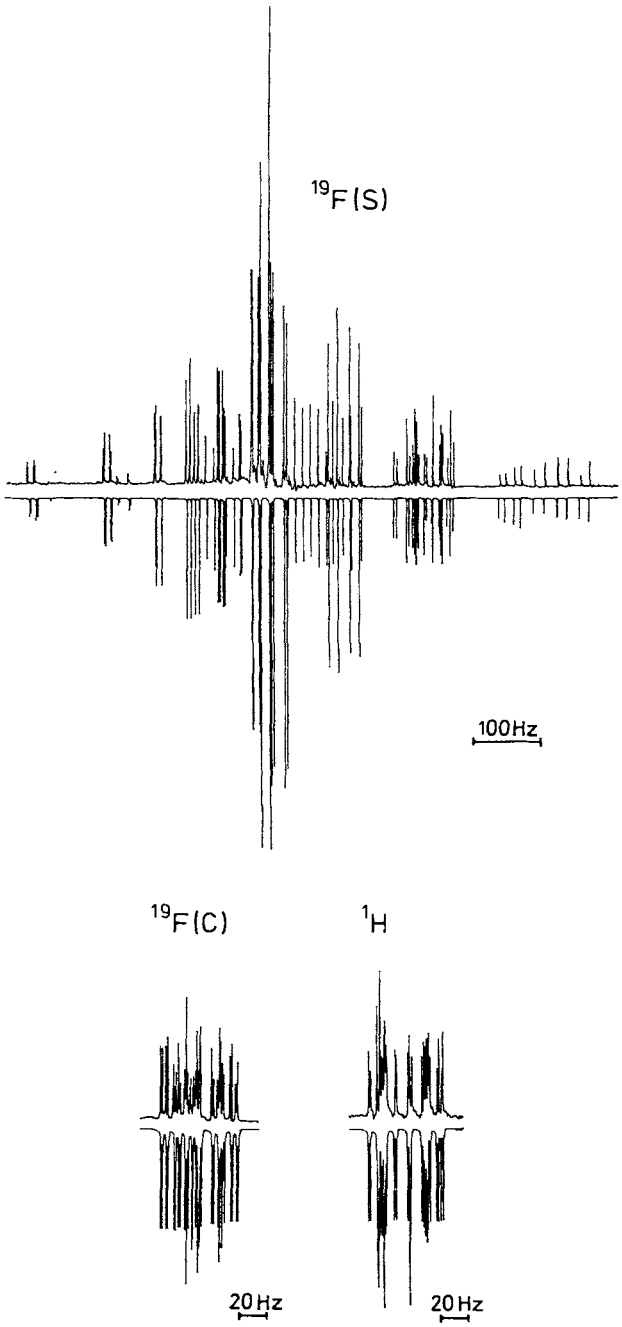

Fig. 2. ^{19}F- and ^{1}H-NMR spectra of F_4S=CH–COF **4** at +25 °C, 84.25 and 90 MHz, respectively, CD_3CN. Top: measured spectrum; bottom: simulation with the following values: A_2BCDX spectrum: $\delta F_A = 60.9$, $\delta F_B = 59.1$, $\delta F_C = 57.0$, $\delta F_D = 42.9$, $\delta H_{(X)} = 4.4$; $J_{AB} = 165.3$, $J_{AC} = 165.9$, $J_{AD} = -4.2$, $J_{BC} = 11.7$, $J_{BD} = -34.2$, $J_{CD} = -14.1$, $J_{AX} = 8.2$, $J_{BX} = -11.1$, $J_{CX} = -38.8$, $J_{DX} = -1.3$ Hz.

A striking feature is that the angle between the equatorial fluorine atoms is markedly larger (101.71°) than in $H_2C{=}SF_4$ (96.6°),[3] while the angle between the axial fluorine atoms is nearly the same in both compounds. It can be concluded from these results that there is a reduction in the π-electron density at the C=S double bond in the equatorial plane.

The complex ^{19}F- and ^1H-nuclear resonance spectra, which are temperature-independent between −130 and +100°C (Fig. 2), reveal the presence of a rigid C=S bond, since torsion about this bonding axis and Berry pseudorotation of the fluorine atoms on the fivefold coordinated sulfur atom would be coupled processes. There are also no indications of a freezable rotation of the COF group.[8] In the case of acryloyl fluoride the rotation of this group is frozen out at −154°C ($\Delta H^{\neq} = 23.8$ kJ/mol).[6]

Experimental

2: A vertically oriented heatable glass tube was loosely packed with Siccapent, P_4O_{10}/sand mixture and P_4O_{10}. The tube was heated with a temperature gradient from 60°C (top) to 160°C (bottom). 15 g of **1** was sublimed at the top of the system and pumped through the tube within two days (10^{-1} mbar) and frozen out at −196°C. Vacuum condensation at −100°C furnished 10.6 g (70%) of pure **2** as a colorless liquid, b.p. 47°C. MS (80 eV): *m/z* 168 ($M^{\oplus}$, 100%). IR (gaseous): $\tilde{\nu}$ = 3135 (w), 2177 (s), 1325 (w), 878 (vs), 720 (m) cm^{-1}. ^{19}F-NMR: AB_4X spectrum $\delta_A = 80.2$, $\delta_B = 88.7$, $J_{AB} = 152.7$ Hz. ^1H-NMR: $\delta = 5.5$ ($J(H\text{-}F_B) = 5.7$ Hz).

4: 2 g of **2** was passed at ca. 10^{-1} bar through a tube packed with glass chips heated to 270–290°C and finally frozen out. Vacuum condensation at −78°C and fractional crystallization at −70°C afforded 1 g (50%) of pure **4**. Colorless liquid, m.p. −29°C. MS (80 eV): *m/z* 168 ($M^{\oplus}$, 56%). IR (gaseous): $\tilde{\nu}$ = 3154 (vw), 1859 (vs), 1818 (m), 1372 (s), 1254 (vw), 1155 (s), 1116 (m), 1089 (m), 932 (s), 860 (vs), 798 (s), 791 (w), 678 (w), 614 (w), 582 (w) cm^{-1}.

Received: April 3, 1987 [Z 2178 IE]
German version: *Angew. Chem. 99* (1987) 808

[1] a) G. Kleemann, K. Seppelt, *Angew. Chem. 90* (1978) 547; *Angew. Chem. Int. Ed. Engl. 18* (1978) 516; b) H. Bock, J. E. Boggs, G. Kleemann, D. Lentz, H. Oberhammer, E. M. Peters, K. Seppelt, A. Simon, B. Solouki, *ibid. 91* (1979) 1008 and *18* (1979) 944.

[2] G. Kleemann, K. Seppelt, *Chem. Ber. 116* (1983) 645.

[3] A. Simon, E. M. Peters, D. Lentz, K. Seppelt, *Z. Anorg. Allg. Chem. 468* (1980) 7.

[4] K. Kuchitsu, T. Fukayama, T. Morino, *J. Mol. Struct. 4* (1969) 41.

[5] a) A. Almenningen, O. Bastiansen, M. Traetteberg, *Acta Chem. Scand. 12* (1958) 1221; b) J. Marais, N. Sheppard, B. P. Stoicheff, *Tetrahedron 17* (1962) 163.

[6] S. Tsuchiya, *J. Mol. Struct. 22* (1974) 77.

[7] F. S. Lin, K. L. Servis, *J. Am. Chem. Soc. 94* (1972) 5794.

[8] The finding that the NMR spectra remain unchanged over the whole temperature range can be interpreted in three ways: 1) The conjugated molecular system is still rigid and flat even at +100°C (unlikely). 2) The COF group still rotates freely even at −140°C (equally unlikely). 3) The difference in energy between the cisoid form and all other conformations is so large that these are present in only smallest amounts in the equilibrium. Hence the NMR signals remain *almost* unchanged on freezing-in the COF rotation.

[9] A 0.3-mm-thick glass capillary was filled to ca. 3 mm high with **4** by vacuum condensation. Low-temperature differential thermal analysis up to −140°C showed no transformation apart from the melting point. The crystals were grown directly on a Siemens four-circle diffractometer according to a method already described in the literature [10]. For the intensity measurement, the sample was cooled to −168°C. **4**, $P2_1/m$, $a = 570.3(3)$, $b = 575.8(3)$, $c = 917.4(4)$ pm, $\beta = 125.35(3)°$, $Z = 2$, $\rho_{calc} = 2.258$ g cm^{-3} at −168°C, 1252 measured reflections up to $2\theta = 72°$, 1207 reflections with $I \geq 2\sigma(I)$, 56 parameters, $R = 0.037$, $R_w = 0.041$. Further details of the crystal structure investigation are available on request from the Fachinformationszentrum Energie, Physik, Mathematik GmbH, D-7514 Eggenstein-Leopoldshafen 2 (FRG), on quoting the depository number CSD-52440, the names of the authors, and the journal citation.

[10] P. Luger, J. Buschmann, *J. Am. Chem. Soc. 102* (1984) 7118.

BOOK REVIEWS

EXAFS: Basic Principles and Data Analysis (Volume 9 in the series **Inorganic Chemistry Concepts**). By *B. K. Theo*. Springer, Berlin 1986. xviii, 349 pp., bound, DM 188.00.—ISBN 3-540-15833-2

Despite the growth of interest in fine structure X-ray spectroscopy (EXAFS), which is due to the availability of synchrotron radiation, there has hitherto been no easily accessible introduction to this topic. This book should now fill that gap.

The author's strategy, based on his considerable experience of experimental and theoretical work, is to lead the reader from fundamental principles and simple analysis of data to more advanced theories and complex calculations. This approach is especially welcome, as it offers both beginners and specialists an appropriate choice of entry points into the material presented. The text and diagrams are very clear, and the derivations of the formulae can be followed without too much effort.

Of the book's eight chapters, the first two introduce the properties of X-rays and electrons, their interactions with matter, the elementary theory of EXAFS, and the analysis of data. In the third chapter the EXAFS parameters (phase shift and E_0) are discussed qualitatively and represented graphically. This is especially useful for beginners wishing to develop a feeling for the technique. The next two chapters present the generalized theory and its refinements (including L-edges), lifetime effects, and in particular static and dynamic disorder effects. Chapter 6 covers practical data analysis and most aspects of filtering, curve fitting and phase information. This is followed by a chapter on theoretical amplitudes and phase functions. The final chapter presents a good review of multiple scattering effects and the determination of bond angles. Information on edge characteristics, Victoreen coefficients, fluorescence yields, scattering amplitudes and phases is contained in seven appendixes.

The book has only two weaknesses, which could easily be remedied in a later edition. It is to be regretted that experimental aspects are not mentioned at all, especially since the book "EXAFS Spectroscopy: Techniques and Applications" (edited by *B. K. Theo* and *D. C. Joy*, 1981) is already out of date. Secondly, the book should include some insight into, and a feeling for, factors such as energy resolution, harmonic contamination, and detector limita-

tions, which affect the quality of the experimental results; this would be especially useful for beginners and non-specialists. On p. 23 it is promised that "details of various experimental methods will be discussed elsewhere", but unfortunately "elsewhere" turns out to be outside this book. Another drawback is that the bibliography, which contains more literature references than are cited in the text—in itself a plus point—gives no indication as to the literature sources actually used in the text. A comment preceding each of these citations would have served the purpose.

Finally, there is a criticism which is addressed more to the publisher than to the author. Only purists would object to the use of the shorter American spellings, but in this age of word processing systems with in-built correction of errors the Springer Press might easily have avoided errors like "revolutionalize" or "parameterization", especially when one takes into consideration the price of this book.

Despite these minor details, the book can be highly recommended, not only to those who use EXAFS or would like to use it, but also to all physicists, chemists and biochemists who are looking for a work of reference which will give them a feeling for this technique and its capabilities and limitations.

M. Koch [NB 808 IE]
EMBL Outstation Hamburg (FRG)

Chemie der Hauptgruppenelemente - Stand und Erwartung (Leopoldina Symposium, Halle GDR, October 9-12, 1985). Edited by *G. Fritz, R. Hoppe,* and *K. Issleib*. Wissenschaftliche Verlagsgesellschaft, Stuttgart 1985. vi, 397 pp. (Nova Acta Leopoldina, New Series no. 264), paperback, DM 36.00.—ISBN 0369-5034

The papers collected together in this volume were presented at a symposium whose purpose was to give an overview of the current situation in the chemistry of the main group elements, and to evaluate the developments reported. In the preface the editors explain that for several reasons it was not possible to treat the whole of the chemistry of the main group elements in a uniform way. The choice of contributors resulted in certain topics being emphasized, but also gave benefits in depth of treatment.

The first quarter of the book is devoted to phosphorus chemistry, with special emphasis on low coordination numbers and on the formation and breaking of phosphorus-phosphorus bonds. It is fascinating to note how rapidly the chemistry of phosphorus with coordination numbers one and two, e.g. in pericyclic reactions, is developing: more is now known about Cope rearrangements in phospha-compounds than in thia-compounds. Equally interesting are the analogies between the nucleophilic degradation of phosphorus and sulfur compounds, e.g. the cleavage of cyclophosphanes by phosphinite to give phosphinyl phosphide, which is related to the formation of thiosulfate by the reaction of elemental sulfur with sulfite. In these phosphorus reactions ^{31}P-NMR spectroscopy might contribute further to an understanding of the chain breaking and reforming steps. Some recent results (on alkylidynephosphanes) lead one to expect that connections between the chemistry of main group elements and that of transition metals in high oxidation states will become more important in the future. Such connections are apparent, for example, in the reactions of 2,2-dimethylpropylidynephosphane (a Becker phosphaalkyne) with 2,2-dimethylpropylidynetri(*tert*-butoxy)tungsten (Schrock carbyne complex), or with $TaCl_5$, giving a polycyclic cation $(t\mathrm{BuCP})_6\mathrm{P}^{\oplus}$ of the 1,3,5-triphosphatris(homocyclopropenylium) type.

The next part of the book contains papers on solid state structural chemistry, with the emphasis on oxides and Zintl phases, these areas of inorganic chemistry being neatly brought together under the title "Zintl phases as complex ligands".

The second part of the book contains four papers on sulfur chemistry, and two each on boron chemistry and on metals in low oxidation states. The book concludes with four papers concerned with silicon. A neat link with synthetic organic chemistry is forged here, in the discussion on acyllithium reagents.

A three-day symposium cannot, of course, cover everything in the chemistry of main group elements which is currently of special interest. Nevertheless, important trends such as reactive species, low coordination numbers and novel types of multiple bonds formed by phosphorus, sulfur and boron to carbon or nitrogen, the effects of "inert" electron lone pairs in main group heavy elements, cluster compounds, and molecular aggregates are all treated by means of numerous examples.

This book, which contains the texts of 26 plenary lectures (three of them, by *J. D. Corbett, N. N. Greenwood,* and *D. Seyferth,* being in English), and consists of 400 pages with nearly 800 literature references, gives a very up-to-date survey of the basic research activities of well-known inorganic chemists of the German-speaking world. Its price is very reasonable (almost comparable in that respect to the inexpensive volumes 100, 200, and 300 of the expensive Journal of Organometallic Chemistry), and this readable and very useful volume can therefore be recommended for purchase even by advanced undergraduate and post-graduate students who are familiar with reading German, to increase the depth of their knowledge of inorganic chemistry.

Wolf-Walther du Mont [NB 805 IE]
Fachbereich Chemie der Universität Oldenburg (FRG)

Organometallic Intramolecular-coordination Compounds. By *I. Omae*. Elsevier, Amsterdam 1986. x, 402 pp., bound, HFl 250.00.—ISBN 0-444-42584-5

The author has assembled together in this book a series of review articles on the topic defined in the title, setting out to bring them up to date with the latest situation (as at the editorial deadline of the end of 1984). He expresses the hope that his book will be useful to undergraduate students, graduate students and research workers. It is arranged in eight chapters followed by two appendixes (1. The Periodic Table and Electronegativity, 2. Atomic masses, van der Waals radii, and Covalent radii) and a subject index.

Chapter 1 deals with general considerations. According to the definition of *Bähr* (1955), organometallic intramolecular complexes are compounds in which a metal atom is covalently bonded to an alkyl or aryl group having a donor atom as a substituent, and also forms a coordinative bond to that donor atom, giving a chelate ring. Such intramolecular complexes are here further classified according to the nature of the donor center. Following an account of the history of such compounds, their general properties are discussed, including ring size, structure, and the types of reactions which produce them.

The chapters which follow relate to the various types of donor centers involved in the coordinative bond. Thus, for

example, Chapter 2 deals with many different chelate complexes containing a metal-nitrogen bond as part of the organometallic ring.

The subdivision of the chapters does not follow a uniform pattern. Chapter 2 (85 pp.) is divided into ten sections according to the classification of the nitrogen-containing ligands. This chapter ends, as do all the others, with a section entitled "Concluding remarks" and a comprehensive bibliography.

Chapters 3, 4 and 6 (phosphorus, arsenic and sulfur compounds respectively) are, in contrast, subdivided according to the size of the chelate ring.

Chapter 5 (43 pp.) has yet a further different construction. First there is a coarse division into carbonyl-oxygen ligands and alkoxy-oxygen ligands, which are then further subdivided according to the compound type of the ligand (e.g. dicarboxylic acid esters, monocarboxylic acid esters, ketones, amides), the relevant complexes in each case being listed according to the type of formation reaction.

Chapter 7 (8 pp.) is devoted to halogen compounds as ligands, and lastly Chapter 8 (126 pp.) to π-complexes, subdivided into vinylene, π-allyl, cyclopentadienyl and aryl compounds.

The individual chapters list compounds, structures and reactions in the style which is familiar from the "Annual Surveys" in the Journal of Organometallic Chemistry. Consequently the book has, taken as a whole, the character of a rather heterogeneous collection of review articles.

A preliminary glance through the book produces a quite favorable impression. The direct reproduction method used for the text allows rapid publication, thus ensuring coverage of very recent literature, and hence topicality. On closer study, however, the initial good impression fades rather quickly. The numerous typographical errors are especially noticeable and tiresome, and where these occur in formulae or equations they often alter the meaning, demanding great vigilance on the part of the reader.

A similar degree of carelessness is, regrettably, also found in the text. Thus, for example, on p. 12 the following comment is made concerning a manganese-nitrogen interatomic distance: "The ability for ring formation of the compounds varies with type of metal and coordinating atom. Where the metal is manganese and the coordinating atom is nitrogen, the metal-nitrogen bond length of, e.g., (tetracarbonyl)-*N,N*-dimethylbenzylamine-manganese 1-33 is 2.139 Å (the sum of the covalent radii ($1.18(r(\mathrm{Mn})+0.7(r(\mathrm{N})=1.88$ Å [68])); therefore, the coordination bond is strong because the length is only 0.26 Å longer than the sum of covalent radii." The author could have spared himself this nonsensical interpretation if he had carefully read the original paper, since the Mn-N distance is there discussed correctly.

Also the author has had some difficulties with the nomenclature of these chelate complexes. This may be excusable with complicated compounds, but ought not to arise with substances such as $AgPF_6$ ("silver hexafluorophosphine"). There are, too, many other places in the book where chemical expressions are carelessly used. Hydrogen halides, carbon monoxide and the benzyl group are all described as "leaving groups" in the formation of chelate rings (p. 17), despite the fact that this term, as used in organic chemistry, is properly defined. Again, the author refers to the decarbonylation of acyl- and arylcarbonyl complexes as two types of "eliminations" (p. 23). On p. 25, chelate-forming reactions of the same type are differentiated under the headings "Insertions" and "Condensations". Phosphanes, amines and "acetylacetone" (by which is meant the acetylacetonate ligand) are regarded by the author as donor ligands of similar strengths (p. 29).

The title of the book is, in this reviewer's opinion, now an outdated terminology. *Bähr* in his definition distinguishes between covalent and coordinative bonding. We now know, however, that so-called coordinative bonds are also covalent in nature. The author's use of the term "intramolecular complex" also leads him to define an "intermolecular complex". This does not mean a complex of several nuclei bridged by ligands, but on the other hand a mono-nuclear compound with, for example, two terminal η^1-nitrogen ligands (pp. 15, 57).

Because of the existence of these many inaccuracies (the list of which could easily be extended), one would definitely not wish to see this book used by "undergraduate and graduate students". In view of its specialized nature this is, in any case, not likely. This leaves only the "research workers" as a potential readership for the book. It is not suited for use as a textbook-type monograph, for the reasons which have been given. For someone beginning work in the field of "organometallic intramolecular complexes" the extensive bibliography (about 1500 references) will certainly be welcome as a means of quick access to the original literature. However, contrary to the author's claims there are significant gaps in the coverage, especially on three-membered ring complexes. Consequently, neither can it be regarded as a reference book on organometallic intramolecular complexes with complete coverage of the literature up to the end of 1984. In view of the shortage of resources in many libraries, avoiding the purchase of this book would not cause much hardship.

Lothar Weber [NB 784 IE]
Institut für Anorganische Chemie
der Universität-Gesamthochschule, Essen (FRG)

Inorganic Solid Fluorides. Chemistry and Physics. Edited by *P. Hagenmüller*. Academic Press, New York 1985. xv, 628 pp., bound, $99.00.—ISBN 0-12-313380-X

This book sets out to collect together knowledge about the preparation and the chemical and physical properties of inorganic solid fluorides. The inclusion of contributions from theoreticians underlines the intention that the book should have an interdisciplinary character, and thus be equally useful from the viewpoints of the solid state chemist and the solid state physicist.

The book consists of 21 chapters as follows: *P. Hagenmüller* General Trends; *J. Grannec, L. Lozano* Preparative Methods; *D. Babel, A. Tressaud* Crystal Chemistry of Fluorides; *B. L. Chamberland* The Crystal Chemistry of Transition Metal Oxyfluorides; *C. R. A. Catlow* Defects in Solid Fluorides; *R. Hoppe* High Oxidation States in Fluorine Chemistry; *J. Videau, J. Portier* Fluoride Glasses; *N. Watanabe, H. Touhara, T. Nakajima, N. Bartlett, T. Mallouk, H. Selig* Fluorine Intercalation Compounds of Graphite; *J.-M. Dance, A. Tressaud* Ferro- and Ferrimagnetism in Fluorides; *G. Ferey, M. Leblanc, R. DePape, J. Pannetier* Competing Spin Interaction and Frustration Effects in Fluorides; *A. Tressaud* Electronic Conduction in Fluorides; *J. M. Réau, J. Crannec* Fast Fluorine Ion Conductors; *J. Ravez* Nonlinear Properties of Fluorides; *C. Fauassier* Optical Properties of Fluorides; *T. Oi, K. Miyauchi, J.-M. Dance* Fluorides for Electrochromic Devices; *G. Villeneuve* Nuclear Magnetic Resonance of Fluofides; *P. B. Fabritchnyi* Mössbauer Spectroscopy of Fluorine Compounds; *D. Reinen, J.-M. Dance* Local and Cooperative Effects in the Electron Paramagnetic Resonance Spectra of

Transition Metal Fluorides; *C. A. Baud* Fluorine Chemistry and Biomineralization; *J. Portier* Fluorine Chemistry and Energy; *J. B. Cochet-Muchy, J. Portier* Industrial Use of Inorganic Fluorides.

An introductory chapter by the editor is followed by a detailed description of methods for synthesizing fluorides, dealing with gas phase reactions, reactions in solution, solid reactions, and syntheses under high pressure. There is also a section discussing the most important crystal growing techniques.

A large part of the book (185 pages) is occupied by Chapters 3 and 4, which discuss the structural chemistry of fluorides and oxyfluorides. For each class of molecular formula or type of structure (e.g. binary fluorides MF_2, MF_3, MF_5), numerous compounds are listed in the form of tables and discussed from a structural standpoint, illustrated by many figures to clarify the discussion. The chapter on oxyfluorides discusses important structures such as those of the pyrochlorite, garnet and scheelite types, and deals with the molecular formula classes MOF, MO_2F, AMO_2F and many others.

A short section on defects in fluorides (e.g. in CaF_2) is followed by Chapter 6, in which *R. Hoppe* reports on fluorides containing elements in "high" oxidation states. In addition to describing such exotic representatives of these compounds as Cs_2CuF_6, AuF_6, AuF_5 and XeF_6, this chapter explains to the reader the problems that arise in understanding the occurrence of compounds of this type and their interrelationships. Chapter 7 discusses the most important fluoride glasses and surveys the properties of these materials. Graphite fluorides and intercalation compounds of binary and ternary fluorides in graphite are dealt with in Chapter 8, with the emphasis on preparation and characterization (by ^{13}C-NMR); their applications (e.g. in lithium batteries) are also discussed.

Chapters 9–15 are concerned mainly with physical properties. *J.-M. Dance* and *A. Tressaud* discuss fluorides with ferromagnetic and ferrimagnetic ordering; *G. Ferey* and co-authors are concerned with fluoro-manganates, -niccolates and -ferrates, which show hysteresis behavior. Chapter 11 deals briefly with semiconducting and (one- and two-dimensional) metallic fluorides. Chapter 12, in contrast, treats good fluoride ion electrical conductors in considerable detail; as well as describing such compounds, the ways of optimizing fluoride ion mobility, and the mechanism of conduction are included.

Chapters 13–15 are very brief, and show that fluorides include some materials with piezoelectric, pyroelectric or ferroelectric properties, or with color centers.

The next three chapters are concerned with physical methods used to study fluorides. *Villeneuve*'s contribution includes some interesting results (from NMR spectra) concerning diffusion of fluoride ions and chemical bonding in fluorides. The importance of EPR spectroscopy in investigating the local properties at paramagnetic centers is explained with the help of examples by *D. Reinen* and *J.-M. Dance*. The chapter by *C. A. Baud* is mainly concerned with the mineralizing effect of fluoride ions on biological apatite. The two concluding chapters review the importance of fluorides in energy technology and industrial production.

Verdict: This book has not been written for students; it is suitable for research workers who are concerned with substances in the solid state, in the broadest sense. The contributions come from authors with a very wide range of research interests, with the natural result that the contents of the chapters do not always have a lot in common with each other—sometimes the only link is that fluorine compounds are discussed. Nevertheless, the book is more than a good collection of original papers, since some of the more topical chapters, containing some of their authors' own ideas, extend well beyond what can be found in journal articles. Unfortunately some of these chapters are quite short owing to limited space. It would have been advantageous to omit from the articles on fluoride-specific aspects some trivial matters which are already adequately covered by numerous books (e.g. crystal growing techniques). From the same point of view one might also have considered leaving out the chapters on topics such as industrial applications and energy technology, which merely serve to extend the research worker's general knowledge.

In summary, the book is recommended for all libraries, and also for individual research workers, though many of the latter will be deterred by its high price.

Jürgen Köhler [NB 810 IE]
Max-Planck-Institut
für Festkörperforschung, Stuttgart (FRG)

Corrigendum

In the communication entitled "A New Low-Temperature Synthesis of 1,2-Dihydro-1,2-diphosphetes" by L. Ricard, N. Maigrot, C. Charrier, and F. Mathey (*Angew. Chem. Int. Ed. Engl. 26* (1987) 548) the headings in Table 1 should read as follows, and not as printed:

Table 1. Substituents of **1** and **3–5**; yields of **5**.

1		**3–5**			**5**
R	R^1	R	R^1	R^2	Yield [%]

Registered names, trademarks, etc. used in this journal, even when not marked as such, are not to be considered unprotected by law.

© VCH Verlagsgesellschaft mbH, D-6940 Weinheim, 1987. - Printed in the Federal Republic of Germany by Zechnersche Buchdruckerei, Speyer/Rhein.

All rights reserved (including those of translation into foreign languages). No part of this issue may be be reproduced in any form - by photoprint, microfilm, or any other means - nor transmitted or translated into a machine language without written permission from the publishers. Only single copies of contributions, or parts thereof, may be made for personal use.

Valid for users in the USA: The appearance of the code at the bottom of the first page of an article in this journal (serial) indicates the copyright owner's consent that copies of the article may be made for personal or internal use, or for the personal or internal use of specific clients. This consent is given on the condition, however, that the copier pay the stated per-copy fee through the Copyright Clearance Center, Inc., for copying beyond that permitted by Sections 107 or 108 of the U.S. Copyright Law. This consent does not extend to other kinds of copying, such as copying for general distribution, for advertising or promotional purposes, for creating new collective works, or for resale. For copying from back volumes of this journal see 'Permissions to Photo-Copy: Publisher's Fee List' of the CCC.

Editorial office: Pappelallee 3, D-6940 Weinheim, Federal Republic of Germany, Telephone (06201) 602315, Telex 465516 vchwh d, Telefax (06201) 602328.

Editor: *P. Gölitz.*

Associate editors: *D. I. Loewus, A. Stimson,* **Editorial assistant:** *E. Schweikart*

Publishers: VCH Verlagsgesellschaft mbH. (Managing Directors: *Prof. Dr. Helmut Grünewald* and *Hans Dirk Köhler*), Pappelallee 3, D-6940 Weinheim, Federal Republic of Germany. Correspondence concerning advertisements should be addressed to VCH Verlagsgesellschaft mbH. (Advertising Manager *R. J. Roth*), Boschstr. 12. P.O. Box 1260/1280, D-6940 Weinheim, Federal Republic of Germany, Telephone Weinheim (06201) 602-0, Telex 465516 vchwh d, Telefax (06201) 602328.

ANGEWANDTE CHEMIE
International Edition in English
Volume 26 · Number 9
September 1987
Pages 805–938

The Generation and Characterization of Molecules by Neutralization-Reionization Mass Spectrometry (NRMS)

New Analytical Methods (33)

By Johan K. Terlouw and Helmut Schwarz*

Dedicated to Professor John H. Beynon FRS

The diluted gas phase within a mass spectrometer is ideally suited for performing collision experiments of fast moving ions with thermalized target atoms. One important reaction which can be brought about with a given cation is its selective reduction, i.e. its neutralization. This allows the synthesis in tailored experiments of a variety of unusual chemical species, which because of intermolecular processes cannot be prepared or studied in solution or in a matrix. Among the molecules which have been generated in this way are hypervalent species (Rydberg radicals) like $H_3^{\odot}$, van der Waals complexes like He_2, mono- or disubstituted acetylene derivatives XC≡CY (X = H, Y = OH, NH_2; X = Y = OH, NH_2), and elusive compounds like carbonic acid (H_2CO_3) or carbamic acid (NH_2CO_2H). Collision experiments can also be used advantageously for the structural analysis of the *neutral molecule N* generated in unimolecular dissociation reactions of the type $m_1^{\oplus} \rightarrow m_2^{\oplus} + N$. The dissociation of ionized aniline for example yields, besides $C_5H_6^{\odot\oplus}$ cations, neutral isocyanic acid, HNC, and not cyanic acid, HCN. The technique of *Neutralization Reionization Mass Spectrometry* (NRMS) is performed in the diluted gas phase, a medium where intermolecular interactions are entirely absent. The method may therefore increasingly be applied to the study of molecular species whose reactivity precludes their characterization in matrices. Molecules in specific excited states and fragments of organometallic compounds with unsaturated valencies are two examples of systems which could fruitfully be studied.

1. Introduction

Quite a few molecular species can only be generated in the gas phase because in solution or even in the solid state intramolecular interactions will make them unstable and lead to isomerization, polymerization or dissociation.[1] Mass spectrometric techniques are commonly employed to study the chemistry of ions in the gas phase and the past ten years have seen an impressive development in methods[2] for the tailor-made generation and characterization of solitary ions with unusual structures and/or intriguing properties. As early as 1966–1968 *Lavertu* et al.[4a] and *Devienne*[4b] demonstrated that the gas phase is also an ideal medium for the mass spectrometric generation of *neutral* molecules by reduction of the corresponding cations. However, the scope of their fundamental collision experiments was not widely recognized and more than ten years passed before the technique of *Neutralization Reionization Mass Spectrometry* (NRMS) was rediscovered by several research groups.[5] This led quickly to the realization that NRMS is a new methodological asset to physical organic chemistry. The discussion of some highlights and typical

[*] Prof. Dr. H. Schwarz
Institut für Organische Chemie der Technischen Universität
Strasse des 17. Juni 135, D-1000 Berlin 12
Dr. J. K. Terlouw
Analytical Chemistry Laboratory, University of Utrecht
Croesestraat 77a, NL-3522 AD Utrecht (The Netherlands)

 © VCH Verlagsgesellschaft mbH, D-6940 Weinheim, 1987 0570-0833/87/0909-0805 $ 02.50/0

examples of results recently obtained with this technique forms the theme of this article. We shall not go into a detailed discussion of the more fundamental aspects of the method and the questions which arise with the interpretation of the spectra. These are the subject of recent review articles by *Wesdemiotis* and *McLafferty*[6a] and *Holmes*.[6b]

A neutralization-reionization experiment consists of the following steps (see Scheme 1):

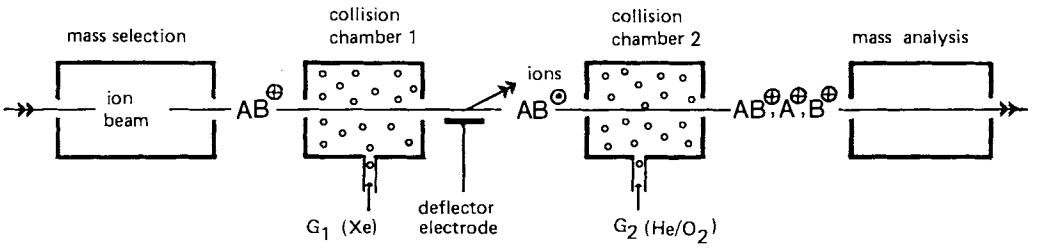

Scheme 1. Schematic diagram of an NRMS experiment.

1) A given open- or closed-shell cation $AB^{\oplus}$ is generated in a mass spectrometer using one of the accepted methods and its structure is determined.[7]
2) Upon acceleration (typically to 8 kV translational energy) and mass selection the ions $AB^{\oplus}$ enter a collision gas chamber 1 (Cell 1) where electron-capture from a target gas G_1 results in their reduction to the neutral species AB [Eqn. (1)]. All $AB^{\oplus}$ ions which have not been neutralized and also (the minor fraction of) their ionic dissociation products [Eqn. (2)] are removed from the beam by a charged deflector electrode. The only species which enter the second collision gas chamber (Cell 2) are therefore the neutral molecules AB (having the momentum of $AB^{\oplus}$) and their uncharged dissociation products $A^{\odot}$ and $B^{\odot}$ (having the momentum of $A^{\oplus}$ and $B^{\oplus}$).
3) The fast moving neutrals AB are reionized by collision with a target gas G_2 in the second chamber [Eqn. (3)]. This oxidation step should be performed in such a way that not only molecular ions $AB^{\oplus}$, but also charged fragments are generated. The spectrum of the latter can conveniently be registered and serves to characterize the structure of $AB^{\oplus}$. Upon its generation in cell 1 it takes ca. 10^{-6} s for a given neutral AB, which is not necessarily in its ground state, to reach the reionization cell. The presence of a signal $AB^{\oplus}$ in a NRM spectrum

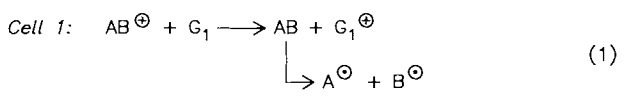

(1)

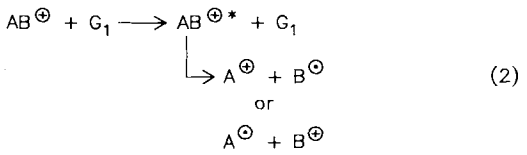

(2)

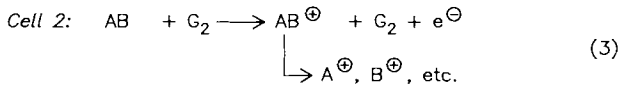

(3)

therefore signifies that the neutral has remained an intact, stable species for $> 10^{-6}$ s.

The cross sections of reactions (1) and (3) and also the lifetimes and electronic states of the reaction products AB and $AB^{\oplus}$ are highly dependent on the nature of the target gases G_1 and G_2 used. For neutralization [Eqn. (1)] *McLafferty* et al.,[5c,d,6a,8a] following the Porter group,[5b] preferentially use metal vapors (Hg, Na), whereas *Holmes*, *Terlouw*, and *Burgers* et al.[5e,f,g,h,6b] have introduced the use of xenon. This inert gas not only allows an efficient electron transfer but it is also more easily manipulated than metal vapors. When metals are used whose ionization energy (*IE*) is much lower than that of AB the charge exchange process of Equation (1) yields highly excited neutral species AB*. Their lifetime *t* can become so much shorter than that of AB that during the transit time required to reach the reionization cell (10^{-7}–10^{-5} s, dependent on the experimental setup) they completely decompose into $A^{\odot}$ and $B^{\odot}$. The NRM spectrum then only shows the signals $A^{\oplus}$ and $B^{\oplus}$ of the reionized dissociation products. However, an efficient neutralization does not require that $IE(G_1) < IE(AB)$; electron transfer upon collision as shown in Equation (1) also readily occurs if $IE(G_1) > IE(AB)$, as is the case with Xe whose *IE* (12.1 eV) is larger than that of most organic molecules. In such neutralization experiments the energy deficit (a few eV) is taken from the translational energy (typically 8000 eV) of the fast moving $AB^{\oplus}$ ions.

For reionization [Eqn. (3)], O_2 seems to have the highest efficiency. This could be related to the formation of $O_2^{\ominus}$ in the electron transfer process. Helium is also frequently used for reionization especially when a high yield of structurally characteristic fragment ions is desired.

Finally, it should be mentioned that instrumentation has been developed in which the intensity of the beam of neutrals AB is sampled as a function of scattering angle. Important structural and spectroscopic data can be derived from the resulting beam profiles including the kinetic energy released by dissociation of AB*. This method—Neutralized Ion Beam Spectroscopy—has been introduced by *Porter* et al.[5b] and it has proved of great value for the characterization of many interesting molecules (hypervalent species, van der Waals clusters, etc.).

2. Hypervalent Molecules (Rydberg Radicals) $XH_2^{\odot}$ (X = H, CH_3, NH_2, OH, F, Cl)

The unorthodox binding properties of hypervalent molecules, i.e. species having more valence electrons than pre-

scribed by the octet rule, have always fascinated chemists and physicists. For the majority of these molecules the electronic ground state is repulsive towards the dissociation products [Eqns. (4) and (5)] but as metastable molecules in highly excited (Rydberg) states they do have a definite lifetime. Leading theoreticians have predicted that the lifetime of these $XH_2^{\odot}$ radicals will increase greatly with substitution of H by D and also with the formation of clusters of $XH_2^{\odot}$ with XH molecules. This will be illustrated by some instructive examples.

$$XH_2^{\odot} \longrightarrow XH + H^{\odot} \quad (4)$$

$$XH_2^{\odot} \longrightarrow X^{\odot} + H_2 \quad (5)$$

The triatomic hydrogen radical $H_3^{\odot}$[9] has been investigated theoretically and experimentally for more than 40 years. The radical is considered to have a repulsive ground state ($H_3^{\odot} \rightarrow H_2 + H^{\odot}$) but, as pointed out by *Herzberg* et al.[9a] it should have a lifetime $t \geq 10^{-8}$ s in some of its excited states. Indeed, the first NRMS experiments on $H_3^{\oplus}$[4b,5a] clearly showed that $H_3^{\odot}$ exists in long-lived states. In subsequent studies the Porter group[10] was able to show that, dependent on the nature of the reducing agent, electron transfer to $H_3^{\oplus}$ according to Equation (6) yields $H_3^{\odot}$ in either its dissociative ground state $2p^2E'$ or the electronically excited dissociative $2s^2A_1'$, and metastable $2p^2A_2''$ states. In particular, $H_3^{\odot}$ molecules populating the nonrotating (N = K = O) level of the $2p^2A_2''$ state were observed to have an appreciable lifetime (87 μs). In going from $H_3^{\oplus}$ to $D_3^{\oplus}$ the lifetime (but not the yield) of neutral species in the metastable $2p^2A_2''$ state greatly increases: e.g. $H_3^{\odot}$ and $D_3^{\odot}$ in the 1,1 rotational level have lifetimes of 3×10^{-11} and 1.7×10^{-7} s, respectively. The $H_3^{\odot}$ radical in its $2p^2A_2''$ state was estimated to have an ionization energy of 4.1 eV.

$$H_3^{\oplus} \xrightarrow{Mg} H_3^{\odot}\ (2\ p^2E') \qquad H_3^{\oplus} \xrightarrow{K} H_3^{\odot}\ (2\ p^2A_2'') \quad (6)$$

Early calculations[11] predict that the $CH_5^{\odot}$ radical is not a minimum on the $CH_5^{\odot}$ hypersurface but that it spontaneously decomposes into $CH_4/H^{\odot}$ or $CH_3^{\odot}/H_2$. This agrees well with the findings of *Porter* et al.,[10c,12] who were not able to detect a signal corresponding to a stable $CH_5^{\odot}$ neutral in their NR spectra; the perdeuterated analogue was estimated to have a lifetime $t < 10^{-8}$ s. Surprisingly, however, *Beynon* et al.[13] in a very recent communication report that the $CH_5^{\odot}$ radical is a stable species with a lifetime $t > 3.9 \times 10^{-7}$ s and an ionization energy of 8.0 ± 0.5 eV. The sources of disagreement between the two experimental results are not yet understood.[*]

The ammonium radical $NH_4^{\odot}$ has also been the subject of numerous experimental and theoretical investigations.[14] Following *Herzberg*'s identification of its visible emission spectrum[15] in 1981, *Porter* et al.[5b,10c,12,16] (see also Refs. [17], [18]) have reported a comprehensive study of this radical from which the following conclusions can be drawn:

1) The $NH_4^{\odot}$ radical (produced by reduction of $NH_4^{\oplus}$ with various metals) has too short a lifetime for its detection with the presently available techniques. This is also the case with the labeled radicals $NH_3D^{\odot}$, $NH_2D_2^{\odot}$ and $NHD_3^{\odot}$ which undergo a very fast loss of $H^{\odot}$. For the perdeuterated radical $ND_4^{\odot}$, however, an undissociated state ($t > 10^{-6}$ s) could be observed, consistent with a tunneling dissociation mechanism for the preferential fast loss of $H^{\odot}$ from the isotopically mixed radicals.

   $$NH_{4-x}D_x^{\odot} \longrightarrow NH_{3-x}D_x + H^{\odot} \quad (x = 1, 2, 3)$$

   The ionization energy of $ND_4^{\odot}$ derived from these experiments is 4.73 eV, close to that predicted by an X_{α} calculation for $NH_4^{\odot}$ (4.85 eV).[17] Should it be possible to stabilize $NH_4^{\odot}$ in a condensed state a compound would become available with interesting metallic properties.[18]
2) For clusters of the type $NH_4(NH_3)_n^{\odot}$ (n = 1–3) and their deuterated analogues stable radicals with $t > 10^{-6}$ s could be obtained by neutralization of the corresponding ionic clusters with potassium. The *IE* of the $NH_4(NH_3)_n^{\odot}$ species decreases drastically with increasing n (n = 0, *IE* = 4.73 eV; n = 1, *IE* = 4.0 eV; n = 3, *IE* = 2.5 eV!).
3) The behavior of the $CH_3NH_3(NH_3)_n^{\odot}$ (n = 0, 1) system closely resembles that of the parent system $NH_4(NH_3)_n^{\odot}$. Substituting all hydrogens in $CH_3NH_3^{\odot}$ by deuterium ($\rightarrow CD_3ND_3^{\odot}$) and/or clustering with an NH_3 molecule significantly increases the lifetime of the neutralized species. The observed ionization energies are 4.3 eV for $CH_3NH_3^{\odot}$ and 3.9 eV for $CH_3NH_3(NH_3)^{\odot}$.

Another fascinating question in this area is the possible existence of the $H_3O^{\odot}$ (oxonium) radical. It has engaged the attention of many a theoretician and experimentalist over the past 25 years[12,19] and the most important results can be summarized as follows: *Gellene* and *Porter*[19] have elegantly demonstrated that neutralization of $D_3O^{\oplus}$ with K vapor produces $D_3O^{\odot}$ in a distribution of dissociative and metastable states with $t > 6 \times 10^{-7}$ s. Upon substitution of D by H the lifetime of the metastable state decreases rapidly (cf. the $NH_4^{\odot}$ system) and neither $H_3O^{\odot}$ nor $HD_2O^{\odot}$ could be observed, i.e. $t < 7 \times 10^{-8}$ s. The stabilizing effect of an H_2O molecule on the $H_3O^{\odot}$ radical is reflected in the increased lifetime of the oxonium monohydrate $H_3O(H_2O)^{\odot}$ which was observed to exist in metastable states for several H/D isotopic variants: $t\ [H_3O(H_2O)^{\odot}] = 2 \times 10^{-7}$ s and $t\ [D_3O(D_2O)^{\odot}] > 7 \times 10^{-7}$ s. The ionization energy is also lowered: *IE* $[D_3O(D_2O)^{\odot}] \geq 3.4$ eV, whereas *IE* $[D_3O^{\odot}] = 4.3 \pm 0.1$ eV.

Isotope effects were also employed for increasing the lifetime of the dihydrogen fluoride radical. $H_2F^{\odot}$ has too brief a lifetime for observation, whereas $D_2F^{\odot}$, produced by the reduction of $D_2F^{\oplus}$ with Na, has a lifetime of over 4×10^{-7} s.[20] Quite unexpected isotope effects were observed by *McLafferty* et al.[21] in the NR mass spectra of chloronium ions. Their findings that the life spans of the

[*] Other recent experiments strongly indicate that both $CH_5^{\odot}$ and $CD_5^{\odot}$ are unstable, separating with a large kinetic energy release into $CH_4/H^{\odot}$ and $CD_4/D^{\odot}$ (*J. L. Holmes*, private communication).

deuterated species follow the order $HDCl^{\odot} \gg H_2Cl^{\odot} > D_2Cl^{\odot}$ and that the spectra strongly depend on the chemical ionization conditions under which the primary ions, $HDCl^{\oplus}$, $H_2Cl^{\oplus}$ and $D_2Cl^{\oplus}$, respectively, are generated led the authors to the suggestion of an exothermic isomerization $H-Cl-H^{\oplus} \rightarrow H-H-Cl^{\oplus}$ prior to neutralization. The neutralization would then lead to a stable chloronium radical $H-H-Cl^{\odot}$, whereas the neutralization of $HClH^{\oplus}$ does not lead to a stable $HClH^{\odot}$ radical. Although this model explains the experimental results, it is at variance with state-of-the-art ab initio calculations[22] which exclude an *exothermic* isomerization $H-Cl-H^{\oplus} \rightarrow H-H-Cl^{\oplus}$. The global minimum on the $H_2Cl^{\oplus}$ hypersurface corresponds to an $H-Cl-H^{\oplus}$ structure with $H-H-Cl^{\oplus}$ at least 80 kcal/mol higher in energy. The radical hypersurface so far shows only one minimum corresponding to $H-Cl-H^{\odot}$ (C_{2v}). Possibly the neutralization populates Rydberg-states, which were not taken into account either in the interpretation of experiments[21] or in the ab initio calculations.[22]

3. Ylides CH_2XH (X = NH_2, OH, Cl, F) and Betaines CH_2CH_2XH (X = NH_2, OH)

The accessibility of ylide cations in the gas phase through dissociative ionization [Eqns. (7)-(9)] or through ion-molecule reactions [Eqn. (10)] has been demonstrated several times over the past few years.[23] Frequently, radical cations **1**, **3**, **5** and many others turn out to be more stable than their tautomers of more conventional structure (**2**, **4**, **6**), from which, moreover, they are separated by significant energy barriers.

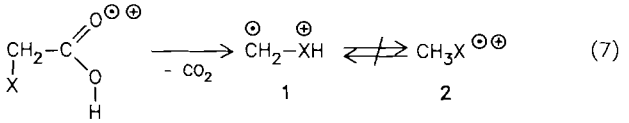

X = F, Cl (7)

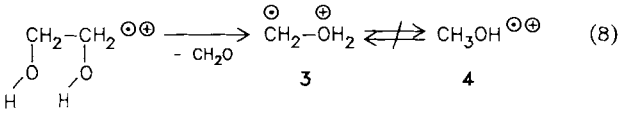

(8)

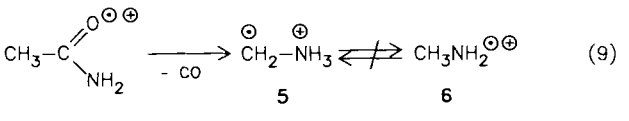

(9)

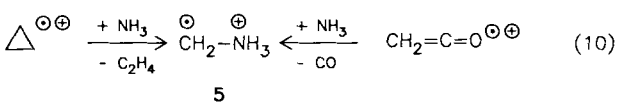

(10)

It goes without saying that NRMS opens an interesting route from the easily accessible radical cations to the *neutral* ylides.[24] And last but not least, this is attractive because many ylides are fundamentally inapproachable in other ways. The NRMS experiment, however, also has its pitfalls. In the first place, the neutralization probably takes place in the form of a near-vertical process; if the geometries of the ion and the neutral differ the latter is therefore not generated in its ground state. Further high level ab initio calculations[25] point to low stabilities of *neutral* ylides such as CH_2OH_2, CH_2ClH or hydrogen bonded isomers like H_2CHF against decomposition into CH_2 and HX (12, 4 and 7 kcal/mol, respectively). Also the same evidence points to low barriers against isomerization $CH_2XH \rightarrow CH_3X$ (X = OH, Cl, F; barriers < 1, 11, 1.5 kcal/mol, respectively). The chances of producing ylides of this kind through gas-phase neutralization of the corresponding ylide ions therefore appear slim,[26] and indeed the Holmes-Terlouw group[27] did not succeed in producing stable neutrals of the CH_2XH (X = F, Cl, OH) type. The signal for CH_2XH found by *Wesdemiotis* et al.[5c,28] in the NR mass spectra of $CH_2XH^{\oplus}$ was shown by *Holmes, Terlouw* et al.[27] to originate, at least in part, from isotope interferences and the presence of conventional CH_3X species.

In the neutralization reionization mass spectra of the distonic[*] ions $\overset{\odot}{C}H_2-CH_2-\overset{\oplus}{O}H_2$ and $\overset{\odot}{C}H_2-CH_2-\overset{\oplus}{N}H_3$ signals are observed at *m/z* 46 ($C_2H_6O^{\odot\oplus}$) and *m/z* 45 ($C_2H_7N^{\odot\oplus}$), respectively.[30] These signals cannot be assigned to $[CH_3CH_2OH]^{\odot\oplus}$ and $[CH_3CH_2NH_2]^{\odot\oplus}$, respectively, since fragment ions characteristic of α-cleavage in ionized ethanol and ethylamine are not present in the NRM spectra. The authors propose that the species produced upon neutralization with Hg are either betaines ($CH_2CH_2OH_2$/$CH_2CH_2NH_3$) or complexes of ethene with H_2O and NH_3, respectively. Irrespective of the actual structures these unusual neutral species must have a lifetime of over 10^{-6} s.

4. Rare Gas Dimers X_2 (X = He, Ne, Ar)

In a detailed study, *Gellene* and *Porter*[31] have shown that rare gas dimer ions $X_2^{\odot\oplus}$ (X = He, Ne, Ar, generated by ion/molecule reactions in a high pressure ion source) react with potassium to yield neutral dimers X_2^* in their first excited singlet ($^1\Sigma_u^+$) and triplet state ($^3\Sigma_u^+$). From the analysis of the beam profiles and additional spectroscopic evidence it follows that both states decay radiatively into the essentially repulsive ground state. The triplet state, however, is sufficiently stable to enable its radiative lifetime to be estimated, viz. He_2^* $t > 3.2 \times 10^{-6}$ s; Ne_2^* $t > 7.2 \times 10^{-6}$ s; Ar_2^* $t > 2.1 \times 10^{-6}$ s. Ion beam attenuation cross sections are particularly large for $He_2^{\oplus}$ and $Ne_2^{\oplus}$ (250 and 180 Å^2, respectively), indicating that electron transfer from K [Eqn. (11)] is very efficient. The relatively intense molecular beams of He_2^* and Ne_2^* thus produced have ca. 18.0 and 16.5 eV of electronic energy, respectively. They may find applications in the investigation of energy transfer reactions.

$$X_2^{\odot\oplus} + K(g) \longrightarrow X_2^* + K^{\oplus} \quad (11)$$

X = He, Ne, Ar

[*] Distonic radical ions are defined [29] as species in which the charge and spin are "located" on different atoms.

5. Neutral Molecules which Cannot Exist in Solution

A prime reason for the attention which the NRMS technique has recently received is its successful application in the gas phase synthesis of small molecules which in solution have an extremely short lifetime only because intermolecular reactions promote their fast conversion into more stable isomers or derivatives. As prototypal examples thereof, long sought after acetylene derivatives, further carbonic acid, carbamic acid, and some acetaldehyde isomers are presented.

Decarbonylation of the radical cations of propiolic acid **7**,[32] its amide **10**,[33] squaric acid **13**[5h] and its derivatives **16** and **19**[5h] yield the substituted acetylene radical cations **8**, **11**, **14**, **17**, and **20**, respectively, whose structures could be unambiguously characterized. An example is presented in Figure 1 where it is seen that the partial collisional activation mass spectrum of ion **11** contains a structure-characteristic signal at *m/z* 16 ($NH_2^{\oplus}$) which is absent in the spectra of all other $C_2H_3N^{\oplus}$ isomeric ions. Upon neutralization, all of the above ions yield stable molecules. Their

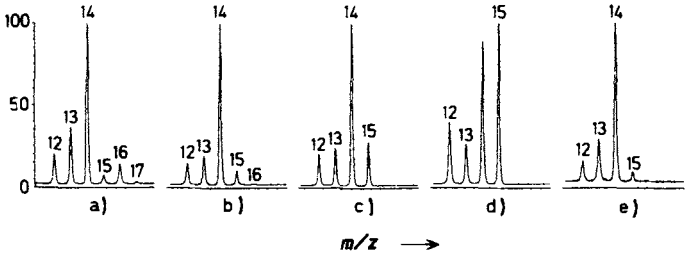

Fig. 1. Collision activation spectra (sections with *m/z* 12 to *m/z* 17) of $C_2H_3N^{\odot\oplus}$ isomers. a) $HC{\equiv}CNH_2^{\odot\oplus}$ **11** [generated according to Eqn. (13)], b) $H_2C{=}C{=}NH^{\odot\oplus}$ (from *n*-$C_3H_7CN^{\odot\oplus}$), c) $H_3CCN^{\odot\oplus}$, d) $H_3CNC^{\odot\oplus}$, e) $H_2C{=}N{=}CH$ (from *n*-$C_4H_9NC^{\odot\oplus}$).

reionization spectra leave no doubt (compare, e.g., the NR spectra of $CH_2{=}C{=}O^{\odot\oplus}$ and $HC{\equiv}COH^{\odot\oplus}$ shown in Fig. 2) that we are dealing with the long sought after acetylene

$$H{-}C{\equiv}C{-}\overset{\overset{O}{\|}}{C}{-}OH^{\odot\oplus} \xrightarrow[-\,CO]{} H{-}C{\equiv}C{-}OH^{\odot\oplus} \longrightarrow H{-}C{\equiv}C{-}OH \quad (12)$$
7 8 9

$$H{-}C{\equiv}C{-}\overset{\overset{O}{\|}}{C}{-}NH_2^{\odot\oplus} \xrightarrow[-\,CO]{} H{-}C{\equiv}C{-}NH_2^{\odot\oplus} \longrightarrow H{-}C{\equiv}C{-}NH_2 \quad (13)$$
10 11 12

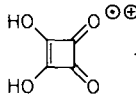
$$\xrightarrow[-\,2\,CO]{} HO{-}C{\equiv}C{-}OH^{\odot\oplus} \longrightarrow HO{-}C{\equiv}C{-}OH \quad (14)$$
13 14 15

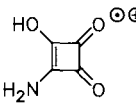
$$\xrightarrow[-\,2\,CO]{} HO{-}C{\equiv}C{-}NH_2^{\odot\oplus} \longrightarrow HO{-}C{\equiv}C{-}NH_2 \quad (15)$$
16 17 18

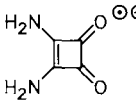
$$\xrightarrow[-\,2\,CO]{} H_2N{-}C{\equiv}C{-}NH_2^{\odot\oplus} \longrightarrow H_2N{-}C{\equiv}C{-}NH_2 \quad (16)$$
19 20 21

derivatives $XC{\equiv}CY$ (X = H, OH, NH_2; Y = OH, NH_2). Some of these are of general interest like ethynylamine, **12**, which may play a role in interstellar chemistry.[34] Considering the theoretical predictions that the barriers for *unimolecular* isomerization and decomposition are quite high, it is not really surprising that these acetylene derivatives can so easily be generated in the gas phase. Finally, it should be mentioned that apart from their reduction to the neutral molecules **9** and **12**, ions **8** and **11** can also be oxidized to their respective dications[32,33] under "charge stripping" conditions.[36]

Statements of the kind that "carbonic acid, $(HO)_2CO$, and carbamic acid, NH_2CO_2H, cannot exist in the free state"[37] are warranted in so far as it has not been possible to prepare these molecules as stable species in solution.

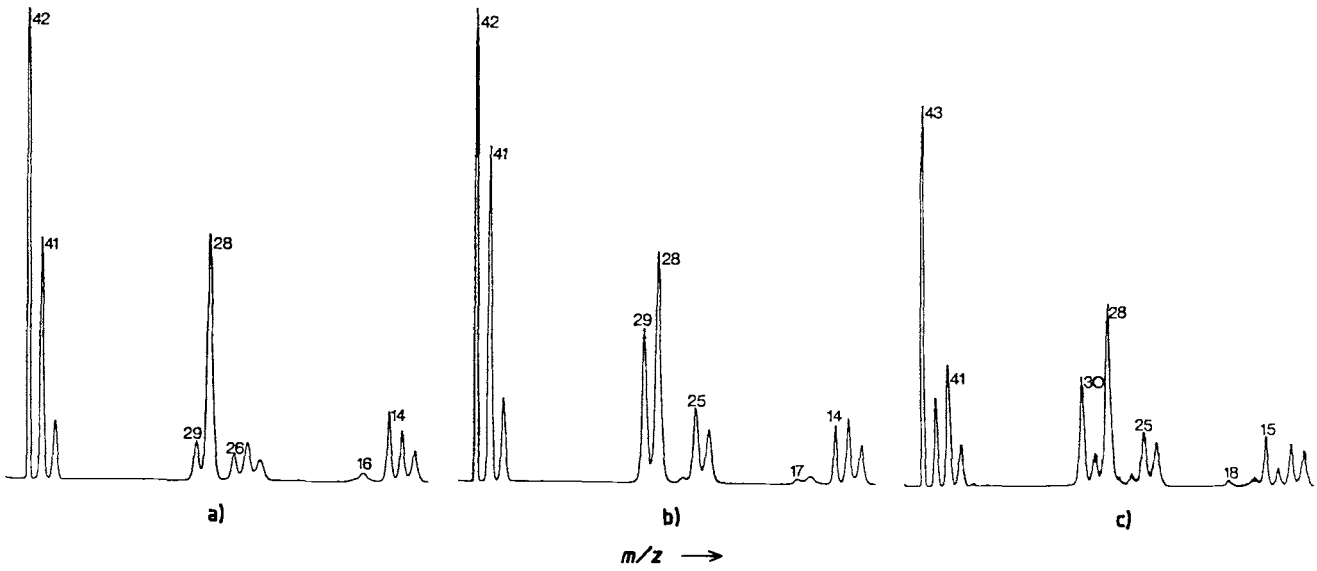

Fig. 2. NRMS of a) $H_2C{=}C{=}O^{\odot\oplus}$, b) $HC{\equiv}COH^{\odot\oplus}$ **8** [generated according to Eqn. (12)], c) $HC{\equiv}COD^{\odot\oplus}$ (generated by decarbonylation of $HC{\equiv}CCO_2D^{\odot\oplus}$): Xe was used for the neutralization and He for the reionization.

This is not due to an inherent instability of these molecules but rather to the fact that, in solution, acid/base or solvent catalysis promotes a rapid decomposition and, in the case of H_2CO_3, also deprotonation into the bicarbonate ion [Eqn. (17), (18)].

$$CO_{2aq} + H_2O \rightleftharpoons [H_2CO_{3aq}] \rightleftharpoons HCO^{\ominus}_{3aq} + H^{\oplus}_{aq} \quad (17)$$

$$CO_{2aq} + NH_{3aq} \rightleftharpoons [H_2NCO_2H_{aq}] \quad (18)$$

In the gas phase, however, quite a different situation obtains: the unimolecular dissociation of H_2CO_3 and H_2NCO_2H into $CO_2 + H_2O$ and $CO_2 + NH_3$ respectively, is predicted by *ab initio* MO studies[38] to be hampered by significant energy barriers (>40 kcal/mol), and thus the free acids should both exist as stable molecules. Indeed, recent reports[39] describe the successful preparation [Eqns. (19), (20)] and chararacterization of both acids and their radical cations in the diluted gas phase: ionization by 70 eV electrons in a mass spectrometer of the gaseous decomposition products from gently heated (T = ca. 120°C) samples of finely powdered ammonium hydrogencarbonate and ammonium carbamate yield signals at *m/z* 62.00002 and 61.01604 Dalton, respectively. These exact mass values are only compatible with the elemental compositions CH_2O_3 and CH_3NO_2, respectively. The experiments further show[39] that the *m/z 62 and m/z 61 ions must originate from the direct ionization of the corresponding neutral molecules*. That the ions have the structure of ionized carbonic acid and carbamic acid (**23** and **25**), respectively, follows from their dissociation characteristics. These further show that, analogously to the neutral counterparts, decomposition or isomerization in the ions is thwarted by sizeable energy barriers. NRMS experiments show that the neutral acids **22** and **24** can readily be regenerated by reduction of the ions **23** and **25** in the gas phase [Eqn. (19), (20)]. The NR mass spectra are only compatible with the structures **22**–**25**.

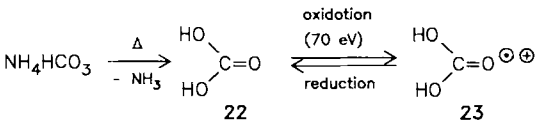

(19)

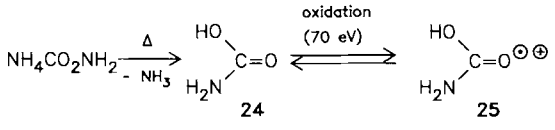

(20)

Vinyl alcohol **28** and hydroxymethylcarbene **31**, two isomers of acetaldehyde, are not accessible as pure species in solution.[40,41d] In the gas phase, however, they can readily be generated by the reduction of their radical cations **27** and **30**.[6] Ions **27** and **30** and also other $C_2H_4O^{\odot\oplus}$ isomers, like the methoxycarbene cation **33**,[41d] are separated by high isomerization barriers and they are accessible from various precursor molecules.[41] As a result a direct route is available for the generation of several neutral isomers on the C_2H_4O hypersurface.

Similarly, the reduction of "closed-shell" ions $M^{\oplus}$ [Eqn. (24)] in the gas phase provides a convenient route

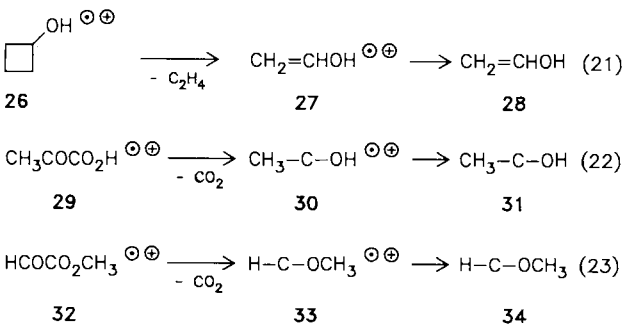

(21)

(22)

(23)

to the formation of free radicals $M^{\odot}$. The following list of radicals generated and characterized by NRMS may illustrate the scope of the method: $CH_3^{\odot}$,[28a,42] $C_2H_5^{\odot}$,[42] $C_3H_7^{\odot}$,[30] $C_4H_9^{\odot}$,[8a] $C_7H_9^{\odot}$ (toluene + $H^{\odot}$),[5c] $CH_2NH_2^{\odot}$,[8b] $CH_2OH^{\odot}$,[28,42] $CH_2F^{\odot}$,[27] $CH_2Cl^{\odot}$,[8b,27] $CH(CH_3)OH^{\odot}$,[6] $CH_2CH_2OH^{\odot}$,[6] $CH(CH_3)NH_2^{\odot}$,[30] $CH_2CH_2NH_2^{\odot}$,[30] $CH_2(CH_2)_3OH^{\odot}$,[30] $HCO^{\odot}$,[5f,43] $CH_3CO^{\odot}$,[5c,15,28] and $CO_2H^{\odot}$.[5f,28]

$$M^{\oplus} \underset{\text{oxidation}}{\overset{\text{reduction}}{\rightleftharpoons}} M^{\odot} \quad (24)$$

Another possibility for the generation of radicals in the gas phase is the *oxidation* of anions via the spontaneous or collision-induced loss of an electron [Eqn. (25)].[5g,44]

$$AB^{\ominus} (+ G_1) \longrightarrow AB^{\odot} + e^{\ominus} (+ G_1) \quad (25)$$

Starting from the easily accessible alkoxide ion $RO^{\ominus}$ (R = C_1 to C_3-alkyl) it indeed proved to be possible in collision processes to first generate alkoxy radicals by removal of an electron and subsequently to ionize these.

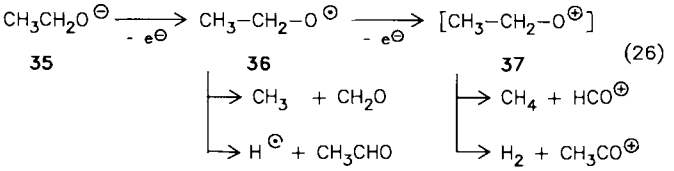

(26)

A typical example is shown in Equation 26 where it is seen that β-cleavage is the preferred dissociation pathway of the intermediate alkoxy radicals **36**. In contrast, the oxenium ions **37** mainly decompose via a 1,1 elimination of H_2 and CH_4. These reactions occur so rapidly that intact oxenium ions are not detected.

6. The Characterization of Neutral Molecules *N* in the Dissociation of Ions $m_1^{\oplus} \rightarrow m_2^{\oplus} + N$

Until recently the question of the structure of the neutral species *N* generated in the unimolecular dissociation of ions $m_1^{\oplus}$ [Eqn. (27)] has received relatively little attention. One reason is that the neutral eliminated often is a small molecule whose structure is not in doubt because only a single isomer exists (e.g. H_2O, $CH_3^{\odot}$, CH_4, CO_2 etc.). Secondly, it is often tacitly assumed (although this is by no means prescribed by theory) that metastable ions dissociate into the thermodynamically most stable products, thus making the question redundant whether energetically less favored neutral species would be (co)-generated. The most important reason perhaps is that, whereas a whole armoury of techniques is available to investigate the struc-

ture of the ions $m_1^{\oplus}$ and $m_2^{\oplus}$,[2,7,36] until recently the structure of N could, given a few exceptions,[45] only be determined indirectly. A recently developed variant of the NRMS technique, CIDI, the collision induced dissociative ionization of neutral molecules,[46] removes this obstacle and it is now possible to obtain a quick answer to mechanistic problems where the structure of the neutral is uncertain.

A CIDI experiment is performed with the instrumental setup for NRMS (Scheme 1) but without using collision gas chamber 1. A small fraction of the beam of fast moving mass selected ions $m_1^{\oplus}$ under investigation will dissociate unimolecularly [Eqn. (27)] during the flight to collision

$$m_1^{\oplus} \longrightarrow m_2^{\oplus} + N \qquad (27)$$

chamber 2. Upon arrival at the charged deflector electrode all ions, i.e. $m_1^{\oplus}$ and the *ionic* dissociation products $m_2^{\oplus}$, are deflected away so that the only species entering the collision chamber are the fast moving neutrals, N. These have a translational energy $E_N = (N/m_1) \times E_{m1}$ (in which E_{m1} is the translational energy, typically 8 kV, of the primary ions $m_1^{\oplus}$).

Within the cell the neutrals are ionized by collision with thermalized inert gas molecules and since we are dealing with an isolated system the energy required for ionization ($IE_{(N)}$) is taken from the translational energy of N, leading to $E_{N^{\oplus}} = E_N - IE_{(N)}$. Thus it is in principle possible to derive $IE_{(N)}$ from an accurate measurement of $E_{N^{\oplus}}$ using the procedures commonly employed for measuring the IE of cations in "charge stripping" experiments ($m^{\oplus} \rightarrow m^{2\oplus} + e^{\ominus}$).[36]

Upon collision part of the ionized neutrals dissociate and the spectrum of ionic dissociation products, which can conveniently be registered with the mass spectrometer, is used to characterize the structure of N. The following three examples from the recent literature may serve to illustrate the potential of the method.

6.1. HCN versus HNC

The major reaction observed for metastable aniline radical cations **38**, $C_6H_5NH_2^{\odot\oplus} \rightarrow C_5H_6^{\odot\oplus} + CHN$, is shown in Equation (28). Earlier work[47] clearly showed that the product ion generated is the cyclopentadiene radical cation **39**, whereas the neutral was presumed to be HCN rather than HNC on the basis of its greater thermodynamic stability.[48]

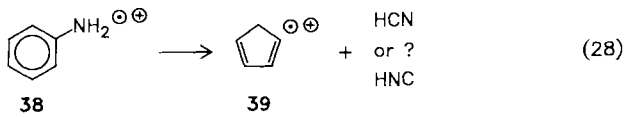

38 **39** (28)

A thorough analysis of the thermochemistry and the appearance energies obtained for reaction (28) allowed *Lifshitz* et al.[49] to conclude that dissociation of **38** yields HNC and not the thermodynamically more stable (by ca. 15 kcal/mol[50]) isomer HCN. This has been proposed earlier[51] on the basis of "chemical plausibility".

The result of the CIDI experiments[46] shown in Figure 3 provides unambiguous experimental evidence that the above proposal is correct: HCN (generated from e.g. ionized pyridine) and HNC (generated from **38**) yield strongly different CIDI spectra with signals in the m/z 12–16 region characteristic of the structure of the two isomers. Thus, it is readily shown that HNC is generated upon dissociation of **38**.

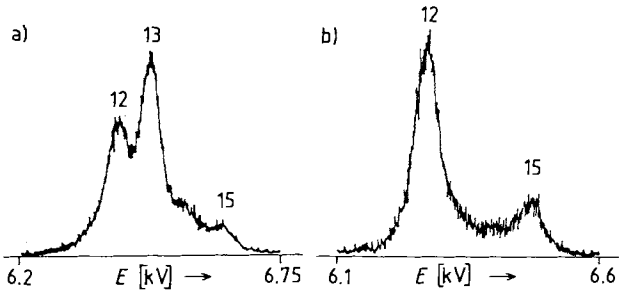

Fig. 3. CIDI spectra of a) HCN (generated from pyridine$^{\odot\ominus}$) and b) HNC (generated from aniline$^{\odot\oplus}$ **38**).

The method was successfully applied to similar cases and it could be established that the radical cations of pyrazole,[52] imidazole,[52] benzonitrile,[53] and benzyl cyanide[53] all eliminate HCN exclusively; in the case of benzonitrile and benzyl cyanide this confirms earlier proposals.[54,55]

6.2. $CH_3O^{\odot}$ versus $CH_2OH^{\odot}$

There is no doubt that the $C_2H_3O^{\oplus}$ ion generated in the unimolecular dissociation of ionized methyl acetate, $CH_3COOCH_3^{\odot\oplus}$, is the acetyl cation, $CH_3CO^{\oplus}$.[56] However, the question of the structure of the neutral generated in this reaction, which could be either the methoxy- ($CH_3O^{\odot}$) or the hydroxymethyl ($CH_2OH^{\odot}$) radical, was not settled until recently.

Results of CIDI experiments reported from several laboratories[42,44,53,57-61] were interpreted differently and for some time a confusing picture existed. However, there now seems to be a consensus that $CH_3O^{\odot}$ and $CH_2OH^{\odot}$ radicals are both generated in the above reaction, in a ratio of ca. 4:1. Whereas $CH_3O^{\odot}$ can readily be generated from $CH_3CO_2CH_3^{\odot\oplus}$ by a simple α-cleavage, a more complex mechanism must be associated with the formation of $CH_2OH^{\odot}$, which is the more stable radical by ca. 10 kcal/mol. The $CH_2OH^{\odot}$ radicals do not originate from isomerization of initially formed $CH_3O^{\odot}$ radicals[42] but are formed from methylacetate molecular ions which have undergone an extensive skeletal rearrangement. As shown in a recent ab initio molecular orbital study[62] the minimal energy requirement path for the dissociation of $CH_3COOCH_3^{\odot\oplus}$ **40** involves isomerization into the distonic ion **41** to yield the hydrogen bridged complex **42**. This ion (probably in its first excited state $^2A''$) then serves as the precursor to the formation of $CH_3CO^{\oplus}$ and $CH_2OH^{\odot}$ by direct bond cleavage (Fig. 4). This multistep pathway

$$CH_3CO_2CH_3^{\odot\oplus} \longrightarrow CH_3CO^{\oplus}/CH_2OH^{\odot}$$

is calculated to be energetically favored over the direct dissociation of **40** into $CH_3CO^{\oplus}/CH_3O^{\odot}$ by ca. 4–5 kcal/mol. The latter is entropically favored and may therefore predominate in the decomposition of methyl acetate ions of higher internal energies.

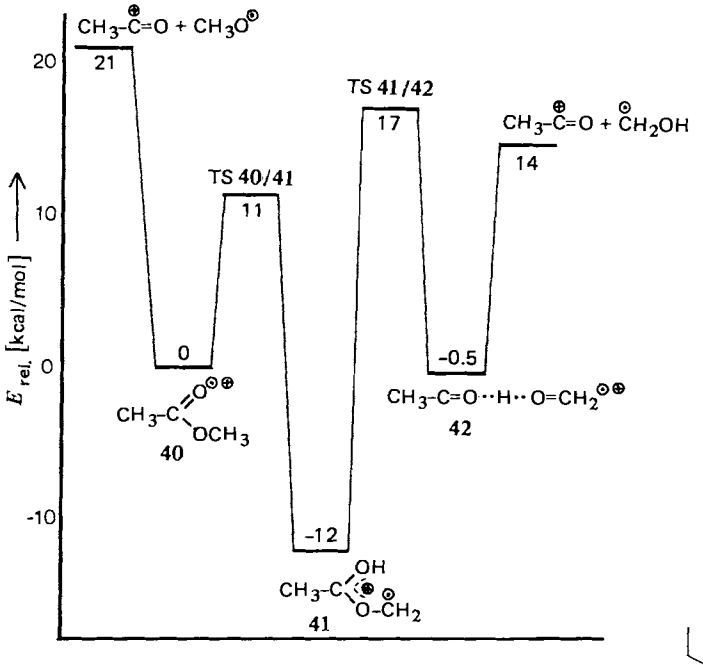

Fig. 4. Minimal energy pathway for the isomerization and decomposition of $CH_3CO_2CH_3^{\odot\oplus}$ **40** (MP2/6-31G(d)//3-21G+ZPE). Relative energies given in kcal/mol. TS = transition structure.

6.3. CH_3COOH versus $CH_2=C(OH)_2$

Because of its widespread occurrence in organic mass spectrometry the McLafferty rearrangement [Eqn. (29)] has been studied extensively.[63] Following the transfer of a γ-hydrogen to the positively charged acceptor group (e.g. a carbonyl group; **43** → **44**) dissociation into a radical cation

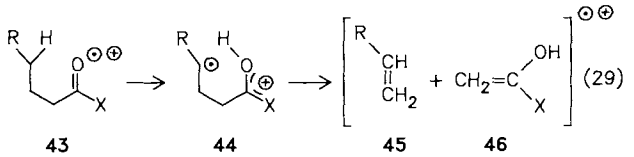

(**46**) and a neutral molecule (**45**) occurs by cleavage of the C_α–C_β bond. Energetic factors (Stevenson-Audier rule) determine which of the two fragments carries the charge.

In this context an interesting case has recently been uncovered[64] which could lead to a reinterpretation of the mechanism of the McLafferty rearrangement.

The mass spectrum of *n*-hexanoic acid **47** displays peaks at *m/z* 60 ($C_2H_4O_2^{\odot\oplus}$) and *m/z* 56 ($C_4H_8^{\odot\oplus}$) which formally are the results of a McLafferty rearrangement. A field ionization kinetics study[65] had already shown that the product ion distribution *m/z* 60 versus *m/z* 56 was strongly dependent on the lifetime *t* (and thus the internal energy) of the precursor ions **47**: ions of low internal energy mainly dissociate into *m/z* 56 ions, i.e. via a McLafferty rearrangement accompanied with transfer of the charge, **47** → $C_4H_8^{\odot\oplus}$ + $C_2H_4O_2$ [Eqn. (30b)]. Apparently the complementary process in which the charge is retained, **47** → $C_2H_4O_2^{\odot\oplus}$ + C_4H_8 [Eqn. (30a)], is thermodynamically less favored. The $C_2H_4O_2^{\odot\oplus}$ product ion generated in this reaction was shown in a CA study to be **48**, the enol of acetic acid radical cation, and the neutral probably has the 2-butene structure, **49**.[66] Thermochemical considerations[64] make it plausible that the reaction **47** → $C_4H_8^{\odot\oplus}$ + $C_2H_4O_2$ can only effectively compete with the process **47** → **48** + **49** [Eqn. (30a)] if its dissociation products are ionized 2-butene, **50**, and neutral acetic acid, **51** [Eqn. (30b)]. CIDI experiments established that the neutral generated from **47** is indeed acetic acid, **51**, and not its enol. This implies that the simple mechanism based on Equation (29) can be ruled out. Combining the results of the CIDI experiments with those of labeling studies[65] one is led to the conclusion[64] that the McLafferty rearrangement is a reaction in which the final dissociation step is preceded by an *intramolecularly catalyzed isomerization* of the dissociation products via long-lived *ion-dipole* and *hydrogen-bridged intermediate ions*. Thus the distonic ion **44** does *not* serve as the direct precursor for the formation of **45** and **46**.

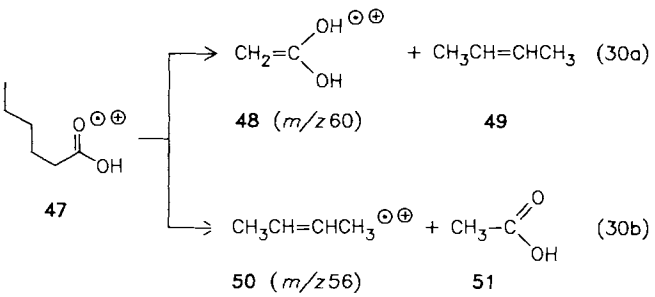

6.4. The $C_2H_3O^{\odot}$ Radicals $CH_2CHO^{\odot}$ and $CH_3CO^{\odot}$[67]

Lossing and *Holmes*[68] have shown that the measurement of the appearance energy (*AE*) of the ionic fragment $A^{\oplus}$ in the dissociative ionization of AB [Eqn. (31a)] can lead to an accurate heat of formation (ΔH_f^0) for the neutral $B^{\odot}$ via Equation (31b) provided $\Delta H^0_{f,A^{\oplus}}$ and $\Delta H^0_{f,AB}$ are well established.

$$AB + e^{\ominus} \longrightarrow A^{\oplus} + B^{\odot} + 2e^{\ominus} \quad (31a)$$

$$\Delta H^0_{f,B^{\odot}} = AE(A^{\oplus}) + H^0_{f,AB} - H^0_{f,A^{\oplus}} \quad (31b)$$

In this way it could be decided which structure the $C_2H_3O^{\odot}$ radical has, which is formed according to Equation (32). That the ΔH_f^0 value of the $C_2H_3O^{\odot}$ radical derived from such a measurement for the dissociation of **52** [Eqn. (32)] does indeed correspond with the oxyallyl radical **54** and not with the (thermodynamically more stable) acetyl radical **55** follows from a comparison of its CIDI spectrum (Fig. 5a) with that of acetyl radicals (Fig. 5b) generated via Equation (33).[44a] Whereas ionization of $CH_3CO^{\odot}$ produces the stable $CH_3CO^{\oplus}$ cation (*m/z* 43), $CH_2CHO^{\odot}$ yields $CH_2CHO^{\oplus}$ ions which, in agreement with theoretical calculations,[69] are unstable and largely dissociate (Fig. 5a).

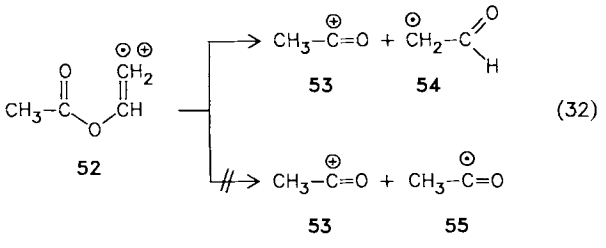

(32)

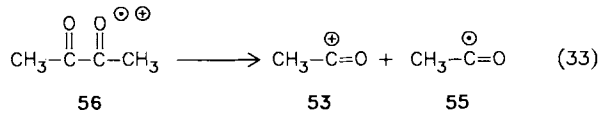

(33)

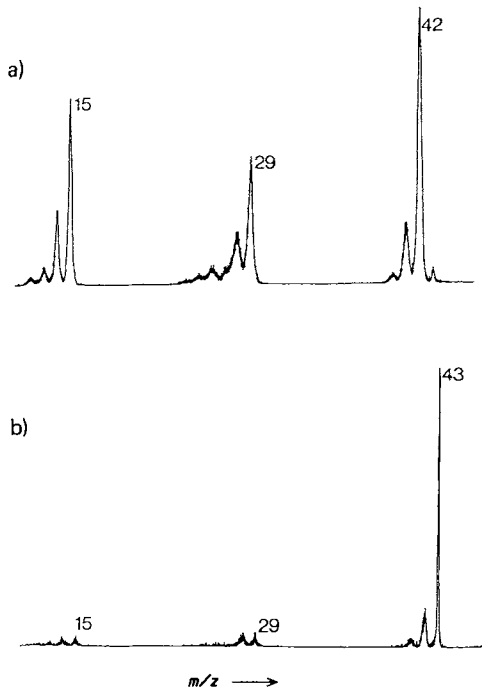

Fig. 5. CIDI spectra of a) $CH_2CHO^{\odot}$ **54** (generated from **52**) and b) $CH_3CO^{\odot}$ **55** (generated from **56**). O_2 was used for the ionization.

7. Outlook

NRMS is a relatively young and promising method for generating and characterizing neutral molecules from cations or anions. It has a greater potential than could be shown in the limited scope of this paper. We refer the reader therefore to the extensive reviews by *Porter*,[5b] *McLafferty*,[6a] and *Holmes*.[6b] We might briefly point out a few interesting fields of investigation.

7.1. Generating Neutrals in Excited States

Reduction of $AB^{\oplus}$ by a metal M with an ionization energy lower than the electron affinity of $AB^{\oplus}$ leads to AB* neutrals excited to levels optically inaccessible due to selection rules. Different sets of levels can be populated by a judicious choice of M as was shown for CH_n^* species obtained in various spin states by neutralization of $CH_n^{\oplus}$ with Na or K atoms in the gas phase.[70]

7.2. Distinguishing Isomeric Ions

Many ions cannot be uniquely characterized by straightforward mass spectrometry. This may be due to too flat a potential hypersurface resulting in a set of equilibrating structures or to the experimental methods discriminating only weakly between isomers. An example of the first category is the $C_2H_5^{\oplus}$ problem (open versus bridged structure). Localizing the site of protonation of substituted aromatics in the gas phase is a typical case of the second category.

When ions are neutralized the geometry is largely frozen because rearrangements occur rarely in the neutrals as compared with ionic species. The radical decompositions may therefore allow conclusions as to the structure of the precursor ion. In this way it was shown for the $C_2H_5^{\oplus}$ case that reaction (34) has a ΔG^0 of 0.8 ± 0.1 kcal/mol[5h,71] and also that electron impact ionization of C_2H_5I generates ionic species **57** and **58** in the ratio 2 : 1.[6]

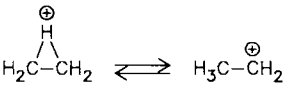

(34)

Equally promising are the first experiments[6,72] for establishing the site of protonation of substituted aromatics by NRMS.

7.3. Electronically Unsaturated Fragments of Organometallic Compounds

Organometallic compounds of the type **59** readily produce ionic fragments **60** through dissociative gas phase ionization [Eqn. (35)]. These are to be considered as coordinatively unsaturated and NRMS experiments on **60** should establish whether *neutral* compounds of type **61** have sufficiently long lifetimes to allow investigation. Results with $Fe(CO)_5$ and $CoNO(CO)_3$[73] justify cautious optimism in the direction of so far inaccessible, ligand-deficient organometallic compounds.

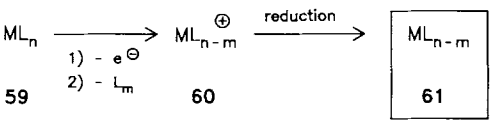

(35)

7.4. Addendum (July 1, 1987)

The NRMS technique has been successfully applied in the first "synthesis" of stable molecules of the type $FeCH_x$ (x = 0–3), species which may well serve as intermediates in homogenous and heterogeneous catalytic reactions.[74]

The radicals $NH_2O^{\odot}$ and $NHOH^{\odot}$, which may play a role in a catalytic cycle destroying ozone in stratospheric chemistry, and also their cations have been unambiguously characterized as stable species in the gas phase.[75] It is also reported in this study that metastable $CH_3CONHOH^{\odot\oplus}$ ions dissociate into $CH_3CO^{\oplus}$ and $NH_2O^{\odot}$ (not $NHOH^{\odot}$). Thus there is an interesting analogy with the behavior of $CH_3COOCH_3^{\odot\oplus}$ discussed in Section 6.2, i.e. the generation of $CH_3CO^{\oplus}/CH_3O^{\odot}$ versus $CH_3CO^{\oplus}/CH_2OH^{\odot}$.

Neutralization of the radical cations of fulminic acid (HCNO) and isocyanic acid (HNCO), compounds which have played a significant role in the historical development of chemistry (concept of isomerism), yields highly structure characteristic NR mass spectra.[76] Finally the first observation has been reported of the imino methyl radical ($HCNH^{\odot}$), a species of astrochemical interest.[77]

The continuous financial support of our work by the Deutsche Forschungsgemeinschaft, the Fonds der Chemischen Industrie, and the Gesellschaft von Freunden der Technischen Universität Berlin is gratefully acknowledged. We are indebted to our co-workers and the colleagues mentioned in the text for valuable contributions, helpful comments, and moral support in the preparation of this article.

Received: May 21, 1987 [A 635 IE]
German version: *Angew. Chem. 99* (1987) 829

[1] a) C. Wentrup: *Reactive Molecules: The Neutral Reactive Intermediate in Organic Chemistry*, Wiley-Interscience, New York 1984; b) W. W. Duley, D. A. Williams: *Interstellar Chemistry*, Academic Press, London 1984; c) G. Winnewisser, E. Herbst, *Top. Curr. Chem. 139* (1987) 119.

[2] a) R. G. Cooks, J. H. Beynon, R. M. Caprioli, G. R. Lester: *Metastable Ions*, Elsevier, Amsterdam 1973; b) M. T. Bowers (Ed.): *Gas Phase Ion Chemistry, Vol. 1-3*, Academic Press, Orlando 1984; c) T. A. Miller, V. E. Bondyberg (Eds.): *Molecular Ions: Spectroscopy, Structure and Chemistry*, North-Holland Publishing Company, Amsterdam 1983; d) F. W. McLafferty (Ed.): *Tandem Mass Spectrometry*, Wiley-Interscience, New York 1983; e) M. B. Comisarow, N. M. M. Nibbering, *Int. J. Mass Spectrom. Ion Processes 72* (1986) 1; f) J. H. Futrell (Ed.): *Gaseous Ion Chemistry and Mass Spectrometry*, Wiley-Interscience, New York 1986; g) C. Lifshitz, *Int. Rev. Phys. Chem. 6* (1987) 35; h) K. Vékey, A. G. Brenton, J. H. Beynon, *Int. J. Mass Spectrom. Ion Processes 70* (1986) 277.

[3] As one of the numerously cited sources might be mentioned: P. Ausloos, S. Lias (Eds.): *Structure/Reactivity and Thermochemistry of Ions* (Proc. NATO ASI), Reidel, Dordrecht 1987.

[4] a) R. Lavertu, M. Catte, A. Pentenero, P. Le Goff, *C. R. Hebd. Séances Acad. Sci. Ser. C263* (1966) 1099; b) F. M. Devienne, *Entropie 24* (1968) 35.

[5] a) M. J. Gaillard, A. G. de Pinho, J. C. Poizat, J. Remillieux, R. Saoudi, *Phys. Rev. A28* (1983) 1267; b) G. I. Gellene, R. F. Porter, *Acc. Chem. Res. 16* (1983) 200; c) P. O. Danis, C. Wesdemiotis, F. W. McLafferty, *J. Am. Chem. Soc. 105* (1983) 7454; d) C. Wesdemiotis, P. O. Danis, R. Feng, E. R. Williams, F. W. McLafferty, *ibid. 107* (1985) 8059; e) J. K. Terlouw, W. M. Kieskamp, J. L. Holmes, A. A. Mommers, P. C. Burgers, *Int. J. Mass Spectrom. Ion Processes 64* (1985) 245; f) J. L. Holmes, A. A. Mommers, J. K. Terlouw, C. E. C. A. Hop, *ibid. 68* (1986) 249; g) S. Villeneuve, P. C. Burgers, *Org. Mass Spectrom. 21* (1986) 733; h) J. K. Terlouw, P. C. Burgers, B. L. M. van Baar, T. Weiske, H. Schwarz, *Chimia 40* (1986) 357; i) R. E. March, A. B. Young, *Int. J. Mass Spectrom. Ion Processes 76* (1987) 11.

[6] a) C. Wesdemiotis, F. W. McLafferty, *Chem. Rev. 87* (1987) 485; b) J. L. Holmes, unpublished.

[7] For reviews of the most important methods presently available for the determination of the structures of ions in the gas phase, where, strictly speaking, structure refers to the constitution of the atoms only: a) J. L. Holmes, *Org. Mass Spectrom. 20* (1985) 169; b) K. Levsen: *Fundamental Aspects of Organic Mass Spectrometry*, Verlag Chemie, Weinheim 1978.

[8] a) P. O. Danis, R. Feng, F. W. McLafferty, *Anal. Chem. 58* (1986) 348; b) *ibid. 58* (1986) 355.

[9] a) G. Herzberg, J. T. Honger, J. K. G. Watson, *Can. J. Phys. 60* (1982) 1261, and references cited therein; b) for the generation and characterization of $H_3^{\oplus}$ on emitter *surfaces* by strong electric fields and further literature see: N. Ernst, J. H. Block, *Phys. Rev. B29* (1984) 7092.

[10] a) G. I. Gellene, R. F. Porter, *J. Chem. Phys. 79* (1983) 5975; b) S.-J. Jeon, A. B. Raksit, G. I. Gellene, R. F. Porter, *ibid. 82* (1985) 4916; c) G. I. Gellene, R. F. Porter, *Int. J. Mass Spectrom. Ion Processes 64* (1985) 55.

[11] W. A. Lathan, W. J. Hehre, L. A. Curtis, J. A. Pople, *J. Am. Chem. Soc. 93* (1971) 6377.

[12] B. W. Williams, R. F. Porter, *J. Chem. Phys. 73* (1980) 5598.

[13] W. J. Griffiths, F. M. Harris, A. G. Brenton, J. H. Beynon, *Int. J. Mass Spectrom. Ion Processes 74* (1986) 317.

[14] For detailed literature data see [5b]. Recently published theoretical work: E. Kassab, E. M. Evleth, *J. Am. Chem. Soc. 109* (1987) 1653.

[15] G. Herzberg, *Faraday Discuss. Chem. Soc. 71* (1981) 165.

[16] a) G. I. Gellene, D. A. Cleary, R. F. Porter, *J. Chem. Phys. 77* (1982) 3471; b) G. I. Gellene, R. F. Porter, *J. Phys. Chem. 88* (1984) 6680; c) S.-J. Jeon, A. B. Raksit, G. I. Gellene, R. F. Porter, *J. Am. Chem. Soc. 107* (1985) 4129.

[17] E. Broclawik, J. Mrozek, V. H. Smith, Jr., *Chem. Phys. 66* (1982) 417.

[18] J. K. S. Wan, *J. Chem. Educ. 45* (1968) 40.

[19] G. I. Gellene, R. F. Porter, *J. Chem. Phys. 81* (1984) 5570, and references cited therein.

[20] A. B. Raksit, S.-J. Jeon, R. F. Porter, *J. Phys. Chem. 90* (1986) 2298.

[21] C. Wesdemiotis, R. Feng, F. W. McLafferty, *J. Am. Chem. Soc. 108* (1986) 5656.

[22] a) W. Koch, H. Schwarz, unpublished results; b) L. Radom, private communication, September 1986.

[23] Reviews and selected examples: a) L. Radom, W. J. Bouma, R. H. Nobes, B. F. Yates, *Pure Appl. Chem. 56* (1984) 1831; b) H. Schwarz, *Mass Spectrosc. (Tokyo) 32* (1984) 3; c) W. J. Bouma, J. K. MacLeod, L. Radom, *J. Am. Chem. Soc. 104* (1982) 2930; d) J. L. Holmes, F. P. Lossing, J. K. Terlouw, P. C. Burgers, *ibid. 104* (1982) 2931; e) H. Halim, B. Ciommer, H. Schwarz, *Angew. Chem. 94* (1982) 547; *Angew. Chem. Int. Ed. Engl. 21* (1982) 528; f) J. K. Terlouw, W. Heerma, G. Dijkstra, J. L. Holmes, P. C. Burgers, *Int. J. Mass Spectrom. Ion Phys. 47* (1983) 147; g) J. L. Holmes, F. P. Lossing, J. K. Terlouw, P. C. Burgers, *Can. J. Chem. 61* (1983) 2305; h) E. Weger, K. Levsen, I. Ruppert, P. C. Burgers, J. K. Terlouw, *Org. Mass Spectrom. 18* (1983) 327; i) F. Maquin, D. Stahl, A. Sawaryn, P. von R. Schleyer, W. Koch, G. Frenking, H. Schwarz, *J. Chem. Soc. Chem. Commun. 1984*, 504; j) T. M. Sack, R. L. Cerny, M. L. Gross, *J. Am. Chem. Soc. 107* (1985) 4562; k) T. Drewello, N. Heinrich, W. P. Maas, N. M. M. Nibbering, T. Weiske, H. Schwarz, *ibid. 109* (1987) 4810; l) S. Hammerum, *Mass Spectrom. Rev.*, in press.

[24] For an excellent review of ylides, see: D. G. Morris, *Surv. Prog. Chem. 10* (1983) 189.

[25] B. F. Yates, W. J. Bouma, L. Radom, *J. Am. Chem. Soc. 106* (1984) 5805; *109* (1987) 2250, and references cited therein.

[26] This does not obtain for the ylides CH_2NH_3, CH_2PH_3 and CH_2SH_2 which theory predicts to exist in potential wells of sufficient depth that it may be expected that the excited neutral species generated by vertical neutralization in a NRMS experiment will not rapidly dissociate into CH_2/X ($X = NH_3$, PH_3, SH_2) or isomerize into CH_3X. Indeed, *McLafferty* et al. [5c 27] have been able to generate CH_2NH_3 from $CH_2NH_3^{\oplus\odot}$ in NRMS experiments.

[27] a) J. K. Terlouw, W. M. Kieskamp, J. L. Holmes, A. A. Mommers, P. C. Burgers, *Int. J. Mass Spectrom. Ion Processes 64* (1985) 245; b) C. E. C. A. Hop, J. Bordas-Nagy, J. L. Holmes, J. K. Terlouw, unpublished.

[28] C. Wesdemiotis, R. Feng, P. O. Danis, E. R. Williams, F. W. McLafferty, *J. Am. Chem. Soc. 108* (1986) 5847.

[29] For the definition of *distonic* see a) B. F. Yates, W. J. Bouma, L. Radom, *J. Am. Chem. Soc. 106* (1984) 5805; b) *Tetrahedron 42* (1986) 6225.

[30] C. Wesdemiotis, P. O. Danis, R. Feng, J. Tso, F. W. McLafferty, *J. Am. Chem. Soc. 107* (1985) 8059.

[31] G. I. Gellene, R. F. Porter, *High Temp. Sci. 17* (1984) 171.

[32] B. van Baar, T. Weiske, J. K. Terlouw, H. Schwarz, *Angew. Chem. 98* (1986) 275; *Angew. Chem. Int. Ed. Engl. 25* (1986) 282.

[33] a) B. van Baar, W. Koch, C. B. Lebrilla, J. K. Terlouw, T. Weiske, H. Schwarz, *Angew. Chem. 98* (1986) 834; *Angew. Chem. Int. Ed. Engl. 25* (1986) 827; b) J. M. Buschek, J. L. Holmes, F. P. Lossing, *Org. Mass Spectrom. 21* (1986) 729.

[34] S. Green, *Annu. Rev. Phys. Chem. 32* (1981) 103.

[35] S. Saebo, L. Farnell, N. V. Riggs, L. Radom, *J. Am. Chem. Soc. 106* (1984) 5047, and references cited therein.

[36] a) R. G. Cooks (Ed.): *Collision Spectroscopy*, Plenum Press, New York 1978; b) T. Ast, C. J. Porter, C. J. Proctor, J. H. Beynon, *Bull. Soc. Chim. Beograd 46* (1981) 135; c) K. Levsen, H. Schwarz, *Mass Spectrom. Rev. 2* (1983) 77; d) W. Koch, F. Maquin, D. Stahl, H. Schwarz, *Chimia 39* (1985) 376.

[37] a) H. Beyer, W. Walter: *Lehrbuch der Organischen Chemie*, 20th edit., S. Hirzel Verlag, Stuttgart 1984, p. 324; b) *Gmelin Handbuch der anorganischen Chemie: Kohlenstoff, Part C3*, 8th edit., Verlag Chemie, Weinheim 1973, p. 117; c) J. Paetsch in *Ullmanns Encyklopädie der technischen Chemie, Vol. 9*, 4th edit., Verlag Chemie, Weinheim 1975, p. 115; d) [37b], *Part D1*, 1973, p. 385; e) D. L. Frasco, *J. Chem. Phys. 41* (1964) 2134.

[38] M. T. Nguyen, T.-K. Ha, *J. Am. Chem. Soc. 106* (1984) 599, and references cited therein.

[39] a) J. K. Terlouw, C. B. Lebrilla, H. Schwarz, *Angew. Chem. 99* (1987) 352; *Angew. Chem. Int. Ed. Engl. 26* (1987) 354; b) K. J. van den Berg, C. B. Lebrilla, J. K. Terlouw, H. Schwarz, *Chimia 41* (1987) 122.

[40] a) H. Hart, *Chem. Rev. 79* (1979) 515; b) B. Capon, A. K. Siddhanta, *J. Org. Chem. 49* (1984) 255; c) see also H. Schwarz, *Adv. Mass Spectrom. 10* (1986) 13.

[41] a) C. C. Van de Sande, F. W. McLafferty, *J. Am. Chem. Soc. 97* (1975) 4613; b) B. Ciommer, G. Depke, G. Frenking, S. Meyn, J. Schmidt, H. Schwarz, *Int. J. Mass Spectrom. Ion Processes 59* (1984) 21; c) J. K. Terlouw, J. Wezenberg, P. C. Burgers, J. L. Holmes, *J. Chem. Soc. Chem.*

Commun. 1983, 1121; d) J. Buschek, J. L. Holmes, J. K. Terlouw, *J. Am. Chem. Soc.*, in press.
[42] C. Wesdemiotis, R. Feng, E. R. Williams, F. W. McLafferty, *Org. Mass Spectrom. 21* (1986) 689.
[43] P. C. Burgers, J. L. Holmes, A. A. Mommers, *J. Am. Chem. Soc. 107* (1985) 1099.
[44] a) R. Clair, J. L. Holmes, A. A. Mommers, P. C. Burgers, *Org. Mass Spectrom. 20* (1985) 207; b) R. S. Mercer, A. G. Harrison, *ibid.*, in press; c) B. L. M. van Baar, N. Heinrich, W. Koch, R. Postma, J. K. Terlouw, H. Schwarz, *Angew. Chem. 99* (1987) 153; *Angew. Chem. Int. Ed. Engl. 26* (1987) 140.
[45] C. A. Liefer, J. A. Brauman, *J. Am. Chem. Soc. 96* (1974) 4028.
[46] P. C. Burgers, J. L. Holmes, A. A. Mommers, J. K. Terlouw, *Chem. Phys. Lett. 102* (1983) 1.
[47] T. Baer, T. E. Carney, *J. Chem. Phys. 76* (1982) 1304.
[48] a) P. N. Rylander, S. Meyerson, E. L. Eliel, J. D. McCollum, *J. Am. Chem. Soc. 85* (1963) 2723; b) D. Proch, D. M. Rider, R. N. Zare, *Chem. Phys. Lett. 81* (1981) 430.
[49] C. Lifshitz, P. Gotchiguon, R. Roller, *Chem. Phys. Lett. 95* (1983) 106.
[50] P. K. Pearson, H. F. Schaefer, U. Wahlgren, *J. Chem. Phys. 62* (1975) 350.
[51] H. Schwarz, K. Levsen in S. Patai (Ed.): *The Chemistry of Functional Groups. Supplement F: The Chemistry of Amino, Nitroso and Nitro Compounds and their Derivatives*, Wiley, Chichester 1985, p. 85.
[52] J. Main-Bobo, S. Olesik, W. Gase, T. Baer, A. A. Mommers, J. L. Holmes, *J. Am. Chem. Soc. 108* (1986) 677.
[53] P. C. Burgers, J. L. Holmes, A. A. Mommers, J. E. Szulejko, J. K. Terlouw, *Org. Mass Spectrom. 19* (1984) 442.
[54] H. M. Rosenstock, R. Stockbauer, A. C. Parr, *J. Chem. Phys. 77* (1980) 745, and references cited therein.
[55] J. van der Greef, T. A. Molenaar-Langeveld, N. M. M. Nibbering, *Int. J. Mass Spectrom. Ion Phys. 29* (1979) 11.
[56] a) H. Schwarz, C. Wesdemiotis, *Org. Mass Spectrom. 14* (1979) 25; b) J. H. Vajda, A. G. Harrison, A. Hiraoka, F. W. McLafferty, *J. Am. Chem. Soc. 103* (1981) 36; c) P. C. Burgers, J. L. Holmes, J. E. Szulejko, A. A. Mommers, J. K. Terlouw, *Org. Mass Spectrom. 18* (1983) 254; d) C. Wesdemiotis, R. Csencsits, F. W. McLafferty, *Org. Mass Spectrom. 20* (1985) 98.
[57] J. L. Holmes, A. A. Mommers, *Org. Mass Spectrom. 19* (1984) 460.
[58] J. K. Terlouw, J. L. Holmes, P. C. Burgers, *Int. J. Mass Spectrom. Ion Processes 66* (1985) 239.
[59] P. C. Burgers, J. L. Holmes, C. E. C. A. Hop, J. K. Terlouw, *Org. Mass Spectrom. 21* (1986) 549.
[60] A. G. Harrison, R. S. Mercer, E. J. Reiner, A. B. Young, R. K. Boyd, R. E. March, C. J. Porter, *Int. J. Mass Spectrom. Ion Processes 74* (1986) 13.
[61] J. L. Holmes, C. E. C. A. Hop, J. K. Terlouw, *Org. Mass Spectrom. 21* (1986) 776.
[62] N. Heinrich, J. Schmidt, H. Schwarz, Y. Apeloig, *J. Am. Chem. Soc. 109* (1987) 1317, and references cited therein.
[63] Review: D. G. I. Kingston, J. T. Bursey, M. M. Bursey, *Chem. Rev. 74* (1974) 216.
[64] B. L. M. van Baar, J. K. Terlouw, S. Akkök, W. Zummack, H. Schwarz, *Int. J. Mass Spectrom. Ion Processes*, in press.
[65] R. Weber, K. Levsen, C. Wesdemiotis, T. Weiske, H. Schwarz, *Int. J. Mass Spectrom. Ion Phys. 43* (1982) 131.
[66] K. Levsen, H. Schwarz, *J. Chem. Soc. Perkin Trans. 2 1976*, 1231.
[67] J. L. Holmes, F. P. Lossing, J. K. Terlouw, *J. Am. Chem. Soc. 108* (1986) 1086.
[68] J. L. Holmes, F. P. Lossing, *Int. J. Mass Spectrom. Ion Processes 58* (1984) 113.
[69] R. H. Nobes, W. J. Bouma, L. Radom, *J. Am. Chem. Soc. 105* (1983) 309.
[70] G. I. Gellene, B. W. Williams, R. F. Porter, *J. Chem. Phys. 74* (1981) 5636.
[71] G. I. Gellene, N. S. Kleinrock, R. F. Porter, *J. Chem. Phys. 78* (1983) 1795.
[72] J. K. Terlouw, H. Schwarz, unpublished.
[73] T. Drewello, C. B. Lebrilla, H. Schwarz, unpublished.
[74] C. B. Lebrilla, T. Drewello, H. Schwarz, *Organometallics*, in press.
[75] C. Lifshitz, P. J. A. Ruttink, G. Schaftenaar, J. K. Terlouw, *Rapid Commun. Mass Spectrom.*, in press.
[76] C. E. C. A. Hop, K. J. van den Berg, J. L. Holmes, J. K. Terlouw, *Rapid Commun. Mass Spectrom.*, in press.
[77] A. B. Raksit, D. M. Hudgins, S. Buchan, R. F. Porter, *Rapid Commun. Mass Spectrom.*, in press.

Liquid Crystalline Polymers

By Heino Finkelmann*

The liquid crystalline behavior of low molecular weight compounds has been known for more than a century; synthetic polymers have been manufactured on a large scale for several decades, but just recently it was found possible to produce polymers using the structural principles of liquid crystalline compounds. The resulting materials have, as expected, unusual properties. Numerous applications, not only in opto-electronics, are already anticipated for such materials.

1. Introduction

Technological progress is directly linked to the demand for specific and efficient materials. Particularly, in the area of macromolecular chemistry, developments in the past few years have shown that specific modification of molecular structure can lead to materials with new potential applications. Alone for linear macromolecules, the number of possibilities for varying the molecular structure is almost inexhaustable. One can vary the chemical constitution of the monomer units of homo- and copolymers or introduce groups with specific chemical, photochemical or pharmacological characteristics. The possibilities are particularly intriguing in the case of block copolymers, whose microphase-separated blocks can lead to ordered super structures.

But polymer behavior is not only determined by molecular architecture; much more crucial is the physical state in which the macromolecular compound exists. For this reason, the crystalline (or partly crystalline) state, the liquid, isotropic melt, and the glassy, amorphous state have been intensively studied in the past decade. In the case of high molecular weight compounds, the gaseous state is not achievable without decomposition.

This list of possible physical states of a polymer is, however, still far from complete. For almost a century, it has been known that certain low molecular weight compounds do not transform directly into the isotropic melt at their melting point.[1] Under constant pressure and within a defined temperature range, these compounds exist in a state, which on the one hand has the low viscosity of liquids, and on the other displays the physical anisotropic characteristics of a crystalline solid. This aggregate phase is known as the liquid crystalline phase, and the substances which form such phases are known as liquid crystals. The liquid crystalline phase of low molecular weight compounds has been intensively researched in the past twenty years, especially after it was discovered that the unusual physical properties of liquid crystals could be exploited in the field of opto-electronics.[2]

It is obvious to pursue the question of whether macromolecular substances could have liquid crystalline phases. The combination of polymer-specific characteristics with the anisotropic, physical characteristics of the liquid crystalline state promises not only interesting novel materials but also opens up new, multi-faceted theoretical, experimental and technological aspects. The chemist is thereby not only faced with constructing specific molecular structures but also with producing a defined physical state of the material.

The intention of this article is to show, with a knowledge of the structural principles of low molecular weight liquid crystals (Section 2), how various types of polymers with potentially liquid crystalline phases can be synthesized (Section 3). Each structural type shows in specific ways the liquid crystalline phase and the properties of the polymer. In Sections 4 to 6, the peculiarities of selected examples will be outlined and their properties and application perspectives will be discussed.

2. The Liquid Crystalline Phase

If an isobaric line is drawn through the phase diagram of a liquid crystal (dashed line in Fig. 1), one finds at lower temperatures ($T < T_m$) the crystalline phase which is characterized by a three-dimensional, long-range positional order of the molecule's center of mass in the crystalline lattice. Furthermore, in non-spherically symmetric molecules, the superior molecular axes, which are usually the longest molecular axes, are oriented with respect to each other

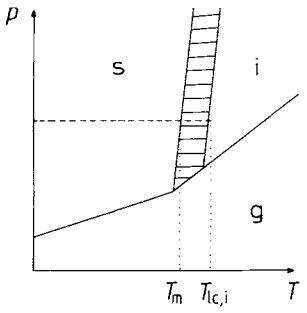

Fig. 1. pT diagram of a substance which shows a liquid crystalline phase (dashed area). s = crystalline; i = isotropic; g = gas; T_m = melting point; $T_{lc,i}$ = liquid crystalline-isotropic phase transformation temperature.

[*] Prof. Dr. H. Finkelmann
Institut für Makromolekulare Chemie der Universität
Stefan-Meier-Strasse 31, D-7800 Freiburg (FRG)

(long-range orientational order of the longitudinal molecular axes). With non-cubic crystals, the positional and orientational long-range order lead to anisotropic physical properties.

At the melting point T_m, the long-range orientational order as well as the long-range positional order for most organic compounds are lost and a melt results in which only short-range ordering between the molecules exists. The physical properties are independent of direction (isotropic).

The long-range orientational and positional order of the molecule need not always spontaneously and completely disappear at the melting point. A step-wise decay with increasing temperature of the long-range positional order in the first, second or third dimension and finally the long-range orientational order can also lead to an isotropic melt. Hence, in the temperature range $T_m < T < T_{l.c.i.}$, aggregate phases (dashed area in Fig. 1) which show a reduced long-range ordering with respect to the crystalline phase can exist between the crystalline phase and the isotropic phase. The loss of long-range positional order in at least one dimension means, however, that the solid phase has been lost and a liquid exists. The existence of long-range positional order and/or long-range orientational order of the molecules leads, on the other hand, to the anisotropic physical characteristics typical for crystals with non-cubic symmetry. This aggregate phase is therefore known as the "liquid crystalline phase."

Systematic investigations have proven that the liquid crystalline phase is found only in those substances whose molecules have a pronounced shape anisometry. They are rod- or disk-shaped molecules. Changes in conformation should not substantially affect the shape anisometry; therefore, a relatively rigid molecular structure is required. Molecules which satisfy these structural principles are known as mesogenic molecules or compounds with mesogenic groups. Simple basic structures of low molar mass, rod-shaped mesogenic compounds are given in Table 1.[3] The various liquid crystalline phases are differentiated with respect to the state of order and the ordering possibilities of the rod- and disc-shaped molecules. The most important of these types for rod-shaped molecules are summarized in Figure 2. The phase structure is determined by the chemical constitution of the mesogenic group and its substituents. In general, for a homologous series of a class of mesogenic compounds, the development of the highly-ordered smectic phase increases with increasing chain length of the flexible substituent located at the end of the longitudinal axis of the mesogen.[3]

Table 1. Selected examples of some basic structures of liquid crystalline compounds with rod-shaped molecular structure.

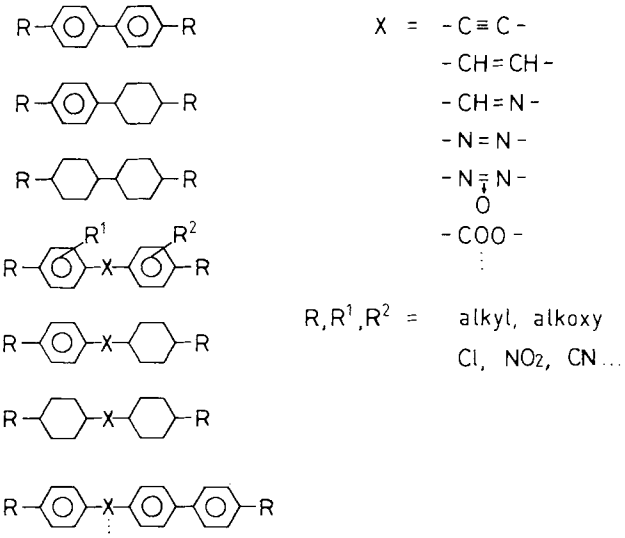

3. Liquid Crystalline Polymers

The existence of the liquid crystalline state requires rigid, shape-anisometric molecules. With the knowledge of these structural principles the construction of polymers with potential liquid crystalline properties is immediately obvious. The macromolecule as a whole must either have a rigid rod-like or disk-like structure or contain mesogenic groups as monomer units. Polymers whose total structures are mesogenic are only achievable when the polymer itself is rod-shaped, for example via a rigid, helical secondary structure. On the other hand, numerous structures are conceivable for polymers with mesogenic groups as monomer units, whereby one can differentiate between two fundamentally different types (Fig. 3):

1. Those in which the mesogenic groups are located in the polymer main chain. These polymers are known as liquid crystalline main chain polymers (see Section 4).
2. Those in which the mesogenic groups are attached to the polymer main chain in a side-chain-like manner. Such polymers are known as liquid crystalline side chain polymers (see Section 5).

Liquid crystalline side chain elastomers are dealt with in Section 6.

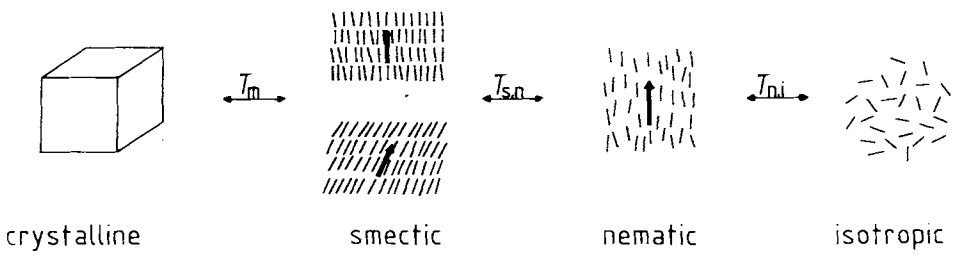

Fig. 2. Phase sequence of a liquid crystalline substance. The arrow shows the preferred direction of the orientation of the long axes of the rod-shaped molecules.

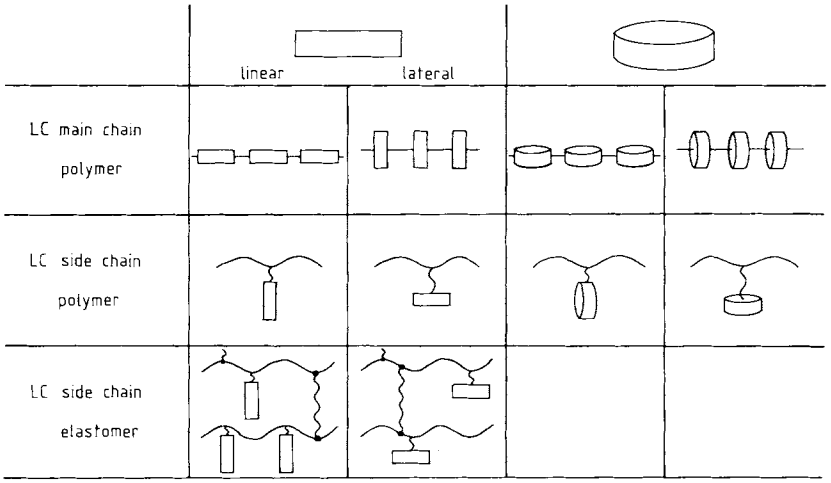

Fig. 3. Types of liquid crystalline polymers derived from rod-shaped and from disk-shaped mesogenic molecules. LC = liquid crystalline.

In comparison to low molar mass liquid crystals, attachment of the mesogenic groups to the polymer generally restricts the translational and rotational motions of the mesogenic groups. Therefore an influence on the temperature range of existence and a change in the physical properties of the liquid crystalline phase is to be directly expected. From the list of possible polymer types given in Figure 3, polymers which contain rod-shaped, mesogenic groups have been synthesized and intensively investigated in the past few years.[4] Polymers with disk-shaped monomer units could only recently be synthesized.[5,6] The same is true for combinations of liquid crystalline main and side chain polymers[7-9] and other structural variations.[8]

In the following, therefore, only selected examples of the synthesis of simple polymers with rod-shaped mesogenic groups in the main or side chain will be discussed. In addition, their characteristic properties and scope of application will be outlined.

4. Liquid Crystalline Main Chain Polymers

4.1. Synthesis and Structure

As shown schematically in Figure 3, the longitudinal axis of a mesogenic element can be laterally or linearly bound to a macromolecule. In the first case, rotations about the transverse axis and in the second case, rotations about the longitudinal axis of the individual mesogenic groups within the main chain are restricted due to polymerization. While linear attachment yields a more or less rigid main chain, with lateral attachment a chain flexibility (at least perpendicular to the mesogenic group) comparable to that of conventional polymers should result. Of these two structural variations, almost exclusively polymers with linearly-attached mesogenic groups have thus far been synthesized. The lateral attachment of mesogenic groups has only recently been described for two examples.[10]

There is a wide variety of possible polycondensation reactions for the synthesis of linear main chain polymers. In the simplest case, already known low molar mass liquid crystals[3] are functionalized with groups able to undergo polycondensation (Scheme 1). This leads to polymers which can be derived from simple basic types of mesogenic groups as shown in Table 1. Polycondensation reactions yielding polyesters, polyamides and polyethers are the most preferred reactions.

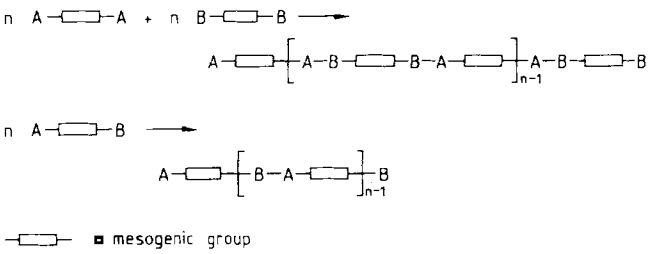

Scheme 1.

The direct, linear, rigid attachment of mesogenic groups, however, leads to problems. Beginning with a low degree of polymerization r ($r < 10$), the liquid crystalline-isotropic phase transformation temperature is quickly shifted to higher temperature with increasing r. This is due to the high anisometry of the molecule. Similarly, the melting point rises to above the decomposition temperature of the compound. As a result, the liquid crystalline phase often cannot be reached in the case of oligomers. A typical example is the polyester of 4-hydroxybenzoic acid:[11]

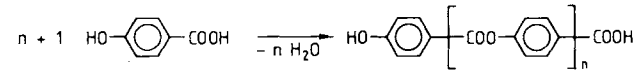

Although the low molar mass phenyl benzoates represent an important class of liquid crystals, the polymers of 4-hydroxybenzoic acid or analogous polycondensates of terephthalic acid and hydroquinone decompose before melting and are processable only as powders via a sintering method.

In order to obtain the liquid crystalline state with these types of polymers, there are three possible ways of modifying the rigid, rod-shaped basic structure[14,15] to decrease the melting point temperature:

1. The linearity of the macromolecule can be reduced by a less symmetric comonomer unit or a voluminous aromatic side group.
2. The rigid mesogenic groups are attached via a "flexible spacer," for example an alkyl or alkoxy chain. With increasing length of the flexible chain between the mesogenic groups, not only is the melting point of the polymer lowered, but the mesogenic groups have an increasing tendency to order in a layer-like manner. Above a specific length of the flexible spacer, which is dependent on the structure of the polymer, the development of a smectic phase can occur.
3. Linear macromolecules are substituted laterally with mesogenic groups via a flexible chain. These groups behave as "chemically-bound solvent molecules" and thereby reduce the polymer–polymer interactions and hence the melting point.

A few examples arbitrarily selected from the several polymers already synthesized are listed in Table 2.

Table 2. Liquid crystalline main chain polymers (examples).

1. Copolymers with non-linear chain segments	Ref.
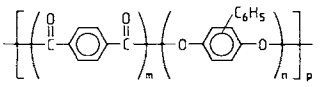	[12]
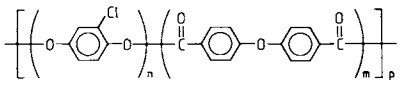	[13]
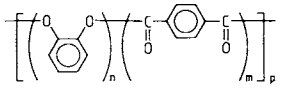	
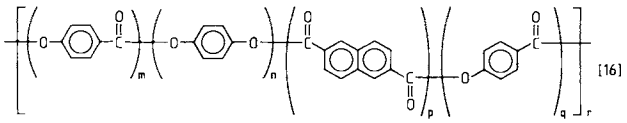	[16]
2. Polymers with flexible chains in the main chain	**Ref.**
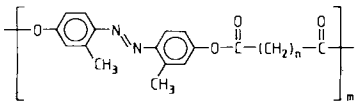	[17, 18]
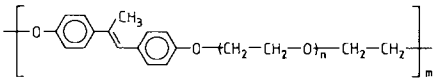	[19]
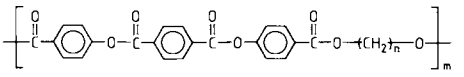	[20]
3. Polymers with laterally-attached flexible side-chain units	**Ref.**
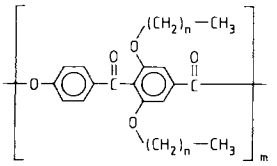	[21]
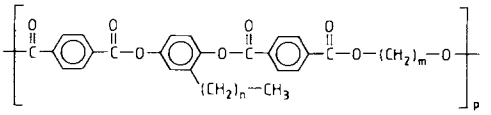	[22]

Decreasing the melting temperature results in the lowering of the liquid crystalline-isotropic phase transformation temperature. Through suitable combinations of different monomer units, an adjustment of a desired phase transition temperature is possible.

Liquid crystalline main chain polymers build, in general, a nematic phase above the melting point. An ordering of the monomer units into a smectic layered structure is prevented, especially in the case of statistically irregular copolymers which are composed of two or more different monomer units. In analogy to low molar mass liquid crystals, the development of the nematic phase is favored over that of the higher ordered smectic phase only after flexible spacers of increasing length have been introduced between the mesogens.

The liquid crystalline phase can also be realized with non-melting, rigid, rod-shaped polymers when a suitable solvent is added to reduce the melting point. This behavior was theoretically predicted in 1949 by *Onsager*[23] and in 1956 by *Flory*.[24] Rod-shaped macromolecules favor the development of nematic phases above a certain ratio of the length of the longitudinal molecular axis (or of the statistical chain segment length) to the length of the transverse axis in solution above a defined concentration of the macromolecule. The suitable solvent is in many cases problematic. Polyesters, for example, are often only soluble in substituted phenols. The most well-known polymer which forms a liquid crystalline phase only in solution is Kevlar (Du Pont).[25] In concentrated sulfuric acid, it forms a nematic phase.

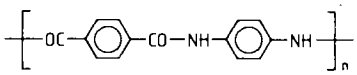

Polymers with laterally-ordered mesogenic molecules in the polymer main chain are an interesting structural variation of the liquid crystalline main chain polymer. With these polymers, the mesogenic group can rotate only about its short molecular axis; rotation about the longitudinal axis is impossible. This restriction of motion has consequences on the nematic phase structure, which will be discussed later with the corresponding side-chain polymers (Section 5). Furthermore, for this type of polymer, the anisometry of the mesogenic unit does not increase with increasing r, so that the length of the macromolecule should not influence the liquid crystalline phase behavior. Only one such polymer has thus far been synthesized which has a liquid crystalline phase.[10] This phase structure has however not yet been clarified.

The characterization of liquid crystalline main chain polymers continues to be problematic. The polydispersity of polymers and copolymers leads to very broad phase transitions. Due to this multicomponent system, isotropic, liquid crystalline and crystalline phases can exist simultaneously. In spite of that, homogeneous polymers with nematic and smectic phases can be clearly identified and character-

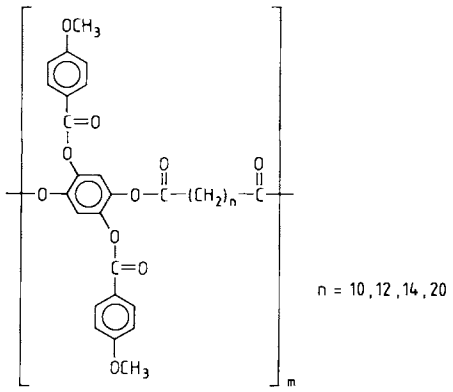

ized.[4] The liquid crystalline phase leads to unusual properties, which will be discussed in the following by considering a model.

4.2. Properties

In the ideal case of the fully rigid polymer main chain, the longitudinal axes of the macromolecules are ordered more or less parallel to one another in the nematic melt. The state of order of this long-range orientation is described through the order parameter

$$S = 3/2(\overline{\cos^2\theta} - 1/3)$$

where the angle θ gives the deviation of the longitudinal axis of the molecule from the preferred direction of the longitudinal axes of all the molecules. For $S = 1$, all molecules are ordered exactly parallel to one another, and for the isotropic melt, $S = 0$. The preferred direction of the orientation of the longitudinal molecular axes is called the director (director = symmetry axis of the orientation distribution function of the longitudinal molecular axes). The position of the director oscillates due to thermal fluctuations within a probe so that over the macroscopic dimension of the probe, no single direction of the director develops. If, however, the polymer is exposed to a shear gradient and, for example, spun through a nozzle, a macroscopically singular orientation of the director—here in the fiber direction—can be obtained (see Fig. 4). If vitrification results upon cooling the flow-oriented polymer, the macroscopically ordered nematic structure is maintained in the glassy state. If this (ideally nematic) glass has the chains ordered fully parallel ($S = 1$), and if the degree of polymerization is high (towards infinity), then a mechanical strength in the fiber direction results due to the strength of the covalent bonds in the direction of the longitudinal molecular axis. The van der Waals interactions between the polymer chains then determine the mechanical properties perpendicular to the fiber direction.

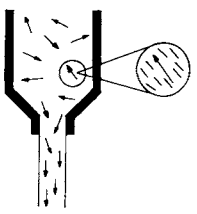

Fig. 4. Flow-orientation process of a liquid crystalline main chain polymer. → = director.

In reality, unusually high mechanical properties in the fiber direction have been found for these polymers; however, the theoretically possible values have not been reached.[15] The reason lies in the imperfect orientation of the director, a degree of order which is less than one ($S < 1$), and the finite molecular weight of the polymer which leads to defects. In addition, most polymers of this type crystallize. Theoretically, this should not reduce the mechanical characteristics of the above model, but apparently the crystallization does heavily influence the mechanical behavior due to defect structures.

Further technological interest in these polymers is based on the lower viscosity of the nematic phase as compared to the isotropic phase.[26] The cause lies in the orientation of the polymer in a shear gradient and in an anisotropic flow process which can no longer be described by one viscosity coefficient.

Due to these unusual mechanical and rheological properties, a series of liquid crystalline main chain polymers has recently become commercially available. Besides their outstanding mechanical properties,[15] they are distinguished by their dimensional stability with a very low thermal expansion coefficient, high temperature stability and low inflammability. Their possible areas of application extend therefore from fibers and composites to injection moulded parts of high tolerance with high thermal stability. Tolerance and thermal stability of electronic and optical components are critical material demands which could be fulfilled by liquid crystalline main chain polymers.

5. Liquid Crystalline Side Chain Polymers

5.1. Synthesis and Structure

In liquid crystalline side chain polymers, the mesogenic molecules are bound as side-chains, usually via a flexible spacer to a desired polymer main chain (Fig. 3). With rod-shaped mesogenic molecules, it is significant whether the liquid crystalline molecule is attached to the macromolecule along its longitudinal or transverse axis. Lateral (with respect to the longitudinal molecular axis) substituents considerably lower the stability of the liquid crystalline state,[27] while linear substituents are, in general, necessary for the existence of the liquid crystalline state.[3] In addition, motions of the mesogens are influenced differently depending on their linkage to the backbone; this will be discussed in detail later.

For the synthesis of liquid crystalline side chain polymers, each of the known low molar mass liquid crystalline molecules can in principle be supplied with functional groups through substitution reactions and then converted into a polymer.

The active species of initiation and chain growth reactions of ionic, radical, insertion and group transfer polymerizations must be carefully selected with respect to the chemical constitution of the mesogenic groups, which lim-

its in most cases the choice of the type of polymerization. No polymerizable liquid crystal has yet been synthesized which can be converted into a high molecular weight polymer through ionic polymerization. Termination reactions in ionic polymerization lead only to oligomeric products.[28, 29] On the other hand, ionic polymerization is of interest because it enables the study of the influence of the tacticity of the polymer main chain on the liquid crystalline phase behavior. This question has yet to be clarified.

Most polymers have thus far been synthesized by radical polymerization.[4] Mesogenic compounds which are esterified with acrylic, methacrylic or chloracrylic acid[30] on the terminal or lateral substituent of the mesogenic group are converted without problem into high molecular weight products via radical polymerization under usual experimental conditions (Scheme 2).

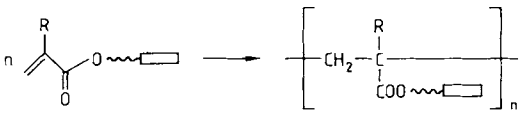

R = H, CH_3, Cl

Scheme 2.

Reactions analogous to polymerizations[31] such as the addition of liquid crystals with terminal C=C double bonds on the mesogenic group to poly[oxy(methylsilylene)], (Scheme 3) afford access to liquid crystalline polysiloxanes.[32-34]

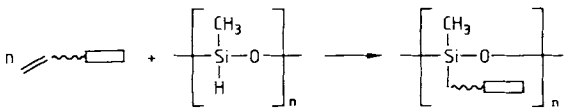

Scheme 3.

These platinum compound-catalyzed reactions have high reaction turnover and can be used to synthesize copolymers using monomer mixtures. Finally, liquid crystalline side chain polymers can be synthesized by polycondensation reactions[35] and group transfer reactions.[36]

Based on experience collected thus far, a few simple predictions can be made concerning the expected liquid crystalline phase of a liquid crystalline side chain polymer which is to be synthesized:

1. The conversion of monomers into a polymer leaves the anisometry of the mesogenic groups unchanged. This is contrary to the liquid crystalline main chain polymers with linearly-ordered mesogenic groups. The specific volume of the material, however, is lowered by polymerization; that is, the packing density of the mesogenic groups increases. Consequently, polymerization shifts the liquid crystalline-isotropic phase transformation to higher temperatures, in analogy to the increase in the packing density of low molar mass compounds with increasing pressure. This effect as a function of the degree of polymerization r of a polymer is shown schematically in Figure 5. The phase transition temperatures shift considerably in the oligomer region ($r < 10$), while for $r > 100$, dependence on the degree of polymerization is in general no longer observed.[37]

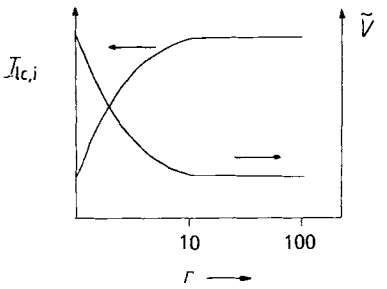

Fig. 5. Dependence of the liquid crystalline-isotropic phase transformation temperature $T_{lc,i}$ and of the specific volume $\tilde{V}$ on the degree of polymerization r of the liquid crystalline side-chain polymer.

2. In general, the attachment of the mesogenic groups on a polymer main chain tends to lead to the development of the highly ordered smectic phase. The known dependence of the polymorphology of the liquid crystalline phases on the substituents of the mesogenic groups for low molar mass liquid crystals is essentially valid also for polymers. With increasing length of the terminal, flexible substituent, development of the smectic phase is favored. This is found, however, only for polymers with flexible spacers which have a minimum length of three to four atoms within the chain. With shorter spacers, packing problems often lead to no liquid crystalline phase, or the polymer main chain forces a smectic ordering of the mesogenic side groups. Under these conditions, nematic phases are in general not found in spite of the short-chain substituents on the mesogenic groups.[38]

A further, theoretically interesting aspect is, as mentioned above, the manner in which the mesogenic group is attached to the polymer main chain. Rotation of the mesogenic group about the longitudinal axis is possible with linear attachment of the mesogenic groups and the spacers, while it is prevented by lateral attachment. Therefore, specific motions which influence the phase structure can be affected by polymer fixation. This is exemplified by the following nematic phase: For low molecular weight liquid crystals, the rather "board-shaped" molecules can be thought of as cylindrically symmetric because they rotate nearly unrestricted about their longitudinal axis. A uniaxial phase structure results from the long-range orientational order of the cylindrically symmetric longitudinal molecular axes. If now the rotation about the longitudinal axis is prevented by the lateral attachment of the mesogenic groups to the polymer main chain, the molecular shape can no longer be thought of as cylindrically symmetric. The molecule structure must be considered as being "board-like." In 1970, it was theoretically predicted[39] that with restricted rotation about the longitudinal axes, the short molecular axes could also develop long-range orientational order to one another. The result is a macroscopically biaxial nematic phase. However, because of the low rotational barrier potential, a biaxial nematic phase for low molar mass liquid crystals has not yet been demonstrated, although it does exist in polymers with laterally-

attached mesogenic groups.[40] Figure 6 shows a photograph, taken under the polarizing microscope, of a biaxial nematic polymer between two surface parallel glass plates. Through changes in the position of the director, which is essentially determined by orientation effects of the polymer at the boundary surface, a characteristic texture of the interference pattern under crossed polarizers results. This texture differs in appearance from that of the uniaxial nematic phase and can be used to identify the phase. This example demonstrates that through the attachment of the liquid crystalline molecule, specific motions can be influenced, resulting not only in new phase structures but also theoretically interesting ones.

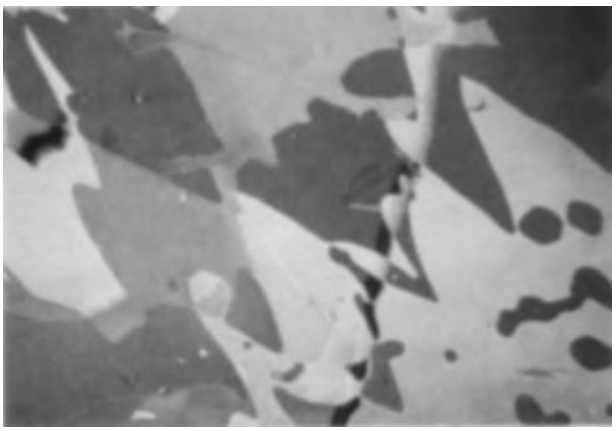

Fig. 6. Photographs, taken under the polarizing microscope, of the biaxially nematic polymer poly[1-{11-[2,5-bis(*p*-anisoyloxy)phenyl]undecyloxycarbonyl}-1-methylethylene] (crossed polarizers, magnification 40×). Original colors: mainly red-violet, light-brown, lime-green.

5.2. Properties

Although the anisotropic phase structure of liquid crystalline main chain polymers results from the long-range ordering of the main chain, only the mesogenic side groups determine the phase structure of side chain polymers. Thus the polymer main chain does not itself need to have long-range ordering. The local chain conformation must only be consistent with the liquid crystalline phase structure of the side chains. For example, a deformed polymer coil in the nematic phase was ascertained to have an axial length of 1.5 times its radius of gyration.[41] As a result, these polymers are similar to conventional amorphous polymers in their mechanical characteristics. They do not show the unusual mechanical properties of liquid crystalline main chain polymers.

Of special interest is the phase behavior of these polymers when the liquid crystalline melt is cooled to lower temperatures. This is shown schematically in Figure 7, in which the order parameter S is given as a function of temperature. With decreasing temperature, the long-range orientational order of the mesogenic side chain continually increases until a defined temperature $T_{g,lc}$ below which it then remains constant. Thermodynamic studies show that at this temperature, the liquid crystalline melt transforms into the glassy state. Optical[38] and NMR spectroscopic

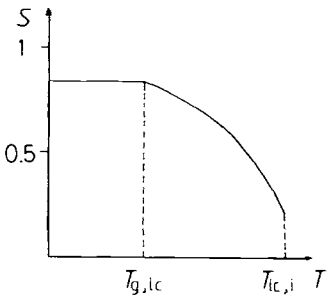

Fig. 7. Order parameter S as a function of temperature for a liquid crystalline side-chain polymer. $T_{g,lc}$ = glass transition temperature; $T_{lc,i}$ = liquid crystalline-isotropic phase transformation temperature.

measurements[42] show that the liquid crystalline structure remains unchanged in the glassy phase. Therefore it is possible to produce *anisotropic glasses* which display a nematic or smectic structure depending on the type of polymer. The glass transition temperature $T_{g,lc}$ essentially depends on the chemical constitution of the polymer main chain.

A further important aspect is the influence of an electric or magnetic field on the position of the director in the liquid crystalline phase.[43–45] In analogy to modern electrooptical display elements of low molar mass liquid crystals, the position of the director can be changed and macroscopically ordered by the application of an external field. In the ordered phase, the optical properties of the polymer correspond to that of a single crystal of the same dimension. By cooling the polymer into the glassy state, this ordered state is permanently frozen in.[46]

The combination of these characteristics—the glassy state and anisotropic physical characteristics—introduces broad application perspectives for these polymers as optical components in linear and non-linear optics.[47] Furthermore, optical memory (storage) elements which can utilize changes in the most diverse physical properties can be realized. As an example, a recording element which gives high resolution suitable for holographic photographs is shown in Figure 8.[48] A uniformly ordered polymer in the

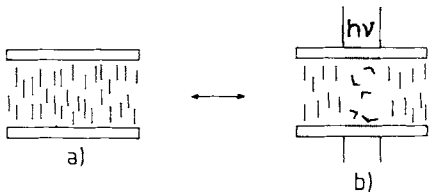

Fig. 8. Recording element with a liquid crystalline side-chain polymer. a) A uniformly ordered polymer in the glassy state; b) a linear *trans*-dye compound isomerized by light radiation into the bent *cis*-form.

glassy state (Fig. 8a) contains a dye which can undergo *trans-cis* isomerization. The glassy polymer is warmed into the liquid crystalline state by exposure to a laser for a short time, and simultaneously the linear *trans*-dye isomerizes to the bent *cis*-dye (Fig. 8b). Due to the bent conformation of the dye, the local ordering of the phase within the radiated area is reduced, thus changing the anisotropic optical

properties. After irradiation, the polymer returns to the glassy state and the given information is permanently stored. It can be retrieved by a minimal laser output. The process is reversible (for example, via a thermal reverse reaction to the *trans*-dye in the glassy state, in which the local state of order of the phase remains unaffected).

A completely different application follows from the anisotropic properties of the polymer and its negligible vapor pressure at high temperatures. As stationary phases in gas chromatography such polymers lead to higher separation efficiencies than conventional materials.[49,50]

6. Liquid Crystalline Elastomers

6.1. Synthesis and Structure

In the liquid crystalline melt above the glass temperature, the linear polymer main chains of the liquid crystalline side chain polymers can move among themselves through translational diffusion. If the linear chains are made into a polymer network by a chemical cross-linking reaction, this translational diffusion is prevented. Disregarding the cross-linkage sites, however, the high flexibility of the chain segments remains in spite of the cross-linking. In addition, the mesogenic molecules which are attached to the network are not prevented from building liquid crystalline phase structures. The networks now show, on the one hand, the anisotropic phase behavior characteristic of low molar mass liquid crystals and, on the other, the nondeformability and rubber elasticity characteristic of conventional elastomers.[51,52]

Liquid crystalline elastomers can be prepared by usual procedures in macromolecular chemistry, but the synthesis of defined networks is extremely difficult. The currently known liquid crystalline elastomers have been synthesized by simple, statistical copolymerization or by statistical polymerization-analogous addition reactions with multifunctional cross-linking molecules. Another simple method is the copolymerization of a mesogenic monomer with a functionalized comonomer to give a linear liquid crystalline copolymer, which in a second reaction step with cross-linking agent B is transformed into a network (Scheme 4).[53]

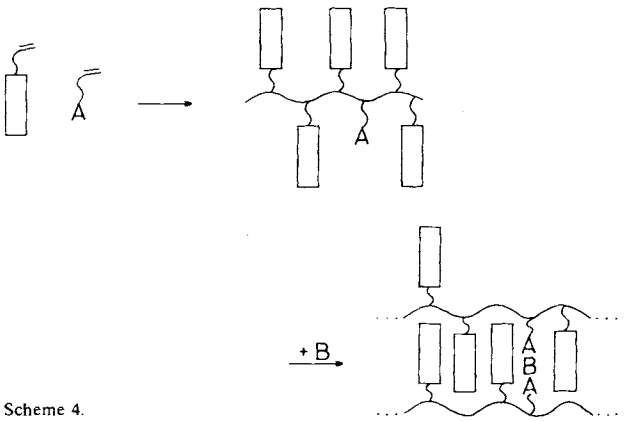

Scheme 4.

6.2. Properties

Elastomers with nematic and smectic phases are known which show the same dependence of the liquid crystalline phase on the chemical structure of the monomer units as the linear liquid crystalline polymers. At the glass transition temperature $T_{g,lc}$ the elastomer freezes into a glass with the liquid crystalline structure.

Of special importance are the mechanical properties of the elastomers. They behave at higher temperatures in the isotropic phase like conventional rubbers, whereas below the isotropic-liquid crystalline phase transformation the mechanical properties are direction dependent. If one considers an undeformed elastomer in the liquid crystalline phase, the preferred direction of the mesogenic side groups varies due to thermal fluctuations, as it does in low molar mass liquid crystals and linear liquid crystalline polymers (Fig. 9). If the elastomer is mechanically deformed by a retractive force, then one obtains a macroscopic ordering of the mesogenic side groups. The orientation of the mesogenic side groups in the direction of the force is determined by the linkage between the mesogenic groups and the network.[54] It has thus far been observed that, depending on the length of the linkage of the flexible spacer, the preferred direction of the longitudinal axes of the mesogenic groups is either parallel to or perpendicular to the deformation axis; other angular positions are not found.

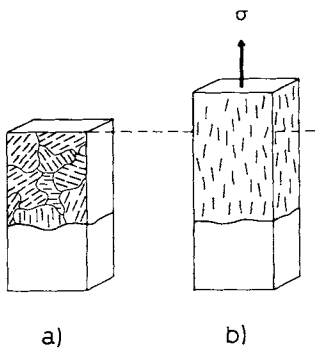

Fig. 9. Orientation of the director of a liquid crystalline elastomer through a mechanical stress σ. a) In the unstressed state, the orientation of the director is non-uniform; b) through mechanical deformation, the director is uniformly ordered. The optical characteristics of the sample correspond to that of a single crystal of the same dimensions.

The elastomer is comparable in its optical properties to a single crystal of the same dimension. A reorientation results from a change in the direction of the stress, in which the direction of the stress and the direction of the long-range orientational order are always directly related. Therefore mechanical deformation of the elastomers has the same influence on the orientation of the liquid crystalline molecules as an electric or magnetic field has on the orientation of low molar mass liquid crystals and linear liquid crystalline polymers.

Combination of the properties of anisotropic phase structure, rubber elasticity and the ability to orient the op-

tical axis through mechanical deformation results in a new class of materials whose scope of application extends beyond the area of optics. For example, thin anisotropic films can be used as separation membranes. Other detailed studies on these new materials are therefore not only of theoretical interest with respect to the interaction between a deformed polymer network and the liquid crystalline phase structure, but also provide the basis for new applications.

7. Summary and Outlook

Liquid crystalline phases always require a rigid, rod- or disk-shaped mesogenic element. The introduction of these structural elements into a polymer main chain or as side groups on the monomer unit of a macromolecule enables the synthesis of polymers which build thermodynamically stable liquid crystalline phases within a defined temperature range. In the liquid crystalline phase, the main chain segments or the mesogenic side groups which are structurally similar to low molar mass liquid crystals show long-range orientational and positional order. The liquid crystalline structure can be frozen into the glassy state of the polymer, thus enabling the preparation of glasses with anisotropic physical properties.

The examples given in this article represent only a small number of the wide spectrum of realizable or conceivable liquid crystalline polymers. The intended aim of this article has been to point out that the combination of those properties specific to polymers with the anisotropic properties of liquid crystalline structures enables the synthesis of a wide variety of new materials. The liquid crystalline polymers not only offer possibilities for new types of application. The interplay between anisotropic phase structure and the properties of the macromolecular system provides the chemist, physical chemist and physicist with many interesting theoretical and experimental problems which remain to be solved.

Received: April 23, 1987 [A 634 IE]
German version: *Angew. Chem. 99* (1987) 840

[1] F. Reinitzer, *Monatsh. Chem. 9* (1888) 421.
[2] H. Kelker, R. Hatz: *Handbook of Liquid Crystals*, Verlag Chemie, Weinheim 1980.
[3] D. Demus, H. Demus, H. Zaschke: *Flüssige Kristalle in Tabellen*, VEB Deutscher Verlag für Grundstoffindustrie, Leipzig 1976; D. Demus, H. Zaschke: *Flüssige Kristalle in Tabellen II*, VEB Deutscher Verlag für Grundstoffindustrie, Leipzig 1984.
[4] Reviews in a) M. Gordon (Ed.): *Liquid Crystal Polymers I-III, Adv. Polym. Sci. 59-61* (1984): C. K. Ober, J.-I. Jin, R. W. Lenz, *Vol. I*, p. 103; M. G. Dobb, J. E. McIntyre, *Vol. II/III*, p. 61; H. Finkelmann, G. Rehage, *Vol. II/III*, p. 99; V. P. Shibaev, N. A. Platé, *Vol. II/III*, p. 173; b) L. L. Chapoy (Ed.): *Recent Advances in Liquid Crystalline Polymers*, Elsevier, Amsterdam 1985; c) A. Blumstein (Ed.): *Polymer Liquid Crystals*, Plenum Press, New York 1985.
[5] W. Kreuder, H. Ringsdorf, *Makromol. Chem. Rapid Commun. 4* (1983) 807.
[6] W. Kreuder, H. Ringsdorf, P. Tschirner, *Makromol. Chem. Rapid Commun. 6* (1985) 367.
[7] B. Reck, H. Ringsdorf, *Makromol. Chem. Rapid Commun. 6* (1985) 291.
[8] M. Engel, B. Hisgen, R. Keller, W. Kreuder, B. Reck, H. Ringsdorf, H. W. Schmidt, P. Tschirner, *Pure Appl. Chem. 57* (1985) 1009.
[9] R. Zentel, G. Reckert, B. Reck, *Liq. Cryst. 2* (1987) 83.
[10] V. Krone, B. Reck, H. Ringsdorf, *Makromol. Chem. Rapid Commun. 7* (1986) 381.
[11] S. G. Cottis, J. Economy, L. C. Wohrer, DBP 2248127 (1973) and 2507066 (1976).
[12] C. R. Payet, DOS 27511653 (1978).
[13] B. Griffin, M. K. Cox, *Br. Polym. J. 12* (1980) 147.
[14] J. I. Jin, S. Antoun, C. Ober, R. W. Lenz, *Br. Polym. J. 12* (1980) 132, and references cited therein.
[15] Gia Huynh-Ba, E. F. Cluff in A. Blumstein (Ed.): *Polymeric Liquid Crystals*, Plenum Press, New York 1985, p. 217.
[16] G. W. Calundann, US-Pat. 4130545 (1978).
[17] A. Blumstein, S. Vilasagar, S. Ponrathnam, S. B. Clough, R. B. Blumstein, *J. Polym. Sci. Polym. Phys. Ed. 20* (1982) 877.
[18] A. Blumstein, *Polym. J.* (Japan) 17 (1985) 277.
[19] T. D. Shaffer, V. Percec, *Polym. Prepr. Am. Chem. Soc. Div. Polym. Chem. 27* (1986) 369.
[20] R. W. Lenz, *Faraday Discuss. Chem. Soc. 79* (1985), paper 2.
[21] M. Ballauf, G. F. Schmidt, *Makromol. Chem. Rapid Commun. 8* (1987) 93.
[22] R. W. Lenz, *Polym. J.* 17 (1985) 105.
[23] L. Onsager, *Ann. N. Y. Acad. Sci. 51* (1949) 627.
[24] P. J. Flory, *Proc. R. Soc. London Ser. A 234* (1956) 60.
[25] J. Preston, *Angew. Makromol. Chem. 109/110* (1982) 1.
[26] K. F. Wissbrun, *Faraday Discuss. Chem. Soc. 79* (1985), paper 13.
[27] W. Weisflog, A. Wiegleben, D. Demus, *Mater. Chem. Phys. 12* (1981) 875.
[28] B. Hahn, J. H. Wendorff, M. Portugall, H. Ringsdorf, *Colloid Polym. Sci. 259* (1981) 875.
[29] F. Cser, K. Nyitrai, J. Horvath, G. Hardy, *Eur. Polym. J. 21* (1985) 259.
[30] a) J. C. Dubois, G. Decobert, P. Barny, *Mol. Cryst. Liq. Cryst. 137* (1986) 349; b) R. Zentel, H. Ringsdorf, *Makromol. Chem. Rapid Commun. 5* (1984) 393.
[31] P. Keller, *Makromol. Chem. Rapid Commun. 6* (1985) 707.
[32] H. Finkelmann, G. Rehage, *Makromol. Chem. Rapid Commun. 1* (1980) 31.
[33] P. A. Gemmel, G. W. Gray, D. Lacey, *Mol. Cryst. Liq. Cryst. 122* (1985) 205.
[34] H. Ringsdorf, A. Schneller, *Makromol. Chem. Rapid Commun. 3* (1982) 557.
[35] B. Reck, *Diplomarbeit*, Universität Mainz 1985.
[36] W. Kreuder, O. W. Webster, H. Ringsdorf, *Makromol. Chem. Rapid Commun. 7* (1986) 5.
[37] H. Stevens, G. Rehage, H. Finkelmann, *Macromolecules 17* (1984) 851.
[38] H. Finkelmann, G. Rehage, *Adv. Polym. Sci. 60/61* (1984) 99.
[39] M. J. Freiser, *Phys. Rev. Lett. 24* (1970) 1041.
[40] F. Hessel, H. Finkelmann, *Polym. Bull. (Berlin) 15* (1986) 349.
[41] H. Mattoussi, R. Ober, M. Veyssie, H. Finkelmann, *Europhys. Lett. 2* (1986) 233.
[42] K. Müller, P. Meier, G. Kothe, *Prog. Nucl. Magn. Reson. Spectrosc. 17* (1985) 211.
[43] H. Finkelmann, U. Kiechle, G. Rehage, *Mol. Cryst. Liq. Cryst. 92* (1983) 49.
[44] G. S. Attard, G. Williams, G. W. Gray, D. Lacey, P. A. Gemmel, *Polymer 27* (1986) 185.
[45] M. S. Sefton, H. J. Coles, *Polymer 26* (1985) 1319.
[46] P. Fabre, C. Casagrande, M. Veyssie, H. Finkelmann, *Phys. Rev. Lett. 53* (1984) 993.
[47] H. Finkelmann, H. Kock, *Display Technol. 1* (1985) 81.
[48] M. Eich, J. H. Wendorff, R. Reck, H. Ringsdorf, *Makromol. Chem. Rapid Commun. 8* (1987) 59.
[49] M. A. Apfel, H. Finkelmann, G. M. Janini, R. J. Laub, B. H. Lühmann, A. Price, W. L. Roberts, T. J. Shaw, C. A. Smith, *Anal. Chem. 57* (1985) 651.
[50] J. S. Bradshaw, C. Schregensberger, K. H. C. Chang, K. E. Markides, M. L. Lee, *J. Chromatogr. 358* (1986) 95.
[51] H. Finkelmann, H. J. Kock, G. Rehage, *Makromol. Chem. Rapid Commun. 2* (1981) 317.
[52] W. Gleim, H. Finkelmann, *Makromol. Chem. 188* (1987) 1489.
[53] R. Zentel, *Liq. Cryst. 1* (1986) 589.
[54] J. Schätzle, H. Finkelmann, *Mol. Cryst. Liq. Cryst. 142* (1987) 85.

harge Transfer and Radical Ions in Photochemistry**

By Jochen Mattay*

Bimolecular photoreactions usually occur via several steps involving "complex-type" intermediates (excimers or exciplexes). Although physical chemists have investigated them for nearly thirty years (*Förster*, *Weller*), and postulated their existence in numerous publications, it is only in the last decade that evidence for an exciplex intermediate in cycloadditions (*Caldwell*) has been obtained, thereby establishing the link between spectroscopy and synthetic photochemistry. Since then, many investigations have confirmed the role of exciplexes as intermediates in bimolecular photoreactions. The photochemically induced charge transfer from a donor to an acceptor substrate determines not only the bond strengths in the primary exciplex but also influences—via the charge-transfer nature of the complex—the structure of the exciplex and thereby the selectivity of subsequent reactions. Such chemical processes between the donor and the acceptor prevent the reverse transfer of electrons, which usually results in regeneration of the starting materials, thereby only causing the dissipation of energy and occasionally—under specific conditions—the generation of molecules of the starting material in the triplet state. Ionic photodissociation also reduces the probability of a reverse transfer of electrons. This process, which produces solvated radical ions, is promoted by polar solvents and salt effects, particularly special salt effects. By this means it is possible to generate specific radical cations from, for example, alkenes and dienes and to study their reactions. Although in some areas, for example physical and biophysical chemistry, discussions of single electron transfer (SET) processes have long been found in the basic textbooks, organic chemistry lags far behind, although—and this is shown by the numerous recent publications—organic chemists are also aware of the fundamental importance of these processes. In this connection photochemistry plays a central role, since its instruments make it possible to carry out specific SET processes, to analyze them, and to use them in chemical reactions.

1. Introduction

"One of the simplest elementary processes in solution is the exchange of an electron between two chemical substrates." This statement by *Eberson*[1] is of fundamental importance for many areas of chemistry.[2–6] In this elementary process, bonds are neither broken nor formed. However, the transfer of an electron has important consequences for the chemical reactivity of the compounds.[1] For example, a nucleophilic reagent R–Nu is transformed by oxidation (i.e., the loss of an electron) into an electrophile. Correspondingly, the reduction of an electrophilic substrate enhances its nucleophilic character. Electron transfer therefore leads to "umpolung" (Fig. 1) with all its consequences for the ensuing reactions.

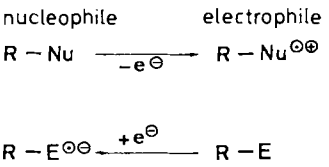

Fig. 1. Umpolung by means of electron transfer.

The importance of electron transfer in photochemistry has been known ever since the fundamental work of *Weller* et al.[7] and, for example, the studies of *Marcus*[8] and *Hush*,[9] but it was not until the 1970s that numerous groups began to approach the problem experimentally. These investigations paralleled the development of highly time-resolved methods of transient analysis, such as laser flash spectroscopy, which made possible the study of chemical processes in the ns[10–13] and ps[13–16] region, and chemically induced dynamic nuclear polarization (CIDNP),[17] which can also be applied in a time-dependent manner.[18,19] Occasionally, time-resolved ESR spectroscopy[13,20] and, most recently, time-resolved Raman spectroscopy[21] have been used. These modern analytical methods can be used to obtain information about the types of reactive intermediates and their kinetics. Simultaneously, interest has been growing in organic syntheses that proceed via electron-transfer processes.[22–24]

2. Basic Principles

2.1. Energetics

Why is there so much activity in the field of photochemistry at the moment? Because specific photochemically initiated electron-transfer processes can be used to carry out chemical reactions involving radical ions in homogeneous solution, and these reactions, in turn, can be studied by the modern analytical techniques mentioned above. Photo-

[*] Prof. Dr. J. Mattay
Institut für Organische Chemie der Technischen Hochschule
Prof.-Pirlet-Strasse 1, D-5100 Aachen (FRG)

[**] Radical Ions and Photochemical Charge Transfer Phenomena, Part 17. – Part 16: J. Mattay, J. Gersdorf, K. Buchkremer, *Chem. Ber. 120* (1987) 307.

 © VCH Verlagsgesellschaft mbH, D-6940 Weinheim, 1987 0570-0833/87/0909-0825 $ 02.50/0

excitation of electron-acceptor (A) or electron-donor (D) substrates leads to well-defined changes in their redox properties (Fig. 2). For example, the donor properties of D

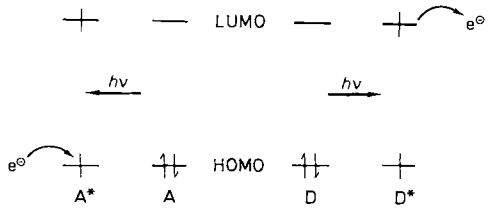

Fig. 2. Photochemical excitation and redox properties of donor (D) and acceptor (A) molecules.

increase proportionally to the excitation energy ($\Delta E(D^*)=h\nu$); i.e., the ionization energy, $IP(D)$, is reduced by the promotion of an electron from the HOMO to the LUMO [Eq. (a)]. The electron affinity of the acceptor, $EA(A)$, behaves similarly [Eq. (b)].[7,25] Electron transfer

$$IP(D^*)=IP(D)-\Delta E(D^*) \quad (a)$$
$$EA(A^*)=EA(A)+\Delta E(A^*) \quad (b)$$

between donor and acceptor substrates should therefore occur more easily after photochemical excitation of one of the reacting species[7] if either $IP(D^*)<EA(A)$ or $IP(D)<EA(A^*)$ holds true (Fig. 3).

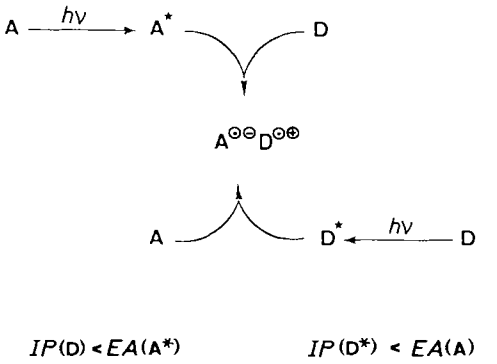

Fig. 3. Photochemically induced electron transfer between donor and acceptor molecules.

Simple energy considerations such as this clarify the dependence of the electron transfer on electronic conditions in the participating substrates. IP and EA are valid only for the gas phase. However, since the oxidation and reduction potentials ($E^{ox}_{1/2}(D)$ and $E^{red}_{1/2}(A)$), which are the corresponding parameters in solution, are easily obtained experimentally[26] and are linearly related to IP and EA, respectively,[27] the conditions for electron transfer between D and A after irradiation can be formulated as follows:

$$\Delta G(A_s^{\odot\ominus}D_s^{\odot\oplus})=F[E^{ox}_{1/2}(D)-E^{red}_{1/2}(A)]-\Delta E_{excit}+\Delta E_{coul} \quad (c)$$

In Equation (c)—the Weller equation—$E^{ox}_{1/2}(D)$ and $E^{red}_{1/2}(A)$ are the oxidation potential of the donor and the reduction potential of the acceptor, respectively, measured in acetonitrile; ΔE_{excit} is the excitation energy of the electronically excited species, and ΔE_{coul} the coulomb interaction energy of the two radical ions at a distance a from one another in a given solvent.[28,29] The exact value of ΔE_{coul} is obtained, according to the Born equation, from Equation (d).[29] With $F=96489$ C, $e=1.602\times10^{-19}$ C,

$$\Delta E_{coul}=\frac{eN}{4\pi\varepsilon_0 a}\left[\frac{1}{\varepsilon}-\frac{2}{37.5}\right] \quad (d)$$

$\varepsilon_0=8.854\times10^{-12}$ CV^{-1} m^{-1}, and $N=6.023\times10^{23}$ mol^{-1}, one obtains the free energy of formation (ΔG) of the solvent-separated radical-ion pair $A_s^{\odot\ominus}D_s^{\odot\oplus}$(SSIP) in a solvent with dielectric constant ε. In general, the distance a for a solvent-separated radical-ion pair is taken as 0.7 nm. The Weller equation therefore allows an estimate, to a first approximation, as to whether electron transfer within a donor-acceptor system is thermodynamically allowed (ΔG negative, exergonic process) or not (ΔG positive, endergonic process). In addition, it shows that the electron-transfer process can be decisively influenced by the polarity of the solvent as well as by the electronic properties of the reacting species. This gives the chemist a number of ways to direct reactions involving radical ions in a desired fashion.

2.2. Radical-Ion Pairs, Exciplexes

While the fate of a donor-acceptor pair in the exergonic region of electron transfer ($\Delta G<0$, Eq. (c)) appears at first glance to be straightforward—namely, the preferred formation of radical-ion pairs—this is not true for the endergonic region. In addition to energy transfer,[6] an exciplex (i.e., a complex in an excited state) may be formed, especially when the energy of the excited species (sensitizer) is greater than the excitation energy of the second species (for the possibility of energy transfer via exciplex intermediates, see, for example, *Kavarnos* and *Turro*[6]). Figure 4

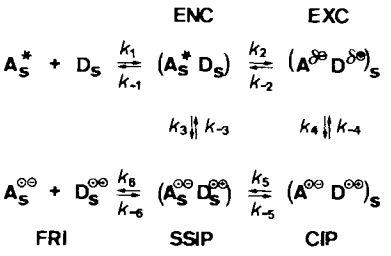

Fig. 4. General kinetic scheme for photochemically induced electron transfer in donor-acceptor systems (according to [30]). ENC complex = collision complex; EXC = exciplex; CIP = contact ion pair; SSIP = solvent-separated radical-ion pair; FRI = free radical ions.

shows various quenching processes that an excited acceptor molecule A* can undergo with a donor molecule D in the ground state (spin multiplicities as well as subsequent processes, e.g., the formation of triplet and product molecules, are not considered here for reasons of simplicity).[30] The path characterized by k_3 shows the direct formation of the SSIP from the collision complex in the exergonic region. However, the electron transfer is also possible via an exciplex intermediate (k_2, k_4, k_5). This possibility

is supported by the observation that, in contrast to the expectations based on the Marcus theory,[8] reductions in the rate constants for electron transfers in highly exergonic regions have not been observed.[30] Recently, however, *Miller, Closs* et al.[31] found clear evidence for the so-called "Marcus inverted region" in intramolecular electron-transfer processes.

According to *Weller* et al.,[27,32,33] exciplexes form because of a coupling of a local excited state with the so-called charge-transfer (CT) state [(e) and (f)]. The weight-

$$(A^*D) \longleftrightarrow (AD^*) \longleftrightarrow (A^{\ominus}D^{\oplus}) \quad \text{(e)}$$

$$\psi = c_1\psi(A^*D) + c_2\psi(AD^*) + c_3\psi(A^{\ominus}D^{\oplus}) \quad \text{(f)}$$

ing of the wave function $\psi(A^{\ominus}D^{\oplus})$ determines the CT character of the exciplex. For $c_3 > c_1$ and c_2, the wave function corresponds to a highly polar exciplex which can easily dissociate in polar solvents to form solvated radical ions (ionic photodissociation[34]). In the extreme case $c_3 \gg c_1$ and c_2, the exciplex can be considered as a contact ion pair.[29]

Exciplexes are often discussed as intermediates in photochemical reactions;[25,35-37] this is also the case for several photochemical reactions of arenes and carbonyl compounds which have been investigated in our laboratory.[38-45] If such an exciplex exhibits a bathochromic shift in emission compared with the monomer luminescence[27,46] (Fig. 5), then the experimental detection of a

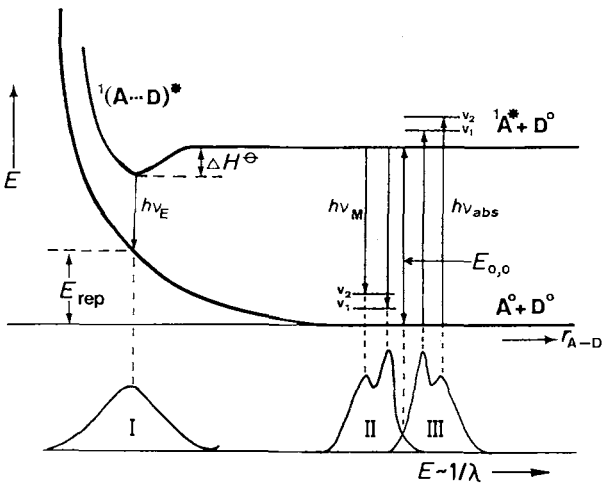

Fig. 5. Schematic potential curves for the formation of exciplexes (from [27]). $\Delta H^{\ominus}$ = enthalpy of exciplex formation; $h\nu_E/h\nu_M$ = emission energy of exciplex/monomer; E_{rep} = repulsion energy in the ground state; v_i = vibrational quantum number. I/II = fluorescence of the exciplex/monomer, III = absorption of the monomer.

reactive intermediate in a photochemical reaction is relatively simple. For example, *Caldwell et al.*[47] were able to quench the 9-phenanthrenecarbonitrile–anethole exciplex specifically with dimethyl acetylenedicarboxylate (quenching of $h\nu_E$, but not $h\nu_M$; cf. Fig. 5) and thereby demonstrate the reactive character of this intermediate. Similar examples have been described by other authors.[35,36,38,39]

Although the observation of exciplex emission is not the rule,[22] the existence of exciplexes and their role as reactive intermediates is nowadays unchallenged. Numerous studies have shown that indirect evidence can also be found. For example, reversibly formed exciplexes have been recognized by the biexponential decay of their monomer luminescence.[48] Similarly, the deviation of fluorescence or phosphorescence quenching from Rehm–Weller behavior [correlation between $\log k_q$ and ΔG: k_q = rate constant for the bimolecular quenching process; ΔG = reaction free energy of the electron transfer, given by Equation (c)] indicates the existence of additional intermediates.[40,41,44,45] Further examples are found in numerous reviews.[6,23,25,32,34-37,43]

2.3. Aim and Scope of This Article

In our studies of the photochemistry of donor–acceptor systems, we have been able to show that reaction selectivity is strongly influenced by photochemically induced charge transfer.[40-45,49,50] Reactions involving radical ions and those involving exciplex intermediates follow different paths. However, the reactions of the latter species are also determined by the degree of charge transfer (i.e., the reactivity of highly polar exciplexes is different from that of weakly polar species). The reaction free energy for the electron transfer (ΔG) calculated from the Weller equation has proved to be an excellent ordering criterion.[41-43,45] In the following discussion, we will present some examples chosen from our own work which demonstrate this correlation between reaction selectivity and ΔG values. Examples from other areas will make the general validity of this ΔG correlation clear. With the help of transient analysis methods, the intermediates involved can be detected and their kinetics investigated. It will be shown in detail how, for example, the equilibrium between contact ion pairs (CIP) and solvent-separated ion pairs (SSIP) or free radical ions (FRI) can be influenced by the suitable choice of the reaction medium and how the course of the reaction can thereby be directed. Borderline cases such as the involvement of ternary complexes in photoreactions will be discussed. This article is restricted to the photochemistry of electron donor–acceptor systems. The generation of radical ions by photoionization[51] will not be dealt with here. Readers who are interested in electron transfer processes in microheterogeneous systems, as well as in the relationship between energy transfer and electron transfer, are referred to other reviews.[5,6,22,52-54] Furthermore, reactions of radical ions in homogeneous solution have been reviewed by *Chanon* et al.,[22] *Farid* et al.,[23] and *Mariano*.[24]

3. The Concept

3.1. Photochemically Induced Charge Transfer, Intermediates, and the Course of Reaction

Table 1 shows, in a simplified manner, possible intermediates and the course of reaction for photoreactions between electron-donor and electron-acceptor molecules. This scheme was developed for the reactions between arenes and alkenes,[42,43] but has, as we shall see, proved valid for other systems. The decisive criterion for the

course of the reaction is the type of intermediate and hence the degree of charge transfer, which can be correlated with the reaction free energy for the formation of SSIPs. A positive or negative ΔG value [calculated by means of Eq. (c)] should show, to a first approximation, whether the formation of SSIPs is allowed or not, i.e.,

Table 1. Photoreactions of electron donor-acceptor systems.

Reaction	ΔG	Intermediate		Product	Example
Donor-acceptor reaction A + D	>0	$(AD)^*_\chi$	nonpolar exciplex	[AD]	cycloaddition
		$(A^{\delta\ominus}D^{\delta\oplus})_\chi$	polar	[AD]'	
	$\lesssim 0$	$(A^{\odot\ominus}D^{\odot\oplus})_\chi$	CIP	[AD]''	
Reactions of radical ions (A)D + D'	$\lesssim 0$	$(A^{\odot\ominus}_\chi D^{\odot\oplus}_\chi)$	SSIP	[DD']	cycloaddition, nucleophilic addition
		$A^{\odot\ominus}_\chi D^{\odot\oplus}_\chi$	FRI		

whether free, or at least solvent-separated, radical ions (pairs) are preferentially formed, assuming that the polarity of the reaction medium suffices for the solvation of the individual species.

The situation in the endergonic region of electron transfer is more complicated. A calculation of the free energy of formation of the exciplex is only possible when molecular parameters such as dipole moment, the radius, and the separation between the components are known.[29] Although these values are not usually known, Equation (c) offers a way out of the dilemma. Figure 6 shows curves for

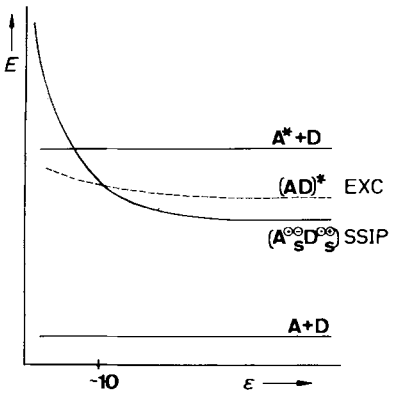

Fig. 6. Dependence of exciplex and SSIP potentials on the dielectric constant (ε) of the solvent (from [55]).

the potential of an exciplex and an SSIP as a function of the polarity of the solvent, as expressed by the dielectric constant ε. Since the curves cross in the region of $\varepsilon \lesssim 10$,[55] the experimentally easily obtainable ΔG(SSIP) value can be used as an approximate estimate of the exciplex free energy. Equation (c) therefore makes it possible to estimate the CT character of an exciplex [cf. Eqs. (e) and (f)]. This method is particularly useful when the correlations with ΔG values for electron transfer are carried out within a substrate series, since the parameters that determine the exciplex energy depend on the type of molecule.

3.2. Influencing Charge Transfer by Solvent Polarity and Salt Effects (Transient Analysis Studies)

The reaction medium plays a decisive part in processes that occur via polar intermediates.[56,57] According to Equations (c) and (d), for example, the formation of solvent-separated ion pairs in acetonitrile ($\varepsilon = 37.5$) is favored by 0.98 eV (=94.4 kJ mol^{-1}) over that in *n*-hexane ($\varepsilon = 1.89$). Ionic photodissociation of donor-acceptor pairs[34] to solvated radical ions therefore requires a polar solvent. The influence of the solvent can often be followed by transient analysis because of the specific UV/VIS absorption of the intermediates involved.

Fluorenone **1** is particularly well suited as an acceptor for such studies since the concentration, solvent, temperature, and cation-radius dependence of the absorption spectra of pairs formed from metal cations and fluorenone radical anions are already known from earlier work.[58,59] The effect of solvent and of added salts on the photoreactions of fluorenone with the electron-rich alkenes **2** and **3** is shown in Figures 7 and 8, respectively.[60] Whereas the formation of solvated radical ions is favored in polar sol-

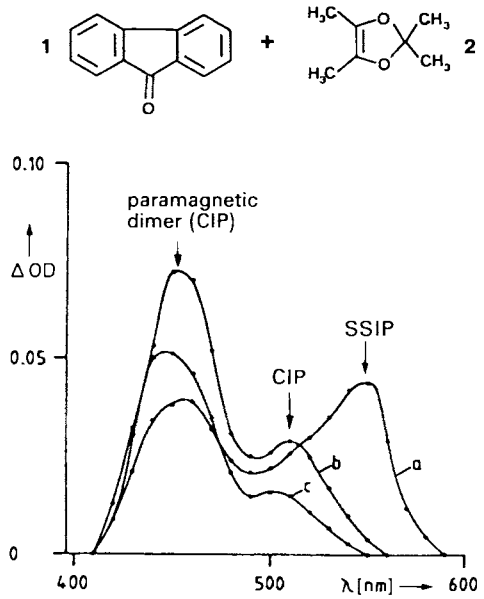

Fig. 7. Transient absorption spectra (ΔOD = absorption difference) 100 μs after flash photolytic excitation of **1** in the presence of tetramethyl-1,3-dioxole **2** in various solvents (from [60]). a) Acetonitrile. b) Benzene. c) Cyclohexane.

vents, only contact ion pairs or paramagnetic dimers could be observed in nonpolar media. It should be noted, in particular, that electron transfer from electron-rich alkenes to **1** even takes place in nonpolar solvents through the formation of contact ion pairs.

Following the fundamental work of *Hughes*, *Ingold* et al.[62] and *Winstein* et al.,[63] salt effects have been frequently investigated in organic chemistry.[57] The so-called normal salt effect is largely determined by the ionic strength; the departure from the "normal" behavior of the reaction rate at low salt concentrations has been called the special salt effect by *Winstein* et al.[63] This effect is presumably due to an ion exchange process that causes a shift in the equilibrium between the SSIP and the CIP. Whereas

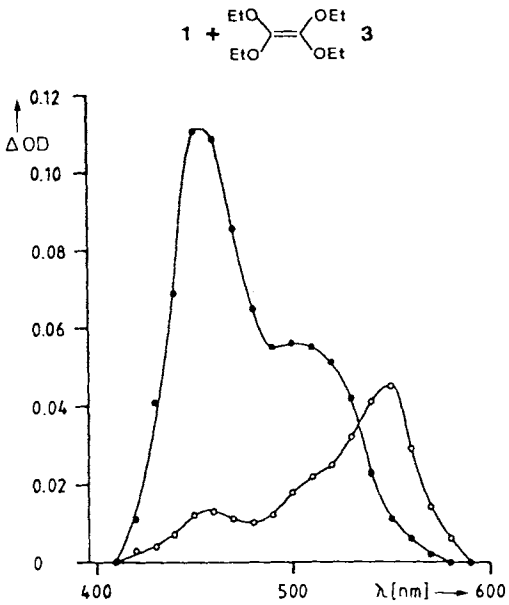

Fig. 8. Dependence of the transient spectra on added lithium perchlorate 100 μs after flash photolytic excitation of **1** in the presence of **3** in acetonitrile—special salt effect (from [60]). ○, no $LiClO_4$; ●, 0.1 M $LiClO_4$.

the long-wavelength absorption at ca. 550 nm in Figure 8 can be ascribed to the SSIP formed by $\mathbf{1}^{\odot\ominus}$ and $\mathbf{3}^{\odot\oplus}$, the addition of lithium perchlorate brings about the formation of a new ion pair (consisting of $\mathbf{1}^{\odot\ominus}$ and $Li^{\oplus}$). The hypsochromic shift of the absorption shows that this species is a contact ion pair [Eq. (g)]. The special salt effect can

$$(A_s^{\odot\ominus} D_s^{\odot\oplus}) + Li^{\oplus} \rightleftharpoons (A^{\odot\ominus} Li^{\oplus})_s + D_s^{\odot\oplus} \qquad (g)$$

therefore be used to influence the equilibrium between the SSIP and the CIP.

The separation between $A^{\odot\ominus}$ and $D^{\odot\oplus}$ makes for a longer lifetime for the radical ions, since the reverse transfer of electrons clearly takes longer. For example, using the benzophenone–alkene and benzil–alkene systems, we could extend the lifetimes by a factor of 15 (as determined by laser flash spectroscopy) by the addition of lithium perchlorate.[44,64] In addition, the special salt effect occasionally results in a greater yield of radical ions.[44,64] In the investigations of the systems so far mentioned, only the formation and decay of the long-wavelength-absorbing radical anions could be followed spectroscopically. Simultaneous analysis of both radical-ion species is possible using *p*-chloranil **4** as the acceptor and 2-methoxy-1,1-diphenylethene **5** as the donor,[44,65] because of their favorable absorption characteristics (Fig. 9). Both the radical anion $\mathbf{4}^{\odot\ominus}$ and the radical cation $\mathbf{5}^{\odot\oplus}$ decay with second-order kinetics and have almost identical lifetimes in the microsecond region, as expected for a reverse transfer of electrons. The addition of lithium perchlorate increases the lifetime by a factor of 10 without affecting the coupling of the two radical ions (Table 2).

Table 2. Effect of $LiClO_4$ on the lifetimes $\tau_{1/2}$ of $\mathbf{4}^{\odot\ominus}$ and $\mathbf{5}^{\odot\oplus}$.

λ [nm]	$\tau_{1/2}$ [μs]	
	without $LiClO_4$	1 M $LiClO_4$
450	0.9	8.9
600	1.3	11.2

Further transient analysis methods such as ESR spectroscopy using in situ photolysis conditions[40,45] can yield information about the structure of the radical-ion intermediates involved but provide little information about their dynamics. It should be noted that salt effects in photochemically induced electron-transfer processes have been investigated by other groups. For example, *Goodman* and *Peters*[66] were able to show, with the help of picosecond laser flash spectroscopy, that both the electron back transfer and the dissociation of contact ion pairs formed between *trans*-stilbene and electron-poor alkenes could be accelerated by the addition of salts. However, these effects,

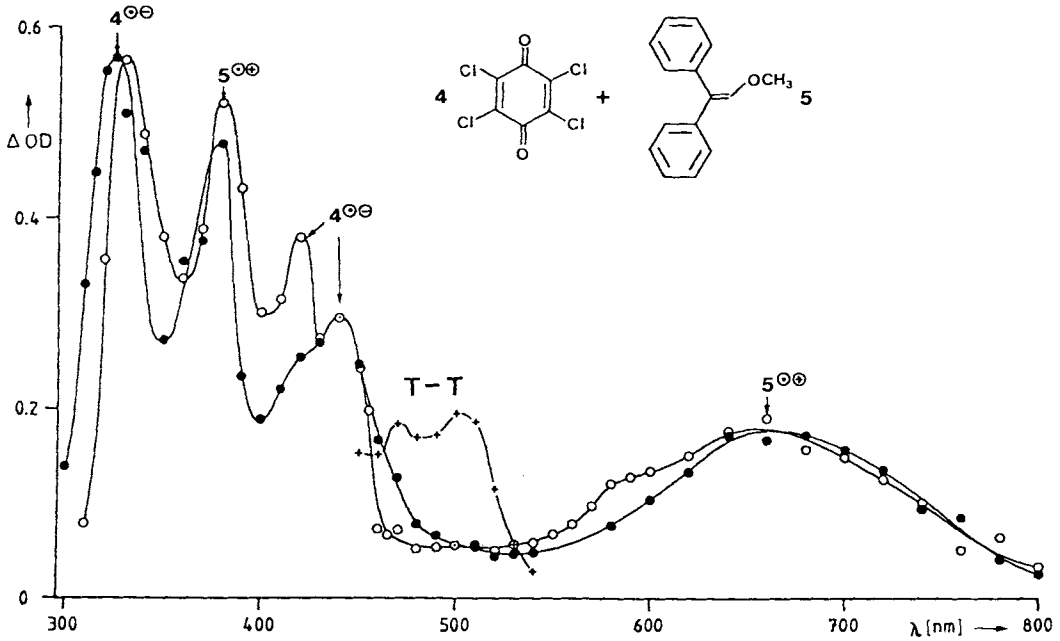

Fig. 9. Transient absorption spectra of **4** and **5** in acetonitrile 50 ns (+, T-T = absorption) and 800 ns after the start of the laser flash (from [44, 61]). ●, no $LiClO_4$; ○, 1 M $LiClO_4$.

ascribed to ionic strength, affect the dissociation more strongly, so that ion-pair separation predominates. *Goodson* and *Schuster*[67] found, moreover, that exciplexes in nonpolar solvents could also dissociate into free radical ions upon addition of ammonium salts. This effect was ascribed to the formation of larger salt aggregates. The same authors showed, in later work, that the lifetimes of 1,4-naphthalenedicarbonitrile radical anions could be dramatically increased by the addition of magnesium salts owing to the formation of complexes.[68] *Masnovi* and *Kochi*[69] investigated, in detail, the dynamic behavior of ion pairs formed by the CT excitation of electron donor-acceptor complexes formed between anthracene and tetranitromethane, and observed both normal and special salt effects in the presence of tetra-*n*-butylammonium trinitromethanide and tetra-*n*-butylammonium perchlorate.

In conclusion, it has been established that solvents and salts strongly influence the ionic dissociation of photochemically excited electron donor-acceptor pairs. Electron acceptors (for example, mixtures of carbonyl compounds or arenecarbonitriles and metal salts) are therefore suitable catalysts for chemical reactions that proceed via radical cations [Eq. (h)].[50,61]

$$A + D \xrightarrow{h\nu} (A^{\delta\ominus}D^{\delta\oplus})_s \xrightarrow{Li^{\oplus}} (A^{\ominus\ominus}Li^{\oplus})_s + D_s^{\oplus\oplus} \xrightarrow{D'} \text{product} \qquad \text{(h)}$$

4. Photochemical Reactions between Donor and Acceptor Compounds

Photoreactions between donor and acceptor molecules proceed mostly via exciplex intermediates (see Section 2.2). A scheme by which numerous reactions can be classified is shown in Figure 10 (cf. Table 1). According to this

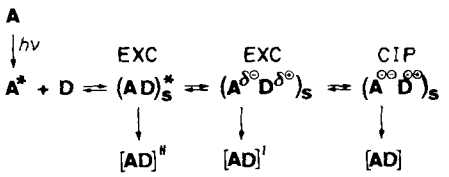

Fig. 10. Reaction between donor and acceptor molecules via exciplex and contact-ion-pair intermediates (alternatively, excitation of the donor is possible)—cf. Table 1.

scheme, the amount of charge transfer determines the type of intermediate and thereby the way in which the reaction proceeds. This concept will be exemplified by the photochemical reaction between arenes and alkenes. Three types of intermediates can be distinguished: polar and nonpolar exciplexes react to give cycloadducts, although with different degrees of selectivity; exciplexes having complete charge transfer (contact ion pairs)[29] usually show a different reaction behavior—if suitably substituted, they undergo heterolytic bond fission to form radical pairs, which then couple with one another ("substitution"), or they decay via the formation of triplet states. Dissociation into solvated radical ions and their synthetic use will be dealt with in Sections 5.1–5.3.

4.1. Photoreactions of Benzene and Monosubstituted Benzenes with Alkenes

4.1.1. The α,α,α-Trifluorotoluene Example

Discussion of the mechanism of the cycloaddition of alkenes **7** to photochemically excited benzene or its derivatives **6** has been carried on ever since the discovery of *ortho* cycloaddition[70–73] (to **9**) and *meta* cycloaddition[74,75] (to **8**).[76] On the basis of the results of various groups, we have been able to show, during the last few years, that the exciplex mechanism most fully explains the current experimental results, especially since it accounts for cycloaddition as well as substitution (to **11** and **12**) (Fig. 11).[42,43]

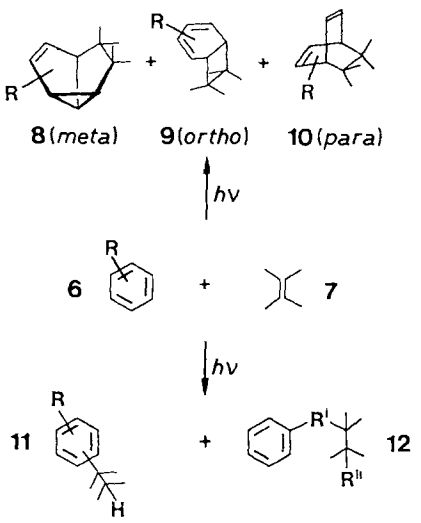

Fig. 11. Photoreactions of arenes with alkenes.

The photoreaction of α,α,α-trifluorotoluene **13** with alkenes results in the formation of all these product types in good yields (50–72%) (Fig. 12).[41] It should be noted that *para* cycloaddition (to **10**) is seldom observed and that **10** in some cases is formed from the *ortho* adducts **9** via secondary photochemical processes.[43]

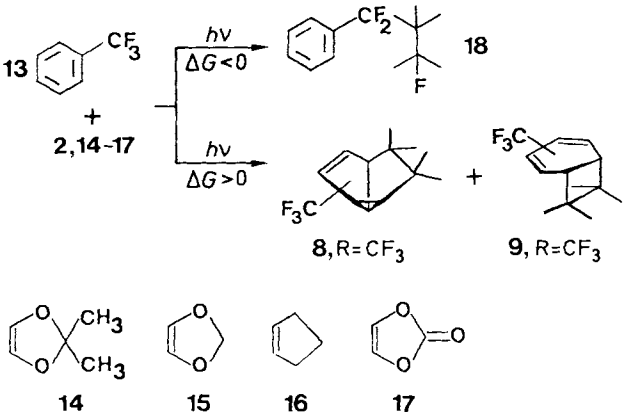

Fig. 12. Photoreactions of **13** with alkenes. Note that in the system **13/17** the alkene **17** acts as an acceptor (Table 3).

Table 3. Preferred reaction type in the photoreaction of **13** with the olefins **2** and **14**-**17** as a function of the oxidation potential of the olefin and ΔG [Eq. (c)] [a].

Olefin	$E_{1/2}$ [V]	ΔG [eV] [b]	Substitution	Cycloaddition
2	0.42	−0.23	+	−
14	0.69	+0.04	+	−
15	0.76	+0.11	+	+
16	1.83	+1.18	−	+
17	−2.64	+1.72	−	+

[a] $E^{red}_{1/2}(\mathbf{13}) = -3.18$ V, $E^{ox}_{1/2}(\mathbf{13}) = 2.91$ V, $\Delta E_{excit} = 4.65$ eV. [b] In dioxane.

After electronic excitation, **13** preferentially forms the substitution products **18** with electron-rich alkenes such as **2** and **14**. With electron-poor reactants such as **16** and **17**, on the other hand, cycloaddition to give **8**, R = CF_3, is mainly observed (Table 3). This trend is reflected in the oxidation potentials of the alkenes. The free energies of electron transfer calculated from Equation (c) show clearly that only substitution will be observed at $\Delta G \approx 0$ in the exergonic region and only cycloaddition in the endergonic region. The reaction of **13** with **15** occupies an intermediate position with respect to both selectivity and charge transfer. In line with its small positive ΔG value (in dioxane, $\varepsilon = 2.2$), the exciplex is very polar (for indirect evidence see Ref. [41]), and, in addition to forming the substitution product **18**, forms mainly the *ortho* and *meta* cycloadducts **8** and **9** (R = CF_3), respectively. According to Equations (c) and (d), the electron transfer for this system should be exergonic in a solvent of $\varepsilon > 3$. Indeed, the cycloaddition is completely suppressed when the photoreaction is carried out in solvents more polar than dioxane (Fig. 13). Only the formation of the substitution products

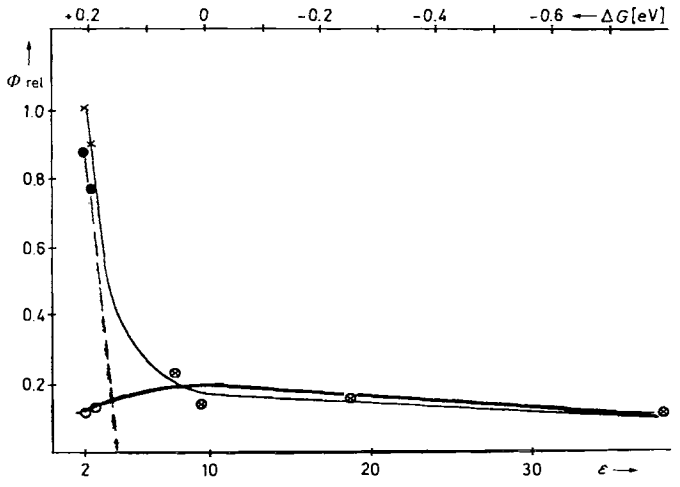

Fig. 13. Reaction selectivity (as measured by product quantum yield Φ_{rel}) as a function of the dielectric constant (ε) in the photoreaction between **13** and **15**. × = overall yield; ○ = yield of **18**; ● = yield of **8** and **9** (R = CF_3).

18 is observed. This "special" solvent effect is overlaid by the "normal" effect; i.e., the product formation is suppressed in favor of ionic photodissociation in polar media—an effect that is observed with all reactions in the exergonic region of electron transfer. The Weller equation, with the inclusion of the coulomb term [Eq. (d)], can therefore be used to control reaction selectivity.

The mechanism that best describes the relationship between photochemically induced charge transfer and the course of the reaction is shown in Figure 14. The key to the

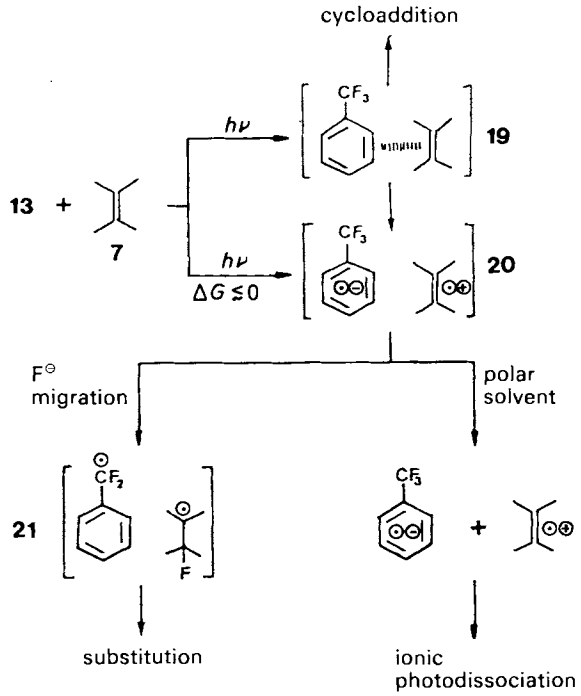

Fig. 14. Mechanism of the reactions of **13** with alkenes.

reaction is the intermediate. For $\Delta G > 0$, cycloaddition occurs via an exciplex **19**. Only when $\Delta G < 0$ is a CIP, **20**, formed; **20** either dissociates in polar media or undergoes heterolytic bond breaking to form a radical pair **21**, which in turn, finally recombines to form substitution products.

4.1.2. *Generalization of the ΔG Correlation*

Figure 15 shows the correlation between mode selectivity (substitution, *ortho* and *meta* cycloaddition) and the ΔG values for the electron transfer, as exemplified by the photoreaction of benzene **6**, R = H, with alkenes **7**.[42]

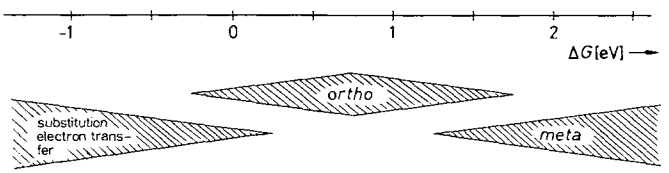

Fig. 15. Mode selectivity as a function of the free energy of electron transfer in the photoreactions of **6**, R = H, with alkenes **7**.

Relatively polar exciplexes (characterized by $\Delta G \lesssim 1.5$ eV) preferentially form *ortho* cycloadducts, while *meta* cycloaddition is mainly observed between reactants with $\Delta G \gtrsim 1.5$ eV). Similar correlations can be established for other arenes.[42] In the case of benzonitrile, for example, even cycloaddition to the nitrile group can be included. One must however always be aware of the empiri-

cal character of these correlations; i.e., their validity may be confined to only a series of related compounds.[42,43]

The classification of photocycloadditions of alkenes to arenes by means of the type of intermediate corresponding to the ΔG value also allows some connections to be drawn concerning stereo- and regioselectivity. Equation (c) can be used, for example, to determine which reagent acts as donor and which as acceptor. In many systems vinylene carbonate is an acceptor since the following relation is valid:[41-43,77]

$$\Delta G(17 = \text{A, arene} = \text{D}) < \Delta G(17 = \text{D, arene} = \text{A})$$

The electronic interactions between the components of such intermediates influence the stereochemical course of the cycloaddition in a dramatic fashion[43] (Fig. 16). Further aspects of the stereo- and regioselectivity have been discussed comprehensively elsewhere.[42,43]

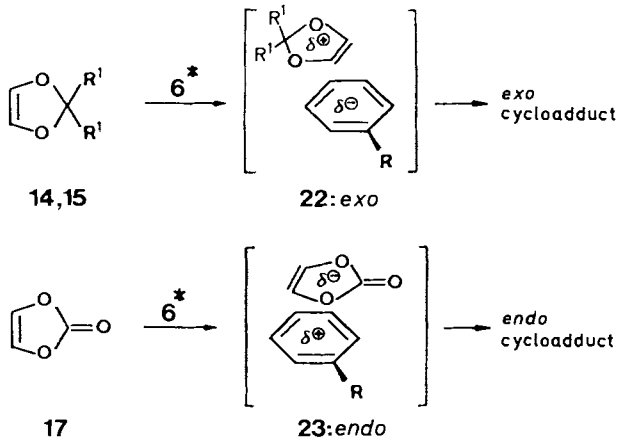

Fig. 16. Direction of electron transfer and selectivity in the photocycloadditions of 1,3-dioxole derivatives **14**, **15**, and **17** to arenes.

4.2. Photoreactions of Multiply Substituted Benzenes and Higher Arenes

The photoreactions of higher, especially acceptor-substituted, arenes with donor substrates have been investigated often. Usually, systems have been dealt with in which electron transfer is thermodynamically allowed according to Equation (c) and which accordingly yield preferentially substitution products. Some typical examples will be presented in the following discussion.

4.2.1. Reactions of Excited Acceptor Arenes

As we have already demonstrated in the case of simply substituted benzene derivatives, the substitution products are not formed by direct coupling of the radical-ion species of the contact ion pairs. In most cases the reaction occurs via a number of steps involving the heterolytic splitting off of an electrofugal or nucleofugal group and the final recombination of the radicals thus formed (exceptions include the reactions of **34** and **35** and of anthracene and *N,N*-dimethylaniline, see below). Very frequently, deprotonation of the radical cation by the radical anion is observed [Eq. (i)]. The first evidence for such a reaction was found in the 1970s by *McCullough* and co-workers[78,79] and by *Arnold* et al.[89] in the photoreactions of arene carbonitriles with alkenes as well as by *Ohashi* et al.[81] and later *Albini* et al.[82] in the corresponding reactions

$$A + DH \xrightarrow{h\nu} (A^{\ominus\ominus}DH^{\oplus\oplus}) \longrightarrow (HA^{\bullet}D^{\bullet}) \longrightarrow HA-D \qquad (i)$$

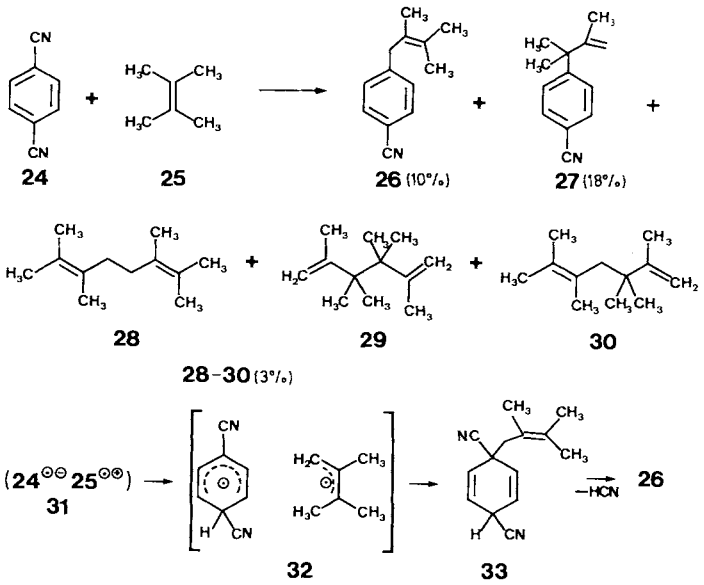

Fig. 17. Photoreaction of **24** with **25** in acetonitrile.

with alkylarenes as electron donors. Photoexcitation of terephthalodinitrile **24** in the presence of 2,3-dimethyl-2-butene **25** results in the formation of the dimerization products of **25** (**28**-**30**),[80] in addition to the substitution products **26** and **27**. The free energies calculated according to Equation (c) for radical-pair formation are -0.96 eV and thus support a mechanism involving electron and subsequent proton transfer to give **31** and **32**, respectively, as the key steps (Fig. 17). Compound **26** is presumably formed via **33**.

The corresponding reactions of 1,4-naphthalenedicarbonitrile[80] and 9-phenanthrenecarbonitrile[83] give similar results. *Mizuno*, *Otsuji* et al. were able to transform these variable-yield photosubstitution reactions into efficient allylation methods by the introduction of the trimethylsilyl group (which is easily split off as a cation) into the olefinic reagent[84,85] (Fig. 18).

Albini et al. have studied in detail the photoreactions of arenecarbonitriles with alkylbenzenes.[82,86] Also in these cases, the first step is photochemically induced electron transfer with the formation of a radical-ion pair, which

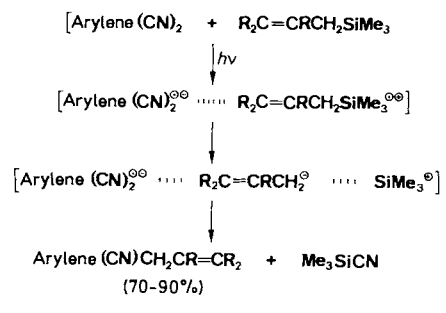

Fig. 18. Photochemical allylation of arenedicarbonitriles with allylsilanes.

then generally undergoes deprotonation and subsequent recombination of the radicals. With peralkylated toluene or dibenzyl derivatives, for which no proton transfer is possible, they even observed heterolytic fission of a C–C bond.[86] The high stereoselectivity of the addition of cumene **35** to 1,4-naphthalenedicarbonitrile **34** to give the products **36** and **37** (Fig. 19) indicates that the reactions

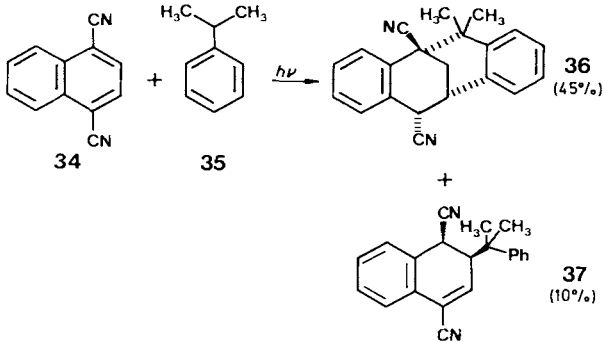

Fig. 19. Photochemical addition of **35** to **34**.

occur within the solvent cage and consequently by means of radical-ion pairs or radical pairs. Only dissociated radicals undergo the typical reactions of free and non-correlated intermediates. The ΔG values calculated by the Weller equation indicate once again that an exergonic electron transfer takes place.[87]

Because of their low oxidation potentials, amines are often used as donor components in photochemical electron-transfer reactions (see also Section 4.3) and also in reactions with excited acceptor arenes. For example, electronically excited anthracene reacts with *N,N*-dimethylaniline, by direct coupling of the radical ions, to give 9-(4′-dimethylaminophenyl)-9,10-dihydroanthracene in 70% yield along with small amounts of dimerization and H addition products.[88] In contrast, *trans*-stilbene reacts with triethylamine via a multistep series of electron and proton transfers to give disproportionation and recombination products (cage reactions) as well as symmetrical dimerization products (escape reactions).[89]

4.2.2. Reactions of Excited Donor Arenes

In 1974 *McCullough* et al.[90] reported on the photoreactions of naphthalene **38** with acrylonitrile **39**, which gave, together with the cycloadduct **40**, the substitution products **41** (Fig. 20). In polar solvents, such as acetonitrile, the electron transfer should, according to Equation (c), be thermodynamically allowed (for the redox potentials and excitation energies, see Refs. [42, 90]). Here again one can assume the formation of an ion pair followed by a proton transfer to the acrylonitrile radical anion (either from the solvent or, with other donor arenes such as indene, from the corresponding radical cation). This assumption is supported by the catalytic effect of protic solvents and isotopic labeling experiments.[90] For weaker donors, such as anthracene and phenanthrene, the electron transfer is endergonic and hence no substitution products are formed.[91]

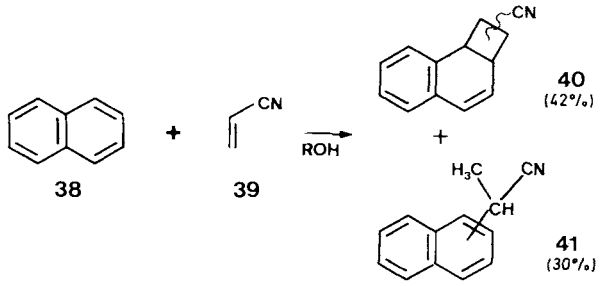

Fig. 20. Cycloaddition and substitution in the photoreaction of **38** with **39**.

Kochi, Rentzepis et al. have carried out comprehensive studies on the role of ion pairs in the photoreactions of CT complexes.[92,93] Irradiation in the long-wavelength absorption bands of CT complexes of 9-substituted anthracenes **42** and tetranitromethane **43** results, in accordance with the Mulliken theory,[95] in a fast electron transfer ($t < 25$ ps) with the formation of a radical-ion pair. Within a few ps the tetranitromethylide fragments. Ionic and radical coupling follow in two slower steps to form **44** and the final product **45**, respectively (Fig. 21). The corresponding steps apply to the nitration of methoxybenzenes[96] and alkenes.[94]

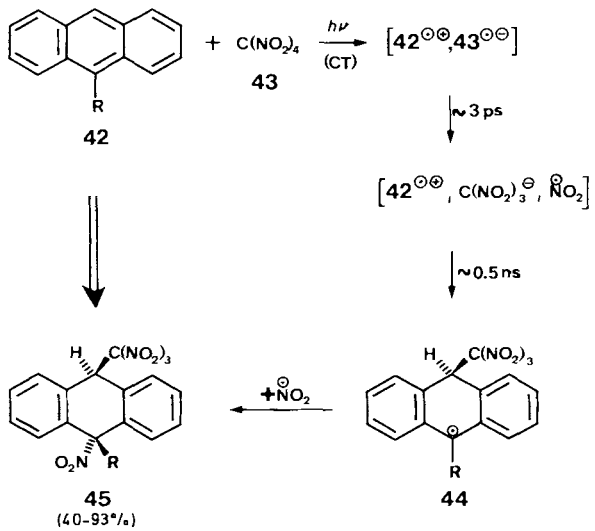

Fig. 21. Ionic coupling within a contact ion pair and radical coupling via free radicals in the photoreactions of **42** and **43**.

With tetracyanoethylene (TCNE), the anthracenes **42** form no products.[93] Transient analyses in the ps region, however, clearly show the formation of ion pairs. A proton transfer from $\mathbf{42}^{\odot\oplus}$ to $TCNE^{\odot\ominus}$ or the formation of Diels–Alder dimers apparently cannot compete with the rapid back transfer of electrons. On the other hand, the system **38**/*N*-methyldihydrotriazoledione is reactive: *Sheridan* et al.[97] were able to show, however, that here the long-wavelength-absorbing alkene component was excited and formed, from the triplet or singlet state, a contact ion pair with **38** as donor. This gave a Diels–Alder adduct in 40% yield. The same photochemical Diels–Alder reaction was observed when the CT complex was directly excited.

Sundberg has a reported, in a comprehensive review,[99] on chloroacetamide cyclization in aromatic systems in

which the initiating step is a photochemically induced electron transfer and which, in other variations, leads to lactam formation.

4.3. Photoreactions of Carbonyl Compounds with Alkenes, Alkylbenzenes, and Amines

The photoreactions of carbonyl compounds have been studied in detail since the early days of photochemistry.[99,100] In particular, the [2+2] cycloaddition with alkenes, which leads to oxetanes **48** (Paterno-Büchi reaction), has assumed great synthetic importance[100-102] although, depending on the substituents, a number of by-products (**46**, **47**, **49**, **50**) can be formed (Fig. 22).

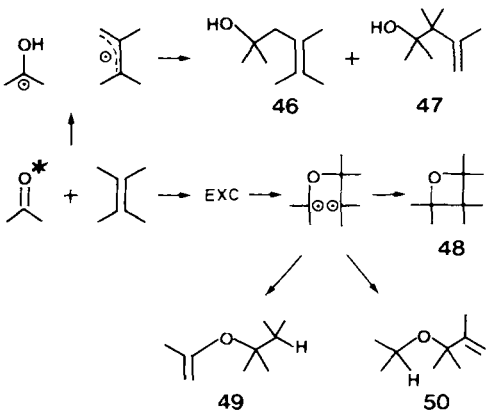

Fig. 22. Products of photoreactions of ketones with alkenes.

In general, the exciplex-diradical mechanism[100] is used to explain the reaction behavior of simple alkenes. However, owing to the ready accessibility of very electron-rich alkenes such as **2**, **14**, and **15**, electron-transfer processes have recently been shown to occur as well.[40,44,45,49] Whereas with "normal" alkenes a large number of products are often observed[100] (Fig. 22), the photochemically induced electron transfer can act as a "regulator" for reactions with electron-rich alkenes. Upon photoexcitation, biacetyl **54** reacts with ketene acetal **53** to form exclusively the oxetane **51**.[45,49] Trapping experiments with the radical cation $\mathbf{53}^{\odot\oplus}$ indicate an electron transfer as the primary photochemical step. The components of the contact ion pair, which show high spin densities at their radical centers, recombine through the radical positions to form first a zwitterion **59** and then **51** (the most important resonance structures of the radical ions taking part are given in Fig. 23). Since **53** and **54** also undergo an aldol-type cycloaddition (via dipolar intermediates) to give the other regioisomeric oxetane **52**,[49,103] the reaction here involves "umpolung" of the reactivity of a carbonyl group by means of photochemically induced electron transfer.[49]

The extremely electron-rich alkenes **2** and **55** show another type of reaction behavior. Because of the allylic hydrogen, $\mathbf{2}^{\odot\oplus}$ and $\mathbf{55}^{\odot\oplus}$, respectively, are deprotonated by $\mathbf{54}^{\odot\ominus}$ with the formation of a radical pair, which then recombines to give the reaction products **57** and **58** [see also Eq. (i)].[40,45] The dependence of the ratio (**57** + **58**) : **56** on

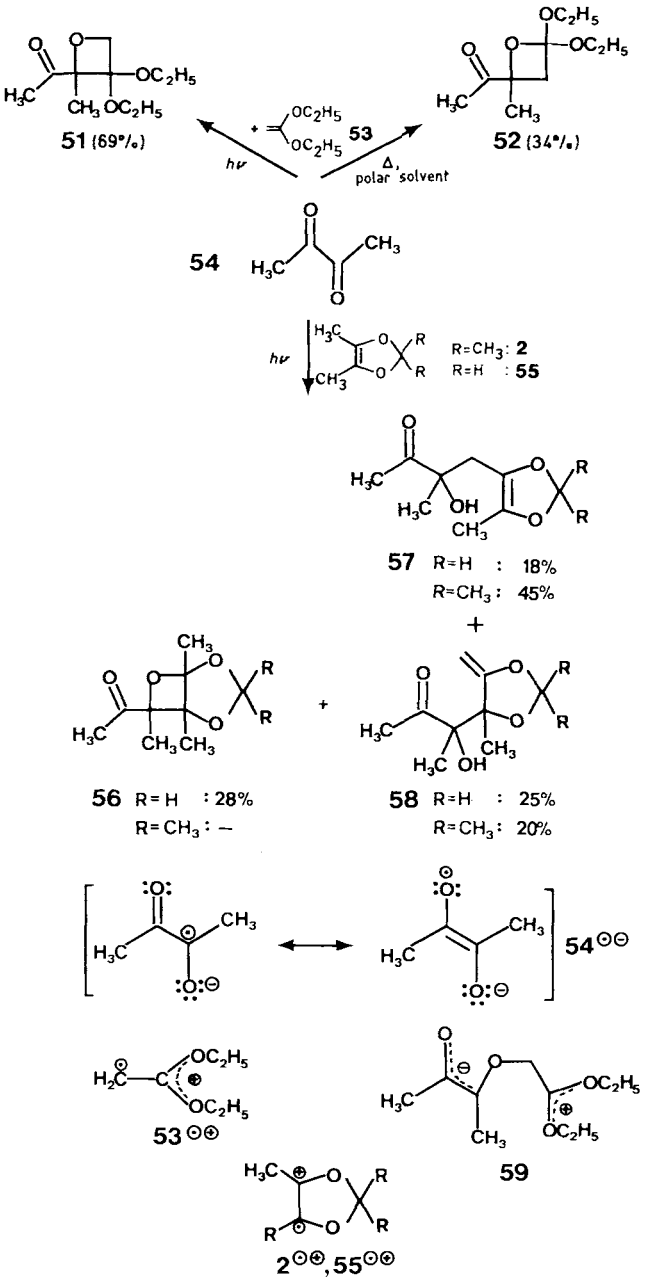

Fig. 23. Photoreactions of **54** with electron-rich alkenes.

the oxidation potential of the alkene and transient analysis investigations by means of ESR spectroscopy support this extended mechanism for the photoreactions between carbonyl compounds and alkenes.[40,45]

In an article summarizing recent results, *Wagner* et al.[104] have described the influence of charge transfer on the photoreactions of phenyl ketones with alkyl benzenes as donors. The ketones react via both the $n\pi^*$ and the $\pi\pi^*$ states by means of a CT mechanism in which the extent of the charge and electron transfer is determined by the electrochemical redox potentials of the species involved. Although $n\pi^*$ and $\pi\pi^*$ states are the same in this respect, they show different reaction behaviors because of the different structures of the exciplexes involved. In addition, H abstraction (the initiating step in the formation of a photoreduction product) can change from a one-step (H transfer) to a two-step ($e^{\ominus}$ and $H^{\oplus}$ transfer) mechanism (cf. the

photoreactions of **54** with **2** and **55**, Fig. 23, and Refs. [40, 45]).

Amines have also been used as powerful electron donors in photoreactions with ketones. An early example[105,106] is shown in Equation (j). *Seebach* et al.[107] were able to use

$$Ph_2CO + H_2NCH_3 \xrightarrow{h\nu} [Ph_2CO^{\ominus\ominus}H_2NCH_3^{\oplus\oplus}] \longrightarrow [Ph_2\overset{\ominus}{C}OH\ H\overset{\oplus}{N}CH_3] \longrightarrow Ph_2C(OH)C(OH)CPh_2 + HNCH_2 \quad (j)$$

this method for an asymmetric photopinacol reaction. The involvement of contact ion pairs was examined in detail by *Peters* et al.[108] The preparative applications of this reaction have been discussed elsewhere.[24,106]

Quinones are powerful oxidizing agents, particularly after photoexcitation, and their reactions have been frequently described.[100,109] Here, the photoreactions of 1,4-naphthoquinones **60** with 1,1-diarylethenes, such as **61**, should be briefly mentioned, since a direct dependence of the course of the reaction on the ΔG values of the electron transfer similar to that found in the case of α,α,α-trifluorotoluene (Section 4.1.1) has been observed (Fig. 24).[110]

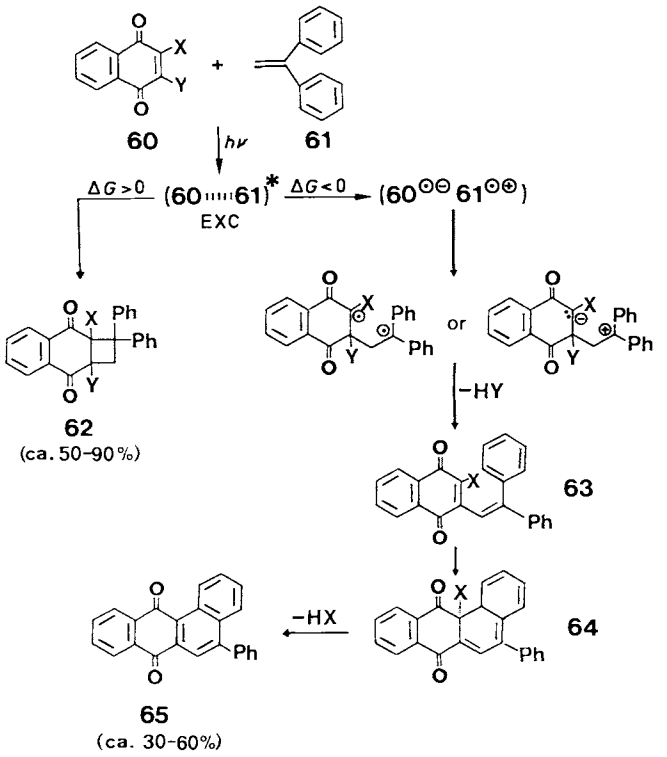

Fig. 24. Charge transfer and the course of reaction in photoreactions of **60** with 1,1-diphenylethene **61**.

Electronically excited naphthoquinones **60** form two types of products with 1,1-diarylethenes of type **61**. The cyclobutanes **62** are formed only when electron transfer is endergonic according to Equation (c), probably via exciplex intermediates. For thermodynamically allowed electron transfer, one observes the formation of the ethene adducts **63** exclusively. The presumed intermediacy of contact ion pairs and diradicals or zwitterions is supported by CIDNP studies. A subsequent photoreaction, via **64**, makes physiologically interesting benz[*a*]anthraquinones such as **65** available by means of this route.

4.4. Photoreactions of Phthalimides

Besides ketones, other carbonyl compounds such as carboxylic acids and their derivatives are of photochemical interest.[111-114] We will restrict ourselves here to the photoreactions of *N*-methylphthalimides **66** with alkenes **7**; the selectivity of these reactions is similarly determined by charge transfer (from the alkene to the imide) and the products are of synthetic interest.

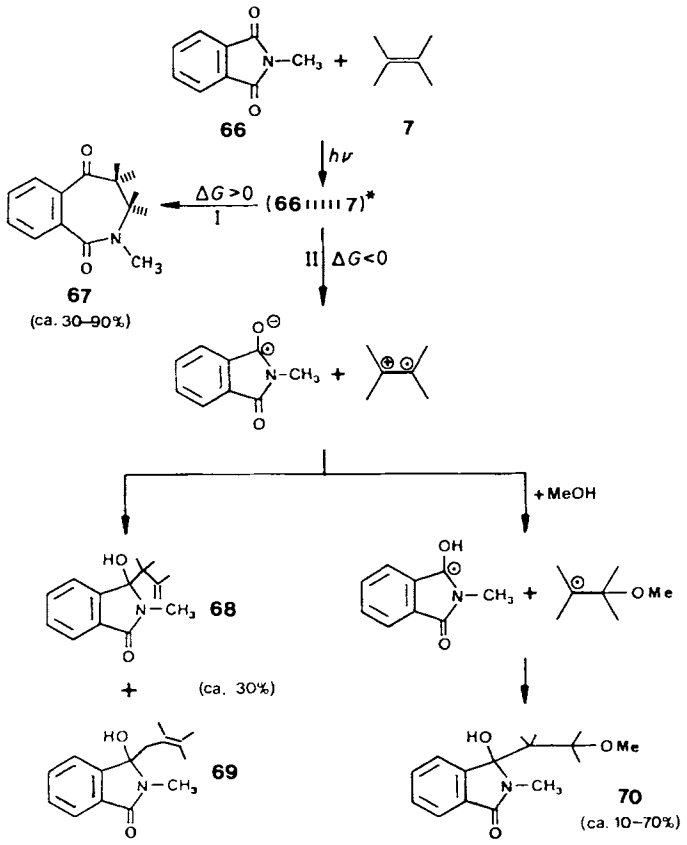

Fig. 25. Addition and reduction in the photoreactions of **66** with alkenes **7**.

In their fundamental work, *Mazzocchi* et al.[115] investigated the photoreactions of **66** with various alkenes **7**. Two types of reaction were observed (Fig. 25); the regio- and stereospecific addition of the alkenes to a carbonyl group of **66** with ring expansion to the dihydrobenzazepinediones **67**[116] (I) and the photoreduction to **68** and **69**, which, in the presence of methanol, leads to **70**[115] (II). The ΔG values, calculated according to Equation (c), clearly demonstrate the regulatory effect of electron transfer: in the endergonic region only the $(\sigma^2+\pi^2)$ addition (I) was observed and in the exergonic region only the photoreduction (II). Trapping experiments with methanol as a nucleophile confirmed the existence of radical-ion intermediates. Only recently have *Mazzocchi* et al. been able to show, with intramolecular systems, that, here too, a direct coupling of the radical ions of the contact ion pair is possible through their radical centers.[117] The synthetic potential of such intramolecular reactions, which produce annelated dihydrobenzazepinediones or macrocyclic spiro com-

pounds, has recently been demonstrated by *Kubo* et al.[118] and *Machida* et al.[119] Other synthetic applications have been described in reviews by *Kanaoka*,[112] *Mazzocchi*,[113] and *Coyle*.[114]

4.5. Photoreactions of Alkylideneammonium Salts

Alkylideneammonium salts such as **71** are powerful electron acceptors even in their ground states. This property should be enhanced in the excited state. Indeed, photochemical electron-transfer processes have even been observed with simple alkenes;[120] they lead to products such as **72**–**78**.

In Figure 26, the probable mechanism is shown; the initiating step is the transfer of an electron from a donor molecule to an alkylideneammonium salt **71** with the formation of an α-aminoradical–radical-cation pair. This recombines either directly through the radical positions or after trapping of the radical cation by nucleophiles (e.g., methanol). The values of ΔG for the electron transfer, calculated

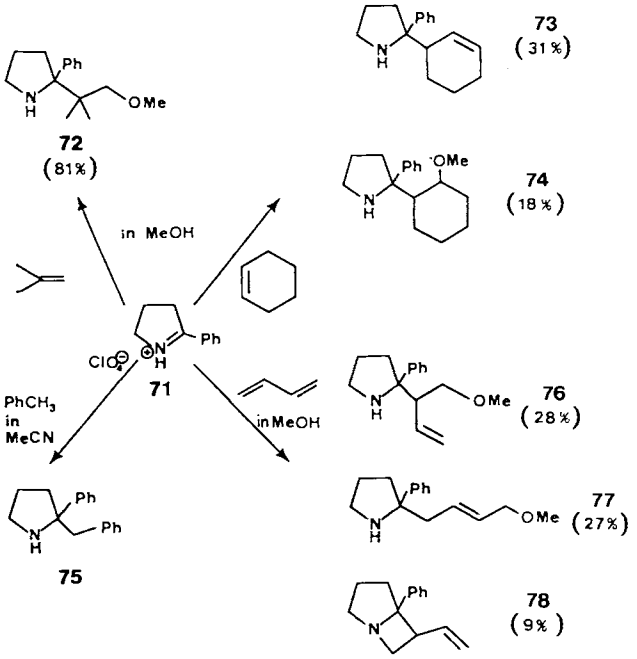

mechanism:

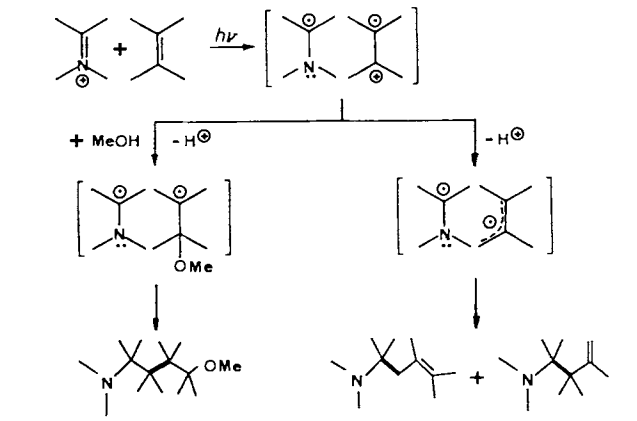

Fig. 26. Photoreactions of alkylideneammonium

from Equation (c), can once again be used as a criterion for the course of the reaction.[120, 121]

This method gives access to a large variety of *N*-heterocycles.[24, 120] The synthetic potential of the already widely used alkylideneammonium salts is thereby enormously increased (see, for example, Refs. [122–124]).

As has already been shown in Section 4.2.1, suitably substituted radical cations can easily split off electrofugal groups with the formation of a radical; the simplest case is deprotonation [see Eq. (i)]. *Mariano* et al. were able to transform this procedure into an efficient method for the allylation of alkylideneammonium salts by means of allylsilanes.[125] An intramolecular variant of this method to form structural units of the isoquinoline alkaloids is shown in Figure 27.[126]

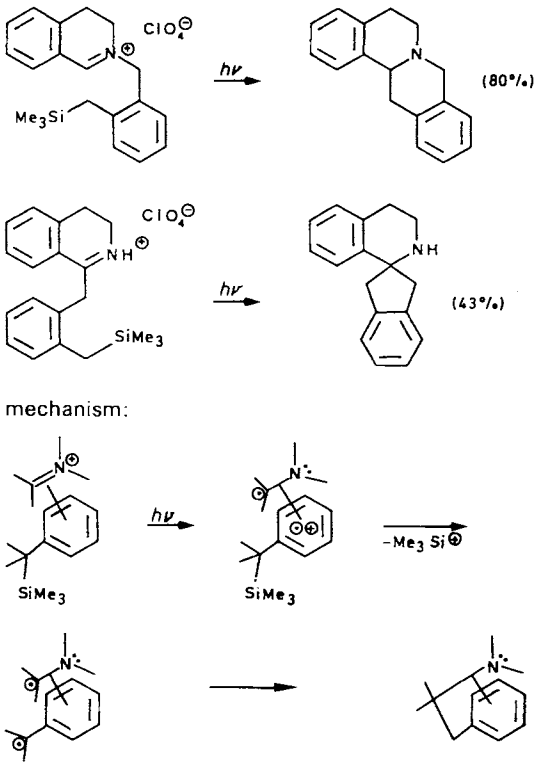

Fig. 27. "Diradical cyclization method" for the synthesis of isoquinoline alkaloid building blocks.

5. Reactions of the Radical Cations of Alkenes and Dienes

In polar solvents the components of a contact ion pair can be "separated" by solvation to form either a solvent-separated radical-ion pair or free radical ions. This process may be enhanced by the salt effect; in some cases the lifetime and the yield can be greatly increased by ion-exchange reactions [special salt effect: see also Section 3.2 and Eq. (g)]. This hindering of the back electron transfer often allows, for the first time, the directed production of radical ions and thereby makes possible the study of their reactions without the involvement of the radical-ion partner, i.e., without chemical reaction [Eq. (h), Fig. 28].

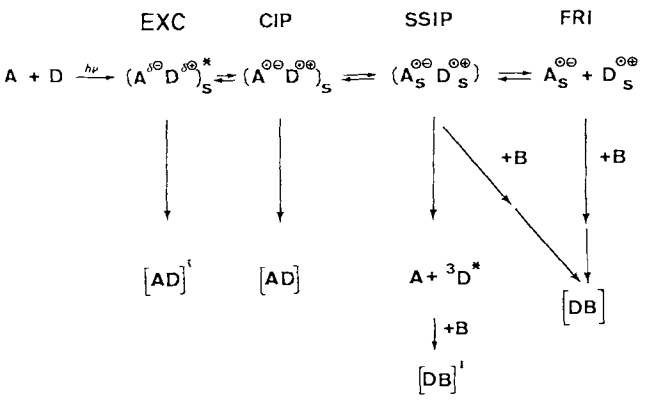

Fig. 28. Intermediates and the course of reaction in electron-transfer processes between donor and acceptor molecules. For abbreviations, see caption to Figure 4.

The following discussion will be restricted to the reactions of radical cations, in particular those of alkenes and dienes.

5.1. Dimerization and Cycloaddition

5.1.1. Reactions of Alkenes

Among the first examples of photochemically induced reactions of alkene radical cations was that of the dimerization of *N*-vinylcarbazole **79**, first discovered by *Ellinger*[127] and later thoroughly investigated by *Ledwith* (Fig. 29).[128,129] The decisive steps are the oxidation of the alkene to a radical cation **79a**$^{\odot\oplus}$ by electron acceptors such as *p*-chloranil **4** or halogenated aromatic ketones (primary electron transfer) and the reduction of an acyclic radical-ionic dimer **80a** or a cyclobutane radical ion **81a**$^{\odot\oplus}$ (secondary electron transfer). Since the quantum yield in these reactions is greater than 100% (maximum value of Φ: 66), a chain reaction is involved (I in Fig. 30) in which the secondary transfer takes place from monomer **79a** to the dimer **80a** or **81a**$^{\odot\oplus}$. The same is true for the enol ether **79b** and the aryl derivative **79c**, although here, because of the lower quantum yield, the chain length must be less.[132] A detailed analysis of the kinetics and thermodynamics of the elementary processes can be found in *Evans* et al.[132]

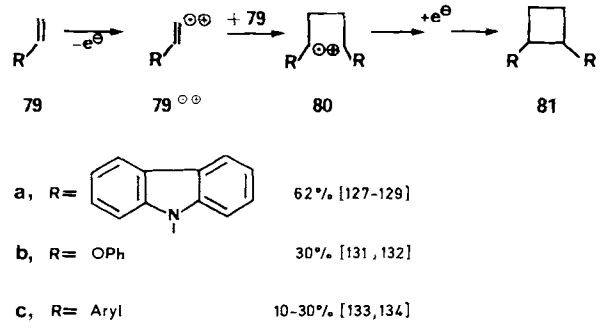

Fig. 29. Dimerization of alkenes via radical cations.

Other dimerizations have been described by *Farid* et al.,[130] *Arnold* et al.,[135] *Pac* et al.,[136,137] and others.[23,24] The regioselectivity of these reactions is generally greater than that of the corresponding triplet reactions involving diradical intermediates, which mostly yield mixtures of regioisomers.[23] Differences in the stereoselectivity have also been observed: for example, 1,3-dioxole **15** dimerizes in an energy-transfer reaction under triplet conditions to give a mixture of *endo*- and *exo*-bis(methylenedioxy)cyclobutanes in the ratio 0.6 : 1,[38] whereas, in a reaction via **15**$^{\odot\oplus}$, the stereoisomer ratio becomes *endo* : *exo* = 1.5 : 1.[51,56] Another mechanism has also been discussed which one can call "electron-transfer sensitization"[138] (II in Fig. 30). Here, the secondary electron transfer takes place between the product radical cation and the radical anion of the acceptor. Since the acceptor is thereby regenerated, it can also be viewed as the sensitizer (Sens in Fig. 30). This mechanism plays a role in many electron-transfer reactions, often in modified form such as the so-called "triplex mechanism."[39,137,139] Quantum yields below 100% are a necessary but not sufficient criterion for mechanism II, since, because of the complex kinetics, a single inefficient elementary process can drastically reduce the quantum yield in mechanism I. Comparison experiments should therefore be carried out with thermal electron acceptors, e.g., ammoniumyl salts $R_3N^{\odot\oplus}X^{\ominus}$,[129,140] for which a chain process is clearly involved. A further criterion in the case

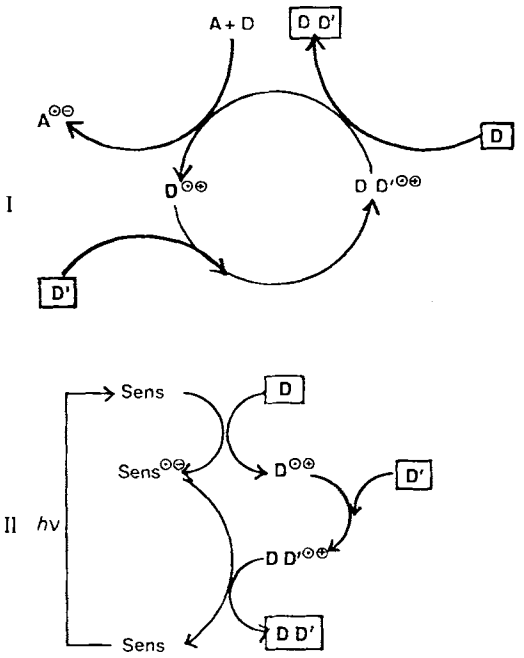

Fig. 30. Chain mechanism (I) and electron-transfer sensitization (II) in radical-cation-catalyzed reactions.

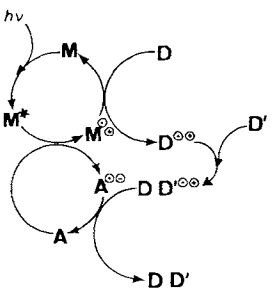

Fig. 31. Redox photosensitization according to *Pac* et al. [136] (M = mediator for "hole transfer," e.g., phenanthrene).

of mechanism I would be chain initiation by means of an independently generated intermediate (for example, by electrolysis).

In some cases the efficiency of the dimerization of alkenes by means of radical cations can be increased by the use of a mediator ("hole transfer"). This mechanism has been investigated by several Japanese groups[136, 141-143] and, according to *Pac* et al.,[136] can be classified as "redox photosensitization" (Fig. 31)—cf. also Ref. [137].

In a fundamental study, *Farid* et al.[144] demonstrated the different reactivities of radical-ion pairs and free radical ions in the dimerization of 1,1-diphenylethene **61** to give the cyclobutane **84** and the "(4+2) dimer" **87** (Fig. 32).

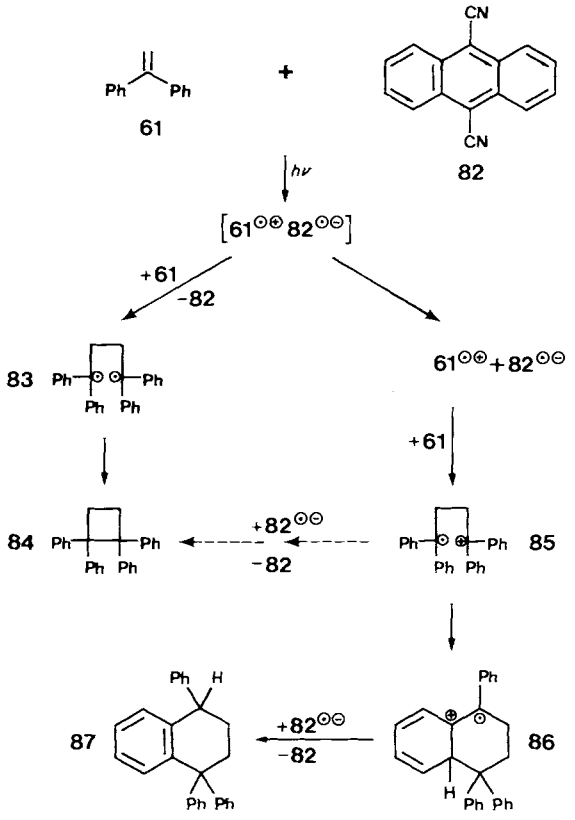

Fig. 32. Electron-transfer-sensitized dimerization of **61** via radical-ion pairs or free radicals to give **84** or [4+2] dimers **87**, respectively.

The initially formed contact ion pair [**61**$^{\odot\oplus}$**82**$^{\odot\ominus}$] reacts further, by the formation of a C–C bond with a neutral alkene **61** and subsequent back electron transfer, to give the 1,4-diradical **83**, which cyclizes to give **84**. This course of reaction largely parallels the triplex mechanism.[39, 137, 139] If, on the other hand, the radical-ion pairs are separated by solvation, the reaction takes a totally different course. In this case, reaction of **61** gives an acyclic radical-cation adduct, **85**, which, because of its longer life, cyclizes to give first the radical-ionic [4+2] dimer **86** and then **87** by means of back electron transfer. Concentration-dependence experiments (higher concentrations of **61** favor the cage reaction giving **84**) and quenching experiments with radical-cation traps support this mechanism.

After the first radical-cation-catalyzed dimerizations of alkenes, there soon followed examples of mixed cycloadditions.[130, 145, 146] A decisive criterion for selectivity is the specific oxidation of only one of the reaction species (Fig. 33), which can be easily accomplished by means of Equation (c). In the most favorable case, the conditions of Equation (k) should apply; i.e., only the oxidation of D

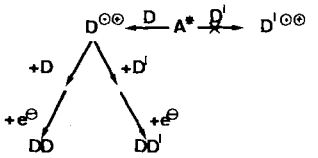

Fig. 33. Possible reaction paths in radical-cation-catalyzed reactions between various donor compounds when only one reactant is oxidized, i.e., when Equations (k) and (l) are satisfied.

$$\Delta G(A^{\odot\ominus}D^{\odot\oplus}) < O < \Delta G(A^{\odot\ominus}D'^{\odot\oplus}) \quad (k)$$

should be thermodynamically allowed. With a sufficiently high concentration of the reaction species D', it is often possible to suppress the undesired dimerization to DD. In the less favorable case, i.e., when both reacting species can undergo oxidation (only Equation (l) is valid), the dimerization to DD can at least be minimized by the optimal choice of concentrations[146] (see also Section 5.1.2). Since the reactions occur via several steps, the course of the reaction can be influenced by other effects, e.g., stabilization of acyclic intermediates by appropriate substituents, the effects of counterion, or even other mechanisms (cf. Section 5.1.2).

$$E^{ox}_{1/2}(D) < E^{ox}_{1/2}(D') \quad (l)$$

5.1.2. Reactions of Dienes (Diels–Alder Reactions)

One of the most important reactions of dienes is the Diels–Alder reaction.[147] Its scope of application, however, is limited by one of the fundamental rules of thermal $(4\pi+2\pi)$ cycloadditions: namely, a sufficiently high reaction rate is only achieved if the frontier orbitals of the starting materials (HOMO and LUMO) are energetically close.[147-149] Such ideal conditions are not always fulfilled, and there has therefore been no lack of attempts to find improvements for Diels–Alder reactions that yield poor results. Examples include reactions under high-pressure conditions,[150-152] catalysis by Lewis acids,[153-155] and the exploitation of the hydrophobic effect for reactions in aqueous media.[156, 157]

A further approach makes use of the following principle: oxidation of one of the reacting species results in an increase in the frontier-orbital interaction, which should in turn lead to an acceleration of the Diels–Alder reaction. As *Freeman* et al.[167b] and *Hammond* et al.[167c] have shown, the radiation-induced dimerization of cyclohexadiene, reported by *Schenck* et al.,[167a] can be explained in this way. A similar effect was also observed by *Mizuno* et al.[158] in the Diels–Alder reaction of furan with indene in the presence of naphthalenecarbonitriles as photochemical electron acceptors; this reaction probably occurs by means of mechanism II (Fig. 30). Later, *Bauld* et al.[159] applied this principle to thermal electron acceptors and coined the term "cation-radical catalyzed Diels–Alder reaction"; this

reaction is based on a chain mechanism (Fig. 30, I). According to theoretical considerations, the radical-cation-catalyzed Diels–Alder reaction should obey the "principle of role selectivity," which states that the cycloaddition ockurs preferably by means of the radical cation of the dienophile.[160] Since then, many groups have concerned themselves with this problem. Although no comprehensive picture has yet emerged, some of the mechanistic aspects will be dealt with here since they are directly related to the subject of this review (cf. Section 3).

The dimerization of simple dienes to Diels–Alder adducts via photochemically generated radical cations does not usually present any great difficulties as long as the diene is oxidizable, which, in turn, can be estimated from Equation (c). One exception is 2-acetoxy-1,3-cyclohexadiene (see Fig. 39 and accompanying text). Various acceptors have been used: arenecarbonitriles,[139, 161, 162] ketones and quinones in the presence of lithium perchlorate (special salt effect),[61, 65, 162–164] and pyrylium salts.[61, 65, 162–165]

The dimerization of 1,3-cyclohexadiene **88** has been investigated under various conditions (Fig. 34, Table 4). Under thermal conditions, in spite of long reaction times, the [4+2] dimers **89** and **90** are formed only in poor yield.[166, 167] The dimerization is only better under high-pressure conditions (up to 7 kbar); however, the cyclobutane adducts **91** and **92** as well as some acyclic dimers, formed by nonconcerted processes, are also produced.[168] The dimerization by means of radical-cation catalysis, on the other hand, occurs very efficiently to give, preferentially, the Diels–Alder adducts **89** and **90**.[61, 65, 139, 159, 162–165]

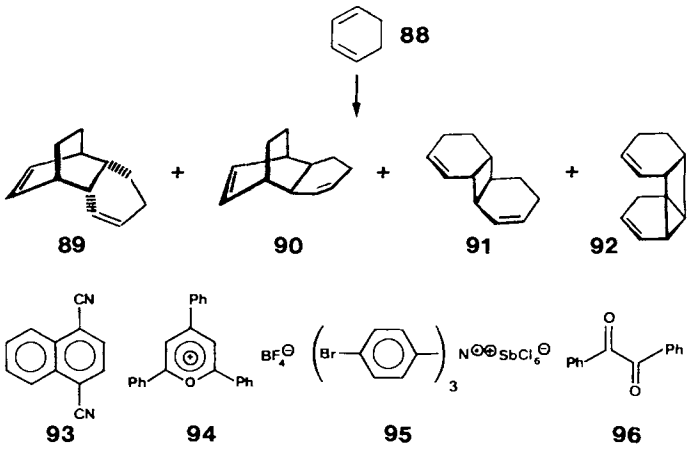

Fig. 34. Dimerization of **88** under thermal conditions and energy- and electron-transfer conditions. **93–96**: electron-acceptor molecules. See also Table 4.

Here, it is unimportant whether one employs thermal acceptors via a chain mechanism (Table 4, No. 8) or whether one uses photochemical acceptors (Nos. 5–7). Only the stereoselectivity (*endo/exo* ratio) changes, which indicates that different mechanisms are operating. It should be noted that the dimerization under energy-transfer conditions yields mainly the cyclobutane adducts **91** and **92** (No. 2, 3).[139, 166, 167]

The question of the validity of the "role selectivity" of radical-cation-catalyzed Diels–Alder reactions cannot be answered by product studies of the dimerization of dienes. For example, the mixed cycloaddition between **88** and 1,3-dioxole **15** provided clear evidence that the Diels–Alder reaction can take place via either the radical cation of the dienophile (here **15**) or the radical cation of the diene (here **88**).[162] Whereas the reaction via $\mathbf{15}^{\odot\oplus}$ forms the *endo* isomer **97** preferentially, both reaction paths are almost equally important in the corresponding cycloaddition via $\mathbf{88}^{\odot\oplus}$ (Fig. 35).

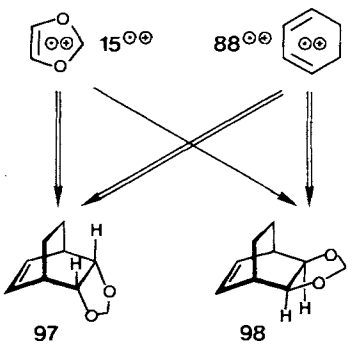

Fig. 35. Reaction paths in the radical-cation-catalyzed Diels–Alder reaction between **88** and **15** (⇒ preferred, → less preferred).

This shows at least that the cycloaddition via the diene radical cation cannot be concerted. The results obtained for the reactions between furan **99** and indene **100**[158, 163] or 1,4-dioxene **103**[163] confirm a multistep mechanism in which the cycloadduct **101** as well as the substitution products **102** and **104** are formed via acyclic radical-ion intermediates (Fig. 36).

Other authors have also found clear evidence for a multistep mechanism: *Gross* et al.[169] in the case of the dimerization of 1,3-butadiene to 4-vinylcyclohexene in the gas phase, which he investigated by means of the collision-activated decomposition (CAD) method in a tandem mass spectrometer; and recently *Roth* et al.[179] in the case of the

Table 4. Reaction conditions and product ratios in the dimerization of **88**.

No.	Reaction	Yield [%]	**89**	: **90**	: **91**	: **92**	Ref.
1	Δ	32	4	1	—	—	[166, 167]
2	*hν*, direct			1	1	1	[167]
3	*hν*, triplet	92	traces	1	3	1	[166, 167]
4	*hν*, **93**, benzene	75	(1	6)	main products		[139]
5	*hν*, **93**	60–80	4	1	minor products		[139]
6	*hν*, **94**, CH_3CN	80	6	1	traces	traces	[61, 162–165]
7	*hν*, R_2CO [a], $LiClO_4$, CH_3CN	60	1	1	traces	traces	[61, 162–165]
8	Δ, **95**, CH_2Cl_2	77	4	1	—	—	[61, 159, 162–164]

[a] R_2CO = **1**, **4**, **96**.

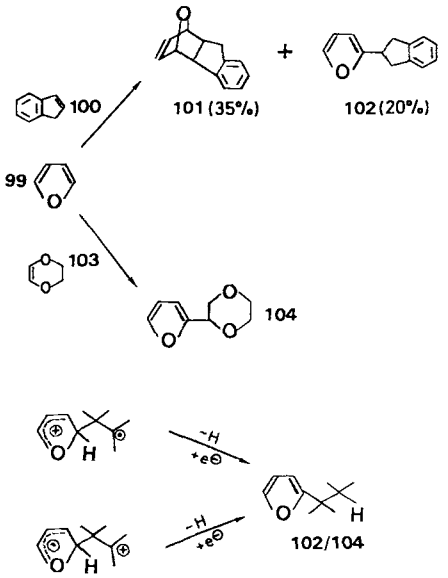

Fig. 36. Multistep reaction between **99** and **100** or **103**; possible radical-cation intermediates involved in the formation of **102** or **104**, respectively.

dimerization of spiro[2.4]heptadiene in solution, which he studied by means of CIDNP techniques.

We have observed different selectivities for contact ion pairs, on the one hand, and solvent-separated ion pairs or free radical ions, on the other hand, in the dimerization of 1,3-cyclohexadienes.[163] A high concentration of the diene and the absence of salts favor the formation of both the cyclobutanes **91** and **92** and the *exo* Diels–Alder adduct **90** even in polar solvents (20% conversion, I in Fig. 37). Addition of lithium perchlorate or a low concentration of the diene, however, result in preferential formation of the *endo* Diels–Alder adduct **89** (II in Fig. 37).

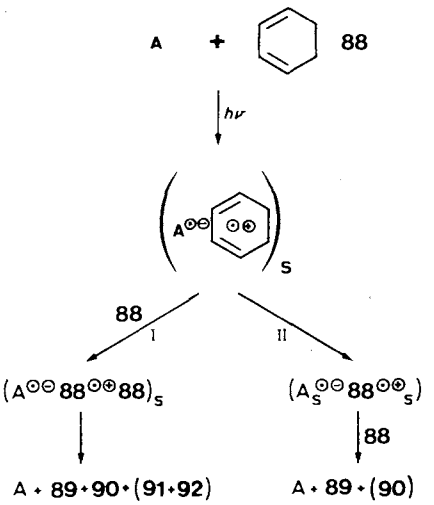

Fig. 37. Dimerization of **88** via contact ion pairs (exciplexes) (I) or via solvated radical ions (II). A: **4** and **93** ($LiClO_4$), **94**; main product **89**.

These effects are even more pronounced in the dimerization of 1-acetoxy-1,3-cyclohexadiene to the corresponding [2+2] and [4+2] adducts. Quenching experiments using 1,2,4-trimethoxybenzene (TMB, $E^{ox}_{1/2} = 0.82$ V versus Ag/$AgNO_3$ in CH_3CN[163]) and methanol confirm our assumption of the involvement of differently solvated radical-ion pairs: both TMB and methanol efficiently quench the type-II reaction but affect the type-I reaction involving contact ion pairs (or exciplexes according to *Weller*, cf. Section 2.2) far less. We have observed similar effects in the dimerization of 1-acetoxy-1,3-cyclohexadiene.

The mechanism described here for the dimerization of dienes via photochemically induced charge transfer resembles the one proposed by *Farid* et al.[144] for the dimerization of 1,1-diphenylethene **61**.[144] Whether so-called triplex intermediates are involved in this case, as suggested by *Schuster* et al.,[139] cannot be decided at present. We also observed the involvement of ternary complexes, in a different context,[39] either as reactive intermediates or simply as transition states; such complexes therefore appear to have general significance in photochemistry.[33, 137, 139, 144]

The stereoselectivity in radical-cation-catalyzed Diels–Alder reactions can also be influenced in other ways, e.g., by the choice of the acceptor (Fig. 38, Table 5). The radi-

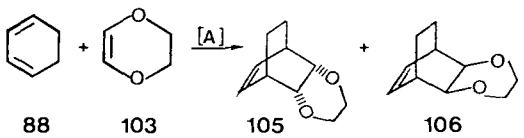

Fig. 38. Diels–Alder reaction between **88** and **103**.

Table 5. Influence of acceptor on the product ratio in the reaction of **88** with **103**.

A	Method	105 : 106	Yield [%]
95	Δ	2 : 1	29% (+40% **89** + **90**)
94	$h\nu$, S_1	10 : 1	29% (+50% **89** + **90**)

cal-cation chain mechanism in the presence of **95** shows only a small *endo* selectivity to form **105**; the selectivity is increased by the use of the photochemical electron acceptor **94** (under singlet conditions). Here, also, an electron-transfer process is probably involved, as is shown by quenching experiments with 1,2,4-trimethoxybenzene,[163, 171] which, because of its low oxidation potential (see above) can trap radical-cation intermediates. On the other hand, a smaller *endo* selectivity is observed under triplet conditions with chloranil **4** as sensitizer. Whether in this case a Diels–Alder reaction via energy transfer is operating or whether contact ion pairs are involved, as we have observed in the dimerization of 1,3-cyclohexadiene (see Fig. 37 and accompanying text), is not yet known.

Although the radical-cation-catalyzed Diels–Alder reaction can take place via various reaction mechanisms, whose relationships are not yet fully understood, radical-cation catalysis offers a new possibility for influencing selectivity and, in addition, often makes it possible to carry out, for the first time, reactions that are impossible under thermal conditions. For example, no Diels–Alder addition occurs between **88** and **103** (Fig. 38) even under high pressure.[172]

Also noteworthy is the so-called triplex mechanism,[39, 137, 139] which could, in the future, offer a further

method of directing selectivity: here, a highly polar exciplex, which does not dissociate in nonpolar solvents into radical ions, is trapped by a second donor molecule with the formation of the product [possibly via a ternary complex as reactive intermediate, see Eq. (m)]. Such exciplexes

$$A + D \xrightarrow{h\nu} [A\cdots D]^* \xrightarrow{D'} [A\cdots D\cdots D']^* \longrightarrow A + DD' \qquad (m)$$

are characterized by relatively strong bonding energies (up to 80 kJ mol^{-1}), a marked CT character (cf. Section 3.1), and a high dipole moment.[33, 39, 175, 176] They are often structured, as, for example, our studies in the field of arene photochemistry have shown, and have a decisive influence on the course of the reaction.[43] By this means it should be possible, even for the [2+2] and [4+2] cycloadditions, to make use of the different diastereomeric interactions in the exciplex formation to direct the reaction. Recently *Lemaire* et al.[177] reported very successful applications—using charge-transfer complexes, however.

Further cycloadditions of 1,3-cyclohexadienes have been investigated by *Bauld* et al.[173] and *Steckhan* et al.[165] as well as in our own laboratory[61, 163, 164, 174] with special emphasis on the correlation between substitution and mechanism, on the one hand, and efficiency and selectivity, on the other. 1-Acetoxy-1,3-cyclohexadiene **107** dimerizes, with high efficiency, to give the Diels-Alder adducts **109** and **110** (A = **94**, 47%; A = **4**, 63%). In contrast, the corresponding reaction of the isomer **111** proceeds very unselectively and in low yield, affording products similar to those obtained in the triplet-sensitized reaction (energy-transfer conditions) (Fig. 39). Assuming a multistep mechanism, a substituent at position 1 of the allylic unit (**108**) stabilizes acyclic radical-ion intermediates more efficiently than one in position 2 (**112**). Consequently, the cycloaddition of **111** and **103** to form the Diels-Alder adducts **114** and **115** (yield: 45%) now competes efficiently with the dimerization of **111**. The carboxonium ion structure of the intermediate **113** apparently favors this mixed reaction.

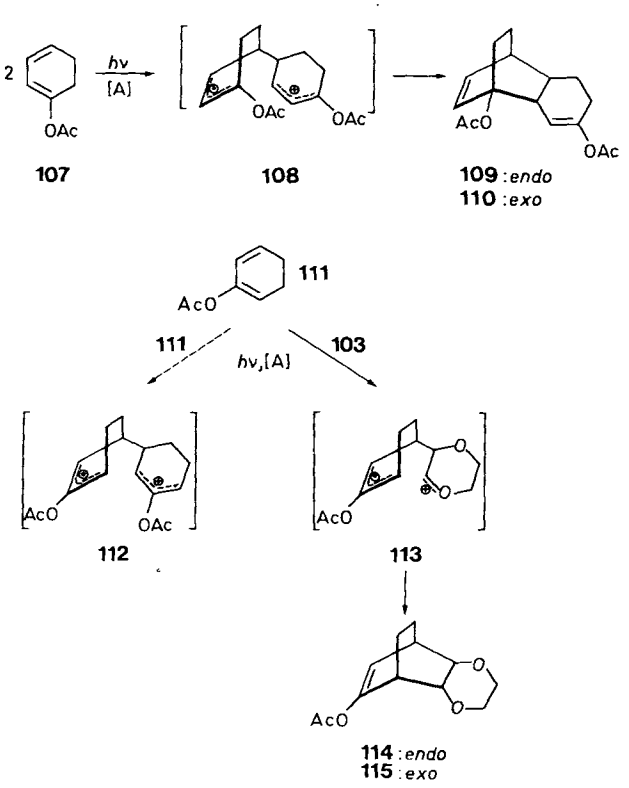

Fig. 39. Dimerizations and cycloadditions of **107** and **111**. A: **1** ($LiClO_4$), **4** ($LiClO_4$), **93** ($LiClO_4$), **94**; main products, **109** and **114**.

5.2. Reactions with Nucleophiles

Alkene radical cations can be captured in nucleophilic solvents as neutral products. This process has been extensively investigated by *Arnold* et al. and extended to the counterpart, i.e., the reactions of the corresponding radical anions with electrophiles[135, 178] (Fig. 40). For example,

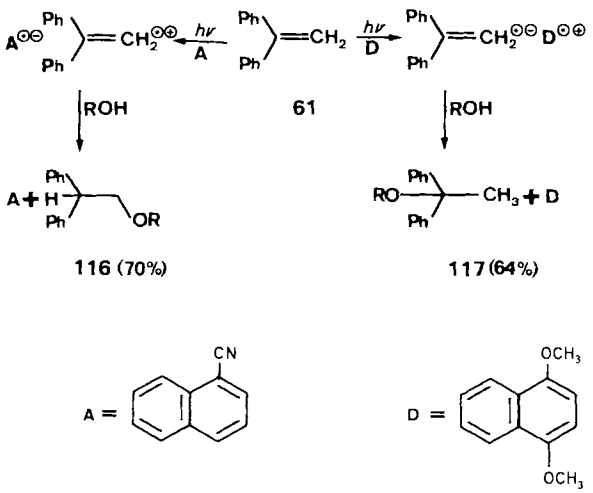

Fig. 40. Reactions of photochemically generated radical cations and anions with alcohols.

whereas the radical cation generated from **61** by electron-transfer sensitization reacts with an alcohol to give the anti-Markovnikov product **116**, the corresponding radical anion shows normal behavior, giving **117**.

Other solvents can also react as nucleophiles with alkene radical cations: e.g., the acyclic radical-ion intermediate in the dimerization of enol ethers can be captured by acetonitrile with the formation of pyridine derivatives.[132] Nitromethane acts, in addition, as an oxygen-transfer agent.[179] Finally, *Arnold* et al. applied this method to other alkene radical-cation capture reactions of synthetic interest, such as the photosensitized cyanidation of alkenes.[180] Other examples can be found in the reviews by *Farid* et al.[23] and *Mariano*.[24]

Attempts to capture radical cations with nucleophiles are not always successful. We have found differences in the reactivity of 1,3-dioxole radical cations on the one hand with $OH^{\ominus}$ and $HPO_4^{2\ominus}$ and on the other with alcohols.[51, 181] Whereas the charged nucleophiles reacted, in part, with the radical cations to form neutral products, this did not occur with alcohols. Although *Arnold* et al. were successful in similar experiments[80, 178] and thus clearly conflicting results have been obtained, there is an interesting parallel between our results and the theoretical considerations of *Pross*.[182] According to the latter, a direct attack

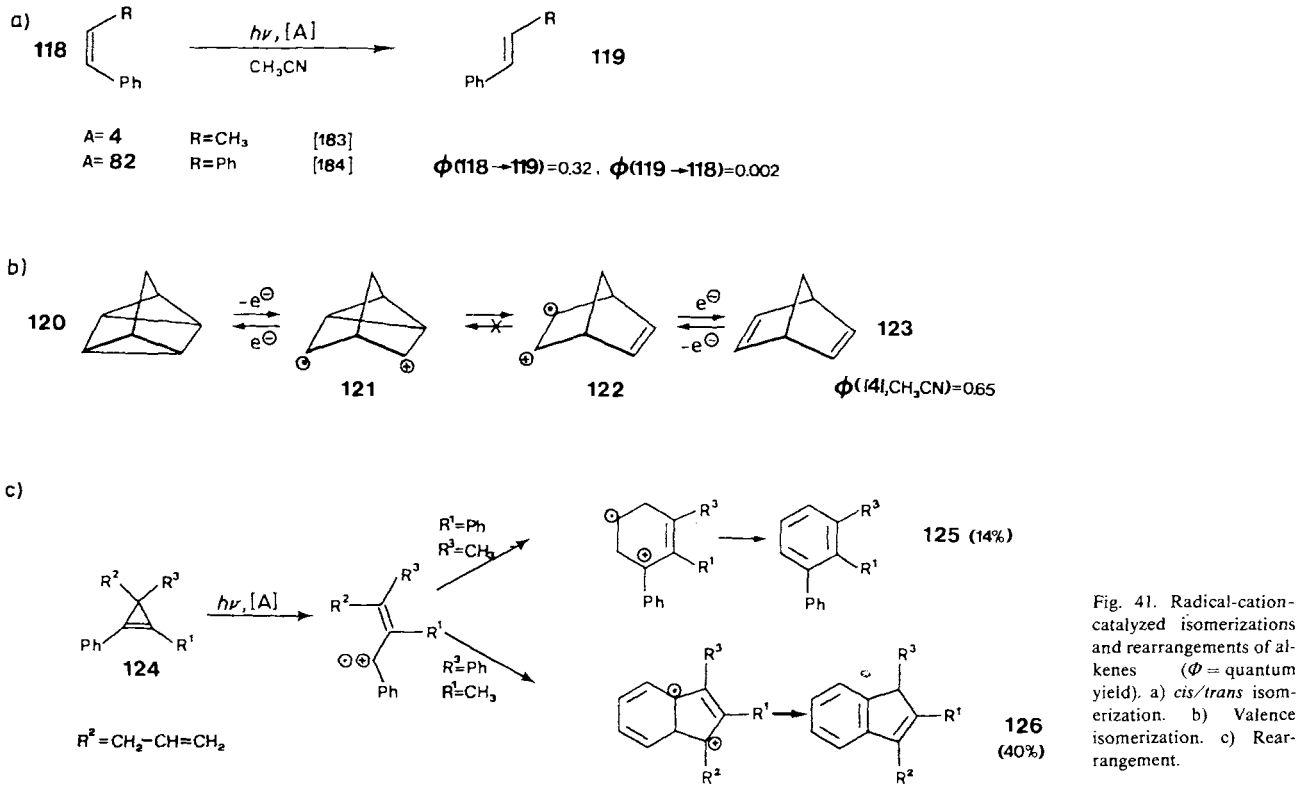

Fig. 41. Radical-cation-catalyzed isomerizations and rearrangements of alkenes (Φ = quantum yield). a) *cis/trans* isomerization. b) Valence isomerization. c) Rearrangement.

of a nucleophile on a radical cation is "forbidden" and therefore has a high activation energy.

5.3. Isomerization and Rearrangement

Since the double-bond character of the alkene has been removed in the radical cation, isomerization and rearrangements are observed, as in the case of the corresponding photoreactions involving energy transfer. Recently, the *cis/trans* isomerization of alkenes has been intensively studied. In Figure 41a, two examples are shown, both of which occur by means of a chain reaction.[183, 184] Increased solvent polarity and the addition of salts increase the efficiency of this isomerization and thus confirm that the mechanism involves solvated radical ions.[184] Here again, the analogous reaction via alkene radical anions is known, but it occurs via an electron-transfer sensitization (cf. II in Fig. 30).[185]

Valence isomerizations by means of radical cations have been observed with Dewar benzene,[186] in the intramolecular cycloaddition of "cage compounds,"[187, 188] and in the norbornadiene (**123**)/quadricyclane (**120**) system.[189–191] The latter, in particular, is of fundamental importance in connection with the storage of solar energy and has therefore been intensively investigated. The valence-isomeric radical cations **121** and **122** can be distinguished by CIDNP methods (Fig. 41b).[189, 190] The energetically unfavorable isomerization **123** → **120** can only be achieved by means of strong electron acceptors. In such a case, the contact ion pair dissociates with the formation of **123** in a triplet state, which then isomerizes to **120**[190] [Eq. (n), cf. Section 5.4).

$$A + \mathbf{123} \xrightarrow{h\nu} (A^{\ominus\ominus}\ \mathbf{123}^{\oplus\oplus}) \longrightarrow A + {}^3\mathbf{123}^* \longrightarrow \mathbf{120} \qquad (n)$$

Two examples of the rearrangement of cyclopropene derivatives (**124**) via radical cations, leading to the formation of **125** and **126**, are shown in Figure 41c.[192] The corresponding energy-transfer reactions, on the other hand, lead to intramolecular [2+2] cycloadducts (triplet) or indene derivatives via the intermediate formation of carbenes (singlet). *Roth* et al.[193] and *Gassman* et al.[194] have reported on the rearrangements of bicyclopropenyl- and bicyclo[1.1.0]butane derivatives.

5.4. Back Electron Transfer with the Formation of Triplets

According to *Weller*,[30] back electron transfer can occur from various intermediates. For example, a contact ion pair in the singlet state should give the starting material predominantly in the singlet (ground) state unless intersystem crossing by means of a hyperfine mechanism can compete with the dissociation of the radical-ion pair. Whereas this process takes place rapidly (ns region), the back electron transfer by recombination of the radical ions takes place slowly (μs region) and gives, corresponding to the number of spin sublevels, 75% of the starting material in the triplet state. Triplet formation is favored by back electron transfer when the energy of the radical-ion pair lies higher than the triplet energy of one of the starting materials. *Farid* et al.[195] have reported such an example in the electron-transfer-sensitized reactions of methyl 1,2-diphenylcyclopropene-3-carboxylate. In nonpolar solvents, it reacts with 9,10-anthracenedicarbonitrile to form the *exo*-Diels–Alder adduct via a luminescent exciplex, whereas in acetonitrile the cyclopropene dimerizes to give an *anti*-tricyclo[3.1.0.0^{2,4}]hexane derivative by means of a back-electron-transfer triplet mechanism.

We have observed similar effects in the photoreactions of electron-poor arenes with 1,3-dioxoles, which often, in the exergonic region of electron transfer, also formed dioxole dimers.[42] Here, solvent polarity plays a decisive role since it strongly affects the energy of the ion pairs [Eqs. (c) and (d)] in a different way than it does the triplet energy of the reactants. The studies of *Bauld* et al.[196] on the dimerization of 1,3-cyclohexadiene **88** and 2,4-dimethyl-1,3-pentadiene in different solvents can be interpreted on this basis. In dichloromethane ($\varepsilon = 8.9$) the proportion of cyclobutane, which is formed via the triplet reaction path according to *Bauld*, is dramatically increased in comparison to the amount formed in acetonitrile ($\varepsilon = 37.5$). Sometimes, however, the specific interaction between the radical ions and the solvent can also influence the competition between the radical-ion and the triplet reaction paths.[196] When sensitizers that are also strong electron acceptors are used, on the other hand, the involvement of differently solvated radical ions (CIP or SSIP) may also lead to the product ratios observed here (cf. Section 5.1.1 and 5.1.2).

6. Conclusions and Prospects

The electrochemical redox potentials and electronic excitation energies of reactants as well as the polarity of the reaction medium determine the amount of charge transfer between electron-donor and electron-acceptor compounds. The free energies of formation calculated according to the Weller equation [Eq. (c)] for solvent-separated radical-ion pairs have proved to be suitable as criteria for the estimation of photochemically induced charge transfer. In the exergonic region of electron transfer, solvated radical ions are formed preferentially after the excitation of donor–acceptor systems (Fig. 42, left). Back electron transfer, already reduced in this way, can be further suppressed by means of salt effects (particularly the special salt effect). This gives rise to new possibilities in the generation of radical ions and the study of their reactions. Impressive proof of this is provided by examples from the currently intensively investigated field of radical-cation-catalyzed cycloadditions of olefins and dienes. Interactions with the acceptor radical anion—either via differently solvated radical ion pairs or by means of the so-called triplex mechanism—the influence of counterions, and the participation of triplet reaction paths can alter the course of the reaction markedly, particularly the stereoselectivity. In this, and in the fact that many reactions are only possible under the conditions of radical-cation catalysis, lies the synthetic potential of these new methods.

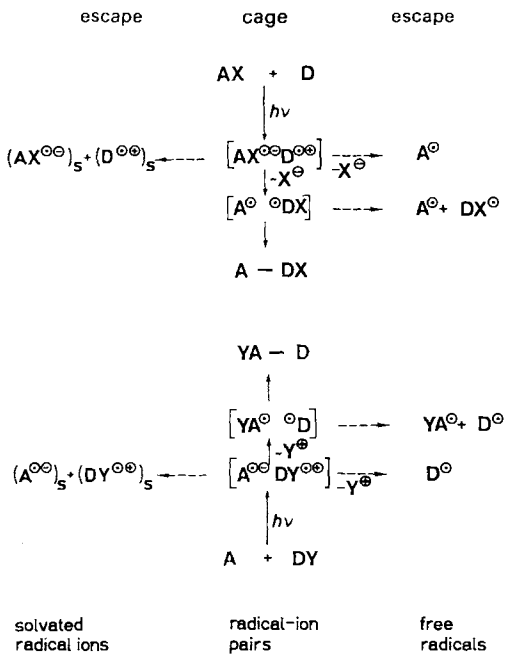

Fig. 42. "Cage" and "escape" processes in photochemical electron-transfer reactions between donor and acceptor molecules.

A further possible method of hindering the back transfer of electrons is offered by the reactions of donor and acceptor radical ions among themselves. In the most common cases, these reactions are initiated by the heterolytic splitting off of a nucleofugal or electrofugal group (Fig. 42, middle). The recombination of the radicals thus formed terminates the process. If the recombination is prevented by the choice of suitable substrates, then a new method for the generation of free radicals by means of photochemically induced electron transfer is obtained[197] (Fig. 42, right).

In the endergonic region, the free energies of electron transfer can be used to estimate the CT character and to determine the direction of the charge transfer within the exciplex. The ΔG values calculated by means of Equation (c) correlate, at least within a substrate series, with the course of the reaction (Figs. 10 and 15). In other words, photochemically induced charge transfer has a regulatory effect on the reactions between electron-donor and electron-acceptor molecules. Here also, it is possible to influence charge transfer and stereoselectivity by a suitable choice of reaction medium.

Many photoreactions in which charge transfer has a decisive influence on the course of the reaction could not be dealt with in this article. These include the diverse photoreactions of metal coordination compounds,[2-6, 22, 198-201] the photoreactions involved in the extensive studies of the storage of solar energy[5] (this area has recently been reviewed by *Fendler*[202]), and many other organic reactions.[6, 24]

The progress made in the field of photochemistry would not have been possible without interaction between individual chemical disciplines. This is particularly true for the study of electron-transfer processes, which play a decisive role in many areas of chemistry, whether they be in biological, inorganic, or organic systems, or whether they take place under thermal conditions or under the influence of light. The enormous increase, in recent years, in the number of publications dealing with electron-transfer processes is less a sign of a short-lived fashion than an indication of growing awareness of chemists that the questions concerning these processes need to be answered. The development of more refined analytical methods, the investigation of fundamental questions such as the applicability of the Marcus theory or Weller's empirical relationship to the kinetics of electron transfer, and synthetic studies by

preparatively oriented organic chemists will give a further impulse to research in this important area.

The personal work referred to here has only been possible thanks to the enthusiastic help of my co-workers Karl Buchkremer, Dr. Joachim Gersdorf, Christel Dittmer, Jürgen Mertes, Gisela Trampe, and Gabi Weber and the cooperation of colleagues working in other areas. I would specially like to thank Dr. H. Görner and Dr. S. Steenken (Max-Planck-Institut für Strahlenchemie, Mülheim) for help with the fundamental transient-analysis studies and Dr. J. Runsink (RWTH Aachen) for help with the NMR analyses. I thank the Deutsche Forschungsgemeinschaft and the Fonds der Chemischen Industrie for their generous financial help and, finally, Bayer and BASF for gifts of materials.

Received: December 2, 1986;
supplemented: May 11, 1987 [A 632 IE]
German version: *Angew. Chem. 99* (1987) 849
Translated by Dr. *Douglas Maas*, Kronberg, Taunus

[1] L. Eberson, *Adv. Phys. Org. Chem. 18* (1982) 79.
[2] H. Taube, *Angew. Chem. 96* (1984) 315; *Angew. Chem. Int. Ed. Engl. 23* (1984) 329.
[3] S. J. Lippard (Ed.): *Prog. Inorg. Chem. 30* (1983) 141, 273, 389, 441; *ibid. 32* (1984) 443.
[4] N. Sutin, *J. Photochem. 10* (1979) 19.
[5] M. Grätzel (Ed.): *Energy Resources through Photochemistry and Catalysis*, Academic Press, New York 1983.
[6] G. J. Kavarnos, N. J. Turro, *Chem. Rev. 86* (1986) 401.
[7] H. Leonhardt, A. Weller, *Ber. Bunsenges. Phys. Chem. 67* (1963) 791.
[8] R. A. Marcus, *Annu. Rev. Phys. Chem. 15* (1964) 155.
[9] N. S. Hush, *Trans. Faraday Soc. 57* (1961) 557.
[10] N. Mataga, M. Mitiga, T. Nishimura, *J. Mol. Struct. 47* (1978) 199.
[11] J. C. Scaiano, *Acc. Chem. Res. 15* (1982) 252.
[12] N. J. Turro, *Tetrahedron 38* (1982) 809.
[13] J. F. Rabeck: *Experimental Methods in Photochemistry and Photophysics, Part 2*, Wiley, New York 1982, p. 822ff.
[14] N. Mataga, *Pure Appl. Chem. 56* (1984) 1255.
[15] J. D. Simon, K. S. Peters, *Acc. Chem. Res. 17* (1984) 277.
[16] E. F. Hilinski, P. M. Rentzepis, *Acc. Chem. Res. 16* (1983) 224.
[17] H. D. Roth in L. T. Muus (Ed.): *Chemically Induced Magnetic Polarisation*, Reidel, Dordrecht 1977, p. 39.
[18] G. L. Closs, R. J. Miller, O. D. Redwine, *Acc. Chem. Res. 18* (1985) 196.
[19] N. J. Turro, *J. Photochem. 25* (1984) 69.
[20] P. J. Hore, C. G. Joslin, K. A. McLauchlan, *Chem. Soc. Rev. 8* (1979) 29.
[21] J. Terner, M. A. El-Sayed, *Acc. Chem. Res. 18* (1985) 331.
[22] M. Julliard, M. Chanon, *Chem. Rev. 83* (1983) 425.
[23] S. L. Mattes, S. Farid in A. Padwa (Ed.): *Organic Photochemistry, Vol. 6*, Dekker, New York 1983, p. 233ff.
[24] P. S. Mariano in W. M. Horspool (Ed.): *Synthetic Organic Photochemistry*, Plenum, New York 1984, p. 145-257.
[25] N. J. Turro: *Modern Molecular Photochemistry*, Benjamin/Cummings, Menlo Park, CA, USA 1978.
[26] J. Heinze, *Angew. Chem. 96* (1984) 823; *Angew. Chem. Int. Ed. Engl. 23* (1984) 831.
[27] D. Rehm, A. Weller, *Z. Phys. Chem. (Munich) 69* (1970) 183.
[28] D. Rehm, A. Weller, *Isr. J. Chem. 8* (1970) 259.
[29] A. Weller, *Z. Phys. Chem. (Munich) 133* (1982) 93.
[30] A. Weller, *Z. Phys. Chem. (Munich) 130* (1982) 129; *Pure Appl. Chem. 54* (1982) 1885.
[31] J. R. Miller, L. T. Calcaterra, G. L. Closs, *J. Am. Chem. Soc. 106* (1984) 3047.
[32] A. Weller in M. Gordon, W. R. Ware (Ed.): *The Exciplex*, Academic Press, New York 1975, p. 23ff.
[33] H. Beens, H. Knibbe, A. Weller, *J. Chem. Phys. 47* (1967) 1183; H. Beens, A. Weller, *Phys. Chem. Lett. 2* (1968) 140.
[34] H. Masuhara, N. Mataga, *Acc. Chem. Res. 14* (1981) 312.
[35] F. D. Lewis, *Acc. Chem. Res. 12* (1979) 152.
[36] R. A. Caldwell, *Acc. Chem. Res. 13* (1980) 45.
[37] S. L. Mattes, S. Farid, *Acc. Chem. Res. 15* (1982) 80.
[38] J. Mattay, H. Leismann, H.-D. Scharf, *Chem. Ber. 112* (1979) 577; *Mol. Photochem. 9* (1979) 119.
[39] H. Leismann, J. Mattay, H.-D. Scharf, *J. Am. Chem. Soc. 106* (1984) 3985.
[40] J. Mattay, J. Gersdorf, H. Leismann, S. Steenken, *Angew. Chem. 96* (1984) 240; *Angew. Chem. Int. Ed. Engl. 23* (1984) 249.
[41] J. Mattay, J. Runsink, J. Gersdorf, T. Rumbach, C. Ly, *J. Am. Chem. Soc. 107* (1985) 2557; *Helv. Chim. Acta 69* (1986) 442.
[42] J. Mattay, *Tetrahedron 41* (1985) 2393, 2405.
[43] J. Mattay, *J. Photochem. 37* (1987) 167.
[44] J. Gersdorf, J. Mattay, H. Görner, *J. Am. Chem. Soc. 109* (1987) 1203.
[45] J. Mattay, J. Gersdorf, K. Buchkremer, *Chem. Ber. 120* (1987) 307.
[46] H. Leismann, J. Mattay, *Tetrahedron Lett. 1978*, 4265.
[47] R. A. Caldwell, L. Smith, *J. Am. Chem. Soc. 96* (1974) 2994.
[48] G. Schmitt, *Dissertation*, Technische Hochschule Aachen 1986.
[49] J. Mattay, J. Gersdorf, U. Freudenberg, *Tetrahedron Lett. 25* (1984) 817.
[50] J. Mattay, J. Gersdorf, J. Mertes, *J. Chem. Soc. Chem. Commun. 1985*, 1088.
[51] J. Mattay, G. Trampe, S. Steenken, *Proc. 11th IUPAC-Symp. Photochem.* (Lissabon 1986), pp. 114-115.
[52] J. H. Fendler: *Membrane Mimetic Chemistry*, Wiley, New York 1982; *Chem. Eng. News 62* (1984) No. 1, p. 25.
[53] M. Grätzel, *Pure Appl. Chem. 54* (1982) 2369.
[54] H. Gerischer, J. J. Katz (Eds.): *Light-Induced Charge Separation in Biology and Chemistry Systems (Life Sci. Res. Rep. 12)*, Verlag Chemie, Weinheim 1979.
[55] Y. Taniguchi, Y. Nishina, N. Mataga, *Bull. Chem. Soc. Jpn. 45* (1972) 764.
[56] L. Reichardt: *Solvent Effects in Organic Chemistry*, Verlag Chemie, Weinheim 1979; *Angew. Chem. 77* (1965) 30; *Angew. Chem. Int. Ed. Engl. 4* (1965) 29; *ibid. 91* (1979) 119 and *18* (1979) 98.
[57] M. Szwarc (Ed.): *Ions and Ion Pairs in Organic Reactions, Vol. 1, 2*, Wiley, New York 1974.
[58] N. Hirota, S. J. Weissmann, *J. Am. Chem. Soc. 86* (1964) 2538; N. Hirota in E. T. Kaiser, L. Kevan (Eds.): *Radical Ions*, Wiley, New York 1968, p. 35.
[59] K. Nakamura, *J. Am. Chem. Soc. 102* (1980) 7846.
[60] J. Gersdorf, J. Mattay, *J. Photochem. 28* (1985) 405.
[61] J. Mattay, G. Trampe, J. Mertes, J. Gersdorf, *Proc. 11th IUPAC-Symp. Photochem.* (Lisbon 1986), pp. 209-210.
[62] L. C. Bateman, M. G. Church, E. D. Hughes, C. K. Ingold, N. A. Taher, *J. Chem. Soc. 1940*, 979.
[63] A. H. Fainberg, S. J. Winstein, *J. Am. Chem. Soc. 78* (1956) 2767.
[64] J. Mattay, J. Gersdorf, H. Görner, *Proc. 10th IUPAC-Symp. Photochem.* (Interlaken, Switzerland 1984), pp. 153-154.
[65] J. Gersdorf, *Dissertation*, Technische Hochschule Aachen 1985.
[66] J. L. Goodman, K. S. Peters, *J. Am. Chem. Soc. 107* (1985) 6459.
[67] B. E. Goodson, G. B. Schuster, *J. Am. Chem. Soc. 106* (1984) 7254.
[68] B. E. Goodson, G. B. Schuster, *Tetrahedron Lett. 27* (1986) 3123.
[69] J. M. Masnovi, J. K. Kochi, *J. Am. Chem. Soc. 107* (1985) 7880.
[70] D. E. Ayer, G. H. Büchi, US Pat. 2805242 (1957), E. I. duPont de Nemours; *Chem. Abstr. 52* (1958) 2904a.
[71] H. J. F. Angus, D. Bryce-Smith, *Proc. Chem. Soc. (London) 1959*, 326; *J. Chem. Soc. 1960*, 4791.
[72] G. O. Schenck, R. Steinmetz, *Tetrahedron Lett. 1960*, 1.
[73] E. Grovenstein, D. V. Rao, J. W. Taylor, *J. Am. Chem. Soc. 83* (1961) 1705.
[74] D. Bryce-Smith, A. Gilbert, B. H. Orger, *Chem. Commun. 1966*, 512.
[75] K. E. Wilzbach, L. Kaplan, *J. Am. Chem. Soc. 88* (1966) 2066.
[76] A. Gilbert in D. Bryce-Smith (Ed.): *Photochemistry (Spec. Period. Rep. Photochem.) 1-17* (1970-1986), The Royal Society of Chemistry, London.
[77] J. Mattay, J. Runsink, R. Hertel, J. Kalbe, I. Schewe, *J. Photochem. 37* (1987) 335.
[78] J. J. McCullough, R. C. Miller, D. Fung, W. S. Wu, *J. Am. Chem. Soc. 97* (1975) 5942.
[79] J. J. McCullough, R. C. Miller, W. S. Wu, *Can. J. Chem. 55* (1977) 2909.
[80] D. R. Arnold, P. C. Wong, A. J. Maroulis, T. S. Cameron, *Pure Appl. Chem. 52* (1980) 2609.
[81] A. Yoshino, K. Yamasaki, T. Yonezawa, M. Ohashi, *J. Chem. Soc. Perkin Trans. 1 1975*, 735.
[82] A. Albini, E. Fasani, R. Oberti, *Tetrahedron 38* (1982) 1027.
[83] F. D. Lewis, R. J. DeVoe, *Tetrahedron 38* (1982) 1069.
[84] K. Mizuno, M. Ikeda, Y. Otsuji, *Tetrahedron Lett. 26* (1985) 461.
[85] K. Mizuno, K. Terasaka, M. Ikeda, Y. Otsuji, *Tetrahedron Lett. 26* (1985) 5819.
[86] A. Albini, E. Fasani, M. Mella, *J. Am. Chem. Soc. 108* (1986) 4119.
[87] A. Albini, E. Fasani, A. Sulpizio, *J. Am. Chem. Soc. 106* (1984) 3562.
[88] M. Yasuda, C. Pac, H. Sakurai, *Bull. Chem. Soc. Jpn. 54* (1981) 2352.
[89] F. D. Lewis, T. I. Ho, *J. Am. Chem. Soc. 102* (1980) 1751.
[90] R. M. Bowman, T. R. Chamberlain, C. W. Huang, J. J. McCullough, *J. Am. Chem. Soc. 96* (1974) 692.
[91] T. Miyamoto, T. Mori, Y. Odaira, *Chem. Commun. 1970*, 1598.
[92] J. M. Masnovi, J. K. Kochi, E. F. Hilinski, P. M. Rentzepis, *J. Am. Chem. Soc. 108* (1986) 1126.
[93] E. F. Hilinski, J. M. Masnovi, J. K. Kochi, P. M. Rentzepis, *J. Am. Chem. Soc. 106* (1984) 8071.

[94] J. M. Masnovi, J. K. Kochi, *J. Org. Chem. 50* (1985) 5245; *Recl. J. R. Neth. Chem. Soc. 105* (1986) 286.
[95] G. Briegleb: *Elektronen-Donor-Acceptor-Komplexe*, Springer, Berlin 1961.
[96] S. Sankararaman, J. K. Kochi, *Recl. J. R. Neth. Chem. Soc. 105* (1986) 278.
[97] D. P. Kjell, R. S. Sheridan, *J. Photochem. 28* (1985) 205.
[98] R. J. Sundberg in A. Padwa (Ed.): *Organic Photochemistry, Vol. 6*, Dekker, New York 1983, pp. 121-176.
[99] P. J. Wagner, *Top. Curr. Chem. 66* (1976) 1.
[100] G. Jones II in A. Padwa (Ed.): *Organic Photochemistry, Vol. 5*, Dekker, New York 1981, pp. 1-122.
[101] M. Braun, *Nachr. Chem. Tech. Lab. 33* (1985) 213.
[102] H.-D. Scharf, H. Herzog, R. Pelzer, unpublished.
[103] J. Mattay, J. Runsink, *J. Org. Chem. 50* (1985) 2815.
[104] P. J. Wagner, R. J. Truman, A. E. Puchalski, R. Wake, *J. Am. Chem. Soc. 108* (1986) 7727. We thank *P. J. Wagner* for a preprint of this article.
[105] S. G. Cohen, R. J. Baumgarten, *J. Am. Chem. Soc. 89* (1967) 3471.
[106] S. G. Cohen, A. Parola, G. H. Parsons, *Chem. Rev. 73* (1973) 141.
[107] D. Seebach, H. Daum, *J. Am. Chem. Soc. 93* (1971) 2795.
[108] J. D. Simon, K. S. Peters, *J. Am. Chem. Soc. 103* (1981) 6403; *ibid. 105* (1983) 4875.
[109] L. M. Bruce in S. Patai (Ed.): *The Chemistry of Quinonoid Compounds, Vol. 1*, Wiley, New York 1974, pp. 465-538.
[110] K. Maruyama, T. Otsuki, S. Tai, *J. Org. Chem. 50* (1985) 52.
[111] J. D. Coyle, *Chem. Rev. 78* (1978) 97.
[112] Y. Kanaoka, *Acc. Chem. Res. 11* (1978) 407.
[113] P. H. Mazzocchi in A. Padwa (Ed.): *Organic Photochemistry, Vol. 5*, Dekker, New York 1981, pp. 421-471.
[114] J. D. Coyle in W. M. Horspool (Ed.): *Synthetic Organic Photochemistry*, Plenum, New York 1984, pp. 259-284.
[115] P. H. Mazzocchi, S. Minamikawa, P. Wilson, *J. Org. Chem. 50* (1985) 2681.
[116] P. H. Mazzocchi, P. Wilson, F. Khachik, L. Klingler, S. Minamikawa, *J. Org. Chem. 48* (1983) 2981.
[117] P. H. Mazzocchi, G. Fritz, *J. Am. Chem. Soc. 108* (1986) 5362.
[118] K. Maruyama, T. Ogawa, Y. Kubo, T. Araki, *J. Chem. Soc. Perkin Trans. 1 1985*, 2025.
[119] M. Machida, K. Oda, Y. Kanaoka, *Tetrahedron 41* (1985) 4995.
[120] P. S. Mariano, *Tetrahedron 39* (1983) 3845; *Acc. Chem. Res. 16* (1983) 130.
[121] P. S. Mariano, J. Stavinoha, E. Bay, *Tetrahedron 37* (1981) 3385.
[122] H. Böhme, H. G. Viehe: *Imminium Salts in Organic Chemistry*, Wiley, New York 1976.
[123] W. N. Speckamp, H. Hiemstra, *Tetrahedron 41* (1985) 4367.
[124] S. D. Larsen, P. A. Grieco, W. F. Fobare, *J. Am. Chem. Soc. 108* (1986) 3512, and references cited therein.
[125] K. Ohga, U. C. Yoon, P. S. Mariano, *J. Org. Chem. 49* (1984) 213.
[126] G. Dai-Ho, A. J. Y. Lan, P. S. Mariano, *Tetrahedron Lett. 26* (1985) 5867.
[127] L. P. Ellinger, *Polymer 5* (1964) 599.
[128] A. Ledwith in M. Gordon, W. R. Ware (Eds.): *The Exciplex*, Academic Press, New York 1975, pp. 209-245.
[129] A. Ledwith, *Acc. Chem. Res. 5* (1972) 133.
[130] S. Farid, S. E. Hartman, T. R. Evans in M. Gordon, W. R. Ware (Eds.): *The Exciplex*, Academic Press, New York 1975, pp. 327-343.
[131] S. Kuwata, Y. Shigemitsu, Y. Odaira, *J. Org. Chem. 38* (1973) 3803.
[132] T. R. Evans, R. W. Wake, O. Jaenicke in M. Gordon, W. R. Ware (Eds.): *The Exciplex*, Academic Press, New York 1975, pp. 345-358.
[133] T. Asanuma, M. Yamamoto, Y. Nishijima, *J. Chem. Soc. Chem. Commun. 1975*, 53, 56, 608.
[134] M. Kojima, H. Sakuragi, K. Tokumaru, *Tetrahedron Lett. 22* (1981) 2889.
[135] R. A. Neunteufel, D. R. Arnold, *J. Am. Chem. Soc. 95* (1973) 4080.
[136] T. Majima, C. Pac, A. Nakasone, H. Sakurai, *J. Am. Chem. Soc. 103* (1981) 4499.
[137] C. Pac, *Pure Appl. Chem. 58* (1986) 1249.
[138] A. Albini, *Synthesis 1981*, 249.
[139] G. C. Calhoun, G. B. Schuster, *J. Am. Chem. Soc. 108* (1986) 8021.
[140] N. L. Bauld, R. Pabon, *J. Am. Chem. Soc. 105* (1983) 633.
[141] T. Asanuma, T. Gotoh, A. Tsuchida, M. Yamamoto, Y. Nishijima, *J. Chem. Soc. Chem. Commun. 1977*, 485.
[142] T. Gotoh, M. Kato, M. Yamamoto, Y. Nishijima, *J. Chem. Soc. Chem. Commun. 1981*, 90.
[143] S. Tazuke, N. Kitamura, *J. Chem. Soc. Chem. Commun. 1977*, 515.
[144] S. L. Mattes, S. Farid, *J. Am. Chem. Soc. 108* (1986) 7356.
[145] K. Mizuno, R. Kaji, Y. Otsuji, *Chem. Lett. 1977*, 1027.
[146] K. Mizuno, H. Ueda, Y. Otsuji, *Chem. Lett. 1981*, 1237.
[147] K. N. Houk, *Acc. Chem. Res. 8* (1975) 361.
[148] J. Sauer, R. Sustmann, *Angew. Chem. 92* (1980) 773; *Angew. Chem. Int. Ed. Engl. 19* (1980) 779.
[149] I. Fleming: *Grenzorbitale und Reaktionen organischer Verbindungen*, Verlag Chemie, Weinheim 1979.
[150] W. J. le Noble, H. Kelm, *Angew. Chem. 92* (1980) 887; *Angew. Chem. Int. Ed. Engl. 19* (1980) 841.
[151] W. J. le Noble, *Chem. Unserer Zeit 17* (1983) 152.
[152] K. Matsumoto, A. Sera, T. Uchida, *Synthesis 1985*, 1, 999.
[153] P. Yates, P. Eaton, *J. Am. Chem. Soc. 82* (1960) 4436.
[154] H. Wollweber in *Houben-Weyl-Müller: Methoden der Organischen Chemie, Band V/1c*, Thieme, Stuttgart 1970, p. 1092.
[155] P. Welzel, *Nachr. Chem. Tech. Lab. 31* (1983) 979.
[156] D. C. Rideout, R. Breslow, *J. Am. Chem. Soc. 102* (1980) 7816.
[157] P. A. Grieco, P. Galatsis, R. F. Spohn, *Tetrahedron 42* (1986) 2847.
[158] K. Mizuno, R. Kaji, H. Okada, Y. Otsuji, *J. Chem. Soc. Chem. Commun. 1978*, 594.
[159] D. J. Beleville, D. D. Wirth, N. L. Bauld, *J. Am. Chem. Soc. 103* (1981) 718.
[160] N. L. Bauld, D. J. Beleville, R. Pabon, R. Chelsky, G. Green, *J. Am. Chem. Soc. 105* (1983) 2378.
[161] C. R. Jones, B. J. Allman, A. Mooring, B. Saphic, *J. Am. Chem. Soc. 105* (1983) 652.
[162] J. Mattay, J. Gersdorf, J. Mertes, *J. Chem. Soc. Chem. Commun. 1985*, 1088.
[163] G. Trampe, *Dissertation*, Technische Hochschule Aachen 1987.
[164] J. Mattay, J. Gersdorf, G. Trampe, *Chemiedozententagung* (Aachen 1985), Proceedings p. 42; *20. GDCh-Hauptversammlung* (Heidelberg 1985), Proceedings p. 111.
[165] J. Mlcoch, E. Steckhan, *Angew. Chem. 97* (1985) 429; *Angew. Chem. Int. Ed. Engl. 24* (1985) 412.
[166] D. Valentine, N. J. Turro, G. S. Hammond, *J. Am. Chem. Soc. 86* (1964) 5202.
[167] a) G. O. Schenck, S. P. Mannsfeld, G. Schomburg, C. H. Krauch, *Z. Naturforsch. B 19* (1964) 18; b) R. Schutte, G. R. Freeman, *J. Am. Chem. Soc. 91* (1969) 3715; c) T. L. Palmer, D. G. Whitten, G. S. Hammond, *ibid. 92* (1970) 2861.
[168] F.-G. Klärner, B. M. J. Dogan, O. Ermer, W. von E. Doering, M. P. Cohen, *Angew. Chem. 98* (1986) 109; *Angew. Chem. Int. Ed. Engl. 25* (1986) 108.
[169] G. S. Groenewald, M. L. Gross, *J. Am. Chem. Soc. 106* (1984) 6569.
[170] H. D. Roth, M. L. M. Schilling, C. J. Abelt, *J. Am. Chem. Soc. 108* (1986) 6098.
[171] J. Mertes, *Diplomarbeit*, Technische Hochschule Aachen 1986.
[172] J. Mattay, G. Trampe, F.-G. Klärner, unpublished.
[173] R. A. Pabon, D. J. Beleville, N. L. Bauld, *J. Am. Chem. Soc. 105* (1983) 5158.
[174] G. Trampe, J. Mattay, *2nd Postgraduate Symp. Photochem.* (Mülheim a. d. Ruhr 1986), Proceedings pp. 34-35.
[175] G. Schmidt, *Dissertation*, Technische Hochschule Aachen 1986.
[176] W. Baumann, H. Bischof, J. C. Frohling, *J. Lumin. 24/25* (1981) 555.
[177] M. Lemaire, A. Guy, D. Imbert, J.-P. Guette, *J. Chem. Soc. Chem. Commun. 1986*, 741.
[178] A. J. Maroulis, D. R. Arnold, *Synthesis 1979*, 819.
[179] S. L. Mattes, S. Farid, *J. Chem. Soc. Chem. Commun. 1980*, 126.
[180] A. J. Maroulis, Y. Shijemitsu, D. R. Arnold, *J. Am. Chem. Soc. 100* (1978) 535.
[181] G. Weber, R. Runsink, J. Mattay, *J. Chem. Soc. Perkin Trans. 1*, in press.
[182] A. Pross, *J. Am. Chem. Soc. 108* (1986) 3537.
[183] H. D. Roth, M. L. M. Schilling, *J. Am. Chem. Soc. 101* (1979) 1898; *ibid. 102* (1980) 4303.
[184] F. D. Lewis, J. R. Petisce, J. D. Oxman, M. J. Nepras, *J. Am. Chem. Soc. 107* (1985) 203.
[185] G. A. Lee, S. H. Israel, *J. Org. Chem. 48* (1983) 4557.
[186] T. R. Evans, R. W. Wake, M. M. Sifain, *Tetrahedron Lett. 1973*, 701.
[187] G. Jones II, W. G. Becker, S. H. Chiang, *J. Photochem. 19* (1982) 245.
[188] K. Okada, K. Hisamitsu, T. Miyashi, T. Mukai, *J. Chem. Soc. Chem. Commun. 1982*, 974.
[189] H. D. Roth, M. L. M. Schilling, G. Jones II, *J. Am. Chem. Soc. 103* (1981) 1246.
[190] H. D. Roth, M. L. M. Schilling, *J. Am. Chem. Soc. 103* (1981) 7210.
[191] G. Jones II, S. H. Chiang, W. G. Becker, A. J. Welch, *J. Phys. Chem. 86* (1982) 2805.
[192] A. Padwa, C. S. Chou, W. F. Rieker, *J. Org. Chem. 45* (1980) 4555.
[193] C. J. Abelt, H. D. Roth, *J. Am. Chem. Soc. 107* (1985) 3840.
[194] P. G. Gassman, B. A. Hay, *J. Am. Chem. Soc. 108* (1986) 4227.
[195] K. A. Brown-Wensley, S. L. Mattes, S. Farid, *J. Am. Chem. Soc. 100* (1978) 4162.
[196] D. W. Reynolds, N. L. Bauld, *Tetrahedron Lett. 26* (1985) 2539.
[197] D. F. Eaton, *Pure Appl. Chem. 56* (1984) 1191.
[198] M. Chanon, M. L. Tobe, *Angew. Chem. 94* (1982) 27; *Angew. Chem. Int. Ed. Engl. 21* (1982) 1.
[199] L. G. Vanquickenborne, A. Ceulemans, *Coord. Chem. Rev. 48* (1983) 157.
[200] M. A. Fox, *Adv. Photochem. 13* (1986) 237.
[201] G. L. Geoffroy, M. S. Wrighton: *Organometallic Photochemistry*, Academic Press, New York 1979.
[202] J. H. Fendler, *J. Phys. Chem. 89* (1985) 2730.

How Chemistry and Physics Meet in the Solid State

By Roald Hoffmann*

To make sense of the marvelous electronic properties of the solid state, chemists must learn the language of solid-state physics, of band structures. An attempt is made here to demystify that language, drawing explicit parallels to well-known concepts in theoretical chemistry. To the joint search of physicists and chemists for understanding of the bonding in extended systems, the chemist brings a great deal of intuition and some simple but powerful notions. Most important among these is the idea of a bond, and the use of frontier-orbital arguments. How to find localized bonds among all those maximally delocalized bands? Interpretative constructs, such as the density of states, the decomposition of these densities, and crystal orbital overlap populations, allow a recovery of bonds, a finding of the frontier orbitals that control structure and reactivity in extended systems as well as discrete molecules.

Introduction

There is no need to provide an *apologia pro vita sua* for solid-state chemistry. Macromolecules extended in one, two, or three dimensions, of biological or natural origin, or synthetics, fill the world around us. Metals, alloys, and composites, be they copper or bronze or ceramics, have played a pivotal, shaping role in our culture. Mineral structures form the base of the paint that colors our walls, and the glass through which we look at the outside world. Organic polymers, be they nylon or wool, clothe us. New materials—ternary inorganic superconductors, conducting organic polymers—exhibit unusual electric and magnetic properties, promise to shape the technology of the future. Solid-state chemistry is important, alive, and growing.

Given the vitality and attractiveness of the field, I take some risk in listing some minor problems that I perceive at the interfaces of solid-state chemistry with physics and with the rest of chemistry. This is done not with the intent to find fault, but constructively—the remainder of this paper tries to resolve some of these perceived difficulties.

What is most interesting about many of the new materials are their electrical and magnetic properties. Chemists have to learn to measure these properties, not only to make the new materials and determine their structures. The history of the compounds that are at the center of today's exciting developments in high-temperature superconductivity makes this point very well. And they must be able to reason intelligently about the electronic structure of the compounds they make, so that they may understand how these properties and structures may be tuned. Here's the first problem then, for such an understanding of solids perforce must involve the language of modern solid-state physics, of band theory. That language is generally not part of the education of chemists. It should be.

I suspect that physicists don't think that chemists have much to tell them about bonding in the solid state. I would disagree. Chemists have built up a great deal of understanding, in the intuitive language of simple covalent or ionic bonding, of the structure of solids. The chemist's viewpoint is often local. Chemists are especially good at seeing bonds or clusters, and our literature and memory are especially well-developed, so that we can immediately think of a hundred structures or molecules related to the compound under study. From much empirical experience, a little simple theory, chemists have gained much intuitive knowledge of the what, how, and why molecules hold together. To put it as provocatively as I can, our physicist friends know better than we how to calculate the electronic structure of a molecule or solid, but often they do not *understand* it as well as we do, with all the epistemological complexity of meaning that "understanding" something involves.

Chemists need not enter a dialogue with physicists with any inferiority feelings at all; the experience of molecular chemistry is tremendously useful in interpreting complex electronic structure. (Another reason not to feel inferior: until you synthesize that molecule, no one can study its properties. The synthetic chemist is quite in control.) This is not to say that it will not take some effort to overcome the skepticism of physicists as to the likelihood that chemists can teach them something about bonding.

Another interface is that between solid-state chemistry, often inorganic, and molecular chemistry, both organic and inorganic. With one exception, the theoretical concepts that have served solid-state chemists well have not been "molecular." At the risk of oversimplification, the most important of these concepts have been the idea that one has ions (electrostatic forces, Madelung energies) and that these ions have a size (ionic radii, packing considerations). The success of these simple notions has led solid-state chemists to use these concepts even in cases where there is substantial covalency. What can be wrong with an idea that works, that explains structure and properties? What is wrong, or can be wrong, is that application of such concepts may draw that field, that group of scientists, away from the heart of chemistry. At the heart of chemistry, let there be no doubt, is the molecule! My personal feeling is that if there is a choice among explanations in solid-state chemistry, one must choose the explanation which permits a connection between the structure at hand

[*] Prof. Roald Hoffmann
Department of Chemistry and Materials Science Center
Cornell University, Baker Laboratory
Ithaca, NY 14853-1301 (USA)

 © VCH Verlagsgesellschaft mbH, D-6940 Weinheim, 1987 0570-0833/87/0909-0846 $ 02.50/0

and some discrete molecule, organic or inorganic. Making connections has inherent scientific value. It also makes "political" sense. Again, if I might express myself provocatively, I would say that many solid-state chemists have isolated themselves (no wonder that their organic or even inorganic colleagues aren't interested in what they do) by choosing not to see bonds in their materials.

Which, or course, brings me to the exception: the marvelous and useful Zintl concept. The simple notion, introduced by *Zintl* and popularized by *Klemm*, *Busmann*, *Herbert Schäfer*, and others,[1] is that in some compounds A_xB_y, where A is very electropositive relative to a main-group element B, one could just think, that's all, think that the A atoms transfer their electrons to the B atoms, which then use them to form bonds. This very simple idea, in my opinion, is the single most important theoretical concept (and how not very theoretical it is!) in solid-state chemistry of this century. And it is so important, not just because it explains so much chemistry, but especially because it builds a bridge between solid-state chemistry and organic or main-group chemistry.

The three problems I have identified, and let me repeat that I think they are relatively minor ones for a lively field, are (1) some lack of knowledge (therefore fear) of solid-state physics language on the part of chemists, (2) insufficient appreciation of the chemists' intuitive feeling for bonding on the part of physicists, and (3) not enough reaching out for connections with molecular chemistry on the part of solid-state chemists. The characterization of these as problems represents a generalization on my part, with the associated danger that any generalization carries. Typologies and generalizations often point not so much to reality as to the weakness of the mind that proposes them.

What can a theoretical chemist contribute to the amelioration of these problems, if they indeed are real ones? A theoretical *chemist* can, in fact, do very much. With his or her firm knowledge of solid-state physics (which he should, in principle, have, but often doesn't) *and* his feeling for bonding and the marvelous bounty of structures that he knows his chemical colleagues have made, the theoretical chemist should be in a wonderful position to serve as a bridge between chemistry and physics. We should certainly be able to help with point (1) above, showing our colleagues that band theory is easy. Points (2) and (3) are more difficult. We need to push our experimental colleagues to see bonds, clusters, molecular patterns in new species. But, they can see these patterns, without our help, better than we do. And to convince physicists that chemists are good for anything except making molecules, that chemists in fact understand what the electrons in molecules and solids are doing—that will take some doing.

In fact, the effort has been under way from the theoretical side for some time. I would like to mention here especially the contributions of *Jeremy Burdett*,[2,3] who is responsible for the first new ideas on what determines solid-state structures since the pioneering contribution of *Pauling*, and of *Myung-Hwan Whangbo*,[4,5] whose analysis of the bonding in low-dimensional materials such as the niobium selenides, tetrathiafulvalene-type organic conductors, and molybdenum bronzes has contributed much to our knowledge of the balance of delocalization and electron repulsion in conducting solids. On the side of physics, let me mention the work of several individuals who have shown an unusual sensitivity to chemistry and chemical ways of thinking: *Jacques Friedel*, *Walter A. Harrison*, *Volker Heine*, *James C. Phillips*, *Ole Krogh Andersen*, and *David W. Bullett*.

In this paper, I would like to work mainly on point (1) mentioned above, the teaching, to chemists, of some of the language of band theory.[6-8] As many connections as possible to our traditional ways of thinking about chemical bonding will be made—it is this aspect which should be of interest to any physicists who might read this article. The approach will be simple, indeed, oversimplified in part. Where detailed computational results are displayed, they will be of the extended Hückel type, or of its solid-state analogue, the tight-binding method with overlap.

Orbitals and Bands in One Dimension

It's usually easier to work with small, simple things, and one-dimensional infinite systems are particularly easy to visualize.[2-5] Much of the physics of three-dimensional solids is there in one dimension. Let's begin with a chain of equally spaced H atoms, **1**, or the isomorphic π-system of a non-bond-alternating, delocalized polyene **2**, stretched out for the moment. And we will progress to a stack of Pt^{II} square-planar complexes, **3**, $[Pt(CN)_4]^{2\ominus}$ or a model $[PtH_4]^{2\ominus}$.

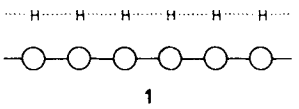

1

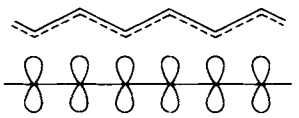

2

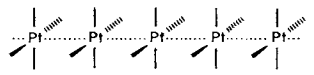

3

A digression here: every chemist would have an intuitive feeling for what that model chain of hydrogen atoms, **1**, would do if we were to release it from the prison of its theoretical construction. At ambient pressure, it would form a chain of hydrogen molecules, **4**. This simple bond-

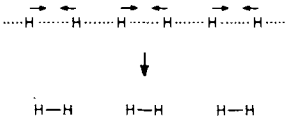

4

forming process could be analyzed by the physicist (we will do it soon) by calculating a band for the equally

spaced polymer, then seeing that it's subject to an instability, called a Peierls distortion. Other words around that characterization would be strong electron-phonon coupling, a pairing distortion, or a $2k_F$ instability. And the physicist would come to the conclusion that the initially equally spaced H polymer would form a chain of hydrogen molecules. I mention this thought process here to make the point, which I will do again and again, that the chemist's intuition is really excellent. But we must bring the languages of our sister sciences into correspondence. Incidentally, whether distortion **4** will take place at 2 Mbar is not obvious, an open question.

Let's return to our chain of equally spaced H atoms. It turns out to be computationally convenient to think of that chain as an imperceptibly bent segment of a large ring (this is called applying cyclic boundary conditions). The orbitals of medium-sized rings on the way to that very large one are quite well known. They are shown in **5**.

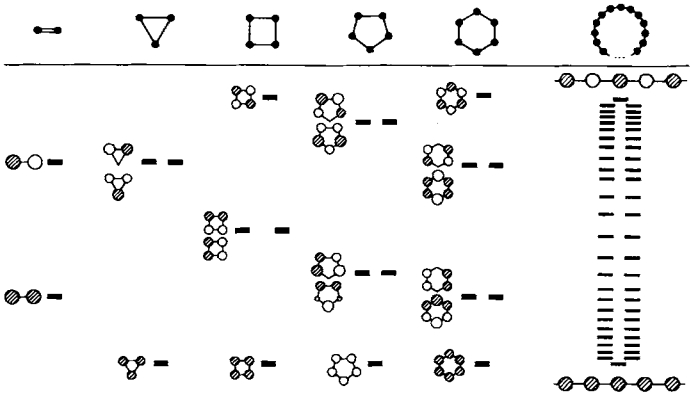

5

For a hydrogen molecule (or ethylene) there is a bonding $\sigma_g(\pi)$ below an antibonding $\sigma_u^*(\pi^*)$. For cyclic H_3 or cyclopropenyl we have one orbital below two degenerate ones; for cyclobutadiene the familiar one below two below one, and so on. Except for the lowest (and occasionally the highest) level, the orbitals come in degenerate pairs. The number of nodes increases as one rises in energy. We'd expect the same for an infinite polymer—the lowest level nodeless, the highest with the maximum number of nodes. In between, the levels should come in pairs, with a growing number of nodes. The chemist's representation of that band for the polymer is given at right in **5**.

Bloch Functions, k, Band Structures

There is a better way to write out all these orbitals, making use of the translational symmetry. If we have a lattice whose points are labeled by an index n = 0, 1, 2, 3, 4, etc., as shown in **6**, and if on each lattice point there is a basis function (a H 1s orbital), χ_0, χ_1, χ_2, etc., then the appropriate symmetry-adapted linear combinations ψ (remember translation is just as good a symmetry operation as any other one we know) are given in **6**. Here a is the lattice spacing (the unit cell being in one dimension) and k is an index which labels which irreducible representation of the translation group ψ transforms as. We will see in a moment that k is much more, but for now, k is just an index for an irreducible representation, just like a, e_1, and e_2 in C_5 are labels.

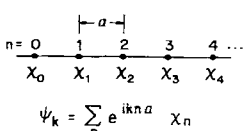

6

The process of symmetry adaptation is called in the solid-state physics trade "forming Bloch functions."[3,5,6,8] To reassure a chemist that one is getting what one expects from **5**, let's see what combinations are generated for two specific values of k, k = 0 and k = π/a (see **7**). Referring

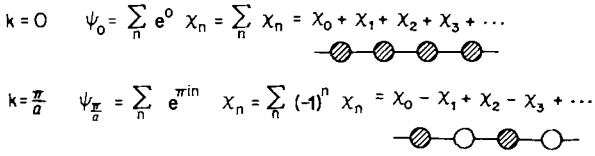

7

back to **5**, we see that the wave function corresponding to k = 0 is the most bonding one, the one for k = π/a the top of the band. For other values of k we get a neat description of the other levels in the band. So k counts nodes as well. The larger the absolute value of k, the more nodes one has in the wave function. But one has to be careful—there is a range of k and if one goes outside of it, one doesn't get a new wave function, but repeats an old one. The unique values of k are in the interval $-\pi/a \leq k < \pi/a$ or $|k| \leq \pi/a$. This is called the first Brillouin zone, the range of unique k.

How many values of k are there? As many as the number of translations in the crystal, or, alternatively, as many as there are microscopic unit cells in the macroscopic crystal. So let us say Avogadro's number (N_A), give or take a few. There is an energy level for each value of k (actually a degenerate pair of levels for each pair of positive and negative k values). There is an easily proved theorem that $E(k) = E(-k)$. Most representations of $E(k)$ do not give the redundant $E(-k)$, but plot $E(|k|)$ and label it as $E(k)$). Also, the allowed values of k are equally spaced in the space of k, which is called reciprocal or momentum space. The relationship between $k = 1/\lambda$ and momentum derives from the de Broglie relationship $\lambda = h/p$. Remarkably, k is not only a symmetry label and a node counter, but it is also a wave vector, and so measures momentum.

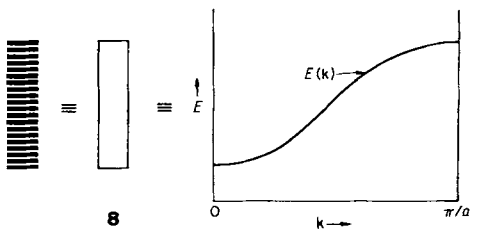

8

So what a chemist draws as a band in **5**, repeated at left in **8** (and the chemist tires and draws ≈20 lines or just a

block instead of N_A lines), the physicist will alternatively draw as an $E(k)$ vs. k diagram at right in **8**. Recall that k is quantized, and there is a finite but large number of levels in the diagram at right. The reason it looks continuous is that this is a fine "dot matrix" printer—there are N_A points jammed in there, and so it's no wonder we see a line.

Graphs of $E(k)$ vs. k are called band structures. You can be sure that they can be much more complicated than this simple one, but no matter how complicated, they can be understood.

Band Width

One very important feature of a band is its *dispersion*, or *band width*, the difference in energy between the highest and lowest levels in the band. What determines the width of bands? The same thing that determines the splitting of levels in a "dimer," ethylene or H_2, namely, the overlap between the interacting orbitals (in the polymer the overlap is that between neighboring unit cells). The greater the overlap between neighbors, the greater the band width. Figure 1 illustrates this in detail for a chain of H atoms

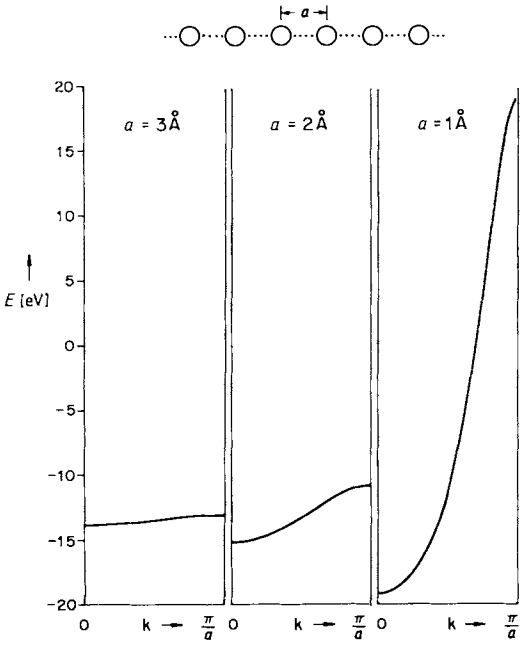

Fig. 1. The band structure of a chain of H atoms spaced 3, 2, and 1 Å apart. The energy of an isolated H atom is −13.6 eV.

spaced 3, 2, and 1 Å apart. That the bands extend unsymmetrically around their "origin," the energy of a free H atom at −13.6 eV, is a consequence of the inclusion of overlap in the calculations. For two levels, a dimer, the energies are given by Equation (a). The bonding E_+ combi-

$$E_{\pm} = \frac{H_{AA} \pm H_{AB}}{1 \pm S_{AB}} \qquad (a)$$

nation is less stabilized than the antibonding one E_- is destabilized. There are nontrivial consequences in chemistry, for this is the source of four-electron repulsions and steric effects in one-electron theories.[8] A similar effect of overlap is responsible for the bands "spreading up" in Figure 1.

See How They Run

Another interesting feature of bands is how they "run." The lovely mathematical algorithm **6** applies in general; it does not say anything about the energy of the orbitals at the center of the zone (k = 0) relative to those at the edge (k = π/a). For a chain of H atoms it is clear that $E(k=0) < E(k=\pi/a)$. But consider a chain of p functions, **9**. The same combinations are given to us by the transla-

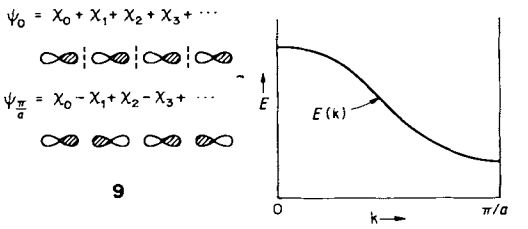

9

tional symmetry, but now it is clearly k = 0 which is high energy, the most antibonding way to put together a chain of p orbitals.

The band of s functions for the hydrogen chain "runs up," the band of p orbitals "runs down" (from zone center to zone edge). In general, it is the topology of orbital interactions which determines which way bands run.

Let me mention here an organic analogue to make one feel comfortable with this idea. Consider the through-space interaction of the three π bonds in **10** and **11**. The

10 **11**

threefold symmetry of each molecule says that there must be an a and an e combination of the π bonds. And the theory of group representations gives us the symmetry-adapted linear combinations: for a, $\chi_1+\chi_2+\chi_3$; for e (one choice of an infinity), $\chi_1-2\chi_2+\chi_3$ and $\chi_1-\chi_3$, where χ_1 is the π orbital of double bond 1, etc. But there is nothing in the group theory that tells us whether a is lower than e in energy. For that, one needs chemistry or physics. It is easy to conclude from an evaluation of the orbital topologies that a is below e in **10**, but the reverse is true in **11**. To summarize: *band width is set by inter-unit-cell overlap, and the way the bands run is determined by the topology of that overlap.*

An Eclipsed Stack of Pt^{II} Square-Planar Complexes

Let us test the knowledge we have acquired on an example a little more complicated than a chain of hydrogen atoms. This is an eclipsed stack of square-planar d^8 PtL_4 complexes, **12**. The normal tetracyanoplatinates (e.g.,

$K_2[Pt(CN)_4]$) indeed show such stacking in the solid state, at the relatively uninteresting Pt–Pt separation of ≈ 3.3 Å.

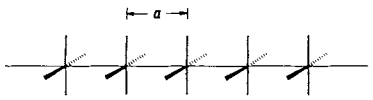

12

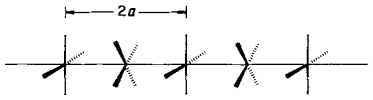

13

More exciting are the partially oxidized materials, such as $K_2[Pt(CN)_4Cl_{0.3}]$ and $K_2[Pt(CN)_4(FHF)_{0.25}]$. These are also stacked, but staggered, **13**, with a much shorter Pt–Pt contact of 2.7–3.0 Å. The Pt–Pt distance had been shown to be inversely related to the degree of oxidation of Pt.[9]

The real test of understanding is prediction. So, let's try to predict the approximate band structure of **12** and **13** without a calculation, just using the general principles we have at hand. Let's not worry about the nature of the ligand L—it is usually $CN^{\ominus}$, but since it is only the square-planar feature which is likely to be essential, let's imagine a theoretician's generic ligand, $H^{\ominus}$. And let's begin with **12**, because the unit cell in it is the chemical PtL_4 unit, whereas in **13** it is doubled, $[(PtL_4)_2]$.

One always begins with the monomer. What are its frontier levels? The classical crystal field or molecular orbital

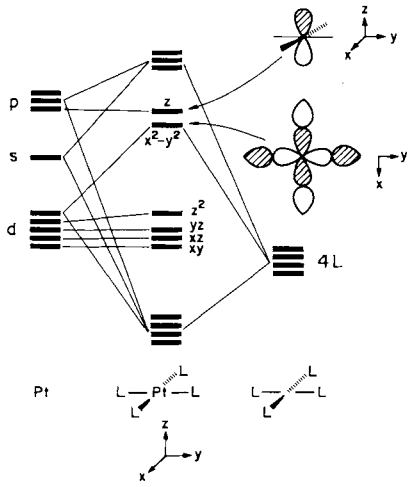

Fig. 2. Molecular-orbital derivation of the frontier orbitals of a square-planar PtL_4 complex.

picture of a square-planar complex (Fig. 2) leads to a four-below-one splitting of the d block.[8] For 16 electrons we have d_{z^2}, d_{xz}, d_{yz}, and d_{xy} occupied and $d_{x^2-y^2}$ empty. Competing with the ligand-field-destabilized $d_{x^2-y^2}$ orbital for being the lowest unoccupied molecular orbital (LUMO) of the molecule is the metal p_z. These two orbitals can be manipulated in understandable ways: π-acceptors push p_z down, π-donors push it up. Better σ-donors push $d_{x^2-y^2}$ up.

We form the polymer. Each MO of the monomer generates a band. There may (will) be some further symmetry-conditioned mixing between orbitals of the same symmetry in the polymer (e.g., s and p_z and d_{z^2} are of different symmetry in the monomer, but certain of their polymer MOs are of the same symmetry). But a good start is made by ignoring that secondary mixing, and just developing a band from each monomer level independently.

First, a chemist's judgment of the band widths that will develop (see **14**): the bands that will arise from d_{z^2} and p_z

14

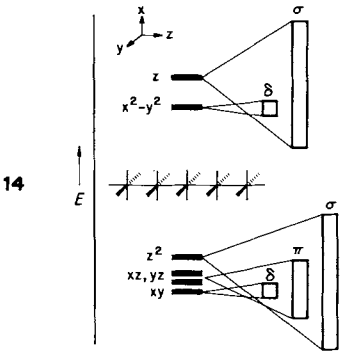

will be wide, those from d_{xz} and d_{yz} of medium width, those from $d_{x^2-y^2}$ and d_{xy} narrow. This characterization follows from the realization that the first set of interactions (p_z, d_{z^2}) is σ type, thus has a large overlap between unit cells. The d_{xz}, d_{yz} set has a medium π overlap, and the d_{xy} and $d_{x^2-y^2}$ orbitals (the latter of course has a ligand admixture, but that doesn't change its symmetry) are δ.

It is also easy to see how the bands run. Let's write out the Bloch functions at the zone center ($k=0$) and zone edge ($k=\pi/a$). Only one of the π and δ functions is represented in **15**. The moment one writes these down, one sees

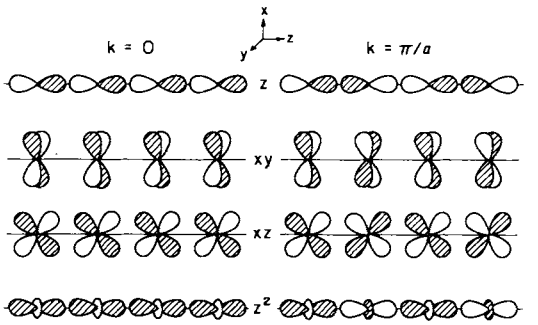

15

that the d_{z^2} and d_{xy} bands will run "up" from the zone center (the $k=0$ combination is the most bonding) while the d_z and d_{xy} bands will run "down" (the $k=0$ combination is the most antibonding).

The predicted band structure, merging considerations of band width and orbital topology, is that of **16**. To make a real estimate of band width, one would need an actual calculation of the various overlaps, and these in turn would depend on the Pt–Pt separation.

The actual band structure, as it emerges from an extended Hückel calculation at Pt–Pt = 3.0 Å, is shown in

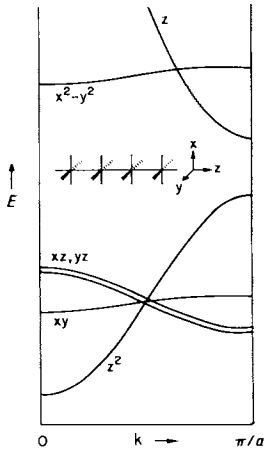

16

Figure 3. It matches our expectations very precisely. There are, of course, bands below and above the frontier orbitals discussed—these are Pt–H σ and σ* orbitals.

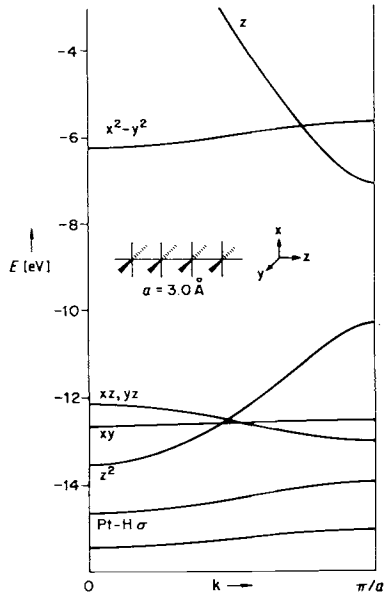

Fig. 3. Computed band structure of an eclipsed $[PtH_4]^{2\ominus}$ stack, spaced at 3 Å. The orbital marked d_{xz}, d_{yz} is doubly degenerate.

To make a connection with molecular chemistry: the construction of **16**, an approximate band structure for a cyanoplatinate stack, involves no new physics, no new chemistry, no new mathematics beyond what every chemist already knows for one of the most beautiful ideas of modern chemistry—*Cotton*'s construct of the metal–metal quadruple bond.[10] If we are asked to explain quadruple bonding, for instance in $[Re_2Cl_8]^{2\ominus}$, what we do is to draw **17**. We form bonding and antibonding combinations from the $d_{z^2}(\sigma)$, $d_{xz},d_{yz}(\pi)$, and $d_{x^2-y^2}(\delta)$ frontier orbitals of each $ReCl_4^{\ominus}$ fragment. And we split σ from σ* by more than π from π*, which in turn is split more than δ and δ*. What goes on in the infinite solid is precisely the same thing. True, there are a few more levels, but the translational symmetry helps us out with that. It's really easy to

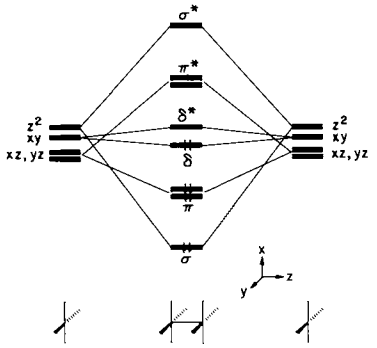

17

write down the symmetry-adapted linear combinations, the Bloch functions.

The Fermi Level

It's important to know how many electrons one has in one's molecule. Fe^{II} has a different chemistry from Fe^{III}, and $CR_3^{\oplus}$ carbocations are different from CR_3 radicals and $CR_3^{\ominus}$ anions. In the case of $[Re_2Cl_8]^{2\ominus}$, the archetypical quadruple bond, we have formally Re^{III}, d^4, i.e., a total of eight electrons to put into the frontier orbitals of the dimer level scheme, **17**. They fill the σ, two π, and the δ level for the explicit quadruple bond. What about the $[\{PtH_4\}^{2\ominus}]_\infty$ polymer **12**? Each monomer is d^8. If there are N_A unit cells, there will be N_A levels in each band. And each level has a place for two electrons. So the first four bands are filled, the xy, xz, yz, and z^2 bands. The Fermi level, the highest occupied molecular orbital (HOMO), is at the very top of the z^2 band. (Strictly speaking, there is another thermodynamic definition of the Fermi level, appropriate both to metals and semiconductors,[6] but here we will use the simple equivalence of the Fermi level with the HOMO.)

Is there a bond between the platinums in this $[\{PtH_4\}^{2\ominus}]_\infty$ polymer? We haven't introduced, yet, a formal description of the bonding properties of an orbital or a band, but a glance at **15** and **16** will show that the bottom of *each* band, be it made up of z^2, xz, yz, or xy, is bonding, and the top antibonding. Filling a band completely, just like filling bonding and antibonding orbitals in a dimer (think of He_2, think of the sequence N_2, O_2, F_2, Ne_2) provides no net bonding. In fact, it gives net antibonding. So why does the unoxidized PtL_4 chain stack? It could be van der Waals attractions, not in our quantum chemistry at this primitive level. I think there is also a contribution of orbital interaction, i.e., real bonding, involving the mixing of the z^2 and z bands.[11] We will return to this soon.

The band structure gives a ready explanation for why the Pt–Pt separation decreases on oxidation. A typical degree of oxidation is 0.3 electron per Pt.[9] These electrons must come from the top of the z^2 band. The degree of oxidation specifies that 15% of that band is empty. The states vacated are not innocent of bonding. They are strongly Pt–Pt σ antibonding. So it's no wonder that removing these electrons results in the formation of a partial Pt–Pt bond.

The oxidized material also has its Fermi level in a band; i.e., there is a zero band gap between filled and empty levels. The unoxidized cyanoplatinates have a substantial

gap—they are semiconductors or insulators. The oxidized materials are good low-dimensional conductors, which is a substantial part of what makes them interesting to physicists.[9, 11]

In general, conductivity is not a simple phenomenon to explain, and there may be several mechanisms impeding the motion of electrons in a material.[6] A prerequisite for having a good electronic conductor is to have the Fermi level cut one or more bands (soon we will use the language of density of states to say this more precisely). One has to beware, however, (1) of distortions which open up gaps at the Fermi level and (2) of very narrow bands cut by the Fermi level, for these will lead to localized states and not to good conductivity.[4, 6]

Density of States

We have already remarked that in the solid, a very large molecule, one has to deal with a very large number of levels or states. If there are n atomic orbitals (basis functions) in the unit cell generating n molecular orbitals, and if in our macroscopic crystal there are N unit cells (N is a number that approaches N_A), then we will have N·n crystal levels. Many of these are occupied and, roughly speaking, they are jammed into the same energy interval in which we find the molecular or unit cell levels. In a discrete molecule we are able to single out one orbital or a small subgroup of orbitals (HOMO, LUMO) as being the frontier, or valence, orbitals of the molecule, responsible for its geometry, reactivity, etc. There is no way in the world that a single level among the myriad N·n orbitals of the crystal will have the power to direct a geometry or reactivity.

There is, however, a way to retrieve a frontier orbital language in the solid state. We cannot think about a single level, but perhaps we can talk about bunches of levels. There are many ways to group levels, but one pretty obvious one is to look at all the levels in a given energy interval. The density of states (DOS) is defined by (b). For a

$$\mathrm{DOS}(E)\,\mathrm{d}E = \text{number of levels between } E \text{ and } E+\mathrm{d}E \qquad \text{(b)}$$

simple band of a chain of hydrogen atoms, the DOS curve takes on the shape of **18**. Note that because the levels are equally spaced along the k axis, and because the E(k)

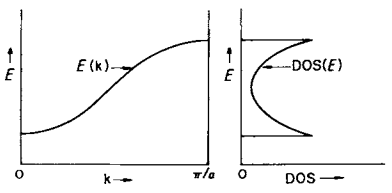

18

curve, the band structure, has a simple cosine curve shape, there are more states in a given energy interval at the top and bottom of this band. In general, DOS(E) is proportional to the inverse of the slope of E(k) vs. k, or to put it into plain English, the flatter the band, the greater the density of states at that energy.

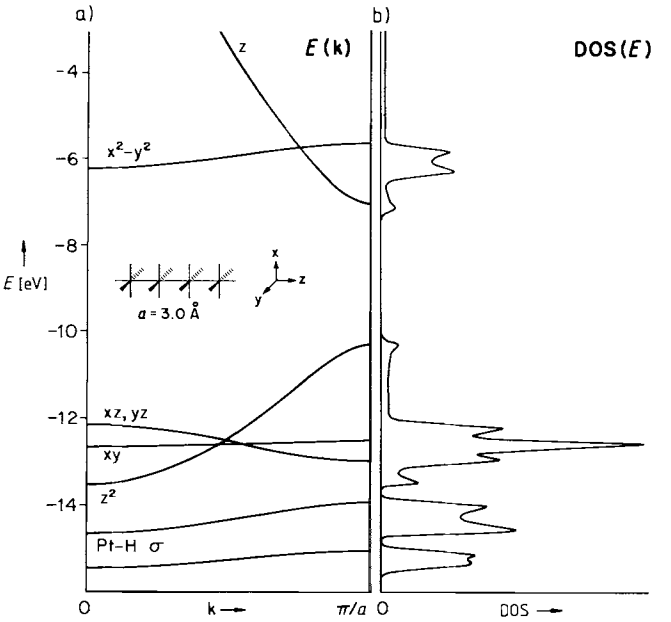

Fig. 4. a) Band structure and b) density of states (DOS) for an eclipsed $[PtH_4]^{2\ominus}$ stack. The DOS curves are broadened so that the two-peaked shape of the xy peak in the DOS is not resolved.

The shapes of DOS curves are predictable from the band structures. Figure 4 shows the DOS curve for the $[PtH_4]^{2\ominus}$ chain. It could have been sketched from the band structure at left. In general, the detailed construction of these is a job best left for computers. The density-of-states curve counts levels. The integral of DOS up to the Fermi level is the total number of occupied MOs. Multiplied by two, it's the total number of electrons. So, the DOS curves plot the distribution of electrons in energy.

One important aspect of the DOS curves is that they represent a return from reciprocal space, the space of k, to real space. The DOS is an average over the Brillouin zone, over all k that might give molecular orbitals at the specified energy. The advantage here is largely psychological. If I may be permitted to generalize, I think chemists (with the exception of crystallographers) by and large feel themselves uncomfortable in reciprocal space. They'd rather return to, and think in, real space.

There is another aspect of the return to real space that is significant: *chemists can sketch the DOS of any material, approximately, intuitively*. All that's involved is a knowledge of the atoms, their approximate ionization potentials and electronegativities, and some judgment as to the extent of inter-unit-cell overlap (usually apparent from the structure).

Let's take the $[\{PtH_4\}^{2\ominus}]_\infty$ polymer as an example. The monomer units are clearly intact in the polymer. At intermediate monomer–monomer separations (e.g., 3 Å) the major inter-unit-cell overlap is between d_{z^2} and p_z orbitals. Next is the d_{xz}, d_{yz} π-type overlap; all other interactions are likely to be small. **19** is a sketch of what we would expect. In **19**, I haven't been careful in drawing the integrated areas commensurate with the actual total number of states, nor have I put in the two-peaked nature of the DOS each level generates—all I want to do is to convey the rough spread of each band. Compare **19** to Figure 4.

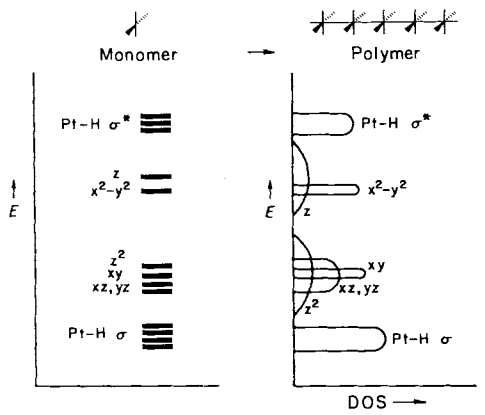

19

This was easy, because the polymer was built up of molecular monomer units. Let's try something inherently three-dimensional. The rutile structure is a relatively common type. As **20** shows, the rutile structure has a nice oc-

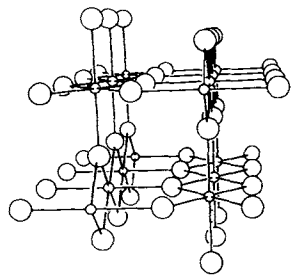

20

tahedral environment of each metal center, each ligand (e.g., O) bound to three metals. There are infinite chains of edge-sharing MO_6 octahedra running in one direction in the crystal, but the metal–metal separation is always relatively long.[12] There are no monomer units here, just an infinite assembly. Yet there are quite identifiable octahedral sites. At each, the metal d block must split into t_{2g} and e_g combinations, the classic three-below-two crystal field splitting. The only other thing we need is to realize that O has quite distinct 2s and 2p levels, and that there is no effective O–O or Ti–Ti interaction in this crystal. We expect something like **21**.

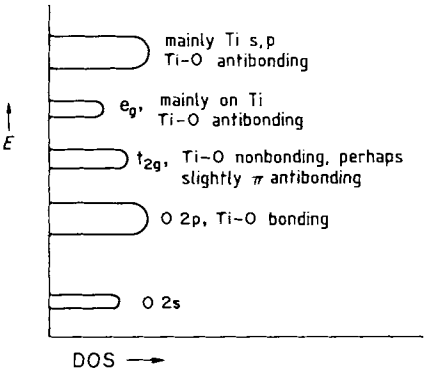

21

Note that the writing down of the approximate DOS curve is done *bypassing* the band structure calculation *per se*. Not that that band structure is very complicated. But it is three-dimensional, and our exercises so far have been easy, in one dimension. So the computed band structure (Fig. 5) will seem complex. The number of bands is doubled (i.e., twelve O 2p, six t_{2g} bands), simply because the unit cell contains two formula units, $[(TiO_2)_2]$. There is not one reciprocal space variable, but several lines ($\Gamma \rightarrow X$, $X \rightarrow M$, etc.) which refer to directions in the three-dimensional Brillouin zone. These complications of moving from one dimension to three we will soon approach. If we glance at the DOS, we see that it does resemble the expectations of **21**. There are well-separated O 2s, O 2p, Ti t_{2g}, and e_g bands.[12]

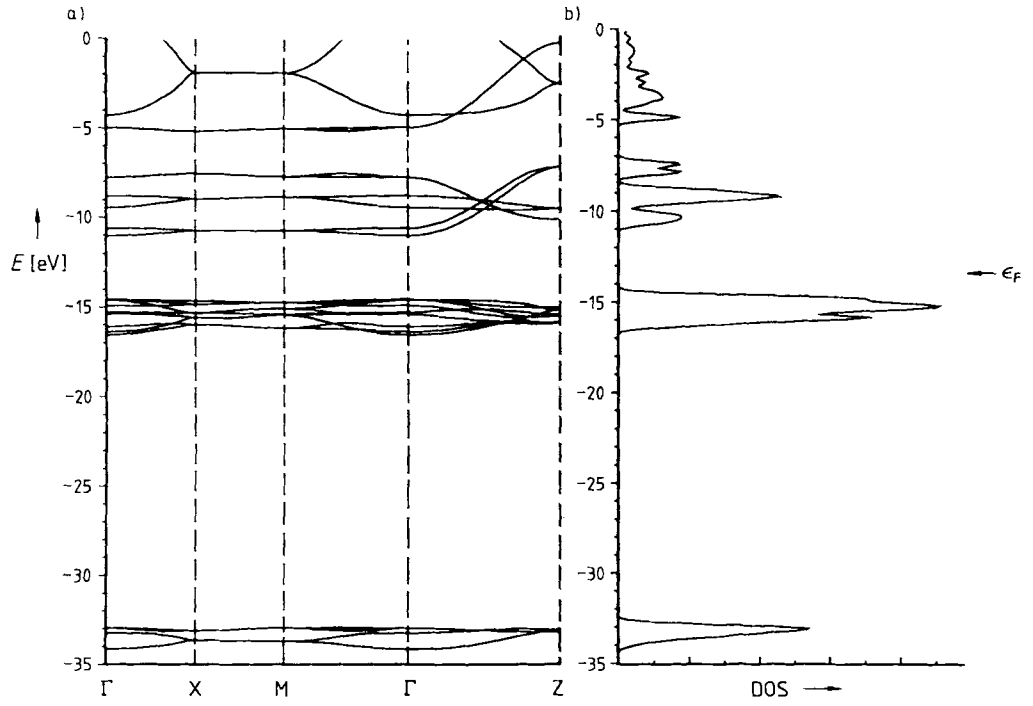

Fig. 5. a) Band structure and b) density of states for rutile, TiO_2. The two Ti–O distances are 2.04 Å (2×), 2.07 Å (4×) in the assumed structure.

Would you like to try something a little (but not much) more challenging? Attempt to construct the DOS of the new superconductors based on the La_2CuO_4 and $YBa_2Cu_3O_7$ structures. And when you have done so, and found that these should be conductors, reflect on how that doesn't allow you yet, did not allow anyone, to predict that compounds slightly off these stoichiometries would be remarkable superconductors.

The chemists' ability to write down approximate density-of-states curves should not be slighted. It gives us tremendous power, and qualitative understanding, an obvious connection to local, chemical viewpoints such as the crystal or ligand field model. I want to mention here one solid-state chemist, *John B. Goodenough*, who has shown over the years, and especially in his prescient book,[13] just how good the chemist's approximate construction of band structures can be.

In **19** and **21**, the qualitative DOS diagrams for $[PtH_4]^{2\ominus}$ and TiO_2, there is, however, much more than a guess at a DOS. There is a chemical characterization of the localization in real space of the states (are they on Pt, on H; on Ti, on O), and a specification of their bonding properties (Pt–H bonding, antibonding, nonbonding, etc.). The chemist sees right away, or asks—where in space are the electrons? Where are the bonds? There must be a way that these inherently chemical, local questions can be answered, even if the crystal molecular orbitals, the Bloch functions, delocalize the electrons over the entire crystal.

Where Are the Electrons?

One of the interesting tensions in chemistry is between the desire to assign electrons to specific centers, deriving from an atomic, electrostatic view of atoms in a molecule, and the knowledge that electrons are not as localized as we would like them to be. Let's take the two-center molecular orbital of Equation (c), where χ_1 is on center 1 and χ_2 on center 2, and let's assume centers 1 and 2 are not identical, and that χ_1 and χ_2 are normalized, but not orthogonal.

$$\psi = c_1\chi_1 + c_2\chi_2 \qquad \text{(c)}$$

The distribution of an electron in this MO is given by ψ^2. ψ should be normalized, so that Equation (d) is valid,

$$1 = \int \psi^2 \, d\tau = \int (c_1\chi_1 + c_2\chi_2)^2 \, d\tau = c_1^2 + c_2^2 + 2c_1c_2S_{12} \qquad \text{(d)}$$

where S_{12} is the overlap integral between χ_1 and χ_2. This is how one electron in ψ is distributed. Now it's obvious that c_1^2 of it is to be assigned to center 1, c_2^2 to center 2. $2c_1c_2S_{12}$ is clearly a quantity that is associated with interaction. It's called the overlap population, and we will soon relate it to the bond order. But what are we to do if we persist in wanting to divide up the electron density between centers 1 and 2? We want all the parts to add up to 1 and $c_1^2 + c_2^2$ won't do. We must assign, somehow, the "overlap density" $2c_1c_2S_{12}$ to the two centers. *Mulliken* suggested (and that's why we call this a Mulliken population analysis[14]) a democratic solution, splitting $2c_1c_2S_{12}$ equally between centers 1 and 2. Thus center 1 is assigned $c_1^2 + c_1c_2S_{12}$, center 2 $c_2^2 + c_1c_2S_{12}$, and the sum is guaranteed to add up to 1. It should be realized that the Mulliken prescription for partitioning the overlap density, while uniquely defined, is quite arbitrary.

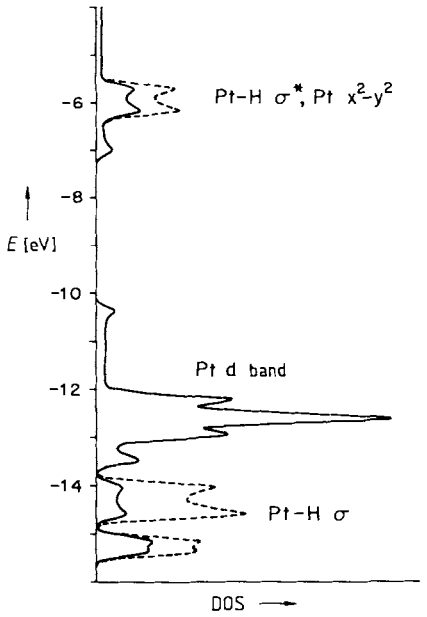

Fig. 6. The solid line is the Pt contribution to the total DOS (dashed line) of an eclipsed $[PtH_4]^{2\ominus}$ stack. What is not on Pt is on the four H's.

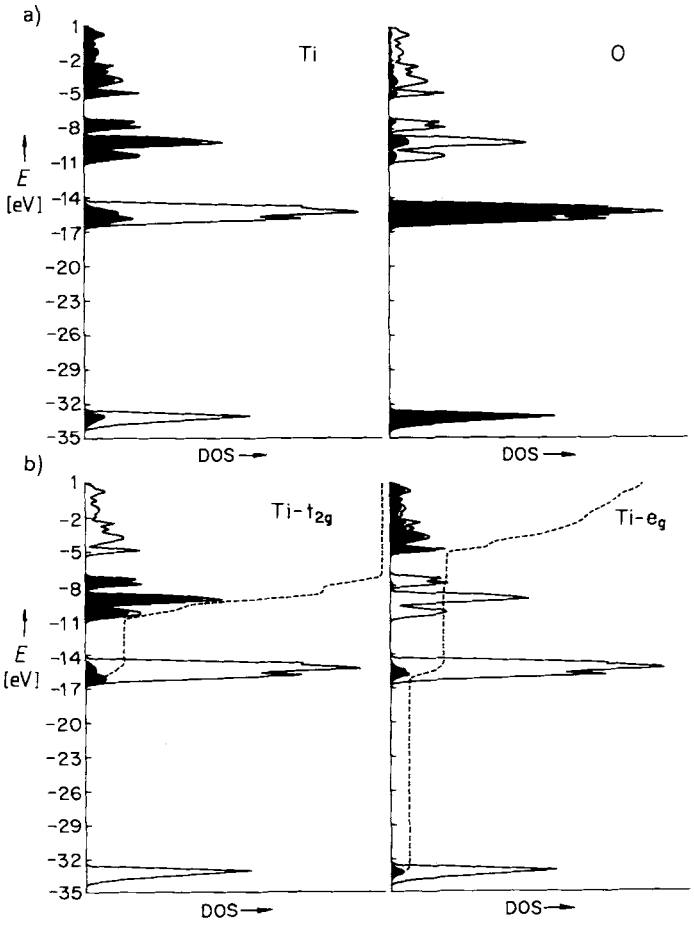

Fig. 7. a) Contributions of Ti and O (dark area) to the total DOS (solid line) of rutile, TiO_2. b) The t_{2g} and e_g Ti contributions (dark area); their integration (on a scale of 0 to 100%) is given by the dashed line.

What a computer does is just a little more involved, for it sums these contributions for each atomic orbital on a given center (there are several), over each occupied MO (there may be many). And in the crystal, it does it for several k points in the Brillouin zone, and then returns to real space by averaging over these.[15] The net result is a partitioning of the total DOS into contributions to it by either atoms or orbitals. In the solid-state trade these are often called "projections of the DOS" or "local DOS." Whatever they're called, they divide up the DOS among the atoms. The integral of these projections up to the Fermi level then gives the total electron density on a given atom or in a specified orbital. Then, by reference to some standard density, a charge can be assigned.

Figures 6 and 7 give the partitioning of the electron density between Pt and H in the $[PtH_4]^{2\ominus}$ stack, and between Ti and O in rutile. Everything is as **19** and **21** predict, as the chemist knows it should be—the lower orbitals are localized in the more electronegative ligands (H or O), the higher ones on the metal.

Do we want more specific information? In TiO_2 we might want to see the crystal field argument upheld. So we ask for the contributions of the three orbitals that make up the t_{2g} (d_{xz}, d_{yz}, d_{xy} in a local coordinate system) and the two orbitals that make up the e_g (d_{z^2}, $d_{x^2-y^2}$) set. This is also shown in Figure 7. Note the very clear separation of the t_{2g} and e_g orbitals. The e_g set has a small amount of density in the O 2s and 2p bands (σ bonding) and the t_{2g} set in the O 2p band (π bonding). Each metal orbital type (t_{2g} or e_g) is spread out into a band, but the memory of the near octahedral local crystal field is very clear.

In $[PtH_4]^{2\ominus}$ we could ask the computer to give us the d_{z^2} contribution to the DOS, or the p_z part (Fig. 8). If we look at the z component of the DOS in $[PtH_4]^{2\ominus}$, we see a small contribution in the top of the z^2 band. This is easiest picked up by the integral in Figure 8b. The dotted line is a simple integration, like an NMR integration. It counts, on a scale of 0 to 100% at the top, what percent of the specified orbital is filled at a given energy. At the Fermi level in unoxidized $[PtH_4]^{2\ominus}$, about 4% of the z states are filled.

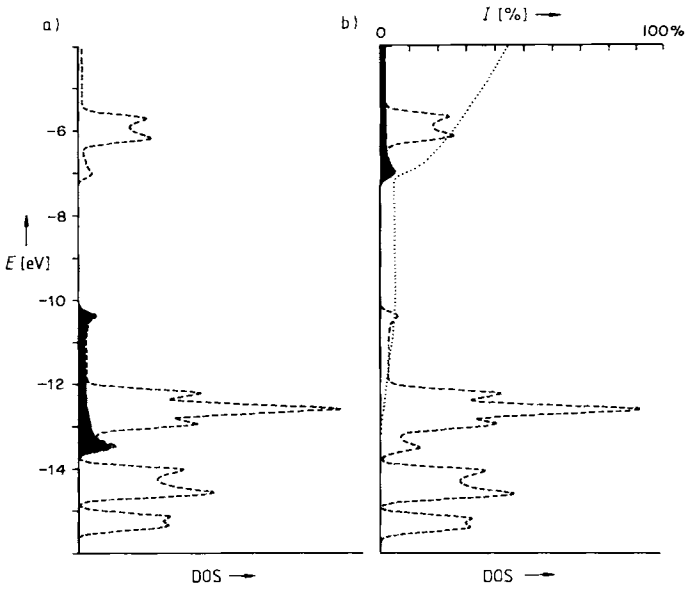

Fig. 8. a) d_{z^2} and b) p_z contributions (dark area) to the total DOS (dashed line) of an eclipsed $[PtH_4]^{2\ominus}$ stack. The dotted line is an integration I of the p_z orbital contribution.

How does this come about? There are two ways to talk about this. Locally, the donor function of one monomer (d_{z^2}) can interact with the acceptor function (p_z) of its neighbor (**22**). The overlap is good, but the energy match is

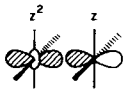

22

poor.[8] So the interaction is small, but it's there. Alternatively, one could think about interaction of the Bloch functions, or symmetry-adapted z and z^2 crystal orbitals. At $k=0$ and $k=\pi/a$, they don't mix. But at every interior point in the Brillouin zone, the symmetry group of ψ is isomorphic to C_{4v},[15] and both z and z^2-Bloch functions transform as a_1. So they mix. Some small bonding is provided by this mixing. But it is really small. When the stack is oxidized, the loss of this bonding (which would lengthen the Pt-Pt contact) is overcome by the loss of Pt-Pt antibonding that is a consequence of the vacated orbitals being at the top of the z^2 band.

We have seen that we can locate the electrons in the crystal. But ...

Where Are the Bonds?

Local bonding considerations (see **19**, **21**) trivially lead us to assign bonding characteristics to certain orbitals and, therefore, bands. There must be a way to find these bonds in the bands that a fully delocalized calculation gives.

It's possible to extend the idea of an overlap population to a crystal. Recall that in the integration of ψ^2 for a two-center orbital, $2c_1c_2S_{12}$ was a characteristic of bonding. If the overlap integral is taken as positive (and it can always be arranged so), then this quantity scales as we expect of a bond order: it is positive (bonding) if c_1 and c_2 are of the same sign, and negative if c_1 and c_2 are of opposite sign. And the magnitude of the "Mulliken overlap population," for that is what $2c_ic_jS_{ij}$ (summed over all orbitals on the two atoms, over all occupied MOs) is called, depends on c_i, c_j, and S_{ij}.

Now we move into the solid. An obvious procedure is to take all the states in a certain energy interval and interrogate them as to their bonding proclivities, measured by the Mulliken overlap population, $2c_ic_jS_{ij}$.[14] What we are defining is an overlap-population-weighted density of states. The beginning of the obvious acronym (OPWDOS) unfortunately has been preempted by another common usage in solid-state physics. For that reason we have called this quantity COOP (pronounced "co-op") for crystal orbital overlap population.[16] The suggestion of orbitals working together to make bonds in the crystal is not accidental.

To get a feeling for this quantity, let's think what a COOP curve for a hydrogen chain looks like. The simple band structure and DOS were given earlier; they are repeated with the COOP curve in **23**.

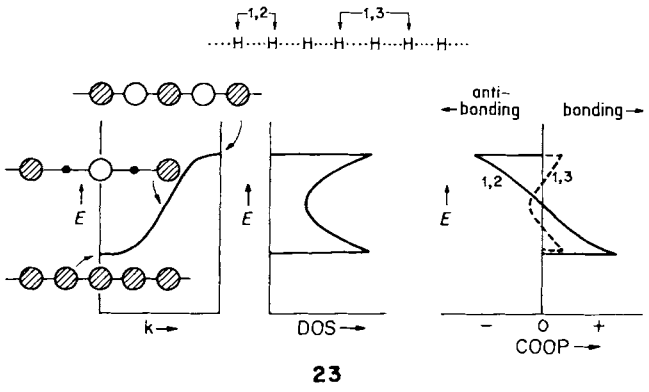

23

To calculate a COOP curve, one has to specify a bond. Let's take the nearest-neighbor 1,2 interaction. The bottom of the band is 1,2 bonding, the middle nonbonding, the top antibonding. The COOP curve obviously has the shape shown at right in **23**. But not all COOP curves look that way. If we specify the 1,3 next-nearest-neighbor bond (silly for a linear chain, not so silly if the chain is kinked), then the bottom *and* the top of the band are 1,3 bonding, the middle antibonding. That curve, the dotted line in the drawing, is different in shape. And, of course, its magnitude is much smaller, because of the rapid decrease of S_{ij} with distance.

Note the general characteristics of COOP curves—positive regions which are bonding, negative regions which are antibonding. The amplitudes of these curves depend on the number of states in that energy interval, the magnitude of the coupling overlap, and the size of the coefficients in the MOs.

The integral of the COOP curve up to the Fermi level is the total overlap population of the specified bond. This points us to another way of thinking of the DOS and COOP curves. These are the differential versions of electron number and bond order indices in the crystal. The integral of the DOS to the Fermi level gives the total number of electrons, the integral of the COOP curve gives the total overlap population, which is not identical to the bond order but which scales like it. It is the closest a theoretician can get to that ill-defined but fantastically useful simple concept of a bond order.

To move to something a little more complicated than the hydrogen or polyene chain, let's examine the COOP curves for the $[PtH_4]^{2\ominus}$ chain. Figure 9 shows both the Pt-H and Pt-Pt COOP curves. The DOS curve for the polymer is also drawn. The characterization of certain bonds as bonding or antibonding is obvious, and matches fully the expectations of the approximate sketch **19**. (1) The bands at -14 and -15 eV are Pt-H σ bonding, the band at -6 eV Pt-H antibonding (this is the crystal-field-destabilized $d_{x^2-y^2}$ orbital). (2) It is no surprise that the mass of d-block levels between -10 and -13 eV doesn't contribute anything to Pt-H bonding. But of course it is these orbitals which are involved in Pt-Pt bonding. The rather complex structure of the -10 to -13 eV region is easily understood by thinking of it as a superposition of σ ($d_{z^2}-d_{z^2}$), π ((d_{xz},d_{yz})$-$(d_{xz},d_{yz})), and δ ($d_{xy}-d_{xy}$) bonding and antibonding, as shown in **24**. Each type of bonding generates a band, the bottom of which is bonding and the top antibonding (see **15** and Fig. 3). (3) The δ contribution to the COOP is small, because of the poor overlap involved. The large Pt-Pt bonding region at -7 eV is due to the bottom of the Pt z band.

We now have a clear representation of the Pt-H and Pt-Pt bonding properties as a function of energy. If we are presented with an oxidized material, then the consequences of the oxidation on the bonding are crystal clear from Figure 9. Removing electrons from the top of the z^2 band at ≈ -10 eV takes them from orbitals that are Pt-Pt antibonding and Pt-H nonbonding. So we expect the Pt-Pt separation, the stacking distance, to decrease, as it does.

The tuning of electron counts is one of the strategies of the solid-state chemists. Elements can be substituted, atoms intercalated, nonstoichiometries enhanced. Oxidation and reduction, in solid-state chemistry as in ordinary molecular solution chemistry, are about as characteristic (but experimentally not always trivial) chemical activities

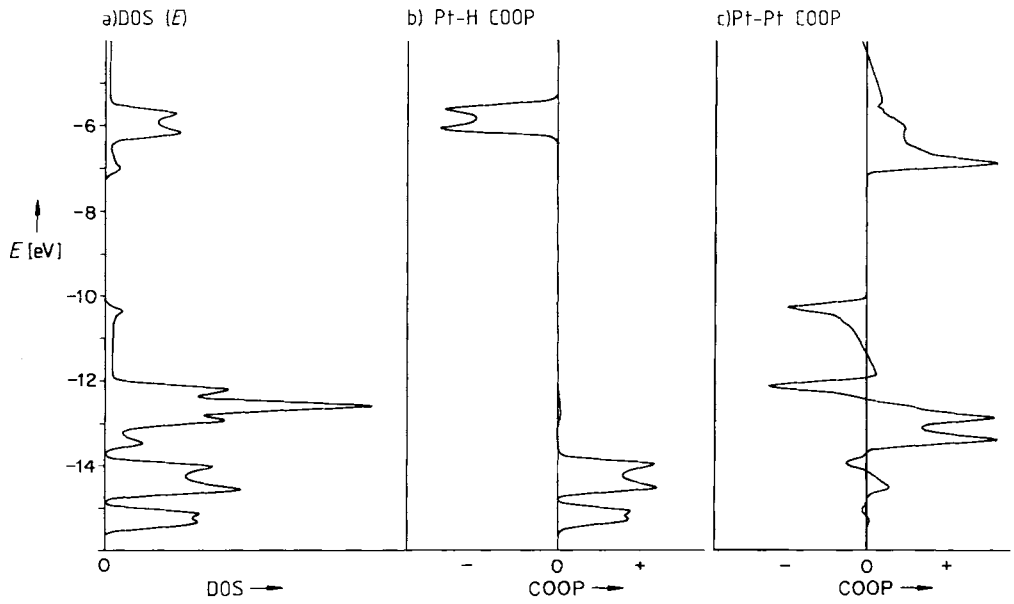

Fig. 9. Total density of states (a), and Pt-H (b) and Pt-Pt (c) crystal orbital overlap population curves for the eclipsed $[PtH_4]^{2\ominus}$ stack.

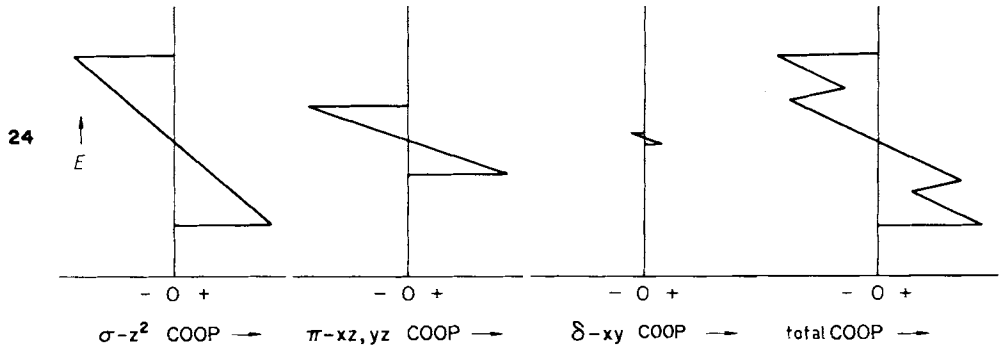

as one can conceive. The conclusions we reached for the Pt–Pt chain were simple, easily anticipated. Other cases are guaranteed to be more complicated. The COOP curves allow one, at a glance, to reach conclusions about the local effects on bond length (will bonds be weaker, stronger) upon oxidation or reduction.

We showed earlier a band structure for rutile (Fig. 5b, repeated in Fig. 10a). The corresponding COOP curve for the Ti–O bond (Fig. 10b) is extremely simple. Note the bonding in the lower, oxygen bands, and antibonding in the e_g crystal-field-destabilized orbital. The t_{2g} is, as expected, Ti–O "π-antibonding."

Let's try our hand at predicting the DOS for something quite different from $[PtH_4]^{2\ominus}$ or TiO_2, namely, a bulk transition metal, the face-centered cubic Ni structure. Each metal atom has as its valence orbitals 3d, 4s, and 4p, ordered in energy approximately as at the left in **25**. Each will spread out into a band. We can make some judgment as to the width of the bands from the overlap. The s,p orbitals are diffuse, their overlap will be large, and a wide band will result. They also mix with each other extensively. The d orbitals are contracted, and so will give rise to a relatively narrow band.

The computed DOS for bulk Ni (bypassing the actual band structure) is shown in Figure 11, along with the Ni s and p contributions to that DOS. What is not s or p is d. The general features of **25** are reproduced. At the Fermi level, a substantial part of the s band is occupied, so that the calculated[17] Ni configuration is $d^{9.15}s^{0.62}p^{0.23}$.

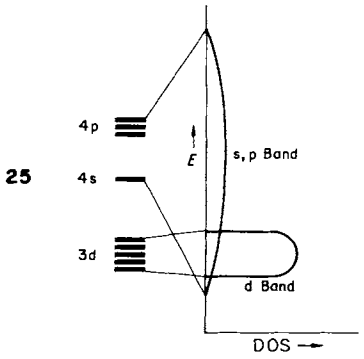

What would one expect of the COOP curve for bulk Ni? As a first approximation we could generate the COOP curve for each band separately (**26a**, **b**). Each band in **25** has a lower Ni–Ni bonding part, an upper Ni–Ni antibonding part. The composite is **26c**. The computed COOP curve is in Figure 12. The expectations of **26c** are met reasonably well.

A metal–metal COOP curve like that of **26c** or Figure 12 is expected for any transition metal. The energy levels

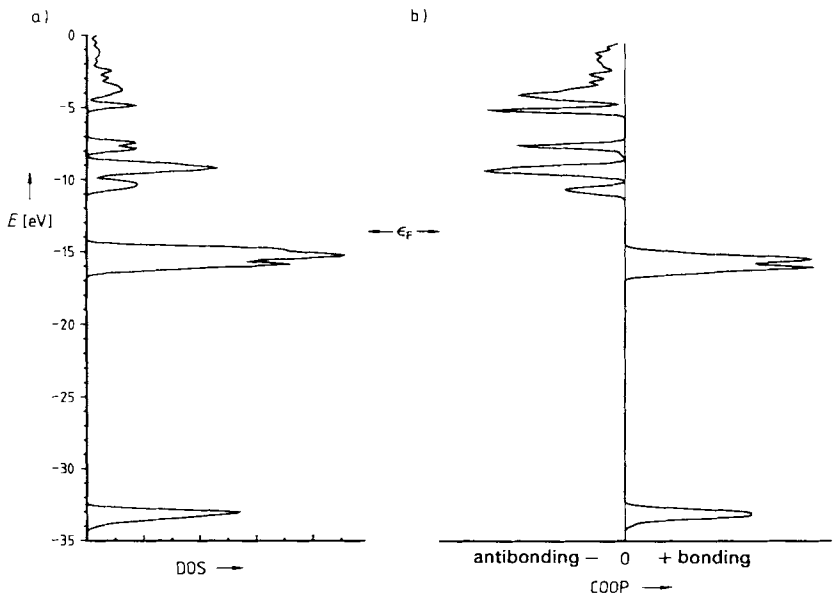

Fig. 10. a) DOS and b) Ti–O COOP for rutile.

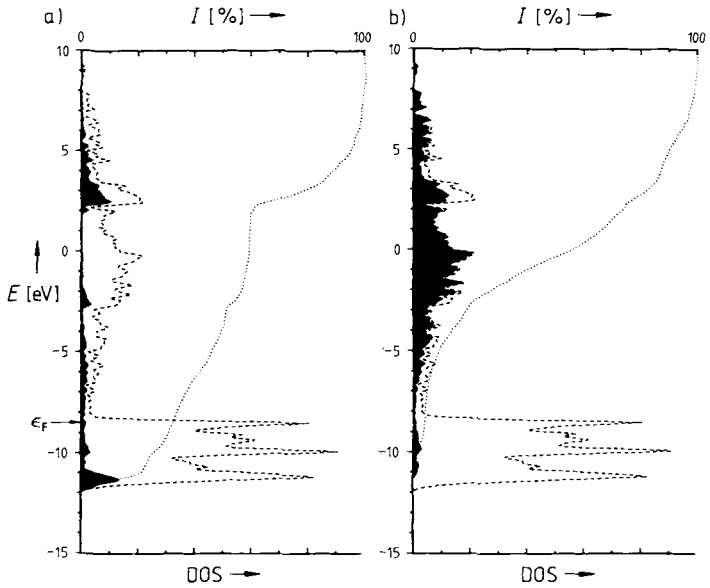

Fig. 11. Total DOS (dashed line) and 4s (a) and 4p (b) contributions to it in bulk Ni. The dotted line is an integration of the occupation of a specified orbital, on a scale of 0 to 100% given at top.

might be shifted up, they might be shifted down, but their bonding characteristics are likely to be the same. If we assume that a similar band structure and COOP curve hold for all metals (in the solid-state trade this would be called the rigid band model), then Figure 12 gains tremendous power. It summarizes, simply, the cohesive energies of all metals. As one moves across the transition series, the M–M overlap population (which is clearly related to the binding or cohesive energy) will increase, peaking at about six electrons per metal (Cr, Mo, W). Then it will decrease toward the end of the transition series and rise again for small s,p electron counts. For more than 14 electrons, a metal is unlikely; the net overlap population for such high coordination becomes negative. Molecular allotropes with lower coordination are favored. There is much more to cohesive energies and the metal–nonmetal transition than this, but

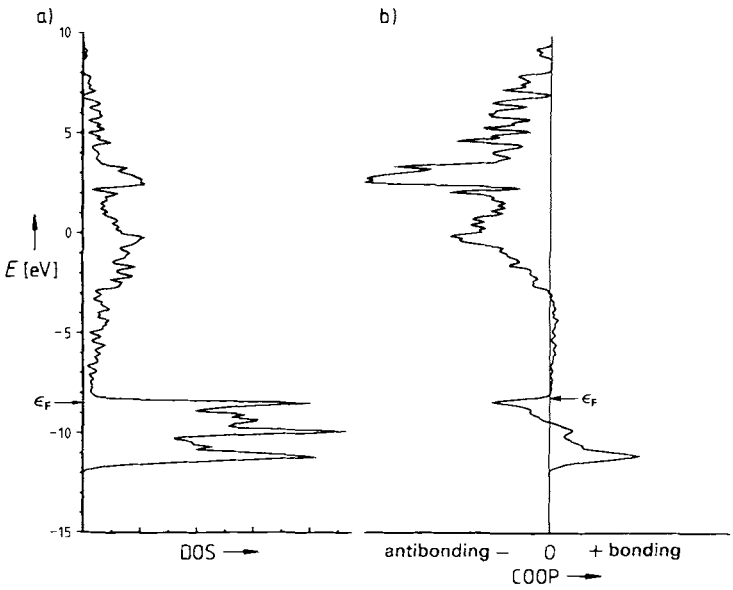

Fig. 12. a) The total DOS and b) nearest-neighbor Ni–Ni COOP in bulk Ni.

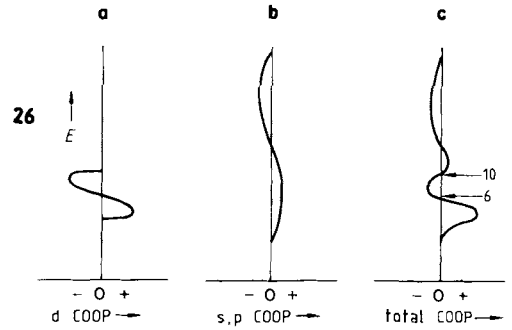

there is much physics and chemistry that flows from the simple construction of **26**.

With a little effort, we have constructed the tools—density of states, its decompositions, the crystal orbital overlap population—which allow us to move from a complicated, completely delocalized set of crystal orbitals or Bloch functions to the localized, chemical description. There is no mystery in this motion. In fact, what I hope I have shown here is just how much power there is in the chemists' concepts. The construction of the *approximate* DOS and bonding characteristics of a $[\{PtH_4\}^{2\ominus}]_\infty$ polymer, or rutile, or bulk Ni, is really easy.

Of course, there is much more to solid-state physics than band structures. The mechanism of conductivity, the remarkable phenomenon of superconductivity, the multitude of electric and magnetic phenomena that are special to the solid state, for these one needs the tools and ingenuity of physics.[6] But as for *bonding* in the solid state, I think (some will disagree) there is nothing new, only a different language.

More Than One Electronic Unit in the Unit Cell: Folding Bands

The oxidized cyanoplatinates are not eclipsed (**27a**), but staggered (**27b**). A polyene is not a simple linear chain, **28a**, but, of course, at least *s-trans* or zigzag, **28b**. Or it could be *s-cis*, **28c**. And obviously that does not exhaust the possibility of arrangements. Nature always seems to

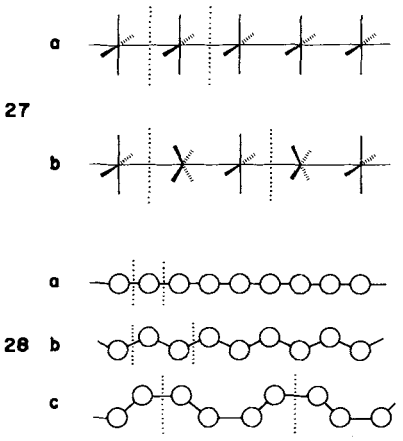

find one we haven't thought of. In **27a** and **28a**, the unit cell contains one basic electronic unit, $[PtH_4]^{2\ominus}$ and a CH group, respectively. In **27b** and **28b**, the unit is doubled, approximately so in unit cell dimension, exactly so in

chemical composition. In **28c**, we have four CH units per unit cell. A purely physical approach might say each is a case unto itself. A chemist is likely to say that probably not much has changed on doubling or quadrupling or multiplying by 17 the contents of a unit cell. If the geometrical distortions of the basic electronic unit that is being repeated are not large, it is likely that any electronic characteristics of that unit are preserved.

The number of bands in a band structure is equal to the number of molecular orbitals in the unit cell. So if the unit cell contains 17 times as many atoms as the basic unit, it will contain 17 times as many bands. The band structure may look messy. The chemist's feeling that the "17-mer" is a small perturbation on the basic electronic unit can be used to simplify a complex calculation. Let's see how this goes, first for the polyene chain, then for the $[\{PtH_4\}^{2\ominus}]_\infty$ polymer.

28a, **b**, and **c** differ from each other not just in the number of CH entities in the unit cell, but also in their geometry. Let's take these one at a time. First prepare for the distortion from **28a** to **28b** by doubling the unit cell, and then, subsequently, distorting. This sequence of actions is indicated in **29**.

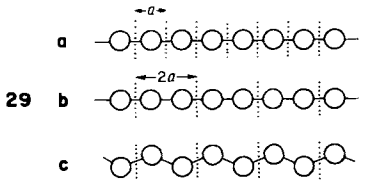

Suppose we construct the orbitals of **29b**, the doubled unit cell polymer, by the standard prescription: (1) get MOs in unit cell, (2) form Bloch functions from them. Within the unit cell the MOs of the dimer are π and π^*, **30**.

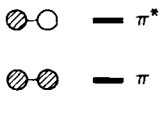

30

Each of these spreads out into a band, that of the π "running up," that of π^* "running down," **31**. The orbitals are written out explicitly at the zone boundaries in **31**. This

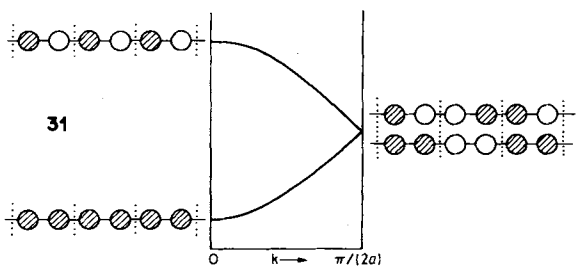

allows one to see that the top of the π band and the bottom of the π^* band, both at $k = \pi/2a$, are precisely degenerate. There is no bond alternation in this polyene (yet), and the two orbitals may have been constructed in a different way, but they obviously have the same nodal structure—one node every two centers.

If we now detach ourselves from this viewpoint and go back and construct the orbitals of the one CH per unit cell linear chain **29a**, we get **32**. The Brillouin zone in **29b** is half as long as it is here, because the unit cell is twice as long.

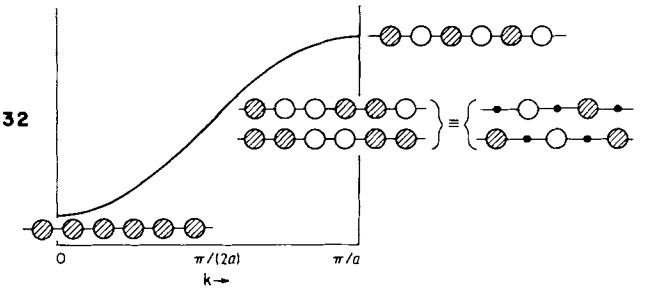

At this point, the realization hits us that, of course, the orbitals of these polymers are the same. The polymers are identical, it is only some peculiar quirk that made us choose one CH unit as the unit cell in one case, two CH units in the other. I have presented the two constructions independently to make explicit the identity of the orbitals.

What we have is two ways of presenting the same orbitals. Band structure **31**, with two bands, is identical to **32**, with one band. All that has happened is that the band of the minimal polymer, one CH per unit cell, has been "folded back" in **32**. The process is shown in **33**.[18]

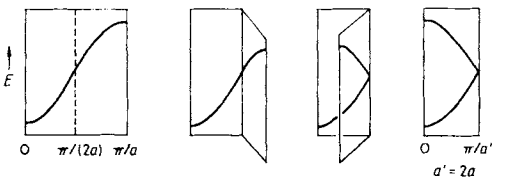

33

The process can be continued. If the unit cell is tripled, the band will fold as in **34a**. If it is quadrupled, we get **34b**, and so on. However, the point of all this is not just

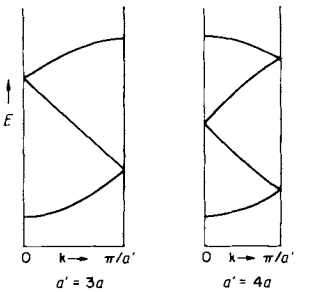

34

redundancy, seeing the same thing in different ways. There are two important consequences or utilizations of this folding. First, if a unit cell contains more than one electronic unit (and this happens often), then a realization of that fact, and the attendant multiplication of bands (remember

32 → **31**, **34a**, or **34b**), allows a chemist to simplify in his or her mind the analysis. The multiplicity of bands is a consequence of an enlargement of the unit cell. By reversing, in our minds in a model calculation, the folding process, by unfolding, we can go back to the most fundamental electronic act—the true monomer.

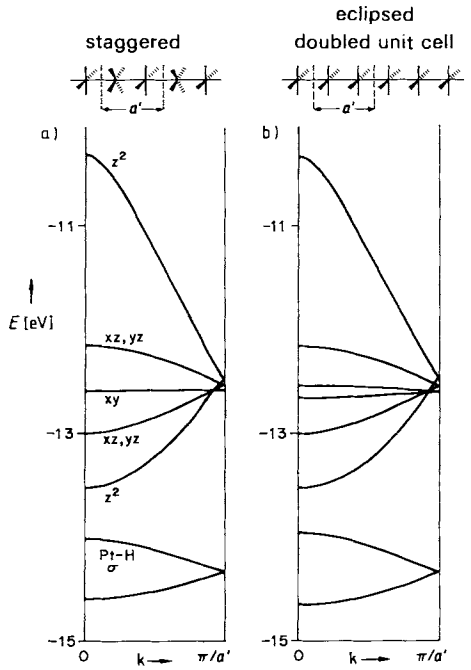

Fig. 13. The band structure of a staggered $[PtH_4]^{2\ominus}$ stack (a), compared with the folded-back band structure of an eclipsed stack, two $[PtH_4]^{2\ominus}$ in a unit cell (b).

To illustrate this point, let me show the band structure of the *staggered* $[PtH_4]^{2\ominus}$ chain, **27b**. This is done in Figure 13a. There are twice as many bands in this region as there are in the case of the eclipsed monomer (the xy band is doubly degenerate). This is no surprise; the unit cell in the staggered polymer is $[\{PtH_4\}^{2\ominus}]_2$. But it's possible to understand Figure 13 as a small perturbation on the eclipsed polymer. Imagine the thought process **35a** → **35b** → **35c**, i.e., doubling the unit cell in an eclipsed polymer and then rotating every other unit by 45° around the z axis. To go

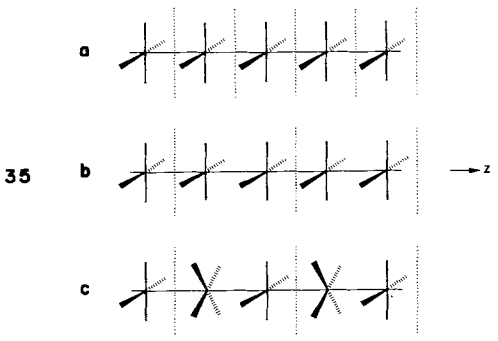

from **35a** to **35b** is trivial, a simple folding back. The result is shown in Figure 13b. Figures 13a and 13b are nearly identical. There is a small difference in the xy band, which is doubled, nondegenerate, in the folded-back eclipsed polymer (Fig. 13b), but degenerate in the staggered polymer. What happened here could be stated in two ways, both the consequence of the fact that a real rotation intervenes between **35b** and **35c**. From a group-theoretical point of view, the staggered polymer has a new, higher symmetry element, an eightfold rotation-reflection axis. Higher symmetry means more degeneracies. It is easy to see that the two combinations, **36**, are degenerate.

Except for this minor wrinkle, the band structures of the folded-back eclipsed polymer and the staggered one are very, very similar. That allows us to reverse the argument, to *understand* the staggered one in terms of the eclipsed one plus the here minor perturbation of rotation of every second unit.

The chemist's intuition is that the eclipsed and staggered polymers *can't* be very different. At least until the ligands start bumping into each other, and for such steric effects there is, in turn, much further intuition. The band structures may look different, for one polymer has one, the other two basic electronic units in the cell. Chemically, however, they should be similar, and we can see this by returning from reciprocal space to real space. Figure 14, comparing the DOS of the staggered (Fig. 14a) and eclipsed (Fig. 14b) polymers, shows just how alike they are in their distribution of levels in energy.

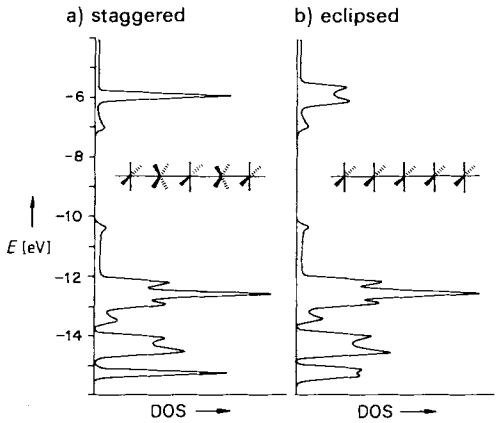

Fig. 14. A comparison of the DOS of staggered (a) and eclipsed (b) $[PtH_4]^{2\ominus}$ stacks.

There is another reason for feeling at home with the folding process. The folding-back construction may be a prerequisite to understanding a chemically significant distortion of the polymer. To illustrate this point, we return to the polyene **29**. To go from **29a** to **29b** involves no distortion. However, **29b** is a way point, a preparation for a real distortion to the more realistic "kinked" chain, **29c**. It behooves us to analyze the process stepwise if we are to understand the levels of **29c**.

Of course, nothing much happens to the π system of the polymer on going from **29a**,**b** to **29c**. If the nearest-neighbor distances are kept constant, then the first real change is

in the 1,3 interactions. These are unlikely to be large in a polyene, since the π overlap falls off very quickly past the bonding region. We can estimate what will happen by writing down some explicit points in the band, and deciding whether the 1,3 interaction that is turned on is stabilizing or destabilizing. This is done in **37**. Of course, in a real CH

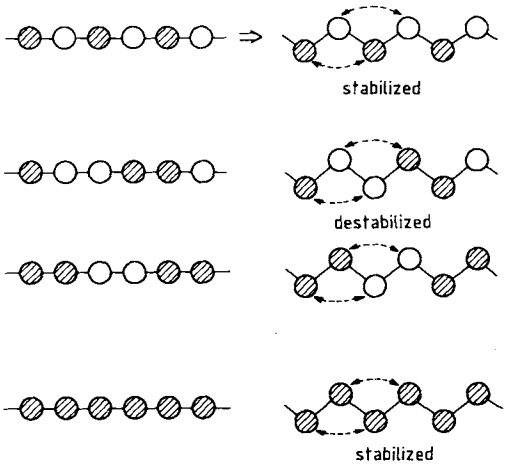

37

polymer this kinking distortion is very much a real thing, but that has nothing to do with the π system, it's a result of strain.

However, there is another distortion which the polyene can and does undergo. This is double-bond localization, an example of the very important Peierls distortion, the solid-state analogue of the Jahn–Teller effect.

Making Bonds in a Crystal

When a chemist sees a molecular structure which contains several free radicals, orbitals with unpaired electrons, his inclination is to predict that such a structure will undergo a geometry change in which electrons will pair up, forming bonds. It is this reasoning, so obvious as to seem almost subconscious, which is behind the chemist's intuition that a chain of hydrogen atoms will collapse into a chain of hydrogen molecules.

If we translate that intuition into a molecular orbital picture, we have **38a**, a bunch (here six) of radicals forming bonds. That process of bond formation follows the H_2 paradigm, **38b**, i.e., in the process of making each bond a level goes down, a level goes up, and two electrons are stabilized by occupying the lower, bonding orbital.

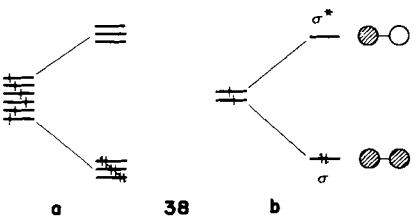

a **38** b

In solid-state physics, bond formation has not stood at center stage, as it has in chemistry. The reasons for this are obvious: the most interesting developments in solid-state physics have been around metals and alloys, and in these often close-packed or nearly close-packed substances, by and large localized chemical viewpoints have seemed irrelevant. For another large group of materials, ionic solids, it also seemed useless to think of bonds. My contention is that there is a range of bonding, including what are usually called metallic, covalent, and ionic solids, and that there is, in fact, substantial overlap between seemingly divergent frameworks of describing the bonding in these three types of crystals. I will take the view that the covalent approach is central and look for bonds when others wouldn't think they're there. One reason for tolerating such foolhardiness might be that the other approaches (metallic, ionic) have had their day—why not give this one a chance? A second reason, one I've mentioned earlier, is that, in thinking and talking about bonds in the crystal, one makes a psychologically valuable connection to molecular chemistry.

To return to our discussion of molecular and solid-state bond formation, let's pursue the trivial chemical perspective of the beginning of this section. The guiding principle, implicit in **38**, is: *Maximize bonding*. There may be impediments to bonding: electron repulsions, steric effects, i.e., the impossibility of two radicals to reach within bonding distance of each other. Obviously, the stable state is a compromise—some bonding may have to be weakened to strengthen some other bonding. But, in general, a system will distort so as to make bonds out of radical sites. Or to translate this into the language of densities of states: *maximizing bonding in the solid state is connected to lowering the DOS at the Fermi level, moving bonding states to lower energy, antibonding ones to high energy.*

The Peierls Distortion

In considerations of the solid state, a natural starting point is high symmetry—a linear chain, a cubic or close-packed three-dimensional lattice. The orbitals of the highly symmetrical, idealized structures are easy to obtain, but they often do not correspond to situations of maximum bonding. These are less symmetrical, deformations of the simplest, archetype structure.

The chemist's experience is usually the reverse, beginning from localized structures. However, there is one piece of experience we have that matches the way of thinking of the solid-state physicist. This is the Jahn–Teller effect,[19] and it's worthwhile to show its working by a simple example.

The Hückel π MOs of a square-planar cyclobutadiene are well known. They are the one-below-two-below-one set shown in **39**.

39

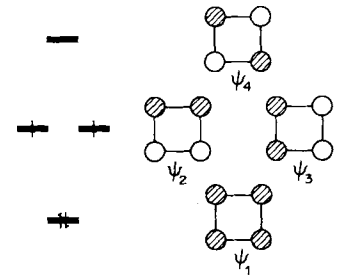

We have a typical Jahn–Teller situation—two electrons in two degenerate orbitals. (Of course, we need worry

about the various states that arise from this occupation, and the Jahn-Teller theorem really applies to only one.[19] The Jahn-Teller theorem says that such a situation necessitates a large interaction of vibrational and electronic motion. It states that there must be at least one normal mode of vibration which will break the degeneracy and lower the energy of the system (and, of course, lower its symmetry). It even specifies which vibrations would accomplish this.

In the case at hand the most effective normal mode is illustrated in **40**. It lowers the symmetry from D_{4h} to D_{2h}, and, to use chemical language, localizes double bonds.

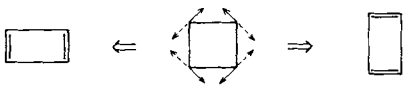

40

The orbital workings of this Jahn-Teller distortion are easy to see. **41** illustrates how the degeneracy of the e orbital is broken in the two phases of the vibration. On forming the rectangle as at right in **40** or **41**, ψ_2 is stabilized:

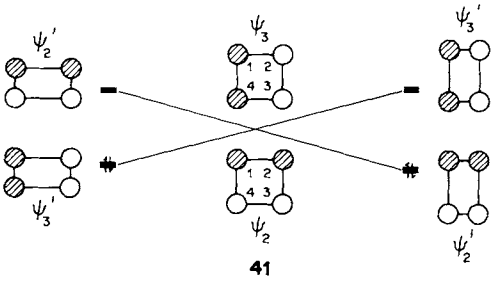

41

the 1-2 and 3-4 interactions, which were bonding in the square, are increased; the 1-4 and 2-3 interactions, which were antibonding, are decreased by the deformation. The reverse is true for ψ_3—it is destabilized by the distortion at right. If we follow the opposite phase of the vibration (to the left in **40** or **41**), ψ_3 is stabilized, ψ_2 destabilized.

The essence of the Jahn-Teller theorem is revealed here: a symmetry-lowering deformation breaks an orbital degeneracy, stabilizing one orbital, destabilizing another. Note the phenomenological correspondence to **38** in the previous section.

One doesn't need a real degeneracy to benefit from this effect. Consider a nondegenerate two-level system, **42**,

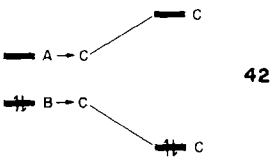

42

with the two levels of different symmetry (here labeled A and B) in one geometry. If a vibration lowers the symmetry so that these two levels transform as the same irreducible representation (call it C), then they will interact, mix, repel each other. For two electrons, the system will be stabilized. The technical name of this effect is a second-order Jahn-Teller deformation.[19]

The essence of the Jahn-Teller effect, first or second order, is: a high-symmetry geometry generates a degeneracy or near degeneracy, which can be broken, with stabilization, by a symmetry-lowering deformation. Note a further point: the level degeneracy is not enough by itself—one needs the right electron count. The cyclobutadiene (or any square) situation of **39** will be stabilized by a D_{2h} deformation for three, four, or five electrons, but not for two or six (e.g., $S_4^{2\oplus}$).

This framework we can take over to the solid. There is degeneracy and near degeneracy for any partially filled band. The degeneracy is that already mentioned, for $E(k)=E(-k)$ for any k in the zone. The near degeneracy is, of course, for k's just above or just below the specified Fermi level. For any such partially filled band there is, in principle, available a deformation which will lower the energy of the system. In the jargon of the trade one says that the partial filling leads to an electron-phonon coupling which opens up a gap just at the Fermi level. This is the Peierls distortion,[20] the solid-state counterpart of the Jahn-Teller effect.

Let's see how this works on a chain of hydrogen atoms (or a polyene). The original chain has one orbital per unit cell, **43a**, and an associated simple band. We prepare it for

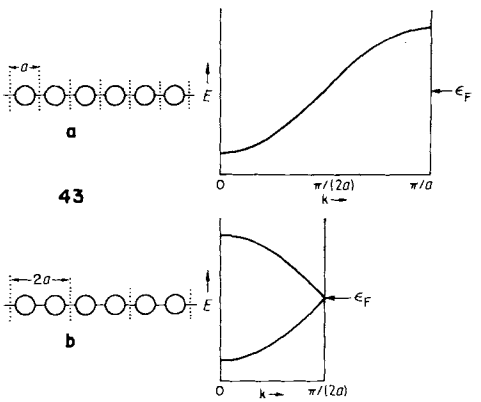

deformation by doubling the unit cell, **43b**. The band is typically folded. The Fermi level is halfway up the band—the band has room for two electrons per orbital, but for H or CH we have one electron per orbital.

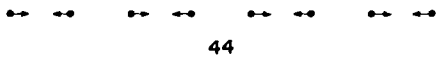

44

The phonon or lattice vibration mode that couples most effectively with the electronic motions is the symmetric pairing vibration, **44**. Let's examine what it does to typical orbitals at the bottom, middle (Fermi level), and top of the band, **45**.

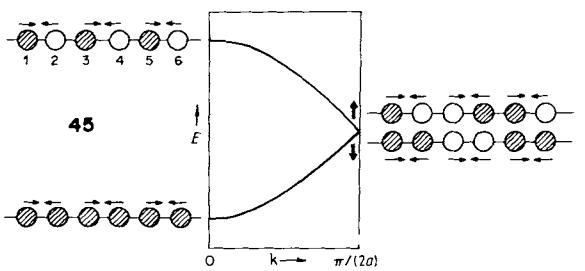

At the bottom and top of the band nothing happens. What is gained (lost) in increased 1-2, 3-4, 5-6, etc. bonding (antibonding) is lost (gained) in decreased 2-3, 4-5, 6-7, etc. bonding (antibonding). But in the middle of the band, at the Fermi level, the effects are dramatic. One of the degenerate levels there is stabilized by the distortion, the other destabilized. Note the phenomenological similarity to what happened for cyclobutadiene.

The action does not take place just at the Fermi level, but in a second-order way the stabilization "penetrates" into the zone. It does fall off with k, a consequence of the way perturbation theory works. A schematic representation of what happens is shown in **46** (I and II represent the

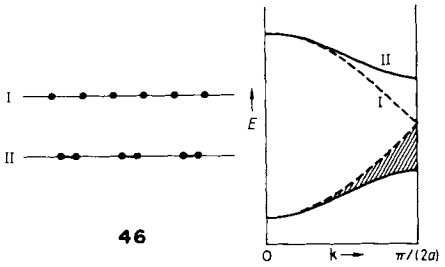

46

chain before and after the distortion). A net stabilization of the system occurs for any Fermi level, but obviously it is maximal for the half-filled band, and it is at the ε_F that the band gap is opened up. If we were to summarize what happens in block form, we'd get **47**. Note the resemblance to **38**.

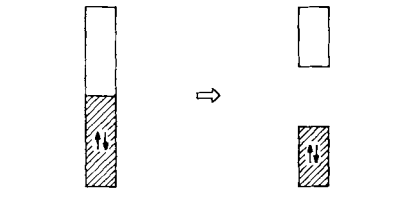

47

The polyene case (today it would be called polyacetylene) is especially interesting, for some years ago it occasioned a great deal of discussion. Would an infinite polyene localize (**48**)? Eventually, *Salem* and *Longuet-Higgins* demonstrated that it would.[21] Polyacetylenes are an exciting field of modern research.[22] Pure polyacetylene is not a conductor. When it is doped, either partially filling the upper band in **45** or emptying the lower, it becomes a superb conductor.

48

There are many beautiful intricacies of the first- and second-order and low- or high-spin Peierls distortion, and for these the reader is referred to the very accessible review by *Whangbo*.[5]

The Peierls distortion plays a crucial role in determining the structure of solids in general; the one-dimensional pairing distortion is only one simple example of its workings. Let's move up in dimensionality.

One ubiquitous ternary structure is that of PbFCl (ZrSiS, BiOCl, Co_2Sb, Fe_2As).[23,24] We'll call it MAB here, because in the phases of interest to us the first element is often a transition metal, the other components, A, B, often main-group elements. **49** shows one view of this structure, **50** another.

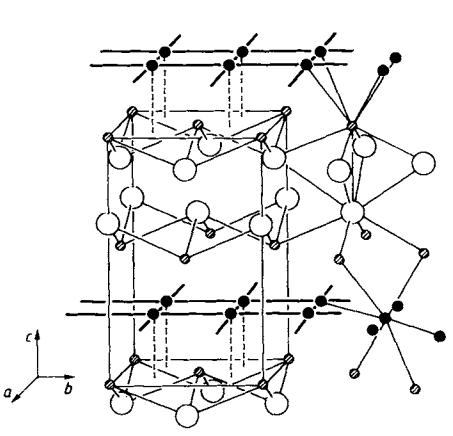

49

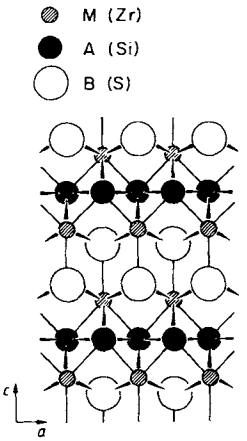

50

In this structure we see two associated square nets of M and B atoms, separated by a square-net layer of A's. The A layer is twice as dense as the others, hence the MAB stoichiometry. Most interesting, from a Zintl viewpoint, is a consequence of that A layer density, a short A-A contact, typically 2.5 Å for Si. This is definitely in the range of some bonding. There are no short B-B contacts.

Some compounds in this series in fact retain this structure. Others distort. It is easy to see why. Take GdPS. If we assign normal oxidation states of $Gd^{3\oplus}$ and $S^{2\ominus}$, we come to a formal charge of $P^{\ominus}$ on the dense-packed P net. From a Zintl viewpoint, $P^{\ominus}$ is like S and so should form two bonds per P. This is exactly what it does. The GdPS struc-

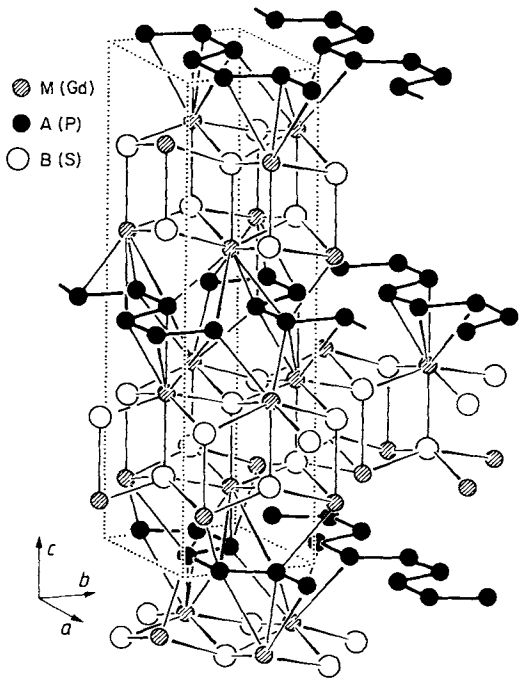

51

ture[25] is shown in **51**, which is drawn after the beautiful representation of *Hulliger* et al.[25] Note the P–P *cis* chains in this elegant structure.

From the point of view of a band structure calculation one might also expect bond formation, a distortion of the square net. **52** shows a qualitative DOS diagram for GdPS.

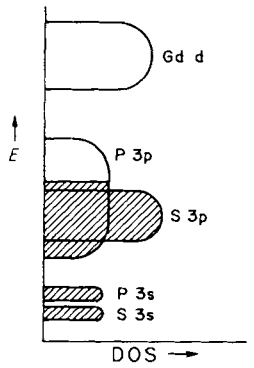

52

What goes into the construction of this diagram is a judgment as to the electronegativities (Gd < P < S). And the structural information that there are short P–P interactions in the undistorted square net, but no short S–S contacts. With the normal oxidation states of $Gd^{3\oplus}$ and $S^{2\ominus}$ one comes to $P^{\ominus}$, as stated above. This means the P 3p band is 2/3 filled. The Fermi level is expected to fall in a region of a large DOS, as **52** shows. A distortion should follow.

The details of what actually happens are presented elsewhere.[24] The situation is intricate; the observed structure is only one likely way for the parent structure to stabilize—there are others. **53** shows some possibilities suggested by *Hulliger* et al.[25] CeAsS chooses **53c**.[26] Nor is the range of geometrical possibilities of the MAB phases exhausted by these. Other deformations are possible; many of them can be rationalized in terms of second-order Peierls distortions in the solid.[24]

An interesting three-dimensional instance of a Peierls distortion at work (from one point of view) is the derivation of the observed structures of elemental arsenic and black phosphorus from a cubic lattice. This treatment is due to *Burdett* and co-workers.[2,27] The two structures are shown in their usual representation in **54**. It turns out that they can be easily related to a simple cubic structure, **55**.

The DOS associated with the band structure of **55**, with one element of the fifth main group per lattice site must

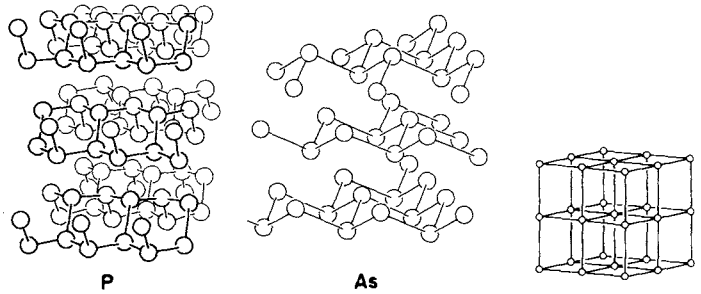

54 **55**

have the block form **56**. There are five electrons per atom, so if the s band is completely filled, we have a half-filled p band. The detailed DOS is given elsewhere.[27] What is significant here is what we see without calculations, namely, a half-filled band. This system is a good candidate for a Peierls distortion. One pairing up of all the atoms along the x, y, and z directions will provide the maximum stabilization, indicated schematically in **57**.

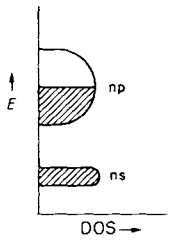

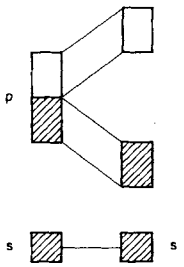

56 **57**

Burdett, *McLarnan*, and *Haaland*[27a,c] have shown that there are no less than 36 different ways to so distort. Two of these correspond to black phosphorus and arsenic, **58**. There are other possibilities.

There is one aspect of the outcome of a Peierls distortion, the creation of a gap at the Fermi level, that might be taken from the last case as being typical, but which is not necessarily so. In one dimension one can always find a Peierls distortion to create a gap. In three dimensions, atoms are much more tightly linked together. In some cases a stabilizing deformation leads to the formation of a real band gap, to an insulator or semiconductor. In other cases, a deformation is effective in producing bonds, pull-

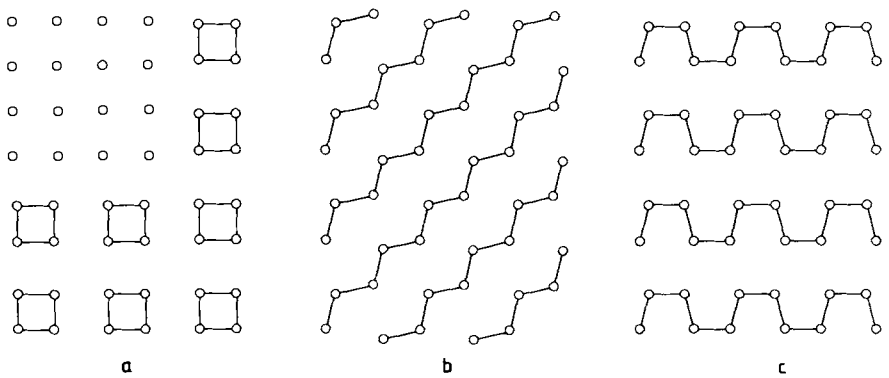

53

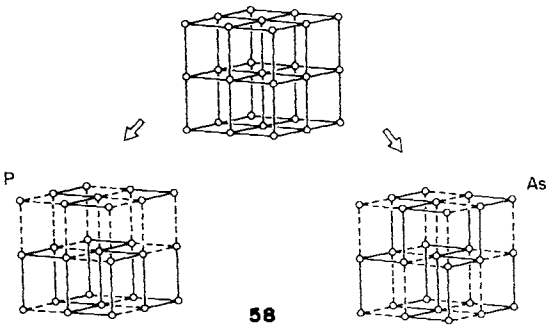

58

ing some states down from the Fermi level region. But because of the three-dimensional linkage it may not be possible to remove all the states from the Fermi level region. Some DOS remains there; the material may still be a conductor.

The applications discussed in this section make it clear that one must know, at least approximately, the band structure (and the consequent DOS) of two- and three-dimensional materials before one can make sense of their marvelous geometrical richness. The band structures that we have discussed in detail have been one-dimensional. Now let's look more carefully at what happens as we increase dimensionality.

More Dimensions

Most materials are two- or three-dimensional, and while one dimension is fun, we must eventually leave it for higher dimensionality. Nothing much new happens, except that we must treat $\vec{k}$ as a vector, with components in reciprocal space, and the Brillouin zone is now a two- or three-dimensional area or volume.[6, 15]

To introduce some of these ideas, let's begin with a square lattice, **59**, defined by the translation vectors $\vec{a}_1$ and

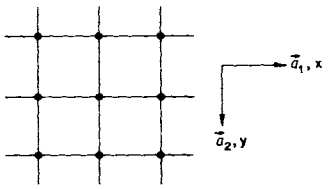

59

$\vec{a}_2$. Suppose there is an H 1s orbital on each lattice site. It turns out that the Schrödinger equation in the crystal factors into separate wave equations along the x and y axes, each of them identical to the one-dimensional equation for a linear chain. There is a k_x and a k_y, the range of each is $0 \leq |k_x|, |k_y| \leq \pi/a$ ($a = |\vec{a}_1| = |\vec{a}_2|$). Some typical solutions are shown in **60**.

The construction of these is obvious. What the construction also shows, very clearly, is the vector nature of k. Consider the $(k_x, k_y) = (\pi/2a, \pi/2a)$ and $(\pi/a, \pi/a)$ solutions. A look at them reveals that they are waves running along a direction which is the vector sum of k_x and k_y, i.e., on a diagonal. The wavelength is inversely proportional to the magnitude of that vector.

The space of k here is defined by two vectors $\vec{b}_1$ and $\vec{b}_2$, and the range of allowed k, the Brillouin zone, is a square.

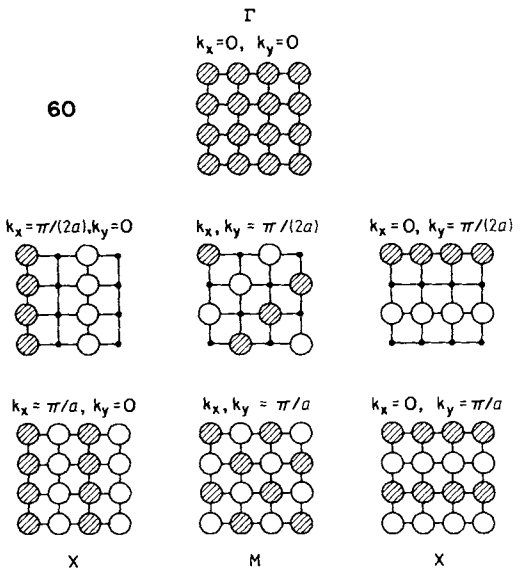

60

Certain special values of k are given names: $\Gamma = (0,0)$ is the zone center, $X = (\pi/a, 0) = (0, \pi/a)$, $M = (\pi/a, \pi/a)$. These are shown in **61**, and the specific solutions for Γ, X, M were so labeled in **60**.

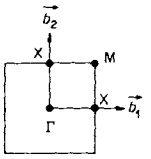

61

It is difficult to show the energy levels, $E(\vec{k})$ for all $\vec{k}$. So what one typically does is to illustrate the evolution of E along certain lines in the Brillouin zone. Some obvious ones are $\Gamma \rightarrow X$, $\Gamma \rightarrow M$, $X \rightarrow M$. From **60** it is clear that M is the highest energy wave function, and that X is pretty much nonbonding, since it has as many bonding interactions (along y) as it does antibonding ones (along x). So we would expect the band structure to look like **62**. A computed band structure and DOS for a hydrogen lattice with $a = 2.0$ Å (Fig. 15) confirms our expectations.

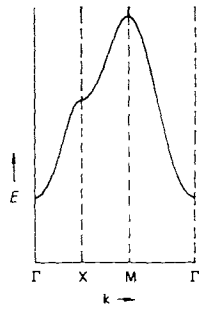

62

The chemist would expect the chessboard of H atoms to distort into one of H_2 molecules (an interesting problem is how many different ways there are to accomplish this). The large peak in the DOS for the half-filled H square-lattice band would make the physicist think of a lattice vibration that would create a gap at ε_F. Any pairwise deformation will do that.

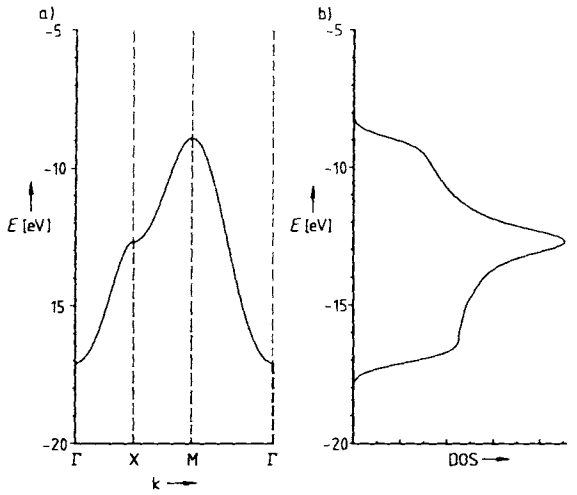

Fig. 15. a) The band structure and b) DOS of a square lattice of H atoms; H-H separation 2.0 Å.

Let's now put some p orbitals on the square lattice, with the direction perpendicular to the lattice taken as z. The p_z orbitals will be separated from p_y and p_x by their symmetry. Reflection in the plane of the lattice remains a good symmetry operation at all k. The $p_z(z)$ orbitals will give a band structure similar to that of the s orbitals, for the topology of the interaction of these orbitals is similar. This is why in the one-dimensional case we could talk at one and the same time about chains of H atoms and polyenes.

The p_x and p_y orbitals present a somewhat different problem. Shown in **63** are the symmetry-adapted combinations of each at Γ, X, Y, and M. (Y is by symmetry equivalent to X; the difference is just in the propagation along x or y.) Each crystal orbital can be characterized by the p, p σ or π bonding present. Thus at Γ the x and y combinations are σ antibonding and π bonding; at X they are σ and π bonding (one of them), and σ and π antibonding (the other). At M they are both σ bonding, π antibonding. It is also clear that the x,y combinations are degenerate at Γ and M (and it turns out along the line Γ→M, but for that one needs a little group theory[15]) and nondegenerate at X and Y (and everywhere else in the Brillouin zone).

Putting in the estimate that σ bonding is more important than π bonding, one can order these special symmetry points of the Brillouin zone in energy, and draw a qualitative band structure (Fig. 16). The actual appearance of any

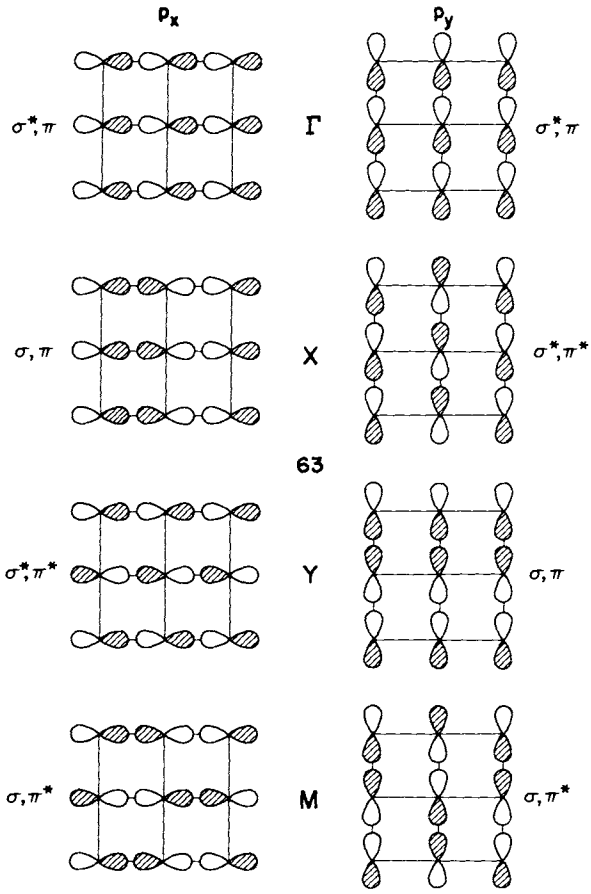

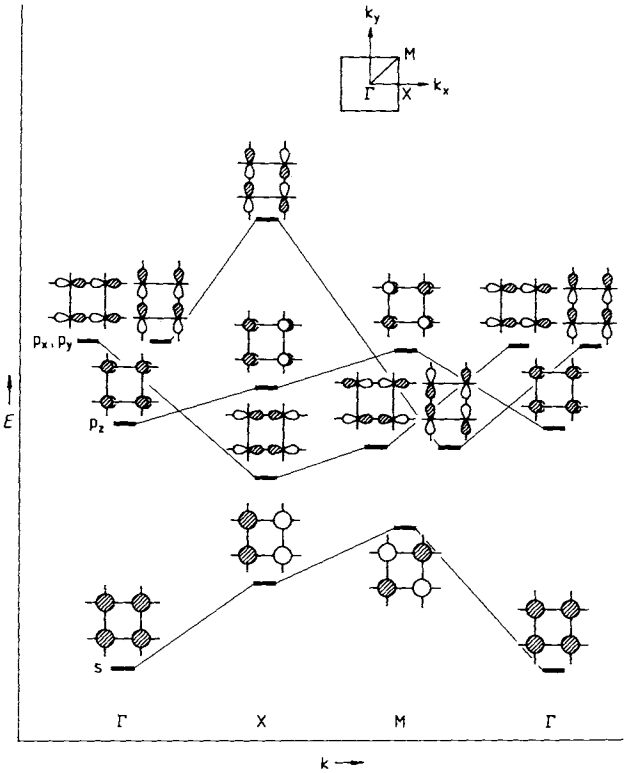

Fig. 16. Schematic band structure of a planar square lattice of atoms bearing ns and np orbitals. The s and p levels have a large enough separation that the s and p bands do not overlap.

real band structure (e.g., the P net in GdPS discussed in the last section) will depend on the lattice spacing. Band dispersions will increase with short contacts, and complications due to s,p mixing will arise. Roughly, however, *any* square lattice, be it the P net in GdPS,[24] a square overlayer of S atoms adsorbed on Ni(100),[28a] the oxygen and lead nets in litharge,[28b] a Si layer in $BaPdSi_3$,[28c] will have these orbitals.

Three dimensions really introduce little new, except for the complexities of drawing and the wonders of group theory in the 230 space groups. The s, p, and d bands of a cubic lattice, or of face-centered or body-centered close-packed structures, are particularly easy to construct.

Let's look at a three-dimensional case of some complexity, the NiAs→MnP→NiP distortion.[29] First, the chemical

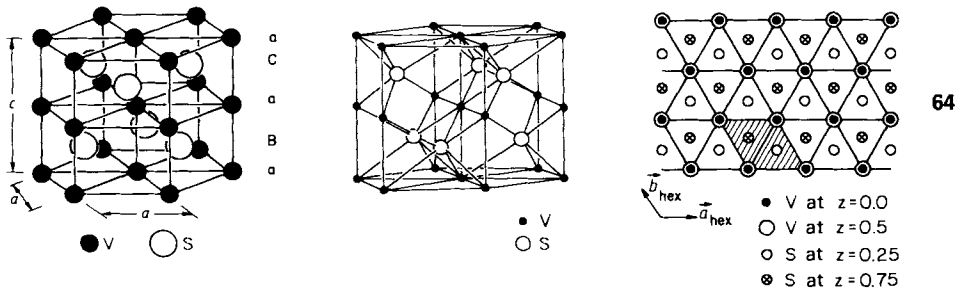

64

motivation. The NiAs structure is one of the most common AB structures, with over a hundred well-characterized materials crystallizing in this type. The structure, shown in three different ways in **64**, consists of hexagonal close-packed layers which alternate metal and non-metal atoms. To be specific, let's discuss the VS representative. The structure contains a hexagonal layer of vanadium atoms at $z=0$, then a layer of sulfur atoms at $z=1/4$, then a second layer of metal atoms at $z=1/2$, superimposable on the one at $z=0$, and, finally, a second layer of main group atoms at $z=3/4$. The pattern is repeated along the c direction to generate a three-dimensional stacking of the type aBaCaBaC. It should not be imagined, however, that this is a layered compound; it is a tightly connected three-dimensional array. The axial V–V separation is 2.94 Å; the V–V contacts within the hexagonal net are longer (3.33 Å).[29]

In terms of local coordination, each sulfur sits at the center of a trigonal prism of vanadiums, which in turn are octahedrally coordinated by six sulfurs. The V–S distances are typical of coordination compounds and, while there is no S–S bonding, the sulfurs are in contact with each other.

This is the structure of stoichiometric VS at high temperatures (>550°C). At room temperature, the structure is a lower symmetry, an orthorhombic MnP one. The same structural transition is triggered by a subtle change in stoichiometry in VS_x, by lowering x from 1 at room temperature.[30]

The MnP structure is a small but significant perturbation on the NiAs type. Most (but not all) of the motion takes place in the plane perpendicular to the hexagonal axis. The net effect in each hexagonal net is to break it up into zigzag chains, as in **65**. The isolation of the chains is

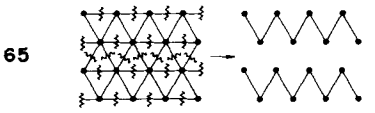

65

exaggerated: the short V–V contact emphasized in **65** changes from 3.33 Å to 2.76 Å, but the V–V distance perpendicular to the plane (not indicated in **65**) is not much longer (2.94 Å).

Still further distortions can take place. In NiP, the chains of Ni and P atoms discernible in the MnP structure break up into Ni_2 and P_2 pairs. For phosphides, it is experimentally clear that the number of available electrons tunes the transition from one structural type to another. Nine or ten valence electrons favor the NiAs structure (for phosphides), 11 to 14 the MnP, and a greater number of electrons prefers the NiP alternative. For the arsenides this trend is less clear.

The details of these fascinating transformations are given elsewhere.[29] It is clear that any discussion must begin with the band structure of the "aristotype," NiAs (here computed for VS). This is presented in Figure 17.

A veritable spaghetti diagram this, seemingly beyond the powers of comprehension of any human being. Why not abdicate understanding, just let the computer spew these bands out and accept (or distrust) them? No, that's too

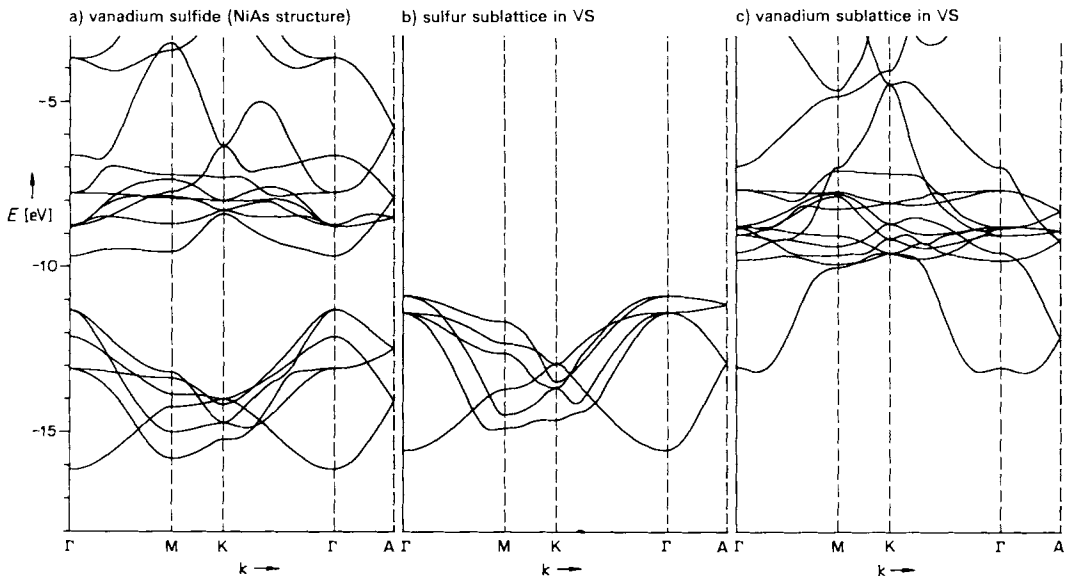

Fig. 17. The band structure for VS in the NiAs structure (a), together with the band structures of its S (b) and V (c) sublattices.

easy a way out. We *can* understand much of this diagram.

First, the general aspects. The hexagonal unit cell is shown in **66**. It contains two formula units V_2S_2. That tells us immediately that we should expect $4\times2=8$ sulfur bands, two 3s separated from six 3p. And $9\times2=18$ vanadium bands, of which 10, the 3d block, should be lowest.

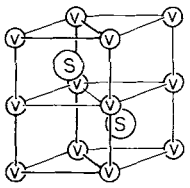

66

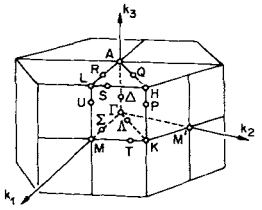

67

The Brillouin zone (**67**) has some special points labeled in it. There are conventions for this labeling.[6, 15] The zone is, of course, three-dimensional. The band structure (Fig. 17) shows the evolution of the levels along several directions in the zone. Count the levels in Figure 17a to confirm the presence of six low-lying bands (which a decomposition of the DOS shows to be mainly S 3p) and ten V 3d bands. The two S 3s bands are below the energy window of the drawing. At some special points in the Brillouin zone there are degeneracies, so one should pick a general point to count bands.

A feeling that this structure is made up of simpler components can be pursued by decomposing it into V and S sublattices (Fig. 17b,c). Note the relatively narrow V d bands around -8 to -9 eV. There is metal-metal bonding in the V sublattice; the widths of the V s,p bands show this. There are also changes in the V d bands on entering the composite VS lattice. A chemist would look for the local t_{2g}-e_g splitting, characteristic of vanadium's octahedral environment.

Each of these component band structures could be understood in further detail.[31] Take the S 3p substructure at Γ. The unit cell contains two S atoms, redrawn in a two-

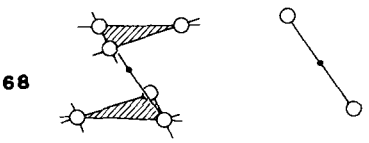

68

dimensional slice of the lattice in **68** to emphasize the inversion symmetry. **69**–**71** are representative x,y and z com-

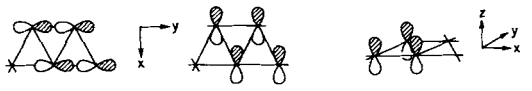

69 **70** **71**

binations of one S two-dimensional hexagonal layer at Γ. Obviously, x and y are degenerate, and the x,y combination should be above z—the former is locally σ antibonding, the latter π bonding. Now combine two layers. The x,y layer Bloch functions will interact less (π overlap) than the z functions (σ antibonding for the Γ point, **72**). These

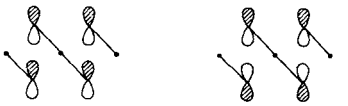

72

qualitative considerations (x,y above z, the z bands split more than the x,y bands) are clearly visible in the positioning of the S 3p bands in Figures 17b and 17a.

With more, admittedly tedious, work, every aspect of these spaghetti diagrams can be understood. And, much more interestingly, so can the electronic tuning of the NiAs→MnP→NiP displacive transition.[29]

A Sample Problem: The $ThCr_2Si_2$ Structure

The preceding sections have outlined some of the theoretical tools for analysis of bonding in the solid state. To see how these ideas can be integrated, let's discuss a specific problem.

More than 400 compounds of AB_2X_2 stoichiometry adopt the $ThCr_2Si_2$ type structure,[32] but you are not likely to find any mention of these in any modern textbook of general inorganic chemistry, which just tells us something about the ascendancy of molecular inorganic chemistry, especially transition-metal organometallic chemistry, in the last three decades. However, these compounds are there, we know their structures and they have interesting properties. A is typically a rare-earth, alkaline-earth, or alkali element, B is a transition metal or main-group element, and X comes from the fifth, fourth, and occasionally third main group. Since the synthesis of AB_2X_2 with A = a rare-earth element, by *Parthé*, *Rossi*, and their co-workers, the unusual physical properties exhibited by these solids have attracted much attention. Physicists speak with enthusiasm of valence fluctuation, p-wave or heavy-fermion superconductivity and of many peculiar magnetic properties of these materials. The very structure of these materials carries much that is of interest to the chemist.

The $ThCr_2Si_2$ structure type for AB_2X_2 stoichiometry compounds is shown in **73**. It consists of B_2X_2 layers interspersed with A layers. The bonding between A and B_2X_2 layers appears largely ionic, which is why we may write the charge partitioning as $A^{2\oplus}$ and $B_2X_2^{2\ominus}$. But in the B_2X_2 layer there is indication not only of covalent B–X bonding, but also some metal–metal B–B bonding. Typical metal–metal distances are in the range of 2.7–2.9 Å.

A way to describe the B_2X_2 layers in these compounds is to imagine a perfect square-planar two-dimensional lattice of metal atoms B, above and below the fourfold hollows of which lie the main-group X atoms. This is shown in **74**.

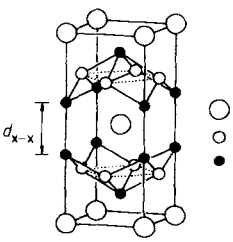

73

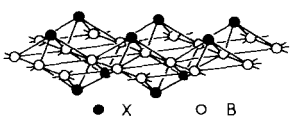

74

The coordination environment of the metal atom B is approximately tetrahedral in the main-group elements X, with four additional square-planar near-neighbor metal atoms B. The coordination of the X atoms is much more unusual—they reside at the apex of a square pyramid.

It may be noted here that there are alternative ways to describe the layer structure. For instance, the B_2X_2 layer may be thought of as being built up by sharing four of the six edges of a BX_4 tetrahedron by infinite extension in two dimensions, as in **75**. Such packing diagrams, or alternative ways of looking at the same structure, are inherently useful—a new view often leads to new insight. I would just introduce a very personal prejudice, voiced above, for views of structure that make as many connections as possible to other subfields of chemistry. On that basis, I would give a slight preference to **74** over **75**—the latter pulls one a little away from bonds.

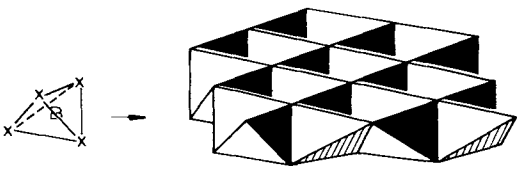

75

There is a long X–X contact within the layer, but what becomes the main focus of this section is a remarkable tunable X–X contact, d_{X-X}, *between* all layers, along the edges (and across the top and bottom faces) of the tetragonal unit cell **73**. This contact is the primary geometrical variable in these structures.

Table 1. The X-X distances in some phosphide compounds of the AB_2X_2 type.

AB_2X_2	d_{X-X} [Å]	AB_2X_2	d_{X-X} [Å]
$CaCu_{1.75}P_2$	2.25	$SrCu_{1.75}P_2$	2.30
$CaNi_2P_2$	2.30		
$CaCo_2P_2$	2.45	$SrCo_2P_2$	3.42
$CaFe_2P_2$	2.71	$SrFe_2P_2$	3.43

Sometimes d_{X-X} is long, sometimes it is short. In Table 1 are shown two series of compounds studied by *Mewis*.[33] In these the cation is kept constant, and so is the main-group element, P. Only the metal varies. For reference the P–P distance in P_4 is 2.21 Å and 2.192 Å in Me_2P-PMe_2. The P–P single-bond distance in many compounds is remarkably constant at 2.19–2.26 Å. The P=P and P≡P bond lengths are around 2.03 Å and 1.87 Å, respectively. It is clear that the short distances in the $ThCr_2Si_2$ type phosphides are characteristic of a full P–P single bond. The long contacts, such as 3.43 Å, imply essentially no bonding at all. All the compounds known with a nonbonding X–X separation contain metals from the left-hand side of the periodic table. In fact, examination of all the structures reveals a trend. As one moves from left to right in the transition series, the P–P contact shortens. Clearly, there is an electronic effect at work here—a P–P bond is made or broken in the solid state. We would like to understand how and why this happens.

Incidentally, let's see what happens if one takes a Zintl viewpoint of these structures. The long P–P contact would be associated with a filled octet, $P^{3\ominus}$, the full P–P single bond with a $P\text{-}P^{4\ominus}$ or $P^{2\ominus}$. For a divalent $A^{2\oplus}$ we would be left with a metal in oxidation state II for the case of no P–P bond, oxidation state I for a single P–P bond. One could make some sense of the trend in terms of the energetics of the various metal oxidation states, but one way or another the Zintl picture has a difficult time with intermediate distances. How does one describe a P–P bond length of 2.72 Å? A delocalized approach has no problems with describing such partial bonding.

Chong Zheng and I[34] approached the AB_2X_2 structure, represented by a typical $BaMn_2P_2$ compound, in stages. First, we looked at a single two-dimensional $Mn_2P_2^{2\ominus}$ layer. Then, we formed a three-dimensional $Mn_2P_2^{2\ominus}$ sublattice by bringing many such layers together in the third dimension.

Consider a single $Mn_2P_2^{2\ominus}$ layer, **74**. The Mn–P distance is 2.455 Å, and the Mn–Mn distance in the square metal lattice is 2.855 Å. The latter is definitely in the metal–metal bonding range, so a wide-band, delocalized picture is inevitable. But in some hierarchy or ranking of interactions, it is clear the Mn–P bonding is stronger than Mn–Mn, so let's construct this solid conceptually or think of it in terms of first turning on Mn–P bonding, and then Mn–Mn interaction.

The local coordination environment at each Mn is approximately tetrahedral. If we had a discrete tetrahedral Mn complex, e.g., $[Mn(PR_3)_4]$, we might expect a qualitative bonding picture such as **76**. Four phosphane lone pairs, a_1+t_2 in symmetry, interact with their symmetry match, mainly Mn 4s and 4p, but also with the t_2 component of the Mn 3d set. Four orbitals, mainly on P, P–Mn σ bonding, go down. Four orbitals, mainly on Mn, P–Mn σ antibonding, go up. The Mn d block splits in the expected two-below-three way.

76

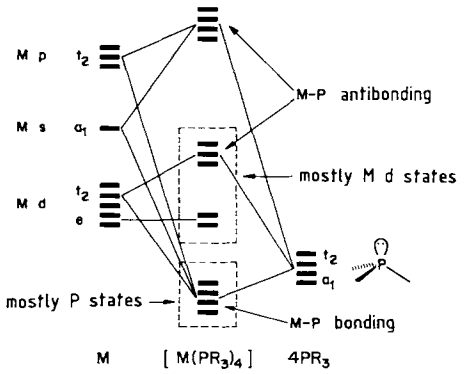

Something like this *must* happen in the solid. In addition, there are Mn–Mn bonding contacts in the layer, and these will lead to dispersion in those bands which are built up from orbitals containing substantial metal character. The combined construction is shown in Figure 18.

Can we see this local, very chemical bonding construction in a delocalized band structure? Most certainly. The calculated (extended Hückel) band structure and total den-

sity of states of a single $Mn_2P_2^{2\ominus}$ layer is illustrated in Figure 19.

The unit cell is a rhomboid of two Mn and two P atoms. P is clearly more electronegative than Mn, so we expect two mainly P 3s bands below six P 3p bands below 10 Mn 3d bands. The number of bands in Figure 19 checks. A decomposition of the DOS (Fig. 20) confirms the assignment.

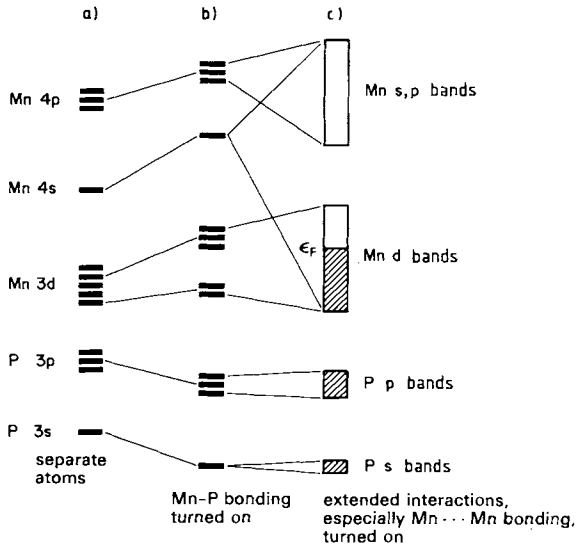

Fig. 18. A schematic picture of the $Mn_2P_2^{2\ominus}$ layer band structure is derived by first turning on local Mn-P interactions and then the two-dimensional periodicity and Mn-Mn interactions. The unit cell contains two Mn and two P atoms, so in reality each of the levels in the first two columns should be doubled.

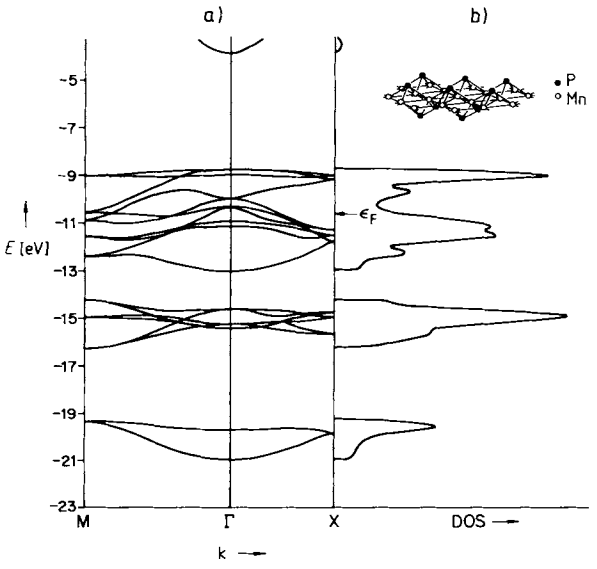

Fig. 19. a) Band structure and b) DOS of a single $Mn_2P_2^{2\ominus}$ layer.

What about the bonding characteristics predicted by the qualitative bonding scheme **76**? This is where a COOP curve is useful (Fig. 21). Note that the two lower bands (at -15 and -19 eV), which by previous decomposition were seen to be mainly P, are Mn-P bonding, whereas the mainly metal bands around -12 eV are Mn-P nonbonding. The bunch of levels at ≈ -9 eV is Mn-P antibonding—it corresponds to the crystal-field-destabilized t_2 level in **76**. The bottom of the mainly metal band is Mn-Mn bonding, the top Mn-Mn antibonding. Everything is as expected.

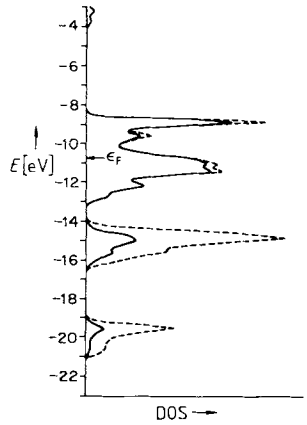

Fig. 20. Total DOS of the composite $Mn_2P_2^{2\ominus}$ layer lattice (dashed line) and the contributions of Mn orbitals to that DOS (solid line). What is not on Mn is on P.

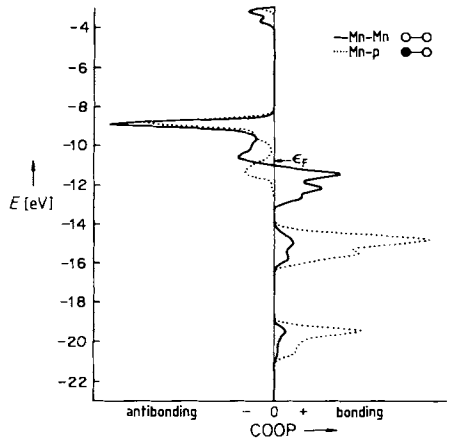

Fig. 21. Crystal orbital overlap population curves for the Mn-Mn bonds (solid line) and Mn-P bonds (dotted line) in the $Mn_2P_2^{2\ominus}$ single layer.

An interesting, slightly different approach to the bonding in the layer is obtained if we, so to speak, turn on Mn-Mn bonding first, then Mn-P bonding by "inserting" or "intercalating" a P sublattice (Fig. 22). In Figure 22a is the P sublattice. We see P 3s (around -19 eV) and P 3p (around -14 eV) bands. Both are narrow, because the P atoms are ≈ 4 Å apart. The Mn sublattice (Fig. 22b) shows a nicely dispersed density of states (DOS). The Mn-Mn separation is only 2.855 Å. Thus we have a two-dimensional metal, with a familiar wide s,p plus narrow d band pattern. The bottom part of the DOS in Figure 22b is the 3d band, the top is the lower part of the 4s,4p band. Figure 22c shows the density of states of the composite $Mn_2P_2^{2\ominus}$ layer. Note how the individual P and Mn bunches of states repel each other on forming the composite lattice. Note how part of the Mn d band stays where it is, part moves up. There is the memory, within this delocalized structure, of the local e-below-t_2 crystal field splitting. There is no more graphic way of showing that what happens in the inorganic solid is similar to what happens in an isolated inorganic molecule.

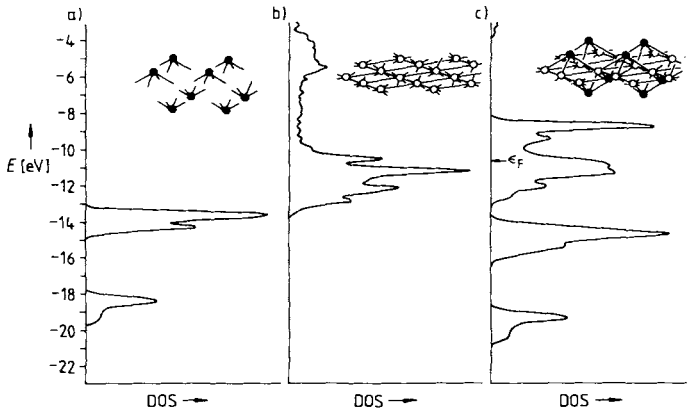

Fig. 22. Total DOS of the P sublattice (a), the Mn sublattice (b), and the composite $Mn_2P_2^{2\ominus}$ layer lattice (c).

Still another, more chemical detail. Each phosphorus in the slab is in an unusual coordination environment, at the apex of a square pyramid of Mn atoms. A chemist looks for a lone pair, **77**, pointing away from the ligands. We can

77

look for it, theoretically, by focusing on its directionality. P $3p_z$ should contribute most to this lone pair, so we interrogate the DOS for its z contribution (Fig. 23). The p_z orbital is indeed well localized, 70% of it in a band at ≈ -15 eV. Here is the lone pair.

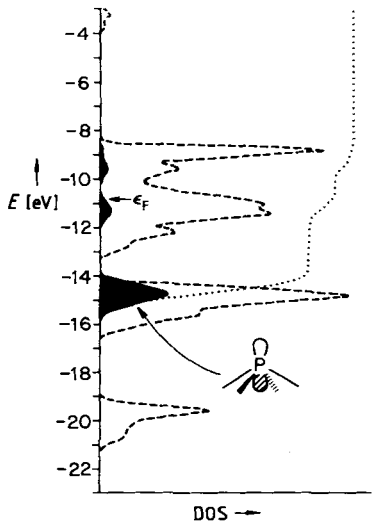

Fig. 23. Phosphorus $3p_z$ orbital contribution (dark area) to the total DOS (dashed line) of the $Mn_2P_2^{2\ominus}$ single layer. The dotted line is an integration of the dark line, on a scale of 0 to 100%.

A point that can be made here is that localization in energy space (such as we see for the P p_z projection) implies localization in real space. The easiest way to think this through is to go back to the construction of bands at the beginning of this paper. The molecular orbitals of a crystal are always completely delocalized Bloch functions. But there is a difference between what we might call symmetry-enforced delocalization (formation of Bloch functions, little overlap) and real, chemical delocalization (overlap between unit cells). The former gives rise to narrow bands, the latter to highly dispersed ones. Turning the argument around, if one sees narrow bands, that's a sign of chemical localization, where as wide bands imply real delocalization.

On to the three-dimensional solid. When the two-dimensional $Mn_2P_2^{2\ominus}$ layers are brought together to form the three-dimensional solid $Mn_2P_2^{2\ominus}$ (still without the counterions), the P $3p_z$ orbitals or lone pairs in one layer form bonding and antibonding combinations with the corresponding orbitals in the layers above or below. Figure 24

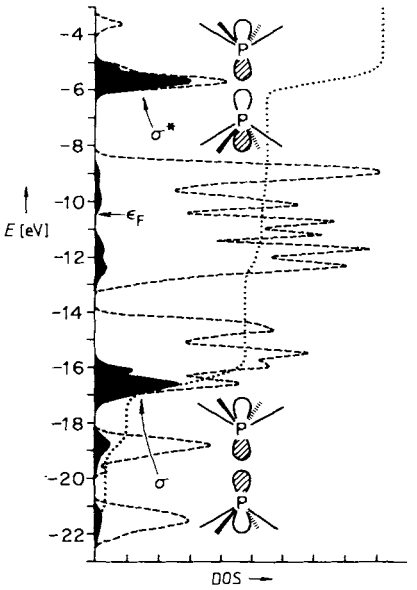

Fig. 24. Phosphorus $3p_z$ orbital contribution (dark area) to the total DOS (dashed line) of the three-dimensional $Mn_2P_2^{2\ominus}$ lattice. The phosphorus-phosphorus bond length here is 2.4 Å. The dotted line is an integration (see Fig. 23).

shows the P $3p_z$ density of states at an interlayer P–P distance of 2.4 Å. The wide band at -8 to -12 eV is Mn 3d. Below and above this metal band are P bands, and in these, quite well localized, are P–P σ and σ^* combinations, **78**. These bands are narrow, because the lateral P–P distance is long.

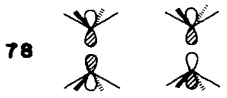

78

Perhaps it's appropriate to stop here and reflect on what has happened. There are N_A levels per atomic orbital in the solid. It's all delocalized bonding, but with our theoretical tools we have been able to see, quite localized in energy, orbitals of a diatomic molecule. The localization in energy reflects the validity of a localization in space, i.e., a bond.

If the three-dimensional calculation is repeated at different interslab or P–P distances, all that happens is that the localized P–P σ and σ^* bands occur at different energies. Their splitting decreases with increasing P–P separation, as one would expect from their respective bonding and antibonding nature.

We are now in a position to explain simply the effect of the transition metal on the P-P separation. What happens when the transition metal moves to the right-hand side of the periodic table? The increased nuclear charge will be more incompletely screened and the d electrons more tightly bound. As a result, the d band comes down in energy and becomes narrower. At the same time, the band filling increases as one moves to the right in the transition series. The balance is complicated, and it is important. **79** shows the result. For details the reader is referred to the definitive work of *O. K. Andersen*.[35]

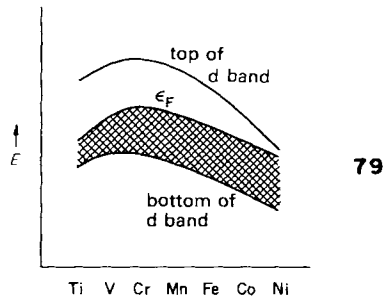

79

79 is the most important single graph of metal physics. It is analogous in its significance to the plot of the ionization potentials of atoms or diatomic molecules. At the right side of the transition series, the area of concern to us, the Fermi level falls as one moves to the right, the work function of the metal increases.

Now imagine superimposed on this variable-energy sea of electrons the P-P σ and σ^* bands for some typical, moderately bonding P-P distance, **80**. In the middle of the

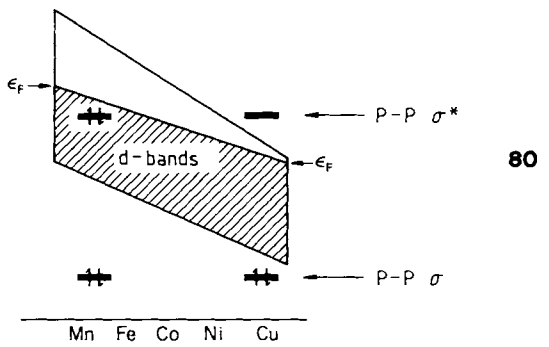

80

transition series, the metal Fermi level is above the P-P σ^*. Both σ and σ^* are occupied; there is no resultant P-P bond. As P-P stretches in response, the σ^* only becomes more filled. On the right side of the transition series, the P-P σ^* is above the Fermi level of the metal, and so is unfilled. The filled P-P σ makes a P-P bond. Making the P-P distance shorter only improves this situation.

The steady, gradual variation of the P-P distance would seem to be as inconsistent with the molecular orbital model shown here as it was with the Zintl concept. This is not so. If we turn on the interaction between the P atoms and the metal layer (and we have seen before that this interaction is substantial), we will get mixing of P and Mn orbitals. The discontinuity of the above picture will be replaced by a continuous variation of the occupation of the P σ and σ^* orbitals between two and zero.

The experimentally observed trend has been explained. There is much more to the AB_2X_2 structures than I have been able to present here,[34] of course. More important than the rationalizations and predictions of the experimental facts that one is able to make in this case, is the degree of understanding one can achieve and the facility of motion between chemical and physical perspectives.

One final comment on the $ThCr_2Si_2$ structure. The reader will note that we did not use a Peierls distortion argument in the resolution of this problem. We could have done so, somewhat artificially, by choosing a structure in which the interlayer P-P separation was so large that the P-P σ and σ^* DOS came right at the Fermi level. Then a pairing distortion could have been invoked, yielding the observed bond. That, however, would have been a somewhat artificial approach. Peierls distortions are ubiquitous and important, but they're not the only way to approach bonds in the solid.

Orbital Interactions in the Solid

I have made use of frontier orbitals and orbital interactions throughout this article—the construct of densities of states restored to us the possibility of utilizing this language. Perhaps it is appropriate to make these ideas explicit.

Consider the interaction of two molecules, A and B, not an extended solid. **81** indicates, schematically, three types of interaction. ① and ② are two-electron stabilizing inter-

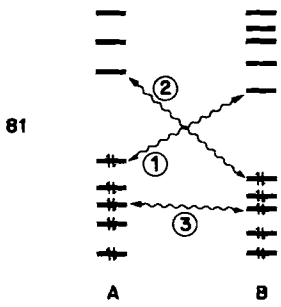

81

actions, ③ is a four-electron destabilizing interaction. The lines are drawn to specific orbitals, the HOMOs and LUMOs of each component. Some degree of frontier orbital control is implied here; in reality we know that all orbitals interact, and that their role is gauged by the overlap and energy factors in Equation (e).[8]

$$\Delta E = \frac{|H_{ij}|^2}{E_i^0 - E_j^0} \qquad \text{(e)}$$

In interaction ①, A acts as a donor, B as an acceptor. In ②, their roles are reversed. The balance of real charge transfer depends on the magnitude of the two interactions, as evaluated by the above-given perturbation expression. If the energy separation $E_i^0 - E_j^0$ were dominant, then, in **81**, A would be a donor relative to B.

It should be realized that this description, while of immense interpretative power, is only a one-electron model. To analyze orbital interactions properly, in a many-electron way, is not easy. The simple picture of **81** seems to be lost; competing interaction or partition schemes have been

suggested.[36] One way to appreciate the problem a true many-electron theory has in analyzing interactions is to realize that the energy levels of A and B are not invariant to electron transfer. They change in energy depending on the charge on fragments A and B: a positive charge makes them go down, a negative charge go up. Actually realizing this, one has learned the most important correction to the simple one-electron picture.

The frontier orbital way of thinking, especially with respect to donor–acceptor interactions, is of substantial utility in the solid state. Let me give two examples here.

The Chevrel phases are a fascinating set of ternary molybdenum chalcogenide materials of varying dimensionality and interesting physical properties.[37] In the parent phase, epitomized by $PbMo_6S_8$, one has recognizable $[Mo_6S_8]$ clusters. In these clusters, shown in three views in **82**, sulfurs cap the eight faces of an octahedron of molyb-

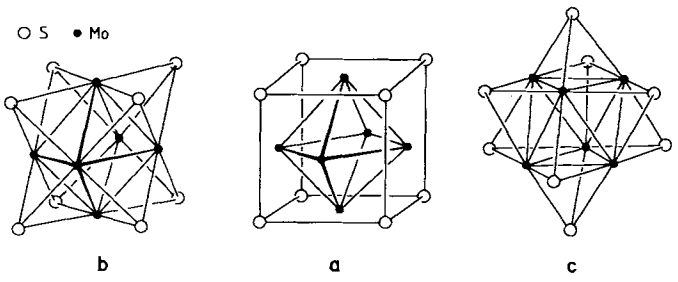

82

denums. The $[Mo_6S_8]$ clusters are then embedded in a substructure of lead cubes (this is a thought construction of the structure!), as in **83**. But the structure doesn't remain here. In every cubical cell, the $[Mo_6S_8]$ rotates by $\approx 26°$ around a cube diagonal to reach structure **84** (Pb's are missing in this drawing, for clarity).

Why? The answer is implicit in **84**. A rotation of roughly this magnitude is required to give each Mo within one unit a fifth bonding interaction with a sulfur of a cluster in the

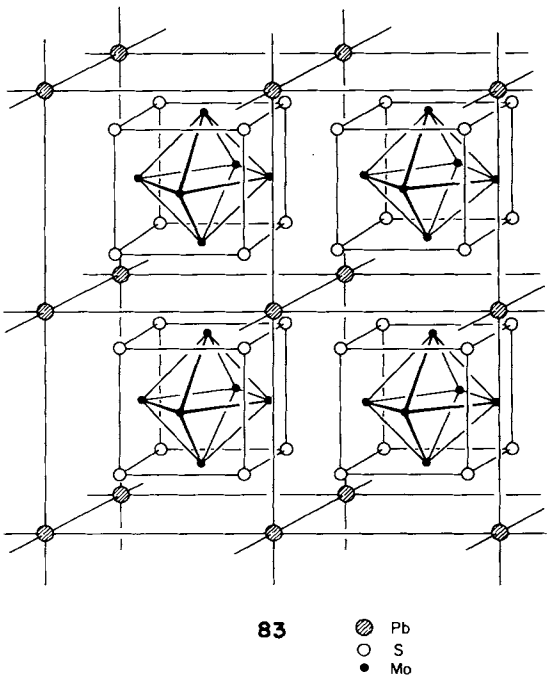

83

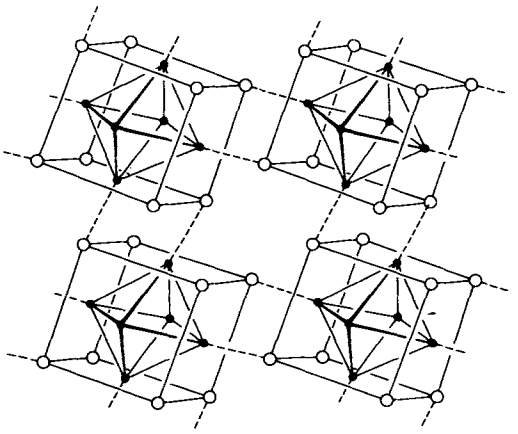

84

neighboring cube. If one does a molecular orbital calculation on the isolated cluster (Fig. 25), one finds that the five lowest empty orbitals of the cluster point out, away from the molybdenums, hungry for the electron density of a neighboring sulfur.[38,39]

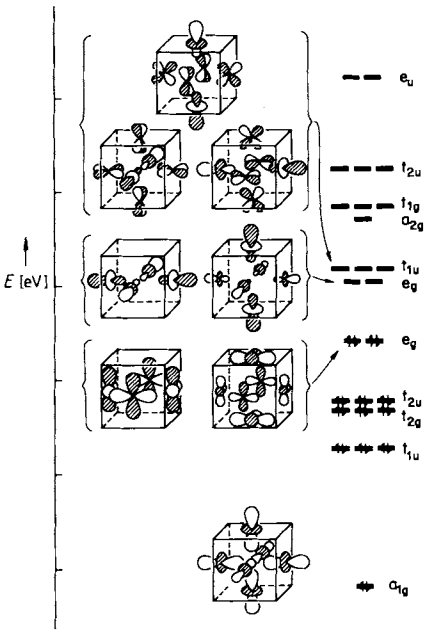

Fig. 25. The frontier orbitals of an $[Mo_6S_8]^{4\oplus}$ cluster, with some selected orbitals sketched. The lowest a_{1g} and the higher e_g and t_{1u} orbitals have substantial local z^2 character, i.e., point "out."

The structure of this material is driven by donor–acceptor interactions. So it is for $In_3Mo_{15}Se_{19}$ and $K_2Mo_9S_{11}$, which contain $[Mo_{12}X_{14}]$ and $[Mo_9X_{11}]$ clusters (**85**).[37] A molecular orbital calculation on each of these clusters shows prominent low-lying unfilled orbitals directed away from the terminal Mo's, just where the dashed lines are. That's how these clusters link and aggregate in their respective solid-state structures.

This donor–acceptor analysis of the crystal structure indicates that if one wants to "solubilize" these clusters as discrete molecular entities, one must provide an alternative, better base than the molecule itself. Only then will one get discrete $[Mo_6X_8 \cdot L_6]^q$ complexes.

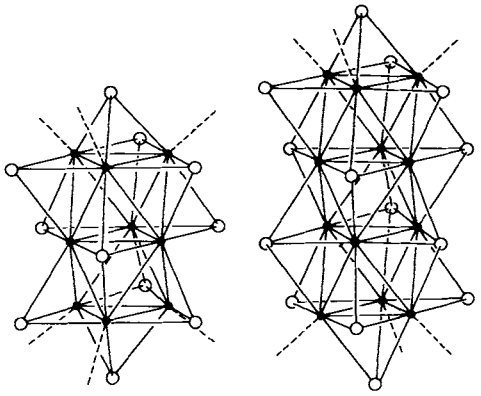

85

One more conclusion easily drawn from Figure 25, one applying what we know: when the clusters assemble into the lattice **83**, the five LUMOs of Figure 25 will be pushed up by interactions with neighboring cube sulfurs. All the cluster levels will spread out into bands. Will the HOMO band be broad or narrow? That band is crucial, because if you do the electron counting in $PbMo_6S_8$ you come to 22 electrons per $[Mo_6S_8]^{2\ominus}$; the top level in Figure 25 is half-filled. A glance at Figure 25 shows that the level in question, of e_g symmetry, is made up of Mo d functions which are of δ type with respect to the Mo–S external axis. Bringing in the neighboring cells will provide little dispersion for this band. The result is a high DOS at the Fermi level, one requirement (of several) for superconductivity.[40]

An interesting variation on the donor–acceptor theme in the solid is that the donor or acceptor need not be a discrete molecule, as one $[Mo_6S_8]$ cluster is toward another in the Chevrel phases. Instead, we can have electron transfer from one sublattice, one component of a structure, to another. We've already seen this in the explanation of the tuning of the X–X contact in the AB_2X_2 $ThCr_2Si_2$ structure. There the entire transition metal or B sublattice, made up of square nets, acts as a donor or acceptor, a reducing or oxidizing agent, for the X sublattice, made up of X–X pairs. A further example is provided by the remarkable $CaBe_2Ge_2$ structure, **86**.[41] In this structure one B_2X_2 layer,

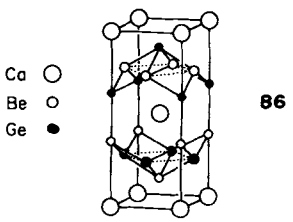

86

87, is identical to the $ThCr_2Si_2$ layer. The other, **88**, has B and X components interchanging places. These layers are

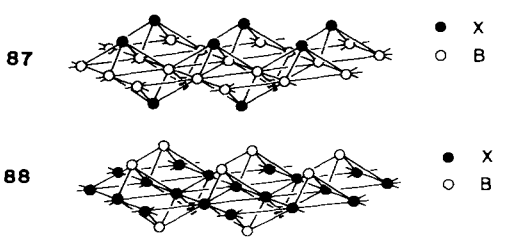

not identical, but isomeric. They will have different Fermi levels. One layer in the crystal will be a donor relative to the other. Can you reason out which will be the donor, which the acceptor layer?

What's New in the Solid?

If all the bands in a crystal are narrow (as they are in molecular and most extremely ionic solids), i.e., if there is little overlap between repeating molecular units, then there is no new bonding to speak of. But if at least some of the bands are wide, then there is delocalization, new bonding; a molecular orbital picture is necessary. This is not to say that we cannot recover, even in such a large-dispersion, delocalized situation, local bonding. The preceding sections have shown that we can see bonds. But there may be qualitatively new bonding schemes that result from substantial delocalization. Recall in organic chemistry the consequences of aromaticity, and in inorganic cluster chemistry of skeletal electron-pair counting algorithms.[42]

The language of orbital interactions, of perturbation theory, provides a tool that is applicable for the analysis of these highly delocalized systems, just as it works for small, discrete, molecules. For instance, take the question posed at the end of the last section. We have two isomeric two-dimensional lattices, **87** and **88**. Which will be a donor relative to the other? And which will be most stable?

These lattices are built up from two elements B and X in equal numbers, occupying two sublattices, I and II in **89**.

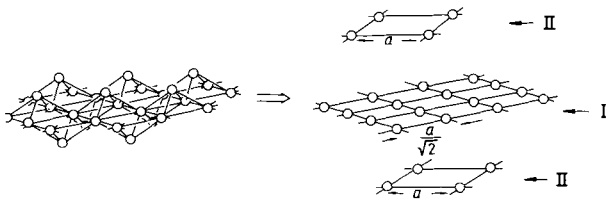

89

The elements are of unequal electronegativity, in the general case. In $ThCr_2Si_2$, one is a transition metal, the other a main-group element, in $CaBe_2Ge_2$ each a main-group element. Let's take, for purposes of discussion, $CaBe_2Ge_2$ as a model and write an interaction diagram, **90**, for what happens locally (Ge is more electronegative than Be). No implication as to band width is yet made—the orbital blocks are just that, blocks, indicating the rough position of the levels. The lower block of levels is obviously derived from

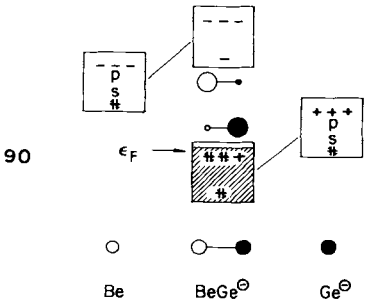

90

or localized in the orbitals of the more electronegative element. The band filling is actually appropriate to the

$CaBe_2Ge_2$ structure, i.e., $Be_2Ge_2^{2\ominus}$, or $BeGe^{\ominus}$, or seven electrons per two main-group atoms.

The orbitals develop into bands. The width of the bands depends on the inter-unit-cell overlap. The site II atoms are much farther apart from each other than the site I atoms (recall here the short metal–metal contacts in the $ThCr_2Si_2$ structure). We can say that sublattice I is more *dispersive* than sublattice II. The orbitals of atoms placed in sublattice I will form wider bands than those in sublattice II.

Now we have two choices: the more electronegative atoms can enter the less dispersive sites (lattice II) or the more dispersive sites (lattice I). The consequences are shown in **91** and **92**.

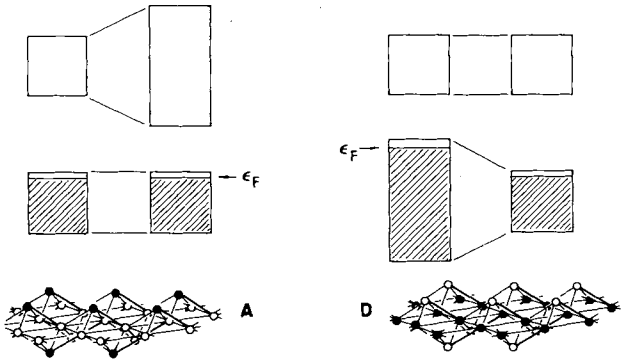

91 **92**

Which layer will be most stable and which will have the higher Fermi level depends on the electron filling. For a case such as $CaBe_2Ge_2$, or in general where the lower band is more than half-filled, the more electronegative atom will prefer the less dispersive site (**91**) and that layer will have a higher ionization potential, be a poorer donor.

The stability conclusion bears a little elaboration. It is based on the same "overlap repulsion" argument that was behind the asymmetric splitting of hydrogen chain bands (Fig. 1). When orbitals interact, the antibonding combinations are more antibonding than the bonding ones are bonding [cf. Eq. (a)]. Filling antibonding combinations, filling the tops of widely dispersed bands, is costly in energy. Conclusions on stability, as is the case in molecular chemistry, depend strongly on the electron count. In this particular case if the lower band were less than half-filled, the conclusion would be reversed, the more electronegative element should prefer the more dispersive site.

For $ThCr_2Si_2$ AB_2X_2 structures the conclusion we reach, that the more electronegative element should enter the less dispersive site, implies that for most cases the main-group X component will prefer the less dispersive, square-pyramidal, sublattice II positions. In $CaBe_2Ge_2$, Ge is more electronegative than Be. That means the layer in which the Ge enters the more dispersive sites (the bottom layer in **86**) should be a donor relative to the upper layer.

A reasonable question to ask is the following. If one layer (the acceptor layer) in $CaBe_2Ge_2$ is more stable than the other, the donor layer, why does the $CaBe_2Ge_2$ structure form at all? Why doesn't it go into a $ThCr_2Si_2$ structure based on the acceptor layer alone? The answer lies in the balance of covalent and dative interactions; for some elements the binding energy gained in donor–acceptor *interlayer* interactions overcomes the inherent stability of one isolated layer.[41]

At times the perturbation introduced by delocalization may be strong enough to upset the local, more "chemical" bonding schemes. Let me sketch two examples here.

Marcasites and arsenopyrites are a common structural choice for MA_2 compounds, where M is a late transition metal and A an element of the fifth or sixth main group. The structure, **93**, is related to the rutile one, in that one can easily perceive in the structure the octahedral coordination of the metal and one-dimensional chains of edge-sharing octahedra. The ligands are now interacting, however; not isolated $O^{2\ominus}$ as in rutile, but $S_2^{2\ominus}$ or $P_2^{4\ominus}$ diatomic units in the marcasites.[43]

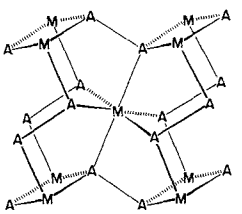

93

Low dimensionality characterizes another set of MS_2 sublattices, now in ternary structures of the type of $KFeS_2$ or $Na_3Fe_2S_4$.[44,45] In these molecules one finds one-dimensional MS_2 chains, consisting of edge-sharing tetrahedra (**94**).

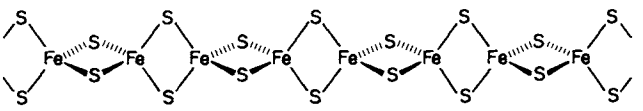

94

In both of these structural types, characterized by their simplicity, the metal–metal separations are in the range (2.6–3.1 Å) where reasonable men, or women, might disagree whether there is much metal–metal bonding. Cases with bridging ligands are ones in which real metal–metal bonding is particularly difficult to sort out from bonding through the bridge. Certainly the metal–metal bonding doesn't look to be very strong, if it's there at all. So a chemist would certainly start out from the local metal site environment, which is strikingly simple.

One would then predict a three-below-two orbital splitting at each metal in the octahedral marcasites and a two-below-three splitting in the tetrahedral MS_2 chains. The magic electron counts for a closed-shell low-spin structure should be then d^6 for the octahedral **93**, d^4 for the tetrahedral **94**. Forming the one-dimensional chains and then the three-dimensional structure will introduce some dispersion into these bands, one might reason. But not much—appropriate electron counts for semiconducting or non-magnetic behavior should remain d^6 for **93** and d^4 for **94**.

The experimental facts are as follows: the d^6 marcasites and arsenopyrites are semiconducting, but, surprisingly, so are the d^4 ones. Most of the AMS_2 structures synthesized to date feature the metal atom in configurations between

d^5 and $d^{6.5}$. The measured magnetic moments are anomalously low.

When calculations on these chains are carried out, one finds, to one's initial surprise, that the octahedral marcasite structure has a band gap at d^4 as well as d^6, and that the tetrahedral chain has a band gap at $d^{5.5}$ and not d^4. It seems that local crystal field considerations don't work. What in fact happens (and here the reader is referred to the detailed explanation in our papers[43,45]) is that the local field is a good starting point, but that further delocalizing interactions (and these are ligand-ligand and metal-ligand, and not so much metal-metal in the distance range considered) must be taken into account. The extended interactions modify the magic or gap electron counts that might be expected from just looking at the metal site symmetry.

In the preceding section, I outlined the orbital interactions that are operative in the solid state. These were the same ones as those that govern molecular geometries and reactivity. There is an interesting new feature in some solids, however. This is an interaction-induced rearrangement of the DOS around the Fermi level.

Suppose that one of the interacting orbital components is localized, with narrow bands, but it is interacting with a metallic sublattice, characterized by a reasonable DOS at the Fermi level. This is indicated schematically in **95**. Perhaps it's best to have a real example to think about. Consider an acetylene chemisorbed in low coverage on a Pt(111) surface, **96**. Here the discrete, narrow-band orbitals are the four π and π^* levels of a low-coverage acetylene layer, and the band is the Pt d band, nearly filled.[46,47]

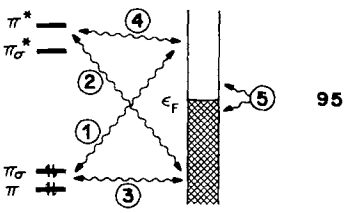

95

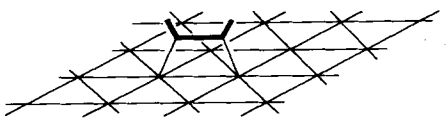

96

The most important two-electron bonding interactions that take place are between two of the acetylene π orbitals, π_σ and $\pi_\sigma{}^*$ (see **97**) and the d band. π_σ and $\pi_\sigma{}^*$ "point"

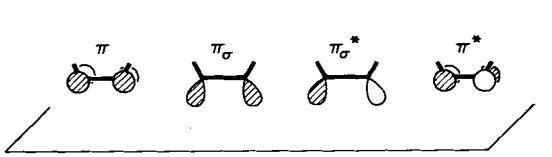

97

toward the surface, have greater overlap with metal orbitals, and they interact preferentially with different parts of the band, picking out those metal surface orbitals which have similar nodal patterns as the adsorbate. **98** shows this—in the "parallel bridging" geometry at hand the π_σ orbital interacts better with the bottom of the surface z^2 band and the $\pi_\sigma{}^*$ with the top of that band.

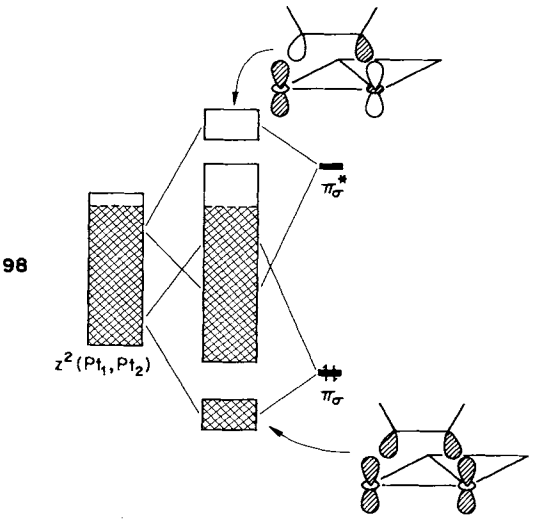

98

Both of these interactions are primarily of type ① and ③ (see **81** or **95**), four-electron repulsive or two-electron attractive interactions. Actually, the energetic and bonding consequences are a little complicated: the z^2-π_σ interaction would be destabilizing if the antibonding component of this interaction remained filled, below the Fermi level. In fact, many z^2-π_σ antibonding states are pushed above the Fermi level, vacated. This converts a destabilizing, four-electron interaction into a stabilizing two-electron one.

A counterpart to this interaction is ④ in **95**. Normally we would not worry about zero-electron interactions, because there is no "power" in them if there are no electrons. However, in the case of a metal with a continuous band of states, some of these levels—these are bonding combinations of $\pi_\sigma{}^*$ with the top of the z^2 band, as indicated in **98**—come below the Fermi level and are occupied. Therefore, they also contribute to bonding the adsorbate to the surface.

It should be noted that a consequence of all of these interactions is not only strengthening of metal-acetylene bonding, but also a weakening of bonding within the acetylene *and* within the metal. Interaction means delocalization, which in turn implies charge transfer. Interactions ①-④ operate to depopulate π_σ, populate $\pi_\sigma{}^*$, both actions weakening the acetylene π bond. Removing electrons from the bottom of the z^2 band and filling better the top of that band both result in a weakening of the Pt-Pt bond.

Interaction ⑤, peculiar to the solid, is a reorganization of the states around the Fermi level as a consequence of primary interactions ①-④. Consider, for instance, the levels that are pushed up above the Fermi level as a result of interaction ③, the four-electron repulsion. One way to think about this is the following: the electrons do not, in fact, go up past the Fermi level (which remains approximately constant), but are dumped at the Fermi level into levels somewhere in the solid. This is shown schematically in **99**.

But where is "somewhere"? The electrons that come in come largely from regions that are not directly involved in the bonding with the adsorbate. In the case at hand, they may come from Pt bulk levels, from Pt surface atoms not

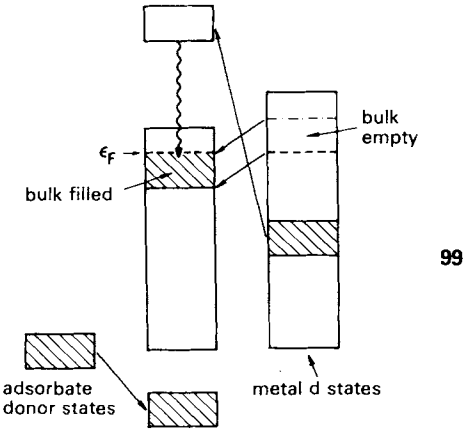

99

involved with the acetylene, from the Pt atoms binding the acetylene, but from orbitals of these atoms not used in that binding. While the metal surface is a nice reservoir of such electrons, these electrons are not innocent of bonding. They are near the top of their respective band (see **99**), and as such are metal–metal antibonding. Thus interaction ⑤ weakens bonding in the surface. Together with the aforementioned electron transfer effects of interactions ①–④ it is responsible for adsorbate-induced surface reconstruction.

In general, non-dissociative chemisorption is a delicate balance between attractive surface–molecule bonding and the consequences of the very same interactions, which weaken bonds in the adsorbed molecule and in the surface. Dissociative chemisorption and surface reconstruction are just two extremes of one and the same phenomenon.

I have discussed an example here of a surface reaction. A more detailed analysis of the theoretical aspects of surface science will be given elsewhere.[48] I bring this example in, because I want to make the point that surface chemistry and physics is not a thing unto itself, but also part of the wondrous continuum of molecular bonding that is chemistry. Surface science, a discipline in an exciting, explosive growth phase over the last decade, occasionally neglects its connections to solid-state chemistry. It shouldn't. Solid-state chemists should also take more advantage of what surface scientists have learned. Rather interestingly, the intellectual connection between surface science and discrete molecular chemistry has remained strong, perhaps because one component of surface chemistry, the adsorbate, is patently a molecule. The cluster–surface analogy has also served to bring together the literatures of surface science and organometallic chemistry.

From the perspective of orbital interactions, surfaces by themselves, and surfaces interacting with molecules, fit perfectly into a continuum of dimensionality of solid-state chemistry and physics. They are two-dimensional, half-solid, half-molecule extended systems—the same tools of orbital analysis apply to surfaces as to other solids.

So what's new in the solid? My straw-man physicist friend thinking of superconductivity, charge and spin density waves, heavy fermions, solitons, nonlinear optical phenomena, ferromagnetism in its various guises—all the fascinating things of interest to him and that I've neglected—he might say "everything." An exaggeration of what I've said in this paper is "not much." There are interesting, novel consequences of delocalization and wide-band formation, but even these can be analyzed in the language of orbital interactions.

It would not surprise anyone if the truth were somewhere in between. It is certainly true that I've omitted, by and large, the origins of most of the physical properties of the solid, especially those like superconductivity and ferromagnetism that are peculiar to that state of matter. Chemists will have to learn much more solid-state physics than I've tried to teach here if they are to understand these observables, and they *must* understand them if they are to make rational syntheses. I have concentrated on the most chemical notion of all—the solid is a molecule, a big one, to be sure, but just a molecule. Let's try to extract from the perforce delocalized picture of Bloch functions the chemical essence, the bonds that determine the structure and reactivity of this large molecule. The bonds must be there.

My graduate students, postdoctoral associates, and senior visitors to the group are responsible both for teaching me solid-state physics and for implementing the algorithms and computer programs that have made this work possible. While in my usual way I've suppressed the computations in favor of explanations, little understanding would have come without those computations. An early contribution to our work was made by Chien-Chuen Wan, but the real computational and interpretational advances came through the work of Myung-Hwan Whangbo, Charles Wilker, Miklos Kertesz, Tim Hughbanks, Sunil Wijeyesekera, and Chong Zheng. This paper owes much to their ingenuity and perseverance. Several crucial ideas were borrowed early on from Jeremy Burdett, such as using special k point sets for properties. Contributions were also made by Christian Minot, Jean-Yves Saillard, Denis Underwood, Georges Trinquier, Santiago Alvarez, Joel Bernstein, Jerome Silvestre, Marja Zonnevylle, Ralph Wheeler, Shen-shu Sung, Wolfgang Tremel, Douglas Keszler, and Jing Li.

In the early stages of this work, very important to me was a renewed collaboration with R. B. Woodward, prompted by our joint interest in organic conductors. It was unfortunately cut short by his death in 1979. Mike Sienko and his students offered gentle encouragement by showing us the interesting structures they worked on, as did Thor Rhodin on the surface science side. It was always instructive to try to provoke John Wilkins.

Over the years my research has been steadily supported by the National Science Foundation's Chemistry Division. I owe Bill Cramer and his fellow program directors thanks for their continued support. A special role in my group's research on extended structures has been played by the Materials Science Center (MSC) at Cornell University, supported by the Materials Research Division of the National Science Foundation. The MSC's activities, especially the interdisciplinary seminars it has supported, and in general the opportunity is has offered for learning of work in other areas of science relevant to this topic, have been crucial in the development of my work. My recent surface work, briefly mentioned in the last section, has been generously supported by the Office of Naval Research.

One reason it is easy to cross disciplines at Cornell is the existence of the Physical Sciences Library, with its broad coverage of chemistry and physics. I would like to thank Ellen Thomas and her staff for her contributions here. Our drawings, a critical part of the way our research is presented, have

been beautifully made over the years by Jane Jorgensen and Elisabeth Fields. I'd like to thank Eleanor Stagg for the typing and secretarial assistance in the past, and Linda Kapitany for the present manuscript.

This manuscript was written while I held the Tage Erlander Professorship of the Swedish Science Research Council NFR. The hospitality of Professor Per Siegbahn and the staff of the Institute of Theoretical Physics of the University of Stockholm is gratefully acknowledged, as well as the assistance of Ralph Wheeler, Jing Li, and Wolfgang Tremel in the writing and computations. The comments of many people on this paper were also very useful, especially those of J. Dunitz and H.-G. von Schnering. I thank W. Tremel and H. Tremel for the German translation.

Received: March 5, 1987 [A 633 IE]
German version: *Angew. Chem. 99* (1987) 871

[1] a) E. Zintl, G. Woltersdorf, *Z. Elektrochem. Angew. Phys. Chem. 41* (1935) 876; E. Zintl, *Angew. Chem. 52* (1939) 1; b) W. Klemm, E. Busmann, *Z. Anorg. Allg. Chem. 319* (1963) 297; W. Klemm, *Proc. Chem. Soc. London 1958*, 329; c) H. Schäfer, B. Eisenmann, W. Müller, *Angew. Chem. 85* (1973) 742; *Angew. Chem. Int. Ed. Engl. 12* (1973) 694; d) H. Schäfer, *Annu. Rev. Mater. Sci. 15* (1985) 1, and references cited therein.

[2] a) J. K. Burdett, *Nature (London) 279* (1979) 121; b) in A. Navrotsky, M. O'Keeffe (Eds.): *Structure and Bonding in Crystals*, Academic Press, New York 1981, p. 255; c) *Acc. Chem. Res. 15* (1982) 34, and references cited therein.

[3] J. K. Burdett, *Prog. Solid State Chem. 15* (1984) 173.

[4] a) M.-H. Whangbo in J. S. Miller (ed.): *Extended Linear Chain Compounds*, Plenum, New York 1982, p. 127; b) *Acc. Chem. Res. 16* (1983) 95, and references cited therein.

[5] M.-H. Whangbo in J. Rouxel (ed.): *Crystal Chemistry and Properties of Materials with Quasi-One Dimensional Structures*, Reidel, Dordrecht 1986, p. 27.

[6] The modern classic solid-state physics text is by N. W. Ashcroft and N. D. Mermin: "Solid State Physics," Holt, Rinehart and Winston, New York, 1976. Three other introductions to the field, ones which I think are pedagogically effective and accessible to chemists are: W. A. Harrison: *Solid State Theory*, Dover, New York 1980; W. A. Harrison: *Electronic Structure and the Properties of Solids*, Freeman, San Francisco 1980; S. L. Altman: *Band Theory of Metals*, Pergamon, New York 1970.

[7] Excellent introductions to this subject, written in the spirit of this article, and with a chemical audience in mind, are to be found in [3, 5, 8.]; M. Kertesz, *Int. Rev. Phys. Chem. 4* (1985) 125.

[8] T. A. Albright, J. K. Burdett, M.-H. Whangbo: *Orbital Interactions in Chemistry*, Wiley-Interscience, New York 1985, Chap. 20.

[9] For a review of this fascinating class of materials, see J. R. Williams, *Adv. Inorg. Chem. Radiochem. 26* (1983) 235.

[10] F. A. Cotton, R. A. Walton: *Multiple Bonds Between Metal Atoms*, Wiley, New York 1982, and references cited therein.

[11] For more information on the cyanoplatinates, see [4, 5].

[12] Fore more on the electronic structure of rutile and related compounds, see: J. K. Burdett, T. Hughbanks, *Inorg. Chem. 24* (1985) 1741; J. K. Burdett, *ibid. 24* (1985) 2244; L. F. Mattheis, *Phys. Rev. B: Solid State 13* (1976) 2433.

[13] J. B. Goodenough: *Magnetism and the Chemical Bond*, Krieger, New York 1976.

[14] R. S. Mulliken, *J. Chem. Phys. 23* (1955) 1833, 2343.

[15] For this task, and for band structure calculation in general, a chemist needs to learn group theory in the solid state. For a lucid introduction, see M. Tinkham: *Group Theory and Quantum Mechanics*, McGraw-Hill, New York 1964; G. Burns, A. M. Glazer: *Space Groups for Solid State Scientists*, Academic Press, New York 1978; O. Madelung: *Introduction to Solid State Theory*, Springer, Berlin 1978.

[16] The extension of overlap population considerations to the solid seems obvious, but I think we first introduced the formalism: a) T. Hughbanks, R. Hoffmann, *J. Am. Chem. Soc. 105* (1983) 3528; b) S. D. Wijeyesekera, R. Hoffmann, *Organometallics 3* (1984) 949; c) M. Kertesz, R. Hoffmann, *ibid. 3* (1984) 949; c) M. Kertesz, R. Hoffmann, *J. Am. Chem. Soc. 106* (1984) 3453.

[17] This is from an extended Hückel calculation: J.-Y. Saillard, R. Hoffmann, *J. Am. Chem. Soc. 106* (1984) 2006. For better calculations, see [35].

[18] This drawing was taken from [8].

[19] Original reference: H. A. Jahn, E. Teller, *Proc. R. Soc. London Ser. A 161* (1937) 220; a discussion of the utility of this theorem in deriving molecular geometries is given by J. K. Burdett: *Molecular Shapes*, Wiley, New York 1980; *Inorg. Chem. 20* (1981) 1959, and references cited therein; see also [3, 5] and R. G. Pearson: *Symmetry Rules for Chemical Reactions*, Wiley, New York 1976. The first application of the Jahn-Teller argument to stereochemical problems, and, incidentally, to condensed phases, was made by J. D. Dunitz, L. E. Orgel, *J. Phys. Chem. Solids 3* (1957) 20, 318; *Adv. Inorg. Chem. Radiochem. 2* (1960) 1; L. E. Orgel, J. D. Dunitz, *Nature (London) 179* (1957) 462.

[20] R. E. Peierls: *Quantum Theory of Solids*, University Press, Oxford 1972.

[21] H. C. Longuet-Higgins, L. Salem, *Proc. R. Soc. London Ser. A 251* (1959) 172.

[22] Review: M. Kertesz, *Adv. Quantum Chem. 15* (1982) 161.

[23] W. B. Pearson, *Z. Kristallogr. 171* (1985) 23, zit. Lit.

[24] For a theoretical analysis of this structural class, see: W. Tremel, R. Hoffmann, *J. Am. Chem. Soc. 109* (1987) 124; *Inorg. Chem. 26* (1987) 118; D. A. Keszler, R. Hoffmann, *J. Am. Chem. Soc. 109* (1987) 118.

[25] F. Hulliger, R. Schmelczer, D. Schwarzenbach, *J. Solid State Chem. 21* (1977) 371.

[26] R. Schmelczer, D. Schwarzenbach, F. Hulliger, *Z. Naturforsch. B36* (1981) 463, and references cited therein.

[27] a) J. K. Burdett, P. Haaland, T. J. McLarnan, *J. Chem. Phys. 75* (1981) 5774; b) J. K. Burdett, S. Lee, *J. Am. Chem. Soc. 105* (1983) 1079; c) J. K. Burdett, T. J. McLarnan, *J. Chem. Phys. 75* (1981) 5764.

[28] a) M. C. Zonnevylle, R. Hoffmann, *Langmuir 3* (1987), in press; b) G. Trinquier, R. Hoffmann, *J. Phys. Chem. 88* (1984) 6696; c) J. Li, R. Hoffmann, *Z. Naturforsch. B41* (1986) 1399; d) P. B. Littlewood, *CRC Crit. Rev. in Solid State Mat. Sci. 11* (1984) 229.

[29] a) W. Tremel, R. Hoffmann, *J. Am. Chem. Soc. 108* (1986) 5174, and references cited therein; b) J. Silvestre, W. Tremel, R. Hoffmann, *J. Less Common Met. 116* (1986) 113.

[30] H. F. Franzen, T. J. Burger, *J. Chem. Phys. 49* (1968) 2268; H. F. Franzen, G. A. Wiegers, *J. Solid State Chem. 13* (1975) 114.

[31] For further elaboration, see [16c, 29].

[32] W. B. Pearson, *J. Solid State Chem. 56* (1985) 278, and references cited therein.

[33] A. Mewis, *Z. Naturforsch. B35* (1980) 141.

[34] a) C. Zheng, R. Hoffmann, *J. Phys. Chem. 89* (1985) 4175; b) *Z. Naturforsch. B41* (1986) 292; c) *J. Am. Chem. Soc. 108* (1986) 3078.

[35] O. K. Andersen in P. Phariseau, W. M. Temmerman (Eds.): *The Electronic Structure of Complex Systems*, Plenum, New York 1984; in F. Bassani, F. Fumi, M. P. Tossi (Eds.): *Highlights of Condensed Matter Physics*, North-Holland, New York 1985.

[36] J. N. Murrell, M. Randic, D. R. Williams, *Proc. R. Soc. London Ser. A 284* (1965) 566; A. Devaquet, L. Salem, *J. Am. Chem. Soc. 91* (1969) 379; K. Fukui, H. Fujimoto, *Bull. Chem. Soc. Jpn. 41* (1968) 1984; M. Baba, S. Suzuki, T. Takemura, *J. Chem. Phys. 50* (1969) 2078; M.-H. Whangbo, S. Wolfe, *Can. J. Chem. 54* (1976) 949; K. Morokuma, *J. Chem. Phys. 55* (1971) 1236.

[37] Review: R. Chevrel in S. Foner, B. B. Schwartz (Eds.): *Superconductor Materials Science: Metallurgy, Fabrication and Applications*, Plenum, New York 1981, Chap. 10.

[38] J.-H. Lin, J. K. Burdett, *Inorg. Chem. 21* (1982) 5.

[39] T. Hughbanks, R. Hoffmann, *J. Am. Chem. Soc. 105* (1983) 1150.

[40] See also O. K. Andersen, W. Klose, H. Nohl, *Phys. Rev. B: Solid State 17* (1977) 1760; H. Nohl, W. Klose, O. K. Andersen in Ø. Fisher, M. B. Maple (Eds.): *Superconductivity in Ternary Compounds*, Springer, Berlin 1981, Chap. 6; D. W. Bullett, *Phys. Rev. Lett. 44* (1980) 178.

[41] See [34c], and references cited therein.

[42] K. Wade, *Chem. Commun. 1971*, 792; *Inorg. Nucl. Chem. Lett. 8* (1972) 559; *Electron Deficient Compounds*, Nelson, London 1971; D. M. P. Mingos, *Nature (London) Phys. Sci. 236* (1972) 99.

[43] For references, see S. D. Wijeyesekera, R. Hoffmann, *Inorg. Chem. 22* (1983) 3287.

[44] W. Bronger, *Angew. Chem. 93* (1981) 12; *Angew. Chem. Int. Ed. Engl. 20* (1981) 52.

[45] J. Silvestre, R. Hoffmann, *Inorg. Chem. 24* (1985) 4108.

[46] J. Silvestre, R. Hoffmann, *Langmuir 1* (1985) 621.

[47] The general principles underlying orbital interactions in chemisorption were analyzed also in our earlier paper on C-H and H-H activation [17].

[48] R. Hoffmann, *Rev. Mod. Phys.*, in press.

When submitting manuscripts, authors of articles intended for publication as "Communications" are requested to read the "Notice to Authors" reproduced in the January issue of the journal following the list of contents; upon request, a copy can be obtained from the editorial office.

[4+2] Cycloadditions of 2,3-Diazido-1,3-butadienes: A Novel Entry to Vicinal Vinyl Diazides and 1,4-Dicyano Compounds**

By *Klaus Banert**

Special interest attaches to the vinyl azides because of the universality of their reactions.[1] Simple methods for the synthesis of 2,3-diazido-1,3-butadienes (**1**, **9**, **10**, **13**–**16**) were reported recently[2–4] which provide access to interesting azirines and biazirinyls by photolysis or thermolysis.[3,4] In the following communication [4+2] cycloadditions of 2,3-diazido-1,3-butadienes are presented which afford a novel route to vicinal vinyl diazides and 1,4-dicyano compounds.

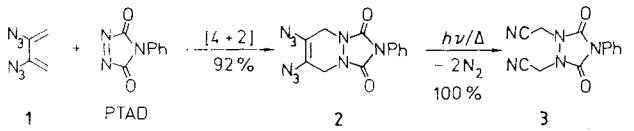

1 2 3

2,3-Diazido-1,3-butadiene **1** reacts with 4-phenyl-1,2,4-triazol-3,5-dione (PTAD) to give the Diels–Alder product **2**, which can be converted photolytically or thermally into the 1,4-dicyano compound **3** (Table 1).[5] Numerous examples for the decomposition of vicinal vinyl diazides to dinitriles have already been reported in the literature.[6–9] Directed syntheses, however, were hitherto only known for such vicinal diazides[10] in which two flanking, electron-attracting substituents facilitate introduction of the azide groups[9,11] or in which the azide groups are arranged *ortho* in an aromatic system.[8,12] The diazide **1** not only reacts with PTAD but also with tetracyanoethylene (TCNE), methyl tricyanoethylenecarboxylate,[13] dimethyl dicyanofumarate,[14] maleic acid anhydride, *N*-phenylmaleimide or fumaric acid dichloride in a [4+2] cycloaddition. Particularly high yields are obtained with TCNE. Initially, the vicinal vinyl diazide **4** is formed; this is then converted by photolysis or thermolysis into the hexacyano compound **5** (Table 1). These reactions, exactly like the sequence **1** + PTAD → **2** → **3**, represent a *cis* addition of two NC–CH_2 groups to an electron-deficient dienophile. On prolonged thermolysis, **5** decomposes into the fragments **7**[15] and **8**.[15] Since this cleavage is catalyzed by bases (such as NEt_3), formation of the intermediate **6** seems plausible.

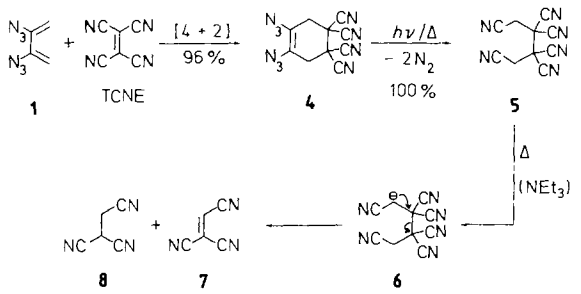

1 4 5 8 7 6

Reaction of PTAD with **9**, like that with **10**, leads to the vicinal vinyl diazide **11**, which upon photolysis or thermolysis is converted into the 1,4-dicyano compound **12** (Table 1). The yield (referred to **9** or **10**) is 91%. The methyl group in the *Z*-position accelerates the cycloaddition, since **9** is more electron-rich than **1**. On the other hand, the methyl group in the *E*-position in **10** hinders a cisoid arrangement of the diene. Hence, in Diels–Alder reactions, **10** reacts more slowly than **1**. Similar differences in reaction rates are observed in the [4+2] cycloadditions of **13**–**16** with TCNE: Thus, **13** reacts much more rapidly than **14**, while

Table 1. Some physical data of the new compounds **2**–**5**, **11**, **12**, and **17**–**20**. ^{1}H-NMR at 400 and 80 MHz, ^{13}C-NMR at 100 MHz. Spectra of **2**, **3**, **11**, and **12** in $CDCl_3$; Spectra of **17**–**20** in [D_6]acetone.

2: Bright-yellow solid; IR: $\tilde{\nu}$ = 2110, 1715, 1420 cm^{-1}; ^{1}H-NMR: δ = 4.22 (s, 4H), 7.49 (m, 5H); ^{13}C-NMR: δ = 43.4 (t, 144 Hz), 116.3 (s), 125.3 (d, 164 Hz), 128.5 (d, 162 Hz), 129.3 (d, 162 Hz), 130.7 (s), 152.2 (s)

3: Colorless solid; IR: $\tilde{\nu}$ = 1740, 1500, 1415 cm^{-1}; ^{1}H-NMR: δ = 4.61 (s, 4H), 7.51 (s, 5H); ^{13}C-NMR: δ = 36.2 (t, 151 Hz), 112.2 (t, 7 Hz), 125.4 (ddd, 165, 7, and 6 Hz), 129.5 (dt, 162 and 7 Hz), 129.6 (dd, 163 and 8 Hz), 129.9 (t, 9 Hz), 153.7 (t, 4 Hz)

4: Light-brown solid; IR (THF): $\tilde{\nu}$ = 2110 cm^{-1}; ^{1}H-NMR ([D_8]THF): δ = 3.60 (s); ^{13}C-NMR ([D_8]THF): δ = 32.2 (t, 140 Hz), 39.7 (tt, 6 and 5 Hz), 111.3 (s), 116.3 (s); ^{15}N-NMR ([D_6]acetone, CH_3NO_2 as external standard): δ = –290.4, –146.1, –142.3, –113.8 (CN)

5: ^{1}H-NMR ([D_8]THF): δ = 4.14 (s); ^{13}C-NMR ([D_8]THF): δ = 26.3 (t, 145 Hz), 42.7 (s), 109.3 (t, 4 Hz), 112.9 (t, 11 Hz); ^{15}N-NMR ([D_6]acetone): δ = –116.6 (2CN), –106.0 (4CN)

11: ^{1}H-NMR: δ = 1.48 (d, 6.3 Hz, 3H), 4.08 (dd, 15.0 and 1.6 Hz, 1H), 4.40 (d, 15 Hz, 1H), 4.54 (q, br, 6.3 Hz, 1H), 7.4–7.55 (m, 5H); ^{13}C-NMR: δ = 16.0 (q), 43.7 (t), 50.7 (d), 116.1 (s), 121.8 (s), 125.2 (d), 128.4 (d), 129.2 (d), 130.8 (s), 151.3 (s), 153.0 (s)

12: ^{1}H-NMR: δ = 1.73 (d, 7 Hz, 3H), 4.66 (s, 2H), 5.21 (q, 7 Hz, 1H, C*H*Me), 7.4–7.55 (m); ^{13}C-NMR: δ = 16.5 (qd, 132 and 5 Hz), 37.3 (t, 151 Hz), 45.5 (dq, 147 and 4 Hz), 112.4 (t, 7 Hz), 116.2 (dq, 9 and 6 Hz), 125.4 (dt, 165 and 6 Hz), 129.4 (dt, 162 and 7 Hz), 129.5 (dd, 164 and 9 Hz), 130.0 (t, 10 Hz), 153.5 (d, 3 Hz), 154.4 (t, 4 Hz)

17: ^{1}H-NMR: δ = 1.72 (d, 7 Hz, 6H), 3.89 (m, 2H); ^{13}C-NMR: δ = 16.4 (q), 38.3 (d), 44.5 (s), 111.0 (s), 112.0 (s), 122.8 (s)

18: ^{1}H-NMR: δ = 1.74 (d, 7 Hz, 6H), 3.87 (m, 2H); ^{13}C-NMR: δ = 15.6 (q), 38.5 (d), 46.7 (s), 109.4 (s), 111.8 (s), 123.9 (s)

19: ^{1}H-NMR: δ = 2.03 (d, 7 Hz, 6H), 4.61 (q, 7 Hz, 2H); ^{13}C-NMR: δ = 17.2 (q), 35.1 (d), 47.2 (s), 108.8 (s), 109.3 (s), 115.9 (s)

20: ^{1}H-NMR: δ = 2.05 (d, 7 Hz, 6H), 4.62 (q, 7 Hz, 2H); ^{13}C-NMR: δ = 17.1 (q), 35.0 (d), 46.9 (s), 108.5 (s), 108.7 (s), 115.4 (s)

[*] Dr. K. Banert
Fachbereich 8, Organische Chemie II
der Universität—Gesamthochschule
Adolf-Reichwein-Strasse, D-5900 Siegen (FRG)

[**] Reactions of Unsaturated Azides, Part 4. This work was supported by the Deutsche Forschungsgemeinschaft. The author thanks Frau *R. Stötzel* for assistance with some of the syntheses.—Part 3: [4].

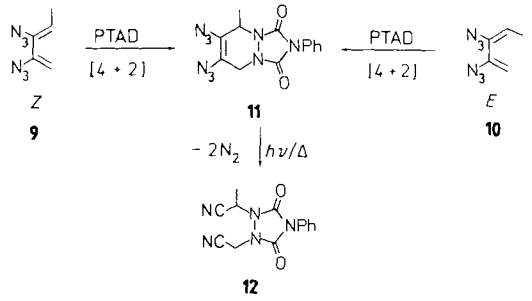

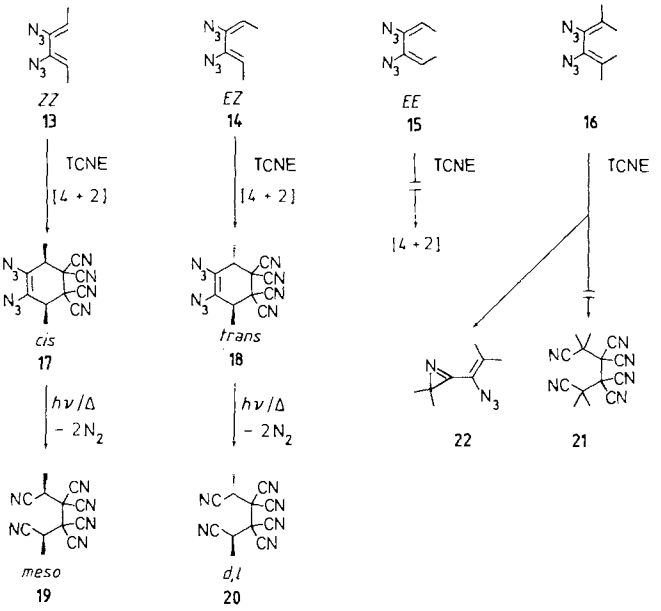

15, like **16**, does not undergo a Diels–Alder reaction.[16, 17] The reaction **16** → **22** requires three months at room temperature. The stereospecificity of the cycloaddition to **13** and **14** is shown by the formation of the diastereomers **17** and **18** (secondary products **19** and **20**) (Table 1) with >95% *de* (NMR).

The reactivities of the dienes **1**, **9**, **10**, and **13**–**16** can be compared with one another by competition reactions, with some hydrocarbons giving a more complete picture.[18] Scheme 1 gives a qualitative comparison of the reactivities.

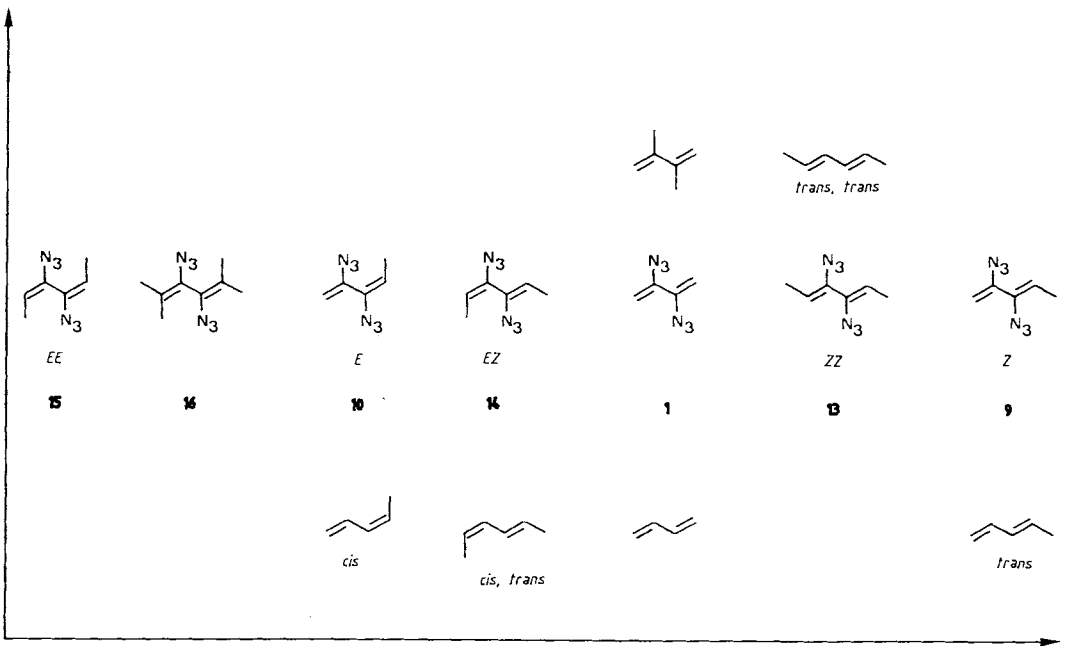

Scheme 1. Reactivity in [4 + 2] cycloadditions with TCNE or PTAD, qualitative comparison. The reactivity increases in the direction of the two arrows.

In the case of the azides, methyl groups in the *E*-position inhibit the [4 + 2] cycloadditions, whereas methyl groups in the *Z*-position have an accelerating effect. A comparison of the diazides with the analogous hydrocarbons shows that the additional azide groups facilitate faster Diels–Alder reactions. This effect is, however, less conspicuous than in the case of replacement of the hydrogen by methyl groups: **1** reacts more rapidly than 1,3-butadiene, but markedly more slowly than 2,3-dimethyl-1,3-butadiene. **13** occupies an unexpected position in Scheme 1. With its two activating methyl groups, **13** shows, on the one hand, a slower cycloaddition than **9** with only one such group; on the other hand, **13** reacts more slowly than the analogous hydrocarbon (*E*,*E*)-2,4-hexadiene.

The synthetic potential of 2,3-diazido-1,3-butadienes of type **1** is still not exhausted by the reactions described here. Preliminary experiments indicate that [2 + 2] cycloadditions and 1,3-dipolar cycloadditions are also possible.

Received: April 7, 1987;
revised: May 26, 1987 [Z 2186 IE]
German version: *Angew. Chem.* 99 (1987) 932

[1] G. Smolinsky, C. A. Pryde in S. Patai (Ed.): *The Chemistry of the Azido Group*. Wiley-Interscience, London 1971, p. 555; G. L'abbé, *Angew. Chem.* 87 (1975) 831; *Angew. Chem. Int. Ed. Engl.* 14 (1975) 775; A. Hassner in E. F. V. Scriven (Ed.): *Azides and Nitrenes*, Academic Press, Orlando, FL (USA) 1984, p. 35.

[2] H. Priebe, *Angew. Chem.* 96 (1984) 728; *Angew. Chem. Int. Ed. Engl.* 23 (1984) 736.

[3] K. Banert, *Tetrahedron Lett. 26* (1985) 5261.
[4] K. Banert, *Chem. Ber.*, in press.
[5] Reactions with PTAD were carried out in chloroform, reactions with TCNE in acetone or THF at room temperature (*if necessary with cooling*). These solvents were also used for the thermolyses (20–60°C) and photolyses (−10 to −40°C, mercury high-pressure lamp, Duran vessels).
[6] G. Smolinsky, C. A. Pryde, *J. Org. Chem. 33* (1968) 2411.
[7] J. H. Hall, *J. Am. Chem. Soc. 87* (1965) 1147; D. S. Pearce, M.-S. Lee, H. W. Moore, *J. Org. Chem. 39* (1974) 1362; A. Yabe, *Bull. Chem. Soc. Jpn. 52* (1979) 789; *54* (1981) 1176.
[8] J. H. Hall, E. Patterson, *J. Am. Chem. Soc. 89* (1967) 5856; M. E. Peek, C. W. Rees, R. C. Storr, *J. Chem. Soc. Faraday Trans. 2 1974*, 1260.
[9] J. A. VanAllen, W. J. Priest, A. S. Marshall, G. A. Reynolds, *J. Org. Chem. 33* (1968) 1100; H. W. Moore, M.-S. Lee, *Tetrahedron Lett. 1971*, 3645; D. S. Pearce, M. J. Locke, H. W. Moore, *J. Am. Chem. Soc. 97* (1975) 6181.
[10] Simple vicinal vinyl diazides (i.e. without directly neighboring electron-attracting substituents or without aromatic structure) have so far never been isolated but only proposed as intermediates: A. Hassner, R. J. Isbister, A. Friederang, *Tetrahedron Lett. 1969*, 2939.
[11] A. Mustafa, S. M. A. D. Zayed, S. Khattab, *J. Am. Chem. Soc. 78* (1956) 145; W. I. Awad, S. M. A. R. Omran, F. Nagieb, *Tetrahedron 19* (1963) 1591; W. L. Mosby, M. L. Silva, *J. Chem. Soc. 1964*, 3990; E. Winkelmann, *Tetrahedron 25* (1969) 2427; H. W. Moore, D. L. Maurer, D. S. Pearce, M. S. Lee, *J. Org. Chem. 37* (1972) 1984; P. Gangneux, E. Marechal, *Bull. Soc. Chim. Fr. 1973*, 1466; W. H. Gilligan, M. J. Kamlet, *Tetrahedron Lett. 1978*, 1675; U. Chandra Singh, M. S. Ramachandran, N. R. Subbaratnam, V. K. Kelkar, *Spectrochim. Acta Part A 35* (1979) 663.
[12] W. L. Mosby, M. L. Silva, *J. Chem. Soc. 1965*, 1003; R. Bolton, J. P. B. Sandall, *J. Chem. Soc. Perkin Trans. 2 1978*, 1288.
[13] T. Gotoh, A. B. Padias, H. K. Hall, Jr., *J. Am. Chem. Soc. 108* (1986) 4920.
[14] C. J. Ireland, J. S. Pizey, *J. Chem. Soc. Chem. Commun. 1972*, 4; C. J. Ireland, K. Jones, J. S. Pizey, S. Johnson, *Synth. Commun. 6* (1976) 185.
[15] C. L. Dickinson, D. W. Wiley, B. C. McKusick, *J. Am. Chem. Soc. 82* (1960) 6132.
[16] Reaction of a mixture of **13**–**15** with TCNE leads, as a result of the large differences in reactivity, to initial formation of **17**, which can be separated from **14** and **15**; **18** can also be easily separated from **15**. NMR studies show that the yields of **17**–**20** are of the same order of magnitude as in the reaction **1**→**4**→**5**.
[17] **21** is not formed on reaction of **16** with TCNE. It has, however, already been synthesized: W. J. Middleton, R. E. Heckert, E. L. Little, C. G. Krespan, *J. Am. Chem. Soc. 80* (1958) 2783.
[18] Detailed kinetic studies have been carried out on the cycloadditions of hydrocarbons with TCNE: C. Rücker, D. Lang, J. Sauer, H. Friege, R. Sustmann, *Chem. Ber. 113* (1980) 1663. As expected (*E,E*)-2,4-hexadiene is converted considerably more rapidly than (*E*)-1,3-pentadiene.

Dynamic Processes on the IR Time Scale: Coalescence of CO Stretching Vibrational Bands in [(η⁴-Diene)Fe(CO)₃] Complexes

By *Friedrich-Wilhelm Grevels,* Jürgen Jacke, Werner E. Klotzbücher, Carl Krüger, Klaus Seevogel,* and *Yi-Hung Tsay*

Coalescence phenomena are often observed in NMR spectra and are routinely used for the investigation of exchange processes or fluctional molecular structures. In vibrational spectroscopy, analogous temperature-dependent changes in the band shapes can only be observed when the processes responsible for these phenomena take place on the picosecond time scale. Accordingly, the few known examples[1–5] involve conformational changes or proton transfer reactions. The possibility that rapid intramolecular rearrangements in metal complexes might also be observed by IR spectroscopy has not yet been considered. We now report on [(η⁴-organo)Fe(CO)₃] compounds[6] as the first such examples.

$LM(CO)_3$ complexes containing three equivalent CO groups exhibit two CO stretching vibrations (C_{3v}: A_1, E) in the IR spectrum, which, in the energy-factored force field model,[7] are described as in (a) by two parameters (k, i). An example is given by the CO bands of [(η⁴-trimethylenemethane)Fe(CO)₃] **1** shown in Figure 1A.

$$A_1: k + 2i - K = 0$$
$$E: k - i - K = 0 \qquad \text{(a)}$$

with

$$K = \frac{4\pi^2 c^2}{\mu_{CO} N_A} \tilde{\nu}_{CO}^2$$

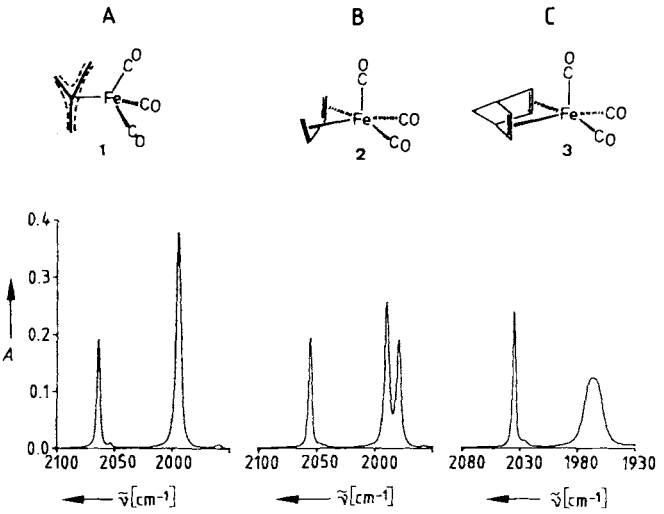

Fig. 1. CO bands of A) **1**: $\tilde{\nu}$ = 2064, 1995 cm⁻¹; B) **2**: $\tilde{\nu}$ = 2056, 1990.5, 1980 cm⁻¹; C) **3**: $\tilde{\nu}$ = 2035.5, 1967 cm⁻¹. *In* isooctane, T = 20°C, c = 0.003 mol L⁻¹, d = 100 μm. A = absorbance.

In [(η⁴-diene)Fe(CO)₃] complexes having square-pyramidal structure, the degeneracy of the out-of-phase CO stretching vibration is removed by the lowering of the symmetry to C_s, resulting in three CO bands (2 A′, A″), as described by (b). These are shown for [(η⁴-1,3-butadiene)Fe(CO)₃] **2** in Figure 1B. The Fe(CO)₃ complexes of

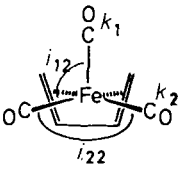

$$A': \begin{vmatrix} k_2 + i_{22} - K & \sqrt{2}\, i_{12} \\ \sqrt{2}\, i_{12} & k_1 - K \end{vmatrix} = 0$$
$$A'': \quad k_2 - i_{22} - K = 0 \qquad \text{b)}$$

norbornadiene (**3**) and 1,5-cyclooctadiene (**4**) belong to the few exceptions. As shown by the X-ray structure analysis of **4** (Fig. 2),[8] these complexes belong to the same square-pyramidal structure type having C_s symmetry as **2**.

[*] Priv.-Doz. Dr. F.-W. Grevels, Dipl.-Chem. J. Jacke, Dr. W. E. Klotzbücher
Max-Planck-Institut für Strahlenchemie
Stiftstrasse 34–36, D-4330 Mülheim a. d. Ruhr (FRG)
Prof. Dr. C. Krüger [+], Dr. K. Seevogel, Dr. Y.-H. Tsay [+]
Max-Planck-Institut für Kohlenforschung
Lembkestrasse 5, D-4330 Mülheim a. d. Ruhr (FRG)
[+] X-ray structure analysis.

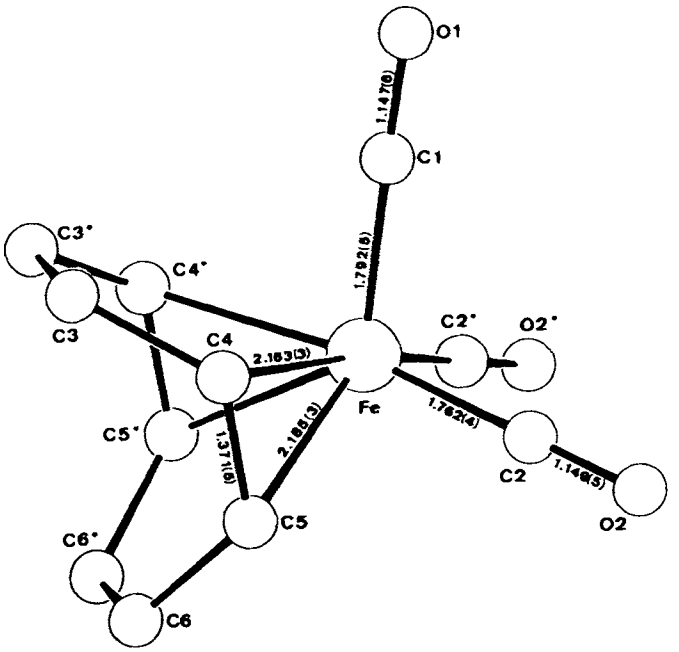

Fig. 2. Molecular structure of **4** [8]. Selected angles [°]: C1-Fe-C2 101.7(1), C2-Fe-C2* 86.6(2), C4-Fe-C4* 81.3(1), C5-Fe-C5* 78.7(1).

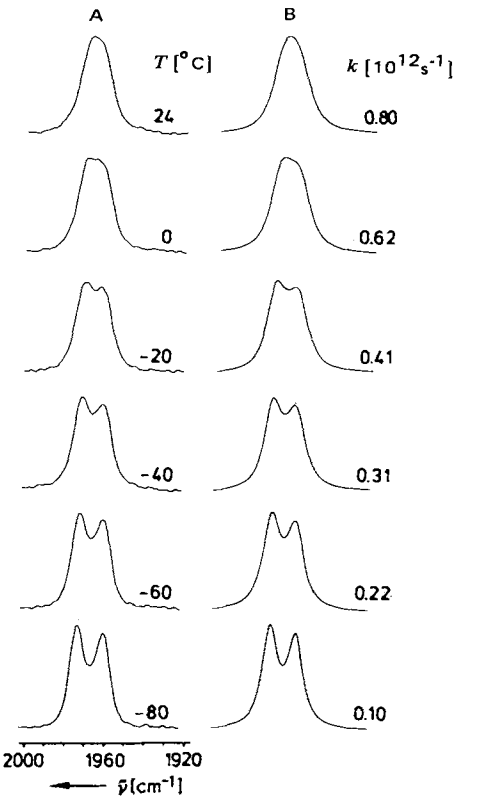

Fig. 3. Temperature-dependent IR spectrum of **3** in isooctane in the region of the two long-wavelength CO stretching bands. A) Measured [10]. B) Simulated [13].

The room-temperature IR spectra of **3** and **4** exhibit only two bands in the region of the CO stretching vibrations (**3**, Fig. 1C; **4**, $\tilde{\nu}=2028$, 1959 cm^{-1}), the long-wavelength band being unusually broad (Fig. 1C). In low-temperature matrices (Ar, $T=10$–12 K), on the other hand, the expected spectrum consisting of three bands of nearly equal intensities and widths is observed in the two cases (**3**: $\tilde{\nu}=2041$, 1980, 1963.5 cm^{-1}; **4**: $\tilde{\nu}=2034$, 1977, 1956.5 cm^{-1}). In order to establish that this marked difference is not due to the effect known as "matrix splitting" (cf. $Fe(CO)_5$[9]), the spectra of **3** and **4** were also recorded in solution (isooctane) at temperatures down to $-80°C$.[10] In both cases, the long-wavelength band was observed to gradually split into two components (Fig. 3A) as the temperature was decreased. In a second series of spectra recorded at temperatures up to 80°C, the long-wavelength band was observed to become narrower and to increase in intensity ($\Delta\tilde{\nu}_{1/2}$: 17.5 cm^{-1} at 20°C, 15 cm^{-1} at 80°C).

The CO bands of **3** and **4** thus exhibit a gradual change between the types of spectra shown in Figures 1B and 1A in the temperature range between $-80°C$ (**3**: $\tilde{\nu}=2035$, 1970.5, 1958.5 cm^{-1}; **4**: $\tilde{\nu}=2027.5$, 1969, 1949.5 cm^{-1}) and $+80°C$ (**3**: $\tilde{\nu}=2035$, 1966.5 cm^{-1}; **4**: $\tilde{\nu}=2028$, 1959.5 cm^{-1}).[11] This temperature dependence in the band shape of the out-of-phase CO stretching vibrations is similar to the known coalescence of NMR signals. It can be interpreted as an equilibration of the three CO groups, assuming that the rate constant for this process lies in the range of the IR time scale. For $k_1=k_2$ and $i_{12}=i_{22}$, the expressions of (b) are transformed to those of (a); i.e., the A″ and out-of-phase A′ vibrations degenerate into the E vibration. That the fully symmetric, high-frequency vibration (in-phase A′) does not participate in this coalescence (it is transformed to the A_1 vibration)[12] is an inevitable consequence of the way in which the three CO vibrations couple [Eq. (a)].

We carried out, as a trial, a simulation of the IR bands shown in Figure 3, in analogy to two NMR signals,[13] by using rate constants of 10^{11}–10^{12} s^{-1} (Fig. 3B). These values, despite all reservations regarding the use of this procedure,[4] should at least be of the correct order of magnitude. Plotting of $\ln k$ and $\lg(k/T)$ vs. $1/T$ gave straight lines, from which the activation parameters $E_a=2.2$ kcal mol^{-1}, $\Delta H^{\neq}=1.7$ kcal mol^{-1}, and $\Delta S^{\neq}\approx 2$ cal mol^{-1} K^{-1} could be derived.[20] The value for E_a lies far below the range that is accessible by NMR spectroscopy. This finding is in agreement with the observation of only one signal for the three CO groups in the ^{13}C-NMR spectra of **3** and **4** at temperatures down to $-110°C$.[14,15]

For the $Fe(CO)_3$ complexes of conjugated dienes, on the other hand, it is known that the equilibration of the CO ligands can be followed by ^{13}C-NMR spectroscopy;[14,16] coalescence occurs in the temperature region between $-40°C$ and $-80°C$ and the activation energies are 7–12 kcal mol^{-1} (e.g., for **2**, $E_a=9.5$ kcal mol^{-1}).

The detailed mechanism of the equilibration (rotation around the metal–diene axis; pseudorotation of the $M(CO)_3$ unit)[17] is not yet clear; however, a species having the structure **I** is a plausible intermediate.[14,15] According

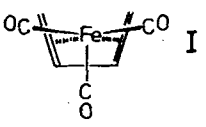

I

to extended Hückel calculations, this structure should be about 7 kcal mol^{-1} higher in energy than the basic structure **2**.[17] However, in the case of the norbornadiene and 1,5-cyclooctadiene complexes **3** and **4**, respectively, **I** is identical with the basic structure. This would adequately explain the unusually low activation energies.

Preliminary measurements carried out on [(η^4-cyclobutadiene)Fe(CO)$_3$] (cf. also Ref. [18]) have shown that this complex behaves similarly to **3** and **4**;[19] however, the long-wavelength, degenerate CO stretching vibration is split in this case only between -110 °C and -120 °C (in 2-methylpentane).

Received: April 22, 1987 [Z 2218 IE]
German version: *Angew. Chem. 99* (1987) 960

[1] M. M. Kreevoy, C. A. Mead, *J. Am. Chem. Soc. 84* (1962) 4596.
[2] M. Eigen, *Angew. Chem. 75* (1963) 489; *Angew. Chem. Int. Ed. Engl. 3* (1964) 1.
[3] B. Cohen, S. Weiss, *J. Phys. Chem. 87* (1983) 3606; *ibid. 88* (1984) 3159.
[4] R. A. MacPhail, H. L. Strauss, *J. Chem. Phys. 82* (1985) 1156.
[5] S. Bratos, G. Tarjus, P. Viot, *J. Chem. Phys. 85* (1986) 803.
[6] Synthesis and structure of [(η^4-organo)Fe(CO)$_3$] complexes: E. A. Koerner von Gustorf, F.-W. Grevels, I. Fischler (Eds.): *The Organic Chemistry of Iron, Vol. 1*, Academic Press, New York 1978, p. 1, 463, and 525.
[7] P. S. Braterman: *Metal Carbonyl Spectra*, Academic Press, London 1975.
[8] Crystal structure analysis of **4**: orthorhombic, *Pnma* (No. 62), $a = 13.906(2)$, $b = 10.300(3)$, $c = 7.562(2)$ Å, $\alpha = \beta = \gamma = 90.0°$, $V = 1083.12$ Å^3, $Z = 4$, $\rho_{calcd} = 1.52$ g cm^{-3}, $\mu(Mo_{K\alpha}) = 13.72$ cm^{-1}, $\lambda = 0.71069$ Å, 1650 reflections, 1078 observed, 122 refined parameters, $R = 0.0457$, $R_w = 0.0450$. Further details of the crystal structure investigation may be obtained from the Fachinformationszentrum Energie, Physik, Mathematik GmbH, D-7514 Eggenstein-Leopoldshafen 2 (FRG), on quoting the depository number CSD-52348, the names of the authors, and the journal citation.
[9] M. Poliakoff, J. J. Turner, *J. Chem. Soc. Dalton Trans. 1973*, 1351.
[10] AgCl microcell GC1 (Research and Industrial Instruments, London), contained in a coolable compartment, Nicolet 7199 FT-IR spectrometer, resolution 0.5 cm^{-1}.
[11] For comparison, the spectra of **1** and **2** were recorded under the same conditions. They remain unchanged over the entire range of temperatures; i.e., the E band of **1** does not undergo splitting at low temperatures and there is no evidence of broadening of the long-wavelength bands of **2** at high temperature.
[12] The frequency of this vibration can change to a small extent by equalization of the force field parameters; cf. [7], p. 45.
[13] Program DNMR5; D. S. Stephenson, G. Binsch, München 1978.
[14] L. Kruczynski, J. Takats, *J. Am. Chem. Soc. 96* (1974) 932; *Inorg. Chem. 15* (1976) 3140.
[15] O. A. Gansow, A. R. Burke, W. D. Vernon, *J. Am. Chem. Soc. 94* (1972) 2550.
[16] J. W. Faller, *Adv. Organomet. Chem. 16* (1977) 211.
[17] T. A. Albright, P. Hofmann, R. Hoffmann, *J. Am. Chem. Soc. 99* (1977) 7546.
[18] P. D. Harvey, I. S. Butler, D. F. R. Gilson, *Inorg. Chem. 25* (1986) 1009.
[19] Investigations in liquid rare gases, including measurements on ^{13}CO-enriched samples, are being carried out in collaboration with *M. Poliakoff* and *J. J. Turner* (Universität Nottingham) as part of a joint project supported by ECC.
[20] *Note added in proof* (August 17, 1987): Recent measurements over a wider range of temperature (down to -140 °C, in 2-methylpentane) indicate that the value determined for E_a is too high, presumably by 0.5–1 kcal mol^{-1}.

5,5-Dimethyl-1,2-dithia-3,7-diselenacycloheptane—A Storable Source of Disulfur, S_2**

By *Max Schmidt** and *Udo Görl*

Singlet oxygen, $^1O_2$, has in principle been known for a long time; its reactivity has been intensively studied.[1,2] The interest in reactions of S_2 was first aroused much later.[3,4] In 1984, *Steliou* et al. were able to produce S_2 for the first time by a method analogous to that used for the production of $^1O_2$ from triphenylphosphane ozonide and to trap it with dienes.[5] Recently, *Steliou* has reported that reaction of 2,2′-dibenzoylbiphenyl with bis(trimethylsilyl) sulfide and boron trichloride affords 2,2′-bis(thiobenzoyl)biphenyl, which spontaneously loses S_2 with C–C coupling and formation of 9,10-diphenylphenanthrene.[6,7]

We have recently synthesized and investigated the first organosubstituted chalcogen chains of the type R–Se–S–S–Se–R.[8] The open-chain compounds are, from our experience, not suitable as a source of S_2. In sharp contrast, however, the cyclic 5,5-dimethyl-1,2-dithia-3,7-diselenacycloheptane **1** undergoes thermal decomposition with ring contraction and formation of 4,4-dimethyl-1,2-diselenacyclopentane **2** and S_2.

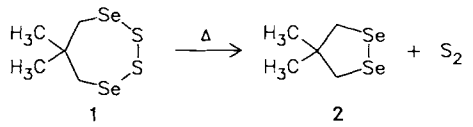

1 **2**

$HSe-CH_2-C(CH_3)_2-CH_2-SeH$ **3**

1 can be prepared from 2,2-dimethyl-1,3-propanediyl di(*p*-toluenesulfonate);[9] on reaction with sodium selenide, the latter is converted into **2**, which can be reduced with phosphorous acid (phosphinic acid)[10] to 2,2-dimethylpropane-1,3-diselenol **3**. Reaction of **3** with S_2Cl_2 then leads to elimination of HCl and formation of **1** in 70% yield as a bright-yellow solid. **1** is air-stable and soluble in the usual solvents. For prolonged storage, however, **1** should be kept at -15 to -20 °C, since it slowly decomposes to **2** and S_2 (which naturally transforms into S_8) at room temperature.

The thermal ring contraction involving cleavage of two selenium–sulfur bonds and formation of a selenium–selenium bond, which can be easily monitored ^{1}H-NMR spectroscopically, requires six days for completion when carried out in boiling toluene but only 90–240 minutes when carried out in boiling chlorobenzene. In the absence of suitable trapping reagents, S_2 is isolated—along with **2**—as S_8. The choice of reaction medium, and thus of the reaction temperature and duration of reaction, depends on the (albeit not always as high as desired) thermal stability of the S_2-adducts that are formed with the unsaturated compounds used in the reaction. Here, we shall only report on attempts to unequivocally detect S_2 by addition to the four 1,3-dienes **4**, **6**, **8**, and **10** in boiling chlorobenzene; presumably the yields can be improved by variation of the reaction time and temperature.

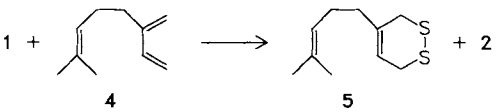

4 **5**

In the decomposition of **1** in the presence of myrcene **4** we obtained 4-(4-methyl-3-pentenyl)-3,6-dihydro-1,2-dithiin **5**, an antibacterial substance recently isolated from beer.[7]

Reaction of 1,1′-bicyclohexenyl **6** with **1** furnished, within 100 min, the complex **7**, 1,2,3,4,5,6,7,8,8a,10a-decahydro-9,10-dithiaphenanthrene, in 48% yield as a bright-yellow oil. In toluene the yield was only 23% after 6 d.

From the reaction of 2,3-dimethyl-1,3-butadiene **8** with **1** we isolated 4,5-dimethyl-3,6-dihydro-1,2-dithiin **9** as a

[*] Prof. Dr. M. Schmidt, Dr. U. Görl
Institut für Anorganische Chemie der Universität
Am Hubland, D-8700 Würzburg (FRG)

[**] This work was supported by the Fonds der Chemischen Industrie.

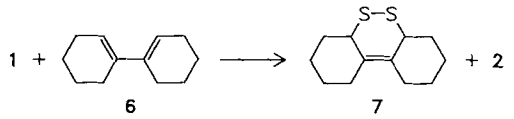

yellow oil in 48% yield. The diphenyl derivative **11** was obtained analogously in 54% yield from **10**.

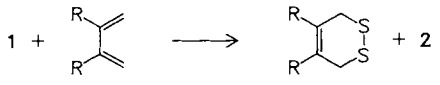

8, R = Me **9**, R = Me
10, R = Ph **11**, R = Ph

Attempts to synthesize pure **1**, which contains two phenyl groups in place of the two methyl groups, have so far failed because of its thermal instability at room temperature. Reaction of **3**, phenyl instead of methyl, with S_2Cl_2 gives the desired product, albeit in admixture with sulfur and the sulfur-free five-membered ring. When myrcene is added to the reaction mixture, the S_2-adduct can be detected but not isolated in sufficient amounts.

Reaction of **1** with the cyclic 1,3-dienes 1,3-cyclohexadiene, 1,2,3,4,5-pentaphenyl-1,3-cyclohexadiene or 1,4-diphenyl-1,3-cyclopentadiene affords **2** again in quantitative yield; however, sulfur and hydrogen sulfide, as well as the two aromatics, benzene and 1,2,3,4,5-pentaphenylbenzene, are also formed. The cyclopentadiene derivative, in which aromatization is not possible, undergoes polymerization.

Experimental:

2: 2,2-dimethyl-1,3-propanediyl di(*p*-toluenesulfonate) [9] (20.04 g, 49.5 mmol) was added portionwise to a Na_2Se_2 solution (prepared from 14.0 g (177 mmol) of Se, 4.20 g (111 mmol) of $NaBH_4$, and 300 mL of ethanol [11]) and the mixture heated under reflux for 72 h. After filtration, the resulting red solution was treated with 200 mL of H_2O and extracted with 250 mL of $CHCl_3$. The extract was dried over $MgSO_4$. Removal of solvent and purification of the remaining red oil by column chromatography (silica gel 400 × 25 mm, room temperature, petroleum ether 30–75 °C, $R_f = 0.17$, N_2 under pressure) afforded 7.9 g of pure **2** (70%). ^{1}H-NMR (60 MHz, CS_2, TMS int.): $\delta = 1.31$ (s, 6H), 3.10 (s, 4H). Correct elemental analysis.

3: A mixture of **2** (7.9 g, 35 mmol), 10 mL of 50% H_3PO_2, and 200 mL of diethylene glycol was heated to 70–80 °C. After 45 min the resulting colorless solution was treated with 100 mL of O_2-free H_2O and the mixture distilled at normal pressure. **3** was extracted from the two-phase distillate with CS_2. After drying over $MgSO_4$ and removal of CS_2 there remained 6.36 g (79%) of **3** as a colorless, foul-smelling oil. ^{1}H-NMR (60 MHz, CS_2, TMS int.): $\delta = -0.9$ (t, 2H, $J_{HCSeH} = 8$ Hz); 1.06 (s, 6H); 2.57 (d, 4H). Correct elemental analysis.

1: Separate solutions of **3** (5.54 g, 24.1 mmol) and S_2Cl_2 (3.24 g, 24.1 mmol) in CS_2 (in each case 50 mL) were cooled to −78 °C, transferred to separate dropping funnels, and added dropwise and simultaneously with stirring into 200 mL of CS_2 at −78 °C. The resulting yellow solution was treated with 4.82 g (48.2 mmol) of triethylamine in one batch. After filtration at −78 °C and removal of solvent at $-40\,°C/10^{-3}$ torr there remained a yellow oil, which was purified by column chromatography (as in the case of **2**) ($R_f = 0.33$). 4.92 g (70%) of pure **1** (m.p. 50–51 °C) was recovered as a yellow solid. ^{1}H-NMR (60 MHz, CS_2, TMS int.): $\delta = 1.10$ (s, 6H), 3.50 (s, 4H). Correct elemental analysis.

5: A mixture of **1** (2.34 g, 8.27 mmol) and **4** (1.13 g, 8.27 mmol) in chlorobenzene (15 mL) was heated under reflux for 90 min. The solvent was removed in a water-jet vacuum and the red oil remaining was separated by column chromatography into five fractions (unchanged **4**, $R_f = 0.75$; S_8, $R_f = 0.64$; unchanged **1**, $R_f = 0.33$; **2**, $R_f = 0.17$; small amounts of **1** and **2** mixed with **5**, $R_f = 0.26$). High-pressure chromatographic separation of the latter fraction yielded 0.66 g (40%) of pure **5** as a bright-yellow oil. ^{1}H-NMR (60 MHz, $CDCl_3$, TMS int.): $\delta = 1.60$ (s, 3H); 1.68 (s, 3H); 2.06 (s, 4H); 3.03–3.33 (m, 4H); 5.07 (m, 1H); 5.72 (m, 1H). Correct elemental analysis.

7: A mixture of **1** (2.145 g, 7.34 mmol) and **6** (1.19 g, 7.34 mmol) was treated and worked-up as described for the preparation of **5**. Yield: 742 mg (48%) of **7** as a bright-yellow oil. ^{1}H-NMR (60 MHz, $CDCl_3$, TMS int.): $\delta = 0.67$–1.03 (m); 1.06–2.06 (m). Correct elemental analysis.

9: **1** (2.76 g, 9.43 mmol) was allowed to react with **8** (2.50 g, 30.3 mmol) in boiling chlorobenzene for 4 h. Excess **8** was then distilled off with the solvent at normal pressure. Column chromatography (as for **2**) and subsequent high-pressure liquid chromatography furnished 675 mg (48%) of pure **9** as a bright-yellow oil. ^{1}H-NMR (60 MHz, CS_2, TMS int.): $\delta = 1.72$ (s, 6H), 3.11 (s, 4H).

11: A mixture of **1** (5.40 g, 18.44 mmol) and **10** (3.80 g, 18.44 mmol) in chlorobenzene (30 mL) was heated under reflux for 90 min. After removal of solvent in a water-jet vacuum, column chromatography afforded 2.68 g (54%) of pure **11** as a colorless solid (m.p. 102 °C). ^{1}H-NMR (60 MHz, $CDCl_3$, TMS int.): $\delta = 3.67$ (s, 4H); 7.10–7.25 (m, 10H). Correct elemental analysis.

Received: April 24, 1987;
revised: May 21, 1987 [Z 2221 IE]
German version: *Angew. Chem. 99* (1987) 917

[1] W. Adam, *Chem. Unserer Zeit 15* (1981) 190.
[2] H. H. Wasserman, R. W. Murray: *Singlet Oxygen*, Academic Press, New York 1979.
[3] R. Jahn, U. Schmidt, *Chem. Ber. 108* (1975) 630.
[4] D. L. Smith, *Diss. Abstr. Int. B37* (1977) 6141.
[5] K. Steliou, Y. Gareau, D. N. Harpp, *J. Am. Chem. Soc. 106* (1984) 799.
[6] K. Steliou, P. Salama, D. Drodeur, Y. Gareau, *J. Am. Chem. Soc. 109* (1987) 926.
[7] *Chem. Eng. News 65* (1987) No. 6, p. 23.
[8] U. Görl, *Dissertation*, Universität Würzburg 1987.
[9] F. Drahowzal, D. Klamann, *Monatsh. Chem. 82* (1951) 464.
[10] M. Schmidt, H. D. Block, *Chem. Ber. 103* (1970) 3348.
[11] I. Kuwajima, M. Shimizu, *H. Urabe, J. Org. Chem. 47* (1982) 837.

Synthesis of *O*-(α-Glyco)peptides by the *N*-Iodosuccinimide Procedure**

By *Horst Kessler,* Matthias Kottenhahn, Andreas Kling,* and *Cenek Kolar**

A large number of proteins found in living organisms are present as glycoconjugates; the elucidation of their structures, the understanding of their functions,[1–3] and their synthesis[4–6] still pose a challenge. One of the main difficulties is the stereoselective linking of the peptide with the carbohydrate. Glycopeptides have so far been prepared almost exclusively by modified Königs–Knorr glycosidation of protected amino acids. The remaining amino acids are subsequently added by standard methods of peptide chemistry. So far, it has not been possible to glycosidate larger peptide fragments stereoselectively in useful yields.

We report here on the use of the *N*-iodosuccinimide (NIS) procedure for the synthesis of glycosidated peptides. This procedure was developed by *Thiem* et al.[7] for the synthesis of 2-deoxy oligosaccharides. In particular, we have found that even pentapeptides react directly to give good yields of products with nearly complete diastereoselectivity.

The procedure consists in the reaction of glycals such as 3,4,6-tri-*O*-acetyl-D-glucal **1** or -galactal **2** with the hydroxyl groups of serine- or threonine-containing peptides in the presence of NIS (Scheme 1). The 2-deoxy-2-iodoglycosides thereby obtained, **3** or **4**, can be converted, via radicalic dehalogenation, into the 2-deoxyglycosides **5** or **6**, respectively.

[*] Prof. Dr. H. Kessler, Dipl.-Chem. M. Kottenhahn,
Dipl.-Chem. A. Kling
Institut für Organische Chemie der Universität
Niederurseler Hang, D-6000 Frankfurt am Main 50 (FRG)
Dr. C. Kolar
Behring-Werke
Postfach 1140, D-3550 Marburg (FRG)

[**] This work was supported by the Fonds der Chemischen Industrie.

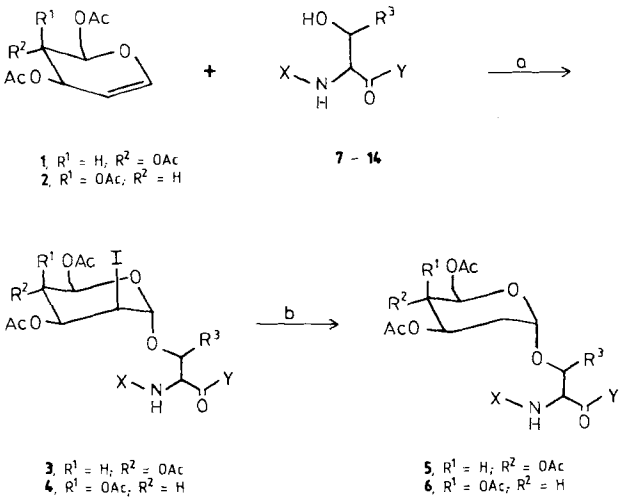

Scheme 1. The reaction of 1,2-didehydro carbohydrates with serine or threonine derivatives according to the NIS procedure followed by dehalogenation of the iodoglycopeptides. R^3 = H, CH_3; X, Y = protecting group, amino acid or peptide derivative (see Table 1). a), b): Experimental procedure, see [15] and [17], respectively.

Application of the NIS procedure has only been reported for the synthesis of di- or oligosaccharides[8] and alkylglycosides.[9] Only C-1 protected 2-deoxyglycosides have been so far prepared with 3,4,6-tri-*O*-acetyl-D-galactal **2**.[10] It is just such reactions, however, that make the method interesting, since galactose is frequently present in naturally occurring glycopeptides.

We first used **1** and **2** to carry out the glycosidation of the building blocks Fmoc-Ser-OBzl and Fmoc-Thr-OBzl, which are readily accessible by the methods of peptide chemistry.[11] Further experiments using model tripeptides and a pentapeptide demonstrate the scope of application and the possibility of using several combinations of protecting groups;[6] the Aloc,[12] Pyoc,[13] and Fmoc[14] groups served as *N*-terminal protecting groups. The yields in Table 1 show that the use of *N*-terminal Pyoc and Aloc protecting groups is not recommended in this procedure, since they give rise to side reactions owing to their chemical structure.

Particularly noteworthy are the good yields obtained in the reactions of the peptides with galactose derivatives and the high α diastereoselectivity.

The glycopeptides of types **3** and **4** thereby obtained are valuable starting materials. For example, some of them were treated with Bu_3SnH/AIBN, according to the known[16] radicalic dehalogenation procedure, to give 2-deoxyglycosides of types **5** and **6**[17] (Table 2; see also Scheme 1). The configuration at the anomeric center is completely retained during this reaction.

Table 2. 2-Deoxyglycopeptides of types **5** and **6** obtained by radical deiodination with Bu_3SnH [17]. TAD-glu = 3,4,6-tri-*O*-acetyl-2-deoxy-α-D-glucopyranosyl; TAD-gal = 3,4,6-tri-*O*-acetyl-2-deoxy-α-D-galactosyl.

Reactant	Product [a]		Yield [%]
3a	Fmoc-Ser(TAD-glu)-OBzl	**5a**	91
4a	Fmoc-Ser(TAD-gal)-OBzl	**6a**	84
3b	Z-Pro-Ser(TAD-glu)-Ala-OBzl	**5b**	82
4d	Z-Pro-Ser(TAD-gal)-Ala-OBzl	**6d**	92
3d	Z-Pro-Thr(TAD-glu)-Ala-OBzl	**5d**	86

[a] The purity of the synthesized compounds was determined by ^{1}H- and ^{13}C-NMR spectroscopy as well as by FAB mass spectrometry.

Of further interest is the replacement of iodine by azide or acetate. The 2-acetamido-2-deoxyglycosides are accessible from the azides (obtainable in the manno or talo configuration so far in yields of 40% by reaction of, e.g., the iodo compound **3a** with $NaN_3/(NH_4)_2Ce(NO_3)_4$).[18]

Deblocking of the glycosidated amino acids and peptides by means of available procedures[19] poses no problems.

Because of its diastereoselectivity, its high yields, and its broad scope of application, the procedure described here is well suited for the direct synthesis of glycopeptides containing various functions at C-2 of the carbohydrate. The non-naturally occurring 2-deoxyglycopeptides thereby formed are of interest as potential glycosidase inhibitors and for improving the pharmacokinetic properties of peptides.

Received: April 23, 1987;
revised: June 5, 1987 [Z 2219 IE]
German version: *Angew. Chem. 99* (1987) 919

[1] J. Montreuil in A. Neuberger, L. L. M. van Deenen (Eds.): *Comprehensive Biochemistry. Vol. 19B*, Part II, Elsevier, Amsterdam 1982, p. 1–187.
[2] N. Sharon, H. Lis, *Chem. Eng. News 59* (1981), No. 13, p. 21.
[3] J. Montreuil, *Adv. Carbohydr. Chem. Biochem. 37* (1980) 157.
[4] H. Paulsen, *Angew. Chem. 94* (1982) 184; *Angew. Chem. Int. Ed. Engl. 21* (1982) 155.

Table 1. 2-Deoxy-2-iodoglycopeptides of types **3** and **4** prepared according to the NIS procedure [15]. TADI-man = 3,4,6-tri-*O*-acetyl-2-deoxy-2-iodo-α-D-mannopyranosyl; TADI-tal = 3,4,6-tri-*O*-acetyl-2-deoxy-2-iodo-α-D-talopyranosyl.

Carbohydrate	Amino acid/peptide [a]		Product [b]		Yield [%]
1	Fmoc-Ser-OBzl	**7**	Fmoc-Ser(TADI-man)-OBzl	**3a**	98
2	Fmoc-Ser-OBzl	**7**	Fmoc-Ser(TADI-tal)-OBzl	**4a**	70
2	Aloc-Ser-OBzl	**8**	Aloc-Ser(TADI-tal)-OBzl	**4b**	41
2	Fmoc-Thr-OBzl	**9**	Fmoc-Thr(TADI-tal)-OBzl	**4c**	78
1	Z-Pro-Ser-Ala-OBzl	**10**	Z-Pro-Ser(TADI-man)-Ala-OBzl	**3b**	quant.
2	Z-Pro-Ser-Ala-OBzl	**10**	Z-Pro-Ser(TADI-tal)-Ala-OBzl	**4d**	79
1	Pyoc-Pro-Ser-Ala-OBzl	**11**	Pyoc-Pro-Ser(TADI-man)-Ala-OBzl	**3c**	31
2	Fmoc-Pro-Ser-Ala-OBzl	**12**	Fmoc-Pro-Ser(TADI-tal)-Ala-OBzl	**4e**	91
1	Z-Pro-Thr-Ala-OBzl	**13**	Z-Pro-Thr(TADI-man)-Ala-OBzl	**3d**	86
2	Z-Pro-Thr-Ala-OBzl	**13**	Z-Pro-Thr(TADI-tal)-Ala-OBzl	**4f**	85
1	Boc-Gly-Phe-Leu-Ser-Gly-OMe	**14**	Boc-Gly-Phe-Leu-Ser(TADI-man)-Gly-OMe	**3e**	>50

[a] Fmoc = 9-fluorenylmethoxycarbonyl, Aloc = allyloxycarbonyl, Pyoc = 2-(2-pyridyl)ethoxycarbonyl. [b] The purity of the synthesized compounds was determined by ^{1}H- and ^{13}C-NMR spectroscopy as well as by FAB mass spectrometry. The presence of β compounds could not be observed within the limits of detection (>97%).

[5] R. R. Schmidt, *Angew. Chem. 98* (1986) 213; *Angew. Chem. Int. Ed. Engl. 25* (1986) 212.
[6] H. Kunz, *Angew. Chem. 99* (1987) 297; *Angew. Chem. Int. Ed. Engl. 26* (1987) 294.
[7] J. Thiem, H. K. Schwentner, J. Schwentner, *Synthesis 1978*, 696.
[8] Example: J. Thiem, *Nachr. Chem. Tech. Lab. 32*, No. 1 (1984), p. 6.
[9] Example: J. Thiem, S. Köpper, J. Schwentner, *Liebigs Ann. Chem. 1985*, 2135.
[10] J. Thiem, B. Meyer, *Chem. Ber. 113* (1980) 3067.
[11] H. Paulsen, M. Schultz, *Liebigs Ann. Chem. 1986*, 1435.
[12] H. Kunz, C. Unverzagt, *Angew. Chem. 96* (1984) 426; *Angew. Chem. Int. Ed. Engl. 23* (1984) 436.
[13] H. Kunz, R. Barthels, *Angew. Chem. 95* (1983) 799; *Angew. Chem. Int. Ed. Engl. 22* (1983) 783; *Angew. Chem. Suppl. 1983*, 39.
[14] H. Kunz, D. Schultheiss-Reismann, *Angew. Chem. 95* (1983) 64; *Angew. Chem. Int. Ed. Engl. 22* (1983) 62, *Angew. Chem. Suppl. 1983*, 39.
[15] *Experimental Procedure* for **3** and **4**: The 3,4,6-tri-*O*-protected glycal **1** or **2** was dissolved in dry CH_3CN or dry CH_3CN/CH_2Cl_2 under inert gas. After addition of one-half to one equivalent of the *C*- and *N*-terminal protected amino acid or the *C*- and *N*-terminal protected peptide, *N*-iodosuccinimide (freshly recrystallized from CCl_4 and dried) was added under inert gas with stirring. The reaction mixture was allowed to warm to room temperature and stirred until no starting material was detected by thin layer chromatography. The reaction mixture was worked up by extracting the product into $CDCl_3$, washing with a 10% solution of sodium thiosulfate and with ice water, and drying the organic phase over magnesium sulfate. After concentration, the residue was chromatographed on silica gel.
[16] K. Tatsuta, K. Fujimoto, M. Kinoshita, *Carbohydr. Res. 54* (1977) 85.
[17] *Experimental Procedure* for **5** and **6**: Compounds **3** and **4**, prepared as described in [15], were dissolved in dry benzene and the stirred solution was treated under inert gas with a catalytic amount of azoisobutyronitrile (AIBN) and then with 1.2 equivalents of tributyltin hydride. The reaction mixture was stirred at 30–40°C under inert gas until no starting material was detected by thin layer chromatography. The mixture was then concentrated under vacuum and the residue was chromatographed on silica gel.
[18] M. Kottenhahn, *Diplomarbeit*, Universität Frankfurt 1986.
[19] H. Kunz, *Nachr. Chem. Tech. Lab. 32* (1984) 11.

Noncovalent Bonding Interactions between Tetraphenylborate Anions and Paraquat and Diquat Dications**

By *Gwilym J. Moody, Richard K. Owusu, Alexandra M. Z. Slawin, Neil Spencer, J. Fraser Stoddart,* J. D. Ronald Thomas,* and *David J. Williams*

The observation[1] that dibenzo[30]crown-10 (DB30C10) complexes with diquat $DQT^{2\oplus}$ but not[2] with paraquat $PQT^{2\oplus}$ has led[3] to the development of an ion-selective electrode for diquat. The sensor, which is used with 2-nitrophenylphenyl ether as a plasticizing solvent mediator in a PVC matrix membrane is based on DB30C10 mixed with diquat bis(tetraphenylborate) **1**. The neutral carrier ligand improves the $DQT^{2\oplus}$-sensing quality, which is also demonstrated by **1** on its own. More recently, a constitutional isomer of DB30C10 containing 1,4-linked benzene rings, namely bisparaphenylene[34]crown-10 (BPP34C10), has been found[4] to complex with $PQT^{2\oplus}$ as well as with $DQT^{2\oplus}$. However, the $PQT^{2\oplus}$ electrode, based on **2**, is surprisingly better when BPP34C10 is absent.[3] The fact that **2** produces orange-colored membranes[5] suggested to us that there is a π–π charge-transfer interaction of the donor–acceptor type[6] between $BPh_4^{\ominus}$ and $PQT^{2\oplus}$ in **2**, in addition to major attractive interactions, involving ion-pairing,[7] and other weaker stabilizing forces arising from van der Waals and dispersive interactions.[8] We now report the confirmation of this hypothesis on the basis of an X-ray structural analysis[9] on a single red crystal[10] of **2**.

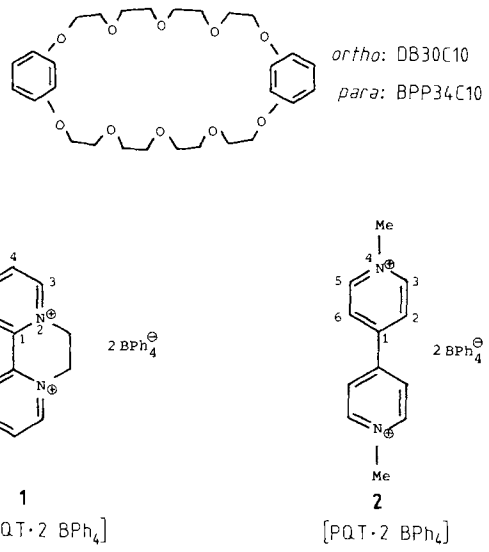

The solid-state structure reveals that the planar $PQT^{2\oplus}$ is sandwiched between two tetraphenylborate anions (Fig. 1) related to each other by a crystallographic center of symmetry which lies at the center of the Cl–Cl′ bond. One of the phenyl rings on each anion is aligned approximately parallel to (10° tilt between mean planes, Fig. 2) and partially overlapping one of the pyridinium rings of $PQT^{2\oplus}$. In the region of ring overlap, the distances of C24 and C25 from the plane of the pyridinium ring are both 3.38 Å and, conversely, those of C2 and C3 from the plane of the phenyl ring are both 3.27 Å. These contacts are consistent[11] with π–π charge-transfer interactions which give rise to the pronounced color observed in both solution[5] and the solid state. In addition to the sandwiching of $PQT^{2\oplus}$ by two anions, the space-filling representation (Fig. 3) illustrates additional edge-to-face interactions between the dication and the orthogonally disposed phenyl rings on the anions. These T-shaped arrangements of the π-electron-de-

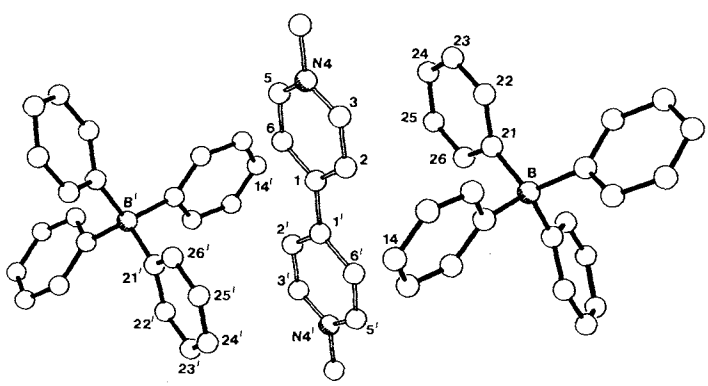

Fig. 1. Structure of paraquat bis(tetraphenylborate) [PQT·2 BPh_4] **2** in the crystal [9].

[*] Dr. J. F. Stoddart, Dr. N. Spencer
Department of Chemistry, The University
Sheffield S3 7HF (UK)
Dr. J. D. R. Thomas, Dr. G. J. Moody, Dr. R. K. Owusu
Department of Applied Chemistry, PO Box 13, UWIST
Cardiff CF1 3XF (UK)
Dr. D. J. Williams, A. M. Z. Slawin
Chemical Crystallography Laboratory
Department of Chemistry, Imperial College
London SW7 2AY (UK)

[**] This work was supported by the Science and Engineering, and Agricultural and Food, Research Councils in the United Kingdom. We thank the Leverhulme Trust for the award of a Research Fellowship to *J. F. S.*

Table 1. ^{1}H-NMR chemical shift data (δ and $\Delta\delta$ values) for **1** and **2** and for reference compounds in [D$_6$]acetone [a].

	$DQT^{2\oplus}$					$PQT^{2\oplus}$			$BPh_4^{\ominus}$		
	H-6	H-5	H-4	H-3	$^{\oplus}NCH_2$	H-3,5	H-2,6	$^{\oplus}NMe$	*ortho*	*meta*	*para*
nBu$_4$NBPh$_4$	—	—	—	—	—	—	—	—	7.27	6.91	6.77
[PQT·2PF$_6$]	—	—	—	—	—	9.36	8.83	4.73	—	—	—
2 [PQT·2BPh$_4$]	—	—	—	—	—	9.03	8.43	4.58	7.34	6.90	6.74
						(−0.33)	(−0.40)	(−0.15)	(+0.07)	(−0.01)	(−0.03)
DQT·2PF$_6$	9.23	9.09	8.59	9.49	5.69	—	—	—	—	—	—
1 [DQT·2BPh$_4$]	8.86	8.86	8.36	9.06	5.31	—	—	—	7.34	6.91	6.76
	(−0.37)	(−0.23)	(−0.23)	(−0.43)	(−0.38)				(+0.07)	(0.00)	(−0.01)

[a] The spectra were recorded at room temperature on a Bruker AM250 spectrometer using CD_2HCOCD_2H in CD_3COCD_3 as reference. The $\Delta\delta$ values (in parentheses, quoted for 0.013 M solutions) indicate the shifts with respect to the appropriate standard (nBu$_4$NBPh$_4$, [PQT·2PF$_6$], or [DQT·2PF$_6$]). The $\Delta\delta$ values for **2** represent the lowest numerical limits, since the salt starts to crystallize in the NMR tube even while the spectrum is being recorded (see [10] and [16]).

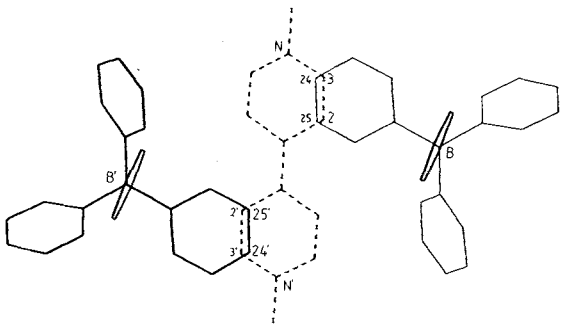

Fig. 2. Schematic representation of the overlap between the pyridinium rings of the dication $PQT^{2\oplus}$ (broken lines) and one of the phenyl rings of each anion $BPh_4^{\ominus}$ (solid lines) of **2**.

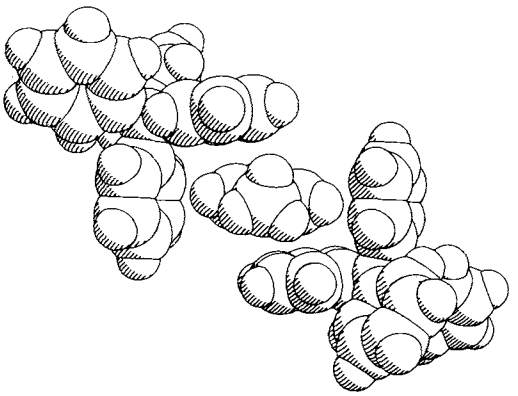

Fig. 3. Space-filling representation of the structure of paraquat bis(tetraphenylborate) **2** highlighting both face-to-face and edge-to-face interactions between the pyridinium rings of the dication and the orthogonally disposed phenyl rings of the anions.

ficient pyridinium and π-electron-rich phenyl rings, coupled with a centroid–centroid distance of 5.0 Å and the 4° inclination of the associated vector to the normal to the phenyl ring in each case, are characteristic of the geometry associated with the global potential energy minimum for two interacting aromatic rings.[11–14]

The ^{1}H-NMR chemical shift data for **1**, **2**, and reference compounds recorded in Table 1 shows that close association is maintained between the $PQT^{2\oplus}$ and $BPh_4^{\ominus}$ ions in solid **2** in acetone solution.[15] All the evidence suggests that a highly structured ternary complex involving a dication and two anions exists[16] in solution as well as in the solid state. The upfield shifts of $\Delta\delta = -0.33$ and -0.40 ppm for H-3,5 and H-2,6, respectively, in $PQT^{2\oplus}$ are compatible with the positioning (see Figs. 2 and 3) of one side of each pyridinium ring in the paratropic regions of both a parallel and an orthogonally disposed phenyl ring of $BPh_4^{\ominus}$. These upfield shifts are accompanied by small downfield shifts of the *ortho* protons of the anions: this reflects the diatropy of the encircled dication. The fact that a similar downfield shift is observed for these protons in **1** suggests that this ternary complex[16] is also a highly structured one in solution.

As a consequence of these results one can envisage a new generation of macrocyclic dianionic receptors and sensors incorporating two tetraarylborate residues.[17]

Received: March 20, 1987;
revised: June 15, 1987 [Z 2151 IE]
German version: *Angew. Chem.* 99 (1987) 939

CAS Registry numbers:
1, 107573-79-5; **2**, 80777-50-0.

[1] H. M. Colquhoun, E. P. Goodings, J. M. Maud, J. F. Stoddart, D. J. Williams, J. B. Wolstenholme, *J. Chem. Soc. Perkin Trans. 2 1985*, 607.
[2] This observation was made for CH_2Cl_2 solutions [1]. However, when equimolar amounts of [PQT·2PF$_6$] and DB30C10 are mixed in acetone, a faint orange coloration is observed, indicating the existence of a weak charge-transfer interaction.
[3] G. J. Moody, R. K. Owusu, J. D. R. Thomas, *Analyst (London) 112* (1987) 121.
[4] B. L. Allwood, N. Spencer, H. Shahriari-Zavareh, J. F. Stoddart, D. J. Williams, *J. Chem. Soc. Chem. Commun. 1987*, 1064.
[5] UV spectra of **1** ([DQT·2BPh$_4$]) and **2** ([PQT·2BPh$_4$]) recorded in acetone show absorptions associated with very broad bands that extend beyond $\lambda = 500$ nm. In the case of **1**, two shoulders are clearly identifiable at $\lambda = 380$ and 480 nm: in the case of **2**, only one shoulder could be identified at $\lambda = 360$ nm. Since neither [PQT·2PF$_6$] or [DQT·2PF$_6$] nor nBu$_4$NBF$_4$ absorb in the visible region, these absorption bands may be attributed to charge-transfer interactions (R. Foster: *Organic Charge-Transfer Complexes*, Academic Press, London 1969).
[6] C. J. Bender, *Chem. Soc. Rev. 15* (1986) 475.
[7] Ion-pair complexation with charge-transfer interactions involving $PQT^{2\oplus}$ and inorganic anions is well established (L. A. Summers: *The Bipyridinium Herbicides*, Academic Press, New York 1980, p. 116). Ion-pair complexation involving large organometallic cations and large organic anions is also well known (for a recent example, see S. Tachiyashiki, H. Yamatera, *Inorg. Chem. 25* (1986) 3209.
[8] R. S. Mulliken, *J. Am. Chem. Soc. 74* (1952) 811; M. Meot-Ner (Mautner), *Acc. Chem. Res. 17* (1984) 186.
[9] **2**: monoclinic, $a = 9.925(2)$, $b = 14.734(3)$, $c = 17.487(5)$ Å, $\beta = 93.85(2)°$, $V = 2549$ Å^3, $P2_1/c$, $Z = 2$ (the complex possesses a center of symmetry), $\rho_{calcd} = 1.10$ g cm^{-3}. Nicolet R3m diffractometer, ω-scan, graphite monochromated $Cu_{K\alpha}$ radiation. The structure was solved by direct methods and refined anisotropically to give $R = 0.085$, $R_w = 0.095$ for 1859 independent observed reflections [$|F_o| > 3\sigma(|F_o|)$, $\theta \leq 50°$]. The R factor is high owing to slight disorder in the phenyl groups of the anion and to the presence of disordered solvent fragments. Further details of the crystal structure investigation are available from the Director of the Cambridge Crystallographic Data Centre, University Chemical Laboratory, Lensfield Road, Cambridge CB2 1EW (England) on quoting the full literature citation.
[10] *Experimental Procedure* for **2** ([PQT·2BPh$_4$]): n-Bu$_4$NBPh$_4$ (10 mg, 0.018 mmol) was dissolved in [D$_6$]acetone (0.7 mL) and the solution was added to [PQT·2PF$_6$] (4.25 mg, 0.009 mmol). The solution instantly

turned deep yellow with a slight precipitation occurring thereafter. The solution was filtered and red single crystals, suitable for X-ray investigation, grew in the filtrate within the following 24 h. M.p. = 215–220 °C (decomp.).

[11] R. O. Gould, A. M. Gray, P. Taylor, M. D. Walkinshaw, *J. Am. Chem. Soc. 107* (1985) 5921.

[12] S. K. Burley, G. A. Petsko, *Science (Washington, DC) 229* (1985) 23; *J. Am. Chem. Soc. 108* (1986) 7995.

[13] It has not escaped our attention that, in the X-ray structure of the benzene complex of a self-adjusting molecular cage containing two 1,1,1-triphenylethane units linked by three $OCH_2C{\equiv}C{-}C{\equiv}CCH_2O$ linkages (E. O'Krongley, S. R. Denmeade, M. Y. Chiang, R. Breslow, *J. Am. Chem. Soc. 107* (1985) 5544), the included benzene molecule is clamped between two phenyl residues both arranged with their edges directed toward the opposite faces of the benzene molecule.

[14] Recently, we have observed edge-to-face stacking of aromatic rings (I) in the macrocycle BPP25C7, an analogue of BPP34C10 (A. M. Z. Slawin, N. Spencer, J. F. Stoddart, D. J. Williams, *J. Chem. Soc. Chem. Commun. 1987*, 1070) and (2) in a 1:2 adduct formed between $[Pt(NH_3)_4]^{2\oplus}$ and two second-sphere bicyclic polyether ligands each incorporating two 2,6-bis(hydroxymethyl)phenol residues (D. R. Alston, A. M. Z. Slawin, J. F. Stoddart, D. J. Williams, R. Zarzycki, *Angew. Chem. 99* (1987) 697, 698; *Angew. Chem. Int. Ed. Engl. 26* (1987) 692, 693. Although, in the first example, the attractive edge-to-face interactions are occurring intramolecularly, in the second example, they exist *intermolecularly* and so are more similar in type to those observed in $[PQT{\cdot}2BPh_4]$ **2** (Figs. 1–3).

[15] We have observed similar significant changes of chemical shifts of specific substrate and receptor protons *in acetone solution* when $DQT^{2\oplus}$ and $PQT^{2\oplus}$ form 1:1 inclusion complexes with DB30C10 and BPP34C10, respectively [1, 4]. It is worthy of note that the 1:1 inclusion complexes formed between numerous *water-soluble macrocyclic receptors* of the cyclophane type, incorporating either diphenylmethane or substituted diphenylmethane residues and aromatic substrates (e.g., 2,7-dihydroxynaphthalene and pyrene) also exhibit strong changes of the chemical shifts of specific protons of receptor and substrate upon complexation (K. Odashima, A. Itai, Y. Iitaka, Y. Arata, K. Koga, *Tetrahedron Lett. 21* (1980) 4347; J. Winkler, E. Coutouli-Argyropoulou, R. Leppkes, R. Breslow, *J. Am. Chem. Soc. 105* (1983) 7198; F. Diederich, K. Dick, *Angew. Chem. 95* (1983) 730; *Angew. Chem. Int. Ed. Engl. 22* (1983) 715; *Angew. Chem. Suppl. 1983*, 957; F. Diederich, D. Griebel, *J. Am. Chem. Soc. 105* (1984) 8037).

[16] In the case of $[PQT{\cdot}2BPh_4]$ **2**, a highly structured ternary complex in acetone solution is indicated by its propensity to crystallize. In the case of $[DQT{\cdot}2BPh_4]$ **1**, ^{1}H-NMR titration curves for all the $DQT^{2\oplus}$ protons obtained by adding nBu_4NBPh_4 to $[DQT{\cdot}2PF_6]$ exhibit "knees" at 2:1 molar ratios of $BPh_4^{\ominus}$ to $DQT^{2\oplus}$.

[17] The distance (6.9 Å) between C14 and C24′ (and C14′ and C24) in **2** could be bridged by, for example, an $OCH_2CH_2OCH_2CH_2O$ or an $OCH_2C{\equiv}C{-}C{\equiv}CCH_2O$ unit. Such compounds, if they can be prepared, will have obvious structural similarities with some of the macrocyclic compounds mentioned in [13] and [14].

Molecular Belts and Collars in the Making: A Hexaepoxyoctacosahydro[12]cyclacene Derivative**

By *Franz H. Kohnke, Alexandra M. Z. Slawin, J. Fraser Stoddart,** and *David J. Williams**

For some time[1] we have been trying to prepare polyunsaturated hydrocarbons of the variety **1** wherein 1,4-cyclohexadiene rings are linked laterally to each other by means of their C=C double bonds in a belt-like manner.[2] Such compounds would provide a facile synthetic entry into a fascinating new range of molecular architectures, e.g. **2** and **3**, where compounds with intellectually-appealing

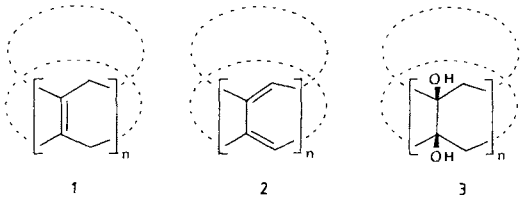

1 2 3

structures[3] promise to exhibit exciting new physical and chemical properties. The first steps towards the making of **1** where n = 12 have now been accomplished by employing repetitive Diels–Alder reactions on the readily-available[4,5] bisdiene **4** and bisdienophile **5**. Here, we disclose our synthetic strategy for the conversion (Scheme 1) of **4** and **5** via the 1:1 adduct **6** and the 2:1 adduct **7** into the hexa-

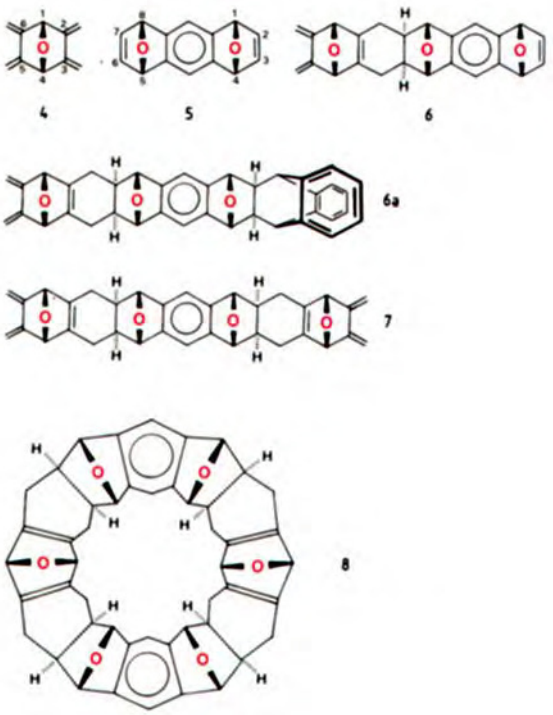

epoxyoctacosahydro[12]cyclacene derivative **8**, emphasizing the importance of (i) the choice of appropriate starting materials, e.g. **4** and **5**, with the required molecular stiffness and curvature,[6] (ii) the role of X-ray crystallography in characterizing the key intermediate **6** as its anthracene adduct **6a** and so removing any nagging doubts concerning the stereochemical options[7] that lie along the synthetic pathways, (iii) the use of high pressures in the liquid-phase[8] to promote, with acceptable efficiency, the crucial intramolecular Diels-Alder reaction[9] that leads to **8**, and (iv) the power of X-ray crystallography, not only to characterize **8** structurally but also, to reveal its exceptional ability to intercalate chloroform molecules in a layer-like manner.

The choice of 2,3,5,6-tetramethylene-7-oxabicyclo-[2.2.1]heptane **4** as one of the starting materials was based on the following features and facts: it can be prepared[4] in gram quantities from the inexpensive Diels–Alder adduct of furan and maleic anhydride: it forms[4,10,11] monoad-

[*] Dr. J. F. Stoddart, Dr. F. H. Kohnke [+]
Department of Chemistry, The University
Sheffield S3 7HF (UK)
Dr. D. J. Williams, A. M. Z. Slawin
Chemical Crystallography Laboratory
Department of Chemistry, Imperial College
London SW7 2AY (UK)

[+] On leave of absence from the University of Messina.

[**] This work was supported by the British Technology Group, the Royal Society, the Agricultural and Food, and Science and Engineering Research Councils in the United Kingdom, as well as by the Accademia dei Lincei and the University of Messina in Italy.

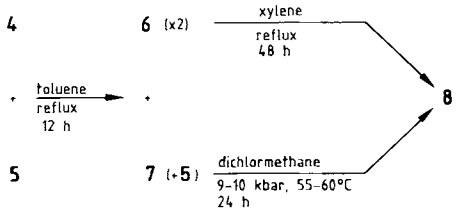

Scheme 1. Strategy for the synthesis of **8**.

ducts much faster (> 100 times) than bisadducts and so reactions can be easily controlled by varying the conditions: in its cycloadditions with bisdienophiles (e.g. benzoquinone), *one* of the two possible diastereoisomers predominates[11] overwhelmingly (e.g. > 95 : < 5). The choice of the *syn*-isomer **5** of 1,4:5,8-diepoxy-1,4,5,8-tetrahydroanthracene as the other starting material was based on the following features and facts: it can be prepared[5] in gram quantities from 1,2,4,5-tetrabromobenzene and furan; the relative configuration has been determined by an X-ray crystal structure analysis;[5] upon reaction with anthracene, only *one* of the three possible diastereoisomeric bisadducts is formed.[5] Both **4** and **5** share another two important characteristics: (i) they are rigid molecules with concave and convex surfaces; (ii) removal of the oxygen bridges at the end of a sequence of Diels–Alder reactions can usually be accomplished[5] with ease.

Inspection of molecular models revealed that, of the four possible diastereoisomeric 1 : 1 adducts which can be formed between **4** and **5**, only the two with all-*syn* oxygen atoms were candidates for macropolycyclization or macropolycyclic dimerization. Indeed, in the cycloaddition, **6** was obtained (Scheme 1) along with a bisadduct, which was assigned tentatively the relative configuration **7** on the basis of ^{1}H- and ^{13}C-NMR data, which are consistent with its C_{2v} molecular symmetry and emphasize its configurational relationship (compare chemical shifts) with **6**, whose relative configuration was established (Fig. 1) by X-ray crystallography[12] performed on the anthracene adduct **6a**. Under more forcing thermal conditions, **6** underwent (Scheme 1) macropolycyclic dimerization to give **8** in very low yield;[13] on the other hand, reaction of **7** with **5** under high pressure gave much better yields (20%) of **8** and established the stereochemistry of **7** beyond any doubt.[14] The X-ray crystal structure[12] of **8** (Fig. 2) reveals a certain structural elegance about this novel molecule with all six oxygen atoms distributed around the outer surface of the stiff molecular collar. The molecule possesses a crystallographic center of symmetry, the two benzene rings being therefore parallel with an interplanar separation of 7.9 Å. As expected, the eight *endo* methine hydrogen atoms, associated with the four benzo-fused oxanorbornene ring systems, are all directed into the center of the rigid molecular cavity. The molecules do not form continuous channels in the crystals but are arranged in parallel approximate edge-to-edge layers with the chloroform molecules sandwiched in between.[17]

The path is now clear for the production of a vast array of macropolycyclic derivatives and analogues of **8**. The synthetic intermediates provide the additional opportunity to increase the availability of rod-like molecules containing linearly-annulated rings[15] and wedge-shaped clefts and grooves.[16] Finally, answers are required to the question of the factors governing the *remote* stereoselectivities observed[18] in Diels–Alder reactions.

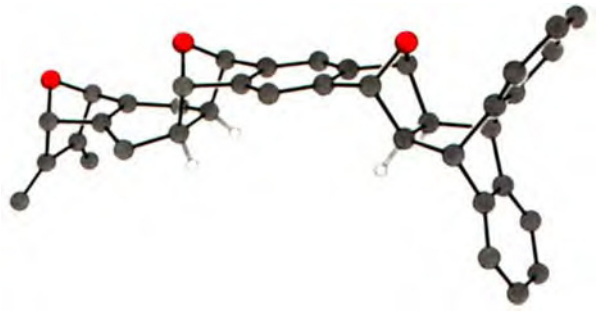

Fig. 1. Structure of **6a** in the crystal (H = white, C = gray, O = red). Crystal data: triclinic, $a = 14.399(4)$, $b = 15.220(7)$, $c = 17.274(8)$ Å, $\alpha = 86.29(4)$, $\beta = 79.63(3)$, $\gamma = 66.38(3)°$, $V = 3412$ Å^3, space group $P\bar{1}$, $Z = 4$ (2 crystallographically independent molecules, both with the same relative configuration), $\rho = 1.20$ g cm^{-3}, $\mu(Cu_{K\alpha}) = 20$ cm^{-1}, 4582 independent reflections [$|F_0| > 3\sigma(|F_0|)$, $\theta \leq 50°$], $R = 0.14$. There are four disordered $ClCH_2CH_2Cl$ molecules in six discrete orientations included in the unit cell. For clarity, only the four methine H atoms are shown.

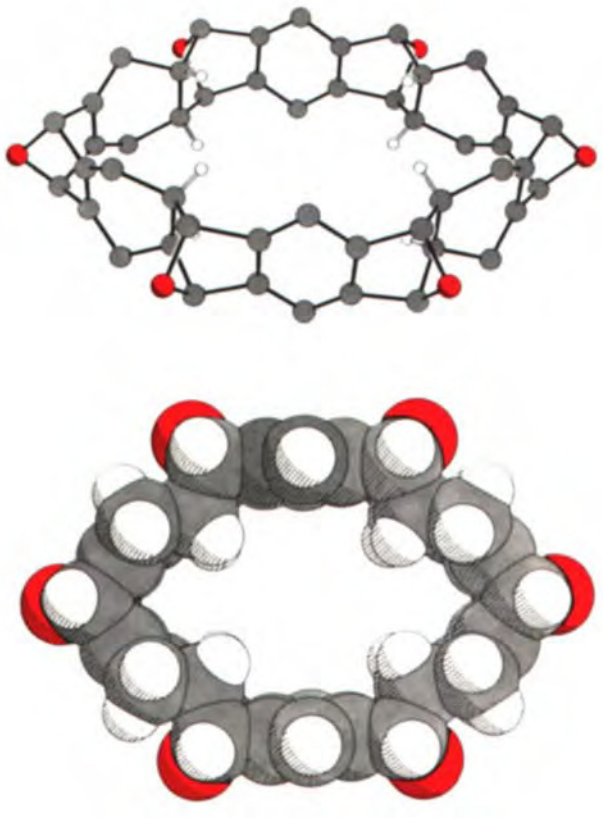

Fig. 2. Top: Structure of **8** in the crystal (H = white, C = gray, O = red). Crystal data: monoclinic, $a = 12.250(5)$, $b = 21.247(12)$, $c = 14.279(11)$ Å, $\beta = 110.59(5)°$, $V = 3479$ Å^3, space group $P2_1/c$, $Z = 2$, $\rho = 1.36$ g cm^{-3}, $\mu(Cu_{K\alpha}) = 70$ cm^{-1}, 1689 independent reflections [$|F_0| > 3\sigma(|F_0|)$, $\theta \leq 50°$], $R = 0.196$. There are 12 disordered $CHCl_3$ molecules included in the unit cell in 16 discrete orientations. For clarity only the eight methine H atoms are shown.—Bottom: Space-filling representation of the structure of **8** (H = white, C = gray, O = red).

Experimental

6/7: The bisdiene **4** (3.37 g, 23.1 mmol) and the bisdieneophile **5** (2.43 g, 11.5 mmol) were heated under reflux (12 h) in toluene (245 mL), affording, after chromatography (SiO_2/$CHCl_3$-EtOAc-light petroleum), the 1 : 1 adduct **6** [1.0 g, 24%, recrystallized from $CHCl_3$-MeOH, m.p. > 300 °C, *m/z* (EIMS) 356; ^{1}H-NMR ($CDCl_3$): $\delta = 1.85$ (m), 2.33 (m), 2.61 (m), 4.91 (s), 4.97 (br.s), 4.98 (s), 5.08 (s), 5.63 (m), 7.02 (m), 7.08 (s) with all signals having equal intensities (2 H); ^{13}C-NMR ($CDCl_3$): $\delta = 23.7$, 43.2, 82.3, 85.1, 85.3, 100.9, 112.0, 143.1, 143.1, 143.3, 144.2, 168.6] and the 2 : 1 adduct **7** [3.63 g, 61%,

crystallized from EtOAc, m.p. >300°C, *m/z* (EIMS) 502; ^{1}H-NMR ($CDCl_3$): $\delta = 1.81$ (m, 4H), 2.33 (m, 4H), 2.61 (m, 4H), 4.92 (s, 4H), 4.97 (bs, 4H), 4.99 (s, 4H), 5.09 (s, 4H), 6.99 (s, 2H); ^{13}C-NMR ($CDCl_3$): $\delta = 25.7$, 43.2, 85.0, 85.3, 100.9, 110.2, 143.1, 144.2, 144.6].

6a: **6** (156 mg, 0.88 mmol) was heated under reflux (48 h, N_2) with anthracene (50 mg, 0.28 mmol) in xylene (5 mL); yield of the crude product: after chromatography (SiO_2/$CHCl_3$-Et_2O) 17 mg, 11%. Colorless crystals [m.p. >300°C), *m/z* (positive ion FABMS) 535 for $(M+H)^{\oplus}$] suitable for X-ray crystallography, were grown by the vapor diffusion method ($CHCl_3$-$ClCH_2CH_2Cl$-light petroleum).

8: Reaction (CH_2Cl_2, 9–10 kbar, 55–60°C, 200 h) of **7** (373 mg, 0.74 mmol) with **5** (156 mg, 0.74 mmol) yielded, after chromatography (SiO_2/$CHCl_3$-MeOH), **8** [105 mg, 20%, recrystallized from $CHCl_3$, m.p. >300°C, *m/z* (positive ion FABMS) 713 for $(M+H)^{\oplus}$; ^{1}H-NMR ($CDCl_3$): $\delta = 1.62$ (m, 4H), 2.32 (m, 8H), 2.63 (m, 8H), 4.89 (s, 8H), 5.08 (s, 4H), 6.98 (s, 4H); ^{13}C-NMR ($CDCl_3$): $\delta = 27.1$, 44.2, 84.8, 86.6, 110.1, 144.6, 152.5], which was also obtained in very low yield (3.5%) by heating **6** under reflux (48 h, N_2) in xylene. Single crystals, suitable for X-ray analysis, were obtained by slow evaporation of a chloroform solution of **8** at room temperature.

Received: June 16, 1987 [Z 2299 IE]
German version: *Angew. Chem. 99* (1987) 941

[1] Champions of highly speculative projects are few and far between; here, they were Dr. *R. D. Handscombe* (University of Sheffield) and Prof. *G. Stagno d'Alcontres* (University of Messina). We thank *them* for their moral support—and for their enthusiastic efforts, *all* the many postgraduate students, who over the years, have received their introduction to the research laboratory in Sheffield making starting materials for "the crazy molecule". One of the authors *(J. F. S.)* also thanks the Leverhulme Trust for the award of a Research Fellowship.

[2] Recently, some force-field calculations have been carried out (R. W. Alder, R. B. Sessions, *J. Chem. Soc. Perkin Trans. 2 1985*, 1849) on molecular belts built from cyclohexa-1,4-diene rings. Compounds of the type **1** were referred to in the above paper as [*n*]beltenes; the strain energy per 2-butene-1,2,3,4-tetrayl unit was found to decrease monotonically from [3]beltene to [12]beltene. Calculations on encapsulated complexes of small molecules led to the prediction that, in the case of acetylene, for example, [9]beltene will be the optimum molecular receptor.

[3] In looking to the future in cyclophane chemistry, *F. Vögtle* (*Top. Curr. Chem.* ("Cyclophanes II") *115* (1983) 157) has highlighted the challenge posed by the synthesis of the [*n*]cyclacenes **2**, which are also of considerable theoretical interest (S. Kivelson, O. L. Chapman, *Phys. Rev. B 28* (1983) 7236) as a class of new materials with possibly novel one-dimensional conducting properties.

[4] In the beginning, we prepared **4** in a six-step synthesis (P. Vogel, A. Florey, *Helv. Chim. Acta 57* (1974) 200) starting from dimethyl 3,4-furandicarboxylate and dimethyl acetylenedicarboxylate. More recently, the highly efficient four-step synthesis (C. Mahaim, P.-A. Carrupt, J.-P. Hagenbuch, A. Florey, P. Vogel, *Helv. Chim. Acta 63* (1980) 1149) of **4** from the Diels-Alder adduct of furan and maleic anhydride has been employed. An X-ray crystal structure analysis (F. H. Kohnke, A. M. Z. Slawin, J. F. Stoddart, D. J. Williams, unpublished results) on single crystals of the intermediate tetramethyl 7-oxabicyclo[2.2.1]heptane-2,3,5,6-tetracarboxylate has indeed confirmed that it has the all-*exo* configuration.

[5] The preparation of 1,4:5,8-diepoxy-1,4,5,8-tetrahydroanthracene from 1,2,4,5-tetrabromobenzene and furan, and the chromatographic isolation of the *syn*-isomer **5** were achieved after the kind provision (Prof. *H. Hart*, personal communication, 1986) of a detailed experimental procedure which provided some essential additional information to that already published (H. Hart, N. Raja, M. A. Meador, D. L. Ward, *J. Org. Chem. 48* (1983) 4357). Identification of the *syn*-isomer **5** in our hands followed from X-ray crystallography on single crystals of a compound isomeric with **5**. Although the crystal data we have obtained (F. H. Kohnke, A. M. Z. Slawin, J. F. Stoddart, D. J. Williams, unpublished results) are totally different to those reported in the above paper by *Hart* et al. for the *anti*-isomer of **5**, determination of the X-ray structure showed that the crystals only contain molecules of *anti* geometry. These two crystal structures must clearly represent alternative polymorphs.

[6] These principles have been capitalized upon by others (see, for example, D. J. Cram, *Science 219* (1983) 1177; H. C. Kang, A. W. Hanson, B. Eaton, V. Boekelheide, *J. Am. Chem. Soc. 107* (1985) 1979; D. J. Cram, K. D. Stewart, I. Goldberg, K. N. Trueblood, *J. Am. Chem. Soc. 107* (1985) 2574) in the synthesis of molecules with enforced cavities.—An example of a molecule similar to **8** with a rigid collar-like structure is cucurbituril which can be readily assembled (W. A. Freeman, W. L. Mock, N.-Y. Shih, *J. Am. Chem. Soc. 106* (1984) 1416) from urea, glyoxal, and formaldehyde. It forms (W. L. Mock, N.-Y. Shih, *J. Org. Chem. 48* (1983) 3618; *51* (1986) 4440) host-guest solution complexes and catalyzes (W. L. Mock, T. A. Mirra, J. P. Wepsiec, T. L. Manimaran, *J. Org. Chem. 48* (1983) 3619) 1,3-dipolar cycloadditions between appropriate substrates in a highly regioselective manner.

[7] The X-ray crystal structure analysis of **6a** (Fig. 1) not only established the stereochemistry in **6** but also demonstrated that the cycloaddition of anthracene occurs preferentially to the *exo*-face of the dienophilic C=C double bond of **6**. This strongly suggests that the 1:2 adduct formed (H. Hart, N. Raju, M. A. Meador, D. L. Ward, *J. Org. Chem. 48* (1983) 4357) between **5** and anthracene has the *exo-exo* configuration.

[8] As a result of their negative volumes of activation, Diels–Alder reactions are accelerated at high pressures (for a recent review, see N. S. Isaacs and A. V. George, *Chem. Br. 23* (1987) 47). We thank Prof. *S. V. Ley* (Imperial College) for removing any hesitation we had about employing this technique and Dr. *N. S. Isaacs* (SERC High Pressure Service Facility, University of Reading) for the superb service and help he has given us in preparing **8**.

[9] Although intramolecular Diels–Alder reactions with flexible trienes have been much studied (for a recent review, see E. Ciganek, *Org. React. 32* (1984) 1) during the last decade, their occurrence in highly rigid molecules containing diene and dienophilic units has, surprisingly, not been investigated.

[10] P.-A. Carrupt, P. Vogel, *Tetrahedron Lett. 1979*, 4533; Y. Bessiére, P. Vogel, *Helv. Chim. Acta 63* (1980) 232.

[11] A. A. Pinkerton, D. Schwarzenbach, J. H. A. Stibbard, P.-A. Carrupt, P. Vogel, *J. Am. Chem. Soc. 103* (1983) 2095; J.-M. Tornare, P. Vogel, A. A. Pinkerton, D. Schwarzenbach, *Helv. Chim. Acta 68* (1985) 2195.

[12] Nicolet R3m diffractometer, ω-scans, $Cu_{K\alpha}$ radiation (graphite monochromator). A crystal of **8** was sealed in a Lindemann capillary tube under chloroform, which was drawn away to opposite ends of the tube thus leaving the crystal in a vapor pressure of solvent: a numerical absorption correction was carried out. Both structures were solved by direct methods and refined anisotropically: the *R*-factors are high as a result of severe disorder involving included chlorinated solvents, which is particularly pronounced in the case of **8**. Further details of these structural investigations can be obtained from the Director of the Cambridge Crystallographic Data Centre, University Chemical Laboratory, Lensfield Road, Cambridge CB2 1EW (England). Any request should be accompanied by the full literature citation for this communication.

[13] The monoadduct **6** is unstable and undergoes polymerization. It is for this reason that we prefer to approach the synthesis of **8** via the bisadduct **7**, which can be stored for several months at −20°C in the dark without detectable decomposition.

[14] All new compounds gave satisfactory elemental analyses and spectroscopic data. We are extremely grateful to Mr. *P. R. Ashton* for obtaining EIMS and FABMS on a Kratos MS80RF spectrometer and to Dr. *C. M. Spencer* for recording high field NMR spectra on a Bruker WH400 spectrometer. We also thank Dr. *A. D. McNaught* (The Royal Society of Chemistry, London) for his freely given advice on trivial—as well as systematic—nomenclature for these new compounds.

[15] See, for example, R. O. Angus, Jr., R. P. Johnson, *J. Org. Chem. 48* (1983) 373; L. L. Miller, A. D. Thomas, C. L. Wilkins, D. A. Weil, *J. Chem. Soc. Chem. Commun. 1986*, 661.

[16] See, for example, G. A. Russell, N. K. Suleman, H. Iwamura, O. W. Webster, *J. Am. Chem. Soc. 103* (1981) 1560; E. Lipczynska-Kochany, H. Iwamura, *Chem. Lett. 1982*, 1075; C. S. Wilcox, L. M. Greer, V. Lynch, *J. Am. Chem. Soc. 109* (1987) 1865.

[17] This clathration phenomenon explains the instantaneous loss of chloroform with concomitant collapse of the crystals on removal from their mother liquor.

[18] For some excellent reviews on this topic see, W. H. Watson (Ed.): *Stereochemistry and Reactivity of Systems containing π-Electrons*, Verlag Chemie International, Deerfield Beach, FL (USA) 1983.

Triphosgene, a Crystalline Phosgene Substitute**

By *Heiner Eckert** and *Barbara Forster*

The "defusing" of dangerous and risky chemicals is exemplified here by the avoidance of the highly toxic, gaseous basic chemical phosgene ($COCl_2$) as a reagent. Liquid trichloromethyl chloroformate ($ClCO_2CCl_3$, "diphosgene"),[1] which has already been used as a phosgene substitute, has proved useful in all common phosgene reactions,[2] but, as a liquid, its transport and storage still pose considerable dangers. Bis(trichloromethyl) carbonate **1** ("triphosgene"),[3] on the other hand, is a crystalline, stable

[*] Dr. H. Eckert, Dr. B. Forster
Organisch-chemisches Institut der Technischen Universität München
Lichtenbergstrasse 4, D-8046 Garching (FRG)

[**] This work was supported by the Deutsche Forschungsgemeinschaft.

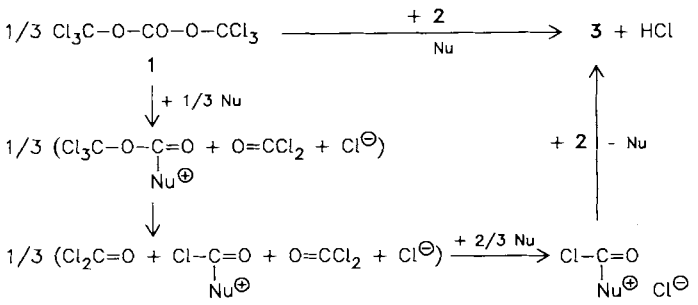

Scheme 1. Triphosgene as a phosgene substitute.

solid (m.p. = 80 °C, b.p. = 206 °C; at the boiling point, only slight decomposition to phosgene occurs[3c]), which is easy to transport and to store. Compound **1** was first prepared in 1880 by *Councler*[3a] by chlorination of dimethyl carbonate and has so far been used in reactions with primary alcohols to give esters,[3c, d] with ammonia and aniline to give ureas,[3c, d] and with aldehydes.[3b]

1/3 mol of **1** reacts under the influence of a nucleophile Nu similarly to 1 mol of phosgene, which can also arise as an intermediate (Scheme 1). Table 1 lists a selection of the reactants **2** and the products **3** thereby obtained. The auxiliary nucleophile Nu can also be identical with **2**. The functions of phosgene, e.g.,

chloroformylation	1/3 **1** + **2a**, **b** ⟶ **3a**, **b**
carbonylation	1/3 **1** + **2c–f** ⟶ **3c–f**
chlorination	1/3 **1** + **2g** ⟶ **3g**
dehydration	1/3 **1** + **2h**, **i** ⟶ **3h**, **i**

can also be performed by **1**. Good to very good yields of **3** are thereby obtained by the use of **2** in equivalent amounts in the usual solvents (dichloromethane, *o*-dichlorobenzene) or without solvent. Phosgene, on the other hand, has to be used in severalfold excess and, even in this case, the yields are often only moderate. A further advantage of **1** is that, as a solid, it can be exactly weighed out in milligram amounts. Furthermore, owing to the relatively low volatility of **1**, only the usual safety precautions are necessary.

Experimental Procedure

1: A stirred, cooled (10–20 °C cooling bath temperature) solution of dimethyl carbonate (45 g, 0.5 mol) in 250 mL of CCl_4 was irradiated with two lamps (Philips MLU 300 W). Chlorine gas was then admitted to the solution so fast that it did not leave the solution. After 28 h of net reaction (interruption of the reaction is possible), which can be followed by ^{1}H-NMR spectroscopy, the CCl_4 was removed in vacuum (200 torr); the remaining crystalline solid was dried at 0.1 torr. Yield: 143 g (97%) **1**. M.p. = 79 °C. IR (KBr): $\tilde{\nu}$ = 1820, 1175, 1115, 820 cm^{-1}. The HCl formed during the reaction is passed by means of a reflux condensor into 1.6 L of a 20% sodium carbonate solution.

Received: April 13, 1987;
supplemented: June 4, 1987 [Z 2196 IE]
German version: *Angew. Chem. 99* (1987) 922

CAS Registry numbers:
1, 32315-10-9; **2a**, 57-15-8; **2b**, 334-22-5; **2c**, 95-53-4; **2d**, 95-69-2; **2e**, 101-77-9; **2f**, 80-05-7; **2g**, 103-82-2; **2h**, 78375-50-5; **2i**, 110172-14-0; **3a**, 66270-36-8; **3b**, 2998-56-3; **3c**, 614-68-6; **3d**, 37408-18-7; **3e**, 101-68-8; **3f**, 24936-68-3; **3g**, 103-80-0; **3h**, 78375-48-1; **3i**, 32755-43-4; CCl_4, 56-23-5; dimethyl carbonate, 616-38-6.

[1] a) W. Hentschel, *J. Prakt. Chem. NF 36* (1887) 99, 305; b) H. C. Ramsperger, G. Waddington, *J. Am. Chem. Soc. 55* (1933) 214; c) K. Kurita, T. Matsuma, Y. Iwakura, *J. Org. Chem. 41* (1976) 2070; d) G. Skorna, I. Ugi, *Angew. Chem. 89* (1977) 267; *Angew. Chem. Int. Ed. Engl. 16* (1977) 259; e) K. Kurita, Y. Iwakura, *Org. Synth. 59* (1979) 195.

[2] a) H. Babad, A. G. Zeiler, *Chem. Rev. 73* (1973) 75; b) R. Gottschlich, *Kontakte 1981*, No. 1, p. 14.

[3] a) C. Councler, *Ber. Dtsch. Chem. Ges. 13* (1880) 1697; b) Bayer & Co., DRP 121223 (1901); *Chem. Zentralbl. 72 II* (1901) 69; c) D. Marotta, *Gazz. Chim. Ital. 59* (1929) 955; d) W. Nekrassow, N. Melnikow, *J. Prakt. Chem. NF 126* (1930) 81.

Table 1. Reaction conditions and yields for the reaction 1/3 **1** + **2** → **3**.

	2	**3**	Nu	**1** : **2**	Reaction conditions t [h]	T [°C]	Yield [%]
a	$Cl_3C-C(CH_3)_2-OH$	$Cl_3C-C(CH_3)_2-O-CO-Cl$	C_5H_5N	1 : 3	96	20	91
b	$(ClCH_2CH_2)_2NH$	$(ClCH_2CH_2)_2N-CO-Cl$	C_5H_5N	1 : 3	72	20	85
c			Et_3N	1 : 3	2	70	82
d	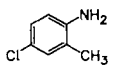	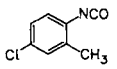	**2d**	1 : 3	1 2	70 130	68
e	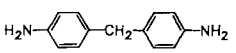	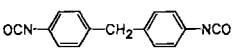	**2e**	2 : 3	2 1	130 180	92
f	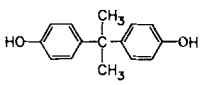	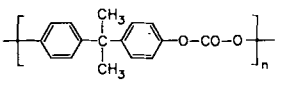	Et_3N	1 : 3	8	20	75
g	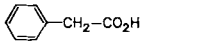	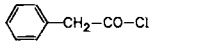	trace DMF [a]	1 : 3	24	60	71
h	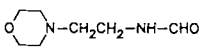	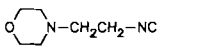	Et_3N	1 : 3	8	20	74
i	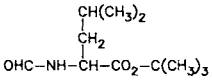	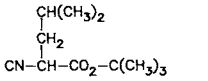	Et_3N	1 : 3	2	20	94

[a] Dimethylformamide.

Changes of Stereoselectivity in Diels-Alder Reactions by Hydrophobic Solvent Effects and by β-Cyclodextrin**

By *Hans-Jörg Schneider* and *Naresh K. Sangwan**

The possibility of controlling the course of Diels-Alder additions by the use of aqueous solvents[1] and by added cyclodextrins is currently attracting considerable interest and probably depends on an externally driven compression or packing of diene and dienophile.[2,3] After having recently been able to correlate the kinetics of such reactions for the first time with solvophobicity parameters and to demonstrate high accelerations as well as enzyme-analogue saturation kinetics with cyclodextrin,[3] we now wish to report on significant changes in the product ratios obtained in such reactions.

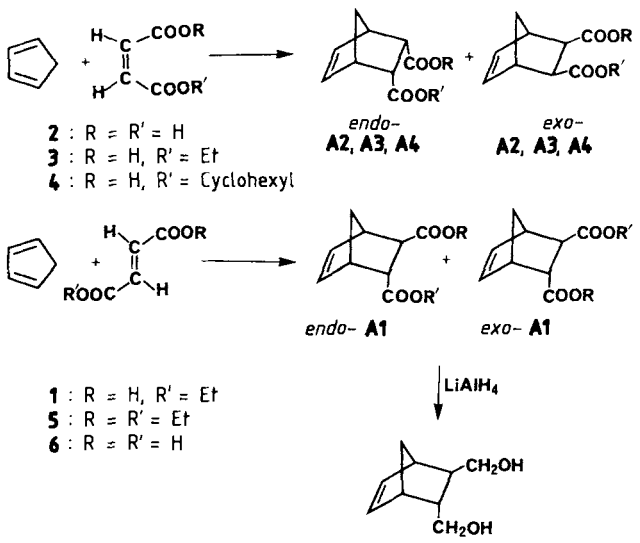

Table 1. Solvent-dependence of the diastereoselectivities (*endo/exo*-product) in Diels-Alder reactions with cyclopentadiene [a].

Dienophile	90% Dioxane 10% H_2O	MeOH	50% MeOH 50% H_2O	30% MeOH 70% H_2O	H_2O
1 [b]	—	1.10 ± 0.05	1.12 ± 0.05	—	1.10 ± 0.05
2	—	30 ± 1.5	36.5 ± 1	—	47 ± 4
3 [c]	20.5 ± 1	23.5 ± 2	39 ± 3	44 ± 4	48.5 ± 4
4	37 ± 2	—	—	60 ± 5	—

[a] In homogeneous solution at 20°C; binary solvent mixture composition given as % v/v, analysis by integration of ^{1}H-NMR signals (400-MHz measurements), whose pattern is in accord with the literature data (N. Kamezawa, K. Sakashita, K. Hayamizn, *Org. Magn. Reson. 1* (1969) 405). [b] *endo*-COOEt/*exo*-COOEt, error: deviation between two signal pair-evaluations. [c] Further measurement in 70% MeOH: 34 ± 2.

In reactions of cyclopentadiene with the maleic acid derivatives **2**–**4** we find an increase in the proportion of the *endo* products **A2** to **A4** by the use of water (Table 1). This increase is of a similar order of magnitude as that observed in earlier investigations.[1,2] Use of the particularly hydrophobic cyclohexyl ester **4** does not lead to any noticeably higher change in selectivity than **2** and **3**, thus indicating the possible increased formation in this case of associates without productive orientation of the π-systems. In contrast to earlier investigations[1,2] it was established that no micelle formation occurs even in water: at the concentrations used (e.g. 5×10^{-3} M in water) the UV extinctions obey the Lambert-Beer law, and the diastereoselectivities (*endo/exo* product) obtained in water fitted the correlation curves determined with binary solvent mixtures (Fig. 1a). This comparison of the log(*endo/exo*) values with solvophobicity parameters Sp, which are based on changes in the free energy ΔG_t^0 of transfer of hydrocarbons from the gas phase into a given solvent,[4] is to our knowledge the first quantitative description of product ratios as a function of hydrophobic solvent properties.

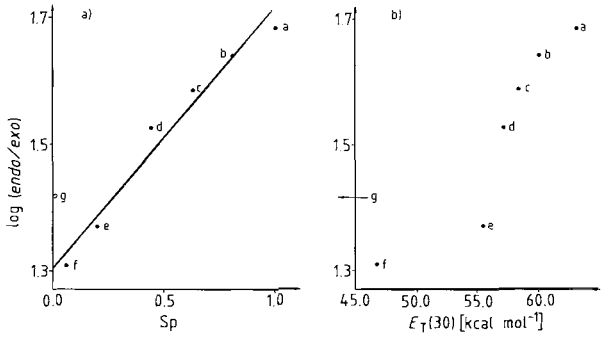

Fig. 1. a) Diastereoselectivities log(*endo/exo*) vs. solvophobicity parameter Sp for the reaction of cyclopentadiene with monoethyl maleate **3**. a: in water; b–e: 30, 50, 70, 100% methanol (v/v); f: 90% dioxane; g: hexane. b) Diastereoselectivities as a function of solvent polarity E_T(30).

The observed correlation clearly supports the aforementioned hydrophobic effect[1,2] as opposed to micelles[1c,5] being responsible for the changes in selectivity. Consistent with this finding is the observed *decrease* rather than increase in the selectivity, both on addition of surfactants as well as on increasing the concentration of starting material above its solubility in water.[2b]

In agreement with earlier results,[1b,7] the significantly poorer correlation with E_T(30)-values[8] (Fig. 1b) argues against polarity effects being the essential factors responsible for the *endo/exo*-product variations.[6] However, in order to check whether solvent polarities might play an *additional* role here,[2c] a multiple correlation for the system **3** + cyclopentadiene was carried out. A comparison of the correlations obtained and the respective errors shows that the inclusion of polarity parameters is of no significance:

with Sp alone:

$\log(endo/exo) = (0.414 \pm 0.038)\,Sp + (1.30 \pm 0.024)$

($r = 0.9835$, $\psi = 5\%$)

with E_T(30) alone:

$\log(endo/exo) = 0.0248 \pm 0.0054)\,E_T(30) + (0.113 \pm 0.306)$

($r = 0.9177$, $\psi = 24\%$)

with Sp *and* E_T(30):

$\log(endo/exo) = (0.364 \pm 0.101)\,Sp + (0.0035 \pm 0.0065)\,E_T(30) + (1.304 \pm 0.322)$

(multilinear correlation coefficient $r = 0.9850$)

[*] Prof. Dr. H.-J. Schneider, Dr. N. K. Sangwan [+]
Fachrichtung Organische Chemie der Universität
D-6600 Saarbrücken 11 (FRG)

[+] Permanent address:
Department of Chemistry and Biochemistry
Haryana Agricultural University, Hissar (India)

[**] Host-Guest Chemistry, Part 13. This work was supported by the Deutsche Forschungsgemeinschaft and the Fonds der Chemischen Industrie. We thank Dr. *M. H. Abraham* for stimulating discussions on the development of a solvophobicity scale, and for useful information.— Part 12: H. J. Schneider, R. Kramer, S. Kumar, U. Schneider, *31st IUPAC Congress, Sofia 1987, Proc. Org. Chem. Sect.* 189–204.

The solvent-dependence of *endo/exo* ratios recently described by *two* separate correlations for protic and aprotic solvents[1c] can also be described by *one* correlation ($r = 0.940$, $\psi = 16\%$) if Sp values—insofar as they are available—instead of $E_T(30)$ values are employed. Only the result in the extremely nonpolar solvent hexane lies significantly above the correlation curves (see Fig. 1a; hence correlation without the value in hexane), thus indicating the formation of associates by hydrogen bonding; the stereoselectivities observed in hexane usually correlate even less satisfactorily with $E_T(30)$ values (see Fig. 1b).

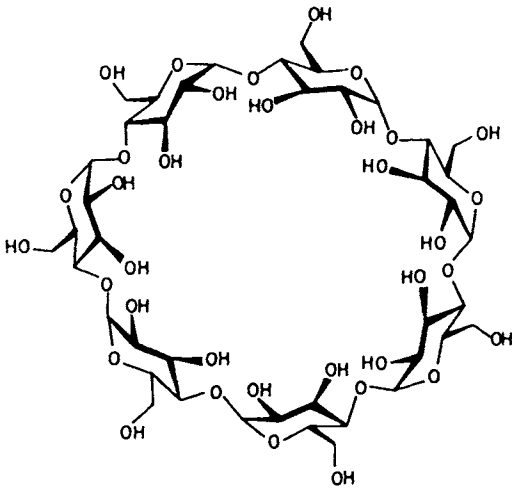

β-CYD

Table 2. Influence of β-cyclodextrin (β-CYD) on diastereo- and enantioselectivity in Diels–Alder reactions with cyclopentadiene.

Dienophile	H_2O Diastereoselectivity [b] (*endo/exo*-product)	0.015 M β-CYD Diastereoselectivity [b] (*endo/exo*-product)	0.015 M β-CYD Enantioselectivity *ee* [%]	
			exo-COOEt	*endo*-COOEt
1	1.10 ± 0.05	2.2 ± 0.08	8.4 ± 0.5	< 2.0
2	47 ± 4	69 ± 4	–	
3	48.5 ± 4	112 ± 5	–	
5	–	–	21.0 ± 5.5 [c]	
6	–	–	< 1	

[a] In homogeneous solution in water at 20°C. [b] For **1** *endo*-COOEt/*exo*-COOEt. [c] With [educt] = 0.001 M; with 0.003 M: 19.5 ± 1% *ee*; with which the specific rotation of the diester obtained with **5** was calculated: $[\alpha]_D^{20} = +87 \pm 2°$ (1.4% in $CHCl_3$).

The influence of cyclodextrins on diastereo- or enantioselectivities in Diels–Alder reactions has so far never been proven. Addition of maleic and fumaric acid derivatives to cyclopentadiene (Table 2) in presence of the highest possible concentration of β-cyclodextrin (0.015 M in water) show a large increase in the amount of *endo* product; this must be interpreted in terms of a more compact transition state being realized in the cavity. Noteworthy is the increase in selectivity of the reaction of the fumaric acid half ester **1**, which cannot be achieved with the use of water alone (cf. Table 1).

The asymmetric induction by the chiral cyclodextrin cavity was investigated for the addition of fumaric acid derivatives (**1**, **5**, **6**) to cyclopentadiene; in the case of the semiester **1** only the product *exo*-**A1** with *exo*-ester group could be completely analyzed. The ^{1}H-NMR spectrum of a 0.2 M solution of **1** in the presence of 0.6 M optically active 1-phenylethylamine showed pairs of signals with separations of 0.04 and 0.05 pm respectively, for the olefinic protons, from whose signal areas the enantiomeric excesses were determined[9] (Table 2). Since the product *endo*-**A1** obtained from **1** showed no splitting (not even with optically active 1-naphthylethylamine[9]), the mixture was reduced to the diol, which, like the diol obtained from the adducts with **5** and **6** in the presence of the chiral camphorato-lanthanoid shift reagent $Eu(tfc)_3$[9] [0.023 M] showed a 0.11 ppm splitting of the olefinic protons (diol concentration 0.09 M; solvent in each case $CDCl_3/CCl_4 = 15/85$). Combination of the 4.2% *ee* for the diols thus obtained from **1** with the known selectivities regarding the *exo*-COOEt compound *exo*-**A1** indicates < 2% *ee* for the isomeric *endo*-**A1** (Table 2). The enantiomeric excesses for the reaction with **5** and **6** could be determined from the area ratios of the respective diol signals in the presence of $Eu(tfc)_3$.

Whereas the enantiomeric excesses achieved in the reaction with **1** and **6** are limited by an incomplete complexation, in the case of **5** the degree of complexation must be > 90% on the basis of the corresponding kinetic analysis;[3] moreover the reaction in the complex proceeds about 70 times faster. An increase in the enantioselectivity is therefore only possible by chemical modification of the cyclodextrin.

Received: May 6, 1987 [Z 2230 IE]
German version: *Angew. Chem. 99* (1987) 924

[1] Recent references in: a) H.-U. Reissig, *Nachr. Chem. Tech. Lab. 34* (1986) 1169; b) A. Lubineau, Y. Quenau, *J. Org. Chem. 52* (1987) 1001; recent work: c) R. Braun, F. Schuster, J. Sauer, *Tetrahedron Lett. 27* (1986) 1285.

[2] a) D. C. Rideout, R. Breslow, *J. Am. Chem. Soc. 102* (1980) 7816; b) R. Breslow, U. Maitra, D. Rideout, *Tetrahedron Lett. 24* (1983) 1901; c) R. Breslow, U. Maitra, *ibid. 25* (1984) 1239.

[3] H.-J. Schneider, N. K. Sangwan, *J. Chem. Soc. Chem. Commun. 1986*, 1787.

[4] Cf. a) M. H. Abraham, *J. Am. Chem. Soc. 104* (1982) 2085; b) *J. Chem. Soc. Faraday Trans. 80* (1984) 153; c) H.-J. Schneider, K. Philippi, J. Pöhlmann, *Angew. Chem. 96* (1984) 907; *Angew. Chem. Int. Ed. Engl. 23* (1984) 908.

[5] P. A. Grieco, P. Garner, Zhen-min He, *Tetrahedron Lett. 24* (1983) 1897; P. A. Grieco, K. Yoshida, P. Garner, *J. Org. Chem. 48* (1983) 3137.

[6] J. A. Berson, Z. Hamlet, W. Mueller, *J. Am. Chem. Soc. 84* (1962) 297.

[7] A. A.-Z. Samii, A. de Savignac, I. Rico, A. Lattes, *Tetrahedron 41* (1985) 3683.

[8] C. Reichardt: *Solvent Effects in Organic Chemistry*, Verlag Chemie, Weinheim 1979.

[9] For methods see P. L. Rinaldi, *Prog. Nucl. Magn. Reson. Spectros. 15* (1982) 291.

Cluster of Clusters: Structure of the 37-Atom Cluster $[(p\text{-}Tol_3P)_{12}Au_{18}Ag_{19}Br_{11}]^{2\oplus}$ and a Novel Series of Supraclusters Based on Vertex-Sharing Icosahedra**

By *Boon K. Teo,* M. C. Hong, Hong Zhang,* and *D. B. Huang*

Basic understanding of the formation and properties of small metal aggregates, or clusters, constitutes a prerequisite to the further progress of many industries, ranging from the materials problems in microelectronics[1-3] to ca-

[*] Prof. Dr. B. K. Teo, M. C. Hong, H. Zhang, D. B. Huang
Department of Chemistry, University of Illinois at Chicago
P.O. Box 4348, Chicago, IL 60680 (USA)

[**] Acknowledgement is made to the donors of the Petroleum Research Fund (No. 18873-AC3), administered by the American Chemical Society, for partial support of this research. *B. K. T.* is also grateful to the University of Illinois at Chicago for a Campus Research Board Award and a start-up fund in partial support of this research.

talysis[4] in chemical industry. Synthetic and structural studies of metal clusters will not only help shed light on the important question of the development of metallic behavior[5] as a function of particle size but will also pave ways for the discovery of novel materials with unusual physical or chemical properties.

Recently, we reported the synthesis and structural characterization of a 25-atom[6] and a 38-atom[7] cluster containing gold and silver. We now wish to report the structure of a novel 37-atom cluster, the title compound **1**, formed as the AsF_6 salt upon reduction of a mixture of p-Tol_3P, Au_2O_3, $AgAsF_6$ and HBr with $NaBH_4$ in ethanol (Tol = tolyl). With 37 metal atoms, it represents the second largest structurally characterized Au–Ag cluster known (second only to **2**[7]). Other examples of metal clusters with similar nuclearities are **3**–**7**.[9–13]

$[(p\text{-}Tol_3P)_{12}Au_{18}Ag_{19}Br_{11}]^{2\oplus}$[8] **1**
$[(p\text{-}Tol_3P)_{12}Au_{18}Ag_{20}Cl_{14}]$[7] **2**
$[Pt_6Ni_{38}(CO)_{48}H_{6-n}]^{n\ominus}$[9] **3**, n = 4, 5
$[Ni_{38}(CO)_{42}C_6H]^{5\ominus}$[10] **4**
$[Ni_{34}Se_{22}(PPh_3)_{10}]$[11] **5**
$[Pd_{38}(CO)_{28}(PEt_3)_{12}]$[12] **6**
$[Pt_{38}(CO)_{44}]^{2\ominus}$[13] **7**

The $[P_{12}Au_{18}Ag_{19}Br_{11}]$ framework of cluster **1**, which conforms to idealized C_{3v} symmetry, is portrayed in Figure 1a. There are two types of Au atoms in the cluster: 12 on the surface and 6 in the interior. There are 12 tri(*p*-tolyl)phosphanes coordinated to the 12 peripheral Au atoms and 11 bromide ligands (six doubly bridging, four triply bridging, and one terminal) coordinated to the Ag atoms.

The metal–metal distances follow the approximate trend Au-Au (2.66–3.20 Å) ≈ Au-Ag (2.73–3.01 Å) < Ag-Ag (2.79–3.34 Å), all of which can be considered as more or less bonding. There are four groups of Ag–Ag distances: 2.79–2.94 Å for unbridged, 2.98–3.26 Å for doubly bridged, and 3.04–3.34 Å for triply bridged Ag–Ag bonds. The Ag···Ag contacts of 3.73–3.82 Å involving the one apical Ag atom (see Fig. 1b) are longer. The distances from Ag to the terminal, doubly bridging, and triply bridging Br ligands are 2.39, 2.52–2.60, and 2.62–2.81 Å, respectively.

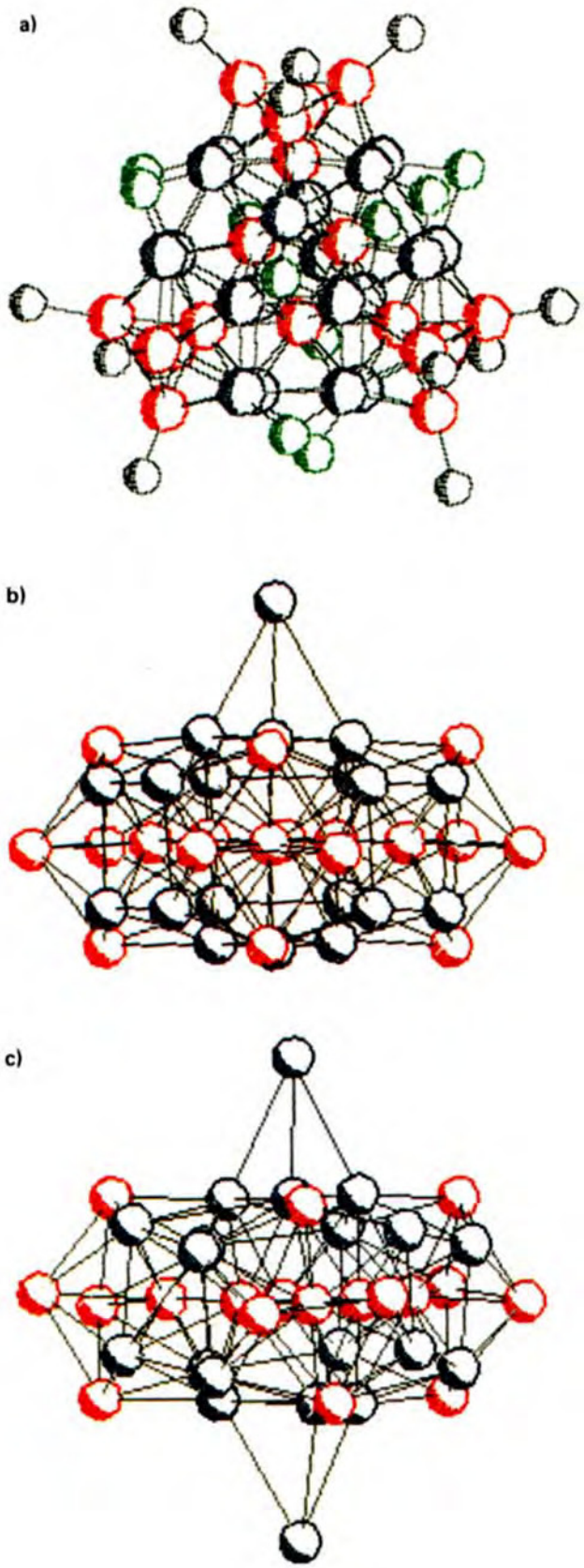

Fig. 1. a) The $[P_{12}Au_{18}Ag_{19}Br_{11}]$ framework of the 37-atom cluster **1**; Au (red), Ag (blue), Br (green), P (black). b) Side views of the metal framework of **1** and c) of **2**; Au (red), Ag (blue).

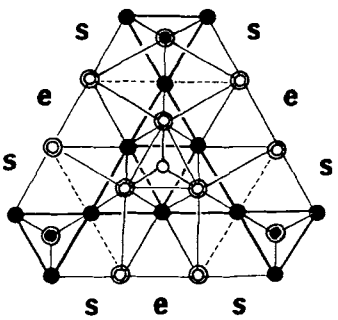

Fig. 2. A schematic representation illustrating the close packing of the metal framework of the 37-atom cluster **1**; Au ●, 2Au ⊙, Ag ○, 2Ag ◎. s = staggered, e = eclipsed.

Cluster **1** can be described in a number of ways. The most obvious description is based on close-packing of metal atoms (Fig. 2). In this description, imagine a two-dimensional close-packing of 12 Au atoms to form a v_2 triangle and three v_1 triangles sharing corners.[14] Above and below the three small triangles are six Au atoms conceptually changing the smaller triangles into trigonal bipyramids. Above the central (large) triangle are four Ag atoms arranged in a v_2 tetrahedral array. Below this trian-

gle are three Ag atoms giving rise to a v_2 tetrahedron truncated at one corner. On the three edges are 12 Ag atoms (not closest-packed), 6 above and 6 below the plane of the 12 Au atoms.

The 37-atom cluster **1** (Fig. 1b) is related to the 38-atom cluster **2** (Fig. 1c) via removal of one of the two apical $Ag^{\oplus}$ ions. The "main frame" of **1** and **2** can be approximated as a three-layer structure. More specifically, replacement of one of the two apical AgX_4 moieties (X = halogen) in cluster **2** by a μ_3-X unit gives rise to cluster **1**. In fact, if **2** is a neutral species, then **1** should be a dication, since replacement of a $[AgX_4]^{3\ominus}$ moiety by $X^{\ominus}$ decreases the charge by 2. We assume here that the 36-atom cluster framework remains unaffected by such a formal replacement.

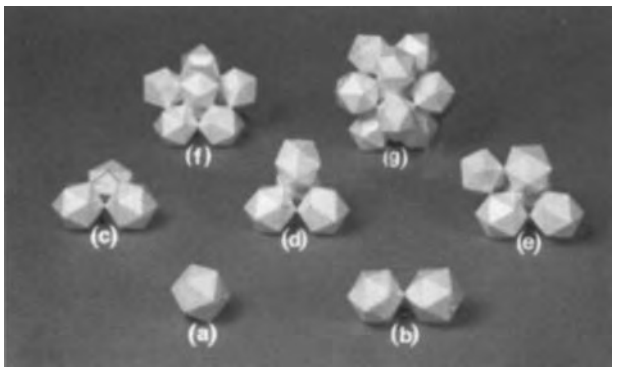

Fig. 3. Supracluster s_n formed by sharing vertices of n centered icosahedra (nuclearity in parentheses): a) s_1 (13); b) s_2 (25); c) s_3 (36); d) s_4 (46); e) s_5 (56); f) s_7 (76); g) s_{12} (127).

The most interesting structural characteristic of the 25-,[6] 37- (**1**), and 38-atom (**2**[7]) clusters is that they can be considered as being built from 13-atom, centered icosahedral cluster units (Fig. 3a). Thus, the 25-atom cluster can be considered as *two* icosahedra sharing a vertex ($2 \times 13 - 1 = 25$, Fig. 3b), the 37- and 38-atom clusters, **1** and **2**, respectively, as *three* isosahedra sharing three vertices in a cyclic manner ($3 \times 13 - 3 = 36$, Fig. 3c) plus one and two capping atoms, respectively. These considerations open up new pathways to larger metal clusters via fusion of smaller cluster units as building blocks. We shall refer to the resulting clusters as supraclusters. For example, we predict that the nuclearity of a supracluster formed by vertex-sharing of centered icosahedra is given by $13n - e$ where n is the number of the cluster units and e is the number of edges of the polyhedron formed by the centers of the icosahedral units. Thus, tetrahedral, trigonal-bipyramidal, and pentagonal-bipyramidal arrays of vertex-sharing icosahedra will give rise to nuclearities of $4 \times 13 - 6 = 46$, $5 \times 13 - 9 = 56$, and $7 \times 13 - 15 = 76$, respectively (see Fig. 3d–f). One exception to this rule is the icosahedral supracluster of I_h symmetry formed by 12 centered icosahedra sharing 30 corners. Here, the icosahedral hole created by the 12 icosahedra is filled with one atom ($12 \times 13 - 30 + 1 = 127$, Fig. 3g). Stereochemical considerations revealed that other n ($n < 13$) values are not favorable.

It is hoped that the idea of cluster of clusters in general, and the structures of the 25-, 37-, and 38-atom clusters in particular, may provide new pathways to novel high-nuclearity supraclusters via vertex-, edge-, and face-sharing and/or by close-packing of smaller cluster units as building blocks.[15, 16]

Received: March 16, 1987;
supplemented: May 18, 1987 [Z 2144 IE]
German version: *Angew. Chem. 99* (1987) 943

[1] For an interesting historical review of microelectronics, see T. R. Reid: *The Chip*, Simon and Schuster, New York 1984, p. 195.

[2] a) F. L. Carter (Ed.): *Molecular Electronic Devices*, Marcel Dekker, New York 1982; b) F. L. Carter, NRL Memo. Rep. 4717 (1982).

[3] T. J. Marks, C. W. Dirk, D. F. Schoch, Jr. in [2a]; S. Etemad, A. J. Heeger, A. G. MacDiarmid, *Annu. Rev. Phys. Chem. 33* (1982) 443.

[4] J. H. Sinfelt in J. R. Anderson, M. Boudart (Ed.): *Catalysis, Science, and Technology, Vol. 1*, Springer, New York 1981, p. 257; J. H. Sinfelt, *Chem. Eng. News 50* (1972) 18; *Acc. Chem. Res. 10* (1977) 15; *Catal. Rev. Sci. Eng. 9* (1974) 147; W. M. H. Sachtler, *J. Mol. Catal. 25* (1984) 1; V. Ponec, *Adv. Catal. 32* (1983) 149; L. Guczi, *J. Mol. Catal. 25* (1984) 13; P. B. Venuto, E. T. Habid, Jr.: *Fluid Catalytic Cracking with Zeolite Catalysts*, Marcel Dekker, New York 1979; J. Scott: *Zeolite Technology and Applications, Recent Advances*, Chemical Technology Review No. 170, Noyes Data Corp., Park Ridge, NJ 1980; J. W. Ward in B. E. Leach (Ed.): *Applied Industrial Catalysis, Vol. 3*, Academic Press, New York 1984, p. 271.

[5] R. P. Messmer, S. K. Knudson, K. H. Johnson, J. B. Diamond, C. Y. Yang, *Phys. Rev. B 13* (1976) 1396; C. Y. Yang, K. H. Johnson, D. R. Salahub, J. Kaspar, R. P. Messmer, *ibid. 24* (1981) 5673; R. C. Baetzoid, M. G. Mason, J. F. Hamilton, *J. Chem. Phys. 72* (1980) 366; R. Kubo, *J. Phys. Soc. Jpn. 17* (1962) 975; A. Kawabata, R. Kubo, *ibid. 21* (1966) 1765; R. Monot, C. Narbel, J.-P. Borel, *Nuovo Cimento B 19* (1974) 253; J.-P. Borel, J.-L. Millet, *J. Phys. (Orsay, Fr.) C 2 1977*, 115; W. D. Knight, *ibid. 1977*, 109; R. Rossetti, S. Nakahara, L. E. Brus, *J. Chem. Phys. 79* (1983) 1086; P. Yee, W. D. Knight, *Phys. Rev. B 11* (1975) 3261; G. A. Ozin, S. A. Mitchell, *Angew. Chem. 95* (1983) 706; *Angew. Chem. Int. Ed. Engl. 22* (1983) 674; T. G. Dietz, M. A. Duncan, D. E. Powers, R. E. Smalley, *J. Chem. Phys. 74* (1981) 6511; E. A. Rohlfing, D. M. Cox, A. Kaldor, *Chem. Phys. Lett. 99* (1983) 161; R. E. Benfield, P. P. Edwards, A. M. Stacy, *J. Chem. Soc. Chem. Commun. 1982*, 525; D. C. Johnson, R. E. Benfield, P. P. Edwards, W. J. H. Nelson, M. D. Vargas, *Nature (London) 314* (1985) 231; B. K. Teo, F. J. DiSalvo, J. V. Waszczak, G. Longoni, A. Ceriotti, *Inorg. Chem. 25* (1986) 2262; M. R. Hoare, P. Pal, *Adv. Phys. 20* (1971) 161; J. J. Burton, *Cat. Rev. Sci. Eng. 9* (1974) 209; M. R. Hoare, P. Pal, *Adv. Phys. 24* (1975) 645; M. R. Hoare, *Adv. Chem. Phys. 40* (1979) 48; M. R. Hoare, P. Pal, *Nature (Phys. Sci.) (London) 236* (1972) 35; *Nature (London) 230* (1971) 5; J. J. Burton, *Chem. Phys. Lett. 3* (1970) 594; *Nature (London) 229* (1971) 335.

[6] B. K. Teo, K. Keating, *J. Am. Chem. Soc. 106* (1984) 2224.

[7] B. K. Teo, M. C. Hong, H. Zhang, D. B. Huang, submitted for publication; see also *Chem. Eng. News 65* (1987) No. 2, p. 21.

[8] Cluster **1** $(AsF_6)_2$ forms dark red prismatic crystals; space group $P\bar{1}$, $a = 24.647(10)$, $b = 26.218(8)$, $c = 30.309(12)$ Å; $\alpha = 77.87(2)$, $\beta = 81.92(4)$, $\gamma = 65.94(4)°$; $V = 17452(2)$ Å^3, $Z = 2$. Enraf-Nonius CAD4 diffractometer, $Cu_{K\alpha}$ radiation, 12984 independent reflections ($1° \leq 2\theta \leq 75°$) with $I > 5\sigma(I)$. Anisotropic refinement (metal atoms only), $R_1 = 0.092$. Though tentatively formulated here as a dication, the overall charge of **1** cannot yet be definitely determined.

[9] A. Ceriotti, F. Demartin, G. Longoni, M. Manassero, M. Marchionna, G. Piva, M. Sansoni, *Angew. Chem. 97* (1985) 708; *Angew. Chem. Int. Ed. Engl. 24* (1985) 697.

[10] A. Ceriotti, A. Fait, G. Longoni, G. Piro, F. Demartin, M. Manassero, N. Masciocchi, M. Sansoni, *J. Am. Chem. Soc. 108* (1986) 8091.

[11] D. Fenske, J. Ohmer, J. Hachgenei, *Angew. Chem. 97* (1985) 993; *Angew. Chem. Int. Ed. Engl. 24* (1985) 993.

[12] E. G. Mednikov, N. K. Eremenko, Y. L. Slovokhotov, Y. T. Struchkov, *J. Chem. Soc. Chem. Commun. 1987*, 218.

[13] A. Ceriotti, P. Chini, G. Longoni, D. M. Washecheck, M. A. Murphy, L. F. Dahl, unpublished results.

[14] B. K. Teo, N. J. A. Sloane, *Inorg. Chem. 24* (1985) 4545; N. J. A. Sloane, B. K. Teo, *J. Chem. Phys. 83* (1985) 6520; B. K. Teo, N. J. A. Sloane, *Inorg. Chem. 25* (1986) 2315; B. K. Teo, *ibid. 23* (1984) 1251; B. K. Teo, G. Longoni, F. R. K. Chung, *ibid. 23* (1984) 1257; B. K. Teo, *ibid. 24* (1985) 1627, 4209.

[15] Recently, *G. Schmid* and *N. Klein* (*Angew. Chem. 98* (1986) 910; *Angew. Chem. Int. Ed. Engl. 25* (1986) 922) explained their transmission electron micrographs and X-ray powder patterns by $(M_{13})_{13}$ and $(M_{13})_{\infty}$. The difference between their idea and ours is that they considered packing of spherical M_{13} cuboctahedra to form supraclusters with the following nuclearities (number of clusters in brackets): [2] $2 \times 13 = 26$, [3] $3 \times 13 = 39$, ... [13] $13 \times 13 = 169$, [∞] $13 \times 13 \times 13 \times$ ... In contrast, we considered vertex-sharing icosahedra to form supraclusters with the following nuclearities: [2] $2 \times 13 - 1 = 25$, [3] $3 \times 13 - 3 = 36$, ... [12] $12 \times 13 - 30 + 1 = 127$ ... The operational test for these two ideas will be

the synthesis and single-crystal structural determination of these two series of supraclusters with distinctly different nuclearities.

[16] Supracluster assemblies of icosahedral symmetry also occur in nature (e.g., viruses). See, for example, E. D. P. deRobertis, E. M. F. DeRobertis: *Cell and Molecular Biology*, 7th ed., Saunders College, Philadelphia, PA 1980, p. 119.

(2,2,8,8-Tetramethyl-5-oxa-4,6-diphospha-3,6-nonadiene)tetrakis[dicarbonyl-(methylcyclopentadienyl)manganese], the First Complexed Bis(phosphavinyl) Ether**

By *Manfred L. Ziegler,* Rainer Balles, Bernd Nuber, Gerd Becker, Helmut Schmidt, Basil Kanellakopulos,* and *Bernhard Powietzka*

The rich complexation chemistry of phosphaalkynes, especially that of 2,2-dimethylpropylidynephosphane **1**,[1] is supported by numerous examples.[2] We have now observed a novel reaction type. Reaction of **1** with the manganese complex **2** surprisingly results in formation of complex **3** (see Experimental Procedure).

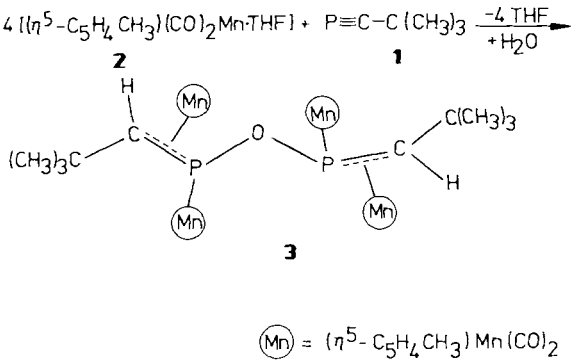

This compound contains the first bis(phosphavinyl) ether ligand, to which four $(C_5H_4CH_3)Mn(CO)_2$ fragments are coordinated. The formation of this ligand can be formally understood as the addition of one molecule of H_2O to two molecules of **1**. Since the reaction was carried out in dried solvents under inert gas, the source of the water is not yet known. The reaction might involve the initial formation of a presumably very reactive complex with the solvent tetrahydrofuran (THF). In view of the diverse reactions of phosphaalkyne complexes, such secondary reactions are certainly conceivable. Unfortunately, the introduction of D_2O into the reaction mixture did not lead to unequivocal results.

The molecular ion is readily apparent in the EI and the FD mass spectra; in addition, **3** was characterized by its elemental analysis and the usual spectroscopic data,[3] as well as by X-ray structure analysis. As revealed in Figure 1, the bis(phosphavinyl) ether ligand functions as an eight-electron donor. Of the four manganese complex fragments, two are bonded to the phosphorus atoms, which thus act as phosphanes, and the other two are bonded η^2-like to the C=P double bond of the ligand.

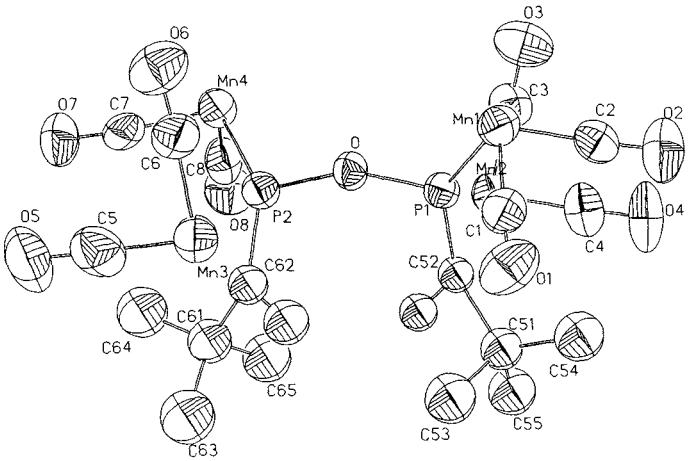

Fig. 1. Molecular crystal structure of **3**; for clarity, the methylcyclopentadienyl moieties are omitted. Selected bond lengths [pm] and angles [°]: Mn1-P1 223.6(4), Mn2-P1 240.2(3), P1-C52 171(1), Mn2-C52 215.7(9), Mn4-P2 222.6(3), Mn3-P2 243.8(3), Mn3-C62 215.6(10), P2-C62 170(1), P1-O 164.3(7), P2-O 166.5(7); O-P1-C52 107.7(7), O-P2-C62 107.2(7), P1-O-P2 154.8(7). Space group $P2_1/c$, $a=1218.6(3)$, $b=1808.2(6)$, $c=2031.4(7)$ pm, $\beta=96.66(2)°$, $Z=4$, $R_{anniso}=0.072$, $R_w=0.053$, $\rho_{calcd}=1.42$ g cm^{-3}, $F_{000}=1960$, AED2 Siemens-Stoe, graphite monochromator, $\lambda=0.7107$ Å ($Mo_{K\alpha}$), measuring range $3°\leq 2\theta\leq 60°$; $h(0/17)$, $k(0/25)$, $l(-29/29)$, 3150 measured, 3070 independent reflections with $I>2.0\sigma(I)$, $R_{merge}=0.056$. Structure solution: Patterson and differential Fourier methods, all non-hydrogen atoms refined anisotropically, H atoms calculated at ideal positions. Further details of the crystal structure investigation may be obtained from the Fachinformationszentrum Energie, Physik, Mathematik GmbH, D-7514 Eggenstein-Leopoldshafen 2 (FRG), on quoting the depository number CSD-52488, the names of the authors, and the journal citation.

The noticeable broadening of the NMR signals prompted us to carry out magnetic measurements. They revealed a field-dependent paramagnetism for **3** between 50 K and room temperature. The magnetic moment increases monotonically between 77.6 K ($\mu_{eff}=4.57\mu_B$ per Mn) and 293.8 K (5.44). The μ_{eff} values correspond to two unpaired electrons per Mn atom. Between 20 and 1.3 K, the paramagnetism is strongly field-dependent; between 50 K and room temperature, the susceptibility obeys the Curie-Weiss law ($\theta=-53.5$ K). Since the 18-electron rule is formally valid for all manganese atoms in **3**, this finding is particularly surprising. Tetragonally or trigonally distorted coordinated Mn^I (d^6) provides a possible explanation, especially since the Mn-Mn distances (Mn1-Mn2 410.6 and Mn3-Mn4 416.0 pm) rule out the possibility of magnetic interactions.

Experimental Procedure

A solution of $[(\eta^5\text{-}C_5H_4CH_3)Mn(CO)_3]$ (1 g, 1.38 mmol) in 400 mL of THF was irradiated under inert gas in a water-cooled photolysis vessel. The evolution of CO ceased after 90 min (≈ 150 mL at 25°C). The solution of the solvent complex **2** thereby obtained was concentrated to 150 mL, cooled in a sodium chloride-ice bath, and then treated with **1** (1 g, 1.10 mmol). The mixture was stirred under constant pressure for 6 h at room temperature and the solvent was then removed in an oil-pump vacuum. The residue was dissolved in 20 mL of *n*-hexane and transferred to a column (silica gel 0.05–0.2, 40 × 2 cm, *n*-hexane). Unreacted **2** was first eluted with *n*-hexane, followed by a second, unstable, uncharacterized brown fraction with hexane/toluene (1:1) and, finally, deep orange **3** with toluene/ether (1:1). The solvent was removed and the residue was recrystallized from toluene/CH_2Cl_2 (1:1). Deep orange crystals: yield 480 mg (25%, based on the total amount of **2**), m.p. = 142–145°C.

Received: February 4, 1987 [Z 2089 IE]
German version: *Angew. Chem.* 99 (1987) 929

[*] Prof. Dr. M. L. Ziegler, R. Balles, Dr. B. Nuber
Anorganisch-chemisches Institut der Universität
Im Neuenheimer Feld 270, D-6900 Heidelberg (FRG)
Prof. Dr. G. Becker, Dipl.-Chem. H. Schmidt
Institut für Anorganische Chemie der Universität
Pfaffenwaldring 55, D-7000 Stuttgart 80 (FRG)
Prof. Dr. B. Kanellakopulos, B. Powietzka
Kernforschungszentrum Karlsruhe, Institut für Heisse Chemie
Postfach 3640, D-7500 Karlsruhe (FRG)

[**] This work was supported by the Fonds der Chemischen Industrie and the Deutsche Forschungsgemeinschaft.

CAS Registry numbers:
1, 78129-68-7; **2**, 51922-84-0; **3**, 109907-06-4; $[(\eta^5\text{-}C_5H_4CH_3)Mn(CO)_3]$, 12108-13-3.

[1] G. Becker, G. Gresser, W. Uhl, *Z. Naturforsch. B36* (1981) 16.

[2] G. Becker, W. A. Herrmann, W. Kalcher, G. W. Kriechbaum, C. Pahl, T. C. Wagner, M. L. Ziegler, *Angew. Chem. 95* (1983) 417; *Angew. Chem. Int. Ed. Engl. 22* (1983) 413; *Angew. Chem. Suppl. 1983*, 501; P. Binger, R. Milczarek, R. Mynott, M. Regitz, W. Rösch, *Angew. Chem. 98* (1986) 645; *Angew. Chem. Int. Ed. Engl. 25* (1986) 644; P. B. Hitchcock, M. J. Maah, J. F. Nixon, *J. Chem. Soc. Chem. Commun. 1986*, 737.

[3] Spectroscopic data of **3**: ^{1}H-NMR (60 MHz, CCl_3D, TMS, 25°C): $\delta = 5.31$ (s, C_5H_4 (8H)), 4.80 (s, C_5H_4 (8H)), 4.26 (s, CH (2H)), 2.11 (s, CH_3 (6H)), 1.96 (s, CH_3 (6H)), 1.36 (s, $C(CH_3)_3$ (18H)); ^{31}P-NMR (90 MHz, H_3PO_4 ext., 25°C): $\delta = +414.89$ (s); IR (ν_{CO} [cm^{-1}], KBr): 1964 vs, 1935 vs, 1929 vs, 1903 s, 1866 vs; FD-MS (160°C, toluene, ether): *m/z* 978 ($M^{\oplus}$).

Selective Molecular Recognition and Separation of Isomeric and Partially Hydrogenated Arenes**

By *Fritz Vögtle,* Walter M. Müller, Ute Werner,* and *Hans-Willi Losensky*

Herein we describe a novel, easily obtainable, efficient host substance **1** having a symmetrical molecular structure, which owing to its large disk-shaped cavity shows remarkable, previously unobserved guest selectivities towards polycyclic arenes, partially hydrogenated and substituted arenes, in aqueous solution.[1,2]

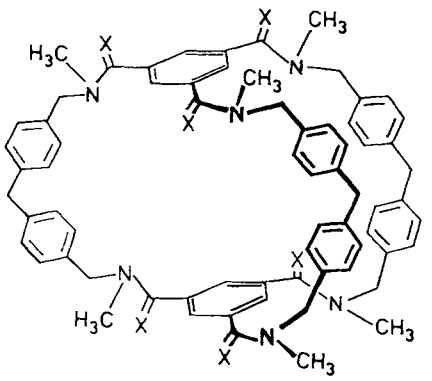

1: X = H
2: 1·6 HCl
3: X = O

The hexamine **1**, which is readily soluble as the hydrochloride **2** in dilute hydrochloric acid, is obtained under dilution principle conditions by cyclization of 1,3,5-benzenetricarboxylic acid trichloride with 4,4′-bis(*N*-methylaminomethyl)diphenylmethane in benzene and subsequent reduction of the crude lactam **3**.[3]

The binding of guest molecules by the hydrochloride **2** was first demonstrated by fluorescence spectroscopy[4] using perylene as fluorescing guest in methanolic solution;[5] the measured data indicated an association constant of about $10^{2.5}$.

[*] Prof. Dr. F. Vögtle, W. M. Müller, U. Werner, Dipl.-Chem. H.-W. Losensky
Institut für Organische Chemie und Biochemie der Universität
Gerhard-Domagk-Strasse 1, D-5300 Bonn 1 (FRG)

[**] This work was supported by the Minister für Wissenschaft und Forschung des Landes Nordrhein-Westfalen. We thank Priv.-Doz. Dr. *K. Müller* (Basel) for molecular modeling calculations, Prof. Dr. *R. H. Mitchell* (University of Columbia, Canada) for a sample of *trans*-10b,10c-dimethyl-10b,10c-dihydropyrene, Mr. *C. Schmidt* for recording the NMR spectra, Mr. *E. Gessi* for carrying out the fluorescence spectroscopy measurements, and Mrs. *S. Geskes* for valuable assistance.

Table 1. Compounds complexed and non-complexed by **1** (in D_2O/DCl).

Complexed compounds	
Acenaphthylene	Perylene
Benzo[*def*]chrysene ("1,2-Benzpyrene")	Phenanthrene
Benzo[*ghi*]perylene ("1,12-Benzperylene")	Pyrene
Fluoranthene	Triphenylene
Non-complexed compounds [a]	
Acenaphthene	3,6-Dimethylphenanthrene
Adamantane	1,2,3,4,5,6,7,8,9,10,11,12-Dodecahydrotriphenylene
Anthracene	Fluorene
Azulene	1,2,3,6,7,8-Hexahydropyrene
Benzene	Hexamethylbenzene
Chrysene	Mesitylene
Coronene	Naphthalene
cis- and *trans*-Decalin	2,6-Naphthalenedicarboxylic acid
9,10-Dihydrophenanthrene	Tetralin
trans-10b,10c-Dimethyl-10b,10c-dihydropyrene	2,3,6,7-Tetramethylanthracene
2,6-Dimethylnaphthalene	Triptycene

[a] Within the limits of detection by ^{1}H-NMR spectroscopy (200 MHz).

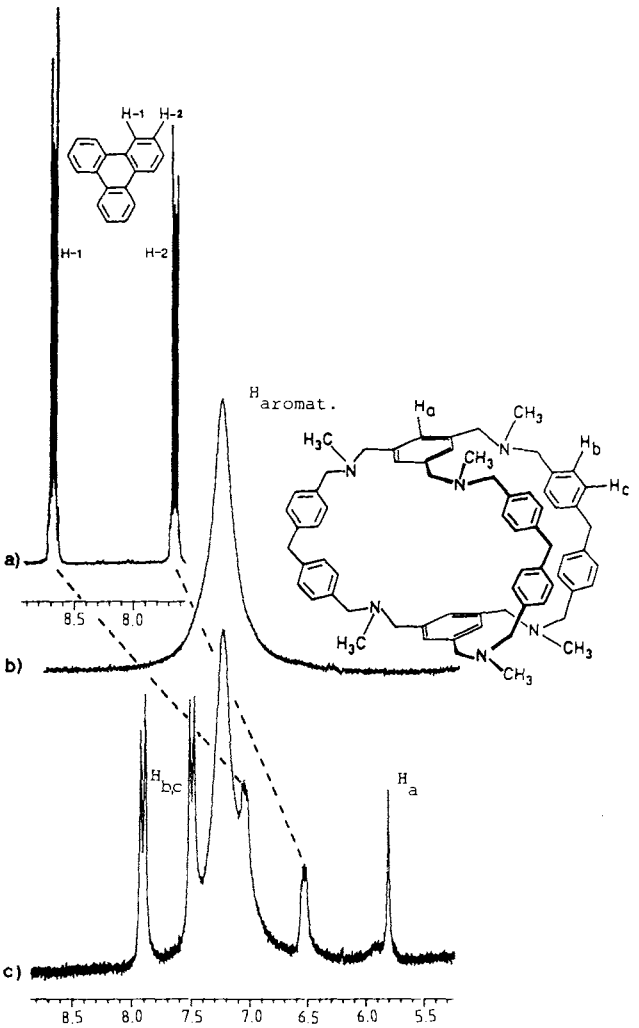

Fig. 1. ^{1}H-NMR spectra (sections; 200 MHz) [6]: a) of the guest triphenylene in CD_2Cl_2/CD_3OD (1:1); b) of the host compound **1** in D_2O/DCl; c) of the host-guest complex (**1** · triphenylene). [The guest was added in excess to a 1×10^{-2} M solution of the host (D_2O/DCl); after 30 minutes' ultrasonication the mixture was filtered.] The spectrum also shows, besides signals of H-1 and H-2 of the guest, signals of protons of the complexed *and* non-complexed host. These two kinds of host signals can be attributed to a slow establishment of the complexation/decomplexation equilibrium.

The ^{1}H-NMR absorptions of the host compound **1** are markedly broadened at room temperature/200 MHz in D_2O/DCl (Fig. 1), and become more sharply defined on increasing the temperature; the process is reversible. Addition of certain aromatic guest compounds (cf. Table 1) not only leads to drastic upfield shifts of the proton absorptions of the guests (cf. Table 2), but also to signal sharpening, splitting, and upfield (NCH_3 protons and H_a-aromatic) as well as downfield shifts ($H_{b/c}$-aromatic) of host signals. This is illustrated in Figure 1 with the example triphenylene as guest. The upfield shifts of some other guest compounds are listed in Table 2.

We explain these findings in terms of the accomodation of ideally fitting guests with complementary topology in the cavity of **1** and of the change in conformational mobility of the host molecule upon accomodating a guest. However, as Table 1 shows, there are substrates which have very little influence, if any, on the ^{1}H-NMR spectrum of the host **1**; these include substrate molecules that are too small or too large for the host's cavity and such molecules whose topology deviates widely from the flat and discoid shape of the condensed arenes.

Table 2. Some significant ^{1}H-NMR upfield shifts $\Delta\delta$ [ppm] of guest protons by the host **1** (in D_2O/DCl, 200 MHz, room temperature) [a].

Guest proton	Triphenylene	Pyrene	Perylene	Acenaphthylene
	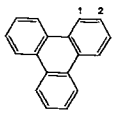	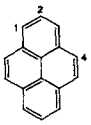	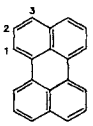	
H-1	+1.61	+1.53	+1.01	+0.75
H-2	+1.14	+0.97	+1.24	
H-3			+1.65	– [b]
H-4		+1.52		+1.60
H-5				+1.35

[a] 0.1 mmol of the guest compound was added to 1 mL of a 1×10^{-2} M solution of the host **1** (D_2O/DCl). After 30 min ultrasonication the mixture was filtered and the filtrate investigated ^{1}H-NMR spectroscopically. [b] Masked by aromatic protons of the host.

That is, the host **1**—consistent with findings on space-filling models—preferably accomodates in its cavity guest molecules with the topology of triphenylene, pyrene, and perylene. Apparently benzene, naphthalene, azulene are too small, while coronene is too large. In contrast, all other previously synthesized host substances known to accomodate larger aromatic molecules complex even naphthalene as well as naphthalene and benzene bearing methyl substituents.[1,2]

Remarkably, phenanthrene is complexed, but the isomeric anthracene is not, a discrimination which has not been observed hitherto—not even with the cyclodextrins. The angularly annelated phenanthrene, with its unilateral "rounded off" shape would appear to find accomodation in the disk-shaped cavity more easily than linear guests. A similar sharp selection obtains in the case of benzo[*def*]chrysene and chrysene: benzo[*def*]chrysene ("1,2-benzpyrene") is complexed—this is the first reported instance—whereas complexation of the elongated chrysene is not detectable.

For partially hydrogenated arenes such as hexahydropyrene, dihydrophenanthrene, acenaphthene, and dodecahydrotriphenylene a complexation is not observed, even though the corresponding arenes fit in the host cavity.

It can be concluded from these substrate selectivities that the cavity of **1** obviously only accomodates such guests in which H atoms of the arene directly project into the rigid angle of the CH_2 group of the diphenylmethane units. Aliphatic CH_2 and CH_3 groups at the periphery of the guest molecule interfere, as demonstrated by the negative results obtained in insertion experiments with hexahydropyrene and dihydrophenanthrene, and even 2,6-dimethylnaphthalene. Adamantane and the decalins also fail to qualify as guests for the same reason.

Such a selective complexation should facilitate a preparative separation of mixtures of the substances by extraction of the potential guests dissolved in *n*-hexane with an aqueous (1×10^{-3} M) solution of the host **1** (host : guest : guest 1 : 0.75 : 0.75). The following mixtures of substances have been employed: I: phenanthrene/anthracene; II: phenanthrene/dihydrophenanthrene; III: pyrene/hexahydropyrene; IV: acenaphthylene/acenaphthene; V: triphenylene/dodecahydrotriphenylene. After the separation, the phases were investigated ^{1}H-NMR spectroscopically. (For this the hexane solution was evaporated to dryness and the residue taken up in CD_2Cl_2.) It was found, upon continuous extraction of the mixtures III and V, that the hydrocarbon (pyrene; triphenylene) is transferred to the extent of more than 70% into the aqueous phase, whereas the respective partially hydrogenated arene is not detectable in the aqueous phase by ^{1}H-NMR spectroscopy. In contrast, no noticeable liquid/liquid phase transfer is observed in the case of the mixtures I, II, and IV. We attribute this to the inferior complementary topology of these guest substances, which, nevertheless, is satisfactory enough for a solid/liquid phase transfer: in each case only the first of the given components is extracted from the crystalline mixtures I–V into the aqueous host phase with an aqueous host solution after two hours ultrasonication.[7]

Thus, to our knowledge, aromatic compounds have been preparatively separated for the first time from related compounds of similar molecular masses by selective molecular complexation. In view of these findings we posed ourselves the question whether one of the components can be selectively extracted from a solution of fluoranthene, chrysene, naphthalene, anthracene, and adamantane in paraffin-oil—as, e.g., are present in tars. Indeed, exclusively pure fluoranthene was obtained in 60% yield from such a mixture in a single extraction (several hours' stirring with the hydrochloric acid solution of **1**).

Further separations are possible by way of the selective transport of various guest compounds according to the U-tube method.[8] For example, when a solution of a 1 : 1 mixture of naphthalene/phenanthrene (4×10^{-2} mol/L of each) in *n*-hexane is placed in one limb of the U-tube, separated from neat *n*-hexane in the other limb by a layer of an aqueous-hydrochloric acid solution of **1**, after 12 hours' stirring only phenanthrene (25% of the amount initially present in the mixture) and no naphthalene could be detected in the previously "empty" (neat) *n*-hexane solution (^{1}H-NMR).

Received: April 13, 1987;
revised: May 27, 1987 [Z 2201 IE]
German version: *Angew. Chem.* 99 (1987) 930

[1] Complexation of hydrocarbons of the benzene and naphthalene series in aqueous solution: a) K. Mori, K. Odashima, A. Itai, Y. Iitaka, K. Koga, *Heterocycles 21* (1984) 388; b) F. Diederich, K. Dick, D. Griebel, *J. Am. Chem. Soc. 108* (1986) 2273; c) S. B. Ferguson, F. Diederich, *Angew. Chem. 98* (1986) 1127; *Angew. Chem. Int. Ed. Engl. 25* (1986) 1127; d) J.

Franke, F. Vögtle, *ibid.* 97 (1985) 224 and *24* (1985) 219; e) H.-J. Schneider, K. Philippi, J. Pöhlmann, *ibid.* 96 (1984) 907 and *23* (1984) 908; f) M. A. Petti, T. J. Shepodd, D. A. Dougherty, *Tetrahedron Lett.* 27 (1986) 807.

[2] Complexation of aromatic hydrocarbons containing at least three rings: see [1b].

[3] Procedure for **1-3**: A solution of 1,3,5-benzenetricarboxylic acid trichloride (4.78 g, 18.0 mmol) in anhydrous benzene (250 mL) and a solution of 4,4'-bis(*N*-methylaminomethyl)diphenylmethane (13.74 g, 54.0 mmol), also in 250 mL of anhydrous benzene, were added dropwise and simultaneously within 8 h to 2 L of anhydrous benzene at room temperature. The hydrochloride precipitate was filtered off, the filtrate evaporated to dryness, and the resulting residue thoroughly dried. For characterization the crude hexalactam **3** (20% yield) was purified by column chromatography on SiO_2 (eluent: dichloromethane/ethanol 20:1): 4% pure yield, m.p. 221-226°C. Crude **3** was heated under reflux with 90 mL of 1 M boranetetrahydrofuran solution for 7 h. Finally, the mixture was carefully hydrolyzed, the THF removed by distillation, and the residue acidified with 15% hydrochloric acid and heated under reflux for a further 2 h. The mixture was then rendered alkaline with solid sodium hydroxide and extracted five times with dichloromethane. The combined dichloromethane extracts were washed with water, dried, and evaporated to dryness. The solid residue was separated on an Al_2O_3 column (basic) with dichloromethane/ethanol (100:35) as eluent. Yield of **1**: 359 mg (2%), m.p. 78°C (decomp.). In some cases the hydrochloride **2** precipitated from the hydrochloric acid solution before neutralization; decomposition above 242°C. Correct elemental analyses and NMR and MS spectra were obtained for **1-3**.

[4] Fluorescence measurements at 20°C with a Perkin-Elmer Model 204-A. Excitation wavelength 440 nm, emission wavelength 470 nm (perylene). The concentration of the fluorescence indicator was 1×10^{-8} M, the host concentration was varied from 0 to 10^{-3} M. Methanol was used as solvent.

[5] Micelle formation could not be observed at a host concentration of 3×10^{-2} M (^{1}H-NMR measurements at various concentrations).

[6] Cf. F. Vögtle, W. M. Müller, *Angew. Chem. 96* (1984) 711; *Angew. Chem. Int. Ed. Engl. 23* (1984) 712.

[7] The differences between solid/liquid and liquid/liquid extraction are attributed to host/guest solvation/desolvation effects, boundary effects, crystal-lattice forces etc.

[8] Cf. F. Diederich, K. Dick, *J. Am. Chem. Soc. 106* (1984) 8024.

Olefinic C=C Double Bond Coordination to a M≡M Triple Bond: Bis(η^2-ethylene)hexakis(neopentyloxy)ditungsten**

By *Malcolm H. Chisholm** and *Mark Hampden-Smith*

Multiple bonds between metal atoms are reactive inorganic functional groups.[1,2] For example, the M-M triple bonds in $[Cp_2Mo_2(CO)_4]$[3] and $[M_2(OR)_6]$[4] (M = Mo or W) have been found to react with CO, alkynes, allenes, carbodiimides, diazoalkanes, and a host of other unsaturated substrates, in addition to showing reactivity toward oxidative-additions and cluster formation reactions. Notably absent from the list of substrates to be activated are N_2, H_2 and olefinic C-C double bonds. We describe here our observation of the binding of ethylene to $[W_2(ONp)_6]$ (Np = CH_2CMe_3).

$[W_2(ONp)_6]$ can be obtained as a yellow crystalline solid by reaction of $[W_2(OtBu)_6]$ with NpOH (>6 equiv.) in hexane at 0°C. The structure of the compound is analogous to that of $[W_2(OiPr)_6]$.[5] $[W_2(ONp)_6]$ is stable in hydrocarbon solutions with respect to cluster formation for a period of days at room temperature.[6] Addition of C_2H_4 (2 equivalents) to a solution of $[W_2(ONp)_6]$ in [D_8]toluene or [D_6]-benzene leads to an immediate darkening of the solution, from pale yellow to deep yellow/brown. The ^{1}H-NMR spectrum reveals, in addition to some unreacted ethylene and $[W_2(ONp)_6]$, the formation of a 1:2 adduct, $[W_2(ONp)_6(C_2H_4)_2]$. The ^{1}H-NMR spectra require that the molecule adopts a relatively rigid structure having a C_2 axis of molecular symmetry. Specifically, there are three types of ONp ligands in the integral ratio 1:1:1 each having diastereotopic methylene protons,[7] and one ethylene moiety per $W(ONp)_3$ unit. This is consistent with a typical Lewis acid-base adduct[8] of the type shown diagrammatically by **I**, given that rotation about the M≡M bond is frozen-out. For alkoxide ligands this barrier to M≡M bond rotation is low (e.g. $\Delta G^{\ddagger} = 9.5$ kcal mol^{-1} for $[W_2(ONp)_6(HNMe_2)_2]$) and typically a "frozen-out spectrum" is only attained at very low temperatures.

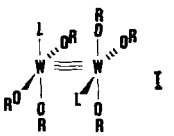

I

Particularly noteworthy are the ^{1}H-NMR signals of the ethylene ligand (four multiplets, see Fig. 1). Again this is indicative of a rather rigid structure in which ethylene rotation about the metal ethylene axis is frozen-out on the NMR time-scale. Coordination of C_2H_4 thus generates an ABCD spin system, a situation rarely encountered in mononuclear complexes.[9]

In the ^{13}C-NMR spectrum (22°C, 75 MHz, [D_6]benzene), there are two resonances (at $\delta = 60.8$ and 63.8) assignable to the ethylene carbon atoms. Both signals show coupling to ^{183}W ($I = 1/2$, 14.5% natural abundance):

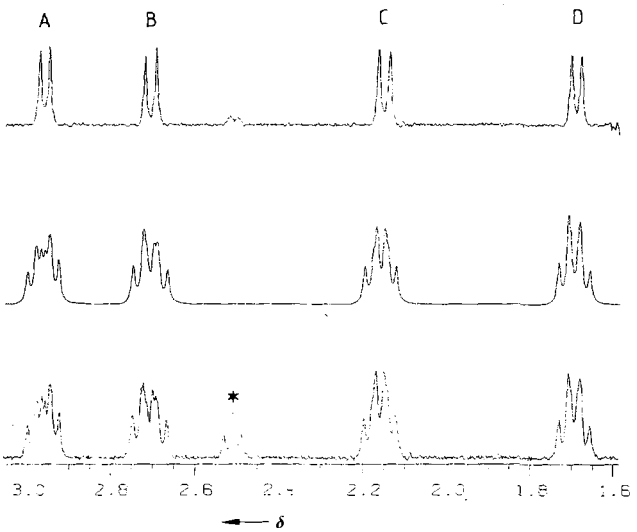

Fig. 1. Bottom: Section of a 360-MHz ^{1}H-NMR spectrum (ethylene region) of $[W_2(ONp)_6(C_2H_4)_2]$ recorded at 10°C in [D_6]benzene. The resonance marked * is due to a derivative of $[W_2(ONp)_6(C_2H_4)_2]$. Top: The ^{1}H-NMR spectrum of the ethylene region of $[W_2(ONp)_6(trans\text{-}CHD{=}CHD)_2]$ shows that statistical distribution of the three possible enantiomers and no scrambling of the label have occurred. Resonances A and D and B and C were shown to be mutually *trans*. Resonances A and C and B and D were shown to be mutually geminal in the isotopomer $[W_2(ONp)_6(CH_2{=}CD_2)_2]$. Decoupling experiments on the protio ethylene complex were employed to determine the remaining coupling constants ($^{cis}J_{AB} = 12.0$, $^{gem}J_{AC} = 6.8$, $^{trans}J_{AD} = 8.5$ Hz, $^{trans}J_{BC} = 9.5$, $^{gem}J_{BD} = 7.9$, $^{cis}J_{CD} = 10.4$ Hz) and to generate the simulated spectrum (middle).

[*] Prof. Dr. M. H. Chisholm, M. Hampden-Smith
Department of Chemistry and Molecular Structure Center
Indiana University
Bloomington, IN 47405 (USA)

[**] This work was supported by the National Science Foundation (USA) and the Indiana University Foundation.

$J_{^{183}W-^{13}C} = 36$ Hz.[10] In the ^{13}C spectrum of the ^{13}C-labeled compound $[W_2(ONp)_6(*C_2H_4)_2]$ where *C represents 99 mol% ^{13}C, $^1J_{C-C} = 28$ Hz, and from the ^1H spectrum, $^1J_{H_A-C} = 150$ Hz, $^1J_{H_B-C} = 163.4$ Hz, $^1J_{H_C-C} = 146$ Hz, and $^1J_{H_D-C} = 154$ Hz.

The bisethylene adduct is formed reversibly and, over a period of days, reacts further, so that a full characterization of the compound by a single crystal X-ray study has thus far been thwarted. It is possible to formulate some satisfactory structures based on the spectroscopic requirements that: 1) the molecule has empirical formula $[W(ONp)_3(C_2H_4)]_n$ and must have C_2 symmetry; 2) there is restricted rotation about the ethylene tungsten bond. One such structure may be envisaged by analogy to **I** in which restricted ethylene rotation can be understood by a consideration of the metal to ethylene back-bonding which competes with the metal-metal triple bond. One such ethylene-W_2 interaction is diagramatically shown in **II**.

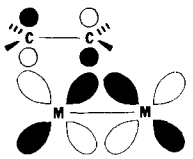

I

If this is the M-M π orbital formed from metal d_{xz}-d_{xz} interactions, it follows that the other ethylene will coordinate to the other metal atom at right angles to that shown in **II** so as to interact with the metal d_{yz}-d_{yz} π bond. In the limit the reaction of two C-C double bonds and one M-M triple bond, $\sigma^2\pi^4$, can be represented by Equation (a), bearing in mind that the M_2C_4 moiety is not flat but folded such that the angle between the two C_2M_2 planes is ca. 90°.

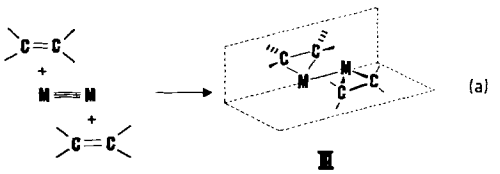

(a)

II

Another structural possibility involves two five-coordinate tungsten atoms in which the plane of ethylene coordination is perpendicular to the metal-metal bond such as is seen in $[W_2R_2(\eta^2\text{-}C_2R'_2)_2(O\mathit{i}Pr)_4]$ compounds.[11]

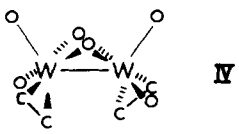

IV

The NMR spectra cannot reliably distinguish between **III** and **IV**, though we are inclined to favor **III** because (i) $[W_2(ONp)_6(C_2H_4)_2]$ is in fact in equilibrium with $[W_2(ONp)_6]$ and free ethylene, and (ii) in compounds of formula $[W_2R_2(\eta^2\text{-}C_2R'_2)_2(O\mathit{i}Pr)_6]$ there is rapid rotation about the W-alkyne C_2 vector. Despite this prejudice in favor of **III** it should be noted that in both **III** and **IV** the ethylene metal interaction may be termed a metallacyclopropane in contrast to **I** where the ethylene merely acts as a Lewis base. **I**, **III**, and **IV** represent limiting bonding modes and evidence in favor of a significant metallacyclopropane contribution is seen by the low value of $^1J_{C-C} = 28$ Hz in $[W_2(ONp)_6(C_2H_4)_2]$ which may be compared with $^1J_{C-C} = 67.6$ and ca. 10 Hz in ethylene[12] and cyclopropane,[13] respectively. Furthermore, from the ^1H-NMR spectrum of the compound employing $CH_2{=}CD_2$ instead of $CH_2{=}CH_2$ we can determine that the two geminal HH couplings are 7.9 and 6.8 Hz. This is significantly larger than the corresponding value for free ethylene (+2.5 Hz; $^{cis}J_{HH} = +11.7$ Hz, $^{trans}J_{HH} = +19.1$ Hz)[12] and for weakly coordinating ethylene ligands such as $[CpMn(CO)_2(C_2H_4)]$ and $[CpCr(CO)(NO)(C_2H_4)]$, where $^{gem}J_{HH}$ values fall in the range 0.5 to 1.0 Hz.[14] On the other hand, the J_{HH} values in phosphirane[15] closely resemble the values measured for $[W_2(ONp)_6(C_2H_4)_2]$.

Received: April 10, 1987;
supplemented: May 29, 1987 [Z 2191 IE]
German version: *Angew. Chem. 99* (1987) 936

[1] F. A. Cotton, *J. Chem. Educ. 60* (1983) 713.
[2] F. A. Cotton, R. A. Walton: *Multiple Bonds Between Metal Atoms*, Wiley, New York 1982.
[3] M. D. Curtis, *Polyhedron 6* (1987) 759.
[4] M. H. Chisholm, *Angew. Chem. 98* (1986) 21; *Angew. Chem. Int. Ed. Engl. 25* (1986) 21.
[5] M. H. Chisholm, D. L. Clark, K. Folting, J. C. Huffman, *Angew. Chem. 98* (1986) 1021; *Angew. Chem. Int. Ed. Engl. 25* (1986) 1014.
[6] M. H. Chisholm, M. Hampden-Smith, unpublished.
[7] 25°C in C_6D_6, methylene protons, $\delta = 4.73$, 4.42, $^2J_{HH} = 10.2$ Hz; 4.18, 4.07, $^2J_{HH} = 9.4$ Hz; 3.95, 3.352, $^2J_{HH} = 9.7$ Hz; methyl protons: $\delta = 1.20$, 1.97, 1.34.
[8] M. H. Chisholm, *Polyhedron 2* (1983) 681.
[9] R. Benn, *Org. Magn. Res. 21* (1983) 723.
[10] This value is substantially smaller than expected for $^1J(^{183}W\text{-}^{13}C)$ of a σ-W-C_{sp^3} alkyl complex, where typical values are 60–105 Hz. M. H. Chisholm, B. W. Eichhorn, K. Folting, J. C. Huffman, unpublished.
[11] M. H. Chisholm, B. W. Eichhorn, J. C. Huffman, *J. Chem. Soc. Chem. Commun.* (1985) 861 and unpublished results.
[12] J. W. Emsley, J. Feeney, L. H. Sutcliffe: *High Resolution Nuclear Magnetic Resonance Spectroscopy, Vol. 2*, Pergamon Press, New York 1966, p. 713 and p. 1029.
[13] F. J. Weigert, J. D. Roberts, *J. Am. Chem. Soc. 94* (1972) 6021.
[14] H. Alt, M. Herberhold, C. Kreiter, H. Strack, *J. Organomet. Chem. 77* (1974) 353.
[15] In phosphiranes, $^{gem}J_{HH} = 5.90$ Hz, $^{trans}J_{HH} = 7.80$ Hz, $^{cis}J_{HH} = 9.26$ and 10.05 Hz. H. Goldwhite, D. Rowsell, L. Vertal, M. T. Bowers, M. A. Cooper, S. L. Maratt, *Org. Magn. Reson. 21* (1983) 494.

Preparation and Structure of $[Mo_4(OMe)_2(O\mathit{i}Pr)_{10}]$; Comments on Why $[W_2(O\mathit{i}Pr)_6]$ Dimerizes, Whereas $[Mo_2(O\mathit{i}Pr)_6]$ Does Not**

By *Malcolm H. Chisholm,* Charles E. Hammond, Mark Hampden-Smith, John C. Huffmann,* and *William G. Van Der Sluys*

Our recent discovery[1] and characterization of $[W_2(O\mathit{i}Pr)_6]$ ($M{\equiv}M$) and its dimeric cluster $[W_4(O\mathit{i}Pr)_{12}]$ has led us to question why such a process does not occur for $[Mo_2(O\mathit{i}Pr)_6]$.[2] We have studied[3] the equilibrium (a) between $[W_4(O\mathit{i}Pr)_{12}]$ and $[W_2(O\mathit{i}Pr)_6]_2$ over the temperature range +20 to +38°C at six different temperatures using two different concentrations for the forward reaction and one concentration for the back reaction in $[D_8]$toluene by ^1H-NMR studies.

[*] Prof. Dr. M. H. Chisholm, C. E. Hammond, M. Hampden-Smith, Dr. C. Huffmann, W. G. Van Der Sluys
Department of Chemistry and Molecular Structure Center
Indiana University
Bloomington, IN 47405 (USA)

[**] This work was supported by the National Science Foundation, the Wrubel Computing Center and the Indiana University Foundation.

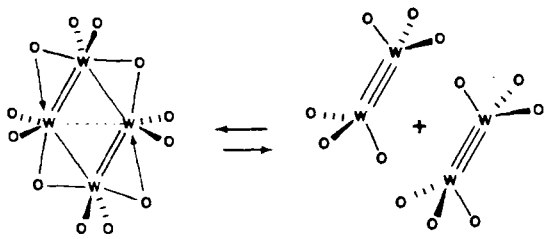

(a)

The tetranuclear cluster is enthalpically favored, ΔH^0, by 22 kcal mol^{-1} but entropically disfavored, ΔS^0, by 61 cal mol^{-1} K^{-1}. The activation parameters for the forward reaction, reveal $\Delta H^* = +30$ kcal mol^{-1} and $\Delta S^* = +17$ cal mol^{-1} K^{-1}, while the back reaction (dimerization) has a small enthalpy of activation, $\Delta H^* = +8$ kcal mol^{-1} but a large entropy of activation, $\Delta S^* = -44$ cal mol^{-1} K^{-1}. These activation parameters for the dimerization led us to propose that alkoxide bridge formation, as seen in

$[Mo_4(\mu\text{-}OMe)_2(\mu\text{-}O\textit{i}Pr)_2(O\textit{i}Pr)_8]$ **1**

represents an important step in cluster formation. Since in the complex $[W_4(O\textit{i}Pr)_{12}]$ there are really only two regular alkoxy bridges (two being semi-bridging[1,4] having long W···O distances of 2.59 Å) it seems that W–W bonding must make a significant contribution to the value of $\Delta H^0 = +22$ kcal mol^{-1} in favoring the cluster. The large ΔS^0 value has several components. The loss of translational entropy on combining two particles of mass of ca. 722 Daltons to give one particle of mass of ca. 1444 Daltons yields -44 cal mol^{-1} K^{-1} at 22 °C using the Sackur-Tetrode equation.[5] In addition there will be negative contributions from the loss of rotational entropy on formation of the $[W_4(O\textit{i}Pr)_{12}]$ cluster. However, it is likely that the coordinatively unsaturated $[W_2(O\textit{i}Pr)_6]$ molecule is more highly solvated, even in [D$_8$]toluene, than is its cluster, giving rise to a release of (positive) entropy for $[W_4(O\textit{i}Pr)_{12}]$ formation. Since it is known that $[W_2(OR)_6]$ compounds bind Lewis bases somewhat more strongly than related $[Mo_2(OR)_6]$ compounds[6] one is led to the conclusion that the tetranuclear compound $[Mo_4(O\textit{i}Pr)_{12}]$ might well be thermodynamically favored at lower temperatures; but at these temperatures the cluster forming reaction would be so slow that $[Mo_2(O\textit{i}Pr)_6]$ would be kinetically inert.

In an attempt to test this hypothesis we have lessened the steric demands at the $[Mo_2(O\textit{i}Pr)_6]$ center by substituting one O*i*Pr ligand by one OMe ligand. This has been achieved by controlled methanolysis [Eqn. (b)].

$$[Mo_2(O\textit{i}Pr)_6] + MeOH \xrightarrow[\text{hexane}]{22\,^\circ C} \tfrac{1}{2}[Mo_4(OMe)_2(O\textit{i}Pr)_{10}] + \textit{i}PrOH \quad (b)$$

1

The red crystalline compound **1** has a centrosymmetric molecular structure in the solid-state (Fig. 1). The rectangular Mo_4 unit has two short (2.238(1) Å) Mo–Mo distances and two long (3.344(1) Å) Mo–Mo distances, corresponding to localized Mo≡Mo bonds and non-bonding distances, respectively. The local geometry about each Mo atom consists of a distorted square planar MoO_4 unit. The four Mo–μ-O distances are essentially equivalent (Mo–O = 2.11(1) Å), while the terminal Mo–O distances (Mo–O = 1.90 Å (av)) are indicative of the retention of some Mo–O double bond character.[7] Note the Mo≡Mo bonds are unbridged by alkoxides and the molecule can be viewed as a dimer $[Mo_2(\mu\text{-}OMe)(\mu\text{-}O\textit{i}Pr)(O\textit{i}Pr)_4]_2$. In [D$_8$]toluene solution the ^{1}H-NMR spectra are indicative of a fluxional molecule and suggestive of rapid and reversible bridge opening and closing. **1** represents the first example of a structurally characterized $[Mo_4(OR)_{12}]$ compound even though the alkoxides are broken into two sets: ten O*i*Pr and two OMe ligands. What is most striking in comparing the W_4 and Mo_4 compounds supported by alkoxide ligands is that the W_4 compound $[W_4(O\textit{i}Pr)_{12}]$ clearly favors a 12-electron W_4 cluster bonding mode while the Mo_4 compound, **1**, retains the two localized Mo≡Mo bonds.

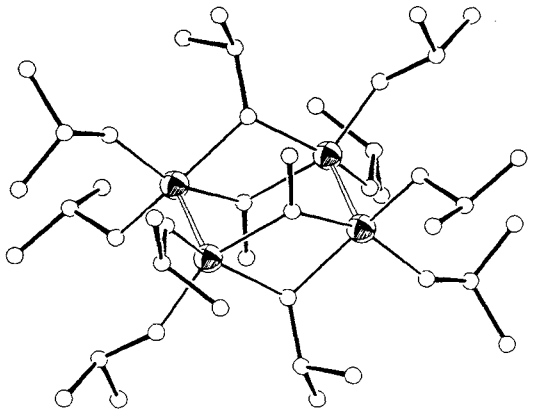

Fig. 1. Crystal structure of $[Mo_4(\mu\text{-}OMe)_2(\mu\text{-}O\textit{i}Pr)_2(O\textit{i}Pr)_8]$ **1**. The unbridged Mo≡Mo bonds (2.238(1) Å) are shown in white. The distance between the bridged Mo atoms is 3.344(1) Å; other distances: Mo-O(terminal) = 1.90(1) Å, Mo-μ-O = 2.11(1) Å.—Space group $P\bar{1}$, cell dimensions at -156 °C, $a = 10.207(4)$, $b = 10.856(4)$, $c = 9.536(3)$ Å, $\alpha = 106.63(1)$, $\beta = 78.06(2)$, $\gamma = 73.76(1)$°, $Z = 1$, $\rho_{calcd} = 1.56$ gm/cm^3 [8].

This leads us to the conclusion that the $[Mo{\equiv}Mo]^{6\oplus}$ unit is thermodynamically more stable than the the corresponding $[W{\equiv}W]^{6\oplus}$ unit with respect to cluster formation. We suggest that this finding can be attributed to core-core repulsions,[9] which has a parallel in triple-bond systems between elements of the 2nd and 3rd main groups (e.g. $2\,N_2$ vs. N_4 and $2\,P_2$ vs. P_4[10]). It is now well recognized that for compounds containing quadruple bonds $[M{\equiv}M]^{4\oplus}$ the W–W distances are longer by ca. 0.1 Å than their Mo–Mo counterparts.[11] Similarly for related $[M{\equiv}M]^{6\oplus}$-containing compounds the W–W distances are ca. 0.08 Å longer than the Mo–Mo distances.[11] In sets of related compounds the M–L distances differ by less than 0.01 Å with the W–L distances generally being shorter.[11] Consequently, for tungsten the drive to cluster formation relieves the problems of core-core repulsion relative to molybdenum for M–M bonds of high order.

Obviously this hypothesis needs considerable further elaboration, but the differences between the molecular structures of $[W_4(O\textit{i}Pr)_{12}]$ and $[Mo_4(OMe)_2(O\textit{i}Pr)_{10}]$ are most noteworthy and warrant general consideration.

Received: May 5, 1987 [Z 2227 IE]
German version: *Angew. Chem. 99* (1987) 937

[1] M. H. Chisholm, D. L. Clark, K. Folting, J. C. Huffman, *Angew. Chem. 98* (1986) 1021; *Angew. Chem. Int. Ed. Engl. 25* (1986) 1014.
[2] M. H. Chisholm, F. A. Cotton, C. A. Murillo, W. W. Reichert, *Inorg. Chem. 16* (1977) 1801.
[3] M. H. Chisholm, D. L. Clark, M. Hampden-Smith, unpublished.
[4] M. H. Chisholm, K. Folting, J. C. Huffman, C. C. Kirkpatrick, *J. Chem. Soc. Chem. Commun. 1982*, 188.
[5] D. A. McQuarrie: *Statistical Mechanics*, Harper and Row, New York 1976, p. 86.
[6] M. Akiyama, M. H. Chisholm, F. A. Cotton, M. W. Extine, D. A. Haitko, D. Little, P. E. Fanwick, *Inorg. Chem. 18* (1979) 2266.

[7] M. H. Chisholm, *Polyhedron 2* (1983) 681.
[8] $Mo_{K\alpha}$, $6° < 2\theta < 45°$. Of the 2917 reflections collected, 2884 were unique, and the 2543 with $F > 2.33\sigma(F)$ were used in the full least squares refinement. Final residuals are $R(F) = 0.028$ and $R_w(F) = 0.032$. — Further details of the crystal structure investigations are available on request from the Fachinformationszentrum Energie, Physik, Mathematik GmbH, D-7514 Eggenstein-Leopoldshafen 2 (FRG), on quoting the depository number CSD-52610, the names of the authors, and the journal citation.
[9] a) T. J. Ziegler, *J. Am. Chem. Soc. 106* (1984) 5901; *ibid. 107* (1985) 4453; b) E. M. Kober, D. L. Lichtenberger, *ibid. 107* (1985) 7199; c) W. C. Trogler, *J. Chem. Educ. 57* (1980) 424.
[10] a) F. A. Cotton, G. Wilkinson, *Advanced Inorganic Chemistry*, 4th Ed., Wiley, New York 1980; b) N. N. Greenwood, A. Earnshaw: *Chemistry of the Elements*, Pergamon Press, Oxford 1984; c) H. Block, H. Muller, *Inorg. Chem. 23* (1984) 4365.
[11] F. A. Cotton, R. A. Walton: *Multiple Bonds Between Metal Atoms*, Wiley-Interscience, New York 1982.

Nonaphenyltristiboxane-1,5-diyl Disulfonates**

By *Robert Rüther, Friedo Huber,** and *Hans Preut*

The long known distiboxanes $(XR_3Sb)_2O$[1] may be regarded as products of the partial hydrolysis of triorganoantimony(v) compounds R_3SbX_2 (X = e.g. Cl). A hydrolysis proceeding beyond the stage of the distiboxanes and accompanied by condensation reactions takes place only under relatively drastic conditions. In such a case polymeric $(R_3SbO)_n$ is formed. Intermediates of this reaction are not known. We have now succeeded in synthesizing and characterizing for the first time the tristiboxanes $XPh_3Sb-O-SbPh_3-O-SbPh_3X$ (X = 2,4-$(NO_2)_2C_6H_3SO_3$, 2,4,6-$(NO_2)_3C_6H_2SO_3$).

Dimeric triphenylantimony oxide **1**[2,3] reacts with the free sulfonic acids **2** (molar ratio 3 : 4) in the presence of 2,2-dimethoxypropane as water-trapping reagent to give the compounds **3** [Eqn. (a)].

$$3(Ph_3SbO)_2 + 4HX \longrightarrow \underset{\mathbf{1}}{} \quad \underset{\mathbf{2a,b}}{} \qquad (a)$$

$$2XPh_3Sb-O-SbPh_3-O-SbPh_3X + 2H_2O$$

$$\underset{\mathbf{3a,b}}{}$$

a, X = 2,4-$(NO_2)_2C_6H_3SO_3$; **b**, X = 2,4,6-$(NO_2)_3C_6H_2SO_3$

3a and **3b** form yellow, air-sensitive crystals which are moderately soluble in alcohol and dimethyl sulfoxide, sparingly soluble in chloroform, and very sparingly soluble in water and hexane. The ^{1}H-NMR spectra of **3a** and **3b** exhibit several multiplets, indicating concomitant presence of various phenylantimony species in solution. Comparable observations on hexaphenyl-1λ^5,3λ^5-distiboxane-1,3-diyl disulfonates in $CHCl_3$ or acetone implicate establishment of rearrangement equilibria.[2] In analogous reactions of **1** with less acidic sulfonic acids (X = $MeSO_3$, $PhSO_3$, 4-$CH_3C_6H_4SO_3$, $HOCH_2CH_2SO_3$) mixtures of the corresponding distiboxanes and excess oxide are formed.

As previously reported,[4] the preparation and structure of the organoantimonyl(v) sulfonates are strongly influenced by the nucleophilicity of the respective sulfonate ion, while the size of the organic moiety of the sulfonate group plays only a subordinate role. Moreover, the electronic properties and the size of the organo-substituents on the antimony atom are of considerable importance.[2] Thus trimethylantimony compounds analogous to **3** cannot be synthesized, and the reaction of CF_3SO_3H with **1** leads only to the distiboxane.

The X-ray structure analysis of **3a**[5] reveals a chain of three O-coupled $SbPh_3$ units; two monodentate bonded 2,4-dinitrobenzenesulfonic acid residues function as terminal groups of this chain (Fig. 1). The trigonal-bypyrimidal

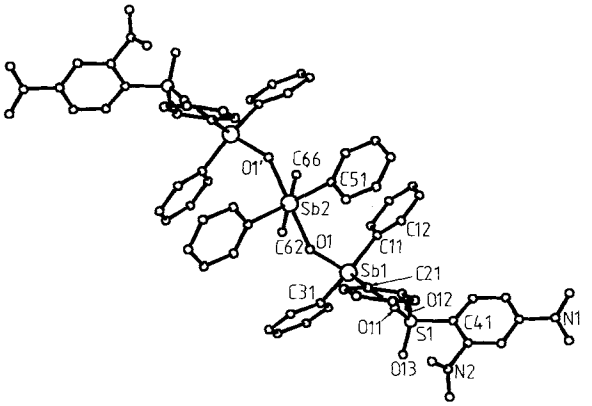

Fig. 1. Crystal structure of **3a** viewed along the C_2 axis, which runs through the atoms Sb2, C61, and C64 (ORTEP II, without H atoms); C61 and C64 are hidden by Sb2, C63 is hidden by C62. Selected bond lengths [pm] and angles [°]: Sb1-O1 192.1(4), Sb2-O1 203.5(5), Sb1-O11 250.9(5), S1-O11 145.8(5), S1-O12 143.0(7), S1-O13 144.9(7); Sb1-O1-Sb2 140.8(3), O1-Sb1-O11 174.4(2), O1-Sb2-O1' 176.8(2).

arrangement of the three equatorial phenyl groups is virtually undistorted, while the phenyl groups of the outer antimony atoms are tilted from the equatorial plane in the direction of the respective sulfonate group (mean value of the O11-Sb-C angle (C = C11, C21, C31): 82.3°), and the O1-Sb1-O11 angle of 174.4(2)° also deviates more from linearity than the O1-Sb2-O1' angle. The large Sb1-O11 distance of 250.9(5) pm (cf. Table 1), the distortion also found in other comparable compounds, and the IR data (Table 2) point to a relatively high degree of ionic character for the Sb-OSO_2 bonds.

Table 1. Typical Sb-O distances in stibonylsulfonates.

Compound	*d*(Sb-O) [pm]	Ref.
$Ph_3Sb(O_3SC_6H_5)_2$	212.8(2) and 210.6(3)	[4]
$Ph_4SbO_3SC_6H_5 \cdot H_2O$	250.6(4)	[6]
$(Ph_3SbO_3SC_6H_5)_2O$	224.7(5) and 228.0(5)	[7a]

Table 2. IR data of the compounds **3** (Nujol; $\tilde{\nu}$ in cm^{-1}).

	$\tilde{\nu}_{as}(SO_2)$	$\tilde{\nu}_{s}(SO_2)$	$\tilde{\nu}$(SO)	$\tilde{\nu}_{as}$(Sb-O-Sb)
3a	1275	1192/1185	1020	750
3b	1290	1212	1030	750

Sb-O-Sb bridges can be linear[8] or bent.[7] In **3a** the angle is 140.8(3)° and thus essentially corresponds to the values observed in bent distiboxanes.[7] Remarkable is the unsymmetric disposition of the Sb-O-Sb bridges. The Sb2-O1 distance (203.5(5) pm) corresponds to the normal Sb-O distance for a covalent bond in organoantimony(v) compounds.[9] The substantially shorter Sb1-O1 bond (192.1(4) pm) is comparable to the μ-O-Sb bonds in the previously known distiboxanes.[7,8] Substantially different μ-O-Sb bonds are also found in the Sb-O-Sb-O four-membered

[*] Prof. Dr. F. Huber, Dr. R. Rüther, Dr. H. Preut
Fachbereich Chemie der Universität
Otto-Hahn-Strasse 6, D-4600 Dortmund 50 (FRG)

[**] This work was supported by the Fonds der Chemischen Industrie.

ring of **1** (mean values 207.3(7) and 192.5(7) pm), which, however, can only be referred to for comparison with care because of the different orientation (apical and equatorial in **1**, apical in **3a**). The formation of unsymmetrical Sb-O-Sb bridges in **3a** can be attributed to the positive partial charge of the outer antimony atoms. This elicits a stronger interaction between metal atom and the lone pair of the bridge oxygen atom and a strengthening of the μ-O-Sb bond.

Experimental

3: A suspension of **1** (1.107 g, 1.5 mmol) [2, 4] and **2a** (0.496 g, 2 mmol) or **2b** (0.586 g, 2 mmol) in acetone (15 mL) was prepared at room temperature. After a short time a clear yellow solution formed, which, after addition of 10 mL of 2,2-dimethoxypropane, was stirred overnight and finally evaporated down under vacuum to about 10 mL. The precipitated microcrystalline, yellow powder was filtered off and washed with a small amount of ether. M.p.: **3a** 204–206 °C (decomp.); **3b** 202–206 °C (decomp.); yield **3a** 30%; **3b** 32%.

Received: March 30, 1987 [Z 2169 IE]
German version: *Angew. Chem. 99* (1987) 948

[1] H. Landolt, *J. Prakt. Chem. 84* (1861) 328; L. Kolditz, M. Gitter, E. Rösel, *Z. Anorg. Allg. Chem. 316* (1962) 270; G. G. Long, G. O. Doak, L. D. Freedmann, *J. Am. Chem. Soc. 86* (1964) 209.
[2] R. Rüther, *Dissertation*, Universität Dortmund 1986.
[3] J. Bordner, G. O. Doak, T. S. Everett, *J. Am. Chem. Soc. 108* (1986) 4206.
[4] R. Rüther, F. Huber, H. Preut, *Z. Anorg. Allg. Chem. 539* (1986) 110.
[5] Single crystals suitable for X-ray structure analysis were obtained by recrystallization of **3a** from chloroform/petroleum ether. Space group $I2/a$, $a = 2443.6(7)$, $b = 1066.5(5)$, $c = 2475(9)$ pm, $\beta = 99.62(5)°$, $Z = 4$. Four-circle diffractometer CAD4 (Enraf-Nonius), $Mo_{K\alpha}$ radiation, graphite monochromator, $2\theta/\omega$ scans, $2 \leq \theta \leq 23.5°$, 3742 observed ($I > 3\sigma(I)$) independent absorption-corrected reflections from 5104 measured reflections, 412 refined parameters, unit weights, $R = 0.03$, $S = 2.8$, residual electron density $= 0.2(1) \times 10^6$ e pm^{-3}. Further details of the crystal structure investigation are available on request from the Fachinformationszentrum Energie, Physik, Mathematik GmbH, D-7514 Eggenstein-Leopoldshafen 2 (FRG) on quoting the depository number CSD-52490, the names of the authors, and the journal citation.
[6] R. Rüther, F. Huber, H. Preut, *J. Organomet. Chem. 295* (1985) 21.
[7] a) H. Preut, R. Rüther, F. Huber, *Acta Crystallogr. Sect. C42* (1986) 1154; b) G. Ferguson, F. L. March, O. R. Ridley, *Acta Crystallogr. Sect. B31* (1975) 1260; G. Ferguson, D. R. Ridley, *ibid. 29* (1973) 2221.
[8] Z. A. Starikova, T. M. Shchegoleva, V. K. Trunov, I. E. Pokrovskaya, *Sov. Phys. Crystallogr. (Engl. Transl.) 23* (1978) 547; H. Preut, R. Rüther, F. Huber, *Acta Crystallogr. Sect. C41* (1985) 358.
[9] a) A. L. Beauchamp, M. J. Bennett, F. A. Cotton, *J. Am. Chem. Soc. 91* (1969) 297; K.-W. Shen, W. E. McEwen, S. J. La Placa, W. C. Hamilton, A. P. Wolf, *ibid. 90* (1968) 1718.

Metal-Promoted Cyclotrimerization of a λ^3-Phosphaalkyne: Formation of a Molybdenum-Coordinated 1,3,5-Triphosphabenzene**

By *Andrew R. Barron* and *Alan H. Cowley**

Despite the fact that phosphaalkynes RC≡P are isovalent with nitriles, their reaction chemistry more closely resembles that of alkynes. Phosphaalkynes thus represent excellent potential building blocks for the facile construction of a wide variety of phosphorus-containing heterocycles. This capability has been demonstrated recently by the synthesis of 1,3-diphosphacyclobutadiene complexes.[1] To the best of our knowledge, **1**, which features two λ^5-phosphorus atoms, is the sole example of a 1,3,5-triphosphabenzene derivative.[2] Since the cyclotrimerization of alkynes on transition-metal centers is well documented,[3, 4] we were prompted to investigate the corresponding chemistry of phosphaalkynes and report herein the first example of a coordinated 1,3,5-triphosphabenzene derivative.[***]

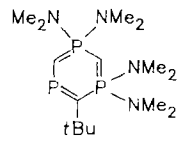

Treatment of the cycloheptatriene-molybdenum complex **2**[5] with *t*BuC≡P[6] afforded the orange, *microcrystalline* Mo complex **3**. Unfortunately, crystals of **3** were unsuitable for X-ray diffraction study.

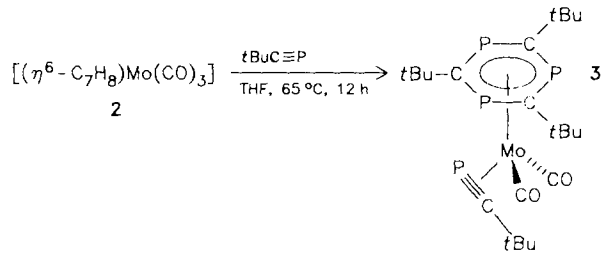

The composition $C_{22}H_{36}MoO_2P_4$ of **3** was established by high-resolution mass spectroscopy ($M^{\oplus}$, calcd 554.0721; found 554.0712, relative intensity 23%). The medium-resolution mass spectral fragmentation pattern revealed peaks at m/z 498 (20%), 497 (19%), and 454 (7%), which correspond to the loss of two CO's, *t*Bu, and *t*BuC≡P, respectively.[7] The lowest m/z peak of significant intensity (12%) corresponds to $[Mo(tBuCP)_3]^{\oplus}$.

The IR spectrum of **3** exhibits two bands in the carbonyl region (1950 and 1890 cm^{-1}), which can be assigned to symmetric and asymmetric CO stretching, respectively. Use of these data leads to a computed[8] inter-carbonyl angle of 89 ± 3°, thus indicating a *cis* disposition of the CO ligands.

The ^{1}H-NMR spectrum of **3** (300 MHz, C_6D_6, TMS ext.) consists of two singlets at $\delta = 1.46$ and 1.30 in a 3 : 1 intensity ratio. In the $^{31}P\{^1H\}$-NMR spectrum (32.2 MHz, C_6D_6, 85% H_3PO_4, ext.) two singlets in the same intensity ratio were detected at $\delta = +25.2$ and -228.2. The high-field resonance falls in a region assigned previously to η^2-attachment of *t*BuC≡P to Mo.[9] The ^{31}P chemical shifts for uncoordinated phosphabenzenes fall in the range $\delta = 150$–300.[2, 10] Although there is no literature precedent, a ^{31}P chemical shift of $\delta = 25.2$ therefore seems plausible for an η^6-coordinated triphosphabenzene.

Experimental Procedure

3: To a solution of **2** (0.476 g, 1.75 mmol) in THF (60 mL) was added *t*BuC≡P (1.05 g, 10.5 mmol). After refluxing for 12 h, the solvent was removed (in vacuo) and the residue extracted with cyclopentane (2 × 50 mL); reduction in volume and cooling (−20 °C) gave an orange solid. Yield: 0.57 g (59%), m.p. = 83 °C (dec.).

Received: May 4, 1987 [Z 2225 IE]
German version: *Angew. Chem. 99* (1987) 956

[*] Prof. A. H. Cowley, Dr. A. R. Barron
Department of Chemistry, The University of Texas at Austin
Austin, TX 78712 (USA)

[**] This work was supported by the National Science Foundation and the Robert A. Welch Foundation.

[***] Note added by the editorial staff: The following communication reports a related cyclotrimerization giving rise to a valence isomer of a 1,3,5-triphosphabenzene derivative in the coordination sphere of vanadium: R. Milczarek, W. Rüsseler, P. Binger, K. Jonas, K. Angermund, C. Krüger, M. Regitz, *Angew. Chem. 99* (1987) 957; *Angew. Chem. Int. Ed. Engl. 26* (1987) 908.

[1] P. Binger, R. Milczarek, R. Mynott, M. Regitz, W. Rösch, *Angew. Chem. 98* (1986) 645; *Angew. Chem. Int. Ed. Engl. 25* (1986) 644; P. B. Hitchcock, M. J. Maah, J. F. Nixon, *J. Chem. Soc. Chem. Commun. 1986*, 737.
[2] E. Fluck, G. Becker, B. Neumüller, R. Knebl, G. Heckmann, H. Riffel, *Angew. Chem. 98* (1986) 1018; *Angew. Chem. Int. Ed. Engl. 25* (1986) 1002.
[3] G. W. Parshall: *Homogeneous Catalysis*, Wiley, London 1980, p. 165.
[4] The formal cyclotrimerization of P_2 has also been demonstrated. O. J. Scherer, H. Sitzmann, G. Wolmershäuser, *Angew. Chem. 97* (1985) 358; *Angew. Chem. Int. Ed. Engl. 24* (1985) 351.
[5] E. W. Abel, M. A. Bennett, R. Burton, G. Wilkinson, *J. Chem. Soc. 1958*, 4559.
[6] G. Becker, G. Gressner, U. Uhl, *Z. Naturforsch. B36* (1981) 16; G. Becker, *Z. Anorg. Allg. Chem. 430* (1974) 66.
[7] The isotope distribution patterns of all fragment ions were computer simulated.
[8] F. A. Cotton, G. Wilkinson: *Advanced Inorganic Chemistry*, 4th ed., Wiley, London 1980, p. 1074; *Anorganische Chemie*, 4th ed., Verlag Chemie, Weinheim 1982, p. 1094f.
[9] R. Bartsch, P. B. Hitchcock, M. F. Meidine, J. F. Nixon, *J. Organomet. Chem. 266* (1984) C41.
[10] K. Dimroth in A. R. Katritzky, C. W. Rees (Eds.): *Comprehensive Heterocyclic Chemistry, Vol. 1*, Pergamon, Oxford 1984, p. 506.

Metal-Promoted Cyclotrimerization of a λ^3-Phosphaalkyne: Formation of Vanadium-Complexed Valence Isomers of a 1,3,5-Triphosphabenzene**

By *Roman Milczarek, Wolfgang Rüsseler, Paul Binger,* Klaus Jonas, Klaus Angermund, Carl Krüger,* and *Manfred Regitz*

tert-Butylphosphaacetylene **1** undergoes cyclodimerization on η^5-cyclopentadienyl metal complexes: Whereas reaction of **1** and cyclopentadienylbis(ethene)cobalt results in the formation of a λ^3-1,3-diphosphacyclobutadienecobalt complex with displacement of the ethene ligands,[1,2] reaction of **1** and the Cp_2Zr fragment (prepared in situ) affords a 1,3-diphosphabicyclo[1.1.0]butane-2,4-diylzirconium complex.[3] Free or complexed cyclotrimers of λ^3-phosphaacetylenes[4] were previously unknown.[***] Herein we report a metal-promoted cyclotrimerization of a λ^3-phosphaalkyne.

Reaction of *tert*-butylphosphaalkyne **1** with the naphthalenevanadium complex **2**,[5] which is a suitable source of Cp*V fragments (Cp* = η^5-pentamethylcyclopentadienyl), results in liberation of naphthalene in an exothermic reaction and formation of a new organovanadium complex as dark brown crystals having the composition $[Cp^*V(PC_tBu)_3]$ **3** (MS, elemental analysis). At room temperature, **3** readily reacts with 1 mol of CO yielding complex **4** (MS, elemental analysis) as dark green crystals.

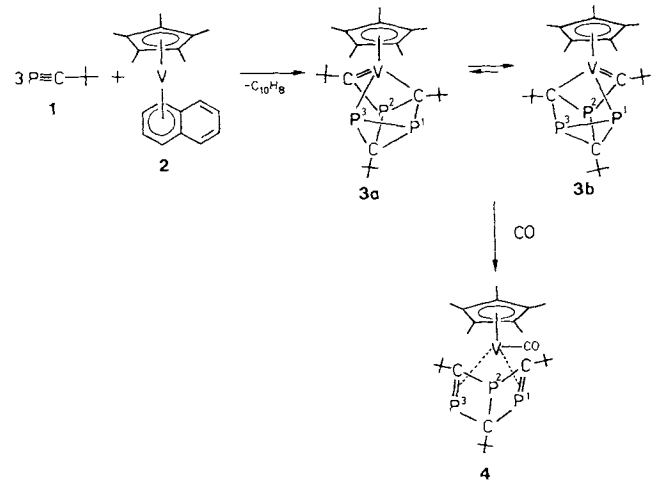

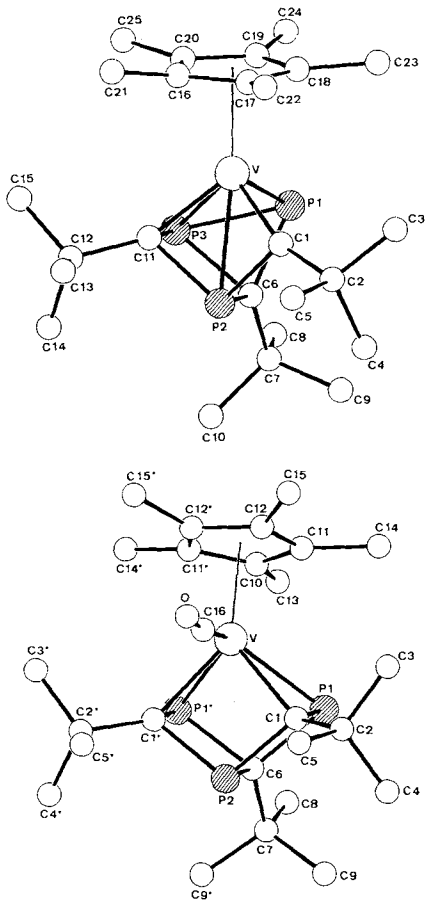

Fig. 1. Top: Molecular structure of **3**. $C_{25}H_{42}P_3V$, $a = 9.664(2)$, $b = 17.935(3)$, $c = 16.015(1)$ Å, $\beta = 101.91(1)°$, $V = 2716.0$ Å^3, $\rho_{calcd} = 1.19$ g cm^{-3}, $\mu(Mo_{K\alpha}) = 5.36$ cm^{-1}, $Z = 4$, space group $P2_1/n$, 6537 measured reflections ($\pm h$, $+k$, $+l$) (averaged according to point group symmetry $2/m$), 6120 unique reflections, 4424 observed ($I > 2\sigma(I)$), empirical absorption correction (min, 0.861; max, 1.083), 262 refined parameters, $R = 0.043$, $R_w = 0.050$. Selected distances [Å] and angles [°]: V-P1 2.382(1), V-P2 2.437(1), V-P3 2.702(1), V-C1 1.849(3), V-C11 1.993(3), P1-P3 2.206(1), P1-C6 1.845(3), P1-C1 3.047(3), P2-C1 1.850(3), P2-C6 1.904(3), P2-C11 1.842(3), P3-C6 1.915(3), P3-C11 1.937(3); C6-P1-P3 55.6(1), C6-P1-V 87.3(1), P3-P1-V 72.1(1), C11-P2-C6 88.9(1), C11-P2-C1 98.1(1), C11-P2-V 53.3(1), C6-P2-C1 104.6(1), C6-P2-V 84.4(1), C1-P2-V 48.8(1), C11-P3-C6 85.9(1), C11-P3-P1 99.5(1), C11-P3-V 47.4(1), C6-P3-P1 52.6(1), C6-P3-V 77.1(1), P1-P3-V 57.0(1), P2-C1-V 82.4(1), P3-C6-P2 91.9(1), P3-C6-P1 71.8(1), P2-C6-P1 107.2(1), P3-C11-P2 93.2(1), P3-C11-V 86.9(1), P2-C11-V 78.8(1) [6]. — Bottom: Molecular structure of **4**. $C_{26}H_{42}OP_3V$, $a = 18.525(1)$, $b = 15.674(1)$, $c = 9.555(1)$ Å, $V = 2774.4$ Å^3, $\rho_{calcd} = 1.23$ g cm^{-3}, $\mu(Mo_{K\alpha}) = 5.31$ cm^{-1}, $Z = 4$. Space group *Pnma*, 4489 measured reflections ($+h$, $+k$, $+l$) (averaged according to point group symmetry *mmm*), 4135 unique reflections, 2995 observed reflections ($I > 2\sigma(I)$). 154 refined parameters, $R = 0.040$, $R_w = 0.047$. Selected distances [Å] and angles [°]: V-P1 2.459(1), V-C1 2.171(2), P1-C1 1.801(2), P1-C6 1.886(1), P2-C1 1.859(2), P2-C6 1.878(3); C6-P1-V 83.3(1), C6-P1-C1 88.0(1), V-P1-C1 58.9(1), C6-P2-C1 86.6(1), C1*-P2-C1 102.6(1), P2-C1-V 85.8(1), P2-C1-P1 94.3(1), V-C1-P1 75.8(1), P2-C6-P1 91.0(1), P1*-C6-P1 105.2(2) [6].

[*] Priv.-Doz. Dr. P. Binger, Dr. R. Milczarek, Dr. W. Rüsseler, Prof. Dr. K. Jonas, Dr. K. Angermund, Prof. Dr. C. Krüger
Max-Planck-Institut für Kohlenforschung
Kaiser-Wilhelm-Platz 1, D-4330 Mülheim a. d. Ruhr
Prof. Dr. M. Regitz
Fachbereich Chemie der Universität
Erwin-Schrödinger-Strasse, D-6750 Kaiserslautern

[**] This work was supported by the Stiftung Volkswagenwerk.

[***] Note added by the editorial staff: A related cyclotrimerization in which a 1,3,5-triphosphabenzene derivative is formed in the coordination sphere of molybdenum is also reported in this issue: A. R. Barron, A. H. Cowley, *Angew. Chem. 99* (1987) 956; *Angew. Chem. Int. Ed. Engl. 26* (1987) 907.

The crystal structure analyses of **3** and **4** show that, in both compounds, the three phosphaalkynes are bound to the vanadium center as valence isomers of 2,4,6-tri-*tert*-butyl-1,3,5-triphosphabenzene (Fig. 1). The C_3P_3 ligand in complex **3** can be derived from a 1,3,5-triphosphaprismane in which no bonding interaction between P1 and C1 or between C1 and C11 (see Fig. 1, top) is present. In complex **4**, the C_3P_3 ligand is unequivocally bound as 1,3,5-triphospha-Dewar-benzene (Fig. 1, bottom).

In contrast to **4**, complex **3** exhibits dynamic behavior in solution. At 20°C, a broad signal for P-1 and P-3 at $\delta = -58.2$ is observed in the ^{31}P-NMR spectrum; only at -100°C is it split into two doublets at $\delta = +140.4$ and -234.4 ($J_{PP} = 219$ Hz). The signal for P-2, on the other hand, is temperature independent, appearing at $\delta = -130.9$ at 20°C and -135.8 at -100°C. Therefore, at room temperature a rapid valence isomerization occurs, which can be described, for example, by the structural formulas **3a** and **3b**. The small differences between the bond lengths in the C_3P_3V framework of **3a** (see caption to Fig. 1, top), however, indicate that other valence isomeric structures exist, such as those found for the structurally similar $P_7^{3\ominus}$ clusters[7] and that these must be considered for a complete description of the structural dynamics. In the ^{31}P-NMR spectrum of the carbonyl complex **4**, the P-1 and P-3 signals are observed at $\delta = -22.4$ (d, $J_{PP} = 6.0$ Hz) and that for P-2 at $\delta = +84.4$ (t); both are temperature independent.

It is remarkable that **1** and **2** react to form vanadium complexes of valence isomers of 1,3,5-triphosphabenzene, since reaction of **2** (Cp instead of Cp*) with diphenylacetylene affords a Cp vanadium complex containing π-bonded hexaphenylbenzene.[8] A possible reason for this is the strong tendency of two-coordinate phosphorus in phosphaalkenes to undergo transformation to the more stable three-coordinate form,[9] but it is not clear what role the transition metal and the Cp or Cp* ligands play.

Experimental Procedure

3: **1** (2.5 g, 25 mmol) [10] in 10 mL of THF was added to a solution of **2** (2.3 g, 7.3 mmol) [5] in 30 mL of THF at room temperature; the solution gradually heats up to boiling accompanied by a color change from dark red to brown. After stirring for 1 h at 20°C, all volatiles were removed at 0.1 torr and then most of the naphthalene was sublimed off at 20°C/0.01 torr. The residue was dissolved in 35 mL of hexane; the crystals precipitating at -78°C were filtered off and the residual naphthalene was removed at 0.001 torr. A second recrystallization from a small amount of hexane gave 1.53 g (43%) of **3** (nearly black crystals, m.p. = 121°C).

4: A solution of **3** (0.95 g, 1.95 mmol) in 15 mL of hexane absorbed 1.95 mmol of CO in 1 h at 20°C, the solution turning green. The green crystals separating out near the end of the reaction were filtered off and recrystallized from ca. 5 mL of diethyl ether at -30°C. After washing with a small amount of cold pentane and drying at 0.1 torr, 0.9 g (90%) of **4** (decomp. at 125°C) was obtained.

Received: May 21, 1987 [Z 2251 IE]
German version: *Angew. Chem. 99* (1987) 957

[1] P. Binger, R. Milczarek, R. Mynott, M. Regitz, W. Rösch, *Angew. Chem. 98* (1986) 645; *Angew. Chem. Int. Ed. Engl. 25* (1986) 644.
[2] P. B. Hitchcock, M. J. Maah, H. F. Nixon, *J. Chem. Soc. Chem. Commun. 1986*, 737.
[3] P. Binger, B. Biedenbach, C. Krüger, M. Regitz, *Angew. Chem. 99* (1987) 798; *Angew. Chem. Int. Ed. Engl. 26* (1987) 764.
[4] Of interest in this connection is the recently described synthesis of a 1,3,5-triphosphabenzene, which, however, contains two λ^5 phosphorus atoms: E. Fluck, G. Becker, B. Neumüller, R. Knebl, G. Heckmann, H. Rittel, *Angew. Chem. 98* (1986) 1018; *Angew. Chem. Int. Ed. Engl. 25* (1986) 1002; cf. the complex stabilization of cyclo-P_6 (hexaphosphabenzene): O. J. Scherer, H. Sitzmann, G. Wolmershäuser, *Angew. Chem. 97* (1985) 358; *Angew. Chem. Int. Ed. Engl. 24* (1985) 351.
[5] K. Jonas, W. Rüsseler, C. Krüger, E. Raabe, *Angew. Chem. 98* (1986) 902; *Angew. Chem. Int. Ed. Engl. 25* (1986) 925.
[6] Further details of the crystal structure investigation may be obtained from the Fachinformationszentrum Energie, Physik, Mathematik GmbH, D-7514 Eggenstein-Leopoldshafen 2 (FRG), on quoting the depository number CSD-52458, the names of the authors, and the journal citation.
[7] a) M. Baudler, *Angew. Chem. 94* (1982) 520; *Angew. Chem. Int. Ed. Engl. 21* (1982) 492; b) H. G. von Schnering, *ibid. 93* (1981) 44 and *20* (1981) 33.
[8] W. Rüsseler, *Dissertation*, Universität Bochum 1986.
[9] See, e.g., the thermal 2-Dewar-phosphinine → 1-Dewar-phosphinine rearrangement: K. Blatter, W. Rösch, U.-J. Vogelbacher, J. Fink, M. Regitz, *Angew. Chem. 99* (1987) 67; *Angew. Chem. Int. Ed. Engl. 26* (1987) 85.
[10] G. Becker, G. Gresser, W. Uhl, *Z. Naturforsch. B36* (1981) 16; improved procedure: W. Rösch, U. Hess, M. Regitz, *Chem. Ber. 120* (1987), in press.

C–S Bond Cleavage in a π-Thiophene Ruthenium Complex**

By *Johannes W. Hachgenei* and *Robert J. Angelici**

Catalytic hydrodesulfurization (HDS), the process by which sulfur is removed from crude oil by treatment with hydrogen over a Mo-Co(γ-Al_2O_3) catalyst, is practiced industrially on a very large scale.[1] However, little is understood about the mechanism of this process, especially for the thiophene-containing organosulfur compounds, which are the most difficult to desulfurize.[2] As a model for the possible reaction of π-adsorbed thiophene with hydride hydrogen bound to the surface of the HDS catalyst, we previously[3] allowed $[Mn(CO)_3(\eta^5\text{-thiophene})](SO_3CF_3)$ to react with hydridometalates ($HFe(CO)_4^{\ominus}$ and $HW(CO)_5^{\ominus}$) and obtained the hydride adduct **1**.

$[Mn(CO)_3(\eta^4\text{-}SC_4H_5)]$ **1**

$[CpRu(\eta^5\text{-}2,5\text{-}Me_2\text{-}C_4H_2S)]PF_6$ **2**·PF_6[4]

$Na[(CH_3OCH_2CH_2O)_2AlH_2]$ **3**

$[CpRu(Me_2C_4H_3S)]$ **4**

We now find that the reaction of **2** (Cp = η-C_5H_5)[4] with hydrides ($LiAlH_4$, **3**, and $NaBHEt_3$) also results in the formation of a hydride adduct, **4**. However, an X-ray crystal structure analysis[5] of **4** (Fig. 1) shows that, in contrast to **1**, a C–S bond has been cleaved to give a butadiene

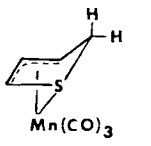

1

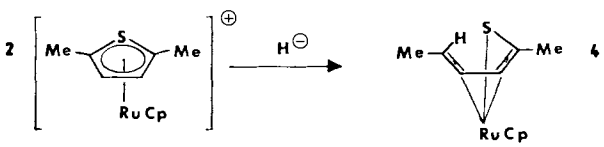

4

[*] Prof. Dr. R. J. Angelici, Dr. J. W. Hachgenei
Department of Chemistry and Ames Laboratory,
Iowa State University
Ames, IA 50011 (USA)

[**] Ames Laboratory is operated for the U.S. Department of Energy by Iowa State University under Contract No. W-7405-Eng-82. This research was supported by the Office of Basic Energy Sciences, Chemical Sciences Division. We thank Prof. *R. A. Jacobson* and *D. Wintergrass* for their help with the X-ray diffraction analysis.

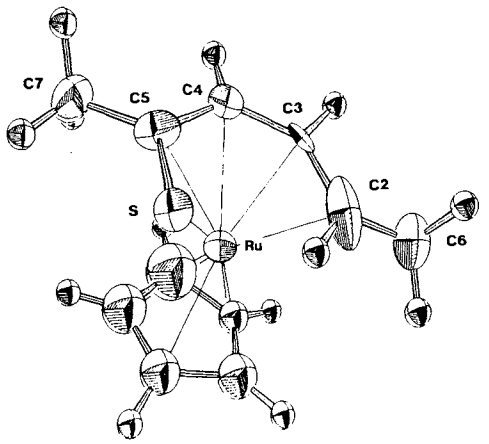

Fig. 1. Crystal structure of **4** showing 50% thermal ellipsoids. Selected bond distances [pm] and angles [°] (±2°): Ru-S 240.1(6), Ru-(C2-C5) 215-220(3), S-C5 170(2), C2-C6 129(3), C2-C3 142(4), C3-C4 140(3), C4-C5 150(3), C5-C7 151(3), Ru-C(Cp) 215-223(5), C-C (within the Cp ring) 131-147(5); C3-C2-C6 128, C2-C3-C4 138, C3-C4-C5 122, C4-C5-C7 118, C4-C5-S 121, C7-C5-S 121.

thiolate ligand. Because of disorder in the crystal,[7] the distances and angles have relatively large errors, but it is clear that the C2–S distance (315 pm) is too long for bonding and that the Ru is coordinated to all four C atoms and the sulfur of the butadiene thiolate ligand. The plane of the four C atoms (C2–C5) is at an angle of 10.7° with respect to the plane of the Cp carbons. The ^{1}H- and ^{13}C-NMR spectra are consistent with the results of the structure analysis (Table 1). Similar hydride addition to the related complexes $[CpRu(\eta^5\text{-}SC_4HR^1R^2R^3)]^{\oplus}$, where $R^1=R^2=R^3=H$ or R^1=2-Me, 3-Me, $R^2=R^3=H$ or R^1+R^2=2,3-Me_2, $R^3=H$ or $R^1+R^2+R^3$=2,3,5-Me_3, yields the analogous butadiene thiolate complexes, as indicated by their NMR spectra. Likewise, other nucleophiles, such as $SEt^{\ominus}$, $OMe^{\ominus}$, and $CH(CO_2Me)_2^{\ominus}$, give similar butadiene thiolate products[8] resulting from nucleophilic addition at a carbon adjacent to the sulfur and C–S bond cleavage. *D. Baudry* et al. report that the reaction of $[(PPh_3)_2ReH_7]$, 3,3-dimethylbutene, and furan yields the related complex $[Re(\eta^5\text{-}C_4H_5O)(PPh_3)_2(CO)]$.[9]

Table 1. NMR data of **4** (C_6D_6, 300 (^{1}H), 75.46 MHz (^{13}C)), δ values in ppm, J in Hz.

^{1}H-NMR: δ = 1.48 (d, 3H; H6), 2.29 (s, 3H; H7), 3.58 (m, 1H; H2), 4.33 (s and m, 6H; Cp and H3), 5.42 (d, 1H; H4), J(H2-H3) = 9.2, J(H2-H6) = 6.1, J(H3-H4) = 6.2

^{13}C-NMR: δ = 22.6 (q, J(CH) = 121; C7), 32.8 (q, 127; C6), 61.9 (d, 166; C2), 79.1 (d, 190; Cp), 87.7 (d, 162; C3), 91.6 (d, 161, C4), 109.9 (s; C5)

Not only do these ring-opening reactions illustrate a new type of π-thiophene reactivity, but they also provide a new model for a possible initial step in the HDS of thiophene, where surface hydride transfer to a π-adsorbed thiophene could lead directly to C–S bond cleavage. It is perhaps especially noteworthy that Ru is an excellent HDS catalyst, whereas Mn is among the worst.[10] The low HDS activity of Mn may be related to its inability to cleave the C–S bond, instead leading only to the partially saturated ring as in **1**.

Experimental Procedure

4: **2**·PF_6 (50 mg, 0.12 mmol) [4, 8] was dissolved in THF (20 mL) and treated with an equimolar amount of **3** ("Red Al," Aldrich, 3.4 M solution in toluene). The solution immediately turned intense yellow. The solvent was removed, the residue was dissolved in benzene, and the solution was chromatographed over basic Al_2O_3 (5 × 80 mm) with benzene as the eluant. Orange crystals of **4** were obtained from hexane at 0°C. The product (60% yield) was sublimed under vacuum. Correct elemental analysis—MS: m/z 280 ($M^{\oplus}$), 265 ($M^{\oplus}-CH_3$).

Received: April 14, 1987 [Z 2204 IE]
German version: *Angew. Chem. 99* (1987) 947

[1] B. C. Gates, J. R. Katzer, G. C. A. Schuit: *Chemistry of Catalytic Processes*, McGraw-Hill, New York 1979.
[2] M. Zdrazil, *Appl. Catal. 4* (1982) 107.
[3] D. A. Lesch, J. W. Richardson, R. A. Jacobson, R. J. Angelici, *J. Am. Chem. Soc. 106* (1984) 2901.
[4] G. H. Spies, R. J. Angelici, *J. Am. Chem. Soc. 107* (1985) 5569.
[5] **4**: Space group $P2_1$, $Z=2$, lattice parameters (255 K): a = 707.8(9), b = 1360.0(12), c = 589.5(7) pm, β = 96.96(10)°, $\mu(Mo_{K\alpha})$ = 16.2 cm^{-1}, Syntex P21, $2\theta < 55°$, 1376 reflections, 1091 with $I > 2\sigma(I)$, absorption correction. Patterson Methods, difference Fourier analysis [6]. Ru, S, C2–C7 anisotropically, Cp isotropically refined, H positions calculated. R = 0.068, R_w = 0.093. Further details of the crystal structure investigation may be obtained from the Fachinformationszentrum Energie, Physik, Mathematik GmbH, D-7514 Eggenstein-Leopoldshafen 2 (FRG), on quoting the depository number CSD-52467, the names of the authors, and the journal citation.
[6] R. A. Jacobson, *J. Appl. Crystallogr. 9* (1976) 115. R. L. Lapp, R. A. Jacobson, U. S. DOE Report IS-4708, ISU, Ames, IA, 1979; D. R. Powell, R. A. Jacobson, U. S. DOE Report IS-4737, ISU, Ames, IA, 1980.
[7] By variation of the occupancy one gets values of 0.85 for S and 1.5 for C2, which means that the crystal contains about 15% of the other enantiomer of **4** where S lies on the position of C2.
[8] G. H. Spies, R. J. Angelici, *Organometallics*, in press.
[9] D. Baudry, J.-C. Daran, Y. Dromzee, M. Ephritikhine, H. Felkin, Y. Jeannin, J. Zakrzewski, *J. Chem. Soc. Chem. Commun. 1983*, 813.
[10] T. A. Pecoraro, R. R. Chianelli, *J. Catal. 67* (1981) 430.

A Novel Heterobimetallic Asymmetric Hydrogenation Catalyst Based Upon a Chiral Rhenium Template Containing Two Phosphido Substituents**

By *Bill D. Zwick, Atta M. Arif, Alan T. Patton*, and *John A. Gladysz**

During the last decade, many pseudotetrahedral, optically active, chiral-at-metal complexes have become available.[1] Surprisingly, few if any applications in catalysis have been reported. Over the same period, terminal metal phosphide complexes, L_nMPR_2, have been shown to be excellent templates for the synthesis of binuclear bridging phosphide complexes,[2] and rhodium(I) complexes of chiral-at-backbone-carbon chelating diphosphanes have seen extensive use in catalytic asymmetric hydrogenation.[3] In this communication, we describe the combination of these *disjecta membra* to give a novel rhodium(I) asymmetric hydrogenation catalyst that contains a chiral *rhenium* in a chelating "diphosphane" backbone.[4] This structurally unique catalyst gives product enantiomeric excesses that are among the highest observed for rhodium(I) systems.

The optically active diphenylphosphide complex (+)-(*S*)-**1** ($[\alpha]^{22}_{589}$ = 220)[5] was synthesized in 89–96% yields from the tosylate complex (−)-(*S*)-[(η^5-C_5H_5)Re(NO)-

[*] Prof. J. A. Gladysz, Mr. B. D. Zwick, Dr. A. M. Arif, Mr. A. T. Patton
Department of Chemistry, University of Utah
Salt Lake City, UT 84112 (USA)

[**] We thank the National Science Foundation (USA) for support of this research.

$(PPh_3)(OTs)]$[6] (>99% *ee*) by a procedure analogous to that previously reported for the racemate.[7] Reaction of (+)-(*S*)-**1** with *n*BuLi (1.1 equiv., THF, −78°C) gave a complex, (*S*)-**2**, that was stable for days at 25°C, and whose reactivity and ^{31}P-NMR spectrum[8] were consistent with the formula shown. Subsequent addition of $ClPPh_2$ (1.0 equiv., −78°C) and work-up gave the phosphidocyclopentadienyl complex (+)-(*S*)-**3** (68–89%, $[\alpha]_{589}^{22} = 216$)[5] as a THF or benzene hemisolvate. The structure of (+)-(*S*)-**3** followed readily from its ^{1}H- and ^{13}C-NMR spectra, which showed patterns characteristic of η^5-C_5H_4X ligands, and from its ^{31}P-NMR spectrum.[8]

Reaction of (+)-(*S*)-**3** with $[Rh(nbd)Cl]_2/AgPF_6$ (1.0 : 0.5 : 1.1, THF)[5,9] gave the heterobimetallic complex (+)-(*R*)-**4** (88%, $[\alpha]_{589}^{22} = 48$)[5] as a THF monosolvate after work-up. The structure of (+)-(*R*)-**4** followed readily from its spectroscopic properties. These included large J_{PRh} for both phosphide phosphorus atoms in the ^{31}P-NMR spectrum.[9] The racemic compound, (±)-**4**, was prepared by an analogous series of reactions (92% from (±)-**3**).

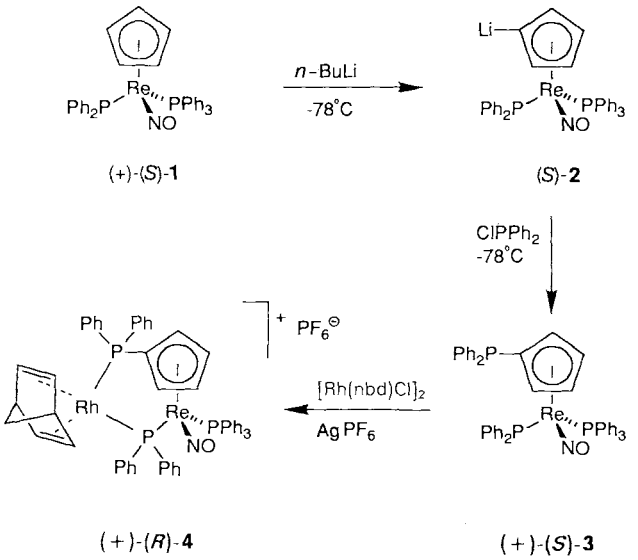

Complex (+)-(*R*)-**4** efficiently catalyzed the asymmetric hydrogenation (1 atm, ambient temperature) of enamide precursors to α-amino acids and esters.[10] Unoptimized turnover rates ranged from 300 to 100/h (see Scheme 1).

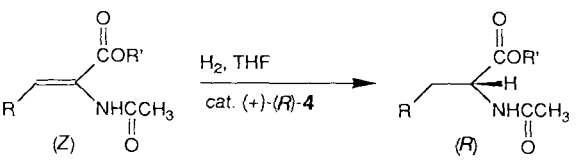

R=H, R'=H:	98% ee	82%
R=Ph, R'=H:	93% ee	70%
R=Ph, R'=CH_3:	88% ee	94%
R=Ph, R'=CH_2CH_3:	82% ee	86%

Scheme 1.

We sought to structurally characterize the catalyst precursor, but suitable crystals were obtained only for the solvated racemate (±)-**4**·$(CHCl_3)_2$ (deep red prisms, $CHCl_3$/hexane).[11] The five-membered chelate ring (Fig. 1) adopts

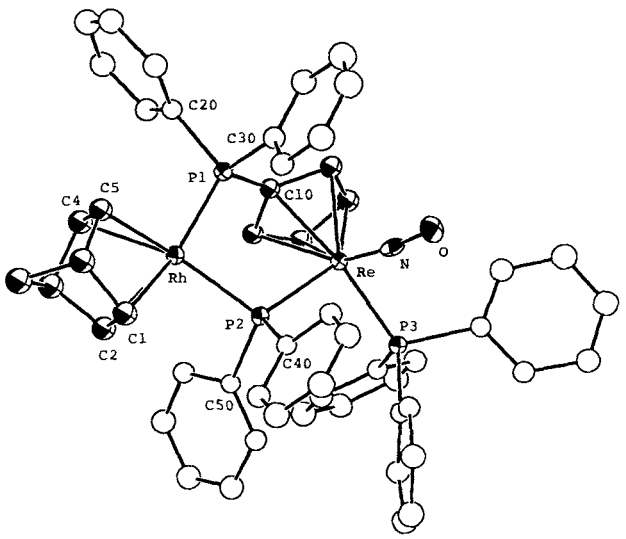

Fig. 1. Structure of the cation of (±)-**4**·$(CHCl_3)_2$. *Selected bond lengths* [Å] *and angles* [°]: Re-C10 2.217(12), Re-P1 2.487(3), Re-P3 2.392(3), Rh-P1 2.276(4), Rh-P2 2.380(3), Rh-C1 2.254(16), Rh-C2 2.258(16), Rh-C4 2.193(15), Rh-C5 2.193(15), P1-C10 1.805(13), Re-N 1.731(13); Re-P2-Rh 113.40(14), P1-Rh-P2 91.35(12), Rh-P1-C10 110.63(44), P1-C10-Re 117.09(59), C10-Re-N 112.88(46), C10-Re-P3 153.94(32), C10-Re-P2 87.42(34), C20-P1-Rh 114.78(44), C30-P1-Rh 113.30(48), C20-P1-C10 106.99(58), C30-P1-C10 106.08(60), C40-P2-Rh 102.42(42), C50-P2-Rh 108.71(40), C40-P2-Re 115.67(43), C50-P2-Re 111.39(39), Re-N-O 171.11(106), P2-Re-P3 99.55(12), P2-Re-N 99.79(38), P3-Re-N 90.81(33).

a distorted "envelope" conformation[12] in which the rhenium and *ipso*-cyclopentadienyl carbon C10 lie 0.338 Å and 0.916 Å below the P1-Rh-P2 plane. This contrasts with five-membered chelate rings in other Rh^I asymmetric hydrogenation catalysts, which adopt "half-chair"[12] (idealized C_2) conformations with one chelate atom below and another above the P-Rh-P plane.[3a,d,f,g] The PPh_3 and NO ligands occupy pseudoequatorial and pseudoaxial positions, respectively. The phenyl rings on P2 bend closer to rhodium than those on P1 (see C-P-Rh angles), most likely due to PPh_3 ligand bulk. These structural features undoubtedly contribute to the unique catalytic activity of (+)-(*R*)-**4**.

Brunner et al. have recently reported an interesting nitrogen-chelated Rh(nbd) complex that contains an asymmetric molybdenum atom in the chelate skeleton, and has briefly examined catalytic hydrosilylation reactions.[4] His study and ours should be the forerunners of a new generation of useful asymmetric catalysts based upon heterobimetallic and polymetallic complexes that contain a chiral metal.

Received: March 31, 1987 [Z 2173 IE]
German version: *Angew. Chem. 99* (1987) 921

[1] a) H. Brunner, *Adv. Organomet. Chem. 18* (1980) 151; b) T. C. Flood, K. D. Campbell, K. D. Downs, S. Nakanishi, *Organometallics 2* (1983) 1590; c) J. H. Merrifield, C. E. Strouse, J. A. Gladysz, *ibid. 1* (1982) 1204; d) J. W. Faller, K.-H. Chao, *ibid. 3* (1984) 927; e) F. Morandini, G. Consiglio, V. Lucchini, *ibid. 4* (1985) 1202; f) S. G. Davies, I. M. Dordor-Hedgecock, K. H. Sutton, J. C. Walker, C. Bourne, R. H. Jones, K. Prout, *J. Chem. Soc. Chem. Commun. 1986*, 607.

[2] See footnote [16] in Ref. [7] and a) J. Powell, J. F. Sawyer, M. V. R. Stainer, *J. Chem. Soc. Chem. Commun. 1985*, 1314; b) R. T. Baker, T. H. Tulip, *Organometallics 5* (1985) 839; c) S. Rosenberg, W. S. Mahonery, J. M. Hayes, G. L. Geoffroy, A. L. Rheingold, *ibid. 5* (1986) 1065.

[3] a) J. Halpern, *Science 217* (1982) 401; b) B. D. Vineyard, W. S. Knowles, J. J. Sabacky, G. L. Bachman, D. J. Weinkauff, *J. Am. Chem. Soc. 99* (1977) 5946; c) W. S. Knowles, *Acc. Chem. Res. 16* (1983) 106; d) M. D. Fryzuk, B. Bosnich, *J. Am. Chem. Soc. 99* (1977) 6262; e) D. P. Riley, R.

E. Shumate, *J. Org. Chem. 45* (1980) 5187; f) J. D. Oliver, D. P. Riley, *Organometallics 2* (1983) 1032; g) E. P. Kyba, R. E. Davis, P. N. Juri, K. R. Shirley, *Inorg. Chem. 20* (1981) 3616; h) J. M. Brown, P. A. Chaloner, G. A. Morris, *J. Chem. Soc. Chem. Commun. 1983*, 664; i) G. Pracejus, H. Pracejus, *J. Mol. Cat. 24* (1984) 227; j) U. Nagel, E. Kinzel, J. Andrade, G. Prescher, *Chem. Ber. 119* (1986) 3326.

[4] See also H. Brunner, J. Wachter, J. Schmidbauer, G. M. Sheldrick, P. G. Jones, *Angew. Chem. 98* (1986) 339; *Angew. Chem. Int. Ed. Engl. 25* (1986) 371; *Organometallics 5* (1986) 2212.

[5] Abbreviations: OTs = OSO_2–*p*-$C_6H_4CH_3$; nbd = norbornadiene. Good precedent exists that all reactions should proceed with retention of configuration at rhenium [6] and *R/S* assignments have been made accordingly; $c = 1.0$ mg/mL (THF) for all $[\alpha]$ values.

[6] J. H. Merrifield, J. M. Fernández, W. E. Buhro, J. A. Gladysz, *Inorg. Chem. 23* (1984) 4022.

[7] W. E. Buhro, S. Georgiou, J. P. Hutchinson, J. A. Gladysz, *J. Am. Chem. Soc. 106* (1985) 3346.

[8] New compounds were characterized by microanalysis, IR, and NMR (^1H, ^{13}C, ^{31}P). Selected $^{31}P\{^1H\}$-NMR data (121 MHz, *J* values): (*S*)-**2** (THF): 21.63 (d, $J_{PP} = 16.0$ Hz, PPh_3), −41.24 (d, $J_{PP} = 16.0$ Hz, PPh_2); (+)-(*S*)-**3** ([D_8]THF): 20.23 (d, $J_{PP} = 14.8$ Hz, PPh_3), −16.20 (s, $CPPh_2$), −45.15 (d, $J_{PP} = 14.8$ Hz, $RePPh_2$); (+)-(*R*)-**4** (CD_2Cl_2): 50.38 (ddd, $J_{PRh} = 182.9$ Hz, $J_{PP} = 18.5$, 5.0 Hz, $CPPh_2$), 9.83 (dd, $J_{PP} = 14.0$, 5.0 Hz, PPh_3), −49.23 (ddd, $J_{PRh} = 126.6$ Hz, $J_{PP} = 18.5$, 14.0 Hz, $RePPh_2$).

[9] a) R. R. Schrock, J. A. Osborn, *J. Am. Chem. Soc. 93* (1971) 2397; b) E. W. Abel, M. A. Bennet, G. Wilkinson, *J. Chem. Soc. 1959*, 3178.

[10] *General hydrogenation procedure:* An oven-dried 50-mL flask was charged (under an inert atmosphere) with a stir bar, (+)-(*R*)-**4** (0.015 g, 0.012 mmol, 0.4 mol%), α-acetamidoacrylic acid (0.616 g, 3.00 mmol), and freshly distilled THF (ca. 25 mL), and connected via a three-way stopcock to a vacuum line and a gas buret. The resulting light orange solution was subjected to a freeze–pump–thaw–degas cycle four times, with H_2 admitted on the final cycle. The reaction solution was vigorously stirred for 6 h, after which H_2 uptake ceased. Work-up [3e] gave (*R*)-*N*-acetylalanine (0.541 g, 2.61 mmol, 87%). The optical purity was assayed both polarimetrically [3b, e] and (after derivatization) chromatographically (5% SP-300 (*N*-lauroyl-L-valine-*t*-butylamide) chiral stationary phase on 100/120 Supelcoport, 130°C, 2 m × 2-mm glass column; see technical bulletin 765G, Supelco Inc., Bellefonte, PA).

[11] Crystal data: monoclinic, $P2_1/C$; $a = 12.980(4)$, $b = 15.832(4)$, $c = 29.117(7)$, $\beta = 91.70(3)°$; $Z = 4$; 12009 reflections ($Mo_{K\alpha}$ radiation, $2\theta_{max} = 29°$), $R = 0.074$, $R_w = 0.083$. Refinement to lower *R* factor was limited by the number of parameters allowed in the programs employed and by disorder in one solvate molecule. Details will appear in B. D. Zwick, *Ph. D. Thesis*, University of Utah, Salt Lake City 1987.

[12] B. Fuchs, *Top. Stereochem. 10* (1978) 1.

Iodophosphonium Salts with Unusual Properties and a Structural Alternative for Halophosphoranes**

By *Wolf-Walther du Mont,* Michael Bätcher, Siegfried Pohl,* and *Wolfgang Saak*

The halogenation of tertiary phosphanes affords dihalophosphoranes, which, in the condensed phase, are present as molecules having a trigonal-bipyramidal arrangement of the substituents, **A**, or as halophosphonium halides, **B** (Fig. 1), depending on the substituent pattern at the phosphorus

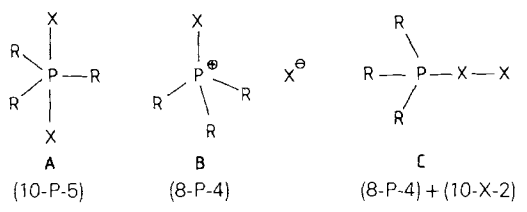

Fig. 1. Structural alternatives for the compounds R_3PX_2 [1].

[*] Prof. Dr. W.-W. du Mont, Dipl.-Chem. M. Bätcher, Prof. Dr. S. Pohl, Dipl.-Chem. W. Saak
Fachbereich Chemie der Universität
Carl-von-Ossietzky-Strasse 9-11, D-2900 Oldenburg (FRG)

[**] This work was supported by the Deutsche Forschungsgemeinschaft and the Fonds der Chemischen Industrie.

atom.[1] In the case of iodophosphonium ions, the proposed structures and the suggestion of equilibria such as (a) are based mainly on conductivity measurements.[2, 3] Io-

$$R_3PI_2 \rightleftharpoons R_3PI^{\oplus}I^{\ominus} \quad (a)$$

dophosphonium ions are isoelectronic with the phosphane tellurides $R_3P{=}Te$, for which rapid transfer of tellurium to tertiary phosphanes is observed. We have suggested that the mechanism of this transfer involves nucleophilic attack on the tellurium atom with formation of (10-Te-2) intermediates.[4] In the correspondingly rapid transfer of $I^{\oplus}$ ions between phosphanes, (10-I-2) intermediates will be energetically favored if, despite its negative polarization, the iodine atom bonded to the phosphonium center is appreciably electrophilic.[4, 6] We have now found that ^{31}P-NMR spectroscopy provides a very sensitive method to detect the significant increase in electrophilic character of the halogen atom in going from chloro- to bromo- to iodophosphonium salts. Furthermore, the first crystal structure analysis of a diiodophosphorane shows that, in the solid state, a linear arrangement P-I-I having a (10-I-2) situation on the central iodine atom, i.e., a new structural type for halophosphoranes (Fig. 1 **C**), is present.[7]

When the reaction of tri-*tert*-butylphosphane **1** with various amounts of elemental iodine in CH_2Cl_2 is followed by ^1H- and ^{31}P-NMR spectroscopy, one observes continuous changes in the chemical shifts and the coupling constants during the addition of the iodine; separate signals for the reaction products are not observed (Table 1). After the

Table 1. ^{31}P-NMR data for the system **1**/iodine (31.91 MHz).

	Solvent	$\delta^{31}P$	$\lvert^3J(^{31}P,^1H)\rvert$ [Hz]
1	CD_2Cl_2	62.0	± 9.8
1 : I_2 = 1 : 1 (= **2**)	CD_2Cl_2	80.8	± 16.0
1 : I_2 = 1 : 1.5	CD_2Cl_2	96	± 16.8
1 : I_2 = 1 : 2 (= **3**)	CH_2Cl_2/C_6D_6	112	± 17.4
$tBu_3PI^{\oplus}I^{\ominus}$ **2B**	H_2O/D_2O	115	± 17.8
$tBu_3PI^{\oplus}BPh_4^{\ominus}$	CD_2Cl_2	110	± 18.0

"equivalence point" (**1** : I_2 = 1 : 1) is attained, the ^{31}P-NMR shift does not remain constant upon continued addition of iodine, but rather is shifted further downfield and the $^3J_{^{31}P,^1H}$ values increase still further. The 1 : 1 adduct **2** formed between **1** and iodine in water (colorless solution) exhibits ^{31}P-NMR shifts and coupling constants $^3J_{^{31}P,^1H}$ that are very close to those of the phosphonium salt $tBu_3PI^{\oplus}BPh_4^{\ominus}$ (colorless in solution and in the solid state) and differ clearly from the NMR data of the yellow solutions of **2** in CH_2Cl_2 or $CHCl_3$ (Table 1). All observations are in accord with a pronounced acceptor character of the iodine atom bonded to the phosphonium center toward soft nucleophiles ($I^{\ominus}$, PR_3, $I_3^{\ominus}$):

1. If **1** is present in excess, **2** undergoes rapid $I^{\oplus}$ exchange [Eq. (b)], so that averaged NMR shifts and coupling constants are measured.[4, 8]

$$tBu_3PI^{\oplus} + P^*tBu_3 \rightleftharpoons tBu_3P + IP^*tBu_3^{\oplus} \quad (b)$$

2. Pure **2** is characterized by a considerable iodine–iodine interaction (**2C**) in aprotic dipolar solvents and in the solid state; these interactions are the apparent cause of

the yellow color of **2** [**2** in CH_3CN: $\lambda_{max}=314$ nm ($\varepsilon=900$), tailing into the visible]. Nucleophilic attack of $I^{\ominus}$ on the iodine atom in $tBu_3PI^{\oplus}$ leads to upfield shift and a reduction in $^3J_{^{31}P,^1H}$.[9] Isolated, hydrated $tBu_3PI^{\oplus}$ and $I^{\ominus}$ ions are probably present in water (**2B**).

3. If iodine is present in excess, iodophosphonium triiodide **3** is formed.[3-5, 10] The $I_3^{\ominus}$ ion is apparently less nucleophilic than $I^{\ominus}$, so that addition of iodine to **2** in CH_2Cl_2 results in a downfield shift of the ^{31}P-NMR signal, namely toward the value for the "free" tri-*tert*-butyliodophosphonium ion [Eq. (c)].

$$\underset{\textbf{2C}}{tBu_3P{-}I{-}I} + I_2 \longrightarrow \underset{\textbf{3}}{tBu_3PI^{\oplus}I_3^{\ominus}} \qquad (c)$$

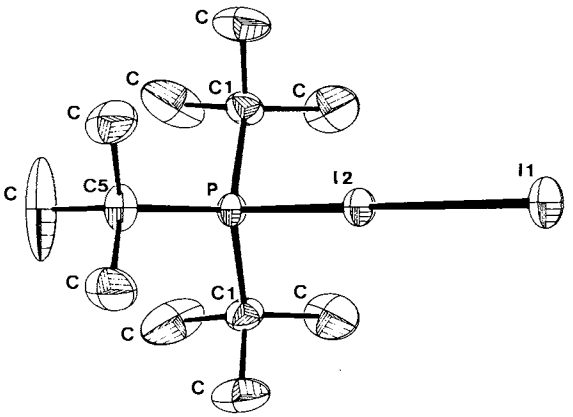

Fig. 2. Crystal structure of **2** (H atoms omitted); thermal ellipsoids at 50% probability. Selected distances [pm] and angles [°]: I1-I2 332.6(1), I2-P 246.1(2), P-C1 190.5(6), P-C5 190.1(9); I1-I2-P 177.6(1), I2-P-C1 106.3(2), I2-P-C5 105.1(3), C1-P-C5 112.5(2).

The X-ray structure analysis (Fig. 2)[11] carried out on a yellow crystal of **2** confirms the existence of significant iodine-iodine interaction in the solid state. The nearly linear P-I-I structural fragment makes **2** comparable with iodine charge-transfer complexes such as the recently described triphenylarsane diiodine.[7, 12] Since the I–I bond in solid **2** is considerably longer than in typical iodine charge-transfer complexes (d(I-I) in **2** 332.6, in Ph_3AsI_2 300.5 pm[7, 13]), **2** can be regarded as an iodophosphonium salt or as a phosphane diiodine charge-transfer complex.[14]

It remains to be shown whether, in the equilibria (a) suggested earlier,[2, 3, 15] the undissociated form R_3PI_2 is indeed present as a (10-P-5) phosphorane or instead as analogue **2** [with hypervalent (10-I-2) iodine].

Received: March 25, 1987;
supplemented: May 5, 1987 [Z 2163 IE]
German version: *Angew. Chem. 99* (1987) 945

[1] (10-P-5) means ten valence electrons around the central atom P, to which five ligands are bonded: C. W. Perkins, J. C. Martin, A. J. Arduengo III, W. Lau, A. Alegria, J. K. Kochi, *J. Am. Chem. Soc. 102* (1980) 7753.
[2] K. Issleib, W. Seidel, *Z. Anorg. Allg. Chem. 288* (1956) 201.
[3] A. D. Beveridge, G. S. Harris, F. Inglis, *J. Chem. Soc. A 1966*, 520.
[4] W.-W. du Mont, H. J. Kroth, *J. Organomet. Chem. 113* (1976) C35.
[5] H. J. Frohn, H. Maurer, *J. Fluorine Chem. 34* (1986) 73.
[6] The first crystallographic evidence for the acceptor behavior of an iodine atom bonded to a phosphonium center was provided by the structure determinations of $PI_4^{\oplus}AlI_4^{\ominus}$ and $P_2I_5^{\oplus}AlI_4^{\ominus}$: S. Pohl, *Z. Anorg. Allg. Chem. 498* (1983) 15, 20.
[7] A compound containing a linear As–I–I structural fragment was recently reported: C. A. McAuliffe, B. Beagley, G. A. Gott, A. G. Mackie, P. P. MacRory, R. G. Pritchard, *Angew. Chem. 99* (1987) 237; *Angew. Chem. Int. Ed. Engl. 26* (1987) 264 and 370.
[8] A correspondingly fast bromine cation transfer is observed in the system **1**/$tBu_3PBr^{\oplus}$: W.-W. du Mont, *Z. Anorg. Allg. Chem. 458* (1979) 85.
[9] The NMR data of bromo-tri-*tert*-butylphosphonium salts are only slightly dependent on the anion and the solvent [10].
[10] M. Bätcher, *Diplomarbeit*, Universität Oldenburg 1987. Correct analytical data obtained for **2** and **3**.
[11] **2**: orthorhombic, space group *Pnma*, $a=1543(1)$, $b=1229.1(1)$, $c=922.0(1)$ pm, $V=1749.6\times10^6$ pm^3, $Z=4$; 1397 unique reflections, 1217 observed ($I>2\sigma(I)$); $R_w=0.038$ (measurement, Siemens-AED-2; solution, SHELX-76). Further details of the crystal structure investigation may be obtained from the Fachinformationszentrum Energie, Physik, Mathematik GmbH, D-7514 Eggenstein-Leopoldshafen 2 (FRG), on quoting the depository number CSD-52635, the names of the authors, and the journal citation.
[12] For the behavior of Ph_3AsI_2 in CH_3CN solution: A. D. Beveridge, G. S. Harris, *J. Chem. Soc. 1964*, 6076.
[13] N. N. Greenwood, A. Earnshaw: *Chemistry of the Elements*, Pergamon, Oxford 1984, p. 940–943.
[14] Similarly as phosphane tellurides $R_3P{=}Te$ can also be regarded as Te^0–phosphane complexes: W.-W. du Mont, *Angew. Chem. 92* (1980) 562; *Angew. Chem. Int. Ed. Engl. 19* (1980) 554.
[15] L. Horner, H. Winkler, *Tetrahedron Lett. 1964*, 445.

Structure and Magnetic Properties of a Gadolinium Hexafluoroacetylacetonate Adduct with the Radical 4,4,5,5-tetramethyl-2-phenyl-4,5-dihydro-1*H*-imidazole 3-Oxide 1-Oxyl**

By *Cristiano Benelli, Andrea Caneschi, Dante Gatteschi,* Jean Laugier,* and *Paul Rey**

Adducts of stable organic radicals with metal ions are currently investigated[1] in order to discover novel types of magnetic interactions and also to study possible models of biologically relevant materials.

In principle, the interaction of radicals with lanthanoid ions can give rise to interesting magnetic properties, because of the high spin values of the metal ions. Indeed, although the f orbitals are relatively shielded, they can nevertheless overlap with the orbitals of the radical in a direct exchange mechanism, thus giving rise to appreciable coupling.

To our knowledge, only a few solution studies of weak interactions between nitroxides and lanthanoid ions have been reported so far,[2] but no stable adducts of a radical ligand directly bound to a lanthanoid ion have been characterized. We wish to report here the synthesis, X-ray crystal structure, and magnetic properties of the adduct formed by gadolinium(III) hexafluoroacetylacetonate, $Gd(hfac)_3$ **1**,[3] with the radical 4,4,5,5-tetramethyl-2-phenyl-4,5-dihydro-1*H*-imidazole 3-oxide 1-oxyl **2**.[4]

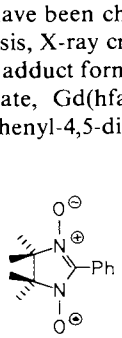

2

[*] Prof. Dr. D. Gatteschi, Prof. Dr. C. Benelli, Dr. A. Caneschi
Università degli Studi di Firenze, Dipartimento di Chimica
Via Maragliano 75, I.50144 Firenze (Italy)
Dr. J. Laugier, Dr. P. Rey
Laboratoires de Chimie, UA 1194 CNRS
Département de Recherche Fondamentale, C.E.N.G.
85 x Grenoble Cédex, F-38041 Grenoble (France)

[**] The financial support of the Italian Ministry of Public Education and of the CNR is gratefully acknowledged.

The X-ray crystal structure analysis[5] of $3 \cdot 0.5\,n\text{-}C_6H_{14}$, performed at room temperature, showed that the asymmetric unit consists of a discrete adduct $[Gd(hfac)_3(\mathbf{2})_2]$ and half a molecule of *n*-hexane (Fig. 1). The Gd ion is eight coordinate to six O atoms of the three hfac molecules and

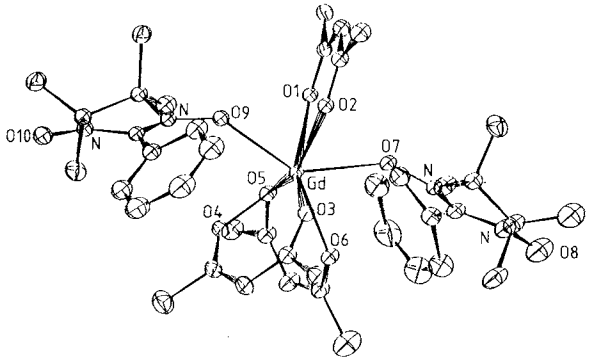

Fig. 1. Molecular structure of $3 \cdot 0.5\,n\text{-}C_6H_{14}$ (ORTEP). The atoms omitted are C atoms. Selected distances [pm] and angles [°]: Gd-O1 237.9(6), Gd-O2 238.5(4), Gd-O3 235.0(6), Gd-O4 240.3(5), Gd-O5 234.8(5), Gd-O6 237.6(5), Gd-O7 232.7(5), Gd-O9 233.7(5); O1-Gd-O9 72.2(1), O2-Gd-O9 75.0(1), O3-Gd-O9 104.1(2), O4-Gd-O9 74.2(1), O5-Gd-O9 91.1(1), O6-Gd-O9 148.1(1), O1-Gd-O7 71.0(1), O2-Gd-O7 75.7(1), O3-Gd-O7 96.3(1), O4-Gd-O7 147.5(1), O5-Gd-O7 97.8(1), O6-Gd-O7 72.7(1).

two O atoms of two different radicals **2**. The bond distances between the Gd ion and the O atoms of the bidentate ligands are in the range 234.8–240.3 pm, while the Gd–O bond distances with the two nitroxides average to 233.2 pm. The coordination polyhedron can be best described as a distorted dodecahedron, according to a procedure suggested in the literature.[6] The pseudo-S_4 axis of the dodecahedron is roughly orthogonal to the O5–O6 and O2–O9 directions. The bond distances within the nitroxides fall in the range usually found for these molecules.[7] The five-membered rings of the nitroxides are to a good approximation planar: the mean deviation of the atoms from the least-squares plane is 10 pm.

The temperature dependence of the inverse molar magnetic susceptibility χ_m^{-1} and of the product $\chi_m T$ for **3** are shown in Figure 2. The experimental points can be fitted to the Curie-Weiss law, with $\theta = 1.468(2)$ K and $C = 8.127(1)$, indicating a weak ferromagnetic interaction between Gd (spin quantum number $S = 7/2$) and the unpaired electrons

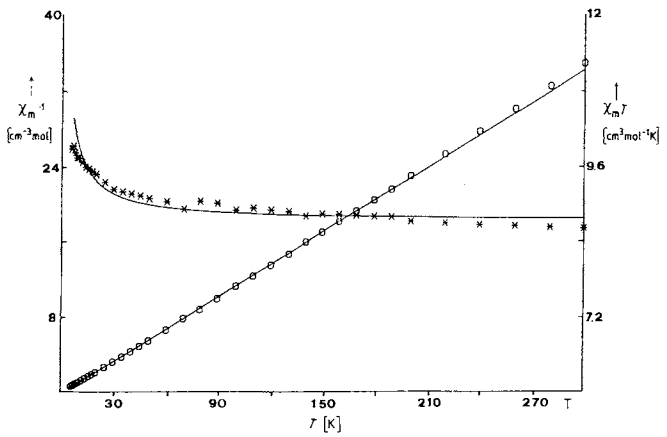

Fig. 2. Temperature dependence of the inverse molar magnetic susceptibility χ_m^{-1} (□) and of the product $\chi_m T$ (*) of **3** in the range 6–300 K.

of the two radicals ($S = 1/2$). This interpretation is confirmed by the temperature dependence of $\chi_m T$, which remains substantially constant down to ca. 20 K and increases steadily below this temperature. The $\chi_m T$ value expected for three non-interacting spins is 8.625 cm^3 mol^{-1} K, while the observed one at $T = 6$ K is $\chi_m T = 9.888$ cm^3 mol^{-1} K.

The experimental points can be fitted with a simple formula[8] which considers only isotropic exchange between gadolinium and the radicals (rad) and between the two radicals. The $\chi_m T$ curve shown in Figure 2 is calculated with the parameters $g_{Gd} = 2.010(1)$, $J_{Gd\text{-}rad} = -1.022(1)$ cm^{-1}, $J_{rad\text{-}rad} = 1.65(2)$ cm^{-1}. This result indicates a weak ferromagnetic interaction between the Gd^{III} ion and the radicals, as well as an antiferromagnetic interaction between the two radicals. The isotropic exchange may not be the only relevant mechanism of interaction and refinements might be introduced using anisotropic exchange and gadolinium zero field splitting, but anisotropic magnetic data must first become available.

In order to determine the possible orbital mechanism of interaction between the metal ions and the radicals, an angular overlap analysis can be performed using the reported matrices.[9]

In fact, the AO parameters are expected to be proportional to the square of the diatomic overlap integral S_λ ($\lambda = \sigma, \pi, \delta \ldots$) of the metal and ligand functions, and also the antiferromagnetic part of the coupling should be proportional to S_λ^2. From the AO analysis we learn that the magnetic orbital of one radical can interact with a linear combination of the f orbitals $(4z^2\text{-}x^2\text{-}y^2)x$ and $(3x^2y\text{-}y^3)$, while that of the other radical interacts with $(4z^2\text{-}x^2\text{-}y^2)y$ and $(x^3\text{-}3xy^2)$, using a reference frame with the *z* axis parallel to the pseudo-S_4 axis. This yields a weak antiferromagnetic contribution, while the interaction with the remaining six combinations of f orbitals may give ferromagnetic contributions. The experimental data show that the latter dominate.

The coupling in **3** can be best compared with manganese–radical complexes,[10] since both are ions having an S ground state. In the manganese complexes, the coupling has been found to be antiferromagnetic, with *J* of the order of 10^2 cm^{-1}. Even in the case of transition-metal ions, therefore, a direct overlap of metal and ligand orbitals does not cause a complete pairing of the spins, and the ferromagnetic contributions of the other metal orbitals become important. The reduced antiferromagnetic component in the lanthanoid ions apparently scales down the coupling, which eventually changes sign.

Experimental Procedure

$1 \cdot 2H_2O$ [3] (718.4 mg, 1 mmol) was suspended in 200 mL of hot *n*-hexane, and **2** (466.6 mg, 2 mmol) [4] was then added; after stirring for 5 min, the solution was filtered, and red-violet crystals, which analyze satisfactorily for $[Gd(hfac)_3(\mathbf{2})_2 \cdot 0.5\,n\text{-}C_6H_{14}]$ ($\mathbf{3} \cdot 0.5\,n\text{-}C_6H_{14}$), were obtained by slow evaporation at room temperature in approximately ten days.

Received: March 30, 1987;
supplemented: May 26, 1987 [Z 2172 IE]
German version: *Angew. Chem. 99* (1987) 958

[1] J. Laugier, P. Rey, C. Benelli, D. Gatteschi, C. Zanchini, *J. Am. Chem. Soc. 108* (1986) 6931.
[2] S. S. Eaton, G. R. Eaton, *Coord. Chem. Rev. 26* (1978) 207.
[3] M. F. Richardson, D. F. Wagner, D. E. Sands, *J. Inorg. Nucl. Chem. 30* (1968) 1275.
[4] M. Lanchen, T. W. Mittag, *J. Chem. Soc. 1966*, 2300; E. F. Ullman, J. H. Osiecki, D. G. B. Boocock, R. Darcy, *J. Am. Chem. Soc. 94* (1972) 7049.
[5] **3**: $P\bar{1}$, $a = 1165.1(4)$, $b = 1269.0(4)$, $c = 1906.2(7)$ pm, $\alpha = 87.50(2)$, $\beta = 73.22(2)$, $\gamma = 85.50(2)$, $Z = 2$, $R = 0.048$ for 5965 independent reflec-

tions with $|F_o| \geq 3\sigma(|F_o|)$ (Enraf-Nonius CAD-4 $Mo_{K\alpha}$). Further details of the crystal structure investigation are available on request from the Fachinformationszentrum Energie, Physik, Mathematik GmbH, D-7514 Eggenstein-Leopoldshafen 2 (FRG), on quoting the depository number CSD-52464, the names of the authors, and the full citation of the journal.

[6] M. G. B. Drew, *Coord. Chem. Rev. 24* (1977) 179.

[7] S. P. Sinha, *Struct. Bonding (Berlin) 25* (1976) 69.

[8] A. Bencini, C. Benelli, A. Caneschi, R. L. Carlin, A. Dei, D. Gatteschi, *J. Am. Chem. Soc. 107* (1985) 8128. A misprint in the reported formula has been corrected.

[9] W. Urland, *Chem. Phys. 38* (1979) 407.

[10] M. H. Dickman, L. C. Porter, R. J. Doedens, *Inorg. Chem. 25* (1986) 2595.

Salicylate-Mediated Assembly of the Discrete Mixed-Valence Nonanuclear Manganese Complex $[Mn_9O_4(O_2CPh)_8(sal)_4(salH)_2(py)_4]$ ($salH_2$ = salicylic acid, py = pyridine)**

By *Cheryl Christmas, John B. Vincent, John C. Huffman, George Christou,* Hsiu-Rong Chang,* and *David N. Hendrickson*

Recent developments in Fe^{III} chemistry have established that high nuclearity (>4) complexes can be prepared with carboxylate or mixed carboxylate/amine ligation even in the expected absence of metal–metal bonds to assist aggregation. Iron complexes of this kind have been prepared by hydrolytic reactions from smaller nuclearity complexes and, to date, octanuclear[1] and undecanuclear[2] species have been structurally characterized. These units are held together by oxide and hydroxide bridges. The efforts of our own research program have been concentrated on the neighboring 3d metal Mn, and we have reported the non-hydrolytic bipyridine(bpy)-mediated conversion of trinuclear $[Mn_3O(O_2CR)_6L_3]^{0,\oplus}$ (R = Me, Ph; L = pyridine(py), H_2O) into tetranuclear species containing the non-planar $[Mn_4O_2]$ core.[3,4] We have now found that use of salicylic acid ($salH_2$) instead of bpy in these reactions leads to still higher aggregation and herein report the preparation of the remarkable nonanuclear complex **1**.

$[Mn_9O_4(O_2CPh)_8(sal)_4(salH)_2(py)_4]$ **1**

To a stirred brown solution of $[Mn_3O(O_2CPh)_6(py)_2(H_2O)]$[5] in MeCN was added solid salicylic acid (3 equiv.) under aerobic conditions. The acid soon dissolved, and the homogeneous dark brown solution was left undisturbed overnight at room temperature. The resulting black crystals of **1** were collected by filtration, washed with hexane, and dried in vacuo;[6] yield ca. 40%.

The X-ray structure[7] of **1** is shown in Figure 1. Charge considerations necessitate a mixed-valence description ($8\,Mn^{III}$, Mn^{II}) and the unique central atom Mn(1) is assigned as the Mn^{II} atom through which there is a crystallographic two-fold axis relating the two halves of the molecule. The average Mn(1)–O distances (2.312 Å) are similar to those in the eight-coordinate Mn^{II} complex $[Mn(NO_3)_4]^{2\ominus}$ (2.306 Å).[8] The eight Mn^{III} atoms are six-coordinate and are disposed in two tetranuclear $Mn_4(\mu_3\text{-}O)_2$ units, each with a butterfly structure. Figure 2a shows a stereoview of **1**; Figure 2b shows a top view of one of the $[Mn_4O_2]$-units, and it can be seen to be similar to that in discrete $[Mn_4O_2]$-containing complexes.[4] The two Mn_4O_2 units and central Mn(1) in **1** are held together via four $\mu_3\text{-}\eta^3\text{-}sal^{2\ominus}$ groups (*o*-oxidobenzoate). Peripheral ligation is by four terminal py, eight bridging $PhCO_2^{\ominus}$ (benzoate), and two bridging $salH^{\ominus}$ groups (salicylate). The latter, one at each end of the molecule, are bound only through their carboxylate functions; the OH-groups with the oxygen atoms O(60) and O(60)′ are not involved in metal ligation. This conclusion is supported by the near coplanarity between the Ph ring and its carboxylate group, and the resulting close approach of O(60) to O(51) (2.59(2) Å), suggesting a hydrogen-bonded O(60)–H···O(51) unit. A similar situation has been seen in Mo^{II} and Rh^{II} complexes containing μ-salH bridges.[9,10] Overall, the Mn_9 unit can be considered a purely inorganic example of a 'sandwich' compound not supported by metal–metal bonding and with the central Mn and two outer $[Mn_4O_2]$ units representing the three layers.

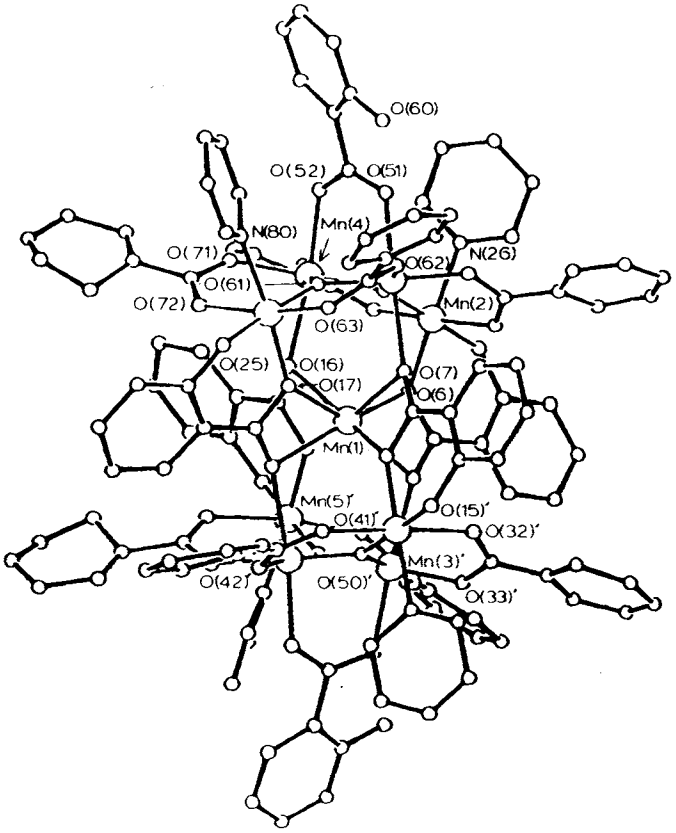

Fig. 1. Crystal structure of complex **1**. To avoid congestion, only one of each symmetry-related pair of Mn and O atoms are labeled. Primed and unprimed atoms are related by the twofold rotation axis through Mn(1). Selected atomic separations: Mn(1)–Mn(2,3,4,5), 3.814(6)–3.983(6) Å; Mn(1)–O(6,7,16,17), 2.240(14)–2.385(14) Å.

Variable temperature, solid-state magnetic susceptibility studies have been performed on powdered samples of **1** in the temperature range 300.9 K to 5.0 K. The effective magnetic moment per molecule, μ_{eff}, gradually decreases from a value of 11.82 μ_B at 300.9 K to a value of 5.83 μ_B at 5.0 K. Extensive coupling is thus indicated and attempts are in progress to elucidate the precise nature and magnitude of the magnetic interactions between the various Mn atoms of

[*] Prof. Dr. G. Christou, Dr. J. C. Huffman, J. B. Vincent, C. Christmas
Department of Chemistry and the Molecular Structure Center,
Indiana University
Bloomington, IN 47405 (USA)
Prof. Dr. D. N. Hendrickson, H.-R. Chang
School of Chemical Sciences, University of Illinois
Urbana, IL 61801 (USA)

[**] This work was supported by the U. S. National Science Foundation (CHE 8507748).

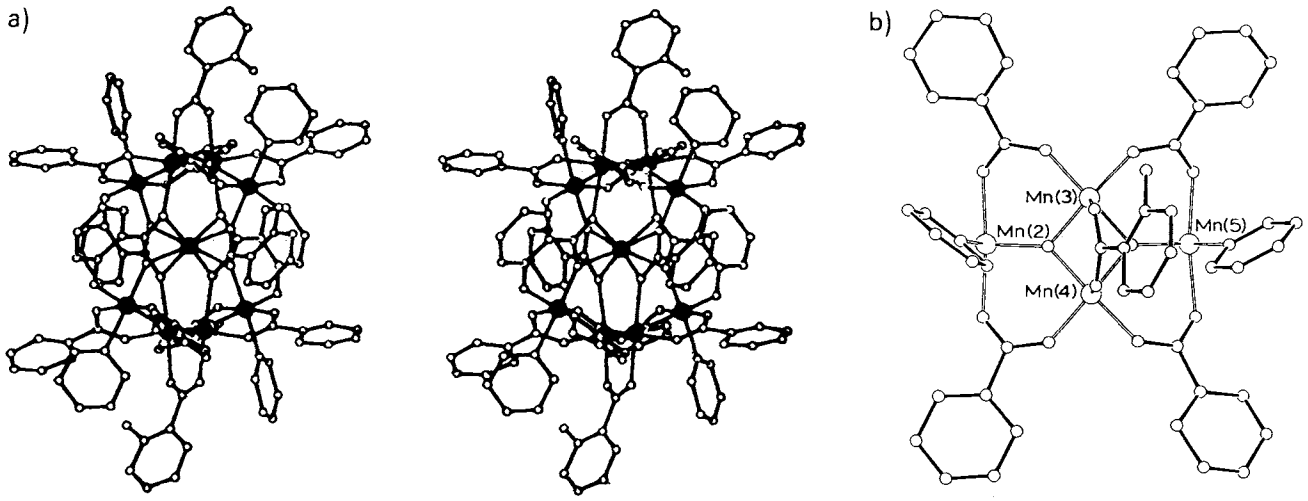

Fig. 2. a) Stereoview of the crystal structure of **1**. b) Top view of one end of complex **1** clarifying the structure of the $[Mn_4(\mu_3\text{-}O)_2]$ unit. Selected atomic separations: Mn(3)-Mn(4), 2.817(6); Mn(3)-Mn(2), 3.406(6); Mn(3)-Mn(5), 3.408(6); Mn(4)-Mn(2), 3.443(6); Mn(4)-Mn(5), 3.425(6); Mn(2)-Mn(5), 5.914(6) Å.

this complicated and relatively low symmetry molecule.[11]

In summary, trinuclear $[Mn_3O(O_2CR)_6L_3]$ complexes continue to prove useful as precursors to higher nuclearity species, and reaction with the bifunctional ligand salicylic acid leads to a convenient non-hydrolytic conversion to a discrete nonanuclear species with an unusual structure. In contrast to the octa- and undecanuclear Fe^{III} complexes, **1** is a mixed-valence compound containing Mn^{II} and Mn^{III}, as found for the recently reported hexanuclear species $[Mn_6O_2(piv)_{10}(pivH)_4]$ (pivH = pivalic acid).[12] It is interesting how these neighboring 3d metals exhibit similar, yet distinctly different, chemistry with such ligands, although it should be added that we have yet to investigate the reaction of salicylic acid with an $[Fe_3O]$-containing complex. Further studies in high nuclearity Mn/carboxylate chemistry are in progress.[13]

Received: May 21, 1987;
revised: June 25, 1987 [Z 2253 IE]
German version: *Angew. Chem. 99* (1987) 934

[1] K. Wieghardt, K. Pohl, I. Jibril, G. Huttner, *Angew. Chem. 96* (1984) 66; *Angew. Chem. Int. Ed. Engl. 23* (1984) 77.
[2] S. M. Gorun, S. J. Lippard, *Nature (London) 319* (1986) 666.
[3] C. Christmas, J. B. Vincent, J. C. Huffman, G. Christou, H.-R. Chang, D. N. Hendrickson, *J. Chem. Soc. Chem. Commun.*, in press.
[4] J. B. Vincent, C. Christmas, J. C. Huffman, G. Christou, H.-R. Chang, D. N. Hendrickson, *J. Chem. Soc. Chem. Commun. 1987*, 236.
[5] J. B. Vincent, H.-R. Chang, K. Folting, J. C. Huffman, G. Christou, D. N. Hendrickson, *J. Am. Chem. Soc.*, in press.
[6] Correct elemental analysis (C, H, N, Mn).
[7] X-ray structure data: monoclinic, space group $C2/c$, $a = 17.625(13)$, $b = 38.314(35)$, $c = 19.886(16)$ Å, $\beta = 99.17(4)°$, $V = 13256.64$ Å^3, $Z = 2$, data collected $6° \leq 2\theta \leq 45°$, 6164 unique reflections with $F > 2.33\sigma(F)$, $R = 0.0970$, $R_w = 0.0992$. Due to the large number of independent atoms, only Mn atoms were refined anisotropically and no hydrogen atoms were included. Full details of the crystal structure determination can be obtained from the director of the Cambridge Crystallographic Data Centre, Lensfield Road, Cambridge CB2 1EW (UK), on quoting the names of the authors and the journal citation.
[8] J. Drummond, J. S. Wood, *J. Chem. Soc. A 1970*, 226.
[9] D. P. Bancroft, F. A. Cotton, S. Han, *Inorg. Chem. 23* (1984) 2408.
[10] F. A. Cotton, G. N. Mott, *Inorg. Chim. Acta 70* (1983) 159.
[11] C. Christmas, J. B. Vincent, G. Christou, H.-R. Chang, D. N. Hendrickson, unpublished.
[12] A. R. E. Baikie, A. J. Howes, M. B. Hursthouse, A. B. Quick, P. Thornton, *J. Chem. Soc. Chem. Commun. 1986*, 1587.
[13] We have now structurally characterized $[Mn_{12}O_{12}(O_2CPh)_{16}(H_2O)_4]$ with a structure similar but not identical to the AcO^- analogue prepared by T. Lis (*Acta Crystallogr. Sect. B 36* (1980) 2042).

Synthesis and Structure of Compounds Containing Ditellurium *Side-on* Bonded to Nickel Complex Fragments

By *Massimo Di Vaira, Maurizio Peruzzini,* and *Piero Stoppioni**

There has recently been increasing interest in the chemistry of the heavier chalcogen atoms.[1] However, metal complexes containing Te ligands are extremely scarce, probably because of their instability and the limited propensity of tellurium to undergo concatenation, compared with the lighter chalcogens.[2] The Te_2 unit has been unambiguously identified so far in three compounds obtained by chance: a trimetal complex where the Te_2 unit is both terminally and *side-on* bonded[3] and two dimetal complexes where the unit is *side-on* bonded[4] or unsymmetrically[5] bridging. Stabilization of Te_2 in such compounds could be due to the presence of various shielding groups and bulky ligands. Very recently, the Te_3 cyclic unit has been identified in a tungsten carbonyl complex.[6]

We report here the synthesis of two monometal compounds containing less shielded Te_2 groups. These have been obtained by reacting a polytelluride solution and LNi^{II} fragments by a similar procedure to that already used to obtain the dinuclear Te_2 compound.[4] This may suggest a general approach to the synthesis of tellurium-rich transition-metal compounds.

The reaction of $Ni(ClO_4)_2 \cdot 6H_2O$ in the presence of the tridentate ligand 1,1,1-tris(diphenylphosphinomethyl)ethane (triphos) or bis(2-diphenylphosphinoethyl)phenylphosphane (ppp) with the stoichiometric amount of sodium telluride (prepared by reduction of tellurium with $NaBH_4$) affords the diamagnetic compounds **1** or **2**, respectively (Scheme 1), in good yield. The compounds are stable in the dark in the solid state and quite insoluble in organic solvents.

[*] Dr. P. Stoppioni, Prof. Dr. M. Di Vaira
Dipartimento di Chimica, Università di Firenze
Via Maragliano 77, I-50144 Florence (Italy)
Dr. M. Peruzzini
Istituto I.S.S.E.C.C., C.N.R.
Via J. Nardi 39, I-50132 Florence (Italy)

The X-ray structural investigations of **1** and **2**[7] showed that each contains one Te_2 unit coordinated as a bidentate ligand to the Ni atom, which is bound in addition by the

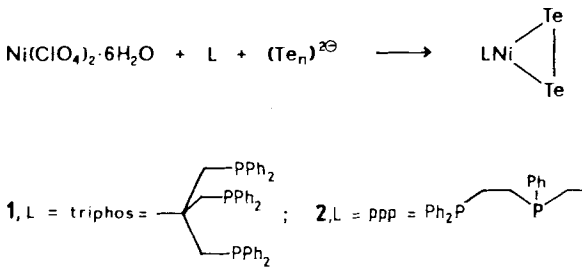

Scheme 1.

three P donor atoms of the L ligand. Figure 1 shows the structure of **2**. The metal atom achieves the 18-electron configuration if the Te_2 unit is considered to behave as a two-electron donor. The $NiTe_2$ fragment, which has practically identical dimensions in the two compounds, is almost perpendicular to the plane through the three P atoms (within 0.9° and 0.8° for **1** and **2**, respectively).

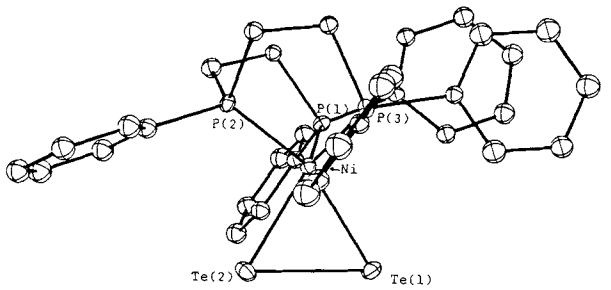

Fig. 1. Molecular structure of **2** (ORTEP). Selected bond lengths [Å] and bond angles [°]: Te1-Te2 2.668(1), Ni-Te1 2.557(2), Ni-Te2 2.555(2), Ni-P1 2.228(4), Ni-P2 2.136(3), Ni-P3 2.203(3); Te1-Ni-Te2 62.9(1), P1-Ni-P2 89.7(1), P1-Ni-P3 108.4(1), P2-Ni-P3 89.0(1).

Although the Ni-Te distances in **1** and **2** (2.570(6) Å and 2.556(2) Å, respectively) are close to those (2.586(14) Å) found for the compound where the Te_2 unit is in a bridging position between two (triphos)Ni moieties,[4] the Te-Te distances in **1** and **2** (2.665(2) Å and 2.668(1) Å, respectively) are significantly shorter than that (2.802(1) Å) existing in this dimer. They compare better with the Te-Te bond length (2.686(4) Å) in the trimetal complex[3] and are slightly closer than the latter to the value for free Te_2 (2.59(2) Å),[8] probably because of the comparatively weak interactions with a single metal center.

The *side-on* coordination of the Te_2 unit should allow such a unit to react with other metal complex fragments and make it suitable for the construction of polynuclear complexes containing "naked" polytellurium ligands. Compound **2** indeed reacts with the [(ppp)Ni^{II}] moiety and with $[(PPh_3)_2Pt(C_2H_4)]$ yielding the dinuclear complexes **3** and **4**, respectively (Scheme 2), which are formed by insertion of an LM fragment (LM = (ppp)Ni or $(PPh_3)_2Pt$) into the Te-Te bond.

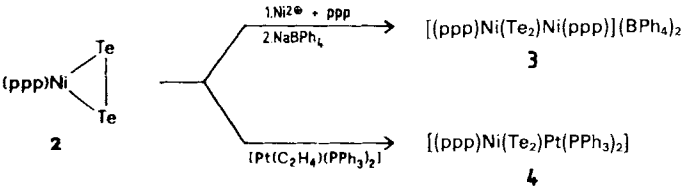

Scheme 2.

Experimental Procedure

All reactions and manipulations, except when otherwise stated, were carried out under purified nitrogen in the dark.

1/2: A clear red solution obtained by refluxing a stirred solution of tellurium (255 mg, 2 mmol) and $NaBH_4$ (75 mg, 2 mmol) in absolute ethanol (35 mL) for 6 h was added to a solution of $Ni(ClO_4)_2 \cdot 6H_2O$ (365 mg, 1.0 mmol) in ethanol (10 mL) and the ligand (1.0 mmol) in THF (40 mL). The deep red crystals of compounds **1** (470 mg, 50% yield) or **2** (595 mg, 70% yield) separated out in a short time together with a small amount of light black powder; the amorphous precipitate was separated from the crystals by washing with ethanol.

3: A solution of $Ni(ClO_4)_2 \cdot 6H_2O$ (73 mg, 0.2 mmol) in ethanol (5 mL) and the ligand ppp (107 mg, 0.2 mmol) in CH_2Cl_2 (15 mL) was added to a suspension of **2** (170 mg, 0.2 mmol) in CH_2Cl_2 (25 mL); the resulting mixture was stirred for 1 h. Complex **3** (250 mg, 60% yield) was obtained as black crystals by adding $NaBPh_4$ (135 mg, 0.4 mmol) in ethanol (15 mL) and concentrating the resulting solution.

4: Solid $[(PPh_3)_2Pt(C_2H_4)]$ (150 mg, 0.2 mmol) was added to a suspension of **2** (170 mg, 0.2 mmol) in CH_2Cl_2 (25 mL) under ethylene (1 atm); the reaction mixture was allowed to stir for 30 min; compound **4** (94 mg, 30% yield) was obtained by adding benzene (10 mL) and concentrating the resulting solution under nitrogen.

All compounds gave correct elemental analyses (C, H, Ni, P, Te).

$^{31}P\{^1H\}$-NMR (32.19 MHz, CD_2Cl_2; standard: H_3PO_4 ext.): **3**: $\delta = 98.9$ (t, 1P, [NiP]), 54.5 (d, 2P, [NiP_2], $J(P\text{-}P) = 20.6$ Hz); **4**: $\delta = 109.7$ (t, 1P, [NiP]), 47.7 (d, 2P, [NiP_2], $J(P\text{-}P) = 43.8$ Hz), −5.6 (s, 2P, [PtP_2], $J(Pt\text{-}P) = 1527$ Hz).

Received: April 21, 1987 [Z 2215 IE]
German version: *Angew. Chem. 99* (1987) 955

CAS Registry numbers:
1, 110026-53-4; **2**, 110026-52-3; **3**, 110026-51-2; **4**, 110026-51-2; **5**, 12120-15-9.

[1] D. Liotta, *Acc. Chem. Res. 17* (1984) 28; W. A. Herrmann, *Angew. Chem. 98* (1986) 57; *Angew. Chem. Int. Ed. Engl. 25* (1986) 56; W. A. Herrmann, J. Rohrmann, *Chem. Ber. 119* (1986) 1437; D. J. Jones, T. Makani, J. Rozière, *J. Chem. Soc. Chem. Commun. 1986*, 1275; A. L. Rheingold, C. M. Bolinger, T. B. Rauchfuss, *Acta Crystallogr. C42* (1986) 1878.

[2] H. Köpf, W. Kahl, A. Wirl, *Angew. Chem. 82* (1970) 814; *Angew. Chem. Int. Ed. Engl. 9* (1970) 801; A. P. Ginsberg, J. H. Osborne, C. R. Sprinkle, *Inorg. Chem. 22* (1983) 1781; M. J. Collins, R. J. Gillespie, J. W. Kolis, J. F. Sawyer, *ibid. 25* (1986) 2057; H. Brunner, W. Meier, B. Nuber, J. Wachter, M. L. Ziegler, *Angew. Chem. 98* (1986) 907; *Angew. Chem. Int. Ed. Engl. 25* (1986) 907; H. Köpf, B. Block, M. Schmidt, *Chem. Ber. 101* (1968) 272; C. M. Bolinger, T. B. Rauchfuss, *Inorg. Chem. 21* (1982) 3947.

[3] O. Scheidsteger, G. Huttner, K. Dehnicke, J. Pebler, *Angew. Chem. 97* (1985) 434; *Angew. Chem. Int. Ed. Engl. 24* (1985) 428.

[4] M. Di Vaira, M. Peruzzini, P. Stoppioni, *J. Chem. Soc. Chem. Commun. 1986*, 374.

[5] W. Herrmann, C. Hecht, E. Herdtweck, H. Kneuper, *Angew. Chem. 99* (1987) 158; *Angew. Chem. Int. Ed. Engl. 26* (1987) 132.

[6] R. Faggiani, R. J. Gillespie, C. Campana, J. W. Kolis, *J. Chem. Soc. Chem. Commun. 1987*, 485.

[7] **1**: $P2_12_12_1$, $a = 18.233(14)$, $b = 15.341(9)$, $c = 13.473(8)$ Å, $V = 3768.6$ Å^3, $Z = 4$. Philips PW1100 diffractometer, $Mo_{K\alpha}$, $5° < 2\theta < 50°$, 2071 independent reflections with $I > 3\sigma(I)$. $R = 0.068$. Important bond lengths [Å] and angles [°]: Te1-Te2 2.665(2), Ni-Te1 2.566(3), Ni-Te2 2.574(3), Ni-P1 2.181(6), Ni-P2 2.307(7), Ni-P3 2.188(6); Te1-Ni-Te2 62.5(1), P1-Ni-P2 92.1(2), P1-Ni-P3 95.5(2), P2-Ni-P3 95.6(2).—**2**: $P1$, $a = 11.088(8)$, $b = 8.579(7)$, $c = 9.186(7)$ Å, $\alpha = 90.40(5)$, $\beta = 112.80(6)$, $\gamma = 94.25(5)°$, $V = 802.7$ Å^3, $Z = 1$. Philips PW1100 diffractometer, $Mo_{K\alpha}$, $5° < 2\theta < 50°$, 2276 independent reflections with $I > 3\sigma(I)$. $R_w = 0.045$. Further details on the crystal structure investigations are available on request from the Fachinformationszentrum Energie, Physik, Mathematik GmbH, D-7514 Eggenstein-Leopoldshafen 2 (FRG), on quoting the depository number CSD-52479, the names of the authors, and the journal citation.

[8] *Interatomic Distances, Supplement*, Chem. Soc., Spcialist Publication, No. 18, London 1965.

Colloidal Bimetallic Catalysts: Pt–Au**

By *Paul A. Sermon,* John M. Thomas,* Kelei Keryou,* and *G. Robert Millward*

Two distinct but related topics constitute the subject of this communication: preparation and characterization of bimetallic colloidal sols which have not hitherto been reported; and the catalytic performance of these bimetallic particles of colloidal dimension after supporting them on graphite.

Monometallic colloidal sols are of ancient lineage[1] with those of Pt[2] and Au[3] receiving particular attention; and it has long been recognized[4] that they are potentially powerful catalysts. Effort is currently being expended in devising new ways of preparing and characterizing[5] such sols. However, as a result of their greater catalytic selectivity and resistance to poisoning, metal *alloys* are of increasing importance.[6] We have therefore explored sol routes to the preparation of bimetallic particles as they could have advantages over the traditional methods of co-impregnation, co-adsorption or co-precipitation. This approach to the production of uniform bimetallic particles of colloidal size has not, to our knowledge, been reported.

We chose $Pt_{100-x}Au_x$ ($0 < x < 100$) because of the wealth of catalytic knowledge on the respective monometallic sols[2,3] and also because, as x increases in bulk alloys of Pt and Au, the activity for hydrocarbon isomerization and hydrogenolysis decreases but activity for dehydrogenation increases.[7] These bimetallic sols were prepared by reducing mixed aqueous solutions of H_2PtCl_6 and $HAuCl_4$ (30 mg·dm^{-3} of each) with a 1% trisodium citrate solution at 373 K in a manner similar to that used for monometallic sols.[2,3,8] Their average particle sizes were found by electron microscopy to be larger than those predicted on the basis of differences in crystallographic lattice energies and surface energies. High resolution electron microscopy was used to examine the internal and surface structure[9] of these sols; the JOEL 200CX electron microscope employed having been fitted with an improved pole-piece and stage[5] with which a point-to-point resolution of 0.196 nm was achievable. The composition of the alloys was determined in two ways: *globally* by means of atomic absorption (AA) analysis of the digested sols and *locally* (2 nm diameter spot) from the intensities of the L_α X-ray emission peaks in a scanning transmission electron microscope (STEM). The catalytic activity of the colloidal particles, after they had been adsorbed onto graphite (Fluka, 99.9% purity) in a manner similar to that used recently[10] for Pt sols, was tested at 633 K in the hydrogenolysis, isomerization and dehydrogenation of *n*-butane and compared with a standard silica-supported Pt sample EuroPt.[11]

Several noteworthy features emerged. First, the individual colloidal particles possess a high degree of crystalline order (see Fig. 1a, b), with well-defined (111) and (200) planes present in sols of all compositions. Second, the size distribution of the sols at each composition is narrow (2.3 ± 0.9 nm, 4.8 ± 1.8 nm, 12.3 ± 1.4 nm, 14.3 ± 4.0 nm, and 24.7 ± 6.4 nm for $x = 0$, 10, 50, 90, and 100, respectively) and the average size increases progressively with Au content. Average radii computed from nucleation theory[12] assuming attainment of equilibrium are much smaller than measured average radii at all compositions. Third, no significant segregation of one metal with respect to the other was noted. Thus in sols prepared with the nominal composition corresponding to $x = 50$ (i.e. $Pt_{50}Au_{50}$) STEM analysis of nine individual particles of diameter 12.0 ± 0.1 nm

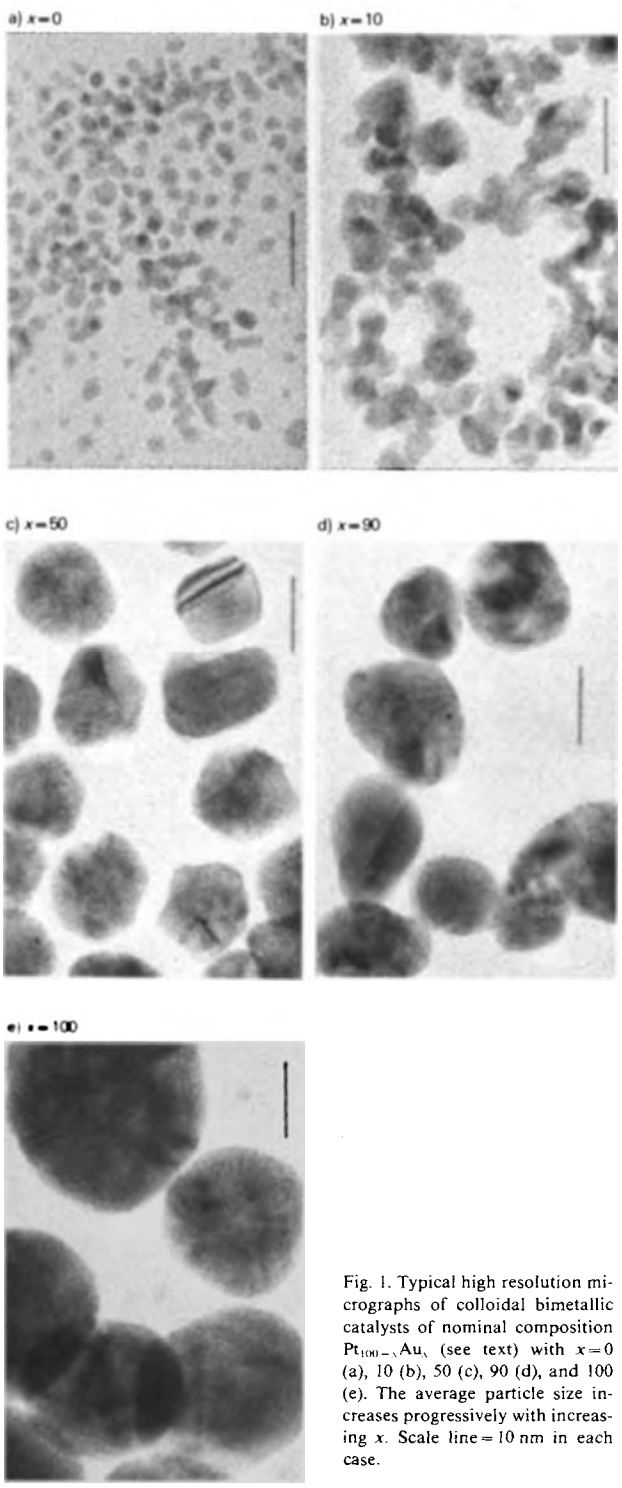

Fig. 1. Typical high resolution micrographs of colloidal bimetallic catalysts of nominal composition $Pt_{100-x}Au_x$ (see text) with $x = 0$ (a), 10 (b), 50 (c), 90 (d), and 100 (e). The average particle size increases progressively with increasing x. Scale line = 10 nm in each case.

[*] Dr. P. A. Sermon, K. Keryou
Department of Chemistry, Brunel University
Uxbridge, Middlesex UB8 3PH (UK)
Prof. Dr. J. M. Thomas
Davy Faraday Research Laboratories
The Royal Institution of Great Britain
21 Albemarle Street, London W1X 4BS (UK)
Dr. G. R. Millward
Department of Physical Chemistry, University of Cambridge
Lensfield Road, Cambridge CB2 1EP (UK)

[**] We thank the University of Gezira (Sudan) and the British Council for support (to *K. K.*), the Science and Engineering Research Council for an equipment grant, and BP for provision of a fellowship (to *G. R. M.*). We are also grateful to Dr. *S. D. Berger* (University of Cambridge) for his helpful assistance.

yielded an average composition corresponding to an x value of 47 ± 3. Particles in Pt-rich sols were somewhat less homogeneous than Au-rich ones. AA analysis revealed total Pt : Au ratios very close to those expected (i.e. for sols with $x = 10$, 25, and 50, Pt: Au ratios were found to be 9.0, 2.7, and 1.0, respectively).

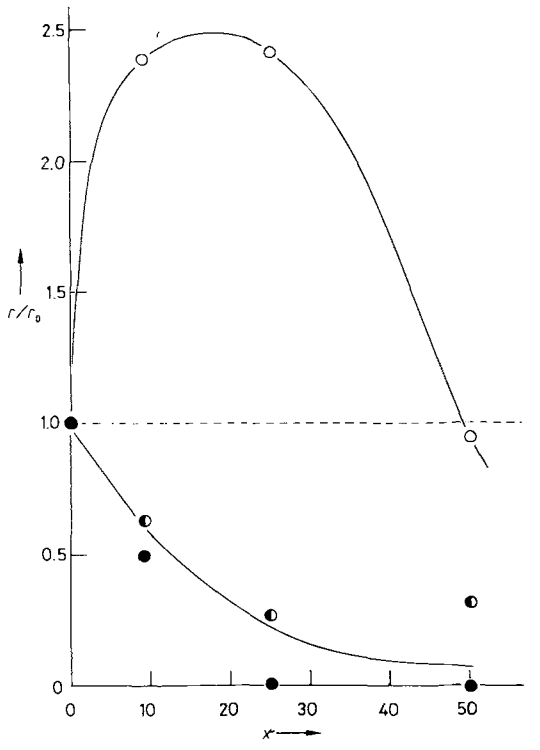

Fig. 2. Rates (r) of dehydrogenation (○), isomerization (◐), and hydrogenolysis (●) of n-butane over graphite-supported sol-derived $Pt_{100-x}Au_x$ particles relative to those exhibited when $x = 0$ (r_0).

Figure 2 shows that the activities of these supported sols towards the hydrogenolysis and isomerization of n-butane decreases steadily as their gold content increases and passes through a maximum. In broad terms these catalytic results are consistent with those for bulk Pt–Au[7] and Ni–Cu[13] alloys. As expected, addition of Au disrupts local Pt–Pt coordination thereby making the structure-sensitive hydrogenolysis[14] less favorable. However, structure-insensitive dehydrogenation, which is sustained on very small ensembles, is seen to be facilitated here. It is encouraging that these bimetallic particles of colloidal size show catalytic properties that can be related to those of the bulk alloys while at the same time offering considerable scope for fine-tuning of their specific performance. It is conceivable that alloys corresponding to the metal/metal oxide colloidal catalysts recently found[15] to be of value in the production of H_2 and O_2 from water might also be amenable to preparations of the kind adopted here.

Received: July 2, 1987 [Z 2278 IE]
German version: *Angew. Chem. 99* (1987) 949

CAS Registry numbers:
Pt-Au, 12633-70-4; graphite, 7782-42-5.

[1] F. Selmi, *Nuovi Ann. Sci. Naturale di Bologna 2. 4* (1845) 146; M. Faraday, *Philos. Trans. R. Soc. London 147* (1857) 145; T. H. Graham, *ibid. 151* (1861) 183.
[2] D. N. Furlong, A. Launikonis, W. H. F. Sasse, J. V. Sanders, *J. Chem. Soc. Faraday Trans. 1 80* (1984) 571; J. Turkevich, R. S. Miner, L. Babenkova, *J. Phys. Chem. 90* (1986) 4765, and references to work by the same group cited therein.
[3] J. Turkevich, P. C. Stevenson, J. Hillier, *Discuss. Faraday Soc. 11* (1951) 55.
[4] E. K. Rideal, *J. Am. Chem. Soc. 42* (1920) 748.
[5] a) D. A. Jefferson, J. M. Thomas, G. R. Millward, K. Tsuno, A. Harriman, R. D. Brydson, *Nature (London) 323* (1986) 428; b) J. L. Tirado, J. M. Thomas, D. A. Jefferson, G. R. Millward, S. W. Charles, *J. Chem. Soc. Chem. Commun. 1987*, 365.
[6] S. Naito, M. Tanimoto, *J. Chem. Soc. Chem. Commun. 1987*, 363.
[7] R. C. Yates, G. A. Somorjai, *J. Catal. 103* (1987) 208; J. K. A. Clark, I. Manninger, T. Baird, *ibid. 54* (1978) 230; A. O. Cinneide, F. G. Gault, *ibid. 38* (1975) 311; J. R. H. van Schaik, R. P. Dessing, V. Ponec, *ibid. 38* (1975) 272; J. W. A. Sachtler, M. A. Van Hove, J. P. Biberian, G. A. Somorjai, *Phys. Rev. Lett. 45* (1980) 1601; W. M. H. Sachtler, G. A. Somorjai, *J. Catal. 89* (1984) 35.
[8] B. V. Enustun, T. Turkevich, *J. Am. Chem. Soc. 85* (1963) 3317.
[9] J. M. Thomas, *Ultramicroscopy 8* (1982) 11; J. M. Cowley, *Prog. Surf. Sci. 21* (1986) 209.
[10] M. Boutonnet, J. Kizling, V. Mintsa-Eya, A. Choplin, R. Touroude, G. Maire, P. Stenius, *J. Catal. 103* (1987) 95.
[11] G. C. Bond, Zu. Yide, *J. Chem. Soc. Faraday Trans. 1 80* (1984) 969.
[12] E. Rideal, *Discuss. Faraday Soc. 11* (1951) 9.
[13] J. H. Sinfelt, J. L. Carter, D. J. C. Yates, *J. Catal. 24* (1972) 283; J. H. Sinfelt, *Adv. Catal. 23* (1974) 147.
[14] J. H. Sinfelt: *Bimetallic Catalysts*, Wiley, New York 1985.
[15] A. Harriman, G. R. Millward, J. M. Thomas, *Nouv. J. Chim.*, in press.

Synthesis and Structure of the Formaldehyde Complex [(tmeda)Ni(C_2H_4)(H_2CO)]**

By *Wolfgang Schröder, Klaus R. Pörschke,* Yi-Hung Tsay*, and *Carl Krüger*

Formaldehyde-transition-metal complexes[3] are attracting increasing interest[4] as conceivable intermediates of the Fischer-Tropsch synthesis,[2] but so far it has not been possible to prepare a nickel complex of this kind despite endorsing MO calculations.[3b, 5a, b] We now report a formaldehyde complex of nickel(0) which also contains π-bonded ethene.[6]

The complex [Ni(C_2H_4)$_3$], **2**,[7b] which can be prepared from (*trans,trans,trans*-1,5,9-cyclododecatriene)nickel(0) [Ni(cdt)] **1**[7a] and ethene,[7b] reacts with TMEDA (= *N,N,N',N'*-tetramethylethylenediamine)[1] and paraformaldehyde at −30 °C slowly (60 h) to give, after filtration, an orange colored solution from which orange-red crystals of the formaldehyde complex **3** separate out in up to 35% yield at −78 °C.[8] The [tmeda)Ni^0] core binds two π-ligands, if they are comparatively weak acceptors.[1]

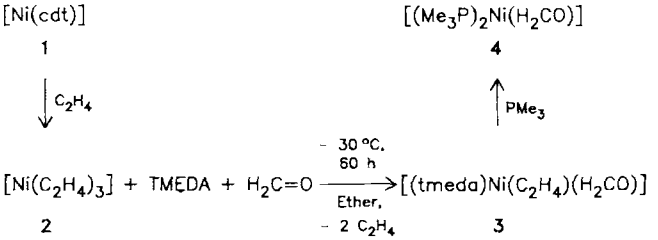

Solid **3** is sensitive toward oxygen and is stable only below −15 °C. At −78 °C the complex dissolves readily in THF and toluene but only moderately in ether and methanol. **3** reacts with CO at −78 °C with release of all ligands

[*] Dr. K. R. Pörschke, Dipl.-Chem. W. Schröder, Dr. Y.-H. Tsay [+], Prof. Dr. C. Krüger [+]
Max-Planck-Institut für Kohlenforschung
Postfach 101353, D-4330 Mülheim a. d. Ruhr 1 (FRG)
[+] Single-crystal structure analysis.
[**] tmeda-Nickel Complexes, Part 2.—Part 1: [1].

to give $Ni(CO)_4$, and with 1,5-cyclooctadiene (cod) at $-20°C$ to give $Ni(cod)_2$. Up to the decomposition temperature in solution ($-20°C$), no reaction could be detected with hydrogen, ethyne, butadiene or butyllithium; with $LiAlH_4$, decomposition with separation of nickel takes place. Removal of the tmeda ligand by reaction with a stoichiometric amount of trimethylphosphane at $-20°C$ leads to $[(Me_3P)_2Ni(H_2CO)]$ **4** (yellow crystals; 25%);[9] in contrast, reaction of $[(Ph_3P)_2Ni(C_2H_4)]$ with paraformaldehyde (20°C) leads, with liberation of hydrogen, to the carbonyl complex $[(Ph_3P)_2Ni(CO)_2]$.[3b,6] A coupling of the ethene and formaldehyde ligands with formation of an oxametallacyclopentane[3d] has not been detected.

Spectroscopically, **3** is characterized by its IR, ^{1}H-NMR and ^{13}C-NMR spectra.[10] The C=O stretching vibration of **3** ($\tilde{\nu}=1605\ cm^{-1}$) is shifted relatively little to smaller wave numbers as compared to that of free formaldehyde ($\tilde{\nu}=1746\ cm^{-1}$);[11a] consequently, a "metallaoxirane" structure[3c] can be ruled out. In the 400-MHz ^{1}H-NMR spectrum ($-110°C$) the protons of the H_2CO ligand give rise to doublets at $\delta=4.58$ and 4.23 ($^2J(H,H)=21$ Hz); in the 75.5-MHz ^{13}C-NMR spectrum ($-120°C$) a signal for the C1 atom is observed at $\delta=82.3$ (t, $J(CH)=163$ Hz).[12] For the ethene ligand, all protons as well as the two C-atoms are nonequivalent at low temperature; however, only two of the four expected ^{1}H-NMR signals were observed at $\delta=2.07$ and 1.81; the ^{13}C-resonances occur at $\delta=46.2$ and 35.8. In the low-temperature NMR spectra the tmeda ligand gives rise to four ^{1}H-NCH_3- and four ^{1}H-NCH_2-resonances as well as different resonances for all six C-atoms.[10] Above $-110°C$, the ^{1}H-resonances of the H_2CO ligand, the ^{1}H- and ^{13}C-NMR signals of the C_2H_4 ligand as well as those of the tmeda-NCH_3 and the tmeda-NCH_2 groups coalesce so that one signal each is obtained for the respective ^{1}H- (200 MHz) and ^{13}C-nuclei at $-80°C$; the signal of the NCH_3 C-atoms is still broad. Accordingly, on increasing the temperature, the H_2CO- and C_2H_4-ligands rotate about the axes between the Ni center and midpoints of the C=O and C=C bonds, respectively, and a change in the conformation of the NCH_2CH_2N bridge occurs. The low-temperature NMR spectra of **3** are consistent with the given structure, which has been found for crystalline **3** (Fig. 1).

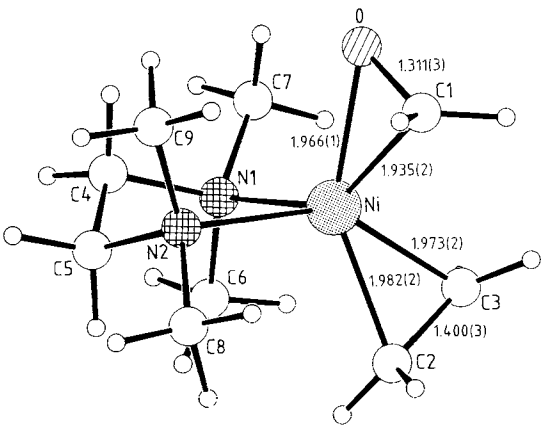

Fig. 1. Crystal structure of **3** [13].

The crystal structure analysis of **3**[13] revealed a pseudo-tetrahedral coordination of the nickel atom, whereby the geometry of the complex is defined by the midpoints (D1, D2) of the formaldehyde C=O and ethene C=C bonds (D1-Ni-D2 121.2°) and the two tmeda N-atoms. The interplanar angles are 84.2° for the Ni,N1,N2/Ni,C1,O planes, 77.9° for the Ni,N1,N2/Ni,C2,C3 planes, and 82.8° for the Ni,C1,O/Ni,C2,C3 planes. The Ni-N distances (2.144(1), 2.167(2) Å) and the Ni-C distances to the ethene ligand (1.973(2), 1.982(2) Å) as well as the C-C bond length (1.400(3) Å) of the latter are as expected.[14] The C=O bond of **3** (1.311(3) Å) is longer than that in uncomplexed formaldehyde (1.209(3) Å);[11e] its length compares with those of other formaldehyde-transition-metal complexes with short C=O bonds.[3b,f] Unlike the H_2CO-complexes of strongly oxophilic metals,[3a-c,e-g] the d^{10}-Ni complex **3** shows for the first time a short metal-carbon bond (1.935(2) Å), and a significantly longer metal-oxygen bond (1.966(1) Å). Intermolecular hydrogen bonding by interaction of the oxygen atom with methyl H-atoms of neighboring tmeda ligands (O···H 2.65-2.8 Å) must be taken into account as a contributory factor to the weak Ni-O bonding.

Received: April 15, 1987 [Z 2206 IE]
German version: *Angew. Chem. 99* (1987) 953

[1] W. Schröder, K. R. Pörschke, *J. Organomet. Chem. 322* (1987) 385.
[2] H. Pichler, H. Schulz, *Chem.-Ing. Tech. 42* (1970) 1162.
[3] Examples: a) $[(Cp_2Zr(H_2CO)]_3]$: K. Kropp, V. Skibbe, G. Erker, C. Krüger, *J. Am. Chem. Soc. 105* (1983) 3353; b) $[Cp_2V(H_2CO)]$: S. Gambarotta, C. Floriani, A. Chiesi-Villa, C. Guastini, *ibid. 104* (1982) 2019; *Organometallics 5* (1986) 2425; c) $[Cp_2Mo(H_2CO)]$: G. E. Herberich, J. Okuda, *Angew. Chem. 97* (1985) 400; *Angew. Chem. Int. Ed. Engl. 24* (1985) 402; S. Gambarotta, C. Floriani, A. Chiesi-Villa, C. Guastini, *J. Am. Chem. Soc. 107* (1985) 2985; d) $[(Me_3P)_4WH_2(H_2CO)]$: M. L. H. Green, G. Parkin, K. J. Moynihan, K. Prout, *J. Chem. Soc. Chem. Commun. 1984*, 1540; $[(Me_3P)_3W(C_4H_6)(H_2CO)]$: M. L. H. Green, G. Parkin, *ibid. 1986*, 90; e) $[Cp(NO)Re(PPh_3)(H_2CO)][PF_6]$: W. E. Buhro, A. T. Patton, C. E. Strouse, J. A. Gladysz, F. B. McCormick, M. C. Etter, *J. Am. Chem. Soc. 105* (1983) 1056; f) $[(MeO)_3P]_2(CO)_2Fe(H_2CO)]$: H. Berke, G. Huttner, G. Weiler, L. Zsolnai, *J. Organomet. Chem. 219* (1981) 353; H. Berke, R. Birk, G. Huttner, L. Zsolnai, *Z. Naturforsch. B39* (1984) 1380; g) $[(Ph_3P)_2(CO)_2Os(H_2CO)]$: K. L. Brown, G. R. Clark, C. E. L. Headford, K. Marsden, W. R. Roper, *J. Am. Chem. Soc. 101* (1979) 503; G. R. Clark, C. E. L. Headford, K. Marsden, W. R. Roper, *J. Organomet. Chem. 231* (1982) 335; h) $[(Et_3P)_2Pt(H_2CO)]$: R. A. Head, *J. Chem. Soc. Dalton Trans. 1982*, 1637.
[4] a) E. L. Muetterties, J. Stein, *Chem. Rev. 79* (1979) 479; b) W. A. Herrmann, *Angew. Chem. 94* (1982) 118; *Angew. Chem. Int. Ed. Engl. 21* (1982) 117.
[5] a) S. Sakaki, K. Kitaura, K. Morokuma, K. Ohkubo, *Inorg. Chem. 22* (1983) 104; b) C. Bianchini, A. Meli, *Organometallics 4* (1985) 1537.
[6] W. Schröder, *Diplomarbeit*, Universität Bonn 1986.
[7] a) B. Bogdanović, M. Kröner, G. Wilke, *Justus Liebigs Ann. Chem. 699* (1966) 1; b) K. Fischer, K. Jonas, G. Wilke, *Angew. Chem. 85* (1973) 620; *Angew. Chem. Int. Ed. Engl. 12* (1973) 565.
[8] *Experimental procedure* (exclusion of oxygen): **3**: A solution of **2** [7b] (prepared from **1** [7a] (1.165 g, 5.0 mmol; 95%) and ethene) in ether (20 mL) was stirred with 2 mL of TMEDA and 1 g of paraformaldehyde for 60 h at $-30°C$. After filtration through a cold frit and cooling to $-78°C$ orange-red crystals slowly separated out, which, after removal of the mother liquor with a capillary pipette, were washed twice with cold pentane and dried under vacuum at $-30°C$. Yield 360 mg (31%). Correct elemental analysis.
[9] **4**: Yield not optimized; correct elemental analysis.—IR (KBr, $-30°C$): $\tilde{\nu}=1595\ cm^{-1}$ ($H_2C=O$); ^{1}H-NMR ([D$_8$]THF, 400 MHz, rel. TMS, $-80°C$): $\delta=3.64$ (t, H_2CO), 1.14 (d, $J(PH)=7.2$ Hz, PMe_3), 1.12 (d, $J(PH)=6.4$ Hz, PMe_3); ^{13}C-NMR ([D$_8$]THF, 75.5 MHz, $-80°C$): $\delta=70.9$ ($J(CH)=165$ Hz, $^2J(PC)=17.8$ Hz, H_2CO), 18.4 ($^1J(PC)=24.0$ Hz, $^3J(PC)=4.0$ Hz, PMe_3), 16.4 ($J(PC)=19.3$ Hz, PMe_3); ^{31}P[^{1}H]-NMR ([D$_8$]THF, 32.4 MHz, rel. 85% aqueous H_3PO_4, $-30°C$): $\delta=-6.6$ (d), -18.3 (d, $J(PP)=57$ Hz).
[10] **3**: IR (KBr, $-40°C$): $\tilde{\nu}=1605\ cm^{-1}$ ($H_2C=O$); ^{1}H-NMR ([D$_8$]THF, 400 MHz, rel. TMS, $-110°C$): $\delta=4.58$ (d), 4.23 (d, $^2J(H1,H1')=21$ Hz, $H_2C=O$), 3.04, 2.85, 2.25, 2.17 (NCH_2, tmeda), 2.64, 2.54, 2.28, 2.07 (NCH_3, tmeda), 2.07, 1.81 ($H_2C=CH_2$); ($-80°C$): 4.45 (H_2CO), 2.55 (NCH_2), 2.38 (NCH_3), 1.92 (C_2H_4); ^{13}C-NMR ([D$_8$]THF, 75.5 MHz, rel. TMS, $-120°C$): $\delta=82.3$ (t, $J(CH)=163$ Hz, $H_2C=O$), 46.2, 35.8 (broad, $H_2C=CH_2$), 59.3, 58.8 (NCH_2, tmeda), 51.8, 49.6, 44.9, 44.3 (NCH_3, tmeda); ($-80°C$): $\delta=82.7$ (H_2CO), 59.15 (NCH_2), 52 to 44 (NCH_3), 41.2 (C_2H_4). We thank Dr. *R. Benn* and Dr. *R. Mynott* for the spectra.

[11] a) H. H. Blau Jr., H. H. Nielsen, *J. Mol. Spectrosc. 1* (1957) 124; b) M. Hesse, H. Meier, B. Zech: *Spektroskopische Methoden in der Organischen Chemie*, Thieme, Stuttgart 1979, p. 158; c) H.-O. Kalinowski, S. Berger, S. Braun: *^{13}C-NMR-Spektroskopie*, Thieme, Stuttgart 1984, p. 173; d) P. C. Lauterbur, *J. Chem. Phys. 26* (1957) 217; e) C. Kato, S. Konaka, T. Iijima, M. Kimura, *Bull. Chem. Soc. Jpn. 42* (1969) 2148.

[12] Monomeric formaldehyde: δ(H) = 9.6 [3c], ^2J(HH) = 42.2 Hz [11b], δ(C) = 197.0 [11c], J(CH) = 172 Hz [11d].

[13] Crystal structure analysis of **3**: crystal dimensions 0.55 mm × 0.052 mm × 0.19 mm, space group $P2_1/n$, a = 8.964(1), b = 11.571(1), c = 11.918(1) Å, β = 107.00(1)°, V = 1182.1 Å^3, Z = 4, ρ_{calcd} = 1.31 g cm^{-3}, $\mu(Mo_{K\alpha})$ = 16.18 cm^{-1}; measurements at −72°C; 9899 reflections measured ($\pm h \pm k + l$), averaged to 4752 independent reflections, 2721 of which considered as observed ($I > 2\sigma(I)$); empirical absorption corrections, heavy atom method; H atoms found and isotropically refined; 206 parameters, R = 0.029, R_w = 0.026. Further details of the crystal structure analysis are available on request from the Fachinformationszentrum Energie, Physik, Mathematik GmbH, D-7514 Eggenstein-Leopoldshafen 2 (FRG), on quoting the depository number CSD-52215, the names of the authors, and the journal citation.

[14] a) K. R. Pörschke, W. Kleimann, G. Wilke, K. H. Claus, C. Krüger, *Angew. Chem. 95* (1983) 1032; *Angew. Chem. Int. Ed. Engl. 22* (1983) 991; b) K. R. Pörschke, K. Jonas, G. Wilke, R. Benn, R. Mynott, R. Goddard, C. Krüger, *Chem. Ber. 118* (1985) 275.

Trifluoromethyl Isocyanide as a Synthetic Building Block—Reaction with Trifluoroacetic Acid and with Hexafluoroacetone**

By *Dieter Lentz,* Irene Brüdgam,* and *Hans Hartl*

Trifluoromethyl isocyanide **1**[1] is of particular interest with respect to its ligand properties.[2] However, the synthesis of *N*-halomethylenetrifluoromethylamines[3] (*N*-trifluoromethyl)halomethanimines) from **1** and hydrogen halides has shown that **1** can also be used as a synthetic building block. This finding prompted us to employ **1** in two other typical isocyanide reactions.

N-Methylformamide was first prepared in 1869 by *Gautier* by the reaction of methyl isocyanide with acetic acid.[4] Its fluorinated analogue, $F_3C-NH-CHO$ **3**, on the other hand, has not been reported.

We have now succeeded in synthesizing **3** from **1**[1] and trifluoroacetic acid **2** [Eq. (a)]. Because **3** was expected to

$$\underset{\mathbf{1}}{F_3C-NC} + 2\,\underset{\mathbf{2}}{F_3C-COOH} \longrightarrow \underset{\mathbf{3}}{F_3C-NH-CHO} + (F_3CCO)_2O \quad (a)$$

have a lower boiling point than that of *N*-methylformamide owing to the fluorine substitution, trifluoroacetic acid **2** was used as the carboxylic acid in order to facilitate the separation of **3**. Unexpectedly, in contrast to trifluoromethylamine, which already decomposes at its melting point (−21°C) to cyanogen fluoride FCN with elimination of HF,[5] **3** is surprisingly stable and can be distilled at 116°C without decomposition (for spectroscopic data see Tables 1 and 2).

Table 1. Spectroscopic data for the new compounds **3** and **7**.

3: IR (gas): $\tilde{\nu}$ = 3456 (m), 3244 (m), 3164 (m), 3051 (w), 2995 (m), 2928 (m), 2768 (w), 1762 (vs), 1744 (vs), 1502 (s), 1476 (s), 1470 (s), 1389 (s), 1302 (vs), 1253 (vs), 1200 (vs), 1176 (vs), 920 (s), 811 (w), 720 (m) cm^{-1}.—Raman (liquid): 3268 (w, br, p), 3127 (vw, p), 2934.5 (m, p), 2789 (vw, p), 1775 (w, p), 1727 (m, p), 1703 (vs, p), 1505.5 (w, p), 1408.0 (s, p), 1310 (w, p), 1255 (vw), 1159.5 (w, dp), 1031 (vw, dp), 924.5 (vs, p), 900 (vs, p), 812.5 (vs, p), 722 (vs, p), 589 (w), 552.5 (vw, dp), 474.5 (w, p), 427.5 (m, p), 375.5 (w, p), 254 (m, br), 195 (m, br) cm^{-1}.—MS (80 eV): *m/z* 113 ($M^{\oplus}$), 85 ($CF_3NH_2^{\oplus}$), 69 ($CF_3^{\oplus}$), 66 ($CF_2NH_2^{\oplus}$), 65 ($CF_2NH^{\oplus}$), 46 ($CFNH^{\oplus}$), 44 ($CH_2NO^{\oplus}$); high-resolution molecular ion: calcd. 113.0088, found 113.0086.

7: ^{19}F-NMR ([D$_6$]acetone, 84.25 MHz): δ = −50.5 (sept, J = 11.0 Hz), −51.9 (sept, J = 11.0 Hz), −54.6 (q, J = 12.8 Hz), −56.6 (q, J = 12.8 Hz), −72.3 (sept, J = 11 Hz).—^{13}C-NMR ([D$_6$]acetone, 67.925 MHz): δ = 94.9 (sept, ^2J(CF) = 37.4 Hz), 118.0 (q, ^1J(CF) = 267.0 Hz), 118.62 (q, ^1J(CF) = 267.0 Hz), 118.65 (q, ^1J(CF) = 266.3 Hz), 120.18 (q, ^1J(CF) = 290.72 Hz), 121.38 (q, ^1J(CF) = 258.1 Hz), 128.79 (s), 136.24 (s), 139.38 (q, ^3J(CF) = 8.8 Hz), 152.1 (s).—MS (80 eV): *m/z* 546 ($M^{\oplus}$, 6%), 527 ($[M-F]^{\oplus}$, 8), 477 ($[M-CF_3]^{\oplus}$, 19) and smaller fragment ions; high-resolution molecular ion: calcd. 545.9785, found 545.9746.

Besides the possibility of *E* and *Z* isomers, which have been well investigated for formamides[6] and are due to hindered rotation around the C–N bond, the possible existence of the isomeric *N*-hydroxymethylidenetrifluoromethylamine must be considered (Scheme 1).

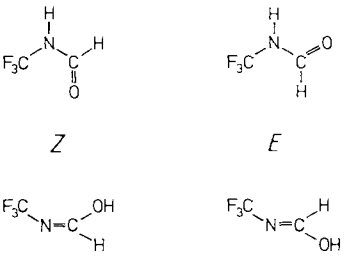

Scheme 1. Possible structural isomers of **3**.

Table 2. NMR data for *Z*- and *E*-**3** in [D$_6$]acetone (89.55-MHz ^{1}H-, 84.25-MHz ^{19}F-, 22.49-MHz ^{13}C-NMR spectra).

	Z-3		*E*-3	
	δ	J [Hz]	δ	J [Hz]
^{1}H-NMR (−50°C)	9.29 (CH, q) 10.0 (NH, br)		9.71 (CH, d) 10.0 (NH, br)	$^3J(HH)_{trans}$ = 8.5
^{19}F-NMR (−50°C)	−57.1 (dd)	^3J(HF) = 3.7 $^4J(HF)_{trans}$ = 3.9	−55.0 (d)	^3J(HF) = 3.2
^{13}C-NMR (−90°C)	160.7 (CO)	^1J(CH) = 207.5 ^2J(CH) = 2.4	161.5 (CO)	^1J(CH) = 209.0 ^3J(CF) = 3.7
	119.0 (CF_3)	^1J(CF) = 259 ^2J(CH) = 2.4 ^3J(CH) = 11.0	120.3 (CF_3)	^1J(CF) = 258 ^2J(CH) = 2.4

A comparison of the NMR data in Table 2 with those of *N*-methylformamide[6] and *N*-methylenetrifluoromethylamines (*N*-(trifluoromethyl)methanamines)[3] shows that **3** exists primarily in the formamide form. For instance, all *N*-methylidenetrifluoromethylamines $F_3C-N=C(H)X$

[*] Priv.-Doz. Dr. D. Lentz, I. Brüdgam, Prof. Dr. H. Hartl
Institut für Anorganische und Analytische Chemie
der Freien Universität
Fabeckstrasse 34-36, D-1000 Berlin 33

[**] This work was supported by the Deutsche Forschungsgemeinschaft and the Fonds der Chemischen Industrie.

(X = F, Cl, Br), regardless of the relative orientation of the protons with respect to the CF_3 group, exhibit a coupling $^4J_{HF}$ of 1–1.5 Hz, which was not observed for the main isomers of **3**. Whereas the *Z* isomer predominates for *N*-methylformamide[6] and only the addition of the shift reagent $Eu(fod)_3$ leads to a noticeable shift in the equilibrium,[7] the relative stability of the isomers of *N*-trifluoromethylformamide is markedly solvent dependent (Table 3). In relatively nonpolar solvents, such as $CDCl_3$ or CD_2Cl_2, the *E* isomer predominates, in contrast to the case observed for the nonfluorinated compound. In [D_6]acetone, which, moreover, is a much better solvent than other solvents for **3** at low temperatures, the amount of the *Z* isomer increases dramatically. From the temperature dependence of the NMR spectra it is possible to determine the free energy of activation for the interconversion of the conformers *Z*/*E*-**3** ($\Delta G^{\neq} = 62$ kJ/mol^{-1}). The hydroxymethylidenamine form is of only minor importance. However, it can be detected in a triethylamine/[D_6]acetone solution by NMR spectroscopy.

Table 3. Ratios of the isomers of **3** in various solvents.

	% *Z*	% *E*
3	43.5	56.5
$CDCl_3$	26.3	73.7
CD_2Cl_2	26.3	73.7
[D_6]acetone	55.6	44.4

The formation of iminodioxolanes **6** from hexafluoroacetone **4** and isocyanides **5** [Eq. (b)][8] can be regarded as a typical isocyanide reaction. We were therefore surprised

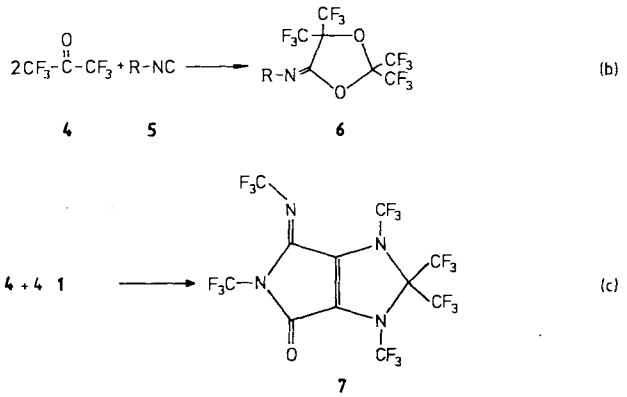

when we isolated yellow crystals of **7** in high yield as sole product of the reaction of **4** with **1** [Eq. (c)]. On the basis of its spectroscopic data (Table 1) and elemental analysis, **7** has the composition $(CF_3NC)_4(CF_3)_2CO$. Despite extensive spectroscopic data, the structure of **7** could not be established. The crystal structure analysis[9] that was therefore carried out yielded a surprising result: **7** was identified as 4-oxo-1,2,2,3,5-pentakis(trifluoromethyl)-6-trifluoromethylimino-1,2,3,4,5,6-hexahydropyrrolo[3,4-d]imidazole (Fig. 1).

The two nearly planar, annelated five-membered rings (maximal deviation from the best planes 4.1 pm) form a mutual angle of 8.2(1.5)°. Both O1 and N2 lie almost in the ring plane. Only the *N*-bonded CF_3 groups are located slightly outside of the planes.

Only a few pyrrolo[3,4-*d*]imidazoles are known and these required multistep syntheses.[10] It was therefore very

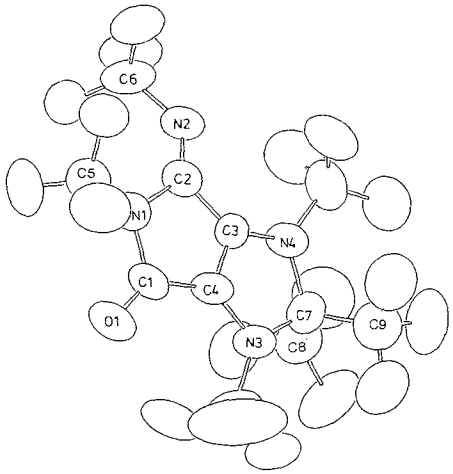

Fig. 1. Molecular structure of **7**. Important bond lengths [pm] and angles [°]: C1-N1 144(2), C1-O1 120(2), C1-C4 145(2), C2-N1 145(2), C2-N2 126(2), C2-C3 145(2), C3-N4 139(2), C3-C4 131(2), C4-N3 140(2), C7-N3 148(2), C7-N4 149(2), N1-C5 142(2), N2-C6 142(2), C-F 127–135(2); N1-C1-C4 103.9(9), C1-N1-C2 110.1(8), N1-C2-C3 102.9(9), C2-C3-C4 112.0(9), C1-C4-C3 111(1), N3-C4-C3 111(1), N4-C3-C4 110(1), C4-N3-C7 108.0(9), C3-N4-C7 108.3(9), N3-C7-N4 102.0(9), C8-C7-C9 112(1), C2-N2-C6 128(1), C2-N1-C5 127.3(9).

surprising to observe nearly quantitative formation of **7** from the simple starting materials **1** and **4**, a reaction involving the formation of several C–C bonds and the migration of the oxygen atom. Only speculation is possible as to the detailed mechanism of the reaction (Scheme 2). Compound **1** tends to form an α polymer $[F_3C-N=C]_n$.[11] Reaction of the oligomer of **1**, n = 4, with **4** could lead to the formation of **8**, which could then isomerize to the stable **7**; all reactions thereby occurring involve the formation of thermodynamically favored five-membered rings.

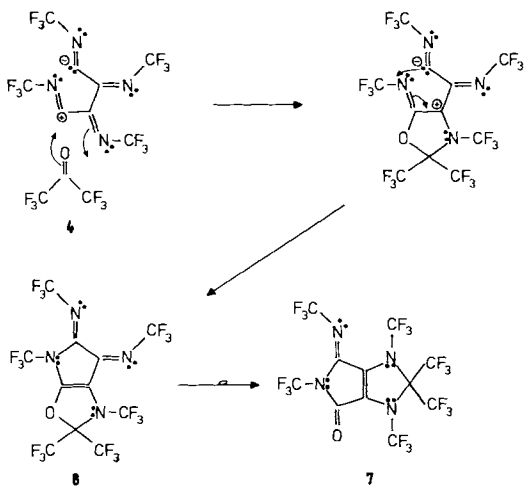

Scheme 2. Possible intermediates in the formation of **7** from **1** and **4**.

Experimental Procedure

3: Compound **1** (9.3 g, 98 mmol) was added in 14-mmol portions over 3 h to **2** (24 g, 210 mmol) in a 250-mL flask equipped with a PTFE stopcock and the reaction mixture was then stirred at room temperature. The volatile reaction products were condensed in vacuum into a 50-mL flask. Distillation through a 30-cm spinning-band column gave 5.1 g of **3** (46%); colorless liquid, b.p. = 116–118 °C, m.p. = – 16 °C. The small amount of **2** still present as an impurity could be removed by preparative gas chromatography (4-m SE 30, 15% on Chromosorb PAW, Ø = 10 mm; temperature program: 12 min 115 °C, 40°/min, 1 min 135°, 40°/min, 6 min 155 °C). In this way, 3.1 g of analytically pure **3** was obtained.

7: Compound **1** (1.5 g, 7 mmol) was condensed into a 250-mL flask equipped with a PTFE stopcock and containing **4** (0.66 g, 7 mmol). The flask was allowed to stand at room temperature. After 1-2 d, yellow crystals began to collect on the walls of the flask. At intervals of 2-3 d, 7 mmol of **1** was condensed three times into the flask. After a further 3 d of reaction, the readily volatile components (0.4 g) were distilled off at room temperature into a 100-mL flask equipped with a stopcock. Their vapor-phase IR spectrum showed exclusively the bands corresponding to unreacted **1** and **4**. The crystalline residue was dissolved in 100 mL of CH_2Cl_2. After removal of the solvent by rotory evaporation, sublimation was carried out in vacuum (10^{-2} mbar) onto a cold finger at -20°C. Yield: 3.6 g **7** (95%); yellow crystals, m.p. = 102°C.

Received: April 6, 1987;
revised: May 18, 1987 [Z 2182/2183 IE]
German version: *Angew. Chem. 99* (1987) 951

[1] D. Lentz, *J. Fluorine Chem. 24* (1984) 523.
[2] D. Lentz, J. Kroll, C. Langner, *Chem. Ber. 120* (1987) 303; D. Lentz, I. Brüdgam, H. Hartl, *J. Organomet. Chem. 299* (1986) C38; D. Lentz, *Chem. Ber. 118* (1985) 560; I. Brüdgam, H. Hartl, D. Lentz, *Z. Naturforsch. B39* (1983) 721; D. Lentz, I. Brüdgam, H. Hartl, *Angew. Chem. 96* (1984) 511; *Angew. Chem. Int. Ed. Engl. 23* (1984) 525; D. Lentz, *Chem. Ber. 117* (1984) 415.
[3] D. Lentz, H. Oberhammer, *Inorg. Chem. 24* (1985) 4665.
[4] A. Gautier, *Ann. Chem. Pharm. 151* (1869) 239; *Beilsteins Handbuch der Organischen Chemie, Band IV* (1922), p. 58.
[5] G. Klöter, W. Lutz, K. Seppelt, W. Sundermeyer, *Angew. Chem. 89* (1977) 754; *Angew. Chem. Int. Ed. Engl. 16* (1977) 707; G. Klöter, K. Seppelt, *J. Am. Chem. Soc. 101* (1979) 347.
[6] J. Dorie, J. P. Gouemard, B. Mechin, N. Naulet, G. J. Martin, *Org. Magn. Res. 13* (1980) 126, and references cited therein; D. E. Dorman, F. A. Bovey, *J. Org. Chem. 38* (1973) 1719.
[7] M. Liler, *J. Chem. Soc. Perkin Trans. 2 1972*, 720.
[8] W. J. Middleton, D. C. England, C. G. Krespan, *J. Org. Chem. 32* (1967) 948; H. W. Roesky, *J. Fluorine Chem. 30* (1985) 123; V. W. Pogatski, H. W. Roesky, *Chem. Ber. 119* (1986) 771; H. W. Roesky, J. Lucas, K.-R. Weber, H. Djarrah, E. Egert, M. Noltemeyer, G. M. Sheldrick, *ibid. 118* (1985) 2396; K. Burger, E. Huber, *Chem. Ztg. 110* (1986) 211.
[9] Single crystals of **7** suitable for an X-ray crystal structure analysis were obtained by vacuum sublimation in a sealed ampoule at 30-40°C. Tetragonal, $I4_1/a$, $a = 2321.4(5)$, $c = 1308.7(4)$ pm, $Z = 16$, $\rho_{calcd} = 2.06$ g cm^{-3}, $\rho_{exp} = 1.92$ g cm^{-3}, $R = 0.073$ [$Cu_{K\alpha} = 154.18$ pm, 1949 reflections, 1052 with $I > 2\sigma(I)$, absorption correction ($\mu = 23.3$ cm^{-1}), anisotropic temperature factors, 307 refined parameters]. Further details of the crystal structure investigation may be obtained from the Fachinformationszentrum Energie, Physik, Mathematik GmbH, D-7514 Eggenstein-Leopoldshafen 2 (FRG), on quoting the depository number CSD-52496, the names of the authors, and the journal citation.
[10] D. E. Casteel, N. J. Leonard, *J. Org. Chem. 50* (1985) 2050, and references cited therein.
[11] R. E. Banks, R. N. Haszeldine, J. Stevenson, B. G. Willoughby, *J. Chem. Soc. C1969*, 2119.

First Synthesis of *N*-Methylene-Ynamines (2-Azabut-1-en-3-ynes)**

By *Ernst-Ulrich Würthwein** and *Reinhard Weigmann*

Ynamines are highly reactive key substances for the synthesis of a great variety of acyclic and heterocyclic compounds.[1] Ynimines (iminoalkynes), wherein a C=N-function (instead of the NH_2-group as in ynamines) is bonded to a CC-triple bond, form *two* isomeric classes of compounds, of which only one, the propargylideneamines **1** (1-azabut-1-en-3-ynes), is known;[2] to our knowledge the isomeric *N*-methylene-ynamines **2** (2-azabut-1-en-3-ynes) have so far never been synthesized. We now report on an easy access to both classes of compounds, starting from alkynyl cuprates and imino derivatives.

The target molecules **2** are best prepared using alkynyl nucleophiles and imine electrophiles. The inverse strategy—alkynyl electrophiles and imine nucleophiles—yields the desired products **2** only in small amounts, because of the competing oxidative coupling of two alkynyl units to give bisalkynes; ynamines however are usually prepared using this approach. In our experience alkynyl cuprates of type **3** are the most suitable alkynyl nucleophiles.[3,4] Among the available imino compounds with electrophilic properties at the nitrogen atom, the *N*-halogenoalkylideneamines are not very useful because of their strong tendency to undergo side reactions. Better yields may be obtained using the oxime esters **4** of arenesulfonic acids,[5] which are sufficiently stable at lower temperatures.

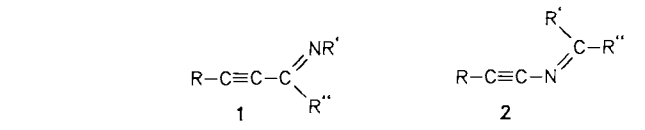

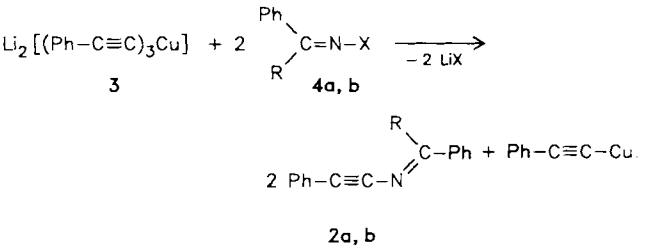

a: R = Ph, X = $OSO_2C_6H_4CH_3(p)$; **b**: R = CH_3, X = $OSO_2C_6H_5$

Reaction of **3** and **4** in diethyl ether at 20°C affords the new isolable compounds **2a** and **2b** as yellow and orange solids, respectively; they are stable in air for only a few hours.[6] In the IR spectra (KBr), the C≡C- and C=N-stretching vibrations appear at 2170-2180 and 1540-1560 cm^{-1}, respectively. The ^{13}C-NMR chemical shifts (25.15 MHz, $CDCl_3$, Standard TMS) of the three C-atoms of the C≡C−N=C-unit of **2a** are $\delta = 94.33$, 91.98, and 177.52, and thus do not show significant interaction (polarization) between the alkyne and imino part of the molecule.—Following the same procedure, alkyl, cycloalkyl, and trimethylsilyl substituted derivatives of **2** can also be synthesized, although they are generally less stable than **2a** and **2b**.

For clear analytical differentiation of the new compounds **2** from the isomers **1**, which, e.g., could have been formed by a Beckmann type rearrangement of the oxime ester **4** to the imidoyl compound **5** and subsequent coupling with **3**, we also synthesized the corresponding propargylideneamine **1a**. In analogy to a procedure described by *Bourgain* and *Normant*[2a] we obtained the stable substance **1a** upon reaction of *N*-phenylbenzimidoyl chloride **5a** with the alkynyl cuprate **6** (46%).[8] With the cuprate **3**, the yield of **1a** increases to ca. 60%; 1,4-diphenylbutadiene was identified as byproduct.

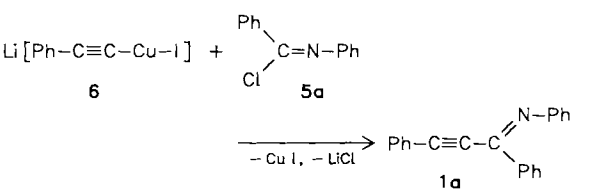

[*] Prof. Dr. E.-U. Würthwein, Dipl.-Chem. R. Weigmann
Institut für Organische Chemie der Universität
Orléansring 23, D-4400 Münster (FRG)

[**] This work was supported by the Fonds der Chemischen Industrie.

If the reactions of oxime esters **4** and the cuprate **3** are carried out at 35 °C (diethyl ether, reflux) instead of 20 °C, compounds of type **1** can also be obtained (ca. 30% **1a**, together with small amounts of **2a**). Hence, the C/N regioselectivity of this reaction, leading to the isomeric products **1** and **2**, respectively, can be influenced remarkably by simple temperature control (mechanism: probably Beckman type rearrangement of an intermediate cuprate imine complex; see also Ref. [7]).

The spectroscopic data of **1a** are significantly different from those of **2a**: in the IR spectrum (KBr), the C≡C-stretching vibration is found at 2200 and the C=N-stretching vibration at 1560 cm^{-1}; thus both absorptions lie ca. 20 cm^{-1} at higher energy than those for **2a**, indicating higher bond orders in the C-C-C-N unit. The ^{13}C-NMR chemical shifts (25.15 MHz, $CDCl_3$, standard TMS) of the alkynyl carbons are 83.15 and 97.74, respectively, revealing strong polarization of the alkyne system; in analogy to the spectra of the corresponding 1-azabutadienes we assign the downfield signal to the terminal carbon atom. The absorption of the imine carbon atom is found at $\delta =$ 149.94.

According to quantum mechanical model calculations (ab initio 6-31G*//6-31G* basis set[9]) on the unsubstituted parent compounds of **1** and **2** (C_3H_3N), the isomer **1** with (*Z*)-C=N-H conformation is thermodynamically more stable ($E_{tot} = -169.70388$ a.u.) than **2** by 7.22 kcal mol^{-1}; the (*E*)-conformer of **1** is predicted to be higher in energy than the (*Z*)-form by ca. 0.8 kcal mol^{-1}. In **1** and **2** the C≡C- and C=N-bonds are almost equal in length (1.187–1.188 Å; 1.253–1.255 Å, respectively), but the charge distribution in the central skeleton of both systems is remarkably different: in **1**, both terminal atoms (N1 and C4) bear high negative charges, whereas C2 and C3 are less charged. In **2** however, alternating charge distribution is found with negative charges at N2 and C4 and positive charges at C1 and C3. This influence of the more electronegative nitrogen atom on the electron distribution in both systems is understandable from perturbation theory arguments.

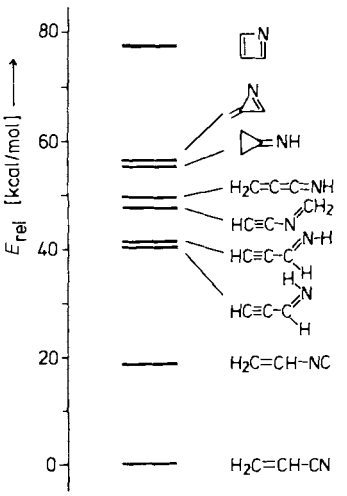

Fig. 1. Relative energies of selected C_3H_3N-isomers [kcal/mol] (ab-initio-6-31G*//6-31G*-results).

Among the substances with the molecular formula C_3H_3N there are some more interesting molecules: a comparison of the calculated total energies allows predictions to be made of the relative stabilities of these molecules (Fig. 1). The most stable isomer is acrylonitrile ($E_{tot} = -169.76801$ a.u., $E_{rel} = 0.00$ kcal mol^{-1}); vinyl isocyanide ($E_{rel} = 18.59$ kcal mol^{-1}) is clearly richer in energy. With a relative energy of more than 40 kcal mol^{-1} the unsubstituted compounds **1** and **2** have almost the high energy content of 1-azabutatriene ($E_{rel} = 49.41$ kcal mol^{-1}), probably combined with similar reactivity. The (*Z*)-form of **1** ($E_{rel} = 40.24$ kcal mol^{-1}) is the most favorable in this group of compounds, followed by the (*E*)-conformer ($E_{rel} = 41.09$ kcal mol^{-1}). **2**, with a relative energy $E_{rel} = 47.53$ kcal mol^{-1} is ca. 7 kcal mol^{-1} more energy-rich than **1**, reflecting the nitrogen perturbation on the wave function in the less favorable 2-position. The recently synthesized (as a tri-*tert*-butyl derivative) azacyclobutadiene[10] is by far the most energy-rich isomer among the closed shell molecules considered here ($E_{rel} = 77.73$ kcal mol^{-1}). The strained three-membered ring systems 2-methylene-2*H*-azirine and cyclopropenimine each assume intermediate positions ($E_{rel} = 56.07$ and 55.31 kcal mol^{-1}, respectively).

Received: April 29, 1987;
revised: May 29, 1987 [Z 2223 IE]
German version: *Angew. Chem. 99* (1987) 918

[1] H. G. Viehe, *Chemistry of Acetylenes*, Marcel Dekker, New York 1969; J. Ficini, *Tetrahedron 32* (1976) 1449; G. Pitacco, E. Valentin in S. Patai (Ed.): *The Chemistry of Amino, Nitroso, and Nitro Compounds and Their Derivatives, Suppl. F, Part I*, Wiley, New York 1982, p. 623 ff; J. Collard-Motte, Z. Janousek, *Top. Curr. Chem. 130* (1986) 89.
[2] a) M. Bourgain, J.-F. Normant, *Bull. Soc. Chim. Fr. 1973*, 2137; b) J. V. Suvorova, M. D. Stadnichuk, *J. Gen. Chem. USSR 52* (1982) 397; c) W. B. Austin, N. Bilow, W. J. Kelleghan, K. S. Y. Lau, *J. Org. Chem. 46* (1981) 2280; d) T.-a. Kobayashi, T. Sakakura, M. Tanaka, *Tetrahedron Lett. 26* (1985) 3463.
[3] G. Posner, *Org. React. 19* (1972) 1; *22* (1975) 253; J.-F. Normant, *Synthesis 1972*, 63.
[4] G. Boche, M. Bernheim, M. Niessner, *Angew. Chem. 95* (1983) 48; *Angew. Chem. Int. Ed. Engl. 22* (1983) 53; *Angew. Chem. Suppl. 1983*, 34.
[5] P. Oxley, W. F. Short, *J. Chem. Soc. 1948*, 1514.
[6] 20 h reaction time at 20 °C. **2a**: 45% yield, m.p.: 70 °C (decomp.); **2b**: 39% yield, m.p.: 75 °C (decomp.).
[7] E. Müller, B. Narr, *Z. Naturforsch. B 16* (1961) 845; H. P. Fischer, C. A. Grob, *Helv. Chim. Acta 46* (1963) 936; C. A. Grob, H. P. Fischer, W. Raudenbusch, J. Zergenyi, *ibid. 47* (1964) 1003.
[8] 48 h reflux in diethyl ether. **1a** (yellow needles): 46% yield, m.p. 60 °C, b.p. 160 °C/0.1 torr.
[9] P. C. Hariharan, J. A. Pople, *Theor. Chim. Acta (Berlin) 28* (1973) 213.
[10] U.-J. Vogelbacher, M. Regitz, M. Mynott, *Angew. Chem. 98* (1986) 835; *Angew. Chem. Int. Ed. Engl. 25* (1986) 842.

The Mechanism of Substitution Reactions at $[LRe(NO)(CO)(CH_3)]^{\oplus}$ in Acid Solution and the Structure of $[\{LRe(NO)(CO)\}_2(\mu\text{-}CH_2OCH_2)]I_2$ (L = 1,4,7-Triazacyclononane)**

By *Christa Pomp, Helmut Duddeck, Karl Wieghardt,* Bernhard Nuber,* and *Johannes Weiss*

Graham et al.,[1] *Gladysz* et al.,[2] and *Casey* et al.[3] have shown that stepwise reduction of *one* carbonyl ligand in

[*] Prof. Dr. K. Wieghardt, C. Pomp
Lehrstuhl für Anorganische Chemie I der Universität
Postfach 102148, D-4630 Bochum (FRG)
Prof. Dr. H. Duddeck
Lehrstuhl für Strukturchemie der Universität
Postfach 102148, D-4630 Bochum (FRG)
Dr. B. Nuber, Prof. Dr. J. Weiss
Anorganisch-chemisches Institut der Universität
Im Neuenheimer Feld 270, D-6900 Heidelberg (FRG)

[**] This work was supported by the Fonds der Chemischen Industrie.

the pseudotetrahedral cation $[CpRe(NO)(CO)_2]^{\oplus}$ ($Cp = \eta^5$-C_5H_5) is possible using $NaBH_4$ in THF/H_2O. The formyl and hydroxymethyl intermediates, as well as the methyl complex, could be synthesized and characterized. In the complex $[CpRe(NO)(PPh_3)(CH_3)]$, the Re–CH_3 bond is cleaved by H–X or by X_2 (X = Cl, Br, I), resulting in the formation of $[CpRe(NO)(PPh_3)X]$ and CH_4 or CH_3X, respectively, with retention of configuration at the Re center.[2] The mechanism of these electrophilic M–C bond cleavage reactions has been suggested to involve protonation of the Re center, reductive elimination of CH_4, and rapid reaction of the 16-electron fragment with $X^{\ominus}$ to give $[CpRe(NO)(PPh_3)X]$. However, kinetic measurements have not been reported.

We recently synthesized the octahedral complex **1** (L = 1,4,7-triazacyclononane)[4] and have now found that **1** reacts with $NaBH_4$ in aqueous solution to give red, racemic **2**. Recrystallization of **2** from H_2O after addition of (1*S*)-(+)-3-bromo-8-camphorsulfonic acid monohydrate afforded enantiomerically pure **3** in 45% yield.

$[LRe(NO)(CO)_2](BF_4)_2$ **1**
$[LRe(NO)(CO)(CH_3)]BF_4$ **2**
$[LRe^*(NO)(CO)(CH_3)][(1S)\text{-}C_{10}H_{14}BrO_4S]\cdot H_2O$ **3**
$[LRe^*(NO)(CO)Cl][(1S)\text{-}C_{10}H_{14}BrO_4S]\cdot H_2O$ **4**
$\{[LRe(NO)(CO)]_2(\mu\text{-}CH_2OCH_2)\}I_2$ **5**
$[LRe(NO)(CO)(CH_2I)]BF_4$ **6**

The crystal structure analysis of **3**[5] reveals that the complex $[LRe^*(NO)(CO)(CH_3)]^{\oplus}$ has the *S* configuration[6] and that the three five-membered rings formed by the Re atom and the coordinated amine ligand have the ($\delta\delta\delta$) conformation (Fig. 1). Reaction of **3** with 1 M HCl smoothly leads to **4** and methane (> 80%) [Eq. (a)].[7]

$$[LRe^*(NO)(CO)(CH_3)]^{\oplus} + HCl \longrightarrow [LRe^*(NO)(CO)Cl]^{\oplus} + CH_4 \quad (a)$$

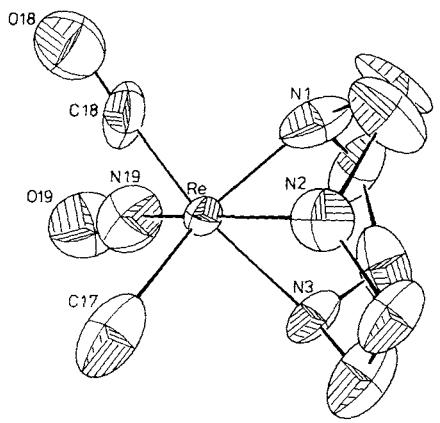

Fig. 1. Molecular structure of the cation of **3**. Selected distances [Å] and angles [°]: Re-N1 2.14(1), Re-N2 2.18(1), Re-N3 2.19(1), Re-C17 2.12(2), Re-C18 1.82(2), Re-N19 1.845(14), N19-O19 1.17(2), C18-O18 1.17(2); O19-N19-Re 173(1); O18-C18-Re 176(1).

The cation of **4** has the *R* configuration,[6] and the five-membered rings have the ($\delta\delta\delta$) conformation, as revealed by an X-ray structure analysis. Reaction (a) therefore proceeds with retention of configuration at the Re center.

From kinetic measurements of reaction (a),[8] the rate law (b) was obtained; this result is in agreement with a mechanism for which the rate-determining step is the reaction of the nucleophile $Cl^{\ominus}$ with a protonated species of the cation of **3** to give CH_4 and $[LRe(NO)(CO)Cl]^{\oplus}$ [Eqs. (c)–(e)]. If the protonation constant K_p is small ($\approx 10^{-2}$ M^{-1}), then, under the conditions selected, $K_p[H^{\oplus}] \ll 1$ and Equation (e) simplifies to Equation (b) with $k = k_1 \cdot K_0$ ($M^{-2}\ s^{-1}$).[8]

$$-d[3]/dt = k[H^{\oplus}][Cl^{\ominus}][3] \quad (b)$$

$$3 + H^{\oplus} \underset{}{\overset{K_p}{\rightleftharpoons}} [3H]^{\oplus} \quad (c)$$

$$[3H]^{\oplus} + Cl^{\ominus} \xrightarrow{k_1} [LRe(NO)(CO)Cl]^{\oplus} + CH_4 \quad (d)$$

$$-d[3]/dt = \{k_1 K_p[H^{\oplus}]/(1 + K_p[H^{\oplus}])\}[Cl^{\ominus}][3] \quad (e)$$

Interestingly, **3** does *not* react with 1 M $HClO_4$ at 25 °C if no other effective nucleophile is present; likewise, no reaction occurs at pH = 7 and 1 M $[Cl^{\ominus}]$. Reaction (a) therefore occurs only in the presence of protons *and* a suitable nucleophile. Three positions of the cation of **3** are possible sites for attack of a proton: (1) the electron-rich, low-valent Re center is protonated (formation of an Re–H species, followed by irreversible reductive elimination of CH_4 and addition of $Cl^{\ominus}$ to the 16-electron fragment formed as an intermediate; (2) Re–NO is protonated to give an Re–N(O)H species; (3) an N atom of the macrocycle is protonated after an Re–N bond is dissociatively broken. The nearly linear, extremely electron-poor Re–NO group in **3** is probably not available for the attack of $H^{\oplus}$;[9] the formation of an Re–H species and the reductive elimination of CH_4 in the rate-determining step is not in accord with the experimental rate law (moreover, the stability of **3** toward $HClO_4$ would not be explainable). We therefore propose a mechanism according to point 3 (Fig. 2), in

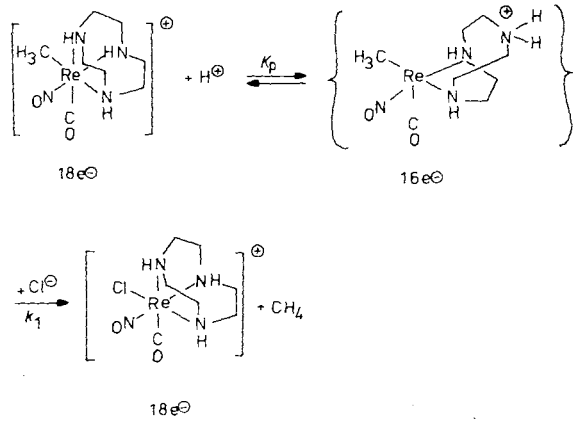

Fig. 2. Proposed mechanism for the substitution reaction (a).

which a 16-electron species is generated by acid-catalyzed cleavage of an $Re\text{-}N_{amine}$ bond. The $Re\text{-}N_{amine}$ bond involving the N atom that is *trans* to the CO ligand in **3** is the weakest. Attack of the nucleophile $Cl^{\ominus}$ and expulsion of $CH_3^{\oplus}$ (which undergoes immediate protonation) is then the rate-determining step, which is followed by rapid reformation of the $Re\text{-}N_{amine}$ bond.

Upon attempting to obtain single crystals of $[LRe(NO)(CO)(CH_3)]I$ from **2** in aqueous NaI solution exposed to the air, we surprisingly obtained, after about ten days, orange-red crystals of **5** in 40% yield. Complex **5** contains the previously unknown 2-oxapropane-1,3-diide bridge, $^{\ominus}CH_2\text{–}O\text{–}CH_2^{\oplus}$ (Fig. 3).[10]

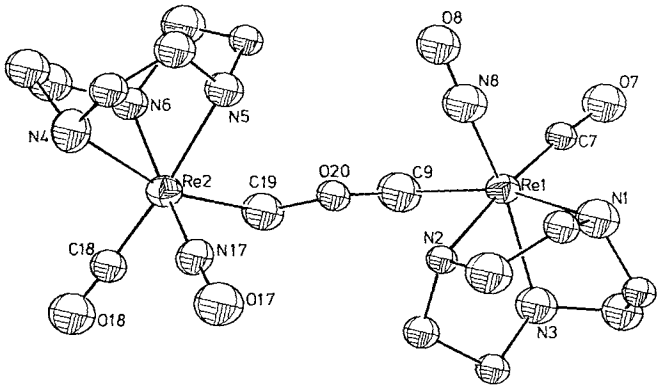

Fig. 3. Molecular structure of the cation of **5**. Selected distances [Å] and angles [°]: Re1-N2 2.19(2), Re1-N3 2.22(2), Re1-N8 1.77(3), Re1-N1 2.20(3), Re1-C7 1.83(3), Re1-C9 2.18(3), Re2-N4 2.20(3), Re2-N5 2.23(2), Re2-N6 2.09(2), Re2-N17 1.70(3), Re2-C18 1.83(2), Re2-C19 2.17(3), C19-O20 1.49(3), C9-O20 1.40(4), N8-O8 1.26(4), C7-O7 1.16(4), N17-O17 1.24(4), C18-O18 1.21(3); Re2-C19-O20 107(2), C19-O20-C9 113(2), O20-C9-Re1 111(2).

Complex **5** crystallizes in the acentric space group $P2_1$.[11] In the crystal investigated, both Re centers have the same configuration *R*,[6] and, in each case, the conformation of the coordinated 1,4,7-triazacyclononane ring is ($\lambda\lambda\lambda$). Thus, racemic resolution occurs spontaneously upon crystallization. Interestingly, the cation of **5** contains two weak N–H···O hydrogen bonds between the O atom of the bridge and one of the N–H groups of the two ligands L (N5···O20 2.98(2) Å; N2···O20 2.95(2) Å). In the solid, the cation is present as a relatively symmetrical rotamer. By examination of a model it is possible to show that an unsymmetrical rotamer of **5** can also exist which is characterized by hydrogen bonds from N2 and N6 to O20 or from N3 and N5 to O20.

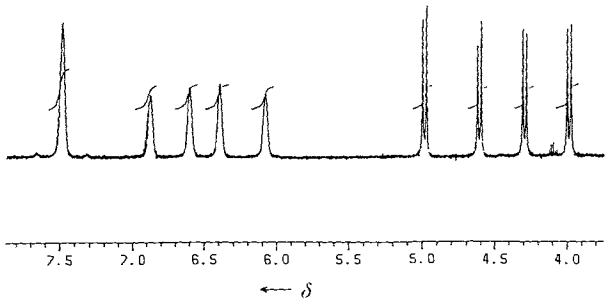

Fig. 4. Signals of the OCH_2 and NH protons in the 400.1-MHz ^{1}H-NMR spectrum of **5** in [D_6]DMSO.

The 400-MHz ^{1}H-NMR spectrum of **5** in [D_6]dimethylsulfoxide ([D_6]DMSO) (Fig. 4) exhibits chemically nonequivalent OCH_2 protons; i.e., the unsymmetrical rotamer is energetically favored in solution. Correspondingly, five N–H signals are observed, that at $\delta = 7.48$ corresponding to two protons. These signals disappear upon addition of D_2O; however, the exchange of the two H atoms whose signal appears at $\delta = 7.48$ is appreciably slower than that of the four other protons—an indication that the two weak intermolecular N–H–O hydrogen bonds are also maintained in solution.

The formation of **5** from **2** involves oxidation of the coordinated methyl group in **2**. It is known that aqueous solutions of **2** are indefinitely stable in the presence of O_2 but in the absence of iodide ions. Likewise, iodide-containing solutions of **2** are stable in the absence of O_2. Presumably, therefore, elemental iodine reacts with the Re–CH_3 unit in the first step to give Re–CH_2I (and $I^{\ominus}$), and this unit then undergoes hydrolysis in H_2O with dimerization to give **5**. The direct oxidation of **2** with I_2 (molar ratio 1 : 1) in dry ethanol gave **6**, which, in aqueous solution indeed reacts to give **5**. Complex **5** is also formed from **2** within 2–3 d after addition of I_2 dissolved in ethanol.

Experimental Procedure

2: Solid $NaBH_4$ (0.038 g, 1 mmol) was added to **1** (0.58 g, 1 mmol) [4] dissolved in 10 mL of H_2O at 20°C. Gas evolved and the solution turned red. Within 24 h, red crystals of **2** formed (ca. 75% yield). Recrystallization from CH_3CN. UV-VIS (H_2O): $\lambda = 496$ nm ($\varepsilon = 52$ L mol^{-1} cm^{-1}), 301 (423).—IR (KBr): $\tilde{\nu} = 1940$ cm^{-1} (CO), 1700 (NO).—^{1}H-NMR (400.1 MHz, CD_3CN): $\delta = 0.65$ (s, 3H; Re–CH_3), 2.70–3.50 (m, 12H; NCH_2), 4.76 (s, 1H; NH), 5.70 (s, 1H; NH), 6.10 (s, 1H; NH).—^{13}C-NMR (100.6 MHz, $CDCl_3$): $\delta = -10.2$ (Re–CH_3), 49.6–59.8 (6 signals, CH_2), 220.0 (CO).

3: (1*S*)-3-bromo-8-camphorsulfonic acid monohydrate (0.659 g, 2 mmol) dissolved in 5 mL of acetone was added to **2** (0.476 g, 1 mmol) in 10 mL of H_2O. Within 3 d, red needles of **3** crystallized (45% yield). CD spectrum (H_2O): $\Delta\varepsilon_{500\,nm} \approx -0.036$.

4: 20 mL of 37% HCl was added to **3** (0.72 g, 1 mmol) and the resulting solution was heated at reflux for 2 h. After concentration of the reaction solution to 10 mL, red crystals of **4** precipitated out within 2 d (92% yield). Recrystallization from H_2O/acetone. UV-VIS (H_2O): $\lambda = 486$ nm ($\varepsilon = 56$ L mol^{-1} cm^{-1}).—IR (KBr): $\tilde{\nu} = 1940$ cm^{-1} (CO), 1700 (NO).—CD spectrum (H_2O): $\Delta\varepsilon_{507\,nm} \approx -0.030$.

5: Method A: 5 mL of a cold, saturated aqueous solution of NaI was added to a solution of **2** (0.576 g, 1 mmol) in 10 mL of H_2O/acetone (1/1). The reaction mixture was then heated to 50°C. The resulting mixture was allowed to stand in the air, resulting in the formation, after 10 d, of orange-red crystals of **5**.

Method B: A solution of iodine (0.25 g, 1 mmol) in ethanol (5 mL) was added to a solution of **2** (0.576 g, 1 mmol) in 10 mL of H_2O. After 3 d of standing under normal atmosphere, the solution was filtered under suction to isolate crystalline **5**, which was then washed with a small amount of ether and allowed to dry in the air (yield obtained by the use of either method, 40% based on **2**.

UV-VIS (H_2O): $\lambda = 482$ nm ($\varepsilon = 89$ L mol^{-1} cm^{-1}).—IR (KBr): $\tilde{\nu} = 3060$ cm^{-1} (m, NH), 2750–2990 (br, w, CH), 1920 (s, CO), 1680 (s, NO).—^{1}H-NMR (400.1 MHz, [D_6]DMSO): $\delta = 4.98$, 4.62, 4.30, 3.99 (d, $J = 10.11$ Hz, 4H; μ-CH_2OCH_2), 6.08, 6.38, 6.62, 6.97 (s, 4H; NH), 7.48 (s, 2H; NH), 2.80–3.50 (m, 24H; NCH_2).—^{13}C-NMR (100.6 MHz, [D_6]DMSO): $\delta = 46.7$–53.8 (m; NCH_2), 71.7, 72.1 (μ-CH_2OCH_2), 220.11, 220.92 (CO).

6: I_2 (0.25 g, 1 mmol) in 10 mL of anhydrous ethanol was added under argon to a solution of **2** (0.576 g, 1 mmol) in 50 mL of anhydrous ethanol. The reaction mixture was stirred for 2 d at 22°C and the solvent was then removed. The product was washed with $CHCl_3$ and dried in the air (97% yield).

UV-VIS (CH_3CN): $\lambda = 361$ nm ($\varepsilon = 98$ L mol^{-1} cm^{-1}).—IR (KBr): $\tilde{\nu} = 1950$ cm^{-1} (s, CO), 1710 (s, NO).—^{1}H-NMR (400.1 MHz, CD_3CN): $\delta = 5.85$, 5.95, 6.11 (s, 3H; NH), 3.70, 3.87 (q, 2H; CH_2I), 2.90–3.52 (m, 12H; NCH_2).

All complexes gave correct elemental analyses (C, H, N, I, Re).

Received: April 7, 1987;
revised: June 2, 1987 [Z 2184/2185 IE]
German version: *Angew. Chem.* 99 (1987) 927

CAS Registry numbers:
1, 101566-55-6; **2**, 109862-88-6; **3** (**3**·H_2O), 110011-95-5; **4**, 109956-57-2; **5**, 109862-90-0; **6**, 109-862-92-2.

[1] a) R. P. Stewart, N. Okamoto, W. A. G. Graham, *J. Organomet. Chem.* *42* (1972) C32; b) J. R. Sweet, W. A. G. Graham, *J. Am. Chem. Soc.* *104* (1982) 2811.

[2] a) J. H. Merrifield, J. M. Fernandéz, W. E. Buhro, J. A. Gladysz, *Inorg. Chem.* *23* (1984) 4022; b) W. Tam, G. Y. Lin, W. K. Wong, W. A. Kiel, V. K. Wong, J. A. Gladysz, *J. Am. Chem. Soc.* *104* (1982) 141; c) J. H. Merrifield, C. E. Strouse, J. A. Gladysz, *Organometallics 1* (1982) 1204.

[3] a) C. P. Casey, M. A. Andrews, D. R. McAlister, J. E. Rinz, *J. Am. Chem. Soc.* *102* (1980) 1927; b) C. P. Casey, M. A. Andrews, D. R. McAlister, *ibid.* *101* (1979) 3371.

[4] K. Wieghardt, C. Pomp, B. Nuber, J. Weiss, *Inorg. Chem.* *25* (1986) 1659.

[5] **3**: Siemens AED II diffractometer, $Mo_{K\alpha}$ radiation, graphite monochromator. Orthorhombic space group $P2_12_12_1$, $a = 10.007(6)$, $b = 10.937(4)$, $c = 22.884(9)$ Å, $V = 2504.6$ Å^3, $\rho_{calcd} = 1.89$ g cm^{-3}, $Z = 4$; $T = 22$°C, $\mu(Mo_{K\alpha}) = 68.3$ cm^{-1}. 3996 unique reflections with $I \geq 2.5\sigma(I)$, empirical absorption correction, anisotropic temperature factors, H at calcu-

lated positions with the exception of the Re–CH_3 group. $R=0.051$; $R_w=0.044$; $w=1/\sigma^2(I)$ for 299 parameters. $\Delta\rho$(max/min) = 4.1/−1.7 e/Å^{-3} (Re); [11b].

[6] In order to determine the configuration, the cyclic triamine L was weighted as a unit having three times the atomic number of N, resulting in the following order of priority: L > NO > CO > CH_3. This resulted in an *S* configuration at the Re center. For determination of configuration, see K. Stanley, M. C. Baird, *J. Am. Chem. Soc. 97* (1975) 6598. Replacement of the CH_3 group in **3** by Cl results in a change in the designation of the configuration at the Re center. In the cation of **4**, the center has the *R* configuration.

[7] The gaseous products of reaction (a) were analyzed by gas chromatography: 85% methane and ca. 15% ethane along with traces of ethene.

[8] Kinetic measurements: $[H^{\oplus}]=0.10$–1.00 M, $[Cl^{\ominus}]=0.10$–1.00 M, [3] = 1.1×10^{-3} M; $k=1.65\times10^{-4}$ M^{-2} s^{-1} at 35°C (*I* (ionic strength) = 1.0 M); $\Delta H^{\neq}=17.7$ (±1.0) kcal mol^{-1}; $\Delta S^{\neq}=-18$ (±3) cal mol^{-1} K^{-1}, determined at five temperatures between 15 and 60°C.

[9] G. La Monica, M. Freni, S. Cenini, *J. Organomet. Chem. 71* (1974) 57.

[10] The monomeric complex [CpRe(NO)(CO)(CH_2OCH_3)] has been reported: [3a].

[11] a) **5**: Siemens AED II diffractometer, $Mo_{K\alpha}$ radiation, $\lambda=0.71069$ Å, graphite monochromator. Monoclinic space group $P2_1$ (C_2, No. 4), $a=7.997(7)$, $b=11.23(1)$, $c=16.38(2)$ Å, $\beta=103.63(7)°$, $V=1429.6$ Å^3, $\rho_{calcd}=2.43$ g cm^{-3}, $Z=2$; $T=22$°C, $\mu(Mo_{K\alpha})=111.2$ cm^{-1}. 1776 reflections with $I\geq2.5\sigma(I)$, empirical absorption correction based on ψ scans of six reflections with $10<2\theta<38°$ with relative transmission 0.67–1.00, anisotropic temperature factors for Re, I, all other atoms with isotropic factors, H atoms of the CH_2 groups at calculated positions. $R=0.049$, $R_w=0.041$, $w=1/\sigma^2(I)$ for 153 parameters. $\Delta\rho$(max/min) = 1.1/−1.2 e/Å^3; b) Further details of the crystal structure investigation may be obtained from the Fachinformationszentrum Energie, Physik, Mathematik GmbH, D-7514 Eggenstein-Leopoldshafen 2 (FRG), on quoting the depository number CSD-52 569, the names of the authors, and the journal citation.

$[\{Co(Cp)_2\}\{CuI_2\}]_n$ (n = 3, 4), Cobaltocenium Iodocuprates(I) with Unusual Anion Structures**

By *Hans Hartl**

The series of compounds containing unusual iodocuprate(I) ions[1] has been extended by two examples involving cobaltocenium $[Co(Cp)]^{\oplus}$ ($Cp=\eta^5$-C_5H_5) as cation. Reaction of CuI with $[Co(Cp)_2]I$ in acetone leads to formation of the two homologous complexes, $[\{Co(Cp)_2\}\{CuI_2\}]_n$ with n = 3 (**1**) and 4 (**2**).

The tetranuclear, centrosymmetric anion $[Cu_4I_8]^{4\ominus}$ consists of two edge-linked CuI_4 tetrahedra; in addition, each tetrahedron shares a common edge with a nearly planar CuI_3 group (Fig. 1). In each case, the face of the CuI_3 unit is oriented with respect to a tetrahedral face in such a way that a strongly distorted tetrahedral coordination results for the copper atom (Cu2). This arrangement of the iodine atoms permits the following, alternative description of the anion structure: The eight iodide ions form two edge-linked trigonal bipyramids. Two of the four Cu^I ions are located at the centers of the two inner iodine tetrahedra and the two others, owing to spatial limitations, are each shifted toward a face of the two external tetrahedra. Since the I–I distances within the CuI_3 units and the CuI_4 tetrahedra are nearly identical, the Cu–I bonds in the CuI_4 tetrahedra (average 269 pm) are significantly longer than those in the CuI_3 units (254 pm). The simultaneous existence of Cu^I of coordination numbers 3 and 4 in a single anion is evidence that the transition of Cu^I from a tetrahedral hole to the planar arrangement CuI_3 is sterically easily possible; this also means, however, that Cu^I ions can migrate through the triangular faces formed by iodide ions without major deformations of the iodine framework, as is required for solid ion conductors based on iodocuprates(I).

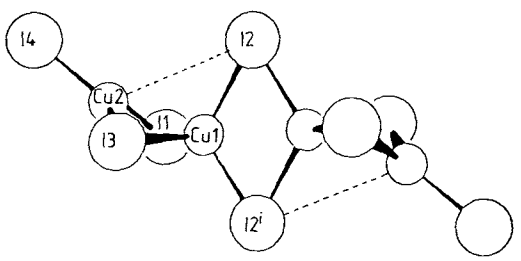

Fig. 1. Crystal structure of the anion $[Cu_4I_8]^{4\ominus}$ [5, 7]. Selected bond distances [pm] and angles [°]: Cu1-I1 270.3(3), Cu1-I2 265.3(2), Cu1-I3 276.1(2), Cu1-I2^i 269.0(3), Cu2-I1 258.0(2), Cu2-I3 255.1(2), Cu2-I4 248.6(2), Cu2···I2 408.7(3), Cu···Cu 269.0(3) and 271.0(3); I-Cu1-I 106.88(8)–118.51(9), I-Cu2-I 117.25(9), 117.62(9), 124.66(9).

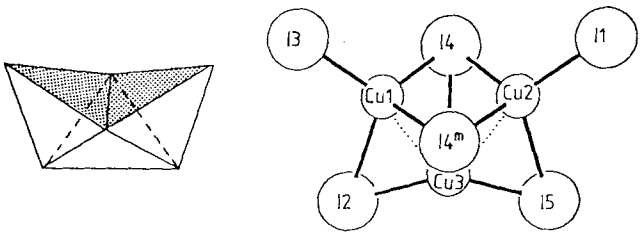

Fig. 2. Crystal structure of the anion $[Cu_3I_6]^{3\ominus}$ [6, 7]. (Left: polyhedron model. Right: Sphere model.) Selected distances [pm] and angles [°]: Cu1-I2 292.2(5), Cu1-I3 251.9(6), Cu1-I4, Cu1-I4^m 271.7(4), Cu2-I1 250.5(5), Cu2-I4, Cu2-I4^m 272.3(4), Cu2-I5 291.1(6), Cu3-I2 252.9(6), Cu3-I5 253.5(6), Cu3-I4 275.7(8), Cu3-I4^m 320.5(8), Cu3···Cu1 251.9(6), Cu3···Cu2 251.8(6), Cu1···Cu2 317.8(6); I-Cu1-I 100.1(1)–116.7(2), I-Cu2-I 100.2(1)–116.6(2), I-Cu3-I 95.3(3)–136.7(3).

The trinuclear anion $[Cu_3I_6]^{3\ominus}$ contains three face-sharing CuI_4 tetrahedra (Fig. 2). Although this structural unit has already been found as a component of an iodocuprate(I) chain $^1_\infty[Cu_3I_4]^{\ominus}$ and in the anion $[Cu_5I_7]^{2\ominus}$,[2] it was unknown as the isolated iodocuprate(I) ion. The structure of $[Cu_3I_6]^{3\ominus}$ can also be described in an alternative way: Two trigonal bipyramids formed from iodide ions are linked in such a way that they share a common iodine tetrahedron. Although the middle copper atom (Cu3) is displaced in the direction of a tetrahedral face, very short Cu–Cu distances (ca. 250 pm) result owing to the face sharing. Such short distances have been found repeatedly for comparable compounds in which this unusual face sharing of CuI_4 tetrahedra is observed (Cu–Cu distance in metallic copper: 256 pm). The short Cu–Cu distances raise the question whether Cu–Cu bonds in this anion play a role or whether the short distance is sterically forced upon the molecule by the threefold iodine bridging. By means of MO calculations on organocopper compounds, *Hoffmann* et al. have shown that bonds between Cu^I are possible by direct overlap of molecular orbitals.[3] The short Cu–Cu bonds in iodocuprates(I) might also involve indirect interactions between the metal atoms such as those assumed, for example, by *C. Haas*[4] for systems in which metal ions are surrounded by an easily polarizable medium—in this case, the iodide ions. The structures of the iodocuprates(I) are determined, above all, by the tendency of the iodine atoms to arrange themselves into the most energetically favorable spherical packings. These packings, in turn, form an easily polarizable matrix, in which the copper atoms oc-

[*] Prof. Dr. H. Hartl
Institut für Anorganische und Analytische Chemie
der Freien Universität
Fabeckstrasse 34-36, D-1000 Berlin 33

[**] Synthesis and Structural Investigation of Iodocuprates(I), Part 7. This work was supported by the Deutsche Forschungsgemeinschaft and the Fonds der Chemischen Industrie.—Part 6: [1].

cupy suitable holes. The nature of the packing and the occupation of the tetrahedral and triangular sites with Cu^{I} ions is influenced by the size, form, and charge distribution of the associated cations. Large cations favor, on the one hand, the formation of isolated iodocuprate(I) ions, since, by means of a kind of dilution effect, they hinder the condensation to give higher molecular units; on the other hand, large cations with low charge stabilize iodocuprate(I) ions that likewise have small charge density, i.e., a large $CuI/I^{\ominus}$ ratio and thus a high degree of condensation. Which of the two influences predominates depends on the relative concentrations and the solvent and precipitation agent employed in the synthesis. High concentrations and a large $CuI/I^{\ominus}$ ratio facilitate the crystallization of higher condensed and polymeric anions, whereas strong dilution and large cations favor the formation of lower-molecular ions. As the size of the cation decreases, the iodocuprates(I) become increasingly unstable and decompose to give the starting components CuI and iodide. An example is provided by the alkali-metal iodocuprates(I), whose stability decreases in the order $Cs^{\oplus} > Rb^{\oplus} > K^{\oplus} > Na^{\oplus}$. Due to its polarizability, the cation $[Co(Cp)_2]^{\oplus}$ is able to stabilize the relatively high negative charge of the anions $[Cu_4I_8]^{4\ominus}$ and $[Cu_3I_6]^{3\ominus}$. Electron delocalization effects or charge transfer processes of the type $Cu^{I} \rightarrow I^{\ominus} \rightarrow$ cation could play a role here. Diffuse reflection spectra and ESR measurements of iodocuprate(I) salts with other cations that are electron acceptors, e.g., *N*-methylpyridinium or dipyridiniomethane, show that such charge transfers are possible.[1b]

The packing of the anions and the cations in the crystals of both compounds confirms what has been found for all iodocuprates(I) investigated so far: The iodide partial structure and the structure of the cation are adjusted to each other in such a way that an optimal spatial packing is achieved. This simple principle of construction explains the structural variety of the iodocuprate(I) ions and suggests the possibility of obtaining other unusual structure types by suitable variation of the cation.

The cyclopentadienyl rings of the $[Co(Cp)_2]^{\oplus}$ ions are eclipsed and arranged parallel (largest dihedral angle 3.1°) in both compounds; in the different $[Co(Cp)_2]^{\oplus}$ ions of the two compounds, the distances of the cobalt atoms from the ring centers deviate by at most 2 pm from the calculated average value (163 pm); the Co-C distances are 202 ± 2 pm. Short intermolecular separations were not observed; one of the three crystallographically independent $[Co(Cp)_2]^{\oplus}$ ions in **1** is disordered.

Experimental Procedure

$[Co(Cp)_2]I$ (1.6 g, 5 mmol) and CuI (1.1 g, 6 mmol) were stirred in 150 mL of dry acetone for several hours. The reactions mixture was filtered and allowed to cool in the refrigerator (4°C), resulting in the precipitation of red-brown, column-shaped crystals of **2**. Additional **2** crystallized upon addition of $CHCl_3$. Slow addition of toluene resulted in the precipitation of **1**, in addition to **2**, with increasing dilution, in the form of thin, likewise red-brown, needle-shaped crystals. At the conclusion of the precipitation reaction, only a small amount of red-brown, leaflets of crystalline $[Co(Cp)_2]_2[CuI_3]$, containing the mononuclear, trigonal-planar anion $[CuI_3]^{2\ominus}$, were formed. Relatively pure **1** can be obtained by the addition of toluene to strongly diluted solutions containing seeding crystals of **1**.

Received: March 20, 1987;
supplemented: May 18, 1987 [Z 2150 IE]
German version: *Angew. Chem. 99* (1987) 925

[1] a) H. Hartl, J. Fuchs, *Angew. Chem. 98* (1986) 550; *Angew. Chem. Int. Ed. Engl. 25* (1986) 569; b) H. Hartl, I. Brüdgam, F. Mahdjour-Hassan-Abadi, *Z. Naturforsch. B40* (1985) 1032.

[2] H. Hartl, F. Mahdjour-Hassan-Abadi, *Z. Naturforsch. B39* (1984) 149; *Angew. Chem. 96* (1984) 359; *Angew. Chem. Int. Ed. Engl. 23* (1984) 378.

[3] P. K. Mehrotra, R. Hoffmann, *Inorg. Chem. 17* (1978) 2187.

[4] C. Haas, *J. Solid State Chem. 59* (1985) 116.

[5] **2**: monoclinic, $P2_1/c$, $a = 1200.2(3)$, $b = 1343.1(3)$, $c = 1809.6(4)$ pm, $\beta = 116.98(8)°$, $Z = 2$, $\rho_{calcd} = 2.59$ g cm^{-3}, $R = 0.057$; $Mo_{K\alpha}$, graphite monochromator, 3175 crystallographically unique reflections, 2762 with $I > 2\sigma(I)$, extinction and absorption correction ($\mu = 78.0$ cm^{-1}), anisotropic temperature factors, no H-atom positions, 254 refined parameters [7].

[6] **1**: monoclinic, $P2_1/m$, $a = 1864.0(5)$, $b = 915.4(5)$, $c = 1144.6(5)$ pm, $\beta = 100.20(8)°$, $Z = 2$, $\rho_{calcd} = 2.62$ g cm^{-3}, $R = 0.08$; $Mo_{K\alpha}$, graphite monochromator, 3740 crystallographically unique reflections, 3421 with $I > 2\sigma(I)$, isotropic extinction correction, anisotropic temperature factors, no H-atom positions, Cu3 refined as split atom above and below the mirror plane, 218 refined parameters [7].

[7] Further details of the crystal structure investigation may be obtained from the Fachinformationszentrum Energie, Physik, Mathematik GmbH, D-7514 Eggenstein-Leopoldshafen 2 (FRG), on quoting the depository number CSD-52484, the names of the authors, and the journal citation.

2,7,12,17-Tetrapropylporphycene—Counterpart of Octaethylporphyrin in the Porphycene Series**

By *Emanuel Vogel,* Metin Balci, Kakumanu Pramod, Peter Koch, Johann Lex,* and *Otto Ermer*

Octaethylporphyrin **1** [H_2(OEP)], first synthesized as early as 1929 by *H. Fischer*,[1] has in recent years acquired great importance as a model compound "par excellence" in the investigation of the porphyrins and metalloporphyrins.[2] In contrast to porphine and its metal complexes, whose study is impaired by solubility problems, many of the complexes derived from **1** are amenable to almost any physical and chemical investigations due to the propensity of the alkyl groups to promote solubilization and crystallization.[3] The symmetrical distribution of the substituents in **1** primarily serves to simplify the interpretation of the spectra, especially in the case of metal complexes.

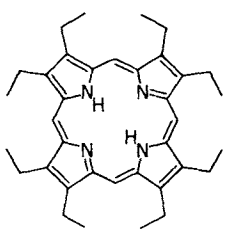

1

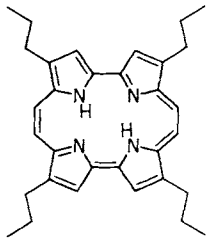

2

The novel porphine structural isomer porphycene recently discovered in this laboratory[4] is actually more soluble than porphine, but metalloporphycenes, similarly to the metalloporphines, could hitherto only be obtained as microcrystalline powders, i.e. in a form unsuitable for X-ray structure analyses. With 2,7,12,17-tetrapropylporphycene **2**, a molecule exhibiting effective D_{2h} symmetry (NMR time scale), we now have found a porphycene derivative, which, in view of its properties, would seem predestined to play the role of a counterpart to H_2(OEP) in opening up porphycene chemistry. We report here on the syn-

[*] Prof. Dr. E. Vogel, Dr. M. Balci, Dr. K. Pramod, P. Koch, Dr. J. Lex, Prof. Dr. O. Ermer
Institut für Organische Chemie der Universität
Greinstrasse 4, D-5000 Köln 41 (FRG)

[**] *K. P.* thanks the Alexander-von-Humboldt-Stiftung for a fellowship.

thesis and molecular structure of **2** and its nickel complex.

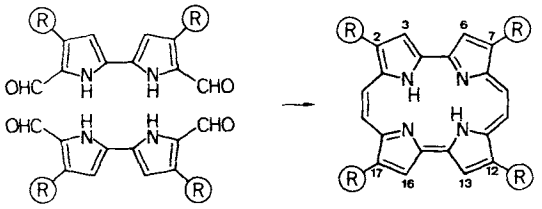

3 R = CH_3
4 C_2H_5
5 C_3H_7

6 R = CH_3
7 C_2H_5
2 C_3H_7

The choice of a 2,7,12,17-tetraalkylporphycene – instead of the octaethylporphycene corresponding to **1** in its substitution pattern – as versatile representative of the new tetrapyrrolic macrocycle was compelling on steric grounds. As follows from model considerations on the porphycene system, 3,6- and 13,16-alkyl substitution lead to considerable non-bonding interactions between substituents, which can be expected to give rise to a more or less severe puckering of the ring skeleton and thus to perturbation of the porphycene chromophore. With the presence of four alkyl groups in the 2,7,12,17-positions, on the other hand, the planarity of the porphycene skeleton should essentially remain unaffected. The question as to what size these four alkyl groups should have in order to render the respective porphycene as comparably soluble as **1** could only be decided by experiment.

The synthesis of porphycene by reductive coupling of 5,5′-diformyl-2,2′-bipyrrole with low-valent titanium can be extended to various alkylated porphycenes. Treatment of the diformylbipyrroles **3**[5] and **4**[6] with titanium tetrachloride and activated zinc in the presence of pyridine in tetrahydrofuran (THF)[7] leads to formation of the tetraalkylporphycenes **6** and **7**, respectively (yields 2 and 4%, resp.), of which, however, even the tetraethyl compound does not have a solubility much better than that of unsubstituted porphycene. In contrast to this, the analogous synthesis of **2** from **5** represented a sort of breakthrough, for not only was **2** formed in considerably higher yield (10%), but it also exhibited a similar solubility and crystallizability as H_2(OEP). **2**, which is air-stable, affords violet needle-shaped crystals from *n*-hexane melting without decomposition at 192–194°C.

The absorption pattern and chemical shifts in the ^{1}H-NMR spectrum (300 MHz, $CDCl_3$) show that **2** is an aromatic porphycene with effective D_{2h} symmetry. The protons H-3,6,13,16 and H-9,10,19,20 of the porphycene skeleton appear as singlets ($\delta = 9.21$ and 9.62, resp.) at very low field (absorption region of corresponding porphyrin protons), whereas the N-protons give rise to a broad signal ($\delta = 3.04$) at relatively high field but are not as strongly shielded as the porphyrin N-protons ($\delta = -3$ to -4) because of the strong N–H···N hydrogen bonding. The protons of the propyl groups appear in the expected region. The simplicity of the spectrum is readily explained by a rapid NH-tautomerism in **2**, which is not noticeably slowed down even at -120°C.[8] Complementary to the ^{1}H-NMR spectrum, eight signals occur in the ^{13}C-NMR spectrum, all of which can be unequivocally assigned. Unlike the IR spectra of the porphyrins, the IR spectrum of **2** shows no NH-stretching vibration in the range of 3300–3360 cm^{-1}, thus supporting the conclusion already drawn from the ^{1}H-NMR spectrum that **2** contains strong N–H···N hydrogen bridges. As expected, **2** has a UV/VIS spectrum very similar to that of porphycene; the alkyl substitution largely manifests itself by the 1–10 nm bathochromic shift of the absorption bands.

According to an X-ray structure analysis (Fig. 1) **2** is present in the crystal as a centrosymmetric molecule with

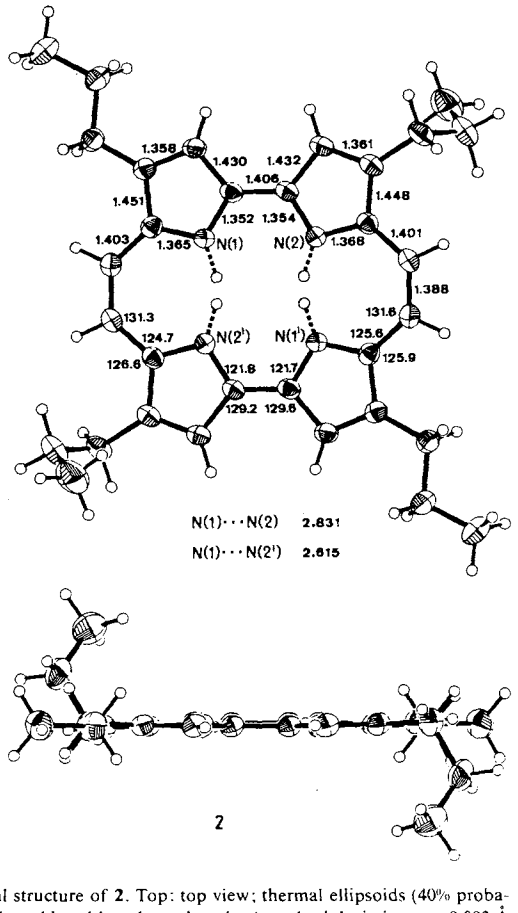

Fig. 1. Crystal structure of **2**. Top: top view; thermal ellipsoids (40% probability) and selected bond lengths and angles (standard deviations ca. 0.003 Å and 0.2°, resp.); inner hydrogen atoms disorded, see Figure 2. Bottom: side view. Crystals from *n*-hexane; monoclinic, space group $P2_1/c$, $Z=2$; $a=9.665(4)$, $b=5.343(2)$, $c=25.694(6)$ Å, $\beta=97.92(2)$°; $\rho_{calc}=1.210$ g cm^{-3}; intensity measurements on a four-circle diffractometer [room temperature, $\lambda_{Mo}=0.71069$ Å, $\theta_{Mo}(max)=27$°]; refinement (C,N anisotropic, H isotropic) including 1692 reflections with $F_0 > 4\sigma(F_0)$; $R=0.040$, $R_w=0.045$. For the two inner H atoms, four positions were refined with half-weights [9].

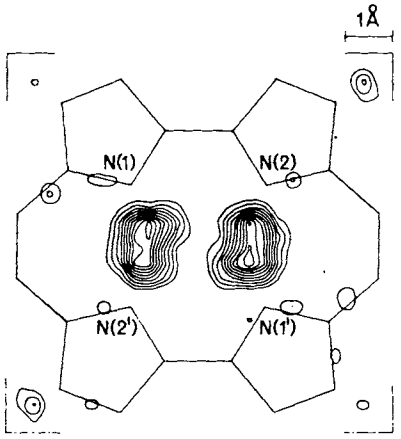

Fig. 2. Difference electron density map in the molecular plane of **2** (propyl substituents omitted). Contributions of all atoms subtracted, except inner hydrogen atoms; contours beginning with 0.05, intervals 0.025 $eÅ^{-3}$.

two pairs of conformationally different propyl groups. In accord with the model considerations, the planarity of the parent compound remains virtually unaltered in the porphycene skeleton of **2** (maximum deviation of the C- and N-atoms from the mean plane: ±0.04 Å). The propyl groups cause only slight changes in bond lengths and angles at the sites of substitution.

The electron density distribution in the N_4 nucleus of **2** (Fig. 2) indicates that the N-hydrogen atoms are partly disordered; this precludes their assignment to individual pyrrole rings. The strong N–H···N hydrogen bonds already established spectroscopically are apparently asymmetric and therefore to be described energetically by double minimum potentials. A similar behavior regarding the localization of the N-hydrogen atoms is encountered in all porphycenes structurally characterized so far (the parent compound,[4a] 2,3-dihydroporphycene,[10] and 9,10,19,20-tetrapropylporphycene[11]).

The properties of **2** would suggest the possible existence of numerous metallotetrapropylporphycenes which should have the afore-mentioned advantages over the complexes of the parent compound. Since the cavity in the porphycene system is smaller than in the porphyrin system and since the orbitals of the lone pairs on the nitrogen atoms are not optimally oriented towards the center of the molecule it was to be expected that the tendency of formation and stability of the metalloporphycenes are generally lower than those of the corresponding metalloporphyrins. Experience gathered in the meantime with complexes of unsubstituted porphycene confirm this supposition.[4a] The good agreement of the distance between N and the center of the molecule in **2** (1.920 and 1.933 Å, resp.) and the NNi distances in square-planar nickel(II) complexes (normal value: 1.95 Å),[12] as a result of which the planar diamagnetic 2,7,12,17-tetrapropylporphycenatonickel(II) **8** should be very stable, encouraged us to test the complexation of **2** with divalent nickel as metal.

The metalation of **2** with nickel was achieved unproblematically by the acetate method[2b] in that the free ligand was heated under reflux with $Ni(OAc)_2 \cdot 4H_2O$ in acetic acid. On cooling the reaction mixture, **8** crystallized out. Recrystallization from ethyl acetate/dichloromethane (1:1) furnished bluish-violet needles; m.p. >300 °C (yield 89%).

The conversion of **2** into **8** is clearly visible in the spectra. In the ^{1}H-NMR spectrum of the complex, apart from the absence of the NH resonance of **2**, a slight high-field shift of the H-3,6,13,16 and H-9,10,19,20 signals (0.4 and 0.2 ppm, resp.) is observed, while in the ^{13}C-NMR spectrum the signals of two types of quaternary C-atoms, with some certainty those of C-1,8,11,18 and C-4,5,14,15, are shifted to lower field ($\Delta\delta = 6.3$ and 9.0 ppm, resp.). Particularly convincing is the mass spectrum of **8**.

According to an X-ray structure analysis (Fig. 3), the complex **8** – like the free ligand – is centrosymmetric in the crystal; this means that the nickel atom and the nitrogen atoms are coplanar. Furthermore, the porphycene skeleton as a whole proves, to a good approximation, to be planar (maximum deviation of the heavy atoms from the mean plane ±0.04 Å). The conformations of the propyl substituents are similar to those in the free ligand. Irrespective of the overall structural similarity of **2** and **8**, the introduction of nickel into **2** obviously distorts the porphycene skeleton considerably. The complexation most strikingly affects the edge lengths of the rectangle of the N_4 nucleus.

In the free ligand **2** (Fig. 1) the distance between N(1) and N(2) is about 0.22 Å greater than that between N(1) and N(2'), whereas conversely, in the complex **8** (Fig. 3)

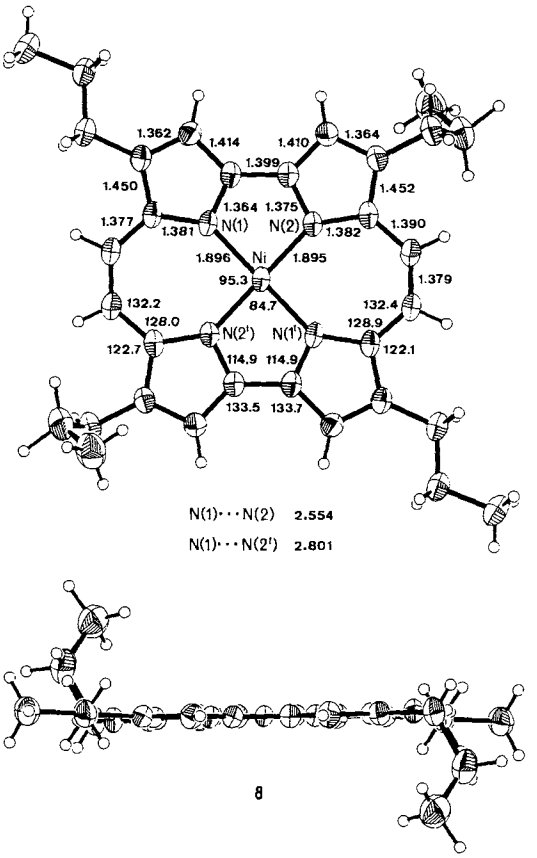

Fig. 3. Crystal structure of **8**. Same presentation as in Figure 1 (standard deviations ca. 0.004 Å and 0.3°, resp., for data involving Ni 0.002 Å and 0.1°, resp.). Crystals from dichloromethane/ethyl acetate; triclinic, space group $P\bar{1}$, $Z = 1$; $a = 5.308(1)$, $b = 9.893(1)$, $c = 12.647(2)$ Å, $\alpha = 98.97(1)$, $\beta = 94.42(2)$, $\gamma = 90.31(1)°$; $\rho_{calc} = 1.359$ g cm^{-3}; measuring conditions as for **2**; refinement (C, N anisotropic, H isotropic) including 2005 reflections with $F_0 > 4\sigma(F_0)$; $R = 0.039$, $R_w = 0.043$ [9].

the distance between N(1) and N(2') is found to be 0.25 Å greater than that between N(1) and N(2). The NiN distances (1.90 Å) are somewhat shorter than those in nickel(II)-porphyrin complexes.[13] Most likely, the geometric changes of the N_4 nucleus are to a large extent ensuing from a rotation of the pyrrole rings in the molecular plane (accompanied by considerable compression of the bond angles of the NCCN segments, Figs. 1 and 3), induced by the propensity of the metal to attain a stereoelectronically favorable square-planar coordination. The relatively long N(1)···N(2') and N(2)···N(1') distances are plausible if one takes into consideration that the two strong hydrogen bonds disappear on metalation.

In the crystal the complex **8** forms stacks of laterally displaced molecules at interplanar distances of 3.45 Å.

Physical data of the new compounds are listed in Table 1.

Experimental

2: 1.36 g (5 mmol) of **5** (see below) was added in one batch to a slurry of the titanium reagent (argon atmosphere), prepared from 9.5 g (50 mmol) of titanium tetrachloride and 6.55 g (100 mmol) of activated zinc in the presence of 2.5 mL of pyridine in 400 mL of tetrahydrofuran (THF), and the reaction mixture was then heated for 30 min under reflux. After hydrolysis with 125 mL of 10% aqueous potassium carbonate solution, repeated extraction with dichloromethane, and chromatography on silica gel (column: 5 × 20 cm) with dichloromethane/hexane (1:1), **2** was obtained as the only non-poly-

meric product. Recrystallization from *n*-hexane afforded fine, violet needles of m.p. 192–194 °C; yield 120 mg (10%).

5: The dipropyl derivative **5** was obtained for the first time analogously to the dimethyl derivative **3** according to the following reaction scheme [5, 14]:

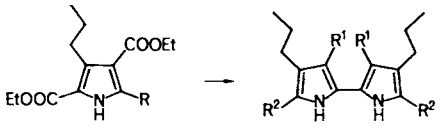

9: [15] R = CH_3 — **12**: $R^1 = R^2 = COOEt$
10: R = COOH — **13**: $R^1 = R^2 = COOH$
11: R = I — **14**: $R^1 = R^2 = H$
5: $R^1 = H$, $R^2 = CHO$

9 → **10**: Br_2, SO_2Cl_2 in $CH_3COOH/HCOOH$, 0 °C, 4 h; H_2O (50–58%); **10** → **11**: KI/I_2 in $EtOH/H_2O$, 75 °C (75–77%); **11** → **12**: Cu, dimethylformamide (DMF), 20 °C, 17 h (62–71%); **12** → **13**: NaOH in $EtOH/H_2O$, 15 h reflux (96%); **13** → **14**: Sublimation at 230 °C, 0.2 torr (89%); **14** → **5**: $POCl_3$/DMF; NaOAc, H_2O (86%).

Table 1. Selected physical data of the new compounds. ^{1}H-NMR: 300 MHz, ^{13}C-NMR: 75.5 MHz, MS: 70 eV.

2: m.p. = 192–194 °C (*n*-hexane); ^{1}H-NMR ($CDCl_3$): δ = 9.62 (s, 4H, H-9,10,19,20), 9.21 (s, 4H, H-3,6,13,16), 3.94 (t, 8H, α-CH_2), 3.04 (br. s, 2H, NH), 2.37 (sext, 8H, β-CH_2), 1.32 (t, 12H, CH_3); ^{13}C-NMR ($CDCl_3$): δ = 144.67, 143.44, 134.05, 122.59, 110.33, 30.42, 25.20, 14.55; MS: *m/z* 478 ($M^{\oplus}$, 100%), 239 ($M^{2\oplus}$, 10); IR (KBr): $\tilde{\nu}$ = 2957, 2926, 2865, 1459, 1363, 1215, 1037, 1010, 968, 878, 807 cm^{-1}; UV/VIS (CH_2Cl_2): λ_{max} = 370 nm (ε = 142000), 381 (100200), 560 (36400), 600 (34100), 633 (48200)

4: m.p. = 270–272 °C (decomp.) (ethanol/dichloromethane); ^{1}H-NMR ([D_6]DMSO): δ = 11.94 (br. s, 2H), 9.60 (s, 2H), 6.75 (d, 2H); 2.74 (q, 4H), 1.20 (t, 6H); MS: *m/z* 244 ($M^{\oplus}$, 100%); IR (KBr): $\tilde{\nu}$ = 3266, 1641 cm^{-1}; UV/VIS ($CHCl_3$): λ_{max} = 270 nm (ε = 16100), 312 (5600), 375 (36300)

5: m.p. = 232–234 °C (decomp.) (ethanol/dichloromethane); ^{1}H-NMR ([D_6]DMSO): δ = 11.94 (br. s, 2H), 9.58 (s, 2H), 6.71 (d, 2H), 2.69 (t, 4H), 1.60 (sext, 4H), 0.91 (t, 6H); MS: *m/z* 272 ($M^{\oplus}$, 100%); IR (KBr): $\tilde{\nu}$ = 3267, 1652 cm^{-1}; UV/VIS ($CHCl_3$): λ_{max} = 271 nm (ε = 16800), 313 (5800), 380 (37000)

6: sublimation > 250 °C; ^{1}H-NMR ($CDCl_3$): δ = 9.73 (s, 4H, H-9,10,19,20), 9.28 (s, 4H, H-3,6,13,16), 3.64 (s, 12H, CH_3), 3.15 (br. s, 2H, NH); ^{13}C-NMR ($CDCl_3$): δ = 144.14, 139.93, 134.06, 123.70, 110.50, 13.94; MS: *m/z* 366 ($M^{\oplus}$, 100%), 183 ($M^{2\oplus}$, 75); IR (CsI): $\tilde{\nu}$ = 2969, 2922, 1463, 1368, 1286, 1226, 1081, 968, 887, 813 cm^{-1}; UV/VIS (CH_2Cl_2): λ_{max} = 368 nm (ε = 141300), 380 (97600), 560 (32400), 599 (28500), 631 (41400)

7: sublimation > 250 °C; ^{1}H-NMR ($CDCl_3$): δ = 9.75 (s, 4H, H-9,10,19,20), 9.33 (t, 4H, H-3,6,13,16), 4.11 (dq, 8H, CH_2), 3.19 (br. s, 2H, NH), 1.99 (t, 12H, CH_3); ^{13}C-NMR ($CDCl_3$): δ = 146.64, 143.37, 134.21, 121.95, 110.32, 21.59, 15.92; MS: *m/z* 422 ($M^{\oplus}$, 100%), 211 ($M^{2\oplus}$, 37); IR (KBr): $\tilde{\nu}$ = 2971, 2934, 2912, 2878, 2838, 1457, 1220, 1024, 973, 812 cm^{-1}; UV/VIS (CH_2Cl_2): λ_{max} = 370 nm (ε = 141900), 381 (103000), 560 (36800), 599 (33300), 632 (48000)

8: m.p. > 300 °C; ^{1}H-NMR ($CDCl_3$): δ = 9.40 (s, 4H, H-9,10,19,20), 8.86 (s, 4H, H-3,6,13,16), 3.90 (t, 8H, α-CH_2), 2.32 (sext, 8H, β-CH_2), 1.31 (s, 12H, CH_3); ^{13}C-NMR ($CDCl_3$): δ = 149.71, 145.72, 143.02, 119.24, 107.26, 31.09, 24.99, 14.53; MS: *m/z* 534/536 ($M^{\oplus}$, 100/53%); IR (KBr): $\tilde{\nu}$ = 2957, 2928, 2867, 1490, 1358, 1303, 1240, 1049, 971, 805, 296 cm^{-1}; UV/VIS (CH_2Cl_2): λ_{max} = 366 nm (ε = 63000) sh, 387 (148700), 558 (15000) sh, 600 (62600), 614 (42400) sh

10: m.p. 136–137 °C (ethanol); ^{1}H-NMR ($CDCl_3$): δ = 14.81 (br. s, 1H), 10.34 (br. s, 1H), 4.49 (q, 2H), 4.39 (q, 2H), 3.08 (dd, 2H), 1.57 (m, 2H), 1.48 (t, 3H), 1.41 (t, 3H), 0.96 (t, 3H); MS: *m/z* 297 ($M^{\oplus}$, 10%), 251 (100); IR (KBr): $\tilde{\nu}$ = 3263, 1735, 1693, 1623 cm^{-1}; UV/VIS ($CHCl_3$): λ_{max} = 245 nm (ε = 10800), 257 (10300), 264 (9700), 290 (8700)

11: m.p. 154–155 °C (ethanol/dichloromethane); ^{1}H-NMR ($CDCl_3$): δ = 10.31 (br. s, 1H), 4.42 (q, 2H), 4.34 (q, 2H), 3.06 (dd, 2H), 1.55 (m, 2H), 1.40 (t, 3H), 1.39 (t, 3H), 0.96 (t, 3H); MS: *m/z* 379 ($M^{\oplus}$, 20%), 276 (100); IR (KBr): $\tilde{\nu}$ = 3244, 1692, 1668 cm^{-1}; UV/VIS ($CHCl_3$): λ_{max} = 266 nm (ε = 16700)

12: m.p. 149–150 °C (ethanol); ^{1}H-NMR ($CDCl_3$): δ = 14.13 (br. s, 2H), 4.39 (q, 4H), 4.35 (q, 4H), 3.07 (dd, 4H), 1.54 (m, 4H), 1.38 (t, 12H), 0.95 (t, 6H); MS: *m/z* 504 ($M^{\oplus}$, 100%); IR (KBr): ν = 1717, 1639 cm^{-1}; UV/VIS ($CHCl_3$): λ_{max} = 250 nm (ε = 23800), 291 (16600), 349 (23200)

14: decomp. above 140 °C; ^{1}H-NMR ([D_6]DMSO): δ = 10.38 (br. s, 2H), 6.39 (m, 2H), 6.01 (m, 2H), 2.32 (t, 4H), 1.50 (sext, 4H), 0.89 (t, 6H); MS: *m/z* 216 ($M^{\oplus}$, 79%), 187 (100); IR (KBr): $\tilde{\nu}$ = 3397 cm^{-1}; UV/VIS (DMSO): λ_{max} = 294 nm (ε = 17700)

CAS Registry numbers:
2, 106562-37-2; **3**, 38220-51-8; **4**, 110078-56-3; **5**, 110078-57-4; **6**, 110078-58-5; 7, 110078-59-6; **8**, 110096-34-9; **9**, 110078-60-9; **10**, 110078-61-0; **11**, 110078-62-1; **12**, 110078-63-2; **13**, 110078-64-3; **14**, 110078-65-4; 4,4'-diethyl-2,2'-bipyrrole, 91556-60-4.

Received: March 12, 1987 [Z 2135 IE]
German version: *Angew. Chem. 99* (1987) 909

[1] H. Fischer, R. Bäumler, *Justus Liebigs Ann. Chem. 468* (1929) 58.
[2] a) H. Scheer, J. J. Katz in K. M. Smith: *Porphyrins and Metalloporphyrins*, Elsevier, Amsterdam 1975, p. 416; b) J. W. Buchler in D. Dolphin: *The Porphyrins, Vol. I*, Academic Press, New York 1978, p. 389; c) J. B. Paine III, W. B. Kirshner, D. W. Moskowitz, D. Dolphin, *J. Org. Chem. 41* (1976) 3857; d) P. J. Brothers, J. P. Collman, *Acc. Chem. Res. 19* (1986) 209.
[3] Cf., e.g. the influence of three *n*-butyl groups on the solubility behavior of dodecahydrohexaazakekulene [J. E. B. Ransohoff, H. A. Staab, *Tetrahedron Lett. 26* (1985) 6179]; T. W. Bell, A. Firestone, *J. Am. Chem. Soc. 108* (1986) 8109.
[4] a) E. Vogel, M. Köcher, H. Schmickler, J. Lex, *Angew. Chem. 98* (1986) 262; *Angew. Chem. Int. Ed. Engl. 25* (1986) 257; b) *Chem. Eng. News 64* (1986), No. 23, p. 27; c) P. F. Aramendia, R. W. Redmond, S. Nonell, W. Schuster, S. E. Braslavsky, K. Schaffner, E. Vogel, *Photochem. Photobiol. 44* (1986) 555; d) in the meantime, further novel tetrapyrrolic macrocycles have been reported: [26]porphyrin: M. Gosmann, B. Franck, *Angew. Chem. 98* (1986) 1107; *Angew. Chem. Int. Ed. Engl. 25* (1986) 1100; [1,5,1,5]platyrin: E. LeGoff, O. G. Weaver, *J. Org. Chem. 52* (1987) 710.
[5] M. J. Broadhurst, R. Grigg, A. W. Johnson, *J. Chem. Soc. Perkin Trans. 1 1972*, 2111.
[6] We obtained the ethyl derivative **4** (for spectral data see Table 1) for the first time by reaction of 4,4'-diethyl-2,2'-bipyrrole [14b] with the Vilsmeier complex of dimethylformamide and phosphorus oxide trichloride employing a procedure analogous to that used for the preparation of 5,5-diformyl-2,2'-bipyrrole [V. J. Bauer, D. L. J. Clive, D. Dolphin, J. B. Paine III, F. L. Harris, M. M. King, J. Loder, S.-W. Chien Wang, R. B. Woodward, *J. Am. Chem. Soc. 105* (1983) 6429].
[7] a) T. Mukaiyama, T. Sato, J. Hanna, *Chem. Lett. 1973*, 1041; b) D. Lenoir, *Synthesis 1977*, 553; c) the reductive coupling of **5** with $TiCl_3$/$LiAlH_4$ [J. E. McMurry, M. P. Fleming, *J. Am. Chem. Soc. 96* (1974) 4708] leads predominantly to tetrahydro derivatives of **2** which have not yet been investigated in detail.
[8] M. J. Crossley, M. M. Harding, S. Sternhell, *J. Am. Chem. Soc. 108* (1986) 3608, and references cited therein.
[9] Further details of the crystal structure investigations are available on request from the Fachinformationszentrum Energie, Physik, Mathematik GmbH, D-7514 Eggenstein-Leopoldshafen 2 (FRG), on quoting the depository number CSD-52592 (for **2** and **8**), the names of the authors, and the journal citation.
[10] E. Vogel, M. Köcher, M. Balci, I. Teichler, J. Lex, H. Schmickler, O. Ermer, *Angew. Chem. 99* (1987) 912; *Angew. Chem. Int. Ed. Engl. 26* (1987) 931.
[11] E. Vogel, M. Köcher, J. Lex, unpublished experiments.
[12] C. Kratky, R. Waditschatka, C. Angst, J. E. Johansen, J. C. Plaquevent, J. Schreiber, A. Eschenmoser, *Helv. Chim. Acta 68* (1985) 1312.
[13] X-ray structure analysis of tetragonal and triclinic Ni(OEP): E. F. Meyer, Jr., *Acta Crystallogr. Sect. B 28* (1972) 2162 and D. L. Cullen, E. F. Meyer, Jr., *J. Am. Chem. Soc. 96* (1974) 2095, resp.; also see the analysis of the H_2(OEP) ligand: J. W. Lauher, J. A. Ibers, *ibid. 95* (1973) 5148.
[14] a) A. H. Corwin, W. A. Bailey, Jr., P. Viohl, *J. Am. Chem. Soc. 64* (1942) 1267; b) R. Grigg, A. W. Johnson, J. W. F. Wasley, *J. Chem. Soc. 1963*, 359.
[15] H. Fischer, M. Goldschmidt, W. Nüssler, *Justus Liebigs Ann. Chem. 486* (1931) 1.

2,3-Dihydroporphycene—an Analogue of Chlorin

By *Emanuel Vogel,* Matthias Köcher, Metin Balci, Ilona Teichler, Johann Lex, Hans Schmickler,* and *Otto Ermer*

Responsible for the aromaticity of porphine, the parent compound of the porphyrins, is the presence of 18 π electrons in the main conjugation pathway (NH-bridged di-

[*] Prof. Dr. E. Vogel, Dipl.-Chem. M. Köcher, Dr. M. Balci, I. Teichler, Dr. J. Lex, Dr. H. Schmickler, Prof. Dr. O. Ermer
Institut für Organische Chemie der Universität
Greinstrasse 4, D-5000 Köln 41 (FRG)

aza[18]annulene).[1] This supposition would further explain why chlorin **1**[2] – the parent system of chlorophyll – and bacteriochlorin **2**,[3] in which respectively one and two of the peripheral double bonds are hydrogenated, likewise exhibit aromatic character.

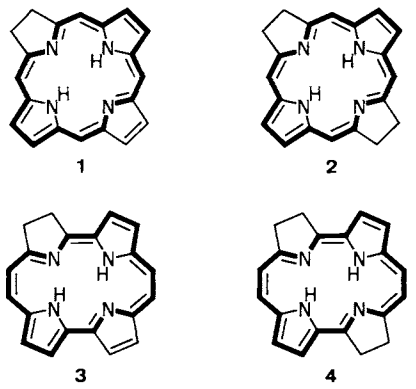

The same structural relationship formally exists between the novel porphine-isomer porphycene **5**[4] and its dihydro and tetrahydro derivatives, the compounds **3** and **4**, respectively, as in the series porphine – **1** – **2**. Having established by spectroscopic and structural investigations that porphycene and porphine exhibit essentially the same type of bonding, especially with regard to the π-electron structure, it followed that **3** and **4** should be regarded as "chlorin- and bacteriochlorin-analogues". The synthesis and properties of **3** reported in the sequel lend support to this interpretation.

Porphycene **5** (10 mg) on catalytic hydrogenation with 10% Pd/C (10 mg) in ethyl acetate (20 mL) afforded, after 45 min, a mixture consisting of 2,3-dihydroporphycene **3** (80–90%) and the starting compound **5**. Attempts to achieve complete conversion by prolonging the reaction time led to reduced yields, presumably as a result of formation of labile, more highly hydrogenated products. The isolation of **3**, which could not be accomplished by normal chromatography, was finally achieved by preparative HPLC.[5] Upon recrystallization from ethyl acetate/cyclohexane (1:1), expediently carried out with the combined products of four HPLC runs, **3** was obtained as small violet rhombs (yield 20 mg; m.p. >300°C).

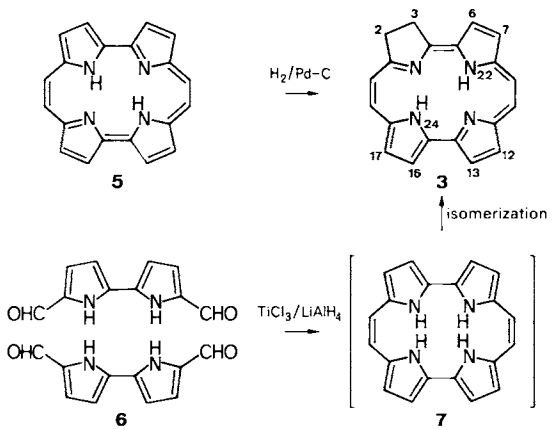

Surprisingly, the synthesis of **3** can also be realized, albeit in only 1% yield, if the reductive coupling of 5,5′-diformyl-2,2′-bipyrrole **6** by low-valent titanium, which leads to porphycene **5** when titanium tetrachloride/zinc in tetrahydrofuran (THF) is used,[6] is instead carried out with titanium trichloride/lithium aluminum hydride (likewise in THF).[7,8] An explanation for this result is provided by the assumption that both titanium coupling reactions proceed via the dihydroporphycene **7** (still to be detected), and that, in the presence of titanium trichloride/lithium aluminum hydride, the prototropic rearrangement **7** → **3** is more rapid than the dehydrogenation **7** → **5**. The possibility that **3** is formed via **5** could be ruled out by control experiments.

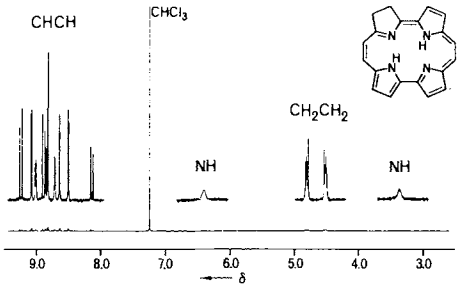

Fig. 1. ^{1}H-NMR spectrum of 2,3-dihydroporphycene **3** (300 MHz, $CDCl_3$).

The structure and the chlorin-like nature of **3** are confirmed by the spectra of the compound.[9] The ^{1}H-NMR spectrum (Fig. 1) shows: a) five AX systems in the region $\delta = 9.3$–8.2 which are easily recognizable by double resonance experiments and which by virtue of the coupling constants can be ascribed to the protons of the three pyrrolic ($J \approx 4$ Hz) and the two non-pyrrolic ($J \approx 11$ Hz) CHCH units, b) an AA′BB′ system at $\delta = 4.9$–4.6 (CH_2CH_2 protons), and c) two broad signals at $\delta = 6.45$ and 3.51 (each one N-proton; H22 and H24, resp.). Of the three AX systems of the pyrrolic protons, two are split further by coupling with an N-proton, from which it can be concluded that the N-protons each belong to a pyrrole ring. The appearance of the NH signals at relatively low field clearly indicates the presence of strong N–H···N hydrogen bonding (cf. the spectra of porphycenes[4,10]). With the aid of decoupling and NOE experiments it was possible to assign the spectrum completely (Table 1). On recording the spectrum at higher temperature (up to 75°C in C_6D_6) a noticeable broadening of the NH signals was observed, but the selective coupling of each of the N-protons to a specific pyrrolic CHCH proton pair remained unaltered. The NH tautomerism in **3** which, for geometric reasons, is presumably very rapid even at room temperature is, according to the NMR findings, apparently characterized by the fact that of the possible tautomers, predominantly one – namely **3** – is present.

Table 1. ^{1}H-NMR data (δ values and H,H coupling constants [Hz]) of 2,3-dihydroporphycene **3** (300 MHz, $CDCl_3$, saturated solution, room temperature).

	H2	H3	H6	H7	H9	H10	H12	H13	H16	H17	H19	H20	H22	H24
δ	4.64	4.94	8.91	8.54	8.90	9.24	8.64	9.08	9.03	8.75	8.91	8.24	6.45	3.51
J_{AX}			4.32		11.46		3.99		4.50		10.75			
$^4J_{A-NH}$			1.46	1.12					1.88	1.76				

The relationship between the systems porphycene **5**/dihydroporphycene **3** and porphine/chlorin **1** manifests itself especially strikingly in the ^{1}H-NMR spectrum, for in

 © VCH Verlagsgesellschaft mbH, D-6940 Weinheim, 1987 0570-0833/87/0909-0932 $ 02.50/0

both cases the transformation of the parent compound into the dihydro derivative results in the spectral centroid of the "arene protons" being slightly shifted to higher field [$\Delta\delta = 0.77$ (**5**/**3**) and 0.62 ppm (porphine/**1**)] and that of the N-protons being shifted downfield ($\Delta\delta = 1.83$ and 1.77 ppm).[11]

The UV/VIS spectrum of **3**, which shows three bands in the Soret region and a characteristic band pattern in the long wavelength region, is closely related to that of porphycene **5**. A pronounced increase in intensity of the longest wavelength band as in the spectrum of chlorin **1**[12] (relative to that of porphine) is not observed. Consistent with the stability and porphinoid nature of the compound, the mass spectrum (electron impact-ionization, 70 eV) exhibits $M^{\oplus}$ and $M^{2\oplus}$ as predominant peaks. The IR spectrum shows no bands for the NH stretching vibration (strong N–H···N bridges).

According to an X-ray structure analysis,[13] **3** has an almost planar ring skeleton (maximum distance of the C- and N-atoms from the central plane ± 0.09 Å; in porphycene ± 0.04 Å), like porphycene **5**, whereby the planarization of the partly hydrogenated pyrrole ring is likely to be attributed to the restricted torsional freedom about the two CN bonds.[14] The close similarity between **3** and **5** also expresses itself in other essential structural features such as the short N–H···N distances, the size of the cavity, and the widening of the CCC angles (to 132°) in the CHCH units linking the five-membered rings (Fig. 2).

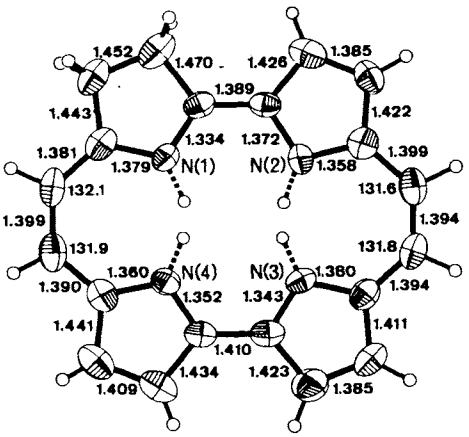

N(1)···N(2)	2.843	N(2)···N(3)	2.632
N(1)···N(4)	2.668	N(3)···N(4)	2.846

Fig. 2. Crystal structure of **3**. Top: top view; thermal ellipsoids (40% probability) and selected bond lengths and angles (standard deviations ca. 0.004 Å and 0.3°, resp.); inner hydrogen atoms presumably disordered, see Figure 3. Bottom: side view.

From a difference electron density map in the plane of the molecule (Fig. 3) and from the shape of the thermal ellipsoids (Fig. 2) it can be concluded that the crystal structure of **3** is partially disordered. This affects, in particular, the two inner hydrogen atoms, which – other than is possible in solution, as shown by the ^{1}H-NMR spectrum – cannot be assigned to individual N-atoms. The electron density distribution in the N_4 nucleus would seem to indicate asymmetric hydrogen bridges, thus suggesting an NH tautomerism describable by double minimum potentials. In the case of porphycene and porphine, such potentials could in the meantime be unequivocally confirmed by solid-state ^{15}N-NMR measurements.[15]

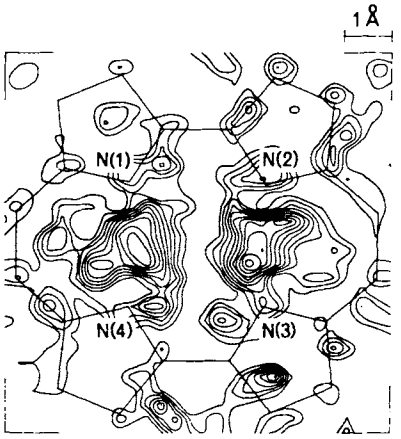

Fig. 3. Difference electron density map in the molecular plane of **3**. Contributions of all atoms subtracted except inner hydrogen atoms; contours beginning with 0.05, intervals 0.025 eÅ^{-3}.

From Figure 3 it is evident that there are a number of residual density maxima remote from atoms or chemical bonds. These maxima may be ascribed to an additional disorder effect, originating in the fact that, apart from the predominant orientation of the molecule, at least one further orientation rotated in the plane of the molecule is present. The unexpected finding that the CC single bond of the partly hydrogenated pyrrole ring is 0.09 Å shorter than normal, whereas the CC bonds of the three pyrrolic CHCH units are 0.04 Å longer than those in porphycene might be attributed to similar effects. An analysis of the anisotropic temperature factors in terms of rigid-body-motions is also in line with such an interpretation of the bond lengths.

Received: March 12, 1987 [Z 2136 IE]
German version: *Angew. Chem. 99* (1987) 912

CAS Registry numbers:
3, 109907-04-2; **5**, 100572-96-1; **6**, 86568-92-5.

[1] a) H. H. Inhoffen, J. W. Buchler, P. Jäger, *Fortschr. Chem. Org. Naturst. 26* (1968) 284; b) H. Scheer, J. J. Katz in K. M. Smith: *Porphyrins and Metalloporphyrins*, Elsevier, Amsterdam 1975, p. 405; c) T. R. Janson, J. J. Katz in D. Dolphin: *The Porphyrins, Vol. IV*, Academic Press, New York 1979, p. 1.

[2] U. Eisner, R. P. Linstead, *J. Chem. Soc. 1955*, 3742.

[3] Unsubstituted metal-free bacteriochlorin **2** and isobacteriochlorin (2,3,7,8-tetrahydroporphine) have, to our knowledge, not been described in the literature so far. For the synthesis of norporphines with bacteriochlorin or isobacteriochlorin chromophore see W. Flitsch, *Pure Appl. Chem. 58* (1986) 153; W. Flitsch, D. Schulz, H.-G. Kneip, *Liebigs Ann. Chem. 1985*, 1004.

[4] a) E. Vogel, M. Köcher, H. Schmickler, J. Lex, *Angew. Chem. 98* (1986) 262; *Angew. Chem. Int. Ed. Engl. 25* (1986) 257; b) P. F. Aramendia, R. W. Redmond, S. Nonell, W. Schuster, S. E. Braslavsky, K. Schaffner, E. Vogel, *Photochem. Photobiol. 44* (1986) 555.

[5] Separation conditions: RP-18 column; 2.5 × 30 cm; acetonitrile/water (8:2); 1.5 bar; 12 mL/min.

[6] a) T. Mukaiyama, T. Sato, J. Hanna, *Chem. Lett. 1973*, 1041; b) D. Lenoir, *Synthesis 1977*, 553.

[7] J. E. McMurry, M. P. Fleming, *J. Am. Chem. Soc. 96* (1974) 4708.

[8] The compound **3** thus obtained is usually accompanied by traces of **5**, so that it is also necessary here to isolate **3** by HPLC.

[9] 3: ^{1}H-NMR see Table 1; ^{13}C-NMR (75.5 MHz, $CDCl_3$): $\delta = 32.14$ (C-2), 36.21 (C-3), 106.54 (C-20), 109.66 (C-9), 117.18 (C-19), 118.91 (C-10), 119.25 (C-16), 121.97 (C-13), 124.16 (C-7), 125.54 (C-6), 126.11 (C-12), 128.16 (C-17), 129.02, 131.18, 133.66, 134.03, 142.86, 144.00, 158.35, 166.84 (quaternary C); MS (70 eV): m/z 312 ($M^{\oplus}$, 100%), 311 ($M^{\oplus}-H$, 25), 156 ($M^{2\oplus}$, 40); UV/VIS (benzene): $\lambda = 360$ nm ($\varepsilon = 71400$), 382 (51700), 402 (74400), 532 (11300) sh, 548 (15300) sh, 560 (17100), 575 (23800), 595 (29900); IR (KBr): $\tilde{\nu} = 3095$, 2921, 1558, 1350, 1213, 1169, 1038, 966, 898, 802 cm^{-1}.

[10] E. Vogel, M. Balci, K. Pramod, P. Koch, J. Lex, O. Ermer, *Angew. Chem. 99* (1987) 909; *Angew. Chem. Int. Ed. Engl. 26* (1987) 928.

[11] 1: ^{1}H-NMR (300 MHz, $CDCl_3$, saturated solution, 20°C): $\delta = 9.81$ (9.62) [H-10,15], 8.99 (8.92) [H-5,20], 9.04 (9.03) [H-12,13], 9.20 (8.63) [H-8,17], 8.87 (8.52) [H-7,18], 4.74 (4.25) [H-2,3], −2.41 (−2.75) [N-H]. Values in parentheses taken from K. N. Solov'ev, V. A. Mashenkov, A. T. Gradyushko, A. E. Turkova, V. P. Lezina, *J. Appl. Spectrosc. USSR 13* (1970) 1106 (see also: H. Scheer, J. J. Katz in K. M. Smith: *Porphyrins and Metalloporphyrins*, Elsevier, Amsterdam 1975, p. 442). The observed deviations might be due to differences in concentration.

[12] J. D. Keegan, A. M. Stolzenberg, Y.-C. Lu, R. E. Linder, G. Barth, A. Moscowitz, E. Bunnenberg, C. Djerassi, *J. Am. Chem. Soc. 104* (1982) 4305.

[13] 3: m.p. >300°C, crystals from chloroform; monoclinic, space group $P2_1/c$, $Z = 4$; $a = 10.369(1)$, $b = 14.456(3)$, $c = 10.535(2)$ Å, $\beta = 102.91(1)°$; $\rho_{calc} = 1.348$ g cm^{-3}; intensities measured on a four-circle diffractometer [room temperature, $\lambda_{Mo} = 0.71069$ Å, $\theta_{Mo}(max) = 27°$]; refinement (C, N anisotropic, H isotropic) including the 1403 reflections with $F_0 > 4\sigma(F_0)$; $R = 0.038$, $R_w = 0.042$. For the two inner H-atoms, four positions were refined with half-weights. Further details of the crystal structure investigation are available on request from the Fachinformationszentrum Energie, Physik, Mathematik GmbH, D-7514 Eggenstein-Leopoldshafen 2 (FRG), on quoting the depository number CSD-52593, the names of the authors, and the journal citation.

[14] The crystal structure of unsubstituted, metal-free chlorin 1 has hitherto not been described. In the crystals of a highly-substituted chlorin derivative (phyllochlorin ester) the partially hydrogenated pyrrole ring is not planar; this may be attributed in part to steric interactions of the substituents; W. Hoppe, G. Will, J. Gassmann, H. Weichselgartner, *Z. Kristallogr. 128* (1969) 18.

[15] B. Wehrle, H.-H. Limbach, M. Köcher, O. Ermer, E. Vogel, *Angew. Chem. 99* (1987) 914; *Angew. Chem. Int. Ed. Engl. 26* (1987) 934.

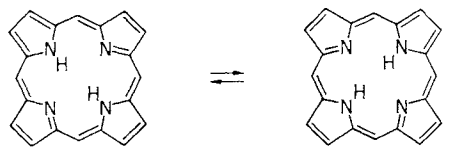

1

Scheme 1. Tautomerism of Porphine 1.

Whereas double minimum potentials have been found by dynamic NMR spectroscopy for dissolved[3] and crystalline[4,5] porphyrins the problem of tautomerism in crystalline porphine 1 has not yet been solved. Two X-ray structure analyses of 1[6,7] also indicate a double minimum potential but are contradictory with respect to the phenomenon of order or disorder of the inner hydrogen atoms.

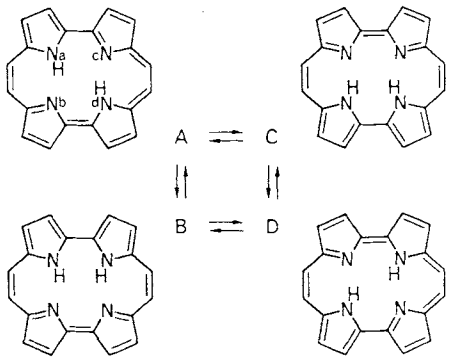

2

Scheme 2. Tautomerism of Porphycene 2.

^{15}N-CPMAS-NMR Study of the Problem of NH Tautomerism in Crystalline Porphine and Porphycene**

By *Bernd Wehrle, Hans-Heinrich Limbach,* Matthias Köcher, Otto Ermer,* and *Emanuel Vogel**

In contrast to porphine 1 (Scheme 1) and many of its derivatives the novel porphine isomer porphycene 2[1] (Scheme 2) is distinguished by the presence of strong N–H···N hydrogen bonds and by an apparently extremely fast NH tautomerism, as indicated by the ^{1}H-NMR and IR spectra of 2. This finding agrees with model considerations because the compound can obviously be formally classified with respect to the arrangement of the N–H···N groups and the short NN distances as a double seven-membered ring H-chelate.[2] Similarly as in the case of such chelates it is also difficult to establish for 2 whether the inner H-atoms are located in a single minimum potential or whether they move along a double minimum potential. An X-ray structure analysis of 2 – although subject to some uncertainties with regard to the position of the H-atoms – indicates a multiple minimum potential.[1]

In view of the experimental[3–8] and theoretical[9] importance of NH tautomerism in the chemistry of porphyrins and related pyrrolic macrocycles we have now investigated the localization and transfer of the N-protons in 1 and 2 using variable-temperature high-resolution ^{15}N-CPMAS-NMR spectroscopy—which has already proven useful in the chemistry of macrocyles.[4,5,10,11]

Figure 1 shows a superposition of the experimental and calculated 9.12-MHz ^{15}N-CPMAS-NMR spectra of ^{15}N-enriched[13] 1 as a function of temperature. At low temperatures we observe a singlet at $\delta_{NH} = 107$ ppm for the imino and a singlet at $\delta_N = 215$ ppm for the azomethine nitrogen atoms.[14] As the temperature is raised the signals broaden and coalesce into one sharp singlet at 161 ppm. From these findings it follows that the proton transfer is very fast at room temperature, but "frozen" at low temperatures. A nitrogen atom m involved in a fast tautomeric process gives rise to a line m in the ^{15}N-NMR spectra at the position

$$\delta_m = p_m \delta_{NH} + (1 - p_m)\delta_N. \qquad (a)$$

p_m is the average proton density on atom m. The observation of only one average line at $\delta = (\delta_{NH} + \delta_N)/2$ means, therefore, that all nitrogen atoms in crystalline 1 are characterized within the margin of error by the same average proton density $p = 1/2$. This result contradicts the proposition of localized inner H-atoms,[7] but supports a disordered structure with two tautomers of almost equal energy[6] shown in Scheme 1. Such a symmetric situation is, however, the exception[4,5,10] rather than the rule, and has

[*] Priv.-Doz. Dr. H.-H. Limbach, Dipl.-Chem. B. Wehrle
Institut für Physikalische Chemie der Universität
Albertstr. 21, D-7800 Freiburg (FRG)
Prof. Dr. E. Vogel, Prof. Dr. O. Ermer, Dipl.-Chem. M. Köcher
Institut für Organische Chemie der Universität
Greinstr. 4, D-5000 Köln 41 (FRG)

[**] This work was supported by the Deutsche Forschungsgemeinschaft, the Stiftung Volkswagenwerk, and the Fonds der Chemischen Industrie.

been observed so far only in the case of *meso*-tetratolylporphyrin (TTP).[4, 15] In the case of triclinic *meso*-tetraphenylporphyrin (TPP) it was found by ^{15}N-CPMAS-NMR spectroscopy that the equilibrium in Scheme 1 was disturbed by crystal effects.[4] By simulation of the experimental spectra (Fig. 1) in the temperature range between 200 and 350 K an energy of activation of 39 kJ mol^{-1} and a frequency factor of 10^{11} s^{-1} were obtained for the exchange in Scheme 1. These values agree well with those found previously for dissolved TPP[3] and crystalline TTP.[4] It is still unclear as to whether the proton motion in **1** takes place along a synchronous pathway or along an asynchronous pathway via tautomers with protons on adjacent nitrogen atoms, and as to whether each inner proton migrates between only two or - as in solution[3] - between all four nitrogen atoms.

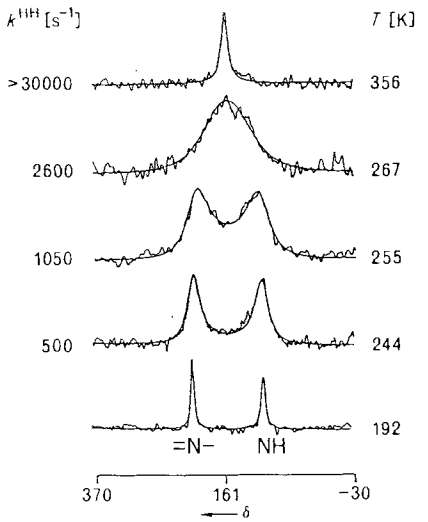

Fig. 1. Superposed experimental and calculated ^{15}N-CPMAS-NMR spectra of 95% ^{15}N-enriched porphine **1** at 9.12 MHz as a function of temperature. 3 to 6 ms CP-time, 7 kHz spectral width, 2.1 s repetition time. Reference: external $^{15}NH_4Cl$. The spectra were obtained with a Bruker CXP-100 NMR spectrometer equipped with a Doty-spinner [12] and a low temperature heat exchanger described previously [5]. k^{HH} is the rate constant of the tautomerism in a symmetric double-minimum potential. The additional simulation parameters, $W_0(N) = 57$ Hz and $W_0(NH) = 75$ Hz (halfwidth in absence of exchange) were taken from the low-temperature spectra.

A comparison of the ^{15}N-CPMAS-NMR spectra of **2** (Fig. 2) at elevated temperatures with the spectra of **1** surprisingly reveals virtually no differences, i.e. at high temperatures a very fast proton transfer apparently takes place not only in **1** but also in **2**. However, in contrast to **1**, **2** does not show line-broadening as the temperature is lowered, i.e. no "freezing" of the proton motions, but a splitting into four sharp singlets a–d, which continously drift away from each other with decreasing temperature. The upfield shift of line a (and of d) matches the downfield shift of line b (and of c). This observation proves the presence of two non-equivalent asymmetric proton transfer systems

$$ab \equiv N_aH\cdots N_b \rightleftharpoons N_a\cdots HN_b$$

and

$$dc \equiv N_dH\cdots N_c \rightleftharpoons N_d\cdots HN_c$$

in which the exchange is still fast with respect to the NMR time-scale even at 107 K. The shifts of the signals with decreasing temperature can be explained in terms of Equation (a) with an increasing proton density p_a on atom a at the expense of the proton density p_b on atom b. The same is true for the system dc, where, however, the effect is less pronounced. Since temperature-dependent proton densities are characteristic for double- or multiple-minimum potentials one can, therefore, exclude the possibility of a single minimum potential for the inner hydrogen atoms of **2**. Note that in the case of a symmetric double minimum potential the proton densities are also independent of temperature, a fact which makes it very difficult in the case of symmetric molecules in the liquid state to distinguish between single- and multiple-minimum potentials by NMR. As shown here for **2**, this distinction is possible nowadays by CPMAS-NMR spectroscopic examination of the molecules in the solid state where symmetries are generally perturbed. In order to calculate values for K_{ab} and K_{dc} in terms of Equation (a) it is necessary to assume values of the unknown quantities δ_{NH} and δ_N. Since the high-temperature ^{15}N-NMR line positions of **1** and **2** agree exactly one can take these values in approximation from **1**. Thus, we obtain from the temperature dependence of K_{ab} and K_{dc} for the tautomerism of crystalline **2** the very small reaction enthalpies $\Delta H_{ab} = 0.69$ kJ mol^{-1} and $\Delta H_{dc} = 0.2$ kJ mol^{-1}, but no entropy differences, i.e. $\Delta S_{ab} \approx \Delta S_{dc} \approx 0$. It cannot be excluded that there are also small energy differences between the two tautomers in crystalline **1** which, however, cannot be observed because of severe dynamic line-broadening when the temperature is lowered.

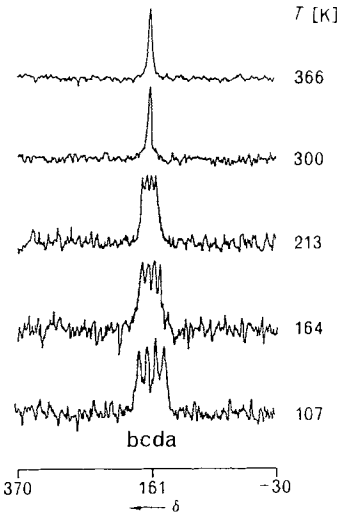

Fig. 2. ^{15}N-CPMAS-NMR spectra of 95% ^{15}N-enriched porphycene **2** at 9.12 MHz as a function of temperature. 6 ms CP-time, 5 kHz spectral width, 2.7 s repetition time. Reference: external $^{15}NH_4Cl$. Average number of scans: 1200. The low-temperature spectra were obtained with a pulse sequence for minimizing artifacts from long radiofrequency pulses [16] by which—as we find here—also acoustic ringing [17] is suppressed.

For an assignment of the nitrogen lines a–d in Figure 2 to atom positions in the unit cell two possibilities are consistent with the NMR spectra: (i) there are two non-equivalent porphycene molecules in the crystal at low temperatures, each of which contains either two equivalent ab or dc proton transfer systems, i.e. has access to only two tautomeric states; (ii) all porphycene molecules in the crystal are equivalent, but each molecule contains both proton transfer systems ab and cd, i.e. exists in all of the four fast interconverting tautomeric states A to B shown in Scheme 2. In both cases the degeneracy of the two tautomers with a

transverse arrangement and of those with a vicinal arrangement of the inner protons is removed in the crystal due to intermolecular interactions.[18] Since only one type of porphycene molecules is observed in the crystal at room temperature,[11] there is a high probability that case (ii) is realized.[19] If one further assumes that the state of lowest energy is characterized by a transverse arrangement of the inner hydrogen atoms one can, tentatively, assign the observed nitrogen lines to the atom positions shown in Scheme 2. The observation that $K_{ab}=p_b/p_a$ and $K_{dc}=p_c/p_d$ are different means that the proton motion in both proton transfer units is asynchronous. A similar situation has been found recently for a tetraaza[14]annulene derivative.[10]

We conclude that the two inner H-atoms in crystalline porphine **1** move with measurable rates in a double minimum potential which is symmetric within the margins of experimental error. In the seven-membered ring H-chelate porphycene **2** an energy barrier exists between the four NH tautomers, which, however, is very small because of the short NH···N distances. The pairwise equivalence of the tautomers is destroyed due to crystal effects. In contrast to the case of **1**, the mutual interconversion of the tautomers is, therefore, so fast that it is no longer possible to measure rate constants for the proton motion by lineshape analysis of the ^{15}N-CPMAS-NMR spectra.

Received: March 12, 1987 [Z 2137 IE]
German version: *Angew. Chem. 99* (1987) 914

CAS Registry numbers:
1, 101-60-0; **2**, 100572-96-1.

[1] E. Vogel, M. Köcher, H. Schmickler, J. Lex, *Angew. Chem. 98* (1986) 262; *Angew. Chem. Int. Ed. Engl. 25* (1986) 257.
[2] B. Bock, K. Flatau, H. Junge, M. Kuhr, H. Musso, *Angew. Chem. 83* (1971) 239; *Angew. Chem. Int. Ed. Engl. 10* (1971) 225; S. Bratan-Mayer, F. Strohbusch, W. Hänsel, *Z. Naturforsch. B31* (1976) 1106; H. M. Pickett, *J. Am. Chem. Soc. 95* (1973) 1770; H. L. Ammon, U. Mueller-Westerhoff, *Tetrahedron 30* (1974) 1437; U. Mueller-Westerhoff, *J. Am. Chem. Soc. 92* (1970) 4849; H. A. Staab, T. Saupe, C. Krieger, *Angew. Chem. 95* (1983) 748; *Angew. Chem. Int. Ed. Engl. 22* (1983) 731.
[3] C. B. Storm, Y. Teklu, *Ann. N. Y. Acad. Sci. 206* (1973) 631; H. H. Limbach, J. Hennig, D. Gerritzen, H. Rumpel, *Faraday Discuss. Chem. Soc. 74* (1982) 229; H. H. Limbach, J. Hennig, J. Stulz, *J. Chem. Phys. 78* (1983) 5432; H. H. Limbach, *ibid. 80* (1984) 5343; M. Schlabach, B. Wehrle, H. H. Limbach, E. Bunnenberg, A. Knierzinger, A. Y. L. Shu, B. R. Tolf, C. Djerassi, *J. Am. Chem. Soc. 108* (1986) 3856.
[4] H. H. Limbach, J. Hennig, R. D. Kendrick, C. S. Yannoni, *J. Am. Chem. Soc. 106* (1984) 4059; H. H. Limbach, D. Gerritzen, H. Rumpel, B. Wehrle, G. Otting, H. Zimmermann, R. D. Kendrick, C. S. Yannoni in H. Sixl, J. Friedrich, C. Bräuchle (Eds.): *Photoreaktive Festkörper*, M. Wahl Verlag, Karlsruhe 1985, p. 19-43.
[5] R. D. Kendrick, S. Friedrich, B. Wehrle, H. H. Limbach, C. S. Yannoni, *J. Magn. Reson. 65* (1985) 159.
[6] L. E. Webb, E. B. Fleischer, *J. Chem. Phys. 43* (1965) 3100.
[7] B. M. L. Chen, A. Tulinsky, *J. Am. Chem. Soc. 94* (1972) 4144; A. Tulinsky, *Ann. N. Y. Acad. Sci. 206* (1973) 47.
[8] S. Völker, J. H. van der Waals, *Mol. Phys. 32* (1976) 1703; J. Friedrich, D. Haarer, *Angew. Chem. 96* (1984) 96; *Angew. Chem. Int. Ed. Engl. 23* (1984) 113.
[9] J. Almlöf, *Int. J. Quantum Chem. 8* (1974) 915; A. Sarai, *J. Chem. Phys. 76* (1982) 5554; *ibid. 80* (1984) 5341; V. A. Kuzmitsky, K. N. Solovyov, *J. Mol. Struct. 65* (1980) 219; G. I. Bersuker, V. Z. Polinger, *Chem. Phys. 86* (1984) 57.
[10] H. H. Limbach, B. Wehrle, H. Zimmermann, R. D. Kendrick, C. S. Yannoni, *J. Am. Chem. Soc. 109* (1987) 929; H. H. Limbach, B. Wehrle, H. Zimmermann, R. D. Kendrick, C. S. Yannoni, *Angew. Chem. 99* (1987) 241; *Angew. Chem. Int. Ed. Engl. 26* (1987) 247.
[11] CP ≡ cross polarization, MAS ≡ magic angle spinning. For reviews on the CPMAS-NMR method see C. A. Fyfe: *Solid State NMR for Chemists*. C. F. C. Press, Guelph, Ontario 1983; J. R. Lyerla, C. S. Yannoni, C. A. Fyfe, *Acc. Chem. Res. 15* (1982) 208. Review on ^{15}N-NMR spectroscopy: W. von Philipsborn, R. Müller, *Angew. Chem. 98* (1986) 381; *Angew. Chem. Int. Ed. Engl. 25* (1986) 383.
[12] P. D. Ellis, F. D. Doty, *Rev. Sci. Instr. 52* (1981) 1868.
[13] ^{15}N-enriched **1** and **2** were synthesized from $^{15}NH_4Cl$ [A. H. Hempel GmbH, D-4000 Düsseldorf (FRG)] using slightly modified versions of the procedures described for the unlabeled compounds. See: R. M. Silverstein, E. E. Ryskiewicz, S. W. Chaikin, *J. Am. Chem. Soc. 76* (1954) 4485; F. R. Longo, E. J. Thorne, A. D. Adler, S. Dym, *J. Heterocycl. Chem. 12* (1975) 1305; see also Ref. [1]. Impurities due to metal complexation could not be detected in the mass-spectra of **1** and **2**.
[14] The larger linewidth of the NH signal at low temperatures is not caused instrumentally but, probably, by slightly different chemical shifts of the two NH atoms in **1** arising from a reduced molecular symmetry in the monoclinic crystal.
[15] R. J. Butcher, G. B. Jameson, C. B. Storm, *J. Am. Chem. Soc. 107* (1985) 2978.
[16] P. DuBois Murphy, *J. Magn. Reson. 70* (1986) 307.
[17] E. Fukushima, S. B. W. Roeder, *J. Magn. Reson. 33* (1979) 199.
[18] K_{ab} and K_{dc} are equilibrium constants in case (i). In case (ii), K_{ab} and K_{dc} are complex quantities which are related to the equilibrium constants K_{mn}, m, n = A, D of tautomerism by

$$K_{ab}=K_{AC}(1+K_{CD})/(1+K_{AB}); \quad K_{dc}=K_{AB}(1+K_{BD})/(1+K_{AC}).$$

[19] A differentiation of both cases by two-dimensional spin diffusion experiments as in the case of 5,14-dihydro-6,8,15,17-tetramethyl-5,9,14,18-tetraazadibenzo[*a,h*]cyclotetradecene(tetramethyldibenzotetraaza[14]annulene) [10] will be attempted in a future study.

BOOK REVIEWS

Ostwalds Klassiker der exakten Wissenschaften 265. Jacobus Henricus van't Hoff: Studien zur chemischen Dynamik (Etudes de dynamique chimique) 1884. Translated by *L. Dunsch*. Akademische Verlagsgesellschaft Geest & Portig, Leipzig 1985. 236 pp., paperback, DM 31.00.—

In the report "Opportunities in Chemistry" (the Pimentel Report, a successor to the Westheimer Report), published recently in the USA, the first item in a list of the most important chemical research tasks suggested for intensive study in the rest of this century is: "Understanding chemical reactivity (... clarification of factors that control the rates of reactions ... to sustain international leadership for the US at the major fundamental frontier of chemistry)". The award of the Nobel Prize for Chemistry last year to *D. Herschbach, Y. Lee* and *J. Polanyi* for their work on the dynamics of chemical reactions underlines this view of the importance of reaction kinetics.

J. H. van't Hoff's "Etudes de dynamique chimique" was published in 1884. These studies of the dynamics of chemical processes are probably the first comprehensive account of reaction kinetics. It is a happy circumstance that this classic work has now been published again (for the first time in German), and it provides a good opportunity to look back on 100 years of growth in the quantitative understanding of chemical reactions, an understanding which, as indicated above, is still open to much further improvement.

Van't Hoff's studies were published at a time when the atomic theory had become common ground to (almost) all chemists, and when thermodynamics was slowly beginning to establish a foothold in chemistry. The measurements by *Wilhemy* on the time-dependence of the inversion reaction in cane sugar, which constitute the first ever study of reaction kinetics in the modern sense, had been made about thirty years previously.

The book begins with a quantitative description of the time-scale of chemical reactions, under the following headings:

Normal reactions: unimolecular, bimolecular, multimolecular—in each case with examples of suitably chosen reactions from the known chemistry of the day, whose kinetics were carefully measured by the author and his collaborators, presented to the reader in such a way that he could follow the evaluation of the data.
Factors influencing reactions: a section which is still as relevant today as then, and from which *van't Hoff*'s working methods and experimental techniques come out especially clearly.
Applications: this section is concerned with "multimolecular" reactions and the use of rate measurements to derive reactant properties. In studying reactions of the type $4\,AsH_3 \rightarrow As_4 + 6\,H_2$, it occurred to *van't Hoff* that "the majority of these (chemical) equations give only a very distorted idea of the mechanism of the reaction ... and the actual mechanism is nearly always uni- or bimolecular". Unfortunately this point does not appear to have become more widely understood at the time.

The effect of temperature on chemical reactions, in terms of the (correct) thermodynamic expressions for temperature dependence of rate constants, is given in this section, and the essential features of the theory of thermal explosions are presented through discussion and diagrams. This too did not become a part of generally accepted knowledge until much later.

The second half of the book is concerned with chemical equilibria, vaporization equilibria, and other matters. Included here are the effects of external variables on such equilibria, and chemical affinity, topics which are still associated today with the name of *van't Hoff*. He introduced the use of twin arrows for describing a chemical equilibrium, to indicate "that the chemical reaction proceeds in two opposing directions simultaneously".

Many of *van't Hoff*'s ideas which are recorded in his "Etudes" were of a pioneering nature, and are now generally accepted knowledge, and some could have been written today. Just a few of these will be cited here, either literally or in summarized form. Time plays a special role in the chemist's thinking, it is usually not perceived. *Van't Hoff* thus concentrated on studying those reactions whose progress could be directly followed. "Reactions which occur in immediate succession or simultaneously make the process complicated, and these must be avoided in order to obtain a clearer understanding of reactions." He thereby defined a problem which still concerns reaction kineticists today. For simple reactions he states the important principle that "The progress of a chemical reaction is characterized entirely by the number of molecules whose interaction produces that reaction."

The extent to which he contributed to ideas about detailed reaction mechanisms does not emerge from the text of this book. In 1884 his papers on the size and shape of molecules had already been published ten years before. Possibly he held back from discussing this topic because conclusive experiments had only been carried out much more recently.

Since 1884 chemists have been able to obtain much further insight into the progress of chemical reactions. Numerous proposed models have been investigated, and in many cases have had to be rejected. The desire which is expressed in the Pimentel Report, perhaps almost impatiently, for more progress in "Understanding chemical reactivity", shows that *van't Hoff*'s view that "the understanding of chemical reactions has not yet been put on to such a firm basis as that of thermodynamics" is still relevant 100 years later. Nevertheless the prospects for attaining this objective have never been so good as they are today.

Herr *L. Dunsch* deserves praise for his translation, and for his explanatory notes to the German edition.

Heinz-Georg Wagner [NB 818 IE]
Institut für Physikalische Chemie
der Universität Göttingen (FRG)

Aspects of Chemical Evolution. XVIIth Solvay Conference on Chemistry. Edited by *G. Nikolis*. Wiley, Chichester 1985. xvi, 286 pp., bound, £ 52.25.—ISBN 0-471-88405-7

The international physics and chemistry institutes founded in 1912 by the Belgian industrialist *Ernest Solvay* can be viewed as unique catalysts in the development of modern science. With a minimum of organization these famous institutes have succeeded again and again up to the present day in bringing together prominent scientists from every conceivable discipline to discuss their work, thereby providing a significant impetus for the progress of science.

The seventeenth Solvay Conference on Chemistry, which was held jointly with the US National Academy of Sciences on the occasion of the 150th anniversary of the Belgian state, was concerned with the current research situation in chemical evolution, a fundamental problem area of modern science, whose development has been greatly influenced by the theoretical work of the Director of the Solvay Institutes, Professor *I. Prigogine*.

This volume in the series "Advances in Chemical Physics" contains the lectures presented by the international experts, together with a brief look back at the history of the Solvay Institutes (*E. Amaldi* and *A. R. Ubbelohde*) and an introduction by *I. Prigogine* on the theme "Nonequilibrium Thermodynamics and Chemical Evolution". We find brilliant essays on "Atmospheric Chemistry" *(M. Nicolet)*, "The Prebiotic Synthesis of Organic Molecules and Polymers" *(S. L. Miller)*, "The Origin and Evolution of Life at the Molecular Level" *(M. Eigen)*, "Optimization of Mitochondrial Energy Conversions" *(J. W. Stucki)*, "Bifurcations and Symmetry Breaking in Far-from-Equilibrium Systems: Towards a Dynamics of Complexity" *(G. Nicolis)*, "Bifurcation in Insect Morphogenesis" *(S. A. Kauffman)*, and "Logical Description, Analysis, and Synthesis of Biological and other Networks Comprising Feedback Loops" *(R. Thomas)*. The volume also includes brief commentaries on problems of chirality, stochastic models, and oscillatory chemical systems. Altogether, this volume truly reflects the breadth of the interdisciplinary fields which are now involved in research on chemical evolution.

Benno Hess [NB 814 IE]
Max-Planck-Institut
für Ernährungsphysiologie, Dortmund (FRG)

A Dictionary of Scientific Units. By *H. G. Jerrard* and *D. B. McNeill*. Chapman, London 1986. ix, 222 pp., paperback, £ 8.95.—ISBN 0-412-28100-7

Did you know the following?
that the name of the French physicist *Jean Baptiste Biot* (1774–1862) has been used no less than three times to describe physical quantities: 1. in the CGS electromagnetic system as the unit of electric current; 2. as a CGS unit of rotator strength, which is a quantity used in describing circular dichorism; 3. as a name for the dimensionless coefficient which characterizes heat transfer between a mobile fluid and a solid surface (now superseded by the Nusselt number)
that Kelvin is not only the name of the SI unit of temperature, but can also be used as a synonym for kilowatt-hour
that the centimeter can be an electromagnetic unit (10^9 cm = 1 henry), an electrostatic unit (9×10^{11} cm = 1 farad), or a unit of length (10^2 cm = 1 m)
that four names have been suggested for the unit of wave number: Balmer, Rydberg and Kayser for cm^{-1}, and permicron for μm^{-1}.

I did not know these facts before opening this dictionary of scientific units, dimensionless numbers, and scales of measurement. This book, having been originally published in 1963, is now appearing in its fifth edition, and contains definitions of more than 850 words, often with the addition of brief historical notes. The introduction reminds us that all non-electrical physical quantities can be defined in terms of the three fundamental mechanical quantities mass, length and time, while for electrical or magnetic quantities one additional quantity (current, permeability, or permittivity) is needed. This makes the existence of the vast number of units described in the dictionary all the more remarkable. Following the introduction there is a brief description of twelve systems that have been used in setting up units (e.g. the SI, British Imperial, and Stroud systems).

The main (dictionary) part of the book is followed by an appendix consisting of five sections: values of physical constants given to the degree of precision at present measurable; a list of committees and conferences which concern themselves with problems of standardization, each with a short paragraph on its history and responsibilities; a list of the common weights and measures units used in the USA and Great Britain; conversion tables between units of the following quantities: length, area, volume, angle, time, mass, force, power, energy (work and heat), pressure, resistance, capacitance, inductance, charge, current, potential, magnetic flux, flux density, e.m.f., magnetic field strength, light intensity, illuminance; conversion factors between units of the SI and CGS systems. Finally there follows a somewhat idiosyncratic, but nevertheless clearly arranged, bibliography.

Although the main emphasis in this dictionary is on physics, it also offers much more besides, as can be seen from this short selection of entries: Ångström, ionic strength, Miller indices, pH value, enzyme unit, Michaelis constant, osmolality, turnover number, amu (= Dalton) with the various reference masses used, Bohr magneton, quantum, clo (a unit used to specify heat transmission through a material, 1 clo = 0.154° $cm^2\ W^{-1}$), misery index (suggested by The Times for classifying rainy English summers), paper sizes (A, B, C; 0–6), pica, point (unit used in typesetting), screw threads, mesh size of sieves, trichromatic or T-coefficients (proportions of red, green and blue in a color).

I greatly enjoyed thumbing through this dictionary, but even so I must make two critical comments, the second of which is more serious than the first: 1. The authors' Anglo-Saxon origin is too evident in the book (a very detailed treatment of the "old" weights and measures units; for a unit such as the cubit only its value in inches is given). 2. Not much care has gone into preparing the index; for example, "henry" cannot be found on the given page numbers 113, 125, and 192, but appears instead on p. 188, which is not listed, "kilogram" is not on pp. 183 and 192 but instead is on p. 184, "grain" is not on p. 175 but instead on p. 177, "gauss" is not on pp. 189 and 192 but appears on the again unlisted p. 190. All of these incorrect listings relate not to the main entry for the word in question but, especially irritatingly, to the cross-references, which are sometimes much harder to find.

Despite these criticisms, I recommend this book to all those who encounter many different units in the course of their work, and also to everyone who wants to find a clearer way through the maze of units.

Elisabeth Weber [NB 815 IE]
Weinheim (FRG)

Registered names, trademarks, etc. used in this journal, even when not marked as such, are not to be considered unprotected by law.
© VCH Verlagsgesellschaft mbH, D-6940 Weinheim, 1987. - Printed in the Federal Republic of Germany by Zechnersche Buchdruckerei, Speyer/Rhein.

All rights reserved (including those of translation into foreign languages). No part of this issue may be be reproduced in any form - by photoprint, microfilm, or any other means - nor transmitted or translated into a machine language without written permission from the publishers. Only single copies of contributions, or parts thereof, may be made for personal use.

Valid for users in the USA: The appearance of the code at the bottom of the first page of an article in this journal (serial) indicates the copyright owner's consent that copies of the article may be made for personal or internal use, or for the personal or internal use of specific clients. This consent is given on the condition, however, that the copier pay the stated per-copy fee through the Copyright Clearance Center, Inc., for copying beyond that permitted by Sections 107 or 108 of the U.S. Copyright Law. This consent does not extend to other kinds of copying, such as copying for general distribution, for advertising or promotional purposes, for creating new collective works, or for resale. For copying from back volumes of this journal see 'Permissions to Photo-Copy: Publisher's Fee List' of the CCC.

Editorial office: Pappelallee 3, D-6940 Weinheim, Federal Republic of Germany, Telephone (06201) 602315, Telex 465516 vchwh d, Telefax (06201) 602328.

Editor: *P. Gölitz.*

Associate editors: *D. I. Loewus, A. Stimson.* **Editorial assistant:** *E. Schweikart*

Publishers: VCH Verlagsgesellschaft mbH. (Managing Directors: *Prof. Dr. Helmut Grünewald* and *Hans Dirk Köhler*), Pappelallee 3, D-6940 Weinheim, Federal Republic of Germany. Correspondence concerning advertisements should be addressed to VCH Verlagsgesellschaft mbH. (Advertising Manager *R. J. Roth*), Boschstr. 12, P.O. Box 1260/1280, D-6940 Weinheim, Federal Republic of Germany, Telephone Weinheim (06201) 602-0, Telex 465516 vchwh d, Telefax (06201) 602328.

ANGEWANDTE CHEMIE
International Edition in English
Volume 26 · Number 10
October 1987
Pages 939–1058

Molecular Beam Studies of Elementary Chemical Processes (Nobel Lecture)**

By Yuan Tseh Lee*

Introduction

Chemistry is the study of material transformations. Yet a knowledge of the rate, or time dependence, of chemical change is of critical importance for the successful synthesis of new materials and for the utilization of the energy generated by a reaction. During the past century it has become clear that all macroscopic chemical processes consist of many elementary chemical reactions that are themselves simply a series of encounters between atomic or molecular species. In order to understand the time dependence of chemical reactions, chemical kineticists have traditionally focused on sorting out all of the elementary chemical reactions involved in a macroscopic chemical process and determining their respective rates.

Our basic understanding of the relation between reactive molecular encounters and rates of reactions (formulated in terms of activation energies, E_a, and pre-exponential factors, A, as elucidated by *Arrhenius* in his rate constant expression, $k = A \cdot \exp(-E_a/RT)$), was deepened some fifty years ago following the discovery of quantum mechanics. Since a chemical reaction is fundamentally a mechanical event, involving the rearrangement of atoms and molecules during a collision, detailed information on the dynamics of simple chemical reactions could be obtained by first carrying out extensive quantum-mechanical calculations of the interaction potential as a function of interatomic distances and then computing classical trajectories based on this potential energy surface.[1] Although these initial theoretical studies were only qualitative, they heralded a new era in the field of chemical kinetics; the chemist could now, in principle, predict the dynamical course of a chemical reaction.

During the past three decades, with the development of many sophisticated experimental techniques, it has become possible to study the dynamics of elementary chemical reactions in the laboratory. For example, detailed information on the nascent quantum state distributions of simple products for some chemical reactions can be derived from the chemiluminescence spectra of reaction products obtained under single collision conditions,[2] the analysis of the threshold operating conditions of a chemical laser,[3] or the spectra obtained using various linear or nonlinear laser spectroscopic techniques.[4,5] However, when one desires to (1) control the energies of the reagents, (2) understand the dependence of chemical reactivity on molecular orientation, (3) explore the nature of reaction intermediates and their subsequent decay dynamics, and (4) identify complex reaction mechanisms involving polyatomic radical products, the crossed molecular beams technique is most suitable.[6,7]

Information derived from the measurements of angular and velocity distributions of reaction products played a crucial role in the advancement of our understanding of the dynamics of elementary chemical reactions. This and the more general investigations of chemical reactions under single collision conditions in crossed molecular beams will be the subject of this lecture.

Crossed Molecular Beams Experiments: Measurements of Angular and Velocity Distributions of Products

If the motion of individual atoms were observable during reactive collisions between molecules, it would be pos-

[*] Prof. Y. T. Lee
Department of Chemistry, University of California
Berkeley, CA 94720 (USA)

[**] Copyright © The Nobel Foundation 1987.—We thank the Nobel Foundation, Stockholm, for permission to print this article.

sible to understand exactly how a chemical reaction takes place by just following the motion of these atoms. Unfortunately, despite recent advances in microscope technology that allow us to observe the static arrangement of atoms in a solid, we are still far from being able to follow the motion of atoms in the gas phase in real time. The idea of crossed molecular beams experiments is in a sense to "visualize" the details of a chemical reaction by tracing the trajectories of the reaction products. This is done by first defining the velocities, approach angle, and other initial conditions of the reactants, and then measuring the velocity and angular distributions of the products. For example, in the investigation of reaction (a),[8] if we let F atoms and

$$F + D_2 \longrightarrow DF + D \qquad (a)$$

D_2 molecules collide at a relative energy of 1.82 kcal mol^{-1} and then measure the angular and velocity distributions of DF products, we will obtain the results shown in Figure 1.

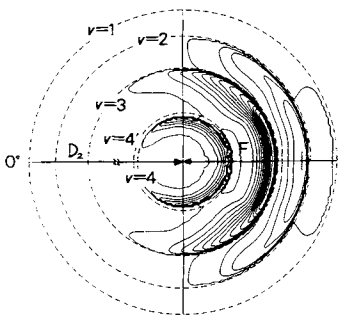

Fig. 1. Center-of-mass velocity flux contour map for reaction (a). F atoms and D_2 molecules move towards each other at a collision energy of 1.82 kcal mol^{-1}, with the F atoms moving from right to left.

This contour map shows the probability of DF products appearing at specific angles and velocities and reveals a great deal about the dynamics of the reaction. 0° corresponds to the initial direction of the F atom beam and the distance between any point and the center is the center-of-mass velocity. The strong backward peaking of DF products with respect to the initial direction of F atoms indicates that not all the collisions between F atoms and D_2 molecules produce DF product. Only those collisions in which the F atom and the two D atoms are nearly linear will react and produce DF. Apparently, if an F atom collides with a D_2 molecule from a direction perpendicular to the molecular axis of the D_2, the F atom will only bounce off elastically. The appearance of DF in several velocity bands (Fig. 1) is due to the fact that DF molecules are produced in several vibrational states (quantum number v) with different recoil velocities as indicated in the figure. Since the total energy released in every reactive encounter between F and D_2 is the same, the maximum energy available for translational motion will depend on the vibrational quantum state of DF. Because the rotational energy spread of DF products is less than the spacings of the vibrational energy levels, the recoil velocities of various vibrational states of DF products are well separated and can be identified easily.

If a crossed molecular beams study of reaction (a) is carried out using the experimental arrangement shown in Figure 2, the rate of production of DF products, dN_{DF}/dt, in

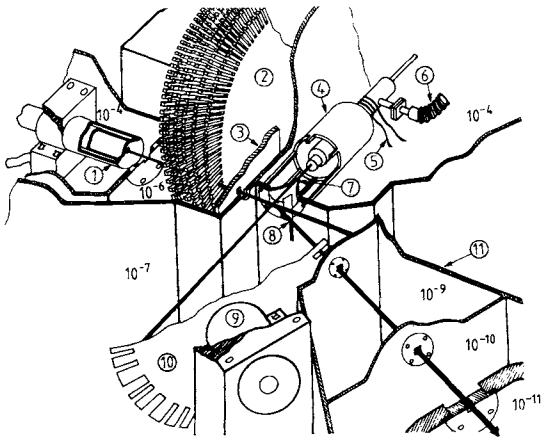

Fig. 2. Experimental arrangement for $F + D_2 \rightarrow DF + D$ and $F + H_2 \rightarrow HF + H$ reactive scattering. Pressures (in torr) for each region are indicated. Components shown by numbers are: (1) effusive F-atom beam source made of nickel, resistively heated; (2) velocity selector; (3) liquid-nitrogen-cooled cold trap; (4) D_2 or H_2 beam source, supersonic expansion; (5) heater; (6) liquid-nitrogen feed line; (7) skimmer; (8) tuning-fork chopper; (9) synchronous motor; (10) cross-correlation chopper for time-of-flight velocity analysis; (11) ultrahigh vacuum, triply differentially pumped, mass-spectrometric detector chamber.

the scattering volume defined by the crossing of two beams can be estimated from Equation (1), where n_F and n_{D_2} are

$$\frac{dN_{DF}}{dt} = n_F n_{D_2} \sigma g \Delta V \qquad (1)$$

the number densities of F atoms and D_2 molecules in the scattering region, σ, g, and ΔV are the reaction cross section, the relative velocity between F and D_2, and the scattering volume, respectively. In an experiment using a velocity-selected effusive F-atom source and a supersonic beam of D_2, the values of n_F, n_{D_2}, and ΔV are typically 10^{10} molecules cm^{-3}, 10^{12} molecules cm^{-3}, and 10^{-2} cm^3, respectively. If the relative velocity g between F and D_2 is 10^5 cm s^{-1} and the reactive cross section σ is 10^{-15} cm^2, then dN_{HF}/dt will have a value of 10^{10} molecules s^{-1}. These DF products with various recoil velocities will scatter into a range of laboratory angles. If the DF is scattered fairly evenly within 1 steradian of solid angle in the laboratory and if the movable detector which scans the angular distribution has an acceptance solid angle of 1/3000 steradian (approximately an angular width of 1° in both directions from the detector axis), the detector will receive approximately 3×10^6 DF molecules per second.

This would certainly constitute a large product signal, assuming we were able to count all of these molecules. Indeed, in a reactive scattering experiment using a beam of alkali atoms, surface ionization could be used to detect the alkali-containing product with nearly 100 percent efficiency and with high specificity. Therefore, even in the presence of a billion times more background molecules, very good signal-to-noise ratios can be obtained in a short time.

To detect the DF products, however, first it is necessary to ionize DF to $DF^{\oplus}$ by electron bombardment. The product ion can then be mass filtered and counted. The typical ionization efficiency for a molecule during the short transit time through the ionizer is about 10^{-4}. 3×10^6 DF s^{-1} reaching the detector will yield only 300 $DF^{\oplus}$ ions s^{-1}. However, this is a large enough number to allow reliable measurements of angular and velocity distributions in a relatively short time if the background count rate is not much greater. Indeed, the success of a crossed molecular beams study of such a chemical reaction depends entirely on whether the background in the mass-spectrometric detector can be reduced sufficiently.[9]

There are two sources of background molecules in the detector that one has to deal with in a crossed molecular beams experiment: the inherent background in the detector chamber and the background caused by the effusion of molecules from the collision chamber into the detector when the beams are on. The former is mainly due to outgassing from the materials used for the construction of the chamber and to limitations imposed by the performance of the ultrahigh vacuum pumping equipment. Reduction of the latter requires many stages of differential pumping using buffer chambers. 3×10^6 molecules s^{-1} entering the detector with a speed of 10^5 cm s^{-1} through a 0.3-cm^2 aperture will establish a steady-state density of only 100 molecules cm^{-3}, which is equivalent to a DF pressure of about 3×10^{-15} torr. This is four orders of magnitude lower than the pressure attainable using conventional ultrahigh vacuum techniques. Since none of the chemical compounds found in a vacuum system give ions with a mass-to-charge ratio (m/z) of 21 ($DF^{\oplus}$) in the ionization process, inherent background will not be a problem for the investigation of reaction (a) even if the ultimate pressure of the detector chamber is around 10^{-11} torr.

Suppose the partial pressure of DF background molecules in the collision chamber after the introduction of beams of F atoms and D_2 molecules reaches about 10^{-9} torr. Then three stages of differential pumping will be required to obtain a partial pressure of about 10^{-15} torr in the ionizer chamber if the partial pressure of DF is reduced by a factor of 100 in each separately pumped buffer chamber. As long as the inherent background in the detector does not contain the species to be detected, extensive differential pumping appears to be the only thing needed to make reactive scattering experiments feasible. This conclusion is unfortunately not quite correct. In order to detect the scattered products, the defining apertures, which are located on the walls of the buffer chambers of the detector, must be perfectly aligned. This limits the reduction of background that would be possible through many stages of differential pumping since some of the DF molecules in the main chamber moving along the axis of the detector will pass straight through all the defining apertures and into the detector chamber. It is important to understand that no matter how many stages of differential pumping are arranged between the collision chamber and the detector chamber, the number of these "straight through" molecules cannot be reduced.

If all the apertures on the walls of the buffer chambers and the detector chamber have the same area, A, the steady-state density of "straight through" molecules in the detector chamber, n', at a distance d from the entrance aperture of the first buffer chamber can be calculated from Equation (2), where n is the number density of background

$$n' = \frac{nA}{4\pi d^2} \tag{2}$$

molecules in the collision chamber. If d is 20 cm and A is 0.3 cm^2, Equation (3) is obtained. If the partial pressure of

$$n' = \frac{0.3}{4\pi \cdot (20)^2} n \approx 6 \times 10^{-5} n \tag{3}$$

DF background molecules in the collision chamber is 10^{-9} torr, the "straight through" molecules will create a steady-state density of 6×10^{-14} torr, which is 60 times larger than what one hopes to accomplish with three stages of differential pumping. Of course, reduction of the partial pressure of DF molecules in the collision chamber will also reduce the "straight through" background, but increasing the pumping speed in the collision chamber to reduce the partial pressure of DF by several orders of magnitude is simply not a practical solution.

Fortunately, there is a way to reduce this background without substantially increasing the pumping speed in the collision chamber. Recognizing that at a pressure of 10^{-7} torr the mean free path between molecular collisions in the collision chamber is more than 100 m, which is two orders of magnitude larger than the size of a typical scattering apparatus, one realizes that almost all of the "straight through" background will come from those molecules that bounce off the surface which is in the line-of-sight of the detector, and not from gas-phase collisions that occur in the viewing window of the detector. Installing a small liquid-helium-cooled surface opposite the detector and behind the collision region, such that the detector line-of-sight always faces a cold surface, will help to eliminate this background since the surface will trap essentially all condensable molecules that impinge on it.

Since the mid-1960s, many "universal" crossed molecular beams apparatuses have been constructed in various laboratories. Since ultrahigh vacuum equipment available twenty years ago could attain an ultimate pressure of only about 10^{-10} torr, and only two stages of differential pumping were needed to reduce the pressure from 10^{-7} torr in the collision chamber to 10^{-10} torr in the detector chamber, almost all mass-spectrometric detectors with electron-impact ionization were constructed with no more than two stages of differential pumping, the principal exceptions being those built in our laboratory.[10] The failure to recognize that for many chemical species the partial pressure in the detector chamber could be reduced well below the ultimate total pressure through additional differential pumping was part of the reason why many of these apparatuses did not perform optimally.

Direct Experimental Probing of Potential Energy Surfaces

For gaseous rare-gas systems, if the interaction potentials between the atoms are accurately known, all bulk

properties and transport phenomena can be predicted theoretically. Similarly, for a simple atom–molecule reaction, the potential energy surface, which describes the interaction potential as a function of the coordinates of the atoms, will be the basis for the understanding of the detailed dynamics of a chemical reaction.

One of the systems that has attracted extensive attention in both experimental and theoretical efforts during the last fifteen years is reaction (b). In the early 1970s, using quasi-

$$F + H_2 \longrightarrow HF + H \qquad (b)$$

classical trajectory calculations, *Muckerman* derived a semiempirical potential energy surface, known as the Muckerman V surface, which gave results in agreement with all experimental data available at that time.[11] These results included rate constants, vibrational-rotational state distributions obtained from chemical laser and chemiluminescence experiments, as well as product angular distributions obtained from experiment involving reaction (a) (see Fig. 1). The potential energy surface obtained from the ab initio quantum-mechanical calculations[12] was still rather limited at that time, but it did show many important features which were in good qualitative agreement with the Muckerman V surface.

If the Muckerman V surface were sufficiently accurate, it would be possible to carry out scattering calculations using this surface under conditions which could not be easily arranged in the laboratory. This would significantly expand the scope of our understanding of the dynamics of this system. However, the accuracy of the Muckerman V surface depends not only on the reliability of the experimental input used in the derivation of the surface, but also on the applicability of classical mechanics in treating reaction (b). This is certainly a major concern for an H-atom transfer reaction.

One-dimensional quantum calculations on the $F+H_2$ reaction, although not necessarily realistic, had in fact shown the inadequacy of classical mechanics in handling this reaction.[13,14] Quantum effects were, indeed, very important, and in all these calculations strong "resonances" were found in the dependence of reaction probability on collision energy.[15] These resonances were later shown to be due to the formation of "quasi-bound" states in the F-H-H reaction intermediate.[16,17] The $F+H_2$ surface has a barrier in the entrance channel, but there is no attractive well in the intimate region near the transition state. The quasi-bound states in the $F+H_2$ reaction are entirely dynamical in nature. Loosely speaking, the first dynamic resonance is due to the formation of a bound state which is a superposition of $F+H_2(v=0)$ and $HF(v=3)+H$ in the intimate region of chemical interaction.

The discovery of dynamical resonances in the collinear "quantal" calculations of the $F+H_2$ system provided new possibilities for probing the critical region of the potential energy surface more directly. In contrast to most other microscopic experiments, in which the influence of the potential energy surface on the final distribution of products is assessed, the experimental observation of resonances is almost equivalent to carrying out vibrational spectroscopy directly on the reaction intermediate. Thus it should offer a more stringent test of the details of the calculated potential energy surface.[16]

In a three-dimensional quantum scattering calculation of $F+H_2$ on the Muckerman V surface, *Wyatt* et al.[18] have shown that as the collision energy is increased beyond the one-dimensional resonance energy, the resonance does not just disappear but occurs at increasingly larger impact parameters. Consequently, resonances cannot be observed in an experiment in which the reaction cross section is measured as a function of collision energy. On the other hand, if the experiment is carried out at a fixed collision energy, and if the reaction probability is measured as a function of impact parameter, the resonance should be observable. Unfortunately, one has no hope of controlling or measuring the impact parameter *in* a scattering experiment. But, for reaction (b), in which the collinear configuration dominates the reactive scattering at lower collision energies, the scattering angle of HF should depend on the impact parameter. In particular, when a quasi-bound state is formed, if the average lifetime of the F-H-H intermediate is an appreciable fraction of its rotational period, HF produced from the decay of the F-H-H quasi-bound state is expected to scatter in a more forward direction compared to the strongly backward peaked HF produced by direct reaction. One of the unique and most important aspects of the measurement of product angular distributions is that one can use the rotational period of the reaction intermediate, typically 10^{-12}–10^{-13} s to judge the lifetime of the reaction intermediate.[6] If the average lifetime of the intermediate is much longer than the rotational period, the angular distribution of products will show forward–backward symmetry. On the other hand, if the lifetime is much shorter, the asymmetric angular distribution reveals the preferred molecular orientation for the chemical reaction to occur.

Experimental measurements of the laboratory angular distribution and time-of-flight velocity distributions of HF products at a collision energy of 1.84 kcal mol^{-1}, using the experimental arrangement shown in Figure 2, are shown in Figures 3 and 4. The velocity and angular distributions in the center-of-mass coordinate system derived from these experimental results are shown in Figure 5.[19] The enhanced forward peaking in the angular distribution of HF in $v=3$ is a strong indication that quasi-bound states are indeed formed in reaction (b) at this energy, and that they seem to decay exclusively into HF in the $v=3$ state.

For reaction (c), quantal collinear calculations give a very striking result. There is a sharp spike in the $HF(v=2)$

$$F + HD \longrightarrow HF + D \qquad (c)$$

reaction probability near threshold and virtually no other product is formed at higher collision energies up to 0.2 eV. The collinear calculations therefore indicate that the formation of HF in this reaction is dominated by resonant scattering while the DF product is formed by direct scattering. As shown in Figure 6, the product angular distribution of HF measured at a collision energy of 1.98 kcal mol^{-1} indeed shows that most of the signal is in the forward direction as expected, in strong contrast to the DF signal which is formed through direct scattering and is

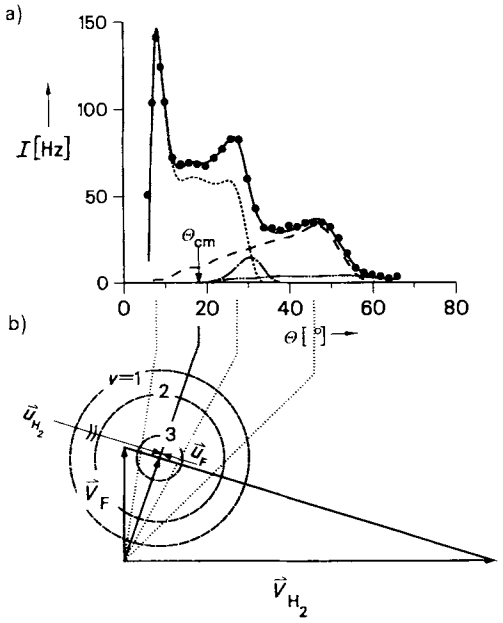

Fig. 3. a) Laboratory angular distribution for F + para-H_2, 1.84 kcal mol^{-1}. b) Velocity diagram. Both the data and calculated laboratory distributions are shown: ● data, — total calculated, — · · · — $v=1$, — — — $v=2$, ------ $v=3$, — · — $v=3'$ (from H_2 ($J=2$). I = signal intensity; Θ_{cm} = laboratory angle of the center-of-mass of the system.

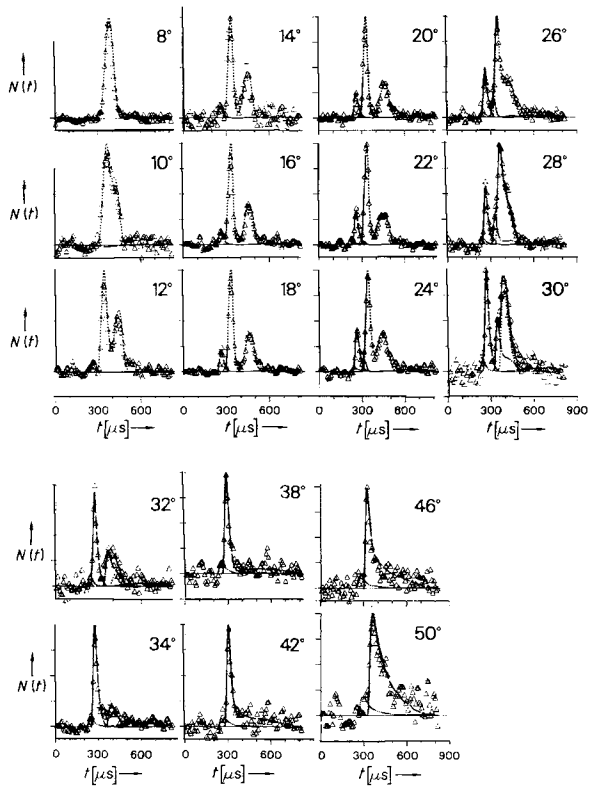

Fig. 4. Time-of-flight spectra for F + para-H_2, 1.84 kcal mol^{-1}: Δ data; for calculated curves, see caption of Fig. 3. $N(t)$ = number of product molecules in arbitrary units.

therefore mainly scattered in the backward direction. Again, the forward-peaked HF products are found to be in the $v=3$ state, rather than $v=2$, as was observed in the quantal calculations on reaction (b). This disagreement is certainly due to the shortcoming in the Muckerman V surface. These vibrationally state-specific angular distributions obtained at various collision energies for F + H_2, HD, and D_2 reactions provide a very stringent test for the ever improving potential energy surfaces obtained from ab initio quantum-mechanical calculations.

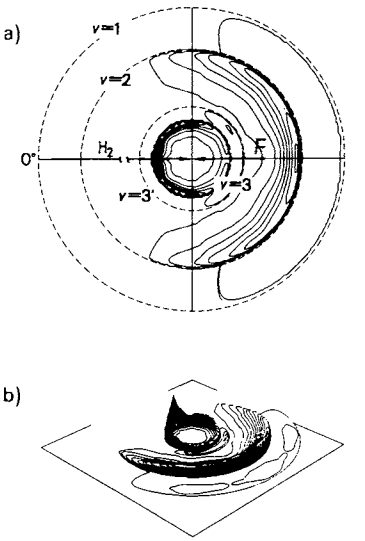

Fig. 5. a) Center-of-mass velocity flux contour map for F + para-H_2, 1.84 kcal mol^{-1}; b) three-dimensional perspective.

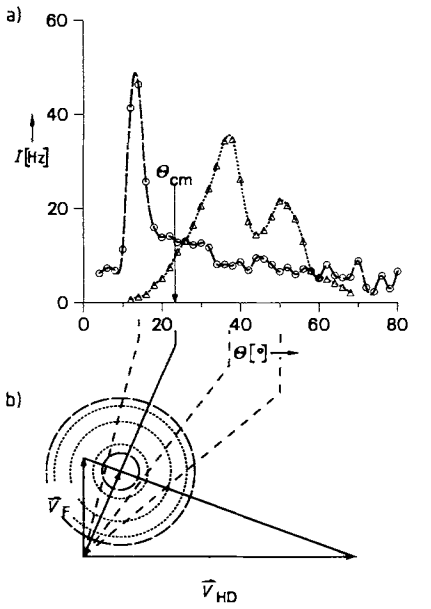

Fig. 6. Laboratory angular distribution for F + HD, at a collision energy of 1.98 kcal mol^{-1} (---O---O--- HF product, · · · · Δ · · · · Δ · · · · DF product). The Newton circles corresponding to HF and DF product are drawn with the same texture as the lines in the angular distributions. The HF($v=3$) and HF($v=2$) circles are shown, as are the $v=4$, 3, and 2 circles for DF.

There is no doubt that through meaningful comparisons with experimental results, more sophisticated and reliable ab initio quantum-mechanical calculation techniques will emerge. In the near future, ab initio calculations of potential energy surfaces and exact scattering calculations on these systems will likely provide more detailed and accurate information on simple reactive systems such as F + H_2 than one could possible learn in the laboratory. The fruit-

ful interplay of theory and experiment will then extend to more complicated systems, making chemistry a more exact science.

Exploration of New Chemistry under Single Collision Conditions

There are many mysterious phenomena in nature which have thus far defied explanation. The mystery is often due to the fact that a certain phenomenon cannot be understood based on our established knowledge or common sense.

The ease with which F_2 and I_2 react to produce electronically excited IF molecules, which relax through photon emission, was a mystery a dozen years ago.[20] A molecule-molecule reaction is supposed to have a high energy barrier and the four-center reaction producing two IF molecules, with either both in the ground state or one of them in an excited state, is a symmetry-forbidden process. The textbook mechanism has either I_2 or F_2 molecules first dissociating into atoms followed by the radical chain reactions (d) and (e). However, neither of these reactions is exothermic enough to produce electronically excited IF.

$$F + I_2 \longrightarrow IF + I \quad (d)$$
$$I + F_2 \longrightarrow IF + F \quad (e)$$

The clue that something new might be happening in this reaction was actually discovered in a crossed molecular beams study of reaction (f).[21] When we found that this

$$F + CH_3I \longrightarrow IF + CH_3 \quad (f)$$

reaction proceeded through the formation of a long-lived complex, we began to increase the collision energy to see whether it was possible to shorten the lifetime enough to make it comparable to the rotational period of the CH_3IF complex. If we could estimate the lifetime of the collision complex using the rotational period as a clock, it would be possible to evaluate the stability of this reaction intermediate using statistical theories for the unimolecular decomposition rate constants. At higher collision energies, the angular distribution of products monitored at m/z 146 ($IF^{\oplus}$) showed a peculiar feature which could not possibly be due to IF produced from the $F+CH_3I$ reaction. This was later shown to be from stable CH_3IF produced in the collision volume of the two beams which yielded additional $IF^{\oplus}$ signal after dissociative ionization.

The stable CH_3IF was in fact formed by the reaction of undissociated F_2 in our F-atom beam with CH_3I [reaction (g)]. The threshold E_0 for this reaction was found to be 11

$$CH_3I + F_2 \longrightarrow CH_3IF + F \quad (g)$$

kcal mol^{-1} as shown in Figure 7. The product angular distribution measured at a collision energy of 25.1 kcal mol^{-1} is shown in Figure 8. Since the dissociation energy of F_2 is 37 kcal mol^{-1}, the dissociation energy of $CH_3IF \rightarrow CH_3I + F$ could be as high as 26 kcal mol^{-1} (Fig. 9). This was certainly a surprising result and was entirely unsuspected.

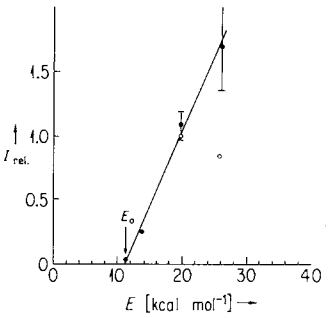

Fig. 7. The kinetic energy dependence of the production of CH_3IF in reaction (g). I_{rel} = amount of CH_3IF in arbitrary units.

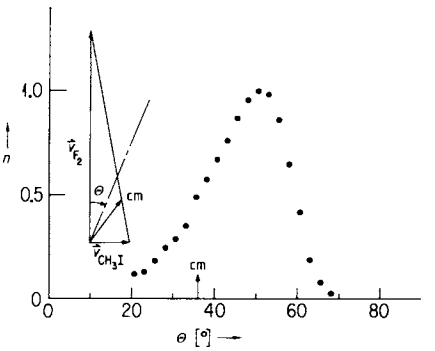

Fig. 8. Laboratory angular distribution of CH_3IF obtained in reaction (g) at a collision energy of 25.1 kcal mol^{-1}. n = number density.

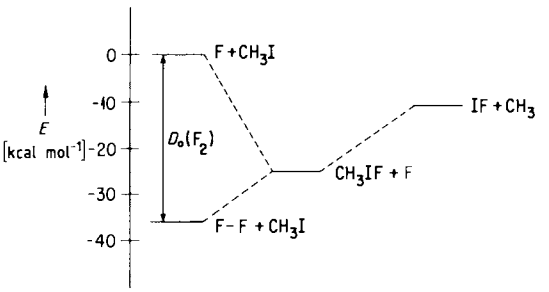

Fig. 9. Energy diagram showing the relative energy of the CH_3IF intermediate formed in reaction (f) and as a product of the endothermic reaction (g).

In the reaction of I_2 and F_2, it was not surprising that the stability of the I_2F radical is the driving force for reaction (h) to proceed. But, what amazed us most was that reaction

$$I_2 + F_2 \longrightarrow I_2F + F \quad (h)$$

(h) had a threshold of only 4 kcal mol^{-1}, and that at 7 kcal mol^{-1} reaction (i) was observed.[22] The production of I

$$I_2 + F_2 \longrightarrow I + IF + F \quad (i)$$

and IF in this reaction is most likely through the secondary decomposition of vibrationally excited I_2F radicals. Later, a careful investigation showed that the threshold energy for producing electronically excited iodofluoride, IF* [reaction (j)],[23] is identical to that for I_2F+F formation

$$I_2 + F_2 \longrightarrow IF^* + IF \quad (j)$$

[reaction (h)]. However, the formation of electronically excited IF* is only a minor channel compared to $I_2F + F$ formation. Apparently, it is a secondary encounter between the departing F atom and the terminal I atom in I_2F which produces IF*. A relatively rare sequential process during a binary collision between F_2 and I_2 is responsible for the production of electronically excited IF, not the symmetry-forbidden four-center reaction which breaks and forms two bonds simultaneously.

The fact that one can control kinetic energy precisely and carry out a synthetic study of delicate new radicals through endothermic reactions is certainly among the most dramatic features of crossed molecular beams experiments. Successful studies of the stabilities of a series of I–F-containing radicals such as HIF, ClIF, and I_2F were carried out by transferring the correct amount of kinetic energy into potential energy, just like an acrobatic performance in a circus in which an acrobat is bounced off of a plank and lands gently on the shoulder of a second acrobat who is standing on top of a third to form a fragile three-acrobat formation (Fig. 10).

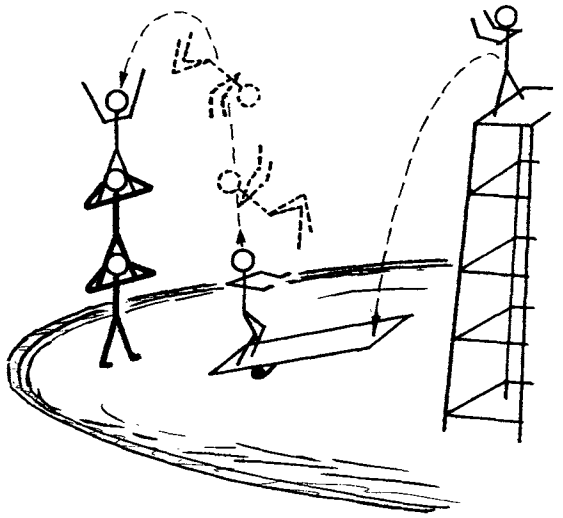

Fig. 10. An acrobat bounced off the plank converts his kinetic energy into potential energy on his way to forming a delicate three-man formation. Many delicate radicals that cannot be synthesized through exothermic channels were synthesized by this method.

The development of the seeded supersonic beam source has been largely responsible for making crossed molecular beams experiments at higher collision energies possible.[24] If a gaseous mixture is expanded into a vacuum chamber through a small nozzle with a sufficiently high stagnation pressure, all molecules, regardless of their molecular weights, attain the same average terminal speed. Consequently, the kinetic energies of molecules in the beam will be proportional to their molecular weights, and for heavier atoms or molecules a very high kinetic energy can be obtained by seeding a small fraction of heavy particles in a very light carrier gas.

Using this aerodynamic acceleration for heavier particles many interesting experiments have been carried out in our laboratory. In the collision-induced dissociation of alkali halides by rare-gas atoms,[25] it was found from classical trajectory simulations of velocity and angular distributions of the products that, for most dissociative collisions at energies near the dissociation threshold, the most efficient means of transferring translational energy into internal energy is through initial bond compression in near collinear collisions. The experimental angular and velocity distributions of $Rb^{\oplus}$ and $I^{\ominus}$ from reaction (k) at a collision

$$Xe + RbI \longrightarrow Xe + Rb^{\oplus} + I^{\ominus} \qquad (k)$$

energy of 5.97 eV are shown in Figure 11. The amount of energy transferred as measured from the final translational energy distributions of dissociated atoms agrees with the estimated initial momentum transfer to one of the atoms in the diatomic molecule using the impulse approximation.

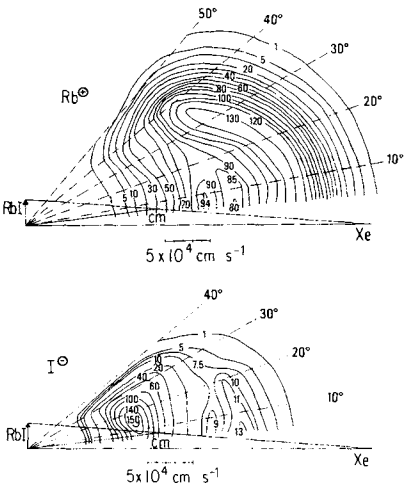

Fig. 11. Cartesian contour map of $Rb^{\oplus}$ and $I^{\ominus}$ angular and velocity distributions resulting from dissociative Xe + RbI collisions at a most probable relative collision energy of 5.97 eV.

In a recent series of investigations of substantially endothermic reactions of Br atoms with *ortho-*, *meta-* and *para*-chlorotoluenes, a beam of energetic Br atoms was used to study the reactivity and dynamics of Cl-atom substitution by Br atoms.[26] The intermediates of these reactions are expected to have potential wells that are much shallower than the endothermicity of reaction. From the measurements of the translational energy dependence of the reaction cross sections and the product translational energy distributions, the extent of energy randomization among various vibrational degrees of freedom was found to be rather limited. Despite the fact that *ortho-* and *para*-chlorotoluenes react easily, no substitution was observed for *meta*-chlorotoluene, indicating that the electron density distribution on the benzene ring strongly influences the reactivity, even though dynamic factors are expected to be more important in endothermic substitution reactions.

Elucidation of Reaction Mechanisms from Product Angular and Velocity Distributions

In elementary chemical reactions involving complicated polyatomic molecules, the unraveling of the reaction

mechanism is often the most important issue. Without the positive identification of primary products, it is not possible to discuss reaction dynamics in a meaningful way. In bulk experiments, the identification of primary products has often been complicated by fast secondary reactions of primary products. Recently, advances in sensitive detection methods and time-resolved laser techniques have allowed single collision experiments to become possible even in the bulk, and complications caused by secondary collisions can be avoided. However, the positive identification of internally excited polyatomic radicals produced under single collision conditions is still a very difficult problem. Spectroscopic techniques, which are so powerful in providing state-resolved detection of atoms or diatomic molecules, are often not very useful, either because of the lack of spectroscopic information or simply because huge numbers of states are involved. The more general mass-spectrometric technique, which depends heavily on "fingerprints" of fragment ions for positive identification, also suffers from the fact that fragmentation patterns for vibrationally excited polyatomic radical products in electron-bombardment ionization are not known. This problem is especially serious because many radicals do not yield parent ions. Even if stable molecules are formed as products, the change in fragmentation patterns with increasing internal energy can be so drastic that erroneous conclusions are often reached. For example, at room temperature both ethanol (C_2H_5OH) and acetaldehyde (CH_3CHO) will yield $C_2H_5OH^{\oplus}$ and $CH_3CHO^{\oplus}$ as major ions by electron-bombardment ionization. However, since both these ions contain a very weak bond and most of the vibrational energy is retained in the ionization process, when highly vibrationally excited C_2H_5OH and CH_3CHO are ionized, even if parent ions are initially produced, they will further dissociate into $C_2H_5O^{\oplus}$ and $CH_3CO^{\oplus}$ by ejecting an H atom.[27]

The problem of product identification caused by the fragmentation of primary products during the ionization process can be overcome if product angular and velocity distributions are measured carefully in high-resolution crossed molecular beams experiments. For example, the reaction between $O(^3P)$ and C_2H_4 under single-collision conditions using a mass spectrometer to detect the products generates signals at *m/z* 43, 42, 29, 27, and 15. The fact that *m/z* 15 ($CH_3^{\oplus}$) and 29 ($HCO^{\oplus}$) are the most intense signals suggests that $CH_3 + HCO$ is the major reaction channel. This conclusion is in agreement with previous studies of the reaction of $O(^3P)$ with C_2H_4 carried out by *Cvetanovic*,[28] *Pruss* et al.,[29] and *Blumenberg* et al.[30] From the analysis of final products in a bulk experiment using photoionization detection of products with hydrogen Lyman-α (10.2 eV) radiation and electron-bombardment ionization mass spectrometry, it was concluded that formation of CH_3 and HCO, resulting from 1,2 migration of a hydrogen atom in the reaction intermediate and subsequent C-C rupture, as shown in reaction (l), provides

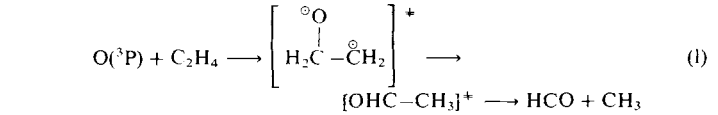

$$O(^3P) + C_2H_4 \longrightarrow \left[\begin{array}{c} {}^{\ominus}O \\ | \\ H_2C-\overset{\oplus}{C}H_2 \end{array}\right]^{*} \longrightarrow [OHC-CH_3]^{+} \longrightarrow HCO + CH_3 \qquad (l)$$

90 percent of the products. The remaining 10 percent is ketene formed by a three-center elimination of an H_2 molecule from the reaction intermediate [reaction (m)].

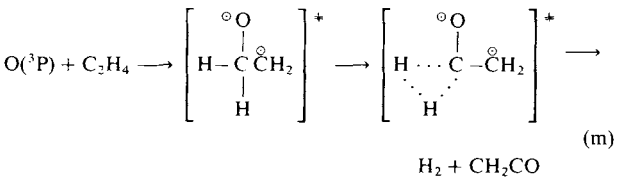

$$O(^3P) + C_2H_4 \longrightarrow \left[\begin{array}{c} {}^{\ominus}O \\ | \\ H-C\overset{\oplus}{C}H_2 \\ | \\ H \end{array}\right]^{*} \longrightarrow \left[\begin{array}{c} {}^{\ominus}O \\ | \\ H\cdots C-\overset{\oplus}{C}H_2 \\ \vdots \\ H \end{array}\right]^{*} \longrightarrow H_2 + CH_2CO \qquad (m)$$

The measurements of product angular distributions in a crossed molecular beams experiment,[31] as shown in Figure 12, gave strong evidence that the above conclusion was not quite correct. The fact that the intense *m/z* 42 signal and the weak *m/z* 43 signal (not shown) have the same angular distributions indicates that the substitution reaction forming vinyloxy radical occurs [reaction (n)]. The *m/z* 42

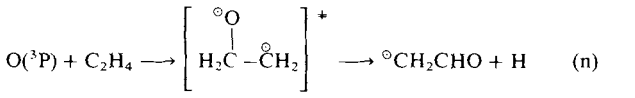

$$O(^3P) + C_2H_4 \longrightarrow \left[\begin{array}{c} {}^{\ominus}O \\ | \\ H_2C-\overset{\oplus}{C}H_2 \end{array}\right]^{*} \longrightarrow {}^{\ominus}CH_2CHO + H \qquad (n)$$

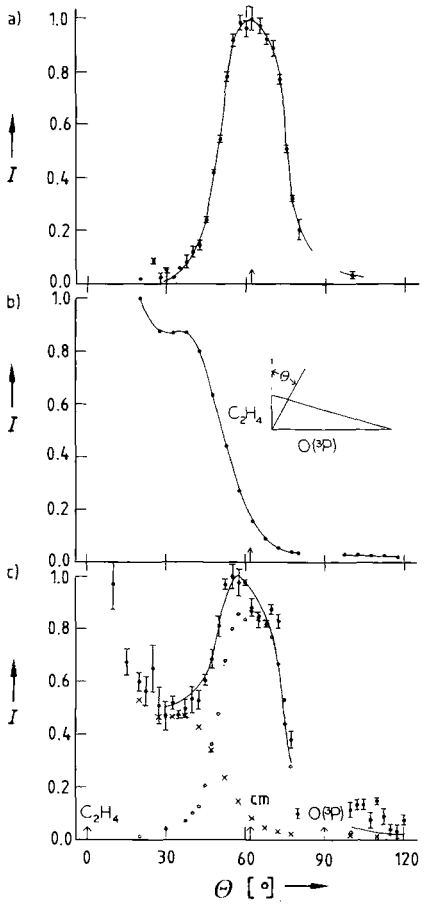

Fig. 12. Laboratory angular distributions from the reaction $O + C_2H_4$ at 10.7 kcal mol^{-1} collision energy. a) CH_2CHO product, monitored at *m/z* 42 ($C_2H_2O^{\oplus}$); b) elastic scattering of C_2H_4 monitored at *m/z* 27 ($C_2H_3^{\oplus}$); c) $CH_3^{\oplus}$ (*m/z* 15, ●), contributions from C_2H_4 and CH_2CHO are indicated by × and ○, respectively.

signal ($C_2H_2O^{\oplus}$) results from dissociative ionization of CH_2CHO product rather than from the formation of CH_2CO and H_2 [reaction (m)]. The formation of CH_2CO through the three-center elimination of a hydrogen mole-

cule is expected to release a larger amount of recoil energy and the fact that CH_2CO is recoiling from H_2 rather than from an H atom will cause the laboratory angular distribution of CH_2CO to be much broader than that of CH_2CHO. The *m/z* 15 ($CH_3^{\oplus}$) angular distribution clearly shows that in addition to reaction products, elastically scattered C_2H_4 molecules also produce $CH_3^{\oplus}$ ions during ionization. The angular distribution of scattered C_2H_4 can be unambiguously measured at *m/z* 27 ($C_2H_3^{\oplus}$). After subtracting the contribution of elastically scattered C_2H_4 from the angular distribution at *m/z* 15, it is quite clear that the residual angular distribution of reactively scattered $CH_3^{\oplus}$ has an identical angular distribution to that measured at *m/z* 43 and 42. Apparently, most of the $CH_3^{\oplus}$ from reactive scattering are also daughter ions of vinyloxy radicals, CH_2CHO. If the product channel $CH_3 + HCO$ were dominant, the angular distribution of $CH_3^{\oplus}$ would be much broader. Without the measurement of product angular or velocity distributions, which reveal the parent-daughter relations, one would not have suspected that the simple substitution reaction (n) forming vinyloxy radical is in fact the major channel.

This was certainly a shocking discovery to chemical kineticists, since the mechanism of reaction (l) was thought to be well established. The important role played by the $CH_2CHO + H$ channel was never suspected. Several recent bulk studies using various time-resolved spectroscopic techniques[32-36] have verified the major role played by the hydrogen-substitution channel indicated by the crossed molecular beams experiments. These were not strictly single-collision experiments, but all showed that the reaction channel $CH_2CHO + H$ accounted for at least half of the products.

For the reaction of oxygen atoms with benzene the story is quite similar.[37] In earlier mass-spectrometric studies of the reaction products under single-collision conditions, it was concluded that in addition to the formation of a stable addition product, CO elimination from the reaction intermediate to form C_5H_6 was another major pathway. The CO elimination mechanism was mostly based on the experimental observation that *m/z* 66 and 65 ($C_5H_6^{\oplus}$ and $C_5H_5^{\oplus}$) were the most intense signals. However, the angular distribution of products monitored at *m/z* 66 and 65 in the crossed molecular beams experiments clearly show that they are different from each other but very similar to those monitored at *m/z* 94 and 93 ($C_6H_5OH^{\oplus}$ and $C_6H_5O^{\oplus}$), respectively. Apparently, the $C_5H_5^{\oplus}$ ions observed are not from neutral C_5H_5 product, but are actually daughter ions of the phenoxy radical C_6H_5O. The fact that the very weak signals at *m/z* 94 and 93 have different angular distributions, as also reflected in the angular distributions of *m/z* 66 and 65 shown in Figure 13, is convincing evidence that the *m/z* 93 signal ($C_6H_5O^{\oplus}$) is not entirely from the dissociative ionization of the addition product, C_6H_5OH. It is the substitution reaction, in which an oxygen atom replaces a hydrogen atom in the benzene molecule, which causes the angular distribution of the phenoxy product, C_6H_5O, to be broader than that of the adduct, C_6H_5OH. The benzene ring does not seem to open up after the initial attack of an oxygen atom. The subsequent decomposition of phenoxy radicals appears to be the important ring-

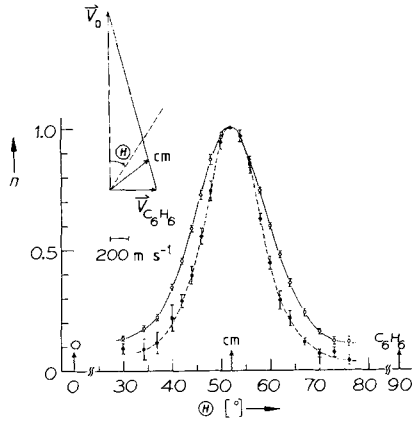

Fig. 13. Laboratory angular distributions from the reaction $O(^3P) + C_6H_6$, at a collision energy of 6.5 kcal mol^{-1}. The primary reaction products formed were C_6H_5O and C_6H_5OH, which subsequently fragmented during electron-bombardment ionization to give $C_5H_5^{\oplus}$ (*m/z* 65, ○) and $C_5H_6^{\oplus}$ (*m/z* 66, ●), respectively.

opening step. Crossed beams studies of substitution reactions of oxygen atoms with a series of halogenated benzenes[38] indeed showed that very highly vibrationally excited phenoxy radicals, produced by substituting bromine and iodine atoms in bromo- and iodobenzene with oxygen atoms, undergo decomposition to eliminate CO.

The fact that each product in a crossed molecular beams experiment has a unique angular and velocity distribution and the requirements that total mass number in a chemical reaction be conserved and that a pair of products from a given channel have the ratio of their center-of-mass recoil velocities inversely proportional to their mass ratio in order to conserve linear momentum are three of the main reasons why measurements of product angular and velocity distributions are so useful in the positive identification of reaction products, even in those cases where none of the products yield parent ions in mass-spectrometric detection.[9] In fact, there is no other general method more useful in elucidating complex gas-phase reaction mechanisms and providing information on the energetics and dynamics.

Molecular Beam Studies of Photochemical Processes

In the investigation of reaction dynamics, lasers have become increasingly important. Not only are they used extensively for the preparation of reagents and quantum-state-specific detection of products, but they have also become indispensable for the investigation of the dynamics and mechanisms of photochemical processes.

One of the more exciting applications of lasers in crossed molecular beams experiments is the control of the alignment and orientation of electronically excited orbitals before a reactive encounter. For example, in the reaction of Na with O_2,[39,40] if linearly polarized dye lasers are used to sequentially excite Na atoms from the 3S to 3P to 4D states, the electronically excited 4d orbital can be aligned along the polarization direction of the electric field vector of the lasers. Consequently, the effect of the alignment of the excited orbital on chemical reactivity can be studied in

detail by simply rotating the polarization of the lasers with respect to the relative velocity vector.

For many atom–molecule reactions that proceed directly without forming long-lived complexes, for example, $K+CH_3I$, $F+H_2$ and D_2, and $Na(4D)+O_2$, the dependence of chemical reactivity on the molecular orientation can be obtained from measurements of product angular distributions. For symmetric top molecules, control of molecular orientation in the laboratory frame is possible, and careful investigations of the orientation dependence of chemical reactivity have been carried out for many systems. The combination of laser-induced alignment of excited atomic orbitals and measurements of product angular distributions provide the first opportunity for the detailed experimental probing of the correlation between the alignment of the excited atomic orbital and the orientation of the molecule in a reactive encounter between an atom and a molecule.

The experimental arrangement for the reactive scattering of electronically excited Na with simple molecules is schematically shown in Figure 14. Because the radiative lifetimes of electronically excited Na are short, excitation and alignment have to be carried out in the intersection region of the two beams.

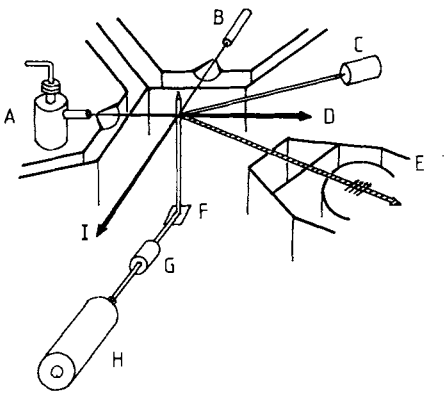

Fig. 14. Cut-out view of the experimental apparatus for the reactive scattering of electronically excited sodium atoms with various molecules. A = Na source, B = molecule source (e.g., HCl), C = fluorescence monitor, D = Na beam, E = rotating mass spectrometric detector, F = mirror, G = polarization rotator, H = dye laser, I = molecule beam.

The reaction of ground state Na atoms with O_2 [reaction (o)] is substantially endothermic. Even if Na is electroni-

$$Na(3S) + O_2 \longrightarrow NaO + O \qquad (o)$$

cally excited to the 3P state, it is still slightly endothermic, and excess translational energy in the reactants was not found to promote NaO formation in our recent experiments. Further excitation of Na from 3P to either the 4D or 5S state, which requires comparable excitation energies, makes NaO formation highly exothermic, but only Na(4D) reacts with O_2 and then only at collision energies greater than 18 kcal mol^{-1}. The NaO produced is sharply backward peaked with respect to the Na-atom beam. As in the low-energy reactive scattering of $F+D_2$ [reaction (a)], the Na(4D) and two O atoms must be lined up collinearly in order for chemical reaction to take place. Such a strict entrance channel configuration with a high threshold energy for $Na(4D)+O_2 \rightarrow NaO+O$ and the lack of chemical reactivity for Na(5S) are quite astonishing for a system in which electron transfer from Na to O_2 is expected to take place at a relatively large separation.

The 4D state of Na prepared by sequential excitation using linearly polarized lasers has an electron-density distribution similar to that of the d_{z^2} orbital in a H atom, if we take the laser polarization axis to be the z axis. Rotation of this excited 4d orbital with respect to the relative velocity vector was found to cause a strong variation in reactivity. The reactively scattered signal reaches a maximum when the d_{z^2} orbital approaches O_2 perpendicularly to the relative velocity vector (Fig. 15). The polarization dependence of products appearing at different scattering angles reflects the strong preference for the d_{z^2} orbital to be aligned perpendicularly to the O_2 molecular axis (Fig. 15b).

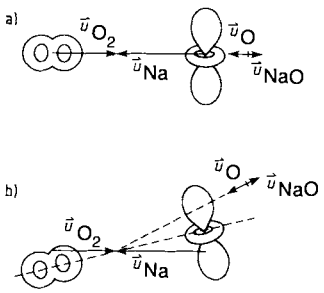

Fig. 15. From the measurements of polarization dependence at various angles, the required geometry for reaction was shown to have the Na–O–O intermediate collinear (a) so that with increasing impact parameter, the Na–O–O axis must be tilted with respect to the relative velocity vector. The Na $4d_{z^2}$ orbital remains perpendicular to the Na–O–O axis as shown (b).

These experimental observations are contrary to what one would expect from simple theoretical considerations. Because O_2 has a finite electron affinity, the $Na(4D)$–O_2 potential energy surface is expected to cross the $Na^{\oplus}$–$O_2^{\ominus}$ surface at a relatively large internuclear distance and the long-range electron transfer from Na(4D) to O_2, to form a $Na^{\oplus}O_2^{\ominus}$ intermediate, should play an important role. If this chemically activated $Na^{\oplus}O_2^{\ominus}$ complex is indeed responsible for the formation of an ionic NaO product, the reaction should proceed with a large cross section at low collision energies. Also, because the most stable structure of $Na^{\oplus}O_2^{\ominus}$ is an isosceles triangle, the angular distribution of the NaO product should show either forward peaking or forward–backward symmetry.

Apparently, this long-range electron transfer, in spite of its importance, is not the mechanism by which NaO product is formed, and may lead only to the quenching of electronically excited Na(4D) through an inelastic scattering process. It appears that only those collinear collisions that have the d_{z^2} orbital of Na(4D) aligned perpendicularly to the molecular axis can effectively avoid the long-range electron transfer. Then, with this configuration and sufficient collision energy, Na and O_2 could follow a covalent surface to reach a very short Na–O distance where the electron from Na(4D) is transferred to an electronically excited orbital of O_2 after which the complex can separate as $Na^{\oplus}O^{\ominus}$ and O.

Reaction (p) is a substantially more exothermic reaction, but it has many features which are similar to those found

$$Na(4D) + NO_2 \longrightarrow NaO + NO \qquad (p)$$

in the $Na(4D) + O_2 \rightarrow NaO + O$ reaction.[41] First of all, the high translational energy requirement, > 18 kcal mol^{-1}, for NaO product formation again indicates that the entrance channel is very restricted and is likely to be along an O–N bond. If a Na(4D) atom must approach an NO_2 molecule along an O–N bond at a high translational energy in order for a chemical reaction to occur, the orbital angular momentum between Na(4D) and NO_2 will overwhelm the molecular angular momentum of NO_2, coplanar scattering will dominate, and NaO product will be scattered in the plane of the NO_2, which also contains the relative velocity vector. In other words, when Na(4D) approaches NO_2 along the NO bond, all the forces between the interacting atoms will lie in the plane of the NO_2, and the scattered NaO will be confined to that plane. Thus, the detector, which rotates in a plane containing both the Na and NO_2 beams, can only detect those NaO products which are produced from NO_2 molecules lying in this plane at the instant when the reactions take place. In contrast to the collinear approach of Na and O_2, there is no cylindrical symmetry about the O–N axis when Na approaches NO_2 along that axis. Because of this, the reaction will depend not only on the d_{z^2} orbital alignment in the plane defined by the beams and the detector, but also on the alignment of the d_{z^2} about the relative velocity vector. This is exactly what we have observed in the laboratory. The reactivity of $Na(4D) + NO_2 \rightarrow NaO + NO$ as a function of the d_{z^2} orbital alignment with respect to the NO_2 molecule is shown in Figure 16. The most favorable approach has the d_{z^2} orbital

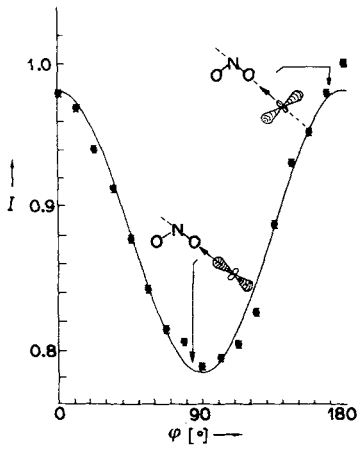

Fig. 16. Polarization dependence of the NaO signal from reaction (p). As the $4d_{z^2}$ orbital of Na was rotated in the plane which contains both beams and the detector, the signal was found to reach a maximum when the $4d_{z^2}$ orbital was perpendicular to the relative velocity vector and reached a minimum when it was parallel.

approaching the O–N axis perpendicularly and lying in the plane of the NO_2. When the alignment of the d_{z^2} orbital is rotated in the plane of the NO_2, the reactivity is reduced as the d_{z^2} orbital comes closer to being collinear with the O–N axis. When the d_{z^2} orbital is rotated out of the NO_2 plane from this collinear configuration, the reactivity decreases further and reaches a minimum when the orbital becomes perpendicular to the NO_2 plane.

The reaction of ground-state Na atoms with HCl is endothermic by 5.6 kcal mol^{-1}. Figure 17 shows the product NaCl angular distributions for Na(3S,3P,4D) at an average collision energy of 5 kcal mol^{-1}. These angular distributions were measured at m/z 23 because most of the NaCl fragments yield $Na^{\oplus}$ in the electron-bombardment ionizer.

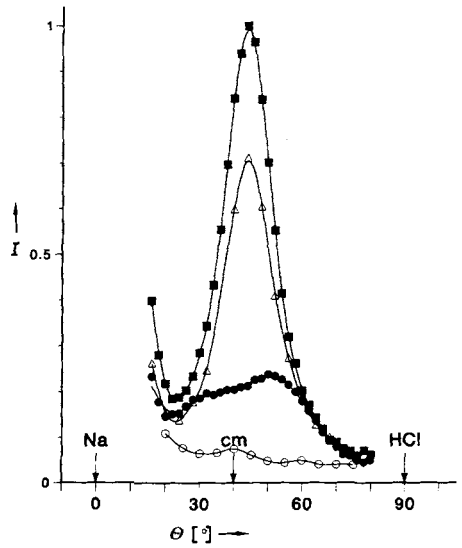

Fig. 17. Laboratory angular distributions for NaCl formed in the reactions of Na(3S) (○), Na(3P) (●), Na(4D) (■), and Na(5S) (△) with HCl at a collision energy of 5.6 kcal mol^{-1}.

The rising signal at low angles is due to elastically scattered Na atoms. The reactive cross section increases with increasing electronic energy. At the collision energy shown, the Na(3S) ground-state atoms react because the high-velocity components of each beam just barely overcome the endothermicity of the reaction. For the reaction of the Na(3P) atoms, NaCl product is observed over the full laboratory angular range possible allowing for the conservation of the momentum and total energy of the system. This implies a broad range of product translational energies, a conclusion which is supported by product velocity measurements. The same is not true of the reaction of the Na(4D) and Na(5S) states, in which the NaCl is scattered over a narrower angular range than that produced from the Na(3P) state, indicating less translational energy despite an additional 2 eV of excess energy. This is illustrated in Figure 18 in which the Na(3P) and Na(4D) angular distributions from Figure 17 have both been normalized.

These interesting results can be explained by invoking electron transfer followed by repulsion of the H atom and NaCl products. HCl is known to be dissociated by slow electrons, and has a *negative* vertical electron affinity of approximately 1 eV. For the reaction of the Na(3P) atoms, this electron transfer becomes energetically possible at 3.5 Å. This is, incidentally, the peak of the Na 3p orbital density. What the departing H atom feels is the repulsion from the Cl atom of the fully developed closed-shell NaCl molecule, and a significant impulse is given to it. In the case of the Na(4D) atoms, the crossing of the neutral and ionic potential curves (the initial point of electron transfer)

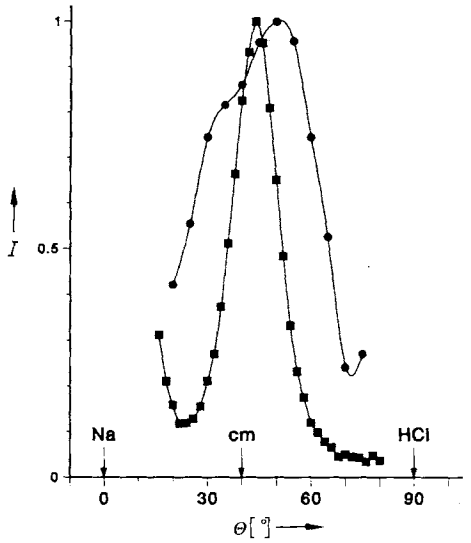

Fig. 18. NaCl angular distributions for the reactions of Na(3P) (●) and Na(4D) (■) with HCl at a collision energy of 5.6 kcal mol^{-1} from Figure 17. The peak intensity of the distribution arising from the reaction of Na(3P) is normalized to that arising from Na(4D) allowing comparison of the angular widths of the two distributions.

moves out to 7.7 Å. Thus, an electron transfers over, $HCl^{\ominus}$ dissociates, the H atom departs, and the $Na^{\oplus}$ and $Cl^{\ominus}$ are drawn together. The highly vibrationally excited NaCl cannot get rid of any of its energy as the H atom is already gone. The H atom has only felt the repulsion of the loosely bound or highly vibrationally excited NaCl. This interpretation is borne out by the polarization measurements in which the favored alignment of the Na 4d orbital for reactive signal at any laboratory detector angle is along the relative velocity vector of the system. This corresponds to pointing the 4d orbital towards the HCl, because at long range the relative velocity vector in the laboratory is from the Na to the HCl.

Such a detailed study of the dependence of reactivity on the orbital alignment and the molecular orientation is possible only by combining the crossed molecular beams method with laser excitation.

Concluding Remarks

The experimental investigation of elementary chemical reactions is presently in a very exciting period. The advancement in modern microscopic experimental methods, especially crossed molecular beams and laser technology, has made it possible to explore the dynamics and mechanisms of important elementary chemical reactions in great detail. Through the continued accumulation of detailed and reliable knowledge about elementary reactions, we will be in a better position to understand, predict, and control many time-dependent macroscopic chemical processes which are important in nature or to human society.

In addition, because of recent improvements in the accuracy of theoretical predictions based on large-scale ab initio quantum-mechanical calculations, meaningful comparisons between theoretical and experimental findings have become possible. In the remaining years of the twentieth century, there is no doubt that the experimental investigation of the dynamics and mechanisms of elementary chemical reactions will play a very important role in bridging the gap between the basic laws of mechanics and the real world of chemistry.

The experimental investigations described in this article would not have been possible without the dedicated efforts of my brilliant and enthusiastic co-workers during the past twenty years. I enjoyed working with them immensely and sharing the excitement of carrying out research together.

I entered the field of reaction dynamics in 1965 as a postdoctoral fellow in the late Bruce Mahan's group at Berkeley, and learned a lot about the art of designing and assembling a complex experimental apparatus from many scientists and supporting staff at the Lawrence Berkeley Laboratory while studying ion-molecule scattering. In February of 1967, I joined Dudley Herschbach's group at Harvard as a postdoctoral fellow. There, I was exposed to the excitement of the crossed molecular beams research and participated in the construction of a universal crossed molecular beams apparatus. Dudley's contagious enthusiasm and spectacular insight motivated not only me, but a whole generation of chemical dynamicists.

Molecular collision dynamics has been a wonderful area of research for all practitioners. This is especially true for those who were following the footsteps of pioneers and leaders of the field twenty years ago. In my early years, I was also inspired by the pioneering research work of Sheldon Datz and Ellison Taylor, Richard Bernstein, John Ross, and Ned Green, as well as the "supersonic" John Fenn. They have been most generous and caring scientists and all of us admire them. Their work is the main reason why the field of molecular beam scattering has attracted many of the best minds in the world and made it a most exciting and rewarding field.

My associations with the University of Chicago (1968–74) and with the University of California, Berkeley (1974–) have been very rewarding. I could not ask for a better environment to pursue an academic career. The stimulating colleagues and excellent facilities as shown in Figure 19 are what made these institutions so wonderful.

Fig. 19. Part of the new molecular beam laboratory at the University of California, Berkeley.

Throughout all these years, my scientific research activities have been supported continuously by the Office of Basic Energy Sciences of the Department of Energy and the Office of Naval Research. The stable and continuing support and the confidence they have shown in my research have been most important and are gratefully appreciated.

Received: February 27, 1987 [A 636 IE]
German version: *Angew. Chem. 99* (1987) 967

[1] H. Eyring, M. Polanyi, *Z. Phys. Chem. B 12* (1931) 279.
[2] J. C. Polanyi, D. C. Tardy, *J. Chem. Phys. 51* (1969) 5717.
[3] J. H. Parker, G. C. Pimentel, *J. Chem. Phys. 51* (1969) 91.
[4] H. W. Cruse, P. J. Dagdigian, R. N. Zare, *Faraday Discuss. Chem. Soc. 55* (1973) 277.
[5] D. P. Gerrity, J. J. Valentini, *J. Chem. Phys. 82* (1985) 1323.
[6] D. R. Herschbach, *Angew. Chem. 99* (1987) No. 12; *Angew. Chem. Int. Ed. Engl. 26* (1987) No. 12.
[7] R. B. Bernstein: *Chemical Dynamics via Molecular Beam and Laser Techniques*, University Press, Oxford 1982.
[8] D. M. Neumark, A. M. Wodtke, G. N. Robinson, C. C. Hayden, K. Shobatake, R. K. Sparks, T. P. Schaefer, Y. T. Lee, *J. Chem. Phys. 82* (1985) 3067.
[9] Y. T. Lee in G. Scoles, U. Buck (Eds.): *Atomic and Molecular Beam Method*, University Press, Oxford 1986.
[10] Y. T. Lee, J. D. McDonald, P. R. LeBreton, D. R. Herschbach, *Rev. Sci. Instrum. 40* (1969) 1402.
[11] J. T. Muckerman in H. Eyring, D. Henderson (Eds.): *Theoretical Chemistry - Advances and Perspectives, Vol. 6A*, Academic Press, New York 1981, pp. 1-77.
[12] C. F. Bender, S. V. O'Neill, P. K. Pearson, H. F. Schaefer III, *J. Chem. Phys. 56* (1972) 4626; *Science (Washington) 176* (1972) 1412.
[13] D. G. Truhlar, A. Kuppermann, *J. Chem. Phys. 52* (1970) 384; *56* (1972) 2232.
[14] S.-F. Wu, R. D. Levine, *Mol. Phys. 22* (1971) 991.
[15] G. C. Schatz, J. M. Bowman, A. Kuppermann, *J. Chem. Phys. 63* (1975) 674.
[16] A. Kuppermann in D. G. Truhlar (Ed.): *Potential Energy Surfaces and Dynamics Calculations*, Plenum, New York 1981.
[17] J. M. Launay, M. LeDourneuf, *J. Phys. B 15* (1982) L455.
[18] R. E. Wyatt, J. F. McNutt, M. J. Redmon, *Ber. Bunsenges. Phys. Chem. 86* (1982) 437.
[19] D. M. Neumark, A. M. Wodtke, G. N. Robinson, C. C. Hayden, Y. T. Lee, *J. Chem. Phys. 82* (1985) 3045.
[20] J. W. Birks, S. D. Gabelnick, H. S. Johnston, *J. Mol. Spectrosc. 57* (1975) 23.
[21] J. M. Farrar, *J. Chem. Phys. 63* (1975) 3639.
[22] M. J. Coggiola, J. J. Valentini, Y. T. Lee, *Int. J. Chem. Kinet. 8* (1976) 605.
[23] C. C. Kahler, Y. T. Lee, *J. Chem. Phys. 73* (1980) 5122.
[24] R. P. Andres, J. B. Fenn, D. R. Miller, *Rarefied Gas Dynamics, Fifth Symp. 1967*, pp. 1317-1336.
[25] F. P. Tully, N. H. Cheung, H. Haberland, Y. T. Lee, *J. Chem. Phys. 73* (1980) 4460.
[26] G. N. Robinson, R. E. Continetti, Y. T. Lee, *Faraday Discuss. Chem. Soc. 84* (1987), in press.
[27] F. Huisken, D. Krajnovich, Z. Zhang, Y. R. Shen, Y. T. Lee, *J. Chem. Phys. 78* (1983) 3806.
[28] R. J. Cvetanovic, *Can. J. Chem. 33* (1955) 1684.
[29] F. J. Pruss, J. R. Slagle, D. Gutman, *J. Phys. Chem. 78* (1974) 663.
[30] B. Blumenberg, K. Hoyerman, R. Sievert, *Proc. XVIth Int. Symp. Combust.* (The Combustion Institute, Pittsburgh 1977), p. 841.
[31] R. J. Buss, R. J. Baseman, G. He, Y. T. Lee, *J. Photochem. 17* (1981) 389.
[32] G. Inoue, H. Akimoto, *J. Chem. Phys. 74* (1981) 425.
[33] H. E. Hunziker, H. Kneppe, H. R. Wendt, *J. Photochem. 17* (1981) 377.
[34] F. Temps, H. G. Wagner, *Ber. Max-Planck-Inst. Strömungsforsch. 1982*, No. 18.
[35] U. C. Sridharan, F. Kaufman, *Chem. Phys. Lett. 102* (1983) 45.
[36] Y. Endo, S. Tsuchiya, C. Yamada, E. Hirota, *J. Chem. Phys. 85* (1986) 4446.
[37] S. J. Sibener, R. J. Buss, P. Casavecchia, T. Hirooka, Y. T. Lee, *J. Chem. Phys. 72* (1980) 4341.
[38] R. J. Brudzynski, A. M. Schmoltner, P. Chu, Y. T. Lee, *J. Chem. Phys. 87* (1987), in press.
[39] H. Schmidt, P. S. Weiss, J. M. Mestdagh, M. H. Covinsky, Y. T. Lee, *Chem. Phys. Lett. 118* (1985) 539.
[40] P. S. Weiss, Ph. D. Thesis, University of California, Berkeley 1986.
[41] B. A. Balko, H. Schmidt, C. P. Schulz, M. H. Covinsky, J. M. Mestdagh, Y. T. Lee, *J. Chem. Phys. 87* (1987), in press.

Some Concepts in Reaction Dynamics (Nobel Lecture)**

By John C. Polanyi*

The objective in this work has been one which I have shared with the two other 1986 Nobel lecturers, *D. R. Herschbach* and *Y. T. Lee*, as well as with a wide group of colleagues and co-workers who have been responsible for bringing this field to its current state. That state is summarized in the title; we now have some concepts relevant to the motions of atoms and molecules in simple reactions, and some examples of the application of these concepts. We are, however, richer in vocabulary than in literature. The great epics of reaction dynamics remain to be written. I shall confine myself to some simple stories.

1. Experimental and Theoretical Approaches

In this section I shall say something about the experimental and theoretical tools we have used, and give some indication of their origins.

Our principal experimental method has been the study of IR chemiluminescence. The most valuable theoretical tool has been, and remains, the computer integration of the classical equations of motion. Though both of these methods belong to the modern period of reaction dynamics, both have clear antecedents in earlier times.

IR chemiluminescence derives from the presence of vibrationally excited molecules in the products of reaction. Indirect evidence for the existence of such species was obtained by *M. Polanyi* and his co-workers in 1928 in the course of studies of the reactions of alkali metal atoms and halogens.[1] Following a suggestion by *Bates* and *Nicolet*[2] and by *Herzberg*,[3] *McKinley*, *Garvin*, and *Boudart*[4] looked for and found visible emission from vibrationally excited hydroxyl radicals formed in the reaction of atomic hydrogen with ozone. This finding was followed soon after by the identification, by absorption spectroscopy, of vibrational excitation in the products of the reactions of atomic oxygen with NO_2 and ClO_2.[5]

Reference [5] appeared in the year that, in collaboration with *J. K. Cashion*, we undertook to look for IR chemiluminescence from vibrationally excited hydrogen halides (and other hydrogen-containing compounds) formed in simple exchange and addition reactions. The first reaction studied was that of atomic hydrogen with molecular halogens.[6,7] IR emission was observed in the region 1.5–4.5 μm arising from the low-pressure ($\approx 10^{-1}$ torr) room temperature reaction

$$H + X_2 \longrightarrow HX^{\dagger} + X \qquad (1)$$

where X was Cl or Br.

At that date there was lively discussion of the possibility of a visible analogue of the maser, that would operate on population-inverted electronic states (a working laser was still in the future).[8] Given our interests it was natural to speculate about the properties of a vibrational laser. In our communication ("Proposal for an Infrared Maser Dependent on Vibrational Excitation")[9] we pointed to a number of virtues of such a device, of which we shall note two here.

(1) Provided that the vibrational temperature, T_V, sufficiently exceeds the rotational temperature, T_R, (both temperatures being positive, in contrast to the negative temperatures associated with population inversion in the discussions of that date), a large number of P-branch transitions will exhibit population inversion (Fig. 1). We gave the name *partial population inversion* to this phenomenon, and noted that lasing based on partial population inversion could ensue shortly after a thermal pulse (arising from a pulsed arc, or shock wave), since "partial cooling" would ensure $T_V \gg T_R$.

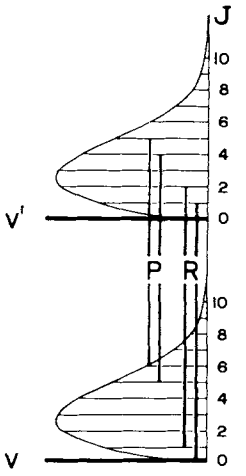

Fig. 1. "Partial population inversion"; $T_V \gg T_R$ (>0) ensures that the population in the upper state, N_u, exceeds that in the optically linked lower state, N_l for the indicated transitions (among others). The condition for lasing, $(N_u/g_u) > (N_l/g_l)$ where g is degeneracy, is only met for the P branch. (From J. C. Polanyi, *Appl. Opt. Suppl. 2* (1965) 109 [10], see also *J. Chem. Phys. 34* (1961) 347 [9b].)

(2) A chemical reaction could be used to obtain either "partial" or "complete" population inversion. We were struck by the fact that the upper atmosphere could constitute a natural laser in the IR favored by its long path length and large number of partially population-inverted transitions.[9,10]

Vibrational lasing was first achieved by *Patel* and coworkers.[11] Chemical reaction as the working material in a vibrational laser followed shortly afterward, through the work of *Pimentel* and his associates.[12] In both cases the major contribution to lasing came from partial population

[*] Prof. J. C. Polanyi
Department of Chemistry, University of Toronto
Toronto M5S 1A1 (Canada)

[**] Copyright © The Nobel Foundation 1987.—We thank the Nobel Foundation, Stockholm, for permission to print this article.

inversion, as indicated by the predominance of P-branch emission.

In our first communication regarding IR chemiluminescence, we expressed the view that the method "promises to provide for the first time information concerning the distribution of vibrational and possibly rotational energy among the products of a three-center reaction."[6] This outcome was not so readily achieved.

By 1962 it was evident that reaction (1), despite the fact that it had proved to be a ready source of IR chemiluminescence, converted its heat of reaction into vibration with the modest efficiency of $\leq 50\%$.[13] This finding met with skepticism, since it was pointed out, correctly, that it implied for the reverse endothermic process that one could have so much vibration in the reagents that the reaction probability would be markedly diminished.[14] The somewhat lame reply at that date was that "though odd, it could still be the case!"[15]

Today we would surmise that it is the case since for the endothermic process $Cl + HCl \rightarrow Cl_2 + H$ a heavy particle (Cl) must approach during the brief time that the H-Cl bond remains extended; too much vibrational excitation can have the consequence that the Cl + HCl interaction is averaged over many vibrational periods, resulting in an "adiabaticity" with respect to the flow of energy into the bond to be broken. At that date the importance of the relative timing of molecular motions (though recognized for other types of inelastic encounters) had not yet been documented for chemical reactions.

It was not until 1967, with the development of the methods of "measured relaxation" (MR)[16] and "arrested relaxation" (AR)[16] that the goals established nine years earlier were truly achieved. The impediment to obtaining full quantitative data by infrared chemiluminescence, or any other means, in regard to what we have termed the "detailed rate constants", $k(V',R')$ (V' is the product vibrational excitation, and R' the product rotational excitation), has been the presence of an undetermined amount of vibrational and rotational relaxation of the reaction product prior to observation.

In the MR approach[16,17-19] this was addressed by measuring the vibrational relaxation at points along the direction of flow, and hence correcting for this effect (see Fig. 2a). In the AR method[16,18-21] relaxation, rather than being measured, was arrested to the fullest extent possible, by the rapid removal of excited products. This was achieved by complete deactivation at a surface, usually cooled in the range 20-77 K (Fig. 2b). Arrest of relaxation yielded detailed rate constants at the level $k(V',R',T')$, where T' is the translational energy distribution in the newly formed product, obtained by subtracting the initial vibrational plus rotational distributions from the total available energy.

Concurrently with the development of these IR chemiluminescence techniques, the crossed molecular beam method was established as a quantitative tool, particularly by *Herschbach* and co-workers. This method obviated problems of relaxation by conducting reaction under single-collision conditions. Since the prime measurables were product angular and translational energy distributions, by 1967 a degree of overlap existed between the approaches. It was not, however, until the incorporation of universal

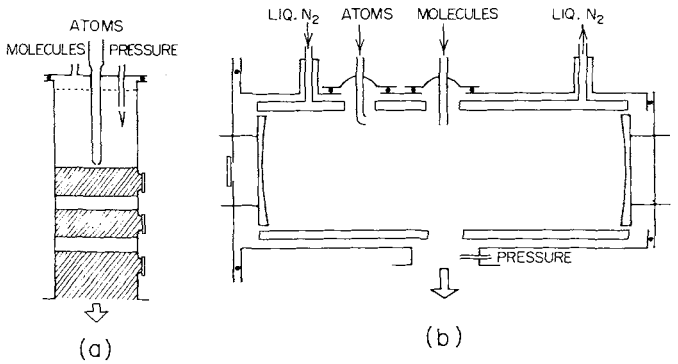

Fig. 2. a) Reaction vessel for "measured relaxation" (MR) (shaded regions indicate internal reflective coating; three sapphire windows at successive sampling points are indicated at the right); b) Reaction vessel for "arrested relaxation" (AR) shown schematically (mirrors at either end of the vessel collect IR radiation and bring it to the sapphire window at the left). (From K. G. Anlauf et al., *Discuss. Faraday Soc. 44* (1967) 183 [16].)

detectors by *Lee* and *Herschbach*, following what we have come to know as the "alkali age" of beam chemistry, that the same systems could be studied by both IR chemiluminescence and molecular beam scattering.

By the time that the first quantitative data began to appear powerful theoretical tools were available which could be used to link the potential field operating between atoms A, B, and C in a reaction

$$A + BC \longrightarrow AB + C \qquad (2)$$

to the motions of the particles. In the original work on the London equation[22] by *Eyring* and *Polanyi*[23] an attempt was made, in collaboration with *Wigner*, to solve the classical equations of motion for the reactive system A + BC. This work was taken up by *Hirschfelder* and *Wigner*,[24] but it was not until the first computer calculations of reaction dynamics by *Wall, Hiller*, and *Mazur*[25] that the full power of the approach became evident.

In parallel with *Blais* and *Bunker*,[26] we[27] employed *Wall, Hiller*, and *Mazur*'s approach in an attempt to map out the major determinants of A + BC reaction dynamics. Both groups were inspired by the proposal made by *M. G. Evans* and *M. Polanyi*,[28] over two decades earlier, that vibration in a newly formed bond might originate from the release of reaction energy as the reagents approached. Detailed computation indicated that this suggestion embodied an important kernel of truth, though the full story, as might have been expected, revealed a substantially richer range of scenarios.

2. Energy Distribution among Reaction Products

2.1. Experiment

In the MR method (see Section 1) several observation windows for recording IR chemiluminescence were located along the line of streaming flow. Provided that the observation windows were situated at distances corresponding to times during which relaxation was moderate, a simple graphical extrapolation back to zero time yielded adequate values for the relative $k(v')$ (v' is the vibrational

quantum number corresponding to the product vibrational energy V').[16,17] Detailed numerical analyses were also made, which included the effects of reaction, diffusion, flow, radiation, and collisional deactivation.[17] A model of this sort permitted, in effect, a more intelligent extrapolation to time $t=0$.

Subsequently, the flow-tube approach was applied to the determination of vibrational energy distributions in a substantial number of IR chemiluminescent reactions, particularly by *Setser* and his co-workers[29] and by *Kaufman*.[30] IR chemiluminescence experiments in flow tubes have also been extended to the elucidation of product energy distributions from ion-molecule reactions.[31]

In the AR method two uncollimated beams of reagent met in the center of a vessel, exhibiting a background pressure, with reagents flowing, of ca. 10^{-4}–10^{-5} torr. Reaction occurred at the intersection of the beams (as demonstrated in Ref. [18]). The products of reaction were transferred, following a few secondary collisions, to a deactivating surface which surrounded the reaction zone. Depending on the reagents, this surface acted as a cryo-pump, as a getter pump (trapping non-condensibles in excess condensible), or simply as an adsorber capable of bringing about complete vibrational deactivation (adsorbing product for a time sufficient to deactivate the material to its ground vibrational state, $v=0$).

The IR chemiluminescence stemming from the small fraction of molecules that emitted early in their lifetimes, was collected by gold front-surface mirrors, freshly coated for each experiment; this procedure increased the effective solid angle being viewed by almost $50\times$.[32] By this means ca. 10^{-9} torr of vibrationally excited product could be detected in one v,J (vibrotational) state, using the liquid-nitrogen-cooled PbS semiconductor detectors that became available in the late 1950s. The emission spectrum (Fig. 3) was recorded in early work on a (NaCl, then LiF) prism spectrometer, later on a grating spectrometer and (from the early 1970s; see, e.g., Ref. [33]) on a variety of Fourier transform interferometric spectrometers.

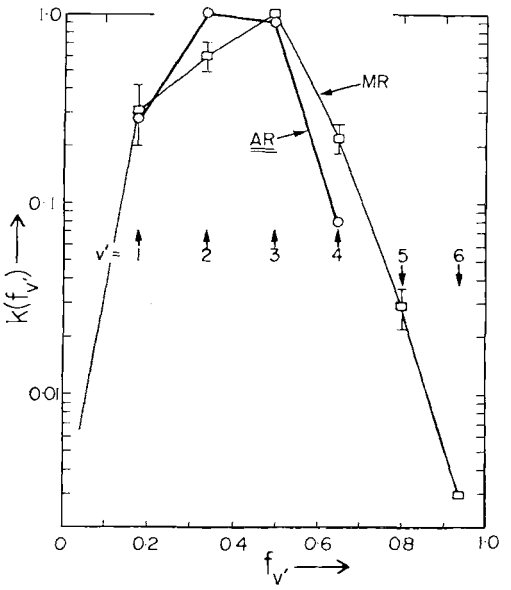

Fig. 3. Semi-logarithmic plot of the probability that a fraction $f_{v'}$ of the energy in the products of the reaction $H+Cl_2 \rightarrow HCl+Cl$ enters vibration in the newly formed bond. The data were obtained independently by the MR and AR methods, as indicated. The vibrational quantum states $v'=1$–6 correspond to the values of $f_{v'}$ indicated by arrows across the center of the figure. (From K. G. Anlauf et al., *Discuss. Faraday Soc. 44* (1967) 183 [16].)

The AR method was adopted by several laboratories, notably *N. Jonathan*'s,[34] *D. W. Setser*'s,[35] and *J. D. McDonald*'s.[36] It is characterized by molecular flow of the reactants and hence low densities in the reaction zone, permitting observation of reaction products with highly non-

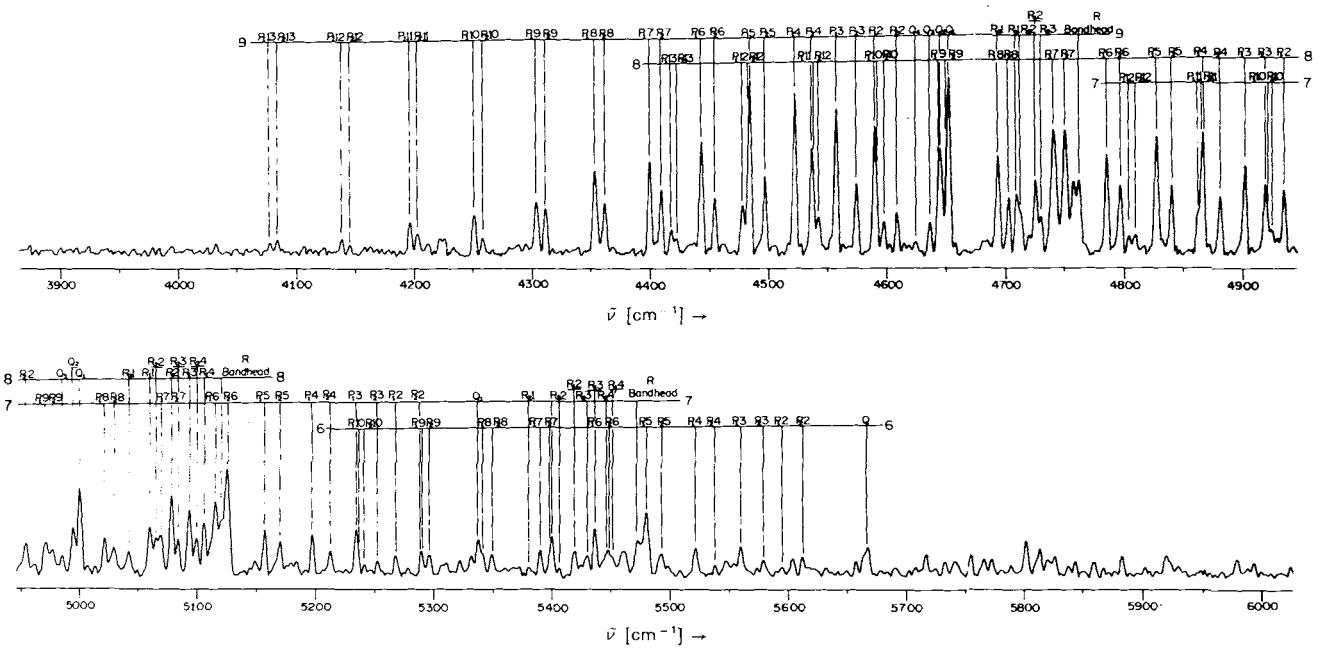

Fig. 4. First-overtone ($\Delta v'=-1$) spectrum of OH formed in the reaction $H+O_3 \rightarrow OH+O_2$, $-\Delta H_0^\circ = 77$ kcal mol^{-1}. Under arrested relaxation conditions, a continuous flow of reagents yields a steady-state distribution of $OH(v')$ that increases with v' up to the highest accessible vibrational level, $v'=9$ ($E(v'=9)=75$ kcal mol^{-1}, i.e., 3.25 eV). This spectrum was recorded by using a Fourier transform spectrometer and AR geometry; emission is from $v'=6$–9 as indicated. (From P. E. Charters et al., *J. Appl. Opt. 10* (1971) 1747 [33]; see also J. C. Polanyi, J. J. Sloan, *Int. J. Chem. Kinet. Symposium 1* (1975) 51.)

Boltzmann rotational distribution, as well as non-Boltzmann vibrational distributions.

The effectiveness of the combination of molecular flow plus rapid removal of reaction products in reducing relaxation to an insignificant amount in the majority of systems studied was indicated by the fact that the steady-state distribution observed under these conditions was in satisfactory agreement with the initial vibrational distribution obtained by the MR method (Fig. 4) and the observed rotational distribution was largely unrelaxed (Fig. 5), indicating that collisional deactivation of vibrators—generally a less efficient process—was insignificant. In the case of a few very fast reactions (notably $F+HBr \rightarrow HF+Br$[29]), $k(v')$ from MR were at variance with those from AR. At the low flows used in the AR machine it appears that reaction and deactivation were occurring within the inlets, invalidating the results;[37] in such a case the AR rotational distributions were also found to have been relaxed.[38]

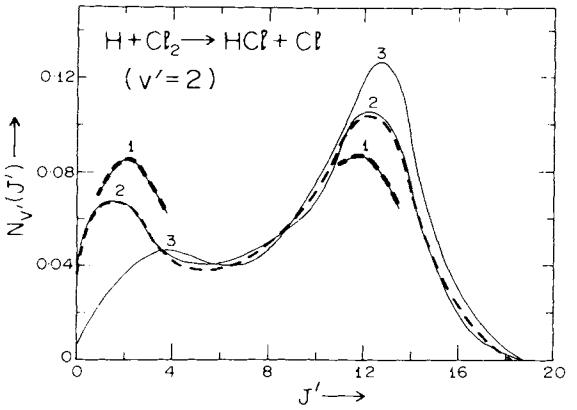

Fig. 5. Solid lines record the decreasing contribution of the peak at low J' to the observed rotational distribution (for $H+Cl_2 \rightarrow HCl(v'=2,J')+Cl$) as the pressure in the beam-crossing region is decreased (in the sequence $3 \rightarrow 2 \rightarrow 1$) in an AR vessel. The broken lines give relaxed distributions computed from 3. (Based on Fig. 1 of J. C. Polanyi, K. B. Woodall, *J. Chem. Phys. 56* (1972) 1563 [39].)

The observed rotational distributions were typically bimodal, comprising a non-thermal distribution at high rotational quantum number (high J') and a thermal distribution peaking at low J'. The contribution of the peak at low J' relative to that at high J' decreased with diminishing pressure in the reaction zone (Fig. 5). Accordingly, the low J' peak was ascribed to collisional relaxation; the relaxation mechanism being analyzed in detail.[39]

Some detailed rate constants, $k(v')$, for the reaction

$$F + H_2 \longrightarrow HF + H \qquad (3)$$

obtained by different procedures and by different workers are given in Table 1. Included among the methods used is one due to *Pimentel* and co-workers which made use of stimulated, rather than spontaneous, IR emission.[34b] This approach was an outgrowth of the first chemical laser, due to the same laboratory.[12] The laser approach[40] gave quantitative data concerning the population in the vibrational ground state $v'=0$, which previously had been unobservable. Also included in Table 1 are the findings from crossed molecular beam studies performed in *Y. T. Lee*'s laboratory.[42a] In these demanding experiments the vibrational distribution was obtained from structure in the product translation energy distribution, which was the measured quantity (the findings are for somewhat different reagent energy distributions than for the other experiments tabulated). The reaction $F+H_2 \rightarrow HF+H$ is of considerable fundamental interest since it involves only eleven electrons, and should therefore be amenable to ab initio computation (see below). The agreement between determinations of $k(v')$ is satisfactory.

When these experiments and those described below were undertaken, quantitative data regarding $k(v')$ did not exist. The prior observation of highly vibrationally excited reaction products in a number of systems, since it was a qualitative finding, left open the question of the form of $k(v')$ which could have peaked anywhere from $v'=0$ to $v'=v'_{max}$ (the highest accessible vibrational state). In fact the distributions observed by IR chemiluminescence were found to peak at intermediate v', so that the mean fraction of the available energy entering vibration in the new bond ranged from $\langle f_{v'}\rangle = 0.39$ for $H+Cl_2$, $\langle f_{v'}\rangle = 0.55$ for $H+Br_2$, $\langle f_{v'}\rangle = 0.53$ for $H+F_2$, and $\langle f_{v'}\rangle = 0.66$ for $F+H_2$ up to $\langle f_{v'}\rangle = 0.71$ for $Cl+HI$ and $\langle f_{v'}\rangle \approx 0.9$ for $H+O_3 \rightarrow OH+O_2$.

An early finding was that the product vibrational energy distribution $k(v')$ altered dramatically with isotopic substitution, but was roughly invariant if represented in the re-

Table 1. Detailed rate constants $k(v')$, for $F+H_2 \rightarrow HF(v')+H$; comparison data from various studies (with some variation in reagent collision energy).

	Collision energy	$v'=1$	$v'=2$	$v'=3$
Parker and Pimentel (1969) [40a]	539 K	0.18	1.00	—
Polanyi and *Tardy* (1969) [84]	300 K	0.29	1.00	0.47
Jonathan et al. (1971) [34b]	300 K	0.28 ± 0.02	1.00	0.58 ± 0.12
Polanyi and *Woodall* (1972) [20]	300 K	0.31	1.00	0.47
Coombe and *Pimentel* (1973) [40b]	236 K	—	1.00	0.505 ± 0.01
	298 K	—	1.00	0.478 ± 0.005
	364 K	—	1.00	0.463 ± 0.006
	172 K	0.222 ± 0.01	1.00	—
	432 K	0.345 ± 0.03	1.00	—
Chang and *Setser* (1973) [35a]	300 K	0.29	1.00	0.56
Berry (1973) [40d]	297 K	0.294 ± 0.01	1.00	0.63 ± 0.04
Perry and *Polanyi* (1976) [47]	279 K	0.28	1.00	0.55
	718 K	0.38	1.00	0.55
	1315 K	0.44	1.00	0.55
Newmark, Lee et al. (1985) [42a]	1.84 kcal mol^{-1}	0.21	1.00	0.67

duced form $k(f_{v'})$.[41] This is what one would expect if classical mechanics applied rather than conservation laws involving quantum states. The finding gave us courage in applying classical mechanics to these reactions (despite the fact that they were characterized by widely spaced vibrational and rotational states), and also encouraged us to record our results in a graphical form that rode roughshod over the quantized nature of $k(v',J')$.

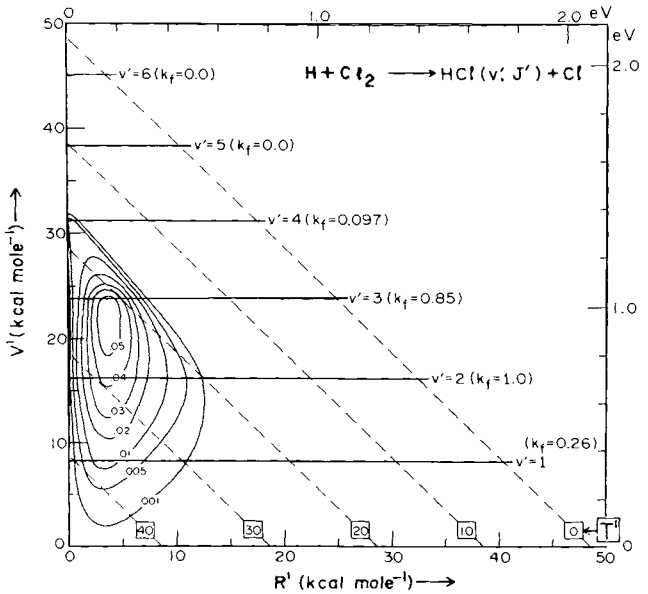

Fig. 6. "Triangle plot" for $H+Cl_2 \rightarrow HCl+Cl$ reaction showing the distribution of vibrational, rotational, and translational energy as contours of equal detailed rate constant $k(V',R',T')$. The ordinate is product vibrational energy, and the abscissa is the product rotational energy. Since the total available energy is approximately constant ($E'_{tot}=48.4$ kcal mol^{-1}), translational energy, T', given by the broken diagonal lines, increases to 34 kcal mol^{-1} at $V'=0$, $R'=0$. The rate constant $k_f \equiv k(v')=\Sigma_{J'}k(v',J')$; the subscript f denotes the "forward," exothermic, direction. Contours have been normalized to $k(v')=1.00$ where v' is the most populated vibrational level. (From K. G. Anlauf et al., *J. Chem. Phys.* *57* (1972) 1561 [19].)

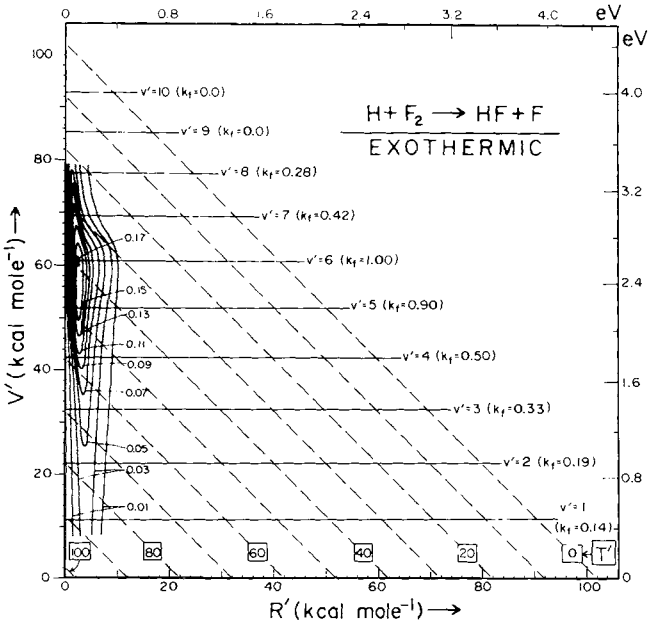

Fig. 7. Triangle plot for $H+F_2 \rightarrow HF+F$ (see caption to Fig. 6). $E'_{tot}=102$ kcal mol^{-1} for this reaction. (From J. C. Polanyi, J. J. Sloan, *J. Chem. Phys.* *57* (1972) 4988 [21].)

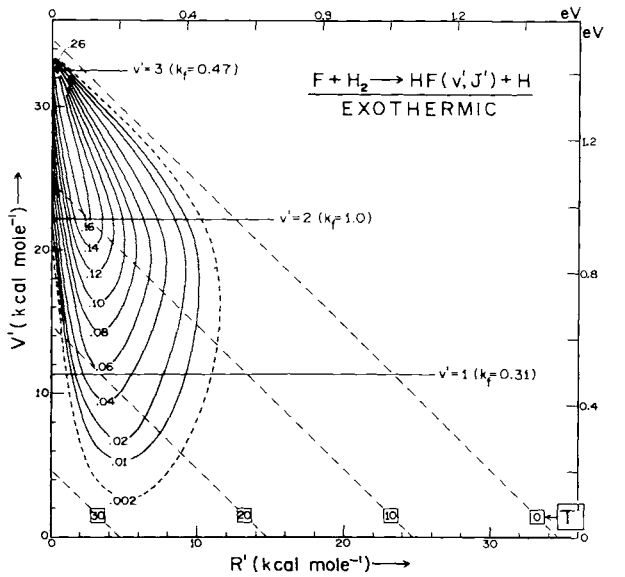

Fig. 8. Triangle plot for $F+H_2 \rightarrow HF+H$ (see caption to Fig. 6). $E'_{tot}=34.7$ kcal mol^{-1} for this reaction. (From J. C. Polanyi, K. B. Woodall, *J. Chem. Phys.* *57* (1972) 1574 [20].)

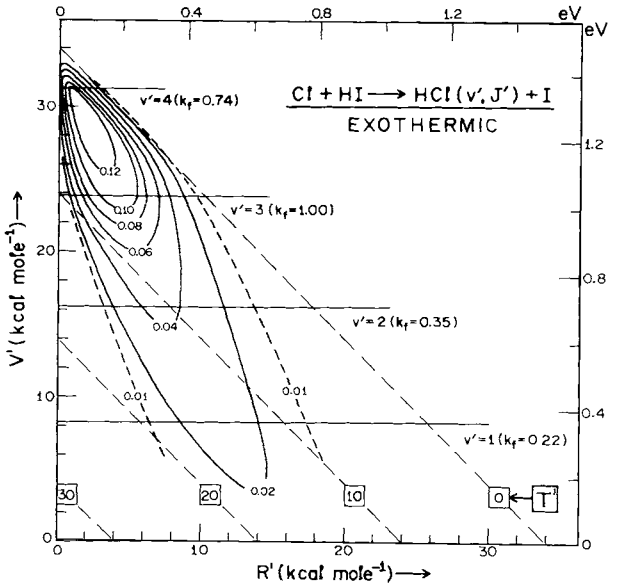

Fig. 9. Triangle plot for $Cl+HI \rightarrow HCl+I$. See caption to Fig. 6. $E'_{tot}=34$ kcal mol^{-1}. (From D. H. Maylotte et al., *J. Chem. Phys.* *57* (1972) 1547 [18].)

Four examples of the graphs that we have used (as a supplement to the tabulation of the actual $k(v',J')$ values) as an aid to the visualization of the experimentally determined product energy distributions, are shown in Figures 6–9. By interpolation between permitted combinations of V', R', and T', we obtain contours of equal $k(V',R',T')$. In these "triangle plots" contours are shown in V',R',T' space. They delineate a "hill" of detailed rate constant in that space. Portions of the hill that lie between vibrational energy states are merely included to guide the eye as to the breadth and shape of the product energy distribution over the axes corresponding to V', R', and T'. Since classical mechanics is widely used in order to interpret energy distributions, these classical "fingerprints" of differing chem-

ical reactions help us to picture contrasting types of behavior.

It is readily apparent that the first two reactions, $H+Cl_2$ and $H+F_2$ (Figs. 6 and 7), though they liberate markedly different energies, both exhibit inefficient vibrational and rotational excitation and consequently efficient translational excitation. The third reaction, $F+H_2$ (Fig. 8), gives rise to highly efficient vibrational excitation together with inefficient rotational excitation. The fourth reaction pictured, Cl+HI (Fig. 9), combines efficient vibrational excitation with exceptionally efficient rotational excitation ($\langle f_{R'}\rangle = 0.13$ for Cl+HI in contrast to $\langle f_{R'}\rangle = 0.03$ for $H+F_2$). In concurrent work, alluded to in the following section, we linked these changes in dynamics tentatively to the release of repulsive energy in systems having differing mass combination and preferred geometries of the intermediate.

The ridge of the "detailed rate constant hill" is almost vertical in the case of the first three reactions, moving out to higher R' at lower V' in the fourth of the reactions pictured (Cl+HI) (for a tabulation of mean $\langle f_{v'}\rangle$, $\langle f_{R'}\rangle$, and $\langle f_{T'}\rangle$ and for the slope of the ridge $\Delta R'/\Delta V'$ for these reactions, see Table IV of Ref. [21]). Leaving aside the dynamical implications of this distinctive behavior (see Section 2.2 below), it is noteworthy that successively lower vibrational states will exhibit marked increases in *translational* energy in the first three cases, but an overlapped "translational energy spectrum" in the fourth case. This finding was seen to have interesting implications for the crossed molecular beam chemistry in which T' (as already noted) is the prime measurable. Figure 10 gives sample distributions over $f_{T'}$ (blending rotational states into a continuum, since they cannot be resolved in molecular beam time-of-flight (TOF) studies). The reaction $H+F_2$, not pictured here, gives rise to eight well-resolved translational peaks (Fig. 5 of Ref. [21]). In the case of the $F+H_2$ reaction and its isotopic analogues, in addition to resolving these peaks by TOF, *Y. T. Lee*'s laboratory has in recent times fully characterized the angular distribution of each.[42]

The triangle plots, exemplified in Figures 6–9, constitute one way of "compacting" the substantial data embodied in $k(v',J',T')$.The information theory, pioneered by *Bernstein* and *Levine*,[43] has provided a widely used alternative method of compaction in terms of parameters which describe the deviation of the observed vibrational and rotational distributions from a statistical outcome. These deviations can be described as vibrational and rotational "surprisals." In those cases for which the surprisal is found to be a linear function of $f_{v'}$ or $f_{R'}$, not only can the data be reduced to only two constants, but extrapolations can be made. We have made use of this in our work in order to estimate the (small) fraction of product formed in the non-emitting state, $v'=0$.

Figures 11a and 11b contrasts the triangle plots for HF and DF formed in the thermal reaction $F+HD \rightarrow HF(v',J')$ or $DF(v',J')$ (+D or +H).[47] These data are included since they shed light on a source of product rotational excitation. The forces operating are very similar but are clearly substantially more effective in rotationally exciting HF (mean fraction of the available energy entering rotation is $\langle f_{R'}\rangle \approx 0.125$) than DF ($\langle f_{R'}\rangle = 0.066$). We postpone discussion to Section 2.2 below.

It is interesting to note that for the family of reactions $F+HD \rightarrow HF$, $F+HD \rightarrow DF$, $F+H_2$, and $F+D_2$, studied by IR chemiluminescence, the first reaction in the list exhibited vibrational excitation that was anomalously low as compared with classical calculation. This (together with

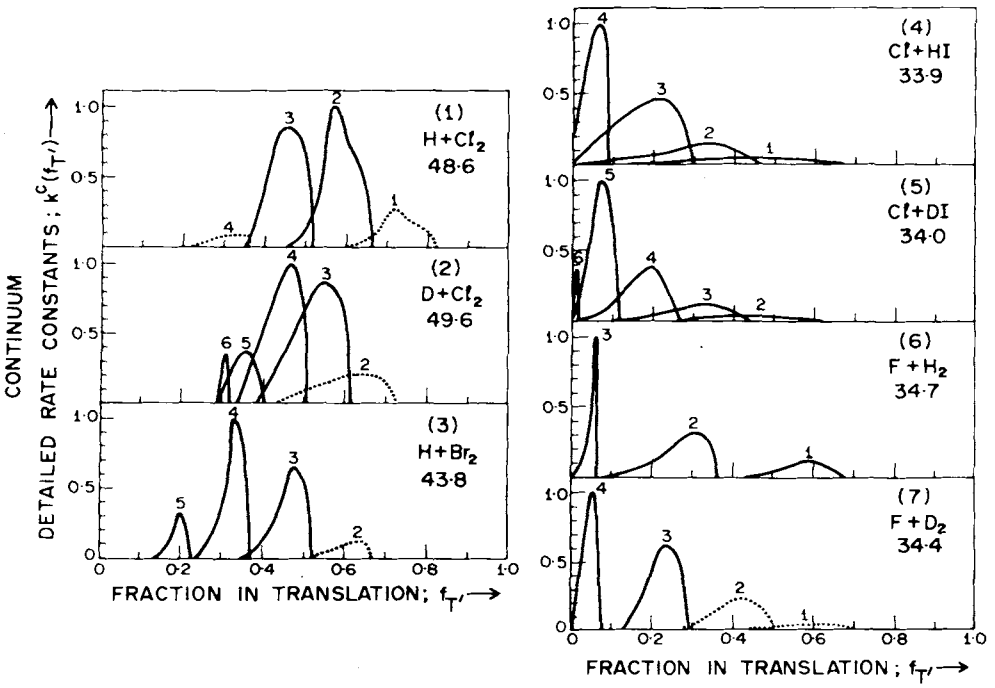

Fig. 10. Translational energy distribution ($f_{T'}$) in the products of some exchange reactions A+BC → AB+C obtained by subtracting the vibrational excitation measured by IR chemiluminescence from the total product energies (indicated in the figure). The vibrational states that contribute to the translational peaks are recorded above each peak (see text). (From K. G. Anlauf et al., *J. Chem. Phys. 53* (1970) 4091 [48a].)

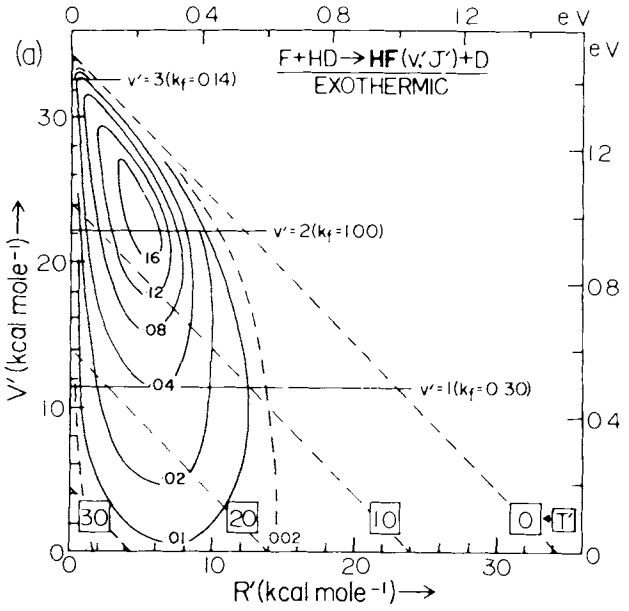

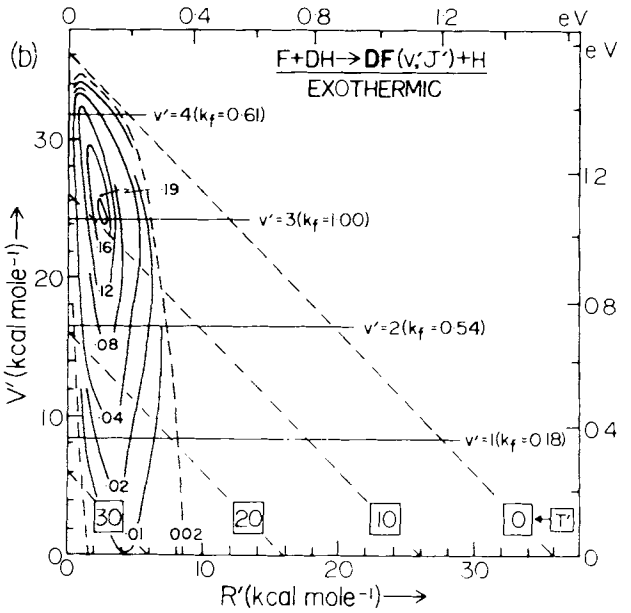

Fig. 11. Triangle plots for both branches of the F+HD exchange reaction. The total available energy in the products was taken to be $E'_{tot}=34.3$ kcal mol^{-1} for the HF product, and $E'_{tot}=36.1$ kcal mol^{-1} for DF, in calculating product translation T'. (From D. S. Perry, J. C. Polanyi, *Chem. Phys. 12* (1976) 419 [47].)

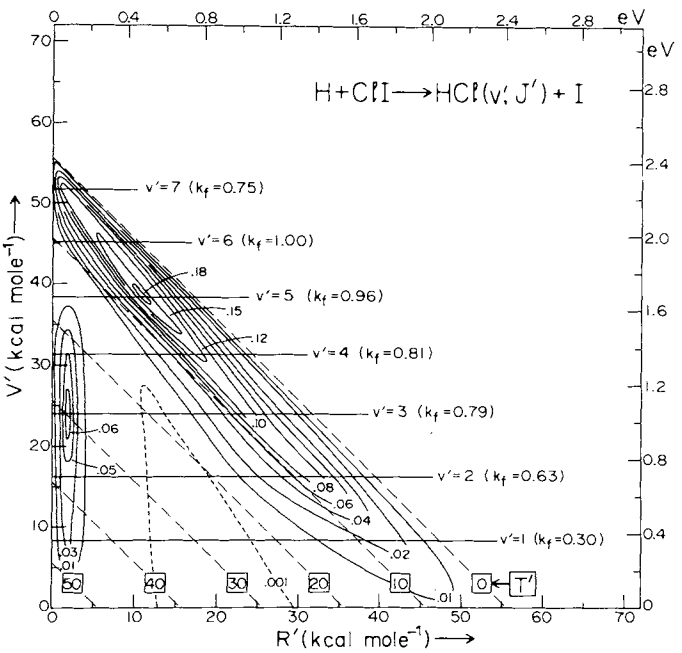

Fig. 12. Triangle plot for the reaction H+ClI → HCl+I at 300 K showing bimodality (18% of the HCl is in the low $-J'$ mode, 82% in the high $-J'$). (From M. A. Nazar, J. C. Polanyi, W. J. Skrlac, *Chem. Phys. Lett. 29* (1974) 473 [48c]; see also J. C. Polanyi, W. J. Skrlac, *Chem. Phys. 23* (1977) 167 [48d].)

the reagent-energy dependence of $k(v'=3)$ was taken to be evidence of a quantum effect at the threshold energy for formation of HF($v'=3$). Molecular beam experiments in *Y. T. Lee*'s laboratory have shown the importance of quantum effects on the dynamics of the first member of this family of reactions.[42]

Figure 12 shows the dramatic influence that atom C can have on the dynamics of a reaction A+BC → AB+C. On paper the reaction illustrated resembles H+ClY → HCl+Y, for which the detailed rate constant $k(V',R',T')$ is given in Figure 6; the difference is that the second halogen atom, Y, has been changed from Y=Cl to Y=I, with the effect on $k(V',R',T')$ recorded in Figure 12. Bimodal product energy distributions were also observed in a number of other studies[48-51] and were regarded as indicative of the existence of two types of reaction dynamics leading to the identical product (HCl in the case illustrated). This phenomenon was termed *microscopic* branching, to distinguish it from the *macroscopic* branching leading to chemically different products (see, for example, Fig. 11). As we shall indicate in Section 2.2, these two types of branching are likely to be linked.

It is interesting to consider the strengths and weaknesses of IR spectroscopy as a tool in the study of reaction dynamics. The major limitations have stemmed from the low transition probabilities in the IR, the insensitivity of IR detectors, and the lack of a sufficiently precise time scale against which to measure the vibrational and especially rotational relaxation. Substantial improvements in sensitivity have been achieved using the important new methods of laser-induced fluorescence (LIF)[44] and resonantly enhanced multiphoton ionization (REMPI).[45] However, since these make use of electronic transitions, they cannot so readily scan the full manifold of product vibrotational energy states to yield data as complete as that exemplified in Figures 7-9, which remains the most complete available.

Tunable IR lasers, combined with adequate time resolution, could give a new lease of life to the vibrotational spectroscopy of reaction products. A promising development, employing IR chemiluminescence is the introduction of time-resolved Fourier transform spectroscopy following the pulsed photolytic initiation of exchange reaction.[46]

2.2. Theory

The origin of these theoretical studies is outlined in Section 1. In the early 1960s two groups[26,27] became interested in using the computer-based classical trajectory method[25] (often called the Monte Carlo approach) to explore, for the first time, a suggestion made over two decades earlier,[28] that energy released as reagents approach is responsible for vibration in the newly formed bond.

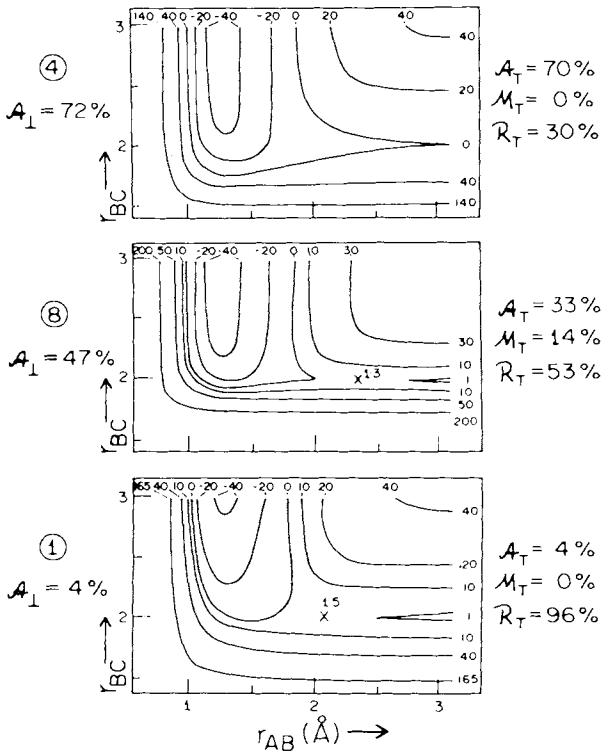

Fig. 13. Three potential-energy surfaces (PES) illustrative of the changes in potential energy as reagents A + BC (lower right) pass through collinear transition states A--B--C to form products AB + C (upper left). Contour energies are in kcal mol^{-1}; all three reactions have the same exothermicity. The PES, designated 1, 8, and 4, are arranged vertically in order of increasing "attractiveness." The PES are indexed at the left according to the percentage attractive energy release taken from a perpendicular path across the surface ($\mathscr{A}_\perp$ = 4, 47, and 72% for surfaces 1, 8, and 4). The same PES are described at the right according to the percentage attractive, mixed, and repulsive energy release, $\mathscr{A}_T$, $\mathscr{M}_T$, and $\mathscr{R}_T$, along a single collinear trajectory; this designation depends upon mass combination, which was L + HH (L = 1 amu, H = 80 amu). The barrier crest, designated x, shifts to "earlier" locations along r_{AB} as the surfaces become more attractive. (Excerpted from P. J. Kuntz et al., *J. Chem. Phys. 44* (1966) 1168 [53].)

Figure 13 shows three potential energy surfaces (PES), all of a modified London, Eyring, Polanyi, Sato (LEPS) variety,[27,52,53] selected from a wider group examined in Ref. [53]. The energy released as the reagents approached (termed the attractive energy release, and defined as $\mathscr{A}_\perp$ or $\mathscr{A}_T$,[53,54] see the caption of Fig. 13) increases as one moves upwards in the figure. There is, in related families of reaction, a concurrent diminution in the height of the energy barrier and a shift of the barrier to earlier locations along the coordinate of approach; it has proved possible to give an empirical expression to these correlations.[55,56]

In Figure 14 it can be seen that for a group of eight PES's moderate percentages of energy release along the

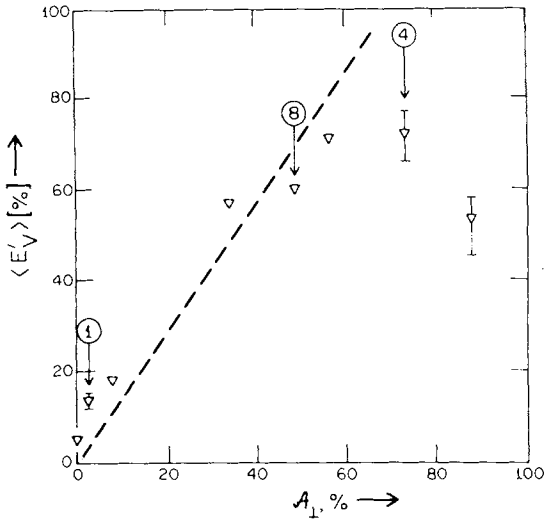

Fig. 14. Mean vibrational excitation in the products of 3D L + HH reaction on eight potential-energy hypersurfaces (PES) plotted against the perpendicular attractive energy release, $\mathscr{A}_\perp$. The collinear cuts through PES 1, 8, and 4 are to be found in the previous figure. The fall-off in $\langle E'_V \rangle$ at high $\mathscr{A}_\perp$ is due to the prevalence of secondary encounters (see text). (From P. J. Kuntz et al., *J. Chem. Phys. 44* (1966) 1168 [53].)

coordinate of approach (% $\mathscr{A}_\perp$) are converted quantitatively into product vibration, for a particular reagent mass combination (L + HH; see caption). For high % $\mathscr{A}_\perp$ the reaction moves into a new regime in which product vibration decreases with increased attractive energy release. Examination of the trajectories indicates that a transition is occurring from predominantly *direct* reaction (products once they start to separate continue to do so[57]) to *indirect* reaction in which subsequent "clutching" and "clouting" secondary encounters drain the incipient vibration out of the new bond into rotation and translation.[58,59] What we are seeing is the onset of statistical behavior, in the limit of which product vibration will receive no more than its modest equipartition allocation.

At the other end of the scale in Figure 14, where repulsive energy release predominates, the low vibrational excitation shown in the figure is by no means the rule; the observed vibrational excitation is strongly dependent on the chosen mass combination. The L + HH mass combination shown here is in fact anomalous in fulfilling the initial expectation that repulsive energy release $\mathscr{R}_\perp$ (energy released along the coordinate of separation of the PES) will be inefficiently channeled into vibration. For L + HH the attacking atom A approaches BC rapidly up to the normal bonding separation before the respulsion is released (dynamics in which r_{AB} decreases to its equilibrium separation, r^0_{AB}, and only then does r_{BC} increase, correspond on the PES to a rectilinear path). Since the repulsion operates on an already existent AB bond, vibrational excitation is indeed inefficient (left end of Fig. 14). This behavior is sufficiently atypical to be described as the "light-atom anomaly."[53]

For the more general case of a heavier attacking atom relative to the molecule under attack, the new bond is still extended ($r_{AB} > r^0_{AB}$) at the time that the bulk of the repulsion is released; we can symbolize this as A--B·C. In this case repulsion between the separating atoms B and C re-

sults in recoil of B, rather than of AB as a whole; i.e., it gives rise to efficient internal excitation of the new bond, AB.

Since the solution of the collinear equations of motion can be pictured in terms of the motion of a sliding mass across a suitably scaled and skewed representation of the PES, it is instructive to consider the characteristic path across the PES in this general case. The fact that r_{AB} decreases at the same time as r_{BC} increases (we term the energy released in this phase "mixed"; $\mathscr{M}_T$) means that the sliding mass, rather than following a rectilinear path, is cutting the corner of the PES. Instead, therefore, of approaching the exit valley from its head, it approaches the valley from the side; consequently it oscillates from side to side of the exit valley indicating that the new bond is vibrationally excited.

The proportion of the energy released during corner-cutting is clearly relevant to the efficiency with which the repulsive energy is channeled into vibration. We have routinely determined the extent of mixed energy release, $\mathscr{M}_T$, from a specimen collinear trajectory employing the appropriate mass combination and the PES in question.[10,53,60] Figure 13 shows that $\% \mathscr{M}_T$ is insignificant for **L + HH**. For other mass combinations it is so great that the points on a plot of the type shown in Figure 14 begin at substantial $\langle E'_V \rangle$, and the region of linearity prior to the falloff in $\langle E'_V \rangle$ due to the onset of indirect dynamics becomes a very short region (see the case of the heavy attacking atom in Fig. 7 of Ref. [53]).

Turning to the experimental findings of Section 2.1, it was evident that the moderate mean fractional conversion of reaction energy into product vibration, $\langle f_{V'} \rangle$, could be explained either by a highly attractive interaction leading to secondary encounters, or by predominantly one source of product rotation. The experimental data in the triangle plots of Figure 11 give persuasive evidence of the significance of this effect in the important reaction $F + H_2$. Product repulsion should be expected[47,67] on the basis of momentum conservation to give rise to decreasing $\langle f_{R'} \rangle$ in the series FH·D > FH·H > FD·D > FD·H (the dot indicated the locus of the repulsion); this is found theoretically, in 3D trajectory studies, and also experimentally (see Fig. 15). The triangle plots of Figure 11 correspond to the extremes of this range of isotopic mass combinations; $\langle f_{R'} \rangle$ for the FH·D pathway substantially exceeds that for FD·H.

Qualitative pictures of the type given in Figure 16 suggest simple models of the reactive event. Several such models are indicated in Figure 17, all of which stress the role of the forces operating along the coordinate of separation of the PES. The implications of each of these models are discussed in Ref. [59]. Despite their crudity, simple models have the important virtue that their "moving parts" are open to inspection. Model (c), called the simple harmonic model, has been used to improve our understanding of the mechanism of mixed energy release, in which a repulsive force operating between particles B and C drives an oscillator joining A to B that is under tension.[60] The model shows that for a wide range of conditions mixed energy release can play a significant role in channeling product repulsion into vibration.

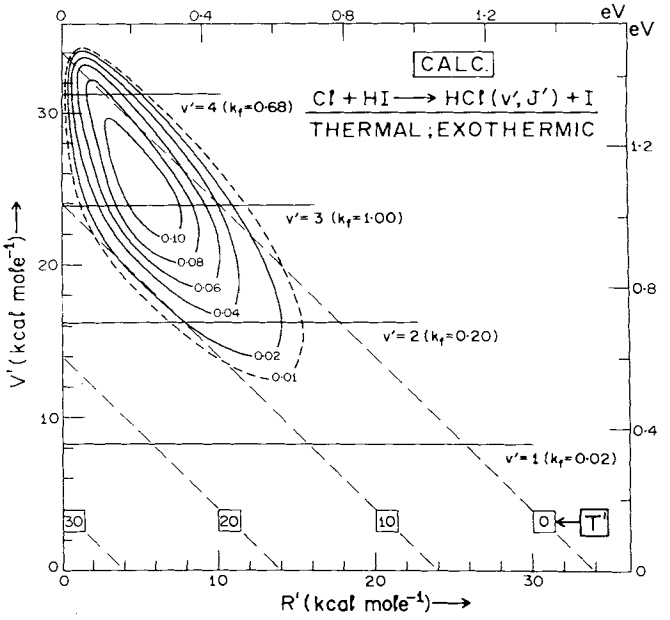

Fig. 15. Computed triangle plot for the reaction Cl + HI → HCl + I at thermal collision energies (300 K). The 3D classical trajectory method was applied to a highly repulsive PES (proposed by K. G. Anlauf et al., *J. Chem. Phys. 49* (1968) 5189 [41]; from C. A. Parr et al., *ibid. 58* (1973) 5 [61]).

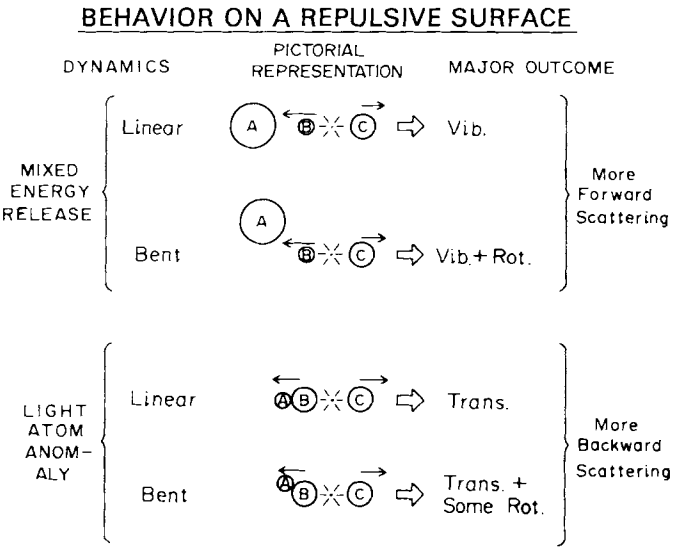

Fig. 16. Pictorial representation of contrasting types of reaction dynamics on a repulsive energy surface. "Mixed energy release" is commonly observed. "The light-atom anomaly" is observed if the attacking atom is very light. (From J. C. Polanyi, *Acc. Chem. Res. 5* (1972) 161 [58].)

Model (d), the direct interaction with product repulsion (DIPR) model,[68] sidesteps consideration of forces in the new bond by obtaining the product vibration, V', from $E'_{tot} - (R' + T')$. From the direction of recoil of atom C relative to the direction of approach of A, angular distributions can readily be generated in three dimensions (3D). The model provides a simple means to expose the link between the angular distribution of reaction products and the internal excitation, as well as the connection between these two quantities and the collision energy.

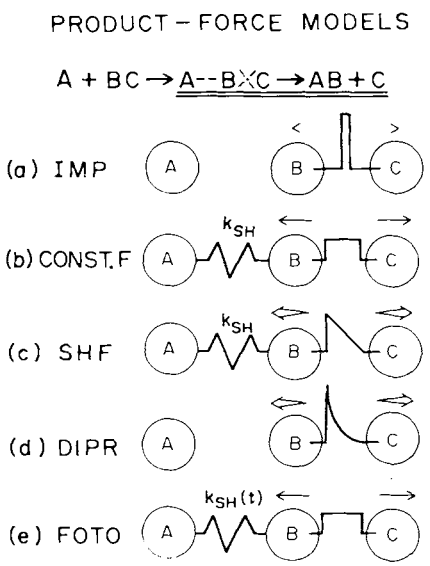

Fig. 17. Five types of simple "product-force models," which interpret product energy distributions in terms of the mode of relaxation of ABC in its retreat from the activated state → AB + C. A repulsive force is assumed to be located between the separating atoms B-C. Various assumptions are made regarding the bond A--B which is forming. a) The impulsive model (IMP); b) the constant force model (CONST. F.); c) the simple harmonic model (SHF); d) the direct interation with product repulsion (DIPR) model; e) the forced oscillation in a tightening oscillator (FOTO) model. (From J. C. Polanyi, *Faraday Discuss. Chem. Soc. 55* (1973) 389 [80].)

Findings for the DIPR model are summarized in Figure 18 (solid lines). Reading from left to right, the interactions become less repulsive (more attractive). This is achieved by systematically decreasing the repulsive impulse (the time integral of the force, $F(t)$, between B and C) which alone governs the dynamics. Since a measure of $\int F(t)\,dt$ can be obtained by a variety of means for any actual reactive PES,[47,67] the model can be applied to cases for which the results of 3D trajectory computation are known. The agreement—see the points for the more repulsive cases in Figure 18—is excellent, so long as the assumption of direct interaction remains valid.

The lessons that can be learned from Figure 18 are that strongly repulsive energy release will tend to give backward scattering of the molecular product (Θ_{mol} is substantial at 180°) coupled with moderate internal excitation, E'_{int}. As the repulsion is decreased, Θ_{mol} shifts forward and E'_{int} increases. The same effect can be achieved by increasing the reactant collision energy, since this too has the effect of decreasing the repulsive impulse $\int F(t)\,dt$.

Herschbach and co-workers have injected physical content into the DIPR model in their DIPR-DIP extension, in which the repulsive impulse is assumed to be "distributed as in photodissociation" (DIP).[69,70] The model then accounts nicely for product distributions observed in a number of reactions.[69] More recently *Zare*'s laboratory has shown how the DIPR approach can be used to understand the plane of rotation of newborn reaction products.[70]

The forced oscillation in a tightening oscillator (FOTO) model (Fig. 17e) gives a fuller rendition of the forces on a colinear PES; the B-C repulsion operates on an AB oscillator whose force constant is in the process of increasing, and whose equilibrium separation, r^0_{AB}, is decreasing. The

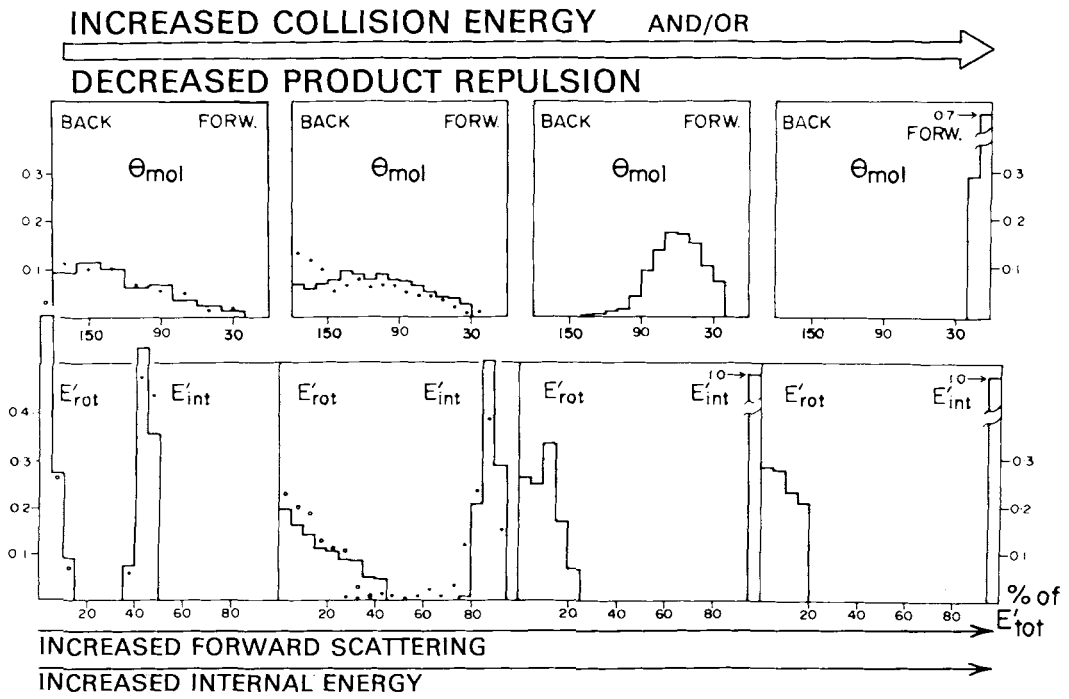

Fig. 18. Effect of repulsive energy release on product angular distribution (top row) and energy distribution (bottom row; E'_{tot} is product rotational excitation and E'_{int} is vibration plus rotation). The solid lines show the results of 3D DIPR model calculations (masses K + Br_2, energy release $E'_{tot} = 53$ kcal mol^{-1}). The total product repulsion used in the DIPR model calculations was decreased in four stages, from left to right in the figure, simulating decreased % $\mathscr{R}$, implying increased % $\mathscr{A}$. According to the DIPR model, this is mathematically equivalent to increasing the reagent collision energy, hence the dual label of the arrow at the top. The *consequences* of these changes are summarized, qualitatively, by the arrows at the foot of the figure. The dots record the distributions obtained from 3D trajectories on potential-energy hypersurfaces with comparable partitioning of the energy release. (Adapted from P. J. Kuntz et al., *J. Chem. Phys. 50* (1969) 4623 [68].)

model, which has been applied to ten reactions for which experimental or theoretical data exist, is sufficiently complete to embody analogues of the "attractive," "mixed," and "repulsive" phases of energy release.

To the extent that the rotation in a newly formed reaction product AB originates in repulsion AB·C, the rotational motion should be coplanar with the repulsive force, and B in AB should recoil away from C. This implies that the angle between the product rotational angular momentum vector, $\vec{J}'$, and the product orbital angular momentum vector, $\vec{L}'$, should be $\Theta_{J'L'} \approx 180°$ (Fig. 19). Analyses of product distributions from 3D trajectory studies[64,71] bear this out. Experimental studies of correlations between such vector attributes will add materially to the mosaic from which our picture of reaction dynamics is composed.

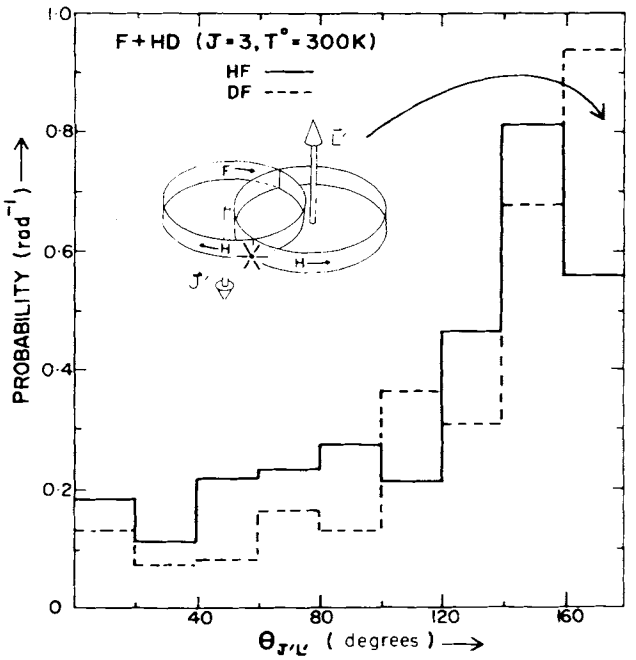

Fig. 19. Computed distribution, $\Theta_{J'L'}$, of the angle between the product rotational angular momentum, $\vec{J}'$, and orbital angular momentum, $\vec{L}'$, following repulsive energy release between the products of the reaction F+HD → HF+D (solid line) and F+HD → DF+H (broken line). At the extreme left $\Theta_{J'L'}=0$ corresponds to $\vec{J}'$ parallel to $\vec{L}'$, while at the extreme right $\Theta_{J'L'}=180°$ corresponds to the favored outcome of $\vec{J}'$ antiparallel to $\vec{L}'$.

The richer the detail in the rate constants $k(V',R',T')$, the clearer the message. The striking bimodality in the product energy distribution from H+ClI → HCl(v',J')+I recorded in Figure 12 can be ascribed to "microscopic branching"; two patterns of molecular dynamics result in the formation of the same reaction product (HCl in this example). The dynamics have been explored in 3D for reasonable PES's.[72] They are shown schematically in Figure 20. In the case of H+ClI, the migratory *microscopic* pathway (at the right of Fig. 20) is thought to dominate. This is for the same reason that *macroscopic* branching favors formation of HI rather than HCl, namely, the existence of a smaller energy barrier for approach from the I end of ICl (see Refs. [72, 73] for the greater stability of ClIH than HClI). In collisions of H with the I end of ICl that fail to yield HI, the H atom can migrate toward the Cl end of the molecule to yield highly internally excited HCl. The HCl

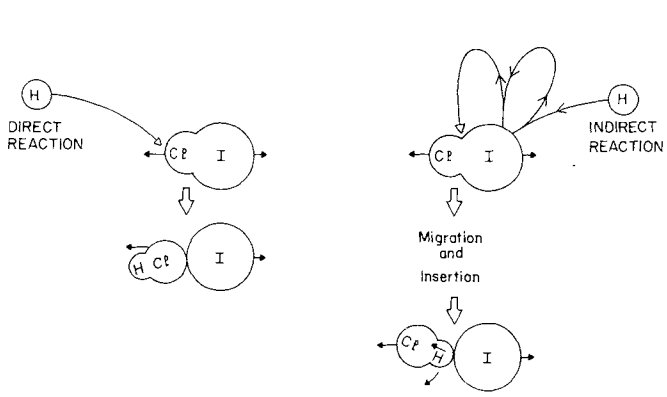

Fig. 20. Pictorial representation of the alternative dynamics—direct and indirect—in the microscopic branching underlying the bimodality of product energy distribution exemplified in Figure 12. (Based on a classical trajectory study; J. C. Polanyi et al., *Faraday Discuss. Chem. Soc.* 67 (1979) 66 [51]).

product with low internal excitation comes from H that have reacted directly at the Cl end of ClI. Since the barrier to this mode of reaction is higher, the yield (at normal reagent energies) is lower. It is evident that the relative yields of HCl and HI in *macroscopic* branching are linked to the yields of low E'_{int} and high E'_{int} HCl by way of *microscopic* branching.

Microscopic branching is though to constitute more than merely an interesting curiosity, since it can contribute to the dynamics in any case where macroscopic branching is possible—a large class of reactions. As would be expected, the importance of microscopic branching, in common with macroscopic branching, depends sensitively on the reagent energy.[49,50,74]

3. Channeling Reagent Energy into Products

3.1. Experiment

In the experiments that will now be briefly described, reagent translational, vibrational, and rotational energies were altered by simple means in order to explore the effect on the product energy distribution. To increase the collision energy we formed the atomic reagent (Cl for Cl+HI,[67,75] F for F+HCl[50] or F+D_2,[50] and H for H+Cl_2[50]) by pyrolysis, rather than using room temperature atoms as in the work described in the previous section. The effect is shown for H+Cl_2 in the triangle plot of Figure 21. Comparison with the earlier 300-K triangle plot (Fig. 6) shows marked changes. The *additional* reagent translation, ΔT, in excess of the barrier to reaction, has been channeled principally into additional product translation.

A second repository for this additional reagent energy was product rotation. (It was interesting to observe in both Cl+HI[75] and H+Cl_2[50] that this enhanced product rotation was associated with the appearance of a second maximum in the product rotational distribution, $k(J')_{v'}$, as if enhanced collision energy had led to *induced microscopic branching*.) The general finding regarding the disposition of additional reagent translation could be summarized as follows:

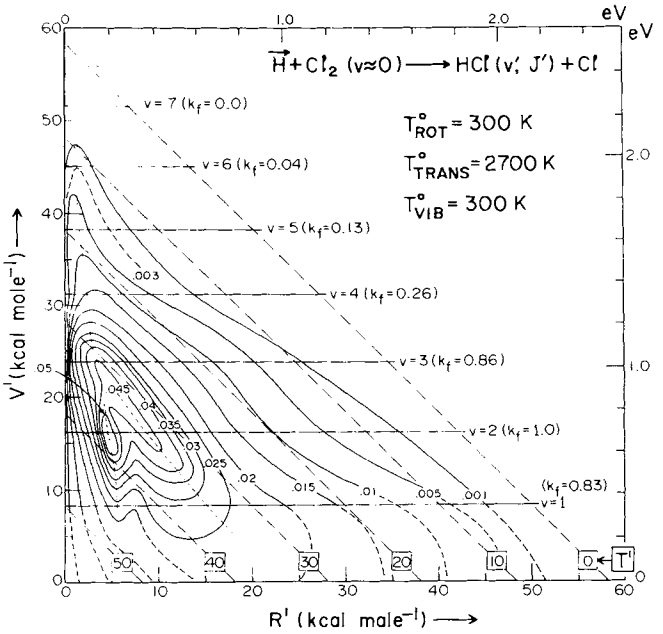

Fig. 21. Effect of enhanced reagent collision energy on the product energy distribution, i.e., experimental $k(V', R', T')$, for $H + Cl_2(v=0) \rightarrow HCl(v', J') + Cl$. Mean collision energy, $\langle T \rangle \approx 10.6$ kcal mol^{-1}. Compare $k(V', R', T')$ for room temperature reaction, in Figure 6. (From A. M. G. Ding et al., *Faraday Discuss. Chem. Soc.* 55 (1973) 252 [50].)

$$\Delta T \longrightarrow \Delta T' + \Delta R' \qquad (4)$$

This describes the average behavior; the breadth of the product energy distribution increased markedly over V', R', and T'.

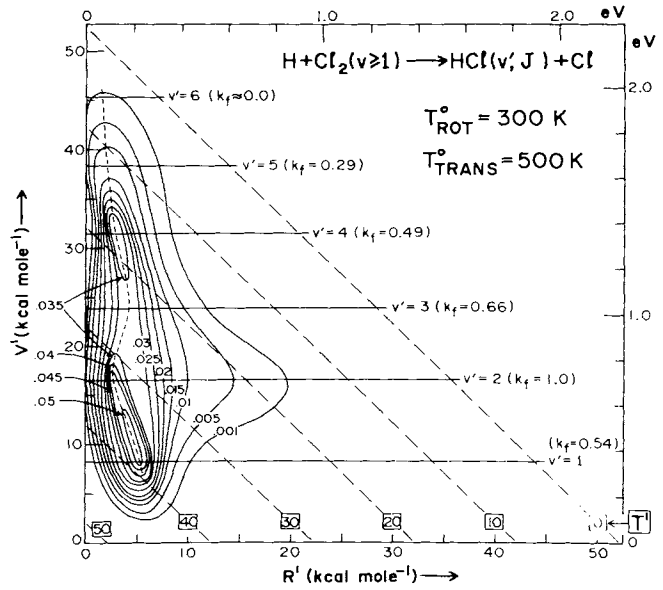

Fig. 22. Effect of enhanced reagent internal energy on the product energy distribution, i.e., experimental $k(V', R', T')$, for $H + Cl_2(v \geq 1) \rightarrow HCl(v', J') + Cl$. This result is approximate since it was obtained by subtracting the detailed rate constants for $H + Cl_2(v \approx 0) \rightarrow HCl + Cl$ from $H + Cl_2(v \geq 0) \rightarrow HCl + Cl$. Mean vibrational energy, $\langle V \rangle \approx 3.3$ kcal mol^{-1}. Compare with Figure 6. (From A. M. G. Ding et al., *Faraday Discuss. Chem. Soc.* 55 (1973) 252 [50].)

By heating the molecular species under attack and recording the change in product energy distribution (see Fig. 22), we found evidence of a similar adiabaticity, on the average, in regard to the conversion of reagent vibration into product excitation,

$$\Delta V \longrightarrow \Delta V' \qquad (5)$$

where the symbol Δ denotes energy in excess of that required for barrier crossing. As before, the breadths of the product energy distributions increased, that over V' appearing to be bimodal.

A more stringent test of this tendency toward vibrational adiabaticity was obtained using the method of IR chemiluminescence depletion (CD; Section 4.1) and IR emission. Vibrationally excited reagent, OH(v), was formed in a selected "pre-reaction." Pulses of a further reagent—Cl in the present case—were introduced, and a record was made of the depletion of chemiluminescence (at the pulsing frequency) in OH(v), as well as of the appearance of chemiluminescence in reaction product HCl(v') (Fig. 23). The reaction responsible for both emissions was

$$Cl + OH(v) \longrightarrow HCl(v') + O \qquad (6)$$

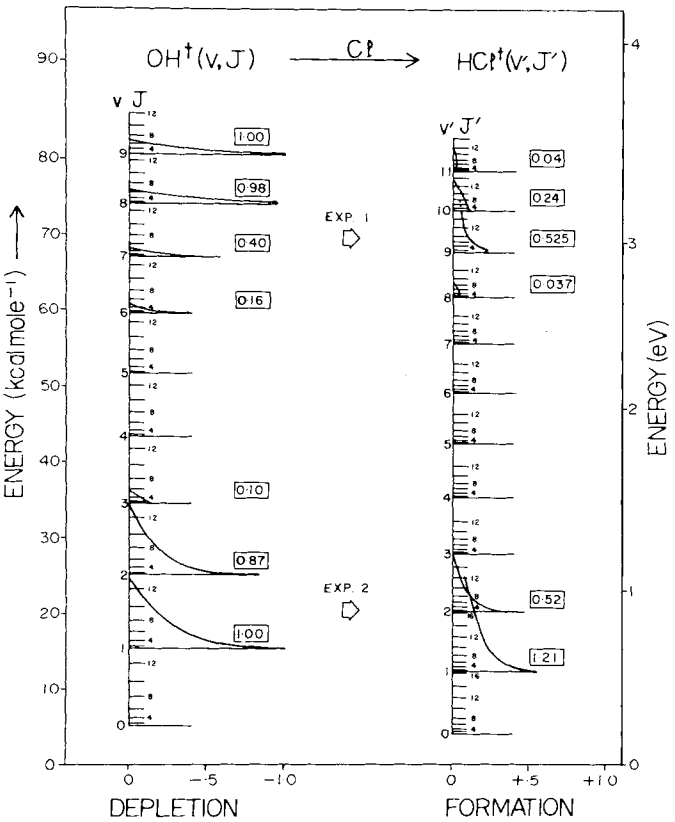

Fig. 23. Experimental evidence for the conversion of high reagent vibrational excitation into the corresponding degree of freedom of the product in the reaction $Cl + OH(v, J) \rightarrow HCl(v', J') + O$. The curves at the left show the *decrease* in population of each OH vibrotational level resulting from the introduction of Cl atoms; the curves at the right were taken from a concurrent record of the amount of HCl formed in each vibrotational level. In experiment 1 (top) the OH was formed in $v = 6$-9 by the pre-reaction $H + O_3$. In experiment 2 (bottom) the OH was formed in $v = 1$-3 by the pre-reaction $H + NO_2$. The numbers in the boxes at the left give the fractional depletions of each OH v level (summed over J), and those at the right give the corresponding information for the product HCl. (From B. A. Blackwell et al., *Chem. Phys.* 24 (1977) 25 [76].)

Using two different pre-reactions (see caption to Fig. 23), the reagent vibrational energy could be given mean values of $\langle V \rangle = 72.1$ kcal mol^{-1} or 20.5 kcal mol^{-1}. For these high vibrational energies, over 90% of the reagent vibration was found to be channeled into product vibration. Once again,

$\Delta V \longrightarrow \Delta V'$[76]

Evidence regarding the fate of reagent rotation was more fragmentary, coming from studies of the reaction $F + H_2(J)$ with J varied systematically from $0 \rightarrow 1 \rightarrow 2$.[77] A small but significant decrease was observed in the fraction of the total energy entering product vibration when $J = 0 \rightarrow 1$, followed by an increase in this fraction as $J = 1 \rightarrow 2$. This finding was in accord with an earlier less detailed study by *Coombe* and *Pimentel*.[78] As is often the case at present with the effects of reagent rotation (see Section 4.2) detailed understanding is lacking.

3.2. Theory

The nature and the origins of the approximate adiabaticity relations (4) and (5) have been discussed in a number of places.[49, 50, 54, 61, 67, 79–82] The success of the 3D classical trajectory method in describing the types of change in detailed rate constant observed experimentally (see Figs. 21 and 22) can be judged from Figure 24.[81] Figure 24b shows a computed triangle plot for the 300-K $H + F_2 \rightarrow HF(v', J') + F$ reaction at the center (see Fig. 7 for the experimental counterpart), and Figures 24c and 24a show the predictions for enhanced reagent translation (Fig. 3 in Ref. [82] has the experimental counterpart) and vibration, respectively. It is evident from inspection of Figure 24 that $\Delta T \rightarrow \Delta T' + \Delta R'$, and $\Delta V \rightarrow \Delta V'$. In addition, the increased breadths of product energy distributions over T' and R' in the former case and over V' in the latter are apparent, as also is the bimodality over V' resulting from enhanced V. (See Ref. [50] for comparable trajectory studies using parameters chosen for $H + Cl_2$.)

The origin of this adiabaticity is evident from an inspection of trajectories with and without the additional reagent energy (Fig. 25). The effect of enhanced translation is to shift the characteristic pathway across the collinear PES (used as a diagnostic of 3D behavior) toward more compressed configurations—the sliding mass impelled by its enhanced momentum along r_{AB} caroms into the corner of the PES in the region of ① in Figure 25. The compressed intermediate A·B·C, if collinear, then flies apart to give translation in AB + C, and, if bent, to give enhanced rotation in AB. For enhanced reagent vibration the most common paths to product are shifted to the region ② in Figure 25; the effect is to favor a more stretched intermediate A--B--C that pulls together along r_{AB} to give $AB(v \gg 0) + C$. The opposite phase of vibration to that pictured in Figure 25 drives the intermediate into region ①, giving rise to the low V' peak in the product distribution. Since energy released along r_{BC} has been characterized as repulsive and that along r_{AB} as attractive, we have termed these changes in dynamics *induced repulsive energy release* in the first case, and *induced attractive energy release* in the second. For a strongly exothermic reaction such as

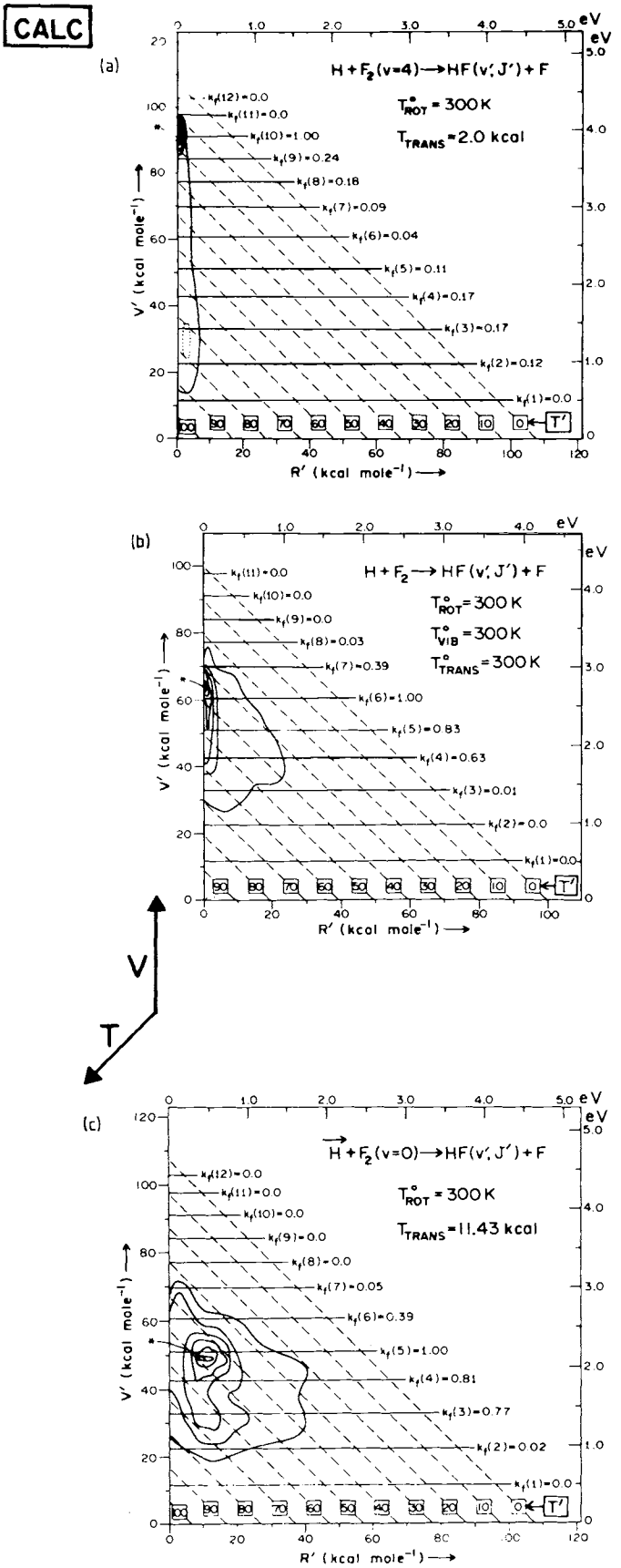

Fig. 24. Computed triangle plots for the $H + F_2 \rightarrow HF + F$ reaction. In (b) the reagents were Monte Carlo selected from a 300-K Boltzmann distribution. In (a) the F_2 reagent vibrational excitation, V, was increased to $v = 4$ (reagent collision energy 2.0 kcal mol^{-1}), and in (c) the reagent relative translational energy, T, was increased to 11.43 kcal mol^{-1} (reagent vibrational energy corresponded to $v = 0$). (From J. C. Polanyi et al., *Chem. Phys.* 9 (1975) 403 [81].)

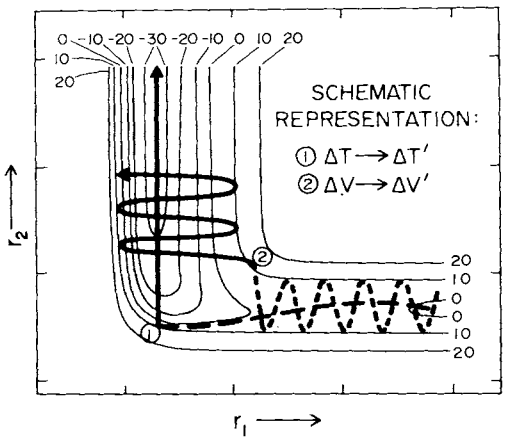

Fig. 25. Schematic representation (on a typical collinear exothermic PES) of the mechanism (1) by which "additional" reagent translation ($\Delta T \gg E_c$, where E_c is the barrier height) is channeled into "additional" product translation ($\Delta T'$), and also (2) the mechanism by which "additional" reagent vibration ($\Delta V \gg E_c$) becomes "additional" product vibration ($\Delta V'$). (These are not actual trajectories since they show neither the exothermic energy release nor the effect on that energy release of changing reagent energy; the intention, which is artificial, is to show the effect of ΔT and ΔV in isolation). (From A. M. G. Ding et al., *Faraday Discuss. Chem. Soc. 55* (1973) 252 [50].)

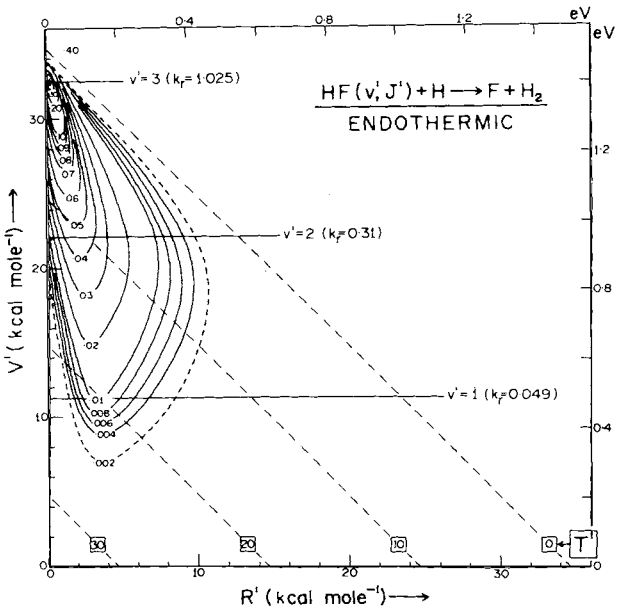

Fig. 26. Contours represent values of *reagent* vibrational, rotational, and translational energies for the endothermic reaction $HF(v',J') + H \rightarrow F + H_2$ which correspond to equal $k_r(\equiv k_{endo})$. The data were obtained by application of microscopic reversibility to the $k_f(\equiv k_{exo})$ given in Figure 8. (From J. C. Polanyi, D. C. Tardy, *J. Chem. Phys. 51* (1969) 5717 [84].)

$H + F_2$ (Fig. 24), these shifts affect not only the channeling of the *additional* reagent energy, but also the channeling of the exothermicity into product excitation, so that $(\Delta T' + \Delta R')/\Delta T$ and $\Delta V'/\Delta V$ exceed unity.[81]

4. Surmounting the Energy Barrier

4.1. Experiment

The most detailed information regarding the relative efficiency of various types of reagent motions in surmounting an energy barrier comes from the application of microscopic reversibility to detailed rate constants for forward reaction, $k_f(V',R',T')$.[83] Detailed rate constants for the reverse reaction obtained in this way, $k_r(V',R',T')$, are recorded in the triangle plot of Figure 26, where V', R', and T' are now the vibrational, rotational, and translational energies of the *reagents* for the endothermic reaction $HF(v',J') + H \rightarrow F + H_2$.[82] The total energy available for distribution is fixed by the nature of the experiment, being equal to the energy made available by the forward exothermic reaction; 34.7 kcal mol^{-1} in the case illustrated. This approach has been tested numerically by applying it to a case where $k_r(V',R',T')$ could be obtained directly from 3D trajectories or by application of microscopic reversibility; the procedures agreed with one another to approximately 10%.[85]

Inspection of Figure 26 indicates that a redistribution of 30 kcal mol^{-1} from T' into V' has the dramatic effect of increasing by ca. $10^3\times$ the rate of reaction in the endothermic direction.[58,84] Endothermic triangle plots of this type are to be found in, for example, Refs. [67, 83, 84]. In a few cases, in other laboratories, direct measurement has been made of the relative efficiency of vibration and translation in surmounting an energy barrier;[86–88] in one of these cases[88] the barrier corresponded to "substantially"[67] endothermic reaction; the reaction was $HF(v') + K \rightarrow H + KF$ (17 kcal mol^{-1} endothermic) and the effect of transferring 11 kcal mol^{-1} from reagent translation to vibration was to give an increase of $> 10^2$ in reaction rate.

The IR "chemiluminescence depletion" (CD) method, already alluded to in Section 3.1, was used to obtain a measure of the efficiency of a high degree of vibrational excitation in promoting endothermic reaction. In contrast to the microscopic reversibility procedure outlined above, by CD the vibrational energy could be varied independently of the collision energy and could be made much larger than the endothermic barrier height. The energies of one family of endothermic reactions investigated in this fashion are shown in Figure 27; $HX^{\dagger} + Y \rightarrow Y + HX$, where X = Cl or F, Y = Br or Cl, and the dagger indicates vibrational excitation.[89] An analogous study has been made of

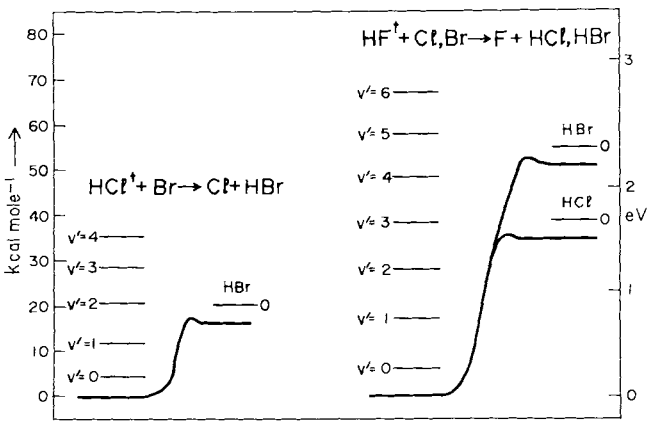

Fig. 27. Endothermicities of three reactions $HX + Y \rightarrow X + HY$; showing kcal mol^{-1} at left, eV at right, and the vibrational spacing of the relevant HX within the figure. Energy profiles are schematic. (From D. J. Douglas et al., *Chem. Phys. 13* (1976) 15.)

the endothermic reactions $HX^{\dagger} + Na \rightarrow H + NaX$, X = Cl, F.[90] For CD experiments the vibrationally excited reagent $HX^{\dagger}$ was formed in a variety of pre-reactions or in a variety of partially relaxed vibrational distributions from a single pre-reaction. The atomic reagent, Y or Na, was pulsed and a concurrent record was made of the IR chemiluminescence from $HX^{\dagger}$ (cw) and of the depletion (CD was measured on an amplifier locked to the pulsing frequency of the Y or Na beam).

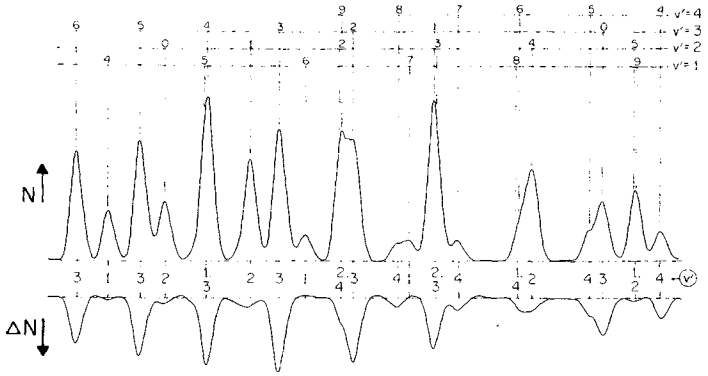

Fig. 28. A portion (20%) of the spectrum recorded in an IR chemiluminescence depletion (CD) study of the endothermic reaction $HCl(v'=1\text{-}4) + Br \rightarrow Cl + HBr$. At the top (labeled N) is the emission from the $HCl(v'=1\text{-}4)$ formed in a pre-reaction. Below (ΔN) is the concurrent record of the depletion, due to pulses of Br (trace enlarged 2.5×). The fraction $\Delta N(v')/N(v') > 0$ for $v' \geq 2$. (Excursions of ΔN above the baseline can be identified with product emission ($HBr(v=1,2)$) rather than reagent depletion.) (From D. J. Douglas et al., *J. Chem. Phys. 59* (1973) 6679 [89].)

A small portion of the concurrent spectral traces from an experiment on $HCl(v',J') + Br$[89] is given in Figure 28. The fractional depletions ($\Delta N(v',J')/N(v',J')$), which should be independent of $N(v',J')$, gave a measure of the endothermic rate constant, $k_{endo}(v',J')$. Values of $k_{endo}(v')$ (summed over J') are shown plotted against the reagent energy expressed as a fraction of the endothermic barrier height, Q^* in Figure 29.[89] The onset of k_{endo} is marked for each reaction by a threshold at the expected Q^* ($Q^* = 16.5$, 34, and 49 kcal mol^{-1} for the reactions discussed here). The reagent translational energy corresponded to 300 K; it follows that approximately 95% of the reagent energy was present as vibration. Calibrations showed that the reactive cross section for high v exceeded 1 Å^2; i.e., the collision efficiencies for reaction approached 0.1. With an analogous preponderance of vibration in the reagents of $HX^{\dagger} + Na$, the collision efficiencies approached unity.[90] We conclude that vibrational excitation is highly efficient in carrying these reactions over their endothermic energy barriers.

The CD approach was also used to map out the dependence of reaction rate on reagent rotational excitation. The results shown in Figure 30 for the endothermic processes $HX(J)_v + Na \rightarrow H + NaX$ are typical of the findings from CD. Comparable results were obtained (by a cruder approach) for the exothermic reaction $F + HCl(J)_v \rightarrow HF + Cl$.[50] There is an initial decline in reaction probability with increasing J, followed by a rise in reaction probability. Similar behavior has been noted in crossed beam experiments.[92,93] Nonetheless our knowledge of $k(J)$ leaves much to be desired.

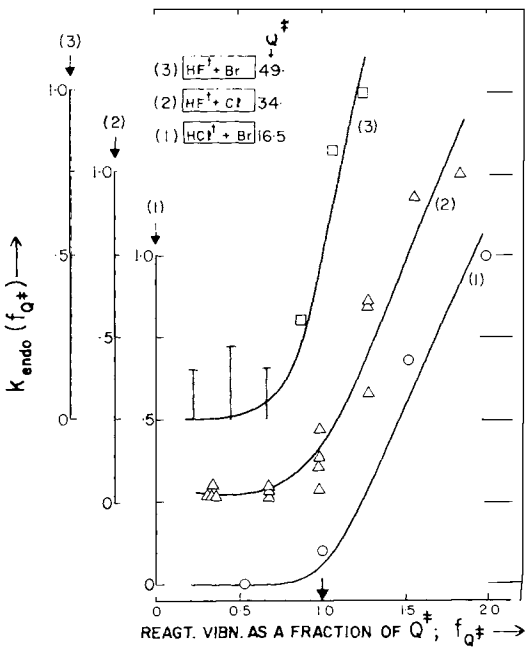

Fig. 29. Endothermic rate constant, $k_{endo}(f_{Q^*})$ is the reagent vibrational energy expressed as a fraction of the endothermicity Q^* for reactions (1)-(3). (From D. J. Douglas et al., *Chem. Phys. 13* (1976) 15.)

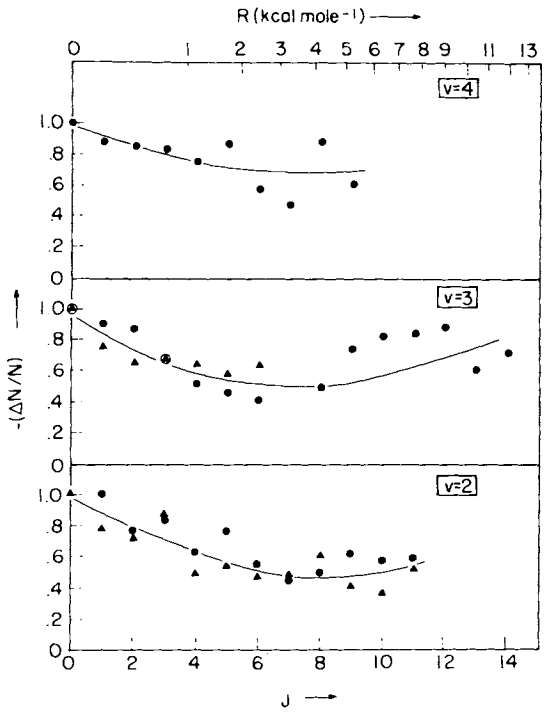

Fig. 30. Fractional depletions of individual J states of $v = 2\text{-}4$ in a CD study of the endothermic reaction $HF^{\dagger} + Na$. (From B. A. Blackwell et al., *Chem. Phys. 30* (1978) 299 [91].)

4.1. Theory

We have found it useful and revealing to link the preferred type of reagent energy distribution to the location of the energy barrier on the collinear PES (termed a "diagnostic cut" through the full hypersurface which gives the 3D dynamics). In the first approximation we have looked

for a correlation between the dynamics of barrier crossing and the location of the barrier crest relative to the point at which the entry and exit valleys of the PES may be said to meet on the collinear PES, namely, the equal-stretch configuration, ρ^*, for which $r_{AB}-r^0_{AB}=r_{BC}-r^0_{BC}$.[94] *Duff* and *Truhlar*[95] have examined an alternative definition of the point where entry and exit valleys meet, namely, the point of maximum curvature, C*, of the minimum-energy path across the collinear PES (a concept prefigured in work of *Hofacker* and *Levine*[96]). Since the two bonds change length with minimum expenditure of energy at their maximum extension, it is understandable that $\rho^* \approx C^*$.[97]

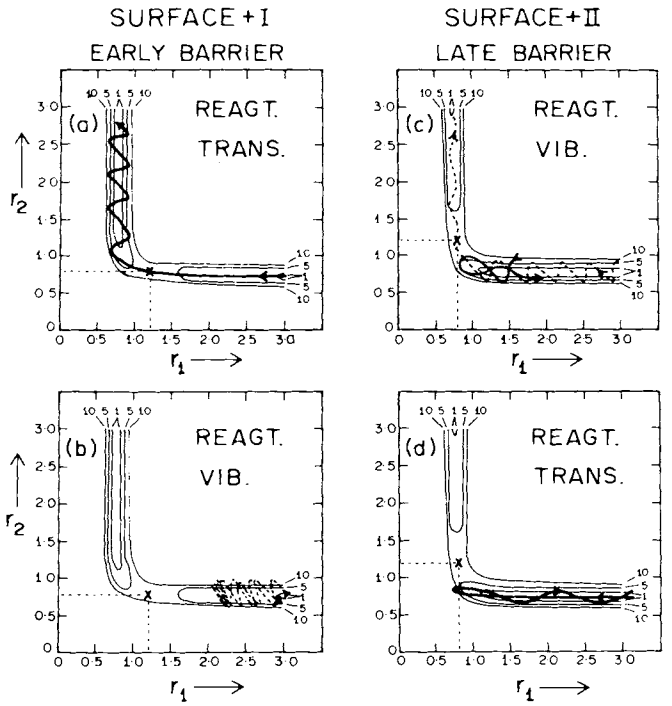

Fig. 31. At the left (a) and (b) show specimen trajectories with (a) largely reagent translation ($T=9$, $V=0$) and (b) largely reagent vibration ($T=1.5$ and $V=14.5$) on an "early barrier" surface, i.e., type I. At the right (c) and (d) show trajectories with (c) largely reagent vibration ($T=1.5$ and $V=7.5$) and (d) largely reagent translation ($T=16.0$, $V=0$). All energies are kcal mol^{-1}; reagent vibration relative to $E(v=0)$. Three equal masses, $m_A=m_B=m_C$. Positive and negative vibrational phases in solid and broken lines. Barrier heights on both surfaces I and II are 7 kcal mol^{-1}; contours are labeled in kcal/mol. (From J. C. Polanyi, W. H. Wong, *J. Chem. Phys. 51* (1969) 1439 [94].)

Figure 31 shows the dynamics characteristic of equal masses reacting across a PES with "early barrier" (surface I) at the left and "late barrier" (surface II) at the right.[44] The barrier crest was located approximately 0.03 Å ahead of ρ^* on surface I and 0.03 Å beyond ρ^* on II (these surfaces are designated +I and +II in Figure 31, since the labels −I and −II were used for potential hollows similarly displaced from ρ^*[58]). The effect of these displacements of the barrier crest upon the preferred mode of motion in the reagents was dramatic. As illustrated in Figure 32, on surface I a reagent translational energy only slightly in excess of the 7 kcal mol^{-1} barrier height gave a calculable cross section, whereas a reagent vibrational energy double the barrier height gave a reactive cross section too small to be computed in our study. The converse behavior

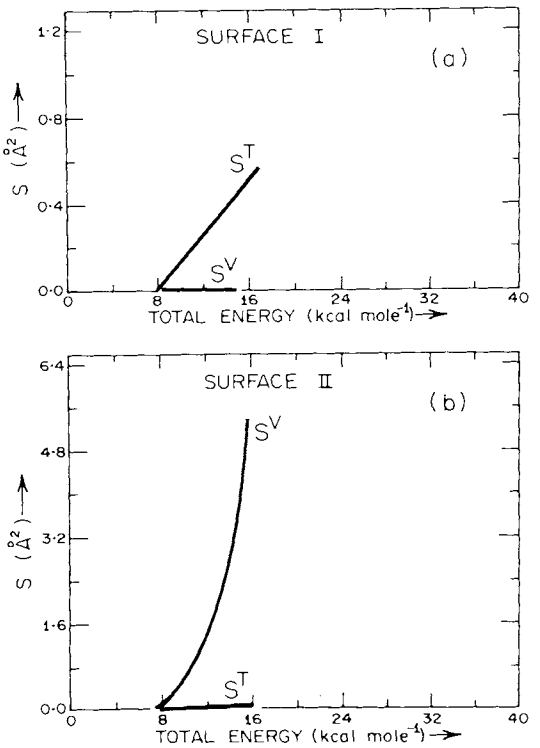

Fig. 32. a) Reactive cross sections S^T (reagent energy in translation (S^V (reagent energy in vibration, + 1.5 kcal mol^{-1} of translation) on the "early barrier" surface depicted at the left of Figure 31. b) Reactive cross sections S^T and S^V on the "late barrier" surface shown at the right of Figure 31. Three equal masses. (From J. C. Polanyi, W. H. Wong, *J. Chem. Phys. 51* (1969) 1439 [94].)

is seen to apply to surface II (Fig. 32); reagent vibrational energy (with a small amount of translation to bring the reagents together) was highly effective in giving reaction, whereas translation was without effect.

As we have remarked, these correlations are of more than empirical value; by focusing attention on certain simple attributes of the PES, we can shed light upon dominant features of the dynamics. In terms of the dynamics of the reaction A+BC the correlations noted in the preceding paragraph reduce to the proposition that a barrier predominantly along the coordinate of approach, r_{AB}, is best traversed by motion in that same coordinate, namely, reagent translation, whereas a barrier predominantly along the coordinate of separation, r_{BC}, is best traversed by motion in that coordinate, i.e., vibration in the bond under attack. The trajectories in Figure 31 (obtained by solution of the equations of motion, but capable of being pictured as the motion of a sliding mass across the PES) illustrate this; the reactive cases are (a) and (c) (early and late barriers), the nonreactive are (b) and (d) (early and late barriers once more). The effect illustrated is sufficiently striking that it may also have relevance to the dynamics of reactions involving many atoms (cf. Ref. [99]), provided that these occur by a direct pathway.

The interest of these correlations is greatly increased if we can link the form of the PES to the nature of the chemical reaction. Though unrecognized by reaction dynamicists, *Hammond*'s postulate[100] that for endothermic reactions the transition state resembles reaction products should have pointed the way to the desired connection.

In fact it was a systematic study of a considerable number of exchange reactions $A+BC \rightarrow AB+C$ in terms of both the London, Eyring, Polanyi, Sato (LEPS) and the bond-energy bond-order (BEBO) methods that led to the conclusion that for substantially exothermic reactions the barrier crest is located in the entrance valley ("early barrier") of the PES, and for substantially endothermic reactions it is in the exit valley ("late barrier").[55] From this and the dynamical study of early and late barriers, it followed (as previously surmised[101]) that the favored degree of freedom for barrier crossing in substantially exothermic reactions would be translation, whereas reagent vibration would be most effective in giving rise to substantially endothermic reaction. (In the BEBO approximation, "substantially" has the meaning ≥ 10 kcal mol^{-1}[67]).

Behavior of the type illustrated in Figure 32a, computed for the well-studied exothermic reaction $F+H_2 \rightarrow HF+H$ is shown in Ref. [64]. Behavior of the type illustrated in Figure 32b is in accord with the evidence of Section 4.1. There is, nonetheless, a clear need for comparisons of what we have termed (Fig. 32) S^T with S^V for a range of reactions and within related series of reactions.

If barrier location is to be made to any degree a quantitative index of the relative efficacy of translation and vibration in bringing about barrier crossing, the location of the barrier must be considered as it appears on a surface skewed and scaled for the appropriate masses m_A, m_B, and m_C, so that a sliding mass will correctly solve the equations of (collinear) motion.[98] The mass combination **H + HL** accentuates surface I behavior while diminishing the surface II effect, whereas **L + HH** has the converse effect. The qualitative behavior noted above remains unaltered.

A further significant refinement in understanding the controlling features of the PES takes note of the fact that in the case of a later barrier crest some part of the energy barrier is located along the coordinate of approach. This further element was included in the picture by distinguishing between type "IIS" and "IIG" barriers, where S and G differentiate late barriers approached by a sudden (S) or gradual (G) potential rise.[97] The gradual rise implies the existence of a significant fraction of the type II barrier in the coordinate of approach, with a corresponding requirement for a minimum reagent translational energy along with the (dominant) vibrational contribution.

A further dividend that accrues from the inclusion of this refinement is that it has the effect of tying in the considerations raised in this section, regarding the favored type of reagent energy for endothermic barrier crossing, with those described in Section 2.2 in regard to the channeling of exothermic energy into product degrees of freedom. The portion of the (late) barrier to endothermic reaction that extends into the coordinate of approach for "reverse" reaction is the portion of the exothermic energy release that occurs in the coordinate of separation for "forward" reaction; we are viewing the same hill from below and above. Similarly, the reagent translational energy required for endothermic reaction is related to the translational energy derived from repulsive energy release in the corresponding exothermic reaction. Since the PES is a single whole, it is to be hoped that the various indices of reactive behavior bear an evident relationship to one another.

The "indices of reactive behavior" referred to in the previous paragraph (see Sections 2.2 and 3.2) make frequent use of the collinear "diagnostic" PES. Since this allows for neither reagent nor product angular momenta, it gives no insight into the sources of product rotation (Section 2.2), nor into the channeling of reagent rotation into motion across the barrier.

The experimentally observed dependence of reaction probability on J can plausibly be explained as follows.[91] In the great majority of reactions there will be a preferred orientation for the required close approach of the attacking atom to the molecule under attack. With increased J the time that the system spends in this orientation will decrease, as will the detailed rate constant, $k(J)$. With further increase in J the preferred orientation will be recovered at short intervals during the approach of A to BC, resulting in a reversal of the downward trend in $k(J)$. At high J the attacking atom responds to an average interaction around BC; $k(J)$ would be expected to level off. There is, however, a further contributing factor at J sufficiently high that the rotational energy is significant in terms of the energy required for barrier crossing; this is the effect of rotation in carrying the system across the barrier to reaction. If the barrier is "late," this would be expected to occur largely through vibration–rotation interaction; if "early," through the component of force along r_{AB} as BC rotates into A (see Ref. [71b] for the geometry of this collision).

These scenarios are speculative. What can be said with assurance is that the ratio of time spent along the approach coordinate to the rotational period of the molecule under attack will play an important role in the outcome of a potentially reactive encounter in addition to the energy vested in rotation.

5. Future Directions

This talk has described the development of one type of "state-specified" chemistry, from which some simple lessons regarding reaction dynamics can be drawn. What we see obscurely today we shall in the future see much more clearly through the more rigorous application of state selection, an increase in the range of attributes being selected, and also an extension in the range of reactions amenable to study. All of this will add up to a maturation of the field of state-to-state chemistry.

In closing, I mention two further approaches which could assist materially in the quest for understanding of the choreography of chemical reaction. In the first, attempts are being made to observe the molecular partners while they are, so to speak, on the stage, rather than immediately prior to and following the reactive dance. This we term "transition-state spectroscopy" (TSS); it is a young but burgeoning field. In the second novel approach, the intention, stated a little grandiosely, is to have a hand in writing the script according to which the dynamics occurs; the reagents are aligned by the forces at a crystal surface and held in a fixed arrangement immediately prior to the initiation of the reaction by light, thus restricting the subsequent pattern of motion. This field of "surface aligned photochemistry" (SAP) has only very recently made its ap-

pearance. SAP may initiate reaction part way across the PES and hence is related to TSS, since the adsorbed reactants can be held together in configurations that locate them at the outset part way up the reactive barrier. In the SAP experiments performed till now the forces holding the reactants to the surface have been physisorptive.

These two approaches, TSS and SAP, will be briefly reviewed.

The impetus for transition-state spectroscopy, TSS, came from a series of theoretical studies of the effect of laser fields on reactive encounters.[102] A variety of intriguing alterations in dynamics were predicted, exemplifying in the reactive domain the effects being explored at that date for nonreactive encounters under the heading of "laser-assisted collisions." However, the laser powers thought to be required lay in the gigawatt to terawatt range (powers associated with the electrical breakdown of gases) so that the outlook for success appeared bleak.

It was pointed out that a simple alternative would be to look for emission from electronically excited transition-state configurations (ABC^{+*}).[103] (In reaction rate theory "transition states" are sets of intermediate configurations variously defined; in the spectroscopic context we use the term to denote the full range of configurations intermediate between reactants A + BC and products AB + C). An example is shown in Figure 33. In collisional line-broaden-

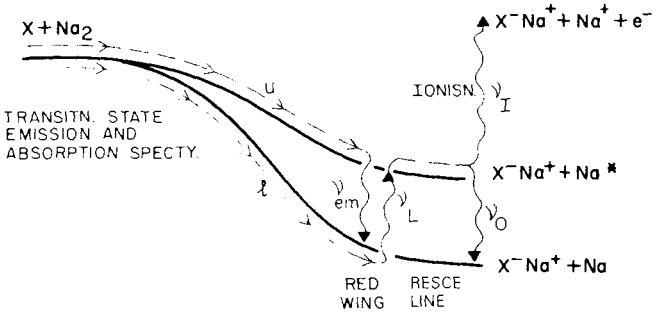

Fig. 33. Illustration of transition state emission and absorption spectroscopy (TSS), in analogy to collisional line-broadening. The reaction is $X + Na_2 \rightarrow NaX + Na^{(*)}$ (X = halogen). Reaction on the upper surface, u, leads to emission as the products separate (ν_{em} constitutes a redshifted "wing" on the D line at ν_0). Reaction on the lower surface, l, may be detected by laser absorption as products separate ($\nu_L < \nu_0$ in the illustration); absorption at ν_L may be evidenced by subsequent emission of Na* at ν_0, or by laser ionization of Na* using a second laser tuned to ν_L. (From J. C. Polanyi, *Faraday Discuss. Chem. Soc.* 67 (1979) 129 [103].)

ing of Na* + NaX the wings on the atomic line emission would be due to the approach of Na* to NaX (moving from right to left in the figure) followed by emission of frequency ν_{em}. In TSS comparable wings should be observed due to the fact that every Na* is formed by separation from NaX (moving from left to right in the figure); separation can be preceded by emission at frequency ν_{em}. A simple calculation showed that the emission intensity at a ν_{em} of ca. 1 cm^{-1} bandwidth, would total approximately 10^{-6} the chemiluminescent intensity of Na*, and that this should be measurable. Observation of wings of this intensity, having the appropriate kinetics, followed shortly thereafter.[104] Preliminary reports of similar measurements in absorption[105-107] have led to more definitive successes[108] at increasing levels of spectroscopic detail.[109]

The relative intensity of the TSS at various ν_{em} or ν_L (corrected for changing transition moment, where warranted) will yield information concerning the relative times that the absorber, ABC^+, spends at successive configurations *en route* from reagents to products.[110-112] This is precisely the information that reaction dynamicists have sought to infer from a knowledge of reagent and product motions. The more direct approach of TSS suffers from the drawback that it is a spectroscopy of two PES's rather than one, namely, the reactive PES and the optically linked PES (preferably a bound state) to which emission or absorption occurs. This complication need no more be fatal to TSS than it was to the study of stable molecules by electronic emission or absorption spectroscopy in decades past. It does however mean that as soon as our experimental virtuosity permits, we should turn our attention to the TSS of the simplest reactive systems, such as that involving only hydrogen atoms ($H + H_2 \rightarrow H_3^+ \rightarrow H_2 + H$).[111, 112]

In regard to surface aligned photochemistry (SAP) we can be brief. In the experiments performed to date[113] a submonolayer of H_2S was adsorbed in ultrahigh vacuum (UHV) on a single crystal of LiF(001), and was irradiated with ultraviolet (UV) at 193 and 222 nm coming from an excimer laser (5 mJ/pulse). At low coverage (ca. 0.01 monolayers), fast-moving $\bar{H}$ photofragments were observed to leave the surface. From their energy and angular distribution these were clearly due to the UV photolysis of H_2S still held at the surface at the instant of photofragmentation. With increasing coverage ($\gtrsim 0.1$ monolayers), the photoproducts included fast-moving $\bar{H}_2$ formed in the reaction $\bar{H} + H_2S \rightarrow \bar{H}_2 + HS$. The yield of $\bar{H}_2$ increased with coverage at a rate and to an extent that could only be explained by the reaction of photorecoiling $\bar{H}$ with *adsorbed* H_2S; accordingly the reaction is ascribed to SAP. The $\bar{H}_2$ product is fast and directional.

This is a small first step along the way to inducing reactions under conditions where the range of reagent angles-of-approach and impact parameters is restricted by surface alignment and (by choice of crystal, crystal face, and coverage) is controllable. A trajectory study[113] illustrates the simplified link between product attributes and reactive geometries that applies under these more disciplined conditions.

Even in the world of molecules the civilizing influence of modest restraints is a cause for rejoicing.

The research described here in so far as it relates to the work of my laboratory was performed over a thirty-year period at the University of Toronto. It is a pleasure to express my indebtedness to my colleagues at this University—most especially to the late Prof. D. J. LeRoy who fostered this work from its inception—and to my students and postdoctoral associates whose talents, generosity, and friendship have made this undertaking possible and fulfilling.

Received: February 27, 1987 [A 637 IE]
German version: *Angew. Chem.* 99 (1987) 981

[1] M. Beutler, M. Polanyi, *Z. Phys. Chem. Abt. B1* (1928) 3; S. von Bogdandy, M. Polanyi, *ibid. 1* (1928) 21; M. Polanyi, G. Schay, *ibid. 1* (1928) 30.
[2] D. R. Bates, M. Nicolet, *J. Geophys. Res. 55* (1950) 301.
[3] G. Herzberg, *J. R. Astron. Soc. Can. 45* (1951) 100.

[4] J. D. McKinley, D. Garvin, M. Boudart, *J. Chem. Phys. 23* (1955) 784; T. M. Cawthorn, J. D. McKinley, *ibid. 25* (1956) 583.
[5] F. J. Lipscomb, R. G. W. Norrish, B. A. Thrush, *Proc. R. Soc. London Ser. A 233* (1956) 455.
[6] J. K. Cashion, J. C. Polanyi, *J. Chem. Phys. 29* (1958) 455.
[7] J. K. Cashion, J. C. Polanyi, *J. Chem. Phys. 30* (1959) 1097; *Proc. R. Soc. London Ser. A 258* (1960) 529, 564, 570.
[8] A. L. Schawlow, C. H. Townes, *Phys. Rev. 112* (1958) 1940; A. M. Prokhorov, *Zh. Eksp. Teor. Fiz. 34* (1958) 1658; *Sov. Phys. - JETP (Engl. Transl.) 7* (1958) 1140.
[9] a) J. C. Polanyi, *Proc. R. Soc. Can. Ser. C 54* (1960) 25; b) *J. Chem. Phys. 34* (1961) 347.
[10] J. C. Polanyi, *Appl. Opt. Suppl. 2* (1965) 109.
[11] C. K. N. Patel, W. L. Faust, R. A. McFarlane, *Bull. Am. Phys. Soc. 119* (1964) 500; C. K. N. Patel, R. J. Kerl, *Appl. Phys. Lett. 5* (1964) 81; C. K. N. Patel, *Phys. Rev. Lett. 12* (1964) 588.
[12] J. V. V. Kasper, G. C. Pimentel, *Phys. Rev. Lett. 14* (1965) 352; G. C. Pimentel, *Sci. Am. 214* (1966) No. 4, p. 32.
[13] P. E. Charters, J. C. Polanyi, *Discuss. Faraday Soc. 33* (1962) 107.
[14] H. O. Pritchard, *Trans. Faraday Soc. 33* (1962) 278.
[15] J. C. Polanyi, *Trans. Faraday Soc. 33* (1962) 279.
[16] K. G. Anlauf, P. J. Kuntz, D. H. Maylotte, P. D. Pacey, J. C. Polanyi, *Discuss. Faraday Soc. 44* (1967) 183.
[17] P. D. Pacey, J. C. Polanyi, *J. Appl. Opt. 10* (1971) 1725.
[18] D. H. Maylotte, J. C. Polanyi, K. B. Woodall, *J. Chem. Phys. 57* (1972) 1547.
[19] K. G. Anlauf, D. S. Horne, R. G. Macdonald, J. C. Polanyi, K. B. Woodall, *J. Chem. Phys. 57* (1972) 1561.
[20] J. C. Polanyi, K. B. Woodall, *J. Chem. Phys. 57* (1972) 1574.
[21] J. C. Polanyi, J. J. Sloan, *J. Chem. Phys. 57* (1972) 4988.
[22] F. London in P. Debye (Ed.): *Probleme der modernen Physik (Sommerfeld-Festschrift)*, Hirzel, Leipzig 1928, p. 104; *Z. Elektrochem. 35* (1924) 552.
[23] H. Eyring, M. Polanyi, *Z. Phys. Chem. Abt. B 12* (1931) 279.
[24] J. O. Hirschfelder, E. Wigner, *J. Chem. Phys. 7* (1929) 616.
[25] F. T. Wall, L. A. Hiller, J. Mazur, *J. Chem. Phys. 29* (1958) 255; *35* (1961) 1284.
[26] N. C. Blais, D. L. Bunker, *J. Chem. Phys. 37* (1962) 2713; *39* (1962) 315.
[27] J. C. Polanyi in R. Stoops (Ed.): *Transfer d'Energie dans les Gaz*, Interscience, New York 1962, p. 177–182, 526–528; J. C. Polanyi, S. D. Rosner, *J. Chem. Phys. 38* (1963) 1028.
[28] M. G. Evans, M. Polanyi, *Trans. Faraday Soc. 35* (1939) 178.
[29] Review: B. S. Agrawala, D. W. Setser in A. Fontijn (Ed.): *Gas Phase Chemiluminescence and Chemi-ionization*, Elsevier, Amsterdam 1985, p. 157.
[30] B. M. Berquist, J. W. Bozzelli, L. S. Dzelzkalns, L. G. Piper, F. Kaufman, *J. Chem. Phys. 76* (1982) 2972; B. M. Berquist, L. S. Dzelzkalns, F. Kaufman, *ibid. 76* (1982) 2984; L. S. Dzelzkalns, F. Kaufman, *ibid. 77* (1982) 3508; *79* (1983) 3836.
[31] J. C. Weisshaar, T. S. Zwier, S. R. Leone, *J. Chem. Phys. 75* (1981) 4873; C. E. Hamilton, S. R. Leone in A. Fontijn (Ed.): *Gas Phase Chemiluminescence and Chemi-ionization*, Elsevier, Amsterdam 1985, p. 139.
[32] H. L. Welsh, C. Cumming, E. J. Stansbury, *J. Opt. Soc. Am. 41* (1951) 712; H. L. Welsh, E. J. Stansbury, J. Romanko, T. Feldman, *ibid. 45* (1955) 338.
[33] P. E. Charters, R. G. Macdonald, J. C. Polanyi, *Appl. Opt. 10* (1971) 1747.
[34] a) N. Jonathan, C. M. Melliar-Smith, D. H. Slater, *Mol. Phys. 20* (1971) 93; b) N. Jonathan, C. M. Melliar-Smith, S. Okuda, D. M. Slater, D. Timlin, *ibid. 22* (1971) 561.
[35] a) H. W. Chang, D. W. Setser, *J. Chem. Phys. 58* (1973) 2298; b) D. J. Bogan, D. W. Setser, *ibid. 64* (1976) 586.
[36] J. C. Moehlmann, J. D. McDonald, *J. Chem. Phys. 62* (1975) 3061; J. W. Hudgens, J. D. McDonald, *ibid. 67* (1977) 3401.
[37] P. M. Aker, D. J. Donaldson, J. J. Sloan, *J. Phys. Chem. 40* (1986) 3110.
[38] D. Brandt, L. W. Dickson, L. N. Y. Kwan, J. C. Polanyi, *Chem. Phys. 39* (1979) 189; L. W. Dickson, *Ph. D. Thesis*, University of Toronto 1982.
[39] J. C. Polanyi, K. B. Woodall, *J. Chem. Phys. 56* (1972) 1563.
[40] a) J. H. Parker, G. C. Pimentel, *J. Chem. Phys. 51* (1969) 91; b) R. D. Coombe, G. C. Pimentel, *ibid. 59* (1973) 251; c) *59* (1973) 1535; d) M. J. Berry, *ibid. 59* (1973) 6229.
[41] K. G. Anlauf, J. C. Polanyi, W. H. Wong, K. B. Woodall, *J. Chem. Phys. 49* (1968) 5189.
[42] a) D. M. Neumark, A. M. Wodtke, G. N. Robinson, C. C. Hayden, Y. T. Lee, *J. Chem. Phys. 82* (1985) 3045; b) D. M. Neumark, A. M. Wodtke, G. N. Robinson, C. C. Hayden, K. Shobotake, R. K. Sparks, T. P. Schaefer, Y. T. Lee, *ibid. 82* (1985) 3067.
[43] R. B. Bernstein, R. D. Levine, *J. Chem. Phys. 57* (1972) 434; *Adv. At. Mol. Phys. 11* (1975); R. B. Bernstein, R. D. Levine in W. H. Miller (Ed.): *Modern Theoretical Chemistry, Vol. 3, Dynamics of Molecular Collisions, Part B*, Plenum Press, New York 1976, Chap. 7.
[44] R. N. Zare, P. J. Dagdigian, *Science (Washington, DC) 185* (1974) 739.
[45] S. H. Lin, Y. Fujimura, H. J. Neusser, E. W. Schlag: *Multiphoton Spectroscopy of Molecules*, Academic Press, New York 1984.
[46] P. M. Aker, J. J. Sloan, *J. Chem. Phys. 85* (1986) 1412; P. M. Aker, J. J. Sloan, J. S. Wright, *Chem. Phys.* (1986).
[47] D. S. Perry, J. C. Polanyi, *Chem. Phys. 12* (1976) 419.
[48] a) K. G. Anlauf, P. E. Charters, D. S. Horne, R. G. Macdonald, D. H. Maylotte, J. C. Polanyi, W. J. Skrlac, D. C. Tardy, K. B. Woodall, *J. Chem. Phys. 53* (1970) 4091; b) H. Heydtmann, J. C. Polanyi, *J. Appl. Opt. 10* (1971) 1738; c) M. A. Nazar, J. C. Polanyi, W. J. Skrlac, *Chem. Phys. Lett. 29* (1974) 473; d) J. C. Polanyi, W. J. Skrlac, *Chem. Phys. 23* (1977) 167; e) D. Brandt, J. C. Polanyi, *ibid. 35* (1978) 23; *45* (1980) 65.
[49] L. T. Cowley, D. S. Horne, J. C. Polanyi, *Chem. Phys. Lett. 12* (1971) 144.
[50] A. M. G. Ding, L. J. Kirsch, D. S. Perry, J. C. Polanyi, J. L. Schreiber, *Faraday Discuss. Chem. Soc. 55* (1973) 252.
[51] J. C. Polanyi, J. L. Schreiber, W. J. Skrlac, *Faraday Discuss. Chem. Soc. 67* (1979) 66.
[52] J. C. Polanyi, *J. Quant. Spectrosc. Radiat. Transfer 3* (1963) 471.
[53] P. J. Kuntz, E. M. Nemeth, J. C. Polanyi, S. D. Rosner, C. E. Young, *J. Chem. Phys. 44* (1966) 1168.
[54] D. S. Perry, J. C. Polanyi, C. Woodrow Wilson, Jr., *Chem. Phys. 3* (1974) 317.
[55] M. H. Mok, J. C. Polanyi, *J. Chem. Phys. 51* (1969) 1451.
[56] T. H. Dunning, Jr., *J. Phys. Chem. 88* (1984) 2469.
[57] J. C. Polanyi, *Discuss. Faraday Soc. 44* (1967) 293.
[58] Review: J. C. Polanyi, *Acc. Chem. Res. 5* (1972) 161.
[59] Review: J. C. Polanyi, J. L. Schreiber in H. Eyring, W. Jost, D. Henderson (Eds.): *Physical Chemistry - An Advanced Treatise, Vol. VIA. Kinetics of Gas Reactions*, Academic Press, New York 1974, Chap. 6, p. 383.
[60] P. J. Kuntz, E. M. Nemeth, J. C. Polanyi, *J. Chem. Phys. 50* (1969) 4607.
[61] C. A. Parr, J. C. Polanyi, W. H. Wong, *J. Chem. Phys. 58* (1973) 5.
[62] J. T. Muckerman, *J. Chem. Phys. 54* (1971) 1155; *56* (1972) 2997; *57* (1972) 3388.
[63] J. C. Polanyi, J. L. Schreiber, *Chem. Phys. Lett. 29* (1974) 319.
[64] J. C. Polanyi, J. L. Schreiber, *Faraday Discuss. Chem. Soc. 62* (1977) 267.
[65] C. F. Bender, S. V. O'Neill, P. K. Pearson, H. F. Schaefer III, *Science (Washington, DC) 176* (1972) 1412.
[66] H. F. Schaefer III, *J. Phys. Chem. 89* (1985) 5336.
[67] D. S. Perry, J. C. Polanyi, *Chem. Phys. 12* (1976) 419.
[68] P. J. Kuntz, M. H. Mok, J. C. Polanyi, *J. Chem. Phys. 50* (1969) 4623.
[69] D. R. Herschbach, *Faraday Discuss. Chem. Soc. 55* (1973) 233.
[70] M. G. Prisant, C. T. Rettner, R. N. Zare, *J. Chem. Phys. 81* (1984) 2699.
[71] a) N. H. Hijazi, J. C. Polanyi, *J. Chem. Phys. 63* (1975) 2249; b) *Chem. Phys. 11* (1975) 1.
[72] A. D. Walsh, *J. Chem. Soc. 1953*, 2266.
[73] J. J. Valentini, M. J. Coggiola, Y. T. Lee, *J. Am. Chem. Soc. 98* (1976) 853; *Faraday Discuss. Chem. Soc. 62* (1977) 232.
[74] J. W. Hudgens, J. D. McDonald, *J. Chem. Phys. 67* (1977) 3401.
[75] L. T. Cowley, D. S. Horne, J. C. Polanyi, *Chem. Phys. Lett. 12* (1971) 144.
[76] B. A. Blackwell, J. C. Polanyi, J. J. Sloan, *Chem. Phys. 24* (1977) 25.
[77] D. J. Douglas, J. C. Polanyi, *Chem. Phys. 16* (1976) 1.
[78] R. D. Coombe, G. C. Pimentel, *J. Chem. Phys. 59* (1973) 1535.
[79] D. L. Thompson, *J. Chem. Phys. 56* (1972) 3570.
[80] J. C. Polanyi, *Faraday Discuss. Chem. Soc. 55* (1973) 389.
[81] J. C. Polanyi, J. L. Schreiber, J. J. Sloan, *Chem. Phys. 9* (1975) 403.
[82] J. C. Polanyi, J. J. Sloan, J. Wanner, *Chem. Phys. 13* (1976) 1.
[83] K. G. Anlauf, D. H. Maylotte, J. C. Polanyi, R. B. Bernstein, *J. Chem. Phys. 51* (1969) 5716.
[84] J. C. Polanyi, D. C. Tardy, *J. Chem. Phys. 51* (1969) 5717.
[85] D. S. Perry, J. C. Polanyi, C. Woodrow Wilson, Jr., *Chem. Phys. Lett. 24* (1974) 484.
[86] T. J. Odiorne, P. R. Brooks, J. V. V. Kasper, *J. Chem. Phys. 55* (1971) 1980; J. G. Pruett, F. R. Grabiner, P. R. Brooks, *ibid. 63* (1974) 3335; *63* (1974) 1173.
[87] A. Gupta, D. S. Perry, R. N. Zare, *J. Chem. Phys. 72* (1980) 6237, 6250.
[88] F. Heismann, H. J. Loesch, *Chem. Phys. 64* (1982) 43.
[89] D. J. Douglas, J. C. Polanyi, J. J. Sloan, *J. Chem. Phys. 59* (1973) 6679.
[90] F. E. Bartoszek, B. A. Blackwell, J. C. Polanyi, J. J. Sloan, *J. Chem. Phys. 74* (1981) 3400.
[91] B. A. Blackwell, J. C. Polanyi, J. J. Sloan, *Chem. Phys. 30* (1978) 299.
[92] H. H. Dispert, M. W. Geis, P. R. Brooks, *J. Chem. Phys. 70* (1979) 5317.

[93] M. Hoffmeister, L. Potthast, H. J. Loesch, *Book of Abstracts, XII International Conference on the Physics of Electronic and Atomic Collisions*, Gatlinburg 1981.
[94] J. C. Polanyi, W. H. Wong, *J. Chem. Phys. 51* (1969) 1439.
[95] J. W. Duff, D. G. Truhlar, *J. Chem. Phys. 62* (1975) 2477.
[96] G. L. Hofacker, R. D. Levine, *Chem. Phys. Lett. 9* (1971) 617.
[97] J. C. Polanyi, N. Sathyamurthy, *Chem. Phys. 33* (1978) 287.
[98] B. A. Hodgson, J. C. Polanyi, *J. Chem. Phys. 55* (1971) 4745.
[99] M. H. Mok, J. C. Polanyi, *J. Chem. Phys. 53* (1970) 4588.
[100] G. S. Hammond, *J. Am. Chem. Soc. 77* (1955) 334.
[101] J. C. Polanyi, *J. Chem. Phys. 31* (1959) 1338.
[102] a) T. F. George, *J. Phys. Chem. 86* (1982) 10, and references cited therein; b) A. M. F. Lau, *Phys. Rev. A 13* (1976) 139; *14* (1976) 279; *Phys. Rev. Lett. 43* (1978) 1009; *Phys. Rev. A 22* (1980) 614; c) V. S. Dubov, L. I. Gudzenko, L. V. Gurvich, S. I. Yakovlenko, *Chem. Phys. Lett. 45* (1977) 330; S. I. Yakovlenko, *Sov. J. Quantum Electron (Engl. Transl.) 8* (1977) 151; d) A. E. Orel, W. H. Miller, *Chem. Phys. Lett. 57* (1979) 362; *J. Chem. Phys. 70* (1979) 4393; e) J. C. Light, A. Altenberger-Siczek, *ibid. 70* (1979) 4108.
[103] J. C. Polanyi, *Faraday Discuss. Chem. Soc. 67* (1979) 129.
[104] P. Arrowsmith, F. E. Bartoszek, S. H. P. Bly, T. Carrington Jr., P. E. Charters, J. C. Polanyi, *J. Chem. Phys. 73* (1980) 5895; H.-J. Foth, J. C. Polanyi, H. H. Telle, *J. Phys. Chem. 86* (1982) 5027; P. Arrowsmith, S. H. P. Bly, P. E. Charters, J. C. Polanyi, *J. Chem. Phys. 79* (1983) 283.
[105] P. Hering, P. R. Brooks, R. F. Curl, Jr., R. S. Judson, R. S. Lowe, *Phys. Rev. Lett. 44* (1980) 657; P. R. Brooks, R. F. Curl, T. C. Maguire, *Ber. Bunsenges. Phys. Chem. 86* (1982) 401.
[106] H. P. Grieneisen, H. Xue-Jing, K. L. Kompa, *Chem. Phys. Lett. 82* (1981) 421.
[107] J. K. Ku, G. Inoue, D. W. Setser, *J. Phys. Chem. 87* (1983) 2989.
[108] T. C. Maguire, P. R. Brooks, R. F. Curl, J. H. Spence, S. Ulrick, *J. Chem. Phys. 85* (1986) 844; *Phys. Rev. A 34* (1986) 4418.
[109] P. D. Kleiber, A. M. Lyyra, K. M. Sando, S. P. Heneghan, W. C. Stwalley, *Phys. Rev. Lett. 54* (1985) 2003; P. D. Kleiber, A. M. Lyyra, K. M. Sando, V. Zafiropolos, W. C. Stwalley, *J. Chem. Phys. 85* (1986) 5493.
[110] J. C. Polanyi, R. J. Wolf, *J. Chem. Phys. 75* (1981) 5951.
[111] H. R. Mayne, R. A. Poirier, J. C. Polanyi, *J. Chem. Phys. 80* (1984) 4025; H. R. Mayne, J. C. Polanyi, N. Sathyamurthy, S. Raynor, *ibid. 88* (1984) 4064.
[112] V. Engel, Z. Bacic, R. Schinke, M. Shapiro, *J. Chem. Phys. 82* (1985) 4844; V. Engel, R. Schinke, *Chem. Phys. Lett. 122* (1985) 103.
[113] E. B. D. Bourdon, J. P. Cowin, I. Harrison, J. C. Polanyi, J. Segner, C. D. Stanners, P. A. Young, *J. Phys. Chem. 88* (1984) 6100; E. B. D. Bourdon, P. Das, I. Harrison, J. C. Polanyi, J. Segner, C. D. Stanners, R. J. Williams, P. A. Young, *Faraday Discuss. Chem. Soc. 82* (1986).

Ether Cleavage with Organo-Alkali-Metal Compounds and Alkali Metals

By Adalbert Maercker*

In memoriam Georg Wittig

Reactions with organo-alkali-metal compounds are mostly carried out in ether-type solvents. It has long been known that ether cleavage takes place at the same time. The mechanism of the cleavage, in particular the fact that dialkyl ethers can be decomposed by a variety of mechanisms acting simultaneously, has only become clear in the most recent investigations. The observation that even with purely aliphatic ethers a considerable amount of Wittig ether rearrangement can occur is remarkable. Unusual secondary reactions can also occur by means of which alkyl- and aryllithium compounds in ether or tetrahydrofuran yield new organolithium compounds—sometimes with rearrangement. The reactions of alkyl aryl ethers with alkali metals are also varied and five different mechanisms for them have been discussed in the literature. It is interesting, for example, that the cleavage of anisole can be directed simply by changing the solvent so that in one case only cleavage of the aryl-oxygen bond occurs and in the other almost 100% cleavage of the alkyl-oxygen bond results. The formation of biphenyl as a by-product upon cleavage of the alkyl-oxygen bond in anisole was also puzzling. This was later shown to occur not through the dimerization of phenyl radicals but via 2-methoxybiphenyl. The number of cleavage mechanisms reduces to two if one assumes two different σ*-radical anions as being intermediates in the kinetically controlled reaction. Comparison of the reactivity of thioethers and ethers reveals not only gradual but also fundamental differences—the cleavage of the thioethers is thermodynamically controlled.

1. Introduction

Review articles concerning ether cleavage, in which also cleavages with organo-alkali-metal compounds and alkali metals are thoroughly dealt with, already appeared in the literature in 1954,[1] 1965,[2] and 1967.[3,4] A later review in 1983,[5] which, however, only touched on these areas, mentioned little which was new. The present review therefore concentrates mainly on developments over the last 20 years and includes many unpublished results from our research group. Older work which has already been mentioned in the earlier reviews[1-3] will only be cited where it is considered necessary for an understanding of newly developed mechanistic concepts. Likewise, the numerous syntheses with metalated benzyl,[6] allyl,[7-12] and vinyl[13-17] ethers, in which the cleavage of the ether bond was first achieved later, using other methods, will not be dealt with here.

2. Ether Cleavage with Organo-Alkali-Metal Compounds

2.1. Primary Reactions

2.1.1. *Protophilic Cleavage*

Theoretically there are four different reaction paths available for the cleavage of any dialkyl ether with a base R″Li (Scheme 1): β-, α-, and α,β′-elimination as well as the Wittig rearrangement. The number of possibilities doubles when R≠R′. It is clear that β-, α-, and α′,β-elimination as well as β′-, α′-, and α,β′-elimination lead to the same end products, respectively, so that only the Wittig rearrangement can be differentiated by product analysis.

An example from the literature in which the ether cleavage probably takes place via a β-elimination is the reaction of 2-methoxyoctane with isopropyllithium [Eq. (1)].[18] α-Eliminations have been observed with dimethyl ether and butyl methyl ether,[19] where the undetectable methylene carbenoid intermediate either combines with the alkyllithium compounds or is trapped, in the presence of cyclohexene, as norcarane [Eq. (2)].[20] If there is a hydrogen atom on the atom adjacent to the carbenoid center, stabilization usually occurs by means of a 1,2-hydride shift (Scheme 1).[21] The first α,β′-elimination was discovered with metalated benzyl ethyl ether,[22] and the mechanism was confirmed by means of isotopic labeling [Eq. (3)].[23] The Wittig ether rearrangement[24] was first observed in the reaction of benzyl methyl ether with phenyllithium [Eq. (4)].[22]

The decomposition of diethyl ether with organolithium compounds to ethylene and lithium ethoxide has been known for a long time.[19] In the literature the α-,[19] β-,[3] and even the α′,β-elimination[25] mechanisms have been postulated (Scheme 2), although, as has been pointed out, a decision on the basis of a product analysis is not possible. In order to clarify the cleavage mechanism we have prepared the α- and the β-deuterated diethyl ethers in a high state of purity and allowed them to react with perdeu-

[*] Prof. Dr. A. Maercker
Institut für Organische Chemie der Universität
Adolf-Reichwein-Strasse, D-5900 Siegen

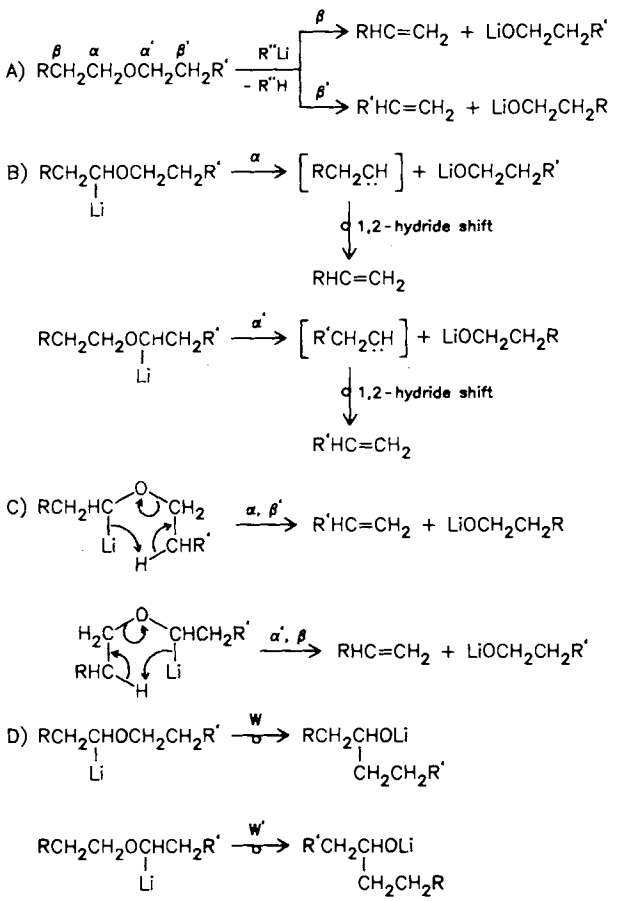

Scheme 1. Mechanism of protophilic dialkyl ether cleavage. A) β- or β′-elimination. B) α- or α′-elimination. C) α,β′- or α′,β-elimination. D) Wittig rearrangement (W or W′).

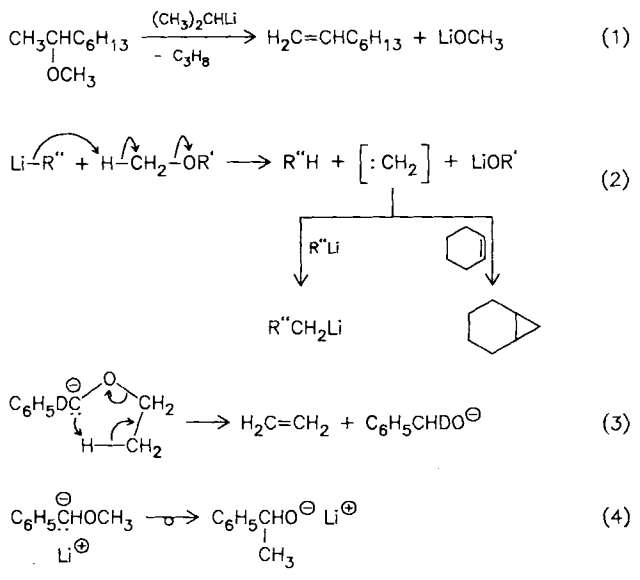

terioethyllithium.[26] Surprisingly, the two ethers are decomposed by different mechanisms. While the α-deuteriated ether undergoes exclusively β-elimination the extent of attack at the β-position in the β-deuteriated ether is reduced to 45% because of the isotope effect.[27] At the same time 10% α- and 45% α′,β-elimination are observed. Competition experiments with 1:1 mixtures of the α- and β-deuteriated diethyl ether on the one hand—in which almost exclusively the α-deuteriated ether was attacked—and α- and non-deuteriated diethyl ethers on the other—in which both ethers were decomposed in equal amounts—show that both the undeuteriated and the α-deuteriated ethers are cleaved by β-elimination.

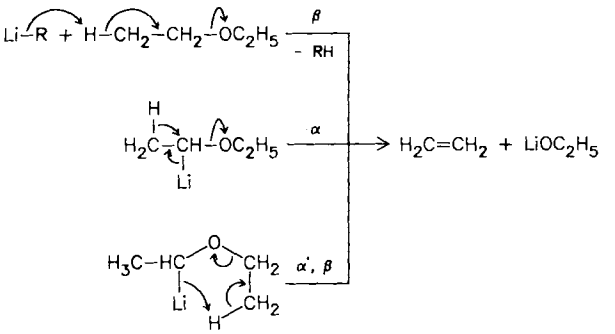

Scheme 2. Proposed mechanisms for the decomposition of diethyl ether by organolithium compounds.

Starting from diethyl ether,[26] ethers with shorter and longer alkyl groups were now systematically investigated, so that finally, with seven further α- and/or β-deuteriated dialkyl ethers, the cleavage mechanism—even for the mixed aliphatic ethers—could be completely elucidated.[28]

With the exception of dimethyl ether, in which exclusively α-elimination occurred, all the dialkyl ethers investigated were decomposed by several mechanisms operating simultaneously, one or other mechanism being preferred depending on the substitution pattern or the position of deuteriation. The following regularities were found for the course of the reaction:[28]

If the ether contained a β-methyl group the attack of the alkyllithium compound took place overwhelmingly at the primary β-C–H bonds, presumably via E2-elimination in which proton removal probably precedes C–O bond breaking. Thus, all ethyl ethers such as diethyl ether or butyl ethyl ether undergo, almost exclusively, β-elimination at the ethoxy group. A similar situation occurs with an α-methyl group, though the reactivity is slightly less, as is evidenced by the cleavage of methyl ethyl ether, in which α-elimination from the methoxy group (ca. 40%) competes with β-elimination from the ethoxy group (ca. 60%). The isotope effect[27] in β-deuteriated ethyl methyl ether is already sufficient to allow α-elimination to become the main reaction (ca. 80%). Here deuteriation has a very similar influence to that of alkyl chain elongation. This is strikingly evident on comparing β-deuteriated ethyl methyl ether and butyl methyl ether, which exhibit almost identical cleavage patterns. Apart from dimethyl ether, where only α-elimination is possible, the highest contribution of α-elimination (90%) is found, as expected, with the combination of alkyl chain elongation and β-deuteriation in β-deuteriated butyl methyl ether. In three β-deuteriated dialkyl ethers, besides α- and β-elimination a considerable amount of α′,β-elimination could also be detected.[28]

Interestingly, whenever the α-, β-, or α′,β-elimination is hindered we find a large amount of Wittig rearrangement taking place. We have observed[28] a maximum of

21%, for example, on using the specifically deuteriated dibutyl and butyl methyl ethers $(C_2H_5CD_2CH_2)_2O$ and $C_2H_5CD_2CH_2OCD_3$ [Eq. (5)]. Apart from in the case of di-

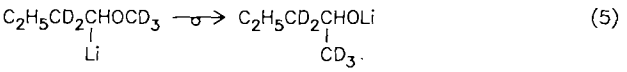

(5)

methyl ether, Wittig rearrangements were found to take place to a small extent with all ethers. Undeuteriated dibutyl ether as well as butyl trideuteriomethyl ether, $C_2H_5CH_2CH_2OCD_3$ still yield 12% of the product of a Wittig rearrangement. At the moment no definite statements can be made about the mechanism of this new form of the Wittig rearrangement for pure aliphatic ethers.[28]

We have not yet investigated the kinetics of the cleavage reactions in detail. However, it was especially interesting to find that the temperature coefficient for the cleavage of diethyl ether with *n*-butyllithium or isobutyllithium is negative[29-31] when the reactions are carried out in *n*-heptane with equimolar amounts of the reactants. The increase in the reaction rate as the temperature is reduced from +30°C to −21°C is explained by the shifting of the solvation equilibrium (6) to the left favoring a kinetically more

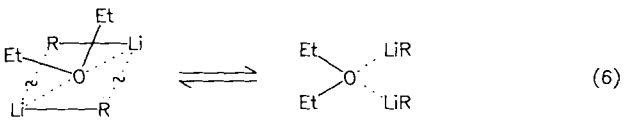

(6)

active solvate. Other simple ethers behave similarly, but not, however, mixed ethers such as *n*-butyl *tert*-butyl ether, where a positive temperature coefficient has been found for the cleavage with *n*-butyllithium.[32]

The investigations were also extended to tetrahydrofuran (THF), which behaves kinetically like the simple ethers, that is the rate of cleavage with *n*-butyllithium decreases on increasing the temperature from −20°C to +20°C.[33,34] The *mechanism* of the cleavage of THF is, however, quite different from that of the open-chain dialkyl ethers: after the α-metalation, a [π4s + π2s] cycloreversion occurs with the formation of ethylene and the enolate of acetaldehyde [Eq. (7)].[35,36] A β-hydrogen atom of the

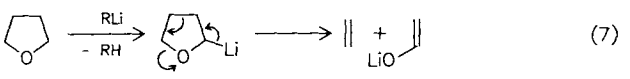

(7)

ring is not attacked, since the steric prerequisites for an E2-elimination in a five-membered ring are unfavorable. A seven-membered ring is the first which can assume the requisite geometry without difficulty [Eq. (8)].[36,37]

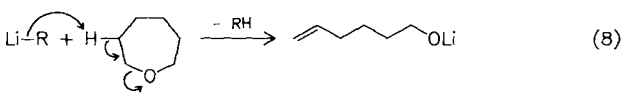

(8)

Alkyl groups in the 2-position of the five-membered ring favor a β-elimination; however, as expected, a side-chain proton is removed exclusively (Scheme 3).[36,38,39] Also in the case of 2-substituted six-membered rings the attack of

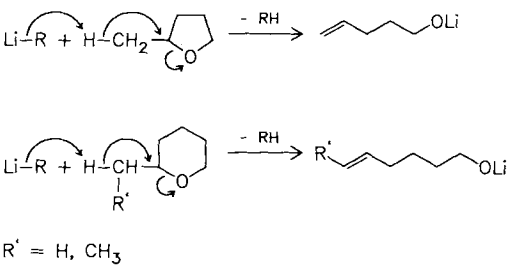

Scheme 3. β-Elimination with *n*-butyllithium in 2-alkyl-substituted THF and tetrahydropyran.

the protophile occurs exclusively on the side chain,[38] even if the methyl group is replaced by an ethyl group.[40] Interestingly, the β-elimination can be suppressed in favor of the α-elimination by using butylpotassium as base.[39]

The course of the reaction with dihydropyrans depends on the position of the double bond in the ring. Dihydropyran with the double bond in the α,β-position can be metalated, with amylsodium, at the β-vinyl position; subsequent β-elimination then leads to formation of 4-pentynolate, which is also obtained from 2-methylenetetrahydrofuran [Eq. (9)].[41] If the double bond is in the β,γ-position, metal-

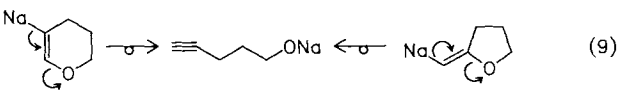

(9)

ation by *n*-butyllithium takes place in the 2-position, and subsequent rearrangement leads to a cyclopropyl-substituted enolate [Eq. (10)].[42]

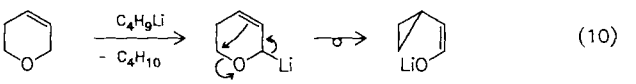

(10)

The course of the reaction of alkyl *aryl* ethers with perdeuteriated ethyllithium has been thoroughly studied, by us, using phenetole.[43] Here again, the cleavage mechanism is—as with diethyl ether[26,28]—strongly dependent on the position of deuteriation. While we were able to confirm, with α-deuteriated phenetole, the β-elimination already found by *Letsinger* et al.[23] on using propylsodium, with β-deuteriated phenetole (Scheme 4) this form of elimination could no longer be detected.[43] The main reaction is, in each case, *ortho*-metalation;[44] the *o'*,β-elimination

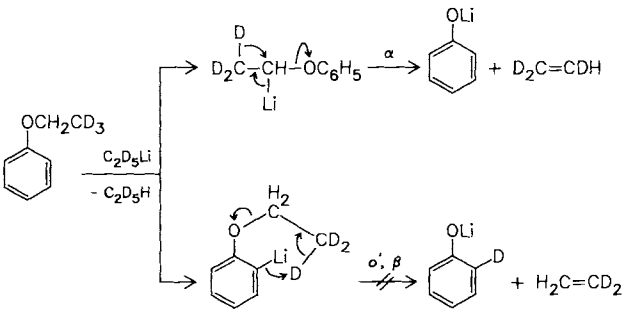

Scheme 4. Reaction of β-deuteriated phenetol with perdeuterioethyllithium.

(here *o'* indicates that the *o* and β positions are situated on different sides of the oxygen atom),[45] which was expected to follow, could be ruled out. This reaction does, however, take place to a small extent (16%) with 1-methoxy-2-phenoxyethane, where *inter*molecular elimination still predominates.[46]

The most interesting subsequent reaction of metalated phenetole is, undoubtedly, the condensation of two molecules of 2-ethoxyphenyllithium with elimination of lithium ethoxide, leading to 2-ethoxy-2'-lithiobiphenyl (Scheme 5).[43] The intermediate formation of dehydrobenzene, i.e. the *intra*molecular elimination of lithium ethoxide, as has been observed in the photolysis[47] of 2-methoxyphenyllithium, can be excluded with THF as the solvent.[48] Only in the presence of *N,N,N',N'*-tetramethylethylenediamine (TMEDA) in the dark was dehydrobenzene formed as an intermediate which could be trapped with anthracene with the formation of triptycene.[43] We formulate the *inter*molecular elimination of lithium alkoxide via the formation of a dimeric species (Scheme 5)

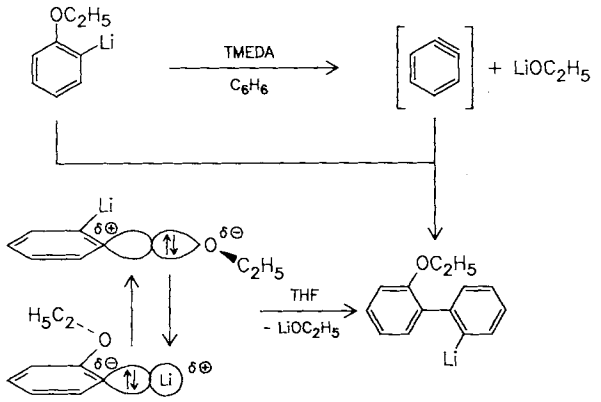

Scheme 5. Condensation reaction of metalated phenetole.

which probably first dissociates under the influence of TMEDA into a monomeric ion pair, which then undergoes reaction according to the aryne mechanism.[49]

Open-chain alkynes are formed by β-elimination from vinyl ethers,[41,50] and also from 2-chloroethyl ethers.[51,52]

2.1.2. *Nucleophilic Cleavages*

Only mesomerically stabilized, soft, organolithium compounds such as tritylithium,[53] 1,1-diphenylhexyllithium,[54] or benzhydryllithium[55,56] are capable of cleaving THF nucleophilically [Eq. (11)].

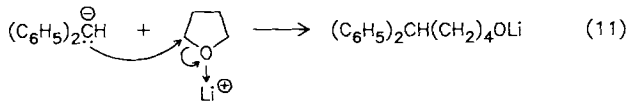

We were unable[40,57] to reproduce the corresponding reaction with ethyllithium.[35] Even benzyllithium tends to prefer protophilic cleavage;[57] however, in perdeuteriotetrahydrofuran this is so suppressed by the isotope effect[27] that nucleophilic cleavage predominates.[58,59]

The counterion is clearly involved in the reaction, since tritylsodium reacts only in the presence of triphenylboron.[60] Radical anions of naphthalene, anthracene, and biphenyl with lithium—but not sodium—as the counterion are also able to cleave THF nucleophilically.[61]

Hard organolithium reagents, even lithium acetylides,[62] can be activated for a nucleophilic attack on THF and smaller rings, if they are used in the presence of boron trifluoride ether [Eq. (12)].[63] On changing over to organo-

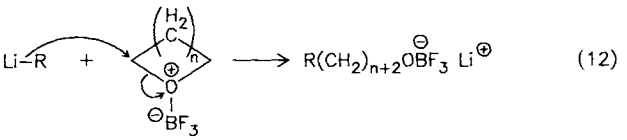

copper compounds,[64] especially in the presence of boron trifluoride,[65] there is a dramatic increase in reactivity.

Interestingly, unlike THF, tetrahydropyran is attacked nucleophilically by butyllithium without the addition of any other reagents; the yield of 1-nonanol at room temperature after 2–3 days is about 20%.[40] Tetrahydropyran is, therefore, less stable than diethyl ether towards butyllithium, although it is not attacked nucleophilically by 1,1-diphenylhexyllithium.[54] Dihydropyran, with the double bond in the α,β-position, reacts with butyllithium to give *trans*-4-nonen-1-ol [Eq. (13)].[40,66] Here, as with the open-

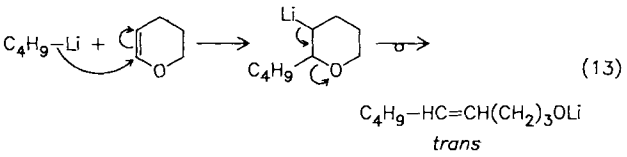

chain vinyl ethers,[50,54,67] an addition-elimination mechanism is probably involved. With hard bases there is competition from protophilic cleavage [cf. Eq. (9)],[50] or metalation occurs in the α-position.[13–17]

The S_N2 or S_N2' attack of organolithium compounds on allyl ethers, which takes place particularly easily,[68] is generally sterically controlled, but also dependent on the solvent used.[54] Conversion of the organolithium compounds into corresponding organocopper compounds or cuprates allows one to steer the reaction in one direction or the other (Scheme 6).[69]

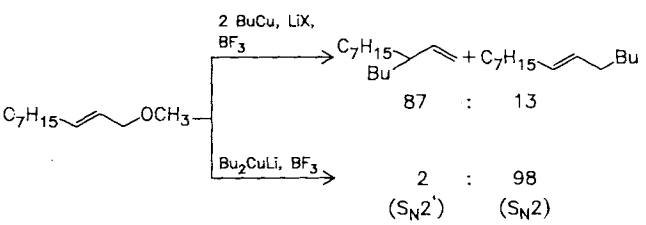

Scheme 6. Influence of the organometallic compound on the course of reaction in allyl ethers.

Even the methyl group in anisole can be attacked by nucleophiles,[54] although, in the case of alkyllithium compounds, only when it is twisted out of the plane of the ar-

ene ring by the presence of two *ortho*-substituents.[70, 71] With phenylcesium prepared in situ, however, we have also observed a nucleophilic attack on unsubstituted anisole.[72]

For the attack of 1,1-diphenylhexyllithium on a variety of ethers the following reactivity series is found:[54] Allyl-O > Vinyl-O > Methyl-O ≫ Aryl-O.

2.2. Secondary Reactions

Metalated dimethyl ether and alkyl methyl ethers metalated on the methyl group undergo an interesting secondary reaction with the unreacted organolithium compound involving a methylene insertion into the Li-C bond.[19] With hexyllithium we have observed up to ten methylene insertions.[28] Presumably this occurs via a direct attack of the alkyllithium compound R″Li on the α-metalated ether [Eq. (14)] without the formation of a free carbene intermediate.[73] This view is supported by the finding[28] that such carbene insertions are only observed with methyl ethers; in the case of secondary alkoxyalkyllithium compounds ROCH(R′)Li, the attack of an alkyllithium compound is hindered both sterically and inductively, and, as a consequence, intramolecular reactions such as α,β′-elimination and the Wittig rearrangement are much more favorable. In addition there is, in general, always the possibility of an α-elimination occurring, followed by an intramolecular 1,2-hydride shift (cf. Scheme 1B)[21]—as has been demonstrated in particular with β-deuteriated diethyl ether and β-deuteriated dibutyl ether.[28]

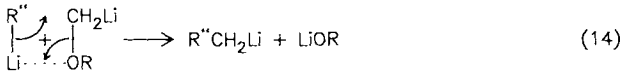

(14)

However, we have, quite accidentally,[74] also observed the gradual formation of higher homologous alkyllithium compounds during the decomposition of organolithium compounds in diethyl ether and THF. A systematic investigation[27] of this secondary reaction showed that the ethylene formed in the primary reaction inserted itself several times into the Li-C bond of the still unreacted organolithium compound [Eq. (15)]. This corresponds to a carbanion-initiated ethylene oligomerization, a reaction which was earlier[75] believed to be possible only under a pressure of several hundred atmospheres. Starting with *n*-butyllithium, up to twelve ethylene insertions could be demonstrated mass spectroscopically, and, after hydrolysis, in contrast to the reaction in dimethyl ether, only *n*-alkanes with an even number of carbon atoms were obtained.[27] The analogous reaction starting from secondary and tertiary alkyllithium compounds,[76] or from naphthalene dianions,[77] strangely comes to a halt after the insertion of one ethylene unit into the Li-C bond. Phenyllithium (Scheme 7) behaves like *n*-butyllithium but only in diethyl ether as solvent. In THF, after two insertions of ethylene into the Li-C bond a 1,4-proton shift occurs, leading to the formation of 1-phenylbutyllithium, which then either reacts further with ethylene or attacks the THF nucleophilically.[57] The intramolecular course of the reaction was confirmed in a later study.[58]

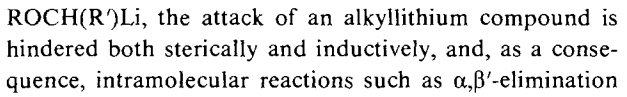

(15)

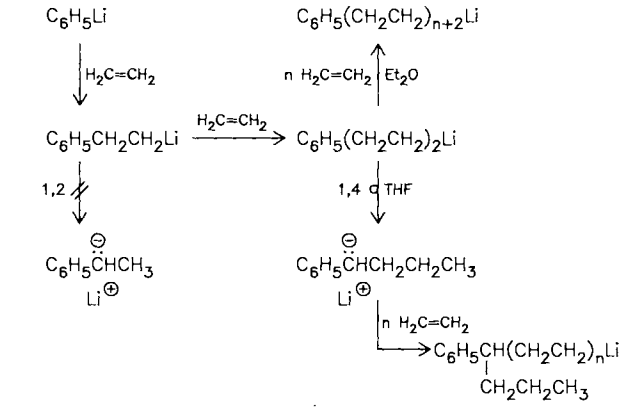

Scheme 7. Insertion of ethylene from Et_2O and THF into the Li-C bond of phenyllithium.

The formation of 1-phenylpropyllithium from benzyllithium and ethylene in THF, however, depends—contrary to earlier opinion[57]—on an *inter*molecular transmetalation of propylbenzene by still unchanged benzyllithium[59] and not on an *intra*molecular 1,3-proton shift [Eq. (16)].[58]

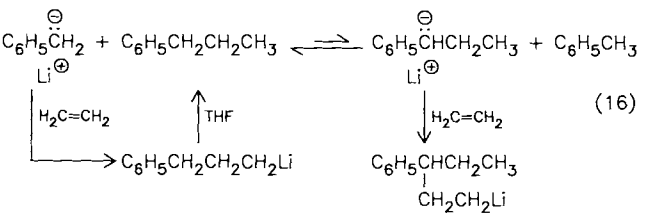

(16)

The equilibrium lies well to the left ($K^{293} = 1.1 \times 10^{-4}$), but since 1-phenylpropyllithium reacts very much faster with ethylene than benzyllithium it is continuously removed from the system, so that eventually the branched molecule is obtained as the major product of the secondary reaction.[59]

Branched products are also obtained from the decomposition of ethyllithium in phenetole.[43] Interestingly however they are derived not from ethyllithium but from *o*-ethoxyphenyllithium (Scheme 8). Here also the rearrange-

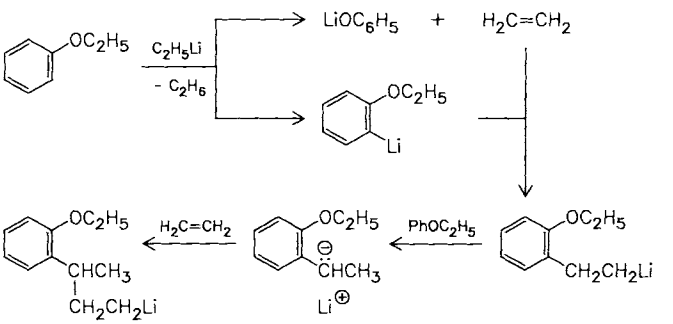

Scheme 8. Branched products from phenetole and ethyllithium.

ment of (2-(*o*-ethoxyphenyl)ethyllithium to 1-(*o*-ethoxyphenyl)ethyllithium) takes place *inter*molecularly, since neither 1,2- nor 1,3-*intra*molecular proton shifts are possible.[58]

In the corresponding, extremely slow reaction of phenyl propyl ether with ethyllithium the propylene generated in the primary reaction inserts itself into the Li-C bond to give, contrary to expectations, the secondary and not the primary organolithium compound [Eq. (17)].[49]

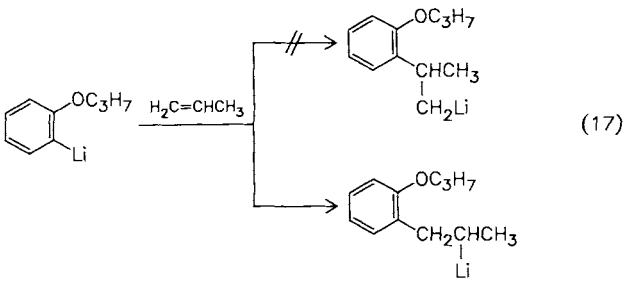

(17)

2.3. Cleavage of Thioethers

Thioethers can also be cleaved protophilically or nucleophilically, but are, however, clearly differentiated from the ethers in their reactivity. In addition, there is the possibility of a thiophilic attack, i.e. a nucleophilic attack on sulfur. What is striking is the ease with which α′,β-eliminations occur even with alkyl methyl sulfides [Eq. (18)].[78]

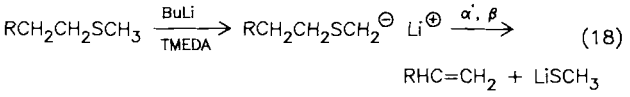

(18)

This is undoubtedly because of the higher acidity of the methylthio group, which is even higher than that of benzylic protons (Scheme 9).[79] The *ortho*-positions of an arene ring are, nevertheless, much less activated by SMe than by OMe (Scheme 9).[80]

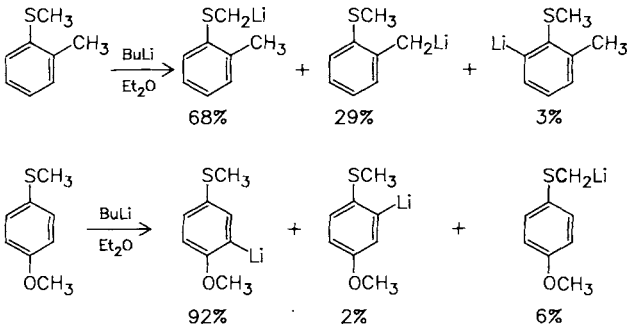

Scheme 9. Comparison of the reactivity of ArylSMe/ArylMe and ArylSMe/ArylOMe.

Protophilic and nucleophilic cleavage often occur simultaneously; with (1-methylthioethyl)benzene, for example, β-elimination, coupling, and Wittig rearrangement occur.[81]

Interestingly, in the metalation of benzyl methyl sulfide with butyllithium both the coupling reaction and the Wittig rearrangement can be suppressed by employing hexane with added TMEDA as the solvent instead of diethyl ether.[82] By varying the solvent, *n*-butyllithium can also be made to react with 2,5-bis(methylthio)thiophene, either as a thiophile or as a protophile [Eq. (19)].[83] Sometimes protophilic and thiophilic steps occur consecutively [Eq. (20)].[84,85]

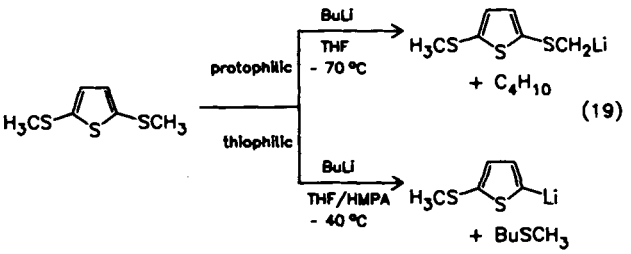

(19)

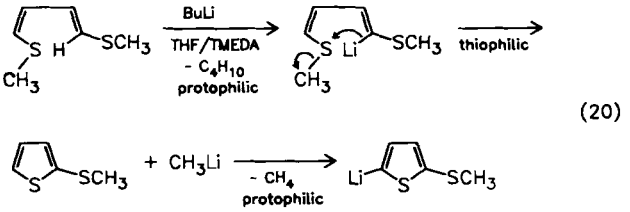

(20)

3. Ether Cleavage with Alkali Metals

3.1. Cleavage with Lithium

Cleavage of certain ethers such as allyl[86] and benzyl[87] ethers with lithium is very important for the synthesis of mesomerically stabilized organolithium compounds, which, because of extensive Wurtz coupling, are not readily available from the corresponding halo-compounds [Eqs. (21) and (22)].

(21)

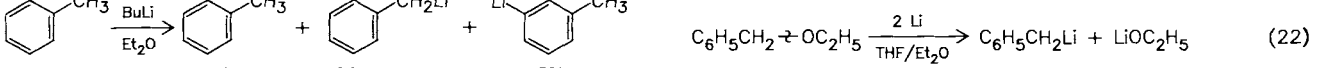

(22)

In order to establish whether the allyl- or the benzyl-oxygen bond is most easily cleaved we allowed allyl benzyl ether to react, under the same conditions, with lithium in THF.[88] Surprisingly, neither allyl- nor benzyllithium were obtained. The benzyl-oxygen bond was indeed cleaved but the benzyllithium formed as a primary product reacted with the simultaneously formed lithium allyl oxide to form an adduct [Eq. (23)][89] whose Li-C bond, as one might ex-

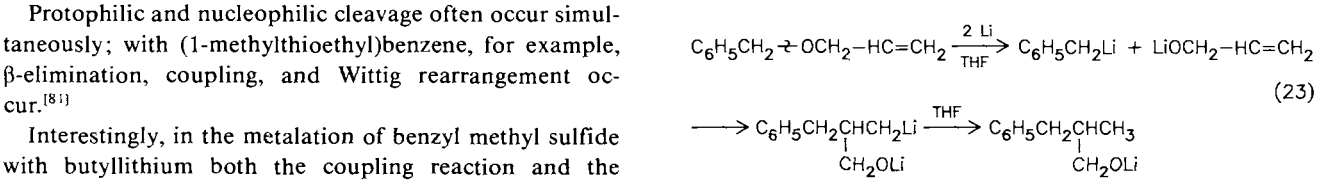

(23)

pect, is not stable in THF.[88] Also when the allyl group in allyl phenyl ether was replaced by a cyclopropylmethyl group, we did not isolate the initially formed alkyllithium compound in analogy to (21).[90] The homoallyllithium formed by rearrangement is, in contrast to allyllithium, so strongly basic that it deprotonates the phenyl ring of the starting material in the *ortho*-position (Scheme 10).[90] We have found a quite similar course of reaction in the case of anisole (Scheme 10).[90] The fact that this *ortho*-metalation

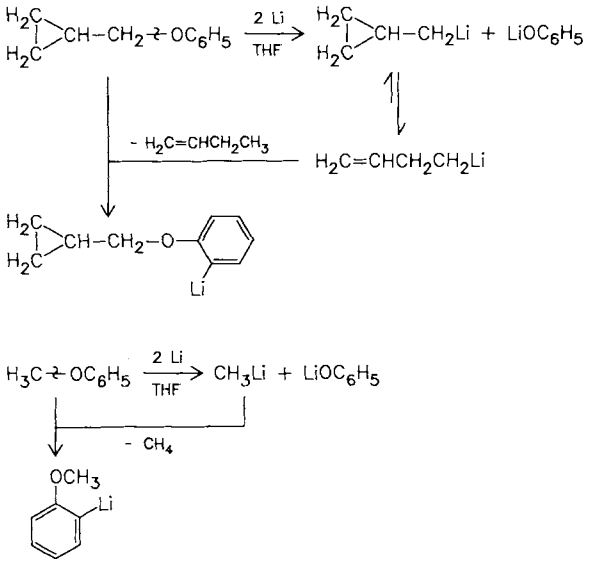

Scheme 10. *ortho*-Metalation as secondary reaction in the reaction of alkyl aryl ethers with lithium.

has not been observed before[91] is probably due to the use of hydrolytic work-up procedures. Our observations were, however, confirmed later—also in the corresponding cleavage of diphenyl ether by lithium.[92]

In order to cleave less reactive ethers it is often useful to catalyze the reaction by making use of electron transfer in the presence of biphenyl,[90-93] naphthalene,[92,93] phenanthrene,[92] or even pyridine.[94] In this way, even THF can be cleaved.[91]

Interestingly, in the cleavage of anisole with lithium in THF we also found biphenyl, although none had been added, especially when the reaction was carried out at relatively high concentrations (>3 molar).[48] It is formed via 2-methoxybiphenyl [Eq. (24), cf. also Scheme 5], which,

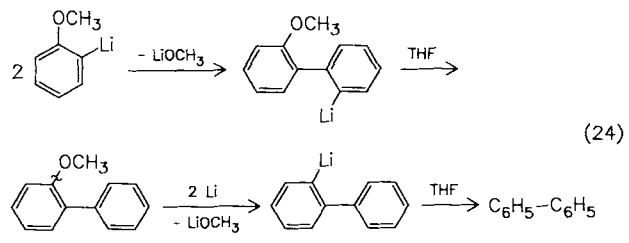

(24)

under the conditions used, suffers aryl-oxygen cleavage only, as was also demonstrated in a separate experiment.[48] Formation of an arene intermediate can be ruled out, since, when starting with 4-methyl-anisole, 3,3'-bitolyl should be found together with the 3,4'-bitolyl that is formed.[48]

As a gross simplification one can say that, under otherwise identical conditions, the degree of aryl-oxygen cleavage is higher, in general, with a more extended aromatic system. Even with anisole (Scheme 11) we do not find exclusive cleavage of the methyl-oxygen bond, although it exceeds 80%—at least in THF.[48] Just how important the solvent is, can be gauged from the observation that for anisole in heptane practically only phenyl-oxygen cleavage takes place, and that the reaction with lithium powder at room temperature only reaches 75% completion after 14 days.[72]

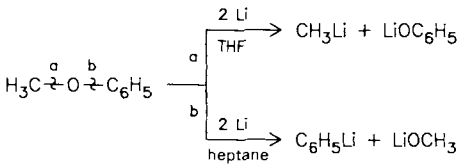

Scheme 11. Influence of solvent on the cleavage of anisole with lithium.

The cleavage of the methoxynaphthalenes in THF [Eq. (25)] lies, with regard to its regioselectivity, between that of

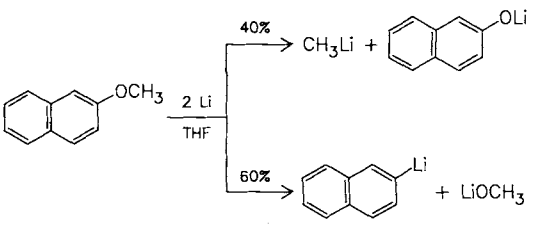

(25)

anisole and 2-methoxybiphenyl. In contrast to anisole, no metalation of the starting materials by the organolithium compounds formed was observed. This is probably because cleavage occurs much more rapidly than metalation, a fact which can be deduced from the exothermic nature of the reaction.[48] In this connection it is interesting to note[92] that diphenyl ether is only *ortho*-metalated if lithium-naphthalene is used in less than molar proportions. This might also be due to competition between cleavage and metalation.

The yield of β-naphthol in the cleavage of nerolin (2-methoxynaphthalene) in THF exceeds 90% if lithium-naphthalene is used instead of lithium.[95] Aryl-oxygen cleavage predominates—also in THF—whenever the methyl group is twisted out of the plane of the aromatic system (**1**),[48] or when it is replaced by a methoxymethyl group (**2**) or other acetal group, e.g. tetrahydropyranyl ether (Scheme 12).[96] A *tert*-butyl group has the opposite

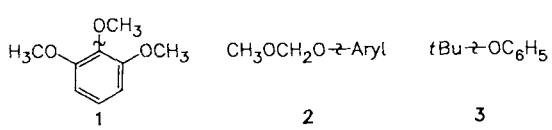

Scheme 12. Types of compounds in which one of the C–O bonds is preferentially cleaved.

effect,[48,96] and in the case of *tert*-butyl phenyl ether (**3**), for example, alkyl-oxygen cleavage predominates to the extent of 99%.[48] The influence of structure and solvent on the regioselectivity of the cleavage will be discussed in more detail later. It should, however, be pointed out here and now that, in the case of methyl substituted dibenzofurans[97] and diphenyl ethers,[98] the bond between the unsubstituted ring and the oxygen atom is preferentially cleaved (Scheme 13).

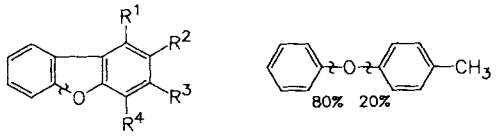

R^1, R^2, R^3, R^4 = H, CH_3

Scheme 13. Mode of cleavage in unsymmetrically substituted diaryl ethers.

The organolithium compound formed in the primary reaction naturally defies detection when the reaction is carried out in ethylenediamine,[98] ethylamine,[99] or HMPA[95,100] as a solvent.

In the cleavage of epoxides with lithium, even different products are obtained depending on whether protic or aprotic solvents are used (Scheme 14). In ethylenediamine,

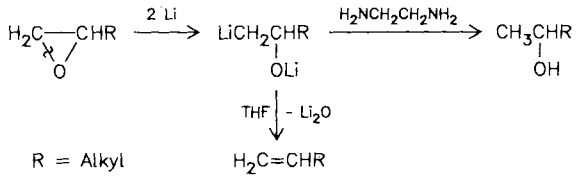

R = Alkyl

Scheme 14. Influence of solvent on the isolable products in the cleavage of epoxides with lithium.

the product of the primary reaction, a β-lithioalkoxide, is protonated to an alcohol,[101,102] whereas in boiling THF it splits off lithium oxide with the formation of the corresponding alkene.[103] Only with lithium-biphenyl or lithium-naphthalene at −80 °C has it been possible to prepare the β-lithioalkoxides unchanged and to derivatize them with nucleophiles.[93] For R = C_6H_5,[93] $CO_2C_2H_5$,[93] or C≡CH[104] the other C-O bond of the epoxide ring (not marked in Scheme 14) is broken.

3.2. Cleavages with Higher Alkali Metals

For many years ether cleavages have been carried out with sodium or potassium in liquid ammonia[105-112] or hexamethylphosphoric acid triamide (HMPA).[113-116] Naturally, no organometallic intermediates can be isolated, since they are immediately protonated by the solvent. Alkyl aryl ethers are usually dealkylated to phenols (alkyl-oxygen cleavage); the ease of splitting off alkyl decreases along the series: $PhCH_2 > CH_3 > n$Pr, iPr.[109,116] Acetals undergo aryl-oxygen cleavage, the breaking of the bond taking place preferentially in the *meta*-position to electron releasing substituents [Eq. (26)] and in the *para*-position to electron withdrawing substituents [Eq. (27)].[107,109] The

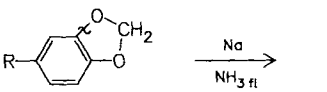

(26a)

R = H, CH_3, C_3H_7, $H_2C=CHCH_2$

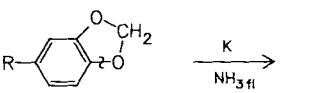

(26b)

R = CO_2H, $H_3C-HC=CH$

methyleneoxy group is released as formaldehyde, as shown in reaction (28) (DME = dimethoxyethane), in which the formaldehyde is incorporated, to some extent, into the primary product.[117] Open chain acetals are decomposed in a corresponding fashion.[109]

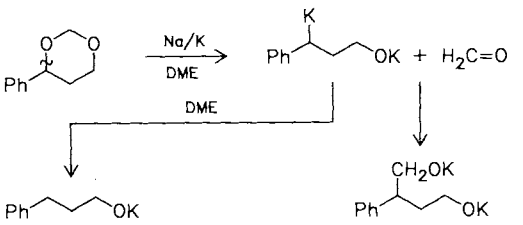

(27)

In HMPA, nerolin yields an almost 1:1 mixture of naphthalene and β-naphthol.[114] 1-Methoxynaphthalene reacts analogously with potassium in DME/THF.[95]

With diphenyl ethers the substituents play a role in determining the direction of cleavage (Scheme 15): electron releasing groups reduce the tendency toward bond breaking between the oxygen atom and the substituted ring in the order p-$CH_3 < p$-$OCH_3 < p$-NH_2, while electron withdrawing groups such as p-CO_2H increase it.[105,106]

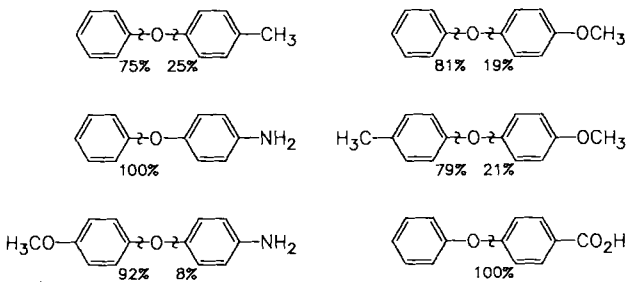

Scheme 15. Influence of substituents on the mode of cleavage in diphenyl ethers.

If the reactions of diaryl ethers[118] or dibenzofuran[119] with alkali metals are carried out in ether-type solvents such as DME or THF then the primarily formed radical anion can be detected by means of ESR-spectroscopy. With aryl *methyl* ethers this is not, however, always possible. Only in six of the eleven ethers investigated (Scheme 16) could we observe the ESR spectrum of the original radical anion $ArylOCH_3^{\odot\ominus}$ after reduction with potassium in THF at 170 K; in the remaining cases it was that of the corresponding cleavage product $ArylH^{\odot\ominus}$.[120]

From these findings there emerges a remarkable dependence of the stability of the primarily formed radical anion $ArylOCH_3^{\odot\ominus}$ on the bond order, calculated by the Hückel method, of the aryl-oxygen bond. As soon as the π-bond order falls below 0.19 only the ESR spectrum of the radical anion $ArylH^{\odot\ominus}$ can be observed, even at low temperatures (170 K).[120] Particularly interesting in this respect was the finding that in the decomposition of 3,4-dimethoxytoluene (4-methylveratrole) only one of the two aryl–oxygen bonds was split, namely that for which a π-bond order of 0.169 was calculated, while the other with a π-bond order of 0.196 remained unaffected.[120] A borderline case is that of 9-methoxyanthracene with a π-bond order of 0.197. Here, one can demonstrate very nicely that the stability of the radical anion is also dependent on the nature of the counterion, the ease of decomposition falling off in the order Li > Na > K > Rb > Cs. With lithium, even at low temperatures, the ESR spectrum of the anthracene radical anion $ArylH^{\odot\ominus}$ appears, while with sodium, between −110 and −30 °C, one observes the radical anion of the starting ether $ArylOCH_3^{\odot\ominus}$ and at room temperature $ArylH^{\odot\ominus}$. With potassium and cesium as counterions the radical anion of 9-methoxyanthracene is stable at room temperature for long periods and the ESR spectrum of $ArylOCH_3^{\odot\ominus}$ is then gradually replaced—more slowly with cesium than with potassium—by that of the anthracene radical anion $ArylH^{\odot\ominus}$.[120] With dibenzofuran also, it has been observed that the decomposition of the radical anion with lithium as the counterion is 25 times faster than with cesium.[119]

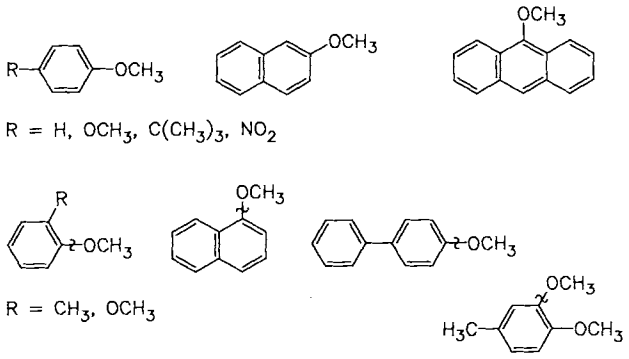

Scheme 16. ESR spectra could be obtained of the aryl methyl ethers of the first row after reduction with potassium in THF. In the case of the ethers of the second row the cleavage was too rapid.

In the presence of dicyclohexyl[18]crown-6, veratrole yields the radical anion of *o*-benzoquinone; that is, both *methyl*-oxygen bonds are cleaved [Eq. (28a)].[121]

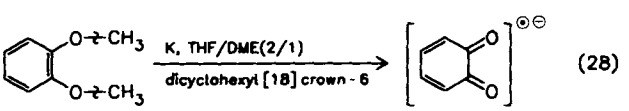

(28)

On the other hand, both *aryl*-oxygen bonds are cleaved in 4,4′- and 2,2′-dimethoxybiphenyl; the intermediate could only be detected (by ESR spectroscopy) in the case of the 4,4′-derivative (Scheme 17).[122]

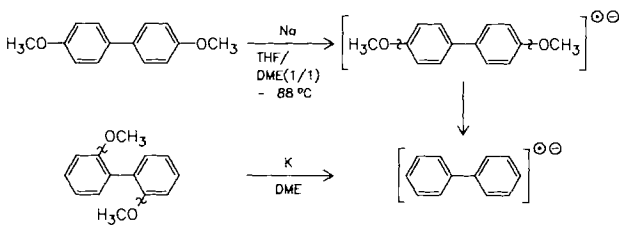

Scheme 17. Ether cleavage in methoxy-substituted biphenyls.

At first the appearance of biphenyl in the cleavage of anisole with potassium in DME was puzzling, since at that time none of the mechanisms under discussion could be reconciled with the results of the isotopic labeling experiments.[123] If the assumptions developed by us for the case of lithium can be extended to the mode of reaction of the higher alkali metals, the "strange behavior of anisole"[124] would be easily explained in terms of the mechanism shown in Equation (29). Clearly, anisole can also act as a proton donor, in place of DME, in the decomposition of the biphenylylpotassium compounds which occur as intermediates—particularly when the solvent is deuteriated. When the reaction is carried out in perdeuteriated DME, no deuterium from the solvent is found in the biphenyl that is formed.[123]

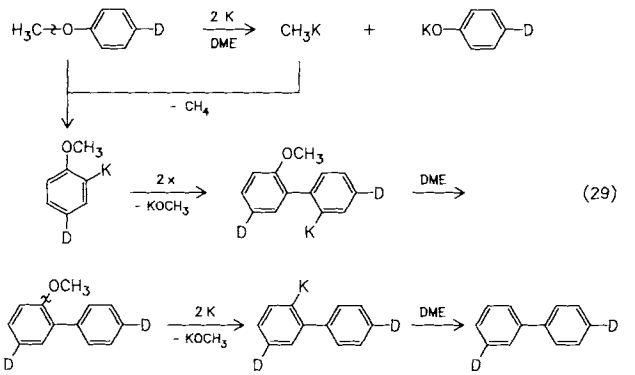

(29)

Even for the preparation of mesomerically stabilized organosodium and -potassium compounds—with the exception of benzhydryl and trityl compounds[125]—ether-type solvents such as THF and DME are not suitable, since Wurtz coupling,[125] Wittig rearrangement,[126] and other secondary reactions[127] can occur—with strongly basic compounds also protonations.[117, 125] Wittig rearrangements have also been observed in HMPA.[114] The best solvents are, therefore, aliphatic hydrocarbons such as hexane[128] and heptane;[129, 130] however, other than in THF, the cleavage of anisole this time takes place at the phenyl-oxygen bond (Scheme 18).[130]

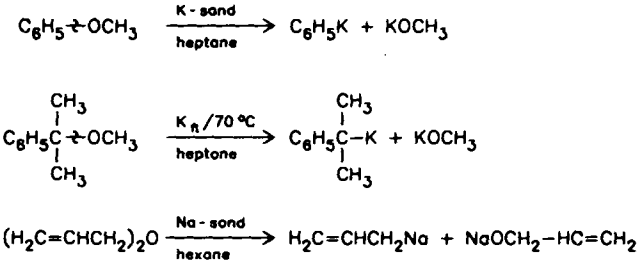

Scheme 18. Syntheses of some organo-sodium and -potassium compounds.

In the preparation of allyl- and benzyltrimethylsilane from allyl- and benzylsodium it is obviously better, even in *n*-decane or toluene, to carry out the ether cleavage in the presence of chlorotrimethylsilane.[131] A secondary reaction, which however only takes place to a large extent at 60°C, has been observed by us in the cleavage of anisole with cesium in heptane.[72] The phenylcesium attacks the methoxy group nucleophilically with the formation of toluene and cesium phenolate [Eq. (30)].

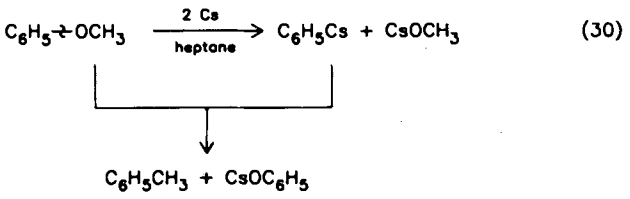

(30)

3.3. Influences on the Direction of Cleavage in Alkyl Aryl Ethers

3.3.1. Influence of Structure

In the reduction of alkyl aryl ethers with alkali metals both the alkyl-oxygen and the aryl-oxygen bond can be broken. In most cases one observes both directions of cleavage [Eq. (31)]. In the ESR spectrum one only sees the

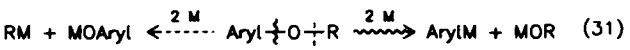

(31)

fragment due to aryl-oxygen cleavage—however little there is—since the phenolate formed by alkyl-oxygen cleavage forms no radical anion and therefore cannot be observed. This is why, in the reduction of anisole with potassium in DME,[123] an unimportant secondary reaction, which leads to the formation of biphenyl [see Eq. (29)], is observed in the ESR spectrum, while the main reaction—cleavage of the methyl-oxygen bond to give methylpotassium and potassium phenolate—is not. Influences on the regioselectivity of the cleavage can therefore only be studied when all the cleavage products can be analytically determined.

For this reason we have taken anisole as the starting point and varied the alkyl residue systematically, and, after carrying out the cleavage with each compound under identical conditions [lithium powder in boiling THF (2 h)], have analyzed the products by gas chromatography[48] (Table 1). It is obvious that the amount of alkyl-oxygen cleavage falls off strongly at first on going from anisole to phenetole but then rises again with isopropyl and *tert*-butyl ethers. A similar pattern is found with the corresponding naphthyl ethers except that it is shifted in favor of the aryl-oxygen cleavage, i.e. here also there is a minimum in the alkyl-oxygen cleavage with the ethyl ether (Table 2). Another important observation is that there is no connection between the rate of the reaction and the cleavage pattern. Ethyl naphthyl and isopropyl naphthyl ethers (1 : 1) react with a substoichiometric amount of lithium at approximately the same rate although they show totally different cleavage patterns.[48]

Table 1. Regioselectivity of the cleavage of alkyl phenyl ethers with lithium in THF [37].

R	% C_6H_5O–R	% C_6H_5–OR
CH_3	82	18
C_2H_5	59	41
$CH(CH_3)_2$	84	16
$C(CH_3)_3$	99	1

Table 2. Regioselectivity of the cleavage of alkyl naphthyl ethers with lithium in THF [37].

R	% Naphthyl–O–R		% Naphthyl–OR	
	α	β	α	β
CH_3	36	40	64	60
C_2H_5	2	1	98	99
$CH(CH_3)_2$	57	53	43	47
$C(CH_3)_3$	87	97	13	3

Substituents on the arene ring also influence the direction of cleavage, as can be shown in the example of the cresol ethers[48] (Table 3). The *para*-compound yields values comparable with those of anisole, whereas the extent of methyl-oxygen cleavage in the *ortho*-compound is clearly higher, and in the case of the *meta*-compound it is considerably lower.

Table 3. Influence of the position of methyl on the cleavage of cresol ethers with lithium in THF [37].

H_3C–C_6H_4–OCH_3	% C_7H_7O–CH_3	% C_7H_7–OCH_3
ortho	91	9
meta	68	32
para	79	21

The introduction of a second methoxy group, particularly in the *para* position, leads in each case to a marked increase in the amount of cleavage of the the aryl-oxygen bond. In addition, we have shown that veratrole is cleaved faster, by a factor of 7, than anisole.[48] Particularly interesting is the influence, in 4-methylveratrole, of an additional methyl group, which favors both types of cleavage, i.e. alkyl-oxygen as well as aryl-oxygen cleavage, in the *meta* position as opposed to the *para* position (Scheme 19).[48] Of the four different types of cleavage only one could be recognized in the ESR spectrum after reaction with potassium in THF.[120]

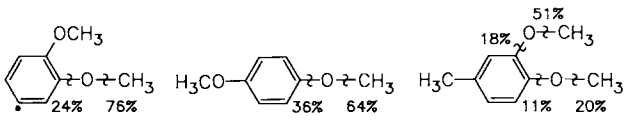

Scheme 19. Mode of cleavage in substituted anisoles.

Aryl methyl ethers, whose methoxy groups are twisted out of the plane of the arene ring by two *ortho*-substituents,[132] show overwhelmingly aryl—oxygen cleavage (Scheme 20)[48]—even upon reduction with potassium in DME.[72] If, however, the orientation in the plane is fixed,

as in 2,3-dihydrobenzo[*b*]furan, alkyl-oxygen cleavage occurs exclusively, but with a much reduced reactivity (Scheme 20).[72]

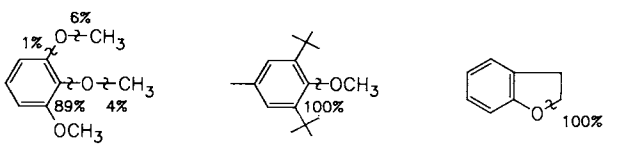

Scheme 20. Steric influence on the mode of cleavage in alkyl aryl ethers.

A mixture of four products—enriched by secondary products such as benzene and phenol—is obtained upon reduction of the mixed hydroquinone ethers **4**–**7** with lithium powder in THF (Scheme 21).[48] Of particular interest is the methyl isopropyl *p*-hydroquinone diether **5**, since the cleavage patterns of methyl phenyl and isopropyl phenyl ethers are very similar (cf. Table 1).

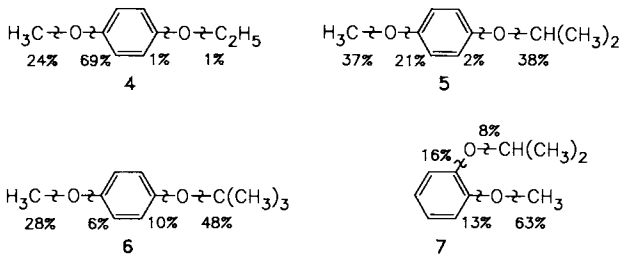

Scheme 21. Pattern of cleavage in diethers with hydroquinones as aryl component.

In fact, the two alkyl-oxygen bonds in **5** are cleaved almost to the same extent, but not so the aryl-oxygen bonds; in the case of the corresponding *o*-hydroquinone diether **7** exactly the opposite is true.[48]

With sodium in HMPA, the preferential cleavage of the methyl group in contrast to the isopropyl group had already been found, both in the case of **5** and **7**, as well as in the *m*-isomer.[116] As expected, in this solvent aryl-oxygen cleavage plays no part, so that the yield of the corresponding isopropyl half ethers of *p*-hydroquinone, pyrocatechol, and resorcinol lies between 72 and 93%.[116] In HMPA even the trimethoxybenzene **8** can be partly dealkylated; however, the two different methyl-oxygen bonds are each only cleaved to the extent of 30%.[116] In the 1,2,4-trialkoxybenzenes, the alkyl group in the 2-position is always preferentially split off—even when it is an isopropyl group (cf. **9** and **10**).[116]

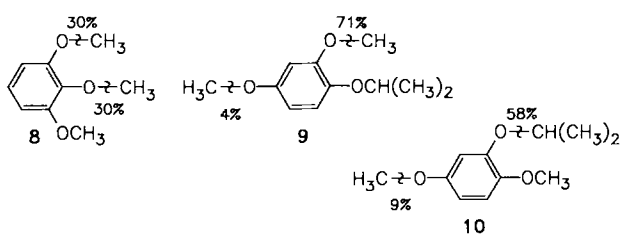

With 2,3-dialkoxynaphthalene we have observed substantial further reduction of the primary reaction products (Scheme 22). β-Naphthol, however, does not undergo further cleavage, as was also shown in a separate experiment.[48]

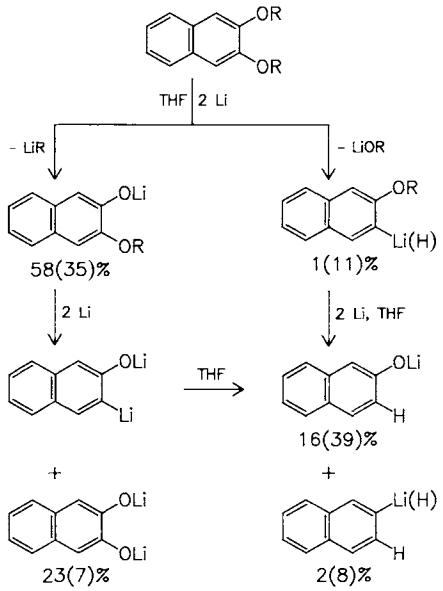

Scheme 22. Cleavage of 2,3-dialkoxynaphthalenes. The product ratios hold true for R = $CH_3(C_2H_5)$.

3.3.2. *Influence of the Solvent*

Once it was known that the solvent had, in some cases, a large influence on the regioselectivity of cleavage[133] we undertook a systematic study of the cleavage of anisole with potassium powder and with sodium/potassium alloy in various solvents.[72] It turns out that one can alter the direction of the cleavage from pure aryl-oxygen cleavage to almost 100% alkyl-oxygen cleavage simply by changing the solvent used.

When the cleavage was carried out in heptane as solvent we were unable to find evidence of there being more than 2–3% phenol when using potassium powder or sodium/potassium alloy [Eq. (32)]. The amount of alkyl-oxygen

$$C_6D_5K + KOCD_3 \xleftarrow[98\%]{2\ K} \underset{\text{in heptane}}{C_6D_5OCD_3} \xrightarrow[2\%]{2\ K} CD_3K + KOC_6D_5 \quad (32)$$

splitting remained just as low even when the reaction temperature was raised to 60–65 °C. The objection could be raised that such traces of phenol could arise from oxidation of phenylpotassium by traces of oxygen in the reaction mixture. We therefore also analyzed the gaseous products after deuteriolysis by mass spectroscopy and indeed found traces of methane—and, starting with perdeuterioanisole, traces of CD_4.[72]

The situation is completely different when even small amounts of THF are added to the heptane (Table 4). The addition of only 1 mmol of THF per mmol of potassium increases the amount of phenol to 13%.[72] Particularly interesting is the finding that the amount of alkyl-oxygen cleavage in pure THF drops from 96% to 71% if the reaction is carried out at 65 °C instead of 20 °C.[72] DME is even more effective than THF in forcing methyl-oxygen cleav-

Table 4. Influence of increasing amounts of THF on the regioselectivity of the cleavage of 25 mmol of anisole with 25 mmol of sodium/potassium alloy in heptane at room temperature [63].

THF	% $C_6H_5O\rightarrow CH_3$	% $C_6H_5\rightarrow OCH_3$
0%	2	98
25 mmol (=7%)	13	87
50%	89	11
100%	96	4

age. In pure DME as solvent, only 1% of benzene was found after the hydrolysis.[72]

A surprising observation was made with TMEDA as solvent. Addition of 5 mmol per mmol of potassium only brought about 32% of alkyl-oxygen cleavage, and even in pure TMEDA it amounted to only 49%.[72] This finding is very important with regard to our concepts of the mechanism of ether cleavage (see Section 3.4).

A large increase in the amount of alkyl-oxygen cleavage was also found in the changeover from THF to THF/HMPA (1:1) in the cleavage of α-naphthyl decyl (from 29 to 63%) and β-naphthyl decyl ethers (from 30 to 56%) with potassium.[134] Upon cleavage of these decyl ethers with sodium, with a change from THF/biphenyl to THF/HMPA as solvent, the increase was even larger: α-naphthyl decyl ether (from 18 to 92%), β-naphthyl decyl ether (from 34 to 92%), and *p*-biphenylyl decyl ether (from 5 to 83%).[134]

There are, however, ethers whose direction of cleavage remains completely uninfluenced by the solvent (Scheme 23). Thus, 2,3-dihydrobenzo[*b*]furan, 2,3-dihydro-2,2-dimethylbenzo[*b*]furan, and *tert*-butyl phenyl ether **3** undergo pure alkyl-oxygen cleavage with potassium in all solvents—heptane, THF, DME—whereas 2,6-di-*tert*-butyl-4-methylanisole is attacked exclusively at the aryl-oxygen bond, even in DME.[72] All these ethers react extremely slowly in heptane at room temperature, even with potassium powder, so that prolonged heating at 80–90 °C is often necessary.

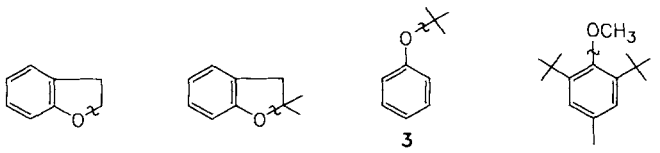

Scheme 23. Ethers in which the mode of cleavage is not influenced by the choice of solvent.

3.3.3. *Influence of the Metal*

In contrast to the solvent, which has a dramatic influence on the direction of cleavage of anisole, the alkali metal (lithium to rubidium) has no significant influence on the regioselectivity of the cleavage; only cesium is at variance.[72] Naturally, one finds great differences in the reactivity. However, it is astonishing that anisole reacts at all with lithium powder at room temperature in heptane, and then largely by phenyl-oxygen cleavage.

Rubidium cleaves ethers in the same way as potassium, i.e. in heptane 98:2 in favor of aryl-oxygen splitting, but in DME the ratio is 7.5:92.5.[72]

In heptane, cesium behaves like potassium only at room temperature. At 60 °C, the initially formed phenylcesium attacks the starting material nucleophilically with formation of toluene and cesium phenolate [Eq. (30)].[72] There is also a marked difference in the behavior of cesium and potassium in THF. Whereas with potassium the amount of alkyl-oxygen scission decreases from 96% to 71% as the temperature is raised from 20 °C to 65 °C, with cesium exactly the opposite is observed; the amount of methyl-oxygen cleavage increases with increasing temperature from 39% at room temperature to 62% at 60 °C.[72]

Larger differences in regioselectivity were observed in the cleavage of aryl decyl ethers with lithium, sodium, or potassium in THF, where, however, biphenyl was added as a catalyst[134] (Table 5). The large differences between the α- and β-naphthyl ethers are striking; these did not come to light in our work. Also striking is the completely different behavior of *p*-biphenylyl decyl ether. In the case of the naphthyl ethers the results with lithium and potassium are very similar, in the case of biphenylyl ethers, however, those with sodium and potassium are very similar.

3.4. Mechanistic Considerations

In the literature one finds diametrically opposed views on the mechanism of ether cleavage by alkali metals (Scheme 24). The only undisputed point is the primary for-

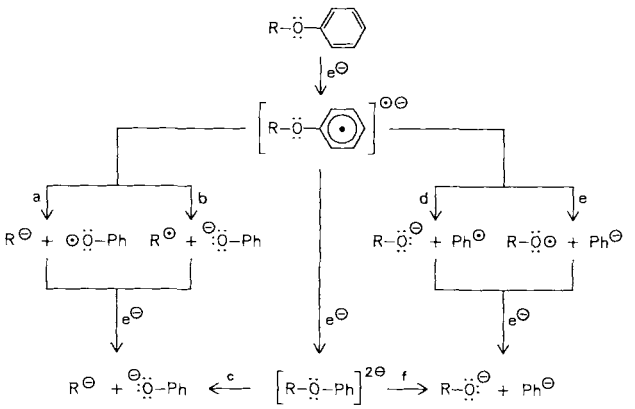

Scheme 24. Proposed mechanisms for the cleavage of ethers with alkali metals.

Table 5. Influence of the metal on the regioselectivity of the cleavage of various aryl decyl ethers in THF/biphenyl [125].

Metal	% Naphthyl$O\rightarrow C_{10}H_{21}$		% Naphthyl$\rightarrow OC_{10}H_{21}$		% *p*-Biphenylyl$O\rightarrow C_{10}H_{21}$	% *p*-Biphenylyl$\rightarrow OC_{10}H_{21}$
	α	β	α	β		
Li	54	36	46	64	69	31
Na	18	34	82	66	5	95
K	54	44	46	56	7	93

mation of a radical anion, which in some cases has been demonstrated by ESR spectroscopy. The radical anion can collapse in four different ways (a, b, d, e) into a radical and an anion, or, before collapsing, it can take up a second electron with the formation of the corresponding dianion. The collapse of this dianion into two anions, which can also occur in two different ways (c, f), completes the spectrum of conceivable mechanisms.

In the case of alkyl aryl ethers, of the six possibile reactions three (paths a–c) lead to alkyl–oxygen scission and three (paths d–f) to aryl–oxygen scission. With the exception of path e all the reaction mechanisms have been discussed in the literature. Confusion often arises upon introducing thermodynamic arguments—stability considerations of the products—although the course of the reaction is undoubtedly kinetically controlled.

For example, path a has been postulated for alkyl–oxygen cleavage[123] on the basis of the following argument: the phenetole radical anion is more stable than the anisole radical anion, because the ethyl anion is less stable than the methyl anion.

Path b, however, has been discussed even more often[92, 134, 135]—partly on the grounds of electrochemical findings.[136, 137] Another group of workers[116] is of the opinion that path b is followed by alkyl aryl sulfides, but not, however, by the alkyl aryl ethers, for whose cleavage path c via the dianion is required. The dianion mechanism (path c) was also favored in the older work[91, 108, 109, 114] for alkyl–oxygen cleavage as well as for the alkyl–sulfur cleavage in thioanisole,[138] which, nevertheless, is said to take path b to the extent of 10% in solvents like benzene.[138]

The dianion also enjoys great popularity as an intermediate in the aryl–oxygen cleavage by path f of diaryl ethers[118] and alkyl aryl ethers.[134]

Nevertheless, the one-electron mechanism via path d has many adherents[92, 119, 123, 139]—also for the cleavage of the aryl–sulfur bond.[116, 140, 141] Through the electrochemical reduction of a suitably substituted diphenyl ether, and with the help of a cyclization reaction characteristic of radical reactions, evidence was even adduced for an intermediate aryl radical [Eq. (33)].[142]

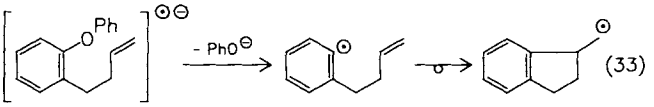

(33)

The intermediacy of the phenyl radical was also held to be plausible in the cathodic reduction of diphenyl ether, when the dianion did not lead to cleavage.[143] The same is true for diphenyl sulfide.[144]

A few phenyl radicals could be trapped during the cleavage of diphenyl ether with potassium in liquid ammonia, when it was carried out in the presence of the acetone enolate anion [Eq. (34)].[139]

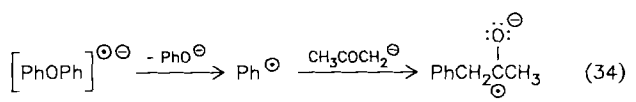

(34)

Unfortunately, under these conditions the cleavage of anisole did not occur.[145] The fact that up until now no aryl radicals have been demonstrated in the cleavage of alkyl aryl ethers does not, of course, mean that path d can be ruled out.

Our mechanistic propositions are shown in Scheme 25. According to this scheme there is only one mechanism for each direction of cleavage and the assumption of a dianion intermediate is not necessary. The reaction paths correspond to paths b and d in Scheme 24, but a major difference is that before the scission of the π*-radical anion a conversion into two different σ*-radical anions has been introduced. σ*-Radical anions are nowadays discussed as intermediates in a wide variety of reactions,[144, 146–152] and that formed from pentafluoroiodobenzene can even be demonstrated by means of ESR spectroscopy at 77 K.[153]

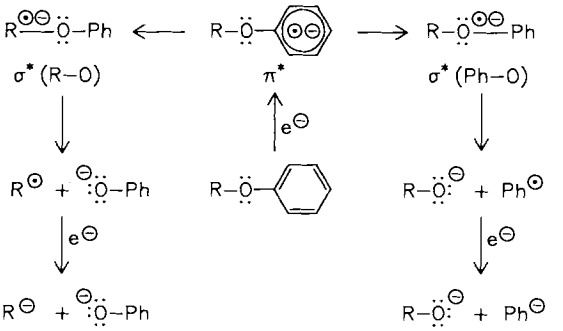

Scheme 25. Probable mechanism of the cleavage of ethers with alkali metals.

The σ*(Ph–O)-radical anion would correspond to the intermediate in an $S_{RN}1$ reaction[154, 155] between an alkoxide anion and a phenyl radical, a reaction which is not, however, observed since the corresponding σ*-orbital probably lies at too high an energy.[156] Corresponding reactions are known, on the other hand, with sulfur,[139, 140, 146, 147, 157] selenium,[158] tellurium,[158] arsenic,[148, 159] and antimony[148] analogues of alkoxides. However, in contrast to the σ*-radical anions discussed in these instances, the case of σ*(R–O) and σ*(Ph–O) radical anions is not one of two limiting mesomeric forms of one and the same radical anion but of two entirely different species of which the σ*(Ph–O) radical anion, because of the stronger—by ca. 170 kJ/mol (40 kcal/mol)—phenyl oxygen bond,[160] lies energetically much higher than the σ*(R–O) radical anion.

With thermodynamic control therefore almost exclusive alkyl–oxygen cleavage must occur, as is observed with the corresponding alkyl aryl sulfides.[161] Kinetically, however, the electron transfer π*→σ*(Ph–O) is much more favorable, probably because the oxygen forms a large barrier. This is reminiscent of the fission of certain benzyl phenyl ethers which—contrary to thermodynamic expectations—only take place unproblematically if the spin density remains on the radical which is split off ("regioconservation") [cf. Eqs. (35) and (36)].[152]

Here also, electrons cross the oxygen only with difficulty. There is much evidence that with the aryl alkyl ethers this occurs well only in a solvent separated ion-pair. Only in this way can we explain why the amount of alkyl–oxy-

gen cleavage with sodium/potassium alloy in THF drops from 96% to 71% when the temperature is raised from

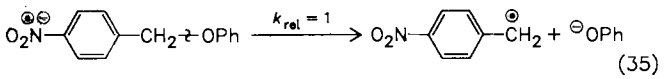

(35)

(36)

20°C to 65°C (see Section 3.3.2),[72] since it is well known that this rise in temperature reduces the number of solvent separated ion-pairs in the solution.[162] This is further supported by the finding that in TMEDA (Section 3.3.2) which has been shown not to favor the formation of solvent separated ion-pairs,[162] alkyl-oxygen cleavage does not even reach 50%.[72] Similarly, the small amount of alkyl-oxygen cleavage with cesium in THF[72] fits into this scheme since $Cs^{\oplus}$, as the largest alkali metal ion, is the one most poorly solvated by THF. The increase in alkyl-oxygen cleavage with increasing temperature,[72] however, indicates that with cesium as the counterion the $\pi^* \rightarrow \sigma^*$(R-O) electron transfer does not only take place within a solvent separated ion-pair.

The kinetic barrier can also be lowered by the addition of naphthalene[95] or biphenyl[134] as catalysts, so that the amount of alkyl-oxygen cleavage increases. The same is true when the solvent is changed to DME[72] or HMPA.[114, 116]

The transfer of electrons into the σ^*(Ph-O) orbital is also made easier by solvation of the counterion, although not to the same extent. This is particularly well illustrated in the case of 9-methoxyanthracene whose radical anion in THF is more stable with cesium as counterion than with lithium.[120]

A hypothetical energy diagram for the two intramolecular electron transfers, which may possibly even take place through space,[163] is shown in Scheme 26.

Only one of the possible 18 resonance formulas[164] which can be written for the π^*-radical anion is shown in Scheme 26, but this is probably, by a wide margin, the most important one. We have established that the reaction with alkali metals takes place best—with both alkyl-oxygen and aryl-oxygen cleavage—if the spin density on the carbon atom which bears the oxygen atom is particularly

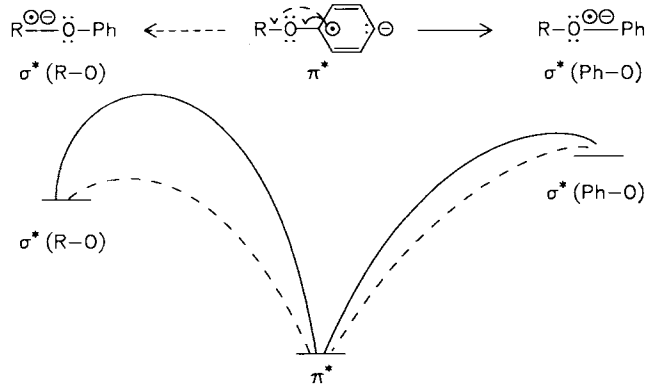

Scheme 26. Hypothetical energy diagram of the transformation of the π^* radical anion of Scheme 25 into the two σ^* radical anions. — non-polar solvent; --- readily solvating solvent.

high and with it the weighting of the mesomer shown. With this as a working hypothesis it is also easy to predict the preferred direction of cleavage of bifunctional ethers. Naturally, one can calculate the relevant bond strengths quite accurately from MO-theory;[120] a glance at the essential resonance formulas (Scheme 27), however, tells us immediately which bond will be preferentially cleaved, for example, in 4-substituted *o*-hydroquinone diethers.

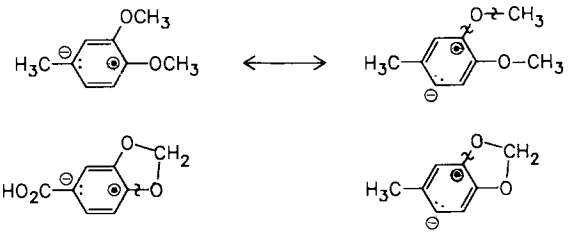

Scheme 27. Establishment of preferred modes of cleavage in dialkyl aryl diethers on the basis of resonance formulas.

As already mentioned in Section 3.3.1, not only the aryl-oxygen bond in 4-methylveratrole but also the *methyl*-oxygen bond *meta* to a methyl group is more easily cleaved, although it should be stronger than that of the methoxy group in the *para* position. This is also an indication that the $\pi^* \rightarrow \sigma^*$ electron transfer takes place intramolecularly and is kinetically controlled. The, at first surprising, results[116] in the cleavage of 1,2,4-trialkoxybenzenes with sodium in HMPA can be explained in the same way.

In diaryl ethers ArylOAryl',[97, 98, 105, 106] too—in contrast to the corresponding thioethers[140, 165]—the strongest bond is preferentially cleaved (Scheme 28), since electron with-

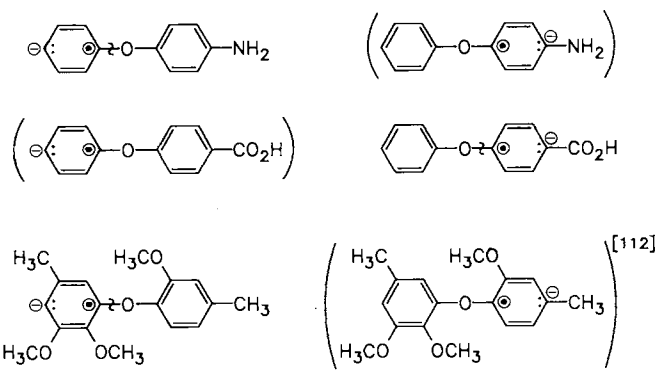

Scheme 28. Establishment of the preferred modes of cleavage in diaryl ethers on the basis of resonance formulas.

drawing substituents, which reduce the energy of the π^*-orbitals, on the one hand facilitate the entry of the electrons but on the other raise the π-bond order to the oxygen atom.

If the σ^*(Aryl-O) and σ^*(Aryl'-O) radical anions were only limiting resonance structures of one and the same species, as is the case with sulfur,[147] then the weaker aryl-oxygen bond would be cleaved preferentially.

If the aryl-oxygen bond in alkyl aryl ethers is especially weak, as when the alkyl residue, for steric reasons, is twisted out of the plane of the arene ring, then cleavage of

the aryl-oxygen bond occurs under conditions which normally lead to alkyl-oxygen scission. On the other hand, the aryl-oxygen bond may be very strong, as in 2,3-dihydrobenzo[*b*]furan, or the alkyl-oxygen bond especially weak, as in *tert*-butyl ethyl ethers, leading to alkyl-oxygen scission under all conditions.

The reason that the methyl group is always more easily split off than the ethyl group is no doubt due to the lower bond dissociation energy of the methyl-oxygen bond in anisole (239 ± 8 kJ mol^{-1} = 57 ± 2 kcal mol^{-1}),[166] as compared with the ethyl-oxygen bond in phenetole (278.8 kJ mol^{-1} = 64.0 kcal mol^{-1}),[167] which in turn affects the energy of the σ^*-orbital involved. However, there are always other influences at work; besides the energy difference between the two σ^*-orbitals, there may be, in the solvent separated ion-pair, steric factors which also play a role.

3.5. The Cleavage of Thioethers

Thioethers are more easily cleaved than ethers. Moreover, the regioselectivity is much greater; for instance alkyl phenyl sulfides are—with few exceptions[161]—almost exclusively cleaved at the alkyl-sulfur bond. This property has been exploited in the synthesis of numerous alkyllithium compounds, including bifunctional ones [Eqs. (37) and (38)].[168, 169]

$$PhCH_2O(CH_2)_3SPh \xrightarrow[\text{THF}\\ -50\,^\circ C]{2\ Li} PhCH_2O(CH_2)_3Li + LiSPh \qquad (37)$$

$$PhS(CH_2)_3O(CH_2)_3SPh \xrightarrow[\text{THF}]{4\ Li} Li(CH_2)_3O(CH_2)_3Li + 2\ LiSPh \qquad (38)$$

To accelerate the reaction—even in the preparation of benzylsodium or -potassium compounds[169]—naphthalene is added, or the metal is used as a dispersion. For the synthesis of allyllithium compounds from allyl phenyl sulfides, the addition of 1-dimethylaminonaphthalene instead of naphthalene is recommended, as this is easily removed from the reaction products by extraction with acid.[170] With lithium di-*tert*-butylbiphenyl,[171] even a trilithio compound could be prepared [Eq. (39)].[172]

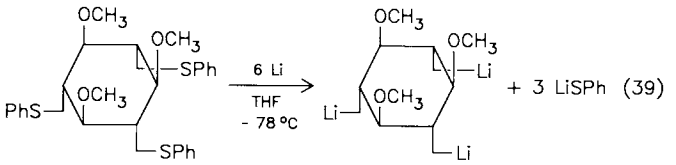

+ 3 LiSPh (39)

These and other examples[91, 116, 140, 173, 174] show that the carbon-sulfur bond can be selectively cleaved even in the presence of ether bonds (see Scheme 29).

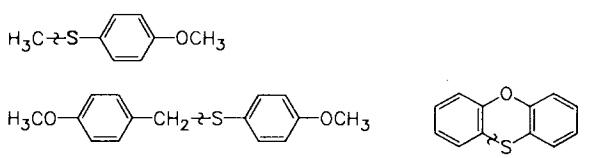

Scheme 29. Selective cleavage of carbon-sulfur bonds in the presence of ether bonds.

Interestingly, diaryl sulfides behave quite differently to the corresponding diaryl ethers in cleavage reactions with lithium in methylamine[165] or potassium in liquid ammonia.[140] In the case of the ethers, electron releasing substituents hinder the cleavage of the substituted ring from oxygen, whereas in the case of the thioethers the sulfur-oxygen cleavage is facilitated (Scheme 30).

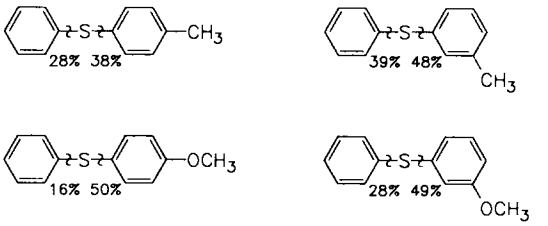

Scheme 30. Influence of substituents on the mode of cleavage in diaryl sulfides.

Naturally, under these conditions, no organometallic compound can be isolated, no more so than in cleavages with lithium or sodium in liquid ammonia.[175-177] However, lithium and sodium do not necessarily lead to the same end products (Scheme 31).[178] Even in ethereal solvents

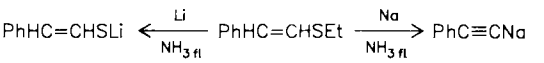

Scheme 31. Influence of the metal on the product in the cleavage of thioethers.

such as diethyl ether, DME[138, 179] or THF,[180] stable organometallic compounds are formed with sodium and potassium only in exceptional cases.[169, 181] The same is true for HMPA as a solvent.[116, 161] A beautiful example of such an exception is reaction (40).[181]

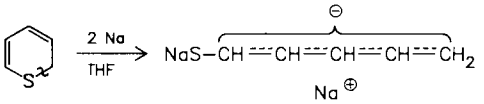

(40)

In the cleavage of thioanisole with potassium in toluene the solvent is metalated by the initially formed methylpotassium and benzylpotassium is obtained in 70% yield [Eq. (41)].[138] It should be noted that under these conditions—

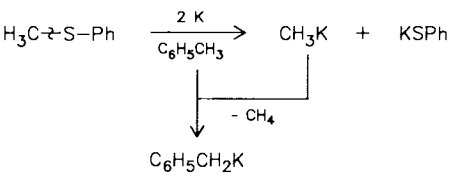

(41)

other than in the case of anisole—no cleavage of the aryl-heteroatom bond occurs. The only exception—even with HMPA as solvent—was observed as a side reaction in the dealkylation of poly(alkylthio)benzenes with sodium, although only when two or three spatially demanding alkyl-

thio groups in the *ortho* position strongly interfered with one another.[161]

A further reaction, which finds no analogy in the corresponding ether cleavages, is the splitting out of K_2S from the thiophenolates which are first formed in the cleavage of mono- or diaryl sulfides, for example, in the cleavage of dibenzothiophene with potassium-naphthalene in THF [Eq. (42)].[180] The collapse of the dibenzothiophene radical

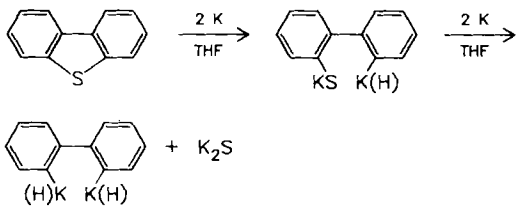

(42)

anion and its conversion into a dianion by electron transfer from another radical anion can be followed spectroscopically.[141] Especially interesting is the reconversion of the reaction products into two molecules of the original radical anion by flash photolysis [Eq. (43)].[141]

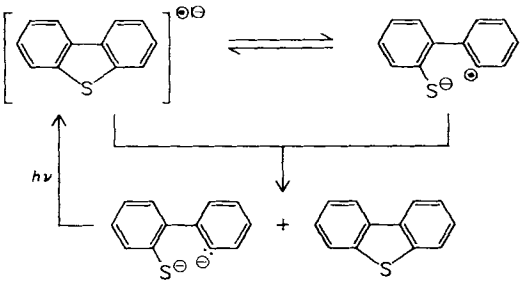

(43)

In the cleavage of dialkyl sulfides (with sodium in liquid ammonia[182, 183]), on the other hand, no sodium sulfide is formed, since the alkyl sulfides formed under these conditions are stable.[182] In the case of ethyl methyl sulfide exclusively the methyl-sulfur bond is cleaved [Eq. (44)].[183]

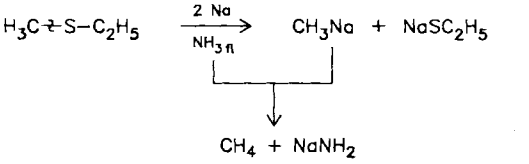

(44)

The easier cleavage of the dialkyl sulfides compared with that of the dialkyl ethers is remarkable, and shows that the transfer of electrons into the corresponding σ^*-orbitals can also occur without difficulty even if no π^*-orbitals are available as a means of transfer. The possibility cannot be excluded, therefore, that the formation of π^*-radical anions—at least in the case of the cleavage of alkyl aryl sulfides—is only a side reaction. What is certain, however, is that the cleavage, in contrast to the corresponding ether cleavage, is thermodynamically controlled.

I wish to thank the Deutschen Forschungsgemeinschaft and the Fonds der Chemischen Industrie, for supporting my work, and the "Stiftung Volkswagenwerk" for financing the collaboration with Professor B. J. Herold, Lisbon, Portugal, whom I would like to thank for many ESR measurements and valuable discussions. I would also like to thank Dr. E. Bartmann, Darmstadt, for generously placing his unpublished results at my disposal. The, largely unpublished, results from my group were made possible only by the unsparing efforts of the co-workers, whose names are given in the literature citations, and to whom I would also like to convey my sincerest thanks.

Received: February 16, 1987;
revised: April 24, 1987 [A 638 IE]
German version: *Angew. Chem. 99* (1987) 1002

[1] R. L. Burwell, Jr., *Chem. Rev. 54* (1954) 615.
[2] H. Meerwein in *Houben-Weyl-Müller: Methoden der Organischen Chemie, Band 6/3*, 4th edit., Thieme, Stuttgart 1965, p. 143 ff.
[3] E. Staude, F. Patat in S. Patai (Ed.): *The Chemistry of the Ether Linkage*, Wiley Interscience, New York 1967, p. 21 ff.
[4] Important information is also to be found in textbooks and in the standard works dealing with organometallic compounds; see for example: U. Schöllkopf in *Houben-Weyl-Müller: Methoden der Organischen Chemie, Band 13/1*, 4th edit., Thieme, Stuttgart 1970, p. 87 ff., H. F. Ebel, A. Lüttringhaus, *ibid.*, p. 255 ff., B. J. Wakefield: *The Chemistry of Organolithium Compounds*, Pergamon, Oxford 1974; cf. also H. Kropf, J. Thiem, H. Nimz in *Houben-Weyl-Müller: Methoden der Organischen Chemie, Band 6/1a/1*, 4th edit., Thieme, Stuttgart 1979, p. 318 ff.
[5] M. V. Bhatt, S. U. Kulkarni, *Synthesis 1983*, 249.
[6] J. Blagg, S. G. Davies, N. J. Holman, C. A. Laughton, B. E. Mobbs, *J. Chem. Soc. Perkin Trans. 1 1986*, 1581.
[7] Y. Leroux, R. Mantione, *Tetrahedron Lett. 1971*, 591.
[8] R. Mantione, Y. Leroux, *Tetrahedron Lett. 1971*, 593.
[9] D. A. Evans, G. C. Andrews, B. Buckwalter, *J. Am. Chem. Soc. 96* (1974) 5560.
[10] W. C. Still, T. L. Macdonald, *J. Am. Chem. Soc. 96* (1974) 5561.
[11] J. Hartmann, M. Stähle, M. Schlosser, *Synthesis 1974*, 888.
[12] W. Oppolzer, R. L. Snowden, *Tetrahedron Lett. 1976*, 4187.
[13] U. Schöllkopf, P. Hänßle, *Justus Liebigs Ann. Chem. 763* (1972) 208.
[14] J. E. Baldwin, G. A. Höfle, O. W. Lever, Jr., *J. Am. Chem. Soc. 96* (1974) 7125.
[15] C. G. Chavdarian, C. H. Heathcock, *J. Am. Chem. Soc. 97* (1975) 3822.
[16] J. E. Baldwin, O. W. Lever, Jr., N. R. Tzodikov, *J. Org. Chem. 41* (1976) 2874.
[17] R. K. Boeckman, Jr., K. J. Bruza, *Tetrahedron 37* (1981) 3997.
[18] R. Letsinger, W. Schnizer, E. Bobko, *J. Am. Chem. Soc. 73* (1951) 5708.
[19] K. Ziegler, H.-G. Gellert, *Justus Liebigs Ann. Chem. 567* (1950) 185.
[20] H. Hoberg, *Justus Liebigs Ann. Chem. 656* (1962) 1.
[21] Review: H. Normant, *J. Organomet. Chem. 100* (1975) 189; cf. also J. Villiéras, C. Bacquet, J.-F. Normant, *Bull. Soc. Chim. Fr. 1974*, 1731.
[22] G. Wittig, L. Löhmann, *Justus Liebigs Ann. Chem. 550* (1942) 260.
[23] R. Letsinger, D. Pollart, *J. Am. Chem. Soc. 78* (1956) 6079.
[24] Reviews: U. Schöllkopf, *Angew. Chem. 82* (1970) 795; *Angew. Chem. Int. Ed. Engl. 9* (1970) 763; T. Nakai, K. Mikami, *Chem. Rev. 86* (1986) 885. Concerning the mechanism cf. also J. F. Garst, C. D. Smith, *J. Am. Chem. Soc. 98* (1976) 1526, and references cited therein.
[25] G. E. Coates, M. L. H. Green, P. Powell, K. Wade: *Einführung in die metallorganische Chemie*, Enke, Stuttgart 1972, p. 52.
[26] A. Maercker, W. Demuth, *Angew. Chem. 85* (1973) 90; *Angew. Chem. Int. Ed. Engl. 12* (1973) 75.
[27] A. Maercker, W. Theysohn, *Justus Liebigs Ann. Chem. 747* (1971) 70.
[28] A. Maercker, W. Demuth, *Justus Liebigs Ann. Chem. 1977*, 1909.
[29] Yu. N. Baryshnikov, G. I. Vesnovskaya, V. A. Shushunov, *Dokl. Akad. Nauk SSSR 185* (1969) 580.
[30] Yu. N. Baryshnikov, G. I. Vesnovskaya, V. N. Mushkarinova, *Dokl. Akad. Nauk SSSR 205* (1972) 1353.
[31] Yu. N. Baryshnikov, G. I. Vesnovskaya, *Zh. Obshch. Khim. 44* (1974) 2538.
[32] Yu. N. Baryshnikov, G. I. Vesnovskaya, *Zh. Obshch. Khim. 42* (1972) 913.
[33] Yu. N. Baryshnikov, N. N. Kaloshina, G. I. Vesnovskaya, *Zh. Obshch. Khim. 47* (1977) 2790.

[34] Kinetics of the cleavage of THF with *n*-butyllithium in less than equimolar amounts cf. S. C. Honeycutt, *J. Organomet. Chem. 29* (1971) 1.
[35] A. Rembaum, S.-P. Siao, N. Indictor, *J. Polym. Sci. 56* (1962) S17.
[36] R. B. Bates, L. M. Kroposki, D. E. Potter, *J. Org. Chem. 37* (1972) 560.
[37] Concerning the stereochemistry of the elimination in open-chain systems - *syn* or *anti* dependence on the solvent - cf. T. Sugita, J. Nakagawa, K. Nishimoto, Y. Kasai, K. Ichikawa, *Bull. Chem. Soc. Jpn. 52* (1979) 871.
[38] R. J. Crawford, *Dissertation*, Pennsylvania State University, University Park, PA 1970.
[39] B. Schaub, M. Schlosser, *Helv. Chim. Acta 58* (1975) 556; R. Lehmann, M. Schlosser, *Tetrahedron Lett. 25* (1984) 745.
[40] W. Demuth, unpublished results.
[41] R. Paul, S. Tchelitcheff, *Bull. Soc. Chim. Fr. 1952*, 808.
[42] V. Rautenstrauch, *Helv. Chim. Acta 55* (1972) 594.
[43] A. Maercker, R. W. Stumpe, *Tetrahedron Lett. 1979*, 3843.
[44] The results of D. A. Shirley, J. R. Johnson, Jr., J. D. Hendrix, *J. Organomet. Chem. 11* (1968) 209, according to which the metalation took place partially also in the *meta*- and *para*-positions, could not be confirmed.
[45] This intramolecular β-elimination had already been postulated as the mechanism for the cleavage of alkyl phenyl ethers as early as 1954 but could not however be verified; cf. A. A. Morton, A. E. Brachman, *J. Am. Chem. Soc. 76* (1954) 2973.
[46] R. A. Ellison, F. N. Kotsonis, *J. Org. Chem. 38* (1973) 4192.
[47] W. H. Glaze, A. C. Ranade, *J. Org. Chem. 36* (1971) 3331.
[48] A. Maercker, G. Schaller, unpublished; cf. G. Schaller, *Dissertation*, Universität Erlangen-Nürnberg, Erlangen 1975.
[49] A. Maercker, R. Stumpe, unpublished; cf. R. Stumpe, *Dissertation*, Universität Erlangen-Nürnberg, Erlangen 1977.
[50] G. Wittig, W. Böll, K.-H. Krück, *Chem. Ber. 95* (1962) 2514.
[51] U. Schöllkopf, J. Paust, A. Al-Azrak, H. Schumacher, *Chem. Ber. 99* (1966) 3391.
[52] G. H. Posner, J.-S. Ting, *Synth. Commun. 5* (1975) 331.
[53] G. Carpenter, A. G. Evans, N. H. Rees, *J. Chem. Soc. Perkin Trans. 2 1972*, 1598.
[54] G. Köbrich, A. Baumann, *Angew. Chem. 85* (1973) 916; *Angew. Chem. Int. Ed. Engl. 12* (1973) 856.
[55] H. Gilman, B. J. Gaj, *J. Org. Chem. 28* (1963) 1725.
[56] A. Maercker, M. Passlack, *Chem. Ber. 116* (1983) 710.
[57] A. Maercker, J. Troesch, *J. Organomet. Chem. 102* (1975) C1.
[58] A. Maercker, M. Passlack, *Chem. Ber. 115* (1982) 540.
[59] A. Maercker, R. Stötzel, *J. Organomet. Chem. 254* (1983) 1.
[60] G. Wittig, G. Kolb, *Chem. Ber. 93* (1960) 1469.
[61] T. Fujita, K. Suga, S. Watanabe, *Synthesis 1972*, 630.
[62] M. Yamaguchi, Y. Nobayashi, I. Hirao, *Tetrahedron 40* (1984) 4261.
[63] M. J. Eis, J. E. Wrobel, B. Ganem, *J. Am. Chem. Soc. 106* (1984) 3693.
[64] J. Millon, G. Linstrumelle, *Tetrahedron Lett. 1976*, 1095.
[65] A. Alexakis, D. Jachiet, J. F. Normant, *Tetrahedron 42* (1986) 5607.
[66] F. L. M. Pattison, R. E. A. Dear, *Can. J. Chem. 41* (1963) 2600.
[67] K. Suga, S. Watanabe, T. P. Pan, *Aust. J. Chem. 21* (1968) 2341.
[68] C. D. Broaddus, *J. Org. Chem. 30* (1965) 4131.
[69] A. Ghribi, A. Alexakis, J. F. Normant, *Tetrahedron Lett. 25* (1984) 3079.
[70] G. Wittig, G. Pieper, G. Fuhrmann, *Ber. Dtsch. Chem. Ges. B 73* (1940) 1193.
[71] K. A. Kun, H. G. Cassidy, *J. Org. Chem. 27* (1962) 841.
[72] A. Maercker, H. Jansen, unpublished; cf. H. Jansen, *Dissertation*, Universität Erlangen-Nürnberg, Erlangen 1978.
[73] Reviews: W. Kirmse, *Angew. Chem. 77* (1965) 1; *Angew. Chem. Int. Ed. Engl. 4* (1965) 1; G. Köbrich, *Angew. Chem. 79* (1967) 15; *Angew. Chem. Int. Ed. Engl. 6* (1967) 41; cf. also P. Beak, A. I. Meyers, *Acc. Chem. Res. 19* (1986) 356.
[74] A. Maercker, *Justus Liebigs Ann. Chem. 732* (1970) 151.
[75] K. Ziegler, H.-G. Gellert, *Justus Liebigs Ann. Chem. 567* (1950) 195.
[76] P. D. Bartlett, S. Friedman, M. Stiles, *J. Am. Chem. Soc. 75* (1953) 1771; P. D. Bartlett, S. J. Tauber, W. P. Weber, *ibid. 91* (1969) 6362; P. D. Bartlett, C. V. Goebel, W. P. Weber, *ibid. 91* (1969) 7425; cf. also L. Spialter, C. W. Harris, *J. Org. Chem. 31* (1966) 4263.
[77] J. C. Carnahan, Jr., W. D. Closson, *J. Org. Chem. 37* (1972) 4469.
[78] J.-F. Biellmann, H. d'Orchymont, J.-L. Schmitt, *J. Am. Chem. Soc. 101* (1979) 3283.
[79] S. Cabiddu, S. Melis, P. P. Piras, F. Sotgiu, *J. Organomet. Chem. 178* (1979) 291.
[80] S. Cabiddu, S. Melis, P. P. Piras, F. Sotgiu, *J. Organomet. Chem. 182* (1979) 155.
[81] S. Cabiddu, C. Floris, S. Melis, P. P. Piras, F. Sotgiu, *J. Organomet. Chem. 236* (1982) 149.
[82] S. Cabiddu, C. Floris, S. Melis, F. Sotgiu, *Phosphorus Sulfur 19* (1984) 61.
[83] R. Gräfing, L. Brandsma, *Recl. Trav. Chim. Pays-Bas 95* (1976) 264.
[84] R. H. Everhardus, H. G. Eeuwhorst, L. Brandsma, *J. Chem. Soc. Chem. Commun. 1977*, 801.
[85] M. Schoufs, J. Meyer, P. Vermeer, L. Brandsma, *Recl. Trav. Chim. Pays-Bas 96* (1977) 259.
[86] J. J. Eisch, A. M. Jacobs, *J. Org. Chem. 28* (1963) 2145.
[87] H. Gilman, G. L. Schwebke, *J. Org. Chem. 27* (1962) 4259.
[88] A. Maercker, J. Troesch, unpublished; cf. J. Troesch, *Dissertation*, Universität Erlangen-Nürnberg, Erlangen 1974.
[89] J. K. Crandall, A. C. Clark, *J. Org. Chem. 37* (1972) 4236.
[90] A. Maercker, *Justus Liebigs Ann. Chem. 730* (1969) 91.
[91] J. J. Eisch, *J. Org. Chem. 28* (1963) 707.
[92] C. G. Screttas, *J. Chem. Soc. Chem. Commun. 1972*, 869.
[93] E. Bartmann, *Angew. Chem. 98* (1986) 629; *Angew. Chem. Int. Ed. Engl. 25* (1986) 653.
[94] V. Prey, *Ber. Dtsch. Chem. Ges. B 76* (1943) 156.
[95] E. Bartmann, unpublished results.
[96] A. N. Cherkasov, K. K. Pivnitskii, *Zh. Org. Khim. 8* (1972) 211.
[97] T. Keumi, C. Murata, Y. Sasaki, H. Kitajima, *Synthesis 1980*, 634.
[98] S. Mejer, K. Gawecka, L. Jabłoński, *Rocz. Chem. 51* (1977) 2477.
[99] T. Kobayashi, H. Tsuruta, *Synthesis 1980*, 492.
[100] W. Kotlarek, *Tetrahedron Lett. 1973*, 67.
[101] H. C. Brown, S. Ikegami, J. H. Kawakami, *J. Org. Chem. 35* (1970) 3243.
[102] R. A. Benkeser, A. Rappa, L. A. Wolsieffer, *J. Org. Chem. 51* (1986) 3391.
[103] K. N. Gurudutt, B. Ravindranath, *Tetrahedron Lett. 21* (1980) 1173.
[104] R. G. Carlson, W. W. Cox, *J. Org. Chem. 42* (1977) 2382.
[105] P. A. Sartoretto, F. J. Sowa, *J. Am. Chem. Soc. 59* (1937) 603.
[106] F. C. Weber, F. J. Sowa, *J. Am. Chem. Soc. 60* (1938) 94.
[107] K. Freudenberg, F. Klinck, E. Flickinger, A. Sobek, *Ber. Dtsch. Chem. Ges. B 72* (1939) 217; K. Freudenberg, W. Lautsch, G. Piazolo, *ibid. 74* (1941) 1879.
[108] A. J. Birch, *J. Chem. Soc. 1944*, 430.
[109] A. J. Birch, *J. Chem. Soc. 1947*, 102.
[110] K. E. Hamlin, F. E. Fischer, *J. Am. Chem. Soc. 75* (1953) 5119.
[111] C. D. Hurd, G. L. Oliver, *J. Am. Chem. Soc. 81* (1959) 2795.
[112] M. Tomita, K. Bessho, *Yakugaku Zasshi 79* (1959) 1097.
[113] H. Normant, T. Cuvigny, J. Normant, B. Angelo, *Bull. Soc. Chim. Fr. 1965*, 3441, 3446.
[114] H. Normant, T. Cuvigny, *Bull. Soc. Chim. Fr. 1966*, 3344.
[115] Cf. M. Larchevêque, *Ann. Chim. (Paris) 1970*, 129.
[116] L. Testaferri, M. Tiecco, M. Tingoli, D. Chianelli, M. Montanucci, *Tetrahedron 38* (1982) 3687.
[117] W. F. Bailey, E. A. Cioffi, *J. Chem. Soc. Chem. Commun. 1981*, 155.
[118] D. H. Eargle, Jr., *J. Org. Chem. 28* (1963) 1703.
[119] A. G. Evans, P. B. Roberts, B. J. Tabner, *J. Chem. Soc. B 1966*, 269.
[120] M. C. Lazana, M. L. Franco, B. J. Herold, A. Maercker, *IX Encontro Anual da Sociedade Portuguesa de Quimica, Estrutura e Reactividade Molecular* (Coimbra, Portugal 1986), Communication 8 CP 15; cf. B. J. Herold, Report to the Stiftung Volkswagenwerk, Spring 1986.
[121] V. Cerri, M. Boyer, P. Tordo, *Gazz. Chim. Ital. 115* (1985) 147.
[122] H. Tylli, *Suom. Kemistiseuran Tied. 82* (1973) 70; *Chem. Abstr. 80* (1974) 132506f.
[123] J. K. Brown, D. R. Burnham, N. A. J. Rogers, *J. Chem. Soc. B 1969*, 1149.
[124] K. W. Bowers in E. T. Kaiser, L. Kevan (Eds.): *Radical Ions*, Wiley Interscience, New York 1968, p. 232ff.
[125] B. Angelo, *Bull. Soc. Chim. Fr. 1966*, 1091.
[126] D. R. Moore, *J. Org. Chem. 26* (1961) 3596.
[127] D. H. Hunter, D. W. Moore, *Can. J. Chem. 49* (1971) 1665.
[128] R. L. Letsinger, J. G. Traynham, *J. Am. Chem. Soc. 70* (1948) 3342.
[129] K. Ziegler, H. Dislich, *Chem. Ber. 90* (1957) 1107.
[130] A. A. Morton, E. J. Lanpher, *J. Org. Chem. 23* (1958) 1636.
[131] D. Tzeng, W. P. Weber, *J. Org. Chem. 46* (1981) 265.
[132] Cf. A. Makriyannis, S. Fesik, *J. Am. Chem. Soc. 104* (1982) 6462; G. M. Anderson III, P. A. Kollman, L. N. Domelsmith, K. N. Houk, *ibid. 101* (1979) 2344.
[133] A. A. Morton, A. E. Brachman, *J. Am. Chem. Soc. 76* (1954) 2973.
[134] M. Itoh, S. Yoshida, T. Ando, N. Miyaura, *Chem. Lett. 1976*, 271.
[135] K. M. Patel, R. J. Baltisberger, V. I. Stenberg, N. F. Woolsey, *J. Org. Chem. 47* (1982) 4250.
[136] E. Santiago, J. Simonet, *Electrochim. Acta 20* (1975) 853.
[137] M. D. Koppang, N. F. Woolsey, D. E. Bartak, *J. Am. Chem. Soc. 106* (1984) 2799.
[138] R. Gerdil, E. A. C. Lucken, *J. Chem. Soc. 1963*, 2857.
[139] R. A. Rossi, J. F. Bunnett, *J. Am. Chem. Soc. 94* (1972) 683.
[140] J. F. Bunnett, X. Creary, *J. Org. Chem. 40* (1975) 3740.
[141] O. Ito, T. Aruga, M. Matsuda, *J. Chem. Soc. Perkin Trans. 2 1982*, 1113.
[142] T. A. Thornton, N. F. Woolsey, D. E. Bartak, *J. Am. Chem. Soc. 108* (1986) 6497.

[143] R. I. Pacut, E. Kariv-Miller, *J. Org. Chem. 51* (1986) 3468.
[144] C. Amatore, C. Combellas, J. Pinson, M. A. Oturan, S. Robveille, J.-M. Savéant, A. Thiébault, *J. Am. Chem. Soc. 107* (1985) 4846.
[145] R. A. Rossi, J. F. Bunnett, *J. Am. Chem. Soc. 96* (1974) 112.
[146] C. Galli, J. F. Bunnett, *J. Am. Chem. Soc. 103* (1981) 7140.
[147] R. A. Rossi, S. M. Palacios, *J. Org. Chem. 46* (1981) 5300.
[148] R. A. Alonso, R. A. Rossi, *J. Org. Chem. 47* (1982) 77.
[149] H. Villar, E. A. Castro, R. A. Rossi, *Can. J. Chem. 60* (1982) 2525.
[150] H. O. Villar, E. A. Castro, R. A. Rossi, *Z. Naturforsch. A 39* (1984) 49.
[151] R. A. Rossi, *J. Chem. Educ. 59* (1982) 310.
[152] P. Maslak, R. D. Guthrie, *J. Am. Chem. Soc. 108* (1986) 2628, 2637.
[153] M. C. R. Symons, *J. Chem. Soc. Chem. Commun. 1977*, 408; cf. also M. C. R. Symons, *Pure Appl. Chem. 53* (1981) 223.
[154] J. F. Bunnett, *Acc. Chem. Res. 11* (1978) 413.
[155] R. A. Rossi, *Acc. Chem. Res. 15* (1982) 164.
[156] R. A. Rossi, A. B. Pierini, *J. Org. Chem. 45* (1980) 2914.
[157] J. F. Bunnett, X. Creary, *J. Org. Chem. 39* (1974) 3173.
[158] A. B. Pierini, R. A. Rossi, *J. Org. Chem. 44* (1979) 4667.
[159] R. A. Rossi, R. A. Alonso, S. M. Palacios, *J. Org. Chem. 46* (1981) 2498.
[160] Cf. *Handbook of Chemistry and Physics*, 59th edit., CRC Press, West Palm Beach 1978-79, p. F-240.
[161] F. Maiolo, L. Testaferri, M. Tiecco, M. Tingoli, *J. Org. Chem. 46* (1981) 3070.
[162] J. Smid, *Angew. Chem. 84* (1972) 127; *Angew. Chem. Int. Ed. Engl. 11* (1972) 112.
[163] Cf. P. Neta, D. Behar, *J. Am. Chem. Soc. 102* (1980) 4798; J. P. Bays, S. T. Blumer, S. Baral-Tosh, D. Behar, P. Neta, *ibid. 105* (1983) 320.
[164] H. E. Zimmerman, *Tetrahedron 16* (1961) 169.
[165] W. E. Truce, D. P. Tate, D. N. Burdge, *J. Am. Chem. Soc. 82* (1960) 2872.
[166] S. Paul, M. H. Back, *Can. J. Chem. 53* (1975) 3330.
[167] A. J. Colussi, F. Zabel, S. W. Benson, *Int. J. Chem. Kinet. 9* (1977) 161.
[168] C. G. Screttas, M. Micha-Screttas, *J. Org. Chem. 43* (1978) 1064.
[169] C. G. Screttas, M. Micha-Screttas, *J. Org. Chem. 44* (1979) 713.
[170] T. Cohen, B.-S. Guo, *Tetrahedron 42* (1986) 2803.
[171] P. K. Freeman, L. L. Hutchinson, *J. Org. Chem. 45* (1980) 1924; *ibid. 48* (1983) 4705.
[172] C. Rücker, *J. Organomet. Chem. 310* (1986) 135.
[173] U. G. Nayak, R. K. Brown, *Can. J. Chem. 44* (1966) 591.
[174] A. R. Krawczyk, J. T. Wróbel, *Rocz. Chem. 51* (1977) 285.
[175] E. P. Zakharov, Ya. L. Gol'dfarb, *Izv. Akad. Nauk SSSR Ser. Khim. 1978*, 1877.
[176] E. P. Zakharov, F. M. Stoyanovich, Ya. L. Gol'dfarb, *Izv. Akad. Nauk SSSR Ser. Khim. 1985*, 2530.
[177] W. G. Blenderman, M. M. Joullié, G. Preti, *Tetrahedron Lett. 1979*, 4985.
[178] M. L. Petrov, N. A. Bunina, A. A. Petrov, *Zh. Org. Khim. 14* (1978) 210.
[179] R. Gerdil, E. A. C. Lucken, *J. Chem. Soc. 1963*, 5444.
[180] T. Ignasiak, A. V. Kemp-Jones, O. P. Strausz, *J. Org. Chem. 42* (1977) 312.
[181] R. Gräfing, L. Brandsma, *Recl. Trav. Chim. Pays-Bas 98* (1979) 520.
[182] F. E. Williams, E. Gebauer-Fuelnegg, *J. Am. Chem. Soc. 53* (1931) 352.
[183] R. L. Jones, R. R. Dewald, *J. Am. Chem. Soc. 96* (1974) 2315.

Di-Grignard Compounds and Metallacycles

By Friedrich Bickelhaupt*

In memoriam Georg Wittig

Just as the by now famous Grignard reaction can be used to prepare organomagnesium halides from organic monohalides, organic dihalides can be used under certain conditions to prepare di-Grignard compounds. Difficulties are encountered in particular when the two halide functionalities are separated by only a short carbon chain (i.e. by 1–3 carbon atoms): in such cases side reactions predominate. It has however recently become possible to obtain such "short" di-Grignard compounds on a preparatively useful scale. This opens up new perspectives for the synthesis of metallacyclic compounds of other main group and transition metal elements and in particular for metallacyclobutanes. The preparation, structure and application of a selected number of di-Grignard reagents will be treated in the present review.

1. Introduction

1.1. Background Perspectives

I should like at the beginning of this article to indicate in the form of a short personal note the (by no means straight) line connecting my apprenticeship in *Georg Wittig*'s laboratory in Tübingen, and the inspiration he provided, with my own work which is discussed in this review.

During his investigations on the formation and behavior of ate complexes,[1] *Wittig* had discovered the formation of a complex between phenyllithium and phenylsodium; he had shown this interaction to have a stabilizing effect on phenylsodium, which is otherwise extremely reactive.[2] The "remarkable stability" of phenylsodium in diethyl ether was interpreted in terms of the formation of diphenyllithium-sodium (or sodium diphenyllithiate) **1** [Eqn. (a)].

$$PhLi + PhNa \longrightarrow \underset{\mathbf{1}}{Na[LiPh_2]} \qquad (a)$$

The task assigned to me in the laboratory in Tübingen was to extend this concept to other combinations of alkyl and aryl derivatives of lithium and sodium. This goal was achieved, but with only a moderate degree of success.[3] When my diploma work was completed, *Wittig* thus suggested another subject for my doctoral thesis, the preparation of *ortho*-dilithiobenzene (**2**) from *ortho*-phenylenemercury (**3**)[4–6] and lithium metal in diethyl ether [Eqn. (b)].

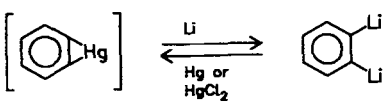

3 **2** (b)

The fascination arising from this deep red, reactive compound[5] has never left me since, even though my active interests often involved completely different topics. Apart from its beautiful red color, the fascination of this compound stems in part from the existence of two highly polarized carbon–metal bonds in one molecule. These lie close together in space, so that one may expect them to influence each other to a high degree and thus to produce a special electronic structure and reactivity. On the other hand, the well-known synthetic potential of reactive organometallic compounds suggests that bifunctional species of this type will have many and varied applications in organic and organometallic chemistry. A simple example is provided by the retro-transformation of **2** into **3** by means of mercury, or better still mercuric chloride;[5] many other examples could be added.[5,7]

1.2. Scope of the Present Review

Organolithium and organomagnesium compounds are of approximately equal importance in preparative chemistry; they are often used interchangeably for comparable purposes. Although organolithium reagents are more reactive, this difference in reactivity is often not decisive: more often it is a question of convenience (the accessibility or the method of preparation) which determines the class of compound to be used.

This survey of bifunctional organometallic compounds will put particular emphasis on those compounds in which the metal functionalities are separated by a short chain consisting of 1, 2 or 3 carbon atoms. These types of compound are at present much more readily accessible in the Grignard series than are the corresponding organolithium reagents. For this reason, and because polylithium compounds have recently been the subject of several reviews,[8–10] the present article will deal mainly with bifunctional organomagnesium compounds.

A second limitation results from the breadth of this area. As already indicated, an important goal in the synthesis of bifunctional organolithium and organomagnesium com-

[*] Prof. Dr. F. Bickelhaupt
Scheikundig Laboratorium, Vrije Universiteit
De Boelelaan 1083, NL-1081 HV Amsterdam (The Netherlands)

pounds is the synthesis of other bifunctional derivatives and in particular the preparation of metal-containing cyclic compounds, the metallacycles. As will be shown, this goal was recognized soon after the discovery by *Grignard* of the reagents bearing his name and was intensively pursued. It is thus not surprising that the synthesis of metallacycles by such routes has led to a plethora of reactions and compounds.[11] For this reason I shall mainly concentrate in the following on results obtained by our own group; these deal in particular with aliphatic compounds and arylalkyl compounds.

2. Di-Grignard Compounds

2.1. Preparation

Of the various methods for the preparation of organomagnesium compounds,[11a,c,12] two in particular are important in the present context. The preparation starting from organic dihalides corresponds to the famous original synthesis of the Grignard reagent[13] [Eqn. (c)] and is also preparatively the most important because of the ready accessibility of the starting materials and because of the (at least in principle!) simple experimental procedure.

$$R-Br + Mg \xrightarrow[Et_2O]{} R-Mg-Br \qquad (c)$$

The preparation starting from organic derivatives of mercury [Eqn. (d)] should also be mentioned, since it yields very pure Grignard reagents.

$$R-Hg-Br + Mg \longrightarrow R-Mg-Br + Mg/Hg \qquad (d)$$

2.1.1. General and Historical Remarks

After Grignard had succeeded in 1900 in preparing the first mono-Grignard reagents [Eqn. (c)], the obvious next step was to use organic dihalides to prepare the corresponding di-Grignard compounds. *Tissier* and *Grignard* in fact carried out the first investigations in this direction in the following year. That they[14] and others[15] were at first unsuccessful was not due to the concept being faulty, but to the starting materials chosen: 1,2-dibromoethane and 1,3-dibromopropane were the only readily available dibromides, but were at the same time the very two which were not suited for the desired synthesis. Instead of the hoped-for di-Grignard compounds **5** [Eqn. (e)] and **7** [Eqn. (f)], ethene and cyclopropane were obtained in high yields. It is very likely[16] that these reactions occur in two

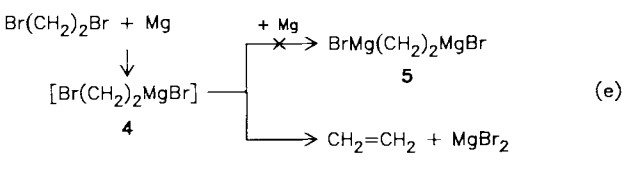

(e)

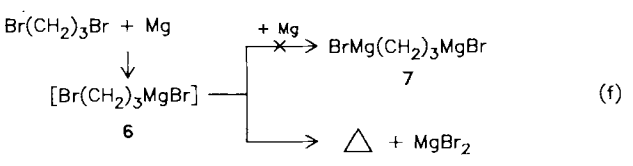

(f)

steps, the initially-formed mono-Grignard reagents **4** and **6** very rapidly eliminating magnesium bromide.

Thus, the truism well known to every chemist showed itself to apply yet again: no product will be obtained without a (suitable) starting material! As in the present case, it is of little importance whether the required starting material is unknown or merely difficult to obtain. Higher homologues, such as the 1,5-dibromopentane (**8**), with which the Grignard reaction can readily be carried out, were in fact already known.[17] But advances towards obtaining di-Grignard compounds were made only after *J. von Braun* had in 1904 shown this compound to be readily available in pure form from the reaction between phosphorus pentabromide and benzoylpiperidine.[18]

However, this process did not occur without tension and a certain amount of drama. *J. von Braun* had certainly immediately recognized the potential of this "synthon" (as we would say today) and studied its reactivity in various directions with great success. As early as 1905, in a publication with *Steindorff*,[19] he mentioned an investigation of its reactivity "towards magnesium in absolute ethereal solution. We intend to report in the near future in more detail on the application of the Grignard reaction to 1,5-dihalogen compounds".

It is not known to me why the publication of these results was delayed. However, the first detailed study of the preparation and of several reactions of 1,5-di(bromomagnesio)pentane (or pentamethylene-1,5-bis(magnesium bromide)) (**9**) appeared only in 1907; it was published by *Grignard* and *Vignon*[20,21]

$$\underset{\mathbf{8}}{Br(CH_2)_5Br} + 2\,Mg \longrightarrow \underset{\mathbf{9}}{BrMg(CH_2)_5MgBr}$$

Grignard made it quite clear that this success was mainly due to the availability of the starting material **8**: "Malheureusement les dihalogénures intermédiaires étaient, jusqu'à ces dernières années, à peu près inaccessibles, lorsqu'en 1904, M. J. v. Braun[1] découvrit un élégant procédé d'obtention du dichloro- et du dibromopentane, ...".[20]

However, it must have been a great disappointment to *von Braun*, as he reacted swiftly and not without bitterness.[22] He first emphasized the key role of the starting material and then derived his own claim[23] from its production: "That I am carrying out such experiments (and, as the discoverer of the method by which the pentamethylenedihalogen compound first became available in larger amounts, I surely had the right to use the Grignard reaction, which has by now become common property), ...". He referred to the publication mentioned above of his intentions[19] and continued: "In the interests of both sides it is to be regretted that the references concerned have escaped the notice of the French colleagues, ..." *Von Braun* did indeed play an important part in the discovery and application of the aliphatic α,ω-di-Grignard compounds.[24] In addition, he was one of the first to use the new dihalogenoalkanes for the synthesis of a metallacycle, the (oligomeric) pentamethylenemercury;[25] however, he used sodium amalgam in its preparation, as did *Hilpert* and *Grüttner*.[26] *Grüttner* and his school, to which the well-

known *E. Krause* also belonged, then rapidly developed the preparation of metallacycles and other organoelement heterocycles using di-Grignard reagents.[27,28]

The experience gained in the course of these earlier studies and of many later ones[29] can be summarized as follows. Di-Grignard compounds can be prepared from the corresponding dihalides (generally the dibromides[12,29]) *with some care* just as well as can the mono-Grignard compounds, when the two halogens are separated by at least four carbon atoms. The necessary *precautions* involve the reaction being carried out relatively slowly, since otherwise intra- and intermolecular Wurtz coupling occurs, as is also the case for the normal Grignard reaction. It will be shown in Section 2.2.1 that the "normality" of this type of di-Grignard compound is expressed not only in its preparation but also in its properties.

In contrast, the Grignard reaction does not succeed, or the yields are very poor, when 1, 2 or 3 carbon atoms separate the halogens. These three cases will now be dealt with in more detail.

2.1.2. *Geminal Di-Grignard Compounds*

It is interesting that the simplest members of the group of "small" di-Grignard compounds are in fact exceptional in that they can be prepared in relatively good yields and have thus been known for the longest time. They were first described by *Emschwiller* in 1926,[30] and their preparation was subsequently considerably improved by *Cainelli* et al.;[31] the most important modifications made by them were to use magnesium amalgam instead of magnesium metal and to use a 1:1 mixture of ether and benzene instead of pure absolute diethyl ether.

$$CH_2X_2 \xrightarrow[Et_2O/C_6H_6]{+Mg/Hg} CH_2(MgX)_2$$

The yields of the methylene di-Grignard reagents were however still not easily reproducible and generally lay no higher than 50–60%;[31,32] the by-products were ethene, propene, cyclopropane and, particularly unwanted for organometallic syntheses, methylmagnesium halide. Better yields were obtained only in reactions which were carried out under "Barbier" conditions, i.e. when a dihalogenomethane was reacted with magnesium amalgam and the substrate (for example a ketone) in a "one-pot" synthesis.[31] We were recently able to improve the synthesis further by using diisopropyl ether as solvent. In this way the methylenedimagnesium dibromide **10** can be obtained in a reproducible yield of 80% and free from unwanted by-products.[33] It has thus become an interesting synthon for the anionic introduction of a methylene group.[34]

$$\underset{}{CH_2Br_2} \xrightarrow[iPr_2O]{+Mg/Hg} \underset{\mathbf{10}}{CH_2(MgBr)_2}$$

The excellent way in which the reaction proceeds when this method is used is even more remarkable since it is an essentially heterogeneous reaction: **10** is practically insoluble in the reaction mixture, just like the amalgam and the magnesium bromide which is formed as a by-product. On the other hand, the success of the reaction is due to exactly these circumstances: all other by-products such as (unsaturated) hydrocarbons and methylmagnesium bromide dissolve in diisopropyl ether and can be removed by simple decantation.

Still to be explained is the (intuitively somewhat unexpected) ready formation of the "1,1-di-Grignard reagent" **10** in contrast to the "1,2-reagent" **5** and the "1,3-reagent" **7**. This is probably due to differences in stability, the carbenoid mono-Grignard **11** (which must be postulated as an intermediate) being much more stable than **4** and **6**. The α-elimination of **11** to give **12** proceeds more slowly since it is enthalpically less favorable than the formation of ethene [Eq. (e)] and cyclopropane [Eq. (f)].

$$\begin{array}{l} CH_2Br_2 \\ \downarrow \\ BrCH_2MgBr \longrightarrow BrMgCH_2MgBr \\ \quad\mathbf{11} \qquad\qquad\quad \mathbf{10} \\ \downarrow \\ MgBr_2 + CH_2{:} \longrightarrow CH_2{=}CH_2 + CH_3CH{=}CH_2 + \triangle \\ \quad\quad\mathbf{12} \end{array}$$

The α-elimination can however not be completely suppressed, and is probably responsible for the formation of ethene, propene, and cyclopropane.[32] It can be reduced to a minimum by the choice of suitable reaction conditions: particularly important is that the magnesium content of the amalgam be as low as possible (0.5–1% magnesium). This results in the main drawback of the synthesis: relatively large amounts of mercury (which, of course, can be recovered) are required.

Although this procedure for the preparation of **10** is successful, in our experience it cannot (with one exception) be extended to the use of other 1,1-dibromo compounds. For example, neither 1,1-dibromoethane, 1,1-dibromoneopentane nor benzal bromide give appreciable amounts of any organomagnesium compounds in an ether/benzene solvent mixture.[35] Only trimethylsilyldibromomethane (**13**) reacts in diisopropyl ether to yield 70% of the di-Grignard compound **14**;[36] even the tin analogue of **13** gives complex product mixtures.[37]

$$\underset{\mathbf{13}}{Me_3SiCHBr_2} \xrightarrow[iPr_2O]{+Mg/Hg} \underset{\mathbf{14}}{Me_3SiCH(MgBr)_2}$$

2.1.3. *Vicinal Di-Grignard Compounds*

The preparation of compounds of this type has until now proven to be the most difficult to realize, particularly in the aliphatic series. The future prospects are also not particularly good, since the β-elimination described as an example in Equation (e) is so strongly favored both by entropy and by enthalpy that the lifetime of an intermediate such as **4** is too short for it to react in a second step with the magnesium surface to give a di-magnesium derivative such as **5**.

Success has thus been limited to cases in which it has been possible to drastically retard the rate of β-elimination. The classical example in the aliphatic series is the preparation of the *cis*-1,2-di-Grignard reagent **18** of cyclopropane by *Wiberg* and *Bartley*[38] from *trans*-1,2-dibromocyclopropane (**15a**). In this case the β-elimination from the mono-Grignard reagent **16** is made difficult by the fact that it leads to cyclopropene [Eqn. (g)]: this process doubles the already high ring strain in cyclopropane.

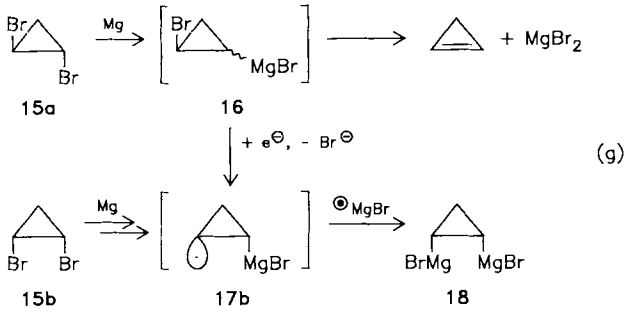

Various aspects of this reaction are remarkable, firstly of course the fact that **18** is formed at all. The yield is low (ca. 10–15%), the main product being the alkene (i.e. cyclopropene), as in Equation (e). The formation of the *cis*-compound **18** from the *trans*-compound **15a** is also surprising; *Wiberg* and *Bartley* assigned this structure on the basis of the carboxylation and deuterolysis of **18**, since they obtained *cis*-products in both cases. They attempted to rationalize the formation of the *cis*-structure by the formulation **19**, but presented no arguments for it.

We have repeated *Wiberg*'s experiments and could in the main confirm their results.[39] In addition we were able to isolate **18** in a pure form, as it is only slightly soluble in diethyl ether. It is interesting that its solubility is increased considerably by the addition of magnesium bromide (see Section 2.2.2); this allowed us to measure the ^{1}H-NMR spectrum of **18** and thus to confirm the *cis*-structure directly. In addition we found that **18** is also formed in a comparable yield from the *cis*-dibromide **15b**. Since the cyclopropyl-magnesium bond is generally configurationally stable,[40] the *cis*-configuration of **18** is either thermodynamically more stable, which would be somewhat surprising (see however the discussion in Section 2.2.2), or the stereochemistry is determined at the stage of the configurationally flexible cyclopropyl radicals.[55] The immediate precursor for **18** is very likely **17b** [Eqn. (g)]. Theoretical calculations show that **17b** is more stable than its *trans*-isomer **17a**,[41] so that the explanation of the favored *cis*-configuration on the basis of *kinetic* factors gains credibility.

It appears questionable at present whether a simple aliphatic 1,2-dimagnesium compound such as **5** can in fact be synthesized. It is also unclear whether it would be thermally stable, since the corresponding organolithium compounds appear to decompose very readily with elimination of lithium hydride.[10]

$$LiCH_2CH_2Li \longrightarrow LiCH{=}CH_2 + LiH$$

From this point of view, the stability of **18** at room temperature is probably due to two factors: firstly the lesser tendency of magnesium to split off hydride and secondly the strain already mentioned in the product of magnesium hydride elimination from **18**, which would be a Grignard derivative of cyclopropene.

It could also be expected that in the aromatic series the β-elimination from *o*-dihalogenobenzenes **20** would be made more difficult by the formation of the strained triple bond of the aryne.

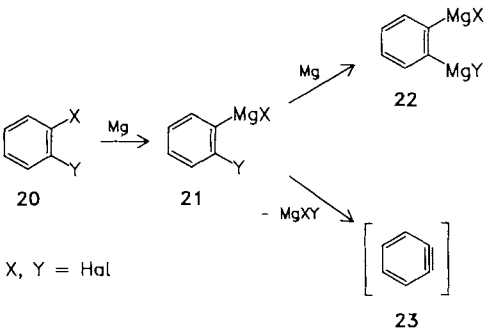

The course taken by the reaction depends on the nature of the halogens X and Y. The first step (**20**→**21**) only occurs in a satisfactory manner when X = Br or I.[42,43] The mono-Grignard compound **21** can be quite stable, especially when Y = Cl or Br.[44,45] This has already been utilized for further reactions of **21**.[42–46] However, there is a more or less distinct tendency for the elimination of magnesium halide to give the aryne (e.g. **23**), as has been shown in particular by *Wittig*.[44] The di-Grignard compounds **22** can be obtained under favorable conditions from **20** (X = Y = Br,[12,47] X = I, Y = Br[48]) in 20–40% yield. This relatively poor yield can however be of preparative interest, since one can obtain bifunctional or cyclic products in a one-pot synthesis from a readily available starting material (**20**). However, pure **22a** can only be obtained via the dilithium compound **2**.[5]

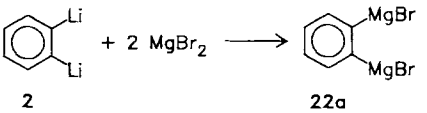

2.1.4. 1,3-Di-Grignard Compounds

The chance that a 1,3-di-Grignard compound can be prepared from the dibromide [Eqn. (f)] is a priori greater than that for a 1,2-di-Grignard compound [Eqn. (e)]. The gain in enthalpy from the successfully competing elimination of magnesium bromide is probably approximately equal in both cases, but the entropy is clearly more favorable for the 1,2-elimination, particularly since the ideal combination of a strongly electrofugal group ($MgBr^{\oplus}$) and a strongly nucleofugal one ($Br^{\ominus}$) makes only small demands on the relative orientation of the groups.

In spite of this, all attempts to prepare **7** were, for a long time, unsuccessful.[15b,c] *Zelinsky* and *Gutt* were able to identify a di-Grignard compound as well as the by-product propene; however, the product was not **7** but 1,6-bis(bromomagnesio)hexane **27**,[15c] the product of a Wurtz reaction. The main product was always cyclopropane. One can generalize by saying that the formation of a three-membered ring from a 1,3-dihalide proceeds so well that it has been developed into a versatile synthesis for cyclopropanes and heterocyclopropanes; zinc and alkali metals can be used as well as magnesium.

The first preparation of **7** was achieved by *Costa* and *Whitesides* in 1977 using an indirect method via organoboron and organomercury compounds.[49]

$$CH_2{=}C{=}CH_2 \xrightarrow{B_2H_6} B(CH_2CH_2CH_2)_3B \xrightarrow{Hg(OAc)_2}$$

$$AcOHg(CH_2)_3HgOAc \xrightarrow{NaCl} ClHg(CH_2)_3HgCl \xrightarrow{CH_3Li}$$

$$CH_3Hg(CH_2)_3HgCH_3 \xrightarrow{Mg/MgBr_2}$$

$$\underset{\mathbf{7}}{BrMg(CH_2)_3MgBr} + CH_3MgBr + n\text{-}C_3H_7MgBr + \underset{\mathbf{24}}{CH_2{=}CHCH_2MgBr}$$

Although the concept of this synthesis is very elegant, it cannot to be recommended for preparative applications because of its complexity, the low yields, and the large number of organomagnesium side products; however, *Costa* and *Whitesides* were able to use **7** to prepare a silacyclobutane.[49]

A chance observation in fact finally led to a breakthrough in the direct synthesis of **7**. In our laboratory *F. A. Hartog* had been studying the Barbier reaction,[50] one goal being to trap unstable Grignard intermediates using carbonyl compounds.[51] Thus he obtained **25**, which can be interpreted as an adduct between **27** and benzophenone, in 6% yield. This indicated the possibility that the lifetime of compounds of type **26**, to which **6** [Eqn. (f)] also belongs, is short, yet long enough to permit further intermolecular reactions.

$$\underbrace{Cl(CH_2)_3Br + Mg}_{\downarrow} + Ph_2C{=}O \xrightarrow{H_2O} \underset{OH}{Ph_2C(CH_2)_3Cl}\ \mathbf{25}$$

$$\mathbf{26}\ [Cl(CH_2)_3MgBr] \xrightarrow{1)\ Ph_2C{=}O,\ 2)\ H_2O} \uparrow$$

This result, together with the demonstrated ability of **7** to exist,[49] removed the psychological barriers which had for so long prevented attempts to synthesize **7** directly from 1,3-dibromopropane.[51,52] The first ray of hope was provided by a signal at $\delta \approx 0$ to -1 ppm in the ^{1}H-NMR spectrum of the reaction mixture: it could only be due to **7**, but the yield was at first below half a percent. Variation of the dihalide, the metal and the solvent led to the procedure which gave the best results [Eq. (h)].[53]

$$Br(CH_2)_3Br \xrightarrow{+Mg} \underset{\mathbf{7}\ (30\%)}{BrMg(CH_2)_3MgBr} + \underset{\mathbf{27}\ (15\%)}{BrMg(CH_2)_6MgBr} + CH_2{=}CHCH_2MgBr + (CH_2)_3 + MgBr_2 \quad \text{(h)}$$

$$\mathbf{24}\ (0\text{–}10\%)$$

It is important for a high yield of **7** (ca. 30%) that the reaction be carried out slowly in diethyl ether using a large excess of magnesium (the latter should preferably be purified and activated by double sublimation). Such conditions can be readily achieved when the dibromopropane is added to the magnesium at room temperature over a period of 2 days in a sealed glass apparatus with an overflow system. Under these conditions, cyclopropane is still the main product. A few percent of other hydrocarbons are also present: propene (1.1%), propane (1.0%), ethene (0.6%), methane (0.4%), and ethane (0.1%). This indicates that the Grignard reaction occurs in a complex manner involving free radicals.[55] If necessary, **7** can easily be purified by treating it with THF (see Section 3).

The range of di-Grignard compounds which can be obtained directly has in this case also proven to be small. The synthesis of the 2,2-dimethyl derivative **28** is preparatively useful; though the yield is only 10–15%, the reagent is almost free from organometallic by-products and can thus be used directly for the synthesis of metallacycles; in addition, the starting material is readily available.[56]

$$BrCH_2CMe_2CH_2Br + Mg \longrightarrow \underset{\mathbf{28}}{BrMgCH_2CMe_2CH_2MgBr}$$

In contrast, the formation of 1,3-di-Grignard reagents does not occur satisfactorily when a hydrogen atom is present in position 2, as is shown by the example of **29** (9%). Remarkable in this reaction is the high yield (70%) of the hydrocarbon **30**, which is formed directly during the

$$BrCH_2CH(t\text{Bu})CH_2Br \xrightarrow{+\ 2\ Mg} \underset{\mathbf{29}\ (9\%)}{BrMgCH_2CH(t\text{Bu})CH_2MgBr} + \underset{\mathbf{30}\ (70\%)}{\text{[structure]}}$$

reaction and not by hydrolysis of an organomagnesium precursor.[56] We still have no completely satisfactory explanation for the formation of **30**.[52]

Similarly, our expectation that it would be possible by using the cyclic dibromides **31** and **32** to reduce the formation of three-membered rings, because of the ring strain generated in such products, and thus favor the formation of the di-Grignard compounds has regrettably not been fulfilled.[52] The products **32** and **34** were obtained in low yields, in each case together with several by-products; in addition **34** decomposes rapidly to give **35** (see also Section 2.2.2).

On the other hand, we have recently succeeded in obtaining the 1,3-di-Grignard reagent **37** in 96–100% yield by slow reaction of *ortho*-bromobenzyl chloride (**36**) with an excess of magnesium (sublimed and sieved to give a par-

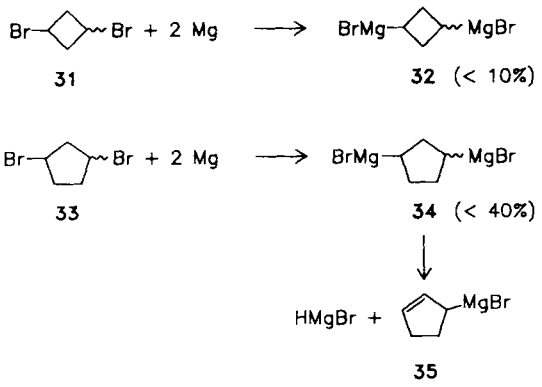

ticle size <2 mesh) in THF. It disproportionates immediately according to the Schlenk equilibrium [Eqn. (l) in Section 2.2.1]. The diorganylmagnesium compound **38**, a nearly insoluble solid, is precipitated and can be easily freed from all impurities by decantation (isolated yield 85–90%) [Eqn. (i)] (see also Section 2.2.2).

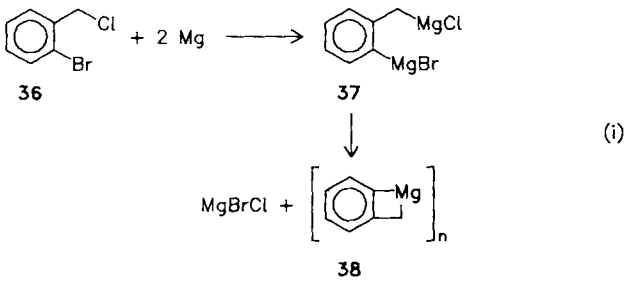

(i)

2.1.5. *Summary of the Previous Results*

We can sum up as follows: it is possible not only to prepare "normal" di-Grignard compounds directly from the corresponding dihalides; a number of such reagents where the two magnesium atoms are separated by one or three carbon atoms is now known. However, 1,2-di-Grignard compounds are rareties, and it appears that this will continue to be the case in the foreseeable future.

2.1.6. *Di-Grignard Reagents from Mercury Compounds*

The preparation of Grignard reagents from the corresponding organomercury compounds [Eqn. (d)] is normally of no preparative importance, since the mercury compounds are themselves obtained from the Grignard compounds (with the exception of the amalgam method). This cumbersome reaction sequence can however become necessary when a Grignard reagent of high purity is required for structural studies. This is always the case when the yield for the reaction of formation from the organic halide is low; dihalides, as we have seen, very often give such low yields.

$$RBr \xrightarrow{Mg} RMgBr \xrightarrow{HgBr_2} RHgBr \xrightarrow{Mg} RMgBr$$

This method has two advantages: firstly the impure Grignard reagents obtained initially can be converted into stable organomercury halides which can be obtained in high purity by recrystallization. The subsequent reaction, carried out by shaking the organomercury compound in THF with an excess of magnesium metal, is slow but practically quantitative. In mechanistic terms there is probably an initial reduction to give the diorganomercury compound, which reacts with further magnesium to give the diorganomagnesium compound; the Schlenk equilibrium is then set up between the latter and the magnesium bromide formed [Eqn. (j)] (see Section 2.2).

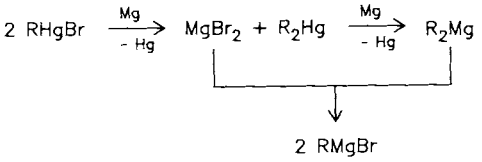

(j)

When the substituents R are sterically demanding, the second step is sterically hindered and the reaction proceeds only as far as the diorganomercury compound.[58]

The last step in Equation (j), the ligand exchange reaction between the diorganomagnesium compound and magnesium bromide, can also be carried out separately: for example, a cyclic organomercury compound can first be converted into the magnesacycle and the latter then treated with the stoichiometric amount of magnesium bromide [Eqn. (k)].

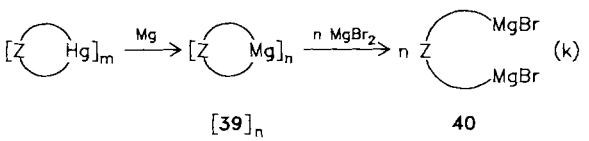

(k)

2.2. Structure and Properties

No X-ray crystal structure determinations have yet been reported for solid di-Grignard compounds, so that the following discussion refers to solutions, mainly in THF.

2.2.1. *"Normal" Di-Grignard Compounds*

The structure of Grignard reagents in solution is complex, since several parallel equilibria are involved.[11c] Apart from a quantitatively unimportant electrolytic dissociation, the so-called Schlenk equilibrium [Eqn. (l)] dominates; all the components of this equilibrium can form associates with themselves or with other components.

$$2\,RMgBr \overset{K}{\rightleftharpoons} R_2Mg + MgBr_2 \qquad (l)$$

The position of these equilibria depends on the organic group R, on the halide and on the solvent. Our structural investigations have been concerned mainly with bromides in THF as solvent. In this case, association is unimportant for all three components; they are monomolecular. In the bifunctional series, the same is true for the di-Grignard compound **40** and for magnesium bromide but not for the diorganomagnesium, which is in this case the magnesacycle **39**. In dilute solution, magnesacycles are either completely dimerized or at least dimerized to a large extent to

$[39]_2$. It was not possible to derive the structure and behavior of the di-Grignard compounds **39** until after the structure of $[39]_2$ was known (see Section 3) [Eqn. (m)].

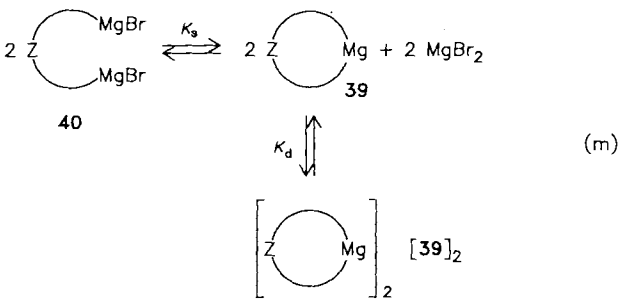

(m)

The position of the equilibrium was determined by very accurate measurements of the osmotic particle number using a stationary isothermal distillation. The results are collected in Table 1 and compared with the values for ethyl magnesium bromide.

Table 1. Thermodynamic parameters of the Schlenk equilibrium in THF at 25 °C [Eqns. (l) and (m), upper part].

Compound	K_s	ΔH_s [kJ mol^{-1}]	ΔS_s [J mol^{-1} K^{-1}]	Ref.
EtMgBr	6.8	25.6	99.2	[59]
$BrMg(CH_2)_4MgBr$	9.3	32.6	127.6	[60]
$BrMg(CH_2)_5MgBr$	9.2	31.4	123.4	[61]

These results show that the mutual influence of the two organomagnesium functionalities is not large in the thermodynamic ground state, since they do not deviate appreciably from the values for the monofunctional model compound and show little dependence on the length of the methylene chain. This probably also means that the situation in solution is the same as that for the mono-Grignard compound. The magnesium usually binds two additional THF molecules to become tetracoordinate.[11e] Association, including that with magnesium bromide, is unimportant; we shall however see in Section 2.2.3 that the situation is very different for the "short" di-Grignard compounds.

The mono- and di-Grignards also resemble each other in diethyl ether in that in both cases the Schlenk equilibrium is shifted completely towards the side of the organomagnesium bromide.[11c,62,63]

2.2.2. *Intramolecular Coordination*

The situation is quite different when, as in **41**, the chain linking the two organomagnesium functionalities carries an oxygen atom which is able to form an intermolecular coordinative bond to the magnesium atom. In these cases

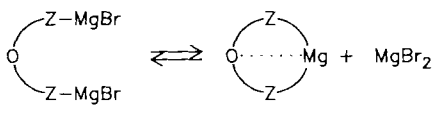

41 42

Z = $(CH_2)_3$[64]; $(CH_2)_4$[65]; o-$C_6H_4CH_2CH_2$[65]

the cyclic diorganomagnesium compound **42** is so stable (see Section 3) that the Schlenk equilibrium is shifted completely to the right-hand side (cf. **55**, **56**, and **57** in Table 2).

2.2.3. *"Short" Di-Grignard Compounds*

Di-Grignard compounds with 1, 2 or 3 carbons between the two magnesium functionalities differ in several characteristic aspects from the "normal" members of this class. These differences probably have a common origin in the relatively short distance between the charges or dipoles of the two polarized carbon–magnesium bonds. However, we have no direct information on the structure of **7**, **10**, and **18**, since their crystal structures have not been determined and no association measurements have been carried out.

In general the solubilities of the "short" Grignard reagents are low. In THF, where the Schlenk equilibrium [Eqn. (l)] is shifted considerably to the right (see Section 2.2.1), disproportionation to the dialkylmagnesium **43** occurs; because of its oligomeric or polymeric character, the latter is practically insoluble [Eqn. (n); compare Eqn. (o)].

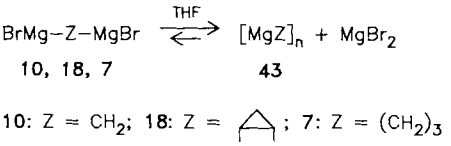

(n)

In the case of **10** this reaction does not go to completion, since magnesium bromide is apparently locked in structures such as $[CH_2Mg \cdot CH_2(MgBr)_2]_n$ (**44**) (for the sake of clarity coordinated solvent molecules have been omitted).[32,36]

$[CH_2Mg \cdot CH_2(MgBr)_2]_n$

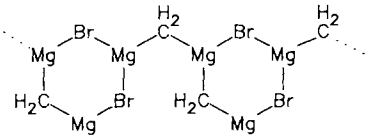

44

In all cases, the insoluble **43** can be redissolved by the addition of an excess of magnesium bromide. This is not due to a shift of the Schlenk equilibrium (n) to the right, since in the case of **18** and 7 exactly two moles of magne-

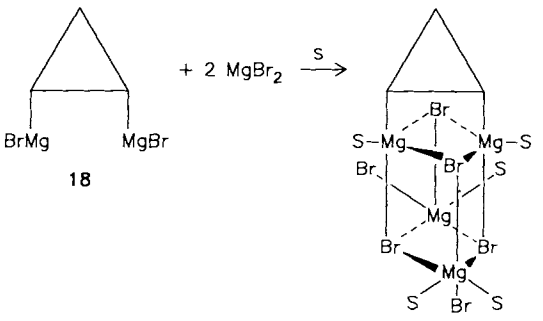

S = THF 45

sium bromide are used; thus the formation of a complex such as **45**[39] must be assumed; analogies are known in the case of simple organomagnesium compounds.[66]

This unusually strong complex formation with magnesium bromide apparently serves to compensate for the high "concentration" of negative charge in a small space.

As has already been mentioned, the Schlenk equilibrium in diethyl ether lies far to the side of the organomagnesium bromides;[62,63] **10**, **18**, and **7** are more soluble in this solvent (where they probably have the structure depicted). However, their solubilities are still not high, particularly in the case of **18** (see Section 2.1.3). What is remarkable, and so far unexplained, is the considerable increase in the solubility of **10** in a 1:1 mixture of diethyl ether and benzene. Since the non-polar benzene normally decreases the solubility of the somewhat polar Grignard compounds, one may speculate that **10** is aggregated [Eqn. (o)] to form the dimer **46**, which has a relatively non-polar outer surface.[67]

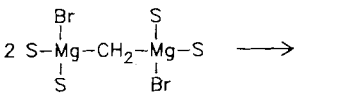

10 · 4S (o)

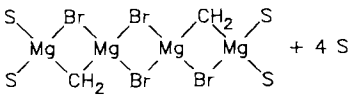

S = Et_2O **46**

We have also observed a tendency for **7** to form charge-compensated bromine bridges in diethyl ether.[34,52] At lower temperatures, coalescence effects are observed in the proton NMR spectra; these can be interpreted as an equilibrium between the two equivalent structures **47a** and **47b** (together 90%), and **48** (10%). The ratio of **47** to **48** is temperature-independent, which means that the enthalpy difference is zero; that **47** is favored must thus be due to entropy factors ($\Delta S = -4.3$ J mol^{-1} K^{-1}), the ring formation in **47** apparently being overcompensated by the fixation of additional solvent molecules **S** in **48**.

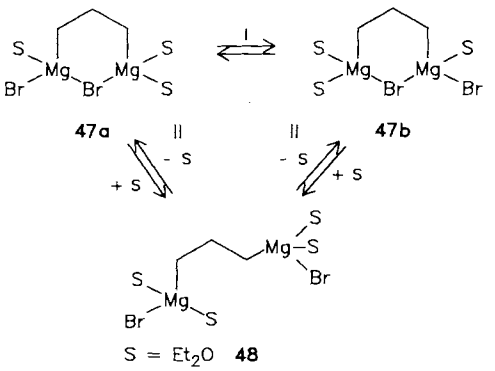

S = Et_2O **48**

Since the two α-methylene groups in **47a** or **47b** and **48** have different chemical shifts, line shape analysis allowed us to determine the activation parameters for the equilibria I ($\Delta H^{\neq} = 21$ kJ mol^{-1}, $\Delta S^{\neq} = -109$ J mol^{-1} K^{-1}) and II ($\Delta H^{\neq} = 28$ kJ mol^{-1}, $\Delta S^{\neq} = -118$ J mol^{-1} K^{-1}). The negative entropy of activation in particular indicates that the initial steps in the rearrangement reactions involve attack by solvent molecules.

Finally, we should comment on a property of **7** which somewhat reduces its stability and usefulness. It was mentioned in Section 2.1.4 that one of the by-products in the preparation of **7** by both *Whitesides'* and our method is allylmagnesium bromide (**24**). Further studies[52,53] have shown that **24** does not arise during the formation of **7**, but is a secondary product formed from **7**.

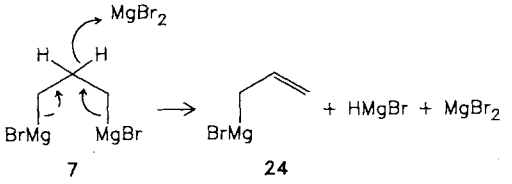

7 **24**

The hydrogens at carbon 2 are hydridically activated from both sides by hyperconjugation with the two electron-rich carbon-magnesium bonds, so that magnesium bromide hydride can be split off. Magnesium bromide functions here as a Lewis acid catalyst, so that the rate of decomposition of **7** depends on the concentration of $MgBr_2$. Since the presence of $MgBr_2$ is unavoidable in both syntheses, a certain amount of **24** is always present. However, when **7** is purified according to Equation (r) and is free from excess magnesium bromide, it is quite stable in solution (half-life ca. 120 days). We shall see, however, that the double hydridic activation can be a great disadvantage in some applications. The 2,2-dimethyl derivative **28** can naturally not split off hydride; it is thus quite stable and also undergoes no side reactions during chemical transformations.

3. Magnesacycles

The preparation and study of magnesacycles is important for two reasons. Firstly, they are of fundamental importance as metal-containing heterocycles: thus, for example, the question can arise as to whether a magnesacyclohexane is stable, and as to its structure. In addition, a knowledge of the structure of magnesacycles is also essential when the structures of the di-Grignard reagents (see Section 2.2) are to be studied, particularly in the most important solvent, THF. The dilemma present is that, because of the unavoidable Schlenk equilibrium (Eqns. (l) and (m)], Grignard compounds can never be obtained in a pure form in this system. This limitation does not apply to the other partner of the Schlenk equilibrium, the dialkylmagnesium compound; thus pure [**39**]$_n$ can be obtained from the corresponding mercury compound, as shown in the first step of Equation (k). A further possibility is the method discovered by *Schlenk* himself during his studies of the equilibrium reaction which bears his name:[68] this involves the removal of the magnesium bromide, formed according to Equation (l), as an insoluble dioxane complex. This method is faster and more convenient for the preparative formation of diorganomagnesium compounds,

but is not to be recommended when extremely pure compounds are required for structural studies. In the case of the magnesacycles there is an additional problem: the dioxane precipitate contains not only magnesium bromide but also organomagnesium compounds (either bonded or only entrained), so that the yields of pure magnesacycles in solution are very low.

It should be remembered that all components of the Schlenk equilibrium [Eqn. (l)] are normally monomeric in THF. In the case of organomagnesium compounds the strong nucleophilicity of the THF molecule towards magnesium usually leads to the formation of a tetracoordinated, saturated species.[11c,69,70]

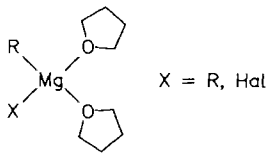

X = R, Hal

It was thus surprising that in the case of magnesacyclohexane an extremely strong tendency to dimerization [cf. k_D in Eqn. (p)] was observed;[63] the monomeric form could only be detected by measurements in extremely dilute solutions (0.001 to 0.02 M). The thermodynamic parameters (Table 2) were determined from the temperature-dependence of the dimerization equilibrium.

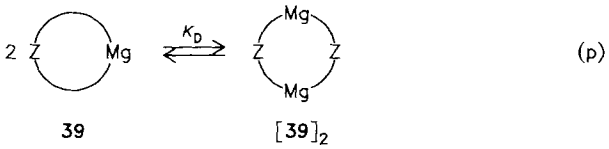

(p)

39 $[39]_2$

Table 2. Association of magnesacycles of type **39** in THF [71].

2 **39** ⇌ $[39]_2$	Z	n [a]	Ref.
49	$(CH_2)_4$	2	[60, 74]
50	$(CH_2)_5$	1-2 [b]	[61]
51	$(CH_2)_6$	2	[72]
52	$(CH_2)_9$	2	[72]
53	*o*-$C_6H_4(CH_2)_3$	1-2 [c]	[72]
54	*o*-$C_6H_4(CH_2)_2$	1	[72]
55	$(CH_2)_3O(CH_2)_3$	1	[64, 65]
56	$(CH_2)_4O(CH_2)_4$	1	[65]
57	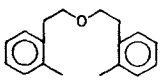	1	[65]

[a] Association number $n = c_f : c_{osm}$, c_f being the formal concentration when 100% monomer is present and c_{osm} the particle concentration determined osmotically. [b] $\Delta H_D = -48.0 \pm 3.0$ kJ mol^{-1}, $\Delta S_D = -106.0 \pm 10.0$ J mol^{-1} K^{-1}. [c] $\Delta H_D = -48.7$ kJ mol^{-1}, $\Delta S_D = -118 \pm 12$ J mol^{-1} K^{-1}.

Two aspects of this result were extremely puzzling: 1) Why is magnesacyclohexane **50** so unstable compared to the dimer $[50]_2$, although a six-membered ring structure with tetracoordinated magnesium could be considered possible? 2) When **50** is so unstable, why does it give only the dimer without polymerizing further?

The answers are supplied by the X-ray structural analysis of $[50]_2$ (Fig. 1).[61] The compound is dimeric in the crystal. As expected, the magnesium is made tetracoordinate by the complexation of two molecules of THF. However, the geometry is not that of an ideal tetrahedron, the

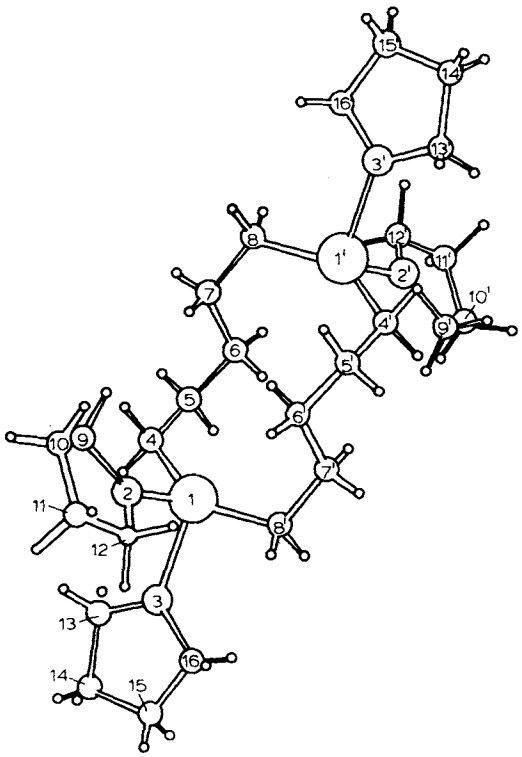

Fig. 1. X-ray crystal structure of 1,7-dimagnesacyclododecane $[50]_2$; 1 and 1′ are the magnesium atoms, 2, 3, 2′ and 3′ the oxygen atoms of the four THF molecules, 4-8 and 4′-8′ the carbons of the two pentamethylene chains, and 9-16 and 9′-16′ the carbon atoms of the four THF molecules.

C-Mg-C angle being very obtuse (141.5°). According to one's taste one can either say that the sp-hybridization of the magnesium (bond angle 180°, see zinc and mercury!) is only slightly perturbed by the ether oxygens, or that according to *Bent*'s rule[73] the magnesium uses much more s-character in the bond to carbon than in that to the more strongly electronegative oxygen.

In any case, the result is a large intraannular angle at magnesium; this cannot be accommodated in the six-membered ring of **50** without introducing strain, but becomes possible in the twelve-membered ring of $[50]_2$. The strain makes itself felt in the form of the exothermal dimerization energy of $\Delta H_D = -48$ kJ mol^{-1}. The entropy loss caused by the dimerization ($\Delta S_D = -107$ J mol^{-1} K^{-1}) compensates only partially for this effect ($\Delta G_D(25\,°C) = -16$ kJ mol^{-1}). However, as soon as the driving force of the ring strain in the six-membered ring has disappeared in the dimerization to the twelve-membered ring, the entropy component opposes any further polymerization. Evaporation of $[39]_2$ followed by slow warming in fact yields modifications of **39** [Eqn. (m)] which can be redissolved only with difficulty on shaking for a long time with THF. Apparently, the removal of the complex-forming THF has led to an extensive polymerization (to $[39]_n$).

The ring strain in **50** has also been confirmed thermochemically. Model experiments first showed that with respect to one carbon-magnesium bond, the enthalpy of reaction according to Equation (q) always has the same value ($\Delta H = -220$ kJ mol^{-1}), independent of the group R.

$$R_2Mg + 2CH_3COOH \longrightarrow 2RH + (CH_3COO)_2Mg \qquad (q)$$

Deviations from this standard value signalize particular effects, for example ring strain. Thus, when the position of the equilibrium $2\,\mathbf{50} \rightleftarrows [\mathbf{50}]_2$ is known the experimentally determined heat of reaction can be used to determine the ring strain in **50**, under the reasonable assumption that $[\mathbf{50}]_2$ is strain-free. The value obtained for **50** was $\Delta H = -45.4 \pm 6.5$ kJ mol^{-1}, which within the (in this case much larger) limits of error agrees with that from the association measurements ($\Delta H = -48.0 \pm 3.0$ kJ mol^{-1}; Table 2). A similar equilibrium position and ring strain was determined for the six-membered benzoannelated magnesacycle **53** (Table 2).

After this detailed discussion of the results for **50**, the other data in Table 2 can be readily explained. It is of course completely clear that a large C–Mg–C bond angle in a five-membered ring will generate even more strain than in a six-membered ring; it is thus not surprising that $[\mathbf{49}]_2$ in THF shows no tendency to form the monomeric five-membered ring **49**. $[\mathbf{49}]_2$ also exists as a ten-membered ring in the crystalline state.[74] We can thus assume that $[\mathbf{51}]_2$ and $[\mathbf{52}]_2$, which exist solely in the dimeric form, also contain fourteen- and twenty-membered rings, respectively. Ths complete dimerization of **52**, which would like $[\mathbf{49}]_2$ contain a ten-membered ring if monomeric, is at first surprising. A detailed analysis of the X-ray structures of $[\mathbf{49}]_2$ and $[\mathbf{50}]_2$, however, shows that the two oligomethylene chains in these compounds are sufficiently separated from each other by the two large magnesium atoms; thus, they cannot cause a transannular van der Waals repulsion. In contrast, **52** as a ten-membered ring would contain only one magnesium atom; therefore, just as for **51**, the well-known ring strain in medium-sized rings plays an unfavorable role.

It is interesting to note that the rapid exchange of bonds between magnesium and carbon or oxygen[11c] is responsible for the fact that the systems mentioned above can and must always seek out the thermodynamically most favorable state. Pure carbocycles or hetero- and metallacycles with stable ring bonds do not have this possibility, so that in such systems strain can only be determined thermochemically and not by means of the experimentally simpler association measurements.

Finally, we should remark on the last four compounds in Table 2. In contrast to the general trend, they exist in a purely monomeric form. We have no completely convincing explanation for this in the case of **54**; probably the ring strain is reduced by benzocondensation (i.e. some unfavorable hydrogen interactions are no longer present; see also [74b]). In the cases of **55**, **56**, and **57** the monomeric state is clearly stabilized by intramolecular coordination (see also Section 2.2.2). Particularly informative is **56**, which without oxygen coordination would have a ten-membered ring as does **52**. While the latter is not stable as the monomer, **56** is, the reason being that it contains not a ten-membered ring but two six-membered rings.

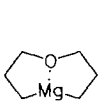

55

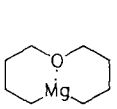

56

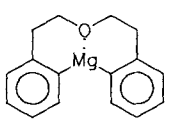

57

The heats of the reaction with acetic acid mentioned above can also be used in conjunction with values for standard dialkylmagnesium compounds to estimate the strength of the intramolecular coordination.[65] This is however only possible to a certain degree of approximation, since compounds **55**–**57** do not have the idealized geometry mentioned above; because of the longer Mg–C and Mg–O bonds, the rings do in fact exhibit ring strain, the value of which is not known. In this manner we arrive at a lower limit of $\Delta H = 90$ and 87 kJ mol^{-1}, respectively, for the strengths of the Mg–O bonds in **55** and **56**.[65] This value lies considerably higher than that of 68 kJ mol^{-1} estimated for the magnesium–oxygen bond in $Et_2Mg \cdot 2\,THF$; it should be remembered that THF is quite a strong base toward magnesium.

Little is known about the structures and properties of the dialkylmagnesium compounds or magnesacycles corresponding to the "short" di-Grignard compounds **10**, **18**, and **7**. They are in general only slightly soluble and appear to be oligomeric or even polymeric. This is in fact understandable, since on the basis of experience with larger systems the formation of smaller rings is extremely unlikely (Table 2).

As already mentioned in Section 2.2.3, **10** can be freed from most of the magnesium bromide by precipitation and washing, though it is not possible in this way to obtain bromine-free methylenemagnesium (**58**).[32b] However, *Ziegler* et al. have prepared **58** as a white insoluble powder by pyrolyzing dimethylmagnesium.[75]

$$n\,Mg(CH_3)_2 \xrightarrow{\Delta} n\,CH_4 + [MgCH_2]_n \quad \mathbf{58}$$

It is also worthy of mention that the bromide-containing **58** obtained by us gives better results in some applications than does **10**, for example in the synthesis of a 1,3-digermacyclobutane[32b] (see Section 4.2.5).

The dialkylmagnesium compound **59** obtained from the di-Grignard **18** also consists of a mixture of oligomers. This is suggested by the following observation: while **59** is almost insoluble in THF, it dissolves in $[D_{18}]$HMPA (hexamethylphosphoric acid triamide). The α-protons in the ^{1}H-NMR spectrum of **59** occur as a broad signal at $\delta \approx -1.7$ (signal width ca. 1 ppm). When the HMPA solution is allowed to stand for several days, a weak unsymmetrical multiplet is observed which overlaps the broad band; eventually the solution decomposes slowly with a half-life of ca. 16 days.[39,52] We assume that **59** is polymeric or highly oligomeric in the solid state; when it dissolves in HMPA, smaller oligomeric units with $n > 3$ are slowly formed.

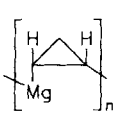

59

The dialkylmagnesium compound **60** corresponding to the di-Grignard **7** is also fairly insoluble in THF and can be obtained in pure form when the impure **7** obtained from 1,3-dibromopropane is evaporated and the magnesium bromide washed out, together with other impurities [Eqn. (h)], using small portions of THF; large volumes of

THF cannot be used, since otherwise too much **60** will be lost as a THF-soluble complex of **7** with $MgBr_2$ (see Section 2.2.3). We thus have a preparatively simple method for the formation of very pure **7**: the pure **60**, a dry white powder obtained by decanting off the THF, is treated with one molar equivalent of magnesium bromide in diethyl ether; since in this solvent the Schlenk equilibrium lies on the side of the Grignard reagent (see Section 2.2.1), **7** is re-formed quantitatively and dissolves [Eqn. (r)].[54]

$$7 + \text{impurities} \longrightarrow \xrightarrow{THF} \longrightarrow \qquad (r)$$

$$1/n(MgCH_2CH_2CH_2)_n \xrightarrow[MgBr_2]{Et_2O} BrMg(CH_2)_3MgBr$$

60 **7**

4. Applications of Di-Grignard Compounds

4.1. "Normal" Di-Grignard Compounds

As has already been noted briefly in Sections 1.2 and 2.1.1, the direct synthesis of readily available "normal" di-Grignard compounds with four or more carbon atoms between the magnesium functionalities was used early on for the synthesis of both acyclic and more particularly cyclic compounds, especially in organometallic chemistry.[11,52] Apart from the syntheses already mentioned,[24–28] the preparation of metallacyclic transition metal compounds by the groups of *Whitesides* (Ti,[76] Pt[77]) and *Grubbs* (Pt,[78] Ni[79]) are worthy of mention as examples of more recent developments; the same holds for our own work on the synthesis of heterocycles of main group elements.[46,80]

4.2. "Short" Di-Grignard Compounds

The 1,1-di-Grignard reagent **10** has been known since 1926,[30] and its application in organic synthesis has already been studied.[31,32] However, apart from one example,[81] its potential for the synthesis of organometallic reagents had not been explored. This is naturally also true for the recently prepared 1,2- and 1,3-reagents. In the following discussion we shall reverse the sequence used in Sections 2 and 3 and start with the applications of the 1,3-di-Grignard reagents **7** and **28**, since they precede those of **10** and, as will be shown, have contributed conceptually to certain developments of the chemistry of **10**.

4.2.1. Organic Compounds from 1,3-Di-Grignard Compounds

We shall first refer to some applications of **7** and **28** in organic synthesis; these will show some interesting possibilities, but also clear limitations. **7** reacts readily with hard nucleophiles such as water and CO_2; as expected, propane and glutaric acid are formed.[53]

Glutaric acid is obtained as the main product only by pouring **7** onto dry ice. When, however, gaseous carbon dioxide is slowly passed into the reaction vessel, the well-known[20,24] double reaction with one molecule of CO_2 occurs, giving the magnesium salt **61** of cyclobutanone hydrate; this in turn gives cyclobutanone **62** on hydrolysis.[82] Although the yield of **62** is only ca. 30% (with respect to **7**), this method for its preparation is one of the simplest and cheapest. It is also simple to execute, since crude **7** [Eqn. (h)] can be used; **61** is the only product in the reaction mixture which is rather insoluble, so that all by-products can be decanted off prior to hydrolysis; **62** can be obtained by simple distillation after the hydrolysis of **61**.

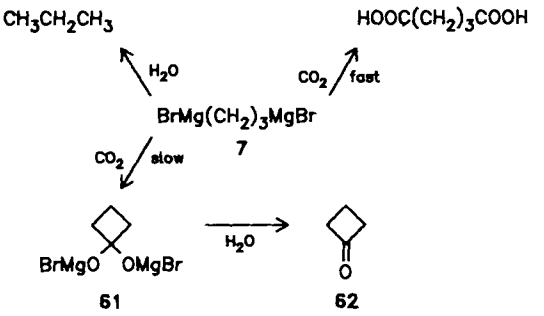

The greatest limitation for the use of **7** is unfortunately to be found in its reactions with carbonyl compounds and in particular with ketones. Here the double hydridic activation of the β-hydrogens takes the upper hand, and for example the reaction with benzophenone yields only its reduction product benzhydrol and the tertiary alcohol 1,1-diphenyl-3-buten-1-ol, the latter arising from addition of the allyl derivative **24** (which is formed as an intermediate) to benzophenone.

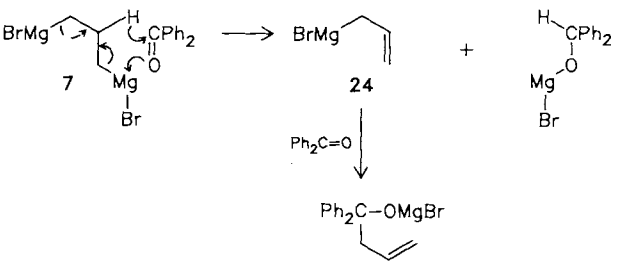

Problems of this type do not arise with **28**, as demonstrated by the reaction with cyclohexanone, which leads to the expected diol **63**.

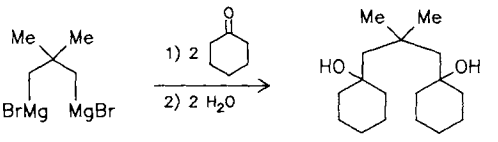

4.2.2. Acyclic 1,3-Dimetal Compounds from 1,3-Di-Grignard Compounds

The reactions of **7** and **28** with chlorotrimethylstannane and mercuric bromide are very clean, and can be used for the determination of the yields of the di-Grignards.

The 1,3-bis(bromomercurio)propanes **64** and **65** in turn offer interesting reaction possibilities, as will be shown using two examples. The two-step reaction with butyllithium afforded the 1,3-dilithiopropanes **66** and **67**,[83] which had

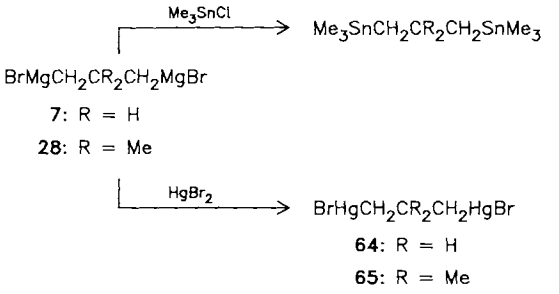

previously been found to be inaccessible by other routes.[10]

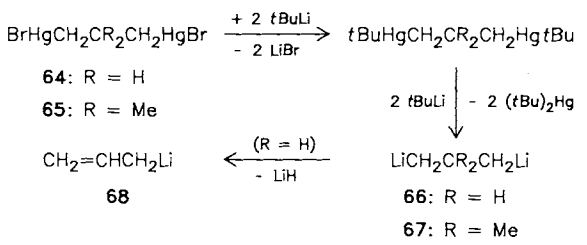

Compound **66** exhibits an even more extreme β-hydride activation than that described for **7** and splits off lithium hydride even at −60 °C to give allyllithium (**68**).

In contrast, compound **67** is extraordinarily stable for an organolithium compound in diethyl ether; according to calculations by *Schleyer* et al., this could be due to the existence of a structure with double lithium bridges.[8, 10, 84]

A second interesting application of **64** and **65** lies in their thermolysis; this occurs with elimination of mercurous bromide, presumably giving trimethylene (**69**) or its 2,2-dimethyl derivative **70**.[53, 85] Interestingly, the product spectrum of the diradicals obtained in this manner differs strongly from those which are normally found for **69** and **70**.[86] This applies not only to the relatively low yield of cyclopropane (or its dimethyl derivative), but also particularly to the unusual formation of **71**, which is perhaps due to a 1,2-methyl migration. A possible explanation could be that the diradicals are formed in a vibronically excited state.[85]

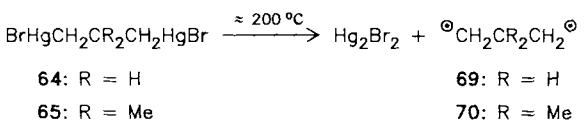

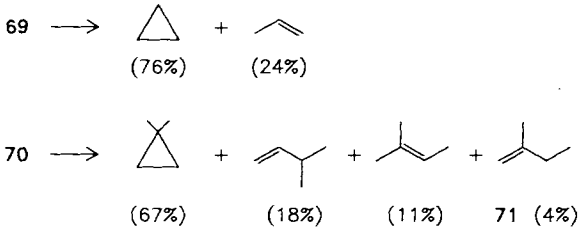

4.2.3. *Metallacyclobutanes from 1,3-Di-Grignard Compounds*

Metallacyclobutanes are of great interest because of their structural and bonding properties and because of their postulated or demonstrated role as catalytic intermediates in important industrial processes such as olefin metathesis.[34, 57, 87, 88] They have thus been extensively studied, although until recently no general route to these compounds was available. The proven di-Grignard route to larger rings suggests itself: as shown by Equation (s), both main group and transition metal element dichlorides **72** should in principle lead to metallacyclobutanes **73**.

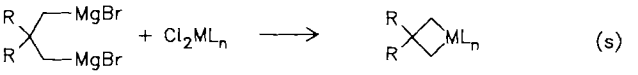

7: R = H
28: R = Me

72

73

As is so often the case, this new procedure is not so universally applicable as had been hoped. The greatest, though trivial, problem is the in some cases inherent instability of **73**, e.g. for M = Ni.[89] However, the route via Equation (s) is useful even in such a case; one can postulate with more confidence than otherwise that **73** is in fact formed and that the secondary products actually detected do arise from **73**.

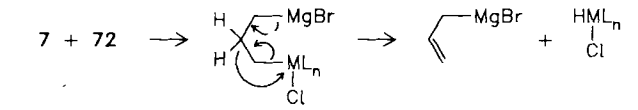

74 **24** **75**

On the other hand, it can happen that the yields of **73** are low although **73** itself is in fact stable.[90] The reason is then to be found in a particularly strong activation of the β-hydrogens in the intermediate **74** by certain transition metals M. While **73** is stable, because the orientation necessary for β-elimination is not possible in the inflexible four-membered ring,[77] **74** can by rotation adopt conformations in which the elimination of **75** is readily possible. In the case of **28**, such a complication cannot occur, so that better results have been obtained using this reagent. Table 3 gives an overview of the results so far obtained.

It is outside the scope of the present review to go into details of the many interesting aspects of the various reac-

Table 3. Metallacyclobutanes of type **73** (from 1,3-di-Grignard compounds).

ML_n	R	Yield [%]	Ref.
$TiCp_2$	H	<5	[90]
$TiCp_2$	Me	89	[90]
$ZrCp_2$	H	<5	[90]
$ZrCp_2$	Me	76	[90]
$HfCp_2$	Me	57	[90]
VCp_2	Me	30 [a]	[56]
$MoCp_2$	Me	80	[37]
WCp_2	Me	18	[37]
Re(O)Cp* [b]	Me	50	[91]
$Ni(PPh_3)_2$	Me	(unstable)	[89b]
$GeMe_2$	H	96	[54]
$GeMe_2$	Me	98	[54]
$SnMe_2$	H	10	[52, 92]
$SnMe_2$	Me	48	[52, 92]

[a] A different decomposition reaction of the intermediate **74** is observed in this case [56]. [b] Cp* = C_5Me_5.

tions and compounds; here we must refer to the original literature (Table 3). We should, however, mention that many of the metallacyclobutanes in Table 3 (M = Hf, Zr, V, Re, Sn) have been prepared for the first time using this method: the hafnium compound has since been obtained by a different procedure. The gaps in Table 3 make it clear that much valuable work remains to be done in this area.

A first example is provided by the spiro compounds **76** [Eqn. (t)].[93]

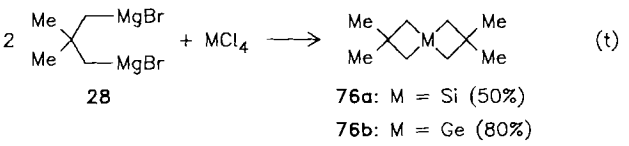

The development of new 1,3-di-Grignard reagents has opened up other possibilities. Apart from the examples to be discussed in Section 4.2.4, the reagent **38** [Eqn. (i)] should be mentioned here; it has been used as the starting material for the preparation of the new metallacyclobutabenzenes **77**[94] and **78**[91] and of corresponding derivatives with Si, Ge, Sn or Pb.[89b]

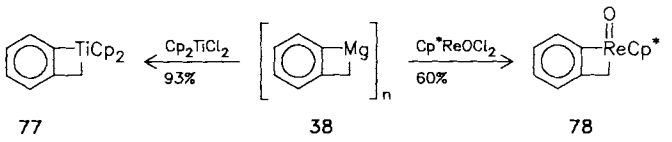

4.2.4. *The Methylene Di-Grignard Reagent*

We have already referred to the possibility of using the methylene di-Grignard reagent **10** in organic synthesis in Section 4.2.[31,32,81] Its use for the preparation of other dimetallomethanes requires only a brief mention; in some cases such compounds are available via other routes. A certain disadvantage is the markedly reduced reactivity of **10** in comparison with other Grignard compounds; thus, while the formation of **79** and **80** occurs readily, **81** is produced only slowly.[32b]

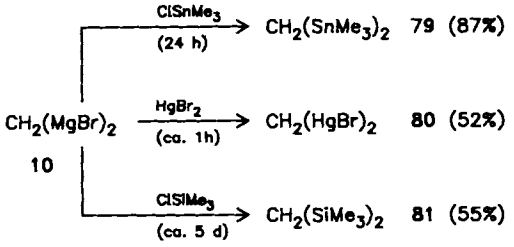

It should also be mentioned that the last ten years have seen the development of the chemistry of the 1,1-dimetal compounds ("methylene complexes") on a broad front;[10,36,95-100] in this connection the by now classical Tebbe reagent **82**[95,96] and the dizinc reagent **83**[97] are worthy of particular mention.

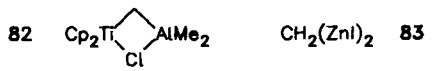

The chemistry of these compounds cannot be discussed here; there is however a certain amount of overlap with that of **10**, so that the decision as to which reagent should be used for a certain reaction is often one of small nuances and in particular of preparative availability. Developments in the coming years will show which approach is the most practical; the recently improved preparation of **10**[33] will certainly put it in a more competitive position.

4.2.5. *1,3-Dimetallacyclobutanes*

The reactions of **10** with Me_2GeCl_2 and Me_2SnCl_2 have so far been successful only in the case of the 1,3-digermacyclobutane **84a**; it is not clear whether the tin analog **84b** was not formed or whether it merely decomposed very rapidly.[32b] The use of the only slightly soluble and largely bromide-free modification **44** gave considerably better yields of the four-membered ring **84a**; the interesting higher ring-homologues **85** and **86** were also obtained.

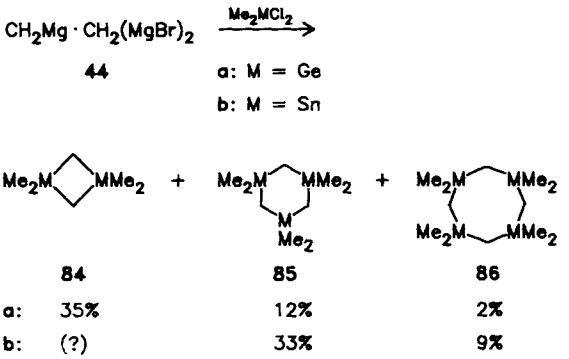

The reactions which have been studied in the most detail are those with cyclopentadienyl derivatives of titanium, zirconium, and hafnium. As the example of the titanocene dichloride [Eqn. (n)] shows, either one or both chloride functions can be allowed to react with **10**, giving the intermediates **87** and **88**, respectively.

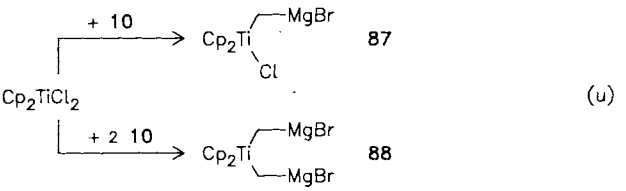

The behavior of **87** will be discussed in Section 4.2.6. Compound **88** can be regarded as a di-Grignard compound in which carbon atom 2 in **7** or **28** has been replaced by the titanocene moiety. It can be used in a completely analogous manner (see Section 4.2.3) for syntheses of four-membered rings [Eqn. (v)]. The same is probably true for **91** and **92**, which are obtained from zirconocene and hafnocene dichlorides [Eqn. (w)].[33]

Only two of the nine 1,3-dimetallacyclobutanes described in Equations (v) and (w), **89a**[101] and **90a**,[102] had previously been prepared in other ways.

It must be noted that some of the four-membered ring compounds were obtained in only poor yields. This is for

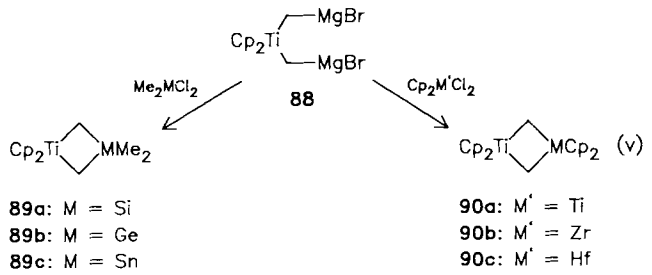

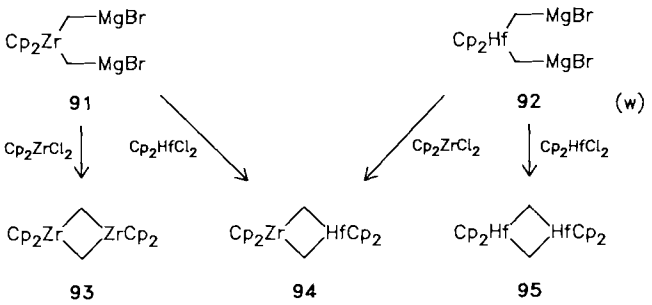

example the case for **89c**, which, however, being a stannacyclobutane is inherently unstable (see Ref. [92]). It also applies for **94** and **95**; in these cases the reasons lie in practical difficulties such as the solubility of **91** and the presence of zirconocene dichloride as an impurity in the hafnocene analogue. We have also since been able to show that the published yields can be improved by modification of the reaction conditions (for example in the case of **95** from 3.5%[33] to 24%[37]). A discussion of the interesting spectral and bonding properties of the 1,3-metallacyclobutanes lies outside the scope of the present survey.[33]

It should, however, be mentioned here that the analogy between the reagents **28** and **88** also applies to the synthesis of the spiro compounds **96**,[103] which can be described as double 1,3-dimetalla-analogues of the double metallacyclobutane **76** [Eqn. (t)].

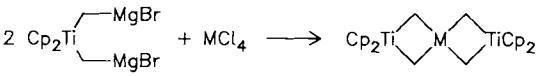

a: M = Si, b: M = Ge, c: M = Sn

4.2.6. Metallaalkenes

Metallaalkenes or metal-carbene complexes contain the structural element $L_nM{=}CR_2$ and are, like the metallacyclobutanes, objects of great interest.[87] A point of contact between the two types of compound can be found in olefin metathesis,[88] for which a mechanism according to Equation (x) is now generally accepted.

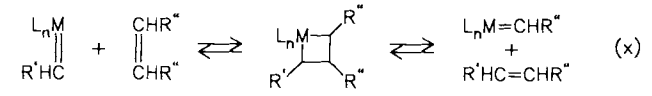

As *Tebbe* et al.[95] and *Grubbs* et al.[96] have shown, the Tebbe reagent **82** provides an easy route to the titanaethene **97**; this can, when prepared in situ, be trapped reversibly by alkenes to give titanacyclobutanes **98** or by carbonyl compounds to give 1-alkenes **99**.

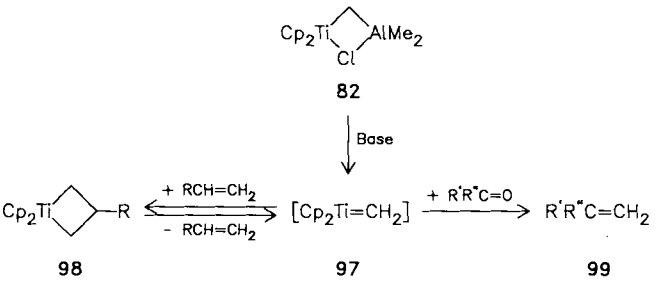

The titanium/zinc compound **100**[97] obtained from the dizinc reagent **83** and compound **87** obtained by us from **10** [Eqn. (u)] undergo completely analogous reactions. Free **97** is extremely unstable and is present in only a very

$$\underbrace{XTi(Cp_2)CH_2ZnX}, \quad X = Cl \text{ or } I \qquad \mathbf{100}$$

low steady state concentration; it can, however, be stabilized at low temperatures as **101** by complexation with tertiary phosphanes. Apart from **82**[104] and **98**,[105] compound **90a** (obtained according to Equation (v)) has been shown to be a good starting material for this reaction [Eqn. (y)].

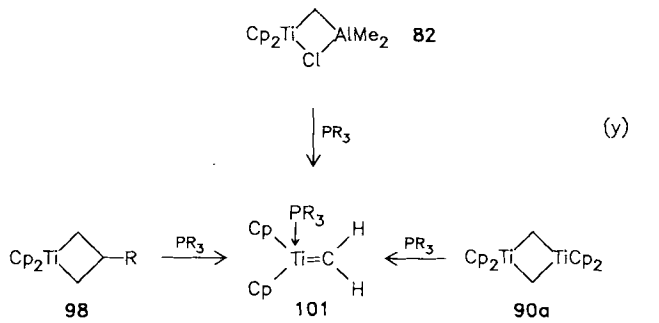

Compounds such as **82**, **87**, **100** and **90a** can thus be regarded as "precarbenes" or as metallaalkenes stabilized by other metal compounds, Me_2AlCl, MgBrCl, ZnX_2 or $Cp_2Ti{=}CH_2$ (**97**), respectively, acting as "stabilizers". Such an approach is justified not only by the reactivity of these compounds [Eqn. (y)] but also by theoretical calculations[107] and by their ^1H- and ^{13}C-NMR spectra; the carbenoid carbon and its attached protons are generally very strongly deshielded (Table 4).

Table 4. Chemical shifts of the methylene hydrogen and carbon nuclei of methylenetitanium compounds.

	Compound	$\delta(^1H)$	$\delta(^{13}C)$	Ref.
82	$\underbrace{ClTi(Cp_2)CH_2}AlMe_2$ [a]	8.49	188	[95]
100	$\underbrace{XTi(Cp_2)CH_2}ZnX$ [b]	8.32	—	[97a]
87	$\underbrace{ClTi(Cp_2)CH_2}MgBr$ [c]	2.93	—	[37]
102	$\underbrace{BrTi(Cp_2)CH_2Mg}\underbrace{CH_2Ti(Cp_2)}Br$ [b]	9.87	223.3	[37]
90a	$\underbrace{CH_2Ti(Cp_2)CH_2}TiCp_2$ [a]	8.72	235.8	[33, 102]
101, R = Me	$(PMe_3)Ti(Cp_2){=}CH_2$ [d]	11.83	285.2	[106]
98, R = H	$\underbrace{CH_2Ti(Cp_2)CH_2}CH_2$ [b]	2.95	76.7	[32, 108]

[a] In [D6]benzene. [b] In [D8]toluene. [c] In [D10]Et_2O/[D6]benzene 1:1. [d] In [D8]THF.

The different NMR behavior of **87**, the structure **87a** of which is at a first glance completely analogous to those of **82** and **100**, shows that there are still problems to be solved in this area. Very recent results[37] have surprisingly shown that **87** can be converted into **102** when a solution of **87** in ether/benzene is evaporated to dryness and the residue so obtained is dissolved in toluene.

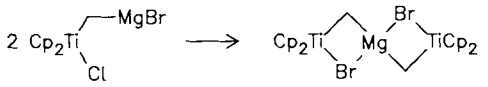

87 **102**

Compound **102** then exhibited the expected low-field shift for the methylene protons (Table 4) and showed itself to be a very good starting material for **97**. The unexpected NMR data for **87** are probably due to the fact that in the ether/benzene solution, which contains excess magnesium halide, **87** exists as **87b** or **87c** and not as **87a** (for the sake of clarity the ether molecules are not shown; both Cl as well as Br are symbolized by X).

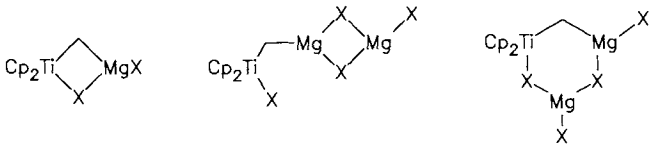

87a **87b** **87c**

It remains astounding that structures such as **87** and **102** are in fact relatively stable, although the differences appear subtle when one considers that bonds between magnesium and carbon or halogen normally undergo rapid exchange in ethereal solution.[11c] It is also surprising that these on paper subtle structural differences apparently have wide-reaching consequences for the bonding situation, as must be concluded from the very different NMR data for the methylene protons (Table 4). Further studies will undoubtedly shed more light on this important question.

Many of the results discussed here were obtained in our own laboratories; they are due mainly to the enthusiasm, the hard work and the great skill of my co-workers, whose names can be found in the list of references. I am very thankful to all of them, but in particular to Dr. O. S. Akkerman and Dr. C. Blomberg, who have been with me for many years, and to Mr. Gerrit Schat who supported the often extremely difficult work by his immeasurable experimental ability and passed on practical experience and traditions in the group to many generations of undergraduate and graduate students. I thank the foundation for Chemical Research in the Netherlands (S.O.N.) for supporting our work with funds from the Organization for Fundamental Scientific Research (Z.W.O.).

Received: February 12, 1987 [A 639 IE]
German version: *Angew. Chem. 99* (1987) 1020

[1] G. Wittig, *Angew. Chem. 70* (1958) 65.
[2] G. Wittig, R. Ludwig, R. Polster, *Chem. Ber. 88* (1955) 294.
[3] G. Wittig, F. Bickelhaupt, *Chem. Ber. 91* (1958) 865.
[4] L. Vecchiotti, *Ber. Dtsch. Chem. Ges. 63* (1930) 2275.
[5] G. Wittig, F. Bickelhaupt, *Chem. Ber. 91* (1958) 883.
[6] While according to [5] the degree of oligomerization of **3** is n = 6, later measurements gave the value n = 3: a) D. S. Brown, A. G. Massey, D. A. Wickens, *Acta Crystallogr. Sect. B 34* (1978) 1695; b) N. A. A. Al-Jabar, A. G. Massey, *J. Organomet. Chem. 275* (1984) 9.
[7] a) H. J. S. Winkler, G. Wittig, *J. Org. Chem. 28* (1963) 1733; b) R. E. Humphries, N. A. A. Al-Jabar, D. Bowen, A. G. Massey, G. B. Deacon, *J. Organomet. Chem. 319* (1987) 59.
[8] P. von R. Schleyer, *Pure Appl. Chem. 56* (1984) 151.
[9] A. Streitwieser, Jr., *Acc. Chem. Res. 17* (1984) 353.
[10] A. Maercker, M. Theis, *Top. Curr. Chem. 38* (1987) 1.
[11] For reviews see: a) *Houben-Weyl-Müller: Methoden der Organischen Chemie, Band XIII*, Thieme, Stuttgart 1970-1978; b) J. P. Collman, L. S. Hegedus: *Principles and Application of Organotransition Metal Chemistry*, University Science Books, Mill Valley, CA (USA) 1980; c) G. Wilkinson, F. G. A. Stone, E. W. Abel: *Comprehensive Organometallic Chemistry*, Pergamon Press, Oxford 1982.
[12] F. Bickelhaupt in J. J. Zuckerman (Ed.): *Inorganic Reactions and Methods, Vol. 10*, VCH, Weinheim, in press.
[13] V. Grignard, *C. R. Hebd. Séances Acad. Sci. 130* (1900) 1322.
[14] L. Tissier, V. Grignard, *C. R. Hebd. Séances Acad. Sci. 132* (1901) 835.
[15] a) F. B. Ahrens, A. Spaler, *Ber. Dtsch. Chem. Ges. 38* (1905) 1296; b) C. A. Bishoff, *ibid. 38* (1905) 2078; c) Z. Zelinsky, J. Gutt, *ibid. 40* (1907) 3049.
[16] W. H. Saunders, Jr., A. F. Cockerill: *Mechanism of Elimination Reactions*, Wiley, New York 1972.
[17] a) Geromont, *Justus Liebigs Ann. Chem. 158* (1871) 370; b) Freund, *Monatsh. Chem. 2* (1881) 639; c) Gustavson, *J. Pr. Chem.* [2] *62* (1900) 294.
[18] J. von Braun, *Ber. Dtsch. Chem. Ges. 37* (1904) 3210.
[19] J. von Braun, A. Steindorff, *Ber. Dtsch. Chem. Ges. 38* (1905) 956.
[20] V. Grignard, G. Vignon, *C. R. Hebd. Séances Acad. Sci. 144* (1907) 1358; see also [21].
[21] It is not clear whether the preparation of the 1,9-di-Grignard reagent of *n*-nonane was achieved earlier; it is claimed without details by E. E. Blaise, Houillon, *Bull. Soc. Chim. Fr.* [3] *31* (1904) 960.
[22] J. von Braun, *Ber. Dtsch. Chem. Ges. 40* (1907) 4065.
[23] One should note that seven years had passed since the discovery of the Grignard reagents, and three years since the discovery of **8**!
[24] J. von Braun, W. Sobecki, *Ber. Dtsch. Chem. Ges. 44* (1911) 1918.
[25] J. von Braun, *Ber. Dtsch. Chem. Ges. 46* (1913) 1782; *47* (1914) 490.
[26] S. Hilpert, G. Grüttner, *Ber. Dtsch. Chem. Ges. 47* (1914) 186.
[27] a) S. Hilpert, G. Grüttner, *Ber. Dtsch. Chem. Ges. 47* (1914) 177; b) G. Grüttner, M. Wiernik, *ibid. 48* (1915) 1473; c) G. Grüttner, E. Krause, *ibid. 49* (1916) 437, 2666; d) G. Grüttner, E. Krause, M. Wiernik, *ibid. 50* (1917) 1549; e) compare also the early example of the synthesis of 1,1-dichlorosilacyclohexane [28].
[28] A. Bygdén, *Ber. Dtsch. Chem. Ges. 48* (1915) 1236.
[29] M. S. Kharash, O. Reinmuth: *Grignard Reactions of Nonmetallic Substances*. Prentice-Hall, New York 1954.
[30] G. Emschwiller, *C. R. Hebd. Séances Acad. Sci. 183* (1926) 665.
[31] F. Bertini, P. Grasselli, G. Zubiani, G. Cainelli, *Tetrahedron 26* (1970) 1281.
[32] a) J. W. Bruin, G. Schat, O. S. Akkerman, F. Bickelhaupt, *Tetrahedron Lett. 24* (1983) 3935; b) J. W. Bruin, G. Schat, O. S. Akkerman, F. Bickelhaupt, *J. Organomet. Chem. 288* (1985) 13.
[33] B. J. J. van de Heisteeg, G. Schat, O. S. Akkerman, F. Bickelhaupt, *J. Organomet. Chem. 308* (1986) 1.
[34] F. Bickelhaupt, *Pure Appl. Chem. 58* (1986) 537.
[35] J. W. Bruin, unpublished results.
[36] B. J. J. van de Heisteeg, G. Schat, M. A. G. M. Tinga, O. S. Akkerman, F. Bickelhaupt, *Tetrahedron Lett. 27* (1986) 6123.
[37] B. J. J. van de Heisteeg, *Dissertation*, Vrije Universiteit Amsterdam 1987.
[38] K. B. Wiberg, W. J. Bartley, *J. Am. Chem. Soc. 82* (1960) 6375.
[39] J. W. F. L. Seetz, O. S. Akkerman, F. Bickelhaupt, *Tetrahedron Lett. 22* (1981) 4857.
[40] H. M. Walborsky, *Tetrahedron 37* (1981) 1625.
[41] T. Clark, A. J. Kos, P. von R. Schleyer, W. P. Cofino, W. H. de Wolf, F. Bickelhaupt, *J. Chem. Soc. Chem. Commun. 1983*, 685.
[42] I. T. Millar, H. Heaney, *Q. Rev. Chem. Soc. 11* (1957) 109.
[43] H. Heaney, *Organomet. Chem. Rev. 1* (1966) 27.
[44] G. Wittig, *Angew. Chem. 69* (1957) 245.
[45] H. Heaney, F. G. Mann, I. T. Millar, *J. Chem. Soc. 1956*, 4692; *1957*, 3930.
[46] F. Bickelhaupt, C. Jongsma, P. de Koe, R. Lourens, N. R. Mast, G. L. van Mourik, H. Vermeer, R. J. M. Weustink, *Tetrahedron 32* (1976) 1921.
[47] O. S. Akkerman, unpublished results.
[48] F. A. Hart, F. G. Mann, *J. Chem. Soc. 1957*, 3939, and references cited therein.

[49] L. C. Costa, G. M. Whitesides, *J. Am. Chem. Soc. 99* (1977) 2390.
[50] C. Blomberg, F. A. Hartog, *Synthesis 1977,* 18.
[51] F. A. Hartog: *The Barbier Reaction, A Mechanistic Study, Dissertation,* Vrije Universiteit Amsterdam 1978.
[52] J. W. F. L. Seetz: *Bifunctionele organometaalverbindingen met korte koolstofketens en metallacyclobutanen, Dissertation,* Vrije Universiteit Amsterdam 1983.
[53] J. W. F. L. Seetz, F. A. Hartog, H. P. Böhm, C. Blomberg, O. S. Akkerman, F. Bickelhaupt, *Tetrahedron Lett. 23* (1982) 1497.
[54] J. W. F. L. Seetz, B. J. J. van de Heisteeg, G. Schat, O. S. Akkerman, F. Bickelhaupt, *J. Organomet. Chem. 277* (1984) 319.
[55] For the free-radical nature of the reaction see: a) H. M. Walborsky, M. S. Aronoff, *J. Organomet. Chem. 51* (1973) 31; b) B. J. Schaart, C. Blomberg, O. S. Akkerman, F. Bickelhaupt, *Can. J. Chem. 58* (1980) 932; c) H. R. Rogers, C. L. Hill, Y. Fujiwara, R. J. Rogers, H. L. Mitchell, G. M. Whitesides, *J. Am. Chem. Soc. 102* (1980) 217, and references cited therein.
[56] J. W. F. L. Seetz, B. J. J. van de Heisteeg, G. Schat, O. S. Akkerman, F. Bickelhaupt, *J. Organomet. Chem. 275* (1984) 173.
[57] J. W. F. L. Seetz, B. J. J. van de Heisteeg, G. Schat, O. S. Akkerman, F. Bickelhaupt, *J. Mol. Catal. 28* (1985) 71.
[58] P. Markies, unpublished results.
[59] M. B. Smith, W. E. Becker, *Tetrahedron 23* (1967) 4215.
[60] H. C. Holtkamp, G. Schat, C. Blomberg, F. Bickelhaupt, *J. Organomet. Chem. 240* (1982) 1.
[61] A. L. Spek, G. Schat, H. C. Holtkamp, C. Blomberg, F. Bickelhaupt, *J. Organomet. Chem. 131* (1977) 331.
[62] M. B. Smith, W. E. Becker, *Tetrahedron 22* (1966) 3027.
[63] H. C. Holtkamp, C. Blomberg, F. Bickelhaupt, *J. Organomet. Chem. 19* (1969) 279.
[64] C. Blomberg, G. Schat, H. H. Grootveld, A. D. Vreugdenhil, F. Bickelhaupt, *Justus Liebigs Ann. Chem. 763* (1972) 148.
[65] F. J. M. Freijee, G. van der Wal, G. Schat, O. S. Akkerman, F. Bickelhaupt, *J. Organomet. Chem. 240* (1982) 229.
[66] J. Toney, G. D. Stucky, *J. Organomet. Chem. 28* (1971) 5.
[67] P. Voorbergen, C. Blomberg, F. Bickelhaupt, *J. Organomet. Chem. 40* (1972) 225.
[68] W. Schlenk, W. Schlenk jun., *Ber. Dtsch. Chem. Ges. 62* (1929) 920.
[69] A. D. Vreugdenhil, C. Blomberg, *Recl. Trav. Chim. Pays-Bas 82* (1963) 453, 461.
[70] F. W. Walker, E. C. Ashby, *J. Am. Chem. Soc. 91* (1969) 3845.
[71] Lower degrees of association are given in the literature for other solvents; it is unclear whether a solvent effect is involved or whether the reason lies in experimental difficulties in handling these extremely sensitive compounds: B. Denise, J. Ducom, F. J. Fauvarque, *Bull. Soc. Chim. Fr. 1972,* 990.
[72] F. J. M. Freijee, G. Schat, O. S. Akkerman, F. Bickelhaupt, *J. Organomet. Chem. 240* (1982) 217.
[73] H. A. Bent, *Chem. Rev. 61* (1961) 275.
[74] a) M. Vallino, *Thèse,* Université de Paris VI 1972; b) on the other hand, *o*-$C_6H_4(CH_2)_2Mg \cdot 2THF$ is trimeric in the crystal; this has been explained on the basis of Bayer strain in the magnesahydrindane skeleton: M. F. Lappert, T. R. Martin, C. L. Raston, B. W. Skelton, A. H. White, *J. Chem. Soc. Dalton Trans. 1982,* 1959.
[75] K. Ziegler, K. Nagel, M. Patheiger, *Z. Anorg. Allg. Chem. 282* (1955) 345.
[76] J. X. McDermott, G. M. Whitesides, *J. Am. Chem. Soc. 96* (1974) 947.
[77] J. X. McDermott, J. F. White, G. M. Whitesides, *J. Am. Chem. Soc. 98* (1976) 6521.
[78] C. G. Bielefeld, H. A. Eick, R. H. Grubbs, *Inorg. Chem. 12* (1973) 2166.
[79] R. H. Grubbs, A. Miyashita, M. Liu, P. Burk, *J. Am. Chem. Soc. 100* (1978) 2418.
[80] C. Jongsma, J. J. de Kok, R. J. M. Weustink, M. van der Ley, J. Bulthuis, F. Bickelhaupt, *Tetrahedron 33* (1977) 205.
[81] M. M. Koton, T. M. Kiseleva, *Zh. Obshch. Khim. 35* (1965) 2036.
[82] J. W. F. L. Seetz, R. Tol, O. S. Akkerman, F. Bickelhaupt, *Synthesis 1983,* 721.
[83] J. W. F. L. Seetz, G. Schat, O. S. Akkerman, F. Bickelhaupt, *J. Am. Chem. Soc. 104* (1982) 6848.
[84] P. von R. Schleyer, A. J. Kos, E. Kaufmann, *J. Am. Chem. Soc. 105* (1983) 7617.
[85] M. A. G. M. Tinga, B. J. J. van de Heisteeg, unpublished results.
[86] R. G. Bergman in J. K. Kochi (Ed.): *Free Radicals, Vol. 1,* Wiley, New York 1973, p. 191.
[87] K. H. Dötz, H. Fischer, P. Hofmann, F. R. Kreissl, U. Schubert, K. Weiss: *Transition Metal Carbene Complexes,* Verlag Chemie, Weinheim 1983.
[88] K. J. Irvin, *Olefin Metathesis,* Academic Press, London 1983.
[89] a) R. H. Grubbs, A. Miyashita, *J. Am. Chem. Soc. 100* (1978) 7418; b) H. J. R. de Boer, unpublished results; c) A. Miyashita, H. Shitara, H. Nohiro, *J. Chem. Soc. Chem. Commun. 1985,* 850, and references cited therein.
[90] J. W. F. L. Seetz, G. Schat, O. S. Akkerman, F. Bickelhaupt, *Angew. Chem. 95* (1983) 242; *Angew. Chem. Int. Ed. Engl. 22* (1983) 248; *Angew. Chem. Suppl. 1983,* 234.
[91] H. J. R. de Boer, B. J. J. van de Heisteeg, M. Flöel, W. A. Herrmann, O. S. Akkerman, F. Bickelhaupt, *Angew. Chem. 99* (1987) 88; *Angew. Chem. Int. Ed. Engl. 26* (1987) 73.
[92] J. W. F. L. Seetz, G. Schat, O. S. Akkerman, F. Bickelhaupt, *J. Am. Chem. Soc. 105* (1983) 3336.
[93] B. J. J. van de Heisteeg, M. A. G. M. Tinga, Y. van den Winkel, O. S. Akkerman, F. Bickelhaupt, *J. Organomet. Chem. 316* (1986) 51.
[94] H. J. R. de Boer, O. S. Akkerman, F. Bickelhaupt, G. Erker, P. Czisch, R. Mynott, J. M. Wallis, C. Krüger, *Angew. Chem. 98* (1986) 641; *Angew. Chem. Int. Ed. Engl. 25* (1986) 639.
[95] a) F. N. Tebbe, G. W. Parshall, G. S. Reddy, *J. Am. Chem. Soc. 100* (1978) 3611; b) U. Klabunde, F. N. Tebbe, G. W. Parshall, R. L. Harlow, *J. Mol. Catal. 8* (1980) 37.
[96] a) J. B. Lee, K. C. Ott, R. H. Grubbs, *J. Am. Chem. Soc. 104* (1982) 7491; b) S. H. Pine, R. Zahler, D. A. Evans, R. H. Grubbs, *ibid. 102* (1980) 3270.
[97] a) J. J. Eisch, A. Piotrowski, *Tetrahedron Lett. 24* (1983) 2043; b) A. M. Piotrowski, J. J. Eisch in R. B. King, J. J. Eisch (Eds.): *Organometallic Syntheses, Vol. 3,* Elsevier, Amsterdam 1986, p. 16.
[98] W. A. Herrmann, *Angew. Chem. 94* (1982) 118; *Angew. Chem. Int. Ed. Engl. 21* (1982) 117; *J. Organomet. Chem. 250* (1983) 319.
[99] J. Hibino, T. Okazoe, K. Takai, H. Nozaki, *Tetrahedron Lett. 26* (1985) 5579.
[100] P. Knochel, J. F. Normant, *Tetrahedron Lett. 27* (1986) 1039, 1043.
[101] a) W. R. Tikkanen, J. Z. Liu, J. W. Egan, Jr., J. L. Petersen, *Organometallics 3* (1984) 825; b) W. R. Tikkanen, J. W. Egan, Jr., J. L. Petersen, *ibid. 3* (1984) 1646.
[102] K. C. Ott, R. H. Grubbs, *J. Am. Chem. Soc. 103* (1981) 5922.
[103] a) M = Si: B. J. J. van de Heisteeg, G. Schat, O. S. Akkerman, F. Bickelhaupt, *Organometallics 5* (1986) 1749; b) M = Ge, Sn: see [37].
[104] a) J. Schwartz, K. I. Gell, *J. Organomet. Chem. 184* (1980) C 1; b) F. W. Hartner, Jr., J. Schwartz, K. I. Gell, *J. Organomet. Chem. 184* (1980) C 1; b) F. W. Hartner, Jr., J. Schwartz, S. M. Clift, *J. Am. Chem. Soc. 105* (1983) 640; S. M. Clift, J. Schwartz, *J. Organomet. Chem. 285* (1985) C 5.
[105] L. R. Gilliom, R. H. Grubbs, *Organometallics 5* (1986) 721.
[106] B. J. J. van de Heisteeg, G. Schat, O. S. Akkerman, F. Bickelhaupt, *J. Organomet. Chem. 310* (1986) C 25.
[107] a) M. M. Francl, W. J. Pietro, R. F. Hout, W. J. Hehre, *Organometallics 2* (1983) 281, 815; b) T. H. Upton, A. K. Rappé, *J. Am. Chem. Soc. 107* (1985) 1206, and references cited therein; c) F. Volatron, O. Eisenstein, *ibid. 108* (1986) 2173, and references cited therein.
[108] J. B. Lee, G. J. Gajda, W. P. Schaefer, T. R. Howard, T. Ikarya, D. A. Strauss, R. H. Grubbs, *J. Am. Chem. Soc. 103* (1981) 7358.

When submitting manuscripts, authors of articles intended for publication as "Communications" are requested to read the "Notice to Authors" reproduced in the January issue of the journal following the list of contents; upon request, a copy can be obtained from the editorial office.

Nonacyclo[10.8.0.0^{2,11}.0^{4,9}.0^{4,19}.0^{6,17}.0^{7,16}.0^{9,14}.0^{14,19}]-icosane, a Double Tetraasterane**

By *Volker T. Hoffmann* and *Hans Musso**

Dedicated to Professor Ulrich Schöllkopf on the occasion of his 60th birthday

Replacement of the cyclohexane chair-form rings in the vertical planes of the diamond lattice by boat-form rings results in the wurzite lattice. If this is also carried out on the horizontal planes, one obtains an unknown carbon modification,[1] whose smallest characteristic structural unit, the tetrasterane **1**, is known.[2] Earlier, we succeeded in enlarging **1** by the addition of two cyclohexane rings to give **2**.[3] We now report the synthesis of the double tetraasterane **9**[4] (Scheme 1).

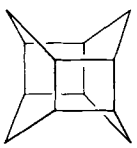

1

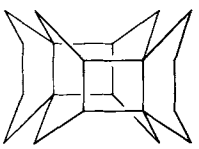

2

Photoexcitation of 1,4,5,8-tetrahydronaphthalene-2,3-dicarboxylic anhydride **3**[5] in dioxane with a high-pressure mercury lamp equipped with a Solidex filter in the presence of benzophenone as photosensitizer results in the formation, in approximately 8% yield, of a sparingly soluble mixture consisting of at least four dimers. Fractional sublimation of this mixture at 10^{-4} torr gave a forerun at about 250°C followed by the desired dimer **4** starting at 310°C (relative amount in the mixture, 46%; m.p. >350°C). Compound **4** was treated with methanol/acetyl chloride to convert it into the tetramethyl ester **6** (Table 1). The *anti* head-head dimer **5** undergoes sublimation already at 190–200°C and was likewise characterized as the tetramethyl ester (**10**). The structures of **6** and **10** were confirmed by X-ray crystal structure analysis.[4,6] Chromatography of the mother liquors of **10** on SiO_2 revealed the presence of two additional compounds. The faster eluting component was isolated and identified spectroscopically as the doubly aromatized derivative of **10**, namely, **12**. The more slowly eluting component could not be obtained in pure form. The tetraasterapropellane structure of **11** can be derived from its ^{1}H-NMR spectrum.

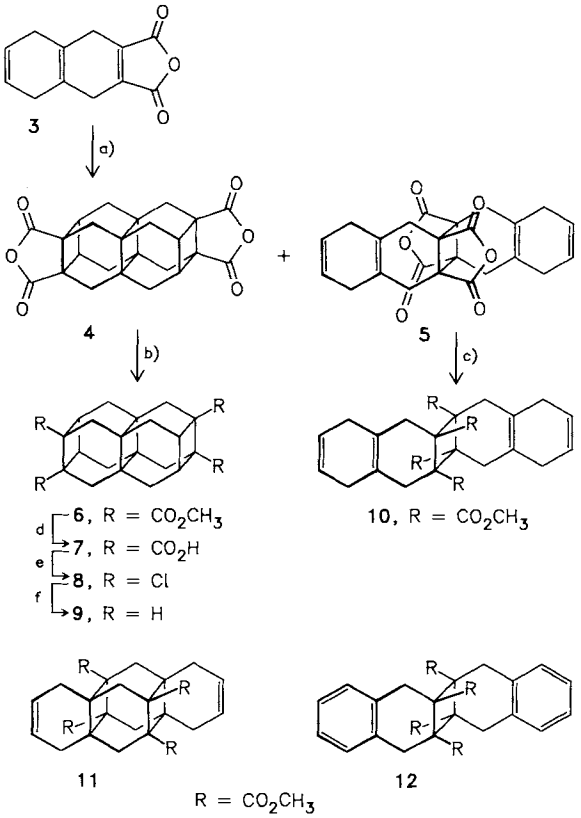

Scheme 1. a) **3** (6.8 g, 33.6 mmol), benzophenone (200 mg), dioxane (200 mL) under N_2. Philips HPK (125 W), Solidex filter, irradiated for 4 d. 560 mg (8%) **4** + **5** (see text). b) **4** (65 mg, 0.16 mmol), methanol (10 mL), acetyl chloride (1.0 mL), refluxed for 5 d, heterogeneous reaction, 69 mg (87%) **6**, m.p. = 324°C. c) **5** (200 mg, 0.48 mmol) was added to a solution containing sodium (50 mg) in methanol (15 mL) and the solution was acidified with dilute H_2SO_4. The monoester was extracted with ether and then treated with diazomethane in ether, affording 124 mg (51%) **10**, m.p. = 230°C. d) **6** (400 mg, 0.99 mmol) dissolved in 2 N NaOH (50 mL) over 30 min. The solution was then acidified with 2 N H_2SO_4, resulting in the formation of a fine, colorless precipitate, 396 mg (90%) **7**. e) A suspension of **7** (690 mg, 1.56 mmol), *N*-chlorosuccinimide (3.22 g, 24 mmol), and $Pb(OAc)_4$ (5.0 g, 6.3 mmol) in dimethylformamide/glacial acetic acid (5:1) (30 mL) was heated under N_2; the reaction occurred at 45–60°C. Workup with water and pentane and sublimation afforded 14 mg (2%) **8**, m.p. >350°C, containing a small amount of a pentachloro derivative. f) A refluxing suspension of **8** (50 mg, 0.13 mmol) in ethanol (40 mL) was treated over 3 h with sodium (3.0 g, 0.13 mmol) added in the form of small pieces. Workup with water and pentane afforded 7.0 mg (21%) **9** as colorless needles, m.p. = 230–235°C (methanol). $M^{\oplus}$ (calcd) = 264.1878, $M^{\oplus}$ (found) = 264.1885.

Alkaline hydrolysis of the tetramethyl ester **6** yields the acid **7** (90%), which, upon heating or drying, is readily converted back into the anhydride **4**. Grob degradation[7] kith lead tetraacetate and *N*-chlorosuccinimide results in the formation of a mixture consisting of three parts of the expected tetrachloride **8** and roughly one part of a pentachloro compound (mass spectrum), which cannot be completely separated by recrystallization. Dehalogenation occurs only slowly with sodium in ethanol and affords the

[*] Prof. Dr. H. Musso, Dr. V. T. Hoffmann
Institut für Organische Chemie der Universität
Richard-Willstätter-Allee 2, D-7500 Karlsruhe

[**] Asteranes, Part 19. This work was supported by the Deutsche Forschungsgemeinschaft and the Fonds der Chemischen Industrie. We thank *A. Kuiper, P. Lang, I. Maier, I. Rossnagel, I. Süss,* and *U. Tanger* for numerous spectra, gas chromatograms, and elemental analyses.— Part 18: A. Otterbach, H. Musso, *Angew. Chem. 99* (1987) 588; *Angew. Chem. Int. Ed. Engl. 26* (1987) 554.

Table 1. Melting points and ^{1}H- and ^{13}C-NMR data [a] for the compounds **1**, **6**, and **9**–**12** [8].

	1	**6**	**9**	**10**	**11**	**12**
M.p. [°C]	324–325	324	230–235	230	— [b]	227–229
^{1}H-NMR						
olefin./ aromat.	—	—	—	5.70	5.71	7.05–7.20
CO_2CH_3	—	3.67	—	3.63	3.61	3.51
CH	2.61	3.12	2.65	—	—	
CH_2	1.60	1.89, 1.61 1.55	1.40	2.84, 2.17 2.49, 2.40	2.56, 2.45 2.55	3.46, 3.29
^{13}C-NMR						
CO		175.76 (s)		173.87 (s)		172.67 (s)
olefin./ aromat.				124.16 (d) 122.21 (s)		136.45 (s) 127.25 (d) 126.54 (d)
OCH_3		51.77 (q)		51.81 (q)		51.73 (q)
other C atoms		48.15 (s) 34.89 (s) 31.93 (d) 30.89 (t) 26.83 (t)	34.75 (s) 30.84 (d) 28.56 (t)	51.70 (s) 33.98 (t) 30.71 (t)		35.47 (t)

[a] ^{1}H-NMR: 250 MHz, $CDCl_3$; ^{13}C-NMR: 250 MHz, $CDCl_3$. [b] Not isolated.

pure, double tetraasterane **9** in only about 21% yield as colorless needles (m.p. = 230–235 °C, methanol). Whereas **1** melts at very high temperature (Table 1) and is thermally stable at temperatures over 300 °C, heating of **9** in the injection part of a gas chromatograph at 270 °C results in the formation of two isomers; however, the structures of the isomers have not yet been determined.

Received: February 2, 1987;
revised: March 6, 1987 [Z 2082 IE]
Publication delayed at authors' request
German version: *Angew. Chem. 99* (1987) 1036

[1] S. Housmans, P. H. Honnef, *Nachr. Chem. Tech. Lab. 32* (1984) 379.
[2] H. G. Fritz, H.-M. Hutmacher, H. Musso, G. Ahlgren, B. Akermark, R. Karlson, *Chem. Ber. 109* (1976) 3781.
[3] G. Kaiser, H. Musso, *Chem. Ber. 118* (1985) 2266.
[4] V. T. Hoffmann, *Dissertation*, Universität Karlsruhe 1987.
[5] W. J. Bailey, J. Rosenberg, *J. Am. Chem. Soc. 77* (1955) 73; R. Askani, Giessen, private communication.
[6] X-ray structure analysis ($Mo_{K\alpha}$, $\lambda = 71.073$ pm, graphite monochromator): **6** (M. Schmidt, *Diplomarbeit*, Universität Karlsruhe 1985): $C_{28}H_{32}O_8$ (496.56); $\rho = 1.43$ g cm^{-3}, $P1$, $Z = 2$; $a = 719.7(4)$, $b = 1115.2(6)$, $c = 1534.0(8)$ pm, $\alpha = 98.8(4)$, $\beta = 89.95$, $\gamma = 107.9(4)°$, $V = 1.15689 \times 10^9$ pm^3; $R = 0.088$ ($R_w = 0.074$). **10** [4]: $C_{28}H_{32}O_8 \cdot 2CH_3OH$ (560.65); $\rho = 1.32$, $C2/c$, $Z = 4$ (−86 °C); $a = 2058.9$, $b = 1109.5$, $c = 1834.6$ pm, $\beta = 137.9°$, $V = 2.8118 \times 10^9$ pm^3, 5705 reflections, $R = R_w = 0.067$. — Further details of the crystal structure investigation may be obtained from the Fachinformationszentrum Energie, Physik, Mathematik GmbH, D-7514 Eggenstein-Leopoldshafen 2 (FRG), on quoting the depository number CSD-52466, the names of the authors, and the journal citation.
[7] K. B. Beder, M. Geisel, C. A. Grob, F. Kuhnen, *Synthesis 1973*, 493.
[8] The spectra and elemental analyses of all other new compounds [4] are in accord with the structures given.

Dimanganese Heptoxide for the Selective Oxidation of Organic Substrates

By *Martin Trömel** and *Manuel Russ*

Mn_2O_7 has been described as a dark red, volatile, unstable oil,[1] which, apart from its strong oxidative ability, can explode unexpectedly (for example, on contact with organic compounds or with dust from the air). There are apparently no reports on controlled oxidation reactions, although the compound has been known for over 125 years. The Mn–O bond lengths,[2] which have been determined experimentally,[3] indicate that Mn_2O_7 should be a stronger oxidizing agent than permanganate.

According to the most detailed investigation carried out so far,[4] solvents such as glacial acetic acid or CCl_4 undergo oxidation by Mn_2O_7 even at low temperature. In contrast, we have been able, by means of a special procedure, to obtain stable solutions of Mn_2O_7 in CCl_4 or 1,1,2-trifluoro-1,2,2-trichloroethane (Freon 113). Mn_2O_7, prepared by reaction of $KMnO_4$ with concentrated sulfuric acid in the presence of the solvent according to the following reaction, is immediately taken up by the organic phase:

$$2\,KMnO_4 + 2\,H_2SO_4 \longrightarrow Mn_2O_7 + 2\,KHSO_4 + H_2O$$

The stability of the solutions is probably due to the fact that oxidizable impurities and traces of water, which cause decomposition of Mn_2O_7, are removed during its formation. The deep red solutions contain approximately 100 mg of Mn_2O_7 per mL, are practically completely stable at room temperature, and, in contrast to undiluted Mn_2O_7, can be handled safely. Our investigations so far have shown that selective oxidation reactions are possible which can be carried out simply with efficient thermal control. The course of the reaction can be observed owing to the intense color of the Mn_2O_7 solution themselves. The reagent is especially suitable for use in aprotic medium.

Aliphatic and alicyclic C–C bonds, C–F and C–Cl bonds, and primary C–H bonds are not usually attacked at room temperature; the same holds true for trimethylsilyl groups.

Primary and secondary alcohols, such as **1** and **2**–**6** (Table 1), respectively, are smoothly oxidized to carboxylic acids and ketones, respectively. The reactions proceed in aprotic medium at temperatures as low as −70 °C, thereby making it possible to react thermally unstable and acid-sensitive compounds such as **2** and **5**, respectively.

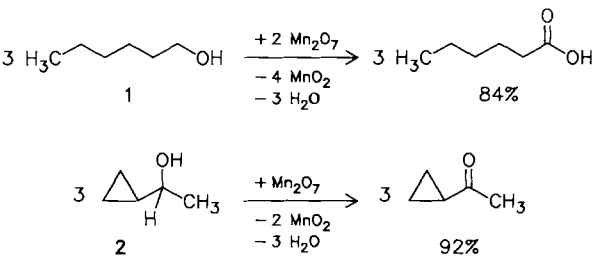

Table 1. Oxidation of selected secondary alcohols with Mn_2O_7.

	Alcohol	Product	Yield [%] [a]
3	cycloheptanol	cycloheptanone	91
4	1-cyclohexylethanol	cyclohexyl methyl ketone	88
5	1-phenylethanol	acetophenone	81
6	3-octanol	3-octanone	84

[a] Yields of isolated product.

Owing to the low temperature, the oxidation of primary alcohols such as **1** can be carried out without accompanying acetalization. Ketones formed from secondary alcohols can be easily separated by filtration from the MnO_2 precipitate. In addition, the MnO_2 binds the water formed dur-

[*] Prof. Dr. M. Trömel, Dipl.-Chem. M. Russ
Institut für Anorganische Chemie der Universität
Niederurseler Hang, D-6000 Frankfurt am Main 50 (FRG)

ing the reaction. Oxidative C–C bond cleavage does not occur at all, and tertiary C–H bonds such as those in **4** and **2** are not attacked. Phenyl and cyclopropyl groups such as those in **5** and **2**, respectively, are stable under the reaction conditions, so that the reactions occur chemoselectively and afford high yields of products.

CC double bonds, such as those in **7**–**13** (Table 2), undergo oxidative cleavage already at −80 °C with formation of the same products, albeit in high yield, as those formed by ozonolysis followed by oxidative workup. These oxidations can also be carried out selectively in the presence of aromatic systems.

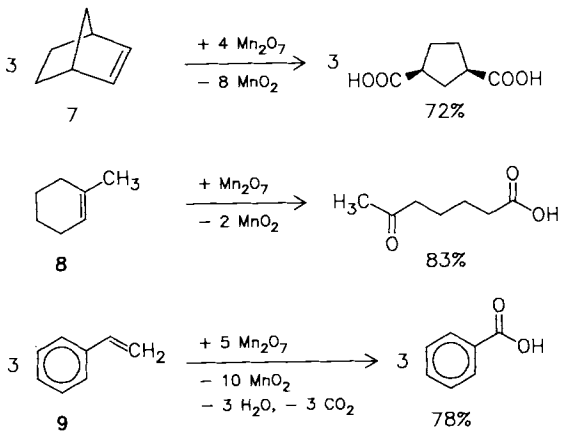

Table 2. Oxidation of selected alkenes with Mn_2O_7.

	Olefin	Product	Yield [%] [a]
10	cyclohexene	adipic acid	69
11	cycloheptene	pimelic acid	82
12	1-octene	heptanoic acid	73
13	heptadecafluoro-1-decene (H_2C=CH–C_8F_{17})	perfluorononoic acid	94

[a] Yields of isolated product.

α-Methylene groups in ethers such as **14**–**16** react at −45 °C to form lactones or esters. Aromatic systems, for example that of benzene, on the other hand, are attacked at temperatures around −20 °C.

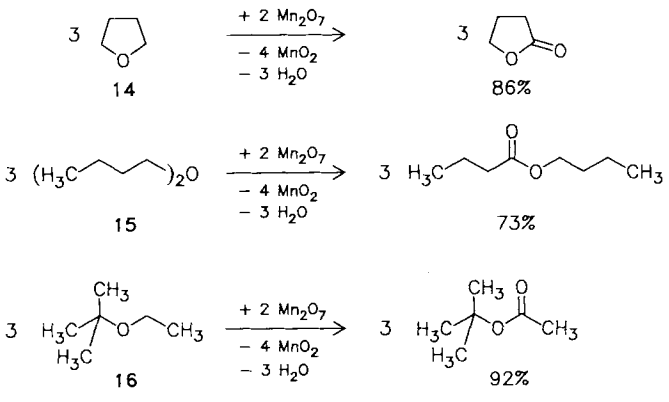

Oxidations with dimanganese heptoxide are, without exception, complete within a short period of time (seconds or minutes) and are characterized by simple operational procedures and a smooth course of reaction. The reaction mixtures can be worked up easily without the necessity of employing extraction procedures. The resulting manganese oxide, which is easily filtered off, binds water formed during the reaction, so that the organic product can be simply isolated by evaporation of the solvent. In all reactions leading to carboxylic acids, the products are bound to the MnO_2 precipitate. They can be separated by reduction with sulfite followed by extraction (see Experimental Procedure). The extraction is unnecessary if the MnO_2 is immediately reduced in the reaction mixture by reaction with a defined mixture of solid $Na_2SO_3 \cdot 7\,H_2O$ and $Na_2S_2O_5$ or, more elegantly, with glyoxylic acid **17**.

$$MnO_2 + (HO)_2CH{-}COOH \longrightarrow Mn(COO)_2 \cdot 2\,H_2O$$

17

The carboxylic acid is thereby released and taken up by the solvent. Glyoxylic acid and the manganese oxalate formed are insoluble in the reaction medium, so that the carboxylic acid may be obtained by filtration and evaporation of the solvent. At temperatures up to approximately +15 °C, solvents such as acetone, methyl and ethyl acetate, CCl_4, Freon 113, and mixtures thereof, are suitable for the oxidations with Mn_2O_7.

In carrying out these reactions, it is important that undiluted Mn_2O_7 not be allowed to collect (e.g., by evaporation of the solvent), since, in the presence of flammable vapors, it can explode. The reactions should therefore be carried out in a stream of inert gas. Moreover, the spout of the dropping funnel should be drawn out to a point and, during prolonged addition, this should be washed with Freon 113 or CCl_4. The ground glass must not be greased.

Experimental Procedure

Preparation of a Mn_2O_7 solution: Powdered $KMnO_4$ (16.3 g) was added in portions to a stirred mixture of concentrated H_2SO_4 (24 mL) and dry CCl_4 (100 mL) in a 250-mL flask kept at 20–25 °C. The resulting reaction mixture was stirred for several hours and the deep red organic phase was then decanted from the lower layer. The solution was stored in the refrigerator at approximately 4 °C.—The procedure can also be carried out using correspondingly larger amounts of reactants (up to approximately 50 g of $KMnO_4$).

Determination of the content: 0.3 mL of the solution was added to approximately 30 mL of water and the resulting mixture was stirred. After addition of KI (1.5 g) and glacial acetic acid (p.a., 4 mL), the solution was titrated. 1 mL of 0.1 N thiosulfate solution corresponds to 2.2 mg of Mn_2O_7.

Oxidations: The reactant (7.8 mmol) in a 1:1 mixture of CCl_4 and acetone (both dry) or of methyl or ethyl acetate and Freon 113 was placed in a 100-mL three-necked flask equipped with a thermometer, a stirrer, a dropping funnel, and an inlet for inert gas. 3 to 4 mL of the solvent was required per 100 mg of the stoichiometrically required Mn_2O_7 amount to ensure easy stirring. After cooling to the reaction temperature (alcohols, −70 °C; alkenes, −80 °C; ethers, −45 °C), Mn_2O_7 in CCl_4 solution was added with stirring in a moderate stream of nitrogen or argon at such a rate that the temperature did not increase by more than 5 °C. Mn_2O_7 was thereby used in a small excess. The reaction mixture was then stirred for 5 min at the same temperature. Excess Mn_2O_7 can be removed by addition of several mL of isopropyl alcohol.

Workup of esters and ketones: After warming to room temperature, the precipitate was filtered off under suction, the filtrate was concentrated, and the crude product was purified by recrystallization or by distillation.

Workup of carboxylic acids (extractive): The MnO_2 precipitate obtained by filtration or evaporation of the solvent was combined with 20–30 mL of water and the resulting slurry was treated with $Na_2S_2O_5$ (0.95 g per 1 g of reacted Mn_2O_7). 50% aqueous H_2SO_4 was then added to the stirred mixture until full dissolution had occurred and the reaction mixture was strongly acidic. The carboxylic acid was extracted and purified according to the standard procedures.

Workup of carboxylic acids (without extraction): After completion of the reaction and warming of the reaction mixture to 0 °C, 0.97 g of $Na_2SO_3 \cdot 7\,H_2O$, 0.76 g of $Na_2S_2O_5$ (both powdered), and 1.25 mL of HCOOH (p.a.) per 1 g of Mn_2O_7 employed were added to the mixture, which was stirred at room temperature. After complete disappearance of the color (ca. 1 h), the salts were

filtered off under suction, the filtrate was concentrated, and the residue was purified by distillation or by crystallization.—Alternatively, after completion of the reaction, 0.94 g of powdered glyoxylic acid monohydrate and 1.25 mL of HCOOH (p.a.) were added per 1 g of reacted Mn_2O_7 at 0°C. The reaction mixture was then worked up as described above.

Received: March 30, 1987;
supplemented: July 10, 1987 [Z 2170/2171]
German version: *Angew. Chem. 99* (1987) 1037

[1] H. Aschoff, *Ann. Phys. Chem. 111* (1860) 217; *J. Prakt. Chem. 81* (1860) 29.
[2] M. Trömel, *Acta Crystallogr. Sect. B 39* (1983) 664.
[3] A. Simon, R. Dronskowski, B. Krebs, B. Hettich, *Angew. Chem. 99* (1987) 160; *Angew. Chem. Int. Ed. Engl. 26* (1987) 139.
[4] O. Glemser, H. Schröder, *Z. Anorg. Allg. Chem. 271* (1953) 293.

$[Fe_4Te_4(TePh)_4]^{3\ominus}$, the First Telluride-Tellurolate Complex**

By *Wolfgang Simon, Alfons Wilk, Bernt Krebs,* and *Gerald Henkel**

Complexes having cubane-like M_4X_4 frameworks and tetrahedral MX_4 centers are of considerable interest, in particular because of their widespread occurrence in iron-sulfur proteins (see, e.g., Ref. [1]). In addition to roughly 40 differently substituted sulfide-thiolate clusters of the type $[Fe_4(\mu_3\text{-}S)_4(SR)_4]^{2\ominus/3\ominus}$ (see, e.g., Ref. [2]), the ion $[Fe_4(\mu_3\text{-}Se)_4(SePh)_4]^{2\ominus}$,[3,4] the first example of a species having a selenide-selenolate ligand sphere has been reported. Tellurium-coordinated soluble cubane clusters, however, were previously unknown.

In our attempts to prepare the first members of this new class of compounds, we initially prepared the precursor **1**, which was reacted with NaHTe in acetonitrile to give the complex salt **2**, containing the cubane-like anion **3**.[5]

$[Et_4N]_2[Fe(TePh)_4]$ **1**
$[Et_4N]_3[Fe_4(\mu_3\text{-}Te)_4(TePh)_4]\cdot 2\,MeCN$ **2**
$[Fe_4(\mu_3\text{-}Te)_4(TePh)_4]^{3\ominus}$ **3**

The X-ray crystal structure analysis[6] revealed that crystals of **2** consist of $Et_4N^{\oplus}$ cations, MeCN molecules, and isolated anions **3**. The arrangement of the cations and MeCN molecules precludes unusually short intermolecular contacts between the anions of **2**. The center of **3** (Fig. 1) contains the characteristic Fe_4Te_4 cage with the cubane-like structure well known from iron-sulfide-thiolate chemistry. This cage consists of two interpenetrating distorted tetrahedra of different size, the smaller one being defined by Fe atoms and the larger one by Te atoms. They are arranged in such a way that the Te atoms are located above the centers of the faces of the iron tetrahedron.

The Fe atoms complete their coordination by each binding a tellurophenolate ligand with an average distance of 2.598 Å, thereby increasing their coordination number to 4. This results in an Fe_4Te_8 framework consisting of four $FeTe_4$ tetrahedra sharing common edges in such a way that three vertices always coincide. Very similarly constructed Fe_4Te_8 units are present in the ternary solid-state compound $Cs_7Fe_4Te_8$ reported by *Bronger* et al.[7] The analogies between soluble clusters and discrete structural units in typical solids extend beyond mere topological relationships. They are also revealed in the oxidation state of iron, which, in both the salt **2** and $Cs_7Fe_4Te_8$, has an average value of +2.25.

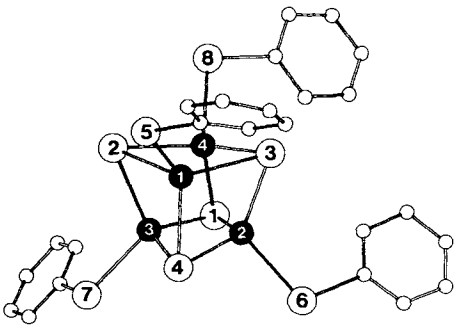

Fig. 1. Molecular structure of the anion **3** in crystals of **2** (hydrogen atoms omitted). Large empty circles, tellurium; large solid circles, iron; −120°C. Important distances [Å]: Fe_4Te_4 framework: Fe1···Fe4 2.640(1), Fe2···Fe3 2.624(2), Fe1···Fe2 2.799(2), Fe1···Fe3 2.781(2), Fe2···Fe4 2.825(2), Fe3···Fe4 2.810(1); Fe1-Te4 2.588(1), Fe2-Te3 2.564(1), Fe3-Te2 2.565(1), Fe4-Te1 2.571(1); Fe1-Te2 2.646(1), Fe1-Te3 2.627(1), Fe2-Te1 2.620(1), Fe2-Te4 2.604(1), Fe3-Te1 2.631(1), Fe3-Te4 2.640(1), Fe4-Te2 2.598(1), Fe4-Te3 2.611(1); Fe-$Te_{term.}$: Fe1-Te5 2.601(1), Fe2-Te6 2.594(2), Fe3-Te7 2.589(1), Fe4-Te8 2.606(1); Angles [°]: Fe_4Te_4 framework: Fe-Te-Fe 60.0(1) to 60.5(1) (average 60.2, 4×) and 64.3(1) to 66.2(1) (average 65.3, 8×); Te-Fe-Te 105.7(1) to 108.9(1) (average 106.8, 8×) and 116.7(1) to 119.1(1) (average 118.0, 4×); $Te_{term.}$-Fe-$Te_{br.}$ 94.3(1) to 100.0(1) (average 96.5, 4×) and 108.0(1) to 118.1(1) (average 114.4, 8×).

The magnetic properties of **2** in solution indicate the existence of antiferromagnetic coupling of the iron atoms. Based on the results of NMR spectroscopy,[5] similar magnetic properties are expected as for the corresponding sulfur-containing trianions.[8] The magnetic properties of crystalline **2** are still under investigation. Values for $Cs_7Fe_4Te_8$ are not available.

The Fe_4Te_4 framework in **3** is significantly distorted from the T_d symmetry of a regular A_4B_4 cubane system towards an idealized D_{2d} symmetry; in addition to four short Fe–Te bonds, which correspond to a set of parallel edges of an undistorted cube and which are 2.572 Å long on the average, the cluster contains eight significantly longer distances with an average value of 2.622 Å. With respect to the $\bar{4}$ axis, which passes through the center of the edges Fe1-Fe4 and Fe2-Fe3, the Fe_4 tetrahedron is clearly stretched (average edge lengths: 2×2.632, 4×2.804 Å), whereas the Te_4 tetrahedron is just as clearly compressed (average edge lengths: 4×4.169, 2×4,496 Å). Both effects are reflected in the observed compression of the overall Fe_4Te_4 cubane unit, the distances Fe1-Fe4 and Fe2-Fe3 (2.632 Å, average) being unusually short for mixed cubane clusters and approaching the iron-ligand distances.

At first sight, these findings appear to violate an empirical rule formulated by *Holm* et al.,[9] which—based on a number of sulfide-thiolate complexes—establishes a relationship between the distortion of the cubane unit and the average oxidation state of the iron atoms. In accordance with this rule, the cubane unit should be stretched along the $\bar{4}$ axis for an average oxidation state of +2.25. The compression observed here, which is also present—albeit to a smaller extent—in $Cs_7Fe_4Te_8$, might be due to electronic factors caused by the specific influence of the tellurium ligands. However, in analyzing electronically induced distortions in solids, one should note that these effects overlap with the effects due to packing. Thus, it is also possible that the molecular $\bar{4}$ axis of the thermodynami-

[*] Priv.-Doz. Dr. G. Henkel, Dipl.-Chem. W. Simon, A. Wilk, Prof. Dr. B. Krebs
Anorganisch-chemisches Institut der Universität
Wilhelm-Klemm-Strasse 8, D-4400 Münster (FRG)

[**] This work was supported by the Bundesminister für Forschung und Technologie under grant number 05339GAB/3, by the Minister für Wissenschaft und Forschung des Landes Nordrhein-Westfalen, and by the Fonds der Chemischen Industrie.

cally stable conformation does not correspond to the 4 axis observed in the crystal, but rather to one of the two twofold axes. In order to clarify this question, we are currently carrying out Fe EXAFS investigations on crystalline phases and on dissolved samples.

Received: February 25, 1987;
supplemented: July 20, 1987 [Z 2123 IE]
German version: *Angew. Chem. 99* (1987) 1039

CAS Registry numbers:
1, 110142-55-7; **2**, 110173-55-2; $[Et_4N]_2[FeCl_4]$, 15050-84-7.

[1] A. J. Thomson in P. Harrison (Ed.): *Metalloproteins—Metal Proteins with Redox-Roles, Part 1*, VCH, Weinheim 1985, Chapter 3.

[2] J. M. Berg, R. H. Holm in T. G. Spiro (Ed.): *Iron-Sulfur Proteins*, Wiley, New York 1982, Chapter 1.

[3] M. A. Bobrik, E. J. Laskowski, R. W. Johnson, W. O. Gillum, J. M. Berg, K. O. Hodgson, R. H. Holm, *Inorg. Chem. 17* (1978) 1402.

[4] W. Simon, B. Krebs, G. Henkel, manuscript in preparation.

[5] *Experimental Procedure:* All operations were carried out under inert gas (N_2 or Ar) in closed apparatus owing to the extreme sensitivity of the components toward oxidation.—**1**: A solution of NaTePh (16 mmol, prepared from Ph_2Te_2 (3.27 g, 8 mmol) and $NaBH_4$ (0.61 g, 16 mmol) in 10 mL of ethanol) was added to a suspension of $[Et_4N]_2[FeCl_4]$ (1.83 g, 4 mmol) in acetone (25 mL). The immediately formed red precipitate was filtered off and dried under vacuum. Quantitative yield; correct elemental analysis (C, H, N).—**2**: A NaHTe solution (prepared by reaction of Te powder (0.51 g, 4 mmol) with $NaBH_4$ in threefold excess in ethanol, removal of the solvent, and dissolving the residue in 30 mL of acetonitrile) was added dropwise to a suspension of **1** (4.54 g, 4 mmol) in acetonitrile (40 mL), resulting in the formation of a deep violet solution. After filtration of this solution and cooling to −25 °C, black crystals of **2** having an edge length of up to several mm separated out. The bound acetonitrile can be removed under vacuum. Yield 30%; correct elemental analysis (C, H, N). ^{1}H-NMR spectrum (CD_3CN, 300 MHz, δ values in parentheses: $(\Delta H/H_0)_{iso}$): *m*-H, 11.8 (−4.6); *o*-H, 3.3 (+4.5); *p*-H, 0.9 (+6.3); diamagnetic standard: Ph_2Te_2; *o*-H, 7.8; *m*-H and *p*-H, 7.2.—UV/VIS (DMF): $\lambda_{max} \approx 269$, 311, 346 (sh), 536 nm (br, w).

[6] Crystal data: Syntex $P2_1$ four circle diffractometer, $Mo_{K\alpha}$ radiation, graphite monochromator, scintillation counter, $2\theta-\theta$ scan, $T = -120$ °C, empirical absorption correction. **2**: triclinic, space group $P\bar{1}$, $a = 11.416(2)$, $b = 13.107(3)$, $c = 13.820(3)$ Å, $\alpha = 112.36(2)$, $\beta = 111.01(2)$, $\gamma = 98.94(2)$°, $V = 1680.2$ Å^3, $Z = 1$, $\rho_{calcd} = 1.97$ g cm^{-3}, $\mu(Mo_{K\alpha}) = 44.3$ cm^{-1}, crystal dimensions 0.23 mm × 0.19 mm × 0.18 mm, $2\theta_{max} \approx 54$°, 7370 unique reflections, $R(R_w) = 0.028$ (0.038) for 7349 reflections with $F_0 > 3.92\sigma(F_0)$. EXTL and SHELXTL programs; structure solution by direct methods, least-squares fit, 351 parameters, H atoms at idealized positions with isotropic temperature factors ($U(H) = 1.2\ U_{eq}$ (C)), all other atoms refined with anisotropic (Fe, Te) or isotropic (N, C) temperature factors, one scaling factor, methylene groups of an Et_4N cation disordered (occupation 1 : 2).Further details of the crystal structure investigation may be obtained from the Fachinformationszentrum Energie, Physik, Mathematik GmbH, D-7514 Eggenstein-Leopoldshafen 2 (FRG), on quoting the depository number CSD-52620, the names of the authors, and the journal citation.

[7] W. Bronger, M. Kimpel, D. Schmitz, *Angew. Chem. 94* (1982) 562; *Angew. Chem. Int. Ed. Engl. 21* (1982) 544; *Acta Crystallogr. Sect. B39* (1983) 235.

[8] J. G. Reynolds, E. J. Laskowski, R. H. Holm, *J. Am. Chem. Soc. 100* (1978) 5315.

[9] E. J. Laskowski, J. G. Reynolds, R. B. Frankel, S. Foner, G. C. Papaefthymiou, R. H. Holm, *J. Am. Chem. Soc. 101* (1979) 6562.

[1+4] Cycloaddition of a Diphosphene to Acrolein: Synthesis and Structure of a Dihydro-1,2λ^5-oxaphosphole with an Exocyclic P=P Bond**

By *Lothar Weber,* Matthias Frebel,* and *Roland Boese*

Iminophosphanes **A** tend to undergo dimerization[2] and react with $(CF_3)_2CO$[3] to give three-membered heterocycles. The phosphanediyl complex **B** can also react in this "carbene-like" way with olefins and alkynes.[4] Furthermore, the cheletropic [1+4] cycloaddition of **B** to cinnamaldehyde has been reported.[4] Such behavior was previously unknown for diphosphenes **C**. Instead, these react in an "olefin-like" way with dienes, undergoing [2+4] cycloaddition.[5] We report here the cheletropic [1+4] cycloaddition of the transition-metal-substituted diphosphene **1**[6] to acrolein, an α,β-unsaturated aldehyde.

R−P=N−R′ (CO)$_5$W=PPh R−P=P−R′

A **B** **C**

Compound **1** reacts with acrolein (molar ratio 1 : 1) in benzene at 0 °C to give the dihydro-1,2λ^5-oxaphosphole **2**, which was isolated as a violet, diamagnetic, air-sensitive solid. The ^{31}P-NMR signals of **1** are shifted strongly upfield on cyclization ($\Delta\delta_{P^1} = 553.9$, $\Delta\delta_{P^2} = 581.7$ ppm). The increase in the coupling constants $^1J_{P1P2}$ from 594.2 to 727.5 Hz is in agreement with the presence of a P=P bond in **2**, but its ylide character is indicated by the marked upfield shift of P2 ($\delta = -28.2$).[7]

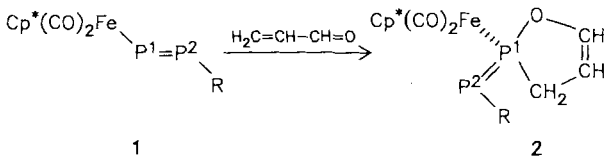

1 **2**

Cp* = C_5Me_5, R = 2,4,6-tBu$_3$C$_6$H$_2$

The $[(\eta^5\text{-}C_5Me_5)Fe(CO)_2]$ fragment of **2** is revealed in the IR spectrum (pentane) by two intense bands at 2018 and 1966 cm^{-1}. The X-ray crystal structure analysis of **2** (Fig. 1) shows[8] that the ring P atom P1 is coordinated in a distorted tetrahedral fashion and is part of a dihydrooxaphosphole.

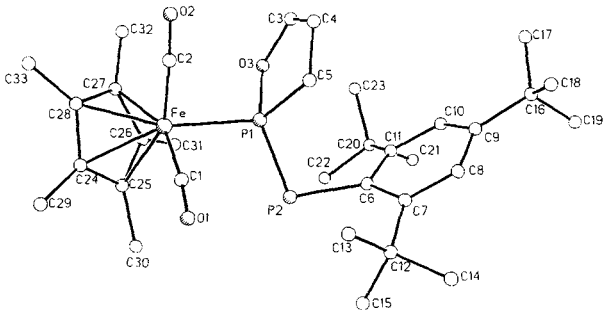

Fig. 1. Molecular structure of **2**. Selected bond lengths [pm] and angles [°]: Fe-P1 224.3(2), Fe-C1 175.0(6), Fe-C2 174.7(6), P1-P2 206.4(2), P1-O3 170.3(5), P1-C5 185.2(7), P2-C6 185.0(5), O1-C1 113.9(7), O2-C2 114.3(8), O3-C3 138.8(11), C3-C4 126.8(12), C4-C5 145.5(11); Fe-P1-P2 111.2(1), Fe-P1-O3 105.9(2), Fe-P1-C5 114.2(2), O3-P1-C5 92.0(3), P1-P2-C6 100.3(2).

The P1–P2 distance in **2** (206.4(2) pm) is significantly larger than that in **1** (202.7(1) pm). In contrast to **1**, C6 does not lie in the same plane as Fe, P1, and P2 in **2**, but is displaced by 0.485 Å out of this plane toward C5 (torsion angle Fe,P1,P2,C6 = 164.6°). The dihydrooxaphosphole ring is slightly tilted along the O3–C5 axis (dihedral angle 169.7°); it is nearly orthogonal to the Fe,P1,P2 plane (interplanar angle 94.5°). In P_2H_2, the n_+ and π orbitals have similar energies.[9] The incorporation of a strongly nucleophilic transition-metal fragment apparently increases the energy level of the n_+ so much relative to the π MO that

[*] Prof. Dr. L. Weber, Dipl.-Chem. M. Frebel, Dr. R. Boese
Institut für Anorganische Chemie der Universität
Universitätsstrasse 5-7, D-4300 Essen 1 (FRG)

[**] Transition-Metal-Substituted Diphosphenes, Part 11. This work was supported by the Fonds der Chemischen Industrie.—Part 10: [1].

"carbene-like" reactions are possible.[10] Other mechanisms for the formation of **2** are also conceivable.

Experimental Procedure

0.7 mL of a solution containing freshly distilled acrolein (2 mL) in benzene (8 mL, 2.95 mmol) was added to a vigorously stirred solution of **1** (1.50 g, 2.70 mmol) in benzene (10 mL) at 0°C. The reaction mixture was then stirred for 2 h at 20°C, the red-brown solution thereby turning deep violet. All volatiles were removed in vacuum and the violet, oily residue was dissolved in pentane (20 mL). The solution was filtered and the filter cake was extracted with pentane until the extracts were colorless. The filtrate and combined extracts were concentrated to ca. 10 mL and stored at −28°C, resulting in the crystallization of violet **2**; yield 0.77 g (47%), m.p. = 151°C (dec.).—^{1}H-NMR (200 MHz, C_6D_6, 22°C): δ = 1.38 (s, 9H, *p*-*t*Bu), 1.56 (s, 15H, $C_5(CH_3)_5$), 1.86 (m, 1H, CH_2), 1.92 (s, 9H, *o*-*t*Bu), 2.01 (s, 9H, *o*-*t*Bu), 2.36 (m, 1H, CH_2), 4.73 (m, 1H, =C*H*−CH_2), 5.95 (m, 1H, =CH−O), 7.47 (d, 2H, ^4J(PH) = 4.2 Hz, *m*-H phenyl).—^{13}C{H}-NMR (C_6D_6, 22°C): δ = 9.99 (d, ^3J(PC) = 5.4 Hz, $C_5(CH_3)_5$), 31.74 (s, *p*-C(CH_3)$_3$), 33.04 (d, ^1J(PC) = 18.8 Hz, CH_2), 33.76 (dd, J(PC) = 10.8 Hz, 2.7 Hz, *o*-C(CH_3), 34.70 (s, *o*-C(CH_3)$_3$), 34.83 (s, *p*-*C*(CH_3)$_3$), 39.00 (s, *o*-*C*(CH_3)$_3$), 39.48 (s, *o*-*C*(CH_3)$_3$), 98.18 (s, $C_5(CH_3)_5$), 103.7 (s, CH_2−*C*H=), 119.69 (d, J(PC) = 3.9 Hz, *m*-C phenyl), 121.0 (d, J(PC) = 3.9 Hz, *m*-C phenyl), 138.46 (dd, J(PC) = 82.0, 20.4 Hz, *ipso*-C phenyl), 143.55 (dd, J(PC) = 7.0, 3.5 Hz, O−*C*H=), 146.93 (d, J(PC) = 4.5 Hz, *p*-C phenyl), 157.5 (d, J(PC) = 9.9 Hz, *o*-C phenyl), 157.8 (d, J(PC) = 8.4 Hz, *o*-C phenyl), 213.45 (dd, J(PC) = 18.6, 4.8 Hz, FeCO), 215.5 (d, J(PC) = 22.8 Hz, FeCO).—^{31}P{H}-NMR (C_6D_6, 22°C): δ = 162.25 (d, $^1J_{P1P2}$ = 727.5 Hz, P1), −28.2 (d, $^1J_{P1P2}$ = 727.5 Hz, P2).—IR (pentane): 2018 s, 1966 s cm^{-1} [ν(CO)].—EI/MS (Varian MAT 312); *m*/*z* 610 ($M^{\oplus}$).

Received: May 8, 1987 [Z 2231 IE]
German version: *Angew. Chem. 99* (1987) 1045

[1] L. Weber, G. Meine, N. Niederprüm, R. Boese, *Organometallics*, in press.
[2] E. Niecke, R. Rüger, W. W. Schoeller, *Angew. Chem. 93* (1981) 1110; *Angew. Chem. Int. Ed. Engl. 20* (1981) 1034.
[3] E. Niecke, D. Gudat, W. W. Schoeller, P. Rademacher, *J. Chem. Soc. Chem. Commun. 1985*, 1050.
[4] Review: F. Mathey, *Angew. Chem. 99* (1987) 285; *Angew. Chem. Int. Ed. Engl. 26* (1987) 275, and references cited therein.
[5] a) J. Escudié, C. Couret, J. D. Andiamizaka, J. Satgé, *J. Organomet. Chem. 228* (1982) C76; b) E. Niecke, R. Rüger, *Angew. Chem. 95* (1983) 154; *Angew. Chem. Int. Ed. Engl. 22* (1983) 155; c) J. Grobe, D. Le Van, J. Schulze, *Z. Naturforsch. B40* (1985) 1753; d) C. Couret, J. Escudié, H. Ranaivonjatovo, J. Satgé, *Organometallics 5* (1986) 113.
[6] L. Weber, K. Reizig, D. Bungardt, R. Boese, *Organometallics 6* (1987) 110.
[7] *Regitz* et al. recently reported phosphoranylidenephosphanes with coupling constants ^1J(PP) = 429 and 433 Hz: F. Zurmühlen, M. Regitz, *Angew. Chem. 99* (1987) 65; *Angew. Chem. Int. Ed. Engl. 26* (1987) 83.
[8] Space group $P2_1/n$, a = 1850.8(4), b = 923.8(3), c = 2057.7(5) pm, β = 99.71(2)°, V = 3467.9(14) pm^3, Z = 4, R = 0.066. Further details of the crystal structure investigation may be obtained from the Fachinformationszentrum Energie, Physik, Mathematik GmbH, D-7514 Eggenstein-Leopoldshafen 2 (FRG), on quoting the depository number CSD-52641, the names of the authors, and the journal citation.
[9] A. H. Cowley, *Polyhedron 3* (1984) 418, and references cited therein.
[10] The oxidation potential of **1** (in THF, vs. SCE) is only +0.45 V (U. Kölle, private communication), whereas for $[Me_3Si-P]_2$ E_{ox} = +1.14 V (in CH_3CN vs. SCE) was measured: M. Culcasi, G. Gronchi, J. Escudié, C. Couret, L. Pujol, P. Tordo, *J. Am. Chem. Soc. 108* (1986) 3130.

Mono- and Diphosphatricyclo[3.2.1.0^{2,7}]oct-3-enes: Synthesis from 1,3- and 1,4-Dienes and a Stable Phosphaalkyne**

By *Eberhard P. O. Fuchs, Wolfgang Rösch,* and *Manfred Regitz**

Phosphaalkynes undergo regiospecific [3+2] cycloaddition with 1,3-dipoles, such as diazo compounds, azides, and nitrile oxides, to give the corresponding phospholes.[1–3] In contrast, only a few examples of Diels–Alder reactions of phosphaalkynes with cyclic 1,3-dienes are known.[4] The reaction of open-chain 1,3-dienes with the phosphaalkyne **2** is—as we report here—much more complex: it proceeds—largely independent of the ratio of reactants—with a 1:2 stoichiometry.

In order to carry out the reaction, the reactants are heated in a glass pressure vessel partly with and partly without solvent (see footnotes to Table 1) to temperatures ≥90°C. Kugelrohr distillation affords the oily 1,7-diphosphatricyclo[3.2.1.0^{2,7}]oct-3-enes **5a–d** in high yields.[5] The reactions of **1b** and **1d** with **2** each afford two isomers, the main products being **5b** and **5d**, respectively (ratio 60:40 and 90:10, respectively, as determined by ^{31}P-NMR spectroscopy). In the minor products, the sequence of the substituents R^1–R^4 is the reverse of that in **5b** and **5d**.

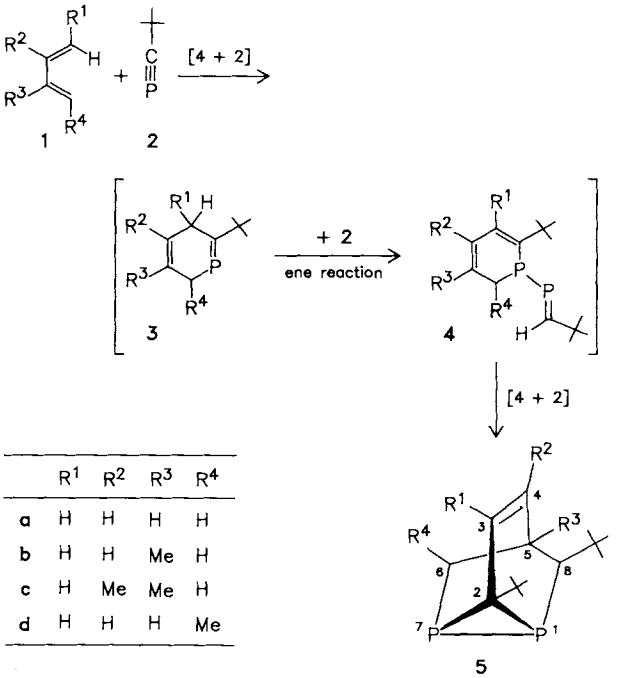

	R^1	R^2	R^3	R^4
a	H	H	H	H
b	H	H	Me	H
c	H	Me	Me	H
d	H	H	H	Me

The products are presumably formed by an initial Diels–Alder reaction (**1** + **2** → **3**) followed by an ene reaction of **3** with a second equivalent of **2** to give **4**,[6] which, in turn, undergoes an intramolecular [4+2] cycloaddition (**4** → **5**). In the case of **1b** and **1d**, the first step is not regiospecific, which explains the formation of the minor products. The ene reaction, in contrast, occurs specifically at the PC double bond. Steps **3** → **4** and **4** → **5** were previously unknown in the chemistry of low-coordinate phosphorus compounds. The mechanistic interpretation of the reaction **1** + **2** → **5** is also supported by the fact that the 1,4-cyclohexadienes **6a–d** react with **2** in a ratio of 1:1 under comparable conditions (see footnotes to Table 1) to give the 1-phosphatricyclo[3.2.1.0^{2,7}]oct-3-enes **8a–d** (colorless to yellow oils).

In the case of **6c** and **6d**—but not of **6b**—approximately 10% (^{31}P-NMR spectroscopy) of an isomer is formed in addition to the main products; this isomer bears the substituents in the 4,5 positions, but it could not be separated. Thus, the ene reaction with **6b** occurs exclusively, and that with **6c** and **6d** with great selectivity, at the substituted, electron-richer CC double bond. In carbon chemistry, it is known that **6a** reacts with dimethyl acety-

[*] Prof. Dr. M. Regitz, E. P. O. Fuchs, Dr. W. Rösch
Fachbereich Chemie der Universität
Erwin-Schrödinger-Strasse, D-6750 Kaiserslautern (FRG)

[**] Phosphorus Compounds with Unusual Coordination, Part 23. This work was supported by the Deutsche Forschungsgemeinschaft and the Fonds der Chemischen Industrie.—Part 22: W. Rösch, M. Regitz, *Synthesis 1987*, 689.

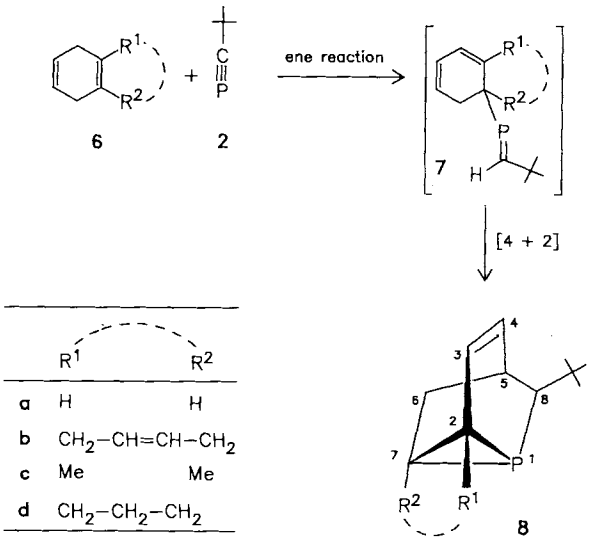

lenedicarboxylate to give correspondingly dimethyl tricyclo[3.2.1.0^{2,7}]oct-3-ene-1,8-dicarboxylate,[7–9] but to our knowledge this reaction has not been extended to other reaction partners.

Table 1. Yields and characteristic NMR data (δ values) for the mono- and diphosphatricyclooctenes **5** and **8**.

Compd	Yield	^{31}P-NMR [a]			^{13}C-NMR [a]				
	[%]	P-1	P-7	C-7	C-2	C-3/C-4	C-5	C-6	C-8
5a [b]	90	−190.0	−194.5	—	43.2	124.2/128.4	32.9	32.5	59.4
5b [b]	85	−165.5	−202.2	—	43.0	128.6/127.7	37.9	44.0	61.7
5c [c]	86	−165.6	−210.6	—	43.4	123.6/131.6	40.7	45.1	61.7
5d [d]	66	−174.2	−176.3	—	42.9	120.1/128.3	37.7	39.5	58.9
8a [b]	90	−234.0	—	19.1	22.2	124.7/124.6	33.8	33.5	56.2
8b [d]	33	−196.9	—	33.6	39.8	124.7/130.3	36.1	41.1	57.5
8c [c]	60	−192.0	—	32.9	37.3	124.6/131.5	35.9	43.3	59.5
8d [d]	46	−204.6	—	41.0	45.8	123.9/129.5	35.6	37.5	58.2

[a] **5a,b** in C_6D_6, all other compounds in $CDCl_3$. [b] Preparation: without solvent, ca. 15 h at 90–120°C. [c] Preparation: benzene, ca. 30 h at 120°C. [d] Preparation: petroleum ether 30–75°C, ca. 30–50 h at 140°C.

Correct elemental analyses were obtained for all products (including the mixtures of isomers). The ^{1}H-, ^{31}P-, and ^{13}C-NMR spectra provided detailed information (for the latter, see Table 1). The signals of both P atoms of **5a–d** appear as a AB system at the expected high field with $^1J_{P,P}$ couplings of 150.0–158.7 Hz.[10] Analogous results were obtained for the constitutional isomers of **5b** and **5d** having the reverse sequence of substituents.[11] The phosphorus of **8a–d** exhibits a comparable chemical shift.[12] The signals of the sp^3 carbon atoms C-2, C-6, and C-8 of **5a–d** and of C-2, C-7, and C-8 of **8a–d** are split owing to $^1J_{P,C}$ couplings (28.2–49.0 Hz).

Received: May 15, 1987 [Z 2242 IE]
German version: *Angew. Chem. 99* (1987) 1058

[1] W. Rösch, M. Regitz, *Angew. Chem. 96* (1984) 898; *Angew. Chem. Int. Ed. Engl. 23* (1984) 900.
[2] T. Allspach, M. Regitz, G. Becker, W. Becker, *Synthesis 1986*, 31.
[3] W. Rösch, U. Vogelbacher, T. Allspach, M. Regitz, *J. Organomet. Chem. 306* (1986) 39.
[4] W. Rösch, M. Regitz, *Z. Naturforsch. B41* (1986) 931.
[5] Only **5a** crystallizes upon removal of the excess 1,3-butadiene; m.p. = 75°C. The constitution of this compound is confirmed by an X-ray structure analysis. Selected bond lengths [Å] and angles [°]: P1-P7 2.183(2), P1-C2 1.886(4), P7-C2 1.888(4); P7-P1-C2 54.7(1), P1-P7-C2 54.6(1), P1-C2-P7 70.7(2).
[6] The reaction of **2** with isobutene at 120°C (pressure vessel) has already shown that phosphaalkynes are capable, in principle, of undergoing ene reactions. However, the phosphaalkene thereby formed adds a second mole of isobutene, according to the same principle, to give bis(2-methylallyl)neopentylphosphane (^{31}P-NMR (C_6D_6): $\delta = -43.9$). Compound **2** reacts with 2,3-dimethyl-2-butene, on the other hand, in a simple ene reaction to give 2,3,3,6,6-pentamethyl-4-phospha-1,4-heptadiene (^{31}P-NMR (C_6D_6): $\delta = +268.4$, $^2J_{P,H} = 24.6$ Hz): E. P. O. Fuchs, M. Regitz, unpublished results, Universität Kaiserslautern 1987.
[7] C. Bong, *Dissertation*, Universität Köln 1952. Discussed in H. Wollweber: *Diels-Alder-Reaktion*, 1st ed., Thieme, Stuttgart 1972, p. 139ff.
[8] K. Alder, F. Brochhagen, C. Kaiser, W. Roth, *Justus Liebigs Ann. Chem. 593* (1955) 1.
[9] C. F. Huebner, E. Donoghue, L. Dorfman, F. A. Stuber, N. Danieli, E. Wenkert, *Tetrahedron Lett. 1966*, 1185.
[10] See L. Quin: *The Heterocyclic Chemistry of Phosphorus*, 1st ed., Wiley, New York 1981, p. 231.
[11] ^{31}P-NMR (C_6D_6): $\delta = -192.5$ and -194.9, $^1J_{P,P} = 152.7$ Hz and -169.2 and -195.5, $^1J_{P,P} = 160.1$ Hz.
[12] ^{31}P-NMR ($CDCl_3$) of the constitutional isomers of **8c**, **d**: $\delta = -208.1$ and -207.9, respectively.

A New 1,3-Diphosphaallylnickel Complex for the Polymerization of Ethene

By *Wilhelm Keim,* Rolf Appel,* Stefan Gruppe,* and *Falk Knoch**

Dedicated to Professor Friedrich Asinger on the occasion of his 80th birthday

There have been few investigations regarding the influence of chelating ligands on the transition-metal-catalyzed formation of C–C bonds under homogeneous conditions. Noteworthy, however, is the controlling effect that has been achieved using PO bidentate ligands.[1] The size of the chelate ring plays an important role in these reactions: for example, PO complexes, **I**, oligomerize ethene selectively to give α olefins (SHOP process).[2]

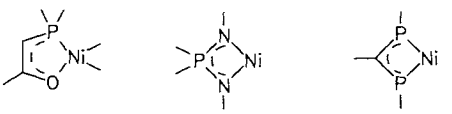

I II III

Using aminobis(imino)phosphorane complexes, **II**, α olefins could be polymerized to give α,ω linkages via a novel mechanism.[3] As shown by the X-ray structure analysis of **II**, the complex contains a four-membered ring in which three electrons are distributed in a η^3-allyl-like fashion. In order to increase our understanding of chelate ligand properties and to discover new ways to carry out C–C bond formation, it seemed of interest to include phosphaalkene complexes, **III**, in our investigations, since it was known that phosphaalkenes can function as η^3-1,3-diphosphaallyl chelating ligands.[4]

Reaction of bis(1,5-cyclooctadiene)nickel with the 1,3-diphosphapropene **1** in toluene affords a catalyst, which, in situ at 70–100°C and 30 bar ethene, polymerizes ethene to give linear polyethylene ($M_r \approx 0.8 \times 10^6$). IR investigations reveal that mostly terminal double bonds are present. Activities of > 1000 mol ethene per mole of nickel per

[*] Prof. Dr. W. Keim, S. Gruppe
Institut für Technische Chemie und
Petrolchemie der Technischen Hochschule
Worringer Weg 1, D-5100 Aachen (FRG)
Prof. Dr. R. Appel, Dr. F. Knoch
Anorganisch-chemisches Institut der Universität
Gerhard-Domagk-Strasse 1, D-5300 Bonn 1 (FRG)

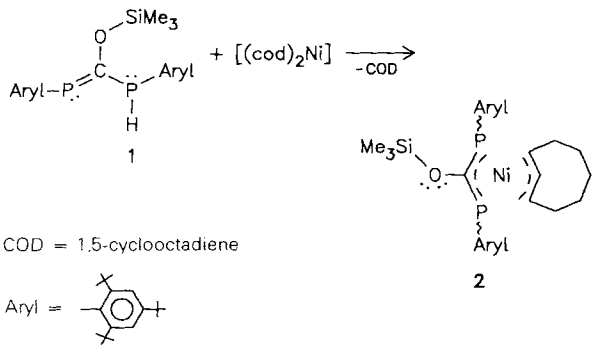

hour were attained. No catalysis was observed for propene.

The stoichiometric reaction of bis(1,5-cyclooctadiene)nickel with **1** gives complex **2**, which also catalyzes the polymerization of ethene.

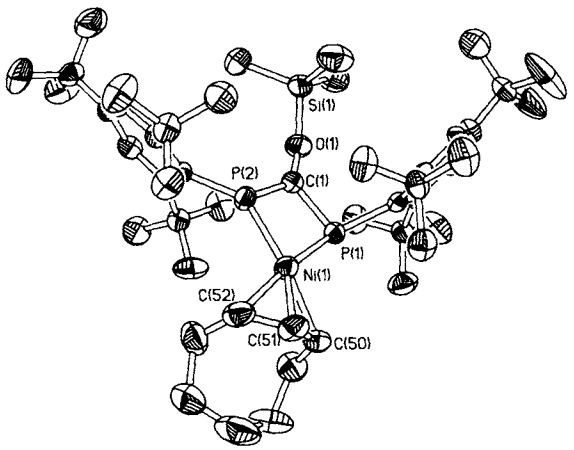

Fig. 1. Molecular structure of complex **2**. Space group $P\bar{1}$, $a=1038.8(2)$, $b=1411.7(3)$, $c=1886.4(5)$ pm, $\alpha=73.26(2)$, $\beta=77.17(2)$, $\gamma=71.09(2)°$, $V=2481(1)\times10^6$ pm^3, $\rho_{calcd}=1.10$ g/cm^3. Solution of the structure by direct methods (SHELXTL); 11060 asymmetric data, 5747 observed with $F>4\sigma(F)$, 556 parameters. $R=0.074$, $R_w=0.056$. Important distances [pm]: P(1)-C(1) 178, P(2)-C(1) 171, P(1)-Ni 227, P(2)-Ni 221, C(50)-Ni 205, C(51)-Ni 198, C(52)-Ni 211, C(50)-C(51) 139, C(51)-C(52) 139. Important angles [°]: P(1)-Ni-P(2) 74.6, P(1)-Ni-C(52) 170.8, P(2)-Ni-C(51) 148.7, P(2)-Ni-C(50) 164.1, P(1)-Ni-C(50) 101.0, P(1)-Ni-C(51) 136.1, P(2)-Ni-C(52) 111.1, C(50)-C(51)-C(52) 122.1.—Further details of the crystal structure investigation may be obtained from the Fachinformationszentrum Energie, Physik, Mathematik GmbH, D-7514 Eggenstein-Leopoldshafen 2 (FRG), on quoting the depository number CSD-52489, the names of the authors, and the journal citation.

An X-ray crystal structure analysis of **2** revealed that the 1,3-diphosphapropene ligand was η^1,η^2-coordinated. This finding is supported by the different P–C and P–Ni distances and the aryl–P–C angle. According to the spectroscopic data (^{1}H- and ^{13}C-NMR)[5] recorded in solution, **2** contains an η^3-1,3-diphosphaallyl ligand, so that equilibrium (a) can be postulated:

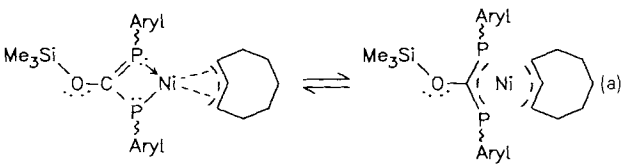

Experimental Procedure

All reactions were carried out under argon.

2: [(cod)$_2$Ni] (5.6 g, 20.35 mmol) and **1** (13.35 g, 20.3 mmol) [6] were each dissolved in 50 mL of toluene and the solutions were cooled to −50°C. The two solutions were combined with stirring and the resulting reaction mixture was stirred at room temperature for ca. 15 h. Toluene was removed in vacuum and the oily residue was dissolved in 10 mL of CH_2Cl_2. After filtration, the filtrate was treated with acetonitrile until it became cloudy. In ca. 15 h, 4.2 g (32%) of **2** crystallized at −15°C.

Received: May 6, 1987 [Z 2229 IE]
German version: *Angew. Chem. 99* (1987) 1042

[1] a) W. Keim, A. Behr, B. Gruber, B. Hoffmann, F. H. Kowaldt, U. Kürschner, B. Limbäcker, F. P. Sistig, *Organometallics 5* (1986) 2356; b) W. Keim in T. Keii and K. Soga (Eds.): *Catalytic Polymerization of Olefins*, Elsevier, Amsterdam 1986, p. 201.

[2] W. Keim, *Chem.-Ing.-Tech. 56* (1984) 850.

[3] a) W. Keim, R. Appel, A. Storeck, C. Krüger, R. Goddard, *Angew. Chem. 93* (1981) 91; *Angew. Chem. Int. Ed. Engl. 20* (1981) 116; b) G. Fink, V. Möhring, *ibid. 97* (1985) 982 and *24* (1985) 1001.

[4] a) R. Appel, W. Schuhn, F. Knoch, *Angew. Chem. 97* (1985) 421; *Angew. Chem. Int. Ed. Engl. 24* (1985) 419; b) H. H. Karsch, F. H. Koehler, H. U. Reisacher, *Tetrahedron Lett. 25* (1984) 3687; c) M. Yoshifuji, I. Shimo, N. Inamoto, *J. Am. Chem. Soc. 105* (1983) 2495.

[5] NMR data: ^{1}H-NMR (200 MHz, C_6D_{12}) $\delta=0.0$ ($SiMe_3$), 1.0–1.8 (*t*Bu and CH_2 groups of the cyclooctenyl ligand), 4.35 (outer allylic CH groups of the cyclooctenyl ligand), 5.35 (middle allylic CH group), 7.3–7.8 (aryl H).—^{13}C-NMR (67.88 MHz, C_6D_{12}): $\delta=5.4$ ($SiMe_3$), 18–33 (*t*Bu and CH_2 groups of the cyclooctenyl ligand), 66.0 (outer allylic C atom of the cyclooctenyl ligand), 100.7 (middle allylic C atom of the cyclooctenyl ligand), 116–151 (C atoms of the aryl group and C1).

[6] R. Appel, P. Fölling, B. Josten, M. Siray, V. Winkhaus, F. Knoch, *Angew. Chem. 96* (1984) 620; *Angew. Chem. Int. Ed. Engl. 23* (1984) 619.

Unusual Ligand Directed Regioselectivity in the Iron Catalyzed Cross Coupling of Allylic Ethers to 2-Substituted 1,3-Dienes**

By *James M. Takacs,** *Lawrence G. Anderson, G. V. Bindu Madhavan,* and *Franklin L. Seely*

Catalytic transition metal mediated carbon–carbon bond forming reactions which enable useful new types of bond constructions, or which exhibit unusual reaction selectivities, have found exceptional use in organic synthesis.[1,2] We have recently reported that soluble (bpy)Fe^0 complexes (bpy = 2,2′-bipyridine) catalyze the selective 1:1 cross coupling of 2,3-dimethyl-1,3-butadiene to allyl benzyl ether to yield (benzene, 25°C, 8 h, 80%) a 1,4-addition product.[3] This new iron catalyzed cross coupling reaction complements the known thermal ene chemistry.[4,5] We now wish to report that by judicious choice of ligand, the (L)Fe^0-catalyzed cross coupling reactions of monosubstituted 1,3-dienes with allylic ethers can be directed toward *either* 1,4-addition or toward the previously unknown 1,2-addition mode. These cross coupling reactions provide an unusually striking example of the effect that coordinated ligands can impose upon the kinetic selectivity of a catalytic metal complex.

Catalytically active soluble iron(0) complexes can be conveniently prepared in situ via reduction of Fe(acac)$_3$ with 3.1 equiv of Et_3Al in the presence of a 1,3-diene and 1.1 equiv of an appropriate ligand.[6] Allyl benzyl ether

[*] Prof. J. M. Takacs, L. G. Anderson, Dr. G. V. B. Madhavan, F. L. Seely
Department of Chemistry, University of Utah
Salt Lake City, UT 84112 (USA)

[**] This work was supported by the National Institutes of Health, the Petroleum Research Fund administered by the American Chemical Society, and the University of Utah Research Committee.

reacts with isoprene (benzene, 25 °C, 3–10 h) in the presence of 5–10 mol-% of (L)Fe^0 catalysts to give a mixture of four isomeric 1:1 coupling products **1**–**4** (Scheme 1, $R^1 = CH_3$, $R^2 = CH_2Ph$). The yields lie between 30 and 90% (Table 1).[7] The product ratio is dramatically influenced by the ligands attached to the metal.

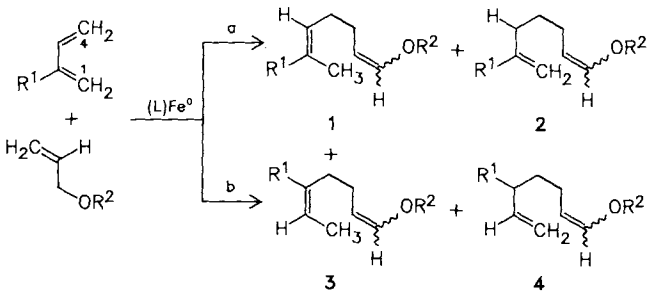

Scheme 1. Fe^0-catalyzed addition of allyl ethers to monosubstituted butadienes. a) Addition to C4; b) addition to C1. **1** and **3** are the products of 1,4-additions, **2** and **4** those of 1,2-additions.

Two unusual types of reaction selectivity are of particular interest in this process. First, the carbon–carbon bond construction is regioselective (C4- vs C1-addition) with respect to the 2-substituted 1,3-diene moiety. Secondly, we have found that within each of the addition modes the selectivity between 1,4- and 1,2-addition products can be varied (Table 1). For example, allyl benzyl ether reacts with isoprene in the presence of 10 mol-% (bpy)Fe^0 (benzene, 25 °C, 8 h) to give a mixture of enol ethers **1**–**4** in 80% yield (Table 1). In this case, about 90% of the carbon–carbon bond formation takes place at the less substituted olefin of the isoprene unit (C4-addition) to yield predominantly products **1** and **2**.[8] In comparison, the known addition of carbanion nucleophiles to the [(η^4-isoprene)$Fe(CO)_3$] complex under kinetic conditions proceeds primarily (90%) at the 3-position of the coordinated isoprene. Under thermodynamic conditions, however, the carbanion additions yield only C4-addition products and no products resulting from C1-addition are observed.[1d] Considering the products derived from the predominant C4-addition mode in the (bpy)Fe^0 catalyzed reaction, we find that greater than 70% is the 1,2-addition product **2** (**1**:**2**, 27:73). The minor coupling products **3** and **4** (< 10% yield), derived from coupling to the more substituted end of isoprene (C1-addition) are formed with little selectivity by this catalyst (**3**:**4** = 56:44). The observed reaction selectivities obtained with the (bpy)Fe^0 catalyst are not highly dependent upon the reaction medium (benzene, ether or THF) nor upon the allylic ether substituent ($R^2 = CH_2Ph$, $CH_2C_6H_{11}$, tetrahydropyranyl (THP); Table 1).

In contrast to the (bpy)Fe^0 catalyzed reaction, the C4-addition product mixture formed from the coupling of allyl benzyl ether to isoprene in the presence of 10 mol-% (pyr)Fe^0 (pyr = pyridine; in benzene, 25 °C, 10 h, 70%) is predominantly the 1,4-addition product **1** (**1**:**2** = 94:6). In the presence of this catalyst, however, the regioselectivity favoring C4- over C1-addition to isoprene is only modest (62:38). Of the isomeric products formed from the latter mode of coupling, about 70% results from the 1,2-addition mode (**3**:**4** = 24:76). Soluble iron catalysts containing 2,2′-biquinoline, 1,10-phenanthroline, or methyl substituted 1,10-phenanthroline ligands, and catalysts prepared in the absence of added ligand show product ratios of **1**–**4** similar to those of (pyr)Fe^0.[9] Table 1 lists the results.

While the origin of the catalyst selectivity cannot yet be fully resolved, preliminary experiments indicate that the isomeric products formed in the presence of these various catalysts are the result of ligand directed kinetic selectivity. We find that the isolated 1,2- and 1,4-addition products do not interconvert when subjected to active (bpy)Fe^0 or (pyr)Fe^0 catalysts [Eq. (a)]. In addition, the observed C4-

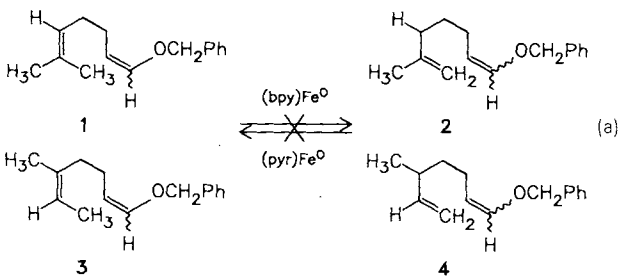

(a)

vs. C1-addition ratios parallel the relative reactivities of isoprene and 2,3-dimethyl-1,3-butadiene toward the (L)Fe^0 catalysts. Treatment of allyl benzyl ether with (bpy)Fe^0 in the presence of a large excess of an equimolar mixture of the two dienes yields a mixture of products in which the isoprene unit is incorporated with about 4:1 selectivity. The corresponding reaction catalyzed by (pyr)Fe^0 is nonselective, consistent with the low C4:C1 selectivity exhibited by this catalyst.

Structurally more complex dienes can also be employed in the coupling reaction of Scheme 1. Myrcene, 2-(2′-phenyl-2′-trimethylsilyloxyethyl)-1,3-butadiene and 2-(trimethylsilylmethyl)-1,3-butadiene yield the corresponding coupled products **1**–**4** when treated with the various (L)Fe^0 catalysts. In each case, the products corresponding

Table 1. The substrate and ligand dependency of the product distribution in the cross coupling of allylic ethers to isoprene (Scheme 1, $R^1 = CH_3$).

R^2	Solvent	Ligand	Product distribution						Yield [%] [9]
			1	**2**	**3**	**4**	C4:C1 addition	**1**:**2**	
CH_2Ph	benzene	2,2′-bipyridine	24.0	65.2	6.1	4.7	89.2 : 10.8	26.9 : 73.1	80
CH_2Ph	ether	2,2′-bipyridine	24.4	64.1	6.7	4.8	88.5 : 11.5	27.6 : 72.4	33
CH_2Ph	tetrahydrofuran	2,2′-bipyridine	32.1	59.7	7.1	1.1	91.8 : 8.2	35.0 : 65.0	—
$CH_2C_6H_{11}$	benzene	2,2′-bipyridine	18.4	71.5	7.2	2.9	89.9 : 10.1	20.5 : 79.5	42
THP	benzene	2,2′-bipyridine	29.6	62.2	4.4	3.8	91.8 : 8.2	32.2 : 67.8	52
CH_2Ph	benzene	2,2′-biquinoline	59.6	4.1	11.8	24.5	63.7 : 36.3	93.6 : 6.4	33
CH_2Ph	benzene	1,10-phenanthroline	59.9	7.4	11.9	20.8	67.3 : 32.7	89.0 : 11.0	46
CH_2Ph	benzene	4,5,6,7-Me_4-1,10-phen	58.6	4.7	11.7	25.0	63.3 : 36.7	92.6 : 7.4	29
CH_2Ph	benzene	pyridine (one equiv)	57.6	3.9	9.3	29.2	61.5 : 38.5	93.7 : 6.3	70
CH_2Ph	benzene	none	60.5	3.9	10.5	25.1	64.4 : 35.6	93.9 : 6.1	88

to isomers **1** and **3** are formed as *single trisubstituted olefin isomers* possessing the indicated *E*-geometry. The selectivity trends are similar to those observed with isoprene. For example, myrcene reacts with allyl benzyl ether in the presence of 10 mol-% (bpy)Fe^0 (benzene, 25°C, 21 h, 79%) to give an 8.0:59.2:13.7:19.1 mixture of **1-4** ($R^1 = CH_2CH_2CH{=}C(CH_3)_2$, $R^2 = CH_2Ph$), while the (pyr)Fe^0-catalyzed reaction (benzene, 25°C, 12 h, 82%) leads to a product mixture of the composition **1**:**2**:**3**:**4** = 63.3:27.1:4.4:5.2. Other dienes such as 1-vinylcyclohexene, 1,3-decadiene and 2-(α-acetoxybenzyl)-1,3-butadiene are not efficiently coupled to allyl benzyl ether under the influence of the (L)Fe^0 catalysts examined to date.

Received: February 3, 1987;
revised: July 9, 1987 [Z 2084 IE]
German version: *Angew. Chem. 99* (1987) 1073

[1] a) R. Scheffold: *Modern Synthetic Methods, Vol. 3*, Wiley, New York 1983; b) S. G. Davies: *Organotransition Metal Chemistry: Application to Organic Synthesis*, Pergamon, New York 1982; c) H. M. Colquhoun, J. Horton, D. J. Thompson, M. V. Twigg: *New Pathways for Organic Synthesis: Practical Application of Transition Metals*, Plenum, New York 1984; for specific examples illustrating the synthetic utility of organoiron chemistry see: d) M. F. Semmelhack, H. T. M. Le, *J. Am. Chem. Soc. 107* (1985) 1455; e) A. J. Pearson, C. W. Ong, *J. Org. Chem. 47* (1982) 3780; f) M. Rosenblum, M. M. Turnbull, B. M. Foxman, *Organometallics 5* (1986) 1062; g) M. E. Wright, G. O. Nelson, R. S. Glass, *ibid. 4* (1985) 245; h) H. tom Dieck, R. Diercks, *Angew. Chem. 95* (1983) 801; *Angew. Chem. Int. Ed. Engl. 22* (1983) 778; *Angew. Chem. Suppl. 1983*, 1138; i) H. Hoberg, K. Jennig, C. Krüger, E. Raabe, *ibid. 98* (1986) 819 and *25* (1986) 810.

[2] For examples illustrating other transition metal mediated olefin cross coupling reactions see: a) B. M. Trost, J. Y. L. Chung, *J. Am. Chem. Soc. 107* (1985) 4586; b) P. A. Wender, N. C. Ihle, *ibid. 108* (1986) 4678; c) B. M. Trost, *Angew. Chem. 98* (1986) 1; *Angew. Chem. Int. Ed. Engl. 25* (1986) 1; d) T. Antonsson, A. Heumann, C. J. Moberg, *J. Chem. Soc. Chem. Commun. 1986*, 518; e) L. E. Overman, A. F. Renaldo, *Tetrahedron Lett. 24* (1983) 2235; f) W. D. Wulff, R. W. Kaesler, G. A. Peterson, P.-C. Tang, *J. Am. Chem. Soc. 107* (1985) 1060; g) B. C. Berris, G. H. Hovakeemian, Y.-H. Lai, H. Mestdagh, K. P. C. Vollhardt, *ibid. 107* (1985) 5670; h) H. Yasuda, K. Tatsumi, A. Nakamura, *Accts. Chem. Res. 18* (1985) 120; i) G. Buono, C. S. G. Peiffer, C. Triantaphylides, P. Denis, A. Mortreux, F. Petit, *J. Org. Chem. 50* (1985) 1782; j) P. Brun, A. Tenaglia, B. Waegell, *Tetrahedron Lett. 24* (1983) 385; k) H. Lehmkuhl, Y. L. Tsien, *Chem. Ber. 116* (1983) 2437.

[3] J. M. Takacs, L. G. Anderson, G. V. B. Madhavan, M. W. Creswell, F. L. Seely, W. F. Devroy, *Organometallics 5* (1986) 2395.

[4] a) H. M. R. Hoffmann, *Angew. Chem. 81* (1969) 597; *Angew. Chem. Int. Ed. Engl. 8* (1969) 556; b) W. Oppolzer, V. Snieckus, *ibid. 90* (1978) 506 and *17* (1978) 476; c) W. Oppolzer, *ibid 96* (1984) 840 and *23* (1984) 876; d) D. F. Taber: *Intramolecular Diels-Alder and Alder-Ene Reactions*, Springer, New York 1984; e) B. B. Snider, *Acc. Chem. Res. 13* (1980) 426; f) W. Oppolzer, P. Schneider, *Tetrahedron Lett. 25* (1984) 3305; g) L. F. Tietze, U. Beifuss, *ibid. 27* (1986) 1767.

[5] B. M. Jacobson, G. M. Arvanitis, C. A. Eliasen, R. Mitelman, *J. Org. Chem. 50* (1985) 194.

[6] A. Carbonaro, A. Greco, G. Dall-Asia, *J. Organomet. Chem. 20* (1969) 177.

[7] Compounds **1-4** are formed as a mixture of *cis/trans* enol ethers (60:40). The ratios of **1-4** are determined by capillary gas chromatography after conversion to their ethylene acetals ($HOCH_2CH_2OH$/TsOH/THF). The ratio of isomeric products **1**:**2**:**3**:**4** does not change with the degree of conversion. Conversions are typically 60-100% after 8 h at 25°C. Cyclooligomerization of the 1,3-diene is competitive with the coupling reaction. No attempt to optimize the catalyst or reaction conditions with respect to this side reaction was made. Typically a three- to fivefold excess of 1,3-diene is employed.

[8] Similar regioselectivity has been observed in the oxidative coupling of tetrafluoroethylene to tricarbonyl(isoprene)iron(0): A. Bond, B. Lewis, M. Green, *J. Chem. Soc. Dalton Trans. 1975*, 1109.

[9] The regioselectivity of carbon-carbon bond formation with respect to the allyl ether component is also highly dependent upon the added ligand [4]. While the (bpy)Fe^0, (pyr)Fe^0, and "ligand-free" catalysts are highly selective toward the formation of products **1-4**, other (L)Fe^0 catalysts which we have examined are not. In those cases, a 30:70 mixture of 1,2- and 1,4-hydrovinylation products, **5** and **6**, can be isolated in addition to the 1,2- and 1,4-addition products, **1-4**. The ratio of addition to hydrovinylation coupling products in the reaction of allyl benzyl ether with isoprene catalyzed by (L)Fe^0 varies as a function of L; L = pyr: >95:5; bpy: >95:5; 2,2'-biquinoline: 55:45; 1,10-phenanthroline: 56:44; 2,9-dimethyl-1,10-phenanthroline: 46:54; 3,4,5,6-tetramethyl-1,10-phenanthroline: 34:66. The chemical yields cited in Table 1 are for the addition products **1-4** only.

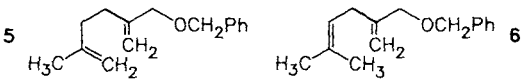

Stereoselective Synthesis of (*E*)-3-Methylene-4-alken-2-ones from Aldehydes and Methyl Vinyl Ketone and Their Spontaneous Dimerization**

By *H. M. R. Hoffmann,* Ulrike Eggert,* and *Wolfgang Poly*

Dedicated to Professor Ulrich Schöllkopf on the occasion of his 60th birthday

3-Methylene-4-alken-2-ones of type **1** were hitherto unknown, although **2**[1] and the trimethylated derivative **3**[2] have been reported.[3,4] The parent compound **1a** (R = H)[5] has also been isolated as the stable tricarbonyliron complex **4**.[2]

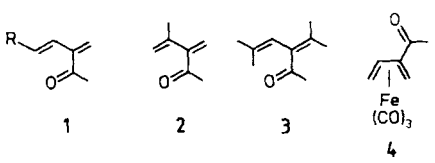

We describe a facile two-step route to *E*-configurated oxodienes **1** and show that such functionalized dienes dimerize spontaneously and regioselectively.

Coupling of aldehydes **5** with methyl vinyl ketone as Michael acceptor in the presence of 1,4-diazabicyclo[2.2.2]octane (DABCO)[6] affords the 4-hydroxy-3-methylene-2-alkanones **6**, whose dehydration should furnish

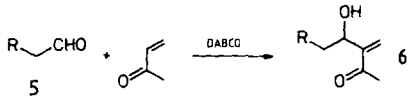

the desired 3-methylene-4-alken-2-ones. However, given rotamers **6A** and **6B** and an antiperiplanar E2 transition state, both the *E*-configurated diene **1** and its *Z*-isomer **7** seem feasible as the reaction products.

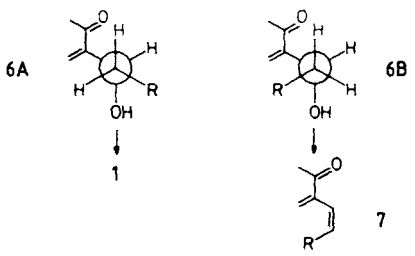

[*] Prof. H. M. R. Hoffmann, U. Eggert, Dipl.-Chem. W. Poly
Institut für Organische Chemie der Universität
Schneiderberg 1 B, D-3000 Hannover 1 (FRG)

[**] DABCO-Catalyzed Coupling of Aldehydes with Activated Double Bonds, Part 7. This work was supported by the Deutsche Forschungsgemeinschaft and the Fonds der Chemischen Industrie. We thank *N. Daude* for experimental contributions.—Part 6: [7].

Orienting experiments showed that mild conditions were necessary in order to suppress *E/Z* isomerization, 1,5-hydrogen shifts, and other undesirable side reactions.

When the β-ketoallyl alcohols **6** were allowed to react with methanesulfonyl chloride/DABCO at 0°C to room temperature and the reaction mixture was worked up after 1 day, neither the monomer **1** nor its *Z*-isomer **7** were obtained. Instead, the functionalized 1,4-diacetylcyclohexenes **8** were isolated in good to very good yields (Table 1).

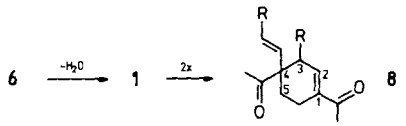

Several stereochemical features of the sequence **6**→**1**→**8** are of interest.

1. *E-Selectivity of the formation of the monomer.* All dimers **8b–i** showed an *E*-configurated exocyclic CC-double bond. No isomer with a *Z*-olefinic bond was detected. Thus, the monomer intermediate is **1** rather than **7**.
2. *Regioselectivity of dimerization.* The dimerization proceeds with unusual ease and is highly *para*-selective to give **8**. No *meta*-oriented dimers (cf. dimerization of **2**[1]) were detected.
3. *Stereochemistry of dimerization.* Column chromatography combined with ^{13}C-NMR allowed us to establish two stereochemical series, consisting of the major and the minor stereoisomer of the dimerization. Table 1 lists the diagnostic ^{13}C-NMR signals for each series. Dimer **8d** (the major stereoisomer) was subjected to a double haloform reaction giving the diacid, which was converted into the diester **9**. Comparison of the spectra (^{1}H-NMR, ^{13}C-NMR, IR) showed the diester **9** to be identical with the major stereoisomer formed in the dimerization of diene ester **10**. The dimer from the latter

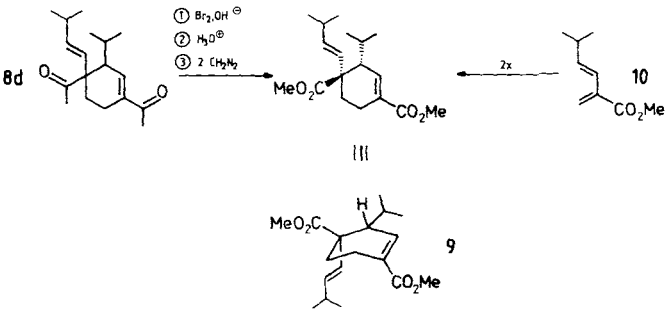

reaction is probably the *endo* dimer,[7] i.e., the alkenyl side chain in **9** is *endo* with respect to a rooflike cyclohexene moiety, and the 3-isopropyl group is *trans* to the 4-methoxycarbonyl group. Thus, the dimerization of **1d** and of the other dienes **1** is moderately *endo*-selective, contrary to that of the corresponding diene esters (e.g. **10**).[7]

The DABCO-catalyzed coupling of methyl vinyl ketone with aldehydes (**5**) to give **6** and in-situ dimerization of the dehydration product **1** to functionalized 1,4-diacetylcyclohexenes **8** is thus an efficient and short procedure, which starts from inexpensive educts and creates four new σ bonds and two new unsaturated CC-bonds in convergent fashion. The products, which are formed *para*-selectively and contain a quaternary carbon, are of interest in terpene synthesis, e.g., for preparing spirocyclic compounds. The

Table 1. Characteristic ^{13}C-NMR signals (in $CDCl_3$) of the major (δ_1) and the minor stereoisomers (δ_2) of **8a–i** and yields after chromatography.

Compd	R	δ_1, δ_2, $\Delta=\delta_1-\delta_2$ C-1	C-2	C-3	C-4	C-5	H/N	$\tilde{\nu}$(C=C) [cm^{-1}]	Yield [%]
8a	H	138.4	139.5 [or	31.9	53.4	—	—	—	41
		—	138.1]	—	—	—			
		—		—	—	—			
8b	Me	136.1	145.6	34.1	55.4	—		1160	62
		138.1	142.5	36.4	56.4		4:1		
		−2.0	+3.1	−2.3	1.0				
8c	Et	136.8	144.1	40.9	56.8	—	—	1160	69
		139.8	140.6	43.4	55.7				
		−3.0	+3.5	−2.5	+1.1				
8d	*i*Pr	138.5	—	43.9	56.6	25.6	5:3	1155	73
		140.5		47.5	55.9	24.5			
		−2.3		−3.6	+0.7	+1.1			
8e	*t*Bu	137.5	—	49.3	57.5	26.0	5:2	1160	40
		140.4		53.1	55.6	23.7			
		−2.9		−3.8	+1.9	+2.3			
8f	CH_2OMe	137.9	141.4	40.0	55.3	26.6	—	1155	78
		139.5	138.4	43.2	54.3	—			
		−1.6	+3.0	−3.2	+1.0	—			
8g	CH_2CO_2Me	137.3	142.2	35.8	56.4	24.5	5:2	—	66
		138.5	140.2	—	55.8	—			
		−1.2	+2.0	—	+0.6	—			
8h	$CH_2CH_2CO_2Me$	137.4	142.5	38.4	56.7	24.7	ca. 2:1	—	70
		139.5	139.3	40.4	55.7	—			
		−2.1	+3.2	−2.0	+1.0	—			
8i	CH_2Ph	—	143.7	41.4	56.8	24.9	8:3	1155	91
			140.8	43.7	56.0	24.1			
			+2.9	−2.3	+0.8	+0.8			

procedure allows also for the introduction of further functionality via the aldehyde **5**.

Experimental procedure

6: Methyl vinyl ketone (7.01 g, 100 mmol), aldehyde **5** (100 mmol), and DABCO (1.68 g, 15 mmol) were dissolved in anhydrous THF (25 mL) and left at room temperature. After 7 days the solution was diluted with diethyl ether, washed with dilute hydrochloric acid and aqueous $NaHCO_3$, and dried ($MgSO_4$). The crude product was purified by chromatography on silica gel (diethyl ether–light petroleum) or distilled in a Kugelrohr apparatus.

8: The coupling product **6** (10 mmol), DABCO (3.37 g, 30 mmol) and *p*-dimethylaminopyridine (120 mg, 1 mmol) were dissolved in anhydrous CH_2Cl_2 (20 mL) and the solution cooled to 0°C. Methanesulfonyl chloride (1.37 g, 12 mmol) in anhydrous CH_2Cl_2 (10 mL) was added dropwise and the reaction mixture stirred for 24 h at room temperature. The mixture was worked up by dilution with CH_2Cl_2, washing with water (3×), drying ($MgSO_4$), and removal of the solvent. The crude mixture of stereoisomers was purified on silica gel/diethyl ether-light petroleum and—when possible—separated (cf. Table 1).

Received: May 18, 1987;
supplemented: July 7, 1987 [Z 2244 IE]
German version: *Angew. Chem. 99* (1987) 1047

[1] R. Lantzsch, D. Arlt, *Justus Liebigs Ann. Chem. 1976*, 1757.
[2] M. Franck-Neumann, D. Martina, F. Brion, *Angew. Chem. 93* (1981) 900; *Angew. Chem. Int. Ed. Engl. 20* (1981) 864.
[3] The synthesis and characterization of a series of *E*-configurated 5-aryl-3-methylene-4-penten-2-ones (**1**: R=aryl) have been claimed [4]. These dienes were thought "not to take part in the Diels-Alder Reaction ... or in polymerization reactions." In the dehydration of **6j** (R=Ph) we obtained dimer **8j** (R=Ph), m.p. 125–128°C, 38% yield.—^{1}H-NMR (200 MHz, $CDCl_3$): δ=2.19 (s, 3H, CH_3CO), 2.31 (s, 3H, CH_3CO), 1.9–2.8 (m, 4H, $2CH_2$), 4.44 (d, J=5.0 Hz, 1H, 3-H), 5.72 (d, J=16.5 Hz, 1H, olefin-H), 6.21 (d, J=16.5 Hz, 1H, olefin-H), 6.98 (m, 1H, olefin-H), 7.05–7.30 (m, 10H, phenyl-H). ^{13}C-NMR ($CDCl_3$, selection): δ=208.6 s, 198.8 s (2×C=O), 141.5 (d, C-2), 57.2 (s, C-4), 46.4 (d, C-3), 25.5 q, 25.3 q (2×CH_3), 24.6 (t, C-5), 20.8 (t, C-6).
[4] M. I. Shevchuk, I. V. Megera, N. A. Burachenko, A. V. Dombrovskii, *Zh. Org. Khim. 10* (1974) 167, English translation. Cf. *Chem. Abstr. 80* (1974) 121064j.
[5] J. F. Honek, M. L. Mancini, B. Belleau, *Synth. Commun. 14* (1984) 483.
[6] H. M. R. Hoffmann, J. Rabe, *Angew. Chem. 95* (1983) 795; *Angew. Chem. Int. Ed. Engl. 22* (1983) 795; J. Rabe, H. M. R. Hoffmann, *ibid. 95* (1983) 796 and *22* (1983) 796; H. M. R. Hoffmann, J. Rabe, *J. Org. Chem. 50* (1985) 3849; C. Grundke, H. M. R. Hoffmann, *Chem. Ber. 120* (1987) 1461; D. Basavaiah, V. V. L. Gowriswari, *Tetrahedron Lett. 27* (1986) 2031; H. Amri, J. Villieras, *ibid. 27* (1986) 4307; F. Ameer, S. E. Drewes, P. T. Kaye, G. Loizou, D. G. Malissar, G. H. P. Roos, *S. Afr. J. Chem. 40* (1987) 35, and references cited therein.
[7] W. Poly, D. Schomburg, H. M. R. Hoffmann, unpublished.

Adsorption and Curvature in Highly Dealuminated Zeolites**

By *Ronnie Thomasson, Sven Lidin,* and *Sten Andersson**

We have recently shown that the silicon and oxygen atoms in a zeolite structure like faujasite reside on a surface parallel to the periodic minimal surface, the so-called *D*-surface.[1] Extensive Ewald calculations of electrostatic point charge distributions by *von Schnering* and *Nesper* have shown that there exist equipotential surfaces in solids which in fact are periodic minimal surfaces.[2]

It has also been shown that when gases are adsorbed by zeolites, the dispersion energy contribution to the physical bond between sorbate and sorbent varies according to the geometry of the local environment. The heats of sorption in zeolite cavities can be as much as eight times larger than those found for a corresponding smooth, planar surface of the same chemical composition.[3]

The total van der Waals force between two molecules is the sum of the van der Waals forces between atoms facing each other in the two molecules. Therefore, it generally, increases with the number of atoms and their atomic numbers and thus often appears to increase with the molecular weight. It is also well known that molecules of a homologue series are adsorbed by zeolites according to their molecular weight. Further, it is found that zeolites of different structures have different heats of sorption for the same molecule at the same temperature.

The purpose of this paper is to describe the adsorption process in a zeolite with the concept of intrinsic curvature. We have already shown in earlier works that the atoms in the faujasite, cristobalite, diamond or silicon structure lie on a surface parallel to the *D*-surface.[1a] This is shown schematically in Figure 1 for a (110) plane of the structure of cristobalite. The curved line corresponds to a principal line of curvature in the *D*-surface.

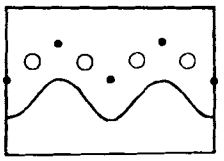

Fig. 1. (110) section of the structure of cristobalite. The small circles represent silicon atoms, and the larger circles oxygen atoms. The curve is the minimal surface D.

If we assume that this surface constitutes the path for molecules being adsorbed by a zeolite, and that such molecules move as particles, the well known equation

$$\boldsymbol{a} = \frac{\mathrm{d}\boldsymbol{v}}{\mathrm{d}t} = \frac{\mathrm{d}v}{\mathrm{d}t} \cdot \boldsymbol{u}_T + v^2 \cdot \kappa \boldsymbol{u}_N \qquad (1)$$

holds true ($\boldsymbol{a}$ is the acceleration, $\boldsymbol{v}$ is the velocity, v is the magnitude of velocity or speed, κ is the curvature, and $\boldsymbol{u}_T$ and $\boldsymbol{u}_N$ are tangent and normal vectors, respectively. If the molecules move on principal lines of curvature, the motion is curvilinear and uniform (the force lines are orthogonal to the curve, speed is constant) there is no tangent acceleration and

$$|a| = v^2\kappa \quad \text{or} \quad F = \mathrm{m}v^2\kappa \qquad (2)$$

The curvature in Figure 1 corresponds to a principal line of curvature for the *D*-surface, and then

$$\kappa = \sqrt{-K}$$

where K is the Gaussian curvature ($K=\kappa_1\cdot\kappa_2$ and for minimal surfaces $\kappa_1 = -\kappa_2$).

F is here a van der Waals force acting on a molecule from the zeolite surface, and is strongest when K is greatest, that is on the saddle points. However, during its motion, the molecule "feels" forces from a surface element and its integral curvature.

One of the most important equations in differential geometry is the Gauss-Bonnet equation

$$\iint_{ABC} K\,\mathrm{d}s = A + B + C - \pi \qquad (3)$$

[*] Prof. Dr. S. Andersson, R. Thomasson, S. Lidin
Chemical Center, University of Lund, Inorganic Chemistry 2
P.O. Box 124, S-221 00 Lund (Sweden)

[**] This work was supported by the Swedish Research Council. We thank Dr. *Zoltan Blum* for valuable discussions.

A, B, and C are here the interior angles in a geodesic triangle (easy to find in minimal surfaces), and K is the Gaussian curvature of a point inside the triangle. The integral curvature of a unit saddle with tetrahedral boundaries for the isometric surfaces D, P, and G is $-2/3\pi$. Required here, however, is an average Gaussian curvature, which we define as follows:

$$K_{av} = \frac{\text{integral curvature}}{\text{area}}$$

We have already reported on the calculation of the cartesian coordinates and Gaussian curvatures of the D, P, and G surfaces by the numerical integration of the Weierstrass equation.[1c] The area of the minimal surface was calculated using a result from elementary differential geometry: If dA is the area of a surface element S and dA' is the Gauss map S* of S, then

$$\lim_{A \to 0} \frac{A'}{A} = K$$

thus

$$\iint dA_S = \int\int_{S^*} \frac{dA'}{K}$$

The area of the surface contained in one unit cell of the dealuminized faujasite structure of $a = 24.20$ Å becomes 2261 Å^2, and a tetrahedral saddle 47.11 Å^2. And the average curvature is

$$K_{av} = -\frac{2}{3}\frac{\pi}{47.11} = -0.0445\ \text{Å}^{-2}$$

Inside a zeolite, molecules should experience an attractive force:

$$F = \text{const} \cdot N \cdot K_{av} \qquad (4)$$

Although mass or molecular weight is useful in explaining adsorption behavior, we use here N, the number of bonding electrons per molecule, which also reflects the nature of interaction between sorbate and sorbent in the group of molecules discussed below. The formula clearly shows how bond force depends on curvature, and the physical meaning of the sign of K_{av} is whether the sorbent surface is convex (+) or concave (−). Valleys or holes in a surface attract molecules, while hills or elevations repel them.

The differential heat of adsorption (ΔH) to be calculated should be valid for small uptake when adsorbate-adsorbate interaction is negligible. The adsorbate-adsorbent interaction should be as "clean" as possible as present in hydrophobic zeolites. The expression for ΔH now includes the distance between the adsorbed molecule and the host structure (harmonic motion) and we assume that it will not vary for a series of related compounds:

$$\Delta H = \text{const}_1 \cdot N \cdot K_{av} \qquad (5)$$

Recently *Stach* et al.[5] reported accurate calorimetric measurements on the adsorption of *n*-paraffins and related compounds in a US-Ex zeolite of the faujasite type with a Si/Al ratio = 95:1.

The peculiar shapes of the enthalpy curves for small adsorbed amounts are obviously due to the fact that the first molecules interact with saddles or sites with maximum curvature. We have therefore calculated integrated enthalpies up to 0.5 mmol adsorbate per gram zeolite from the data given by *Stach* et al.[5] This concentration corresponds to slightly less than 50% occupancy of the internal interface for the faujasite structure, and slightly more than 50% for the silicalite structure.

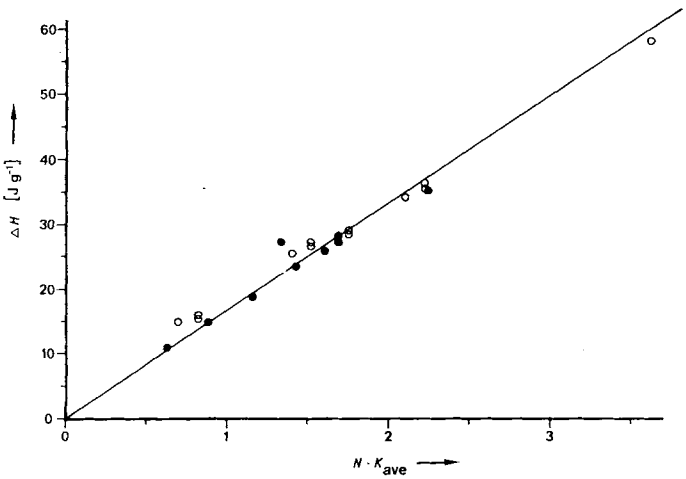

Fig. 2. Integrated heats of adsorption for various hydrocarbons vs. the product of curvature K_{av} and N (number of bonding electrons) in US-Ex and silicalite. Filled circles, in US-Ex, from left to right ethane, propane, *n*-butane, *n*-pentane, benzene, cyclohexane, *n*-hexane, *n*-hexane, *n*-octane; empty circles, in silicalite, from left to right ethene, ethane, ethane, 1-butene, *n*-butane, *n*-butane, cyclopentane, benzene, *n*-hexane, *n*-hexane, toluene, *n*-decane.

The product of N and curvature K_{av} is plotted versus ΔH in Figure 2 [cf. Eq. (5)]. *Stach* et al.[5] also made accurate measurements on the adsorption of some hydrocarbons on silicalite. This zeolite has a orthorhombic structure with ten-membered rings, for which we do not yet have a periodic minimal surface. However, with the knowledge of const_1 in Equation (5), and with known integrated ΔH and N for several different hydrocarbons, an average curvature for silicalite has been calculated to be -0.0584 Å^{-2} (see Fig. 2).

In conclusion it should be mentioned that the concept of curvature is useful for explaining why zeolites of different structures have different adsorption properties. We hope to be able to extend our studies to the ordinary alkali zeolites and their properties.

Received: April 27, 1987 [Z 2213 IE]
German version: *Angew. Chem.* *99* (1987) 1056

[1] a) S. Andersson, S. T. Hyde, H. G. von Schnering, *Z. Kristallogr. 168* (1984) 1; b) S. T. Hyde, S. Andersson, *ibid. 168* (1984) 221; c) *ibid. 170* (1985) 225; d) *ibid. 174* (1986) 225.
[2] R. Nesper, H. G. von Schnering, *Z. Kristallogr. 170* (1985) 138; *Angew. Chem. 98* (1986) 111; *Angew. Chem. Int. Ed. Engl. 25* (1986) 110; H. G. von Schnering, *Z. Kristallogr. 174* (1986) 182; review: H. G. von Schnering, R. Nesper, *Angew. Chem. 99* (1987) No. 11, *Angew. Chem. Int. Ed. Engl. 26* (1987) No. 11.
[3] L. V. C. Rees, *Chem. Ind. (London) 1984*, 252.
[4] N. E. Christiansen, *Phys. Rev. B32* (1985) 6490.
[5] H. Stach, U. Lohse, H. Tamm, W. Schirmer, *Zeolites 6* (1986) 74.

 © VCH Verlagsgesellschaft mbH, D-6940 Weinheim, 1987

Stereocontrolled Total Synthesis of Lipoxins A_5 and B_5**

By *K. C. Nicolaou,* S. E. Webber, J. Ramphal,* and *Y. Abe*

A recent report by *Wong* et al.[1] described the isolation of lipoxins A_5 (LXA_5, 5,6,15-trihydroxy-7,9,11,13,17-eicosapentaenoic acid) and B_5 (LXB_5, 5,14,15-trihydroxy-6,8,10,12,17-eicosapentaenoic acid) from incubation mixtures of porcine leukocytes and 15-hydroperoxyeicosapentaenoic acid (15-HPEPE). In view of the current nutritional and biomedical interest[2] in eicosapentaenoic acid (EPA) and its metabolites and the minute quantities in which these substances are available from biosynthetic schemes coupled with the uncertainty regarding their precise structures and biological profiles, we undertook their total synthesis. We now report the first total synthesis of (5*S*,6*R*,15*S*)-5,6-15-trihydroxy-7,9,11,13,17-eicosapentaenoic acid (LXA_5) and (5*S*,14*R*,15*S*)-5,14,15-trihydroxy-6,8,10,12,17-eicosapentaenoic acid (LXB_5), the two structures suspected of being the natural stereoisomers by analogy to the structures of lipoxins A_4 (LXA_4)[3] and B_4 (LXB_4).[4]

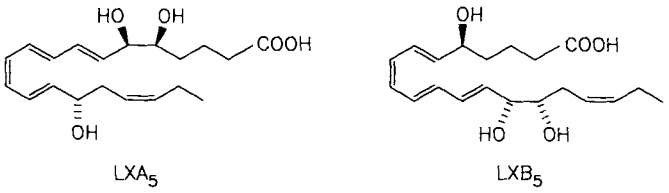

The synthetic schemes for the construction of LXA_5 and LXB_5 were based on our recently established general strategy towards linear eicosanoids.[5] This efficient strategy involves Pd^0–Cu^I catalyzed coupling of terminal acetylenes with vinyl halides[6] to construct the eicosanoid skeleton and Lindlar hydrogenation to secure the *Z* olefins stereoselectively. Scheme 1 outlines the synthesis of LXA_5 starting with the readily available *R*-epoxyalcohol **1**.[7] Thus, 1-lithiobutyne reacts with the THP ether of **1** in the presence of TMEDA in THF (−78→25 °C) to afford compound **3** in 77% yield. Selective hydrogenation of the triple bond in **3** ((Lindlar catalyst, Fluka, hexane) led to olefin **4** (91%), which was transformed by standard chemistry to aldehyde **7** via intermediates **5** and **6**. The *E*-vinyl iodide **8** was then prepared from **7** using $CrCl_2$–CHI_3 according to

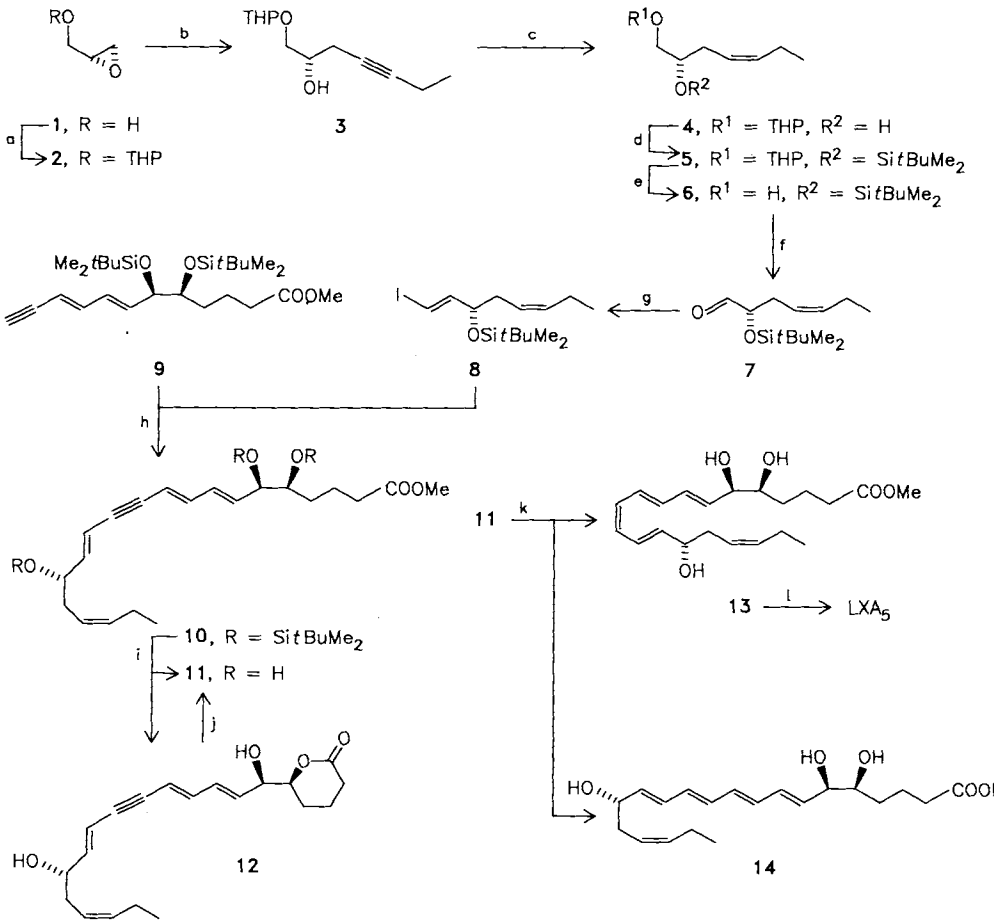

Scheme 1. Synthesis of LXA_5. Reagents and conditions. (a) 1.5 equiv. dihydropyran, TsOH catalyst, CH_2Cl_2, 0 °C, 2 h, 88%; (b) 5.0 equiv. 1-butyne, 1.1 equiv. *n*BuLi, 1.0 equiv. TMEDA, THF, −78→−20 °C, 1 h then add 0.5 equiv. **2**, −78→25 °C, 12 h, 77%; (c) 12% by weight Lindlar catalyst (Fluka), 1.0 equiv. quinoline, H_2, hexane, 25 °C, 91%; (d) 1.2 equiv. *t*$BuMe_2SiCl$, 2.5 equiv. imidazole, DMF, 25 °C, 12 h, 98%; (e) 4.0 equiv. Me_2AlCl, CH_2Cl_2, −30→25 °C, 95%; (f) 9.0 equiv. SO_3·pyridine, 20.0 equiv. Et_3N, DMSO, 25 °C, 85%; (g) 6.0 equiv. $CrCl_2$, 1.2 equiv. CHI_3, THF, 0 °C, 45%; (h) 1.0 equiv. **8**, 0.04 equiv. $[Pd(Ph_3P)_4]$, 1.4 equiv. *n*$PrNH_2$, benzene (degassed) then add 1.0 equiv. **9**, 0.16 equiv. CuI, 25 °C, 3 h, 94%; (i) excess HF·pyridine, THF, 0→25 °C, 3 h then saturated aqueous $NaHCO_3$ work-up, **11** (60%), **12** (24%); (j) 5.0 equiv. Et_3N, MeOH, 25 °C, 4 h, 83%; (k) 10% by weight (Lindlar catalyst (Fluka), 0.5 equiv. quinoline, H_2, CH_2Cl_2, 25 °C, 5 h, **11** (30%), **13** (51%), **14** (9%); (l) 2.0 equiv. LiOH, THF : H_2O (4 : 1), 25 °C then dilute aqueous H_2SO_4, pH 5–6, 90%.

the recently reported method of *Takai* et al.[8] in 45% yield. Coupling of **8** with the previously prepared[5b] terminal acetylene **9** under the standard Pd^0–Cu^I conditions[5] led to compound **10** in 94% yield. Desilylation of **10** with pyridinium fluoride gave, in addition to the expected product **11** (60%), the δ-lactone **12** (24%). Compound **12** was con-

[*] Prof. K. C. Nicolaou, Dr. S. E. Webber, J. Ramphal, Dr. Y. Abe
Department of Chemistry, University of Pennsylvania
Philadelphia, PA 19104 (USA)

[**] This work was financially supported by the National Institutes of Health, Merck Sharp and Dohme, Smith Kline & French, and Hoffmann-La Roche, USA.

verted into **11** by exposure to Et_3N in MeOH (83%). Finally, controlled hydrogenation of **11** (Lindlar catalyst, Fluka, quinoline, CH_2Cl_2), gave LXA_5 methyl ester **13** (51%), its all-*trans* isomer **14** (9%), and unreacted starting material **11** (30%), which were separated by HPLC [reverse phase; altex-ultrasphere ODS, 5-μm particle size; MeOH : H_2O (70 : 30); 3.5 mL/min; retention times: 9.4 min (**11**); 11.6 min (**14**); 12.7 min (**13**)]. LXA_5 methyl ester **13** was found to isomerize slowly at ambient temperatures to the all-*trans* isomer **14**, a conversion which was accelerated by catalytic amounts of iodine. Hydrolysis of **13** to LXA_5 was carried out with LiOH in aqueous THF.[5a]

The synthesis of LXB_5 and its methyl ester **29** utilized the readily accessible optically active hydroxyepoxide **15**[9] and vinyl bromide **25**[10] as starting materials and proceeded along similar lines as described above for the synthesis of LXA_5. Scheme 2 summarizes the chemistry involved in this synthesis including reagents, conditions, and yields. LXB_5 methyl ester (**29**) was purified by HPLC as described above (retention time = 13 min) and was also observed to isomerize slowly to its all-*trans* isomer (**30**) at ambient temperatures, a process found to be catalyzed by trace amounts of iodine. LXB_5 itself could be generated from **29** by saponification as in the case of LXA_5. Some

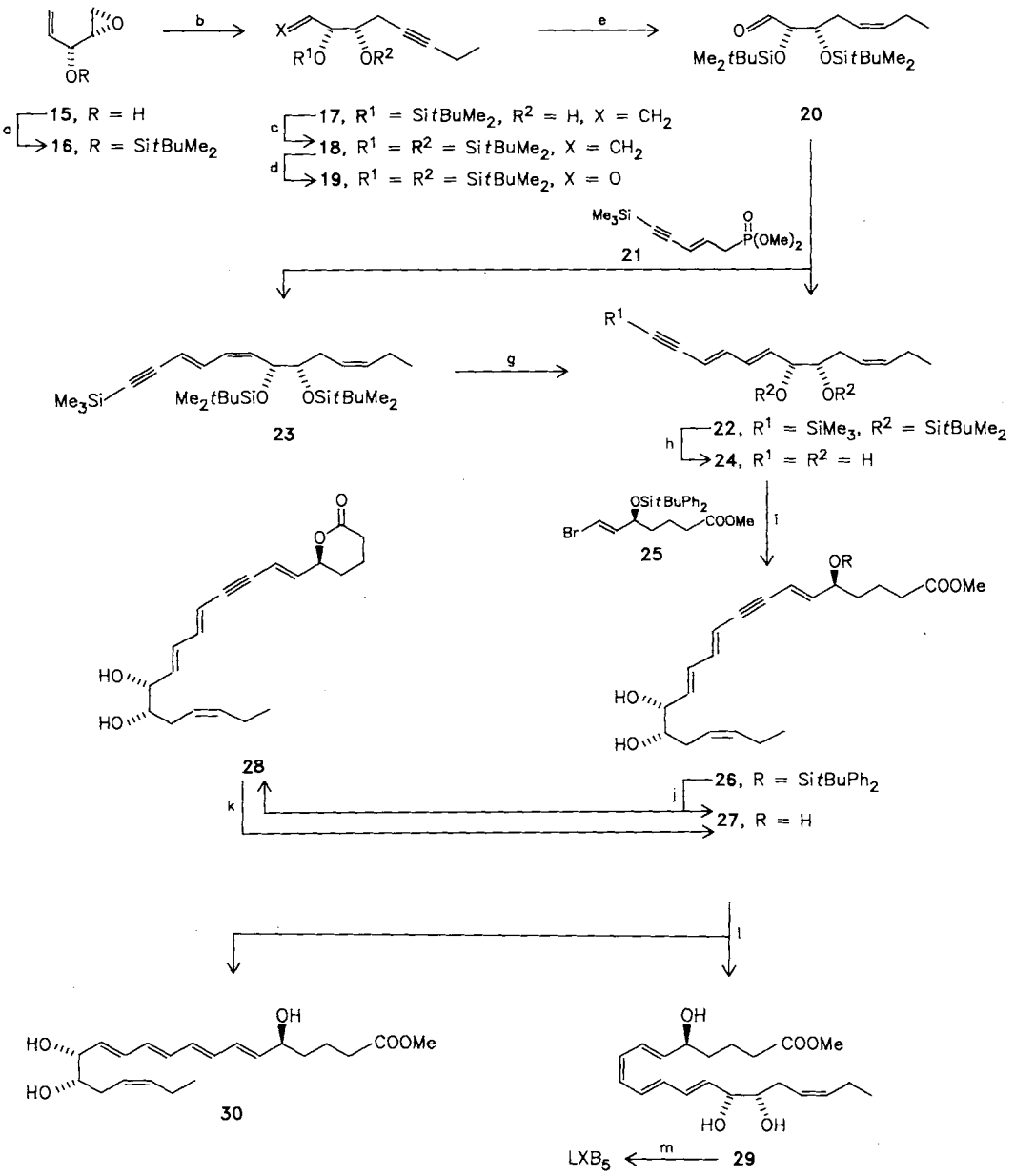

Scheme 2. Synthesis of LXB_5. Reagents and conditions. (a) 1.1 equiv. *t*$BuMe_2SiCl$, 2.0 equiv. imidazole, DMF, 25 °C, 12 h, 90%; (b) 5.0 equiv. 1-butyne, 1.3 equiv. *n*BuLi, 1.8 equiv. Et_2AlCl [11], toluene, 0→25 °C, then add 1.0 equiv. **16**, 25→60 °C, 4 h, 77%; (c) same as (a) above, 88%; (d) O_3, CH_2Cl_2, −78 °C, then add 1.1 equiv. Ph_3P, −78→25 °C, 2 h, 82%; (e) 20% by weight, Lindlar catalyst (Fluka), EtOAc : hexane (4 : 1), 25 °C, 4 h, 85%; (f) 1.5 equiv. **21**, 1.3 equiv. $LiN(SiMe_3)_2$, THF, −78 °C, 0.5 h then 0 °C, 5 min, then add 1.0 equiv. **20**, −78→25 °C, 2 h, 80%; (g) 0.007 equiv. I_2, benzene, 25 °C, 4 h, 93%; (h) 5.0 equiv. *n*Bu_4NF, THF, 0→25 °C, 1 h, 81%; (i) 1.2 equiv. **24**, 0.02 equiv. $[Pd(Ph_3P)_4]$, Et_2NH (solvent, 1.4 M, degassed) then add 1.0 equiv. **25**, 0.16 equiv. CuI, 25 °C, 4 h, 82%; (j) excess HF·pyridine, THF, 0→25 °C, 14 h then saturated aqueous $NaHCO_3$ work-up, **27** (70%), **28** (15%); (k) 5.0 equiv. Et_3N, MeOH, 25 °C, 4 h, **27** (85%); (l) 10% by weight Lindlar catalyst (Fluka), 0.5 equiv. quinoline, H_2, CH_2Cl_2, 25 °C, 6 h, **27** (25%), **29** (55%), **30** (8%); (m) 2.0 equiv. LiOH, THF : H_2O (4 : 1), 25 °C then dilute aqueous H_2SO_4, pH 5–6, 92%.

 © VCH Verlagsgesellschaft mbH, D-6940 Weinheim, 1987 0570-0833/87/1010-1020 $ 02.50/0 Angew. Chem. Int. Ed. Engl. 26 (1987) No. 10

important spectral and other physical data for compounds **10**, **13**, **26**, and **29** are summarized in Table 1.

Table 1. Selected physical data of the compounds **10**, **13**, **26**, and **29**.

10: $R_f = 0.38$ (silica gel, petroleum ether:ether (95:5)); $[\alpha]_D^{23} = -8.1°$ ($c = 1.17$, $CHCl_3$); IR (film): $\tilde{\nu}_{max} = 3020$ (m), 2965 (vs), 2925 (vs), 2890 (s), 2860 (vs), 2180 (w), 1745 (s), 1425 (m), 1365 (m), 1255 (s), 1105 (s), 840 (vs), 775 (vs) cm^{-1}; ^1H-NMR (500 MHz, $CDCl_3$): $\delta = 6.55$ (dd, $J(9,10) = 15.4$ Hz, $J(8,9) = 10.8$ Hz, 1H, H-9), 6.16 (dd, $J(7,8) = 15.3$ Hz, $J(8,9) = 10.8$ Hz, 1H, H-8), 6.13 (dd, $J(13,14) = 15.7$ Hz, $J(14,15) = 5.3$ Hz, H-14), 5.80 (dt, $J(13,14) = 15.7$ Hz, $J(13,15) = J(10,13) = 1.9$ Hz, 1H, H-13), 5.72 (dd, $J(7,8) = 15.3$ Hz, $J(6,7) = 7.1$ Hz, 1H, H-7), 5.68 (dd, $J(9,10) = 15.6$ Hz, $J(10,13) = 2.1$ Hz, 1H, H-10), 5.46 (m, 1H, H-17), 5.32 (m, 1H, H-18), 4.19 (m, 1H, H-15), 3.97 (m, 1H, H-6), 3.66 (s, 3H, $COOCH_3$), 3.56 (m, 1H, H-5), 2.28 (t, $J(2,3) = 7.4$ Hz, 2H, H-2), 2.24 (m, 2H, H-16), 2.02 (m, 2H, H-19), 1.68 (m, 2H, H-3), 1.50 (m, 2H, H-4), 0.95 (t, $J(19,20) = 7.5$ Hz, 3H, H-20), 0.89–0.86 (theee singlets, total 27H, Si*t*Bu), 0.05–0.00 (six singlets, total 18H, $SiMe_2$); UV (qualitative, MeOH): $\lambda_{max} = 282$, 296, 314 nm

13: $R_f = 0.16$ (silica gel, CH_2Cl_2:MeOH (95:5)); $[\alpha]_D^{23} = +11.2°$ ($c = 1.76$, $CHCl_3$); IR ($CHCl_3$): $\tilde{\nu}_{max} = 3610$ (m), 3020 (s), 2965 (m), 2935 (m), 2880 (m), 1735 (vs), 1440 (m), 1380 (m), 1220 (s), 1075 (m), 1000 (s), 980 (vs), 665 (m) cm^{-1}; ^1H-NMR (500 MHz, $CDCl_3$): $\delta = 6.58$ (m, 2H, H-10,13), 6.35 (dd, $J(7,8) = 15.0$ Hz, $J(8,9) = 10.8$ Hz, 1H, H-8), 6.21 (dd, $J(9,10) = 14.5$ Hz, $J(8,9) = 10.8$ Hz, 1H, H-9), 5.99 (m, 2H, H-11, 12), 5.76 (dd, $J(13,14) = 15.0$ Hz, $J(14,15) = 5.7$ Hz, 1H, H-14), 5.75 (dd, $J(7,8) = 15.0$ Hz, $J(6,7) = 7.8$ Hz, 1H, H-7), 5.56 (m, 1H, H-17), 5.33 (m, 1H, H-18), 4.24 (m, 1H, H-15), 4.11 (m, 1H, H-6), 3.66 (m, 1H, H-5), 3.63 (s, 3H, $COOCH_3$), 2.32 (m, 5H, H-2,16, O*H*), 2.04 (m, 2H, H-19), 1.85 (br. s, 2H, O*H*), 1.81–1.66 (m, 2H, H-4), 1.40 (m, 2H, H-3), 0.94 (t, $J(19,20) = 7.5$ Hz, 3H, H-20); UV (qualitative, MeOH): $\lambda_{max} = 278$, 288, 302, 316 nm

26: $R_f = 0.29$ (silica gel, CH_2Cl_2:MeOH (95:5)); $[\alpha]_D^{23} = -89.9°$ ($c = 0.525$, $CHCl_3$); IR (film): $\tilde{\nu}_{max} = 3605$ (s), 3010 (s), 2980 (s), 2930 (vs), 2190 (w), 1735 (vs), 1440 (m), 1360 (m), 1255 (m), 1080 (m), 990 (s), 870 (m) cm^{-1}; ^1H-NMR (500 MHz, $CDCl_3$): $\delta = 7.63$ (m, 4H, aromatic), 7.40 (m, 6H, aromatic), 6.56 (dd, $J(11,10) = 15.4$ Hz, $J(11,12) = 10.9$ Hz, 1H, H-11), 6.34 (dd, $J(12,13) = 15.4$ Hz, $J(12,11) = 10.8$ Hz, 1H, H-12), 6.03 (dd, $J(6,7) = 15.7$ Hz, $J(6,5) = 5.95$ Hz, 1H, H-6), 5.82 (dd, $J(12,13) = 15.2$ Hz, $J(13,14) = 6.7$ Hz, 1H, H-13), 5.73 (d, $J(10,11) = 15.4$ Hz, 1H, H-10), 5.67 (d, $J(7,6) = 15.8$ Hz, 1H, H-7), 5.55 (m, 1H, H-17), 5.35 (m, 1H, H-18), 4.21 (m, 2H, H-5, 14), 5.70 (m, 1H, H-15), 3.59 (s, 3H, $COOCH_3$), 2.26 (m, 2H, H-16), 2.11 (t, $J(2,3) = 7.2$ Hz, 2H, H-2), 2.03 (m, 2H, H-19), 1.54 (br. s, 2H, O*H*), 1.43 (m, 4H, H-3, 4), 1.04 (s, 9H, Si*t*Bu), 0.95 (t, $J(20,19) = 7.5$ Hz, 3H, H-20); UV (MeOH): $\lambda_{max} = 283$, 297, 314 nm

29: $R_f = 0.22$ (silica gel, CH_2Cl_2:MeOH (95:5)); $[\alpha]_D^{23} = +14°$ ($c = 0.570$, MeOH); IR (film): $\tilde{\nu}_{max} = 3610$ (s), 3020 (m), 2970 (m), 2940 (m), 2880 (m), 1730 (vs), 1445 (m), 1380 (m), 1250 (m), 1075 (m), 1000 (s), 980 (s), 870 (m) cm^{-1}; ^1H-NMR (500 MHz, $CDCl_3$): $\delta = 6.68$ (m, 2H, H-10, 12), 6.36 (dd, $J(7,6) = 14.9$ Hz, $J(7,8) = 10.5$ Hz, 1H, H-7), 6.23 (m, 2H, H-8, 9), 5.99 (m, 1H, H-11), 5.78 (dd, $J(6,7) = 15.2$ Hz, $J(6,5) = 6.9$ Hz, 1H, H-6), 5.72 (dd, $J(13,12) = 15.1$ Hz, $J(13,14) = 6.6$ Hz, 1H, H-13), 5.55 (m, 1H, H-17), 5.33 (m, 1H, H-18), 4.20 (m, 2H, H-5, 14), 3.69 (m, 1H, H-15), 3.64 (s, 3H, $COOCH_3$), 2.33 (t, $J(2,3) = 7.2$ Hz, 2H, H-2), 2.24 (m, 2H, H-16), 2.15 (m, 2H, H-19), 2.02 (m, 2H, H-4), 1.73–1.61 (m, 2H, H-3), 1.57 (br. s, 3H, O*H*), 0.93 (t, $J(20,19) = 7.5$ Hz, 3H, H-20); UV (MeOH): $\lambda_{max} = 315$, 301, 288 nm

The described chemistry renders these two new metabolites of eicosapentaenoic acid (EPA), LXA_5 and LXB_5, readily available and in optically active form. Comparisons of the synthetic compounds with naturally derived LXA_5 and LXB_5 and biological investigations with these compounds are currently in progress.[12]

Received: June 10, 1987;
revised: July 20, 1987 [Z 2292 IE]
German version: *Angew. Chem. 99* (1987) 1077

[1] P. Y.-K. Wong, R. Hughes, B. Lam, *Biochem. Biophys. Res. Commun. 126* (1985) 763.
[2] M. H. Davidson, P. R. Liebson, *Cardiovasc. Rev. Rep. 7* (1986) 461.
[3] C. N. Serhan, K. C. Nicolaou, S. E. Webber, C. A. Veale, S.-E. Dahlen, T. J. Pulustinenen, B. Samuelsson, *J. Biol. Chem. 261* (1986) 16840.
[4] C. N. Serhan, M. Hamberg, B. Samuelsson, J. Morris, D. G. Wishka, *Proc. Natl. Acad. Sci. USA 83* (1986) 1983.
[5] a) K. C. Nicolaou, S. E. Webber, *J. Am. Chem. Soc. 106* (1984) 5734; b) K. C. Nicolaou, C. A. Veale, S. E. Webber, H. Katerinopoulos, *ibid. 107* (1985) 7515; c) K. C. Nicolaou, S. E. Webber, *Synthesis 1986*, 453; d) K. C. Nicolaou, S. E. Webber, *J. Chem. Soc. Chem. Commun. 1986*, 1816.
[6] a) K. Sonogashira, Y. Tohda, N. Hogihara, *Tetrahedron Lett. 1975*, 4467; b) V. Ratovelomana, G. Linstrumelle, *Synth. Commun. 11* (1981) 917.
[7] J. M. Klunder, S. Y. Ko, K. B. Sharpless, *J. Org. Chem. 51* (1986) 3710.
[8] T. Takai, K. Nitta, K. Utimoto, *J. Am. Chem. Soc. 108* (1986) 7408.
[9] a) S. L. Schreiber, T. S. Schreiber, D. B. Smith, *J. Am. Chem. Soc. 109* (1987) 1525; b) R. E. Babine, *Tetrahedron Lett. 27* (1986) 5791; c) B. Hafele, D. Schroter, V. Jager, *Angew. Chem. 98* (1986) 89; *Angew. Chem. Int. Ed. Engl. 25* (1986) 87.
[10] This vinyl bromide was prepared according to the procedure described in Ref. [5c] for its *tert*-butyldimethylsilyl counterpart.
[11] R. S. Matthews, D. J. Eickhoff, *J. Org. Chem. 50* (1985) 3923.
[12] New compounds exhibited satisfactory spectral and analytical/exact mass data. Yields refer to spectroscopically and chromatographically homogeneous materials.

1,8-Naphthalene-Linked Cofacial Dimeric Phthalocyanines**

By *Clifford C. Leznoff,* Herman Lam, W. Andrew Nevin, Nagao Kobayashi, Pavel Janda,* and *A. B. P. Lever*

Binuclear phthalocyanines covalently linked by five,[1,2] four,[3] two,[3] one,[4] and "−1"[5] atom bridges have been recently described. We now report new cofacial binuclear phthalocyanines **1a–d** linked by a triatomic bridge on a rigid naphthalene framework. These compounds complement 1,8-anthracene bridged porphines,[6,7] and provide entry to a new class of pillared phthalocyanines. They

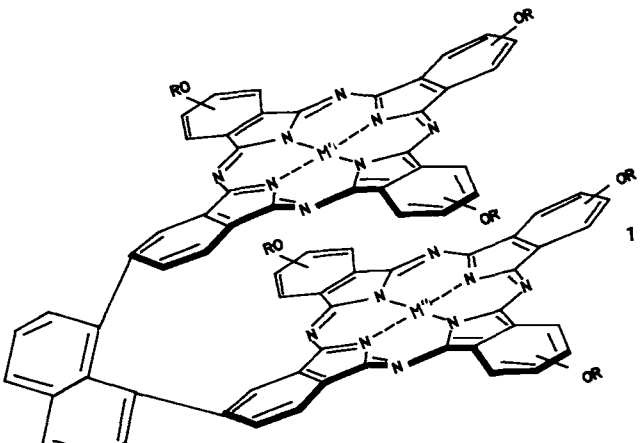

1

a: R = $CH_2C(CH_3)_3$, M' = M'' = H_2
b: R = $CH_2C(CH_3)_3$, M' = M'' = Co^{II}
c: R = $CH_2C(CH_3)_3$, M' = M'' = Cu^{II}
d: R = $CH_2C(CH_3)_3$, M' = M'' = Zn^{II}
e: R = $CH_2C(CH_3)_3$, M' = Co^{I}, M'' = Co^{II}
f: R = $CH_2C(CH_3)_3$, M' = M'' = Co^{I}

[*] Prof. C. C. Leznoff, H. Lam, Dr. W. A. Nevin, Prof. N. Kobayashi [+], Dr. P. Janda [++], Prof. A. B. P. Lever
Department of Chemistry, York University
4700 Keele Street, North York, Ontario M3J 1P3 (Canada)
[+] Visiting Professor from the Pharmaceutical Institute, Tohoku University, Japan.
[++] Visiting research associate from the Heyrovsky Institute of the Czech Academy of Sciences, Prague, Czechoslovakia.

[**] This work was supported by grants from the Natural Sciences and Engineering Research Council (Ottawa) and the Office of Naval Research (Washington). It was also partially funded by the Midwest Center for Mass Spectroscopy and the National Science Foundation Regional Instrumentation Facility (Grant No. CHE 8211164).

should prove of value in the photo- or electroactivation of small molecules, such as dioxygen, carbon or sulfur dioxide.

Treatment of 4-iodophthalonitrile **2** (4.0 g, 16 mmol) with 1,8-diiodonaphthalene **3** (2.0 g, 5.3 mmol) in a mixed coupling reaction, in the presence of elementary nickel powder under conditions described for homocoupling reactions[8,9] led to 1,8-bis(3,4-dicyanophenyl)naphthalene **4** (310 mg, 15.5% yield) as a mixture of *syn* and *anti* isomers due to restricted rotation about the 1,8-positions of the naphthalene nucleus. Conversion of **4** (380 mg, 1 mmol) into its dihydroisoindole **5** and a mixed condensation of **5** with the dihydroisoindole **6** prepared from 4-neopentyloxyphthalonitrile (6.0 g, 28 mmol) gave, following standard reaction conditions and chromatography,[1-5] the desired 1,8-bis-2'-(9',16',23'-trineopentyloxyphthalocyaninyl)naphthalene **1a** in 15.5% yield. The dicobalt, dicopper, and dizinc derivatives (**1b-d**) of **1a** were prepared by refluxing **1a** with $CoCl_2$, $Cu(OAc)_2$ and $Zn(OAc)_2$, respectively, as previously described.[1-5]

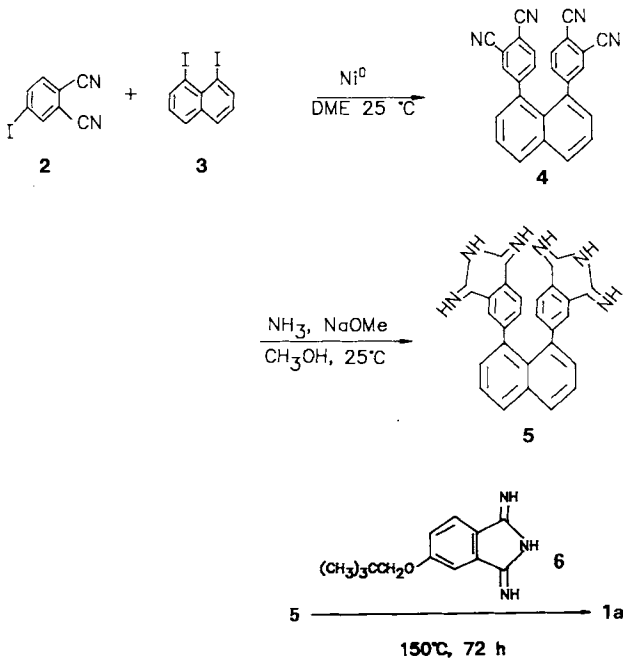

1a-d and **4** have been fully characterized.[10] The fast atom bombardment[11] (FAB) mass spectra **1a-d** were most informative, exhibiting parent ions as the base peak. Furthermore, no evidence of partially or half-metalated derivatives of **1b-d** were detected in their mass spectra. The ^{1}H-NMR spectrum of **1a** exhibited the upfield shifted NH protons which were absent in the spectrum of the zinc derivative **1d**.

Electrochemical and spectroelectrochemical results show that the rigid geometry of the naphthalene bridge induces important changes in the cofacial dicobalt derivative **1b**, compared with previously studied mononuclear and "clamshell" binuclear cobalt phthalocyanines.[1-4,12] The halves of the molecule of **1b** do not oxidize and reduce at the same potential, resulting in clear splitting of the redox couples. Cyclic and differential pulse voltammetry of **1b** in *o*-dichlorobenzene (0.2 M nBu_4NClO_4) revealed a series of three oxidation and four reduction waves with halfwave potentials of +0.53, +0.14, 0.00, −0.90, −1.29, −1.68, and −2.08 V vs $Fc^{\oplus}/Fc$ (Fc = ferrocene).[13,14] Comparison with the cyclic voltammogram of the mononuclear parent compound (2,9,16,23-tetrapentyloxyphthalocyaninato)cobalt CoTNPc ($E_{1/2}$ = +0.59, +0.03, −0.91, and −2.07 V in *o*-dichlorobenzene[12]) indicates splitting of the first oxidation ($L^{\oplus}/L$), and first reduction (Co^{II}/Co^{I}) couples by 140 and 390 mV, respectively. This is the first example of clearly observed splitting of the redox waves in a ring bridged binuclear metal-phthalocyanine and indicates a high degree of coupling between the halves of the molecule. Mixed valence $L^{\oplus}/L$ and Co^{II}/Co^{I} species are thus potentially available.

In contrast to **1b**, the splitting of the corresponding redox couple in the case of a so-called (−1) binuclear derivative (two phthalocyanine rings sharing a common benzene ring)[5] was less than 100 mV (shoulder) in the mixed valence Co^{II}-Co^{I} species. The reduction couples at −0.90 and −1.29 V were investigated by controlled potential electrolysis in an optically transparent thin layer electrode (OTTLE) cell utilizing a gold minigrid or platinum mesh working electrode. Stepwise reduction across each of the couples in turn gives the spectroscopic changes shown in Figure 1. Reduction over the first wave gives a green solution, with isosbestic points occurring at 322, 348, 545, 642, 664, and 760 nm (Fig. 1a). The spectrum is unlike any seen previously for a reduced cobalt-phthalocyanine, having a Q band at 650 nm. It does however exhibit a new absorption band in the region of 450–470 nm associated with metal-to-ligand charge transfer (MLCT) [Co^{I}Pc[d(xz,yz)]→π*($1b_{1u}$)Pc] of a Co^{I}Pc species,[12,15,16] as well as a blue shift and increase in intensity of the Soret band.

The second reduction at −1.29 V (Fig. 1b) gives a yellow solution, with isosbestic points at 332, 395, 566, 678, and 758 nm. The final spectrum is very similar to that of the mononuclear Co^{I}TNPc species,[12] indicating that both cobalt atoms have been reduced to Co^{I}. The spectra are fully reversible by stepwise oxidation to the initial species.

Nernst plots of the spectroelectrochemical data over each of the reductions give slopes approaching 59 mV, showing that each step involves a one-electron transfer. Thus, the product of the reduction at −0.90 V must be a mixed valence species **1e**, of mainly [Co^{II}-Co^{I}] character. The intensity of the MLCT band is only 35% of that of the fully reduced Co^{I}-Co^{I} species **1f**, so that some delocalization of the added electron over the phthalocyanine ring system may be occurring. The presence of the well resolved Q band at 650 nm, rather than ca. 710 nm, may also indicate extensive delocalization throughout the molecule. A weak absorption occurs in **1e**, in the region of 800–900 nm (Fig. 1a), absent from the spectra of both **1b** and **1f** and which may be an intervalence band. The Q band region of the spectrum of **1e** mixed valence species is very different from that observed for the −1-bridged mixed valence Co^{II}-Co^{I} compound,[5] which has a split Q band at 700 and 760 nm.

Neither of the species **1b** or **1f** exhibit ESR absorption in *o*-dichlorobenzene. Species **1e**, however, exhibits typical low spin $(dz^2)^1Co^{II}$ ESR absorption when 2-methylimidazole is added to the solution. The spectrum (g = 2.25) is very similar to that observed for the mixed valence Co^{II}/Co^{II} species of a cofacial dicobaltporphyrin[17] in the presence of *N*-methylimidazole.

In comparing these findings with those for the corresponding cofacial binuclear dicobalt porphyrins[17-20] note that the latter also show splitting of the Co^{II}/Co^{I} couple by up to 290 mV; however, unlike the phthalocyanines, no

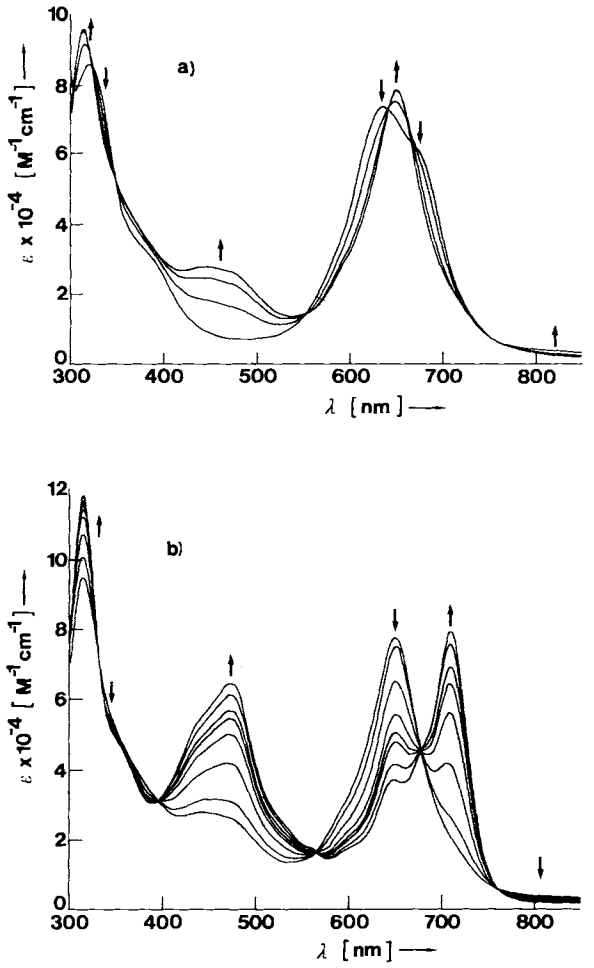

Fig. 1. Development of the electronic spectra with time (in *o*-dichlorobenzene), showing the formation of (a) the mixed valence Co^{II}-Co^{I} compound **1e**, and (b) the doubly reduced Co^{I}-Co^{I} species **1f** obtained by reduction of **1b** at potentials between -0.9 and -1.2 V, and -1.3 and -1.6 V, respectively, (vs $Fc^{\oplus}$/Fc). [**1b**] = 1×10^{-4} M, [TBAP] = 0.3 M.

distinct changes in the electronic spectra were observed for the mixed valence species.[19]

Electrocatalytic reduction of oxygen was examined at electrodes (glassy carbon and ordinary pyrolytic graphite) covered with adsorbed **1b**. Oxygen reduction occurred at -0.34 V (vs SCE, cyclic voltammogram, pH 1 to pH 13), and the limiting current corresponding to two-electron reduction of oxygen to hydrogen peroxide was observed in rotating disc experiments. Logarithmic analysis of the wave yielded a Tafel plot of -120 mV/decade, which corresponds to a charge-transfer coefficient of 0.5 and a one-electron transfer rate-determining step.

Received: April 21, 1987;
revised: July 8, 1987 [Z 2214 IE]
German version: *Angew. Chem. 99* (1987) 1065

[1] C. C. Leznoff, S. Greenberg, S. M. Marcuccio, P. C. Minor, P. Seymour, A. B. P. Lever, K. B. Tomer, *Inorg. Chim. Acta 89* (1984) L35.
[2] C. C. Leznoff, S. M. Marcuccio, S. Greenberg, A. B. P. Lever, K. B. Tomer, *Can. J. Chem. 63* (1985) 623.
[3] C. C. Leznoff, S. M. Marcuccio, P. I. Svirskaya, S. Greenberg, A. B. P. Lever, K. B. Tomer, *Can. J. Chem. 63* (1985) 3057.
[4] S. Greenberg, S. M. Marcuccio, C. C. Leznoff, K. B. Tomer, *Synthesis 1986*, 406.
[5] C. C. Leznoff, H. Lam, S. M. Marcuccio, W. A. Nevin, P. Janda, N. Kobayashi, A. B. P. Lever, *J. Chem. Soc. Chem. Commun. 1987*, 699.
[6] C. K. Chang, H. Y. Liu, I. Abdalmuhdi, *J. Am. Chem. Soc. 106* (1984) 2725.
[7] C. K. Chang, I. Abdalmuhdi, *J. Org. Chem. 48* (1983) 5388.
[8] H. O. House, D. Kreopsell, W. Campbell, *J. Org. Chem. 37* (1972) 1003.
[9] H. Matsumoto, S. Inaba, R. Rieka, *J. Org. Chem. 48* (1983) 840.
[10] The new compounds **4** and **1a–d** were completely characterized by the following physical and spectroscopic data. **4**: m.p. 285°C; MS (EI): *m/z* 380 (100%, $M^{\oplus}$, 253 ($M^{\oplus}-C_8H_3N_2$); ^{1}H-NMR (300 MHz, [D$_6$]DMSO); complex absorptions from $\delta = 7.3$–8.5 analyzed as a 1:1 mixture of *syn* and *anti* isomers; IR (KBr): $\nu = 3060$, 2240 (CN), 1600, 1490, 835, 780 cm^{-1}; UV/VIS (CH_2Cl_2): $\lambda_{max} = 238$ ($\varepsilon = 21900$), 265 sh (17000), 340 (11000) nm; correct elemental analysis (C, H, N).— **1a**: MS (FAB): *m/z* 1670 (100%, $M^{\oplus}$, molecular ion cluster); ^{1}H-NMR (300 MHz, $CDCl_3$): $\delta = -6.9$, -6.1, -5.5 (br. weak NH), 1.0–1.6 (br., 36H, CH_3), 3.3–3.8 (br., 8H, OCH_2), 7.0–8.5 (br., aromatic); IR (KBr): $\nu = 3300$ (NH), 1615, 1245, 1100, 1020 (NH), 750 cm^{-1}; UV/VIS (*o*-dichlorobenzene): $\lambda_{max} = 340$ ($\varepsilon = 79500$), 648 (77600) nm; correct elemental analysis (C, H, N).— **1b**: MS (FAB): *m/z* 1784 (100%, $M^{\oplus}+1$, molecular ion cluster); IR (KBr): $\nu = 2950$, 1610, 1100, 740 cm^{-1}; UV/VIS (*o*-dichlorobenzene): $\lambda_{max} = 306$ ($\varepsilon = 141000$), 638 (123000), 674 (102000) nm.— **1c**: MS (FAB): *m/z* 1793.6 (100%, $M^{\oplus}+1$, molecular ion cluster); IR (KBr): $\nu = 2950$, 1610, 1100, 740 cm^{-1}; UV/VIS (*o*-dichlorobenzene): $\lambda_{max} = 300$ ($\varepsilon = 63100$), 338 (102000), 640 (95500), 686 (93300).— **1d**: MS (FAB): *m/z* 1797.6 (100%, $M^{\oplus}+1$, molecular ion cluster); ^{1}H-NMR (300 MHz, $CDCl_3$): $\delta = 1.0$–1.6 (br., 36H, CH_3), 3.3–4.3 (br., 8H, OCH_2), 7.5–8.5 (br., aromatic); IR (KBr): $\nu = 2950$, 1610, 1100, 740 cm^{-1}; UV/VIS (*o*-dichlorobenzene): $\lambda_{max} = 298$ ($\varepsilon = 72400$), 340 (112000), 640 (107000), 686 (93300) nm.
[11] M. Barber, R. S. Bordoli, R. D. Sedgwick, A. N. Tyler, *J. Chem. Soc. Chem. Commun. 1981*, 325.
[12] W. A. Nevin, M. R. Hempstead, W. Liu, C. C. Leznoff, A. B. P. Lever, *Inorg. Chem. 26* (1987) 570.
[13] R. R. Gagne, C. A. Koval, D. C. Lisensky, *Inorg. Chem. 19* (1980) 2854.
[14] G. Gritzner, J. Kuta, *Electrochim. Acta 29* (1984) 869.
[15] M. J. Stillman, A. J. Thompson, *J. Chem. Soc. Faraday Trans. 2 70* (1974) 790.
[16] P. C. Minor, M. Gouterman, A. B. P. Lever, *Inorg. Chem. 24* (1985) 1890.
[17] Y. Le Mest, M. L'Her, J. Courtot-Coupez, J. P. Collman, E. R. Evitt, C. S. Bencosme, *J. Electroanal. Chem. 184* (1985) 331.
[18] R. R. Durand Jr., C. S. Bencosme, J. P. Collman, F. C. Anson, *J. Am. Chem. Soc. 105* (1893) 2710.
[19] J. P. Collman, M. Marrocco, C. M. Elliott, M. L'Her, *J. Electroanal. Chem. 124* (1981) 113.
[20] J. P. Collman, F. C. Anson, S. Bencosme, A. Chong, T. Collins, P. Denisevich, E. Evitt, T. Geiger, J. A. Ibers, G. Jameson, Y. Konai, K. Meier, P. Oakley, R. B. Pettman, E. Schmittov, J. Sessler in B. M. Trost, C. R. Hutchinson (Eds.): *Organic Synthesis Today and Tomorrow*. Pergamon Press, Oxford 1981.

Pentacyclo[11.3.0.0^{1,5}.0^{5,9}.0^{9,13}]hexadecane ([4.5]Coronane)**

By *Lutz Fitjer** and *Ulrike Quabeck*

Dedicated to Professor Ulrich Schöllkopf on the occasion of his 60th birthday

As has recently been reported,[1] reaction of the dispiroketone **1** with anhydrous *p*-toluenesulfonic acid in benzene leads via a fourfold 1,2-shift to formation of the propellanone **3**. The rearrangement proceeds via the β-hydroxy carbenium ion **2** and is quantitative.

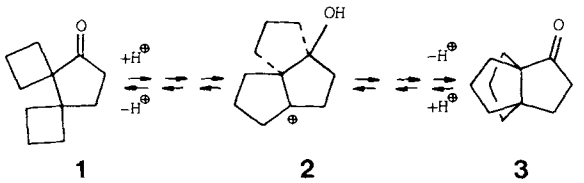

[*] Prof. Dr. L. Fitjer, Dipl.-Chem. U. Quabeck
Institut für Organische Chemie der Universität
Tammannstrasse 2, D-3400 Göttingen (FRG)

[**] Polyspiranes, Part 13, Cascade Rearrangements, Part 8. This work was supported by the Deutsche Forschungsgemeinschaft and the Fonds der Chemischen Industrie.—Parts 12 and 7, respectively: [3].

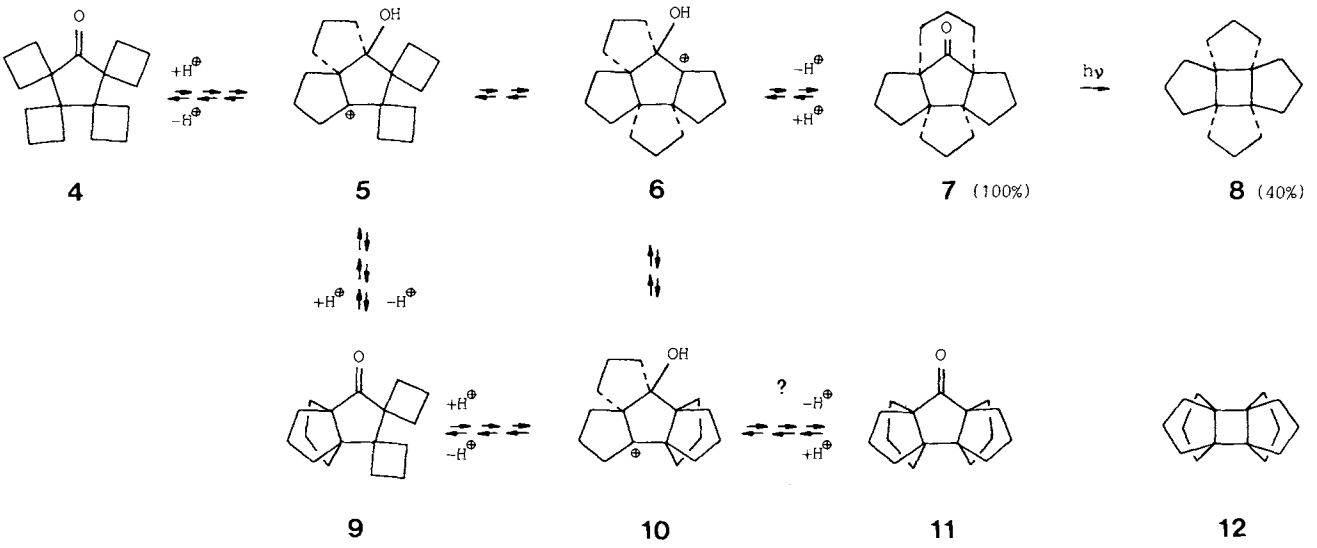

This finding led us to question whether the previously unknown tetraspiroketone **4** would be converted under comparable conditions into the bispropellanone **11** related to **3** (**4**→**5**→**6**(**9**)→**10**→**11**) or into the bridged pentacyclic ketone **7** (**4**→**5**→**6**→**7**). Both ketones appeared to be amenable to a photochemical decarbonylation and thus to a conversion into the novel pentacyclic hydrocarbons **12**[2] and **8** ([4.5]coronane),[3] respectively. According to force field calculations[4] **8** ($\Delta H_f^0 = -3.2$ kcal/mol) proved to be slightly favored over **12** ($\Delta H_f^0 = -0.8$ kcal/mol); however there proved to be no significant preference with regard to the rearrangement of **4** ($\Delta H_f^0 = 25.8$ kcal/mol) into **7** ($\Delta H_f^0 = -53.1$ kcal/mol) and/or **11** ($\Delta H_f^0 = -53.5$ kcal/mol). Since the boundary kinetics of a rearrangement of **4** also appeared to be difficult to estimate, we sought an experimental explanation.

The synthesis of the tetraspiroketone **4** was accomplished by cycloaddition of carbonylcyclobutane (trimethyleneketene)[5], generated in situ, to bi(cyclobutylidene) **13**[6] and subsequent ring-expansion of the trispiroketone **14** via the β-hydroxyselenide **15**.[7]

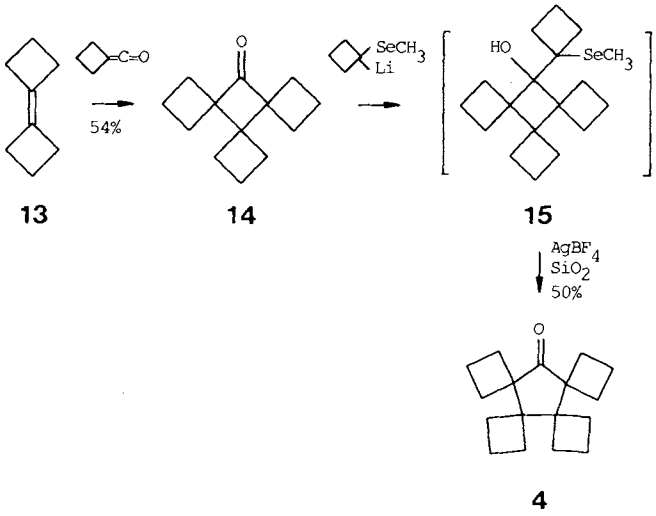

For the cycloaddition, a solution of triethylamine (0.15 mol) in bi(cyclobutylidene) **13**[6] (100 mL) was treated with cyclobutanecarboxylic acid chloride (0.10 mol) and the mixture heated for 5 h at 120°C; after washing with 2 N hydrochloric acid and saturated sodium bicarbonate solution, **14** (b.p. 76°C/0.6 torr; yield 54%)[8] was isolated by fractional distillation. Unchanged **13** (b.p. 145–148°C)[6] could be recovered as first fraction. For the homologization[9] the trispiroketone **14** (25 mmol) was added dropwise to a solution of 1-lithio-1-(methylseleno)cyclobutane (prepared from 1,1-bis(methylseleno)cyclobutane[10]) (30 mmol) in ether/pentane at −78°C, the mixture worked-up after 2 h at −78°C, and the crude β-hydroxyselenide **15** (yellow foul-smelling oil) rearranged without further purification with silver tetrafluoroborate (25 mmol) and aluminum oxide (200 mmol) in carbon tetrachloride (100 mL). **15** was completely consumed after 36 h at 20°C. Filtration and chromatography on silica gel in pentane/ether (9 : 1) afforded pure **4** (m.p. 78°C; yield 50%).[8]

As expected, the tetraspiroketone **4** proved to be unstable toward acids. A 0.25 M solution of anhydrous *p*-toluenesulfonic acid in benzene (molar ratio **4** : acid = 1 : 1) isomerized it quantitatively within 30 min at 80°C to a new ketone (b.p. 144–145°C), which, according to the ^{13}C-NMR spectrum (50.3 MHz, $CDCl_3$): $\delta = 18.30$, 25.86, 25.88, 30.01, 34.12, 37.79, 38.16 (C_{sec}), 57.47, 63.56, 222.66 (C_{quart}) was the bridged compound **7**.[8] The same ketone could also be obtained within 10 h at 80°C by reaction of Nafion-H[11] with a 0.25 M solution of **4** in benzene (w/w ratio of **4** : Nafion-H = 1 : 1). In both cases no intermediates were detectable; **7** remained unaltered on prolonging the reaction times. This does not mean, however, that **7** had to be formed in a thermodynamically controlled reaction.

For the decarbonylation, a solution of 200 mg of **7** ($\lambda_{max} = 289$ nm, $\varepsilon = 20$) in 35 mL of cyclohexane was irradiated with a 150W mercury high-pressure lamp in a Duran ring reactor. After 14 d at 20°C, 40% of **7** was consumed and a single product was formed, which was recognized by the presence of only three lines in the ^{13}C-NMR spectrum [(50.3 MHz, $CDCl_3$): $\delta = 26.54$, 35.48 (C_{sec}), 55.06 (C_{quart})] as the desired [4.5]coronane **8** (m.p. 186–188°C.[8] It is the second [m.n]coronane,[3] and, according to force field calculations,[4] has S_4 symmetry. Non-bonding interactions seem to be minimized by a slight folding of the

central ring ($\theta = 11.0°$), which cause the peripheral rings to be crossed pairwise.

Received: February 13, 1987 [Z 2102 IE]
German version: *Angew. Chem. 99* (1987) 1054
Publication delayed at authors' request

CAS Registry numbers:
4, 108451-21-4; **7**, 108451-22-5; **8**, 108451-23-6; **13**, 6708-14-1; **14**, 108451-19-0; **15**, 108451-20-3; 1-lithio-1-(methylseleno)cyclobutane, 78814-62-7; trimethylenketene, 59078-45-4; cyclobutanecarboxylic chloride, 5006-22-4; **11**, 109865-47-6; **12**, 109865-48-7

[1] L. Fitjer, A. Kanschik, M. Majewski, *Tetrahedron Lett. 26* (1985) 5277.
[2] Bis- and trispropellanes related to **12** are described by D. Ginsburg in *Top. Curr. Chem. 137* (1987) 1.
[3] For the definition and synthesis of [6.5]coronane, cf. D. Wehle, L. Fitjer, *Angew. Chem. 99* (1987) 135; *Angew. Chem. Int. Ed. Engl. 26* (1987) 130.
[4] Program MM2: N. L. Allinger, *J. Am. Chem. Soc. 98* (1977) 8127; we thank Dr. *D. Wehle* for carrying out the calculations.
[5] Cycloadditions of carbonylcyclobutane (trimethyleneketene) to other compounds were to our knowledge not known. Its dimerization, on the other hand, has been described: H. M. Walborsky, *J. Am. Chem. Soc. 74* (1952) 4962; J. L. E. Erickson, F. E. Collins, Jr., B. L. Owen, *J. Org. Chem. 31* (1966) 480.
[6] L. Fitjer, U. Quabeck, *Synthesis 1987*, 299.
[7] Ring expansions via β-hydroxyselenides are known: D. Labar, A. Krief, *J. Chem. Soc. Chem. Commun. 1982*, 564; D. Labar, J. L. Laboureur, A. Krief, *Tetrahedron Lett. 23* (1982) 983; J. L. Laboureur, A. Krief, *ibid. 25* (1984) 2713. The insertion of a cyclobutane described here is new.
[8] All the new compounds (**4**, **7**, **8**, **14**) gave correct analyses and/or correct values in the high resolution mass spectrum. The IR, ^{1}H-NMR, and mass spectroscopic data are consistent with the given structures. ^{13}C-NMR data (as far as not mentioned in text): **4**: (20 MHz, $CDCl_3$): $\delta = 15.63$, 15.92, 23.36, 26.99, 50.71, 56.53, 224.25; **14**: (25.2 MHz, $CDCl_3$): $\delta = 16.20$, 16.42, 24.48, 26.24, 45.49, 65.97, 216.66.
[9] The homologization of **14** was carried out analogously to the homologization of hexamethylcyclobutanone with 2-lithio-2-(methylseleno)propane: L. Fitjer, D. Wehle, H.-J. Scheuermann, *Chem. Ber. 119* (1986) 1162.
[10] M. Clarembeau, A. Cravador, W. Dumont, L. Hevesi, A. Krief, J. Lucchetti, D. van Ende, *Tetrahedron 41* (1985) 4793.
[11] Nafion-H is a polymer of tetrafluoroethylene and sulfur dioxide with SO_3H terminal groups; review: G.-A. Olah, *Synthesis 1986*, 513.

9,10-(1′-Magnesiapropano)-9,10-dihydroanthracene, Synthesis, Structure, and Reactivity**

By *Borislav Bogdanović,* Nikolaus Janke, Carl Krüger, Klaus Schlichte,* and *Joachim Treber*

The high reactivity of the Mg–C bonds in the strained metallacycle of magnesiumanthracene·3THF **1a**[1,2] and the known insertion of alkenes into the Mg–C bonds of certain Grignard compounds[3] prompted us to investigate the reaction of **1a** and its methyl derivative **1b**[4] with ethene. We report herein on the synthesis of 9,10-(1′-magnesiapropano)-9,10-dihydroanthracene·2THF **2a** and its methyl derivative **2b** from **1a** and **1b**, respectively, and ethene, as well as on the crystal structures of the new compounds and on a few reactions of **2a** with electrophiles.

When the reactions of **1a** and **1b** were carried out at 85 °C and 60 bar ethene in THF, **2a** and **2b** were obtained in 72% and 45% yields, respectively. The protolysis of **2a** afforded 9-ethyl-9,10-dihydroanthracene **3a**[5] and that of **2b** the corresponding methyl derivative **3b**. This means

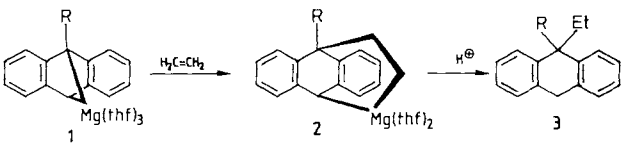

a, R = H; b, R = Me

that in the case of **1b**, ethene is inserted only into the Mg–C_{tert} bond. Further insertion of ethene does not take place under the given conditions. Presumably this can be attributed to removal of ring strain in the metallacycle system upon conversion of **1** into **2** and to the resulting reduced reactivity of the Mg–C bond. Products of the insertion of ring-opened THF into the Mg–C bond of **1a**[1] and **2a** are formed in side reactions with the solvent (ca. 10%). Due to their insolubility, however, these can be readily removed from the reaction solution. The compounds **2** already lose one equivalent of THF at room temperature in toluene.

The monomeric structures of **2** could be confirmed, both by NMR investigations and structure analyses on single crystals.[6] Compounds **2a** and **2b** (Fig. 1) have com-

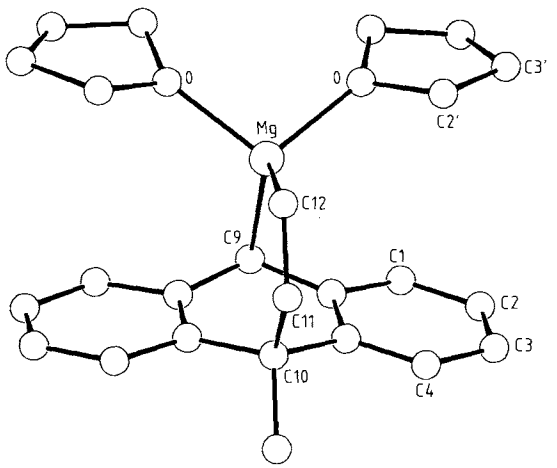

Fig. 1. Crystal structure of **2b**.

parable structures. In each case the coordination geometry about the magnesium atom is distorted tetrahedral with the metal attached via one coordination site directly to the anthracene skeleton. Moreover, a σ-Mg–C bond is also formed (mean value 2.113(9) Å). The two remaining coordination sites of the magnesium are occupied by the THF molecules, whereby the THF rings are not only puckered differently, but, depending on the molecular packing in the lattice, exhibit different torsional angles with respect to the C–Mg–O bonds. Both compounds are chiral; in **2a** there are two molecules in the asymmetric unit which differ slightly in the anthracene skeleton. The anthracene moieties of both compounds are folded along the C9–C10 vector, with the interplanar angle in **2b** being smaller (11.1°) than in **2a** (26.0°) for steric reasons (methyl group on C10).

Further metallapropano compounds analogous to **2a** are accessible by reaction of **2a** with organometal dihalides. Thus, reaction of **2a** with dichloromethylsilane or

[*] Prof. Dr. B. Bogdanović, Dr. N. Janke, Prof. Dr. C. Krüger, K. Schlichte, Dipl.-Chem. J. Treber
Max-Planck-Institut für Kohlenforschung
Kaiser-Wilhelm-Platz 1, D-4330 Mülheim a. d. Ruhr (FRG)

[**] Magnesium-Anthracene Systems, Part 3.—Part 2: [2].

dichlorodiphenylgermane in dioxane (20°C/5 d) leads, via elimination of $MgCl_2$, to the sila- and germapropano derivatives **4** and **5**, respectively, in 80 and 50% yield,[7] the structures of which could be deduced by comparison of the NMR spectra with those of **2a** (see *Experimental Procedure*).

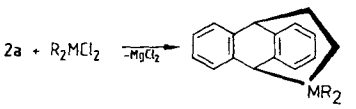

4, M = Si, R = Me
5, M = Ge, R = Ph

Owing to the different Mg-C distances in **2a**, the two carbanion centers can be expected to exhibit different reactivities. Whereas **1a** is characterized by its ambivalent character,[8] **2a** behaves chemically as a "normal" diorganomagnesium compound, but with a markedly increased reactivity of the long Mg-C9 bond compared to that of the short Mg-C12 bond. Thus, **2a** can react chemoselectively with two different electrophiles E^1X^1 and E^2X^2 in succession to give 9,10-disubstituted 9,10-dihydroanthracenes **7** (Scheme 1). With electrophiles EX in excess, 9,10-disubstituted 9,10-dihydroanthracenes of type **6** are formed (Scheme 1). Since the compounds **6** and **7** are *Z*-configurated[9] (exception: reaction with CO_2 to give the *E*-dicarboxylate) it can be concluded that the Mg-C9 bond participates in the S_E reaction with retention of the configuration on C9. With one exception,[12] these are the first examples for the elucidation of the stereochemical course of S_E reactions with C-C coupling.[13]

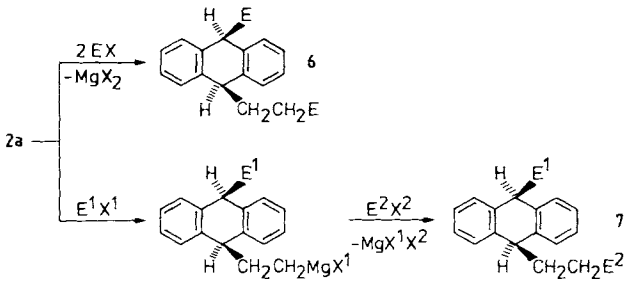

Scheme 1. Reactants and reaction temperatures: EX = MeI (70°C) [14], EtI (20°C), Me_3SiCl (50°C), CO_2 (20°C); E^1X^1 = MeI, EtI, *i*PrBr, oxacyclobutane; $E^2X^2 = H_2O$, CO_2. All compounds **7** were prepared at 20°C.

Experimental Procedure

2a: A solution of **1a** [1] (32.5 g, 77.6 mmol) in THF (300 mL) was stirred for 3 d at 60 bar ethene pressure and 80°C in a 500-mL autoclave in the absence of air and moisture. The solution was filtered, the solvent removed, and the resulting residue stirred for 3 h in 250 mL of toluene. The pale-yellow mono-THF adduct thus obtained was filtered off, washed with toluene and pentane, and dried in a vacuum. Yield: 16.0 g (72%). Correct elemental analysis. For the crystallization 40 mL of the THF-filtrate was cooled to −78°C and the precipitated crude product separated off and dissolved in a THF/pentane mixture (1/1). After 48 h at −30°C, **2a** was obtained as pale-yellow platelet-shaped crystals.

^{13}C-NMR (7.5 MHz, [D$_8$]THF, $\delta \pm 1$ rel. TMS, ^1J(CH) ±1 in Hz): δ = 129.0 (C1; ^1J(CH) = 151.0), 117.9 (C2; 158.0), 125.5 (C3; 155.0), 119.5 (C4; 153.0), 51.7 (C9; 141.0), 51.0 (C10; 124.0), 133.3 (C11), 149.2 (C12), 44.3, −0.85 (THF C-atoms).

2b is obtained analogously from 15.79 g (36.5 mmol) of **1b** [4] in 250 mL of THF at 54 bar ethene pressure (60°C, 6 d). Yield: 4.0 g (45%). Correct elemental analysis; pale-yellow platelet shaped crystals.

Received: May 14, 1987 [Z 2241 IE]
German version: *Angew. Chem. 99* (1987) 1046

[1] B. Bogdanović, S. Liao, R. Mynott, K. Schlichte, U. Westeppe, *Chem. Ber. 117* (1984) 1378.
[2] B. Bogdanović, N. Janke, C. Krüger, R. Mynott, K. Schlichte, U. Westeppe, *Angew. Chem. 97* (1985) 972; *Angew. Chem. Int. Ed. Engl. 24* (1985) 960.
[3] Review: H. Lehmkuhl, *Bull. Soc. Chim. Fr. II 1981*, 87.
[4] N. Janke, *Dissertation*, Universität Bochum 1986.
[5] A. W. Brinkmann, M. Gordon, R. G. Harvey, P. W. Rabideau, J. B. Stotzers, A. L. Ternay, Jr., *J. Am. Chem. Soc. 92* (1970) 5912.
[6] **2a**: $a = 18.336(1)$, $b = 10.791(1)$, $c = 22.776(1)$ Å, $\beta = 105.99(1)°$, $V = 4332.2$ Å^3, $Z = 8$, $\rho_{calc} = 1.15$ g cm^{-3}, $\mu(Cu_{K\alpha}) = 7.89$ cm^{-1}, space group $P2_1/a$, 8370 independent reflections, 5034 observed ($I > 2\sigma(I)$), 727 refined parameters, $R = 0.071$, $R_w = 0.090$. Disordered THF rings. **2b**: $a = 8.165(1)$, $b = 13.757(3)$, $c = 19.608(3)$ Å, $V = 2202.3$ Å^3, $Z = 4$, $\rho_{calc} = 1.17$ g cm^{-3}, $\mu(Mo_{K\alpha}) = 0.92$ cm^{-1}, space group $P2_12_12_1$, 2832 independent reflections, 1325 observed ($I > 2\sigma(I)$), 253 refined parameters, $R = 0.039$, $R_w = 0.036$. Further details of the crystal structure investigations are available on request from the Fachinformationszentrum Energie, Physik, Mathematik GmbH, D-7514 Eggenstein-Leopoldshafen 2 (FRG), on quoting the depository number CSD-52216, the names of the authors, and the journal citation.
[7] J. Treber, *Diplomarbeit*, Universität Kaiserslautern 1986.
[8] Review: B. Bogdanović, *Angew. Chem. 97* (1985) 253; *Angew. Chem. Int. Ed. Engl. 24* (1985) 262.
[9] The identification as *Z* isomers (E^1 = Me, Et; E^2 = H) was possible on the basis of known data [10] and crystal structure analyses [11].
[10] a) R. G. Harvey, L. Arzadon, J. Grant, K. Urberg, *J. Am. Chem. Soc. 91* (1969) 4535; b) N. Ahmad, C. Cloke, I. K. Hatton, N. J. Lewis, J. MacMillan, *J. Chem. Soc. Perkin Trans. 1 1985*, 1859.
[11] a) N. Ahmad, R. J. Goddard, I. K. Hatton, J. A. K. Howard, N. J. Lewis, J. MacMillan, *J. Chem. Soc. Perkin Trans. 1 1985*, 1859; b) J. Bordner, R. H. Stanford, Jr., H. E. Zieger, *Acta Crystallogr. Sect. B29* (1973) 313.
[12] H. M. Walborsky, A. E. Young, *J. Am. Chem. Soc. 83* (1961) 2595.
[13] a) M. H. Abraham in M. Gielen (Ed.): *Topics in Physical Organometallic Chemistry, Vol. 1*, Freund Publishing House, London 1985, p. 143; b) M. H. Abraham, P. L. Grellier in F. R. Hartley, S. Patai (Eds.): *The Chemistry of the Metal Carbon Bond, Vol. 2*, Wiley, New York 1985, p. 25.
[14] Longer reaction times at room temperature with MeI in excess led via radical mechanisms to 1,4-bis(10-dimethyl-9,10-dihydro-9-anthryl)butane, methane, and ethane. For an undoubted analogous reaction see: H. D. Becker, K. Anderson, *Tetrahedron 42* (1986) 1555.

Anodic Grob Fragmentation of Bicycloalkylcarboxyl Acids to Specifically Disubstituted Cycloalkenes**

By *Ralf Michaelis, Ulrich Müller,* and *Hans J. Schäfer**

Dedicated to Professor Kenneth B. Wiberg on the occasion of his 60th birthday

The anodic oxidation of carboxylates leads, depending on the reaction conditions and the structure of the carboxylic acid, to radicals (Kolbe electrolysis[1]) or—in a secondary oxidation—to carbocations (non-Kolbe electrolysis[1,2]).

We have now found that stereospecifically 3,4-disubstituted cyclopentenes can be obtained from 3-substituted 6-hydroxy-2-norbornanecarboxylic acids by non-Kolbe electrolysis (Scheme 1). The reaction course resembles that observed by *Grob* et al. in the fragmentation of norbornyl tosylates.[3] Depending on whether there is an *exo*- or *endo*-substituent in the 3-position, either a *trans*- [Eq. (a)] or a *cis*-disubstituted cyclopentene [Eq. (b)] is obtained. Of additional preparative advantage is the fact that the two substituents do not have to be the same. Table 1 shows the broad spectrum of applications of the reaction.

The starting substances were obtained in a few steps in high yield by Diels-Alder reaction and hydrolactonization

[*] Prof. Dr. H. J. Schäfer, Dr. R. Michaelis, Dr. U. Müller
Organisch-chemisches Institut der Universität
Correns-Strasse 40, D-4400 Münster (FRG)

[**] Anodic Oxidation, Part 35. This work was supported by the Fonds der Chemischen Industrie.—Part 34: [4].

Table 1. Anodic fragmentation of γ-hydroxy- and γ-oxocarboxylic acids.

Educt	Product	Yield [%] [a] Product	Recovered educt
1	**2**	27	31
3	**4**	38	20
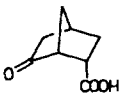 **5**	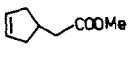 **6**	71	0
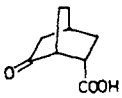 **7**	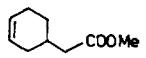 **8**	44	23
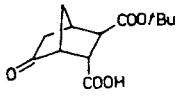 **9**	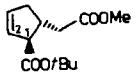 **10**	55	16
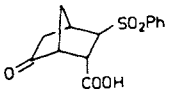 **11**	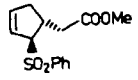 **12**	63	8
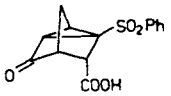 **13**	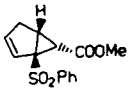 **14**	47	22
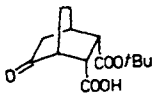 **15**	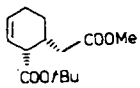 **16**	49	8
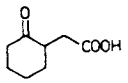 **17**	**18**	61	6
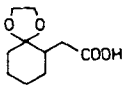 **19**	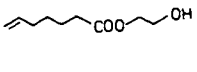 **20**	47	14
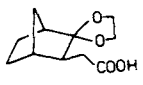 **21**	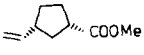 **22**	76 [b]	11

[a]Based on conversion. [b] After acid-catalyzed transesterification in methanol.

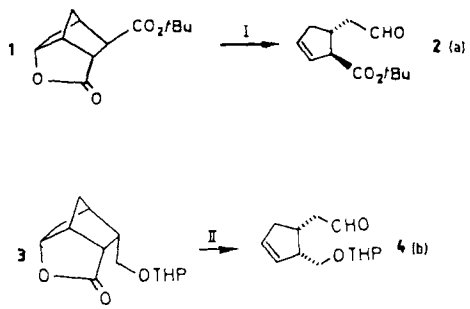

Scheme 1. I) LiOH in methanol, $-e^{\ominus}$, 0°C, graphite anode. II) KOH in acetonitrile/ethanol (5/1), $-e^{\ominus}$, 10°C, graphite anode. THF = tetrahydrofuran.

(**1**, **3**) and oxidation of the γ-lactones at a nickel hydroxide electrode[4] (**5**, **7**, **9**, **11**, **13**, **15**). **17** and **19** were obtained by α-alkylation of cyclohexanone with bromoacetate. **21** is the product of the Mn^{III}-acetate-oxidation of norbornene and subsequent oxidation of the γ-lactone.[4]

As shown in Table 1, the lactones, which open under the conditions of the non-Kolbe electrolysis to give γ-hydroxycarboxylic acids, fragment to cyclopenteneacetaldehydes (**2**, **4**). The γ-oxocarboxylic acids correspondingly form cycloalkeneacetic acids, which are isolated in the form of their methyl esters (**6**, **8**, **10**, **12**, **14**, **16**). In the case of **17** an elimination with subsequent double-bond isomerization takes place, but also here the fragmentation can be achieved—by ketalization of the carbonyl group (**19**). **21** fragments analogously.

The readily and specifically accessible products are suitable, inter alia, for the synthesis of cyclopentanoid natural products.

Experimental Procedure

The experimental procedure is described for the example **10**. A solution of **9** (0.25 g, 1.00 mmol) in methanol (50 mL) was neutralized to 100% with 1 M NaOH in methanol and electrolyzed at graphite electrodes in an undivided cell using a current density of 10 mA cm^{-2} at 0°C until consumption of 4 F mol^{-1}. The solution was then evaporated to dryness, treated with saturated NaCl solution, and extracted five times with CH_2Cl_2. After drying ($MgSO_4$) and removal of the CH_2Cl_2, 0.11 g (55%) of **10** was obtained as a colorless oil by column filtration (silica gel, petroleum ether/ether = 2/1). After acidification with conc. HCl to pH = 1 and threefold extraction with CH_2Cl_2, 0.04 g (16%) of **9** was recovered from the aqueous phase.— **10**: IR (film): $\tilde{\nu}$ [cm^{-1}] = 3040, 1720 (C=O). ^{1}H-NMR ($CDCl_3$): δ = 1.45 (s, 9H; *t*Bu), 2.06 (J = 14.4, 6.1, 4.5, 2.2 Hz, 1H; 4-H), 2.41 (J = 15.4, 8.4 Hz, 1H; 6-H), 2.58 (J = 15.4, 6.1 Hz, 1H; 6-H), 2.70 (J = 14.3, 8.5, 4.7, 2.1 Hz, 1H; 4-H), 2.87 (J = 9.5, 8.4, 6.3, 6.3, 1H; 5-H), 3.18 (J = 6.3, 4.8, 2.4 Hz, 1H; 1-H), 3.67 (s, 3H; Me), 5.65 (J = 5.8, 4.6, 2.2 Hz, 1H; 3-H), 5.78 (J = 5.8, 4.6, 2.1 Hz, 1H; 2-H). — MS (70 eV): *m/z* (%) 184 (15, $M^{\oplus} - C_4H_8$), 167 (13, $M^{\oplus} - OC_4H_9$).

Received: May 21, 1987 [Z 2252 IE]
German version: *Angew. Chem. 99* (1987) 1049

[1] The Kolbe electrolysis is favored by high current density, platinum as anode material, a low degree of neutralization (< 5%) of the acid, as well as hydrogen, and −M and −I substituents in the α-position of the carboxylic acid: S. Torii: *Electroorganic Syntheses, Part I*, VCH Verlagsgesellschaft, Weinheim 1985, p. 50–53, and references cited therein.

[2] The non-Kolbe electrolysis or Hofer-Moest reaction is favored by graphite as anode material, addition of salts (e.g. $NaClO_4$), pyridine/water as solvent, a high degree of neutralization of the acid, as well as +M and +I substituents in the α-position of the carboxylic acid: J. P. Coleman, R. Lines, J. H. P. Utley, B. C. L. Weedon, *J. Chem. Soc. Perkin Trans. 2 1974*, 1064.

[3] C. A. Grob, *Angew. Chem. 94* (1982) 87; *Angew. Chem. Int. Ed. Engl. 21* (1982) 87; W. Fischer, C. A. Grob, G. von Sprecher, A. Waldner, *Helv. Chim. Acta 63* (1980) 928.

[4] H. Ruholl, H. J. Schäfer, *Synthesis 1987*, 408.

Regio- and Stereoselective Carbosulfenylation of Olefins**

By *Manfred T. Reetz,** and *Thomas Seitz*

Dedicated to Professor Ulrich Schöllkopf on the occasion of his 60th birthday

Lewis acidic organotitanium reagents[1] such as CH_3TiCl_3[2] or trichlorotitanium enolates[3] undergo C-C coupling reactions with S_N1-active alkylating agents, e.g. with tertiary or aryl-activated secondary alkyl halides. Since carbocations occur as intermediates, mixtures of enantiomers[4] or diastereomers are formed in stereochemically relevant cases.[1] However, if the alkylating agent contains a suitable neighboring group, then not only is an increased reaction rate to be expected, but also retention of configuration (double inversion).[3,5] In the following communication we report on regio- and stereoselective reactions of Lewis acidic methylmetal reagents with β-chlorosulfides, in which the sulfur residue functions as the neighboring group.[6]

When the *trans*-β-chlorosulfides **2** obtained from cyclic olefins **1** are allowed to react in a one-pot process with dimethylzinc in the presence of 20 mol-% $TiCl_4$ in dichloromethane, the C-C coupling products **4** are formed with complete *retention* of configuration.[7] The same holds true for the carbosulfenylation of the prochirally pure olefin **5** to **6**. Since $(CH_3)_2Zn$ reacts spontaneously with $TiCl_4$ to give CH_3TiCl_3 and $(CH_3)_2TiCl_2$,[2] the latter are probably the alkylating reagents. Supported by the PhS-neighboring groups they effect the formation of episulfonium ions **3**,[8] which are attacked stereospecifically by the complex counterion (e.g. $[CH_3TiCl_4]^{\ominus}$). The only by-products are the starting olefins and CH_3SPh, which are formed by nucleophilic attack at the sulfur in the episulfonium ion **3**. Besides $(CH_3)_2Zn/TiCl_4$, the more reactive $(CH_3)_3Al$ (CH_2Cl_2, 0°C, 22°C/5 h) is also an effective reagent (80% **4b**).

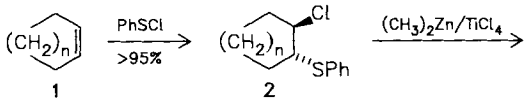

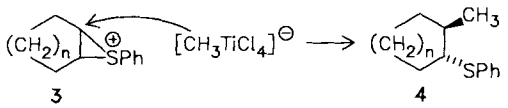

a, n = 1(78%); b, n = 2(68%); c, n = 3(50%)

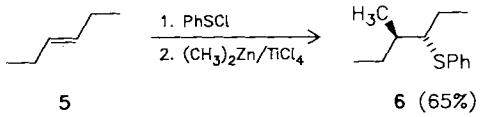

Noteworthy is the regioselectivity of the C-C coupling in the case of di- and trisubstituted olefins: the methyl group is always placed at the higher substituted C-atom. The regioselectivity of the reversible chlorosulfenylation is incomplete, but this is of no importance, since both adducts (e.g. **8**/**9**) lead to the same episulfonium ion (e.g. **10**). Charge control determines the regioselectivity of the subsequent irreversible methylation. In the case of **13a**, the use of $(CH_3)_3Al$ was also examined: the mixture **14**/**15** (97 : 3) was formed in 68% yield.

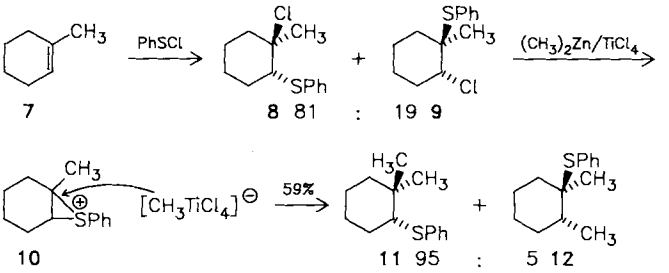

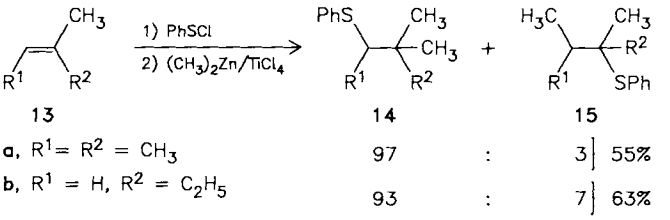

Finally, the regioselectivity as well as the 1,2-asymmetric induction in the case of α-chiral 1,2-disubstituted olefins were investigated. In the case of the cyclic olefin **16** the regioselectivity is 85% and **19** is formed with >99% diastereofacial selectivity. Probably two episulfonium ions **17** and **18** are formed in equilibrium. For stereoelectronic reasons, only **17** undergoes a *trans*-1,2-diaxial ring opening to give **19** in the chair conformation.[7]

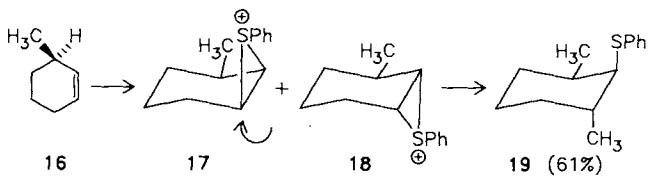

In the case of the acyclic olefins **20** with electronegative moieties at the chiral center, the carbosulfenylations are likewise regio- and, depending on the nature of the protective group on the oxygen, stereoselective (Table 1). The regioselectivity can be explained in terms of steric and electronic effects. More difficult is an interpretation of the 1,2-asymmetric induction.[9,10] As a possible model we postulate the preferred formation and reaction of the episulfonium ion **21**, in which an electrostatic attraction between

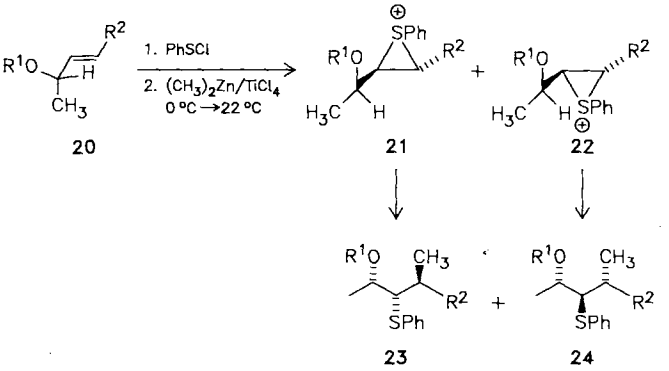

[*] Prof. Dr. M. T. Reetz, Dipl.-Chem. T. Seitz
Fachbereich Chemie der Universität
Hans-Meerwein-Strasse, D-3550 Marburg (FRG)

[**] This work was supported by the Deutsche Forschungsgemeinschaft (Sonderforschungsbereich 260).

Table 1. Carbosulfenylation of allyl ethers **20** [a].

R^1	R^2	T [°C]	Yield [%]	**23** : **24**
CH_3	CH_3	0	50	99 : 1
CH_3	CH_3	−78	50	94 : 6
CH_2Ph	CH_3	0	60	85 : 15
CH_2Ph	CH_3	−78	61	74 : 26
$SiMe_3$	CH_3	0	69	84 : 16
$SiMe_3$	CH_3	−78	70	60 : 40
$SitBuPh_2$	CH_3	0	77	60 : 40
$SitBuPh_2$	CH_3	−78	77	50 : 50
$SitBuMe_2$	CH_3	0	70	47 : 53
$SitBuMe_2$	CH_3	−78	72	32 : 68
CH_3	C_2H_5	0	40	99 : 1

[a] The carbosulfenylation was carried out at the given temperatures, the methylation immediately thereafter with $(CH_3)_2Zn/TiCl_4$ at 0°C→22°C/15 h.

the positive sulfur atom and the electron-rich oxygen residue has a stabilizing effect.[11] Consistent with this hypothesis is the significantly smaller 1,2-asymmetric induction with larger protective groups which hinder this interaction. The influence of the temperature of the PhSCl addition on the stereochemistry of the subsequent methylation points to a possible equilibration of diastereomeric β-chlorosulfides.[11] The diastereoselectivity can even be reversed with the *tert*-butyldimethylsilyl protective group. The results are preparatively important, since the interplay of 1,2-asymmetric induction and *trans*-stereospecificity leads to a well-defined 1,3-stereorelation.[7]

Preliminary experiments with further organometallic reagents as well as other arylsulfenyl chlorides can be summarized as follows: ethyl moieties can be stereospecifically introduced with $AlEt_3$ (e.g. **2b**→**25**).

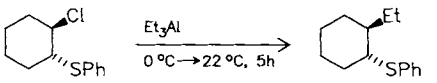

2b **25** (85%)

Organoaluminum reagents are less suited for allyl ethers, since, inter alia, ether cleavages occur. Cuprates such as $(CH_3)_2CuLi$ do not effect methylation. Replacement of PhSCl by 2,4,6-triisopropylphenylsulfenyl chloride leads to adducts which afford fewer by-products with $(CH_3)_2Zn/TiCl_4$ (starting olefins/CH_3SPh). For example, the adduct of cyclohexene can be methylated to the extent of 90% (82% isolated, in contrast to 68% in the case of **4b**). The bulky residue on the sulfur suppresses the undesired thiophilic attack. It remains to be seen whether these steric effects also influence regio- and stereoselectivity.[12]

Received: May 25, 1987 [Z 2258 IE]
German version: *Angew. Chem. 99* (1987) 1081

[1] M. T. Reetz: *Organotitanium Reagents in Organic Synthesis*, Springer, Berlin 1986.
[2] M. T. Reetz, J. Westermann, R. Steinbach, *Angew. Chem. 92* (1980) 933; *Angew. Chem. Int. Ed. Engl. 19* (1980) 901.
[3] For a review of the α-alkylation of carbonyl compounds with S_N1-active alkylating agents: M. T. Reetz, *Angew. Chem. 94* (1982) 97; *Angew. Chem. Int. Ed. Engl. 21* (1982) 96.
[4] G. H. Posner, T. P. Koga, *J. Chem. Soc. Chem. Commun. 1983*, 1481.
[5] M. T. Reetz, M. Sauerwald, P. Walz, *Tetrahedron Lett. 22* (1981) 1101.
[6] For the carbosulfenylation of olefins with introduction of cyano groups see: B. M. Trost, M. Preckel, L. M. Leichter, *J. Am. Chem. Soc. 97* (1975) 2224, and for those with introduction of enolates and allyl moieties see: M. A. Ibraginov, W. A. Smit, *Tetrahedron Lett. 24* (1983) 961; R. P. Alexander, I. Paterson, *ibid. 24* (1983) 5911).
[7] The *trans* arrangement in **4** was demonstrated ^{1}H-NMR spectroscopically. In the case of **19**, desulfurization (Raney nickel) led exclusively to the known *trans*-1,3-dimethylcyclohexane. The assignment of the compounds **23/24** was achieved as follows: after removal of the protective group on the oxygen, the sulfur residue was methylated with $(CH_3)_3OBF_4$ and an epoxide was formed stereospecifically (**23** gave the *cis*-epoxide, **24** the *trans*-isomer).
[8] W. A. Smit, N. S. Zefirov, I. V. Bodrikov, M. Z. Krimer, *Acc. Chem. Res. 12* (1979) 282; E. Kühle, *Synthesis 1971*, 617.
[9] Electrophilic additions to chiral olefins with electronegative substituents at the allyl position proceed stereochemically differently depending on the electrophile and substrate. For a survey of the literature on this theme as well as an attempted explanation [10] see: S. D. Kahn, W. H. Hehre, *J. Am. Chem. Soc. 109* (1987) 666.
[10] Alternative theories: K. N. Houk, S. R. Moses, Y.-D. Wu, N. G. Rondan, V. Jäger, R. Schoke, F. R. Fronczek, *J. Am. Chem. Soc. 106* (1984) 3880; K. N. Houk, M. N. Paddon-Row, N. G. Rondan, Y. D. Wu, F. K. Brown, D. C. Spellmeyer, J. T. Metz, Y. Li, R. J. Loncharid, *Science 231* (1986) 1108.
[11] Of course, **22** can also assume a conformation in which the alkoxy group is situated near the sulfur residue; this would, however, cause an unfavorable steric interaction between the methyl group and the three-membered ring. Use of the Hehre model in which the entering electrophile is guided by the alkoxy residue [9] would require a kinetically controlled reaction.
[12] *Typical procedure:* Phenylsulfenyl chloride (2.9 g, 20 mmol) is added at 0°C (or −78°C) (see Table 1) to a solution of cyclohexene (2 mL, 20 mmol) in anhydrous CH_2Cl_2 under argon until a permanantly pale-yellow colored solution is obtained (quantitative conversion). After 10 min, 5 mL of a 4 M $(CH_3)_2Zn$-solution in CH_2Cl_2 (1.9 g; 20 mmol of pure $(CH_3)_2Zn$) is syringed into the stirred reaction solution at 0°C. Upon subsequent addition of $TiCl_4$ (0.44 mL, 4 mmol) the solution turns blood red. Thereafter the solution is stirred for 15 h at room temperature. The black-brown mixture is poured into 100 mL of ice-water, treated with 2 N HCl to dissolve any precipitate, and the aqueous phase extracted several times with ether. The combined organic phases are washed with $NaHCO_3$ and NaCl solutions and dried over $MgSO_4$. After removal of the solvent the residue is distilled in a Kugelrohr (80–82°C/1 torr). Yield: 2.7 g (68%) of pure **4b**. The same procedure using 2,4,6-triisopropylsulfenyl yields, after column chromatographic purification, 82% of the analogous product.

Control of the Relative Electrophilicity of Alkylating Agents by Variation of the Lewis Acid Concentration**

By *Herbert Mayr**, *Christian Schade*, *Monika Rubow*, and *Reinhard Schneider*

Dedicated to Professor George A. Olah on the occasion of his 60th birthday

The Lewis acid-catalyzed addition of alkyl halides **1** to alkenes **2** represents a straightforward method for the formation of CC-bonds.

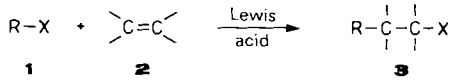

1 **2** **3**

When only small equilibrium concentrations of carbenium ions are generated during such reactions, the selective formation of 1 : 1 products can only be achieved if the reactants **1** ionize faster than the products **3**.[1] Other regularities result when the condition ΔG^0 (ionization) ≫ 0 is abandoned, and the foregoing rule turns out to be a special case of a more general principle.[2] We now demonstrate

[*] Prof. Dr. H. Mayr, Dipl.-Chem. C. Schade, M. Rubow, Dipl.-Chem. R. Schneider
Institut für Chemie der Medizinischen Universität
Ratzeburger Allee 160, D-2400 Lübeck 1 (FRG)

[**] This work was supported by the Deutsche Forschungsgemeinschaft and the Fonds der Chemischen Industrie. *C. S.* thanks the Stiftung Volkswagenwerk for a Kekulé fellowship.

for a model reaction, how to invert the relative reactivities of alkylating agents by varying the concentration of the Lewis acid (see Scheme 1).

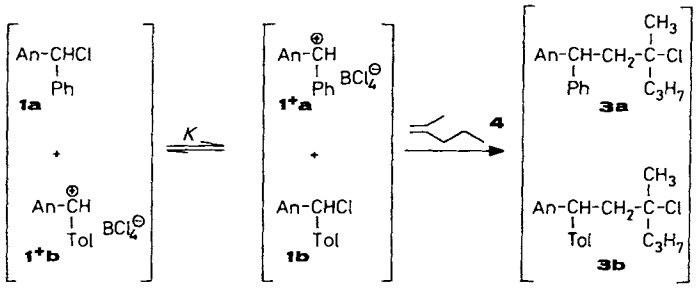

Scheme 1. An = *p*-methoxyphenyl, Tol = *p*-tolyl.

When 5 equivalents of BCl_3 (6.0 mmol) and 0.20 mmol of 2-methyl-1-pentene **4** are added successively to a solution of the diarylmethyl chlorides **1a** (0.40 mmol) and **1b** (0.80 mmol) in dichloromethane, the 1 : 1 adducts **3a** and **3b** are formed in the ratio 2.98 : 1. From this experiment, a competition constant $k_a/k_b = 7.2$ is derived,[3] which is closely similar to the ratio of the rate constants directly measured for the reactions of $\mathbf{1}^+\mathbf{a}$ and $\mathbf{1}^+\mathbf{b}$ with **4** (7.06);[4] under these conditions both diarylmethyl chlorides are fully ionized.

Reduction of the BCl_3 concentration causes a decrease of the reactivity ratio *a/b* (Fig. 1), and a value of 0.18 is achieved when 0.05 equivalents of BCl_3 are used. The less reactive carbenium ion $\mathbf{1}^+\mathbf{b}$ now reacts preferentially, because of its higher concentration in the preceding equilibrium (Curtin Hammett situation[5]). A theoretical value of 0.18 is obtained for the competition constant at low catalyst concentrations by multiplication of the ratio $k(\mathbf{1}^+\mathbf{a})/k(\mathbf{1}^+\mathbf{b})$ with the NMR spectroscopically determined equilibrium constant $K = ([\mathbf{1}^+\mathbf{a}][\mathbf{1b}])/([\mathbf{1a}][\mathbf{1}^+\mathbf{b}]) = 0.025$.

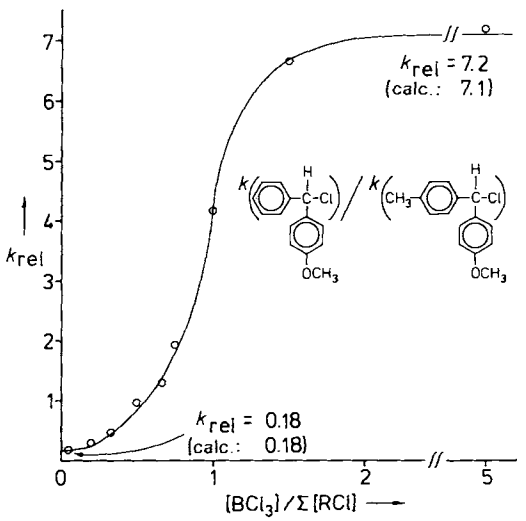

Fig. 1. Relative reactivity of the diarylmethyl chlorides **1a/b** towards 2-methyl-1-pentene in CH_2Cl_2 at −70°C as a function of the Lewis acid concentration.

In this system, the difference between the reactivities of two electrophiles increases with increasing difference of the ionization standard free enthalpies ($\Delta\Delta G^0_{ionization}$) of the two competitors. Under conditions of prevailing ionization, the *p*-phenoxy-substituted benzhydryl cation is 5400 times more reactive than the bis(*p*-methoxy)-substituted benzhydryl cation, while in presence of catalytic amounts of Lewis acid the relative reactivity is 0.016 (Fig. 2).

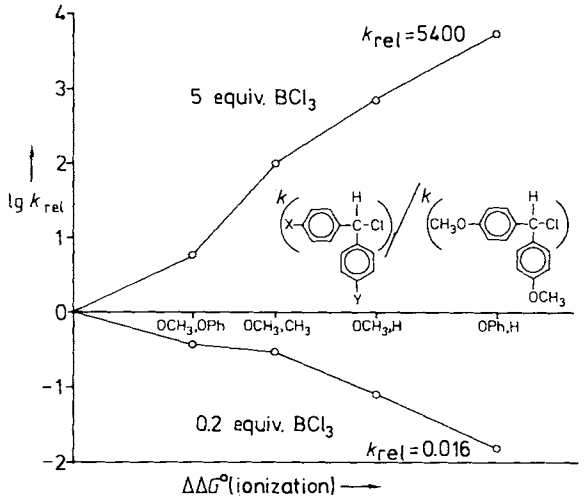

Fig. 2. Relative reactivity of *para*-substituted diarylmethyl chlorides towards 2-methyl-1-pentene in presence of catalytic amounts of Lewis Acid (bottom) and under conditions of complete ionization (top) (CH_2Cl_2/ −70°C).

A situation as described above is generally encountered in electrophilic alkylations of the type $\mathbf{1} + \mathbf{2} \rightarrow \mathbf{3}$. The $\mathbf{1}/\mathbf{1}^+$ and $\mathbf{3}/\mathbf{3}^+$ couples compete for the alkene **2**, and it depends on the magnitude of the particular competition constant, whether selective formation of $\mathbf{3}/\mathbf{3}^+$ or polymerization takes place. Hence the following rules result:

A: *If the carbenium ion* $\mathbf{1}^+$ *is less stabilized than* $\mathbf{3}^+$ [i.e. $\Delta G^0_{ionization}(\mathbf{1}) > \Delta G^0_{ionization}(\mathbf{3})$] *the selective formation of 1 : 1 products requires at least an equivalent amount of a completely ionizing Lewis acid.*

B: *If the carbenium ion* $\mathbf{1}^+$ *is better stabilized than* $\mathbf{3}^+$ [i.e. $\Delta G^0_{ionization}(\mathbf{1}) < \Delta G^0_{ionization}(\mathbf{3})$] *the 1 : 1 products are formed most selectively with (catalytic amounts of) the weakest possible Lewis acid.*

Since ΔH^0 ($\approx \Delta G^0 + \text{const.}$) of the ionization of alkyl chlorides and ΔG^+ of the corresponding solvolysis reactions are proportional to each other,[6] rule B is equivalent to the earlier alkylation rules,[1a,b] which were restricted to systems with a small degree of ionization. These rules have proven useful in the case of electrophilic carboxylations and carbonylations of alkenes[7a] and for a new cyclopropene-cyclopropenone synthesis by addition of trichloropropenylium ions to olefins.[7b]

Received: May 26, 1987 [Z 2261 IE]
German version: *Angew. Chem. 99* (1987) 1059

[1] a) H. Mayr, *Angew. Chem. 93* (1981) 202; *Angew. Chem. Int. Ed. Engl. 20* (1981) 184; b) H. Mayr, W. Striepe, *J. Org. Chem. 48* (1983) 1159; c) H. Mayr, H. Klein, G. Kolberg, *Chem. Ber. 117* (1984) 2555.
[2] H. Mayr, R. Schneider, R. Pock, *Makromol. Chem. Macromol. Symp. 3* (1986) 19.
[3] a) R. Huisgen: *Ausführung kinetischer Versuche* in *Houben-Weyl, Methoden der Organischen Chemie, Band III/1*, Thieme, Stuttgart 1970, p. 144; b) C. K. Ingold, F. R. Shaw, *J. Chem. Soc. 1949*, 575.
[4] R. Schneider, U. Grabis, H. Mayr, *Angew. Chem. 98* (1986) 94; *Angew. Chem. Int. Ed. Engl. 25* (1986) 89.
[5] a) D. Y. Curtin, *Rec. Chem. Progr. 15* (1954) 111; b) L. P. Hammett: *Physical Organic Chemistry*, McGraw-Hill, New York 1970; c) J. I. Seeman, *Chem. Rev. 83* (1983) 83.
[6] E. M. Arnett, C. Petro, P. von R. Schleyer, *J. Am. Chem. Soc. 101* (1979) 522.
[7] a) H. Mayr, M. von der Brüggen, *Chem. Ber.*, in press; b) K. Musigmann, H. Mayr, A. de Meijere, *Tetrahedron Lett. 28* (1987) 4517.

Electrocatalytic Deposition of Polypyrrole**

By *Manfred Oberst* and *Fritz Beck**

Ever since it was demonstrated that durable films are produced on electropolymerization of pyrrole in aqueous[1] and non-aqueous[2] electrolytes, polypyrrole has been the subject of intensive study. In the past few years particular attention has been paid to reversible discharging and recharging of primarily co-deposited anions in view of a possible application as battery electrodes or in electrochromic displays (cf. Refs. [3, 4]). Other possible applications, e.g. in corrosion protection are being studied. The continuous preparation of polymer films by electrochemical deposition on slowly rotating anode cylinders has been described.[5] For the mechanism of the electrochemical deposition the primary formation of a radical cation is assumed as a direct electrode process [Reaction (a)].

$$\text{pyrrole} \longrightarrow \text{pyrrole}^{\oplus\ominus} + e^{\ominus} \qquad \text{(a)}$$

As second reaction step there follows a C–C coupling in the 2-position, either between two radical cations or between a radical cation and a neutral molecule.[6, 7] Since these dimers can (at less positive potentials) be readily further oxidized, the oxidative synthesis of the polymer proceeds according to a scheme 2+2, 2+4, 4+4, etc. When the solubility limit of the oligomers is reached a solid phase forms.

Our voltammetric measurements for the electrodeposition of polypyrrole at a rotating platinum disk electrode reveal a primary step (Fig. 1a), which is partially kinetically determined, even when using freshly distilled, highly pure pyrrole. Polypyrrole is deposited both in the region of the prewave as well as in the positive main branch. The prewave is also observed with Bu_4NBF_4 as supporting electrolyte. It is independent of the pyrrole concentration down to small values (0.01 M). From these findings we conclude that the pyrrole is reacting in the adsorbed state. A polypyrrole layer behaves thereby like platinum.

We have now surprisingly found that a bromine-catalyzed electrodeposition of polypyrrole is also possible. The current-voltage curve in the presence of 1 mM $Br^{\ominus}$ is reproduced in Figure 1b. Once again a prewave can be recognized, but at still more negative potentials. In the course of this primary step *no* film formation is observed. The deep-colored polypyrrole is already clearly recognizable at a layer thickness of 100 nm. During this prewave a polypyrrole film of about 0.5 μm thickness could have been formed. Polypyrrole first grows in the steeply rising part, which coincidentally occurs at the same potential as the prewave in Figure 1a. As experiments on large platinum sheets have shown, the current efficiency is almost 100% (referred to the theoretical value of 2.4 F/mol). The current-voltage curve in the absence of pyrrole, i.e. with 1 mM $Br^{\ominus}$ in acetonitrile (0.1 M Bu_4NBF_4 as supporting electrolyte) shows two steps in the ratio 2 : 1 (cf. Fig. 1c). Consistent with earlier measurements in acetonitrile[8, 9] we assign the first step, which appears at the same potential as the prewave in Figure 1b, to the formation of the tribromine anion [Reaction (b)].

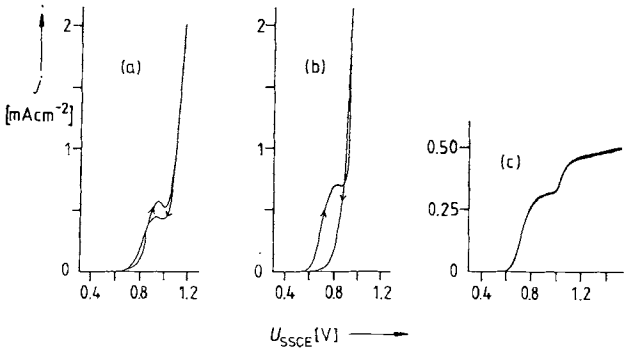

Fig. 1. Current-voltage curves at the rotating Pt-disk electrode ($A = 0.5$ cm^2 at 200 rpm and a voltage scan rate of $v_s = 2$ mV s^{-1}. Solvent: anhydrous acetonitrile; 20°C). a) Bromide-free system, 0.1 M pyrrole, 0.05 M $NaBF_4$; b) 0.1 M pyrrole, 0.1 M Bu_4NBF_4, 1 mM Bu_4NBr; c) pyrrole-free system. Potentials "U_{SSCE}" versus the calomel electrode with $NaCl_{sat}$, which is 236 mV more positive than the standard hydrogen electrode.

$$3\,Br^{\ominus} \longrightarrow [Br_3]^{\ominus} + 2e^{\ominus} \qquad \text{(b)}$$

Only in the course of the second step is free bromine formed [Reaction (c)].

$$[Br_3]^{\ominus} \longrightarrow 3/2\,Br_2 + e^{\ominus} \qquad \text{(c)}$$

The free bromine, here formulated as tribromine complex can oxidize pyrrole radical cations according to [Reaction (d)].

$$\text{pyrrole} + Br_3 \xrightarrow{k} \text{pyrrole}^{\oplus\ominus} + [Br_3]^{\ominus} \qquad \text{(d)}$$

The anion is reoxidized at the electrode. The homogeneous reaction (d) takes place in a reaction boundary layer in front of the electrode. At higher pyrrole concentrations it is quasi first order. This means that the thickness of the reaction layer can be calculated using the simple relationship

$$\rho = \sqrt{D/k} \qquad \text{(e)}$$

where D = diffusion coefficient and k = first order chemical rate constant; ρ concomitantly determines the rate of back diffusion of the $[Br_3]^{\ominus}$ to the electrode. That is, with the assumption of a rapid electrochemical partial step, there is a current amplification proportional to $\sqrt{k}$ and to the concentration of pyrrole.

When a dilute solution of bromine in acetonitrile is mixed with a solution of pyrrole in acetonitrile a sudden decoloration is observed, followed by a slow coloration to dark-green and subsequent separation of a black precipitate of pyrrole black; its formation with chemical oxidizing agents has been investigated by *Gardini*.[10]

Experiments with the rotating ring-disk electrode reveal the presence of reducible oligomeric radical cations, but no Br_2. This means that reaction (d) is rapid. Our mechanism is also supported by the finding that, in the galvanostatic deposition progressively less substance is deposited on the rotating disk with increasing speed of rotation. Since the height of the two steps in Figure 1c and that of the primary step in Figure 1b increases proportionally to $\sqrt{\omega}$ (ω = angular velocity), and thus (according to *Levich*) there is a limiting diffusion, it follows that an ever greater increasing percentage of the current is involved in the ineffective reaction (b) with increasing ω.

A homogeneous redox catalysis by electrolytically generated bromine is also observed in other electroorganic

[*] Prof. Dr. F. Beck, Dipl.-Chem. M. Oberst
Fachbereich 6—Elektrochemie der Universität—Gesamthochschule
Lotharstr. 1, D-4100 Duisburg 1 (FRG)

[**] This work was supported by the Arbeitsgemeinschaft Industrieller Forschungsvereinigungen (AIF) and the Nordrhein-Westfälische Ministerium für Wissenschaft und Forschung.

reactions, e.g. in the anodic methoxylation of furan[11] and the anodic oxidation of propylene to propylene oxide.[12] Even pyrrole has already been electropolymerized in aqueous HBr[13] and NaBr solution.[14] In this case, however, the polymer contains considerable amounts of bromine (up to 0.8 mol Br per pyrrole unit), which may in part be covalently bound. We use bromide in only small concentration, and the polymeric product contains practically no bromine; that is, bromide is a real catalyst. *Bidan* et al. have recently reported on the polymerization of 2-bromopyrrole to polypyrrole with cleavage of HBr.[15] Under our conditions, the intermediary formation of a bromine-substitution product can, however, be ruled out on kinetic grounds.

The practical significance of the electroanalytical deposition of polypyrrole lies in the realization of higher current densities. Whereas small current densities (below 1 mA cm^{-2}), which obviously lie in the region of the primary step in Figure 1a, are usually recommended,[16] a deposition is possible at essentially higher current densities in the presence of small bromide concentrations. In this way the scan times can be substantially decreased.

Received: May 27, 1987 [Z 2263 IE]
German version: *Angew. Chem. 99* (1987) 1061

CAS Registry numbers:
$[Br_3]^{\ominus}$, 14522-80-6; $Br^{\ominus}$, 24959-67-9; pyrrole, 109-97-7; pyrrole black, 62449-68-7; polypyrrole, 30604-81-0; pyrrole radical cation, 34468-30-9.

[1] A. Dall'Olio, Y. Dascota, V. Varacca, V. Bocchi, *C. R. Acad. Sci. Ser. C 267* (1968) 433.
[2] A. F. Diaz, K. K. Kanazawa, G. P. Gardini, *J. Chem. Soc. Chem. Commun. 1979*, 635; cf. A. Stanienda, *Z. Naturforsch. B 22* (1967) 1107.
[3] G. Wegner, *Angew. Chem. 93* (1981) 352; *Angew. Chem. Int. Ed. Engl. 20* (1981) 361.
[4] T. A. Skotheim (Ed.): *Handbook of Conducting Polymers, Vol. 2*, Marcel Dekker, New York 1986.
[5] H. Naarmann, *Makromol. Chem. Macromol. Symp. 8* (1987) 1.
[6] E. M. Genies, G. Bidan, A. F. Diaz, *J. Electroanal. Chem. 149* (1983) 101.
[7] J. Heinze, K. Hinkelmann, M. Dietrich, J. Mortensen, *DECHEMA-Monogr. 102* (1986) 209.
[8] M. Michlmayr, D. T. Sawyer, *J. Electroanal. Chem. 23* (1969) 387.
[9] T. Iwasita, M. C. Giordano, *Electrochim. Acta 14* (1969) 1045.
[10] G. P. Gardini, *Adv. Heterocycl. Chem. 15* (1973) 67.
[11] N. Clauson-Kaas, F. Limborg, K. Glens, *Acta Chem. Scand. 6* (1952) 531.
[12] F. Beck, *Pure Appl. Chem. 5* (1974) 111.
[13] G. Mengoli, M. M. Musiani, M. Fleischmann, D. Pletcher, *J. Appl. Electrochem. 14* (1984) 285.
[14] S. Tokito, T. Tsutsui, S. Saito, *Chem. Lett. 1985*, 531.
[15] P. Audebert, G. Bidan, *Synth. Met. 15* (1986) 9.
[16] A. F. Diaz, K. K. Kanazawa, J. I. Castillo, J. A. Logan in R. B. Seymour (Ed.): *Conductive Polymers*, Plenum Press, New York 1981, p. 149.

cis- and *trans*-1,2-Dilithioethylene**

By *Adalbert Maercker,** *Thomas Graule,* and *Wolfgang Demuth*

Dedicated to Professor Ulrich Schöllkopf on the occasion of his 60th birthday

We recently found that vicinal dilithioalkenes are accessible by addition of lithium to alkynes.[1] When the reaction is carried out with open-chain alkynes in diethyl ether, insoluble *trans*-products are formed, whereas cyclooctyne affords the soluble *cis*-1,2-dilithiocyclooctene. All attempts to prepare the 'parent compounds' *cis*- and *trans*-1,2-dilithioethylene have so far failed, even though at least the *trans*-compound has been estimated calculationally to have a higher stability than methyl- and vinyllithium.[2] Inconsistent with this proposal was the finding that only one stannyl moiety in the *trans*-1,2-bis(tributylstannyl)ethylene **1** ($R = n\text{-}C_4H_9$) can be replaced by lithium upon reaction with *n*-butyllithium.[3] We are therefore of the opinion that even *n*-butyllithium is more stable than *trans*-1,2-dilithioethylene **6**.[4]

Switching over to *tert*-butyllithium for the R_3Sn/Li exchange in **1** had little hope of success, however, since the ate-complex intermediate with four *tert*-butyl groups attached to the five-coordinate tin necessary for the second exchange would be sterically too demanding. Thus, e.g., even in the case of tetramethylstannane in this way maximally two methyl groups can be replaced by *tert*-butyl residues.[5] We have therefore replaced the four-coordinate tin by two-coordinate mercury prior to the reaction with *tert*-butyllithium and thus indeed have been able to achieve a double metal-metal exchange. The compounds **6** and **7** already formed at −75 °C in diethyl ether or THF were derivatized with dimethyl sulfate, which had the advantage that the gaseous reaction products *trans*- **9** and *cis*-2-butene **10** could be driven out of the reaction mixture and quantitatively determined as *meso*- **8** and *d,l*-2,3-dibromobutane **11**, respectively, after passage into a solution of bromine in chloroform. The analysis was accomplished gas chromatographically as well as by combined GC/MS.

One could argue that the derivatization might also have proceeded stepwise, i.e. that the second Hg/Li exchange has taken place only after the introduction of the first methyl group. This argument can easily be invalidated: It could be shown that the metal-metal exchange in the presence of dimethyl sulfate functions very poorly, since *tert*-butyllithium reacts much more rapidly with dimethyl sulfate than with the mercury compounds.[6] The finding that the amount of di-*tert*-butylmercury in the reaction mixture before and after the derivatization is the same, also speaks against a mercury-lithium exchange during the addition of the dimethyl sulfate. Crystallization of the 1,2-dilithioethylenes and thus the separation from the di-*tert*-butylmercury has so far not been accomplished. No statements can be made therefore about the exact structure and degree of association of the compounds.

Interestingly, it was observed that reaction of *cis*-1,2-bis(chloromercurio)ethylene **3** containing 7% **2** at −75 °C does indeed afford the 2-butenes **10** and **9** in the ratio 93 : 7, but, after 10 min at 0 °C, the amount of *trans* product increases to 65%. This first suggested a rapid rearrangement of the *cis*-1,2-dilithioethylene **7** into the *trans*-isomer **6**.[7] In the meantime it has emerged that this *cis-trans* rearrangement **7** → **6** is only simulated due to a very much higher *kinetic* stability of **6** in comparison to **7**. Namely, *cis*-1,2-dilithioethylene **7** decomposes particularly rapidly, splitting off lithium hydride,[8] and, as expected, the lithioacetylene **12** formed thereby is immediately metalated to dilithioacetylene **14**. Not only is excess *tert*-butyllithium suitable as metalating reagent, but also the dilithioethylenes themselves. The resulting vinyllithium **13**, like the dilithioacetylene **14**, was derivatized by dimethyl sulfate, so that finally the bromination products of propene **15** and 2-butyne **16** could be detected gas chromatographically in addition to **8** and **11**. The methane formed by reaction of lithium hydride with dimethyl sulfate was detected mass spectrometrically.

[*] Prof. Dr. A. Maercker, Dipl.-Chem. T. Graule, Dr. W. Demuth
Institut für Organische Chemie der Universität
Adolf-Reichwein-Strasse, D-5900 Siegen (FRG)

[**] Polylithium Organic Compounds, Part 6. This work was supported by the Fonds der Chemischen Industrie.—Part 5: [1].

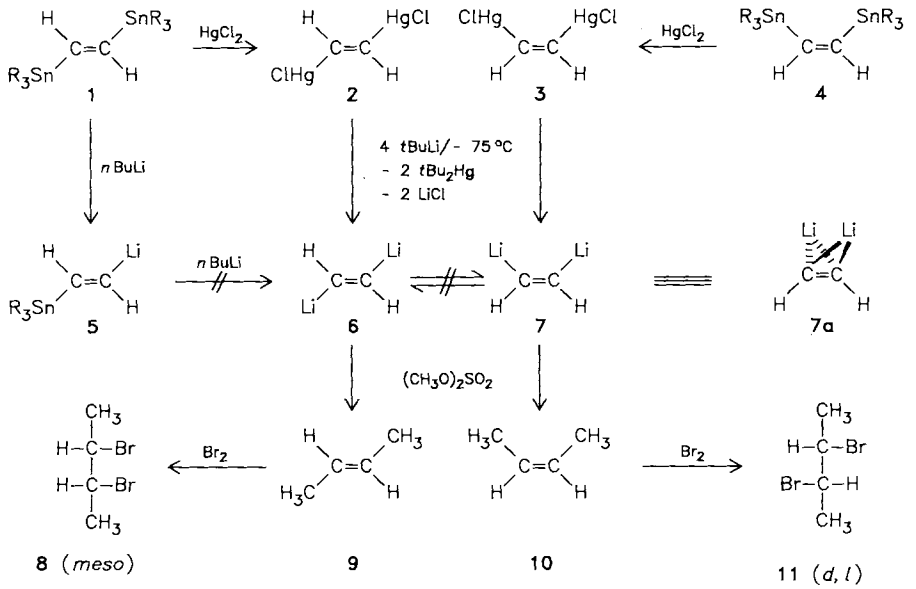

8 (*meso*) 9 10 11 (*d, l*)

Indications that the rearrangement **6** ⇌ **7** does not take place were already provided in experiments in which *n*-decane had been added as standard. Despite varying yields it was recognizable that with increasing portions of *trans*-2-

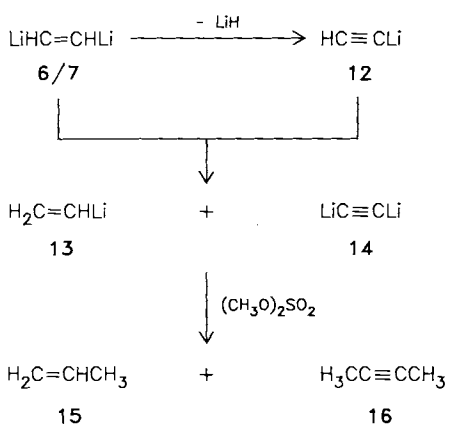

butene **9** in the reaction mixture the overall yield of 2-butene **9** + **10** decreased, whereas the amount of propene **15** and 2-butyne **16** became greater and greater.[9]

Final proof of this conception was then possible however with the help of the isotope technique. Doubly deuteriated **2** and doubly deuteriated **3** were each prepared and allowed to react in the form of a 4 : 1 *cis-trans*-mixture consisting of [D_2]-**3** + **2** and **3** + [D_2]-**2**, respectively, with *tert*-butyllithium. In none of the cases was there any appreciable change in the isotopic composition of the *trans*-1,2-dilithioethylene **6** upon enrichment in the reaction mixture, i.e. a rearrangement **6** ⇌ **7** can be ruled out. Interestingly, in an incompletely deuteriated sample of *cis*-1,2-dilithioethylene, the deuterium is enriched; this can be attributed to an isotope effect during lithium hydride elimination (LiH > LiD). In the decomposition of an undeuteriated sample of **7** in deuteriated diethyl ether, no deuterium was incorporated in the vinyllithium **13**, i.e. the solvent is comparatively slowly decomposed.[10]

Experimental Procedure

6: 0.50 g (1.0 mmol) of **2**, prepared from **1** (R = *n*-C_4H_9) [11] by reaction with $HgCl_2$ [12], was slurried with 2.0 mL of anhydrous THF under argon in a 10 mL Schlenk tube. 2.8 mL (4.0 mmol) of a 1.44 M solution of *tert*-butyllithium in pentane (Metallgesellschaft, Frankfurt am Main) was then added to the vigorously stirred slurry (magnetic stirrer) within 15 min at −75 °C from a gas-tight syringe and the mixture stirred for a further 15 min at this temperature. Derivatization was then carried out with 0.6 g (4.76 mmol) of dimethyl sulfate in 2.0 mL of diethyl ether at −75 °C, whereby the gas formed was passed into a solution of 1.2 mmol of bromine in 10.0 mL of chloroform with *n*-decane as standard. To ensure complete transfer of the dissolved gas the reaction mixture was warmed slowly to room temperature, heated to reflux (35 °C), and a weak flow of argon passed through the apparatus for ca. 10 min. Gas chromatographic analysis revealed an overall yield of 84.3% of dibromo adducts: 9.5% ethylene (at least partly from the solvent), 14.2% propene **15**, 13.0% 2-butyne **16**, 47.3% *trans*-2-butene **9**, and 0.3% *cis*-2-butene **10**.

3, prepared from **4** (R = CH_3) [13], was allowed to react in an analogous way with *tert*-butyllithium.

The starting material for [D_2]-**2** and [D_2]-**3** was the corresponding *cis*-1,2-dideuterio-1,2-bis(trimethylstannyl)ethylene [D_2]-**4** (R = CH_3), which was prepared from dideuterioacetylene and from which the corresponding *trans*-compound [D_2]-**1** (R = CH_3) can be synthesized by photoisomerization [13].

Received: June 4, 1987;
revised: July 21, 1987 [Z 2282 IE]
German version: *Angew. Chem. 99* (1987) 1075

[1] A. Maercker, T. Graule, U. Girreser, *Angew. Chem. 98* (1986) 174; *Angew. Chem. Int. Ed. Engl. 25* (1986) 167.
[2] Y. Apeloig, T. Clark, A. J. Kos, E. D. Jemmis, P. von R. Schleyer, *Israel J. Chem. 20* (1980) 43.
[3] D. Seyferth, S. C. Vick, *J. Organomet. Chem. 144* (1978) 1.
[4] A. Maercker, M. Theis, *Top. Curr. Chem. 138* (1987) 1.
[5] D. Farah, T. J. Karol, H. G. Kuivila, *Organometallics 4* (1985) 662.
[6] Small amounts of 2-butene are indeed also formed, but no 2-butyne, since, in contrast to 1,2-dilithioethylene, the monolithioethylene precursors do not split off lithium hydride.
[7] According to ab-initio calculations carried out in 1979 [2], **6** should be 1.4 kcal/mol less stable than **7**. The energies of the two 1,2-dilithioethylenes were therefore recently recalculated using improved methods, with the result that the *trans*-compound is now 1.6 kcal/mol more stable than the *cis*-isomer **7a**. A computerized determination of the reaction mechanism of the *cis-trans* isomerization has also been proposed. Cf. P. von R. Schleyer, E. Kaufmann, A. J. Kos, T. Clark, J. A. Pople, *Angew. Chem. 98* (1986) 164; *Angew. Chem. Int. Ed. Engl. 25* (1986) 169.
[8] The easy elimination of lithium hydride from 1,2-dilithioethylene is remarkable, since according to calculations [2] it should proceed strongly endothermally, much more unfavorably than the elimination of H_2 or Li_2, neither of which have we been able to observe. We presume that lithioacetylene initially forms a relatively stable complex with lithium hydride. This could be similar to the case of 1,2-dilithioethane, where the experimental results could also be only explained theoretically after assuming formation of an extremely stable complex of vinyllithium with lithium hydride.
[9] Some vinyllithium **13** and dilithioacetylene **14** are already formed during the synthesis at −75 °C, presumably by splitting off lithium hydride

from the second ate complex intermediate, as we have previously observed also in other Hg/Li exchange reactions [4].
[10] A. Maercker, W. Demuth, *Justus Liebigs Ann. Chem. 1977*, 1909.
[11] E. J. Corey, R. H. Wollenberg, *J. Org. Chem. 40* (1975) 3788; J. C. Bottaro, R. N. Hanson, D. E. Seitz, *ibid. 46* (1981) 5221.
[12] A. N. Nesmeyanov, A. E. Borisov, Chi-Hua Wan, *Izv. Akad. Nauk SSSR, Ser. Khim. 1967*, 1141.
[13] T. N. Mitchell, A. Amamria, H. Killing, D. Rutschow, *J. Organomet. Chem. 241* (1983) C45; *ibid. 304* (1986) 257.

chain extension of optically active 2-oxyalkanals by a 2-hydroxy-3-methylpropanal unit **A** to give branched deoxyhexoses in three steps (including a simple diastereomer separation; Scheme 1).

(*S*)-2-Benzyloxypropanal **5**,[5,6] obtained from (*S*)-ethyl lactate, reacts with **2**[3,4] to give two enantiomerically pure (*Z*)-3,4-*anti*-adducts[7,8] **6** and **7** in the ratio 53:47 (42.5% of **6** and 37.5% of **7** after a simple chromatographic separation on silica gel). As expected, the chiral center of the aldehyde **5** does not effect a diastereofacial differentiation, since the topicity of the carbonyl attack is determined by the stereogenic α-C-atom of the racemic reagent **2**.[9]

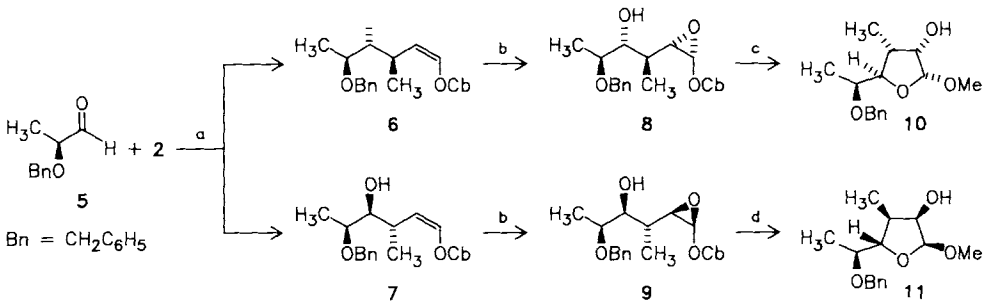

Scheme 1. a) 1.1 equiv. **2**, 16 h at −78°C, Et_2O; column chromatography (LC) on silica gel, ether/hexane. b) 1.5 equiv. *t*BuOOH [10], 2 mol% $VO(acac)_2$; 0.07 M in CH_2Cl_2, 16 h, 0→20°C; c) unpurified **8** in 5 mL of anhydrous CH_3OH and 5 mL CH_2Cl_2/mmol, 1.0 equiv. Et_3N, LC [1b]. d) As for c), but without CH_2Cl_2.

Enantioselective Synthesis of Methylfuranosides of Unnatural 3,6-Dideoxy-3-methylaldohexoses from Lactates by Homoaldol Reactions**

By *Dieter Hoppe,* Gerhard Tarara, Marcus Wilckens, Peter G. Jones, Dieter Schmidt,* and *John J. Stezowski*

Dedicated to Professor Ulrich Schöllkopf on the occasion of his 60th birthday

As we have recently shown,[1] simple racemic 1-oxyoxiranes of type **4** with four contiguous chiral centers are accessible with high diastereoselectivity (>98% *ds*) in only two steps by homoaldol reactions:[2] addition of the α-titanated[3] (*E*)-2-butenylcarbamate **2**[4] to prochiral aldehydes yields the *anti*-enolcarbamates **3**, which are converted via vanadyl-catalyzed oxidation into the reactive epoxides **4**. Depending on the reaction conditions, nucleophiles open the three-membered ring either at C-2 (inversion of configuration) or at C-1 (retention at C-2[1b]). We now report the

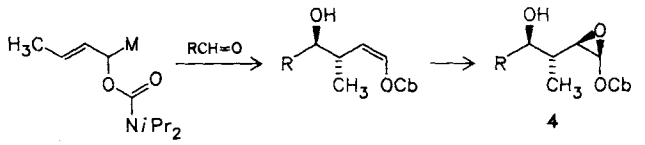

1, M = Li · tmeda
2, M = $Ti(NEt_2)_3$
Cb = $CNiPr_2$; racemates

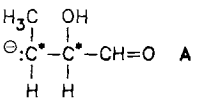

The reaction of the more polar 4,5-*anti*-diastereomer **6** with di(*tert*-butyl) hydroperoxide via $VO(acac)_2$-catalysis[10,2a] yields the diastereomerically pure crystalline epoxide **8** (yield 92%), whose relative—and thus absolute—configuration was confirmed by an X-ray structure analysis. **7** correspondingly afforded the epoxide **9** in 97% yield. Acid-catalyzed methanolysis[1b] of the oxirane **8** at −78°C leads in 75% yield to a single methylfuranoside **10**,[12] whose α-L-*allo* configuration followed from that of the precursor **6** and comparison of the ^{1}H-NMR spectrum with that of an analogue whose structure had been confirmed by a crystal structure analysis.[1b] In the same way, the diastereomer **9** furnishes β-L-*talo*-furanoside **11** in 79% yield.

The method outlined here should be generally applicable to the de-novo synthesis[13] of 3-*C*-branched deoxyaldoses. Few steps are necessary since the terminal C-atom in the homoenolate reagent **2** is already present as a masked carbonyl group and, in addition, the (1*Z*)-substituent in the adduct **6** and **7** permits subsequent reactions that are highly stereoselective. Further advantages are the formation of anomerically pure furanosides and the chemical differentiation of all hydroxy groups. The free 2-hydroxy group in **10** and **11** allows inversion of configuration at C-2 in a few steps. Thus *ent*-**10**[14] affords the α-D-*altro*-furanoside *ent*-**12** in 65% yield by successive trifluoromethanesulfonylation, acetolysis with cesium acetate,[15,16] and hydrolysis. Correspondingly, *ent*-**11**[14] furnishes the β-D-*galacto*-furanoside *ent*-**13** (yield 67%) (Scheme 2). Table 1 contains selected physical and NMR spectroscopic data for **8**–**11** as well as *ent*-**12** and *ent*-**13**.

The only drawback of the simple racemic reagent **2** is that two diastereomers are formed in similar amounts; this disadvantage does not apply to the enantiomerically pure 1-alkylated homoenolate reagents (e.g. CH_3 for 1-H in **2**).[9,17,18]

[*] Prof. Dr. D. Hoppe, G. Tarara, M. Wilckens
Institut für Organische Chemie der Universität
Olshausenstr. 40, D-2300 Kiel 1 (FRG)
Prof. Dr. P. G. Jones, D. Schmidt
Institut für Anorganische Chemie der Universität
Tammannstr. 4, D-3400 Göttingen (FRG)
Prof. Dr. J. J. Stezowski
Institut für Organische Chemie der Universität
Pfaffenwaldring 55, D-7000 Stuttgart 80 (FRG)

[**] This work was supported by the Deutsche Forschungsgemeinschaft and the Fonds der Chemischen Industrie. We thank Schering AG (Bergkamen) and BASF AG (Ludwigshafen) for generous gifts of chemicals.

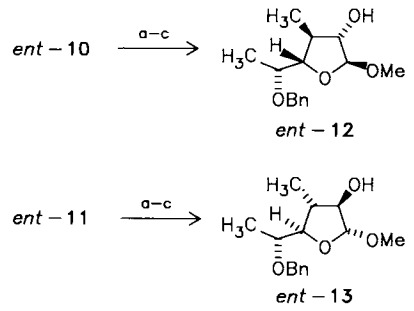

Scheme 2. a) 2.0 equiv, $(CF_3SO_2)O$, pyridine, $-15 \rightarrow 10°C$, 5 h; aqueous work-up. b) 5.0 equiv. CsOAc, DMSO, 15 h at 50°C [16]. c) 2.0 equiv. KOH in CH_3OH, 4 h at 20°C; LC on silica gel.

Table 1. Some physical data of **8**–**11** and *ent*-**12** and *ent*-**13**. ^1H- and ^{13}C-NMR: δ values ($CDCl_3$).

8: m.p. = 122°C (ether/pentane); $[\alpha]_D^{21} = +35.7$ ($c = 1.5$, CH_3OH). ^1H-NMR: 5.63 (d, $J_{1,2} = 2.5$ Hz, 1-H); 3.06 (dd, $J_{2,3} = 9.5$ Hz, 2-H); 2.0 (m, 3-H); 3.5–4.2 (m, 4-H and 5-H); 2.90 (s, OH) [8]. ^{13}C-NMR: 77.00 (C-1); 57.74 (C-2); 35.38 (C-3); 78.00 (C-4); 75.83 (C-5); 15.90 (C-6); 14.16 (3-CH_3)

9: oil; $[\alpha]_D^{20} = +16.4$ ($c = 3$, CH_3OH). ^1H-NMR: 5.6 (d, $J_{1,2} = 2.5$ Hz, 1-H); 3.16 (dd, $J_{2,3} = 9$ Hz, 2-H); 1.86 (m, 3-H); 3.5 (dd, $J_{4,3} = 3$ Hz, $J_{4,5} = 8$ Hz, 4-H); 2.25 (s, OH) [8]. ^{13}C-NMR: 77.24 (C-1); 56.00 (C-2); 34.00 (C-3); 78.37 (C-4); 74.99 (C-5); 15.39 (C-6); 14.00 (3-CH_3)

10: oil; $[\alpha]_D^{21} = -80.8$ ($c = 4$, CH_3OH). ^1H-NMR: 4.88 (d, $J_{1,2} = 4.5$ Hz, 1-H); 4.18 (ddd, $J_{2,3} = 7.5$ Hz, $J_{2,OH} = 9.0$ Hz, 2-H); 2.25 (m, H-3); 3.77 (dd, $J_{4,3} = 5.8$ Hz, $J_{4,5} = 3.8$ Hz, 4-H); 3.62 (dq, 5-H); 1.19 (d, $J_{6,5} = 6.4$ Hz, 6-H_3). ^{13}C-NMR: 103.42 (C-1); 73.20 (C-2); 35.92 (C-3); 87.77 (C-4); 76.36 (C-5); 15.95 (C-6)

11: oil; $[\alpha 7_D^{20} = +97.3$ ($c = 4$, CH_3OH). ^1H-NMR: 4.95 (d, $J_{1,2} = 4.4$ Hz, 1-H); 4.17 (ddd, $J_{2,3} = 7.6$ Hz, $J_{2,OH} = 7.5$ Hz, 2-H); 2.20 (m, 3-H); 3.74 (dd, $J_{4,3} = 7.2$ Hz, 4-H); 3.55 (dq, $J_{5,4} = 3.5$ Hz, 5-H); 1.25 (d, $J_{6,5} = 6.4$ Hz, 3-H_3). ^{13}C-NMR: 103.49 (C-1); 73.35 (C-2); 36.54 (C-3); 86.83 (C-4); 74.21 (C-5); 15.78 (C-6)

ent-**12**: oil; $[\alpha]_D^{20} = +59.1$ ($c = 4$, CH_3OH). ^1H-NMR: 4.83 (d, $J_{1,2} = 0.7$ Hz, 1-H); 3.69 (m, 2-H); 2.19 (m, 3-H); 3.75 (dd, $J_{4,3} = 3.5$ Hz, $J_{4,5} = 2.3$ Hz, 4-H); 3.82 (dq, $J_{5,6} = 7.5$ Hz, 5-H); 1.21 (d, 6-H_3); 1.16 (d, $J = 6.5$ Hz, 3-CH_3); 3.62 (s, OH), 3.34 (s, OCH_3). ^{13}C-NMR: 110.51 (C-1); 80.88 (C-2); 41.00 (C-3); 89.27 (C-4); 75.94 (C-5); 18.62 (C-6); 15.96 (3-CH_3); 54.48 (OCH_3)

ent-**13**: oil; $[\alpha]_D^{19} = -88.9$ ($c = 4$, CH_3OH). ^1H-NMR: 4.82 ("s", $J_{1,2} < 0.3$ Hz, 1-H); 3.60 (m, 2-H); 2.50 (m, 3-H); 3.75 (dd, $J_{4,3} = 5.9$ Hz, $J_{4,5} = 4.0$ Hz, 4-H); 3.55 (dq, $J_{5,6} = 6.4$ Hz, 5-H); 1.36 (d, 6-H_3); 1.15 (d, $J = 7.4$ Hz, 3-CH_3); 3.72 (d, $J = 9.5$ Hz, OH); 3.33 (s, OCH_3). ^{13}C-NMR: 110.47 (C-1); 81.12 (C-2); 43.08 (C-3); 88.74 (C-4); 74.54 (C-5); 17.43 (C-6); 15.38 (3-CH_3); 54.54 (OCH_3)

Received: June 1, 1987 [Z 2273 IE]
German version: *Angew. Chem. 99* (1987) 1079

CAS Registry numbers:
2, 110455-87-3; **5**, 81445-44-5; **6**, 110418-30-9; 7, 110455-86-2; **8**, 110418-31-0; **9**, 110418-32-1; **10**, 110418-33-2; **11**, 110418-34-3; *ent*-**12**, 110418-35-4; *ent*-**13**, 110418-36-5.

[1] a) D. Hoppe, J. Lüssmann, P. G. Jones, D. Schmidt, G. M. Sheldrick, *Tetrahedron Lett. 27* (1986) 3591; b) J. Lüssmann, D. Hoppe, P. G. Jones, C. Fittschen, G. M. Sheldrick, *ibid. 27* (1986) 3595.

[2] Reviews: D. Hoppe, *Angew. Chem. 96* (1984) 930; *Angew. Chem. Int. Ed. Engl. 23* (1984) 932; D. Hoppe in M. P. Schneider (Ed.): *Enzymes as Catalysts in Organic Synthesis*, Reidel, Dordrecht 1986, p. 176.

[3] Reviews: D. Seebach, B. Weidmann in R. Scheffold (Ed.): *Modern Synthetic Methods 1983*, Salle, Frankfurt 1983; M. T. Reetz: *Organotitanium Reagents in Organic Synthesis*, Springer, Berlin 1986.

[4] D. Hoppe, R. Hanko, A. Brönneke, F. Lichtenberg, E. van Hülsen, *Chem. Ber. 118* (1985) 2822.

[5] **5**: $[\alpha]_D^{20} = -63.1$ (neat); D. C. Baker, L. D. Hawkins, *J. Org. Chem. 47* (1982) 2179, prepared by diisobutylaluminum hydride reduction [6a] of ethyl (*S*)-2-benzyloxypropionate [6b].

[6] a) S. K. Massad, L. D. Hawkins, D. C. Baker, *J. Org. Chem. 48* (1983) 5180; b) K. Mislow, R. E. O'Brien, H. Schaefer, *J. Am. Chem. Soc. 84* (1962) 1940.

[7] 6 and 7, R_f(ether/pentane 1:1) = 0.25 and 0.37, respectively. $[\alpha]_D^{19}$: **6**: −16.0; 7: +56.1 ($c = 2$, $CHCl_3$). In contrast to *rac*-**6** and *rac*-7, no splitting is observed in the ^1H-NMR spectra of (−)-**6** and (+)-7 with Eu(hfc)$_3$. ^1H-NMR ($CDCl_3$, δ): **6**: 2.05 and 7: 2.65 (each s, OH) [8].

[8] ^1H-NMR spectroscopic assignment of *syn*- and *anti*-diols: B. Landmann, R. W. Hoffmann, *Chem. Ber. 120* (1987) 331.

[9] **1** and **2** are chiral and configurationally stable at the reaction temperature; cf. D. Hoppe, T. Krämer, *Angew. Chem. 98* (1986) 171; *Angew. Chem. Int. Ed. Engl. 25* (1986) 160.

[10] E. D. Mihelich, K. Daniels, D. J. Eickhoff, *J. Am. Chem. Soc. 103* (1981) 7690.—Review: K. B. Sharpless, T. R. Verhoeven, *Aldrichim. Acta 12* (1979) 63.

[11] Crystal structure analysis of **8**: tetragonal, $P4_32_12$, $a = 877.6(1)$, $c = 5767.1(8)$ pm, $V = 4.442$ nm^3, $Z = 8$, $\rho_{calc} = 1.13$ Mg m^{-3}, $Cu_{K\alpha}$ radiation, $\mu = 0.6$ mm^{-1}, $R = 0.046$, $R_w = 0.052$ for 2618 extinction-corrected reflections with $F > 4\sigma(F)$. The absolute configuration (and thus the space group) was chosen to agree with the known configuration of **5**. Further details of the crystal structure investigation are available on request from the Fachinformationszentrum Energie, Physik, Mathematik GmbH, D-7514 Eggenstein-Leopoldshafen 2 (FRG), on quoting the deposition number CSD-52585, the names of the authors, and the journal citation.

[12] The anomeric ratio here is determined kinetically. The acidic reaction mixtures isomerize at room temperature to give 1-*epi*-**10** and 1-*epi*-**11**, respectively.

[13] Reviews: R. R. Schmidt, *Pure Appl. Chem. 59* (1987) 415; A. Zamojski, A. Banaszek, G. Grynkiewicz, *Adv. Carbohydr. Chem. Biochem. 40* (1982) 1.

[14] Obtained from *ent*-**5**, which was prepared from biotechnologically accessible (*R*)-isobutyl lactate.

[15] Review: B. Klieser, L. Rossa, F. Vögtle, *Kontakte (Darmstadt) 1984*, No. 1, p. 3.

[16] Alternative: Step a) 2.0 equiv. CH_3SO_2Cl, pyridine, 24 h at $0°C \rightarrow 20°C$; step b) 10 equiv. KOAc, 22 h at 120°C in DMSO, yield 40–45% *ent*-**12** and *ent*-**13**, respectively; partial thermal elimination of the acetates to give the furan.—Acetolyses or formolyses according to the method of *Mitsunobu* failed; D. M. Mitsunobu, *Synthesis 1981*, 1.

[17] T. Krämer, D. Hoppe, *Tetrahedron Lett. 28* (1987), in press.

[18] Whether the known asymmetric *n*-butanal-β-enolate equivalents are suitable for this purpose is unknown. a) V. S. Jephcote, A. J. Pratt, E. J. Thomas, *J. Chem. Soc. Chem. Commun. 1984*, 800. b) H. Roder, G. Helmchen, E.-M. Peters, K. Peters, H.-G. von Schnering, *Angew. Chem. 96* (1984) 895; *Angew. Chem. Int. Ed. Engl. 23* (1984) 898. c) R. W. Hoffmann, S. Dresely, *ibid. 98* (1986) 186 and *25* (1986) 189.

Cobalt-Mediated [2+2+2]Cycloadditions of Alkynes to the Imidazole 4,5-Double Bond. First Synthesis of the 3*a*,7*a*-Dihydrobenzimidazole Nucleus and Its Preliminary Chemistry Including a Novel Quinoline Construction**

By *Roland Boese, Hans-Joachim Knölker,* and *K. Peter C. Vollhardt**

We recently reported that the aromatic 2,3-double bonds in indole[1] and pyrrole[2] could be activated by $(C_5H_5)Co$ to enter into [2+2+2]cycloadditions[3] with alkynes giving rise to hitherto unknown heterocycles. An application of this methodology to the imidazole nucleus was deemed significant as: 1) it provided the opportunity to test the relative reactivities of a C–C versus a C–N double bond, 2) it represented a significant expansion of the substrate pool available to this reaction, and 3) it involved a heterocycle abundant not only in ordinary natural and/or medicinal products[4] but also in two of the nucleic acid bases, adenine and guanine. Herein we describe a novel mode of

[*] Prof. Dr. K. P. C. Vollhardt, Dr. H.-J. Knölker
Department of Chemistry, University of California,
The Materials and Chemical Sciences Division,
Lawrence Berkeley Laboratory, Berkeley, CA 94720 (USA)
Dr. R. Boese
Institut für Anorganische Chemie der Universität-Gesamthochschule
Universitätsstrasse 5-7, D-4300 Essen 1 (FRG)

[**] This work was supported by the National Institutes of Health (GM 22479). *H.-J. K.* was the recipient of a DFG postdoctoral fellowship (1986). *K. P. C. V.* was a Miller Research Professor in Residence (1985–1986).

reactivity[5] (Scheme 1) of this readily available moiety mediated by cobalt which allows its extensively chemo-, regio-, and stereospecific elaboration to other oligoheterocycles. Table 1 summarizes our results.[6]

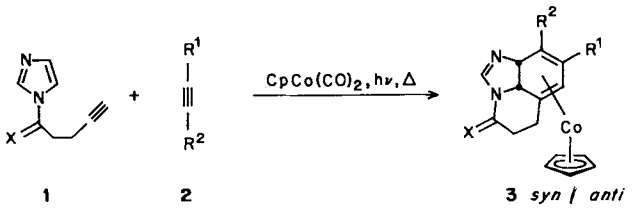

Scheme 1. *syn* and *anti* give the position of Co relative to tertiary bridgehead hydrogens.

Table 1. Preparation of **1** and results of their (C_5H_5)Co-mediated cyclization with **2** to give **3** [6].

1	Method of preparation [Ref.] (Yield [%])	2	3 (Yield [%])
1a, (X = O)	[7] (91)	**2a** $R^1 = R^2 = Si(CH_3)_3$	**3a** (*anti*) (72)
1b, (X = H_2)	[8] (85)	**2a** $R^1 = R^2 = Si(CH_3)_3$	**3b** (*anti*) (18) **3b** (*syn*) (18)
1a	[7] (91)	**2b** $R^1 = CH_2CH_3$, $R^2 = Si(CH_3)_3$	**3c** (*anti*) (22) $R^1 = CH_2CH_3$, $R^2 = Si(CH_3)_3$
1a	[7] (91)	**2c** $R^1 = OCH_3$, $R^2 = Si(CH_3)_3$	**3d** (*anti*) (25) $R^1 = OCH_3$, $R^1 = Si(CH_3)_3$
1a	[7] (91)	**2d** $R^1 = COOCH_3$, $R^2 = Si(CH_3)_3$	**3e** (*anti*) (35) $R^1 = COOCH_3$, $R^2 = Si(CH_3)_3$ **3f** (*anti*) (10) $R^1 = Si(CH_3)_3$, $R^2 = COOCH_3$

Several comments are in order to amplify our data. 1) Some optimization of the efficiency of the reaction was carried out only for **3a** leading to an improvement of the initial yield from 26% (cyclization executed at 25 °C) to 72%. We have remarked earlier[2] that variation of the reaction conditions (temperature, solvent, addition rates, substrate ratios, use of $[(C_5H_5)Co(CH_2{=}CH_2)_2]$) can affect yields dramatically, and have refrained here from such an optimization for each case of **3**. Instead, the yields reported refer to a standard set of conditions [high dilution in 1,2-dimethoxyethane, reflux (with the exception of the cyclization of **1b**, which was carried out at room temperature), irradiation with a Sylvania ELH 300W tungsten lamp], under which the starting materials **1** are unstable. 2) The reaction is extensively chemoselective, none of the other possible cyclization products[3] being observed. 3) It is similarly stereoselective, the *cis*-stereochemistry around the 4,5-imidazole bond being preserved in the novel 3*a*,7*a*-dihydrobenzimidazole product, and the metal usually (with the exception of **3b**) emerging *anti*. 4) It is also highly regioselective, the trimethylsilyl group in **3** preferring the terminal diene position, in accord with mechanistic expectations;[3] an electronic effect[9] appears to be strongly influential in the formation of **3f**. 5) The structural assignments of **3** are based on spectral data[6] in comparison with model systems,[1,2] an X-ray structural analysis of **3e** (Fig. 1),[10] and chemical transformations.

Thus, complexes **3** (and also **5**, vide infra) could be demetalated [$CuCl_2$, $CH_3OCH_2CH_2OCH_3$, H_2O, 0 °C] to the free ligands (with the exception of **3d** *anti*, vide infra) in high yield.[6] In contrast to the analogous indole-derived

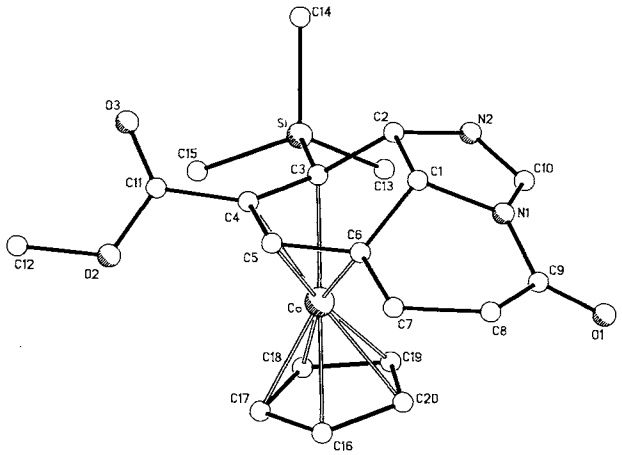

Fig. 1. Crystal structure of **3e** [10]. Important bond lengths [Å] and angles [°]: Co-C3 2.058(2), Co-C4 1.967(2), Co-C5 1.981(3), Co-C6 2.067(3), C2-C1-C6 113.8(2), C1-C2-C3 111.1(2), C2-C3-C4 116.1(2), C3-C4-C5 116.3(2), C4-C5-C6 115.9(2), C1-C6-C5 118.9(2).

complex,[1] but in agreement with the related pyrrole system,[2] recomplexation of the free ligand derived from **3a** *anti* gave the original complex exclusively. While the new functional arrangement in **3a** *anti* is surprisingly inert to treatment with $NaBH_4$ or even $LiAlH_4$, exposure to $NaBH_4$ (2 equiv.) in 1,2-dimethoxyethane, followed by addition of $CuCl_2$ (4 equiv.)[11] in water gave rise selectively to the surprisingly stable **4** (72%).[6] Selective protodesilylation of **3a** *anti* to **5** (and also of **3f** *anti* to the analogous complex) could also be achieved [nBu_4NF, THF, 2 h, 25 °C, 91% **5**, m.p. 134 °C], a significant result in view of

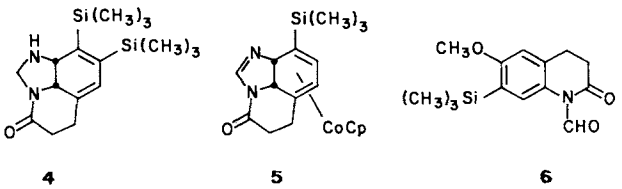

4 **5** **6**

the number of related bis(trimethylsilylated) diene complexes that have become accessible by this technology.[1-3] Finally, and of clear relevance to further synthetic applications, the methoxy derivative **3d** *anti* was converted into the quinolone **6**[6] (ca. 60%), the result of a combined demetalation, aromatization, and imine hydrolysis process during which the original imidazole auxiliary is unravelled to leave a heterobicycle, constructed entirely in the cobalt-mediated step. Support for this sequence is derived from the isolation of the intermediate imine (6%) of **6** in this transformation. The generality of this process is under active investigation.

Received: June 3, 1987 [Z 2280 IE]
German version: *Angew. Chem.* 99 (1987) 1067

[1] D. B. Grotjahn, K. P. C. Vollhardt, *J. Am. Chem. Soc.* 108 (1986) 2091.
[2] G. S. Sheppard, K. P. C. Vollhardt, *J. Org. Chem.* 51 (1986) 5496.
[3] K. P. C. Vollhardt, *Angew. Chem.* 96 (1984) 525; *Angew. Chem. Int. Ed. Engl.* 23 (1984) 539.
[4] J. S. Glasby: *Encyclopedia of the Alkaloids*, Vol. 1-4, Plenum Press, New York 1979, 1982, 1983; D. Lednicer, L. Mitscher: *The Organic Chemistry of Drug Synthesis, Vol. 1-3*, Wiley-Interscience, New York 1977, 1980, 1984.
[5] M. R. Grimmett, *Adv. Heterocycl. Chem.* 12 (1970) 103; 27 (1980) 241; M. P. Sammes, A. R. Katritzky, *ibid.* 35 (1984) 375, 413.

[6] All new compounds gave correct elemental analytical and/or high resolution mass-spectral data. Selected spectral data: **3a** *anti:* red crystals, m.p. 170–173°C; IR ($CHCl_3$): $\tilde{\nu}$=2990, 2980, 2900, 2850, 1730, 1670, 1612, 1450, 1390, 1245, 855, 835 cm^{-1}; ^{1}H-NMR (300 MHz, $CDCl_3$): δ=7.86 (d, J=1.6 Hz, 1H), 4.98 (s, 1H), 4.74 (s, 5H), 3.14 (dd, J=7.7, 1.6 Hz, 1H), 2.91 (d, J=7.7 Hz, 1H), 2.59 (m, 2H), 1.97 (m, 1H), 1.70 (m, 1H), 0.37 (s, 9H), 0.29 (s, 9H); ^{13}C-NMR (75 MHz, $CDCl_3$): δ=169.1, 145.3, 84.22, 81.22, 80.71, 74.27, 66.83, 63.80, 59.17, 30.75, 29.42, 3.26, 2.90; MS (70 eV): m/z 442 ($M^{\oplus}$, 100), 73 (39). **3a** (free ligand): colorless crystals, m.p. 110°C; IR ($CHCl_3$): $\tilde{\nu}$=3000, 2960, 2930, 2860, 1685, 1622, 1380, 1340, 1270, 1253, 865, 842 cm^{-1}; ^{1}H-NMR (300 MHz, $CDCl_3$): δ=7.77 (d, J=3 Hz, 1H), 5.97 ("t", J=1.1 Hz, 1H), 5.18 (dd, J=14, 3 Hz, 1H), 4.52 (dd, J=14, 0.8 Hz, 1H), 2.8–2.4 (m, 4H), 0.30 (s, 9H), 0.21 (s, 9H); ^{13}C-NMR (75 MHz, $CDCl_3$): δ=169.0, 144.5, 143.2, 142.7, 126.2, 122.5, 70.60, 52.48, 31.83, 25.62, 1.95, 1.34; MS (70 eV): m/z 318 ($M^{\oplus}$, 30), 317 (90), 73 (100). **4**: colorless oil; IR ($CHCl_3$): $\tilde{\nu}$=3400, 3000, 2960, 2930, 2860, 1650, 1450, 1420, 1252, 990, 870, 845 cm^{-1}; ^{1}H-NMR (300 MHz, $CDCl_3$): δ=5.92 (d, J=1.4 Hz, 1H), 4.72 (d, J=10.1 Hz, 1H), 3.98 (dd, J=9.5, 1.4 Hz, 1H), 3.81 (d, J=9.5 Hz, 1H), 3.66 (d, J=10.1 Hz, 1H), 2.8–2.4 (m, 4H), 0.26 (s, 9H), 0.21 (s, 9H); MS (70 eV): m/z 320 ($M^{\oplus}$, 100). **6**: colorless crystals, m.p. 106°C; IR ($CHCl_3$): $\tilde{\nu}$=3030, 3010, 2960, 2900, 2850, 1733, 1710, 1605, 1490, 1465, 1410, 1390, 1330, 1312, 1295, 1250, 1235, 1170, 1105, 1065, 950, 850 cm^{-1}; ^{1}H-NMR (300 MHz, $CDCl_3$): δ=9.67 (s, 1H), 7.83 (s, 1H), 6.65 (s, 1H), 3.79 (s, 3H), 2.95–2.85 (m, 2H), 2.77–2.68 (m, 2H), 0.25 (s, 9H); ^{13}C-NMR (75 MHz, $CDCl_3$): δ=174.4, 161.9, 160.6, 131.4, 128.6, 126.8, 112.6, 108.7, 55.33, 33.55, 25.46, −1.09; MS (70 eV): m/z 277 ($M^{\oplus}$, 24), 249 (94), 204 (100).

[7] G. Eglinton, M. C. Whiting, *J. Chem. Soc. 1953*, 3052; B. C. Holland, N. W. Gilman, *Synth. Commun. 4* (1974) 203; H. A. Staab, *Angew. Chem. 74* (1962) 407; *Angew. Chem. Int. Ed. Engl. 1* (1962) 351.

[8] By alkylation of imidazole with 5-iodopentyne (G. Büchi, H. Wüest, *J. Org. Chem. 44* (1979) 546) using NaH, dimethoxyethane, 25°C, 2 h.

[9] See: Y. Wakatsuki, S. Miya, H. Yamazaki, S. Ikuta, *J. Chem. Soc. Dalton Trans. 1986*, 1201.

[10] Monoclinic, $P2_1/c$, a=17.662(3), b=8.434(2), c=13.980(2) Å, $\alpha=\gamma=90°$, β=109.00(1)°, V=1968.9(6) $Å^3$, Z=4, ρ_{calcd}=1.445 g/cm^3, μ=9.50 cm^{-1}; $Mo_{K\alpha}$ radiation (graphite monochromator); scan range $3° \le 2\theta \le 55°$; independent reflections 4513, observed 3835 ($F_0 \ge 3.5\sigma(F_0)$), R=0.041, R_w=0.044. Further details of the crystal structure investigation may be obtained from the Fachinformationszentrum Energie, Physik, Mathematik GmbH, D-7514 Eggenstein-Leopoldshafen 2 (FRG), on quoting the depository number CSD-52700, the names of the authors, and the journal citation.

[11] T. Satoh, K. Nanba, S. Suzuki, *Chem. Pharm. Bull. 19* (1971) 817; J. A. Cowan, *Tetrahedron Lett. 27* (1986) 1205; J. O. Osby, S. W. Heinzman, B. Ganem, *J. Am. Chem. Soc. 108* (1986) 67.

2,6-Diaza-*s*-indacenes**

By *Fritz Closs, Rudolf Gompper,* Ulrich Nagel,* and *Hans-Ulrich Wagner*

Donor and acceptor substituents in cyclopolyolefins generally reduce the HOMO-LUMO gap in (4n+2) π-systems and increase it in (4n) π-systems. This enables the synthesis of stable (4n) π-electron systems; examples are diethyl 2,4-bis(diethylamino)cyclobutadiene-1,3-dicarboxylate,[1] 1,3-bis(dimethylamino)-2-azapentalenes,[2,3] donor-acceptor-substituted cyclopentadienylium salts,[4,5] and azacyclopentadienylium salts.[6–8] The attachment of benzene rings to cyclopentadienylium salts naturally leads to a weakening of antiaromatic effects,[9] yet the NMR and MO data of the 1,3-bis(diethylamino)isoindolylium perchlorate **1** still show that a part of the positive charge is delocalized in the benzene ring in the sense of an 8π-electron system. This therefore raises the question of what sort of an effect the annelation of a positively charged ring element to **1**, as shown, e.g., in **2**, would have on the system. In contrast to **1**, **2** is a 10π-electron system. Its reduction ought to lead to 1,3,5,7-tetrakis(diethylamino)-2,6-diaza-*s*-indacene (**5**), a representative of the hitherto unknown class of diaza-*s*-indacenes. The Dewar resonance energies ($E^{\pi}_{ring} - E^{\pi}_{open\ chain}$ [HMO]) of *s*-indacene (1.639β), 2,6-diaza-*s*-indacene (1.738β), 1,3,5,7-tetraamino-*s*-indacene (1.700β), and 1,3,5,7-tetraamino-2,6-diaza-*s*-indacene (1.756β) show that *s*-indacene is an aromatic system and document an increase in aromaticity in **5** by the donor-acceptor effect. **5** has a very high-lying HOMO (according to HMO: 0.141β) and should thus be a strong reducing agent.

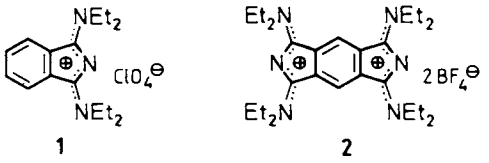

1 **2**

The convergence of the properties of donor-acceptor-substituted antiaromatic systems to those of aromatic ones also brings about, inter alia, a reduction or complete removal of the tendency to undergo double bond localization characteristic of antiaromatic systems. Evidence of this effect is provided by diethyl-2,4-bis(diethylamino)cyclobutadiene-1,3-dicarboxylate[10] and the 4,8-bis(dimethylamino)- and 1,3,5,7-tetra-*tert*-butyl-*s*-indacenes synthesized by *Hafner* et al.[11,12] Also in the case of 1,3,5,7-tetradonor-2,6-diacceptor-substituted *s*-indacenes, the MNDO heats of formation show that a tendency to undergo double-bond localization no longer exists. The double-bond localization parameters "λ_{max}" calculated according to the method of *Binsch* and *Heilbronner*[13,14] show the same trend: *s*-indacene (1.36), 1,3,5,7-tetraamino-*s*-indacene (1.18), 1,3,5,7-tetraamino-2,6-diaza-*s*-indacene (1.22).

The method developed earlier by us for the synthesis of **1**[6] from 1,1,3-trichloro-1*H*-isoindole opens up a route to **2** and **5**. Similarly to the conversion of phthalimide into trichloroisoindole,[15] pyromellitimide **3** can be converted into 1,1,3,5,5,7-hexachloro-2,6-diaza-1,5-dihydroindacene **4** (or into the 1,1,3,5,7,7-isomer) by heating with PCl_5/$POCl_3$ (yield of crude product almost quantitative). **4** reacts with diethyl(trimethylsilyl)amine in THF to give a blue product mixture, from which the yellow salt **2** can be separated (see Table 1) in 31% yield after treatment with sodium tetrafluoroborate/acetonitrile, stripping of the acetonitrile, addition of cold water and extraction of the aque-

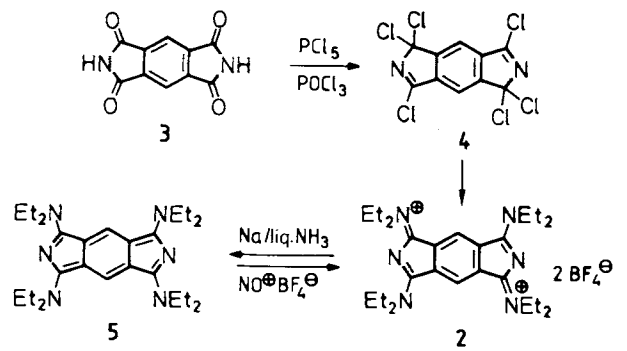

3 **4** **5** **2**

[*] Prof. Dr. R. Gompper, Dipl.-Chem. F. Closs, Dr. H. U. Wagner
Institut für Organische Chemie der Universität
Karlstrasse 23, D-8000 München 2 (FRG)
Dr. U. Nagel
Institut für Anorganische Chemie der Universität
Meiserstrasse 1, D-8000 München 2 (FRG)

[**] This work was supported by the Fonds der Chemischen Industrie.

ous phase with dichloromethane. Although one could expect that **2**, as a 10π-electron system, fundamentally differs from **1**, as an 8π-electron system, no significant difference is observable, at least in the electronic spectrum ($\lambda_{max}(CHCl_3)$: **1**: 375 nm; **2**: 440 nm; λ_{max} calculated according to PPP: **1**: 385 nm; **2**: 415 nm), and even the positions of the signals of H-4 and H-8 in the ^{1}H-NMR spectrum of **2** ($\delta = 8.05$) differs very little from the positions of the signals of H-4 to H-7 in **1** ($\delta = 7.96$). According to this, the interaction of the two azavinamidinium moieties in **2** appears to be relatively weak.

Table 1. Selected data of the compounds **2** and **5**–**11**.

2: m.p. = 276 °C; UV/VIS (CH_2Cl_2): $\lambda_{max}(\log\varepsilon) = 260$ nm (4.66), 269 (4.66), 326 (4.20), 352 (4.13), 420 (3.99), 434 (3.99), 440 (3.99); ^{1}H-NMR (80 MHz; CD_3CN): $\delta = 1.45$ (t; 12H, CH_2CH_3), 1.53 (t; 12H, CH_2CH_3), 4.00 (q; 8H, CH_2CH_3), 4.10 (q 8H, CH_2CH_3), 8.05 (s; 2H, H-4, H-8)

5: Violet rods with green-gold shiny surface decomp. > 120 °C; UV/VIS (hexane): $\lambda_{max} = 223$ nm, 260, 295, 306, 327, 343, 395, 609; (benzene): $\lambda_{max} = 313$ nm, 334, 376, 614; calculated according to PPP: $\lambda_{max} = 233$ nm, 249, 293, 596); ^{1}H-NMR (360 MHz; [D$_8$]THF): $\delta = 1.00$ (t; 24H, CH_2CH_3), 2.55 (q; 16H, CH_2CH_3), 7.66 (s; 2H, H-4, H-8)

6: m.p. > 350 °C; UV/VIS (CH_3CN): $\lambda_{max}(\log\varepsilon) = 337$ nm (4.37), 627 (4.16)

7: m.p. > 350 °C; UV/VIS (DMF): $\lambda_{max}(\log\varepsilon) = 314$ nm (4.62), 356 (4.52), 440 (sh), 464 (4.50), 497 (4.57), 610 (sh), 650 (4.64)

8: m.p. 295 °C; UV/VIS ($CHCl_3$): $\lambda_{max}(\log\varepsilon) = 320$ nm (4.62), 350 (sh), 375 (4.07), 390 (sh), 395 (4.09), 460 (sh), 484 (4.37), 506 (4.25), 518 (4.28)

9: m.p. > 350 °C; UV/VIS (CH_3CN): $\lambda_{max}(\log\varepsilon) = 333$ nm (4.38), 361 (4.25), 400 (sh), 484 (4.10), 507 (4.10), 545 (4.01)

10: m.p. > 350 °C; UV/VIS (DMF): $\lambda_{max}(\log\varepsilon) = 347$ nm (sh), 362 (4.76), 394 (4.50), 419 (4.39), 520 (4.51), 543 (4.50)

11: m.p. 293 °C; λ_{max} (DMF) = *290* nm, *310*, 364, 395, 419, *490*, 520, 540, *800*, *880* (bands in italics occur in addition to the bands in **2** and **10**)

A series of colored by-products as well as **2** are formed from **4**. The violet compound **6** (see Table 1) can be separated in 3–5% yield from the mixture by column chromatography on silica gel (eluent $CHCl_3/CH_3OH$ 9 : 1).

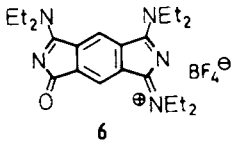

6

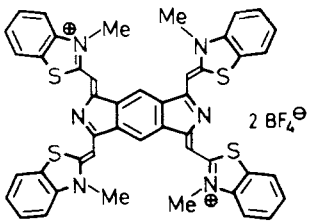

7

4 can also be reacted with enamines instead of with tertiary amines. If, e.g., 2,3-dimethylbenzothiazolium tetrafluoroborate is used as enamine precursor the dark green cyanine dye **7** results (see Table 1). The two chromophores of this compound are, as in the case of **2**, only weakly coupled. For comparison: the cyanine dye[16] prepared from aminoimino-1*H*-isoindole and a 2,3-dimethylbenzthiazolium salt absorbs at only about 25 nm shorter wavelength ($\lambda_{max} = 625$ nm) than **7**, which is somewhat less than the corresponding difference observed in the spectra of **2** and **1**.

2 can also be used for reactions with nucleophiles. For example, reaction with sodium malononitrile leads, depending on the molarity of the reactants, to **8**, **9** or **10** (see Table 1).

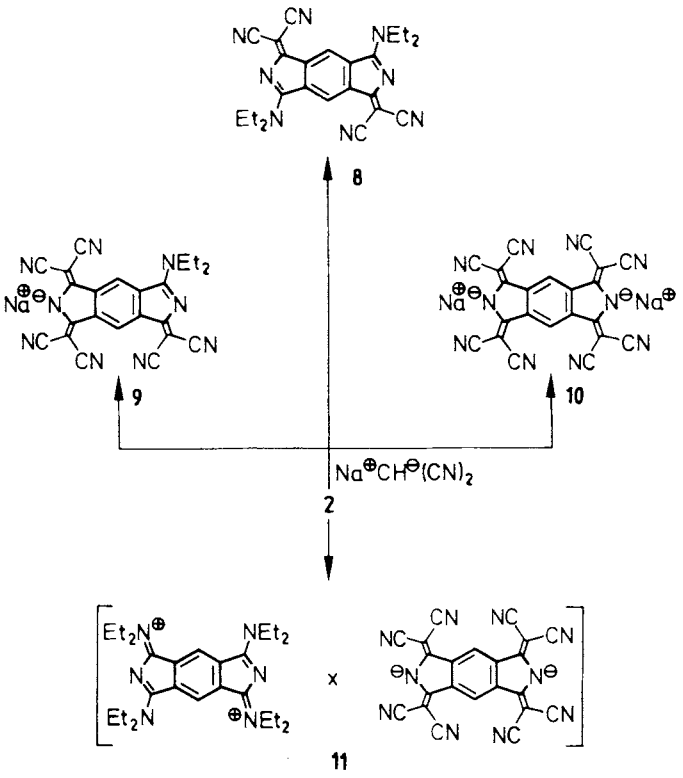

8, **9**, **10**, **2**, **11**

10, as dianion salt, is the electronic counterpart of the dication salt **2**. Combination of the aqueous solutions of **2** and **10** results in formation of the red compound **11** in 89% yield (see Table 1), which is predominantly present as the dication-dianion salt. However, **11** also partly contains radical cations, formed from **2** under the influence of **10**, as can be concluded from the UV/VIS spectrum. Namely, the bands at 800 and 880 nm also appear (in THF at 795 and 875 nm) when equimolar amounts of **2** and **5** are combined in THF.

The cyclic voltammogram of **2** shows two reversible one-electron transitions at −0.10 and −0.56 V (THF, 0.1 M tetrabutylammonium hexafluorophosphate, gold electrode versus Ag/Ag$^{\oplus}$). So far only the diaza-*s*-indacene **5** could be isolated in the reduction of **2**. On reaction of **2** in liquid ammonia with sodium in the ratio 1 : 2 a violet solid is ob-

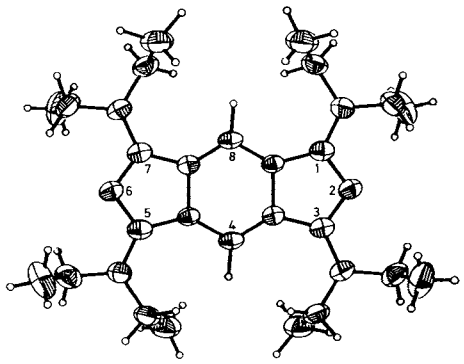

Fig. 1. Crystal structure of **5** at 0 °C; bond lengths (in pm, standard deviations: 0.5 pm [17]) [MNDO results]: C1-N2 136.0, [139.9], N2-C3 135.8 [137.9], C3-C3a 142.5 [144.0], C3a-C4 138.8 [139.8], C8-C8a 139.2 [139.8], C3a-C8a 148.7], C1-NEt_2 136.4 [136.6], C3-NEt_2 136.6 [136.6].

tained from which **5** can be extracted with *n*-pentane under argon (yield 47%). The X-ray structure analysis (Fig. 1; measurement at 0°C) shows **5** to be a planar molecule (apart from the methyl groups) with approximate D_{2h} symmetry.

The observed bond lengths are in good agreement with the MNDO results for 1,3,5,7-tetraamino-2,6-diaza-*s*-indacene and also with the bond lengths found in the case of 1,3,5,7-tetra-*tert*-butyl-*s*-indacene.[12, 13] The dipolar resonance structure **12** illustrates the bonding situation in **5**. However, further investigations are necessary in order to clarify whether **5** has a delocalized structure or whether a very rapid valence isomerization between two localized structures takes place.

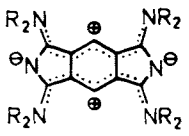

12, R = Et

As an electron-rich π-electron system, **5** is a strong reducing agent and air-sensitive, even in the crystalline state. Solutions in hexane or THF show traces of radicals (ESR signal). A radical cation salt has so far not been isolated. **5** can be oxidized to **2** in good yields with nitrosyl tetrafluoroborate. **5** and **2** show consistent cyclovoltammograms.

Received: May 11, 1987 [Z 2232 IE]
German version: *Angew. Chem. 99* (1987) 1068

[1] R. Gompper, G. Seybold, *Angew. Chem. 80* (1968) 804; *Angew. Chem. Int. Ed. Engl. 7* (1968) 824.
[2] H. J. Gais, K. Hafner, *Tetrahedron Lett. 1974*, 771.
[3] K. Hafner, F. Schmidt, *Angew. Chem. 85* (1973) 450; *Angew. Chem. Int. Ed. Engl. 12* (1973) 418.
[4] R. Gompper, H. Glöckner, *Angew. Chem. 96* (1984) 48; *Angew. Chem. Int. Ed. Engl. 23* (1984) 53.
[5] R. Gompper, T. Gessner, *Angew. Chem. 97* (1985) 996; *Angew. Chem. Int. Ed. Engl. 24* (1985) 982.
[6] R. Gompper, K. Bichlmayer, *Angew. Chem. 91* (1979) 170; *Angew. Chem. Int. Ed. Engl. 18* (1979) 156.
[7] R. Gompper, M. Junius, *Tetrahedron Lett. 21* (1980) 2883.
[8] R. Gompper, R. Guggenberger, R. Zentgraf, *Angew. Chem. 97* (1985) 998; *Angew. Chem. Int. Ed. Engl. 24* (1985) 984.
[9] E. C. Friedrich, T. M. Tam, *J. Org. Chem. 47* (1982) 315; E. C. Friedrich, G. De Lucca, *ibid. 48* (1983) 4563.
[10] R. Gompper, J. Kroner, G. Seybold, H.-U. Wagner, *Tetrahedron 32* (1976) 629.
[11] K. Hafner, *Pure Appl. Chem. 54* (1982) 939.
[12] K. Hafner, B. Stowasser, H. P. Krimmer, S. Fischer, M. C. Böhm, H. J. Lindner, *Angew. Chem. 98* (1986) 646; *Angew. Chem. Int. Ed. Engl. 25* (1986) 630.
[13] G. Binsch, E. Heilbronner, *Tetrahedron 24* (1968) 1215).
[14] E. Heilbronner, Z.-z. Yang, *Angew. Chem. 99* (1987) 369; *Angew. Chem. Int. Ed. Engl. 26* (1987) 360.
[15] H. Vollmann, F. Baumann, B. Bienert, US-Pat. 2701252 (1955), Bayer AG; *Chem. Abstr. 49* (1955) P10374b.
[16] G. E. Fecken, J. D. Kendall, *Chimia 15* (1961) 110.
[17] **5**: monoclinic, space group $C2/c$, $Z=4$, $a=2703(2)$, $b=1102.7(6)$, $c=918.3(5)$ pm, $\beta=106.31(4)°$, $V=2.627\times10^9$ pm^3, $\rho_{calcd}=1.109$ g cm^{-3}; $4°<2\theta<50°$ ($Mo_{K\alpha}=71.07$), 1284 independent reflections, Lorentz and polarization corrections, molecules on crystallographic inversion centers, positions of the hydrogen atoms calculated for ideal geometry and optimized, anisotropic refinement of the carbon and nitrogen atoms, $R=0.0662$, $R_w=0.0607$. Further details of the crystal structure investigation are available on request from the Fachinformationszentrum Energie, Physik, Mathematik GmbH, D-7514 Eggenstein-Leopoldshafen 2, on quoting the depository number CSD-52575, the names of the authors, and the journal citation.

Propellanes of the Glycoluril Series and Bridged Tetrazocines**

By *Rudolf Gompper,* Heinrich Nöth,* Wilfried Rattay, Marie-Luise Schwarzensteiner, Peter Spes,* and *Hans-Ulrich Wagner*

Dedicated to Professor Ulrich Schöllkopf on the occasion of his 60th birthday

The search for semibullvalenes and diazasemibullvalenes with bishomo-aromatic ground states[1, 2] has hitherto been virtually unsuccessful (cf. Ref. [3]; surprisingly, tetramethyl 1,5-hexamethylenesemibullvalene-2,4,6,8-tetracarboxylate has previously been reported to have a symmetrical structure with a delocalized electron system[4]). We had attempted the preparation, not of the hitherto inaccessible 2,4,6,8-tetracyanosemibullvalenes[5] but of the structurally related 2,4,6,8-tetraazasemibullvalenes **1** (Do = donor) (cf. 2,6-diazasemibullvalenes[6]). A bishomoaromatic ground

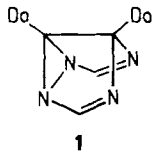

1

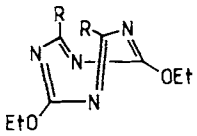

2

state should be formed in the case of **1** due to the tendency of the NN bond in the diaziridine ring to undergo cleavage. Instead of tetraazasemibullvalenes, however, we obtained 1,3,5,7-tetrazocines **2**[7] on oxidation of glycoluril derivatives. Apparently, either the 3a–6a bond of the glycoluril derivative or the 1–5 bond of intermediary tetraazasemibullvalenes (bishomoaromatic structure?) is cleaved during the course of the oxidation. In order to prevent this cleavage we have now synthesized 3a,6a-bridged glycolurils and investigated their oxidation.

The reaction of cyclic α-diketones **3** (cyclopentane-, cyclohexane-, cycloheptane-1,2-dione, *cis*-5-cyclooctene-1,2-dione, acenaphthenequinone, camphorquinone; benzocyclobutenedione reacts differently[8]) with urea in ethanol-water in the presence of some hydrochloric acid (**4a** is obtained by heating the components in benzene in the presence of ethereal tetrafluoroboric acid) affords the sparingly soluble, bridged glycolurils **4** in good yields (only **4b** was known[9]), which can be converted by reaction with triethyloxonium tetrafluoroborate (cf. Ref. [10]; 110°C; after cooling the melt, addition of 50% aqueous potassium carbonate solution and extraction with chloroform) into the bisimidates **6** (cf. Table 1). The bisimidates **6** can be oxidized in various ways: 1) with one equivalent of *tert*-butyl hypochlorite in dichloromethane and subsequent addition of potassium *tert*-butoxide; 2) successive addition of two equivalents of potassium *tert*-butoxide and iodine in tetrahydrofuran; 3) heating in carbon tetrachloride with *N*-bromosuccinimide in the presence of azobisisobutyronitrile; 4) reaction with two equivalents of *tert*-butyl hypochlorite to give the dichloro compounds **7** and their reduction with naphthalene-sodium. All these methods, howev-

[*] Prof. Dr. R. Gompper, Dr. M.-L. Schwarzensteiner
Dipl.-Chem. P. Spes, Dr. H.-U. Wagner
Institut für Organische Chemie der Universität
Karlstrasse 23, D-8000 München 2 (FRG)
Prof. Dr. H. Nöth, Dr. W. Rattay
Institut für Anorganische Chemie der Universität
Meiserstrasse 1, D-8000 München 2 (FRG)

[**] This work was supported by the Fonds der Chemischen Industrie.

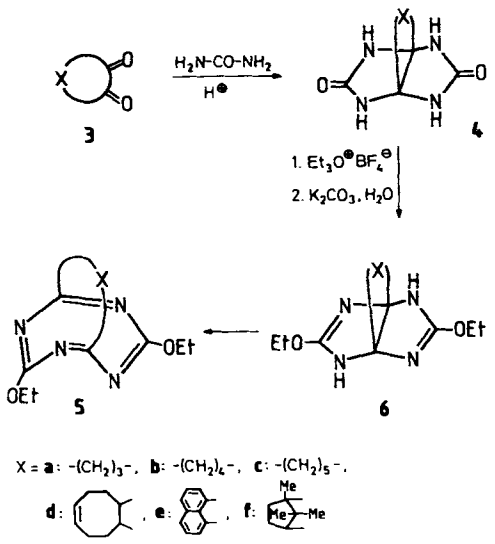

er, do not give 1,5-bridged tetraazasemibullvalenes, but 2,6-bridged 1,3,5,7-tetrazocines **5** (cf. Table 1). That the products **5** are in fact tetrazocines and not tetraazasemibullvalenes follows from the X-ray structure analysis of **5c** (Fig. 1).[11] It should be emphasized that the distance between the atoms C-2 and C-6 is 278 pm; the corresponding distance in 2,6-diethoxy-4,8-diphenyl-1,3,5,7-tetrazocine is 301 pm;[7] i.e., in comparison to the monocyclic compound, the eight-membered ring of **5c** is slightly distorted in the manner expected in a tetraazasemibullvalene.

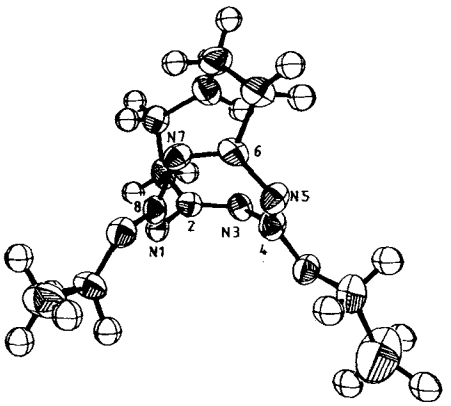

Fig. 1. Crystal structure of **5c**; bond lengths (in pm, standard deviations 0.8–0.9 pm [11]): N1-C2 128.0, C2-N3 140.9, N3-C4 125.3, C4-N5 139.1, N5-C6 127.9, C6-N7 140.8, N7-C8 130.0, C4-O 134.6, C8-O 134.5; sum of angles at C2 and C6 359.9°.

The NMR data of **5a** and **5b** compare with those of **5c**, thus indicating that **5a** and **5b** are also tetrazocines. In the ^{13}C-NMR spectra of **5** the signals of C-3a/6a of the starting substances **6** at $\delta \approx 90$ have disappeared and in their place the signals of the bridgehead C-atoms appear at $\delta = 160$–170. Most surprising is that the tetraazasemibullvalene structure does not even occur in **5a**. Actually, it is a derivative of bicyclo[3.3.3]undec-1-ene, which is counted among the "isolable" bridgehead olefins (cf. Refs. [12, 13]), but which, aside from 2-azabicyclo[3.3.1]nonene[14] is the only "anti-Bredt" bridgehead imine isolated so far (cf. Ref. [15]). The greater ring strain in **5a** compared to that in **5b** and **5c** is evidenced by the shift of the C=N stretching vibration to lower frequencies ($\nu_{C=N} = 1560$ cm^{-1} vs. 1610 and 1614 cm^{-1}, resp.), as has also been observed in 4-aza-

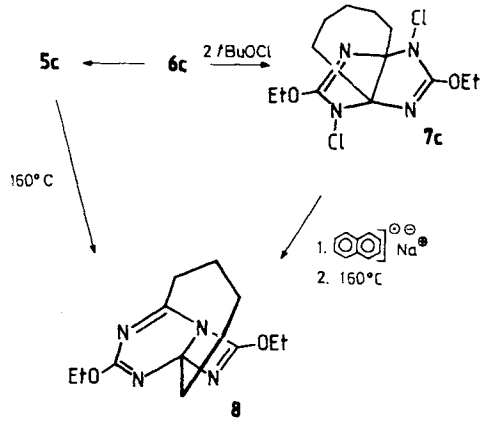

Table 1. Selected data of the compounds **5**, **6**, and **9**–**11**. ^1H-NMR spectra: 60/80 MHz, $CDCl_3$; ^{13}C-NMR spectra: 20 MHz, $CDCl_3$; IR spectra: KBr.

5a: b.p. 160°C (0.1 torr); ^1H-NMR: $\delta = 1.42$ (t; 6H, OCH_2CH_3), 2.26, 2.80 (mc; 6H, $(CH_2)_3$), 4.46 (q; 4H, OCH_2CH_3); ^{13}C-NMR: $\delta = 14.27$ (OCH_2CH_3), 23.00, 37.54 ($(CH_2)_3$), 64.14 (OCH_2CH_3), 171.98 (C-4/8), 182.38 (C–OEt); IR: 2934, 1560 cm^{-1}

5b: m.p. 50–52°C; ^1H-NMR: $\delta = 1.40$ (t; 6H, OCH_2CH_3), 2.21, 2.43 (mc; 8H, $(CH_2)_4$), 4.28 (q; 4H, OCH_2CH_3); ^{13}C-NMR: $\delta = 14.30$ (OCH_2CH_3), 28.77, 39.25 ($(CH_2)_4$), 64.94 (OCH_2CH_3), 158.47 (s; C-4/8), 178.83 (C–OEt); IR: 2960, 1610 cm^{-1}

5c: m.p. 64°C; ^1H-NMR: $\delta = 1.35$ (t; 6H, OCH_2CH_3), 1.87, 2.36 (mc; 16H, $(CH_2)_5$), 4.21 (q; 4H, OCH_2CH_3); ^{13}C-NMR: $\delta = 14.09$ (OCH_2CH_3), 23.89, 28.90, 38.49 ($(CH_2)_5$), 64.55 (OCH_2CH_3), 159.19 (C-4/8), 177.20 (C–OEt); IR: 2985, 2933, 1614 cm^{-1}

6a: m.p. 217°C; ^1H-NMR: $\delta = 1.30$ (t, 6H, OCH_2CH_3), 1.86 (mc; 6H, $(CH_2)_3$, 4.16 (q; 4H, OCH_2CH_3), 5.16 (s; 2H, NH); ^{13}C-NMR ($CDCl_3/CF_3CO_2H$): $\delta = 13.96$ (OCH_2CH_3), 24.96, 39.98 ($(CH_2)_3$), 74.97 (OCH_2CH_3), 91.08 (C-3a/6a), 164.35 (C–OEt); IR: 3156, 1616 cm^{-1}

6b: m.p. 219°C; ^1H-NMR: $\delta = 1.31$ (t; 6H, OCH_2CH_3), 1.53, 1.80 (mc; 8H, $(CH_2)_4$), 4.15 (q; 4H, OCH_2CH_3), 5.29 (s; 2H, NH)

6c: m.p. 225°C; ^1H-NMR: $\delta = 1.33$ (t; 6H, OCH_2CH_3), 1.46, 1.83 (mc; 10H, $(CH_2)_5$), 4.12 (q; 4H, OCH_2CH_3), 5.20 (s; 2H, NH); ^{13}C-NMR: $\delta = 14.27$ (OCH_2CH_3), 25.26, 30.54, 36.22 ($(CH_2)_5$), 75.39 (OCH_2CH_3), 88.35 (C-3a/6a), 164.80 (C–OEt); IR: 3150, 2923, 1630 cm^{-1}

6d: m.p. 195–197°C; ^1H-NMR: $\delta = 1.33$ (t; 6H, OCH_2CH_3), 2.31 (mc; 8H, CH_2-Brücke), 4.20 (q; OCH_2CH_3), 5.50 (s; 2H, NH), 5.90 (mc; 2H, CH=CH)

6e: m.p. 208–210°C; IR: 3250, 1726, 1605 cm^{-1}

6f: m.p. 178–180°C

8: m.p. 130°C; ^1H-NMR: $\delta = 1.23$ (t; 3H, OCH_2CH_3), 1.40 (t; 3H, OCH_2CH_3), 1.73, 2.63 (mc; $(CH_2)_5$), 4.26 (mc; 4H, OCH_2CH_3); ^{13}C-NMR: $\delta = 14.63$ (OCH_2CH_3), 22.63, 22.86, 23.11, 23.44, 32.44 ($(CH_2)_5$), 62.52 (OCH_2CH_3), 116.95 (sp^3 bridgehead), 158.20 (C=N bridgehead), 161.44 (four-membered ring C–OEt), 165.98 (six-membered ring C–OEt); IR: 1630, 1560 cm^{-1}

9a: ^{13}C-NMR ([D$_6$]DMSO): $\delta = 18.02$ (OCH_2CH_3), 20.81, 38.89 ($(CH_2)_3$), 61.09 (OCH_2CH_3), 100.83 (C-3a/6a), 167.92 (C–OEt)

9c: ^1H-NMR ([D$_6$]DMSO): $\delta = 1.20$ (mc; 6H, OCH_2CH_3), 1.46, 1.80 (mc; 10H, $(CH_2)_5$), 4.01 (mc; 4H, OCH_2CH_3); ^{13}C-NMR ([D$_6$]DMSO/18-crown[6]): $\delta = 15.08$ (OCH_2CH_3), 25.23, 31.05, 36.53 ($(CH_2)_5$), 61.00 (OCH_2CH_3), 96.11 (C3a/6a), 167.50 (C–OEt)

10a/11a: ^1H-NMR: $\delta = 1.30$ (mc; 6H, OCH_2CH_3), 1.50, 1.86 (mc; 10H, $(CH_2)_5$), 2.73, 2.83 (s; 6H, NCH_3), 4.20 (mc; 4H, OCH_2CH_3); ^{13}C-NMR: $\delta = 14.57$ (OCH_2CH_3), 24.26, 24.38, 25.96, 27.75, 29.80, 31.11, 34.71, 39.16 ($(CH_e)_5$), 64.27, 64.49 (OCH_2CH_3), 89.29, 91.81, 96.29 (C-3/6a), 161.23, 161.71 (C–OEt)

10b/11b: ^1H-NMR: $\delta = 1.40$ (t; 6H, OCH_2CH_3), 1.56, 1.91 (mc; 10H, $(CH_2)_5$), 2.36, 2.53 (s; 6H, $NCOCH_3$), 4.43 (q; 4H, OCH_2CH_3)

homoadamant-3-ene[15] as a result of twisting of the C=N bond. Although no pyramidalization of the N atoms is observed in **5c**, $\nu_{C=N}$ is somewhat smaller in the case of **5c** than in the case of 2,6-diethoxy-4,8-dimethyl-1,3,5,7-tetrazocine ($\nu_{C=N}$ = 1648, 1625 cm^{-1}).[7] On heating to 160°C (Kugelrohr distillation), **5c** is converted into **8** (cf. Table 1), which is also obtained when the N^1,N^4-dichloro compound **7c** (88%; m.p. 133°C; obtained by chlorination of **6c** with two equivalents of *tert*-butyl hypochlorite in dichloromethane) is reduced with naphthalene-sodium and the resulting product distilled.

The X-ray structure analysis of **7b**[16] (m.p. 131°C) affords insights into the bonding situation in a tetraazapropellane. The N-atoms are pyramidalized; the 3a–6a distance (154.9 pm) is much smaller than the distance between the bridgehead C-atoms in **5c**.

Reduction of **5** with potassium in liquid ammonia leads to dipotassium salts **9** (cf. Table 1), which can also be generated from **6** by treatment with potassium *tert*-butoxide. According to the ^{13}C-NMR spectra of **9** these salts contain dianions of **6**. The signals of the bridge C-atoms of **9** are shifted significantly upfield but still appear downfield compared to those of **5**. Decisive, however, is that the signals of *C*-OEt in **9** and **6** appear at practically the same field strength. Had tetrazocine dianions been present then the signals would have been shifted significantly upfield.

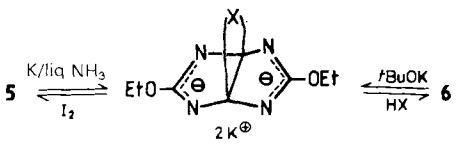

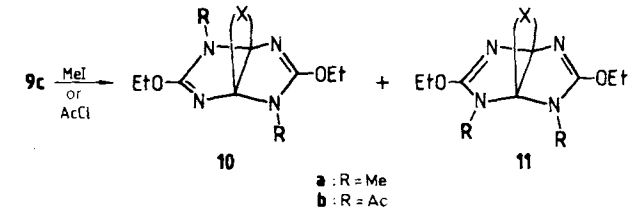

The formation of **9**, which can be regarded as a bishomoantiaromatic[17] 12π-electron system, instead of an aromatic 10π-electron tetrazocine dianion is in no way associated with the 3a,6a bridge. The disodium salt obtained by reduction of 2,6-diethoxy-4,8-dimethyl-1,3,5,7-tetrazocine[7] with sodium in liquid ammonia is, according to the ^{13}C-NMR data, a salt of 2,5-diethoxy-3a,6a-dimethyl-3a,6a-dihydro-1,4*H*-imidazo(5,4-*d*)imidazole and not, as originally presumed,[18] a tetrazocine dianion salt. Dianions of tetrahydropentalenes normally rearrange into cyclooctatetraene dianions.[6, 19–21] The formation of dianions of the type **9** from **5** or **6** now affords examples for the opposite case (MNDO heats of formation also show that donor-acceptor substituted bicyclo[3.3.0]octadiendiyl dianions are generally preferred over the corresponding cyclooctatetraene dianions).

The fact that no tetrazocine derivatives have been found in any of the reactions with electrophiles, apart from the oxidation with iodine leading to **5**, can also be considered as evidence for the tricyclic structure **9**. In the reaction of **9** with methyl iodide a 1:1 mixture of **10a** and **11a** is formed, in that with acetyl chloride a mixture of **10b** and **11b** (cf. Table 1).

Received: June 9, 1987;
revised: July 29, 1987 [Z 2288 IE]
German version: *Angew. Chem. 99* (1987) 1071

[1] R. Hoffmann, W. D. Stohrer, *J. Am. Chem. Soc. 93* (1971) 6941.
[2] a) M. J. S. Dewar, D. H. Lo, *J. Am. Chem. Soc. 93* (1971) 7201; b) M. J. S. Dewar, Z. Náhlovská, B. D. Náhlovská, *J. Chem. Soc. Chem. Commun. 1971*, 1377.
[3] a) H. Quast, J. Christ, E.-M. Peters, K. Peters, H. G. von Schnering, *Chem. Ber. 118* (1985) 1154; b) H. Quast, J. Christ, *Angew. Chem. 96* (1984) 606; *Angew. Chem. Int. Ed. Engl. 23* (1984) 631.
[4] K. Grühmann, R. Iyengar, L. S. Miller, R. Piña in *Abstract of papers, No. 3 of the 193rd ACS National Meetings*, April 5–10, 1987.
[5] C. Schnieders, H.-J. Altenbach, K. Müllen, *Angew. Chem. 94* (1982) 639; *Angew. Chem. Int. Ed. Engl. 21* (1982) 637; *Angew. Chem. Suppl. 1982*, 1353.
[6] L. S. Miller, K. Grohmann, J. J. Dannenberg, *J. Am. Chem. Soc. 105* (1983) 6862.
[7] R. Gompper, M.-L. Schwarzensteiner, *Angew. Chem. 95* (1983) 553; *Angew. Chem. Int. Ed. Engl. 22* (1983) 543; *Angew. Chem. Suppl. 1983*, 812.
[8] So far we have been unable to prepare compounds of the type **6** with smaller 3a,6a bridges. Reaction of benzocyclobutenedione with urea (12 hours' heating under reflux in benzene in the presence of trifluoroacetic acid; water separator) did not afford a glycoluril derivative but surprisingly 4-amino-6-(2-carboxyphenyl)-*s*-triazin-2-one (34%; m.p. 250°C), which can be converted—by heating with triethyloxonium tetrafluoroborate to 110°C and treatment of the cold melt with 50% aqueous potassium carbonate solution—into 2-amino-4-(2-carboxyphenyl)-6-ethoxy-*s*-triazine (36%; m.p. 219°C (decomp.); the constitution has been confirmed by an X-ray structure analysis).
[9] a) D. F. Kutepov, A. A. Potashnik, D. N. Khokhlov, V. A. Tuzhilkina, *Zh. Obsh. Khim. 29* (1959) 855; *Chem. Abstr. 54* (1960) 1481f; b) D. F. Kutepov, S. S. Dupov, O. G. Struhov, *Zh. Strukt. Khim. 5* (1964) 309; *Chem. Abstr. 61* (1964) 3819g.
[10] L. I. Suvorova, L. V. Epishina, O. V. Lebedev, L. I. Khmel'nitskii, S. S. Novikov, *Izv. Akad. Nauk SSSR, Ser. Khim. 10* (1979) 2282, 2286; *Chem. Abstr. 92* (1980) 94365x, 94366y.
[11] **5c**, $C_{13}H_{20}N_4O_2$, MW = 264.3, *Pbca*, $Z = 8$, $a = 935.2(3)$, $b = 1497.8(6)$, $c = 2059.7(7)$ pm, $V = 2.885 \times 10^9$ pm^3, $\rho = 1.217$, $Cu_{K\alpha}$ radiation, $2 < 2\theta < 58°$, 1941 symmetry independent reflections $F_0 > 3\sigma(F)$. Solution by direct methods. $R = 0.096$. We thank Herrn Dr. *H. Lotter* for carrying out the measurement.—Further details of the crystal structure investigation are available on request from the Fachinformationszentrum Energie, Physik, Mathematik GmbH, D-7514 Eggenstein-Leopoldshafen 2 (FRG), on quoting the depository number CSD-52604, the names of the authors, and the journal citation.
[12] W. F. Maier, P. von R. Schleyer, *J. Am. Chem. Soc. 103* (1981) 1891.
[13] G. Szeimies in R. A. Abramovitch (Ed.): *Reactive Intermediates*. Plenum, New York 1983, p. 329–359.
[14] M. Toda, Y. Hirata, S. Yamamura, *J. Chem. Soc. Chem. Commun. 1970; Tetrahedron 28* (1972) 1477.
[15] J. G. Radziszewski, J. W. Downing, M. Jawdosiuk, P. Kovacic, J. Michl, *J. Am. Chem. Soc. 107* (1985) 594.
[16] **7b**: The molecule has almost C_2 point symmetry. Bond lengths in pm, standard deviations: 0.3–0.4 pm): C3a-C6a 154.9, C8a-N1 149.7, N1-C2 126.9, C2-N3 140.0, C2-O 133.7, N3-C3a 148.6, C3a-N4 147.9, N4-C5 126.9, C5-N6 140.0, N6-C6a 148.5; Sum of angles at N3 337.6°, at N6 339.7°. The cyclohexane ring has a twist conformation. $C_{12}H_{18}Cl_2N_4O_2$, MW = 321.2, rhombic, *Pna*2$_1$, $Z = 4$, $a = 994.2(3)$, $b = 1128.6(2)$, $c = 1341.1(2)$ pm, $V = 1.5047 \times 10^9$ pm^3, $\rho = 1.418$, $Mo_{K\alpha}$ radiation, $2 < 2\theta < 45°$, 1854 symmetry independent reflections $F_0 > 3\sigma(F)$, Lp correction. Solution by direct methods $R = 0.033$, $R_w = 0.036$. Further details of the crystal structure investigation are available on request from the Fachinformationszentrum Energie, Physik, Mathematik GmbH, D-7514 Eggenstein-Leopoldshafen 2 (FRG), on quoting the depository number CSD-52604, the names of the authors, and the journal citation.
[17] M. J. Goldstein, R. Hoffmann, *J. Am. Chem. Soc. 93* (1971) 6193.
[18] R. Gompper, *Bull. Soc. Chim. Belg. 92* (1983) 781.
[19] K. Müllen, private communication; cf. [5].
[20] D. Wilhelm, T. Clark, P. von R. Schleyer, A. G. Davies, *J. Chem. Soc. Chem. Commun. 1984*, 558.
[21] M. Goldstein, T. T. Wenzel, *J. Chem. Soc. Chem. Commun. 1984*, 1655.

IR Emission Analysis of Temperature Profiles in Pt/SiO_2 Catalysts during Exothermic Reactions**

By *George Georgiades, Valerie A. Self,* and *Paul A. Sermon**

Although the excess temperature of the active sites in supported catalysts during catalysis could be several hundred degrees higher than that measured by a thermocouple,[1] theoretical and experimental results have been contradictory. Indirect evidence may come from catalyst sintering[2] (attributed to local heating and consequent Pt mobility during oxidation-reduction) and the fact that in CO oxidation a Pd/SiO_2 catalyst without external heating remained at 150–190 K above the temperature of the reactant stream.[3] Unfortunately, 150-K temperature excursions of Pt/SiO_2 are probably representative of the support rather than the active sites (see Ref. [4]).

Infrared emission can, however, provide direct evidence of the temperature of the more important supported phase if at the relevant wavelengths the "black" active metal emits more strongly than the support. It has been shown that (1) the temperature of Ni crystallites exhibits an average transient increase of 165 K above that of the silica support within 3 s on O_2 chemisorption,[5] (2) during CO oxidation at 573 K the temperature of Pd is at least 190 K above that of its SiO_2 support,[3] and (3) temperature variations of 28 K exist across Pt/Al_2O_3 catalysts during H_2 oxidation.[6] However, it is now necessary to concentrate on temperature profiles produced under flow conditions using porous impregnated catalysts, operating in flow reactors with residence times of a few seconds, at partial pressures close to the stoichiometric composition of reactants[7] and to consider their significance for analysis of the kinetics of heterogeneous reactions.[8] We report here on the Pt/SiO_2-catalyzed oxidation of H_2 and hydrogenation of cyclohexene.

This particular catalyst (see *Experimental Procedure*) was selected because (1) the size of its pores might be large enough to reduce pore diffusion limitation, (2) the support would increase thermal and chemical isolation of the Pt active sites, (3) the activity of Pt was high and well known in the reactions selected, and (4) the Pt was finely dispersed (i.e., hydrogen chemisorption revealed[10] that it existed as 4-nm particles) throughout the internal pore structure of the support with sizes much smaller than the support pore size, thereby possibly allowing relatively ready access of reactants and release of products.

Platinum is one of the most active metals for H_2 oxidation[11] ($-\Delta H = 241.8$ kJ/mol H_2O) and has been studied in the unsupported[12] and supported[13] states. On supported catalysts a thermal feedback from the heat generated by the reaction may affect the chemical rate and cause oscillations and bistability.[14, 15] Interestingly, the higher activity for smaller SiO_2-supported Pt particles during H_2 oxidation[13] could not be explained by their heating up more than the larger ones. In cyclohexene hydrogenation ($-\Delta H = 117.8$ kJ/mol[16]) supported and unsupported Pt have been found[17–20] to show structure insensitivity (i.e., the turnover numbers remained constant at 2–3 cyclohexane molecules produced per Pt site per second[21] and independent of Pt particle size) with an activation energy of about 30 kJ/mol.

In the past many surface reactions have been probed by IR spectroscopy.[22] However, here IR emission analysis during catalysis has been carried out (see *Experimental Procedure*). Temperature profiles within catalysts during use can be predicted,[23] but precise catalyst parameters[24, 25] define the magnitude of the temperature rises of microscopic active centers and, inevitably, such analyses require assumptions concerning rates of generation, conduction, radiation, and convection of heat. As a result, widely varying excess temperatures[26] have been calculated and measurement[1] by IR emission[27] must be preferable (noting when external gas-film mass-transfer limitation[28] or stagnant gaseous boundary layers adjacent to the catalyst particle[29] are significant).

Figure 1 shows the temperature profiles of the Pt particles at the external surface of the Pt/SiO_2 catalyst particle during catalysis of H_2 oxidation (above) and cyclohexene hydrogenation (below), where the catalyst particle was initially at 294 K and 300 K, respectively. In view of the par-

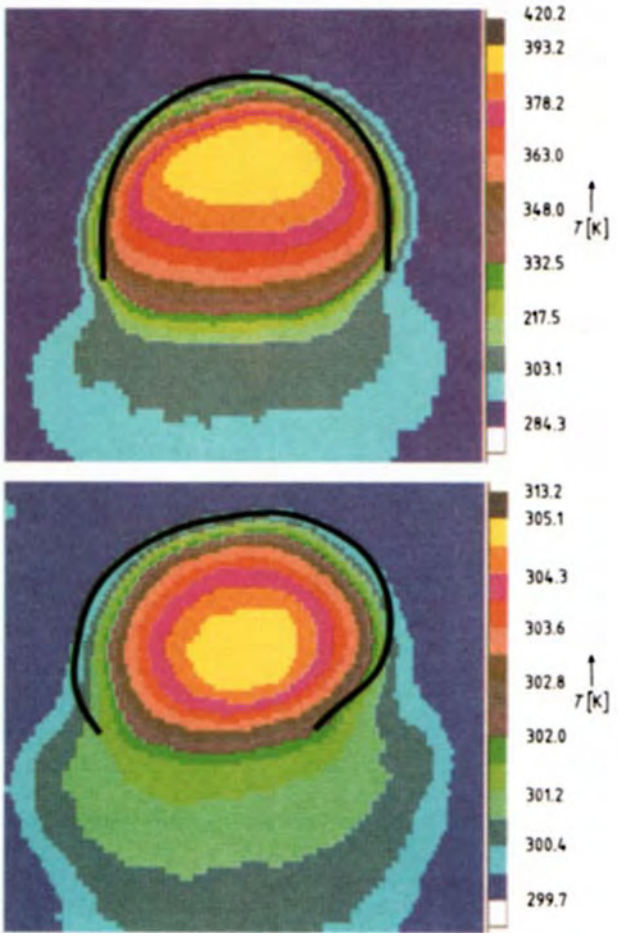

Fig. 1. Thermal profile observed for a 2.5-mm spherical particle of the Pt/SiO_2 catalyst, whose position is indicated by the dark line. The temperature of the SiO_2-supported Pt crystallites is predominantly assessed by IR emission. Above: Catalyst (which was predominantly at 293.7 K before reaction in flowing N_2) 13.0 min after initiation of hydrogen oxidation. Clearly, the temperature of the supported Pt crystallites rises as a result of the reaction to a maximum of 393.2 K. Interestingly, the gas stream temperature hardly appears to rise at all.—Below: Catalyst (which was predominantly at 300.3 K before reaction in flowing N_2) 3.25 min after initiation of cyclohexene hydrogenation. Here, 21% of the cyclohexene was hydrogenated by this catalyst particle. The temperature of the SiO_2-supported Pt crystallites clearly rises as a result of the reaction, but only modestly to 305.1 K.

[*] Dr. P. A. Sermon, Dr. G. Georgiades, Dr. V. A. Self
Department of Chemistry, Brunel University
Uxbridge, Middlesex, UB8 3PH (UK)

[**] The authors gratefully acknowledge the provision of the Thermovision 782 IR emission analytical facility by Agema Infrared Systems Ltd. and the financial support of *V. A. S.* by SERC.

ticle position indicated (black outline), there is no evidence of a stagnant boundary layer[29] surrounding the catalyst particle. However, there are a number of notable features which require comment. First, the temperature of the SiO_2-supported Pt crystallites (which is preferentially assessed by the IR emission method used here, unlike thermoelectric methods used previously,[13-14] which measure essentially the insulator support temperature), does increase as a result of sustained catalysis for both exothermic reactions, but to a much greater extent for H_2 oxidation than for cyclohexene hydrogenation. It should, however, be noted that excess temperatures of the obscured Pt particles within the catalyst pores may be higher than those noted at the external surface. Second, such excess Pt temperatures are stable as a function of reaction time. Third, there is a very wide range of Pt temperatures on the catalyst particles (which are not affected by the direction of reactant flow, but which are affected a little by the presence of the Pyrex pedestal which produces a vertical thermal asymmetry).

Despite the trend to design reactors with minimal concentration and temperature gradients, these temperature distributions are those that may exist during real heterogeneous catalysis. It has been shown here that the excess temperature of the SiO_2-supported Pt increases during catalysis of exothermic reactions to an extent which appears to vary from one reaction to another. This is unexpected for reactions whose overall enthalpies differ by only a factor of about two. Why it should be so remains uncertain. It is possible that in H_2 oxidation energy released is dissipated by radiation and so transfer to the gas phase is minimized, but that the reverse is the case for cyclohexene hydrogenation. If the reactant flow within the catalyst pores is a Knudsen flow, then the effective diffusion coefficients of oxygen and cyclohexene (0.025 and 0.015 $cm^2\ s^{-1}$ at 300 K) are significantly lower than in the bulk gases. However, turnover numbers of both reactions are approximately one product molecule per surface Pt atom per second. Therefore, the entire catalyst surface appears active and so with the present catalyst the differences in temperature are unlikely to result from larger cyclohexene molecules being hydrogenated at the outer edge of the catalyst and H_2 being oxidized through the porous structure catalyst particle, with radiation losses being greater in the former case. Bearing in mind the catalyst pore size, it is more likely to be attributable to the mechanisms of the two reactions being radically different, leading to different predominant modes of energy release. Thus, H_2 oxidation will result in formation of surface OH groups and adsorption of product water under these conditions is also quite likely.

The fact that the temperatures of the active crystallites in heterogeneous catalysts during exothermic reactions are raised relative to those of the support and of the gas phase is bound to affect the kinetics of catalyzed reactions. This means that measurement of the kinetics of reactions promoted by heterogeneous catalysts are made more complex by being a summation of the kinetics of processes occurring at reaction centers having a distribution of temperatures.[8] At least it may now be that these excess temperatures can be measured and controlled better than previously during catalysis under realistic conditions. They may then be found to affect the activity, selectivity, and reactivity of catalysts.

Experimental Procedure

Catalyst: A representative spherical particle (0.0124 g; 2.5 mm diameter) of 3% Pt/SiO_2 was used. This catalyst had been prepared by impregnation of SiO_2 (Shell, 2.5 S980-2.5 3; 211 m^2/g by N_2 BET analysis; 83% of its pore volume (0.94 cm^3/g) within the range 6-10 nm) with an aqueous H_2PtCl_6 (Johnson Matthey, Secpure) solution to the point of incipient wetness at 373 K and drying at the same temperature, calcining in air (543 K, 3 h), and reducing in flowing hydrogen at (713 K, 1 h) [9]. Since the catalyst had only a slightly lower pore volume (but a very similar surface area (205 m^2/g) and pore size range) compared to the support itself, support pore blocking on introduction of Pt was not great.

Methods: IR emission analysis was carried out using an Agema Thermovision 782 instrument (operating at 3-5.6 μm using a 7° lens and extension rings and image analysis on an IBM XT P/C with TIC 8000 cats software) and a Pyrex flow reactor. The emissivity of the supported metal particles was assumed to be 1 here and previously [5]. The catalyst sphere was placed in the reactor (in the center of an IR transparent window on a Pyrex pedestal) and around this flowed the reactant stream at constant flow rate and temperature (294 K or 300 K). The prepurified [7] reactant streams selected were (1) 4.05 kPa H_2 and 2.03 kPa O_2 (with the balance to 101 kPa being N_2) at a total flow rate of 100 ± 0.1 cm^3/min and (2) 4.05 kPa H_2 and 2.03 kPa cyclohexene (with the balance to 101 kPa being N_2) at a total flow rate of 40 ± 0.1 cm^3/min. These catalytic conditions were selected because of their previous use[7] and the prediction that they would result in identical excess temperatures of Pt in these reactions.

Received: January 23, 1987;
revised: May 15, 1987 [Z 2065 IE]
German version: *Angew. Chem. 99* (1987) 1050

CAS Registry numbers:
H_2, 1333-74-0; Pt, 7440-06-4; cyclohexane, 110-83-8.

[1] H. Heinemann in G. C. Bond, P. B. Wells, F. C. Tompkins (Eds.): *Proc. Int. Congr. Catal. 6th (1976), Vol. 2*, R. Soc. Chem., London 1977, p. 778.
[2] G. A. Mills, S. Weller, E. B. Cornelius, *Actes Congr. Int. Catal. 2nd (1960), Vol. 2* (1961) 2221.
[3] D. R. Kember, N. Sheppard, *J. Chem. Soc. Faraday Trans. 2 77* (1981) 1309, 1321.
[4] D. J. Kaul, E. E. Wolf, *J. Catal. 91* (1985) 216.
[5] J. A. Cusumano, M. J. D. Low, *J. Catal. 17* (1970) 98.
[6] J. R. Brown, G. A. D'Netto, R. A. Schmitz, *Springer Ser. Synergetics 29* (1985) 86; G. A. D'Netto, J. R. Brown, R. A. Schmitz, *Inst. Chem. Eng. Symp. Ser. 87* (1986) 247.
[7] P. A. Sermon, G. Georgiades, M. S. W. Vong, M. A. M. Luengo, P. N. Reyes, *Proc. R. Soc. London A 410* (1987) 353.
[8] P. A. Sermon, unpublished.
[9] M. A. M. Luengo, P. A. Sermon, K. S. W. Sing in B. Delmon, P. Grange, P. A. Jacobs, G. Poncelet (Eds.): *Proc. IV. Int. Symp. Sci. Basis Prep. Heterogeneous Catal.*, Elsevier, Amsterdam 1987, p. 29.
[10] M. A. M. Luengo, P. A. Sermon, A. T. Wurie, *J. Chem. Soc. Faraday Trans. 1 83* (1987) 1651.
[11] V. V. Gorodetskii, V. A. Sobyanin, N. N. Bulgakov, Z. Knor, *Surf. Sci. 82* (1979) 120.
[12] P. R. Norton in D. A. King, D. P. Woodruff (Eds.): *Fundamental Studies of Heterogenous Catalysis*, Elsevier, Amsterdam 1982, p. 27.
[13] E. Wicke, P. Kummann, W. Keil, J. Schiefler, *Ber. Bunsenges. Phys. Chem. 84* (1980) 315.
[14] Yu. Sh. Matros (Ed.): *Unsteady Processes in Catalytic Reactors (Stud. Surf. Sci. Catal. 22* (1985)).
[15] F. V. Hanson, M. Boudart, *J. Catal. 53* (1978) 56.
[16] D. R. Stull, E. F. Westrum, G. C. Sinke: *The Chemical Thermodynamics of Organic Compounds*, Wiley, New York 1969.
[17] E. Segal, R. J. Madon, M. Boudart, *J. Catal. 52* (1978) 45.
[18] S. M. Davis, G. A. Somorjai, *J. Catal. 65* (1980) 78; *Surf. Sci. 91* (1980) 73.
[19] M. S. W. Vong, *Ph. D. thesis*, Brunel University 1981.
[20] G. Georgiades, *M. Phil. thesis*, Brunel University 1984.
[21] D. J. O'Rear, D. G. Loffler, M. Boudart, *J. Catal. 94* (1985) 225.
[22] L. H. Little: *Infra-red Spectra of Adsorbed Species*, Academic Press, London 1966; M. L. Hair: *Infra-red Spectroscopy in Surface Chemistry*, Marcel Dekker, New York 1967.
[23] A. Moise, H. O. Pritchard, *Can. J. Chem. 60* (1982) 2012.
[24] J. Wei, *Chem. Eng. Sci. 21* (1966) 1171.
[25] C. D. Prater, *Chem. Eng. Sci. 8* (1958) 284.
[26] W. L. Holstein, M. Boudart, *Rev. Latinoam. Ing. Quim. Quim. Appl. 13* (1983) 107; D. Luss, *Chem. Eng. J. Lausanne 1* (1970) 311; S. H. Chan, M. J. D. Low, W. K. Mueller, *AIChEJ 17* (1971) 1499; C. Steinbruchel, L. D. Schmidt, *Surf. Sci. 40* (1973) 693; E. Ruckenstein, C. A. Pretty, *Chem. Eng. Sci. 27* (1972) 937.
[27] R. T. Matyi, J. B. Butt, L. H. Schwartz, *J. Catal. 91* (1985) 185; T. S. Cale, *ibid. 90* (1984) 40.
[28] S. P. S. Andrews in G. C. Bond, P. B. Wells, F. C. Tompkins (Eds.): *Proc. Int. Congr. Catal. (1976) Vol. 2*, R. Soc. Chem., London 1977, p. 778.
[29] W. J. Thomas, *Proc. Int. Congr. Catal. 6th (1976) Vol. 2*, R. Soc. Chem., London 1977, p. 778.

Novel Bimetallic Macrocyclic Polymer Structures Incorporating Deprotonated 2-Pyrrolidone Bridges: The Crystal Structures of $[\{Hg_2Cu(C_4H_6NO)_4\}X_2]_n$ ($X = NO_3$ or ClO_4)**

By *David M. L. Goodgame,* David J. Williams,** and *Richard E. P. Winpenny*

Polynuclear complexes involving different metal ions are currently of appreciable interest because, *inter alia*, of their possible role in catalysis, their involvement in metalloenzyme activity, and the unusual magnetic and electron transfer behavior they often exhibit. In the case of heterobimetallic complexes, easy electron transfer and the formation of metal centers with less-common oxidation states should be favored by the use of metals capable of ready redox behavior. With this in mind, we have been studying the formation of new polynuclear complexes involving combinations of mercury(II) ions with various transition metal ions.

Herein we report the syntheses and structural characterization of polynuclear complexes of stoichiometry $[Hg_2Cu(C_4H_6NO)_4X_2]$ with $X = NO_3$ (**1**) and ClO_4 (**2**); where C_4H_6NO = deprotonated 2-pyrrolidone **3**.

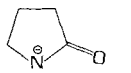

3

In both cases the X-ray structure analyses[1] show the Cu atoms to be coordinated to four 2-pyrrolidone units and two counterion oxygen atoms in an elongated octahedral arrangement (Fig. 1). The distances to the apical (counterion) oxygen atoms are significantly longer (ca. 2.6 Å) than those to the equatorial, pyrrolidone oxygens (ca. 1.9 Å). Additionally, the Hg atoms form strong bonds to the pyrrolidone nitrogen atoms,[2] producing linear N–Hg–N units linking pyrrolidone rings.

The consequence of these combined interactions is the formation of a unique polymeric, bimetallic, macrocyclic array (Fig. 2). The array is comprised of contiguous 32-membered macrocyclic rings, each ring being formed of 4 Cu, 4 Hg, 8 O, 8 N, and 8 C atoms. Within each macrocycle there are two counterions. In addition to their role of occupying the apical coordination sites on the Cu atoms, these form, in **1**, stabilizing ONO-bridges between opposite Hg atoms within each macrocycle, but in **2** they bridge only between the mercury and copper atoms.[3] In both structures the corrugated macrocyclic arrays are two-dimensional with, in each case, no significant inter-layer interactions.[4]

The formation of these structures may be thought to arise from the pronounced tendency of mercury(II) to favor deprotonation of the ring nitrogen atom of the 2-pyrrolidone and adoption of a linear N–Hg–N arrangement, accompanied by coordination of the exocyclic oxygen atom to copper(II). Conceptually, this behavior is related to that in some trinuclear species of the type

$[(NH_3)_2Pt^{II}L_2Cu^{II}Pt^{II}_2(NH_3)_2]^{n\oplus}$

where L represents 1-methylcytidine, or the anions of 1-

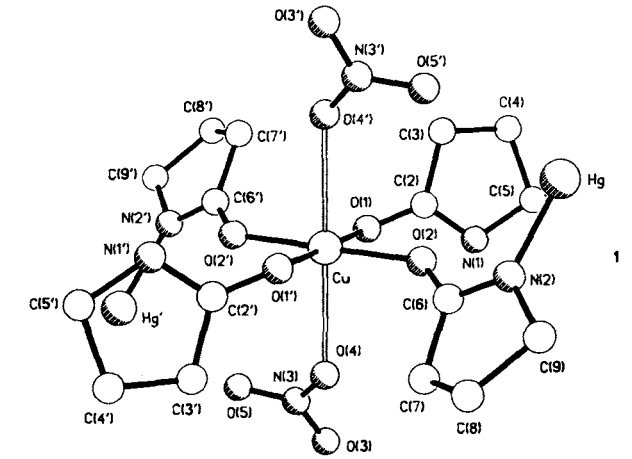

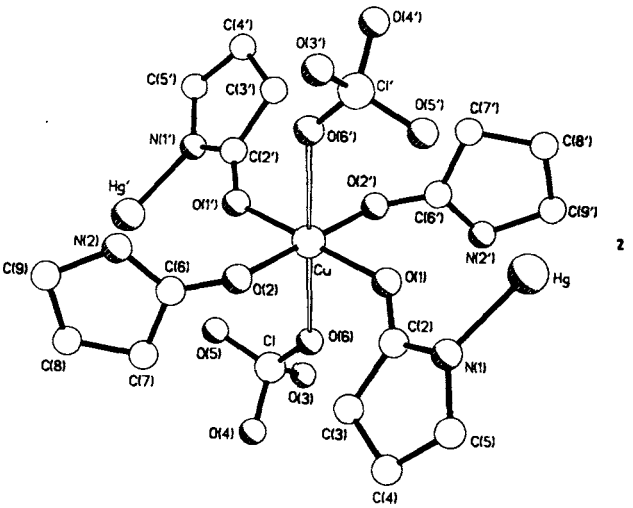

Fig. 1. The structures of **1** and **2** in the crystal. In **1** Cu-O1 = 1.960(7), Cu-O2 = 1.920(8) and Cu-O4 = 2.552(7) Å. In **2** Cu-O1 = 1.931(10), Cu-O2 = 1.955(10) and Cu-O6 = 2.681(10) Å.

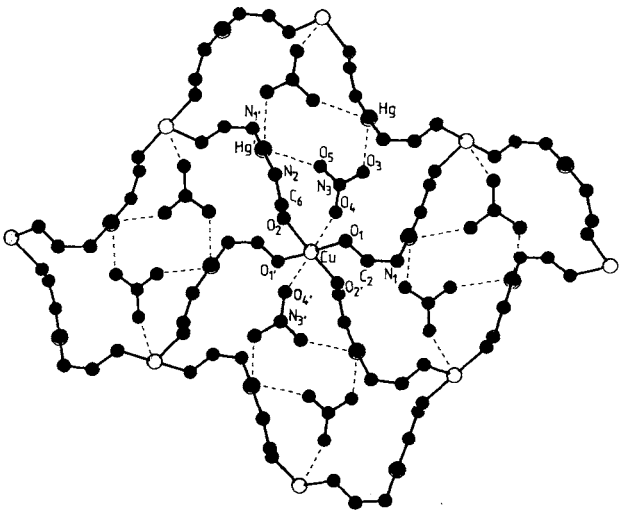

Fig. 2. Part of the contiguous macrocyclic array in the crystal structure of **1** showing also the $NO_3^{\ominus}$ stabilizing bridges. For clarity, only the atoms comprising the macrocyclic skeleton are shown (the pyrrolidone carbon atoms C3 to C5 and C7 to C9—see Fig. 1—have been omitted).

[*] Dr. D. M. L. Goodgame, Dr. D. J. Williams, R. E. P. Winpenny
Chemistry Department, Imperial College of Science and Technology
London SW7 2AY (UK)

[**] This work was supported by the Science and Engineering Research Council.

methyluracil or 1-methylthymine,[5] in which Pt^{II} binds to the ring nitrogen atom and Cu^{II} to the exocyclic oxygen atoms of the heterocyclic ligand (see **4**). In **1** and **2**, however, discrete units of low nuclearity are not formed.[6] Instead, the described contiguous, polymeric ring structure results.

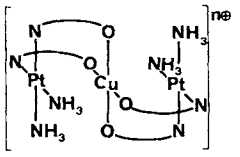

4

Magnetic and spectral measurements[7] show that there is no strong coupling between the unpaired electrons on the copper(II) centers. There is evidence for a small degree of copper–copper interaction in **1**, as its g_z band in the ESR spectrum shows no evident Cu hyperfine coupling; this is in contrast to that observed in **2** (Fig. 3). However, no 'half-field' ($\Delta M_s = 2$) line, often observed for strongly coupled binuclear Cu^{II} systems,[8] was detected. The distance between nearest copper centers in both **1** and **2** is similar and is > 8 Å, so direct Cu–Cu interaction is unlikely. The poorer magnetic dilution in **1**, compared with **2**, may originate via a weak Cu–nitrate–Hg–nitrate–Cu mediated interaction (Fig. 2). Rhombicity is apparent in both spectra but is noticeably better resolved in the spectrum of **1**.

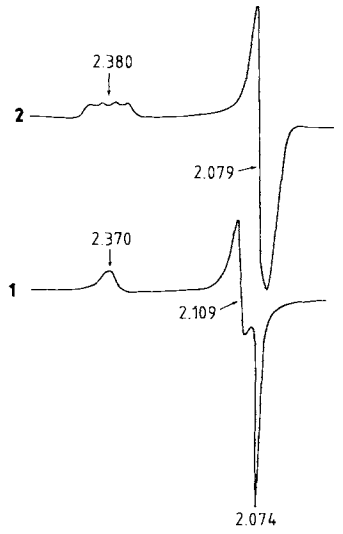

Fig. 3. Q-Band (≈34 GHz) ESR spectra of polycrystalline samples of **1** and **2**.

It is also of interest that the ν(C=O) bands, due to the bridging 2-pyrrolidones, in the IR spectra of **1** and **2** are much lower than those in complexes in which these ligands bind in monodentate fashion,[9] and this may provide a useful diagnostic guide for related compounds not amenable to single crystal X-ray analysis.

In view of the fairly loosely bound environment of the counterions in these structures there is potential for the development of analogous systems, with the possibility for anion exchange. It is perhaps noteworthy that the acetate used in the preparation of these complexes is not incorporated into either structure.

Experimental

Mercury(II) acetate (2 mmol), 2-pyrrolidone (8 mmol) and the appropriate ($X = NO_3$ or ClO_4) hydrated copper(II) salt (2 mmol) were refluxed in methanol (120 cm^3) for 3 d. The solutions were concentrated to ca. 20 cm^3, filtered and allowed to evaporate at room temperature when pale blue crystals suitable for X-ray analysis were obtained. Yields of **1** and **2** 49 and 56%, respectively. Both compounds gave satisfactory elemental analyses.

Received: April 14, 1987;
supplemented: July 8, 1987 [Z 2205 IE]
German version: *Angew. Chem. 99* (1987) 1053

[1] **1**: monoclinic, $a = 20.998(7)$, $b = 12.680(4)$, $c = 9.971(3)$ Å, $\beta = 117.53(2)°$, $V = 2354$ Å^3, $C2/c$, $Z = 4$, $\mu(Cu_{K\alpha}) = 263$ cm^{-1}, $\rho_{calcd} = 2.61$ g cm^{-3}. **2**: monoclinic, $a = 9.558(2)$, $b = 12.862(2)$, $c = 10.334(2)$ Å, $\beta = 100.28(2)°$, $V = 1250$ Å^3, $P2_1/c$, $Z = 2$, $\mu(Cu_{K\alpha}) = 269$ cm^{-1}, $\rho_{calcd} = 2.61$ g cm^{-3}. Nicolet R3m diffractometer, ω-scan, graphite-monochromated $Cu_{K\alpha}$ radiation. Both structures were solved by heavy atom methods, corrected for absorption, and refined anisotropically to give $R = 0.036$ ($R_w = 0.038$) and $R = 0.050$ ($R_w = 0.050$), respectively, for 1457 and 1304 independent observed reflections [$\theta \leq 58°$ (**1**), 58° (**2**), $|F_o| > 3\sigma(|F_o|)$]. Further details of the crystal structure investigations can be obtained from the Director of the Cambridge Crystallographic Data Centre, Lensfield Road, Cambridge, CB2 1EW (England), by quoting the full literature citation.

[2] **1** Hg–N 2.021(7) and 2.027(6) Å; **2**, Hg–N 2.02(1) and 2.03(1) Å.

[3] In **1** Hg···O3 = 2.77, Hg···O5′ = 2.88 Å. There is also a slightly longer (2.98 Å) contact between Hg and O5. In **2** Hg···O3 = 2.75 Å. The only other Hg···O contacts are to the ClO_4 oxygen O5 (3.07 Å) and to the pyrrolidone oxygen O1 (3.07 Å). Interestingly these weak interactions do not seriously perturb the linearity of the N–Hg–N units, 178.0(4)° in **1** and 178.2(5)° in **2**.

[4] In **1** the shortest inter-layer contact is 3.53 Å between one of the nitrate oxygens, O3, in one layer and a pyrrolidone carbon atom, C9, in the next. In **2** the shortest inter-layer contact is 3.34 Å between the perchlorate oxygen, O4, and the pyrrolidone carbon atom C4.

[5] D. M. L. Goodgame, M. A. Hitchman, B. Lippert, *Inorg. Chem. 25* (1986) 2191, and references cited therein.

[6] Tetranuclear platinum complexes of 2-pyrrolidone containing the platinum in mixed oxidation states have been described by Matsumoto (K. Matsumoto, *Chem. Lett. 1984*, 2061, and references cited therein).

[7] Magnetic moments at room temperature, by Gouy method are unexceptional: **1**, 2.01; **2**, 1.83. Electronic spectra by reflectance technique (Beckman DK2 spectrometer): **1**, 8700 sh, 10800 sh, 12500 cm^{-1}; **2**, 8400, 11000 sh, 13000 cm^{-1}. ESR spectra (polycrystalline samples at room temperature, Bruker ER200 spectrometer at Q-band frequency, ≈34 GHz): **1**, $g_x, g_y = 2.074, 2.109$, $g_z = 2.370$. **2**, $g_{xy} = 2.079$, $g_z = 2.380$ ($a_z = 128$ gauss).

[8] Example: D. M. L. Goodgame, Y. Nishida, R. E. P. Winpenny, *Bull. Chem. Soc. Jpn. 59* (1986) 344.

[9] ν(C=O) for **1** 1580 cm^{-1}, for **2** 1575 cm^{-1}; cf. 1691 cm^{-1} for the free ligand, and 1638–1649 cm^{-1} in typical monodentate metal complexes (S. K. Madan, W. V. Miller, and K.-W. Kuo, *J. Inorg. Nucl. Chem. 32* (1970) 3855).

Spherical Mixed-Valence $[V_{15}O_{36}]^{5\ominus}$, an Example from an Unusual Cluster Family

By *Achim Müller,* Erich Krickemeyer, Michael Penk, Heinz-Jürgen Walberg,* and *Hartmut Bögge*

Intramolecular electron transfer processes in $M_xS_yM'_z$ clusters (M = V, Mo, W, Re; M′ = Fe, Co), and especially in the thioanions $VS_4^{3\ominus}$, $MoS_4^{2\ominus}$, $WS_4^{2\ominus}$ and $ReS_4^{\ominus}$, are of interest regarding a knowledge of the component 1 of the enzyme system nitrogenase[1] and HDS catalysis.[2] Remarkably, reduction of V^V by the $S^{2\ominus}$ ligands *and* rapid S–O exchange already take place on gently heating $VS_4^{3\ominus}$ (in contrast, e.g., to $MoS_4^{2\ominus}$) in H_2O. We have now been able to prepare black

$[NMe_4]_6[V_{15}O_{36}]\cdot Cl\cdot 4H_2O$ **1**

[*] Prof. Dr. A. Müller, E. Krickemeyer, M. Penk, H.-J. Walberg, Dr. H. Bögge
Fakultät für Chemie der Universität
Postfach 8640, D-4800 Bielefeld 1 (FRG)

in high yields by this reaction[3] and to characterize it by elemental analysis, manganometric titration of the V^{IV}, DTA/TG analysis, IR spectroscopy,[4] magnetic measurements, and single-crystal X-ray structure analysis.[5]

The spherical anion $[V_{15}O_{36}]^{5\ominus}$ (Fig. 1), which has the high crystallographic symmetry $\bar{6}m2(D_{3h})$, is formed by linkage of fifteen tetragonal VO_5 pyramids. The different V-O distances ($V\text{-}O_{term} < V\text{-}(\mu_2\text{-}O) < V\text{-}(\mu_3\text{-}O)$; Fig. 1) are in the expected range. The 15 V atoms are arranged on the surface of a sphere at a distance of 343 ± 10 pm from the center of the cluster, where the $Cl^{\ominus}$ ion resides. Eighteen V-V distances in the range 293 to 300 pm indicate spin-spin interactions. Owing to significant spin coupling and the delocalized electronic ground state, the 8-electron cluster can *only formally* be referred to as a $V_7^V V_8^{IV}$-system[6] ($\mu_{eff} = 3.9\,\mu_B$ at room temperature). Probably the electronic interaction of the metal centers is optimized on a spherical surface.

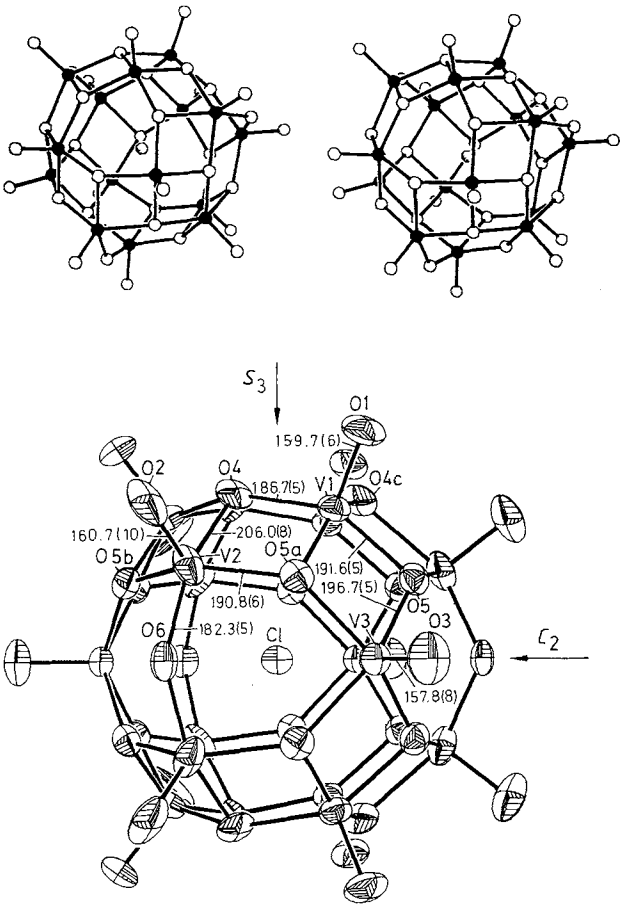

Fig. 1. Structure of the $[V_{15}O_{36}]^{5\ominus}$ anion with entrapped $Cl^{\ominus}$ ion in the crystals of **1**. Top: stereodiagram for clarification of the geometry: six VO_5 pyramids are each linked via three edges and two corners, six further are each linked via two edges and three corners and three are each linked via two edges and four corners. All μ_3-O atoms concomitantly participate in two edge linkages and one corner-linkage; the μ_2-O atoms form a corner linkage (V = black, O = white, Cl = shaded). Bottom: Ellipsoid plot with view perpendicular to the crystallographic S_3 and to one of the C_2 axes with bond lengths [pm]. Symmetry operations *a*: $-y, -x, z$; *b*: $y-x, -x, z$; *c*: $-y, x-y, z$; V-V distances [pm]: V1···V2 293.3(2), V1···V3 300.0(2); Bond angle ranges [°]: O_{term}-V-(μ-O) 101.0(4)-110.7(2), (μ-O)-V-(μ-O) 77.3(3)-93.0(6), 136.1(4)-156.1(4), V-(μ_3-O)-V 96.5(2)-101.2(2), 138.7(3)-140.8(5), V-(μ_2-O)-V 130.2(6).

The mixed-valence isopolyanions of vanadium probably form a structurally unusually versatile cluster family, since the metal-metal interaction is not very marked (in contrast to clusters of the 4d and 5d metals such as e.g., Mo with d^n configuration, in which the number of the d-electrons is structure-determining due to the formation of strongly covalent metal-metal bonds[7]), but can be highly modified by variable amounts of V^{IV} and V^V, and, moreover, the coordination geometries at the V centers are highly variable (tetrahedral (V^V), tetragonal-pyramidal (V^{IV}/V^V), and octahedral (V^{IV}/V^V)).

Received: May 29, 1987 [Z 2271 IE]
German version: *Angew. Chem. 99* (1987) 1060

[1] A. Müller, R. Jostes, E. Krickemeyer, H. Bögge, *Naturwissenschaften 74* (1987) 388; A. Müller, W. E. Newton: *Nitrogen Fixation. The Chemical-Biochemical-Genetic Interface*, Plenum Press, New York 1983.

[2] Suitable bimetallic sulfides can be obtained, e.g., from 3d metal complexes with the quoted thioanions as ligands: A. Müller, *Polyhedron 5* (1986) 323.

[3] A solution of Me_4NCl (5 g, 45.6 mmol) in H_2O (75 mL) was treated at 60°C with $[NH_4]_3[VS_4]$ (1 g, 4.29 mmol) in a 100-mL Erlenmeyer flask (wide-necked, covered with a watch glass) and allowed to stand on a hotplate at 60–65° (internal temperature) without stirring for 16 h (color change from red-violet to dark brown). After filtration, the filtrate was allowed to stand at 60–65°C for a further 5 days. The black crystals of **1** that precipitated were separated from the supernatant, almost colorless solution, washed with H_2O, 2-propanol, CS_2, and diethyl ether, and dried in air. Yield 0.46 g (85%). Elemental analysis: found C 15.10, Cl 2.02, H 4.28, N 4.40, V_{total} 39.6, V^{IV} 21.6; calculated C 15.23, Cl 1.87, H 4.26, N 4.44, V_{total} 40.38, V^{IV} 21.53.

[4] IR spectrum (solid/CsI pellet): $\tilde{\nu}(V\text{-}O_{term}) = 980$ (s); $\tilde{\nu}(V\text{-}O\text{-}V) = 790$ (m), 720 (m), 660 (s) cm^{-1}.

[5] $P6_3/mmc$; $a = 1383.2(4)$, $c = 2007.4(4)$ pm, $V = 3326.2 \times 10^6$ pm^3; $\mu = 20.64$ cm^{-1}; $Z = 2$; $R = 0.080$ for 946 independent reflections ($F_0 > 3.92\sigma(F_0)$); Syntex-$P2_1$ diffractometer, $Mo_{K\alpha}$ radiation, graphite monochromator). The water molecules are highly disordered in the crystal lattice. The powder diffraction pattern calculated from single-crystal data agrees with the measured one. Further details of the crystal structure investigation are available on request from the Fachinformationszentrum Energie, Physik, Mathematik GmbH, D-7514 Eggenstein-Leopoldshafen 2 (FRG), on quoting the depository number CSD-52557, the names of the authors, and the journal citation.

[6] The only previously known and structurally unequivocally characterized mixed-valence isopolyvanadate is $[V_{10}O_{26}]^{4\ominus}$; A. Bino, S. Cohen, C. Heitner-Wirguin, *Inorg. Chem. 21* (1982) 429. A further "reduced" isopolyvanadate, $[V_{18}O_{42}]^{12\ominus}$, contains *only* V^{IV} centers: G. K. Johnson, E. O. Schlemper, *J. Am. Chem. Soc. 100* (1978) 3645, and references cited therein; F. A. Cotton, G. Wilkinson: *Anorganische Chemie*, 4th Edit., Verlag Chemie, Weinheim 1982, p. 728.

[7] A. Müller, S. Sarkar, R. G. Bhattacharyya, S. Pohl, M. Dartmann, *Angew. Chem. 90* (1978) 564; *Angew. Chem. Int. Ed. Engl. 17* (1978) 535.

A Non-Stereospecific Diels-Alder Reaction**

By *Herbert Meier,* Heinz-Ludwig Eckes, Hans-Peter Niedermann,* and *Heinz Kolshorn*

Dedicated to Professor Ernst Bayer on the occasion of his 60th birthday

Since its discovery some 60 years ago[1] the Diels-Alder reaction has been a major subject of study in organic chemistry both from the preparative as well as mechanistic point of view.[2] At an early stage, *Diels* and *Alder* highlighted stereospecificity as a very important aspect of this [4+2] cycloaddition. According to present-day textbooks by far the majority of such cycloadditions involve a concerted mechanism. Very few cases are known in which the configuration of diene or dienophile is not retained during product formation.[3]

On the basis of frontier orbital theory it can be assumed that large energy differences HOMO(diene)-LUMO(die-

[*] Prof. Dr. H. Meier, Dipl.-Chem. H.-L. Eckes, Dr. H.-P. Niedermann, Dipl.-Chem. H. Kolshorn
Institut für Organische Chemie der Universität
Johann-Joachim-Becher-Weg 18-22, D-6500 Mainz 1 (FRG)

[**] This work was supported by the Fonds der Chemischen Industrie.

nophile) and HOMO(dienophile)-LUMO(diene) can be a decisive prerequisite for a two step mechanism being able to compete with the concerted mechanism.[2] *Huisgen* et al. recently demonstrated with an impressive example that this effect together with a strong steric hindrance reduces the stereoselectivity in the closely related 1,3-dipolar cycloaddition.[10] All the more surprising is that the heterodiene **2** reacts *stereo-unspecifically*—despite energetically favorably lying frontier orbitals and the absence of significant hindrance.

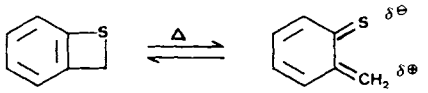

1 **2**

Because of its ease of thermal ring-opening to **2**, benzothiete **1** is suitable as synthon for the synthesis of numerous heterocycles.[11] According to MNDO calculations the *o*-quinoid form **2** has a low-lying LUMO and a relatively high-lying HOMO (Fig. 1); it can therefore be used as 4π (or 8π) component in cycloadditions with electron-rich or electron-deficient olefins **3** (2π components).

From the orbital coefficients it is clear that **2** should be attacked at the exocyclic positions; also evident in Figure 1 is the mode of addition for electron-rich olefins. The substituents X should assume the α-position to the sulfur in the cycloadduct (correlation A). In the case of electron-deficient olefins both modes of addition appear to be possible, whereby a slight preference for the β-position in the adduct can be assumed for the substituents Z (correlation B).

While the predicted periselectivity is rigidly retained, only in case A do the reactions proceed completely regioselectively; in case B, apart from the predicted main product, a by-product with inverse orientation of the dienophile is observed. In all cases the cycloaddition of **2** to **3** to give the products **4** and/or **5** competes with the cyclodimerization of **2** to **6**.

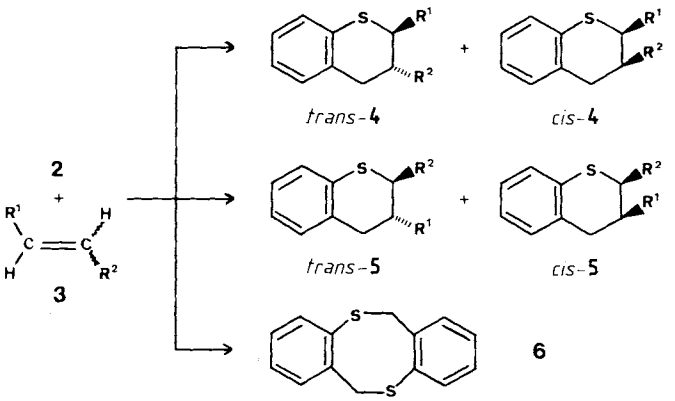

Table 1. Yields in the cycloadditions of **2** (from **1**) to **3** (toluene, 80–110°C, molar ratio **1** : **3** = 1 : 1.5).

3	Dienophile R¹	Dienophile R²	Total yield [%] (based on 1)	Rel. yields *trans*-4	*cis*-4	*trans*-5	*cis*-5	6	Regioselect. [%]	Retention of configuration [%]
E-**3a**	C_6H_5	OCH_3	92	—	—	80 [a]	—	20	99	≥99
Z-**3a**	C_6H_5	OCH_3	94	—	—	76	—	24	99	≤ 1
E-**3b**	CH_3	CO_2CH_3	63	57 [b]	—	11 [c]	—	32	84	≥99
Z-**3b**	CH_3	CO_2CH_3	44	2 [d]	23 [c]	—	7 [c]	68	79	93
E-**3c**	$CO_2C_2H_5$	$CO_2C_2H_5$	97	97 [c]	—			3	— [e]	≥99
Z-**3c**	$CO_2C_2H_5$	$CO_2C_2H_5$	59	10	22 [c]			68	— [e]	68
			63 [f]	13	27			60	— [e]	68

[a] M.p. 71°C. [b] M.p. 65°C. [c] Oily liquid. [d] Detection by capillary-GC. [e] **4** ≡ **5** for $R^1 = R^2$. [f] Reaction in pure diethyl maleate.

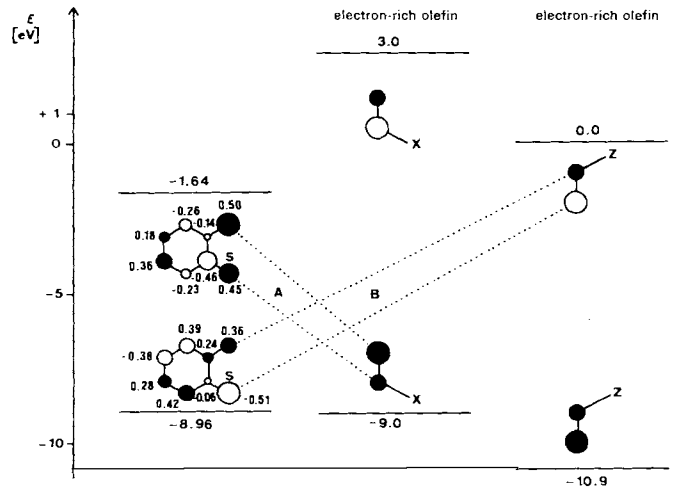

Fig. 1. Frontier orbitals of **2**, calculated according to the MNDO method [12], and estimation of the regio- and peri-selectivity of $[\pi 4_s + \pi 2_s]$ cycloadditions. (A, B: see text.)

Table 1 lists the total yields and the percentage distribution for the products of the reaction of **1** (via **2**) with the *E*- and *Z*-configurated dienophiles **3a–c**. It can be seen that the *E*-olefins are added strictly stereospecifically; in the case of the more sluggishly reacting *Z*-olefins the amount of **6** is larger and the configuration of the olefin can even be completely inverted. This is so in the case of *Z*-**3a**, which affords exclusively *trans*-**5**. In the case of *Z*-**3b** the configuration is up to 93% retained and in the case of *Z*-**3c** 68% retained.

A mechanistic explanation for these observations is given for the example **2** + **3a** (Scheme 1). In its behavior **2** is reminiscent of a weakly polar diradical.[13] It adds *Z*-**3a** with formation of *one* bond (C–S or C–C). **7a** should be more stable than the 1,6-diradical, which is formed by primary C–C linkage. When $k_r \gg k_2'$ the *Z*-configuration is lost by rotation prior to the CC coupling. The isomeric diradical **8a** can cyclize to *trans*-**5a** ($k_2 \gg k_2'$), but also be cleaved to *E*-**3a** and **2** ($k_1 \gg k_2'$). In the case of unused *Z*-**3a** a partial isomerization to *E*-**3a** is indeed observed. Under these circumstances the reaction path to *cis*-**4a** is not followed at all. At the beginning of the reaction the concentration of *E*-**3a** is very low, and it follows from the rate of formation of *trans*-**5a** that the process *Z*-**3a** + **2** → **7a** → **8a** → *trans*-**5a**

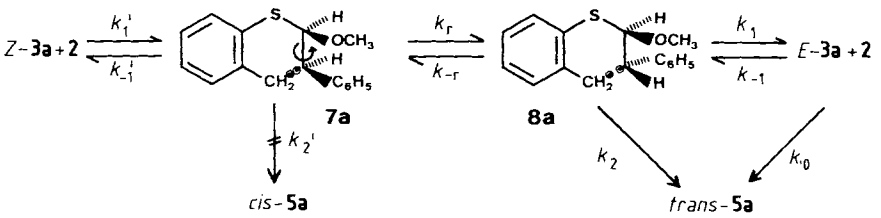

Scheme 1.

dominates. It is still unclear to what extent *E*-**3a** reacts in a concerted reaction (k_0) or via **8a** to give *trans*-**5a**. If one starts with *E*-**3a** no isomerization to *Z*-**3a** can be observed (k_0 or $k_2 \gg k_{-r}$). In any case, in the process *Z*-**3a** + **2** → *trans*-**5a** a *Diels–Alder reaction takes place via a non-concerted reaction with loss of the Z-configuration of the added olefin*; in control experiments it can be unequivocally demonstrated that neither a direct isomerization *Z*-**3a** ⇄ *E*-**3a** nor an isomerization *cis*-**4** ⇄ *trans*-**4** or *cis*-**5** ⇄ *trans*-**5** is possible under the given reaction conditions.

The degree of stereoselectivity in the other examples likewise depends on the ratio of the partial rate constants. Apparently, favorable HOMO(diene)–LUMO(dienophile) or LUMO(diene)–HOMO(dienophile) interactions still do not suffice to ensure a concerted reaction. The asymmetry of the transition state may here be crucial: the C–S and C–C bonds to be formed have quite different lengths and therefore have different resonance integrals $\beta = f$ (distance *d*) on approach of **2** and **3**. This explanation is supported by the finding that the related *o*-quinodimethane system reacts stereospecifically with fumarates and maleates.[14]

Table 2. ^{1}H-NMR data of the cycloadducts **4** and **5** (δ values, TMS, vicinal *trans*- or *cis*-coupling $^3J_{2,3}$ in Hz). Solvents in brackets in the first column.

Cyclo-adduct	2-H	3-H	$^3J_{2,3}$	4-H (AB)	5,6,7,8-H (ABCD)	R^1 and R^2
trans-**5a** ($CDCl_3$)	4.99	3.20	5.8	3.03, 3.12	7.1–7.3	3.38 (OCH_3), 7.1–7.3 (C_6H_5)
trans-**4b** ($CDCl_3$)	3.57	2.67	9.3	3.06, 3.99	7.0–7.1	1.33 (CH_3), 3.73 (OCH_3)
cis-**4b** (C_6D_6)	3.41	2.86	3.2	2.80, 3.01	6.8–7.1	1.17 (CH_3), 3.22 (OCH_3)
trans-**5b** ($CDCl_3$)	3.62	2.36	7.7	2.50, 2.86	7.0–7.2	1.12 (CH_3), 3.73 (OCH_3)
cis-**5b** (C_6D_6)	3.62	2.15	3.5	2.43, 2.84	6.8–7.1	0.90 (CH_3), 3.20 (OCH_3)
trans-**4c** ($CDCl_3$)	4.30	3.22	8.5	2.88, 3.13	7.0–7.2	1.24, 1.26 (CH_3), 4.17, 4.19 (OCH_2)
cis-**4c** (C_6D_6)	4.10	2.80	3.7	3.05, 3.75	6.7–7.1	0.89, 0.90 (CH_3), 3.88, 3.90 (OCH_2)

The cycloadducts **4** and **5** were characterized by elemental analysis and by their IR, ^{1}H-NMR, ^{13}C-NMR and mass spectra; Table 2 lists the important ^{1}H-NMR data for the *cis-trans* assignment.

Received: April 3, 1987;
supplemented: July 1, 1987 [Z 2179 IE]
German version: *Angew. Chem. 99* (1987) 1040

CAS Registry numbers:
1, 63559-01-3; **2**, 59130-11-9; *E*-**3a**, 4110-75-2; *Z*-**3a**, 14371-19-8; *E*-**3b**, 623-43-8; *Z*-**3b**, 4358-59-2; *E*-**3c**, 623-91-6; *Z*-**3c**, 141-05-9; *trans*-**4b**, 110472-34-9; *cis*-**4b**, 110472-35-0; *trans*-**4c**, 110472-37-2; *cis*-**4c**, 110472-38-3; *trans*-**5a**, 110472-33-8; *trans*-**5b**, 110472-39-4; *cis*-**5b**, 110472-36-1; **6**, 263-06-9.

[1] O. Diels, K. Alder, *Justus Liebigs Ann. Chem. 460* (1928) 98.
[2] Review: J. Sauer, R. Sustmann, *Angew. Chem. 92* (1980) 773; *Angew. Chem. Int. Ed. Engl. 19* (1980) 779.
[3] Most frequently cited is the example described by *Mark* [4], according to which (*E*)-1,2-dichloroethylene affords predominantly an adduct with *cis*-chloro-substituents on reaction with hexachlorocyclopentadiene. *Mark* has further qualified this result in a later work [5]. For other examples of stereo-unspecific Diels–Alder reactions cf. Refs. [6–9].
[4] V. Mark, *J. Org. Chem. 39* (1974) 3179.
[5] J. B. Lambert, C. D. McLaughlin, V. Mark, *Tetrahedron 32* (1976) 2075; see especially footnote 8 therein.
[6] L. M. Stephenson, R. V. Gemmer, S. Current, *J. Am. Chem. Soc. 97* (1975) 5909.
[7] P. D. Bartlett, J. J.-B. Mallet, *J. Am. Chem. Soc. 98* (1976) 143.
[8] G. Huybrechts, B. van Mele, *Int. J. Chem. Kinet. 10* (1978) 1183.
[9] P. Magnus, C. Walker, P. R. Jenkins, K. A. Menear, *Tetrahedron Lett. 27* (1986) 651.
[10] R. Huisgen, G. Mloston, E. Langhals, *J. Am. Chem. Soc. 108* (1986) 6401.
[11] D. Jacob, H.-P. Niedermann, H. Meier, *Tetrahedron Lett. 27* (1986) 5703, and references cited therein.
[12] M. J. S. Dewar, W. Thiel, *J. Am. Chem. Soc. 99* (1977) 4907.
[13] Cf. also *V. Bonačić-Koutecký, J. Koutecký, J. Michl, Angew. Chem. 99* (1987) 216; *Angew. Chem. Int. Ed. Engl. 26* (1987) 170.
[14] Y. Ito, M. Nakatsuka, T. Saegusa, *J. Am. Chem. Soc. 104* (1982) 7609.

Imaging Oxygen Vacancies in Superconducting $YBa_2Cu_3O_{7-\delta}$ by High Resolution Electron Microscopy**

By *Dong Tang, Wuzong Zhou,* and *John M. Thomas**

Recent studies by high-resolution powder diffractometry[1,2] indicate that, in the perovskite-based superconductor $YBa_2Cu_3O_{7-\delta}$, there is a tendency for the oxygen anion vacancies to be preferentially ordered. It is thought that the arrangement of vacancies in the *ab* plane is such that CuO_4 planar groups constitute one-dimensional chains running parallel to the *b* axis (Fig. 1). High-resolution electron microscopic studies have also been brought to bear on the question of oxygen vacancy ordering;[3,4] but, owing to the inherent features of this technique (summarized below), less firm conclusions have hitherto been drawn concerning the preferential nature of these vacancies. Extensive computations, using the multislice procedure for coping with multiple electron scattering, along with high-resolution electron microscopic imaging, is shown here to yield strong supportive evidence for the recently proposed structural model.[2] In particular, we show that under certain well-defined conditions of imaging—sample thicknesses 60 to 80 Å, defocus settings of +600 to −1800 Å and resolutions close to 2.0 Å—the ordering of oxygen vacancies

[*] Prof. Dr. J. M. Thomas, Dr. Dong Tang, [+] Dr. Wuzong Zhou [+]
Davy Faraday Research Laboratory,
The Royal Institution of Great Britain
21, Albemarle Street, London W1X 4BS (UK)
[+] Second Address:
Department of Physical Chemistry, University of Cambridge
Lensfield Road, Cambridge, CB2 1EP (UK)

[**] We thank the Royal Society for an Elizabeth Scholarship to enable one of us (*D. T.*) to come from the Institute of Physics, Academia Sinica, Beijing to London and Cambridge, Fudan and Cambridge Universities for support (to *W. Z.*) and the SERC for an equipment grant (to *J. M. T.*).

can be experimentally identified. Images projected along either [010] or [100] zone axes reveal direct evidence for the alignment of vacancies; those along either [001] or [110] do not. Such vacancies are crucially implicated in proposed[2,5] interpretations of the superconductivity of these mixed oxides.

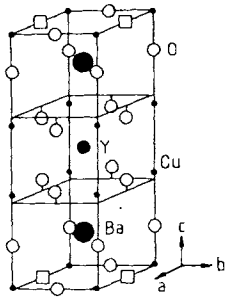

Fig. 1. Representation of the idealized structure of $YBa_2Cu_3O_{7-\delta}$ with the oxygen vacancies designated by □.

Experimental determinations of the structure of the high-temperature superconductor $YBa_2Cu_3O_{7-\delta}$ by X-ray and neutron scattering or by high-resolution electron microscopy leave little doubt as to the location of cations in the unit cell (Fig. 1). The arrangement of the anion vacancies in the oxygen sub-lattice is, however, more difficult to determine. And although there can be certain circumstances when the presence or absence of light atoms may be unambiguously detected either from superlattice spots[6,7] in electron diffraction patterns or by rather special conditions of high-resolution imaging,[8] it is no mean task unambiguously to characterize the nature of the arrangement of light atoms or vacancies by electron microscopy. We have tested the currently accepted structural model by comparing our observed images—recorded under conditions described in an earlier paper[9] dealing with crystalline defects in $YBa_2Cu_3O_{7-\delta}$—with the results of several hundred image computations covering a wide range of observational conditions.

High-resolution electron microscopy can nowadays achieve point-to-point resolutions of better than 1.6 Å. But there is no ready intuitive way of reading off structural detail from projected images of relatively tightly packed structures. Why this is so has been amply described elsewhere.[10,11] One of the main reasons stems from the multiple scattering of electron waves so that, even with ideal electron lenses, the structural information transferred to the Gaussian image plane is complex, and is, in any case, further affected by imperfections in the lenses and by processes other than diffraction which occur when the monochromatic electron waves pass through the sample. Fortunately, a well-tried method—the multislice procedure—of image computation is available. It transpires that, depending upon the suspected feature in the sample that one seeks to characterize, a specific imaging condition, or 'window' of conditions is found, by numerical computation, to be appropriate. Thus, in endeavouring to locate exchangeable cations, for example, in zeolitic catalysts, it is found[12] that a lower rather than higher resolution (fewer diffracted beams) is advantageous.

Samples of the material $YBa_2Cu_3O_{7-\delta}$ were kindly supplied by Dr. *W. Y. Liang* of the Cavendish Laboratory, University of Cambridge. The preparation, composition, superconducting properties ($T_c \approx 93$ K; $\Delta T_c \approx 1$ K) of this material and our electron-microscopic and computational procedures have been described elsewhere.[9]

Using the atom coordinates given by *David* et al.,[2] we have computed images projected along all the principal high symmetry directions. Sample thickness has been varied systematically up to 120 Å, lens defocus from 400 to −2300 Å and image resolutions from 1.90 to 2.40 Å, the accelerating voltage being 200 keV throughout.

Not surprisingly, with thin specimens, computed projected images of the structure containing aligned vacancies show no difference as between the [010] and [100] projections for a resolution of 1.90 Å. At 80 Å thickness, however, significant differences begin to emerge for the [010] and [100] projections (see Fig. 2). But images along [001] and [110] do not yield any information about oxygen vacancies. When the oxygen occupancy factors are all set equally at

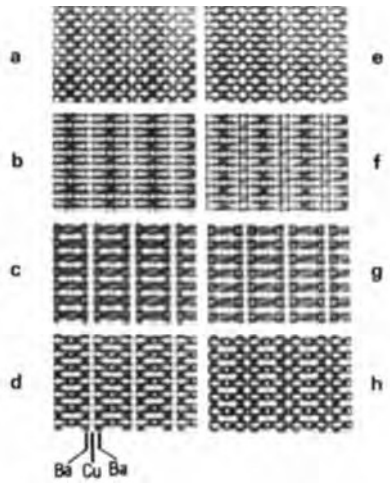

Fig. 2. Computed images along [010] (*a*, *b*, *c*, *d*) and [100] (*e*, *f*, *g*, *h*) zone axes. From top to bottom, specimen thickness: 20, 40, 60 and 80 Å; resolution = 1.90 Å; defocus = −600 Å. Note the difference between *d* and *h*. Along [010], the Cu-O "plane" is imaged to be more as a continuous line than in *h*, where discrete white spots are visible.

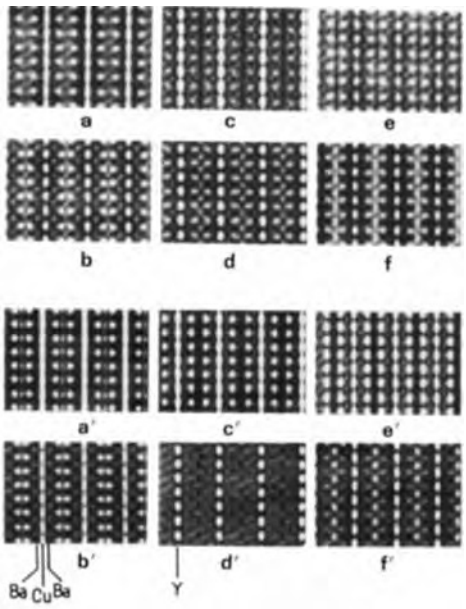

Fig. 3. Computed images along [100] projection (*a* to *f*) and [010] projection (*a'* to *f'*). Resolution = 1.98 Å; defocus = −600 Å (*a*, *b*, *a'*, *b'*), −1200 Å (*c*, *d*, *c'*, *d'*) and −1800 Å (*e*, *f*, *e'*, *f'*); thickness = 60 Å (*a*, *c*, *e*, *a'*, *c'*, *e'*) and 80 Å (*b*, *d*, *f*, *b'*, *d'*, *f'*).

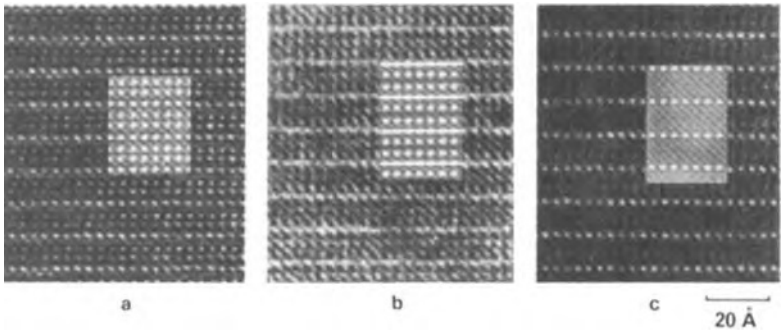

Fig. 4. Experimental images of $YBa_2Cu_3O_{7-\delta}$. a) [100] projection, the computation conditions of the inset: resolution of 1.98 Å; defocus of −1800 Å and thickness of 60 Å; b) und c) [010] projection, the computation conditions of the insets: resolution of 1.98 Å; defocus of −1200 Å; thickness of 60 Å (b) and 80 Å (c).

0.5 at the four sites on the *ab* plane, the differences in the images along the [010] and [100] directions is much reduced.

By choosing a resolution for the computed image close to that used by us experimentally (1.98 to 2.00 Å) we find that there are now clear-cut differences between the computed images of the structure containing aligned oxygen vacancies for the [100] and [010] projections (see Fig. 3).

Our experimental results, Figure 4a from one particle and Figures 4b,c from other regions of another particle, show different details of image contrast. The inset of Figure 4a is identical to that shown in Fig. 3e. None of the images calculated along [010] matches this experimental result. The insets of Figures 4b and c are identical to those from Figures 3c′ and d′ respectively. The sample-thickness dependence of these two images match only with those found experimentally for projections along [010].

In summary, we have demonstrated that, in principle, it is possible by high resolution electron microscopy, to observe contrast effects arising from the presence of a given oxygen vacancy arrangement in the *ab* plane of $YBa_2Cu_3O_{7-\delta}$. Further studies of this system, with larger[13–15] values of δ, are underway.

Received: June 23, 1987 [Z 2308 IE]
German version: *Angew. Chem.* 99 (1987) 1063

[1] R. M. Hazen, L. W. Finger, R. J. Angel, C. T. Prewit, H. K. Mao, C. G. Gadidiacos, P. H. Hor, R. L. Meng, C. W. Chu, *Phys. Rev. B35* (1987) 7238.
[2] W. I. F. David, W. T. A. Harrison, J. M. F. Gunn, O. Moze, A. K. Soper, P. Day, J. D. Jorgensen, D. G. Hinks, M. A. Beno, L. Soderholm, D. W. Capone, I. K. Schuller, C. U. Segre, K. Zhang, J. D. Grace, *Nature (London) 327* (1987) 310.
[3] A. Ourmazd, J. A. Rentschler, J. C. H. Spence, M. O'Keeffe, R. J. Graham, D. W. Rhodes, W. W. Rhodes, *Nature (London) 327* (1987) 308.
[4] E. A. Hewat, M. Dupuy, A. Bourret, J. J. Capponi, M. Marezio, *Nature (London) 327* (1987) 400.
[5] A. Simon, *Angew. Chem. 99* (1987) 602; *Angew. Chem. Int. Ed. Engl. 26* (1987) 579.
[6] J. M. Thomas in M. H. Chisholm (Ed.): *Inorganic Chemistry Towards the 21st Century ACS Monograph 211* (1983) 445.
[7] A. Reller, J. M. Thomas, D. A. Jefferson, M. K. Uppal, *Proc. R. Soc. A 394* (1984) 223.
[8] D. Tang, C. M. Tang, J. Zhou, F. H. Li, *Acta Crystallogr. B42* (1986) 340.
[9] W. Zhou, J. M. Thomas, D. A. Jefferson, I. van Damme, K. D. Mackay, T. H. Shen, W. Y. Liang, *J. Phys. F17* (1987) 173.
[10] P. Goodman, A. F. Moodie, *Acta Crystallogr. A30* (1974) 280.
[11] R. Gruehn, W. Mertin, *Angew. Chem. 92* (1980) 531; *Angew. Chem. Int. Ed. Engl. 19* (1980) 531.
[12] M. K. Uppal, O. Terasaki, J. M. Thomas, *Zeolites*, in press.
[13] G. N. Subbana, P. Gauguly, C. N. R. Rao, *Mod. Phys. Lett. B*, in press.
[14] D. C. Johnston, A. J. Jacobson, J. M. Newsam, J. T. Lewandowski, D. P. Goshorn, D. Xie, W. B. Yelon in: *Chemistry of High-Temperatue Superconductors (ACS Symp. Ser. 351* (1987)), p. 136.
[15] M. A. Alario-Franco, C. Chaillout, J. J. Capponi, J. Chenevas, *Mater. Res. Bull. 12* (1987), in press.

BOOK REVIEWS

Clusters and Catalysis

The above title has in recent years become a catchphrase used in support of research on clusters, especially in the USA. Although opinions may differ about the use of a phrase which contains such promises, it has nevertheless gained attention and funding for cluster research, and led to increased activity in this area. Consequently the appearance of monographs on the theme "Clusters and Catalysis" was only a question of time. That has now occurred in the two books

Metal Clusters in Catalysis. Edited by *B. C. Gates, L. Guczi,* and *H. Knözinger.* Elsevier, Amsterdam 1986, xxv, 648 pp., bound, HFl 195.00.—ISBN 0-444-42708-2, and **Metal Clusters.** Edited by *M. Moskovits.* Wiley, Chichester 1986. ix, 313 pp., bound, £ 47.95.—ISBN 0-471-89388-9

and more will probably follow. In both cases the editors do not come from the field of preparative cluster chemistry, which is mostly associated with inorganic chemistry, but instead come from physical chemistry. The book of over 600 pages edited by *Gates, Guczi,* and *Knözinger*

states its aims in the title, whereas in the volume of 300-odd pages edited by *Moskovits* the definition of subject matter first appears in the list of contents. Both books are priced at a level which today is normal for monographs of this kind, both give about the same amount of paper in relation to the price, and both can be described as collections of review articles. In both cases the editors have enlisted a competent team of authors (seventeen in "Metal Clusters in Catalysis" and ten in "Metal Clusters"), from whose names specialists in the field will be able to predict the subjects covered, and also those that receive little attention. Altogether one can say of both these books that they deal with the essential highlights of the chemistry of cluster compounds, mainly those without organic ligands.

"Metal Clusters in Catalysis" is divided into three sections, which can be defined as molecular cluster chemistry, clusters in and on supports, and some analogies between clusters and surfaces. In the first part *G. L. Geoffroy* gives a short but complete survey of synthetic methods for molecular clusters, which is followed by a very brief article by the same author on cluster structures. Likewise very brief is the article by *J. A. Connor* on thermochemistry and binding energies in clusters. The essay on reactivities of molecular clusters by *G. Lavigne* and *H. D. Kaesz* which comes next is well organized and essentially complete. The article by *L. Markó and A. Vizi-Orosz* on homogeneous catalysis by metal clusters is the fullest review yet to appear on this topic. The second part of the book contains its main emphasis, in accordance with the editors' chief area of interest. The chapter by *H. Knözinger, L. Guczi,* and *R. F. Pettifer* on characterization by physical methods is very detailed, carefully written, and longer than all the preceding five chapters put together. The chapter by *G. A. Ozin* and *M. P. Andrews* on clusters produced by the condensation of metal vapors is authoritative and comprehensive. The treatment by *P. A. Jacobs* of clusters in zeolites emphasizes the great hopes which are held for developments in this area. This is followed by the second principal chapter of the book, to which *B. C. Gates, R. Psaro, R. Ugo, G. Maire,* and *H. Knözinger* have contributed; this is concerned with clusters immobilized on surfaces, their preparation from molecular clusters, and the associated organometallic surface chemistry. The following chapter by *L. Guczi* on surface bound bimetallic catalysts is actually a sub-chapter of the preceding one. The third section of the book consists of only a single essay, in which *G. Ertl*—impressive as always—discusses relationships between clusters and surfaces. Although the book, with 648 pages, is by no means thin, it cannot be said that any of the eleven chapters is unduly long.

In "Metal Clusters" the emphasis is very unevenly distributed between individual topics. General themes are treated very briefly: bonding theory considerations (by *R. C. Baetzold*), structures (by *D. H. Farrar* and *R. J. Goudsmit*), organometallic chemistry involving clusters (by *J. S. Bradley*), and catalysis by surface bound clusters (by *B. C. Gates*). In contrast, two chapters on individual special topics, namely reaction kinetics of metal carbonyl clusters (by *A. J. Poë*) and optical methods for identifying cluster compounds in the gas phase (by *J. L. Gole*), are very detailed. The book is rounded off by an account of methods for identifying matrix-isolated clusters (by the editor, *M. Moskovits*), and two applications-oriented chapters, on clusters in zeolites (by *P. Gallezot*) and on a comparison of the catalytic activities of surface bound clusters (by *A. Brenner*). Thus the book's rather general title conceals a collection of essays on particular aspects of cluster chemistry, determined by the choice of authors, the main emphasis being on describing the properties of metal atom aggregates.

The field of cluster chemistry as a whole is already so large that these two books, even when taken together, can present only a selection from it. Regarding the selections that have been made, they are to some extent complementary, but they overlap on matrix isolation, clusters in zeolites, structure geometry, and clusters on supports. On the last topic we also find the same author, *B. C. Gates,* in both books. Both books are attractively produced; the detailed index in "Metal Clusters in Catalysis" is an additional good feature. Both books have their strengths and weaknesses, of course, since they can be no better than the individual contributions of their authors. As monographs, however, they offer a very good account of the present state of knowledge on the topics treated, and therefore should not be omitted from any library. So far as purchase by individuals is concerned, though, they will only be of interest to specialists, particularly in the case of "Metal Clusters". Even when one accepts that the very brief treatment of molecular cluster chemistry is in accord with the editors' stated aims, it would nevertheless have been desirable to include some discussions of the chemistry of soluble cluster compounds with inorganic ligands, the redox properties of clusters, the extensive topic of clusters in solid state compounds, and the biological importance of clusters. Since the phase of frantic activity in cluster chemistry is coming to an end and the matter is becoming somewhat settled now, perhaps some author should risk writing a textbook type monograph on the subject.

Heinrich Vahrenkamp [NB 825 IE]
Institut für Anorganische Chemie
der Universität Freiburg (FRG)

Analytical Methods in Human Toxicology, Part 2. Edited by *A. S. Curry.* VCH Verlagsgesellschaft, Weinheim 1986. x, 354 pp., bound, DM 170.00.—ISBN 3-527-26285-7

The second volume of "Analytical Methods in Human Toxicology" deals with HPLC, fluorescence analysis and radioimmunoassay methods, and their application to solving toxicological problems. In addition it familiarizes the reader with pharmaco-kinetic investigations. Using examples from the literature, the large differences often found in metabolization of pharmaceutical substances are discussed, together with the related concept of the "effective dose". Lastly, procedures used to test for the presence of some toxicologically important classes of compounds, such as narcotics and combustion gases, are described in detail; other classes of substances, e.g. barbiturates, benzodiazepines and tricyclic antidepressants, are included in the discussion of practical examples.

The book includes references to a considerable amount of literature which is important to the toxicologist. Some chapters contain a wealth of very useful advice, e.g. in the section on the elimination of errors in HPLC. Unfortunately, though, the editor has not succeeded in this second volume in avoiding some duplication of material, e.g. the analysis of tricyclic antidepressants has already been treated thoroughly in volume 1. Despite this lack of complete coordination, every toxicological laboratory will find that this second volume too is a valuable addition to its library.

Gerhard Spiteller [NB 827 IE]
Lehrstuhl für Organische Chemie
der Universität Bayreuth (FRG)

Schrödinger. Centenary Celebration of a Polymath. Edited by *C. W. Kilminster*. Cambridge University Press, Cambridge 1987. 253 pp., bound, £30.00.—ISBN 0-521-34017-9

To mark the centenary of the birth of *Erwin Schrödinger* a conference was held in the spring of 1987 at Imperial College, London. Most of the papers presented at the meeting are contained in this volume. They are all, without exception, written by internationally recognized scientists.

Schrödinger, who, together with *Einstein* and *Planck*, is one of the best known of the founders of twentieth century physics, was born in Vienna and studied physics at the city's university. Towards the end of an eventful life, he returned in 1957 to his native country. The places where *Schrödinger* did his most important work were Zürich (1921–1927), where his achievements included the publication of his six famous papers on wave mechanics, Berlin (1927–1933) and Dublin (1940–1957), where, after years of fleeing from the Nazis, he found a secure intellectual home in the Institute of Advanced Studies. In 1933 he was awarded a Nobel Prize in physics for his work on wave mechanics.

This collection of articles is, by the nature of its theme, very heterogeneous. There are two contributions (by *Flamm* and *McCrea*) on biographical aspects and on the background to *Schrödinger*'s scientific works, while the rest of the articles are mainly concerned with the current state of knowledge in those fields which were given a new theoretical basis by the *Schrödinger* equation. Readers unfamiliar with the methods of theoretical physics will find considerable difficulty with many of the articles. Nevertheless, even the layman will be impressed by the enormous range of influence that *Schrödinger*'s work has on modern physics.

Schrödinger, like *Einstein*, was never entirely satisfied with the then generally accepted interpretation of quantum mechanics according to the Copenhagen school. For this reason the three papers (by *Dorling, Bell,* and *Yang*) that are concerned with the modern view of *Schrödinger*'s interpretation of wave mechanics, are especially interesting. I have the impression that the front of resistance to "unconventional" interpretations of the quantum theory is gradually beginning to weaken.

From the chemist's point of view the greatest interest lies in the significance of the *Schrödinger* equation for questions of chemistry, to which four papers are devoted (*Karplus, Fukui, Buckingham, Pauling*). Understanding of chemical bonding and chemical reactions would be highly inadequate without the basis provided by *Schrödinger*'s work. Further, the numerical methods of calculation that are based on the *Schrödinger* equation are now an indispensable source of exact data on molecules and molecular aggregates. Molecular dynamics too has its origins in quantum mechanics. In this field laborious quantum-mechanical calculations are nowadays often replaced by classical approximations which are sufficiently accurate. Some of the most important modern applications are to understanding chemical reactions of small molecules in the gas phase, to the structure and dynamics of liquids, and to the study of biologically important macromolecules.

The little book "What is Life?", which *Schrödinger* wrote during his time in Dublin, undoubtedly introduced many young physicists to interesting unsolved problems in biology. The reservations expressed by those experts (*Perutz, Pauling*) who criticize the eminent physicist for superficiality and insufficient knowledge of the literature were therefore somewhat unexpected, though justified on closer scrutiny. These minor complaints, though, cannot shake the overall picture of *Schrödinger* as a widely ranging scholar. This book is written mainly with physicists in mind, but the chemist or biochemist with interests in this field will also find it profitable reading.

Peter Schuster [NB 850 IE]
Institut für Theoretische Chemie und Strahlenchemie
der Universität Wien (Austria)

Trace Analysis. Spectroscopic Methods for Molecules. Edited by *G. D. Christian* and *J. B. Callis*. Wiley, Chichester 1986. XII, 406 pp., hard cover, £ 52.75.—ISBN 0-471-87583-X

The identification and quantitative analysis of molecular trace components in (usually) complex mixtures belongs to the most important tasks in modern Analytical Chemistry, particularly in areas like environmental, clinical, agricultural, food and biochemistry. In order to obtain reliable and accurate results, separation methods (like GC, HPLC) are often combined with spectroscopic techniques which enable one to obtain qualitative and quantitative information.

This volume presents four of these spectroscopic techniques—photometry, luminescence spectroscopy, IR spectrometry and NMR spectroscopy. The most important technique for trace analysis of molecules, mass spectrometry, is not included, obviously to keep the number of pages limited. The limitation of the content to these four techniques should have been stated in the title!

The chapters have been written by different authors, consequently the chapters differ somewhat in style and structure: While the chapter on IR (*A. L. Smith*, Dow Corning Corp.) does not cover the fundamentals of IR spectrometry but centers on aspects of trace analysis with this technique, the other chapters on photometry (*K. L. Ratzlaff*, University of Kansas), luminescence spectroscopy (*R. J. Hurtubise*, University of Wyoming) and NMR (*D. L. Rabenstein*, University of California, and *T. T. Nakashima*, University of Alberta) provide more a presentation of fundamentals, instrumentation and application of the individual techniques. Relation to trace analysis is provided to a variable extent. The chapter on NMR shows a particular emphasis on the fundamental principles of the technique: only 10 out of 108 pages are devoted to trace analysis.

Nevertheless—all of the chapters are of interest for those who want to make themselves acquainted with the principles and basic potential of these spectroscopic techniques. The presentations are clear and illustrative and much specific information about measurement techniques etc. is given. Major recent progress in each area—e.g. the use of lasers in photometry—is included as well as a list of references (between 86 and 395 per chapter) which refers either to fundamental literature or specific information.

The general impression can be summarized as follows: a good presentation of four major spectroscopic techniques for trace analysis of molecules. The book is useful for separation scientists who want to get to know such spectroscopic techniques. It may also serve as a rather good textbook on photometry, luminescence spectroscopy and NMR for analytical chemistry courses.

M. Grasserbauer [NB 851 IE]
Laboratorium für Physikalische Analyse
Institut für Analytische Chemie
Technische Universität Wien (Austria)

Inorganic High Pressure Chemistry. Kinetics and Mechanisms. Edited by *R. van Eldik*. Elsevier, Amsterdam 1986. x, 448 pp., bound, HFl 280.00.—ISBN 0-444-42682-2

High pressure kinetics has become more and more important in the last years. Especially in coordination chemistry it brought new insights into the reaction mechanisms. The editor *Rudi van Eldik* is one of the leading experts in high pressure kinetics of coordination compounds. The reader will notice his experience and competence. He himself has written a large part of the book, thus making it very coherent. There are almost no repetitions.

The introductory chapter by *van Eldik* describes the high pressure techniques and methods of analysis comprehensively. The experimental results are arranged according to reaction types: Solvent Exchange Reactions (*Y. Ducommun* and *A. E. Merbach*); Substitution, Isomerization and Related Reactions of Octahedral Complexes (*R. van Eldik*) and of Four-Coordinate Complexes (*M. Kotowski* and *R. van Eldik*); Electron Transfer Reactions (*T. W. Swaddle*); Photochemical and Photophysical Processes (*P. C. Ford*); as well as Bioinorganic Systems (*K. Heremans*). The final chapter by *van Eldik* demonstrates how much the subject is in a state of flux. Simple transition state theory is used to discuss the high pressure data almost all over the book. It is only in the last chapter that *van* Eldik shows what consequences the simplifications have and which extensions were suggested. These difficulties become evident especially in high pressure photochemistry. Here, the application of transition state theory is not justified a priori. In the introduction to his chapter *Ford* explicitly stressed this point: "the processes subsequent to photoexcitation have to be treated somewhat differently". However, he also uses the simple transition state theory to discuss the experimental results. Obviously there is nothing better.

I am sure this monograph will remain the standard work on high pressure kinetics for years. Everyone working in this field will use it and quote from it. The nonspecialist might be discouraged by size and price. But there is hope, its contents will get into text books on reaction kinetics and thus will become widely known. For, the pressure dependence of rate constants will soon become as important as the Arrhenius diagram is to-day.

Fritz Wasgestian [NB 829 IE]
Institut für Anorganische Chemie
der Universität Köln (FRG)

Stereoselective Synthesis. By *Mihály Nógrádi*. VCH Verlagsgesellschaft, Weinheim 1987. xiv, 356 pp., bound, DM 168.00.—ISBN 3-527-26467-1

The area of stereoselective synthesis has been intensively studied for a good decade, and has thus reached some degree of maturity. Therefore both outsiders and those working in the field have an equal need for a critical review which sets out the principles and highlights the reliable methods. We already have, from the years 1983-1985, the five volume work "Asymmetric Synthesis", edited by *J. D. Morrison* (see *Angew. Chem. Int. Ed. Engl. 25* (1986) 848), which describes the essence of the more important methods. What can the present book offer us?

The introduction, which discusses the basic concepts of stereochemistry, shows the author to be a scientist who proceeds in a systematic way. This is followed by chapters on stereoselective catalytic hydrogenations, stereoselective non-catalytic reductions, stereoselective oxidations and stereoselective C-C bond-forming reactions. Finally there are two shorter chapters on stereoselective pericyclic reactions and stereoselective carbon-heteroatom bond formation. However, the critical evaluation which we had hoped for constitutes only a small insignificant part of the book, which being simply a collection of data is scarcely more exciting to read than a telephone directory. The author has, however, assembled, under types of reactions, all the important factual information on stereoselective syntheses from recent years, and a large amount of additional data. Is this book then to be regarded as the "Beilstein" of stereoselective synthesis? The scandalously long time interval between the end of literature coverage in 1984 and the book's publication in 1987 is reminiscent of that. But that is the only resemblance—whereas Beilstein is recognized for the proverbial reliability of the data, *Nógrádi*'s book contains many incorrect structural formulas. These, regrettably, include quite a number of errors which alter the intended meaning. Worse still, some reactions which superficially look correct are in fact given wrongly, e.g. because the configuration of a stereogenic center in a product is shown wrongly, or the description of the reaction as a whole does not correspond to that in the papers cited. Of course, the reader only notices such errors in those topics with which he is familiar. It is unfair, but understandable, to draw conclusions from this about the treatment of other topics. In short, viewed in this light the book is a source of irritation.

Despite these criticisms I must give the author credit where it is due. Behind this collection of data there lies an immense amount of work, and the book is certainly of value insofar as it contains a wealth of well organized data on stereoselective syntheses. This includes much factual information and examples which the reader interested in this field could not otherwise readily find. Nevertheless, all users of the book are strongly advised to check the data by consulting the original papers!

It may occur to the reader of this review that minor defects of presentation and inaccuracies, which one would usually criticize, have not been mentioned here. Such faults pale into insignificance compared with the lack of care in presenting structural information. It is perhaps typical of the book that the page devoted to advertising by VCH Verlagsgesellschaft shows an sp^2 hybridized carbon atom with tetrahedral bond angles!

Reinhard W. Hoffmann [NB 838 IE]
Fachbereich Chemie
der Universität Marburg (FRG)

Transient Techniques in NMR of Solids. An Introduction to Theory and Practice. By *B. C. Gerstein* and *C. R. Dybowski*. Academic Press, New York 1985, xi, 295 pp., bound, $59.00.—ISBN 0-12-281180-1

As the authors state this book is written for students working in the field of high resolution NMR spectroscopy of solids, who wish to gain a thorough understanding of this specialized topic. They have sought to convey to the reader their own, quite individual view of this subject, the fascination which it generates, and their own pleasure in the scientific concepts involved. To this end they use a very lively style of language rich in individual idioms and expressions. They treat at length with very detailed calculations the fundamental topics, including some rather trivial ones. Time and again the authors feel obliged to lead the reader into digressions, e.g., into complex numbers, alter-

nating current circuits, selected topics in magnetostatics, some of the fundamentals of quantum mechanics and linear algebra, and into the mathematics of exponential operators.

However, accuracy sometimes becomes lost in the authors' enthusiasm for the subject. Thus, for example, they talk about "decoupling of differential equations," where what they actually mean are *linear first-order* differential equations. A more bizarre example is seen on p. 21, where the symbol τ is used with two different meanings within the same simple equation. The misprint demon has struck in a particularly malicious way on p. 167, where, as a result of a "0" (zero) having been converted into the letter "O", the whole thing has turned into a hopeless mess.

In a sense the impression is conveyed that the book has been compiled in such a way as to make it superfluous for a student working on solid state NMR spectroscopy to study any other text. The essential problem of the book is, though, that it is addressed to a fictitious readership.

At the beginning of Chapter 5, on p. 198 (of a total of 275 pages), the authors state that all that has gone previously is only a preparation for the real objective, which is to understand the mechanism of multipulse cycles. I am sorry to have to say, though, that the heyday of multipulse cycles took place ten years ago. Throughout the world there are now only a few groups working in this particular field and their number is decreasing rather than growing. *Gerstein* and *Dybowski* mainly ignore the successes of the multipulse technique, which in my view are best seen in single crystal studies. It thus seems an ironic accident that in the one example relating to single crystal measurements, data containing systematic errors are used. It is casually stated that in any case most samples are in the form of powders. The hope is expressed that a combination of multipulse cycles with rapid rotation of the sample about the "magic angle" (here dealt with only briefly) will yield a method equivalent in information content and ease of interpretation to true high resolution liquid state NMR spectroscopy, which is so outstandingly successful as an analytical technique. However, one hardly finds in this volume any convincing example to support such a hope.

The final chapter is devoted to heteronuclear pulse experiments. The style here is different. We no longer have detailed analyses and a complete understanding, but instead a more or less traditional presentation of well-known techniques. It is clearly apparent that the authors are here no longer drawing on their own store of experience and knowledge to the extent that they are in the earlier chapters.

The literature citations are a peculiar feature of the book. On the grounds that this is a textbook, *Gerstein* and *Dybowski* avoid citing original papers so far as possible. In some places, however, original work is deliberately cited. The reader may easily guess at the system which is used. Writing a whole chapter on multipulse cycles and homonuclear pulse experiments in solids without mentioning the name of *J. S. Waugh* even once in the text, is, to say the least, a strange thing—and this is by no means an isolated example.

Research libraries concerned about full coverage will not be able to avoid buying this book, but I fear that there will not be many students, at least in Germany who will give themselves the "pleasure" of studying it systematically.

U. Haeberlen [NB 801 IE]
Max-Planck-Institut für medizinische Forschung,
Heidelberg (FRG)

Low Energy Electrons and Surface Chemistry. By *G. Ertl* and *J. Küppers*. VCH Verlagsgesellschaft, Weinheim 1986. XII, 374 pp., hard cover, DM 168.00.—ISBN 3-527-26056-0

If *Irving Langmuir* were to appear again on the scene in surface science he would be captivated by many things, not the least important of which is the ability we now have of being able to probe the composition and structure of solid surfaces with great dexterity and precision. To test the theory of monolayer saturation in adsorption, proposed by *Langmuir*, it was necessary to use high-area solids, typically activated charcoal or silica gel which have areas ranging from 20 to 400 $m^2 g^{-1}$. Only by boosting the extent of the adsorbed phase in this way was it possible to cope experimentally with the reliable measurement of adsorption from the gas phase or solution. Nowadays, however, it is routinely possible to monitor the build-up of monolayer volumes, Vm, from fractions of coverage of 10^{-4} to unity when the surface area is no more than a few $cm^2 g^{-1}$. The principal cause of the revolutionary advance has been the use of electron, and other beams (including soft X-rays, and ions of light elements) as primary probes for arriving at the composition, stoichiometry and structure of two dimensional ordered or disordered two-dimensional structures at solid surfaces. Low-energy monoenergetic electrons (1 to 5 eV) beams are ideal for exciting the vibrations of chemisorbed and physically adsorbed layers; and from the diffraction of monoenergetic electrons of energy in the range 60 to 300 eV, a great deal can be inferred about the atomic disposition of the exterior surface of a bulk solid and of overlayers that can form upon it.

It would be difficult to overemphasize the importance of the study of such systems: they are deeply implicated in the phenomenology of catalysis, corrosion, epitaxy, and the vast ramifying technologies that hinge upon these including the fashioning of new devices from quantum well lasers to fast transistors. At the fundamental level, too, a great deal needs to be learned about the basics of surface science. Why does the sticking coefficient of a given gaseous species vary so enormously from one crystal face to another on a simple solid such as tungsten. For graphite, for example, the 'anisotropy' in sticking coefficient of oxygen as between the prismatic and basal faces is a factor of some 10^{15}.

In the last two decades major progress has been accomplished in enlarging our understanding and control of the properties of surfaces. There have been dramatic improvements ever since the first edition of this very fine monograph appeared in 1974. The reader is given concise, expert guidance in numerous facets of surface science, and, in particular, is introduced to all the principal ways in which the strong interaction of electrons with matter are turned to good advantage in gaining further insights into surface properties and behavior. Only a fastidious concern for perfection leads one to discover minor almost trivial, faults with this book. The reviewer is a little disappointed (and perhaps a few students who will read this text avidly, will be too) that a more specific definition of work function (introduced on page 101) is not spelled out. The work function is a notion that often causes confusion for those that encounter the surface properties of solids for the first time. A minor omission is a detailed discussion of low-resolution, high-energy electron energy loss spectroscopy which is currently finding increasing relevance as a tool in the science of catalysts. But this is understandable if the title is to be interpreted literally.

The book is lavishly illustrated with the important points

of theory, experiment and, where appropriate, instrumentation is thoroughly discussed. It is moreover, up-to-date, as evidenced by the treatments of topics as fast-moving and disparate as inverse photoemission, Auger neutralization and extended- and near-edge X-ray absorption fine structure.

Drs. *Ertl* and *Küppers* are to be complimented on producing an excellent monograph, the lifetime of which should, on present trends, substantially exceed that of the first edition.

John M. Thomas [NB 849 IE]
The Royal Institution, London

Gaseous Ion Chemistry and Mass Spectrometry. Edited by *J. H. Futrell.* Wiley, Chichester 1986. xii, 335 pp., bound, £ 57.50.—ISBN 0-471-82803-3

A workshop, from which this book takes its title, took place in 1983, organized by the Department of Chemistry of the University of Utah along the lines of a Gordon Conference. The participants wished to put the contributions on record by publishing a book, lest the matters discussed should be forgotten. However, it is open to doubt whether that was a useful aim, and whether it has been achieved.

The papers, written by scientists who in some cases are of the first rank in their fields, cover thirteen topics, and are arranged under four groups. They vary greatly in their length, content, presentation, and coverage of literature for further study. Some of the papers, such as that by *Futrell* on ion cyclotron resonance (11 pages with 23 references), are concise but informative; on the other hand some are quite weak, such as those by *Morrison* on photoionization and multiphoton ionization (11 pp., 33 refs.), and on instrumentation (18 pp., 35 refs.). The paper on clusters by *Castleman* and *Märk* (44 pp., 160 refs.) is well worth reading, and also has the advantage that the bibliography is up-to-date, although it is marred by too much emphasis on the authors' own published work, and insufficient coverage of important contributions from other groups. In fact it seems to be a general shortcoming of the book that the attention given to papers from other research groups is inadequate and unduly selective. Considering the level of competence and the high standing of the authors, one might have expected a more balanced presentation of the various topics. Two examples may suffice to illustrate this: in the treatment of doubly charged cations there is not a word about *Beynon*'s charge-stripping experiments, and in the discussion of laser-induced fluorescence in ions one looks in vain for a reference to the work of *J. P. Maier* and collaborators.

All the authors are either physicists or physical chemists, with only one exception (*D. C. Smith*, who contributes a chapter on biochemical applications which is inappropriate for this book, and is also too superficial). I am afraid that the book will not appeal to chemists, and it would have been more appropriate if the title had mentioned ion physics rather than ion chemistry. It is doubtful whether students of chemistry or physics will be able to follow the text easily without some guidance, and since the specialists have access to other sources of information, I fear that the effort expended on this book will turn out to have been in vain.

Helmut Schwarz [NB 843 IE]
Institut für Organische Chemie
der Technischen Universität Berlin (FRG)

Mikrobiologische und biochemische Verfahrenstechnik; eine Einführung. By *A. Einsele, W. Samhaber,* and *R. K. Finn.* VCH Verlagsgesellschaft, Weinheim 1985. x, 248 pp., bound, DM 88.00.—ISBN 3-527-26117-6

The appearance of this book constitutes a highlight in German scientific literature. The authors have succeeded in drawing together the interdisciplinary character of biotechnology into a single textbook. The book is in eight chapters. After an introduction to microbiology and a survey of microbial processes, we reach the subject of the kinetics of such processes. The chapters on "Mass transfer in biological systems", "Sterilization", "Bioreactors" and "Process control" lay the foundations for the technology of these processes, by enabling the reader to understand the process engineering principles which are followed by the discussion of Downstream processing.

Each chapter is a complete unit in itself, so that the reader, depending on his interests and previous knowledge, can concentrate on individual topics, without being tied to a particular sequence. Readers already familiar with microbiology will skip the first three chapters, as these provide a short introduction to the topics of metabolization and regulation, and classify microbial processes so as to illustrate the many possibilities offered by microorganisms. From their complex nutritional requirements and the main growth-determining factors we come to the determination of biomass. This section on the kinetics of biological processes concludes with the kinetic description of a batch and a continuous culture.

The supply of oxygen plays a key role in bioreactors, and the fourth chapter therefore deals with mass transfer. The fundamental aspects are the solubility of oxygen in water (Henry's law), and the oxygen transport coefficient K_La; three methods for calculating the latter are described, with their advantages and disadvantages. The theoretical relationships are explained by means of several examples. The effects of other hindrances to transport, such as cell agglomerates, biofilms, and the rheological properties of the system, are also considered.

The excursion into sterilization which follows is comparatively brief; besides two examples of calculations it covers continuous steam sterilizing and sterilization of gases.

Much space is given to the bioreactor and techniques of measurement and control. The reader has to work through a good 100 pages on the aeration, mixing and oxygen transfer rates, and on the more important of the dimensionless numbers (e.g. the Newton number). This is followed by other reactor systems, problems of scaling up the process, and the uses of special types of reactors (carrier immobilization, animal cell culture). The essential peripheral devices such as sensors, gas probes, enzyme electrodes, analytical instruments, and the introduction of computers, which are covered under process control technology, are absolutely essential for monitoring the complex reactions occurring in the fermenter. There is a particularly detailed examination of the types of electrodes. Downstream processing in biotechnology is a topic large enough to justify a textbook by itself; consequently in the final chapter here only general considerations and the principles of the methods can be given. Certain unit operations are common to the various work-up processes used, e.g. the separation of solids from liquids as a first step. Filtration methods are central to this topic, as they have recently undergone much development. The book describes the potential applications of these and the difficulties. Sedimentation, centrifugation and chromatographic separation are also discussed.

The instructional style of the book makes it easier for the newcomer to biotechnology to quickly and easily familiarize himself with the subject matter, so as to gain an understanding of the field or assimilate new knowledge. For those already working in the field this book will serve as a work of reference, and it is therefore suitable as an addition to one's personal library. The good organization of the contents and the excellent typographic presentation contribute to this favorable impression. As a reviewer I have read this book with interest, as the text is clear, comprehensible, and very readable in style. In scarcely 250 pages it is, of course, only possible to present a small section of the field of biotechnology. Those who wish to go into the subject in greater depth will need to consult more detailed works. If this book should later form the basis for a considerably more extensive work, it is to be hoped that its good qualities will not be lost in the "scale-up". I wish to recommend this book, though its price gives some cause for concern, the ratio of usefulness to price being very unfavorable compared with other textbooks.

Gunnar Pommerening [NB 739 IE]
Kernforschungsanlage Jülich

Polymer Synthesis. By *P. Rempp* and *E. W. Merrill.* Hüthig & Wepf Verlag, Heidelberg 1986. 315 pp., bound, DM 96.00.—ISBN 3-85739-116-2

This textbook has arisen out of the notes for lectures given by the two authors during the past twelve years in the Department of Chemical Engineering at the Massachusetts Institute of Technology. As the title indicates, it is principally concerned with polymer synthesis. Problems of characterization (structure and properties), and the physico-chemical aspects of polymer science, are dealt with only insofar as they are important in synthesis.

The authors have divided the writing between them. *P. Rempp* has prepared the first part of the book, which is concerned with polymer synthesis on a laboratory scale. It deals with reaction mechanisms, kinetic aspects, and their consequences as regards molecular weight distribution and molecular structure. *E. W. Merrill* has written the second part of the book, dealing with industrial polymerization processes, in which heterogeneous systems and continuous processes assume special importance.

The first part of the book follows the classical pattern of subdivision of an excellent lecture entitled "Introduction to Macromolecular Chemistry". After a general chapter introducing the basic concepts, there follows a relatively short section on addition polymerization. Next come chapters on free radical polymerization (including copolymerization), anionic and cationic polymerization (including polymerization-depolymerization equilibria), and finally stereospecific polymerization. The book concludes with chapters on chemical reactions involving polymers, and on functional polymers, including block and graft copolymers and model networks.

The second part of the book is concerned with reactors and processes for the homogeneous phase and multiphase free radical polymerization (including suspension polymerization and emulsion polymerization), heterogeneous ionic polymerization, reaction injection molding, and polymerization in the presence of heterogeneous catalysts. This part of the book is unusual for a textbook, at least in its orientation towards industrial processes, though in Germany too this ought to be an essential part of a training in macromolecular chemistry. Here one finds descriptions not only of the polymerization of ethylene with heterogeneous catalysts in the fluidized bed process, but also of the manufacture of a glass fiber reinforced polyester and of motor tires.

Appendices are provided which, for example, make it easier to understand the derivation of molecular weight distribution functions. Problems included at the ends of the chapters, in the well-established style of American textbooks, allow the reader to test the knowledge which he has gained. Altogether this is a useful and convenient book, but one which regrettably includes no references to original literature, nor to material for further reading. Surprising is the small number of polymer pioneers' names the authors require.

Hartwig Höcker [NB 834 IE]
Lehrstuhl für Textilchemie
und Makromolekulare Chemie,
RWTH Aachen (FRG)

Affinity Chromatography: A Practical Approach. Edited by *P. D. G. Dean, W. S. Johnson,* and *F. A. Middle.* IRL Press, Oxford 1985. xv, 215 pp., paperback, £ 11.00.—ISBN 0-904147-71-1

As a result of the progress in genetic engineering, effective methods for separation of proteins are becoming increasingly important. In addition to the conventional methods of ion exchange and gel chromatography, HPLC has in recent years come into use as a preparative technique to an ever greater extent. Affinity chromatography, on the other hand, plays only a subsidiary role, as it has hitherto been regarded as a complicated technique which is only useful in special cases.

These reservations concerning affinity chromatography are certainly not justified, for it is an outstandingly effective method, and there are many proteins whose isolation could not have been performed without it. The principle of affinity chromatography is very simple. Specific enzyme inhibitors, ligands or antibodies are covalently bonded to a gel matrix. Under optimal conditions only the desired protein then bonds to the column, with the result that a very high degree of enrichment can be obtained in a single stage of purification. Affinity chromatography has become an indispensable tool for isolating proteins which occur in very low concentrations and those that are attached to membranes. It is also of great interest as a means of isolating proteins made by genetic engineering methods, since here the separation of the desired protein from a mixture of intermediate products, which have the same amino-acid sequence but different chain folding, can be achieved very neatly, and often in a single step, by using a suitable ligand or antibody which is bonded to the gel matrix.

Against this background the book under review is greatly to be welcomed. It is a strongly application-orientated handbook which includes a reasonable amount of directly applicable instructional content, while not neglecting the theoretical aspects, and it forms a good contribution to making affinity chromatography more widely known. The book is divided into eight main chapters, and consists of contributions from 25 authors. It is to the credit of the three editors that the book nevertheless reads well, and there are only a few instances of repetition.

The first chapter is a useful survey of the more important gel matrices now in common use, with their properties and methods of preparation. In most cases, though, it is more sensible and economical to buy ready prepared gel

materials; newcomers to the field are particularly advised against preparing their own.

The strongest features of the book are in Chapters 2, 3, and 5, which deal in detail with techniques of activation and bonding. The methods given are mostly within the capabilities of any biochemical laboratory with the usual facilities. It has, of course, not been possible to describe every special case, but the methods given here can be adapted by analogy to cover many of them. Chapter 4 describes particular chromatographic procedures, and the associated methods for determining the degree of substitution of the stationary phase material. Chapters 6 and 7, which are concerned with affinity chromatography as a method of quantitative analysis, seem rather too long. The use of affinity chromatography for separating cell populations is an economical alternative to installing cell sorting equipment. This application, discussed in the final chapter, is, however, limited to only a few cell types.

Altogether this is a very interesting book, which gives valuable guidance on planning and setting up affinity chromatography methods. An additional reason for recommending its purchase is the comparatively low price.

Jan Verdenhalven [NB 767 IE]
Pflanzenschutzforschungs-Biochemie
Hoechst AG, Frankfurt

Computer-Aided Chemical Thermodynamics of Gases and Liquids—Theory, Models, Programs. By *P. Benedek* and *F. Olti*. Wiley, Chichester 1985. xxvii, 731 pp., bound, £ 86.95.—ISBN 0-471-87825-1

To begin with, the title of this book is annoying. Too much of what is published lately is given the honor of being described as "computer-aided". One might well have guessed that thermodynamics, the classic discipline of physical chemistry, would not escape this treatment.

It has also become the practice in chemistry to treat complex problems by computer modelling calculations, so that the calculations are used in a sense to carry out "experiments", to define limits, or to test particular approximations. The unique step forward which computers have brought is in facilitating the solution of lengthy and complex problems by appropriate fast mathematical techniques. A great deal can now be achieved with personal computers, which is especially important for the chemist because he likes to be able to do the work himself and understand its details.

The chemist therefore welcomes books which provide him with an introduction to practical work on physicochemical calculations using computers. The present book claims to do this for chemists and chemical engineers, mainly in the field of classical thermodynamics, and certainly it should be able to meet this objective within its considerable space of more than 700 pages. In classical reversible thermodynamics the requirements for the numerical mathematical toolkit are relatively modest, being limited to the solution of algebraic equations and expansions in infinite series, both of these operations being easy to program in any of the common computer languages.

In its subtitle "Theory, Models, Programs", the book makes sweeping claims with regard to the depth of treatment. This may well be justified for certain chapters (equations of state, phase equilibria, systems of one substance). However, the chapter on chemical equilibria, which is particularly important for the chemist, treats this topic in a rather offhand way, and the only example given in the chapter (methane conversion) ought to have been complemented by including other types of reactions.

The theory is treated in a very formal way, without any descriptions of related phenomena of practical importance. This may be sufficient for the working chemist who has already covered this material in his previous studies, but for chemistry students the treatment will certainly seem too dry and uninteresting. Nevertheless, it is sufficiently detailed and thorough, so that the student need seldom refer to more comprehensive works on thermodynamics.

The programs for calculating thermodynamic quantities are written in BASIC, and are rather odd in appearance, as they have been written for a computer which has only 32 characters per line. Unfortunately too the programs are not structured conventionally, especially with regard to repeat loops, which makes them less easy to follow. This again is probably a result of using an obsolescent computer. No explanatory notes are provided with the programs, which means that the user needs either to have the required knowledge of BASIC beforehand, or to acquire it elsewhere. On the other hand, a lot of examples are provided with the programs, though here the authors have perhaps given us too much of a good thing. The examples are often set out at great length without attention to economy of space, and consequently they take up a not inconsiderable proportion of the book. The thermodynamic data needed in conjunction with the examples are given alongside. In addition the data for more than 200 substances are collected together in an appendix, which also has its own index.

By "models" the authors apparently mean the equations whereby the values of the various thermodynamic quantities and functions are calculated. For this purpose they reproduce well-known and proven formulas. The authors are to be complimented in this on having produced an exhaustive compilation.

The book is definitely of considerably more value to the chemical engineer than to the chemist. It is well suited for the training of chemical engineers, and as additional material on which to base a course in engineering thermodynamics. The chemist could more appropriately use it as a reference book and additional source of information when he is looking for a quick solution to a practical problem in thermodynamics, and does not want to have to write his own program.

Klaus Ebert, Hanns J. Ederer [NB 806 IE]
Institut für Heisse Chemie,
Kernforschungszentrum Karlsruhe

Biotechnology. A Comprehensive Treatise in 8 Volumes. Series Editors: *H.-J. Rehm* and *G. Reed*. **Vol. 4. Microbial Products II.** Volume Editors: *H. Pape* and *H.-J. Rehm*. VCH Verlagsgesellschaft, Weinheim 1986. XIII, 673 pp., bound, subscription price: DM 425.00; series price: DM 495.00.—ISBN 3-527-25766-7

This is the 6th volume to be published in the series.[*] Its publication helps complete the sequence from Volume 1 to Volume 6a. Volumes 3 and 5 covered a number of "microbial products" that are compounds for the food and feed production industries. The primary focus of Volume 4 is on secondary metabolites from microorganisms represented by the actinomycetes which are gram positive fil-

[*] Cf. *Angew. Chem. Int. Ed. Engl. 22* (1983) 893; *22* (1985) 436.

amentous bacteria, and to a lesser extent, fungi. The intent is to cover the era after the development of industrial production of penicillin in the 1940's during which other medically useful metabolites were sought.

The first three chapters are an excellent introduction to the concepts and genetics of secondary metabolism by *R. Hütter, L. C. Vining,* and *V. S. Malik.* Factors affecting production of the secondary metabolites, control mechanisms, and the strategies used for isolation of *Streptomyces* genes are discussed. A discussion of recombinant DNA work with fungi such as *Aspergillus, Penicillium,* and *Cephalosporium* is also presented. Most readers would find this section highly useful.

Five chapters are devoted to the so called "complex" products. The term "complex" is used for nucleic acids and related compounds, vitamins, coenzymes, lipids, and iron-complex compounds (siderophores). The emphasis varies from chapter to chapter depending on the author's background. Those with private industry have tended to provide at least a very cursory commercial research perspective. This reviewer feels perhaps more should have been done along those lines. Generally, the style in each chapter is that of a research review article. Most of these chapters are very readable. With bacteria and yeast as the source, the production of nucleic acids, nucleotides, nucleosides, and pyrimidine compounds is reviewed by *A. Kuninaka.* Vitamins B12, B2, C, provitamins A and D2, and biotin are discussed by *J. Florent.* ATP gets some coverage twice, once in the nucleotides chapter and once in a chapter on coenzymes. The latter chapter also touches upon NAD, NADP, and Coenzyme A.

A very readable chapter from a "practice" viewpoint on lipids is presented by *C. Ratledge*, who reviews the patterns and pathways of lipid synthesis with examples for triacylglycerols, sterols, carotenoids, esters, and the use of esterases and lipases. The isolation and characterization of siderophores from bacteria and fungi is reviewed by *G. Winkelmann* in the last chapter on "complex" compounds.

The last twelve chapters in this volume deal with secondary metabolites. These chapters generally review compounds that are either considered antibiotics or are "bioactive" in some sense. By "bioactive" we mean the compounds have one or more of the following activities: antimycobacterial, antifungal, antibacterial, antitumor, antiviral, or immunomodulatory. Those interested in this area should find this group of chapters quite useful. Penicillins, cephalosporins, clavams, carbaphenems, nocardicins, monobactams, peptide antibiotics, aminoglycoside antibiotics, macrolide antibiotics, tetracyclines, rifamycins, chloramphenicol, lincomycin, novobiocin, fusidic acid, vancomycin, griseofulvin, blasticidin S, polyoxins, cycloheximide, feed additive antibiotics, antitumor substances such as actinomycin D, bleomycin etc., are covered in several chapters.

The last four chapters attend to a slightly different group of secondary metabolites other than antibiotics. Inhibitors of glycosidases such as acarbose, including their isolation procedures, are presented by *L. Müller.* These compounds have potential as antihyperglycemic compounds.

The physiology, genetics, and commercial production of ergot alkaloids is covered by *H. Kobel* and *J.-J. Sanglier.* Metabolites from *Streptomyces* known to be inducers (factors A, L, B), immunomodulators, enzyme inhibitors for use as antihypercholesterolemic drugs, plant growth regulators such as gibberellic acid, compounds useful as insecticides and as animal growth promoters are reviewed in another chapter in this set. As a preview of soon to come Volume 6b, the subject of plant cell culture is introduced. Here, *J. Berlin* covers cinnamic acid derivatives, naphtho- and anthraquinones, alkaloids, pigments, steroidal compounds, ubiquinone-10, and nicotine as well as compounds tissue culturists would *like to make* via plant cultures. An important point is made here that conventional techniques of screening for highly productive variants are not sufficient and new approaches must be found on the way to commercial success. Anyone starting out in plant cell culture would find this chapter very insightful.

Bhavender Paul Sharma [NB 819 IE]
Genencor, South San Francisco, California (USA)

Registered names, trademarks, etc. used in this journal, even when not marked as such, are not to be considered unprotected by law.

© VCH Verlagsgesellschaft mbH, D-6940 Weinheim, 1987. - Printed in the Federal Republic of Germany by Zechnersche Buchdruckerei, Speyer/Rhein.

All rights reserved (including those of translation into foreign languages). No part of this issue may be be reproduced in any form - by photoprint, microfilm, or any other means - nor transmitted or translated into a machine language without written permission from the publishers. Only single copies of contributions, or parts thereof, may be made for personal use.

Valid for users in the USA: The appearance of the code at the bottom of the first page of an article in this journal (serial) indicates the copyright owner's consent that copies of the article may be made for personal or internal use, or for the personal or internal use of specific clients. This consent is given on the condition, however, that the copier pay the stated per-copy fee through the Copyright Clearance Center, Inc., for copying beyond that permitted by Sections 107 or 108 of the U.S. Copyright Law. This consent does not extend to other kinds of copying, such as copying for general distribution, for advertising or promotional purposes, for creating new collective works, or for resale. For copying from back volumes of this journal see 'Permissions to Photo-Copy: Publisher's Fee List' of the CCC.

Editorial office: Pappelallee 3, D-6940 Weinheim, Federal Republic of Germany, Telephone (06201) 602315, Telex 465516 vchwh d, Telefax (06201) 602328.

Editor: *P. Göltitz.*

Associate editors: *D. J. Loewus, A. Stimson.* **Editorial assistant:** *E. Schweikart*

Publishers: VCH Verlagsgesellschaft mbH. (Managing Directors: *Prof. Dr. Helmut Grünewald* and *Hans Dirk Köhler*), Pappelallee 3, D-6940 Weinheim, Federal Republic of Germany. Correspondence concerning advertisements should be addressed to VCH Verlagsgesellschaft mbH, (Advertising Manager *R. J. Roth*), Boschstr. 12, P.O. Box 1260/1280, D-6940 Weinheim, Federal Republic of Germany, Telephone Weinheim (06201) 602-0, Telex 465516 vchwh d, Telefax (06201) 602328.

ANGEWANDTE CHEMIE

Volume 26 · Number 11
November 1987
Pages 1059–1200

How Nature Adapts Chemical Structures to Curved Surfaces

By Hans Georg von Schnering* and Reinhard Nesper

Dedicated to Professor Rudolf Hoppe on the occasion of his 65th birthday

Guided by the symmetry in a natural way, periodic potential surfaces partition the space in solid crystalline compounds. The arrangement of atoms, clusters and molecules obviously follows the (in general) curved shape of these 'space partitioners'. In structures, the atoms therefore choose only a very limited subset of the infinite set of possible positions. In collective structures the periodic surfaces separate areas of different interactions between atoms, clusters, and molecules. In a certain sense, they can be considered as inner surfaces, a knowledge of which reveals insights into the organization of crystalline matter. There are many good indications that the weakly bonded electrons in the highest occupied orbitals are preferably localized in the region of the space partitioners. Dynamic processes as well can be correlated to the shape of the periodic surfaces. Moreover, the surfaces are didactically very helpful in making accessible the complicated three-dimensional relations in collective structures because the main features are projected onto (although curved) two-dimensional creations. The application of periodic potential surfaces to such a variety of compounds as quartz, brass and alpha-amylose underscores their general significance. Simple qualitative considerations already reveal the manifold relations to animate and inanimate nature through to mathematics, art and architecture. It appears that, in a very universal sense, the adaption of structures to a collective order finds a natural solution through curvature.

1. How Do Structures Organize Themselves?

The recognition, generalization and utilization of relationships between structures of compounds and their properties has long ranked as one of the great tasks in chemistry. Simple concepts (8-electron rule, Zintl-Klemm rule, radii ratios etc.) and complex methods (e.g. force field, MO and band structure calculations) are qualified for manifold, far-reaching statements. They can be tested, and if necessary improved by means of a large number of precisely determined structures. On the other hand, one feels that, despite the elucidation of many details, decisive comprehensive correlations are not yet recognized or cannot be formulated clearly. Besides, a big obstacle arises by frequently using very different terms for the description of the facts.

Three years ago, while preparing a seminar about *periodic minimal surfaces* (PMS), we conceived the idea of investigating, whether in electrostatic charge distributions of a given crystal symmetry coherent potential surfaces exist, and what they might look like. In the meantime new insights into the comprehensive correlations essential for the organization of crystalline solids are occurring daily,[1–5]

[*] Prof. Dr. H. G. von Schnering, Dr. R. Nesper
Max-Planck-Institut für Festkörperforschung
Heisenbergstr. 1, D-7000 Stuttgart 80 (FRG)

making a detailed representation appropriate. Above all, there emerges a notably close relationship between the course of potential surfaces and the spatial distribution of electrons in crystals.[6] Close collaboration with *S. Andersson* (Lund) and *S. T. Hyde* (Canberra) has given us many fruitful ideas.[7-12] It is not yet certain, whether the things seen through the authors spectacles[*] will be bearing in the long run. However, even if only the beauty in the structures of solids should remain, it will have been worth it.

Chemical structures of molecules and crystals are fascinating, not only because of their local symmetry but also because of the symmetry of the periodical translational patterns extending into crystal space. In a comprehensive sense, it is the symmetry that unites chemical structures with objects of inanimate and animate nature, the architecture and the art by virtue of governing mathematical relationships. This is not a new discovery, and in all areas one repeatedly finds the phenomenon of *optimal form*, apparently dominant over all and a challenge to an interdisciplinary bridging. From the manifold literature, the monographs of *Pearce*,[13] *Duarte*,[14] *Frei Otto* et al.,[15] *Stevens*,[16] as well as of *Hildebrandt* and *Tromba*[17] are highly recommended.

Quite frequently, the symmetry of single objects does not fit the symmetry of an arrangement of such objects. However, by the development of curved structures, an adaption is then possible. Just as hexagons and pentagons are arranged in a nearly unconstrained way to form the cover of a soccer ball, a chemical molecule of the corresponding structure can be formed. In both cases the local symmetry of the building units remains, however without appearing in the arrangement. It can be shown that also in chemical structures in a very general way, the curvature plays an important role in the adaption of parts to the whole!

Atoms with four bonds are regarded as centers of local tetrahedral symmetry. Objects of such a symmetry cannot be connected for example to a three-membered ring (ring tension) without loss of the local symmetry. Usually, in the theoretical treatment the local symmetry of the bonding functions is then adapted to the total symmetry. However, if the local symmetry is retained, the arrangement of the three-membered ring can only be produced by a curvature of the bonds. The curvature of bonds, following the symmetry only locally at the centers has a significant consequence: The usual bond angles are only of topological meaning, but the "true" values can be obtained by a measurement on non-euclidean surfaces, which are spanned by the curved bonds. This concept can also be extended to certain collective crystal structures and contributes to the understanding of peculiar experimental observations.

In the crystalline state, the topology of chemical structures is substantially influenced by the symmetry of the periodical translations. While the latter organize the packing of the building units in molecular crystals, in true collective structures primary connections between the atoms of the collective arrangement are also produced by the translation (in collective structures molecular units cannot be delimited informally). Also, in these arrangements, the point symmetry of local aggregations in general does not correspond to the crystal symmetry. In the structures, the adaption of local aggregations to the demand of the crystal symmetry then seems to take place by nestling the periodically curved surfaces. Let the building units be atoms, molecules, clusters or even blackberries (Fig. 1a) [even humans?]; their aggregations are to some extent regulated similarly by a balance between the rigidity of the individual and the force of the collective law. The self-similarity, e.g. between a single blackberry (packet of tiny blackberries) and a pile of blackberries (packet of blackberries), is called *fractal* in mathematics.[18,19] In nature it appears in multifarious ways and is also found in the combination of curved single building units and their collective.

S. Andersson is credited with recognizing the general significance of periodic minimal surfaces as being curved space partitioners.[7-9] Such surfaces are creations of extraordinary harmony and fascination, which one can hardly escape. Also *Mackay*[20] had already alluded to connections between PMS and the macrostructure of silicate membranes. Recently, a number of papers have been published which refer to the general application of PMS to crystal structures.[21-31]

We were able to show that *p*eriodic *e*qui-*p*otential *s*urfaces (PEPS) and, of these, especially the *p*eriodic *zero p*otential *s*urfaces (POPS) of appropriate Coulomb fields are very similar to such minimal surfaces. They are of more comprehensive importance, because they contain the PMS, and, moreover, permit space partitions for which corresponding PMS do not exist. With PEPS and POPS direct correlations to physical properties result. In addition, we can show that the concept of periodic potential surfaces (PEPS) generates a general relationship between crystallography and PMS, which is also important for mathematicians. This is because PEPS are determined by symmetry-adapted distributions of points and point charges. Such distributions are known by the term *point configurations* (PK),[32,33] and they represent the fundamental point patterns in the corresponding symmetry groups. According to *Fischer* and *Koch* some of these PK's form so-called sphere packings, which means graphs of spheres touching each other.[34-36] POPS are connected in a natural manner with such sphere packings, because they span the space partitioner between non-touching interpenetrating sphere packings. Thus, e.g., as in Figure 2c, where the bridging Nb-Cl-Nb bonds (yellow) of one partial structure (violet side) never touch those of the other (blue side). This is especially important for the fragmentation of space into unequal parts, because the mathematical prerequisites for the derivation of PMS are still missing in this case. The same is true for sphere packings with spheres of different size.

We believe that with PEPS and POPS we have put aside a real component to the fascination which comes from the idea of space partitioning periodic minimal surfaces and their curvature properties. Numerous examples demonstrate the surprising consequence by which nature obviously correlates chemical structures with the topology of periodic equi-potential surfaces and with the curved labyrinths generated by the latter acting as space partitioners.

[*] Cf. Figure 16 in H. G. von Schnering, *Angew. Chem. Int. Ed. Engl. 20* (1981) 33.

2. Generation and Representation of Periodic Equi-Potential Surfaces PEPS

Periodic equi-potential surfaces PEPS, and among these also the periodic zero-potential surfaces (POPS), are quite simply obtained using a Coulomb ansatz. For this, in a defined three-dimensional (3D) distribution of point charges $q_1=(m+)$ and $q_2=(n-)$ the electrostatic potentials $P(xyz)=\sum_i q_i \cdot r_i^{-1}$ are calculated for a large number of mesh points (xyz) (q_i = given point charges; r_i = distance between q_i and (xyz)) and then the equi-potential contours are determined and plotted. The distribution of the generating point charges q_i is selected according to typical point configurations, as they are characteristic for the symmetry of the given space groups.[33] In the simplest case two symmetry equivalent point configurations are occupied by the charges (+) and (−). Such arrangements are especially important, because the charge distributions are *commutable*, i.e., with an exchange of (+) and (−) the trace of the POPS does not change. The chosen point configurations are connected with each other by a translation vector $-\vec{s}$, whose sign takes into consideration the change in the charges. For the CsCl structure type, e.g., $-\vec{s}$ is $(\frac{1}{2}\frac{1}{2}\frac{1}{2})$ [space group $Pm\bar{3}m$, (+) at position 1a (000), (−) at position 1b $(\frac{1}{2}\frac{1}{2}\frac{1}{2})$].

For the mathematical evaluation the program system OBERFLEX[37] was developed, which combines a whole series of different functions. First of all the program MADKUG[38] calculates the lattice potentials according to the Ewald-method,[39] whose convergence behavior is controlled by the eligible numerical accuracy *GN*. The accuracy is selected after test calculations ($4 \leqq GN \leqq 7$ valid digits) and it essentially determines the computing time. Crucial for the determination of the entire potential space $P(xyz)$ is the introduction of a probe S_0 with the charge $q_s=0$[38] which is suitable for the calculation of vacancy potentials, especially on those positions (xyz) which are *not* occupied by one of the generating point charges q_i. The probe S_0 moves through the 3D space in chosen steps,[37] whose width is a compromise between the desired accuracy and computing time. Usually 20–40 steps along the main lattice directions are sufficient, and this rather rough mesh yields around 8000 potentials to be calculated per asymmetric unit.

The following interpolation using the program LINES[37] or POLYGON,[37] supplies sufficiently smooth PEPS and POPS surface elements in the asymmetric unit, which can be expanded if desired via the symmetry elements of the appropriate space group within a chosen parallelepiped or a sphere of any size (program EXPAND[37]). The representation is done in the form of open nets or closed polygons (POLYGON[37]), which allows graphical and topological evaluations, e.g. the determination of the surface area. The complete representation of the surfaces is stored explicitly and can be used in modules. In this way the modular assembly of surfaces with correspondingly scaled and stored structures and convex polyhedra is possible (STRUKTUR[37]; KVEXPOL[37]). Two new graphic programs finally allow the preparation and interactive alteration of the pictorial representations on a two-dimensional graphic terminal (AED767[*]; FNETZ[37]) and on a three-dimensional RASTER graphics station (RASTER TECHNOLOGIES, MODEL ONE/380[*]; RAPTURE[37]).

Finally, by means of a scenario, the graphical representations can be recorded as a movie picture. The automatic recording of single pictures is controlled by the program FNETZ[37] for SUPER 8 film, 16 mm film and/or videocamera (U-MATIC). A further option allows to display suitable representations (without undercuts) of closed surfaces and structures to such an extent that they can be used by numerically controlled milling machines for an automatic generation of molds for models (FNETZ[**], FRAES[37]).

3. Topology of Zero-Potential Surfaces

In the following we will point out the properties of POPS in connection with the generating point configurations (PK) of the symmetry groups and also the relationships between POPS and periodic minimal surfaces PMS. First of all, two completely different types of POPS have to be distinguished, namely those which are based on *commutable* PK's and those which are based on *non-commutable* PK's.

3.1. POPS of Commutable Point Configurations

Independently of the actual symmetry, POPS of commutable point configurations fulfill some boundary conditions: a) The symmetry of the charge distribution and the potential space obey a so-called *black-white symmetry group*.—b) Positive and negative partial spaces are topologically exchangeable and therefore have the same volume.—c) Thus, the respective POPS divide the space into equivalent halves, and POPS are therefore *invariant* against an exchange of the generating charges and contain exactly those symmetry elements which perform the exchange of complete partial spaces.—d) Therefore, these POPS belong to a supergroup (normalizer) of the generating symmetry group (space group) and in the limiting case to the corresponding Cheshire group. If we take $Cs^{\oplus}Cl^{\ominus}$ as the generating structure with the symmetry $Pm\bar{3}m$ then the POPS ($Cs^{\oplus}Cl^{\ominus}$) has the higher symmetry $Im\bar{3}m$; if we choose $Na^{\oplus}Tl^{\ominus}$ with the symmetry $Fd\bar{3}m$, again POPS ($Na^{\oplus}Tl^{\ominus}$) has the higher symmetry $Pn3m$ ($a'=a/2$).—e) Among all equi-potential surfaces PEPS of a given charge distribution, POPS has the smallest maximum curvature and also the smallest average curvature *at each point* of the surface.—f) The integral curvature taken over the asymmetric unit is $\bar{H}=0$, because of the interchangeability of the partial spaces.

These particular properties make POPS very similar to the mathematical periodic minimal surfaces PMS of the same symmetry. In certain cases they presumably are even

[*] CIS Graphic & Bildverarbeitung, D-4060 Viersen (FRG).

[**] Uses the DI 3000-graphic package, Precision Visuals, D-8000 München (FRG).

exactly identical (which has to be proven separately). For PMS, the average curvature, e.g. the sum of both principal curvatures *at each point* of the surface, vanishes: $H=(\kappa_1+\kappa_2)=0$ and trivially $\overline{H}=0$, just like the POPS, for which exact conditions for the average local curvature cannot be given; here, only positive and negative curvatures of the same absolute value must appear at any but not necessarily at identical points of the POPS. Nevertheless, PMS and POPS are exactly identical in special points (xyz) and at certain straight lines, because of the relationships mentioned in (c) and (d) above, which are valid for both PMS and POPS. Thus, twofold axes form straight lines on PMS and POPS, which are needed as boundary conditions for the mathematical derivation of the PMS. Inversion centers at both types of surfaces are always flat points, however not saddle points.

3.2. POPS of Non-Commutable Point Configurations

If POPS are generated from non-commutable PK's then the listed (a priori) conditions in 3.1a) - f) are not applicable. For POPS of this type (type 2) only the following holds: They belong to the symmetry group of the generating charge distribution; they separate the two *unequal* partial spaces in such a manner that the volume integrals over the potentials of both partial spaces have the same absolute value but opposite sign $\left(\int_0^{V(-)} P(-)\,\mathrm{d}V = -\int_0^{V(+)} P(+)\,\mathrm{d}V\right)$. The more the volume difference between both partial spaces increases the more the average potentials of both parts differ. In general, for $V(+)>V(-)$ in the (larger) positive partial space a family of PEPS should exist which show smaller average and integral curvatures than POPS. Again, among the PEPS, there has to be a PEPS_{min} for which the integral curvature vanishes ($\overline{H}=0$). Their space partitioning properties are also worth further investigations, which, however, we could not carry out systematically, because the determination of such PEPS turned out to be very difficult.

No mathematical boundary conditions for the derivation of equivalent PMS can be given because PEPS of type 2 do not contain any symmetry elements—a substantial difference when compared to the surfaces of type 1. Nevertheless, today one knows some PMS of this type which divide space into non-equivalent parts such as the surfaces *I-WP* and *OC-TO*.[40] As a rule they were obtained empirically by stochastic methods.

Of course these surfaces also obey—even if not parameter-free—boundary conditions if they are intersected by symmetry elements. For example, all rotation axes and mirror planes intersect the POPS and PMS of type 2 perpendicular to the surface. Each twofold axis perpendicular to the surfaces generates at least one saddle point on the intersection point, all rotation axes of higher order produce a flat point. However, these points are not fixed along the rotation axis (cf. the mobility of a soap bubble along a penetrating straw). Intersection lines of POPS (PMS) with mirror planes are plane lines, because all their normal vectors lie in one plane, namely the mirror plane.

3.3. Topology

Very important topological information is obtained from the POPS and PMS about the existence, shape and orientation of tunnel connections between cavities *of the same* potential (cf. Fig. 1c, CsCl). They show the direction in which structure elements of the same type "can see each other" and therefore show the direction in which interactions between such units may occur. We also believe that these tunnels define symmetry determined polarization directions, which always exist (if symmetry allowed) but become more or less effective depending on the type of participating atoms and aggregates. Especially strong interactions between units of the same kind correspond to covalent bonds with short distances between neighboring atoms. Such structures often belong to space groups whose symmetry generates POPS with marked tunnel systems (e.g. D^* with NaTl or diamond (Fig. 1b); Q^* with quartz or α-amylose (Fig. 1j)).

In contrast to this only a few POPS exist *without* any tunnel connections, i.e. "positive" and "negative" areas are optimally shielded. Typical examples are the F^* surface of the $Na^{\oplus}Cl^{\ominus}$ charge distribution or the W^* surface (Table 1; Fig. 1g, h), which contributes to an understanding of the substitutional behavior of certain clathrate structures (cf. Section 5.7). A POPS with this exceptional property was also found with hexagonal symmetry (cf. E^*, Table 1, Fig. 1k).

Finally, a family of surfaces exists among the POPS of type 2 which contains neither tunnel nor shielding planes but bubbles (*F-P*$_2$; *I-W*). For these, the Gaussian curvature is always positive, a fundamental difference to the continuous surfaces. However, even in these cases there exists between the bubbles a PEPS with vanishing integral curvature. POPS with the bubble structure correspond to strained PMS, perhaps a regular structure of isolated soap bubbles.

3.4. How Many POPS can Be Generated?

The answer to this important question is disillusioning at first: There are infinitely many! Let us take a charge distribution corresponding to the NaTl structure and generate the D^* surface in the space group $F\bar{4}3m$ with the parameters: (1+) at 000, (1+) at $\frac{1}{4}\frac{1}{4}\frac{1}{4}$, (1−) at $\frac{1}{2}\frac{1}{2}\frac{1}{2}$ and (1−) at $\frac{3}{4}\frac{3}{4}\frac{3}{4}$. By reducing the charges at $\frac{1}{4}\frac{1}{4}\frac{1}{4}$ (+) and at $\frac{3}{4}\frac{3}{4}\frac{3}{4}$ (−) one *continusouly* reaches the F^* surface of NaCl. Beginning (D^*) and end (F^*) of this transformation differ drastically! However, in the course of this continuous transformation *no topological new* type appears (cf. Section 7). This must be explained in more detail: The topology distinguishes bodies by their *genus*, namely the amount of tubes (tunnels, channels) which originate from the bodies. Therefore, each sphere has the genus = 0, spheres with a handle have the genus = 1 (= 2/2) etc. Each periodic infinite surface which divides the space in any form has the genus = n, which is just the number of channels leading from one unit cell to neighboring cells (e.g. "CsCl", n = 6/2 = 3, Fig. 1c). The surface D^* mentioned above has a four-armed tunnel system which envelops the diamond structure and according to the Cheshire group $Pn\bar{3}m$ ($a'=a/2$), to which the D^*

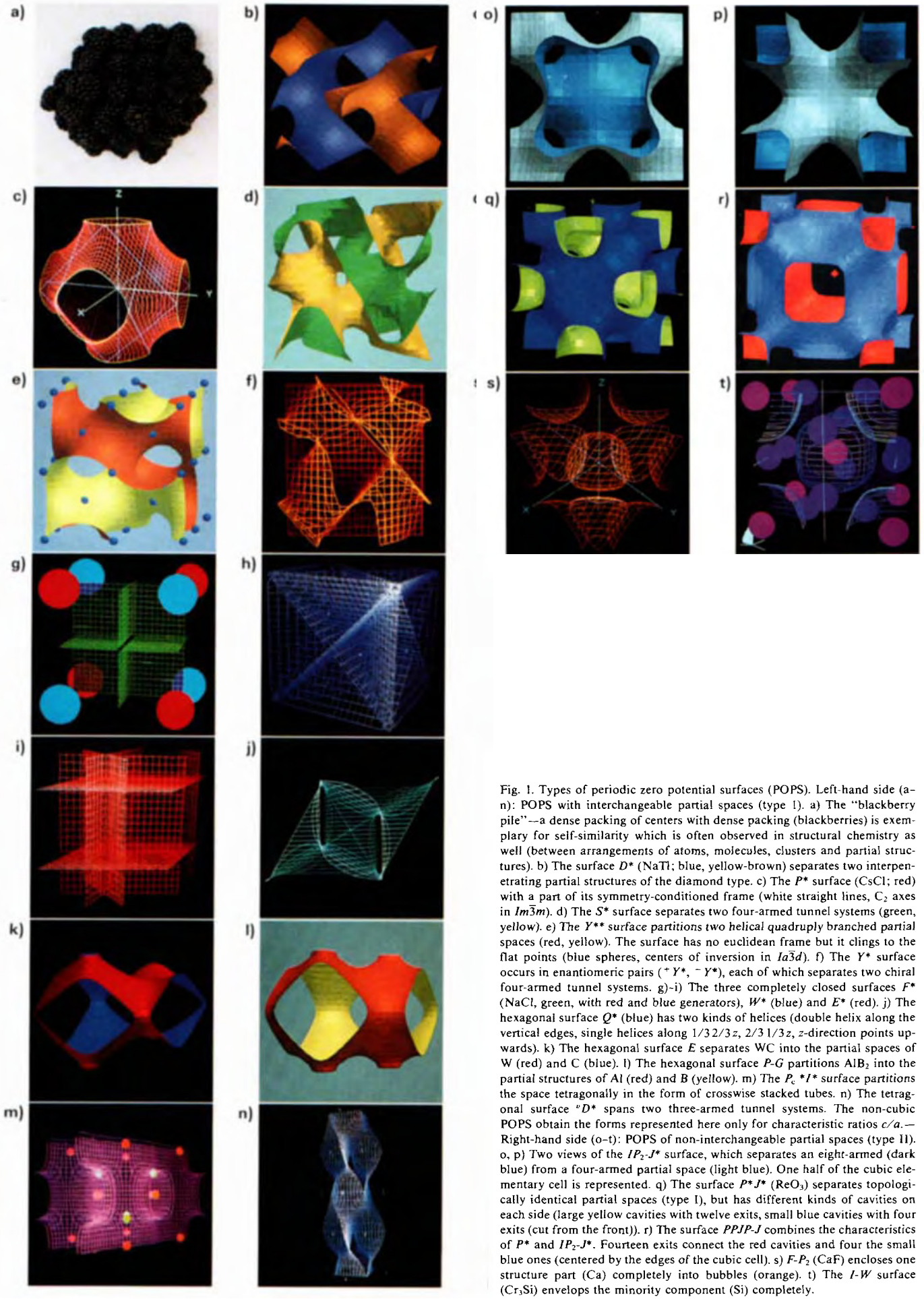

Fig. 1. Types of periodic zero potential surfaces (POPS). Left-hand side (a–n): POPS with interchangeable partial spaces (type I). a) The "blackberry pile"—a dense packing of centers with dense packing (blackberries) is exemplary for self-similarity which is often observed in structural chemistry as well (between arrangements of atoms, molecules, clusters and partial structures). b) The surface D^* (NaTl; blue, yellow-brown) separates two interpenetrating partial structures of the diamond type. c) The P^* surface (CsCl; red) with a part of its symmetry-conditioned frame (white straight lines, C_2 axes in $Im\bar{3}m$). d) The S^* surface separates two four-armed tunnel systems (green, yellow). e) The Y^{**} surface partitions two helical quadruply branched partial spaces (red, yellow). The surface has no euclidean frame but it clings to the flat points (blue spheres, centers of inversion in $Ia\bar{3}d$). f) The Y^* surface occurs in enantiomeric pairs ($^{+}Y^*$, $^{-}Y^*$), each of which separates two chiral four-armed tunnel systems. g)–i) The three completely closed surfaces F^* (NaCl, green, with red and blue generators), W^* (blue) and E^* (red). j) The hexagonal surface Q^* (blue) has two kinds of helices (double helix along the vertical edges, single helices along $1/3\,2/3\,z$, $2/3\,1/3\,z$, z-direction points upwards). k) The hexagonal surface E separates WC into the partial spaces of W (red) and C (blue). l) The hexagonal surface P-G partitions AlB_2 into the partial structures of Al (red) and B (yellow). m) The P_c $^{*}I^*$ surface partitions the space tetragonally in the form of crosswise stacked tubes. n) The tetragonal surface $^{v}D^*$ spans two three-armed tunnel systems. The non-cubic POPS obtain the forms represented here only for characteristic ratios c/a.—Right-hand side (o–t): POPS of non-interchangeable partial spaces (type II). o, p) Two views of the IP_2-J^* surface, which separates an eight-armed (dark blue) from a four-armed partial space (light blue). One half of the cubic elementary cell is represented. q) The surface P^*J^* (ReO_3) separates topologically identical partial spaces (type I), but has different kinds of cavities on each side (large yellow cavities with twelve exits, small blue cavities with four exits (cut from the front)). r) The surface $PPJP$-J combines the characteristics of P^* and IP_2-J^*. Fourteen exits connect the red cavities and four the small blue ones (centered by the edges of the cubic cell). s) F-P_2 (CaF) encloses one structure part (Ca) completely into bubbles (orange). t) The I-W surface (Cr_3Si) envelops the minority component (Si) completely.

surface belongs, has the genus = 4 (for the entire NaTl unit cell as generator, the genus = $32 = 4 \times 2^3$; $a = 2a'$). The $Na^{\oplus}Cl^{\ominus}$ distribution, on the other hand, yields the POPS F^* without any tunnels: genus = 0. But all intermediate stages in the above described transformation maintain the genus = 4 typical for the D^* surface, i.e. the infinite set of POPS of this transformation only belongs to *two* topologically different types.

It is obvious that only the discussion of topological *types* is of general interest in the investigation of structures and their properties. Only these provide a small and surveyable group of principally different forms: A very encouraging discovery!

3.5. Distinctions between POPS and PMS

It should be pointed out that for certain symmetry groups no PMS can be generated, e.g. for the space group $Fd\bar{3}m$. If, e.g., in the space group $F4\bar{3}m$ a charge distribution $\langle F^{(+)}|\frac{1}{4}\frac{1}{4}\frac{1}{4}|F^{(-)}\rangle$ is chosen, then without any difficulties the POPS D of the symmetry $Fd\bar{3}m$ (Table 1) is obtained. It has the same genus = 4 as the surface D^* (= PMS "D" of *Schwarz*) and also the same system of C_2 axes, which lie on the surface as straight lines. If this system of straight lines were to be dipped into a soap solution, *only one* stable PMS would be obtained, namely PMS "D" which corresponds to POPS D^*. In a given framework only that surface which produces an additional set of C_2 axes perpendicular to the surface is also a PMS, because this is the only way to obey the condition $H = 0$ at all points of the surface (the symmetry of this PMS is therefore $Pn\bar{3}m$ with $a' = a/2$). Consequently, the $Fd\bar{3}m$ frame, built from C_2 axes, cannot generate a PMS equivalent to the POPS D. On the other hand, the POPS D only has to fulfill the weaker condition $\overline{H} = 0$ and, therefore, in the given frame, equivalent surface elements (just like, e.g., a sail) can be alternately more or less inflated without losing the character of the tunnel structure. This is due to the fact that, for the generation of the POPS, not all equivalent positions have to be occupied by charges (and usually they are not), and the POPS is able to respond topologically, which is impossible for a PMS under the same boundary conditions. The family of POPS is therefore larger than the family of PMS. Analyzing in detail the topological changes during the transition from D^* to D one gets the impression that the D surface ($Fd\bar{3}m$, ZnS) might be a variant of D^* modulated by a periodical variation of pressure in the labyrinths.

Another important difference is that POPS are always orientable surfaces. Because of their construction, namely the separation of positive and negative space, a situation like on a Möbius strip can never occur, i.e. one cannot move continuously from the positive to the negative side of the surface. However, PMS with this particular property are well-known.

4. The Periodic Zero-Potential Surfaces POPS

Table 1 compiles the current state of our knowledge of such surfaces. The graphical representations are illustrated in different figures and are each given abbreviated symbols. One always has to keep in mind that the POPS only reflect the symmetry of the corresponding space group and by that also characterize the space partitioning properties of the related point configurations PK. They are generated from only a few special point positions xyz, which with a few exceptions don't have anything to do with a real structure. Primarily they also have nothing to do with structures that may be connected with the generating charge distribution. Characterizations such as 'CsCl surface' are merely used as obviously short symbols. The striking similarities of POPS and PMS show again that the electrostatic ansatz only represents a well manageable procedure to determine the space partitioning surfaces ($P(xyz) = 0$). There can be no doubt that in principle the same forms would be reached if it were possible to formulate mathematically where a "blue" partial space switches into a "red" one. The same holds for other potential ansaetze. If for instance balloons are pumped up, which are fixed at constant distances according to a cubic body centered structure, then the partitioning skin finally has the form of the so-called P surface (= POPS P^*).

To label the POPS (Table 1) we have chosen symbols which follow the well-known PMS or produce other simple relationships (Q^* for the symmetry group of *quartz*). Furthermore, a detailed symbol will be used to establish the connection to the generation of the surfaces. Example D^*: Generating symmetry group is $Fd\bar{3}m$ with the equivalent positions (8a) and (8b), which both have the point configuration D (cf. Ref. [33]). $D_{(8a)}$ is occupied by (1+) and $D_{(8b)}$ by (1−). The resulting POPS symmetry is $Pn\bar{3}m$, and accordingly, the symbol $cP\ \langle D|\frac{1}{2}\frac{1}{2}\frac{1}{2}|D\rangle$ is chosen because the POPS has cubic P translation and separates two D configurations from each other shifted by $\frac{1}{2}\frac{1}{2}\frac{1}{2}$. The latter fact is described by the symbol D^*, and simultanously the analogy to *Schwarz*'s minimal surface D is set up (D is by the way a wrong symmetry declaration).

Today, all cubic space groups are investigated systematically for the existence of PMS and POPS of type 1, for which all pairs of generating PK's show the same point symmetry, even if more than one PK belongs to the same partial space. In contrast, only minimal information is available for surfaces of type 2, even for the cubic systems. As already mentioned, especially for the PMS, systematic statements are missing for the mathematical boundary conditions. However, with the help of suitable POPS it would seem that there is the possibility of expanding our knowledge of this subject.

Leaving the cubic systems, from the variable axial ratios additional free parameters are gained for the lower crystal classes. Because of such anisotropy effects in certain directions, tunnels can merge and in other directions they can completely break off. Related crystal structures as a rule also show the character of layer structures (cf. Section 7). However, all in all our knowledge of POPS and PMS for these 194 symmetry groups is, at present, very limited.

How is the topology of POPS's affected by the splitting of a high symmetry position occupied by a charge? This question is equally important for structural chemistry and crystallography. This process corresponds to the replacement of an atom by a cluster or a molecule respectively.

Table 1. Periodic zero potential surfaces POPS, their correspondence to point configurations PK and known periodic minimal surfaces PMS. The charges of the PK's are in the upper parentheses, the Wyckoff positions of the space group are in the lower parentheses. c, h and t indicate cubic, hexagonal and tetragonal Bravais lattices ($\wedge$ = logical 'and').

POPS	POPS symmetry	Generating SG for POPS	Generating PK	Complete POPS symbol	Synonym	PMS
P^*	$Im\bar{3}m$	$Pm\bar{3}m$	$P^{(1+)}_{(1a)} \wedge P^{(1-)}_{(1b)}$	$cI\langle P\vert\frac{1}{2}\frac{1}{2}\frac{1}{2}\vert P\rangle$	CsCl	Schwarz's *P* surface
D^*	$Pn\bar{3}m$	$Fd\bar{3}m$	$D^{(1+)}_{(8a)}fD^{(1-)}_{(8b)}$	$cP\langle D\vert\frac{1}{2}\frac{1}{2}\frac{1}{2}\vert D\rangle$	NaTl	Schwarz's *D* surface
P^*J^*	$Im\bar{3}m$	$Pm\bar{3}m$	$P^{(3+)}_{(1a)}J^{(1+)}_{(3c)} \wedge P^{(3-)}_{(1b)}J^{(1-)}_{(3c)}$	$cI\langle PJ\vert\frac{1}{2}\frac{1}{2}\frac{1}{2}\vert PJ\rangle$	$2\,ReO_3$	Neovius's surface
IP_2-J^*	$Im\bar{3}m$	$Im\bar{3}m$	$I^{(2+)}_{(2a)}P_2{}^{(1+)}_{(8c)} \wedge J^{*(2-)}_{(6h)}$	$cI\langle IP_2\vert 000\vert J^*\rangle$	—	*Schoen*'s *I-WP* surface
Y^{**}	$Ia\bar{3}d$	$I4_132$	$Y^{*(1+)}_{(8a)} \wedge Y^{*(1-)}_{(8b)}$	$cI\langle Y^*\vert\frac{1}{2}\frac{1}{2}\frac{1}{2}\vert Y^*\rangle$	—	*Schoen*'s gyroid
F^*	$Pm\bar{3}m$	$Fm\bar{3}m$	$F^{(1+)}_{(4a)} \wedge F(1-)(4b)$	$cP\langle F\vert\frac{1}{2}\frac{1}{2}\frac{1}{2}\vert F\rangle$	NaCl	
F-P_2	$Fm\bar{3}m$	$Fm\bar{3}m$	$F^{(2+)}_{(4a)} \wedge P_2{}^{(1-)}_{(8c)}$	$cF\langle F\vert 000\vert P_2\rangle$	CaF_2	
S^*	$Ia\bar{3}d$	$I\bar{4}3d$	$S^{(1+)}_{(12a)} \wedge S^{(1-)}_{(12b)}$	$cI\langle S\vert\frac{1}{2}\frac{1}{2}\frac{1}{2}\,x\,S\rangle$	$2\beta'$-Ga	*Fischer Koch*'s *S* surface
I-W	$Pm\bar{3}n$	$Pm\bar{3}n$	$I^{(3+)}_{(2a)} \wedge W^{(1-)}_{(6c)}$	$cP\langle I\vert 000\vert W\rangle$	Cr_3Si	
D	$Fd\bar{3}m$	$F\bar{4}3m$	$F^{(1+)}_{(4a)} \wedge F^{(1-)}_{(4b)}$	$cF\langle F\vert\frac{1}{4}\frac{1}{4}\frac{1}{4}\vert F\rangle$	ZnS	
$^+Y^*$	$I4_132$	$P4_332$	$^+Y^{(1+)}_{(4a)} \wedge {}^+Y^{(1-)}_{(4b)}$	$cI\langle {}^+Y\vert\frac{1}{2}\frac{1}{2}\frac{1}{2}\vert {}^+Y\rangle$	—	*Fischer Koch*'s *Y* surface
$^-Y^*$	$I4_132$	$P4_132$	$^-Y^{(1+)}_{(4a)} \wedge {}^-Y^{(1-?}_{(4b)}$	$cI\langle {}^-Y\vert\frac{1}{2}\frac{1}{2}\frac{1}{2}\,x\,{}^-Y\rangle$	—	*Fischer Koch*'s *Y* surface
W^*	$Im\bar{3}m$	$Pm\bar{3}m$	$W^{(1+)}_{(6c)} \wedge W^{(1-)}_{(6d)}$	$cI\langle W\vert\frac{1}{2}\frac{1}{2}\frac{1}{2}\vert W\rangle$	—	
$PPJP$-J	$Pm\bar{3}m$	$Pm\bar{3}m$	$P^{(2+)}_{(1a)}P^{(2+)}_{(1b)}J^{(1+)}_{(3c)}P^{(1+)}_{(8g)}x=\frac{1}{8} \wedge J^{(5-)}_{(3d)}$	$cP\langle P^*JP8(1/8)\vert 000\vert J\rangle$	—	*Schoen*'s *OC-TO* surface
$F^*Y^*[x]$	$I2_13$	$P2_13$	$FY^{(1+)}_{(4a)}[x] \wedge FY^{(1-)}_{(4a)}[x+\frac{1}{2}]$	$cI\langle FY\vert\frac{1}{2}\frac{1}{2}\frac{1}{2}\vert FY\rangle$	—	x = 0: F^*, x = 1/8 Y^*
$P^*Y^{**}[x]$	$I\bar{4}3d$	$I2_13$	$P_2Y^{*(1+)}_{(8a)}[x] \wedge P_2Y^{*(1-)}_{(8a)}[x+\frac{1}{4}]$	$cI\langle P_2Y^*\vert\frac{1}{4}\frac{1}{4}\frac{1}{4}\vert P_2Y^*\rangle$	—	x = 0: Schwarz's *P*, x = 1/8: *Schoen*'s gyroid
$^+Q^*$	$P6_222$	$P6_422$	$^-Q^{(1+)}_{(3c)} \wedge {}^-Q^{(1-)}_{(3d)}$	$hP\langle {}^-Q\vert 00\frac{1}{2}\vert {}^-Q\rangle$	Quartz	
$^-Q^*$	$P6_422$	$P6_222$	$^+Q^{(1+)}_{(3c)} \wedge {}^+Q^{(1-)}_{(3d)}$	$hP\langle {}^+Q\vert 00\frac{1}{2}\vert {}^+Q\rangle$	Quartz	
E	$P6_3/mmc$	$P\bar{6}m2$	$P^{(1+)}_{(1a)} \wedge P^{(1-)}_{(1d)}$	$hP\langle P\vert\frac{1}{3}\frac{2}{3}\frac{1}{2}\vert P\rangle$	WC	
E^*	$P6_3/mcm$	$P\bar{6}2c$	$E^{(1+)}_{(2c)} \wedge E^{(1-)}_{(2d)}$	$hP\langle E\vert 00\frac{1}{2}\vert E\rangle$	2 WC	
P-G	$P6/mmm$	$P6/mmm$	$P^{(2+)}_{(1a)} \wedge G^{(1-)}_{(2d)}$	$hP\langle P\vert 000\vert G\rangle$	AlB_2	*Schoen*'s *H'-T* surface (with c/a = 1)
R^*	$I\bar{3}m$	$R\bar{3}m$	$R^{(1+)}_{(3a)} \wedge R^{(1-)}_{(3b)}$	$hR\langle R\vert 00\frac{1}{2}\vert R\rangle$	—	
$^vD^*$	$C4_2/amd$	$I4_1/amd$	$^vD^{(1+)}_{(4a)} \wedge {}^vD^{(1-)}_{(4b)}$	$tC\langle {}^vD\vert 00\frac{1}{2}\vert {}^vD\rangle$	NbAs	*Schoen*'s D_T surface (with c/a = 2)
$P^*_cI^*$	$C4_2/mmc$	$P4_2/mmc$	$P_{c(2a)}I^{(1+)}_{(2c)} \wedge P_{c(2b)}I^{(1-)}_{(2d)}$	$tC\langle P_cI\vert\frac{1}{2}\frac{1}{2}0\vert P_cI\rangle$	—	*Schoen*'s *CLP* surface (with c/a = $1/\sqrt{2}$
$F_c[x]$	$I4_1/acd$	$I4_122$	$^vD2xx^{(1+)}_{(8d)}[x] \wedge {}^vD2x\bar{x}^{(1-)}_{(8e)}[x+\frac{1}{2}]$	$tI\langle {}^vD2xx\vert\frac{1}{2}\frac{1}{2}0\vert {}^vD2x\bar{x}\rangle$	—	$\begin{cases}(x=0,\ c/a=\sqrt{2})\text{: } D^*,\ (x=1/8,\ c/a=1)\text{: } Y^{**},\\ (x=1/4,\ c/a=2)\text{: } F^*\end{cases}$
$^vD[x]$	$I4_1$/amd	$I4_122$	$^vD2xx^{(1+)}_{(8d)}[x] \wedge {}^vD2x\bar{x}^{(1-)}_{(8e)}[x]$	$tI\langle {}^vD2xx\vert 000\vert {}^vD2x\bar{x}\rangle$	—	

One may for example think of the transition $CsCl \rightarrow CaB_6$. The invariant symmetry-controlled boundary conditions (space group $Pm\bar{3}m$) are maintained in any case and independent of the choice of the multipole. From some selected examples it can be assumed[41] that the topology might in fact change locally, but it still keeps its essential features, i.e. the type. Finally, we would like to point out the important relations between POPS and PMS on the one hand and the Dirichlet partitions with the conception of the convex polyhedra on the other.[31,42-49] Often the facet surfaces, which were determined by the polyhedra method, represent very good approximations for POPS and PMS (Fig. 2p), and with this method even partitions of the 3D space in *four* interpenetrating labyrinths (four colors) can be derived, for which equivalent PMS and POPS cannot as yet be given.

5. POPS and Structures

What do zero-potential surfaces POPS (or periodic minimal surfaces PMS) have to do with chemical structures? In this section we would like to show how the surfaces, which are solely formed by the symmetry, separate chemical structures in crystals in an almost natural way, and how this partitioning accounts for the obviously different interactions between the partial structures. Figures 1-6 show the most important POPS presently known, together with an arbitrary selection of structures of completely different character, which are adjusted solely by a scaling factor into the affiliated POPS.

5.1. The P^* Surface

This surface, besides those of the type IP_2-J^* and P^*J^* (Table 1), is a representative of the symmetry group $Im\bar{3}m$, and at the same time it is suitable for the topology of structures in the subgroups $I\bar{4}3m$, $I432$, $Im\bar{3}$, $I23$, $Pm\bar{3}m$, $P\bar{4}3m$, $P\bar{4}3n$, $P432$, $Pm\bar{3}$, $P23$, etc. In Figure 2a a part of the structure of the zeolite sodalite is shown ($Na_4Al_3Si_{12}O_{26}Cl$; $P\bar{4}3n$). Na and Cl form a partial structure of the type of the intermetallic phase $PtHg_4$. The entire aluminosilicate framework lies, in very good approximation, on the P^* surface, while the few $Na^{\oplus}$ cations are centering the cavities and the $Cl^{\ominus}$ anions lie above the twelve-membered rings of the silicate framework. The O atoms are bonded such that the lone electron pairs are on both sides of the surface, and directed towards the cations in the cavities. They practically form a double layer along the P^* surface, which primarily participates in the polar interactions with the cations, while the more covalent partial structure matches the surfaces. The sodalite structure can be described analogously with the help of the surfaces IP_2-J^* (group-subgroup relationship: $Im\bar{3}m$-$I\bar{4}3m$-$P\bar{4}3m$).

Because Al and Si fulfill equivalent functions, they can be unified in $Pm\bar{3}m$ symmetry. Indeed the aluminosilicate framework coincides with the intersection lines of the surfaces P^* and IP_2-J^*. The latter one possesses tunnel openings in the region of the twelve-membered rings and is closed where the openings of P^* lie, namely above the eight-membered rings. Both surfaces are topologically combined in the surface *PPJP-J* (Fig. 1r); however, their symmetry group is only $Pm\bar{3}m$. For the latter the $(Al,Si)O_2$ framework lies on the surfaces and all tunnel passages are open. Apparently all three POPS (PMS) belonging to the above mentioned symmetry branch describe in the same way the spatial separation of the different chemical interactions.

In the CaB_6 structure ($Pm\bar{3}m$, Fig. 2b) $Ca^{2\oplus}$ and the three-dimensional net of connected B_6 octahedra form two cubic primitive partial structures, which are separated by P^*. Here P^* apparently represents an inner surface, which to some extent centers the ionic interactions between $Ca^{2\oplus}$ and the electrons of the boron framework. Because of the larger expansion of the B_6 net into the volume, the curved surface also marks the area in which the weakest bonded electrons of the entire structure are found, namely those between the Ca and B atoms.[6] The important perovskite structure ($CaTiO_3$, $Pm\bar{3}m$) can be described analogously with the help of P^*.

At first glance the complicated α-Mn structure ($I\bar{4}3m$) seems to be somewhat obscure. A topological classification of different atoms is difficult for the element even though it is known that the four distinguishable crystallographic positions are occupied by Mn atoms of different magnetic moments. About 60 binary and ternary phases are known with this structure, and for a few of them exact structure information has been documented.

Obviously nature separates the four crystallographic positions in analogy to a POPS into such positions which lie close to the POPS (position 24(g), 24(g)) and into such which are further away (positions 2(a), 8(c)). As a result $A_{17}B_{12}$ structures are observed (A = Mg, Ta, Re; B = Al, Ta),[50] in which the more electronegative element often forms Friauf polyhedra (Fig. 2d) that are separated by P^*. However, in compounds like Ti_5Re_{24},[50] the electropositive element forms the Friauf polyhedra and occupies the positions on the P^* surface. The fragmentation of $Li_5Mg_{12}Al_{12}$[5] is an especially good example. Here Al forms the Friauf polyhedra, Mg occupies the surface, and Li lies in the cavities.

The metal cluster compound Nb_6F_{15}[52] (Fig. 2c) is an impressive example for two interpenetrating identical structures. The $[Nb_6F^i_{12}]$ clusters are linked via six bridging F atoms forming two independent three-dimensional nets ${}^3_\infty[Nb_6F^i_{12}]F^{a-a}_{6/2}$, which are inserted into each other just like a catena-compound. Mainly covalent forces predominate within the complex networks, but the interaction between the two independent nets is exclusively of van der Waals type. The linked clusters are large octahedra with triangular faces formed by six F atoms (Fig. 2c). Caused by the organization of the interpenetrating partial structures, two large triangular faces of neighboring cluster nets always meet in all cubic space diagonals, and they are separated by a layer of empty F_6 octahedra. This is the van der Waals gap, typical for layer structures, but in the present structure these layers change their orientation in space, going from one layer piece to the next. Therefore the Nb_6F_{15} structure is a non-euclidean layer structure whose van der Waals layers completely follow the course of the POPS P^*,[9] and again the highest occupied orbitals of the covalent bonded structure units are facing the P^* surface.

5.2. The D^* Surface

Up to now the D^* surface (Fig. 1b) is the only representative of the space group $Pn\bar{3}m$ and of the respective symmetry branch with the subgroups $Fd\bar{3}m$, $F\bar{4}3m$, $F4_132$, $Fd\bar{3}$, $F23$, $Fd\bar{3}c$, $F\bar{4}3c$, $F4_132$, etc. The large zeolite structure of faujasite ($Fd\bar{3}m$, $M^1_{57}Al_{57}Si_{135}O_{384}$[53]) can be understood with the help of D^*. The few isolated cations occupy cavities or at most tunnels while the covalent aluminosilicate network nestles closely to the surface. By doing this, the lone electron pairs of the O atoms are again aligned towards the surface in the direction of the cations.

The cubic Laves phase $MgCu_2$ ($Fd\bar{3}m$) is a typical representative of the intermetallic compounds. In Figures 2g, h the structure is shown together with the D^* surface. The Mg atoms center that partial space (Fig. 2h) which is enclosed by the green side of the surface. In the "blue" part the Cu atoms form a network of linked tetrahedra, and their centers set up a diamond structure which is equivalent to the arrangement of the Mg atoms. This structure is especially interesting, because it directly refers to the above discussed question about the splitting of point charges distributed at high symmetry positions into multipoles. If we choose for the generation of the POPS the real $MgCu_2$ structure ($Mg^{2\oplus}Cu^{\ominus}$, $D^{(2+)}_{(8a)} \wedge T^{(-)}_{(16d)}$) instead of the high symmetry ansatz ($Na^{\oplus}Tl^{\ominus}$, $D^{(+)}_{(8a)} \wedge D^{(-)}_{(8b)}$) then the resulting POPS hardly looks different. Therefore the splitting of the generating charges (cf. Section 4) into multipoles causes only marginal changes of the POPS! Apparent relations exist between structures formed by single atoms and structures formed by clusters, particularly because these often show the same basic patterns. Does the topological space partitioner therefore have a chemical meaning, too? In fact one can assume that the weakest bound electrons (in a metal the conduction electrons) reside close to the affiliated surface.[54] The expression 'interstitial' is almost a synonym for a weak bond with a flat course of the potential at points located *as far* away as possible from the atomic cores. Quantum mechanical investigations for this are in progress.

$Li_{21}Si_5$ is a γ-brass phase built of main group elements ($F\bar{4}3m$,[55] see Figs. 2i-l). The 416 atoms of the huge structure form as fundamental units 16 A_{26} clusters of two different types, namely $[Li_{22}Si_4]$ and $[Li_{20}Si_6]$. The centers of each of the eight clusters of both kinds form two interpenetrating structures of the diamond type. In other words, a NaTl structure of higher order (A_{26} clusters instead of atoms) is formed for which the D^* surface is likewise the space partitioner.[55] The periphery of the clusters is built by twelve Li atoms forming a cuboctahedron, and the mutual spatial arrangement leads to an interlocking of all cuboctahedra in such a way that all (!) these Li atoms lie on

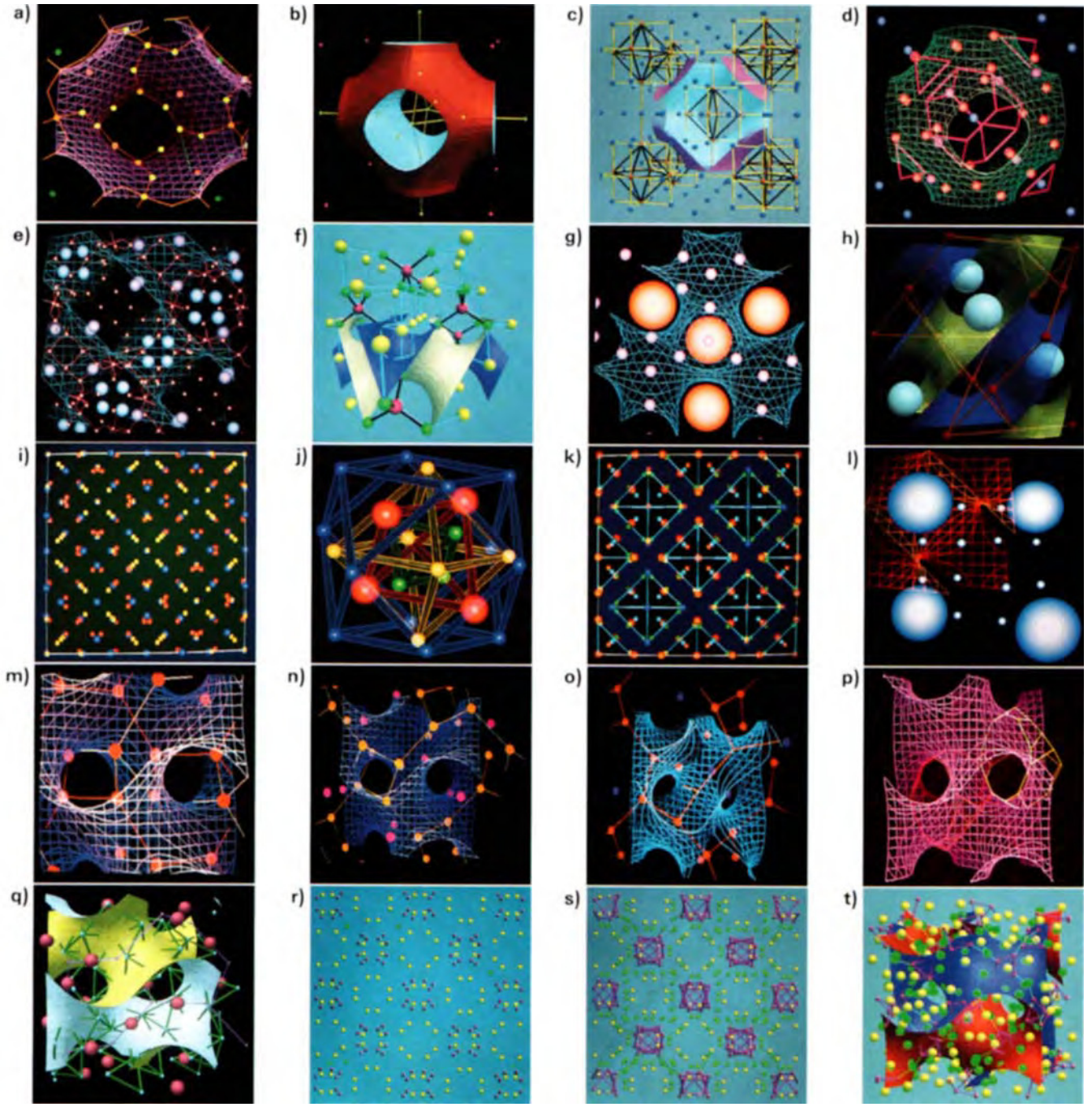

Fig. 2. Structures and POPS. a)–d) The surface P^*. a) In the sodalite structure (section of the cubic elementary cell) the aluminosilicate framework (yellow, red) lies on the P^* surface. Cl (green) and Na (not plotted, in the center of the cell) form a partial structure of the CsCl-type. b) CaB_6 is partitioned by P^* (red, light blue, transparent representation) into the boron framework (yellow, light-blue space) and the cation part (Ca, red). c) Nb_6F_{15} consists of two interpenetrating partial structures of $[Nb_6F_{12}]F_{6/2}$ clusters (Nb red, F blue) which are separated from each other by a "van der Waals skin". d) Partition of the α-Mn structure like in $Li_5Mg_{12}Al_{12}$ into Friauf polyhedra (Al pink, not complete at the corners of the cell), whose centers (Li blue) as well as the atoms (Mg orange) are located close to P^* (light blue).—e)–h) The surface D^*: e) In the zeolite faujasite the aluminosilicate network (red) reproduces the essential contours of D^* (blue). The large cations (e.g. $La^{3\oplus}$ light blue) fill the tunnels on both sides of D^*. f) Spinel in a perspective [110] projection. D^* separates the connected AlO_6-octahedra (blue, Al yellow, O green) from the partial structure of the MgO_4-tetrahedra (black, Mg red). g) The Laves phase $MgCu_2$ in [111] projection. D^* (blue) separates the Mg atoms (orange) from the Cu atoms (pink) that are connected to tetrahedra. h) $MgCu_2$ and D^* in another representation (Mg (light blue) in the green and Cu (red) in the dark blue space). i)–l) $Li_{21}Si_5$ and the surface D^*. i) $Li_{21}Si_5$; the projection of the elementary cell only reveals the $6\times6\times6$ superstructure of a cubic body-centered cell. j) The building unit of $Li_{21}Si_5$ is a 26-atom-cluster consisting of an inner tetrahedron (IT), outer tetrahedron (OT), octahedron (OH) and cuboctahedron (CO). k) Distribution of the clusters in the structure of $Li_{21}Si_5$ (half cell in the direction of viewing). l) The CO positions (small light-blue spheres) of all clusters are interlocked and lie on D^*, the cluster nuclei consisting of IT, OT, OH (large light-blue spheres) center the tunnels.—m)–t) The surface Y^{**}: m) Y^{**} (blue) partitions the γ-Si structure, a high-pressure modification of silicon, into helix-type systems (orange). n) In $SrSi_2$, one of the Si partial structures is missing and this part is replaced by the $Sr^{2\oplus}$ cations (red). The other Si partial structure remains virtually unchanged. o) A part of the β-Mn structure (red) exactly corresponds to the arrangement of the Si-atoms in $SrSi_2$. p) The Y^{**} surface (red) and a convex polyhedron (yellow) generated via the Dirichlet-construction. A dense packing of such polyhedra approaches the POPS (and PMS) in the form of facets [31]. q) The garnet structure (Ca red, O light blue, O octahedra and tetrahedra green, Al and Si center the O polyhedra on Y^{**}). The whole structure arranges itself in the form of non-euclidean layers around the graphs (violet) connecting the Ca cations (see also Fig. 6a). r) Projection of the complex structure of Ta_6Cl_{15} (Ta violet, Cl green, yellow) in which the separation into centers with clusters (Ta octahedra, red) and channels with van der Waals-packing of the Cl atoms already becomes perceptible. t) The centers of the Ta_6 octahedra lie on Y^{**}, while the Cl atoms form a dense non-euclidean packing on both sides of the surface.

the D^* surface, which acts as the topological space partitioner. The significance of this detail for the spatial distribution of the highest occupied orbitals is discussed in Section 8.

5.3. The Y^{**} Surface

From the highest cubic space group $Ia\bar{3}d$ originate two symmetry branches, the characteristic point configurations of which are Y^*, Y, V and S. The symmetry groups $Ia\bar{3}d$, $I4_132$, $Ia\bar{3}$, $I23$, $P4_132$, $P4_332$, P23 belong to the first group and only $Ia\bar{3}d$, $I\bar{4}3d$, $I2_13$, and $P2_13$ to the second. The combination $Y^*\{^{+}_{(8a)}\} \wedge Y^*\{^{-}_{(8b)}\}$ in $I4_132$ generates the POPS Y^{**} (Type 1, symmetry $Ia\bar{3}d$, see Figs. 2m–t), which is a surface of aesthetic beauty. Their counterpart is *Schoen*'s gyroid (gyros (Greek) = twisted) and was discovered stochastically about 20 years ago as one of the cubic PMS.[40] The particular difficulty for the derivation of this minimal surface is the absence of any euclidean frame (straight lines). The surface is exclusively spanned by flat points of $\bar{3}$ symmetry—that is an all-over open frame results, which lets any experiment with soap films fail! However the POPS Y^{**} is generated without special efforts; it can even be obtained in three different ways, namely by taking all three possible combinations of the PK's Y^* and V (cf. Table 1). It is true that the three generating potential spaces are different, but not the resulting POPS, and that again is a nice example for the minor influence of the splitting of a generating pole into a multipole (PK $Y^* \rightarrow$ PK V).

We would like to discuss a few structures in connection with the Y^{**} surface. Today, compounds with the garnet structure $Ca_3[Al_2Si_3O_{12}]$ ($Ia\bar{3}d$[56]) are important materials. Because of their extraordinary physical properties[57,58] they are used as opto-electronic color displays and as magnetic bubble memories for computers. The garnet structure seems to be complex and difficult to survey.[59] This is simply due to the fact that its topology is also subject to the complicated twists, which are characterized by the POPS Y^{**} and the gyroid respectively. In Figures 2q and 6a the garnet structure and the Y^{**} surface are mapped on top of each other. The immediate question arises, which divine principle distributes and orientates the AlO_6 octahedra in such a terrible-but-beautiful way. Guided visually by the space partitioning POPS, one recognizes at once that all atoms are arranged on concentric non-euclidean layers of increasing surface area (Ca < O < Al, Si). The $Ca^{2\oplus}$ cations can be connected via two interpenetrating Y shaped graphs. The first structure-chemical envelope of each graph is formed by the O atoms (or by their lone electron pairs) and the following envelope is the Y^{**} surface (with Al, Si) which already belongs to both Y graphs. Developing the curved POPS the coordination polyhedra of Al and Si (tetrahedra, octahedra) therefore form a non-euclidean double layer with more covalent bonds in the center and the lone electron pairs of the O atoms on the outer skin. One immediately gets the impression that the plastic insulation of a slightly angled copper wire with Y shaped knots could be a pattern for the POPS Y^{**}. In other words: One should be able to pack such plastic pieces to a space-filling cube!

Ta_6Cl_{15} is a fascinating example to demonstrate how in the space group $Ia\bar{3}d$, 336 atoms can be organized into a harmonic structure with a few positional parameters. In contrast to Nb_6F_{15} the $[Ta_6Cl^i_{12}]$ clusters form a single continuous 3D net $^3_\infty[Ta_6Cl^i_{12}]Cl^a_{6/2}{}^a$ (Figs. 2r, s), which follows the curvature of the Y^{**} surface (Fig. 2t). In both structures, the centers of the clusters are arranged according to a simple bcc structure.[59,60] A part of the Cl^i atoms lies on Y^{**}, almost desperately following its curvature in detail and therefore breaking the internal octahedral symmetry of the cluster. The other atoms envelop the surface and form a curved optimal non-euclidean sphere packing (Figs. 2t and 6d).

As further examples we mention γ-Si (Fig. 2m), $SrSi_2$ (Fig. 2n) and β-Mn (Fig. 2o), that is completely different materials. γ-Si is formed from a hexagonal high pressure modification of silicon by pressure release. Three of four Si–Si bonds either belong to one *or* to the other of the two 3D nets which exclusively extend in one *or* the other labyrinth of the Y^{**} surface. The fourth bond crosses the surface and connects both interpenetrating nets to the complete structure. Both threefold bonded partial nets are related to each other like left-handed and right-handed systems (Fig. 2m). In the $SrSi_2$ structure the Si atoms still form *one* of the partial nets of γ-Si, while the Sr atoms now lie in the second labyrinth (Fig. 2n). One might speculate whether the bonds crossing the Y^{**} surface are those which are most open to attack in the structure of γ-Si at all and consequently the most vulnerable in case of an electron transfer. However, this plausible assumption has to be proven by a quantum mechanical investigation. The structure is certainly highly strained, and only with great efforts can it be joined together from tetrahedral knots and flexible bonds (Prentice-Hall Model Kit, Minit Model System). However, the result can then be taken as that of an analogue computation (Structure Model Analogue Computer[61]). The three bonds in the labyrinths are extremely bent, and the intersecting bond is straight. Since the tension can *only* be released by lengthening of the least bent bond, the cleavage of just this bond seems to be necessary. It is noted that the transition of γ-Si to the polyanion $^3_\infty[Si^{\ominus}]$ refers to a special case in which a tetrahedral structure[62] develops a completely threefold bonded net by the removal of *half* of all atoms (3D net of neighboring defects[63]).

Nobody would assume that β-Mn has anything to do with γ-Si or $SrSi_2$. However, part of the Mn atoms (Fig. 2o) form a very similar partial structure to that of the Si atoms in $SrSi_2$. The others lie close to the Sr positions. It isn't misleading to assume a tendentiously similar polarization between both partial structures even for the β-Mn. Hence it follows that during the phase transition α-Mn ⇄ β-Mn, something like a disproportionation takes place (cf. Section 8).

5.4. The S^* Surface

Actually the S^* surface (Fig. 1d) was discovered at first as a POPS,[1] and just recently the corresponding PMS could also be established.[31] It is a surface of type 1 with

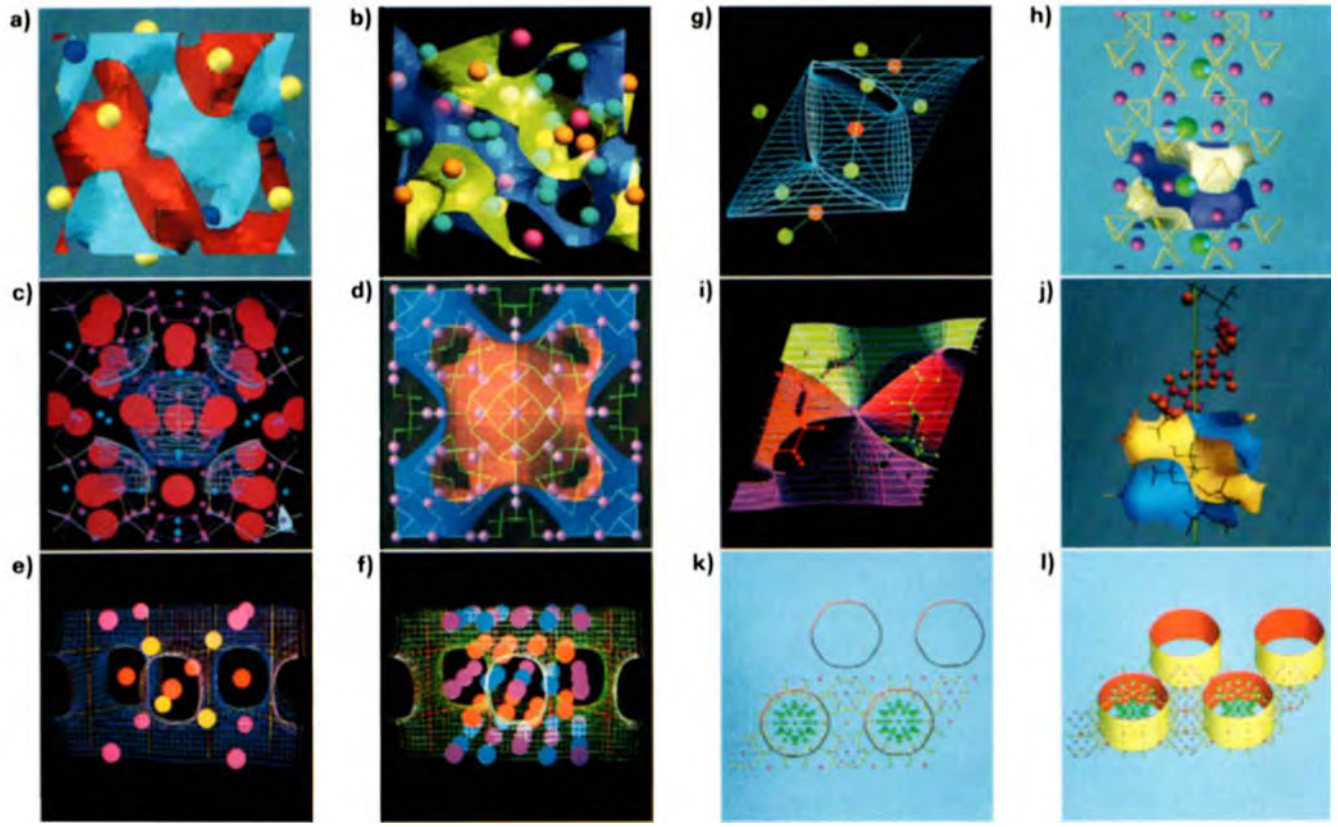

Fig. 3. Structures and POPS. a) The structure Th_3P_4 (Th yellow, P dark blue) and the surface S^* (light blue, red; only one half of unit cell is shown in direction of viewing). b) $Li_{14}MgSi_4$ (Li green-blue, Li/Mg orange, Si red; only one half of unit cell shown in direction of viewing). c) The clathrate-I structure (e.g. $K_8Ge_{44}\square_2$, K large red circles, Ge and □ small blue and violet circles, clathrate framework blue and violet lines) and the bubble surface *I-W* (blue). d) The complex structure of $BaCuO_2$ (Ba violet, Cu–O framework green) and the surface IP_2-J^*. e) $CdIn_2Se_4$ (Cd pink, In orange, Se yellow) and the surface $P_c^*I^*$ (blue, skew [100]-projection). f) $Cu_9Fe_9S_{16}$ (Cu blue, Fe violet, S orange) and the $P_c^*I^*$ surface (green, skew [100]-projection). g) Quartz structure (Si orange, O yellow-green, [001]-projection) and the surface Q^*. Si and O atoms center one of the tunnel systems, while the free electron pairs of the O atoms are directed through Q^* into the empty partial space. h) $CaSO_4(H_2O)_{0.5}$ (Ca violet, sulfate anion yellow tetrahedra) and the surface Q^* (light, dark blue, section around [00z] in the area of the double helix). Q^* separates the space of the $SO_4^{2\ominus}$ anions from the space of the $Ca^{2\oplus}$ cations, to which, the lone electron pairs are directed through Q^*. The H_2O molecules follow a wing of the helix (O green, H light blue). i) The double helix in the structure of α-amylose (red and green single helix) optimally follows the surface Q^* (violet and green wing); [001]-projection). The brown and the red wing mark the "van der Waals-skin" between the chains (see also Fig. 6b). j) The helix in α-amylose follows the different gradients on Q^* (yellow portion of the surface, black part of amylose, top: C red, O orange, H violet (small); [001]-projection). k) Zeolite L (Al,Si yellow, O green (small), H_2O green (large), cations red; [001]-projection) has large tubes containing the water molecules. The surface *P-G* (red hexagonal rings) distinctly changes its character (cf. Fig. 11) for the axial ratio $c/a = 0.408$ to a marked tubular topology. l) Oblique view of Zeolite L and *P-G* (red, yellow).

$Ia\bar{3}d$ symmetry and can be applied to structures of the symmetry $Ia\bar{3}d$, $I\bar{4}3d$, $I2_13$, and $P2_13$. It has the same flat points as Y^{**}, but in addition it also has straight lines (position 48g in $Ia\bar{3}d$; twofold axes). An important structure of suitable symmetry is the Th_3P_4 type (Fig. 3a). The eightfold coordinated Th atoms occupy a point configuration *S* and thus center one of the two tunnel systems, while the phosphorus atoms lie on the other side close to the POPS S^* and are coordinated from the direction of the thorium space. In this description the Th_3P_4 structure is a non-euclidean tube structure, in which two tunnel systems of Th atoms and of P atoms respectively interpenetrate without intersections. The S^* surface separates and connects both tunnel systems. The $Cu_{15}Si_4$ structure is a stuffed derivative of Th_3P_4 (Fig. 3a). It represents the basic structure type of a series of chemically unusual compounds, e.g. $Li_{15}Ge_4$, $Na_{15}Sn_4$ and $Na_{15}Pb_4$, for which one would actually expect the composition $A_{16}B_4$ with completely filled electron octet of the semi-metal. $H_{15}Th_4$ forms this structure, too, but now the B positions are occupied by the electropositive component.

The A atoms occupy two point configurations, namely the general position 48(e) and the position 12(b) in the space group $I\bar{4}3d$. The first one spans a multipole around one of the generating *S* PK's, the last one is the other PK of type *S* generating the S^* surface. On the other hand, the B atoms have the same PK as the P atoms of Th_3P_4 and therefore lie close to the S* surface which now separates both labyrinths of the A component. Whether this arrangement of the B component can "save" electrons, has to be studied in further detail. However, if additional electrons are offered to a phase like $Li_{15}Ge_4$, e.g. by replacing Li by Mg, salt-like Zintl phases of the same structure, like $Li_{14}MgSi_4$, are obtained[51] (see Figs. 3b and 6c). As expected, extended Hückel-calculations also show a distinct band gap at 16 electrons per formula unit.[54]

5.5. The Y^* Surface

This surface has $I4_132$ symmetry and was first discovered as a POPS. Recently, it was also shown that a corresponding and until now unknown PMS exists.[31] The Y^* surface has a remarkable property. It can be generated

from the two enantiomorphic space groups $P4_132$ and $P4_332$ and therefore exists in two enantiomeric forms ($^{-}Y^*$ and $^{+}Y^*$), but with the same symmetry. Only in the gyroid Y^{**} are both enantiomers united (non-euclidean mirror, cf. Section 5.3). Ag_3AuTe_2 is a structure with the Y^* surface as space separator. Due to the described symmetry conditions one can choose either to put the PK $^{-}Y^*$ *in the labyrinth* of a $^{-}Y^*$ surface or *on the enantiomeric* $^{+}Y^*$ surface. They both meet the symmetry, but more experience has to be gained to carefully consider the propositions of both representations. On the other hand, exactly such symmetry groups provide knowledge about "the Right in the Left" and vice versa.

5.6. The Surfaces IP_2-J^* and P^*J^*

Schoen's I-WP minimal surface[40] belongs to one of the very few surfaces discovered up to now which separate the space into two non-commutable and therefore different parts (type 2). The POPS IP_2-J^* corresponds to this surface (Figs. 1o, p). Both belong to the symmetry $Im\bar{3}m$ and separate the PK's I and J^* from each other (000, $\frac{1}{2}\frac{1}{2}\frac{1}{2}$ and $\frac{1}{2}00$ cyc., $\frac{1}{2}\frac{1}{2}0$ cyc.). They can be used for the analysis of structures of the symmetry branches $Im\bar{3}m$, $I\bar{4}3m$, $I\bar{4}32$, and $Im\bar{3}$. As an example the complicated structure of $BaCuO_2$ might be named.[64] The cavities around the PK I are filled by large spherical clusters, in which a net of square-planar coordinated Cu atoms encompasses a single Ba atom. Eight characteristic tunnels—their bounds are the generating elements of the entire surface, a "Wendehals" (turn-neck) of $\bar{3}$ symmetry—are centered by the eight pairs of isolated Cu_6O_{12} crowns surrounded by Ba atoms which lie close to the surface. Both structure parts lie together in the larger labyrinth. The smaller labyrinth is a four-armed tunnel system with a square planar tunnel cross and with extended flat points as bounds. Located in this labyrinth is that part of the $CuO_2^{2\ominus}$ partial structure which is distinguished by disorder.

The POPS P^*J^* belongs to the type 1 but has a certain relationship to the POPS IP_2-J^*, because it is also generated by a combination of PK's with different point charges (Table 1, Fig. 1q). Generators here are two interpenetrating equivalent partial structures of the ReO_3 type. This surface also has $Im\bar{3}m$ symmetry, is generated in $Pm\bar{3}m$, and can be related to the so-called Neovius' surface.[65] The special property of this surface is the appearance of enveloped areas of completely different extension (Fig. 3q), a consequence of the different charges on both sides used for the generation of the POPS. Because both substructures are topologically identical, P^*J^* divides the space into two equal halves.

The larger cavities show twelve exits to the neighboring small cavities, and each of these has four tunnels in square planar arrangement to the large cavities. The surface P^*J^* (and the Neovius' PMS) is a complementary surface of P^* (*Schwarz*'s "P" surface), because the tunnels of P^* are closed by the extended flat points of P^*J^*, but for that twelve saddle points of P^* are opened. An example is the simple Mg_3NF_3 structure. Here P^*J^* separates the cations from the anions and therefore again describes an internal surface.

5.7. The Bubble Surface I-W

The surface I-W (Table 1) is discussed as an example of a non-connected POPS (general context cf. Section 3.3). It is generated by the distribution of charges onto the positions of the Cr_3Si structure (A15). Therefore, these positions are trivially located in both partial spaces with the minority component in the bubble (Fig. 1t). Apparently, bubble surfaces are typical for the generators $A^{n+} \wedge nB^{1-}$ with $n \geqq 3$. Surprising is the topological correspondence of these POPS I-W with the framework structure of the clathrates-I,[2] whose atoms, with one exception, lie on the surface. In defect clathrates (e.g. $K_8Ge_{44}\square_2$, Fig. 3c) the only position off the surface is exactly the location of deficiencies.[66]

5.8. The Surfaces F^*, W^* and E^*

These surfaces are distinguished by a complete enclosure *of all* generating points (Figs. 1g–i). The consequences for an understanding of very polar structures was already discussed previously.[2] The NaCl structure is the typical representative for F^*, while for W^* and E^* no simple examples are known. This is probably due to the coordination properties in these arrangements. However, there are filled-up derivatives in which there are polar centers as parts of a predominately non-polar structure separated by W^*.

5.9. The Quartz Surface Q^*

At this stage it should be pointed out again that the *generation* of POPS has *nothing* to do with real structures, which could possibly be assigned to the generating charge distribution. In particular, the "quartz surface" has nothing to do with the quartz structure except for the symmetry group and the axial ratio c/a, a free parameter. This remark is important, because we would like to show that the Q^* surface is an adequate space partitioner for SiO_2 as well as for α-amylose. Q^* is generated in $P6_222$ ($P6_422$), has the symmetry $P6_422$ ($P6_222$) with $c' = c/2$, and belongs to type 1. It was the first POPS of hexagonal symmetry,[1] and, during the calculation and representation, information about the general topology was obtained which later on allowed for the derivation of the extraordinarily important equivalent PMS,[67] because Q^* has a euclidean frame. This surface represents a novel variant, which in many respects exhibits special features. Q^* contains two surface regions which can serve as topological models for two different helical systems (Fig. 1j) and are centered by 3_1 axes and 6_2 axes in the ratio 2:1. The combination of these symmetry elements generates intersections, i.e. intersecting lines of surfaces, if the symmetry elements lie on the POPS (or PMS). Areas with 3_1 screw axes avoid the intersections, because the surface does not actually touch the helix axis, but winds around it—even if hardly noticeable. The corresponding region of the surface can, on the one hand, be understood as an equalizing (average) surface of a helix and, on the other, as the partitioning surface of two helices. In contrast to this, an intersection line lies in the center of the second screw type, coincident with the 6_2 axis. In

addition to this combination of a helical surface and double helix, the POPS Q^* has a further property of general meaning for structural chemistry. Q^* divides the space into two *four-armed* labyrinths, which is an unexpected feature for the hexagonal symmetry. However, it corresponds to the properties of the point configuration Q.[68]

In the structures of high-quartz (β) and low-quartz (α) the SiO_4 tetrahedra form a 3D network $^3_\infty[SiO_{4/2}]$ for which the four-armed feature of the Q^* labyrinths is tailor-made. At the same time, the tetrahedral network belongs to all three helical areas, which are in a certain way linked by the POPS Q^* as a common skin (Fig. 3g). All atoms lie *in one* of the partial spaces which are separated by the POPS. In $BaZnO_2$, a stuffed derivative of the α-quartz structure,[69] the corresponding atoms of the polymeric anions $^3_\infty[ZnO_2]^{2\ominus}$ lie in one labyrinth and the $Ba^{2\oplus}$ cations in the other. The O atoms are located exactly at the necks of the labyrinths, and concerning the scale of the interatomic distances it is clear that their lone electron pairs should almost lie on Q^*. Therefore, the free labyrinth in α-quartz is also a non-euclidean layer structure with exclusively van der Waals interactions. The $BaZnO_2$ structure contains cations intercalated in this labyrinth, and the surface Q^* now acts so to speak as a donor.

Calcium sulfate hemihydrate $CaSO_4(H_2O)_{0.5}$[70,71] does not have much in common with α-SiO_2 in a purely chemical sense. The two structures merely crystallize trigonally in the same space group with a similar c/a ratio. They become comparable through the POPS Q^* common for both structures. The $SO_4^{2\ominus}$ anions fill one partial space, whereby the modified orientation of the tetrahedra (90° compared to SiO_2) provides optimal distances between the O atoms of neighboring $SO_4^{2\ominus}$ groups. The O atoms now lie close to Q^*, and from Figure 3h there is hardly any doubt that their lone electron pairs are directed through Q^* towards the $Ca^{2\oplus}$ cations in the other partial space. Therefore Q^* divides the space in SiO_2, $BaZnO_2$ and in $CaSO_4(H_2O)_{0.5}$ into two parts of different interactions. The H_2O molecules finally squeeze themselves into the tight area of the intersections of Q^* (6_2 axis) and are therefore able to form hydrogen bonds for two parts of the $SO_4^{2\ominus}$ labyrinth and coordinate $Ca^{2\oplus}$ in two parts of the $Ca^{2\oplus}$ labyrinth (Fig. 3h).

From the structures treated so far, one continuously has the feeling that adequate things are combined with each other, e.g. P^* with CaB_6 and sodalite, or D^* with $MgCu_2$ and faujasite, or Q^* with quartz and gypsum. The compounds are inorganic, and the surfaces would more likely be assigned to the non-organic objects, just for once using common short terms for things of importance and unimportance—not to mention the bio-aspect.

With α-amylose Nature presents us a welcome interdisciplanary example for the extensive and obligate rules which symmetry imposes on all things that attempt to organize themselves in the solid state. The α-amylose impressively reveals the role of POPS and PMS as a continuous mediator between local and collective forms. This very large organic molecule crystallizes in three forms (α, β, γ), which are distinguished by their water content. The α-form crystallizes orthorhombically; however, the axial ratio and the presently known details of the structure[72–74] show a surprisingly close relationship to high quartz. In particular the amylose molecules follow the 6_2 axis as double helices (if idealized), and, in a natural way, through their quasi-hexagonal rod packing, generate intermediate areas with two 3_1 screws in which the unsettled (but presumably also helical) water structure is built up. In Figures 3i and 6b a part of the presently known partial structure of the α-amylose together with the POPS Q^* is shown. (Q^* was fitted to the dimension of the α-amylose by merely applying a minimal distortion of the mean hexagonal c/a ratio, namely a pseudo hexagonal angle $\gamma = 112.5°$ and by introducing *one single* scaling factor.) With surprising precision the surface area around the 6_2 axis characterizes the mean helical surface of the gigantic molecule intersecting the centers of the glycosidic six-membered rings. One should bear in mind that no uniformly curved helix is present, but rather that steep and flat parts alternate! Because of the polar screw axes, structures can be fitted into the Q^* surface in steps of $c/6$. Therefore the gigantic molecules of the α-amylose can either be centered *on* Q^* (as mentioned above) or they are centered *between* two successive subspaces (Fig. 3i). With this second equivalent representation Q^* forms approximately the "van der Waals skin" of the amylose chains.[72]

At some time in the course of the enzymatic construction of amylose chains, bifurcations develop on the primary helices, which then begin to wind up in the neighborhood of parallel secondary helices (in the present model neighboring 6_2 screws of the rod packing). Until now there is nothing known about the structure of these interconnections. However, we expect with the knowledge of the Q^* surface that the marked saddles of Q^*, which appear between the 6_2 screws, carry the connecting glycosidic unit (and/or are "enclosed" by them). In any case, a model structure yields an extraordinarily satisfying interconnected structure with respect to symmetry spatial expansion and orientation.

For biochemistry another aspect might still be of importance.[75] The Q^* surface gains its special features from the combination of double helices and simple screws in the ratio 1:2 (cf. above). Precisely this ratio is typical for the composition of muscular fibers with the building units myosin (large double helix) and actin (small helices). One might imagine that in the course of the contraction, these different helical structures move against each other, controlled and mediated by the suitable space partitioner Q^*.

Finally, there is another general aspect of this remarkable surface which essentially deals with the translational symmetry, through which certain symmetry elements are generated half-way to the translational identity quasi from nothing. In this way, all symmetry elements appear again after one half rotation (because of the double helix $\pi/2$), suited to wind a second double helix of the same kind or of a different kind (e.g. a helical water structure). A close packing of double helices comes close to a hexagonal rod packing, and again this arrangement produces by translation the above mentioned *two* additional helical areas in the interspace (centers of triangles), and it naturally also produces intersections of the space partitioning surfaces. In general the Q^* surface is, therefore, the space separator for "successful" rod packing of double helices. Not much is changed concerning the principal topological properties,

even if neighboring double helices are out of phase with regard to their windings.

5.10. The Hexagonal *P-G* Surface

The fundamental type of this POPS can be directly compared with the PMS *H'-T* (*Schoen*[40]). Especially in this case, with the help of POPS (Fig. 1k) the dominant influence of the axial ratio *c/a* can be studied. For $c/a \approx 0.5$ the POPS consists of modulated tubes along *c*. In the zeolite structure ($K_6Na_3Al_9Si_{27}O_{72}H_2O$[77]) with $c/a = 0.41$ the aluminosilicate framework fills the area between the tubes. In the tubes the water molecules (large tube) and the cations are distributed according to the modulation. At $c/a \approx 0.9$ the POPS *P-G* is very similar to the PMS *H'-T* and forms a 3D labyrinth with wide and narrow necks along *c* (ratio 1:2). With $c/a \geqq 1.05$ the necks tear off and the two-dimensional character now corresponds to the AlB_2 structure (cf. also BN).

This width of variation of the POPS *P-G* with *c/a* permits the modelling of completely different structure branches, a capability which the PMS do not have to that extent.

5.11. The Tetragonal Surfaces ${}^{v}D^*$ and $P_c{}^*I^*$

The two POPS apparently obtain their topological type independent of the axial ratio *c/a* — a very important property. For $c/a = 2.0$ and $1/\sqrt{2}$ they correspond to the already known PMS D_T and *CLP*, respectively (*Schoen*[40]). The POPS ${}^{v}D^*$ (Fig. 1n) separates at $c/a = 2\sqrt{3}$, inter alia, the substructures of α-$ThSi_2$. The Th atoms occupy the centers of one labyrinth, while the 3D net of the Si atoms fills the other. Two Si atoms form poles (PK ${}^{v}T$) around the PK ${}^{v}D$, which is equivalent to Th (Fig. 3b). ${}^{v}D^*$ is discussed in Section 8 in connection with the unusual electron density distribution of Cs-IV. With $c/a \approx 2$ the ${}^{v}D^*$ surface separates the partial structures of scheelite $CaWO_4$ into $Ca^{2\oplus}$ and $WO_4^{2\ominus}$, or those of anatase TiO_2 and $LiInO_2$.

Approximately 20 different crystal structures correspond to the POPS $P_c^*I^*$ (Fig. 1m, PMS *CLP*). In most cases the following holds true: 1) the anions always occupy the position of the largest curvature at the intersection point of twofold axes; 2) in complex structures, polyhedral splittings are found around the same positions, e.g. in $Cu_9Fe_9S_{16}$;[78] 3) the ratio *c/a* almost does not influence this arrangement of cations and anions; 4) the cations lie in both labyrinths, which are arranged in crosswise stacked tubes (Figs. 3e, 3f).

6. POPS and Dynamical Processes

After investigating numerous crystal structures, for which very close relationships between structure elements and zero-potential surfaces occur, we are encouraged to use this instrument to investigate other phenomena than pure structural phenomena. Even if the surfaces PEPS and POPS are used as relatively easily accessible substitutes for the PMS, they nevertheless represent definite physical quantities, which contain an important aspect of the kaleidoscope of all interactions in real structures. PEPS and POPS are based on quite a simple potential ansatz, however they are particularly suited for our purpose to demonstrate the general influence of the symmetry on the topology of structures. Just the really simple ansatz for the individual allows to demonstrate in an exceptionally clear way the influence of the collective—which no member of a structure can escape. Therefore, when interpreting physical properties we concentrate on the global topological links without forgetting that each substitution of an atom by another one or by a defect generates a local change in the structure. Only when such local changes are very large does one expect a phase transformation, i.e. another symmetry then optimally joins the units together.

Earlier we pointed out the fact that the $Ag^{\oplus}$ ions in the optimized ionic conductor α-AgI ($Pm\bar{3}m$,[76]) are located on the POPS P^*. It is noted that the silver ions apparently do not occupy the largest interstitial positions on the face centers of the cubic unit cell, but rather those indicated in Figure 4a. These are the locations of the highest probability density, which is depopulated with increasing temperatures for the benefit of other positions. So far we have not found exact information in the literature about the trace of the hopping paths, nevertheless we do not believe that these are straight lines, as is often suspected. Rather they should follow the POPS's curvature as in PbF_2 and β-eucryptite (cf. below). What relationship does the POPS P^* have to the hopping paths of the silver anions in a cubic body-centered partial structure of $I^{\ominus}$ ions? The largest gradients that are "felt" by a positively charged particle on a POPS, are always perpendicular to the surface and point in the direction of the anions. By definition, no potential changes and also no gradient occur along the POPS. However the occurrence of preferred positions for $Ag^{\oplus}$ means that gradients along the surface are present in β-AgI. The reason for this still needs to be clarified. But it is clear that the curvature of the POPS is maximal at the favored positions i.e. the neighboring equi-potential surfaces follow one another very closely.

At higher temperatures NaOH (NaOD) forms the CsCl structure, in which the $OH^{\ominus}$ ions apparently behave spherically symmetric. This high symmetry is produced by a dynamic orientational disorder. As far as the preferred orientations of the dipoles are concerned, it might be said, that the H atoms should rarely point in the direction of the space diagonal ($Na^{\oplus}$), but should prefer the orientation along the cubic axes. By means of neutron diffraction it was shown[79] that precisely this arrangement, which appears to be optimal, is completely avoided, and, instead, orientations of the D atoms follow a probability distribution which reproduces the basic features of the POPS P^* suitable for the symmetry of the CsCl structure.

Here, we again refer to the fast ionic-conductors PbF_2 ($F^{\ominus}$ conduction) and ZrO_2 ($O^{2\ominus}$ conduction)[80,81] both having the CaF_2 structure. Some time ago the controversy whether the hopping $F^{\ominus}$ ions in PbF_2 prefer to occupy the favorable vacancies of the structure ($\frac{1}{2}\frac{1}{2}\frac{1}{2}$ fcc) or not was settled with the experimental determination of the $F^{\ominus}$ hopping paths.[82] On their diffusion path they follow the topology of the POPS *F* (CaF_2; cf. Table 1 and Fig. 4e). This

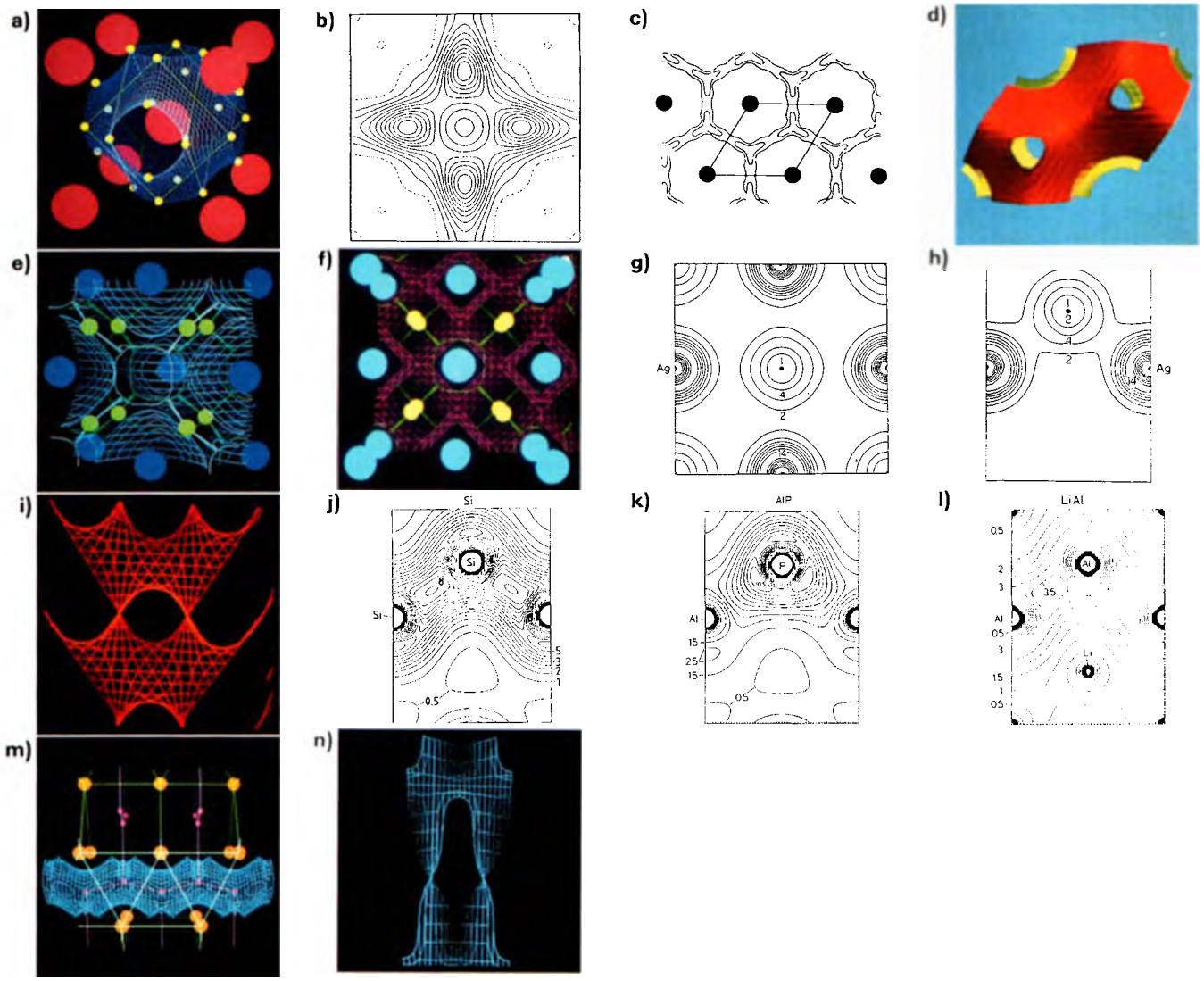

Fig. 4. Ionic conduction and electron density distribution. a) The $Ag^{\oplus}$ ions (yellow) in α-AgI ($I^{\ominus}$ red) lie on P^* (blue). b) Experimentally determined electron density for the surface $(x, y, 0)$ [76]. c) Electron density distribution of $Na^{\oplus}$ ions in (001) plane of β-eucryptite [83, 84]. d) The surface P-G partitioning the space of the cation partial structure (yellow) and of the O atoms (red). e) The bubble surface F-P_2 (blue) and the $F^{\ominus}$ ionic conductor PbF_2 (Pb dark blue, F light green, experimentally determined hopping paths [82] green). f) A negative PEPS (violet) which only leaves opened narrow tunnels between $F^{\ominus}$-$F^{\ominus}$ (yellow) and $Pb^{2\oplus}$-$Pb^{2\oplus}$ (light blue) through which the paths of the anion movement proceed. g, h) Calculated electron density distributions for AgI [95]. In the NaCl structure (g) only almost spherical densities appear; in the zinc blende structure (h), on the other hand, distinctly polarized densities occur. i) The surface D^* with a (110) section. j)-l) Calculated electron densities ((110) sections) for silicon [101], AlP [98] and LiAl [99] between the atoms the densities follow the local circumstances. In the interstitial range the equi-density lines follow D^*. m) Structure and calculated valence electron density (blue) for the high pressure modification Cs-IV (yellow) [105]. The positions of the Cs atoms correspond to the positions of the Th atoms in $ThSi_2$ (Si violet). The highest densities are found in the range where they are observed in $ThSi_2$ too, along the Si chains. n) A part of the "D^* surface with a tunnel structure corresponding to the density distribution.

zero-potential surface is not an interconnected unit, but forms isolated bubbles around the $M^{2\oplus}$ poles, whose outer shape has flat regions related to a formation of octahedra ($m\bar{3}m$). Only the following neighboring PEPS in the negative partial space form increasingly closed surfaces between the positive and negative poles. One of these surfaces finally comes close to the form of connected tetrahedra (around $F^{\ominus}$) and octahedra (around $Pb^{2\ominus}$). The topological development of the PEPS and the experimental $F^{\ominus}$ hopping paths are clearly correlated. Both correspond optimally where the largest distance to the neighboring ions is reached, e.g. in the area of the "neck" connecting the $Pb^{2\oplus}$ in the center of Figure 4f. Obviously the $F^{\ominus}$ ions try not to "descend", or also not to "ascend" in the potential of the neighborhood while hopping. In any case, they circle around the "favorable" potential holes at $\frac{1}{2}\frac{1}{2}\frac{1}{2}$ etc.! This example also follows the general trend, which we would like to demonstrate with the help of the POPS.

β-Eucryptite $Na_xAl_2O_3$ (Figs. 4c, d) is famous for its properties as a $Na^{\oplus}$ ionic conductor and has been studied extensively.[83, 84] Reliable information about the paths of the hopping $Na^{\oplus}$ ions come from diffraction experiments. *Schoen*'s H'-T surface[40] belongs to the matching symmetry branch and is topologically equivalent to the POPS P-G (Table 1). The POPS P-G is generated by a charge distribution of the AlB_2 structure type, and it partitions the space in non-commutable labyrinths. The $O^{2\ominus}$ partial structure of β-eucryptite lies in one part and the cations $Al^{3\oplus}$ and $Na^{\oplus}$ in the other, with the latter ones one upon the other along the c-axis (channels). With its tunnel system the sur-

face models the optimal paths of the hopping ions (the tunnels themselves are "blocked" by $Al^{3\oplus}$), and in this structure the POPS can be regarded as topological approximation of the inner surface of the $O^{2\ominus}$ anion in the crystal.

7. POPS and Phase Transitions

Second order phase transitions proceed continuously without activation and often have extended induction periods. Structural changes can be very easily observed, because the transformation takes place without destoying the crystals. The local motions of the atoms and especially their coordinative variations refer directly to the reaction paths in molecular reactions. With first order phase transitions the circumstances are complicated. On the one hand, at T_c, two separated and principally different solid phases are in equilibrium, and therefore there is no need for any structural relationships between the two. On the other hand, local structural changes are frequently observed in such transitions when approaching T_c, which show all the important synonyms of cooperative second order transformations. Only at T_c each reference is lost between the beginning- and end-states, because no symmetry relationships are necessary according to *Landau-Lifschitz*. For the phase transformations, the discussion can be limited to thermodynamic variables of state as a driving force; hence, one is always on the safe side. On the other hand, chemists show a preference for kinetic pictures. They "know" exactly when and why such bonds open and close, at least in molecules. While in the first case one retreats to the space of the observables—it is the reciprocal space—one acts in the second case freely and easily in the real space of the surrounding objects. Especially here the cooperative is not easily examinable, and therefore all efforts are concentrated on the local process. We believe that at least in the crystalline phases the POPS (and PMS) can bridge the gap, because they are a part of the real structure, however they describe the global characteristics of collective forms of organization. Thus, it is not surprising that the POPS reveal details during the process of phase transformations, which seem to be in obvious contradiction to the local variations at positions which are occupied by atoms.

First of all, we analyzed how the POPS react to changes of symmetry, and how they behave at phase transformations. Often principal topological changes in the POPS occur regarding the number of tunnels (genus of the POPS, cf. Section 3.4) and their position to each other. Even a complete break off of the continuous surface in one, two or three directions can occur, which leads to forms that are characteristic for layer structures, one-dimensional arrangements, and locally more or less closed systems.

For the transition between the CsCl and NaCl structure there are several models,[86,87] which we only partly have pursued with POPS. Even though it concerns a transition of first order, as discussed in the following, it can be regarded as a continuously proceeding mechanism, in which the interface between the phases moves through the structure. For this, both cubic structures are set up trigonally along the space diagonal. This has the advantage that the positional parameters do not change during the transition and the entire relative shift of all atoms can be described by one single parameter, namely by the axial ratio c/a: $CsCl \triangleq \sqrt{3/2} = 1.2247 \leqq c/a \leqq 2.4495 = \sqrt{6} \triangleq NaCl$. As c/a increases the symmetry groups $Pm\bar{3}m$, $R\bar{3}m$, $Fm\bar{3}m$ are passed through, i.e. only both terminal members are cubic, while the phase transition itself proceeds under rhombohedral symmetry. The calculations for this simple process show how differently the changes act *locally* and *globally*. Looking at the potentials on the positions of the point charges (via the Partial Madelung Factors[88,89] they supply the Madelung Part of Lattice Energy MAPLE according to *Hoppe*[90]), one immediately gets the impression that the NaCl structure is maintained for wide regions of c/a, before the CsCl structure almost appears as a singularity.[91] However, the topology of the affiliated POPS as a measure for the course of the potential *between* the ions behaves completely different. *All* rhombohedral intermediate stages belong to a six-armed tunnel system (genus = 3) which is *continuously* modelled from the P^* surface that is typical for CsCl (Figs. 5a-j[92]). Only the tunnel cross sections become increasingly narrow, and they change from almost circular to small slit-shaped graphs and finally close to cube edges, typical for the F^* surface (Table 1, Figs. 5g, h). Now the topology of the NaCl surface F^* is a singularity which can only be established accurately with the correct c/a ratio. If one looks again at the last step before reaching the NaCl structure it can be seen that each time six of the cube edges open the one partial space, and six edges open the other partial space. Close to the POPS, as 'inner surface', these atoms touch each other, and here the outer electron shells are located, which easily can be polarized. With minor distortions produced by lattice vibrations tunnels are opened in the NaCl structure, and thus polarization is induced which is able to drive the phase transition.

If c/a is increased and exceeds the value $\sqrt{6}$, then immediate neighboring cube edges open to form puckered layers perpendicular to the trigonal c axis, and a POPS with the characteristic topology of a layer structure develops. Indeed for $c/a > 2.45$ the typical layer structures are found, like e.g. α-$Zn(OH)_2$ (2.51), Bi (2.61), Sb (2.62), As (2.81), α-Ga_2O_3 (2.70) etc. The structure of bismuth together with the POPS R^* ($c/a = 2.61$) is shown in Figure 5j. The correlation between structure and surface requires no further comments.

By maintaining the cubic symmetry a continuous transition can be demonstrated for the POPS P^* and Y^{**}. For this one generates in the space group $P2_13$ with the PK $FY1xxx$ according to ($FY^{(+)}_{(4a)}[x]$, $FY^{(1+)}_{(4a)}[x+1/2] \wedge FY^{(1-)}_{(4a)}[x+1/4]$, $FY^{(1-)}_{(4a)}[x+3/4]$). The transition occurs by the selection of x. P^* develops for $x = 0$, the gyroid Y^{**} for $x = 1/8$. The point configurations change from a F-type into a Y-type, and at the same time the tunnel system of the resulting POPS continuously changes from a six-armed (P^*) into a three-armed (Y^{**}). In Figures 5k-p it can be seen clearly how the F^*Y^* surfaces change little by little and finally lock into the higher symmetric POPS. The generating operation by the way is a remarkable structural chemical procedure. By variation of x the components of an interpenetrating fourfold rod packing, that is non-crossing

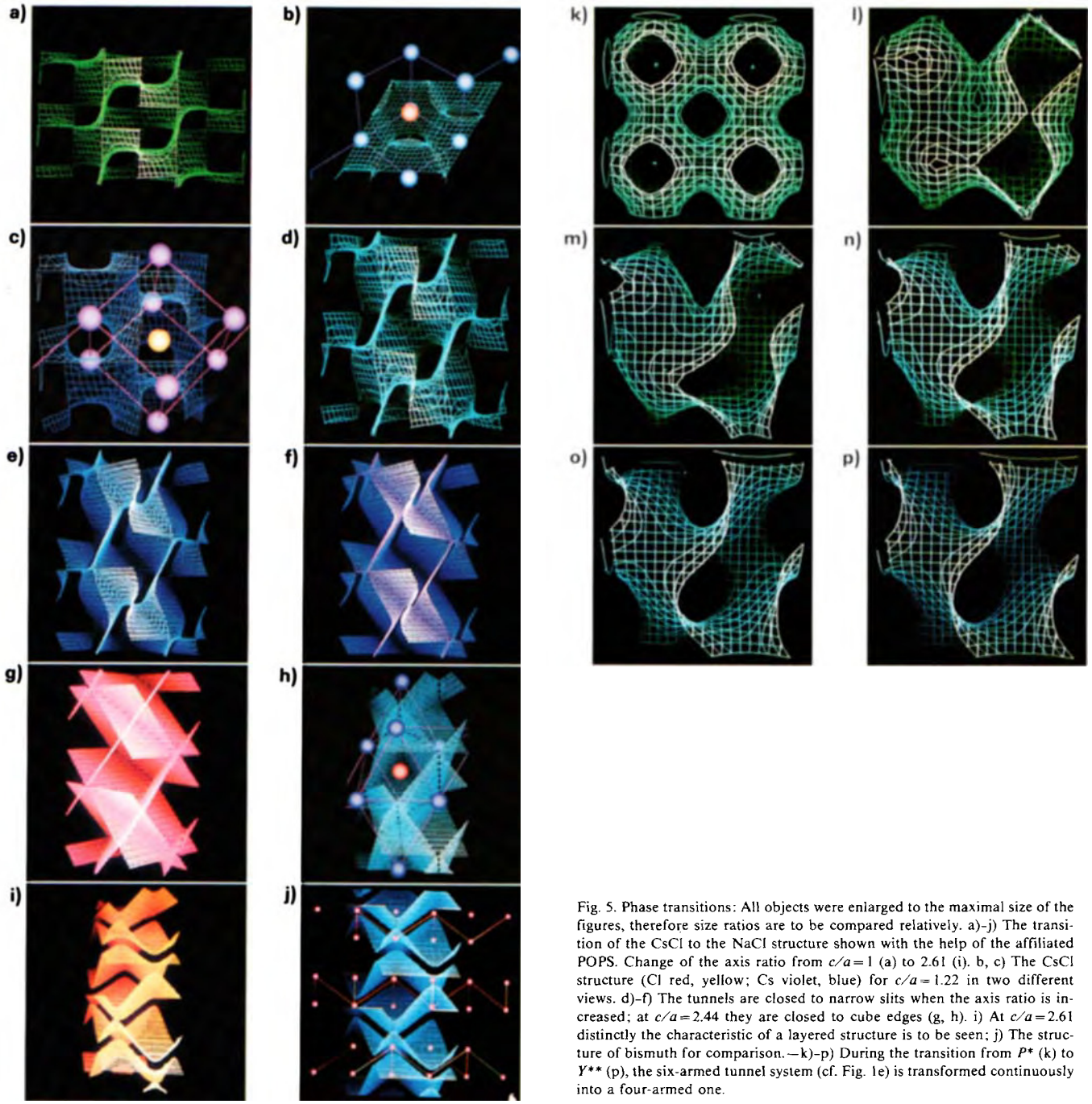

Fig. 5. Phase transitions: All objects were enlarged to the maximal size of the figures, therefore size ratios are to be compared relatively. a)–j) The transition of the CsCl to the NaCl structure shown with the help of the affiliated POPS. Change of the axis ratio from $c/a = 1$ (a) to 2.61 (i). b, c) The CsCl structure (Cl red, yellow; Cs violet, blue) for $c/a = 1.22$ in two different views. d)–f) The tunnels are closed to narrow slits when the axis ratio is increased; at $c/a = 2.44$ they are closed to cube edges (g, h). i) At $c/a = 2.61$ distinctly the characteristic of a layered structure is to be seen; j) The structure of bismuth for comparison.—k)–p) During the transition from P^* (k) to Y^{**} (p), the six-armed tunnel system (cf. Fig. 1e) is transformed continuously into a four-armed one.

stacks, are shifted.[9] The displacement of the rod shaped components is polar along the four cubic space diagonals. Only at $x = 0$ a *local* cubic symmetry is obtained. In the remaining range $0 < x \leqq 1/8$ only the *global* symmetry is cubic, but the local symmetry is at most trigonal! An interesting example for this transition would be the transformation of the Nb_6F_{15} structure into the Ta_6Cl_{15} structure (which unfortunately has not been observed yet). Although in both structures the M_6X_{12} clusters are linked to six other M_6X_{12} clusters, in Nb_6F_{15} a system of two interpenetrating nets is present, while in Ta_6Cl_{15} all clusters are connected directly or indirectly to a common net (cf. Sections 5.1 and 5.3). The transformation would have to be accompanied by a drastic change of the network but could topologically still be forseeable.

It should be mentioned that a continuous transition from Q^* to P^* is possible. A four-armed tunnel system is transferred into a six-armed one by removal of the intersections in the space partitioners. Both compounds $BaZnO_2$ and $CaTiO_3$ exemplarily show that there are important relations to be discovered between perovskites and defect perovskites with statistical defect distribution on the one hand and ordered and reorganized defect distribution on the other.

Such investigations could become important, if successive cooperative displacements of a large number of atoms (which lie e.g., on the POPS) are to be described by a few parameters, just as are needed for the generation of POPS. A nice example is the investigation of martensitic transformations with the help of D^* and Y^{**} as were carried out

by *Andersson* and *Hyde*.[22] The authors look at the PMS and not the POPS. For the PMS a mathematical transformation exists, the so-called Bonnet transformation,[94] in which no changes of lengths appear on the surfaces, but the angles do. One can think of it as a surface of chain links which doesn't allow compression and expansion (knight's chain mail). The Bonnet transformation is derived from a representation of the surface in the complex Gaussian plane, and consequently in certain cases a further reduction of the number of parameters is possible. In the present case therefore not even the definition of a fixed-point in real space is necessary. That is, during the transformation all the atoms shift at the same time and continuously against each other—apparently a very realistic description of the actual processes.

8. Electron Density and POPS

In structures with small unit cells there are only a few atoms, mostly at special positions. Direct relationships to the POPS and PMS can hardly be seen, because the atoms are often subjected to the high local symmetry and are not able to follow the global forces of the entire arrangement. On the other hand, exactly these structures present themselves for the investigation of very fine structural details, as, e.g., the formation of specific electron density contours of the different atoms under the influence of the symmetry (e.g., in homoemorphic series).

The surfaces F^* and D^* (Fig. 1, Table 1) differ drastically. F^* consists of a space-filling pack of closed cubes—each center of the cubes is therefore surrounded by a closed "cube skin"—while for D^* a four-armed "tetrahedral" tunnel system is typical. AgI and AgBr appear in two modifications, namely the NaCl structure and the ZnS structure.[95,96] How will the electron density distribution adapt to both of these crystal fields? 50 years ago, *Brill* et al. carried out directive experiments[97] and until now in principle nothing has changed in their statement. In the NaCl structure essentially spherical electron densities are found around the atoms (Fig. 4g) and this corresponds to the concept that the atoms are optimally shielded from each other and are surrounded by a closed POPS (F^*). In contrast to that the compounds having the ZnS structure (blende) clearly show a direction-dependent density distribution,[95] which as expected extends in the direction of the tunnel opening of the D^* surface. In this connection the inspection of the valence electron densities obtained in quantum mechanical calculations is impressive for such analogues of the diamond structure and its partial structures (Si (Fig. 4j), LiAl (Fig. 4l), LiAlSi,[98–101] LiZnAs).[102] In all cases the electron density on the short connection lines (chemical bond) is increased but very differently according to height and shape. This is to be expected because of the substantial differences between the investigated systems. However, the electron density is almost equal or at least more similar on the interstitial range for all the compounds (Fig. 4) and its progress is as if the electron density was modelled onto the D^*-surface in this range. Obviously there are areas in the structures in which the global overall symmetry gains the greater influence over the localized central forces of the atoms. How strong this collective effect finds its expression in different structures can't be estimated yet.

However, one thing seems to be well established, namely that structures with a trigonal-prismatic arrangement preferably 'house' d-electrons. We will illustrate this with the example Cs-IV, a high pressure modification of cesium. At a pressure of 44 kbar a tetragonal structure with the relative volume $V/V_0 = 0.39$ is formed,[103] in the picture of *Biltz*'s volume increments, this corresponds to $Cs^{\oplus}$.[104] Despite the enormous collapse in volume, none of the usual 'dense packings' are realized, but a packing of trigonal prisms directly comparable to the arrangement of the Th atoms in α-$ThSi_2$. In their publication the authors themselves recognized neither the trigonal prisms nor the connection to α-$ThSi_2$. An extensive quantum mechanical treatment shows that Cs with this curious structure has no electrons in s-states any more[105] but has transformed into a d^1 metal. The distribution of the valence electrons is really surprising (Fig. 4m): The areas with highest density are *not* located in the proximity of the Cs core but have the form of bent tubes (caterpillar shape) crossing the centers of the prisms. The highest accumulation is found on the square faces and at the centers of the prisms. This distribution shows a striking reference to the α-$ThSi_2$ structure, in which the electronegative Si atoms form a threefold bonded framework which exactly reproduces the topology of the electron density distribution of Cs-IV (Fig. 4m). Maximum densities are found at the centers of the Si–Si bonds in α-$ThSi_2$ and where the Si atoms are located. From this simple electronic system one gets the impression that trigonal-prismatic arrangements of atoms generate optimal positions for electrons, which are "localized" in the centers or on the square faces of the prisms respectively. Finally, the symmetry adapted POPS ${}^{c}D^*$ ($c/a = 3.73$) in addition presents the three-dimensional topological model for exactly this peculiar density distribution—it contains a three-armed tunnel system and separates the $Cs^{\oplus}$ ions from their valence electrons!

In a broader sense this description implies the concept of understanding this Cs modification as cesium electride $Cs^{\oplus}e^{\ominus}$. Perhaps one has to take into consideration that despite high pressure, no optimal packing of the atoms is reached, because additional quasi-particles need appropriate coordination polyhedra and therefore take part in determining the structure. Apparently the electrons are more strongly localized in Cs-IV than in α-Cs, an observation which demonstrates clearly that with increasing

Fig. 6. Stereo representations. a) The structure of garnet, $Ca_3[Al_2Si_{12}O_{12}]$ (Ca red, O light blue, Si inside the green octahedra, Al inside the green tetrahedra), consisting of two interpenetrating partial structures, which are centered by the Y shaped graph (violet) and which are separated by the surface Y^{**} (yellow and light blue side of the surface, respectively). b) One chain of the double helix in α-amylose (C pink, O orange, H small pink spheres) and a section of the Q^* surface (green, blue). c) The structure of $Li_{14}MgSi_4$ is partitioned by the S^* surface into a yellow and a blue labyrinth in which Li (green), Mg (orange) and Si (red) lie. The silicon atoms are located above the flat points of the surface. d) The structure of Ta_6Cl_{15} and the surface Y^{**}. The Ta atoms (red) form octahedra (black), which are linked by one type of the chlorine atoms (green) to a three-dimensional network. The other Cl atoms (dark blue) mold Y^{**} in the form of a non-euclidean sphere packing.

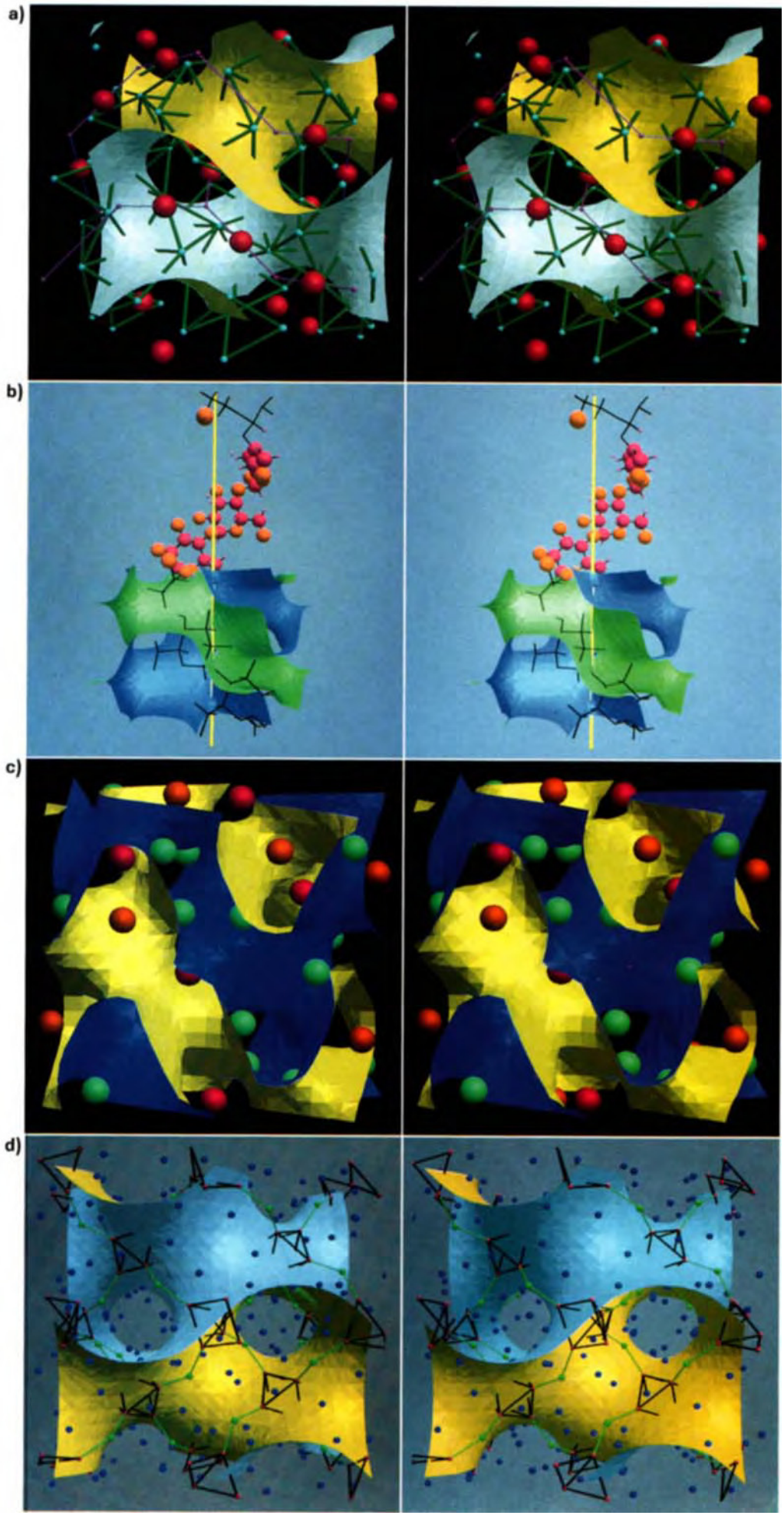
a)
b)
c)
d)

pressure not necessarily the stronger degenerate (metallic) state is favored.

As already mentioned from the adaption of certain structure fragments to the POPS it can be derived that in this area predominantly the highest occupied orbitals (HOMO) are located.[6] Once again we go back to the structure of $Li_{21}Si_5$ (cf. Section 5.2 and Figs. 2i-l[55]) which is fragmented by the D^* surface. By application of the Zintl-Klemm rule in the usual form, according to $[Li_{22}Si_4]^{4\oplus}$ and $[Li_{20}Si_6]^{4\ominus}$ two electrons remain in the first cluster, which can not be placed into Si states.[55] Because of these electrons metallic conductivity would be expected. Quantum mechanical cluster calculations have shown that these excess electrons are in fact (de-)localized on the surface of the cluster in a *cage orbital* over the outer Li atoms.[106, 107] Exactly these Li atoms lie on the correctly scaled D^* surface, which is the topological space partitioner. Therefore it is definitely proven that the weakest bonded electrons (the cage orbitals are highest in energy) essentially are localized around this surface. At this time it is emphasized again that the POPS of type 1 like D^* represent a higher symmetry than the overall structure actually has. In this respect one might as well think of a symmetry conditioned stabilization of the cage orbital.[6]

Band structure calculations for the structure of $Li_5Mg_{12}Al_{12}$ show (cf. Section 5.1) that the electrons essentially occupy the Al states and the highest occupied states substantially mediate the Mg-to-Al interactions and are therefore located between the Al and Mg atoms. This is again the interstitial area which topologically follows the P^* surface.[6]

Finally, another remark about CsCl and β-AgI (cf. Sections 5.1 and 6). For both structures imbedded in P^* it equally applies that the electrons feel the smallest potential and thus experience the weakest bond on or close to the POPS P^*. This means that the highest occupied states in CsCl as well as those in β-AgI are spatially to be expected where P^* partitions the space. In the first case this is caused by the balance of the attractive forces, $Cs^{\delta\oplus}$–$Cl^{\delta\ominus}$, in the second case by those of the repulsive $I^{\delta\ominus}$–$I^{\delta\ominus}$. We assume that the characteristic partition of the space in directions of symmetry conditioned different qualities, even for complicated realistic potential conditions, maintains the topological features of the POPS. This means directions distinguished by tunnels are different in their structural-chemical meaning, e.g., from such which are perpendicular to the POPS. Nature uses this discrimination of the different directions for an optimal arrangement of different interactions.

In any case it would be interesting to carry out an analysis of the spatial distribution of the HOMO's. Their result possibly gives preference to one or the other description.

9. Epilogue

The experiences in this relatively new field are still limited, and a systematic investigation of the structures of solids is out of the question. However even the kaleidoscopic glance into the world of collective forms of organization, which is gained from the investigation carried out up to now, already permits a few general statements.

1. Important knowledge is gained from the interplay between periodic potential surfaces and chemical structures namely the following: Apparently from the threefold infinite set of positional parameters *xyz* Nature chooses only this small subset, which lies in the close spatial area of the POPS, and only in a few special cases in the centers of the labyrinths. It still has to be examined if this phenomenon can be used for the derivation of phase relationships between structure factors. Relevant investigations are already under way.[108]

2. The importance of POPS (PMS) in structural chemistry results from the natural separation of different interactions in collective chemical structures. Such spatial separations are typical for molecules (intra-insular covalence, van der Waals skin) and can be recognized in cluster compounds, in which the covalent intra-cluster interactions can be distinctly spatially delimitated from the localized inter-cluster bonds or from the ionic inter-cluster interactions. Crystals of molecules and cluster-anions and cluster-cations have in common that the intra-insular interactions are based on non-directional ("delocalized") central forces of the van der Waals type or Coulomb type, respectively. In both cases the demarcations to the interstitial space are formed by the lone electron pairs of the substituents or the outer ligands, respectively. In metallic phases with the formation of clusters, there is reason to believe that the weakest bound electrons populate just these interstitial areas.[6]

3. One finds that distinguished regions are centered by the POPS, e.g. double layers, where either especially strong (covalent, ionic) or especially weak interactions (metallic, van der Waals) appear in the overall structure. Therefore POPS serve as topological concepts for structural basic models or even as concept for space partitioner of structures.

4. As a rule the majority component forms the inner surface (POPS, PMS) in a structure, where stoichiometry and space requirements play an important role. Therefore, for the formation of interpenetrating structures, it can be considered that even with suitable symmetry certain boundary conditions have to be fulfilled. The conservation of sufficient atomic distances between the interpenetrating partial structures is absolutely necessary. The more atoms take part in building the net-forming units (Nb_6F_{15}) the easier it is. In small structures this can only be achieved, if simultaneously the majority component provides the smaller atoms (Cu_2O, but not cristobalite SiO_2).

5. A few words about the curvature in structures: The question whether everything is curved will of course always be asked. A glance at the phenomena of Nature teaches us very quickly that the construction of curved structures is actually the norm, and for the formation of linear or plane arrangements considerable efforts are needed. A two-dimensional plane form needs exact relationships of radial and lateral extensions (growth rules). In the language of interatomic distances of a net this means exact relationships for all vectors. A plane NaCl net is only obtained for $q = d(\text{Cl-Cl})/d(\text{Na-Cl}) = \sqrt{2}$. However, in the free interplay of the forces deviations like $q < \sqrt{2}$ (surface of positive curvature; spherical cap) and $q > \sqrt{2}$ (surface of negative curvature, "pleated skirt"; PMS) are more likely. An in-

structive experiment is the pasting of five, six, seven etc. equilateral triangles around a common center. In crystalline compounds the translation period (elementary cell) forms the outer frame of a net. Only if this frame is small $q=\sqrt{2}$ can not be avoided. Therefore, only structures with very small translational periods are typical collectives: Here, the individual has no chance and even the electron density has to obey. In a natural way larger unit cells give space for free development to the variety of curved structures.

Chemistry is alive and essentially profits from the creative intuition as a successful strategy as well as from the pronounced feeling of a chemist for compounds and their structures, which even enables him to see electrons. Our contribution to this is the partition of structures by means of non-euclidean periodic curved surfaces, which separate fragments from each other and at the same time connect them. In view of their chemical meaning they can be analyzed as structure increments and therefore serve for a better understanding of the collective laws. These surfaces express the translational symmetry and play an important role in the hierarchy of the organization of organisms, comparable with the homoetic genes in biological systems. These determine, e.g., *where* legs grow, but have nothing to do with the growth of organs. Quite analogously, in crystalline phases the translational symmetry determines *where* building units lie and has nothing to do with the construction of the units. With the application of periodic potential surfaces to crystal structures we believe that we have found a new, strong strategy for an understanding of larger correlations in structures and for the interpretation of their properties. It helps and inspires us daily, hourly—may it be of use!

We would like to thank Dipl.-Chem. M. Oehme for the calculations of the phase transitions, Dr. R. Wedig and B. Koerner for extensive help in setting up the computational facilities and Mrs. C. Fowler for typing this manuscript. Special thanks are addressed to Prof. S. Andersson for numerous fruitful discussions on firm (diagonal support) and on uncertain grounds (not only around Öland) and to Prof. W. Jeitschko for sacrificing his kitchen for wet mathematics. The incomparable support of our work by the Fond der Chemischen Industrie is gratefully acknowledged.

Received: July 18, 1987 [A 640 IE]
German version: *Angew. Chem. 99* (1987) 1097

[1] R. Nesper, H. G. von Schnering, *Z. Kristallogr. 170* (1985) 138.
[2] R. Nesper, H. G. von Schnering, *Angew. Chem. 98* (1986) 111; *Angew. Chem. Int. Ed. Engl. 25* (1986) 110.
[3] H. G. von Schnering, *Conference Report Heidelb. Akad. Wiss. Math.-Naturwiss. Kl. 1985*, 90.
[4] H. G. von Schnering, *Z. Kristallogr. 174* (1986) 182.
[5] H. G. von Schnering, R. Nesper, *Jahrb. Max-Planck-Ges. 1986*, 509.
[6] R. Nesper, *Z. Kristallogr.*, in press; presented in part at the Intern. 'Hemdsärmel-Koll.', Universität Lund, March 1987.
[7] L. Faelth, S. Andersson, *Z. Kristallogr. 160* (1982) 313.
[8] S. Andersson, S. T. Hyde, *Angew. Chem. 95* (1983) 67; *Angew. Chem. Int. Ed. Engl. 22* (1983) 69.
[9] S. T. Hyde, S. Andersson, H. G. von Schnering, *Z. Kristallogr. 168* (1984) 1.
[10] S. T. Hyde, S. Andersson, *Z. Kristallogr. 168* (1984) 213; *ibid. 170* (1985) 225.
[11] S. Andersson, S. T. Hyde, *Z. Kristallogr. 173* (1985) 97.
[12] A.-C. Eliasson, L. Larsson, S. Andersson, S. T. Hyde, R. Nesper, H. G. von Schnering, *Stärke*, in press.
[13] P. Pearce: *Structure in Nature as a Strategy for Design*, MIT Press, Cambridge, MA, USA 1979.
[14] *Angel Duarte, Exhibition Catalogue*, Städtische Galerie zum Strauhof, Zürich, Musee' des Beau Arts Vidomat, Sion 1981.
[15] R. Bach, B. Burkhardt, F. Otto: *Seifenblasen-Foaming Bubbles (Mitteilungen des Instituts für leichte Flächentragwerke Nr. 18)*, 1987, in press.
[16] P. S. Stevens: *Zauber der Formen in der Natur*, R. Oldenbourg Verlag, München 1983.
[17] S. Hildebrandt, A. Tromba: *Mathematics and Optimal Form*, Scientific American Books/Freeman, New York 1985.
[18] B. Mandelbrot: *The Fractal Geometry of Nature*, Freeman, New York 1982.
[19] M. Kolb, *Phys. Bl. 42* (1986) 123.
[20] A. L. Mackay, *5th Eur. Crystallogr. Meet.*, Collected Abstracts 73-P1-5a, Copenhagen 1979.
[21] K. Larsson, S. Andersson, *Acta Chem. Scand. Ser. B 40* (1986) 1.
[22] S. T. Hyde, S. Andersson, *Z. Kristallogr. 174* (1986) 225.
[23] S. T. Hyde, S. Andersson, *Z. Kristallogr. 174* (1986) 237.
[24] S. T. Hyde, *Solid State Ionics*, in press.
[25] J. Klinowski, *Compu. & Math. Appl. 12B* (1986) 803. A. L. Mackay, *Nature (London) 314* (1985) 604.
[26] A. L. Mackay, *Physica B+C (Amsterdam) 131* (1985) 300.
[27] A. L. Mackay, *Nature 314* (1985) 604.
[28] A. L. Mackay, *Compu. & Math. Appl. 12B* (1986) 19.
[29] A. L. Mackay, *Compu. & Math. Appl. 12B* (1986) 21.
[30] A. L. Mackay, *J. Phys. (Les Ulis, Fr.) C3* (1986) 153.
[31] W. Fischer, E. Koch, *Z. Kristallogr.* (1987), in press.
[32] W. Fischer, E. Koch: *On 3-periodic minimal surfaces*, Lecture at the 10th Eur. Crystallogr. Meet., Coll. Abstr., Wroclaw, Poland, 1986, p. 564.
[33] T. Hahn (Ed.): *International Tables for Crystallography, Vol. A*, Reidel, Dordrecht, Holland 1983, p. 819ff.
[34] W. Fischer, *Z. Kristallogr. 133* (1971) 18.
[35] W. Fischer, *Z. Kristallogr. 138* (1983) 129.
[36] W. Fischer, E. Koch, *Acta Crystallogr. A 32* (1976) 225.
[37] R. Nesper, B. Koerner, U. Wedig: *OBERFLEX, Programmsystem zur flexiblen Darstellung von dreidimensionalen Strukturen und Oberflächen*, Max-Planck-Institut für Festkörperforschung, Stuttgart (FRG), 1986.
[38] G. Roch, H. G. von Schnering, B. Neukäter: *MADKUG, Programm zur Berechnung von Gitterpotentialen und Madelung-Konstanten*, Universität Münster 1962.
[39] P. P. Ewald, *Ann. Physik 64* (1920) 253.
[40] A. H. Schoen, *NASA Technical Note D-5541*, Cambridge Mass. 1970.
[41] R. Nesper, H. G. von Schnering, unpublished results.
[42] W. Fischer, E. Koch, E. Hellner, *Neues Jahrb. Mineral., Monatsh. 1971*, 227.
[43] W. Fischer, E. Koch, *Neues Jahrb. Mineral., Monatsh. 1973*, 252.
[44] E. Koch, W. Fischer, *Neues Jahrb. Mineral., Monatsh. 1973*, 361.
[45] E. Koch, *Z. Kristallogr. 138* (1973) 196.
[46] W. Fischer, E. Koch, *Z. Kristallogr. 150* (1979) 245.
[47] E. Koch, W. Fischer, *Z. Kristallogr. 153* (1980) 255.
[48] W. Nowacki, *Z. Kristallogr. 143* (1976) 360.
[49] P. Engel: *Geometric Crystallography*, Reidel, Dordrecht, Holland 1986, p. 13ff.
[50] P. Villars, L. D. Calvert: *Pearson's Handbook of Crystallographic Data for Intermetallic Phases*, American Society for Metals, Metals Park, OH 44073, USA 1985, p. 740.
[51] R. Nesper, unpublished.
[52] H. Schäfer, H. G. von Schnering, K.-J. Niehues, H. G. Nieder-Vahrenholz, *J. Less-Common Met. 9* (1965) 59.
[53] W. Nowacki, F. Laves, K. Löhberg, P. Rahlfs, *Nachr. Ges. Wiss. Göttingen Math.-Phys. Kl. N.F. 1* (1984) 67; W. Trzebiatowski, J. Niemiec, *Rocz. Chem. 29* (1955) 277. *Neues Jahrb. Mineral., Monatsh. 1958*, 193.
[54] R. Nesper, unpublished.
[55] R. Nesper, H. G. von Schnering, *J. Solid State Chem. 1987*, in press.
[56] S. C. Abrahams, S. Geller, *Acta Crystallogr. A 11* (1958) 437.
[57] A. Paoletti (Ed.): *Physics of Magnetic Garnets (Proc. Int. School Phys. 'Enrico Fermi')*, North Holland, Amsterdam, The Netherlands 1978.
[58] P. Hansen, M. Hartmann, *Phys. Magn. Mater. Proc. Int. Conf., 2nd, 1984* in *Acta Phys. Polonia A 68* (1985) 158.
[59] *Z. Kristallogr., Strukturbericht 1* (1931) 15.
[60] D. Bauer, H. G. von Schnering, *Z. Anorg. Allg. Chem. 361* (1968) 259.
[61] H. G. von Schnering, unpublished.
[62] E. Parthé: *Cristallochimie des Structures Tétraédriques*, Gordon and Breach, Paris 1972.
[63] R. Nesper, H. G. von Schnering, *TMPM, Tschermaks Mineral. Petrogr. Mitt. 32* (1983) 195.
[64] R. Kipka, H. Müller-Buschbaum, *Z. Naturforsch. B32* (1977) 121.
[65] R. E. Neovius: *Determination of two special periodic minimal surfaces upon which an infinitely large number of straight lines and an infinitely large number of flat geodetic lines lie.*
[66] H. G. von Schnering, J. Llanos, R. Nesper, J. Curda, unpublished; H. G. von Schnering, *Nova Acta Leopold. 264* (1986) 165.
[67] S. Andersson, private communication; cf. also [12].
[68] W. Fischer, E. Koch, *Z. Kristallogr. 139* (1974) 268.

[69] H. G. von Schnering, R. Hoppe, J. Zemann, *Z. Anorg. Allg. Chem. 305* (1960) 241.
[70] W. Abriel, *Acta Crystallogr. C39* (1983) 956.
[71] K. Reisdorf, W. Abriel, R. Nesper, *Z. Kristallogr.* (1987), in press.
[72] H.-C. H. Wu, A. Sarko, *Carbohydr. Res. 61* (1978) 7.
[73] H.-C. H. Wu, A. Sarko, *Carbohydr. Res. 61* (1978) 27.
[74] D. L. Wild, J. M. V. Blanshard, private communication.
[75] K. Larsson, Lund, private communication.
[76] R. J. Cava, F. Reidinger, B. J. Wuensch in P. Vashishta, J. N. Mundy, G. K. Shenoy (Eds.): *Fast Ion Transport in Solids*, North Holland, Amsterdam 1979.
[77] R. M. Barrer, H. Villiger, *Z. Kristallogr. 128* (1969) 352.
[78] S. R. Hall, J. F. Rowland, *Acta Crystallogr. B29* (1973) 2365.
[79] H. J. Bleif, H. Dachs, *Acta Crystallogr. A38* (1982) 470.
[80] C. E. Derrington, A. Navrotsky, M. O'Keeffe, *Solid State Commun. 18* (1976) 47.
[81] T. M. Gur, I. D. Raistrick, R. A. Huggins, *Solid State Ionics 9/10* (1983) 251.
[82] R. Bachmann, H. Schulz, *Solid State Ionics 9/10* (1983) 521.
[83] J. O. Thomas, M. Alden, G. C. Farrington, *Solid State Ionics 9/10* (1983) 301.
[84] W. Carillo-Cabrere, J. O. Thomas, G. C. Farrington, *Solid State Ionics 9/10* (1983) 245.
[85] L. D. Landau, E. M. Lifshitz: *Statistical Physics*, Pergamon Press, Oxford 1959.
[86] B. G. Hyde, M. O'Keeffe in H. K. Henisch, R. Roy, L. E. Cross (Eds.): *Phase Transitions, Proc. Conf. Phase Transitions Their Appl. Mater. Sci. 1973*, Pergamon, New York 1973, p. 345.
[87] O. Blaschko, G. Ernst, G. Quittner, G. Pepy, M. Roth, *Phys. Rev. B20* (1979) 1157.
[88] R. Hoppe, *Habilitationsschrift*, Universität Münster 1958.
[89] H. G. von Schnering, *Habilitationsschrift*, Universität Münster 1964.
[90] R. Hoppe, *Angew. Chem. 78* (1966) 52; *Angew. Chem. Int. Ed. Engl. 5* (1966) 15.
[91] R. Hoppe, H. G. von Schnering, *Bull. Soc. Chim. Fr. 1965*, 1115.
[92] M. Oehme, *Diplomarbeit*, Universität Stuttgart 1986.
[93] J. D. H. Donnay, G. Donnay, E. G. Cox, O. Kennard, M. V. King: *Crystal Data*, Williams and Heintz Map. Corp., Washington, D.C., USA 1973.
[94] O. Bonnet, *C. R. Acad. Sci. Paris 37* (1853) 529.
[95] W. Andreoni, K. Maschke, *Solid State Ionics 9/10* (1983) 1389.
[96] M. J. Gillan, *Solid State Ionics 9/10* (1983) 761.
[97] R. Brill, H. G. Grimm, C. Hermann, Cl. Peters, *Ann. Phys. 34* (1939) 393.
[98] S. Pawlowska, N. E. Christensen, S. Satpathy, O. Jepsen, *Phys. Rev. B34* (1986) 7080.
[99] N. E. Christensen, *Phys. Rev. B32* (1985) 207.
[100] N. E. Christensen, *Phys. Rev. B32* (1985) 6490.
[101] O. K. Andersen, S. Pawlowska, O. Jepsen, *Phys. Rev. B34* (1986) 5253.
[102] S. H. Wei, A. Zunger, *Phys. Rev. Lett. 56* (1986) 528.
[103] K. Takemura, S. Minomura, O. Shimomura, *Phys. Rev. Lett. 49* (1982) 1772.
[104] W. Biltz: *Raumchemie der festen Stoffe*, Verlag L. Voss, Leipzig 1934.
[105] N. E. Christensen, O. K. Andersen, S. Pawlowska, unpublished.
[106] R. Ramirez, R. Nesper, H. G. von Schnering, M. C. Böhm, *Z. Naturforsch. A41* (1986) 1267.
[107] R. Ramirez, R. Nesper, H. G. von Schnering, M. C. Böhm, *J. Phys. Chem. Solids 48* (1987) 51.
[108] R. Nesper, K. Vogel, H. G. von Schnering, unpublished.

Fluorides of Copper, Silver, Gold, and Palladium

By Bernd G. Müller*

Dedicated to Professor Rudolf Hoppe on the occasion of his 65th birthday

Fluorine, by far the most reactive of the non-metals, is capable of forming a large number of compounds with nearly all other elements (exceptions (so far): He, Ne, and Ar), even under comparatively "mild" reaction conditions. These compounds usually differ markedly from those of the heavier halogens in composition, structure, and chemical and physical properties. Thus, for example, it is generally quite easy to prepare fluorides containing elements in high oxidation states (often their maximum), as in AgF_2, $CsAgF_4$, PdF_3, $CsAuF_6$ etc., whereas the corresponding chlorides, bromides or iodides are in many cases (still) unknown. Conversely, the synthesis of fluorides containing these elements in middle or low oxidation states often meets with considerable difficulty, even where it is possible at all, as, e.g., in the case of CuF, AuF, PtF_2, SeF_2. Finally, there are also some examples of compounds MX_n, which with X = F are stable, but with X = Cl are unstable or decompose easily (e.g. $CoF_3/CoCl_3$, VF_4/VCl_4, $PbF_4/PbCl_4$, $AsF_5/AsCl_5$). Consequently, fluorine compounds are of great general interest.

1. Introduction

The nineteen-fifties heralded a new phase of development in fluorine chemistry. It began, on the one hand, with the preparation of complex transition metal fluorides (and oxides) in high and in some cases previously unknown oxidation states (K_2NiF_6, K_3CuF_6, $CsAgF_4$ etc.),[1-3] first by *W. Klemm*, then later by *R. Hoppe* and co-workers, and, on the other, with the use of BrF_3 as a solvent and fluorinating agent (e.g. by *H. J. Emeléus* et al.). It culminated in the (independent) discovery of the first noble gas fluorides by *N. Bartlett* ("$XePtF_6$")[4] and *R. Hoppe* et al. (XeF_2)[5] in 1962. In the following years it became possible, using more sophisticated methods of fluorination (e.g. high pressure fluorination, or the use of KrF_2 as a fluorinating agent) to synthesize further compounds of unusual constitution, some likewise in previously unknown oxidation states, for example $Cl_6^+PtF_6^-$,[6], $KrF^+AuF_6^-$,[7] and Cs_2CuF_6,[8] (see also Refs. [9, 10]).

However, despite the remarkable progress that has been made regarding preparative methods, our knowledge of this area of inorganic fluorine chemistry, where single crystal X-ray diffraction measurements are essential for the unambiguous characterization of the constitution and structure of the compounds, is still only fragmentary. Up to now such investigations have mainly been restricted to thermally stable, involatile and, in most cases, ionic fluorides which are capable of being grown in the form of single crystals from the melt, with air and moisture excluded if necessary, and using flasks or crucibles of appropriate materials (the Bridgman/Czochralski technique and its variants).[11] Only seldom is it possible to prepare anhydrous monocrystalline fluorides without decomposition:

1. from concentrated HF solutions (e.g. Cs_2PtF_6, K_2MnF_6,[12, 13] or under hydrothermal conditions;[14]
2. by crystallization from anhydrous HF as solvent (e.g. $XeF_4 \cdot SbF_5$,[15] $H_3O^+TiF_5^-$,[16] $AgF_2 \cdot 2SbF_5$[17])—a method whose application is limited by the sparing solubility of many (ionic) fluorides in HF;
3. by growing crystals from the melt,[18] either by transport or by gel crystallization;[11]
4. by sublimation without decomposition, under an inert atmosphere (e.g. Ar), under fluorine, or in a high vacuum (e.g. RhF_5,[19] AuF_3,[20] $(XeF_5)_2^+PdF_6^{2-}$[21]).

Very few examples of the preparation of single crystals of fluorides which are easily decomposed thermally (especially in the absence of F_2) have thus far been reported in the literature.

As already known, the structures of many metal fluorides can be derived from those with the most densely packed anions, as a result of their essentially ionic bond character, with the cations distributed between the available sites (usually octahedral, less frequently tetrahedral) in a usually ordered manner corresponding to the molecular formula.

Following this simple building principle, many classes of compounds can be assigned to a small number of basic structural types. Thus, for example, in the VF_3 structure vanadium can be replaced by any of the similarly charged ions (Al^{3+}, Ga^{3+}, Ti^{3+}, Cr^{3+}, etc.), or by M^{II}/M^{IV} ($\triangleq M^{II}M^{IV}F_6$ with M^{II} = Zn, Ni, Co, ..., M^{IV} = Ti, Sn, Pd, Pt ...), or by M^{I}/M^{V} ($\triangleq M^{I}M^{V}F_6$ with M^{I} = Li, Na ..., M^{V} = Sb, Pt ...)[22] without altering any basic structural features.

The same holds true for complex fluorides, an example being the $RbNiCrF_6$-type structure derived from the pyrochlores.[23] Here substitution of other metals in place of Rb, Ni and Cr gives a remarkably large number of new quaternary fluorides with the same structure and arrangement of cations. With fluorides, therefore, one is often in

[*] Priv.-Doz. Dr. B. G. Müller
Institut für Anorganische und Analytische Chemie der Universität
Heinrich-Buff-Ring 58, D-6300 Giessen (FRG)

the fortunate situation of being able to dispense with single crystal measurements and to limit oneself to interpreting the generally less informative powder diffraction data, providing an exact single crystal structure determination is already available for at least one example.

There are, nevertheless, certain exceptions which do not allow such simplified analogies and isostructural considerations. These are the cases where one or more of the cations involved in building up the structure require a less symmetrical arrangement of the ligands, owing to the existence of e_g states with odd-numbered occupancy (Jahn-Teller effect). Those which are relevant for fluorides include Cr^{2+} and Mn^{3+} ($3d^4$ "high spin" configuration: $t_{2g}^3e_g^1$), Cu^{2+} and Ag^{2+} ($3d^9/4d^9$ configuration: $t_{2g}^6e_g^3$), and Ni^{3+}, Cu^{4+}, and Pd^{3+} ($3d^7/4d^7$ "low spin" configuration: $t_{2g}^6e_g^1$).

Unusual structures are sometimes also found in the case of fluorine complexes of Cu^{3+}, Pd^{2+}, Ag^{3+}, and Au^{3+} (nd^8 configuration, where $n=3, 4, 5$), as a result of the rarely occurring coordination number C.N. $[M^{n+}]=4$ in relation to fluorine (with F^- ions in a square planar configuration around the central ion).

Because of these special structural characteristics, such fluorides have already been the subject of many of the early studies, but there are some further reasons why the fluorides of the coinage metals seem a particularly attractive subject for investigation:

1. The elements Cu, Ag, and Au lie on the border between transition metals and Main Group metals ("meta-metals"), but are "true" transition metals in the narrower sense insofar as, in contrast to the elements Zn, Cd, and Hg, d-electrons can still be involved in their bonding.
2. They are the only elements (apart from, in the widest sense, a few lanthanoids, e.g., Ce, Pr ...) which occur in oxidation states higher than that corresponding to their position in the Periodic System of the Elements, i.e. their outer electron shell configuration.
3. The individual physical and chemical properties of the elements differ more widely, and are less susceptible to extrapolation than in any other group of the Periodic System—one need only consider their chemistry in aqueous solution.
4. The fluorides are of particular importance insofar as they are the only compounds in which certain oxidation states can exist.

An interpretation of the, in some cases remarkable, physical properties (magnetism, spectra, conductivity etc.) of these compounds requires a detailed knowledge of the structures; consequently, careful single-crystal measurements are essential.

However, there are usually considerable difficulties in preparing pure microcrystalline samples of the fluorides of interest in this connection, and the production of suitable single crystals poses even greater problems. The following report describes some methods for synthesizing thermally less stable fluorides of the coinage metals and palladium, and outlines the associated problems (e.g. side reactions and decomposition of products) that are commonly met with; it also gives an overview, mainly in the form of tables, of our present state of knowledge of this area of chemistry.

2. Copper Compounds

Copper occurs in combination with fluorine in the oxidation states +1, +2, +3, and +4, with the +2 state as clearly the predominating one. Fluorine complexes of mono-, tri- and tetravalent copper are listed in Table 1. Because of the very large number of known copper(II) compounds, Tables 2 and 3 (p. 1084) list only a few representative examples chosen more or less arbitrarily, but limited to those whose structures have been determined on single crystals.

It is surprising that, apart from $CuAsF_6$,[24] fluorides of Cu^I (including CuF itself) are so far totally unknown, despite numerous attempts at producing them. This contrasts with copper(I) oxides, e.g. Cu_2O, $K_4[Cu_4O_4]$,[35] or chlorides such as CuCl and $KCuCl_2$. Copper differs markedly in this respect from the homologous element silver, in which it is well known that the +1 oxidation state predominates, and not only as regards its chemistry in aqueous solutions. Copper is also unique amongst the coinage metals (even though based on only a few examples) in its ability to form compounds having the +4 oxidation state, namely $M^I_2[CuF_6]$, where $M^I=$(K), Rb, Cs.[8,29,30,31] These are of particular interest from the structural chemistry standpoint in having (according to original powder diffraction data) a slightly distorted orthorhombic (and from more recent single-crystal data tetragonal) structure of the same type as K_2PtCl_6. Thus, single crystal studies are necessary in this case to determine the Cu^{4+} coordination sphere more exactly (d^7 "low spin/high spin" configuration), and to give a deeper understanding of other features, e.g. magnetic properties. Understandably, however, their preparation is by no means easy. This is related to the fact that pure samples of, for example, Cs_2CuF_6, can only be obtained by (in solid reaction terms) rapid conversion of, e.g., Cs_2CuF_4 using F_2. If one attempts prolonged annealing (in order to grow crystals), decomposition occurs by uncontrollable and incompletely understood mechanisms which are affected by pressure, temperature, and the material of the crucible. Some of the possible products from side-reactions or decomposition are indicated in Scheme 1.

One is therefore limited to either carrying out experiments over longer periods at relatively low temperatures, or to repeated annealing for short periods (at higher temperatures) on the same sample. This also applies for all other compounds which can only be prepared under similar conditions. Using the second (rather laborious) method, it has recently been possible to prepare single crystals even of Cs_2CuF_6, and to determine the structure in detail.

The basic problems involved in synthesizing single crystals of thermally sensitive, highly reactive fluoro-complexes of the transition metals (especially those containing alkali metals or alkaline earth metals) are already evident from the above discussion, namely the large number of possible side-products or decomposition products, and of reactions between one or more components (especially CsF) and the walls of the vessel during lengthy experi-

Table 1. Copper fluorides with oxidation states +1, +3, +4.

Compound	Ref.	Color	Structure	Lattice constants [Å]	Angles [°]	C.N. [Cu^{n+}]	$d[Cu^{n+}\text{-}F]$ [Å] [a]	Magnetic properties
$CuAsF_6$	[24]	colorless	$LiSbF_6$ ($R\bar{3}$)	$a = 5.49$	$\alpha = 55.7$	(6)	—	diamagnetic
Na_3CuF_6	[25, 26]	green	cryolite ($P2_1/n$)	$a = 5.454$ $b = 5.667$ $c = 7.843$	$\beta = 90.2$	6	1.845(2×) 1.917(2×) 1.919(2×)	$\mu = 2.66$ B.M. (contaminated with NaF/CuF_2)
K_3CuF_6	[26]	pale green	K_3FeF_6 [b] ($Fm3m$)	$a = 8.51$		(6)	—	$\mu = 3.03$ B.M.
Cs_2KCuF_6 [c, d]	[26, 27]	pale green	elpasolite ($Fm3m$)	$a = 8.894$		6	1.830	$\mu = 2.83$ B.M.
$Cs[CuF_4]$	[28]	orange	$KrBrF_4$ ($I4/mmm$)	$a = 5.58$ $c = 12.04$		4	1.730	diamagnetic
$CsCuCuF_6$	[26]	black	$CsNiNiF_6$ ($Imma$)	$a = 7.067$ $b = 7.277$ $c = 10.32$		Cu^{2+} 4+2 Cu^{3+} 6	1.980(4×) 2.130(2×) 1.900	—
[d] Cs_2CuF_6	[8, 29]	orange-red	K_2PtCl_6 Variant ($I4/mmm$)	$a = 6.282$ $c = 8.885$		4+2	1.772(2×) 1.750(4×)	$\mu = 1.76$ B.M.
Rb_2CuF_6	[30, 31]	orange-red	K_2PtCl_6 Variant ($Immm$?)	$a = 8.835$ $b = 5.978$ $c = 6.007$		—	—	—

[a] Interatomic distances found from powder data, where these are given, are by their nature inaccurate (except in structures without F parameters, eg. AgF), and are often based on analogy considerations, or (occasionally) on MAPLE calculations. The same remarks apply to the rest of the tables. [b] The structures which have been postulated for these and other compounds of the form $M^I_3M^{III}F_6$ (M^I = K, Rb, Cs; M^{III} = Ga, Fe, Co ...) are in need of correction, as shown by a number of studies (see, for example, [26, 32-34]). [c] Isostructural type: $M^I_2M^ICuF_6$, light green to beige (M^I = K, Rb, Cs; M^I = Li, Na, K, Rb) [26]. [d] Single crystal data available for this compound.

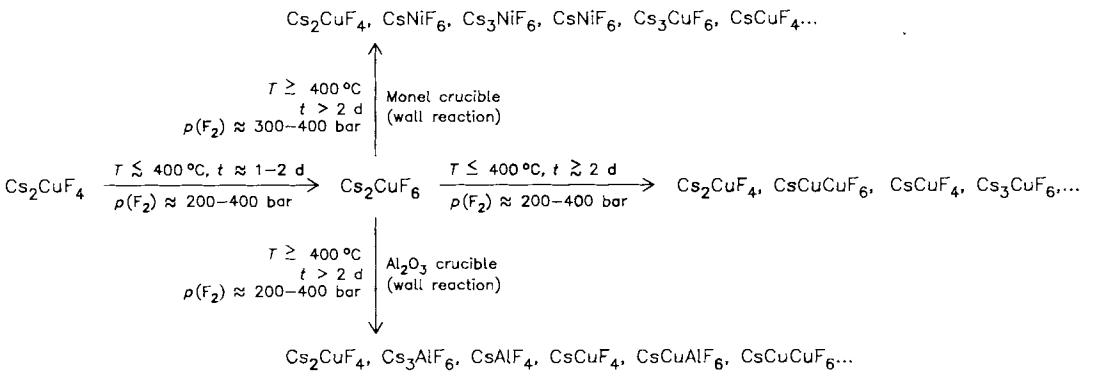

Scheme 1. Side-reactions in attempts to prepare Cs_2CuF_6 single crystals.

ments. Further, a reduction in F_2 partial pressure (as a result of fluorine being lost through reaction with the autoclave material) can cause thermal decomposition of those compounds which are particularly sensitive.

Also, owing to the fact that practically all the fluorides of interest here are insoluble (without causing hydrolysis or decomposition) in the usual solvents, and that other more appropriate methods of purification such as distillation or sublimation are not available, it is impossible in principle to remove impurities from samples after preparing them.

The fluorine complexes of trivalent copper are generally much more stable, and have consequently been more thoroughly studied. A notable example is the successful preparation of single crystals of Cs_2KCuF_6 in closed copper crucibles (under argon!). In this case the basic elpasolite structure of the complex evidently permits an "optimal" arrangement of the individual ions (stable matrix with a high lattice energy) which gives exceptional thermal stability.[27] Other examples too support this conclusion.

In addition to these, copper(III) fluorides are known, namely $Cs[CuF_4]$[28] and $CsCuCuF_6$,[26] but these can only be made under more extreme conditions (F_2 pressures above 400 bar), and are correspondingly lacking in stability. The existence of $Cs[CuF_4]$ (isostructural with $K[BrF_4]$) is "reassuring", since in this respect copper follows the behavior of the two other coinage metals, which in their +3 oxidation states with fluorine show predominantly (for Ag^{3+}) or exclusively (for Au^{3+}) a coordination number of 4, with a square planar arrangement of F^- ions around M^{3+}.

$CsCuCuF_6$ is interesting as regards its structural chemistry, being a very sensitive compound of mixed valency Cu^{2+}/Cu^{3+}. According to powder diffraction data it is isostructural with $CsNiNiF_6$,[36] but the results do not allow one to determine either the positions of the Cu^{2+} ($3d^9$, Jahn-Teller effect) and Cu^{3+} ions or the F parameters (proximity to the strongly scattering Cs^+ ions) and thus to calculate reliable values for the distances $d[Cu^{n+}\text{-}F]$. Nor is it easy in such cases to propose plausible structural mod-

els, as the structures of $CsPdPdF_5$,[37] $RbCuPdF_5$,[38] and $CsAgFeF_6$[39] show, and single crystal data are therefore essential.

In general, a considerable amount of knowledge exists concerning the structure and constitution of copper(II) fluorides, which, as a result of their $3d^9$ configuration, differ markedly from compounds of similar formula (so far as these are known) formed by the adjacent elements nickel and zinc. The reason for this is that CuF_2 and fluorine complexes of Cu^{2+} (compared with Cr^{2+}, Mn^{3+}, or Ag^{2+} compounds) can usually be prepared without difficulty, even as single crystals, and there exists a correspondingly large amount of exact (single crystal) structural data—see Tables 2 and 3. Ternary and quaternary systems containing Cu^{2+} are usually obtained by annealing suitably chosen mixtures in copper bombs or Au/Pt tubes (welded under Ar). The only exceptions to this are compounds in which one or more of the cations involved (in polynary complexes) is thermally sensitive, that is decomposes with change of oxidation state upon heating, or can be readily split off in the form of a binary volatile fluoride. This is the case in the $CuMF_6$ series (M = Ti, Sn, Mn, Cr, Pt ...), for example, and as a result it has only recently been possible to determine the structure of $CuPtF_6$ single crystals.[38] The synthesis of $CuPtF_6$ must be carried out in a closed autoclave, because of the volatility of PtF_5 and PtF_6; however, for the same reason too high a pressure of F_2 must be avoided. Once made, however, $CuPtF_6$ has—apart from its

Table 2. Copper fluorides with oxidation state +2 (cationic). Single-crystal data measured for all compounds.

Compound	Ref.	Color	Structure	Lattice constants [Å]	Angles [°]	C.N. [Cu^{2+}]	d[Cu^{2+}-F] [Å]	Magnetic properties
CuF_2	[40]	colorless	rutile variant ($P2_1/n$)	a = 3.307 b = 4.546 c = 4.599	β = 96.57	4+2	1.910(2×) 1.929(2×) 2.305(2×)	—
$CuPtF_6$	[38]	orange	$LiSbF_6$ variant ($P\bar{1}$)	a = 4.952 b = 4.982 c = 9.624	α = 89.9 β = 104.2 γ = 120.4	2+2+2	1.930(2×) 2.007(2×) 2.122(2×)	μ = 2.06 B.M.
α-$CuZrF_6$	[41, 42]	colorless	ReO_3 (variant) ($Fm3m$, disorded)	a = 5.613		(6)	1.985	μ = 1.84 B.M.
$FCu[AuF_4]$	[43]	yellow	unique type ($P\bar{1}$)	a = 5.536 b = 4.979 c = 3.707	α = 107.6 β = 98.77 γ = 98.63	2+2+2	1.854(2×) 2.021(2×) 2.221(2×)	antiferromagn. μ(251 K) = 1.32 B.M.
$RbCuPdF_5$	[38]	orange	$CdPdPdF_5$ variant ($Pnma$)	a = 6.296 b = 7.199 c = 10.76		4+2	1.928(2×) 1.959(2×) 2.190(2×)	—
$KCuAlF_6$	[44a]	colorless	$CsAgFeF_6$ type ($Pnma$)	a = 6.731 b = 7.040 c = 9.743		2+4	1.873 1.881 2.121(4×)	—
$KCuCrF_5$	[44b]	green	unique type ($P2_1/c$)	a = 7.266 b = 9.945 c = 6.769	β = 92.79	2+2+2	1.872 2.007 1.878 2.239 1.999 2.261	—

Table 3. Copper fluorides with oxidation state +2 (anionic). Single-crystal data measured for all compounds.

Compound	Ref.	Color	Structure	Lattice constants [Å]	Angles [°]	C.N. [Cu^{2+}]	d[Cu^{2+}-F] [Å]
$KCuF_3$	[45]	colorless	perowskite variant ($I4/mcm$)	a = 5.863 c = 7.847		2+2+2	1.888(2×) 1.962(2×) 2.258(2×)
$K_3Cu_2F_7$	[46]	colorless	unique type ($I4/mmm$)	a = 4.156 c = 20.52		1+2+1+2	1.907 1.927 1.960(2×) 2.225(2×)
Cs_2CuF_4	[47]	pale blue	K_2NiF_4 ($I4/mmm$)	a = 4.403 c = 14.03		4(+2)	1.933(2×) 1.961(2×) 2.474(2×)
$Cs_4Cu_3F_{10}$	[29]	bluish cast/ colorless	unique type ($P\bar{1}$)	a = 8.505 b = 7.740 c = 6.268	α = 113.9 β = 111.8 γ = 103.1	Cu(1) 4+2 Cu(2) 2+2+2	1.902(2×) 1.944(2×) 2.251(2×) 1.865-2.226
$Cs_7Cu_6F_{19}$	[29]	pale blue	unique type ($P2_1/c$)	a = 11.73 b = 6.266 c = 15.68	β = 99.19	Cu(1) 2+2+2 Cu(2) 3+2+1 Cu(3) 1+1+1+1+1+1	1.853-2.171 1.850-2.405 1.845-2.353
$SrCuF_4$	[48]	blue-green	$KBrF_4$ ($I4/mcm$)	a = 5.643 c = 10.67		4	1.858
Ba_2CuF_6	[49]	colorless	unique type ($Bbma$)	a = 5.937 b = 5.837 c = 15.85		4+2	1.862(2×) 1.867(2×) 2.320(2×)
α-$Ba_2Cu_5F_{14}$	[50]	colorless	unique type ($C2/c$)	a = 18.17 b = 6.652 c = 10.328	β = 117.1	Cu(1) 2+2+2 Cu(2) 4+1+1 Cu(3) 2+2+2	1.875-2.372 1.911(4×) 2.275 2.469 1.865(2p) 2.056(2×) 2.148(2×)

susceptibility to hydrolysis—surprisingly good thermal stability, and single crystals can be grown in welded platinum tubes (under Ar) at about 750 °C (!).

Generally speaking, the coordination sphere of Cu^{2+} is of most interest. Usually one expects this to occupy an elongated octahedral environment with a coordination number C.N.$[Cu^{2+}]=4+2$, but in the limiting case C.N.$[Cu^{2+}]=4$ (square planar). Here, though, it is to some extent a "philosophical" question as to whether one describes the environment as (still) octahedral or (already) square planar—the transition is a gradual one. Numerous examples are known—Tables 2 and 3 list just a few, with the corresponding interatomic distances. In addition, however, quite a few fluorides have been reported, mainly in recent work, in which Cu^{2+} has been found to be in an "abnormal" coordination state, or in which different coordination states occur alongside each other in the same compound. Abnormally coordinated are, e.g., $KCuAlF_6$[44a] and $KCuCrF_6$[44b] with C.N.$[Cu^{2+}]=2+4$, and $FCu[AuF_4]$[43] and $CuPtF_6$[38] with C.N.$[Cu^{2+}]=2+2+2$; mixed coordination is found in $Cs_7Cu_6F_{19}$[47b] with C.N.$[Cu^{2+}]\simeq 3+2+1$; $2+2+2$; $1+1+1+1+1+1$ (this assignment is, of course, arbitrary—but some evidence is obtainable from ECoN calculations[51, 52]). Other phases exist in the CsF/CuF_2 system besides $Cs_7Cu_6F_{19}$; in this case Cu^{2+} resembles its neighbor element nickel, which similarly forms numerous compounds with CsF (cf., e.g., Ref. [53]), rather than the homologous element silver, for which only $CsAgF_3$[54] and Cs_2AgF_4[44] are known up to now.

The copper fluorides, considered as a whole in comparison with those of the other coinage metals, remain the most thoroughly characterized, especially those of Cu^{2+}.

The surprising results that are occasionally found (especially concerning the stoichiometry and environment of Cu^{2+}, as for example in $Cs_7Cu_6F_{19}$ or $FCu[AuF_4]$) on the one hand, and some yet unsolved problems (e.g. regarding the existence of copper(I) fluorides, or the exact structures of Cs_2CuF_6 and $CsCuCuF_6$) on the other, show that it is certainly worthwhile to take a fresh look at problems regarded as already solved, or at systems believed to be fully understood.

3. Silver Compounds

Silver, like copper, shows valencies of +1, +2, +3 and (formally) +4 in its fluorides. In contrast to copper, however, compounds of Ag^+ are by far the most stable, while those in the remaining oxidation states are all very unstable thermally (in the absence of fluorine), and are accordingly difficult to prepare as pure samples or single crystals.

In addition to these "chemical" differences one also often finds, in comparable systems with the same oxidation states, differences in constitution and structure, and associated differences in the coordination geometry at the central ion.

Table 4 lists a few selected silver(I) compounds, together with all the known fluorides containing silver in the +3

Table 4. Silver fluorides with the oxidation states (+0.5), +1, +3, +4 (+3/+5).

Compound	Ref.	Color	Structure	Lattice constants [Å]	Angles [°]	C.N. $[Ag^{n+}]$	$d[Ag^{n+}-F]$ [Å]	Magnetic properties
Ag_2F [a]	[56]	bronze	*anti*-CdI_2 ($R\bar{3}m$)	$a=2.916$ $c=5.691$		6	2.451	—
AgF-I	[57]	colorless	NaCl ($Fm3m$)	$a=4.395$		6	2.467	diamagnetic
AgF-II	[57]	colorless	CsCl ($Pm3m$)	$a=2.945$		8	2.550	(diamagnetic)
AgF-III	[58]	colorless	inverse NiAs-type ($P6_3mc$)	$a=3.264$ $c=6.226$		6	2.436	(diamagnetic)
$AgCuF_3$	[59]	colorless	perowskite variant monoclinic	$a=4.06$ $b=3.83$ $c=4.06$	$\beta=91.2$	—	—	—
Ag_2CuFeF_7 [b]	[60]	colorless	weberite ($Imm2$)	$a=7.243$ $b=10.47$ $c=7.769$		4+4	2.421(2×) 2.540(2×) 2.788(2×) 2.907(2×)	—
$AgPdZr_2F_{11}$ [a]	[61]	blue	unique type ($C2/m$)	$a=9.351$ $b=6.991$ $c=7.801$	$\beta=115.7$	4+4	2.355(4×) 2.798(4×)	paramagnetic $\mu=2.83$ B.M.
AgF_3	[62]	red-brown	unique type	—		—	—	paramagnetic $\mu=1.15$B.M.
$KAgF_4$ [c]	[63, 64]	yellow	$KBrF_4$ ($I4/mmm$)	$a=5.90$ $c=11.15$		4	1.90	diamagnetic
Cs_2KAgF_6	[65]	purple-red	elpasolite ($Fm3m$)	$a=9.175$		6	2.13	paramagnetic $\mu=2.6$ B.M.
„Cs_2AgF_6"	[66]	orange	K_2PtCl_6 ($Fm3m$)	$a=8.907$		—	—	paramagnetic $\mu=1.39$ B.M.
$Cs_2Ga_{0.5}Ag_{0.5}F_6$	[66]	orange	K_2PtCl_6 ($Fm3m$)	$a=9.01$		—	—	paramagnetic
$XeF_5^+AgF_4^-$	[67]	yellow	unique type ($I4/mmm$)	—		—	—	diamagnetic

[a] Single-crystal data measured for this compound. [b] Isostructural are $Ag_2M^{II}M^{III}F_7$, colorless (M^{II} = Mg, Co, Ni ...; M^{III} = Al, Ga, Sc, In ...) [60]. [c] Isostructural are M^IAgF_4, yellow (M^I = Na, Rb) [64].

and +4 (or +3/+5) oxidation states, insofar as these have already been described in detail.

Ag_2F is anomalous and is unique in its stoichiometry, being the only subfluoride so far known. Ag_2F can be prepared, for example, by reaction of AgF with finely divided silver, or by electrolysis of AgF in HF; it is obtained as bronze-colored platelet-like crystals,[56] and is an electrical conductor. The structure is of the same type as that of *anti*-CdI_2, and consists of alternating Ag double layers (metallic bonds) and intercalated fluorine (F^-) layers (ionic bonding). Ag_2F is thus one of the very few examples of cluster compounds (in the broadest sense) containing F^-. It is reminiscent—with a little imaginative licence—of the suboxides of Rb and Cs,[68] although in these cases $Rb_9O_2^{5+}$ or $Cs_{11}O_3^{5+}$ clusters are present (two Rb_6 or three Cs_6 face-sharing octahedra with an O^{2-} ion at the center of each octahedron).

Fluorides of Ag^+ are (mainly) ionic. As might be expected on comparing atomic radii (for C.N. = 6, $r[Ag^+] = 1.15$ Å and $r[Na^+] = 1.02$ Å[69]), they are often found to resemble the corresponding Na^+ compounds (this is true, for example, for the binary fluorides AgF and NaF). A detailed description of the Ag^+ fluorides in this respect is therefore unnecessary. Furthermore, their preparation does not usually call for any special precautions; they can be obtained (similarly to the copper(II) fluorides, which are entirely comparable in this respect) by heating intimately mixed samples of the corresponding binary fluorides under Ar in sealed Ag bombs or welded tubes. Only the preparation of dry AgF presents some difficulties; direct fluorination of finely divided silver at room temperature (using a 1:10 mixture of F_2 with N_2) has proved to be a suitable method. The presence of some AgF_2 here causes no problems; on the contrary, by evolving fluorine it inhibits the partial decomposition to elemental silver (probably caused by a reaction with the container walls) at high temperatures.

It can further be seen from Table 4 that fluorine complexes of silver in the +3 and +4 (+3/+5) oxidation states are rare; so far, only a few have been prepared as pure samples and studied in detail. Such complexes include, aside from Cs_2KAgF_6,[65] the species M^IAgF_4 (M^I = Na, K, Rb),[64] for all of which there exist X-ray powder data.[64] Also magnetic data are available for Cs_2KAgF_6,[65] and spectroscopic data for M^IAgF_4 (M^I = K, Rb[42]). Other compounds which have been reported[71] are $CsAgF_4$ and "$BaAgF_5$" (or "$Ba[AgF_4]_2$", which is analogous to $Ba[AuF_4]_2$[70]), but no further details of these are yet available.

The purple-red paramagnetic complex Cs_2KAgF_6 (with an elpasolite structure!) occupies a special position, being up to now the only confirmed example of a fluoroargentate(III) with Ag^{3+} being 6-coordinative with F^-. The rest of the silver(III) fluorides, which again are not many in number, contain silver in a square planar environment (C.N.$[Ag^{3+}] = 4$, with the possible exception of AgF_3); this certainly also holds true for $CsAgF_4$, "$BaAgF_5$" ($Ba[AgF_4]_2$), and the recently reported $XeF_6 \cdot AgF_3$ ($= XeF_5^+ AgF_4^-$),[67] all of which are yellow and diamagnetic, with still unknown structures.[*]

Little is known, at least with regard to structure, about the red-brown compound AgF_3, which is by far the most sensitive and most difficult of the trivalent silver compounds to isolate; it is prepared by the oxidation of AgF_2 with KrF_2 in HF (20 °C, 2 d), but the product may still contain some impurities. Its color and magnetic properties indicate an octahedral Ag^{3+} environment, comparable with the isoelectronic Pd^{2+} in PdF_2 (C.N.$[Pd^{2+}] = 6$[72]) rather than (as in the case of the mainly planar fluoroargentates(III)) with Au^{3+} in AuF_3 (C.N. $[Au^{3+}] = 4$[20]). The mixed valency formula $Ag^{2+}[Ag^{4+}F_6]^{2-}$ has also been proposed (somewhat analogous to $PdF_3 = Pd^{II}Pd^{IV}F_6$), although this to some extent conflicts with the findings for Cs_2AgF_6 (here the replacement of Ag^{4+} by Ag^{3+}/Ag^{5+} should explain some experimental results).

For Cs_2AgF_6[66] (obtained as an orange-colored, light-sensitive, and very unstable substance by high pressure fluorination of, for example, Cs_2AgF_4), the formula $Cs_2Ag^{III}_{0.5}Ag^{V}_{0.5}F_6$ appears entirely plausible (the isoelectronic PdF_3 too can be envisaged as a mixed valency compound $Pd^{II}Pd^{IV}F_6$,[73] and Ag^{3+} can also be replaced by Ga^{3+}, as in $Cs_2Ga^{III}_{0.5}Ag^{V}_{0.5}F_6$[66]), but the actual structure, as also in the case of AgF_3, can be clarified only by single crystal studies. It is surprising in this context that it has not yet been possible to obtain any pure Ag^V compounds (such as "$CsAgF_6$"), although $CsAuF_6$[74] and the (isoelectronic) Cs_2PdF_6[75] can be prepared without difficulty at normal pressure ($p_{F_2} \leq 1$ bar).

It is easy enough to emphasize on paper the importance of synthesizing single crystals of these very unstable substances, but putting this into practice may still be only a distant prospect, at least with the techniques currently available. It appears that for these compounds (and also for PrF_4,[76] Cs_2KNdF_7 and Cs_2KDyF_7[77,78] and others) a frontier has now been reached, with further progress hindered by the difficulties of synthesizing single crystals using existing methods. The decomposition (with release of F_2), which already commences at room temperature or slightly above leads one to suspect that the substances described here are already thermodynamically unstable toward decomposition to "low valency" fluorides and elemental fluorine in the temperature ranges specified.

Although AgF_2 was first described more than fifty years ago, and its magnetic properties were also investigated soon afterwards,[79,80] there was for a long time uncertainty about its true nature. At first it was envisaged, by analogy with AgO ($= Ag^IAg^{III}O_2$[81]) as a mixed valency compound ($= Ag^I[Ag^{III}F_4]$), and it was only later shown, by more precise magnetic measurements (combined with a thorough understanding of collective magnetic properties), and by a neutron diffraction structure determination (on powder samples),[82] that silver in AgF_2 is actually in the +2 oxidation state.

Surprisingly, fluorine complexes of Ag^{2+}—in contrast to those of Ag^{3+}[63]—were not synthesized until comparatively recently. Then, however, their intense colors (at least

[*] In the meantime the structure of $XeF_5^+AgF_4^-$ has been determined by a single-crystal structure analysis; as suspected Ag^{3+} has C.N. = 4 and resides in a square planar environment (*B. Zemva*, private communication).

for simple inorganic fluorides, and in comparison, e.g. with copper(II) fluorides), their widely varying magnetic properties, and their individual structural properties with sometimes unusual stoichiometry, stimulated the preparation of further silver(II) compounds in rapid succession (Table 5).

In a few cases it was possible to derive the crystal structures from powder diffraction data (based on isostructural types), while "plausibility" considerations and MAPLE calculations[51] led to "credible" interatomic distances $d[Ag^{2+}\text{-}F]$, and gave the first indications concerning the coordination behavior of divalent silver. As a rule, however, more exact information on structure could not be obtained, and spectroscopic data[83] or magnetic measurements[55] provided little further clarification.

Divalent silver is particularly interesting, at least from the structural chemistry standpoint, for several reasons:

1. Ag^{2+}, with its $4d^9$ outer electron configuration, is like Cu^{2+} a cation in which, owing to the Jahn-Teller effect, the ligands need to be less symmetrically arranged around the central ion (Ag^{2+}) than in other M^{2+} ions of comparable size.
2. In the series Pd^{2+}, Ag^{2+}, Cd^{2+} one finds, as a result of the increase in the radius $r_{M^{2+}}$ (or in the ratio $r_{M^{2+}}/r_{F^-}$), a transition from the rutile structure with C.N.$[M^{2+}]=6$ (PdF_2) to the fluorite structure with C.N.$[M^{2+}]=8$ (CdF_2). $CdPdF_4$,[90] which is (formally) "isoelectronic" with AgF_2, and the isostructural high pressure modifications of PdF_2[91,92] and of AgF_2[91] already crystallize in a CaF_2-type structure with C.N.$[M^{2+}]=6$ (+2), with a highly distorted octahedral arrangement of F^- around M^{2+}; for AgF_2 itself and for the corresponding fluoride complexes one therefore might expect to find (at the transition) an essentially singular structural behavior.
3. Neither binary nor simply constructed complexes (i.e. those in which there is no additional stabilization from organic ligands such as py, bpy etc.) of Ag^{2+} are yet known, and, as is shown by the high redox potential of Ag^{2+} ($\varepsilon_0(Ag^+/Ag^{2+})=1.98$ V in aqueous solution!), they are scarcely to be expected. The highly unstable

Table 5. Silver fluorides with oxidation state +2.

Compound	Ref.	Color	Structure	Lattice constants [Å]	Angles [°]	C.N. $[Ag^{2+}]$	$d[Ag^{2+}\text{-}F]$ [Å]	Magnetic properties
AgF_2	[54, 82]	blue-black	unique type (*Pbca*)	$a=5.548$ $b=5.834$ $c=5.094$		4	2.07 (2.59)	antiferromagn. $\mu=1.07$ B.M.
$KAgF_3$ [a]	[54]	brown	perowskite variant (*Pbnm*)	$a=6.186$ $b=6.207$ $c=8.300$		2+4	2.08(2×) 2.20(4×)	antiferromagn. $\mu=0.81$ B.M.
Cs_2AgF_4 [b]	[55]	violet	K_2NiF_4 (*I4/mmm*)	$a=4.581$ $c=14.192$		4	—	weakly ferromagn. $\mu=1.49$ B.M.
$BaAgF_4$ [c]	[84]	violet	$KBrF_4$ (*I4/mmm*)	$a=6.038$ $c=11.46$		4	2.05	paramagnetic $\mu=1.92$ B.M.
$CsAgFeF_6$ [d, e]	[39]	blue-green	unique type (*Pnma*)	$a=7.338$ $b=7.564$ $c=10.554$		2+4	2.049 2.277(2×) 2.055 2.300(2*)	antiferromagn. $\mu=5.95$ B.M.
$CsAgAlF_6$ [d]	[39]	ultramarine blue	$CsAgFeF_6$ (*Pnma*)	$a=7.380$ $b=7.241$ $c=10.352$		2+4	2.063 2.293(2×) 2.081 2.297(2×)	antiferromagn. $\mu=1.30$ B.M.
$RbAgFe_xAl_{1-x}F_6$ [d]	[39]	blue-green	$CsAgFeF_6$ (*Pnma*)	$a=7.19$ $b=7.39$ $c=10.32$		2+4	2.045 2.311(2×) 2.051 2.316(2×)	(antiferromagn.)
$CsAgScF_6$ [f]	[85]	green	$RbNiCrF_6$ (*Fm3m*)	$a=10.79$		6	2.05	antiferromagn. $\mu=1.16$ B.M.
$AgSnF_6$ [g]	[86]	light-blue	($CuPtF_6$) ($P\bar{1}$)	—		—	—	paramagnetic $\mu=1.99$ B.M.
$Ag_3Hf_2F_{14}$ [h]	[87]	blue-violet	unique type (*C2/c*)	$a=9.248$ $b=6.677$ $c=9.064$	$\beta=91.14$	Ag(1) 4+2 Ag(2) 4+2+2	2.066(4×) 2.354(2×) 1.998 2.147(2p) 2.092 2.608(2×) 2.789(2×)	antiferromagn.
$NaAgZr_2F_{11}$ [d]	[61]	blue	unique type ($P\bar{1}$)	$a=7.809$ $b=5.700$ $c=5.832$	$\alpha=106.1$ $\beta=111.5$ $\gamma=96.62$	2+2+2	2.048(2×) 2.181(2×) 2.339(2×)	paramagnetic $\mu=1.87$ B.M.
$Ag[TaF_6]_2$ [d, i]	[88]	light blue	unique type ($P\bar{1}$)	$a=9.044$ $b=5.596$ $c=5.518$	$\alpha=118.76$ $\beta=91.53$ $\gamma=102.42$	4+2	2.067(4×) 2.367(2×)	$\mu=1.95$ B.M.
$AgF_2\cdot 2SbF_5$ [d]	[89]	green	$Ag[TaF_6]_2$ (?) ($P\bar{1}$)	$a=5.224$ $b=5.446$ $c=8.779$	$\alpha=75.78$ $\beta=78.02$ $\gamma=65.29$	5(+2)	2.09(4×) 2.43(2×)	—

[a] Structurally related are: M^IAgF_3, brown (M^I = Rb, Cs) [54]. [b] $M^I_2AgF_4$, violet (M^I = K, Rb) structure not yet known [55]. [c] Isostructural type: $M^{II}AgF_4$, violet (M^{II} = Ca, Sr, Cd, Hg) [84]. [d] Single-crystal data measured for this compound. [e] Isostructural type: $M^IAgM^{III}F_6$, blue to green (M^I = K, Rb, Cs; M^{III} = K, Fe, Ga) [39]. [f] Isostructural type: $M^IAgM^{III}F_6$, green (M^I = Cs; M^{III} = In, Tl) [85]. [g] Probably of isostructural type: $AgM^{IV}F_6$, light blue to black (M^{IV} = Ti, Pb, Pd, Pt ...) [86]. [h] Isostructural type: $Ag_3Zr_2F_{14}$, blue-violet (single crystal data), related are: $M^{II}Ag_2M^{IV}_2F_{14}$, red-violet (M^{II} = Mg, Ni, Zn; M^{IV} = Zr, Hf) and $AgM^{II}_2M^{IV}_2F_{14}$, emerald-green (M^{II} = Ca, Cd, Hg; M^{IV} = Zr, Hf) [87]. [i] Isostructural type: $Ag[NbF_6]_2$, light blue [88] and possibly $AgF_2\cdot 2SbF_5$, green [89].

oxides Ag_3O_4[89] and Ag_2O_3,[93] which have recently been prepared as single crystals by anodic oxidation at low temperatures (about 0°C), do show, however, that oxoargentate(II), or oxoargentate(III) complexes are conceivable. Consequently, if information about the spectroscopic, magnetic or structural chemical properties of Ag^{2+} is required, one has in principle to rely on studies of the corresponding fluorides.

The synthesis of microcrystalline (powder) samples of AgF_2 and complex fluorides of Ag^{2+} is now relatively easy, by direct reaction of suitable starting mixtures with elemental fluorine ("Klemm/Hoppe fluorinations"[94]). Growing single crystals suitable for X-ray structure analysis, on the other hand, sometimes involves considerable difficulties. The reason for this is simple: fluorides of divalent silver decompose with loss of fluorine (in the absence of F_2) at temperatures between 150 and 200°C depending on the particular compound, and, if crystals are required, prolonged annealing (6–10 weeks or longer) at relatively high temperatures (above 580°C, say) under a partial pressure of F_2 (depending on the compound) is necessary. There is, of course, much corrosion of the vessel (with associated impurities and side-reactions) if common materials are used, and it is therefore not surprising that structure determinations from single crystal data have only been successfully achieved in recent times.

The first such success was achieved with silver(II) compounds of the composition $M^IAg^{II}M^{III}F_6$ (M^I = Cs, Rb; M^{III} = Al, Fe).[39] Owing to the high reactivity of MF (wall reactions) and the possibility of silver being oxidized further with the formation of $M[AgF_4]$, careful attention to maintaining correct reaction conditions (F_2 partial pressure, crucible material, temperature) was essential.

It was found that Mg boats "passivated" with fluorine (formation of MgF_2) were especially suitable as sample receptacles, since MgF_2 forms neither mixed crystals nor any kind of ternary compounds with AgF_2, and is also very stable towards other fluorides, especially those of the alkali metals (cf. Scheme 2).

In the first structure determinations carried out on $CsAgFeF_6$, Ag^{2+} was found to have a compressed octahedral environment (an unusual situation for a "Jahn-Teller ion"; cf. Table 5). In order to confirm this unexpected result, the investigations were repeated (with similar results in each case) on $CsAgAlF_6$ and $RbAgAl_{1-x}Fe_xF_6$ (Fe^{3+} being partially replaced in the latter case by Al^{3+} from the corundum boats used!). However, since in parallel with this the same structure was also found in the case of $NH_4Fe^{II}Fe^{III}F_6$[95] (same space group, same occupancy of the corresponding lattice positions, comparable interatomic distances), with no involvement of a cation with d^4 or d^9 configuration in this case, the compression of the octahedron around Ag^{2+} could well be mainly a structural effect. It appears that in both the elpasolites and the pyrochlores (and variants thereof), the Cu^{2+} ion (cf. Table 3) or Ag^{2+} ion adapts to the usually less favorable environment with C.N.$[M^{2+}] = 2+4$, so as to optimize the overall arrangement of the differently charged ions.

This rather vague notion is, however, substantiated to some extent by the existence and structure of $CsPd^{II}Pd^{II}F_5$ and $RbCu^{II}Pd^{II}F_5$. In both these compounds the distribution of all the atoms at the lattice positions corresponds exactly with that in $CsAgFeF_6$ and NH_4FeFeF_6, except that one F^- position remains unoccupied to preserve the electric charge balance. This leads to half the number of Pd^{2+} ions having a square planar configuration with

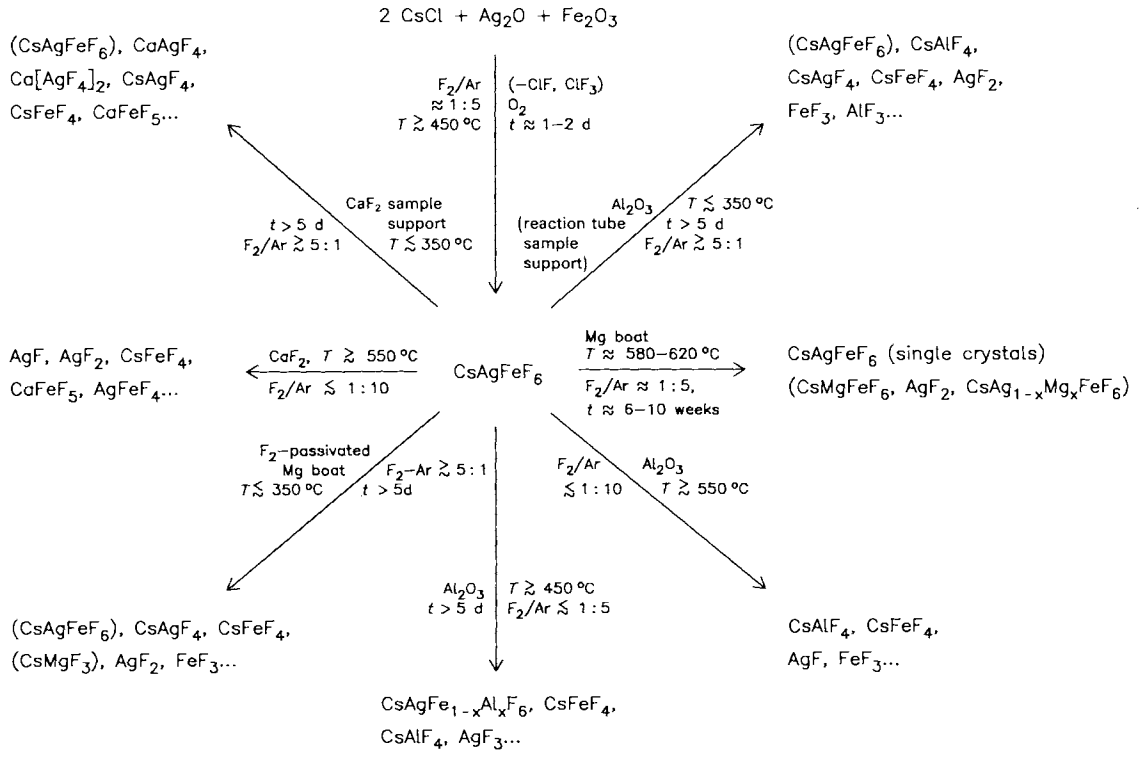

Scheme 2. Conditions needed for preparing $CsAgFeF_6$ single crystals, with side reactions.

C.N.$[Pd^{2+}]=4$ in relation to F^-, instead of being in a compressed octahedral environment (like Ag^{2+}, Fe^{2+}).[37,38] Figures 1a and 1b show the similarity of the two structures.

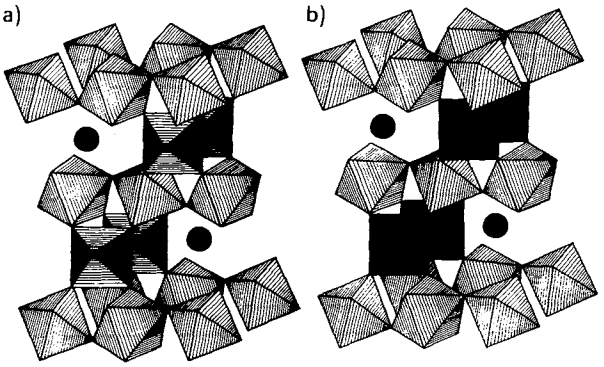

Fig. 1. a) Crystal structure of $CsAgFeF_6$ with chains of $[FeF_6]$ and $[AgF_6]$ octahedra; b) crystal structure of $CsPdPdF_5$ with chains of $[PdF_6]$ octahedra and planar $[PdF_4]$ units.

The synthesis of $Ag_3Hf_2F_{14}$ single crystals is somewhat more difficult, as we here have a phase which is comparatively rich in silver. Accordingly, the compound readily decomposes and annealing must therefore be performed under nearly pure fluorine (cf. Scheme 3). Any small variations in the fluorine concentration above the sample cause partial decomposition with the formation of Ag^+, and the sample melts and "creeps" over the edges of the boat.[87]

The existence of a compound with the composition $Ag_3Hf_2F_{14}$ is quite surprising, since in the case of Cu^{2+}, or the appreciably larger ions Sr^{2+}, Pb^{2+} and Ba^{2+}, under similar conditions one obtains only $M^{II}M^{IV}F_6$ (M^{II} = Cu, Sr, Pb, Ba; M^{IV} = Zr, Hf).[41,96] Its structure too is very unusual, as Ag^{2+} is found to have markedly different coordination numbers at adjacent sites (namely 4+2 and 4+2+2). Consequently, it is possible to selectively replace[87] the first of these two types of Ag^{2+} ions by Cu^{2+}, Ni^{2+}, Zn^{2+} or Mg^{2+} and the other type by Ca^{2+}, Cd^{2+} or Hg^{2+} (although not by Sr^{2+} or Ba^{2+}, which produce bright blue compounds of unknown structure).

This compound, whose structure at first sight appears so complicated, provides a further example of the stability of certain types of ionic structures, which, as was mentioned at the outset, remain essentially unchanged on substituting many different cations. It is therefore not surprising that this structural principle continues to hold true for other compounds of completely different stoichiometry. This is so, not only for $AgPdZr_2F_{11}$ (cf. Tables 5 and 8) and $NaM^{II}Zr_2F_{11}$ (M^{II} = Ag, Pd), formally derived from $Ag(1)Ag(2)_2Zr_2F_{14}$ by replacing $Ag^{2+}(1)$ by Na^+ and "eliminating" AgF_3), but also for $CaMnF_5$,[97] and for $NaMn_3F_{10}$,[98] as can be seen from Figures 2–5.

All these crystal structures are based on coordination polyhedra sharing edges or corners in the "equatorial plane" (i.e. octahedral, pentagonal and hexagonal bipyramids) and all have nearly planar layers, built up in a "base on peak" arrangement (i.e. they are linked through F^- ions in a *trans* position).

It can be seen from this description that loosely packed layers containing only F^- ions (e.g. with a shortest interatomic distance $d[F^-\text{-}F^-]=3.48$ Å in $AgPdZr_2F_{11}$ (Fig. 2)) alternate with layers which, in addition to F^-, contain all the cations (shortest fluorine-fluorine distance in the above compound: d[F-F] = 2.27 Å!). The individual structures differ only in the order of stacking, according to the various stoichiometries.

As a final example of the synthesis of single crystal samples containing Ag^{2+}, we consider $Ag[TaF_6]_2$. Owing to the ease of decomposition into the binary components (in a stream of fluorine gas at temperatures above 150 °C) and the volatility of TaF_5, one must in this case use a closed system (autoclave). The production of single crystals is briefly outlined in Scheme 4.

It is interesting here to note that single crystals of $Ag[TaF_6]_2$ are always found in the cooler, upper part of the autoclave. Since AgF_2 (m.p. $\gtrsim$ 620 °C, under F_2) certainly does not sublime under these conditions ($T \lesssim 400$ °C), TaF_5 must participate (with the formation of volatile complexes of unknown constitution that are stable only at high pressures) in the transport through the gaseous phase.

The layer structure is very simple: three AgF_6 octahedra (with approximate D_{4h} symmetry—see also Table 5) are attached in the *cis* position above a very obviously distorted TaF_6 octahedron (cf. Fig. 6). The remaining three F^- of the TaF_6 octahedron are terminal, i.e. no linkage via further cations takes place between each of the layers. Thus each AgF_6 octahedron has six different TaF_6 octahedra, each TaF_6 octahedron, however, only three different AgF_6 octahedra as ligands (for further details cf. Ref. [90]).

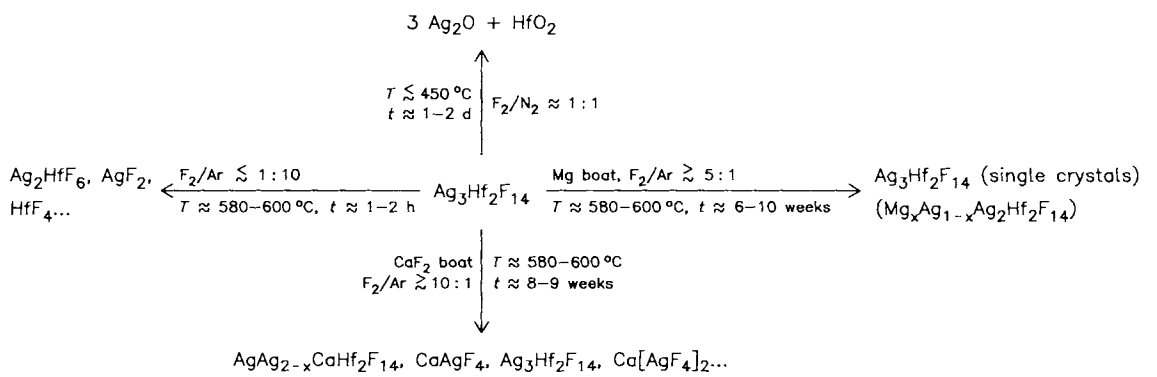

Scheme 3. Conditions for the synthesis of $Ag_3Hf_2F_{14}$ single crystals, with side reactions.

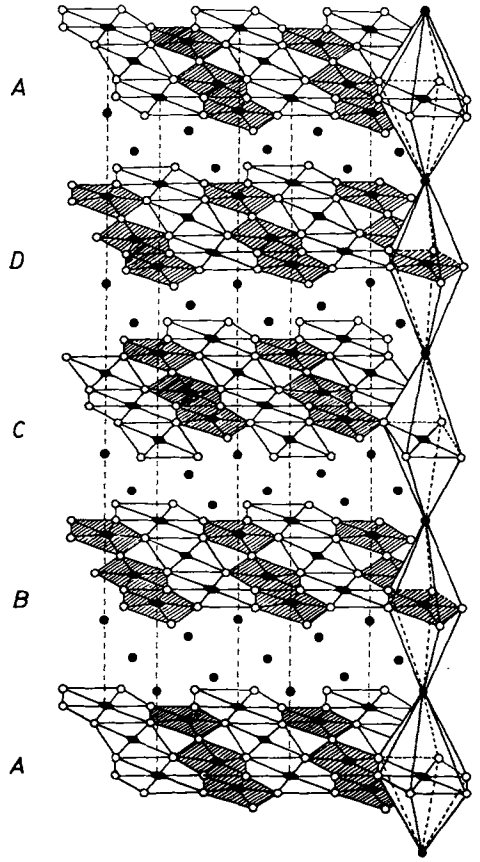

Fig. 2. Layer structure and layer sequence in $AgPdZr_2F_{11}$ ($NaAgZr_2F_{11}$). Black squares: Pd^{2+}; black hexagons: Ag^+; black pentagons: Zr^{4+}; circles: F^-.

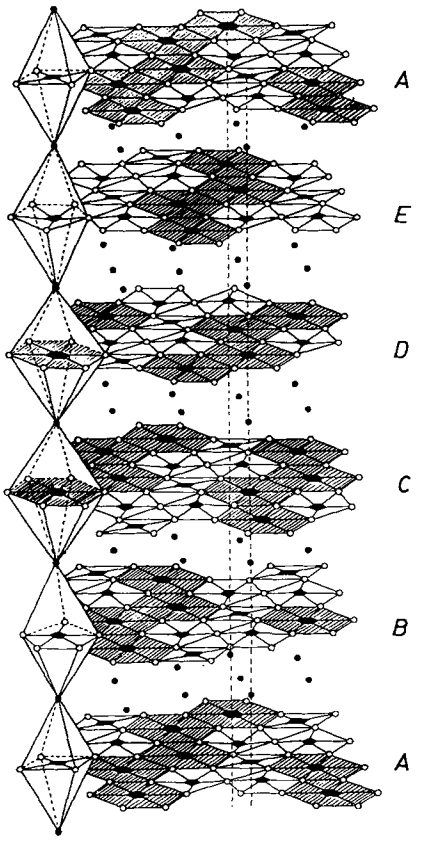

Fig. 3. Layer structure and layer sequence in $Ag_3Hf_2F_{14}$. Black squares: $Ag^{2+}(1)$; black hexagons: $Ag^{2+}(2)$; black pentagons: Hf^{4+}; circles: F^-.

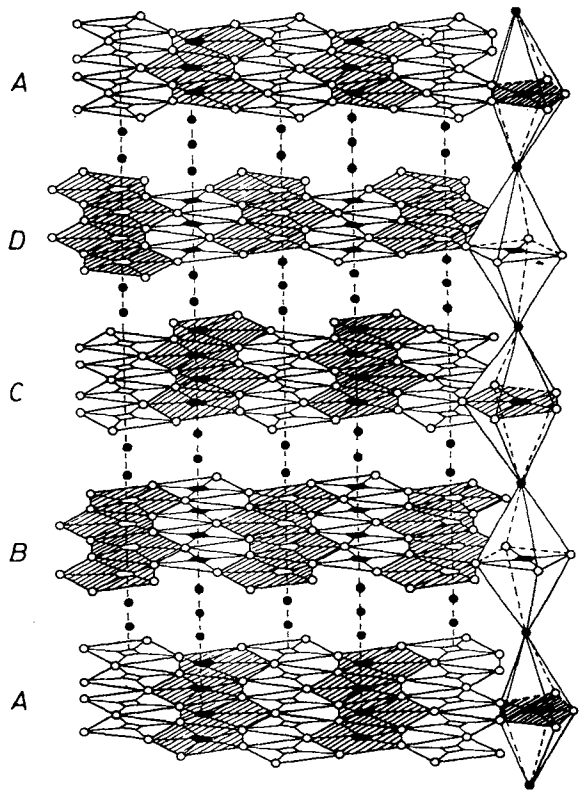

Fig. 4. Layer structure and layer sequence in $CaMnF_5$. White squares: Mn^{3+}; white pentagons: $Ca^{2+}(1)$; black pentagons: $Ca^{2+}(2)$; circles: F^-.

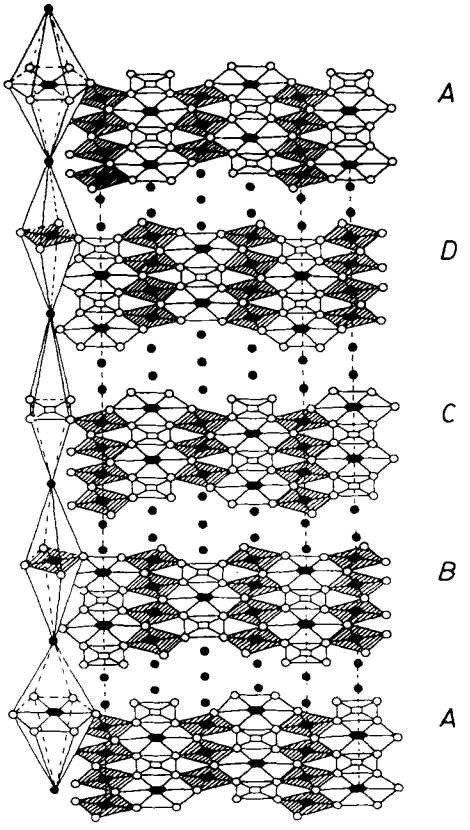

Fig. 5. Layer structure and layer sequence in $NaMn_3F_{10}$. Black hexagons: Na^+; white squares: $Mn^{3+}(1)$; black squares $Mn^{3+}(2)$; circles: F^-.

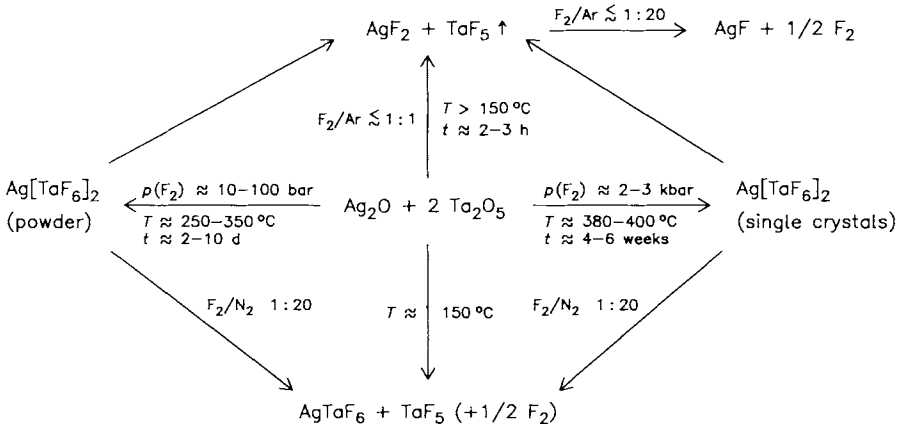

Scheme 4. Conditions for the synthesis of $Ag[TaF_6]_2$ single crystals, with side-reactions.

As we can see from the examples given here, silver(II) compounds are actually quite unpredictable in their structural chemical behavior. The conditions needed to prepare them—at least for single crystals—vary considerably and cannot be simply extended from one to another, so that one must treat each case individually and find the optimal conditions, sometimes through a tedious succession of experiments calling for much patience.

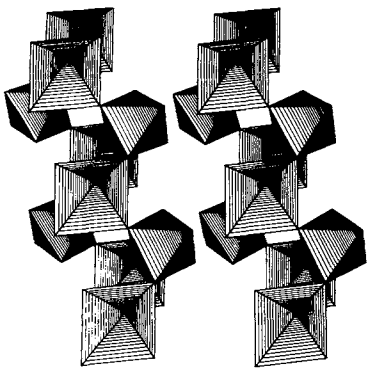

Fig. 6. The layer structure of $Ag[TaF_6]_2$, consisting of corner-sharing $[AgF_6]$ and $[TaF_6]$ octahedra.

4. Gold Compounds

In contrast to the rather "enigmatic" behavior of silver fluorides, and to a lesser extent that of copper fluorides, the chemistry and especially the structural chemistry of gold fluorides are remarkably lacking in surprises. This is largely due to the fact that neither gold(I), gold(II) nor (clearly defined) gold(IV) fluorides have thus far been described. Only fluoroaurates(III) and a few fluoroaurate(V) complexes are known. They are all yellow, the coordination number relative to fluorine being always $C.N.[Au^{3+}]=4$ for the trivalent gold compounds (square planar configuration), and $C.N.[Au^{5+}]=6$ for the pentavalent gold compounds (octahedral environment).

Further, all the compounds are diamagnetic, excepting where one of the other cations is paramagnetic. Their preparation too is generally comparatively easy, and is carried out under similar conditions for the different compounds.

In the case of the ternary gold(III) fluorides, the volatility of AuF_3 in the stream of fluorine ($T>350°C$) causes something of a problem; nevertheless it is possible[20] to obtain AuF_3 as orange-red needle-shaped crystals up to several mm in length. Single crystals of the ternary fluorides listed in Table 6 can be obtained (similarly to the Cu^{2+} and Ag^{2+} compounds) by annealing fine mixtures of the starting components in welded Au tubes (under dry Ar).

It is interesting from a crystallographic point of view that so many different structure types are found for the same empirical formula $M^{II}[AuF_4]_2$. It appears that here the structure is determined (in a subtly graded way) by the sizes (i.e. ionic radii) of the individual cations. Thus for $M^{II}[AuF_4]_2$ with different metals one finds different types of structures as follows: $M^{II}=Mg$, Ni or Zn (monoclinic), $M^{II}=Pd$ (orthorhombic), $M^{II}=Ca$ or Sr (monoclinic), $M^{II}=Cd$, Hg or Pb (tetragonal-P), $M^{II}=Ba$ (tetragonal-I), with coordination numbers ranging from $C.N.[M^{2+}]=6$ (e.g. Mg^{2+}) to $C.N.[M^{2+}]=12$ (Ba^{2+}).[42] Copper, instead of forming "$Cu[AuF_4]_2$", forms the compound $FCu[AuF_4]$, in which only one of the F^- ions in CuF_2 is formally replaced by $[AuF_4]^-$. The structure of this compound (see Fig. 7) is surprisingly simple: linear [-F-Cu-F-] chains lie along the [001] direction, around which, at the same "height" as Cu^{2+}, four isolated square planar $[AuF_4]$ units are so arranged that one F^- ion of each such unit completes the (highly distorted) octahedron around the Cu^{2+}.[43] In contrast the structures of $FM^{III}_2[AuF_4]_5$—in which we again see that the F^- ions of MF_3 are only partly formally replaced by $[AuF_4]^-$—are extraordinarily complicated. Remarkable is the occurrence of $[M^{III}_2F_{17}]$ units (two corner-sharing trebly capped trigonal prisms), which are linked by (isolated) $[AuF_4]^-$ units to form a three-dimensional structure (cf. Fig. 8).

Comparatively little is known about gold(V) fluorides; the first known gold(V) compound was described only quite recently.[102] This is rather surprising, since $CsAuF_6$ can be obtained by the direct conversion of $CsAuCl_4$ with elemental fluorine at about 300°C; to prepare homogeneous samples, however, increased fluorine pressures are recommended.[101] It appears that the surprisingly easy formation and the (relatively) good stability of $CsAuF_6$ (toward decomposition into $CsAuF_4+F_2$) were so unexpected that the results of early experiments led, at first, to wrong inter-

Table 6. Gold fluorides with oxidation states +3 and +5.

Compound	Ref.	Color	Structure	Lattice constants [Å]	Angles [°]	C.N. [Au^{n+}]	d[Au^{n+}-F] [Å]	Magnetic properties
AuF_3 [a]	[20]	red-orange	unique type ($P6_122$)	$a=5.149$ $c=16.26$		4	1.91(2×) 2.04(2×)	diamagnetc
$Rb[AuF_4]$ [a, b]	[42]	yellow	$KBrF_4$ ($I4/mmm$)	$a=6.182$ $c=11.911$		4	1.915	diamagnetic
$Zn[AuF_4]_2$ [a, c]	[70]	yellow	unique type ($P2_1/c$)	$a=5.847$ $b=5.518$ $c=10.83$	$\beta=109.3$	4	1.892(2×) 1.924 1.928	diamagnetic
$Ba[AuF_4]_2$ [a]	[70]	yellow	unique type ($I\bar{4}$)	$a=9.788$ $c=7.600$		4	1.898(2×) 1.931 1.937	diamagnetic
$FCu[AuF_4]$ [a]	[43]	yellow	unique type ($P\bar{1}$)	$a=5.536$ $b=4.979$ $c=3.707$	$\alpha=107.6$ $\beta=98.77$ $\gamma=89.63$	4	1.907(2×) 1.930(2×)	antiferromagn. $\mu=1.32$ B.M.
$FPr_2[AuF_4]_5$ [a, d]	[99]	yellow	unique type ($P4_12_12$)	$a=8.310$ $c=25.897$		4	1.889 1.905 1.890 1.926	paramagnetic $\mu=7.47$ B.M.
$FEr_2[AuF_4]_5$ [a, e]	[100]	yellow	unique type ($P2_1/n$)	$a=8.955$ $b=7.960$ $c=7.960$	$\beta=90.83$	4	1.883 1.975 1.885 2.008	paramagnetic $\mu=11.45$ B.M.
AuF_5	[74]	orange	(RhF_5?)	—		—	—	diamagnetic
$CsAuF_6$ [f]	[101]	yellow	$LiSbF_6$ ($R\bar{3}$)	$a=5.24$	$\alpha=96.5$	—	—	diamagnetic
$Xe_2F_{11}^+AuF_6^-$ [a]	[102, 103]	yellow-green	$Xe_2F_{11}^+RuF_6^-$ ($Pnma$)	$a=9.115$ $b=8.542$ $c=15.726$		6	1.85 1.86(4×) 1.90	diamagnetic
$O_2^+AuF_6^-$	[101]	lemon-yellow	$LiSbF_6$ ($R\bar{3}$)	$a=5.001$	$\alpha=99.5$	—	—	paramagnetic $\mu=1.66$ B.M.
$IF_6^+AuF_6^-$	[101]	yellow	unique type	$a=9.573$		—	—	diamagnetic

[a] Single-crystal data measured for this compound. [b] Isostructural are $M^I[AuF_4]$, yellow (M^I = Na–Cs) [104]. [c] Isostructural are $M^{II}[AuF_4]_2$, yellow (M^{II} = Mg, Ni); (M^{II} = Cd, Hg, Pb, Pd, Ag) have unknown structure [70]. [d] Isostructural $FM_2^{III}[AuF_4]_5$, yellow (M^{III} = In, Tl, Bi, La–Tb) [99]. [e] Isostructural are $FM_2^{III}[AuF_4]_5$, yellow (M^{III} = Dy–Lu) [100]. [f] Isostructural are $MAuF_6$, yellow ($M=NO^+$, K) [101].

pretations ("$CsAuF_4 \cdot 1.5\,HF$"); the same also applies in the case of "$M[AuF_4] \cdot x\,HF$" (M = K, Rb; $x = 1.5$–2.0).[105]

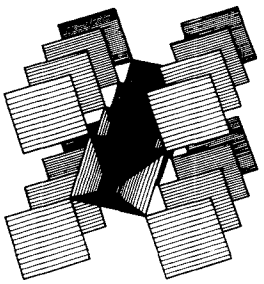

Fig. 7. Crystal structure of $FCu[AuF_4]$, with corner-sharing chains of $[CuF_6]$ octahedra and planar $[AuF_4]$ units.

Single crystal studies have so far only been carried out on $[Xe_2F_{11}]^+[AuF_6]^-$,[103] whose preparation under comparatively "mild" conditions ($T \approx 400$ °C, $p_{F_2} \approx 70$ bar, $t \approx 48$ h) is possibly made easier by the volatility (and high mobility) of XeF_6, or perhaps of both components (AuF_5, XeF_6).

In AuF_6^-, as in all other examples which have been studied in detail, Au^V is in an octahedral environment; the interatomic distances $d[Au^{5+}\text{-}F^-] = 1.85$–$1.90$ Å are of the expected order of magnitude. Other fluorine complexes of pentavalent gold, e.g. $M^{II}[AuF_6]_2$ (M^{II} = Ca, Sr) and "$FM_2^{III}[AuF_6]_5$" (M^{III} = La, Pr ...), can be prepared by high-pressure fluorination ($p_{F_2} > 3$ kbar) of $M^{II}[AuF_4]_2$ or $FM_2^{III}[AuF_4]_5$ respectively, but up to now they have only been obtained as microcrystalline powders, owing to increasing instability.[100]

Only sparse information exists as yet on gold pentafluoride, which is, as expected, the most unstable of the gold(v) compounds. It is obtained in the form of a dark orange-red, diamagnetic X-ray amorphous solid upon careful thermal decomposition of $O_2^+AuF_2^-$ (or $KrF^+AuF_6^-$). In the solid state (m.p. ≈ 75 °C) tetrameric units are probably present (as in RhF_5 and other pentafluorides[19]), and elec-

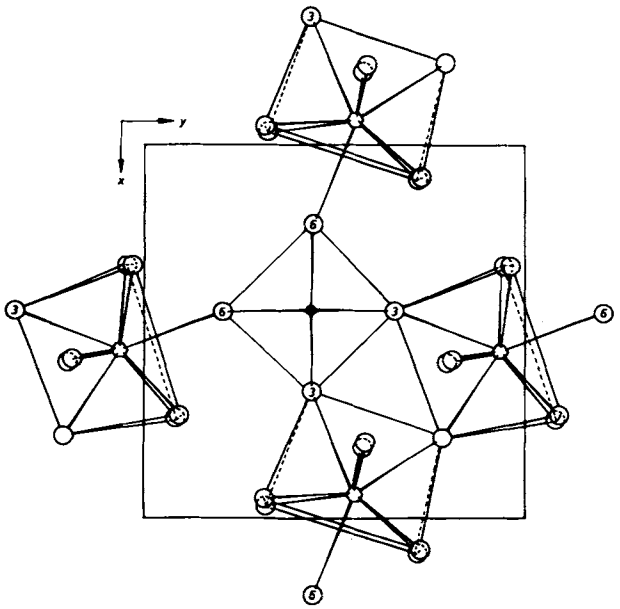

Fig. 8. The $[M_2^{II}F_{17}]/[AuF_4]$ units in $FM_2[AuF_4]_5$ (M = In, La-Tb) and their interlinkage. Filled circles: Au^{III}; open circles, F^-; hexagons, Mn^{III}.

tron diffraction studies (at 493 K) have provided evidence for the existence of $[AuF_5]_2$ and $[AuF_5]_3$ species.[106]

Viewed as a whole, the fluoroaurate(V) complexes are comparatively difficult to prepare, with increased fluorine pressures being generally necessary, but most of them (e.g. $MAuF_6$, where M = K, Rb, Cs) are appreciably more stable than, for example, Cs_2AgF_6 or Cs_2CuF_6.

In the interest of completeness it should also be mentioned here that in Raman spectroscopic measurements on a mixture of $NO^+AuF_4^-$ and $NO^+AuF_6^-$ also the yellow compound $[NO^+]_2[AuF_6]^{2-}$ was identified. However, in view of the comparatively small amount of information available, further more detailed studies are needed (especially magnetic measurements) to confirm the existence of this only known example of a gold(IV) compound.[107] The same applies to the recently reported compound "AuF_7" (prepared by the reaction of AuF_5 with F_2 in vacuum (!)), for which again there exists only spectroscopic evidence.[108]

5. Palladium Compounds

The existence of fluorides of di-, tri- and tetravalent palladium is firmly established (cf. Table 7). Results on $O_2^+PdF_6^-$ containing Pd^V (identified by Raman spectroscopy) need to be definitely substantiated, since under comparable reaction conditions ($p_{F_2} \gtrsim 4$ kbar, $T \approx 300$–400°C, $t \approx 2$ h–3 d) no evidence has so far been found for the formation of "$CsPdF_6$".

Further, the X-ray powder diffraction patterns of $O_2^+PdF_6^-$, containing many lines, are considerably different from those of the structurally related dioxygen(1+) compounds $O_2^+MF_6^-$ (M = Rh, Pt, Au ...) having the same general formula.[109]

There is little difficulty in synthesizing alkali metal and alkaline earth metal fluoropalladates(IV) (by conversion of the appropriate starting mixtures with dilute fluorine at temperatures of 300–500°C)[75,110] and the compounds $M^{II}PdF_6$ (with M^{II} = Ni, Mg, Zn ...),[111] including $Pd[PdF_6]$ itself.[73] The brick-red, diamagnetic, very unstable compound PdF_4 is, in contrast, obtainable only by high-pressure fluorination of PdF_3.[112] Its structure (determined by neutron diffraction on powder samples) is unusual, and consists—in contrast to SnF_4[113]—of $[PdF_6]$ octahedra linked at their corners with terminal F^- ions in the *cis* position.[114] The interatomic distances $d[M^{4+}\text{-}F^-]$ are comparable to those in SnF_4.

Up to now, single crystal studies have only been carried out on $[XeF_5^+]_2[PdF_6]^{2-}$, prepared under conditions identical to those for single crystals of $Xe_2F_{11}^+AuF_6^-$.[117] Like the isoelectronic Au^{5+} ion, Pd^{4+} here has an octahedral environment of fluorine ions; the interatomic distances have been found to be in the range $d[Pd^{4+}\text{-}F^-] = 1.86$–$1.92$ Å, as expected and previously estimated from known Pd^{IV} complexes.[75]

The constitution of PdF_3—similarly as in the case of AgF_2—was at first in doubt, but one can now regard the mixed valency formula $Pd^{II}[Pd^{IV}F_6]$ as proven, despite the lack of any single-crystal data. On the other hand, "true" palladium(III) fluorides are extraordinarily rare, having been reported for the first time only recently.[115,116] Their preparation is sometimes not easy, and in certain cases one needs to use high pressures (inert gas, e.g. Ar at about 4 kbar). The compounds $M_2^IM'^{II}PdF_6$ (elpasolites!), however, can be prepared by heating the binary fluorides under argon at atmospheric pressure.[115]

In view of the fact that Co^{2+} (with an identical arrangement of valence electrons) always has the $t_{2g}^5e_g^1$ ("high spin") configuration in fluorides, and that magnetic measurements on Ni^{3+} compounds (e.g. on Cs_2KNiF_6[119]) indicate a thermal equilibrium between "high spin" and "low spin" configurations (with the possibility of a Jahn-

Table 7. Palladium fluorides with the oxidation states +3 and +4.

Compound	Ref.	Color	Structure	Lattice constants [Å]	Angle [°]	C.N. $[Pd^{n+}]$	$d[Pd^{n+}\text{-}F]$ [Å]	Magnetic properties
"PdF_3" $= Pd^{II}Pd^{IV}F_6$	[73]	black-violet	$LiSbF_6$ ($R\bar{3}$)	$a = 5.01$ $c = 14.12$		6	2.04	paramagnetic $\mu = 2.88$ B.M.
K_2NaPdF_6 [a]	[115]	light green	elpasolite variant ($F4/mmm$)	$a = 8.30$ $c = 8.72$		4+2	1.95(4×) 2.14(2×)	(paramagnetic)
$NaPdF_4$	[116]	gray	$KBrF_4$ variant (monoclinic)	$a = 11.84$ $b = 5.36$ $c = 5.86$	$\beta = 114$	(4)	—	(paramagnetic)
PdF_4	[112, 114]	brick red	unique type ($Fdd2$)	$a = 9.339$ $b = 9.240$ $c = 5.828$		6	1.91(2×) 1.94(2×) 2.00(2×)	diamagnetic
$PbPdF_6$ [b]	[110]	yellow	$BaGeF_6$ ($R\bar{3}m$)	$a = 7.213$ $c = 6.989$		6	1.82	diamagnetic
$MgPdF_6$ [c]	[111]	yellow	$LiSbF_6$ ($R\bar{3}$)	$a = 4.98$ $c = 13.48$		6	1.85	diamagnetic
Cs_2PdF_6 [d]	[75]	yellow	K_2PtCl_6 ($Fm3m$)	$a = 9.00$		6	1.89	diamagnetic
$[XeF_5^+]_2[PdF_6]^{2-}$ [e]	[117]	yellow	unique type ($Pca2_1$)	$a = 9.346$ $b = 12.78$ $c = 9.397$		6	1.860–1.902	diamagnetic

[a] Isostructural or structurally related are $M_2^IM'^{II}PdF_6$, light green to beige (M^I = K, Rb, Cs; M'^{II} = Li, Na, K, Rb) [115]. [b] Isostructural are $M^{II}PdF_6$, yellow (M^{II} = Ba, Sr) [118]. [c] Isostructural are $M^{II}PdF_6$, yellow ocher (M^{II} = Ni, Mg, Zn ...) [112]. [d] Isostructural or structurally related are $M_2^IPdF_6$, yellow (M^I = K, Rb, Cs) [110]. [e] Single-crystal data measured for this compound.

Teller distortion involving Ni^{3+}), there is naturally great interest in the comparable palladium(III) fluorides. ESR and magnetic measurements indicate the existence of the "low spin" case ($t_{2g}^6 e_g^1$). If the arrangement of F^- ions around the Pd^{3+} ion could be determined, with exact values for the distances $d[Pd^{3+}\text{-}F^-]$, this would give information concerning the nature and magnitude of the Jahn-Teller distortion, which would be of considerable importance.[115]

Divalent palladium behaves in complex fluorides as an inorganic "chameleon", i.e. it adapts its coordination number, and accordingly the structure, color, and magnetic properties in the compounds concerned, to the situation imposed by the type and number of the accompanying cations.

In the alkali metal and alkaline earth metal fluoropalladate(II) complexes one generally finds a square planar environment (C.N.$[Pd^{2+}]=4$), e.g. in $M_2^IPdF_5$ (M^I = K, Rb, Cs) (yellow),[37] and in $M^{II}[PdF_4]$ (M^{II} = Ba (orange), Sr (red), Ca, Pb (purple)),[120] all of which are diamagnetic. In the compounds $M^IPd^{II}Pd^{III}F_5$ (M^I = K, Rb, Cs), which are orange-brown and antiferromagnetic, Pd^{2+} occupies a half octahedral and half square planar environment of F^- ions; the Pd^{2+} ions in octahedral positions can be selectively replaced by M^{2+}, [$M^{2+}=Mg^{2+}$ or Zn^{2+} (yellow, diamagnetic) and $M^{2+}=Ni^{2+}$ or Cu^{2+} (yellow and orange-brown respectively, antiferromagnetic)].[37,38]

Fluorides in which Pd^{2+} has regular octahedral coordination can be violet colored (PdF_2[72,120,121]), brown-violet ($RbPdF_3$[90]) (both antiferromagnetic), or blue ($NaPdZr_2F_{11}$, $AgPdZr_2F_{11}$, paramagnetic[61]). In addition, we have dark blue $CdPdF_4$, black $HgPdF_4$,[122] and HP-PdF_2[91,92] (antiferromagnetic) with a highly distorted octahedral arrangement of F^- around Pd^{2+}.

As a rule, the divalent palladium compounds listed in Table 8 are quite easy to prepare. If required, they can be obtained as single crystals by annealing mixtures of the appropriate binary fluorides under inert gas (Ar) in welded Pd tubes. The preparation of pure samples of PdF_2, however, presents something of a problem; PdF_3 (obtained by fluorination of, e.g., metallic Pd) is allowed to react with powdered palladium (which has previously had all traces of oxygen removed by heating in high vacuum), under inert gas (Ar) in welded Pd tubes at temperatures between 600 and 950 °C. By this method, using $T \gtrsim 950$ °C and $t \approx 4$-6 weeks, it has been possible to grow excellent millimeter-sized, amethyst-colored single crystals of PdF_2.[120]

Of the many palladium(II) fluorides which are now known, and which, in some cases, have been characterized by single crystal measurements, aside from those already mentioned, the compounds $CsPdPdF_5$, $M_3^IPdF_5$ (M^I = K, Rb, Cs), and $CdPdF_4$ are especially noteworthy. In Rb_3PdF_5, which is an "alkali-rich" phase, unusual amongst fluorometalate(II) complexes, two crystallogra-

Table 8. Palladium fluorides with oxidation state +2.

Compound	Ref.	Color	Structure	Lattice constants [Å]	Angles [°]	C.N. $[Pd^{2+}]$	$d[Pd^{2+}\text{-}F]$ [Å]	Magnetic properties
PdF_2 [a]	[72,120,121]	amethyst	rutile ($P4/mnm$)	$a=4.961$ $c=3.391$		4+2	2.15(4×) 2.17(2×)	antiferromagn. $\mu=1.90$ B.M.
HP-PdF_2	[91,92]	black	$CdPdF_4$ ($Pa3$)	$a=5.327$		6	2.175	antiferromagn. $\mu=2.10$ B.M.
$CdPdF_4$ [a, b]	[122]	dark blue	CaF_2 variant ($Pa3$)	$a=5.403$		6	2.205	antiferromagn. $\mu=2.58$ B.M.
$CaPdF_4$ [a, c]	[120]	purple	$KBrF_4$ ($I4/mmm$)	$a=5.521$ $c=10.570$		4	1.991	diamagnetic
$RbPdF_3$ [d]	[90]	brown-violet	perowskite variant ($Pm3m$)	$a=4.298$		6	2.15	antiferromagn. $\mu=1.32$ B.M.
$CsPdInF_6$ [e]	[123]	brown-violet	$RbNiCrF_6$ ($Fd3m$)	$a=10.89$		—	—	antiferromagn. $\mu=1.79$ B.M.
$CsPdPdF_5$ [a, f]	[37]	orange-brown	unique type ($Imma$)	$a=6.53$ $b=7.862$ $c=10.79$		4	1.951	antiferromagn. $\mu=1.56$ B.M.
Rb_3PdF_5 [a, g]	[37]	yellow	unique type ($P4/mbm$)	$a=7.462$ $c=6.457$		4	1.926	diamagnetic
$CsRb_2PdF_5$ [a, g]	[37]	yellow	Rb_3PdF_5 ($P4/mbm$)	$a=7.579$ $c=6.455$		4	1.940	diamagnetic
$RbCuPdF_5$ [a, h]	[38]	orange-brown	unique type ($Pnma$)	$a=6.269$ $b=7.199$ $c=10.76$		4	1.944(2×) 1.975(2×)	(antiferromagn.)
$NaPdZr_2F_{11}$ [a]	[61]	blue	$NaAgZr_2F_{11}$ ($P\bar{1}$)	$a=7.910$ $b=5.746$ $c=5.745$	$\alpha=106.7$ $\beta=112.2$ $\gamma=97.9$	6	2.154(4×) 2.165(2×)	paramagnetic $\mu=2.88$ B.M.
$AgPdZr_2F_{11}$ [a]	[61]	blue	unique type ($C2/m$)	$a=9.351$ $b=6.991$ $c=7.801$	$\beta=115.7$	6	2.160(2×) 2.172(4×)	paramagnetic $\mu=2.83$ B.M.
$PdPtF_6$ [a]	[38,73]	green	$LiSbF_6$ ($R\bar{3}$)	$a=5.038$ $c=14.31$		6	2.176	paramagnetic $\mu=2.88$ B.M.

[a] Single-crystal data measured for this compound. [b] Isostructural are $HgPdF_4$, black [90]. [c] Isostructural are $M^{II}PdF_4$, purple to orange (M^{II} = Sr, Ba, Pb) [120]. [d] Structurally related are M^IPdF_3, brown-violet (M^I = K, Tl) [90]. [e] Isostructural are $CsPdM^{III}F_6$ (M^{III} = Fe, Sc ...) [92]. [f] Isostructural are $M^IM^{II}PdF_5$, yellow to orange-brown (M^I = K, Rb, Cs, Tl; M^{II} = Pd, Mg, Ni) [37]. [g] Isostructural are $M_3^IPdF_5$ and $M^IM_2^{II}PdF_5$, yellow (M^I = K, Rb, Cs, Tl) [37]. [h] Isostructural are M^ICuPdF_5 (M^I = K, Cs) [100].

phically different types of Rb^+ and F^- ions are present. Those rubidium ions which occupy sufficiently large holes in the lattice can be specifically replaced by cesium (to give $CsRb_2PdF_5$), with no appreciable change in the lattice constants, but attempts to carry out a similar partial exchange of Cl^- for F^- have so far been unsuccessful. Most surprisingly, however, the same types of compounds and structures have recently been found in complex platinum hydrides, e.g. Rb_3PtH_5 or $CsRb_2PtH_5$.[124] Figure 9 shows a pictorial impression of the structure of the palladium compounds, consisting of channels with square and triangular cross sections.

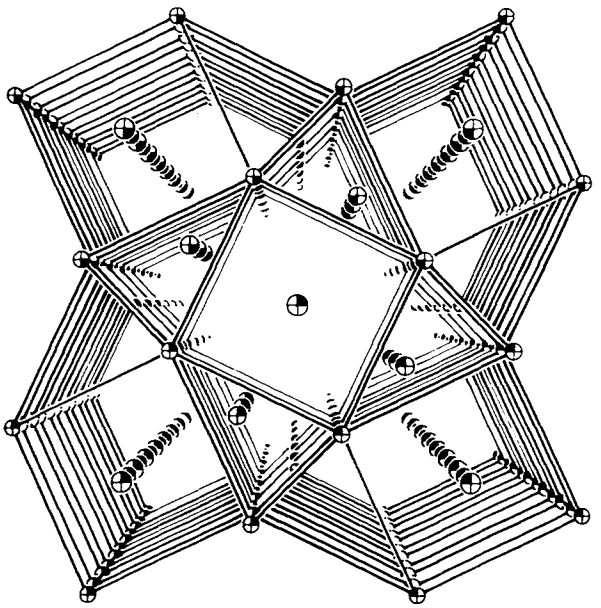

Fig. 9. Crystal structure of Rb_3PdF_5 and $CsRb_2PdF_5$ with tetragonal and trigonal channels.

Finally, $CdPdF_4$ (and also $HgPdF_4$) is of interest from a structural chemical standpoint, since it undergoes the transition from a $KBrF_4$-type structure, through a variant of the CaF_2 type ($CdPdF_4$), to the pure CaF_2 type (CdF_2), as has already been suggested in the case of $CdAgF_4$[84] (with $c/a \approx 1.99$). In view of this, it seems plausible that high pressure modifications of PdF_2 and AgF_2, metastable at normal pressure and isostructural with $CdPdF_4$, can exist.

6. Concluding Remarks

Despite the remarkable progress that has been made in this area of inorganic solid state chemistry the present state of our knowledge regarding the fluorides of copper, silver, gold and platinum, which has here been described only selectively, still leaves much to be desired. In the first place there is a shortage of available methods for preparing pure homogeneous samples (partly due to a lack of suitable methods of purification), and secondly the growing of single crystals (especially those of fluorides with poor thermal stability) is often hindered by severe problems in finding suitable materials, and by the occurrence of obscure or unpredictable side reactions.

It is possible in some cases that the presence of one or more volatile substances (even when one can only speculate about their existence as intermediate products or species of unknown composition) plays an important or even a crucial role. Two final examples will again serve to illustrate this.

1. When one tries to make single crystals of $Ba[AuF_6]_2$ (F_2 pressure >3 kbar) one obtains, in addition to crystals of that compound (of moderate quality), ruby-red single crystals of $BaNiF_6$ (formed by Ni from the monel-metal crucible!). This compound can normally be prepared (under comparable conditions, but without Au) only with difficulty, and always in microcrystalline form.[125, 126] A possible cause of this surprising occurrence of $BaNiF_6$ crystals is the formation of AuF_5 (as a "mobile phase" side-product) during the preparation. However, in the absence of firm evidence this remains mere speculation.
2. Single crystals of MnF_4 are only obtained (under an F_2 pressure of >3 kbar) if traces of O_2 are present (leading to formation of the volatile, structurally related compound $O_2^+Mn_2F_9^-$). In oxygen-free experiments under otherwise identical conditions, the samples produced are X-ray amorphous.[127, 128]

Finally, we are still far from having a deeper understanding of these structures, even in such simple systems which are formed predominantly by ionic bonding.

Thus, it remains unclear (and incomprehensible) why, in the system MF_2/ZrF_4 with both small (M^{II} = Ni, Co, Fe ... through to Cu) and large (M^{II} = Ca, Cd, Eu ...) cations, compounds of the type $M^{II}ZrF_6$ are formed (usually variants of the ReO_3 structure), whereas with Ag^{2+}, $Ag_3Zr_2F_{14}$ is formed (with a noticeably more complicated structure), and—even less comprehensible—why no compounds at all are formed with Pd^{2+}.

Simple models or concepts based on purely ionic bonding are inadequate to explain these results. Consequently, even in fluorides of metals in low oxidation states, there must be additional factors (apart from simple geometrical influences such as those of ionic radii or local distortions of the immediate environment due to the Jahn-Teller effect). For example, there could be a definite space requirement for occupied d orbitals (with a preferred orientation), as has been suggested for NbF_4,[129] or there may be significant contributions from covalent bonding (considering the volatility of AuF_3 and HgF_2!).

This is quite at variance with the view expressed by *Wilhelm Klemm* (on the occasion of a tribute in 1940 to the work of *O. Ruff* in fluorine chemistry): "*Ruff*'s work on the preparation of fluorides was so complete and thorough that little more remains to be done. In future research in this field the emphasis must increasingly be on determining their physical properties".[130] On the contrary, now as then we need new or more refined and sophisticated methods for preparing purer, well-characterized samples, including single crystals (as indeed *Klemm* himself shortly afterwards demonstrated when he introduced new fluorination techniques). The substances so prepared will then

lay down the basis for measuring their real physical properties and interpreting them correctly.

I wish to thank Herrn Dipl.-Chem. D. Kissel, Herrn Dr. M. Serafin, Herrn Dr. K. H. Wandner and, in particular, Frau W. Schmidt for their extremely valuable help in preparing this review.

Received: June 25, 1987 [A 641 IE]
German version: *Angew. Chem. 99* (1987) 1120
Translated by Dr. *J. K. Becconsall*, Northwich (UK)

[1] W. Klemm, *Angew. Chem. 63* (1951) 396.
[2] W. Klemm, E. Huss, *Z. Anorg. Allg. Chem. 258* (1949) 221.
[3] R. Hoppe, *Z. Anorg. Allg. Chem. 292* (1957) 28.
[4] N. Bartlett, *Proc. Chem. Soc. (London) 1962*, 218.
[5] R. Hoppe, H. Mattauch, K.-M. Rödder, W. Dähne, *Z. Anorg. Allg. Chem. 74* (1962) 903.
[6] K. O. Christe, *Inorg. Chem. 12* (1973) 1580.
[7] H. Selig, J. H. Holloway, *Top. Curr. Chem. 124* (1984) 33.
[8] W. Harnischmacher, R. Hoppe, *Angew. Chem. 85* (1973) 590; *Angew. Chem. Int. Ed. Engl. 12* (1973) 582.
[9] *J. Fluorine Chem. 33* (1986) (Special issue on the history of fluorine chemistry).
[10] P. Hagenmüller: *Inorganic Solid Fluorides*, Academic Press, New York 1985.
[11] J. Grannec, L. Locano, P. Hagenmüller in [10], Chap. 2.
[12] L. Grosse, R. Hoppe, *Naturwissenschaften 69* (1982) 447.
[13] P. Bukovec, R. Hoppe, *J. Fluorine Chem. 23* (1983) 579.
[14] G. Ferey, M. Leblanc, R. de Pape, M. Passaret, M. P. B. Razzazi, *J. Cryst. Growth 29* (1975) 209.
[15] D. E. McKee, N. Bartlett, *Inorg. Chem. 12* (1973) 1722.
[16] S. Cohen, H. Selig, R. Gut, *J. Fluorine Chem. 20* (1982) 349.
[17] D. Gantar, J. H. Holloway, I. Leban, B. Frlec, *11th Int. Symp. Fluorine Chem. 1985*, Berlin (East), Abstracts P 10.
[18] R. Domesle, R. Hoppe, *Angew. Chem. 92* (1980) 499; *Angew. Chem. Int. Ed. Engl. 19* (1980) 489.
[19] B. K. Morell, A. Zalkin, A. Tressaud, N. Bartlett, *Inorg. Chem. 12* (1973) 2640.
[20] F. Einstein, P. R. Rao, *J. Trotter, N. Bartlett, J. Chem. Soc. A 1967*, 478.
[21] K. Leary, D. H. Templeton, A. Zalkin, N. Bartlett, *Inorg. Chem. 12* (1973) 1726.
[22] D. Babel, A. Tressaud, P. Hagenmuller in [10], Chap. 3.
[23] D. Babel, G. Pausewang, W. Viehbahn, *Z. Naturforsch. B22* (1967) 1219.
[24] C. D. Desjardins, J. Passmore, *J. Fluorine Chem. 6* (1975) 379.
[25] J. Grannec, J. Portier, M. Pouchard, P. Hagenmuller, *J. Inorg. Nucl. Chem. Suppl. 1976*, 119.
[26] R. Hoppe, G. Wingefeld, *Z. Anorg. Allg. Chem. 519* (1984) 195.
[27] D. Kissel, R. Hoppe, *Z. Anorg. Allg. Chem. 532* (1986) 17.
[28] T. Fleischer, R. Hoppe, *Z. Anorg. Allg. Chem. 492* (1982) 76.
[29] D. Kissel, R. Hoppe, unpublished.
[30] P. Sorbe, J. Grannec, J. Portier, P. Hagenmuller, *C. R. Hebd. Séances Acad. Sci. Ser. C282* (1976) 663.
[31] T. Fleischer, *Dissertation*, Universität Giessen 1981.
[32] E. Alter, *Diplomarbeit*, Universität Giessen 1970.
[33] G. Wingfield, *Diplomarbeit*, Universität Giessen 1982.
[34] K.-H. Wandner, *Diplomarbeit*, Universität Giessen 1982.
[35] H. Klassen, R. Hoppe, *Z. Anorg. Allg. Chem. 483* (1982) 101.
[36] T. Fleischer, R. Hoppe, *J. Fluorine Chem. 19* (1982) 529.
[37] B. G. Müller, *Z. Anorg. Allg. Chem. 491* (1982) 245.
[38] B. G. Müller, *Z. Anorg. Allg. Chem.*, in press.
[39] B. G. Müller, *J. Fluorine Chem. 17* (1981) 317.
[40] J. C. Taylor, P. W. Wilson, *J. Less-Common Met. 34* (1974) 257.
[41] V. Probach, F. Steffens, *Z. Naturforsch. B33* (1978) 268.
[42] B. G. Müller, unpublished; *Habilitationsschrift*, Universität Giessen 1981.
[43] B. G. Müller, *Angew. Chem. 99* (1987) 685; *Angew. Chem. Int. Ed. Engl. 26* (1987) 688.
[44] a) G. Wingefeld, R. Hoppe, *Z. Anorg. Allg. Chem. 516* (1984) 223; b) D. Kissel, R. Hoppe, *ibid.*, in press.
[45] K. Tanaka, M. Komishi, F. Morumo, *Acta Crystallogr. Sect. B35* (1979) 1303.
[46] E. Herdtweck, D. Babel, *Z. Anorg. Allg. Chem. 474* (1981) 113.
[47] a) D. Kissel, R. Hoppe, *Z. Anorg. Allg. Chem. 540* (1986) 135; b) part of a Dissertation by D. Kissel, Universität Giessen 1987.
[48] H. G. von Schnering, B. Kolloch, A. Kolodziejezyck, *Angew. Chem. 83* (1971) 440; *Angew. Chem. Int. Ed. Engl. 10* (1971) 413.
[49] H. G. von Schnering, *Z. Anorg. Allg. Chem. 400* (1976) 201.
[50] A. de Kozak, M. Samonel, J. Renandin, G. Ferey, *Rev. Chim. Miner. 23* (1986) 352.
[51] R. Hoppe, *Angew. Chem. 82* (1970) 7; *Angew. Chem. Int. Ed. Engl. 9* (1970) 25.
[52] R. Hoppe, *Z. Kristallogr. 150* (1979) 23.
[53] R. E. Schmidt, D. Babel, *Z. Anorg. Allg. Chem. 516* (1984) 187.
[54] R. H. Odenthal, R. Hoppe, *Monatsh. Chem. 102* (1971) 1340.
[55] R. H. Odenthal, D. Paus, R. Hoppe, *Z. Anorg. Allg. Chem. 407* (1974) 144.
[56] G. Argany, F. Náray-Szabó, *Acta Chim. Acad. Sci. Hung. 49* (1966) 329.
[57] P. M. Halleck, J. C. Jarieson, C. W. T. T. Pistorius, *J. Phys. Chem. Solids 33* (1972) 769.
[58] J. C. Jarieson, P. M. Halleck, R. B. Roof, C. W. T. T. Pistorius, *J. Phys. Chem. Solids 36* (1975) 939.
[59] J. Portier, A. Tressaud, J. L. Dupin, *C. R. Hebd. Séances Acad. Sci. Serie C270* (1970) 216.
[60] J. Koch, C. Hebecker, *Naturwissenschaften 72* (1985) 431.
[61] B. G. Müller, *Z. Anorg. Allg. Chem.*, in press.
[62] R. Bougon, T. Bai Huy, M. Lance, H. Abazli, Inorg. Chem. 23 (1984) 3667.
[63] R. Hoppe, *Z. Anorg. Allg. Chem. 292* (1957) 28.
[64] R. Hoppe, R. Homann, *Z. Anorg. Allg. Chem. 379* (1970) 193.
[65] R. Hoppe, R. Homann, *Naturwissenschaften 53* (1966) 501.
[66] P. Sorbe, J. Grannec, J. Portier, P. Hagenmuller, *J. Fluorine Chem. 11* (1978) 243.
[67] K. Lutar, A. Jesih, B. Žemva, *Rev. Chim. Miner. 23* (1986) 565.
[68] A. Simon, *Struct. Bonding (Berlin) 36* (1979) 81.
[69] R. D. Shannon, *Acta Crystallogr. Sect. A 32* (1976) 751.
[70] B. G. Müller, *Z. Anorg. Allg. Chem.*, in press.
[71] R. Hoppe, *Dissertation*, Universität Münster 1954.
[72] N. Bartlett, J. W. Quail, *J. Chem. Soc. 1961*, 3728.
[73] N. Bartlett, P. R. Rao, *Proc. Chem. Soc. (London) 1964*, 393.
[74] A. J. Edwards, W. E. Falconer, J. E. Griffith, W. A. Sunder, M. J. Vasile, *J. Chem. Soc. Dalton Trans. 1974*, 1129.
[75] R. Hoppe, W. Klemm, *Z. Anorg. Allg. Chem. 268* (1952) 364.
[76] V. I. Spitzin, L. I. Martynenko, J. U. M. Kiselow, *Z. Anorg. Allg. Chem. 495* (1982) 39.
[77] K. Feldner, *Dissertation*, Universität Giessen 1979.
[78] R. Hoppe in G. J. MacCarthy, H. B. Silber, J. J. Rhynne (Eds.): *The Rare Earth Modern Science and Technology, Vol. 3*, Plenum Press, New York 1982, p. 315.
[79] O. Ruff, M. Giese, *Z. Anorg. Allg. Chem. 219* (1934) 143.
[80] E. Gruner, W. Klemm, *Naturwissenschaften 4* (1937) 59.
[81] K. Yvon, A. Betzinge, P. Tissot, P. Fischer, *J. Solid State Chem. 65* (1986) 225.
[82] P. Charpin, P. Plurien, P. Meriel, *Bull. Soc. Fr. Mineral. Cristallogr. 93* (1970) 7.
[83] C. Friebel, D. Reinen, *Z. Anorg. Allg. Chem. 413* (1975) 51.
[84] R. H. Odenthal, R. Hoppe, *Z. Anorg. Allg. Chem. 385* (1971) 92.
[85] B. G. Müller, R. Hoppe, *Z. Anorg. Allg. Chem. 395* (1973) 239.
[86] B. G. Müller, R. Hoppe, *Z. Anorg. Allg. Chem. 392* (1972) 37.
[87] B. G. Müller, *Z. Anorg. Allg. Chem.*, in press.
[88] B. G. Müller, *Angew. Chem. 99* (1987) 685; *Angew. Chem. Int. Ed. Engl. 26* (1987) 689.
[89] B. Standke, M. Jansen, *Angew. Chem. 97* (1985) 114; *Angew. Chem. Int. Ed. Engl. 24* (1985) 118.
[90] E. Alter, R. Hoppe, *Z. Anorg. Allg. Chem. 408* (1974) 115.
[91] B. G. Müller, *Naturwissenschaften 66* (1979) 519.
[92] A. Tressaud, J. L. Soubereaux, H. Touhara, G. Demazean, F. Langlais, *Mater. Res. Bull. 16* (1981) 207.
[93] B. Standke, M. Jansen, *Angew. Chem. 98* (1986) 78; *Angew. Chem. Int. Ed. Engl. 25* (1986) 77.
[94] R. Hoppe, *Angew. Chem. 93* (1981) 64; *Angew. Chem. Int. Ed. Engl. 20* (1981) 63.
[95] G. Ferey, M. Leblanc, R. de Pape, *J. Solid State Chem. 40* (1981) 1.
[96] B. Mehlhorn, R. Hoppe, *Z. Anorg. Allg. Chem. 425* (1976) 180.
[97] K. H. Wandner, R. Hoppe, *Rev. Chim. Miner. 23* (1986) 565.
[98] K. H. Wandner, R. Hoppe, *Z. Anorg. Allg. Chem.*, in press.
[99] B. G. Müller, Chemiedozententagung Aachen 1985, B39.
[100] B. G. Müller, unpublished.
[101] N. Bartlett, K. Leary, *Rev. Chim. Miner. 13* (1976) 82.
[102] K. Leary, N. Bartlett, *J. Chem. Soc. Chem. Commun. 1972*, 903.
[103] K. Leary, A. Zalkin, N. Bartlett, *J. Chem. Soc. Chem. Commun. 1973*, 113; *Inorg. Chem. 13* (1974) 775.
[104] R. Homann, R. Hoppe, *Z. Anorg. Allg. Chem. 379* (1970) 193.
[105] R. Homann, *Dissertation*, Universität Giessen 1970.
[106] J. Brunvoll, A. A. Ischenko, A. A. Ivanov, G. V. Romanov, V. B. Sokolov, V. P. Spiridonov, T. G. Strand, *Acta Chem. Scand. A36* (1982) 705.
[107] W. A. Sunder, A. L. Wayda, D. Distefano, W. E. Falconer, J. E. Griffith, *J. Fluorine Chem. 14* (1979) 299.
[108] A. A. Timakov, V. N. Prusakov, Yu. V. Drobysheskii, *Dokl. Akad. Nauk SSSR 291* (1986) 125.

[109] W. E. Falconer, F. J. Disalvo, A. J. Edwards, J. E. Griffith, W. A. Sunder, M. J. Valile, *J. Inorg. Chem. Suppl. 1976*, 59.
[110] B. G. Müller, *Dissertation*, Universität Giessen 1972.
[111] H. Henkel, R. Hoppe, *Z. Anorg. Allg. Chem. 359* (1968) 160.
[112] P. R. Rao, A. Tressaud, N. Bartlett, *Inorg. Nucl. Chem. Lett. 1976*, 23.
[113] R. Hoppe, W. Dähne, *Naturwissenschaften 49* (1962) 254.
[114] A. F. Wright, B. E. Fender, N. Bartlett, K. Leary, *Inorg. Chem. 17* (1978) 748.
[115] A. Tressaud, S. Khairoun, J. M. Dance, P. Hagenmuller, *Z. Anorg. Allg. Chem. 517* (1984) 43.
[116] A. Tressaud, S. Khairoun, J. M. Dance, G. Demazean, P. Hagenmuller, *C. R. Hebd. Séances Acad. Sci. Serie II 295* (1982) 183.
[117] K. Leary, D. H. Templeton, A. Zalkin, N. Bartlett, *Inorg. Chem. 12* (1973) 1726.
[118] D. W. A. Sharp, B. Cox, *J. Chem. Soc. 1956*, 877.
[119] E. Alter, R. Hoppe, *Z. Anorg. Allg. Chem. 405* (1974) 167.
[120] B. G. Müller, R. Hoppe, *Mater. Res. Bull. 16* (1981) 207.
[121] O. Ruff, E. Ascher, *Z. Anorg. Allg. Chem. 183* (1929) 204.
[122] B. G. Müller, *J. Fluorine Chem. 20* (1982) 291.
[123] R. R. Jesse, R. Hoppe, *Z. Anorg. Allg. Chem. 428* (1977) 91.
[124] W. Bronger, G. Auffermann, P. Müller, *Z. Kristallogr.*, in press.
[125] B. G. Müller, R. Hoppe, *Z. Anorg. Allg. Chem. 498* (1983) 128.
[126] R. Hoppe, T. Fleischer, *J. Fluorine Chem. 11* (1978) 251.
[127] B. G. Müller, *J. Fluorine Chem. 17* (1981) 409.
[128] B. G. Müller, M. Serafin, *Z. Naturforsch.*, in press.
[129] H. G. von Schnering, Solid-State Colloquium, Kiel 1987.
[130] W. Klemm, *Angew. Chem. 53* (1940) 25.

Homoatomic d^{10}–d^{10} Interactions: Their Effects on Structure and Chemical and Physical Properties

By Martin Jansen*

Dedicated to Professor Rudolf Hoppe on the occasion of his 65th birthday

The distinction between valence electrons and essentially inactive core electrons is the basis of many classifying concepts in chemistry. However, it has recently been recognized that this is an oversimplification and should, at least in some areas of chemistry, be modified. Many cases are known where cations with closed d^{10} configurations are subject to homoatomic interactions that influence structure and properties. A characteristic and surprisingly uniform structural feature (e.g., of a number of compounds containing monovalent coinage metals) is a clusterlike assembly of d^{10} cations that corresponds in geometry and bond lengths to fragments of the metal structures themselves. Further evidence for a special type of bonding in such compounds is provided by their physical properties; for example, the absorption in the UV/VIS region shows a drastic redshift and the compounds are often conductors or semiconductors. The d electrons in such cases have obviously lost their pure "core" nature. All bonding models so far proposed for such systems involve mixing of higher orbitals.

1. Introduction

The nature of chemical bonding was unclear until, after the proposal of *Bohr*'s atomic theory and before the development of wave mechanics, *W. Kossel* and *G. N. Lewis* published descriptions of the limiting cases of ionic[1] and covalent[2] bonding that were plausible and consistent with concepts of atomic structure. Some of the underlying assumptions of these bonding theories are still valid today. This is true in particular for the subdivision of the electron cloud into valence electrons, which largely determine the type, strength, and number of bonds formed by an atom, and core electrons, which do not contribute to the bonding. This simple concept has proved extraordinarily useful for teaching purposes and in descriptive chemistry for the classification and qualitative explanation of new experimental results. All the empirical rules that are based on the number of electrons in a bonding system should also be mentioned here; e.g., the noble gas rule in transition metal chemistry, the concepts derived from the $(8-N)$ rule by *Zintl–Klemm*[3] and *Grimm–Sommerfeld*,[4] the introduction of the "paraelement" concept[5] as a generalization of *Grimm*'s "hydride shift rules" (a special case of a "diagonal relationship"), and the role of "valence electron concentration" in the metallic state.

Core and valence electrons are also handled differently in quantum-chemical bonding calculations. The contributions of the core electrons are regarded as angle-independent in the form of a pseudopotential.[6] Similar considerations lie behind the experimental determination of bonding electron distribution ("deformation density") using diffraction methods: a spherically symmetrical contribution ("core") is subtracted at each atom from the total density.[7]

Although the precise treatment of a bonding system should involve the consideration of all states whose interaction integrals could, by symmetry, be nonzero under the given conditions, the more approximate treatment involving only the valence electrons in the ground state proves to be astonishingly good in practice. There are few experimental results (temperature-independent paramagnetism, for instance) that can only be interpreted when higher energy states are considered. It is also a commonly held view that an increase of the coordination number above four in covalent compounds requires an expansion of the valence shell.

Until recently there were no experimental results that needed a consideration of the core electrons for their interpretation. This situation changed, however, on the discovery of several curious features in compounds with d^{10} or $d^{10}s^2$ cations. In addition to the known bonding patterns, these species seem to involve homoatomic interactions that influence their structure and properties (cf. Ref. [8]), despite the fact that their electron configurations are generally regarded as closed-shell.

It often happens in chemistry, when modern developments generate principles of general validity, that a closer examination of the literature shows related evidence published long before. *A. Byström* and *L. Evers*, in a 1950 report on Ag_2PbO_2 and $Ag_5Pb_2O_6$, drew attention to the short Ag^+–Ag^+ contacts and discussed a form of "covalent" bonding.[9] In 1963, *G. A. Barclay* and *B. F. Hoskins* noted marked differences in the crystallochemical behavior of potassium and silver in $KAgCO_3$ and did not exclude the possibility of bonding between the d^{10} Ag^+ ions.[10] In 1973, *H.-L. Keller* and *Hk. Müller-Buschbaum* described assemblies of silver atoms in the novel compounds $SrAg_6O_4$ and $BaAg_6O_4$ as "metallic regions."[11]

[*] Prof. Dr. M. Jansen
Institut für Anorganische Chemie der Universität
Callinstrasse 9, D-3000 Hannover (FRG)
New address:
Anorganisch-Chemisches Institut
Gerhard-Domagk-Str. 1
D-5300, Bonn (FRG)

 © VCH Verlagsgesellschaft mbH, D-6940 Weinheim, 1987 0570-0833/87/1111-1098 $ 02.50/0

Parallel to this development in solid-state chemistry, corresponding results from coordination chemistry became available. The most remarkable was certainly the synthesis and structure of $[Pt(PPh_3)_2]_2$.[12] The crystal structure of this compound shows a short platinum(0)–platinum(0) contact that, in the absence of bridging ligands, can only be interpreted as a metal–metal bond.

These observations, originally regarded as exceptions, have now attained significance both in number and in consistency[13] and are worthy of detailed classification. This article will review those results that provide evidence for the d^{10}–d^{10} interactions, present correlations between structure and properties, and discuss proposed bonding models. Most examples will be drawn from inorganic solid-state chemistry; it will not be possible to discuss more than isolated examples from the no less extensive and interesting field of related molecular systems.

2. Structural Chemistry

The structure of a solid is determined by the sum of the forces present in it and thus represents an observable property important for the characterization of chemical bonding. Unfortunately, it is in principle impossible to associate particular structural features (e.g., coordination polyhedra, bond lengths and angles) unambiguously or exclusively with a particular set of bonds. However, this is still possible to a good approximation in molecular crystals; the molecular structure is determined by the predominantly covalent bonding between the constituent atoms, whereas the molecular packing is determined by molecular shape and van der Waals forces.[14] Such distinctions, the limitations of which already become apparent on comparing crystal structures of small molecules such as Cl_2, Br_2, and I_2, become invalid for "collective" solids such as ionic crystals or intermetallic phases. This in turn places limitations on the significance of the following discussion of d^{10} systems in crystalline solids. To minimize these limitations, we shall present structural comparisons of compounds that differ only in one component.

2.1. Ternary Silver(I) Oxides

Monovalent silver is in many respects (e.g., transport properties in dilute aqueous solution, crystal chemistry in compounds such as elpasolites[15]) intermediate in properties between sodium and potassium. It thus seems worthwhile to compare ternary silver(I) oxides with their sodium and potassium analogues in order to discover any structural peculiarities of the silver compounds. Such comparisons reveal almost without exception drastic differences in the tertiary structure (the packing of the anionic and cationic components to form a three-dimensional framework), and sometimes even in the secondary and primary structure of the complex anions present in some of these oxides. Whereas crystal structures with cations of noble-gas configuration display (in addition to the usual tendency to form characteristic cation–anion contacts) a tendency to maximize the cation–cation distances and thus the lattice energy, the structures with Ag^+ are distinguished by a separation of the anionic and cationic components of the structure—an "aggregation" of the silver cations to form extended silver assemblies.[13] The peculiar resulting microheterogeneous structure and the special nature of monovalent silver become all the more apparent on comparison with alkali metal ions in formally similar environments; the crystal structure of $KAgCO_3$[10] fulfills this requirement ideally. The complete separation of potassium and silver "substructures" by layers of $CO_3^{2\ominus}$ ions (Fig. 1) is striking. The potassium ions achieve substantial interionic separations, but the silver ions aggregate to form two-dimensional, close-packed assemblies. The shortest K^+–K^+ distance is 404 pm, much longer than the shortest Ag^+–Ag^+ contact (297 pm).

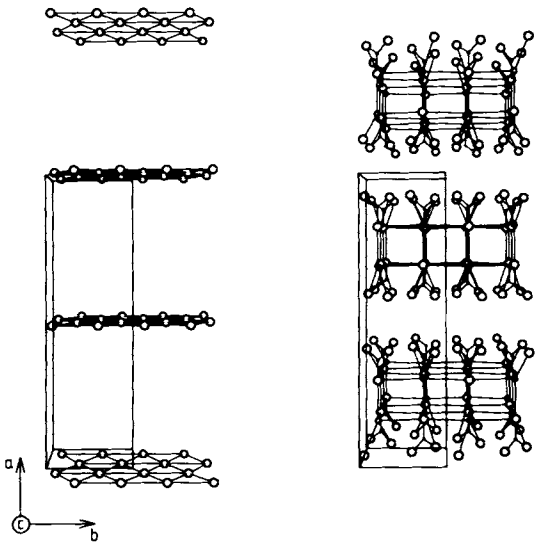

Fig. 1. Crystal structure of $KAgCO_3$; left, silver aggregate; right, KCO_3 grouping.

Further illustrations of this structural tendency are shown in Figures 2–4, where the silver and anion structures are presented separately. These examples ($Ag_6Si_2O_7$,[16] Ag_2CO_3,[17] and $LiAg_3O_2$[18]) show that the aggregation of silver ions is essentially independent of the particular coordination at silver and also of the "cationic" or "anionic" (oxoargentate) role of silver.

Although the general tendency of silver ions to form aggregates is noteworthy, the silver–silver distances within the aggregates are even more impressive; they are approximately constant, the shortest being ca. 280 pm (shorter than the 289 pm in metallic silver) and the longest not longer than 330 pm (i.e., less than the van der Waals diameter of 340 pm[19]). A more detailed examination of the crystal structures shows in addition that the silver aggregates are based on a uniform motif, namely, an approximately equilateral triangle of silver atoms. The triangles are then "condensed" to form ribbons, layers, and three-dimensional frameworks (cf. Figs. 5–8). The crystal structures of the ternary silver oxides known so far show a preference for two-dimensional aggregates (ribbon or layer structures). The silver substructures thus correspond to fragments of the structure of metallic silver, both in geom-

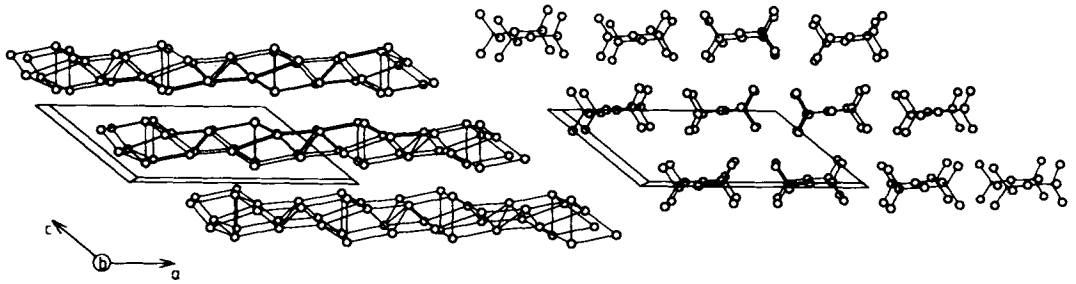

Fig. 2. Anionic (right) and silver components of $Ag_6Si_2O_7$ (I).

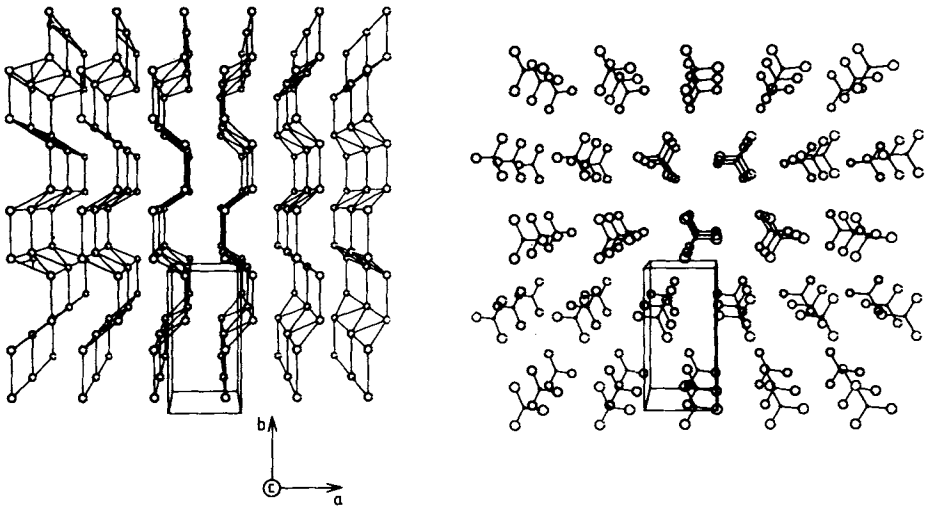

Fig. 3. Anionic (right) and silver components of Ag_2CO_3.

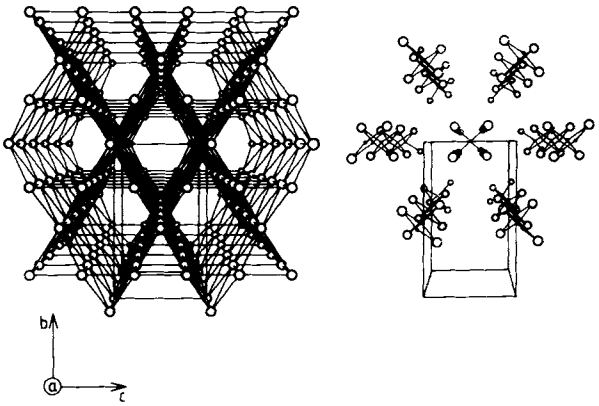

Fig. 4. LiO_2 (right) and silver components of $LiAg_3O_2$.

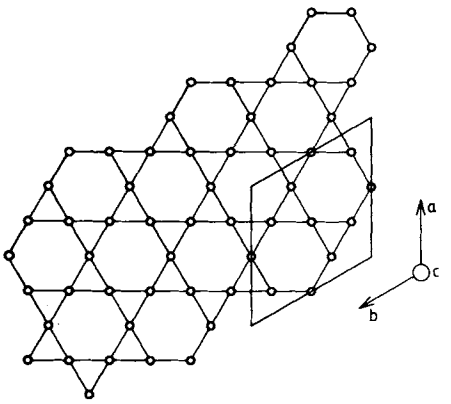

Fig. 6. Silver aggregate in Ag_3BO_3 (projection on (001)).

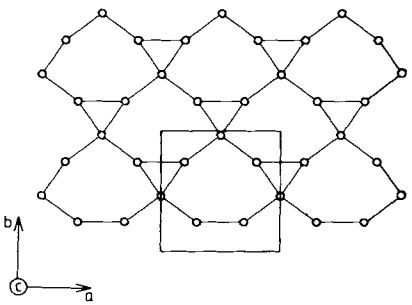

Fig. 5. Part of the silver aggregate in $AgBO_2$.

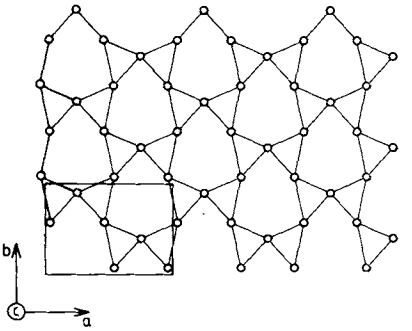

Fig. 7. Part of the silver aggregate in $SrAg_6O_4$.

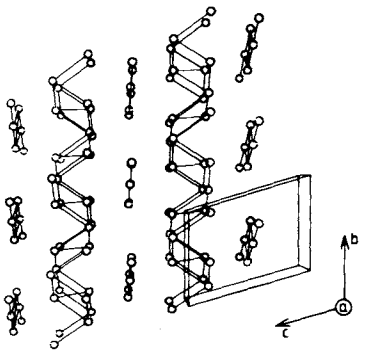

Fig. 8. Silver aggregate in $[Ag_4SiO_4]_2 \cdot AgNO_3$.

etry and in interatomic distances. Table 1 presents a summary of silver compounds in which the shortest Ag–Ag distance lies below 300 pm.

The formation of silver aggregates influences not only the packing of anions and cations but can also govern the secondary structure of condensed oxoanions. The first known example of the tetrasilicate ion in a crystalline solid was the silver salt $Ag_{10}Si_4O_{13}$;[20] $AgBO_2$ contains a polyanion with tetrahedral and trigonal-planar boron in the ratio 1 : 1,[21] previously known only in the high-pressure form of $Ca(BO_2)_2$; and $Ag_2Ge_2O_5$ involves a three-dimensional framework of a kind previously unknown for oxoanions of the composition $Ge_2O_5^{2-}$.[22]

Table 1. Shortest distances between d^{10} cations in compounds of monovalent copper, silver, and gold [pm].

Compound	Distance	Ref.	Compound	Distance	Ref.
$Rb_3Cu_5O_4$	258.1	[67]	$AgSbS_2$	272.5	[47]
$NH_4Cu_7S_4$	240.3	[68]	LaAgOS	286.4	[48]
Cu_4SnS_4	245.3	[69]	Ag_8SiS_6	288.0	[49]
$Cs_3Cu_8Se_6$	246.3	[70]	$K_2Ag_4S_3$	290.9	[50]
$K_3Cu_8S_6$	254.3	[71]	Ag_9GaSe_6	290.9	[51]
$BaCu_4S_3$	255.6	[73]	Ag_2S	294.0	[52]
$Na_2Cu_4S_3$	257.6	[72]	$AgAsS_3$	297.4	[53]
$[C_5H_6N]_2[Cu_3I_5]$	279.0	[77]	Ag_3AuSe_2	297.4	[46]
$[C_{12}H_{28}N]_2[Cu_5I_7]$	240.7	[78]	$Cs_2Ag_4S_3$	298.9	[54]
Ag_6O_2	275.1	[23]	$Ag_3S(NO_3)$	299.9	[55]
$SrAg_6O_4$	281.0	[11]	KAgSe	276.0	[56]
$BaAg_6O_4$	283.8	[11]	$RbAg_3Se_2$	285.9	[57]
Ag_2CO_3	287.2	[17]	$CsAg_3Se_2$	287.3	[57]
$Ag_6Si_2O_7$(II)	288.0	[8a]	$SrAg_2I_4 \cdot 8H_2O$	278.0	[38]
$Ag_{10}Si_4O_{13}$	287.7	[20]	$Ag_2IF \cdot H_2O$	281.2	[39]
2H-$AgAlO_2$	289.6	[26]	$Ag_7I_5F_5 \cdot 2.5\,H_2O$	291.8	[40]
CsAgO	290.3	[27]	Ag_2INO_3	294.0	[41]
KAgO	291.4	[28]	$Ag_3I(NO_3)_2$	294.2	[42]
$Ag_6(SO_4)SiO_4$	292.3	[29]	$Tl_6Ag_2I_{10}$	298.3	[43]
RbAgO	292.9	[30]	AgNCO	274.6	[58]
Ag_2SO_3	292.4	[31]	Na_2AgAs	279.6	[59]
$LiAg_3O_2$	294.7	[18]	$AgHg_2PO_4$	282.0	[60]
$Ag_6Si_2O_7$(I)	294.8	[16]	AgCNO	282.3	[61]
$AgCrO_2$	294.6	[32]	Na_2AgSb	286.3	[62]
$AgBO_2$	295.6	[21]	$Ag_4SO_2N_2$	287.0	[63]
Na_3AgO_2	296.0	[33]	$Ag_3(HN_2O_2S)(NH_3) \cdot H_2O$	290.3	[64]
$Ag_2Li(NO_2)_3$	296.2	[34]	$AgCuPO_4$	294.0	[65]
$KAgCO_3$	297.5	[10]	$K_3Ag_3As_2$	299.5	[66]
$Ag_4V_2O_7$	298.9	[35]	$AgNO_3 \cdot C_2H_5O_2N$	287.7	[25]
$NaAg_3O_2$	298.0	[36]	$Ag_2C_2HS_2O_6$	289.1	[24]
Ag_3PO_4	297.0	[37]	$Ba[Au_2SnS_4]$	293.3	[74]
$[Ag_4SiO_4]_2 \cdot AgNO_3$	293.0	[44]	Ag_3AuS_2	286.4	[75]
$[Ag_4GeO_4]_2 \cdot AgNO_3$	294.4	[44]	Ag_3AuSe_2	297.6	[75]
$Ag_2Ge_2O_5$	284.2	[22]	$Rb_2AgAu_3I_8$	304	[45]
Ag_3AuS_2	256.4	[46]	$Tl[Au(CN)_2]$	303.7	[76]

2.2. Ternary Copper(I) and Gold(I) Oxides

In contrast to the considerable amount of information (mostly stemming from the last few years) on ternary silver oxides, few corresponding examples with similar structural features are known for monovalent copper and none for gold. This difference may simply be attributable to the more intensive preparative studies of ternary silver(I) oxides; even the more silver-rich species[*] are now accessible, thanks to developments in high-pressure oxygen technique that permit solid-state reactions involving Ag_2O.[8a]

Ternary oxides in which univalent gold would be cationic in nature have, to the best of our knowledge, not yet been systematically investigated. Our group has made extensive efforts to synthesize copper-rich species such as $Cu_6Si_2O_7$ or Cu_3BO_3—as yet without success, but our attempts are continuing. This lack of success is difficult to explain, particularly since a series of less metal-rich ternary oxides have been described (e.g., $Cu_6Mo_5O_{18}$[79] and $Cu_4Mo_5O_{17}$[80]), and new representatives of the type $CuMO_2$ (with the delafossite structure) have been obtained without great difficulty.[81] Furthermore, *R. Hoppe* and coworkers have synthesized numerous alkali metal oxocuprates(I), including the only known copper-rich ($Cu : O > 1$) species, $Rb_3Cu_5O_4$.[67] This compound, with a shortest Cu–Cu distance of 257 pm (cf. copper, 254 pm), is clearly related to the silver compounds described above. The assumption that copper(I) oxides could also form clusterlike metal aggregates is therefore not so unreasonable; however, it remains essential to confirm the assumption experimentally.

2.3. Halides and Further Chalcogenides of the Monovalent Coinage Metals

The current knowledge of ternary coinage-metal compounds involving other nonmetal components, such as the halogens or the higher homologues of oxygen, is limited and thus only isolated cases can be discussed here. *Bronger* and co-workers have described silver- and copper-rich sulfides and selenides such as $K_2Ag_4Se_3$,[82] $Cs_2Cu_5Se_4$,[83] and $K_3Cu_8S_6$,[71] in which the singly charged coinage-metal ions are again segregated from the rest of the structure. Figure 9 shows that the copper and silver substructures represent fragments of the cubic face-centered metal lattices. The structural relationship becomes even clearer through the transition to three-dimensional aggregates. The metal–metal distances in the cited compounds are approximately equal to those in the metals themselves, although generally somewhat longer. A comparison with smaller metal fragments (e.g., pairs or isolated groups of atoms) can give the impression that—as with ions of opposite charge—the M^+–M^+ distances increase with coordination number.

An examination of halide structures yields fewer examples of similar phenomena; however, they present some re-

[*] The silver compounds prepared at high oxygen pressure (6 kbar) are not quenched high-pressure phases; they were tested by tempering below their decomposition temperatures at normal pressure and did not revert to "normal-pressure" phases.

markable features. $SrAg_2I_4 \cdot 8H_2O$[38] displays chains of silver atoms with an unusually short Ag-Ag distance of 278 pm. The metal atoms are tetrahedrally coordinated by iodine, as is the case in some iodocuprates(I),[77] where the short Cu^+-Cu^+ distances (241 pm) arise from the linking of coordination polyhedra via common edges or faces. The AuI_2 "dumbbells" in $Rb_2AgAu_3I_8$[45] are not linear; the narrowing of the bond angle at Au^+ to 173° is associated with a short Au^+-Au^+ distance of 304 pm. Except for Au^+-Au^+ interactions, no other reasons for the distortion are detectable.

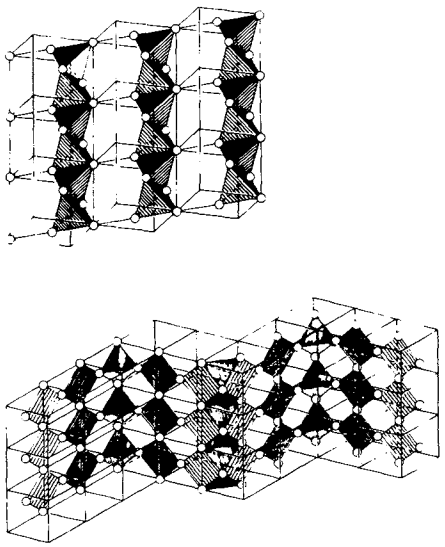

Fig. 9. Coinage-metal aggregates in $K_2Ag_4Se_3$ (above) and $Cs_2Cu_5Se_4$ (below).

2.4. The Structures of Zinc, Cadmium, and Silver Subvalent Compounds

A classical problem (still unsolved) from the structural chemistry of metals is that of the anomalous *c/a* ratios in the hexagonal close-packed crystal structures of zinc and cadmium. There are about 20 metals that crystallize, at least in one allotropic form, in close-packed hexagonal structures; all except zinc and cadmium display *c/a* ratios in the narrow range 1.57-1.64 (the ideal value is 1.63). The deviations for zinc (1.856) and cadmium (1.886) are extreme (over 15%).[84] The distances to the 12 nearest neighbors distort into six shorter ones within the layers and three longer ones both above and below the layers. Proposed explanations of this anomaly, such as the assumption of ellipsoidal Zn^{2+} and Cd^{2+} cores,[85] have not met with general acceptance.[86] Since the conduction band of these two metals can be shown to contain two electrons per atom, the cores must have d^{10} configurations; furthermore, the bonding interactions discussed in this article act preferentially in two dimensions. The zinc and cadmium anomalies therefore correspond perfectly to the structural results described in the preceding section. This is the first time that they have been classified in terms of a more general context.

Silver subfluoride, Ag_2F,[87] was also viewed very much as an exception. It was the only known subvalent compound of silver for a long time and is still the only known subfluoride. The compound is formed by electrochemical reduction of silver(I) fluoride and possesses the *anti*-CdI_2 structure. The distances between silver atoms in the layers are 290 pm, and those between silver atoms of different layers 285 pm. Ag_2F is no longer quite so unusual because Ag_3O, the first silver sub*oxide*, has also been described.[23] The structure is to a first approximation an *anti*-BiI_3 type. The influence of the remaining valence electrons (1/3 per silver atom) causes a deformation of the silver substructure to form Ag_6^{4+} octahedra. The bond lengths within the cluster are significantly shorter than those between clusters (275 and 285, compared with 297 pm). There is an interesting parallel here to the silver germanium phosphide $Ag_6Ge_{10}P_{12}$,[88] which also contains "isolated" Ag_6 groups; if the nonmetals germanium and phosphorus are allocated oxidation states corresponding to their chemical and structural roles, the Ag_6 cluster is also formally 4+, with a valence electron concentration of two per structural unit. The newest member of the small family of silver subvalent compounds, $Bi_4Ag_{18}O_{12}$,[89] also contains silver in the oxidation state 2/3 (a coincidence?). It possesses a three-dimensional silver framework in which, remarkably, no shortening of the silver-silver distances is observed, as compared to the ternary silver(I) oxides discussed in Section 2.1. The published crystal structure of $Ag_5Pb_2O_6$ describes it as a subvalent compound,[9] but the inadequate accuracy of the structure determination precludes an unambiguous assessment.

We believe that there is a connection between the existence of subvalent silver compounds and the tendency of univalent silver to engage in homoatomic interactions. The substructures thereby formed have empty s and p conduction bands, which can easily accommodate further electrons on reduction. The subvalent compounds thus represent a structural link with classical metal cluster compounds, which, however, lie outside the scope of this review.

2.5. Coordination Compounds

Numerous coordination compounds of copper(I), silver(I), and gold(I) have been prepared and structurally investigated.[90] Their crystal structures generally consist of "isolated" molecules, but they nevertheless show remarkable similarity to the compounds discussed above in terms of their cation substructures; the M^+-M^+ contacts are of similar length to the interatomic distances in the elements themselves, sometimes even shorter. Table 2 presents a summary of the shortest contacts so far observed. There are however significant differences between the coordination compounds and the more highly "polymeric" ternary oxides and sulfides. The d^{10} atoms are often held together in pairs by 1,3-bifunctional bidentate ligands; aggregates of more than two d^{10} centers are observed only in isolated cases, and extended two- or three-dimensional cation structures not at all.

The reservations mentioned in Section 2 with respect to structure-bonding relationships are therefore particularly serious. Possible metal-metal interactions cannot be distin-

Table 2. Shortest Cu-Cu, Ag-Ag, and Au-Au distances in coordination compounds [pm].

Compound	Distance	Ref.
$[C_{42}H_{42}Cu_3N_{15}]\cdot C_4H_8O\cdot 0.5C_6H_{14}$	234.8	[92]
$[Cu(CN)(NH_3)]$	241.7	[92]
$[C_{20}H_{37}Cu_2N_4O_3][C_{24}H_{20}B]$	241.8	[93]
$[C_{40}H_{40}Cu_4MgO]$	241.4	[94]
$[C_{17}H_{32}Cu_2N_4O_5]\cdot CH_2Cl_2$	242.1	[95]
$[C_{48}H_{40}Cu_2N_{12}]$	244.1	[96]
$[C_{36}H_{40}Cu_2N_8][ClO_4]_3$	244.4	[97]
$[C_{108}H_{96}Cu_6P_6][C_3H_7NO]$	249.3	[98]
$[C_4H_6Cu_2O_4]$	255.6	[99]
$[C_{14}H_{19}Cu_2I_2N_5]$	258.5	[100]
$[C_{36}H_{44}Ag_4]$	273.3	[101]
$[C_6H_{24}Ag_2N_{12}S_6][ClO_4]_2$	284.5	[102]
$[C_{126}H_{19}Ag_6Cl_6P_5S_6]\cdot 2C_7H_8$	287.5	[108]
$[(C_6H_7N_2O_2)Ag]$	287.4	[109]
$[C_{48}H_{104}Ag_8S_8]$	288.6	[110]
$[C_{10}H_{12}Ag_2N_2O_4]$	289.4	[107]
$[C_{42}H_{84}Ag_6N_2Si_2]$	290.5	[103]
$[C_6H_{11}AgS]$	291.1	[104]
$[C_{50}H_{46}Ag_4Br_4N_2P_4]$	296.4	[105]
$[C_{42}H_{84}Ag_6N_4O_6S_6]$	294.2	[106]
$[C_{126}H_{105}Au_7P_7]OH$	258.2	[111]
$[C_{108}H_{96}Au_2N_4P_4Pt_2][PF_6]_2$	258.9	[112]
$[C_{126}H_{105}Au_8P_7][NO_3]_2\cdot 2CH_2Cl_2$	262.9	[113]
$[C_{80}H_{60}Au_6CO_2O_8P_4]$	262.8	[114]
$[C_{108}H_{104}Au_6P_8][NO_3]_2\cdot 2CH_2Cl_2$	263.0	[115]
$[C_{135}H_{130}Au_{11}P_{10}][CNS]_3$	266.9	[116]
$[C_{14}H_{28}Au_2N_2S_4]$	275.9	[117]
$[C_{35}H_{43}Au_2P_3]$	296.7	[118]
$[C_{38}H_{34}Au_2Cl_2P_2]$	296.2	[121]
$[C_{20}H_{20}Au_4I_4N_4]$	299.5	[119]
$[C_{28}H_{28}Au_2P_2]$	297.7	[120]

guished from the effects of the ligands. Even the deviations from 180° at the metal atom allow no unambiguous conclusions to be drawn; they are associated with both longer and shorter metal-metal contacts (compared with an ideal linear geometry), and no systematic relationship can be recognized at present. It is possible that crystal packing effects are important in view of the generally small deformation energy of linear systems, but such effects are generally ill-defined. The dimeric Pt^0 complex $[Pt(PPh_3)_2]_2$ is a key compound in this respect, since the two d^{10} metal atoms are only 276.5 pm apart despite the absence of bridging ligands.[12] The existence of this complex thus lends weight to the assumption that bonding interactions are present between d^{10} centers in complexes with bridging ligands, too.

2.6. Systematic Structural Comparisons

A structural comparison of related compounds, with systematic variation of anionic or cationic moieties, is more profitable than an amorphous presentation of isolated results. A sufficient number of structures have now been investigated to allow such comparisons for the following compounds:

1. isotypic compounds differing only in the nature of the complex anion (e.g., analogous silver(I) silicates and germanates)
2. salts of the same anion with differing coinage-metal content (e.g., silver(I) sulfamides)
3. compounds that retain the same structural type while allowing the metal-metal distance to vary over a wide range (e.g., copper delafossites)

For the silver silicates and germanates, the following compounds have been shown to be isotypic: $Ag_{10}X_4O_{13}$, $Ag_6X_2O_7$, and $[Ag_4XO_4]_2\cdot AgNO_3$, where X = Si or Ge.[122,44] However, quantitative structural data are available only for the ortho salts. Figure 10 shows the corresponding contacts in the silicate and germanate. Whereas the X-O bond lengths vary markedly and uniformly, the Ag-O bond lengths are not significantly different. Surprisingly, the latter is also true for the silver-silver contacts below 330 pm (within a margin of $\pm 3\sigma$); the average contacts are 308 (Ge) and 309 (Si) pm. The increase in volume in going from the silicate to the germanate is clearly not uniform over the whole crystal structure. Since the Ag-Ag contacts, like the Ag-O distances, are more or less constant, it is possible to speak of a silver-silver "bond length." Moreover, the average deviation (1.4 pm) from the mean value of the shortest Ag-Ag contact (<330 pm) is much lower than that of those contacts between 330 and 400 pm (8.2 pm). We regard these observations as evidence that the metal-metal interactions are indeed bonding.

The silver(I) salts of sulfamide, $O_2S(NH_2)_2$, and their structures are known for all possible stoichiometries (mono- to tetrasilver salts). Apart from the differing degree of protonation, the anions show no marked changes in this series, and a comparison of the silver substructures should therefore provide, to a first approximation, information about the silver-silver interactions. The comparison shows characteristic trends as regards both the extent of the silver aggregates (see Fig. 11) and the interatomic distances within them; for the mono-,[123] di-,[124] tri-,[64] and tetra-

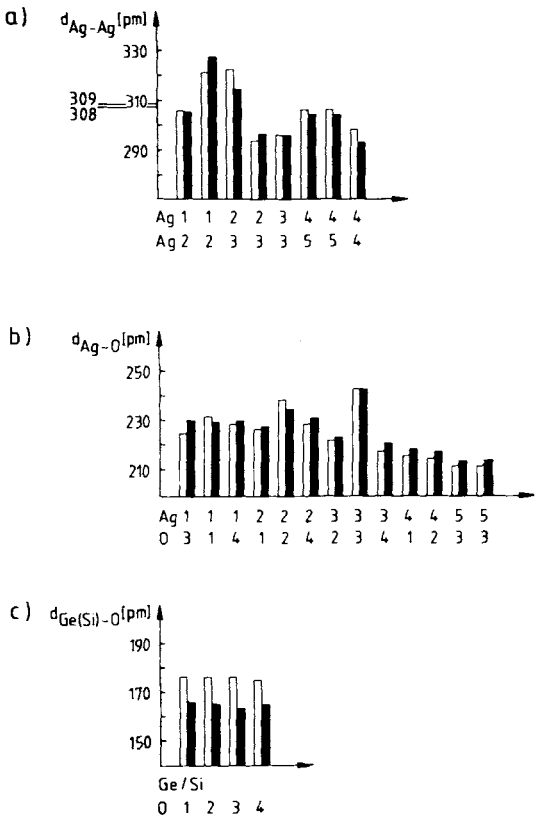

Fig. 10. Comparison of bond lengths in $[Ag_4XO_4]_2\cdot AgNO_3$ with X = Si (dark bars) and Ge.

silver sulfamides,[63] the silver atoms occur singly, in pairs, and in two- and three-dimensional infinite arrangements, respectively (taking 330 pm as the upper limit for an Ag–Ag contact). The variations in, and averages of, the Ag–Ag distances (Fig. 12) also indicate increasing Ag–Ag interactions in going from the mono- to the tetrasilver salt.

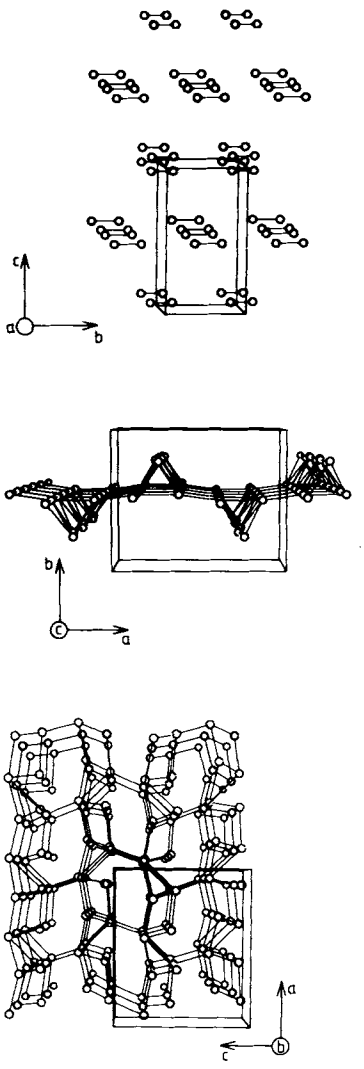

Fig. 11. Silver aggregates in (from above) di-, tri-, and tetrasilver sulfamide.

The delafossites (general formula $A^+B^{3+}O_2$) display two-dimensional infinite networks of d^{10} cations based on equilateral triangles. This can be readily explained in terms of the preferred coordination geometries of the constituent metal ions (octahedral and linear coordination by oxygen). In the context of this article, however, the aggregation phenomenon appears in a different light. The structure can accommodate different sizes of B^{3+} ions, thereby allowing systematic comparison of the ensuing variations; the A^+–A^+ distances are identical with the value of a for the hexagonal crystal system, which is in turn determined by the radius of B^{3+}. The known Cu(I) delafossites have a values of 280–380 pm and thus form a structural group in which the Cu^+–Cu^+ distances also vary over this wide range. If Cu^+–Cu^+ interactions are present, these should vary systematically with the Cu–Cu distance, and the physical properties dependent on the band structure should vary uniformly with the value of a.

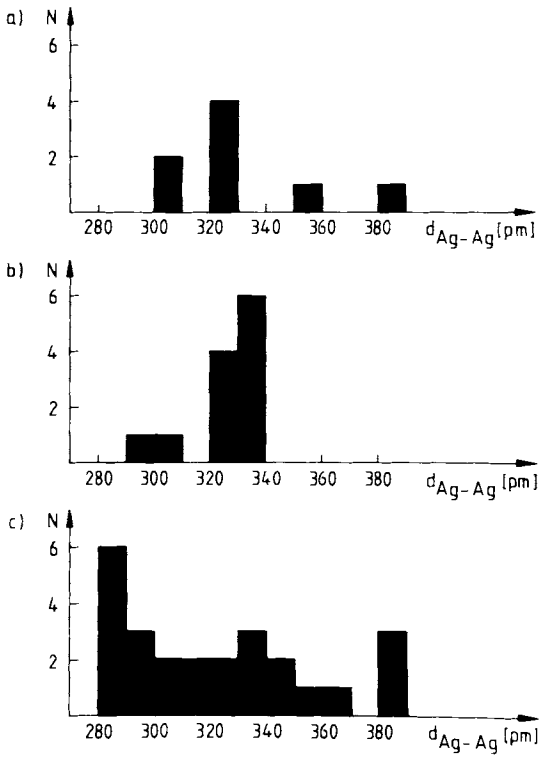

Fig. 12. Distribution of silver–silver distances in di- (a), tri- (b), and tetrasilver sulfamide (c).

A study of bond lengths in delafossite structures determined by single-crystal X-ray analysis reveals a previously unknown tendency: the Cu–O bond lengths decrease significantly with increasing radius of B^{3+}. The obvious assumption that the shortening of the Cu–O bonds occurs at the expense of the B^{3+}–O bonds can be shown to be invalid using the bond length/bond strength concept.[125] The contributions of the trivalent cations to the valence sum (s) of oxygen remain constant.[81] Accordingly, the expected valence sum of 2 for oxygen would constrain the contribution from copper to remain constant at 0.5. Copper would then display the expected valence sum of 1 for all compounds of the series. This conclusion is unfortunately not consistent with the experimental observation that the Cu–O bond lengths decrease with increasing radius of B^{3+}.

Table 3. Contributions of various bonds to the valence sum of copper in some copper delafossites.

	$2H\text{-}CuAlO_2$	$3R\text{-}CuGaO_2$	$2H\text{-}CuScO_2$	$3R\text{-}CuYO_2$
Cu-O[pm]	186.5	185.2	183.5	182.6
Cu-Cu [pm]	286.29	297.66	322.27	353.33
2·s(Cu-O)	0.796	0.850	0.927	0.970
6·s(Cu-Cu)	0.204	0.147	0.073	0.030

Since the valence s of the Cu–O bond in $CuYO_2$ has a higher value than in $CuAlO_2$ (according to the observed bond lengths), the question arises as to the origin of the additional valence needed to saturate the copper atom.

The only possibility is Cu–Cu interactions, since all other contacts outside the inner coordination sphere are too long. An estimate based on *Brown*'s work[125] is that the Cu–Cu interactions contribute 3% to the valence sum of copper in $CuYO_2$ but the impressive amount of more than 20% in $CuAlO_2$ (cf. Table 3).

3. Physical Properties as Indicators of d^{10}–d^{10} Interactions

As already stated, unambiguous conclusions regarding chemical bonding cannot always be drawn from structural data. This can be demonstrated clearly in the case of Na_3AgO_2, which, with a shortest Ag–Ag distance of 296 pm, can reasonably be classified with the compounds discussed in this article. However, the best description of the structure (as published by *R. Hoppe*[33]) is as a structural variant of Na_2O; the shortest distances between all cations (Na^+ and Ag^+) are practically equal and are determined by the matrix of oxide ions. Bond lengths alone are plainly unreliable indicators of bonding interactions between d^{10} cations and it becomes necessary to back up the structural data with evidence from additional sources. Suitable properties to study are clearly those that unambiguously demonstrate marked changes in the electronic structure of the d^{10} cations associated with the homoatomic interactions.

3.1. Absorption in the UV/VIS Region

One change in properties associated with the structural features discussed here is qualitatively apparent; intensely colored compounds are formed, even with anions that (like the "isolated" univalent coinage-metal cations) do not themselves absorb in the visible region. Figure 13 summarizes the known UV/VIS spectroscopic studies[126] and presents the reflection spectrum of Ag_2SO_4 for comparison. The spectra typically show absorption edges with relatively steep gradients (explaining the brilliant coloration of the compounds), the position of the absorption edge corresponding to the particular color. Compared with Ag_2SO_4, which has "isolated" Ag^+ ions, the absorption edges of the compounds described in Section 2.1 are shifted by up to 18000 cm^{-1} (!) to lower wavenumber. This represents a striking correlation between structure and properties, rendered even more significant by the increase in redshift with increasing silver content and with increasing metal aggregation (Table 4). A more rigorous quantitative treatment of this correlation is impossible because we do not yet understand the complicated mutual effects of metal–metal distances and extent of aggregation. A pressure increase also brings about a shift to lower wavenumber, which identifies the associated transitions as those between bands. The UV shift on cooling could then be attributed to a reduction of thermally induced band broadening.

Table 4. Silver content and energy of the absorption edge in selected silver compounds.

Compound	Color	Absorption edge ν [cm^{-1}]	Proportion of silver (per formula unit)
$Ag_2H_2N_2O_2S$	colorless	33300	0.22
Ag_2SO_4	colorless	33100	0.29
Ag_3PO_4	yellow	25600	0.38
Ag_2CO_3	yellow	24600	0.33
$AgBO_2$	yellow	23700	0.25
$(Ag_3HN_2O_2S)NH_3 \cdot H_2O$	yellow	24400	0.19
$Ag_2Ge_2O_5$	pale yellow	23300	0.22
Ag_3BO_3-(II)	yellow	23000	0.43
$Ag_6Si_2O_7$	red	17900	0.40
$Ag_4N_2O_2S$	red	17500	0.44
$Ag_{10}Si_4O_{13}$	red	17300	0.37
$LiAg_3O_2$	red	—	0.50
$Ag_{10}Ge_4O_{13}$	black	13500	0.37

3.2. Electrical Conductivity

Electrical conductivity is a physical property dependent on band structure. The conductivities of several compounds have been determined,[127] allowing for the effects of ionic conductivity, which can be appreciable for d^{10} univalent cations. In contrast to Ag_2SO_4, which is essentially a complete insulator, all compounds with d^{10} cation aggregates so far investigated have proved to be semiconductors. Figure 14 presents Arrhenius diagrams of the conduc-

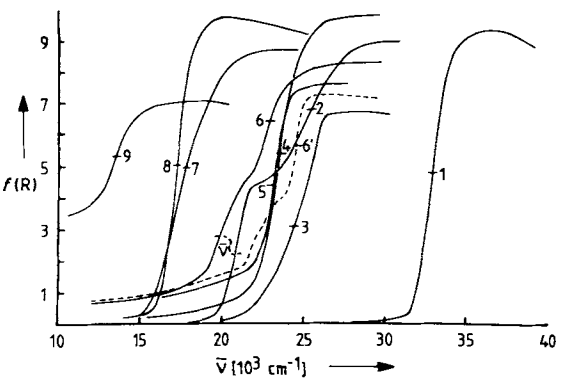

Fig. 13. Reflection spectra of oxoanionic silver(I) compounds: Ag_2SO_4 (1), Ag_3PO_4 (2), Ag_2CO_3 (3), $AgBO_2$ (4), $Ag_2Ge_2O_5$ (5), Ag_3BO_3 at room temperature and at 5 K (6 and 6'), $Ag_6Si_2O_7$ (7), $Ag_{10}Si_4O_{13}$ (8), $Ag_{10}Ge_4O_{13}$ (9).

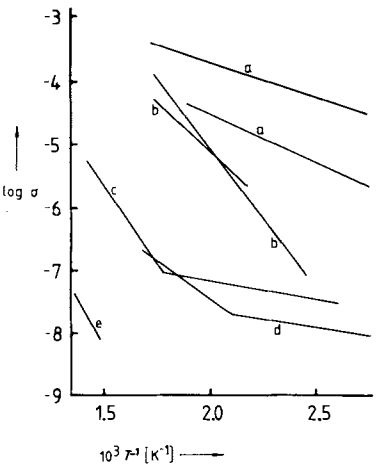

Fig. 14. Electrical conductivity of $Ag_6Ge_2O_7$ (a), Ag_3BO_3 (b), $Ag_2Ge_2O_5$ (c), $Ag_6Si_2O_7$ (d), and $AgBO_2$ (e).

tivity of some representative compounds. An analysis of the intrinsic conductivity curves gives the corresponding activation energy, which is compared in Figure 15 with the optical band gap. The relationship between spectroscopic band gaps and those determined by conductivity measurements is unmistakable. As would be expected, the agreement extends only to relative changes, not to absolute values; the optical transitions with the selection rule $\Delta k = 0$ and the induction of electrical conductivity are governed by different mechanisms.

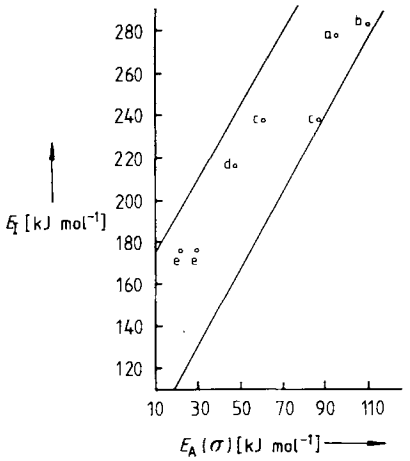

Fig. 15. Optical and conductivity-determined band separations in $Ag_2Ge_2O_5$ (a), $AgBO_2$ (b), Ag_3BO_3 (c), $Ag_6Si_2O_7$ (d), and $Ag_6Ge_2O_7$ (e). E_I = energy of the optical absorption edge; $E_A(\sigma)$ = activation energy of the electrical conductivity.

The silver substructures of the oxides investigated so far differ appreciably in structural detail and are thus difficult to compare quantitatively. Conductivity measurements were therefore carried out on a series of copper delafossites, in which the copper substructures remain qualitatively the same but the Cu-Cu distances vary. It was essential to prevent the formation of Cu^{2+} defects in order to obtain reliable results; this was to a large extent achieved by fixing the oxygen activity during the synthesis.[81] Samples prepared in this way show a very low ionic conductivity and give purely intrinsic electrical conductivity curves. The conductivities vary over the range $\sigma = 10^{-2}$–10^{-6} S cm^{-1} at 273 K. The plot of electrical conductivity against Cu-Cu distance (Fig. 16) shows a practically linear correlation. Since the conductivities of the constitutive sesquioxides are three orders of magnitude smaller, and the conductivity of the delafossites is thus almost entirely attributable to the Cu/O part of the structure, this is a further independent confirmation of interactions between centers with "closed" d^{10} configurations.

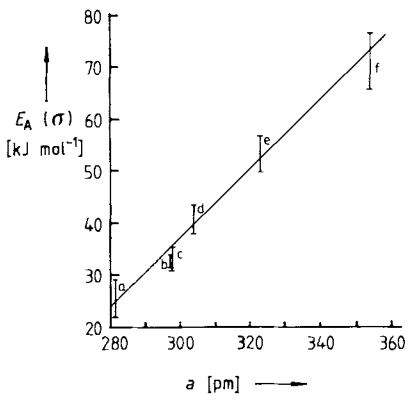

Fig. 16. Activation energy of the electrical conductivity, $E_A(\sigma)$, as a function of the cell constant a in copper(I) delafossites $CuAlO_2$ (a), $CuCrO_2$ (b), $CuGaO_2$ (c), $CuFeO_2$ (d), $CuScO_2$ (e), and $CuYO_2$ (f).

It should be possible to induce electrical conductivity optically as well as thermally; silver sulfamides indeed show a photoinduced rise in conductivity over several orders of magnitude when the wavelength of the irradiated light reaches a value corresponding to the position of the absorption edge (determined independently by reflection spectroscopy)[128,129] (Fig. 17). The observed reduction in the band gap with increasing silver content is consistent with the associated changes in the silver substructures (see above).

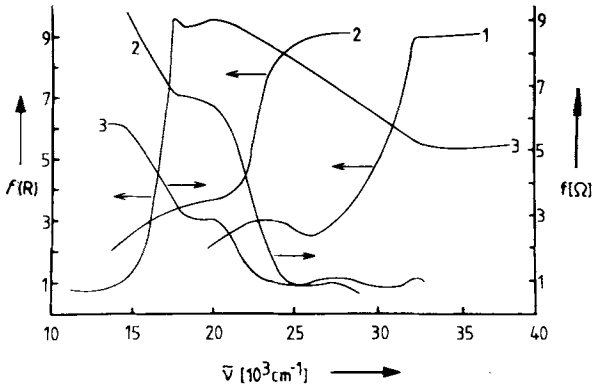

Fig. 17. UV/VIS absorption and photoinduced conductivity of $Ag_2H_2N_2O_2S$ (1), $(Ag_3HN_2O_2S)NH_3 \cdot H_2O$ (2), and $Ag_4N_2O_2S$ (3).

3.3. Other Physical Properties

The bistable switching of amorphous silver(I) silicates[130] and phosphates[131] may also be connected with their microheterogeneous structure and d^{10}–d^{10} interactions. Such materials can, after suitable pretreatment, be reversibly switched between high and low resistance by the application of short square-wave electrical pulses. This behavior is illustrated for a silver(I) silicate glass in Figure 18.

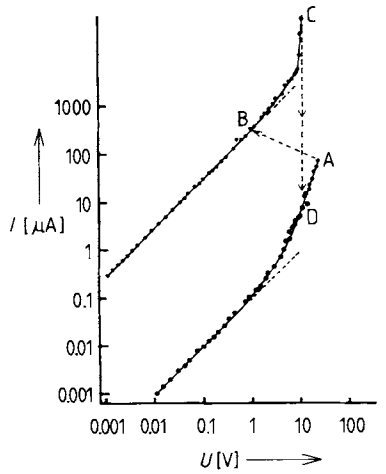

Fig. 18. Current/voltage characteristic of a silver(I) silicate glass after pretreatment. A–D = switching cycle.

Investigations using dielectric methods have given some indication of the presence of silver "clusters" in such glasses.[132]

Solid-state ^{109}Ag-NMR spectroscopy can also be a sensitive probe of changes in bonding; this is shown by the drastic changes in chemical shift between Ag_4RbI_5 and Ag_2F compared with AgF.[133] Our own preliminary studies of $Ag_{10}Si_4O_{13}$ with ^{109}Ag MAS NMR spectroscopy have shown a shift to low field of 320 ppm compared with solid $AgNO_3$.[134]

Anomalies in the dynamic behavior of Ag^+, manifested for example in the phonon spectra[135] of AgCl or AgBr, have been discussed for a long time. Although no unusual Ag^+-Ag^+ contacts are involved (NaCl structure), it is generally agreed that the difference between silver and alkali metal halides is due to attractive interactions between Ag^+ ions.[136]

Finally, it should be remembered that the dominant defect type in silver halides is the Frenkel defect, the formation of which requires the accommodation of short metal-metal contacts.

4. Correlations and Models

There is now enough empirical material to permit initial attempts to (1) establish conditions under which interactions between d^{10} electron systems, usually regarded as closed, become effective, (2) demonstrate correlations between structure and properties, and (3) set up preliminary bonding models.

4.1. Conditions for the Existence of d^{10}-d^{10} Interactions

The influence of homoatomic interactions is regarded as decisively less than that of classical bonding between "anions" and "cations." The tendency of d^{10} cations to undergo aggregation is only realized when their primary coordination requirements are satisfied. An analysis of available structural information shows that a high ratio of electropositive to electronegative species (e.g., the cation-to-oxygen ratio in the ternary silver oxides) is a necessary condition for the development of the characteristic collective bonding that essentially determines the tertiary structure. The excess of cations forces them into mutual proximity, which is clearly necessary in order that the attractive forces should become effective. A high proportion of d^{10} cations alone is not a necessary requirement, as is shown, for example, by the case of $KAgCO_3$. At present, the lowest known cation/oxygen ratio capable of producing d^{10} aggregation is 4/5 (in $Ag_2Ge_2O_5$).

The various classes of compounds are represented by widely varying numbers of known examples (a fact largely determined by the amount of preparative study invested in the individual systems); we believe that it is not yet possible to derive systematic correlations. General tendencies are already recognizable, however, in that the necessary cation/anion ratio is more difficult to attain with highly charged cations or with anions of low charge (halides)—a result of simple arithmetic. This could be the explanation for the readily formed metal aggregates involving the univalent coinage metals and the chalcogenides. For divalent cations, the mutual electrostatic repulsion would be highly disadvantageous; it is therefore not surprising that indications of bonding relationships between the core electrons of divalent atoms have only been obtained for zinc, cadmium, and mercury. Accordingly, the crystal structures of these elements are of key interest because they are ideally suited for studying pure d^{10}-d^{10} interactions. The influence of bonds to the anions on metal-metal distances, which could be critical, obviously plays no part in metallic zinc, cadmium, and mercury.

4.2. The Causes of Color and Conductivity

We have already shown that there are correlations between the structures of the compounds discussed here and their properties. However, the correlations alone provide no information on the nature of the electronic transitions involved. Classical ligand field transitions can be ruled out because of their localized nature, and, particularly, because the absorption phenomena in the visible and ultraviolet regions have proved to be independent of the ligand and of the coordination geometry. Another explanation[137] of the color of silver(I) compounds based on the covalent character of the Ag-X bond (as indicated by bond length) proved to be insupportable[138] because many compounds are now known that have equal Ag-X bond lengths but different colors. There remain two feasible explanations: (1) band transitions between a valence band of predominantly d character and a conduction band with predominantly s and p character within the silver substructure or (2) transitions between the highest occupied molecular orbital in the anionic part of the structure and the s or p band in the silver substructure, or in other words, a charge-transfer phenomenon. There are two main objections to the first explanation that are not easy to refute: first, it is improbable that the transition $^1S_0(4d^{10}5s^0) \rightarrow {}^3D_3(4d^95s^1)$ is lowered from 39000 cm^{-1} in the free silver ion[139] to 12000 cm^{-1} by band broadening induced by the Ag-Ag interactions, and, secondly, it is becoming clear that the position of the absorption edge also depends on the nature of the complex anion. In the isotypic silicates and germanates previously discussed, for example, the silver aggregates are the same, but there is an IR shift of the order of 1000-3800 cm^{-1} on going from a silicate to a germanate. On the other hand, there are drastic changes in groups of related compounds with differing cation content but similar anions—e.g., in the series $Ag_2Ge_2O_5$, $Ag_6Ge_2O_7$, $Ag_{10}Ge_4O_{13}$, and $[Ag_4GeO_4]_2 \cdot AgNO_3$. The absorption therefore clearly depends on the type of silver aggregates (its extent and bond lengths) and on the type of anions. Since the bonding between Ag^+ and silicate ions, for example, is mainly ionic (the irregular coordination of silver by oxygen and the similarity of the silicate dimensions to those in alkali metal silicates support this assumption), it seems easiest to explain the experimental observations in terms of charge-transfer transitions between the HOMOs of the complex anions and the acceptor levels of the metal aggregates, the latter being lowered in energy by the d^{10}-d^{10} interactions.

It should be pointed out, however, that this interpretation is in one respect in conflict with published views. According to *C. K. Jørgensen*, the energy of a charge-transfer process is dependent on the differences in the optical electronegativities of the electron donors and acceptors,[140] as described by the following equation: $\tilde{\nu}=30000\ \mathrm{cm}^{-1}\,(\chi_{opt}(A)-\chi_{opt}(D))$. This concept was modified by *J. A. Duffy*[141] for complex anions, χ_{opt} for oxygen in such anions being determined by the electronegativity of the central nonmetal atom. A comparison of isotypic silver silicates and germanates having the same electron acceptor (the Ag^+ aggregates) but different donors (silicate or germanate) should therefore show a lower energy absorption edge in the silicate because of the lower electronegativity of silicon.[142] The opposite is observed experimentally. This discrepancy should not be regarded too seriously, however, because the postulated transition involves the energy level of the highest occupied state with preponderantly "anionic" character, and this cannot be determined entirely by the electronegativity of the central nonmetal atom.

4.3. Bonding Models

L. E. Orgel[143] suggested a valence-bond model for bonding in compounds of d^{10} ions such as Cu^+, Ag^+, and Hg^{2+}. He postulated hybrid orbitals $1/\sqrt{2}(d_{z^2}-s)$ and $1/\sqrt{2}(d_{z^2}+s)$; the former occupies a position in the xy plane and contains two electrons, while the latter, directed along the z axis, can accept electrons from ligands and so stabilize the linear coordination that these ions generally display. According to *Jørgensen*, linear coordination is rendered more favorable by a small energy separation between the ground state ($^1S_0$) and the first excited state ($^3D_3$). *Rogers* et al.,[144] using the Orgel model as a basis, have stressed the importance of the increased electron density in the xy plane (associated with the d_{xy}, $d_{x^2-y^2}$, and $1/\sqrt{2}(d_{z^2}-s)$ orbitals) as regards the possibility of forming corresponding bands with preponderantly metallic character. A deformation electron density study of $CuAlO_2$ indeed showed the expected increased electron density in the xy plane[145] (Fig. 19); an unexpected feature of the study was that the maxima were located not on the Cu–Cu vectors but at the centers of the equilateral triangles of copper atoms. A detailed analysis of the results suggested the formation of a partially hybridized valence orbital $(0.97\,d_{z^2}-0.24\,s)$.

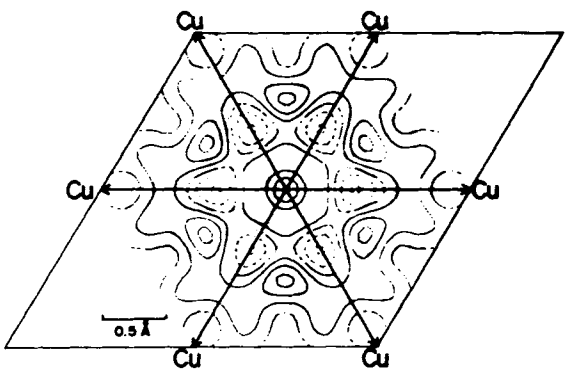

Fig. 19. Difference electron density in $CuAlO_2$, section at $z=0$.

This model seems, at least for the delafossite structures, to be self-consistent and to have been confirmed experimentally. However, it depends on the assumption that the Cu–O bonds are exactly perpendicular to the planes defined by the metal atoms, which is the case in very few compounds in which d^{10}–d^{10} interactions have been postulated. For example, the silver layers in $LiAg_3O_2$ are planar and the coordination at silver is exactly linear, but the angle between the AgO_2 units and the silver plane is only 32°.

Independently of such chemical considerations, and before the discovery of the numerous examples of the particular cation substructures, *H. Bilz* came to the conclusion that d^{10} ions with low-lying excited states—especially Ag^+—should be liable to attractive interactions.[8c] His considerations were prompted by differences in the phonon spectra of AgCl and AgBr compared with alkali metal halides.[135] The model involved polar interactions; it assumed the ready excitation of d valence electrons into s states of the conduction band associated with the formation of a quadrupole moment at the d^{10} centers. Although this model was intended to explain dynamic effects, it also seems suitable for the static phenomena observed; quadrupole–quadrupole interactions between several centers preferentially lead to two-dimensional assemblies, just as were found to predominate in the crystal structures. The shift in optical absorption would then be explicable in that the excited quadrupole state would be lowered in energy by the interactions. This concept reminds one qualitatively of dispersion interactions. Incidentally, it should be noted that *Bilz*'s quadrupole deformation model of d^{10} cations relates also to their marked mobility in ionic crystals.[146]

R. Hoffmann et al. have concerned themselves, in a series of publications, with an explanation of the bonding in the short metal–metal contacts frequently observed in bi- and polynuclear complexes of d^{10} species.[147] An EHMO analysis showed that, even when perturbations of the d^{10} systems by the ligands were neglected, bonding interactions between fully occupied d shells could arise if single-electron d functions were allowed to have partial s and p character. *R. Hoffmann* et al. and *J. K. Burdett* showed that such considerations of localized systems can also be extended to "collective" structures, e.g., the silver substructures in silver-rich oxides.[148]

Although the bonding models so far postulated differ greatly in detail, they all lead to the same conclusion: the presence of a low-lying excited state destroys the pure "core" nature of the "closed" d^{10} shell and also destroys its spherical symmetry. This is illustrated by the determination of deformation electron density at Zn^{2+} in a tetrachloro complex (Fig. 20);[149] the electron density distribution is easiest to reconcile with a configuration $(3d-e)^4(3d-t_2)^{6-x}(4s)^x$. Since the d–s separation is clearly of central importance, Ag^+ should assume a special position with respect to the effects discussed here (Table 5). This is consistent with our current state of knowledge: short Cu^+–Cu^+ and Au^+–Au^+ contacts have so far been observed mainly in the presence of strongly covalently bonded ligands and, in contrast to silver, have less ten-

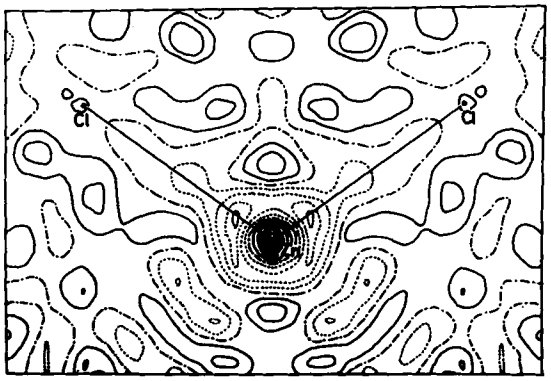

Fig. 20. Difference electron density in the region of the Zn^{2+} ion in $[NH_4]_3[(ZnCl_4)Cl]$.

Table 5. Some energy separations [cm^{-1}] in the free ions Cu^+, Ag^+, and Au^+.

	$^1S_0(d^{10}s^0) \rightarrow {}^3D_3(d^9s^1)$	$^1S_0(d^{10}s^0) \rightarrow {}^3P_2(d^9p^1)$
Cu^+	21928	66418
Ag^+	39163	80172
Au^+	15039	63052

dency to form extended, clusterlike aggregates. Isolable subvalent compounds of copper and gold analogous to those of silver (see Section 2.4) are unknown. The high ionic mobility associated with the unusual bonding interactions discussed here is also most marked for silver.

5. Conclusions

The empirical results presented in this article furnish convincing evidence that d^{10} cations can interact with each other in a way that influences both structure and physical properties. This capability is to a first approximation independent of the type of ligand and the geometry of the ligand field: it is unimportant whether the cations display linear coordination, with strongly covalent ligands, or an irregular geometry involving ionic bonds. The only precondition so far recognizable is that other influences (e.g., bridging ligands or an excess of cations) must first force the d^{10} ions into mutual proximity. "Isolated" d^{10} cations do not display the characteristic phenomena mentioned in this article.

It is not yet clear what causal role the interactions play in determining structure; do they "actively" lead to a weak bond or do the d^{10} species "tolerate" the short homoatomic contacts? It seems that no general answer can be given to this question and to others concerned with the type of bonding. The molecular systems (coordination compounds) will have to be treated differently from the more "collective" (polymeric) structures, and other treatments again will be necessary to describe dynamic effects such as the high mobility of such ions in a solid matrix in detail. Furthermore, it can be seen from the first excitation energies of the free ions Cu^+, Ag^+, and Au^+ (Table 5) that no uniform picture can be expected for the group of coinage metals because of their intrinsic heterogeneity. The only common feature to which the postulated interactions and their consequences can be attributed is the combination of a "closed" d^{10} ground state with low-lying excited states.

I would like to thank the co-workers and colleagues, listed in the references, who were involved with the individual contributions to this field. I am grateful to Dipl.-Chem. Konrad Heidebrecht, Berndt Ullrich Köhler MSc, and Dr. Hartmut Ehrhardt for helpful and fruitful discussions. The Deutsche Forschungsgemeinschaft supported this work financially.

Received: June 6, 1986 [A 642 IE]
German version: *Angew. Chem. 99* (1987) 1136

[1] W. Kossel, *Ann. Phys. (Leipzig) 49* (1916) 229.
[2] G. N. Lewis, *J. Am. Chem. Soc. 38* (1916) 762.
[3] E. Zintl, *Angew. Chem. 52* (1939) 1; W. Klemm, *Proc. Chem. Soc. London 1958*, 329.
[4] H. G. Grimm, *Z. Elektrochem. 31* (1925) 474.
[5] A. Haas, *Chem.-Ztg. 106* (1982) 239.
[6] V. Heine, *Solid State Phys. 35* (1980) 1; P. Gombas: *Pseudopotentiale*, Springer, Wien 1967.
[7] P. Coppens, M. B. Hall: *Electron Distributions and Chemical Bond*, Plenum, New York 1982.
[8] a) M. Jansen, *Habilitationsschrift*, Universität Giessen 1978; b) O. Mundt, G. Becker, H. J. Wessely, H. J. Breunig, H. Kischkel, *Z. Anorg. Allg. Chem. 486* (1982) 70; c) N. G. Kleppmann, H. Bilz, *Commun. Phys. 1* (1976) 105.
[9] A. Byström, L. Evers, *Acta Chem. Scand. 4* (1950) 613.
[10] G. A. Barclay, B. F. Hoskins, *J. Chem. Soc. 1963*, 2807.
[11] H. L. Keller, Hk. Müller-Buschbaum, *Z. Naturforsch. B28* (1973) 263; *Z. Anorg. Allg. Chem. 393* (1972) 266.
[12] D. M. Blake, C. J. Nyman, *J. Am. Chem. Soc. 92* (1970) 5359; A. J. Layton, R. S. Nyholm, G. A. Pneumaticakis, L. Tobe, *Chem. Ind. (London) 1967*, 465.
[13] M. Jansen, *J. Less-Common Met. 76* (1980) 285.
[14] A. I. Kitaigorodski: *Molekülkristalle*, Akademie-Verlag, Berlin 1979.
[15] G. Meyer, P. Linzmeier, *Rev. Chim. Miner. 14* (1977) 52.
[16] M. Jansen, *Acta Crystallogr. Sect. B33* (1977) 3585.
[17] R. Masse, J. C. Guitel, A. Durif, *Acta Crystallogr. Sect. B35* (1979) 1428.
[18] M. Jansen, *Z. Naturforsch. B30* (1975) 854.
[19] A. Bondi, *J. Phys. Chem. 68* (1964) 441.
[20] M. Jansen, H. L. Keller, *Angew. Chem. 91* (1979) 500; *Angew. Chem. Int. Ed. Engl. 18* (1979) 464.
[21] M. Jansen, G. Brachtel, *Z. Anorg. Allg. Chem. 478* (1981) 13; M. Jansen, G. Brachtel, *Naturwissenschaften 67* (1980) 606.
[22] M. Jansen, B. Standke, *Z. Anorg. Allg. Chem. 510* (1984) 143.
[23] W. Beesk, P. G. Jones, H. Rumpel, E. Schwarzmann, G. M. Sheldrick, *J. Chem. Soc. Chem. Commun. 1981*, 664.
[24] F. Charbonnier, R. Faure, H. Loiseleur, *Acta Crystallogr. Sect. B37* (1981) 822.
[25] J. K. H. Rao, H. A. Visewamitra, *Acta Crystallogr. Sect. B28* (1972) 484.
[26] G. Brachtel, M. Jansen, *Cryst. Struct. Commun. 10* (1972) 484.
[27] W. Losert, R. Hoppe, *Z. Anorg. Allg. Chem. 524* (1985) 7.
[28] H. Klassen, R. Hoppe, *Z. Anorg. Allg. Chem. 485* (1982) 101.
[29] H. L. Keller, Hk. Müller-Buschbaum, *Z. Anorg. Allg. Chem. 408* (1974) 207.
[30] W. Losert, R. Hoppe, *Z. Anorg. Allg. Chem. 524* (1985) 7.
[31] L. O. Larsson, *Acta Chem. Scand. 23* (1969) 2261.
[32] H. Hahn, C. Delorent, *Z. Anorg. Allg. Chem. 290* (1957) 68.
[33] F. Schenk, R. Hoppe, *Naturwissenschaften 56* (1969) 44.
[34] S. Ohba, F. Matsumoto, M. Ishihrara, Y. Saito, *Acta Crystallogr. Sect. C42* (1986) 1.
[35] R. Masse, M. T. Averbuch-Pouchot, A. Durif, J. C. Guitel, *Acta Crystallogr. Sect. C39* (1983) 1608.
[36] M. Jansen, *Z. Naturforsch. B31* (1976) 1544.
[37] H. N. Ng, C. Calvo, R. Faggiani, *Acta Crystallogr. Sect. B34* (1978) 898.
[38] S. Geller, T. O. Dudley, *J. Solid State Chem. 26* (1978) 321.
[39] K. Persson, B. Holmberg, *J. Solid State Chem. 42* (1982) 1.
[40] K. Persson, B. Holmberg, *Acta Crystallogr. Sect. B38* (1982) 1065.
[41] K. Persson, *Acta Crystallogr. Sect. B35* (1979) 302.
[42] R. Birnstock, D. Britton, *Z. Kristallogr. 132* (1970) 87.
[43] W. Stoeger, A. Rabenau, *Angew. Chem. 90* (1978) 627; *Angew. Chem. Int. Ed. Engl. 17* (1978) 599.

[44] K. Heidebrecht, M. Jansen, *Z. Kristallogr.*, in press.
[45] W. Werner, J. Strähle, *Z. Naturforsch. B34* (1979) 952.
[46] P. Messien, M. Baiwir, *Bull. Soc. R. Sci. Liege 35* (1966) 234.
[47] R. C. Knowles, *Acta Crystallogr. 17* (1964) 847.
[48] M. Palazzi, S. Jaulmes, *Acta Crystallogr. Sect. B37* (1981) 1337.
[49] B. Krebs, J. Mandt, *Z. Naturforsch. B32* (1977) 373.
[50] W. Bronger, C. Burschka, *Z. Anorg. Allg. Chem. 425* (1976) 109.
[51] J. P. Deloume, R. Faure, H. Loiseleur, M. Roubin, *Acta Crystallogr. Sect. B34* (1978) 3189.
[52] R. Sadanage, S. Sueno, *Mineral. J. 5* (1967) 124.
[53] P. Engel, W. Nowacki, *Acta Crystallogr. Sect. B24* (1968) 77.
[54] C. Burschka, W. Bronger, *Z. Anorg. Allg. Chem. 430* (1977) 61.
[55] G. Bergerhoff, *Z. Anorg. Allg. Chem. 299* (1959) 328.
[56] G. Savelsberg, H. Schäfer, *J. Less-Common Met. 80* (1981) 59.
[57] W. Bronger, J. Eyck, H. Schils, *J. Less-Common Met. 60* (1978) 5.
[58] T. C. Waddington, *J. Chem. Soc. 1959*, 2499.
[59] G. Savelsberg, H. Schäfer, *Z. Naturforsch. B33* (1978) 711.
[60] R. Masse, J. C. Guitel, A. Durif, *J. Solid State Chem. 23* (1978) 369.
[61] D. Britton, J. D. Dunitz, *Acta Crystallogr. 19* (1965) 662.
[62] H. U. Schuster, C. Müs, W. Jung, *Z. Naturforsch. B34* (1979) 354.
[63] C. Kratky, A. Popitsch, *Acta Crystallogr. Sect. B36* (1980) 1044.
[64] C. Kratky, E. Naubaur, A. Popitsch, *Acta Crystallogr. Sect. B37* (1981) 654.
[65] M. T. Oumba, M. Quarton, *Mater. Res. Bull. 18* (1983) 967.
[66] G. Savelsberg, H. Schäfer, *Z. Naturforsch. B34* (1979) 1033.
[67] H. Klassen, R. Hoppe, *Z. Anorg. Allg. Chem. 494* (1982) 20.
[68] G. Gattour, *Acta Crystallogr. 16* (1957) 549.
[69] S. Jaulmes, J. Rivet, P. Laruelle, *Acta Crystallogr. Sect. B33* (1977) 540.
[70] H. Schils, W. Bronger, *Z. Anorg. Allg. Chem. 456* (1979) 187.
[71] C. Burschka, *Z. Naturforsch. B34* (1979) 675.
[72] G. Savelsberg, H. Schäfer, *Mater. Res. Bull. 16* (1981) 1291.
[73] J. E. Iglesias, E. K. Pachali, *H. Steinfink, Mater. Res. Bull. 7* (1972) 147.
[74] C. L. Teske, *Z. Anorg. Allg. Chem. 445* (1978) 193.
[75] P. Messien, M. Baiwir, *Bull. Soc. R. Sci. Liege 35* (1966) 234.
[76] N. Blom, A. Ludi, *Acta Crystallogr. Sect. C40* (1984) 1767.
[77] H. Hartl, J. Fuchs, *Angew. Chem. 98* (1986) 550; *Angew. Chem. Int. Ed. Engl. 25* (1986) 569.
[78] H. Hartl, F. Mahdjour-Hassan-Abadi, *Angew. Chem. 96* (1984) 359; *Angew. Chem. Int. Ed. Engl. 23* (1984) 378.
[79] K. Koop, Hk. Müller-Buschbaum, *Z. Anorg. Allg. Chem. 531* (1985) 140.
[80] K. Koop, Hk. Müller-Buschbaum, *Z. Anorg. Allg. Chem. 530* (1985) 7.
[81] B. U. Köhler, M. Jansen, *Z. Anorg. Allg. Chem. 534* (1986) 73.
[82] W. Bronger, H. Schils, *J. Less-Common Met. 83* (1982) 287.
[83] W. Bronger, H. Schils, *J. Less-Common Met. 83* (1982) 279.
[84] A. F. Wells: *Structural Inorganic Chemistry*, 4th ed., Clarendon Press, Oxford 1975.
[85] K. Herrmann, *Nature (London) 15* (1936) 290.
[86] G. W. Brindley, *Nature (London) 22* (1936) 789.
[87] G. Argay, F. Naray-Szabo, *Acta Chim. Acad. Sci. Hung. 1966*, 329.
[88] H. G. von Schnering, K.-G. Häusler, *Rev. Chim. Miner. 13* (1976) 71.
[89] R. Masse, I. Tordjiman, A. Durif, *C. R. Séances Acad. Sci., Ser. 2, 302* (1986) 631.
[90] H. Schmidbaur, *Angew. Chem. 88* (1976) 830; *Angew. Chem. Int. Ed. Engl. 15* (1976) 728; J. P. Fackler, *Prog. Inorg. Chem. 21* (1976) 55; P. G. Jones, *Gold Bull. 19* (1986) 46.
[91] J. Beck, J. Strähle, *Angew. Chem. 97* (1985) 419; *Angew. Chem. Int. Ed. Engl. 24* (1985) 409.
[92] D. T. Comer, A. C. Larson, R. B. Roof, *Acta Crystallogr. 19* (1965) 192.
[93] M. Pasquali, C. Floriani, A. G. Manfredotti, C. Guastini, *J. Am. Chem. Soc. 103* (1981) 185.
[94] S. I. Khan, P. G. Edwards, H. S. A. Yuan, R. Bau, *J. Am. Chem. Soc. 107* (1985) 1682.
[95] G. Doyle, K. A. Eriksen, M. Modrick, G. A. Ansell, *Organometallics 1* (1982) 1613.
[96] M. Corbett, B. F. Hoskins, N. J. Mcleod, B. P. O'Day, *Aust. J. Chem. 28* (1975) 2377.
[97] K. P. Dancey, P. A. Tasker, R. Price, W. E. Hatfield, D. C. Brower, *J. Chem. Soc. Chem. Commun. 1980*, 1248.
[98] M. R. Churchill, S. A. Bezman, J. A. Osborn, J. Wormald, *Inorg. Chem. 11* (1972) 1818.
[99] R. D. Mounts, T. Ogura, Q. Fernando, *Inorg. Chem. 13* (1974) 802.
[100] J. A. Campbell, C. L. Raston, A. H. White, *Aust. J. Chem. 30* (1977) 1937.
[101] S. Gambarotta, C. Floriani, A. Chiesi-Villa, C. Guastini, *J. Chem. Soc. Chem. Commun. 1983*, 1087.
[102] N. R. Udupa, B. Krebs, *Inorg. Chim. Acta 7* (1973) 271.
[103] R. Hesse, L. Nilson, *Acta Chem. Scand. 23* (1969) 825.
[104] H. S. Hong, A. Olin, R. Hesse, *Acta Chem. Scand. Ser. A29* (1975) 583.
[105] K. Schubert, D. Neugebauer, A. A. M. Aly, *Z. Anorg. Allg. Chem. 464* (1980) 217.
[106] P. Jennische, R. Hesse, *Acta Chem. Scand. 25* (1971) 423.
[107] J. Perron, A. L. Beauchamp, *Can. J. Chem. 62* (1984) 1287.
[108] I. G. Dance, L. J. Fitzpatrick, M. L. Scudder, *Inorg. Chem. 23* (1984) 2276.
[109] F. Guay, A. L. Beauchamp, *J. Am. Chem. Soc. 101* (1979) 6260.
[110] I. G. Dance, L. J. Fitzpatrick, A. D. Rae, M. L. Scudder, *Inorg. Chem. 22* (1983) 3785.
[111] J. Van-der-Velden, P. T. Beuskens, J. J. Bour, W. P. Bosman, J. H. Noordik, K. Kolenbrander, J. Buskes, *Inorg. Chem. 23* (1984) 146.
[112] C. E. Briant, D. I. Gilmour, D. M. P. Mingos, *J. Organomet. Chem. 267* (1984) C 52.
[113] J. Van-der-Velden, J. J. Bour, W. P. Bosman, J. H. Noorduk, *J. Chem. Soc. Chem. Commun. 1981*, 1218.
[114] J. Van-der-Velden, J. J. Bour, W. P. Bosman, J. H. Noorduk, *Inorg. Chem. 22* (1983) 1913.
[115] J. Van-der-Velden, J. J. Bour, J. J. Steggerda, P. T. Beurskens, M. Roseboom, J. H. Noordik, *Inorg. Chem. 21* (1982) 4321.
[116] J. M. M. Smits, J. J. Bour, F. A. Vollenbroek, P. T. Beurskens, *J. Crystallogr. Spectrosc. Res. 13* (1983) 355.
[117] R. Hesse, P. Jennische, *Acta Chem. Scand. 26* (1972) 3855.
[118] H. Schmidbaur, J. R. Mandl, J. M. Bassett, G. Blaschke, B. Zimmer-Gasser, *Chem. Ber. 114* (1981) 433.
[119] H. Adams, W. Hiller, J. Strähle, *Z. Anorg. Allg. Chem. 485* (1982) 81.
[120] J. D. Basil, H. H. Murray, J. P. Fackler, J. Tocher, A. M. Mazany, B. Trzcinska-Bencroft, H. Knachel, D. Dudis, T. J. Delord, D. O. Harler, *J. Am. Chem. Soc. 107* (1985) 6908.
[121] H. Schmidbaur, A. Wohlleben, U. Schubert, A. Frank, G. Huttner, *Chem. Ber. 110* (1977) 2751.
[122] M. Jansen, *Z. Naturforsch. B37* (1982) 265.
[123] F. Belay, C. Kratky, E. Nachbaur, A. Popitsch, *Monatsh. Chem. 118* (1987) 19.
[124] H. Greschonig, E. Nachbaur, A. Krischner, *Acta Crystallogr. Sect. B33* (1977) 3585.
[125] I. D. Brown in M. O'Keefe, A. Navrotsky (Eds.): *Structure and Bonding in Crystals, Vol. II*, Academic Press, New York 1981, p. 1.
[126] C. Friebel, M. Jansen, *Z. Naturforsch. B39* (1984) 739.
[127] B. U. Köhler, W. Weppner, M. Jansen, *J. Solid State Chem. 57* (1985) 227.
[128] H. Gruber, H. Hess, A. Popitsch, A. P. Fischer, *J. Electrochem. Soc. 129* (1982) 369.
[129] A. Popitsch, *J. Crystallogr. Spectrosc. Res. 15* (1985) 603.
[130] M. Jansen, H. H. Käs, *Angew. Chem. 92* (1980) 386; *Angew. Chem. Int. Ed. Engl. 19* (1980) 386.
[131] H. H. Käs, *Naturwissenschaften 64* (1977) 434; H. H. Käs, W. Platzer, J. Tille, *Glastech. Ber. 52* (1979) 25.
[132] H. H. Käs, H. Herwig, *Sci. Electr. 24* (1978) 124.
[133] K. D. Becker, E. von Goldammer, *Chem. Phys. 48* (1980) 193.
[134] K. Heidebrecht, H. Ehrhardt, M. Jansen, unpublished.
[135] W. von der Osten, B. Dorner, *Solid State Commun. 16* (1975) 431.
[136] K. Fischer, H. Bilz, R. Haberkorn, W. Weber, *Phys. Status Solidi B54* (1972) 285.
[137] K. S. Pitzer, J. A. Hildebrand, *J. Am. Chem. Soc. 63* (1941) 2472.
[138] C. Kratky, E. Nachbaur, A. Popitsch, *Monatsh. Chem. 112* (1981) 529.
[139] C. E. Moore: *Atomic Energy Levels, Vol. I-III, Nat. Bur. Stand. U.S. Circ. 467* (1971).
[140] C. K. Jorgensen: *Oxidation Numbers and Oxidation States*, Springer, Berlin 1969, Chap. 7.
[141] J. A. Duffy, *Struct. Bonding (Berlin) 32* (1977) 147.
[142] L. Pauling, *J. Am. Chem. Soc. 54* (1932) 3570.
[143] L. E. Orgel, *J. Chem. Soc. 1958*, 4186.
[144] D. B. Rogers, R. D. Shannon, C. T. Prewitt, J. L. Gillson, *Inorg. Chem. 10* (1971) 723.
[145] N. Kijima, K. Tanaka, F. Maruma, *Acta Crystallogr. Sect. B39* (1983) 569.
[146] H. Bilz, *Cryst. Lattice Defects Amorphous Mater. 12* (1985) 31.
[147] P. K. Mehrotra, R. Hoffmann, *Inorg. Chem. 17* (1978) 2187; A. Dedieu, R. Hoffmann, *J. Am. Chem. Soc. 100* (1978) 2074.
[148] Y. Jiang, S. Alvarez, R. Hoffmann, *Inorg. Chem. 24* (1985) 749; J. K. Burdett, *Prog. Solid State Chem. 15* (1984) 173.
[149] S. Ohba, K. Shiokaira, Y. Saito, *Acta Crystallogr. Sect. C43* (1987) 189.

Carbosilanes**

By Gerhard Fritz*

Dedicated to Professor Rudolf Hoppe on the occasion of his 65th birthday

Carbosilanes are compounds in which the elements carbon and silicon occupy alternate positions in the molecular framework. Formal replacement of every second carbon atom in the diamond lattice by a silicon atom gives silicon carbide, which exists, however, in several modifications characterized by different stacking orders. The SiC lattice is the basis of most carbosilanes.[1] These are divided on the basis of structural differences into carborundanes, silascaphanes, and molecules that no longer contain elements of the silicon carbide structure. In the carborundanes the Si-C six-membered rings are arranged in the chair form, in the silascaphanes in the boat form. The molecular framework of the third group is derived from barrelane and asterane. The reactivity of the carbosilanes is determined mainly by the substituents on the skeletal atoms. The presence of SiH or Si-halogen groups leads to a high reactivity, while derivatives with organic groups on the silicon atoms and CH_2 or CH groups in the skeleton are much less reactive. However, even such CH_2 and CH groups permit certain characteristic reactions. Because of their structural features and the range of substituents that can be introduced, the carbosilanes are presently of considerable interest with respect to technological developments as precursors for ceramics.

1. Introduction

The first organosilicon compounds were obtained in the second half of the last century by reaction of chlorosilanes with alkylzinc or alkylmercury compounds and by Wurtz-Fittig syntheses (reaction of R_3SiCl with R'Cl and sodium). Their systematic study, however, only began after the discovery of Grignard reagents.[2] The "direct synthesis" of the methylchlorosilanes by reaction of silicon and methyl chloride in the presence of a copper catalyst in the 1940s led to the industrial preparation of Me_2SiCl_2 and thus to the development of the chemistry of silicones.[3] Compounds whose molecular framework consists of alternating silicon and carbon atoms have only been synthesized in the last 30 years;[4] the impetus for their study did not come from syntheses involving organosilicon compounds but through studies of the free radical reactions initiated by the thermal decomposition of silanes in the gas phase: e.g., the formation of H_3Si-PH_2 from SiH_4 and PH_3[5] or the reactions of ethylene with thermally produced silyl radicals.[5] The thermal decomposition of methylsilanes and methylchlorosilanes ($Me_{4-x}SiY_x$; Y = Cl, H) in the gas phase leads to the preferential formation of liquid, glassy, or crystalline compounds with an Si-C-Si skeleton.[6]

Another route to carbosilanes is provided by reactions of elemental silicon with CH_2Cl_2 or $CHCl_3$ or with *C*-chlorinated carbosilanes such as $(Cl_3Si)_2CCl_2$ in the presence of a copper catalyst.[7]

Routes involving organometallic synthesis can also be used for the construction of various carbosilanes.[8] Cyclization reactions of *Si*-methylated, linear or monocyclic carbosilanes under the influence of $AlBr_3$ provide a route to oligocyclic carbosilanes.[9]

The silicon and/or carbon atoms of the carbosilanes can be functionalized (e.g., as SiH, SiCl, or SiF, or as CCl, CF, or CLi). Such functionalizations open up further synthetic possibilities. Furthermore, they permit studies of the directing influence of the substituents on the reaction course.

2. Formation of Carbosilanes

2.1. Carbosilanes by Gas-Phase Pyrolysis of $SiMe_4$ and $Me_{4-x}SiCl_x$ (x = 1-3)

2.1.1. Experimental

The synthesis of carbosilanes on a preparative scale is carried out using an apparatus of the type shown in Figure 1. The pump P transfers $SiMe_4$ (b.p. = 26 °C), which evaporates from K into the (initially evacuated) apparatus, in the direction of the arrows through the reaction vessel (720 ± 5 °C) at such a rate that the contact time is ca. 1 min. Shortly after commencement of the reaction, white fumes exit from the reaction vessel and condense out at room temperature in the traps F_1-F_3. At a later stage, molten yellow products emerge from the reaction vessel and crystals are deposited on the walls of the vessel below the oven.[10] At the same time, H_2, CH_4, C_2H_4, and C_2H_6 are formed. Since the vapor pressure of $SiMe_4$ at 20 °C is ca. 720 torr, atmospheric pressure is built up in the apparatus after 2-3 h (excess pressure is released via a mercury valve). The vapor pressure of $SiMe_4$ remains constant in the system as long as liquid $SiMe_4$ is present in the reservoir, so that steady-state conditions are maintained in the apparatus. $SiMe_4$ and (in small amounts) product molecules such as H_2, CH_4, C_2H_4, C_2H_6, SiH-containing alkylsilanes, and some very low-boiling carbosilanes are continuously

[*] Prof. Dr. G. Fritz
Institut für Anorganische Chemie der Universität
Postfach 6380, D-7500 Karlsruhe (FRG)

[**] For a definition of the term "carbosilanes," see Ref. [1].

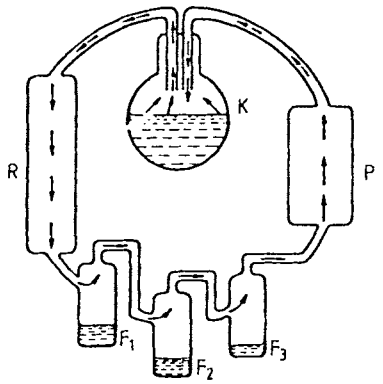

Fig. 1. Pyrolysis apparatus. R, reaction vessel (Rotosil, diameter 12 cm, length 80 cm); K, reservoir containing $SiMe_4$ or the methylchlorosilane; P, circulation pump; F_1–F_3, condensation traps.

forced through the reaction vessel. The pyrolysis of other methylsilanes occurs in an analogous manner.

2.1.2. *Carbosilanes by Pyrolysis of $SiMe_4$*

The complex product mixtures obtained upon pyrolysis of $SiMe_4$ can be separated using chromatographic techniques.[11] The products containing two and three silicon atoms are both linear and cyclic (Scheme 1).

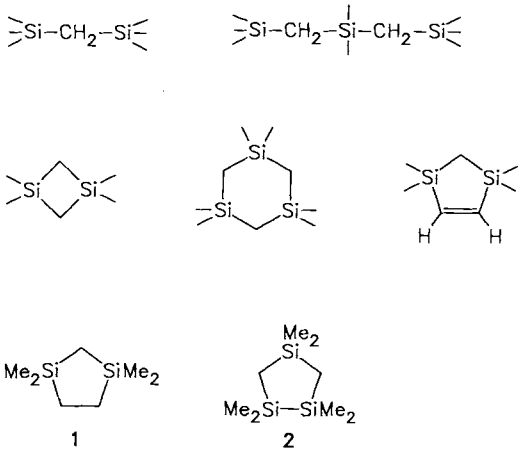

Scheme 1. — = Me or H.

Schemes 2–4 show characteristic silicon-richer compounds, the molecular skeletons of which contain the 1,3,5,7-tetrasilaadamantane unit; this unit can formally be derived from β-SiC (zinc blende type). Scheme 2 contains substituted 1,3,5,7-tetrasilaadamantanes,[12] some of which have an annelated Si–C ring, and Scheme 3 contains compounds in which such skeletons are linked by CH_2 bridges.

Scheme 4 contains the carborundanes, a group of compounds whose molecular skeletons contain two, three, and four annelated 1,3,5,7-tetrasilaadamantane units.[13]

The structural unit of α-SiC (wurtzite-type ZnS) appears in compounds **6** and **7**. Compound **6** contains the adamantane and wurtzitane units, **7** in addition the barrelane unit. Compound **7** represents all essential features of the

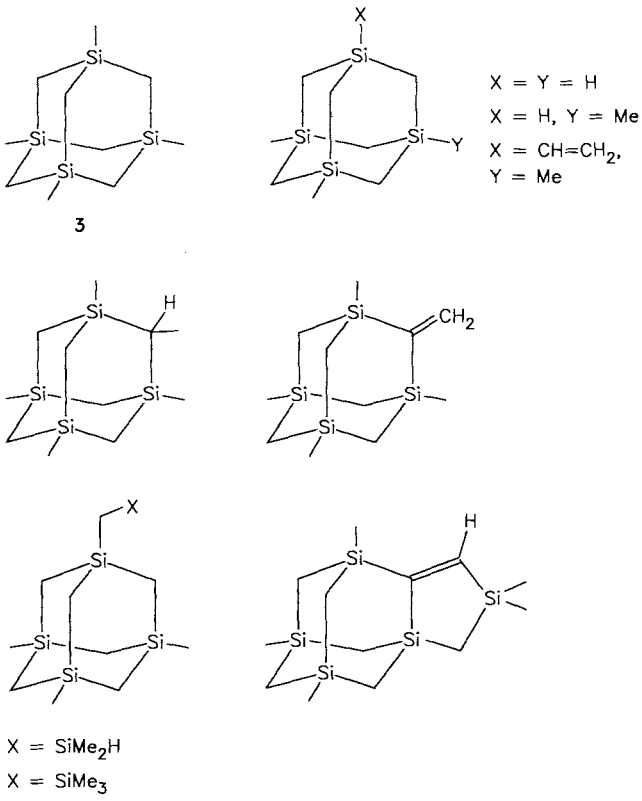

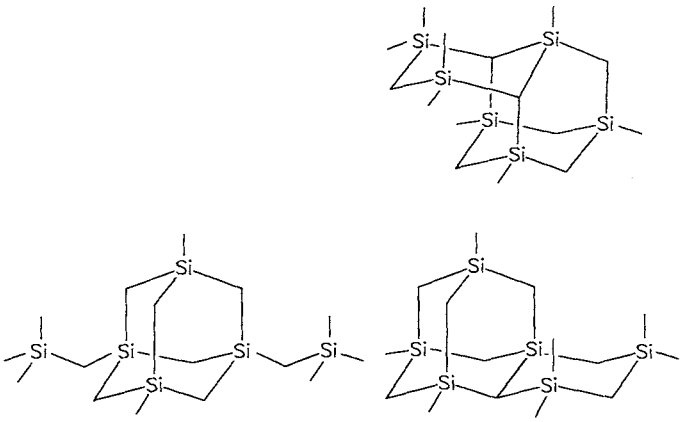

Scheme 2. — = Me.

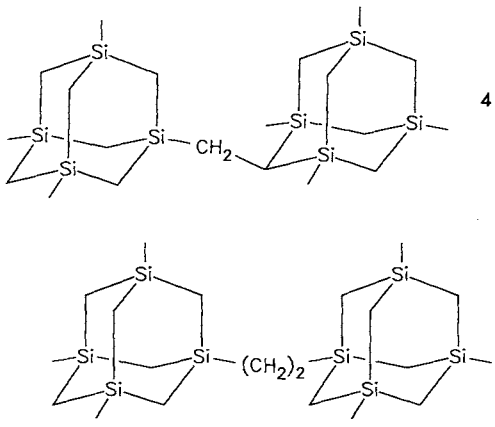

Scheme 3. — = Me.

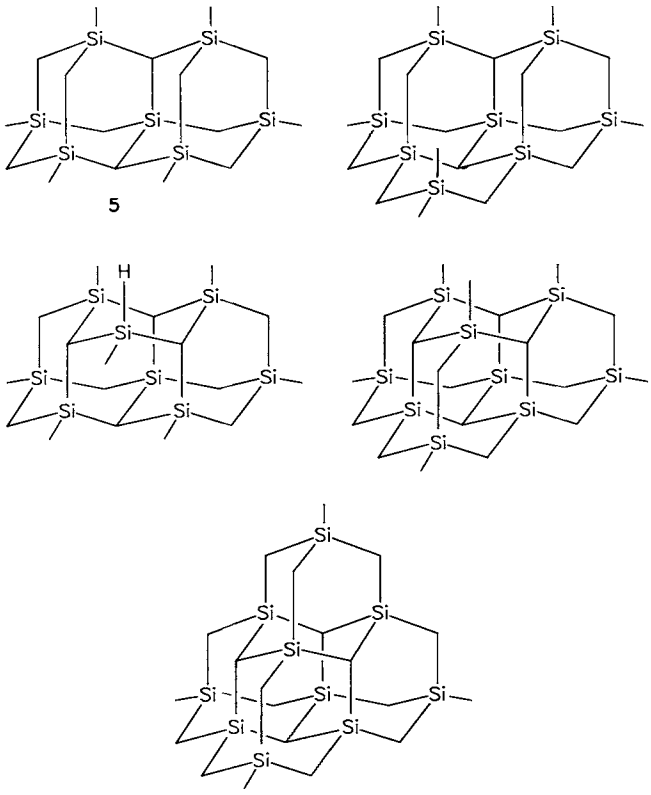

5

Scheme 4. — = Me.

4H-SiC structure: the adamantane unit and the complete wurtzitane skeleton.[14]

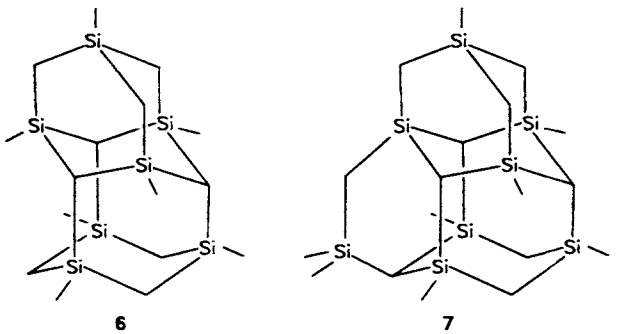

6 7

— = Me

While the carborundanes contain structural elements of silicon carbide, compounds **8** and **9** are members of the silascaphanes, a group whose Si-C six-membered rings are arranged in the boat form.[12, 15]

2.1.3. *Carbosilanes by Pyrolysis of Chloro(methyl)silanes*

The carbosilanes obtained by pyrolysis of tetramethylsilane are mostly unreactive, since (apart from SiH groups in a few cases) they are not functionalized. Carbosilanes containing SiCl functional groups can however be obtained by pyrolysis of the three methylchlorosilanes.[16]

The thermal decomposition of the methylchlorosilanes in the gas phase occurs with sufficient rapidity at ca. 700°C. 60 vol% of the pyrolysate obtained from Me_3SiCl consists of a fraction boiling between 160 and 200°C at atmospheric pressure, the remainder being oils and solids which are soluble in nonpolar solvents. $MeSiCl_3$ yields a pyrolysate of which 85% is liquid and colorless and 15% oily or solid (fusible).

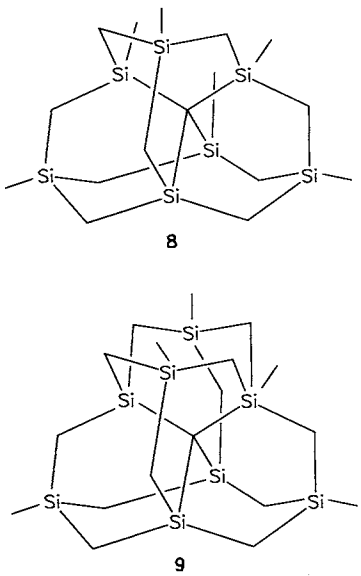

8 9

— = Me

The main products obtained from the methylchlorosilanes include partially methylated 1,3-disilapropanes. Their contribution to the total pyrolysate is 32% in the case of Me_3SiCl, 43% in the case of Me_2SiCl_2, and 60% in the case of $MeSiCl_3$. The pyrolysate from Me_3SiCl contains all the possible chloro- and methyl-substituted compounds with the basic structure $\geqslant Si-CH_2-Si\leqslant$. The main product from Me_3SiCl is **10**, while that from Me_2SiCl_2 and $MeSiCl_3$ is **11**. Isolation and identification of these products

$Me_3Si-CH_2-SiCl_3$ **10** $Cl_3Si-CH_2-SiCl_3$ **11**

was accomplished after reduction with $LiAlH_4$, whereby complete Cl/H exchange occurs without any change in molecular structure. This is also true for the silicon-richer compounds. In the latter case, the 1,3,5-trisilacyclohexane and 1,3,5,7-tetrasilaadamantane structures are increasingly favored when more methyl groups are present in the starting material. Thus, the 1,3,5,7-tetrasilaadamantanes **12**-**15** are formed from Me_3SiCl in the ratio 170 : 26 : 3 : 1.

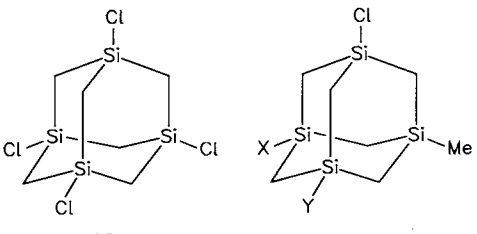

12

13, X = Y = Cl
14, X = Cl, Y = Me
15, X = Y = Me

The silicon-richer compounds formed upon pyrolysis of Me_3SiCl have not been studied in more detail. Those com-

pounds formed upon pyrolysis of Me_2SiCl_2 or $MeSiCl_3$ that contain four to eight silicon atoms have been better characterized.[17] Separation of the products forming the pyrolysate of Me_2SiCl_2 yielded forty compounds containing five to seven silicon atoms; the separation was carried out by chromatography following the conversion of the SiCl groups to SiH groups, and the products were identified on the basis of NMR and MS studies[18]. Figure 2 shows the types of compound obtained, with some examples. Compound **22** is the first known carbosilane with carbon atoms forming the bridgeheads of an adamantane skeleton; i.e., a 2,4,6,8,9,10-hexasilaadamantane derivative.

The polycyclic products formed in the pyrolysis of $MeSiCl_3$ are mostly carbosilanes with the asterane structure[18, 19] (Scheme 5).

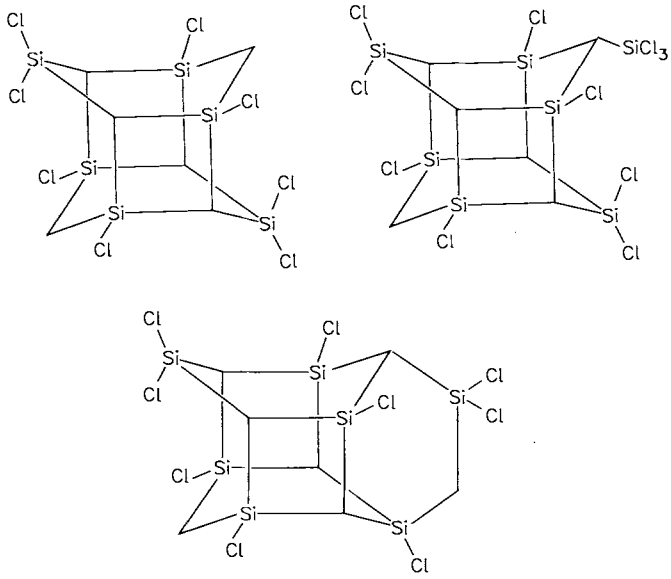

Scheme 5.

The Si:C ratio of the methylsilanes has a considerable influence on the structure of the pyrolysis products. As the number of methyl groups in the starting material is reduced in the series $SiMe_4$, $MeSiCl_3$, $MeCl_2Si-CH_2-SiCl_3$, the formation of carbosilanes with an Si:C ratio of 1:1 is increasingly favored. Carbosilanes with an adamantane structure are formed preferentially from $SiMe_4$, but never from $MeSiCl_3$; in support of this finding, no carbosilanes with the asterane structure are formed from $SiMe_4$. The Si:C ratios of some molecular skeletons are given in Scheme 6.

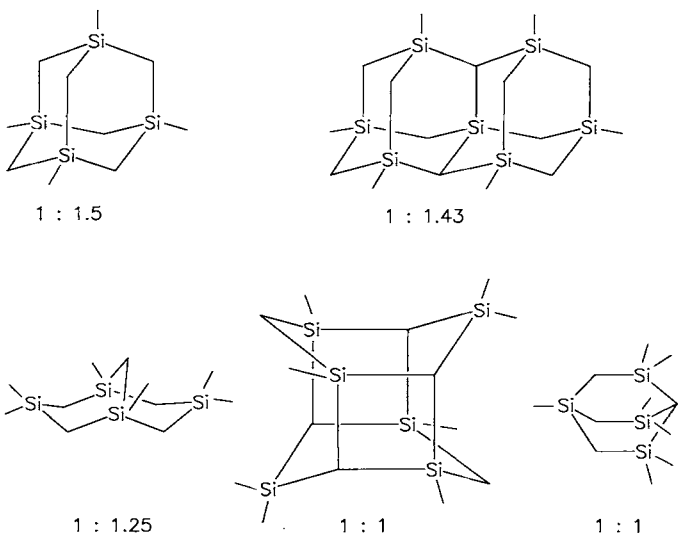

Scheme 6.

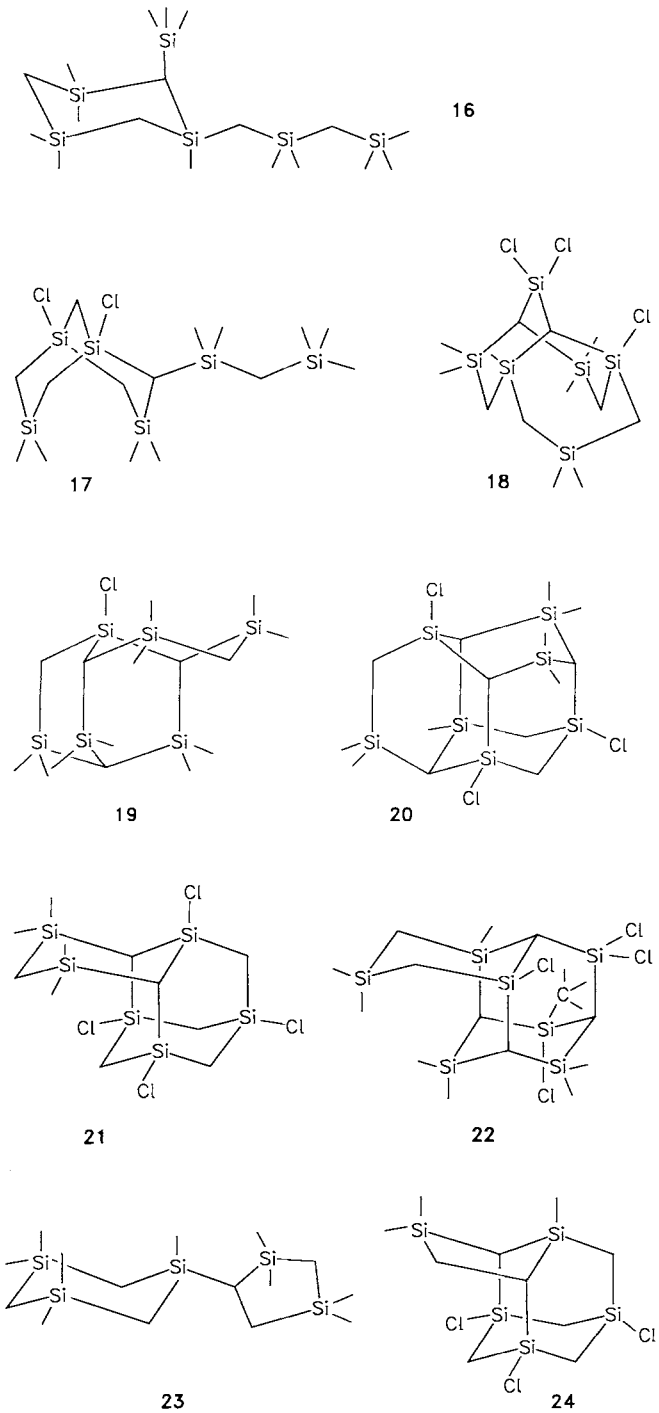

Fig. 2. Types of compound with five to eight silicon atoms formed upon pyrolysis of Me_2SiCl_2. **16**, example of a substituted 1,3,5-trisilacyclohexane; **17**, **18**, examples of substituted 1,3,5,7-tetrasilabicyclo[3.3.1]nonanes; **19**, **20**, examples of substituted 1,3,5,8-tetrasilabicyclo[2.2.2]octanes; **21**, **22**, molecules with the adamantane skeleton; **23**, **24**, molecules containing the 1,3-disilacyclopentane unit. — = H.

2.1.4. *Mechanism of the Formation of Carbosilanes in the Gas-Phase Pyrolysis of Methylsilanes*

Prior to the discussion of the mechanism we should note the following observations. The compounds formed from $SiMe_4$ contain methyl groups and, to a lesser extent, hydrogen atoms as the substituents on the silicon atoms: only in a few cases are structures with Si–Si bonds observed. The compounds derived from methylchlorosilanes bear methyl and chlorine substituents on the silicon atoms. Neither *C*-chlorinated carbosilanes nor carbon polymers are observed. The formation of the pyrolysate occurs via complex reaction sequences which have until now not been sufficiently clarified in detail. Clearly, the preparative method used permits low-molecular-weight reaction products to participate in the overall reaction, owing to the permanent circulation of volatile molecules through the apparatus. The formation of silicon-rich products of higher molecular weight is favored by a thermal aftertreatment. Taking into account the experimental facts, the discussion of the mechanism has to include the following considerations:

a) the primary reaction in the thermal decomposition of the methylsilanes in the gas phase;
b) the importance of insertion of the CH_2 group into the Si–Si bond;
c) the possible participation of initially produced, simple carbosilanes in the formation of higher-molecular-weight ones.

a) The first step in the thermolysis of $SiMe_4$ is described by reaction (1). In order to account for the formation of

$$SiMe_4 \longrightarrow Me_3Si + Me \qquad (1)$$

compounds with the $\geqslant Si-CH_2-Si\leqslant$ skeleton, reaction (2) also seems likely. Of particular importance is the isola-

$$Me_3Si-Me + Me \longrightarrow Me_3Si-CH_2 + CH_4 \qquad (2)$$

tion of the cyclic compounds **25** and **26**. These are also formed when the methylsilanes are decomposed in a cold plasma;[20] under these conditions, thermally induced sec-

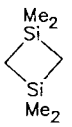

25

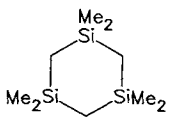

26

ondary reactions cannot occur. These compounds are presumably formed via reaction (3), followed by dimerization and trimerization.

$$Me_3Si-CH_2 \longrightarrow Me_2Si-CH_2 + Me \qquad (3)$$

Helm and *Mack*[21a] and later *Davidson* et al.[21b] have suggested a primary reaction in which radicals or reactive intermediates with a silicon–carbon double bond are formed, respectively. The existence of radicals has not yet been proved, and species with Si–C double bonds formed at 700 °C in the gas phase should be regarded in a more general sense as reactive intermediates. However, it appears correct to define the primary reaction as one in which an Si–C bond undergoes homolysis to give a silyl and a methyl radical.

b) It is noteworthy that compounds with SiH groups are found among the pyrolysis products of $SiMe_4$. Since silyl radicals are formed in the pyrolysis of the methylsilanes, their recombination to give compounds with Si–Si bonds is to be expected. The formation of the SiH groups is due to the insertion of the CH_2 group into the Si–Si bond according to reaction (4). Examples are provided by hexamethyl-

$$\geqslant Si-Si\leqslant CH_3 \longrightarrow \geqslant Si-CH_2-Si\leqslant H \qquad (4)$$

disilane [reaction (5)][22] and trisilacyclopentane **2**[23,24] [reaction (6)].

$$Me_3Si-SiMe_3 \longrightarrow Me_3-CH_2-SiMe_2H \qquad (5)$$

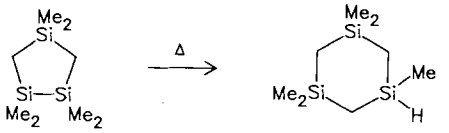

(6)

2

c) In order to obtain information pertinent to the participation of simple carbosilanes in the total pyrolysis reaction, the thermal behavior of the linear compounds $(Me_3Si)_2CH_2$, $(Me_3Si-CH_2)_2SiMe_2$, and $(Me_3Si-CH_2-SiMe_2)_2CH_2$ and the cyclic compounds **25**, **26**, and **27** was studied. Ther-

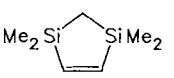

27

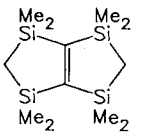

28

mally induced rearrangements are most likely to occur when the molecular framework of the compound is strained. The studies on the disilacyclobutane derivative **25** show the influence of temperature;[25] while at 300–320 °C polymeric Si–C–Si chains are formed, at 480–500 °C molecular structures are formed which correspond to those observed in the pyrolysis of $SiMe_4$. The six-membered ring compound **26**, in contrast, is much more stable. At 500 °C the disilacyclopentene **27** yields 1,3,5,7-tetrasilaadamantanes and the bicyclooctene **28** as well as further products of the $SiMe_4$ pyrolysis. Thus it appears that some of the compounds formed in the pyrolysis of $SiMe_4$ react further, under the reaction conditions, as intermediates in the construction of the silicon-richer compounds. The studies carried out until now have not permitted a complete characterization of the higher-molecular-weight carbosilanes in the methylsilane pyrolysates; they occur as solid, glasslike, fusible products.

2.2. Carbosilanes by Reaction of Silicon with CH_2Cl_2, $CHCl_3$, and CCl_4

2.2.1. *Reaction of CH_2Cl_2 with Silicon*

As early as 1945, following the direct synthesis of the methylchlorosilanes, a US patent reported the reaction of silicon with CH_2Cl_2 in the presence of copper;[26] the products were stated to include linear compounds, $X_3Si(CH_2)_nSiX_2Y$ (X = Cl, Y = H or Cl, n = 1–4) and cyclic compounds $(SiCl_2CH_2)_x$ (x = 3 and larger). We were later able to isolate the crystalline six-membered ring com-

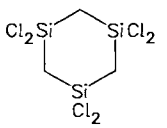

29

30

pound $(Cl_2Si{-}CH_2)_3$ **29** and the eight-membered ring compound $(Cl_2Si{-}CH_2)_4$ **30** from such reactions.[17,27] Apart from these and the linear compounds **11** and **31**, only viscous and nondistillable products are formed. The reaction of silicon with CH_2Cl_2 in a fluidized bed at 350 °C favors the formation of such substances. Since SiCl groups hinder chromatographic separation, they were first converted into SiH groups by reduction with $LiAlH_4$. The compounds obtained (see Fig. 3) were then separated by HPLC[7,11] (for further details see Refs. [4, 7]).

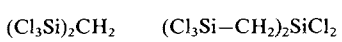

11 **31**

a) $Si_nC_{n-1}H_{4n}$ n = 4–12 (two terminal SiH_3 groups)
b) $Si_nC_nH_{4n+2}$ n = 4–9 (one terminal SiH_3 and one terminal CH_3 group)

c)

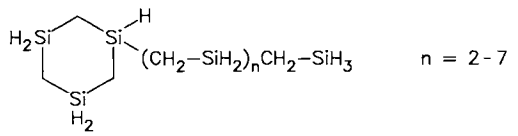

n = 2–7

d)

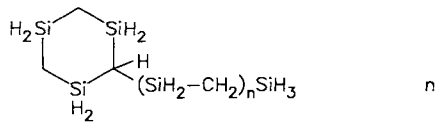

n = 3–8

Fig. 3. Types of substances formed in the reaction of silicon with CH_2Cl_2 (Cu catalyst).

The products of the reaction of silicon with CH_2Cl_2 contain the corresponding *Si*-chlorinated compounds. Those of higher molecular weight are honeylike, tarry, or solid glassy substances. The proportion of such substances is ca. 20%. The viscosity of the SiH-containing compounds is considerably lower.

2.2.2. *Reaction of $CHCl_3$ and CCl_4 with Silicon*

R. Müller et al.[28] studied the reaction of silicon with $CHCl_3$ and were able to identify the compounds shown in Figure 4a. In this case, too, the reaction in a fluidized bed favors the formation of higher-molecular-weight products; these could be separated by chromatography and identified after transforming the SiCl groups into SiH groups (see Refs. [7, 4] and Fig. 4b–d).

a) $(Cl_3Si)_2CH_2$ **11**, $HCl_2Si{-}CH_2{-}SiCl_3$, $Cl_3Si{-}CHCl{-}SiCl_3$, $HCl_2Si{-}CH(SiCl_3)_2$, $(Cl_3Si)_3CH$, $(Cl_3Si{-}CH_2)_2SiCl_2$ **31**, $Cl_3Si{-}CHCl{-}SiCl_2{-}CH_2{-}SiCl_3$, $(Cl_3Si)_2CH{-}SiCl_2{-}CH_2{-}SiCl_3$, $(Cl_3Si{-}CH_2{-}SiCl_2)_2CH_2$,

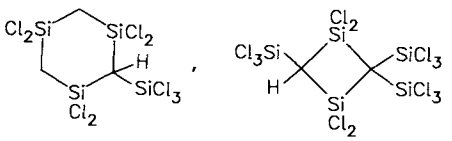

b) Unbranched carbosilanes with terminal SiH_3 groups, e.g., $H_3Si(CH_2{-}SiH_2)_4CH_2{-}SiH_3$
c) Carbosilanes with one or two C branches, e.g.,
$H_3Si{-}CH_2{-}SiH_2{-}CH(SiH_3){-}SiH_2{-}CH_2{-}SiH_3$,
$H_3Si(CH_2{-}SiH_2)_2CH(SiH_3){-}SiH_2{-}CH_2{-}SiH_3$,
$H_3Si(CH_2{-}SiH_2)_3CH(SiH_3)_2$,
$(H_3Si)_2CH{-}SiH_2{-}CH(SiH_3)_2$,
$H_3Si{-}CH_2{-}SiH_2{-}CH(SiH_3){-}SiH_2{-}CH(SiH_3)_2$,
$H_3Si{-}CH_2{-}SiH_2{-}CH(SiH_3){-}SiH_2{-}CH(SiH_3){-}SiH_2{-}CH_2SiH_3$
d) 1,3,5-Trisilacyclohexanes with one, two, or three Si substituents at the C atoms, e.g.,

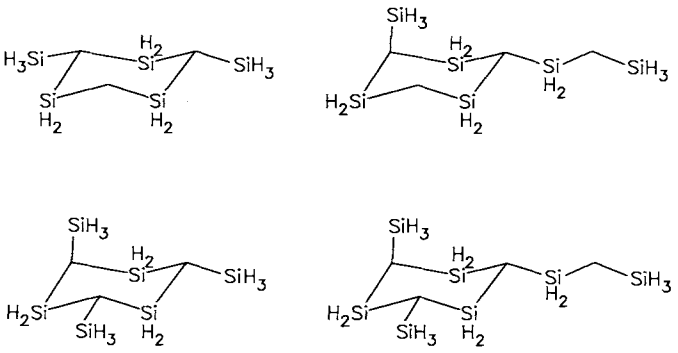

Fig. 4. Compounds formed in the reaction of $CHCl_3$ with silicon (Cu catalyst).

R. Müller and co-workers[29,30] also studied the reaction of silicon with CCl_4. In agreement with *Müller*'s results, the reaction in a fluidized bed[7] leads mainly to the following substituted methane, ethylene, and acetylene derivatives:

$Cl_3Si{-}C{\equiv}C{-}SiCl_3$, $(Cl_3Si)ClC{=}CCl(SiCl_3)$, $(Cl_3Si)_3CH$, $(Cl_3Si)_3CCl$, $(Cl_3Si)_4C$,

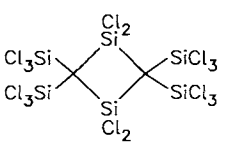

32

2.2.3. *Mechanism of the Reaction of CH_2Cl_2, $CHCl_3$, and CCl_4 with Silicon*

The reactions of silicon (Cu catalyst) with CH_2Cl_2 and $CHCl_3$ in a fluidized bed afford almost solely carbosilanes. With CH_2Cl_2, 70–80% of the products consist of non-branched carbosilanes, while with $CHCl_3$ similar amounts of *C*-branched carbosilanes and *C*-substituted trisilacyclohexanes are formed; no bi- and polycyclic carbosilanes are observed. An increase in the reaction temperature always leads to a decrease in the amounts of Si-richer carbosilanes. These results can be understood on the basis of the mechanism proposed by *Klebanskij* and *Fikhtengol'ts*[31,32] for the reaction of silicon (Cu catalyst) with MeCl. The adsorption of the CH_2Cl_2 molecules on the catalyst surface is a crucial step, the complete reaction occurring at this surface. The possibility that further reaction steps occur in the gas phase, leading finally to the observed products, can be excluded. This hypothesis is supported by the following observations: no further reaction occurs when isolated carbosilanes, such as $(Cl_3Si{-}CH_2{-}SiCl_2)_2CH_2$, are passed over activated silicon (Cu catalyst) at 350°C; changes occur only at 500°C after three days. Linear carbosilanes with four or more Si atoms undergo degradation to give the six-membered ring compound **29**, which is not formed from **31**.[33]

2.2.4. *C-Spirocyclic Carbosilanes from Perchlorinated Carbosilanes and Silicon (Cu Catalyst)*

The reactions of chlorinated methanes with silicon described in Sections 2.2.1 and 2.2.2 can be applied to *C*-chlorinated carbosilanes. Thus, $(Cl_3Si)_2CCl_2$ **33** reacts at 300–350°C with silicon (Cu catalyst) to give the carbosilanes shown in Figure 5 (white crystals); the four-membered rings are joined in a spirocyclic manner via carbon atoms.[34]

$(Cl_3Si)_2CCl_2$ **33**

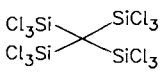

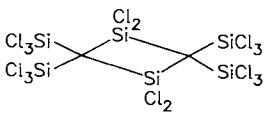

32

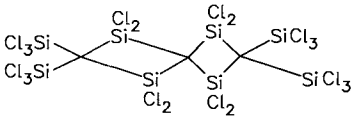

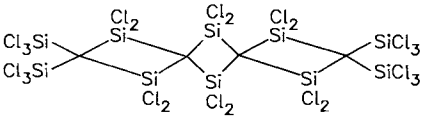

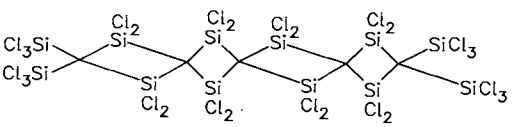

Fig. 5. Carbosilanes formed by reaction of **33** with silicon (Cu catalyst).

The replacement of the chlorines on silicon by methyl groups has a considerable effect on this reaction, as can be seen by the reaction of **34**

$(Me_3Si)_2CCl_2$ **34**

and of the partially methylated derivatives. A $\geqslant Si{-}CHCl{-}Si\leqslant$ unit is formed which prohibits the formation of cyclic compounds. Thus, $Me_3Si{-}CCl_2{-}SiMe_2Cl$ gives (among other compounds) isomers of composition $Si_3C_6H_{16}Cl_4$, e.g., compound **35**.[33] The formation of the spiro arrangement from perchlorinated carbosilanes appears to be favored; thus the products of the reaction of the octachloro derivative **36** with elemental silicon at

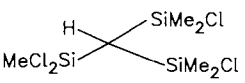

35

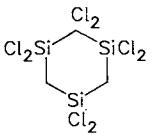

36

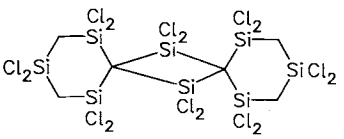

37

330°C include the spirocyclic compound **37** as well as further compounds such as those having the empirical formulas $Si_7C_6H_9Cl_3$ and $Si_{11}C_9H_{12}Cl_{20}$, whose structures are not completely clear.[35] These reactions, the mechanism of which is not known, lead to a new group of carbosilanes.

3. The Organometallic Synthesis of Carbosilanes

Functional substituents on silicon are of great importance for the synthesis and chemical behavior of the carbosilanes. Most substitution reactions with organometallic compounds occur via the Si–halogens, particularly via the SiCl group.[36] The cleavage of phenyl groups from silicon with HBr or HI has proved to be extremely useful for the synthesis of carbosilanes from organosilicon compounds and for the preparation of halosilanes with SiH groups (such as SiH_3Br)[37] [reaction (7)]. The cleavage of phenyl

$$\geqslant Si{-}Ph + HBr \longrightarrow \geqslant SiBr + C_6H_6 \qquad (7)$$

groups is slowed down, or even prevented, by the introduction of electronegative substituents on the Si atom.

3.1. The Synthesis of Oligocyclic Carbosilanes

The organometallic synthesis of cyclic and polycyclic carbosilanes has been reviewed.[8] It is made possible by

the introduction of Si-protecting groups (e.g., phenyl), which are transformed into functional groups in the step preceding the final one of ring formation. An example is the synthesis of *trans*- and *cis*-nonamethyl-1,3,5,7,9-pentasiladecalin **40**: construction of the linear, protected carbo-

$(PhMe_2Si-CH_2-SiMe_2-CH_2)_2SiPhMe$ **38**
$(BrMe_2Si-CH_2-SiMe_2-CH_2)_2SiMeBr$ **39**

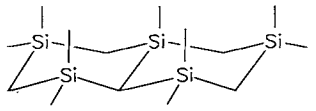

40, — = Me

silane **38**; cleavage of the Si-phenyl bonds with the formation of the bromo compound **39**; reaction of **39** with $CHBr_3$ and lithium to give the *trans* and *cis* compounds **40**.[38] A further example is the synthesis of the *trans-trans* and *cis-trans* perhydrophenalene derivatives **45** and **46**, respectively:[39] synthesis of the chain **41**; Br_2 cleavage of one phenyl group on each Si atom to give **42**; reduction with $LiAlH_4$ to give **43**; ring formation with lithium to yield **44**; once again, Si-Ph cleavage; bromination of the SiH groups and reaction with $CHBr_3$ and lithium to give a product mixture from which the isomers **45** and **46** are isolated.

$XPhMeSi-CH_2(SiMe_2-CH_2-SiMeX-CH_2)_2SiMe_2-CH_2Br$
41, X = Ph; **42**, X = Br; **43**, X = H

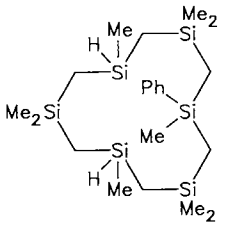

44

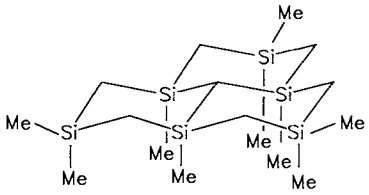

45

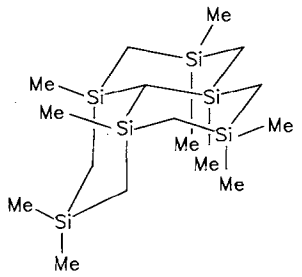

46

The synthesis of the heptasila[4.4.4]propellane **48**[40] was achieved in an analogous manner from **47** (after replacing the phenyl groups by bromine), CCl_4, and lithium.

$PhSi(CH_2-SiMe_2-CH_2-SiMe_2Ph)_3$ **47**

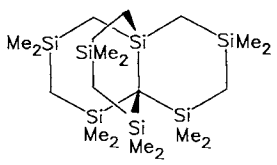

48

3.2. Synthesis of C-Bridged Carbosilanes

So far, the syntheses of oligocyclic carbosilanes always make use of functional substituents at silicon and thus lead to bridging via silicon atoms. The pyrolysis of methylsilanes (Section 2.1) and the rearrangement reactions of carbosilanes induced by $AlCl_3$ (Section 4) also lead in general to similar Si-bridged carbosilanes. The situation is illustrated in Scheme 7.

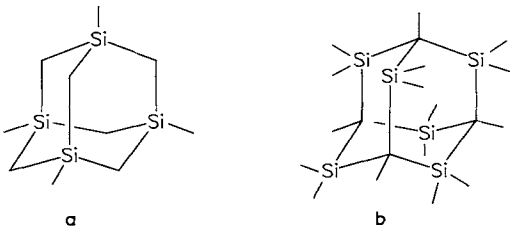

a b

Scheme 7.

In the isolated carborundanes the Si atoms occupy bridgehead positions (a). The formation of compounds with carbon bridgeheads and the Si_6C_4 skeleton (b) is an exception[18] (cf. **22**). An approach to compounds of this type requires further progress in the syntheses of *C*-functional carbosilanes. In Sections 3.2.1 and 3.2.2 suitable reactions at the carbon atoms of the carbosilane skeleton will be described.

3.2.1. Lithiation at Skeletal Carbon Atoms of Si-Methylated Carbosilanes

In contrast to the possibilities for reactions involving the substituents on the Si atom, the CH_2 group in the carbosilanes appears unreactive. In order to expand the scope of carbosilane synthesis it is necessary to incorporate the latter group into the synthetic scheme. Reactions of perchlorinated carbosilanes with alkyllithium or alkylmagnesium compounds are not suitable, since the reactivity of the CCl_2 group is enhanced by its position between the two $SiCl_2$ groups: for example, reactions with MeMgCl lead to skeletal changes (see Section 5.1.3). However, one possibility lies in the selective acid-base reaction[41] according to reaction (8).

$$-Me_2Si-CH_2-SiMe_2- + LiR \longrightarrow -Me_2Si-CHLi-SiMe_2- + RH \quad (8)$$

Reaction (8) requires a reagent that selectively lithiates $\geqslant Si-CH_2-Si\leqslant$ groups but does not react with either $(\geqslant Si)_3CH$, $\geqslant SiMe$, $>SiMe_2$, or $-SiMe_3$ groups. These criteria are satisfied by the complex between *n*BuLi and *N,N,N',N'*-tetramethylethylenediamine (TMEDA).[42] The model substance used for our studies was 1,1,3,3,5,5-hexamethyl-1,3,5-trisilacyclohexane **26**, which can undergo several successive lithiations and silylations.[41] The reaction of **26** with *n*BuLi/TMEDA in hexane at 30°C gives the monolithiated compound **49** quantitatively in 2-3 h (Scheme 8).

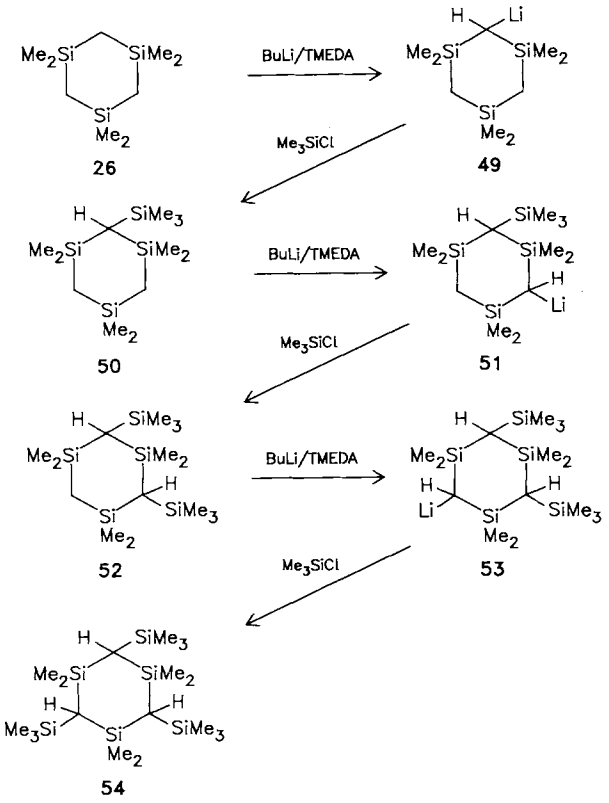

Scheme 8. Stepwise lithiation and silylation of compound **26** to give **54**.

The reaction is thermodynamically controlled, the carbanion formed being stabilized by two $SiMe_2$–CH_2 groups. No further metalation occurs with an excess of BuLi at 20 °C. Compound **49** is stable for several weeks; it undergoes quantitative silylation with Me_3SiCl to afford **50**. The treatment of **50** with BuLi can in principle lead to two products, the formation of either the thermodynamically more stable arrangement $(\geqslant Si)_3CLi$ (stabilization of the carbanion) or the kinetically preferred arrangement $\geqslant Si-CHLi-Si\leqslant$.

The use of *n*BuLi/TMEDA leads to compound **51**, owing to the large size of the reagent and the high shielding of the $(\geqslant Si)_3CH$ group. The reaction of **51** with Me_3SiCl gives compound **52**: the *cis* and *trans* isomers are formed in a ratio of 1 : 2.[43] The further reaction of **52** (80% *trans* and 20% *cis* isomer) with *n*BuLi/TMEDA at 20 °C confirms the selectivity of the lithiation; compound **53** is formed. Silylation of **53** gives compound **54** (94% *cis-trans* and 6% *cis*-is isomer[43]). The lithium compounds **51** and **53** are the kinetically controlled reaction products and are formed quantitatively. The thermodynamically favored lithium compounds are **55** and **56**, in which the anion is stabilized by three methylated silyl groups. The rearrangement of **51** to **55** or of **53** to **56** occurs in TMEDA/hexane at higher temperatures.

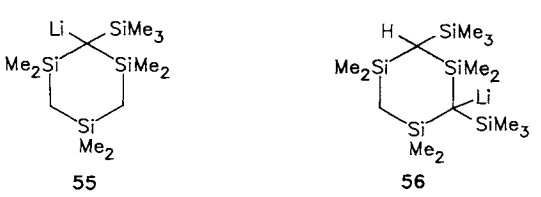

Compound **50** contains primary, secondary, and tertiary C atoms and is thus a model substance for studying the thermodynamic acidity of this class of compound: $(\geqslant Si)_3CH > \geqslant Si-CH_2-Si\leqslant > \geqslant SiMe$. Since MeLi in THF is a weaker base than BuLi in TMEDA, but sterically less demanding, the reaction with MeLi should be thermodynamically controlled. Indeed, the reaction of **50** with

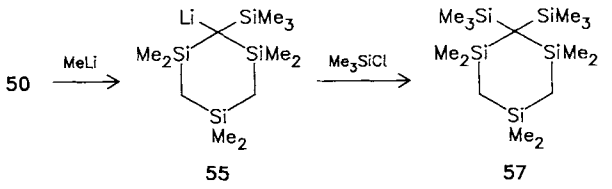

MeLi in THF/ether (7 : 1) is complete in 24 h at 20 °C. Subsequent reaction with Me_3SiCl leads, as expected, to **57**. Further examples are provided by the lithiation of nonamethyl-1,3,5,7,9-pentasiladecalin **40** and of the silabarrelane **62**.[50]

3.2.2. *Metalation of the CBr_2 Group*

The photobromination of the trisilacyclohexane **26** permits the conversion of a CH_2 group into a CBr_2 group.[44] The product **58** can be metalated at −100 °C in a mixture of THF, ether, and pentane (4 : 1 : 1) according to Scheme 9.

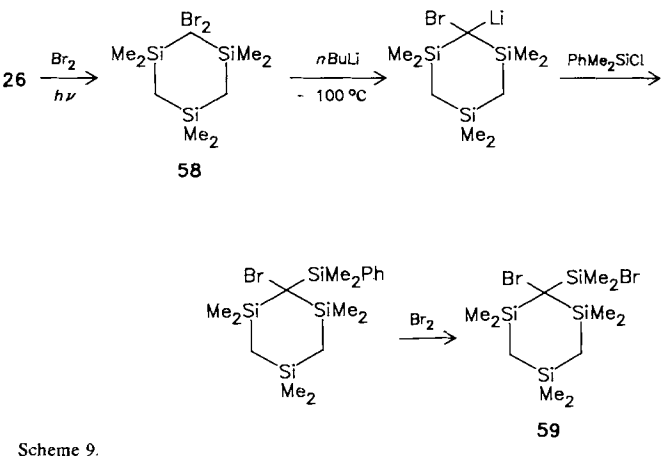

Scheme 9.

This reaction principle leads to various synthetic possibilities, e.g., that shown in Scheme 10.[45] The spirocyclic compound **60** is formed extremely selectively (cf. Section 2.2.4).

As *N. Wiberg* and *G. Wagner* have shown,[46] *C*-lithiation at a position next to a Si-halogen group and subsequent elimination of LiX leads to the formation of a silaalkene when the necessary sterically demanding groups are pres-

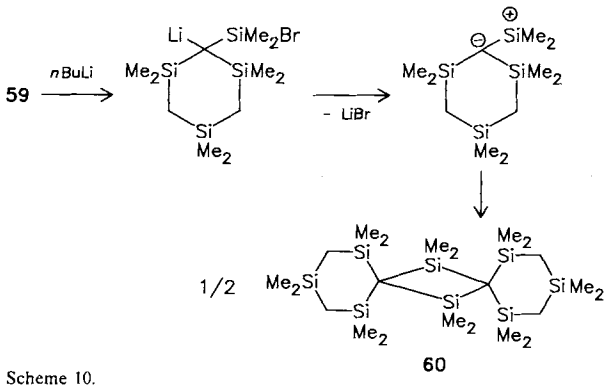

Scheme 10.

ent. They prepared compound **61**, which contains a SiC double bond.

$Me_2Si{=}C(SiMe_3)SiMe(tBu)_2$ **61**

4. Polycyclic Carbosilanes via Rearrangement of *Si*-Methylated Linear and Monocyclic Carbosilanes with $AlBr_3$ or $AlCl_3$

The organometallic syntheses of carbosilanes have not yet opened a convenient route to the 1,3,5,7-tetrasilaadamantanes: thus cyclization reactions that proceed without pyrolysis are of interest. Such a reaction is that of $(Me_2Si{-}CH_2)_3$ **26** with $AlBr_3$ to give 1,3,5,7-tetrasilaadamantane **3** and $SiMe_4$.[47] Linear carbosilanes react under similar conditions with $AlBr_3$ to give **26** and thence **3**.[9] *Si*-methylated carbosilane chains as substituents at the tertiary C atom of a carbosilane form an additional six-membered ring with $AlBr_3$, as shown in Scheme 11. Both *cis* and *trans* isomers of pentasiladecalin **40** were formed.

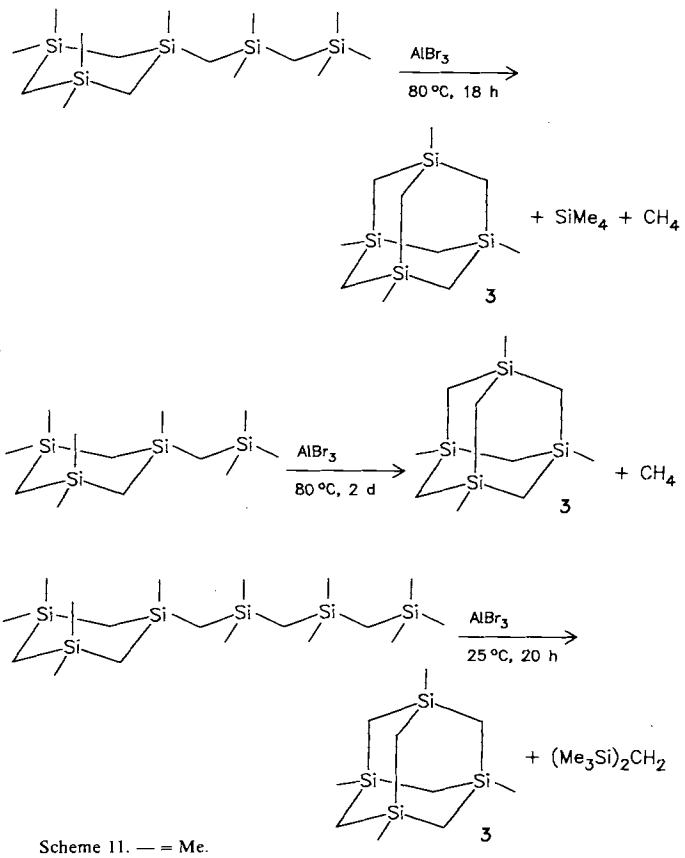

Scheme 11. — = Me.

In contrast, if the side chain is shortened so that ring closure to give a six-membered ring is no longer possible, carbosilanes with the barrelane (**62**), decalin (**40**, *cis* and *trans*), or diadamantane (**5**) skeleton are formed[9] (Scheme 12).

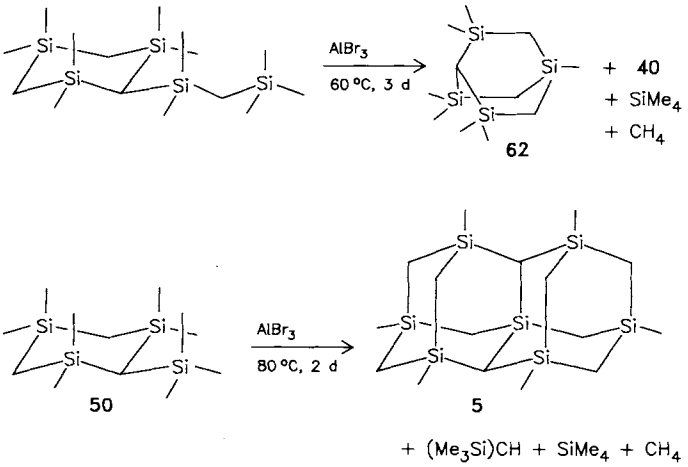

Scheme 12. — = Me.

According to this principle, compound **63** can be converted via a double ring closure into the all-*trans* compound **45** [reaction (9)].

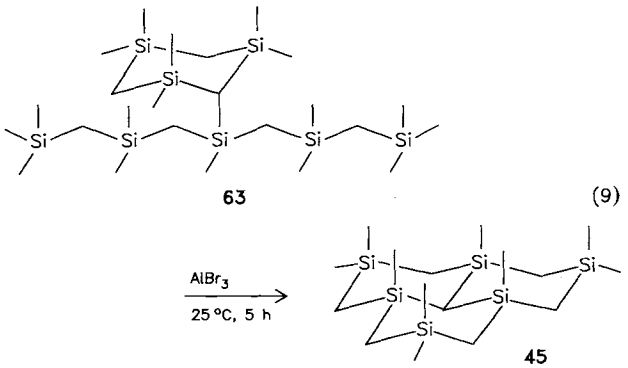

(9)

Compound **45** is a convex molecule (the cap of a sphere) in which all axial methyl groups point upwards, the axial CH_2 protons and the CH group downwards.[48]

Steric factors play an important part in these ring closure reactions. While the transformation of the *C*-substituted compound **57** into the carbosilane **64** occurs with elimination of CH_4 (Scheme 13),[9] a corresponding reaction of compounds **65** and **66** (with further $SiMe_3$ substituents on the skeletal carbon atoms) no longer occurs on steric grounds.[49] The sole reaction is a partial bromination with substitution of a methyl group.

This steric hindrance is not present in compound **67**, so that it can eliminate methane to give the silascaphane **68**[50] (Scheme 14).

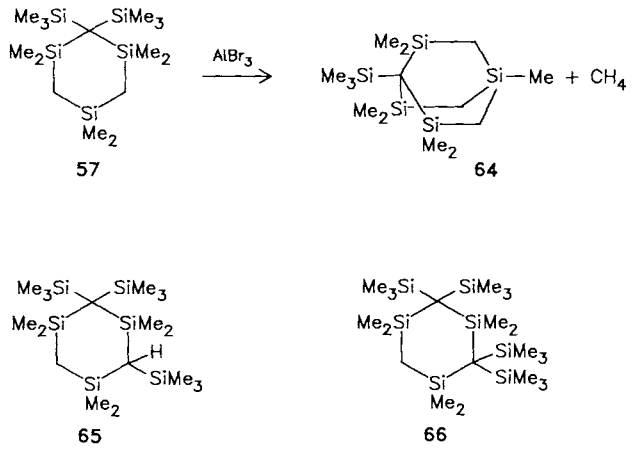

Scheme 13.

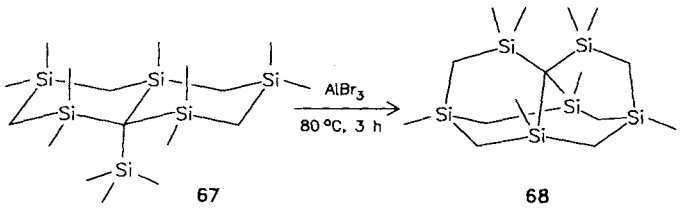

Scheme 14. — = Me.

Ring formation accompanied by methane elimination also occurs when carbosilane chains of varying lengths are attached to a Si atom of a carbosilane ring (Scheme 15).

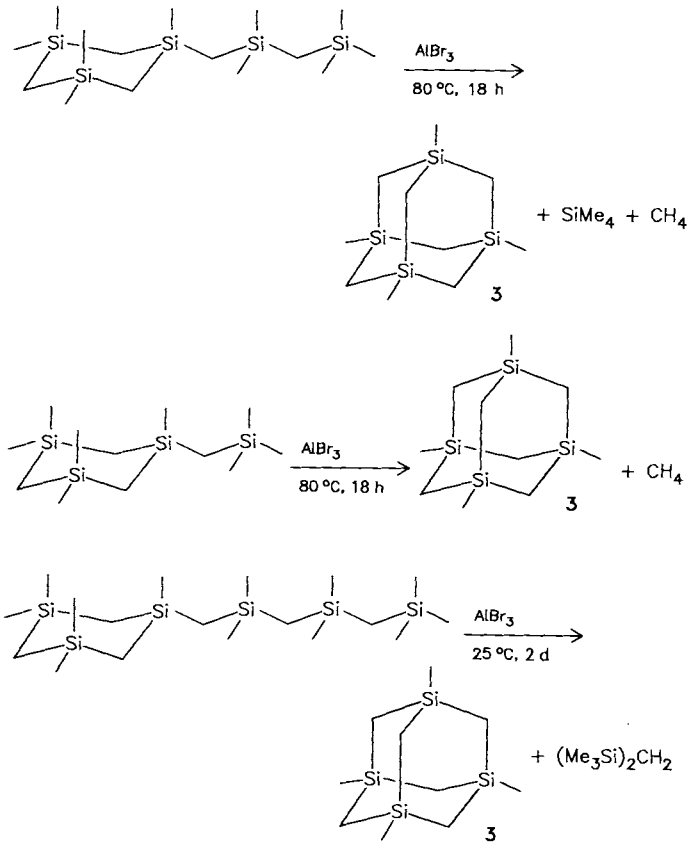

Scheme 15. — = Me.

This provides a relatively simple route to *Si*-methylated 1,3,5,7-tetrasilaadamantane **3**.[49]

In many cases the compounds initially formed are further transformed when they are subjected to the influence of $AlBr_3$ for a longer time. Thus, compound **40**, which is formed in a yield of ca. 90% according to Scheme 11, reacts further in the reaction mixture to give derivatives of 1,3,5,7-tetrasilaadamantane, along with **26** and $SiMe_4$.[51] The barrelane derivative **62** rearranges under similar conditions to give derivatives of **3**.[52] The 1,3,5,7-tetrasilaadamantane structure element is stable towards $AlBr_3$. The reaction without solvent leads after 8 d at 80 °C to the compounds shown in Scheme 16.

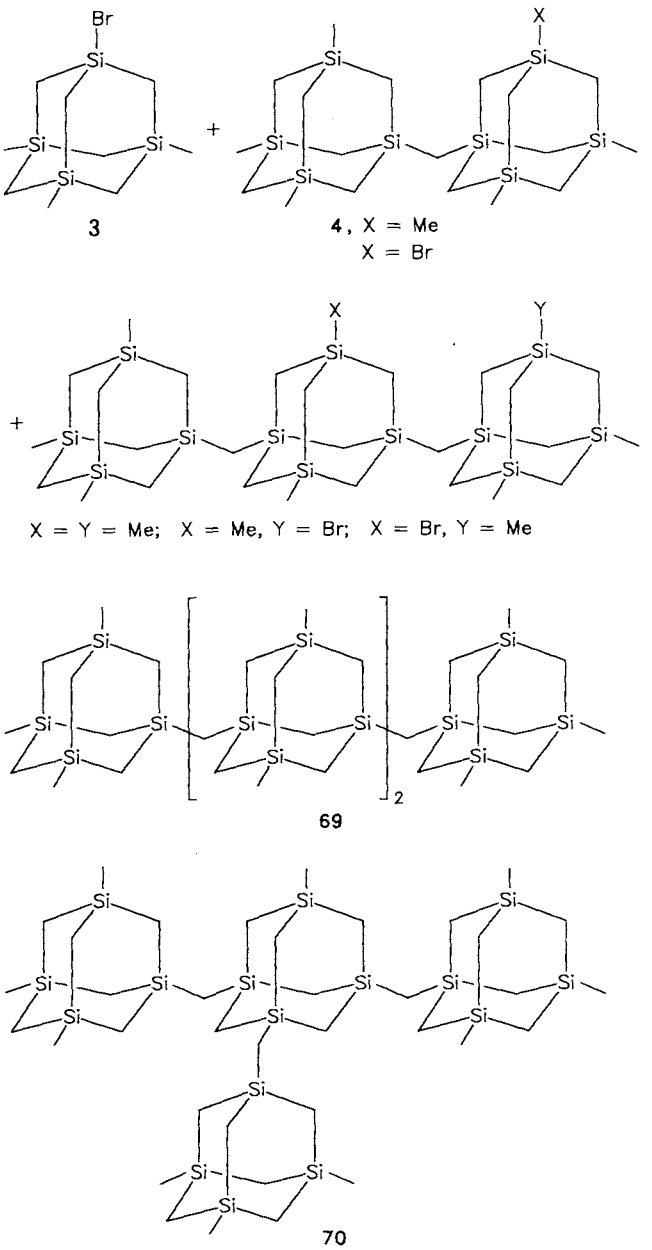

Scheme 16. — = Me.

An increase in the reaction time leads to the formation of insoluble polycarbosilanes of this type. The reaction with $AlCl_3$ is slower, so that the isolation of the isomers **69** and **70** is possible.[52]

The ring formation of *Si*-methylated carbosilanes with concurrent elimination of $SiMe_4$ is induced by the polarization of the Si–C bond by $AlBr_3$ (Scheme 17), as has been shown for partially deuterated carbosilanes.[51]

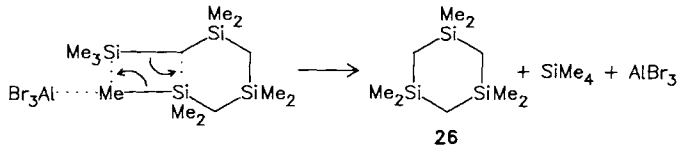

Scheme 17.

The ring closure reaction with $SiMe_4$ elimination is sometimes accompanied by a ring closure with methane elimination; in some cases the latter is the sole reaction. It is due to an initial cleavage of a Si–Me bond by $AlBr_3$ to give $\geqslant$Si–Br and $MeAlBr_2$ **72**. Thus, the pure compounds **71** and **72**, synthesized independently, react in a molar ratio of 1 : 1 with the formation of almost no side products[53] to give the tetrasilaadamantane **3** and CH_4.

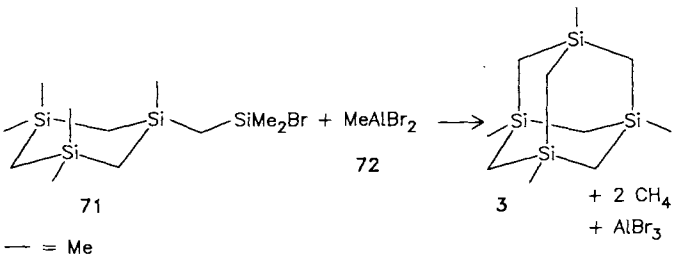

Very pure $AlBr_3$ and $AlCl_3$ do not induce the ring closure reaction; this only occurs when small amounts of Br_2 or HBr are added or with commercially available $AlBr_3$.

5. Reactions of Carbosilanes

The question arises as to whether the known reactions of functionalized silanes also occur for carbosilanes; in particular, what influence is exerted by groups such as CH_2, CCl_2, SiCl, SiF, and SiH. The following model compounds were chosen to give an answer to this question:

$(Cl_3Si)_2CH_2$ **11**, $(Cl_3Si{-}CH_2)_2SiCl_2$ **31**, $(Cl_2Si{-}CH_2)_3$ **29**, 1,3,5,7-tetrachloro-1,3,5,7-tetrasilaadamantane **12**.

5.1. Reactions of *Si*- and *C*-Chlorinated Carbosilanes with MeMgCl and RLi

The conversion of CH_2 groups into CCl_2 or CHCl groups in carbosilane skeletons can be carried out via photochlorination without cleavage of the Si–C–Si skeleton. The photochlorination can be controlled in such a way that intermediates with one and two CCl_2 groups can be preparatively isolated. Examples of such products are:

$(Cl_3Si)_2CCl_2$ **33**,[54] $(Cl_3Si{-}CCl_2)_2SiCl_2$ **73**, $SiCl_3{-}CCl_2{-}SiCl_2{-}CH_2{-}SiCl_3$ **74**,[55] $(Cl_2Si{-}CCl_2)_3$ **75**[56]

5.1.1. Reactions of $(Cl_3Si)_2CCl_2$ with MeMgCl and MeLi

The reactions of $(Cl_3Si)_2CCl_2$ **33**, the simplest member of this series, with MeMgCl or MeLi (excess with respect to the total number of Cl atoms) leads to the compounds shown in Scheme 18.[57]

$(Me_3Si)_2C{=}CH_2$ **76** (85%) {3%}, $(Me_3Si)_2CHMe$ **77** (2%) {23%}, $(Me_3Si)_2CMe_2$ (2%) {25%}, $(Me_3Si)_2CHCl$ (2%) {28%}

Scheme 18. Yields of the reactions with MeMgCl in parentheses; yields of the reactions with MeLi in curly brackets.

When **33** is treated with MeMgCl, a total of 55 different 1,3-disilapropanes can be detected depending on the molar ratio of the reactants. These products have varying chlorine content and can be divided into six groups according to changes in the carbon bridge (CCl_2, CHMe, C=CHMe, CHCl, CH_2, $C{=}CH_2$).[58]

The reaction with MeLi occurs in a more straightforward manner: it is initiated by the methylation of the CCl_2 group:

$$(Cl_3Si)_2CCl_2 + MeLi \longrightarrow (Cl_3Si)_2CMeCl + LiCl$$
33 **78**

Reaction of **33** with 1–1.5 molar equivalents of MeLi gives **78** in 93% yield, while reaction with 2 molar equivalents gives $(Cl_3Si)_2CMe_2$ in 90% yield. Only then does the methylation of the $SiCl_3$ groups occur, so that the reaction of **33** with 4 molar equivalents of MeLi gives $(ClMe_2Si)_2CMe_2$ in 86% yield.[58]

The study of the course of reaction was first concentrated on the formation of the methylidene group in the main product **76** of the reaction with MeMgCl. The formation of methylidene groups is always observed when an isolated Si–CCl_2–Si group is present in a carbosilane, as is shown for example by 2,2-dichlorohexamethyl-1,3,5-trisilacyclohexane and the carbosilane **79**.[67,68] The only pos-

$Me_3Si{-}CCl_2{-}SiCl_2{-}C{\equiv}C{-}SiMe_3$
79

sible intermediates for their formation from **33** are derivatives with CCl_2 or CMeCl groups, as all others can be excluded because of their low reactivity. The study of the reaction mechanism was thus carried out using 2,2-dichloro-1,3-disilapropanes chlorinated and methylated at silicon to different degrees as well as 2-chloro-2-methyl-1,3-disilapropanes, which were available as pure compounds.[59,60] The compounds **80** are indeed precursors for the formation of $(\geqslant Si)_2C{=}CH_2$.

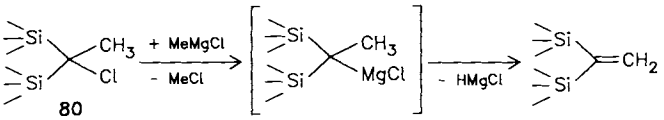

— = Me, Cl

C-metalation of **81** does not occur with MeMgCl or MeLi, but can be carried out with magnesium or lithium.

Complete reaction of **81** with lithium in cyclohexane or benzene gives **76** and **77** in the ratio of 55 : 45 (see Scheme 19).

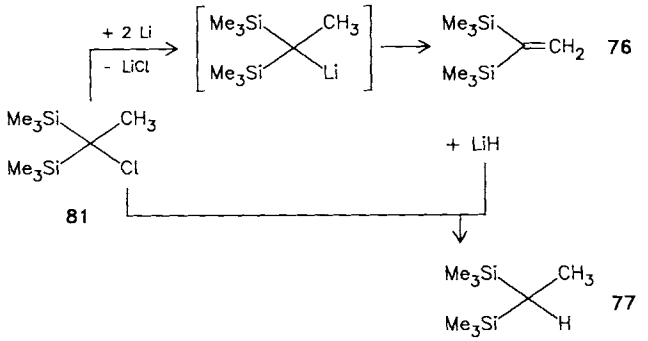

Scheme 19.

The reaction with magnesium in ether occurs in an analogous manner, but the compounds **76** and **77** are formed in the ratio of 43 : 57. This change in product ratio is explained by Scheme 20.

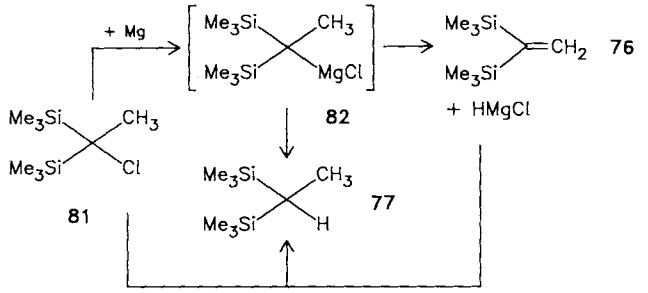

Scheme 20.

The intermediate **82** formed initially reacts further with elimination of HMgCl, which in turn reduces unreacted **81** to **77**; these reactions are accompanied by reaction of ether with the intermediate and subsequent ether cleavage, which also leads to **77**. This mechanism is confirmed by the reaction of $(Me_3Si)_2CCl(CD_3)$ with magnesium in ether: according to Scheme 20, this compound should split off DMgCl to give $(Me_3Si)_2C{=}CD_2$. The reaction of $(Me_3Si)_2CCl(CD_3)$ with DMgCl should give $(Me_3Si)_2CD(CD_3)$, while ether cleavage by the intermediate gives $(Me_3Si)_2CH(CD_3)$. The three compounds $(Me_3Si)_2C{=}CD_2$, $(Me_3Si)_2CD(CD_3)$, and $(Me_3Si)_2CH(CD_3)$ are indeed formed in the ratio of 3 : 3 : 1.[60]

Si-chlorinated derivatives of **81** form the methylidene group even with MeMgCl, since the intermediate is formed more readily when the partial negative charge on carbon is stabilized more strongly by electronegative substituents on silicon.

$(Me_3Si)_2CCl_2$ **34** reacts with MeMgCl about as fast as **81** with Mg to give the final product **76**. However, **34** reacts faster to give the intermediate **82** than does **81**. The reaction of **34** can thus not begin with a methylation at the CCl_2 group followed by a metalation, but must occur in the reverse manner (Scheme 21); this can also be understood in terms of the better stabilization of the carbanionic intermediate.

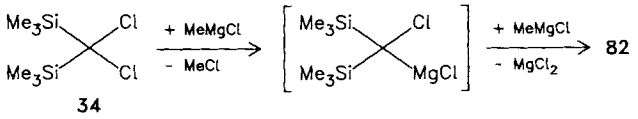

Scheme 21.

Either *Si*-methylation or *C*-metalation can occur upon reaction of the 2,2-dichloro-1,3-disilapropanes with MeMgCl. *C*-metalation dominates when the degree of chlorination at silicon is low, while *Si*-methylation is more important when it is high. Thus, for example, all products obtained from $Me_3Si{-}CCl_2{-}SiMe_2Cl$ are formed by attack at the bridging C atom, while ca. 40% of those from $MeCl_2Si{-}CCl_2{-}SiCl_3$ are due to *Si*-methylation. The metalation, and thus the formation of the methylidene and CHCl groups, however, is much faster if, besides methyl groups, chlorine substituents are still present on silicon.

5.1.2. *Formation and Reaction of $Me_3Si{-}CCl(Li){-}SiMe_2Cl$*

Great importance was attached to the proof of the *C*-lithiation of perchlorinated carbosilanes, which has been verified for $(Cl_3Si)_2CCl_2$ **33** and $(Cl_2Si{-}CCl_2)_3$ **75** by subsequent trapping reactions at $-100\,^{\circ}C$ with MeI or Me_3SiI. Thus, starting from **33**/*n*-BuLi, it is possible in this way to prepare $(Cl_3Si)_2C(Cl)Me$ **78** and $(Cl_3Si)_2C(Cl)SiMe_3$ preparatively (yield 80%). Compound **75** behaves in a corresponding manner.[61] Warming of $(Cl_3Si)_2CCl(Li)$ leads to the formation of LiCl, the chlorine atom of which is derived from one of the $SiCl_3$ groups. In this way, the disilabicyclo[1.1.0]butane **85** (white crystals, m.p. = 28 °C) is obtained as the end product of the *C*-lithiation.[62]

The precursors of **85** are two 1,3-disilacyclobutanes formed initially from the carbenoid **84**. They are lithiated by **84** in THF according to Scheme 22.[63]

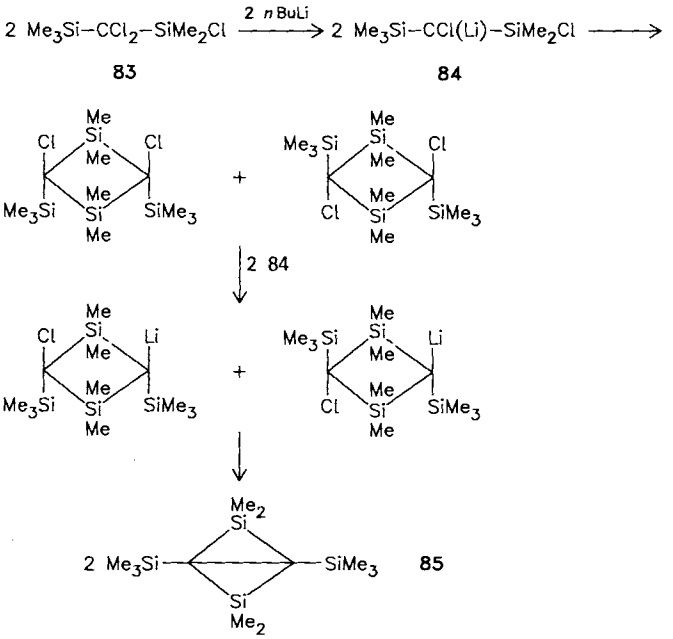

Scheme 22.

5.1.3. *Reactions of $(Cl_3Si-CCl_2)_2SiCl_2$ with MeMgCl and MeLi*

The reaction of the trisilapentane **73** with an excess of MeMgCl (molar ratio 1:18) in ether leads to the compounds shown in Scheme 23; the main products are **86** and $SiMe_4$.[64]

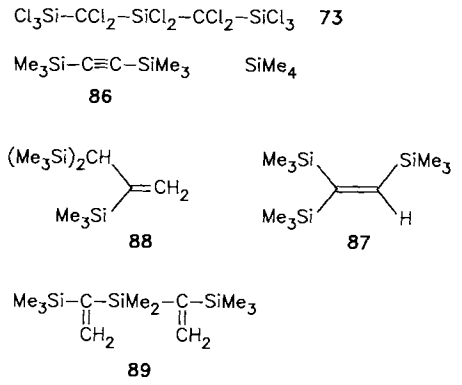

Scheme 23.

Reactions of **73** with lesser amounts of MeMgCl give less of the compounds shown in Scheme 23, and at a molar ratio of 1:1 the product is **90**.

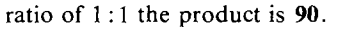

The number of CCl_2 groups in the 1,3,5-trisilapentane determines the course of the reaction. Thus the reaction of **74** with MeMgCl leads to **91** (70%) and that of **90** to **87** as

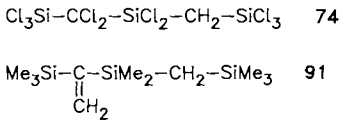

the major product. The reaction of **73** with an excess of MeLi[65] occurs in a similar manner to give $SiMe_4$, **87**, **88**, **92**, and **93** as the main products, which are shown along with the byproducts in Scheme 24.

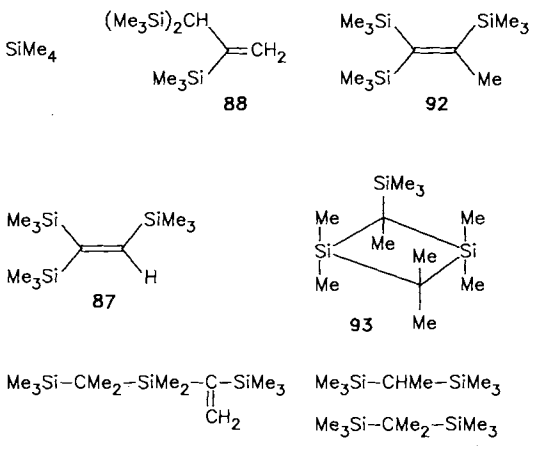

Scheme 24.

The reaction of **73** with MeMgCl can be explained by the mechanism in Scheme 25.

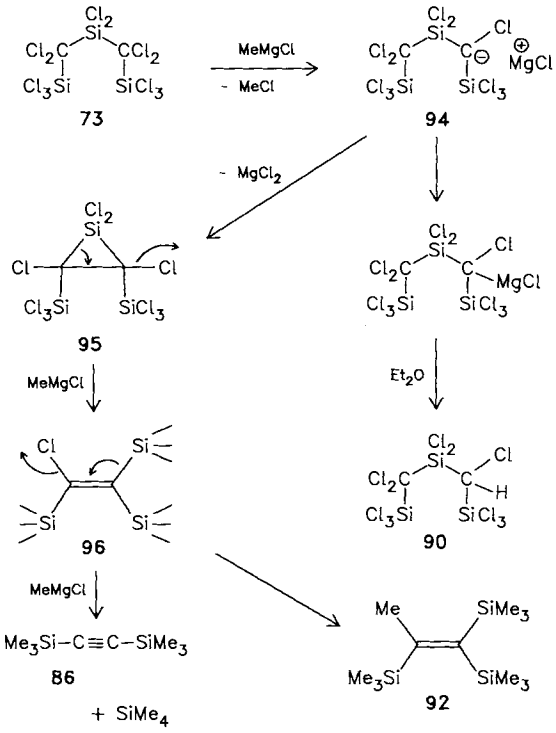

Scheme 25.

The first step is a metalation at a CCl_2 group to give **94**. It is followed by an intermolecular elimination of $MgCl_2$ to give **95**, which undergoes β-elimination and *Si*-methylation to give **86** and $SiMe_4$. The initial reaction of **73** with MeLi is analogous. Compound **86** reacts with an excess of MeLi according to reaction (10), as is shown by the formation of acetylene in the hydrolysis of the reaction product **97**. The vinylic Cl atom in the intermediate **96**, which is not isolated, can be methylated by MeLi to give **92** (Scheme 24), so that no further reaction occurs. The formation of **87** is due to the reaction of **90** (CCl_2-lithiation and subsequent ether cleavage). An important difference between the behavior of MeLi and MeMgCl with respect to **73** lies in the formation of **93**; it is formed via the *C*-lithiated intermediate **98** (Scheme 26).

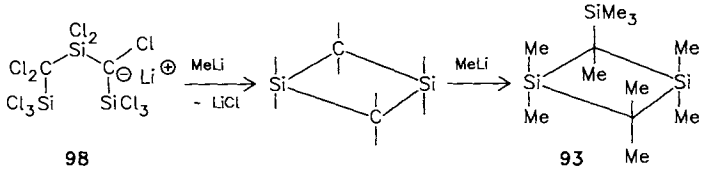

Scheme 26. — = Me or Cl.

The carbanion of the Li compound **98** is much more reactive than the corresponding Mg derivative **94** and attacks not only at the CCl_2 group but also at the terminal Si atom with the formation of **93**. Compound **92** rearranges catalytically, undergoing 1,3-isomerization in the presence of traces of moisture or acids, to give **88** (Scheme 27).

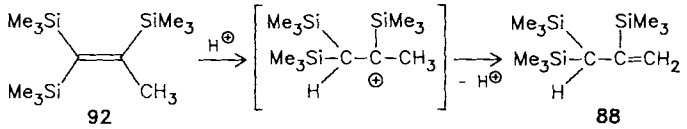

Scheme 27.

The product ratio is strongly influenced by the MeLi concentration during the reaction.

5.1.4. *Reactions of $(Cl_2Si-CCl_2)_3$ with MeMgCl*

The perchlorinated compound **75** reacts with MeMgCl to give the products of ring contraction and ring cleavage[66,67] shown in Scheme 28.

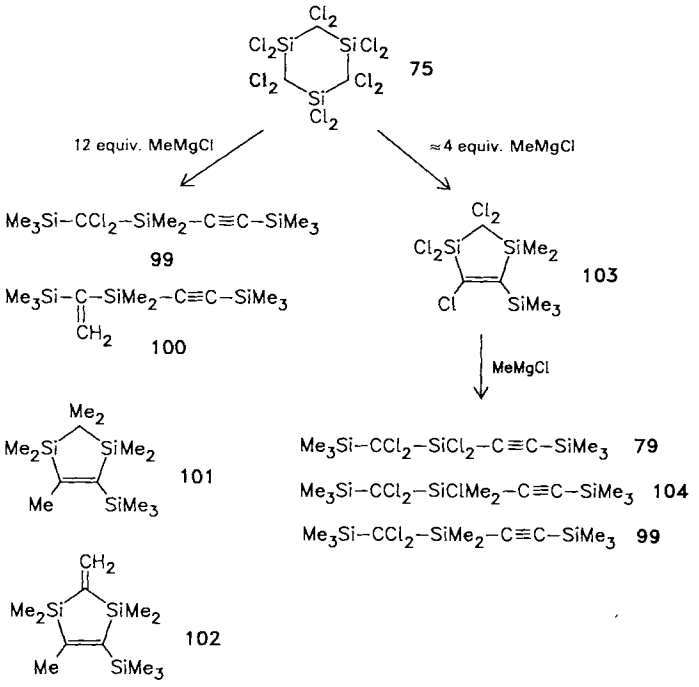

Scheme 28.

The linear derivatives **99** and **100** are formed preferentially when MeMgCl is used in excess (for the transformation of **99** to **100**, compare Scheme 20). The formation of the 1,3-disilacyclopentene **103** is the decisive step in the reaction sequence: **103** is formed as white crystals in ca. 98% yield when **75** is treated with MeMgCl (molar ratio 1:4) and reacts with further MeMgCl to give mainly the acetylene derivatives **79**, **104**, and **99**,[66] which are also formed directly when **75** is treated with an excess of MeMgCl. This reaction proceeds via **103** (Scheme 29; for the reaction **75** → **103**, see Scheme 30).

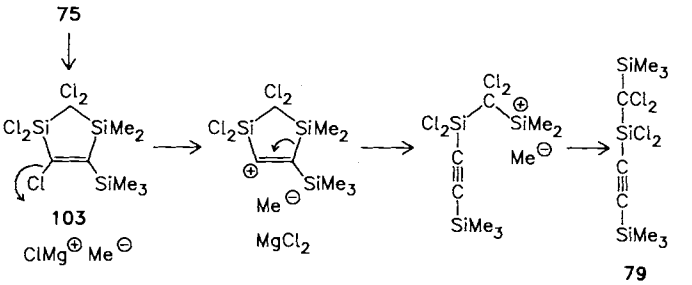

Scheme 29.

The initial step is the cleavage of the vinylic chlorine atom under the influence of MeMgCl: the cation thus formed rearranges to the energetically more favored C≡C linkage and then adds the nucleophilic anion $Me^{\ominus}$ with concomitant methylation at silicon to give **79**.

The experiment gives the following information regarding the ring contraction of **75** to **103**: the reaction begins

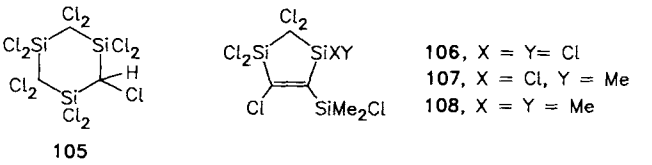

106, X = Y = Cl
107, X = Cl, Y = Me
108, X = Y = Me

with a magnesium–halogen exchange at a skeletal carbon atom. The primary reaction products **105**–**108** have been detected.

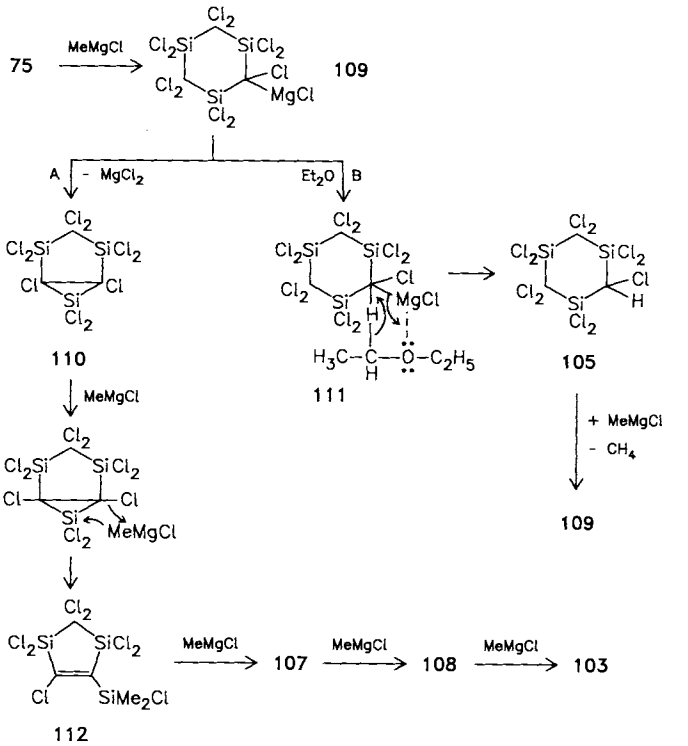

Scheme 30.

Scheme 30 describes the course of the reaction. The first step is the magnesium–halogen exchange of **75** to give **109**, which can react further by two routes. Route A results

in a rearrangement under the influence of MeMgCl of the bicyclic intermediate formed to give **112**; *Si*-methylation by further MeMgCl gives **103**. Route B leads from **109** via ether cleavage to **105**. The acidic CH proton of **105** reacts with MeMgCl to give CH_4 and **109**, provided that no metalation of a CCl_2 group in **105** by MeMgCl occurs. Whether route A or route B is preferentially followed depends on the concentration of MeMgCl; if it is low, **105** containing the CHCl group is formed, while if it is high the rearrangement via route A is favored. The complete course of the subsequent reactions is determined by the key compound **103**[68] [reaction (11)].

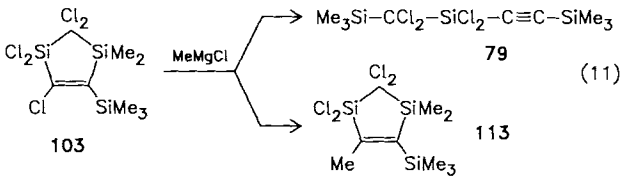

(11)

The cleavage reaction giving **79** (Scheme 29) starts from the vinylic chlorine substituent: if this position is methylated (here a side reaction), no cleavage takes place, and the disilacyclopentenes **114**, **101**, and **102** are formed. All

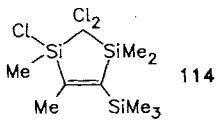

114

the linear reaction products can be explained by the reactions of the functional groups in **79**.

5.1.5. *Reactions of SiCl-Containing and Partially C-Chlorinated Carbosilanes with MeMgCl*

The reaction of $(Cl_2Si–CCl_2)_3$ **75** with MeMgCl to give the 1,3-disilacyclopentene skeleton (such as **103**) according to Scheme 30 requires the presence of at least two CCl_2 groups for the ring contraction: it should not occur when only one such group is present. Thus, the reaction of compound **36** with an excess of MeMgCl proceeds without any change in ring size to give **115** (Scheme 31). Compound **36** thus reacts like an acyclic compound containing an $–SiCl_2–CCl_2–SiCl_2–$ group.[59,60]

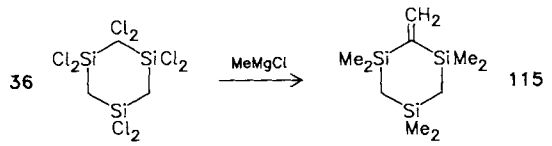

Scheme 31.

However, compound **116** (with two CCl_2 groups) undergoes ring contraction with an excess of MeMgCl to give **117** (Scheme 32) in ca. 80% yield. This reaction proceeds analogously to that shown in Scheme 30.[67] Rearrangement with formation of linear compounds according to

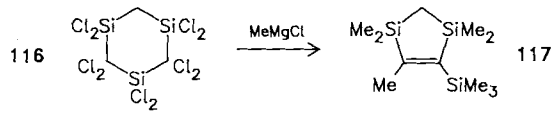

Scheme 32.

reaction (11) does not occur, apparently because of the favored methylation of the vinylic Cl atom.

5.2. Reactions of *C*-Chlorinated SiH-Containing Carbosilanes

The SiCl groups in CH_2-containing carbosilanes can be converted by $LiAlH_4$ into SiH groups without any change in the molecular structure.[69] Examples are provided by the transformations of **31** and **29**.

$$(Cl_3Si–CH_2)_2SiCl_2 \longrightarrow (H_3Si–CH_2)_2SiH_2$$
31

$$(Cl_2Si–CH_2)_3 \longrightarrow (H_2Si–CH_2)_3$$
29

This reaction also permits the formation of SiH- and CCl-containing derivatives from perchlorinated compounds, as shown below:

$$(Cl_3Si–CCl_2)_2SiCl_2 \longrightarrow (H_3Si–CCl_2)_2SiH_2$$
73 **118**

$$(Cl_2Si–CCl_2)_3 \longrightarrow (H_2Si–CCl_2)_3$$
75

However, side reactions such as cleavage of the Si–C bond and formation of CH groups are always observed. It must be noted that violent explosions will occur when pure SiH- and CCl-containing compounds (such as **118**) are heated above room temperature: however, their solutions in ether or hydrocarbons have shown themselves to be safe. Their reactivity is due to hydrogen–chlorine exchange [reaction (12)]. This reaction can be used for the formation

$$\geqslant SiH + \geqslant CCl \longrightarrow \geqslant SiCl + \geqslant CH \qquad (12)$$

of partially chlorinated SiH-containing compounds, as the example in Scheme 33 shows.[70]

$(Cl_2Si–CCl_2)_3$ **75** $(Cl_2Si–CH_2)_3$ **29**

\+ ⟶ +

$3(H_3Si–CH_2)_2SiH_2$ $3H_2ClSi–CH_2–SiHCl–CH_2–SiH_3$

Scheme 33.

The influence of the CCl_2 group on the SiH bond is shown by the following comparison: while in $(H_2Si–CH_2)_3$ the SiH group can only be methylated with extreme difficulty by MeMgCl in Et_2O, such a methylation does occur

under analogous conditions for derivatives containing the CCl_2 group (e.g., formation of **120** from **119**).

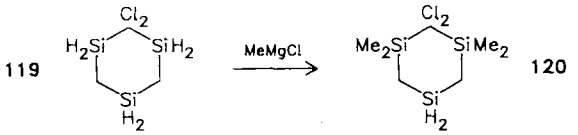

Derivatives containing SiHMe groups are also formed, but there is no formation of the $C{=}CH_2$ group (cf. Scheme 31). The reaction of the 1,3,5-trisilacyclohexane **121** (containing two CCl_2 groups) with MeMgCl gives **122**; thus the reactions shown in Schemes 31 or 32 do not occur.

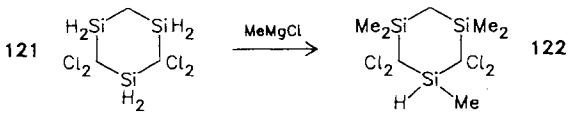

The studies thus present the following picture: $(Cl_2Si{-}CH_2)_3$ reacts with MeMgCl to give $(Me_2Si{-}CH_2)_3$ **23**, while $(H_2Si{-}CH_2)_3$ does not react under these conditions. Methylation of the neighboring SiH_2 groups is only possible when a CCl_2 group is introduced; the latter does not undergo substitution. However, the route from $(H_2Si{-}CCl_2)_3$ to $(Me_2Si{-}CCl_2)_3$ with MeMgCl is not feasible, since the introduction of three CCl_2 groups favors cleavage of the Si–C–Si skeleton during the reaction with MeMgCl.

5.3. Reactions of *C*-Chlorinated SiF-Containing Carbosilanes

The fluorination of SiCl groups in carbosilanes can be carried out using ZnF_2; almost no Si–C bond cleavage is observed. The preparation of $(F_3Si{-}CH_2)_2SiF_2$ and $(F_3Si{-}CCl_2)_2SiF_2$ is most readily carried out by reaction of the corresponding chlorinated compounds with ZnF_2 in hexachlorobutadiene.[71] In a similar manner, $(F_2Si{-}CH_2)_3$ is formed from $(Cl_2Si{-}CH_2)_3$ **29** and the adamantane **123** from **12**.[72]

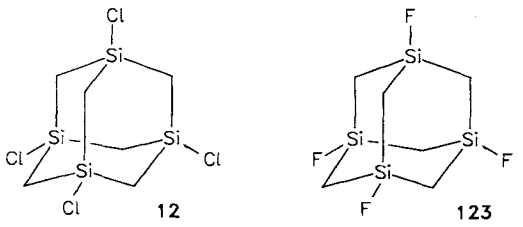

However, it is not possible to use perchlorinated carbosilanes and ZnF_2 to form cyclic SiF- and CCl-containing carbosilanes, since decomposition reactions occur which may even lead to the formation of SiF_4. Such carbosilanes can be formed via photochlorination of SiF-containing derivatives; e.g., reaction of $(F_2Si{-}CH_2)_3$ gives $(F_2Si{-}CCl_2)_3$.[72]

The SiF groups in *Si*-fluorinated, *C*-chlorinated carbosilanes determine the course of their reactions. Thus, **124** reacts with MeLi according to reaction (13).

$$(F_3Si)_2CCl_2 + MeLi \longrightarrow (Me_3Si)_2CCl_2 + LiF \quad (13)$$

124 **34**

$F_3Si{-}CCl_2{-}SiFMe_2$ **125** $Me_2FSi{-}CCl_2{-}SiFMe_2$ **126**

Additional products are **125** and **126** as well as further partially methylated derivatives.[71] Similarly, **127** reacts to give **128**.

$$F_3Si{-}CCl_2{-}SiF_2{-}CH_2{-}SiF_3 \longrightarrow$$

127

$Me_3Si{-}CCl_2{-}SiMe_2{-}CH_2{-}SiMe_3$

128

In contrast, **129**, which, unlike **127**, contains no CH_2 groups, behaves in a quite different manner; the products of three different methylation reactions are shown in Scheme 34.

$(F_3Si{-}CCl_2)_2SiF_2$ **129**

a) $F_3Si{-}CCl_2H$, $MeF_2Si{-}CCl_2{-}SiMeF_2$, $Me_2FSi{-}CCl_2{-}SiMeF_2$

b) $Me_3Si{-}CCl_2{-}SiMe_3$ **34**, $Me_3Si{-}CCl_2{-}SiMe_2{-}CH_2{-}SiMe_3$, $(Me_3Si{-}CCl_2)_2SiMeF$, $Me_3Si{-}CH_2{-}SiMe_2{-}CCl_2H$, $Me_3Si{-}CCl_2{-}SiMeF{-}CH_2{-}SiMe_3$, $(Me_3Si{-}CCl_2)_2SiMe_2$

c) $Me_3Si{-}C{\equiv}C{-}SiMe_3$ **86**, **34**, $Me_3Si{-}C{\equiv}C{-}SiMe_2{-}C{\equiv}C{-}SiMe_3$, $Me_3Si{-}CCl_2{-}SiMe_2{-}C{\equiv}C{-}SiMe_3$ **99**, $SiMe_4$

Scheme 34. Reaction of **129** in Et_2O with a) MeMgCl in a molar ratio of 1 : 1, b) excess MeMgCl, and c) MeLi in excess (1 : 10).

In this case the cleavage of the molecular skeleton is the predominant reaction; it is followed by *Si*-methylation. The reaction with MeLi leads to, among other compounds, **86** and shows that this stronger metalating agent is also capable of *C*-metalation and thus is able to induce the accompanying skeletal changes.[71]

The initial reaction of *Si*-fluorinated 1,3,5-trisilacyclohexanes (e.g., **130**) is also *Si*-methylation.[73] As with the linear derivatives, ring cleavage is favored by polar solvents (e.g., THF) and MeLi.

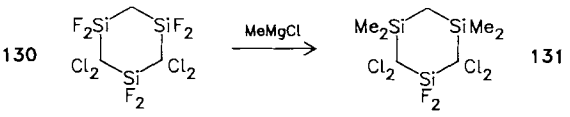

$(F_2Si{-}CCl_2)_3$ can be methylated by MeMgCl, affording $(MeFSi{-}CCl_2)_3$ in 86% yield. Further reaction with MeMgCl or MeLi leads to changes in the ring structure. The reaction of **130** with an excess of MeMgCl (Scheme 35) makes this clear. The initial reaction is the *Si*-methylation to give **131**. At this degree of methylation the metalation of the CCl_2 group occurs; it leads via ring contraction to **133**, which rearranges to give **117** and **134**. Thus, above a certain degree of *Si*-methylation, the reaction occurs according to Scheme 30 and reaction (11).

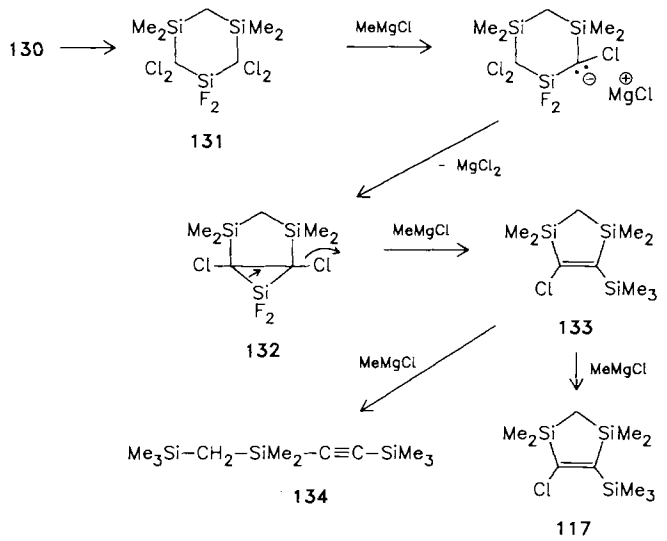

Scheme 35.

5.4. Reactions of CF_2-Containing Carbosilanes

Carbosilanes containing the $\geqslant Si-CF_2-Si\leqslant$ group can be prepared via the insertion of difluorocarbene into the Si–Si bond.[74]

$$FMe_2Si-SiMe_2F + CF_2 \longrightarrow FMe_2Si-CF_2-SiMe_2F$$
135 **136**

The carbene CF_2 is formed by thermolysis of Me_3SnCF_3.[75] Further examples are provided by the reactions of **137** and **138** and of the trisilane **139**.[74] This insertion into the Si–Si bond is only observed when the terminal Si atoms bear one or more $-I$ substituents

$$XMe_2Si-SiMe_3 \longrightarrow XMe_2Si-CF_2-SiMe_3$$
137 (X = F, Cl, Br, OMe)

$$F_2MeSi-SiMe_2F \longrightarrow F_2MeSi-CF_2-SiMe_2F$$
138

$$(FMe_2Si)_2SiMe_2 \longrightarrow$$
139
$$FMe_2Si-CF_2-SiMe_2-SiMe_2F + (FMe_2Si-CF_2)_2SiMe_2$$

(F, Cl, Br, OMe). These substituents weaken the Si–Si bonds and favor the CF_2 insertion. In the absence of such substituents (e.g., for Si_2Me_6) the CF_2 insertion does not occur, and more highly fluorinated disilanes (such as $F_2MeSi-SiMeF_2$ and Si_2F_6) decompose at temperatures below that required to generate CF_2 from $MeSnCF_3$.

In contrast to comparable *C*-chlorinated carbosilanes, **136** reacts with MeMgCl or MeLi even at lower temperatures not with *C*-metalation but with *Si*-alkylation, the products being **140** and **141**. Similarly, reaction with PhLi and PhMgBr gives **142** and **143**. Compound **136** and its derivatives react with $LiAlH_4$ with formation of SiH groups; e.g., $(HMe_2Si)_2CF_2$ is formed. Reaction with $LiPMe_2$ leads to substitution at the silicon atom: reaction of **136** gives $Me_2P-SiMe_2-CF_2-SiMe_2F$ and $(Me_2P-SiMe_2)_2CF_2$.[74]

$Me_3Si-CF_2-SiMe_2F$ $(Me_3Si)_2CF_2$
140 **141**

$PhMe_2Si-CF_2-SiMe_2F$ $(PhMe_2Si)_2CF_2$
142 **143**

5.5. The Cleavage of the Si–Me Bond in Carbosilanes

The clean cleavage of the Si–C bond and the influence of substituents on this reaction are of considerable interest. The alkaline cleavage is favored by the chlorination of the α-carbon atoms.[54,75] The Si–Ph bond is cleaved in aqueous HCl solution.[76] These reactions have the disadvantage that the SiOH groups thereby formed condense to form $\geqslant Si-O-Si\leqslant$ units and therefore the functionality at silicon is lost. The cleavage of the Si–Ph bond by pure HBr is a basic requirement for the organometallic synthesis of carbosilanes (see Section 3).[37] Under these conditions the Si–Me bond is stable. Its cleavage by Me_3SiCl or acetyl chloride with $AlCl_3$ as a catalyst has been described by *Kumada* and co-workers.[77] A cleavage reaction using $HSiCl_3$ and catalyzed by H_2PtCl_6 was described by *Benkeser* et al.[78] and extended by *Hengge* et al.[79] to the *Si*-chlorination of methylated silanes with Si–Si bonds. *Calas* et al.[80] reported the formation of Me_3SiCl from $SiMe_4$ and ICl (Scheme 36); *Eaborn* et al.[87] have reported similar reactions.

$$Me_3Si(CH_2)_nSiMe_3 + 2\,Me_3SiCl \xrightarrow{AlCl_3}$$
$$ClMe_2Si(CH_2)_nSiMe_2Cl + 2\,SiMe_4 \;(n = 1\text{–}4)$$

$$SiMe_4 + CH_3COCl \xrightarrow{AlCl_3} Me_3SiCl + CH_3COCH_3$$

$$R_3SiMe + HSiCl_3 \xrightarrow{Pt\ cat.} R_3SiCl + MeHSiCl_2$$

$$SiMe_4 + 2\,ICl \longrightarrow Me_3SiCl + MeCl + I_2$$

Scheme 36.

These reactions convert the unreactive SiMe group into a functional SiCl group. The reaction with ICl can be extended to numerous *Si*-methylated carbosilanes,[81] leading in each case to the replacement of at the most one methyl group at each silicon atom.[81] Thus, the end product of the reaction of $(Me_2Si-CH_2)_3$ **26** is $(ClMeSi-CH_2)_3$, while in 1,3,5,7-tetramethyl-1,3,5,7-tetrasilaadamantane **3** all SiMe groups are converted into SiCl groups. Further examples for the reaction with ICl are:

$$(Me_3Si-CH_2)_2SiMe_2 \longrightarrow (ClMe_2Si-CH_2)_2SiMeCl$$

$$HC(SiMe_3)_3 \longrightarrow HC(SiMe_2Cl)_3$$

A higher degree of chlorination is possible with ICl and catalytic amounts of $AlBr_3$:[81]

$(Me_2Si-CH_2)_3 \longrightarrow (Cl_2Si-CH_2)_3$

26 **29**

$(Me_3Si-CH_2)_2SiMe_2 \longrightarrow$

$(ClMe_2Si-CH_2)_2SiMeCl \longrightarrow (Cl_2MeSi-CH_2)_2SiCl_2$

$(Me_3Si)_2CH_2 \longrightarrow (Cl_2MeSi)_2CH_2$

The CH_2-SiMe_3 group in compound **144** is not degraded by ICl; instead, one Cl atom is introduced at each Si atom. The initial reaction is the formation of **145**, which

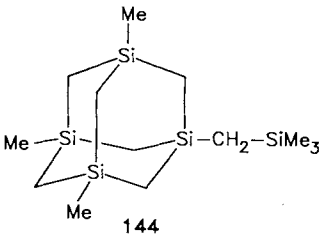

144

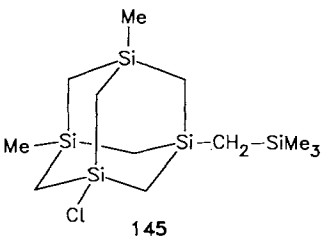

145

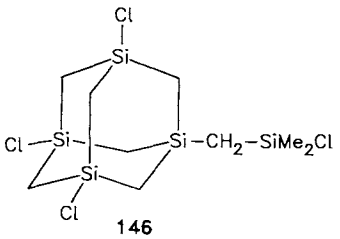

146

is then converted into the end product **146**. Compound **147** behaves similarly, though in a side reaction (8%) there is ring opening at the Si atom bearing the side chain. *C*-silylated derivatives behave similarly: for example, **54**

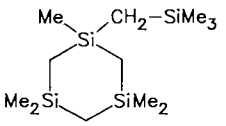

147

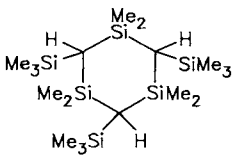

54

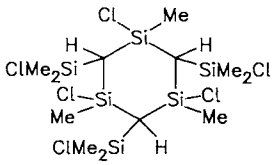

148

reacts with ICl to give **148**, and $(Me_2Si-CHMe)_3$ forms $(ClMeSi-CHMe)_3$.[81]

Not only Cl substituents at silicon atoms but also the CBr_2 group stabilizes the neighboring Si-Me bonds, as is

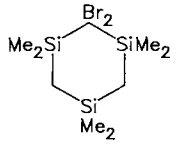

58

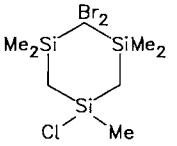

149

shown by the reaction of **58** to give **149**: ICl causes the selective cleavage of an Si-Me bond at the silicon atom in the position "*para*" to the CBr_2 group.[81]

6. The Influence of Substituents on Carbosilanes

The substituents on the Si and C atoms of carbosilanes have an effect on both the reactivity of the remaining groups and the stability of the molecular skeleton, as shown by the following examples:

a) The SiH group in carbosilanes such as $(H_2Si-CH_2)_3$ reacts only slowly with MeMgCl in Et_2O to give *Si*-methylated products. However, if the SiH group is in a position next to a CCl_2 group, it can be relatively easily substituted (with *Si*-methylation); the CCl_2 group is not attacked.

b) The SiCl group is normally much more readily alkylated by RLi or RMgCl than is the CCl_2 group. However, in the case of perchlorinated carbosilanes such as **73** or **75** the reaction with MeMgCl commences at the CCl_2 group; the primary reaction is followed by further characteristic reactions. At $-100\,^{\circ}C$ *n*BuLi lithiates the C atom of **33** without attacking the SiCl groups. The behavior of *C*-chlorinated carbosilanes containing either SiF or SiH groups towards MeMgCl is quite different: in these cases the initial reaction occurs at the SiF or SiH groups, and the CCl_2 group is at first not involved in the reaction (e.g., conversion of $(F_3Si)_2CCl_2$ into $(Me_3Si)_2CCl_2$ **34**).

$(Cl_3Si-CCl_2)_2SiCl_2$ $(Cl_2Si-CCl_2)_3$ $(Cl_3Si)_2CCl_2$

73 **75** **33**

c) In carbosilanes with CCl_2 groups the cleavage of an Si-C bond in the molecular skeleton occurs relatively readily, e.g., when one attempts to convert **33** into $(H_3Si)_2CCl_2$ or **75** into $(H_2Si-CCl_2)_3$ using an excess of $LiAlH_4$. Such cleavages of Si-C bonds are also observed in reactions of SiH- and CCl-containing carbosilanes with organometallic compounds, such as in the reaction of $(H_2Si-CCl_2)_3$ with MeMgCl.

d) *Si*-methylated linear carbosilanes or *Si*-methylated cyclic carbosilanes with *Si*-methylated side chains rearrange under the influence of $AlBr_3$ (formation of six-membered rings with elimination of $SiMe_4$). This cyclization reaction does not occur with the corresponding compounds that are partially chlorinated at silicon.

e) The reaction of linear and cyclic *Si*-methylated carbosilanes with ICl leads only to the substitution of one SiMe group at the Si atom concerned: thus $(ClMeSi-CH_2)_3$ is formed from $(Me_2Si-CH_2)_3$ **26**, while the reaction with $ICl/AlBr_3$ gives $(Cl_2Si-CH_2)_3$

29. Here the second Si–Me bond is also cleaved, but the Si–C–Si skeleton of the molecule is not attacked.

The behavior of the carbosilanes is mainly determined by the polarity of the Si–C bond, which is influenced by the substituents. Because of the electronegativities of the elements concerned, the bond polarizations in a carbosilane such as $(H_3Si-CH_2)_2SiH_2$ are as follows:

$\overset{\oplus}{Si}-\overset{\ominus}{H}$, $\overset{\ominus}{C}-\overset{\oplus}{H}$, $\overset{\oplus}{Si}-\overset{\ominus}{C}$

C-chlorination leads via the electron withdrawal by chlorine to a decrease in the shielding at the C atom and thus to a decrease in the shielding at the Si atom. This in turn causes an increase in the polarity of the Si–H bond. Thus the increased reactivity of the SiH group caused by *C*-chlorination is explained, as well as the fact that the Si–C bond in such compounds is more readily cleaved. Similarly, methylation at silicon must (since Me acts as an electron-donating substituent) decrease the reactivity of the H atoms on the silicon concerned and thus reduce the tendency for Si–C cleavage. The *Si*- and *C*-chlorinated derivatives differ from those that are SiH-containing and *C*-chlorinated in that the reactivity of the CCl_2 groups is increased. The reason for this is that with increased *C*-chlorination more electrons of the chlorines in SiCl groups are available for an increased shielding of the Si atom, so that the SiCl group becomes less polar and less reactive. The behavior of the SiF- and CCl-containing carbosilanes, such as **150**, more nearly approaches that of SiH- and CCl-containing carbosilanes (e.g., **118**) than that of SiCl- and CCl-containing derivatives (e.g., **73**). The reaction of **127** with MeMgCl commences with *Si*-methylation and not with the *C*-metalation observed in the corresponding *Si*- and *C*-chlorinated compounds.

$(F_3Si-CCl_2)_2SiF_2$ **150** $(H_3Si-CCl_2)_2SiH_2$ **118**

$(Cl_3Si-CCl_2)_2SiCl_2$ **73** $F_3Si-CCl_2-SiF_2-CH_2-SiF_3$ **127**

Polarity variations of the Si–C bond also determine the chemical behavior observed in the reactions of *Si*-methylated carbosilanes with ICl and $ICl/AlBr_3$. In the reaction with ICl, only one methyl group in the $SiMe_3$ group is substituted by Cl. The introduction of such an SiCl group decreases the polarity of the remaining Si–Me bonds, so that the possibility of a nucleophilic cleavage is decreased. This is also the reason that the ring closure reaction of methylated carbosilanes with elimination of $SiMe_4$ no longer occurs when an SiCl group is present. The generally lower bond polarity of the $Si-CH_2-Si$ bonds in comparison with that of the Si–Me bond explains the observed stability of the carbosilane skeleton with respect to cleavage. Aluminum halides polarize not only the Si–Me bond but also the ICl molecule and thus make possible further Si–Me cleavage and higher degrees of chlorination. These experimental results and their qualitative interpretation are in agreement with quantum-mechanical calculations for simple silicon-carbon compounds.[82]

7. Polycarbosilanes

The favorable properties of silicon carbide (chemical resistance, density 3.2 g cm^{-3}, hardness 9.5) for use in modern ceramics have also led to an increasing interest in polymeric carbosilanes. These substances are obtained either via pyrolysis of methylsilanes[4,6] or via prolonged thermal treatment of polysilanes.[83] *S. Yajima*[84] has reported the formation of SiC fibers by thermal treatment of methylpolysilanes. Polysilanes of the type $(Me_2Si)_n$ (n = 5–35) are formed from Me_2SiCl_2 and Na/K in THF; various cyclic and polycyclic polycarbosilanes are obtained by the cocondensation of Me_2SiCl_2 and $MeSiCl_3$ with Na/K.[83] On heating to ca. 450 °C these polysilanes rearrange: CH_2 derived from $SiCH_3$ groups inserts into Si–Si bonds with concomitant formation of SiH groups according to reactions (5) and (6). The polycarbosilanes so formed[85] are converted into β-SiC at 1300 °C. Because of the formation of volatile products, this stepwise procedure involves considerable material loss. The mechanism of the formation of these polycarbosilanes as well as their further structural variations are not yet well understood.

In the pyrolysis of $SiMe_4$ (Fig. 1, Section 2) the Si-poor carbosilanes initially formed are involved in the subsequent reactions to give the Si-richer products: an example is provided by $(Me_2Si-CH_2)_2$ **25** (Section 2.1.4). The studies showed that in a closed system **25** is converted at temperatures between 200 and 280 °C without gas evolution into linear polycarbosilanes of the type $Me_3Si(CH_2-SiMe_2)_n-CH_2-SiMe_3$ ($M_r \approx 250\,000$, temperature-dependent; colorless gel-like substances, still soluble in toluene).[25] When these are subjected to higher temperatures (650 °C, 4 h), a partial degradation to give low-molecular-weight carbosilanes is accompanied by the formation of insoluble products.

The polycarbosilanes obtained by the pyrolysis of methylsilanes are not linear (as revealed by their composition); however, their structures have not been unambiguously determined. Since the lower-molecular-weight carbosilanes formed from the various methylsilanes (varying Si : C ratios) have different structures, differences in the structures of the polymers are also to be expected. This becomes clear in the thermal treatment of the compounds in Figure 2 (Section 2.1.3) obtained from Me_2SiCl_2. Between 420 and 620 °C there is a marked increase in viscosity, accompanied by elimination of $SiCl_4$ and $MeSiCl_3$; low-molecular-weight carbosilanes are formed. Since most of the end groups of the compounds in Figure 2 are initially $SiCl_3$ groups, the formation of $SiCl_4$ indicates a condensation with formation of additional Si–C bonds which link these molecular skeletons: they thus become structural elements in the polymers.[18]

8. Summary and Outlook

An extremely large number of structurally different carbosilanes have now been synthesized in different ways. Be-

cause of their chemical behavior, the carbosilane frameworks can be described neither as "quasi-C-skeletons" nor as silicone-like systems (despite the fact that the Si–CH_2–Si grouping is isoelectronic with Si–O–Si). It is noteworthy that the chemical stability of the Si–C–Si molecular structures is higher than that of SiMe end groups and that their stability increases still further when electronegative substituents are introduced at the Si atoms. Numerous questions however remain to be answered. Thus the formation of Si-richer and high-molecular-weight carbosilanes in the pyrolysis of methylsilanes is still not sufficiently well understood. Further studies on the reaction of silicon with CH_2Cl_2 to give unbranched linear carbosilanes should serve to increase considerably our knowledge of catalytic processes at Si surfaces. The same is true for the catalyzed reactions of perchlorinated carbosilanes with silicon, which will provide routes to new carbosilane structures. Organometallic synthesis from organosilicon compounds alone appears to be of only limited use for the construction of polycyclic carbosilanes, though the possibilities provided by its combination with cyclization reactions induced by $AlBr_3$ are extremely interesting. In many ways a more quantitative physicochemical foundation for carbosilane chemistry is required; for example, calorimetric studies could provide valuable information.

Studies on the construction and structure of polymeric carbosilanes are at present mainly of only a qualitative nature. The use of carbosilanes in high-performance ceramics[86] requires not only the formation of polymers of different types and information on the structures of such polymers but also a complete understanding of the reactions that they undergo on further thermal treatment. This is a challenge for both the chemist and the materials scientist.

I thank my co-workers (whose names appear in the list of references) for their dedication. The work discussed here could not have been carried out without the support of the Fonds der Chemischen Industrie and the Deutsche Forschungsgemeinschaft. I feel myself particularly indebted to these institutions.

Received: May 22, 1987 [A 643 IE]
German version: *Angew. Chem. 99* (1987) 1150
Translated by Prof. *T. N. Mitchell*, Dortmund

[1] G. Fritz, *Angew. Chem. 70* (1958) 701.
[2] F. Kipping, *Proc. Chem. Soc. (London) 20* (1904) 15; C. Eaborn: *Organosilicon Compounds*, Butterworths, London 1960.
[3] E. G. Rochow: *Einführung in die Chemie der Silicone*, Verlag Chemie, Weinheim 1952.
[4] G. Fritz, E. Matern: *Carbosilanes, Syntheses and Reactions*, Springer, Berlin 1986.
[5] G. Fritz, *Z. Anorg. Allg. Chem. 280* (1955) 332; *Z. Naturforsch. B 7* (1952) 207.
[6] G. Fritz, J. Grobe, D. Kummer, *Adv. Inorg. Chem. Radiochem. 7* (1965) 349.
[7] G. Fritz, A. Wörsching, *Z. Anorg. Allg. Chem. 512* (1984) 131; G. Fritz, S. Lauble, unpublished results.
[8] G. Fritz, *Top. Curr. Chem. 50* (1974) 44.
[9] G. Fritz, J. Neutzner, H. Volk, *Z. Anorg. Allg. Chem. 497* (1983) 21.
[10] G. Fritz, B. Raabe, *Z. Anorg. Allg. Chem. 299* (1959) 232.
[11] G. Fritz, N. Götz, *Z. Anorg. Allg. Chem. 375* (1970) 54; G. Fritz, H. Reuss, K.-P. Wörns, A. Wörsching, *ibid. 512* (1984) 93.
[12] G. Fritz, G. Marquardt, *Z. Anorg. Allg. Chem. 404* (1974) 1; H. G. von Schnering, G. Sawitzki, K. Peters, K.-F. Tebbe, *ibid. 404* (1974) 38.
[13] G. Fritz, F. Diem, H. Köhler, D. Kummer, H. Scheer, *Angew. Chem. 82* (1970) 445; *Angew. Chem. Int. Ed. Engl. 9* (1970) 464; G. Fritz, H. Köhler, D. Kummer, *Z. Anorg. Allg. Chem. 374* (1970) 54; G. Sawitzki, H. G. von Schnering, *ibid. 425* (1976) 1; G. Fritz, K.-P. Wörns, *ibid. 512* (1984) 103.
[14] G. Fritz, K.-P. Wörns, K. Peters, E.-M. Peters, H. G. von Schnering, *Z. Anorg. Allg. Chem. 512* (1984) 126; R. O. Klaus, H. Tobler, C. Ganter, *Helv. Chim. Acta 57* (1974) 2517.
[15] G. Fritz, G. Marquardt, H. Scheer, *Angew. Chem. 85* (1973) 587; *Angew. Chem. Int. Ed. Engl. 12* (1973) 654.
[16] G. Fritz, D. Habel, D. Kummer, G. Teichmann, *Z. Anorg. Allg. Chem. 302* (1959) 60; G. Fritz, D. Ksinsik, *ibid. 322* (1963) 46; G. Fritz, H. Buhl, D. Kummer, *ibid. 327* (1964) 165; G. Fritz, W. König, H. Scheer, *ibid. 377* (1970) 240.
[17] G. Fritz, R. Haase, D. Kummer, *Z. Anorg. Allg. Chem. 365* (1969) 1.
[18] G. Fritz, D. Tögel, unpublished results.
[19] G. Fritz, H. J. Dannappel, E. Matern, *Z. Anorg. Allg. Chem. 399* (1973) 263; G. Sawitzki, H. G. von Schnering, *ibid. 399* (1973) 257.
[20] G. Fritz, J. Maas, A. Hornung, *Z. Anorg. Allg. Chem. 460* (1980) 115.
[21] a) D. F. Helm, E. S. Mack, *J. Am. Chem. Soc. 59* (1937) 60; b) A. C. Baldwin, I. M. T. Davidson, M. D. Reed, *J. Chem. Soc. Faraday Trans. I 74* (1978) 2171.
[22] I. M. T. Davidson, C. Eaborn, *J. Chem. Soc. Faraday Trans. I 70* (1974) 249.
[23] G. Fritz, B. Grunert, *Z. Anorg. Allg. Chem. 419* (1976) 249.
[24] I. M. T. Davidson, F. T. Lawrence, G. Fritz, E. Matern, *Organometallics 1* (1982) 1453.
[25] G. Fritz, N. Götz, *Z. Anorg. Allg. Chem. 375* (1970) 171; W. R. Hörmann, *Diplomarbeit*, Universität Karlsruhe 1970; G. Fritz, C. Hill, unpublished results.
[26] W. I. Patnode, R. W. Schiessler, US-Pat. 2381000, 2381001, 2381002 (1945); *Chem. Abstr. 39* (1945) 4889.
[27] G. Fritz, H. Thielking, *Z. Anorg. Allg. Chem. 306* (1960) 39.
[28] R. Müller, G. Seitz, *Chem. Ber. 91* (1958) 22.
[29] R. Müller, H. Beyer, *Chem. Ber. 92* (1959) 1018.
[30] R. Müller, W. Müller, *Chem. Ber. 96* (1963) 2894; *97* (1964) 1111.
[31] V. S. Fikhtengol'ts, A. L. Klebanskij, *J. Gen. Chem. USSR (Engl. Transl.) 27* (1957) 2535; *26* (1956) 2795; R. J. H. Voorhoeve, J. A. Vlugter, J. A. Lipe, *J. Catal. 3* (1964) 414; *4* (1965) 220.
[32] R. J. H. Voorhoeve: *Organohalosilanes*, Elsevier, Amsterdam 1967.
[33] G. Fritz, S. Lauble, unpublished results.
[34] G. Fritz, S. Lauble, K. Peters, H. G. von Schnering, unpublished results.
[35] G. Fritz, P. Fusik, K. Peters, H. G. von Schnering, unpublished results.
[36] C. Eaborn, R. W. Bott: *Organometallic Compounds of the Group IV Elements, Vol. 1, Part 1, 1*, Marcel Dekker, New York 1968.
[37] G. Fritz, D. Kummer, *Z. Anorg. Allg. Chem. 308* (1961) 105.
[38] G. Fritz, M. Hähnke, *Z. Anorg. Allg. Chem. 390* (1972) 137.
[39] G. Fritz, M. Hähnke, *Z. Anorg. Allg. Chem. 390* (1972) 157.
[40] G. Fritz, H. J. Vogt, *Z. Anorg. Allg. Chem. 419* (1976) 1; A. Lipka, H. G. von Schnering, *ibid. 419* (1976) 9.
[41] G. Fritz, U. Finke, *Z. Anorg. Allg. Chem. 424* (1976) 238.
[42] G. G. Eberhard, W. A. Butte, *J. Org. Chem. 29* (1964) 2928.
[43] G. Fritz, U. Finke, *Z. Anorg. Allg. Chem. 430* (1977) 121.
[44] G. Fritz, U. Finke, W. Speck, *Z. Anorg. Allg. Chem. 481* (1981) 51; G. Fritz, W. Schick, M. Keuthen, unpublished results.
[45] G. Fritz, W. Speck, *Z. Anorg. Allg. Chem. 481* (1981) 60.
[46] N. Wiberg, G. Wagner, *Angew. Chem. 95* (1983) 1027; *Angew. Chem. Int. Ed. Engl. 22* (1983) 1005.
[47] C. L. Frye, D. R. Weyenberg, J. M. Klosowski, *J. Am. Chem. Soc. 92* (1970) 6379; *Intra-Sci. Chem. Rep. 7* (1973) 4, 147; C. L. Frye, J. M. Klosowski, *J. Am. Chem. Soc. 94* (1972) 7186.
[48] G. Fritz, H. Volk, M. Straub, K. Peters, E.-M. Peters, H. G. von Schnering, *J. Organomet. Chem.*, in press.
[49] G. Fritz, H. Volk, unpublished results.
[50] G. Fritz, H. Volk, K. Peters, E.-M. Peters, H. G. von Schnering, *Z. Anorg. Allg. Chem. 497* (1983) 119.
[51] G. Fritz, G. Brauch, *Z. Anorg. Allg. Chem. 497* (1983) 134.
[52] G. Fritz, G. Brauch, unpublished results.
[53] G. Fritz, M. Straub, unpublished results.
[54] G. Fritz, J. Grobe, D. Ksinsik, *Z. Anorg. Allg. Chem. 302* (1959) 175.
[55] G. Fritz, H. Fröhlich, *Z. Anorg. Allg. Chem. 382* (1971) 217.
[56] G. Fritz, D. Habel, G. Teichmann, *Z. Anorg. Allg. Chem. 303* (1960) 85.
[57] G. Fritz, J. Grobe, *Z. Anorg. Allg. Chem. 309* (1961) 77.
[58] G. Fritz, R. Riekens, T. Günther, M. Berndt, *Z. Naturforsch. B 26* (1971) 480.
[59] G. Fritz, W. Himmel, *Z. Anorg. Allg. Chem. 448* (1979) 40.
[60] G. Fritz, W. Himmel, *Z. Anorg. Allg. Chem. 448* (1979) 55.
[61] G. Fritz, S. Wartanessian, *J. Organomet. Chem. 178* (1979) 11.
[62] G. Fritz, S. Wartanessian, E. Matern, W. Hönle, H. G. von Schnering, *Z. Anorg. Allg. Chem. 475* (1981) 87.
[63] G. Fritz, J. Thomas, *J. Organomet. Chem. 271* (1984) 107.

[64] G. Fritz, E. Bosch, *Z. Anorg. Allg. Chem. 404* (1974) 103.
[65] G. Fritz, J. W. Chang, N. Braunagel, *Z. Anorg. Allg. Chem. 416* (1975) 211.
[66] G. Fritz, N. Szczepanski, *Z. Anorg. Allg. Chem. 367* (1969) 44.
[67] G. Fritz, N. Braunagel, *Z. Anorg. Allg. Chem. 399* (1973) 280.
[68] G. Fritz, P. Böttinger, *Z. Anorg. Allg. Chem. 395* (1973) 159.
[69] G. Fritz, H. Fröhlich, *Z. Anorg. Allg. Chem. 382* (1971) 9.
[70] G. Fritz, H. Fröhlich, *Z. Anorg. Allg. Chem. 382* (1971) 217.
[71] G. Fritz, W. H. Dresel, *Z. Anorg. Allg. Chem. 439* (1978) 116.
[72] G. Fritz, M. Berndt, R. Huber, *Z. Anorg. Allg. Chem. 391* (1972) 219.
[73] G. Fritz, M. Portner, *Z. Naturforsch. B 30* (1975) 965.
[74] G. Fritz, H. Bauer, *Angew. Chem. 95* (1983) 740; *Angew. Chem. Int. Ed. Engl. 22* (1983) 730.
[75] R. H. Krieble, J. R. Elliott, *J. Am. Chem. Soc. 68* (1046) 2291.
[76] V. Chvalovsky, V. Bazant, *Collect. Czech. Chem. Commun. 21* (1956) 93.
[77] M. Ishikawa, M. Kumada, H. Sakurai, *J. Organomet. Chem. 23* (1970) 63; H. Sakurai, T. Watanabe, M. Kumada, *ibid. 7* (1967) P15.
[78] K. R. Beck, R. A. Benkeser, *J. Organomet. Chem. 21* (1970) P35.
[79] E. Hengge, W. Peter, *J. Organomet. Chem. 148* (1978) C22.
[80] M. Bordeau, S. M. Djamei, J. Dunoguès, R. Calas, *Bull. Soc. Chim. Fr. 1982*, II-159.
[81] G. Fritz, J. Honold, *Z. Anorg. Allg. Chem.*, in press.
[82] H. Schiffer, R. Ahlrichs, unpublished results.
[83] L. F. Brough, R. West, *J. Am. Chem. Soc. 103* (1981) 3049; R. West, C. D. David, P. I. Djurovich, K. L. Stearley, K. S. Srinivasan, H. Yu, *ibid. 103* (1981) 7352; R. West, *J. Organomet. Chem. 300* (1986) 327.
[84] S. Yajima, *Am. Ceram. Soc. Bull. 62* (1983) 893.
[85] S. Yajima, Y. Hasegawa, J. Hayashi, M. Iimura, *J. Mater. Sci. 13* (1978) 2569; Y. Hasegawa, M. Iimura, S. Yajima, *ibid. 15* (1980) 720; Y. Hasegawa, K. Okamura, *ibid. 18* (1983) 3633; *21* (1986) 321.
[86] F. Aldinger, H.-J. Kalz, *Angew. Chem. 99* (1987) 381; *Angew. Chem. Int. Ed. Engl. 26* (1987) 371.
[87] C. Eaborn, P. D. Lickiss, *J. Organomet. Chem. 294* (1985) 305.

The 100th anniversary issue of ANGEWANDTE CHEMIE (January 1988) will contain the following articles:

A. Eschenmoser	Vitamin B_{12}: Experiments Concerning the Origin of Its Molecular Structure
J. Falbe et al.	Natural Fats and Oils—Renewable Raw Materials for Chemical Industry
H. Gerischer	Light as a Probe for the Investigation of Electrochemical Surface Reactions
R. Huber	Flexibility and Rigidity of Proteins and Protein-Pigment Complexes
J.-M. Lehn	Supramolecular Chemistry—Molecules, Supermolecules, and Molecular Devices
H. Ringsdorf	Molecular Architecture and Function of Polymeric Oriented Systems
A. Simon	Clusters of Valence-Electron-Deficient Metals—Structure, Bonding, and Properties
G. Wilke	100 Years of Organonickel Chemistry

When submitting manuscripts, authors of articles intended for publication as "Communications" are requested to read the "Notice to Authors" reproduced in the January issue of the journal following the list of contents; upon request, a copy can be obtained from the editorial office.

A Sulfene Umpolung**

By *Rudolf Allmann, Wolfgang Hanefeld,* Magda Krestel,* and *Bernd Spangenberg*

Sulfenes are very reactive intermediates which are usually generated from sulfonic acid chlorides such as **1**—which contain an α-hydrogen atom—and bases, and are trapped in situ. Stable sulfenes are unknown.[1]

We report here the first direct demonstration of a sulfene umpolung (charge reversion), which facilitates a nucleophilic attack at the sulfene C atom.

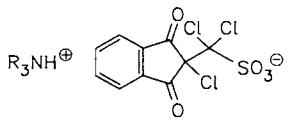

4a, b

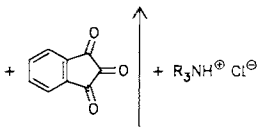

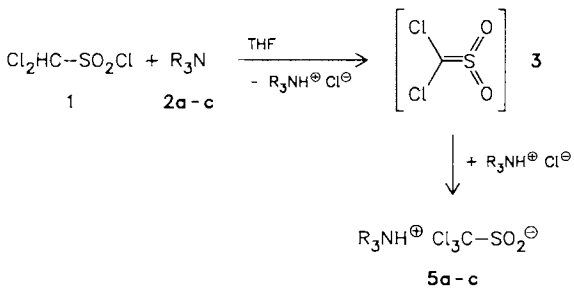

2a, R_3N = $(C_2H_5)_3N$; 2b, R_3N = ; **2c, R_3N** = 1/2

In connection with our studies on the preparation of novel β-sultones[2] we were able to trap **3** in a typical sulfene reaction with indanetrione to give **4**.[3] The intermediary dichlorosulfene **3** reacts in a manner typical for sulfenes, namely as a 1,2-dipole with a nucleophilic carbon atom (see **3A**).

If the reaction is carried out under the same conditions but in the absence of indanetrione,[4] the salt **5** containing a trichloromethanesulfinate ion is surprisingly formed almost quantitatively; this finding could be confirmed by an X-ray structure analysis of **5c**.[5] The spectroscopic data show that **5a** and **5b** also contain the trichloromethanesulfinate ion (Table 1).

Table 1. Selected spectroscopic data of **4** and **5**. IR: **4a, 4b** (KBr), **5a** (NaCl platelets), **5b, 5c** (KBr), $\tilde{\nu}$ [cm^{-1}]; ^{13}C-NMR (25 MHz, $CDCl_3$; **5a, 5b**: solvent as standard; **5c**: in D_2O, dioxane ext.).

Cpd.	**4**: IR (SO_2^s) **5**: IR (SO_2^s)	^{13}C-NMR δ values
4a	1278, 1256, 1216, 1055	
4b	1282, 1255, 1214, 1190, 1050	
5a	1125, 1023	114.89
5b	1118, 1012, 997	113.83
5c	1098, 1005, 966	113.50

The reaction presented here, and described by *J. F. King* et al. as an "abnormal addition", has been postulated on several occasions for sulfenes,[6,7] but could never be conclusively demonstrated.[7,8] In particular, the reaction of camphorsulfonic acid chlorides with triethylamine[9] to give alkyl-substituted α-chlorosulfines (!), first reported as long ago as 1923, requires involvement of a sulfene umpolung.[10]

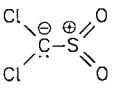

3A

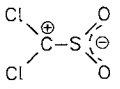

3B

The proof that dichlorosulfene can react as a "normal" form **3A** and as a form **3B** with umpolung now supports, after 64 years, the presumption that the first sulfine was obtained via an intermediary sulfene.[9] The weakness of the explanation given at that time for the reaction—the formulation of an atypical sulfene reaction—no longer comes into question.

Received: June 4, 1987
revised: July 7, 1987 [Z 2281 IE]
German version: *Angew. Chem. 99* (1987) 1175

CAS Registry numbers:
1, 41197-29-9; **2a**, 121-44-8; **2b**, 110-86-1; **2c**, 280-57-9; **3**, 110852-75-0; **4a**, 81054-77-5; **4b**, 110852-76-1; **5a**, 53799-69-2; **5b**, 53799-68-1; **5c**, 110852-77-2.

[*] Prof. Dr. W. Hanefeld, Dr. B. Spangenberg
Pharmazeutisch-chemisches Institut der Universität
Marbacher Weg 6, D-3550 Marburg (FRG)
Prof. Dr. R. Allmann, M. Krestel
Fachbereich Geowissenschaften der Universität
Hans-Meerwein-Strasse, D-3550 Marburg (FRG)

[**] This work was supported by the Deutsche Forschungsgemeinschaft.

[1] B. G. Lenz, B. Zwanenburg in *Houben-Weyl-Müller: Methoden der Organischen Chemie, Band E11*, Thieme, Stuttgart 1985, p. 1326.
[2] W. Hanefeld, D. Kluck, *Arch. Pharm. (Weinheim, FRG) 315* (1982) 57.
[3] B. Spangenberg, *Dissertation*, Universität Marburg 1987.
[4] *Procedure:* A solution of dichloromethanesulfonic acid chloride **1** (1.83 g, 10 mmol; for the synthesis of **5c**: 20 mmol) in THF (10 mL) was treated slowly at 0 °C with 10 mmol of the respective bases **2** (**2a**: 1.0 g; **2b**: 0.79 g; **2c**: 1.12 g). **5a** separated as a yellow oil and was purified over silica gel 60 (THF/$CHCl_3$ 1:1); yield 81%, m.p. 6 °C. **5b** precipitated as a colorless solid and was recrystallized from THF; yield 95%, m.p. 109–112 °C (decomp). **5c** precipitated as a colorless solid and was recrystallized from water; yield 63%, m.p. 145–147 °C.
[5] Crystal structure of **5c**: $P2_1/m$, $a = 18.079(1)$, $b = 10.773(2)$, $c = 9.809(5)$, Å, $\alpha = 92.57(1)°$, $\rho_{calc} = 1.4136$ gcm^{-3}, $Z = 4$, 2729 reflections, $R = 0.088$,

$R_w = 0.098$. Selected structural data: S-O 1.46(9) and 1.54, S-C 1.91, C-Cl 1.75(3), 1.76(1), 1.79(1) Å; O-S-O 106.3(4)°. Further details of the crystal structure investigation are available on request from the Fachinformationszentrum Energie, Physik, Mathematik GmbH, D-7514 Eggenstein-Leopoldshafen 2 (FRG), on quoting the depository number CSD-52574, the names of the authors, and the journal citation.

[6] G. Opitz, *Angew. Chem. 79* (1967) 161; *Angew. Chem. Int. Ed. Engl. 6* (1967) 107.

[7] J. F. King, R. P. Beatson, J. M. Buchshrieber, *Can. J. Chem. 55* (1977) 2323, and references cited therein.

[8] T. Kempe, T. Norin, *Acta Chem. Scand. B28* (1974) 609. The authors presumed that a trichloromethanesulfinate is formed in the reaction of **1** with triethylamine, but they could not conclusively demonstrate this. Moreover, at that time the formation of the dichlorosulfene from **1** was not confirmed experimentally.

[9] E. Wedekind, D. Schenk, R. Stüsser, *Ber. Dtsch. Chem. Ges. 56* (1923) 633.

[10] J. F. King, T. Durst, *Tetrahedron Lett. 1963*, 585, and references cited therein.

Valence Isomerization between 1-Phosphanorcaradienes and 1-Phospha-2*H*-tropylidenes (2*H*-Phosphepines)

By *Gottfried Märkl,* Hans J. Beckh, Manfred L. Ziegler,* and *Bernd Nuber*

In the case of the parent compounds the norcaradiene/tropylidene equilibrium lies on the side of the monocycle; electron-withdrawing substituents in the 7-position effect a shift in favor of the norcaradiene structure.[1] 1-Azanorcaradienes and thus also their valence isomerism with 1-azatropylidenes (2*H*-azepines) are still unknown.[2]

We describe here results which indicate a 1-phosphanorcaradiene/1-phospha-2*H*-tropylidene valence isomerization equilibrium [Eq. (a)].

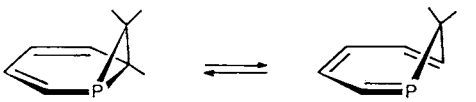

(a)

We recently reported that the pentacyclic phosphachiropteradienes **2** are formed in the reaction of 3,5-diphenyl-λ^3-phosphinine **1** with diazomethane, monosubstituted diazomethanes, and dialkyl-substituted diazomethanes.[3] In contrast, with diphenyldiazomethane, the 1-phosphanorcaradiene derivative **3** is formed (Scheme 1).

The $M(CO)_5$ complexes **5**[4] of **1** react with diphenyldiazomethane to give the 1-phosphanorcaradiene complexes **6**, corresponding to **3** (Table 1), but with diazomethane and monosubstituted diazomethanes to give the $M(CO)_5$ complexes of the [5.3.0]-bicycles **7**. Other than would appear to be the case, there is a causal relation between the formation of **6** and **7**. The chemistry of **6**, as well as the formation of **7**, affords arguments for the assumption that the reaction of **5** with diazoalkanes $RR'C{=}N_2$ generally first leads to the 1-phosphanorcaradienes **8**, which are in equilibrium with the valence isomeric 1-phosphatropylidene complexes **9**. This equilibrium must, however, lie so far on the side of the thermodynamically more stable phosphane **8** that a spectroscopic detection of **9** is impossible.

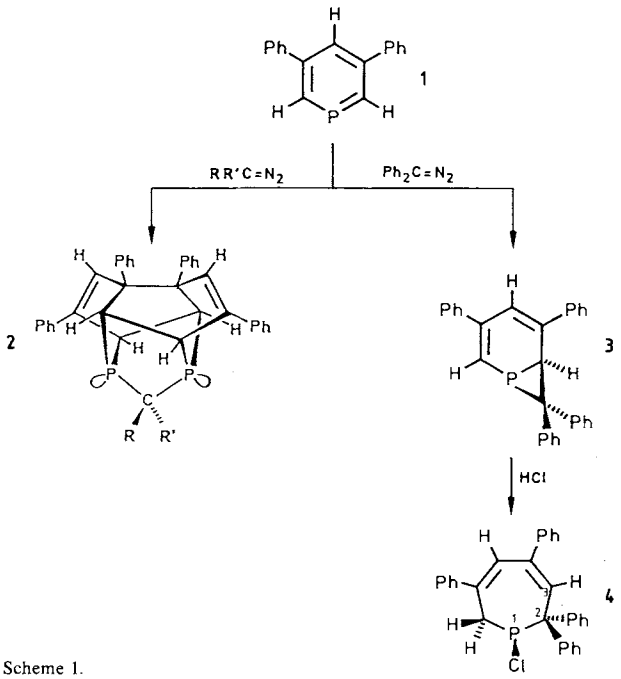

Scheme 1.

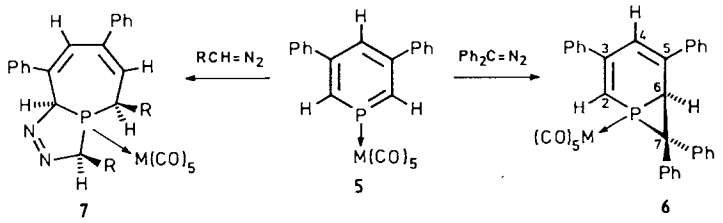

a, M = Cr; **b**, M = Mo; **c**, M = W; **7a**, **b**, R = H; **7c**, R = Me

An equilibrium between **8** and **9**, in which a reactive PC double bond with $\lambda^3\sigma^2$ phosphorus is present, is indicated by the fact that the 1-chlorodihydrophosphepine **10** is obtained upon addition of hydrogen chloride to **8** (Table 1).

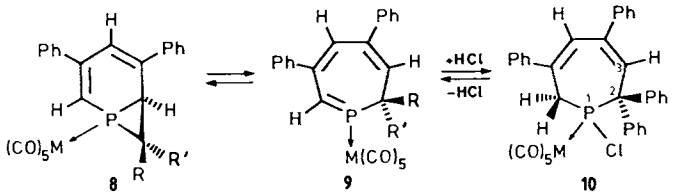

The non-complexed bicycle **3** reacts analogously with hydrogen chloride to give **4** (Scheme 1, Table 1). Compound **10** can be quantitatively reconverted into **8** by base-induced (NEt_3) dehydrochlorination.

That the equilibrium **8**⇄**9** is actually established and the formation of **10** is not the result of a direct, ring-opening HCl-addition to **8**, underscores the result of the reaction of **5** with diazomethane and diazoethane: the 1-phosphanorcaradienes **8** formed with the first molecule of diazomethane with elimination of nitrogen can react further with a second molecule of diazoalkane only via the valence isomeric 1-phosphatropylidenes **9** in a 1,3-dipolar cycloaddition to give **7**. The cycloadducts **7** are not isolable as such; depending on R and the solvent from which they

[*] Prof. Dr. G. Märkl, Dipl.-Chem. H. J. Beckh
Institut für Organische Chemie der Universität
Universitätsstrasse 31, D-8400 Regensburg (FRG)
Prof. Dr. M. L. Ziegler, Dr. B. Nuber
Institut für Anorganische Chemie der Universität
Im Neuenheimer Feld, D-6900 Heidelberg (FRG)

Table 1. Yields and physical and spectroscopic properties of **4**, **6**, **10**–**12** (101.25-MHz $^{31}P\{^1H\}$-NMR, 250-MHz ^1H-NMR, 70-eV MS). J values in Hz.

4: 98%; m.p. 64–68 °C; ^1H-NMR: $\delta = 7.00$ (d, $J(PH) = 3.60$; H-3), 6.10 (d, J(H-5, H-7) = 3.60; H-5), 3.35 (d, J(P, H) = 17.99; H-7, H-7'); ^{31}P-NMR: $\delta = 128.1$

6a: 61%; m.p. 162–163 °C; ^1H-NMR: $\delta = 6.63$ (d, J(P, H) = 43.7; H-2), 6.41 (s; H-4), 4.03 (s; H-6); ^{31}P-NMR: $\delta = 66.2$; FD-MS: m/z 606 ($M^{\oplus\oplus}$ for ^{52}Cr)

6b: 87%; m.p. 175–177°; ^1H-NMR: $\delta = 6.23$ (d, J(P, H) = 43.6; H-2), 6.43 (s; H-4), 4.19 (s; H-6); ^{31}P-NMR: $\delta = -111.8$ (d, $J(^{31}P, ^{183}W) = 267.1$); FD-MS: m/z 736 ($M^{\oplus\oplus}$ for ^{182}W)

10a: 84%; m.p. 53–56 °C; ^1H-NMR: $\delta = 6.71$ (d, J(P, H) = 8.88 (H-3), 6.32 (dd, J(P, H) = 1.39, J (H-5, H-7) = 130; H-5), 3.62 (br, s; H-7, H-7')

10b: 96%; oil; ^1H-NMR: $\delta = 6.71$ (d, J(P, H) = 9.17; H-3), 6.34 (d, J(H-5, H-7) = 1.25; H-5), 3.83 and 3.79 (each dd, J (H-7, H-7') = 16.1, J (P, H) = 2.82, J (P, H) = 9.0; H-7, H-7'); ^{31}P-NMR: $\delta = +80.2$ ($J(^{31}P, ^{183}W) = 290.9$)

11b: 65%; m.p. 147 °C (yellow platelets, form MeOH); ^1H-NMR: $\delta = 6.71$ (dd, J(P, H) = 5.90, J(H, H-8a) = 3.70; NH), 7.15 (d, J(P, H) = 50.5; H-3), 2.99 (ddd, J(P, H) = 13.4, J(H-4, H-4') = 14.7, J(H-4, H-5) = 6.71; H-4 (H-4')), 2.58 (dd, J(H-4', H-5) = 8.04, J(P, H) = 0; H-4' (H-4)), 6.40 (ddd, J(P, H) = 3.28; H-5), 6.61 (s; H-7), 5.16 (m; H-8); ^{31}P-NMR: $\delta = +89.52$ ($J(^{31}P, ^{183}W) = 227.50$)

12a: 78%; m.p. 117–119 °C (yellow needles from $CHCl_3$/petroleum ether); ^1H-NMR: $\delta = 6.32$ (sbr; NH), 3.08 (d, J(P, H) = 5.24; H-4), 3.05 (d, J(P, H) = 7.23; H-4'), 4.33 (t, J(P, H) = 11.10, J(H-3, H-3') = 12.5θ; H-3), 3.95 (ψt, J(P, H) = 11.65; H-3'), 6.17 (quint, J(P, H) = 5.82, J(H-5, H-4) = 7.28, J(H-5, H-4') = 7.28; H-5), 6.60 (s; H-7)

12b: 68%; m.p. 165 °C (yellow needles); ^1H-NMR: $\delta = 6.31$ (dd, J(P, H) = 10.1, J(NH, H-3) = 2.63; NH), 4.09 (dd, J(P, H) = 10.7, J(H-3, H-3') = 12.66; H-3), 4.50 (ddd, J(P, H) = 10.1, J(NH, H-3') = 2.63; H-3'), 3.07 (ddd, J(P, H) = 3.72, J(H-4, H-4') = 14.97, J(H-4, H-5) = 9.47; H-4), 3.19 (dd, J(H-4', H-5) = 5.37; H-4'), 6.17 (ddd, J(P, H) = 5.45; H-5), 6.62 (d, J(P, H) = 1.65; H-7); ^{31}P-NMR; $\delta = 54.45$ ($J(^{31}P, ^{183}W) = 240$)

12c: 31%; m.p. 209–210 °C; ^1H-NMR: NH not observable, 4.76 (dq, J(P, H) = 6.93, $J(CH_3, H) = 6.86$; H-3), 1.63 (dd, J(P, H) = 15.97; CH_3-3), 3.69 (ddq, J(P, H) = 14.6, $J(CH_3, H) = 7.20$, J(H-4, H-5) = 4.59; H-4), 1.43 (dd, J(P, H) = 18.1; CH_3-4), 5.85 (dd, J(P, H) = 11.27; H-5), 6.42 (d, J(P, H) = 2.14; H-7)

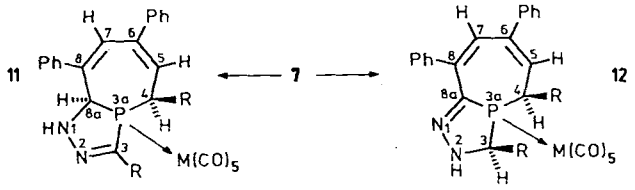

are recrystallized, they undergo 1,3 H-shifts to give the isomeric hydrazones **11** and **12**.

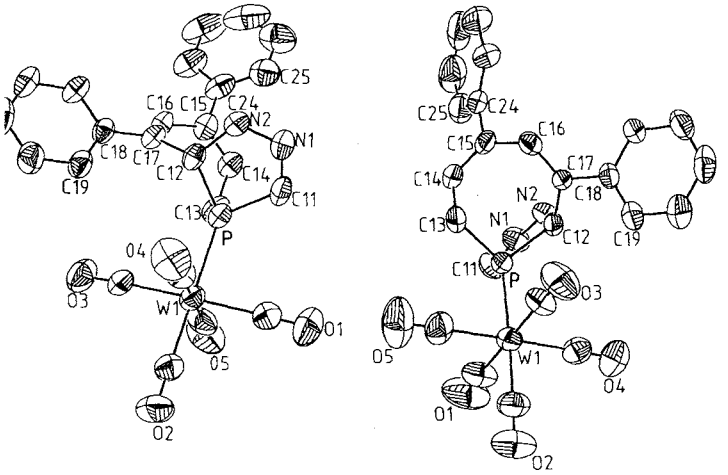

Fig. 1. Crystal structure of **11b** (two views). Selected bond lengths [Å] and angles [°] P-W1 2.492(2), P-C11 1.818(5), P-C12 1.863(7), P-C13 1.829(8), C11-N1 1.287(9), N1-N2 1.352(6), N2-C12 1.456(7); C11-P-C12 87.0(3), C11-P-C13 103.1(3), C12-P-C13 102.7(3).

Whereas both tautomers [**11b** from methanol (Table 1), **12b** from $CHCl_3$/petroleum ether (Table 1)] are obtained from **7b**, so far only the hydrazones **12a** and **12c** are formed from **7a** and **7c** (Table 1). The proposed structure is confirmed by spectroscopic data as well as the result of an X-ray structure analysis of **11b**[5] (Fig. 1).

The disrotatory, electrocyclic valence isomerization **8**⇆**9**, similarly as the Cope rearrangements of phospha-1,5-hexadienes[6] and the electrocyclic isomerization of 1,4-diphospha-1,3-butadienes in diphosphacyclobutenes,[7] demonstrates that the mutual conversion of $\lambda^3\sigma^3$- and $\lambda^3\sigma^2$-phosphorus in pericyclic reactions is possible (Scheme 2).

Scheme 2.

Received: June 5, 1987 [Z 2287 IE]
German version: *Angew. Chem.* 99 (1987) 1214

CAS Registry numbers:
1, 90543-75-2; **3**, 107175-04-2; **4**, 110798-32-8; **5a**, 110825-83-7; **5b**, 110825-90-6; **5c**, 110825-92-8; **6a**, 110825-84-8; **6c**, 110825-91-7; **7a**, 110825-85-9; **7b**, 110825-93-9; **7c**, 110825-94-0; **10a**, 110825-87-1; **10b**, 110825-95-1; **11b**, 110825-88-2; **12a**, 110825-89-3; **12b**, 110850-47-0; **12c**, 110825-86-0.

[1] See, e.g., G. Maier, *Angew. Chem.* 79 (1967) 446; *Angew. Chem. Int. Ed. Engl.* 6 (1967) 402.
[2] See, e.g., C. Wentrup, *Adv. Heterocycl. Chem.* 28 (1981) 231.
[3] G. Märkl, H. J. Beckh, K. K. Mayer, M. L. Ziegler, T. Zahn, *Angew. Chem.* 99 (1987) 255; *Angew. Chem. Int. Ed. Engl.* 26 (1987) 236.
[4] G. Märkl, H. J. Beckh, *Tetrahedron Lett.* 28 (1987) 3475.
[5] Crystal data of **11b**: space group C_i^1-$P\bar{1}$ (2), $a = 10.116(4)$, $b = 16.133(7)$, $c = 16.595(8)$ Å, $\alpha = 116.12(4)$, $\beta = 94.18(4)$, $\gamma = 98.83(4)°$, $V = 2372.6$ Å^3, $Z = 4$, $\rho_{calc} = 1.76$ g cm^{-3}, $F_{000} = 1208$, $\mu(Mo_{K\alpha}) = 1.57$ cm^{-1}. In the region surveyed (h 0/14, k −23/23, l −23/23; $3° < 2\theta < 60°$) 7313 measured reflections (ω scans; $J > 2\sigma(J)$), 6603 independent ($R_{merge} = 0.026$) Lp and absorption correction (empirical, six reflections ($9.7° \leq 2\theta \leq 36.6°$), ψ scans). Transmission factors: min 0.75, max 1.0 $Mo_{K\alpha}$ ($\lambda = 0.71069$ Å), graphite monochromator, AED-II Siemens-Stoe. The structure was solved by direct methods (SHELXTL program; residual electron density: max. 0.86, min. −0.77 e/Å^3; there are two independent molecules in the triclinic unit cell; $R = 0.037$, $R_w = 0.030$. Further details of the crystal structure investigation are available on request from the Fachinformationszentrum Energie, Physik, Mathematik GmbH, D-7514 Eggenstein Leopoldshafen 2 (FRG), on quoting the depository number CSD-52487, the names of the authors, and the journal citation.
[6] R. Appel, V. Barth, F. Knoll, I. Ruppert, *Angew. Chem.* 91 (1979) 936; *Angew. Chem. Int. Ed. Engl.* 18 (1979) 873; R. Appel, F. Knoll, I. Ruppert, *ibid.* 93 (1981) 771 and 20 (1981) 731.
[7] R. Appel, V. Barth, F. Knoch, *Chem. Ber.* 116 (1983) 938.

Stereoselective Synthesis of β-Amino Alcohols from Optically Active α-Amino Acids**

By *Manfred T. Reetz,* Mark W. Drewes,* and *Alfred Schmitz*

Optically active β-amino alcohols with two stereocenters not only occur as natural products[1] and are used as drugs,[2] but are also components of amino sugars[1] and of certain peptides and peptide analogues[3] which function as enzyme inhibitors. An attractive synthetic strategy con-

[*] Prof. Dr. M. T. Reetz, M. W. Drewes, A. Schmitz
Fachbereich Chemie der Universität
Hans-Meerwein-Strasse, D-3550 Marburg (FRG)

[**] This work was supported by the Fonds der Chemischen Industrie. *M.W.D.* thanks the Deutsche Akademische Austauschdienst and the Council for Scientific and Industrial Research for fellowship grants.

sists in the conversion of protected natural or unnatural α-amino acids into the α-amino aldehydes followed by stereoselective Grignard or aldol addition. The most frequently used protective group is *tert*-butoxycarbonyl (Boc), which, however, may lead to configurational lability at the stage of the aldehyde and only seldom allows a high degree of diastereoselectivity to be achieved.[4] The 9-phenyl-9-fluorenyl protective group guarantees configurational stability and thus the easy manipulation of the aldehyde, but Grignard and aldol additions afford only 1:1 and 1:3 mixtures, respectively.[5] We report here on a general solution of both problems using the benzyl protective group and suitable organometallic reagents.

When the natural L-amino acids **1** are allowed to react with benzyl bromide in the presence of K_2CO_3/NaOH, the *N,N*-dibenzylamino benzyl esters **2** are formed (67–73%),[6] which can be reduced to the >99% optically active alcohols **3** (69–75%).[7] Swern oxidation affords the aldehydes **4** (88–92%), which are configurationally stable at room temperature.[8]

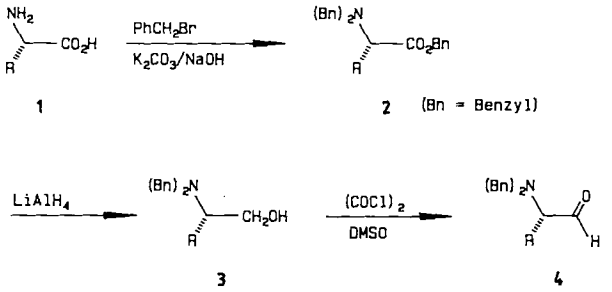

Surprisingly, Grignard and alkyllithium reagents react highly diastereoselectively with **4** with non-chelation control[9] to give the amino alcohols **6**[10] (Table 1). The degree of diastereoselectivity can even be further increased in some cases—by titanation of RMgX or RLi with $ClTi(OiPr)_3$ or $ClTi(NEt_2)_3$[11] (Entries 3, 12, 15, 20, 25, 27, 31, 34 in Table 1). In contrast, cuprates reduce the stereoselectivity (cf. Entry 10 in Table 1). Reversal of diastereoselectivity (cf. **5**) can be achieved with special Lewis acidic or chelating agents[9,11] of the type CH_3TiCl_3 or allyl-$SiMe_3/SnCl_4$ (Entries 9, 13, 21, 22, 28, 32, 35 in Table 1). Control experiments show that **5** and **6** are at least >99% enantiomerically pure, i.e. no racemization occurs during the reaction.[12] The protecting groups can be hydrogenolytically cleaved with H_2/Pd-black with formation of **7** and **8** (70–90%).[13]

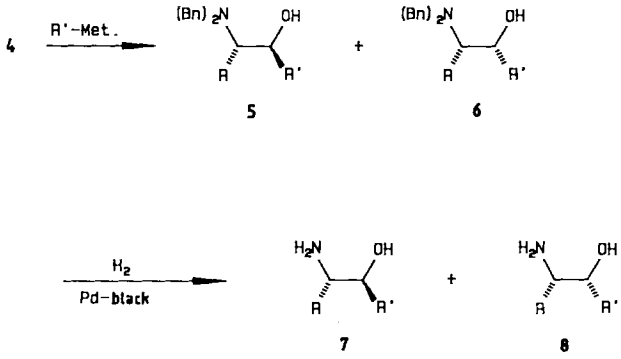

Why do RMgX, RLi, and R_2CuLi[14] show *no* chelation effects, even though amino groups are known to have excellent donor properties? Perhaps "tieing up" the molecules by these metals to give a five-membered ring chelate is prevented on steric grounds, the *Cornforth* or *Felkin-Anh* model therefore being relevant.[9] Chelation is only possible by use of very strong Lewis acidic reagents. Remarkable is the finding that aldehydes such as **9**, which contain sterically less-demanding protective groups, undergo chelate-controlled reaction even with $(CH_3)_2CuLi$, thereby leading preferentially to **10** instead of **11** (75–78% yield).

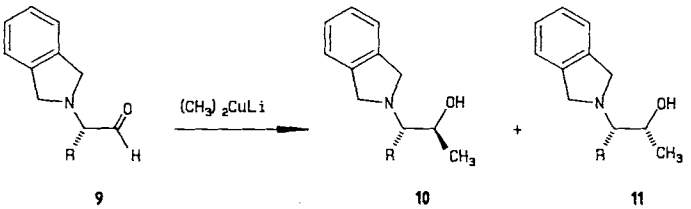

R = CH_3	90	:	10
R = CH_2Ph	95	:	5

The addition of lithium enolates to **4** takes place under non-chelation control without any racemization (cf. **13**)[10] (Table 2). Here again, reversal of diastereoselectivity (formation of **12**) is the more difficult task. In the presence of Lewis acids such as $TiCl_4$, enolsilanes add with chelation control, but the yield of aldol is low (Entry 3 in Table 2).

Table 1. Stereoselective Grignard and Grignard-like additions to α-amino-aldehydes **4** [a].

No.	R	Reagent	*T*/*t* [°C/h]	5+6 Yield [%]	5:6
1	CH_3	CH_3MgI	0/1	87	5: 95
2	CH_3	CH_3Li	−10/1	91	9: 91
3	CH_3	$CH_3Ti(OiPr)_3$	20/5	78	3: 97
4	CH_3	PhMgBr	0/1	85	3: 97
5	CH_3	EtMgBr	0/1	85	5: 95
6	CH_3	*i*PrMgBr	0/1	75	<3: >97
7	CH_3	*t*BuMgBr	0/1	72	5: 95
8	CH_3	*t*BuLi	−60/1	88	<3: >97
9	CH_3	CH_3TiCl_3	[b]/6	82	94: 6
10	CH_3	$(CH_3)_2CuLi$	−78/4	80	25: 75
11	CH_3	CH_3CeCl_2	[c]/2	70	10: 90
12	CH_3	$allylTi(NEt_2)_3$	−78/4	74	4: 96
13	CH_3	$allylSiMe_3/SnCl_4$	−78/2	85	84: 16
14	CH_2Ph	CH_3MgI	0/1	85	8: 92
15	CH_2Ph	$CH_3Ti(OiPr)_3$	20/5	89	7: 93
16	CH_2Ph	PhMgBr	0/1	84	3: 97
17	CH_2Ph	PhC≡CLi	−78/2	72	<4: >96
18	CH_2Ph	$PhCH_2CH_2MgBr$	−78/1	84	<4: >96
19	CH_2Ph	allylMgCl	−78/2	82	28: 72
20	CH_2Ph	$allylTi(NEt_2)_3$	−78/4	81	7: 93
21	CH_2Ph	$allylSiMe_3/SnCl_4$	−78/2	79	87: 13
22	CH_2Ph	CH_3TiCl_3	[b]/6	63	78: 22
23	*i*Bu	CH_3MgI	0/1	85	10: 90
24	*i*Bu	CH_3Li	−10/1	89	20: 80
25	*i*Bu	$CH_3Ti(OiPr)_3$	20/5	80	6: 94
26	*i*Bu	PhMgBr	0/1	84	3: 97
27	*i*Bu	$allylTi(NEt_2)_3$	−78/4	81	3: 97
28	*i*Bu	$allylSiMe_3/SnCl_4$	−78/4	78	90: 10
29	*i*Pr	CH_3MgI	0/1	87	5: 95
30	*i*Pr	CH_3Li	−10/1	81	14: 86
31	*i*Pr	$CH_3Ti(OiPr)_3$	20/5	77	3: 97
32	*i*Pr	CH_3TiCl_3	[b]/6	65	65: 35
33	*i*Pr	PhMgBr	0/1	69	9: 91
34	*i*Pr	$allylTi(NEt_2)_3$	−78/4	83	4: 96
35	*i*Pr	$allylSiMe_3/SnCl_4$	−78/2	79	95: 5

[a] No. 9, 13, 21, 22, 28, 32, 35: CH_2Cl_2 as solvents; No. 10–12, 19, 20, 27, 34: THF; all others: diethyl ether. [b] −78→−30 °C. [c] −78→−20 °C.

 © VCH Verlagsgesellschaft mbH, D-6940 Weinheim, 1987 0570-0833/87/1111-1142 $ 02.50/0 Angew. Chem. Int. Ed. Engl. 26 (1987) No. 11

The main product is formed by aldol condensation, i.e., under the reaction conditions water is eliminated.[15] Since the allyl residue represents a latent carbonyl unit,[16] the reaction of allyl$SiMe_3$/$SnCl_4$ provides a chelation-controlled aldol-analogous addition (Entries 13, 21, 28, 35 in Table 1).

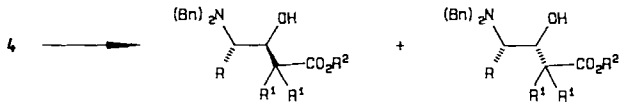

12 **13**

Table 2. Aldol additions to α-amino aldehydes **4**; conditions: −78 °C, 15 min, in THF.

No.	R	Enolate	Yield **12**+**13** [%]	**12**:**13**
1	CH_3	$H_2C{=}C(OCH_3)OLi$	82	5:95
2	CH_3	$(CH_3)_2C{=}C(OCH_3)OLi$	84	3:97
3 [a]	CH_3	$H_2C{=}C(OPh)OSiMe_3/TiCl_4$	25	95: 5
4	CH_2Ph	$H_2C{=}C(OCH_3)OLi$	83	10:90
5	*i*Bu	$H_2C{=}C(OEt)OLi$	74	7:93

[a] Conditions: −78→−40 °C, 3.5 h, in CH_2Cl_2.

Our results show that optically active *N,N*-dibenzylated α-amino aldehydes are readily accessible and that *optional* chelation or non-chelation-controlled Grignard and aldol additions free of racemization are possible for the first time. The potential of the natural L-amino acid chiral pool has thus been enlarged considerably.[17] Since many synthetic D-amino acids are also available, the mirror-image products are also accessible.

Experimental

Typical procedure for Grignard addition to **4**: the solution of (*S*)-α-(*N,N*-dibenzylamino)propionaldehyde **4**, R = CH_3, (1.0 g, 4 mmol) in ether (3 mL) was added dropwise under N_2 to a solution of methylmagnesium iodide (4.8 mmol) in ether (4 mL). After one hours' stirring the reaction mixture was hydrolyzed with 8 mL of saturated NH_4Cl solution; the organic phase was separated off and the aqueous phase was extracted with ether. The combined ether phases were washed with NaCl solution and dried over $MgSO_4$. After removal of ether the residue (**5**:**6** = 5:95 according to the ^{13}C-NMR spectrum) was purified by flash chromatography (silica gel/ethyl acetate, petroleum ether); yield 925 mg (87%) of pure (2*R*,3*S*)-3-(*N,N*-dibenzylamino)-2-butanol **6**, R = R′ = CH_3, white crystals of m.p. 76–77 °C.

Received: July 6, 1987;
supplemented: August 13, 1987 [Z 2329 IE]
German version: *Angew. Chem. 99* (1987) 1186

[1] K. Nakanishi, T. Goto, S. Ito, S. Natori, S. Nozoe: *Natural Products Chemistry, Vol. 3*, Oxford University Press, Oxford 1983; J. F. Kennedy, C. A. White: *Bioactive Carbohydrates*, Ellis Horwood, Chichester 1983.
[2] See, e.g. Chloramphenicol: *Merck Index*, 10th Edit., Merck and Co., Rahway, NJ (USA) 1983, p. 289.
[3] Cf. the hypertensive action of renin inhibitors: D. H. Rich, *J. Med. Chem. 28* (1985) 263.
[4] See, e.g.: M. W. Holladay, D. H. Rich, *Tetrahedron Lett. 24* (1983) 4401; G. H. Hanson, T. Lindberg, *J. Org. Chem. 50* (1985) 5399; B. Rague, J. A. Fehrentz, R. Geugan, Y. Chapleur, B. Castro, *Bull. Soc. Chim. Fr. 1983*, II 230; S. Danishefsky, S. Kobayashi, J. F. Kerwin, *J. Org. Chem. 47* (1982) 1983; P. W. K. Woo, *Tetrahedron Lett. 26* (1985) 2973; P. Garner, *J. Org. Chem. 51* (1986) 2609.
[5] W. D. Lubell, H. Rapoport, *J. Am. Chem. Soc. 109* (1987) 236.
[6] L. Velluz, G. Amiard, R. Heymes, *Bull. Soc. Chim. Fr. 1954*, 1012.
[7] All alcohols **3** were characterized ^1H- and ^{13}C-NMR spectroscopically and gave correct C, H analyses. The optical purity was determined by the Mosher method: esterification with (+)- and (−)-3,3,3-trifluoro-2-methoxy-2-phenylpropionic acid chloride and NMR spectroscopic investigation of the products. Cf. J. A. Dale, D. L. Dull, H. S. Mosher, *J. Org. Chem. 34* (1969) 2543.
[8] A. J. Mancuser, S. L. Huang, D. Swern, *J. Org. Chem. 43* (1978) 2480. The aldehydes **4** are obtained almost pure and are used without purification in further reactions with the organometallic reagents.
[9] Review of chelation- and non-chelation controlled additions to α- and β-alkoxycarbonyl compounds: M. T. Reetz, *Angew. Chem. 96* (1984) 542; *Angew. Chem. Int. Ed. Engl. 23* (1984) 556.
[10] All products gave correct C, H analyses. They were characterized ^1H- and ^{13}C-NMR spectroscopically. The assignment of the relative configuration was made by: a) conversion into known compounds, e.g. **6**, R = CH_3, R = Ph, in norephedrine; b) synthesis of comparison compounds, e.g. by stereospecific *trans*-ring opening of configurationally defined epoxides with dibenzylamine; or c) conversion of **7**/**8** or the deprotected forms of **12**/**13** into 2-oxazolidones, followed by NMR spectroscopic investigations. The chelation-controlled products **5** and **12** move more rapidly on the thin-layer chromatographic plate than the non-chelation-controlled products **6** and **13**.
[11] M. T. Reetz: *Organotitanium Reagents in Organic Synthesis*, Springer, Berlin 1986.
[12] **5**/**6** and **12**/**13** were each esterified according to the Mosher method (cf. [7]) and investigated NMR spectroscopically.
[13] B. El Amin, G. Anantharamaiah, G. Royer, G. Means, *J. Org. Chem. 44* (1979) 3442.
[14] G. H. Posner, C. E. Whitten, P. E. McFarland, *J. Am. Chem. Soc. 94* (1972) 5106; W. C. Still, J. A. Schneider, *Tetrahedron Lett. 21* (1980) 1035.
[15] α,β-Unsaturated esters with a chiral center at the allylic position are also interesting building blocks.
[16] R. W. Hoffmann, *Angew. Chem. 94* (1982) 569; *Angew. Chem. Int. Ed. Engl. 21* (1982) 555.
[17] J. Martens, *Top. Curr. Chem. 125* (1984) 165.

High Stereoselectivity in Lewis-Acid-Catalyzed and Uncatalyzed Diels-Alder Reactions of the Fumarate of (S)-Ethyl Lactate**

By *Horst Hartmann, Abdel Fattah Abdel Hady, Karina Sartor, John Weetman,* and *Günter Helmchen**

Dedicated to Professor Ulrich Schöllkopf on the occasion of his 60th birthday

Asymmetric Diels-Alder reactions with α,β-unsaturated esters of chiral alcohols have been the subject of numerous studies.[1] Whereas a wide variety of excellent results have been reported for Lewis-acid-catalyzed reactions, very little has so far been achieved for the uncatalyzed variant. We have now found a dienophile, namely the title compound **1**, which exhibits both high stereoselectivity and inverse stereoselectivity for both variants.

The acrylate **3** of (*S*)-ethyl lactate reacts diastereoselectively (80:20) with cyclopentadiene at 0 °C in hexane to give the *endo*-adduct.[2] Under the same conditions, the fumarate **1** yields the adducts **2a** and **2b** in the ratio

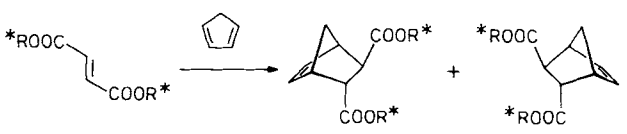

1 **2a** **2b**

[*] Prof. Dr. G. Helmchen, Dipl.-Chem. H. Hartmann, A. F. Abdel Hady M. Sc., K. Sartor, Dr. J. Weetman
Organisch-chemisches Institut der Universität
Im Neuenheimer Feld 270, D-6900 Heidelberg (FRG)

[**] This work was supported by the Deutsche Forschungsgemeinschaft and the Fonds der Chemischen Industrie.

95.5 : 4.5, clearly indicating a cooperative effect[3] of the auxiliary groups. At −54 °C (cf. Table 1) the ratio **2a : 2b** is even 98 : 2.[4] To explain these results we assume that **1** reacts as C_2 symmetric species **5** with *anti*-enoate conformation[5] (cf. Formula), for which attack from the sterically more accessible back face is favored.

For $TiCl_4$-catalyzed additions of the acrylate **3**, which yield preferred products of opposite configuration compared to the uncatalyzed reactions, the complex **4** with *syn*-enoate conformation is postulated as reactive species.[6] On extending this mechanistic model to the fumarate **1** one would expect the 1 : 1 complex **6** with *syn*- and *anti*-enoate conformation as reactive species, and therefore antagonistic action of the auxiliary groups, and/or the 2 : 1 complex **7** with *syn*-planar enoate conformation on both

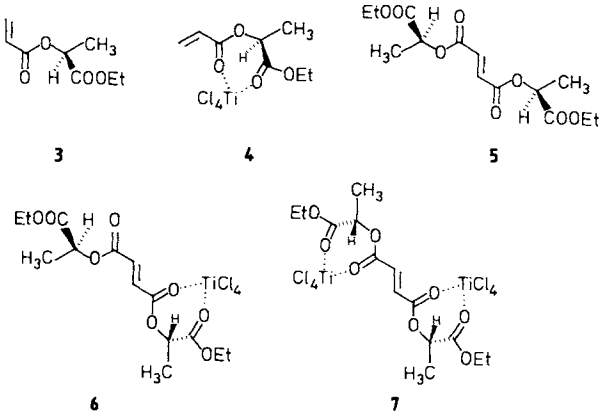

3 **4** **5**

6 **7**

R*−OH= (*S*)-ethyl lactate.

sides, and therefore synergistic action of the auxiliary groups. For differentiation of these complexes, **1** was allowed to react with cyclopentadiene using various $TiCl_4$: **1** ratios and the ratio **2a : 2b** was analyzed by HPLC. We interpret the results of this series of experiments (Fig. 1) as follows: at low $TiCl_4$: **1** ratios (A) **6** determines the course of reaction, hence the unselective reaction. In the range B, competition of the complex **7** becomes noticeable, which in range C finally dominates and gives the ester **2b** with 95 : 5 selectivity.

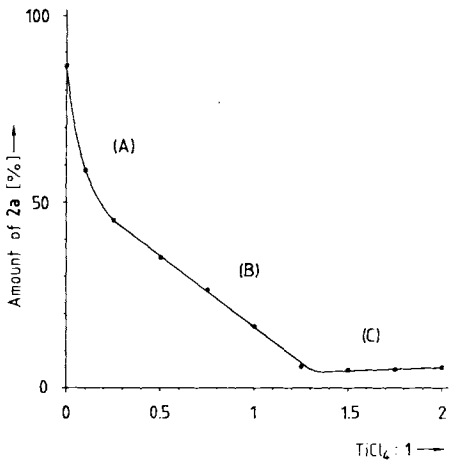

Fig. 1. Dependence of the diastereoselectivity (content of **2a** in product mixture) in the $TiCl_4$-catalyzed reaction of the fumarate **1** with cyclopentadiene on the molar ratio $TiCl_4$: **1** (solvent: CH_2Cl_2, $T = -40$ °C, concentration of 1 : 0.05 mol/L, ratio **1** : cyclopentadiene = 1 : 4).

Analogous results (Table 1) were obtained with cyclohexadiene, butadiene, and anthracene, although in uncatalyzed reactions these dienes require reaction temperatures above ca. 75 °C. Generally, high selectivity is achieved in the uncatalyzed reaction only with unpolar solvents, preferably hexane.[2] Increasing the pressure to 7 kbar allows the reaction temperature to be considerably lowered, leading to a significant increase in diastereoselectivity (Table 1).

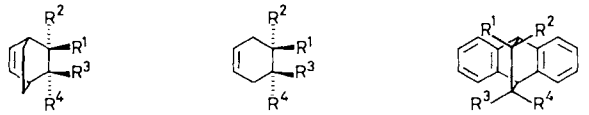

8 **9** **10**

R*−OH = (*S*)-ethyl lactate
a, $R^1 = R^4 = COOR^*$, $R^2 = R^3 = H$
b, $R^1 = R^4 = H$, $R^2 = R^3 = COOR^*$

Table 1. $TiCl_4$-catalyzed and uncatalyzed Diels-Alder reactions of the fumarate **1** to give the adducts **2** and **8–10** (in each case as diastereomers **a** and **b**) [a].

Diene (→ Product)	$TiCl_4$: **1**	T [°C]	Solvent	t	**a : b**	Yield [%]
Cyclopentadiene	—	−54	*n*-hexane/ CCl_4 6 : 4	23 h	98 : 2	99
→**2**	1.5 : 1	−40	CH_2Cl_2	18 h	5 : 95	99
Cyclohexadiene	[b] —	25	*n*-hexane	16 h	94.5 : 5.5	96 [c]
→**8**	—	77	CCl_4	48 h	90 : 10	96
	1.4 : 1	−24	CH_2Cl_2/ *n*-hexane 1 : 1	20 h	8 : 92	97
Butadiene	—	130	*n*-hexane	20 h	75 : 25	96
→**9**	1.4 : 1	−50	CH_2Cl_2	6 h	10 : 90	95
Anthracene	[b] —	70	xylene	0.7 h	92 : 8	62
→**10**	—	110 [d]	toluene	6 d	87 : 13	[e]
	2.0 : 1	0	CH_2Cl_2	6 d	34 : 66	[f]

[a] Reaction conditions: In the uncatalyzed reaction a solution of **1** (0.3 M) and diene in the given solvent was heated under reflux or in an autoclave at the given temperature until complete conversion was achieved (DC control). The molar ratio **1** : diene was 1 : 1.5 to 1 : 5. In the catalyzed variant a 1 M solution of $TiCl_4$ in CH_2Cl_2 was added at room temperature to a 0.05 M solution of **1** in CH_2Cl_2. 5 min later, at the given temperature, the diene was slowly added to the well stirred solution. The molar ratio of **1** : diene was 1 : 1.5 to 1 : 5. [b] Carried out in a high-pressure autoclave at 7 kbar. [c] Single recrystallization from *n*-hexane yielded diastereomerically pure **8a** in 84% yield. [d] At 140 °C the reaction was clearly reversible. [e] Diastereomerically pure **10a** was obtained in 50–60% yield by recrystallization from ethyl acetate/hexane. [f] Not determined.

Diels Alder reactions with the inexpensive fumarate **1** are of interest for preparative applications—e.g., the (2*S*,3*S*)-5-norbornene-2,3-dicarboxylic acid readily obtainable[4] from the adduct **2b** is a valuable starting material for the synthesis of prostaglandins.[7] It is advantageous for such applications that the diastereomeric adducts can generally be easily separated by liquid chromatography.[8] With **8** and **10**, in each case one of the diastereomers, **8a** and **10a**, respectively, is crystalline and can be obtained pure by recrystallization of the crude product.

Received: July 15, 1987;
revised: August 14, 1987 [Z 2360 IE]
German version: *Angew. Chem.* 99 (1987) 1188

[1] a) Review: G. Helmchen, R. Karge, J. Weetman in R. Scheffold (Ed.): *Modern Synthetic Methods 1986, Vol. 4*, Springer, Heidelberg 1986, p.

262; b) K. Furuta, K. Iwanaga, H. Yamamoto, *Tetahedron Lett. 27* (1986) 4507; c) H. Kunz, B. Müller, D. Schanzenbach, *Angew. Chem. 99* (1987) 269; *Angew. Chem. Int. Ed. Engl. 26* (1987) 267.
[2] T. Poll, G. Helmchen, B. Bauer, *Tetrahedron Lett. 25* (1984) 2191.
[3] L. M. Tolbert, M. B. Ali, *J. Am. Chem. Soc. 106* (1984) 3806.
[4] For the preparative utilization of the Diels-Alder adducts **2** and their analogues it is important to obtain enantiomerically pure secondary products with differentiated COOR groups. Both problems are solved by hydrolysis (LiOH in THF/water) to the dicarboxylic acid, preparation and recrystallization of the iodolactone, esterification or reduction of the COOH group, and reduction with zinc (cf. [1a]).
[5] The conformation of the chiral ester group was chosen on the basis of force-field calculations on **3**, which were carried out by Prof. *H.-J. Lindner*, Darmstadt.
[6] T. Poll, J. O. Metter, G. Helmchen, *Angew. Chem. 97* (1985) 116; *Angew. Chem. Int. Ed. Engl. 24* (1985) 112.
[7] J. S. Bindra in J. ApSimon (Ed.): *The Total Synthesis of Natural Products. Vol. 4.* Wiley-Interscience, New York 1981, p. 414.
[8] All the new compounds were characterized by elemental analysis and spectroscopic data. Diastereomers were separated by medium pressure liquid chromatography and separately characterized.

Estimation of the Configurational Stability of Chiral Organometallic Reagents**

By *Reinhard W. Hoffmann,* Joachim Lanz, Rainer Metternich, Gerhard Tarara,* and *Dieter Hoppe**

Dedicated to Professor Ulrich Schöllkopf on the occasion of his 60th birthday

Information about the degree of configurational stability of organometallic compounds is of great importance for their use in stereoselective synthesis. Thus, the configurational stability of, e.g., vinyllithium[1] and (α-alkoxyalkyl)lithium compounds is well documented.[2,3] The configurational stability is frequently investigated by using a second stereogenic center in the organometallic compound as a reference point and observing the occurrence or absence of an epimerization by way of the secondary products.[2] We wish to present here another simple method for this purpose involving reaction of the organometallic compound in its racemic form with a chiral aldehyde.—This aldehyde is reacted once in enantiomerically pure form and once as a racemate with the organometallic reagent. Reaction of the allenyltitanium compound **2**[4] with α-benzyloxypropionaldehyde **3** serves as example. The reagent **2** was generated by metalation of 3-methoxy-1,2-butadiene **1**[5] with *n*-butyllithium at −30 °C and titanation with titanium tetraisopropoxide at −78 °C. The solution of **2** was then allowed to react at −78 °C with one equivalent of the aldehyde **3** [*rac*- or (*S*)-(−)-**3** (α_D^{20} = 66.35° neat, l = 1 dm], whereupon a mixture of the diastereomeric adducts **4**–**7**[6] was obtained in 70–90% yield.[7] The product ratios were determined by gas chromatography.

The inference that the establishment of equilibrium between the enantiomers of **2** is slow compared to addition of **2** to **3**, is based on the fact that the product ratios in the two experiments are different. Furthermore, one can recognize that the numbers in Experiment **A** can be combined pairwise, so that, within the accuracy of the determination (± 1%), the ratio 50 : 50 results (50 + 1 and 35 + 14).

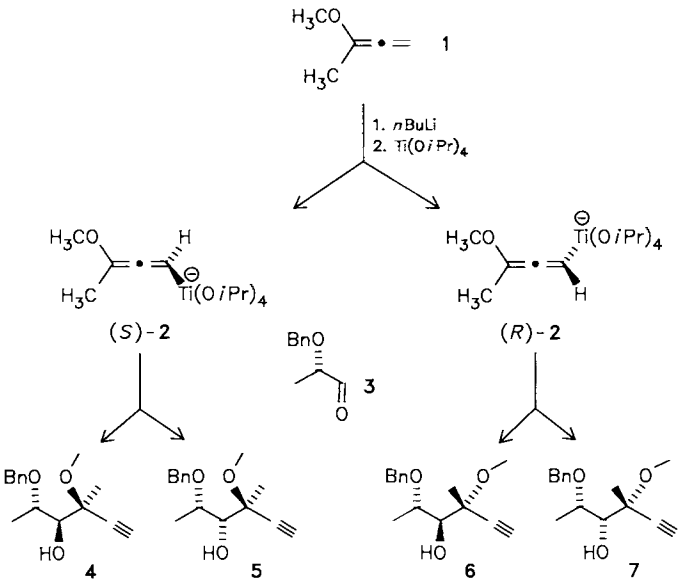

A	(*S*)-(−)-**3**:	**4**		**5**		**6**		**7**
		50	:	1	:	35	:	14
B	*rac*-**3**:	*rac*-**4**		*rac*-**5**		*rac*-**6**		*rac*-**7**
		92	:	< 1	:	6	:	2

This is based on the fact that (*S*)-**2** leads to the products **4** and **5**, while the enantiomer (*R*)-**2** leads to the products **6** and **7**. Since the two enantiomers of **2** are present in the ratio 50 : 50, this must, after complete reaction of **2**, also be true for the products **4**+**5** and **6**+**7**. Experiment **A** thus represents the limiting case in which the enantiomer-equilibrium (racemization) of **2** is very much slower than the addition to **3**.

However, the combinations (*R*)-**2** + (*S*)-**3** and (*S*)-**2** + (*S*)-**3** react at different rates, as can be seen from Experiment **B**: Here, in the reaction of the racemates eleven times more of the product **4** (+**5**) was formed (92%) than of the products **6**+**7** (8%) by mutual kinetic resolution.[8] The combinations (*S*)-**2** + (*S*)-**3** and (*R*)-**2** + (*R*)-**3** thus reacted considerably more rapidly than the *R*/*S* pairs.

Returning to the question of the configurational stability of **2**: In the other limiting case—the enantiomer-equilibration of **2** be rapid compared to its addition of **3**—as also in the case of an achiral organometallic compound, in Experiment **A** the same number ratios ought to result as in Experiment **B**[9], because due to rapid enantiomer-equilibration of **2** the faster, reacting enantiomer would be immediately re-formed, i.e. it makes no difference whether the reaction partner (aldehyde) is racemic or enantiomerically pure. In the third case—the enantiomer-equilibration of the reagent and its addition to the aldehyde proceeding at a similar rate—in Experiment **A** a product ratio 92 : 8 > [**4**+**5**] : [**6**+**7**] > 50 : 50 should result.[10]

This method should be generally applicable for checking the configurational stability of chiral organometallic reagents. The example described here is comparatively complicated because four diastereomeric products are formed. The reason for this is the low *syn*/*anti* selectivity of **2** with respect to the relative configuration of the two new stereocenters. If this type of diastereoselectivity of the reagent is high, one has practically only to deal with two diastereo-

[*] Prof. Dr. R. W. Hoffmann, Dipl.-Chem. J. Lanz, Dr. R. Metternich
Fachbereich Chemie der Universität
Hans-Meerwein-Strasse, D-3550 Marburg (FRG)
Prof. Dr. D. Hoppe, Dipl.-Chem. G. Tarara
Institut für Organische Chemie der Universität
Olshausenstrasse 40, D-2300 Kiel 1 (FRG)

[**] This work was supported by the Deutsche Forschungsgemeinschaft and the Fonds der Chemischen Industrie.

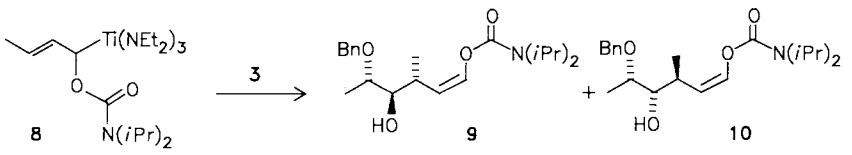

C	(*S*)-(−)-**3**:	53	:	47
D	*rac*-**3**:	68	:	32

meric products, which in the reaction of a configurationally stable racemic reagent with racemic aldehyde should be obtained as a mixture of two racemic diastereomers in a ratio ≠50:50, and with enantiomerically pure aldehyde[10] as a 50:50 pair of enantiomerically pure diastereomers. This was realized in the addition of the carbamoyltitanium compound **8**[3] to the aldehyde **3**. The product ratio **9**:**10** in Experiment **C** corresponds almost to the expected value of 50:50.

The enantiomers of **2**, probably allenylmetal compounds **11**, could equilibrate via a metallotropic shift[11] to give **12**. Such an isomerization is found in the case of the

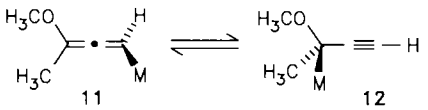

lithium compound corresponding to **2**, which added with low regioselectivity to aliphatic aldehydes.[4, 12] The configurational stability of **2** at −78 °C reported here indicates that titanation presumably not only shifts the equilibrium in favor of **2** but also raises the isomerization threshold.[3]

Received: June 19, 1987;
revised: August 21, 1987 [Z 2301 IE]
German version: *Angew. Chem. 99* (1987) 1196

[1] H. M. Walborsky, R. B. Banks, *Bull. Soc. Chim. Belg. 89* (1980) 849; E. Lattke, R. Knorr, *Chem. Ber. 114* (1981) 1600, and references cited therein.

[2] W. C. Still, C. Sreekumar, *J. Am. Chem. Soc. 102* (1980) 1201; J. S. Sawyer, T. L. Macdonald, G. J. McGarvey, *ibid. 106* (1984) 3376; V. J. Jephcote, A. J. Pratt, E. J. Thomas, *J. Chem. Soc. Chem. Commun. 1984*, 800; P. Lesimple, J.-M. Beau, P. Sinay, *ibid. 1985*, 894.

[3] Cf. also D. Hoppe, T. Krämer, *Angew. Chem. 98* (1986) 171; *Angew. Chem. Int. Ed. Engl. 25* (1986) 160; D. Hoppe, G. Tarara, M. Wilckens, P. G. Jones, D. Schmidt, J. J. Stezowski, *ibid. 99* (1987) 1079 and *26* (1987) 1034.

[4] Allenylmetal compounds can be in equilibrium with propargylmetal compounds (cf. **11** ⇌ **12**). The addition to aldehydes is assumed to proceed with allenyl (propargyl) inversion: K. Furuta, M. Ishiguro, R. Haruta, N. Ikeda, H. Yamamoto, *Bull. Chem. Soc. Jpn. 57* (1984) 2768. Since only products with an alkyne structure were obtained in the addition of **2** to the aldehyde **3**, we assume that the titanium compound possesses the allenic structure **2**.

[5] R. W. Hoffmann, R. Metternich, *Liebigs Ann. Chem. 1985*, 2390.

[6] The structures of **4** and **7** were confirmed by conversion into 2,6-dideoxy-3-*O*-methyl-3-methyl-L-hexoses: J. Lanz, *Dissertation*, Universität Marburg 1987.

[7] For the addition of other (alkoxyallenyl)metal compounds to aldehydes see: K. Mutsuoka, Y. Horiguchi, I. Kuwajima, *Tetrahedron Lett. 28* (1987) 1299; F. Mercier, R. Epsztein, S. Holand, *Bull. Soc. Chim. Fr. 1972*, 690.

[8] Cf. C. H. Heathcock, *Asymmetric Synth. 3* (1984) 199.

[9] In Experiment **B** a large deficiency of optically active aldehyde can also be used in place of the racemic aldehyde: cf. G. Schmid, W. Hofheinz, *J. Am. Chem. Soc. 105* (1983) 624.

[10] In the reaction with the optically active aldehyde it is important that at least one molar equivalent of the aldehyde is employed and that the organometallic reagent undergoes complete reaction.

[11] J. Klein in S. Patai (Ed.): *The Chemistry of the Carbon Carbon Triple Bond, Vol. 1*, Wiley, New York 1978, p. 343; R. W. Hoffmann, *Angew. Chem. 94* (1982) 569; *Angew. Chem. Int. Ed. Engl. 21* (1982) 555; cf. also the literature cited in K. K. Wang, S. S. Nikam, C. D. Ho, *J. Org. Chem. 48* (1983) 5376.

[12] R. Metternich, *Dissertation*, Universität Marburg 1985.

Isovalent and Mixed-Valent Ylide Complexes of Gold: The Synthesis of Trinuclear Compounds Having Double Paddlewheel Structure**

By *Hubert Schmidbaur,* Christoph Hartmann, Gabriele Reber,* and *Gerhard Müller*

Since their first synthesis,[1] gold complexes of phosphorus ylides have repeatedly been the subject of preparative, mechanistic, and theoretical studies,[2-5] because they are superbly suited as models for the investigation of the reactions of polynuclear coordination compounds. Of particular interest is the course of the oxidative additions to binuclear complexes of type **A**, since these reactions can lead to either isovalent Au^{II} compounds **B** having a Au–Au bond or mixed-valent Au^{I}–Au^{III} compounds **C**.[6-8] In favorable cases, reaction with XY may even lead to simultaneous formation of both isomers.

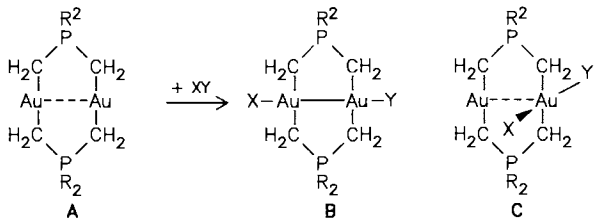

Herein we report on the reactions of **B** (R = phenyl; X = Y = halogen; ≙ **1**) with several phosphorus ylides R'_3PCH_2 ($R'_3 = Me_3$, Ph_3, and Ph_2Me), which result in the initial formation of mono- and disubstituted intermediates and which finally lead to the unexpected formation of novel, mixed-valent trinuclear complexes.

Reaction of the gold(II) complex **1b** with Ph_3PCH_2 in a 1:1 molar ratio affords **2b** as the main product. Likewise, reaction of the complex **1c** with Me_3PhCH_2[9] and with Ph_3PCH_2[10] affords **2a** and **2c**, respectively. The yellow, ionic products were obtained in high yields. Their structure was established by spectroscopic data as well as by

[*] Prof. Dr. H. Schmidbaur, Dipl.-Chem. C. Hartmann, Dipl.-Chem. G. Reber, Dr. G. Müller
Anorganisch-chemisches Institut der Technischen Universität München
Lichtenbergstrasse 4, D-8046 Garching (FRG)

[**] This work was supported by the Deutsche Forschungsgemeinschaft (Leibniz program), by the Fonds der Chemischen Industrie, and by Degussa AG.

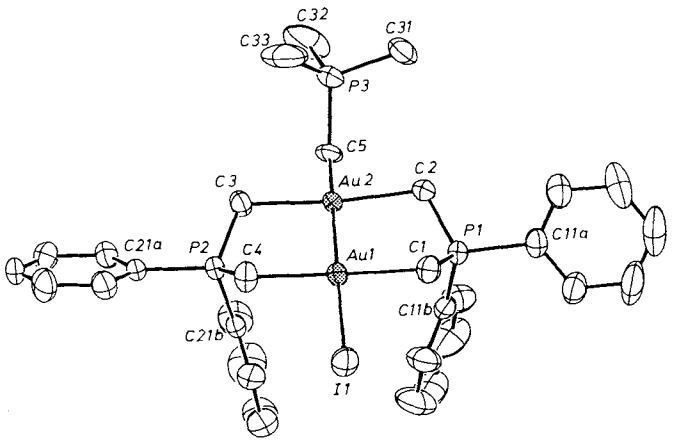

Fig. 1. Molecular structure of the cation of **2a** (ORTEP, thermal ellipsoids 50%, H atoms omitted). The eight-membered $Au_2C_4P_2$ heterocycle is in boat conformation with a nearly planar $C_2Au_2C_2$ moiety. The Ph_2P and PMe_3 groups point away from one another. Important distances [Å] and angles [°]: Au1-Au2 2.681(1), Au1-I1 2.822(1), Au1-C1 2.096(7), Au1-C4 2.100(7), Au2-C2 2.107(7), Au2-C3 2.106(7), Au2-C5 2.083(8); Au2-Au1-I1 172.4(1), C5-Au2-Au1 173.1(2), C1-Au1-C4 175.4(3), C2-Au2-C3 173.8(3) [11].

an X-ray structure analysis of **2a**.[11] Their diamagnetic character, the short Au–Au distance (Fig. 1), and the ^{197}Au Mössbauer spectrum[12] show unequivocally that the isovalent structure [$Au^{II}Au^{II}$] has been retained.

In contrast, reaction of **1c** with the ylides Me_3PCH_2, $MePh_2PCH_2$,[13] or Ph_3PCH_2 in a 1:2 molar ratio results in formation of the bright yellow, dicationic complexes **3a–c**, which have a $Au^{I}Au^{III}$ constitution, as shown, for example, by the Mössbauer spectra.[12] This result is in agreement with the finding that oxidative addition of CH_3I to **A** affords a product of type **B** (X = CH_3, Y = I), whereas attempts to carry out further alkylation with $LiCH_3$ afford only a mixed-valent isomer of type **C** (X = Y = CH_3).[1] Apparently, the strong *trans* influence of two alkyl groups on the Au–Au bond results in destabilization of this structural unit and induces disproportionation. The introduction of two onium charges—as in **3**—does not change this situation appreciably, and multiple fluorine substitution is necessary in order to generate dialkylated compounds of type **B**.[18]

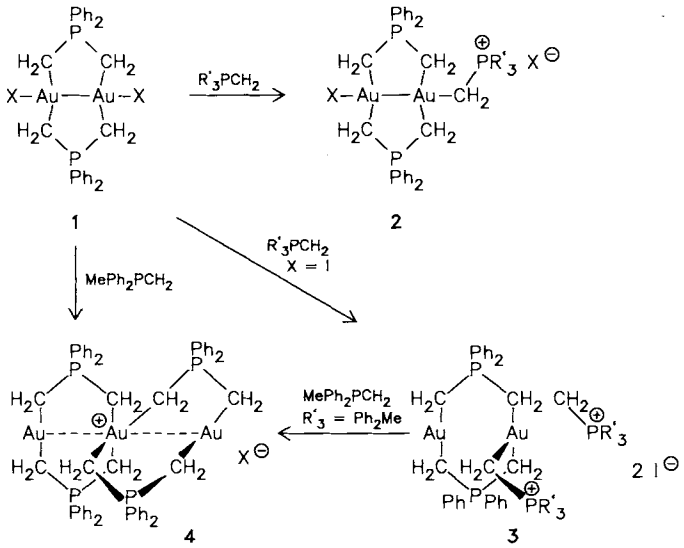

	X		X	R'_3		R'_3
1a, 4a	Cl	**2a**	I	Me_3	**3a**	Me_3
1b, 4b	Br	**2b**	Br	Ph_3	**3b**	Ph_2Me
1c, 4c	I	**2c**	I	Ph_3	**3c**	Ph_3

Reaction of **1a–c** and **3b** with excess $MePh_2PCH_2$ leads, regardless of the nature of the halogen, to formation of the colorless, air-stable salts **4a–c** and **4c**, respectively, each of which contains the same trinuclear complex cation. For this reason, the NMR spectra of the solutions are nearly identical. The electrical conductivity corresponds to that of a 1:1 electrolyte. The ^{197}Au Mössbauer spectrum of **4c** shows that gold is present in two oxidation states.[12] The very simple NMR spectra, which exhibit, for example, only a single ^{31}P resonance and only two $^{13}CH_2$ resonances of equal intensity, indicate that the cation complex has a highly symmetrical structure. Indeed, the X-ray structure analysis of **4c**[11] (which crystallizes with four molecules of dichloromethane) shows a spirocyclic arrangement of two diauradiphosphacycles of type **A**, which are oriented at 90° relative to each other, resulting in a double paddlewheel with a Au···Au···Au shaft (Fig. 2). The spiro atom is a Au^{III} center coordinated in a square-planar fashion, whereas the other two gold atoms are present as linear doubly coordinated Au^{I} centers. The cation has no symmetry in the crystal. Its eight-membered rings are both present in boat conformation, as has already been observed for various examples of **A** and **B**. Moreover, the Au···Au···Au unit is not linear (Au1-Au2-Au3 163.6(1)°). In solution, however, the effective symmetry presumably corresponds to the point group D_2 owing to the flexibility of the skeleton.

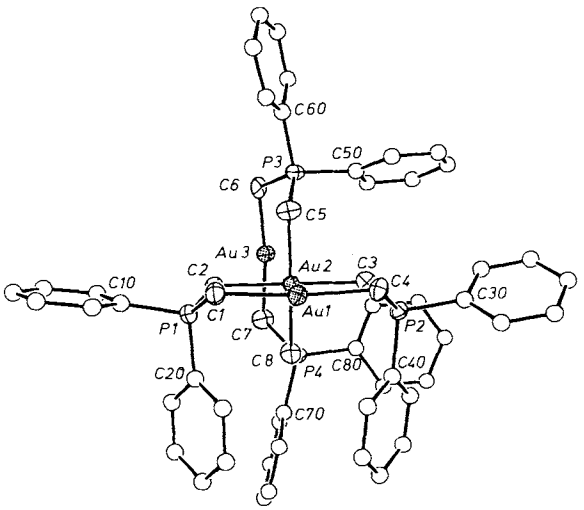

Fig. 2. Molecular structure of the cation of **4c** · $4CH_2Cl_2$ (ORTEP, phenyl C atoms with arbitrary radii). Two of the phosphorus centers (P1/P3) of the nearly perpendicularly oriented eight-membered rings point away from each other and the other two centers (P2/P4) point toward each other. Important distances [Å] and angles [°]: Au1-Au2 3.052(1), Au2-Au3 3.049(1), Au1-C1 2.10(2), Au1-C4 2.10(1), Au2-C2 2.12(1), Au2-C3 2.09(1), Au2-C5 2.13(1), Au2-C8 2.13(1), Au3-C6 2.09(1), Au3-C7 2.10(1); Au1-Au2-Au3 163.6(1), C1-Au1-C4 174.3(5), C2-Au2-C3 176.6(5), C5-Au2-C8 176.7(5), C6-Au3-C7 172.4(6) [11].

As side products of the reactions leading to **4**, ylide complexes of trivalent gold are formed, examples of which are already known:[2] [(ylide)$_2$AuX$_2$]X. Mass and redox balance, which require one Au^{III} equivalent for the transformation of two moles of **1** into one mole of **4**, is thereby

achieved. The structure of the side products, which may involve isomers, were not investigated further.

Experimental Procedure

Each type of complex is exemplified by one preparation.

2c: **1c** (220 mg, 0.21 mmol) was dissolved in THF (50 mL) and the resulting solution was treated at −35 °C with a solution of Ph_3PCH_2 (58 mg, 0.21 mmol) in the same solvent. After the reaction mixture had warmed to room temperature, the orange-yellow precipitate was filtered off, washed with diethyl ether, and dried under vacuum (yield 210 mg, 75%); m.p. = 174–177 °C (dec.), soluble in CH_2Cl_2, $CHCl_3/CH_3OH$; the solutions in $CHCl_3/CH_3OH$ are yellow at 20 °C, green at −30 °C.—^{31}P-NMR(CD_2Cl_2): δ = 44.5, 29.1 (each s, int. 2 : 1). ^{1}H-NMR (CD_2Cl_2): δ = 1.02, 1.76 (each virtual d, N = 10.99 and 9.89 Hz, ring CH_2), 3.18 (d, J = 11.4, CH_2PPh_3), 7.37–7.73 (m, Ph). ^{13}C-NMR (CD_2Cl_2): δ = 4.3, 4.5, 11.1 (all d, J = 51.3, 41.5, and 54.8 Hz, CH_2); 128.9, 130.4, 132.0, 133.5 (Ph_2); 121.7, 129.8, 133.8, 134.3 (Ph_3). ^{197}Au Mössbauer spectrum: *IS* 2.92 and 3.26 mm s^{-1}, *QS* 6.26 and 6.94 mm s^{-1} (4 K, int. 1 : 1).

2b: yield 81%, m.p. = 186–190 °C (dec.).

2a: yield 77%, m.p. = 170–173 °C (dec.) (see Fig. 1).

3a: **1c** (184 mg, 0.17 mmol) was dissolved in THF (50 mL) and the resulting solution was treated at −100 °C with a solution of Me_3PCH_2 (31 mg, 0.34 mmol) in THF. The color became lighter. At −90 °C, after further disappearance of the color, an almost colorless precipitate formed, which was filtered off, washed with ether, and recrystallized from CH_2Cl_2 (yield 146 mg (68%), m.p. = 166–174 °C (dec.), soluble in CH_2Cl_2, $CHCl_3$).—^{31}P-NMR ($CDCl_3$): δ = 26.9, 31.1 (each s, int. 1 : 1). ^{13}C-NMR ($CDCl_3$): δ = 11.34, 18.11, 18.82 (all "d," N = 56.2, 69.9 and 55.7 Hz, int. 1 : 1 : 1, CH_2); 14.65 (d, J = 54.8, CH_3); 129.0–134.6 (m, Ph). ^{1}H-NMR ($CDCl_3$): δ = 0.84, 1.34, 2.23 (all "d," N = 13.9, 12.9, and 14.6 Hz, CH_2); 1.95 (d, J = 13.3, CH_3); 7.2–8.1 (m, Ph). ^{197}Au Mössbauer spectrum: *IS* 3.59 and 3.69 mm s^{-1}, *QS* 6.49 and 9.40 mm s^{-1} (4 K, int.: 2 : 1).

3b: yield 82%, m.p. = 181–184 °C (dec.).

3c: yield 89%, m.p. = 173–176 °C (dec.).

4c: **1c** (464 mg, 0.432 mmol) was dissolved in THF (60 mL) and treated at −105 °C with a solution of $MePh_2PCH_2$ (643 mg, 3 mmol, large excess) in THF (5 mL). After the solution had warmed to room temperature, the colorless precipitate was filtered off, washed with ether, and dried under vacuum. Significant losses occurred upon recrystallization from CH_2Cl_2 (yield 165 mg (48%), m.p. = 195–197 °C (dec.), see Fig. 2)).—^{31}P-NMR ($CDCl_3$): δ = 31.4 (s). ^{13}C-NMR ($CDCl_3/CH_3OH$): δ = 7.45 and 11.37 ("d," N = 50.7 and 49.4 Hz, CH_2); 129.5, 132.1, 132.6, 133.1 (Ph). ^{1}H-NMR ($CDCl_3/CH_3OH$): δ = 1.26 and 1.33 (d, J = 12.2 and 12.7 Hz, CH_2); 7.36–7.57 (Ph). ^{197}Au Mössbauer spectrum: *IS* 3.43 and 3.79 mm s^{-1}, *QS* 5.61 and 9.67 mm s^{-1} (4 K; int. 1 : 1). Solutions in CH_2Cl_2 exhibit the electrical conductivity of a 1 : 1 electrolyte such as **2c**.

4b: decomposition temperature 198–204 °C.

4a: decomposition temperature 200–206 °C.

Satisfactory elemental analyses were obtained for all compounds.

Received: June 29, 1987 [Z 2317 IE]
German version: *Angew. Chem. 99* (1987) 1189

[1] H. Schmidbaur, R. Franke, *Angew. Chem. 85* (1973) 449; *Angew. Chem. Int. Ed. Engl. 12* (1973) 416; *Inorg. Chim. Acta 13* (1975) 84; H. Schmidbaur, *Inorg. Synth. 18* (1978) 136.

[2] H. Schmidbaur, *Angew. Chem. 95* (1983) 980; *Angew. Chem. Int. Ed. Engl. 22* (1983) 907; *Acc. Chem. Res. 8* (1975) 62; *Gmelin Handbook of Inorganic Chemistry, Organogold Compounds*, Springer, Berlin 1980; H. Schmidbaur, P. Jandik, *Inorg. Chim. Acta 74* (1983) 97; H. Schmidbaur, C. Hartmann, *Angew. Chem. 98* (1986) 573; *Angew. Chem. Int. Ed. Engl. 25* (1986) 575 (and references cited therein).

[3] Y. Yamamoto, Z. Kanda, *Bull. Chem. Soc. Jpn. 52* (1979) 2560; Y. Yamamoto, *Chem. Lett. 1980*, 311; W. Ludwig, W. Meyer, *Helv. Chim. Acta 65* (1982) 934; R. Uson, A. Laguna, M. Laguna, A. Uson, M. C. Gimeno, *Inorg. Chim. Acta 116* (1986) 91; R. Uson, A. Laguna, M. Laguna, A. Uson, *ibid. 73* (1983) 63.

[4] J. P. Fackler, *ACS Symp. Ser. 211* (1983) 201; J. P. Fackler, H. H. Murray, J. Basil, *Organometallics 3* (1984) 821; H. H. Murray, A. M. Mazany, J. P. Fackler, *ibid. 4* (1985) 154; H. H. Murray, J. P. Fackler, B. Trzcinska-Bancroft, *ibid. 4* (1985) 1633; J. P. Fackler, B. Trzcinska-Bancroft, *ibid. 4* (1985) 1891; H. H. Murray, J. P. Fackler, D. A. Tocher, *J. Chem. Soc. Chem. Commun. 1985*, 1278.

[5] Y. Jiang, S. Alvarez, R. Hoffmann, *Inorg. Chem. 24* (1985) 749.

[6] H. Schmidbaur, J. R. Mandl, W. Richter, V. Bejenke, A. Frank, G. Huttner, *Chem. Ber. 110* (1977) 2236; H. Schmidbaur, J. R. Mandl, A. Frank, G. Huttner, *ibid. 109* (1976) 466.

[7] H. Schmidbaur, P. Jandik, *Inorg. Chim. Acta 74* (1983) 97; P. Jandik, U. Schubert, H. Schmidbaur, *Angew. Chem. 94 (1982) 74; Angew. Chem. Int. Ed. Engl. 212* (1982) 73; *Angew. Chem. Suppl. 1982*, 1.

[8] D. S. Dudis, J. P. Fackler, *Inorg. Chem. 24* (1985) 3758; H. H. Murray, J. P. Fackler, L. C. Porter, A. M. Mazany, *J. Chem. Soc. Chem. Commun. 1986*, 321; H. H. Murray, J. P. Fackler, L. C. Porter, D. A. Briggs, M. A. Guerra, R. J. Lagow, *Inorg. Chem. 26* (1987) 357.

[9] H. Schmidbaur, W. Tronich, *Chem. Ber. 101* (1968) 595.

[10] H. Schmidbaur, H. Stühler, W. Vornberger, *Chem. Ber. 105* (1972) 1084.

[11] **2a**: Enraf-Nonius CAD4 diffractometer, $Mo_{K\alpha}$ radiation, λ = 0.71069 Å, graphite monochromator, T = 22 °C; triclinic, space group $P\bar{1}$, a = 10.563(1), b = 11.215(1), c = 15.132(2) Å, α = 93.55(1), β = 89.83(1), γ = 92.33(1)°, V = 1787.7 Å^3, Z = 2, ρ_{calcd} = 2.162 g cm^{-3}, $\mu(Mo_{K\alpha})$ = 100.3 cm^{-1}. 6988 unique reflections, 5659 "observed" with $I \geq 2.0\sigma(I)$ (+h, ±k, ±l, $(\sin\theta/\lambda)_{max}$ = 0.616). Lp and empirical absorption correction; solution by Patterson methods (SHELXS-86), $R(R_w)$ = 0.029(0.031), $w = 1/\sigma^2(F_0)$ for 352 refined parameters (SHELX-76). $\Delta\rho_{fin}$ = 0.82/−1.32 e/Å^3 at Au.—**4c** · 4 CH_2Cl_2: Syntex $P2_1$ diffractometer, T = −40 °C, monoclinic, space group $P2_1/c$, a = 10.160(1), b = 19.981(3), c = 35.540(5) Å, β = 98.48(1)°, V = 7136.0 Å^3, Z = 4, ρ_{calcd} = 1.778 g cm^{-3}, $\mu(Mo_{K\alpha})$ = 69.8 cm^{-1}. 10544 reflections, 8188 with $I \geq 2.0\sigma(I)$ (+h, +k, ±l, $(\sin\theta/\lambda)_{max}$ = 0.561). Patterson methods, $R(R_w)$ = 0.054 (0.056) for 493 refined parameters. $\Delta\rho_{fin}$ = 1.76/−2.09 e/Å^3 at the disordered CH_2Cl_2.—Further details of the crystal structure investigation may be obtained from the Fachinformationszentrum Energie, Physik, Mathematik GmbH, D-7514 Eggenstein-Leopoldshafen 2 (FRG), on quoting the depository number CSD-52624, the names of the authors, and the journal citation.

[12] H. Schmidbaur, C. Hartmann, F. E. Wagner, *Angew. Chem. 99* (1987) 1191; *Angew. Chem. Int. Ed. Engl. 26* (1987) 1148.

[13] H. Schmidbaur, M. Heimann, *Z. Naturforsch. B 29* (1974) 485.

The Recoil-Free Fraction of the γ Resonance in ^{197}Au Mössbauer Spectroscopy; Findings from Measurements of Polynuclear, Mixed-Valent Ylide Complexes**

By *Hubert Schmidbaur,* Christoph Hartmann,* and *Friedrich E. Wagner**

^{197}Au Mössbauer spectroscopy provides a useful method for elucidating the structure and bonding of gold compounds.[1] Progress in the interpretation of the spectra has resulted, in particular, from the availability of increasingly reliable correlations of the parameters for the isomeric shift *(IS)* and the quadrupole coupling *(QS)* with chemical characteristics such as the oxidation state and coordination number of gold as well as with the electronic influence of the ligands.[2–6] On the other hand, the interpretation of the absolute and relative intensities of the Mössbauer lines remains a problem, since—in contrast to NMR spectroscopy, for example—the intensities often do not agree with expectations based on stoichiometry. These discrepancies are ascribed to variations in the recoil-free fraction *(RFF)*[1,6] of the γ resonance, which depends on the "intermolecular" lattice vibrations as well as on the "intramolecular" vibrational motions of the gold atoms.[1,6,7]

Our investigations were prompted by the following observations:[8] The newly prepared trinuclear gold complex **1** exhibits two quadrupole doublets in its Mössbauer spec-

[*] Prof. Dr. F. E. Wagner
Physik-Department der Technischen Universität München
Lichtenbergstrasse 4, D-8046 Garching (FRG)
Prof. Dr. H. Schmidbaur, Dr. C. Hartmann
Anorganisch-chemisches Institut der Technischen Universität München
Lichtenbergstrasse 4, D-8046 Garching (FRG)

[**] This work was supported by the Deutsche Forschungsgemeinschaft (Leibniz Progam), the Fonds der Chemischen Industrie, and Degussa AG.

trum, each doublet being composed of two equal-intensity components (Fig. 1). In the binuclear complex **2**, in contrast, the components of the doublet appear in an intensity ratio of 1 : 2 (Fig. 2). Thus, there seems to be no relationship to the stoichiometry, an observation that resulted initially in the proposal of incorrect structures.

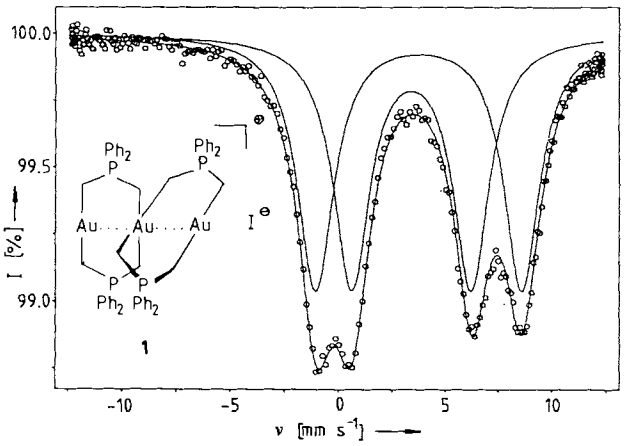

Fig. 1. ^{197}Au Mössbauer spectrum of the trigold compound **1** recorded at 4 K.

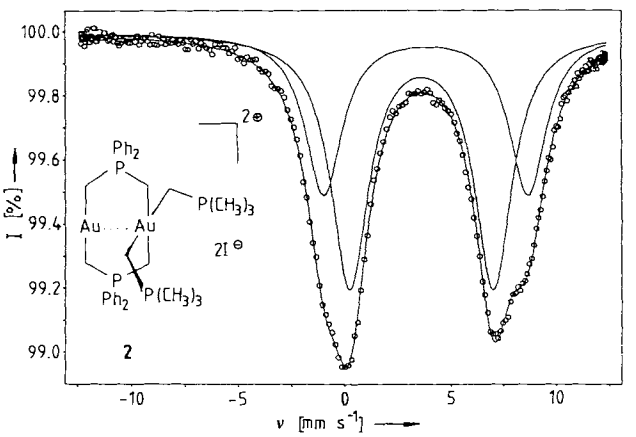

Fig. 2. ^{197}Au Mössbauer spectrum of the digold compound **2**.

Examination of the other measured values then showed that the ^{197}Au Mössbauer intensities are also strongly dependent on the oxidation state, and thus on the coordination number, since, at least for organogold compounds, an increase in the oxidation state is generally associated with an increase in the coordination number.[4]

This conclusion is established by a simple control experiment. The simultaneous measurement of exactly equimolar amounts of the crystalline reference compounds **3**[9] and **4**[10] affords a Mössbauer spectrum (Fig. 3) in which the components of the two doublets do not exhibit a 1 : 1 intensity ratio but rather a 1 : 1.25 ratio, the higher intensity being assigned to the gold(III) complex. With respect to the problem discussed above, this means that the *RFF* of the γ resonance of both **1** and **2** is larger for the Au^{III} centers than for the Au^{I} centers, so that the resonances of the Au^{I} centers are less intense. Otherwise, in the case of **1**, the Au^{I} resonance, which is assigned on the basis of the large *QS* value, should exhibit twice the intensity and, in the case of

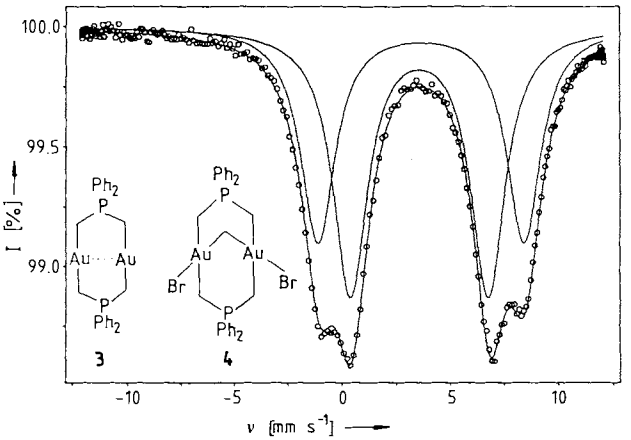

Fig. 3. ^{197}Au Mössbauer spectrum of a mixture of the digold compounds **3** and **4** in a molar ratio of 1 : 1.

2, it should exhibit the same intensity as the Au^{III} resonance.

In contrast, binuclear gold compounds in which the gold atoms are in similar (but not identical) environments, e.g., **5** and **6**,[11] give rise to two equal-area doublets (Fig. 4; the *IS* and *QS* values correspond to those of other di- and trivalent gold compounds[2-4]).

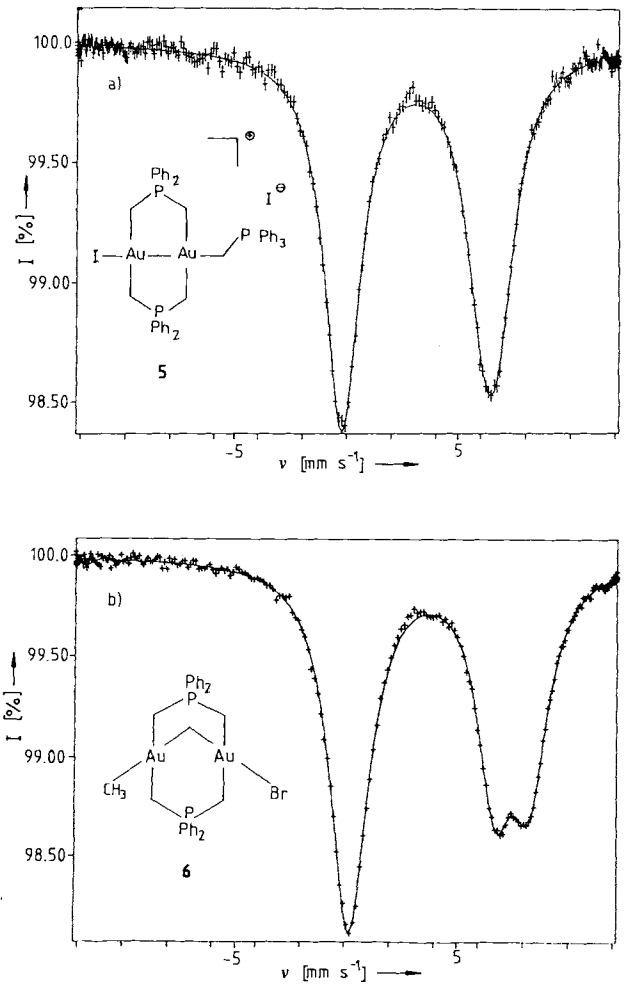

Fig. 4. ^{197}Au Mössbauer spectrum of the digold compounds a) **5** and b) **6**.

The significance of the new data for cations such as **1** and **2** lies in the fact that two gold atoms having different configurations are each present in a common structural unit. *RFF* values are usually broken down in a reasonable way into the aforementioned inter- and intramolecular components, provided that the solid is composed of larger individual structural units:[1]

$$f = f_L \cdot f_M$$

f_L and f_M are the Debye-Waller factors of the lattice and molecular effects, respectively.[1] In the mixed-valent gold compounds reported so far, Au^I and Au^{III} were present in separate species, for example in cation and anion, so that the two *RFF* terms for the individual units were not separable.[1] In the case of **1** and **2**, however, f_L can be assumed to be similar, to a good approximation, for each of the two types of gold atoms, particularly since **1** and **2** are loosely packed in the crystal without discrete interactions between the ions.[8] The dramatic increase in the *RFF* values of the gold atoms in the complexes under consideration on going to higher oxidation states/coordination numbers (C.N.) (Au^I/C.N. 2; Au^{III}/C.N. 4) is thus a direct consequence of the change in the immediate environment of the metal atoms and therefore of f_M.

These results clearly revealed that, in contrast to earlier assumptions,[12] f_L is not the dominant *RFF* term; instead, f_M is primarily responsible for determining the relative intensities of the Mössbauer lines.

The vibrational motions of simple organogold compounds have been the subject of numerous investigations.[12] Normal mode analyses show how the energies and amplitudes of the fundamental vibrations change on going from the one-dimensional (linear) to the two-dimensional (square) coordination. These changes differ particularly in their strong anisotropy from those observed on going to a tetrahedral or a pseudo trigonal-bipyramidal coordination. The situation in ylide complexes is complicated further in that the neighboring gold atoms appreciably approach each other perpendicular to the C-Au-C axis to within distances of under 3.00 Å,[4] resulting in a further increase in the effective coordination number at each gold atom. Although these interactions, indicated by dotted lines in the formulas, are weaker than normal coordinative bonds, they are sufficient, for example, to influence the conformations of complexes and their packing in the crystal.[4, 5] This phenomenon, which is the result of a relativistic effect,[13] presumably also affects the recoil behavior and thus enters into the *RFF* values.

These components are no longer present for **4** owing to the Au-CH_2-Au linkage, so that it is not surprising that the intensity ratio for **4/3** is smaller (Fig. 3) than for **1** or **2** (internal in each case).

It is noteworthy that the ellipsoids of thermal vibration of the gold atoms in **1**, determined by X-ray analysis, also directly reveal the stronger motion of the two Au^I atoms. Obviously, however, a quantitative evaluation is not possible.[9]

Overall, the data show that, in the case of **1** and **2**, the coordinative bonding of the gold atom in a square array of ligands with secondary bonding to further gold atoms causes the *RFF* parameter f_M to increase strongly and thereby results in considerable shifts in the intensities of the Mössbauer lines. Owing to the special geometries of **1** and **2**, these shifts are much larger than analogous effects in other complexes.

In one of the few reported studies in this area, the Debye-Waller factors f_{Au} were correlated with the molecular weight; however, satisfactory results were obtained for only some of the compounds studied.[1, 12] Apparently, the contribution of coordination number and coordination geometry[12] discussed above is still considerably underestimated.

Received: June 29, 1987 [Z 2318 IE]
German version: *Angew. Chem. 99* (1987) 1191

[1] R. V. Parish in G. J. Long (Ed.): *Mössbauer Spectroscopy Applied to Inorganic Chemistry*, Plenum, New York 1984, Chap. 17.
[2] H. Schmidbaur, J. R. Mandl, F. E. Wagner, D. F. van de Vondel, G.P. van der Kelen, *J. Chem. Soc. Chem. Commun. 1976*, 170.
[3] R. V. Parish, *Gold Bull. 15* (1982) 51; M. Melnik, R. V. Parish, *Coord. Chem. Rev. 70* (1986) 157.
[4] H. Schmidbaur in *Gmelin Handbook of Inorganic Chemistry, Organogold Compounds*, Springer, Berlin 1980.
[5] R. J. Puddephatt: *The Chemistry of Gold*, Elsevier, Amsterdam 1980.
[6] N. G. Greenwood, T. C. Gibb: *Mössbauer Spectroscopy*, Chapman and Hall, London 1971, p. 9ff.
[7] A. J. Rein, R. H. Herber, *J. Chem. Phys. 63* (1975) 1021; and earlier references cited therein.
[8] H. Schmidbaur, C. Hartmann, G. Reber, G. Müller, *Angew. Chem. 99* (1987) 1189; *Angew. Chem. Int. Ed. Engl. 26* (1987) 1146.
[9] J. D. Basil, H. H. Murray, J. P. Fackler, J. Tocher, A. M. Mazany, B. Trzcinska-Bancroft, H. Knachel, D. Dusis, T. J. Delord, D. O. Marler, *J. Am. Chem. Soc. 107* (1985) 6908.
[10] P. Jandik, U. Schubert, H. Schmidbaur, *Angew. Chem. 94* (1982) 73; *Angew. Chem. Int. Ed. Engl. 21* (1982) 73; *Angew. Chem. Suppl. 1982*, 1.
[11] H. Schmidbaur, C. Hartmann, J. Riede, B. Huber, G. Müller, *Organometallics 5* (1986) 1652.
[12] T. P. A. Viegers, J. M. Trooster, P. Bouten, T. P. Rit, *J. Chem. Soc. Dalton Trans. 1977*, 2074.
[13] P. Pyykkö, J. P. Desclaux, *Acc. Chem. Res. 12* (1979) 276.

Conformational Transitions between Enantiomeric 3_{10}-Helices

By *Rolf-Peter Hummel, Claudio Toniolo,* and *Günther Jung**

Dedicated to Professor Manfred Rothe on the occasion of his 60th birthday

In the following we report on the ^{13}C-NMR study of an enantiotopomerization of 3_{10}-helices. This conformational change of a peptide, which occurs rapidly at room temperature, has been detected by us on a decapeptide consisting of α-aminoisobutyric acid (Aib), $Me_2C(NH_2)CO_2H$ residues. Our results are of relevance for those engaged in conformational energy calculations, molecular modeling, or the dynamics of peptides or who, for example, wish to use enzyme-resistant, nontoxic α-amino acid residues such as Aib in drug design.

In proteins 3_{10}-helices are found rarely and usually as short segments at the end of α-helices.[1] On the other hand, partial sequences of the peptaibol antibiotics[2] from tri- to octapeptides containing L-amino acids and a large amount of α,α-dialkylated, achiral Aib residues strongly prefer the *right*-handed 3^r_{10}-helical conformation.[2a, 3a-e] When the *N*-terminal -X-Aib sequence is in the type-II β-bend conformation, the adjacent segment of the peptide

[*] Prof. Dr. G. Jung, Dipl.-Chem. R.-P. Hummel
Institut für Organische Chemie der Universität
Auf der Morgenstelle 18, D-7400 Tübingen (FRG)
Prof. Dr. C. Toniolo
Centro di Studi sui Biopolymeri, CNR
Dipartimento di Chimica Organica, Università di Padova
Via Marzolo 1, I-35131 Padova (Italy)

 © VCH Verlagsgesellschaft mbH, D-6940 Weinheim, 1987

chain is forced to adopt the *left*-handed 3^{l}_{10}-helix even if it is formed partially by L-residues.[3a,d] The protected achiral -(Aib)$_n$- (n = 5, 8) homopeptides[3b,c,d] and poly(Aib)$_n$[3f] form enantiomeric 3_{10}-helices in the crystal (Fig. 1).

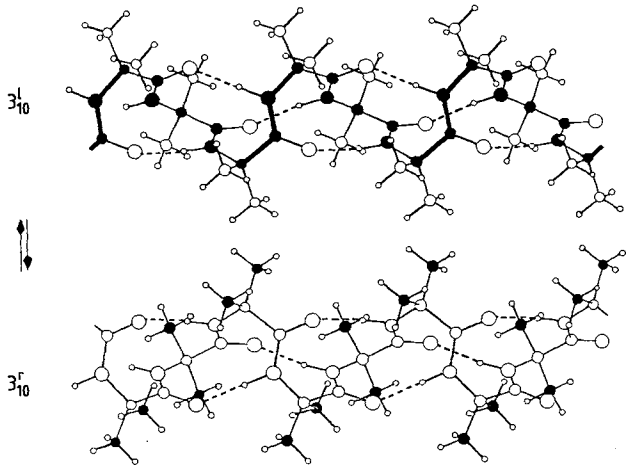

Fig. 1. Enantiomeric homopeptide 3_{10}-helices of Aib residues. In the 3^{l}_{10}-helix the backbone and in the 3^{r}_{10}-helix the α,α-dimethyl groups are emphasized (after [3f]).

In contrast to the short Aib peptides, the icosapeptide antibiotic alamethicin[4a] and three Aib-rich oligopeptides containing from nine to eleven residues[3a,4b,c] adopt mainly α-helical conformations. Solution studies revealed that the α-helical conformation[4b] is manifested at a chain length of about eight amino acids and is stabilized by Aib residues. In α-helices of comparable chain length this stabilizing effect is proportional to the Aib content (from 30 to 50%).[5] Thus, alamethicin and long model compounds possess α-helices of remarkable solvent and temperature stability,[6] which constitute the rigid macrodipole of peptaibols for voltage-dependent, ion-channel formation in membranes.[7] Obviously, at very high Aib content (more than 50%) and in particular in peptides with (Aib)$_n$ (n > 2) insertions, the helix-stabilizing effect is shifted in favor of the narrower 3_{10}-helix.

In a 3_{10}-helix the dipole vectors of the peptide bonds are not parallel to the helix axis and the 4→1 hydrogen bonds are not linear. The side chains of the amino acids are staggered in energetically unfavorable positions along the edges of the three-faced prism (Fig. 1). One of the diastereotopic, geminal Aib methyl groups is almost staggered with respect to the Aib CO group of the following peptide bond in contrast to the eclipsed position of the *pro-R* methyl group in the α-conformation (Fig. 2).[8]

On the NMR time scale conformationally stable, enantiomeric homopeptide 3_{10}-helices ($\Delta G^{\neq} \geqq 92$ kJ mol^{-1})[9] should exhibit a diastereotopic splitting of α-methyl signals,[8] because each methyl group is in a different chiral environment along the helix. Diastereotopicity should also be observable in samples of equal amounts of 3^{l}_{10}- and 3^{r}_{10}-helices, i.e., in a racemate that cannot be studied by chiroptical methods. In view of the strong steric restriction of Aib residues compared with protein amino acids, the question arises whether 3_{10}-helix⇄coil transitions can occur at all, or whether a $3^{l}_{10} \rightleftarrows 3^{r}_{10}$-helix interconversion (enantiotopomerization) occurs without intermediate states.

For the first time we have been able to prove a $3^{r}_{10} \rightleftarrows 3^{l}_{10}$ helix interconversion in the decapeptide **12** via temperature-dependent ^{13}C-NMR measurements between 200 and 300 K in dichloromethane (Fig. 3). At room temperature the conformationally uniform homopeptides **10**–**14**[10] show a sharp Aib-C$_\beta$ signal which broadens to $\Delta = 0.9$ ppm at maximum with increasing chain length (Fig. 2). Thus, the peak resulting from the 20 C$_\beta$ atoms of **12** exhibits a half-height width of only 0.7 ppm (Fig. 2). Its position at $\delta = 25.1$ is exactly halfway between the mean α-helical values of 26.8 and 23.2 ppm known for *pro-R*- and *pro-S*-C$_\beta$, respectively.[5,8]

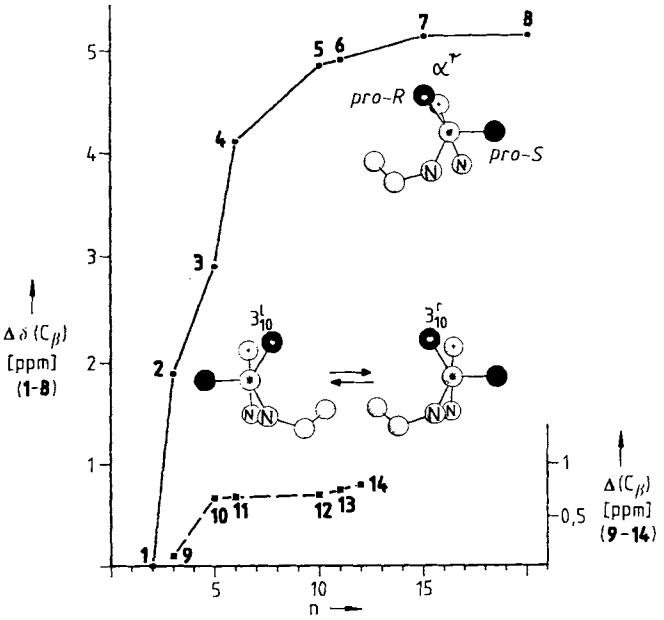

Fig. 2. Magnetic nonequivalence (Δδ) of the diastereotopic Aib C$_\beta$ atoms as a function of the main chain length in the ^{13}C-NMR spectra of the heteropeptides **1**–**8** with alternatingly positioned Aib residues between L-Ala or D-isovaline (Iva). **1**, Boc-Ala-Aib-OMe; **2**, Boc-Ala-Aib-Ala-OMe [8b]; **3**, Boc-Ala-Aib-Ala-Aib-Ala-OMe; **4**, Z-Iva-Ala-Aib-Ala-Aib-Ala-OMe; **5**, Boc-(L-Ala-Aib-Ala-Aib-Ala)$_2$-OMe; **6**, Boc-L-Ala-Aib-Ala-Aib-Ala-D-Iva-Ala-Aib-Ala-Aib-Ala-OMe; **7**, Boc-(L-Ala-Aib-Ala-Aib-Ala)$_3$OMe; **8**, Boc-(L-Ala-Aib-Ala-Aib-Ala)$_4$-OMe [5, 6a]. For comparison, the half-height widths Δ of the Aib C$_\beta$ signals of the homopeptides **9**–**14**, Z-(Aib)$_n$-OrBu (n = 3, 5, 6, 10–12) [70 mg/0.6 mL $CDCl_3/CD_3OD$ (1:1), 27 °C, 100.6 MHz, Bruker WM 400] are given. The inserts show a comparision of the positions of the methyl groups of an Aib residue (* = C$_\alpha$, + = carbonyl O) with respect to the carbonyl group of the following peptide bond.

Upon cooling of the decapeptide solution to 203 K, *two* distinct enantiomeric signal groups at $\delta = 26.7$ and 21.4 originate out of the 20 prochiral C$_\beta$ atoms of each enantiomeric 3_{10}-helix (Fig. 3), as found for the α^r-helices of alamethicin[8a,c] as well as **5**, **7** and **8**.[5] A marked increase in Δδ was seen with decreasing temperature and a maximum value of 5.3 ppm was measured at 203 K (Fig. 3). This finding agrees well with that for α-helical structures at room temperature with increasing chain length (Fig. 2).

At this point one could raise the question whether the decapeptide, known to fold into the 3_{10}-helical conformation in the *solid* state,[10] could eventually adopt the α-conformation in solution at very low temperature. Indeed $\alpha \rightleftarrows 3_{10}$ helix interconversions of alamethicin have been discussed in the context of the potential-dependent channel formation. However, besides vibrational data, several NMR spectroscopic results do not support the contention that Aib homopeptides form α-helices in *solution*. The strongly diverging T_1 relaxation time differences of gemi-

nal Aib C_β atoms between α-helical alamethicin ($\Delta T_1 = 250$–290 ms, 298 K)[8c] and **12** ($\Delta T_1 = 51$ ms, 240 K) at comparable $\Delta\delta$ values (4.5 and 4.6 ppm, respectively) are strongly in favor of the 3_{10}-helix for **12**. The exact evaluation would require additional α-helical T_1 data at 240 K. The energy barrier of the 3_{10}-helix interconversion of **12** at $T_c = 265$ K (Fig. 3) could be estimated rather accurately by the coalescence method.[9] The free energy of activation is $\Delta G^{\neq} = 46$ kJ mol^{-1}, i.e., 4.6 kJ mol^{-1} per Aib residue. This value is much lower than the mean values determined for α-helices.

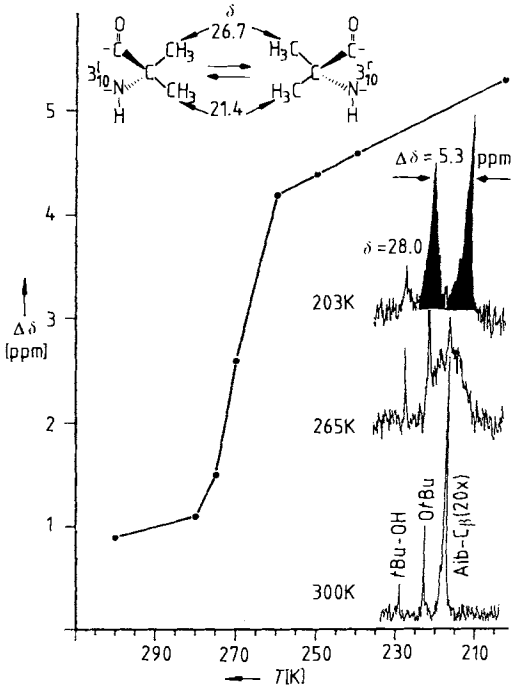

Fig. 3. Temperature dependence of the ^{13}C-NMR of **12** [70 mg/0.5 mL CD_2Cl_2; internal standards CD_2Cl_2 ($\delta = 53.8$) and *tert*-butyl alcohol (*t*Bu-OH) ($\delta = 30.0$) at room temperature; 50 MHz, Bruker MSL 200]. In the insert, spectrum in the region of the Aib-C_β signals at three temperatures: $T = 203$ K, $\delta = 21.4$, 26.7, $\Delta\delta = 5.3$ ppm, frozen 3_{10}-helix interconversion; $T_c(T_m) = 265$ K, broad coalescence signal (from which $\Delta G^{\neq} = 46$ kJ mol^{-1} is derived); $T = 300$ K, single Aib-C_β signal at $\delta = 25.1$ due to fast $3^l_{10} \rightleftarrows 3^r_{10}$ helix interconversion. The sharp signal at $\delta = 28.0$ corresponds to the methyl groups of the *tert*-butyl ester protecting group (O*t*Bu).

A corollary comparison between results from high-resolution and solid-state ^{13}C-NMR spectroscopy (CPMAS) gave further support to our interpretation. The effect of freezing the $3^l_{10} \rightleftarrows 3^r_{10}$ interconversion at very low temperature was found to be comparable to that of shorter Aib homopeptides in the solid state such as Z-(Aib)$_3$-OH ($\Delta\delta = 2.5$ ppm) and Z-(Aib)$_6$-OtBu (4.0 ppm). On the other hand, the Aib residues between the protein amino acid residues in the conformationally more stable α-helices show $\Delta\delta$ values of 3–5 ppm already *in solution at room temperature* (Fig. 2).

The 3_{10}-helix interconversion can be described as a fast monomolecular all-or-nothing process between enantiomeric P- and M-helical forms. A decision cannot be made so far whether measurable amounts of other conformations exist at and above the melting temperature T_m ($= T_c$). Our findings may be of relevance for short 3_{10}-helical segments of peptaibols particularly rich in Aib, e.g., trichotoxin,[11] which could be conformationally labile at room temperature. Inter alia, this could be one reason for the burstlike pore formation of trichotoxin in current/voltage experiments in lipid bilayer membranes,[11] in contrast to the stabile pore system of the α-helical and rigid alamethicin.[7] In addition, the surprising experimental results for this 3_{10}-helix enantiotopomerization, which indicate, e.g., 1200 interconversions per second at room temperature for **12**, appear to be of particular interest for conformational energy calculations.

Received: April 24, 1987 [Z 2220 IE]
German version: *Angew. Chem. 97* (1987) 1180

[1] J. S. Richardson, *Adv. Protein Chem. 34* (1981) 167.
[2] a) E. Benedetti, A. Bavoso, B. Di Blasio, V. Pavone, C. Pedone, C. Toniolo, G. M. Bonora, *Proc. Natl. Acad. Sci. USA 79* (1982) 7951; b) H. Brückner, H. Graf, *Experientia 39* (1983) 528.
[3] a) R. Bosch, G. Jung, H. Schmitt, G. M. Sheldrick, W. Winter, *Angew. Chem. 96* (1984) 440; *Angew. Chem. Int. Ed. Engl. 23* (1984) 450, and references cited therein; b) C. Toniolo, G. M. Bonora, A. Bavoso, E. Benedetti, B. Di Blasio, V. Pavone, C. Pedone, *Biopolymers 22* (1983) 205; c) A. Bavoso, E. Benedetti, B. Di Blasio, V. Pavone, C. Pedone, C. Toniolo, G. M. Bonora, *Proc. Natl. Acad. Sci. USA 83* (1986) 1988; d) B. V. Venkataram Prasad, P. Balaram, *CRC Crit. Rev. Biochem. 16* (1984) 307; e) M. Kokkonidis, D. Tsernoglóu, H. Brückner, *Biochem. Biophys. Res. Commun. 136* (1986) 870; f) B. R. Malcolm, M. D. Walkinshaw, *Biopolymers 25* (1986) 607.
[4] a) R. D. Fox, Jr., F. M. Richards, *Nature (London) 300* (1982) 325; b) R. Bosch, G. Jung, H. Schmitt, W. Winter, *Biopolymers 24* (1985) 961, 979; c) I. L. Karle, M. Sukumar, P. Balaram, *Proc. Natl. Acad. Sci. USA 83* (1986) 9284.
[5] G. Jung, R. Bosch, E. Katz, H. Schmitt, K.-P. Voges, W. Winter, *Biopolymers 22* (1983) 241.
[6] a) K.-P. Voges, G. Jung, W. H. Sawyer, *Biochim. Biophys. Acta 896* (1987) 64; b) G. Jung, N. Dubischar, D. Leibfritz, *Eur. J. Biochem. 54* (1975) 395; c) G. Esposito, J. A. Carver, J. Boyd, I. D. Campbell, *Biochemistry 26* (1987) 1043.
[7] a) G. Boheim, W. Hanke, G. Jung, *Biophys. Struct. Mech. 9* (1983) 181; b) G. Menestrina, K.-P. Voges, G. Jung, G. Boheim, *J. Membr. Biol. 93* (1986) 111.
[8] a) H. Schmitt, G. Jung, *Liebigs Ann. Chem. 1985*, 345; b) R. Bosch, G. Jung, K.-P. Voges, W. Winter, *ibid. 1984*, 1117; c) G. Jung, H. Schmitt in U. Ragnarsson (Ed.), *Peptides 1984*, Almquist & Wiksell, Uppsala 1984, S. 569; d) the chiral 2-trideuteriomethylalanine (*R*)-[D_3]Aib, which is particularly suitable for NMR studies, has been synthesized by *T. Weihrauch* and *D. Leibfritz* (*Liebigs Ann. Chem. 1985*, 1917), but not yet introduced into peptides.
[9] a) H. Kessler, *Angew. Chem. 82* (1970) 237; *Angew. Chem. Int. Ed. Engl. 9* (1970) 219; b) G. Binsch, H. Kessler, *ibid. 92* (1980) 445 and *19* (1980) 411.
[10] C. Toniolo, G. M. Bonora, V. Barone, A. Bavoso, E. Benedetti, B. Di Blasio, G. Grimaldi, F. Lelj, V. Pavone, C. Pedone, *Macromolecules 18* (1985) 895.
[11] W. Hanke, C. Methfessel, H.-U. Wilmsen, E. Katz, G. Jung, G. Boheim, *Biochim. Biophys. Acta 727* (1983) 108.

A Novel Route to Cyclopentane Derivatives: A Radical Chain Reaction**

By *Klaus Weinges** and *Wolfgang Sipos*

Dedicated to Professor Hermann Schildknecht on the occasion of his 65th birthday

Dienes whose double bonds exhibit variable reactivity because of substituent effects can undergo an intramolecular cyclization when subjected to solvomercuration and subsequent reduction with complex boron or tin hydrides.[1-3] We have now found that a mixture of the cyclopentane derivatives *cis*-**4a** and *trans*-**4a** in the ratio 8 : 2 is

[*] Prof. Dr. K. Weinges, Dipl.-Chem. W. Sipos
Organisch-chemisches Institut der Universität
Im Neuenheimer Feld 270, D-6900 Heidelberg 1 (FRG)

[**] This work was supported by the Land Baden-Württemberg (FRG) (Forschungsschwerpunkt No. 35).

formed in 90% yield upon reaction of ethyl 8-methoxy-2,7-octadienoate **3** with mercury acetate in the presence of calcium oxide and methanol and subsequent reduction with $NaBH_4$ (Scheme 1).

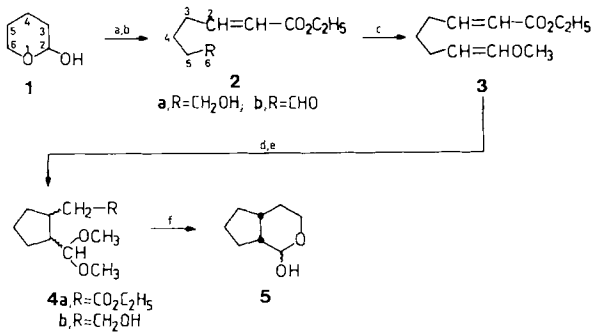

Scheme 1. a) $(C_6H_5)_3P{=}CH{-}CO_2C_2H_5$ in DMF, 90 °C, 12 h; 65% **2a**. b) $pyH^{\oplus}ClCrO_3^{\ominus}$ in CH_2Cl_2, room temperature, 2 h; 95% **2b**. c) $[(C_6H_5)_3P{-}CH_2OCH_3]Cl$ with *t*BuOK in THF added dropwise to the solution of **2b** in THF, reflux, 1 h; 68% **3**. d) $Hg(OAc)_2$ and CaO in MeOH, room temperature, 2 h; $NaBH_4$, 0 °C, 5 min; 90% **4a**. e) $LiAlH_4$ in THF, reflux, 1 h; 72% **4b**. f) 2 N HCl, extraction with ether; 70% **5**.

As starting material for the preparation of **3** we used the commercially available 2-hydroxytetrahydropyran **1**, whose hemiacetal reacts with ethoxycarbonylmethylenetriphenylphosphorane in a Wittig reaction to give **2a**. Oxidation of the initially formed CH_2OH group of **2a** with pyridinium chlorochromate affords aldehyde **2b**. Reaction of **2b** with methoxymethylenetriphenylphosphorane in a second Wittig reaction affords **3** in good yield. Under identical conditions optically active, C-3, C-4- or C-5-substituted 2-hydroxytetrahydropyrans furnish optically active, substituted ethyl 8-methoxy-2,7-octadienoates. These are of special interest, since the chiral centers should influence the stereoselectivity of the subsequent cyclization.

Under the reaction conditions given for the cyclization in Scheme 1 the methanol attacks as intermolecular nucleophile during the mercuration step in such a way that the acetal **6** is formed (Scheme 2). Reaction of **6** with $NaBH_4$, in accord with previous studies on intermolecular C–C coupling,[4–7] affords the alkylmercury hydride **7**, which is converted by loss of a hydrogen atom into the reactive alkylmercury radical **8**. The radical **8** decomposes spontaneously into the carbon radical **9** and mercury. Intramolecular C–C coupling in **9** leads to formation of **10**. The function of the hydrogen donor, which traps the radical **10** as **4a** before a polymerization can take place, is assumed by the alkylmercury hydride **7**. The reactive alkylmercury radical **8** is thereby set free and a radical chain reaction takes place. It can be concluded from the ^1H-NMR spectrum of **4a** that the reaction proceeds with 80% *cis*-stereoselectivity.

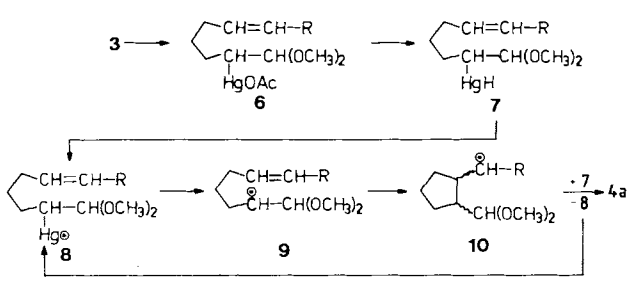

Scheme 2. Mechanism of the radical chain reaction leading to the formation of **4a**. $R{=}CO_2C_2H_5$.

The cyclization reaction is of interest for many reasons. The *cis*-1-hydroxyoctahydrocyclopenta[c]pyran **5**, which represents the basic carbon skeleton of the natural iridoids, can be obtained directly from **4a** by $LiAlH_4$-reduction of the ester group to give **4b**, followed by acid hydrolysis in order to free the aldehyde group.[8] Accordingly, it should be possible to prepare enantiomerically pure iridoids from appropriate optically active starting compounds. Furthermore, **4a** contains already useful potentialities for the construction of a new diene by simple reactions. Further cyclizations would then lead to polycyclopentanes, a class of compounds to which naturally occurring di- and triquinanes belong.[9]

Received: June 19, 1987 [Z 2303 IE]
German version: *Angew. Chem. 99* (1987) 1177

CAS Registry numbers:
1, 694-54-2; **2a**, 110935-49-4; **2b**, 59612-36-1; **3**, 110935-50-7; **4a** (*cis* isomer), 110744-16-6; **4a** (*trans* isomer), 110744-17-7; **4b**, 110935-51-8; **5**, 110744-18-8.

[1] Y. Matsuka, M. Kodama, S. Ito, *Tetrahedron Lett. 1979*, 4081.
[2] S. Danishefsky, S. Chakalamannil, B.-J. Uang, *J. Org. Chem. 47* (1982) 2331.
[3] Review: B. Giese, *Angew. Chem. 97* (1985) 555; *Angew. Chem. Int. Ed. Engl. 24* (1985) 553.
[4] G. M. Whitesides, J. San Filippo, *J. Am. Chem. Soc. 92* (1970) 6611.
[5] C. L. Hill, G. M. Whitesides, *J. Am. Chem. Soc. 96* (1974) 870.
[6] M. Devaud, *J. Organomet. Chem. 220* (1981) C27.
[7] B. Giese, G. Kretzmar, *Chem. Ber. 117* (1984) 3160.
[8] Review: J. M. Bobbitt, K.-P. Segebarth in A. R. Battersby, W. I. Taylor (Eds.): *Cyclopentanoid Terpene Derivatives, Vol 1*, Dekker, New York 1969, p. 1.
[9] Review: L. A. Paquette, *Top. Curr. Chem. 119* (1984) 84.

$[(\eta^5\text{-}C_5Me_5)_2Ti_2P_6]$, a Distorted Dimetallaphosphacubane**

By *Otto J. Scherer,* Herbert Swarowsky, Gotthelf Wolmershäuser, Wolfgang Kaim,* and *Stephan Kohlmann*

Conceptual replacement of the diagonally opposite corner atoms of the unknown cubic P_8 **A**[1] by two transition-metal complex fragments **M** gives the cubane-like M_2P_6 structure type **B**.

Cothermolysis of **1** and white phosphorus (P_4) affords **2** in ca. 20% yield. Complex **2** was obtained in the form of red-brown crystals, which could be handled in the air and

[*] Prof. Dr. O. J. Scherer, Dipl.-Chem. H. Swarowsky, Dr. G. Wolmershäuser [+]
Fachbereich Chemie der Universität
Erwin-Schrödinger-Strasse, D-6750 Kaiserslautern (FRG)
Priv.-Doz. Dr. W. Kaim, Dipl.-Chem. S. Kohlmann
Institut für Anorganische Chemie der Universität
Niederurseler Hang, D-6000 Frankfurt am Main 50 (FRG)

[+] X-ray structure analysis

[**] This work was supported by the Fonds der Chemischen Industrie (doctoral fellowship for *H.S.*).

$$[(\eta^5\text{-}C_5Me_5)_2Ti(CO)_2] \xrightarrow[3\text{ h, ca. }150\,^\circ C]{P_4,\ \text{xylene}} [(\eta^5\text{-}C_5Me_5)_2Ti_2P_6] \qquad \text{(a)}$$

1 **2**

which were moderately soluble in pentane and readily soluble in benzene, toluene, and dichloromethane.

The ^{1}H-NMR spectrum (200 MHz, 293 K, C_6D_6, int. TMS) of **2** exhibits a singlet at $\delta = 2.60$, a region that differs significantly from that found for the triple-decker sandwich complexes **3** [δ **(3a)** = 0.47 (sept.),[2,3] δ **(3b)** = 0.54 (sept.),[3] δ **(3c)** = 1.32(s)[3]]. Even more striking are the differences in the ^{31}P{^{1}H}-NMR chemical shifts (80.82 MHz, CH_2Cl_2, 85% H_3PO_4 ext.): **2**: 386.7(s), **3a**: -315.6(s)[2,3], **3b**: -338.2(s)[3], **3c**: 164.9(s, $W_{1/2} = 540$ Hz[3]). P_2 elimination is observed in the mass spectrum [(EI-MS, 70 eV, 40 °C) *m/z* 552 $M^\oplus$, 89%), 490 ($M^\oplus - P_2$, 100%), 124 ($P_4^\oplus$, 10%), 62 ($P_2^\oplus$, 22%)] along with other lines.

$[(Cp^*M)_2(\mu,\eta^6\text{-}P_6)]$ **3** ($Cp^* = \eta^5\text{-}C_5Me_5$)

3a, M = Mo (28 valence electrons (VE))
3b, M = W (28 VE)
3c, M = V (26 VE)

The neutral 24-VE system **2** undergoes ready cyclovoltammetric oxidation[4] (irreversible, $E_{pa} = 0.70$ V) and reduction (ideally reversible one-electron reduction, $\Delta E = 60$ mV, $E_{red} = -1.31$ V). The redox potential difference (ca. 2.0 V) and the energy of the optical excitation (longest-wavelength band maximum observed as a shoulder at 430 nm ≙ 2.88 eV) exhibit significantly larger differences in this case than for the triple-decker complexes **3** having a planar middle deck (differences of 0.2–0.4 (e)V[3]). This observation is presumably due to a relatively large structural change on going from the crystallographically determined ground state to the first electronic excited state.

The 25-VE anion of **2** is well-characterizable by ESR spectroscopy. The *g* factor of the spectrum, which shows no splitting at room temperature, is 1.9967 and is thus in the range found for Ti^{III}.[5] By computer simulation it is possible to estimate an upper limit of 6 Gauss for the ^{47,49}Ti coupling, which is in agreement with the presence of a delocalized mixed-valent system (cf. **4**[6] and $[Cp_2Ti(\mu\text{-}H)_2TiCp_2]^\ominus$[5,7]). At low temperature, the solution ESR spectrum of the 25-VE anion of **2** exhibits coupling of the unpaired electron with six equivalent ^{31}P nuclei. The coupling of 3.8 Gauss, which is very small for a coupling to ^{31}P, is once again in agreement with the mainly metal character of the singly occupied molecular orbital; the parallels to the 27-VE complex **4** make it likely that the P_6 ring is at least flattened. The ESR results support a model containing high-valent titanium and a reduced P_6 ring. Reasonable alternatives to the 25-VE anion are: a planar $P_6^{4\ominus}$ ring (cf. M_4P_6[8]) and titanium in the oxidation states II and III or a puckered $P_6^{6\ominus}$ ring and Ti^{III}/Ti^{IV}.

$[(Cp^*Cr)_2(\mu,\eta^5\text{-}P_5)]$ **4**

The X-ray structure analysis[9] reveals the skeleton of **2** to consist of a distorted Ti_2P_6 cubane, which can be conceptually derived from a P_6 ring (chair conformation) and two Cp*Ti "caps" (Fig. 1). If **2** is regarded as a titanium–polyphosphide derivative with μ,η^3,η^3 coordination of the P_6 ring, then the following formal charges are obtained: *cyclo*-$P_6^{6\ominus}$ (isoelectronic with cyclo-S_6), $C_5Me_5^\ominus$, and $Ti^{4\oplus}$. This way of looking at the complex reveals an interesting analogy to the μ,η^3,η^3-*cyclo*-$P_6^{6\ominus}$ partial structure of the Th_2P_{11}.[10] The mean values of the P–P distances (2.23 Å) as well as the PPP angles (105.9°) in the P_6 ring of **2** differ by only small amounts from those in the *cyclo*-$P_6^{6\ominus}$ moiety of Th_2P_{11}.[10] They are also comparable with those in orthorhombic black phosphorus,[11] *cyclo*-$(PPh)_6$ (chair conformation),[12] the chair-like P_6 rings of Re_6P_{13} (partial structure),[13] and some MP_3 polyphosphides[14] (e.g., SnP_3[15]). A P–P distance of 2.26–2.31 Å was calculated for cubic P_8.[1] The Ti–P bonds (mean value 2.36 Å) are shorter in **2** than in titanium polyphosphides.[14]

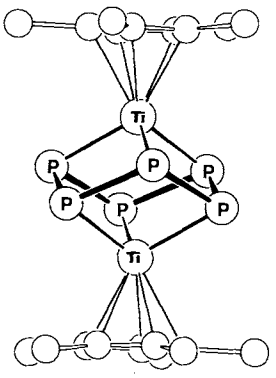

Fig. 1. Molecular structure of **2** (for simplicity, only one orientation is shown). Selected distances [Å] and angles [°]: P-P 2.217(17)-2.251(16), P-Ti 2.358(11)-2.375(13), Ti-Cp*$_{(centr.)}$ 2.00, P...Ti 2.867(12)-2.906(12), Ti...Ti 3.187(4); P-P-P 105.1(6)-106.9(7), Pi-Ti-P 97.3(4)-98.5(4), Ti-P-P 77.0(5)-78.5(5), Ti-Ti-Cp*$_{(centr.)}$ 179.1.

Although attempted generation of P_8 from **2** and two molar equivalents of PX_3 (X = Cl, Br) yielded Cp^*TiX_3 already at room temperature, ^{31}P-NMR spectroscopic analysis has so far only revealed small amounts of unreacted PX_3 in the soluble products.

Experimental Procedure

1 (700 mg, 1.9 mmol) [16] and P_4 (240 mg, 1.9 mmol) in xylene (40 mL) were heated at reflux for 3 h with stirring (monitored by IR; the ^{31}P-NMR spectrum showed only the signal of **2**). Subsequently, ca. 30 mL of xylene was distilled off and the remaining solution was allowed to stir with ca. 5 g of silica gel (Merck, 60, 0.063–0.200 mm; activity II) and then evaporated to dryness under an oil-pump vacuum until the resulting solid flowed freely. This mixture of substances was placed on a column filled with silica gel/pentane ($d = 2$ cm, $l = 40$ cm). Excess P_4 was eluted with pentane and a red-brown fraction was eluted with a 5 : 1 mixture of pentane/toluene. The latter fraction was evaporated to dryness (oil-pump vacuum) and the product was recrystallized from boiling toluene, which, upon cooling to -20 °C, afforded 98 mg of **2** (19%). A correct elemental analysis was obtained.

Received: July 7, 1987 [Z 2337 IE]
Germany version; *Angew. Chem. 99* (1987) 1178

CAS Registry numbers:
1, 11136-40-6; **2**, 110935-04-1.

[1] Most recent theoretical studies: E. A. Halevi, H. Bock, B. Roth, *Inorg. Chem. 23* (1984) 4376; G. Trinquier, J.-P. Daudey, N. Komiha, *J. Am. Chem. Soc. 107* (1985) 7210; R. Ahlrichs, S. Brode, C. Ehrhardt, *ibid. 107* (1985) 7260; K. Raghavachari, R. C. Haddon, J. S. Binkley, *Chem. Phys. Lett. 122* (1985) 219; M. W. Schmidt, M. S. Gordon, *Inorg. Chem. 24* (1985) 4503.

[2] O. J. Scherer, H. Sitzmann, G. Wolmershäuser, *Angew. Chem. 97* (1985) 358; *Angew. Chem. Int. Ed. Engl. 24* (1985) 351.

[3] O. J. Scherer, J. Schwalb, H. Swarowsky, G. Wolmershäuser, W. Kaim, R. Gross, *Chem. Ber.*, in press.

[4] 1,2-Dichlorethane, 0.1 M Bu_4NClO_4 vs. SCE, 100 mV s^{-1}.

[5] B. A. Goodman, J. B. Raynor, *Adv. Inorg. Chem. Radiochem. 13* (1970) 135.

[6] O. J. Scherer, J. Schwalb, G. Wolmershäuser, W. Kaim, R. Gross, *Angew. Chem. 98* (1986) 349; *Angew. Chem. Int. Ed. Engl. 25* (1986) 363.

[7] G. Henrici-Olivé, S. Olivé, *Angew. Chem. 80* (1968) 398; *Angew. Chem. Int. Ed. Engl. 7* (1968) 386.
[8] H.-P. Abicht, W. Hönle, H. G. von Schnering, *Z. Anorg. Allg. Chem. 519* (1984) 7; H. G. von Schnering, T. Meyer, W. Hönle, W. Schmettow, U. Hinze, W. Bauhofer, G. Kliche, *ibid.*, in press.
[9] **2**: The centrosymmetric molecules are disordered. The two equally populated arrangements differ only in the orientation of the P_6 rings (distances and angles are largely identical) relative to the Cp* rings (rotated by ca. 40° with respect to each other around the metal-metal axis). The poor quality of the crystal is responsible for the small number of reflections observed, the relatively high R values, and the large thermal parameters of the the C atoms. Space group $P\bar{1}$, $a = 8.387(2)$, $b = 10.615(3)$, $c = 8.348(2)$ Å, $\alpha = 102.30(2)$, $\beta = 112.76(2)$, $\gamma = 101.74(2)°$, $Z = 1$, $\rho_{calcd} = 1.443$ g cm^{-3}. 1718 unique reflections ($Mo_{K\alpha}$, $3° \leq 2\theta \leq 50°$), 1133 observed with $F_0^2 \geq 2.0\sigma(F_0^2)$. 170 parameters, $R = 0.099$, $R_w = 0.094$. Further details of the crystal structure investigation may be obtained from the Fachinformationszentrum Energie, Physik, Mathematik GmbH, D-7514 Eggenstein-Leopoldshafen 2 (FRG), on quoting the depository number CSD-52609, the names of the authors, and the journal citation.
[10] H. G. von Schnering, M. Wittmann, R. Nesper, *J. Less Common Met. 76* (1980) 213.
[11] A. Brown, S. Rundqvist, *Acta Crystallogr. 15* (1965) 684.
[12] J. J. Daly, *J. Chem. Soc. A 1966*, 428.
[13] R. Rühl, W. Jeitschko, *Z. Anorg. Allg. Chem. 466* (1980) 171; R. Guérin, M. Potel, M. Sergent, *Mater. Res. Bull. 14* (1979) 1335.
[14] For example, D. E. C. Corbridge: *The Structural Chemistry of Phosphorus*. Elsevier, New York 1974.
[15] J. Gullman, O. Olofsson, *J. Solid State Chem. 5* (1972) 441.
[16] D. J. Sikora, K. J. Moriarty, M. D. Rausch, *Inorg. Synth. 24* (1986) 152.

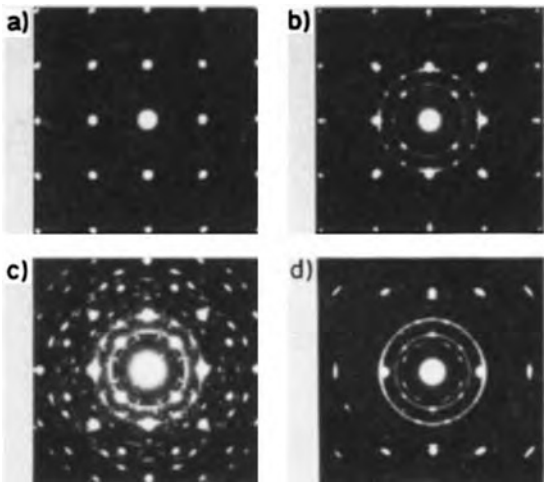

Fig. 1. Selected area diffraction patterns of single crystal Au foils before and after reaction [6] with ethylenediamine solutions of K_4Sn_9: a) $[001]_{Au}$, unreacted; b) $[001]_{Au}$ after a "light dip" in the K_4Sn_9 solution; c) $[001]_{Au}$ after a "heavy dip"; d) same as specimen b) but tilted to the $[112]_{Au}$ orientation. Note that unlike b) and c), the innermost diffraction ring now has sharp well defined spots (see text).

Reaction of Sn_9^{4-} with Single Crystal Au: Textured Fiber Epitaxial Growth of AuSn at Room Temperature

By *Robert C. Haushalter,* Michael M. J. Treacy,* and *Stephen B. Rice*

Since the report on the isolation of Sn_9^{4-},[1] and its decomposition reaction with large organic cations,[2] there have been few studies dealing with the chemical reactivity of these p-block polyanions. Recently, we have shown that many novel solid state materials can be obtained from these clusters such as surface metallized organic polymers[3] and inorganic solids,[4] and a new type of amorphous metallic spin glass.[5] When examining the reactivity of the more electronegative transition metals with the p-block polyanions, it was noted that Sn_9^{4-} or Pb_9^{4-} reacted instantly with clean metals like Au or Pt.[4] However, these reaction products were not completely characterized, so a study of the reaction of Sn_9^{4-} with single crystal Au foils was undertaken using transmission electron microscopy (TEM).

When single crystal gold foils, which were 20 nm thick and oriented with the Au[001] direction normal to the plane of the foil, were immersed in a solution of K_4Sn_9 in ethylenediamine (en), the characteristic gold color of the foil immediately turned to silver-gray. Examination of the reacted foils[6] in the TEM[7] gave the diffraction patterns shown in Figure 1. Even with very short residence times in dilute solutions, the diffraction patterns (Fig. 1b) show the presence of a new crystalline phase in which, except for unreacted Au and the very small spots sprinkled over the pattern which are due to β-tin, all of the spots and rings can be indexed as hexagonal AuSn.

At first glance the AuSn diffraction pattern appears puzzling as it shows rings, normally considered as arising from polycrystalline material, as well as sharp spots with a definite geometrical relationship to the underlying Au substrate indicative of epitaxial growth. The observation of both spots and rings could be explained simply as a mixture of epitaxial growth and polycrystalline deposition except that one of the AuSn reflections, the $[10\bar{1}0]$, has essentially no intense sharp spots, but spots do appear on this ring when the foil is tilted relative to the electron beam (Fig. 1d). To determine the cause of this mixture of spots and rings, the foils were examined by several additional electron microscopy techniques.

Normal bright field imaging immediately after reaction shows the Au to be covered by a thin layer of AuSn. Longer reaction time gives thicker films but eventually a passivating layer is formed as evidenced by the presence of Au reflections (Fig. 1c) even after prolonged exposure to saturated solutions of the Sn_9^{4-} anion. The microdiffraction patterns recorded from many individual AuSn crystallites revealed that none of them had exactly the same crystallographic orientation. The data suggested a form of textured fiber epitaxy[8] where the hexagonal c axis of the AuSn, $[0001]_{AuSn}$, is confined to lie in the plane defined by the $[001]_{Au}$ and $[110]_{Au}$ directions. This means that the $[1\bar{2}10]_{AuSn}$ axis tends to be colinear with the $[1\bar{1}0]_{Au}$ axis (or the other symmetry equivalent Au axes, [110], $[\bar{1}10]$ or $[1\bar{1}0]$) except when $[0001]_{AuSn}$ is parallel to $[001]_{Au}$. If this assumption is valid, then it should be possible to recreate the diffraction pattern using these criteria.

As shown in Figure 2 (top) diffraction vectors originating from each of the $[10\bar{1}1]$, $[10\bar{1}2]$, and $[20\bar{2}1]$ orientations are labelled as dots, squares, and hexagons respectively, and related diffraction spots arising from the fourfold symmetry imposed by the Au support are indicated by the hollow symbols. As the angle, θ, between the $[001]_{Au}$ axis and the $[0001]_{AuSn}$ axis of the various crystallites increases, these major AuSn crystallographic axes will become colinear with the incident beam and thus be brought into the proper condition for diffraction. In this way we can account for most of the sharp AuSn diffraction spots observed in Figures 1b and 1c, except for some of the faint satellites seen on the $(20\bar{2}1)$ ring, and for the rings themselves. The rings can be explained if one assumes that

[*] Dr. R. C. Haushalter, Dr. M. M. J. Treacy, Dr. S. B. Rice
Exxon Research and Engineering Company
Annandale, NJ 08801 (USA)

when the [0001] axis of AuSn is parallel to the [001] axis of Au, it can adopt any azimuthal angle without deviating from the Au [001]/[110] plane. In this unique orientation the constraint for $[1\bar{2}10]_{AuSn}$ to be parallel to $[1\bar{1}0]_{Au}$ disappears, thus producing rings for this reflection as shown in Figures 1b and 1c.

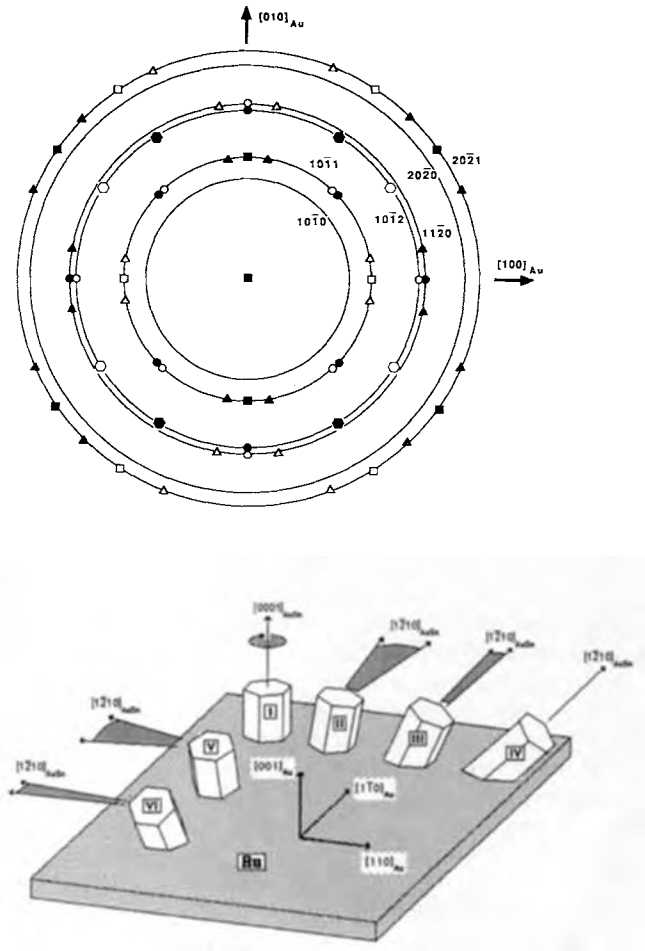

Fig. 2. Top: Reconstructed diffraction pattern based on the textured fiber epitaxy model. Diffraction vectors: ● $[10\bar{1}1]$, ■ $[10\bar{1}2]$, ● $[20\bar{2}1]$, ▲ $[10\bar{1}2]$, 10° misaligned. Note the excellent agreement with the experimental diffraction patterns in Figures 1b and 1c (see text). Bottom: The model for the textured fiber epitaxial growth of AuSn on Au (see text). Particles I–IV show one orientation of the $[1\bar{2}10]_{AuSn}$ to the Au substrate while particles V and VI show an orientation 90° away. The other two possible orientations are not shown.

The epitaxial model is sketched in Figure 2 (bottom). As the $[0001]_{AuSn}$ axis approaches being parallel to the $[001]_{Au}$ axis (i.e. $\theta = 0°$), such as the particle labelled I, the AuSn crystallites are free to adopt any azimuthal angular orientation. As the $[0001]_{AuSn}$ axis tilts within the plane defined by the $[001]/[110]_{Au}$ directions (particle II), or the $[001]/[1\bar{1}0]_{Au}$ directions (particle V), the $[1\bar{2}10]_{AuSn}$ is constrained to align with the $[1\bar{1}0]_{Au}$ or $[110]_{Au}$ directions, respectively. As the angle of declination increases the constraint strengthens (see particles III and IV). It is the weakening of the azimuthal constraint (i.e. that $[1\bar{2}10]_{AuSn}$ be parallel to $[1\bar{1}0]_{Au}$) as the angle of declination decreases that gives rise to the peculiar mixture of spots and rings in the diffraction patterns.

At this point, the precise mechanism for the formation of the epitaxial growth of the AuSn from the reaction of Sn_9^{4-} with Au is not clear, mainly due to our inability to determine the fate of the potassium. In our earlier studies of the reaction of the p-block polyanions with the surface of organic polymers,[3] the element from which the polyanion was composed was oxidized to the metallic state on the surface of the polymer while the polymer underwent concomitant reduction and was intercalated by the polyanion's countercation. If there is a potassium-containing phase present in the Au/AuSn system under consideration here, then it is either amorphous and thus not detectable in the diffraction experiments or it was destroyed by exposure to the air during the time it took to load the sample into the microscope (ca. 1 min). Another possibility is that the Au reacts with the Sn_9^{4-} and produces more reduced Sn clusters. Situations involving the production of transitory Au/Sn anions which rapidly decompose onto the substrate surface or the participation of the solvent in the reaction can be envisioned but all of these mechanisms remain speculative at this point. Furthermore, it is not known if the free metallic Sn found on the surface of the reacted foils is one of the reaction products or derives from the reaction of the highly reducing Sn_9^{4-} with the solvent or solvent impurities. The nature of the mechanism is further complicated by the fact that Sn and Au, and their intermetallic alloy phases, can undergo interdiffusion at relatively low temperatures[9] which could obscure the composition of the initially formed phases.

In summary, the polyanion Sn_9^{4-} reacts instantly with oriented single crystals foils of Au to give AuSn. The growth is such that $[0001]_{AuSn}$ always lies in the plane defined by $[110]_{Au}$ and $[001]_{Au}$ such that the $[1\bar{2}10]_{AuSn}$ is parallel to the $[1\bar{1}0]_{Au}$ (and its symmetry equivalent axes) within the plane of the foil. As the $[0001]_{AuSn}$ axis becomes closer to parallel to the $[001]_{Au}$ axis this restraint is weakened until it vanishes when the two axes are exactly parallel. At this point the AuSn axis is free to adopt any azimuthal angle with respect to the Au surface. This form of strong textured fiber epitaxial growth gives rise to a mixture of sharp spots and rings in selected area electron diffraction patterns.

Received: January 18, 1987 [Z 2049 IE]
German version: *Angew. Chem. 99* (1987) 1172

[1] D. Kummer, L. Diehl, *Angew. Chem. 82* (1970) 881; *Angew. Chem. Int. Ed. Engl. 9* (1970) 895; L. Diehl, K. Kodadedeh, D. Kummer, J. Strähle, *Chem. Ber. 109* (1976) 3404.

[2] L. Diehl, K. Kodadedeh, D. Kummer, J. Strähle, *Z. Naturforsch. B 31* (1976) 522.

[3] R. C. Haushalter, L. Krause, *Thin Solid Films 102* (1983) 161; R. Haushalter, L. Krause in K. Mittal (Ed.): *Polyimides Vol. 2*, New York 1984, p. 735.

[4] R. C. Haushalter, *Angew. Chem. 95* (1983) 560; *Angew. Chem. Int. Ed. Engl. 22* (1983) 558; *Angew. Chem. Suppl. 1983*, 766.

[5] R. C. Haushalter, C. O'Connor, J. Haushalter, A. Umarji, G. Shenoy, *Angew. Chem. 96* (1984) 147; *Angew. Chem. Int. Ed. Engl. 23* (1984) 169.

[6] The Au foils were supported on 200 mesh Au grids and immersed into solutions of K_4Sn_9 in purified ethylenediamine (en): the "light dip" sample was treated for 5 s in a 10^{-4} M solution while the "heavy dip" sample was treated for 30 min in a saturated solution. The samples were then rinsed several times in fresh en. All work was performed under helium (< 1 ppm O_2).

[7] The instruments used were: a) a Philips 400T (FEG) TEM at 100 kV with an energy dispersive X-ray detector; b) a Philips 430T (LaB_6) TEM at 300 kV and c) a VG HB 501A STEM at 100 kV.

[8] L. Reimer, *Transmission Electron Microscopy* (Springer Series in Optical Sciences 36), Springer, Berlin 1984, p. 407.

[9] L. Buene, *Thin Solid Films 43* (1977) 285; S. Nakahara, R. McCoy, *Appl. Phys. Lett. 37* (1980) 42; D. Dufner, L. Eyring, *J. Sol. State Chem. 62* (1986) 112.

Generation of β-, γ-, δ-, ε-, and ζ-Zinc Ketones and Their Transition-Metal-Catalyzed Reactions with Carbon Electrophiles**

By *Yoshinao Tamaru,* Hirofumi Ochiai, Tatsuya Nakamura,* and *Zen-ichi Yoshida**

For organic chemistry, the behavior of compounds possessing both a nucleophilic and an electrophilic center has been a great concern, not only conceptually but also practically. Metallocarbonyl compounds are typical examples.[1] Recently, *Kuwajima*[2] and we[3] have shown that β- and γ-metalloesters (M = Ti, Zn) serve as carbon nucleophiles to form C–C bonds at the β and γ positions of the esters, respectively.[4] However, all β-metalloketones so far reported are either too unstable (forming cyclopropanolates **3** (n = 2))[5] or too unreactive[6] (M = Sn,[2d,7] Hg,[8] Mn),[9] to form C–C bonds with carbon electrophiles.[10] Some β-metalloketones (M = Pd,[11] Ni,[12] Cu,[13] Ag),[13] have been proposed as intermediates for carbonylation and oxidative dimerization.

Here we wish to report that β-zinc ketones and their higher homologues (**1**; X = alkyl, aryl; n = 2–6) are rather stable and undergo neither an intramolecular proton abstraction to form zinc enolates **2** nor nucleophilic attack at the keto carbonyl to form zinc cycloalkanolates **3**.[14] However, these zinc ketones **1** react with various carbon electrophiles by virtue of transition-metal catalysis, which serves either to activate the electrophiles [Eqs. (a)–(d)] or to activate **1** or to activate both species [Eq. (e)]. These zinc ketones **1** directly react with tri-*n*-butylchlorostannanes [Eq. (f)].[14]

In Table 1 are summarized the results of the reactions of **1** with saturated and unsaturated (aromatic and nonaromatic) acid chlorides, catalyzed by Pd^0 [Eq. (a)].[3a] For the generation of **1**, the use of HMPA as a co-solvent (HMPA : iodide = 1.67 : 1) is essential. In the absence of HMPA, no metalation took place. Dimethylformamide and dimethylacetamide (DMA) may serve as a co-solvent, but HMPA is by far the most satisfactory, since it not only greatly facilitates the metalation, which is therefore complete at lower temperatures, but also seems to stabilize **1** (compare reactions 9 and 10 in Table 1).[15] Generally, the larger the number n of CH_2 groups in the iodide, the higher the temperature required for the metalation. The low yields for the reactions 1 and 2 may partly be ascribed to an instability of the starting iodide.[16] Since use of an excess amount of acid chloride results in a complex reaction, a less than stoichiometric amount of acid chloride was routinely used.

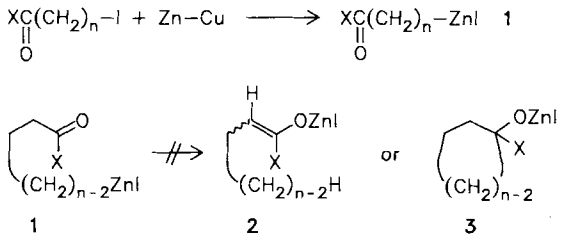

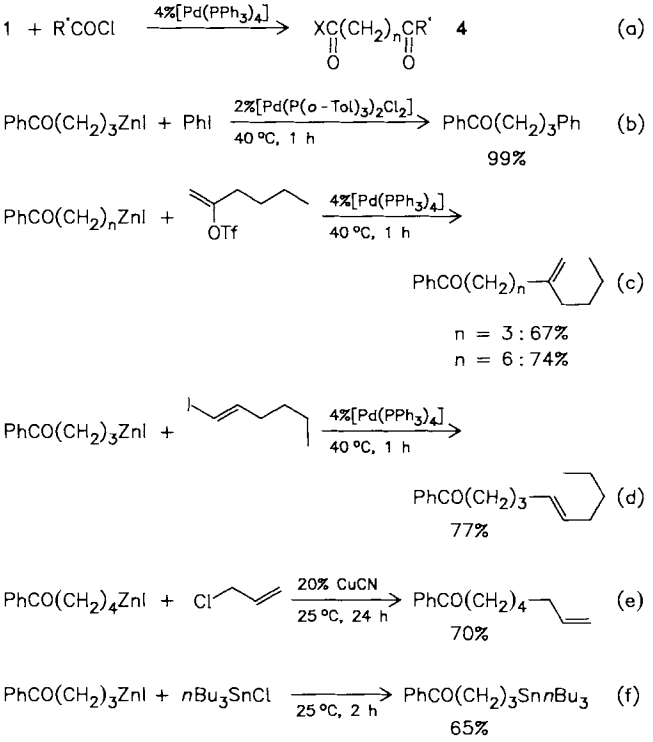

Table 1. Acylation of **1** catalyzed by Pd^0.

Reaction	1 n	1 X	Reaction conditions [a]	R' in R'COCl	γ [b]	Yield of 4 [%] [c]
1	2	Et	25 °C, 1 h, HMPA	Ph	1.3	53 (40)
2	2	Et	25 °C, 1 h, HMPA	C_7H_{15}	1.8	62 (34)
3	3	Ph	40 °C, 1 h, HMPA	C_7H_{15}	1.3	80 (61)
4	3	Ph	40 °C, 1 h, HMPA	*p*-MeO-C_6H_4	1.3	90 (69)
5	3	Me	25 °C, 2 h, HMPA	H_2C=CH	1.7	85 (50)
6	4	Ph	40 °C, 2 h, HMPA	Ph	1.3	76 (58)
7	4	Ph	40 °C, 2 h, HMPA	C_2H_5	1.3	77 (59)
8	4	Et	40 °C, 1 h, HMPA	CH_3	1.1	74 (67)
9	5	Ph	40 °C, 2 h, HMPA	C_2H_5	1.2	85 (71)
10	5	Ph	50 °C, 2 h, DMA	C_2H_5	1.2	63 (53)
11	6	Ph	50 °C, 2 h, HMPA	C_2H_5	1.1	91 (82)

[a] For the generation of **1**, all reaction mixtures were pretreated at 25 °C for 1 h. [b] The ratio of the starting iodide to carbon electrophile. [c] Yields based on acid chlorides. The figures in parentheses refer to the isolated yields based on the starting iodides.

Reactions (b), (c),[18] (d), and (e)[19] were performed according to a similar procedure.[20] Reaction (d) is stereospecific: *cis*- and *trans*-4-nonenyl phenyl ketone in 68% and 77% yield (≧95% purity each), respectively, were obtained from *cis*- (99% purity)[21] and *trans*-1-iodo-1-hexene (98% purity).[22]

The present zinc ketone methodology undoubtedly provides a short-cut for the synthesis of target compounds. The regio- and stereoselectivity for the Cu^I-catalyzed allylation [Eq. (e)] and reactions with other electrophiles are under extensive study.

Finally, the structure of **1** is worth mentioning.[15] The IR spectrum of **1** (n = 3, X = Ph) in benzene/HMPA showed one very strong CO absorption at $\tilde{\nu} = 1675\ cm^{-1}$, the same wavenumber as the starting iodoketone, while **1** (n = 2, X = Et) exhibited its CO absorption at a slightly lower wavenumber ($1690\ cm^{-1}$) compared with the starting iodoketone ($\tilde{\nu} = 1710\ cm^{-1}$). These data suggest that these zinc ketones do not form, or form very weakly, a chelating structure.[23]

[*] Dr. Y. Tamaru, Prof. Dr. Z. Yoshida, Dr. H. Ochiai, T. Nakamura
Department of Synthetic Chemistry, Kyoto University
Yoshida, Kyoto 606 (Japan)

[**] We are grateful for partial financial support from the Ministry of Education, Science and Culture, the Japanese Government (Grant-in-Aid for Special Project No. 60119002 and 61125002 and Scientific Research B No. 61470094).

Experimental Procedure

The generation of **1** and their reactions with acid chlorides were performed in one flask as typified in the following example (reaction 3 in Table 1).

A mixture of Zn-Cu couple [17] (110 mg, 1.7 mmol) and 3-iodopropyl phenyl ketone (356 mg, 1.3 mmol) in dry benzene (4 mL) and HMPA (0.5 mL) was stirred at room temperature for 1 h and then at 40 °C for 1 h under nitrogen. Then, solutions of $[Pd(PPh_3)_4]$ (46 mg, 0.04 mmol) in benzene (1 mL) and octanoyl chloride (163 mg, 1.0 mmol) in benzene (1 mL) were successively added at 40 °C and the mixture was stirred at the same temperature for 2 h. After dilution with ether, successive washing with 1N HCl and aqueous $NaHCO_3$, and drying over $MgSO_4$, followed by evaporation of the solvents, the residue was purified by column chromatography over silica gel (hexane-ethyl acetate gradient) to provide 1-phenyl-1,5-dodecanedione in 80% yield.

Received: April 21, 1987;
revised: July 27, 1987 [Z 2208 IE]
German version: *Angew. Chem. 99* (1987) 1193.

CAS Registry numbers:
4 (n=2, X=Et, R'=Ph), 4437-46-1; **4** (n=2, X=Et, R'=C_7H_{15}), 110743-58-3; **4** (n=3, X=Ph, R'=C_7H_{15}), 110719-02-3; **4** (n=3, X=Ph, R'=*p*-$MeOC_6H_4$), 110719-03-4; **4** (n=3, X=Me, R'=H_2C=CH), 51297-43-9; **4** (n=4, X, R'=Ph), 3375-38-0; **4** (n=4, X=Ph, R'=C_2H_5), 110743-59-4; **4** (n=4, X=Et, R'=C_3), 103260-26-0; **4** (n=5, X=Ph, R'=C_2H_5), 110719-04-5; **4** (n=6, X=Ph, R'=C_2H_5), 110719-05-6; $PhCO(CH_2)_3Ph$, 5407-91-0; $PhCO(CH_2)_3C(CH_2)C_4H_9$, 110719-06-7; $PhCO(CH_2)_6C(CH_2)C_4H_9$, 110719-07-8; (*E*)-$PhCO(CH_2)_3CH$=$CHC_4H_9$, 110719-08-9; (*Z*)-$PhCO(CH_2)_3CH$=$CHC_4H_9$, 110719-11-4; $PhCO(CH_2)_5CH$=CH_2, 110719-09-0; $PhCO(CH_2)_3SnnBu_3$, 110719-10-3; $EtCO(CH_2)_2I$, 72357-44-9; $PhCO(CH_2)_3I$, 65488-05-3; $MeCO(CH_2)_3I$, 3695-29-2; $PhCO(CH_2)_4I$, 66860-64-8; $EtCO(CH_2)_4I$, 110719-00-1; $PhCO(CH_2)_5I$, 71919-91-0; $PhCO(CH_2)_6I$, 110719-01-2; PhCOCl, 98-88-4; $C_7H_{15}COCl$, 111-64-8; *p*-$MeOC_6H_4COCl$, 100-07-2; H_2C=CHCOCl, 814-68-6; C_2H_5COCl, 79-03-8; CH_3COCl, 75-36-5; PhI, 591-50-4; H_2C=C(OTf)C_4H_9, 37555-23-0; (*E*)-ICH=CHC_4H_9, 16644-98-7; (*Z*)-ICH=CHC_4H_9, 16538-47-9; $ClCH_2CH$=CH_2, 107-05-1; nBu_3SnCl, 1461-22-9; $Pd(P(o\text{-}Tol)_3)_2Cl_2$, 40691-33-6; $Pd(PPh_3)_4$, 14221-01-3; CuCN, 544-92-3.

[1] Leading reviews on synthetic equivalents of β-metallocarbonyls; a) N. H. Westiuk, *Tetrahedron 39* (1983) 205; b) D. Hoppe, *Angew. Chem. 96* (1984) 930; *Angew. Chem. Int. Ed. Engl. 23* (1984) 932; c) I. Ryu, N. Sonoda, *Yuki Gosei Kagaku Kyokaishi 43* (1985) 112.

[2] a) E. Nakamura, I. Kuwajima, *J. Am. Chem. Soc. 99* (1977) 7360; b) *106* (1984) 3368; c) H. Oshino, E. Nakamura, I. Kuwajima, *J. Org. Chem. 50* (1985) 2802; d) E. Nakamura, J. Shimada, I. Kuwajima, *Organometallics 4* (1985) 641; e) E. Nakamura, H. Oshino, I. Kuwajima, *J. Am. Chem. Soc. 108* (1986) 3745; see also f) H.-U. Reissig, *Tetrahedron Lett. 22* (1981) 2981.

[3] a) Y. Tamaru, H. Ochiai, T. Nakamura, K. Tsubaki, Z. Yoshida, *Tetrahedron Lett. 26* (1985) 5559; b) Y. Tamaru, H. Ochiai, T. Nakamura, Z. Yoshida, *ibid. 27* (1986) 955.

[4] For β-lithiated amides, see: a) P. Beak, J. E. Hunter, Y. M. Jun, *J. Am. Chem. Soc. 105* (1983) 6350; b) P. E. Eaton, G. Castaldi, *ibid. 107* (1985) 724.

[5] a) D. P. G. Hamon, R. W. Sinclair, *Chem. Commun. 1968*, 890; b) A. A. Ponaras, *Tetrahedron Lett. 1976*, 3105.

[6] Neither tri-n-butyl-3-benzoylpropylstannane nor tri-n-butyl-2-ethoxycarbonylethylstannane, prepared according to reaction (f), reacted with benzoyl chloride under the conditions shown in the text.

[7] a) R. E. Hutton, J. W. Burley, *J. Organomet. Chem. 156* (1978) 369; b) R. A. Howie, E. S. Paterson, J. L. Wardell, J. W. Burley, *ibid. 259* (1983) 71.

[8] a) A. DeBoer, C. H. DePuy, *J. Am. Chem. Soc. 92* (1970) 4008; b) I. Ryu, K. Matsumoto, M. Ando, S. Murai, N. Sonoda, *Tetrahedron Lett. 21* (1980) 4283.

[9] a) M. A. Bennet, G. B. Robertson, R. Watt, P. O. Whimp, *Chem. Commun. 1981*, 752; b) B. L. Booth, S. Casey, R. P. Critchley, R. N. Haszeldine, *J. Organomet. Chem. 226* (1982) 301; see also c) P. DeShong, G. A. Slough, *Organometallics 3* (1984) 636.

[10] For the addition reaction of a β-keto radical, generated from the corresponding mercuric compounds, to olefins, see: a) B. Giese, G. Kretzschmar, *Angew. Chem. 93* (1981) 1015; *Angew. Chem. Int. Ed. Engl. 20* (1981) 965; b) B. Giese, H. Horler, W. Zwick, *Tetrahedron Lett. 23* (1982) 931.

[11] a) S. Brewis, P. R. Hughes, *Chem. Commun. 1965*, 489; *ibid. 1966*, 6; *ibid. 1967*, 71; b) Y. Tamaru, Z. Yoshida, *J. Org. Chem. 44* (1979) 1188; c) T.-W. Lai, A. Sen, *Organometallics 3* (1984) 866.

[12] I. Ryu, I. Rhee, M. Ryang, H. Omura, S. Murai, N. Sonoda, *Synth. Commun. 14* (1984) 1175.

[13] I. Ryu, M. Ando, A. Ogawa, S. Murai, N. Sonoda, *J. Am. Chem. Soc. 105* (1983) 7192.

[14] The reaction of **1** (n=4, X=Ph) with 2.3 molar equivalents of Me_3SiCl gave 1-phenylcyclopentene in 51% yield. This result indicates that Me_3SiCl assists the cyclization of **1** to zinc cycloalkanolates **3**.

[15] During ^{1}H-NMR measurement in $CDCl_3$/benzene/DMA, gradual decomposition of **1** (n=3, X=Ph) was detected by the weakening and broadening of the signal for the methylene protons attached to zinc (δ=0.29 ppm (t), J=7.3 Hz). No such behavior was observed in $CDCl_3$/benzene/HMPA.

[16] R. D. Miller, D. R. McKean, *Tetrahedron Lett.* (1979) 2305.

[17] R. D. Smith, H. E. Simmons in H. E. Baumgarten (Ed.): *Organic Syntheses. Col. Vol. V*. Wiley, Newy York 1973, p. 855.

[18] J. K. Stille, *Angew. Chem. 98* (1986) 504; *Angew. Chem. Int. Ed. Engl. 25* (1986) 508.

[19] Before the addition of allyl chloride, the zinc ketone was filtered under nitrogen to remove unreacted zinc metal.

[20] For these experiments, the factor γ is 1.05, and the yields in the equations refer to the isolated ones, based on the electrophiles. All the products presented here were properly characterized by spectral data (IR, ^{1}H-NMR, ^{13}C-NMR, high-resolution MS) and elemental analyses.

[21] A. Alexaxis, G. Cahiez, J. F. Normant, *Org. Synth. 62* (1984) 1.

[22] G. Zweifel, C. C. Whitney, *J. Am. Chem. Soc. 89* (1967) 2753.

[23] Chelation generally causes the absorption of the CO stretching to shift by 40–80 cm^{-1} to lower wavenumbers: [2d, 7].

Anthracyclinone Ring C Synthesis via Chelate Carbene Complexes**

By *Karl Heinz Dötz** and *Michael Popall*

Dedicated to Professor Ulrich Schöllkopf on the occasion of his 60th birthday

Anthracyclinones, the aglycone components of the antitumor-active anthracyclines,[2] usually feature neighboring central quinone and hydroquinone structures in their linear tetracyclic skeleton and are therefore potential targets of syntheses involving annelation of chromium carbonyl carbene complexes.[3] The most important anthracyclinone is daunomycinone **1**, whose B and C rings should be accessible in principle by a variety of routes—each starting from an unsaturated carbene ligand, a carbonyl ligand, and an alkyne (Scheme 1).

After the B ring had been constructed via routes (a) and (b),[4-6] we directed our attentions to the synthesis of the C ring.

The starting point was the carbene complex **2** [route (c)], which underwent decarbonylation in refluxing *tert*-butyl methyl ether to give quantitatively the chelate carbene complex **3**.[7] Crucial for the annelation of the carbene to the alkyne to afford the hydroquinone skeleton is the long chromium-oxygen bond,[8] which can be opened under mild conditions (ca. 40 °C). In the presence of the alkynes **4a** or **4b**, regiospecific annelation of the carbene ligand occurs to give the coordinated naphthols **5a** or **5b**, respectively. The metal carbonyl fragment is conveniently cleaved off under CO atmosphere, affording hexacarbonylchromium in practically quantitative yield. The latter, in turn, can be used again to generate the carbene complex **3**.

Functionalization of the ketone **6** to give the carboxylic acid **7** is necessary for the formation of ring B. It is achieved, following *O*-methylation, with isocyanomethyl(*p*-tolyl)sulfone.[10] Finally, the carboxylic acid is cyclized to the diketone **8** in acid (trifluoroacetic acid(TFA)/trifluoroacetic anhydride (TFAA)). This reaction was used earlier by *Sih* et al.[11] and by *Rao* et al.[12] as part of a longer route leading to intermediates in the synthesis of

[*] Prof. Dr. K. H. Dötz, Dr. M. Popall
Fachbereich Chemie der Universität
Hans-Meerwein-Strasse, D-3550 Marburg (FRG)

[**] Carbene Ligands as Anthracyclinone Synthons, Part 5. This work was supported by the Deutsche Forschungsgemeinschaft and the Fonds der Chemischen Industrie.—Part 4: [1].

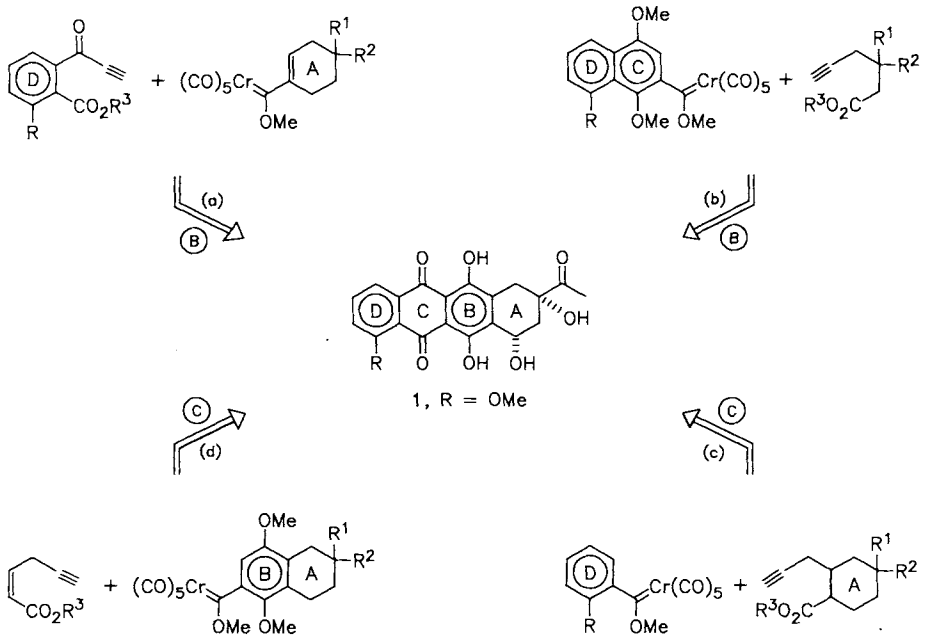

Scheme 1. Synthesis of daunomycinone **1**, R = OMe, via carbene complexes.

11-deoxyanthracyclinones. Thus, the chromium-induced carbene annelation via the chelate carbene complex has been integrated into a formal total synthesis of 11-deoxydaunomycinone **9**; the synthetic route outlined here is overall appreciably shorter than the routes employed so far.

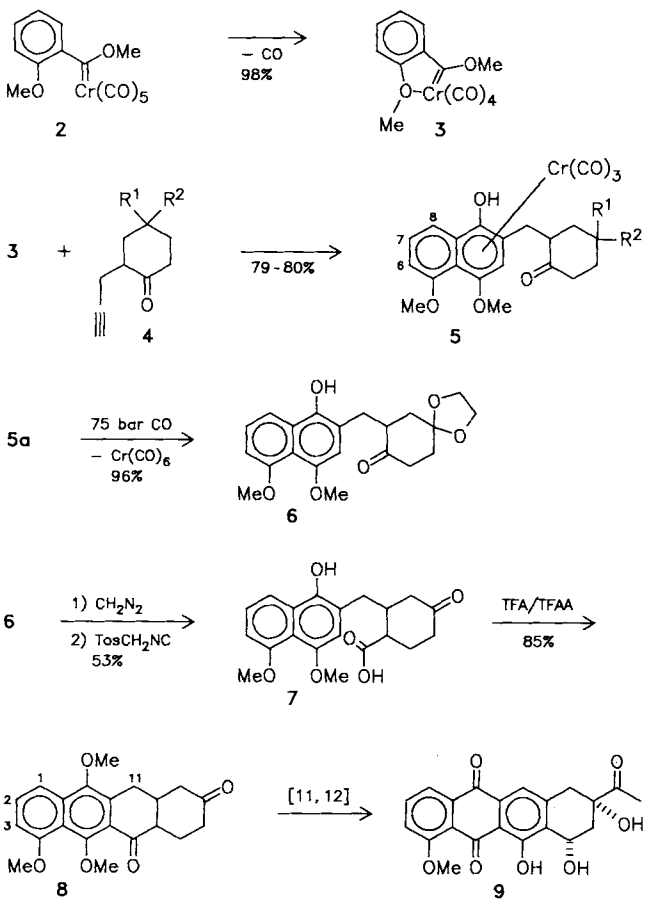

a: R^1, R^2 = OCH_2CH_2O; **b**: R^1, R^2 = O

Experimental Procedure

5a, b: The alkyne **4a** or **4b** [13] (7.5 mmol, 1.46 g or 1.13 g, respectively) was added to a solution of **3** (1.57 g, 5 mmol) [7] in *tert*-butyl methyl ether (50 mL). After stirring for 1 h at 40 °C, an orange-red suspension was obtained. Removal of the solvent and precipitation by addition of CH_2Cl_2/pentane yielded an orange-yellow crystalline powder. Yields: 2.02 g **5a** (79%) and 1.86 g **5b** (80%).—**5a**: IR (KBr): $\tilde{\nu}$(C=O) = 1952, 1864.—^{1}H-NMR (CD_3COCD_3): δ = 7.3–7.9 m, 6.6–7.2 m (3 H, H6-H8); 4.07 (s, 1 H, H3); 3.97 (s, 3 H, 4-OCH_3); 3.82 (s, 3 H, 5-OCH_3); 3.88 (s, 4 H, OCH_2); 3.37 (m, 2 H, CH_2); 1.4–2.9 (m, 7 H, H (cyclohexyl).—**5b**: IR (KBr): $\tilde{\nu}$(C=O) = 1947, 1866.—^{1}H-NMR (CD_3COCD_3): δ = 7.79 (d, 1 H, H8); 7.35 (m, 1 H, H7); 6.91 (m, 1 H, H6); 3.89 (s, 3 H, 4-OCH_3); 3.83 (s, 3 H, 5-OCH_3); 3.37 (m, 2 H, CH_2); 2.1–2.9 (m, 7 H, H (cyclohexyl)).

6: A solution containing **5a** (1.01 g, 2 mmol) in CH_2Cl_2 (100 mL) was heated to 70 °C in a steel autoclave equipped with a glass insert. CO (75 bar) was admitted and the solution was allowed to stir for 72 h. After cooling and careful release of pressure, the solvent was removed and the residue was dissolved in a small amount of ether. The $Cr(CO)_6$ formed was filtered off at −50 °C. Addition of CH_2Cl_2/pentane to the solution afforded a yellow crystalline powder. Yield: 0.82 g (96%).—^{1}H-NMR (CD_3COCD_3): δ = 7.74 (d, 1 H, H8); 7.33 (m, 1 H, H7); 6.91 (m, 1 H, H6); 6.63 (s, 1 H, H3); 3.95 (s, 3 H, 4-OCH_3); 3.88 (s, 4 H, OCH_2); 3.81 (s, 3 H, 5-OCH_3); 3.37 (m, 2 H, CH_2); 2.1–2.9 (m, 7 H, H (cyclohexyl)).—MS: *m/z* 372 ($M^{\oplus}$).

8: **6** (0.24 g, 0.65 mmol) was methylated with an excess of a 0.05 M diazomethane solution. The reaction product in THF was then added at −10 °C to a THF solution containing 0.65 mmol of both potassium *tert*-butoxide and isocyanomethyl(*p*-tolyl)sulfone. The mixture was stirred for 10 min and then treated with 0.4 g of glacial acetic acid. After removal of the solvent, the residue was dissolved in water and extracted with CH_2Cl_2. The crude product was deesterified with 2 N HCl. Extraction with CH_2Cl_2 at pH 1 afforded a yellow powder, which was treated carefully at 0 °C with 7.5 mL of TFA/TFAA (1:2). The red solution was worked up with $NaHCO_3$ and water; extraction with chloroform and evaporation of the solvent gave an orange-red powder, which was purified by preparative thin layer chromatography on silica gel with CH_2Cl_2/THF (2:1) and whose analytical and spectroscopic data are in agreement with those reported for the products described in Refs. [11] and [12]. Yield: 0.10 g (45%).—^{1}H-NMR ($CDCl_3$): δ = 7.72 (d, 1 H, H1); 7.43 (t, 1 H, H2); 6.83 (d, 1 H, H3); 3.98 (s, 3 H), 3.93 (s, 3 H), 3.89 (s, 3 H) (4-, 5-, 12-OCH_3); 3.6 (m, 2 H, CH_2); 2.0–2.9 (m, 8 H, CH_2, CH).—MS: *m/z* 354 ($M^{\oplus}$).

Received: July 6, 1987 [Z 2327 IE]
German version: *Angew. Chem.* 99 (1987) 1220

[1] K. H. Dötz, M. Popall, G. Müller, K. Ackermann, *Angew. Chem.* 98 (1986) 909; *Angew. Chem. Int. Ed. Engl.* 25 (1986) 911.
[2] Recent reviews: a) F. Arcamone: *Doxorubicin Anticancer Antibiotics*, Academic Press, New York 1981; b) H. S. El Khadem (Ed.): *Anthracycline*

Antibiotics, Academic Press, New York 1982; c) K. Krohn, *Angew. Chem. 98* (1986) 788; *Angew. Chem. Int. Ed. Engl. 25* (1986) 790.
[3] Review: K. H. Dötz, Angew. Chem. 86 (1984) 573; *Angew. Chem. Int. Ed. Engl. 23* (1984) 587.
[4] W. D. Wulff, P. C. Tang, *J. Am. Chem. Soc. 106* (1984) 434.
[5] K. H. Dötz, M. Popall, *J. Organomet. Chem. 291* (1985) C 1.
[6] K. H. Dötz, M. Popall, *Tetrahedron 41* (1985) 5797.
[7] K. H. Dötz, W. Sturm, M. Popall, J. Riede, *J. Organomet. Chem. 277* (1984) 267.
[8] The Cr-O bond in **3** (2.182(2) Å [7]) is significantly longer than that in $[(CO)_5Cr(thf)]$ (2.123(3) Å [9]), which usually serves as a source of coordinatively unsaturated chromium carbonyl fragments.
[9] U. Schubert, P. Friedrich, O. Orama, *J. Organomet. Chem. 144* (1978) 175.
[10] U. Schöllkopf, R. Schröder, *Angew. Chem. 84* (1972) 289; *Angew. Chem. Int. Ed. Engl. 11* (1972) 311.
[11] J. Yadav, P. Corey, C.-T. Hsu, K. Perlman, C. J. Sih, *Tetahedron Lett. 22* (1981) 811.
[12] A. V. Rama Rao, V. H. Deshpande, N. L. Reddy, *Tetrahedron Lett. 23* (1982) 775.
[13] The alkynes **4a** and **4b** were synthesized from 1,4-cyclohexanedione monoethylene acetal via 4-pyrrolidino-3-cyclohexen-1-one ethylene acetal [14] and propargyl bromide.
[14] P. Nedenskov, W. Taub, D. Ginsburg, *Acta Chem. Scand. 7* (1958) 1405.

Methyl (*E*)-2-(1-Aryl-4,5-dihydro-1*H*-tetrazol-5-ylidene)-2-cyanoacetate from Methyl 3,3-Diazido-2-cyanoacrylate and Primary Aromatic Amines**

By *Rolf W. Saalfrank,* Michael Fischer, Uwe Wirth,* and *Helmuth Zimmermann**

Dedicated to Professor Ulrich Schöllkopf on the occasion of his 60th birthday

Open-chain systems having the general structure **1**[***] can in principle undergo isomerization to give the corresponding cyclic systems **2**. Whether formula **1** or **2** represents the more stable structure depends on the substituents X and R.[2] For example, acyl azides **1**, X = O, exist exclusively in the open-chain form,[2,3] whereas thioacyl azides **1**, X = S, cyclize to give 1,2,3,4-thiatriazolones **2**, X = S.[2,4] In the case of imino azides **1**, $X=NR^1$, only electron-accepting substituents R^1 are capable of stabilizing the azide form, tetrazoles **2**, $X=NR^1$, being obtained otherwise.[2,5] Whereas this imino azide-tetrazole isomerization[6] is documented by numerous examples, there have been only a few reports on the vinyl azide-4*H*-triazole isomerization (**1**→**2** for $X=CR^1R^2$).[1,7]

Vinyl azides **1** [$R=NR^3R^4$, $X=CCN(CO_2CH_3)$] substituted with donor groups in the 4 position can undergo both 1,5 and 3,5 ring-closure reactions. Depending on the substituents R and the reaction conditions, either stable 1,2,3-triazoles are formed via the 4*H*-1,2,3-triazoles **2**, $R=NR^3R^4$, $X=CCN(CO_2CH_3)$, or 2*H*-azirines **3**, $R=NR^3R^4$, $R^1=CN$, $R^2=CO_2CH_3$, are formed with elimination of nitrogen.[1]

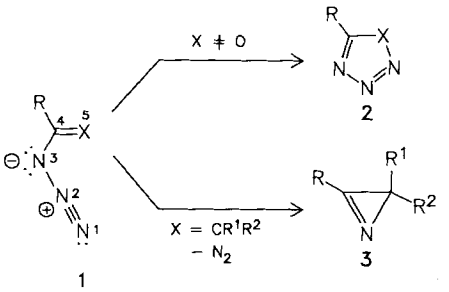

X = O, S, NR^1, CR^1R^2

The thermal transformation of vinyl azides **1** [$X=CR^1R^2$], with R, R^1, R^2 = H, alkyl, aryl, leads exclusively to 2*H*-azirines **3**. As the reaction mechanism, a 3,5 ring closure of **1** with concurrent elimination of nitrogen is favored over a pathway involving a free nitrene or one involving a 1,5 ring closure to give 4*H*-1,2,3-triazoles followed by elimination of nitrogen.[2a,8]

A detailed investigation of the vinyl azides **6**[***] [= **1** with $R=NHR'$, $X=CCN(CO_2CH_3)$] revealed that, for suitable substituents in the 4 position, these compounds could undergo novel, intermolecular reactions (1,5′ ring closure to give **7**,[***] nitrene addition to a C=C bond to give **9**).

Reaction of methyl 3,3-diazido-2-cyanoacrylate **4** with the primary arylamines **5a–c** at −25 °C leads initially to donor-substituted vinyl azides **6a–c** (for experimental data, see Table 1), which undergo base-catalyzed isomerization in dichloromethane to afford the methyl dihydrotetrazolylidenecyanoacetates **7a–c** (Table 1).[9,12]

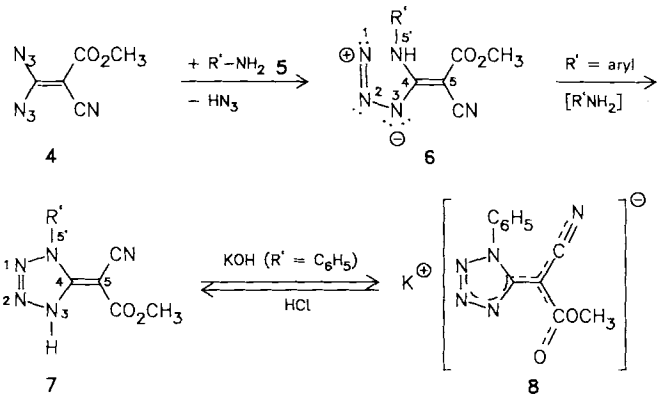

5–7	a	b	c	d
R′	C_6H_5	4-H_3C–C_6H_4	4-H_3CO–C_6H_4	CH_2

Compound **7a** dissolves in aqueous potassium hydroxide as the salt **8** (yield 74%, m.p. = 263 °C (from water/acetone)), which can be converted back into **7a** by reaction with hydrochloric acid.

The constitution of the heterocycles **7** could not be established unequivocally from the spectroscopic data. These data would also be in agreement with the methyl *N*-aryl-*N*-(5-cyano-1*H*-1,2,3-triazol-4-yl) carbamidates iso-

[*] Prof. Dr. R. W. Saalfrank, Dipl.-Chem. M. Fischer, Dipl.-Chem. U. Wirth
Institut für Organische Chemie der Universität Erlangen-Nürnberg
Henkestrasse 42, D-8520 Erlangen (FRG)
Priv.-Doz. Dr. H. Zimmermann
Institut für Angewandte Physik (Kristallographie)
der Universität Erlangen-Nürnberg
Bismarckstrasse 10, D-8520 Erlangen (FRG)

[**] Geminal Vinyl Azides, Part 5. This work was supported by the Deutsche Forschungsgemeinschaft and the Fonds der Chemischen Industrie. We wish to thank Prof. *H. Fritz*, Ciba-Geigy (Basel), for the ^{15}N-NMR spectrum, and Prof. *R. Carrié* and Dr. *D. Danion*, Université Rennes, for stimulating discussions. — Part 4: [1].

[***] The (unsystematic) numbering of the compounds **1**, **6** and **7** assists in discussing the substituent effects and in assigning the spectroscopic data.

Table 1. Data for the compounds **6a–d**, **7a–c**, and **10** [a].

6a: 0.47 g (78%), m.p. = 84 °C (dec.; from dichloromethane).—IR: $\tilde{\nu}$ = 2205 (CN), 2140 (N_3), 1660 cm^{-1} (C=O).—^{1}H-NMR: δ = 3.83 (s, 3 H; OCH_3), 7.36 (s, 5 H; C_6H_5), 11.40 (s, br, 1 H; NH).—^{13}C-NMR: δ = 52.02 (OCH_3), 66.59 (=C), 119.94 (CN), 124.10, 127.10, 129.17, and 134.96 (C_6H_5), 158.38 (=C), 168.42 (C=O).—^{15}N-NMR: δ = 98.4 (N-3), 118.6 (NH), 227.5 (N-1), 242.4 (N-2), 269.8 (CN).—MS: *m/z* 243 ($M^{\oplus}$)

6b: 0.48 g (75%), m.p. = 71 °C (dec.; from dichloromethane).—IR: $\tilde{\nu}$ = 2198 (CN), 2136 (N_3), 1672 cm^{-1} (C=O).—^{1}H-NMR: δ = 2.39 (s, 3 H; CH_3), 3.83 (s, 3 H; OCH_3), 7.19 (s, 4 H; C_6H_4), 11.23 (s, br, 1 H; NH).—^{13}C-NMR: δ = 21.02 (CH_3), 52.18 (OCH_3), 66.43 (=C), 115.30 (CN), 124.38, 129.96, 132.51, and 137.56 (C_6H_4), 158.72 (=C), 168.72 (C=O).—MS: *m/z* 257 ($M^{\oplus}$)

6c: 0.41 g (60%), m.p. = 76 °C (dec.; from dichloromethane).—IR: $\tilde{\nu}$ = 2200 (CN), 2130 (N_3), 1660 cm^{-1} (C=O).—^{1}H-NMR: δ = 3.83 (s, 6 H; two overlapping OCH_3), 7.08 (m, 4 H; C_6H_4), 11.18 (s, br, 1 H; NH).—^{13}C-NMR: δ = 52.15 and 55.51 (OCH_3), 66.07 (=C), 115.43 (CN), 114.51, 126.28, and 127.68 (3 aryl-C), 158.84 and 158.96 (1 aryl-C and =C), 168.75 (C=O).—MS: *m/z* 273 ($M^{\oplus}$)

6d: 0.48 g (93%), m.p. = 65 °C (dec.; from dichloromethane).—IR: $\tilde{\nu}$ = 2200 (CN), 2140 (N_3), 1670 cm^{-1} (C=O).—^{1}H-NMR: δ = 3.78 (s, 3 H; OCH_3), 4.00 (m, 2 H; NCH_2), 5.27 (m, 2 H; $=CH_2$), 5.90 (m, 1 H; =CH), 9.58 (s, br, 1 H; NH).—^{13}C-NMR: δ = 44.80 (NCH_2), 51.63 (OCH_3), 64.43 (=C), 115.21 (CN), 117.37 ($=CH_2$), 131.81 (=CH), 160.10 (=C), 168.51 (C=O).—MS: *m/z* 207 ($M^{\oplus}$)

7a: 0.41 g (84%), m.p. = 176 °C (from dichloromethane).—IR: $\tilde{\nu}$ = 2200 (CN), 1643 (C=O), 1572 cm^{-1} (N=N).—^{1}H-NMR ([D$_6$]DMSO): δ = 3.73 (s, 3 H; OCH_3), 7.67 (s, 5 H; C_6H_5), 15.66 (s, br, 1 H; NH).—^{13}C-NMR (100.5 MHz, [D$_6$]DMSO): δ = 48.49 (=C), 51.08 (OCH_3), 115.91 (CN), 127.60, 129.22, 131.26, and 132.76 (C_6H_5), 148.84 (=C), 166.69 (C=O).—UV (acetonitrile): λ_{max} = 270 nm (ε = 14580).—MS: *m/z* 243 ($M^{\oplus}$)

7b: 0.42 g (82%), m.p. = 193 °C (dec.; from dichloromethane).—IR: $\tilde{\nu}$ = 2200 (CN), 1650 (C=O), 1568 cm^{-1} (N=N).—^{1}H-NMR ($CDCl_3$/[D$_6$]DMSO): δ = 2.48 (s, 3 H; CH_3), 3.98 (s, 3 H; OCH_3), 7.42 (s, br, 4 H; C_6H_4), 13.70 (s, br, 1 H; NH).—MS: *m/z* 257 ($M^{\oplus}$)

7c: 0.41 g (75%), m.p. = 182 °C (dec.; from dichloromethane).—IR: $\tilde{\nu}$ = 2200 (CN), 1640 (C=O), 1585 cm^{-1} (N=N).—^{1}H-NMR ($CDCl_3$/[D$_6$]DMSO): δ = 3.71 and 3.90 (each s, each 3 H; $2OCH_3$), 7.34 (m, 4 H; C_6H_4), 14.28 (s, br, 1 H; NH).—MS: *m/z* 273 ($M^{\oplus}$)

10: 0.32 g (74%), m.p. = 230 °C (dec.; from acetonitrile).—IR: $\tilde{\nu}$ = 2185 (CN), 1640 cm^{-1} (C=O).—^{1}H-NMR ([D$_6$]DMSO): δ = 2.13 (s, 3 H; CH_3), 3.65 (s, 3 H; OCH_3), 6.72 (m, 1 H; =CH), 11.73 (s, br, 2 H; 2NH).—^{13}C-NMR (100.5 MHz, [D$_6$]DMSO): δ = 9.69 (CH_3), 48.33 (=C), 49.96 (OCH_3), 111.13 (=CH), 120.51 (CN), 124.34 ($=CCH_3$), 147.41 (=C), 167.92 (C=O).—MS: *m/z* 179 ($M^{\oplus}$)

[a] ^{1}H-NMR-spectra: JNM-PMX-60 and C-60 (both 60 MHz, TMS int.) (Jeol).—^{13}C-NMR-spectra: JNM-PS-100 and JNM-GX-400-FT (25.15 and 100.5 MHz, TMS int.) (Jeol).—^{15}N-NMR-spectrum: WM-400-spectrometer [40.55 MHz, CH_3NO_2 ext. (380.23 ppm with respect to $NH_{3(l)}$] (Bruker).—Solvent for all NMR spectra: $CDCl_3$ if not stated otherwise. A positive δ value always indicates a downfield shift. Mass spectra: Varian MAT-CH-4B, direct inlet, 70 eV. IR spectra: KBr

meric with **7**. For this reason, an X-ray structure analysis of **7a** was carried out (Table 2).[10]

Table 2. Structure data for the 1,4-dihydro-5-tetrazole skeleton of **7a**.

Bond lengths [pm]		Bond angles [°]	
N5′-N1	137.87 ± 14	N1-N5′-C4	110.1
N1-N2	126.59 ± 16	N2-N1-N5′	107.8
N2-N3	134.65 ± 14	N3-N2-N1	108.3
N3-C4	135.60 ± 15	C4-N3-N2	111.4
C4-N5′	135.47 ± 15	N5′-C4-N3	102.3

So far, it has not been possible to isomerize **6d** to **7d** using *base catalysis*. Upon *thermal* treatment (boiling toluene), **6d** undergoes nitrogen elimination. The nitrene thereby formed presumably reacts initially to give the bicyclic aziridine **9**, which, under the reaction conditions, undergoes spontaneous isomerization to give methyl (*E*)-2-(2,3-dihydro-4-methyl-1*H*-imidazolyidene)-2-cyanoacetate **10** (Table 1).[11, 12]

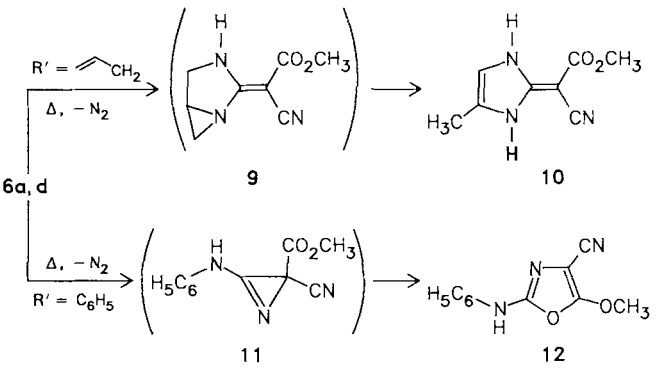

In contrast, thermolysis of **6a** affords the 2-anilino-5-methoxyoxazole-4-carbonitrile **12** (yield 78%, m.p. = 139 °C (from ethanol)), presumably via the azirine **11**.[8b, 13]

General Experimental Procedure

6a–d: The amine **5** (2.5 mmol) in dichloromethane (20 mL) was added under nitrogen to a solution of **4** (0.5 g, 2.6 mmol) [1,14] in dichloromethane (40 mL) at −25 °C. The resulting mixture was allowed to stir for 14 h at −25 °C and filtered. The solvent was then removed under vacuum.

7a–c: Vinyl azide **6** (2.0 mmol) and a catalytic amount of the arylamine **5** were allowed to stir together for 5–10 min at 40 °C in dichloromethane (50 mL). The solvent was then removed under water-aspirator vacuum.

Received: July 1, 1987 [Z 2323 IE]
German version: *Angew. Chem. 99* (1987) 1218

[1] R. W. Saalfrank, E. Ackermann, M. Fischer, U. Wirth, *Chem. Ber. 120* (1987), in press.
[2] Reviews: a) R. Huisgen, *Angew. Chem. 92* (1980) 979; *Angew. Chem. Int. Ed. Engl. 19* (1980) 947; b) M. Tisler, *Synthesis 1973*, 123; c) R. N. Butler, *Adv. Heterocycl. Chem. 21* (1977) 323.
[3] E. Lieber, R. L. Minnis, Jr., C. N. R. Rao, *Chem. Rev. 65* (1965) 377.
[4] A. Holm, *Adv. Heterocycl. Chem. 20* (1976) 145; E. Lieber, C. N. Pillai, *J. Org. Chem. 22* (1957) 1054; E. Lieber, J. Ramachandran, *Can. J. Chem. 37* (1959) 101.
[5] W. von Philipsborn, R. Müller, *Angew. Chem. 98* (1986) 381; *Angew. Chem. Int. Ed. Engl. 25* (1986) 383; W. E. Hull, M. Küstlinger, E. Breitmaier, *ibid. 92* (1980) 957 and *19* (1980) 924; R. Neidlein, E. Henkelbach, *ibid. 78* (1966) 548 bzw. *5* (1966) 520; R. Huisgen, *ibid. 72* (1960) 359.
[6] Used instead of the term "azido/tetrazolo isomerization" [2b].
[7] M. Henriet, M. Hontekie, B. Techy, R. Touillaux, L. Ghosez, *Tetrahedron Lett. 21* (1980) 223; C. Bernard, L. Ghosez, *J. Chem. Soc. Chem. Commun. 1980*, 941.
[8] a) H. Bock, R. Dammel, *Angew. Chem. 99* (1987) 518; *Angew. Chem. Int. Ed. Engl. 26* (1987) 505; H. Bock, R. Dammel, S. Aygen, *J. Am. Chem. Soc. 105* (1983) 7681; H. Bock, R. Dammel, *Z. Naturforsch. B 42* (1987) 301; *Inorg. Chem. 24* (1985) 4427; A. Hassner, N. H. Wiegand, H. E. Gottlieb, *J. Org. Chem. 51* (1986) 3176; T. Yamabe, M. Kaminoyama, T. Minato, K. Hori, K. Isomura, H. Taniguchi, *Tetrahedron 40* (1984) 2095; L. A. Burke, G. Leroy, M. T. Nguyen, M. Sana, *J. Am. Chem. Soc. 100* (1978) 3668; b) G. L'abbé, *Angew. Chem. 87* (1975) 831; *Angew. Chem. Int. Ed. Engl. 14* (1975) 775.
[9] See R. N. Butler in A. R. Katritzky, C. W. Rees (Eds.): *Comprehensive Heterocyclic Chemistry, Vol. 5, Part 4A*, Pergamon, Oxford 1984, p. 791; H. Quast, B. Seifering, *Tetrahedron Lett. 23* (1982) 4681; H. Quast, L. Bieber, G. Meichsner, *Liebigs Ann. Chem. 1987*, 469; H. Quast, L. Bieber, *Angew. Chem. 87* (1975) 422; *Angew. Chem. Int. Ed. Engl. 14* (1975) 428; H. Quast, G. Meichsner, B. Seiferling, *Chem. Ber. 120* (1987) 225; H. Quast, G. Meichsner, *ibid. 120* (1987) 1049.
[10] H. Zimmermann, U. Wirth, M. Fischer, R. W. Saalfrank, unpublished.
[11] See W. Lwowski in W. Lwowski (Ed.): *Nitrenes*, Wiley, Interscience, New York 1970, Kap. 6, p. 185ff; K. Hafner, W. Kaiser, *Tetrahedron Lett. 1964*, 2185.
[12] The vinyl azides **6a–d** and the 1,3-dihydroimidazole **10** are presumably present as the *E* isomers.
[13] A. Hassner in E. F. V. Scriven (Ed.): *Acides and Nitrenes*, Academic Press, New York 1984, Chap. 2, p. 35ff.
[14] *Warning:* Crystals of **4** placed on a Kofler bank decomposed explosively at about 70 °C. For safety reasons, we have therefore only synthesized this substance on a 0.5-g scale or less.

Simultaneous Primary and Secondary Coordination of a Neutral Guest within a Macrocyclic Complex of Rhodium(III)**

By *George Ferguson,* Karen E. Matthes,* and *David Parker**

The binding of a neutral ligand to a metal center within a macrocyclic complex is a common feature of the coordination chemistry of macrocyclic systems. However, there are very few examples[1] in which the complex is stabilized by secondary binding of the neutral ligand to the receptor molecule. During the course of studies directed towards an exploration of the receptor properties of heterotopic macrocyclic ligands,[2] we have characterized a remarkable Rh^{III} complex **1**, in which a water molecule is bound to the metal center and stabilized by intramolecular hydrogen bonding to the polyether chain.

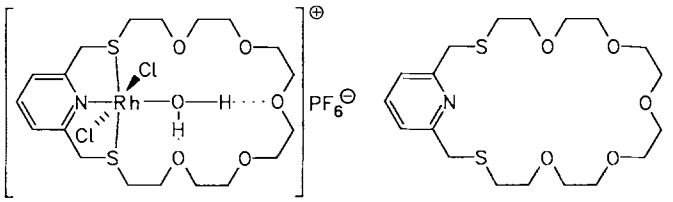

1

2

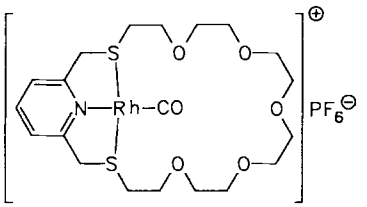

3

Reaction of the ditopic macrocycle **2**[3] with rhodium trichloride in refluxing methanol followed by addition of NH_4PF_6 yielded an orange crystalline complex, **1**, whose fast atom bombardment mass spectrum (8 keV, Ar atoms, glycerol) revealed peaks at m/z 608 [$M^{\oplus}$], 573 [$M^{\oplus}-Cl$], 555 [$M^{\oplus}-Cl$, $-H_2O$], and 520 ($M^{\oplus}$ is the cation of **1** − H). The same complex could also be formed by aerial oxidation of the cationic rhodium(I) carbonyl complex **3** in chloride-saturated methanol. In the ^1H-NMR spectrum of **1** (298 K, CD_2Cl_2) the benzylic methylene protons were diastereotopic ($\delta = 4.92$, 4.70), consistent with stereogenic sulfur centers with a stable configuration. Such behavior was in contrast to the behavior of **3** in solution, which gave an exchange-broadened spectrum (CH_2S and CH_2O resonances) at 298 K (CD_2Cl_2) which sharpened on cooling ($\Delta G_c^{+} = 63.8$ kJ mol^{-1}). The inversion of sulfur may be attributed to a "ring-skip" of the polyether chain over the Rh–CO vector.

[*] Prof. G. Ferguson
Department of Chemistry, University of Guelph
Guelph NG1 2W1, Ontario (Canada)
Dr. D. Parker, K. E. Matthes
Department of Chemistry, University of Durham
South Road, Durham DH1 3LE (UK)

[**] This work was supported by the Science and Engineering Research Council of the United Kingdom and NSERC (Canada).

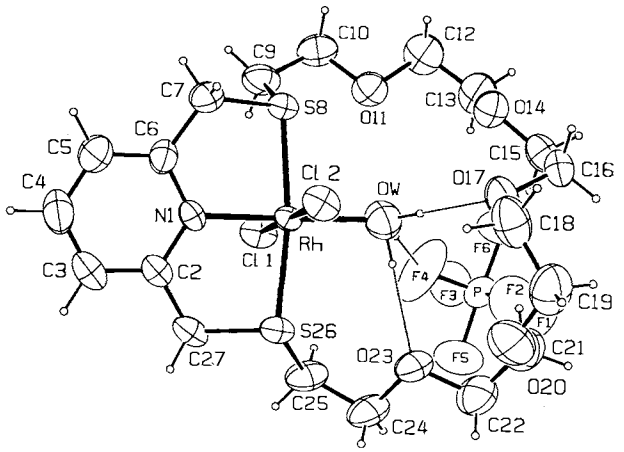

Fig. 1. Structure of **2** in the crystal. Monoclinic, $P2_1/n$, $a = 10.767(2)$, $b = 23.479(4)$, $c = 11.577(2)$ Å, $\beta = 95.04(1)°$, $V = 2915.4$ Å^3, $Z = 4$, $\rho_{calcd} = 1.72$ g cm^{-3}, $F(000) = 1528$, $\mu(Mo_{K\alpha}) = 10.3$ cm^{-1}; 4637 unique reflections were measured on a CAD4 diffractometer, $2\theta < 54°$. After correction for Lorentz polarization and absorption effects, 2103 were labeled "observed" and used in structure solution and refinement to give $R = 0.024$, $R_w = 0.032$. Selected bond lengths [Å] and bond angles [°]: Rh-N1 2.025(4), Rh-OW 2.070(4), Rh-Cl1 2.332(1), Rh-Cl2 2.330(1), Rh-S8 2.329(1), Rh-S26 2.327(1), OW...F4 3.133(6), OW...O17 2.986(6), OW...O23 3.128(6); S8-Rh-S26 166.76(5), OW-Rh-N1 178.2(2); Cl1-Rh-Cl2 179.50(5). Further details of the crystal structure investigation may be obtained from director of the Cambridge Crystallographic Data Centre, University Chemical Laboratory, Lensfield Road, Cambridge, CB2 1EW (UK).

The crystal structure of **1** (Fig. 1) revealed an octahedral coordination for the Rh^{III} center, in which the main distortion arises from the S8–Rh–S26 bond angle of 166.76(5)° due to the intrinsically small bite angles of the two five-ring chelates. The coordinated water molecule is strongly bound to the Rh^{III} center[4] (Rh-OW: 2.070(4) Å), increasing the polarization of the O–H bonds which are directed towards the polyether chain. Electron-density difference-maps at $R = 0.025$ showed that the water hydrogens are disordered over three sites (occupancies from peak densities are 0.72, 0.80, and 0.48) and form three hydrogen bonds. Two of these are intramolecular bonds to O17 and O23 and the third is to a fluorine atom of the PF_6 counterion. This secondary binding is a consequence of the enhanced acidity of the coordinated water molecule.

Given that the Rh–Cl bonds may be easily cleaved by addition of $Ag^{\oplus}$ in solution, complex **1** (and its noble-metal analogues[5]) may afford access to some coordinatively unsaturated d^8 complexes, of potential catalytic activity, in which a neutral molecule (H_2O, NH_3, C_2H_4) or cationic guest ($Na^{\oplus}$, $K^{\oplus}$) may be closely bound within the macrocyclic ring.[6]

Received: June 15, 1987 [Z 2297 IE]
German version: *Angw. Chem. 99* (1987) 1195

[1] N. W. Alcock, J. M. Brown, J. C. Jeffery, *J. Chem. Soc. Dalton Trans. 1976*, 583; H. M. Colquhoun, S. M. Doughty, A. M. Z. Slawin, J. F. Stoddart, D. J. Williams, *Angew. Chem. 97* (1985) 124; *Angew. Chem. Int. Ed. Engl. 24* (1985) 135.

[2] D. Parker, J. M. Lehn, J. Rimmer, *J. Chem. Soc. Dalton Trans. 1985*, 1517; D. Parker, *J. Chem. Soc. Chem. Commun. 1985*, 1129; see also A. Carroy, J. M. Lehn, *ibid. 1986*, 1232.

[3] E. Weber, F. Vögtle, *Chem. Ber. 109* (1976) 1803; G. Weber, *Inorg. Chim. Acta 58* (1982) 27.

[4] Other Rh^{III} aquo complexes: C. K. Thomas, J. A. Stanko, *J. Coord. Chem. 2* (1973) 211, 231; K. Wieghardt, W. Schmidt, B. Nuber, B. Prikner, B. Weiss, *Chem. Ber. 113* (1980) 36; G. H. Y. Lin, J. D. Leggett, R. M. Wing,

Acta Crystallogr. Sect. B 29 (1973) 1023; T. Glowiak, M. Kubiak, T. Szymanska-Buzar, *ibid. B 33* (1977) 1732.

[5] **2** forms well-defined cationic complexes with other noble metals, e.g., [**2** · PdCl]$^{\oplus}$Cl$^{\ominus}$ and [**2** · PtCl]$^{\oplus}$Cl$^{\ominus}$. All new compounds and complexes gave satisfactory microanalytical and spectroscopic data (^{1}H, IR, FAB MS) in accord with the proposed structures.

[6] H. M. Colquhoun, J. F. Stoddart, D. J. Williams, *Angew. Chem. 98* (1986) 483; *Angew. Chem. Int. Ed. Engl. 25* (1986) 487.

Trithiodeltate: a New, Aromatic Thioxocarbon Dianion**

By *Gerhard Baum, Franz-Josef Kaiser, Werner Massa,* and *Gunther Seitz**

Replacement of the oxygen atoms in the dianion deltate **1**[1,2] with other functional groups leads to pseudooxocarbon dianions of the C_3 series,[3] e.g., **2**[4] and **3**,[5] which are

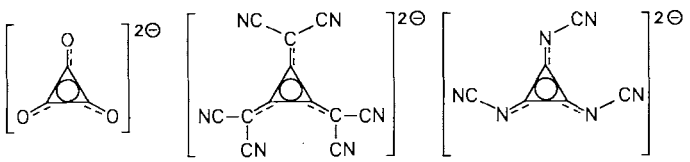

1 **2** **3**

novel, aromatic systems[6] having delocalized π electrons and exhibiting interesting properties. As part of our continuing studies, we have now succeeded in synthesizing the sulfur analogue, trithiodeltate, $C_3S_3^{2\ominus}$ **8**, which, along with tetrathiosquarate $C_4S_4^{2\ominus}$, is the first member of the series $C_nS_n^{2\ominus}$.[7]

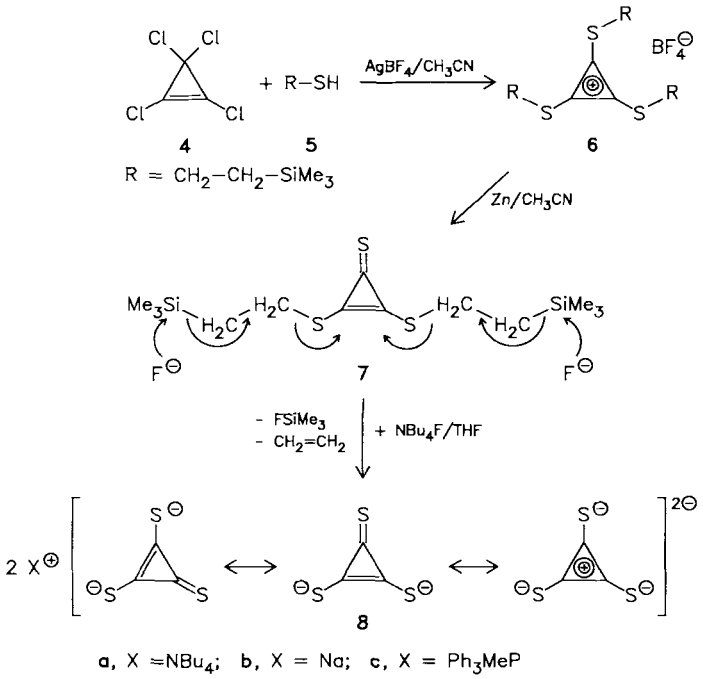

4 **5** **6** **7** **8**

R = CH_2–CH_2–$SiMe_3$

a, X = NBu_4; **b**, X = Na; **c**, X = Ph_3MeP

To introduce three sulfur functions into the deltic acid system,[8] tetrachlorocyclopropene **4** was allowed to react with 2-trimethylsilylethanethiol **5**[9] in the presence of silver ions. This results in formation of the triply thioalkyl-substituted cyclopropenylium salt **6** (yield 20%, m.p. = 114 °C), which contains sulfur functions capable of undergoing elimination reactions to form the dianion trithiodeltate. Before these elimination reactions are performed, however, **6** must be reduced to the thione **7**, which can be achieved with zinc powder in acetonitrile[10] (yield 54%, m.p. = 60 °C). Subsequent fluoride-promoted fragmentation of **7** results in elimination of fluorotrimethylsilane and ethylene to give the tetrabutylammonium salt **8a**, which, by addition of sodium perchlorate solution, is converted into the more readily isolated sodium salt **8b** (yield 62%). Dissolving **8b** in an aqueous methyltriphenylphosphonium bromide solution results in formation of the readily crystallizable salt **8c**. Chemical proof of the structure of **8b** was accomplished by treatment of **8b** with methyl iodide in acetonitrile in order to alkylate all three sulfur functions. The initially formed iodide **9a** reacts with sodium tetrafluoroborate to give the known salt **9b**.[8]

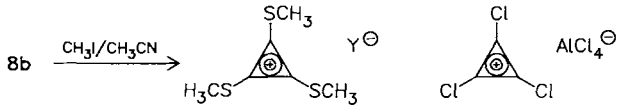

9 **10**

a, Y = I; **b**, Y = BF_4

The ^{13}C-NMR spectrum of **8b** in D_2O consists of a single signal at $\delta = 176.5$. The electronic absorption spectrum of an aqueous solution of **8b** exhibits a long-wavelength maximum at 268 nm (lg $\varepsilon = 4.32$).

The Raman and IR data[11] of the dianion of **8b** are similar to those of the isoelectronic cation of trichlorocyclopropenylium **10**[12] and are in agreement with a planar structure as well as with the expected D_{3h} symmetry.[13] This is also supported by the X-ray structure analysis[14] of **8c** (Fig. 1), which crystallizes along with three molecules

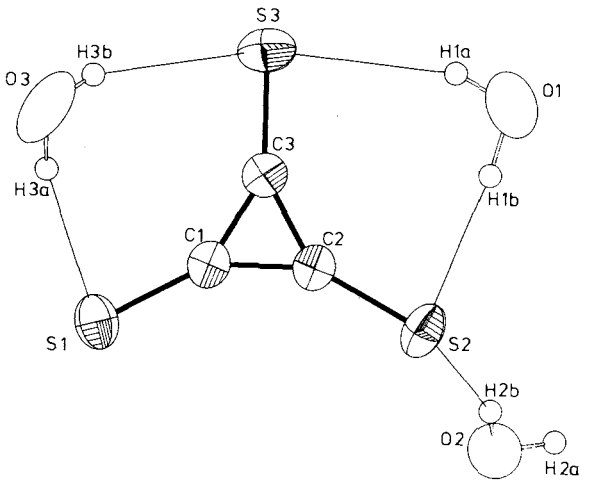

Fig. 1. ORTEP plot [19] of the molecular structure of the dianion of **8c** with surrounding molecules of water. The thermal ellipsoids are drawn at the 50% probability level. Important distances [Å] and angles [°] with vibrational correction in parentheses: C1-C2 1.402(3) [1.406], C1-C3 1.408(3) [1.413], C2-C3 1.406(4) [1.406], C1-S1 1.678(2) [1.684], C2-S2 1.680(3) [1.685], C3-S3 1.669(3) [1.674]; C2-C1-C3 60.0(5), C1-C2-C3 60.2(5), C1-C3-C2 59.8(5), S1-C1-C2 151.3(6), S1-C1-C3 148.7(6), C1-C2-S2 151.3(7), S2-C2-C3 148.5(7), C2-C3-S3 150.7(6), C1-C3-S3 149.6(6). H bonds: S2...O1 3.26, S2-H1b-O1 174; S3...O1 3.34, S3-H1a-O1 157; S3...O3 3.35, S3-H3b-O3 156; S1...O3 3.29, S1-H3a-O3 156; S2...O2 3.40, S2-H2b-O2 161.

[*] Prof. Dr. G. Seitz, Apotheker F.-J. Kaiser
Pharmazeutisch-chemisches Institut der Universität
Marbacher Weg 6, D-3550 Marburg (FRG)
G. Baum, Priv.-Doz. Dr. W. Massa
Fachbereich Chemie der Universität
Hans-Meerwein-Strasse, D-3550 Marburg (FRG)

[**] This work was supported by the Deutsche Forschungsgemeinschaft and the Fonds der Chemischen Industrie.

of water. The bond lengths and bond angles of the crystallographically nonsymmetric dianion trithiodeltate exhibit only minor deviations from those expected for D_{3h} symmetry. The deviations of the "best" plane containing the six atoms of the dianion are all smaller than 0.015 (8) Å.

Trithiodeltate may therefore be regarded as virtually planar with the following mean distances and angles (with vibrational correction in parentheses): C-C 1.405 (1.408), C-S 1.676 (1.681) Å, C-C-C 60.0°, C-C-S 150.0°.

The C-C distances are equal within experimental error and similar to those in triphenylcyclopropenylium perchlorate[15] (1.373 Å) or 1,2,3-tris(dimethylamino)cyclopropenylium perchlorate[16] (1.363 Å). The C-S distance hardly differs from that in the next-highest homologue tetrathiosquarate (1.664 Å)[17] and corresponds to a partial double bond, such as that observed in thiocarboxylic acids and their derivatives.[18] It therefore seems reasonable to describe the ground state of the dianion trithiodeltate with resonance formulas containing cyclopropenylium and displaying C=S character.

Experimental Procedure

8b: A 1M solution (6 mL) of tetrabutylammonium fluoride in THF was added under a stream of nitrogen to a stirred solution of 7 (335 mg, 1 mmol) in $CHCl_3$ (1.5 mL) at 0 °C. After cessation of gas evolution, the cooling bath was removed and the solution was stirred for an additional 10 min under a stream of nitrogen and then for a further 12 h under nitrogen atmosphere. The dark solution was concentrated in a rotory evaporator. The residue was dissolved in $CHCl_3$ (7 mL) and washed six times with 4 mL of water. After drying over sodium sulfate, the organic phase was filtered; the solvent was removed under vacuum and the oily residue was taken up in acetonitrile (5 mL). Addition of a solution of $NaClO_4 \cdot H_2O$ (420 mg, 3 mmol) in acetonitrile (2 mL) resulted in precipitation of the sodium salt **8b** as a beige to grey solid. The grey impurity was removed by dissolving **8b** in water, filtering the resulting solution, and removing the solvent. Yield: 110 mg (62%) crude product; m.p. > 300 °C.

Received: June 24, 1987 [Z 2309 IE]
German version: *Angew. Chem. 99* (1987) 1199

[1] D. Eggerding, R. West, *J. Am. Chem. Soc. 98* (1976) 3641; see also M. A. Pericas, F. Serratosa, *Tetrahedron Lett. 1977*, 4430, 4437; R. West, D. Eggerding, J. Perkins, D. Handy, E. C. Tuazon, *J. Am. Chem. Soc. 101* (1979) 1710.

[2] Reviews: a) R. West: *Oxocarbons*, Academic Press, New York 1980; b) F. Serratosa, *Acc. Chem. Res. 16* (1983) 170; c) A. H. Schmidt, *Chem. Unserer Zeit 16* (1982) 57.

[3] G. Seitz, *Nachr. Chem. Tech. Lab. 28* (1980) 804.

[4] T. Fukunaga, *J. Am. Chem. Soc. 98* (1976) 610.

[5] B. Gerecht, G. Offermann, G. Seitz, *Synthesis 1982*, 727.

[6] For discussions of the aromaticity of the oxocarbon dianions, see J. Aihara, *J. Am. Chem. Soc. 103* (1981) 103; K. Jug, *J. Org. Chem. 48* (1983) 1344.

[7] Review: G. Seitz in [2a], p. 15.

[8] Z. Yoshida, *Top. Curr. Chem. 40* (1973) 48; R. Gompper, U. Jersak, *Tetrahedron Lett. 1973*, 3409; Z. Yoshida, S. Miki, S. Yoneda, *ibid. 1973*, 4731.

[9] T. I. Ito, W. P. Weber, *J. Org. Chem. 39* (1974) 1694.

[10] Application of this reaction principle: Z. Yoshida, Jap. Kokai 75 62,954 (29. May 1975), Mitsubishi Chemical Industries; *Chem. Abstr. 83* (1975) 113752d.

[11] **8b**, Raman spectrum: $\tilde{\nu}$ = 1678w, 1212w, 354s cm^{-1}; IR (Nujol): $\tilde{\nu}$ = 1223vs, 694s, 220m, 198m, 157s, 139w, 115w cm^{-1}.

[12] R. West, A. Sado, S. W. Tobey, *J. Am. Chem. Soc. 88* (1966) 2488.

[13] We thank Herrn Prof. Dr. *K. Dehnicke*, Marburg, for recording the IR and Raman spectra of **8b** and for stimulating discussions.

[14] **8c**, $(Ph_3MeP)_2C_3S_3 \cdot 3H_2O$, space group $P\bar{1}$, $Z = 2$, $a = 10.106(5)$, $b = 11.845(5)$, $c = 18.478(4)$ Å, $\alpha = 72.03(3)$, $\beta = 101.93(3)$, $\gamma = 115.27(3)°$; 6616 unique reflections with $F_o > 3\sigma(F_o)$ measured on a four-circle diffractometer (CAD4, Enraf-Nonius) with $Cu_{K\alpha}$ radiation at −70 °C; numerical absorption correction ($\mu = 27.5$ cm^{-1}), H atoms refined using isotropic temperature factors. 608 parameters, $R_w = 0.049$ (weighting $w = 1/\sigma^2(F_o)$). Further details of the crystal structure investigation may be obtained from the Fachinformationszentrum Energie, Physik, Mathematik GmbH, D-7514 Eggenstein-Leopoldshafen 2 (FRG), on quoting the depository number CSD-52696, the names of the authors, and the journal citation.

[15] M. Sundaralingam, L. H. Jensen, *J. Am. Chem. Soc. 85* (1963) 3302; *88* (1966) 198.

[16] A. T. Ku, M. Sundaralingam, *J. Am. Chem. Soc. 94* (1972) 1688.

[17] R. Allmann, T. Debaerdemaeker, K. Mann, R. Matusch, R. Schmiedel, G. Seitz, *Chem. Ber. 109* (1976) 2208.

[18] Examples: G. Adiwidjaja, H. Gunther, J. Voß, Liebigs Ann. Chem. 1983, 1116, and references cited therein; H. Lund, E. Hoyer, R. G. Hazell, *Acta Chem. Scand. B 36* (1982) 207; R. Mattes, F. Waldmann, *Z. Naturforsch. B 38* (1983) 335.

[19] C. K. Johnson: *ORTEP, A Fortran Thermal-Ellipsoid Plot Program for Crystal Structure Illustrations*, Oak Ridge 1965.

Tricyclic 2,4-Diaminovinamidines—Readily Accessible, Very Strong CHN Bases**

By *Reinhard Schwesinger**

Amidine bases such as 1,8-diazabicyclo[5.4.0]undec-7-ene (DBU) and 1,4-diazabicyclo[4.3.0]non-5-ene[1] and guanidine bases such as tetramethylguanidine and 1,5,7-triazabicyclo[4.4.0]dec-5-ene[2] have so far been the strongest available neutral auxiliary bases. Because of the better charge distribution in the conjugate cation, the so far unknown, completely alkylated 2,4-diaminovinamidines would be expected to exhibit an even higher basicity. Owing to steric interactions, the corresponding open-chain cations,[3] however, exist in a twisted conformation, which is unfavorable for optimal conjugation.[4] The cations **1**, on the other hand, should be largely planar and the conjugate bases **2** should therefore be stronger bases.

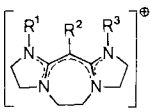

1a, $R^1 = R^2 = R^3 = H$
b, $R^1 = CH_3$, $R^2 = R^3 = H$
c, $R^1 = R^3 = CH_3$, $R^2 = H$
d, $R^1 = Ac$, $R^2 = H$, $R^3 = CH_3$

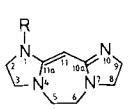

2a, R = H
b, $R = CH_3$
c, R = Ac

1a · Cl can be prepared on a large scale by the one-pot reaction of technical triethylenetetramine, malonodinitrile, and NH_4Cl. The free base **2a** is obtained by reaction of **1a** · Cl with NaOMe and is purified by crystallization (from dimethylformamide) or sublimation (130 °C/0.001 torr).

In contrast to the open-chain systems,[3] **2a** exists (largely) as 2,4-diaminovinamidine and not as malonodiamidine **2a'** according to ^{1}H-NMR analysis (Table 1, also in CD_3CN). This is presumably due to the more effective conjugation in **2a**.

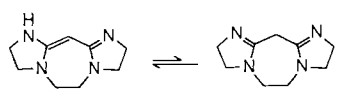

2a ⇌ **2a'**

Monomethylation of **2a** to give **2b** is accomplished in good yield by monoacetylation (*N*-acetylimidazole/tetrahydrofuran/room temperature) to give **2c**, methylation (MeBr/acetonitrile) to give **1d** · Br, and deacetylation to

[*] Dr. R. Schwesinger
Chemisches Laboratorium der Universität
Institut für Organische Chemie und Biochemie
Albertstrasse 21, D-7800 Freiburg (FRG)

[**] This work was supported by the Deutsche Forschungsgemeinschaft and the Fonds der Chemischen Industrie.

give **1b**·Br (Me_2NH/MeOH). The base **2b** (Table 1) is obtained by treatment of **1b**·Br with NaOMe and purified by distillation (b.p. = 172 °C/0.01 torr) or crystallization (from Et_2NH).

Table 1. Melting points and ^{1}H-NMR data for the compounds **1a,b**·ClO_4 and **2a,b** [5].

Compound	M.p. [°C]	250-MHz ^{1}H-NMR (δ in [D$_6$]dimethyl sulfoxide ([D$_6$]DMSO))
2a	137–139	3.25 (10 H, m), 3.47 (2 H, m; H-9), 4.07 (1 H, s; H-11), 5.3 (1 H, br.s; H-10)
1a·ClO_4	260–265	3.48 (4 H, s; H-2, H-9), 3.53 (8 H, m), 4.17 (1 H, s; H-11), 7.73 (2 H, br.s; H-1, H-10)
2b	102–104	2.61 (3 H, s; CH_3), 3.0–3.4 (12 H, m), 3.98 (1 H, s; H-11)
1b·ClO_4	145–147	2.79 (3 H, s; CH_3), 3.3–3.8 (12 H, m), 4.13 (1 H, s; H-11), 7.71 (1 H, br.s; H-10)

The extreme upfield shift (also compared with the open-chain permethyl compound[6]) of the NMR signal for the methine carbon atom in **1a** and **1c** ($\delta(^{13}C) = 61.1$ and 56.7, respectively) indicates the presence of a high charge density at C-11; the nucleophilicity of C-11 is supported by the identification of ca. 16% of **3e** ($R^1 = R^3 = H$, $R^2 = CH_3$) in the reaction of **1a** with methyl *p*-toluenesulfonate (in Me_2SO_2, 130 °C). The cations **1** (analogous to the open-chain cations[3]) are protonated by strong acids at C-11 to give **3**.[5]

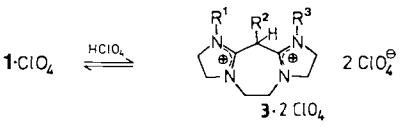

The pK_a values of **2a** and **2b** in acetonitrile (26.22 and 26.95,[7] respectively; DBU, 24.32) are only slightly smaller than those of triaminomonophosphazene bases;[8] however, as dehydrohalogenation reagents and with respect to their (hydrolytic) stability, **2a** and **2b** are appreciably inferior to the latter.

Because of the sparing solubility and excellent crystallizability of the salts of **1a** and **1b**, the bases **2a** and **2b** are useful as proton trapping agents in aprotic medium. We are currently investigating to what extent the rigid skeleton of **2** is suitable for the construction of chiral, strong bases. Very strongly basic "proton sponges" structurally derived from **2** have already been synthesized and studied.[9]

Experimental Procedure

1a·Cl: NH_4Cl (185 g, 3.46 mol) was added in portions to a mixture of technical triethylenetetramine (235 g, ca. 1.13 mol of linear triethylenetetramine) in dry MeOH (330 mL) and anhydrous, peroxide-free diethylene glycol monomethyl ether (400 mL) at ca. 50 °C. A solution of malonodinitrile (66 g, 1 mol) in MeOH (170 mL) was then added over 2 h to the refluxing solution. At the end of the addition, a precipitate began to form. MeOH was distilled off under normal pressure. The residue was heated to 180 °C for 1.5 h (vigorous evolution of ammonia). A hot solution of butylamine (100 mL) in 2-propanol (1.7 L) was then added to the hot mixture (80–100 °C). After ca. 24 h at 0 °C, 176 g (82%) of **1a**·Cl, m.p. ≈ 290 °C (dec.), was isolated.

Received: July 10, 1987;
revised: August 26, 1987 [Z 2343 IE]
German version: *Angew. Chem. 99* (1987) 1209

[1] K. Eiter, H. Oediger, *Justus Liebigs Ann. Chem. 682* (1965) 62.
[2] A. F. McKay, M. E. Kreling, *Can. J. Chem. 35* (1957) 1438; C. Leumann, T. Früh, M. Göbel, A. Eschenmoser, *Angew. Chem. 99* (1987) 273; *Angew. Chem. Int. Ed. Engl. 26* (1987) 261.
[3] H. G. Viehe, Z. Janousek, *Angew. Chem. 85* (1973) 837; *Angew. Chem. Int. Ed. Engl. 12* (1973) 806.
[4] E. Oeser, *Chem. Ber. 107* (1974) 627.
[5] ^{1}H-NMR, UV, and IR data and correct C,H,N,Cl analyses were obtained for all **1**·ClO_4. Owing to their explosive behavior the diperchlorates **3**·2ClO_4 gave unsatisfactory analytical data. The same was true of the free bases **2** owing to their sensitivity toward water. An ^{1}H-NMR spectrum of **3a** in [D$_6$]DMSO shows only very broad, structureless signals. The diperchlorates were only characterized by their melting points. **3a**·2ClO_4, m.p. = 210 °C; **3b**·2ClO_4, m.p. = 233–236 °C (dec.).
[6] H.-U. Wagner, *Chem. Ber. 107* (1974) 634.
[7] Absolute scale determined by UV/VIS-monitored titration with [Et*i*Pr$_2$NH]BPh_4 (0.01 M solution, 25 °C) against indicators; R. Schwesinger, unpublished.
[8] R. Schwesinger, *Chimia 39* (1985) 269.
[9] R. Schwesinger, M. Mißfeldt, K. Peters, H. G. von Schnering, *Angew. Chem. 99* (1987) 1210; *Angew. Chem. Int. Ed. Engl. 26* (1987) 1165.

Novel, Very Strongly Basic, Pentacyclic "Proton Sponges" with Vinamidine Structure**

By *Reinhard Schwesinger,* Michael Mißfeldt, Karl Peters,* and *Hans Georg von Schnering*

The basicity of "proton sponges" is determined by the degree of repulsion between the lone pair electrons, the strength of the hydrogen bond in the conjugate cation, and the proton affinity of the chelating groups. X-ray structure analyses of bases containing two tertiary amino groups and of their cations[1,2] often provide insight into the first two factors and spectroscopic measurements afford information concerning the symmetry of the hydrogen bond.[3] In these systems a high thermodynamic basicity can only be achieved at the expense of a very low kinetic basicity;[4] presumably, it cannot be realized at all with sterically nondemanding, less basic groups.[5] Further extension of the strongly basic system **1**[6] by one dihydroimidazole unit offered a possible route to bases that would be both thermodynamically strong and kinetically active.

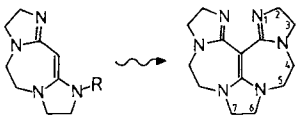

1a, R = H; **1b**, R = CH_3 **2**

Whereas **3** can be obtained directly from **4**[7] and diethylenetriamine, **2**, and its structural analogues **5** and **6** are readily accessible only by symmetrical construction from **4** via **7**, **8**, and **9** (Scheme 1). Compounds **9a–c** are products of "zip reactions";[8] their asymmetrical structures are confirmed by the ^{1}H- and ^{13}C-NMR data. The melting points and ^{1}H-NMR data of the new compounds **2**, **5**, and **6** are summarized in Table 1.

[*] Dr. R. Schwesinger, Dipl.-Chem. M. Mißfeldt
Chemisches Laboratorium der Universität
Institut für Organische Chemie und Biochemie
Albertstrasse 21, D-7800 Freiburg (FRG)
Dr. K. Peters, Prof. Dr. H. G. von Schnering
Max-Planck-Institut für Festkörperforschung
Heisenbergstrasse 1, D-7000 Stuttgart 80 (FRG)

[**] This work was supported by the Deutsche Forschungsgemeinschaft and the Fonds der Chemischen Industrie.

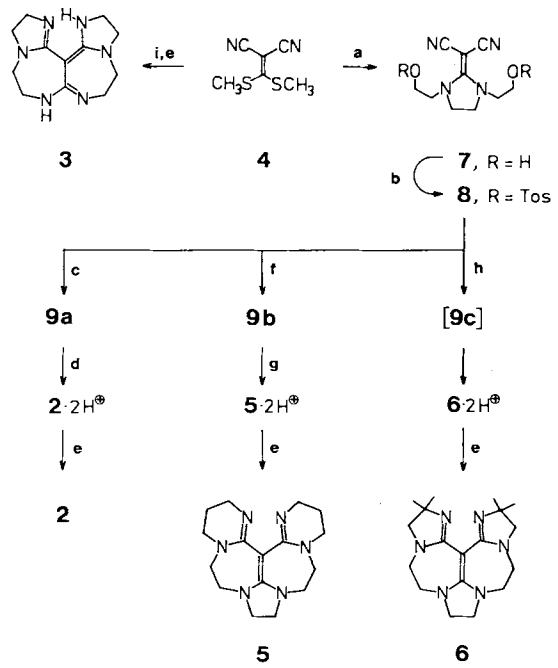

Scheme 1. Synthesis of **2**, **3**, **5**, and **6** [9]: a) 1.1 equiv. $(HO-C_2H_4-NH-CH_2)_2$, CH_3OH, 14 h reflux (92% from H_2O, m.p. = 137–139 °C). b) Pyridine, 0 °C, 3.5 equiv. TosCl in CH_2Cl_2, 16 h, 20 °C; 2 equiv. H_2O, 0 °C; 2 h, 20 °C (88% from CH_2Cl_2/CH_3OH, m.p. = 122–123 °C). c) 20 equiv. ethylenediamine, 2 h 20 °C; high vacuum; precipitation with TosOH/H_2O (91%). d) Dry glycol, 2 equiv. $LiOCH_3$, 15 min, 150 °C, high vacuum; precipitation with $LiClO_4/H_2O$ (m.p. = 250–251 °C (dec.)); renewed precipitation with Li-picrate/H_2O (overall yield 60%). e) Strongly basic anion exchanger, $Cl^{\ominus}$ form, CH_3OH (**2**, **3**) or LiBr, CH_3CN (**5**, **6**), 2 equiv. $NaOCH_3/CH_3OH$, 220 °C/5 × 10^{-4} torr (Table 1). f) 40 equiv. 1,3-propanediamine, 2 h, 60 °C; precipitation with TosOH/H_2O (40%). Dry glycerin, 2 equiv. $LiOCH_3$, 1 h, 200 °C, high vacuum; precipitation with $HClO_4/H_2O$ (67% from CH_3CN, m.p. = 330–334 °C (dec.)). h) 12 equiv. 1,2-diamino-2-methylpropane, 4 h, 60 °C, high vacuum; dry glycol, 1 h, 180 °C, high vacuum; precipitation with $NaPF_6/H_2O$ (68% from CH_3OH, m.p. = 300–305 °C). i) 3 equiv. NH_4Cl, 3 equiv. diethylenetriamine, glycerin, 35 h, 135 °C, high vacuum; precipitation with $HClO_4/H_2O$ (22%, m.p. = 273–274 °C).

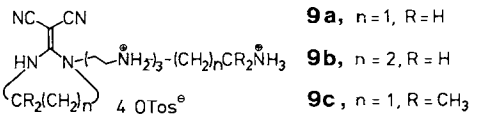

9a, n = 1, R = H
9b, n = 2, R = H
9c, n = 1, R = CH_3

Table 1. Melting points and ^{1}H-NMR data of **2**, **5**, and **6**.

Compound [9]	M.p. [°C]	250-MHz ^{1}H-NMR (δ in CD_3CN)
2	228–231	3.17(4 H; AA′ part of AA′BB′), 3.23–3.29 (8 H, m), 3.33 (4 H, s), 3.44 (4 H; BB′ part of AA′BB′)
5	255–258 (dec.)	1.71 (4 H, m), 3.13–3.18 (4 H, m), 3.21–3.31 (12 H, m), 3.28 (4 H, s), 3.36–3.43 (4 H, m)
6	192–194	1.07 (12 H, s), 2.94 (4 H, s), 3.21–3.24 (8 H, m), 3.31 (4 H, s)

The bases **2** and **5** are moderately stable and moderately soluble in aprotic solvents; **6** is stable and more soluble. With one equivalent of acid, they form monocations, e.g., **2**·H$^{\oplus}$; with two equivalents, dications, e.g., **2**·2H$^{\oplus}$.

In order to carry out an X-ray structure analysis (Fig. 1), crystals of **2**·2HClO$_4$ were obtained by precipitation from water and crystals of **2**·HBPh$_4$ by successive addition of 2-*tert*-butylimino-2-diethylamino-1,3-dimethyl-1,3,2-diaza-

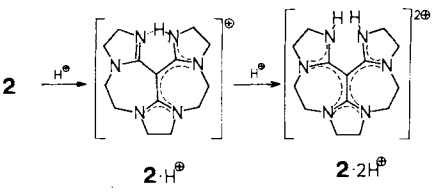

phosphinane[10] and a solution of $NaBPh_4$ in acetonitrile to an acetonitrile solution of **2**·2HClO$_4$. We assumed that the conformation of **2**·2H$^{\oplus}$ might be similar to that of the (less easily handled) base **2**.

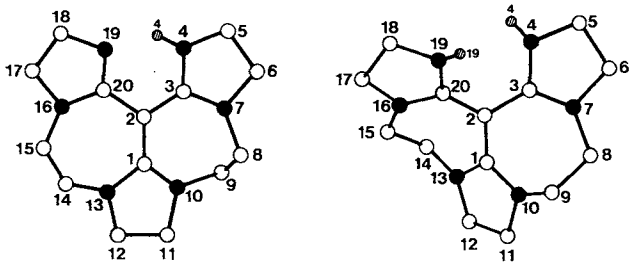

Fig. 1. Structures of **2**·HBPh$_4$ (left) and **2**·2HClO$_4$ (right), anions and *C*-bonded hydrogen atoms omitted (○ = C, ● = N, ⊘ = H) [11]. The numbering does not correspond to systematic nomenclature, but rather to computational parameters.

It was possible to localize approximately the chelate-bonded proton of **2**·H$^{\oplus}$ and to assign it unequivocally to N-4 (Fig. 1, left). Despite the extremely short N-4/N-19 distance (254.1 pm),[2] the hydrogen bond is asymmetric, presumably owing to the structurally imposed nonlinearity[12] ($\sphericalangle$ N-4/H-4/N-19 = 137.6°). This asymmetry also holds true for the chromophore system of **2**·H$^{\oplus}$. The part of the molecule delimited by N-4, C-2, and N-13 corresponds to a delocalized system with significant bond-length equalization; C-2/C-20, on the other hand, is unambiguously a single bond between two C_{sp^2} atoms and C-20/N-19 corresponds to a double bond (Table 2).

Table 2. Important bond lengths [pm] in **2**·HBPh$_4$ and **2**·2HClO$_4$.

Bond	**2**·HBPh$_4$	**2**·2HClO$_4$
C-20/N-19	127.0 (5)	132.6 (6)
C-3/N-4	131.0 (4)	133.6 (6)
C-3/N-7	133.7 (4)	132.2 (6)
C-1/N-10	133.6 (3)	132.3 (6)
C-1/N-13	133.5 (3)	130.6 (6)
C-20/N-16	133.5 (4)	134.6 (6)
C-2/C-20	146.9 (4)	141.2 (6)
C-2/C-3	143.1 (4)	143.0 (6)
C-1/C-2	141.5 (4)	143.9 (6)
N-4/H-4	92.0 (3)	86.0 (34)
N-19/H-4 and N-19/H-19	178 (1)	86.0 (49)

The conformations of the perimeters in **2**·H$^{\oplus}$ and **2**·2H$^{\oplus}$ can be described as sequences of sp^2 nitrogen atoms and ethylene units of planar dihydroimidazole rings (with the exception of the 1,10,11,12,13-ring of **2**·H$^{\oplus}$) and ethylene units of 2,3-dihydro-1,4-diazepinylium rings in the half-chair conformation.[13] Whereas a nearly planar six-membered ring (N-19/C-20/C-2/C-3/N-4/H-4) is present in **2**·H$^{\oplus}$, the C-2/C-20 and C-2/C-3 bonds in **2**·2H$^{\oplus}$ are twisted away from each other by ca. 26°. The N-4/N-19 distance is thereby 30.4 pm longer than that in

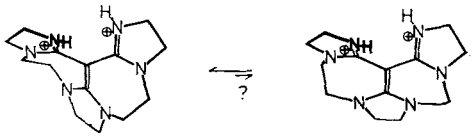

$2 \cdot 2H^{\oplus}$ $2 \cdot 2H^{\oplus\prime}$

$2 \cdot H^{\oplus}$. There is significant twisting around the C-1/C-2 bond in both $2 \cdot H^{\oplus}$ and $2 \cdot 2H^{\oplus}$ (26 and 39°, respectively). Since the C-1/C-2 bond in **2**, which is a pure double bond, should be largely planar—thus corresponding to the conformer $2 \cdot 2H^{\oplus\prime}$ (coupled, double inversion of the dihydrodiazepinylium half-chairs in $2 \cdot 2H^{\oplus}$) that had been expected for $2 \cdot 2H^{\oplus} - 2 \cdot 2H^{\oplus}$ cannot be viewed as a structural model for the free base **2**.

The pK_a values of the new bases in acetonitrile[14,15] (1,8-bis(dimethylamino)naphthalene: $pK_a = 18.18$[16]) allow the following conclusions to be drawn: an additional amidine function exerts a $-I$ effect [comparison of **1b** (26.95) with **3** (25.18)]; the chelate effect amounts to ca. four pK_a units [comparison of **3** with **2** (29.22)]; methyl groups have a $+I$ effect [comparison of **2** with **6** (30.03)]. The difference in the values for **2** and **5** (29.51) can only be interpreted when the structures are better understood.

Compounds **2** and **6** are kinetically active bases.[5] Only averaged signals are apparent in the ^{1}H-NMR spectrum of a mixture of **6** and $6 \cdot H^{\oplus}$ in CD_3CN at ca. 0 °C. Whereas only ca. 15% alkylation is observed by ^{1}H-NMR spectroscopy upon dehydrochlorination of β-phenylethyl chloride with **1b**, compound **2** surprisingly undergoes 43% alkylation in a reaction that is three times slower. Even isopropyl bromide alkylates **2** to a greater extent than **1b**. Compound **2** reacts with 1,2-dibromoethane to give **10** [$10 \cdot 2ClO_4$: m.p. = 323–325 °C; ^{1}H-NMR (CD_3CN): $\delta = 3.66$ (s), 3.75 (s)], which presumably exists in a D_3 conformation.

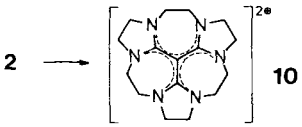

2 **10**

In a competition experiment, **6** is methylated three times faster than *N-tert*-butylpentakis(dimethylamino)diphosphazene[17] ($pK_a = 33.42$!). The relatively high nucleophilicity of **2** and **6** is presumably due to an interaction of the lone electron pairs on the chelate-forming nitrogen atoms (similar to the case of hydrazines). In their scope of application as auxiliary bases, **2** and **6** (and certainly **5**, as well) are thus far inferior to the phosphazene bases.

Received: July 10, 1987;
revised: September 16, 1987 [Z 2344 IE]
German version: *Angew. Chem. 99* (1987) 1210

[1] H. Einspahr, J.-B. Robert, R. E. Marsh, J. D. Roberts, *Acta Crystallogr. Sect. B29* (1973) 1611; M. R. Truter, B. L. Vickery, *J. Chem. Soc. Dalton Trans. 1972*, 395; H. A. Staab, T. Saupe, C. Krieger, *Angew. Chem. 95* (1983) 748; *Angew. Chem. Int. Ed. Engl. 22* (1983) 731.

[2] T. Saupe, C. Krieger, H. A. Staab, *Angew. Chem. 98* (1986) 460; *Angew. Chem. Int. Ed. Engl. 25* (1986) 451; R. W. Alder, A. G. Orpen, R. B. Sessions, *J. Chem. Soc. Chem. Commun. 1983*, 999.

[3] R. W. Alder, R. E. Moss, R. B. Sessions, *J. Chem. Soc. Chem. Commun. 1983*, 1000; E. Haselbach, A. Henriksson, F. Jachimowicz, J. Wirz, *Helv. Chim. Acta 55* (1972) 1757.

[4] R. W. Alder, P. S. Bowman, W. R. S. Steele, D. R. Winterman, *Chem. Commun. 1968*, 723; R. W. Alder, N. C. Goode, N. Miller, *J. Chem. Soc. Chem. Commun. 1978*, 89; P. S. Smith, J. L. Dye, J. Cheney, J.-M. Lehn, *J. Am. Chem. Soc. 103* (1981) 6044; R. W. Alder, A. Casson, R. B. Sessions, *ibid. 101* (1979) 3652.

[5] M. A. Zirnstein, H. A. Staab, *Angew. Chem. 99* (1987) 460; *Angew. Chem. Int. Ed. Engl. 26* (1987) 460.

[6] R. Schwesinger, *Angew. Chem. 99* (1987) 1209; *Angew. Chem. Int. Ed. Engl. 26* (1987) 1164.

[7] R. Gompper, W. Töpfl, *Chem. Ber. 95* (1962) 2871; D. Borrman in *Houben-Weyl-Müller: Methoden der Organischen Chemie Bd. VII, 4*. Thieme, Stuttgart 1968, p. 421.

[8] U. Kramer, H. Schmid, A. Guggisberg, M. Hesse, *Helv. Chim. Acta 62* (1979) 811.

[9] Correct C,H,N(Cl,S) analyses as well as UV, IR, and ^{1}H-NMR data were obtained for all new compounds except for **9a–c** (presumably amorphous).

[10] R. Schwesinger, *Chimia 39* (1985) 269.

[11] $2 \cdot HBPh_4$: monoclinic, space group $P2_1/n$, $a = 2148.4(12)$, $b = 1557.2(11)$, $c = 965.9(10)$ pm, $\beta = 98.52(7)°$; $Z = 4$, $\rho_{calcd} = 1.232$ g cm^{-3}, 5499 reflections with $F > 3\sigma(F)$, $R = 0.076$. $2 \cdot 2HClO_4$: orthorhombic, space group *Pccn*, $a = 1750.2(8)$, $b = 1911.1(8)$, $c = 1194.3(7)$ pm; $Z = 8$, $\rho_{calcd} = 1.574$ g cm^{-3}, 2145 reflections with $F > 3\sigma(F)$, $R = 0.061$. Further details of the crystal structure investigation may be obtained from the Fachinformationszentrum Energie, Physik, Mathematik GmbH, D-7514 Eggenstein-Leopoldshafen 2 (FRG), on quoting the depository number CSD-52674, the names of the authors, and the journal citation.

[12] S. Schreiner, *J. Phys. Chem. 86* (1982) 376.

[13] J. P. Declercq, G. Germain, M. van Meersche, *Acta Crystallogr. Sect B35* (1979) 1175; D. Lloyd, R. K. Mackie, H. McNab, D. R. Marshall, *J. Chem. Soc. Perkin Trans. 2 1973*, 1729.

[14] Absolute scale determined by UV/VIS-monitored titration with $[EtiPr_2NH]BPh_4$ (0.01 M solution, 25 °C) against indicators; R. Schwesinger, unpublished.

[15] The synthesis of the 6,7-didehydro compounds of **2** and **6** as the dications was also successful. The pK_a values of the thermally unstable bases were determined by generation of the free bases by treatment with a phosphazene base [17] in acetonitrile (31.94 and 32.88, respectively) [14]. These values are appreciably higher than those of **2** and **6**.

[16] L. A. Kurasov, A. F. Pozharskii, V. V. Kuz'menko, *Zh. Org. Khim. 19* (1983) 859.

[17] R. Schwesinger, H. Schlemper, *Angew. Chem. 99* (1987) 1212; *Angew. Chem. Int. Ed. Engl. 26* (1987) 1167.

Peralkylated Polyaminophosphazenes—Extremely Strong, Neutral Nitrogen Bases**

By *Reinhard Schwesinger** and *Helmut Schlemper*

Neutral nitrogen bases such as sterically hindered tertiary amines[1] or 1,8-diazabicyclo[5.4.0]undec-7-ene (DBU)[2] play an important role in synthesis; peralkylated, sterically hindered amidine[3] and guanidine bases[1b,4] have been described recently. It seemed of interest to us, therefore, to extend the collection of readily accessible, broadly applicable bases, which can be arranged in order of strength and steric hindrance, to higher pK_a values. The amino-substituted iminophosphoranes (monophosphazenes) **1**[5,6] and **2–4**[6] constituted the first step in this direction.

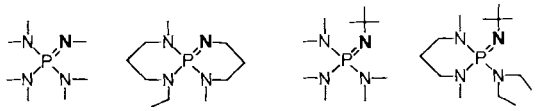

1 **2** **3** **4**

The question we posed was whether completely dialkylamino-substituted (with respect to the phosphazene chain),

[*] Dr. R. Schwesinger, Dipl.-Chem. H. Schlemper
Chemisches Laboratorium der Universität
Institut für Organische Chemie und Biochemie
Albertstrasse 21, D-7800 Freiburg (FRG)

[**] This work was supported by the Fonds der Chemischen Industrie.

noncyclic *N*-alkyl oligophosphazenes,[7] such as the simplest example **5**, would be even stronger bases owing to the better charge delocalization in the conjugate cation[8] $5 \cdot H^{\oplus}$.

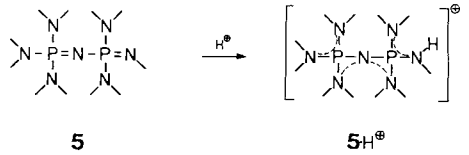

5 **5H$^{\oplus}$**

Compound **5** (Table 2) was easily obtained as a waxlike, distillable solid in 80–90% yield by reaction of **6**[9] with **7**[10] to give **8**·X [in MeCN, 40 °C, 2 h reflux; **8**·ClO_4,[11] m.p. = 280 °C (dec.), ^{1}H-NMR (CD_3CN): $\delta = 2.64$ (m)] followed by demethylation ($KSC_{12}H_{25}$, 180 °C, high vacuum).

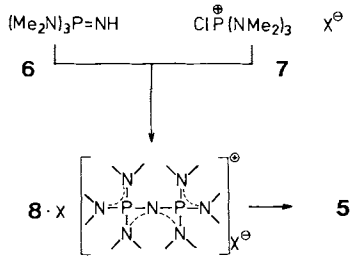

The increase in basicity on going from **1** to its "homologue" **5** is much greater than expected. Compound **5** is thus a very efficient dehydrohalogenation reagent of low nucleophilicity (Table 1).

Table 1. pK_a values of **5** and other bases and rate constants k for the reaction of β-phenylethyl chloride with these bases in MeCN at 25 °C and the percentage of alkylated bases formed upon reaction with excess isopropyl bromide.

Base	pK_a [12, 13]	$k \times 10^4$ [L mol^{-1} s^{-1}]	% Alkylation
4	27.58	0.011	0
NaOEt/EtOH		0.045 [14]	
DBU	24.32	0.047	21
1	27.53	2.2	13
2	28.27	15.5	49
$[Bu_4N]F$		38.9 [14]	
5	32.66	≈600	5

The cation **8** is suitable as a very stable phase-transfer catalyst, especially for strongly nucleophilic anions, as shown by the drastic demethylation conditions. However, salts of **8** are also more stable toward hydroxide ions than the corresponding tetrabutylammonium or tetrabutylphosphonium salts (and slightly more lipophilic):[15] the half-lives of the corresponding chlorides in 50% NaOH/chlorobenzene at 100 °C are 8 h, 20 min, and < 10 min, respectively. Alkylation of **5** results in the formation of more lipophilic cations.[16]

The sterically hindered bases **9–11**, which are "homologous" to **3**, can be prepared on a mole scale in a one-pot procedure from **6** and **12**[17] and isolated as the HBF_4 or $HClO_4$ salts, which are only sparingly soluble in water. Compounds **9** and **10** can be liberated by treatment of these salts with KOMe or NaOMe; **11** is best obtained using KNH_2 (Scheme 1). The most important physical and spectroscopic data for compounds **9–11** and for their $HClO_4$ salts are presented in Table 2.

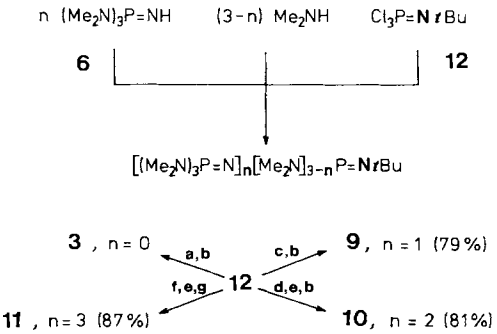

Scheme 1. Synthesis of the bases **3** and **9–11** (data for **9–11**, see Table 2): a) 6 equiv. of Me_2NH(g) added at −15 °C, 24 h reflux. b) H_2O/NH_4BF_4; KOMe/MeOH (exactly 1 equiv.), filter, remove solvent, distill. c) MeCN/tetrahydrofuran (THF); 2.06 equiv. Me_2NH, 2.06 equiv. Et_3N at −60 °C, 24 h 20 °C; 3.03 equiv. **6** at 0 °C, 3 h reflux. d) 1 equiv. $Me_2NH \cdot HCl$, MeCN/THF; 2.06 equiv. Et_3N at −60 °C, 24 h 20 °C; 5.25 equiv. **6** at 0 °C, 2 d reflux. e) H_2O/NH_4BF_4; strongly basic anion exchanger, $Cl^{\ominus}$ form, MeOH; high vacuum 100 °C. f) 5.25 equiv. **6**, MeCN/THF, −60 °C; addition of **12**, 24 h 20 °C, 5 d reflux. g) THF,$KNH_2/NH_{3(l)}$, sublimation (130 °C/0.001 torr).

Table 2. Melting points (and boiling points) as well as ^{1}H-NMR data for the compounds **5** and **9–11** and for their $HClO_4$ salts [11].

Compound	M.p. [°C] (B.p. [°C])	250-MHz ^{1}H-NMR (δ, J[Hz])
5	42 (92 [a])	2.56 (12 H, d, J = 9.5), 2.61 (3 H, d, J = 24), 2.63 (18 H, d, J = 10) [b]
5 · $HClO_4$	> 235 (dec.)	2.50 (3 H, dd, J = 12.5, 6), 2.65 (18 H, d, J = 10.5), 2.65 (12 H, d, J = 10.5), 3.33 (1 H, br.s; NH) [b]
9	76 (83 [a])	1.13 (9 H, d, J = 0.8), 2.53 (12 H, d, J = 9.8), 2.55 (18 H, d, J = 9.8) [b]
9 · $HClO_4$	266–267	1.26 (9 H, d, J = 0.8), 2.62 (12 H, d, J = 10.2), 2.65 (18 H, d, J = 10.2), 3.23 (1 H, br.d, J ≈ 10; NH) [b]
10	57 (155 [a])	1.78 (9 H, d, J = 0.8), 2.60 (36 H, d, J = 10.2), 2.90 (6 H, d, J = 11.4) [c]
10 · $HClO_4$	232–233	1.22 (9 H, d, J = 0.9), 2.25 (1 H, br.d, J = 7; NH), 2.60 (6 H, d, J = 12.3), 2.64 (36 H, d, J = 9.9) [b]
11	207 (subl. [a])	1.73 (9 H, d, J = 0.8), 2.67 (54 H, d, J = 10.5) [c]
11 · $HClO_4$	260–261	1.29 (9 H, d, J = 0.8), 2.07 (1 H, br.d; NH), 2.64 (54 H, d, J = 10.2) [b]

[a] At 0.001 torr. [b] In CD_3CN. [c] In C_6D_6.

The strongly hygroscopic, colorless, crystalline bases **9–11** are, like **1–5**, unusually stable and are very soluble in the conventional solvents. In 1 M D_2O solution, **10**, like **1–5**, undergoes hydrolysis only at about 160 °C ($t_{1/2} \approx 40$ h); even under these conditions, **9** and **11** remain unchanged over 20 h. However, aqueous mineral acids hydrolyze **9–11** readily.

Compound **11** is probably the strongest neutral nitrogen base known at present (Table 3); in THF solution, it is comparable to potassium bis(trimethylsilyl)amide, but less nucleophilic. It deprotonates acetone to a large extent and establishes a clear equilibrium with triphenylmethane. In acetonitrile (pK_a(MeCN) ≈ 44), **10** and **11** cannot be titrated, since they catalyze a rapid self-condensation with "self-buffering." Reaction of **9–11** with *n*-alkyl halides af-

Table 3. pK_a values of **9–11** and of other sterically hindered bases at 25 °C.

Compound	pK_a value	
	In MeCN [13]	In THF [a]
Pentaisopropylguanidine [1b, 4]	(23.2) [b]	
3	26.89 [12]	
4	27.58 [12]	
9	33.42 [12]	19.19 [c]
10	(38.35) [d]	24.18 [e]
11	(42.1) [f]	28.0 ± 0.2 [g]

[a] "Ion-pair pK_a value" [c], relative scale. [b] Estimated from the difference between the pK_a value of pentaisopropylguanidine and pentamethylguanidine in methoxyethanol [1b] and the value for the latter in MeCN [6, 12]. [c] Correlated with 9-phenylfluorene (PFH) [18] via the definition $pK_a = \lg[\mathbf{9}^- \cdot PFH] - \log[\mathbf{9}^-] - \log[PFH] + 18.59$. [d] By extrapolation of the difference of the "ion-pair pK_a values" of **9** and **10** in THF to the MeCN scale. [e] By titration of **9** and **10** in THF; the difference in the pK_a values of the two indicators used was extrapolated from the MeCN scale. [f] By extrapolation from the difference of the "ion-pair pK_a values" of **10** and **11** in THF to the MeCN scale. [g] Estimated by titration in THF against Ph_2NH, from the pK_a value of Ph_2NH in dimethyl sulfoxide (DMSO) [19], and by comparison of the heats of solution of Ph_2NH and Ph_2CH_2 in THF and DMSO in order to estimate the solvent correction factor.

fords 1-alkenes under exceptionally mild conditions (Table 4).

Table 4. Conditions and yields of 1-octenes in the reaction of *n*-octyl bromide (1 mmol) with **9** and **11** in comparison to a known procedure [20].

Base/solvent	Conditions	Yield [a] [%]	Alkylation of the base [%]
KO*t*Bu/[18]crown-6/petroleum ether [20]	60 °C/3 h	75	18
1.1 mmol **9**	70 °C/5 h	74	18
1.1 mmol **11**/0.5 mL THF	25 °C/6 h	96	3

[a] Determined by gas chromatography using a reference.

The extreme basicity of oligophosphazene bases such as **10**, **11**, and higher "homologues" and the high stability of the extremely soft phosphazenium ions should make it possible to modify in a specific manner the reactivity, stability, and selectivity of hard anions (obtainable so far only with hard counterions). Preliminary results have shown that the course of alkylation can indeed be influenced.[21]

Received: July 10, 1987;
revised version: August 26, 1987 [Z 2345/2346 IE]
German version: *Angew. Chem. 99* (1987) 1212

[1] a) S. Hünig, M. Kiessel, *Chem. Ber. 91* (1958) 380; b) G. Wieland, G. Simchen, *Liebigs Ann. Chem. 1985*, 2178.
[2] K. Eiter, H. Oediger, *Justus Liebigs Ann. Chem. 682* (1965) 62; *Kontakte (Darmstadt) 1983*, 46.
[3] F. Heinzer, M. Soukup. A. Eschenmoser, *Helv. Chim. Acta 61* (1978) 2851.
[4] D. H. R. Barton, J. D. Elliott, S. D. Géro, *J. Chem. Soc. Perkin Trans. 1 1982*, 2085.
[5] a) K. Issleib, M. Lischewski, *Synth. Inorg. Met. Org. Chem. 3* (1973) 255; b) P. Haasemann, J. Goubeau, *Z. Anorg. Allg. Chem. 408* (1974) 293.
[6] R. Schwesinger, *Chimia 39* (1985) 269.
[7] *N*-Unsubstituted and silylated diphosphazenes of this type are known: a) A. P. Marchenko, G. N. Koidan, A. M. Pinchuk, *Zh. Obshch. Khim. 53* (1983) 670; b) O. Schlak, W. Stadelmann, O. Stelzer, R. Schmutzler, *Z. Anorg. Allg. Chem. 419* (1976) 275.
[8] R. Schwesinger, *Angew. Chem. 99* (1987) 1209; *Angew. Chem. Int. Ed. Engl. 26* (1987) 1164.
[9] G. N. Koidan, A. P. Marchenko, A. A. Kudryartsev, A. M. Pinchuk, *Zh. Obshch. Khim. 52* (1982) 2001.
[10] H. Nöth, H. J. Vetter, *Chem. Ber. 98* (1965) 1981; B. Castro, J.-R. Dormoy, B. Dourtoglou, G. Evin, C. Selve, J.-C. Ziegler, *Synthesis 1976*, 751; J.-R. Dormoy, B. Castro, *Tetrahedron Lett. 1979*, 3321.
[11] IR data and correct C, H, N analyses are available for all perchlorates; the perchlorates were chosen over the tetrafluoroborates on account of their better analytical results and higher thermal stabilities. The free bases are hygroscopic and therefore do not afford satisfactory analytical data.
[12] Determined by titration (followed by UV/VIS spectroscopy) with $[EtiPr_2NH]BPh_4$ (0.01 M solution, 25 °C) against an indicator; R. Schwesinger, unpublished.
[13] Absolute scale, with respect to pK_a (1,4-diaminobutane) = 20.12: J. F. Coetzee, *Prog. Phys. Org. Chem. 4* (1967) 45.
[14] J.-i. Hayami, N. Ono, A. Kaji, *Tetrahedron Lett. 1970*, 2727.
[15] Salts of **11** should be chemically even more stable. The most stable organic cation of all is presumably the tetrakis[tris(dimethylamino)phosphoranylidenamino]phosphonium ion $[(Me_2N)_3P{=}N]_4P^{\oplus}$ ($ClO_4^{\ominus}$ salt: m.p. = 290 °C (dec.); ^{1}H-NMR ($CDCl_3$): $\delta = 2.62$ (d, $J = 9$ Hz)); R. Schwesinger, H. Schlemper, unpublished.
[16] Several lipophilic hexaminodiphosphazenium salts have been obtained via other routes: [7a].
[17] C. Glidewell, *Angew. Chem. 87* (1975) 875; *Angew. Chem. Int. Ed. Engl. 14* (1975) 826.
[18] A. Streitwieser, Jr., D. A. Bors, M. Kaufman, *J. Chem. Soc. Chem. Commun. 1983*, 1394.
[19] F. G. Bordwell, D. L. Hughes, *J. Am. Chem. Soc. 106* (1984) 3234.
[20] E. von Dehmlow, M. Lissel, *Synthesis 1979*, 372.
[21] In the presence of **11** as base, benzothiazole was *C*-alkylated for the first time. With benzyl bromide in THF at −78 °C, ca. 50% of 2-(benzothiazol-2-yl)-1,2,3-triphenylpropane **13** is obtained. With potassium bis(trimethylsilyl)amide as base, on the other hand, little reaction occurs at −78 °C, possibly because of the poor solubility of the organopotassium compound. After thawing, **13** was isolated in ca. 2-3% yield along with ca. 12% of 1-(benzothiazol-2-yl)-1,2-diphenylethane. Presumably, 2-lithiobenzothiazole cannot be alkylated: H. Chikashita, K. Itho, *Heterocycles 23* (1985) 295.

The Synthesis and Catalytic Properties of Some Open-Sided Binuclear Complexes of Rh^I: The Structure of $[Rh_2(CO)_2(CH_3CN)_2\{CH(PPh_2)_3\}](CF_3SO_3)_2$

By *Hani El-Amouri, Ali A. Bahsoun, Jean Fischer,* and *John A. Osborn**

Binuclear rhodium(I) complexes have attracted attention of late in part because as hydrogenation catalysts they appear to differ in properties from the corresponding mononuclear species. For example, the complex $[Rh_2H_2\{P(OiPr)_3\}_4]$ has been reported to catalyze the *trans* addition of H_2 to diphenylacetylene, whereas monomeric Rh catalysts gave *cis* products.[1] Further, mechanistic studies on the transfer of hydrogen from $[Rh_2H_2(CO)_2(dppm)_2]$ (dppm = methylene(diphenylphosphane)) to acetylenes indicate the presence of a biradical mechanism which is not accessible to mononuclear analogues.[2] We report here on studies involving the synthesis and properties of some dirhodium(I) compounds assembled by the ligand $CH(PPh_2)_3$, and the X-ray determination of one such complex.

Treatment of **1**[3] with 0.5 equivalents of $CH(PPh_2)_3$ yields orange crystals of **2**. The IR spectrum (Nujol) shows

$[Rh(CO)_2S_2]CF_3SO_3$ **1**

$[Rh_2(CO)_3\{CH(PPh_2)_3\}](CF_3SO_3)_2$ **2**

terminal carbonyl absorptions at 2000(s), 2010(sh), 2015(s), and 2085(s) cm^{-1} as well as peaks at 1330 and 1250 cm^{-1}, suggesting the presence of coordinated triflate[4,5] in the solid state. The ^{31}P-NMR data (Table 1) indicate that, in solution, two equivalent phosphorus nuclei,

[*] Prof. J. A. Osborn, H. El-Amouri, Dr. A. A. Bahsoun, Prof. J. Fischer
UA au CNRS 424, Institut Le Bel, Université Louis Pasteur
4 rue Blaise Pascal, F-67000 Strasbourg (France)

P_a, are bound to one rhodium atom, Rh_a, the other, P_b, being coordinated to the second rhodium atom, Rh_b. The ^{13}C-NMR data show three carbonyls binding solely to Rh_b,[6] the sites on Rh_a other than phosphorus being occupied by solvent molecules or weakly coordinated triflates. Further, we propose that a Rh-Rh bond is also present (vide infra). Complex **2** loses CO reversibly to produce **3** (Scheme 1), where the stereochemical change from trigonal bipyramidal to square planar about Rh_b is accompanied by a downfield shift of ca. 27 ppm in the ^{13}P-NMR spectrum of P_b (Table 1).

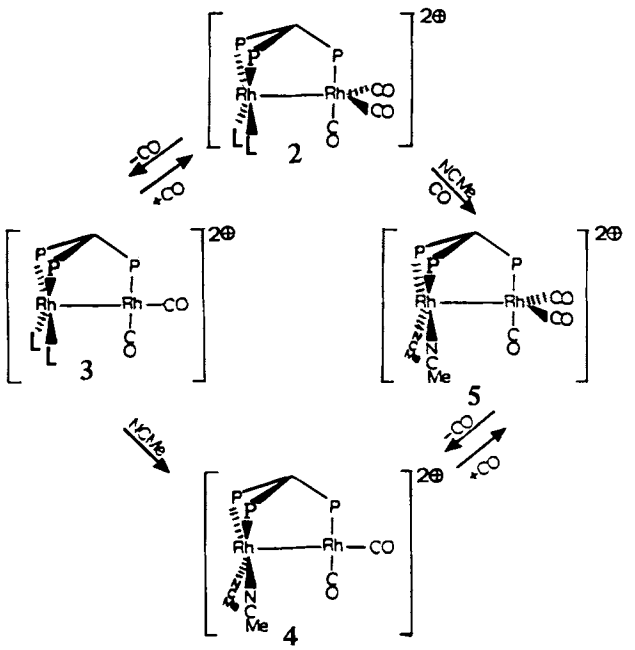

Scheme 1. L = solvent molecule.

Treatment of **3** (or **2** in the absence of CO) with CH_3CN yields **4**, which is spectroscopically very similar to **3**. Yellow crystals were subjected to an X-ray structural determination, which is presented in Figure 1.[7] Notably, the dimeric structure is confirmed, with a Rh–Rh distance of 2.745 Å (single bond), and with the $CH(PPh_2)_3$ ligand holding the two rhodium atoms in a clamplike fashion on one side of the molecule, leaving one side open for the coordination of reactant molecules. In **4**, this side is occupied by CH_3CN and CO ligands. The coordinating geometry about Rh_a is thus approximately square pyramidal, the Rh–Rh bond occupying the apical site on Rh_a and completing the square arrangement about Rh_b. The metal–metal bond appears to be of a strong donor–acceptor character, creating sufficient electron deficiency on Rh_a such that its affinity for π-acid ligands is greatly reduced despite the presence of electron-donating P_a groups. Accordingly, on treatment of **4** with CO, coordination to Rh_b and *not* to Rh_a occurs to form **5** (Scheme 1). This is shown by the similarity of the ^{31}P-NMR spectra of **5** and **2** (Table 1).

$[Rh_2(cod)\{CH(PPh_2)_3\}](CF_3SO_3)_2 \cdot (CH_3)_2CO$ **6**
(cod = 1,5-cyclooctadiene)

Analogously, the dirhodium diene complex **6** can be isolated as burgundy red crystals from acetone using two equivalents of $[Rh(cod)S_2]CF_3SO_3$[3] and one equivalent of

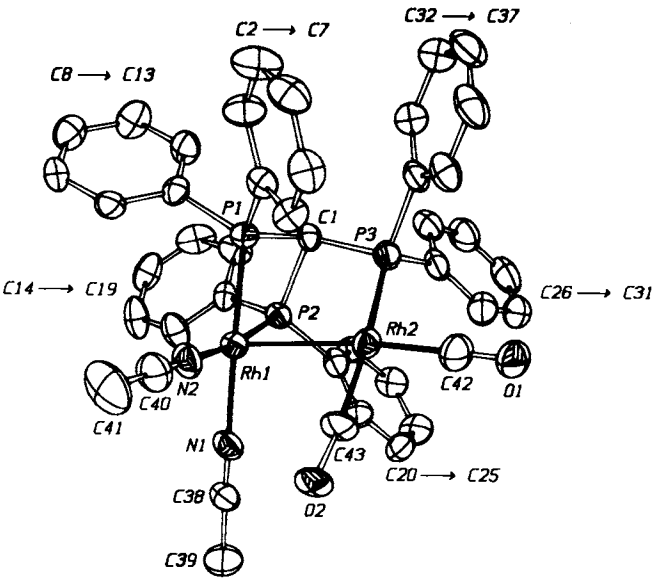

Figure 1. X-ray structure of the cation of **1** (ORTEP plot). Ellipsoids are scaled to enclose 50% of the electronic density. Hydrogen atoms are omitted (Rh1 = Rh_a, Rh2 = Rh_b, P1 + P2 = P_a, P3 = P_b). Bond lengths [Å] and bond angles [°]: Rh1-Rh2 2.745(1), Rh1-P1 2.212(1), Rh1-P2 2.214(1), Rh1-N1 2.106(5), Rh1-N2 2.071(5), Rh2-P3 2.248(1), Rh2-C42 1.834(6), Rh2-C43 2.023(6), ⟨C1-P_i, i = 1,3⟩ 1.853(4); P1-Rh1-N1 171.5(1), P1-Rh1-N2 99.1(1), P1-Rh1-P2 72.81(5), N1-Rh1-N2 89.1(2), P1-Rh1-Rh2 81.18(4), P2-Rh1-Rh2 81.36(4), P3-Rh2-Rh1 94.01(6), P3-Rh2-C42 91.1(2), P3-Rh2-C43 175.5(2), Rh1-Rh2-C42 173.4(3), Rh1-Rh2-C43 81.7(3), C42-Rh2-C43 92.2(3). Further details of the crystal structure investigation are available on request from the Director of the Cambridge Crystallographic Data Centre, University Chemical Laboratory, Lensfield Road, Cambridge CB2 1EW (England) on quoting the names of the authors and the full journal citation.

Table 1. ^{31}P-NMR data of **2**–**6** ($(CD_3)_2CO$ + cosolvent; *J* values in Hz).

Compound	Cosolvent	δ(P_a) [a]	δ(P_b) [b]	*J*(Rh-P_a)	*J*(Rh-P_b)	*J*(P_a-P_b)
2	THF	7.8	12.8	125	141	13
3	THF	7.5	39.6	134	176	8
4	CH_3CN	3.7	32.0	132	161	11
5	CH_3CN	2.3	10.2	126	131	14
6	$(CH_3)_2CO$	13.0	−1.25	143	151	16

[a] Each dd. [b] Each dt.

$CH(PPh_2)_3$. ^{31}P-NMR data (Table 1) show **6** to be isostructural with **3**, the diene ligand replacing the two carbonyl groups. Complex **6** reacts with H_2 in acetone to liberate cyclooctane, and on addition of 1-hexene, catalytic hydrogenation proceeds (25°, 1 atm H_2). Complex **6** possesses two formally coordinatively unsaturated rhodium(I) atoms in close proximity, and interestingly the hydrogenation rate is increased about fivefold on addition of one equivalent of PPh_3. Investigations of the mechanistic details of this reaction are in progress.

Experimental Procedure

All reactions and operations including the distillation of the solvents were carried out under N_2.

2: A solution of $[Rh_2Cl_2(CO)_4]$ (389 mg, 1 mmol) in acetone (4 mL) was added to a solution of $AgCF_3SO_3$ (550 mg, 2.14 mmol) in acetone (3 mL). The white AgCl salt was filtered off, and to the clear yellow filtrate a solution containing $CH(PPh_2)_3$ (510 mg, 0.9 mmol) in benzene (6 mL) was added drop by drop until the solution turned orange-red. The solvent was removed under vacuum and the residue washed several times with benzene and ether. Recrystallization from acetone/ether; yield 550 mg (65%). ^{13}C-NMR ($(CD_3)_2CO$): δ = 188 (dd, *J* (C-Rh) = 70, *J* (C-P_{trans}) = 104 Hz), 170 (dd, *J* (C-Rh) = 66, *J* (C-P_{cis}) = 16 Hz).

4: **1** (50 mg, 0.043 mmol) was dissolved in acetone (4 mL) and to this orange solution acetonitrile (2 mL) was added to yield an immediate color change to

 © VCH Verlagsgesellschaft mbH, D-6940 Weinheim, 1987 0570-0833/87/1111-1170 $ 02.50/0

yellow. Yellow-orange crystals suitable for X-ray investigation were obtained by slow diffusion using ether as cosolvent.

Received: May 14, 1987;
supplemented: July 31, 1987 [Z 2238 IE]
German version: *Angew. Chem. 99* (1987) 1208

CAS Registry numbers:
2, 110827-57-1; **3**, 110827-58-2; **4**, 110827-60-6; **5**, 110827-62-8; **6**, 110827-63-9; $Rh_2Cl_2(CO)_4$, 14523-22-9; COD, 111-78-**4**; PPh_3, 603-35-0; H_2, 1333-74-0; cyclooctane, 292-64-8; 1-hexene, 592-41-6.

[1] R. R. Burch, E. L. Muetterties, *J. Am. Chem. Soc. 104* (1982) 4257.
[2] S. I. Hommeltoft, D. H. Berry, R. Eisenberg, *J. Am. Chem. Soc. 108* (1986) 5345.
[3] R. R. Schrock, J. A. Osborn, *J. Am. Chem. Soc. 93* (1971) 3089.
[4] N. E. Dixon, W. G. Jackson, M. J. Lancaster, G. A. Lawrence, A. M. Sargeson, *Inorg. Chem. 20* (1981) 471.
[5] J. Nitzschke, S. P. Schmidt, W. C. Trogler, *Inorg. Chem. 24* (1985) 1972.
[6] C. P. Casey, R. M. Bullock, F. Nief, *J. Am. Chem. Soc. 105* (1983) 7574.
[7] Crystal data: triclinic, $a=14.218(4)$, $b=16.052(4)$, $c=13.543(4)$ Å, $\alpha=96.80(2)$, $\beta=109.16(2)$, $\gamma=84.38(2)°$, $V=2893$ Å^3, $Z=2$, $\rho_{calcd}=1.527$. 12636 reflections ($\pm h \pm k$l, $3° < \theta < 27°$) measured at -100 °C; 7302 with $I > 3\sigma(I)$ used for structure determination and refinement. Experimental absorption corrections. H atoms in computed cooordinates (C-H = 0.95 Å, B(H) = 1 + Beqv(c) Å^2. No hydrogen atom parameter was allowed to vary during refinement. Anisotropic temperature factors for all non-hydrogen atoms. $R(F)=0.068$, $R_w(F)=0.081$, with $\sigma(F^2)=[\sigma^2_{count.}+(0.08\,F^2)^2]$, GOF = 1.34.

Mo^{II} and Mo^0 Complexes of 3,3,7,7,11,11,15,15-Octamethyl-1,5,9,13-tetrathiacyclohexadecane**

By *Toshikatsu Yoshida,* Tomohiro Adachi, Tatsuo Ueda, Megumi Watanabe, Manabu Kaminaka,* and *Taiichi Higuchi**

Recently, macrocyclic polythioethers as a ligand in transition-metal complexes have received considerable interest in view of the enormously high redox petentials found for the Cu^{II} [1] and Co^{II} [2,3] complexes and the ability to stabilize the metals in low oxidation states such as Rh^I.[4,5] The high nucleophilicity of the square-planar Rh^I cationic complexes of 1,4,8,11-tetrathiacyclotetradecane and its 6,6,13,13-tetramethyl analogue as proved by a facile oxidative addition of CH_2Cl_2 is also remarkable since $[RhCl(PPh_3)_3]$ and $[Rh(tBuNC)_4]^{\oplus}$ are inert toward CH_2Cl_2.[5] These salient features may promise a rich chemistry of macrocyclic polythioether complexes of transition metals, particularly in low oxidation states. In view of current interest in Mo complexes of sulfur ligands, we have prepared the novel monomeric Mo^{II} dihalo complexes **1** and **2** of 3,3,7,7,11,11,15,15-octamethyl-1,5,9,13-

[*trans*-MoX_2L_A] **1**, X = Br; **2**, X = Cl

tetrathiacyclohexadecane, L_A. The Mo^{II} halo complexes of thioethers so far reported, e.g., $[Mo_2Cl_4(SEt_2)_4]$ and $[Mo_6Cl_{12}(dithiahexane)_2]$ are polymeric.[6]

[*] Prof. Dr. T. Yoshida, T. Adachi, T. Ueda, M. Watanabe, M. Kaminaka
Department of Chemistry, Faculty of Integrated Arts and Sciences
University of Osaka Prefecture
Sakai, Osaka 591 (Japan)
Prof. Dr. T. Higuchi
Department of Chemistry, Faculty of Science, Osaka City University
Sumiyoshi, Osaka 588 (Japan)

[**] This work was supported by a Grant-in-Aid (60470048 and 61125005) for Scientific Research from the Ministry of Education, Japan. *T. A.* and *T. H.* are indebted to the Crystallographic Research Center, Institute of Protein Research and Computation Center, Osaka University, for computer calculations.

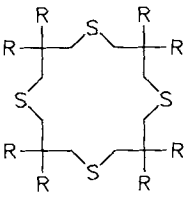

L_A, R = Me
L_B, R = H

Cyclic voltammetry shows that both **1** and **2** exhibit extraordinarily high redox potentials for the Mo^{III}/Mo^{II} (ca. +1.2 V vs. SCE) and Mo^{II}/Mo^I (ca. −0.2 V) couples, which emphasizes the possibility that **1** and **2** might serve as potential precursors for syntheses of lower-valent molybdenum complexes containing the thioether as ligand. In fact, both chemical and electrochemical reductions of **1** under CO atmosphere afforded **3**. Complex **3** represents

[*trans*-$Mo(CO)_2L_A$] **3**

the first example of a Mo^0 *di*carbonyl complex of a thioether ligand, since all known complexes $[Mo(CO)_n(SR_2)_{6-n}]$ contain more than three CO ligands.[7] The dimeric complex $[Mo_2(SH)_2(L_B)_2]^{2\oplus}$ [8] is the only known Mo^{II} complex of a 16-membered cyclic tetrathioether. However, this complex cannot be a candidate for the starting material mentioned above.

The Mo^{II} dibromo complex **1** [9] was prepared by treating $[MoBr_2(CO)_4]_2$ with two molar equivalents of L_A [10] in toluene under reflux as paramagnetic, orange crystals (50% yield based on the ligand). Since the physical properties of **1**,[12] including magnetic, electronic spectral, and electrochemical data are similar to those of the dichloride **2**, a *trans* geometry was proposed for **1**. A similar reaction of $[MoCl_2(CO)_4]_2$ with L_A did not produce **2**; instead, **4** was obtained as paramagnetic, orange crystals (25% yield).[9,12] The formation of **4** is rather expected since the reaction of

[*fac*-$MoCl_3L_A$] **4**

$[MoCl_2(CO)_4]$ with a ligand of poor π-acceptor ability has been known to proceed via disproportionation of Mo^{II} to Mo^{III} and Mo^0 affording CO-free Mo^{III} complexes.[13] Alternatively, **4** was obtained in a higher yield (71%) by treating $[MoCl_4(MeCN)_2]$ with L_A in CH_2Cl_2 at room temperature. Reduction of **4** with Zn powder in CH_2Cl_2 took place readily at room temperature to give **2** as paramagnetic, yellow crystals (51% yield).[9,12] The observation of a single Mo-Cl stretching band ($\tilde{\nu}=306$ cm^{-1}) in the IR spectrum of **2** is consistent with a *trans* geometry.

The cyclic voltammogram of **1** and **2** measured in MeCN (0.1 M nBu_4NBF_4) at a scan rate of 100 mV s^{-1} shows two essentially reversible redox couples due to Mo^{II}/M^I ($E_{1/2}=-0.15$ V vs. SCE, $\Delta E=100$ mV, $I_{pa/pc}=0.92$ for **1** and $E_{1/2}=-0.28$ V, $\Delta E=75$ mV, $I_{pa/pc}=1.08$ for **2**) and Mo^{III}/Mo^{II} ($E_{1/2}=+1.21$ V vs. SCE, $\Delta E=120$ mV, $I_{pa/pc}=1.00$ for **1** and $E_{1/2}=+1.19$ V, $\Delta E=80$ mV, $I_{pa/pc}=1.22$ for **2**). The high redox potentials compared with those of [*trans*-$MoX_2(Ph_2PCH_2CH_2PPh_2)_2$] [$Mo^{II}/Mo^I$, $E_{1/2}=-1.51$ V vs. SCE for X = Br and −1.68 V for X = Cl; Mo^{III}/Mo^{II}, $E_{1/2}=+0.01$ V for X = Br and −0.05 V for X = Cl][14] are remarkable and probably due to the weak σ-donating property of thioethers.[6] In addition, the ring size of the thioether may be responsible for the high potentials as found for a series of the related Cu^{II} complexes.[1]

Reduction of **1** with Na/Hg in THF under CO atmosphere (1 atm CO) occurred at ambient temperature to give **3** as diamagnetic, red crystals quantitatively. Controlled-potential electrolysis of **1** at -2.2 V vs. SCE in MeCN under CO also afforded **3**. Despite the similar redox potentials of **1** and **2**, reduction of **2** under similar conditions employed for **1** gave only traces of **3**. The ^{1}H- and ^{13}C-NMR spectra of **3**[12] indicate a planar coordination of L_A with "all up" conformation, the four 6-membered $MoSCH_2CMe_2CH_2S$ rings assuming the chair form. This is confirmed by an X-ray structural study of **3** (Figure 1).[15]

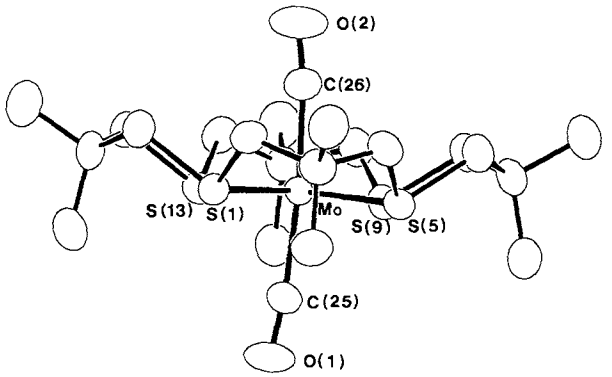

Fig. 1. Molecular structure of **3**. Selected bond distances [Å] and angles [°]: Mo-S(1) 2.434(2), Mo-S(5) 2.439(2), Mo-S(9) 2.432(2), Mo-S(13) 2.438(2); S(1)-Mo-S(5) 90.5(1), S(5)-Mo-S(9) 89.1(1), S(9)-Mo-S(13) 90.1(1), S(1)-Mo-S(13) 90.0(1), S(1)-MoS(9) 175.1(1), S(5)-Mo-S(13) 175.5(1), C(25)-Mo-C(26) 174.3(3), Mo-C(25)-O(1) 174.3(7), Mo-C(26)-O(2) 173.0(7).

The geometry around the Mo atom is slightly distorted octahedral with two CO ligands in the axial positions, and the molecule possesses approximately C_{4v} symmetry. The Mo atom is displaced toward the ring C atoms from the least-squares plane defined by the four S atoms by 0.093(2) Å. The plane defined by the four S atoms is strictly planar, the deviation of the S atoms from the plane being less than 0.002(2) Å. The two Mo–C (Mo-C(26) 1.979(8) and Mo-C(25) 2.002(8) Å) and C–O distances (C(26)-O(2) 1.161(10) and C(25)-O(1) 1.144(10) Å of two mutually trans CO ligands are not significantly different. The Mo–S distances (average 2.436(2) Å) are considerably shorter than those found in the Mo^0 complexes [*fac*-$Mo(CO)_3$(1,4,7-trithiacyclononane)] (mean 2.520(6) Å)[7] and [*trans*-$Mo(N_2)_2(Ph_2PCH_2CH_2SMe)(PMePh_2)_2$] (2.483(3) Å).[16] Furthermore, the short Mo–S distances in **3** compared with the corresponding lengths in $\{Mo_2(SH)_2(L_B)_2\}^{2\oplus}$ (mean 2.493(2) Å)[8] are consistent with the stronger d_π–d_π interaction in the Mo^0–S bond than in the Mo^{II}–S bond. It is to be noted that the *trans* geometry of **3** is stable at room temperature, while [*trans*-$Mo(CO)_2(Ph_2PCH_2CH_2PPh_2)_2$] is known to isomerize readily into the *cis* isomer.[17]

Received: May 19, 1987;
revised: August 31, 1987 [Z 2250 IE]
German version: *Angew. Chem. 99* (1987) 1182

CAS Registry numbers:
1, 110935-32-5; **2**, 110935-33-6; **3**, 110935-34-7; **4**, 110935-35-8; L_A, 110935-37-0; $[MoBr_2(CO)_4]_2$, 80594-72-5; $[MoCl_2(CO)_4]_2$, 12655-17-3; $[MoCl_4(MeCN)_2]$, 19187-82-7; disodium salt of 2,2-dimethyl-1,3-propanedithiolate, 110935-36-9; 1,3-dibromo-2,2-dimethylpropane, 5434-27-5.

[1] T. E. Johnes, D. R. Rorabacher, L. A. Ochrymowycz, *J. Am. Chem. Soc. 98* (1976) 4322.
[2] J. R. Hartman, E. J. Hintsa, S. R. Cooper, *J. Am. Chem. Soc. 108* (1986) 1208.
[3] H.-J. Küppers, A. Neves, C. Pomp, D. Ventur, K. Wieghardt, B. Nuber, J. Weiss, *Inorg. Chem. 25* (1986) 2400.
[4] W. D. Lemke, K. E. Travis, N. E. Takvoryan, D. H. Busch, *Adv. Chem. Ser. 150* (1976) 358.
[5] T. Yoshida, T. Ueda, T. Adachi, K. Yamamoto, T. Higuchi, *J. Chem. Soc. Chem. Commun. 1985*, 1137.
[6] S. G. Murray, F. R. Hartley, *Chem. Rev. 81* (1981) 365.
[7] M. T. Ashby, D. L. Lichtenberger, *Inorg. Chem. 24* (1985) 636, and references cited therein.
[8] J. Cragel, V. B. Pett, M. D. Glick, R. E. DeSimmone, *Inorg. Chem. 17* (1978) 2885.
[9] Satisfactory elemental analyses for all new compounds were obtained.
[10] L_A was prepared by treating disodium 2,2-dimethyl-1,3-propanedithiolate and 1,3-dibromo-2,2-dimethylpropane in EtOH by a similar procedure to that employed for the preparation of 1,5,9,13-tetrathiacyclohexadecane [11]. Purification of the concentrated reaction mixture by chromatography (silica gel, *n*-hexane as eluent) gave colorless crystals (16% yield), m.p. = 165–166 °C. ^{1}H-NMR (60 MHz, $CDCl_3$); $\delta = 1.01$(s, Me), 2.63(s, CH_2).
[11] L. A. Ochrymowycz, C.-P. Mak, J. D. Michna, *J. Org. Chem. 39* (1974) 2079.
[12] **1**: m.p. = 261–262 °C (dec.); $\mu_{eff}(CHCl_3) = 3.1\ \mu_B$; UV/VIS ($CHCl_3$): $\lambda_{max}(\varepsilon) = 320(5900)$, 495 nm (45); MS: *m/z* 666($M^\oplus$), 586($M^\oplus - Br$), 506($M^\oplus - 2Br$). **2**: m.p. = 212 °C(dec); $\mu_{eff}(CHCl_3) = 3.1\ \mu_B$; UV/VIS ($CHCl_3$): $\lambda_{max}(\varepsilon) = 334(4200)$, 457 nm (33); IR(CsBr): $\tilde{\nu}_{Mo\text{-}Cl} = 306\ cm^{-1}$; MS: *m/z* 576($M^\oplus$), 541($M^\oplus - Cl$), 506($M^\oplus - 2Cl$). **3**: m.p. = 160 °C(dec.); ^{1}H-NMR (270 MHz, [D_8]toluene); $\delta = 0.71$ (s, 12 H; Me), 1.12 (s, 12 H; Me), 2.11 (d, $J = 11.0$ Hz, 8 H; CH_2), 2.46 (d, $J = 11.0$ Hz, 8 H; CH_2); ^{13}C-NMR (67.8 MHz, [D_8]toluene): $\delta = 23.0$ (Me), 35.2 (Me), 38.5 (CH_2), 53.5 (CMe_2), 222 (CO); IR (THF): $\tilde{\nu}_{CO} = 1902$ (m), 1767 (vs) cm^{-1}. **4**: m.p. = 155 °C(dec); $\mu_{eff}(CHCl_3) = 3.9\ \mu_B$; UV/VIS ($CHCl_3$): $\lambda_{max}(\varepsilon) = 290(2800)$, 453(160), 750 nm (25); IR(CsBr): $\tilde{\nu}_{M\text{-}Cl} = 290$, 305 cm^{-1}.
[13] D. Westland, N. Muriithi, *Inorg. Chem. 11* (1972) 2971.
[14] T. I. Al-Salih, C. J. Pickett, *J. Chem. Soc. Dalton Trans. 1985*, 1255.
[15] Crystal data for **3**; orthorhombic, space group $P2_12_12_1$, $a = 14.380(5)$, $b = 10.876(5)$, $c = 17.123(5)$ Å, $V = 2678.0(17)$ Å^3, $\rho_{calcd} = 1.391$ g cm^{-3} for $Z = 4$; $\mu(Mo_{K\alpha}) = 7.93\ cm^{-1}$; Rigaku AFC-6 with $Mo_{K\alpha}$ radiation ($\lambda = 0.71069$ Å); 2687 independent reflections ($2 < 2\theta < 50°$), no absorption correction; Patterson method (UNICS), block-diagonal least-squares refinement with anisotropic temperature factors for non-hydrogen atoms (263 parameters) with fixed positional and thermal ($B = 4.0$ Å^2) parameters for hydrogen atoms, 2049 reflections used ($I > 3\sigma(I)$), $R = 0.035$, $R_w = 0.045$, Goodness of Fit = 0.554; $\Delta\rho$(max/min) = 0.42/−0.30 e/Å^3. Further details of the crystal structure investigation may be obtained from the Fachinformationszentrum Energie, Physik, Mathematik GmbH, D-7514 Eggenstein-Leopoldshafen 2 (FGR), on quoting the depository number CSD-52750, the names of the authors, and full citation of the journal.
[16] R. H. Morris, J. M. Ressner, J. F. Sawyer, M. Shiralian, *J. Am. Chem. Soc. 106* (1984) 3683.
[17] M. Sato, T. Tatsumi, T. Kodama, M. Hidai, T. Uchida, Y. Uchida, *J. Am. Chem. Soc. 100* (1978) 4447.

$[As_3Br_{12}]^{3-}$ and $[As_8I_{28}]^{4-}$ — Structurally Novel, Discrete Halogenoarsenate(III) Ions

By *William S. Sheldrick** and *Hans-Joachim Häusler*

The trihalides EX_3 of the elements E = P, As, Sb, Bi are capable of adding further halide ions X^- to give a variety of halogeno anions $[EX_{3+n}]^{n-}$ (in mononuclear anions with n = 1, 2, 3, in polynuclear anions with n = 1/4, 1/2, 2/3, 3/2 inter alia). In the case of the intensively studied halogenoantimonate(III) complexes,[1] both discrete anions[2] such as $[Sb_2Cl_9]^{3-}$ or $[Sb_4Cl_{16}]^{4-}$ as well as polymeric anions, for example $[Sb_2F_7^-]_n$ or $[Sb_3I_{10}^-]_n$,[3] are known. Characteristic of the stereochemistry of the individual Sb atoms is an octahedral coordination with three shorter and three considerably longer *trans*-sited (secondary) Sb-X bonds.

[*] Prof. Dr. W. S. Sheldrick, Dipl.-Chem. H.-J. Häusler
Fachbereich Chemie der Universität
Erwin-Schrödinger-Strasse, D-6750 Kaiserslautern (FRG)

In contrast to the halogenoantimonate(III) complexes only a few of the analogous anions of trivalent arsenic have hitherto been characterized.[4] The data available for arsenic(III) indicate a lesser tendency for the coordination number to increase to six, as well as weaker secondary bonding. We now report on the structurally novel, discrete anions $[As_3Br_{12}]^{3-}$ and $[As_8I_{28}]^{4-}$.

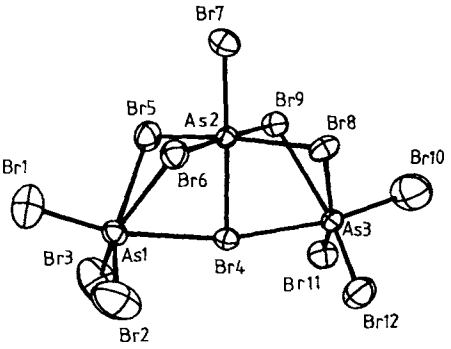

Fig. 1. Crystal structure of the anion of $[Et_3NH]_3[As_3Br_{12}]$. Bond lengths [pm]. As1-Br1 234.9(9), As1-Br2 233.6(9), As1-Br3 230.9(9), As1-Br4 313.8(8), As1-Br5 331.0(7), As1-Br6 312.6(9), As2-Br4 282.3(7), As2-Br5 248.3(7), As2-Br6 271.6(7), As2-Br7 252.2(7), As2-Br8 286.2(6), As2-Br9 258.2(7), As3-Br4 302.2(7), As3-Br8 317.0(7), As3-Br9 335.5(7), As3-Br10 236.1(9), As3-Br11 237.0(8), As3-Br12 236.4(7).

Both anions could be obtained as crystalline triethylammonium salts by cooling equimolar solutions of Et_3NHX and AsX_3 (X = Br, I) in CH_3NO_2 and CH_3CN, respectively.[5] The anion $[As_3Br_{12}]^{3-}$ consists of a central $AsBr_6$ octahedron which is connected via two faces with a common corner to two further $AsBr_6$ octahedra (Fig. 1).[6] The dimensions of the anion also allow the alternative description as a weak complex between a central $[AsBr_6]^{3-}$ ion and two attached $AsBr_3$ molecules. Thus, three very short bonds to terminal Br atoms (range 230.9–237.0 pm) as well as three very long bonds to bridging Br atoms (range 302.2–335.5 pm) are found in each case for the As1 and As3 octahedra. In the central, only slightly distorted As2 octahedron *trans* As-Br bonds expectedly show a characteristic interdependence, yet all bond lengths lie between 248.3 and 286.2 pm. Discrete $[AsX_6]^{3-}$ ions could hitherto not be unequivocally characterized.[4]

According to *Rundle*'s model the bonds of the *trans* X-E-X moieties in halogeno anions $[EX_{3+n}]^{n-}$ can be regarded as electron-rich three-center bonds. A bonding (σ_u^+), through participation of the s-valence orbital, a weak antibonding (σ_g^+), as well as a strongly antibonding (σ_u^+) molecular oribital are formed. The antibonding character of the σ_g^+ orbital can be reduced by asymmetrization of the X-E-X bond (2nd order Jahn-Teller effect); the bonding σ_u^+ interaction is concomitantly weakened. Such an X-E···X asymmetrization should be energetically more favorable for arsenic than for antimony, since an increasing relative s-participation at the σ_g^+ orbital with decreasing atomic number is to be expected for elements of the fifth main group of the Periodic System. However, the non-bonding electron pair does not seem to be stereochemically effective for the central $AsBr_6$ octahedron in the anion $[As_3Br_{12}]^{3-}$, as also in the known anion $[SbCl_6]^{3-}$.[7] All Br-As-Br angles for As2 lie between 87.1 and 93.8°, all angles between the three longer As-Br distances being smaller than 90°.

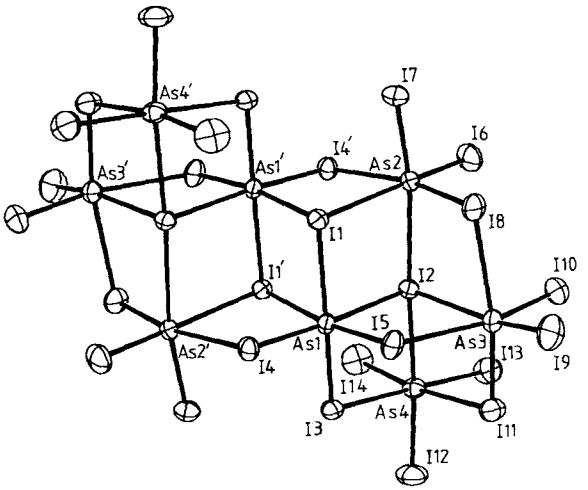

Fig. 2. Crystal structure of the anion of $[Et_3NH]_4[As_8I_{28}]$. Bond lengths [pm]. As1-I1 307.4(2), As1-I1' 306.8(2), As1-I2 316.3(2), As1-I3 272.3(2), As1-I4 269.0(2), As1-I5 273.6(2), As2-I1 320.4(2), As2-I2 334.9(2), As2-I4' 330.1(2), As2-I6 264.2(2), As2-I7 260.6(2), As2-I8 264.0(2), As3-I2 318.2(2), As3-I5 338.8(2), As3-I8 339.6(2), As3-I9 264.8(2), As3-I10 261.3(2), As3-I11 261.9(2), As4-I2 326.0(2), As4-I3 326.4(2), As4-I11 350.7(2), As4-I12 262.7(2), As4-I13 264.4(2), As4-I14 257.8(2).

The surprisingly large centrosymmetric anion $[As_8I_{28}]^{4-}$, which consists of eight edge-bridged AsI_6 octahedra, displays a close relationship with the recently characterized polymeric anion $[Sb_3I_{\bar{10}}]_n$.[3b] Both anions contain centrosymmetric E_6I_{22} units (the octahedra around As1-As3 and As1'-As3' in Fig. 2). In the $[Sb_3I_{\bar{10}}]_n$ anion (Fig. 3) the I atoms I9 and I10 are also related with each other by a symmetry center and thus bridge $[Sb_6I_{20}]^{2-}$ units to give an infinite chain. In contrast, in the discrete $[As_8I_{28}]^{4-}$ anion two further symmetry related AsI_3 units (octahedra As4 and As4') are attached in an edge-bridging fashion. The As-I distances to the μ_3- and μ_4-bridging I atoms I1 and I2 lie between 306.8 and 334.9 pm, whereas the individual As atoms each show three short As-I bonds in the range between 357.8 and 373.6 pm. The recently characterized $[As_8Cl_{28}]^{4-}$ has a completely different structure:[4g] four $AsCl_3$ molecules are very loosely attached to a central $[As_4Cl_{16}]^{4-}$ unit with cubane-like structure.

The common building principle in $[As_8I_{28}]^{4-}$ and $[Sb_3I_{\bar{10}}]_n$ would indicate that other, similarly built iodoar-

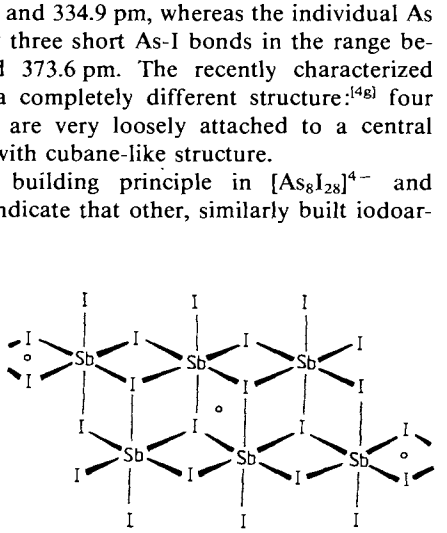

Fig. 3. For comparison: Crystal structure of the polymeric anion $[Sb_3I_{\bar{10}}]_n$ of $[C_3(NMe_2)_3][Sb_3I_{10}]$ [3b].

senate(III) and -antimonate(III) ions may be expected to be obtained by variation of the cation.

Received: June 5, 1987;
revised: July 22, 1987 [Z 2285 IE]
German version: *Angew. Chem. 99* (1987) 1184

CAS Registry numbers:
$[Et_3NH]_3[As_3Br_{12}]$, 110904-89-7; $[Et_3NH]_4[As_8I_{28}]$, 110934-53-7; $AsBr_3$, 7784-33-0; AsI_3, 7784-45-4; Et_3NHBr, 636-70-4; Et_3NHI, 4636-73-1.

[1] J. F. Sawyer, R. J. Gillespie, *Prog. Inorg. Chem. 34* (1986) 65.
[2] a) M. Hall, M. Nunn, M. J. Begley, D. B. Sowerby, *J. Chem. Soc. Dalton Trans. 1986*, 1231; b) U. Ensinger, W. Schwarz, A. Schmidt, *Z. Naturforsch. B 37* (1962) 1584.
[3] a) S. H. Mastin, R. R. Ryan, *Inorg. Chem. 10* (1971) 1757; b) S. Pohl, W. Saak, P. Mayer, A. Schmidpeter, *Angew. Chem. 98* (1986) 813; *Angew. Chem. Int. Ed. Engl. 25* (1986) 825.
[4] a) J. L. Hoard, L. Goldstein, *J. Chem. Phys. 3* (1935) 117; b) A. J. Edwards, S. N. Patel, *J. Chem. Soc. Dalton Trans. 1980*, 1630; c) M. R. Churchill, A. G. Landers, A. L. Rheingold, *Inorg. Chem. 20* (1981) 849; d) J. Kaub, W. S. Sheldrick, *Z. Naturforsch. B 39* (1984) 1952, 1957; e) A. T. Mohammed, U. Müller, *Acta Crystallogr. Sect. C 41* (1985) 329; f) *Z. Anorg. Allg. Chem. 523* (1985) 45; g) W. Willing, U. Müller, J. Eicher, K. Dehnicke, *ibid. 537* (1986) 145.
[5] *Procedure:* $[Et_3NH]_3[As_3Br_{12}]$, yellow crystals; cooling of a solution of 1.57 g (5 mmol) of $AsBr_3$ and 0.91 g (5 mmol) of Et_3NHBr in CH_3NO_2 (yield 86% based on $AsBr_3$); $[Et_3NH]_4[As_8I_{28}]$, red crystals. Cooling of a solution of AsI_3 and Et_3NHI in CH_3CN (yield 82% based on AsI_3); satisfactory C, H, N analyses.
[6] $[Et_3NH]_3[As_3Br_{12}]$ crystallizes monoclinically, $P2_1$, $a=1119.9(3)$, $b=1832.4(3)$, $c=1118.5(2)$ pm, $\beta=99.00(3)°$; 1959 reflections with $F_0^2 \geq 3\sigma(F_0^2)$, $R=0.072$. $[Et_3NH]_4[As_8I_{28}]$ crystallizes triclinically, $P\bar{1}$, $a=1464.8(3)$, $b=1507.2(8)$, $c=1160.6(3)$ pm, $\alpha=110.49(2)$, $\beta=91.14(2)$, $\gamma=104.49(3)°$; 5047 reflections with $F_0^2 \geq 2\sigma(F_0^2)$, $R=0.055$. Further details of the crystal structure investigations are available on request from the Fachinformationszentrum Energie, Physik, Mathematik GmbH, D-7514 Eggenstein-Leopoldshafen 2 (FRG) on quoting the depository number CSD-52596, the names of the authors, and the journal citation.
[7] D. R. Schroeder, R. A. Jacobson, *Inorg. Chem. 12* (1973) 210.

High-Pressure Synthesis and Crystal Structure of Neodymium(III) Oxide Peroxide, $Nd_2O_2(O_2)$**

By *Klaus-Jürgen Range,* Maximilian Stadler, Franz Rau,* and *Ulrich Klement*

Dedicated to Professor Rudolf Hoppe on the occasion of his 65th birthday

Although the spectroscopically determined trend of the fourth ionization energies I_4[1a,b] in the lanthanoid series[1a,b] and the standard electrode potentials for the transition Ln^{III}-Ln^{IV} would make the existence of neodymium(IV) oxides appear possible, at least in the absence of water, all attempts to prepare binary neodymium-oxygen compounds with $O:Nd > 1.5:1$ have so far failed.[2] The stable oxide Nd_2O_3 is neither oxidized further by atomic oxygen[3] nor by $NaBrO_4$ or XeF_2.[4] In contrast, the stabilization of Nd^{IV} is possible by partial incorporation in perowskite host lattices such as $BaCeO_3$, $BaPrO_3$, $BaThO_3$, and $BaZrO_3$.[5] In (so far unsuccessful) attempts to prepare pure $BaNdO_3$ we have now obtained a compound of empirical composition NdO_2, which, however, according to the result of a structural analysis, is not a neodymium(IV) dioxide but a neodymium(III) oxide peroxide.

[*] Prof. Dr. K.-J. Range, Dr. M. Stadler, F. Rau, Dr. U. Klement
Institut für Anorganische Chemie der Universität
Universitätsstrasse 31, D-8400 Regensburg (FRG)

[**] This work was supported by the Deutsche Forschungsgemeinschaft and the Fonds der Chemischen Industrie.

Nd_2O_3/BaO_2 mixtures react under high pressure/high temperature conditions only incompletely to give $Ba_2Nd_2O_5$. The formation of $Nd_2O_2(O_2)$ was first observed in the reaction of Nd_2O_3/BaO_2 mixtures to which KF had been added as flux. After the reaction at 40 kbar and 1500 °C (30 min, modified belt apparatus,[6] Pt crucible) it was found in the form of small, light-blue crystals in a partly white, partly dirty-violet matrix, albeit in a very low yield, which could not be noticeably increased even by drastic variation of the reaction conditions. Following the X-ray spectrographic detection of BaF_2 in the white matrix, it was immediately clear that an oxygen-rich potassium oxide formed from BaO_2 and KF in the melt, and not the relatively unreactive BaO_2, was the actual supplier of oxygen in the formation of $Nd_2O_2(O_2)$. This finding prompted us to react Nd_2O_3 with KO_2. Indeed, in this way it was possible to carry out the complete oxidation of Nd_2O_3 by reaction with KO_2 at 40 kbar and 1500 °C

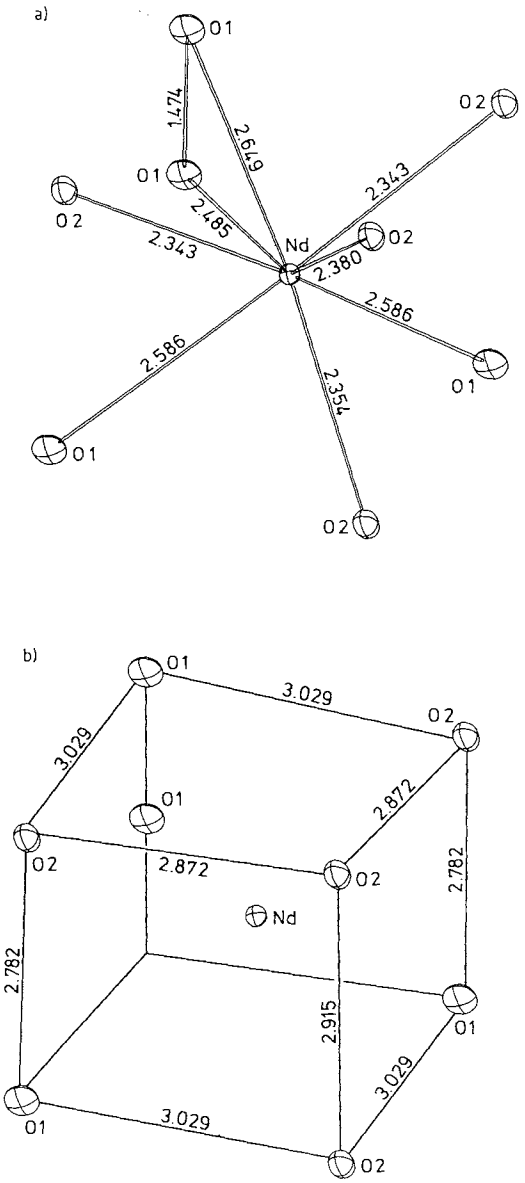

Fig. 1. Section of the crystal structure of $Nd_2O_2(O_2)$. a) Environment of Nd (bond lengths in Å); b) approximate cubic arrangement of O1 and O2 (O1 and O2 signify peroxidic and oxidic O atoms, respectively).

 © VCH Verlagsgesellschaft mbH, D-6940 Weinheim, 1987 0570-0833/87/1111-1174 $ 02.50/0

(30 min, then finally slow cooling to 1000 °C). $Nd_2O_2(O_2)$, which can be easily isolated from the reaction product by treatment with water, forms pleochroic crystals which appear light blue or violet-pink depending on the direction of the incident light. The empirical composition NdO_2 was confirmed by EDX (Energy-Dispersive X-ray analysis) (no cations except Nd present) and chemical analysis (Nd: found 81.5%, calcd 81.8%). Remarkable is the stability of $Nd_2O_2(O_2)$ toward water and air. Upon heating to 420 °C (O_2 or argon atmosphere, 10 K/min) the compound is converted via elimination of oxygen into Nd_2O_3 (cubic C-form). 2 N H_2SO_4 attacks $Nd_2O_2(O_2)$ very slowly with formation of H_2O_2.

The crystal of $Nd_2O_2(O_2)$[7] contains O^{2-} ions and $(O_2)^{2-}$ ions (O-O distance in O_2^{2-}: 1.474(4) Å). Each neodymium ion is coordinated by four oxide (O2) and four peroxide (1) oxygen atoms (Fig. 1a), the peroxide groups assuming almost side-on positions (distances Nd-O: 2.485(3), 2.649(3) Å) and functioning as bridge ligands to other neodymium ions (Nd-O: $2 \times 2.586(2)$ Å). The distances Nd^{3+}-O^{2-} are significantly shorter ($2 \times 2.343(1)$, 2.354(2), 2.380(3) Å).

Figure 1b illustrates a crystallochemical peculiarity of the structure: seven of the eight oxygen neighbors of a neodymium ion are arranged at the corners of an almost regular cube, only the eighth ligand is shifted from a corner (with formation of the O_2^{2-} ion) in the direction of a cube edge. The close relationship to the fluorite structure, which is to be expected for a hypothetical neodymium(IV) dioxide is immediately apparent. The reduced volume for the latter, extrapolated from the ionic radii for Ce^{4+} and Pr^{4+},[8] is about 9.7% smaller than that of $Nd_2O_2(O_2)$. A conversion of $Nd_2O_2(O_2)$ into NdO_2 under still higher pressures than those used here also seems possible.

Received: June 12, 1987 [Z 2294 IE]
German version: *Angew. Chem. 99* (1987) 1176

CAS Registry numbers:
$Nd_2O_2(O_2)$, 12164-76-0; Nd_2O_3, 1313-97-9; KO_2, 12030-88-5.

[1] a) J. Sugar, J. Reader, *J. Chem. Phys. 59* (1973) 2083; b) K. L. van der Sluis, L. J. Nugent, *ibid. 60* (1974) 1927; c) L. J. Ugent, *Int. Rev. Sci. Inorg. Chem. Ser. two 7* (1975) 195.
[2] D. A. Johnson, *Adv. Inorg. Chem. Radiochem. 20* (1977) 1.
[3] D. M. Gruen, W. C. Koehler, J. J. Katz, *J. Am. Chem. Soc. 73* (1951) 1475.
[4] R. B. Nikodem, *Dissertation, Virginia Polytechnic Institute 1969; Diss.-Abstr. Int. B 30* (1969) 2590.
[5] a) A. J. Jacobsen, B. C. Tofield, B. E. F. Fender, *Proc. 10th Rare Earth Res. Conf. Carefree, AZ (USA) 1973*, Vol. 1, p. 194; b) G. Brauer, H. Kristen, *Z. Anorg. Allg. Chem. 456* (1979) 41.
[6] K.-J. Range, R. Leeb, *Z. Naturforsch. B 30* (1975) 889.
[7] Crystal structure data: Enraf-Nonius CAD-4 diffractometer, $Mo_{K\alpha}$ radiation, $\lambda = 0.71073$ Å, graphite monochromator, $T = 23$ °C; monoclinic, space group $C2/m$, $a = 6.6495(7)$, $b = 4.0173(3)$, $c = 6.5174(9)$ Å, $\beta = 98.11(1)°$, $V = 172.36$ Å^3, $\rho_{calc} = 5.79$ g cm^3, $Z = 2$. $(Mo_{K\alpha}) = 297.5$ cm^{-1}. 1785 measured intensities, 1711 "observed" with $I > 2\sigma(I)$, 1027 thereof independent ($R_{int} = 0.015$), ω-2θ scan $\Delta\omega = 1.5 + 0.4 \tan\theta$, $(\sin\theta/\lambda)_{max} = 1.22$, $-16 \leq h + 16$, $-2 < k \leq +9$, $-1 < l \leq +15$. Empirical absorption correction via ψ scans of selected reflections. Heavy atom method, anisotropic refinement of all atoms (Program system SDP 3.0), $R = 0.033$, $R_w = 0.045$ (including unobserved reflections), $S = 1.86$, 19 parameters, $\Delta\rho_{max} = 1.7$ e/Å^3. Further details of the crystal structure investigation are available on request from the Fachinformationszentrum Energie, Physik, Mathematik GmbH, D-7514 Eggenstein-Leopoldshafen 2 (FRG) on quoting the depository number CSD-52565, the names of the authors, and the journal citation.
[8] R. D. Shannon, *Acta Crystallogr. Sect. A 32* (1976) 751.

Observation of an Eclipsed C_{sp^3}-CH_3 Bond in a Tricyclic Orthoamide; Experimental and Theoretical Evidence for C–H ··· O Hydrogen Bonds**

By *Paul Seiler, Gary R. Weisman,* Eric D. Glendening, Frank Weinhold,* Van B. Johnson,* and *Jack D. Dunitz**

Although the conformations of many thousands of methyl groups have been determined in crystals by X-ray and neutron diffraction analyses, we do not know of a single example where the eclipsed arrangement has been established for a C_{sp^3}-CH_3 bond (in contrast to XC_{sp^2}-CH_3 bonds, where eclipsing of a C-H bond with the C=X double bond is the rule, as in propene,[1] acetaldehyde,[2] and numerous other examples). We now report the occurrence of a nearly eclipsed methyl group in the tricyclic orthoamide **1a**, as found by low-temperature (81 K) X-ray analysis

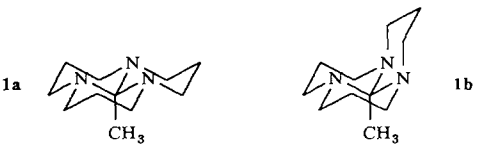

of its crystalline trihydrate,[3] where all H positions have been unambiguously determined. The tricyclic orthoamide molecule (Fig. 1) sits on a crystallographic threefold rotation axis and hence has the all-*trans* configuration with the three N lone pairs antiperiplanar (*app*) to C-CH_3 (with C-C bond distance lengthened to 1.561(1) Å). To our surprise, the conformation about this bond is nearly eclipsed, with N-C-C-H torsion angles of 8.0(9)°.

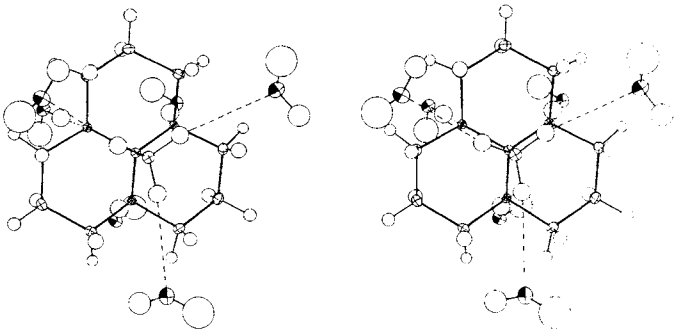

Fig. 1. Stereoview of the tricyclic orthoamide trihydrate in the cubic crystal modification, showing the three water molecules hydrogen-bonded to the nitrogen atoms (below) and the three water molecules hydrogen-bonded to the hydrogen atoms of the methyl group (above, dashed lines). The various atoms are represented by 50% probability ellipsoids (spheres for the hydrogen atoms).

[*] Prof. Dr. J. D. Dunitz, P. Seiler
Laboratorium für Organische Chemie der
Eidgenössischen Technischen Hochschule
ETH-Zentrum, Universitätstrasse 16, CH-8092 Zürich (Switzerland)
Prof. G. R. Weisman, Dr. V. B. Johnson
Department of Chemistry
University of New Hampshire
Durham, NH 03824 (USA)
Prof. F. Weinhold, E. D. Glendening
Theoretical Chemistry Institute and Department of Chemistry
University of Wisconsin, Madison
Madison, WI 53706 (USA)

[**] *G.R.W.*, acknowledges the support of the Petroleum Research Fund administered by the American Chemical Society. Portions of this work were carried out on the San Diego Supercomputer Center Cray X-MP, supported by the National Science Foundation. We thank Dr. *T. Laube* for his help in obtaining the anhydrous material.

In the crystal structure, each N atom is involved in hydrogen bonding to a water molecule (N···O, 2.855 Å; N···H-O angle, 162°). The water molecules then make additional hydrogen bonds among themselves in such a way that the two triads related by the crystallographic inversion center form a chair-like $(H_2O)_6$ ring with O···O distances of 2.770 Å and O-H···O angles of 171°.[4] On the other side of the tricyclic orthoamide, we find that each C-H bond of the methyl group points nearly at an O atom of a neighboring triad (H···O, 2.67 Å; C-H···O angle, 170°). If the observed C-H distance of 1.00 Å is adjusted to correct for the characteristic X-ray shortening effect, the H···O distance in question decreases by about 0.1 Å. While the corrected distance is still somewhat on the long side for C-H···O hydrogen bonding,[7] the nearly linear angle is highly suggestive. Moreover, while the N-C-C-H torsion angle is 8.0° the N-C-C···O torsion angle is only 0.6°. All these features support the idea that C-H···O hydrogen bonding is largely responsible for the unusual methyl conformation.

In any case, we have good evidence that the nearly eclipsed methyl group is not an intrinsic property of the molecule. On the experimental side, after much effort, a solitary single crystal of the anhydrous material has been secured and its structure determined, also at 81 K.[8] Here the asymmetric crystal unit consists of two independent molecules of the tricyclic orthoamide. One has the same all-*trans* configuration as occurs in the trihydrate; the other has the *cis,cis,trans* configuration **1b** (Figure 2),

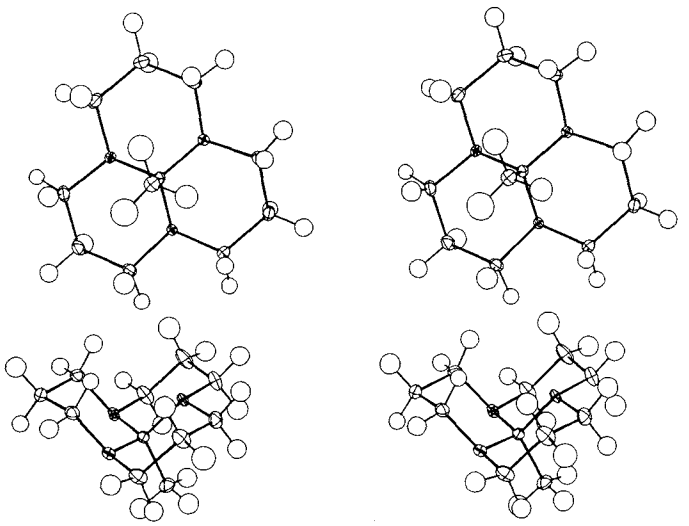

Fig. 2. Stereoview of the two independent cyclic orthoamide molecules **1a** and **1b** in the monoclinic crystal modification. The various atoms are represented by 50% probability ellipsoids (spheres for the hydrogen atoms).

known from NMR evidence[9] to be present in small amounts in dilute solution. In both molecules, the methyl groups are staggered.[10] The C-CH_3 bond distances are 1.555(1) Å in staggered **1a** and 1.539(1) Å in **1b**, both shorter than in eclipsed **1a**. Insofar as hydrogen bonding to the three *app* lone pairs in the trihydrate must surely weaken their stereoelectronic effect on the C-CH_3 bond, the slightly longer bond distance in the trihydrate has to be attributed to the effect of eclipsing.

These unexpected experimental results have prompted us to look into some calculated properties of suitable model systems. Ab initio 6-31G* SCF calculations for model 1,1,1-triaminoethane (N lone pairs *app* to C-C bond, crystal geometrical parameters) show the staggered conformation more stable than the eclipsed by 5.52 kcal mol^{-1}. If the torsion potential is approximated as $V=(V_{max}/2)(1+\cos 3\theta)$ where $V_{max}=5.52$ kcal mol^{-1} and $\theta=8°$, the minimum strength of each of the three C-H···O hydrogen bonds required to produce the eclipsed conformation is ca. 1.8 kcal mol^{-1}, far in excess of the reported $CH_4\cdots OH_2$ interaction strength (ca. 0.5 kcal mol^{-1}) calculated using similar basis sets.[11] Indeed, we calculate at 6-31G* an interaction energy of only −0.63 kcal mol^{-1} for the $CH_4\cdots OH_2$ supermolecule constrained to model the hydrate C-H···O geometry. This failure of the SCF calculations to account for the experimental structure led us to investigate the use of larger basis sets as well as the effect of electron correlation upon the C-H···O hydrogen bond in the $CH_4\cdots OH_2$ system. As can be seen from the results in Table 1, a correlation effect

Table 1. Calculated interaction energies of the $CH_4\cdots OH_2$ complex (kcal mol^{-1}). $E(\text{int})=E(\text{complex})-E(CH_4)-E(H_2O)$.

Basis	SCF	MP2	MP4
6-31G*	−0.634	−1.447	−1.359
6-311G**	−0.936	−1.872	−1.698
6-311G(2d,p)	−0.919	−1.935	−1.726

of unprecedented magnitude for hydrogen bonds significantly enhances the interaction strength (by 0.7–1.0 kcal mol^{-1}) at all levels of calculation. The physical reason for this effect is probably not typical dispersion attraction but rather the generalized contraction of electron density that reduces the effective van der Waals radius of the C-H group, thus allowing the ca. 2 kcal mol^{-1} hyperconjugative n_O-σ^*_{CH} interaction to fully assert itself.[12] We have also investigated the cooperative effect upon C-H···O hydrogen bonding in a model $CH_4\cdots O(H)H\cdots NH_3$ complex. At the MP2/6-31G* level, the C-H···O interaction energy was calculated to be −1.98 kcal mol^{-1}, more than 0.5 kcal mol^{-1} more negative than that of the $CH_4\cdots OH_2$ complex and in the range necessary to reverse the orthoamide methyl rotation barrier. Further extensions of the theoretical model lead to similar net values of C-H···O interaction strength.[13] We believe that the calculational results taken as a whole provide theoretical support for the notion of directed C-H···O hydrogen bonds of sufficient strength to qualitatively account for the anomalous methyl conformation in the orthoamide trihydrate crystal. Furthermore, we believe that the hydrogen bonding and methyl-eclipsing are not significantly dependent on stereoelectronic factors associated with orientation of nitrogen lone pairs (which affect mainly the C-CH_3 bond).

The fact that a suitable arrangement of water molecules can invert the rotation barrier of a methyl group through hydrogen bonding has obvious implications for interaction between "hydrophobic" regions of molecules and aqueous environments. The water molecule arrangements will, in general, be determined by the directional properties of the stronger O-H···O and N-H···O hydrogen bonds. This arrangement, in turn, may affect the conformation of aliphatic chains, etc., through the formation of weaker, but still direction specific, C-H···O hydrogen bonds. Hence, conformational regularities observed for aliphatic portions of molecules in non-aqueous environments may not be ap-

plicable without reservations when the molecules are embedded in a matrix of water molecules.

Received: June 19, 1987 [Z 2304 IE]
German version: *Angew. Chem. 99* (1987) 1216

[1] I. Tokue, T. Fukuyama, K. Kuchitsu, *J. Mol. Struct. 17* (1973) 207.
[2] R. W. Kilb, C. C. Lin, E. B. Wilson, *J. Chem. Phys. 26* (1957) 1695.
[3] Obtained by slow cooling of the liquid (believed pure!) enclosed in a capillary mounted directly on the diffractometer. Space group *Pa*3 (No. 205), $a = 13.719$ Å (at 81 K), $Z = 8 \times C_{11}H_{21}N_3 \cdot 3H_2O$, $Mo_{K\alpha}$ radiation ($\lambda = 0.7107$ Å), intensity measurements out to $\theta = 40°$, $R = 0.032$ [14].
[4] Similar chair-like rings are known to occur, e.g. in ice II [5] and the crystalline trihydrate of 1,3,5-triaza-2,4,6-trimethylcyclohexane [6].
[5] B. Kamb, W. C. Hamilton, S. J. La Placa, A. Prakash, *J. Chem. Phys. 55* (1971) 1934.
[6] E. W. Lund, *Acta Chem. Scand. 5* (1951) 678; *12* (1958) 1768.
[7] R. Taylor, O. Kennard, *J. Amer. Chem. Soc. 104* (1982) 5063; Z. Berkovitch-Yellin, L. Leiserowitz, *Acta Cryst. B40* (1984) 159; J. A. R. P. Sarma, G. R. Desiraju, *Acc. Chem. Res. 19* (1986) 222.
[8] Obtained by distillation of the orthoamide trihydrate from CaH_2 and slow cooling of one drop of liquid distillate in a capillary mounted on the diffractometer. Space group $P2_1/c$, $a = 17.502$, $b = 8.537$, $c = 17.674$ Å, $\beta = 125.89°$ at 81 K, $Z = 8 \times C_{11}H_{21}N_3$, intensity measurements as for the trihydrate, $R = 0.034$ [14].
[9] G. R. Weisman, V. B. Johnson, M. B. Coolidge, *Tetrahedron Lett. 22* (1981) 4365.
[10] Preliminary electron-density difference maps for the anhydrous crystal form show small diffuse residual density peaks (0.05–0.10 eÅ^{-3}) close to the positions expected for H atoms in the alternative eclipsed methyl conformation of the all-*trans* molecule. These could arise from the inadequacy of the isotropic temperature factor formalism used for the H atoms in the least-squares refinements.
[11] Several ab initio calculations of the methane-water system agree that C-H ··· O hydrogen bonding is significant but disagree about details. See for example, S. R. Ungemach, H. F. Schaefer III, *J. Amer. Chem. Soc. 96* (1974) 7898; H. Umeyama, K. Morokuma, *J. Am. Chem. Soc. 99* (1977) 1316; P. Ruelle, G. Leroy, G. Louterman-Leloup, *Bull. Soc. Chim. Belg. 87* (1978) 867.
[12] A. E. Reed, F. Weinhold, L. A. Curtiss, D. J. Pochatko, *J. Chem. Phys. 84* (1986) 5687.
[13] Two extensions are particularly important: Inclusions of diffuse ('+') functions reduces the C-H ··· O interaction by about 1 kcal mol^{-1}. Inclusion of higher-order cooperative effects [e.g., in the model complex $H_2NCH_2CH_3 \cdots O(H)H \cdots NH_3$] strengthens the interaction by an approximately compensating amount.
[14] Further details of the crystal structure investigations are available on request from the Fachinformationszentrum Energie, Physik, Mathematik GmbH, D-7514 Eggenstein-Leopoldshafen 2 (FRG), on quoting the depository number CSD-52487, the names of the authors, and the journal citation.

Aromatic Nitration at the Encounter Rate in the Gas Phase

By *Marina Attinà,* Fulvio Cacace,* and *Giulia de Petris*

Despite the overwhelming amount of attention devoted to aromatic nitration in condensed media, important mechanistic aspects remain far from defined, largely owing to the complicating effects of the reaction environment, which prevent the construction of a unified mechanistic model.[1] This has stimulated extension of the study to the gas phase, where solvation, ion pairing, viscosity, and other complicating factors are largely absent, and the results are directly comparable with those of theoretical calculations. Recently, an integrated approach based on the combination of mass spectrometry with atmospheric-pressure radiolytic techniques allowed us to characterize reaction (a) as the first nitration by a gaseous cation whose

[*] Prof. M. Attinà, Prof. Dr. F. Cacace, Dr. G. de Petris
Università degli Studi di Roma "La Sapienza"
Istituto di Chimica Farmaceutica e Tossicologica
P. le delle Scienze, 5, I-00185 Rome (Italy)

$$[RNO_3H]^{\oplus} + PhX \longrightarrow ROH + [PhXNO_2]^{\oplus} \quad (a)$$
1

substrate and positional selectivity conform to those of electrophilic substitution in solution.[2] A salient anomaly of the preliminary results, confirmed by the present, more detailed study,[3] is the unexpectedly low nitration rate of anisole, PhOMe, comparable to that of toluene, PhMe. It is tempting to ascribe this finding to competitive proton transfer (b) to strongly activated, hence highly basic, sub-

$$\mathbf{1} + PhX \longrightarrow RNO_3 + [PhXH]^{\oplus} \quad (b)$$

strates. This explanation, particularly fit for anisole, which contains an n-type nucleophilic center,[4] is less satisfactory when extended to pure π systems—e.g., polymethylbenzenes—which are characterized, as now we find, by the same behavior (Table 1). Such observations suggest an al-

Table 1. Relative reactivity and isomeric composition of products from the nitration of activated substrates with $[MeNO_3H]^{\oplus}$ and $[CF_3CH_2NO_3H]^{\oplus}$ ions in methane at 37.5 °C, 720 torr [a].

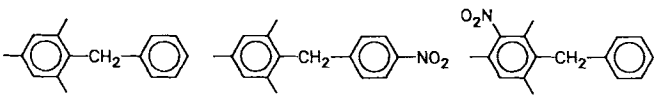

2 **3** **4**

Arene A	k_A/k_{PhH}	Isomeric composition of products [%]		
		ortho	*meta*	*para*
Anisole [3]	7.6	41	–	57
Toluene [3]	5.1 (2.1)	59(50)	7(15)	34(35)
Diphenylmethane	5.7	41	4	55
Mesitylene	8.1			
Isodurene	7.7 (2.2)			
Pentamethylbenzene	7.8			
Benylmesitylene **2**	8 (2.4)	**3** < 5(8)	**4** > 95(92)	

[a] Values in parentheses refer to nitration by $[CF_3CH_2NO_3H]^{\oplus}$. Standard deviation of the data ca. 10%, except in the case of **2**, whose extremely low vapor pressure prevents accurate concentration measurements.

ternative explanation: namely, above a certain activation level all substrates undergo nitration at the encounter rate, kinetically controlled by the formation of an "early" ion-molecule complex [Eq. (c)].

$$\mathbf{1} + PhX \underset{k_{-1}}{\overset{k_1}{\rightleftharpoons}} \text{early complex} \xrightarrow{k_2} \sigma \text{ complexes} \quad (c)$$

A decision between alternatives (b) and (c) cannot be made simply on the grounds that increasingly activated arenes, from toluene to pentamethylbenzene, are nitrated at comparable rates (Table 1), since the trend fits both hypotheses.

Crucial evidence was sought via a different approach, based on nitration of a suitable model molecule, benzylmesitylene **2**, where the activation of the aromatic rings is considerably different, roughly corresponding to that of toluene and isodurene (1,2,3,5-tetramethylbenzene), respectively. If the nitration rate is actually limited by incursion of process (b), one would expect a low isodurene/toluene intermolecular selectivity, and a correspondingly low intramolecular selectivity in the nitration of **2**, since the nitration rate of the more basic isodurene moiety should be limited by process (b) in both systems. On the other hand, if a limiting nitration rate is established by the kine-

tically determining formation of an early complex [Eq. (c)], a low isodurene/toluene intermolecular selectivity should be contrasted by the retention of intramolecular selectivity in the nitration of **2**. The latter has been studied, as in the case of the other substrates, by chemical ionization (CI) mass spectrometry (in CH_4, 0.5 torr, 160 °C) and by a radiolytic technique[5] (in CH_4, 720 torr, 37.5 °C). The nitrating reactant **1** (R=Me, CF_3CH_2) has been obtained in both cases by protonation of the corresponding alkyl nitrate with the $C_nH_5^{\oplus}$ (n=1,2) ions from the ionization of CH_4. The CI spectra reveal formation of the expected $[Arene\cdots NO_2]^{\oplus}$ adducts, of unknown structure. The radiolytic results provide clear-cut evidence for the rate-limiting formation of an early adduct [Eq. (c)] since the $k_{isodurene}:k_{toluene}$ ratio is as low as 1.5, while the intramolecular selectivity in the nitration of **2** is much higher, the activated ring reacting at least 20 times faster than the unsubstituted one, despite the unfavorable (2:5) statistical factor. Nor can such a result be traced to isomerization of primary arenium ions, i.e., to the energetically favored intramolecular migration of $NO_2^{\oplus}$ to the more activated ring. Convincing evidence against such a process is provided by control experiments based on metastable-ion kinetic energy (MIKE) and collisionally induced dissociation (CID) spectrometry of suitable model ions.[6]

In conclusion, the results show that in the nitration of sufficiently activated substrates by gaseous $[RNO_3H]^{\oplus}$ ions the rate-determining and the product-controlling steps are kinetically distinct, according to the scheme outlined in Equation (c).

Whenever k_2 exceeds k_{-1} (i.e., the activation barrier to Wheland intermediates is *lower* than that to dissociation of the complex), nitration occurs at the encounter rate and substrate selectivity is lost. Such a state of affairs is analogous to that prevailing in solution, where the reactants are confined within a solvent cage, forming an "encounter pair" whose separation requires overcoming a viscosity barrier. In the gas phase, formation of the early complex can be traced to the intense electrostatic forces between the free nitrating cation and the aromatic molecule.[7] In a dense gas (e.g., in CH_4 at 720 torr), the energy released in the formation of the complex is rapidly removed by thermalyzing collisions, and the reactants are trapped in a sort of "electrostatic cage," kinetically, if not physically, equivalent to the viscosity cage envisaged in solution.[8]

Experimental Procedure

CH_4 (720 torr), RNO_3 (5–10 torr), and the aromatic substrates (0.1–1 torr) were irradiated in a 220 Gammacell (Nuclear Canada Ltd.) to a dose of 2×10^3 Gy in the presence of O_2 (10 torr) and SF_6 (5 torr), the products being analyzed by GLC and GLC/MS. The ionic nature of the nitration is demonstrated by the negligible yields of nitrated products from irradiations where CH_4 was replaced by isobutane, whose $tBu^{\oplus}$ ions are unable to protonate RNO_3, and by the depression of the yields caused by the presence of ionic interceptors, such as NMe_3, apart from the direct observation of the charged intermediates by CIMS.

The CID experiments were carried out in a ZAB-2F mass spectrometer (VG Micromass Ltd.), whose source was operated in the CI mode, using He as the collision gas.

Received: May 4, 1987;
revised: July 29, 1987 [Z 2226 IE]
German version: *Angew. Chem. 99* (1987) 1174

[1] K. Schofield: *Aromatic Nitration*, University Press, Cambridge 1980 and references cited therein.

[2] a) M. Attinà, F. Cacace, M. Yañez, *J. Am. Chem. Soc. 109* (1987) 5092; b) M. Attinà, F. Cacace, *ibid. 108* (1986) 318. Previous low-pressure mass spectrometric results where hardly consistent with solution-chemistry trends, e.g., pointing to the lack of nitrating ability of $NO_2^{\oplus}$ (S. A. Benezra, M. K. Hoffman, M. M. Bursey, *J. Am. Chem. Soc. 92* (1970) 7501) and to anomalous activating effects of substituents (P. Ausloos, S. G. Lias, *Int. J. Chem. Kinet. 10* (1978) 657).

[3] The irradiation conditions and the analytical techniques have considerably been improved over those reported in Ref. [2]. A sixfold decrease of the dose, aimed at evaluating *initial* nitration rates, and use of SF_6 as a thermal-electron scavenger have provided more accurate selectivity data for activated substrates and a significant decrease of the standard deviation. The changes, concerning in particular the k_A/k_{PhH} ratio for A=toluene and anisole (2.9 and 3.2 [2b]), do not significantly affect the overall selectivity pattern, nor the conclusions from this study.

[4] Most exothermic proton-transfer reactions between n-type nucleophilic centers occur at a collisional rate in the gas phase, T. Su, M. T. Bowers in M. T. Bowers (Ed.): *Gas Phase Ion Chemistry, Vol. 2*, Academic Press, New York 1979, p. 83.

[5] For a recent survey of the integrated mass spectrometric-radiolytic approach, see F. Cacace in P. Ausloos, S. G. Lias (Eds.): *Structure/Reactivity and Thermochemistry of Ions*, Reidel, Dordrecht 1987, p. 467.

[6] a) MIKE = metastable-ion kinetic energy; CID = collisionally induced dissociation; b) Protonated (*p*-nitrobenzyl)mesitylene **3** and protonated benzylnitromesitylene **4** obtained from the corresponding neutral precursors under methane-CI conditions give different MIKE and CID spectra. The fragment at *m/z* 133 (loss of $C_6H_5NO_2$) is detectable only in the MIKE and CID spectra of **3**, and that at *m/z* 178 (loss of C_6H_6) is significant only in the spectra of **4**. Furthermore, the fragments at *m/z* 119 and 241 are present only in the spectra of **3**, and those at *m/z* 160 and 226 in the spectra of **4**. Such conspicuous differences show that **3** fails to rearrange to **4**, despite conditions highly favorable to intramolecular isomerization, including the high exothermicity of the formation process, the high temperature (180 °C), the low pressure (0.5 torr), and the long delay (10^{-5} s) before structural assay.

[7] The stabilization energy of ion-molecule electrostatic complexes are of the order of 10 kcal mol^{-1}, or higher: a) D. K. Sen Sharma, P. Kebarle, *J. Am. Chem. Soc. 104* (1982) 19; b) P. Politzer, K. Jaysauriya, P. Sjoberg, P. R. Laurence, *ibid. 107* (1985) 1174; c) W. Bäther, H.-F. Grützmacher, *Int. J. Mass Spectrom. Ion Processes 64* (1985) 193.

[8] A reaction environment consisting of an inert gas at sufficiently high pressure, e.g., CH_4 at 720 torr, is essential for meaningful comparison with condensed-phase kinetics. At the low pressures typical of mass spectrometric approaches, the energy released in the formation of the ion-molecule complex, unaffected by thermalyzing collisions, often allows the reactants to overcome the barrier to products. This explains the apparent lack of activation energy and the negative temperature coefficient of many exothermic ion-molecule reactions in the low-pressure domain.

Photo- and Thermochromic Liquid Crystal Polysiloxanes**

By *Ivan Cabrera, Valeri Krongauz,** and *Helmut Ringsdorf**

Dedicated to Professor Ernst Fischer on the occasion of his 65th birthday

The combination of photochromic and liquid crystalline properties in one molecule might lead to an unusually versatile material for practical applications.[1] The attempts to synthesize such materials failed because the combination of photochromic and mesogenic moieties in one molecule led to impairment of one or both of the properties.[2,3]

Earlier[3–5] we reported "hybrid" low-molar-mass molecules containing spiropyran and mesogenic groups. The molecules are thermochromic and give a very peculiar metastable mesophase (we named them quasi-liquid crystals). However, they do not exhibit photochromism.

Recently we reported[6] structural transformations occurring in side-chain liquid crystal polyacrylates containing spiropyran side groups. The polymers were synthesized by copolymerization of vinyl monomers with spiropyran and

[*] Prof. Dr. V. Krongauz, Dr. I. Cabrera
Department of Structural Chemistry
The Weizmann Institute of Science
Rehovot 76100 (Israel)
Prof. Dr. H. Ringsdorf
Institut für Organische Chemie der Universität
J.-J. Becher-Weg 18-20, D-6500 Mainz (FRG)

[**] This work was supported by the Minerva Foundation, Munich (FRG).

p-cyanophenylbenzoate groups. The thermochromic spiropyran-to-merocyanine dye conversion occurs on heating of the copolymers. The mesophase could be observed in the copolymers containing more than 20 mol% of spiropyran side groups. Cross-linking of the macromolecules due to aggregation of the dye moieties gives rise to formation of a network, which is responsible for the appearance of a new rheo-optical effect: strong dynamic birefringence, observed above the clearing point.

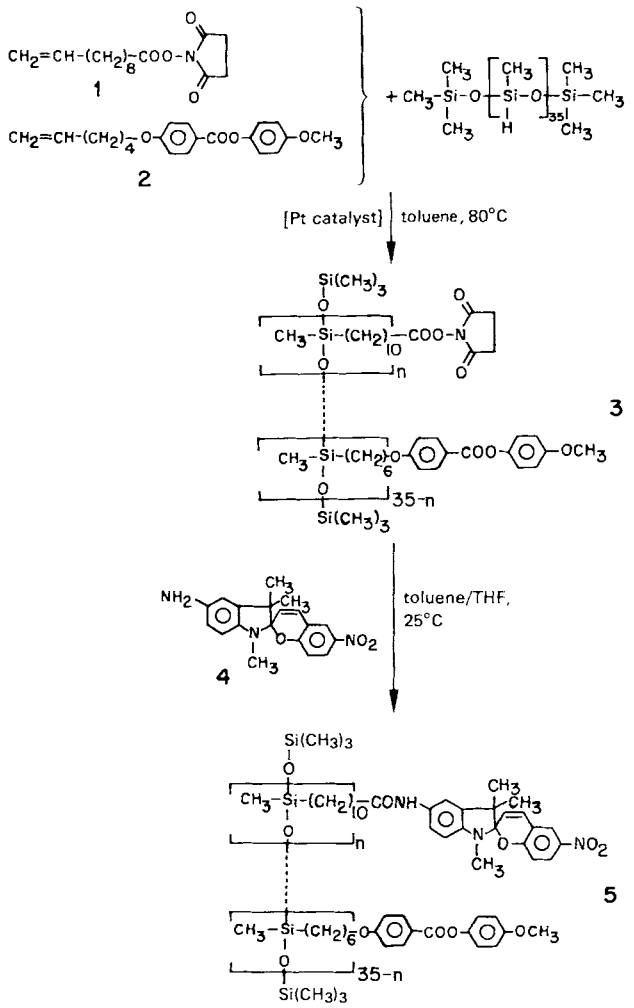

Scheme 1. Synthesis of photochromic polysiloxanes. 5'-amino-1',3',3'-trimethyl-6-nitro-2',3'-dihydrospiro[2*H*-chromen-2,2'-indene] **4** was synthesized according to Ref. [12]. 4-Methoxyphenyl-[4-(5-hexenyloxy)benzoate] ester **2** was prepared by standard methods published in the literature [8]. The *N*-hydroxysuccinimide ester of 10-undecenoic acid **1** was synthesized by the direct esterification of the acid with *N*-hydroxysuccinimide [13]. The product was purified by recrystallization from *n*-hexane (yield 72%, m.p. = 53–55 °C). All compounds were characterized by elemental analysis, ^{1}H-NMR, and mass spectrometry. The copolymers **3** were prepared by addition of the olefins **1** and **2** to polysiloxanes containing SiH groups [7, 8]. The copolymers with spiropyran groups, **5**, were obtained by reacting in situ the copolymers **3** with **4** at room temperature in toluene/THF. The polymers were isolated by preparative gel permeation or by repeated precipitation with methanol (yields 60–70%). The composition of the copolymers was determined by elemental analysis.

Here we report for the first time the photochromic behavior of similar hybrid materials, obtained by the synthesis of liquid crystal polysiloxanes containing spiropyran groups. Since the many organic functions of the spiropyran groups interfere in the hydrosilylation reaction by which the liquid crystal polysiloxanes are usually prepared,[7, 8] the spiropyran-containing polymers were synthesized via the active ester copolymers (Scheme 1). The synthesis through the active ester copolymers can be used in general as a way of preparing polyfunctional liquid crystal polysiloxanes. The phenylbenzoate copolymers with the spiropyran side chains give a mesophase whose clearing temperature decreases with increasing spiropyran content. The phase diagram is given in Figure 1.

The copolymer films cast from solution acquire a pink color at room temperature and exhibit strong birefringence. Irradiation with visible light ($\lambda > 500$ nm) brings about a pale yellow color (Fig. 2a, b), while irradiation of

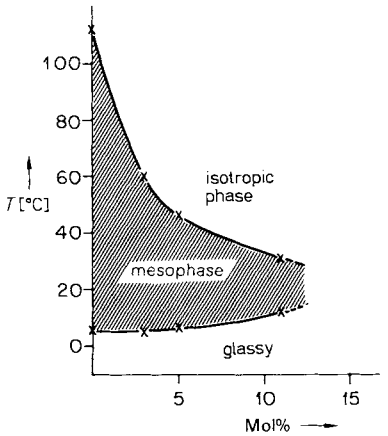

Fig. 1. Phase diagram of the polysiloxanes containing spiropyran. The composition of the copolymers is given as mol% of spiropyran groups.

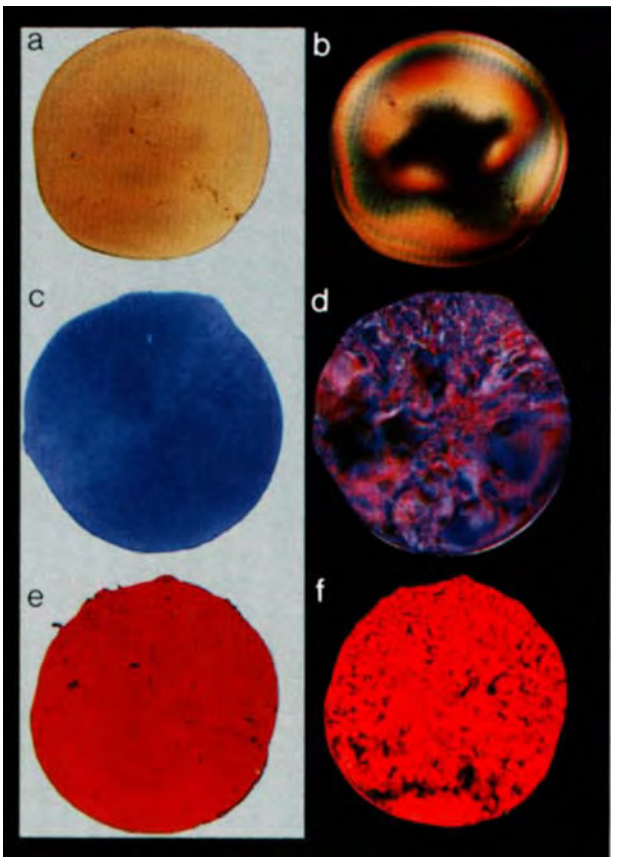

Fig. 2. Photocolored films of the copolymer with 11 mol% of spiropyran units observed without (a,c, e) and between (b, d, f) crossed polarizers (x18). a, b) After irradiation with visible light (> 500 nm) at 25 °C. c, d) After UV irradiation (365 nm) at −20 °C. e, f) After UV irradiation at 25 °C.

the yellow film with UV light ($\lambda = 365$ nm) results in a deep red color (Fig. 2e, f). A yellow film irradiated with UV light at $-20\,^{\circ}C$ turns blue (Fig. 2c, d), and can be converted back to yellow by irradiation with visible light. The blue film is stable in the dark at $-20\,^{\circ}C$ but turns red on heating above $-10\,^{\circ}C$. The red film is thermally stable below the glass transition temperature (see Fig. 1), but turns yellow on irradiation with visible light. Below $-10\,^{\circ}C$, however, the red film is not affected by irradiation with visible light. At room temperature the fading of the red color takes several days, but less than a minute above the clearing point.

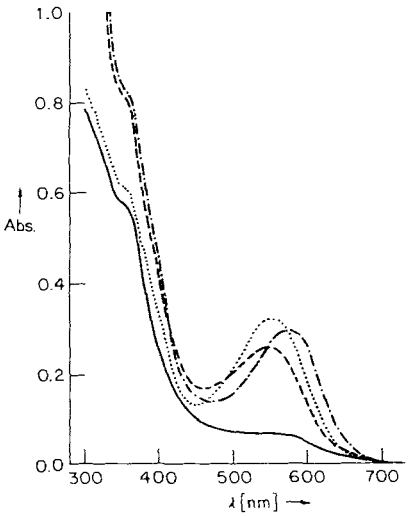

Fig. 3. Absorption spectra of films of the copolymer with 11 mol% of spiropyran units: (——) yellow film at 25 °C; (· · ·) red film at 25 °C; (— · —) blue film at −20 °C; (- - -) red film obtained by heating the blue film to 25 °C. Abs, absorption in arbitrary units.

The electronic absorption spectra of the polymer films are shown in Figure 3. The maximum at 550 nm (red) corresponds to aggregated merocyanines, which cause physical cross-linking of the macromolecules, while the maximum at 580 nm (blue) has been ascribed to isolated merocyanine groups.[6,9] The yellow color ($\lambda_{max} \approx 370$ nm) corresponds to the spiropyran absorption (Scheme 2).

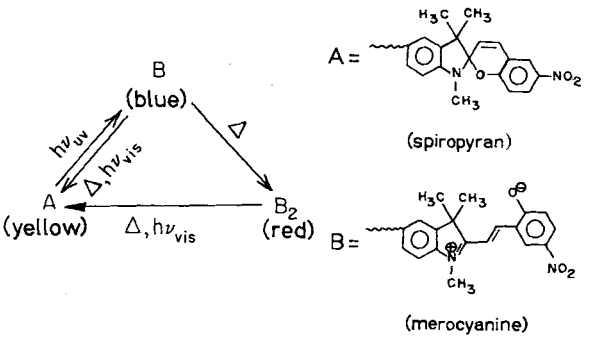

Scheme 2. Scheme for the conversion of the photochromic side groups.

Apparently at temperatures below $-10\,^{\circ}C$ the side chains are immobilized[10] and neither thermal dimerization of the merocyanine groups nor photochemical dissociation of their dimers occurs under these conditions.

The possibility of controlling with light and temperature the formation of the three primary colors may make it possible to tailor these liquid crystal polymers for new applications in imaging technologies.[11]

Received: June 15, 1987;
supplemented: July 24, 1987 [Z 2296 IE]
German version: *Angew. Chem. 99* (1987) 1204

[1] R. Bertelson in G. Brown (Ed.): *Photochromism*, Wiley-Interscience, New York 1971, p. 289.
[2] I. Cabrera, F. Shvartsman, O. Veinberg, V. Krongauz, *Science (Washington) 226* (1984) 341.
[3] F. Shvartsman, V. Krongauz, *Nature (London) 309* (1984) 608.
[4] a) E. Meirovitch, F. Shvartsman, V. Krongauz, H. Zimmermann, *J. Phys. Chem. 89* (1985) 5522; b) F. Shvartsman, I. Cabrera, A. Weis, E. Wachtel, V. Krongauz, *J. Phys. Chem. 89* (1985) 3941.
[5] D. A. Holden, H. Ringsdorf, V. Deblauwe, G. Smets, *J. Phys. Chem. 88* (1987) 716.
[6] I. Cabrera, V. Krongauz, *Nature (London) 326* (1987) 582.
[7] H. Finkelmann, G. Rehage, *Makromol. Chem. Rapid Commun. 1* (1980) 31.
[8] H. Ringsdorf, A. Schneller, *Makromol. Chem. Rapid Commun. 3* (1982) 557.
[9] H. Eckhardt, A. Bose, V. Krongauz, *Polymer*, in press.
[10] K. Horie, M. Tsukamoto, I. Mita, *Eur. Polym. J. 21* (1985) 805.
[11] G. Attard, G. Williams, *Nature (London) 326* (1987) 544.
[12] F. Shvartsman, V. Krongauz, *J. Phys. Chem. 88* (1984) 6448.
[13] A. Hassner, V. Alexanian, *Tetrahedron Lett. 46* (1978) 4475.

Structure and Color of Pentaphenylbismuth**

By *Arno Schmuck, Jürgen Buschmann, Joachim Fuchs,* and *Konrad Seppelt**

The pentaphenyl compounds of phosphorus, arsenic, antimony, and bismuth synthesized in quick succession by *Wittig* et al,[1] $P(C_6H_5)_5$, $As(C_6H_5)_5$, and $Sb(C_6H_5)_5$, whose crystal and molecular structures have in the meantime been characterized, are colorless, stable solids at room temperature. The phenyl groups of $P(C_6H_5)_5$ and $As(C_6H_5)_5$ in the crystalline state are almost ideally oriented towards the corners of a trigonal bipyramid with longer axial element-C bonds,[2] whereas the geometry of the $Sb(C_6H_5)_5$ molecule very much resembles a square pyramid with a particularly short axial Sb-C bond.[3] In contrast, $Bi(C_6H_5)_5$ is violet colored; because of its sensitivity to light, heat, and moisture, however, its crystal and molecular structures have thus far not been determined. The color is very unusual for a compound of a main-group element in its highest valence state and this prompted us to examine it in more detail.

We established that the violet color of $Bi(C_6H_5)_5$ is almost the same in the dissolved state as in the solid state and cannot be attributed to paramagnetism or impurities. The color is due to a weak, broad absorption in the green-yellow region ($\lambda_{max} = 532$ nm, $\log \varepsilon = 2.4$).

Blue needle-shaped crystals containing THF separate out from dilute THF solutions of $Bi(C_6H_5)_5$ at $-25\,^{\circ}C$; on warming to room temperature, however, they rapidly lose THF. Solvate-free $Bi(C_6H_5)_5$ can be isolated in the form of large, rhombic, violet crystals from concentrated THF solutions. Figure 1 shows the molecular structure of $Bi(C_6H_5)_5$ in the crystal at $-96\,^{\circ}C$. It can be seen that $Bi(C_6H_5)_5$ and $Sb(C_6H_5)_5$ have very similar triclinic unit cells ($P\bar{1}$, $Z = 2$). $P(C_6H_5)_5$ and $As(C_6H_5)_5$ also have similar unit cells;[2] they are monoclinic.

[*] Prof. Dr. K. Seppelt, Dipl.-Chem. A. Schmuck, Dr. J. Buschmann, Prof. Dr. J. Fuchs
Institut für Anorganische und Analytische Chemie
der Freien Universität
Fabeckstrasse 34-36, D-1000 Berlin 33

[**] This work was supported by the Deutsche Forschungsgemeinschaft and the Fonds der Chemischen Industrie.

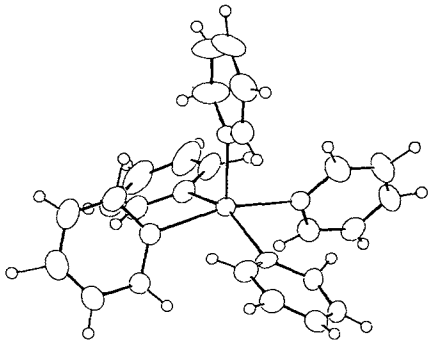

Fig. 1. Crystal structure of $Bi(C_6H_5)_5$ at $-96\,^{\circ}C$ [10]. Vibrational ellipsoids at the 50% probability level. Hydrogen atoms located by difference Fourier analysis. Bi-C_a: 222.1(9), Bi-C_e: 232.9, 232.4, 232.7, 232.2 (9–11) pm; C_a-Bi-C_e: 100.1, 96.4, 103.8, 105.9(4)°; C_e-Bi-C_e: adjacent C_e: 88.1, 87.3, 88.3, 87.8; opposite C_e: 163.5, 150.3(4)°. $P\bar{1}$, $a = 1020.2(2)$, $b = 1064.1(3)$, $c = 1352.5(5)$ pm, $\alpha = 67.54(3)$, $\beta = 78.19(3)$, $\gamma = 62.16(2)°$, $Z = 2$, $V = 1199 \times 10^6$ pm^3. 4650 reflections, 4225 observed with $I > 2\sigma(I)$, $R = R_w = 0.039$, after numerical absorption correction $R = R_w = 0.38$. Further details of the crystal structure investigation are available on request from the Fachinformationszentrum Energie, Physik, Mathematik GmbH, D-7514 Eggenstein-Leopoldshafen 2 (FRG), on quoting the depository number CSD-52633, the names of the authors, and the journal citation.

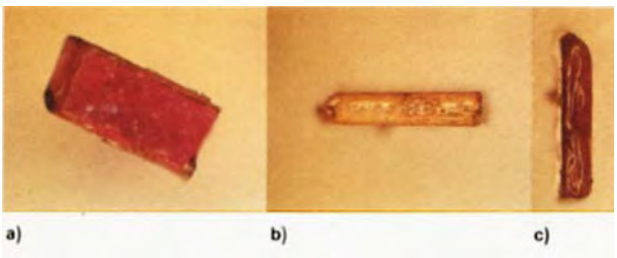

Fig. 2. A $1 \times 0.5 \times 0.2$ mm^3 crystal of $Bi(p\text{-}CH_3C_6H_4)_3(p\text{-}CH_3C_6H_4)_2$, which shows the optical phenoma described in the text better than the multifaceted $Bi(C_6H_5)_5$ crystals. Because of twinning, the exact structure of this compound is not known. a) Large face of crystal; b) same crystal seen from the edge; c) as b) but crystal rotated 90° against the plane of polarization of light. The increasing diffuseness of the surface is real and a result of hydrolytic decomposition within a period of ca. 20 min.

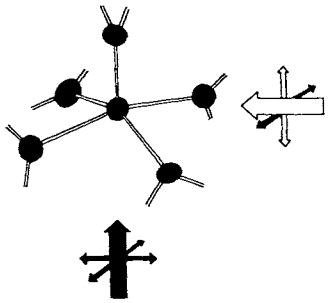

Fig. 3. Optical behavior of a $Bi(C_6H_5)_5$ crystal relative to the molecular orientation. The large arrows indicate the direction of light, the small arrows the vibration plane of the electric vector. Bold arrows: absorption; open arrows: no absorption. It can be seen that a beam of light is polarized after passing parallel to the basal plane of the square pyramid.

$Bi(C_6H_5)_5$ crystallizes in molecules—there is but little evidence of intermolecular interactions. The molecule has an almost regular square pyramidal geometry. The angles between opposite equatorial phenyl groups (163.5 and 150.3°) are quite similar, but deviate markedly from those of an ideal trigonal pyramid (120 and 180°). The four equatorial bonds are significantly longer (232 pm) than the axial bond (221 pm). The four equatorial phenyl groups are oriented propeller-like, that is equidirectionally *twisted*. The structure of $Sb(C_6H_5)_5$ is exactly the same,[3] yet it is colorless! After it had been established that the colorless $Sb(p\text{-}CH_3C_6H_4)_5$ has a trigonal-pyramidal structure[4] it was concluded beyond doubt that the different structures are to be attributed to a slightly different distribution of intermolecular forces in the crystal. In any case, the knowledge of the structure gives no indication of the origin of the color. Even the positions of the hydrogen atoms are completely normal (no agostic H atoms).

We came nearer to solving the color problem when a violet/colorless dichroism was observed with well-formed crystals. Despite the multifacetted surface of the crystals and the triclinic crystal system, we were able to study the phenomenon. Maximum absorption was found in the direction parallel to the axial Bi–C bond and maximum transmission in the plane perpendicular thereto. Light is apparently transmitted unhindered through the crystal in this plane; however, it is strongly polarized; when the electric vector vibrates parallel to this plane, the crystal appears violet, when perpendicular the crystal again appears colorless (see Fig. 2). In this orientation such a crystal is a very effective polarization filter! Since the electric vector always vibrates in the basal plane of the square pyramid in the case of absorption, it must be the excitation of the four long equatorial Bi–C bonds that causes the absorption (see Fig. 3).

So far, the nature of the chromophore is still a matter of speculation: We propose a charge-transfer transition from the phenyl ligand to the bismuth. The pentavalent state is energetically much more unfavorable in the case of bismuth than in the case of antimony, because of poorer shielding of the nucleus by the filled 4f shell (lanthanoid contraction), i.e. bismuth is strongly electronegative in this state. The long bonds are strongly polarized to the bismuth and hence closely approach the excited charge-transfer state:

$$(C_6H_5)_4\overset{\delta^{\ominus}}{Bi}\text{-}\overset{\delta^{\oplus}}{C_6H_5} \longrightarrow (C_6H_5)_4Bi^{\ominus}C_6H_5^{\oplus}$$

Model calculations with inclusion of relativistic effects could confirm both this and the difference from the bonding in $Sb(C_6H_5)_5$. Interestingly, $Bi(C_6H_5)_5$ can be used as an arylating reagent. Acidic hydrogen atoms are thereby replaced by phenyl groups.[5,6] The mechanism of this reaction is presumably not a radical one, but rather an aryl cation has been assumed to be involved in the transition state.[5] It is also remarkable that $Bi(C_6H_5)_5$ produces significant amounts of benzene on heating, whereas $Sb(C_6H_5)_5$ cleaves off only diphenyl.[1] This also indicates a heterolytic Bi–C bond fission.

Since the color of $Bi(C_6H_5)_5$ is in no way connected with the aggregate state, and since the molecule is certainly not rigid in solution and thus present in several different structures, one can predict that trigonal bipyramidal pentaarylbismuth compounds should also be colored. Structural investigations of this kind have hitherto not been described, but $Bi(C_6H_5)_3(p\text{-}ClC_6H_4)_2$[7] and $Bi(p\text{-}CH_3C_6H_4)_5$[8] are likewise violet. Strong electron-withdrawing groups on the ligand should render the charge-transfer transition more difficult. Consistent with this hypothesis, $Bi(C_6H_5)_3(C_6F_5)_2$[9] and $Bi(C_{12}H_8)(C_6H_5)_3$[7] are yellow to orange.

Received: July 14, 1987 [Z 2353 IE]
German version: *Angew. Chem.* 99 (1987) 1206

[1] G. Wittig, M. Rieber, *Justus Liebigs Ann. Chem. 562* (1949) 187; G. Wittig, K. Clauß, *ibid. 577* (1952) 26, *578* (1952) 136.
[2] P. J. Wheatley, G. Wittig, *J. Chem. Soc. 1962*, 251; P. J. Wheatley, *ibid. 1964*, 2206.
[3] P. J. Wheatley, *J. Chem. Soc.* 1964, 3718; A. L. Beauchamp, M. J. Bennett, F. A. Cotton, *J. Am. Chem. Soc. 90* (1968) 6675.
[4] C. Brabant, J. Hubert, A. L. Beauchamp, *Can. J. Chem. 51* (1979) 2952.
[5] D. H. R. Barton, J. P. Finet, *Pure Appl. Chem. 59* (1987) 937.
[6] D. H. R. Barton, N. Y. Bhatnagar, J.-C. Blazejewski, B. Charpiot, J.-P. Finet, D. J. Lester, W. B. Motherwell, M. T. B. Papoula, S. P. Stanforth, *J. Chem. Soc. Perkin Trans. 1 1985*, 2657, 2667.
[7] D. Hellwinkel, M. Bach, *Justus Liebigs Ann. Chem. 720* (1969) 198.
[8] $Bi(p\text{-}CH_3C_6H_5)_5$ is apparently formed as a finely crystalline, violet powder by the reaction of $Bi(p\text{-}CH_3C_6H_4)_3Cl_2$ with $p\text{-}CH_3C_6H_4Li$ in the molar ratio 1:2 in ether below −10 °C. It decomposes with decoloration already at −10 °C.
[9] $Bi(C_6H_5)_3(C_6F_5)_2$: A solution of C_6H_5Li (freshly prepared from C_6F_5Br and $n\text{-}C_4H_9Li$) in ether was added dropwise at −78 °C to a suspension of $Bi(C_6H_5)_3Cl_2$ in anhydrous ether. The mixture was slowly warmed to room temperature, filtered, and the recovered solid recrystallized from ether. Pure $(C_6H_5)_3(C_6F_5)_2$ was obtained in the form of orange, water-sensitive crystals, m.p. 104 °C ^{19}F-NMR (ether, $CHCl_3$ ext.): $\delta(o) = -118.6$, $\delta(m) = -160.2$, $\delta(p) = -155.5$. Correct elemental analysis. The crystals are triclinic and (systematically) twinned.
[10] Siemens diffractometer with low-temperature facility, after H. Dietrich, H. Dierks, *Messtechnik 78* (1970) 184.

Catalytic Dehydrogenation of Cyclohexene on Silica Overlayer Films**

By *Jeffrey M. Cogen, Khosro Ezaz-Nikpay, Ronald H. Fleming, Scott M. Baumann,* and *Wilhelm F. Maier**

Heterogeneous dehydrogenation of cyclohexene **1** to benzene **3** has received attention as a model reaction for dehydrogenation processes.[1] This reaction is not stoichiometric (see temperature dependence of the product distribution in Fig. 3) and requires the presence of dihydrogen.

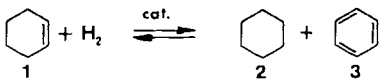

The reaction is not only catalyzed by noble metals, but also by spillover hydrogen[2] as well as on carbonaceous overlayers on Pt.[3,4] Chemically bound hydrogen atoms on Te were proposed as active sites for cyclohexene dehydrogenation in Te-NaX zeolites.[5] The reaction also occurs on gold covered Pt[6] and may be due to active spillover hydrogen on the Au surface.[7] These studies indicate that an exposed transition metal surface may not be necessary to catalyze this reaction.

To test the importance of an exposed transition metal surface the catalytic properties of Pt films supported on Si wafers with and without silica overlayers were compared (see Fig. 1). It was hoped that dihydrogen would diffuse readily through the overlayer to become activated (dissociated) at the underlayer. This activated hydrogen could then migrate back to the oxide surface and was expected to exhibit catalytic reactivity different from that of the exposed transition metal surface.

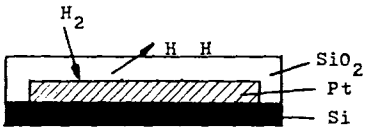

Fig. 1. Schematic representation of the overlayer catalysts.

The film catalysts were prepared by deposition of 10 ± 1.5 nm of Pt by electron beam evaporation at 10^{-7} torr onto polished silicon single-crystal wafers. Overlayers were deposited at a rate of 30–40 nm/min by electron beam evaporation of SiO_2 (from quartz) and the thickness was followed by a quartz crystal thickness monitor. The films were then transferred to a gas-phase flow reactor to test the catalytic activity at atmospheric pressure with dihydrogen or dideuterium as carrier gas. These SiO_2/Pt/Si films catalyze the hydrogenation and dehydrogenation of cyclohexene, while in control experiments SiO_2/Si proved to be catalytically inert.

The effect of the silica overlayer thickness on the rate of conversion of **1** to **2** and **3** at 250 °C was studied for SiO_2/Pt/Si.[8] The reaction rate per unit of geometric surface area drops exponentially with increasing overlayer thickness up to about 30 nm after which the rate stabilizes at about 1/100 (3 orders of magnitude above the background) of the activity of exposed metal and becomes nearly independent of thickness (overlayer thicknesses up to 2200 nm were investigated). During this study we noted that the activity decreases with decreasing deposition rate of the SiO_2 overlayer. Annealing of the overlayer catalyst prior to the reaction also results in a reduction of activity. These data suggest that catalytic activity requires defects in the overlayer film which can serve as carriers of the dissociated hydrogen and/or dihydrogen.

To exclude edge effects the Pt was deposited through a window leaving an outer frame (2 mm) of uncovered silicon so that the subsequent SiO_2 deposition completely covered the edges of the Pt film. On such films the masked (Pt-free) area showed no catalytic activity providing evidence against lateral Pt diffusion. As expected from the low concentration (based on simple geometrical estimates) of exposed edge platinum on unmasked films there was no detectable difference in the activity of masked and unmasked overlayer films. Scanning electron microscopy (SEM) of new and used overlayer catalysts gave no evidence for cracks or pores in the overlayer. Subsequent deposition of silica or gold onto used overlayer films (to fill any cracks or pores) did not decrease catalytic activity. Relative rates of deuteriation of *n*-hexane and *n*-octane (first order in hydrocarbon) on overlayer catalysts correlate with boiling point (as with Pt[9]) and not with hydrocarbon diffusion rates. These experiments are evidence against cracks or pores as carriers of catalytic activity.

The dependence of catalytic activity on SiO_2 overlayer thickness is most likely due to hydrogen recombination processes. However, due to analytical limitations we can not rule out partial accessibility of the Pt films with thin silica overlayers. For this reason subsequent experiments were conducted on thicker (>60 nm) SiO_2 overlayers for which possible exposure of Pt could be addressed.

Auger electron spectra (AES) and thickness profiles of such films are very clean and no transition metal diffusion into the overlayer or to the surface has been detected.[10]

[*] Prof. Dr. W. F. Maier, J. M. Cogen, K. Ezaz-Nikpay
Department of Chemistry
University of California
Berkeley, CA 94720 (USA)
Dr. R. H. Fleming, Dr. S. M. Baumann
Charles Evans & Associates
Redwood City, CA 94063 (USA)

[**] This study was supported by the National Institutes of Health (Grant GM-33386-01). We thank Dr. *R. S. Rai* for the SEM analyses.

However, the rather low sensitivity of AES (about 0.5% for Pt) is not suitable for trace analysis. The most sensitive method for trace analysis of such layered thin films is secondary ion mass spectrometry (SIMS, sensitivity limit <0.0005 atom-% for Pt),[11] which was used to analyze representative thin film catalysts before and after use. Rutherford back scattering spectrometry (RBS, sensitivity limit ≈ 0.005 atom-% for Pt)[12] was also used for chemical analysis and thickness measurements of the overlayer films. SIMS depth-profiling is based on sputtering which leads to unavoidable tailing of one layer into the next, while RBS is nondestructive and provides a much better depth resolution and accuracy. The RBS data confirmed film thicknesses in all cases. RBS and SIMS (see Figure 2) gave no evidence for Pt at or near the oxide surface. The RBS profiles show that the thickness of the films is homogeneous and that the surface of the SiO_2 is continuous and not rough. Although very close to exact stoichiometry, a slight oxygen deficiency in the silica overlayer was sometimes noted by RBS (33–36% Si : 67–64% O). Catalytic activity due to platinum on the silica surface at concentrations below the detection limit of our analytical techniques ($\approx 10^8$ Pt atoms/cm^2) was excluded by the lack of activity after impregnation and activation of SiO_2/Si films with readily detectable Pt concentrations of 10^8–10^{14} Pt/cm^2.[13]

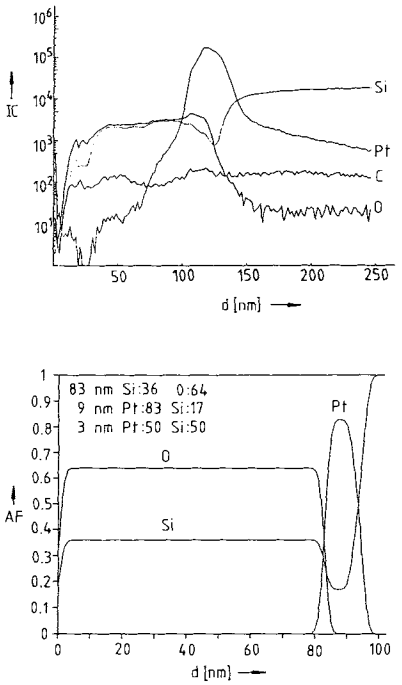

Fig. 2. Representative SIMS (left) and RBS (right) depth profiles of a used, active SiO_2/Pt/Si catalyst. Chemical composition of overlayers is given in atom-% in the upper left corner of the RBS profile. IC = ion counts, d = layer thickness, AF = atomic fraction.

Single crystal experiments have shown that prompt and extensive carbonation occurs on Pt during dehydrogenation of **1** while the reaction continues.[3] To test for sensitivity of SIMS for carbon at the SiO_2-Pt interface, we used a Pt/Si film for the catalytic reaction and then deposited the silica overlayer. The SIMS profile of this film indicated extensive carbonation at the SiO_2-Pt interface showing that SIMS can detect low carbon concentrations in these overlayers. Other overlayer films show no detectable increase of the carbonation below the SiO_2 surface upon use. This also serves as evidence against catalysis at the interface due to cracks or pores or diffusion of hydrocarbons through the silica layer.

Upon prolonged use of these films RBS and SIMS indicate sometimes that there is a slow diffusion of Pt into the silica overlayer (concentration 30 ppm Pt in SiO_2) which is currently under investigation. In this study each experiment was run on an unused film for time periods too short for significant Pt diffusion (confirmed by SIMS and RBS).

The effect of temperature on the rate (turnover frequency, N_f, molecules cm^{-2} sec^{-1}) and selectivity of a 72 nm SiO_2/Pt/Si was remarkably similar to that on a Pt/Si catalyst (Fig. 3). Over the temperature range studied the **3**/**2** ratio was slightly lower on the SiO_2/Pt/Si. The activation energies for the overall reaction of cyclohexene are: Pt/Si $= 2.09 \pm 5$ kJ/mol, SiO_2/Pt/Si $= 16.3 \pm 5$ kJ/mol; for formation of benzene: Pt/Si $= 82.8 \pm 14$ kJ/mol, SiO_2/Pt/Si $= 92.5 \pm 6$ kJ/mol. The differences between the exposed Pt and the overlayer films are not believed to be significant.

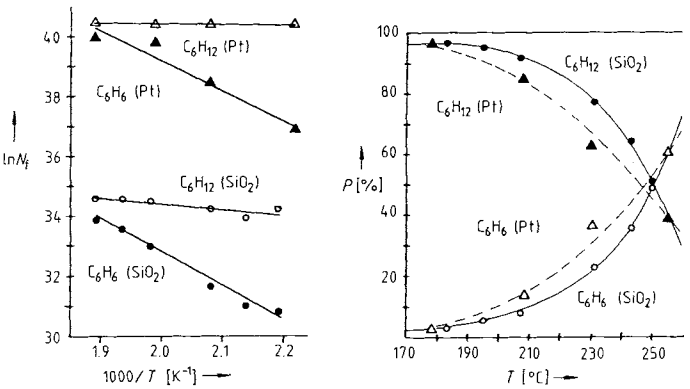

Fig. 3. Comparison of the Arrhenius plots (left) and the temperature dependence of the product composition (right) of cyclohexene conversion (low conversion conditions) on a 72 nm SiO_2/Pt/Si film with that on an exposed Pt/Si film.

Since isotopic product distributions have been useful as characteristic fingerprints for substrate catalyst interactions it was hoped to observe differences between the deuteriation patterns obtained on the oxide and on the Pt surface upon substitution of dideuterium for dihydrogen as carrier gas. However, the isotopic distributions of the products benzene and cyclohexane are very similar and show only a slightly higher deuterium content on Pt/Si relative to the products obtained on SiO_2/Pt/Si.

The similarity of the catalysis on the oxide overlayer to that on the Pt film suggests that this dissociated hydrogen[14] (whatever its nature on the surface) and not the exposed metal represents the active site for this catalytic reaction. The presence of active hydrogen on a surface may then be more important than the chemical nature of the surface. This conclusion is consistent with the wide variety of surfaces known to catalyze this reaction.[1–6]

In summary, inert silicon dioxide thin films become catalytically active in the presence of a platinum underlayer. Additional studies in our laboratory have shown that this phenomenon is not limited to SiO_2 on Pt, but has been observed with many other over-underlayer combinations. The most promising potential features of such catalysts—induction of catalytic activity on new surfaces and the resistance to poisoning due to protection of the transition metal by the overlayer—have now to be investigated.

Received: June 16, 1987;
revised: September 3, 1987 [Z 2298 IE]
German version: *Angew. Chem.* 99 (1987) 1222

[1] P. Tetenyi, K. Schachter, *Acta Chim. Acad. Sci. Hung. 50* (1966) 129; J. E. Germain, M. Cathala, *Chem. Ind. (London) 58* (1971) 1389; V. V. Lunin, A. E. Agronomov, L. K. Denisov, *Vestn. Mosk. Univ. Ser. 2 Khim. 17* (1976) 103; J. K. S. Wang, K. Wolf, R. D. Heydine, *Stud. Surf. Sci. Catal. 19* (1984) 561; A. Clearfield, *J. Mol. Catal. 27* (1984) 251; S. A. Nyarady, R. E. Sievers, *J. Am. Chem. Soc. 107* (1985) 3726; R. H. Crabtree, C. P. Parnell, *Organometallics 4*(1985) 519.
[2] W. C. Conner, Jr., G. M. Pajonk, S. J. Teichner, *Adv. Catal. 34* (1986) 1; S. Khoobiar, *J. Phys. Chem. 68* (1964) 411; S. Khoobiar, R. E. Peck, B. J. Reitzer, *Proc. Int. Congr. Catal. 3rd. 1965*, 338; P. A. Sermon, G. C. Bond, *J. Chem. Soc. Faraday Trans. 1 76* (1980) 889.
[3] S. M. Davis, G. A. Somorjai, *J. Catal. 65* (1980) 78; S. M. Davis, F. Zaera, G. A. Somorjai, *ibid. 77* (1982) 439.
[4] E. Segal, R. J. Madon, M. Boudart, *J. Catal. 52* (1978) 45.
[5] G. L. Price, Z. R. Ismagilov, J. W. Hightower, *J. Catal. 73* (1982) 361.
[6] J. W. A. Sachtler, M. A. Van Hove, J. P. Biberan, G. A. Somorjai, *Phys. Rev. Lett. 45* (1980) 1601.
[7] B. J. Wood, H. Wise, *J. Catal. 5* (1966) 135.
[8] Unless otherwise mentioned, conditions used in all experiments were: atmospheric pressure; dihydrogen flow rate of 4.5×10^{-4} mol/min; cyclohexene addition rate of 2.6×10^{-6} mol/min (syringe pump); catalyst (previously unused) prereduction for 15 min at 250 °C. Capillary GC was used for product analysis. Dideuterium was substituted for hydrogen in deuteriation experiments (analyzed by GC-MS).
[9] C. B. Lebrilla, W. F. Maier, *J. Am. Chem. Soc. 108* (1986) 1606.
[10] A. B. McEwen, G. P. Meeker, W. F. Maier, unpublished results.
[11] W. Heiland, E. Taglauer, *Methods Exp. Phys. 22* (1985) 299.
[12] C. A. Evans, Jr., R. J. Blattner, *Annu. Rev. Mater. Sci. 8* (1978) 181; W. K. Chu, J. W. Mayer, M. A. Nicolet: *Backscattering Spectrometry*, Academic Press, New York 1978.
[13] A. B. McEwen, W. F. Maier, R. H. Fleming, S. M. Baumann, *Nature (London) 329* (1987) 531.
[14] Artifacts due to Brønsted sites can safely be excluded due to the lack of activity of the oxide overlayer in the absence of transition metal underlayer and the lack of detectable rearrangement to methylcyclopentane or methylcyclopentene.

Transition State π-Solvation by Aromatic Rings: An Electronic Contribution to Diels-Alder Reaction Diastereoselectivity**

By *David A. Evans,* Kevin T. Chapman, Deborah Tan Hung,* and *Alan T. Kawaguchi*

"π-Stacking" interactions between aromatic rings and prochiral carbon atoms have been implicated as stereochemical control elements in a broad range of stereodifferentiating organic reactions.[1-8] In each of the cited cases, enhanced reaction diastereoselection *could* be attributed to the imposition of a transition state π-interaction between a resident aromatic ring and prochiral carbon(s). It has proven difficult, however, to unequivocally dissect such noncovalent interactions from the accompanying steric effects which together define reaction stereoselectivity. In the most comprehensive study reported to date for a given system, *Whitesell* et al. have established that the presence of a proximal phenyl group is essential for high diastereoselectivity in certain glyoxylate ene reactions.[3a-e] As was concluded in this study, however, these results do not demand the presence of an electronic effect, but imply that some property of the phenyl ring, be it size, shape, or electronic character, is essential for high stereoselectivity. In view of the tremendous potential utility of such π-stacking interactions in asymmetric synthesis design, we have attempted to define a protocol which might unequivocally demonstrate the presence of such a transition state electronic effect for a given reaction of interest. In the present study we have focused on the Diels-Alder reactions recently reported from this laboratory.

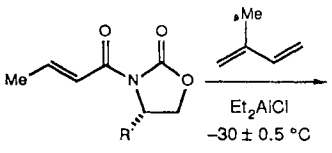

1 a-j

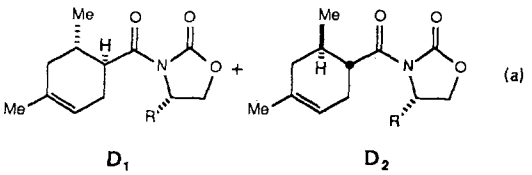

(a)

D_1 **D_2**

During the course of our investigations of the Diels-Alder cycloaddition reactions of α,β-unsaturated acyloxazolidinones **1** [Eq. (a)] we observed that oxazolidinone dienophile **1g** (R = benzyl) consistently provided diastereofacial discrimination superior to that of the closely related congener **1d** (R = isopropyl; cf. Table 1).[12m,n] Since we expected the steric requirements of an appended isopropyl group to exceed those of a benzyl group, we attributed the enhanced facial bias provided by **1g** to "π-tacking". In an effort to verify that we were observing an electronic interaction which was associated with the aromatic π-system, the reaction diastereoselectivity of the fully reduced cyclohexylmethyl derivative **1e** was also evaluated. We noted a significant decrease in the diastereoselectivity of this cycloaddition relative to that of **1g** despite the increased steric bulk of the appended side-chain (Table 1). Thus, some property of the phenyl ring of **1g** is important to the observed diastereofacial bias. It seemed reasonable to expect that a charge-transfer interaction between the aromatic ring and the electron deficient dienophilic moiety in **1g** should manifest itself not only in *increased* diastereoselectivity, but also in *decreased* reactivity. Accordingly, a relative rate comparison between **1e** and **1g** in the cycloaddition with isoprene was carried out. Contrary to expectation, it was found that the phenyl-substituted dienophile **1g** actually reacts slightly faster (rate ratio: 1.3) than does its fully saturated counterpart **1e**. This result suggests that little, if any, electronic reorganization accompanies the alleged π-stacking in the cycloaddition of **1g**. Addi-

Table 1. Variation of diastereoface shielding in oxazolidinone crotonate/isoprene Diels-Alder cycloadditions and oxazolidinone butyrate/methyl iodide alkylations [Eq. (a) and (b)].

1/2	R	Ratio D_1/D_2 [a]	Ratio A_1/A_2 [a]
a	Ph	2.06	4.24
b	Me	3.83	6.95
c	Et	5.50	9.21
d	i-C_3H_7	5.34	9.85
e	$CH_2(c\text{-}C_6H_{11})$	9.68	17.4
f	t-C_4H_9	> 100 [b]	67.7
g	CH_2Ph	20.7	16.7
h	$CH_2(p\text{-}MeOC_6H_4)$	23.3	16.9
i	$CH_2(p\text{-}ClC_6H_4)$	22.8	15.8
j	$CH_2(p\text{-}CF_3C_6H_4)$	21.0	16.8

[a] Ratios determined by capillary vapor phase chromatography. [b] Diastereoselectivity beyond the limits of detection.

[*] Prof. D. A. Evans, Dr. K. T. Chapman, D. T. Hung, A. T. Kawaguchi
Department of Chemistry, Harvard University
Cambridge, MA 02138 (USA)

[**] This work was supported by the National Science Foundation, Washington DC (USA).

tional support for this assertion was derived from an examination of the reaction diastereoselectivities of dienophiles **1h–1j** containing electronically perturbed benzyl substituents. The observed reaction diastereoselectivities of these analogues were insignificantly different from that of the parent crotonate **1g** (Table 1). A similar observation has been made by *Oppolzer* et al. in the Diels-Alder reactions of 8-arylmenthyl acrylates.[2d]

In order to gain more insight into the origin of these substituent effects, a set of experiments was designed to unambiguously dissect the steric from the electronic contributions to reaction diastereoselectivity. We chose to compare the Diels-Alder reaction [Eq. (a)] to an unrelated process which possessed gross transition state topographical similarities but which would not be expected to benefit from π-stacking. In this regard we have previously reported the relevant diastereoselective alkylation reactions of the lithium enolates of *N*-acyl-2-oxazolidinones **2**.[9] Al-

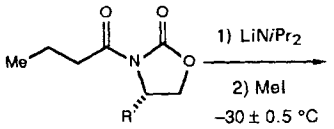

2 a-j

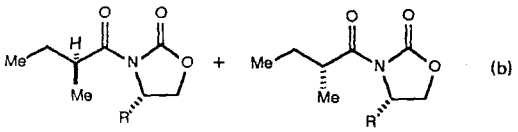

(b)

A$_1$ **A$_2$**

though lithium enolate **3** is topographically quite similar to Lewis acid complex **4**, the presumed reactive species in these Diels-Alder reactions, the electron rich nature of the enolate π-system was presumed to disfavor the π-stacking interaction. Direct comparison of the diastereoselectivities in analogous alkylation and Diels-Alder reactions should

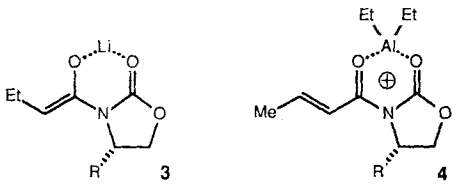

3 **4**

expose any stereochemical control element not common to both sets of transition states. The illustrated enolate methylations [Eq. (b)] and isoprene Diels-Alder reactions of (*E*)-crotyloxazolidinones [Eq. (a)] were selected for comparison at a common reaction temperature (−30 °C). Product diastereomer ratios for these reactions are listed in Table 1 and are plotted against each other in Figure 1.[10] Oxazolidinone substituents which cannot π-solvate the Diels-Alder transition state (Ph, Me, Et, *i*-C_3H_7, CH_2(*c*-C_6H_{11})) lie on a line representing the purely steric contribution to diastereofacial differentiation in both reactions. The excellent linear correlation ($r = 0.997$) for this set of substituents validates this direct comparison. The *para*-substituted benzyl substituents (four cases) fall well off this line in the direction of higher Diels-Alder diastereoselectivity. As would be expected on purely steric grounds, the cyclohexylme-

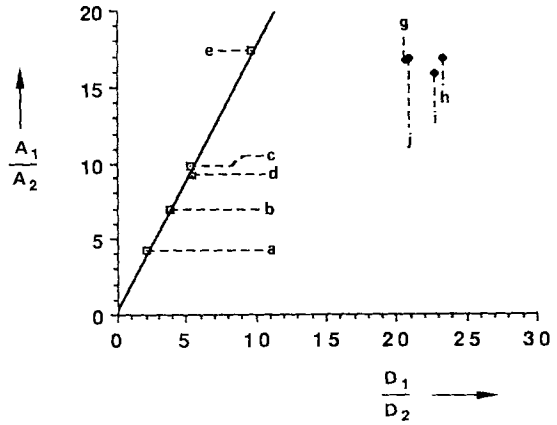

Fig. 1. Plot of crotonate oxazolidinone/isoprene Diels-Alder diastereomer ratio versus corresponding butyrate oxazolidinone/methyl iodide alkylation diastereomer ratio (see Table 1).

thyl- and benzyl-substituted oxazolidinones afford similar distereoselectivities in their butyrate alkylation reactions. They differ dramatically, however, in their corresponding crotonate Diels-Alder diastereoselectivities. *This direct alkylation/Diels-Alder comparision provides compelling evidence that π-facial differentiation, which is electronic in origin, occurs in these Diels-Alder transition states.* Alteration of the π-donor ability of the phenyl group has little effect on the stereselectivity of the Diels-Alder reaction and, as would be expected, has essentially no effect on the corresponding alkylation process. In view of these observations, we believe that the electronic contribution of the benzyl substituent associated with the cycloaddition process results largely from dipole-dipole and Van der Waals attractions and not from a charge-tansfer interaction. Similar conclusions have been reached by *Rebek* et al. with respect to π-π molecular recognition of aryl-substituted amino acids.[11]

In conclusion, we have unambiguously established that appropriately oriented aromatic rings contribute to the enhanced diastereoselectivity of Diels-Alder reactions of α,β-unsaturated *N*-acyloxazolidinones by processes having both steric *and* electronic components. The electronic component to diastereofacial shielding does not appear to have significant charge-transfer character. The method of analysis, which involves the comparison of corresponding alkylation and Diels-Alder reactions, directly provides information about the transition states themselves without recourse to ground state conformational arguments.

Received: June 22, 1987 [Z 2305 IE]
German version: *Angew. Chem. 99* (1987) 1197

[1] E. J. Corey, K. B. Becker, R. K. Varma, *J. Am. Chem. Soc. 94* (1972) 8616.

[2] a) H. E. Ensley, Ph. D. Thesis, Harvard University, Cambridge, MA, USA 1976; b) E. J. Corey, H. E. Ensley, *J. Am. Chem. Soc. 97* (1975) 6908; c) H. E. Ensley, C. A. Parnell, E. J. Corey, *J. Org. Chem. 43* (1978) 1610; d) W. Oppolzer, M. Kurth, D. Reichlin, C. Chapuis, M. Mohnhaupt, F. Moffat, *Helv. Chim. Acta 64* (1981) 2802; e) W. Oppolzer, C. Chapuis, G. M. Dao, D. Reichlin, T. Godel, *Tetrahedron Lett. 23* (1982) 4781; f) B. M. Trost, D. O'Krongly, J. L. Belletire, *J. Am. Chem. Soc. 102* (1980) 7595. Rebuttals: S. Masamune, W. Choy, J. S. Petersen, L. R. Sita, *Angew. Chem. 97* (1985) 1; *Angew. Chem. Int. Ed. Engl. 24* (1985) 1 (see footnote page 12) J. L. Charleton, *Tetrahedron Lett. 26* (1985) 3413; g) B. M. Trost, *Chem. Brit. 20* (1984) 315; h) K. De Jesus, Ph. D. Thesis, University of Wisconsin, Madison, WI, USA 1986; i) W. G. Dauben, R. A. Bunce, *Tetrahedron Lett. 23* (1982) 4875; j) A. B. Smith, N. J. Liverton, N. J. Hrib, H. Sivaramakrishnan, K. Winzenberg, *J. Am. Chem. Soc. 108*

(1986) 3040; k) Y. Ito, Y. Amino, M. Nakatsuka, T. Saegusa, *ibid. 105* (1983) 1586; Rebuttal: J. L. Charlton, *Can. J. Chem. 64* (1986) 720; l) D. A. Evans, K. T. Chapman, J. Bisaha, *J. Am. Chem. Soc. 106* (1984) 4261; m) D. A. Evans, K. T. Chapman, J. Bisaha, *Tetrahedron Lett. 25* (1984) 4071.

[3] a) J. K. Whitsell, A. Battacharya, D. A. Aguilar, K. Henke, *J. Chem. Soc. Chem. Commun. 1982*, 989; b) J. K. Whitesell, D. Deyo, A. Battacharya, *ibid. 1983*, 802; c) J. K. Whitesell, J. N. Younathan, J. R. Hurst, M. A. Fox, *J. Org. Chem. 50* (1985) 5499; d) J. K. Whitesell, *Acc. Chem. Res. 18* (1985) 280; e) J. K. Whitesell, R. M. Lawrence, H. H. Chen, *J. Org. Chem. 51* (1986) 4779; f) W. Oppolzer, C. Robbiani, K. Battig, *Helv. Chim. Acta 63* (1980) 2015; g) W. Oppolzer, *Pure. Appl. Chem. 53* (1981) 1181.

[4] a) G. L. Lange, M. Lee, *Tetrahedron Lett. 26* (1985) 6163; b) H. Herzog, H. Koch, H.-D. Scharf, J. Runsink, *Tetrahedron 42* (1986) 3547.

[5] J. d'Angelo, J. Maddaluno, *J. Am. Chem. Soc. 108* (1986) 8112.

[6] P. Binger, A. Brinkmann, J. Richter, *Tetrahedron Lett. 24* (1983) 3599.

[7] J. Kallmerton, T. J. Gould, *J. Org. Chem. 51* (1986) 1152.

[8] a) J. K. Whitesell, A. Bhattacharya, K. Henke, *J. Chem. Soc. Chem. Commun. 1982*, 988; b) Y. Yamamoto, H. Yatagai, Y. Ishihara, N. Maeda, K. Maruyama, *Tetrahedron 40* (1984) 2239; c) P. Grossen, P. Herold, P. Mohr, C. Tamm, *Helv. Chim. Acta 67* (1984) 1625.

[9] D. A. Evans, M. D. Ennis, D. J. Mathre, *J. Am. Chem. Soc. 104* (1982) 1737.

[10] The diastereoselectivity of the cycloaddition of crotonate **1f** bearing the 4-*tert*-butyl substituent was beyond the limits of our capillary VPC detection and could not be used for these comparisons.

[11] J. Rebek, B. Askew, D. Nemeth, K. Parris, *J. Am. Chem. Soc. 109* (1987) 2432.

Natural Fecapentaene-14 and One Fecapentaene-12 Component are all-*trans* Stereoisomers**

By *José Baptista, Jiri J. Krepinsky,** and *Hans Rudolf Pfaendler**

Fecapentaenes are very effective, directly acting mutagens present in the feces of a large section of European and North American communities, and are suspected of being colon carcinogens.[1] Their structures were elucidated recently as **1** and **2**.[2,3] The absolute configuration of the single chiral center has been determined to be *S*,[4] but the full geometry of the large, conjugated double bond system allowing 32 stereoisomers (excluding enantiomers) has thus far remained unclear. Only the *trans* configuration

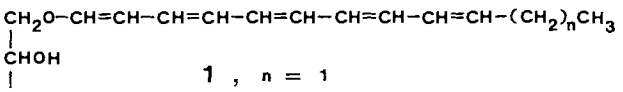

1, n = 1

2, n = 3

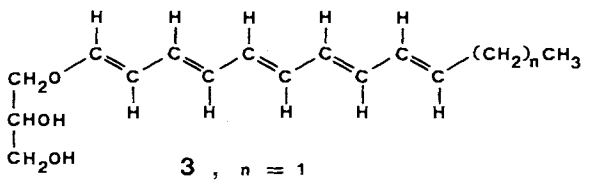

3, n = 1

4, n = 3

[*] Prof. Dr. J. J. Krepinsky, Dr. J. Baptista
Ludwig Institute for Cancer Research, Toronto Branch
Toronto, Ontario M4Y 1M4 (Canada) and
Departments of Medical Genetics and Biophysics
University of Toronto
Toronto, Ontario M5S 1A8 (Canada)
Prof. Dr. H. R. Pfaendler
Institut für Organische Chemie der Universität
Karlstrasse 23, D-8000 München 2 (FRG)

[**] The synthetic part of this work was financially supported by the Deutsche Forschungsgemeinschaft and the Fonds der Chemischen Industrie.

of the CC double bond adjacent to the glyceryl moiety could be deduced from the H-NMR coupling constant (12 Hz) of the isolated O–C*H*=CH– signal ($\delta = 6.84$ in [D$_7$]DMF.[2,3]

Our investigation of many fecal samples by HPLC revealed the occurrence of three fecapentaene-12 isomers (cf. Fig. 1a, peaks **A**, **B**, and **C**). In contrast fecapentaene-14 exists in only one geometric form (Fig. 1a, peak **D**). The ratio of the components can vary considerably from sample to sample depending on the donors.

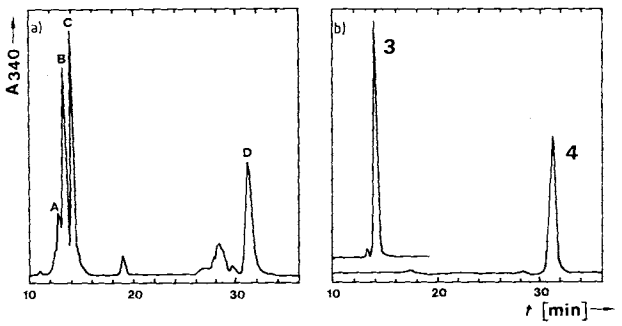

Fig. 1. a) HPLC profiles of fecapentaene fractions from human feces. **A**, **B**, **C**: fecapentaene-12 isomers; **D**: fecapentaene-14 isomer. b) HPLC profiles of the synthetic fecapentaenes **3** and **4**. A_{340}: absorption at 340 nm. Column: Ultrasphere ODS, 25 cm × 4.6 mm; mobile phase: $CH_3CN:CH_3OH:H_2O$:tetrahydrofuran 36.2:25.4:32.0:6.4; diode array detector LKB, model 2140.

The fecapentaenes are very unstable compounds; the mixture of fecapentaenes-12 could not be separated on a preparative scale. However, the three components, corresponding to the peaks **A**, **B**, and **C** in Figure 1a, were shown to have the same CI mass spectrum using a combined HPLC-mass spectrum unit. Thus, it became evident, that they were true stereoisomers. However, the exact identification of the isomers was not possible.

Fecapentaene-14 (peak **D** in Fig. 1a) is isomerically pure. Nevertheless, the geometry of its double bonds could not be defined because of the complexity of the olefin H signals in the ^{1}H-NMR spectrum.[2] Fecapentaene-14 is even less stable than the fecapentaenes-12 and the spectrum of the natural material was always adversely affected by decomposition products.

Through the total synthesis of crystalline, racemic all-*trans*-fecapentaene-12[5] and -14[6] it became possible for the first time to compare synthetic and natural materials and thus to clarify which natural products, if any, are all-*trans*. The HPLC system used for the separation of fecal samples was also suitable for making a comparison of these materials.

A mixture of fecapentaenes from feces was freshly prepared using a procedure previously described in the literature[2] (for HPL chromatogram, see Fig. 1a). Synthetic all-*trans*-fecapentaene-12 (**3**) (cf. Fig. 1b) showed exactly the same retention time as the component **C** of the fecapentaenes-12 and also co-eluted with it. The UV spectrum of the component **C** (recorded with the diode array detector) and the UV spectrum of **3** were likewise identical. This proves that the component **C** is all-*trans*-fecapentaene-12 (**3**).

Similarly, synthetic all-*trans*-fecapentaene-14 (**4**) (cf. HPL chromatogram, Fig. 1b) exhibited identical retention time as the component **D**, and both co-eluted. The H-

NMR spectra (in $[D]_7DMF$) of natural **D** and synthetic **4** were essentially identical, particularly in the region representing olefinic protons ($\delta = 5.6$–6.8). This, in turn, proves that the the component **D** is pure all-*trans*-fecapentaene-14 (**4**).

We have also established that the CI mass spectra of the natural and the synthetic compounds are identical. These spectra, however, show very little fragmentation, and thus are not sufficiently informative.

These investigations enable us for the first time to assign the complete structural formulas to two naturally occurring fecapentaenes. The geometry of the CC double bonds may play a role in the degree of mutagenicity exhibited by both types of fecapentaenes.[7,8] Interestingly, the two identified components, all-*trans*-fecapentaene-12 (**3**)[9] and all-*trans*-fecapentaene-14 (**4**)[7] belong to the most potent mutagens so far known. Their occurrence in human feces and their accessibility by chemical synthesis raise hopes that they might serve to answer the question whether the fecapentanes are carcinogens.

Received: July 1, 1987 [Z 2322 IE]
German version: *Angew. Chem. 99* (1987) 1183

[1] W. R. Bruce, A. J. Varghese, R. Furrer, P. C. Land in H. N. Hiatt, J. D. Watson, J. A. Winsten (Eds.): *Origins of Human Cancer*, Cold Spring Harbor Laboratory, Cold Spring Harbor, NY, 1977,p. 1641.
[2] a) I. Gupta, J. Baptista, W. R. Bruce, C. T. Che, R. Furrer, J. S. Gingerich, A. A. Grey, L. Marai, P. Yates, J. J. Krepinsky, *Biochemistry 22* (1983) 241; b) W. R. Bruce, J. Baptista, T. Che, R. Furrer, J. S. Gingerich, I. Gupta, J. J. Krepinsky, A. A. Grey, P. Yates, *Naturwissenschaften 69* (1982) 557.
[3] N. Hirai, D. G. I. Kingston, R. L. Van Tassel, T. D. Wilkins, *J. Am. Chem. Soc. 104* (1982) 6149.
[4] N. Hirai, D. G. I. Kingston, R. L. Van Tassel, T. D. Wilkins, *J. Nat. Prod. 48* (1985) 622.
[5] H. R. Pfaendler, F. K. Maier, S. Klar, *J. Am. Chem. Soc. 108* (1986) 1338.
[6] H. R. Pfaendler, F. K. Maier, S. Klar, unpublished.
[7] I. Gupta, K. Suzuki, W. R. Bruce, J. J. Krepinsky, P. Yates, *Science* (Washington, DC) *225* (1984) 521.
[8] P. P. DeWit, M. van der Steeg, A. van der Gen, *Tetrahedron Lett. 27* (1968) 6263.
[9] W. Göggelmann, F. K. Maier, H. R. Pfaendler, *Mutation Res. 174* (1986) 165.

Lithium-Tellurium Exchange: A New Entry to Organolithium Compounds**

By *Tomoki Hiiro, Nobuaki Kambe,* Akiya Ogawa, Noritaka Miyoshi, Shinji Murai,* and *Noboru Sonoda**

Since organolithium compounds,[1] as well as Grignard reagents, are most commonly used for the introduction of carbon moiety into organic molecules, the development of efficient methods for the synthesis of organolithium compounds is of vital importance. Organolithium compounds can be prepared directly by hydrogen abstraction or lithium-halogen exchange reaction; when these reactions fail, however, metal-metal exchange is widely resorted to.

We report here on a new method providing access to organolithium compounds **3** from organic tellurides **1** via lithium-tellurium exchange. Alkyl-, benzyl- and allyllithium compounds can be synthesized in a one-pot operation from halides without isolation of the tellurides [see Reaction (c)].

Diorganotellurides **1** react with butyllithium at $-78\,^{\circ}C$ in THF to give the more stable organolithium compounds **3**, which are subsequently trapped with benzaldehyde to give the alcohols **4**. In this way several types of organolithium compounds can be obtained in good yields [Reaction (a), see Table 1]. (*Z*)-Phenyl styryl telluride **1c** afforded exclusively the (*Z*)-olefin **4c**. It should be noted that benzyloxymethyllithium **3e** and trimethylsilylmethyllithium **3f** are synthetically useful as alkoxymethylating[2] and silylmethylating[3] reagents, respectively.

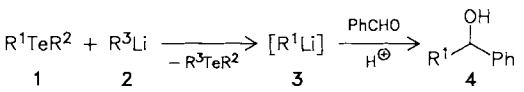

(a)

R^3 = *n*Bu

When the telluride **1** and the alkyllithium **2** are allowed to react in the ratio 1:2, both organic groups on the tellurium are converted into carbanions. For example, reaction of 1 mmol of dibutyl telluride **1h** with 2 mmol of *sec*-butyllithium affords 1.73 mmol of the adduct **4h** [Reaction (b), see Table 1]. This result suggests that the method described here is even suitable for the preparation of nonstabilized carbanions. Phenyllithium **3b** can be generated under identical conditions using *n*- or *tert*-butyllithium.

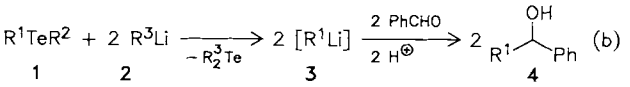

(b)

$R^1 = R^2$

Since alkyl aryl and dialkyl tellurides are readily accessible by reaction of lithium tellurolates **6**[4] with alkyl halides **5**, we then attempted a one-pot synthesis of the organolithium compounds **3** from the corresponding halides without isolation of the tellurides **1** [Reaction (c), see Table 1]. With benzyl, allyl and alkyl halides as starting materials, we obtained the products **4a**, **4i** and **4j** in good yields. When methyl vinyl ketone was used as an electro-

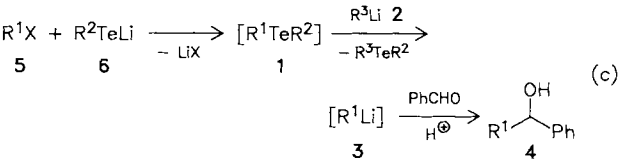

(c)

Table 1. Lithium-tellurium exchange; reaction types (a)–(c). For conditions see *Experimental procedure*.

Type	R^1	R^2	R^3	X	Reaction	Yield [%]
(a)	$PhCH_2$	*n*Bu	*n*Bu	—	**1a→4a**	74
(a)	Ph	*n*Pr	*n*Bu	—	**1b→4b**	77
(a)	PhCH=CH (*Z*)	Ph	*n*Bu	—	**1c→4c**	89
(a)	PhC≡C	Ph	*n*Bu	—	**1d→4d**	89
(a)	$PhCH_2OCH_2$	*n*Bu	*n*Bu	—	**1e→4e**	66
(a)	Me_3SiCH_2	*n*Bu	*n*Bu	—	**1f→4f**	89
(b)	Ph	Ph	*n*Bu	—	**1g→4b**	80
(b)	Ph	Ph	*t*Bu	—	**1g→4b**	72
(b)	*n*Bu	*n*Bu	*s*Bu	—	**1h→4h**	86
(c)	$PhCH_2$	Ph	Ph	Br	**5a→4a**	72
(c)	CH_2=$CHCH_2$	Ph	Ph	Br	**5i→4i**	96
(c)	*n*Pr	*s*Bu	*s*Bu	I	**5j→4j**	84

[*] Prof. Dr. N. Sonoda, Dr. N. Kambe, T. Hiiro, Dr. A. Ogawa, Dr. N. Miyoshi, Dr. S. Murai
Department of Applied Chemistry, Faculty of Engineering
Osaka University
Suita, Osaka 565 (Japan)

[**] This work was supported in part by a grant-in-aid from the Ministry of Education, Science, and Culture, Japan.

phile instead of benzaldehyde, reaction with butyllithium under identical conditions proceeded via 1,2-addition to the carbonyl group to give 2-methyl-1-phenyl-3-buten-2-ol (44% yield based on **5a**).

This one-pot procedure is operationally convenient and will be especially useful when direct lithium-halogen exchange cannot be resorted to—as in the preparation of benzyl- and allyllithium compounds.[5]

Although lithium-selenium exchange has been reported on several occasions,[6] examples of lithium-tellurium exchange were hitherto rare.[7] Studies on the scope and limitation of this reaction are currently in progress.

Experimental Procedure

Preparation of the telluride **1**, $R^1 \neq R^2$: **1a,e,f** from lithium butanetellurolate [4] and benzyl bromide, benzyloxymethyl chloride and trimethylsilylmethyl iodide, respectively, in THF; **1b** from lithium benzenetellurolate and propyl iodide in THF; **1c** from benzenetellurol and phenylacetylene [8]; **1d** by a similar method as described in the literature [9] from benzenetellurenyl iodide (PhTeI) [10] and lithium phenylacetylide.

Typical reaction starting from a diorganyl telluride **1**: A solution of **1f** (1 mmol, 272 mg) in THF (5 mL) was treated at −78 °C with a 1.6 M solution of butyllithium **2** (1 mmol, 0.63 mL), $R^3 = n$Bu, in hexane. After stirring for 15 min, benzaldehyde (1 mmol, 106 mg) was added by a syringe in one portion, and the reaction mixture then warmed to 25 °C over a period of 1 h. Et_2O (30 mL) and dil. aq. HCl (ca. 0.1 M, 50 mL) were added to the mixture, and the product was extracted with Et_2O (50 mL × 3). The ethereal solution was dried over $MgSO_4$ and the solvent removed by evaporation. Subsequent radial layer chromatography (silica gel, Et_2O/hexane) afforded 171 mg (0.89 mmol; 89%) of **4f** together with 238 mg (0.99 mmol) of dibutyl telluride.

Typical reaction starting from a halide **5**: To a solution of lithium benzenetellurolate **6**, $R^2 = Ph$ [4] (prepared in situ from tellurium (2 mmol) and phenyllithium (2 mmol, 1 mL 2.0 M solution in cyclohexane/Et_2O) in THF (5 mL) was added 342 mg (2 mmol) of benzyl bromide **5a** at −78 °C. The mixture was warmed to 25 °C and stirred for 30 min. At this stage, the conversion to the benzyl phenyl telluride **1a** is complete. Further conversion and work-up are the same as in the case of **1f**.

Received: July 10, 1987;
revised: August 17, 1987 [Z 2340 IE]
German version: *Angew. Chem. 99* (1987) 1221

CAS Registry numbers:
1a, 110935-05-2; **1b**, 55776-35-7; **1c**, 82296-87-5; **1d**, 56950-09-5; **1e**, 110935-06-3; **1f**, 110935-07-4; **1g**, 1202-36-4; **1h**, 38788-38-4; **4a**, 614-29-9; **4b**, 91-01-0; **4c**, 62839-70-7; **4d**, 1817-49-8; **4e**, 838-66-4; **4f**, 17993-97-4; **4h**, 583-03-9; **4i**, 936-58-3; **4j**, 614-14-2; PhCHO, 100-52-7; $PhCH_2Br$, 100-39-0; PrBr, 106-94-5; allyl bromide, 106-95-6; lithium, 7439-93-2; tellurium, 13494-80-9.

[1] a) B. J. Wakefiled: *The Chemistry of Organolithum Compounds*, Pergamon, New York, 1974; b) E. Negishi: *Organometallics in Organic Synthesis, Vol. 1*, Wiley, New York, 1980.

[2] The benzyloxymethyl group could easily be converted into the hydroxymethyl group by hydrogenation. Only scattered examples of nucleophilic oxymethylating agents have been reported, see a) E. J. Corey, T. M. Eckrich, *Tetrahedron Lett. 24* (1983) 3163, 3165; b) T. Cohen, J. R. Matz, *J. Am. Chem. Soc. 102* (1980) 6900; c) N. Meyer, D. Seebach, *Chem. Ber. 113* (1980) 1290; d) P. Beak, B. G. McKinnie, *J. Am. Chem. Soc. 99* (1977) 5213; e) D. Seebach, N. Meyer, *Angew. Chem. 88* (1976) 484; *Angew. Chem. Int. Ed. Engl. 15* (1976) 438; f) W. C. Still, *J. Am. Chem. Soc. 100* (1978) 1481; g) W. C. Still, A. Mitra, *ibid. 100* (1978) 1927.

[3] a) C. Tessier-Youngs, O. T. Beachley, Jr., *Inorg. Synth. 24* (1986) 95; b) S. Murai, I. Ryu, J. Iriguchi, N. Sonoda, *J. Am. Chem. Soc. 106* (1984) 2440; c) D. E. Seitz, A. Zapata, *Synthesis 1981*, 557; d) W. Dumont, A. Krief, *Angew. Chem. 88* (1976) 184; *Angew. Chem. Int. Ed. Engl. 15* (1976) 161; e) J. W. Connolly, G. Urry, *Inorg. Chem. 2* (1963) 645.

[4] a) L. Engman, M. P. Cava, *Synth. Commun. 12* (1982) 163; b) J. L. Piette, M. Renson, *Bull. Soc. Chim. Belg. 79* (1970) 353, 367, 383; *Chem. Abstr. 73* (1970) 66199, 66200, 66201; c) N. Petragnani, M. de Moura Campos, *Chem. Ber. 96* (1963) 249.

[5] In the case of benzyl and allyl halides lithium-halogen exchange usually results in the formation of coupling products, see Ref. [1].

[6] For recent reports on lithium-selenium exchange, see: a) C. Paulmier in J. E. Baldwin (Ed.): *Selenium Reagents and Intermediates in Organic Synthesis*, Pergamon, New York, 1986, p. 105, p. 260; b) M. Clarembeau, A. Krief, *Tetrahedron Lett. 26* (1985) 1093; c) M. Clarembeau, A. Krief, *ibid. 25* (1984) 3629; d) J. N. Denis, A. Krief, *ibid. 23* (1982) 3411; e) A. Krief, *Tetrahedron 36* (1980) 2531 and references cited therein.

[7] a) T. Kauffmann, H. Ahlers, *Chem. Ber. 116* (1983) 1001; b) D. Seebach, A. K. Beck, *ibid. 108* (1975) 314; c) D. Hellwinkel, G. Fahrbach, *ibid. 101* (1968) 574.

[8] a) S. Uemura, S. Fukuzawa, S. R. Patil, *J. Organomet. Chem. 243* (1983) 9; b) S. Uemura, S. Fukuzawa, *Tetrahedron Lett. 23* (1982) 1181.

[9] N. Petragnani, L. Torres, K. J. Wynne, *J. Organomet. Chem. 92* (1975) 185.

[10] P. Schulz, G. Klar, *Z. Naturforsch. B30* (1975) 40.

Control of the Superconducting Properties of $YBa_2Cu_3O_7$ by Topotactic Redox Reactions

By *Heinz Eickenbusch, Werner Paulus, Elmar Gocke, Joachim Friedrich March, Hans Koch,* and *Robert Schöllhorn**

Dedicated to Professor Rudolf Hoppe on the occasion of his 65th birthday

A series of ternary copper oxides with perovskite type structures have recently been shown to exhibit unusual superconducting properties with critical temperatures significantly higher than those measured so far for superconducting materials.[1,2] For the defect perovskite system $YBa_2Cu_3O_7$ with the highest confirmed transition temperature it has become obvious that the oxygen stoichiometry plays a major role with respect to the electronic behavior.[3-5] We report here on the modification of the superconducting properties of this compound by topotactic intercalation and deintercalation of oxygen which demonstrates that the temperature of the phase transition normal conductivity/superconductivity can be controlled reversibly in a continuous mode between 93 K and 30 K. Since solids characterized by electronic conductivity, vacant lattice sites, and redox active transition elements may undergo electron/cation transfer reactions,[6] we have, moreover, performed a study on the intercalation of small cations into the lattice of $YBa_2Cu_3O_7$ which shows that both hydrogen and lithium can be inserted.

The starting material $YBa_2Cu_3O_{7\pm0.05}$ **1** was prepared from the corresponding high purity binary oxides in oxygen atmosphere at 950 °C with subsequent controlled cooling and annealing; details of preparation and characterization have been described elsewhere.[5,7] Polycrystalline pressed samples of **1** were annealed under equilibrium conditions at defined temperatures between 25 °C and 900 °C in oxygen atmosphere (1 bar) for 24 h and subsequently quenched in liquid nitrogen. Analytical data (gravimetry, differential thermal gravimetry, reduction in H_2 atmosphere) reveal a continuous decrease of the oxygen content with increasing temperature [Eq. (a)] and a change in

$$YBa_2Cu_3O_7 \rightleftharpoons YBa_2Cu_3O_x + (7-x)/2\,O_2 \qquad (a)$$

stoichiometry from $YBa_2Cu_3O_7$ at 25 °C to $YBa_2Cu_3O_{6.5}$ at 750 °C (Fig. 1); equilibrium is observed after a few hours above 350 °C. The superconducting transition temperatures T_c were measured by ac susceptibility with lead sam-

[*] Prof. Dr. R. Schöllhorn, H. Eickenbusch, Dipl.-Chem. W. Paulus, E. Gocke
Institut für Anorganische und Analytische Chemie
der Technischen Universität
Strasse des 17. Juni 135, D-1000 Berlin 12
Dr. J. F. March, Dr. H. Koch
Physikalisch-Technische Bundesanstalt, Institut Berlin
Abbestrasse 2-12, D-1000 Berlin 10

ples of identical volume for evaluation of the volume susceptibility. Additional measurements of the resistivity were made for comparison reasons with the four probe *(van der Pauw)* technique. Figure 1 shows that the transition tem-

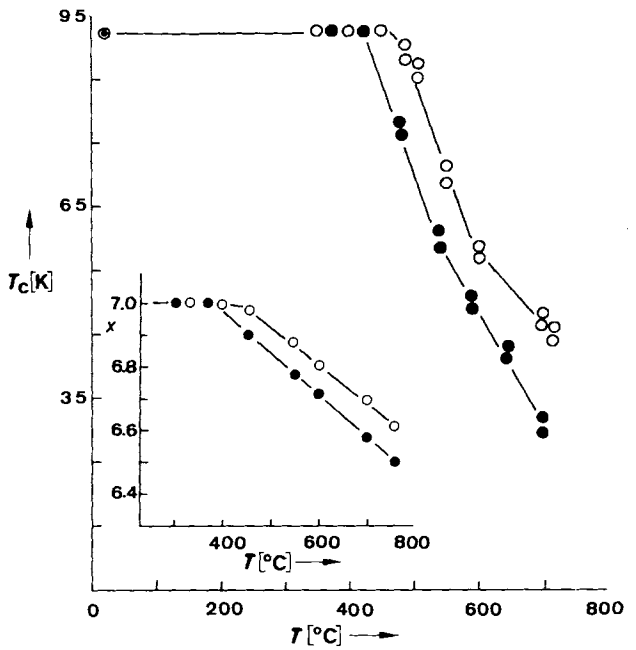

Fig. 1. Outer: Onset temperatures T_c (measured by susceptibility) of the transition normal conductivity/superconductivity for $YBa_2Cu_3O_x$ as a function of the annealing temperature T under oxygen atmosphere (○) and air (●). Inset: change in stoichiometry x with T. In the case of the samples at 760 °C, no phase transition was found up to 4.2 K.

perature can in fact be varied continuously between 93 K and 30 K. This effect is entirely reversible; on treatment of the samples with lower T_c in oxygen atmosphere at 400 °C the original value of $T_c = 93$ K is restored. Annealing at temperatures above 750 °C leads to samples which show semiconducting behavior down to 4 K. At higher temperatures the oxygen content decreases first down to $x \approx 6$, thereafter, non-topotactic processes occur with the appearance of several phases in agreement with earlier reports.[4] The transition width—defined as the temperature difference between 10% and 90% of the susceptibility signal—changes from 1 K at $x = 7.0$ to 3 K at $x = 6.58$. Similar results with slightly different stoichiometry and T_c values at equal annealing temperatures were obtained upon performing the reaction in air. The decrease of the volume susceptibility at $T > 580$ °C and X-ray measurements, however, indicate side reactions leading to increasing fractions of non-superconducting phases.

The change of the lattice parameters with x in $YBa_2Cu_3O_x$ is illustrated in Figure 2. With decreasing x the orthorhombic c axis increases linearly, while a and b change their magnitude such that they finally become identical for $x = 6.5$, where the symmetry of the system converts from orthorhombic to tetragonal. The entire unit cell volume change from $x = 7$ to $x = 6.5$ corresponds to a relatively small increase of 1%.

The orthorhombic distortion of **1** is related to an ordered arrangement of O^1 in the basal plane of the defect perovskite (Fig. 3).[8] Oxygen loss leads for $x = 6.5$ to tetragonal symmetry as a consequence of the selective removal of 50% of O^1 and a statistical distribution of the remaining

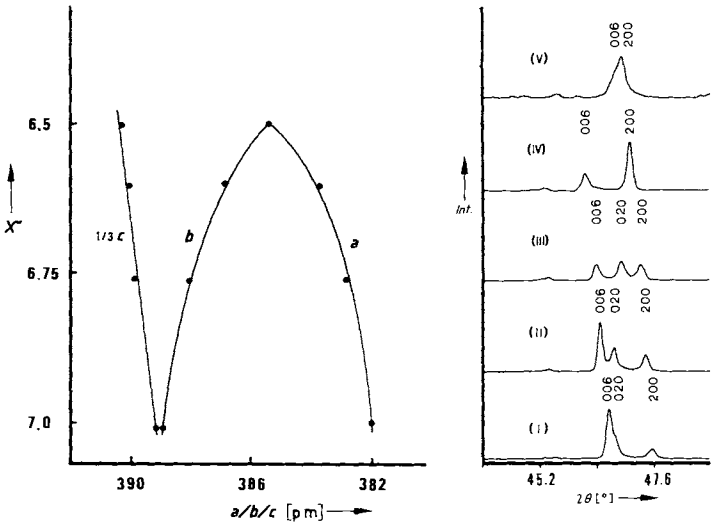

Fig. 2. Left: Change in lattice parameters of $YBa_2Cu_3O_x$ with the oxygen stoichiometry x. Right: X-ray diffractometer scans showing the transition from orthorhombic to tetragonal symmetry: (I) $x = 7.0$; (II) $x = 6.76$; (III) $x = 6.6$; (IV) $x = 6.5$; (V) pseudocubic metastable phase (c.f. text).

oxygen in this plane. The formal oxidation state of Cu in **1** is 2.33 or $YBa_2Cu_2^{2\oplus}Cu^{3\oplus}O_7$ in terms of integral valencies. It is reasonable to assume that $Cu^{3\oplus}$ is preferentially located on the Cu^1 positions (short Cu^1-O^2 distances) forming chains along the b axis, while $Cu^{2\oplus}$ is on sites with distorted pyramidal coordination close to the oxygen free $Y^{3\oplus}$ planes. The position of $Cu^{2\oplus}$ presents a favorable geometry for an interaction of the partially filled d_{z^2} orbitals across the central plane of the unit cell (Fig. 3) leading to distorted pseudooctahedral coordination of $Cu^{2\oplus}$ with a weakly coupled electron pair as the sixth ligand.

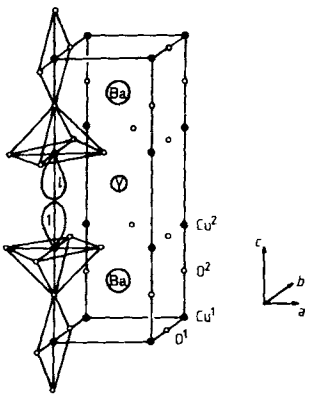

Fig. 3. Stucture model of $YBa_2Cu_3O_7$. Unit cell scheme indicating the coordination of Cu and partially filled d_{z^2} orbitals.

This model could actually explain recent observations on the absence of temperature-dependent magnetism in **1** in spite of the presence of $Cu^{2\oplus}$.[9] At the transition orthorhombic/tetragonal the stoichiometry corresponds formally to bivalent Cu only, i.e. $YBa_2Cu_3^{2\oplus}O_{6.5}$; the magnetic properties of this phase have not been studied in detail so far.

A most interesting phenomenon—also with respect to potential application in catalysis—is the high mobility of oxygen at relatively low temperatures in $YBa_2Cu_3O_x$. The quenched metastable phase $YBa_2Cu_3O_{6.5}$ may take up oxygen already at temperatures as low as 285 °C[5] and convert

to $YBa_2Cu_3O_7$. We now have observed the appearance of an intermediate "pseudocubic" phase under these conditions with $a=b=c/3=388$ pm, which demonstrates that the low temperature reaction mechanism is different from that under equilibrium conditions (Fig. 2), where this phase does not appear. This observation is most likely a consequence of the different positional selectivity of the oxygen anion mobility under the corresponding reaction conditions. Recently the existence of holes in the anion valence band of $YBa_2Cu_3O_x$ due to the equilibrium $Cu^{3\oplus}/O^{2\ominus} \rightleftharpoons Cu^{2\oplus}/O^{\odot\ominus}$ has been discussed.[5] We suggest here a model for the high oxygen mobility on grounds of the presence of monovalent $O^{\odot\ominus}$ ions which must have a considerably lower activation energy for site change as compared to bivalent $O^{2\ominus}$ anions.

Investigations on the intercalation of hydrogen were based on the assumption that $Cu^{3\oplus}$ in **1** can be reduced to $Cu^{2\oplus}$ in a topotactic process with formation of a hydrogen bronze [Eq. (b)]. The maximum value of x can be calculated according to Equation (c) as $x=1.0$.

$$xH^{\oplus} + xe^{\ominus} + YBa_2Cu_3O_7 \rightarrow H_x[YBa_2Cu_3O_7] \quad (b)$$

$$Cu_2^{2\oplus}Cu^{3\oplus} + e^{\ominus} \rightarrow Cu_3^{2\oplus} \quad (c)$$

The electrochemical reaction by galvanostatic cathodic reduction of pressed polycrystalline electrodes of **1** in a galvanic cell with aqueous electrolyte (pH = 6.5) was characterized by a continuous decrease in potential. After an electron transfer of $n=0.3\ e^{\ominus}/YBa_2Cu_3O_7$ the potential of hydrogen discharge was reached. The value for x obtained under these conditions is thus equivalent to $x=1/3$. Direct intercalation of hydrogen gas was performed in a closed system with activation of **1** by sputtering with platinum (1 wt.-% Pt, "overspill" technique[6]). Volumetric determination of the hydrogen taken up at 25 °C/1 bar corresponded in agreement with the electrochemical data to $x=1/3$. The lattice parameters of the resulting hydrogen bronze $H_{1/3}[YBa_2Cu_3O_7]$ (orthorhombic, $a=382.5$ pm, $b=388.5$ pm, $c=1169$ pm) were close to those of the starting phase **1**. Susceptibility measurements revealed that the hydrogen phase exhibits a broad transition with an onset temperature of 89 K. Further reduction with H_2 using extended reaction time or higher temperatures resulted in irreversible structural changes.

$$xLi + xe^{\ominus} + YBa_2Cu_3O_7 \longrightarrow Li_x[YBa_2Cu_3O_7] \quad (d)$$

The intercalation of lithium into **1** according to Equation (d) was carried out in a galvanic cell $Li//LiClO_4$, propylene carbonate$//YBa_2Cu_3O_7$ under galvanostatic and potentiostatic conditions. The reaction proceeds topotactically up to $x=1/3$, i.e. $Li_{0.33}[YBa_2Cu_3O_7]$ (tetragonal, $a=388.1$ pm, $c=1172.6$ pm); beyond a charge transfer of $n=1/3$ irreversible side reactions have been observed. The same phase could also be prepared by reaction of **1** with butyllithium (1.5 M solution in hexane) at ambient temperature. ^{7}Li-NMR line-width studies of $Li_{0.33}[YBa_2Cu_3O_7]$ showed a chemical shift of $\delta=-2$ vs $LiCl/H_2O$ at 300 K and a narrow line width (450 Hz) indicating a rather high lithium mobility comparable with that of Li in the framework lattice of molybdenum cluster chalcogenides $Li_xMo_6X_8$.[10] The electronic properties of the highly susceptible lithium phase are presently under investigation.

The results discussed demonstrate that the new oxide high-temperature superconductors are most interesting systems not only with respect to the correlation between electronic properties, structure and bonding but also in terms of their chemical reactivity as a means for controlling the physical properties of these systems.

Received: July 31, 1987;
revised: September 9, 1987 [Z 2384 IE]
German version: *Angew. Chem. 99* (1987) 1201

[1] J. G. Bednorz, K. A. Müller, *Z. Phys. B 64* (1987) 189.
[2] M. K. Wu, J. R. Ashburn, C. J. Tong, P. H. Hor, R. L. Wong, L. Gao, Z. J. Huang, Y. Q. Wang, C. W. Chu, *Phys. Rev. Lett. 58* (1987) 908.
[3] P. Strobel, J. J. Capponi, C. Chaillout, M. Marezio, J. L. Tholence, *Nature (London) 327* (1987) 306.
[4] P. K. Gallagher, H. M. O'Bryan, S. A. Sunshine, D. W. Murphy, *Mater. Res. Bull. 22* (1987) 995.
[5] H. Eickenbusch, W. Paulus, R. Schöllhorn, R. Schlögl, *Mater. Res. Bull.* (1987), in press.
[6] R. Schöllhorn, *Angew. Chem. 92* (1980) 1015; *Angew. Chem. Int. Ed. Engl. 19* (1980) 983; in J. L. Atwood, J. E. D. Davies, D. D. MacNicol: *Inclusion Compounds, Vol 1*, Academic Press, New York 1984, p. 249.
[7] H. Koch, R. Cantor, J. F. March, H. Eickenbusch, R. Schöllhorn, *Phys. Rev. B36* (1987) 722; R. Cantor, H. Eickenbusch, U. Gernert, H. Koch, R. Schöllhorn, *PTB-Mitt. 97* (1987) 187.
[8] M. A. Alario-Franco, C. Chaillout, J. J. Capponi, J. Chenavas, unpublished.
[9] K. Kadowaki, Y. K. Huang, M. van Sprang, E. Salomons, A. C. Moleman, A. A. Menowsky, *J. Less Common Metals*, in press.
[10] E. Gocke, R. Schöllhorn, G. Aselmann, W. Müller-Warmuth, *Inorg. Chem. 26* (1987) 1805.

Hexacarbonylzirconate(2−), $[Zr(CO)_6]^{2-}$: The First Binary Carbonyl Complex of Zirconium**

By *Kai Ming Chi, Scott R. Frerichs, Stephen B. Philson,* and *John E. Ellis**

Since the pioneering work of *Walter Hieber*,[1] mono- and/or polynuclear binary carbonylmetalates have been isolated for practically all d-block transition metals, except those of the 3rd, 4th and 11th triads, and have proven to be extremely important materials in chemical synthesis.[2] We now report on the synthesis, isolation and characterization of the first binary carbonylzirconium complex $[Zr(CO)_6]^{2-}$ as salt **1**, which contains zirconium in an unprecedented formal oxidation state of −2.[3] Except for important modifications (vide infra) this material was obtained by the alkali-metal naphthalenide method we originally developed for the reductive carbonylation of MCl_5 to $[M(CO)_6]^-$ (M = Nb and Ta) at atmospheric pressure.[4] The ready availability of $[Zr(CO)_6]^{2-}$ should facilitate general studies on the carbonyl chemistry of zirconium, which has been previously limited almost exclusively to cyclopentadienyl derivatives such as $[(C_5H_5)_2Zr(CO)_2]$[5] and $[(C_5H_5)Zr(CO)_4]^-$[6] and other related carbocyclic derivatives.

The reaction sequence for the preparation of **1** is given in Equation (1) (THF = tetrahydrofuran, $C_{10}H_8$ = naphthalene, 15-C-5 = [15]crown-5 = 1,4,7,10,13-pentaoxacyclopentadecane and DME = 1,2-dimethoxyethane). Further details are given under *Experimental procedure*.

$$ZrCl_4 \cdot 2THF + 6KC_{10}H_8 + 4\,15\text{-C-}5 + 6CO \longrightarrow$$
$$[K(15\text{-C-}5)_2]_2[Zr(CO)_6]\downarrow + 4KCl + 6C_{10}H_8 + 2THF \quad (1)$$
1, 25–35%

[*] Prof. Dr. J. E. Ellis, K. M. Chi, S. R. Frerichs, Dr. S. B. Philson
Chemistry Department, University of Minnesota
Minneapolis, MN 55455 (USA)

[**] Highly Reduced Organometallics, Part 22. This work was supported by the U.S. National Science Foundation and the Petroleum Research Fund administered by the American Chemical Society.—Part 21: B. K. Stein, S. R. Frerichs, J. E. Ellis, *Organometallics 6* (1987) 2017.

 © VCH Verlagsgesellschaft mbH, D-6940 Weinheim, 1987 0570-0833/87/1111-1190 $ 02.50/0

It is important to note that in the absence of an effective alkali-metal complexant such as a crown ether or a cryptand,[7] the carbonylation reaction step fails to provide any isolable $[Zr(CO)_6]^{2-}$. Although the formation of **1** is undoubtedly aided by its insolubility in this medium, the product dissolves in strongly polar aprotic solvents such as acetonitrile to provide fairly stable solutions at ambient temperature. The presence of weakly solvated alkali metal cations appears to either prevent formation or cause decomposition of $[Zr(CO)_6]^{2-}$ at low temperature. In contrast, effective alkali-metal complexants need not be present during the aforementioned synthesis of the isoelectronic $[Nb(CO)_6]^-$.[4]

Crystallization of **1** from acetonitrile/THF provides dark purple, extremely air-sensitive microcrystals which appear to be indefinitely stable under argon at room temperature (decomp. pt. ca. 140 °C). The spectroscopic properties of **1** are consistent with the proposed formula.[8] Thus **1** shows a single intense band in the IR spectrum at 1757 cm^{-1} (cf. $[Na_2Ru(CO)_4]$ in $(Me_2N)_3PO$, 1736 cm^{-1}), a single ^{13}C-NMR resonance at $\delta = 245.2$ (cf. $[HV(CO)_5]^{2-}$ in NH_3, $\delta = 250.3$[9] and $[W(CO)_5]^{2-}$ in THF, $\delta = 247.4$[10]), and an extremely narrow ($W_{1/2}$ = ca. 20 Hz) single ^{91}Zr-NMR resonance expected for a molecule of cubic or octahedral symmetry.[11] Although attempts to obtain single crystals of **1** for an X-ray structural determination have so far failed, the presence of octahedral $[Zr(CO)_6]^{2-}$ in **1** has been corroborated by the ^{91}Zr-NMR spectrum of 99% ^{13}C-enriched $[Zr(^{13}CO)_6]^{2-}$ (Fig. 1), which shows the binomial septet predicted for six equivalent carbonyl groups bound to a central zirconium atom.[12] To our knowledge this is the first example of a compound for which ^{91}Zr-^{13}C coupling has been resolved.

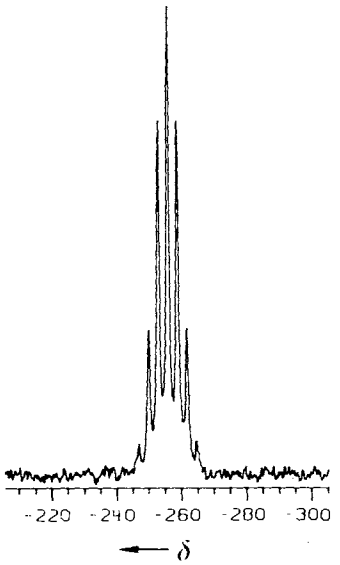

Fig. 1. The ^{91}Zr-NMR spectrum of $[K([15]\text{-Crown-5})_2]_2[Zr(^{13}CO)_6]$ (cf. [12]).

Experimental Procedure

1: A solution of $ZrCl_4 \cdot 2THF$ (2.0 g, 5.30 mmol) was prepared in 50 mL of cold DME at −70 °C and transferred under argon by cannula to a magnetically stirred solution/slurry of $KC_{10}H_8$ (5.35 g, 32.0 mmol) and $C_{10}H_8$ (1.28 g, 10 mmol) in 150 mL of DME at −70 °C. The red-brown solution containing presently uncharacterized intermediate(s) was allowed to slowly warm in a Dewar flask to near ambient temperature over a period of about 12 h. It was then filtered into a Morton flask, anaerobic [15]-Crown-5 was added (4.75 g, 21.6 mmol) and the resulting solution was mechanically stirred at ambient temperature for 2 h. After cooling to −60 °C, the argon atmosphere was removed by evacuation and replaced by ≥99.9% carbon monoxide (free of CO_2, O_2, H_2O). Stirring was continued for 40 h at −60 °C, during which time much purple solid precipitated. The slurry was then warmed to room temperature. After filtration, the solid was thoroughly washed with DME (2 × 20 mL), dried in vacuo, and recrystallized from CH_3CN-DME at 0 °C. In this way we obtained 2.15 g (1.77 mmol, 33% yield) of dark purple microcrystalline product which provided satisfactory elemental analyses (C, H and K). A very similar compound of the formula $[Cs([18]\text{Crown-6})_2]_2[Zr(CO)_6]$ (satisfactory C, H, Cs analysis, decomp. pt 130 °C) has been prepared by the same procedure. Syntheses of $[Zr(CO)_6]^{2-}$ in THF generally provide 10–15% lower yields than those conducted in DME.

Received: August 24, 1987 [Z 2409 IE]
German version: *Angew. Chem. 99* (1987) 1203

CAS Registry numbers:
1, 111004-77-4; $ZrCl_4 \cdot 2THF$, 21959-01-3; $[Cs([18]\text{crown-6})_2]_2[Zr(CO)_6]$, 111004-78-5.

[1] W. Hieber, W. Beck, G. Braun, *Angew. Chem. 72* (1960) 795.
[2] J. Collman, L. Hegedus, J. Norton, R. Finke: *Organotransition Metal Chemisty, 2nd Ed.*, University Science Books, Mill Valley, CA, 1987.
[3] N. N. Greenwood, A. Earnshaw: *Chemistry of the Elements*. Pergamon Press, Oxford 1984, p. 1117, 1133.
[4] C. G. Dewey, J. E. Ellis, K. L. Fjare, K. M. Pfahl, G. F. P. Warnock, *Organometallics 2* (1983) 388.
[5] D. Sikora, D. W. Macomber, M. D. Rausch, *Adv. Organometal. Chem. 25* (1986) 317.
[6] B. A. Kelsey, J. E. Ellis, *J. Am. Chem. Soc. 108* (1986) 1344.
[7] J. M. Lehn, *Acc. Chem. Rs. 11* (1978) 49.
[8] **1**: IR (CH_3CN, $\tilde{\nu}(^{12}CO)$ [cm^{-1}]): 1757 s; (Nujol): 1738 s, 1730 s. ^1H-NMR (300 MHz, 23 °C, CD_3CN): $\delta = 3.58$ (15-C-5), ^{13}C-{^1H}-NMR (85.5 MHz, 23 °C, CD_3CN): $\delta = 245.2$ (CO), 69.5 (15-C-5). ^{91}Zr-NMR (27.9 MHz, 23 °C, CD_3CN/CH_3CN: 1/5; rel. to $[Cp_2ZrBr_2]$ in C_6D_6/C_6H_6 1/10): $\delta = -256.0$, s, $W_{1/2}$ = ca. 20 Hz. See Ref. [11] for further information on ^{91}Zr-NMR spectroscopy.
[9] G. F. P. Warnock, S. B. Philson, J. E. Ellis, *J. Chem. Commun. 1984*, 893.
[10] J. M. Maher, R. P. Beatty, N. J. Cooper, *Organometallics 4* (1985) 1354.
[11] a) R. Benn, A. Rufińska, *Angew. Chem. 98* (1986) 851; *Angew. Chem. Int. Ed. Engl. 25* (1986) 861; b) *J. Organomet. Chem. 273* (1984) C51.
[12] $[K(15\text{-C-5})_2]_2[Zr(^{13}CO)_6]$ was prepared by the same method as **1** except 99% ^{13}CO was employed. Spectral data: IR (CH_3CN, $\tilde{\nu}(^{13}CO)$ [cm^{-1}]): 1719 s. ^{13}C-{^1H}-NMR (75.5 MHz, 23 °C, CD_3CN): $\delta = 245.2$ (CO, satellite $J(^{91}Zr\text{-}^{13}C) \approx 80$ Hz), 69.7 (15-C-5). ^{91}Zr-NMR (27.9 MHz, 23 °C, CD_3CN/CH_3CN = 1/5; relative to $[Cp_2ZrBr_2]$ in C_6D_6/C_6H_6 1/10): $\delta = -256.1$ (septet, $J(^{91}Zr\text{-}^{13}C) = 81.5 \pm 0.5$ Hz).

Two-Dee or not to be*

In the seminar room at the Hotel Alem, which lies in an idyllic situation on the Jugoslavian Adriatic coast near Baska Polje, the Belgian physicist *J. Jeener* wrote on the small blackboard just a few lines in the abstract language of the density matrix. It was enough, however, to sketch out his idea for a two-dimensional NMR spectrum, whose spectral lines would stand out like the mountains in a relief map of the Alps, showing the couplings between the hydrogen nuclei of a molecule and allowing its structural formula to be directly determined. On that day, the 4th of September 1971, none of the 136 participants at the NMR Summer School realized that this idea was actually, in every sense, opening up a second dimension for NMR spectroscopy. It led to a new way of interpreting spectra, which 13 years later made it possible even to determine the tertiary structure of a protein molecule.

It must be remembered that in 1971 the pulsed FT method, nowadays used routinely, was bringing about a revolution in ^{13}C-NMR spectroscopy, which up to then had been withering away. In ^{1}H-NMR spectroscopy the FT method was at first seen by most practitioners as interesting but inappropriate for general use. One important reason for this was the inability with FT NMR spectroscopy to easily and independently change the resolution and spectral range. Another was the lack of adequate on-line data storage capacity, magnetic tapes and disks being not yet available. In these circumstances *Jeener*'s proposal seemed utopian. One had to use, instead of one r.f. pulse, two pulses separated by an interval t_1, to record the signal following the second pulse, and then to repeat the process with a new t_1 value. In this way one would record several hundred FID's, each with around 1000 data points, then carry out a 2D Fourier transformation on the entire data. According to *Jeener* the resulting 2D NMR spectrum would contain complete information on the coupled system of the molecule. However, it appeared that the same information could also be obtained with the double resonance techniques in common use at the time. Since these could be used to study single transitions and selected regions of the spectrum, it was thought that *Jeener*'s proposed method, owing to its heavy demands on data storage capacity and computing power, did not offer any improvement in chemical structure determination.

The Sleeping Beauty of 2D NMR was awakened by the kiss not of one prince, but of several, who finally helped *Jeener*'s idea to make its breakthrough. *Richard Ernst* in Zürich was the first to carry out the experiment. The chemical information yielded was small because of the inadequate computing power available, but nevertheless this experiment was of such fundamental importance that *Ernst*'s joint paper with *Aue* and *Bartholdi* (*J. Chem. Phys. 64* (1976) 2229) determined the course of research for many years to follow. The decisive point for chemistry, however, came with a joint paper by *Richard Ernst* and *Kurt Wüthrich* (*Biochem. Biophys. Res. Commun. 78* (1977) 99), in which they used 2D techniques to study a mixture of five amino acids. These results demonstrated the great potential of 2D NMR spectroscopy, and stimulated its accelerated development, helped by important contributions from *Ray Freeman*'s group in Oxford. During the years 1978 to 1982, many efforts were made to apply the technique to chemically important problems, in spite of the limitations of the available equipment. The phrase "Two Dee or not to be" eloquently summarizes the concerns which occupied many NMR spectroscopists at that time.

We can now recognize that two parallel developments during the last ten years have brought about enormous advances in NMR spectroscopy. Progress in hardware has come from the development of spectrometers with increased sensitivity and spectral dispersion, based on reliable high field cryomagnets and improved r.f. receivers, and of much more powerful on-line computers. Simultaneously, on the techniques side, many new and highly informative experimental procedures have grown out of a deeper understanding of spin dynamics, i.e. the behavior of spin systems under the influence of r.f. pulses. 2D NMR measurements occupy a particularly important position amongst these, the development of the methods and their early applications having been documented in around 1000 publications up to the beginning of 1986. Since then the number of applications has grown rapidly, and 2D NMR spectroscopy now belongs to the armoury of routinely used analytical techniques. However, these modern NMR techniques demand from the spectroscopist a level of knowledge far beyond that which was common in 1980, and one that cannot be gained from the older standard works on NMR spectroscopy. The need arising from this situation is taken into account in the books reviewed here, namely

(1) **Nuclear Magnetic Resonance. Basic Principles.** By *Attaur-Rahman*. Springer, Berlin 1986. ix, 358 pp., bound, DM 128.00.—ISBN 3-540-96243-3

(2) **Modern NMR Techniques for Chemistry Research.** By *A. E. Derome*. Pergamon Press, Oxford 1987. xvii, 280 pp., paperback, $ 35.00.—ISBN 0-08-032513-0

(3) **Modern Techniques in High Resolution FT NMR.** By *N. Chandrakumar* and *S. Subramanian*. Springer, Berlin 1986. ix, 388 pp., bound, DM 136.00.—ISBN 3-540-96327-8

(4) **Principles of Nuclear Magnetic Resonance in One and Two Dimensions** (International Series of Monographs on Chemistry 14). By *R. E. Ernst, G. Bodenhausen,* and *A. Wokaun*. Clarendon Press, Oxford 1987. xxiv, 610 pp., bound, £ 60.00.—ISBN 0-19-855629-2

together with a few more which have appeared in the past year*.

First, some general remarks relating to these books. The direction of rotation which corresponds to a positive angle

[*] Abbreviations used in this review: 1D—one-dimensional, 2D—two-dimensional, r.f.—radiofrequency, H,H-COSY and H,X-COSY—homonuclear and heteronuclear correlation spectroscopies, respectively, CT—coherence transfer, PT—polarization transfer, CP—cross-polarization, MAS—magic angle spinning, DCPL—decoupling, δ—chemical shift, J—coupling constant, T_1, T_2—relaxation times, FID—free induction decay, DQ—double quantum, MQ—multiple quantum, FT—Fourier transform, CW—continuous wave, NOE—nuclear Overhauser effect.

[*] W. R. Croasmun, R. M. K. Carlson: *Two-dimensional NMR Spectroscopy: Applications for Chemists and Biochemists*, VCH Publishers, New York 1987, DM 197.00; K. Wüthrich: *NMR Studies of Proteins*, Wiley, New York 1987, $ 49.95; J. K. Whitesell, M. A. Minton: *Stereochemical Analysis of Aliphatic Compounds by ^{13}C NMR*, Chapman & Hall, London 1987, £ 25.00; J. K. M. Saunders, B. K. Hunter: *Modern NMR. A Guide for Chemists*, Oxford University Press, Oxford 1987, £ 45.00 (h.c.), £ 19.95 (s.c.); W. W. Paudler: *Nuclear Magnetic Resonance*, Wiley, New York 1987, ca. $ 49.00.

is not uniquely defined in the NMR literature. According to the "left hand rule" (LHR) which has been generally used up to now in the chemically-oriented NMR literature, an r.f. magnetic field vector along the positive x-axis causes the magnetization vector to turn from the positive z-axis to the positive y-axis (e.g. for a 90°_x pulse, the thumb is in the direction of the positive x-axis, and the direction of rotation is given by the bending of the fingers). The "right hand rule" (RHR) gives an opposite rotation, i.e. from the positive z-axis to the positive y-axis. Books (1) and (2) use the LHR, while books (3) and (4) use the RHR. Although the procedures in NMR experiments and the interpretation of results are unaffected by the direction of rotation, a universal convention is desirable. It may well be that the RHR convention will now become generally accepted, following the publication of the "Zürich" book (4).

Book (1) is intended as an introduction to modern NMR spectroscopy for students of chemistry and biochemistry. In its 358 pages it describes conventional techniques (Chapters 1-4, 200 pp.), 1D and 2D pulse sequences (Chapter 5, 104 pp.), together with exercises and solutions (26 on ^{1}H NMR, 13 on ^{13}C NMR). The index contains about 1700 entries, of which about half are chemical compounds; some important abbreviations do not appear in the index, even though they are mentioned in the text, i.e. CT, PT and DCPL. Literature references are occasionally included as footnotes, whilst a bibliography for further reading is given at the end of each chapter. It is baffling to find that Chapter 2 (H-H couplings, 53 pp., dealing with systems of two to five spins and giving J-values) cites only twelve references, of which the last seven have already been given in Chapter 1 (δ in ^{1}H NMR, principles, tables, 33 pp.). Of the preceding five references, four relate to ^{13}C NMR, and would therefore be expected to appear instead in Chapter 4 (δ and J in ^{13}C NMR, tables, CP/MAS, 60 pp.)—and indeed we do find them there too! Chapter 4 contains, rather oddly, half a page on NMR imaging, as a paragraph to CP/MAS. On page 89 of Chapter 3 we are told that both permanent and electromagnets are used, and that instruments for both CW and FT operation exist; cryomagnets are not mentioned.

Many of the spectra shown have been copied by hand, and consequently have a rather "sick" appearance. Some of the figures are already familiar to me, but the original papers are not cited. I have the impression that some have been redrawn so as to get around the copyright. There are also some inaccuracies, e.g. in the discussion of CP in liquids, which equates CP to PT and fails to explain the importance of the Hartmann-Hahn condition. The book certainly contains much useful information, and also one or two teaching points worthy of special note, e.g. the reference to geostationary satellites in the explanation of the rotating frame. All the modern pulse sequences are mentioned and explained with vector diagrams. Nevertheless, I felt dissatisfied with the book as a whole, and particularly with the way in which it relates traditional NMR knowledge to modern techniques. I cannot recommend it to my students, as better books are available.

Book (2) is addressed to chemists who are concerned with structure determination in organic and inorganic chemistry. Some knowledge of ^{1}H and ^{13}C NMR spectroscopy is assumed, with regard to the effects of the properties and environments of the molecules under observation on δ, J, T_1 and T_2; books of proven value are available covering these basic topics. However, it is not necessary to be a δ, J virtuoso to benefit from the book, since the modern NMR techniques actually make it easier to interpret spectra. The book therefore concentrates mainly on the practical aspects of the newer pulse methods, dealing with the setting up of the spectrometer conditions, the principles and execution of the experiments, illustrative examples, and even performance tests for a spectrometer, being either available or considered for purchase. The basic construction of the spectrometer is illustrated by photographs. The material is presented in a clear instructive way, with an attractive text written in a user-friendly "I/you/we" style. This is combined with vector diagrams for the rotating frame (to which a detailed introduction is given), and simple energy level diagrams. So as to keep the explanations simple, the author avoids using spin operators in describing the experiments. Consequently the book does not allow one to gain a deeper understanding of zero quantum and multiple quantum processes. The only fall from grace in the presentation of the theory occurs when the off-resonance case is discussed in terms of the Bloch equation without relaxation. The rest of the 61 equations given are all simple, and provide quantitative relationships between quantities to be measured or evaluated. Through the 275 pages, the reader willingly follows the author on his journey through the ideas involved. The ten chapters are as follows: Introduction (8 pp.), Pulsed and FT NMR (30 pp.), Basic experimental techniques—sample preparation, solution concentrations and sensitivity (30 pp.), Theoretical description of pulsed NMR—vector model, relaxation (34 pp.), NOE—mechanism calculations, measurements, applications (32 pp.), Polarization transfer and spectral editing—INEPT, DEPT (24 pp.), Other experimental techniques—pulse length and r.f. field strength in homo- and heteronuclear experiments, composite pulses, broad-band decoupling, T_1 measurements, quantitative measurements, selective excitation, suppression of signals (30 pp.), Homonuclear chemical shift correlations (62 pp.), Heteronuclear chemical shift correlations (14 pp.), Spin echoes and δ,J correlation spectroscopy (18 pp.). Each chapter ends with a short bibliography; a total of 130 references is a far from adequate coverage of the relevant literature, especially in Chapter 8 which contains only 29 references. The subject index contains 600 key words; important examples such as CT, PT and DCPL have adequate ranges of sub-headings. Regrettably there is no list of abbreviations, which would have been especially helpful to the reader in view of the author's tendency to employ some unusual ones (RuSH = *Rubens, States* and *Habekorn*, HSC = heteronuclear shift correlation, nOe = NOE, etc.). Also, of course, the misprint demon has been at work—for example, on p. 74 the legends for the figures have been interchanged. This is already a disaster page, since the author here associates the absorption and dispersion parts of the signal with the x and y components of the magnetization, rather than as arising from the decay of the individual x (or y) component of the FID signal.

Altogether this is a very commendable book in which the author has undoubtedly achieved his objective, and it should be available in every chemistry department. It can be most warmly recommended for anyone wishing to acquire a deeper knowledge of modern NMR spectroscopy, whether as an introduction to practical use of the techniques, or as preparatory reading before a study based on more theoretically oriented monographs. It seems especially suitable for use in research groups which have a considerable turnover of people, for providing newcomers with a minimum basis of NMR knowledge. The paperback is reasonably priced, and should be within the means even of students.

Book (3) is a good complement to Book (2), as it describes the basic pulse experiments in product operator formalism. The 380 pages contain 671 equations! Chapter 1 (18 pp.) briefly introduces the basic theory and relates it to the experiment. A particularly elegant derivation is given leading to the equations for the development of the spin system under the influence of r.f. pulses and the effects of δ and J, for spins of 1/2 and 1, using the Baker-Campbell-Hausdorff equation for exponential operators. Chapter 2 (34 pp.) deals with 1D experiments (transverse magnetization, echoes, J-spectroscopy, spectral editing, decoupling, NOE, J-scaling, selective excitation). The treatment in Chapter 3 of the various PT/CT methods, and of DQ/MQ/z filters, provides the NMR spectroscopist with a very useful account of these important techniques; here the authors' own research interests clearly show to advantage (see *J. Magn. Reson. 71* (1987) 322 and refs. cited therein). In Chapter 4, the longest in the book (102 pp.), the authors deal with the types of 2D experiments currently used for liquids (2D NMR spectra in general, δ,J-spectroscopy, H,H-COSY and H,X-COSY, MQ filtering, relayed COSY, NOESY). Even some quite exotic variations are discussed, such as SuperCOSY, COCONOESY and ACCORDION, but I was surprised to find no mention of such a useful experiment as COLOC. The neat formal description of 2D experiments, which is made possible by using product operators, shows to great advantage in the introduction to the COSY techniques on p. 154. Multiple quantum NMR for liquids and solids is treated succinctly in Chapter 5 (34 pp.), and includes multiplicity-selective excitation and MQ imaging. The final chapter on "Experimental Methods" (20 pp.) is not what one excpects from its title, as it deals mainly with the compensation of r.f. field inhomogeneities (using composite pulses), and—one reads with amazement—11 pages (!) on NMR imaging and in vivo NMR.

The content of the book, except for the last chapter, achieves its aims very well. The book should appeal especially to the physical chemistry oriented reader who needs a survey of the fundamentals of modern NMR spectroscopy. Nevertheless, it falls short of the ideal in some respects. For example, the list of contents tells one little more than one already expects from the title. Nor is it clear from the title itself that most of the book is concerned with the underlying theory of the experiments and techniques. The bibliography, which is divided into fundamentals, books and monographs, CT, 2D NMR in liquids, MQ spectroscopy, high resolution NMR in solids, composite pulses and NMR imaging, contains only 116 references, and therefore does not represent the current literature at all adequately. There are no literature citations at all in the text, apart from the sources given for most of the 259 figures. This means that one has to engage in detective work in trying to identify references, e.g. for interesting applications of ^{2}H NMR spectroscopy which are introduced on p. 226. The index, which for 380 pages of text contains only 140 key words, many of them acronyms, appears as a perfunctory duty to satisfy the publishers rather than as an aid to the reader. It soon fails one, e.g. in looking for "phase sensitive 2D spectrum", WALTZ-16, or MLEV-16, although all these are discussed in the text. Here again, as in Books (1) and (2), there is no list of abbreviations.

To summarize, the shortcomings mentioned here ought not to deter anyone from reading this informative book, which gives an outstandingly good introduction to modern pulse experiments, using the product operator formalism. One could profit greatly from working through it in the manner of a course of lectures; for liquids NMR only this amounts to about 260 pages. I can strongly recommend buying this book although it is not suitable as a reference source.

Finally, *Book (4)* can be regarded as *the* complete 2D NMR book, or even as several books combined into one. Whether or not it deserves to be regarded as the NMR spectroscopist's "New Testament"—the "Old Testament" being *Abragam*'s book—remains to be seen. At least it is almost identical in color, format, number of pages and weight (and also comes from the same publisher). The competence of the new apostles is beyond question, and their charisma is overwhelming, especially when they are shedding light on to spectral chaos (Chapter 7, Separation of the interactions, 42 pp.), reporting from the NMR tree of knowledge (Chapter 8, H,H-COSY and H,X-COSY, 90 pp.), or even offering the forbidden fruit of spectroscopy (Chapter 5, MQ transitions, 41 pp.). After an introductory chapter (9 pp.), Chapter 2 (60 pp.) relates the story of the dynamics of nuclear spin systems. Density matrix operators and superoperators within and outside Liouville space provide us with energy and relaxation. Chapter 3 (20 pp.) describes the manipulation of the Hamiltonian operator and stroboscopic observations. In Chapter 4 (152 pp.) we have the book of 1D FT NMR spectroscopy, including system theory, classical and quantum-mechanical descriptions, non-ideal pulses, sensitivity, heteronuclear PT and investigation of the dynamics of molecular processes, and double resonance. Chapter 6 (75 pp.) is a concise, but mathematically demanding, treatment of the principles of 2D FT NMR spectroscopy (coherence transfer mechanisms, 2D FT experiments, line shapes, and 2D data manipulation). Chapter 9 (50 pp.) deals with dynamic processes such as PT, cross-relaxation (NOE) and chemical exchange, and lastly Chapter 10 (26 pp.) describes NMR imaging techniques. Altogether there are 596 pages, containing 1260 equations. The literature references have been carefully checked and arranged according to chapters; there are 971 references in all. It must be mentioned, though, that two years elapsed between the writing of the preface (March 1985) and the publication of the book. Some of the most recent work, e.g. on fast NMR imaging (FLASH, for example) is therefore not covered. The index contains about 1500 entries; incredibly, though, "exponential operator" does not appear in the list of key words.

The Zürich book, what else would one expect, offers a comprehensive theoretical description of modern pulsed NMR spectroscopy, and includes the relaxation of MQ coherence. Although the principles set out are of quite general validity, the main emphasis of the treatment is on applications to liquids. The discussion of solid samples deals with the separation of δ effects from dipolar coupling effects, and of δ(isotropic) from δ(anisotropic). It may well be useful for chemists to make themselves familiar with exponential operator methods before working through the book, by using either Book (3) or Slichter: *Principles of Magnetic Resonance*, Harper & Row, New York (1963), just as it used to be necessary to first understand pages 22–24 of Abragam. However, the book has a lot to offer even to those less versed in the theoretical background, e.g. the discussions on signal optimization in 1D NMR (the Ernst angle, p. 125), spectral editing (p. 192), a review of methods for measuring T_1 (p. 202), chemical reactions occurring during recording of the FID (p. 211), spin filtering (p. 431) and the important "seven golden rules" for 2D NMR measurements (p. 357). There is a particularly instructive discussion on p. 468 of sensitivity in H,X-COSY

measurements for the case where an insensitive nucleus which is coupled to a proton is to be observed using 1D or 2D pulse sequences. For ^{15}N the relative signal to noise ratios vary in proportion to 1, 10, 30 and 300, depending on the pulse sequence used, requiring measurement times of 25 h, 15 min, 100 s or 1 s, respectively.

The book by *Ernst, Bodenhausen*, and *Wokaun* is undoubtedly to be regarded as the standard work on modern NMR spectroscopy, presenting the basic theory which underlies the newer pulse experiments used in structure elucidation. It will be indispensable for all scientists who wish to learn "at first hand" about these advanced techniques, and no departmental library should be without it. It is likely to become required reading for all physical chemistry oriented NMR spectroscopists.

What, then, is the overall impression? In the last ten years new methods have been introduced into NMR spectroscopy which allow quicker solutions to standard types of chemical problems, and make it possible for the first time to answer questions concerning the structures of such complex systems as proteins in solution. Up to now one has had to rely mainly on reading the original papers for the principles of these methods and examples of their applications. There has been a lack of monographs on the subject, apart from the doctoral thesis by *Ad Bax*, which was successfully published in book form. This situation is now changing rapidly, perhaps more so than people responsible for libraries would wish, in view of their limited budgets. In addition to the four books reviewed here, more are already on the way[*]. With the availability of these, the cost of updating the book stock in NMR alone could easily exceed DM 1000. With regard to the four books reviewed, however, the choice is not too difficult. The purchase of Book (1) is subject of personal preference. Book (2) is highly recommended to everyone who is engaged in the application of modern NMR techniques. No chemistry department should be without it. Book (3) will please anyone who already has NMR experience, and wishes to gain a deeper understanding of the theory of modern pulsed NMR methods using the product operator formalism. Finally, Book (4) is the standard work which belongs in every library and on the desk of the NMR specialist.

Dieter Ziessow [NB 853 IE]
Institut für Physikalische Chemie
der Technischen Universität Berlin

Zuckermans Compendium of Inorganic Chemistry—"timely, critical, comprehensive"?

For some time now it has been well known amongst those involved with the subject that VCH Verlagsgesellschaft was planning a multivolume work in which the wealth of experience in synthetic methods and experimental skills in inorganic chemistry would be brought together in an orderly presentation. At a very early stage well known inorganic chemists were invited to serve on an "Editorial Advisory Board", or as "Editorial Consultants to the Series", so as to take part in managing this truly monumental project under the direction of an experienced editor. Of course, authors were also needed, and some years had passed by the time these were found, and eventually the first contributions arrived and were assembled together in their appropriate individual volumes. Of the 18 volumes on "Reactions" which are planned (with a further six on "Methods" to follow), volumes 1 and 15 have now appeared, namely:

Inorganic Reactions and Methods. Edited by *J. J. Zuckerman*. VCH Verlagsgesellschaft, Weinheim/VCH Publishers, Deerfield Beach 1986. **Vol. 1: The Formation of Bonds to Hydrogen (Part 1).** xxv, 326 pp., bound, DM 275.00.—ISBN 3-527-26259-8/0-89573-251-3; **Vol. 15: Electron-Transfer and Electrochemical Reactions; Photochemical and Other Energized Reactions.** xxiii, 399 pp., bound, DM 298.00.—ISBN 3-527-26273-3/0-89573-250-5

This reviewer anticipated seeing the result of this long gestation with as much curiosity as must the many others who at various times have taken interest in the preparation of the volumes. How would those in charge cope with the almost impossible task which they had been given?

The first chapter of Vol. 1 ("How to Use this Book") begins with an explanation under the title "Organization of Subject Matter". We learn that reactions and techniques are grouped together under "Formation of Bonds" according to the elements involved. Thus we begin in Vol. 1 with "Formation of Bonds to Hydrogen", the elements of the halogen and chalcogen groups being the first bonding partners dealt with. Vol. 2 accordingly deals with hydrides formed by the remaining elements, and this is followed by "Formation of Bonds to Halogens", "Formation of Bonds to Chalcogens", and so on (Vols. 3–13). The material in these volumes is supplemented by special volumes (Vols. 14–18) on themes such as "Insertion Reactions and Their Reverse" (in Vol. 14), and "The Formation of Intercalation Compounds" (in Vol. 17). Vol. 15 deals with "Electron-Transfer and Electrochemical Reactions" and "Photochemical and Other Energized Reactions".

What, then are one's observations after using these "sample volumes"? Vol. 1 turned out to be largely unreadable: if one wishes to get an overview on methods for forming a particular type of bond or compound, one finds that the "iron discipline" which has been followed in the arrangement of the material severs all the usual connections. As an example, in a section which has the subtitles "1.2 The Formation of Hydrogen—1.2.2 By Reactions of Hydride Ions—1.2.2.2 With OH Groups and Acids in OH Systems", one finds on pages 5–11 descriptions of reactions which include that of NaH with water or carboxylic acids, the decomposition of methylberyllium hydride or $B_{20}H_{18}^{2-}$ by acids, the hydrolysis of UH_3 and Th_4H_{15}, the reaction of $Sn(OCH_3)_4$ with diborane, and the catalytic steam reforming reaction (production of hydrogen from alkanes and steam). Under each of these topics there are only a few lines and one equation, and only eight literature references *in total*, then we push on further with the systematic treatment! Again, under the series of headings "1.4 The Formation of Bonds between Hydrogen and Elements of Group VIB (O, S, Se, Te, Po)—1.4.5 By Reactions of Protonic Acids—1.4.5.2 With Sulfides—1.4.5.2.3 In Preparations of Anhydrous Acids of Sulfur", one finds the formation of $H_2S_2O_3$ from sodium thiosulfate and HCl, together with an (incorrect) formula. Would one have looked for it there?—and does it belong there anyway? The next reaction, which follows in the same section without a sentence to bridge the transition, is the formation of CF_3SH.

Since this first volume contains virtually no easily digestible sections which make for easy reading (such as are still found in "Houben-Weyl", for example), this part of the handbook is best treated as a work of reference. It is in fact ideally suited for this purpose, as the author, compound and subject indexes to the first volume occupy 90 of the

326 pages, and are excellent. The more specialized the subject on which one wants information, the better the book serves one as a reference source; for example, the information given on HSeD is faultless, while on the other hand to seek out a critical survey of essential facts about H_2O_2 is a time-consuming task which yields no satisfactory result. There is some compensation, however, in the convenient reading list given at the end of each chapter, even though it is not always fully up to date. This reflects the wide variation between the many individual authors as regards their competence and specialized knowledge in the topics covered.

Quite a different picture emerges in Vol. 15, which contains long reviews on specialized topics by only a few authors, with coverage of even very recent results. The test is enriched by the inclusion of many structural formulas, diagrams and numerical results, and the physical-chemical basis is also treated. The publishers' advertisement of the work as "timely, critical and comprehensive" is certainly true of this volume, while it is not of Vol. 1. The two parts entitled "Electron-Transfer and Electrochemical Reactions" (*N. Sutin, R. G. Linck, C. Creutz, W. E. Geiger, M. J. Weaver*) and "Photochemical and Other Energized Reactions" (*G. L. Geoffroy, P. C. Ford, H. B. Abrahamson, M. Z. Hoffman*) are concerned virtually exclusively with the chemistry of transition metals. Provided that one accepts this limitation, it can be said that the material has been put together in an exemplary way and presented in a very useful and readable form. Presumably in these "late" volumes the shortcomings which result from the rigidly systematic treatment of the d and f blocks elements in only one short volume (Vol. 14) must be remedied.

These first two samples of the new series are thus of very different quality. It is to be hoped that, in the volumes to come, it will still be possible to correct some negative aspects. The external appearance of the books is faultless.

Hubert Schmidbaur [NB 830 IE]
Anorganisch-chemisches Institut
der Technischen Universität München, Garching (FRG)

Houben-Weyl - Controversial

"Houben-Weyl" is one of the central pillars of the chemical literature; it is an authoritative source book of the first rank—and not only in the German-speaking world. The blue cloth-bound volumes command respect, and provide comprehensive and clearly set out information about the methods of organic chemistry. They contain a wealth of treasures, with carefully prepared synopses edited for ease of use. Such, for example, are the volumes on organophosphorus and organoboron chemistry. It is a pleasure to extract information from these, just as much for the experienced specialist as for the newcomer in unfamiliar territory. Two new supplementary volumes have just appeared to join the series on the bookshelf.

Houben-Weyl. Methoden der Organischen Chemie. Vol. E 18/Parts 1 and 2. Organo-π-metall-Verbindungen als Hilfsmittel in der organischen Chemie. Edited by *J. Falbe*. Thieme, Stuttgart 1986. DM 1580.00 (subscription price DM 1422.00). Part 1: xxvii, pp. 1–749, bound, ISBN 3-13-218804-2; Part 2: xv, pp. 750–1428, bound, ISBN 3-13-218804-2

which deal with the use of organometallic π-complexes in organic chemistry. After well over thirty years of productive research in this field, it was high time that it should be thoroughly reviewed from the organic chemist's viewpoint. Because of the large number of topics to be covered, working systematically through all the material has been a laborious and time-consuming task and it is to the credit of the editor *Jürgen Falbe* that these two new volumes have been so rapidly written. The team of sixteen authors has covered all the material, each from has own specialist viewpoint, in 1234 pages (not counting the indexes). They offer the user well-informed summaries of the various aspects, and a mine of information on experimental methods. Amongst these the contributions on hydroformylation by *B. Cornils* and *L. Markó* are outstanding.

However, the volumes fall short of the objective of being a systematically ordered handbook, of the sort that we are accustomed to in "Houben-Weyl". This reviewer struggled on bravely and hopefully through the chapters, at first filled with curiosity, but then with teeth clenched, grim determination. This perseverance yielded only pages of notes containing errata, inconsistencies, and information which was sometimes incomprehensible. According to the jacket synopsis, Part 1 describes preparative methods "arranged according to the various hapto forms". From the outset, however, the book runs into trouble with the hapto nomenclature: as early as the contents list we find "η^2-carbene complexes", an incorrect hapto form which is surpassed on page 58 by "η^3-carbynes". This is definitely taking liberties with the system of nomenclature. Nowadays one expects such a handbook to use nomenclature which conforms to the Chemical Abstracts standards, but these two volumes pay no regard to that. Here alkenyl ligands are usually described by a dehydroolefin nomenclature which, in the absence of a structural formula, is understood by nobody—certainly not by the computer, judging by the "η^3-3-dehydro-cyclooctene" group (p. 1001). Elsewhere, though, we find the more generally accepted form "η^5-cyclopentadienyl-" rather than "dehydrocyclopentadiene". An amusing example found on page 850 is [η^5-cyclopentadienyl]-(η^3-3-dehydro-cyclopentene)-nickel. On page 182 a decision has even been made in favour of "η^5-dehydropyrrolyl-", whereas on page 228 the same ligand is called "dehydropyrrole". What is intended to be a guide through the literature thus instead becomes a labyrinth from the user's point of view.

Presumably it was pressure of time that allowed the misprint gremlin to create havoc by changing "thorium" into "thor", inventing on page 481 a "tris-η^6-pyridine-rhodium", transforming a η^6-phenylborinato ligand into a η^5-ligand, and showing $CO + D_2O$ in equilibrium with $CO_2 + H$ (p. 659). The pressures given in the preparative methods have mostly been converted to kPa, but sometimes incorrectly, as for example on page 1002. For variety, though, they are sometimes measured in bar or torr, while other obsolete units such as "Stde." and "Schmp." have been allowed to pass uncorrected. By referring to an addition as a "silanation" (German: "Silanierung") it becomes instead a substitution, and alongside silylation we find also "disilylation" (German: "Disilylierung"). As for the possible meanings of the (German) words "Carborierung" and "Hydrocarborierung" which have been coined in the list of contents, we can discover them only by studying the relevant chapter in Part 2.

Theophrastus Paracelsus, commenting in 1538 on the chemical literature of his day, wrote in his Labyrinthus Medicorum "Die Tintenbücher haben kein Kunst in ihnen, sondern Sudelns und Kudelns durch einander und machen dann Schwaderlappen, daß die Säu lieber Dreck fressen,

denn ihr Geköcht ..."—i.e. he complained the books were so full of meaningless squiggles and obfuscations that if they were stewed up and fed to the pigs the latter would leave them alone and go on eating filth. The present reviewer cannot express his disappointment in language of such baroque eloquence, but must instead sum up his verdict on these two volumes in just one short sad phrase: What a shame!

Helmut Bönnemann [NB 842 IE]
Max-Planck-Institut für Kohlenforschung,
Mülheim/R. (FRG)

Houben-Weyl: Methoden der Organischen Chemie. Vol. XIII/9a: Organometallverbindungen von Mn, Re, Fe, Ru, Os und Pt. Thieme, Stuttgart 1986. Approx. 1000 pp., bound, DM 1100.—ISBN 3-13-214804-0; **Vol. XIII/9b: Organometallverbindungen von Co, Rh, Ir, Ni und Pd.** 1984. lviii, 1057 pp., bound, DM 1190.—ISBN 3-13-215004-5

In Volumes XIII/9a and XIII/9b, and Volumes XIII/4 and XIII/7 which were published a short time earlier, "Houben-Weyl" steps into new territory, thereby earning praise and respect. Twenty years ago, organometallic compounds of transition metals still belonged in the curiosities cabinet for most preparative organic chemists, but their outlook has since changed (even if hesitantly for some), and now to an ever increasing extent one reads of new syntheses being carried out using transition metals. One need not be much of a prophet to forecast that this trend will intensify.

Volume XIII/9a is devoted to preparations and transformations of organomanganese, -rhenium, -iron, -ruthenium, -osmium and -platinum compounds containing at least one M–C σ-bond (insofar as these reactions are of interest to organic chemists), while Volume XIII/9b deals in a similar way with organometallic compounds of the cobalt series (Co, Rh, Ir) together with nickel and palladium. In both volumes the compounds are arranged under individual metals, first in order of increasing oxidation state of the metal atom, then further divided within these groups according to classes of substances, i.e. organometallic alkyls, ylides, 1-alkenyls, aryls, acyls, alkoxycarbonyls, and aminocarbonyls. The next method of classification is by method of preparation. The foremost of these is the principle of "double substitution" (e.g. in metal halides using Grignard reagents or organolithium compounds). After this π→σ transformations (e.g. of allyl-metal complexes), and methods of synthesis starting from other organometallic transition metal compounds are discussed. Each chapter includes information on the relative importance of the compounds discussed, their properties and relative stabilities, and the transformations which they can undergo. An additional noteworthy feature is the inclusion in Volume XIII/9b of information about the importance of intermediates containing Co–C, Rh–C and Pd–C σ-bonds in large-scale processes such as hydroformylation, the Monsanto acetic acid process, and the Wacker process. Potential applications to synthesizing natural products, e.g. by the use of organopalladium complexes, are also mentioned.

Apart from the use of some rather idiosyncratic expressions, which even most organometallic chemists will fail to understand (e.g. "σ-C→carbene rearrangement"), there is little to find fault with in these two volumes. The usual high standard of the Houben-Weyl series has been maintained, which is saying a great deal with regard to quality. The individual chapters are illustrated throughout with very good structural formulas, enabling the reader to quickly grasp the significance of the results given. The bibliography is remarkably up-to-date for a work of this scale (complete up to 1985 in some cases), indicating a very good degree of collaboration between authors and publisher.

It is difficult to understand why Volume XIII/9a includes platinum organometallic compounds. In spite of all attempts at rearranging the Periodic Table, platinum still remains in the nickel triad of elements, and the platinum compounds ought, therefore, to have been in Volume XIII/9b. It is true that this volume would then have been somewhat thicker than the first one, but that ought not to worry anyone. In any case, the cost of both volumes is—unfortunately—such that only libraries will be able to afford them, and nowadays they are surely groaning not only under the weight of thick volumes, but also under financial burdens such as this. One can only hope that, despite these difficulties, "Houben-Weyl" will maintain its high standards, and will continue to bring about a closer liaison between organometallic chemists of organic and inorganic color.

Helmut Werner [NB 835 IE]
Institut für Anorganische Chemie
der Universität Würzburg (FRG)

Structural Methods in Inorganic Chemistry. By *E. A. V. Ebsworth, D. W. H. Rankin* and *S. Cradock*. Blackwell Scientific Publications, Oxford 1987. xi, 456 pp., hardback, £ 13.50.—ISBN 0-632-01603-5

The authors have written this book with the aim of familiarizing advanced chemistry students in a selective way with the most important physical methods of structure investigation used in inorganic chemistry. An important part of this task is to enable the student to apply the most appropriate combination of techniques to a given structural problem. On the whole the authors fulfill this need, but shortcomings are apparent in some matters of detail.

Following an introductory chapter, which includes a nine page table reviewing the various physical methods, with notes on their use, the methods themselves are treated in eight chapters as follows: nuclear magnetic resonance spectroscopy, electron spin resonance spectroscopy, nuclear quadrupole resonance spectroscopy, rotational and vibrational spectroscopy, electronic spectroscopy and photoelectron spectroscopy, Mössbauer spectroscopy, diffraction methods, and mass spectrometry. A good balance is maintained in the importance accorded to the various methods; thus NMR and vibrational spectroscopies are treated in considerable detail, and mass spectrometry only briefly. It is notable, however, that there is no chapter on magnetochemistry. For each of the techniques covered there is a theoretical introduction; the impression is given in each case that this treatment is sufficient for understanding and using the technique, even though the preface certainly does not make such a claim. Anyone who has little previous knowledge of a technique will discover the limitations of the treatment as soon as he begins to apply what he has read. Thus, for example, in the chapter on vibrational spectroscopy the degeneracy of a vibrational mode is mentioned but not explained, and symmetry operations are treated in a very labored fashion. Again, in the section on diffraction methods, although one is told of the importance of determining the correct space group, the details of this are nowhere explained; reflection planes and

axes of rotation are not mentioned. Crucially important explanations are often dismissed too briefly, e.g. that of Miller indices. Occasionally there appears without warning an unexplained term such as "difference maps".

Yet despite all the criticisms of individual topics, the book is a considerable success, and a useful addition to the major resources available for the study of chemistry. A final, particularly impressive, chapter is entitled "Case Histories", and gives instructive examples of the practical application of what has been learned previously. The reader can also test how well he has learned the material by means of the problems that are set, with answers given at the end only for every second one; this contributes to a useful dialogue between student and teacher.

Kurt Dehnicke [NB 844 IE]
Fachbereich Chemie
der Universität Marburg (FRG)

The Organic Chemistry of Nucleic Acids (Volume 24 in the series **Studies in Organic Chemistry**). By *Y. Mizuno*. Elsevier, Amsterdam 1986. 342 pp., bound, HFl 245.00.—ISBN 0-444-99521-8

The compactness of this book and its broadly worded title lead one to expect a standard reference work rather than an introduction. The preface restricts the scope implied by the title by stating that the length of the chapters is not related to their importance, and furthermore that the main emphasis is on Japanese papers.

The short introduction recalls the history of nucleic acids in chemistry and elaborates the important role which they play in nature. It culminates with a description of the synthesis of the gene for somatostatin, and its expression in *E. coli*. This topic is again taken up briefly in the chapter on "Genetic Engineering" at the end of the book.

The main emphasis of the book and at the same time its best chapters are those on synthesis and reactions of nucleosides, which is the author's speciality. Here also the outstanding contributions made by Japanese investigators become evident. Apart from the mainly historical considerations and those that are included for the sake of completeness, an especially useful feature is the evaluation of the various synthetic routes to purine and pyrimidine nucleosides. The advantages and disadvantages of the individual methods are given, together with the currently preferred method for each case. A great many compounds of pharmacological interest, which are obtained by isolation from microorganisms, by chemical synthesis, or by enzymatic or microbial processes, are listed.

Of the chapters on nucleic acid syntheses, that on the RNA synthesis is almost more instructive than that on the DNA synthesis, as the former is more elaborated on from a chemical point of view. The informative chapter on "DNA Drug Interaction", which provides the pharmaceutical chemist with a short review of the interaction mechanisms of both covalent and non-covalent intercalators, crosslinkers, and DNA splitting agents, deserves special mention. A weak point is the analytical section, which besides the sequencing of DNA and RNA includes only a brief mention of ^{13}C and ^{31}P NMR spectroscopy.

It is a pity that this book, which, according to the author, aims to provide students, lecturers and interested organic chemists in general with a readily comprehensible insight into nucleic acid chemistry, will probably fail to attain that objective because of its considerable cost. For the expert the book gives an overview of the extent of the Japanese contributions in this field. So far as the presentation of the book is concerned, I would have liked to see the many printing errors corrected, and a clear numbering system used for the formulae so that a non-specialist might follow the formulae charts more easily. This book can definitely be recommended for those pharmaceutical chemists who have an interest in what is going on in the area of nucleosides and nucleotides of pharmacological importance.

Joachim Engels [NB 803 IE]
Institut für Organische Chemie
der Universität Frankfurt/Main (FRG)

Chemistry and Structure at Interfaces: New Laser and Optical Techniques. Edited by *R. B. Hall* and *A. B. Ellis*. VCH Publishers, Deerfield Beach 1986. xiv, 351 pp., bound, DM 175.00.—ISBN 0-89573-311-0

The development of lasers and the availability of synchrotron radiation have had an enormous influence on all those fields of research in which electronic excitation can be used either to trigger physical or chemical processes, or to detect them. This book was stimulated by a three-day symposium held by the American Chemical Society in March 1983 on the theme "Photoprocesses at Solid Surfaces". It contains six seminar papers from this symposium, which have been updated by the authors to mid-1985.

"Examination of the Gas-Solid and Metal-Support Interfaces in Supported Catalysts by Near Edge X-ray Absorption Spectroscopy", by *J. A. Horsley* and *F. W. Lytle*, is a comparatively short contribution (23 pp.) dealing mainly with results obtained using synchrotron radiation on small clusters of platinum, iridium and rhodium. The interpretation of the results emphasizes the role played by the *d*-electrons of such clusters in their interaction with adsorbates.

In the next paper "Final-State-Resolved Studies on Molecule-Surface Interactions" (59 pp.), *D. S. King* and *R. R. Cavanagh* describe a very demanding, but highly informative technique, whereby one can get an insight into the distribution of energy between the different modes of excitation of a molecule following its interaction with a surface. For this purpose one makes use of either the fluorescence of the molecules following selective excitation by lasers, or the resonance ionization which generates ions with single or multiple charges, as determined by the absorption of the molecule. Up to now the molecule used as a model has in nearly all cases been NO, whose spectroscopic properties are especially well understood. In this article the authors describe studies of the energy distribution following thermal desorption or after scattering of a molecular beam at single crystal surfaces.

R. B. Hall and *S. J. Bares*, in their paper "Pulsed-Laser-Induced Desorption Studies of the Kinetics of Surface Reactions" (65 pp.), deal exclusively with the thermal desorption of adsorbed molecules by heating of the support. By using a laser beam the heating can be confined to a very small region, thus allowing one to sample small parts of surfaces and follow the progress of chemical reactions which take place during a gradual heating process. Using this technique one can also, by repeated irradiation of a small surface region, monitor the transport of material by surface diffusion.

Second order processes in non-linear optics can occur at boundary surfaces as a consequence of asymmetry. In the article "Applications of Optical Second-Harmonic Generation to Surface Science" by *Y. R. Shen* (56 pp.), some examples are given showing how this process can be used to

study adsorbed molecules, particularly with regard to their orientations. Since this effect depends on the strength of the local electromagnetic field at the surface, it can be used to measure the field, a capability which is important for the SERS effect discussed in the next paper.

Surface-enhanced Raman spectroscopy (SERS) has already been reviewed in numerous articles. *D. A. Weitz, M. Moskovits,* and *J. A. Creighton,* in their article "Surface-Enhanced Raman Spectroscopy with Emphasis on Liquid-Solid Interfaces" (51 pp.), support the view that the only significant factor in the SERS effect is the amplification of the electromagnetic field by resonance phenomena in small particles or at rough surfaces, which is highly controversial. There are many indications that a considerable contribution to the very high enhancement factors of 10^5–10^6 arises from specific chemical interactions between the adsorbate and the substrate. The SERS effect is of importance in its application to investigating problems of practical interest, some of which are briefly discussed here. An example is adsorption on small catalyst particles.

The luminescence observed from semiconductors, either following excitation by absorption of light or as a result of the injection of minority carriers, comes from the bulk material. However, its intensity is surface-dependent, since the radiation yield is determined essentially by the amount of radiationless recombination occurring at the surface. In his contribution "Luminescent Properties of Semiconductor Electrodes" (100 pp.), *A. B. Ellis* describes the experimental requirements for observing the phenomena that occur at semiconductor electrodes, and the theoretical models used to analyze the results. The main interest in such experiments is in evaluating semiconductors for energy conversion purposes, as the yield in photoelectrochemical cells is limited essentially by surface recombination.

All these articles provide interesting and stimulating ideas on the use of lasers and other optical techniques for the characterization of interfaces. The techniques that are proposed are still undergoing development, but undoubtedly have great potential for the future.

Heinz Gerischer [NB 812 IE]
Fritz-Haber-Institut
der Max-Planck-Gesellschaft, Berlin-Dahlem

Molecular Structure and Energetics. Edited by *J. F. Liebman* and *A. Greenberg.* VCH Verlagsgesellschaft, Weinheim/VCH Publishers, Deerfield Beach, FL 1986. **Vol. 1: Chemical Bonding Models.** XIV, 360 pp., bound, DM 240.00 (subscription price DM 210.00).—ISBN 3-527-26344-6/0-89573-139-8; **Vol. 3: Studies of Organic Molecules.** XIV, 385 pp., bound, DM 240.00 (subscription price DM 210.00).—ISBN 3-527-26477-9/0-89573-141-X

A new "open-end" series has been started and the volumes 1 and 3 published first – in the meantime volumes 2 and 4 also appeared – contain 360 und 385 pages respectively; they have been published by the US subsidiary of VCH Verlagsgesellschaft, our old friend Verlag Chemie, in the same esthetic way to which we have become accustomed. (The binding is not to my taste but *de gustibus not est disputandum*).

Each of the two volumes has a general heading and the contributions chosen fit in reasonably well. Each author was given much latitude in the relative blending of theory and experiment and in style. This is perhaps most evident in the chapters written or co-authored by the editors themselves. The standard of the contents, almost without exception, is very high.

In comparing two similar series, published as beautifully as this one by a competing publisher ("Structure and Bonding" and "Topics in Current Chemistry"), one finds similar breadth and homo- or heterogeneity. It is evident that it is cheaper to print in East or even in West Germany per individual volume than in the U. S.

Not as a matter of modesty, but as a matter of fact, I have checked my opinions on chapters further from my realm of understanding with trusted expert colleagues. Though they remain unidentified, any misjudgements are solely my responsibility.

Volume 1 contains nine chapters, the first of which (15 pages) is by *L. Pauling* and *Z. S. Herman.* What a nice idea for the opening chapter of a book on chemical bonding! Although one can always learn from *Pauling*, I, of course, included (albeit Vitamin C is unmentioned), I must abjectly confess my disappointment. I was looking forward to a much greater treat upon reading the first half of the title: "Nature of the Chemical Bond Fifty Years Later:" I expected from the Master a deeper evaluation and perspective than actually touched. The purpose of sub-heading "The Relative Electronegativity of Atoms Seen in Perspective" is achieved. I expected a wider overview on the nature of the chemical bond, 50 years later, perhaps employing more of "the work of such investigators as *Roald Hoffmann*". Perhaps my judgement is clouded by the nature of the first chapter (by *D. J. Cram*) in a two-volume set on cyclophanes.

Chapter 2 by *H. A. Bent* on "Isoelectronic Molecules" treats the subject in an incredibly terse manner (30 pages!), as can be done only by a leading expert; it explains the concepts involved with well chosen examples. I was sorry when the beautifully written chapter ended. I should have been glad to see included the word isolobal.

Chapter 3 by *J. F. Liebman* and *J. Simons* discusses "Carbenes: A Study in Quantitative and Qualitative Theory" (49 pages). Since reviews of carbenes emphasizing the synthetic viewpoint are plentiful, this one is particularly valuable.

In Chapter 4, *M. S. Gordon* considers "Theoretical Studies of Multiple Bonding to Silicon" (22 pages). The author's first sentence makes the point of how rapidly this new field is developing. The length of the chapter is due to the novelty of the field and though coverage is very good Si=N bonding might have been added when Si=P is discussed. The author even manages to cite some 1985 references which were available to him, but much has already appeared in the interim. It is a pity that in this case there is no addendum (as in Vol. 3) to catch up a bit more. Nevertheless, here is the place to mention that publication has been relatively fast and many 1984 references are cited throughout.

In contradistinction, Chapter 5 by *R. B. King* on "Topological Relationships in Molecular Structures and Energetics" (26 pages) is disappointing. It not only skims the surface but its latest 1983 reference is to a chapter elsewhere by the same author on the same general theme. I should have thought that a chapter with this title ought to have contained a bit more about graph theory to simple planar organic compounds if not to those few that cannot be accommodated by a planar graph. Perhaps a more limiting title could not have led to great expectations.

Chapter 6 by *T. P. Fehlner* and *C. E. Housecroft* discusses "Boranes and Heteroboranes" (59 pages). It is a good introduction to the uninitiated as to structures of

cluster compounds, those of boron being perhaps the most versatile examples. Other clusters are mentioned in Chapter 5. This is a place where the editors might have had a bit more substantive inter-connection between the two rather than just placing them adjacently.

J. K. Burdett writes about "Structural-Electronic Relationships in the Solid State" in Chapter 7 (65 pages). It is here again unfortunate that other than two (self) citations from 1985. Nevertheless, this is an excellent review on the subject with examples from a variegated array of molecules. This chapter is one of the best in the Series.

Chapter 8 by two excellent authors, *L. J. Schaad* and *B. A. Hess, Jr.* on "A Detailed Derivation of the Schrödinger Equation" (42 pages) is out of place even in a book with such a broad subtitle, the explanation in its first paragraph notwithstanding. Nor do several theoreticians whom I consulted see any justification for its inclusion.

Chapter 9 by *J. E. Del Bene* on "Quantum Chemical Reaction Enthalpies" need not scare away any organic chemist. Added to the interesting discussion is a very helpful appendix regarding basis set and method notation.

Volume 3 contains seven chapters on almost entirely unrelated subjects. Though heterogeneous we have a collection of interesting discussions, some more specific, some more general. I have found the latter generally useful but I predict that readers will rate the more specific subjects in accord with their interests.

Chapter 1 is an authoritative review by *S. F. Nelsen* on "Hydrazine-Hydrazine Cation Electron Transfer Reactions" (56 pages), a field in which the author is the major contributor. It is a goldmine of information while explaining relative behavior principally by conformational means.

Chapter 2 by *G. R. Stevenson* on "Stabilization and Destabilization of Aromatic and Antiaromatic Compounds" (27 pages) is to me another in a long chain of books and chapters still flogging this creature. I say this seriously but the tongue-in-cheek statement by *E. Heilbronner* about "schizoaromaticity" (a compound believes itself aromatic by one criterion, not so by another) summarizes my feelings about this subject. Annulenes are emphasized and other than a handful of references to his own more recent work the citations are mainly from the 60's and 70's. I do not see the need for a chapter such as this.

Chapter 3 by *R. P. Johnson* on "Structural Limitations in Cyclic Alkenes, Alkynes, and Cumulenes" (56 pages) cites a great many from the late 70's and the 80's including some from 1985. Thus it is a useful up-to-date review nicely blending theory and experiment. I missed explicit citation of *Sondheimer*'s classic work. It ought, perhaps, to have been fitted into the discussion.

Chapter 4 by *B. F. Smart* on "Fluorinated Organic Molecules" (51 pages). (As an aged conservative I enjoyed the note explaining how to convert kcal/mol into SI units! This is dealt with in Chapter 6 in a more kosher manner.) The review is an excellent addition to another by the same author (Ref. 2). Troubles with experimental accuracy and problems in calculations are well illustrated.

Chapter 5 by *A. Greenberg* and *T. A. Stevenson* discusses "Structures and Energies of Substituted Strained Organic Molecules" (74 pages); it is an expectedly fitting sequel to the Liebman-Greenberg monograph on the same topic and a rich source of updated experimental and calculated data.

Chapter 6 by *J. F. Liebman* has relatively little to do with strain. It is entitled "Macroincrementation Reactions: A Holistic Estimation Approach for the Properties of Organic Compounds" (62 pages). Graduate students in chemistry as well as their teachers would do well to enjoy the well written story of heats of formation and their correct application, remembering not to compare apples with pears. They might even learn the meaning of some words in the title. Here again many recent citations are given. The use of comments bracketed by the symbol ≪ ≫ are an original way for emphasis.

Chapter 7 by *E. Ōsawa* and *K. Kanematsu* discusses "Generation of Long Carbon–Carbon Single Bonds in Strained Molecules by Through-Bond Interactions" (41 pages; the ≪ ≫ method employed). It is not surprising that such a fine theoretician-experimentalist team has produced such a valuable chapter. All in all: The Series is a must for every chemical library.

David Ginsburg [NB 833 IE]
Department of Chemistry
Israel Institute of Technology
Haifa (Israel)

Registered names, trademarks, etc. used in this journal, even when not marked as such, are not to be considered unprotected by law.

© VCH Verlagsgesellschaft mbH, D-6940 Weinheim, 1987. – Printed in the Federal Republic of Germany by Zechnersche Buchdruckerei, Speyer/Rhein.

All rights reserved (including those of translation into foreign languages). No part of this issue may be be reproduced in any form – by photoprint, microfilm, or any other means – nor transmitted or translated into a machine language without written permission from the publishers. Only single copies of contributions, or parts thereof, may be made for personal use.

Valid for users in the USA: The appearance of the code at the bottom of the first page of an article in this journal (serial) indicates the copyright owner's consent that copies of the article may be made for personal or internal use, or for the personal or internal use of specific clients. This consent is given on the condition, however, that the copier pay the stated per-copy fee through the Copyright Clearance Center, Inc., for copying beyond that permitted by Sections 107 or 108 of the U.S. Copyright Law. This consent does not extend to other kinds of copying, such as copying for general distribution, for advertising or promotional purposes, for creating new collective works, or for resale. For copying from back volumes of this journal see 'Permissions to Photo-Copy: Publisher's Fee List' of the CCC.

Editorial office: Pappelallee 3, D-6940 Weinheim, Federal Republic of Germany, Telephone (06201) 602315, Telex 465516 vchwh d, Telefax (06201) 602328.

Editor: *P. Gölitz.*

Associate editors: *D. I. Loewus, A. Stimson.* **Editorial assistant:** *E. Schweikart*

Publishers: VCH Verlagsgesellschaft mbH. (Managing Directors: *Prof. Dr. Helmut Grünewald* and *Hans Dirk Köhler*), Pappelallee 3, D-6940 Weinheim, Federal Republic of Germany. Correspondence concerning advertisements should be addressed to VCH Verlagsgesellschaft mbH. (Advertising Manager *R. J. Roth*), Boschstr. 12, P.O. Box 1260/1280, D-6940 Weinheim, Federal Republic of Germany, Telephone Weinheim (06201) 602-0, Telex 465516 vchwh d, Telefax (06201) 602328.

ANGEWANDTE CHEMIE
International Edition in English
Volume 26 · Number 12
December 1987
Pages 1201–1302

Chemistry of the Silicon–Silicon Double Bond

By Robert West*

Disilenes, compounds containing silicon–silicon double bonds, can be isolated as thermally stable, yellow- or orange-colored crystalline compounds; the substituent groups at silicon must be large (mesityl, *tert*-butyl, etc.) to prevent polymerization. Structural and spectroscopic studies indicate many similarities between the 3p–3p π bonding in disilenes and the 2p–2p π bonding in olefins, but disilenes are much more reactive than alkenes. The reactions of disilenes lead to many new classes of silicon compounds, including three- and four-membered rings which present novel problems in chemical bonding.

1. Introduction

Much of the richness and diversity of organic chemistry results from the ability of carbon to form multiple bonds, with itself or with other elements. Since silicon is the element most closely related to carbon, it seemed likely to early researchers that silicon should also form multiple bonds. However, all attempts to synthesize doubly bonded compounds of silicon early in this century proved unsuccessful, leading instead to cyclic oligomers or polymers containing only single covalent bonds.[1] Similar results were obtained for other second- and third-row elements, especially phosphorus and arsenic.[2] These findings led to the view that compounds containing multiple bonds involving silicon or other heavier main-group elements must be unstable: the so-called "double-bond rule."[3,4] According to this concept, weakness of multiple bonds between second-row elements was rationalized as resulting from the large radii of these atoms, leading to poor overlap between adjacent p orbitals.

Evidence for several transient species containing multiple bonds between second-row elements began however to accumulate in the late 1960s and 1970s. And in the single year 1981, the double-bond rule was decisively overthrown when the isolation of stable compounds containing P=P,[5] Si=C,[6] and Si=Si[7] bonds was announced.[*] The key to synthesis of these compounds was the use of sterically hindering substituent groups to block polymerization. Thus the first compound containing a Si=Si double bond to be prepared was tetramesityldisilene, **1**. The same principle has subsequently been used in the synthesis of several other new kinds of multiple bonds, including, inter alia, As=As,[8] Ge=Ge,[9] and for silicon, Si=N[10] and Si=P.[11]

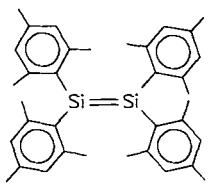

1

This review deals with the disilenes (Si=Si compounds), concentrating on the stable compounds, whose chemistry has undergone considerable development in the last six

[*] Prof. R. West
Department of Chemistry, University of Wisconsin
Madison, WI 53706 (USA)

[*] Note added by the editorial staff: For a short comment on this area of research, see a letter from J. Goubeau (*Angew. Chem. 98* (1986) 944; *Angew. Chem. Int. Ed. Engl. 25* (1986) 1038).

years.[12] Some mention will be made also of the several marginally stable disilenes obtained only in solution.[13] In addition many other disilenes have been isolated in argon or hydrocarbon matrices.[14] The less stable disilenes, and multiple bonds to silicon generally, have been comprehensively reviewed elsewhere.[15] A valuable review of Si=C double bonds has also appeared recently.[16]

2. Si=Si and C=C Bonds: An Overview

Now that compounds containing Si=Si double bonds are readily available, it is fascinating to compare their properties with those of their carbon analogues, the alkenes, which are so well known and understood. In this section the differences and similarities between Si=Si and C=C double bonds will be summarized; details will be given in the sections following.

Structurally, the formation of Si=Si double bonds is accompanied by a marked shortening from the normal Si–Si single-bond distance; the decrease is quite similar to the bond shortening observed on going from C–C to C=C. However, the disilenes may exhibit deviation from the regular planar structure of olefins, because the Si=Si double bond is much more flexible toward distortion than C=C. Appropriately substituted disilenes such as the di-*tert*-butyldimesityl compound **2** exist as *Z* and *E* stereoisomers,

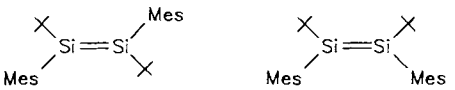

(*E*)-**2** (*Z*)-**2**

Mes = mesityl = 2,4,6-trimethylphenyl

which can be separated but undergo slow thermal isomerization. The barrier to rotation at Si=Si is about 70% as large as that for comparable alkenes. In sharp contrast to alkenes, the disilenes are yellow or orange, with electronic absorption bands between 400 and 470 nm. The visible spectra of disilenes are due to $3p\pi \rightarrow 3p\pi^*$ transitions, which have energies only about half as great as those for typical olefins, whose $2p\pi \rightarrow 2p\pi^*$ absorptions fall in the vacuum ultraviolet region. This difference is understandable in terms of a crude molecular orbital model. As shown in Figure 1, the π orbital for disilenes lies much higher than for alkenes, and the π^* level much lower.

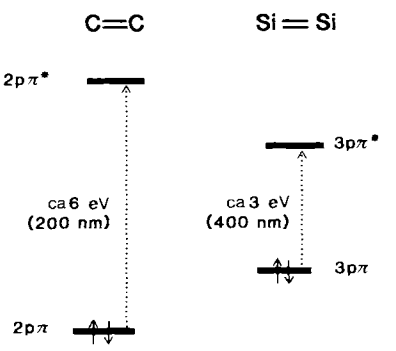

Fig. 1. Qualitative MO diagram showing relative energies of π and π^* levels for alkenes and disilenes.

From the MO diagram of Figure 1, it follows that disilenes should be both more electron-deficient *and* more electron-rich than alkenes. Indeed, the stable disilenes, in spite of their sterically hindering substituents, react readily with a variety of both nucleophilic and electrophilic reagents, and also take part in free-radical reactions. Disilenes undergo the typical addition reactions found for alkenes, but in addition take part in many reactions not normally observed for olefins.

Although the reactions of disilenes are known only very incompletely, they have led to a number of classes of compounds with previously unknown structures. Examples are shown in Figure 2. Some of these new compound types present unusual problems in chemical bonding theory.

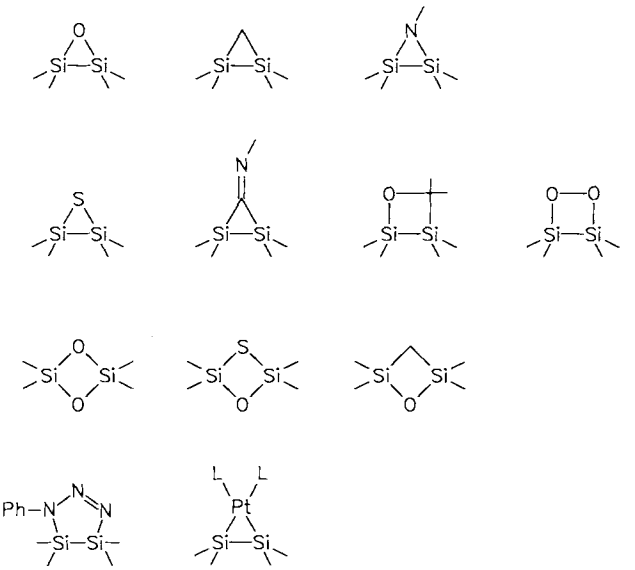

Fig. 2. New structural types obtained from disilenes.

^{29}Si-NMR spectroscopy is of particular importance in the study and characterization of disilenes and their derivatives, just as ^{13}C-NMR spectroscopy has been important for alkenes and other hydrocarbons. Disilenes show ^{29}Si resonances which are strongly deshielded and (for **1**, the only case yet studied) highly anisotropic; also, the $^{1}J_{Si,Si}$ coupling constants are nearly twice as great for Si=Si as for Si–Si. All of these observations are closely paralleled in the ^{13}C-NMR spectra of olefins.

3. Historical: The Discovery of Stable Disilenes

The first evidence for transient disilenes was presented in 1972 by *Roark* and *Peddle*.[17] In a now-classic experiment they heated the $Me_2Si–SiMe_2$ bridged precursor molecule **3** with anthracene, obtaining a high yield of the

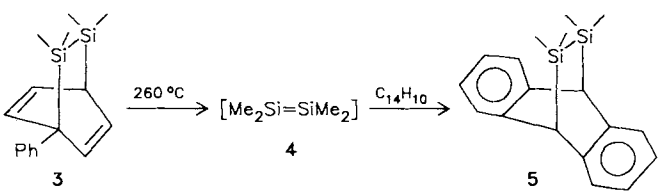

3 **4** **5**

adduct **5**. The result can be explained as due to a retro-Diels–Alder fragmentation of **3** leading to tetramethyldisilene **4**, which undergoes 9,10-addition to anthracene. Subsequently, important work on transient disilenes was carried out by *Barton* et al.,[18] *Gaspar* et al.,[19] and *Sakurai* et al.[20,21]

Our original experiments were also directed toward the synthesis of **4**, which we hoped to trap in an argon matrix for identification. However, these attempts, involving dehalogenation of $ClMe_2SiSiMe_2Cl$ or $BrMe_2SiSiMe_2SiMe_2Br$, were completely unsuccessful; if any disilene was formed, it did not survive long enough to be trapped in the matrix. We then turned our attention to matrix isolation of divalent silicon species (silanediyls or "silylenes"), beginning with Me_2Si generated photolytically from the six-membered ring $(Me_2Si)_6$.[22] This reaction proceeded smoothly at 10 K in argon, permitting a detailed study of the spectroscopy of dimethylsilanediyl.[22]

It soon became evident that photolysis of polysilicon compounds could be used for generation of many different silanediyls, and that these divalent silicon compounds are indefinitely stable not only in argon matrices near 10 K but also in hydrocarbon glasses at liquid nitrogen temperature.[14] Upon melting of the matrix or glass, most silanediyls polymerized, forming cyclic or linear polymeric polysilanes. Dimesitylsilanediyl, however, behaved abnormally. Photolysis of trisilane **6** in 3-methylpentane (3-MP) at 77 K led to the intensely blue-colored silylene **7**. When the hydrocarbon glass was melted a yellow solution was formed which gave reactions consistent with the presence of tetramesityldisilene, **1**, formed by dimerization of **7**. Ultimately, **1** was isolated as a bright yellow crystalline solid when the hydrocarbon was evaporated.[7] In practice, isolation of the silanediyl is not necessary. Simple photolysis of **6** in hydrocarbon solution at −60 °C leads directly to **1**, which crystallizes from solution as it is formed.[23]

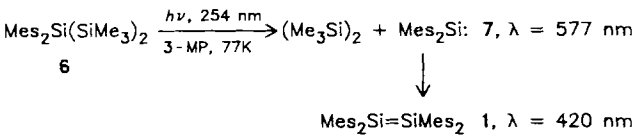

Later experiments have shown that when matrices containing silanediyls are annealed, dimerization to disilenes is the usual first step in polymerization.[14]

4. Synthesis and Properties of Stable Disilenes

4.1. Photolysis of Linear Trisilanes (Method A)

Ultraviolet irradiation at 254 nm of precursors like **6** is a general method for the preparation of stable disilenes.[24] The required trisilanes can be made by standard coupling reactions, illustrated for the synthesis of tBu(Mes)Si($SiMe_3$)$_2$, **8**. Photolysis of **8** leads to the *E* isomer of 1,2-di-*tert*-butyl(dimesityl)disilene, (*E*)-**2** (HMPA = hexamethylphosphoramide).[23]

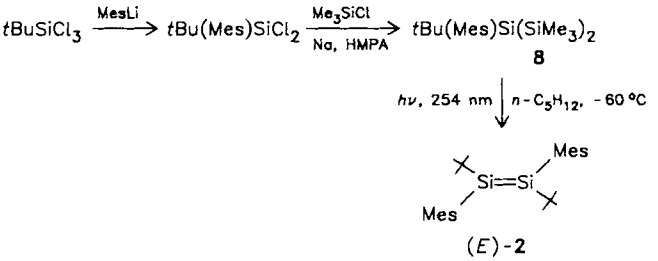

4.2. Photolysis of Cyclic Trisilanes (Method B)

A general method for the synthesis of trisilanes has been developed by *Masamune* et al.[25,26] Cyclic trisilanes are made from hindered diorganodihalosilanes and lithium naphthalide, then photolyzed to give the disilene. The first example was the synthesis of disilene **9**.[27] Presumably, photolysis of the cyclotrisilane produces disilene **9** and the corresponding silanediyl, with the latter undergoing dimerization to give more disilene. Both methods A and B have been used to make unstable as well as stable disilenes.

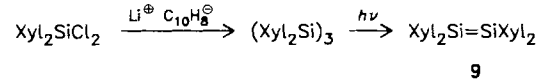

Xyl = 2,6-dimethylphenyl

Table 1. Stable disilenes [a].

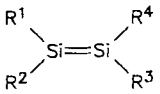

Compd	R^1	R^2	R^3	R^4	Method	d (Si=Si) [pm]	$\delta(^{29}Si)$	λ_{max} [nm]	Ref.
1	Mes	Mes	Mes	Mes	A, C	216.0	63.68	420	[23]
(*E*)-**2**	Mes	*t*Bu	Mes	*t*Bu	A, B	214.3	90.3	400 sh, 338	[23, 26]
(*Z*)-**2**	Mes	*t*Bu	*t*Bu	Mes	[b]		94.7		[26, 31]
9	Xyl	Xyl	Xyl	Xyl	A, B		64.06	422, 340, 272	[27, 30]
10	DEP	DEP	DEP	DEP	B	214.0			[25]
11	Mes	1-Ad	Mes	1-Ad	A		87.1	392 sh, 338	[46]
(*E*)-**12**	Mes	$N(SiMe_3)_2$	$N(SiMe_3)_2$	Mes	A		49.4	468, 362	[31]
(*Z*)-**12**	Mes	$N(SiMe_3)_2$	Mes	$N(SiMe_3)_2$	[c]		61.9	483, 351	[31]
13	Mes	Mes	Xyl	Xyl	A		65.19, 62.56		[32]
(*E*)-**14**	Mes	Xyl	Mes	Xyl	A		63.86		[30]
(*Z*)-**14**	Mes	Xyl	Xyl	Mes	A		63.87		[30]

[a] DEP = 2,6-diethylphenyl; 1-Ad = 1-adamantyl. [b] By UV irradiation of the *E* isomers. [c] By thermal isomerization of the *Z* isomer.

4.3. Dehalogenation of Dihalosilanes (Method C)

The preparation of **1** from the corresponding dichloride has been reported, using either controlled-potential electrochemical reduction or ultrasound-promoted dehalogenation with lithium metal.[28a] These syntheses, however, appear to produce rather impure disilene, and have not been widely used.[28b]

In Table 1 the known stable disilenes are listed with their ^{29}Si-NMR chemical shift values, UV/VIS absorption maxima, and where known, the Si=Si distances.

4.4. Photolytic [2+4] Cycloreversion

Recently it has been shown that irradiation of a disilabicyclo[2.2.2]octadiene precursor is a route to the nearly stable disilenes, tetra-*tert*-butyl-[29] and tetra-*iso*-propyldisilene.[30] The reaction used for the latter is illustrated in Equation (a). Probably the same method could be used to synthesize disilenes that are fully stable at room temperature.

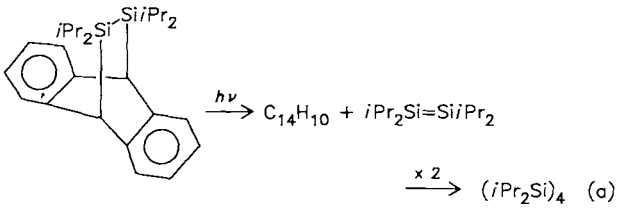

(a)

4.5. Physical Properties of Disilenes

The stable disilenes are pale-yellow to orange-red crystalline solids with remarkable thermal stability. Some disilenes are strongly thermochromic. For example, when tetramesityldisilene (**1**) is heated as a solid, its color changes from bright yellow to orange to red; it melts to a red liquid at 176 °C.[23] The reason for the color changes is not known, but they probably result from temperature-dependent conformational changes affecting the Si=Si chromophore[33]. All of the color changes are reversible if the sample is cooled promptly, but molten **1** decomposes fairly rapidly according to Equation (b).[34]

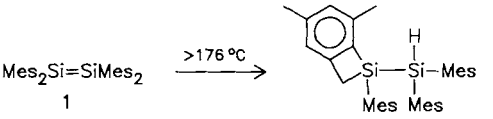

(b)

Other disilenes are even more stable thermally. (*E*)-1,2-Bis(1-adamantyl)-1,2-dimesityldisilene, **11**, apparently survives brief heating to 275 °C.[46]

5. Molecular Structures

X-ray crystal structures have been determined for three disilenes, **1**[23] and (*E*)-**2**[23] (Fig. 3) as well as tetrakis(2,6-diethylphenyl)disilene, **10**.[25] The Si=Si distances in the three compounds fall between 214 and 216 pm (Table 1), about 20 pm less than the normal Si-Si single bond length. The decrease is slightly larger than that observed on going from C–C to C=C in the carbon series (ca. 18 pm).

Each of the three compounds has a slightly different structural arrangement at the Si=Si double bond. In (*E*)-**2**, the two silicon atoms and the four carbons attached to them are coplanar, just as in a normal olefin structure. For **10**, the arrangement at each silicon is coplanar, but the two halves of the molecule are twisted by 10°. In **1**, there is a slight (6°) twist of the double bond and, in addition, the two silicon atoms are pyramidal rather than planar, in an *anti* fashion to one another. The pyramidalization may be measured by the 18° angle formed between the C-Si-C planes and the Si-Si vector.

The slight distortions from planar geometry found for **1** and **10** are consistent with theoretical calculations on $H_2Si{=}SiH_2$[36a] and $(CH_3)_2Si{=}Si(CH_3)_2$,[36b] which indicate that the potential energy surface is quite flat for both *anti*-pyramidalization and for twisting about the Si-Si axis. Therefore, the small differences in structure around the double bond for **1**, (*E*)-**2**, and **10** may reflect preferences due to packing in the crystal lattice, as well as relief of steric strain.

In (*E*)-**2**, the two phenyl rings are inclined at angles of 88° to the plane of the silicon and attached carbon atoms. In this conformation little conjugation can occur between the aromatic rings and the Si=Si double bond. In **1**, two of the aromatic rings, *cis* to each other, are similarly rotated

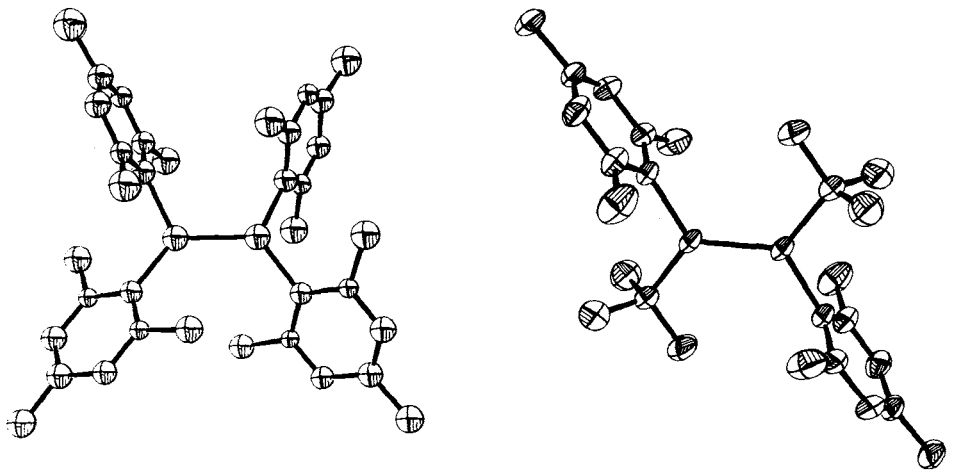

Fig. 3. ORTEP diagrams of X-ray crystal structures for tetramesityldisilene **1** (left) and (*E*)-1,2-di-*tert*-butyl(dimesityl)disilene (*E*)-**2** (right).

so that they are nearly orthogonal to the Si=Si double bond, but the other two rings are much more nearly coplanar with the mean plane of the silicon and attached carbon atoms so that conjugation with the Si=Si double bond is possible. In **10**, all of the aromatic rings are rotated relative to the respective C–Si–Si plane by 62–64°.

The conformations described are those present in the crystals, but of course other conformations are possible in solution. In fact, both the variable-temperature NMR spectra and the emission spectra of **1** suggest coexistence of more than one conformation.

6. Isomerism of Disilenes

6.1. *Z* and *E* Stereoisomers

The isolation of *Z* and *E* stereoisomers of disilenes has made possible studies of the rotational barrier at the silicon-silicon double bond, as well as permitted some beginning studies of reaction stereochemistry. Syntheses of disilenes sometimes produce mainly or exclusively one stereoisomer. For example, photolysis of the trisilane precursor **8** at −60°C produces the thermodynamically stable *E* isomer, (*E*)-**2**, which precipitates from solution almost isomerically pure. Irradiation of a solution of (*E*)-**2** at 350 nm converts it into a photostationary mixture of isomers (63:37 *E*:*Z*). When irradiation is ceased, interconversion of (*Z*)-**2** to (*E*)-**2** takes place slowly to give the equilibrium mixture of isomers (99:1 *E*:*Z*).[31]

For disilene **12**, irradiation of the trisilane precursor produces initially the *less* stable isomer (*Z*)-**12**, which can be crystallized from the photolysis solution in >97% isomeric purity. In solution (*Z*)-**12** slowly transforms to the equilibrium mixture (94:6 (*E*)-**12**:(*Z*)-**12**), from which the pure *E* isomer can be obtained by recrystallization.

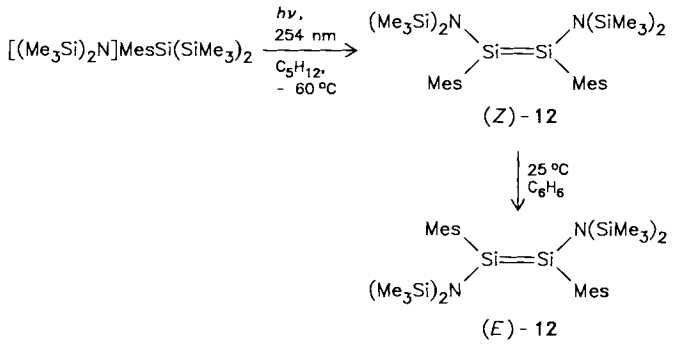

The *Z*/*E* interconversion of disilenes **2** and **12** has been followed using ^{1}H- and ^{29}Si-NMR spectroscopy. From rate measurements as a function of temperature, the rotational energy barriers E_A have been determined. For (*Z*)-**2**/(*E*)-**2**, the barrier is 131 kJ mol^{-1}.[31,35,36] It is of interest to compare this value with the corresponding barriers for C=C double bonds; however, rotational barriers for olefins depend greatly upon the substituent groups present. For DHC=CHD the barrier is 272 kJ mol^{-1}, but for some highly hindered olefins the value is even lower than that for **2**.[36] Perhaps a good molecule for comparison is (*Z*)-stilbene, for which E_A is 179 kJ mol^{-1}, about 30% greater than for (*Z*)-**2**.[37]

For (*Z*)-**12**, E_A for rotation is lower, 107 kJ mol^{-1}, perhaps because interactions of the nitrogen lone pair with the silicon π system reduce the Si–Si bond strength, or lower the energy of the transition state for rotation.[38] Additional data on rotational barriers in disilenes would clearly be desirable.

6.2. 1,2-Migration of Aryl Groups

The first disilene containing silicon atoms that are differently substituted, **13**, was recently synthesized. As shown in Equation (c), cophotolysis of two different trisilane precursors gave initially a 1:2:1 mixture of **1**, **13**, and **9**. It was surprising to find that the composition

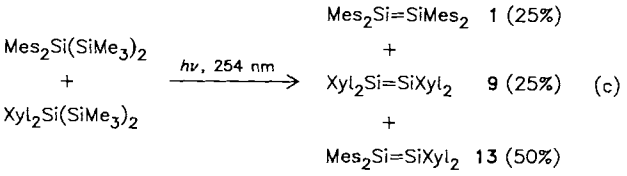

changed with time; **1** and **9** remained constant but the amount of **13** slowly decreased, being replaced by its isomer Mes(Xyl)Si=Si(Xyl)Mes, **14**. As shown in Equation (d), the *Z* isomer of **14** is formed first, but eventually isomerizes to give a *Z*/*E* mixture. At equilibrium, approximately equal amounts of **13**, (*Z*)-**14**, and (*E*)-**14** are present.[30]

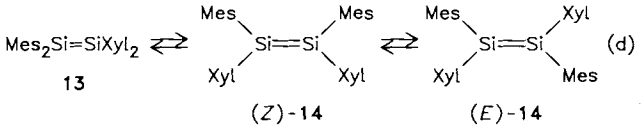

This unusual rearrangement appears to be dyotropic,[39] involving a concerted intramolecular migration of two σ-bonded aryl groups across the Si=Si double bond. Since 1,2-aryl migration is observed to be more rapid than *Z*/*E* interconversion, it must proceed through a different and lower-energy transition state. Presumably, similar rearrangements take place in all tetraaryldisilenes, but are unobservable except in special cases like **13** ⇌ (*Z*)-**14**. On the other hand, no such rearrangement occurs for **2** or **12**; apparently *t*Bu and $(Me_3Si)_2N$ groups do not undergo the 1,2-migration, at least under ordinary conditions.

7. Spectroscopy of Disilenes

7.1. UV/VIS Spectroscopy

The electronic absorption spectra for three disilenes are shown in Figure 4.[40] For (*E*)-**2**, which has no aryl groups in a position suitable for conjugation with the Si=Si bond, the lowest-energy absorption is found at 400 nm, identical to λ_{max} recorded for many tetraalkyldisilenes.[41] In the tetraaryldisilenes, where conjugation between aryl groups and Si=Si is possible, λ_{max} occurs near 420 nm, and in the

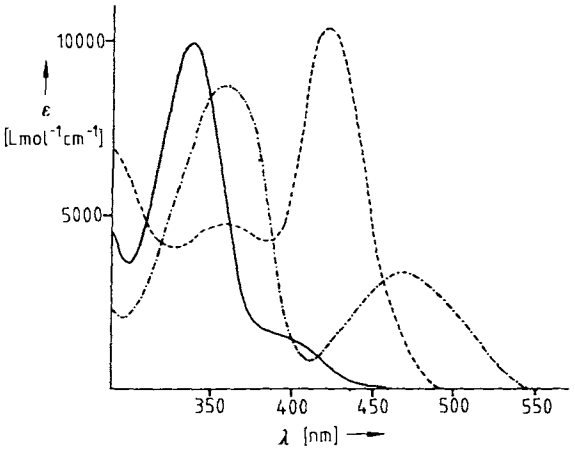

Fig. 4. Electronic absorption spectra for **1** (----), (*E*)-**2** (——), and (*E*)-**12** (—·—·—).

disilene isomers containing $(Me_3Si)_2N$ groups a much larger shift occurs to ca. 475 nm (Table 1).

The absorption and emission spectra of **1** have been investigated in somewhat greater detail.[33] At 77 K in a hydrocarbon glass, the additional absorptions shown in Figure 5 are found for **1**. Also displayed in Figure 5 are the

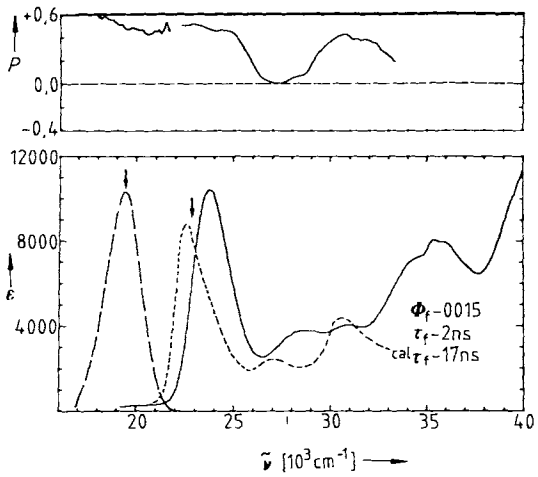

Fig. 5. Absorption (———), emission (— — —), and excitation (----) spectra for **1** in 3-methylpentane at 77 K. Above, polarization of the absorption and emission spectra.

emission and excitation spectra for **1**, as well as their polarizations. The identical value of 0.5 for the emission and excitation spectra indicates that a single electronic transition is involved. The curious feature of the spectra is that the excitation spectrum, although it follows the absorption spectrum closely, is shifted to longer wavelength. Moreover, the fluorescence lifetime of 2 ns is much shorter than the theoretical lifetime of 17 ns calculated from the integrated intensity of the long-wavelength absorption band. The likely explanation of these anomalies is that more than one conformer of **1** is present in solution; nonfluorescing conformer(s) are mainly responsible for the absorption spectrum, and the emission is due to a minor amount of a strongly fluorescent isomer. Similar effects have been observed for conformers of molecules related to stilbene.[42]

7.2. IR and Raman Spectroscopy

The vibrational spectra of disilenes have not been investigated in any detail, but resonance Raman experiments have established that lines at 539 cm^{-1} for **1** and at 525 cm^{-1} for (*Z*)-**2** are associated with Si=Si stretching vibrations.[43] These frequencies are about 30% higher than those for Si–Si single-bond stretching vibrations, consistent with increased Si–Si bond strength in the disilenes.

7.3. NMR Spectroscopy

^{29}Si-NMR spectra are particularly important in the characterization of disilenes. As seen in Table 1, ^{29}Si chemical shift values for disilenes are strongly deshielded, falling between $\delta = +49$ and $+95$. The ^{13}C chemical shift for olefins is similarly deshielded compared with that for alkanes. A study of the ^{29}Si-NMR spectrum of **1** in the solid state revealed a very large anisotropy of the ^{29}Si chemical shift tensor, due to the Si=Si π bond.[44] The ^{29}Si anisotropy for the corresponding disilane $Me_2HSiSiHMes_2$, lacking the π bond, is low. As shown in Table 2, similar effects are seen in the ^{13}C-NMR spectra of olefins versus alkanes.

Table 2. Principal values of chemical shift tensors.

Nucleus	Compound	σ_{11}	σ_{22}	σ_{33}
^{29}Si	$Mes_2Si{=}SiMes_2$	180	27	−15
^{29}Si	$Mes_2HSi{-}SiHMes_2$	−31	−56	−73
^{13}C	$H_2C{=}CH_2$	234	120	24
^{13}C	$H_3C{-}CH_3$	14	14	10

NMR coupling constants are also consistent with π-bonding in disilenes. The one-bond coupling constant, $^1J_{Si,Si}$, was recently measured as 155 Hz for **13**,[32] compared with ca. 85 Hz for typical aryldisilanes. The increase indicates much greater s character in the σ Si–Si bond in disilenes than in disilanes, consistent with approximate sp^2 hybridization of the Si atoms in the disilenes.[45]

^{1}H-NMR spectra of disilenes are normal at room temperature. For **1**[1] and **13**[25] splittings appear as the temperature is lowered, indicating the freezing-out of some motions and possibly also slow equilibration between conformers. Further study of the temperature dependence of the NMR spectra for disilenes seems warranted.

7.4. Cyclic Voltammetry and ESR Spectroscopy

The electrochemistry of several disilenes has recently been studied by cyclic voltammetry. In tetrahydrofuran, disilenes undergo irreversible one-electron oxidations and reductions; a typical voltammogram is shown in Figure 6, and half-wave potentials are listed in Table 3. As expected, both oxidation and reduction occur more easily than for alkenes.[46]

Radical anions or radical cations formed directly from disilenes have not been reported, but *Weidenbruch* et al. have published ESR spectra assigned to disilene radical anions obtained indirectly.[47] Reduction of tetra-*tert*-butyl-1,2-dichlorodisilane or the corresponding dibromo com-

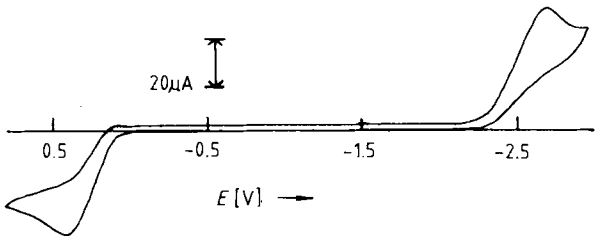

Fig. 6. Cyclic voltammogram for MesAdSi=SiAdMes **11**.

Table 3. Oxidation and reduction peak potentials for disilenes RR'Si=SiR'R.

R	R'	E^p_{red} [V] [a]	E^p_{ox} [V] [a]
Mes	Mes	−2.12	+0.38
2,6-Xyl	2,6-Xyl	−2.03	+0.47
Bdmp [b]	Bdmp [b]	−2.20	+0.48
Mes	*t*Bu	−2.67	+0.63
Mes	1-Ad	−2.64	+0.36

[a] Potentials are vs. standard calomel electrode. [b] 4-*tert*-butyl-2,6-dimethylphenyl.

pound with alkali metals gives an ESR signal assigned to the radical anion $[t\mathrm{Bu_2Si{=}Si}t\mathrm{Bu_2}]^{\odot\ominus}$. The main peak and ^{29}Si sidebands show hyperfine splitting corresponding to interaction with 36 equivalent protons, indicating delocalization of the unpaired electron over the entire molecule (Fig. 7). Similar reduction of 1,2-dichlorotetramesityldisi-

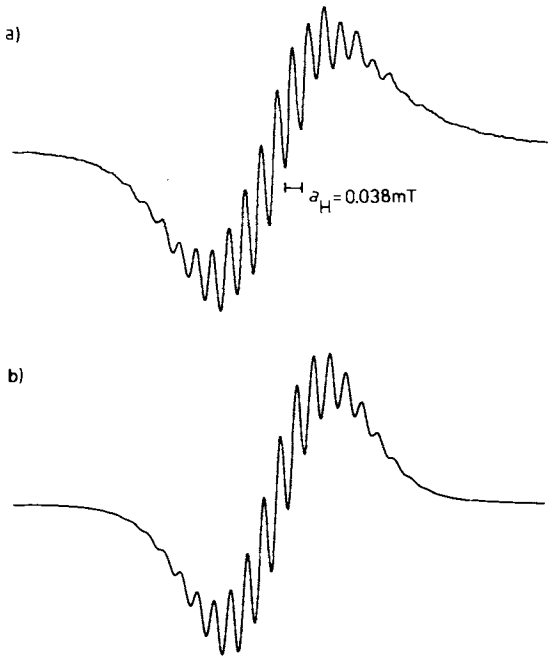

Fig. 7. a) Measured and b) simulated ESR spectrum of tetra-*tert*-butyldisilene radical anion.

lane gave eventually a single-line ESR spectrum attributed to $[\mathrm{Mes_2Si{=}SiMes_2}]^{\odot\ominus}$. For both of these radical anions, the intensity of the ^{29}Si sidebands indicated interaction of the unpaired electron with two silicon atoms. Alkali metal reduction of $t\mathrm{Bu_2ClSi{-}SiClMes_2}$ produced a signal with no hyperfine structure and coupling to only one silicon, explained as due to a localized radical anion, $[t\mathrm{Bu_2Si{=}SiMes_2}]^{\odot\ominus}$.[48]

Reduction of dichlorodisilanes photolytically in the presence of an electron-rich amine produced ESR signals assigned to the chloro-bridged neutral radicals [Eq. (e)].

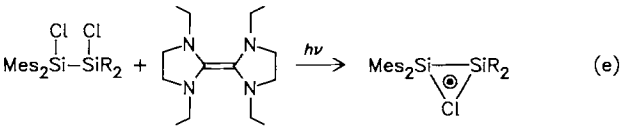

R = Mes, *t*Bu

8. Reactions of Disilenes

8.1. 1,2-Additions

Disilenes readily add hydrogen halides[34,49] and halogens,[27,49] just as olefins do. When these reactions were carried out with the stereoisomeric disilene (*E*)-**2**, HCl added to give a 2.5 : 1 mixture of *meso* and *R,S* diastereomers, indicating that Si–Si rotation takes place during the addition. Reaction with chlorine (in benzene), however, produced only one of the two possible stereoisomers, showing that no Si–Si rotation occurs [see Eq. (f)].[49] The

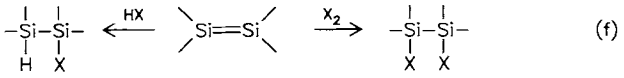

X = Cl, Br

results are consistent with a polar stepwise mechanism for addition of HCl, and a pathway involving a bridged radical or a chloronium ion for addition of Cl_2. However, further study of the mechanisms for these addition reactions is needed.

Addition of Cl_2 to **1** in alkanes takes a different course, producing $\mathrm{Mes_2HSi{-}SiClMes_2}$ as the major product along with products of free-radical chlorination of the alkane. Evidently the disilene catalyzes free-radical chlorination, and then reacts with the liberated HCl.

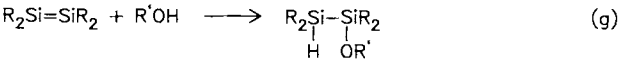

Unlike olefins, disilenes add OH compounds across the Si=Si bond, slowly at room temperature but rapidly at 60 °C [Eq. (g)].[29,34] Addition of alcohols to (*E*)-**2** produces a 1 : 1 mixture of stereoisomers, and so doubtlessly proceeds stepwise.[49] Additional 1,2-addition reactions reported for **1** include those with $n\mathrm{Bu_3SnH}$[49] and $LiAlH_4$ [Eq. (h)].

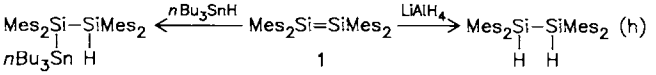

8.2. [2 + 2] Cycloadditions

Tetramesityldisilene reacts readily with aldehydes and ketones to give 1,2,3-oxadisiletanes [Eq. (i)].[28,34] As shown

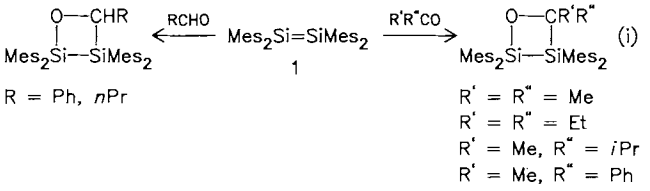

R = Ph, *n*Pr

R' = R'' = Me
R' = R'' = Et
R' = Me, R'' = *i*Pr
R' = Me, R'' = Ph

(i)

in Equation (j), photolysis of the 3-pentanone adduct of **1** in the presence of ethanol leads to cleavage products which suggest the intermediacy of silanone and silaethene species.[50]

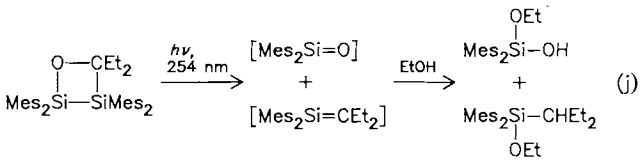

(j)

Tetra-*tert*-butyldisilene also adds to ketones to give 1,2,3-oxadisiletanes.[51] For the acetone and acetophenone adducts interesting further rearrangement reactions have been reported [Eq. (k)].

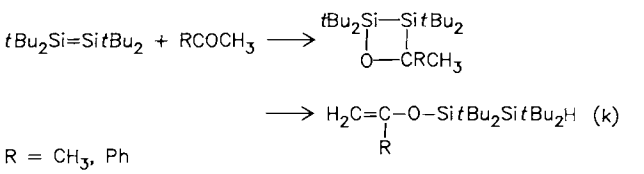

R = CH_3, Ph

(k)

Disilenes also undergo [2+2] cycloadditions with certain 1-alkynes [Eq. (l)].[49] Cycloaddition takes place slowly at room temperature and rapidly at 80°C in benzene. However, no reaction was observed between **1** and

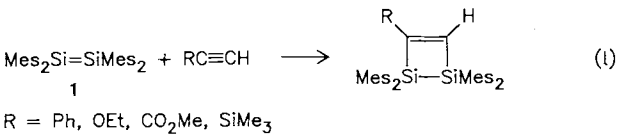

R = Ph, OEt, CO_2Me, $SiMe_3$

(l)

*n*BuC≡CH, $CH_3C{\equiv}CH$, PhC≡CPh, PhC≡CSiMe$_3$, or $MeO_2CC{\equiv}CCO_2Me$, even under forcing conditions. When phenylacetylene or ethynyl ethyl ether was added to (*E*)-**2**, the products were mixtures of equal amounts of diastereomers, indicating that the cycloaddition cannot be concerted.[52] An open-chain, diradical or dipolar intermediate seems likely.[53]

8.3. Other Cycloaddition Reactions

Diels–Alder cycloadditions between disilenes and 1,3-dienes have not been observed. In fact, with 1,3-cyclohexadiene, tetra-*tert*-butyldisilene is reported to react to give the [2+2] rather than the [2+4] cycloadduct.[51] However, both this disilene and **1**[28] react in a [2+4] fashion with benzil [Eq. (m)].

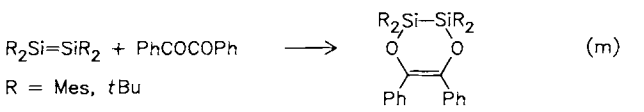

R = Mes, *t*Bu

(m)

One clear example of [2+3] cycloaddition is known. Disilene reacts with aryl azides to give triazadihydrodisiloles along with azadisiliranes [Eq. (n)].[54] These com-

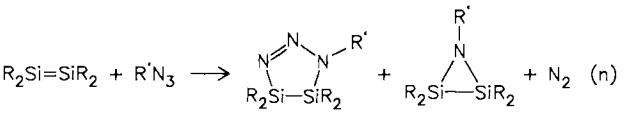

R' = Ph, Mes

(n)

pounds, like other silyl diazenes, are deeply colored.[55] As shown in Equation (o), the reaction of **9** with diazomethane may also proceed through a [2+3]-cycloaddition intermediate, **15**. The isolated product is the disilacyclopropane **16**, which can be oxidized with *m*-chloroperbenzoic acid (MCPA) to give the 1,2,3-oxadisiletane **17**.[56]

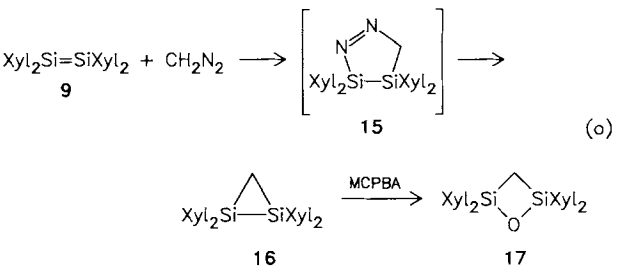

(o)

It is also possible that **16** arises from direct reaction of methylene with the Si=Si double bond. Recently, a [2+1] cycloaddition of a carbene-like molecule to a disilene was discovered. Reaction of **9** with 2,6-dimethylphenyl isocyanide yields the three-ring disilaketimine **18**, as a stable, bright red crystalline compound.[57]

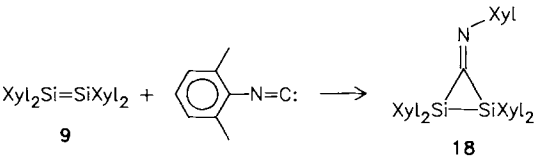

Reactions of disilenes with sulfur[58] or selenium, or with the single-oxygen transfer agents N_2O or azoxybenzene,[59] give three-membered rings containing two silicons and a chalcogen atom [Eq. (p)]. The structure of the sulfur com-

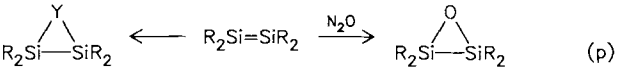

19a, Y = S
19b, Y = Se

(p)

pound, **19a**, has been determined by X-ray crystallography and is of unusual interest. The Si–Si bond is rather short (228.9 pm, compared with Si=Si 215, Si–Si 235 pm). Even more striking, the arrangement of the C, C, and Si atoms attached to each silicon is nearly planar, the sum of the bond angles at Si being 357.4°. The structure of disilacyclopropane **16** is similar, with Si–Si = 227.2 pm and angle sums between 357 and 358°. These features suggest that for both compounds, the σ-bond hybridization at silicon

may be better represented as sp^2 than sp^3, and that partial π-bonding may persist between the silicon atoms. In other words, in compounds **16** and **19** the bonding may be intermediate between a normal three-membered ring and a π-complex (Scheme 1).[60]

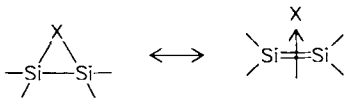

Scheme 1. X = CH_2, S, Se.

8.4. Metal Complexes of Disilenes

Olefin complexes of metals date back to the famous preparation of Zeiss' salt in 1827.[61] The first probable metal complex of a disilene was reported only in 1986.[62] At −70°C, **1** reacts with $Hg(OCOCF_3)_2$ to form a complex[26] observed by NMR and IR spectroscopy. The spectral data suggest a three-membered ring or π-complex structure for **21**. As shown in Equation (q), upon warming of the solution to room temperature, **21** decomposes to give a 1,2-bis(trifluoroacetoxy)disilane.

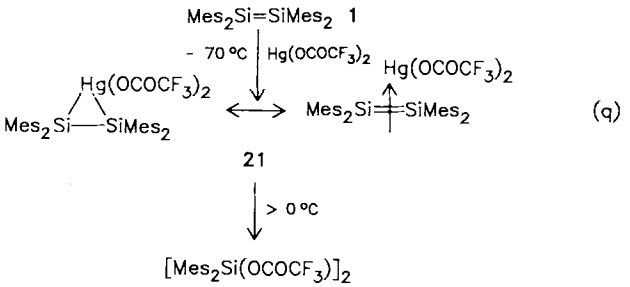

(q)

Very recently, metal complexes of **1** have been isolated at room temperature.[63] Photolysis of a bis(phosphane)platinum(II) oxalate in the presence of **1** produces an orange-yellow crystalline product, identified by its NMR and other spectroscopic properties as the disilene–platinum complex **22**. The same product is obtained by the reaction of ethylenebis(phosphane)platinum(0) with **1**. The characterization of **22** is provided by its reaction with ethanol, leading to the Pt–Si σ-bonded product **23** (Scheme 2).

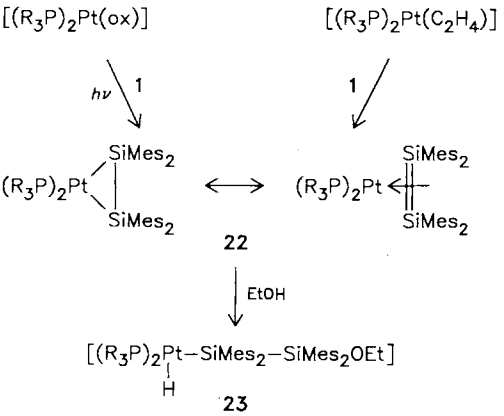

Scheme 2. R = Et, Ph; ox = oxalate.

8.5. Oxidation of Disilenes

Solid disilenes react with dioxygen of the air, rather rapidly for **1** and similar tetraaryldisilenes, but slowly for the more hindered disilenes **2** and especially **11**. The half-time for oxidation of **11**, exposed to the air, is many hours.[64] In all cases the principal products are the novel 1,3-cyclodisiloxanes[*] **26**.[34,65] Cyclic siloxanes are important materials of commerce, made in multiton quantities as intermediates in the silicone industry, but all previously known compounds have six-membered or larger rings.

In solution the oxidation reaction is more complex.[59] Initially two compounds are rapidly produced: A major (ca. 80%) amount of the 1,2-dioxetane **25**, and a minor quantity of the oxadisilirane **20**. The latter compound slowly undergoes further oxidation to the 1,3-cyclodisiloxane **26**, which is also produced by slow intramolecular rearrangement of **25**.[32,59] Both of the pathways to the end product **26** are stereospecific; oxidation of (*E*)-**2** gives, by either route, the *trans*-1,3-cyclodisiloxane.

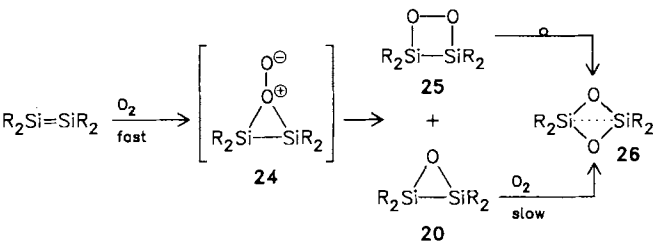

Although 1,2-dioxetanes in the carbon series are formed from (hindered) olefins and singlet oxygen, the analogous silicon compounds **25** are produced from disilenes with triplet oxygen. Spin-pairing must occur at some point in the latter case. The rearrangement of **25** to **26** is unparalleled in carbon chemistry; organic 1,2-dioxetanes instead undergo cleavage to give carbonyl compounds in a photoluminescent reaction.[66] Conversion of **25** to **26** does not go through the silanone ($R_2Si{=}O$) species as an intermediate, because the identical rearrangement takes place in ethanol (which would be expected to trap silanone $R_2Si{=}O$ rapidly). Since both **20** and **25** are formed simultaneously in the initial oxidation, it is possible that they arise from a common intermediate such as the perepoxide **24**.

X-ray crystal structures have not yet been determined for **20** or **25**, but structures are known for three 1,3-cyclodisiloxanes and these are of unusual interest.[67] An ORTEP diagram for the *trans*-1,3-di-*tert*-butyl-1,3-dimesityl compound is shown in Figure 8. Within the nearly planar four-membered rings, the Si–O–Si angles are quite small, ranging from about 86 to 91°. As shown in Figure 9, the effect is to bring the silicon atoms very close to one another. The most extreme case is the tetramesityl compound, in which the Si–Si distance of 230.6 pm is substantially shorter than the normal single bond distance of ca. 235 pm.

[*] According to IUPAC rules, 1,3-cyclodisiloxanes are named 1,3-dioxa-2,4-disiletanes. The trivial name is used in this article.

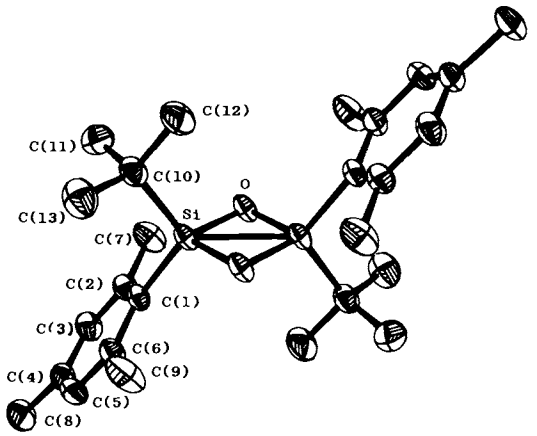

Fig. 8. ORTEP diagram of the X-ray crystal structure for *trans*-1,3-di-*tert*-butyl-1,3-dimesitylcyclodisiloxane.

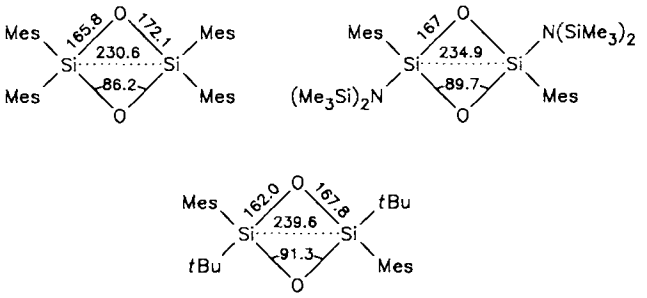

Fig. 9. Bond lengths [pm] and angles [°] in the central four-membered rings in 1,3-cyclodisiloxanes, **26**.

These remarkable structures raise serious questions concerning the chemical bonding in 1,3-cyclodisiloxanes. If there were actually a single covalent bond between the silicon atoms, the Si–O bonds would have to be partially electron-deficient. In fact the Si–O distances are slightly larger than normal siloxane bond lengths (161–165 pm). Another model would be that O–O lone-pair repulsions or other factors are dominant, determining the structure and forcing the silicon atoms close together without any Si–Si bonding.

Several theoretical papers have appeared on the structure and bonding in the (unknown) parent molecule, $(H_2SiO)_2$.[68–72] Most of these studies have concluded that there is no bonding between the silicons, but according to recent work by *Grev* and *Schaefer*,[72] the structure can also be accounted for in terms of an "unsupported pi-bond" with no σ component. The one item of evidence concerning the structure is the $J_{Si,Si}$ coupling constant determined recently in our laboratories for the 1,3-cyclodisiloxane $Mes_2Si(O)_2SiXyl_2$.[32] The observed coupling constant, 3.8 Hz, is about the same as the value of $^2J_{SiOSi}$ found for open-chain siloxanes (1–5 Hz). This result indicates that there is essentially no s-orbital component to the bonding between the silicon atoms in this cyclodisiloxane. It is therefore consistent with the model of *Grev* and *Schaefer* as well as with the other theoretical treatments which propose no bonding between the silicons.

9. Looking to the Future

Although significant progress has been made in the six years since the discovery of stable disilenes, much more remains to be done. The conformations of disilenes in solution are not understood, and the thermochromism of some disilenes is not yet explained. The structures and chemical bonding of many of the known reaction products of disilenes require further investigation. In addition, numerous potentially interesting reactions of disilenes remain to be tried, for example those with carbenes, carbanions, nitroso compounds, amines, imines, sulfoxides and sulfones, azo compounds, and various 1,3-dipolar reagents. Further reactions of the many new kinds of compounds made from disilenes have scarcely been looked at, and almost no work has yet been done on mechanisms of disilene reactions. The potentially large area of disilene–metal complexes has only just been opened up.

It seems clear that the chemistry of disilenes is just in its earliest stages, and that interesting new developments may be expected for many years to come.

Addendum

Since this article was written, several notable developments in disilene chemistry have been reported. The very stable compound tetrakis(2,4,6-triisopropylphenyl)disilene was obtained by the direct reaction of the corresponding dichloro compound with lithium naphthalenide.[73] The first stable tetra*alkyl*disilene, tetrakis[bis(trimethylsilyl)-methyl]disilene, was prepared by a similar lithium naphthalenide reduction of the dialkylsilyl diiodide.[74]

In addition, the crystal structure of oxadisilirane **20** has been determined; the structure resembles that of the sulfur compound **19a** but is even more extreme.[75] The Si–Si bond length is only 222.7 pm, and the arrangement of C, C, and Si atoms around each silicon is *coplanar*.

This work was supported by the Air Force Office of Scientific Research Air Force Systems Command, USAF, under contract No. F49620-86-0010 and by the National Science Foundation Grant No. CHE-8318820-02. I am most grateful to my able and industrious co-workers in our disilene investigations, to my collaborator Professor Josef Michl, now of the University of Texas at Austin, and to H. B. Yokelson for a critical reading of the manuscript.

Received: February 24, 1987 [A 646 IE]
German version: *Angew. Chem. 99* (1987) 1231

[1] F. S. Kipping, *Proc. R. Soc. 27* (1911) 143; *J. Chem Soc. 125* (1924) 2291; *Proc. R. Soc. 159* (1937) 139.
[2] For reviews see: A. H. Cowley, *Polyhydron 3* (1984) 389; A. H. Cowley, N. C. Norman, *Prog. Inorg. Chem. 34* (1986) 2.
[3] P. Jutzi, *Angew. Chem. 87* (1975) 269; *Angew. Chem. Int. Ed. Engl. 14* (1975) 232.
[4] L. E. Gusel'nikov, N. S. Nametkin, *Chem. Rev. 79* (1979) 529.
[5] M. Yoshifuji, I. Shima, N. Inamoto, K. Hirotsu, T. Higuchi, *J. Am. Chem. Soc. 103* (1981) 4587.
[6] A. G. Brook, F. Abdesaken, B. Gutekunst, G. Gutekunst, R. K. Kallury, *J. Chem. Soc. Chem. Commun. 1981*, 191.
[7] R. West, M. J. Fink, J. Michl, *Science (Washington) 214* (1981) 1343.
[8] A. H. Cowley, J. Lasch, N. C. Norman, M. Pakulski, *J. Am. Chem. Soc. 105* (1983) 5506.
[9] S. Collins, S. Murakami, J. T. Snow, S. Masamune, *Tetrahedron Lett. 26* (1986) 1281.
[10] N. Wiberg, K. Schurz, G. Fischer, *Angew. Chem. 97* (1985) 1058; *Angew. Chem. Int. Ed. Engl. 24* (1985) 1053.

[11] C. N. Smit, F. M. Lock, F. Bickelhaupt, *Tetrahedron Lett. 25* (1984) 3011.

[12] For earlier reviews on disilenes, see: a) R. West, *Pure Appl. Chem. 56* (1984) 163; b) R. West, M. J. Fink, M. J. Michalczyk, D. J. De Young, J. Michl in H. Sakurai (Ed.): *Organosilicon and Bioorganosilicon Chemistry*, Ellis Horwood, Chichester, England 1985, p. 3 ff; c) R. West, *Science (Washington) 225* (1984) 1109.

[13] Examples are a) tetraneopentyldisilene: H. Watanabe, T. Okawa, M. Kato, Y. Nagai, *J. Chem. Soc. Chem. Commun. 1983*, 781; b) tetrakis(1-ethylpropyl)disilene: S. Masamune, H. Tobita, S. Murakami, *J. Am. Chem. Soc. 105* (1983) 6524; c) tetra-*tert*-butyldisilene: A. Schäfer, M. Weidenbruch, S. Pohl, *J. Organomet. Chem. 282* (1985) 305; see also a [27] und [51].

[14] M. J. Michalczyk, M. J. Fink, D. J. De Young, C. W. Carlson, K. M. Welsh, R. West, J. Michl, *Silicon Germanium Tin Lead Compd. 9* (1986) 75.

[15] G. Raabe, J. Michl, *Chem. Rev. 85* (1985) 470.

[16] A. G. Brook, K. M. Baines, *Adv. Organomet. Chem. 24* (1985) 179.

[17] D. N. Roark, G. J. D. Peddle, *J. Am. Chem. Soc. 94* (1972) 5837.

[18] W. D. Wulff, W. F. Goure, T. J. Barton, *J. Am. Chem. Soc. 100* (1978) 6236, and references cited therein.

[19] R. T. Conlin, P. P. Gaspar, *J. Am. Chem. Soc. 98* (1982) 868; Y.-S. Chen, P. P. Gaspar, *Organometallics 1* (1982) 1410.

[20] H. Sakurai, Y. Nakadaira, T. Kobayashi, *J. Am. Chem. Soc. 101* (1979) 487; H. Sakurai, H. Sakaba, Y. Nakadaira, *ibid. 104* (1982) 6156.

[21] H. Sakurai, Y. Nakadaira, H. Sakaba, *Organometallics 3* (1984) 1484; H. Sakurai, K. Sakamoto, M. Kira, *Chem. Lett. 1984*, 1379.

[22] T. J. Drahnak, J. Michl, R. West, *J. Am. Chem. Soc. 103* (1981) 1845; C. A. Arrington, R. West, J. Michl, *ibid. 105* (1983) 6176; C. A. Arrington, K. A. Klingensmith, R. West, J. Michl, *ibid. 106* (1984) 525; G. Raabe, H. Vancik, R. West, J. Michl, *ibid. 108* (1986) 677.

[23] M. J. Fink, M. J. Michalczyk, K. J. Haller, J. Michl, R. West, *Organometallics 3* (1984) 793.

[24] R. West, G. R. Gillette, H. B. Yokelson, *Inorg. Synth.*, in press; G. R. Gillette, H. B. Yokelson, R. West, *Organomet. React. Synth.*, in press.

[25] S. Masamune, S. Murakami, J. T. Snow, H. Tobita, D. J. Williams, *Organometallics 3* (1984) 3330.

[26] S. Murakami, S. Collins, S. Masamune, *Tetrahedron Lett. 25* (1984) 2131.

[27] S. Masamune, Y. Hanazawa, S. Murakami, T. Bally, J. F. Blount, *J. Am. Chem. Soc. 104* (982) 1150.

[28] a) P Boudjouk, B.-H. Han, K. R. Anderson, *J. Am. Chem. Soc. 104* (1982) 4992; b) P. Boudjouk, *Nachr. Chem. Tech. Lab. 31* (1983) 798.

[29] S. Masamune, S. Murakami, H. Tobita, *Organometallics 2* (1983) 1464.

[30] H. B. Yokelson, J. Maxka, D. A. Siegel, R. West, *J. Am. Chem. Soc. 108* (1986) 4239.

[31] M. J. Michalczyk, R. West, J. Michl, *Organometallics 4* (1985) 826.

[32] H. B. Yokelson, A. Millevolte, B. Adams, R. West, *J. Am. Chem. Soc. 109* (1987) 4116.

[33] M. J. Fink, R. West, J. W. Downing, H. J. Dewey, G. Radziszewski, J. Michl, unpublished work.

[34] M. J. Fink, D. J. De Young, R. West, J. Michl, *J. Am. Chem. Soc. 105* (1983) 1070.

[35] A lower value is reported in Ref. [25], but may be less accurate since it is based on rate measurements at only two temperatures.

[36] a) The rotational barrier for PhMeSi=SiMePh has been estimated from the rate of stereoisomerization of the thermally generated disilenes as > 108 kJ mol^{-1}. See G. Olbrich, P. Potzinger, B. Reimann, R. Waslh, *Organometallics 3* (1984) 1267; b) K. Krogh-Jespersen, *J. Am. Chem. Soc. 107* (1985) 537.

[37] H.-O. Kalinowski, H. Kessler, *Top. Stereochem. 7* (1973) 300.

[38] Since solvent polarity has little effect on the rate, a nonpolar transition state is implied. From the normal values for the preexponential factors, it is unlikely that a triplet state is involved in the isomerization.

[39] M. Reetz, *Adv. Organomet. Chem. 16* (1977) 33.

[40] M. J. Michalczyk, R. West, J. Michl, *J. Am. Chem. Soc. 106* (1984) 821.

[41] H. Watanabe, Y. Kougo, M. Kato, H. Kuwabara, T. Okawa, Y. Nagai, *Bull. Chem. Soc. Jpn. 57* (1984) 3019.

[42] E. Fischer, *J. Photochem. 17* (1981) 331.

[43] M. J. Fink, R. West, J. W. Downing, H. J. Dewey, J. G. Radisewski, J. Michl, unpublished results.

[44] K. W. Zilm, M. J. Fink, D. M. Grant, R. West, J. Michl, *Organometallics 2* (1983) 193.

[45] a) The values for $^1J(^{29}Si,^{13}C)$ in tetraaryldisilenes are also large (90 Hz, compared with about 50 Hz for alkylsilanes), consistent with sp^2 hybridization at silicon in the disilenes: for a discussion see Ref. [12a]; b) For theoretical calculations of $^1J(^{29}Si,^{29}Si)$ in disilenes see G. Fronzoni, V. Galasso, *Chem. Phys. 103* (1986) 29.

[46] B. Shepherd, R. West, *Chem. Lett.*, in press.

[47] M. Weidenbruch, K. Kramer, A. Schäfer, J. K. Blum, *Chem. Ber. 118* (1985) 107.

[48] M. Weidenbruch, K. Kramer, K. Peters, H. G. von Schnering, *Z. Naturforsch. B 40* (1985) 601.

[49] D. J. De Young, M. J. Fink, J. Michl, R. West, *Main Group Met. Chem., 1* (1987) 19.

[50] D. J. De Young, R. Winslow, R. West, unpublished results.

[51] See Ref. [13c]; M. Weidenbruch, A. Schäfer, K. L. Thom, *Z. Naturforsch. B 38* (1983) 1695.

[52] D. J. De Young, R. West, *Chem. Lett. 1986*, 883.

[53] Y. Nakadaira, R. Sato, H. Sakurai, *Chem. Lett. 1985*, 643.

[54] G. R.Gillette, R. West, presented at the 19th Organosilicon Symposium, Baton Rouge, LA, USA, April 26–27, 1985.

[55] N. Wiberg, *Adv. Organomet. Chem. 24* (1985) 179.

[56] S. Masamune, S. Murakami, H. Tobita, *J. Am. Chem. Soc. 105* (1983) 7776.

[57] H. B. Yokelson, A. J. Millevolte, K. J. Haller, R. West, *J. Chem. Soc. Chem. Commun.*, in press.

[58] R. West, D. J. De Young, K. J. Haller, *J. Am. Chem. Soc. 107* (1985) 4942.

[59] H. B. Yokelson, A. J. Millevolte, G. R. Gillette, R. West, *J. Am. Chem. Soc.*, in press.

[60] For an exeptionally lucid discussion of bonding in three-membered rings, see D. Cremer, E. Kraka, *J. A. Chem. Soc. 107* (1985) 3800.

[61] W. C. Zeise, *Poggendorfs Ann. Phys. Chem. 9* (1827) 632.

[62] C. Zybill, R. West, *J. Chem. Soc. Chem. Commun. 1986*, 857.

[63] E. K. Pham, R. West, unpublished results.

[64] B. Shepherd, R. West, unpublished results.

[65] M. J. Michalczyk, R. West, J. Michl, *J. Chem. Soc., Chem. Commun. 1984*, 1525.

[66] K. P. Kopecky, J. E. Filby, C. Mumford, P. A. Lockwood, J.-Y. Ding, *Can. J. Chem. 53* (1975) 1103.

[67] M. J. Michalczyk, M. J. Fink, K. J. Haller, R. West, J. Michl, *Organometallics 5* (1986) 531.

[68] M. O'Keefe, G. V. Gibbs, *J. Chem. Phys. 81* (1984) 876; *84* (1985) 4574.

[69] S. M. Bachrach, A. Streitweiser Jr., *J. Am. Chem. Soc. 107* (1985) 1186.

[70] T. Kudo, S. Nagase, *J. Am. Chem. Soc. 107* (1985) 2589.

[71] R. J. Brenstein, S. Scheiner, *Int. J. Quantum Chem. 29* (1985) 1191.

[72] R. S. Grev, H. F. Schaefer III, *J. Am. Chem. Soc.*, in press.

[73] H. Watanabe, K. Takeuchi, N. Fukawa, M. Kato, M. Goto, Y. Nagai, *Chem. Lett. 1987* 1341.

[74] S. Masamune, Y. Eriyama, T. Kawase, *Angew. Chem. 99* (1987) 601; *Angew. Chem. Int. Ed. Engl. 26* (1987) 584.

[75] H. B. Yokelson, A. J. Millevolte, G. R. Gillette, R. West, *J. Am. Chem. Soc.*, in press.

Modern NMR Spectroscopy of Organolithium Compounds

By Harald Günther,* Detlef Moskau, Peter Bast, and Dietmar Schmalz

Dedicated to Professor Emanuel Vogel on the occasion of his 60th birthday

Modern methods of NMR spectroscopy, in particular the two-dimensional techniques, offer new chances for structure determinations in the field of organolithium compounds, where the combination of ^{1}H-, ^{13}C-, and $^{6(7)}Li$-NMR spectroscopy is an especially useful feature. Chemical shift correlations which also include the lithium nuclei allow a complete assignment of the ^{1}H-, ^{13}C-, and ^{6}Li-NMR spectra and thereby a better characterization of the various aggregates and complexes present in solution. Spatial proximities of ^{6}Li and ^{1}H can be detected by nuclear Overhauser experiments, and $^{6(7)}Li$-NMR exchange spectroscopy can provide new information with regard to the mechanisms and energetics of dynamic processes like aggregate interchange and complexation. After a short resumé of the experimental aspects of the NMR spectroscopy of organolithium compounds and a discussion of the NMR parameters of these systems, new experimental techniques are presented. Areas of application of these newly conceived one- and two-dimensional NMR experiments are illustrated with selected examples. The results show that even more detailed information about the structure and reactivity of organolithium compounds, which are so important for organic synthesis, can be expected in the future.

1. Introduction

In the last ten years a large number of new experimental techniques have been developed for nuclear magnetic resonance spectroscopy, the most important of which already belong to the standard repertoire of NMR investigations of molecular structure.[1] Structure determinations of dissolved organolithium compounds, which are valuable reagents for organic synthesis,[2] also profit from this development. Numerous X-ray structure investigations performed in recent years have shown that this class of compounds presents a fascinating variety of structures in the solid state.[3] The same is true even more in solution, where organolithium compounds of the type RLi usually do not exist as monomers but rather form oligomeric aggregates $(RLi)_n$. Association in hydrocarbon solvents leads to dimers, tetramers, hexamers, and even nonamers, which very often coexist in fast, reversible equilibria (Fig. 1). In basic solvents like ethers or upon the addition of complex-forming amines like tetramethylethylenediamine (TMEDA) oligomerization is repressed in favor of complex formation with the solvent or the amine. Much more complicated situations can be expected for polylithium compounds, where research on structures is only at its beginning.[4]

The reactivity of dissolved organolithium compounds[2c] also varies with the structure, consequently a knowledge of the structure is very important for planning synthetic strategies. NMR spectroscopy, as the most important physical method for the determination of molecular structures in solution, has therefore long occupied a dominating position in this field,[5] all the more so because various nuclei can be employed as probes. Besides the well-known nuclides ^{1}H and ^{13}C, which are used for the characterization of the organic ligands, two additional attractive magnetic nuclei are available with the isotopes ^{6}Li and ^{7}Li. Despite their quadrupole moment, both are well suited for NMR measurements.[6] Because of the above mentioned equilibrium reactions between aggregates, the dynamic NMR spectroscopy of organolithium compounds is likewise of great importance, since temperature-dependent NMR spectra enable the elucidation of the exchange mechanisms as well as the determination of the thermodynamic and kinetic parameters of the equilibria.

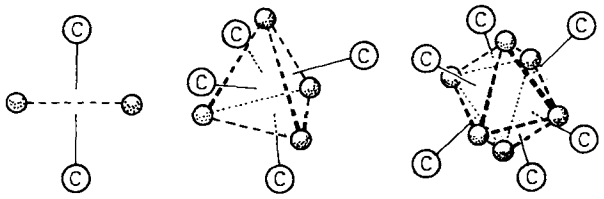

Fig. 1. Schematic representation of the structures of dimeric, tetrameric, and hexameric aggregates of organolithium compounds $(RLi)_n$ in solution [5].

Two-dimensional NMR spectroscopy (2D-NMR) will undoubtedly have a significant impact on further progress in the fields mentioned above. Thus, on the one hand, the ^{1}H- and ^{13}C-NMR spectra of the ligands may be assigned more precisely with the help of homo- and heteronuclear shift correlations, and, on the other, polarization transfer and multiple quantum spectroscopy enable the development of new measuring techniques incorporating the lithium isotopes. The detection of nuclear Overhauser effects between ^{6}Li and neighboring protons provides a new approach for the measurement of Li–H distances in solution and thus allows conclusions to be drawn about the regioselectivity during second metalation reactions. Finally,

[*] Prof. Dr. H. Günther, Dr. D. Moskau, Dipl.-Biol. P. Bast, Dipl.-Chem. D. Schmalz
Fachbereich 8, Organische Chemie II der Universität Gesamthochschule Postfach 10 12 40, D-5900 Siegen (FRG)

two-dimensional exchange spectroscopy should gain importance for the study of the dynamic processes of solute organolithium compounds. This progress report outlines and critically evaluates the potential of these new experimental techniques. Technical aspects are emphasized and a number of experiments are described for the first time.

2. Nuclear Properties

Table 1 lists the nuclear properties of the nuclides ^1H, ^{13}C, ^6Li and ^7Li which are most important for NMR spectroscopy. Those of ^1H and ^{13}C are well-known and serve here only for comparision.

Table 1. Nuclear properties of the lithium isotopes ^6Li and ^7Li in comparision to ^1H and ^{13}C [a].

Nucleus	N [%]	Spin I	γ	Q	ν_0	R (^{13}C)
^6Li	7.42	1	3.9366	-8×10^{-4}	14.72	3.58
^7Li	92.58	3/2	10.396	-4.5×10^{-2}	38.86	1.54×10^3
^1H	99.985	1/2	26.751	—	100.00	5.68×10^3
^{13}C	1.108	1/2	6.7263	—	25.15	1.00

[a] Abbreviations and symbols: N = natural abundance; γ = gyromagnetic ratio in 10^7 rad T^{-1} s^{-1}; Q = quadrupole moment in 10^{-28} m^2; ν_0 resonance frequency (MHz) at field strength B_0 of 2.35 T; $R(^{13}C)$ = signal strength (receptivity), $\gamma^3 N I(N+1)$, rel. to ^{13}C.

Both lithium nuclei have a nuclear spin $I > 1/2$ and therefore a quadrupole moment, which in the case of the isotope ^6Li, however, is so small that this nucleus behaves nearly like a spin-1/2 nucleus and thus is well suited for NMR investigations on organolithium compounds.[7] Line broadening, a disturbing feature often found in the case of nuclei with $I > 1/2$ because of fast quadrupole relaxation, is rarely observed in ^6Li-NMR spectra, and is also always within reasonable limits in ^7Li-NMR spectra. The resonance signals of both nuclei can easily be measured; however, scalar spin-spin couplings J to neighboring nuclei are usually better resolved in the case of ^6Li. This is especially true for low-temperature measurements, which are indispensable for investigations dealing with the dynamics of solute organolithium compounds, because faster ^7Li quadrupole relaxation leads to line broadening and thereby masks line splittings.[8] Thus, it is only ^6Li-labeling which in general paves the way for the measurement of the important structural parameter $^1J(C,Li)$, as the pioneering work of *Fraenkel* et al.[9] and *Seebach* et al.[10] has shown. If high sensitivity is important, additional ^{13}C-labeling is advisable, which then provides optimal NMR conditions for the spin system in question. Since ^6Li labeling can be achieved relatively easily—in the majority of the synthetic routes metallic lithium is used directly or indirectly through a practicable lithium reagent like *n*-butyllithium[2a]—and since this isotope is easily obtainable,[11] the reduced receptivity[6a] of ^6Li as compared to ^7Li presents no problems for the NMR experiment. Furthermore, ^6Li has the advantage that its resonance frequency is close to that of the deuteron (58.86 as compared to 61.40 MHz at a magnetic field strength of 9.4 T), so that with many spectrometers the ^2H-lock channel can be used for ^6Li-NMR experiments, as for instance $^{13}C\{^6Li\}$ decoupling.

2.1. Spin Lattice Relaxation Mechanisms

Because of its small quadrupole moment, other mechanisms besides the mechanism of quadrupole relaxation must contribute to a considerable extent to the spin lattice relaxation of ^6Li. This was first shown by *Wehrli*,[7] who found up to 35% dipolar relaxation through ^6Li-^1H interactions in the case of alkyllithium compounds and who was able to measure $^6Li\{^1H\}$ nuclear Overhauser effects (NOEs) for the first time. NOE measurements provide a valuable supplement to structural information obtained through spin-spin couplings. ^7Li relaxes almost completely via the quadrupole mechanism and exhibits much shorter spin lattice relaxation times T_1 than ^6Li, for which values of 125 s are possible[12] even in organolithium compounds. In case of solvated $^6Li^{\oplus}$ ions T_1 values of up to 1000 s have been measured![13] Therefore, for the determination of the 90° excitation pulse length, which is indispensible in FT-NMR spectroscopy, the steady-state method[14] is suitable in the case of ^6Li because it allows high repetition rates despite long T_1 values. The different contributions of ^6Li and ^7Li to the spin lattice relaxation of neighboring nuclei also provide a means for the determination of Li-C and Li-H distances in aggregates of solute organolithium compounds through the use of the isotopic substitution method,[16] as has been shown by *Jackman* et al. for phenyllithium.[15] If one replaces a nucleus ^nX (spin quantum number I) with strong dipole-dipole interaction by its isotope ^mX (spin quantum number S) with weak dipole-dipole interaction, the difference in the spin lattice relaxation rate R_1 of the neighboring ^{13}C nucleus is given by

$$R_1^{exp}(^nX) - R_1^{exp}(^mX) = R_1^{DD}(^nX)\left[1 - \frac{\gamma_{^mX}^2\, S(S+1)}{\gamma_{^nX}^2\, I(I+1)}\right] \qquad (a)$$

If the correlation time τ_c is known, the distance $r_{C\text{-}X}$ can be determined according to

$$r_{C\text{-}X} = \sqrt[6]{\hbar^2 \gamma_{^{13}C}^2 \gamma_{^nX}^2 \tau_c / R_1^{DD}(^nX)} \qquad (b)$$

τ_c is obtained from the dipolar relaxation rate R_1^{DD} of another ^{13}C nucleus in the same molecule measured under identical conditions and its respective C-H distance.

2.2. Chemical Shifts

The chemical shifts of the lithium nuclides have thus far been the subject of very few investigations. Calculations[17] and measurements on aryllithium compounds[18] have shown that the diamagnetic anisotropy effect of the organic ligands strongly influences the ^7Li resonance frequency in these systems. Since the chemical shift range is extremely small (ca. 2–3 ppm, i.e. ca. 65 Hz for ^6Li and ca. 120 Hz for ^7Li at 2.35 T according to Table 1) and since the resonance frequencies strongly depend on the medium and concentration effects owing to aggregate formation, chemical shifts are not very informative for structure investigations on organolithium compounds. Furthermore, measurements are usually made with external references, and, in addition, various reference compounds are used, thus causing further uncertainties. Nevertheless, a diamagnetic

ring current effect has been detected for the ^{6}Li resonance of lithium salts of charged π-electron systems.[19] In these cases the ^{7}Li shift can also be used for the study of ion pair structures.[20] The ^{1}H and ^{13}C shifts in the organic groups follow the well-known trends, where the charge density plays no major role in the case of aryllithium compounds RLi. Much more important are the anisotropy of the C–Li bond (for ^{1}H)[21] and the local paramagnetism caused by n→π* transitions (for ^{13}C).[22] Typically, the situation for phenyllithium is similar to that in pyridine.[23]

The ^{13}C resonance frequencies of alkyllithium compounds RLi have recently been analyzed in more detail.[24] Compared to the data for the corresponding hydrocarbons RH, low-field shifts of 5.3 ± 0.7 and 7.7 ± 0.5 ppm have been observed for the β- and γ-carbon atoms, respectively. Steric interactions in branched alkyl groups diminish the γ-effect and can even give rise to high-field shifts. The resonance of the δ-carbon atom is not influenced by the metalation, while the effects on the α-carbon atom vary strongly. For primary alkyl groups a shielding of 5.9 ± 0.9 ppm was found which increases on α branching, i.e. in the case of secondary and tertiary alkyllithium compounds. For secondary systems a relationship between $\delta(^{13}C_\alpha)$ and the degree of aggregation was found: the shielding is larger for tetramers than for hexamers.

2.3. Scalar Spin–Spin Coupling

The measurement of ^{13}C,$^{6(7)}$Li coupling constants[25] and the determination of ^{13}C-NMR signal multiplicities has in recent years considerably increased our knowledge of the structure of solute organolithium compounds.[9,10,26] An overview of the rules which have been established, based on the data collection published by *Seebach* et al.,[10a] is presented in Table 2. The values for the $^1J(^{13}C,^6Li)$ coupling constant range from 2 to 18 Hz, whereby the smaller values are a consequence of exchange processes within individual aggregates which are still fast on the NMR time scale even at low temperature. Under these conditions, on time average, each ^{13}C nucleus has contact with all lithium atoms of the aggregate in question so that the coupling with the ^{6}Li nuclei is averaged effectively over all positions. The magnitude of the ^{13}C,^{6}Li coupling constants measured and the multiplicity of the ^{13}C signal are directly related to the degree of aggregation, *n*.[10a] For such dynamic systems the empirical rule $|J| \approx 18/n$ holds true. In the case of fast exchange between different aggregates the line splitting disappears. At room temperature the $^{6(7)}$Li-NMR spectra of organolithium compounds therefore typically show a singlet, because the chemical shifts are averaged as well. "Static" spectra are obtained, on the other hand, if the exchange rates are so small that ^{13}C,$^{6(7)}$Li coupling is limited to next neighbors within one aggregate.

Scalar couplings to ^{7}Li are, according to the relation $\gamma(^7Li)/\gamma(^6Li)$, larger by a factor of 2.64 than coupling to ^{6}Li. Besides coupling to ^{13}C scalar interactions of the lithium nuclides with other nuclei have also been demonstrated; thus, for instance, $^1J(^7Li,^{31}P)$ (39–40 Hz),[27,28] $^1J(^{6(7)}Li,^{29}Si)$ (20–29, 51 Hz),[29] and for highly diluted solutions (0.01 M) of the complex **1**

$(C_5(CH_3)_5)IrHLi$-PMDETA **1**
PMDETA = pentamethyldiethylenetriamine

in the temperature range between 20 and −40°C even $J(^7Li,^1H)$ (8.4 Hz).[30]

3. Applications of New Measuring Techniques

For the NMR spectroscopy of the organic ligands in organolithium compounds the entire arsenal of one and two-dimensional pulse techniques[1] available for ^{1}H- and ^{13}C-NMR spectroscopy can be employed. This has already been demonstrated in a few cases for the important homo- and heteronuclear shift correlations.[31,32] Absolute assignments of ^{13}C resonances are obtained most reliably through the two-dimensional INADEQUATE experiment,[33] which, however, because of its insensitivity—the ^{13}C satellites in the ^{13}C NMR spectrum are detected—requires concentrated samples. The experiment fails if the relative chemical shift between neighboring ^{13}C resonances falls below a critical value which depends on the field strength and the resolution obtained.[33] In the case of organolithium compounds a further limit must be seen in the fact that it is difficult or even impossible to detect the

Table 2. Compilation of $^{13}C,^6Li_x$ spin systems for aggregates of organolithium compounds of the type $(RLi)_n$ with characteristic data for the dependence of the $^1J(^{13}C,^6Li)$ coupling constants on the degree of aggregation *n* (*n*-propyllithium [36, 26d], *tert*-butyllithium [70a], phenyllithium [10], trichloromethyllithium [10]).

Aggregate	$(RLi)_9$		$(RLi)_8$		$R(Li)_6$		$(RLi)_4$		$(RLi)_2$	RLi
Structure									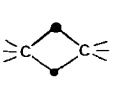	
State	dynamic [a]	static [a]	dynamic	static	dynamic	static	dynamic	static	static	static
x	9	?	8	?	6	3	4	3	2	1
^{13}C-Multiplicity	19	—	17	—	13	7	9	7	5	3
J [Hz]	2.2	—	2.5	—	3.3	—				
n-C_3H_7–Li							4.1	5.4		
t-C_4H_9–Li									8.0	
C_6H_5–Li										17.0
Cl_3C–Li										

[a] "Dynamic" implies interaction with all lithium atoms of the aggregate in the fast exchange region; "static" implies selective interactions with a reduced number of lithium atoms in the sense of a multicenter bond. The ^{13}C-multiplicity is given by $2x+1$ (x = number of lithium nuclei); for ^{7}Li by $3x+1$.

resonance of the metalated carbon atom which is broadened because of coupling to ^{6}Li,^{7}Li. If the assignment of this carbon is uncertain, the experiment should be repeated with ^{7}Li decoupling or, in the case of ^{6}Li-labeled samples, with ^{6}Li decoupling. The scope and the limits of the INADEQUATE method are demonstrated in Figure 2 with the ^{13}C-NMR spectrum of the 1-naphthyllithium-TMEDA complex.[34]

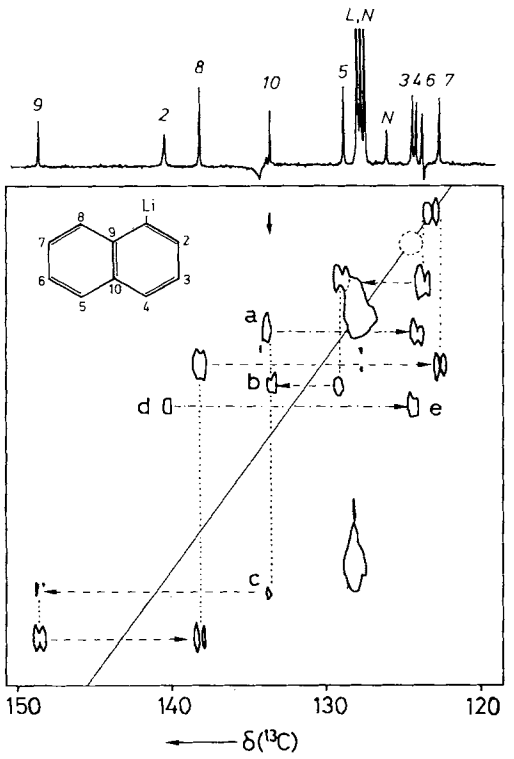

Fig. 2. Two-dimensional INADEQUATE-experiment [33] for 1-naphthyllithium-TMEDA in the region of the resonances of C-2 to C-10 (contour diagram; measuring frequency 100.61 MHz; reference TMS; ca. 1 M in C_6D_6 total experimental time 37 h; additional signals N = naphthalene, L = solvent). The resonances at $\delta = 148.6$ and 133.7 have been identified as those of quaternary carbons by a DEPT-experiment [35]. The assignment starts at C-10, since only this carbon can show three correlation signals with direct neighbors (a, b, c). The C,C connection proceeds from signal c via C-9 as the only quarternary neighbor to C-4. It is then interrupted, because the strongly coupled AB-system of C-3 and C-4 ($\Delta\delta$ 24.3 Hz, $J \approx 60$ Hz), degenerated to a singulet, cannot be detected [33]. The remaining pair of signals d, e must belong to C-2 and C-3 and the absolute assignment follows from the fact that only the signal at $\delta = 124.39$ can yield a strongly coupled AB system (B part at $\delta = 124.15$). The results of this experiment are in agreement with the results of a combined ^{1}H- and ^{13}C,^{1}H-shift correlation [31].

In the following we deal with experimental techniques which have been developed on the basis of the new pulse methods especially for the spectroscopy of the metalated carbon atom and the metal, that is for the spin systems ^{13}C,^{6}Li and ^{13}C,^{7}Li. Because of the far more favorable NMR properties of ^{6}Li the system ^{13}C,^{6}Li stands to the fore.

3.1. Multiplicity Selection and *J,δ* Spectroscopy

The signal multiplicity of scalar coupled $^{13}C_yLi_x$ spin systems can be determined best in the ^{13}C-NMR spectrum (determination of x) for ^{6}Li labeled compounds. If y is also to be determined, the ^{13}C satellite signals in the ^{6}Li-NMR spectrum have to be detected. This measurement is facilitated by ^{13}C labeling of the metalated position. In general, for aggregates of organolithium compounds with labeled α-carbon atom $y = 1$, since spin-spin coupling between individual organic groups in the aggregate is absent. In this case, therefore, the simple first order multiplet patterns for spectra of the $^{13}C^6Li_x$ type are observed for the ^{13}C resonances (Table 2). This situation is met with aggregates of monolithium compounds of type $(RLi)_n$, where the labeled carbon atom on time average can have contact with up to nine lithium atoms.[36] In the case of static spectra one finds coordination with up to three ^{6}Li nuclei. On the other hand, more complicated signal patterns result if different lithium neighbors are present, a situation encountered in the case of polylithium compounds (see Section 2.3). In contrast, in the ^{6}Li-NMR spectrum simple multiplets can always be expected, because homonuclear ^{6}Li,^{6}Li couplings are negligibly small (see Section 2.2) and the metalated carbon atoms have no homonuclear coupling partner if, as is usual, only this position in the molecule is ^{13}C-labeled.

For the recognition of spin multiplets the *J*-modulated spin echo techniques (attached proton test[37]) have proven of value in the case of ^{13}C-NMR spectroscopy. They yield for CX_n groups (X = spin-1/2 nucleus) signal phases of -1 (CH), $+1$ (CH_2), and -1 (CH_3). Through gated ^{13}C-decoupling a similar phase selection can be achieved for ^{6}Li signals which are coupled to ^{13}C, as is shown in Figure 3a with two signals from the ^{6}Li-NMR spectrum of dilithio(phenylsulfonyl)trimethylsilylmethane (**2**).[38]

$C_6H_5-SO_2-CLi_2-Si(CH_3)_3$ **2**

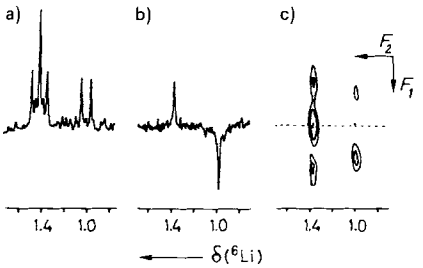

Fig. 3. a) Triplet ($J = 4.1$ Hz) and doublet ($J = 5.6$ Hz) for a $^{13}C_2{}^6Li$- and a $^{13}C^6Li$-spin system in the 58.86-MHz ^{6}Li-NMR spectrum of ^{6}Li- and ^{13}C-labeled dilithio(phenylsulfonyl)trimethylsilylmethane (**2**) (measuring frequency 58.86 MHz; ext. ref. 1 M LiBr/[D_8]THF). b) Phase selection with the technique of gated ^{13}C-decoupling (measuring time 1 h). c) Two-dimensional $^1J(^{13}C,^6Li)$-resolved ^{6}Li-NMR spectrum (measuring time 5.7 h).

If the ^{13}C,^{6}Li-coupling constants over one bond differ strongly, several experiments are necessary for optimal phase selection. If one carries out a two-dimensional *J,δ*-NMR experiment,[39] the $^1J(^{13}C,^6Li)$-resolved ^{6}Li-NMR spectrum shown in Figure 3c is obtained.

Phase selection in the ^{13}C-NMR spectrum through gated ^{6}Li decoupling corresponds to the spin echo methods developed for ^{13}C,^{2}H spin systems,[40] whereby the intensities of the CX_n signals (X = spin-1 nucleus) with an evolution time $t_1 = 1/2J$ are given by Equation (c):[40c]

$$I = I_0(-1/3)^n \qquad (c)$$

For practical applications this procedure is less well suited, since the signal intensity is strongly reduced already for $n=3$ and the ^{13}C signal disappears practically completely for $n>3$.

Besides the determination of multiplicity the two-dimensional J,δ spectroscopy allows a simplification of complicated spectra, because coupling to other nuclei only appears in the F_2 dimension.[41] In this way the $^{31}P,^{6}Li$-coupling constants have been seperated from the homonuclear $^{31}P,^{31}P$-coupling constants in the ^{31}P-NMR spectra of lithiated organophosphorus compounds.[28]

Since scalar spin-spin coupling constants—and only these can be measured in isotropic media—are transmitted in general through covalent bonds, it seems reasonable to ask whether the observation of $^{6(7)}Li,X$ coupling allows conclusions to be drawn about the nature of the corresponding Li-X bonds (ionic or covalent). In this connection *Streitwieser* et al.[42] pointed out for the first time that scalar spin-spin coupling between carbon and lithium does not necessarily imply covalent bonding. The mechanism which they termed spin polarization and which is known in NMR spectroscopy as through-space coupling[43] is believed to operate in several cases where ^{19}F nuclei are involved. In general it is more an exception than the rule. It requires non-bonded interactions of neighboring orbitals which are close in space. Also in the case of a purely ionic Li-X bond scalar Li,X coupling could therefore operate, if only the orbital contact is sufficient.

Several arguments can be cited in favor of this interpretation. It appears, that $^{13}C,^{6(7)}Li$ couplings over more than one bond have, to the best of our knowledge, so far not been observed. In case of a through-bond mechanism however, also geminal and vicinal $^{13}C,^{6(7)}Li$ couplings are to be expected. Furthermore, many well resolved ^{7}Li couplings are not compatable with a high covalent character of the carbon lithium bond, since the unsymmetrical charge distribution should increase the ^{7}Li quadrupole relaxation rate and broaden the ^{13}C-NMR lines.[44] Considering the mechanistic dichotomy for the scalar spin-spin interaction (through-bond or through-space) it cannot so far be decided if the experimentally measured scalar spin-spin couplings of the lithium nuclides are a consequence of a covalent contribution to the respective Li-X bonds or if they are transmitted by a pure through-space mechanism. In view of the dominancy of the through-bond mechanism with other nuclei the second possibility would certainly be unusual.

3.2. Homonuclear Shift Correlations

Shift correlations are without doubt the most important two-dimensional pulse techniques. One distinguishes between scalar and dipolar correlated spectra. The origin of the cross peaks observed in the 2D-NMR spectrum is scalar spin-spin coupling in the first case and the nuclear Overhauser effect in the second. That is, information is obtained, on the one hand about the bonding in the molecule under study, and, on the other, about the spatial surroundings.

Homonuclear δ,δ or COSY spectra[45] for ^{6}Li or ^{7}Li rest on corresponding homonuclear spin-spin coupling. So far this type of coupling has not been observed conventionally, that is by line splitting. Since most organolithium compounds, for reasons of symmetry, show only *one* ^{6}Li- or ^{7}Li-NMR signal for the individual aggregates, even at low temperature (see Fig. 1), such measurements had to be performed on systems with a $^{6}Li/^{7}Li$ isotope ratio of ca. 1:1. From the line width in the ^{7}Li-NMR spectrum of methyllithium, which forms a tetramer,[46] *Brown* et al.[47] concluded that in this case a $^{6}Li,^{7}Li$ coupling over one bond of about 0.3 Hz exists.

With the COSY experiment,[48] we were able to detect a homonuclear $^{6}Li,^{6}Li$ coupling for the first time for 3,4-dilithio-2,5-dimethyl-2,4-hexadiene (**3**).[49] The crystal structure of this compound (Fig. 4)[50] revealed two different Li

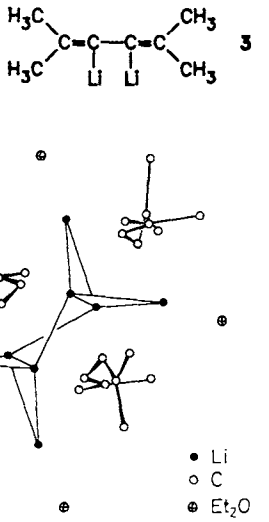

Fig. 4. Crystal structure of 3,4-dilithio-2,5-dimethyl-2,4-hexadiene (**3**) [50].

positions. In THF as solvent, **3** shows two ^{6}Li-NMR signals at $-78\,^{\circ}C$; the COSY experiment (Fig. 5) proves that a scalar spin-spin coupling exists between the two ^{6}Li signals. This suggests that **3** has the same structure in both the solid state and in solution. Both ^{6}Li-NMR signals must be assigned to the same aggregate, which, therefore, like the molecule in the crystal, must contain two types of lithium atoms. The $^{6}Li,^{6}Li$ coupling should be of the order of 0.1 Hz. This is in good agreement with the value estimated by *Brown* et al. for the $^{6}Li,^{7}Li$ coupling, if the corresponding γ factors are taken into account. So far, it is unknown if the coupling is a one-bond or a geminal interaction which includes the metalated carbon in the coupling path.

COSY experiments for quadrupole nuclei have so far been successfully performed for ^{11}B,[51] ^{51}V,[52] ^{2}H[53] and in a few cases for ^{14}N.[54] Broad lines and/or small scalar couplings have negative consequences and may prevent the detection of cross peaks. According to the product operator formalism[55] the dependency of the cross peak intensity, I_k, on the evolution time t_1 for COSY experiments with spin-1 nuclei is governed by the following equation:

$$I_k = I_o \sin 2\pi J t_1 \exp(-t_1/T_2) \qquad \text{(d)}$$

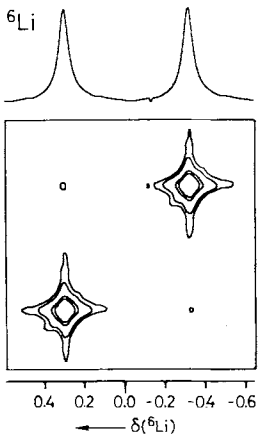

Fig. 5. ^{6}Li,^{6}Li COSY spectrum of 3,4-dilithio-2,5-dimethyl-2,4-hexadiene (**3**) [49], recorded with the pulse sequence proposed for emphasizing small couplings $90°_x - t_1 - \Delta$, $90°_x$, Δ, FID(t_2) [45] (measuring frequency 58.86 MHz; measuring time 1.2 h).

A plot of Equation (d) (Fig. 6) shows that for small couplings and short transverse relaxation times T_2 the cross peak intensity has a maximum if the condition $t_1 = T_2$ holds. Experiments with the quadrupole nucleus ^{2}H show good results with the pulse sequence (1),[45] which was developed in order to emphasize small couplings and to suppress diagonal signals.

$$90°_x - t_1 - \Delta, 45°_x, \Delta - \mathrm{FID}(t_2) \qquad (1)$$

where $t_1(\max) + \Delta = T_2$

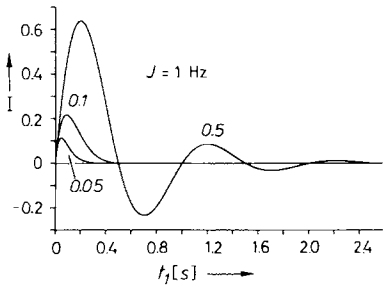

Fig.6. Cross-peak intensity for COSY experiments with nuclei of spin $I = 1$ and small couplings as a function of the transverse relaxation time T_2 (0.5, 0.1, 0.05 s) and the evolution time t_1.

As expected, the COSY experiment for ^{7}Li with the larger quadrupole moment is less favorable. Nevertheless, homonuclear ^{7}Li,^{7}Li couplings for **3** were also successfully detected, even if less clear then in the case of ^{6}Li.[54]

3.3. Heteronuclear Shift Correlations

In principle, there are two pulse sequences available today for the measurement of heteronuclear shift correlations: the standard technique, which is based on polarization transfer (Fig. 7a),[56] and a variant (Fig. 7b),[57] which uses the possibilities of multiple quantum coherences. In the case of organolithium compounds the ^{6}Li,^{13}C correlation is of primary interest, because the identification of ^{6}Li,^{13}C spin pairs via the multiplicities in the ^{13}C- or ^{6}Li-NMR spectra is no longer possible in more complicated cases. Only selective decoupling or one of the two-dimensional methods mentioned above, where one can choose between ^{6}Li or ^{13}C detection, are then applicable. Such experiments form the basis for a successful simulation of the respective ^{13}C,^{6}Li spin systems.

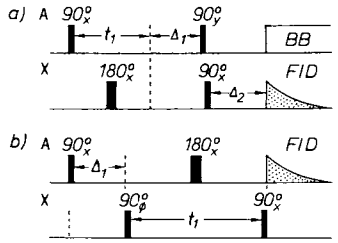

Fig. 7. Pulse sequences for two-dimensional heteronuclear shift correlations on the basis of polarization transfer (a) [56] and multiple quantum coherences (b) [57].

The dilithiosulfone **2** already mentioned above offered the possibility of testing the use of the ^{6}Li,^{13}C shift correlation, because the ^{13}C- as well as the ^{6}Li-NMR spectrum of this compound displays a number of simple as well as complicated multiplets (Fig. 8).[58] Considering the spectrometer configuration available, the two-dimensional experiments could be performed in either case (a) or (b) only with ^{6}Li detection. Method (a) failed, apparently because of fast transverse relaxation, and difficulties with the correct choice of the Δ_1 interval, while method (b) was successful (Fig. 8d). All correlations obtained were confirmed by selective ^{13}C decoupling. The double-resonance technique yielded two additional correlations which were not found in the 2D-NMR experiments, apparently because of small scalar couplings.

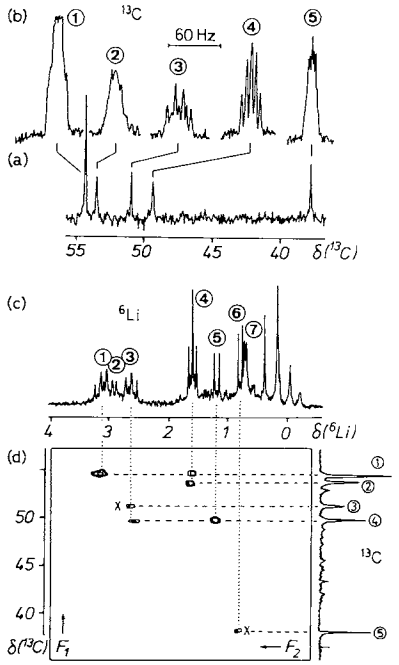

Fig. 8. a) ^{1}H,^{6}Li decoupled 100.61-MHz ^{13}C-NMR spectrum of the dilithiosulfone **2** (−103 °C in [D$_8$]THF); b) ^{13}C multiplets with ^{6}Li coupling; c) 58.86-MHz ^{6}Li-NMR spectrum of ^{13}C-labeled **2** with ^{13}C,^{6}Li coupling (ext. reference, see Fig. 3); d) Two-dimensional ^{6}Li,^{13}C-shift correlation for **2** with the pulse sequence of Figure 7b; the correlations X have been detected with selective ^{6}Li{^{13}C}-spin decoupling [58] (measuring time 4.7 h).

The potential of the $^6Li,^{13}C$-shift correlation experiment is also demonstrated by its application to the dilithium compound **3**.[59] Here, the ^{13}C-NMR spectrum shows all signals of the tetramethylbutadiene structure twice, and the task was to assign the individual resonance lines to the "inner" and "outer" ligands (Fig. 4). This was achieved through the finding that one of the metalated carbon atoms couples to two different lithium nuclei, namely to one of the "inner" and to one of the "outer" positions. The two-dimensional $^6Li,^{13}C$ double quantum spectrum (Fig. 9) shows two cross peaks for the high-field ^{13}C and for the high-field ^6Li signal. Considering the direction of the carbanion orbitals at C-3 and C-4 given by the geometry of the ligands as found in the crystal (Fig. 4), only the carbon of the "outer" ligand can take part in two different scalar interactions and thus show two correlation signals. The results of dynamic NMR spectroscopy, 2D-^1H exchange and 2D-$^{13}C,^1H$-δ,δ-NMR spectroscopy completed the assignment of the resonance signals.

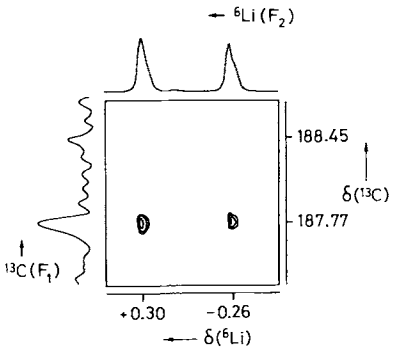

Fig. 9. Two-dimensional $^6Li,^{13}C$-shift correlation based on multiple quantum coherences for 3,4-dilithio-2,5-dimethyl-2,4-hexadiene (**3**) [59] (measuring time 8.7 h).

3.4. Nuclear Overhauser Effects

The nuclear Overhauser enhancement (NOE)[60] is based on dipolar cross relaxation between closely spaced nuclei, which have no chemical bond in common. It is therefore an important supplement for the identification of chemical structures on the basis of scalar spin-spin coupling constants, which are transmitted nearly without exception through bonding pathways. Consequently, NMR spectroscopy is the only method which allows one to determine three-dimensional molecular structures in solution.

For the NMR spectroscopy of solute organolithium compounds it is important that neighboring protons can make a significant contribution to the relaxation of ^6Li through dipolar interactions[7] (see Section 2.1). The proximity of ^6Li and ^1H can, therefore, be detected by heteronuclear $^6Li\{^1H\}$-NOE spectroscopy, where a maximum signal enhancement of 340% would result for the ^6Li nucleus if no competing relaxation mechanisms were available. For ^7Li such experiments are impossible because of its different relaxation behavior.

Heteronuclear NOE experiments can be performed one-dimensionally (1D), best employing the method of difference spectroscopy[61] or, as was first shown by *Rinaldi*[62] for the pair $^{13}C,^1H$ and by *Yu* and *Levy*[63] for $^{31}P,^1H$ two-dimensionally with the pulse sequence (2) (HOESY[63]); ($I = ^1H, ^{19}F, ^{31}P$; $S = ^{13}C, ^{15}N, ^6Li$):

$$\begin{array}{ll} \text{I:} & 90^\circ_x - t_1 - 90^\circ_x - t_m - \text{BB} \\ \text{S:} & \text{——}\ 180^\circ_x\ \text{———}\ 90^\circ_x, \text{FID}(t_2) \end{array} \qquad (2)$$

In this way hydrogen bridges between lithium and boron as well as aluminum, indium or gallium in hydrido[tris(trimethylsilyl)methyl]metalates could be detected[64]. 2D-NMR experiments with the pulse sequence (2) and a 1:1 aggregate of methyl- and 1-naphthyllithium[31] as well as 2-lithio-1-phenylpyrrole[65] allowed the localization of spatially closely related ^6Li and ^1H nuclei (< ca. 350 nm). Since short ^6Li-^1H distances correlate with the activation of the respective CH bond for a second metalation, NOE spectroscopy also yields information about the reactivity of the organic ligands. Quantitative measurements of NOE build-up rates should here, as in the case of ^1H-NMR spectroscopy,[66] enable a more exact determination of nuclear distances. Figure 10 shows the result of a 1D-$^6Li\{^1H\}$-NOE difference experiment for the complex 1-naphthyllithium-TMEDA. Compared to the 2D-NMR experiment[31] the selective detection of ^6Li-^1H neighborhoods is simpler, because a better digital resolution can be achieved.

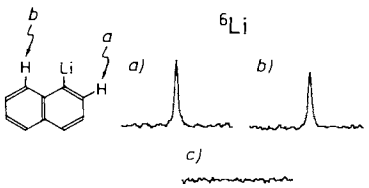

Fig. 10. Selective 58.86-MHz $^6Li\{^1H\}$ nuclear Overhauser difference spectrum for 1-naphthyllithium-TMEDA with natural ^6Li abundance; a) irradiation at 2-H, b) irradiation at 8-H, c) control experiment with off-resonance decoupling (measuring time 4 h each). The NOE effects are 8.5% and 7%, respectively. The decoupler power was calibrated with the SPI-experiment for chloroform[68]; for the assignment of the ^1H-resonances see Ref. [31].

3.5. 2D-$^6Li,^6Li$- and $^7Li,^7Li$-NMR Exchange Spectroscopy (EXSY)

Whether homonuclear NOE effects for $^6Li,^6Li$ nuclear pairs can be detected or not has so far not been investigated. However, *Wehrli* estimated only 6% for the dipolar contribution to the ^6Li relaxation in $^6Li,^7Li$ pairs in methyllithium.[7] For $^6Li,^6Li$ pairs this contribution reduces further to less then 1% and is thus practically negligible. On the other hand, 2D-$^6Li,^6Li$ and 2D-$^7Li,^7Li$-NMR exchange spectra for dynamic systems can be measured without difficulty in the region of slow exchange with the pulse sequence (3),[67]

$$90^\circ_x - t_1 - 90^\circ_x - t_m - 90^\circ_x, \text{FID}(t_2) \qquad (3)$$

as is shown in Figure 11a for ^6Li in the case of **3** and in Figure 11b for ^7Li in the case of an interaggregate exchange process. The investigation of dynamic processes of solute organolithium compounds by NMR line shape analysis[70] thus receives valuable support through 2D-NMR experiments, since not only can exchange mechanisms be

recognized, but, in addition, quantitative analysis of cross peak intensities allows the determination of rate constants.[71]

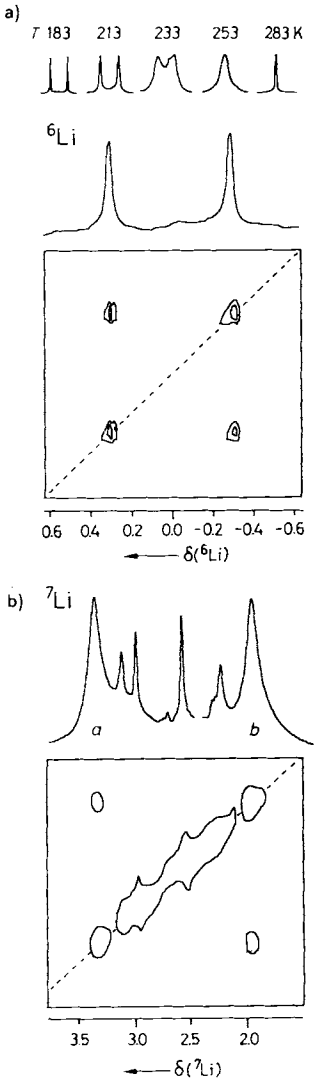

Fig. 11. a) 2 D-^{6}Li,^{6}Li-NMR exchange spectrum for the *intra*-aggregate ^{6}Li exchange in 3,4-dilithio-2,5-dimethyl-2,4-hexadiene (3) ([D$_8$]THF, −83 °C, measuring frequency 58.86 MHz, ext. reference, see Fig. 3, mixing time 1 s, measuring time 1 h); above, the 1D-NMR spectrum for comparision). b) Two-dimensional ^{7}Li,^{7}Li-NMR exchange spectrum for the *inter*-aggregate ^{7}Li exchange between the diethyl ether complex of the dimer of 8-dimethylamino-1-naphthyllithium (signal b) and the ether-free aggregate (signal a) ([D$_8$]toluene [69], −15 °C; measuring frequency 155.51 MHz; ext. reference 1 M LiCl/D$_2$O; mixing time 0.1 s; measuring time 45 min).

3.6. High Resolution Solid State NMR Spectroscopy

This timely and promising technique[72] is without doubt also of interest for the field of organolithium compounds, despite the fact that so far only one investigation has been reported.[73] The reason for this may be seen in the relatively large amount of material necessary for such measurements (200–300 mg) and in the more complicated sample preparation required for compounds that are sensitive to air and moisture. ^{13}C- as well as ^{6}Li-NMR measurements on solids should furnish important structural information bridging the gap between the results of crystal structure analysis on the one hand and NMR spectroscopy in solution on the other. The investigation of methyllithium and dilithiomethane[73] mentioned above shows that ^{6}Li decoupling is also possible in solid state NMR spectroscopy and that the quality of the ^{13}C-NMR spectra thereby increases considerably.

4. Outlook

The experiments discussed in the foregoing sections demonstrate how the structure of organolithium compounds in solution may be determined even more confidently and in more detail in the future. Our knowledge about the reactivity of this important class of compounds can thus be deepened and defined more exactly. More emphasis should be devoted to the elucidation and the quantitative investigation of the mechanisms of the dynamic processes present in solution. 2D-NMR methods can certainly yield new insights in this respect. From the standpoint of bonding theory further investigations of the mechanism of ^{13}C,$^{6(7)}$Li spin–spin coupling as well as the dependence of this parameter on structure are desirable. This is even more true for couplings between lithium nuclei. Finally, interesting results can be expected from the solid state NMR spectroscopy of organolithium compounds, especially since this method can also detect dynamic phenomena in the crystal.[74,75] Organolithium compounds will therefore remain exciting subjects for demanding NMR studies in the future.

We are indebted to Prof. Dr. A. Maercker, Siegen, for a number of important references. Our thanks are due to him and Prof. Dr. H.-J. Gais, Freiburg, as well as to their coworkers Dr. R. Dujardin and Dipl.-Chem. F. Brauers, Siegen, and Dipl.-Chem. J. Vollhardt, Freiburg, for gifts of valuable compounds and exciting collaboration. Generous support of our investigations by the Fonds der Chemischen Industrie, is gratefully acknowledged.

Received: July 24, 1987;
revised: August 21, 1987 [A 644 IE]
German version: *Angew. Chem. 99* (1987) 1242

[1] a) J. K. M. Sanders, B. K. Hunter: *Modern NMR Spectroscopy*, Oxford University Press, Oxford 1987; b) R. R. Ernst, G. Bodenhausen, A. Wokaun, *Principles of Nuclear Magnetic Resonance in One and Two Dimensions*, Clarendon Press, Oxford 1987; c) R. Benn, H. Günther, *Angew. Chem. 95* (1983) 381; *Angew. Chem. Int. Ed. Engl. 22* (1983) 351; d) G. A. Morris, *Magn. Reson. Chem. 24* (1985) 371; e) review on metal NMR spectroscopy: R. Benn, A. Rufińska, *Angew. Chem. 98* (1986) 851; *Angew. Chem. Int. Ed. Engl. 25* (1986) 861.

[2] a) L. Brandsma, H. Verkruijsse: *Preparative Polar Organometallic Chemistry, Vol. 1*, Springer, Berlin 1987; b) B. J. Wakefield: *The Chemistry of Organolithium Compounds*, Pergamon Press, Oxford 1974; c) M. Schlosser: *Polare Organometalle*, Springer, Heidelberg 1973.

[3] a) P. von R. Schleyer, *Pure Appl. Chem. 56* (1984) 151; b) W. N. Setzer, P. von R. Schleyer, *Adv. Organomet. Chem. 24* (1985) 353.

[4] A. Maercker, M. Theis, *Top. Curr. Chem. 138* (1987) 1.

[5] T. L. Brown, *Acc. Chem. Res. 1* (1968) 23.

[6] a) B. Lindman, S. Forsén in R. K. Harris, B. E. Mann (Eds.): *NMR and the Periodic Table*, Academic Press, London 1978, p. 129-194; b) P. Laszlo in J. B. Lambert, F. G. Riddell (Eds.): *The Multinuclear Approach to NMR Spectroscopy*, Reidel, Dordrecht 1982, p. 261-308; c) F. W. Wehrli, *Annu. Rep. NMR Spectrosc. 9* (1979) 125.

[7] F. W. Wehrli, *Org. Magn. Reson. 11* (1978) 106.

[8] G. E. Hartwell, A. Allerhand, *J. Am. Chem. Soc. 93* (1971) 4415.

[9] G. Fraenkel, A. M. Fraenkel, M. J. Geckle, F. Schloss, *J. Am. Chem. Soc. 101* (1979) 4745.

[10] a) D. Seebach, R. Hässig, J. Gabriel, *Helv. Chim. Acta 66* (1983) 308; b) D. Seebach, H. Siegel, J. Gabriel, R. Hässig, *ibid. 63* (1980) 2046.
[11] Martin Marietta Energy System Inc., Oak Ridge, TN (USA).
[12] R. D. Thomas, D. H. Ellington, M. T. Clarke, unpublished, cited in [70a].
[13] F. W. Wehrli, *J. Magn. Reson. 23* (1976) 527.
[14] J. R. Wesener, H. Günther, *J. Magn. Reson. 62* (1985) 158.
[15] L. M. Jackman, L. M. Scarmoutzos, *J. Am. Chem. Soc. 106* (1984) 4627.
[16] L. M. Jackman, J. C. Trewella, *J. Am. Chem. Soc. 98* (1976) 5712; *ibid. 101* (1979) 6428.
[17] P. A. Scherr, R. J. Hogan, J. P. Oliver, *J. Am. Chem. Soc. 96* (1974) 6055.
[18] J. A. Ladd, J. Parker, *J. Chem. Soc. Dalton Trans. 1972*, 930.
[19] R. H. Cox, H. W. Terry, Jr., L. W. Harrison, *Tetrahedron Lett. 1971*, 4815.
[20] R. H. Cox, H. W. Terry, Jr., L. W. Harrison, *J. Am. Chem. Soc. 93* (1971) 3297.
[21] G. Fraenkel, D. G. Adams, R. R. Dean, *J. Phys. Chem. 72* (1968) 944; G. Fraenkel, S. Dayagi, S. Kobayashi, *ibid. 72* (1968) 953.
[22] A. J. Jones, D. M. Grant, J. G. Russell, G. Fraenkel, *J. Phys. Chem. 73* (1969) 1624.
[23] V. M. S. Gil, J. N. Murrell, *Trans. Faraday Soc. 60* (1964) 248.
[24] R. D. Thomas, M. T. Clarke, T. C. Young, *J. Organomet. Chem. 328* (1987) 239; see also J. P. C. M. van Dongen, H. W. D. van Dijkman, M. J. A. de Bie, *Recl. Trav. Chim. Pay-Bas 93* (1974) 29.
[25] L. D. McKeever, R. Waack, M. A. Doran, E. B. Baker, *J. Am. Chem. Soc. 90* (1968) 3244.
[26] a) G. Fraenkel, H. Hsu, B. M. Su in R. O. Bach (Ed.): *Lithium: Current Applications in Science, Medicine, and Technology*, Wiley, New York 1985, p. 273; b) G. Fraenkel, P. Pramanik, *J. Chem. Soc. Chem. Commun. 1983*, 1527; c) R. Hässig, D. Seebach, *Helv. Chim. Acta 66* (1983) 2269; d) D. Seebach, J. Gabriel, R. Hässig, *ibid. 67* (1984) 1083; e) R. D. Thomas, R. M. Jensen, T. C. Young, *Organometallics 6* (1987) 565; f) W. Bauer, W. R. Winchester, P. von R. Schleyer, *ibid. 6* (1987), in press.
[27] I. J. Colquhoun, H. C. E. McFarlane, W. McFarlane, *J. Chem. Soc. Chem. Commun. 1982*, 220.
[28] I. J. Colquhoun, H. C. E. McFarlane, W. McFarlane, *Phosphorus Sulfur 18* (1983) 61.
[29] U. Edlund, T. Lejon, T. K. Venkatachalam, E. Buncel, *J. Am. Chem. Soc. 107* (1985) 6408.
[30] T. M. Gilbert, R. G. Bergmann, *J. Am. Chem. Soc. 107* (1985) 6391.
[31] W. Bauer, T. Clark, P. von R. Schleyer, *J. Am. Chem. Soc. 109* (1987) 970.
[32] A. Rajca, L. M. Tolbert, *J. Am. Chem. Soc. 109* (1987) 1782.
[33] A. Bax, R. Freeman, T. A. Frenkiel, *J. Am. Chem. Soc. 103* (1981) 2102; A. Bax, R. Freeman, T. A. Frenkiel, M. H. Levitt, *J. Magn. Reson. 44* (1981) 212; review: J. Buddrus, H. Bauer, *Angew. Chem. 99* (1987) 642; *Angew. Chem. Int. Ed. Engl. 26* (1987) 625.
[34] Synthese: W. Neugebauer, T. Clark, P. von R. Schleyer, *Chem. Ber. 116* (1983) 3283.
[35] D. M. Doddrell, D. T. Pegg, M. R. Bendall, *J. Magn. Reson. 48* (1982) 323; D. T. Pegg, D. M. Doddrell, M. R. Bendall, *J. Chem. Phys. 77* (1982) 2745.
[36] G. Fraenkel, M. Henrichs, M. Hewitt, M. J. Geckle, B. M. Su, *J. Am. Chem. Soc. 102* (1980) 3345.
[37] S. L. Patt, J. N. Shoolery, *J. Magn. Reson. 46* (1982) 318.
[38] J. Vollhardt, H.-J. Gais, K. L. Lukas, *Angew. Chem. 97* (1985) 695; *Angew. Chem. Int. Ed. Engl. 24* (1985) 696.
[39] a) G. Bodenhausen, R. Freeman, D. L. Turner, *J. Chem. Phys. 75* (1976) 839; b) R. Freeman, S. P. Kempsell, M. H. Levitt, *J. Magn. Reson. 34* (1979) 663; c) see also H. Günther, P. Schmitt, *Kontakte Darmstadt 1985*, No. 2, p. 3.
[40] a) P. Schmitt, J. R. Wesener, H. Günther, *J. Magn. Reson. 52* (1983) 511; b) J. R. Wesener, H. Günther, *Org. Magn. Reson. 21* (1983) 433; c) J. R. Wesener, P. Schmitt, H. Günther, *J. Am. Chem. Soc. 106* (1984) 10.
[41] L. D. Hall, S. Sukumar, *J. Am. Chem. Soc. 101* (1979) 3120; see also [39c].
[42] A. Streitwieser, Jr., J. E. Williams, Jr., S. Alexandratos, J. M. McKelvey, *J. Am. Chem. Soc. 98* (1976) 4778.
[43] J. Hilton, L. H. Sutcliffe, *Prog. NMR Spectrosc. 10* (1975) 27.
[44] E. Buncel, T. K. Venkatachalam, U. Edlund, *Can. J. Chem. 64* (1986) 1674.
[45] A. Bax, R. Freeman, *J. Magn. Reson. 44* (1981) 542; A. Bax: *Two-Dimensional NMR in Liquids*, Reidel, Dordrecht 1983; see also H. Günther, D. Moskau, *Kontakte Darmstadt 1986*, No. 2, p. 41.
[46] L. D. McKeever, R. Waak, M. A. Doran, E. B. Baker, *J. Am. Chem. Soc. 91* (1969) 1057.
[47] T. L. Brown, L. M. Seitz, B. Y. Kimura, *J. Am. Chem. Soc. 90* (1968) 3245.
[48] A. Maercker, R. Dujardin, *Angew. Chem. 97* (1985) 612; *Angew. Chem. Int. Ed. Engl. 24* (1985) 571.
[49] H. Günther, D. Moskau, R. Dujardin, A. Maercker, *Tetrahedron Lett. 27* (1986) 2251.
[50] A. Maercker, R. Dujardin, B. Engelen, W. Buchmeier, M. Jung, unpublished results.
[51] T. L. Venable, W. C. Hutton, R. N. Grimes, *J. Am. Chem. Soc. 106* (1984) 29.
[52] P. J. Domaille, *J. Am. Chem. Soc. 106* (1984) 7677.
[53] D. Moskau, H. Günther, *Angew. Chem. 99* (1987) 151; *Angew. Chem. Int. Ed. Engl. 26* (1987) 156.
[54] D. Moskau, Dissertation, Universität-Gesamthochschule Siegen 1987.
[55] O. W. Sorensen, G. W. Eich, M. H. Levitt, G. Bodenhausen, R. R. Ernst, *Prog. NMR Spectrosc. 16* (1984) 163.
[56] A. A. Maudsley, L. Müller, R. R. Ernst, *J. Magn. Reson. 28* (1977) 463; G. Bodenhausen, R. Freeman, *ibid. 28* (1977) 471.
[57] L. Müller, *J. Am. Chem. Soc. 101* (1979) 4481; A. Bax, R. H. Griffey, B. L. Hawkins, *J. Magn. Reson. 55* (1983) 301.
[58] H.-J. Gais, J. Vollhardt, H. Günther, D. Moskau, H. J. Lindner, D. Braun, *J. Am. Chem. Soc.*, in press.
[59] D. Moskau, F. Brauers, H. Günther, A. Maercker, *J. Am. Chem. Soc. 109* (1987) 5532.
[60] J. H. Noggle, R. E. Schirner: *The Nuclear Overhauser Effekt*, Academic Press, New York 1971.
[61] J. K. M. Sanders, J. D. Mersh, *Prog. NMR Spectrosc. 15* (1983) 353.
[62] P. L. Rinaldi, *J. Am. Chem. Soc. 105* (1983) 5167.
[63] C. Yu, G. C. Levy, *J. Am. Chem. Soc. 105* (1983) 6995.
[64] A. G. Avent, C. Eaborn, M. N. A. El-Kheli, M. E. Molla, J. D. Smith, A. C. Sullivan, *J. Am. Chem. Soc. 108* (1986) 3854.
[65] W. Bauer, G. Müller, R. Pi, P. von R. Schleyer, *Angew. Chem. 98* (1986) 1130; *Angew. Chem. Int. Ed. Engl. 25* (1986) 1103.
[66] A. Kumar, G. Wagner, R. R. Ernst, K. Wüthrich, *J. Am. Chem. Soc. 103* (1981) 3654.
[67] B. H. Meier, R. R. Ernst, *J. Am. Chem. Soc. 101* (1979) 6441; J. Jeener, B. H. Meier, P. Bachmann, R. R. Ernst, *J. Chem. Phys. 71* (1979) 4546; review: R. Willem, *Prog. NMR Spectrosc. 20* (1987) 1.
[68] K. G. R. Pachler, P. L. Wessels, *J. Magn. Reson. 12* (1973) 337.
[69] J. T. B. H. Jastrzebski, G. van Koten, K. Goubitz, C. Arlen, M. Pfeffer, *J. Organomet. Chem. 246* (1983) C75.
[70] Recent examples: a) R. D. Thomas, M. T. Clarke, R. M. Jensen, T. C. Young, *Organometallics 5* (1986) 1851; b) J. Heinzer, J. F. M. Oth, D. Seebach, *Helv. Chim. Acta 68* (1985) 1848.
[71] E. W. Abel, T. P. J. Coston, K. G. Orrell, V. Sik, D. Stephenson, *J. Magn. Reson. 70* (1986) 34, and references cited therein.
[72] C. A. Fyfe: *Solid State NMR for Chemists*, C. F. C. Press, Guelph, Canada 1983.
[73] J. A. Gurak, J. W. Chinn, Jr., R. J. Lagow, H. Steinfink, C. S. Yannoni, *Inorg. Chem. 23* (1984) 3717.
[74] J. R. Lyerla, C. S. Yannoni, C. A. Fyfe, *Acc. Chem. Res. 15* (1982) 208.
[75] a) B. H. Meier, C. B. Storm, W. L. Earl, *J. Am. Chem. Soc. 108* (1986) 6072; b) R. Benn, H. Grondey, G. Erker, R. Nolte, *Organometallics*, in press.

Molecular Dynamics of Elementary Chemical Reactions (Nobel Lecture)**

By Dudley R. Herschbach

Introduction

The vast field of chemical kinetics embraces three distinct levels of understanding or abstraction.[1] The broadest level is qualitative description. Here the emphasis is on *substances:* what products are obtained from what reagents under what conditions. The information gathered is encyclopedic, but quite feeble in predictive power. This is because the overall observed transformation in most reactions comprises a more or less complex sequence or network of elementary steps.

At the next level, the aim is to identify the distinct *elementary steps* and to determine quantitatively the rate factors of the Arrhenius equation, $k=A\exp(E_a/RT)$, a remarkably durable formula now nearly a century old! Some steps involve intermediate species that do not appear among the final products; whenever possible, these intermediates are also characterized by structural, spectral, and thermodynamic properties. Over about the past 70 years, immense effort has been devoted to compiling such quantitative data. It is of great practical value because predictions can be made for many reaction systems, on the usually reliable assumption that the rate parameters for each indivisible elementary step can be carried over from one system to another.

As well as mapping the cooperation and competition among elementary processes, kinetic studies at this level also gave rise to many key chemical ideas. These include such concepts as chain reactions carried by free radical intermediates, collisional energy transfer, and the time lag for energy flow within an excited molecule. Most fundamental was the idea introduced by *Henry Eyring* and *Michael Polanyi* of a transition state on a potential energy surface. This has guided qualitative reasoning about molecular mechanisms, and when augmented by resourceful semitheoretical approximations for potential parameters has enabled limited but useful estimates of rate factors. However, these valuable insights were won despite frustrating handicaps. The basic experimental variables of concentration and temperature are not incisive enough to allow further progress. Postulated elementary steps or intermediates often prove incomplete or illusory. The observable rate factors, which represent averages over myriad random collisions, are too remote from the molecular interactions.

[*] Prof. D. R. Herschbach
Department of Chemistry, Harvard University
Cambridge, MA 02138 (USA)

[**] Copyright © The Nobel Foundation 1987.—We thank the Nobel Foundation, Stockholm, for permission to print this article.

Emergence of Chemical Dynamics

Over the past 30 years a new level has been attained by study of the intimate *molecular dynamics* of individual reactive collisions. One of the chief experimental approaches is molecular beam scattering. This involves forming the reagent molecules into two collimated beams, each so dilute that collisions within them are negligible. The two beams intersect in a vacuum and the direction and velocity of the product molecules emitted from the collision zone are measured. A host of reactions can now be studied readily in this way, by virtue of an extremely sensitive mass spectrometric detector and the use of supersonic nozzles which generate beams with greatly enhanced intensity and with collision energies much higher than provided by ordinary thermal sources. The coupling of spectroscopic techniques with molecular beams has provided further advances in selectivity and sensitivity, particularly by use of intense laser light sources.

The reaction properties now accessible include the disposal of energy among translation, rotation, and vibration of the product molecules; angles of product emission; angular momentum and its orientation in space; and variation of reaction yield and other attributes with impact energy, closeness of collision, rotational orientation or vibrational excitation of the target molecule. From the earliest stages these experiments have stimulated and responded to a vigorous outburst of theoretical developments. Especially helpful are computer simulations in which dynamical properties are predicted for various postulated forces by Monte Carlo sampling of huge numbers of calculated collision trajectories. Both the laboratory experiments and computer simulations have prompted a variety of insightful mechanical models as well as very useful diagnostic procedures based on information theory. Ab initio electronic structure calculations have also begun to contribute significantly to the exploration of reaction dynamics, although (except for $H+H_2$) satisfying overall accuracy has yet to be achieved for potential energy surfaces.

As urged by my students, on this occasion I want both to view our still youthful field of research from a wider perspective and to recount some favorite, instructive episodes from its infancy. I will also briefly discuss several prototype reactions that have served to develop heuristic models and to reveal how electronic structure governs the reaction dynamics. More technical and systematic surveys are abundant.[2] Particularly recommended are recent books by *Bernstein* and by *Levine* and *Bernstein*.[3] The latter, about to appear in its second edition, contains references to 500 review articles in the field of molecular reaction dynamics! Nobody has tried recently to count the research papers in this prolific field; these probably now exceed 5000. This

does not include kindred developments in the study of molecular dynamics in solution or the solid phase.

The emergence of chemical dynamics captivated many enterprising scientists and imbued them with a sense of historical imperative. Figure 1 indicates this in the wider context of physical chemistry. The subject began with thermochemistry, still its foundation. The thermochemical era can be considered to reach a pinnacle in 1923, with the publication of the classic text by *Lewis* and *Randall*. This was shortly before the discovery of quantum mechanics ushered in the new structural era (and spawned chemical physics). In turn, the grand pursuit of molecular structure and spectra reached a twin pinnacle in 1951 and 1953 with the monumental discoveries of the alpha-helix by *Pauling* and the DNA double helix by *Watson* and *Crick*. This was shortly before the early molecular beam and infrared chemiluminescence experiments appeared as harbingers of the dynamics era. It is striking that the prequantum models of *Lewis* and *Langmuir*, still valued today, came well before the onset of the structural era. Likewise, the potential surface and transition-state concepts of *Eyring* and *Polanyi* anticipated the dynamics era.

Not evident in Figure 1, and in contrast to the scientific continuity, are cultural chasms between the eras. *Linus Pauling* once told me of the gulf his students encountered in the late 1920s when, as candidates for an academic position, they presented seminars describing molecular structures they had determined by electron diffraction. All the faculty in the audience had done their Ph.D.'s in thermochemistry, and so imbibed a tradition which emphasized that it did not need to postulate the existence of molecules! Worse, interpretation of the diffraction rings then relied entirely on the so-called "visual method." A densitometer tracing showed only monotonically decreasing intensity curves; the rings could only be seen because the human eye can detect slight changes in intensity. The molecular structures obtained thus depended on an "optical illusion," incomprehensible and reprehensible to many professors of thermodynamics. Forty years later, my own students encountered a similar gulf when presenting seminars describing our early crude molecular-beam reactive-scattering studies. Almost all the incumbent faculty then had done their Ph.D.'s in structure or spectroscopy. They were dubious about work that depended on drawing velocity vector diagrams to interpret bumps on scattering curves.

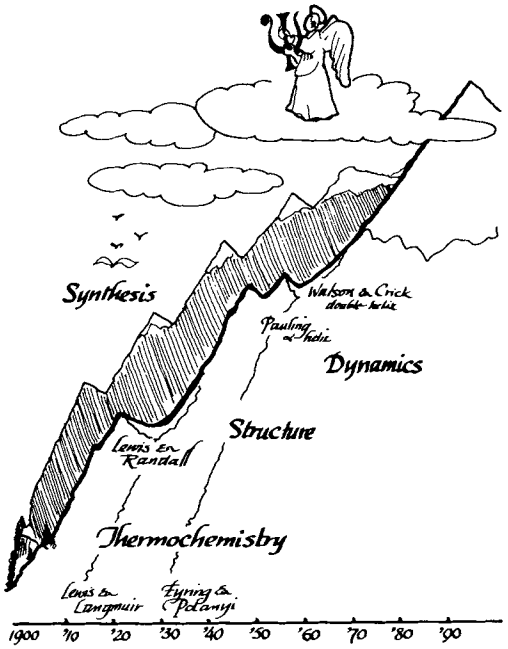

Fig. 1. Historical perspective. Ascending mountains represent three eras, since *thermochemistry* was prerequisite for the *structure* era and both underlie the *dynamics* era. All three connect to a vast range representing *synthetic* chemistry, which draws closest to dynamics as both disappear heavenwards into clouds symbolizing the ultimate triumph of *ab initio* quantum chemistry.

Molecular Beams before Chemical Dynamics

The first molecular beam experiments were carried out 75 years ago, immediately after the invention of the high-speed vacuum pump had made it possible to form directed "rays" of neutral molecules at sufficiently low pressures to prevent their disruption by collisions with background gas. Figure 2 indicates the historical progression. Systematic research began with *Otto Stern*, who developed many aspects of beam techniques. He had retired and was living in Berkeley when I arrived there in 1959. Occasionally, *Stern* attended seminars, and I had the opportunity to hear from him several memorable stories about his work. Two of these are pertinent here.

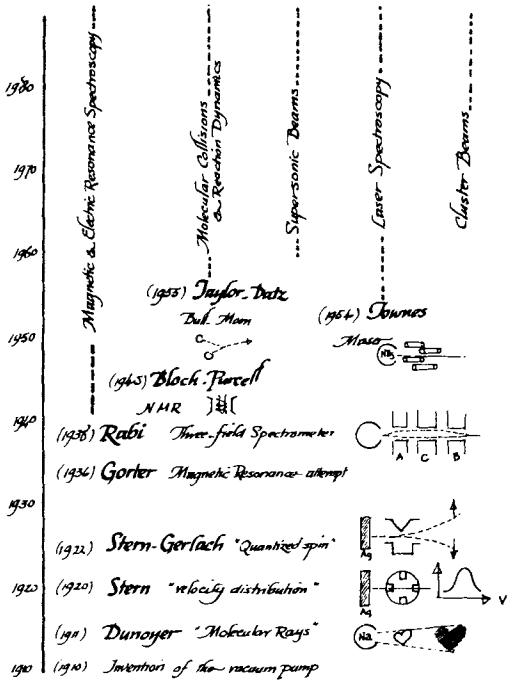

Fig. 2. Evolution of molecular beam and kindred methods.

In his first work, done at Frankfurt in 1920, *Stern* undertook to test the Maxwell-Boltzmann velocity distribution by analyzing the speeds of a silver atom beam with a rotating device. Gleefully, he described how the money to build the apparatus was supplied by *Max Born*; the great theoretical physicist was renowned as a public speaker and gave

a special lecture series to raise the funds. *Stern* found that his experimental results were in approximate agreement with the Maxwell-Boltzmann distribution, but deviated from it in a systematic way. He said:[4]

> After my paper was sent off, I received a letter pointing out that I had overlooked an extra factor of v (the velocity) which enters because the detected atoms must pass through a slit. When this factor was inserted, the agreement became quantitative. That letter came from *Albert Einstein*!

The "extra factor" represents the Jacobian for the transformation from number density (atoms cm^{-3}) to flux density (atoms $cm^{-2}\ s^{-1}$). That same factor and Jacobians for numerous other transformations often appear in chemical dynamics, so I've had reason to tell *Stern*'s story to many bedeviled students. As noted below, some striking effects in molecular collisions are due entirely to a Jacobian factor.

The other favorite story concerns the celebrated Stern-Gerlach experiment, in which a beam of silver atoms was sent through an inhomogeneous magnetic field and discovered to split into two, thereby revealing the space-quantization of the electron spin. This is how *Stern* told the story:[4]

> The question whether a gas might be magnetically birefringent (in the words we used in those days) was raised at a seminar. The next morning I awoke early, too early to go to the lab. As it was too cold to get out of bed, I lay there thinking about the seminar question and had the idea for the experiment. When I got to the lab, I recruited *Gerlach* as a collaborator. He was a skilful experimentalist, while I was not. In fact, each part of the apparatus that I constructed had to be remade by *Gerlach*.
>
> We were never able to get the apparatus to work before midnight. When finally all seemed to function properly, we had a strange experience. After venting to release the vacuum, *Gerlach* removed the detector flange. But he could see no trace of the silver atom beam and handed the flange to me. With *Gerlach* looking over my shoulder as I peered closely at the plate, we were surprised to see gradually emerge two distinct traces of the beam. Several times we repeated the experiment, with the same mysterious result. Finally we realized what it was. I was then the equivalent of an assistant professor. My salary was too low to afford good cigars, so I smoked bad cigars. These had a lot of sulfur in them, so my breath on the plate turned the silver into silver sulfide, which is jet black so easily visible. It was like developing a photographic film.

Although I've rarely tried a cigar, our first reactive scattering work also benefited from lucky contamination of the detector, as described later.

Soon *Stern* could afford good cigars, as he was appointed professor of physical chemistry at Hamburg. His Institute there conducted a series of remarkable molecular beam studies, including invention of the surface ionization detector that was to be so vital in the "alkali age" of chemical dynamics. This detector, derived from *Langmuir*'s studies of surface ionization, has since been used in thousands of experiments. It consists simply of a heated filament of a metal such as tungsten and will ionize with nearly 100% efficiency materials having ionization potentials lower than about 4 or 5 eV, such as alkali atoms. *Stern* had to abandon his splendid work at Hamburg in 1933 when *Hitler* took office.

Other epochal molecular beam contributions to physics came from *Isidor Rabi*. He had also been educated as a chemist and worked with *Stern* as a postdoctoral fellow before joining the physics faculty at Columbia. In 1938 he invented his magnetic resonance method. This followed a seminar by *Gorter* from Leiden describing his failed attempt to detect nuclear magnetic resonance in a crystal. It was then not obvious that the tiny nucleus, with dimensions of the order 10^{-13} cm, would interact appreciably with the external atomic electron distribution, with dimensions of the order 10^{-8} cm. If not, the different nuclear spin orientations (favorable "up" or unfavorable "down") would remain equally probable even when subjected to an external magnetic field. There would then be no net absorption of radiofrequency radiation in the magnetic resonance experiment. Spin flips induced by the radiation are equally likely up or down, so net absorption cannot occur unless interactions permit the spins to relax toward thermal equilibrium where more will be up than down.

Rabi immediately realized how to exploit beams to escape this constraint. He introduced two opposing Stern-Gerlach fields. A beam traversing the first field (denoted A) is split into its nuclear spin components, but on passing through the second field (denoted B) these are recombined. Between these fields, which act like diverging and converging lenses, *Rabi* introduced a third field (the C-field). This was homogeneous and so had no lens action, but it served the role of *Gorter*'s field in defining "up" and "down." Since there are no collisions in the beam, there is no means to relax the spin component populations. But now none is needed. Radiofrequency radiation in the C-field region will at resonance flip equal numbers of spins up or down; but now any spin changing its orientation after the A-field will not be refocused in the B-field. In this ingenious way, *Rabi* could detect which frequencies produced resonances. He thus created a versatile new spectroscopy with extremely high resolving power. It has provided a wealth of information about nuclear structure. An analogous electric resonance spectroscopy operates with rotational states of polar molecules. This has likewise been very fruitful for molecular structure. It has also been used to fully analyze the quantum states of products in some reactive scattering experiments.

Shortly before inventing his resonance spectroscopy, *Rabi* undertook some simple elastic scattering studies by observing the attenuation of an alkali atom beam sent through a gas-filled chamber and detected on a surface ionization filament. If *Gorter* had not come by, perhaps *Rabi* would have continued on to develop reactive scattering. Another quirk of fate was only revealed in 1945, when nuclear magnetic resonance was successfully done in li-

quids and solids by *Purcell* at Harvard and *Bloch* at Stanford. Only then did it become clear that *Gorter*'s original experiment would have worked if he had used a material with magnetic impurities which would have induced the necessary relaxation. Yet another epilogue, also of great portent, was the invention of the maser in 1954 by *Townes* at Columbia. In this device, the precursor of lasers, he sent a beam of ammonia molecules through an electric quadrupole focusing field which selected an energetically unfavorable state. When illuminated with microwave radiation, the molecule reverted to the energetically favorable state, emitting the excess energy as a photon. Thus was born molecular amplifiers and oscillators and the now vast industry of quantum electronics. The idea came to *Townes* on a sunny park bench, 33 years after *Stern* woke up early in his warm bed.

My First Encounters with Kinetics and Beams

Within days of my arrival at college, I first learned something of the challenging field of chemical kinetics from my freshman advisor, *Harold S. Johnston*. He was then a young assistant professor at Stanford University, applying new methods of his own devising to measure rates of fast gas-phase reactions in regimes previously inaccessible. In the summer after my sophomore year, and again after my junior year, *Hal* hired me as a lab assistant for his research group. One project involved weeks of glassblowing, silver soldering, and plastering with great quantities of asbestos paste (now outlawed!) to install a large-volume reaction vessel that could be maintained at a high and uniform temperature. I was greatly impressed with the care and attention to detail shown by *Hal* and his graduate students, and his emphasis on testing theory. He stressed that this could only be done with a reaction known to be an elementary step—and that we could never be entirely certain that all steps and intermediates had been correctly identified.

In my senior year, I took *Hal*'s excellent course in chemical kinetics, and the following year a study of transition-state theory begun there became my master's thesis. In this, we calculated the Arrhenius A factors for twelve well-characterized bimolecular reactions involving only four to six atoms. Necessary assumptions about the properties of the transition state were made uniform for the whole set and consistent with similar stable molecules. Internal rotations of the reaction complexes received special attention, thanks to the help of *Kenneth Pitzer* at Berkeley, who kindly showed me how to design a sensible approximation. Previous tests had been piecemeal and often capricious about internal rotations; *Hal* expected our test might prove embarassing for the theory. In fact, the agreement with experiment was good. This persuaded *Hal* that the theory deserved further development; over the next decade he carried this out and produced an exemplary book. Although *Hal*'s contagious enthusiasm had long since convinced me that I wanted to pursue kinetics, the thesis project made me decide to study first the dynamics of stable molecules. Thus I applied to the chemical physics program at Harvard in order to do Ph. D. research with *E. Bright Wilson, Jr.*

A few weeks before turning in the master's thesis, I first heard of molecular beams. In his course on statistical thermodynamics, *Walter Meyerhof* briefly described *Stern*'s test of the Maxwell-Boltzmann velocity distribution. It was love at first sight. I remember a flush of excitement at the thought that this was *the way* to study elementary reactions, the unequivocal way to know a reaction is elementary and to study directly its properties. This was the spring of 1955. I did not imagine that five years later my own first beam apparatus would be nearly complete at Berkeley and I would have met *Otto Stern* himself.

On arrival at Harvard in the fall, I was delighted to discover that *Norman Ramsey* was offering a seminar course based on the proof sheets of his book on molecular beams. *E. B. Wilson* was giving a course using his just published book on molecular vibrations. *Roy Glauber* provided a rigorous treatment of electromagnetic theory, working through all the mathematical derivations in class with no notes at all. The dessert course of this remarkable academic menu was entitled "Chemical Physics," and given by the legendary *Peter Debye*, a visitor that year. His course had 40 or more auditors, but only 3 of us took it for credit and thus had individual oral exams with *Debye*. I still relish the memory of his lucid lectures and the twinkle in his eye as he so often began, "Let me tell you a story ..." Early in *Ramsey*'s course, he too discussed *Stern*'s velocity analysis study and actually announced, in his booming voice: "This would be a wonderful way to do chemistry!" In the spring term I took among others *Kenneth Bainbridge*'s course on nuclear physics to learn something about nuclear reactions; this was indeed to prove very useful later.

Even more exhilarating that year and thereafter was my experience in *Bright Wilson*'s research group. With microwave spectroscopy, he and his students were developing an elegant new way to study internal rotation by exploiting the tunnel effect. Typical systems had a methyl group attached to an asymmetric molecular frame. The torsion or internal rotation of the methyl group about its axis is hindered by a sinusoidal potential barrier with three equivalent minima. If the barrier is very high, then essentially there are only small torsional oscillations in three separate potential wells, and to good approximation the microwave spectrum is that of a rigid rotor molecule. If the barrier is low enough, however, tunneling between the wells occurs and this causes the microwave rotational transitions to split into doublets. These splittings are very sensitive to the barrier height, so an approximate dynamical theory is adequate to extract an accurate value for the barrier. Since I already had seen how prevalent internal rotation is, not only in stable molecules but in transition states for reaction, I was very excited about this new method. It was such a fresh and powerful approach that almost every day some member of the group had an unanticipated result to report. Because the microwave spectra display a forest of transitions, there was ample need to work out variations on the basic theme and satisfying opportunity for definitive tests.

Although this research was entirely different in character from molecular collisions, I learned invaluable lessons from it and from working with *Bright* and his extremely

able group. A microwave spectroscopist simply must calculate as much as possible before plunging into the forest; for a molecular beamist, the need is less obvious but just as vital. *Bright*'s high standards and absolute integrity had great impact on his students. Thus he put strong emphasis on analyzing and clearly stating what is well-established and what is really based on unproven assumptions. He also gave strong emphasis to blocking out the big questions and on coupling theoretical investigations with experiments.

Microwaves soon led to my first work with beams, in collaboration with an ebullient young instructor, *Bill Klemperer*. He had developed a technique for high-temperature infrared spectroscopy and was using it to study alkali halides (later to become my favorite molecules). *Bill* invited me to help build a high-temperature microwave spectrometer, again a project requiring much asbestos paste. One day *Bill* came in with a paper just published by *Marple* and *Trischka* reporting an electric resonance study of lithium chloride. They had used the venerable tungsten surface ionization filament as a detector. Depending on resonance field settings, the apparatus could resolve four vibrational states. However, the vibrational frequency derived from the relative intensities was much lower than *Bill* had measured in the IR. We examined various possibilities and concluded that most likely was an increase in the efficiency of the surface reaction (dissociation of the salt molecule to ions) with vibrational excitation of the incident molecule.[5] This was near Christmas, 1956. Almost 15 years later, the vibrational excitation mechanism was confirmed and recently it has become a leading issue in surface chemistry.

We were eager to study the surface ionization process experimentally. Since an electric resonance apparatus was not available (at that time only three existed, none closer than 300 miles of Cambridge), we could not study alkali halide molecules. Hence we decided to study ionization of alkali atoms as a function of the surface temperature. *Ramsey* kindly lent us one of his machines over Christmas vacation and we quickly obtained a hundred pages or so of data from which we derived residence times and heats of adsorption for atoms on tungsten and platinum surfaces. Then we discovered that very similar data existed in the Russian literature, so did not publish our results. However, this was a key episode for both *Bill* and me. He too fell in love with molecular beams, and immediately undertook to build an electric resonance apparatus. *Bill* and his students have since turned this into a cornucopia for molecular spectroscopy, unprecedented in resolution and chemical scope. Especially revealing have been their studies in recent years of molecules held together by weak van der Waals forces. This work is building an understanding of these ubiquitous forces which may help elucidate the specificity and selectivity of interactions in biomolecules.

In studying the literature on surface ionization, I was elated to discover[6] a paper by *Taylor* and *Datz* from Oak Ridge describing an actual crossed-beam study of the reaction $K + HBr \rightarrow KBr + H$. Although the traditional tungsten surface ionization detector is about equally sensitive to K and KBr, *Taylor* and *Datz* found that a platinum alloy is much more effective for K than for KBr. From the difference in the signals read on the two detector filaments, they were able to distinguish the small amount of reactively scattered KBr from the large background of elastically scattered K atoms. Small as it was, the little difference bump was a joyful sight. In a series of classic studies in the 1920s, *Michael Polanyi* had shown that many alkali reactions proceeded at rates corresponding to "reaction at every collision." With this differential surface ionization detector, there was now prospect that crossed-beam studies of many of these reactions could be made with relatively simple apparatus.

Soon I found another intriguing crossed-beam study, published two years before by *Bull* and *Moon* at Birmingham. They bombarded a stream of Cs vapor with a pulsed accelerated beam of CCl_4 produced by swatting with a paddle attached to a high-speed rotor. The intense CCl_4 beam could be monitored with a simple ionization gauge and signal pulses due to scattered Cs or CsCl were detected by surface ionization on a tungsten filament. Although there was no direct means to distinguish between Cs and CsCl, the observed signal pulses appeared to come primarily from reactively scattered CsCl, on the basis of time-of-flight analysis and blank runs with the CCl_4 replaced by Hg vapor. Unjustly, these experiments were long discounted or ignored. This was due to the misconception that elastic scattering would always predominate. The high-speed rotor technique also intimidated other prospective experimenters; thus this fine early work did not have the impact it deserved.

During the spring of 1958, while completing my Ph. D. thesis, I visited several universities as a faculty candidate. My seminar about internal rotation was always well received, but my plans for beam experiments sometimes produced outright dismay. Yet the response was often enthusiastic from faculty young in either age or spirit. I was delighted to accept an assistant professorship at Berkeley, especially since *Hal Johnston* was now there and also *Bruce Mahan*, who had the year before completed his Ph. D. at Harvard in kinetics with *George Kistiakowsky*. My appointment was to take effect a year later; meanwhile I continued at Harvard as a Junior Fellow of the Society of Fellows. The intervening year was extremely useful. It gave me time to work out detailed calculations for design of the beam apparatus and a kinematic theory for interpreting crossed-beam experiments. Membership in the Society of Fellows was also a great pleasure because it brought together intense people from all academic disciplines. Monday night dinners included the two dozen Junior Fellows, ten Senior Fellows, and typically ten guests, in a "neo-Pickwickian atmosphere" with ample wine and cigars too good to have saved the *Stern-Gerlach* experiment.[7]

Just before departing to Berkeley, I went to say goodbye to *Kistiakowsky*. Like so many others, I revered him as a scientist and a sage as well as an awesome personality. He confirmed a legendary story about a molecular beam experiment he and *Slichter* had tried in 1951 to test early theoretical calculations on the properties of supersonic expansions.[8] Because of inadequate pumping speed, the experiment was inconclusive and a miserable struggle. Afterwards, *Kisty* destroyed the apparatus with an ax! He said to me, with his extra heavy Russian accent (conveying

whimsey—or so I hoped): "So you have been bitten by the molecular beam bug. Too bad! The trouble is that there are no collisions in one beam, and no collisions in the other beam, so when you cross them there are still no collisions!"

Early Alkali Age of Reactive Scattering

At Berkeley, I was soon joined by two graduate students, *George Kwei* and *Jim Norris*. Space was in short supply, and we were content with a corner (only 4 m × 6 m) of a lab in Lewis Hall. Our first task was to remove a large calorimeter that had long occupied that corner; this we viewed as a rite of passage, with the historical perspective of Figure 1 already in mind. The beam apparatus we installed (dubbed *Big Bertha*) was almost rudimentary. As shown in Figure 3, the beams were formed by thermal effusion from ovens mounted on a turntable which could be rotated to sweep the angular distribution of scattered atoms and molecules past the surface ionization detector. Typically, the distance from the scattering center to the alkali oven was 10 cm, to the other oven 1.5 cm, and to the detector 10 cm. Use of a double-chamber oven for the alkali allowed the temperature of the beam emerging from the upper chamber to be varied by about 300 degrees independently of the vapor pressure established in the lower chamber (about 0.1 torr), which governed the beam intensity. The oven for the reactant gas was connected to an external barostat by a supply tube which passed through the support column in the rotatable lid. Cold shields and collimating slits hid both ovens from the scattering center, and a cold shield also surrounded the detector. The entire scattering chamber was enclosed in a copper box attached to a large liquid nitrogen trap. Since the reactants are condensable, the cold shields and trap provided very high pumping speed. This kept the background vacuum in the scattering chamber low enough (of the order 10^{-7} torr) to ensure that collisions with background gas were negligible for both the reactant beams and the product molecules in flight to the detector.

In typical experiments, the concentration of alkali atoms within the volume defined by the intersection of the beams was about 10^{10} cm^{-3}, equivalent to a pressure of 10^{-6} torr, and that of the reactant gas molecules was about 100-fold

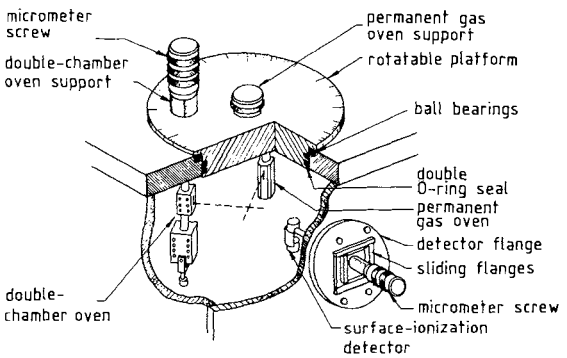

Fig. 3. Crossed-beam apparatus *Big Bertha* for study of alkali atom reactions. Cold shields, collimating slits, shutters to interrupt the beams, and other details omitted.

greater. About 10^{15} alkali atoms s^{-1} entered the reaction volume, of which roughly 0.1–1% reacted to form products while about 10% underwent elastic scattering. The steady-state concentration of products in the reaction volume was roughly 10^{7} to 10^{8} molecules cm^{-3}, the pressure about 10^{-9} to 10^{-10} torr. At the peak of the angular distribution of reactive scattering about 10^{10} to 10^{11} product molecules cm^{-2} s^{-1} arrive at the detector. Since conversion to ions on a hot tungsten or platinum surface is nearly 100% efficient for alkali species, such yields gave readily measurable signals of the order of 10^{-13} A. For many of the reactions studied more than a month would be required to deposit a monolayer of product molecules, so it was essential to have a detector far more sensitive than *Stern*'s cigar.

Experiments Revealing Product Recoil

Our first experiments were begun in the fall of 1960. On the basis of simple theoretical considerations, we decided to try reaction (a). From the angular distribution of the

$$K + CH_3I \longrightarrow KI + CH_3 \qquad (a)$$

reactively scattered KI we hoped to learn whether there was any preferred direction relating the reactant and product relative velocity vectors and also to get some idea how the reaction energy is partitioned between internal excitation of the product molecules and their relative translational motion. Our rationale was based on the CH_3/KI mass ratio. A simple kinematic calculation (see Fig. 5) showed that this ratio was large enough to permit the detected product KI to recoil sufficiently far away from the centroid to reveal any directional preference, but small enough to inhibit the KI from spraying out so widely that the reactive scattering became too weak to observe. Happily, even the first experiments worked nicely. Our kinematic rationale was vindicated, but it was not until three years later that we learned how lucky was this choice of reaction system; it turned out that CH_3I played the role of *Stern*'s cigar.

Figure 4 shows typical results. In Figure 4a, the parent K beam was attenuated 7% by the perpendicularly crossed

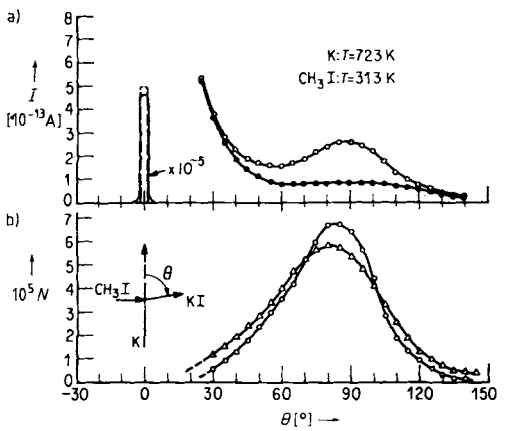

Fig. 4. Reactive scattering data: a) Parent K beam of 5×10^{-8} A attenuated 7% by crossed CH_3I beam. Readings on Pt detector (•) normalized to W (○) at parent beam peak. I = intensity. b) KI distributions; ○ derived from a), △ from a replicate experiment several months later. Area under curves gives collision yield. N = yield.

CH_3I beam; that represents chiefly elastic scattering. Readings on the platinum detector (solid points) were normalized to those on tungsten (open points) at the parent beam peak. In this case, the use of differential detection was not crucial, as the KI distribution (Fig. 4a, right) is displaced far enough from the K beam to appear as a pronounced bump in the signal from the tungsten detector. In Figure 4b, the KI distribution is normalized so that the area under the curve gives the collision yield (integrated intensity of KI divided by total K scattered out of the parent beam). This is about 5×10^{-4} and indicated the reaction cross section (or effective target area) is about 7 Å^2. Measurements at several temperatures of the incident beams indicated that the activation energy for reaction (a) is negligibly small, less than 0.3 kcal mol^{-1}. The new dynamical information we were after is contained in the location and shape of the product angular distribution, however. To extract that information we used a kinematic analysis derived from conservation laws that hold regardless of the forces governing the collision.

Kinematic Analysis Via Newton Diagrams

Velocity vector diagrams such as Figure 5 are a convenient aid in the kinematic analysis. The vectors pertain to the asymptotic initial and final states of the collision. By virtue of momentum conservation, the center-of-mass velocity vector $\boldsymbol{C}$ remains constant throughout; only motion relative to $\boldsymbol{C}$ involves chemical interactions. The recoil velocity vector $\boldsymbol{u}$, which carries the product KI away from $\boldsymbol{C}$, can have any direction, but energy conservation limits its magnitude. Thus, the possible spectrum of recoil vectors $\boldsymbol{u}$ is represented by a set of spheres, one for each accessible value of the final relative translational energy of the products. This energy ranges up to a maximum determined by the initial collision energy and the difference in dissociation energy of the new bond formed and the old bond broken.

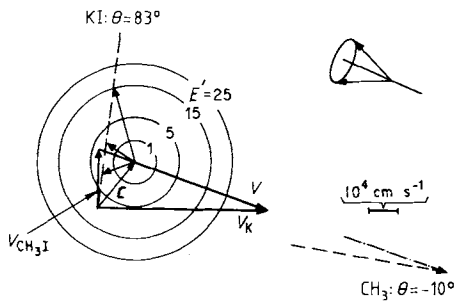

Fig. 5. Newton diagram corresponding to most probable velocities of reactants in Figure 4. Spheres indicate range of KI recoil vectors allowed by conservation of energy and linear momentum; each is labeled by value of E' [kcal mol^{-1}], the final relative translational kinetic energy. Distribution of recoil vectors must have cylindrical symmetry about initial relative velocity vector, by virtue of "dart board" randomness of collisions. Three sample recoil vectors are shown that correspond to the KI observed at the peak of the angular distribution. Also shown is estimate of most probable recoil vector for CH_3 product.

From the velocity vector diagram we see that the broad peak observed near 83° in the laboratory corresponds to reactive scattering in which an observer riding with the center of mass would see the product KI recoil into the backward hemisphere (and the CH_3 forwards) with respect to the incoming K beam. Markedly anisotropic scattering of this kind evidently corresponds to a "hard" collision dominated by repulsion, as the K atom, the CH_3 group, and the center of mass of KI must all reverse direction. We called this the *rebound* mechanism. It was later found for many other reactions dominated by repulsion.

Comparison with the velocity vector diagram also permits an estimate of the energy in product relative translation. This affects the displacement of the laboratory angular distribution from that of $\boldsymbol{C}$ as computed from the initial conditions. In assessing the displacement, it is necessary to take proper account of a Jacobian factor which enhances the intensity of the laboratory scattering at low recoil velocities. We failed to include this Jacobian in our early work (thereby unwittingly emulating *Otto Stern*) and hence underestimated the product translation. The correct analysis showed that for reaction (a) about half of the available energy appears in recoil of the products. This result, later confirmed by direct measurement of the KI velocity distributions, again exhibited the dominant role of repulsive forces in a *rebound* reaction.

For kinematic analysis, Newton's laws suffice. In the asymptotic translational states the beam molecules are too far apart to interact, hence need not be precisely localized in space and can be assigned definite momenta despite *Heisenberg*'s principle. Accordingly, we named our velocity vector constructions "Newton diagrams." These are still much used today, as kinematic analysis is an essential part of the design and interpretation of any collision experiment.

Frustrations and Preparations

We were very happy to find this clear evidence for a preferred range of product recoil angle and energy and were eager to study other alkali atom reactions to look for variations in the scattering patterns that might be correlated with electronic structure. However, we encountered frustrating difficulties with the surface ionization detector. Many reactant gases (other than alkyl halides) poisoned the Pt filament, inducing spurious and irreproducible responses that precluded measurement of reactive scattering. This difficulty stymied us until the fall of 1963, when we finally eliminated it by means of a procedure due to *Touw* and *Trischka*. They demonstrated that the Pt filament could be stabilized in either of two distinct modes. The Pt filament becomes essentially *nondetecting* for alkali compounds (but still detects alkali atoms) if it is preheated while doused with methane or another hydrocarbon. The Pt filament becomes *detecting* for alkali compounds and acts just like a W filament if it is instead preheated while doused with oxygen or merely operated in a sufficiently clean vacuum. The nondetecting mode evidently requires a stable carbon layer on the filament. Thus, the differential detection so useful for alkali reactive scattering results from a dirty surface. Before the preheating procedure was developed, the carbon deposit was a matter of luck, supplied either by pump-oil vapor if the vacuum were poor or

by hydrocarbon-rich reactant species such as methyl iodide; either acted like *Stern*'s cigar.

During the lean period of more than two years before rescue by a dirty detector, our only successful reactive scattering experiments dealt with variants of reaction (a), involving other alkali atoms and alkyl groups with up to seven carbon atoms. However, in this period our research group expanded rapidly and we constructed much new apparatus, experimental and theoretical, that was destined to bring a harvest of results. *Jim Kinsey, Ken Cashion, Mark Child,* and *Malcolm Fluendy* joined as postdoctoral fellows, and *Phil Brooks, Kent Wilson, John Birely, Ron Herm, Jim Cross,* and *Dick Zare* as graduate students. Figure 6 provides a succinct summary, indicating the chief projects pursued by this distinguished roster during our Berkeley era.

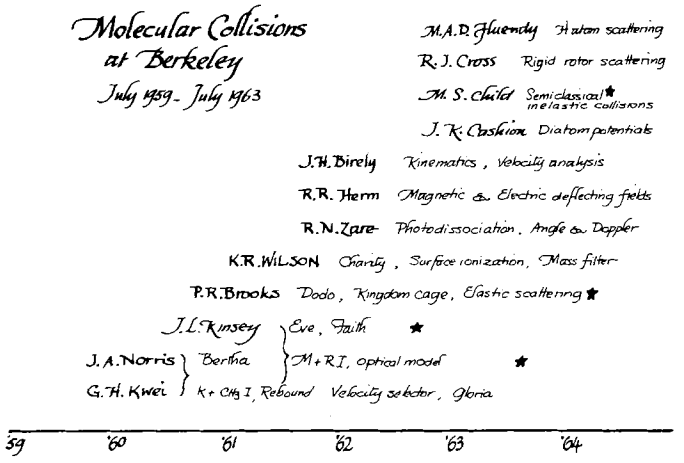

Fig. 6. Roster of graduate students and *postdoctoral fellows* with chief research projects during Berkeley era. Our first apparatus was a helium leak detector called Annie; hence our successive beam machines were named Bertha, Charity, Dodo, Eve, Faith, Gloria, etc. Stars indicate completion of Ph.D. theses or postdoctoral term.

In particular, we note among the apparatus construction projects three analyzing devices: rotating slotted-disk velocity selector, inhomogeneous magnetic deflecting field, and inhomogeneous electric deflecting field. These devices are quite similar to those used by *Otto Stern*; we liked to say that reactive scattering followed the evolutionary principle, "ontogeny recapitulates phylogeny." As seen already, velocity analysis was essential to obtain quantitative data for the recoil angle and translational energy distributions. Magnetic analysis provided, among other things, a definitive test of our detection technique, immune to poisoning of the filaments. By deflecting away most of the paramagnetic alkali atoms, we could measure directly the distribution of diamagnetic alkali halide molecules produced by reactive scattering. Electric deflection of these polar molecules enabled us to determine the rotational angular momentum. This had special appeal for me because of my background in rotational spectroscopy. Furthermore, since mass, velocity, and position all enter into angular momentum, it was clearly a key property for theoretical models of reaction dynamics.

Among our theoretical studies of this period was a treatment of the velocity vector distribution of fragments from molecular photodissociation. This was undertaken because already we had vague notions of a kinship between chemical reactions and photodissociation. In electronic excitation by photons, the angular dependence is determined simply by the dipole selection rule whereas the exit velocity of the photofragments is determined by the repulsive potential of the excited state. This "half-collision" model, worked out nicely by *Dick Zare*, provided rather general "form factors" for numerous properties.[9] Subsequently, this has served as the basis for extracting a lode of information about dissociative excited states by means of laser spectroscopy, and the suspected link with reaction dynamics did indeed emerge.

Our Berkeley days also included several memorable visits with others captivated by reaction dynamics. One of these occurred in the early summer of 1961, when I visited *Don Bunker* at Los Alamos. He had undertaken the first realistic Monte Carlo calculations of classical trajectories for chemical reactions, and his initial aim was to interpret our results for the $K+CH_3I$ system in terms of potential surface features. The scene in his office comes back vividly:[10]

> ... He was decorating the walls with strips of recorder chart paper several yards long, on which were plotted a series of undulating, intertwined curves. These were the first results of his Monte Carlo calculations. ... The room was bright with sunshine and the varicolored curves seemed to shimmer and dance about, as if choreographed to *Don*'s crisp and witty description. It was an exhilarating moment. Henceforth the mechanics of molecular collisions for any postulated force field could be computed, as he liked to say, "in instructive and entertaining detail."

Such classical trajectory calculations, as developed especially by *Martin Karplus* and *John Polanyi*, have indeed proven invaluable for interpreting data and testing concepts of reaction dynamics.

Other inspiring encounters came in April, 1962, at a Faraday Society Discussion held at Cambridge University, where I met many leading workers in chemical kinetics. Equally inspiring was a solo visit to Berkeley a few months later by *Michael Polanyi*. He witnessed an unsuccessful scattering experiment on the $K+Br_2$ reaction while he described to us his prescient speculations of 30 years before that it might proceed by a stripping mechanism with high vibrational excitation of the KBr product. He also mentioned that he liked to think that the attacking alkali atom used its valence electron to "harpoon" the halogen. Later I adopted this term to enliven numerous discussions of electron-transfer reactions.

From Rebound to Stripping with Rainbows Between

Within a few months my group was discussing an unanticipated transfer to Harvard. We had expected to relocate in a new lab about 100 m away in the basement of the nearly completed Latimer Hall, but in the late summer of 1963 instead moved 5000 km to the basement of Mallinckrodt Laboratory. I went even further that summer, as I'd agreed to present a lecture course on molecular collisions

at Göttingen University. There I strolled daily along the path atop the encircling medieval wall, the path taken by many of the pioneers of quantum mechanics during ambulatory debates. But only by communing with the charming little Goose Girl in the Rathaus fountain was I reconciled to the quantumlike dualities of the Harvard/Berkeley choice.

Our new lab was in nearly full swing by Halloween and soon we learned how to avoid poisoning our detector filaments. Thereafter results were rapidly obtained for a wide range of alkali reactions. As illustrated in Figure 7, many showed striking contrasts to reaction (a). We found that for reaction (b) and similar systems the reaction cross section

$$K + Br_2 \longrightarrow KBr + Br \qquad (b)$$

is remarkably large, ca. 200 Å^2, and most of the alkali halide product recoils into the forward hemisphere with respect to the incident alkali atom. These features indicate dominantly attractive interaction in which the bond exchange can occur for quite large impact parameters. This suggests a *stripping* mechanism of the type familiar in nuclear physics. In an independent study of reaction (b), *Minturn* and *Datz* obtained similar results and many other examples of *stripping* reactions were soon found.

Before long, we had examples for which the reaction cross section is of intermediate size and the product peaks sideways, giving a conical angular distribution about the direction of the initial relative velocity vector. Such a case is reaction (c) (see Fig. 7).

$$K + CCl_4 \longrightarrow KCl + CCl_3 \qquad (c)$$

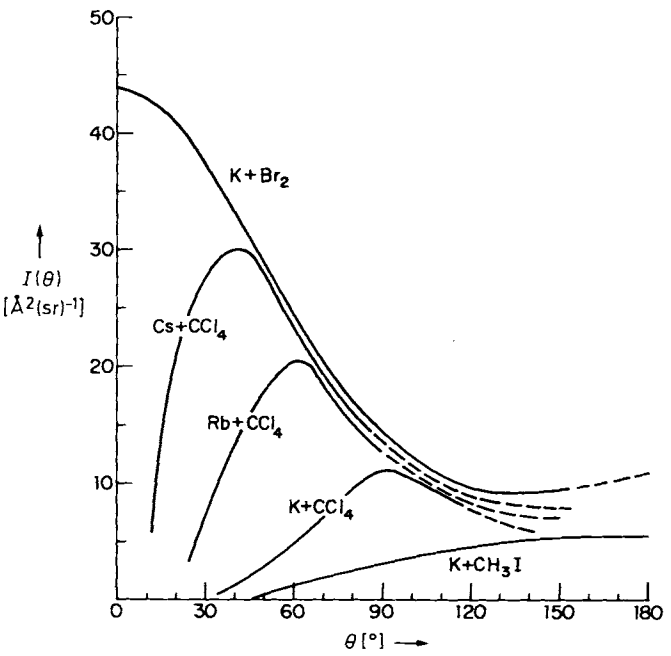

Fig. 7. Comparison of scattering angle distributions, $I(\theta)$, for reactions of alkali atoms with Br_2, CCl_4, and CH_3I, illustrating stripping, transitional, and rebound behavior. Ordinate scale indicates approximate normalization to total reaction cross sections. Distributions show angular variation that would be seen by a hypothetical observer traveling with the center of mass. Scattering angle, θ, indicates deviation of product relative velocity from reactant relative velocity; for $\theta = 0°$, the alkali halide emerges in same direction as incident alkali atom.

A strong correlation emerged: as the magnitude of the total reaction cross section increases, the preferred recoil direction of the alkali halide product shifts forwards. This is exemplified as K→Rb→Cs for the CCl_4 reaction (Fig. 7), whereas the angular distributions do not change much with the identity of the alkali atom for the CH_3I case or the Br_2 case. Velocity analysis experiments likewise show a nice contrast. The product translational energy is large for the CH_3I case and small for the Br_2 case, but the angular distributions do not change much with the exit energy. For the CCl_4 reaction, the preferred direction of the product moves forward rapidly as the translational recoil energy increases. The form of this strong angle–energy coupling resembles the *rainbows* familiar in elastic scattering of molecules and in sunny but moist skies.

The marked anisotropy of the product angular distributions for this family of reactions, ranging between rebound and stripping, indicates that all proceed by a *direct* or *impulsive* mechanism. The duration of the reactive collisions must be so short that most of the transient collision complexes decompose before rotating through 180°. Since the rotational velocities are quite high, roughly half or more of the complexes must decompose within about 5×10^{-13} s, a time not much longer than a vibrational period.

The dynamical properties and chemical variations found for these alkali reactions were well suited to the early Monte Carlo trajectory studies and also prompted several insightful heuristic models. Ironically, trajectory studies of product angular distributions suffered at first from an instructive malady akin to the poisoning problem that had held up our experiments. The calculations for atom exchange reactions, A+BC→AB+C, used plausible forms of potential energy surfaces with empirical parameters. These surfaces were constructed by adding up pairwise interactions modulated by switching functions to weaken each bond as the collision partner draws nigh. *Blais* and *Bunker* found that reactive trajectories for such surfaces gave chiefly backward scattering, in satisfying agreement with our first experiments. But this rebound behavior was unduly prevalent; for about two years after the discovery of stripping and rainbow-like reactive scattering, trajectory calculations remained unable to obtain anything but backward scattering. *Godfrey* and *Karplus* cured this affliction using potential surfaces derived from approximate quantum-mechanical secular equations. This ensured a smooth surface, free from spurious bumps and wrinkles that appeared in surfaces constructed by adding piecewise interactions. It was "contamination by such warts" that induced too much backward scattering. By varying the repulsive or attractive character of the wartless surfaces, the trajectory calculations nicely elucidated the various trends associated with transition from rebound to stripping. Likewise, trajectory studies by *John Polanyi* and his students mapped out the systematics of energy disposal among product translation, vibration, and rotation.

We now could also relate these general dynamical properties of alkali reactions to the electronic structure of the target molecules. All these reactions involve converting a covalent bond into an ionic bond, and in effect are gas-phase acid–base or ion–recombination processes, via reaction (d).

$$A + BC \longrightarrow A^{\oplus} + (BC)^{\ominus} \longrightarrow A^{\oplus}B^{\ominus} + C \qquad (d)$$

According to *Michael Polanyi*'s *harpooning* model, the attacking alkali atom tosses out its valence electron, hooks the halogen-containing molecule, and hauls it in with the Coulomb force. The basic features of the initial electron transfer had been examined as early as 1940 in an exemplary theoretical study by *Magee*. As pictured schematically in Figure 8, the transfer occurs in the vicinity of "curve crossing" between zeroth-order "purely covalent" and "ion-pair" potential surfaces. When the crossing radius r_c is large enough, Coulombic attraction is dominant there and this radius may be estimated from Equation (e),

$$e^2/r_c = IP(A) - EA(BC) \qquad (e)$$

the difference in the ionization potential of the alkali atom and the electron affinity of the target molecule. This relates the size of the reaction cross section to the energy required to create the ion pair.

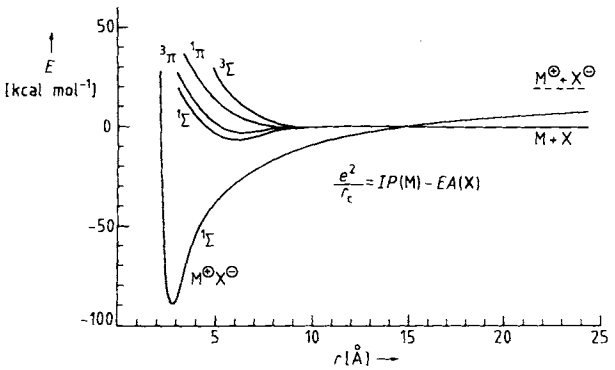

Fig. 8. Potential energy curves for an alkali halide molecule (drawn for KBr) showing the "zeroth-order" crossing of the ionic and covalent states.

However, the dynamical properties are also greatly influenced by the exit interaction as the $A^{\oplus}$ ion approaches the intermediate molecule-ion $BC^{\ominus}$, which is severely distorted by the strong electric field and dissociates [cf. reaction (d)]. Accordingly, many dynamical features will differ with the shape and particularly the location of the asymptote of the potential curve for the negative molecule ion. Often we could estimate the relevant potential curves for the $BC^{\ominus}$ ion from data obtained in electron impact experiments or by means of arguments developed by *Mulliken* for the analysis of charge-transfer spectra. Figure 9 classifies some of the possibilities.

For instance, the case designated $I^{\ominus}C$ pertains to the CH_3I reaction and many other examples of rebound reactions. The negative ion is then formed in a strongly repulsive state, because the harpooning electron enters a strongly antibonding molecular orbital with a node between the originally bonded atoms. This is usually the same orbital that governs photodissociation of the parent molecule, so we could derive the location and shape of the exit potential curve from its absorption spectrum.

In contrast, the case designated $I^{\oplus}A$ pertains to the Br_2 reaction and many of the prototype stripping systems. These involve exceptionally large electron affinities, which

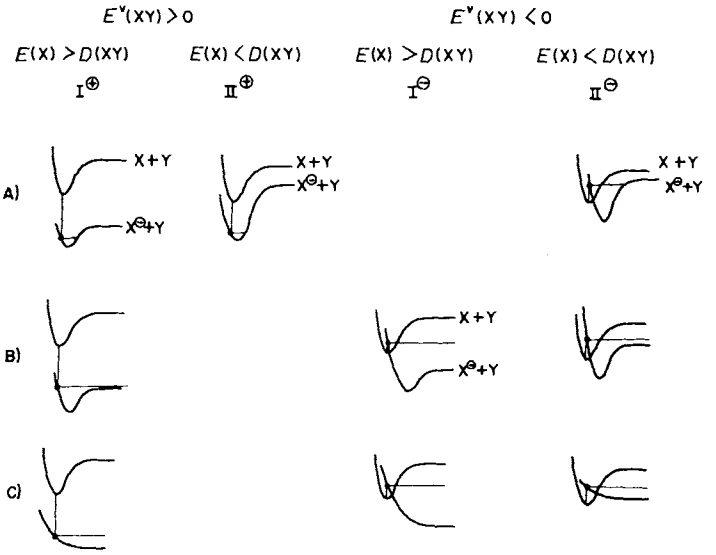

Fig. 9. Classification of electron attachment processes producing negative molecule ions ($XY + e \rightarrow XY^{\ominus}$). Here D denotes the bond dissociation energy, E the adiabatic and E^v the vertical electron affinity.

accounts for the very big reaction cross section and the long-range attraction that gives forward scattering. Here the intermediate negative molecule ion would be stable in the absence of the positive ion, although highly excited vibrationally. But when the ions are within the crossing radius of about 7 Å^2, the Coulomb field exceeds 3×10^9 V cm^{-1} and thus the negative ion will be pulled apart in a time comparable to a vibrational period, or ca. 10^{-13} s. This accounts for the direct character of the reaction. However, the transient attractive coupling between $B^{\ominus}$ and C in the exit channel has a major role in the energy disposal.

The harpooning model prompted treatments of many other properties, such as the mechanics of curve crossing and dissociative electron attachment, orientation dependence, and orbiting outside a centrifugal barrier at the crossing radius. But in terms of chemical perspective, the most striking aspect was the connection to charge-transfer spectra. In retrospect, the detection-imposed limitation of early beam studies was fortunate, as this alkali family was ideally suited for relating reaction dynamics to the electronic structure of reactant molecules.

Elucidating Polanyi Flame Reactions

As well as demonstrating very large reaction rates, the classic studies of alkali–halogen reactions by *Michael Polanyi* also revealed intense emission from electronically excited alkali atoms. This had a major role in early discussions about interaction of electronic and nuclear motions, as the Polanyi flames preceded by a few years the Born–Oppenheimer and Franck–Condon approximations, both found in 1925. Some central questions concerning the chemiluminescence remained unresolved 40 years later, however, when we undertook beam experiments to examine each of the postulated elementary steps in the flame mechanism. Again, the results exemplified prototypical aspects of electronic structure.

One of the key steps producing chemiluminescence involves *vibrational-to-electronic* energy transfer. This we studied by means of a "triple-beam" experiment. Vibrationally excited $KBr^{\dagger}$ was formed at the intersection of crossed beams of K and Br_2 and sent into a second scattering chamber containing a Na crossed beam, where fluorescence from K* was observed. The cross section found for this *reactive transfer* process [reaction (f)] is very large, 10–100 Å^2, whereas that for *nonreactive transfer* [reaction (g)]

$$Na + KBr^{\dagger} \longrightarrow NaBr + K^* \quad (f)$$

$$K + NaBr^{\dagger} \longrightarrow K^* + NaBr \quad (g)$$

is at least tenfold smaller. (The dagger denotes high vibrational energy, the asterisk denotes the lowest ^2P excited electronic state.) This result is interesting because the initial energy distributions of the reactants are nearly the same in the $Na + KBr^{\dagger}$ and the $K + NaBr^{\dagger}$ experiments and the same set of potential surfaces is accessible in both cases. On energetic or statistical grounds, both processes might have been expected to form $K^* + NaBr$ with the same probability. The interpretation becomes clear when the ionic character of the bonding is considered. If in the intermediate $(AB)^{\oplus}X^{\ominus}$ complex the $(AB)^{\oplus}$ ion decomposes rapidly and irreversibly in the field of the $X^{\ominus}$ ion, configurations in which both A and B are symmetrical with respect to both charge-sharing and interaction with $X^{\ominus}$ may seldom be traversed. The chemical exchange process ($A + B^{\oplus}X^{\ominus} \rightarrow A^{\oplus}X^{\ominus} + B^*$) is then more favorable for electronic excitation because it involves charge transfer ($B^{\oplus} + e \rightarrow B^*$), whereas the nonreactive process ($A + B^{\oplus}X^{\ominus} \rightarrow A^* + B^{\oplus}X^{\ominus}$) does not involve charge transfer. Later, we found *translational-to-electronic* energy transfer for these systems exhibits the same strong preference for reactive over nonreactive transfer, although the cross sections are a thousandfold smaller. Potential surface calculations indicate this preference appears to involve a "stereospecific" orientation dependence. The potential surfaces for the ground and excited states remain widely separated except for nearly collinear configurations with the halogen between the two alkali atoms.

In the other major chemiluminescent step, the same potential surface complex is reached via harpooning, $X + AB \rightarrow (AB)^{\oplus}X^{\ominus} \rightarrow A^{\oplus}X^{\ominus} + B^*$. This we studied by generating a beam of halogen atoms from thermal dissociation in a graphite oven and a beam of alkali dimers from a supersonic expansion. Contrary to previous indirect evidence, our beam experiments showed that this step occurs with a large cross section, ca. 10 Å^2. A "degeneracy-induced" excitation mechanism proposed long before by *Magee* was thereby vindicated. The reactant halogen atom has threefold orbital degeneracy, corresponding to location of its valence-shell "hole" in the p_x, p_y, or p_z orbital, whereas the reactant and product molecules are in nondegenerate electronic states. Thus the reactants give rise to three distinct potential energy surfaces but only one of these can lead to the nondegenerate ground state of the product alkali atom and the other two surfaces must lead to electronically excited states.

Many other aspects of the harpooning mechanism were revealed in subsequent studies of electronic excitation processes.[11] Particularly striking was evidence for an "internal reflection" mechanism. This is illustrated in Figure 10 for $K + SO_2$ collisions. Intense emission of $K^*(^2P)$ fluorescence is seen at collision energies above the endoergicity (1.6 eV) for this excitation. The emission increases strongly up to the threshold (3 eV) for formation of $K^{\oplus} + SO_2^{\ominus}$ ion pairs and then declines steeply. At energies above the $A^* + X$ asymptote but below the $A^{\oplus} + X^{\ominus}$ asymptote, trajectories that make the $A + X \rightarrow A^{\oplus}X^{\ominus}$ crossing and intend to exit via the ion-pair channel find it closed. This flux must be reflected back and redistributed at the $A^{\oplus}X^{\ominus} \rightarrow A^* + X$ and $A^{\oplus}X^{\ominus} \rightarrow A + X$ crossings until ultimately it escapes via either the excitation channel or the original entrance channel.

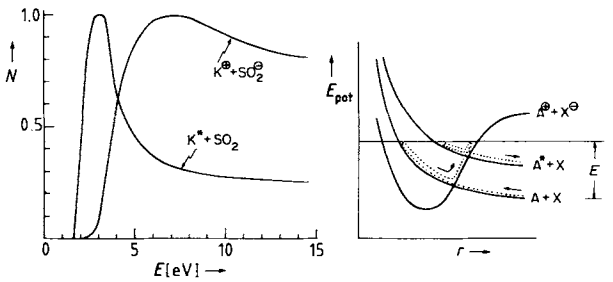

Fig. 10. Cross sections for electronic excitation and ion-pair formation on impact of K atoms with SO_2 molecules, as functions of initial relative kinetic energy E; N = normalized ion and light yields. Schematic potential curves at right show reaction path illustrating "internal reflection" mechanism.

Persistent Collision Complexes with Glorys Galore

Until late 1966, the alkali reactions studied in crossed beams or in Polanyi flames all converted a *covalent* bond into an *ionic* bond, and all appeared to involve abrupt, *impulsive* reaction dynamics. Likewise, by then trajectory calculations for A + BC reactions had explored a variety of "mountain-pass" and "ski-run" potential energy surfaces, and found that the lifetime of the transient A-B-C complex is usually too short for rotational or even vibrational motions; the products typically emerge within 10^{-13} s or less. However, we expected that suitable systems would form a lingering or *persistent* complex with lifetime long compared to rotational as well as vibrational periods. In this regime, the angle and energy distributions of the scattered products would give information about the *unimolecular* decomposition of the complex.

Among alkali reactions, likely candidates were the exchange reactions with alkali halides [reaction (h)] at ordi-

$$A + X^{\ominus}B^{\oplus} \longrightarrow A^{\oplus}X^{\ominus} + B \quad (h)$$

nary thermal energies, too low to permit electronic excitation. For these *ionic + ionic* reactions, since an ion pair is present throughout, electron transfer can enhance attraction rather than induce exit repulsion. Furthermore, the near equality of the $A^{\oplus}X^{\ominus}$ and $B^{\oplus}X^{\ominus}$ bond strengths and the exceptional stability of the diatomic alkali molecule ions (just then confirmed in the Ph. D. work of *Yuan Lee*

with *Bruce Mahan*) favor formation of an $(AB)^{\oplus}X^{\ominus}$ complex of appreciable lifetime. Electronic structure calculations subsequently demonstrated that the potential energy surfaces for dialkali halides indeed have a pronounced basin, corresponding at its minimum to a triangular complex stable by about 10 kcal mol^{-1} or more with respect to the separated products.

With the aim of studying these alkali atom + alkali halide reactions, before departing Berkeley we had begun constructing an apparatus with a mass spectrometer behind the surface ionization filament, to provide differential detection for both of the product species and both of the reactant species. *Walter Miller* and *Sanford Safron* completed the apparatus at Harvard and obtained lovely evidence for persistent collision complexes in more than a dozen of these exchange reactions. In each case, the angular distribution of products has symmetry about 90° and peaks very strongly near 0° and 180°. Furthermore, at wide angles the nonreactive scattering shows a "sticky collision bump" arising from breakup of the complex to reform the reactants rather than proceed to products.

We found the angular distributions could be nicely interpreted in terms of a statistical model adapted from the compound nucleus treatment of nuclear fission. The symmetry about 90° indicates that the complex persists for at least a few rotational periods and hence many vibrational periods. This permits a rough estimate of 5×10^{-12} s as a lower limit for the mean lifetime of the complex. The strong peaking at 0° and 180° indicates that the typical complex forms and dissociates with centrifugal angular momentum much larger than the rotational momenta of the reactant or product salt molecules. As illustrated in Figure 11, the products emerge with equal probability at all azimuthal angles about the total angular momentum vector J of the complex, like water from a lawn sprinkler. The complete angular distribution is obtained by averaging uniformly over all orientations of the sprinkler about the relative velocity vector V of the reactants. The result corresponds to the intersections of circles of latitude and longitude on a globe. The product intensity is low in the equatorial regions but becomes very high in the polar regions, near 0° and 180°. This prominent peaking forward or backward along V is called a "glory," after an analogous effect in light scattering from raindrops.

The glory peaks are rounded off when much of the angular momentum J appears in rotational tumbling of the reactant or product molecules rather than centrifugal motion. As seen in Figure 11, this tilts the spinning sprinkler away from the polar regions. The shape of the product angular distributions thus reveals the relative contribution of the centrifugal and tumbling motions. This is illustrated in Figure 12. In turn, the statistical model links the angular momentum disposal to the moments of inertia of the complex in the transition states for formation and decomposition. The arrangement of atoms and the rotational motions in the transition state thereby can leave its imprint in the product angular distribution, even though the complex may dissociate after only a few rotations.

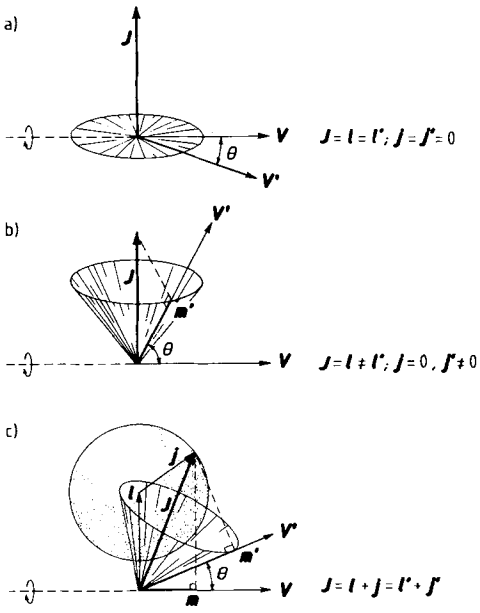

Fig. 11. Relationships among initial and final angular momenta and relative velocity vectors for a long-lived collision complex. In case a) there is no rotational momentum for either the reactant or product molecules; in b) it is present only for the products; in c) for both reactants and products. For fixed magnitudes of the total angular momentum J and the projections m and m' on the relative velocity vectors, the product angular distribution is generated by uniform precessions of V' about J and J about V.

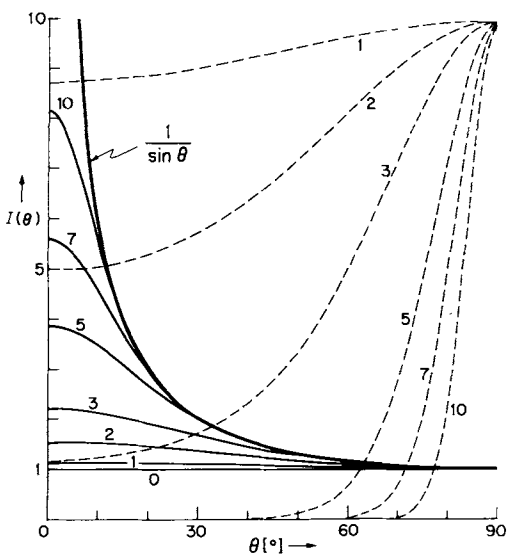

Fig. 12. Angular distributions for the statistical complex model, averaged over distributions of angular momenta appropriate to a prolate complex (solid curves) or an oblate complex (dashed curves), for case b) of Figure 11. All the curves are symmetric about 90°. The index gives the ratio of the maximum value of reactant orbital angular momentum l_{max} to the average value of the projection m' for the dissociating complex; thus the index indicates the relative contribution of centrifugal and tumbling motions.

The product energy distributions are more directly related to properties long familiar in the theory of unimolecular reaction rates. The main features are governed primarily by the statistical densities of rotational and vibrational states at the transition state, as in the Rice-Ramsberger-Kassel-Marcus (RRKM) treatment of unimolecular rates. Qualitative aspects are illustrated in Figure 13. In partitioning the available energy among relative translation, vibration, and rotation of the products, the statistically favored situation puts only a small part into transla-

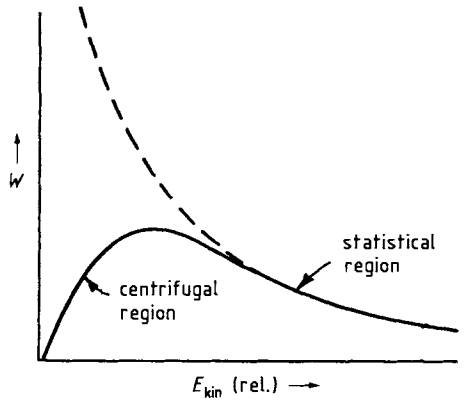

Fig. 13. Schematic distribution of product relative kinetic energy as predicted from statistical theory, without (dashed) and with (solid) the centrifugal contribution that enters for a rotating complex. W = probability.

tion, since the vibrational and rotational modes are more numerous. Thus, the probability distribution declines rather rapidly with increase in product translation energy. This decline becomes more rapid as the number of atoms in the complex increases and hence the number of vibrational modes increases. Another effect enters when the complex is rotating, however. The energy in centrifugal motion is not available for statistical distribution among the other modes. On decomposition of the complex this centrifugal energy is converted into relative motion of the emerging product molecules. This changes the shape of the product translational energy distribution. The low-energy region is determined by the centrifugal contribution, the high energy region by the statistical contribution.

As outlined here, the statistical model pertains to a "loose" complex defined by the exit and entrance centrifugal barriers associated with long-range attraction. Within these barriers, the energy disposal is assumed to be statistical; outside, the collision partners are assumed to rotate freely and travel like point masses subject to two-body forces. This simple model has worked well for many reactions, although various refinements are needed for quantitative analysis. Other basic factors enter for a "tight" complex. The transition state then occurs at a potential barrier rather than a centrifugal barrier, and bond deformations are required to surmount the barrier. This implies that energy can be exchanged between different degrees of freedom as the system moves from the transition state to the separated products. With allowance for such effects, statistical treatments akin to the RRKM theory usually prove adequate in the persistent complex realm.

A major, instructive discrepancy appeared for the dialkali halide systems, however. Despite its good agreement with the angle and energy distributions, the statistical model overestimated the ratio of reactive to nonreactive decay of the collision complex, often by a factor of 3 to 5 or more. This striking discrepancy is attributed to preferred reaction geometry. The potential energy surfaces predict that the preferred direction of approach is collinear, with the incoming alkali atom attacking the "wrong end" of the salt molecule. This corresponds to linear $(AB)^{\oplus}X^{\ominus}$ and reflects the stability of the dialkali ion. By virtue of the strong long-range attraction, most complexes are formed in collisions with large impact parameters and thus the centrifugal momentum often restrains the roughly collinear $(AB)^{\oplus}X^{\ominus}$ configurations from bending into the triangular configurations required for reaction. Later, we found many similar instances of preferred reaction geometry.

In search of another prototypical deviation from the statistical case, we looked for a collision complex with lifetime comparable to its mean rotational period. This is called an *osculating* complex, a term applied by *Wigner* to an analogous realm in nuclear reactions. As indicated in Figure 14, our model calculations for this case assume that during rotation about its total angular momentum J the complex is subject to decomposition with a random lifetime distribution, $\exp(-t/\tau)$. This gives an angle-dependent form factor governed by the ratio τ/τ_r of the mean lifetime to a typical rotational period. The angular distribution is approximated by multiplying that for a persistent complex by this factor. For $\tau \gtrsim 5\,\tau_r$, we thus expect the forward and backward glory peaks to be about equally strong, whereas for $\tau \approx \tau_r$ the backward peak should be attenuated by about 40%. Reactions of alkali atoms with thallium halides were examined as likely candidates. We expected the lifetime of the complex might be shortened by the higher ionization potential of the Tl atom, which inhibits the sharing of charge, and by the higher reaction exoergicity. Indeed, *George Fisk* and *Doug McDonald* found these systems show the glory peaks characteristic of a complex, but the backward peak is substantially weaker, by 30% to 50%. Again, similar behavior was later found for many other reactions. Attractive chemistry often yields not a persistent coupling but just a flirtatious whirl.

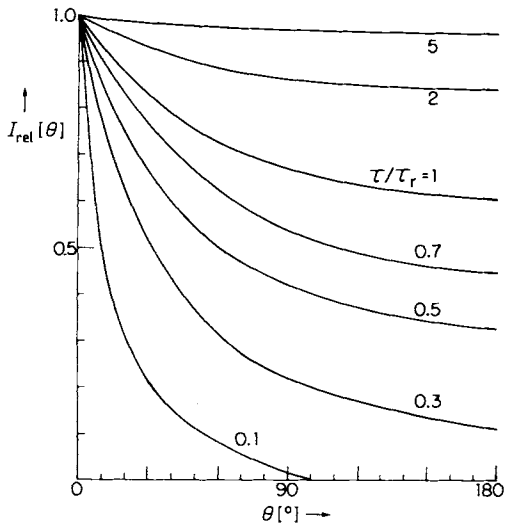

Fig. 14. Ratio of intensity, I_{rel}, appearing at angle θ to the peak intensity for forward scattering ($\theta = 0°$) as calculated for the *osculating model*. The corresponding angular distribution is obtained by multiplying this "falloff function" I_{rel} by the appropriate curve from Figure 12. The falloff curves are labeled by the ratio of the mean lifetime of the complex to a typical rotational period, τ/τ_r.

Another aspect of unimolecular kinetics explored with alkali reactions is the dependence on the number of degrees of freedom. Even some *covalent + ionic* reactions with sizable exoergicity proved to involve persistent or osculat-

ing complexes when six or eight atoms are involved. The most fully characterized example is the $Cs+SF_6$ reaction; in addition to angle and velocity distributions, we measured the CsF rotational excitation by electric deflection and the vibrational populations by electric resonance spectroscopy. Although the available energy is rather large, 40–50 kcal mol^{-1}, the reaction appears thoroughly statistical. It has symmetrical forward and backward glory peaks and the same effective temperatures for translation, rotation, and vibration, corresponding to equipartition of energy. In this study a miniature crossed-beams apparatus was joined with *Klemperer*'s electric resonance spectrometer. This enabled quantum states of the reactively scattered CsF to be completely identified with respect to vibrational level, rotational angular momentum, and space orientation of the angular momentum. It also completed another link with the saga of *Stern* and *Rabi*.

Beyond the Alkali Age

From the beginning, we spoke of the "early alkali age," a phrase both wistful and whimsical. It was intended to suggest that broader ages would inevitably follow, without predicting how soon. Skeptics discounted alkali reactions as an eccentric, unrepresentative family, but we gladly persisted because they revealed such instructive dynamical variety. Meanwhile, an unduly pessimistic view of prospects for beam studies of nonalkali reactions arose elsewhere. This came from attempts to use mass spectrometric detection which failed to reduce sufficiently the interfering background in the electron bombardment region. In March of 1967 we began designing a new apparatus, to be named *Hope*. Only nine months later it would take us "beyond the alkali age."

Universal Detector and Supersonic Nozzles

Hope was undertaken when *Yuan Lee* joined our group as a postdoctoral fellow. With *Bruce Mahan* at Berkeley, he had already built a major apparatus for beam studies of ion–molecule reactions. In this, as in *Hope*, he made elegant use of ion counting techniques adapted from nuclear physics. *Yuan* was teamed with two beginning graduate students, *Pierre LeBreton* and *Doug McDonald*, and several machinists in our Departmental Shop, headed by *George Pisiello*. It was a group of extraordinary skill and zeal, inspired by *Yuan*'s genius and fervent sense of mission. Blissfully, as each of the myriad design questions was settled, we all relished his verdict: "Should be all right."

The main features of *Hope* are shown in Figure 15. The entire detector unit is mounted on a rotatable lid and the beam sources are fixed, to facilitate changing the source modules and strong pumping of the source chambers. The key component of the detector, the electron bombardment ionizer, is located within three nested chambers, each differentially pumped by ion pumps and cryogenic traps. This fulfills two vital design criteria for the ionization region. (1) The background gas (at the mass of interest) that diffuses in from the scattering chamber must be reduced to a

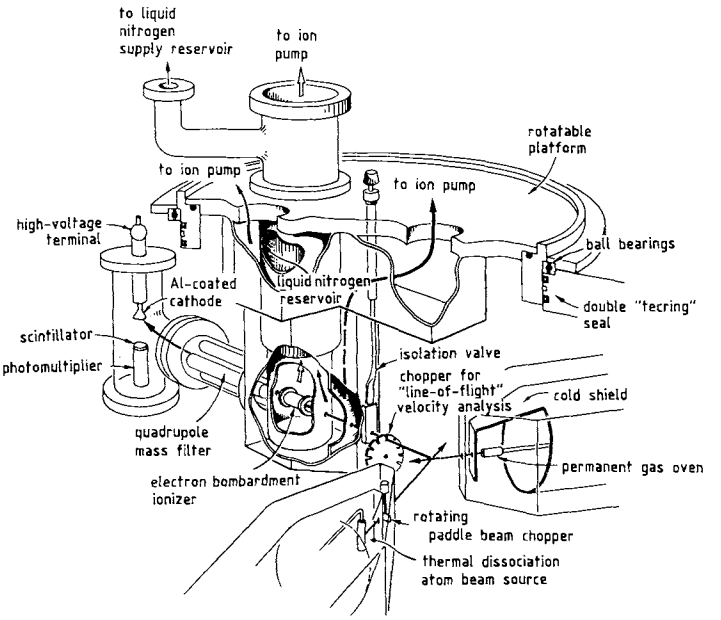

Fig. 15. Cutaway view of crossed-beam apparatus *Hope* with mass spectrometric detector, showing beam geometry and arrangement of differential pumping for detector and source chambers.

partial pressure comparable to or lower than the product species which enters in free flight. This partial pressure is typically ca. 10^{-14} torr, only tenfold above the vacuum in interstellar space. (2) Background from deposit of product molecules on surfaces near the ionizer must be avoided. This is accomplished by the nested design, which permits product molecules that pass through the ionizer without being ionized (the fate of 99.9%!) to fly on to another differentially pumped region before hitting a surface. In practice, *Hope* and its successors made accessible reactions with much smaller yields as well as greatly extending the chemical scope. Respectable reactive scattering data are now often obtained with product fluxes of only ca. 10^3 molecules s^{-1}.

Supersonic nozzles also greatly expanded the variety and scope of beam experiments. Beyond providing very high intensity (typically ca. 10^{18} molecules $(sr\ s)^{-1}$, beams generated from such nozzles can be aptly viewed as a "new state of matter," with special properties much different from the old trinity of gas, liquid, and solid. The collisions occurring in the high-pressure region of a supersonic nozzle organize the beam molecules to a remarkable extent. The exiting crowd of molecules may have mean separations of only 50 diameters, yet have nearly the same velocity and direction and hence suffer almost no collisions. Likewise, the temperatures associated with relative translation and rotation of molecules within the beam are typically very low (of the order of 1 K or less) whereas the vibrational temperature can be kept high or made low by choice of conditions. Another option is translational acceleration by "seeding." The reactant gas is mixed with a large excess (typically 100-fold) of light diluent gas such as helium or hydrogen. Collisions during the supersonic expansion then bring the seeded molecules to the same exit velocity as the diluent gas, and also concentrate the heavier species along the beam axis. Intense beams are thereby

obtained with kinetic energy readily variable over a wide range extending well above typical activation energies for chemical reactions.

Like many others since, our adoption of supersonic nozzles was spurred by *John Fenn* and *Jim Anderson*, ardent evangelists among the chemical engineers then exploring fluid flow in nozzles. Again, there was a cultural gap to be bridged; at a 1965 ecumenical meeting:[12]

> The engineers spoke only to one another and only about Reynolds numbers; the chemists likewise talked just to each other about harpooning electrons.

The *Kistiakowsky* ax story also prompted us to try nozzles and indeed we had already used them in a modest way in alkali studies. Later we extended the scope of the seeding technique by a nozzle design suitable for solid or liquid substances, and others have developed many variants that have found wide application in both collision and spectroscopic experiments. The splinters from *Kisty*'s ax sprouted into a bountiful garden.

Recognizing Covalent and Ionic Cousins

For our first experiments with Hope, we chose to study reaction (i) and other exchange reactions of halogen atoms

$$Cl + Br_2 \longrightarrow BrCl + Br \qquad (i)$$

and molecules. These were inviting because the reactant beams were easy to produce and all species could be very effectively pumped cryogenically. Furthermore, trihalogen complexes had long been postulated as intermediates in the mechanism of halogen atom recombination and other processes. Such complexes had not been detected in the gas phase, and the only rate constants available for the exchange reactions had been derived from the always equivocal analysis of multistep processes in photochemical systems.

Our first attempt to study reaction (i) gave data of excellent quality and revealed instructive dynamical features. Although the total reaction cross section is ca. 10 Å^2, smaller than the hard-sphere cross section, the BrCl angular distribution peaks strongly in the forward hemisphere. This indicates that the dominant interaction is short-range and yet attractive. In previous beam experiments and trajectory calculations, the reactive scattering had always peaked backwards when the cross section was smaller than the hard-sphere value. However, despite its much smaller reaction cross section, the $Cl + Br_2$ reaction gives product angle and translational energy distributions quite similar in form to the $K + Br_2$ reaction. We suggested this was evidence for an osculating complex mechanism.

Only a few months after our results for reaction (i) were announced, groups at Freiburg and Los Alamos had confirmed our study, using mass spectrometric apparatus of appreciably different design. This illustrates the value of choosing an amenable system to test new apparatus or to extend an experimental domain. Yet the reaction cross sections found in the beam studies indicated that the rate constants derived from the photochemical experiments were about 100-fold too low. Later the photochemical studies were repeated, with results in agreement with the beam work.

In studies of other trihalogen systems, we obtained further evidence for an osculating complex with preferred reaction geometry. The wide-angle reactive scattering indicates complexes containing iodine are more stable than those with only bromine or chlorine, in accord with simple electronic structure arguments. Likewise, for complexes containing different atoms, the most stable configuration has the least electronegative atom in the central position. One of the striking results attributed to this preferred geometry appeared in the Br + ClI case. The yield of BrCl is about fivefold smaller than otherwise expected and its angular distribution peaks backwards, indicating repulsive interaction. Subsequent studies, including variation of collision energy, brought out other dynamical features. Often these could also be interpreted by analogy to alkali reactions, despite the marked contrast in covalent and ionic bonding.

Next we pursued the reaction that *John Polanyi* had employed as the prototype in developing his IR chemiluminescence method [reaction (j)].

$$H + Cl_2 \longrightarrow HCl + Cl \qquad (j)$$

This system proved to have a gratifying kinship both to photodissociation of Cl_2 and to the $K + CH_3I$ reaction. Angle-velocity contour maps displaying this comparison are shown in Figure 16. For the Polanyi reaction, the product

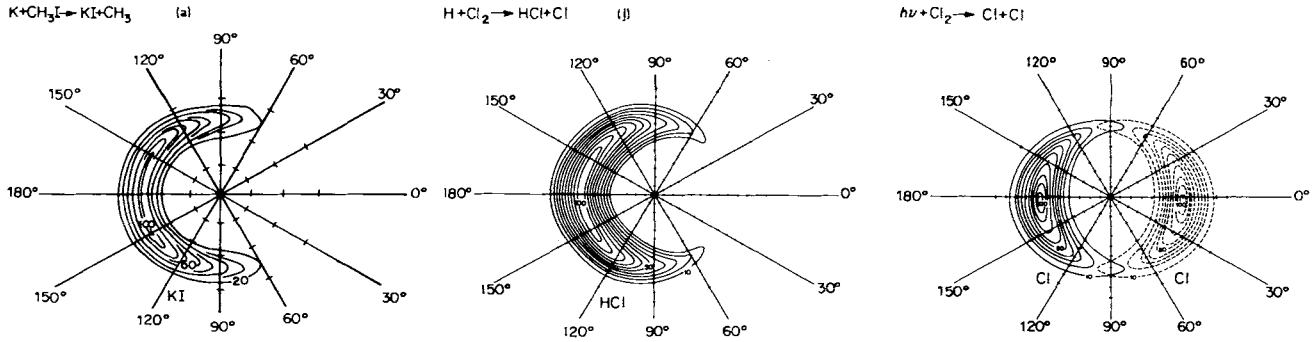

Fig. 16. Comparison of contour maps for photodissociation of the Cl_2 molecule and for reactions (a) and (j). Map for the latter case from work of *A. M. Rulis* and *R. B. Bernstein* [3]. For each map, origin is at center of mass and horizontal axis is along reactant relative velocity vector, with direction of incident atom or photon designated $\theta = 0°$. Tic marks along radial lines indicate velocity intervals of 200 m s^{-1}.

angular distribution is broad but quite anisotropic, with the HCl recoiling backwards and Cl forwards with respect to the incident H atom. The product velocity is very high, about 1600 m s^{-1} at the peak of the distribution. This corresponds to release of about half of the available energy (reaction exoergicity of ca. 45 kcal mol^{-1} plus initial collision energy of ca. 10 kcal mol^{-1}) in the translational recoil of HCl and Cl. The rest appears in vibrational and rotational excitation of HCl, which is observed in the IR luminescence. The form of the angular distribution indicates collinear H-Cl-Cl as the preferred reaction geometry and the high recoil energy shows that strong repulsive forces are abruptly released.

The contour map for photodissociation was constructed from the continuous absorption spectrum of Cl_2, which shows directly the distribution of relative translational energy of the fragment Cl atoms and hence the repulsive energy release. The spectrum can be closely approximated by simply "reflecting" the Gaussian vibrational distribution of the ground electronic state from the steep (ca. 7 eV $Å^{-1}$) repulsive wall of the dissociative excited electronic state. The angular distribution is governed by the dipole selection rule for absorption, which makes the transition probability vary as the square of the cosine of the angle between the Cl-Cl axis and the photon beam direction. We see that reaction (j) and $h\nu + Cl_2$ give remarkably similar angle-velocity maps.

More remarkable still is the close resemblance of reactions (j) and (a); except for a change of scale, the contour maps are almost congruent. In terms of electronic structure, as already noted, the analogy to photodissociation is obvious in the reaction (a) case because the harpooning electron enters the same strongly antibonding molecular orbital excited in photodissociation. In the reaction (j) case the analogy is not obvious, since the very high ionization potential of the H atom prohibits electron transfer. However, we found a molecular orbital rationale using the "frontier orbital" concept of *Fukui*. This is indicated in Figure 17. Collinear approach of the H atom generates three σ orbitals for the H-Cl-Cl complex. The middle one of these, 2σ, is expected to be the highest occupied orbital in the reaction complex. This frontier orbital has one node, resulting from the superposition of two components, one H-Cl antibonding and Cl-Cl bonding, the other vice versa. Simple calculations based on empirical data indicate the latter component is dominant. Thus, the frontier node lies roughly midway between the chlorine atoms, just as in the lowest-lying unoccupied orbital of Cl_2, the orbital excited during photodissociation. The similarity in the contour

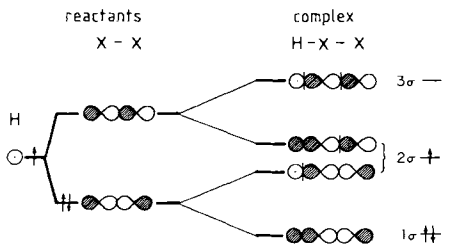

Fig. 17. Schematic construction of the three σ molecular orbitals of collinear H-X-X. The *frontier orbital*, 2σ, may be regarded as a superposition of two components, one H-X antibonding and X-X bonding, the other vice versa.

maps stems from the congruence in frontier nodes which govern the repulsive energy release in both reaction and photodissociation.

It is uncanny that reactions (j) and (a), seminal in developing the IR chemiluminescence and molecular beam methods, proved to be so closely related; not only are both rebound reactions, they are even "kissing cousins." The nineteenth century notation still used to write down chemical reactions gives no hint of such kinships, whereas electronic structure interpretations often bring out the underlying simplicity and broad scope of reaction dynamics.

Other hydrogen atom + halogen reactions provide instructive contrasts. As $Cl_2 \rightarrow Br_2 \rightarrow I_2$, the repulsive-energy release becomes a smaller fraction of that in photodissociation and the hydrogen halide angular distribution shifts from backwards to sideways with respect to the H-atom direction. These aspects are illustrated in Figure 18. The molecular orbital treatment relates both trends to the decrease in halogen electronegativity. This enhances the p character of hybrid orbitals involving the central atom and thereby favors a bent configuration. The frontier node also shifts from about midway between the halogen atoms in H-Cl-Cl to close to the central atom in H-I-I. Many analogous stable molecules are known which have one more or one less valence electron than these H-X-X systems. The molecules with one more electron are linear or nearly so; those having one less electron are strongly bent, with bond angles of 90° to 110°. The shift of the frontier node might be expected to make H-I-I resemble a case with one less electron. Thus it is plausible that decreasing the halogen electronegativity fosters bent reaction geometry and reduces the repulsive energy release.

The H + ICl reaction is especially interesting. On an energetic or statistical basis, reaction at the "Cl-end" would be more favorable than at the "I-end," since the H-Cl bond strength (102 kcal mol^{-1}) is much larger than H-I (70 kcal mol^{-1}). The molecular orbitals suggest the H atom should prefer to attack the I-end, however. As a consequence of the electronegativity difference, in ICl both the highest occupied orbital (π*) and the lowest unoccupied orbital (σ*) are predominantly I atom orbitals. The beam studies find the HI yield is at least comparable to HCl and probably substantially higher (although the effect of some experimental factors that discriminate against HCl remains unresolved). The angular distribution of HI peaks sideways, the HCl backwards. The IR chemiluminescence detects only HCl and not HI, but this is compatible with the beam results because the dipole derivative of HI is exceptionally small and hence the IR emission is very weak. The HCl energy distribution has a very unusual bimodal form. Comparison with trajectory calculations suggests that some of the HCl results from direct attack at the Cl-end but most comes from indirect reaction after initial attack at the I-end. These two reaction modes produce HCl in low and high rotation-vibration states, respectively. Analogous steric preferences for many other reactions can likewise be attributed to *orbital asymmetry* arising from differences in electronegativity.

Further aspects of this theme were examined by studying reactions of oxygen atoms with halogen molecules. We found that reaction (k) goes via a persistent com-

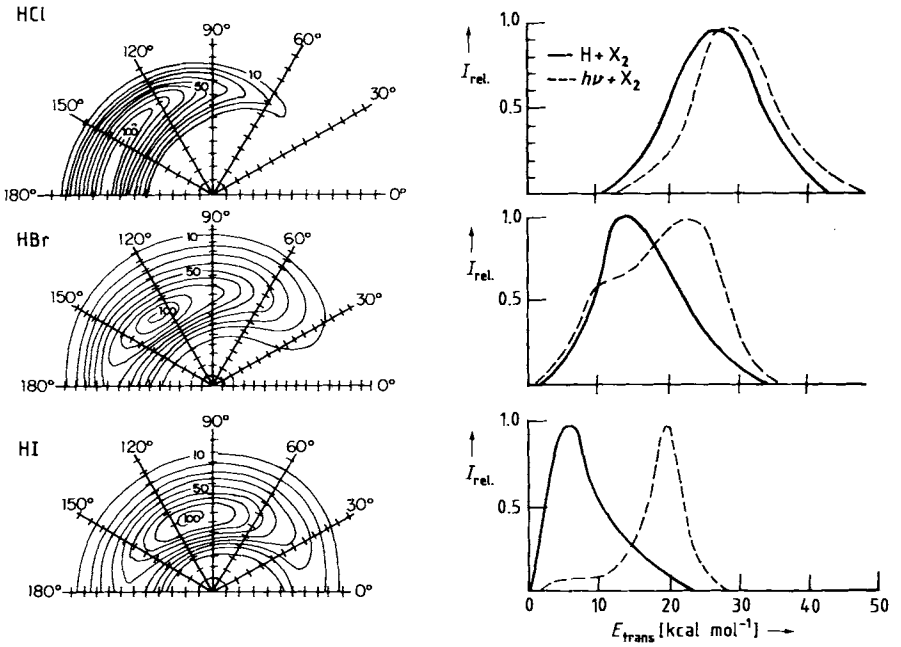

Fig. 18. Comparison of angle-velocity contour maps for reactions of H atoms with halogen molecules. Since maps must be symmetric with respect to the horizontal axis, only upper halves are shown. Tic marks along radial lines indicate velocity intervals of 200 m s^{-1} for Cl_2 case, 100 m s^{-1} for Br_2 and I_2. Panels at right compare distributions of product relative translational energy (solid curves) with continuous absorption spectra of halogen molecules (dashed curves). Abcissa scales for spectra are shifted to place origin at the dissociation asymptote, and thus show directly the repulsive energy release in photodissociation.

$$O + Br_2 \longrightarrow BrO + Br \qquad (k)$$

plex with large yield and no activation energy. The product contour map shows prominent glory peaks. For other reactions with such maps, the intermediate complex usually corresponds to a stable molecular species which correlates with the ground-state reactants and products. Here, however, different spin states are involved. The reactants approach on a triplet surface, whereas the products can depart on either a singlet or triplet surface. The known, stable OBr_2 molecule has a symmetric, strongly bent geometry and a singlet ground state. Qualitative electronic structure arguments suggest that the reaction goes predominantly via a less stable, triplet O-Br-Br potential surface without transition to the more stable, singlet Br-O-Br surface. Likewise, the O + ICl reaction would be expected to give primarily IO + Cl rather than ClO + I, although the latter path is much more exoergic. We indeed found a large yield of IO but no detectable ClO, nice evidence that the reaction involves end-on attack rather than insertion. These results led us to the unorthodox prediction that the $O + F_2$ reaction should prefer the F-O-F geometry rather than O-F-F, since oxygen is less electronegative than fluorine. This implies a relatively high activation energy, associated with the switch to an insertion mechanism, despite the large reaction exoergicity and the notorious chemical personalities of the reactants. Subsequent experiments[13] indeed confirmed that $O + F_2$ is inhibited by a large activation energy.

Migratory Atoms and Bonds

With the mass spectrometric detector, we could now also proceed to "the organic age" and thereby pursue many further aspects of reaction dynamics. Particularly inviting were unimolecular reactions involving isomerizations or rearrangements. Figure 19 shows the contour maps obtained for a favorite pair of examples, the displacement reactions of chlorine atoms with vinyl bromide and with allyl bromide. In these systems [reaction (l)], where R de-

$$Cl^{\odot} + RBr \longrightarrow ClRBr^{\odot} \longrightarrow RCl + Br^{\odot} \qquad (l)$$

notes CH_2=CH or CH_2=CH-CH_2, respectively, the intermediate bromochloroalkyl radical is a known, stable species. It is vibrationally excited by ca. 30 kcal mol^{-1}, the sum of the initial collision energy and thermal excitation of the reactant olefin, the loss in bond strength in converting the double bond into a single bond (ca. 57 kcal mol^{-1}), and the gain in forming the new C-Cl bond (80 kcal mol^{-1}). Under our single-collision conditions, the excited radical cannot be deactivated by a subsequent collision and thus must undergo unimolecular decomposition. The

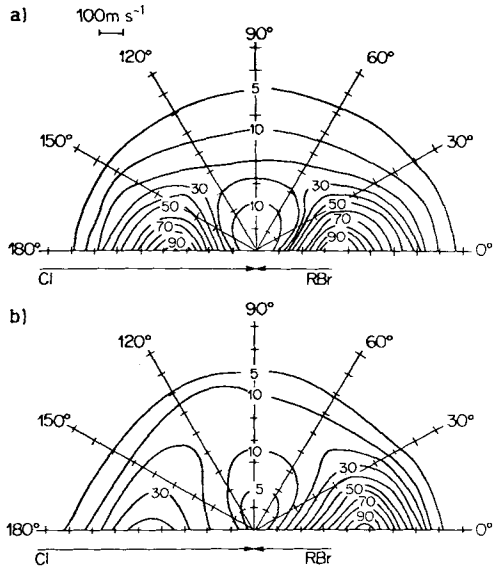

Fig. 19. Comparison of contour maps for chloroolefin products from reactions of chlorine atoms with a) vinyl bromide and b) allyl bromide. Tic marks along radial lines indicate velocity intervals of 100 m s^{-1}.

net energy available to the products on reforming the double bond and releasing the Br atom is ca. 19 kcal mol^{-1}. These energetic aspects are the same for the vinylic and the allylic reactions.

The customary theory of unimolecular processes predicts that the allylic reaction should proceed more slowly and hence show more nearly statistical behavior, since it involves more atoms and therefore the excitation energy shuffles among more vibrational modes than in the vinylic reaction. On the contrary, the contour map for the vinylic reaction indicates a persistent complex, that for the allylic reaction an osculating complex. Some special feature must intervene to make the vinylic reaction more nearly statistical than the allylic reaction. Indeed, this was anticipated in choosing these systems for study. According to a large body of work on organic reaction mechanisms, the initial stage in both reactions should involve addition of the Cl atom to the carbon atom "most distant" from that with the Br atom. As pictured in Figure 20, this implies that a "free valence" appears on the carbon linked to Br in the vinylic case, but not in the allylic case. Thus, the vinylic reaction seems likely to proceed via a 1,2 chlorine *atom migration*, whereas the allylic reaction can go via a 1,3 *bond migration*. Since the heavy atom migration would be much slower than the bond migration, this might provide a rate-limiting process which makes the vinylic reaction more statistical than the allylic one.

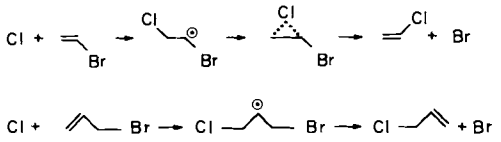

Fig. 20. Stereoselective mechanisms for 1,2 chlorine *atom migration* in vinylic reaction (above) and 1,3 *bond migration* in allylic reaction (below).

These mechanisms require the product chloroolefin to have Cl on the carbon to which Br was originally bonded in the vinylic case, but to remain on the "most distant" carbon in the allylic case. We verified this by analysis of the fragment-ion mass spectra of chloroolefins formed in corresponding reactions with a methyl group added to "label" one or another carbon atom. The methyl substitutions also produced revealing changes in the reactive scattering. For the vinylic cases, the angular distributions show variations which reflect changes in the rotational motions caused by the methyl group. For the allylic cases, the product translational energy distributions become statistical, as if the methyl group diverts the intramolecular energy flow and thereby makes it more random.

Further tests of the migration mechanisms were later obtained by *Rowland* using radioactive tracers.[114] In this work, the same vinylic and allylic reactions examined in the beam experiments were studied under "bulb" conditions. At low pressures, the products obtained were those expected for the atom- and bond-migration mechanisms, respectively. At high pressures, however, different products were obtained. These corresponded to the species expected from collisional stabilization of the intermediate bromochloroalkyl radicals, followed by standard reactions of those radicals.

A host of other organic reactions have now been studied by beam methods, especially by *Yuan Lee* and his students. Often the intermediates and initial elementary steps have proven to be quite different than those postulated in conventional mechanistic studies. The wide range of bonding and stereochemical situations in organic systems ensures vast scope for dynamical detective work in this domain.

Facile Molecular Reactions

The reaction systems discussed so far all involve attack by an open-shell atom or free radical. One of the chief criteria invoked in postulating elementary steps in reaction mechanisms is that only such processes have very low activation energies, less than 5 or 10 kcal mol^{-1}. The advent of the Woodward-Hoffmann rules focused attention on reactions of molecules with molecules, which involve the concerted making and breaking of two or three pairs of bonds. These processes typically have activation energies above 20 kcal mol^{-1} when fully "allowed" by the rules and above about 40 kcal mol^{-1} when "forbidden." In this context, we sought instructive examples of facile bimolecular and termolecular reactions of diatomic molecules.

The simplest case is the exchange reaction of two alkali halides [reaction (m)].

$$Cs^{\oplus}Cl^{\ominus} + K^{\ominus}I^{\ominus} \longrightarrow Cs^{\oplus}I^{\ominus} + K^{\ominus}Cl^{\ominus} \qquad (m)$$

This might be termed a "no-electron" reaction, since the salt molecules are essentially closed-shell ion pairs. Accordingly, no restraints are imposed by the molecular orbital correlations involved in the Woodward-Hoffmann rules. Yet a contemporary theoretical paper had concluded that even this alkali halide reaction would be subject to a high activation energy of ca. 50 kcal mol^{-1}. This seemed unlikely in view of the strong long-range dipole-dipole attraction. Since alkali halides form rhombic quadrupolar dimers with dissociation energy ca. 30–50 kcal mol^{-1}, the potential surface for the exchange reaction has a deep basin. Our beam experiments indeed found the reaction proceeds via a persistent complex. There is no activation energy and the reaction cross section is extremely large, corresponding to formation of the complex in collisions with impact parameters up to ca. 8–9 Å. We therefore spoke of a "vacuum cleaner" potential. The product angle and velocity distributions conform nicely to the usual statistical model, but the ratio of nonreactive to reactive decay of the complex was two or three times larger than statistical. As in the analogous atom + salt case, this can be attributed to geometrical isomerism. Ionic model calculations predict less stable, linear chain isomers exist in addition to the rhombic dimer. These linear chain isomers may often dissociate nonreactively rather than rearrange to the cyclic form required for the exchange process, especially when the centrifugal angular momentum in the collision keeps the chain "ends" apart. It is like two pairs of ice skaters playing "crack the whip." Extensive trajectory calculations by *Brumer* and *Karplus* confirmed this striking role of geometrical isomerism.

Since the four-center ionic + ionic reaction proved facile whereas the typical covalent + covalent case was for-

bidden according to *Hoffmann*'s orbital correlations, we examined several reactions involving ionic + covalent reactions. These also proved facile at thermal collision energies; for example, reaction (n). This reaction very likely

$$Cs^{\ominus}Br^{\circ} + ICl \longrightarrow Cs^{\oplus}Cl^{\ominus} + IBr \qquad (n)$$

involves formation of an alkali trihalide salt, $Cs^{\oplus}(BrICl)^{\ominus}$, and charge migration within the trihalide anion. Although apparently unknown in the gas phase, trihalides have been much studied in solution and in the solid state. In agreement with molecular orbital theory, the trihalide anions are linear or nearly linear, the middle atom is always the least electronegative (I, in this case) and it acquires a small positive charge whereas the end atoms share the negative charge. Clear evidence for this structure appears in the reactive scattering. There is no observable yield of $Cs^{\oplus}I^{\ominus} + BrCl$, even at collision energies more than 20 kcal mol^{-1} above the energetic threshold for this channel. Furthermore, as seen in Figure 21, the IBr angle-velocity contour map has a very unusual skewed shape. The lefthand product peak has distinctly higher intensity and velocity than the righthand peak. This shows that collisions from which IBr and CsCl rebound backwards with respect to the incident ICl and CsBr, respectively, are more probable and involve more repulsive energy release than collisions from which IBr and CsCl emerge in the same direction as the incident ICl and CsBr, respectively. These properties are consistent with the expectation that in $Cs^{\oplus}Br^{\ominus} + ICl$ reactive configurations, $Br^{\ominus}$ tends to be collinear with ICl while $Cs^{\ominus}$ is likely to collide with the central I atom. The positive charge acquired by I as the trihalide forms then repels $Cs^{\oplus}$, which picks up the emerging $Cl^{\ominus}$ and departs quickly in the direction opposite to the incident salt. Similar ionic + covalent reactions such as CsF + HCl and NaO + HCl[15] likewise go with near zero activation energy.

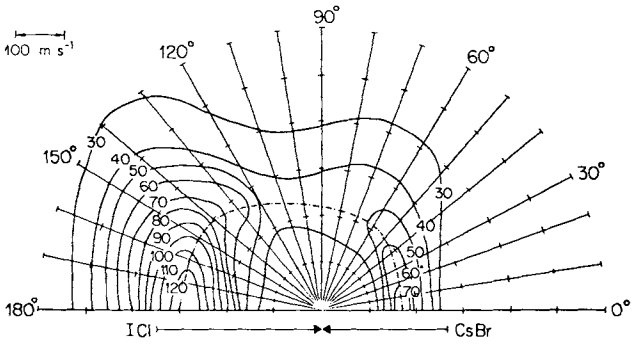

Fig. 21. Contour map of IBr product distribution from CsBr + ICl reaction at collision energy of 3.9 kcal mol^{-1}.

In the domain of four-center covalent + covalent reactions, the landmark is the classic work of Sullivan on the favorite "textbook" case, reaction (o).

$$H_2 + I_2 \longrightarrow 2\,HI \qquad (o)$$

In 1967 he showed reaction (o) does not occur as a four-center reaction but involves dissociation or near-dissociation of I_2 followed by $I + H_2 + I$. Soon after, *Jaffe* and *Anderson* studied HI + DI using the seeded supersonic beam technique and found no detectable HD yield at collision energies far above the empirical activation energy. This is certainly an allowed reaction, at least as the reverse of I + HD + I, but apparently vibrational rather than translational activation is required. Likewise, in our laboratory *David Dixon* and *David King* found no evidence for the four-center exchange reaction (p). Their experiment em-

$$Br_2 + Cl_2 \longrightarrow 2\,BrCl \qquad (p)$$

ployed two supersonic nozzles and scanned the collision energy up to ca. 25 kcal mol^{-1}. Formation of BrCl is readily observed on mixing the reactants in a bulb, and rate studies had indicated a relatively low activation energy, only ca. 15 kcal mol^{-1}. However, this was suspect because of "possible catalysis by moisture or surfaces," a traditional lament in kinetic studies. *Hoffmann*'s molecular orbital correlation diagram predicts a much larger activation barrier, comparable to the promotion energy of two electrons from a bonding to an antibonding orbital and thus above the dissociation energy of the weaker reactant bond (45 kcal mol^{-1}).

Since a six-center, termolecular reaction is allowed by the orbital correlations, we decided to look for reaction (q). Scattering experiments using three crossed beams are

$$Br_2 + Cl_2 \cdots Cl_2 \longrightarrow 2\,BrCl + Cl_2 \qquad (q)$$

utterly impractical, but appreciable fluxes of reactant dimer molecules, linked by a weak van der Waals bond, can readily be generated by a supersonic expansion. We were encouraged by tantalizing evidence obtained by *Noyes* for a third-order reaction of halogen molecules in solution. Yet analogy to other allowed six-center cases (such as Diels-Alder reactions) suggested that the activation barrier might well be ca. 20 kcal mol^{-1}, and it might also require chiefly vibrational rather than translational excitation. Thus, we were startled when *King* and *Dixon* found large yields of BrCl that appeared to come from the termolecular process even at thermal collision energies of only ca. 3 kcal mol^{-1}. However, velocity analysis data for this system and the analogous HI reaction provided several kinematic consistency tests which even indicated that three sequential bond scissions can be resolved in the termolecular exchange process. Soon another example of a facile molecular reaction fostered by a van der Waals dimer was provided by *Durana* and *McDonald*.[16] They found that $F_2 + (HI)_2$ yields intense HF infrared chemiluminescence whereas $F_2 + HI$ gives none. Whether or not these processes actually involve six-center transition states, the weak van der Waals link is remarkably effective in promoting a reaction that otherwise does not go.

Subsequently, we undertook potential surface calculations to examine termolecular, six-center bond exchange processes. For Cl_6 a traditional semiempirical treatment[17] indicates facile reaction but the approximations involved are dubious. For hexagonal H_6 ab initio calculations of high quality were carried out by *Dixon* and *Stevens*[18] and show that a termolecular path is indeed accessible without

breaking an H–H bond whereas there appears to be no such path for a bimolecular, four-center exchange. The results for H_4 and H_6 thus conform to the rule, amply demonstrated in organic chemistry, that cycloaddition reactions involving 4m electrons are forbidden as concerted processes while those involving 4m+2 electrons are allowed. But it turns out that H_6 obeys this rule only through configuration interaction, not by virtue of the usually invoked nodal properties.

The special role of H_6 was elucidated further by comparison with several previous calculations for larger H_n polygons, available for $n=4m+2$ extending from $n=14$ to 62. These calculations, pertinent to model treatments of metallic hydrogen, found the bond length and cohesive energy (binding per atom) to be nearly constant for the whole series. Since our values for H_6 proved to be practically the same, we can reliably estimate the stability of H_{10} and higher polygons by taking the cohesive energy as constant. This shows that H_6 is the only H_{4m+2} polygon that is stable with respect to dissociation of an H_2 bond and hence the only polygon that can serve as transition state for a concerted bond exchange. The customary orbital symmetry criterion thus fails for all the higher 4m+2 polygons; it must be supplemented by an energetic criterion in order to predict whether a reaction is concerted.

The unique stability of H_6 relative to dissociation of an H_2 bond also suggests that solid molecular hydrogen might undergo a high-pressure transition to form a new phase involving termolecular complexes before transition to the long-sought atomic or metallic phase (predicted in 1948 by *Wigner*). This possibility was examined by *Rich LeSar* by means of lattice-energy calculations employing approximate pair potentials.[19] Although uncertainties in the potentials prevent a definite conclusion, the results obtained for a range of parameters indicate that a phase comprising a "partly dissociated" form of the six-center transition state may be stable at pressures above a few hundred kilobars. As shown in Figure 22, repulsive forces from the neighboring units in the crystal prevent dissociation of this complex to diatoms. A marked drop in the H_2 stretching frequency observed at high pressure is qualitatively consistent with formation of molecular clusters but by no means a clear test. In any case, these calculations serve to illustrate how pursuit of reaction dynamics can lead to far distant domains!

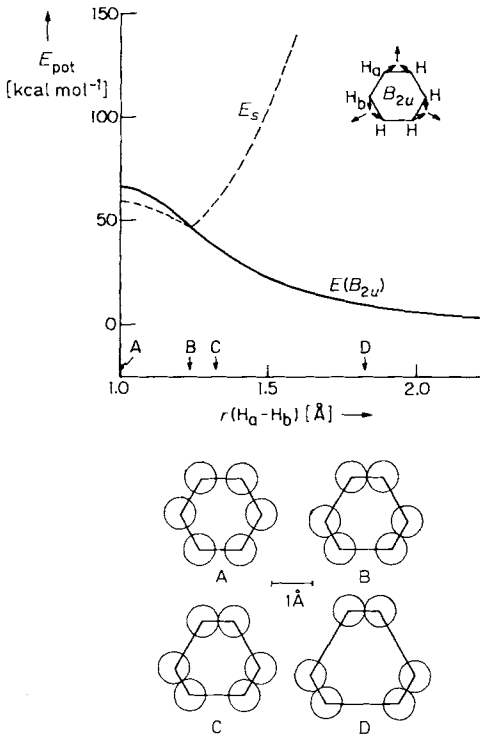

Fig. 22. Above: Potential energy profile for dissociation of a hexagonal H_6 complex in free space (solid curve) and in a hexagonal closest-packed crystal (dashed curve, computed for pressure of 400 kbar) in which repulsive interactions with neighbors prevent the dissociation. Below: Configurations of the termolecular complexes corresponding to positions marked along abcissa. The circles for each H atom have a radius of half of the free H_2 bond length.

Van der Waals Dimers and Clusters

Supersonic expansions make accessible a vast range of species and processes involving feeble bonds. In effect, the very low internal temperatures in supersonic beams circumvent the Second Law, since the entropy term in the free energy, $\Delta H - T\Delta S$, can be made negligible. Even a weakly favorable enthalpy term then suffices to produce large yields of dimers or bigger clusters. This permits studies involving "solvation" of reactant species and other interactions akin to condensed phase or surface chemistry. In the past few years such work has created a major new field, with particular emphasis on metal clusters.[20] Here we describe some of our experiments to illustrate a few favorite themes.

In solution kinetics, much attention has been devoted to photodissociation and recombination processes. These are usually interpreted in terms of "the cage effect," in which the solvent inhibits diffusive separation of the photofragments. A different perspective has now emerged from beam experiments.[21] Complexes of I_2 with various solvent species such as Ar, N_2, benzene, etc. were formed by supersonic expansion and excited with a laser in a spectral region above the dissociation threshold for the bare I_2 molecule. This produced intense fluorescence, showing that, instead of dissociating, much of the iodine relaxes into bound vibrational levels of the electronically excited B state. Energy balance is maintained by breaking the van der Waals bond(s) of the original solvent complex and releasing some repulsion into relative translation of the product fragments. In solution photodissociation must likewise be mollified by energy transfer to the solvent and the surviving excited iodine molecules may account for features previously attributed to recombination of caged atoms.

Another typical role of solvation is exemplified in reactions of ammonia clusters with hydrogen halides. For unclustered ammonia, proton transfer is endoergic to form the ionic salt, $NH_4^{\oplus}X^{\ominus}$, increasingly so for $X=I\rightarrow Br\rightarrow Cl$. In crossed-beam scattering with clustered ammonia, new mass peaks appear that correspond to $(NH_3)_nHX$ adducts with n as large as 15 or more. Fragmentation of these peaks appears to decrease markedly on completion of the first solvation shell. For sufficiently large clusters the complex formation probably involves proton transfer and is

driven by solvation of the resulting $NH_4^{\oplus}X^{\ominus}$ ion pair by the "extra" ammonia molecules in the reactant cluster.

Although solvated ions govern a host of solution phenomena, the individual molecular species and processes often cannot be resolved or characterized in condensed phases. Thus studies of molecular cluster ions in the gas phase have become another major field; for instance, the elusive hydrated electron has now been produced in beams of unfragmented water clusters.[22] In related work, we studied collisional electron transfer from alkali atoms to molecular clusters. Since the process is endoergic, fast atoms are generated from a seeded supersonic expansion. Because the electron transfer can only occur within the crossing radius for the ionic-covalent potential curves, the time scale becomes very short, typically ca. 0.3 ps. This limits use of the method for electron affinity studies but also provides a means to probe the size of cluster subunits involved in impulsive interactions.[23]

For small clusters, particularly dimers, it is feasible to study the exchange of van der Waals bonds by the same methods employed for chemical bonds. Figure 23 shows an angle-velocity contour map obtained by *Worsnop* and *Buelow*[24] for the $Xe + Ar_2$ reaction. Since thermal collision energies are typically several times larger than the dimer well depth, conservation of energy and momentum constrain the scattered diatom product to a narrow circular band centered on the center-of-mass velocity; only within that band can XeAr be formed with low enough internal excitation to hang together. However, several other features provide dynamical information. These include the pronounced "hole" in the reactive scattering in the forward direction, which is accompanied by strong peaking near 50°, and an even stronger backward scattering.

This pattern is remarkably similar to that found for some ion-molecule reactions, such as the $O^{\oplus} + HD \rightarrow OH^{\oplus} + D$ reaction, for which the collision energies and bond strengths are more than 100-fold higher. As illustrated in Figure 23, we find several properties are in nearly quantitative agreement with an impulsive model based on pairwise hard-sphere interactions. Two distinct collision modes give the chief contributions. In the mode that accounts for the forward pitched scattering, A + BC interact via *sequential* hard-sphere elastic collisions (A off B, then B off C); the exchange reaction occurs only when the final relative velocity of A and B corresponds to an energy less than the AB bond strength. For this mode, the angular distribution may be found from a geometric construction devised by *Mahan* et al. for high-energy ion-molecule reactions.[25] The other mode gives strong backward scattering by a process familiar in billiards; A *knocks out* B and thereby comes nearly to rest with respect to the C atom, so the resulting AC molecule moves briskly backward with respect to the center of mass. This study of an exchange of feeble bonds thus helped develop a more comprehensive asymptotic model applicable to any atom-transfer reaction when the ratio of collision energy to bond strength becomes large.

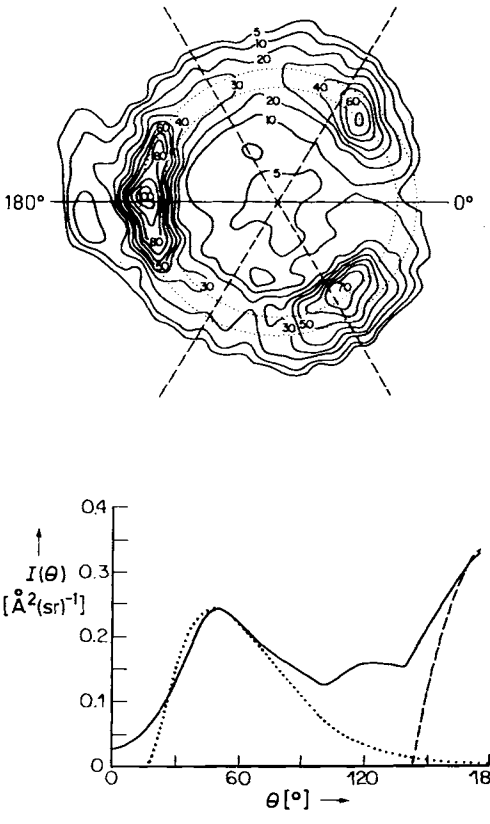

Fig. 23. Above: Contour map for XeAr from $Xe + Ar_2$ reaction at collision energy of 1.3 kcal mol^{-1}. The dotted circular band shows the kinematically allowed scattering region for nominal parent-beam velocities. Below: Angular distribution derived from experimental map (solid curve) is compared with predictions from the hard-sphere model, including *knock-out* (dashed curve) and *sequential impulse* (dotted curve) contributions.

Pursuit of Vector Correlations

In addition to the product angular distribution, many other directional or vector properties of reactions are now accessible in beam experiments, especially by means of laser-induced fluorescence techniques developed by *Zare* which exploit the orientation dependence of the dipole selection rule for electronic excitation.[26] These vector properties offer much information not provided by energetic or other scalar properties, and their study is now emerging as a vigorous field referred to as dynamical stereochemistry or *stereodynamics*. For instance, as indicated in Figure 24,

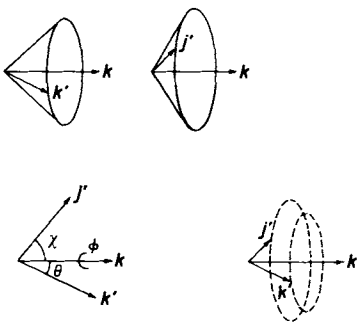

Fig. 24. Three-vector correlation among initial and final relative velocity vectors, here denoted by $\boldsymbol{k}$ and $\boldsymbol{k}'$, and product rotational angular momentum vector $\boldsymbol{j}'$. Upper pair of diagrams indicate the azimuthal symmetry about $\boldsymbol{k}$ of the $\boldsymbol{k}'$ and $\boldsymbol{j}'$ product vectors inherent when these are observed separately, as in the two-vector correlations $(\boldsymbol{k}, \boldsymbol{k}')$ and $(\boldsymbol{k}, \boldsymbol{j}')$. Lower pair of diagrams indicates how the three-vector correction $(\boldsymbol{k}, \boldsymbol{k}', \boldsymbol{j}')$ can give information about the dihedral angle ϕ, in effect undoing the azimuthal averaging about the initial relative velocity.

of special interest is the *triple-vector correlation* among the initial and final relative velocities and the product rotational angular momentum. In principle, this vector correlation offers a means to undo the "dart-board" averaging over the random azimuthal orientations of initial impact parameters. The distributions of both $\boldsymbol{k}'$ and $\boldsymbol{j}'$ must have azimuthal symmetry about $\boldsymbol{k}$, but when a subset is selected of $\boldsymbol{k}'$ vectors with particular $\boldsymbol{j}'$ (or vice versa), this subset in general will not have azimuthal symmetry about $\boldsymbol{k}$. Model calculations and an early electric deflection study by *Hsu* and *McClelland* of the $Cs+CH_3I$ reaction revealed marked asymmetry; as the freshly formed CsI recoils from the collision, its internuclear axis tends to rotate in or near the plane of the initial and final relative velocity vectors. Far more detailed information of this kind is in prospect from studies using laser-induced fluorescence, especially since the great sensitivity of the method may allow the alignment of individual rotation-vibration states to be measured as a function of the scattering angle.

We may even be optimistic about measuring some properties of the four-vector correlation involving both the velocity vectors and the reactant as well as product rotation. This correlation of course contains still more information than found in the six two-vector and four three-vector correlations involving pairs or triads of the four vectors. As exhibited in a model calculation,[27] such information includes the azimuthal asymmetry with respect to both $\boldsymbol{k}$ and $\boldsymbol{k}'$, the preferred rotational orientation of both the reactant and product molecules with respect to the $\boldsymbol{k},\boldsymbol{k}'$ plane, and even the relative sense of rotation (parallel or contrary). Several averages implicit in lower-order vector correlations are thus undone. The loss of information otherwise imposed by the random aspects of the initial conditions resembles the celebrated "phase problem" encountered in X-ray scattering. Thus the complications required to unravel phases for a molecular structure determination are heuristically analogous to undoing impact-parameter averaging by observing one or two "extra angles" in collision experiments. In such ways, a further level of molecular resolution awaits reaction dynamics.

This paper is a tour through a family album. The frequent mentions of work by "we" pertain to my colleagues listed in Table 1, a roster of 51 graduate students and 35 postdoctoral fellows (in italics) listed in order of their "graduation" from our research group. Their work totals about 250 years of research, 150 of that in reaction dynamics. The investment of human resources is far greater, however. Beyond the direct contributions by the machine shop and other staff, all of us received vital help along the way from our teachers, our relatives, and many friends and colleagues. Sustained financial support was likewise vital, including many scholarship and fellowship awards as well as research grants from several agencies, especially the National Science Foundation. To all who made our research possible, I am deeply grateful.

In revisiting the album, I have lingered fondly on the early episodes because, as in dynamics generally, the initial conditions are often as important as the force field. I hope that students and young researchers starting their own work might be encouraged to see how simple and naive were our first steps. I hope also that some research administrators and funding agencies might be encouraged to take a longer-range view of quixotic projects. In our work the essential impetus was the evangelical fervor of young scientists captivated by new vistas. But to pursue such distant vistas we had to have freedom and support. In many quarters this seems less forthcoming today. In expressing thanks for our good fortune, I must urge renewed efforts to foster enterprising work on fundamental problems.

The family album contains far more than shown here, including many intriguing chapters from other laboratories. Again I recommend an admirable pair of texts[3] which survey much work deserving of honor at this forum. Over 30 years of reaction dynamics, the fellowship of striving and joy of discovery have created an intense sense of community. Perhaps in emulation of our molecular friends, recruits to this field seem unusually excitable, zestful, and generous. Working in such a community in pursuit of new insights is a splendid prize, enhanced in the sharing. Thereby we offer thanks for the privilege of studying our ever mysterious atoms and molecules.

Table 1. Roster of graduate students and postdoctoral fellows.

Vintage	Alumni
1962	*J. L. Kinsey, M. S. Child*
1963	J. A. Norris, P. R. Brooks
1964	R. N. Zare, K. R. Wilson, *M. A. D. Fluendy, R. J. McNeal*
1965	M. C. Moulton, R. J. Cross, R. R. Herm, *R. M. Martin, J. Chryusochoos*
1966	J. H. Birely, E. A. Gislason, *M. Cosandey, J. R. Jordan, A. Niehaus*
1967	G. H. Kwei, R. Grice, E. A. Entemann, *H. D. Cohen, P. M. Strudler, P. B. Empedocles*
1968	W. C. Stwalley, R. W. Anderson, *Y. T. Lee, Ch. Ottinger, G. A. Fisk, J. F. Wilson, V. Aquilanti*
1969	S. A. Safron, W. B. Miller, P. E. Siska, H. L. Kramer, C. Maltz, *T. Kitagawa*
1970	P. R. LeBreton, R. J. Gordon, S. J. Riley, R. H. Harris, S. M. Freund, *K. Lacmann*
1971	J. D. McDonald, *R. M. Düren*
1972	N. D. Weinstein, S. A. Adelman, W. S. Struve, *H. J. Loesch*
1973	R. P. Mariella, *D. L. McFadden, D. D. Parrish, J. R. Krenos*
1974	D. L. King, D. S. Y. Hsu, J. T. Cheung, R. A. Larsen, D. M. Lindsay, P. E. McNamee
1975	S. K. Neoh, D. A. Dixon
1976	D. A. Case, *R. A. Sanders*
1977	K. H. Bowen
1978	L. D. Trowbridge, *G. W. Liesegang, J. J. Valentini*
1979	G. M. McClelland, *W. Lee*
1980	E. L. Quitevis, *R. Naaman*
1981	K. L. Saenger, R. A. LeSar, *N. Agmon, O. Cheshnovsky*
1982	D. R. Worsnop, *S. Raynor, A. Yokozeki*
1983	S. J. Buelow, J. D. Barnwell
1984	J. G. Loeser, *C. J. Sandroff*
1986	M. R. Zakin, D. J. Doren, D. Z. Goodson, *S. G. Grubb*

Received: May 14, 1987 [A 649 IE]
German version: *Angew. Chem.* 99 (1987) 1251

[1] H. S. Johnston: *Gas Phase Reaction Rate Theory*, Ronald Press, New York 1966.

[2] For most of the work described here, references to the original literature may be obtained readily from a few reviews. Early chemical applications are discussed by S. Datz, E. H. Taylor in I. Estermann (Ed.): *Recent Research in Molecular Beams*, Academic Press, New York 1959. We have surveyed the development of our studies and allied work in: *Discuss. Faraday Soc. 33* (1962) 149; *Appl. Optics Suppl. 2* (1965) 128; *Adv. Chem. Phys. 10* (1966) 319; *Faraday Discuss. Chem. Soc. 55* (1973) 233; *Pure Appl. Chem. 47* (1976) 61. Usually we will omit specific citation except for papers not referenced in these reviews.

[3] R. B. Bernstein: *Chemical Dynamics via Molecular Beam and Laser Techniques*, Clarendon, Oxford 1982; R. D. Levine, R. B. Bernstein: *Molecular Reaction Dynamics*, 2nd ed., Oxford University Press, New York 1987.

[4] Of course, these are not *Stern*'s exact words, although my memory of him is vivid. I have presented his stories in first person as an attempt to capture his way of telling them.

[5] W. Klemperer, D. R. Herschbach, *Proc. Natl. Acad. Sci. US 43* (1957) 429. The response to vibrational excitation was shown by K. T. Gillen, R. B. Bernstein, *Chem. Phys. Lett. 5* (1970) 275.
[6] This had been published about a year before but somehow I had missed seeing that issue of the *Journal of Chemical Physics*. In the same volume I also found an exceptional paper on transition-state theory by another author new to me: *J. C. Polanyi*!
[7] The Pickwickian phrase is a typically Polanyian comment by *John* delivered when he and his father *Michael* visited the Society of Fellows in 1966.
[8] G. B. Kistiakowsky, W. P. Slichter, *Rev. Sci. Instrum. 22* (1951) 333.
[9] R. N. Zare, D. R. Herschbach, *Proc. IEEE 51* (1963) 173; R. N. Zare, *Mol. Photochem. 4* (1972) 1; C. H. Greene, R. N. Zare, *Annu. Rev. Phys. Chem. 33* (1982) 119.
[10] D. R. Herschbach, *J. Phys. Chem. 83* (1979) 4A.
[11] K. Lacmann, D. R. Herschbach, *Chem. Phys. Lett. 6* (1970) 106.
[12] C. E. Kolb, D. R. Herschbach, *J. Phys. Chem. 88* (1984) 4447.
[13] R. H. Krech, G. J. Diebold, D. L. McFadden, *J. Am. Chem. Soc. 99* (1977) 4605.
[14] R. S. Iyer, F. S. Rowland, *Chem. Phys. Lett. 103* (1983) 213; *Faraday Discuss. Chem. Soc. 67* (1979) 250; see also *J. Phys. Chem. 89* (1985) 2042, 3730; this article reports evidence for a less stereospecific addition as well as for a bromine atom migration.
[15] J. A. Silver, C. E. Kolb, *J. Phys. Chem. 90* (1986) 3267.
[16] J. F. Durana, J. D. McDonald, *J. Am. Chem. Soc. 98* (1976) 1289.
[17] D. A. Dixon, D. R. Herschbach, *Faraday Discuss. Chem. Soc. 62* (1977) 162; D. L. Thompson, H. H. Suzukawa, *J. Am. Chem. Soc. 99* (1977) 3614.
[18] D. A. Dixon, R. M. Stevens, D. R. Herschbach, *Faraday Discuss. Chem. Soc. 62* (1977) 110.
[19] R. LeSar, D. R. Herschbach, *J. Phys. Chem. 85* (1981) 3787.
[20] See, for example, F. Träger, G. zu Putlitz (Eds.): *Metal Clusters* (*Z. Phys. D 3* (1986)).
[21] K. L. Saenger, G. M. McClelland, D. R. Herschbach, *J. Phys. Chem. 85* (1981) 3333; J. J. Valentini, J. B. Cross, *J. Chem. Phys. 77* (1982) 572.
[22] H. Haberland, H.-G. Schindler, D. R. Worsnop, *J. Phys. Chem. 88* (1984) 390.
[23] K. H. Bowen, G. W. Liesegang, B. S. Sanders, D. R. Herschbach, *J. Phys. Chem. 87* (1983) 557.
[24] D. R. Worsnop, S. J. Buelow, D. R. Herschbach, *J. Phys. Chem. 90* (1986) 5121.
[25] B. H. Mahan, W. E. W. Ruska, J. S. Winn, *J. Chem. Phys. 65* (1976) 3888.
[26] D. A. Case, G. M. McClelland, D. R. Herschbach, *Mol. Phys. 35* (1978) 541.
[27] J. D. Barnwell, J. G. Loeser, D. R. Herschbach, *J. Phys. Chem. 87* (1983) 2781.

When submitting manuscripts, authors of articles intended for publication as "Communications" are requested to read the "Notice to Authors" reproduced in the January issue of the journal following the list of contents; upon request, a copy can be obtained from the editorial office.

Molecular Recognition: Stacking Interactions Influence Watson-Crick vs. Hoogsteen Base-Pairing in a Model for Adenine Receptors

By *Julius Rebek, Jr.,* Kevin Williams, Kevin Parris, Pablo Ballester,* and *Kyu-Sung Jeong*

Hydrogen bonding and aromatic stacking interactions are the principal stabilizing forces of double-stranded nucleic acids. In recent disclosures[1] from this laboratory, we have shown how model systems can be used to assess the individual contributions of the two types of interactions. The new model systems consist of imides and aromatic surfaces which converge from perpendicular directions to provide a microenvironment complementary to adenine derivatives (Scheme 1). We have shown that **1a** and **1b** can form from **1** and 9-ethyladenine **6a**; thus the hydrogen bonding is a composite of Watson-Crick (**1a**) and Hoogsteen (**1b**) base-pairing[2] and bifurcated hydrogen bonds can also be involved. We describe here how refinements that influence the nature of base-pairing may be engineered into the model.

Condensation of the imide acid chloride **2** with either β-naphthol **3a** or the di-*tert*-butyl derivative[3] **3b** gave high yields of the corresponding esters **4a** and **4b**, respectively (Scheme 2). Crystallographic studies[4] revealed the conformation shown in which a nearly perpendicular arrangement exists between the planes of the naphthalene nucleus and the imide function in the solid state (Fig. 1; dihedral angle 70° for **4a** and 80° for **4b**). Intermolecular stacking is observed in the crystal structure of **4a** but not in that of **4b**. Apparently, the bulky *t*Bu groups prevent this form of self-association in **4b**.

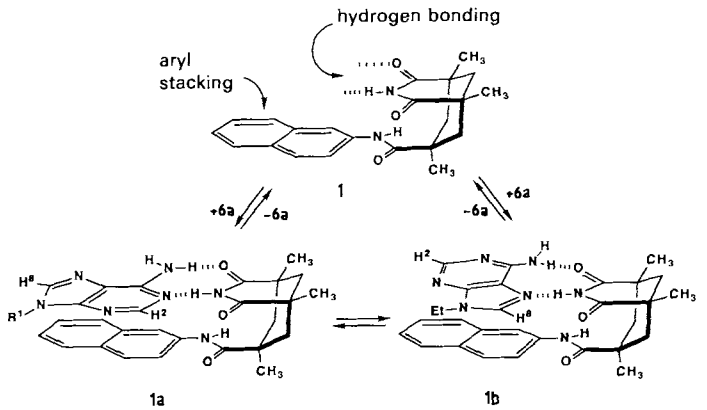

Scheme 1.

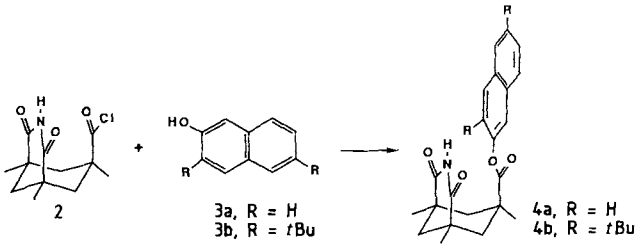

Scheme 2. Reaction conditions: NaH, THF, 25°C, 2 h.

Association constants for binding of 9-ethyladenine **6a** to **4a** and **4b** were measured in $CDCl_3$ using NMR titration; corresponding values for **1** and the anthracene **5** have been reported.[1] In addition, titrations were performed with the *N*-methyladenine derivative **6b**. Steric effects involving N^7 in such structures result in the preference of conformer **6b** over **6b'**,[5] and thus favor base-pairing in the Hoogsteen mode.[6]

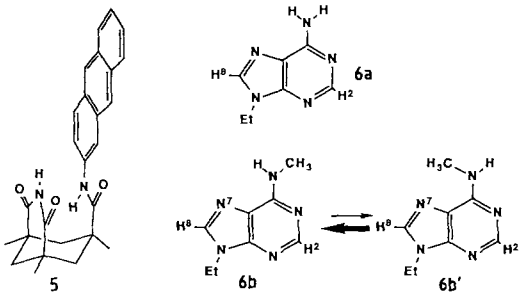

The results are presented in Table 1, with intermolecular nuclear Overhauser enhancements (NOEs) obtained from irradiation of the imide N-H resonance in the various complexes;[7] the estimates of Hoogsteen vs. Watson-Crick base-pairing are calculated from the NOEs.

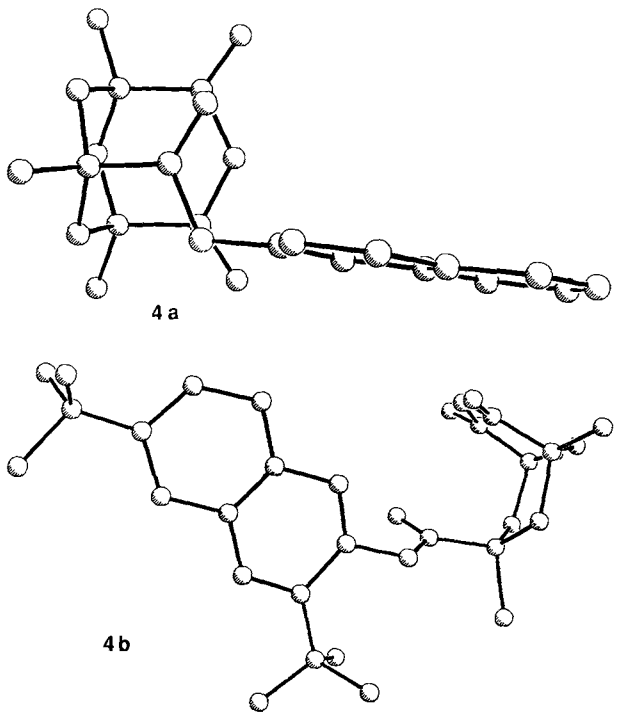

Fig. 1. Molecular structures of **4a** and **4b** [4].

[*] Prof. J. Rebek, Jr., K. Williams, Dr. K. Parris, Dr. P. Ballester, Dr. K.-S. Jeong
Department of Chemistry, University of Pittsburgh
Pittsburgh, Pennsylvania 15260 (USA)

[**] This work was supported by a grant from the National Science Foundation, Washington, D.C. (USA).

 © VCH Verlagsgesellschaft mbH, D-6940 Weinheim, 1987 0570-0833/87/1212-1244 $ 02.50/0

Table 1. Association constants for the binding of **6a** and **6b** to the model receptors **1**, **4a,b**, and **5**, NOE values (see text), and base-pairing preferences in complexation reactions.

Entry	Receptor	K_a [L mol^{-1}] **6a**	**6b**	NOE value [%] $H^8 : H^2$	Hoogsteen : Watson–Crick
1	**1**	220	—	5.3 : 4.2	55 : 45
2	**1**	—	115	1.7 : 0.3	85 : 15
3	**4a**	90	—	2.1 : 1.9	55 : 45
4	**4a**	—	45	3.3 : 0.6	85 : 15
5	**4b**	123	—	2.9 : 1.8	70 : 30
6	**4b**	—	88	3.4 : <0.5	>85 : <15
7	**5**	440	—	5.1 : 8.5	35 : 65
8	**5**	—	142	3.7 : 1.1	75 : 25

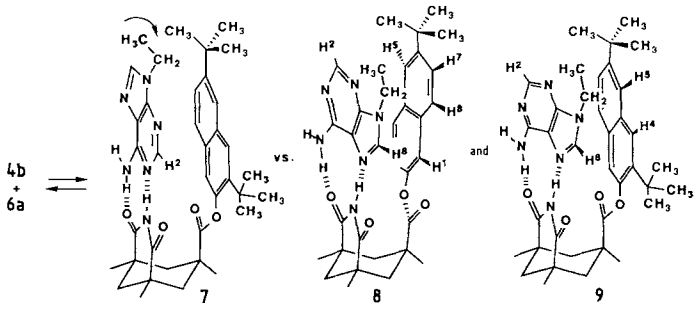

Scheme 3.

The relative sizes of the NOEs observed at H^2 and H^8 relate to the Watson–Crick (**1a**) and Hoogsteen (**1b**) base-pairing, respectively. Only the extended surface of the anthracene derivative **5** favors the Watson–Crick mode (Table 1, entry 7); the shorter naphthyl amide **1** or ester **4a** show comparable amounts of both types of base-pairing with **6a** (entries 1 and 3). Binding of the *N*-methyl derivative **6b** to either **1** or **4a** results in about a 50% diminution in K_a since the Watson–Crick component is largely removed (entries 2 and 4). Accordingly, the NOEs observed for H^2 in complexes with **6b** are much reduced compared with H^8. With the anthracene derivative **5** a larger fraction of the binding is lost with **6b** as the Watson–Crick component is reduced.

The di-*tert*-butyl derivative **4b** provides an example of remote steric effects on base-pairing. Molecular models (CPK) indicate that interactions between the ethyl side chain of the adenine derivative **6a** and the distal *tert*-butyl at C-6 of **4b** prevent close stacking in the Watson–Crick mode but not in the Hoogsteen mode (Scheme 3, **7** vs. **8**, and Fig. 2). Experimentally, two lines of evidence support this surmise. First, only a 30% reduction in K_a is observed for **4b** when the substituted **6b** is bound (instead of ca. 50% as observed for **1** and **4a**) even though the NOEs show most of the Watson–Crick component has been removed (entries 3 and 4). Second, 2D NOESY experiments indicate that H^8 of the adenine shows correlation only with H^1 of the naphthalene, while H^2 of the adenine shows correlation only with H^5 of the naphthalene; this is implicit in structure **8**. Therefore, bulky substituents on the naphthalene nucleus can orient hydrogen bonding elsewhere in the complex.

The model receptors **1**, **4a,b**, and **5** can be used to probe further details concerning multiple, weak intermolecular forces. The esters are intrinsically less attractive to adenine derivatives than amides (Table 1, entry 1 vs. 3 and 5) because bifurcation can be observed with the NH group of adenine and amides[1] but is not observed with the less basic ester carbonyls of **4a,b**. The enhanced binding of **4b** vs. **4a** is also significant. We suggest that the *t*Bu groups of **4b** render its structure more polarizable and result in greater π-stacking interactions.

Finally, the model receptor and NOE techniques reveal an additional subtlety concerning aryl–aryl interactions. *Petsko* et al.[8] have shown that perpendicular (edge-to-face) aryl–aryl interactions are common between aromatic side chains of phenylalanine and tyrosine residues in protein structures. Such interactions combine to provide a significant means of structural stabilization. The solid-state conformations of **4a** and **4b** are in an ideal geometry for such binding, yet irradiation of the CH_2 of 9-ethyladenine **6b** in contact with **4b** shows 1% enhancements in both H^4 and H^5 resonances of the naphthalene. Accordingly, **9** is a contributor to the complex, and face-to-face rather than edge-to-face interactions are indicated in these systems. This is presumably a result of the permanent dipoles featured by these heterocyclic compounds.[9]

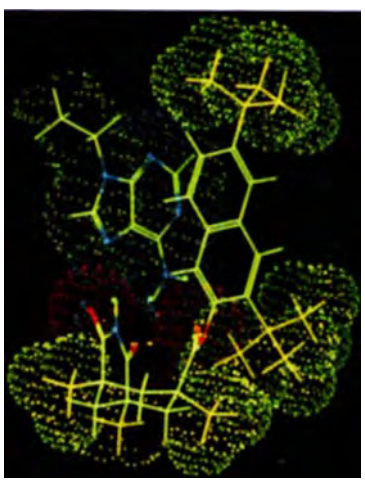

Fig. 2. Structure of the complex formed between **4b** and **6a**. Molecular modeling program: MACROMODEL (*W. C. Still*, Columbia University). Regions of high polarity are drawn in red (O) and blue (N), other regions in yellow [10].

Received: July 23, 1987;
supplemented: October 5, 1987 [Z 2373 IE]
German version: *Angew. Chem. 99* (1987) 1297

[1] J. Rebek, Jr., B. Askew, P. Ballester, C. Buhr, S. Jones, D. Nemeth, K. Williams, *J. Am. Chem. Soc. 109* (1987) 5033; J. Rebek, Jr., B. Askew, P. Ballester, C. Buhr, A. Costero, *ibid.*, in press.

[2] a) W. Saenger, *Principles of Nucleic Acid Structure*, Springer, New York 1984, Ch. 6; b) K. Hoogsteen, *Acta Crystallogr. 16* (1963) 907.

[3] R. W. Layer, *Tetrahedron Lett. 1974*, 3459; D. W. Chasar, *J. Org. Chem. 49* (1984) 4302. We thank Dr. *Chasar* for a generous sample of **3b**.

[4] A dihedral angle of 60° is more common for aryl esters: R. J. Abraham, G. H. Barnett, G. G. E. Hawkes, K. M. Smith, *Tetrahedron 32* (1986) 2949. The crystallographic studies of **4a** (m.p. = 214–216°C) and **4b** (m.p. = 260–263°C) will be published elsewhere. Further details of the crystal structure investigations are available on request from the Director of the Cambridge Crystallographic Data Centre, University Chemical Laboratory, Lensfield Road, Cambridge CB2 1EW (England) on quoting the names of the authors and the full literature citation.

[5] G. Dodin, M. Dreyfus, J.-E. Dubois, *J. Chem. Soc. Perkin 2 1979*, 439.

[6] R. G. Lord, A. Rich, *Proc. Nat. Acad. Sci. USA 57* (1967) 250; see also Ref. [2a], Chap. 7.

[7] Enhancements were determined by integration of the difference spectra; this technique easily permits observation of NOEs as low as 0.5% (L. D. Hall, S. K. M. Sanders, *J. Am. Chem. Soc. 102* (1980) 5703). The low solubility of **1** made the NOE determination of entry 2 difficult. For a similar application of this technique see W. H. Pirkle, T. C. Pochapsky, *ibid. 108* (1986) 5627.

[8] S. K. Burley, G. Petsko, *Science (Washington) 229* (1985) 23; S. K. Burley, G. Petsko, *J. Am. Chem. Soc. 108* (1986) 7995.

[9] Structures **8** and **9** represent Hoogsteen and reverse Hoogsteen conformations; Low-temperature (260 K) NOESY experiments indicate **9** is slightly more populated than **8**.

[10] J. Rebek, Jr., unpublished.

2,3,9,10-Tetrakis(trimethylsilyl)[5]phenylene. Synthesis via Regiospecific Cobalt-Catalyzed Cocyclization of 1,6-Bis(triisopropylsilyl)-1,3,5-hexatriyne**

By *Luis Blanco, Harold E. Helson, Michael Hirthammer, Helene Mestdagh, Spyros Spyroudis,* and *K. Peter C. Vollhardt**

New developments in cobalt-mediated [2+2+2]cycloaddition methodology[1] have provided synthetic access to a series of novel benzenoid hydrocarbons, the [n]phenylenes.[2] In the linear members, electronic spectral data reveal a decreasing incremental bathochromic shift of the longest-wavelength absorption ($\Delta\lambda_{max}$([2]- to [3]phenylene) $\approx$ 75 nm, $\Delta\lambda_{max}$([3]- to [4]phenylene) $\approx$ 54 nm)[2a,c] in accord with MMP2 and MNDO calculations[3] predicting similarly attenuated HOMO–LUMO gaps and ionization potentials. On the other hand, and in contrast to trends expected based on the alternating π electron count between 4n and 4n+2, the ^{1}H-NMR spectra show equally sized upfield shifts ($\Delta\delta \cong 0.35$ ppm) of the inside benzenic hydrogens, whereas their peripheral counterparts resonate at approximately the same positions along the series. The preparation of the next higher "benzocyclobutadienolog" is imperative in order to corroborate these trends and to establish whether the inside benzene nuclei would become eventually olefinic, or more and more antiaromatic as reflected by their increasing paratropism. We report two syntheses of the title compound **6**, the second involving a considerable simplification of our iterative annelation scheme by the use of 1,6-bis(triisopropylsilyl)-1,3,5-hexatriyne as a regioselective cocyclization partner in cobalt-catalyzed alkyne cyclotrimerizations.

Scheme 1 depicts our first synthetic approach to the target, based on methodology employed successfully in the preparation of the [4]phenylene system,[2c] relying on the trimethylstannyl group as a masked halogen to gain access to the crucial cyclization intermediate **1**. Cocyclization with bis(trimethylsilyl)acetylene then gave[4] complex **2**, in addition to small amounts of **3** (<5%), only the second example of a seeming Diels–Alder adduct to a phenylene.[2c] Structural assignments rest on spectral data[4] and their comparison with those of model systems.[2]

Because the decomplexation of **2** proved difficult (treatment with CO[2c] was unsuccessful), a testament to the activated electronic nature of the ligand, a more expeditious route to **6** was sought, one that would also facilitate the synthesis of even higher linear phenylenes. This strategy had its cornerstone in triyne **5**, designed to furnish **1**, and hence **2**, much more rapidly (Scheme 2)[4] by exploiting the greater accessibility of the central triple bond in the cyclization with an *o*-diethynylarene unit, thus regenerating the latter directly in one step.

Demetalation of **2** required the mildest oxidative conditions, found by preliminary cyclic voltammetry experiments and necessitating the presence of eight equivalents of Et_3N to attenuate the oxidizing power of Cu^{II} ion (four

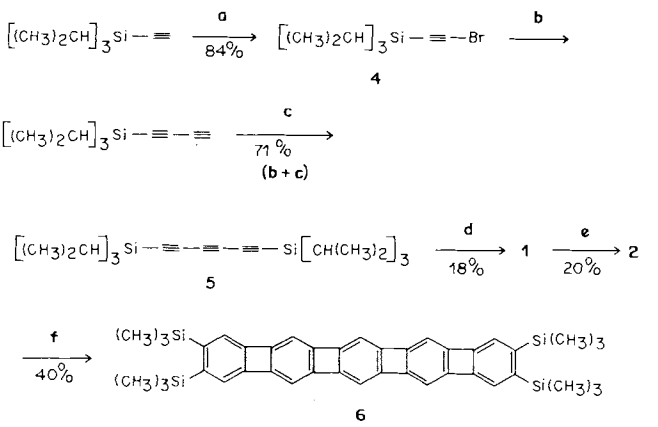

Scheme 2. a) 1. Butylmagnesium chloride, THF, 40°C, 1 h; 2. Br_2, 1 h; b) 1. 2-methyl-3-butyn-2-ol, CuCl, $NH_2OH \cdot HCl$, H_2O, CH_3OH, $CH_3(CH_2)_3NH_2$, 25°C, 20 h; 2. KOH, toluene, 75°C, 2 h; c) **4**, CuCl, $NH_2OH \cdot HCl$, toluene, $CH_3(CH_2)_3NH_2$, 0°C, 3 h; d) 1. 1,2,4,5-tetraethynylbenzene, $[(C_5H_5)Co(CO)_2]$, *N,N*-dimethylformamide, toluene, 16 h, reflux, *hv*; 2. tetrabutylammonium fluoride, THF, EtOH, 1 h, 25°C; e) bis(trimethylsilyl)acetylene, $[(C_5H_5)Co(CO)_2]$, THF, 16 h, reflux, *hv*; f) $CuCl_2 \cdot 2H_2O$ (4 equiv.), 1,2-dimethoxyethane, Et_3N (8 equiv.), H_2O, 3 h, 0°C.

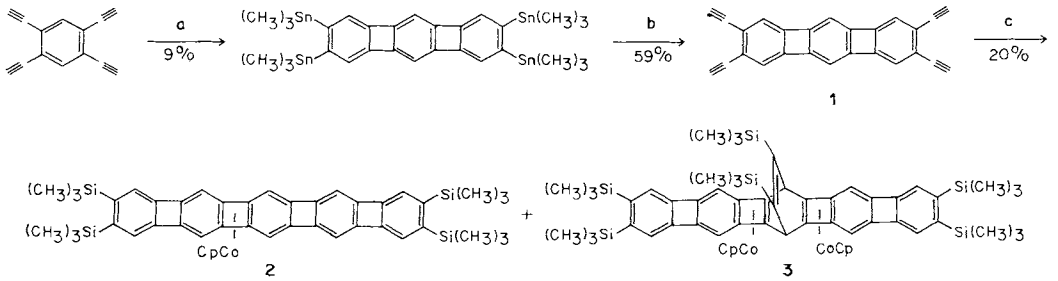

Scheme 1. a) Bis(trimethylstannyl)acetylene, $[(C_5H_5)Co(CO)_2]$, 1,3-dimethylbenzene, THF, 2 h, reflux, *hv*; b) 1. I_2, $CHCl_3$, 25°C, 1 h; 2. trimethylsilylacetylene, $[PdCl_2(PPh_3)_2]$, CuI, PPh_3, Et_3N, piperidine, 25°C, 24 h; 3. CH_3OH, KOH, 3 h; c) bis(trimethylsilyl)acetylene, $[(C_5H_5)Co(CO)_2]$, THF, 16 h, reflux, *hv*.

equivalents). The [5]phenylene derivative **6** is obtained as deep red, highly air-sensitive crystals, which decompose on attempted melting. The most significant spectral data are the positions of its UV and ^{1}H-NMR absorptions. The UV spectra, while exhibiting a pattern identical to that found in the electronic spectra of other linear phenylenes, reveal an even further attenuated bathochromic shift for the longest-wavelength band ($\Delta\lambda_{max}$([4]- to [5]phenylene) = 38 nm). The ^{1}H-NMR spectra, on the other hand, show an upfield shift for the central ring hydrogens ($\delta = 5.56$) by the same increment ($\Delta\delta = 0.33$ ppm) as that observed on going from

[*] Prof. Dr. K. P. C. Vollhardt, Dr. L. Blanco, H. E. Helson, Dr. M. Hirthammer, Dr. H. Mestdagh, Dr. S. Spyroudis
Department of Chemistry, University of California, Berkeley,
and the Materials and Chemical Sciences Division,
Lawrence Berkeley Laboratory
Berkeley, California 94720 (USA)

[**] This work was supported by the National Institutes of Health (CA 20173). *K. P. C. V.* was a Miller Research Professor in Residence (1985–1986). *L. B.* was a NATO (OTAN) (1985–1986) and *H. M.* a C.N.R.S. (France) postdoctoral associate (1983–1984). *M. H.* was the recipient of a postdoctoral fellowship (1984–1985) from the Minna-James-Heinemann-Stiftung, FRG, and *S. S.* of a sabbatical leave fellowship (1986–1987) from the University of Thessaloniki, Greece.

[2]- to [3]phenylenes and from [3]- to [4]phenylenes, and virtually unchanged chemical shifts for the other hydrogens.

The increasingly activated character of the [5]phenylene nucleus compared with the lower members is evident in its sensitivity to oxidizing agents, the tenacity with which it remains attached to $(C_5H_5)Co$, the relative facility with which it breaks through-conjugation by (formal) cycloaddition, as in **3**, and the profound aromatizing effect of metal complexation,[2c] which leads to dramatic downfield shifts of the ^{1}H-NMR absorptions of all the hydrogens, including those at considerable distances from the metal.

A strategy analogous to that depicted in Scheme 2 but starting with 2,3,6,7-tetraethynylbiphenylene[2c] has provided access to 2,3,8,9-tetraethynyl[4]phenylene (35%). So far, despite extensive experimentation, this molecule has failed to function as a precursor to [6]phenylene, perhaps signaling the limit of stability in this class of compounds.

Received: May 14, 1987;
revised: September 23, 1987 [Z 2240 IE]
German version: *Angew. Chem. 99* (1987) 1276

CAS Registry numbers:
1, 111409-78-0; **2**, 111409-84-8; **3**, 111435-11-1; **4**, 111409-79-1; **5**, 111409-80-4; 6, 111409-81-5; $[(CH_3)_2CH]_3SiC{\equiv}CH$, 89343-06-6; $[(CH_3)_2CH]_3SiC{\equiv}CC{\equiv}CH$, 111409-83-7; bis(trimethylstannyl)acetylene, 2117-50-2; piperidine, 110-89-4; trimethylsilylacetylene, 1066-54-2; 1,2,4,5-tetraethynylbenzene, 70603-31-5; 2-methyl-3-butyn-2-ol, 115-19-5; bis(trimethylsilyl)acetylene, 14630-40-1; 2,3,7,8-tetra(trimethylstannyl)benzo[3,4]cyclobuta[1,2-b]biphenylene, 111409-82-6; bis(triphenylphosphane)palladium dichloride, 13965-03-2.

[1] K. P. C. Vollhardt, *Angew. Chem. 96* (1984) 525; *Angew. Chem. Int. Ed. Engl. 23* (1984) 539.

[2] a) B. C. Berris, G. H. Hovakeemian, Y.-H. Lai, H. Mestdagh, K. P. C. Vollhardt, *J. Am. Chem. Soc. 107* (1985) 5670; b) R. Diercks, K. P. C. Vollhardt, *Angew. Chem. 98* (1986) 268; *Angew. Chem. Int. Ed. Engl. 25* (1986) 266; c) M. Hirthammer, K. P. C. Vollhardt, *J. Am. Chem. Soc. 108* (1986) 2481; d) R. Diercks, K. P. C. Vollhardt, *ibid. 108* (1986) 3150.

[3] G. R. Nakayama, D. J. Pernich, K. P. C. Vollhardt, unpublished results.

[4] All new compounds gave satisfactory analytical and/or spectral data. **2**: high-resolution mass spectrum: *m/z* ($C_{47}H_{51}CoSi_4$: 786.2400); 786.2436; ^{1}H-NMR (C_6D_6, 250 MHz): δ = 0.29 (s, 18 H), 0.32 (s, 18 H), 4.58 (s, 5 H), 6.30 (s, 2 H), 6.31 (s, 2 H), 6.75 (s, 2 H), 6.99 (s, 2 H), 7.46 (s, 2 H); ^{13}C-NMR (C_6D_6, 50 MHz): δ = 1.837, 72.62, 74.03, 79.59, 100.34, 110.52, 111.71, 114.65, 124.83, 141.20, 142.88, 147.57, 148.17, 148.60, 149.46, 150.03, 153.64; UV (THF): λ_{max} (lg ε) = 278 (3.54), 315 (3.41), 3.52 (3.49), 412 (3.42) nm.—**3**: MS: *m/z* 910 [$M^{\oplus}-(CH_3)_3SiC_2Si(CH_3)_3$]; ^{1}H-NMR ($C_6D_6$, 250 MHz): δ = 0.28 (s, 36 H), 0.37 (s, 18 H), 4.13 (s, 2 H), 4.69 (s, 5 H), 6.32 (s, 4 H), 7.05 (s, 4 H); ^{13}C-NMR (C_6D_6, 50 MHz): δ = 1.38, 2.25, 51.18, 55.59, 79.98, 80.15, 81.42, 111.30, 121.95, 149.75, 150.81, 151.95.—**5**: m.p. = 156 °C; MS: *m/z* 386 ($M^{\oplus}$, 3), 343 (100); IR (CCl_4): $\tilde{\nu}$ = 2155 cm^{-1}; ^{1}H-NMR (C_6D_6, 300 MHz): δ = 1.01 (m); ^{13}C-NMR (C_6D_6, 50 MHz): δ = 11.54, 18.65, 62.22, 85.00, 90.62.—**6**: MS: *m/z* 662 ($M^{\oplus}$); ^{1}H-NMR (C_6D_6, 300 MHz): δ = 0.31 (s, 36 H), 5.56 (s, 2 H), 5.90 (s, 4 H), 6.81 (s, 4 H); UV (THF): λ_{max} (ε_{rel}) = 304 (sh, 1.00), 315 (1.41), 329 (1.35), 495 (0.50), 530 (0.88) nm.

Cyclohepta[*a*]phenalene: A Highly Electron-Donating Nonalternant Hydrocarbon**

By *Yoshikazu Sugihara, Hiromasa Yamamoto, Kenji Mizoue,* and *Ichiro Murata**

Dedicated to Professor Klaus Hafner on the occasion of his 60th birthday

Two nonalternant hydrocarbons, cyclohepta[*a*]phenalene, **1**, and cyclopenta[*a*]phenalene, **2**,[1] formally derived from azulene by replacing one of its two rings by phenalene, are known as *Reid*'s hydrocarbons, since he first suggested[2] that these two molecules could represent new, azulene-like, polar aromatic structures.[3] Based on Hückel MO treatment,[4] both molecules were predicted to be aromatic[5] with a high-energy HOMO (+0.1055 β) for **1** and a

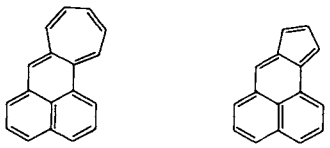

1 **2**

low-energy LUMO (−0.1154 β) for **2**.[4b] Although some derivatives of **2** are known in the literature,[1,6] neither the parent molecule **1** nor any derivatives have been synthesized.[7] We present here the synthesis and some properties of **1** which reveal its high electron-donating ability.

The key step of the synthesis (Scheme 1) is based upon the benzene ring expansion by means of intramolecular ketocarbene reaction (**7**→**8**), which has been used for the synthesis of azulene by *Scott* et al.[8] Methyl 1-(8-phenyl)naphthyl ketone, **6**, easily prepared from 1,8-diiodonaphthalene, **3**,[9] via **4** and **5**, was converted into the diazoketone **7** utilizing a diazo group transfer reaction[10] with $TosN_3$. As expected, reaction of **7** with a catalytic amount of $Rh_2(OAc)_4$[11] in benzene afforded the desired ring-expanded ketone **8** (89% yield). Although transformation of

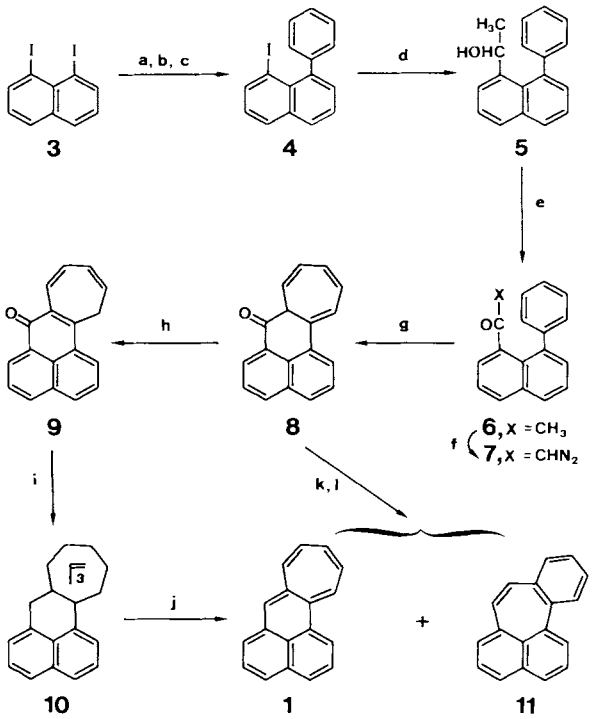

Scheme 1. Synthesis of **1**. a) 1 equiv. of *n*BuLi in Et_2O, 2.0 equiv. of cyclohexanone, −78 °C→room temperature, 2 h (85%); b) catalytic amount of TosOH in benzene, reflux 0.5 h (72%); c) 2.1 equiv. of DDQ in toluene, reflux 1 h (91%); d) 1.2 equiv. of *n*BuLi in Et_2O, 1.2 equiv. of CH_3CHO, −78 °C→room temperature, 1.5 h (83%); e) 3.4 equiv. of pyridinium chlorochromate in CH_2Cl_2, 0 °C, 4 h (80%); f) 4.0 equiv. of lithium diisopropylamide in THF, 3.0 equiv. of $TosN_3$, −78 °C→room temperature, 4 h (80%); g) catalytic amount of $Rh_2(OAc)_4$ in benzene, room temperature, 0.5 h (89%); h) Al_2O_3 with CH_2Cl_2/benzene (64%); i) 5.0 equiv. of DIBAH in benzene, 0 °C, 2 h (42%); j) 1.0 equiv. of DDQ in hexane/benzene (1:8), 0 °C, 1 h (31%); k) 2.9 equiv. of $NaBH_4$ in benzene/MeOH (1:1), room temperature, 1 h (97%); l) 9.7 equiv. of KO*t*Bu, 4.5 equiv. of $MeSO_2Cl$ in THF, −20 °C, 3 h (6%).

[*] Prof. Dr. I. Murata, Dr. Y. Sugihara, H. Yamamoto, K. Mizoue
Department of Chemistry, Faculty of Science, Osaka University
Toyonaka, Osaka 560 (Japan)

[**] This work was supported by a Grant-in-Aid for Special Project Research (60129030) from the Ministry of Education, Science and Culture, Japan.

8 into **1** could be accomplished by way of reduction with $NaBH_4$ and subsequent dehydration, considerable benzo[4,5]cyclohepta[1,2,3-*de*]naphthalene, **11**,[12] was formed along with **1** in a ratio of 1:1 to 1:5. To avoid a tedious purification of **1**, the ketone **8** was isomerized to the phenalenone **9**, which in turn was reduced with diisobutylaluminum hydride to a hydrocarbon mixture **10**. Without separation, **10** was oxidized with 2,3-dichloro-5,6-dicyanobenzoquinone (DDQ) to afford **1**, which, in this case, could easily be purified by simple filtration through basic silica gel (eluant: hexane) followed by recrystallization from benzene/hexane (1:4).[13] Although compound **1**, as dark green needles (m.p. = 60.5 °C (dec.)), is fairly labile,[14] it could be stored under nitrogen in a refrigerator.

The UV/VIS spectrum of **1** exhibits a long-wavelength absorption up to approximately 850 nm. The ^{1}H-NMR resonances of **1** (Fig. 1) are fully consistent with the assigned structure and, at the same time, provide interesting insight into the bonding characteristics of this novel hydrocarbon, which, at first glance, seems to be a perturbed heptafulvene/naphthalene.

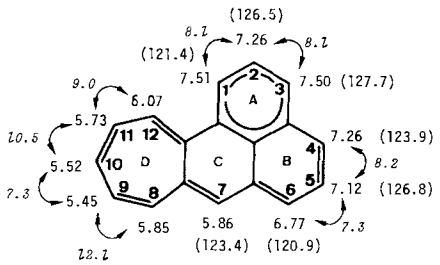

Fig. 1. ^{1}H- (CD_2Cl_2, 400-MHz, complete) and ^{13}C-NMR ($CDCl_3$, 100-MHz, selected, in parentheses) parameters of **1**. Chemical shifts in ppm downfield from internal TMS; *J* in Hz.

In comparison to the proton chemical shifts of naphthalene ($\delta = 7.46$ and 7.81), the signals of H-4, -5, and -6 (ring B) of **1** appear at higher magnetic field ($\delta = 6.77$–7.26) with H-6 being in the olefinic region. On the other hand, the chemical shifts of the ring-A protons might be regarded as appearing in a normal aromatic region. Furthermore, the vicinal proton coupling constants, $J_{4,5}$ and $J_{5,6}$, observed for the ring-B protons, are different by 0.9 Hz, whereas those for the ring-A protons are equivalent, indicating some bond alternation only in ring-B. As for the protons on the seven-membered ring-D, both the chemical shifts ($\delta = 5.45$–6.07) and the vicinal coupling constants ($J = 7.3$–12.1 Hz) are more similar to those of 8,8-diphenylheptafulvene ($\delta = 5.42$–6.10, $J = 7.3$–12.2 Hz)[15] than to those of the parent heptafulvene[16] and its derivatives having electron-withdrawing group(s) at C-8.[17] Based on these findings, the molecule **1** seems to represent a composite of an extended heptafulvene and a benzene ring (Fig. 1). The ^{13}C-NMR data (Table 1) also support this view.[18] Compound **1** is susceptible to protonation at C-7 in trifluoroacetic acid to give the conjugate acid **12**.

The most intriguing property of **1** is its electron-donating ability as borne out by cyclic voltammetry,[19] which reveals three oxidation waves at 0.39, 0.74, and 1.08 V (vs. SCE).[20] The first oxidation potential of **1** is far more negative than that of an alternant isomer, naphthacene (0.77 V),[21] and compares better with that of tetrathiafulvalene (0.34 V).[22] The small separation between E_1^{ox} and E_2^{ox} indicates a small coulombic repulsion that must be overcome in forming the dicationic species.[7] Interestingly,

Table 1. Spectral data of compounds **1**, **12**, and **13**.

1: FD-MS: *m/z* 228 ($M^{\oplus}$); UV (acetonitrile): λ_{max} (lg ε) = 252 (4.46), 298 (3.96), 327 (3.93), 383 (sh, 3.75), 402 (sh, 3.81), 431 (sh, 3.92), 447 (3.93), 602 (3.16) nm, with long tailing up to 850 nm; 400-MHz-^{1}H-NMR (CD_2Cl_2): $\delta = 7.51$ (d, 1H, $J = 8.1$ Hz, H-1 or -3), 7.50 (d, 1H, $J = 8.1$ Hz, H-3 or -1), 7.26 (d, 1H, $J = 8.2$ Hz, H-4), 7.26 (t, 1H, $J = 8.1$ Hz, H-2), 7.12 (dd, 1H, $J = 8.2$, 7.3 Hz, H-5), 6.77 (d, 1H, $J = 7.3$ Hz, H-6), 6.07 (d, 1H, $J = 9.0$ Hz, H-12), 5.86 (s, 1H, H-7), 5.85 (d, 1H, $J = 12.1$ Hz, H-8), 5.73 (ddd, 1H, $J = 10.5$, 9.0, 1.3 Hz, H-11), 5.52 (dd, 1H, $J = 10.5$, 7.3 Hz, H-10), 5.45 (ddd, 1H, $J = 12.1$, 7.3, 1.3 Hz, H-9); 100-MHz-^{13}C-NMR ($CDCl_3$): $\delta = 140.5$, 132.6, 131.3, 128.8, 127.7 (seven-membered ring), 127.7 (C-3), 126.8 (C-5), 126.5 (C-2), 123.9 (C-4), 123.4 (C-7), 121.4 (C-1), 120.9 (C-6), 141.6, 139.8, 134.4, 134.1, 134.0, 131.7 (quaternary C atoms)

12: 400-MHz-^{1}H-NMR (CF_3COOD): $\delta = 9.40$ (d, 1H, $J = 9.2$ Hz, H-12), 8.70 (d, 1H, $J = 9.3$ Hz, H-8), 8.63 (t-like, 1H, H-11), 8.52–8.44 (m, 2H, H-9, -10), 8.40 (d, 1H, $J = 7.2$ Hz, H-1), 8.14 (d, 1H, $J = 8.3$ Hz, H-3), 7.75 (d, 1H, $J = 8.3$ Hz, H-4), 7.63 (dd, 1H, $J = 8.3$, 7.2 Hz, H-2), 7.53 (dd, 1H, $J = 8.3$, 6.4 Hz, H-5), 7.44 (d, 1H, $J = 6.4$ Hz, H-6), 5.00 (bs, 1H)

13: Orange prisms, m.p. = 210–212 °C; MS: *m/z* 329 ($M^{\oplus}$, 100%), 303 ($M^{\oplus} - CN$, 28%), 302 ($M^{\oplus} - HCN$, 10%); IR (KBr): $\tilde{\nu} = 2190$ cm^{-1}; UV-VIS (CH_2Cl_2): λ_{max} (lg ε) = 247 (sh, 4.17), 272 (4.36), 291 (sh, 3.90), 337 (3.99), 462 (4.28); 100-MHz-^{1}H-NMR (CD_2Cl_2): $\delta = 8.98$ (dd, 1H, $J = 1.0$, 7.5 Hz), 8.30–7.35 (m, 6H), 6.91 (dd, 1H, $J = 5.6$, 12.1 Hz), 6.40 (ddd, 1H, $J = 2.1$, 5.6, 10.1 Hz), 6.08 (dd, 1H, $J = 3.9$, 10.1 Hz), 4.06 (dd, 1H, $J = 3.9$, 2.1 Hz)

1 reacts with tetracyanoethylene (TCNE) by single electron transfer[23] to form an [8+2] cycloadduct **13**[13] in 21% yield.

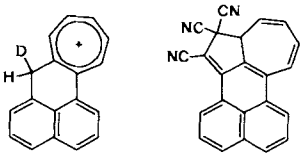

12 **13**

This study provides insight on the bonding of a *peri*-condensed nonalternant molecule and it suggests a way to design novel hydrocarbons of high electron-donating ability.

Received: May 19, 1987;
supplemented: August 12, 1987 [Z 2247 IE]
Publication delayed at authors' request
German version: *Angew. Chem. 99* (1987) 1283

[1] Methoxy derivative of **2**: Y. Sugihara, H. Fujita, I. Murata, *J. Chem. Soc. Chem. Commun. 1986*, 1130.

[2] a) D. H. Reid, *Angew. Chem. 67* (1955) 761; b) I. M. Aitken, D. H. Reid, *J. Chem. Soc. 1956*, 3487; c) D. H. Reid, *Tetrahedron 3* (1958) 339; d) D. H. Reid, *The Chem. Soc. Spec. Publ. 12* (1958) 69.

[3] Dipole moments of **1** and **2** calculated according to the π-SCF force field method are 1.340 and 1.345 D, respectively: cf. H. J. Lindner, *Tetrahedron 30* (1974) 1127; Program PIMM 82. We thank Professor *H. J. Lindner* for these calculations.

[4] a) R. Zahradník, J. Michl, J. Koutecky, *Collect. Czech. Chem. Commun. 29* (1964) 1932; b) R. Zahradník, J. Michl, *ibid. 30* (1965) 520; c) R. Zahradník, *Angew. Chem. 77* (1965) 1097; *Angew. Chem. Int. Ed. Engl. 4* (1965) 1039.

[5] a) B. A. Hess, Jr., L. J. Schaad, *J. Org. Chem. 36* (1971) 3418; b) J. P. Gastmans, D. F. Gastmans, M. H. Mendes Ferraz, *Tetrahedron 33* (1977) 2205; c) J. Aihara, *Bull. Chem. Soc. Jpn. 53* (1980) 2689; d) P. Yang, *Fenzi Kexue Yu Huaxue Yanjiu 3* (1983) 25.

[6] Benzo-annelated derivatives: a) J. Ipaktschi, H. A. Staab, *Tetrahedron Lett. 1967*, 4403; b) R. H. Mitchell, F. Sondheimer, *ibid. 1968*, 2873; c) E. Müller, J. Heiss, M. Sauerbier, D. Streichfuss, R. Thomas, *ibid. 1968*, 1195; d) R. R. Houltson, W. Kemp, *ibid. 1968*, 4093; Naphtho-annelated derivative: W. Kemp, I. T. Storie, C. D. Tulloch, *J. Chem. Soc. Perkin Trans. 1 1980*, 2812.

[7] 6,12-Dihydroxycyclohepta[*a*]phenalene dication: S. Kuroda, Y. Fukuyama, T. Tsuchida, E. Tanaka, S. Hirooka, *Angew. Chem. 97* (1985) 770; *Angew. Chem. Int. Ed. Engl. 24* (1985) 757.

[8] L. T. Scott, *J. Chem. Soc. Chem. Commun. 1973*, 882; L. T. Scott, M. A. Minton, M. A. Kirms, *J. Am. Chem. Soc. 102* (1980) 6311; L. T. Scott, W. R. Brunsvold, M. A. Kirms, I. Erden, *Angew. Chem. 93* (1981) 282; *Angew. Chem. Int. Ed. Engl. 20* (1981) 274.

[9] H. O. House, D. G. Koepsell, W. J. Campbell, *J. Org. Chem. 37* (1972) 1003.
[10] M. Regitz, *Synthesis 1972*, 351.
[11] A. J. Anciaux, A. Demonceau, A. F. Noels, A. J. Hubert, R. Warin, P. Teyssié, *J. Org. Chem. 46* (1981) 873.
[12] J. F. Muller, D. Cagniant, P. Cagniant, *Bull. Soc. Chim. Fr. 1972*, 4364; J. T. Craig, M. A. Pitt, K. W. Wan, A. D. Woolhouse, *Aust. J. Chem. 25* (1972) 837; R. M. Pagni, M. burnett, A. C. Hazell, *Tetrahedron Lett. 1977*, 163.
[13] Correct elemental analyses and satisfactory spectral data were obtained for all the compounds described.
[14] It has been pointed out that "the systems in which the phenalene moiety has to accept a partial negative charge are very sensitive to oxidation": H. Prinzbach, *Pure Appl. Chem. 28* (1971) 281.
[15] K. Komatsu, M. Fujimori, K. Okamoto, *Tetrahedron 33* (1977) 2791.
[16] W. von E. Doering, D. W. Wiley, *Tetrahedron 11* (1960) 183; M. Neuenschwander, W. K. Schenk, *Chimia 26* (1972) 194.
[17] T. Nozoe, T. Mukai, K. Osaka, N. Shishido, *Bull. Chem. Soc. Jpn. 34* (1961) 1384; D. J. Bertelli, T. G. Andrew, Jr., P. O. Crews, *J. Am. Chem. Soc. 91* (1969) 5286; M. Oda, Y. Kitahara, *Chem. Commun. 1969*, 352.
[18] This conclusion is also supported by theoretical calculations [4] which predict that partial negative charges are distributed mainly on C-4 ($q = 1.029$), C-6 (1.032), and C-7 (1.062) in agreement with their carbon chemical shifts.
[19] The cyclic voltammetry measurements were carried out in CH_3CN at $-50\,^{\circ}C$ with 0.1 M $n Bu_4NClO_4$ as the supporting electrolyte with a platinum working electrode and SCE reference electrode. The peak separations are 50, 110, and 170 mV for the 1st, 2nd, and 3rd waves, respectively.
[20] The observation of the 3rd oxidation wave (irreversible) at 1.08 V may be interpreted in terms of an association of the radical cation $\mathbf{1}^{\odot\oplus}$ formed in the primary step to give a charge-transfer complex which is more difficult to oxidize than the radical cation $\mathbf{1}^{\odot\oplus}$; M. Baier, J. Daub, A. Hasenhündl, A. Merz, K. M. Rapp, *Angew. Chem. 93* (1981) 196; *Angew. Chem. Int. Ed. Engl. 20* (1981) 198.
[21] E. S. Pysh, N. C. Yang, *J. Am. Chem. Soc. 85* (1963) 2124.
[22] D. C. Green, *J. Org. Chem. 44* (1979) 1476.
[23] When **1** was mixed with TCNE in benzene under vacuum, strong ESR signals could be observed.

The "Wheel of Mainz" as a Liquid Crystal?—Structural Variation and Mesophase Properties of Trimeric Discotic Compounds**

By *Willi Kreuder, Helmut Ringsdorf,** *Otto Herrmann-Schönherr,* and *Joachim H. Wendorff*

Liquid crystals—which are of great interest from both a theoretical and a practical point of view—are currently the subject of interdisciplinary research.[1] The reasons are the fascinating ability of anisotropic molecules to form supramolecular systems through self-organization and the resulting properties of such systems. The type and extent of this molecular order can be largely predetermined by the synthesis of molecules having appropriate molecular geometries. The first liquid crystals—discovered in 1888[2]—were formed from rodlike molecules (calamitic mesogens A, Fig. 1); the first discotic mesophases formed from disclike molecules were identified only ten years ago[3] (discogens B, Fig. 1). In both mesophase systems, the characteristic molecular axes are on average parallel (director): in the case of rods the long axes and in the case of discs the short axes.[4] If this is the only principle of organization, then there exists a nematic phase (*n* for calamitic-nematic phases formed from rodlike molecules, N_D for discotic-nematic phases formed from disclike molecules[5]). An additional positional order of the molecules gives rise to the different layer structures of the smectic phases in the calamitic system.[6] The analogues in the discotic system are the stack structures of the columnar phases.[4] These elementary geometries have been expanded recently: dimeric discogens[7] ("discotic twins"[8]) can form stable discotic phases; molecules with pyramid-shaped central moieties give rise to "pyramidal mesophases";[9] discogens with a small "hole" in the flat central moiety give rise to "tubular phases";[10] rodlike mesogens, the ends of which rigidly bear one or two half-discogens, form "phasmidic phases."[11]

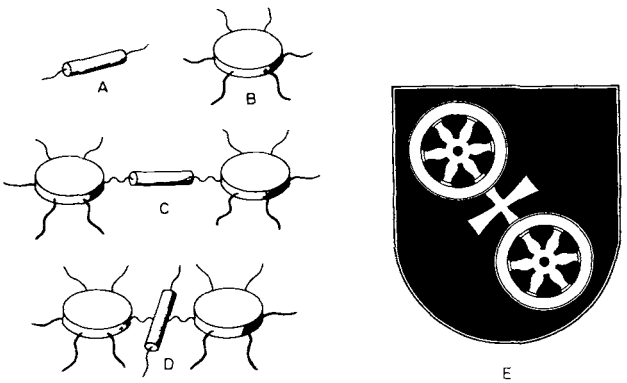

Fig. 1. Schematic representation of the geometry of liquid crystal molecules. A, rod-shaped mesogen (calamitic mesophases); B, disc-shaped mesogen = discogen (discotic mesophases); C, two discogens and a rodlike mesogen *terminally* linked; D, two discogens and a rodlike mesogen *laterally* linked; E, for comparison, the "Wheel of Mainz," the coat of arms of Mainz.

Structural variation of polymeric liquid crystals[12a] and, in particular, of discotic polymers bearing the discogens either as side groups[12b,c] or in the main chain[12c-e] led to the synthesis of monofunctional triphenylene derivatives. These derivatives provide access to compounds formed from disc- *and* rod-shaped mesogens. Such materials are of interest, for example, in integrated optics, since they might form macroscopically biaxial nematic phases. This state, which has been theoretically predicted[13] and recently discussed for polymers as well,[14] is characterized by the existence of a second director axis. Optical biaxiality has not been achieved so far in simple mixtures of an *n* phase and an N_D phase owing to their immiscibility.[5,15] Our goal, therefore, was to prevent phase separation by covalently combining one or more molecules having different geometric anisotropies.

We report here the syntheses and properties of compounds **4**, **5**, and **9**, each of which consists of one rodlike and two disclike mesogens (C and D in Fig. 1). However, none of the three substances fulfilled our expectations. The "trimesogen" **4** (structure C in Fig. 1) is amorphous; the homologous trimesogen **5** forms a novel, highly ordered mesophase; finally, **9**, which, owing to the similarity of its global geometry (structure D in Fig. 1) with the coat of arms of Mainz (E in Fig. 1), has been described as the chemical equivalent of the "Wheel of Mainz," is characterized by excellent crystallizability. Scheme 1 outlines the synthetic route leading to **4** and **5** and Scheme 2 that leading to **9**.

[*] Prof. Dr. H. Ringsdorf, Dr. W. Kreuder
Institut für Organische Chemie der Universität
J.-J.-Becher-Weg 18-20, D-6500 Mainz (FRG)
Prof. Dr. J. H. Wendorff [+], Dipl.-Phys. O. Herrmann-Schönherr [+]
Deutsches Kunststoff-Institut
Schlossgartenstrasse 6 R, D-6100 Darmstadt (FRG)

[+] Structural investigations.

[**] This work was supported by the Deutsche Forschungsgemeinschaft as part of the study of thermotropic liquid crystals (Discotic Polymers project).

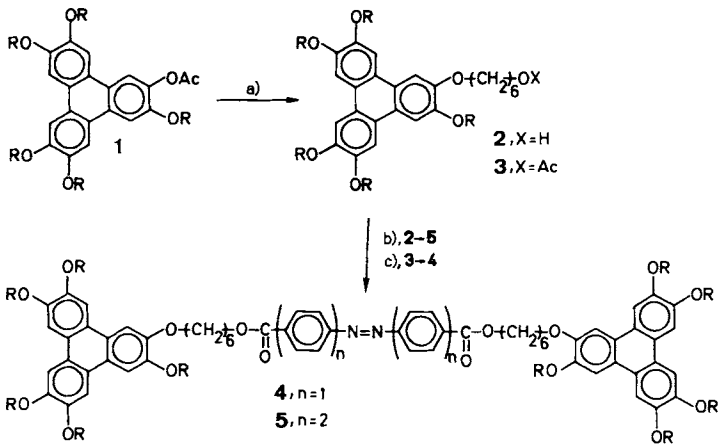

Scheme 1. R = C_5H_{11}. a) 6-Chlorohexanol (4 equiv.), K_2CO_3 (4 equiv.), KI (1 equiv.) in acetone, Ar, 5 d reflux, Ag_2O (wet) in THF, 20 h at room temperature; dissolve in ethyl acetate/water; lyophilized from benzene, chromatography (silica gel 60, CH_2Cl_2), R_f($CHCl_3$ + 6‰ EtOH): 0.2 (**2**) 0.5 (**3**); b) azobiphenyl-4′,4‴-bis(carbonylchloride) [16] (0.46 equiv.), 1,2-dichlorobenzene, pyridine, 60 h at room temperature, crystallization from $CHCl_3$/EtOH (2 + 5); chromatography ($CHCl_3$, ethanol-free) R_f ($CHCl_3$ + 6‰ EtOH) = 0.5–0.6 (owing to *cis-trans* isomerism); c) diethyl 4,4′-azobenzenedicarboxylate [17] (0.48 equiv.), (iPrO)$_4$Ti (0.4 equiv.) [18], Ar, 10 h 140 °C, 10 h 170 °C; repeated precipitation from THF/MeOH (1 + 1) in MeOH (4), flash chromatography (CH_2Cl_2/EtOH, 98 + 2), R_f = 0.7, precipitation from MeOH; flash chromatography (toluene/ethyl acetate, 49 + 1), R_f(*trans*) = 0.32, R_f(*cis*) = 0.2. Precipitation from THF/EtOH (1 + 1) in EtOH (4).

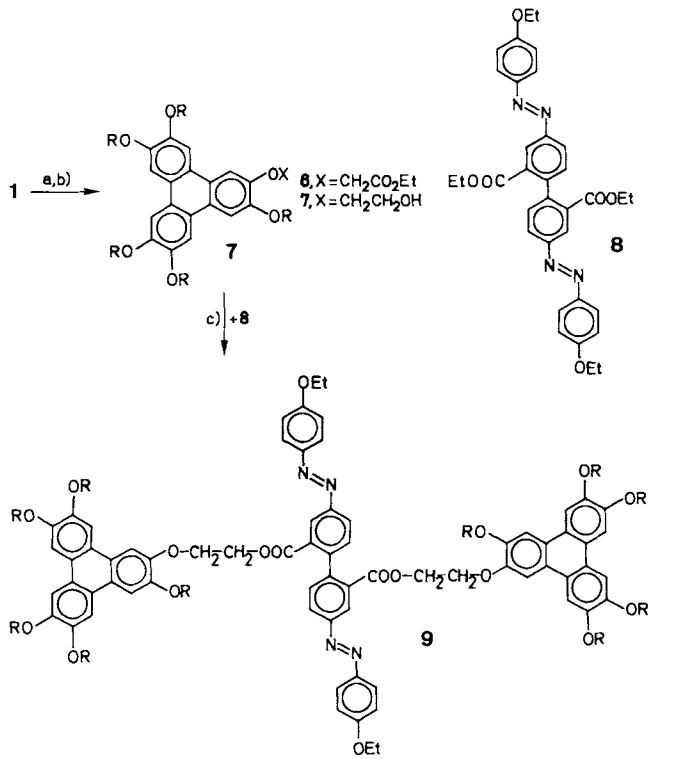

Scheme 2. R = C_5H_{11}. a) Ethyl bromoacetate (4 equiv.), K_2CO_3 (4 equiv.) in acetone, Ar, 5 h reflux. R_f(CH_2Cl_2): 0.4 (**1**), 0.2 (**6**). Dissolve in ethyl acetate + HOAc/water, crystallization from EtOH. Flash chromatography (CH_2Cl_2), crystallization from EtOH; b) $LiAlH_4$ (4 equiv.), THF, 3 h reflux, MeOH, ethyl acetate/1 N HCl/water; flash chromatography (first CH_2Cl_2, finally CH_2Cl_2/EtOH, 49 + 1), crystallization from EtOH; c) diethyl 4,4′-bis(*p*-ethoxyphenylazo)-2,2′-biphenyldicarboxylate **8** [19] (0.49 equiv.), (iPrO)$_4$Ti (0.1 equiv.), Ar, 2 h 130 °C, p = 0.5 mbar slow change to 180 °C, p = 0.005 mbar. Flash chromatography (toluene/ethyl acetate, first 99 + 1, finally 97 + 3). R_f(*trans*) = 0.55, R_f(*cis*) = 0.4. Recrystallization from THF/EtOH (1 + 17).

The yields and the liquid crystal properties obtained from polarization microscopic and differential calorimetric investigations of the new substances are listed in Table 1. The ^{1}H-NMR data are summarized in Table 2. Correct elemental analyses were obtained for all compounds. The monofunctional triphenylene derivatives **2**, **3**, **6**, and **7** display the columnar D_{ho} phase (cf. footnote [a] of Table 1). This corresponds to the observation[12b,d,21] that the high molecular symmetry of the reference compound 2,3,6,7,10,11-hexakis(pentyloxy)triphenylene—phase sequence: k 69 D_{ho} 122 i[22]—is not necessary for formation of the highly symmetric D_{ho} phase. In the case of **6**, the polar ethoxycarbonylmethyl side group, which may be regarded as a nearly isosteric replacement for a pentyl group, even results in enlargement of the mesophase region.[23] In contrast, the long acetoxyhexyl side group in **3**

Table 1. Phase transitions. Yields, relative molecular weights, and mass spectrometric data for **2**–**9**.

Compd	Phase transitions T [°C] [a] (ΔH [J g^{-1}])	Yield [%]	M_r [g mol^{-1}]	m/z [b]
2	k_1 41 k_2 66 D_{ho} 77 i (33) (3) (2)	66 [c]	775.1	774 ($M^{\oplus}$)
3	k 45 D_{ho} 50 i (36) (6)	27 [c]	817.2	816 ($M^{\oplus}$)
4	amorphous at T > 0 °C	73	1784.4	1784 ($MH^{\oplus}$)
5	k 72 lc 120 i (10) (12)	69	1936.6	1936/1952
6	k 65 D_{ho} 140 i	65	761.0	761 ($MH^{\oplus}$)
7	k 69 D_{ho} 101 i	78	719.0	719 ($MH^{\oplus}$)
8	k 198 (n 169) i [d]	72	594.7	594 ($M^{\oplus}$) [e]
9	k 167 i	61	1940.6	1938 ($M^{\oplus}$)

[a] Abbreviations: k, k_1, k_2, crystalline; D_{ho}, *d*iscotic mesophase with *h*exagonally packed columns and *o*rder (= regular distances) of the molecules in a column; lc,*l*iquid *c*rystalline; new mesophase, see Fig. 3 and the explanation in the text; n, *n*ematic phase; i, *i*sotropic phase. [b] Field desorption MS for **2**, **3**, **6**, and **7**; intensity of the molecular ion always at 100%. Fast atom bombardment (FAB) MS for **4**, **5**, and **9**: matrix, *m*-nitrobenzaldehyde; **5** contains azoxy homologue [28]. [c] **2** and **3** are formed together. [d] Clearing point only observable in the supercooled melt; monotropic phase. [e] Electron-impact-ionization MS; relative intensity of the molecular ion: 38%.

Table 2. ^{1}H-NMR data for selected compounds ($CDCl_3$, 400 MHz) [a].

2: δ = 7.82 (s; arom., 6 H), 4.22 (t, J = 6.6 Hz; CH_2O, 12 H), 3.66 (t, J = 6.5 Hz; CH_2OH, 2 H), 1.94 (m; CH_2–CH_2O, 12 H), 1.7–1.3 (ms; $-(CH_2)_n-$, 26 H), 0.97 (t, J = 7 Hz; CH_3, 15 H)

4: δ = 8.16 (d, J = 8.5 Hz; 4 H) and 7.88 (d, J = 8.5 Hz; $-C_6H_4-$, 4 H), 7.82, 7.81, 7.80 (ss; arom. triphenylene, 12 H), 4.39 (t, J = 6.5 Hz; CH_2–O–CO, 4 H), 4.21 (ts; CH_2O, 24 H), 1.93 (m; CH_2–CH_2O, 28 H), 1.9–1.5 (ms; $-(CH_2)_n-$, 48 H), 0.96 (t, J = 7 Hz; CH_3, 30 H)

5: δ = 8.32–7.53 (m; $-C_6H_4-$, 16 H), 7.82 (s; arom. triphenylene, 12 H), 4.40 (t; CH_2OCO, 4 H), 4.26 (t; $CH_2(-CH_2)_5OCO$, 4 H), 4.21 (t; CH_2O, 20 H), 2.1–1.8 (ms; CH_2–CH_2O, 28 H), 1.8–1.4 (ms; $-(CH_2)_n-$, 48 H), 0.97 (m; CH_3, 30 H)

6: δ = 7.91 (s; arom., *ortho* to CH_2CO, 1 H), 7.82 (s; arom., 1 H), 7.81 (s; arom., 3 H), 7.77 (s; arom., 1 H), 4.85 (s; CH_2CO, 2 H), 4.30 (q, J = 5.4 Hz; $COOCH_2$, 2 H), 4.21 (2t; CH_2O, 10 H), 1.94 (m; CH_2–CH_2O, 10 H), 1.31 (t, J = 7 Hz; $COOCH_2CH_3$, 3 H), 0.96 (t, J = 7 Hz; CH_3, 15 H)

8: δ = 8.54 (d, J_{meta} = 2 Hz; C-2 *ortho* to COO, 2 H), 8.03 (q, J_{ortho} = 8.2 Hz, J_{meta} = 2 Hz; C-5 *ortho* to N=N, 2 H), 7.94 (sex., J_{ortho} = 9 Hz, J_{meta} = 3 Hz, J_{para} = 2 Hz; C-3,5 *ortho* to OEt, 4 H), 7.36 (d, J_{ortho} = 8.2 Hz; C-6 *meta* to COO, 2 H), 7.01 (sex., J_{ortho} = 9 Hz, J_{meta} = 3 Hz, J_{para} = 2 Hz, C-2,6 *meta* to OEt, 4 H), 4.12 and 4.10 (2q, J = 5.5 Hz and 7.1 Hz; CH_2, 8 H), 1.45 (t, J = 7 Hz; $COOCH_2CH_3$, 6 H), 1.05 (t, J = 7 Hz; OCH_2CH_3, 6 H)

9: δ = 8.52–6.64 (s and ms; arom., 26 H), 4.5 (m; CH_2OOC, 4 H), 4.3–4.0 (ms, ts (not resolved); CH_2O, 28 H), 2.0–1.8 (ms; CH_2CH_2O, 20 H), 1.6–1.2 (ms; $-(CH_2)_n-$, 40 H), 1.05–0.8 (ts; CH_3, 36 H)

[a] Correct ^{13}C-NMR spectra were obtained for all new compounds.

results in considerable reduction in the stability range of the mesophase.

The "Wheel of Mainz" **9** proved to be a spherolithic crystalline compound. The isotropic melt can be supercooled to 120 °C (m.p. = 167 °C). This rules out the existence of a monotropic, i.e., metastable, mesophase. Contact preparations[24] with typical liquid crystals of the *n* and D_{ho} type do not have any observable effect on the crystalline phase of **9**. It might be possible to prepare a liquid crystalline "Wheel of Mainz" by the introduction of lateral substituents on the molecular axis so as to hinder crystallization.

The most interesting compound proved to be **5**, in which two triphenylene moieties are joined via a mesogenic azobiphenyl moiety. It exhibits a highly viscous mesophase, which is reminiscent of an S_B texture as observed by polarization microscopy.[25] The relatively high enthalpy change at the clearing point (1c→i, 12 J g^{-1}) also points to the existence of an ordered mesophase structure. This was confirmed by X-ray structural analysis using flat camera diagrams of mechanically oriented samples (suppression of crystallization at room temperature) and goniometric diagrams of macroscopically nonoriented samples (Fig. 2).[26]

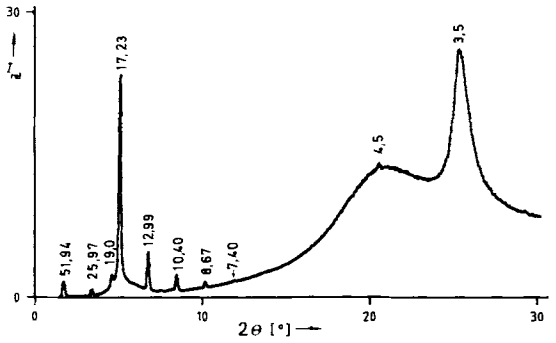

Fig. 2. X-ray goniometric diagram ($\lambda = 1.54$ Å) of **5** (nonoriented); the numbers give the corresponding Bragg distances in Å.

A diffuse halo ($d_{Bragg} = 4.5$ Å) appears in the wide-angle region; in the scattering diagrams of the oriented samples, it appears as a diffuse ring. This behavior is due to liquid-like arrangement of alkyl chains and is typical of discotic phases.[27] At small angles, reflections are observed corresponding to a one-dimensional lattice with a lattice constant of $a = 51.94$ Å. The Bragg distances correspond to 1 : 1/2 : 1/3 : 1/4 : 1/5 : 1/6 : 1/7. The intensities of the reflections indicate that, within a repeat unit *a* of the lattice, two triphenylene moieties are located at approximately 0 and 2/3 *a*. Two further reflections are observed perpendicular to the basis vectors of this lattice, corresponding to the distances $b = 19$ Å and $c = 3.5$ Å. These distances are comparable, respectively, with the diameter of a triphenylene mesogen and with the separations of regularly stacked triphenylene moieties in the D_{ho} phase of hexapentoxytriphenylene.[27] This novel liquid crystalline phase is characterized, on the one hand, by a layer structure typical for smectic phases.[6] On the other hand, the regular stacking of molecular discs observed for discotic phases is also found (similar to D_{ho}). The structure of the mesophase of **5** is shown schematically in Figure 3.

The amorphous substance **4** apparently cannot form a mesophase structure. The reason is presumably the reduction of the anisotropy of the linking azobenzene segment,

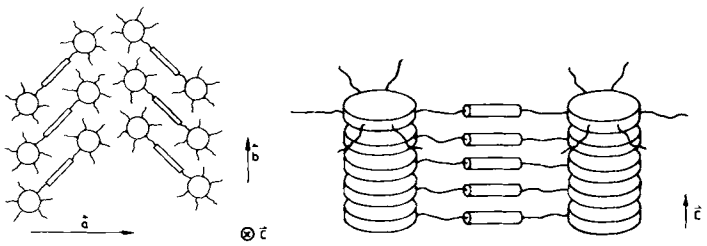

Fig. 3. Structure of the mesophase of **5**. Left: Layer structure of the trimesogens stacked regularly along the *c* axis ($\vec{a}$, layer vector). Right: Stack structure.

which, compared with that in **5**, is two phenylene moieties shorter. The azobenzene segment behaves almost the same as the usual flexible alkyl spacers. This axial mesogen in **4**, together with the two hexylene spacers, is too long, however, for the formation of a normal discotic phase. It is known for discotic main-chain polymers that a very long spacer segment is capable of preventing the formation of anisotropic long-range order.[12d]

Although no nematic phases, and, in particular, none with optical biaxiality, were obtained, we have been able to show that new and unexpected supramolecular structures can be generated by joining different structural elements in a single molecule. The substances discussed here are also model compounds for polymers consisting of alternating rod- and disc-shaped mesogens.

Received: May 27, 1987 [Z 2266 IE]
Publication delayed at authors' request
German version: *Angew. Chem. 99* (1987) 1300

[1] H. Kelker, R. Hatz: *Handbook of Liquid Crystals*, Verlag Chemie, Weinheim 1980.
[2] F. Reinitzer, *Monatsh. Chem. 9* (1888) 421.
[3] S. Chandrasekhar, B. K. Sadashiva, K. A. Suresh, *Pramana 9* (1977) 471; *Chem. Abstr. 88* (1978) 30566y.
[4] C. Destrade, P. Foucher, H. Gasparoux, Nguyen Huu Tinh, A.-M. Levelut, J. Malthête, *Mol. Cryst. Liq. Cryst. 106* (1984) 121.
[5] Nguyen Huu Tinh, C. Destrade, H. Gasparoux, *Phys. Lett. A 72* (1979) 251.
[6] H. Sackmann, *Prog. Colloid Polym. Sci. 69* (1984) 73.
[7] W. Kreuder, *Dissertation*, Universität Mainz 1986.
[8] C. P. Lillya, Y. L. N. Murthy, *Mol. Cryst. Liq. Cryst. Lett. 2* (1985) 121.
[9] a) H. Zimmermann, R. Poupko, Z. Luz, J. Billard, *Z. Naturforsch. A 40* (1985) 149; b) A. M. Levelut, J. Malthête, A. Collet, *J. Phys. (Les Ulis, Fr.) 47* (1986) 351.
[10] J.-M. Lehn, J. Malthête, A. M. Levelut, *J. Chem. Soc. Chem. Commun. 1985*, 1794.
[11] J. Malthête, Nguyen Huu Tinh, A. M. Levelut, *J. Chem. Soc. Chem. Commun. 1986*, 1548.
[12] a) B. Reck, H. Ringsdorf, *Makromol. Chem. Rapid Commun. 7* (1986) 389; S. Berg, V. Krone, H. Ringsdorf, *ibid. 7* (1986) 381; O. Herrmann-Schönherr, J. H. Wendorff, H. Ringsdorf, P. Tschirner, *ibid. 7* (1986) 791; review: H. Finkelmann, *Angew. Chem. 99* (1987) 840; *Angew. Chem. Int. Ed. Engl. 26* (1987) 816; b) W. Kreuder, H. Ringsdorf, *Makromol. Chem. Rapid. Commun. 4* (1983) 807; c) M. Engel, B. Hisgen, R. Keller, W. Kreuder, B. Reck, H. Ringsdorf, H.-W. Schmidt, P. Tschirner, *Pure Appl. Chem. 57* (1985) 1009; d) W. Kreuder, H. Ringsdorf, P. Tschirner, *Makromol. Chem. Rapid Commun. 6* (1985) 367; O. Herrmann-Schönherr, J. H. Wendorff, W. Kreuder, H. Ringsdorf, *ibid. 7* (1986) 97; e) G. Wenz, *ibid. 6* (1985) 577.
[13] a) M. J. Freiser, *Phys. Rev. Lett. 24* (1970) 1041; b) Y. Rabin, W. E. McMullen, W. M. Gelbart, *Mol. Cryst. Liq. Cryst. 89* (1982) 67.
[14] F. Heßel, H. Finkelmann, *Polym. Bull. (Berlin) 15* (1986) 349.
[15] R. Pratibha, M. V. Madhusudana, *Mol. Cryst. Liq. Cryst. Lett. 1* (1985) 111.
[16] The starting material, disodium azobiphenyldicarboxylate, was obtained from Cassella, Frankfurt. Acid chloride: *Beilstein E III, Bd. 16*, p. 235.
[17] Substance provided by B. Reck: *p*-nitrobenzoic acid → azo-4,4'-dibenzoic acid → azo-4,4'-dibenzoyl chloride → diethyl azo-4,4'-dibenzoate, m.p. = 141–142 °C (recrystallized three times from toluene); cf. M. L. Tomlinson, *J. Chem. Soc. 1946*, 756; H. E. Bigelow, D. B. Robinson, *Org. Syn. Coll. Vol. 3* (1955) 103.

[18] D. Seebach, E. Hungerbühler, R. Naef, P. Schnurrenberger, B. Weidmann, M. Züger, *Synthesis 1982*, 138.
[19] 4,4'-Diamino-2,2'-biphenyldicarboxylic acid from 3-nitrobenzaldehyde [20], tetrazotization, phenol, crystallization from acetone; fourfold ethylation with $(EtO)_2SO_2/K_2CO_3$ (1.5 equiv.) in acetone, 24 h reflux, crystallization from acetone and toluene, R_f(toluene/ethyl acetate, 24 + 1) = 0.46.
[20] DRP 69541, Farbwerke Hoechst; see also P. Friedländer, *Fortschr. Theerfarbenfabr. verw. Industriezweige 3* (1896) 26.
[21] Nguyen Huu Tinh, M. C. Bernaud, G. Sigaud, C. Destrade, *Mol. Cryst. Liq. Cryst. 65* (1981) 307.
[22] J. Billard, J. C. Dubois, Nguyen Huu Tinh, A. Zann, *Nouv. J. Chim. 2* (1978) 535.
[23] Hexaethyl (2,3,6,7,10,11-triphenylenehexaylhexaoxy)hexaacetate exhibits k 122 D_{ho} 172 i: R. Wüstefeld, *Diplomarbeit*, Universität Mainz 1987; H. Ringsdorf, R. Wüstefeld, *Int. Conf. Liq. Cryst. Polym.*, Bordeaux, July 20–24, 1987.
[24] L. Kofler, A. Kofler: *Thermomikromethoden*, Verlag Chemie, Weinheim 1954.
[25] D. Demus, L. Richter: *Textures of Liquid Crystals*, Verlag Chemie, Weinheim 1978; G. W. Gray, J. W. G. Goodby: *Smectic Liquid Crystals: Textures and Structures*, Leonhard Hill, Glasgow 1984.
[26] O. Herrmann-Schönherr, J. H. Wendorff, W. Kreuder, H. Ringsdorf, unpublished.
[27] A. M. Levelut, *J. Phys. Lett. 40* (1979) 81.
[28] We thank *P. Fonrobert* and Prof. Dr. *M. Przybylski* for MS investigations.

Relay Conjugation via Twisted Six- and Seven-Membered Rings**

By *Rolf Gleiter,** *Bernd Kissler*, and *Camille Ganter*

Dedicated to Professor Klaus Hafner on the occasion of his 60th birthday

Four-membered rings have been proposed to be good relays for the interaction between two perpendicular π systems.[1] Recent investigations on the tricyclic systems **1**–**3** have supported the concept of relay conjugation between remote π systems.[2,3]

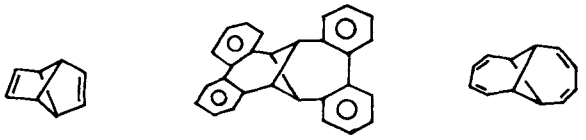

1 **2** **3**

To further extend these studies, we have investigated the spectroscopic properties of the compounds **4**–**6** in which two π moieties are separated by either a six- or seven-membered twisted ring.

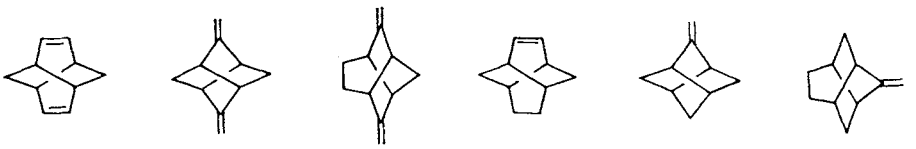

4 **5** **6** **7** **8** **9**

Twistadiene, **4**, was first reported by *Ganter* et al.[4] The synthesis of **6**[6] has been carried out according to the one of **5**[5] (Scheme 1). Compound **14**, prepared from **10** via the intermediates **11**–**13**, was converted by a procedure analogous to that described by *Sauers* et al.[7] Intramolecular addition of the ketene yielded only the tetracyclic ketone **15**, which could be cleaved to the key intermediate **16**, the twistbrendane structure of which was proven by

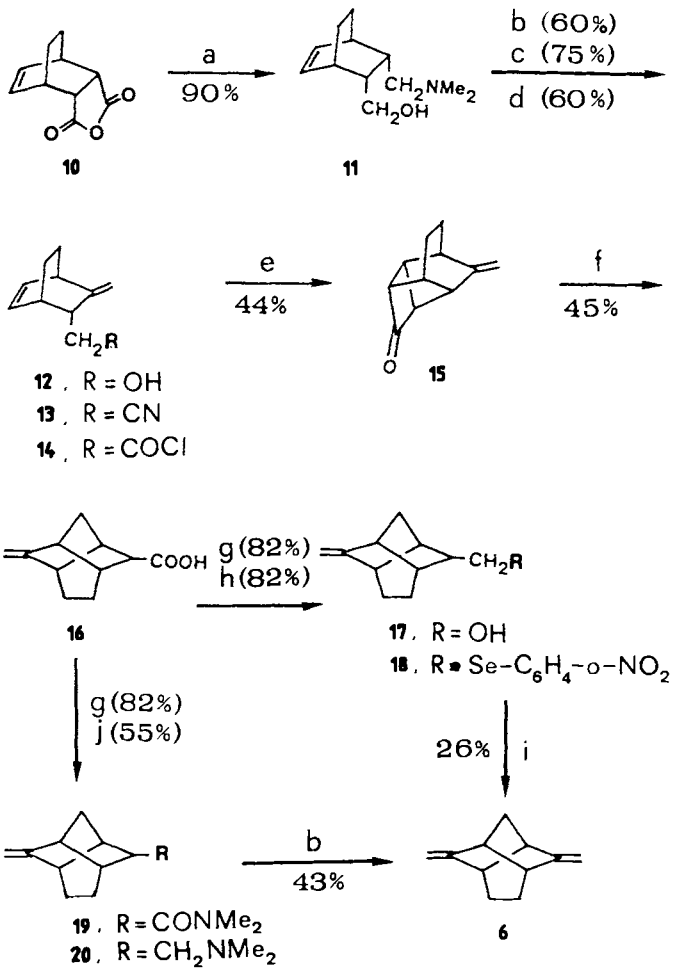

Scheme 1. a) $HNMe_2$, $LiAlH_4$. b) H_2O_2. c) TosCl/pyridine, NaCN/DMF. d) KOH, $SOCl_2$. e) NEt_3/benzene. f) *t*BuOK. g) $LiAlH_4$. h) *o*-NO_2–C_6H_4–SeCN, *n*Bu_3P. i) H_2O_2/THF. j) $SOCl_2$, $HNMe_2$.

[*] Prof. Dr. R. Gleiter, Dr. B. Kissler
Institut für Organische Chemie der Universität
Im Neuenheimer Feld 270, D-6900 Heidelberg (FRG)
Prof. Dr. C. Ganter
Laboratorium für Organische Chemie der
Eidgenössischen Technischen Hochschule
Universitätsstrasse 16, CH-8092 Zürich (Switzerland)

[**] We are grateful to the Fonds der Chemischen Industrie, the DFG, and the BASF Aktiengesellschaft for financial support. *B. K.* thanks the state Baden-Württemberg for a "Graduiertenstipendium."

X-ray investigations on the dimethylamide **19**.[8] Diene **6**[6] could be prepared from **16** via two different routes; in both cases elimination proceeded without rearrangement as was observed in the corresponding synthesis of **5**.[5]

The method of choice to investigate the electronic interactions of the two C=C moieties is HeI_α photoelectron (PE) spectroscopy. In order to interpret the PE spectra of **4**–**6**, we also investigated the monoenes **7**–**9**.[9–11] In Table 1 the first ionization energies are compared to orbital ener-

gies obtained from ab-initio (4-31G[12]) and semiempirical SCF calculations (MINDO/3[13,14]), assuming the validity of *Koopmans*' theorem.[15]

Table 1. Comparison between the first vertical ionization energies, $I_{v,j}$, and the calculated orbital energies, ε_j, of **4**–**9**. Values in eV. j = 1-3 (**4**–**6**) and 1, 2 (**7**–**9**).

Compound	$I_{v,j}$	Assignment	$-\varepsilon_j$
4[a]	8.46	$7b_3(\pi)$	8.24
	9.8	$6b_2(\pi)$	9.54
	10.5	$6b_3(\sigma)$	10.52
5 [a]	8.49	$7b_3(\pi)$	8.87
	9.40	$6b_2(\pi)$	9.76
	10.05	$6b_3(\sigma)$	10.95
6 [a]	8.60	$14b(\pi)$	9.01
	9.30	$15a(\pi)$	9.66
	10.35	$14a(\sigma)$	11.10
7 [b]	8.74	$13b(\pi)$	9.02
	9.57	$12b(\sigma)$	9.47
8 [b]	8.96	$12b(\pi)$	9.34
	10.2	$11b(\sigma)$	9.92
9 [b]	9.00	$13b(\pi)$	9.40
	9.75	$12b(\sigma)$	9.73

[a] Orbital energies calculated with 4-31G. [b] Orbital energies calculated with MINDO/3.

The PE spectra of **4**–**6** reveal a strong splitting of the first two bands ($\Delta \approx 0.7$–1.3 eV). From the observation that the π-ionization energies of **7**–**9** lie between the first two bands of **4**–**6** and from the large separation between the π units in **4**–**6** (> 3 Å), we conclude that the splitting in **4**–**6** has its origin in strong electronic interactions between the central ring and both symmetry-adapted linear combinations of the π orbitals.

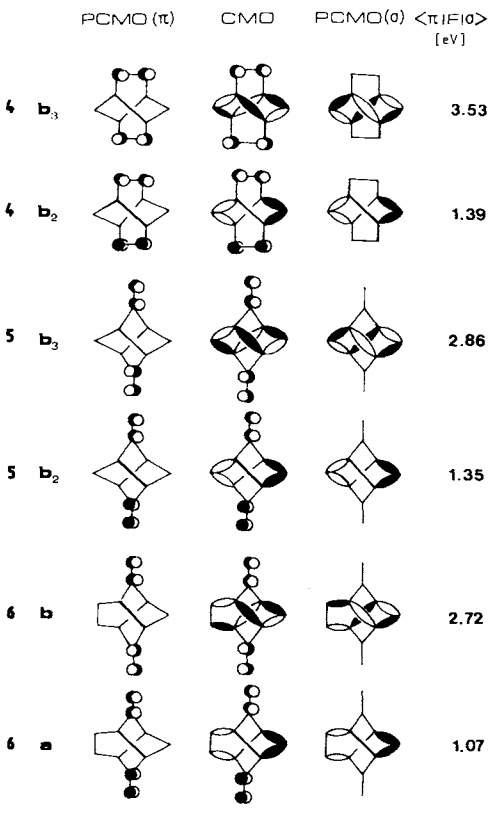

Fig. 1. Schematic representation of the symmetry-adapted precanonical π MOs and the precanonical σ MOs (PCMOs) of the twisted ring moiety together with the resulting two highest canonical MOs (CMOs). The symmetry assignments are given in the first column, the matrix elements $\langle\pi|F|\sigma\rangle$ between the PCMOs in the last column.

A quantitative analysis of this interaction was performed applying the procedure proposed by *Heilbronner* and *Schmelzer*.[16] In Figure 1 we show the precanonical orbitals (PCMOs) of the π and σ type, the resulting canonical MOs, and the matrix element $\langle\pi|F|\sigma\rangle$, the latter being a measure for the intensity of the π,σ mixing. This analysis reveals a strong interaction between the $b_3(\pi)$ (**4**,**5**) and the $b(\pi)$ (**6**) linear combination with the corresponding σ orbitals. Interestingly, the σ orbital that is responsible for the strong π/σ interaction does not belong to the set of ribbon orbitals[17] of the twisted six- or seven-membered ring.

Received: May 29, 1987;
revised: July 22, 1987 [Z 2269 IE]
Publication delayed at authors' request
German version: *Angew. Chem. 99* (1987) 1292

CAS Registry numbers:
4, 58594-24-4; **5**, 96322-97-3; **6**, 111410-43-6; **7**, 25107-15-7; **8**, 111467-19-7; **9**, 111410-44-7.

[1] P. Bischof, R. Gleiter, R. Haider, *J. Am. Chem. Soc. 100* (1978) 1036.
[2] R. Gleiter, T. Kobayashi, *Helv. Chim. Acta 54* (1971) 1081; J. Spanget-Larsen, R. Gleiter, R. Haider, *ibid. 66* (1983) 1441.
[3] L. A. Paquette, J. Dressel, K. L. Chasey, *J. Am. Chem. Soc. 108* (1986) 512; J. Dressel, *Dissertation*, The Ohio State University 1987; R. Gleiter, A. Toyota, P. Bischof, G. Krennrich, J. Dressel, P. D. Pansegrau, L. A. Paquette, unpublished.
[4] H.-G. Capraro, C. Ganter, *Helv. Chim. Acta 59* (1976) 97.
[5] B. Kissler, R. Gleiter, *Tetrahedron Lett. 26* (1985) 185.
[6] Most relevant spectroscopic data of **6**: ^{1}H-NMR (300 MHz, $CDCl_3$): δ = 4.69 (2H, t, J = 1.1 Hz), 4.49 (2H, br. s), 2.78-2.75 (2H, m), 2.49-2.46 (2H, m), 1.72-1.61 (2H, m), 1.52 (2H, br. s), 1.50-1.41 (2H, m). ^{13}C-NMR (75 MHz, $CDCl_3$): δ = 158.8, 98.6, 47.3, 41.9, 28.9, the large half-width of the signal at δ = 41.9 suggests the superposition of two resonances. High-resolution MS: $M^{\oplus}$ 146.1086 (calcd 146.1077).
[7] R. R. Sauers, K. W. Kelly, *J. Org. Chem. 35* (1970) 3286.
[8] We thank *C. Krieger*, Heidelberg, for an X-ray analysis of **19**: R. Gleiter, unpublished.
[9] M. Tichý, J. Sicher, *Collect. Czech. Chem. Commun. 37* (1972) 3107. We thank Dr. *Tichý*, Prague, for a sample of twistene.
[10] M. Nakazaki, K. Naemura, N. Arashiba, *J. Org. Chem. 43* (1978) 888.
[11] R. Gleiter, B. Kissler, unpublished.
[12] R. Ditchfield, W. J. Hehre, J. A. Pople, *J. Chem. Phys. 54* (1971) 724. We thank Prof. *D. Cremer*, Köln, for performing the 4-31G calculation on **6**.
[13] R. C. Bingham, M. J. S. Dewar, D. H. Lo, *J. Am. Chem. Soc. 97* (1975) 1285.
[14] The geometrical parameters adopted for these calculations were obtained from MINDO/3 calculations in which all degrees of freedom were minimized with regard to inherent symmetry restrictions. In those cases where X-ray investigations of derivatives were available (**5**, **6**), we found a good agreement between experimental and calculated geometries.
[15] T. Koopmans, *Physica 1* (1934) 104.
[16] E. Heilbronner, A. Schmelzer, *Helv. Chim. Acta 58* (1975) 936.
[17] R. Hoffmann, P. D. Mollère, E. Heilbronner, *J. Am. Chem. Soc. 95* (1973) 4860.

Low-Temperature Photolysis of Peracetylated Dodecanoyl Peroxides of Tartaric Acid and D-Gluconic Acid in the Solid State— A Diastereoselective Radical Coupling

By *Rainer Lomölder* and *Hans J. Schäfer**

Dedicated to Professor Ulrich Schöllkopf on the occasion of his 60th birthday

Kolbe electrolysis is an attractive method for CC coupling reactions, because it allows a large variety of compounds to be prepared easily and in high yields from inexpensive carboxylic acids.[1] A disadvantage, however, is the lack of selectivity for unsymmetrical products upon coelec-

[*] Prof. Dr. H. J. Schäfer, Dipl.-Chem. R. Lomölder
Organisch-chemisches Institut der Universität
Corrensstrasse 40, D-4400 Münster (FRG)

trolysis of two carboxylic acids and the loss of optical activity observed for carboxylic acids having an asymmetric center at the α-carbon atom. We recently showed that, by solid-state photolysis of unsymmetrical diacyl peroxides, it is possible to obtain unsymmetrical coupling products with high selectivity.[2] We have now found that the configuration at the α-C atom also remains largely unchanged when the optically active diacyl peroxides **1b**–**4b** are photolyzed in the crystal at low temperature.[3]

The peroxides **1b**, **2b**, and **4b** were synthesized, starting from the corresponding acid chlorides peroxydodecanoic acid, and pyridine, in yields of 83–95%. Compound **3b** was obtained, starting from the monomethyl ester of *rac*-bis-*O*-acetyltartaric acid (obtained from *meso*-tartaric acid),[4] peroxydodecanoic acid, and dicyclohexylcarbodiimide (DCC) in 73% yield. Photolysis of **1b**–**4b** afforded the acetates **1c**–**4c** (Table 1).

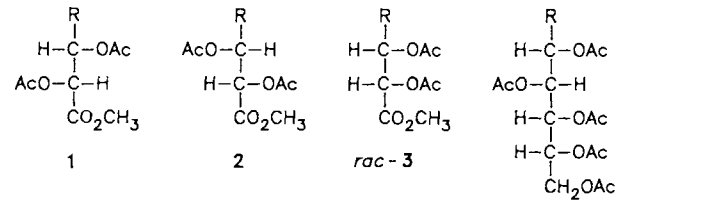

1 2 *rac*-3 4

a, R = COCl bzw. CO_2H (3); b, R = CO–OO–$COC_{11}H_{23}$; c, R = $C_{11}H_{23}$

Table 1. Diastereoselective synthesis of **1c**–**4c** by photolysis of the diacyl peroxides **1b**–**4b**.

No.	Diacyl peroxide	*T* [°C] (*t* [h]) [a]	Undecyl derivative	Yield [%]	Diastereoselectivity [b] [% *de*]
1	**1b**	−60 (4.5–7)	**1c** [c]	44–64	89–95.6
2	**1b**	−20 (3.5)	**1c**	25	35.7
3	**2b**	−60 (5.5)	**2c**	48	95.6
4	**2b**	5 (2)	**2c**	17	3.4
5	**3b**	−60 (7.5)	**3c** [d]	57	92.3
6	**4b**	−60 (5–7.5)	**4c**	34–41	81.6–87
7	**4b**	10 (2)	**4c**	22	6.6

[a] 2.6–8.9 mmol of the solid peroxide, as a suspension in petroleum ether (34–40°C), was irradiated with a medium-pressure Hg lamp in a circulation apparatus. [b] Determination of the diastereoselectivity: **1c**–**3c**, gas chromatography (FFAP, 50 m, 200°C); **4c**, gravimetrically after column chromatography. [c] After saponification, **1c** was converted into the 2,3-di-*O*-isopropylidene methyl ester, whose $J_{2,3} < 1.6$ Hz indicates the *threo* configuration according to the Karplus rule, i.e., the configuration at C3 remains unchanged. [d] **3c** was likewise converted into the 2,3-di-*O*-isopropylidene methyl ester, whose $J_{2,3} = 6.7$ Hz supports the existence of the *erythro* configuration, i.e., the configuration at C3 is presumably also retained in this case.

The high diastereoselectivity observed at −60°C is nearly completely lost at 5–10°C. Furthermore, the fair chemical yields obtained at low temperature decrease upon raising the temperature owing to competing disproportionation (undecane, 1-undecene), symmetrical coupling (docosane), and presumably ionic decomposition.[5]

Diacyl peroxides undergo photochemical decarboxylation to give radical pairs.[6] The cause of the diastereoselectivity, which is unusual for radical couplings, is presumably the restricted motion of the radicals in the solid state.[7] This would also explain the loss in stereoselectivity at higher temperatures. The reaction is mechanistically noteworthy because of the usually complete racemization observed for radical coupling in solution.[8] Furthermore, it permits the decarboxylative alkylation of carboxylic acids from the chiral pool in a simple way with retention of optical activity.

Experimental Procedure

4b: A solution of peroxydodecanoic acid (2.71 g, 12.5 mmol) and dry pyridine (1 mL) in anhydrous ether (70 mL) was treated dropwise at −30°C with a solution of **4a** (5.32 g, 12.6 mmol) in anhydrous ether (120 mL) and the resulting reaction mixture was allowed to stir for 3 h at −30°C. After filtering off the pyridinium hydrochloride, the ether solution was washed (3 × 30 mL 2N HCl, 3 × 20 mL saturated $NaHCO_3$, 3 × 20 mL H_2O) and dried over sodium sulfate. After removal of the solvent at ca. 5°C), the crude product was filtered at 5°C on silica gel (deactivated with 5% H_2O; eluent, ether with 0.1% triethylamine). After removal of the solvent, 6.63 g (11 mmol, 87%) of **4b** was obtained.—Photolysis of **4b** at −60°C: **4b** (2.2 g, 3.6 mmol), dissolved in ether (10 mL), was added to 300 mL of petroleum ether in a circulation apparatus at −60°C. The resulting suspension [9] was photolyzed with a medium-pressure Hg lamp (TQ 150, Hanau) in the well of a photolysis vessel made of quartz glass and equipped with a vacuum jacket. After removal of the petroleum ether, the crude product was dissolved in 300 mL of ether, washed (3 × 30 mL saturated $NaHCO_3$ solution, 3 × 20 mL H_2O), and dried over Na_2SO_4. Flash chromatography (silica gel deactivated with 5% H_2O, ether/petroleum ether (34–40°C) = 2 : 1, v/v) afforded 594 mg (1.2 mmol, 32%) of **4c** along with 41 mg (0.079 mmol, 2%) of the C5 epimer of **4c**.

Received: June 29, 1987;
supplemented: September 8, 1987 [Z 2316 IE]
German version: *Angew. Chem.* 99 (1987) 1282

Table 2. Selected physical data for the compounds discussed here. DCI = direct chemical ionization.

1b, **2b**: DCI, NH_3: *m/z* 464, 42% ($MNH_4^{\oplus}$); $[\alpha]_D^{25} = +45.54$, $CHCl_3$ ($c = 0.993$) (**1b**); $[\alpha]_D^{25} = -45.90$, $CHCl_3$ ($c = 1.563$) (**2b**)

1c, **2c**: GC/CI-MS (FFAP, 50 m, 200°C), isobutane: *m/z* = 359, 100% ($MH^{\oplus}$).—Optical rotations measured for the pure compounds obtained by saponification, recrystallization, and esterification: $[\alpha]_D^{25} = -32.40$, $CHCl_3$ ($c = 1.38$) (**1c**); $[\alpha]_D^{25} = +32.29$, $CHCl_3$ ($c = 1.88$) (**2c**)

3b: DCI, NH_3: *m/z* 420, 100% ($MNH_4^{\oplus} - CO_2$)

3c: GC/CI-MS (FFAP, 50 m, 200°C), isobutane: *m/z* 359, 52% ($MH^{\oplus}$)

4b: DCI, NH_3: *m/z* 578, 30% ($MNH_4^{\oplus} - CO_2$); $[\alpha]_D^{25} = +19.65$, $CHCl_3$ ($c = 2.655$)

4c: GC/CI-MS, isobutane: *m/z* 457, 100% ($MH^{\oplus} - CH_3CO_2H$); $[\alpha]_D^{25} = +7.71$, $CHCl_3$ ($c = 1.82$)

C5-epimer of **4c**: DCI, isobutane: *m/z* 517, 25% ($MH^{\oplus}$); $[\alpha]_D^{25} = +30.27$, $CHCl_3$ ($c = 0.985$)

[1] J. H. P. Utley in N. Weinberg: *Technique of Electroorganic Synthesis Vol. 5, Part 1*. Wiley, New York 1974, p. 793.
[2] M. Feldhues, H. J. Schäfer, *Tetrahedron 41* (1985) 4195.
[3] The corresponding peroxides of α-amino acids proved to be unsuitable. *N*-Boc-, *N*-trifluoroacetyl-, *N*-acetyl-, *N*-lauroyl-L-alanine, and *N*-Boc- and *N*-*p*-tosyl-L-proline were treated with DCC and peroxydodecanoic acid. However, the diacyl peroxides decomposed during the synthesis, presumably via an ionic pathway, to give unstable products that were not characterized further.
[4] The crude nonisolated diacetylated anhydride of *meso*-tartaric acid was treated with methanol; purification of the products by flash chromatography gave the monoester as a colorless oil (67% via two steps).
[5] GC/MS indicated the probable presence of 1-dodecanoyloxy derivatives of **1** and **2** ($R = C_{11}H_{23}CO_2$).
[6] R. A. Sheldon, J. K. Kochi, *J. Am. Chem. Soc. 92* (1970) 4395.
[7] The topochemical principle (reactions in the crystal proceed with a minimum of atomic and molecular motion (M. D. Cohen, *Angew. Chem. 87* (1975) 439; *Angew. Chem. Int. Ed. Engl. 14* (1975) 386)) is not always valid for photolyses of solid diacyl peroxides (J. M. McBride, B. E. Segmüller, M. D. Hollingsworth, D. E. Mills, B. A. Weber, *Science (Washington) 234* (1986) 830). However, the large degree of retention at −60°C indicates a restricted rotation around the C1–C2 bond in the radicals **1**–**4** ($R = \odot$). The diastereoselectivity of the coupling cannot be explained by an equilibrium between diastereomeric radicals, since, if this were the case, the same products or product mixtures would be obtained from **1b** and **3b** or from **2b** and **3b**. Moreover, the activation energies for attaining the diastereomeric transition states are probably not sufficiently different because the radical combination, which requires practically no activation energy, leads to early transition states.
[8] Another example of a diastereoselective radical coupling was described earlier: P. D. Bartlett, J. M. McBride, *Pure Appl. Chem. 15* (1967) 89.
[9] Crystalline **4b** (powder photograph at −58°C), suspended in petroleum ether, leads to the same diastereoselectivity and comparable yields. Compounds **1b**–**3b** were suspended in petroleum ether as solids and then photolyzed.

Polystannanes $Ph_3Sn\text{-}(tBu_2Sn)_n\text{-}SnPh_3$ (n = 1–4): A Route to Molecular Metals?**

By *Stefan Adams* and *Martin Dräger**

Two modifications of elemental tin exhibiting fundamentally different bonding exist, the semimetallic α form and the metallic β form. In the 4th main group of the periodic table, this dimorphism constitutes a stage between non- and semimetallic elements (C, Si, Ge) on the one hand and metallic lead on the other. In the inorganic chemistry of tin, Zintl phases and cluster anions with homonuclear Sn–Sn bonds reveal a continuous transition from metallic to covalent bonding.[1] The structural investigations of organopolystannanes[2a] carried out so far have shown a relationship between these compounds and alkanes; the structure of a distannene has also been described.[2b] Further linking of Sn centers, beyond that studied so far, should build a bridge between the organic and inorganic chemistry of tin.

$$2\,Ph_3SnLi + I\text{-}(tBu_2Sn)_n\text{-}I \xrightarrow[-2\,LiI]{} Ph_3Sn\text{-}(tBu_2Sn)_n\text{-}SnPh_3 \quad (a)$$

1 **2**, n = 2–4 **3**

a, n = 1; **b**, n = 2; **c**, n = 3; **d**, n = 4

With this goal in mind, we allowed the 1,n-diiodo compounds **2**[3] to react with Ph_3SnLi **1** [reaction (a)]. This chain-lengthening reaction is more complicated than the stoichiometry would at first lead one to expect. Variation of the molar ratio of the starting materials as well as of the solvent and the concentration (Table 1[4]) made it possible to isolate the tri- (**3a**), tetra- (**3b**), penta- (**3c**), and hexastannane (**3d**). The solutions of the iodine components react as equilibrium mixtures of different 1,n-diiodopolystannanes; only when nonpolar toluene is used in excess relative to added THF is **3d** obtained in good yield.

Table 1. Reactions and yields for the syntheses of **3a–d**.

1/THF [mmol]/[mL]	**2** n/[mmol]	Solvent ([mL])	Yields [mmol]/[%] [a] **3a** n = 1 [b]	**3b** n = 2 [b]	**3c** n = 3	**3d** n = 4
8.3/170	4/4.1	toluene (120)	1.36/33	0.68/16	—	—
6.0/ 50	4/3.0	THF (20)	0.51/17	0.26/9	0.63/21	
9.6/ 80	4/4.7	toluene (200)	—	—	—	2.1/45
16.0/100	3/8.0	THF (100)	1.52/19	0.76/10	3.7/47	—
12.0/110	2/6.0	THF (30)	—	2.2/37 [c]	—	—

[a] In addition, 2 to 3 mmol of $tBu_2Sn(OH)Cl$ from remaining tBu_2Sn units; yields based on **1**. [b] Mostly as a mixed phase **3a** · 0.5 **3b**. [c] In addition, 2.0/33 Ph_6Sn_2.

X-ray structure analyses[6] of **3a–d** revealed the molecular conformations, bond angles, and Sn–Sn distances shown in Figure 1. Bulky, electron-rich substituents on the Sn–Sn units generally effect an increase of the Sn–Sn bond length.[2a] This is confirmed by the series of *t*Bu-substituted compounds investigated here. The central bond in **3d** (296.6(3) pm; +15.6 ppm (5.6%) versus α-tin) is the longest Sn–Sn bond so far found in organopolystannanes. The same is true for *t*Bu-substituted polysilanes.[7a,b] In all compounds **3** as well as in $I\text{-}(tBu_2Sn)_4\text{-}I$[3a] the Sn_n unit exhibits the *trans* conformation. Intermolecular interactions are not present in the crystal.

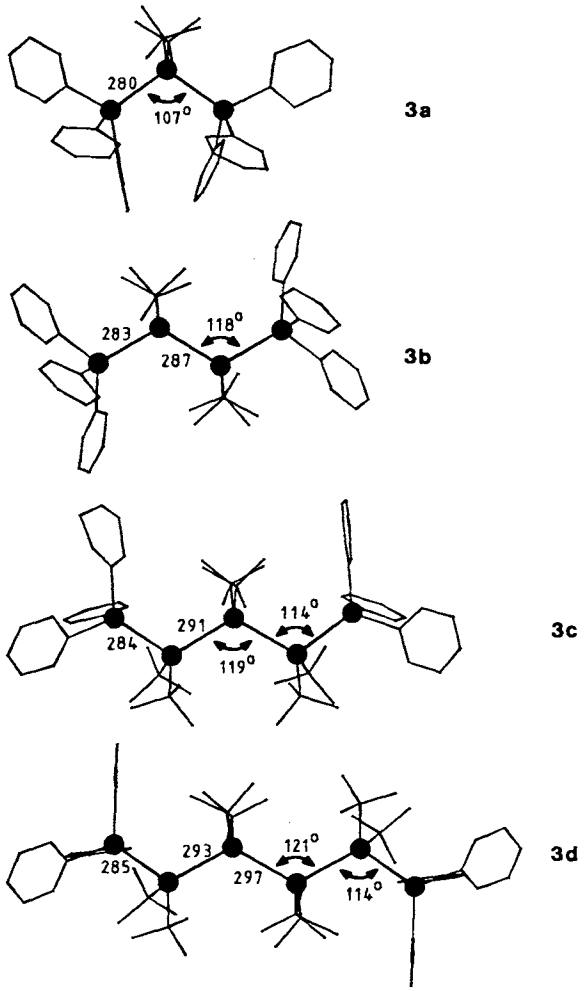

Fig. 1. Molecular structures of **3a–d** with average Sn–Sn bond lengths [pm] and Sn–Sn–Sn bond angles [6].

The polystannanes **3** are relatively soluble in $CDCl_3$; in the ^{119}Sn-NMR spectra, two (**3a**,**b**) or three (**3c**,**d**) major signals are surrounded by numerous well-resolved coupling satellites. Plotting of $^1J(^{119}Sn\text{-}^{119}Sn)$ versus d(Sn-Sn) (eight independent pairs of values) reveals a correlation that shows opposite signs for couplings via short (positive) or long (negative) bonds (change in sign at about 285 pm); data measured earlier by us (13 pairs of values[3a,5b]) and data from the literature (15 pairs of values[8]) fit this relation (Fig. 2). A linear relationship[5a] between $^2J(^{119}Sn\text{-}^{119}Sn)$ and the "nonbonding" distance $d(Sn\cdots Sn)$ was confirmed; in this case, too, the series **3a** to **3d** reveals a change in the sign of the coupling constants (at about 500 pm; 513 pm and −92 Hz for the central bonds in **3d**).

The UV spectra (Fig. 3) exhibit strong absorption maxima with marked redshift with increasing chain length.[7c] Parallels exist with conjugated polyenes, except that the HOMO in Sn_n chains is determined by σ Sn–Sn bonds. The HOMO/LUMO energy difference decreases with increasing chain length. We interpret this as the onset of formation of a metal-like electronic band and thus propose the term "molecular metals" for these compounds. In ad-

[*] Prof. Dr. M. Dräger, Dr. S. Adams
Institut für Anorganische Chemie und Analytische Chemie
der Universität
Johann-Joachim-Becher-Weg 24, D-6500 Mainz (FRG)

[**] Polystannanes, Part 5. This work was supported by the Deutsche Forschungsgemeinschaft and the Fonds der Chemischen Industrie.—Part 4: [5b].

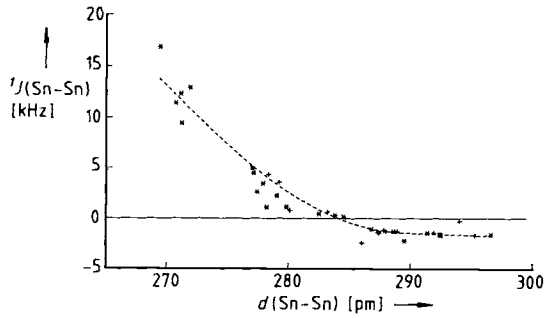

Fig. 2. Plot of the coupling constants $^1J(^{119}Sn\text{-}^{119}Sn)$ versus the bond lengths d(Sn-Sn); * pairs of values from our research, + literature data [8].

dition, Figure 3 shows a relationship between electronic excitation and ^{119}Sn-NMR chemical shift of the central Sn atom: an increase in the wavelength of the absorption is associated with a downfield shift of the NMR signals.

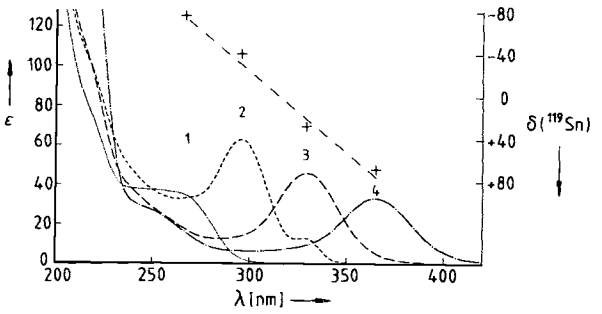

Fig. 3. UV spectra of the compounds **3a-d** (extinction coefficient ε for mol m^{-3}) and plot of the ^{119}Sn-NMR chemical shift [ppm] of the central Sn atom versus the corresponding excitation wavelength of the Sn_n chain (+).

The correlations described here and several empirical correlations for the series of compounds **3a** to **3d** point to a smooth transition between covalently bonded polystannanes and metallic tin. An analogous transition between molecular clusters and metallic microparticles of transition-metal elements has recently been the subject of frequent discussion.[9]

Received: July 15, 1987 [Z 2359 IE]
German version: *Angew. Chem. 99* (1987) 1280

[1] Review: H. G. von Schnering, *Angew. Chem. 93* (1981) 44; *Angew. Chem. Int. Ed. Engl. 20* (1981) 33.

[2] a) Cambridge Crystallographic Data Base, update January 1987 (eight distannanes, twenty cyclostannanes, seven compounds containing cluster anions); b) D. E. Goldberg, P. B. Hitchcock, M. F. Lappert, K. M. Thomas, A. J. Thorne, T. Fjeldberg, A. Haaland, B. E. R. Schilling, *J. Chem. Soc. Dalton Trans. 1986*, 2387.

[3] a) S. Adams, M. Dräger, *J. Organomet. Chem. 288* (1985) 295; b) H. Puff, C. Bach, W. Schuh, R. Zimmer, *ibid. 312* (1986) 313.

[4] *Experimental procedure:* The iodine components **2** [3] were dissolved and cooled to -78°C, resulting in partial precipitation. A freshly prepared and filtered Ph_3SnLi solution [5a] was then added sufficiently slowly so that the green color vanished before the next addition (ca. 1-2 h). The reaction mixture was stirred for several hours without cooling. Isolation: in analogy to [5a]. The polystannanes are stable under normal conditions and are colorless (**3a**) to yellow (**3d**), crystalline solids; in each case, a sharp (**3a**) to broad (**3d**), intense Raman signal was observed for the completely symmetric Sn_n stretching vibration (**3a**, 136; **3b**, 113; **3c**, 117; **3d**, 114 cm^{-1}).

[5] a) S. Adams, M. Dräger, *J. Organomet. Chem. 323* (1987) 11; b) S. Adams, M. Dräger, B. Mathiasch, *ibid. 326* (1987) 173.

[6] *Crystal structure analyses:* a) mixed phase **3a** × 0.5 **3b**, $P2_1/c$, $a = 1118.2(3)$, $b = 3368.0(4)$, $c = 1789.1(3)$ pm, $\beta = 91.61(2)°$, $V = 6735 \times 10^6$ pm^3, $Z = 4$, 8599 reflections with $I > 2\sigma(I)$, 328 variables, $R = 0.060$; b) **3c**, data at -80°C, *Pbca*, $a = 2005.9(10)$, $b = 2587.3(7)$, $c = 2290.9(6)$ pm, $V = 11890 \times 10^6$ pm^3, $Z = 8$, 5690 reflections with $I > 2\sigma(I)$, 288 variables, $R = 0.067$; c) **3d** · 3 cyclohexane, data at -59°C, $P\bar{1}$, $a = 1090.0(12)$, $b = 1091.5(4)$, $c = 1985.9(15)$ pm, $\alpha = 103.45(4)$, $\beta = 101.59(11)$, $\gamma = 92.95(8)°$, $V = 2239 \times 10^6$ pm^3, $Z = 1$, 7444 reflections with $I > 3\sigma(I)$, 195 variables (one cyclohexane molecule disordered), $R = 0.065$. — Further details of the crystal structure investigation may be obtained from the Fachinformationszentrum Energie, Physik, Mathematik GmbH, D-7514 Eggenstein-Leopoldshafen 2 (FRG), on quoting the depository number CSD-52672, the names of the authors, and the journal citation.

[7] a) N. Wiberg, H. Schuster, A. Simon, K. Peters, *Angew. Chem. 98* (1986) 100; *Angew. Chem. Int. Ed. Engl. 25* (1986) 79; b) M. Weidenbruch, B. Blintjer, K. Peters, H. G. von Schnering, *ibid. 98* (1986) 1090 and *25* (1986) 1129; c) compare the corresponding, but less marked, redshifts in organosubstituted polysilanes: C. G. Pitt in A. L. Rheingold (Ed.): *Homoatomic Rings, Chains and Macromolecules of Main-Group Elements*, Elsevier, Amsterdam 1977, p. 203.

[8] B. Wrackmeyer, *Annu. Rep. NMR Spectrosc. 16* (1985) 73.

[9] Cf. e.g. a) G. Schmid, *Nachr. Chem. Tech. Lab. 34* (1987) 249; b) B. K. Teo, K. Keating, Y.-K. Kao, *J. Am. Chem. Soc. 109* (1987) 3494; B. K. Teo, M. C. Hong, H. Zhang, D. B. Huang, *Angew. Chem. 99* (1987) 943; *Angew. Chem. Int. Ed. Engl. 26* (1987) 897.

A 3,7-Diaza-1,2,4,5,6,8-hexaphosphatricyclo-[4.2.0.0^{2,5}]octane, a [2 + 2] Dimer of a 1,2-Dihydro-1-azatriphosphete containing a Planar P_4 Substructure**

By *Edgar Niecke,* Oliver Altmeyer, Martin Nieger,* and *Fritz Knoll*

$R_2N-PH-P(NR_2)-P(NR_2)-PH-NR_2$ ($R = SiMe_3$), a 1,2,3,4-tetrakisaminotetraphosphane, undergoes amine elimination to afford the tetraphosphabicyclobutane **B** instead of the tetraphosphabutadiene **A**.[1] In addition, calculations showed that **B** is the more stable isomer.[2]

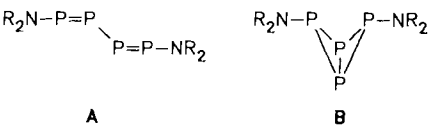

A **B**

When we attempted to convert the diphosphene derivative **3**, obtained by reaction of the hydrazine derivative **1** with the diphosphene **2**, into the azatriphosphabicyclobutane **5** by elimination of chlorotrimethylsilane to give the azatriphosphabutadiene **4**, followed by isomerization,[3] we surprisingly obtained the tricyclic N_2P_6 system **7**.

We believe that electrocyclic ring closure of the azatriphosphabutadiene **4** leads to the intermediary formation of the 1,2-dihydro-1-azatriphosphete **6**, which, in turn, undergoes [2 + 2] cyclodimerization to give **7**.[4] In solution, **7** slowly decomposes to give the thermodynamically stable products P_4 and the iminophosphane **8**. The composition and constitution of compounds **1**, **2**, and **7** were established by elemental analysis, mass spectrometry, and NMR spectroscopy. The existence of the intermediate **3** is supported by the ^{31}P-NMR spectrum. The X-ray structure analysis of **7**[5] confirms the tricyclic structure of the compound (Fig. 1).

[*] Prof. Dr. E. Niecke, O. Altmeyer, M. Nieger, Dr. F. Knoll
Anorganisch-chemisches Institut der Universität
Gerhard-Domagk-Strasse 1, D-5300 Bonn 1 (FRG)

[**] This work was supported by the Fonds der Chemischen Industrie.

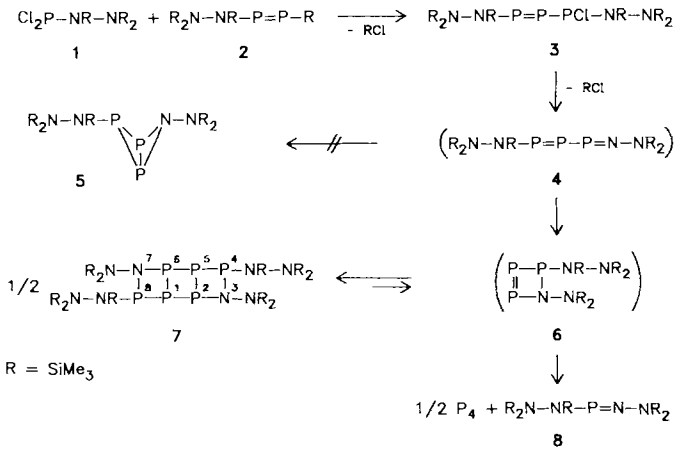

1 2 3 4 5 6 7 8

The molecule exhibits C_i symmetry in the solid. The bonding of the two azatriphosphetidine rings, which are present in a *trans* configuration and are arranged nearly orthogonally to the central P_4 framework, is in accord with expectations.[6] However, in comparison to other *cyclo*-P_4 compounds,[7] the planar arrangement of the central ring system is unusual. Noteworthy is also the relatively long P(2)–P(3) bond (228 pm), which provides an explanation for the retroreaction $7 \rightarrow 6 \rightarrow P_4 + 8$ occurring in solution. Experiments directed at stabilizing the azatriphosphete **6** as a complex ligand are currently in progress.

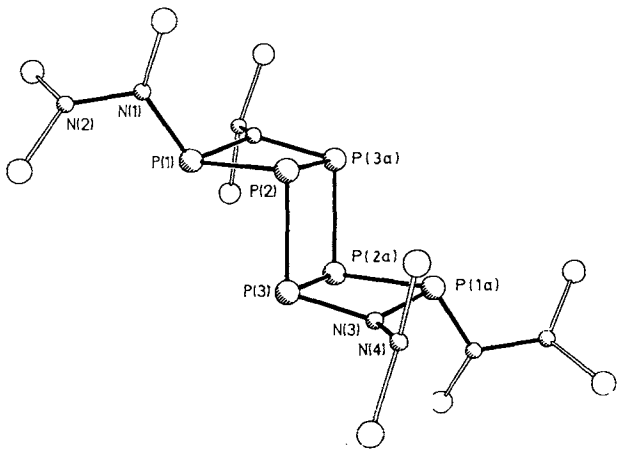

Fig. 1. Structure of **7** (without CH_3 groups). Important bond lengths [Å] and angles [°]: P(1)-P(2) 2.265(5), P(1)-N(3a) 1.745(8), P(2)-P(3) 2.281(6), P(2)-P(3a) 2.236(4), P(3)-N(3) 1.742(8); P(1)-P(2)-P(3) 93.5(2), P(2)-P(3)-N(3) 106.2(4), P(3)-P(2)-P(3a) 92.8(2), P(2)-P(3)-P(2a) 87.2(2), P(2)-P(1)-N(3a) 82.7(3), P(1)-P(2)-P(3a) 78.9(2), N(3)-P(3)-P(2a) 83.7(3), P(3)-N(3)-P(1a) 110.2(4).

Experimental Procedure

1: A solution of PCl_3 (6.0 g, 44 mmol) in ether (100 mL) was treated dropwise at −40 °C with a solution of lithium tris(trimethylsilyl)hydrazide (10.2 g, 40 mmol) in ether (200 mL). The resulting reaction mixture was then allowed to warm to room temperature with stirring. It was stirred for an additional 12 h, after which the solvent and unreacted PCl_3 were removed under vacuum, the residue was dissolved in 150 mL of pentane, and the precipitated LiCl was filtered out. Yield 12.0 g (92%); m.p. = 114–116 °C. MS: $m/z = 348$ $M^{\oplus}$ (5%), 333 $M^{\oplus}$ − Me (15%), 313 $M^{\oplus}$ − Cl (20%), 247 $M^{\oplus} - PCl_2$ (50%), 73 $SiMe_3^{\oplus}$ (100%). $^{31}P\{^1H\}$-NMR (pentane/C_6D_6): $\delta = 165$ (s); ^1H-NMR (C_6D_6): $\delta = 0.23$ (s, 18 H, $SiMe_3$), 0.4 (s, 9 H, $SiMe_3$); $^{29}Si\{^1H\}$-NMR (C_6D_6): $\delta = 13.4$ (d, $J = 6.6$ Hz, PNSi), 19.4 (s, NSi_2).

2: A solution of **1** (6.9 g, 20 mmol) in pentane (40 mL) was treated at −60 °C with a solution of $LiPR_2 \cdot 1.8\,THF$ (6.3 g, 20 mmol) in ether (30 mL) and the resulting reaction mixture was allowed to warm to room temperature. The diphosphane prepared in situ in this way, $R_2N-NR-PCl-PR_2$ (^{31}P-NMR: $\delta = 176$, −146.9, $J_{PP} = 288$ Hz) was stirred at room temperature until chlorosilane elimination was complete (ca. 3 h). Removal of the solvent and the chlorosilane afforded 3.5 g (91%) of **2** as a yellow oil. MS: m/z 382 $M^{\oplus}$ (9%), 367 $M^{\oplus}$ − Me (7%), 309 $M^{\oplus}$ − $SiMe_3$ (12%), 247 $M^{\oplus}$ − $PPSiMe_3$ (25%), 73 $SiMe_3^{\oplus}$ (100%). $^{31}P\{^1H\}$-NMR: $\delta = 542$ (d), 210.3 (d), $J_{PP} = 540$ Hz.

7: A solution of **2** (2 g, 5.2 mmol) in pentane (10 mL) was treated with a solution of **1** (1.8 g, 5.2 mmol) dissolved in pentane (20 mL). The resulting reaction mixture was allowed to stir at room temperature until **7** began to precipitate (ca. 24 h). ^{31}P-NMR spectroscopy, used to follow the reaction, indicated the intermediary formation of **3** ($-P_A=P_BP_C<$, ^{31}P-NMR: $\delta_A = 529.9$, $\delta_B = 292.2$, $\delta_C = 174$; $J_{AB} = 524$, $J_{AC} = 559$, $J_{BC} = 233$ Hz). Recrystallization twice from a small amount of hot toluene afforded **7** as a yellow crystalline solid, which underwent decomposition in solution to form P_4 ($^{31}P\{^1H\}$-NMR: $\delta = -520$) and **8** ($^{31}P\{^1H\}$-NMR: $\delta = 377$). Yield 0.9 g (16.8%), m.p. = 145–146 °C. MS: m/z 1028 $M^{\oplus}$ (< 0.1%), 708 $M^{\oplus} - 2NR_2$ (0.5%), 677 $M^{\oplus} - 2NR_2 - P$ (1%), 646 $M^{\oplus} - 2NR_2 - 2P$ (0.5%), 615 $M^{\oplus} - 2NR_2 - 3P$ (0.25%), 607 $M^{\oplus} - N_4R_5$ (5%), 576 $M^{\oplus} - PN_4R_5$ (2%), 545 $M^{\oplus} - P_2N_4R_5$ (5%), 514 $M^{\oplus}/2$ (30%), 483 $M^{\oplus}/2 - P$ (5%), 452 $M^{\oplus}/2 - 2P$ (20%), 309 $R_3N_2P_2^{\oplus}$ (5%), 205 $R_2N_2P^{\oplus}$ (100%). $^{31}P\{^1H\}$-NMR: $AA'B_2CC'$ spin system (numbering corresponds to Fig. 1) $\delta = 216.4$ (P(1)/(1a)), −48.8 (P(2)/(2a)), 108.4 (P(3)/(3a)); $J_{P(1),P(2)} = -162$ Hz, $J_{P(1),P(3)} = +172$ Hz, $J_{P(2),P(3)} = -100$ Hz, $J_{P(2),P(3a)} = -147$ Hz. Further couplings not observed owing to insufficient resolution.

Received: July 7, 1987 [Z 2336 IE]
German version: *Angew. Chem.* *99* (1987) 1299

[1] E. Niecke, R. Rüger, B. Krebs, *Angew. Chem.* *94* (1982) 553; *Angew. Chem. Int. Ed. Engl.* *21* (1982) 544.
[2] W. W. Schoeller, private communication.
[3] In contrast to **4**, the corresponding 1,2,3-triphosphabutadiene, $R_2N-NR-P=P-P=CR_2$ affords the bicyclic compound: E. Niecke, O. Altmeyer, M. Nieger, unpublished.
[4] Such an isomerization has only been observed so far for 1,3-diphospha- and 1,4-diphospha-1,3-dienes: R. Appel, V. Barth, F. Knoch, *Chem. Ber.* *116* (1983) 938.
[5] **7** ($C_{30}H_{90}N_8P_6Si_{10}$): Yellow crystals from pentane. Crystal dimensions: $0.1 \times 0.2 \times 0.35$ mm^3, triclinic, $P\bar{1}$, $a = 9.244(2)$, $b = 12.052(3)$, $c = 15.033(4)$ Å, $\alpha = 76.82(2)$, $\beta = 83.64(5)$, $\gamma = 68.28(2)$°, $V = 1.514$ nm^3, $Z = 1$, $\rho_{calcd} = 1.17$ g cm^{-3}, $\mu = 0.40$ mm^{-1} ($Mo_{K\alpha}$); 3940 unique reflections ($2\theta_{max} = 45$°), 2171 $|F| > 4\sigma(F)$ used in the structure solution (direct methods) and refinement (244 parameters); non-hydrogen atoms anisotropic, H atoms (localized by difference electron density determination) refined with a "riding" model, $R = 0.088$ ($R_w = 0.082$, $w^{-1} = \sigma_F^2 + 0.0005F^2$). Further details of the crystal structure investigation may be obtained from the Fachinformationszentrum Energie, Physik, Mathematik GmbH, D-7514 Eggenstein-Leopoldshafen 2 (FRG), on quoting the depository number CSD-52570, the names of the authors, and the journal citation.
[6] E. Niecke, R. Rüger, B. Krebs, M. Dartmann, *Angew. Chem.* *95* (1983) 570; *Angew. Chem. Int. Ed. Engl.* *22* (1983) 552.
[7] Cf. M. Baudler, *Angew. Chem.* *99* (1987) 429; *Angew. Chem. Int. Ed. Engl.* *26* (1987) 419, and references cited therein.

The First 2*H*-Phosphirene**

By *Oliver Wagner, Gerhard Maas,* and *Manfred Regitz**

Unsaturated three-membered ring compounds are an attractive object of investigation for both theoretical and synthetic chemists. 1*H*-Azirines **1a** have proved to be transient, antiaromatic 4π-electron systems,[1] whereas the isomeric 2*H*-azirines **2a** are even of importance as synthetic building blocks.[2] The situation with the phosphorus analogues is completely different. Whereas 1*H*-phosphirenes **1b** may be regarded as well-studied, stable compounds,[3] nothing is known yet about 2*H*-phosphirenes **2b**. We re-

[*] Prof. Dr. M. Regitz, Dipl.-Chem. O. Wagner, Prof. Dr. G. Maas
Fachbereich Chemie der Universität
Erwin-Schrödinger-Strasse, D-6750 Kaiserslautern (FRG)

[**] Phosphorus Compounds with Unusual Coordinations, Part 27. This work was supported by the Fonds der Chemischen Industrie and the Deutsche Forschungsgemeinschaft. — Part 26: U. Annen, M. Regitz, *Tetrahedron Lett.* *28* (1987) 5141.

port here the first phosphorus/carbon three-membered ring containing a P=C double bond. The key intermediate involved in its synthesis is the 3*H*-1,2,4-diazaphosphole **5**.

1a, X = NR **2a**, X = N
1b, X = PR **2b**, X = P

The phosphaalkyne **3**[4] undergoes [3+2] cycloaddition with the diazocyclohexane **4**[5] in pentane at −40 °C. After the reaction mixture loses its color, it was evaporated (20 °C, 15 mbar) to give the spirocyclic 3*H*-1,2,4-diazaphosphole **5** as an analytically pure, yellow oil (100%; ^{13}C-NMR (C_6D_6): $\delta = 129.3$ (C-3), 214.5 (d, $^1J(P,C) = 47.2$ Hz, C-5); ^{31}P-NMR (C_6D_6): $\delta = 269.9$).[6] The thermally unstable compound **5** undergoes [1,5]-sigmatropic migration at 20 °C in $CDCl_3$ (12 h) to afford the 4*H*-1,2,4-diazaphosphole **6**, also as an oil (86%; ^{13}C-NMR ($CDCl_3$): $\delta = 189.5$ (d, $^1J(P,C) = 26.0$ Hz, C-3), 186.5 (d, $^1J(P,C) = 39.8$ Hz, C-5)); as expected, the transition from $\lambda^3\sigma^2$ to $\lambda^3\sigma^3$ phosphorus is associated with a marked upfield shift of the ^{31}P-NMR signal (**6**: ^{31}P-NMR ($CDCl_3$), $\delta = 50.0$).

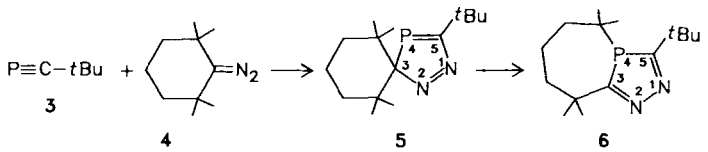

3 **4** **5** **6**

Photolysis of **5** at −40 °C in pentane (2 h, $\lambda \geq 280$ nm, Philips HPK 125 W)[7] affords, after distillative workup (kugelrohr, 130 °C oven temperature/10^{-2} mbar), a 5:1 mixture of the 1-phospha-1-cyclopentene **11** and the 2*H*-phosphirene **10** (Scheme 1). The two isomers were separated by medium-pressure column chromatography (silica gel (Merck, 15–25 μm), pentane, pressure ca. 20 bar); **11**, 54%;[8] **10**, 11%[9]). Compounds **10** and **11** are colorless liquids which can be readily handled in air.

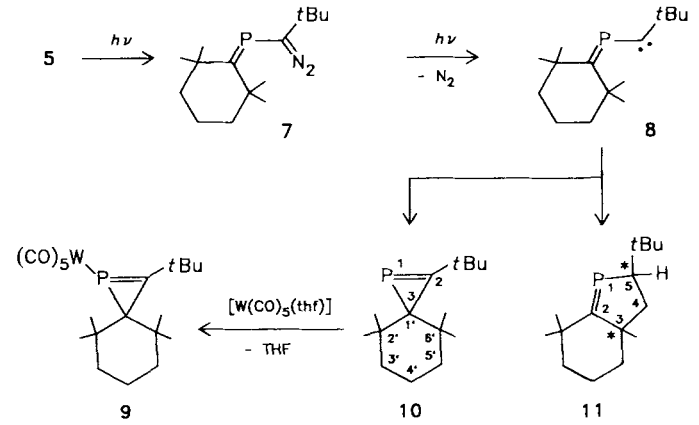

5 **7** **8** **9** **10** **11**

Scheme 1. Arbitrary numbering of **10** and **11**.

Presumably, the photochemical ring opening **5** → **7**[10] is followed by the carbene formation **7** → **8**, at which stage the reaction branches to form **11** (C–H insertion) and **10** (1, 3 ring closure). Compared with the ^{31}P-NMR signals of **11**[8] and other cyclic phosphaalkenes containing four-[11] or six-membered[12] ring frameworks ($\delta \geq 225$), the signal of **10** ($\delta = 71.7$) is shifted far upfield. A comparable effect is observed for the ^{31}P-NMR resonances of cyclotriphosphanes relative to those of the open-chain triphosphanes and large-ring cyclophosphanes.[13] An X-ray crystal structure analysis should remove any remaining doubts concerning the constitution of **10**. The tungsten pentacarbonyl complex **9**[14] proved to be a suitable compound. It was formed from **10** and $[W(CO)_5(thf)]$[15] in tetrahydrofuran at room temperature (45%, yellow crystals, m.p. = 61 °C). The end-on coordination of the $(CO)_5W$ fragment results in an upfield shift of 23 ppm of the ^{31}P-NMR signal ($CDCl_3$). In the corresponding chromium complex (**9**, Cr instead of W),[16] on the other hand, a paramagnetic shift of 37 ppm is observed.[17]

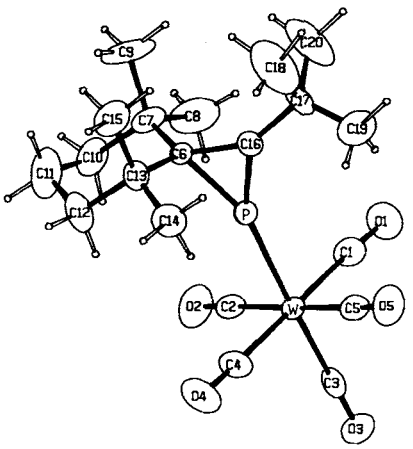

Fig. 1. Molecular structure of **9** (ORTEP). The thermal ellipsoids correspond to the 27% probability level. Selected bond lengths [Å] and angles [°]: W-P 2.458(1), W-C1 2.004(6), W-C2 1.997(6), W-C3 1.965(5), W-C4 2.029(6), W-C5 1.999(5), P-C6 1.881(4), P-C16 1.634(4), C6-C16 1.482(6); W-P-C6 157.7(2), W-P-C16 153.1(2), C6-P-C16 49.2(2), P-C6-C16 56.7(2), P-C16-C6 74.1(3), C7-C6-C13 116.4(4). The *t*Bu group is poorly defined owing to large thermal vibration amplitudes [18].

As revealed in Figure 1, the phosphirene ligand in **9**[18] occupies a site in the coordination octahedron around the tungsten atom. As found for other metal complexes of $\lambda^3\sigma^2$ phosphorus compounds (phosphaalkenes,[19,20] 1,2,3-σ^2-diazaphosphole[17]), the phosphorus atom exhibits nearly planar coordination (angle between P–W vector and the three-membered ring, 1.4°). In comparison to other free[11,21,22] and complexed[19,20] phosphaalkenes, the P=C bond (1.634(4) Å) is strikingly short; on the other hand, the P–C bond in the phosphirene three-membered ring is ca. 0.03 Å longer than the P–C_{sp^3} bond in a phosphaalkene.[21] The P–W distance is ca. 0.03 Å shorter than that in a 2*H*-phosphole, in which the P=C bond, however, functions as a four-electron donor.[23] The shortening of the W–C_{trans} bond (1.965 Å) compared with the W–C_{cis} bonds (mean 2.007 Å) is in accord with expectations.

Received: July 13, 1987 [Z 2349 IE]
German version: *Angew. Chem.* 99 (1987) 1328

[1] M. Regitz, B. Arnold, D. Danion, H. Schubert, G. Fusser, *Bull. Soc. Chim. Belg.* 90 (1981) 615; G. Mitchell, C. W. Rees, *J. Chem. Soc. Perkin Trans. 1* 1987, 413.
[2] See, for example, D. Obrecht, H. Heimgartner, *Helv. Chim. Acta* 70 (1987) 329 and earlier publications of this group.
[3] A. Marinetti, F. Mathey, J. Fischer, A. Mitschler, *J. Chem. Soc. Chem. Commun.* 1984, 45; S. Lochschmidt, F. Mathey, *Tetrahedron Lett.* 27 (1986) 2635.
[4] G. Becker, G. Gresser, W. Uhl, *Z. Naturforsch. B36* (1981) 16; improved procedure: W. Rösch, U. Hees, M. Regitz, *Chem. Ber.* 120 (1987) 1645.

[5] A. Krebs, W. Rüger, B. Ziegenhagen, M. Hebold, I. Hardtke, R. Müller, M. Schütz, M. Wietzke, M. Wilke, *Chem. Ber. 117* (1984) 277.
[6] The same dipolar orientation is also observed in the additions of other diazo compounds to **3**: W. Rösch, M. Regitz, *Angew. Chem. 96* (1984) 898; *Angew. Chem. Int. Ed. Engl. 23* (1984) 900.
[7] For the photolysis of 3*H*-pyrazoles, see, for example, M. Franck-Neumann, C. Buchecker, *Tetrahedron Lett. 1969*, 15.
[8] **11** is a mixture of two diastereomers in a ratio of 5:1 (^{31}P-NMR spectroscopy), in which the bulky groups at the chirality centers are presumably present in the *trans* arrangement. ^{13}C-NMR ($CDCl_3$): major isomer: $\delta = 50.9$ (s, C-4), 53.0 (d, $^2J(P,C) = 11.7$ Hz, C-3), 55.4 (d, $^1J(P,C) = 30.7$ Hz, C-5), 225.7 (d, $^1J(P,C) = 38.6$ Hz); minor isomer: $\delta = 47.5$ (s, C-4), 55.7 (d, $^2J(P,C) = 8.6$ Hz, C-3), 56.5 (d, $^1J(P,C) = 31.2$ Hz, C-5), 223.0 (d, $^1J(P,C) = 40.2$ Hz). ^{31}P-NMR ($CDCl_3$): major isomer: $\delta = 238.5$; minor isomer: $\delta = 236.3$.
[9] ^{1}H-NMR ($CDCl_3$): $\delta = 0.58$, 1.02 (each s, each 6H, Me-cyclohexane), 1.31 (d, $^4J(P,H) = 0.6$ Hz, 9H, *t*Bu), 1.55 (m, 6H, CH_2-cyclohexane). ^{13}C-NMR ($CDCl_3$): $\delta = 19.5$ (C-4'), 30.8 (CH_3-cyclohexyl), 32.2 (d, $^3J(P,C) = 6.1$ Hz, C(*C*H$_3$)$_3$), 34.4 (d, $^3J(P,C) = 9.0$ Hz (CH_3-cyclohexyl)), 37.4 (d, $^2J(P,C) = 7.6$ Hz, C-2'/C-6'), 39.0 (s, *C*(CH$_3$)$_3$), 42.6 (C-3'/C-5'), 56.2 (d, $^1J(P,C) = 35.0$ Hz, C-3 (≡C-1')), 215.4 (d, $^1J(P,C) = 50.9$ Hz, C-2),. ^{31}P-NMR ($CDCl_3$): $\delta = 71.7$.
[10] It is even possible to isolate the diazo isomer (corresponding to **7**) formed upon irradiation of 3,5-di-*tert*-butyl-3-methyl-3*H*-1,2,4-diazaphosphole; red oil, IR (film): $\tilde{\nu} = 2030$ cm^{-1} (C=N$_2$).
[11] J. Fink, W. Rösch, U.-J. Vogelbacher, M. Regitz, *Angew. Chem. 98* (1986) 265; *Angew. Chem. Int. Ed. Engl. 25* (1986) 280.
[12] W. Rösch, M. Regitz, *Z. Naturforsch. B41* (1986) 931.
[13] M. Baudler, *Pure Appl. Chem. 52* (1980) 755.
[14] IR (pentane): $\nu = 1960$, 2095 cm^{-1} (CO). ^{1}H-NMR ($CDCl_3$): $\delta = 0.80$, 1.16 (each s, each 6H, Me-cyclohexane), 1.43 (d, $^4J(P,H) = 1.2$ Hz, 9H, *t*Bu), 1.63 (m, 6H, CH_2-cyclohexane). ^{31}P-NMR ($CDCl_3$): $\delta = 48.7$ (d, $^1J(W,P) = 233$ Hz).
[15] W. Strohmeier, F. J. Müller, *Chem. Ber. 102* (1969) 3608.
[16] Synthesis analogous to **9** (78%, yellow crystals, m.p. = 44°C). IR (pentane): $\tilde{\nu} = 1959$, 2067 cm^{-1} (CO). ^{1}H-NMR ($CDCl_3$): $\delta = 0.75$, 1.05 (each s, each 6H, Me-cyclohexane), 1.42 (d, $^4J(P,H) = 1.2$ Hz, 9H, *t*Bu), 1.61 (m, 6H, CH_2-cyclohexane). ^{31}P-NMR ($CDCl_3$): $\delta = 107.2$.
[17] For similar shift effects observed for phosphole complexes, see J. H. Weinmaier, H. Tautz, A. Schmidpeter, S. Pohl, *J. Organomet. Chem. 185* (1980) 53.
[18] **9**: monoclinic, space group $P2_1/c$, $a = 10.654(2)$, $b = 17.011(7)$, $c = 12.734(2)$ Å, $\beta = 90.23(1)°$, $\rho_{calcd} = 1.618$ g cm^{-3}, $Z = 4$. Enraf-Nonius CAD4 diffractometer, monochromatic $Cu_{K\alpha}$ radiation, 3108 unique reflections with $2.0 \le \theta \le 57.0°$, absorption correction ($\mu = 102.6$ cm^{-1}), full-matrix refinement with 2890 reflections [$I > 2\sigma(I)$] and 244 variables; $R = 0.051$, $R_w = 0.050$ ($P = 0.007$). Further details of the crystal structure investigation may be obtained from the Fachinformationszentrum Energie, Physik, Mathematik GmbH, D-7514 Eggenstein-Leopoldshafen 2 (FRG), on quoting the depository number CSD-52573, the names of the authors, and the journal citation.
[19] T. C. Klebach, R. Lourens, F. Bickelhaupt, C. H. Stam, A. van Herk, *J. Organomet. Chem. 210* (1981) 211.
[20] R. Appel, C. Casser, M. Immenkeppel, F. Knoch, *Angew. Chem. 96* (1984) 905; *Angew. Chem. Int. Ed. Engl. 23* (1984) 895.
[21] G. Becker, O. Mundt, *Z. Allg. Anorg. Chem. 443* (1978) 53.
[22] M. Yoshifuji, K. Toyota, N. Inamoto, K. Hirotsu, T. Higuchi, *Tetrahedron Lett. 26* (1985) 6443; A. H. Cowley, R. A. Jones, J. G. Lasch, N. C. Norman, C. A. Stewart, A. L. Stuart, J. L. Atwood, W. E. Hunter, H.-M. Zhang, *J. Am. Chem. Soc. 106* (1984) 7015; R. Appel, U. Kündgen, F. Knoch, *Chem. Ber. 118* (1985) 1352; T. A. van der Knaap, T. C. Klebach, F. Visser, F. Bickelhaupt, P. Ros, E. J. Baerends, C. H. Stam, M. Konijn, *Tetrahedron 40* (1984) 765.
[23] S. Holand, C. Charrier, F. Mathey, J. Fischer, A. Mitschler, *J. Am. Chem. Soc. 106* (1984) 826.

$[\{(C_5H_5)Co\}_3(C_6H_5CH{=}CHCH_3)]$, an Organometallic Cluster with a Face-Bridging Arene Ligand**

By *Hubert Wadepohl,* Klaus Büchner,* and *Hans Pritzkow*

Molecular complexes in which an arene is bound to more than one metal atom are still rare.[1] Although numerous transition-metal clusters containing η^6-arene ligands are known,[1] the first complexes with a μ_3-η^2:η^2:η^2-benzene ligand attached to a M_3-face was reported only two years ago.[2] Herein we report the one-pot synthesis of the arene complex $[(CpCo)_3(\mu_3\text{-}\eta^2\text{:}\eta^2\text{:}\eta^2\text{-}trans\text{-}\beta\text{-methylstyrene})]$ **1** (Cp = C_5H_5), in the course of which the trinuclear metal cluster is assembled on the arene bearing an unsaturated side chain. The Jonas reagent $[CpCo(C_2H_4)_2]$[3] smoothly reacts with *trans*-β-methylstyrene at 20–60°C to give **1** in high yield;[4] allylbenzene, which is quantitatively rearranged in the course of the reaction, likewise affords **1** under similar conditions. With benzene or toluene no reaction takes place.

$$3[CpCo(C_2H_4)_2] + C_6H_5CH{=}CHCH_3 \xrightarrow{-6C_2H_4} \underset{\mathbf{1}}{[(CpCo)_3(C_6H_5CH{=}CHCH_3)]}$$

The constitution of **1** clearly follows from the spectra:[5] the absence of ^{1}H-NMR signals in the region typical of free arenes points to an arene complex. The mass spectrometrically determined composition [(CpCo)$_3$(methylstyrene)], however, is reconcilable with the NMR spectra only in terms of the arene ligand freely rotating on top of the triangular $(CpCo)_3$ moiety on the NMR time scale.[6] The ^{13}C-NMR signals of the arene are noticeably shifted upfield compared to the values found in η^6-arene complexes.[7] The *trans*-configuration of the side chain is unequivocally confirmed by the ^{1}H-^{1}H-coupling pattern of the olefinic protons H6 and H7. To obtain more detailed information about the bonding, an X-ray crystal structure analysis was carried out on **1**.[8]

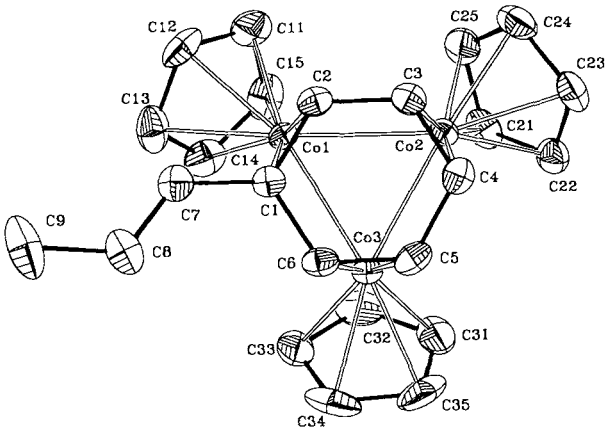

Fig. 1. Molecular structure of **1**. Selected bond lengths [Å] (standard derivations Co-C 0.002, C-C 0.005): Co1-Co2 2.501, Co1-Co3 2.503, Co2-Co3 2.496, Co1-C1 2.059, Co1-C2 2.019, Co2-C3 2.027, Co2-C4 2.027, Co3-C5 2.023, Co3-C6 2.017, C1-C2 1.432, C2-C3 1.435, C3-C4 1.412, C4-C5 1.438, C5-C6 1.415, C6-C1 1.466, C1-C7 1.461, C7-C8 1.317, C8-C9 1.512.

An equilateral triangle of Co atoms is bridged symmetrically by the planar (largest deviation 0.02 Å) arene; The Co_3-triangle and the C_6-ring are coplanar and staggered with respect to each other (Fig. 1). The plane of the 1-propenyl side chain is twisted by 17.4° with respect to the ring plane. Surprisingly, the C–C bond lengths in the aromatic ring show only slight, scarcely significant alternance (mean values 1.420(5) and 1.446(5) Å). The substituents on C1–C6 are displaced from the ring plane away from the Co atoms (C7 0.45 Å, H1 to H5 0.2 to 0.3 Å). In comparison the crystal structure analysis of **2**[2] does not allow an assessment of bond alternance in the benzene ring. However, alternat-

[*] Dr. H. Wadepohl, K. Büchner, Dr. H. Pritzkow
Anorganisch-chemisches Institut der Universität
Im Neuenheimer Feld 270, D-6900 Heidelberg (FRG)

[**] This work was supported by the Land Baden-Württemberg (Forschungsschwerpunkt No. 31).

ing longer and shorter bonds (mean values 1.39(2) and 1.48(2) Å), corresponding to a cyclohexatriene, are present in the μ_3-bridging ligand of **3**.[2]

$[Os_3(CO)_9(\mu_3\text{-}\eta^2:\eta^2:\eta^2\text{-}C_6H_6)]$ **2**
$[Ru_6C(CO)_{11}(\mu_3\text{-}\eta^2:\eta^2:\eta^2\text{-}C_6H_6)(\eta^6\text{-}C_6H_6)]$ **3**

On metal single crystals benzene and other aromatic hydrocarbons are adsorbed molecularly parallel to the close-packed surfaces (e.g. Ni(111) or Rh(111)).[9] However, there is some uncertainty about the orientation relative to the surface metal atoms (C_6 centroid above a metal atom, a 2-fold (M_4) or 3-fold (M_3) metal site).[9, 10] According to LEED investigations (LEED = low energy electron diffraction) of coadsorbates C_6H_6/CO and C_6H_6/2CO on Rh(111) (planar benzene fixed in 3-fold coordination sites) benzene has, at least in these cases, the Kekulé structure with strongly alternating bond lengths.[11] In contrast, a planar arene with virtually equal bonding fixed in a 3-fold metal coordination site is present in **1** — a remarkable finding in view of the postulated analogy between metal surfaces and clusters.[12]

The unsaturated side chain on the benzene ring appears to be the prerequisite for the formation of **1**. We assume initial attack of a CpCo fragment at this site. Assembly of the metal cluster could then proceed (if necessary after shifting of the double bond into the α-position to the arene) via an intermediate with methylstyrene as a doubly η^4-coordinating diene (3-6-η, 1-2:7-8-η). Related structures, albeit with metal atoms coordinating the bridging ligands from opposite sides, were derived from NMR spectroscopic data for $[\{Fe(CO)_3\}_2]$-complexes of substituted styrenes[13] and $[\{(C_5Me_5)Co\}_3(\eta^4:\eta^4:\eta^4\text{-biphenyl})]$.[14] Reaction of the intermediate with a further CpCo fragment and rearomatization of the arene could then lead to **1**.

Received: July 20, 1987 [Z 2367 IE]
German version: *Angew. Chem. 99* (1987) 1294

[1] E. L. Muetterties, J. R. Bleeke, E. J. Wucherer, T. A. Albright, *Chem. Rev. 82* (1982) 499. For more recent studies on compounds with doubly bridging arene ligands see: K. Jonas, *Angew. Chem. 97* (1985) 292; *Angew. Chem. Int. Ed. Engl. 24* (1985) 295, and references cited therein.

[2] M. P. Gomez-Sal, B. F. G. Johnson, J. Lewis, P. R. Raithby, A. H. Wright, *J. Chem. Soc. Chem. Commun. 1985*, 1682.

[3] K. Jonas, C. Krüger, *Angew. Chem. 92* (1980) 513; *Angew. Chem. Int. Ed. Engl. 19* (1980) 520; K. Jonas, E. Deffense, D. Habermann, *Angew. Chem. 95* (1983) 729; *Angew. Chem. Int. Ed. Engl. 22* (1983) 716; *Angew. Chem. Suppl. 1983*, 1005.

[4] *Procedure: trans*-β-methylstyrene (6.31 g, 53.4 mmol) was added dropwise at room temperature to a solution of $[CpCo(C_2H_4)_2]$ (4.81 g, 26.7 mmol) in petroleum ether (100 mL, b.p. 40–60°C). After 1 h the mixture was heated for a further 3 h at 60°C, then cooled to room temperature again and all volatile components removed in a vacuum. The residue was dissolved in toluene/petroleum ether (1:1) and chromatographed on Al_2O_3/5% H_2O. Dark brown needles of **1** (3.49 g, 7.12 mmol, 80% based on Co) were obtained from the eluate at 5°C; m.p. 182°C; correct C,H analyses).

[5] ^{1}H-NMR (200.1 MHz, [D$_8$]toluene, 25°C): δ = 5.76 (dq, J_{HH} = 15.6, 1.5 Hz, 1H; H-6), 5.44 (dq, J_{HH} = 15.6, 6.5 Hz, 1H; H-7), 4.58 (s, 15H; Cp), 4.4 (m, 2H; arene-H), 4.2 (m, 3H; arene-H), 1.57 (dd, J_{HH} = 6.5, 1.5 Hz, 3H; CH_3). ^{13}C-NMR (50.3 MHz, [D$_6$]benzene, 25°C): δ = 140.1 (d; olefin-C), 116.4 (d; olefin-C), 82.7 (d; Cp), 56.1 (s; C-1), 41.8 (d; arene-C), 40.9 (d; arene-C), 39.2 (d; arene-C), 18.4 (q; CH_3). MS (direct chemical ionization) *m/z* 490 (43% rel. int., $M^{\oplus}$), 370 (100, $[(CpCo)_3-2H]^{\oplus}$), 247 (20, $[(CpCo)_2-H]^{\oplus}$), 207 (22), 189 (87, $[Cp_2Co]^{\oplus}$), 124 (28, $[CpCo]^{\oplus}$), 118 (15, $[PhC_3H_5]^{\oplus}$), 117 (19, $[PhC_3H_4]^{\oplus}$), 91 (8, $[C_7H_7]^{\oplus}$), 59 (15, $Co^{\oplus}$), 44 (19).

[6] Two ^{13}C-NMR signals in the intensity ratio 1:2 are observed for the C_5H_5 carbon atoms at 220 K.

[7] B. E. Mann, B. F. Taylor: *^{13}C NMR Data for Organometallic Compounds*, Academic Press, London 1981, p. 247.

[8] Crystal structure analysis of **1**: Space group $P2_1$, a = 8.725(5), b = 7.542(5), c = 15.151(6) Å, β = 103.17(4)°, V = 970.7 Å^3, Z = 2; 3030 reflections measured (Weissenberg diffractometer, $Mo_{K\alpha}$, ω scan), 2893 observed ($I \geq \sigma(I)$), numerical absorption correction; 337 parameters refined (Co, C anisotropically, H isotropically, CH_3 as rigid group), R = 0.026, R_w = 0.027. Further details of the crystal structure investigation are available on request from the Fachinformationszentrum Energie, Physik, Mathematik GmbH, D-7514 Eggenstein-Leopoldshyfen 2 (FRG), on quoting the depository number CSD-52636, the names of the authors, and the journal citation.

[9] E. L. Muetterties, *Pure Appl. Chem. 54* (1982) 83.

[10] R. F. Lin, R. J. Koestner, M. A. Van Hove, G. A. Somorjai, *Surf. Sci. 134* (1983) 161.

[11] M. A. Van Hove, R. Lin, G. A. Somorjai, *Phys. Rev. Lett. 51* (1983) 778; *J. Am. Chem. Soc. 108* (1986) 2532.

[12] E. L. Muetterties, *Bull. Soc. Chim. Belg. 84* (1975) 959; *85* (1976) 451; *Science 196* (1977) 839; *Chem. Rev. 79* (1979) 91, and references cited therein.

[13] R. Victor, R. Ben-Shoshan, S. Sarel, *Chem. Commun. 1970*, 1680; *J. Org. Chem. 37* (1972) 1930.

[14] H. Lehmkuhl, H. Nehl, R. Benn, R. Mynott, *Angew. Chem. 98* (1986) 628; *Angew. Chem. Int. Ed. Engl. 25* (1986) 646.

Reactions of 2,2,4,4-Tetramethyl-3-methylenecyclobutylidene; Thermal Rearrangements of a 2-Methylenebicyclo[2.1.0]pentane**

By *Udo H. Brinker** and *Wolfgang Erdle*

Dedicated to Professor Emanuel Vogel on the occasion of his 60th birthday

Small ring carbenes are important reactive building blocks for the synthesis of highly strained, polycyclic compounds.[1] Cyclobutylidenes preferentially undergo ring contractions to give methylene cyclopropanes.[2] We have examined the extent to which possible interactions between carbene center and an *exo*-methylene group in the 2-[3] or 3-position influence the rearrangement behavior of 2,2,4,4-tetramethyl-3-methylenecyclobutylidene **4**. Besides ring contraction to give **7** there are further intramolecular reactions open to **4**, e.g. insertion into a C–H bond of the neighboring CH_3 groups with formation of the strained 2-methylenebicyclo[2.1.0]pentane **6**. A spectacular addition of the carbene **4** or of the diazo group in **3** to the *exo* double bond could result in formation of the tetramethyl-substituted [1.1.1]propellane **8** or the corresponding 4,5-dihydro-3*H*-pyrazole. That is, the highly-strained propellane skeleton[4] would either have to be formed directly via the structurally integrated allylcarbene[5] in **4** with concomitant formation of *three* cyclopropane rings or only after cleavage of N_2 from the dihydropyrazole.

The 3-methylenecyclobutanone **1**[6] required for the formation of the tosylhydrazone-sodium salt **2** was synthesized from commercially available 2,2,4,4-tetramethyl-1,3-cyclobutanedione.[6] The reaction of **1** with *p*-toluenesulfonylhydrazide afforded the corresponding tosylhydrazone in 92% yield, which on reaction with sodium hydride furnished the sodium salt **2** in almost quantitative yield (97%).

Upon flash pyrolysis[4] of **2** at 240–290°C (10^{-4}–10^{-5} torr) a pink-colored pyrolyzate was obtained whose IR spectrum (CCl_4) showed a strong band at 2020 cm^{-1} ($R_2C{=}N{=}N$ valence vibration). The diazo compound **3**

[*] Prof. Dr. U. H. Brinker, Dipl.-Chem. W. Erdle
Fakultät für Chemie der Universität
Universitätsstrasse 150, D-4630 Bochum-Querenburg (FRG)

[**] Carbene Rearrangements, Part 23. This work was supported by the Deutsche Forschungsgemeinschaft (Br 667/6) and the Fonds der Chemischen Industrie. *W. E.* thanks the Land Nordrhein-Westfalen for a graduate fellowship. We thank Dr. *W. Dietrich* for the ^{1}H- and ^{13}C-NMR spectra of **6** and Prof. *W. R. Roth* for valuable discussions. — Part 22: I. Fleischhauer, U. H. Brinker, *Chem. Ber. 120* (1987) 501.

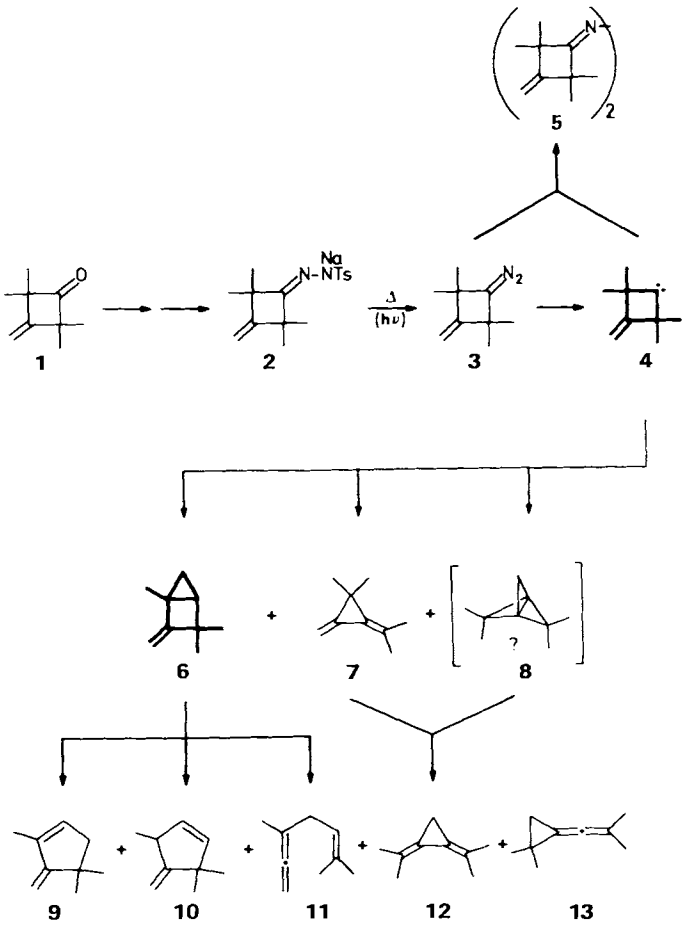

could be enriched if the decomposition of **2** took place between 120 and 130 °C ($<10^{-4}$ torr). The half-life of ca. 6700 s at 31.5 °C shows that **3** is kinetically highly stabilized in comparison to the diazocyclobutane, which is unstable at room temperature.[7] The "longevity" of **3** at 240–290 °C is also reflected in the relatively high yield of azine **5** (20–30%). At these temperatures in addition to some toluene (ca. 3%) seven hydrocarbons are formed in a total yield of 72% (isolated by preparative gas chromatography). 1-Isopropylidene-2,2-dimethyl-3-methylenecyclopropane **7**,[8] which could be formed by a cyclobutylidene-methylenecyclopropane rearrangement of **4**, is isolated in 35% (42% relative) yield. A 1,3-insertion of the carbene carbon into one of the C–H bonds of the four methyl groups results in formation of the strained 1,3,3-trimethyl-2-methylenebicyclo[2.1.0]pentane **6**[8] (27% relative, 15% isolated). As will be shown below, the methylenecyclopentenes **9** (10%, 8%)[8] and **10** (6%, 3%)[8] as well as the allene **11** (11%, 7%)[8] are secondary products of **6**. In addition, diisopropylidenecyclopropane **12**,[9] which could not be formed directly from the carbene **4**, was isolated in 2–3% (4% relative) yield.

Two possible routes come into consideration for the formation of **12** from **4**: 1. The intermediary tetramethyl[1.1.1]propellane **8** resulting from the intramolecular carbene addition (or a 1,3-dipolar cycloaddition of **3** via 4,5-dihydro-3*H*-pyrazole and subsequent N_2 cleavage) rearranges directly to **12**. The parent compound [1.1.1]propellane[5] yields exclusively dimethylenecyclopropane at 430 °C under flow pyrolysis conditions![10] 2. An isomerization of **7** takes place, and the geminal cyclopropane methyl groups are moved to the terminal carbon of the double bond via methylenecyclopropane rearrangement.[11] In the flow pyrolysis[12,13] of **7** at 550 °C (0.1 torr, quartz tube filled with quartz chips)[12] **12** is formed in 61% yield. This result suggests that 2–3% of **7** is also converted into **12**[14] under the conditions of the flash pyrolysis.[3,12]

In addition, 1,1-dimethyl-2-(2-methyl-1-propenylidene)cyclopropane **13**[13b,14] could be identified as a further product (<1%) of the pyrolysis. In the carbene **4** the 1,3-C–H insertion to give **6** (+**9**+**10**+**11**) dominates over the ring contraction to **7** (+**12**) in the ratio of ca. 1.2:1.

The photolysis (Pyrex, Philips HPK, 125W) of an ethereal suspension of **2** between 0 and 20 °C afforded the hydrocarbons **7** and **6** in 40 and 35% yield, respectively. In addition, ca. 5–10% azine **5**, 0.8% **12** and ca. 1% ketone **1** were isolated. **2** was decomposed thermally and photochemically also in the presence of styrene and α-methylstyrene. In the photolysis the spiro[2.3]hexanes **14** are formed in yields of 28–35%. The long lifetime of the diazo compound **3** suggests that spirohexane formation takes place by 1,3-dipolar cycloaddition of **3** via intermediary dihydropyrazoles.[15]

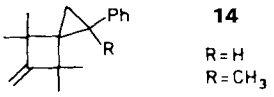

The thermolysis of **6** in the gas phase at 140–190 °C leads to formation of **9**, **10**, and **11**; their formation follows a first order rate law with the given activation parameters (see formula). This suggests formulating the formation of **9**, **10**, and **11**—as in the case of the unsubstituted bicyclo[2.1.0]pentane[16]—via a diradical **15**. Consistent with this interpretation the flow pyrolysis[13a] of the allene **11** affords, besides *p*-xylene, the isomers **9** and **10** (**9**:**10**:**11** = 7:4:89). The assumption of an intermediary diradical also makes the markedly lower activation energies compared to the parent system understandable. For the formation of **9** and **10** these are ca. 11 kcal mol^{-1} lower compared to the cyclopentene formation (E_a = 45.6 kcal mol^{-1}),[16] whereby the resonance stabilization of the allyl radical should make the greatest contribution.

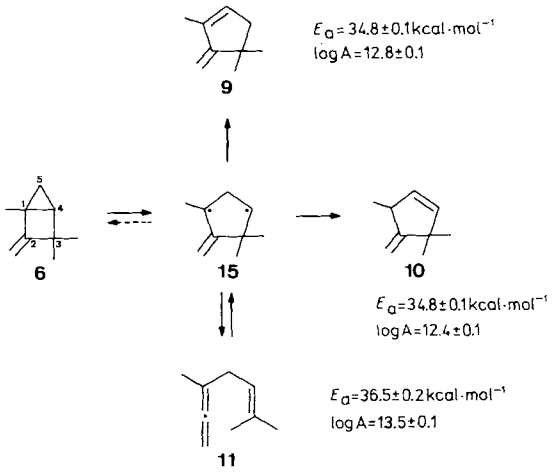

Received: July 14, 1987 [Z 2355 IE]
German version: *Angew. Chem.* 99 (1987) 1290

[1] A. Greenberg, J. F. Liebman: *Strained Organic Molecules*, Academic Press, New York 1978; A. P. Krapcho, *Synthesis 1978*, 77.
[2] W. Kirmse: *Carbene Chemistry*, 2nd Edit., Academic Press, New York 1971, p. 473; L. Friedman, H. Shechter, *J. Am. Chem. Soc. 82* (1960) 1002; U. H. Brinker, G. Schenker, *J. Chem. Soc. Chem. Commun. 1982*, 679; W. W. Schoeller, *J. Am. Chem. Soc. 101* (1979) 4811.
[3] U. H. Brinker, L. König, *Chem. Ber. 116* (1983) 882.
[4] K. B. Wiberg, F. H. Walker, *J. Am. Chem. Soc. 104* (1982) 5239.
[5] Z. Majerski, M. Zuanic, *J. Am. Chem. Soc. 109* (1987) 3496, and references cited therein.
[6] E. Lee-Ruff, *Can. J. Chem. 50* (1972) 952; D. R. Morton, N. J. Turro, *J. Am. Chem. Soc. 95* (1973) 3947.
[7] D. E. Applequist, D. E. McGreer, *J. Am. Chem. Soc. 82* (1960) 1965.
[8] The new compounds are characterized by their spectra (^{1}H-NMR, ^{13}C-NMR, IR, MS) and elemental analyses (**5**, **6**, **7**, **11**, **14**). **6**: ^{1}H-NMR (400 MHz, $CDCl_3$): $\delta = 0.79$ (dd, A part of the ABX system, $J_{5a,5s} = -4.5$ Hz, $J_{4,5a} = 5.5$ Hz, 1H; H5a), 0.85 (s, 3H; CH_3), 1.12 (dd, B part, $J_{4,5s} = 1.5$ Hz, 1H), 1.22 (s, 3H; CH_3), 1.35 (s, 3H; CH_3), 1.70 (dd, X part, 1H), 4.48 (s, 1H; H7), 4.52 (s, 1H; H7); ^{13}C-NMR (100.6 MHz, $CDCl_3$): $\delta = 16.1$ (q), 20.0 (q), 22.9 (t, $J(^{13}C,^1H) = 159$ Hz; C5), 28.0 (s; C1), 29.0 (q), 31.9 (d; C4), 41.8 (s; C3), 96.1 (t; C7), 162.7 (s; C2); UV (*n*-hexane): $\lambda_{max} = 204$ nm ($\varepsilon = 24500$).—**7**: ^{1}H-NMR (400 MHz, $CDCl_3$): $\delta = 1.20$ (s, 6H; aliphat. CH_3), 1.86 (q, $J = 0.7$ Hz; CH_3), 1.89 (q, $J = 0.65$ Hz; CH_3), 5.06 ("s", 1H, olef. H), 5.18 ("s", 1H, olef. H); ^{13}C-NMR (100.6 MHz, $CDCl_3$): $\delta = 21.7$ (s), 21.9 (q), 22.9 (q, $2CH_3$), 23.5 (q), 96.0 (t), 123.2 (s), 124.4 (s), 138.5 (s).—**9**: ^{1}H-NMR (400 MHz, $CDCl_3$): $\delta = 1.09$ (s, 6H; aliphat. CH_3), 1.74–1.77 (m, 3H, CH_3), 2.20–2.24 (m, 2H; H5), 4.62 ("s", 1H; H7), 4.74 ("s", 1H; H7), 5.67–5.71 (m, 1H; H1); ^{13}C-NMR (100.6 MHz, $CDCl_3$): $\delta = 13.0$ (q), 30.0 (q, $2CH_3$), 41.2 (s), 47.2 (t), 98.6 (t), 131.4 (d), 138.6 (s), 165.3 (s).—**10**: ^{1}H-NMR (400 MHz, $CDCl_3$): $\delta = 1.09$ (s, 3H; CH_3), 1.12 (s, 3H; CH_3), 1.12 (d, $J = 7$ Hz, 3H; CH_3), 3.29 (q, each signal exhibits additional fine splitting, 1H; H5), 4.89 ("d", $J = 2.5$ Hz; H8), 4.93 (d, $J = 2.5$ Hz, 1H; H8), 5.03 ("s", 2H; H1, H2); ^{13}C-NMR (100.6 MHz, $CDCl_3$): $\delta = 21.4$ (q), 29.2 (q), 30.0 (q), 44.3 (d), 48.1 (s), 103.6 (t), 132.0 (d), 139.4 (d), 165.1 (s).—**11**: IR (film): $\nu = 1960$ cm^{-1} (C=C=C); ^{1}H-NMR (400 MHz, $CDCl_3$): $\delta = 1.60$ (s, 3H; CH_3), 1.65 (t, $J = 3$ Hz, 3H; CH_3), 1.70 (d, $J = 1.5$ Hz, 3H; CH_3), 2.58–2.65 (m, 2H; H4), 4.56 (sext., $J = 3$ Hz, 2H; H1), 5.18 (t sept., $J_{4,5} = 7$ Hz, $J = 1.5$ Hz, 1H; H5).
[9] R. F. Bleiholder, H. Shechter, *J. Am. Chem. Soc. 86* (1964) 5032.
[10] J. Belzner, G. Szeimies, *Tetrahedron Lett. 27* (1986) 5839.
[11] R. J. Crawford, H. Tokunaga, *Can. J. Chem. 52* (1974) 4033; J. J. Gajewski: *Hydrocarbon Thermal Isomerizations*, Academic Press, New York 1981, p. 51ff.
[12] The results of the flow and the flash pyrolyses [3] cannot be compared with each other directly. Thus, the dry sodium salt of the tosylhydrazone is transferred in solid form into the reaction flask, where it decomposes on the hot glass surface. In contrast, the liquid hydrocarbons must be passed in the gas phase through a furnace-heated quartz tube.
[13] a) Under flow pyrolysis conditions (0.1 torr, quartz tube, $l = 30$ cm, $\varnothing = 1$ cm, packed with quartz chips) **12** first begins to convert into **7** above 400°C (575°C; **12** : **7** = 43 : 57); b) **3** rearranges completely to **12** at 300°C.
[14] G. Leandri, C. Santelli-Rouvier, *Bull. Chem. Soc. Fr. 1970*, 1515.
[15] U. H. Brinker, M. Boxberger, *Angew. Chem. 96* (1984) 971; *Angew. Chem. Int. Ed. Engl. 23* (1984) 974.
[16] C. Steel, R. Zand, P. Hurwitz, S. G. Cohen, *J. Am. Chem. Soc. 86* (1964) 679.

Annelated Isoindoles with an 18π-Electron System**

By *Richard P. Kreher** and *Thomas Hildebrand*

Dedicated to Professor Klaus Hafner on the occasion of his 60th birthday

The radialenes **1** and **2** of naphthalene[2] have been postulated as reactive intermediates and have been suggested as precursors for tetrahydrodicyclobuta[*a,f*]- and tetrahydrodicyclobuta[*a,c*]naphthalenes, respectively. By bridging with two alkylimino groups, it is possible to establish the labile radialene structure. The corresponding tetracyclic heteroarenes **3** and **4** are stabilized by cyclic conjugated 18π-electron systems. Noteworthy in the heteroarene **3** are the annelated 2*H*-isoindole moieties and the central triene system; the isoelectronic heteroarene **4**, on the other hand, is characterized by a "nonperturbed" peripheral benzenoid ring system.[3]

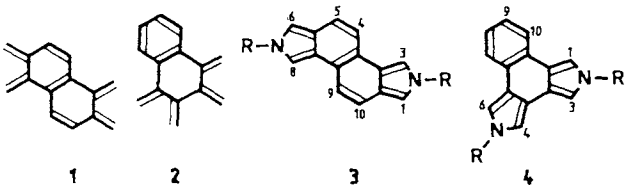

1 **2** **3** **4**

The convergent synthesis of the tetracyclic heteroarenes **3** and **4** makes use of the *N*-oxide route[4] for formation of the pyrrole rings. The preparative effort involved is mainly determined by the requirement of obtaining the corresponding tetrafunctional naphthalenes.

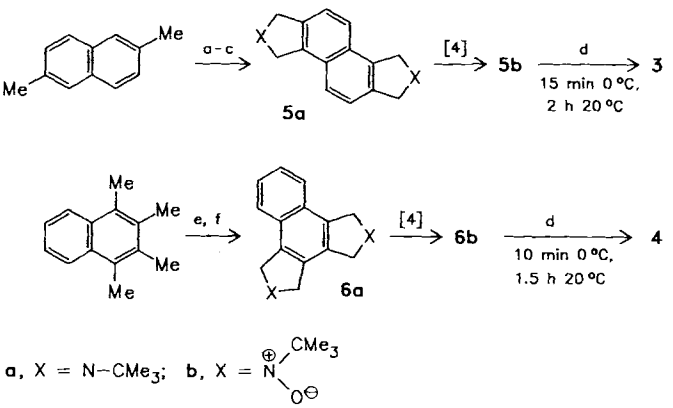

Scheme 1. Synthesis of **3** and **4**, R = CMe_3. a) HBr/formaldehyde in acetic acid/phosphoric acid, 6.5 h reflux. b) *N*-Bromosuccinimide in CCl_4, 45 min reflux. c) *tert*-Butylamine in benzene added over 3 d under reflux, 16 h room temperature. d) Acetic anhydride/triethylamine in $CHCl_3$; 15 min 0°C, 2 h room temperature. e) *N*-Bromosuccinimide in CCl_4, 1 h reflux. f) *tert*-Butylamine in $CHCl_3$ added over 3 d under reflux, 2 h reflux. **5b**: 98% yield, m.p. 163–164°C; **6b**: 71% yield, m.p. = 151°C.

The synthesis of the heteroarene **3**, R = CMe_3, starts from commercially available 2,6-dimethylnaphthalene (Scheme 1). An acceptable yield is obtained by halomethylation[5] of the reactive 1,5 positions. Radical bromination of the methyl groups in the 2,6 positions is followed by facile cyclization with *tert*-butylamine leading to **5a**. Acetolysis of the *N,N*-dioxide **5b**, which is likewise easily carried out, results in aromatization to form **3**.

In order to synthesize the heteroarene **4**, R = CMe_3, synthetically accessible 1,2,3,4-tetramethylnaphthalene[6] is substituted via radical bromination (Scheme 1). The subsequent ring closure occurs in spite of competing reactions with a satisfactory yield of **6a**. Compound **6a** is converted into the *N,N*-dioxide **6b**, which, in turn, is caused to undergo aromatization.

The structural differences in the isoelectronic heteroarenes **3** and **4** are manifested in their chemical behavior. Cycloaddition reactions, which are expected for **3**, are indeed observed. Treatment with *N*-methylmaleimide results, via addition to a pyrrole ring, in the formation of a 1 : 1 cycloadduct having the topology of 2*H*-benz[*e*]isoindole; the reactivity of this 14π-electron system is decreased by

[*] Prof. Dr. R. P. Kreher, Dipl.-Chem. T. Hildebrand
Lehrstuhl für Organische Chemie II der Universität
Postfach 5005 00, D-4600 Dortmund 50 (FRG)

[**] Structure and Reactivity of Isoannelated Heterocyclic Systems with 4nπ and (4n+2)π Electrons, Part 13. This work was supported by the Fonds der Chemischen Industrie.

the *tert*-butyl groups,[7] so that dienophiles no longer react with the *o*-quinonoid diene system of the second pyrrole ring. On the other hand, **4** does not react with *N*-methylmaleimide, even though the 2*H*-benz[*e*]isoindole moiety should also be formed in the reaction with the diene system of a pyrrole ring. This behavior is presumably determined by the vicinal annelation of the pyrrole rings on the naphthalene framework and the resulting steric repulsion.

Chemical proof of the twofold *o*-quinonoid structure was achieved by reaction of the heteroarenes **3** and **4** with activated alkynes. Reaction of dimethyl acetylenedicarboxylate with **3** results in the formation of a crystallizable 2:1 cycloadduct. In this cooperative process, the *anti* arrangement predominates to the extent of ca. 80%. The reaction with the isoelectronic heteroarene **4**, on the other hand, does not occur in a uniform manner, presumably for steric reasons.

Both **3** and **4** react with 3,4,5,6-tetramethyl-1,2-dehydrobenzene, generated from 1,2-dibromo-3,4,5,6-tetramethylbenzene and methyllithium. No topological selectivity is observed in this cycloaddition, since the *o*-quinonoid 14π-electron system of the intermediate 2*H*-benz[*e*]isoindole also undergoes reaction. In the twofold cycloaddition yielding **7** and **8**, the *anti* arrangement of the annelated rings predominates; less than 3% of the *syn* product can be detected by ^{1}H-NMR spectroscopy in the case of the heteroarene **3**, which has isolated reactive centers. The constitution and configuration of the cycloadduct **8** were confirmed by X-ray structure analysis.[8]

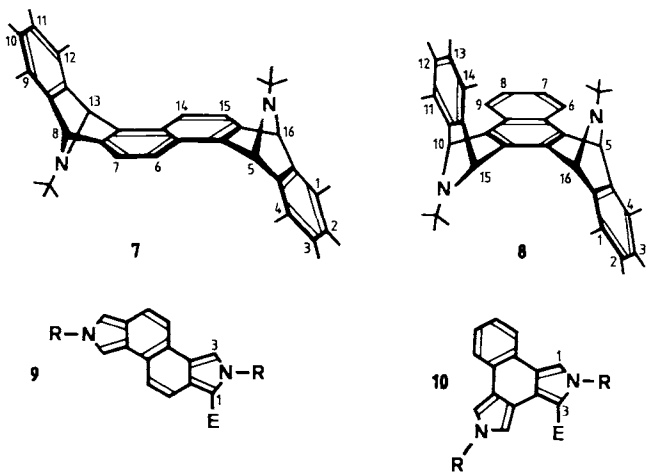

E = N=N-C_6H_4-NO_2, R = CMe_3

4-Nitrobenzenediazonium tetrafluoroborate is a suitable reagent for S_E reactions. Monosubstitution of **3** and **4** leads to the heteroarenes **9** and **10**, respectively; the same regioselectivity is observed for 2*H*-benz[*e*]isoindole.[7] The disubstitution reaction in the case of **9** apparently depends on electronic factors, whereas in the case of **10** steric factors are important.

Selected data for the new compounds are listed in Table 1.

In summary, the tetracylic heteroarenes **3** and **4** behave like systems with localized isoindole structures;[9] the topology of the π system is the determining factor for the chemical reactivity and selectivity. Thermodynamic stabilization of radialene structures by the incorporation of alkylimino groups is obvious; this promising stabilization concept should be generalizable to other carbocylic intermediates.

Table 1. Yields, melting points, and characteristic spectroscopic data for the compounds **3** and **4** (R = CMe_3) and for **7**–**10** [10]. 300-MHz ^{1}H-NMR spectra in $CDCl_3$, 70-eV mass spectra.

3, R = CMe_3: 65%, 276–277 °C.—^{1}H-NMR: δ = 1.70 (s, 18H; 2C(CH_3)$_3$), 7.29 (d, J = 2.2 Hz, 2H; H-1, H-6), AB signal (δ_A = 7.53, δ_B = 7.60, J = 8.8 Hz, 4H; H-4, H-5, H-9, H-10), 7.59 (d, J = 2.2 Hz, 2H; H-3, H-8).—High-resolution MS: $M^{\oplus}$ = 318.2099 (calcd 318.2096)

4, R = CMe_3: 51%, 203–204 °C.—^{1}H-NMR: δ = 1.64 (s, 18H; 2C(CH_3)$_3$), 7.21–7.24 (m, 2H; from H-7–H-10), 7.22 (d, J = 2.2 Hz, 2H; H-3, H-4), 7.49 (d, J = 2.2 Hz, 2H; H-1, H-6), 7.87–7.90 (m, 2H; from H-7–H-10).—MS: *m/z* 318 ($M^{\oplus}$, 94%)

7 (*anti*/*syn* = 97:3): 78%, 320 °C (dec.).—(*anti*): ^{1}H-NMR: δ = 0.92 (s; 18H; 2C(CH_3)$_3$), 1.95 (s, 6H; 2CH_3), 1.97 (s, 6H; 2CH_3), 2.23 (s, 6H; 2CH_3), 2.26 (s, 6H; 2CH_3), 5.44 (br. s, 2H; H-8, H-16), 5.76 (br. s, 2H; H-5, H-13).—MS: *m/z* 582 ($M^{\oplus}$, 35%)

8 (*anti*): 76%, 256–257 °C (from diethyl ether).—^{1}H-NMR: δ = 0.77 (s, 18H; 2C(CH_3)$_3$), 2.00 (s, 6H; 2CH_3), 2.03 (s, 6H; 2CH_3), 2.29 (s, 6H; 2CH_3), 2.40 (s, 6H; 2CH_3), 5.54 (d, J(15/10,16/5) = 1.1 Hz, 2H; H-15, H-16), 5.76 (d, J(10/10,5/16) = 1.1 Hz, 2H; H-5, H-10).—MS: *m/z* 582 ($M^{\oplus}$, 67%)

9: 46%, 215–218 °C (dec.).—^{1}H-NMR: δ = 1.75 (s, 9H; C(CH_3)$_3$), 2.01 (s, 9H; C(CH_3)$_3$), 7.40 (d, J(6/8) = 2.1 Hz, 1H; H-6), AB signal (δ_A = 7.61, δ_B = 7.69, J = 8.9 Hz, 2H; H-4, H-5), 7.75 (d, J(8/6) = 2.1 Hz, 1H; H-8), 8.19–8.24 (m, 2H; H-3, H-9), 8.71 (m_c, 1H; H-10).—MS: *m/z* 468 ($M^{\oplus}$, 29%)

10: 30%, 281 °C (dec.).—^{1}H-NMR: δ = 1.78 (s, 9H; C(CH_3)$_3$), 1.96 (s, 9H; C(CH_3)$_3$), 7.73 (d, J(6/4) = 2.4 Hz, 1H; H-6), 8.18 (s, 1H; H-1), 8.79 (d, J(4/6) = 2.4 Hz, 1H; H-4).—MS: *m/z* 468 ($M^{\oplus}$, 31%)

Received: May 25, 1987 [Z 2256 IE]
Publication delayed at authors' request
German version: *Angew. Chem. 99* (1987) 1325

[1] R. P. Kreher, G. Dyker, *Z. Naturforsch. B 42* (1987) 473.
[2] H. Hart, A. Teuerstein, M. Jeffares, W.-J. Hu Kung, D. L. Ward, *J. Org. Chem. 45* (1980) 3731.
[3] 7*H*-pyrrolo[3,4-*e*]isoindole, which displays similar structural features, is an isolable, tricyclic heteroarene: R. Kreher, K. J. Herd, *Angew. Chem. 90* (1978) 65; *Angew. Chem. Int. Ed. Engl. 17* (1978) 68.
[4] R. P. Kreher, N. Kohl, *Chem. Ztg. 110* (1986) 299, and references cited therein.
[5] *Experimental procedure for chloromethylation:* L. Westfelt, *Acta Chem. Scand. 20* (1966) 2852.
[6] D. Hausigk, *Synthesis 1971*, 307.
[7] N. Kohl, *Dissertation*, Universität Dortmund 1984.—2-*tert*-Butyl-2*H*-benz[*e*]isoindole (b.p. = 180 °C/0.03 torr, n_D^{20} = 1.6403) does not react under the usual conditions with *N*-methylmaleimide. The reaction with dimethyl acetylenedicarboxylate results in the formation of a 1:1 cycloadduct (yield 73%, m.p. = 109–110 °C).
[8] H. Preut, T. Hildebrand, R. P. Kreher, *Acta Crystallogr. Sect. C*, in press. Single-crystal X-ray structure analysis. Cell data: space group *P*1, a = 1170.1(9), b = 1179.6(15), c = 1553.8(8) pm, α = 69.12(7), β = 62.27(7), γ = 67.15(7)°, Z = 2; R = 0.062 for 3466 observed reflections and 398 refined parameters.
[9] E. Heilbronner, Z.-z. Yang, *Angew. Chem. 99* (1987) 369; *Angew. Chem. Int. Ed. Engl. 26* (1987) 360.
[10] The compounds described here afforded correct elemental analyses.

Alkyne Complexes of Rhenium in Intermediate Oxidation States; Synthesis and Molecular Structure of a Rhenium(v)–Allenylidene Complex**

By *Wolfgang A. Herrmann,* Roland A. Fischer,* and *Eberhardt Herdtweck*

Alkynes can be converted with the organorhenium oxide [(η^5-C_5Me_5)ReO_3] according to Scheme 1 into furan deriva-

[*] Prof. Dr. W. A. Herrmann, R. A. Fischer, Dr. E. Herdtweck
Anorganisch-chemisches Institut der Technischen Universität München
Lichtenbergstrasse 4, D-8046 Garching (FRG)

[**] Multiple Bonds between Main Group Elements and Transition Metals, Part 51. This work was supported by the Deutsche Forschungsgemeinschaft, the Bundesministerium für Forschung und Technologie, and the Fonds der Chemischen Industrie.—Part 50: [2].

tives.[1] A catalytic realization of this novel oxidative coupling of two alkynes, which is also possibly useful for the synthesis of thiophenes and pyrroles, has so far not been achieved due to a lack of detailed information about the mechanism involved. There are indications that formation of the two O-C bonds occurs before that of the C-C bond,[1] and apparently involves several reaction steps at rhenium centers in medium oxidation states. Since organorhenium oxides related to $[(\eta^5\text{-}C_5Me_5)ReO_3]$ have proven to be useful catalysts for the metathesis of open-chain alkenes as well as for the metathetical ring-opening polymerization of cycloalkenes to polyalkenamers with elastomeric properties,[2] we have concerned ourselves with gaining a better insight into the mechanisms involved in such catalytic reactions. We now report on the synthesis and structures of relevant model compounds.

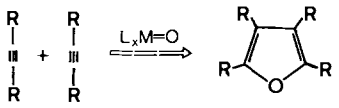

Scheme 1. $L_xM{=}O$ = $(\eta^5\text{-}C_5Me_5)ReO_3/PPh_3/I_2$.

The organorhenium(V) halides

$[(\eta^5\text{-}C_5Me_5)ReX_4]$ **1a**, X = Cl; **1b**, X = Br

obtainable from the organorhenium(VII) oxide $[(\eta^5\text{-}C_5Me_5)ReO_3]$[3] by reductive halogenation can be reduced with HgX_2-activated aluminum powder in the presence of alkynes to rhenium(III) complexes of the type $[(\eta^5\text{-}C_5Me_5)ReX_2(\eta^2\text{-}RC{\equiv}CR)]$ **5**. In the absence of coordinating ligands, however, the reduction of **1a** first leads selectively to the dinuclear Re^{IV} complex **2**, which is further reduced to the chlorine-deficient Re^{III} derivative

$[(\eta^5\text{-}C_5Me_5)_2Re_2Cl_4]$ **3**

containing a ReRe double bond between two Cl bridges. The two diamagnetic compounds were characterized by X-ray structure analyses.[4] Whereas the complex **3** generally proved to be less reactive, the Re^{IV} derivative **2** was found to be a convenient source for a variety of mononuclear products. Thus, its reaction with 2-butyne in the absence of oxygen and moisture leads with disproportionation according to Scheme 2 to formation of the Re^{III} complex **5a** and the novel rhenium(V)-allenylidene complex **4** (each in 50% yield; Table 1); the unexpected constitution of **4** was established by an X-ray structure analysis (Fig. 1).[5]

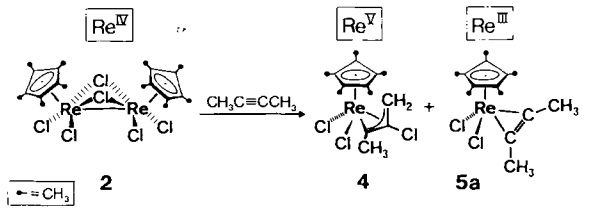

Scheme 2.

The structure of the product **4**, which can be separated from the 2-butyne complex **5a** by column chromatography on silylated silica gel (−10 °C), consists of a $[(\eta^5\text{-}C_5Me_5)ReCl_2]$ moiety which forms a non-planar four-membered ring geometry with the ligand derived from 2-butyne (Fig. 1). Interesting here is that an H atom is cleaved from one of the two methyl groups. Moreover, a Cl atom originally attached to the metal migrates to C2 of the alkyne. The C_4-ligand resulting from the alkyne can best be described as a substituted allyl system, with a carbene/olefin resonance structure (C3 and C1, C2, respectively) contributing to its metal-fixation. The alternative metallacyclobutene structure[6] can be ruled out because of the

Table 1. IR and NMR data of some new compounds.

Cpd.	IR (KBr) [cm^{-1}]	^{1}H-NMR (270 MHz) [δ values]	^{13}C-NMR (68 MHz) [δ values]
4	ν(Re–Cl): 325, 290	4.31 (dq, 1H; ^2J = 3.29 Hz, ^5J = 0.32 Hz) 3.27 (dq, 1H; ^2J = 3.29 Hz, ^5J = 1.93 Hz) 2.76 (dd, 3H; ^5J = 1.93 Hz, ^5J = 0.32 Hz) 1.99 (s, 15H) [a]	265.2, 102.6, 102.4, 51.5, 27.1, 10.9 [c]
5a	ν(Re–Cl): 335	3.42 (s, 6H) 1.98 (s, 15H) [b]	217.3, 107.3, 19.4, 11.7 [b]
5c	ν(C≡C): 1665	3.42 (s, 6H) 2.06 (s, 15H) [c]	216.3, 106.1, 20.8, 11.9 [c]
7	ν(C≡C): 1665 ν(C=C): 1607 ν(Re–Cl): 345	8.77 (m, 2H), 8.16 (m, 1H), 7.73 (m, 2H), 3.17 (s, 6H), 1.87 (s, 15H) [c]	220.3, 141.3, 127.2, 127.1, 108.9, 19.4, 10.7 [c]
8b	ν(C≡C): 1774	3.23 (s, 6H), 2.86 (s, 6H), 1.96 (s, 15H) [d]	176.4, 166.4, 111.7, 17.6, 15.0, 10.7 [d]
8c	ν(C≡C): 1780	3.52 (q, 2H), 3.43 (q, 2H), 3.21 (s, 3H), 2.86 (s, 3H), 1.96 (s, 15H), 1.43 (t, 3H), 1.07 (t, 3H) [d]	178.8, 176.9, 169.2, 166.7, 111.9, 26.7,23.8, 17.8, 15.2, 14.2, 13.9, 10.8 [d]

[a] 400 MHz, $CDCl_3$, 20 °C. [b] CD_2Cl_2, 30 °C. [c] $CDCl_3$, 20 °C. [d] $CDCl_3$, −20 °C; coalescence of the methyl group signals of the butyne ligands in **8b** observed at ca. 30 °C upon heating, $\Delta G^{\neq} = 60 \pm 5$ kJ/mol; further heating to 50 °C: δ = 3.06 (s, 6H), 1.99 (s, 15H); **8c** exhibits similar behavior.

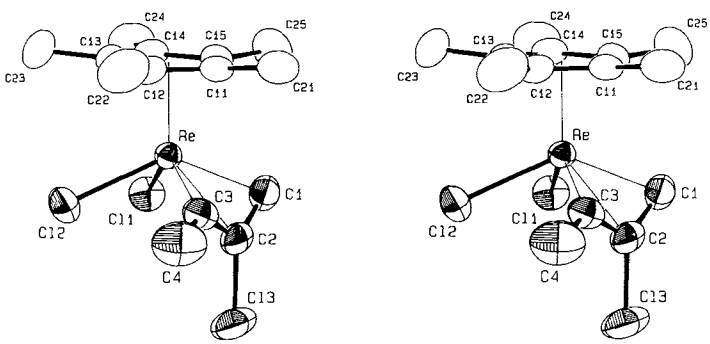

Fig. 1. Stereoview (ORTEP diagram) of the crystal structure of **4** (without H atoms). The vibration ellipsoids are at the 50% probability level.—Selected bond lengths [pm] and angles [°]: Re-C1 219.2(3), Re-C2 224.2(3), Re-C3 196.7(3), C1-C2 141.0(4), C2-C3 136.3(4), C3-C4 147.7(5), Cl3-C2 178.8(3), Re-Cl1 239.1(1); Re-Cl2 241.9(1); C1,C2,C3 117.3(3), C2,C3,C4 131.9(3), Cl3,C2,C1 121.7(3), Cl3,C2,C3 119.7(3), Cl1,Re,Cl2 82.27(3), C1,Re,C3 69.2(1). The C_5Me_5 ligand is decentrally coordinated to the metal (Re–C_{ring} 220.4–237.5 pm).—Further details of the crystal structure investigation are available on request from the Fachinformationszentrum Energie, Physik, Mathematik GmbH, D-7514 Eggenstein-Leopoldshafen 2 (FRG), on quoting the depository number CSD-52602, the names of the authors, and the journal citation.

non-planarity of the ReC_3 substructure (cf. Fig. 1). Thus, the Re-C1 and Re-C2 distances (219.2(3) and 224.2(3) pm, respectively) differ very little from the bond lengths in related allyl complexes such as the Re^{IV}-compound $[(\eta^5\text{-}C_5Me_5)ReBr_2(\eta^3\text{-}C_3H_5)]$.[7] The Re-C3 distance, on the other hand, is shorter (196.7(3) pm) and indicative of double bond character (Re-C distances in carbene complexes of rhenium are 192–197 pm). The system apparently chooses a compromise between the coordination geometry to be expected for a pure allyl and that for a pure carbene-ligand. This is reflected quite markedly in the angle and bond-length deformation in the corresponding structural units. The position of the rhenium atom, 130 pm above the plane through C1C2C3 and 70 pm above the plane through C2C3C4 (interplanar angle 21.0°) is also consistent with this concept.[7,8]

The π-bonded alkyne ligands, as 4e ligands with considerable multiple-bond character in the complexes **5a–5d**, are not easily cleaved from the metal atom, but the rhenium–halogen bonds permit a variety of secondary reactions. Thus, the corresponding diiodo derivatives are smoothly obtainable with sodium iodide in acetone, a typical example being the complex

$[(\eta^5\text{-}C_5Me_5)ReI_2(CH_3C{\equiv}CCH_3)]$ **5e**

Stepwise alkylation and hydrolysis reactions with formation of the complexes

$[(\eta^5\text{-}C_5Me_5)ReCl(CH_3)(CH_3C{\equiv}CCH_3)]$ **6a**
$[(\eta^5\text{-}C_5Me_5)Re(CH_3)_2(CH_3C{\equiv}CCH_3)]$ **6b**
$[(\eta^5\text{-}C_5Me_5)Re(=O)(CH_3C{\equiv}CCH_3)]$ **6c**

are also possible. Reaction of **5a–5d** with $Ag[SbF_6]$ according to Scheme 3 affords access to cationic species stabilized by σ or π ligands. The pyridine- and alkyne complexes **7** and **8**, respectively, which are not interconvertable exemplify the efficiency of this simple synthetic principle.

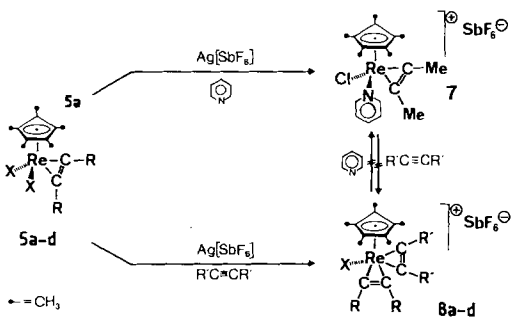

	5a	5b	5c	5d	5e	8a	8b	8c	8d
X	Cl	Cl	Br	Br	I	Cl	Br	Br	Br
R	Me	Et	Me	Et	Me	Et	Me	Me	Me
R'	–	–	–	–	–	Et	Me	Et	C_6H_5

Scheme 3.

The diamagnetism of the bis(π-alkyne) complexes **8** and the upfield shift of the ^{13}C-NMR signals of their alkyne C-atoms compared to the corresponding resonances of the mono(π-alkyne) complexes **5** can only be interpreted in terms of these two ligands contributing a total of six electrons to the bonds to the central metal. Temperature-dependent NMR investigations on the 3-hexyne and 2-butyne omplexes **8a** and **8b**, respectively, confirm the chemical equivalence of the alkyne ligands and rule out different bonding mechanisms or electron-balances. The especially easily accessible bis(π-alkyne) complexes **8** belong to the hitherto lesser known systems of this type[9] which serve as model compounds for intermediates of the rhenium-based furan synthesis of Scheme 1.

Experimental

4: A solution of **2** (410 mg, 0.5 mmol) in dichloromethane (10.0 mL) and dry 2-butyne (3.0 mL) was heated under reflux for 1 h. The volatile components were then removed in a vacuum and the green residue subjected to column-chromatography on silylated silica gel/*n*-hexane ($l = 40$ cm; $d = 1.5$ cm; −10°C). **4** was eluted as a lime-green broad zone with *n*-hexane/dichloromethane (10+1 parts by volume). **5a** was then eluted as a golden yellow zone with *n*-hexane/dichloromethane (10+3 parts volume). Yields after recrystallization from *n*-hexane/dichloromethane: 170 mg of **4** (decomp. at 145°C) and 140 mg of **5a** (decomp. at 75°C).—**5a** is more conveniently accessible in analogy to the procedure for **5c** (yield 90%).

5c: A suspension of **1b** (1.5 g, 2.3 mmol) in 12 mL of THF and 8.0 mL of 2-butyne was treated with 400 mg of granulated aluminum. After addition of a catalytic amount of $HgBr_2$ the mixture was vigorously stirred for 30 min at room temperature. After removal of unused aluminum by filtration, the reddish orange solution was evaporated to dryness in a vacuum. The residue was repeatedly extracted with 20 mL portions of *n*-hexane/dichloromethane (4+1 parts by volume). The combined extracts were evaporated down in a vacuum and the desired product **5c** allowed to crystallize out at −25°C. Yield 1.10 g (90%) (decomp. at 85°C).

8b: 110 mg (0.2 mmol) of **5c** and 0.5 mL of dry 2-butyne were dissolved in 5 mL of dichloromethane at −78°C and the mixture treated in the dark with a solution of 60 mg (0.18 mmol) of $Ag[SbF_6]$ in 1 mL of dichloromethane. Upon slowly heating to room temperature the color of the solution changed from reddish brown to brilliant orange. After removal of precipitated AgBr by filtration the solution was evaporated to dryness and the residue repeatedly washed with 10 mL portions of diethyl ether. Recrystallization from *n*-hexane/dichloromethane (1/1 parts by volume) furnished 120 mg (80%) of **8b** (decomp. at 165°C).

Received: July 22, 1987 [Z 2370 IE]
German version: *Angew. Chem. 99* (1987) 1286

[1] E. J. M. de Boer, J. de With, A. G. Orpen, *J. Am. Chem. Soc. 108* (1986) 8271.
[2] W. A. Herrmann, J. Kuchler, J. K. Felixberger, W. Wagner, E. Herdtweck, *Angew. Chem.*, in press.
[3] Reviews: a) W. A. Herrmann, E. Herdtweck, M. Flöel, J. Kulpe, U. Küsthardt, J. Okuda, *Polyhedron 6* (1987) 1165; b) J. Okuda, W. A. Herrmann, *J. Mol. Catal. 41* (1987) 109; c) W. A. Herrmann, *J. Organomet. Chem. 300* (1986) 111; d) W. A. Herrmann, *Comm. Inorg. Chem.*, in press.
[4] a) W. A. Herrmann, J. K. Felixberger, E. Herdtweck, A. Schäfer, J. Okuda, *Angew. Chem. 99* (1987) 466; *Angew. Chem. Int. Ed. Engl. 26* (1987) 466; b) J. K. Felixberger, unpublished results; c) W. A. Herrmann, R. A. Fischer, E. Herdtweck, *J. Organomet. Chem. 329* (1987) C1.
[5] Green-brown prisms from *n*-hexane/dichloromethane (−35°C); crystal dimensions: 0.42 × 0.17 × 0.10 mm; triclinic, $P\bar{1}$ (Int. Tab. No. 2); $a = 791.4(1)$, $b = 879.7(1)$, $c = 1219.2(4)$ pm, $\alpha = 88.63(2)$, $\beta = 84.69(2)$, $\gamma = 71.42(1)°$; $V = 801 \times 10^6$ pm^3; empirical formula: $C_{14}H_{20}Cl_3Re$; $Z = 2$; $F(000) = 460$; $\rho_{calcd} = 1.993$ g·cm^{-3}; $\lambda = 71.073$ pm ($Mo_{K\alpha}$ radiation); no systematic extinctions; $T = 24 \pm 1$°C; Enraf-Nonius CAD-4; measurement: $2.0° \leq \theta \leq 25.0°$, ω-scan; scan width: $(1.10 + 0.30 \tan\theta)° \pm 25\%$ before and after each reflection; $t(\max) = 60$ s; 5588 measured reflections ($\pm h$, $\pm k$, $\pm l$), 2796 independent reflections, 75 reflections with $I > 0.5\sigma(I)$ suppressed; 230 parameters full-matrix refined; $R = \Sigma(||F_o| - |F_c||)/\Sigma|F_o|$: 0.021; $R_w = [\Sigma w(|F_o| - |F_c|)^2/\Sigma w|F_o|^2]^{1/2}$: 0.022 with $w = 1/\sigma^2(F_o)$, GOF $= [\Sigma w(|F_o| - |F_c|)^2/(NO - NV)]^{1/2}$: 3.024. Structure solution according to Patterson methods. Numerical absorption correction: $\mu = 81.8$ cm^{-1} (eight faces). Correction for decomposition (103 h: −8.7%). The hydrogen positions were successively taken from the difference Fourier syntheses and refined with (per C-atom collectively) individual isotropic temperature factors. Anomalous dispersion taken into account. Shift/error: <0.00 in the last refinement cycle; residual electron density: +1.16 e/Å^3; 92 pm next to the heavy atom.
[6] Examples: a) F. N. Tebbe, R. L. Harlow, *J. Am. Chem. Soc. 102* (1980) 6149; b) R. J. McKinney, T. H. Tulip, D. L. Thorn, T. S. Coolbaugh, F. N. Tebbe, *ibid. 103* (1981) 5584.
[7] E. Herdtweck, M. Flöel, W. A. Herrmann, unpublished results 1986/87. Selected distances: Re-C1,C2,C3 223.5(6), 212.1(5), 219.9(5) pm; distance of Re to plane C1,C2,C3: 183 pm.
[8] F. R. Kreissl, P. Friedrich, *Angew. Chem. 89* (1977) 553; *Angew. Chem. Int. Ed. Engl. 16* (1977) 545 (planar partial structure Re=CR^1, R^2).
[9] Cf. J. M. Mayer, T. H. Tulip, J. C. Calabrese, E. Valencia, *J. Am. Chem. Soc. 109* (1987) 157.

Luminescence Probes: The $Eu^{3\oplus}$- and $Tb^{3\oplus}$-Cryptates of Polypyridine Macrobicyclic Ligands

By *Béatrice Alpha, Vincenzo Balzani,* Jean-Marie Lehn,* Siglinda Perathoner,* and *Nanda Sabbatini*

There is currently a growing interest in the luminescence properties of lanthanoid complexes because of their importance as probe ion species,[1-6] especially for biological applications. Particularly promising are the cryptate complexes[7] where the luminescent lanthanoid ion is encapsulated into the ligand structure.[8-12] In this way, one may reach some important goals: (1) inertness of the complex;[8,12] (2) protection towards deactivating interactions between the luminescent lanthanoid ion and solvent (water);[9-11] (3) efficient energy transfer from the (strongly absorbing) ligand chromophore to the luminescent metal ion.[12,13] These three features are combined in the lanthanoid cryptates[12,14] of macrobicyclic ligands containing the 2,2′-bipyridine (bpy) or 1,10-phenanthroline chromophoric groups.[15]

We have carried out a systematic investigation on the photophysical properties of the $Eu^{3\oplus}$ and $Tb^{3\oplus}$ complexes **1** and **2**[12] and we have found that these species are efficient molecular devices for the conversion of the UV light absorbed by the ligands into visible luminescence of the lanthanoid ions. In view of their interest, in particular as luminescent labels in aqueous solution, we briefly report here some results of our measurements.

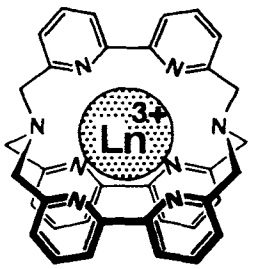

1, Ln = Eu
2, Ln = Tb

Absorption and emission data for **1** and **2** in aqueous solution are shown in Table 1 where data for the corresponding aquo ions[16,17] are also reported for comparison purposes. The cryptate complexes exhibit strong ligand-centered (LC) absorption bands in the near UV region, 10^4-10^5 times more intense than the metal-centered (MC) f-f bands characteristic of the lanthanoid ions. The wavelength of the luminescence emission originating from the $^5D_0$ and $^5D_4$ levels of $Eu^{3\oplus}$ and $Tb^{3\oplus}$, respectively,[3] is almost unaffected by the coordinating environment (water or cryptand ligands), whereas the excited-state lifetimes and the luminescence quantum yields are strongly modified (Table 1). From the lifetime values in H_2O or D_2O solution it is possible to evaluate[2,3] the average number of coordinated water molecules (estimated error, ±0.5): **1**, 2.5; $Eu^{3\oplus}_{aq}$, 9.6; **2**, 3.0; $Tb^{3\oplus}_{aq}$, 9.0. These figures show the capability of the cryptand ligand to shield the metal ion from the solvent molecules.

Table 1. Absorption and emission data for $Eu^{3\oplus}$ and $Tb^{3\oplus}$ aquo ions and cryptates **1** and **2** in aqueous solution.

Complex	Absorption [a]		Emission [b]					
	λ_{max} [nm]	ε_{max} [M^{-1} cm^{-1}]	λ_{max} [nm]	$\tau^{300K}_{H_2O}$ [ms]	$\tau^{300K}_{D_2O}$ [ms]	$\tau^{77K}_{D_2O}$ [ms]	Φ [c]	η [d]
1	304 (LC)	25000	615 [e]	0.34	1.7	1.7	0.02	0.1
$Eu^{3\oplus}_{aq}$	393 (f-f)	3	616 [e]	0.11	3.2	3.3	0.006	—
2	304 (LC)	29000	542 [f]	0.33	0.43	3.8	0.03	0.3
$Tb^{3\oplus}_{aq}$	308 (f-f)	0.3	543 [f]	0.40	3.8	3.8	0.08 [g]	—

[a] Excitation wavelength; LC, ligand-centered band; f-f, metal-centered band. [b] Experimental uncertainties: lifetimes, < 10%; quantum yields, ca. 30%. [c] H_2O solution, room temperature. [d] Energy-transfer efficiency, given as the ratio between the emission quantum yield for LC excitation and excitation into the $^5D_0$ (for $Eu^{3\oplus}$) or $^5D_4$ (for $Tb^{3\oplus}$) emitting levels. The latter quantity has been evaluated from the ratio between the emission lifetime in H_2O at 300 K and the emission lifetime in D_2O at 77 K, taken as the radiative lifetime. [e] Assigned to the $^5D_0 \rightarrow {}^7F_2$ transition (most intense emission band). [f] Assigned to the $^5D_4 \rightarrow {}^7F_5$ transition (most intense emission band). [g] Excitation in the emitting $^5D_4$ level [17].

In H_2O solution at room temperature, the quantum yields of luminescence emission on excitation in the high-intensity ligand-centered band at ca. 300 nm are 0.02 for **1** and 0.03 for **2**. The reason for the lower than unity luminescence quantum yield is the competition between intraligand radiationless decay of ^3LC to the ground state and intramolecular $^3LC \rightarrow (MC)^5D_0$ (for $Eu^{3\oplus}$) or $^3LC \rightarrow (MC)^5D_4$ (for $Tb^{3\oplus}$) energy transfer (for details see Ref. [18]).

In conclusion, because of their very intense absorption bands, which collect incident light, and because of their reasonably high ligand-to-metal energy transfer and luminescence efficiencies, the cryptates **1** and **2** are excellent molecular devices to play the role of luminescence probes and luminescence concentrators (antenna effect). Even in very diluted *aqueous* solutions (ca. 10^{-5} M), they are able to convert about 1% of the *incident* UV photons into emitted visible photons, a quite interesting result for several applications, in particular for labeling of biological materials. Higher conversion efficiency may be attained if structural modifications are found which increase both the shielding of the enclosed ion and the yield of intramolecular energy transfer.

Received: July 27, 1987 [Z 2376 IE]
German version: *Angew. Chem. 99* (1987) 1310

[*] Prof. Dr. V. Balzani, Dr. S. Perathoner, Dr. N. Sabbatini
Departimento di Chimica "G. Ciamician" dell'Università
and Istituto FRAE-CNR
I-20126 Bologna (Italy)
Prof. Dr. J.-M. Lehn, B. Alpha
Institut Le Bel, Université Louis Pasteur
4, rue Blaise Pascal, F-67000 Strasbourg (France)

[**] We wish to thank *V. Cacciari* and *G. Gubellini* for technical assistance. This work was supported by the Consiglio Nazionale delle Ricerche, Ministero della Pubblica Istruzione (Italy), and by ORIS-Industrie (France).

[1] F. S. Richardson, *Chem. Rev. 82* (1982) 541.
[2] W. D. Horrocks, Jr., D. R. Sudnick, *Acc. Chem. Res. 14* (1981) 384.
[3] W. D. Horrocks, Jr., M. Albin in S. J. Lippard (Ed.): *Prog. Inorg. Chem. 31* (1984) 1.
[4] J.-C. G. Bünzli, D. Wessner, *Coord. Chem. Rev. 60* (1984) 191.
[5] V. Balzani, N. Sabbatini, F. Scandola, *Chem. Rev. 86* (1986) 319.
[6] J.-M. Lehn in V. Balzani (Ed.): *Supramolecular Photochemistry*, Reidel, Dordrecht, The Netherlands, 1987, p. 29.
[7] J.-M. Lehn, *Acc. Chem. Res. 11* (1978) 49.
[8] E. L. Yee, O. A. Gansow, M. J. Weaver, *J. Am. Chem. Soc. 102* (1980) 2278.
[9] N. Sabbatini, S. Dellonte, M. Ciano, A. Bonazzi, V. Balzani, *Chem. Phys. Lett. 107* (1984) 212.
[10] G. Blasse, M. Bujs, N. Sabbatini, *Chem. Phys. Lett. 124* (1986) 538.
[11] N. Sabbatini, S. Dellonte, G. Blasse, *Chem. Phys. Lett. 129* (1986) 541.
[12] B. Alpha, J.-M. Lehn, G. Mathis, *Angew. Chem. 99* (1987) 269; *Angew. Chem. Int. Ed. Engl. 26* (1987) 266.
[13] M. J. Weber in K. A. Gschneidner, L. Eyring (Eds.): *Handbook on the Physics and Chemistry of Rare Earths, Vol. 4*, North-Holland, Amsterdam 1979, p. 275.

[14] The structure of these complexes has been confirmed by the determination of the crystal structure of the $La^{3\oplus}$ cryptate of the [bpy·bpy·bpy] macrobicyclic ligand: J. Guilhem, C. Pascard, unpublished results.
[15] J.-C. Rodriguez-Ubis, B. Alpha, D. Plancherel, J.-M. Lehn, *Helv. Chim. Acta 67* (1984) 2264.
[16] Y. Haas, G. Stein, *J. Phys. Chem. 75* (1971) 3668.
[17] G. Stein, E. Würzberg, *J. Chem. Phys. 62* (1975) 208.
[18] N. Sabbatini, S. Perathoner, V. Balzani, B. Alpha, J.-M. Lehn in V. Balzani (Ed.): *Supramolecular Photochemistry*, Reidel, Dordrecht, The Netherlands, 1987, p. 187, and unpublished results.

Pentasila[1.1.1]propellane. Predictions Concerning Structure, Bonding, and Strain Energy**

By *Paul von Ragué Schleyer** and *Rudolf Janoschek**

Because of its inverted carbons, high ring strain, the nature of the bonding between the bridgehead atoms, and, most certainly, its availability through synthesis, [1.1.1]propellane, **1**, is an exceptionally intriguing species.[1-4] Whether or not there is a central bond in **1**, or, if so, to what extent, is being hotly debated.[1-4] Similar questions pertain to pentasila[1.1.1]propellane (tricyclo[1.1.1.0]pentasilane, **2**), the silicon analogue of **1**. Small-ring silicon systems are providing instructive comparisons and contrasts with their carbocyclic analogues. In particular, we have predicted recently that two "bond stretch" isomers of bicyclo[1.1.0]tetrasilane, **3** and **4**, should be capable of existence.[5,6] One of these, **3**, with an essentially classical structure, has an experimental precedent,[6b] but derivatives of the more stable **4**, which can be regarded as a singlet diradical requiring a multiconfigurational description, are not yet known. As we mentioned,[5] similar structural possibilities exist for **2**. We now describe the nature of this species.

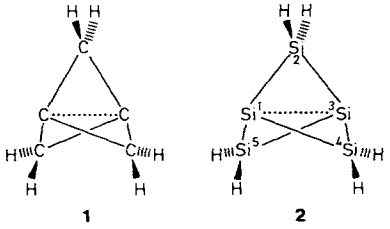

1 **2**

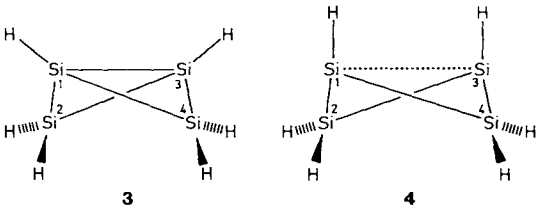

3 **4**

At all ab initio levels investigated, which include single-determinant optimizations with the 3-21G (sp), 3-21G* (spd), and pseudopotential-21G* (spd) basis sets, as well as multiconfigurational (MC-SCF) treatment with the latter method,[7] no minimum corresponding to a "classical" structure of **2** could be located. Like **3**, a classical geometry of **2** would be expected to have nearly equal Si1Si2 and Si1Si3 bond lengths. Instead, when these distances were set to 2.3 Å, optimization led automatically to extension of the central bond (see equilibrium values in Table 1). In order to rule out the possibility of a second minimum with a shorter Si–Si bridge distance, a series of two-configuration MC-SCF (spd) calculations were carried out with various fixed Si1Si3 distances, all other parameters being allowed to vary within the restriction of D_{3h} symmetry. As the results in Table 2 indicate, there was no second minimum. Thus, particularly with regard to the length of the central bond, the structure of **2** is similar to that of **4**, but not to **1** or to **3**. This conclusion is supported by the analysis of the two-configuration wave function:

Table 1. The geometry of **2** at various theoretical levels.

Method	*d*(Si1Si2) [Å]	*d*(Si1Si3) [Å]	Ref.
SCF-21G* (spd) [a]	2.325	2.686	
CEP-31G* [a]	2.347 [b]	2.729 [b]	[3]
MC-SCF (spd) [a]	2.330	2.735	
3-21G	2.443 [c]	2.885 [c]	
3-21G*	2.331 [d]	2.692 [d]	
6-31G*	2.347	2.719	[10]

[a] Pseudopotential method employed. [b] For comparison, the CEP-31G* values for **4** are 2.362 and 2.915 Å [3b]. [c] For comparison, the 3-21G values for **4** are 2.406 and 2.972 Å. [d] For comparison, the 3-21G* values for **4** are 2.305 and 2.731 Å [5].

$$\psi_{MC\text{-}2} = 0.97\,\psi_b(\sigma^2) - 0.25\,\psi_a(\sigma^{*2})$$

Table 2. Search for a second minimum of **2**, MC-SCF (spd).

d(Si1Si2) [Å]	*d*(Si1Si3) [Å]	E_{rel} [kcal mol^{-1}]
2.330	2.735	0.0 [a]
2.309 (opt.)	2.600 (fixed)	1.7
2.305 (opt.)	2.500 (fixed)	5.4
2.305 (opt.)	2.400 (fixed)	11.9

[a] From Table 1.

This wave function indicates substantial singlet diradical character.[8] Hence, it would be misleading to represent **2** by drawing a line between the bridgehead atoms. The 3-21G atom–atom overlap-weighted natural atomic orbital bond order[9] for the central Si1Si3 bond is only 0.176 vs. 0.677 for the Si1Si2 bonds. These are almost identical with the values for **4** (Si1Si3 = 0.173, Si1Si2 = 0.693) but contrast with those for **3** (0.600 and 0.765, respectively). The corresponding results for bicyclo[1.1.1]pentasilane, **5**, are 0.013 for Si1Si3 and 0.762 for Si1Si2.

As with **1**, the formally bonding σ-MO involving the central bond (HOMO) is higher-lying (but only by 0.02

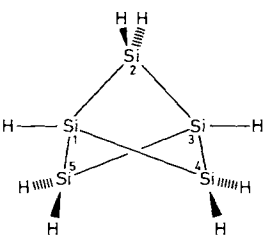

5

[*] Prof. Dr. P. von R. Schleyer
Institut für Organische Chemie der Universität Erlangen-Nürnberg
Henkestrasse 42, D-8520 Erlangen (FRG)
Prof. Dr. R. Janoschek
Institut für Theoretische Chemie der Universität
Mozartgasse 14, A-8010 Graz (Austria)

[**] This work was supported by the Deutsche Forschungsgemeinschaft and the Fonds der Chemischen Industrie. We thank Professor *L. C. Allen* and Professor *S. Nagase* for preprints of their related papers (Ref. [3b] and [10], respectively).

hartree), than the formally anti-bonding degenerate π^*-MOs. The latter are stabilized by interaction with the three peripheral silicon atoms. These are the "σ-bridged-π" interactions described and depicted by *Jackson, Allen* et al.,[3] the importance of which, however, has been discounted in some other analyses of the bonding in **1**.[4]

As we have pointed out in the case of **3** vs. **4**,[5] the difference in behavior of corresponding polycyclic carbon and silicon ring systems can be attributed to differences in strain contributions. While three-membered silicon ring systems are more strained than their carbon counterparts, the opposite is true for four-membered rings.[5] Thus, the ring-opening process, which, in effect, converts the three-membered rings in **3** into the four-membered ring in **4**, results in a higher relief of strain energy than would be possible with the corresponding carbocyclic system. Hence, bicyclobutane prefers a closed structure akin to **3**. The same situation pertains in **2** with its four-membered rings and roughly 100° Si1Si2Si3 bond angles. The geometry with a short Si1Si3 distance, which we find *not* to be minimum, would be higher in energy (see Table 2) due to the presence of three 3-membered silicon rings.

Despite the singlet diradical character of the bridgehead silicons and the weak Si1Si3 bonding, the strain energy in **2** (62.2 kcal mol^{-1} at pseudopotential MC-SCF-21G*)[10-12] is relatively low, particularly in comparison with the strain energy of [1.1.1]propellane **1** (102 kcal mol^{-1}).[2a,c] This difference also is apparent in the much higher strain energy of bicyclo[1.1.1]pentane **6** (67 kcal mol^{-1})[2c] than bicyclo[1.1.1]pentasilane **5** (37 kcal mol^{-1} at 3-21G*).[3b,11] While the bridgehead–bridgehead distance in **6** (1.88 Å) is much longer than that in **1** (1.60 Å),[2,3] the two separations are closer in **2** (ca. 2.73 Å) and in **5** (2.92 Å),[13] especially when the inherently larger silicon distances are taken into account.

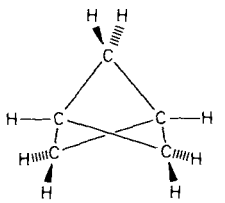

6

In view of the relatively low strain energy predicted for **2** and the considerable recent experimental success in the preparation of **1**, **3**,[6b] and **5**,[13] as well as many small-ring silicon systems, the synthesis of appropriate derivatives of **4** affords an experimental challenge. Generally similar conclusions have been reached by *Allen* et al.[3b] and by *Nagase* et al.[10] who also have studied these systems.

Received: July 31, 1987 [Z 2385 IE]
German version: *Angew. Chem. 99* (1987) 1312

[1] a) For a comprehensive analysis of the bonding in hydrocarbons, see K. B. Wiberg, R. F. W. Bader, C. D. H. Lau, *J. Am. Chem. Soc. 109* (1987) 985; b) Other analyses of the bonding in **1** include: W. Stohrer, R. Hoffmann, *ibid. 94* (1972) 779; M. D. Newton, J. M. Schulman, *ibid. 94* (1972) 773; N. D. Epiotis, *ibid. 106* (1984) 3170; P. Politzer, K. Jayasuriya, *J. Mol. Struct. 135* (1986) 245; R. P. Messmer, P. A. Schultz, *ibid. 108* (1984) 7407, and Ref. [2]-[4].

[2] a) K. B. Wiberg, *Acc. Chem. Res. 17* (1985) 379, and references cited therein; b) K. B. Wiberg, *ibid. 105* (1983) 1227; c) K. B. Wiberg, *Angew. Chem. 98* (1986) 312; *Angew. Chem. Int. Ed. Engl. 25* (1986) 312.

[3] a) J. E. Jackson, L. C. Allen, *J. Am. Chem. Soc. 109* (1984) 591; b) D. B. Kitchen, J. E. Jackson, L. C. Allen, to be published.

[4] a) A. B. Pierini, H. F. Reale, J. Medrano, *J. Mol. Struct. 148* (1986) 109; b) D. Feller, E. R. Davidson, *J. Am. Chem. Soc. 109* (1987) 4133.

[5] P. von R. Schleyer, A. F. Sax, J. Kalcher, R. Janoschek, *Angew. Chem. 99* (1987) 374; *Angew. Chem. Int. Ed. Engl. 26* (1987) 364, and references cited therein.

[6] a) For a theoretical study of **3** (but not **4**) see S. Collins, R. Dutler, A. Rauk, *J. Am. Chem. Soc. 109* (1987) 2564; b) for the X-ray structure of a derivative of **3**, see R. Jones, D. J. Williams, Y. Kabe, S. Masamune, *Angew. Chem. 98* (1986) 176; *Angew. Chem. Int. Ed. Engl. 25* (1986) 79; c) for a theoretical study of **4** (but not **3**), see T. Dabisch, W. Schoeller, *J. Chem. Soc. Chem. Commun. 1986*, 896.

[7] The standard HF calculations were carried out with the Gaussian 82 program; see W. J. Hehre, L. Radom, P. von R. Schleyer, J. A. Pople: *Ab Initio Molecular Orbital Theory*, Wiley, New York 1986. The MC-SCF treatment employed was similar to that described in Ref. [5].

[8] The MC-SCF wave-function obtained for **4** is quite similar, $\psi_{MC} = 0.95\,\psi_b - 0.30\,\psi_a$[5], ψ_b/ψ_a denotes that configuration in which the bonding/antibonding σ-MO of the Si1-Si3 bridge is doubly occupied.

[9] A. E. Reed, F. Weinhold, *J. Chem. Phys. 83* (1985) 1736; A. E. Reed, R. B. Weinstock, F. Weinhold, *ibid. 83* (1985) 735. These bond orders may vary somewhat at higher levels of theory (the 3-21G* bond orders for **2** are: Si1Si3 = 0.245, Si1Si2 = 0.834), but should be interpreted on a relative, rather than on an absolute basis.

[10] S. Nagase, T. Kudo (*Organometallics 6* (1987) 2456) give a strain energy of 70 kcal mol^{-1} for **2** (SCF/6-31G* calculations). These authors call attention to the negatively charged bridgehead silicon, Si1, in **2**. However, this is generally found when a silicon is bound to several SiH_3 or SiH_2 groups. For example, the 3-21G natural charges [9] on the central Si atoms are: −0.106 in **2** (−0.163 at 3-21G*) but −0.378 in $Si(SiH_3)_4$, +0.019 in **5**, +0.028 in **3**, +0.072 in **4**, and +0.19 in $HSi(SiH_3)_3$. In all these molecules, the SiH_2 silicons have charges $+0.34 \pm 0.1$ and the SiH_3 silicons $+0.55 \pm .02$.

[11] Ref. [3b] gives 71.3 and 37.4 kcal mol^{-1} for **2** and **5**, respectively, using a pseudopotential SCF-31G* (spd) basis. Our pseudopotential SCF-21G* value for **2** (72.4 kcal mol^{-1}) agrees well; also the SCF 69 kcal mol^{-1} estimate of *Nagase* [10]. However, an electron-correlation-corrected ring-strain energy was evaluated by "two-configuration (σ^2, σ^{*2})-per-SiSi-bond" wave functions. The decrease of total energy for a normal SiSi bond is 4.7 kcal mol^{-1} whereas that for the diradical central SiSi bond in **2** is 14.9 kcal mol^{-1}. Thus, SCF overestimates ring strain energies in **2**, and also in **4**, by more than 10 kcal mol^{-1}.

[12] All these strain energies are evaluated by the use of the unusual homodesmotic equations [3b, 5, 10].

[13] The first preparation of a derivative of **5** has been reported by *S. Masamune* et al. (*Fifth Int. Symp. Organosilicon Chem.*, St. Louis, MO, USA, June 1987).

Electrocyclic Opening of 2,3-Benzo- and 2,3;7,8-Dibenzobicyclo[4.2.0]octa-2,4,7-triene; Benzoannelated Transition States**

By *Wolfram Grimme,* Johann Lex,* and *Thomas Schmidt*

Dedicated to Professor Emanuel Vogel on the occasion of his 60th birthday

The electrons participating in pericyclic reactions are aromatically stabilized in the transition state before they form new bonds in the product. When an electron pair of a benzene ring participates in a pericyclic reaction, the transition state is benzoannelated and "isoconjugate" with naphthalene, whereas the product has lost all aromaticity. Hence, energy-rich intermediates which rapidly undergo further reaction can be generated relatively easily by pericyclic reactions with benzenoid double bonds. Frequently, the reverse of their formation is the preferred reaction, and it requires special analytical methods in order to detect the occurrence of these processes.

An example of a hidden pericyclic reaction with participation of a benzene ring is the electrocyclic ring-opening of benzonorcaradiene **1** to give the bicyclo[5.4.0]undeca-

[*] Prof. Dr. W. Grimme, Dr. J. Lex, Dr. T. Schmidt
Institut für Organische Chemie der Universität
Greinstrasse 4, D-5000 Köln 41 (FRG)

[**] This work was supported by the Deutsche Forschungsgemeinschaft and the Fonds der Chemischen Industrie.

1,3,6,8,10-pentaene **2**.[1] The reaction already occurs at room temperature, but the product with the *o*-quinodimethane partial structure undergoes back reaction so rapidly that its detection is only possible via the racemization of the benzonorcaradiene, which is very rapid on the NMR time scale at 180°C.

1 2

We report here on the corresponding ring opening of benzo- and dibenzobicyclo[4.2.0]octa-2,4,7-triene. The synthesis of the 2,3-benzobicyclo[4.2.0]octa-2,4,7-triene-2′-carbonitrile **4** was achieved starting from the photoproduct **3**[2] of β-naphthonitrile and ethyl vinyl ether; **3** was obtained in 63% yield as a 5:1 mixture of the *anti*- and *syn*-isomer. Since several steps are involved in the formation of **3** and another skeletal structure has been proposed for the product of the corresponding reaction with methyl vinyl ether,[3] we have confirmed the structure of **3** by an X-ray diffraction analysis of the Diels–Alder adduct **5**.[4] Compound **5** is formed upon heating a solution of **3** in hexachlorocyclopentadiene at 100°C for 14 h and can be isolated by chromatography ($CHCl_3$, silica gel) and purified by recrystallization from hexane. The ether **3** eliminates ethanol on heating to 105°C (3 h) in a mixture of glacial acetic acid, 85% phosphoric acid and water (5:2.75:1 parts by volume) and affords the benzobicyclo[4.2.0]octatriene derivative **4** (72%). Physical data of **4** and the other new compounds are given in Table 1.

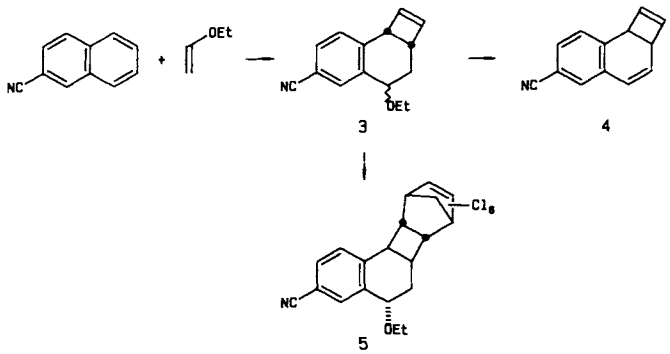

3 4 5

Table 1. Some physical data of the compounds **4**, **5**, **7**, **8**-D, and **8′**-D. The NMR spectra were recorded at 90 MHz in CCl_4 (those of **4** and **5** at 300 MHz in $CDCl_3$ and $CCl_4+CD_2Cl_2$, respectively).

4, m.p. 64–66°C; ^{1}H-NMR: $\delta=7.28$ (AB, $\Delta\nu=71$ Hz, $J=7.8$ Hz; H-3′,4′), 7.27 (d, $J=1.9$ Hz; H-1′), 6.13 (AB, $\Delta\nu=64$ Hz, $J=9.9$ Hz; H-4, 5), 6.09 (AB, $\Delta\nu=50$ Hz, $J=2.7$ Hz; H-7, 8), 4.12 (d, $J=4.5$ Hz; H-1), 3.68 (t, $J=4.5$ Hz; H-6); ^{13}C-NMR: $\delta=140.82$ (C-3), 140.66 (C-7), 138.82 (C-8), 132.87 (C-2), 130.92 (C-3′), 130.47 (C-1′, 5), 128.46 (C-4′), 124.16 (C-4), 118.93 (CN), 110.22 (C-2′), 43.78 (C-1), 42.97 (C-6); UV (hexane): $\lambda_{max}=275$ nm ($\varepsilon=3930$), 285 (3360) sh, 302 (1330) sh, 313 (890) sh

5, m.p. 173°C; ^{1}H-NMR: $\delta=7.65$ (d, $J=1.4$ Hz, 1H), 7.39 (AB, $\Delta\nu=114.5$ Hz, $J=7.9$ Hz, 2H), 4.38 (m, 1H), 3.52 (AB, $\Delta\nu=47$ Hz, $J=9$ Hz, 2H–Et), 3.18 (m, 1H), 3.06 (AB, $\Delta\nu=18$ Hz, $J=8.4$ Hz, 2H), 2.66 (m, 1H), 1.97 (AB, $\Delta\nu=51$ Hz, $J=13.4$ Hz, 2H), 1.22 (t, 3H–Et)

7, ^{1}H-NMR: $\delta=7.30$ (s, 1H), 7.28 (AB, $\Delta\nu=39.3$ Hz, $J=9$ Hz, 2H), 6.32 (AB, $\Delta\nu=37.5$ Hz, $J=12$ Hz, 4H), 5.90 (s, 2H); UV (hexane): $\lambda_{max}=275$ nm ($\varepsilon=2300$) sh

8-D, ^{1}H-NMR: $\delta=7.4$–6.8 (m, 8H), 6.02 (d, $J=4.7$ Hz, 1H), 4.51 (AB, $\Delta\nu=34$ Hz, $J=6$ Hz, 2H)

8′-D, ^{1}H-NMR: $\delta=7.4$–6.8 (m, 8H), 6.13 (AB, $\Delta\nu=15.6$ Hz, $J=9$ Hz, 2H), 4.73 (s, 1H)

Above 100°C, **4** rearranges uniformly in a first-order reaction into 2′-benzocyclooctatetraenecarbonitrile **7**; the NMR-spectroscopically measured rate constant in CD_3CN at 110.3°C is $k_i=(3.80\pm0.06)\times10^{-5}\,s^{-1}$. The energy-rich primary product **6** of the electrocyclic opening of the six-membered ring rapidly forms the arene by a double-bond shift in the eight-membered ring. To check whether recyclization to the starting compound is a competing process, **4** was resolved into the enantiomers by chromatography on microcrystalline triacetylcellulose.[5] The decrease in rotation of (−)-**4** ($[\alpha]_{575}=-360$, $c=0.44$) in CH_3CN at 110.3°C, too, is a first-order process with the rate constant $k_\alpha=(3.54\pm0.03)\times10^{-5}\,s^{-1}$. Since it is found, within the limits of error, that $k_i=k_\alpha$, it must be concluded that back reaction of **6** to racemic **4** does not take place. Likewise the intermolecular trapping reaction with reactive dienophiles cannot compete with the double-bond shift in **6**, so the occurrence of the mechanistically plausible intermediate **6** had to be substantiated in another way.

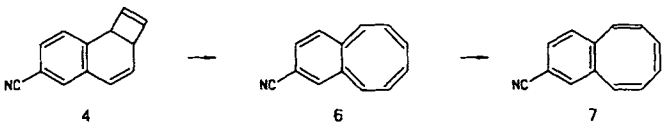

4 6 7

In 2,3;7,8-dibenzobicyclo[4.2.0]octa-2,4,7-triene **8**[6] the electrocyclic opening should occur analogously to that in **4** with participation of an electron pair of the benzene ring annelated to the six-membered ring. In the intermediate **9**, however, the double-bond shift in the eight-membered ring is degenerate and leads to **9′**; here a stabilization can only occur through recyclization. If the racemization of **8** or its automerization to **8′**, both of which are possible only via the *o*-quinoid intermediate, occurs under similar conditions as the rearrangement of **4**, the formation of such an intermediate can also be expected in the case of the latter.

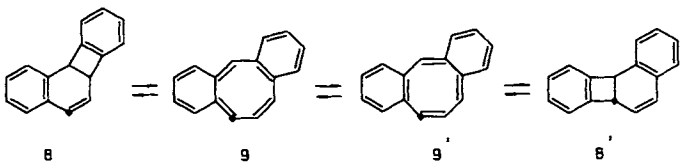

8 9 9′ 8′

The position marked with a black dot is deuteriated.

We first investigated the automerization by means of the compound **8**-D deuteriated in position 4. This was obtained from 4-bromo-2,3;7,8-dibenzobicyclo[4.2.0]octa-2,4,7-triene[7] by metal–halogen exchange with *n*-butyllithium in THF at −70°C and subsequent hydrolysis with D_2O. NMR spectroscopic studies revealed that **8**-D is in equilibrium with its positional isomer **8′**-D at 100°C in CCl_4. The equilibrium constant is $K=1.13$ and the rate constant for the formation of the equilibrium was found to be $(k_a+k'_a)=(7.45\pm0.06)\times10^{-5}\,s^{-1}$ at 100.6°C. Thus the automerization of **8** takes place just as easily as the rearrangement of **4**, indicating the formation of an *o*-quinoid intermediate in both cases.

The question as to whether in the intermediate **9** the recyclization to **8** can compete with the energetically neutral double-bond shift to give **9′** was determined with help of enantiomerically enriched **8**. Partial hydroboration of racemic **8** with diisopinocampheylborane[8] (0.5 molar equivalents, prepared from (−)-α-pinene) in 1.5 M ethereal solu-

tion at °C furnished optically active (+)-**8** with $[\alpha]_{575} = 108.4$ ($c = 9.15$ in benzene). Its racemization in benzene at 100.6 °C is a reaction of first order with the rate constant $k_\alpha = (7.67 \pm 0.03) \times 10^{-5}\ s^{-1}$. Thus, the racemization is equally rapid as the establishment of the equilibrium between the labeled isomers, and the *o*-quinoid intermediate **9** preferentially undergoes a double bond shift to give **9'**.

The free enthalpies of activation for the electrocyclic ring opening of the benzoannelated cyclohexadienes in the compounds **1**, **4**, and **8** can be compared with those for the parent compounds. Table 2 shows that the participation of a benzenoid electron pair increases the free enthalpy of *activation* by 11 ± 1 kcal mol^{-1}. Incremental calculations,[12] on the other hand, indicate that the loss of aromaticity increases the free enthalpy of *reaction* of the benzoannelated compounds by 25 ± 1 kcal mol^{-1}. The introductory concept that benzoannelated transition states of pericyclic reactions are still aromatically stabilized is thus confirmed.

Table 2. Free enthalpies of activation for the ring-opening of cyclohexadienes and their benzoannelated derivatives.

		1		4		8
T [°C]	0	0	110	110	100	100
$\Delta G^{\neq}$ [kcal mol^{-1}]	7.7 [9]	20.2 [1]	20.4 [10]	30.5	19.2 [11]	29.6
$\Delta\Delta G^{\neq}$ [kcal mol^{-1}]	12.5		10.1		10.4	

Received: August 18, 1987 [Z 2403 IE]
German version: *Angew. Chem. 99* (1987) 1277

[1] E. Vogel, D. Wendisch, W. R. Roth, *Angew. Chem. 76* (1964) 432; *Angew. Chem. Int. Ed. Engl. 3* (1964) 443.
[2] K. Mizuno, C. Pac, H. Sakurai, *J. Chem. Soc. Perkin Trans. 1 1975*, 2221.
[3] T. R. Chamberlain, J. J. McCullough, *Can. J. Chem. 51* (1973) 2578.
[4] Triclinic crystals, space group $P\bar{1}$, $Z = 2$, $a = 7.833(1)$, $b = 10.818(2)$, $c = 14.195(3)$ Å, $\alpha = 71.84(2)°$, $\beta = 79.77(2)°$, $\gamma = 69.59(2)°$. $\rho_{calcd} = 1.549$ g cm^{-3}, 3652 reflections observed; $R = 0.033$. Further details of the crystal structure investigation are available on request from the Fachinformationszentrum Energie, Physik, Mathematik GmbH, D-7514 Eggenstein-Leopoldshafen 2 (FRG), on quoting the depository number CSD-52735, the names of the authors, and the journal citation.
[5] We thank Prof. Dr. *F.-G. Klärner*, Bochum, for carrying out the separation.
[6] M. P. Cava, D. R. Napier, *J. Am. Chem. Soc. 78* (1956) 500.
[7] M. P. Cava, D. R. Napier, *J. Am. Chem. Soc. 79* (1957) 1701.
[8] G. Zweifel, H. C. Brown, *J. Am. Chem. Soc. 86* (1964) 393.
[9] M. B. Rubin, *J. Am. Chem. Soc. 103* (1981) 7781.
[10] E. Vogel, H. Kiefer, W. R. Roth, *Angew. Chem. 76* (1964) 432; *Angew. Chem. Int. Ed. Engl. 3* (1964) 442.
[11] M.-E. Günther, R. Aydin, W. Buchmeier, B. Engelen, H. Günther, *Chem. Ber. 117* (1984) 1069.
[12] S. W. Benson: *Thermochemical Kinetics*, Wiley, New York 1968.

Synthesis and X-Ray Structure of $(2,4,6\text{-}Me_3C_6H_2BPC_6H_{11})_3$: A Boron-Phosphorus Analogue of Borazine**

By *H. V. Rasika Dias* and *Philip P. Power**

The isoelectronic nature of the BN and CC pairs has generated considerable interest in various boron-nitrogen compounds. Perhaps the best known species of this type are the borazines[1] and related derivatives. These have many of the characteristics of aromatic compounds exemplified by the close similarity in physical properties of borazine and benzene. In sharp contrast, boron-phosphorus compounds are not nearly as thoroughly studied and no stable boron-phosphorus analogue of borazine has been described. We have recently published the syntheses and structural studies of a monomeric phosphinoborane[2] and some phosphinideneborates[3] to gain some insight on the nature of BP single and multiple bonds. We now report a further addition to the known classes of BP compounds in the form of the first structurally characterized BP analogue of a borazine; this is the title compound $(MesBPC_6H_{11})_3$, **1** (Mes = 2,4,6-$Me_3C_6H_2$, C_6H_{11} = cyclohexyl), which has been characterized by X-ray crystallography, and ^{31}P- and ^{11}B-NMR spectroscopy.

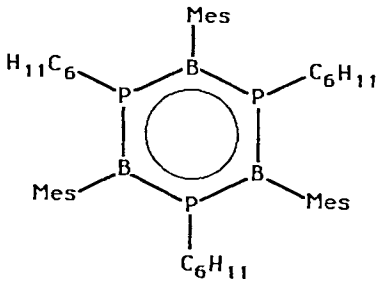

The B_3P_3 compound **1** was formed as pale yellow crystals in moderate yield during the attempted synthesis of $MesB(PH{-}C_6H_{11})_2$. The X-ray crystal structure[4] is illustrated in Figure 1. It consists of a planar[5-7] $B_3P_3C_6$ array in which all the BP bonds are essentially equal, averaging 1.84 Å in length. This distance is considerably shorter than

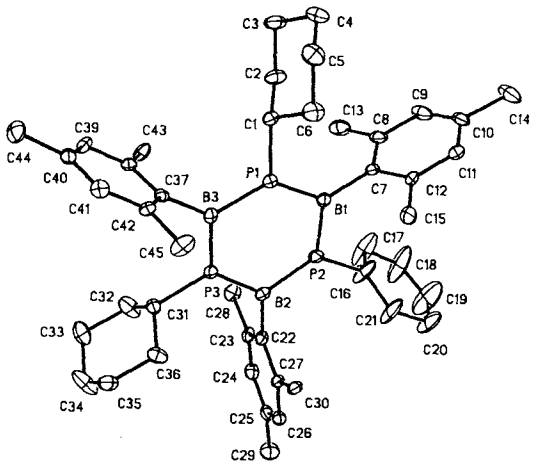

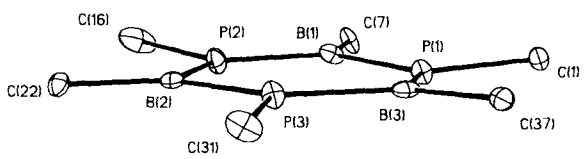

Fig. 1. Two views of the crystal structure of **1** (H atoms omitted for clarity). Selected bond distances [Å] and angles [°]: B1-P1 1.838(6), P1-B3 1.833(6), B3-P3 1.835(6), P3-B2 1.851(6), B2-P2 1.837(7), P2-B1 1.844(7), B1-C7 1.577(8), B2-C22 1.570(8), B3-C37 1.577(8), P1-C1 1.837(6), P2-C16 1.842(7), P3-C31 1.836(6); P1-B1-P2 114.8(3), P2-B2-P3 113.8(3), P1-B3-P3 116.0(3), B1-P1-B3 124.2(3), B1-P2-B2 126.0(3), B2-P3-B3 125.0(3).

[*] Prof. P. P. Power, H. V. R. Dias
Department of Chemistry, University of California
Davis, California 95616 (USA)

[**] This work was supported by the National Science Foundation and the A. P. Sloan Foundation.

the 1.92–1.96 Å range corresponding to a bond order of unity[8] and falls between the 1.859(3) Å seen in the monomeric phosphinoborane Mes_2BPPh_2, **2**,[2] and the 1.82–1.83 Å in the phosphinideneborate species $[Mes_2BPMes]^{\ominus}$, **3**, and $[Li(Et_2O)Mes_2BPR]$, **4** (R = Ph, C_6H_{11}, or Mes).[3] The monomer **2**, on the basis of its structure, has a significant interaction between the phosphorus lone pair and the empty boron p orbital, while the species **3** and **4** are thought to have a large amount of double-bond character. The B_3P_3 ring has thus at least three aromatic characteristics; (1) planarity, (2) equal BP bond lengths, (3) shortened BP bonds. It is also significant that the electronegativities of B and P are almost identical so that the B_3P_3 array should be much less polar than the corresponding B_3N_3 compound. Unfortunately, in the absence of comparative data, neither ^1H-, ^{13}C-, ^{11}B-, nor ^{31}P-NMR spectroscopy could provide evidence supporting the presence of a ring current.

^{31}P- and ^{11}B-NMR data are consistent with the X-ray structure. The ^{31}P-NMR shift ($\delta = 51.85$) of the singlet seen for **1** appears at much lower field than that of Mes_2BPPh_2 (**2**, $\delta = 30.2$) or $MesB(PPh_2)_2$,[9] ($\delta = -0.02$) suggesting less electron density at P, consistent with lone-pair delocalization. The broad singlet at $\delta = 52.6$ in the ^{11}B-NMR spectrum is very close to the value in **2** ($\delta = 51.7$). It is, however, further downfield than that found for $MesB(PPh_2)_2$ ($\delta = 30.1$), the closest compound available for comparison. In contrast, borazines generally absorb at higher ($\Delta\delta \approx 10$ ppm) field than monoaminoboranes whereas they absorb at similar fields to diaminoboranes.[10] Efforts to synthesize other derivatives related to **1** involving different substituents and heavier congeners are in progress.

Experimental Procedure

1: $MesBBr_2$ [11] (3.55 g, 12 mmol) in hexane (20 mL) was added to a solution of $C_6H_{11}PHLi$ (from $C_6H_{11}PH_2$ (2.86 g, 25 mmol) and *n*BuLi in hexane (15.5 mL of a 1.6 M solution)) in Et_2O (80 mL) at 0°C. Stirring for 12 h at ambient temperature afforded a yellow solution. Removal of volatiles under reduced pressure and extraction into hexane at 50°C gave, after filtration and concentration under reduced pressure and cooling to 0°C, pale yellow crystals of the title compound, **1**. Yield: 1.45 g, 48%; m.p. > 275°C. ^{31}P-NMR (THF/C_6D_6; H_3PO_4 ext.), $\delta = 51.85$; ^{11}B-NMR (THF/C_6D_6; $BF_3 \cdot OEt_2$ ext.), $\delta = 52.6$.

Received: August 25, 1987 [Z 2412 IE]
German version: *Angew. Chem. 99* (1987) 1320

[1] A. Stock, E. Pohland, *Chem. Ber. 59* (1926) 2215. See also P. Paetzold, C. von Plotho, G. Schmid, R. Boese, *Z. Naturforsch. 39 B* (1984) 1069 for the structure of a Dewar-type borazine.

[2] a) X. Feng, M. M. Olmstead, P. P. Power, *Inorg. Chem. 25* (1986) 4616. A monomeric phosphinoborane with an amino group on boron, (tmp)ClBPHMes (tmp = 2,2,6,6-tetramethylpiperidine), has also been reported [2b]. The bond distances and angles suggest that the boron p orbital is occupied in bonding to nitrogen rather than phosphorus. b) A. M. Arif, A. H. Cowley, M. Pakulski, J. M. Power, *J. Chem. Soc. Chem. Commun. 1986*, 889.

[3] R. A. Bartlett, X. Feng, P. P. Power, *J. Am. Chem. Soc. 108* (1986) 6817.

[4] Crystal data for **1**, at 130 K with $Mo_{K\alpha}$ ($\lambda = 0.71069$ Å); $a = 14.136(5)$, $b = 14.078(6)$, $c = 22.303(8)$ Å, $\beta = 90.45(3)°$, monoclinic, $P2_1/n$, $Z = 4$, 4185 unique observed ($I > 2\sigma(I)$) data, $R = 0.077$. Further details of the crystal structure investigation may be obtained from the Fachinformationszentrum Energie, Physik, Mathematik GmbH, D-7514 Eggenstein-Leopoldshafen 2 (FRG), on quoting the depository number CSD-52671, the names of the authors, and the journal citation.

[5] Thus, **1** differs from the diphosphadiboretanes $[\{(tmp)BPMes\}_2]$ [2b], $[\{(tmp)BP(2,4,6\text{-}tBu_3C_6H_2)\}_2]$ [6], and $[\{(tmp)BPCEt_3\}_2]$ [7] in which all the phosphorus centers are pyramidal.

[6] A. M. Arif, J. E. Boggs, A. H. Cowley, J.-G. Lee, M. Pakulski, J. M. Power, *J. Am. Chem. Soc. 108* (1986) 6083.

[7] R. T. Paine, P. Kölle, H. Nöth, *Chem. Ber. 119* (1986) 2681.

[8] For example the BP distance in boron phosphide, BP, is 1.96 Å: J. A. Perri, S. La Placa, B. Post, *Acta Crystallogr. 11* (1958) 310. For further discussion see Ref. [3].

[9] H. V. R. Dias, P. P. Power, unpublished work.

[10] H. Nöth, B. Wrackmeyer in P. Diehl, E. Fluck, R. Kosfeld (Eds.): *NMR Basic Principles and Progress, Vol. 14*, Springer, Berlin 1978.

[11] O. Exner, U. Folli, S. Marcaccioli, P. Vivarelli, *J. Chem. Soc. Perkin Trans. 2 1983*, 757.

Proof of the (*S,S*) Configuration of (−)-Bissetone by Synthesis from D-Glucose**

By *Manfred Brehm, William G. Dauben, Peter Köhler,* and *Frieder W. Lichtenthaler**

Dedicated to Professor Klaus Hafner on the occasion of his 60th birthday

The synthesis of enantiomerically pure non-carbohydrate natural products from readily available sugars is only of practical value if the reactions utilized and the number of steps lead to a high overall yield of product, if simple reagents and no complex separations are used, and if the reaction sequence can be transformed to a 10–100-g scale. Such practical criteria normally make it necessary to transform a sugar overfunctionalized with chirality and hydroxyl groups into an enantiomerically pure building block containing one or two chiral centers and suitable functional groups. The efficiency of the preparation of this building block is decisive for the practical utility of the planned total synthesis.

A building block meeting these criteria is the dihydropyranone **3**, which is available from D-glucose in six steps.[1] We report here a greatly improved procedure[2] which can be run on a 100-g scale and which reduces the former six-step reaction sequence to two one-pot reactions (Scheme 1): D-glucose → hydroxyglucal ester **1** (80%)[3] and hydroxylaminolysis → deoximation → elimination (84% for **1** → **2a** → **2b** → **3**).

Selective monooximation of dihydropyranone **3** liberates, without any side reactions, the second carbonyl group blocked as an enol ester and makes possible the synthesis of (*S,S*)-palythazine, **10**,[4,5] a compound isolated from the salt-water invertebrate *Palythoa tuberculosa*.[6] An isolated

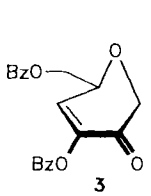

3

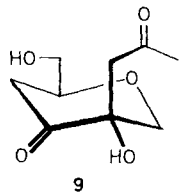

9

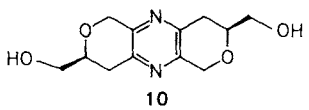

10

[*] Prof. Dr. F. W. Lichtenthaler, Dipl.-Ing. M. Brehm
Institut für Organische Chemie der Technischen Hochschule
Petersenstrasse 22, D-6100 Darmstadt (FRG)
Prof. Dr. W. G. Dauben, Dr. P. Köhler
Department of Chemistry, University of California
Berkeley, California 94720 (USA)

[**] Enantiomerically Pure Building Blocks from Sugars, Part 5. Partially presented at the 4th Eur. Carbohydr. Symp. in Darmstadt, July 13–17, 1987, Abstract A-67. This investigation was supported by the Deutsche Forschungsgemeinschaft (THD) and the National Institute of General Medicine (UCB).—Part 4: F. W. Lichtenthaler, K. Lorenz, W. Y. Ma, *Tetrahedron Lett. 28* (1987) 47.

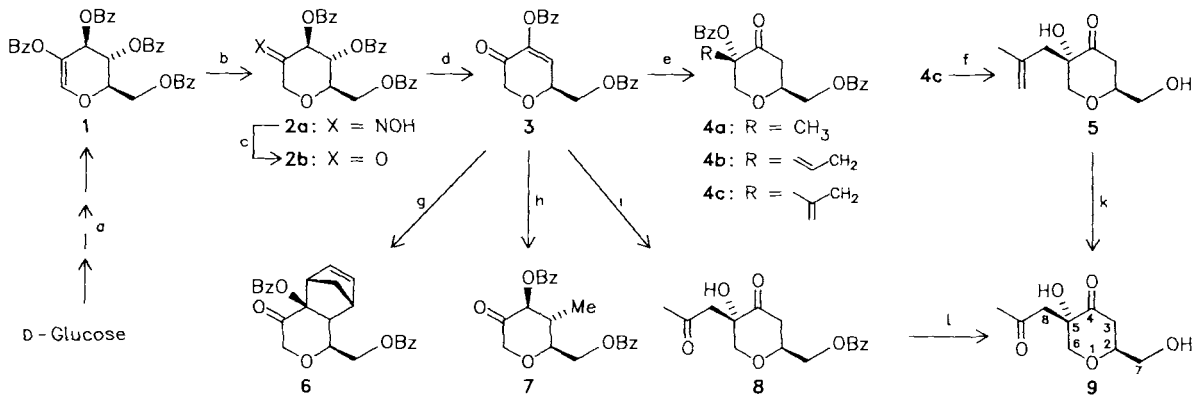

Scheme 1. Synthesis of (−)-bissetone, **9**, from D-glucose. a) Three steps, [3] (80%); b)→c)→d) [2] (84%); e) **3**→**4a**: MeMgI/Et_2O, −78°C, 15 min (69%); **3**→**4b**: $(CH_2{=}CH{-}CH_2)Ti(O\,iPr)_3$, CH_2Cl_2, 15 min, −78°C (85%); **3**→**4c**→**5**: $(CH_2{=}C(CH_3){-}CH_2)Ti(O\,iPr)_3$, CH_2Cl_2, −78°C, then f) NaOMe/MeOH, 15 min, 25°C (83%); g) cyclopentadiene, CH_2Cl_2, 15 kbar, 48 h, 25°C (53%); h) $Li_2Cu_3Me_5$, Et_2O, 30 min, −78°C (40%); i) $MeC(OLi){=}CH_2$, THF, −78°C, 10 min, then H_2O, 2 h, −20°C (60%); k) O_3/HOAc/Zn, 2 h, 25°C (84%); l) NaOMe/MeOH, 12 h, 0°C (92%).

study of the regio- and diastereoselectivities obtainable on **3** with C nucleophiles[7] now led to two different syntheses of (*S,S*)-bissetone, **9**, a constituent of the gorgonian soft coral *Briareum polyanthes*.[8]

The regioselectivities available in addition reactions of **3** naturally depend on the type of reagent and the reaction conditions employed. The steric course of these additions, however, is clearly determined by the envelope-conformation °E of **3**, five nearly coplanar carbon atoms with the ring oxygen above the plane.[9] The cycloaddition of cyclopentadiene to **3** under high-pressure conditions (15 kbar) occurs predominantly (4:1 selectivity) from the α side, i.e., opposite to the ring oxygen, to yield the α-*endo* product **6** (sirup, $[\alpha]_D^{20} = -103$ ($c = 1$, $CHCl_3$),[10] which is of importance for the synthesis of cyclopentanoid natural products by the facile cleavage of the olefinic double bond or by the opening of the pyranoid ring.[7b]

As expected, organocuprates give 1,4-addition products but the reaction leads to a variety of products. However, with $Li_2Cu_3Me_5$, a 40% yield of *C*-methyl-branched tetrahydropyranone **7** as the monohydrate (m.p. = 118–120°C, $[\alpha]_D^{20} = -38$, $CHCl_3$) can be obtained, thus indicating also a definite α selectivity.

With methyllithium or Grignard reagents, the addition to the carbonyl group of the enolone system clearly is the preferred reaction, the primary adduct rearranges by an $O^4 \rightarrow O^3$ benzoyl group migration, normally base-induced during workup,[12] to give a 4-tetrahydropyranone, e.g., **3**→**4a** (m.p. = 125–127°C, $[\alpha]_D^{20} = -89$, $CHCl_3$). The observed (^{1}H-NMR) 4:1 preference of nucleophilic attack from the β side strongly indicates a complexation of Mg in MeMgI with the ring oxygen and the carbonyl groups of **3** in the dominant °E conformation. The lithium enolate of acetone, a suitable C_3 synthon with regard to a synthesis of bissetone, adds with analogous stereoselectivity, affording after aqueous workup the 2-oxopropyl-branched tetrahydropyranone **8**[11] in crystalline form and in a 60% yield, together with 12% of its 5-epimer (syrup, $[\alpha]_D^{20} = -24$, $CHCl_3$). Distinctly higher selectivity of 10:1 in favor of the β-adducts **4b** and **4c** is found with allyl- and methylallyl titanium triisopropoxide, as expected,[13] due to the stronger complexation of the organotitanate with the ring and carbonyl oxygen of **3**. The allyl-branched adduct **4b** (m.p. = 105–106°C, $[\alpha]_D^{20} = 86$, $CHCl_3$) crystallizes from the reaction mixture (85%) whereas the syrupy methylallyl compound **4c**, as a result of its difficult separation from its 5-epimer, is better isolated after debenzoylation to **5**[11] (83% from **3**).

The diketone **8**, of which the configuration of the tertiary C-5 hydroxyl group was unequivocally established by an X-ray structure analysis,[14] constitutes the 7-*O*-benzoyl derivative of bissetone **9**, into which it is converted (92%) upon Zemplén saponification. The methylallyl derivative **5** is also converted into **9** via ozonation followed by reductive workup. The identity of the synthetic **9** with the product isolated from *Briareum polyanthes*[8] is proved by the identity of ^{1}H- and ^{13}C-NMR spectra and by the sign of the rotation. The considerably lower $[\alpha]_D^{20}$ value of the isolated product (oil, −43.6, $c = 4.25$, EtOH)[8] compared with synthetic **9** (sirup, −69.4, $c = 1$, EtOH) clearly indicates that the product isolated from the soft coral (73 mg from 31.3 g of water-soluble material via gel chromatography[8]) was not completely pure. Irrespective of the absolute value, the correspondence of the negative rotations of the synthetic and natural **9** now establishes the absolute configuration, until now unknown, to be (2*S*,5*S*), because the relative configuration was already established[8] and the only possible (*R,R*) alternative would have a positive rotation of at least 43°.

Since both soft-coral constituents palythazine **10** and bissetone **9** possess the (*S,S*) configuration, it is suggestive that the biosynthesis of both compounds proceeds from D-glucose via oxidation and elimination of water, together with transamination and C-branching, most likely through a biosynthetic equivalent of the building block **3**. In this case, the highly efficient syntheses of **9** and **10** from D-glucose (yields of 37% over eight and 26%[4] over nine steps, respectively) follow to a significant degree their biogeneses.

Received: August 18, 1987 [Z 2404 IE]
German version: *Angew. Chem.* 99 (1987) 1318

[1] a) F. W. Lichtenthaler, P. Jarglis, *Tetrahedron Lett.* 21 (1980) 1425; b) F. W. Lichtenthaler, E. S. H. El Ashry, V. H. Göckel, *ibid.* 21 (1980) 1429.

[2] *Experimental procedure* for **1**→**3**: A solution of **1** (115 g, 0.2 mol) [3] and $NH_2OH \cdot HCl$ (55 g, 0.8 mol) in 550 mL of absolute pyridine is kept at 70°C for 14 h and then evaporated to dryness. The residue is dissolved in CH_2Cl_2, extracted repeatedly with 2 N HCl, then aqueous $NaHCO_3$ solution, and dried (Na_2SO_4). Concentration in vacuo and crystallization from ethanol afforded 91 g of **2a** (needles, m.p. = 176–177°C, $[\alpha]_D^{20} = -53$ ($c = 0.5$, $CHCl_3$)), which is suspended in a mixture of 2 N

HCl (100 mL), acetaldehyde (43 mL, 0.75 mmol), and CH_3CN (500 mL) and kept at ambient temperature for 10 h. The resulting solution, containing only **2b** (TLC, silica gel, CCl_4/EtOAc (2:1)), is stirred vigorously with 200 g of solid $NaHCO_3$ for 6 h and then poured into 1.5 L of water. Extraction with CH_2Cl_2 (2 × 300 mL), washing of the combined organic layers with water, drying (Na_2SO_4), and evaporation of the solvent leaves a yellowish syrup, which crystallizes when dissolved in 250 mL of hot methanol: 59.4 g of **3** (84% from **1**), colorless crystals, m.p. = 104–105 °C, $[\alpha]_D^{20} = -16$ ($c = 1$, $CHCl_3$); ^{1}H-NMR (300 MHz, $CDCl_3$): $\delta = 4.35$ (dd, 2-H_a), 4.54 (d, 2-H_b), 4.55 and 4.65 (2 dd, 1 H each, 7-H_2), 5.01 (m, 6-H), 6.86 (d, 5-H), $J(2a,2b) = 16.4$, $J(2a,6) = 1.9$, $J(5,6) = 2.0$, $J(6,7) = 4.8$, and 5.9, $J(7,7) = 11.8$ Hz.

[3] The preparation of **1** from D-glucose by benzoylation [3b], treatment with HBr/acetic acid [3c], and elimination of HBr [3d] gives total yields around 60%, which, after our experience with mole-scale reactions, can be raised to 80% by renouncing purification of the intermediates; b) K. Maurer, R. Böhme, *Ber. Dtsch. Chem. Ges. 69* (1936) 1399; c) H. G. Fletcher, Jr., *Methods Carbohydr. Chem. 2* (1963) 226; d) R. J. Ferrier, G. H. Sankey, *J. Chem. Soc. C 1966*, 2339.

[4] P. Jarglis, F. W. Lichtenthaler, *Angew. Chem. 94* (1982) 140; *Angew. Chem. Int. Ed. Engl. 21* (1982) 141.

[5] F. W. Lichtenthaler in Atta-ur-Rahman (Ed.): *Natural Products Chemistry*, Springer, Heidelberg, New York 1986, p. 227 ff.

[6] D. Uemura, Y. Toya, I. Watanabe, Y. Hirata, *Chem. Lett. 1979*, 1481.

[7] a) P. Köhler, planned *Dissertation*, Technische Hochschule Darmstadt; b) B. Kowalczyk, *Ph. D. Thesis*, University of California, Berkeley 1988.

[8] J. H. Cardellina II, R. L. Hendrickson, K. P. Manfredi, S. A. Strobel, J. Clardy, *Tetrahedron Lett. 28* (1987) 727.

[9] This conformation is in agreement with the $J(5,6)$ values of about 2 Hz, and X-ray structure analyses of a series of analogous pyranoid enolone esters as well as force field calculations with the π-SCF-LCAO-MO method further confirm the conclusion.

[10] The configurational assignment was made by means of the position of the olefinic protons, which resonate at $\delta = 6.12$ and 6.59 in **6**, whereas they collapse to a singlet at $\delta = 6.48$ in the α-*exo* product (sirup, 12%, $[\alpha]_D^{20} = -35$, $CHCl_3$) [7b].

[11] The new compounds are characterized by ^{1}H-NMR, ^{13}C-NMR, IR, and MS spectra and elemental analysis. For example **5**: syrup, $[\alpha]_D^{20} = -148.6$ ($c = 1.1$, $CHCl_3$), ^{1}H-NMR (300 MHz, $CDCl_3$): $\delta = 4.87$ and 4.77 (2 m, 1 H each, $=CH_2$), 4.08 and 3.34 (2 d, 1 H each, 6-H_2), 2.89 and 2.45 (2 dd, 1 H each, 3-H_2), 2.76 and 2.52 (2 d, 1 H each, 8-H_2), 2.17 (t, 1 H, 7-OH), 1.75 (s, 3 H, Me), 1.69 (s, 1 H, 5-OH), $J(2,3) = 2.4$ and 11.5, $J(3,3) = 13.9$, $J(6,6) = 11.2$ Hz.—**8**: needles, m.p. = 103–105 °C, $[\alpha]_D^{20} = -31.6$ ($c = 1.2$, $CHCl_3$), ^{1}H-NMR (300 MHz, $CDCl_3$): $\delta = 2.20$ (s, 3 H, 10-H_3), 2.72 and 2.84 (2 dd, 1 H each, 3-H_2), 3.13 and 3.34 (2 d, 1 H each, 9-H_2), 3.26 and 4.04 (2 d, 1 H each, 6-H_2), 4.00 (m, 1 H, 2-H), 4.2 (br. s, 1 H, OH), 4.41 and 4.48 (2 dd, 1 H each, 7-H_2), $J(2,3e) = 3.1$, $J(2,3a) = 11.5$, $J(2,7) = 4.0$ and 5.5, $J(3,3) = 13.3$, $J(6,6) = 11.4$, $J(7,7) = 11.9$, $J(8,8) = 16.6$ Hz.

[12] F. W. Lichtenthaler, U. Kraska, S. Ogawa, *Tetrahedron Lett. 1978*, 1323; F. W. Lichtenthaler, S. Nishiyama, P. Köhler, H. J. Lindner, *Carbohydr. Res. 136* (1985) 13.

[13] M. T. Reetz, *Top. Curr. Chem. 106* (1982) 24; B. Weidmann, D. Seebach, *Angew. Chem. 95* (1983) 18; *Angew. Chem. Int. Ed. Engl. 22* (1983) 37.

[14] H. J. Lindner, Technische Hochschule Darmstadt, unpublished results.

A New Mechanism For Superconductivity**

By *Michael J. S. Dewar**

The recent discovery[1,2] of high temperature superconductivity in certain mixed copper oxides has aroused much attention, not only because of possible practical applications but also because it cannot easily be explained in terms of the conventional Bardeen-Cooper-Schrieffer (BCS) mechanism.[3] Here, a radically different alternative is suggested, based on electron hopping between atoms of a metal in two different valence states under the control of two cooperating lattice vibrations. Other interpretations have involved variants of BCS theory, being likewise based on the conventional band theory of solids and electron–phonon coupling. The mechanism suggested here postulates a strong coupling between pairs of lattice vibrations and electron hopping, leading to a breakdown of the Born-Oppenheimer approximation in a manner reminiscent of that involved in the Jahn-Teller effect. Such a situation cannot be discussed in terms of conventional band theory because this rests on the Born-Oppenheimer approximation. While the possibility that electron hopping might be involved in these new materials has been recognized,[4,5] the essential feature of the mechanism suggested here is novel.

The basic idea will be illustrated by a specific example, i.e. a possible interpretation of superconduction in the species of greatest current interest, yttrium barium copper oxide (YBCO). Its optimum composition ($YBa_2Cu_3O_7$) corresponds to a situation where the copper atoms are in a mixed valence state, one-third trivalent (Cu^{III}) and two-thirds divalent (Cu^{II}). Recent studies[2,4] indicate that YBCO has a layer structure. Two layers (A) consist of square arrays of copper atoms linked by oxygen, while a third (B) contains parallel linear arrays of CuO_2 units linked by oxygen. The A layers are separated by the yttrium ions and the A and B layers by barium. The optimum composition and crystal symmetry suggests that either the copper atoms in the A layers are divalent and those in the B layer trivalent, or that the copper in the A layers is in a mixed valence state, half Cu^{II} and half Cu^{III}, while that in the B layer is Cu^{II}. We assume the latter. Each copper atom in each layer is linked to four oxygen atoms in an approximately square planar geometry, with longer spacings to the atoms (copper or oxygen) above and below. This is the geometry that would be expected for Cu^{II} or Cu^{III}, the d_{z^2} AO being doubly occupied while the $dCu_{x^2-y^2}$ AO is singly occupied (Cu^{II}) or empty (Cu^{III}).

Consider a linear array, $(-Cu-O-)_n$, of CuO units along the x direction in an A layer, with Cu^{II} and Cu^{III} alternating (Fig. 1). The valence states are expected to alternate because of the coulombic repulsions between the Cu^{III} ions. In situations of this kind, the distinction between different valence states is usually eliminated by resonance between them. Here, however, the two states differ in geometry, the CuO bonds being shorter for Cu^{III} than for Cu^{II}, and the coupling between the Cu atoms is small. It is therefore reasonable to suppose that Peierls-type distortion will lead to localization (Fig. 1a).

Consider the antisymmetric lattice vibration (ν_1) indicated by the full arrows in Figure 1a. In the phase indicated, the y-Cu^{II}–O bonds are shrinking while the y-Cu^{III}–O bonds are stretching. If the amplitude is sufficient to reverse the average CuO bond lengths round the two Cu atoms, electron transfer will occur, leading to an interchange of Cu^{II} and Cu^{III} with a parallel change in the lengths of the x-CuO bonds (see Fig. 1b). Furthermore, *all* the electron transfers in the array will take place in the same direction, leading to a net transfer of negative charge. If the amplitude of the corresponding zero point vibration is sufficient, the transfer of charge will take place spontaneously, without any need for external stimulus. Each half cycle of the vibration will lead to a similar transfer of charge between adjacent Cu atoms.

The direction in which charge transfer occurs will, however, be random because at the instant when the CuO distances are equal, the Cu atoms are equivalent. The direction of each electron transfer is not related to the previous one nor are the transfers in different arrays correlated. An applied electric field will bias the transfers and so lead to a flow of electrons—but only so long as the potential is ap-

[*] Prof. Dr. M. J. S. Dewar
Department of Chemistry, The University of Texas at Austin
Austin, TX 78712 (USA)

[**] This work was supported by the Air Force Office of Scientific Research and the Robert A. Welch Foundation.

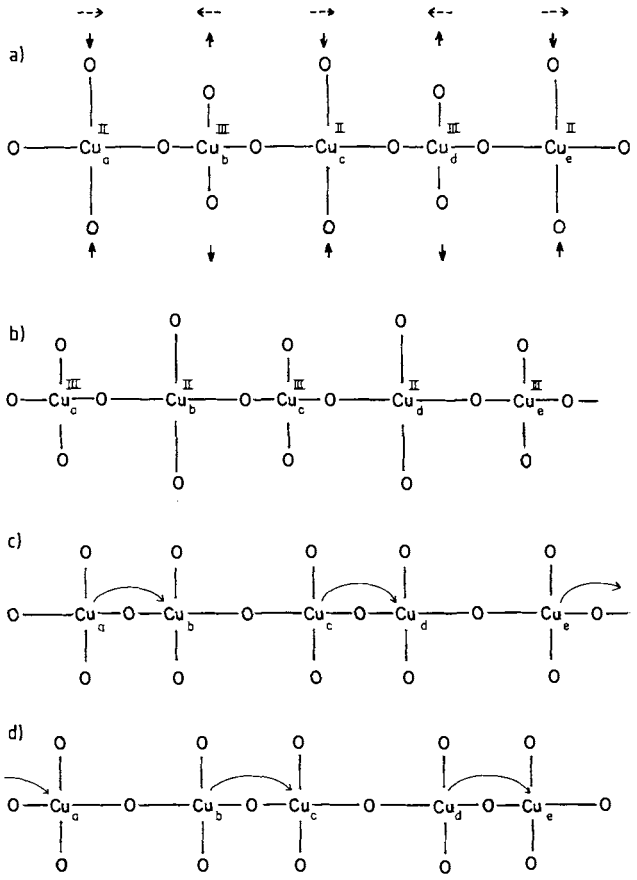

Fig. 1. Schematic representation of the proposed mechanism for superconductivity by application to a copper oxide chain. The differences between the CuO bond lengths are exaggerated, for clarity.

plied. Biassing each transfer involves a decrease in randomness and hence of entropy. For current to continue to flow, this must be continuously compensated. This mechanism, which is similar to that suggested by *Simon*,[3] thus provides a possible mode of conduction, not of superconduction.

Consider now the second lattice vibration (ν_2) indicated by broken arrows in Figure 1a. This leads to an alternate increase and decrease in the distance between pairs of adjacent Cu atoms. If these distances are unequal at the instant when ν_1 has made the Cu atoms equivalent, electron transfer will take place preferentially between pairs of Cu atoms that are closer together as indicated by the curved arrows in Figure 1c. If the two vibrations ν_1 and ν_2 have identical frequencies, the Cu-Cu distances will have inverted at the time of the next electron transfer, which will consequently tend to take place *in the same direction as the first* (see Fig. 1d). Cooperation of the two vibrations thus leads to a continuous unidirectional flow of electrons, which will continue as long as the vibrations remain synchronized. Establishing the flow of current will require energy both to compensate for the decrease in entropy involved in synchronizing the vibrations and to establish the corresponding magnetic field. Once the situation is established, the flow of current will continue without any need for further stimulus.

Consider one of the A (copper oxide) layers in YBCO. For reasons indicated above, alternate Cu atoms should be divalent (Cu^{II}) and trivalent (Cu^{III}) (see Fig. 2). The lattice vibration ν_1 (vertical arrows in Fig. 2) will lead to an oscillation of charge between adjacent Cu atoms along each x-$(CuO)_n$ array. The direction of transfer will be modulated by the lattice vibration ν_2 (horizontal arrows in Fig. 2). If the vibrations have similar frequencies and if the phase relation between them is appropriate, charge transfer will occur not only in the same direction at every vibration but also in the same direction for all the x-$(CuO)_n$ arrays in the crystal. Furthermore, once the vibrations have been synchronized, the flow of electrons will continue without any further stimulus. This clearly provides a mechanism for superconduction.

The situation considered here bears an obvious parallel to that involved in the Jahn-Teller effect. In both cases, a vibration, involving nuclear motion, leads to large changes in the electronic wave function and the Born-Oppenheimer approximation is therefore inapplicable. Neither of the two vibrations can be treated in conventional terms, involving separation of electronic and nuclear variables in the respective wave functions. The motions of electrons and atomic nuclei are strongly coupled in the superconducting state. For the proposed mechanism to operate, ν_1 and ν_2 have to be exactly synchronized. Since both involve similar kinds of vibration, their frequencies would be expected to be similar in a classical model, but not identical. The strong electron-phonon coupling should pull them into resonance. Note again that no work has to be done to maintain this relationship; only to establish it in the first place.

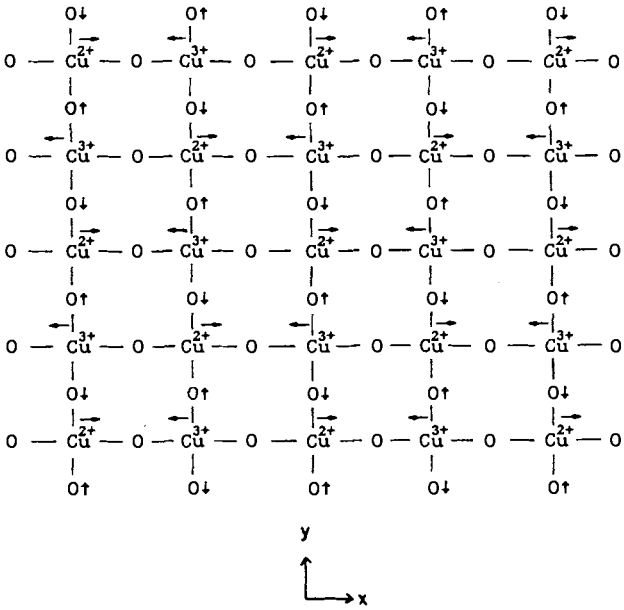

Fig. 2. Suggested mechanism for superconductivity in an A-type plane of YBCO (see text).

In this mechanism, superconduction involves the motion of single electrons along linear CuO arrays. It is possible that the electrons in adjacent A-type layers in YBCO may be coupled. If so, the electron transfers could be regarded as taking place in pairs, corresponding to conduction by a pair-hopping mechanism. However, there seems no advantage in this, particularly since, in the present model, *all* the migrating electrons in the whole crystal move in concert. Even if electron pairs are involved, these would in any case bear no relation to the Cooper pairs of BCS theory.

In the present model, superconduction can be interrupted only by the intervention of other lattice vibrations

that disrupt the phase relationship between ν_1 and ν_2. If this could be effected by other zero point lattice vibrations, the material in question would not be a superconductor in the first place. Higher vibrational modes must therefore be involved whose wavelengths resemble the short wavelength vibrations involved in superconduction (see Fig. 2). The energies of the corresponding quanta will be large, corresponding to frequencies near the top of the phonon band, and the temperature needed to excite them will be correspondingly high. The high transition temperature of YBCO, which has proved difficult to explain in terms of BCS theory, can thus be understood immediately in terms of the mechanism presented here. Indeed, superconduction by the present mechanism might well take place at higher temperatures than 90 K. The critical temperature will depend not only on the energies of interfering phonon quanta but also on the ease with which ν_1 and ν_2 can be uncoupled. This in turn should depend on the frequencies in the uncoupled state. Similar remarks apply to the remarkable insensitivity of YBCO to magnetic fields. Since a magnetic field does not alter the vibration frequencies of a crystal significantly, it should not easily interfere with superconduction by the present mechanism.

Note that above the critical temperature, where the electron-two-phonon coupling is disrupted, materials of this kind should show no unusual behavior. YBCO acts in fact as a poor metallic conductor at higher temperatures.

Another significant feature of YBCO is the insensitivity of its transition temperature to $^{16}O/^{18}O$-isotopic exchange. This finding is inconsistent with a BCS-type mechanism involving electron-phonon coupling. With the mechanism presented here, however, it would be expected, since such an exchange should affect the critical vibration frequencies to comparable extents. For superconduction to be possible, the frequencies only need to be similar. Their absolute values are irrelevant.

The present mechanism need not be confined to copper compounds. The only requirement is a crystal containing a linear array of a metal in two valence states where cooperation of two lattice vibrations leads to conduction by unidirectional electron-hopping. An analogous mechanism may operate in the case of bismuth oxide superconductors[6]—with participation of Bi^{III} and Bi^{V} centers.[5] There is also no need for the two valence states to alternate. The same mechanism could apply in YBCO if every third Cu atom in each A layer were trivalent. The wavelengths of the two relevant vibrations in the crystal would, however, be one-and-a-half times greater and the energies required to excite interfering vibrations should be correspondingly less. Samples of YBCO with compositions $YBa_2Cu_3O_{7-x}$ ($x > 0$) still superconduct, but less effectively, the larger x, i.e. the transition temperature decreases with increasing x.

In conclusion, one possible experimental test for the mechanism which I have presented here may be noted: Since the critical temperature is set by the point at which specific lattice vibrations are excited, superconductivity might be interrupted by irradiation with a tuned infrared laser at an appropriate frequency without heating the sample above its critical temperature.

Received: August 20, 1987;
revised: September 25, 1987 [Z 2407 IE]
German version: *Angew. Chem. 99* (1987) 1313

[1] K. A. Müller, J. D. Bednorz, *Proc. Natl. Acad. Sci. USA 84* (1987) 4678.
[2] C. W. Chu, *Proc. Natl. Acad. Sci. USA 84* (1987) 4681.
[3] W. Buckel: *Supraleitung. Grundlagen und Anwendung*. Physik Verlag, Weinheim 1977.
[4] H. Steinfink, J. S. Swinnea, Z. T. Sui, H. M. Hsu, J. B. Goodenough, *J. Am. Chem. Soc. 109* (1987) 3348.
[5] A. Simon, *Angew. Chem. 99* (1987) 602; *Angew. Chem. Int. Ed. Engl. 26* (1987) 579.
[6] A. W. Sleight, J. L. Gilsson, P. E. Bierstedt, *Solid State Commun. 17* (1975) 27.

Superconductivity—a New Classification of the Chemical Bonding in the Solid Allows to Understand Its Occurrence**

By *Werner Urland**

The chemical bonding in the solid state is traditionally divided into ionic, covalent, and metallic bonding. Compounds are classified according to these three types of bonding and their transitions,[1] a classification which is conveniently represented by a triangular plot corresponding to the phase diagrams of ternary systems.[2] The main aim of this communication is to present a new classification of the chemical bonding in the solid state which provides an insight into the occurrence of superconductivity.[3] The superiority of the new classification, which is *not* tied to the Periodic Table, lies in the fact that, in addition to the electric properties, also the magnetic properties of the solid as well as intermolecular forces are taken into consideration. The classification presented here represents a consequent further development of the ideas of *Anderson*[4] and *Woolley*.[5]

The bonding energy and therefore the chemical bonding in the solid is mainly determined by delocalization, correlation and localization of s, p, and d electrons with the respective energy contributions E_{Del}, E_{Cor}, and E_{Loc}.

E_{Del} means the sum of the energies of the electrons moving with a certain momentum $(h/2\pi)k$ (itinerant electrons with the energy $E(k)$) and arises theoretically as a one-electron problem from band theory. The width of the corresponding incompletely occupied band can be regarded as a measure of the magnitude of E_{Del} and increases with the overlap of the atoms. In the case of free electrons E_{Del} equals the kinetic energy of the electrons.

E_{Cor} is the energy of the spin-dependent electron-electron interaction. It takes into account that the equally-charged electrons avoid each other and favors, in accord with Hund's first rule, high-spin arrangements and therefore paramagnetism in isolated ions. Paramagnetism is theoretically treated by different versions of the formalism of ligand field theory, e.g. by the angular overlap model.[6,7] E_{Cor} leads in solid compounds with more or less strong overlapping of atomic orbitals—beginning delocalization and therefore increase of the ratio E_{Del}/E_{Cor}—to magnetic interaction and the appearance of cooperative magnetic phenomena, e.g. antiferromagnetism, ferromagnetism, as well as spin-density waves. Antiferromagnetism can be described in terms of the formalism of superexchange, which increases with increasing E_{Del}/E_{Cor}.[4] A large increase in the overlap of the atomic orbitals (large increase in E_{Del}/E_{Cor}) finally leads to such a large gain of kinetic energy of the electrons that the repulsion energy of the closely approaching electrons will be overcome and a complete delocalization will result.

[*] Prof. Dr. W. Urland
Institut für Anorganische Chemie der Universität
Callinstrasse 9, D-3000 Hannover 1 (FRG)

[**] This work was supported by the Fonds der Chemischen Industrie.

E_{Loc} means the electron-phonon interaction energy (vibronic coupling energy). If E_{Loc} is larger than E_{Del} a localization of electrons will occur such that the delocalized (itinerant) electrons become electron pairs with antiparallel spins. If we imagine a hypothetical hydrogen metal with a half-filled 1s band (E_{Del}), strong electron-phonon interaction (E_{Loc}) will lead to a Peierls distortion with the formation of H↑↓H-molecules held together by intermolecular forces.[8] (The Peierls distortion corresponds to the known Jahn-Teller distortion in coordination chemistry.) The electron pairs formed by Peierls distortion are the well-known Lewis electron pairs of classical covalent bonding in molecular chemistry. The Peierls instability helps a great deal in undestanding the bonding and structure of elements and compounds like, e.g. P (black), As, Sb, Bi, β-Sn, C (diamond), NaCl and $(SN)_x$.[8,9] Besides the demonstrated localization of an electron pair by dimerization because of electron-phonon coupling in H_2 (E_{Loc}), a localization owing to inner disproportionation is possible in the case of linear metal-anion-metal groups, leading to mixed-valence compounds like, e.g. $(Ag^{I}Ag^{III})O_2$,[10,11] $Ba_2(Bi^{III}Bi^{V})O_6$,[12] or $Cs_2(Au^{I}Au^{III})Cl_6$.[13]

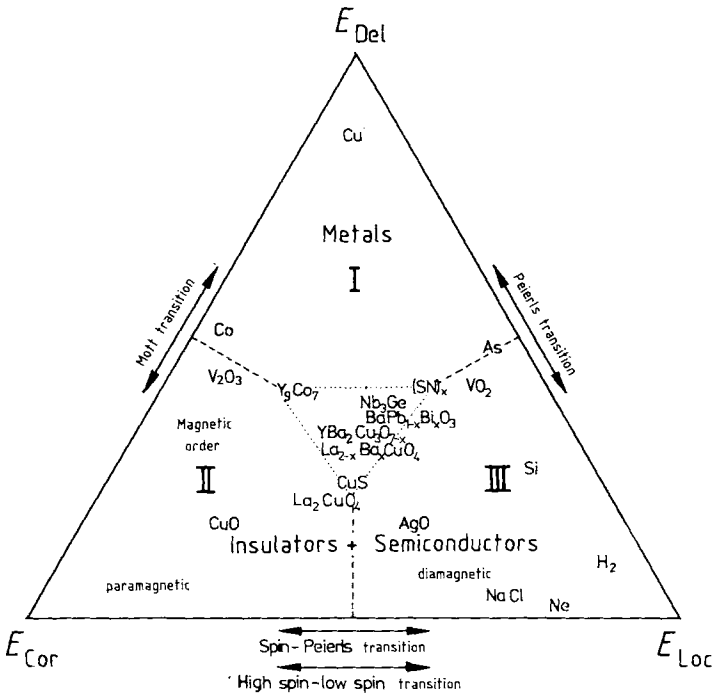

Fig. 1. "Phase diagram of chemical bonding in the solid state" providing an explanation for the occurrence of superconductivity. (Approximate values for x in the formulas are given in the text.)

The chemical bonding in the solid state will now be classified in a new fashion according to the energies E_{Del}, E_{Cor}, and E_{Loc} and their transitions. The classification is again conveniently represented by an equilateral triangle, with the vertices corresponding to the three energies (cf. Fig.1). Solid elements and compounds can now be classified in this "phase diagram" (for atmospheric pressure) according to respective magnitudes of E_{Del}, E_{Cor}, and E_{Loc}. One distinguishes between three 'phase regions':

I $E_{Del} > E_{Cor}, E_{Loc}$: metals, e.g. Cu, Ag

II $E_{Cor} > E_{Del}, E_{Loc}$: paramagnetic and magnetically ordered insulators (and semiconductors), e.g. complex compounds of transition metals; CuO, NiO[14]

III $E_{Loc} > E_{Cor}, E_{Del}$: diamagnetic insulators (and semiconductors), e.g. ionic crystals (NaCl), solid noble gases (Ne), molecular crystals (H_2), covalent crystals ($C_{diamond}$, Si), and mixed-valence compounds of class I[15] (AgO)

Solids with especially interesting physical properties are found to lie near to the broken 'boundary lines' (cf. Fig. 1), i.e. there, where the transitions between the 'phase regions' lie:

Transition I-II $E_{Cor} \approx E_{Del} > E_{Loc}$: compounds showing the Mott transition, e.g. V_2O_3[14]; magnetically ordered metals, e.g. α-Fe, Co, Ni, Cr[14]

Transition II-III $E_{Cor} \approx E_{Loc} > E_{Del}$: compounds showing high-spin (paramagnetic) -low-spin (diamagnetic) transition, e.g. complexes of $Fe^{2\oplus}$[16] or spin-Peierls transition, e.g. tetrathiafulvalene—$Au[S_2C_2(CF_3)_2]_2$[17]

Transition I-III $E_{Del} \approx E_{Loc} > E_{Cor}$: Peierls systems, e.g. semimetals: P (black), As, Sb, Bi[8]; VO_2[14] as well as substances exhibiting the phenomena of charge-density-waves[18] and bipolarons[19]

Solids which have to be classified near to the 'triple point' (cf. dotted triangle in Fig. 1) show superconductivity at low temperatures (transition temperature T_c):

$E_{Del} \approx E_{Cor} \approx E_{Loc}$: for example Y_9Co_7 ($T_c = 2.7$ K)[20], Nb_3Ge ($T_c = 23.2$ K)[3], CuS ($T_c = 1.35$ K)[15], $(SN)_x$ ($T_c = 0.26$ K)[3], $BaPb_{1-x}Bi_xO_3$ with $x \approx 0.3$ ($T_c = 13$ K)[21], $La_{2-x}Ba_xCuO_4$ with $x \approx 0.2$ ($T_c \approx 30$ K)[22], and $YBa_2Cu_3O_{7-x}$ with $x \approx 0.2$ ($T_c \gtrsim 90$ K)[23].

Thus, the occurrence of superconductivity in the solid would appear to be associated with the cooperative action of electron delocalization, localization and correlation with comparable energy contributions. High transition temperatures are found for solids where this cooperative action concerning the energy contributions is an optimum. The energy contributions can be roughly estimated from the chemical and physical properties as well as from theoretical and experimental work on the given or analogous compounds.[8,14,15,20,24-27] After what has been said the phenomenon of superconductivity can be understood in terms of the basis of the theory of *Bardeen*, *Cooper*, and *Schrieffer*—the formation of Cooper pairs[3]—as follows: localization leads to the pairing of electrons, delocalization to conduction, and correlation maintains the pairing of electrons in the superconducting state.

This may be exemplified more closely in the case of the high-temperature superconductors $La_{2-x}Ba_xCuO_4$ ($x \approx 0.2$)[22] and $YBa_2Cu_3O_{7-x}$ ($x \approx 0.2$).[23] Electron delocalization is given by the formation of a nearly half-filled Cu-$3d_{x^2-y^2}$-O 2p band. The bandwidth is maximal as the energies of the Cu 3d and O 2p orbitals practically agree.[28] Electron correlation can be assumed with reference to the compounds CuO and La_2CuO_4, where magnetic susceptibility measurements[25,26] indicate antiferromagnetism (Cu-O-Cu-superexchange). Electron localization can be understood as a Peierls distortion of a nearly half-filled band, as in the case of the above described hydrogen, or as an inner disproportionation if one compares $Cu^{II}O$ with homologous $(Ag^{I}Ag^{II})O_2$ (disproportionation in a linear metal-O-metal group). This all comes practically true also for La_2CuO_4 with copper in the oxidation state +2 which shows no superconductivity at the investigated temperatures.[26] Obviously in this case the influence of correlation is too large and that of delocalization is too small. Only the

increase in the ratio E_{Del}/E_{Cor} by the formation of mixed-valence systems with copper in the oxidation state $\approx +2.2$ bring the compounds discussed here near to the "triple point" (cf. Fig. 1).[29] But why does $YBa_2Cu_3O_{7-x}$ ($x \approx 0.2$) have a higher transition temperature than $La_{2-x}Ba_xCuO_4$ ($x \approx 0.2$)? An answer to this lies in the different structures of the two compounds. $YBa_2Cu_3O_{7-x}$ ($x \approx 0.2$) crystallizes in an orthorhombic structure which is characterized by stacked slabs separated by $Y^{3\oplus}$ ions. In turn the slabs consist of alternate Cu-O and Ba-O layers the Cu-O layers being about 4.2 Å apart.[30] $La_{2-x}Ba_xCuO_4$ ($x \approx 0.2$) crystallizes in the K_2NiF_4-structure, where Cu-O layers are separated by two La/Ba-O layers leading to a distance of about 6.6 Å from each other.[31] In the yttrium compound antiferromagnetic correlations (increase of E_{Del}/E_{Cor} by superexchange) between the Cu-O layers should be significantly larger than in the lanthanum compound; this would mean a closer approach to the "triple point" in Figure 1, and thus a higher transition temperature. Replacement of barium by the smaller strontium in this yttrium compound should therefore lead, as in the case of the lanthanum compound,[32] to a further increase in the transition temperature if no change of the structure occurs.

The concepts developed here embrace those of other authors,[33] e.g. the resonating-valence-bond model (cooperative action of correlation and delocalization),[34] the bipolaron model (localization and delocalization)[35] and the 'chemical model' (localization and delocalization).[36] The theoretical considerations outlined here do not allow the calculation of transition temperatures, but lay out the framework for a comprehensive theory of superconductivity.

Received: September 30, 1987 [Z 2451 IE]
German version: *Angew. Chem. 99* (1987) 1316

[1] Holleman-Wiberg: *Lehrbuch der Anorganischen Chemie*, de Gruyter, Berlin 1985, p. 116ff.
[2] W. L. Jolly: *Modern Inorganic Chemistry*, McGraw-Hill, New York 1984, p. 264ff.
[3] W. Buckel: *Supraleitung, Grundlagen und Anwendung*, Physik-Verlag, Weinheim 1984.
[4] P. W. Anderson in G. T. Rado, H. Suhl (Eds.): *Magnetism, Vol. 1*, Academic Press, New York 1963.
[5] R. G. Woolley, *Int. Symp. Molecules in Physics, Chemistry and Biology dedicated to Prof. R. Daudel*, Paris 1986.
[6] W. Urland, *Chem. Phys. Lett. 46* (1977) 457.
[7] W. Urland, S. R. Niketić, *Chem. Phys. Lett. 129* (1986) 592.
[8] a) R. Hoffmann, *Angew. Chem. 99* (1987) 871; *Angew. Chem. Int. Ed. Engl. 26* (1987) 846; b) T. A. Albright, J. K. Burdett, M. H. Whangbo: *Orbital Interactions in Chemistry*, Wiley, New York 1985.
[9] J. K. Burdett, *Prog. Solid State Chem. 15* (1984) 173.
[10] V. Scatturin, P. L. Bellon, A. J. Salkind, *J. Electrochem. Soc. 108* (1961) 819.
[11] H. P. Fischer, *Diplomarbeit*, Universität Hannover 1987.
[12] D. E. Cox, A. W. Sleight, *Acta Crystallogr. B35* (1979) 1.
[13] J. C. M. Tindemans-van Eijndhoven, G. C. Verschoor, *Mater. Res. Bull. 9* (1974) 1667.
[14] J. B. Goodenough: *Magnetism and the Chemical Bond*, Interscience, New York 1963.
[15] M. B. Robin, P. Day, *Adv. Inorg. Chem. Radiochem. 10* (1967) 247.
[16] P. Gütlich, *Struct. Bonding (Berlin) 44* (1981) 83.
[17] L. J. de Jongh, H. B. Brom, H. J. M. de Groot, T. W. Hijmans, W. H. Korving, *J. Magn. Magn. Mater. 54-57* (1986) 1447.
[18] R. L. Withers, J. A. Wilson, *J. Phys. C: Solid State Phys. 19* (1986) 4809.
[19] B. K. Chakraverty, *J. Phys. (Paris) 42* (1981) 1351.
[20] B. V. B. Sarkissian, J. L. Tholence, *J. Magn. Magn. Mater. 54-57* (1986) 1525.
[21] A. W. Sleight, J. L. Gillson, P. E. Bierstedt, *Solid State Commun. 17* (1975) 27.
[22] J. G. Bednorz, K. A. Müller, *Z. Phys. B64* (1986) 189.
[23] M. K. Wu, J. R. Ashburn, C. J. Torng, P. H. Hor, R. L. Meng, L. Gao, Z. J. Huang, Y. Q. Wang, C. W. Chu, *Phys. Rev. Lett. 58* (1987) 908.
[24] T. M. Rice, L. Sneddon, *Phys. Rev. Lett. 47* (1981) 689.
[25] B. N. Figgis, J. Lewis, *Prog. Inorg. Chem. 6* (1964) 37.
[26] R. L. Greene, H. Maletta, T. S. Plaskett, J. G. Bednorz, K. A. Müller, *Solid State Commun. 63* (1987) 379.
[27] D. Vaknin, S. K. Sinha, D. E. Moncton, D. C. Johnston, J. M. Newsam, C. R. Satinya, H. E. King, Jr., *Phys. Rev. Lett. 58* (1987) 2802.
[28] C. M. Varma, S. Schmitt-Rinck, E. Abrahams, *Solid State Commun. 62* (1987) 681.
[29] K. Sreedhar, T. V. Ramakrishnan, C. N. R. Rao, *Solid State Commun. 63* (1987) 835.
[30] W. I. F. David, W. T. A. Harrison, J. M. F. Gunn, O. Moze, A. K. Soper, P. Day, J. D. Jorgensen, D. G. Hinks, M. A. Beno, L. Soderholm, D. W. Capone II, I. K. Schuller, C. U. Segre, K. Zhang, J. D. Grace, *Nature (London) 327* (1987) 310.
[31] H. H. Wang, U. Geiser, R. J. Thorn, K. D. Carlson, M. A. Beno, M. R. Monaghan, T. J. Allen, R. B. Proksch, D. L. Stupka, W. K. Kwok, G. W. Crabtree, J. M. Williams, *Inorg. Chem. 26* (1987) 1190.
[32] R. J. Cava, R. B. van Dover, B. Batlogg, E. A. Rietman, *Phys. Rev. Lett. 58* (1987) 408.
[33] T. M. Rice, *Z. Phys. B67* (1987) 141.
[34] P. W. Anderson, *Science 235* (1987) 1196.
[35] N. Mott, *Nature (London) 327* (1987) 185.
[36] A. Simon, *Angew. Chem. 99* (1987) 602; *Angew. Chem. Int. Ed. Engl. 26* (1987) 579. See also M. J. S. Dewar, *ibid. 99* (1987) 1313 and *26* (1987) 1273.

A Facile, General Route to Bridge-Annelated [2.2]Paracyclophanedienes**

By *Oliver Reiser, Stefen Reichow,* and *Armin de Meijere**

Dedicated to Professor Klaus Hafner and to Professor Emanuel Vogel on the occasion of their 60th birthdays

The [2.2]paracyclophanediene **7a**,[1] benzoannelated at both bridges, contains two rigid, orthogonally oriented biphenyl moieties and thereby not only exhibits unusual structural features but can also be expected to have interesting chemical and physical properties. However, in the recently reported synthesis[2] **7a** was formed in such moderate yields as to make a detailed investigation of its chemical behavior rather cumbersome.[3] We report here on the first results of a new synthetic strategy which not only allows the parent compound **7a** but also a whole series of analogous bridge-annelated [2.2]paracyclophanedienes to be synthesized with little effort.

The *1,9- and 1,10-dibromodienes* **1**[5] were readily obtained from a mixture of the 1,1,9,9- and 1,1,10,10-tetrabromo[2.2]paracyclophanes[4,5] by dehydrobromination with potassium *tert*-butoxide (*t*BuOK) in *tert*-butyl methyl ether (MTBE). Subsequent addition of two Br_2 gave a mixture of the hexabromides **2**[6] (71% yield), which upon renewed dehydrobromination (*t*BuOK, MTBE) smoothly afforded (56%) 1,2,9,10-tetrabromo[2.2]paracyclophanediene **3** (Scheme 1). The four vinylic bromine substituents in **3** could be conveniently replaced by alkenyl substituents in a Heck-type[7] palladium-catalyzed reaction suitably modified as described by *T. Jeffery*[8] (see Table 1). Whereas the coupling with styrene **4c**, *p*-fluorostyrene **4d**, and methyl acrylate **4f** proceeds in good yields with potassium carbonate as base, sodium hydrogencarbonate was found to

[*] Prof. Dr. A. de Meijere, Dipl.-Chem. O. Reiser, S. Reichow
Institut für Organische Chemie der Universität
Martin-Luther-King-Platz 6, D-2000 Hamburg 13 (FRG)

[**] This work was supported by the Stiftung Volkswagenwerk, by the Fonds der Chemischen Industrie, and by Hoechst AG, BASF AG, Hüls AG, and E. Merck GmbH (gifts of chemicals). *O. R.* thanks the Studienstiftung des Deutschen Volkes for a stipend. We thank Prof. Dr. *W. Lüttke*, Göttingen, for recording the UV spectra of **7c** and **9**.

be more suitable for the reaction with trimethylvinylsilane **4b** and the readily polymerizable acrolein **4e**. Nevertheless, under the reaction conditions (DMF, Bu_4NBR, $NaHCO_3$, $Pd(OAc)_2$, 40°C), the vinylic silyl groups in **6b**, and probably also in **4b**, were in most part split off. The main product formed thereby, the tetravinyl derivative **6a**, can also be obtained directly—albeit in poorer yield—by reaction of **3** with ethylene under 5 bar excess pressure in a glass autoclave.

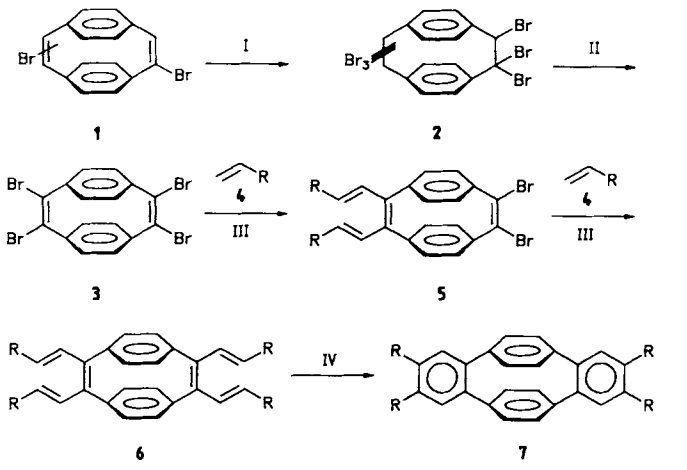

Scheme 1. I: Br_2, $CHCl_3$, Δ. II: *t*BuOK, MTBE, 20°C. III, except for **a**, **b**, and **e**: $Pd(OAc)_2$, Bu_4NBr, K_2CO_3, dimethyl formamide (DMF). IV: Pd/C ($+O_2$) or S, xylene, Δ.

As has already been reported the Heck coupling proceeds in particularly good yields with acceptor-substituted olefins.[7,9] One may assume therefore that predominantly the 1,2-dialkenyl derivatives **5** occur as intermediates in the stepwise alkenylation of **3**: in a prematurely interrupted reaction with **4c**, exclusively the vicinal dibromide **8** was isolated after cyclization and aromatization (vide infra).

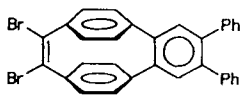

8

According to the ^{1}H-NMR spectra the double bonds in the side chains of **6c**–**f**, are, without exception, *trans*-configurated ($^3J = 15.2$–15.6 Hz). All the derivatives **6**, with exception of **6e**, smoothly underwent 6π-electrocyclization and aromatization to the benzoannelated products **7** upon heating with palladium/active charcoal in the presence of air or with sulfur (see Table 1).

The tetraphenyl derivative **7c** is particularly interesting in that it contains eight orthogonal biphenyl moieties. Four of these are rigidly fixed in the molecular framework, while the other four constitute units of the *o*-terphenyl moieties on both sides of the framework, with the *ortho* phenyl rings—as to be expected in *o*-terphenyls[10]—being perpendicular or almost perpendicular to the rings annelated to the phane skeleton. This is confirmed by the magnitude of the $^6J_{C,F}$ long-distance coupling[11] of the *p*-fluoro derivative **7d** of ≤0.5 Hz and by the UV spectrum of **7c**, in which the long wavelength maximum with $\lambda_{max}(\varepsilon_{max}) = 249$ nm (44200) is clearly hypsochromically shifted compared to that of the 4′,5″-diphenyl derivative[5] with $\lambda_{max}(\varepsilon_{max}) = 257$ (56600).

Table 1. Palladium-catalyzed fourfold coupling of **3** to give tetraalkenyl-[2.2]paracyclophanedienes **6** and their cyclization + dehydrogenation to **7** [6].

	R	6 Conditions	6 Yield [%]	7 Conditions	7 Yield [%]
a	H	100°C (3 d)	— [a]	Pd/C (150°C)	14 [b]
b	$SiMe_3$	40°C (3 d)	—	Pd/C (150°C)	12 [b, c]
c	C_6H_5	70°C (2 d)	50	S (150°C)	55
d	p-F–C_6H_4	70°C (2 d)	—	S (150°C)	22 [b]
e	CHO	40°C (2 d)	32	Pd/C (150°C)	0
f	CO_2Me	70°C (2 d)	40	S (150°C)	45

[a] Not isolated. [b] Yields based on **3**. [c] Product still contained only 5% of the original four trimethylsilyl groups per molecule.

Because of the unusual structure of **7c** and analogous derivatives of **7a**, anions accessible from them by reduction with alkali metals are expected to have interesting chemical properties.[12]

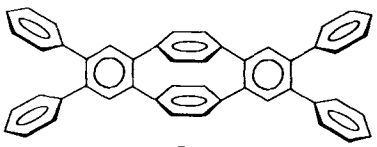

7c

The double Heck-coupling of alkenes with vicinal dibromoalkenes presented here is of more general importance for the synthesis of (*E*,*Z*,*E*)-1,3,5-hexatrienes and the annelation of six-membered rings.[13]

Received: June 26, 1987 [Z 2313 IE]
German version: *Angew. Chem. 99* (1987) 1285

[1] Systematic name: 1,2:9,10-dibenzo[2.2]paracyclophanediene.
[2] C. W. Chan, H. N. C. Wong, *J. Am. Chem. Soc. 107* (1985) 4790.
[3] Structure of **7a**: H. N. C. Wong, C. W. Chan, T. C. W. Mak, *Acta Crystallogr. Sect. C42* (1986) 703; ESR data of the radical anion of **7a**: F. Gerson, W. B. Martin, H. N. C. Wong, C. W. Chan, *Helv. Chim. Acta 70* (1987) 79; PE spectrum of **7a**: Z.-z. Yang, B. Kovac, E. Heilbronner, J. Lecoultre, C. W. Chan, H. N. C. Wong, H. Hopf, F. Vögtle, *ibid. 70* (1987) 299.
[4] K. C. Dewhirst, D. J. Cram, J. Am. Chem. Soc. 80 (1958) 3115.
[5] M. Stöbbe, O. Reiser, R. Bäder, A. de Meijere, *Chem. Ber. 120* (1987) 1667.
[6] All new compounds gave satisfactory elemental analyses and were characterized on the basis of their IR, ^{1}H-NMR, and, in part, ^{13}C-NMR spectra.
[7] H. Dieck, R. R. Heck, *J. Org. Chem. 40* (1975) 1083.
[8] T. Jeffery, *Tetrahedron Lett. 26* (1985) 2667.
[9] Cf. review: H.-U. Reissig, *Nachr. Chem. Tech. Lab. 34* (1986) 1066.
[10] Cf. H. A. Staab: *Einführung in die theoretische organische Chemie*, 3rd edit., Verlag Chemie, Weinheim 1962, p. 374; S. Ozasa, Y. Fujioka, M. Okada, H. Izumi, E. Ibuki, *Chem. Pharm. Bull. 29* (1981) 370.
[11] Cf. D. Vikic-Topic, Z. Meic, *J. Mol. Struct. 142* (1986) 371.
[12] Cf. also [3].
[13] Cf. A. J. Ashe, F. J. Drone, *J. Am. Chem. Soc. 109* (1987) 1879; O. Reiser, A. Lansky, A. de Meijere, unpublished results.

High-Resolution CP-MAS ^{13}C-NMR Spectra of Allylzinc Compounds—Structural Similarities and Differences in the Solid State and in Solution

By *Reinhard Benn,* Hiltrud Grondey, Herbert Lehmkuhl, Hans Nehl, Klaus Angermund,* and *Carl Krüger*

The structure of simple Li-, Mg-, and Zn-allyl compounds has been the subject of numerous NMR[1] and IR/Raman spectroscopic[2] investigations, X-ray analyses,[3] and theoretical calculations.[1f,4] We have now succeeded for the first time in obtaining high-resolution CP-MAS ^{13}C-NMR spectra of 3,3-dimethylallylzinc chloride **1**, bis(2-methylallyl)zinc **2**, bis(allyl)zinc **3**, and 2-methylallylzinc chloride **4**, and a crystal structure analysis of **2**, and in demonstrating that the organic ligand in **1** is bound in an η^1, in **2** in an η^1, η^2, and in **3** and **4** in an η^3 fashion. In contrast, in donor solvents the allyl groups in **1**–**4** are always bound η^1-like to zinc.

Table 1. ^{13}C-chemical shifts of **1**–**4** in the solid state and dissolved in THF (in brackets); cf. also Ref. [2].

Compound	C1	C2	C3	Me
[(3,3-dimethylallyl)ZnCl] **1** [a]	21.4 (14.6)	135.7 (129.1)	127.4 (117.1)	18.8, 28.5 (17.3, 26.0)
[(2-methylallyl)$_2$Zn] **2** [b]	31.0 (24.3)	174.4 (153.0)	91.8 (98.1)	30.0 (26.7)
[(allyl)$_2$Zn] **3** [c]	52 (20.0)	170 (145.4)	52 (99.8)	— —
[(2-methylallyl)ZnCl] **4** [d]	55 (21.2)	207 (152.5)	55 (100.1)	29 (26.6)

[a] At 300 K. [b] In THF at 173 K; in the solid state at 300 K. [c] At 183 K. [d] In THF at 173 K, in the solid state at 300 K.—Central $\delta(^{13}C)$ value in the CP-MAS ^{13}C-NMR spectra.

The ^{13}C-NMR data of **1**–**4** determined by the CP-MAS technique[5] and high power proton decoupling at 50.2 MHz are collected in Table 1. The ^{13}C chemical shifts for **1** in the solid state and in solution differ only slightly, i.e. in each case an η^1-allyl structure is present. According to two-dimensional NMR spectra[6] a slow chemical exchange of the methyl groups takes place in **1** in solution at 300 K, whereas such a process cannot be detected in the solid state at up to $T = 360$ K. Apparently the barrier for the σ-π rearrangement [Eq. (a)] is higher in the solid state

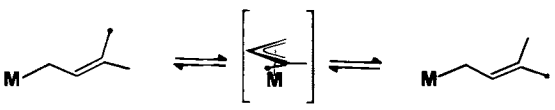

(a)

than in solution. This is also supported by the ^{13}C-NMR spectra of **2** (Fig. 1). In THF solution σ-π rearrangements prevent the typical signals for an η^1-allyl structure from being observed above 173 K, but in the solid state spectrum different signals are found for the terminal allyl C-atoms at 300 K. The halfwidths of these signals are unusually narrow for solid state NMR spectra. The differences between the positions of the signals in the solid state and the solution spectrum lie outside the usual tolerances and cannot be explained in terms of conformational changes. Significant in the CP-MAS spectrum of **2** are, in particular, the strong deshielding of the central allyl C-atom ($\Delta\delta(C2) = +21.4$) and the increased deshielding and shielding of the terminal allyl C-atoms ($\Delta\delta(C1) = +6.7$, $\Delta\delta(C3) = -6.3$).[7] We interpret this finding in terms of a complexation of the double bond to zinc, such that the allyl C-atoms in **2** are unsymmetrically bound in an η^1,η^2 fashion.[8,9] This is confirmed by the crystal structure analysis of **2** (Fig. 2).[10] In the single crystal each symmetry-equivalent methylallyl ligand is σ-bonded via the atom C1 to one Zn atom and is also π-complexed via the C2–C3 bond to another Zn atom. Whereas the two types of bonding can be distinguished at C1 and C3 by the very different

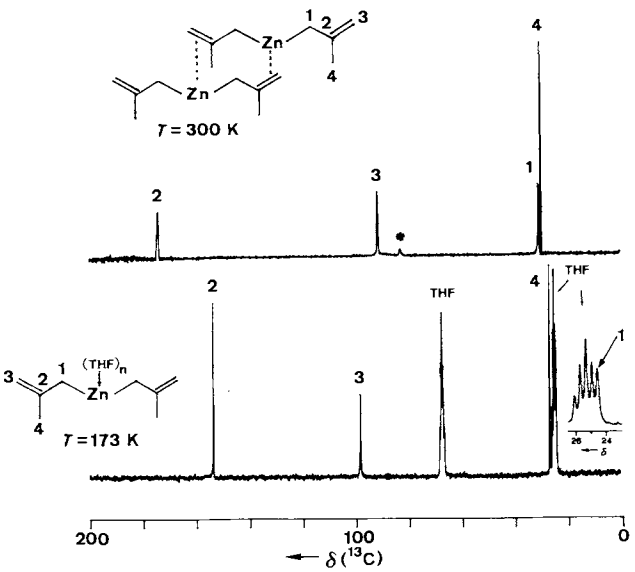

Fig. 1. 50.2-MHz ^{13}C-NMR spectra of bis(2-methylallyl)zinc **2** in THF (ca. 10%) at 173 K (bottom) and CP-MAS spectrum at 300 K (top). Spin frequency ca. 4600 Hz, 90°-^{1}H-pulse 5 μs, contact time 4000 μs. * denotes ^{13}C-signal of the rotor.

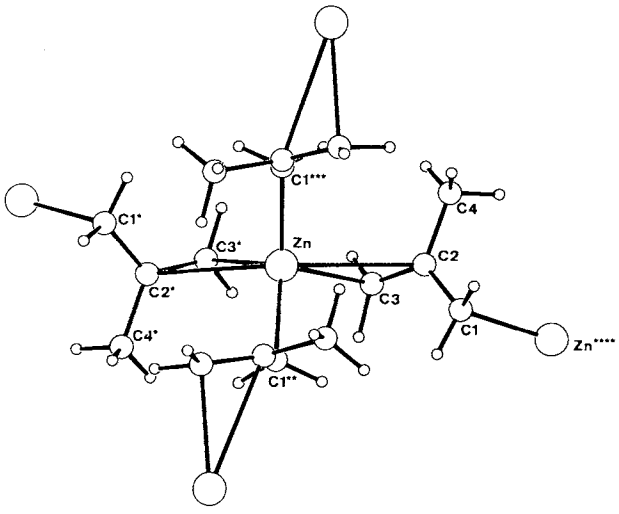

Fig. 2. Molecular structure of **2** in the crystal; space group $P3_221$, $a = b = 8.3452(4)$, $c = 10.565(1)$ Å, $V = 637.2$ Å^3, $Z = 3$, $T = 109$ K, $\mu(Mo_{K\alpha}) = 28.78$ cm^{-1}, $\rho_{calc} = 1.37$ g cm^{-3}, 19280 measured reflections ($\pm h$, $\pm k$, $+l$), averaged to 2602 independent reflections, 2374 observed ($I > 2\sigma(I)$), 70 refined parameters, $R = 0.025$, $R_w = 0.022$ ($w = 1/\sigma^2(F_o)$), residual electron density 0.62 eÅ^{-3}, H positions refined isotropically. Selected bond lengths [Å] and angles [°]: Zn-C1** 2.043(1), Zn-C2 2.919(1), Zn-C3 2.441(1), Zn****-C2 2.906(1), C1-C2 1.460(1), C2-C3 1.367(1), C2-C4 1.511(1); C1**-Zn-C1*** 139.4(1), Mp(C2*,C3*)-Zn-Mp(C2,C3) 113.9 (Mp = midpoint) [10].

[*] Priv.-Doz. Dr. R. Benn, Dipl.-Phys. H. Grondey, Prof. Dr. H. Lehmkuhl, Dr. H. Nehl, Dr. K. Angermund, Prof. Dr. C. Krüger
Max-Planck-Institut für Kohlenforschung
Kaiser-Wilhelm-Platz 1, D-4330 Mülheim/Ruhr (FRG)

Zn-C distances and the differing deviations of the hydrogen atoms from the allyl plane, the *meso* C-atoms are practically equidistant from the two Zn atoms. (Difference 0.013 Å.) The Zn–C2 bond lengths are very long for a Zn–C π-bonding and can possibly be explained in terms of a very unsymmetric (distorted) π-complexation of the C2–C3 bond, caused by the simultaneous σ-bonding of C1 to a further Zn atom, or a frozen-in dynamic process, in the course of which C1 and C3 are each alternately π- and σ-coordinated. The Zn atoms themselves lie on twofold axes of rotation and are each surrounded pseudotetrahedrally by four methylallyl ligands. The overall result is a three-dimensional polymeric structure.

In the case of **3** and **4** the terminal C-atoms of the allyl moiety absorb at $\delta = 52$ and 55, respectively, in the solid-state ^{13}C-NMR spectrum. The spectra of **3** and **4** in THF solutions already show signals characteristic for an η^1-allyl structure at 200 K, whereas no changes in the ^{13}C-chemical shifts and signal halfwidths are observed up to 180 K ($B_0 = 7.0$ T) in the solid state spectrum of **3**. Since it is unreasonable to assume that the barrier for a π-σ allyl rearrangement (in **3** and **4** compared to **2**) is considerably lowered by the methyl group on C2 or the Cl-substituents on Zn, we conclude, in agreement with IR/Raman spectroscopic results,[2] that in the absence of donors the allyl groups of **3** and **4** are symmetrically η^3-complexed to zinc in the solid state.

The results show that in the solid state the simple allyl compounds of zinc can be of quite different structure types **A**, **B**, or **C**, depending upon the alkyl substituent attached to the allyl moiety and the ligand attached to the metal.

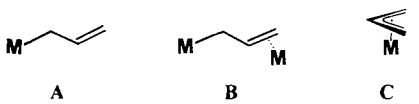

A B C

The differences in the ground state energies for **A**, **B** and **C** are obviously only small, so that upon dissolution in donor solvents exclusively the structure type **A** is found. Moreover, it is clear in the case of **2** that a classification of the allyl structure type merely on the position of the C=C valence vibrations is problematic.

Received: August 5, 1987 [Z 2388 IE]
German version: *Angew. Chem. 99* (1987) 1303

[1] a) G. Wilke, B. Bogdanović, P. Hardt, P. Heimbach, W. Keim, M. Kröner, W. Oberkirch, K. Tanaka, E. Steinrücke, D. Walter, H. Zimmermann, *Angew. Chem. 78* (1966) 157; *Angew. Chem. Int. Ed. Engl. 5* (1966) 151; b) K. Vrieze in L. M. Jackman, F. A. Cotton (Eds.): *Dynamic Nuclear Magnetic Resonance Spectroscopy*, Academic Press, New York 1975, p. 441; c) R. Benn, A. Rufińska, *Organometallics 4* (1985) 221; d) M. Schlosser, M. Stähle, *Angew. Chem. 94* (1982) 142; *Angew. Chem. Int. Ed. Engl. 21* (1982) 145; *Angew. Chem. Suppl. 1982*, 198; e) G. Fraenkel, H. F. Halasa, V. Mockel, R. Stumpe, D. Tate, *J. Org. Chem. 50* (1985) 4563; R. T. McDonald, S. Bywater, *Organometallics 5* (1986) 1529; f) W. R. Winchester, W. Bauer, P. von R. Schleyer, *J. Chem. Soc. Chem. Commun. 1987*, 117, and references cited therein.

[2] E. G. Hoffmann, H. Nehl, H. Lehmkuhl, K. Seevogel, W. Stempfle, *Chem. Ber. 117* (1985) 1364, and references cited therein.

[3] a) H. Köster, E. Weiss, *Chem. Ber. 115* (1982) 3422; b) M. Marsch, K. Harms, W. Massa, G. Boche, *Angew. Chem. 99* (1987) 706; *Angew. Chem. Int. Ed. Engl. 26* (1987) 696; c) U. Schürmann, E. Weiss, H. Dietrich, W. Mahdi, *J. Organomet. Chem. 322* (1987) 299, and references cited therein.

[4] T. Clark, G. Rhode, P. von R. Schleyer, *Organometallics 2* (1983) 1344.

[5] a) C. S. Yannoni, *Acc. Chem. Res. 15* (1982) 201; b) J. R. Lyerla, C. S. Yannoni, C. A. Fyfe, *ibid. 15* (1982) 208; c) E. Oldfield, J. R. Kirkpatrik, *Science 227* (1985) 1537.

[6] a) R. R. Ernst, G. Bodenhausen, A. Wokaun: *Principles of Nuclear Magnetic Resonance in One and Two Dimensions*, Clarendon Press, Oxford 1987; b) for the two-dimensional CP-MAS ^{13}C-NMR exchange spectroscopy of organometallic compounds cf. R. Benn, H. Grondey, R. Nolte, G. Erker, *Organometallics*, in press.

[7] We have observed a similarly strong deshielding of C2 in the solid-state ^{13}C-NMR spectra of allylmagnesium halides. In contrast, no significant shift changes are observed between the solution and the solid-state spectrum for the central allyl carbon atom in $[(\eta^3\text{-allyl})_4\text{Mo}]$, $[(\eta^3\text{-2-methylallyl})_2\text{Pd}]$ or in ether-free $[(\eta^3\text{-allyl})\text{Li}]$. We tentatively attribute the strong deshielding of C2 in the CP-MAS NMR spectra (compared to in solution) to a change in the allyl-metal bonding in the solid state, as has been found for example in the case of **2**.

[8] The IR and Raman spectra of solid **2** and **3** [2] (**2**: IR 1540; Raman 1550; **3**: IR 1520; Raman 1535 cm^{-1}) have been interpreted as being consistent with symmetrically delocalized η^3-bound allyl groups. In the case of **2**, the CP-MAS ^{13}C-NMR spectra clearly contradict this interpretation, whereas in the case of **3** they support it.

[9] Regarding the intramolecular zinc/CC double bond interaction cf. also: A. Haaland, H. Lehmkuhl, H. Nehl, *Acta Chem. Scand. A 38* (1984) 547.

[10] Further details of the crystal structure investigation are available on request from the Fachinformationszentrum Energie, Physik, Mathematik GmbH, D-7514 Eggenstein-Leopoldshafen 2 (FRG), on quoting the depository number CSD-52617, the names of the authors, and the journal citation.

Dipyrrolo[1,2-*a* : 2′,1′-*c*]quinoxalines: A Novel Heterocyclic System**

By *Gerd Kaupp,** *Heike Voss*, and *Herbert Frey*

Dedicated to Professor Ulrich Schöllkopf on the occasion of his 60th birthday

Whereas open-chain nitrones are highly reactive partners for 1,3-dipolar cycloadditions to di- and tetrahydro oxazoles,[1] no cycloadditions have thus far been reported for the quinoxaline dioxides, which are currently the subject of intensive studies because of their wide-ranging biological activities.[2,3] In the reaction of 2,3-dimethylquinoxaline dioxides **1** with phenylpropiolate **2** we have now found a convenient method for the synthesis of the first derivatives of the new heterocycle dipyrrolo[1,2-*a* : 2′,1′-*c*]-quinoxaline.[4]

Reaction of **1**[5] with an excess of **2** for 3 d at 115 °C (Scheme 1) leads to elimination of water and regioselective formation of **3** (35% **3a**, 20% **3b**; no regioisomers). The structure of the reaction product was derived from the ^{1}H-NMR spectra of **3** and the derivative **4**, which was obtained by saponification and decarboxylation of **3a**. In particular the singlet at $\delta = 6.78$ ($\Delta\nu_{1/2} = 2$ Hz) in the spectrum of **4** is reconcilable only with a 2,4-relationship of the H atoms of the pyrrole ring.[6] By-products of the reaction include, inter alia, dimethyl-1-phenylnaphthalene-2,3-dicarboxylate, the dimer of **2** which presumably is formed by [4+2]-cycloaddition in conjunction with a 1,3 H-shift.

As expected this novel mode of reaction (eliminating cycloaddition) is not restricted to 2,3-dimethylquinoxaline dioxides. Thus, the monoxide **5** also reacts regioselectively with **2** to give **6** (115 °C, 4 d, 44%; no regioisomers).

The yellow compounds **3** and **4** containing the new heterocyclic ring system[4] are stable and exhibit the expected structured UV/VIS spectra, the molecular ions as the most intense signals in the mass spectra, and unequivocally as-

[*] Prof. Dr. G. Kaupp, Dipl.-Chem. H. Voss, Dr. H. Frey
Fachbereich Chemie—Organische Chemie I—der Universität
Postfach 2503, D-2900 Oldenburg (FRG)

[**] This work was supported by the Deutsche Forschungsgemeinschaft, the Fonds der Chemischen Industrie, and the Bundesministerium für Forschung und Technologie (Project 10 IVS 325).

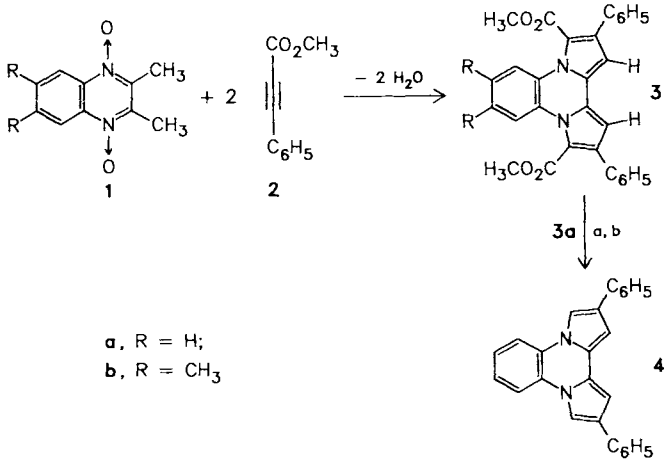

Scheme 1. a) Benzyltrimethylammonium hydroxide. b) Thermal decarboxylation.

signable NMR signals (Table 1). They are potential partners for the construction of highly condensed heterocycles and promise useful biological activities, as do numerous alkaloids of the indolizine type.

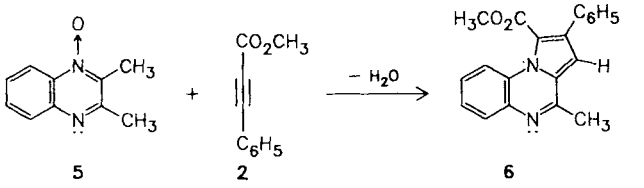

Table 1. Important physical and spectroscopic data of the compounds **3**, **4**, and **6** [7]. UV spectra in CH_2Cl_2, 80-MHz ^{1}H-NMR and 20-MHz ^{13}C-NMR spectra in $CDCl_3$; 70 eV mass spectra.

3a: m.p. 243 °C; UV: $\lambda_{max}(\lg\varepsilon)=375$ (4.13), 358 (4.19), 345 (sh, 4.10), 307 (sh, 4.33), 300 (4.35), 272 nm (4.57).—^{1}H-NMR: $\delta=7.65$–7.2 (14H), 6.72 (2H, s), 3.79 (6H, s).—^{13}C-NMR: $\delta=162.6$ (C=O), 138.1, 134.5, 129.5, 129.5, 128.4, 127.9, 127.7, 127.7, 126.7, 124.9, 120.4, 117.2, 105.3, 51.6 (CH_3).—MS: *m/z* 474 ($M^{\oplus}$, 100%), 443 (7), 416 (32), 358 (28), 355 (22), 320 (5), 289 (9), 279 (3), 237 (4), 221 (9), 177 (16)

3b: m.p. 151 °C; UV: $\lambda_{max}(\lg\varepsilon)=371$ (sh, 4.25), 357 (4.32), 345 (sh, 4.22), 307 (sh, 4.41), 301.5 (4.43), 269 nm (4.68).—^{1}H-NMR: $\delta=7.6$–7.3 (12H), 6.71 (2H, s), 3.78 (6H, s), 2.34 (6H, s).—MS: *m/z* 502 ($M^{\oplus}$, 100%), 472 (2), 444 (9), 443 (1), 384 (6), 383 (9), 251 (4), 236 (1), 235 (2), 184 (4)

4: m.p. 222 °C; UV: $\lambda_{max}(\lg\varepsilon)=313.5$ (1.61), 287.5 (3.60), 264 (4.63), 249 nm (sh, 4.52).—^{1}H-NMR: $\delta=7.7$–7.15 (16H), 6.78 (2H, s).—MS: *m/z* 358 ($M^{\oplus}$, 100%), 332 (1), 330 (3), 328 (2), 282 (1), 280 (3), 254 (3), 179 (12), 178 (4), 140 (1), 102 (1), 77 (2)

6: m.p. 118 °C; UV: $\lambda_{max}(\lg\varepsilon)=334$ (3.96), 345 (sh, 3.90), 265 nm (4.54).—^{1}H-NMR: $\delta=7.95$–7.25 (9H), 6.85 (1H, s), 3.79 (3H, s), 2.67 (3H, s).—^{13}C-NMR: $\delta=163.6$ (C=O), 152.6, 136.5, 134.0, 133.6, 129.1, 128.5, 128.5, 127.8, 127.8, 127.4, 127.1, 126.7, 126.5, 125.2, 118.0, 116.0, 106.2, 51.8 (CH_3), 21.4 (CH_3).—MS: *m/z* 316 ($M^{\oplus}$, 100%), 285 (42), 258 (61), 257 (11), 242 (5), 158 (3), 128 (8), 77 (11)

Since compounds of the types **1** and **5** are accessible in a large variety of ways the reactions presented here may prove to be preparatively very productive. Care should be taken, however, that the heterocyclic α-alkyl *N*-oxides are not too nucleophilic, otherwise predominantly alternative products like **7**[7] (from 2,6-dimethyl- or 2,4,6-trimethylpyridine *N*-oxide and **2**) are formed, in which **2** is incorporated in reversed orientation.[8] The scope and mechanism of this condensation reaction involving ring closure is presently under investigation.

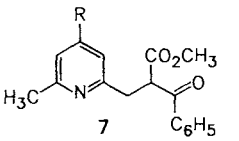

a, R = H; **b**, R = CH_3

Experimental

3a: A mixture of **1a** (1.0 g, 5.3 mmol) and **2** (8.5 g, 53 mmol) was heated in a flask fitted with a condenser for 3 d at 115 °C; the color of the liquid changed from yellow through green and red to greenish black. On cooling, **3a** crystallized out; it was recrystallized from 2-propanol: 0.77 g, m.p. 243 °C. From the mother liquor, a further 0.10 g of **3a** (total yield 35%) could be separated from **2**, its dimer, a green compound (80 mg, $M^{\oplus}=618$), by-products, 2,3-dimethylquinoxaline monoxide (24%), and 2,3-dimethylquinoxaline (24%) by chromatography on silica gel with dichloromethane and ethyl acetate.

Received: June 9, 1987;
revised: September 10, 1987 [Z 2289 IE]
German version: *Angew. Chem. 99* (1987) 1327

[1] See for example J. Hamer, A. Mahaluso, *Chem. Rev. 64* (1964) 473; R. Huisgen, A. Eckell, *Tetrahedron Lett. 1960*, 5; R. Huisgen, *Angew. Chem. 75* (1963) 604, 742; *Angew. Chem. Int. Ed. Engl. 2* (1963) 565, 633.

[2] Numerous derivatives have trade names (Mecadox, Quindoxin, Grofas, Carbadox, Dioxidine, etc.); they are employed, inter alia, as growth-promoting food additives, bactericides (hair and body conditioners), fungicides, and herbicides as well as medicaments (drugs).

[3] A contrary report (M. Ungureanu, I. Druta, I. Zugravescu, *An. Stiint. Univ. "Al. I. Cuza" Iasi Sect. 1C 20* (1974) 29; *Chem. Abstr. 82* (1974) 125351q) could not be duplicated; the compounds formulated therein should not be stable but undergo prototropic rearrangements (see, for example, M. J. Haddadin, M. A. Atfah, *J. Org. Chem. 47* (1982) 1772).

[4] CAS Registry number of the parent compound: 37694-85-2; possible substituted tetrahydro derivatives have not been constitutionally confirmed: R. M. Acheson, M. S. Verlander, *J. Chem. Soc. Perkin Trans. 1 1972*, 1577; *ibid. 1974*, 430.

[5] J. K. Landquist, *J. Chem. Soc. 1953*, 2816.

[6] Cf. M. Hesse, H. Meier, B. Zeeh: *Spektroskopische Methoden in der Organischen Chemie*, 2nd edit., Thieme, Stuttgart 1984, p. 153; the characteristic values for 1-methylpyrrole are $J(2/3)=2.6$, $J(3/4)=3.5$, $J(2/4)=1.3$ Hz.

[7] All the new compounds gave satisfactory spectroscopic data and elemental analyses.

[8] G. Kaupp, H. Voss, unpublished.

Regioselective Protonation of Allylic Anions**

By *Siegfried Hünig,** *Norman Klaunzer,* and *Rüger Schlund*

Dedicated to Professor Klaus Hafner on the occasion of his 60th birthday

Because of the great preparative importance of substituted allylic anions, numerous studies have appeared on the α/γ selectivity of their reaction with electrophiles such as alkylating agents and carbonyl compounds.[1] However, systematic investigations on the regioselectivity of protonation exist only with respect to substituent effects on allylic anions,[2] solvent effects,[3] and the use of various bases;[3] several allylmetal compounds have also been studied.[4] The influence of the proton source XH, on the other hand, has either not been studied at all or only examined within

[*] Prof. Dr. S. Hünig, Dipl.-Chem. N. Klaunzer, Dipl.-Chem. R. Schlund
Institut für Organische Chemie der Universität
Am Hubland, D-8700 Würzburg (FRG)

[**] This work was supported by the Deutsche Forschungsgemeinschaft (as part of the program on "Noncovalent Interactions").

narrow limits.[2,4,13] The goal of this investigation was therefore to determine the regioselectivity of protonation of a substituted allylic anion as a function of the proton source.

We chose the anions **1** and **4** as models—protonation of these anions leads to the isomer pairs **2/3** and **5/6**—for the following reasons: (1) The dithianes **2**[5] and **5** used as educts are smoothly deprotonated by *n*BuLi. This avoids the necessity of using LDA as base, the conjugate acid of which, diisopropylamine, can interfere in the protonation process after addition of a proton source—as has been shown for other examples.[6] (2) The anions **1** and **4** are so strongly basic[7] that they are protonated even by very weak bases. (3) Since water protonates the anion **1** exclusively in the α position,[5] the halogen-substituted derivative **4** was also included, since significant differences in the α/γ protonation ratio would be expected for waterlike proton sources XH.

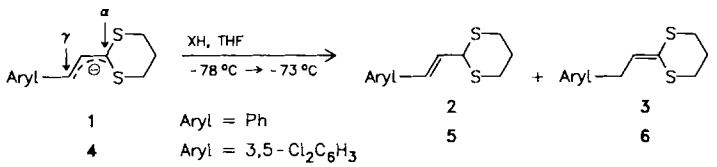

Our results so far are collected in Table 1.[8] They reveal at first glance that the regioselectivity of electrophilic attack on allylic anions can be controlled in principle by the choice of proton source to the same extent as by the choice of alkylating agent.[5] Subsequent equilibration under the experimental conditions can be ruled out. The equilibrium was determined to be **2** : **3** = 35 : 65 and **5** : **6** = 20 : 80 (refluxing methanol/KOH).

Table 1. Product ratios in the protonation of the anions **1** and **4** (as 0.1 M solution in THF, generated by treatment of the conjugate bases with *n*BuLi) with XH at −78 °C to give the isomer pairs **2/3** [9] and **5/6** [10], respectively.

No.	XH	**2** : **3**	**5** : **6**
1	D_2O	> 99 : 1	95 : 5
2	H_2O	> 99 : 1	87 : 13
3	CD_3OD	> 99 : 1	95 : 5
4	CH_3OH	> 99 : 1	77 : 23
5	*t*BuOH	> 99 : 1	
6	2,4,6-$Me_3C_6H_2OH$	> 99 : 1	
7	CH_3CO_2H	95 : 5	84 : 16 [a]
8	PhSH	92 : 8	90 : 10
9	$CH_2(CO_2Me)_2$	92 : 8	79 : 21
10	*i*Pr−$CH(CO_2Me)_2$	88 : 12	44 : 56
11	Et−$CH(CO_2Me)_2$	74 : 26	31 : 69
12	Me−$CH(CO_2Me)_2$	66 : 34	
13	Me−$CH(CO_2Et)_2$	66 : 34	10 : 90
14	Me−$CH(CO_2Et)_2$	> 99 : 1 [b]	

[a] $C_2H_5CO_2H$ instead of CH_3CO_2H. [b] +4 equiv. HMPA.

The exclusive α protonation of **1** by H_2O to give **2** initially provides confirmation of the reported findings.[5] The α protonation of **1** is so strongly preferred that no differences were observed for all OH and OD acids employed (Nos. 1–6 in Table 1). On the other hand, differences are observed for **4**, if the electron density at the α position is reduced by the chlorine substituents.[11] Both deuterium effects (Nos. 1 and 2 as well as 3 and 4) and the effects of small structural differences for XH (Nos. 2 and 4) are now evident. It was surprising, therefore, that the stronger, quite different acids CH_3CO_2H and PhSH display roughly the same differentiation between α and γ protonation (Nos. 7 and 8).

Especially noteworthy are the effects obtained with malonic esters. The amount of γ-protonation product is only small in the case of malonic ester (No. 9); it increases for the monoalkyl malonic esters (with decreasing size of the alkyl group) to surprisingly large values (Nos. 10–12), whereas no difference is observed between methyl and ethyl esters (Nos. 12 and 13).

In the case of **4** the regioselectivity of the α/γ protonation can be forced to two extremes: from 90 : 10 (thiophenol, No. 8) to 10 : 90 (methylmalonic ester, No. 13). This corresponds to a difference of 7.9 kJ mol^{-1} in the energies of the transition states. For **1**, a difference of at least 6.4 kJ mol^{-1} is evident (> 99 : 1 to 66 : 34).

Thus, it is possible in principle to control the regioselectivity of α/γ protonation of allylic anions to an unprecedented extent merely by varying the proton source.

Since no concrete ideas exist concerning the structure of the transition states formed in the kinetically controlled protonation of ambident anions, a detailed interpretation of our results is premature. The counterion ($Li^{\oplus}$) plays an important role in α protonations, since addition of HMPA suppresses this protonation completely (No. 14). Thus, the complexation of the proton sources (e.g., malonic ester derivatives) by the ion pairs Li-**1** and Li-**4** is probable.

It remains to be shown whether the lower rate (by a factor of 10^5 to 10^{12}) of proton transfer from CH acids compared with that from OH acids[12] is also a reason for the increased rate of γ protonation.

Received: July 29, 1987 [Z 2380 IE]
German version: *Angew. Chem. 99* (1987) 1322

[1] Reviews: J. F. Biellmann, J.-B. Ducep, *Org. React. (NY) 27* (1982) 1; H. Ahlbrecht, *Chimia 31* (1977) 391; see also S. Hünig, H. Reichelt, *Chem. Ber. 119* (1986) 1772.
[2] R. J. Bushby, G. J. Ferber, *J. Chem. Soc. Perkin Trans. 2 1976*, 1695.
[3] Y. Ikeda, J. Ukai, N. Ikeda, H. Yamamoto, *Tetrahedron 32* (1987) 743.
[4] Review: G. Courtois, L. Miginiac, *J. Organomet. Chem. 69* (1974) 1.
[5] W. S. Murphy, S. Wattanasin, *J. Chem. Soc. Perkin Trans. 1 1980*, 2678.
[6] Evidence for incomplete deuteration of carbanions; cf. T. Laube, J. D. Dunitz, D. Seebach, *Helv. Chim. Acta 68* (1985) 1373; U. Gerlach, S. Hünig, *Angew. Chem. 99* (1987) 1323; *Angew. Chem. Int. Ed. Engl. 26* (1987) 1283.
[7] p*K* of 2-*p*-biphenylyl-1,3-dithiane = 28 in cyclohexylamine, 25 °C: A. Streitwieser, Jr., S. P. Ewing, *J. Am. Chem. Soc. 97* (1975) 190.
[8] *K. T. Nguyen* and *N. H. Anderson* also have protonated **1** (having a different counterion) with D_2O, H_2O, AcOH, and aqueous HCl to give **2** and **3**. However, their results cannot be discussed here since only a lecture synopsis is available (ACS meeting 1983).
[9] Reproducibility ± 1%, total yields 94–100%. A *n*BuLi solution (1.2 equiv.) in hexane was added to **2** (1.0 mmol) in THF at −40 °C. After 30 min, the reaction mixture was cooled to −78 °C, and XH (3–10 equiv.) in 1 mL of THF was added dropwise to the red solution of Li-**1**. Samples were taken from the colorless reaction mixture and analyzed by HPLC.
[10] The α/γ ratio was determined by ^{1}H-NMR spectroscopy (60 MHz, $CDCl_3$; **5**: δ = 4.8 (d, 1H; CH=CH−C*H*S_2); **6**: δ = 3.5 (d, 2H; $Cl_2C_6H_3$−C*H*$_2$); error limits for multiple integration 5%). Deprotonation of **5** in 45 min under the same reaction conditions as for **2** [9]. The reaction mixture was extracted by shaking with Et_2O; if necessary, XH was removed by kugelrohr distillation.
[11] Compare the "allopolarization" principle: R. Gompper, H.-U. Wagner, *Angew. Chem. 88* (1976) 389; *Angew. Chem. Int. Ed. Engl. 15* (1976) 321.
[12] M. Eigen, *Angew. Chem. 75* (1963) 489; *Angew. Chem. Int. Ed. Engl. 3* (1964) 1.
[13] J. Tanaka, M. Nojima, S. Kusabayashi, *J. Chem. Soc. Perkin Trans. 2 1987*, 673.

Enantioselective Protonation of Carbanions with Chiral Proton Sources**

By *Uwe Gerlach* and *Siegfried Hünig**

Dedicated to Professor Emanuel Vogel on the occasion of his 60th birthday

One of the most important routes for the enantioselective construction of carbon frameworks proceeds via carbanions having chiral auxiliary groups, which must be removed after diastereoselective reaction of the carbanion with alkylating agents or carbonyl compounds.[1] In contrast, only a few reactions of prochiral carbanions with electrophiles are known, in which the nucleofugal leaving group X* functions as a chiral auxiliary group. Examples are X*Me[2] and X*NMe$_2$.[3] An enantioselective protonation of broad scope would also be highly desirable, especially since it should be possible in most cases to recover the chiral proton source X*H. However, no experimental results are available at present in order to develop synthetic applications of such a protonation.

Systematic studies have only been reported by *Duhamel*'s group[4] for the Schiff bases of amino acid esters, e.g., (*R,S*)-**1**-H.[5] Their salts **1**-Li, accessible by reaction of the esters with secondary lithium amides R^{1}R^{2}NLi, react with (*R,R*)-diacyltartaric acids **2** to afford the *S* enantiomer with 4–53% *ee*, the reaction occurring with "deracemization"[4] and the enantiomeric selectivity depending on the lithium amide used and the acyl moiety selected. For example, **2a** protonates prochiral **1**-Li—generated by reaction of the ester with lithium diisopropylamide (LDA)—with 50% *ee* to give (*S*)-**1**-H; on the other hand, reaction with **2b** affords a product with 12% *ee*.[4]

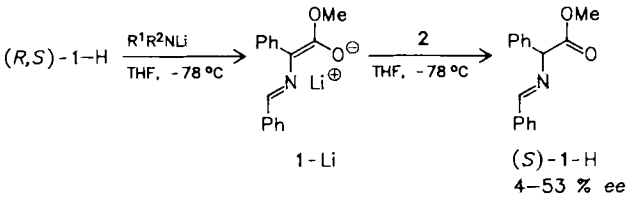

We present here the first results of an extensive study on the enantioselective protonation of the synthetically important ester enolates of α-hydroxycarboxylic acids. As a model, we chose **3**-Li, the cyclic ester enolate of mandelic acid. In contrast to **1**-Li, **3**-Li is neither stabilized by an additional double bond nor by an atom capable of undergoing chelation, but its configuration is unambiguously fixed by its ring structure. (*R,S*)-**3**-H,[6] (*S*)-**3**-H,[7] and (*R*)-**3**-H are readily accessible from the corresponding mandelic acids and acetone. In addition, **3**-Li was prepared via the silyl enol ether **4**, in order to exclude the influence of amines, as well as directly from (*R,S*)-**3**-H by reaction with various amide bases R^{1}R^{2}NLi, in order to clarify the effect of the corresponding amine (Scheme 1). The results are collected in Table 1.

Only 5–7% *ee* was attained for (*R*)-**3**-H when the diacyltartaric acids **2a** and **2b** were employed. Although these acids had afforded good results with **1**-Li. On the other

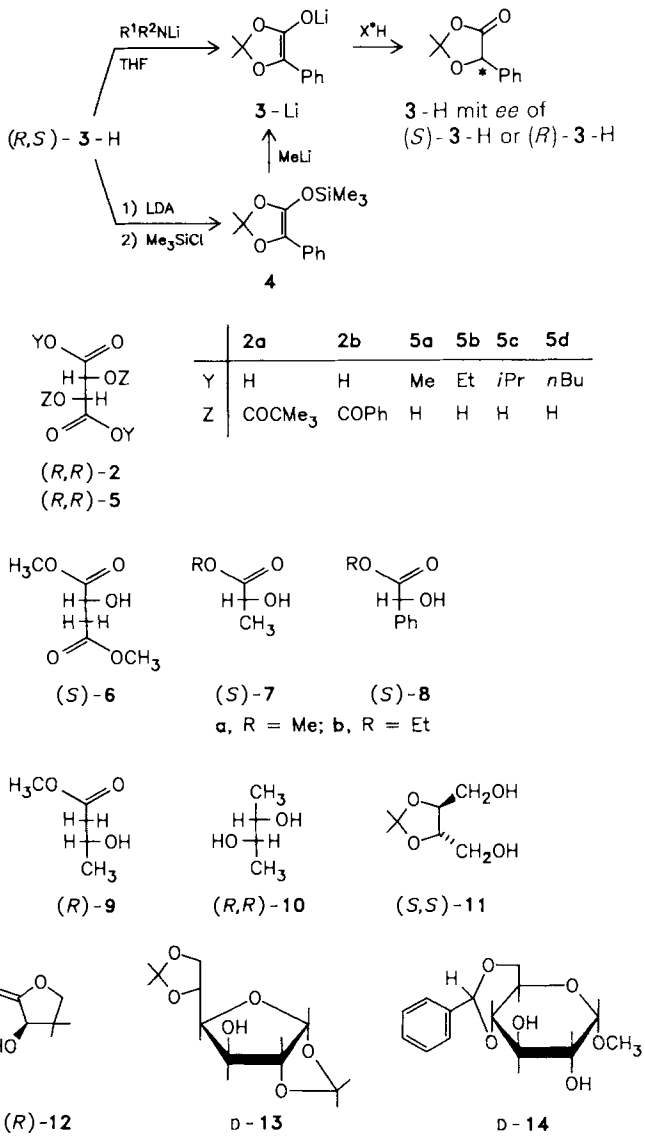

Scheme 1. Enantioselective protonation of **3**-Li. R^{1}R^{2}NLi: (*i*Pr)$_2$NLi (LDA), (Me$_3$Si)$_2$NLi (LiHMDS), lithium 2,2,6,6-tetramethylpiperidide (LiTMP). **2** and **5**–**14** are the chiral proton sources X*H used.

Table 1. Protonation of **3**-Li, generated from **4** with MeLi or from (*R,S*)-**3**-H with LiHMDS, with chiral proton sources X*H in THF at ca. −78 °C [8].

X*H	% *ee* (excess enantiomer of **3**-H) [a]	[b]
(*R,R*)-**2a**	7 (*R*)	6 (*R*)
(*R,R*)-**2b**	—	5 (*R*)
(*R,R*)-**5a**	29 (*S*)	35 (*S*)
(*R,R*)-**5b**	37 (*S*)	42 (*S*)
(*R,R*)-**5c**	43 (*S*)	47 (*S*)
(*S,S*)-**5c**	42 (*R*)	46 (*R*)
(*R,R*)-**5d**	46 (*S*)	42 (*S*)
(*S*)-**6**	21 (*R*)	23 (*R*)
(*S*)-**7a**	—	7 (*R*)
(*S*)-**7b**	—	7 (*R*)
(*S*)-**8a**	43 (*R*)	49 (*R*)
(*S*)-**8b**	48 (*R*)	52 (*R*)
(*R*)-**9**	3 (*R*)	—
(*R,R*)-**10**	3 (*S*)	—
(*S,S*)-**11**	9 (*S*)	—
(*R*)-**12**	53 (*S*)	53 (*S*)
D-**13**	31 (*S*)	—
D-**14**	15 (*S*)	—

[a] Reaction of **3**-Li (generated from (*R,S*)-**3**-H) with X*H. [b] Reaction of **3**-Li (generated from **4**) with X*H.

[*] Prof. Dr. S. Hünig, Dipl.-Chem. U. Gerlach
Institut für Organische Chemie der Universität
Am Hubland, D-8700 Würzburg (FRG)

[**] This work was supported by the Deutsche Forschungsgemeinschaft (as part of the program on "Noncovalent Interactions"). *U. G.* thanks the Fonds der Chemischen Industrie for a doctoral fellowship.

hand, the tartaric esters **5a–d** are very effective, affording products with 29–46% *ee*, (*S*)-**3**-H predominating. The enantioselectivity increases slightly with increasing size of the alkoxy groups. As expected, the enantiomeric excess for **3**-H reverses by using (*R,R*)-**5c** instead of (*S,S*)-**5c**. To determine the effective structural elements of **5a–d**, other proton sources were employed. For malic ester (*S*)-**6**, the enantiomeric excess decreases to approximately one-half the value; for lactic esters **7a** and **7b**, approximately one sixth of the value is obtained. Replacement of the methyl group in **7** by a phenyl group (**8**), however, results in a ca. 50% *ee* of (*R*)-**3** for the mandelic esters (*S*)-**8a** and (*S*)-**8b**, thus exceeding even (*R,R*)-**5c**. On the other hand, the chiral induction is almost completely lost when the β-hydroxybutyric ester (*R*)-**9** is used as X*H. In addition, the absence of alkoxycarbonyl groups ((*R,R*)-**10** and (*S,S*)-**11**) lowers the *ee* value to less than 10%. The front runner in the present series of chiral proton sources is the pantolactone (*R*)-**12**,[9] which produces (*S*)-**3**-H with 53% *ee*. Carbohydrate derivatives, which are obvious candidates, have so far shown only moderate selectivity: diacetoneglucose D-**13**[10, 11] affords (*S*)-**3**-H with only 31% *ee* and the 4,6-*O*-benzylidene-α-D-glucopyranoside D-**14**[11] yields only half this value.

Evidently, chiral proton sources having the α-hydroxycarboxylic acid structural element are of particular importance. Since only (*S*)-**3**-H is formed with *R* proton sources (and vice versa), the (*R,S*) or (*S,R*) arrangement in the transition states formed from X* and **3**-Li is always preferred over the (*R,R*) or (*S,S*) configurations (**5–8**, **12**).

Moreover, Table 1 shows that, in the presence of the amine HMDS-H, the *ee* values are usually only slightly smaller and, in one reproducible case, even a little higher, so that several X*H were allowed to react only with **3**-Li generated from (*R,S*)-**3**-H by reaction with LiHMDS. Table 2 even confirms these results for the bases LDA and LiTMP.

Table 2. Generation of **3**-Li with various bases and its protonation or deuteration with the diisopropyl (*R,R*)-tartarates **5c** or [D]**5c**, respectively, in THF at −78°C.

Base	X*H(D)	% **3**-D	% *ee* of (*R*)-**3**-H
MeLi [a]	**5c**	—	47
MeLi [a]	[D]**5c**	>95	55
LiHMDS [b]	**5c**	—	42
LiHMDS [b]	[D]**5c**	>95	57
LDA [b]	**5c**	—	45
LDA [b]	[D]**5c**	41	51
LiTMP [b]	**5c**	—	41
LiTMP [b]	[D]**5c**	57	48

[a] Reaction with **4**. [b] Reaction with (*R,S*)-**3**-H.

This result is surprising, since it is not in agreement with the deuteration experiments on **3**-Li. In the reaction of **3**-Li (generated with LDA[12] or LiTMP) with [D]**5c**, only ca. 50% of **3**-D is formed (Table 2). Several examples of this effect are known.[13] In those cases, the results are ascribed to the rapid addition of $D^{\oplus}$ to the strong bases $i Pr_2NH$ ($pK_a = 35.7$[14]) and TMPH ($pK_a = 37.3$[14]), whose onium ions can then transfer either protons or deuterons. It is remarkable that this undesired reaction is already completely suppressed on going to HMDS-H ($pK_a = 25.8$[15]) when weak acids such as D_2O or ROD are used. We were also able to smoothly deuterate other compounds after deprotonation with LiHMDS.

On the basis of these results, one would have expected lower *ee* values for (*R*)-**3**-H in the reaction of **3**-Li (generated with LDA or LiTMP) with **5c** and [D]**5c**. As discussed above, however, that is not the case. Furthermore, a significant deuterium effect is observed (also for **3**-Li generated from **4**), presumably owing to the different transition states (distances!) for $H^{\oplus}$ and $D^{\oplus}$ transfer.[16]

According to Table 2, the amount of (*R*)-**3**-H increases, for complete deuteration (LiHMDS as base), from 42 to 57%; for ca. 50% deuteration, the *ee* difference is, as expected, only half as large. All these results support the conclusion that the secondary amine (actually the amount of ammonium ion) does not contribute to the protonation (deuteration) of **3**-Li. Instead, a rapid exchange reaction as shown in (a) presumably occurs. The reason for this course

$$[D]\mathbf{5c} + R_2NH \rightleftharpoons \mathbf{5c} + R_2NHD^{\oplus} \rightleftharpoons \mathbf{5c} + R_2ND \qquad (a)$$

of the enantioselective protonation of **3**-Li is presumably the better coordination (compared with secondary amines) of OH (or OD) acids **5c** to the lithium ion (see below).

As shown by protonations of **3**-Li with (*R,R*)-**5c**, the chiral induction is lower both in ether (27% *ee*) and in THF + 4 HMPA (11% *ee*), owing, in the latter case, to the generation of a solvent-separated ion pair. The necessity of forming a close ion pair with the lithium ion is evident from the decrease in the *ee* value to 2% with NaHMDS and KHMDS. The generation of an ate complex with $Ti(OiPr)_4$, on the other hand, results in an increase in the amount of (*S*)-**3**-H to even 61% *ee*, whereas with $Ti(NEt_2)_4$ only 31% is attained and the mixed titanyl ester expected from **3**-Li and $ClTi(OiPr)_3$ affords only 15% *ee* for (*S*)-**3**.

Thus, the decisive role of the cation is clearly revealed. Presumably, the cation complexes with the carbonyl group of the chiral α-hydroxycarboxylic ester. It is thereby possible for the proton of the α-hydroxyl group perpendicular to the double bond of the enolate to be transferred directly to its α-C atom, as has been shown for the ketonization of enols (enolates).[17] On the basis of this simplified working hypothesis, it should be possible to vary the enantioselectivity by specific structural changes in the proton source, resulting in values even larger than those obtained so far. However, rapid O-protonation, especially when solvent-separated ion pairs are present, might result in formation of the prochiral enol. Since this species can undergo ketonization only intermolecularly,[17, 19] it might itself act as an undesired proton source.

Received: July 29, 1987 [Z 2382 IE]
German version: *Angew. Chem.* *99* (1987) 1323

[1] a) J. W. A. Simon, T. L. Collier, *Tetrahedron 42* (1986) 5157; b) S. Masamune, *Angew. Chem. 97* (1985) 1; *Angew. Chem. Int. Ed. Engl. 24* (1985) 1; c) D. Enders, R. W. Hoffmann, *Chem. Unserer Zeit 19* (1985) 177; d) D. A. Evans in J. D. Morrison: *Asymmetric Synthesis, Vol. 3, Part B*, Academic Press, New York 1984, Chap. 1, p. 1; e) G. Quinkert, H. Stark, *Angew. Chem. 95* (1983) 651; *Angew. Chem. Int. Ed. Engl. 22* (1983) 637; f) H. S. Mosher, J. D. Morrison, *Science (Washington) 221* (1983) 1013.

[2] P. Duhamel, J.-Y. Valnot, J. Jamal Eddine, *Tetrahedron Lett. 23* (1982) 2863; P. Duhamel, J. Jamal Eddine, J.-Y. Valnot, *ibid. 25* (1984) 2355 (also includes a classification of enantioselective reactions); *ibid. 28* (1987) 3801.

[3] G. Boche, W. Schrott, *Tetrahedron Lett. 23* (1982) 5403.

[4] Review: a) L. Duhamel, P. Duhamel, J. C. Launay, J. C. Plaquevent, *Bull. Soc. Chim. Fr. II 1984*, 421; b) L. Duhamel, J. C. Plaquevent, *Tetrahedron Lett. 21* (1980(2521; c) *Bull. Soc. Chim. Fr. II 1982*, 75; d) L. Duhamel, S. Fouquay, J. C. Plaquevent, *Tetrahedron Lett. 27* (1986) 4975; e) L. Duhamel, L. Plaquevent, *J. Am. Chem. Soc. 100* (1978) 7415.

[5] Enantioselective reactions of Li enolates with chiral, nonprotic electrophiles in the presence of chiral secondary amines (D. Seebach, *Proc. Welch Foundation*, Houston 1984, p. 93) are not completely comparable because of the special role of the proton.
[6] M. Farines, J. Soulier, *Bull. Soc. Chim. Fr. 1970*, 332.
[7] The mild synthetic method according to [6] (reaction of (*S*)- or (*R*)-mandelic acid in acetone with $BF_3 \cdot OEt_2$, 4 h at room temperature, chromatographic workup) affords (*S*)-**3**-H with $[\alpha]_D^{20} = +52.7$ or (*R*)-**3**-H with $[\alpha]_D^{20} = -52.9$ ($c = 2$, CCl_4), m.p. = 74°C. For (*S*)-**3**-H, $[\alpha]_D^{20} = 41$ ($c = 2$, CCl_4), m.p. = 71°C (T. Polonski, *Tetrahedron 39* (1983) 3131). The enantiomeric purity was checked by gas chromatographic separation of the enantiomers. We thank Dr. *K. Günther*, Degussa AG, for performing these analyses.
[8] a) **3**-Li from (*R,S*)-**3**-H: (*R,S*)-**3**-H (1.0–1.3 mmol) in THF (4 mL) was added to a solution of LiHMDS (1.5–2.0 mmol, prepared from 1.8–2.1 mmol of HMDS-H and 1.5–2.0 mmol of *n*BuLi in hexane) in THF (4 mL) at −40°C. After the reaction mixture had stirred for 30 min, X*H (3.5–4.1 mmol) in THF (2 mL) was added at −78°C to −72°C. After 15 min, the resulting mixture was allowed to warm to room temperature and then treated with 10 mL of ether and 5 mL of saturated $NaHCO_3$ solution. The washed ether phase was dried over Na_2SO_4 and evaporated and the reaction product was purified by radial chromatography (eluent, petroleum ether/diethyl ether 9/1; yield, 70–90%). The enantiomeric excess was determined polarimetrically and, in certain cases, after addition of a chiral solvent ((*R*)-1-(9-anthryl)-2,2,2-trifluoroethanol), by NMR spectroscopy [18]. b) **3**-Li from **4**: **4** (0.9–1.5 mmol) in THF (4 mL) was treated at −40°C with MeLi (1.1–2.0 mmol) in Et_2O and the reaction mixture was allowed to stir for 30 min at this temperature. The protonation, workup, and analysis were carried out as described in [8a]. The reported enantiomeric excesses are average values from two or three independent experiments (reproducibility ±1.5%).
[9] We thank BASF AG, Ludwigshafen, for a sample of (*R*)-**12**.
[10] The protonation of a pentenoic ester derivative with D-**13** afforded the *S* form with 53% *ee*: F. M. Stoyanovich, E. P. Zakharaov, Y. L. Goldfarb, M. M. Krayushkin, *Izv. Akad. Nauk SSSR Ser. Khim. 1986*, 1455.
[11] We thank Prof. *H. Kunz*, Mainz, for samples of this derivative.
[12] The deprotonation of compounds analogous to **3**-H by treatment with LDA is known: G. Frater, U. Müller, W. Günther, *Tetrahedron Lett. 22* (1981) 4221; D. Seebach, R. Naef, G. Calderari, *Tetrahedron 40* (1984) 1313.
[13] P. E. Pfeffer, L. S. Silvert, J. M. Chirinko, *J. Org. Chem. 37* (1972) 451; D. Seebach, M. Boes, R. Naef, W. B. Schweizer, *J. Am. Chem. Soc. 105* (1983) 5390; T. Laube, J. Dunitz, D. Seebach, *Helv. Chim. Acta 68* (1985) 1373; R. Ehrler, *Diplomarbeit*, Universität Würzburg 1982.
[14] R. R. Fraser, T. S. Mansour, *J. Org. Chem. 49* (1984) 3443; cf. Ref. [15] therein.
[15] R. R. Fraser, T. S. Mansour, S. Savard, *J. Org. Chem. 50* (1985) 3232; since the pK_b of HMDS-H is not known, the basicity of the corresponding amide was used for comparison.
[16] Cf. C. F. Bernasconi, D. E. Fairchild, C. J. Murray, *J. Am. Chem. Soc. 109* (1987) 3409.
[17] Review: H. E. Zimmermann, *Acc. Chem. Res. 20* (1987) 263; J. Toullec, *Adv. Phys. Org. Chem. 18* (1982) 1.
[18] W. H. Pirkle, D. L. Sikkenga, M. S. Pavlin, *J. Org. Chem. 42* (1977) 384.
[19] M. Zakowa, J. Leska, *Collect. Czech. Chem. Commun. 47* (1982) 1897.

2,2-Dimethyl-4,5-dimethylene-1,3-cyclopentanediyl**

By *Wolfgang R. Roth,* Udo Kowalczik, Günther Maier, Hans Peter Reisenauer, Reiner Sustmann,* and *Wolfgang Müller*

Dedicated to Professor Emanuel Vogel on the occasion of his 60th birthday

Theoretical calculations indicate that a singlet ground state can be expected for tetramethyleneethane in its planar as well as its energetically more favorable non-planar conformation.[1] Contrary to this prediction, *Dowd* et al.[2] have recently shown that the parent molecule does have a triplet ground state. If one assumes the orthogonal geometry to be expected for this molecule from calculations,[1] then there remains the question of the multiplicity of the planar system. The aim of the present study is to try to resolve this problem with 2,2-dimethyl-4,5-dimethylene-1,3-cyclopentanediyl **17** as model substrate.

Three precursors of **17** were prepared: 1. The ketoester **1** was converted by α-bromination and Favorskii ring contraction into the cyclopentene derivative **2**, which after bromination with *N*-bromosuccinimide (NBS) and elimination of HBr with 1,8-diazabicyclo[5.4.0]undec-7-ene (DBU) furnished **3**. Reduction to the diol, mesylation and reaction with methyltriazolinedione (MTAD) afforded **4**. Subsequent 1,4-elimination with NaI/acetone furnished **5**, which was converted in the usual way into the diazo compound **6**[3]—a starting compound for **17**—in a total yield of ca. 15% (Scheme 1).

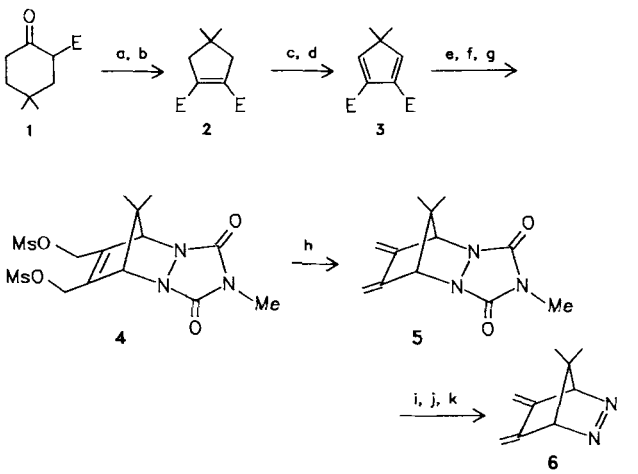

Scheme 1. E = COOMe; a) Br_2, ether, 0°C; b) Na, CH_3OH, room temperature; c) NBS, CCl_4; d) DBU, benzene, 0°C; e) $LiAlH_4$, ether; f) $MeSO_2Cl$, CH_2Cl_2, Et_3N, 0°C; g) MTAD, CH_2Cl_2, room temperature; h) NaI, acetone, room temperature; i) KOH, CH_3OH, 60°C; j) $CuCl_2$; k) NH_3.

2. Starting from 3,3-dimethyl-1,4-pentadiene **7** the **17**-precursor **10**[4] was obtained in a total yield of 27% via the diyne **8**, chain-lengthening to the diyne **9**, and subsequent hydrogen shift reactions (Scheme 2).

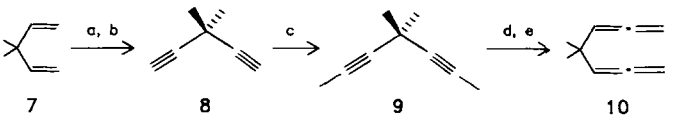

Scheme 2. a) Br_2, CCl_4; b) KOH, 180°C; c) BuLi, hexane, CH_3I; d) *t*BuLi, ether, *N,N,N',N'*-tetramethylethylenediamine (TMDA), Me_3SiCl [5]; e) CF_3COOH, CH_2Cl_2 [6].

3. Starting from the ketoester **11**, the diethynylcyclopropane derivative **13** was obtained via the diketone **12**. Thermolysis of **13** at 500°C led to the extremely labile triene

[*] Prof. Dr. W. R. Roth, Dr. U. Kowalczik
Fakultät für Chemie der Universität
Universitätsstrasse 150, D-4630 Bochum 1 (FRG)
Prof. Dr. G. Maier, Dr. H. P. Reisenauer
Institut für Organische Chemie der Universität
Heinrich-Buff-Ring 58, D-6300 Giessen (FRG)
Prof. Dr. R. Sustmann, Dipl.-Chem. W. Müller
Institut für Organische Chemie der Universität
Postfach 103764, D-4300 Essen 1 (FRG)

[**] This work was supported by the Deutsche Forschungsgemeinschaft and the Fonds der Chemischen Industrie.

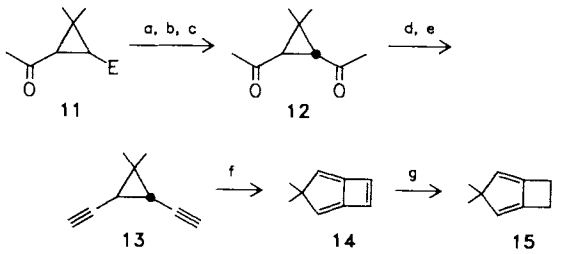

Scheme 3. E = COOMe; a) KOH; b) $SOCl_2$; c) *Collmans* reagent [8], THF, CH_3I, hexamethylphosphoric triamide (HMPT); d) lithium diisopropylamide (LDA), $ClPO(OEt)_2$ [9], THF; e) LDA, THF; f) 500 °C; g) Ph_3RhCl, benzene, H_2.

14, selective hydrogenation of which afforded **15**[7]—the third source of **17**—in a total yield of ca. 10% (Scheme 3).

The diradical **17** can be generated from all three precursors **6**, **10**, and **15** thermally, and from **6** also photochemically, whereby only the dimers **19** and **20** are formed as final products. The diazo compound **6** already decomposes at 40 °C, whereas the bisallene **10** requires temperatures of ca. 150 °C ($E_a = 26.3 \pm 0.1$ kcal mol^{-1}; $A = (1.2 \pm 0.1) \times 10^{11}$ s^{-1}) and the bicycle **15** of ca. 220 °C ($E_a = 40.1 \pm 0.8$ kcal · mol^{-1}; $A = (1.2 \pm 0.9) \times 10^{14}$ s^{-1}). When these reactions are carried out in the presence of oxygen, the peroxide **18** is formed as well as **19** and **20**. If **17** is generated in solution in the presence of *N*-phenylmaleimide (NPM) or SO_2, the trapping products **21**, **22**, and **23** are formed.

The diradical **17** establishes equilibrium with **15** at temperatures above 160 °C. The gas-phase thermolysis of **10** at 160 °C leads to the dimers **19** and **20** *and* to the bicycle **15**, which at temperatures in excess of 200 °C reacts further to give **19** and **20**. If the photolysis of **6** (directly or sensitized) is carried out at temperatures below −20 °C, not only **19** and **20** but also the bicycle **16**[10] is formed, which at temperatures above −20 °C decomposes again to the diradical **17**.

Upon irradiation of **6**[11] in an argon matrix ($\lambda = 350$ nm, $T = 10$ K), the formation of the diradical **17** can be demonstrated both UV and IR spectroscopically. In the UV spectrum an absorption band appears at 463 nm ($\varepsilon \approx 400$) with shoulders at 497 and 520 nm, whose position is comparable with that observed for the absorption band of 2,3-dimethylene-1,4-cyclohexanediyl ($\lambda_{max} = 427$ nm ($\varepsilon = 2400$), 480 (sh)).[15] The IR spectrum, with an intense out-of-plane CH vibration at 767 cm^{-1}, is also consistent with the structure of **17**.[12] The bands of **17** disappear on prolonged irradiation of the matrix (slowly at 350 nm, rapidly at 450 nm), and a new substance is formed which shows no absorption above 300 nm in the UV spectrum. The IR spectrum of this new substance shows two intense bands at 868 and 886 cm^{-1}, indicating the presence of *exo*-methylene groups and a cyclization of **17** to **16**.

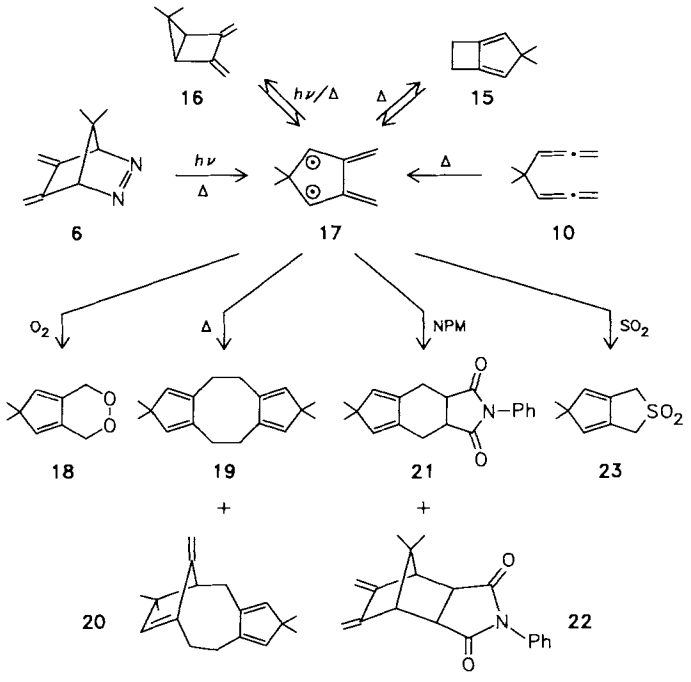

Informative regarding the multiplicity of the diradical **17** is its ESR spectrum. Irradiation[13] of **6** in an argon matrix ($\lambda = 330$ nm, $T = 22$ K) furnished a triplet spectrum (Fig. 1, $\Delta m = 1$: 3387 G, $\Delta m = 2$: 1690 G), from which the

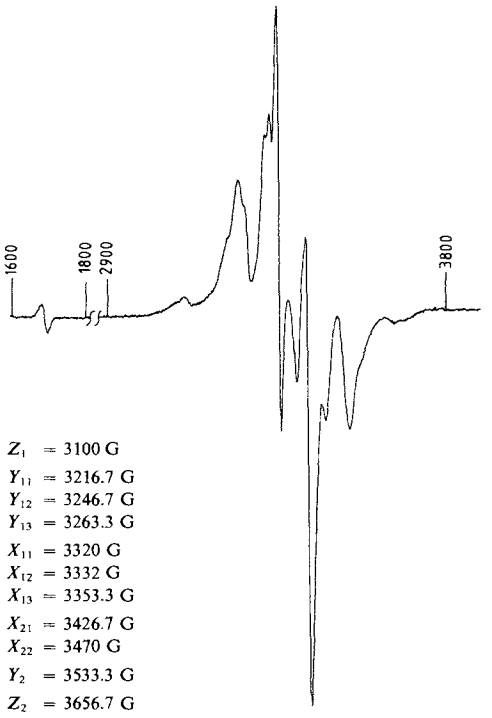

Fig. 1. ESR spectrum of **17** in an argon matrix at 22 K.

zero field parameters were found to be $|D|/(hc) = 0.0259$ and $|E|/(hc) < 0.001$ cm^{-1}. A linear dependence ($r = 0.988$) of the signal intensity on $1/T$ was observed between 15 and 115 K ([D_{16}]adamantane matrix). Thus, contrary to theoretical expectations the singlet and triplet states are either practically degenerated, or, what is more likely, the diradical has a triplet ground state.

Consistent with this interpretation is the observation of polarized ^{1}H-NMR spectra upon thermolysis of **6** (at 40 °C) and **16** (at 0 °C), with the polarized signals appearing exclusively in the emission. The direction of polarization together with the strong dependence of the intensity on the field (no polarization at field strengths above 80 MHz) is consistent with a $T_{\pm} \rightarrow S$ transition,[14] thus requiring thermally achievable triplet states.

The triplet ground state of **17** is also supported by the trapping experiments. Only very reactive dienophiles can compete with the dimerization of the triplet diradical.[15]

 © VCH Verlagsgesellschaft mbH, D-6940 Weinheim, 1987 0570-0833/87/1212-1286 $ 02.50/0 Angew. Chem. Int. Ed. Engl. 26 (1987) No. 12

Thermal as well as photochemical decomposition of **6** in 1,2-dichloroethylene, styrene or fumarates (as solvent) leads exclusively to the dimers **19** and **20**, and even with *N*-phenylmaleimide the dimerization can only be suppressed with excess of the reagent. Since the ratio of trapping products to dimers is not changed in the sensitized photolysis of **6**, the trapping products most likely are formed from the singlet-species present in equilibrium with the triplet species. If one assumes that dimerization and trapping reaction are diffusion controlled, the singlet state must lie at least 4–5 kcal mol^{-1} above that of the triplet state; if the trapping reaction were slower the energy difference would be even greater.

Received: August 7, 1987 [Z 2393 IE]
German version: *Angew. Chem. 99* (1987) 1330

[1] P. Du, W. T. Borden, *J. Am. Chem. Soc. 109* (1987) 930.
[2] P. Dowd, W. Chang, Y. H. Paik, *J. Am. Chem. Soc. 108* (1986) 7416.
[3] IR (CCl_4): $\nu(CH_2)=898$ cm^{-1}; ^{1}H-NMR (400 MHz, $CDCl_3$): $\delta=5.40$ (s, 2H), 5.30 (s, 2H), 5.15 (s, 2H), 0.95 (s, 3H), 0.85 (s, 3H); UV/VIS (pentane): $\lambda_{max}=224$ nm ($\varepsilon=3500$), 354 (80).
[4] IR (CCl_4): $\nu(C=C=C)=1960$ cm^{-1}; ^{1}H-NMR (80 MHz, $CDCl_3$): $\delta=$ 5.3–5.1 (dd, 2H), 4.8 (s, 2H), 4.7 (s, 2H), 1.2 (s, 6H).
[5] G. Zweifel, *J. Org. Chem. 47* (1982) 3364.
[6] T. Flood, P. E. Peterson, *J. Org. Chem. 45* (1980) 5006.
[7] IR (CCl_4): $\nu=3030$, 2980, 2920, 1610, 1500, 1460, 1340, 1285, 1090, 780 cm^{-1}; ^{1}H-NMR (60 MHz, C_6D_6): $\delta=5.6$ (s, 2H), 2.8 (s, 4H), 1.3 (s, 6H).
[8] J. P. Collman, R. G. Finke, J. N. Cawse, J. I. Brauman, *J. Am. Chem. Soc. 100* (1978) 4766.
[9] E. Negishi, A. O. King, W. L. Klima, *J. Org. Chem. 45* (1980) 2526.
[10] ^{1}H-NMR (400 MHz, $CDCl_3$): $\delta=4.86$ (s, 2H), 4.56 (s, 2H), 2.45 (s, 2H), 1.10 (s, 3H), 0.98 (s, 3H).
[11] Radiation source: Osram HBO (200W) Hg high-pressure lamp with monochromator (halfwidth 10 nm) (Bausch and Lomb); cooling equipment: Displex Closed Cycle Refrigeration System 202 (Air Products).
[12] IR: out-of-plane CH vibration of 2,3-dimethylene-1,4-cyclohexanediyl: 770 cm^{-1} [15].
[13] 1000W Hg/Xe high-pressure lamp (Hanovia: 977B-1); uranium glass filter (Schott: UG 5); monochromator (Yvon Jobin: H10-UV).
[14] G. L. Closs, *Adv. Magn. Reson. 7* (1974) 157.
[15] W. R. Roth, M. Biermann, G. Erker, K. Jelich, W. Gerhartz, H. Görner, *Chem. Ber. 113* (1980) 586.

X-Ray Structure Analysis of the Li_2-Compound of Bis(trimethylsilyl)methyl Phenyl Sulfone; Structural Units of an α-Sulfonyl- and a Complex-Stabilized *ortho*-Sulfonyl-"Carbanion"**

By *Werner Hollstein, Klaus Harms, Michael Marsch,* and *Gernot Boche**

Dedicated to Professor Ulrich Schöllkopf on the occasion of his 60th birthday

Regio- and stereo-control by complexation in reactions with organolithium compounds (directed lithiation) not only led to a "new arene chemistry"[1] (*ortho*-lithiation), but also to the selective preparation of other lithium compounds (complex-induced proximity effects).[2] Herein we report on the lithiation of bis(trimethylsilyl)methyl phenyl sulfone **1a**, which furnishes 1,*o*-dilithiobis(trimethylsilyl)methyl phenyl sulfone **3**. Compound **3** crystallizes as the dimer $[\mathbf{3}\cdot(OEt_2)_2]_2$, which contains the structural units of an α-sulfonyl "carbanion"[3] as well as those of an *ortho*-"carbanion" complex-stabilized by the sulfonyl group.[4,5]

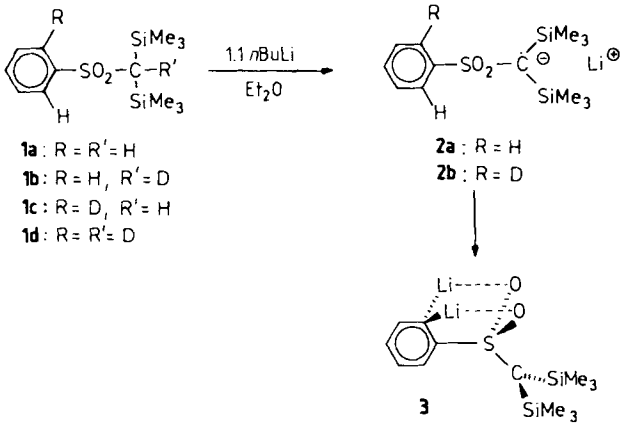

A 1,*o*-dilithio compound of this kind was first characterized chemically and NMR spectroscopically by *Gais* et al. in 1985.[6]

The remarkable formation of the crystalline 1,*o*-dianion $[\mathbf{3}\cdot(OEt_2)_2]_2$ upon reaction of **1a** with 1.1 molar equivalents of *n*BuLi in ether[8] is not fully understood at the moment.[6,7] It can be shown that the sulfones **1a** and **1b** are first completely deprotonated to the dissolved monoanion **2a**,[9] but just how **2a** transforms into **3** and $[\mathbf{3}\cdot(OEt_2)_2]_2$ is still unclear. The dianion character of $[\mathbf{3}\cdot(OEt_2)_2]_2$ was confirmed by deuteriation to **1d**; its structure is reproduced in Figure 1.

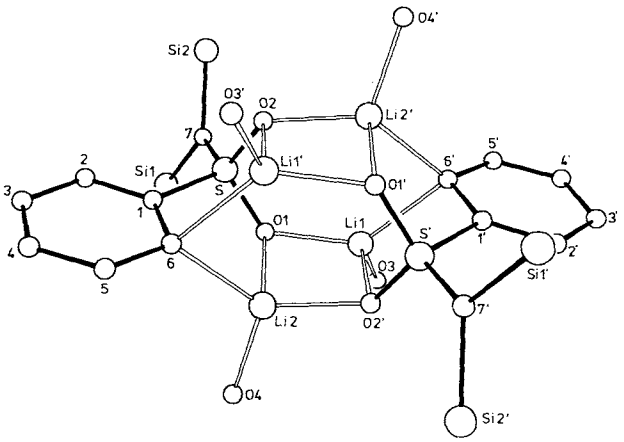

Fig. 1. Crystal structure of $[\mathbf{3}\cdot(OEt_2)_2]_2$. The atomic radii are arbitrary. For clarity, all H atoms, the CH_3 groups of the trimethylsilyl substituents and the CH_3CH_2 groups of the ether molecules are omitted. One CH_3 position of a diethyl ether ligand is disordered. $[\mathbf{3}\cdot(OEt_2)_2]_2$ has an inversion center; symmetry-dependent atoms are primed. Space group $P2_1/c$, $a=11.195(3)$, $b=21.374(5)$, $c=12.619(3)$ Å, $\beta=112.66(3)°$, $Z=4$ (referred to the monomer). Measurements on an Enraf-Nonius CAD4 four-circle diffractometer with graphite monochromated $Cu_{K\alpha}$ radiation at 210 K. 4328 measured reflections (2θ 4–100°); after Lp correction and averaging there remained 2061 observed reflections with $F_o > 3\sigma(F_o)$, which were used for the calculations. Solution by direct methods, refinement according to the least-squares method to $R=0.048$, non-hydrogen atoms anisotropic, hydrogen atoms isotropic [$B(H)=1.3\,B_{equ}(C)$] at calculated positions with a riding model. Some important bond lengths [pm] and angles [°]: C1-S 180.1(5), C7-S 163.7(5), S-O 149.4(3), C7-Si 183.9(4), C6-Li2 215.8(9), C6-Li1' 217.8(9), Li2-O1 204.8(8), Li2-O2' 199.3(8), Li2-O4 195.0(8), Li1-O1 193.8(8), Li1-O2' 214.2(8), Li1-O3 196.4(8); O1-S-O2 109.6(2), Li2-C6-Li1' 83.3(3); torsion angles: O1-S-C1-C6 −47.8(4), O2-S-C1-C6 65.4(4), O1-S-C7-Si1 −50.8(4), O2-S-C7-Si2 13.3(4), C1-S-C7-Si1 66.6(4), C1-S-C7-Si2 −103.1(3), C7-S-C1-C6 −171.8(4), S-C1-C6-Li2 37.8(5), S-C1-C6-Li1' −47.1(4).—Further details of the crystal structure investigation are available on request from the Fachinformationszentrum Energie, Physik, Mathematik GmbH, D-7514 Eggenstein-Leopoldshafen 2 (FRG), on quoting the depository number CSD-52656, the names of the authors, and the journal citation.

[*] Prof. Dr. G. Boche, Dipl.-Chem. W. Hollstein,
Dr. K. Harms, M. Marsch
Fachbereich Chemie der Universität
Hans-Meerwein-Strasse, D-3550 Marburg (FRG)

[**] This work was supported by the Deutsche Forschungsgemeinschaft (SFB 260) and the Fonds der Chemischen Industrie.

Coupling to the dimer takes place via two Li–O–Li–O four-membered rings. Each $Li^{\oplus}$ (e.g. Li2) is bound to an *ortho* C atom (C6), to two O atoms of two different sulfonyl groups (O1 and O2′) and to one diethyl ether O atom (O4). The sp^2 orbital at C6 is oriented almost centrally between Li2 and Li1′ (the torsion angles S-C1-C6-Li2 and S-C1-C6-Li1′ are 37.8(5) and −47.1(4)°, respectively). The two $Li^{\oplus}$ (e.g. Li2 and Li1′) which are coupled to an *ortho* C atom (C6) are complexed by the neighboring sulfone O atoms O1 and O2 such that five-membered rings are formed (e.g. C6-Li1′-O2-S-C1).[10] The ease of *ortho*-lithiation of arenes with an RSO_2 group[4] is thus understandable. The structure computed for $Li_2CHSO_2CH_3$ by *Streitwieser* et al.[11] is very similar to that of $[\mathbf{3}\cdot(OEt_2)_2]_2$ in one respect: the two $Li^{\oplus}$ are bound to the two sulfone O atoms and an "anionic" C (α-C).

The structural characteristics of the α-sulfonyl anion moiety of $[\mathbf{3}\cdot(OEt_2)_2]_2$ are not influenced to any great extent but, nevertheless, noticably so by the dianion formation: the C7–S bond is shortened from 174.7(5) pm in the sulfone **1a**[12] to 163.7(5) pm, and the S–O bonds are lengthened from 144.3(3) pm to 149.4(3) pm; hence, the S–O bonds here are ca. 3 pm longer than in the known α-sulfonyl "carbanions".[3] This could be due to the fact that each O atom in the "dianion" $[\mathbf{3}\cdot(OEt_2)_2]_2$ is coordinated to two $Li^{\oplus}$, but in the monoanions to only one $Li^{\oplus}$. The dihedral angles O1-S-C7-Si1 (−50.8(4)°) and O2-S-C7-Si2 (13.3(4)°) would indicate that the lone pair on C7 assumes a *gauche* conformation to the sulfone O atoms, which is rotated through ca. 18.5° from the ideal position; the same situation is found in monoanions.[3a] C7 is almost planar coordinated: the sum of the torsion angles C1-S-C7-Si1 and C1-S-C7-Si2 is 169.7°. Further, the eight-membered ring (e.g. S-O1-Li1-O2′-S′-O1′-Li1′-O2), which characterizes α-sulfonyl "carbanion" dimers, is also still present.

The X-ray structure analysis of $[\mathbf{3}\cdot(OEt_2)_2]_2$ thus confirms the structural characteristics found in α-sulfonyl "carbanions"; further, the five-membered ring complexation of $Li^{\oplus}$ by the O atoms of an RSO_2 group in an aromatic *ortho* anion is recognizable which contributes to its ease of formation.

Received: August 17, 1987 [Z 2401 IE]
German version: *Angew. Chem. 99* (1987) 1279

[1] D. Seebach, R. Hässig, J. Gabriel, *Helv. Chim. Acta 66* (1983) 308.

[2] The significance of these selective reactions is covered in a series of new reviews: a) P. Beak, D. B. Reitz, *Chem. Rev. 78* (1978) 275; H. W. Gschwend, H. R. Rodriguez, *Org. React. 26* (1979) 1; c) P. Beak, V. Snieckus, *Acc. Chem. Res. 15* (1982) 306; d) P. Beak, A. I. Meyers, *Acc. Chem. Res. 19* (1986) 356; e) G. W. Klumpp, *J. R. Neth. Chem. Soc. 105* (1986) 1.

[3] X-ray structure data have recently become available for some α-sulfonyl "carbanions": a) $[(PhCHSO_2Ph)Li(tmeda)]_2$: G. Boche, M. Marsch, K. Harms, G. M. Sheldrick, *Angew. Chem. 97* (1985) 577; *Angew. Chem. Int. Ed. Engl. 24* (1985) 573; b) $[(CH_2SO_2Ph)Li(tmeda)]_2$: H.-J. Gais, H. J. Lindner, J. Vollhardt, *ibid. 97* (1985) 865 and *24* (1985) 859; c) $[(CH_2{=}CHCHSO_2Ph)Li(diglyme)]_2$: H.-J. Gais, H. J. Lindner, J. Vollhardt, *ibid. 98* (1986) 916 and *25* (1986) 939; d) the structure of $[(Me_3SiCHSO_2Ph)Li(tmeda)]_2$ corresponds in many respects to the structures of the compounds mentioned under (a-c): G. Boche, W. Hollstein, M. Marsch, K. Harms, unpublished.

[4] The strong directing effect of the RSO_2 group (R = aryl, *tert*-butyl, NR_2^1, $NLiR^1$) is known: a) W. E. Truce, M. F. Amos, *J. Am. Chem. Soc. 73* (1951) 3013; b) H. Gilman, S. H. Eidt, *ibid. 78* (1956) 2633; c) H. Watanabe, C. R. Hauser, *J. Org. Chem. 33* (1968) 4278; d) H. Watanabe, R. A. Schwarz, C. R. Hauser, J. Lewis, D. W. Slocum, *Can. J. Chem. 47* (1969) 1543; e) F. M. Stoyanovich, R. G. Karpenko, Y. L. Gol'dfarb, *Tetrahedron 27* (1971) 433; f) J. G. Lombardino, *J. Org. Chem. 36* (1971) 1843; g) D. Hellwinkel, M. Supp, *Chem. Ber. 109* (1976) 3749; h) D. W. Slocum, D. I. Sugarman, *Adv. Chem. Ser. 130* (1974) 222; i) S. J. Shafer, W. D. Closson, *J. Org. Chem. 40* (1975) 889; j) D. W. Slocum, C. A. Jennings, *ibid. 41* (1976) 3653; k) γ-deprotonation of α,β-unsaturated sulfones: E. Block, V. Eswarakrishnan, K. Gebreyes, *Tetrahedron Lett. 25* (1984) 5468.

[5] *ortho*-Li compounds which are complexed intramolecularly by RO- or R_2N-groups have been investigated X-ray crystallographically: a) J. T. B. H. Jastrzebski, G. van Koten, M. Konijn, C. H. Stam, *J. Am. Chem. Soc. 104* (1982) 5490; b) I. R. Butler, W. R. Cullen, J. Reglinski, S. J. Rettig, *J. Organomet. Chem. 249* (1983) 183; c) J. T. B. H. Jastrzebski, G. van Koten, K. Goubitz, C. Arlen, M. Pfeffer, *ibid. 246* (1983) C75; d) H. Dietrich, D. Rewicki, *ibid. 205* (1981) 281; e) see also: W. Neugebauer, A. J. Kos, P. von R. Schleyer, *ibid. 228* (1982) 107.

[6] a) In the reaction of allyl phenyl sulfone with *two* molar equivalents of *n*BuLi in THF at low temperatures the initially formed α-sulfonyl "carbanion" reacts further to give the 1,*o*-dianion corresponding to **3**. Transprotonation to the 1,1-dianion takes place at 50°C [7]; see J. Vollhardt, H.-J. Gais, K. L. Lukas, *Angew. Chem. 97* (1985) 607; *Angew. Chem. Int. Ed. Engl. 24* (1985) 608; b) the second lithiation of (trimethylsilyl)methyl phenyl sulfone proceeds exclusively to the 1,1-dianion; see J. Vollhardt, H.-J. Gais, K. L. Lukas, *ibid. 97* (1985) 695 and *24* (1985) 696; c) the α-sulfonyl "carbanions" mentioned under [3a-d] are formed from the sulfone and one molar equivalent of *n*BuLi; nothing has been reported about a further reaction product. 2,*o*-Dilithio compounds are also known: J. E. Mulvaney, S. Groen, L. J. Carr, Z. G. Garlung, *J. Am. Chem. Soc. 91* (1969) 388; H. M. Walborsky, P. Ronman, *J. Org. Chem. 43* (1978) 731.

[7] 1,1-Dilithiosulfones have been known for some time: a) E. M. Kaiser, L. E. Solter, R. A. Schwarz, R. D. Beard, C. R. Hauser, *J. Am. Chem. Soc. 93* (1971) 4237; b) J. B. Evans, G. Marr, *J. Chem. Soc. Perkin Trans. 1 1972*, 2502; c) K. Kondo, D. Tunemoto, *Tetrahedron 1975*, 1397; d) A. Roggero, T. Salvatori, A. Proni, A. Mazzei, *J. Organomet. Chem. 177* (1979) 313; e) S. P. J. M. van Nispen, C. Mensink, A. M. van Leusen, *Tetrahedron Lett. 21* (1980) 3723; f) M. C. Mussatto, D. Savoia, C. Trombini, A. Umani Ronchi, *J. Org. Chem. 45* (1980) 4002; g) J. J. Eisch, S. K. Dua, M. Behrooz, *ibid. 50* (1985) 3674.

[8] *Procedure* for $[\mathbf{3}\cdot(OEt_2)_2]_2$: A solution of **1a** (90 mg, 0.30 mmol) in diethyl ether (1 mL) was treated at room temperature with 0.33 mmol of *n*BuLi in hexane. After 10 min the solution was evaporated down to about 0.5 mL in an oil-pump vacuum. Single crystals suitable enough for an X-ray analysis could be isolated from the solution after 1 hour. Yield: 44 mg (0.05 mmol), 30%.

[9] The exclusive formation of **2a** from **1b** additionally shows that the deprotonation of **1** does not initially lead to an *ortho* anion that is transprotonated in a second step to the α-anion **2**. Otherwise **2b** and, after protonation, **1c** would have to be formed; deuterium determinations were carried out mass spectrometrically. A corresponding experiment was carried out for the first time by *Gais* et al., see [6b]. A related problem has recently been investigated by other authors: A. I. Meyers, K. B. Kunnen, W. C. Still, *J. Am. Chem. Soc. 109* (1987) 4405. For the mechanism of the second lithiation in some other compounds see: W. Bauer, T. Clark, P. von R. Schleyer, *J. Am. Chem. Soc. 109* (1987) 970; W. Bauer, G. Müller, R. Pi, P. von R. Schleyer, *Angew. Chem. 98* (1986) 1130; *Angew. Chem. Int. Ed. Engl. 25* (1986) 1103.

[10] 1-Magnesio-2-pivaloyl-1,2,3,4-tetrahydroisoquinoline is characterized by a structurally related five-membered ring formation by intramolecular complexation of the carbonyl O atom with the C-bonded Mg: D. Seebach, J. Hansen, P. Seiler, J. M. Gromek, *J. Organomet. Chem. 285* (1985) 1.

[11] D. A. Bors, A. Streitwieser, Jr., *J. Am. Chem. Soc. 108* (1986) 1397.

[12] Structure of **1a**: W. Hollstein, M. Marsch, K. Harms, G. Boche, unpublished.

Coupling of Two Ethyne Molecules at a Nickel Center to Form a Nickelacyclopentadiene Complex

By *Klaus-Richard Pörschke**

The nickel catalyzed cyclooligomerization reactions of acetylene discovered by *Reppe* presumably proceed stepwise by a mechanism involving a nickelacyclopentadiene intermediate.[1] Compounds of this type are already known for other metals,[2] whereas with nickel so far only substituted derivatives have been obtained.[3] Continuing our investigations on ethyne complexes of nickel(0)[4] we have now observed for the first time a coupling of two ethyne molecules on nickel(0) at −78°C (!), leading to formation

[*] Dr. K.-R. Pörschke
Max-Planck-Institut für Kohlenforschung
Postfach 101353, D-4330 Mülheim a. d. Ruhr 1 (FRG)

of a nickelacyclopentadiene complex with bis(diisopropylphosphino)ethane as stabilizing ligand.

When tris(ethene)nickel(0)[5] is treated with stoichiometric amounts of iPr$_2$PC$_2$H$_4$PiPr$_2$ in pentane the crystalline ethene complexes [(μ-iPr$_2$PC$_2$H$_4$PiPr$_2$){Ni(C$_2$H$_4$)$_2$}$_2$] (**1**) and (iPr$_2$PC$_2$H$_4$PiPr$_2$)Ni(C$_2$H$_4$) (**2**) can be isolated. **1** reacts with ethyne in THF at −78°C to yield the mixed ethene/ethyne dinuclear complex [(μ-iPr$_2$PC$_2$H$_4$PiPr$_2$)-{Ni(C$_2$H$_4$)(C$_2$H$_2$)}$_2$] (**3**)[6] as a colorless crystalline and rather sensitive compound. A similar reaction proceeds in ether at −30°C to afford yellow crystals of [(μ-iPr$_2$PC$_2$H$_4$PiPr$_2$){Ni(C$_2$H$_4$)}$_2$(μ-C$_2$H$_2$)] (**4**),[7] in which only one ethyne ligand is present, bridging the nickel atoms. From **2** and ethyne the complex [(iPr$_2$PC$_2$H$_4$PiPr$_2$)Ni(C$_2$H$_2$)] (**5**; C$_2$H$_2$: ν = 1598 cm^{-1}, δ_H = 7.29, δ_C = 123.8, ^1J(CH) = 202 Hz) is obtained, which, particularly in solution, is comparatively stable. **5** reacts with the ethene complex **2** at 0°C with liberation of ethene to afford [{(iPr$_2$PC$_2$H$_4$PiPr$_2$)Ni}$_2$(μ-C$_2$H$_2$)] (**6**; μ-C$_2$H$_2$: ν = 1315 cm^{-1}, δ_H = 5.52, δ_C = 86.3, ^1J(CH) = 188 Hz), in which the ethyne ligand bridges two bis(phosphane)nickel(0) moieties. **6** is cleaved by ethyne at 0°C into two molecules of **5**. Single crystal X-ray structure analyses have been carried out on **5** (d(C≡C) 1.287(7) Å) and **6** (d(C≡C) 1.335(7) Å).[8]

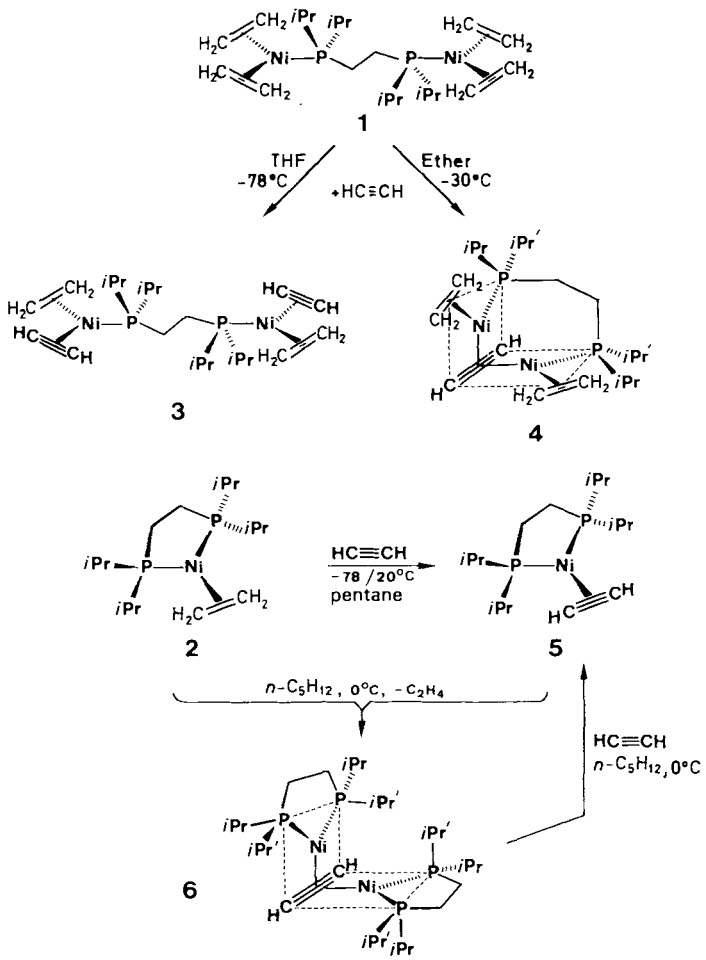

When iPr$_2$PC$_2$H$_4$PiPr$_2$ and excess ethyne are added to a pentane solution of **1** at −78°C, fine yellow crystals of the nickelacyclopentadiene complex **7** separate out in the course of 48 h. Apparently, **7** is formed via **3**: presumably the bridging iPr$_2$C$_2$H$_4$PiPr$_2$ ligand of **3** transforms under the influence of the added iPr$_2$PC$_2$H$_4$PiPr$_2$ into the chelating binding mode and in the course of this reorientation two of the ethyne molecules combine to form the nickelacyclopentadiene group, while a third ethyne molecule forms a bridging ligand between the formal nickel(II) ion and the nickel atom.

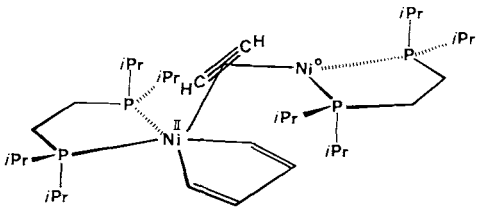

7

7 has been characterized by its ^{1}H-, ^{13}C-, ^{31}P-NMR, and IR spectra[9]. The C≡C stretching vibration of the bridging ethyne ligand of **7** occurs at the same wave number ν = 1315 cm^{-1} as that of **6**. The ^{1}H- and ^{13}C-NMR data of the ethyne ligand of **7** (δ_H = 5.96, δ_C = 98.8, ^1J(CH) = 190 Hz) are similar to those of **6** and also indicate a bridging ethyne ligand (cf. values of **5**). For the μ-C$_4$H$_4$ ligand the chemical shifts and coupling constants of δ_H = 5.09, 4.85 and δ_C = 115.6 (^1J(CH) = 151 Hz, NiCH=*C*H−), 110.8 (^1J(CH) = 143 Hz, Ni−*C*H=) are in the range expected for a metal alkenyl group. In the ^{31}P-NMR spectrum two singlets for the iPr$_2$PC$_2$H$_4$PiPr$_2$ ligands show that the P atoms of each ligand do not couple with those of the neighboring ligand. We are currently studying further reactions of **7**.

Received: September 4, 1987;
revised: October 8, 1987 [Z 2422 IE]
German version: *Angew. Chem. 99* (1987) 1321

CAS Registry numbers:
1, 111497-32-6; **2**, 111497-33-7; **3**, 111497-34-8; **4**, 111524-69-7; **5**, 111497-35-9; **6**, 111556-66-2; **7**, 111524-70-0; iPr$_2$PCH$_2$CH$_2$PiPr$_2$, 87532-69-2; tris(ethene)nickel(0) 50696-82-7.

[1] P. W. Jolly in G. Wilkinson, F. G. A. Stone, E. W. Abel (Eds.): *Comprehensive Organometallic Chemistry, Vol. 8*, Pergamon Press, Oxford 1982, p. 653f.

[2] Examples: a) Ti: H. G. Alt, H. E. Engelhardt, M. D. Rausch, L. B. Kool, *J. Organomet. Chem. 329* (1987) 61; b) Mo: M. H. Chisholm, K. Folting, J. C. Huffman, I. P. Rothwell, *J. Am. Chem. Soc. 104* (1982) 4389; c) W: M. H. Chisholm, K. Folting, D. M. Hoffman, J. C. Huffman, J. Leonelli, *J. Chem. Soc. Chem. Commun. 1983*, 589; M. H. Chisholm, D. M. Hoffman, J. C. Huffman, *J. Am. Chem. Soc. 106* (1984) 6806; d) Fe: G. Dettlaf, E. Weiss, *J. Organomet. Chem. 108* (1976) 213; e) Co: H. Yamazaki, Y. Wakatsuki, *J. Organomet. Chem. 272* (1984) 251.

[3] H. Hoberg, W. Richter, *J. Organomet. Chem. 195* (1980) 355.

[4] a) K. R. Pörschke, R. Mynott, K. Angermund, C. Krüger, *Z. Naturforsch. B40* (1985) 199; b) K. R. Pörschke, R. Mynott, *ibid. 42* (1987) 421; c) K. R. Pörschke, Y.-H. Tsay, C. Krüger, *Angew. Chem. 97* (1985) 334; *Angew. Chem. Int. Ed. Engl. 24* (1985) 323; d) K. R. Pörschke, *XIIth Int. Conf. Organomet. Chem.*, September 8-13, 1985, Abstracts No. 207.

[5] K. Fischer, K. Jonas, G. Wilke, *Angew. Chem. 85* (1973) 620; *Angew. Chem. Int. Ed. Engl. 12* (1973) 565.

[6] **3**: ^{1}H-NMR (200 MHz, [D$_8$]THF, −30°C): δ = 7.10, 6.34 (m, 4H, C$_2$H$_2$), 2.72 (8H, C$_2$H$_4$), 2.25 (m, 4H, PCH), 1.93 (4H, PCH$_2$), 1.08 (m, 24H, kCH$_3$); ^{31}P-NMR (32.4 MHz, [D$_8$]THF, −30°C): δ = 51.6.

[7] **4**: ^{1}H-NMR (200 MHz, [D$_8$]THF, −30°C): δ = 6.08 (1H, C$_2$H$_2$), 4.86 (t, J(PH) = 17.2 Hz, 1H, C$_2$H$_2$), 2.49, 2.27 (m, 8H, C$_2$H$_4$), 2.25 (m, 4H, PCH), 2.1 (m, 4H, PCH$_2$), 1.1 (m, 24H, PCH$_3$); ^{31}P-NMR (32.4 MHz, [D$_8$]THF, −30°C): δ = 34.7.

[8] K. R. Pörschke, W. Bonrath, Y.-H. Tsay, C. Krüger, *Z. Naturforsch. B*, in press.

[9] 7: IR (KBr, −30°C): ν=3010 cm^{-1} (≡C–H or =C–H), ν=1315 cm^{-1} (C≡C), γ=756 cm^{-1} (C–H); ^{1}H-NMR (400 MHz, [D$_8$]THF, rel. TMS, −30°C): δ=5.96 (m, 2H, C$_2$H$_2$), 5.09 (m, 2H, Ni–CH=), 4.85 (m, 2H, =CH–), 2.20, 2.16 (m, 4H, PCH), 1.94, 1.91 (m, 4H, PCH), 1.5–0.9 (8 multiplets, 48H, PCH$_3$); ^{13}C-NMR (75.5 MHz, [D$_8$]THF, rel. TMS, −30°C): δ=115.6 (m, 2C, ^1J(CH)=151 Hz, =CH–), 110.8 (m, 2C, ^1J(CH)=143 Hz, Ni–CH=), 98.8 (m, ^1J(CH)=190 Hz, HC≡CH); ^{31}P-NMR (32.4 MHz, [D$_8$]THF, rel. 85% aqueous H$_3$PO$_4$, −30°C): δ=83.6, 71.4, intensity ratio 1:1.

The Dependence of Intramolecular Electron Transfer on Structure in a Spiro Compound Containing Two Cyclooctatetraene Moieties**

By *Günter Krummel, Walter Huber,* and *Klaus Müllen**

Dedicated to Professor Emanuel Vogel on the occasion of his 60th birthday

The rate constants of the intramolecular electron transfer between separate redox units[1] are not only dependent on the substrate and ion-pair structure[2] but also on the length and conformation of the bridging group.[3,4] We have generated extended redox sequences of several "bis-electrophoric" systems and have been able to alter the energy profiles of intramolecular electron transfers.[5,6]

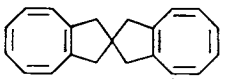

1

The previously unknown compound **1**, 10,10′-spirobi(bicyclo[6.3.0]undeca-2,4,6,8-tetraene), offers the following advantages over already investigated model systems: 1) the subunits are fixed orthogonally to each other by the spiro coupling;[3,6] 2) both a direct π,π conjugation[7–9] as well as a through-space conjugation[6] between the subunits are ruled out; 3) because of the planarization of the cyclooctatetraene (COT) necessary for ion formation,[10] the reorganization energy required for an intramolecular electron transfer between the subunits should be increased.

We describe here the synthesis of **1** and structurally related compounds, the generation of $\mathbf{1}^{\odot\ominus}$, $\mathbf{1}^{2\ominus}$, and $\mathbf{1}^{4\ominus}$ and discuss the possibility of electron transfer between COT subunits of these anions. The method of choice for the preparation of **1** (Scheme 1) is that previously used by us on several occasions: cycloannelation by reaction of dianions with bifunctional electrophiles.[11] After alkylation of the cyclooctatetraene dianion Li_2-**2** (2 equiv.) with tetrabromoneopentane **3b** and aqueous work-up the polycycle **5** is isolated in 56% yield. Apparently a twofold cycloannelation takes place, but the primary product undergoes a valence isomerization under the reaction conditions. The ^{13}C-NMR spectrum of **5** (Table 1) shows that only one species of several conceivable configurational isomers exists. Photolysis of **5** leads via cleavage of benzene to formation of the previously unknown spiro[4.4]nona-2,7-diene **6** as sole product (Table 1).

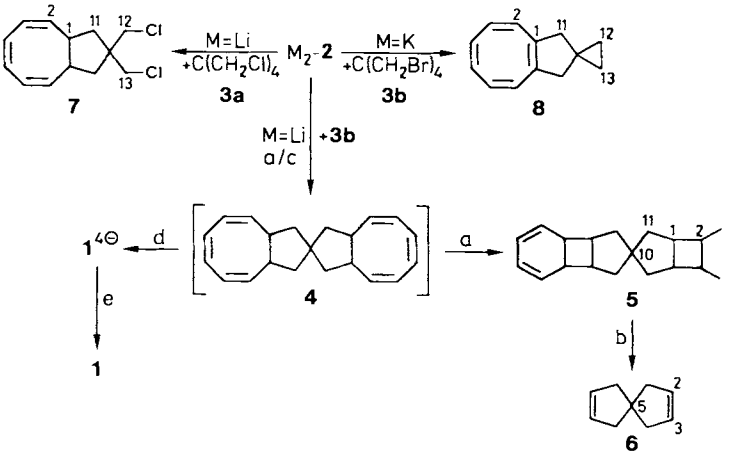

Scheme 1. a) NH_3, −33°C; H_2O, 20°C. b) Pentane, 3×10^{-3} M, Pyrex lamp. c) NH_3, −60°C; d) NH_3, −60°C, KNH_2. e) $CdCl_2$.

The course of the cycloannelation reaction depends on the structure of the ion pair of the nucleophile and on the leaving group of the electrophile **3** (Scheme 1). Alkylation of Li_2-**2** with the chloride **3a** instead of with the bromide **3b** leads to formation of only the monoadduct **7** (Table 1). On the other hand, if the potassium salt K_2-**2** is allowed to react with **3b** only the polycycle **8** is obtained after dehydrogenation (cf. **4** → $\mathbf{1}^{4\ominus}$ → **1**) (Table 1), i.e., here a reductively induced three-membered ring formation follows the cycloannelation.

The conversion of **4** into **5** can be partially suppressed by working at lower temperatures (Scheme 1), and the target compound **1** is obtained via the tetraanion $\mathbf{1}^{4\ominus}$.[12]

Table 1. Melting points (**5**, 7) and ^{13}C-NMR data [a] of **5**–**8**.

5: 83°C; δ=127.6, 127.5, 120.6 (C3–C6, C3′–C6′), 57.6 (C10), 52.0, 51.1 (C2, C7, C2′, C7′), 47.4, 46.3 (C1, C8, C1′, C8′), 37.0, 36.8 (C9, C11, C9′, C11′)

6: δ=130.1 (C2, C3, C7, C8), 48.7 (C5), 47.5 (C1, C4, C6, C9)

7: 84–85°C; δ=134.8, 128.2, 127.7 (C2–C7), 51.5, 50.6 (C12, C13), 46.3 (C10), 43.0, 41.8 (C1, C8, C9, C11)

8: δ=140.2 (C1, C8), 132.5, 131.7, 131.2 (C2–C7), 47.3 (C9, C11), 19.0 (C10), 14.7 (C12, C13)

[a] $CDCl_3$; **5**, **6** 100 MHz; 7, **8** 50 MHz.

The spectroscopic characterization of **1** at room temperature (Table 2) indicates a structure with effective D_{2d} symmetry. Cooling leads to a line-broadening of the singlet signal of the methylene protons and finally at −60°C to the appearance of the signals of two AB systems. This dynamic behavior confirms that both rings are present in a tub conformation.

When a solution of **1** in [D$_8$]tetrahydrofuran is brought into contact with lithium the tetraanion $\mathbf{1}^{4\ominus}$ is formed again. The number and position of the NMR signals (Table 2) indicate a structure with D_{2d} symmetry which contains two planar $COT^{2\ominus}$ units. If one monitors the reduction of **1** NMR spectroscopically it is possible to detect the dianion $\mathbf{1}^{2\ominus}$ as intermediate. The number of the ^{1}H- and ^{13}C-NMR signals (Table 2) shows beyond doubt that the

[*] Prof. Dr. K. Müllen, Dipl.-Chem. G. Krummel
Institut für Organische Chemie der Universität
J.-J.-Becher-Weg 18–20, 6500 Mainz 1 (FRG)
Priv.-Doz. Dr. W. Huber
Institut für Physikalische Chemie der Universität
Klingelbergstrasse 80, CH-4056 Basel (Switzerland)

[**] Reductive Transformations, Part 9. This work was supported by the Deutsche Forschungsgemeinschaft and the Fonds der Chemischen Industrie.—Part 8: G. Neumann, K. Müllen, *J. Am. Chem. Soc. 108* (1986) 4105.

Table 2. $^1H[\delta_H]$- and $^{13}C[\delta_C]$-NMR chemical shifts of **1**, Li_2**1**, and Li_4**1** [a].

	T [°C]	H2–H7, H2′–H7′	H9a, H9b, H11a, H11b	H9a′, H9b′, H11a′, H11b′
δ_H (**1**)	10	5.68–5.55	2.36 (s)	
	−60	5.75–5.53	2.42 (AB), 2.25 (AB)	
δ_H ($\mathbf{1}^{2\ominus}$)	10	5.72–5.40	2.42 (s)	3.48 (s)
	−60	5.66–5.20	2.38 (AB)	3.53 (s), 3.33 (s)
δ_H ($\mathbf{1}^{4\ominus}$)	−50	5.67–5.45	3.52 (s)	

	T [°C]	C1, C8	C1′, C8′	C2–C7	C2′–C7′	C9, C11	C9′, C11′	C10
δ_C (**1**)	10	140.5		133.2, 132.7, 132.1		52.2		48.3
δ_C ($\mathbf{1}^{2\ominus}$)	10	141.3	98.7	133.6, 133.2, 131.1	87.0, 86.7, 85.0	60.7	52.0	47.4
δ_C ($\mathbf{1}^{4\ominus}$)	−50	99.3		86.7, 85.7, 85.0		59.9		45.9

[a] [D_8]THF; 200 MHz (^1H), 50 MHz (^{13}C).

excess charge remains localized in a single eight-membered ring and, as a consequence, a charged and a neutral π-unit are present alongside each other. The equivalence of H9a and H11a and non-equivalence of H9a′ and H11a′ observable at −60°C points to planarity of the charged eight-membered ring and the tub conformation of the uncharged eight-membered ring (Scheme 2). Above 10°C, a rapid inversion of the uncharged ring, recognizable by the coalescence of the signals of H9a′ and H11a′, takes place. No change in the ^{13}C-NMR spectra is observed on heating to 40°C, so that an intramolecular electron transfer on the time scale accessible in the experiment can be ruled out.

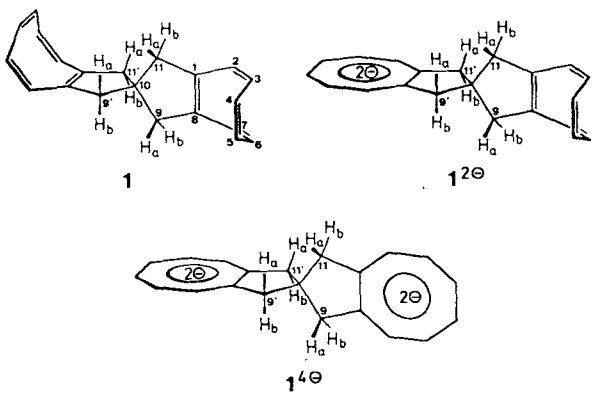

Scheme 2. NMR spectroscopically derived structures of **1**, $\mathbf{1}^{2\ominus}$, and $\mathbf{1}^{4\ominus}$.

During the reduction of **1**, the NMR signals of **1** and $\mathbf{1}^{2\ominus}$ are observed alongside each other without significant line-broadening. This shows that no rapid intermolecular electron transfer takes place and that the intermediate radical anion $\mathbf{1}^{\odot\ominus}$ disproportionates. The ion $\mathbf{1}^{\odot\ominus}$, which apparently is present in only low concentration, cannot be detected ESR spectroscopically. Its characterization can only be achieved if it is generated from the dianion by photooxidation. The ESR coupling constants a_H (0.40 (6 H, COT-ring), 0.40 (2 H, CH_2), 0.88 mT (2 H, CH_2)) show that the unpaired electron is localized in one COT moiety.

Take-up of an electron by **1** forces, as also in COT **2**, a planarization of the eight-membered ring, which contains the additional electron. Such a change of conformation would have to occur alternately in the two eight-membered rings if an intramolecular charge fluctuation between the subunits were to take place in $\mathbf{1}^{\odot\ominus}$ or $\mathbf{1}^{2\ominus}$. As a result of the associated increased reorganization energy,[8–10] the excess charge of $\mathbf{1}^{\odot\ominus}$ and $\mathbf{1}^{2\ominus}$ therefore remains localized in one subunit. The activation energy for the ring inversion of the uncharged ring of $\mathbf{1}^{2\ominus}$, which we determined as 12 kcal mol^{-1}, should comply with the activation barrier of the charge fluctuation. This is also consistent with the fact that the spatial separation of COT subunits is not solely responsible for the charge localization, since rapid intramolecular electron transfer processes can take place in ion pairs with separate rigid subunits.[13]

Received: June 30, 1987;
revised: September 9, 1987 [Z 2320 IE]
German version: *Angew. Chem. 99* (1987) 1305

[1] J. R. Miller, L. T. Calcaterra, G. L. Closs, *J. Am. Chem. Soc. 106* (1984) 3047.
[2] S. Mazur, V. M. Dixit, F. Gerson, *J. Am. Chem. Soc. 102* (1980) 5343.
[3] W. Huber, H. Unterberg, K. Müllen, *Angew. Chem. 95* (1983) 239; *Angew. Chem. Int. Ed. Engl. 22* (1983) 242.
[4] W. Huber, K. Müllen, *Acc. Chem. Res. 19* (1986) 300.
[5] J. Fiedler, W. Huber, K. Müllen, *Angew. Chem. 98* (1986) 444; *Angew. Chem. Int. Ed. Engl. 25* (1986) 443.
[6] W. Irmen, W. Huber, J. Lex, K. Müllen, *Angew. Chem. 96* (1984) 800; *Angew. Chem. Int. Ed. Engl. 23* (1984) 818.
[7] L. Echegoyen, R. Maldonado, J. Nieves, A. Alegria, *J. Am. Chem. Soc. 106* (1984) 7692.
[8] S. W. Staley, C. K. Dustman, K. L. Facchine, G. E. Linkowsky, *J. Am. Chem. Soc. 107* (1985) 4003.
[9] B. Eliasson, U. Edlund, S. W. Staley, *EUCHEM Conf. Electron Transfer React. Org. Chem.*, Visby (Sweden), June 1987.
[10] L. A. Paquette, S. V. Ley, R. H. Meisinger, R. K. Russell, M. Oku, *J. Am. Chem. Soc. 96* (1974) 5806.
[11] K. Müllen, *Angew. Chem. 99* (1987) 192; *Angew. Chem. Int. Ed. Engl. 26* (1987) 204.
[12] The yield of **1** of only 6% referred to **2** is explained by the formation of **5** also occurring under these reaction conditions and by the large losses in the HPLC separation of **1** and **5**.
[13] F. Gerson, W. Huber, W. B. Martin, Jr., P. Caluwe, T. Pepper, M. Szwarc, *Helv. Chim. Acta 67* (1984) 416.

Dibenzo[*fg,mn*]octalene and Cycloocta[*def*]phenanthrene. New Models for the Conformational Analysis of Biphenyl Systems**

By *Willi Heinz, Peter Langensee,* and *Klaus Müllen**

Dedicated to Professor Klaus Hafner on the occasion of his 60th birthday

An important step in the conformational analysis of biphenyl systems is the bridging of the *ortho* positions.[1,2] The compounds **1**, **2**, and **3**[3,4] are particularly attractive

[*] Prof. Dr. K. Müllen, Dipl.-Chem. W. Heinz, Dr. P. Langensee
Institut für Organische Chemie der Universität
J.-J.-Becher-Weg 18–20, D-6500 Mainz 1 (FRG)

[**] This work was supported by the Deutsche Forschungsgemeinschaft and the Fonds der Chemischen Industrie.

because rotation about the biphenyl single bond occurs simultaneously with the inversion of the octalene and/or cyclooctatetraene moieties. Compounds **1**–**3** are of addi-

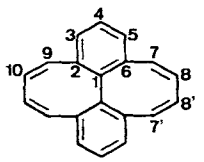

1

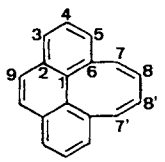

2

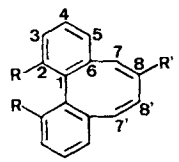

3a, R=R'=H
3b, R=H, R'=CHMe$_2$
3c, R=CH$_3$, R'=CHMe$_2$

tional importance in view of the recently described finding that the energy profiles of conformational conversions can be influenced by electron transfer processes.[5–7] Herein we describe the synthesis, structure, and redox chemistry of the new compounds dibenzo[*fg,mn*]octalene **1** and cycloocta[*def*]phenanthrene **2** and the saturated analogues **5a**, **6** and **8**, and **10**–**12**, respectively, derived therefrom. In the case of the dianion of **1** it was possible to demonstrate a symmetry deformation by charge localization.

The key step of the synthesis of **1** is the reaction of 2,2′,6,6′-tetra(bromomethyl)biphenyl **4** with the dipotassium salt of ethyl ethanetetracarboxylate to give the octaester **5b**, in which two condensed eight-membered rings are formed in one step (Scheme 1). For transformation into **1** the diene **6** obtainable from **5b** by hydrolysis/decarboxylation and subsequent oxidative decarboxylation[4] was converted by bromine addition into a tetrabromide, dehydrobromination of which however, for conformational reasons, did not furnish **1** but only **7**. Therefore **6** was first subjected to a base-induced isomerization. The resulting 7:3 mixture of **8** (*syn/anti*) and **9** after bromination with *N*-bromosuccinimide (NBS) and dehydrobromination affords compound **1** [m.p. 188°C (hexane), colorless needles]. The cycloocta[*def*]phenanthrene **2** is synthesized analogously from 4,5-di(bromomethyl)phenanthrene via **10** (Scheme 1). The partially hydrogenated analogues **5a** as well as **11** and **12** are formed upon reduction of the precursors **6** and **10**, respectively, with H_2. Characteristic data of the new compounds are listed in Tables 1 and 2.

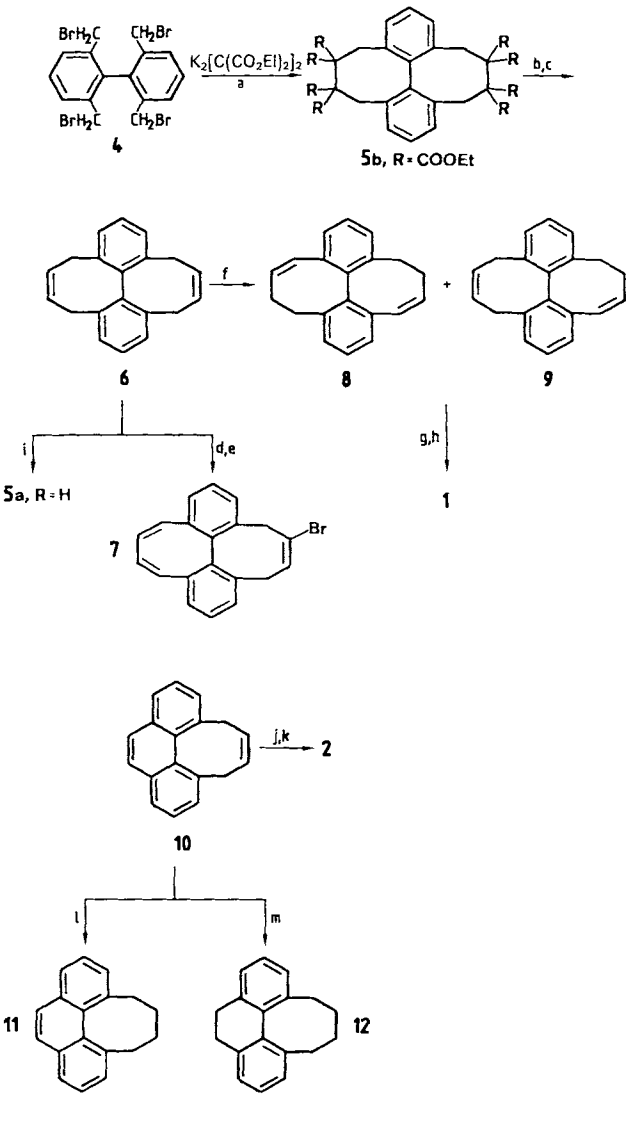

Scheme 1. a) Dimethoxyethane/toluene (1/1), 110°C; 25%. b) KOH, ethylene glycol, 200°C; 84%. c) Pb(OAc)$_4$, pyridine, 65°C; 23%. d) Br_2, CCl_4, 0°C. e) 1,5-diazabicyclo[4.3.0]non-5-ene, toluene, 110°C; 27% referred to **6**. f) *t*BuOK, THF, 65°C. g) NBS, CCl_4, 80°C. h) *t*BuOK, THF, 20°C; 40% referred to **6**. i) H_2 (2 equiv.), Pd/C (5%), ethyl acetate, 25°C; 81%. j) Br_2, CCl_4/hexane, −80°C; 90%. k) 1,8-Diazabicyclo[5.4.0]undec-7-ene, benzene, 80°C; 43%. l) Analogous to (i) (1 equiv. H_2); 80%. m) Analogous to (i); 91%.

Table 1. Melting points (apart for **15**) and ^{1}H-NMR spectroscopic data of the compounds **5a**, **6**, **10**–**13**, and **15**.

5a, m.p. 123°C; ^{1}H-NMR ($C_2D_2Cl_4$, 300 MHz, 110°C): δ=7.31 (t, 2H; *p*-$H_{arom.}$), 7.15 (d, 4H; *m*-$H_{arom.}$), 2.69 (m, 4H), 2.15–2.05 (m, 8H), 1.56 (m, 4H)

6, m.p. 204–205°C; ^{1}H-NMR ($CDCl_3$, 400 MHz): δ=7.29 (t, 2H; *p*-$H_{arom.}$), 7.05 (d, 4H; *m*-$H_{arom.}$), 5.81 (m, 4H; $H_{olef.}$), 3.09, 2.90 (AB system, 8H)

10, m.p. 86.5°C; ^{1}H-NMR (CD_2Cl_2, 300 MHz, 20°C): δ($H_{arom.}$)=7.68 (d, 2H), 7.55 (t, 2H), 7.51 (s, 2H), 7.38 (d, 2H), δ=6.32 (t, 2H; $H_{olef.}$), 3.22 (d, 4H)

11, m.p. 88.5°C; ^{1}H-NMR (CD_2Cl_2, 300 MHz, −30°C): δ($H_{arom.}$)=7.66 (d, 2H), 7.52 (s, 2H), 7.56–7.47 (m, 4H), δ($H_{aliph.}$)=2.91 (m, 2H), 2.33 (m, 2H), 2.21 (m, 2H), 1.99 (m, 2H)

12, m.p. 87°C; ^{1}H-NMR ($CDCl_3$, 300 MHz, 20°C): δ=7.30–7.16 (m, 6H; $H_{arom.}$), 2.89–2.66 (m, 6H), 2.23–2.15 (m, 4H), 1.80–1.73 (m, 2H)

13, m.p. 149–150°C; ^{1}H-NMR ($C_2D_2Cl_4$, 300 MHz, 120°C): δ=7.39–7.26 (m, 8H; $H_{arom.}$), 2.74 (m, 2H), 2.25–2.10 (m, 4H), 1.60 (m, 2H)

15, ^{1}H-NMR ($CDCl_3$, 200 MHz, 20°C): δ=7.27–6.90 (m, 6H; $H_{arom.}$), 6.73, 6.03 (AA′BB′ system, 4H; "butadiene" H), 5.84 (m, 2H; $H_{olef.}$), 3.57 (m, 2H; 2C*H*–CH_3), 0.47 (d, 6H; 2CH_3)

The twisting with respect to the C8–C8′ bond brought about by the tub conformation of the unsaturated eight-membered rings of **1** and **2** as well as the bond alternation are confirmed by the small value for the vicinal coupling constant ^3J(H8,H8′) (see Table 2). According to the X-ray structure analysis[8] the eight-membered ring subunit of **2** is more flattened than that of **3a**[9] (twist angles of the biphenyl moiety: 33.0 and 68.5°; of the butadiene moiety: 51.2 and 58.0°).

If one takes the position of the conjugation band of the respective biphenyl unit[1] in the UV spectrum as a measure of the twist [λ [nm] (ε): **1**, 217 (32000); **3a**, 230 (24000); **5a**, 220 (13000); **12**, 260 (12300); **13**, 235 (11800)], the interplanar angle of the biphenyl system should, firstly, be greater in **1** than in **3a**, secondly, remain unaltered in the transition from **1** and **3a** to **5a** and **13**, respectively, and, thirdly, be smallest in the dihydrophenanthrene system **12**.

Table 2. $^1H[\delta_H]$- and $^{13}C[\delta_C]$-NMR chemical shifts as well as the magnitudes of the vicinal couplings ^3J [Hz] of **1**, **2**, **3a** and K_2-**1**, Li_2-**2**, K_2-**3a** [a].

H/C	1	2	3	4	5	6	7	8	9	10	^3J(H7,H8)	^3J(H8,H8')
δ_H (**1**)	—	—	6.96	7.25	6.96	—	6.65	6.00	6.65	6.00	11.6	2.5
δ_H (**1**$^{2\ominus}$)	—	—	5.03	6.36	7.66	—	6.04	5.90	5.60	6.17	10.8	12.9
δ_C (**1**)	140.9	139.7	127.2	126.1	127.2	139.7	133.8	130.7	133.8	130.7		
δ_C (**1**$^{2\ominus}$)	111.3	144.3	100.0	115.3	133.5	114.8	90.2	96.2	135.2	130.4		
δ_H (**2**)	—	—	7.72	7.57	7.25	—	6.25	6.47	7.53	—	10.9	3.3
δ_H (**2**$^{2\ominus}$)	—	—	6.34	6.43	7.58	—	5.40	6.19	7.14	—	9.6	10.1
δ_C (**2**)	137.9	131.0 [b]	126.8–128.2			134.2 [b]	133.1	131.8	[c]	—		
δ_C (**2**$^{2\ominus}$)	109.5	139.5	106.2	111.1	129.4 [b]	118.0	88.4 [b]	88.7 [b]	129.9 [b]	—		
δ_H (**3a**$^{2\ominus}$)	—	8.02	5.93	6.37	7.78	—	6.12	6.43	—	—	10.2	10.6
δ_C (**3a**$^{2\ominus}$)	108.1	134.9	104.9	113.2	135.9	115.3	91.1	95.3	—	—		

[a] Measurement conditions: **1**: [D$_8$]THF, 200 MHz (^{1}H), 50 MHz (^{13}C), 25°C; **1**$^{2\ominus}$: [D$_8$]THF, 200 MHz, −80°C (^{1}H), 50 MHz, 50°C (^{13}C); **2**: CD_2Cl_2; 300 MHz (^{1}H), 75 MHz (^{13}C), 25°C; **2**$^{2\ominus}$: [D$_8$]THF, 300 MHz, −60°C (^{1}H), 75 MHz, −20°C (^{13}C); **3**$^{2\ominus}$: [D$_8$]THF, 200 MHz, −80°C (^{1}H), 50 MHz, −40°C (^{13}C). [b] Assignment not confirmed experimentally. [c] One of the signals between $\delta = 126.8$ and 128.2.

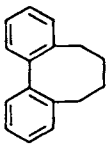

13

The synthesis of the salts M_2-**1** and M_2-**2** was achieved by treatment of **1** and **2**, respectively, with alkali metal (M = Li, K) in [D$_8$]THF. The NMR spectroscopic characterization of the ions (see Table 2) revealed the relationship of **2**$^{2\ominus}$ and **3a**$^{2\ominus}$.[10,11] Characteristic of both species are the distribution of the charge over the *whole* π-electron system (as derived from the chemical shifts), the diatropism of the ions, and the formation of *planarized* eight-membered rings with π-bond delocalization [see the adjustment of the vicinal H,H couplings ^3J(H7,H8) and ^3J(H8,H8')].

Whereas the number of the NMR signals is consistent with a D_2 symmetry for the neutral compound **1**, a lowering of the symmetry is observed in **1**$^{2\ominus}$. The number and position of the signals of **1**$^{2\ominus}$ can only be interpreted in terms of the excess charge of the dianion remaining localized in a dibenzocyclooctene moiety (see **1a**$^{2\ominus}$). Whereas the charged substructure becomes more planar, the uncharged butadiene bridge remains bent. The strain associated with a flattening of the whole molecule is apparently so great that it does not permit a symmetric structure with electrostatically preferred charge delocalization. Even at room temperature there is no fluctuation of charge between charged and uncharged subunits in **1**$^{2\ominus}$.

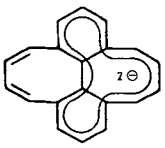

1a$^{2\ominus}$

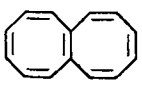

14

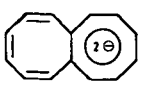

14a$^{2\ominus}$

The conformationally determined charge localization in **1**$^{2\ominus}$ invites comparison with **3b**, **3c**, and **14**:

- ion formation in **3b** effects a flattening or drastically reduces the inversion barrier of the eight-membered ring;[6,7] only strong steric interactions as in **3c** lead to non-planar dianions;[7]
- the dianion of octalene **14** has D_{2h} symmetry even at −145°C; i.e. should structures with charge localization (**14a**$^{2\ominus}$) occur, then they rapidly interconvert.[12]

The charge localization in **1**$^{2\ominus}$ has characteristic chemical consequences. The kinetically controlled attack of electrophiles on dianion-intermediates[13] preferentially takes place at the site of highest charge density; in the case of a charge delocalization in **1**$^{2\ominus}$ (D_{2h}), this would, according to a simple MO consideration, be at C1 and C1'. These bridgehead centers are the centers of highest charge density in **14**$^{2\ominus}$, as has been shown by preparatively useful reductive transformations via Li_2-**14**.[14] That the charge distribution in **1**$^{2\ominus}$ corresponds to that in **3a**$^{2\ominus}$ but not to that in **14**$^{2\ominus}$, follows from the reaction of K_2-**1** with dimethyl sulfate: exclusively the dimethyl adduct **15** is formed.

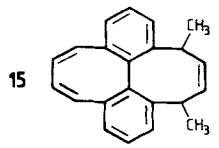

15

Received: June 30, 1987;
revised version: September 9, 1987 [Z 2321 IE]
German version: *Angew. Chem. 99* (1987) 1306

CAS Registry numbers:
1, 111409-90-6; K_2-**1**, 111410-04-9; **2**, 111409-91-7; Li_2-**2**, 111410-08-3; K_2-**3a**, 111410-06-1; **4**, 257-55-6; **5a**, 111409-92-8; **5b**, 111410-02-7; **6**, 111409-93-9; **7**, 111409-94-0; **8**, 111409-95-1; **9**, 111409-96-2; **10**, 111409-97-3; **11**, 111409-98-4; **12**, 111409-99-5; **13**, 1082-12-8; **15**, 111410-01-6.

[1] K. Mislow, M. A. W. Glass, H. B. Hopps, E. Simon, G. H. Wahl, Jr., *J. Am. Chem. Soc. 86* (1964) 1710.
[2] P. Rashidi-Ranjbar, J. Sandström, *Tetrahedron Lett. 28* (1987) 1537.
[3] E. Vogel, W. Frass, J. Wolpers, *Angew. Chem. 75* (1963) 979; *Angew. Chem. Int. Ed. Engl. 2* (1963) 625.
[4] F. Sondheimer, H. N. C. Wong, *J. Org. Chem. 45* (1980) 2438.
[5] R. H. Baughman, I. L. Bredas, R. R. Chance, R. L. Elsenbaumer, L. W. Shacklette, *Chem. Rev. 82* (1982) 209.
[6] W. Huber, K. Müllen, *Acc. Chem. Res. 19* (1986) 300.
[7] W. Heinz, P. Langensee, K. Müllen, *J. Chem. Soc. Chem. Commun. 1986*, 947.
[8] W. Heinz, P. Langensee, J. Lex, K. Müllen, unpublished.
[9] N. Z. Huang, T. C. W. Mak, *J. Mol. Struct. 101* (1983) 135.
[10] K. Müllen, *Helv. Chim. Acta 61* (1978) 1296.
[11] H. Günther, A. Shyouk, D. Cremer, K.-H. Frisch, *Justus Liebigs Ann. Chem. 1978*, 165.
[12] K. Müllen, J. F. M. Oth, H.-W. Engels, E. Vogel, *Angew. Chem. 91* (1979) 251; *Angew. Chem. Int. Ed. Engl. 18* (1979) 229.
[13] K. Müllen, *Angew. Chem. 99* (1987) 192; *Angew. Chem. Int. Ed. Engl. 26* (1987) 204.
[14] E. Vogel, H.-W. Engels, W. Huber, J. Lex, K. Müllen, *J. Am. Chem. Soc. 104* (1982) 3729.

1,5-Electrocyclization in Homofuran, Homopyrrole, and Homothiophene**

By *Frank-Gerrit Klärner** and *Dietmar Schröer*

Dedicated to Professor Emanuel Vogel on the occasion of his 60th birthday

Carbonyl ylides and azomethyne ylides—the products of oxirane and aziridine ring-opening, respectively—are presently attracting considerable interest (e.g. as reaction partners in 1,3-dipolar cycloadditions).[1] The 1,5-electrocyclic ring-opening[2] of the heterocycles homofuran **1a**,[3] homopyrrole **1b**,[4] and homothiophene **1c**[3]—isoelectronic with the bicyclo[3.1.0]hexenyl anion **1d**—should lead to ylide intermediates of the type **2**, which can also be regarded as vinylogous carbonyl ylides, azomethine ylides, and thiocarbonyl ylides **2'**, respectively.

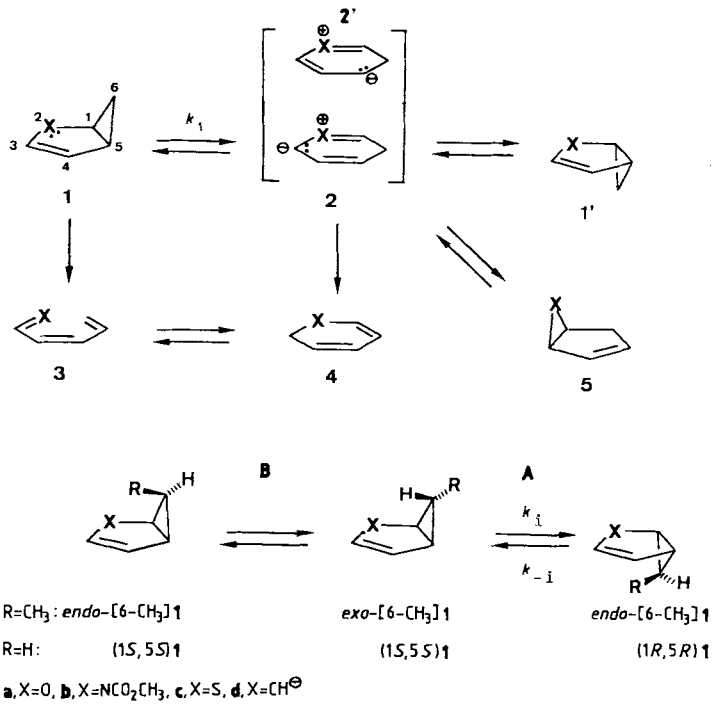

Scheme 1. Valence tautomerizations starting from **1**.

Hitherto, only the epimerization of *exo*- and *endo*-6-methylhomofuran (Scheme 1, bottom) was known,[5] but it was not known whether it takes place, as required for the electrocyclic process, by cleavage of the central cyclopropane bond C^1–C^5 (Route **A**) or by cleavage of one of the peripheral cyclopropane bonds C^1–C^6 or C^5–C^6 (Route **B**). With optically active **1** it should be possible to establish which one of the two alternatives applies, since the epimerization via Route **A** should proceed with concomitant racemization, that via Route **B**, on the other hand, without racemization.

We partially separated racemic **1a** and **1b** into the enantiomers by medium-pressure chromatography on microcrystalline triacetylcellulose (with 95% ethanol as eluant, (−)-**1a** and (−)-**1b**, respectively, were obtained as first fraction and (+)-**1a** and (+)-**1b**, respectively, as second fraction).[6] The enantiomeric excess (*ee*) of (+)-**1a** ($[\alpha]_D^{20} = 194.5°$) could be determined ^{1}H-NMR spectroscopically using the chiral shift reagent Eu(hfc)$_3$ to be 34%.[7,8]

Optically active homofuran **1a** racemizes without side reactions at about 70°C. The temperature-dependence of the rate constants (in dioxane) determined from the decrease of $[\alpha]_D$ with time between 60 and 90°C can be described with the Arrhenius equation (a).

$$k_{rac} = (3.7 \pm 1.3) \times 10^{13} \exp[-(118.6 \pm 1.0)\,\mathrm{kJ\,mol^{-1}(RT)^{-1}}]\,\mathrm{s^{-1}} \quad \text{(a)}$$

Optically active homopyrrole **1b** already slowly racemizes at room temperature. The rate constants determined between 28 and 61°C fit the Arrhenius equation (b).

$$k_{rac} = (1.9 \pm 0.6) \times 10^{13} \exp[-(102.5 \pm 0.4)\,\mathrm{kJ\,mol^{-1}(RT)^{-1}}]\,\mathrm{s^{-1}} \quad \text{(b)}$$

In the case of the homothiophene system all attempts to separate racemic **1c** chromatographically or its methyl derivatives *exo*-[6-CH_3]**1c** and *endo*-[6-CH_3]**1c**, which are formed in the ratio 65 : 35[9] in the copper(I) chloride-catalyzed reaction of thiophene and diazomethane, gas chromatographically, met without success. An explanation for this is found in the ^{1}H-NMR spectra of **1c** recorded at several temperatures (Fig. 1). Above 80°C the exchange of the cyclopropane H atoms *exo*-6-H and *endo*-6-H is rapid on the NMR time scale. The signals of the olefinic H atoms 3-H and 4-H, however, remain unchanged over the whole temperature range, as to be expected for the epimerization process.[10] The rate of exchange of *endo*-6-H and *exo*-6-H at the coalescence temperature of 120°C is estimated with an approximation formula to be $k_{coal} = 205\ \mathrm{s^{-1}}$.[11]

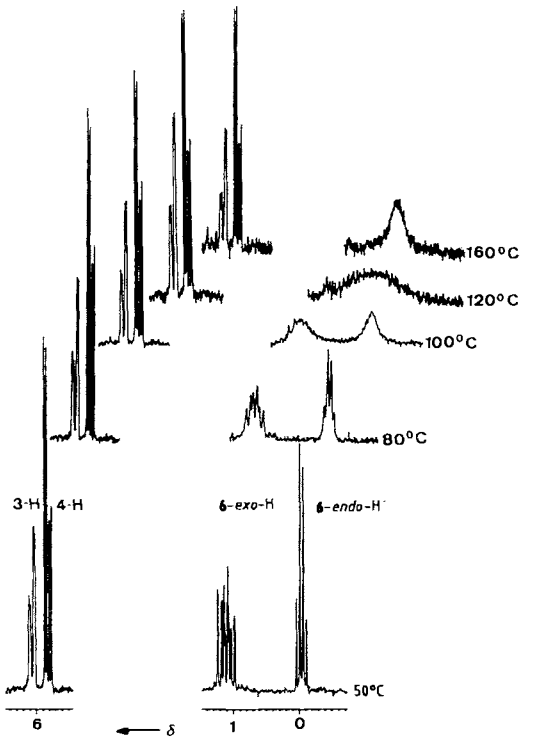

Fig. 1. Sections from the ^{1}H-NMR spectra of **1c** at temperatures between 50 and 160°C (80 MHz, [D_6]Me_2SO).

[*] Prof. Dr. F.-G. Klärner, Dr. D. Schröer
Fakultät für Chemie der Universität
Postfach 102148, D-4630 Bochum 1 (FRG)

[**] This work was supported by the Deutsche Forschungsgemeinschaft and the Fonds der Chemischen Industrie.

That the racemization of optically active **1a** and the epimerization of *exo*-[6-CH_3]**1a** proceed at comparable rates (Table 1) affords evidence for the opening of the central cyclopropane bond (Route **A**) and rules out any significant participation of Route **B**.[12] The disrotatory course of the ring-opening is consistent with the Woodward–Hoffmann rules.[13] An electrocyclic process involving participation of a lone pair on the heteroatom leads to the formal dipolar intermediate of type **2**,[14] but its small dependence on the pressure and solvent polarity (Table 1) indicates

Table 1. Dependence of the racemization of optically active **1a** and the epimerization *exo*-[6-CH_3]**1a** ⇄ *endo*-[6-CH_3]**1a** on solvent and pressure.

	$k \times 10^5$ [s^{-1}] [a]	K [b]	Solvent	p [bar]
[c]	3.49 ± 0.12	1	benzene	1
[c]	2.97 ± 0.03	1	acetonitrile	1
[c]	2.88 ± 0.09	1	acetone	7000
[d]	6.67 ± 0.11	2.12	acetone	1
[d]	2.97 ± 0.05	1.42	acetone	7000

[a] $k = (k_i + k_{-i})$. [b] $K = k_{-i}/k_i$. [c] Racemization. [d] Epimerization.

that the transition state of the reaction **1** → **2** is isopolar with the ground state. Surprisingly, the nature of the heteroatom has a large influence on the rate. From the kinetic parameters it can be estimated by extrapolation that the ring-opening of homothiophene **1c** ($k_i = 2k_{coal}$) and of homopyrrole **1b** ($\Delta G^{\neq} = 77.4$ kJ mol^{-1} and 99.6 kJ mol^{-1}, respectively) occur 63 100 times and 72 times faster, respectively, than that of homofuran **1a** ($\Delta G^{\neq} = 113.4$ kJ mol^{-1}) ($k_i = k_{rac}$). These effects afford proof, for the first time, that the heteroatoms (O, N, and S) stabilize carbonyl-ylide-like intermediates very differently. The surprisingly strong influence of sulfur indicates that the stabilization in the case of **2c** is similar to that in the case of sulfur ylides.[15] However, a quantitative analysis is not possible without a knowledge of the influence which the heteroatom has on the stability of the ground state.

The heterocycles **1a–c** are thermally very stable and only begin to rearrange irreversibly into **3a**,[16] **4b** or **4c**[1] and their secondary products above 250 °C (in a static system) or 400 °C (in a flow system). With the aid of the C-6 labeled compounds [6-CH_3]**1a**,[5] [6,6-D_2]**1b**,[4] and [6-CH_3]**1c** it was established that **4b** is formed from **2b** by a sigmatropic 1,4-H shift, whereas in **1a** and **1c** the cleavage of the C^1–X and C^5–C^6 bonds competes with the H-shift in the ratio 4.8 : 1 and 4.4 : 1, respectively.[17] In no case has a rearrangement to the bicycle **5** been observed, for which an orbital symmetry-forbidden disrotatory ring closure of the intermediate **2** would be required. The rearrangement **1a** → **5a** (besides other reactions) was observed only in a shock tube at 700 °C and with a reaction time of 1.2 ms.[18] The Gibbs activation energy of the reaction **1a** → **5a** can be estimated thereby to be 209 kJ mol^{-1}. Thus, the activation barrier of the orbital symmetry-forbidden ring closure **2a** → **5a** could therefore be at least 96 kJ mol^{-1} higher than that of the allowed reaction **2a** → **1a**.

Received: June 1, 1987;
revised: July 22, 1987 [Z 2275 IE]
German version: *Angew. Chem.* 99 (1987) 1295

[1] a) Review: R. Huisgen, *Angew. Chem.* 89 (1977) 589; *Angew. Chem. Int. Ed. Engl.* 16 (1977) 572; b) theoretical studies: F. Volatron, N. Trong Anh, Y. Jean, *J. Am. Chem. Soc.* 105 (1983) 2359; D. Feller, E. R. Davidson, W. T. Borden, *ibid.* 106 (1984) 2513, and references cited therein.

[2] Review of 1,5-electrocyclizations: R. Huisgen, *Angew. Chem.* 92 (1980) 979; *Angew. Chem. Int. Ed. Engl.* 19 (1980) 947.

[3] E. Müller, H. Kessler, H. Fricke, H. Suhr, *Tetrahedron Lett. 1963*, 1047.

[4] S. R. Tanny, J. Grossmann, F. W. Fowler, *J. Am. Chem. Soc.* 94 (1972) 6495.

[5] J. Wolfhugel, A. Maujean, J. Chuche, *Tetrahedron Lett. 1973*, 1635.

[6] Review: G. Hesse, R. Hagel, *Justus Liebigs Ann. Chem. 1976*, 996.

[7] Tris-[3-(heptafluoropropyl-hydroxymethylene)-(−)-camphorato]europium; H. L. Goering, J. N. Eikenberry, G. Koermer, S. Lattimer, *J. Am. Chem. Soc.* 96 (1974) 1493.

[8] The catalytic hydrogenation (Pd-C, isooctane) of (+)-**1a** (*ee* = 34%) furnished optically active 2- and 3-methyltetrahydrofuran and tetrahydropyran in the ratio 12 : 54 : 34. The analyses of the hydrogenation products carried out on a chiral GC column by Prof. Dr. *V. Schurig* and Frau *D. Wistuba* show that (*S*)-2-methyltetrahydrofuran (*ee* = 32%) is formed. Hence, the (1*S*,5*S*)-configuration can be assigned to the (+)-**1a** enantiomer; cf. W. Kirmse, P. V. Chiem, V. Schurig, *Tetrahedron Lett. 26* (1985) 197.

[9] ^{1}H-NMR (400 MHz, $CDCl_3$) of *exo*-[6-CH_3]**1c**: $\delta = 0.42$ (m; 6-H), 1.09 (d; CH_3), 2.16 (m, $J(1,5) = 7.5$, $J(5,6) = 3.0$ Hz; 5-H), 2.58 (m, $J(1,6) = 3.3$ Hz; 1-H), 5.75 (dd, $J(4,5) = 3.0$ Hz; 4-H), 5.90 (dd, $J(1,3) = 1.6$, $J(3,4) = 5.8$ Hz; 3-H); of *endo*-[6-CH_3]**1c**: $\delta = 0.79$ (d; CH_3), 0.90 (m; 6-H), 2.58 (m, $J(5,6) = 7.4$ Hz; 5-H), 3.00 (td, $J(1,5) = J(1,6) = 7.4$, $J(1,3) = 1.8$ Hz; 1-H), 5.50 (dd, $J(3,4) = 5.8$, $J(4,5) = 3.0$ Hz; 4-H), 6.02 (m; 3-H).

[10] This finding rules out that 1,3- or 1,4-shifts of C-6, leading to an exchange of 1-H and 3-H as well as of 4-H and 5-H, compete with the epimerization at C-6 observed here.

[11] H. Günther: *NMR-Spektroskopie*, 2nd Edit., Thieme, Stuttgart 1985, p. 229.

[12] The small difference in the racemization and epimerization barriers could be attributed to the effect of the methyl group at C-6.

[13] R. B. Woodward, R. Hoffmann, *Angew. Chem. 81* (1969) 797; *Angew. Chem. Int. Ed. Engl. 8* (1969) 781.

[14] Still further resonance structures can be formulated for **2**. According to quantum mechanical calculations [1b] a diradical structure participates up to more than 50% in the structure of the parent carbonyl ylide.

[15] The unusual stability of sulfur ylides is commonly attributed to a dπ–pπ interaction (for example, J. March: Advanced *Organic Chemistry*, 3rd edition, Wiley, New York 1985, p. 36); see also W. Kutzelnigg, *Angew. Chem. 96* (1984) 262; *Angew. Chem. Int. Ed. Engl. 23* (1984) 272.

[16] In the thermolysis of **1a** we obtained essentially the same products as are formed in the thermolysis of 3,4-epoxycyclopentene: P. Schiess, P. Radimerski, *Helv. Chim. Acta 57* (1974) 2583, and references cited therein.

[17] **1c** and [6-CH_3]**1c** were thermolyzed in a flow system (550 °C, 1 torr and 500 °C, 0.1 torr, respectively). Product ratios: **1c** : **4c** : unidentified products = 6 : 84 : 10; [6-CH_3]**1c**: [2-CH_3]**4c** : [3-CH_3]**4c** : unidentified products = 33 : 51 : 12 : 4. The spectroscopic data of the 2*H*-thiopyran derivatives **4c**, [2-CH_3]**4c** and [3-CH_3]**4c** agree with the values given in the literature (D. Schuijl-Laros, P. J. W. Schuijl, L. Brandsma, *Recl. Trav. Chim. Pays-Bas 91* (1972) 785).

[18] We thank Prof. Dr. *W. R. Roth* and Dr. *R. Schmidt*, Bochum, for carrying out the shock tube experiments.

Stereocontrolled Formation of Annelated Cyclopentanes by Intramolecular Hetero-Diels–Alder Reaction. Synthesis of Deoxyloganin from Citronellal**

By *Lutz F. Tietze,* Horst Denzer, Xenia Holdgrün,* and *Manfred Neumann*

Dedicated to Professor Ulrich Schöllkopf on the occasion of his 60th birthday

Deoxyloganin, **4a**, is a member of the large class of iridoidglycoside natural products,[1] whose characteristic

[*] Prof. Dr. L. F. Tietze, Dr. H. Denzer, Dipl.-Chem. X. Holdgrün, Dr. M. Neumann
Institut für Organische Chemie der Universität
Tammannstrasse 2, D-3400 Göttingen (FRG)

[**] Inter- and Intramolecular Hetero-Diels-Alder Reactions, Part 20. This work was supported by the Deutsche Forschungsgemeinschaft and the Fonds der Chemischen Industrie. We wish to thank Professor *Hiroyuki Inouye*, Kyoto, for an authentic sample of deoxyloganin for comparison. Part 19: [7].

structural feature is a cyclopenta[*c*]pyran framework having a β-glycosidically linked glucose at C1. In plants, **4a** is formed from the monoterpene geraniol, **1**, and is a biosynthetic precursor of secologanin, which is a key intermediate in the biosynthesis of a large variety of alkaloids. *Arigoni* et al.[2] postulated that **4a** is formed via the tricarbonyl compound **2b**. It was assumed that **2b** first undergoes a stereoselective hydrogenation to give **3**, which then reacts to yield **5b**. Recently, however, *Inouye* et al.[3] showed that the dialdehyde **2a**, identified by us as a biosynthetic precursor,[4] undergoes a direct cyclization to give **5a**, which, in turn, is transformed into **4** via **5b**.

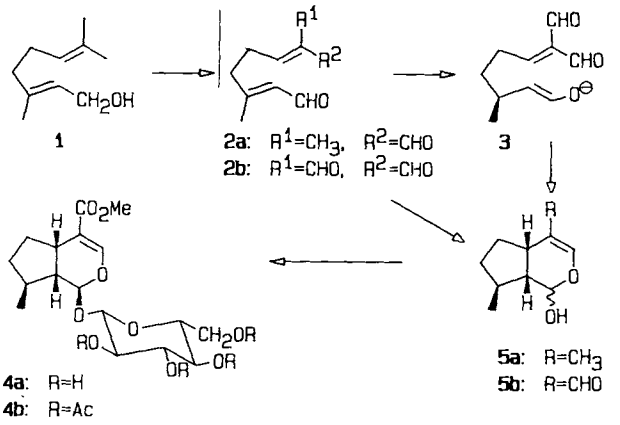

We synthesized in situ compound **12**, as an analogue of **3**, by condensation of the aldehyde (*E*)-**8c** with meldrum's acid **9**. Compound **12** undergoes a hetero-Diels–Alder reaction[5] to give the cyclopenta[*c*]pyran derivatives **11a** and **11b** in 77% yield in a ratio of 10:1 (Scheme 1). The synthesis of (*E*)-**8c** was carried out by first converting (*S*)-citronellal **6a** (*ee* = 86%) via the dimethyl acetal **6b** into the aldehyde **7a**, which, without isolation, was reduced to the alcohol **7b** and subsequently acetylated to give **7c**. Acid-catalyzed elimination afforded a 1:1 mixture of the enol ethers (*E*)-**8a** and (*Z*)-**8a** in good yield, which can be separated by distillation. The (*E*)-enol ether was employed in the subsequent reactions, since the product of its condensation with **9** (**12**, *E*-dienophile moiety) underwent cycloaddition to give **11** with higher selectivity. (*Z*)-**8a** can be reconverted into a 5:4 mixture of (*E*)-**8a** and (*Z*)-**8a** by acid-catalyzed isomerization ($KHSO_4$, 30 min, 180–200 °C; 89%). Solvolysis of (*E*)-**8a** followed by Swern oxidation[6] gives the aldehyde **8c**, which, because of its relative instability, was not isolated but instead allowed to react directly with meldrum's acid **9**.

The *endo-E-syn* (**12**-KI) and *exo-E-anti* (**12**-KII) orientations of the heterodiene moiety of the Knoevenagel product **12** formed as an intermediate must be considered as possible transition states for the cycloaddition. An *exo-Z-syn* arrangement can also be taken into account, but it would lead to a product that was not detected. Moreover, it has been shown for other systems that this transition state is of minor importance.[7] The preferential formation of the *cis*-linked cyclopenta[*c*]pyran derivative **11a** (Table 1)[8] is surprising, since, for comparable compounds bearing two methyl groups on the dienophile moiety, the *trans*

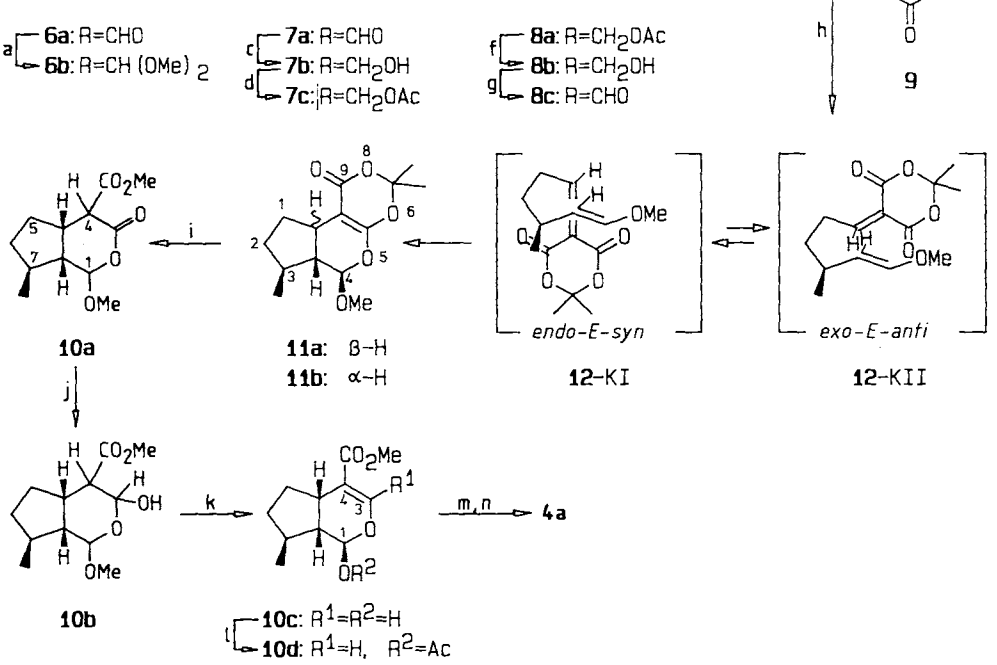

Scheme 1. a) $CH(OMe)_3$, K-10 montmorillonite, 10 min, 20 °C; 95% **6b** ($b.p._{0.5\,torr}$ = 70 °C). b) O_3 in CH_2Cl_2/MeOH, −70 °C, 25 min (ozone content, 58.3 mg/L; rate of gas flow, 20 L/h). c) $NaBH_4$, →20 °C, 20 min; 65%; **7b** ($b.p._{0.2\,torr}$ = 82 °C). d) $(MeCO)_2O$, pyridine, 1 h, 20 °C; 98% **7c** ($b.p._{0.25\,torr}$ = 87 °C). e) $KHSO_4$, 1 h, 120 °C, 6 torr; 80% of a 1:1 mixture of (*E*)-**8a** and (*Z*)-**8a**, separation on a Fischer Spaltrohr column ((*Z*)-**8a**: $b.p._{4\,torr}$ = 76 °C, $[\alpha]_D^{20} = +0.52°$ (*c* = 5, $CHCl_3$); (*E*)-**8a**: $b.p._{4\,torr}$ = 83.4 °C, $[\alpha]_D^{20} = +31.0°$ (*c* = 5, $CHCl_3$)). f) K_2CO_3/MeOH, 20 °C, 4 h. g) $(COCl)_2$, DMSO, CH_2Cl_2, 20 min, −70 °C, Et_3N, 0 °C; (*E*)-**8c** not isolated, crude yield 80–90%. h) Toluene, ethylenediammoniumdiacetate, Na_2SO_4, 20 °C, 2 h; 52% **11a** after chromatography (relative to (*E*)-**8a**, R_f = 0.5 (silica gel, ether/petroleum ether = 1/1)). i) MeOH, 1 h, 64 °C; 7:3 mixture of the C4-isomeric lactones **10a** (R_f = 0.33 (silica gel, ether/petroleum ether = 1/1)). j) DIBAH, ether, 2 h, −70 °C. k) *p*-toluenesulfonic acid, 1 h, 20 °C; 62% **10c** ($[\alpha]_D^{20} = -21.2°$ (*c* = 0.8, $CHCl_3$)). l) Ac_2O, pyridine; 95% **10d**. m) 1-*O*-trimethylsilyl-2,3,4,6-tetra-*O*-acetyl-β-D-glucopyranoside, trimethylsilyltriflate, SO_2 (l), −40 °C, 48 h; 44% **4b** and 43% starting material **10c**. n) NaOMe/MeOH, 20 °C, 2 h, 95% **4a**.

cycloadduct was detected as the major product.[9] Also noteworthy is the high diastereoselective induction (*i-de*[10] > 98%).

To synthesize the deoxyloganin aglycone **10c**, compound **11a** was subjected to solvolysis to give the lactone

Table 1. NMR data for **10a** and **11a**. 200 MHz (^{1}H), 50.3 MHz (^{13}C), in $CDCl_3$.

10a: ^{1}H-NMR: $\delta = 1.10$ (d, $J = 6.0$ Hz, 3H; 7-CH_3), 1.16–1.36 (m, 2H; 5α-H, 6α-H), 1.73–1.90 (m, 2H; 6β-H, 7-H), 1.93 (m, 1H; 7a-H), 2.08 (m, 1H; 5β-H), 3.18 (m, 1H; 4a-H), 3.34 (d, $J = 4.8$ Hz, 0.7H; 4-H), 3.36 (d, $J = 7.5$ Hz, 0.3H; 4-H), 3.48 (s, 3H; OCH_3), 3.80 (s, 3H; CO_2CH_3), 5.03 (d, $J = 3.0$ Hz, 1H; 1-H)

11a: ^{1}H-NMR: $\delta = 1.09$ (d, $J = 6.0$ Hz, 3H; 3-CH_3), 1.1–1.3 (m, 1H; 2β-H), 1.50–1.70 (m, 1H; 1β-H), 1.71 (s, 6H; 2 × 7-CH_3), 1.78–1.98 (m, 3H; 3-H, 3a-H, 2α-H), 2.1–2.3 (m, 1H; 1α-H), 3.02 (m, 1H; 9b-H), 3.57 (s, 3H; OCH_3), 4.97 (d, $J = 3.6$ Hz, 1H; 4-H). — ^{13}C-NMR: $\delta = 20.31$ (3-CH_3), 23.97 (7-CH_3), 26.04 (7-CH_3), 31.21, 32.84 (C1, C2), 32.30, 34.91 (C9b, C3), 49.87 (C3a), 57.30 (OCH_3), 83.00 (C7), 104.69 (C4), 105.44 (C9a), 161.42 (C5a), 168.82 (C9)

ester **10a** (present in the keto form shown; Table 1). Subsequent reduction with two molar equivalents of diisobutylaluminum hydride (DIBAH) afforded the 1,3-diol **10b**, which was treated with acid to obtain **10c**. The unusual cleavage of the acetal moiety of **10a** is due to the fact that the ring of the cyclic hemiacetal (lactol) formed upon reduction undergoes opening between O2 and C3 to form an aluminum enolate and an acyclic hemiacetal moiety. Hydrolysis of the complex affords a dialdehyde, which, presumably as the monohydrate, cyclizes to give **10b**. This reaction course would also explain why two molar equivalents of DIBAH are required for the reduction of the lactone **10a**. Selective glycosidation of **10c** to give **4b** was accomplished using a method developed by us.[11] Compound **10c** was acetylated to give **10d**, which was then allowed to react with peracetylated β-D-trimethylsilylglucose and trimethylsilyl triflate. The peracetylated β-glycoside **4b** was obtained in 44% yield (based on conversion: 83%) and was subsequently converted by solvolysis into deoxyloganin **4a**.[12]

Received: July 17, 1987;
revised: September 16, 1987 [Z 2362 IE]
German version: *Angew. Chem. 99* (1987) 1309

[1] L. F. Tietze, *Angew. Chem. 95* (1983) 840; *Angew. Chem. Int. Ed. Engl. 22* (1983) 828; H. Rimpler, *Planta Med. 33* (1978) 313; O. Sticher, U. Junod-Busch, *Pharm. Acta Helv. 50* (1975) 127; J. B. Bobbitt, K. P. Segebarth in W. I. Taylor, A. R. Battersby (Eds.): *Cyclopentanoid Terpene Derivatives*, Dekker, New York 1969.

[2] S. Escher, P. Loew, D. Arigoni, *Commun. 1970*, 823.

[3] H. Inouye, S. Uesato, *Prog. Chem. Org. Nat. Prod. 50* (1986) 169; S. Uesato, S. Matsuda, H. Inouye, *Chem. Pharm. Bull. 32* (1984) 1672; cf. also J. Balsevich, W. G. W. Kurz, *Planta Med. 49* (1983) 79.

[4] A. R. Battersby, M. Thompson, K.-H. Glüsenkamp, L. F. Tietze, *Chem. Ber. 114* (1981) 3430.

[5] L. F. Tietze in W. Bartmann, B. M. Trost (Eds.): *Selecctivity—a Goal for Synthetic Efficiency*, Verlag Chemie, Weinheim 1984, p. 299; D. F. Taber: *Intramolecular Diels-Alder and Alder Ene Reactions*, Springer, New York 1984; E. Ciganek, *Org. React. 32* (1984) 1.

[6] A. J. Mancuso, D. Swern, *Synthesis 1981*, 165.

[7] L. F. Tietze, T. Brumby, M. Pretor, G. Remberg, *J. Org. Chem.*, in press.

[8] Compound **11b** cannot be isolated in pure form by chromatography, since it readily undergoes isomerization to give **11a**, which is also a *cis*-annulated product. In this process, the C4–O5 bond is presumably cleaved, giving possibly an enol ether as intermediate. Such isomerizations, in which the meldrum's acid moiety remains unchanged, have also been observed for the products of the intermolecular hetero-Diels–Alder reaction of alkylidenemeldrum's acids and enol ethers (W. Holla, *Dissertation*, Universität Göttingen 1985): (3*S*,3a*S*,4*S*,9b*R*)-**11** (*cis*-annulated): $R_f = 0.43$ (silica gel, ether/petroleum ether = 1/1). — ^{1}H-NMR ($CDCl_3$): $\delta = 1.06$ (d, $J = 7.0$ Hz, 3H; 3-CH_3), 1.20–1.40 (m, 1H; 2-H), 1.50–1.65 (m, 2H; 1-H, 3-H), 1.71 (s, 6H; 2 × 7-CH_3), 1.65–2.22 (m, 2H; 1-H, 2-H), 2.22–2.42 (m, 1H; 3a-H), 3.06 (m, 1H; 9b-H), 3.54 (s, 3H; OCH_3), 5.05 (d, $J = 4.0$ Hz, 1H; 4-H). The *trans*-annulated cycloadduct analogous to **11b** can be obtained in pure form by reaction of **8c** with *N,N*-dimethylbarbituric acid: (3*S*,3a*R*,4*R*,9b*R*)-1,2,3,3a,4,6,7,8,9,9b-decahydro-4-methoxy-3,6,8-trimethyl-7,9-dioxacyclopenta[4,5]pyrano[2,3-*d*]pyrimidine: $R_f = 0.5$ (silica gel, diethyl ether). — M.p. = 76 °C (from *n*-pentane). — ^{1}H-NMR ($CDCl_3$): $\delta = 1.12$ (d, $J = 6.5$ Hz, 3H; 3-CH_3), 1.34–1.54 (m, 3H; 1α-H, 2-H, 3a-H), 1.76–2.00 (m, 2H; 3-H), 2.04–2.22 (m, 1H; 1β-H), 2.42–2.68 (m, 1H; 9b-H), 3.32 (s, 3H; N–CH_3), 3.38 (s, 3H; N–CH_3), 3.68 (s, 3H; OCH_3), 5.24 (d, $J = 9.1$ Hz, 1H; 4-H). The *trans* annulation is supported by the relatively high upfield shift of the 9b-H signal and a strong nuclear Overhauser effect between 4-H and 9b-H (*cis*-annulated cycloadduct: 3a-H, $\delta = 1.76$–1.98; 9b-H, $\delta = 3.10$).

[9] We assume that, in analogy to the formation of cyclohexanes, the *exo-E-anti* arrangement of an ω-disubstituted dienophile is preferred in the formation of cyclopentanes for steric and stereoelectronic reasons. However, for ω-monosubstituted dienophiles having the *E* configuration, the steric interactions are less in an *endo-E-syn* arrangement. This is supported by the fact that the corresponding dienophiles having the *Z* configuration afford more *trans*-annulated product and that a 1:1 mixture of *cis*- and *trans*-annulated cycloadducts was obtained upon reaction of **8c** with methyl 3-(trimethylsilyloxy)propenoate; cf. S. Takano, S. Satoh, K. Ogasawara, *Heterocycles 23* (1985) 41.

[10] For an explanation of *i-de* and *ni-de* see L. F. Tietze, U. Beifuss, *Angew. Chem. 97* (1985) 1067; *Angew. Chem. Int. Ed. Engl. 24* (1985) 1042.

[11] L. F. Tietze, R. Fischer, *Angew. Chem. 95* (1983) 902; *Angew. Chem. Int. Ed. Engl. 22* (1983) 888.

[12] Identity was shown by comparison of the NMR spectrum of synthetic **4a** with that of an authentic sample. Glycosidation of **10c** also afforded ca. 7% of a different, chromatographically separable β-glycoside, which is formed from *ent*-**10c**, present as an impurity. This is in accord with the amount of *ent*-**6a** present in the (*S*)-citronellal **6a** employed, which was obtained from commercially available citronellol (Fluka). The *ee* of citronellol was determined by oxidation to citronellic acid and gas chromatographic determination of the diastereomers obtained therefrom by reaction with (*S*)-1-phenylethylamine: E. J. Corey, G. Schmidt, *Tetrahedron Lett. 1979*, 399; K. Mori, S. Masuda, T. Suguro, *Tetrahedron 37* (1981) 1329; T. Kikukawa, M. Amaida, A. Tai, *Bull. Chem. Soc. Jpn. 57* (1984) 1954.

CORRESPONDENCE

Back to the Structure of Benzene

By *R. Janoschek**

In a communication entitled "On the Structure of Benzene", *Ermer*[1] recently demonstrated in an impressive way that still questionable properties of the benzene molecule trace back to seemingly well-founded fundaments such as the D_{6h} symmetry of the structure. In particular, neither our present experimental nor theoretical knowledge can precisely exclude a structure with CC bond alternation (D_{3h} symmetry), he notes.

The term "Back" in the above title should, however, be understood in another sense—namely as referring to a supplement to *Ermer*'s review. Obviously, certain much discussed topics make a periodical appearence, possibly reflecting a change of generation and a changing consciousness with time. For, in the mid-sixties, it was *Rogowski* whose papers and lectures[2] on the D_{6h}–D_{3h} problem were the subject of heated discussions, although the corresponding electron diffraction experiments or at least their assignments were widely unaccepted. At the time also *Rogowski* turned to quantum chemistry for help. Relevant computations were performed and published.[3] A D_{3h} structure could certainly not be found, but the smooth increase in energy of only 4.6 kcal·mol^{-1} on going from D_{6h} (1.39/1.39 Å) to D_{3h} symmetry (1.35/1.43 Å) was remarkable.

A renewed call for quantum chemical calculations on the structure of benzene is not unwarranted, for such calculations can nowadays be performed more accurately and, therefore, more reliably than 20 years ago. The new calculations have been investigated in the following way: starting from the optimized D_{6h} structure, geometries with CC bond alternation have been generated by choosing a fixed length for three short CC bonds and a complete optimization of all other structural parameters. This procedure yields the optimal energy curve for a $D_{6h} \rightarrow D_{3h}$ distortion which is much more informative than the calculation of the complete set of harmonic force constants,[4] in particular that of the B_{2u} vibration, which unequivocally indicates a D_{6h} structure, but cannot exclude a D_{3h} structure.

$C{=}C_{short}$ (fixed) [Å]	1.383	1.370	1.340	1.325
$C{-}C_{long}$ (optim.) [Å]	1.383	1.388	1.402	1.409
ΔE [kcal·mol^{-1}]	0.0	0.2	2.4	4.5

These ab initio calculations at the SCF level with the 3-21G* basis set (spd) indicate again no energy minimum with D_{3h} symmetry. The use of an ethylene C=C bond length (1.339 Å) and a butadiene C–C bond length (1.483 Å) for a D_{3h} structure causes a surprisingly slight destabilization of only 8 kcal·mol^{-1} relative to D_{6h} (1.396 Å).

Prof. Dr. R. Janoschek
Institut für Theoretische Chemie der Universität
Mozartgasse 14, A-8010 Graz (Austria)

[1] O. Ermer, *Angew. Chem. 99* (1987) 791; *Angew. Chem. Int. Ed. Engl. 26* (1987) 782.
[2] F. Rogowski, *Dtsch. Apoth.-Ztg. 39* (1965) 1334; U. Krüger, F. Rogowski, *Z. Naturforsch. B19* (1964) 1157.
[3] R. Janoschek, H. Preuss, G. Diercksen, *Int. J. Quantum Chem. I S* (1967) 209.
[4] P. Pulay, G. Fogarasi, J. E. Boggs, *J. Chem. Phys. 74* (1981) 3999.

CORRIGENDUM

The manuscript of the Nobel Lecture "Concepts in Reaction Dynamics" by *John C. Polanyi* (*Angew. Chem. Int. Ed. Engl. 26* (1987) 952) was inadvertently incomplete. The third full paragraph on p. 960 should read:

Turning to the experimental findings of Section 2.1, it was evident that the moderate mean fractional conversion of reaction energy into product vibration, $\langle f_{V'} \rangle$, could be explained either by a highly attractive interaction leading to secondary encounters, or by predominantly repulsive energy release. The first of these alternatives appeared implausible since it implied a substantially broader distribution over product vibrational and also rotational states than was observed.[16] Instead the evidence favored a strongly repulsive PES, with the light-atom anomaly explaining the markedly reduced $\langle f'_V \rangle$ for $H + X_2$ as compared with $X + H_2$ or $X + HY$, and the lower barrier leading to a slightly increased HA in $H + Br_2$ as compared with $H + Cl_2$ (cf. the correlation noted above) accounting for the greater $\langle f'_V \rangle$ observed for $H + Br_2$ than for $H + Cl_2$.[16]

The success of a strongly repulsive PES in accounting for the general form of the triangle plot for $Cl + HI \rightarrow HCl + I$ is illustrated, by way of an example, in Figure 15,[61] which should be compared with Figure 9 above. Similar success has been obtained for the reaction $F + H_2 \rightarrow HF + H$ (Fig. 8) using a strongly repulsive PES.[62-64] In this case there is now dependable evidence from ab initio variational treatments of FHH[65,66] that the energy release is indeed substantially repulsive. The success of a repulsive PES in describing **L + HH** dynamics will be demonstrated (for $H + F_2 \rightarrow HF + F$; cf. Fig. 7) in Section 3.2.

The discussion of the previous paragraphs as it relates to repulsive energy release is summarized pictorially in Figure 16. Though visualization of reaction dynamics is generally, and often adequately, based on the collinear PES to which the sliding-mass analysis applies, tests of the validity of PESs are made by 3D trajectories.

Product rotational excitation is eliminated from the picture in the collinear world. Though this is a minor constituent of the product energy, it is revealing of the dynamics. In the visualization of Figure 16, we have included the effect of repulsive energy release in bent configurations as one source of product rotation. The experimental data in the triangle plots of Figure 11 give persuasive evidence of the significance of this effect in the important reaction $F + H_2$. Product repulsion should be expected[47,67] on the basis of momentum conservation to give rise to decreasing $\langle f_{R'} \rangle$ in the series FH·D > FH·H > FD·D > FD·H (the dot indicated the locus of the repulsion); this is found theoretically in 3D trajectory studies, and also experimentally (see Fig. 15). The triangle plots in Figure 11 correspond to the extremes of this range of isotopic mass combinations; $\langle f_{R'} \rangle$ for the FH·D pathway substantially exceeds that for FD·H.

Methods of Enzymatic Analysis. Edited by *H. U. Bergmeyer, J. Bergmeyer,* and *M. Grassl.* 3rd edit., VCH Verlagsgesellschaft, Weinheim 1986. **Vol. X: Antigens and Antibodies 1.** Editorial Consultant: *R. F. Masseyeff.* XXII, 509 pp., bound, DM 295.00 (subscription price DM 260.00). - ISBN 3-527-26050-1; **Vol. XI: Antigens and Antibodies 2.** Editorial Consultant: *R. F. Masseyeff.* XXV, 508 pp., bound, DM 315.00 (subscription price DM 280.00). - ISBN 3-527-26051-X; **Vol. XII: Drugs and Pesticides.** Editorial Consultant: *M. Oellerich.* XXIII, 520 pp., bound, DM 315.00 (subscription price DM 280.00. - ISBN 3-527-26052-8

Volumes X and XI of this handbook[*] provide instructions for the enzymatic assay of antibodies and antigens. These two volumes provide a compendium of model enzyme-immunoassays for immunochemistry rather than attempting to cover the growing field completely. They will be useful for many years.

The five chapters of Volume X cover assay procedures for immunoglobulins and immune complexes, for antigens and antibodies in allergic and autoimmune diseases, and for antigens and antibodies in viral diseases. The first chapter discusses the problems of standardizing enzyme-immunoassays for antibodies, particularly with respect to the treatment and expression of data, much as Volume II discusses the interpretation of more classical assays. The chapter also discusses general methods for the assay of antibody- and antigen-secreting cells as well as an ELISA technique for screening monoclonal antibodies.

The remaining chapters of Volume X are a collection of working procedures for the determination of specific antigens and antibodies such as red blood cell autoantibodies, anti-DNA antibodies, and antibodies against herpes simplex virus, measles virus, or the HTLV III virus. A description of these sections appears below.

Volume XI, the companion handbook, treats antigens and antibodies in chlamydial and bacterial diseases, such as various *Clostridia* species or bacterial endotoxins, as well as antigens and antibodies in fungal and parasitic diseases, such as aflatoxins or *Pneumocystis carinii* antigen. The third and final section of this volume comprises a short section devoted to a related and emerging field: that is, the use of enzyme-immunoassays to identify plant viruses such as potato viruses or the soybean mosaic virus.

As in previous volumes, treatment of each antigen or antibody rigidly follows a standard format. This approach makes the two volumes and the entire twelve volume series a convenient and informative reference. One may locate the section covering the desired antigen or antibody using the index at the end of each volume; unfortunately these indices are not cross-referenced to each other or to other volumes. A typical section begins with a general introduction describing the purpose and applications of the assay, properties of the antigen or antibody relevant to the analysis, other methods of determination, and mention of international reference methods and standards, when available.

The assay forms the core of each section, and its documentation is detailed. In standardized format are listed the design of the method, the equipment required, where to obtain and how to prepare the reagents and solutions, and the complete assay procedure from collecting and preparing the sample to interpreting the results. The next unit explains how to validate the method and includes a discussion of sources of error in the assay. Appendices usually provide further detailed information regarding procedures such as how to prepare and purify monoclonal or enzyme-labeled antibodies or how to coat the assay plates.

Graphics illustrating the principle of each method are particularly valuable. Also useful are the graphs and illustrations providing information on optimization of procedures, such as well coating, or on the results of the methods described. Each section closes with a list of references.

These two volumes, containing assay procedures for over 75 substances, provide a solid reference to specific and illustrative methods useful for the analysis of antigens, antibodies and viruses. Clinicians and epidemiologists in particular will find them useful, although the wealth of information presented will assist those interested in using or designing enzyme-immunoassays in biochemistry and biology.

The final volume of "Methods of Enzymatic Analysis," Volume XII, describes the relatively recent applications of enzyme-immunoassays to the quantitative analysis of drugs and pesticides. The first two chapters focus on the determination of serum concentrations of therapeutic drugs and drugs of abuse. The final chapter on pesticides is meant "to stimulate analysts involved in environmental investigations to design simple enzyme-immunoassays".

The eighteen sections of chapter 1, "Drugs Monitored during Therapy", provide information and assay procedures for 25 drugs ranging from the bronchodialator, theophylline, to various aminoglycosides such as gentimycin or tobramycin. The next chapter, "Drugs of Abuse and of Toxicological Relevance," provides similar information for substances such as benzodiazepines or barbiturates in its 16 sections. The final chapter on pesticides, containing six sections of environmental applications of enzyme assays, mainly focusses on the determination of cholinesterase inhibitors such as organophosphorus compounds.

The organization of each of the three chapters is similar. Each opens with a brief, general introduction describing the importance of enzyme-immunoassays to the particular topic. As in previous volumes of the series, the bulk of each chapter is a collection of sections giving information for a particular drug or pesticide, one or more assay methods, and techniques to validate the method. Many sections also include an appendix giving additional information regarding the assay, such as how to prepare enzyme conjugates or antibodies or antigens for the assay. A typical section for a drug is described below; the sections on pesticides have the same format.

Information for a given drug usually includes its chemical structure, mention of the physiological affects and clinical use of the drug, some of its pharmacokinetic parameters, and the reasons for monitoring the drug. Also pro vided is a short summary of chemical properties relevant in analysis (FW, values of pK_a, solubility) and a listing and discussion of other methods of determination. The inclusion of references is helpful because, although the presentation of the information is clear and well organized, it does not attempt to replace descriptions found in more detailed clinical handbooks because the focus of the volume is not on drug description but on drug analysis; the collec-

[*] *Angew. Chem. Int. Ed. Engl. 26* (1987) 368.

tion of clearly explained and well-documented assays meets this goal.

The presentation of the assays is standardized as in previous volumes and typically includes the following information: the method design, equipment needed, how to make up the reagents and solutions, and the assay procedure. Information on the validation of the method is also given, including data on the specificity of the assay and therapeutic ranges of the drug.

This final volume should be a useful handbook for the biochemical, biomedical and clinical laboratory, and will be helpful to those involved in the measurement of drugs or pesticides.

The third edition of "Methods in Enzymatic Analysis"—comprising 6821 pages in twelve volumes—is greatly expanded from the the 2302 pages in the four volumes of the second English edition (1974). This change reflects the increasing importance of enzymatic analyses in the analytical laboratory. As various contributors mention, assays based on enzymes often supplement or replace more lengthly procedures requiring expensive equipment and a high level of technical expertise. The specificity of enzyme assays often means that sample purification can be simplified. In some cases no other reliable analytical method exists.

As with previous editions, this one is primarily designed for those who need to conduct analyses of biological substances, ranging from oxidoreductases to pesticides. The expanded coverage of this edition also collects important material on the theory, design, implementation and interpretation of enzymatic assays, thus making the series of useful reference for scientific and medical libraries as well as a handbook for the laboratory worker.

The great strength of the collection is its adherence to a standard format when presenting the assays. This organizes an immense amount of practical information. The clear and detailed explanations given for each assay allow the procedures to be followed easily and should stimulate the development of new assays, particularly in the rapidly expanding areas of determination of immunological, pharmacological and environmental analytes.

A weakness of the individual volumes of this edition is the lack of cross-referencing to other volumes or to previous editions. Fortunately, work on an index volume is in progress. Complete indexing of the series will make it an even more valuable reference. Overall, this series is a foundation of modern biological analysis. It will be used heavily by those conducting analyses of biological substances.

Ethan S. Simon and *George M. Whitesides* [NB 831 IE]
Harvard University, Cambridge (USA)

Modern Synthetic Methods 1986. Vol. 4. Edited by *R. Scheffold*. Springer, Berlin 1986. viii, 356 pp., paperback, DM 68.00.—ISBN 3-540-16526-6

"Modern Synthetic Methods 1986" contains the texts of the papers presented at the Fourth International Seminar on Modern Synthetic Methods, which was held at Interlaken in April 1986. The general themes of this seminar were "Sound and Light in Synthesis" and "Synthesis of Enantiomerically Pure Compounds". The book contains three papers on each of these two themes, as follows: first theme—"Ultrasound in Synthesis" by *K. S. Suslick* (University of Illinois, Urbana), "Photochemically Generated Building Blocks: Part I—The Tricyclooctanone Approach to Polyquinane Synthesis: The Underlying Photochemistry" by *K. Schaffner*; Part II—"The Tricyclooctane Approach: Photochemical Methods in Cyclopentanoid Natural Products Synthesis—A Comparison" by *M. Demuth* (both authors at Max-Planck Institut für Strahlenforschung, Mülheim); second theme—"EPC Synthesis with C,C-Bond Formation via Acetals and Enamines" by *D. Seebach* (ETH, Zürich), "Asymmetric Diels-Alder Reactions with Chiral Enoates as Dienophiles" by *G. Helmchen* (Heidelberg University), "Enantiomerically Pure Compounds via Chiral Organoboranes" by *H. C. Brown* (Purdue University, West Lafayette).

The papers are not so much review articles of the usual kind as progress reports on important developments in synthetic methods, by authors closely involved in the work; this applies even to the first paper, which reviews the applications of ultrasound in chemistry. In accordance with the "workshop" character of the conference, the book is without doubt mainly of value to the practical researcher; beginning with the basic principles and background and continuing through to the latest results, some still unpublished, it contains a wealth of practical information, and in some cases even a critical evaluation of alternative methods, with full experimental details for representative examples, some of which have not been generally available before. There are plentiful literature references (up to 365 citations), with a coverage which appears to extend to the end of 1985. This is without doubt where the book's greatest value lies. The authors are all leading exponents of their specialist fields, and direct reproduction of their typescripts has made it possible to publish the material rapidly, thereby disseminating it at first hand, as it were, even to those who did not participate in the conference. It would be difficult to find a more competent, topical and comprehensive survey of the themes treated here, emphasizing as they do some important current trends in organic synthesis. For this reason it is certain that the book, like the reports of the previous Interlaken meetings, will be frequently cited.

To summarize, this is an outstandingly informative book, which is a must for all chemists interested in the topics discussed, and it also makes stimulating reading. Working through it reinforces one's impression of the enthusiasm which characterizes these Interlaken conferences.

Hans-J. Altenbach [NB 839 IE]
Fachbereich 13 der Universität-Gesamthochschule
Paderborn (FRG)

High Resolution NMR Spectroscopy of Synthetic Polymers in Bulk. Edited by *R. A. Komoroski*. VCH Publishers/VCH Verlagsgesellschaft, Deerfield Beach and Weinheim 1986. xi, 379 pp., bound, DM 185.00.—ISBN 0-89573-146-0, 3-527-26464-7

The macroscopic properties of polymers are closely connected with their molecular structure and dynamics. Therefore the behavior of the macromolecules in the solid state is of particular interest. In addition to rigid glassy polymers, elastomers, in which the polymer chains in network structures can have mobilities similar to those in liquids have to be considered.

Nuclear magnetic resonance (NMR) spectroscopy, which now plays such a prominent role in elucidating the chemical structures of liquids or solutions, has in the past

been severely limited in its application to solid polymers, because in *solids*, owing to dipolar coupling, one could only obtain poorly resolved spectra with broad signals. In the last ten years, however, techniques have been developed to overcome this deficiency and can now be used in various ways for polymer studies. The most important method is undoubtedly the CP-MAS procedure, in which cross-polarization (CP), proton decoupling, and rotation of the sample at the "magic angle" (magic angle spinning, MAS) enhance the sensitivity and resolution of ^{13}C-NMR spectroscopy sufficiently to justify the description "high resolution NMR spectroscopy of solids".

By this technique, for example, conformational changes can be studied. Furthermore, the anisotropic couplings which exist in the solid state offer various possibilities for using NMR spectroscopy to give information on the important questions of molecular ordering, e.g. alignment of the polymer chains in stretched fibers, and phase separation in block copolymers. One can also use these effects to study molecular dynamics, e.g. segmental mobility in crystalline and amorphous polymers, and in elastomers above the glass transition temperature.

This book edited by *R. A. Komoroski*, gives an outstandingly good review of the application of the newer NMR techniques to solid polymers. The authors of the individual chapters are experts in polymer NMR spectroscopy. Most of them are from the academic world, but others are from industrial research laboratories in the United States, which further underlines the importance of the above mentioned developments to polymer research. Following two introductory chapters, a detailed description is given of the study of chain conformation and mobility in rigid glassy polymers and partly crystalline polymers using ^{13}C-NMR methods. After a chapter on elastomers, the last four chapters of the book have a more physical emphasis, being concerned with local motions in the glassy state, oriented polymers, and two other important techniques, namely ^{1}H multi-pulse NMR spectroscopy and ^{2}H-NMR spectroscopy.

The book is intended mainly for polymer chemists who wish to obtain an overview of the capabilities of solid state NMR techniques for polymer research. It includes enough background information to enable one to understand the newer NMR techniques, and most importantly it contains a wealth of practical examples. It can therefore be highly recommended for all laboratories engaged in the study of the physical chemistry of polymers.

Hans Wolfgang Spiess [NB 828 IE]
Max-Planck-Institut für Polymerforschung,
Mainz (FRG)

Mechanisms of Inorganic Reactions. By *D. Katakis* and *G. Gordon*. Wiley, New York 1987, 384 pp., hand cover, $ 53.15.—ISBN 0-471-84258-3

This book was written to serve as a basis for a one-semester course on this topic for advanced undergraduate and starting level graduate students. It was not intended as a comprehensive review of the current literature, but does contain a brief list of relevant books and review papers at the end of each chapter. In addition, appropriate problems are given such that students can check their ability to analyse kinetic data and to asign mechanisms.

The nine chapters of the book are devoted to: introduction, mechanisms, kinetics and equilibria; events at the molecular level—the activated complex; experimental methods and handling of the data; mechanism and structure; group transfer and atom-transfer reactions; electron-transfer reactions; catalysis; inorganic photochemistry. In general the authors treat more classical type inorganic complexes with little information on organometallic systems. In this respect the book nicely complements *Jim Atwood*'s "Inorganic and Organometallic Reaction Mechanisms" (Brooks/Cole 1985) which mainly concentrates on organometallic systems.

Some sections of this book are extremely well written and the reader will appreciate the authors' efforts. Other sections, for instance the introductory chapter, are rather unsatisfactory. In general the book presents a good course on inorganic reaction mechanisms. Interesting systems dealing with the reactions of dioxygen, antitumor activity and catalysis, demonstrate the applicability of the mechanistic information. A number of shortcomings are: too little information on the meaning of the transmission coefficient (p. 59); an organic example is used to demonstrate the effect of pressure on a rate constant (p. 67) where so many inorganic examples are available; important fast reaction techniques such as stopped-flow (p. 102) and *T*-jump (p. 104) are only treated in a few sentences.

After having read this book. I did experience the need for a comprehensive treatment of inorganic and organometallic reaction mechanisms, an update of the *Basolo* and *Pearson*, *Tobe* or *Wilkins* treatment of the subject. With all the activity in this field, such an undertaking will be a major task and hopefully this book will encourage an inorganic/organometallic kineticist to tackle this challenge in the near future.

Rudi van Eldik [NB 869 IE]
Institut für Anorganische Chemie
Universität Witten/Herdecke

Chemical Modification of Enzymes: Active Site Studies. Edited by *J. Eyzaguirre*. John Wiley, New York 1987. 187 pp., bound, £21.50.—ISBN 0-7458-0023-8

This book describes the classical methods of enzyme chemistry, with special reference to their use for modifying active sites; it consists of eleven chapters written by ten authors. The papers were presented at a conference held in Chile in 1984, and have been edited by *Jaime Eyzaguirre* and published here in book form. The conference report has thereby become a textbook-style description of known techniques with selected examples. In relation to the present state of the techniques it is, unfortunately, already out of date to some extent. For example, it fails to cover any of the DNA techniques for protein modification, in particular that of *in vitro* mutagenesis, and the analytical use of two-dimensional NMR spectroscopy is not included. The book thus suffers from a fault common to many conference publications, in being partly outdated by the time it has appeared.

The book can be recommended for advanced students of biochemistry and for newcomers to the proteins field. It is written in a comprehensible style, is well illustrated and edited, and the individual chapters contain literature references up to 1986. To summarize: easy reading for newcomers to protein chemistry, but containing nothing new for specialists in this field.

Hans Günter Gassen [NB 864 IE]
Institut für Organische Chemie und Biochemie
der Technischen Hochschule Darmstadt (FRG)

Principles of Electrochemistry. By *J. Koryta* and *J. Dvořák*. John Wiley, Chichester 1987. xi, 447 pp., bound, $ 84.40.—ISBN 0-471-91211-5

"Koryta" has long occupied an assured position amongst textbooks on electrochemistry. The authors have now thoroughly revised and updated their book to take account of the rapid progress made during the last 15 years in this area of physical chemistry. Once again, they have produced an excellent book which is easy to read and understand. However, the authors' claim in the preface that they have picked out and emphasized problems of modern electrochemistry, including materials, electrodes, electrochemistry in non-aqueous media, and relevant spectroscopic techniques, does not seem to me to be fully justified. Instead the first three chapters, which constitute almost half the book, mainly treat themes of classical thermodynamics which can be found in physical chemistry textbooks, though usually in significantly less detail.

The book starts with a detailed introduction to electrolyte equilibria. It includes the theory of strong (Debye-Hückel) and weak electrolytes, acids and bases, and models for polyelectrolytes and ionic association phenomena. Chapter 2 discusses transport processes in electrolyte solutions, including a skillful development of the central idea of the ionic flux from the thermodynamics of irreversible processes. It is noteworthy that, besides the phenomenology of mass transport, there is also a separate section discussing the dynamic causes of such processes. This is followed in Chapter 3 by a quite conventional treatment of the thermodynamic principles involved in mass transport at the interface between the electrode and electrolyte phases, including the concepts of EMF, Volta and Galvani potentials, and reversible electrodes with their numerous variations. Practical applications are also discussed, in relation to pH measurements and the determination of activity coefficients and dissociation constants.

In Chapter 4 the electrical double layer is described, together with all the essential thermodynamic and structural properties of this interface, which plays such an important part in electrochemistry. In addition to the familiar Gouy-Chapman theory, there is also a short section devoted to the "jellium" model developed in recent years. Non-metallic interfaces such as occur in semiconductors and immiscible electrolytes are treated in detail.

This is followed in Chapter 5 by a thorough treatment of the electrode reactions themselves, with detailed discussions both of the electrode kinetics in the narrower sense and of transport phenomena. The many different forms current overvoltage curves can take, depending on the type of transient signal are discussed. A welcome feature is the treatment of not only the phenomenological Butler-Volmer equation, the basic equation of electrochemical kinetics, but also the principles of the Marcus theory in relation to other topical problems; they thus present a modern view of elementary processes in charge transfer. Further sections provide information on dynamic electrochemical measurement techniques, including spectroscopic methods, and on coupled chemical reactions which can either precede or follow the charge transfer. Special electrode processes, such as occur in electrocrystallization or in photoelectrochemistry, are also included. The book concludes with a chapter on membrane electrochemistry and bioelectrochemistry. This is mainly concerned with the thermodynamics of charge transfer and transport phenomena in biological and synthetic membranes, and with a description of their applications in ion-selective electrodes. Topics in pure bioelectrochemistry, such as photosynthesis and redox reactions in enzymes, are touched on only in passing.

This textbook by its nature, provides a concise, but complete survey of the fundamentals of electrochemistry. Hence, there is little space for details; but this lack is alleviated by the bibliography at the end of each section, each expertly compiled with a view to topicality. All those who wish to embark on a study of electrochemistry via the classical thermodynamic route will find the new "Koryta" a dependable guide. For a textbook it is, however, expensive, and this will not help it to achieve the wide use which it deserves.

Jürgen Heinze [NB 854 IE]
Institut für Physikalische Chemie
der Universität Freiburg (FRG)

Registered names, trademarks, etc. used in this journal, even when not marked as such, are not to be considered unprotected by law.

© VCH Verlagsgesellschaft mbH, D-6940 Weinheim, 1987. - Printed in the Federal Republic of Germany by Zechnersche Buchdruckerei, Speyer/Rhein.

All rights reserved (including those of translation into foreign languages). No part of this issue may be be reproduced in any form – by photoprint, microfilm, or any other means – nor transmitted or translated into a machine language without written permission from the publishers. Only single copies of contributions, or parts thereof, may be made for personal use.

Valid for users in the USA: The appearance of the code at the bottom of the first page of an article in this journal (serial) indicates the copyright owner's consent that copies of the article may be made for personal or internal use, or for the personal or internal use of specific clients. This consent is given on the condition, however, that the copier pay the stated per-copy fee through the Copyright Clearance Center, Inc., for copying beyond that permitted by Sections 107 or 108 of the U.S. Copyright Law. This consent does not extend to other kinds of copying, such as copying for general distribution, for advertising or promotional purposes, for creating new collective works, or for resale. For copying from back volumes of this journal see 'Permissions to Photo-Copy: Publisher's Fee List' of the CCC.

Editorial office: Pappelallee 3, D-6940 Weinheim, Federal Republic of Germany, Telephone (06201) 602315, Telex 465516 vchwh d, Telefax (06201) 602328.

Editor: *P. Gölitz.*

Associate editors: *D. I. Loewus, A. Stimson.* **Editorial assistant:** *E. Schweikart*

Publishers: VCH Verlagsgesellschaft mbH. (Managing Directors: *Prof. Dr. Helmut Grünewald* and *Hans Dirk Köhler*), Pappelallee 3, D-6940 Weinheim, Federal Republic of Germany. Correspondence concerning advertisements should be addressed to VCH Verlagsgesellschaft mbH. (Advertising Manager *R. J. Roth*), Boschstr. 12. P.O. Box 1260/1280, D-6940 Weinheim, Federal Republic of Germany, Telephone Weinheim (06201) 602-0, Telex 465516 vchwh d, Telefax (06201) 602328.

AUTHOR INDEX [*Angew. Chem. Int. Ed. Engl. 26* (1987)]

The page numbers in square brackets refer to the German edition [*Angew. Chem. 99* (1987)] of Angewandte Chemie. In the case of book reviews the names of the authors are given; the corresponding GE reference can be found in the Author Index of the German Edition.

ABE, Y. 1019 [1077]
Adachi, T. 1171 [1182]
Adam, W. 796, 797 [817, 818]
Adamek, C. 347 [371]
Adams, R. D. 685 [691]
Adams, S. 1255 [1280]
Akkerman, O. S. 73 [88]
Albiez, T. 572 [561]
Aldinger, F. 371 [381]
Allmann, R. 1133 [1175]
Alpha, B. 266, 1266 [259, 1310]
Alston, D. R. 692, 693 [697, 698]
Altmeyer, O. 1256 [1299]
Alvanipour, A. 485 [476]
Anderegg, G. 545 [570]
Anderskewitz, R. 683 [717]
Anderson, L. G. 1013 [1073]
Andersson, S. 1017 [1056]
Angelici, R. J. 909 [947]
Angermund, K. 153, 563, 666, 908, 1279 141, 587, 708, 957, 1303]
Apell, H.-J. 793 [813]
Appel, R. 779, 1012 [810, 1042]
Arif, A. M. 910 [921]
Arsenault, G. J. 86 [79]
Ashe, A. J. 229 [249]
Atta-ur-Rahman 1192
Attinà, M. 1177 [1174]
Attygalle, A. B. 784 [784]
Atwood, D. A. 485 [476]
Atwood, J. L. 485 [476]
Aumann, R. 357, 563 [361, 587]
Autze, V. 362 [363]

BABIN, J. E. 685 [691]
Bahsoun, A. A. 1169 [1208]
Bakar, M. A. 474 [497]
Balaban, A. T. 270
Balci, M. 928, 931 [909, 912]
Balles, R. 900 [929]
Ballester, P. 1244 [1297]
Balzani, V. 1266 [1310]
Bambal, R. 668 [710]
Banert, Klaus 879 [932]
Baptista, J. 1186 [1183]
Bär, T. 793 [813]
Barron, A. R. 907 [956]
Bartmann, M. 256 [271]
Bast, P. 1212 [1242]
Bätcher, M. 912 [945]
Bats, J. W. 61, 362 [82, 363]
Baudler, M. 347, 348, 419 [371, 372, 429]
Bauer, H. 625 [642]
Baum, G. 546, 798, 1163 [559, 790, 1199]
Baumann, S. M. 1182 [1222]
Bayer, E. 545 [570]
Beagley, B. 264 [237]
Beck, F. 1031 [1061]
Beck, K. 670, 672 [694, 695]
Becker, G. 900 [929]
Becker, H.-O. 76 [69]
Beckh, H. J. 236, 1134 [255, 1214]
Beckhaus, H.-D. 573, 770 [592, 807]
Behrens, U. 147 [134]
Beinhauer, A. 796 [817]
Bell, M. N. 250 [253]
Benedek, P. 1057
Benelli, C. 913 [958]
Benn, R. 67, 1279 [73, 1303]
Bennett, M. A. 258, 260 [261, 262]
Berger, S. 546 [559]
Bergmeyer, H. U. 272, 368, 1299
Bergmeyer, J. 272, 368, 1299
Berndt, A. 546, 798 [559, 790]
Bestmann, H. J. 79, 784 [64, 784]
Betz, P. 145 [131]
Bhargava, S. K. 258, 260 [261, 262]
Bianchini, C. 767 [821]
Bickelhaupt, F. 73, 990 [88, 1020]
Biedenbach, B. 764 [798]
Billhardt, U.-M. 362 [363]
Binger, P. 764, 908 [798, 957]
Binnig, G. 606 [622]
Birkhahn, M. 72 [80]
Birkhofer, H. 573 [592]
Blake, A. J. 250 [253]
Blanch, H. W. 590
Blanco, L. 1246 [1276]
Bläser, D. 245 [239]
Blatter, K. 85 [67]
Boche, G. 78, 696, 1287 [62, 706, 1279]
Bock, H. 461, 504, 791 [492, 518, 811]
Bodenhausen, G. 1192
Boehm, H.-P. 253 [266]
Boekelheide, V. 700 [715]
Boese, R. 245, 1010, 1035 [239, 1045, 1067]
Bogdanović, B. 1025 [1046]
Bögge, H. 72, 1045 [80, 1060]
Böhn, K. H. 78 [62]
Bolte, T. 331 [362]
Bonačić-Koutecký, V. 170 [216]
Börner, U. 789 [788]
Bott, S. G. 485 [476]
Böttger, H. 92
Braun, M. 24 [24]
Braunstein, P. 88, 768 [77, 802]
Brehm, M. 1271 [1318]
Bremer, M. 761 [795]
Bretz, N. 345 [357]
Breuer, O. 461 [492]
Brinker, U. H. 577, 1260 [585, 1290]
Brown, J. M. 190 [169]
Brück, T. 59 [59]
Brüdgam, I. 921 [951]
Brunner, H. 230 [268]
Bryksin, V. V. 92
Bublak, W. 234 [248]
Büchner, K. 1259 [1294]
Buddrus, J. 625 [642]
Büldt, G. 699 [707]
Bull, A. T. 588
Büllesbach, P. 470 [459]
Burghard, H. 672 [695]
Buschmann, J. 799, 1180 [808, 1206]
Butz, T. 110 [113]

CABRERA, I. 1178 [1204]
Cacace, F. 1177 [1174]
Callis, J. B. 1052
Caneschi, A. 913 [958]
Cardin, D. J. 592
Casado, A. 797 [818]
Casser, I. 586 [597]
Caulton, K. G. 135 [147]
Chandrakumar, N. 1192
Chang, H.-R. 915 [934]
Chapman, K. T. 1184 [1197]
Charrier, C. 548 (804) [590]
Chawla, A. S. 159
Chi, K. M. 1190 [1203]
Chiesi-Villa, A. 68, 70 [84, 86]
Chisholm, M. H. 903, 904 [936, 937]
Chrambach, A. 370
Christian, G. D. 1052
Christl, M. 449, 690 [474, 720]
Christmas, C. 915 [934]
Christou, G. 915 [934]
Ciriano, M. A. 444 [452]
Ciurli, S. 70 [86]
Clark, T. 158
Closs, F. 552, 1037 [564, 1068]
Cogen, J. M. 1182 [1222]
Cohen, S. 717 [738]
Coleman, A. W. 485 [476]
Cooney, C. L. 589
Cowley, A. H. 907 [956]
Cradock, S. 1197
Cuenca, T. 697 [687]
Curry, A. S. 1051
Curtis, A. C. 676 [688]

DALTON, H. 588
Dammel, R. 504 [518]
Danishefsky, S. J. 15 [15]
Dauben, W. G. 1271 [1318]
Dean, P. D. G. 1056
de Boer, H. J. R. 73 [88]
Deger, S. 344 [349]
Dehmlow, E. V. 72, 329 [80, 340]
Deiseroth, H.-J. 687 [701]
de Meijere, A. 1277 [1285]
de Méric de Bellefon, C. 88 [77]
Demuth, W. 1032 [1075]
DeNinno, M. P. 15 [15]
Denzer, H. 1295 [1309]
de Petris, G. 1177 [1174]
Derome, A. E. 1192
Dettmeier, U. 468 [470]
Deubelly, B. 673, 674 [703, 705]
Dewar, M. J. S. 1273 [1313]
Dias, H. V. R. 1270 [1320]
Dickert, F. L. 228 [238]
Dickson, R. S. 271
Diehl, F. 343 [348]
Dieringer, H. 551 [578]
Dietrich-Buchecker, C. O. 661 [711]
DiMaio, A.-J. 244 [252]
Dimonie, M. 270
Di Vaira, M. 916 [955]
Döhren, H. von 367
Donn, G. 382 [392]
Döpp, D. 146 [142]

Dornauer, H. 367
Dötz, K. H. 1158 [1220]
Dräger, M. 1255 [1280]
Dragutan, V. 270
Drew, S. 590
Drewes, M. W. 1141 [1186]
Driess, M. 781 [789]
Dronskowski, R. 139 [160]
Duddeck, H. 924 [927]
Duff, D. G. 676 [688]
du Mont, W.-W. 780, 912 [820, 945]
Dunitz, J. D. 1175 [1216]
Dunsch, L. 160, 936
Dürner, G. 61, 362 [82, 363]
Dvořák, J. 1302
Dybowski, C. R. 1053
Dyrbusch, M. 480, 683 [480, 717]
Dziallas, M. 248 [277]

EBSWORTH, E. A. V. 1197
Eckert, H. 894 [922]
Eckes, H.-L. 1046 [1040]
Eckes, P. 382 [392]
Edwards, P. P. 676 [688]
Effenberger, F. 142, 458 [146, 491]
Egert, E. 480, 683 [480, 717]
Eggert, U. 1015 [1047]
Eichler, K. 468 [470]
Eickenbusch, H. 1188 [1201]
Einsele, A. 1055
El-Amouri, H. 1169 [1208]
Ellis, A. B. 1198
Ellis, J. E. 1190 [1203]
Elschenbroich, C. 229, 704 [249, —]
Elsner, M. 345 [357]
Emrich, R. 356 [356]
Enders, D. 351 [359]
Engelhardt, H. 705
Engelhardt, L. M. 81, 681 [61, 702]
Epstein, A. J. 287 [332]
Erdle, W. 1260 [1290]
Eriyama, Y. 584 [601]
Erker, G. 666 [708]
Ermer, O. 446, 782, 929, 931, 934 [455, 791, 909, 912, 914]
Ernst, R. E. 1192
Ertl, G. 1054
Eschenmoser, A. 261 [273]
Evans, D. A. 1184 [1197]
Evers, J. 76 [69]
Eyzaguirre, J. 1301
Ezaz-Nikpay, K. 1182 [1222]

FACHINETTI, G. 680 [681]
Falbe, J. 1196
Feldmann, G. 570 [560]
Felixberger, J. K. 466 [466]
Fenske, D. 148 [155]
Ferguson, G. 1162 [1195]
Fessner, W.-D. 451, 452, 455, 457 [482, 484, 486, 488]
Field, J. S. 352 [373]
Fietzek, P. P. 551 [578]
Fink, J. 85 [67]
Finkelmann, H. 816 [840]
Finn, R. K. 1055
Fischer, G. 672 [695]
Fischer, J. 1169 [1208]
Fischer, M. 1160 [1218]
Fischer, R. 796 [817]
Fischer, R. A. 1263 [1286]
Fitjer, L. 130, 1023 [135, 1054]
Fleming, R. H. 1182 [1222]
Flöel, M. 73, 787 [88, 787]
Floriani, C. 68, 70 [84, 86]
Fochi, G. 680 [681]
Folkhard, W. 551 [578]
Forster, B. 894 [922]
Förster, S. 458 [491]
Franck, B. 64 [74]
Frank, W. 74 [68]
Frebel, M. 1010 [1045]
Frerichs, S. R. 1190 [1203]
Frey, H. 1280 [1327]
Frim, R. 232 [243]
Fritz, G. 802, 1111 [—, 1150]
Fritz, H. 452, 455, 668 [484, 486, 710]
Früh, T. 261 [273]
Frühbeis, H. 403 [413]
Fuchs, E. 74 [68]
Fuchs, E. P. O. 1011 [1058]
Fuchs, J. 1180 [1206]
Fuhrhop, J.-H. 699 [707]
Funaioli, T. 680 [681]
Futrell, J. H. 1055

GAA, H. G. 794 [822]
Gaines, Jr., G. L. 341 [346]
Ganter, C. 1252 [1292]
Gates, B. C. 1050
Gatteschi, D. 913 [958]
Geissler, M. 587 [569]
Georgiades, G. 1042 [1050]
Gerlach, U. 1283 [1323]
Germeshausen, J. 348 [372]
Gerson, F. 457 [488]
Gerstein, B. C. 1053
Gescheidt, G. 457 [488]
Gieren, A. 82 [81]
Giese, B. 233, 369, 479 [246, —, 475]
Giuffrè, L. 137 [149]
Gladysz, J. A. 910 [921]
Glasbrenner, J. 784 [784]
Gleiter, R. 347, 763, 1252 [371, 805, 1292]
Glendening, E. D. 1175 [1216]
Glenneberg, J. 362 [363]
Gmeiner, W. 228 [238]
Göbel, K. 59 [59]
Göbel, M. 261 [273]
Göbel, T. 151 [143]
Gocke, E. 1188 [1201]
Gompper, R. 552, 1036, 1039 [564, 1068, 1071]
González-Gómez, J. A. 479 [475]
Goodgame, D. M. L. 1044 [1053]
Gordon, G. 1301
Görl, U. 887 [917]
Göstl, G. 442 [467]
Gott, G. A. 264 [237]
Grabley, S. 664 [692]
Grassi, A. 137 [149]
Grassl, M. 272, 368, 1299
Grätzel, M. 567 [572]
Graule, T. 1032 [1075]
Greenberg, A. 1199
Grevels, F.-W. 885 [960]
Griffiths, K. D. 258, 260 [261, 262]
Grimme, W. 1268 [1277]
Grondey, H. 1279 [1303]
Gröninger, K. S. 233 [246]
Gross, R. 251 [257]
Gross, S. 571 [567]
Gruppe, S. 1012 [1042]
Grüttner, S. 683 [717]
Guarino, N. 88 [77]
Guastini, C. 68, 70 [84, 86]
Guczi, L. 1050
Guilhem, J. 661 [711]
Guldner, K. 82 [81]
Gumbrecht, W. 228 [238]
Günther, Harald 156, 1212 [151, 1242]
Günther, Helmut 128 [139]

HAASE, D. 467 [462]
Haber, L. F. 90
Hachgenei, J. W. 909 [947]
Hädrich, J. 573 [592]
Hady, A. F. A. 1143 [1188]
Hagenmüller, P. 803
Hager, R. 338 [354]
Haines, A. H. 593
Hall, R. B. 1198
Hammond, C. E. 904 [937]
Hampden-Smith, M. 903, 904 [936, 937]
Hampel, B. 583 [563]
Hanack, M. 344 [349]
Hanefeld, W. 1133 [1175]
Harms, K. 696, 1287 [706, 1279]
Harrison, P. 91
Härter, P. 787 [787]
Hartl, H. 921, 927 [951, 925]
Hartmann, C. 1146, 1148 [1189, 1191]
Hartmann, H. 1143 [1188]
Hassel, T. 359 [368]
Hauer, H. 796 [817]
Hauptmann, S. 271
Haushalter, R. C. 549, 1155 [576, 1172]
Häusler, H.-J. 1172 [1184]
Hazeu, W. 151 [143]
Hecht, C. 132 [158]
Heck, R. F. 593
Heilbronner, E. 360 [369]
Heim, N. 362 [363]
Heinrich, N. 140 [153]
Heinz, W. 1291 [1306]
Heinze, J. 352, 457 [373, 488]
Hellwinkel, D. 794 [822]
Helmchen, G. 1143 [1188]
Helson, H. E. 1246 [1276]
Hench, L. L. 706
Hendrickson, D. N. 915 [934]
Henkel, G. 145, 1009 [131, 1039]
Henrici-Olivé, G. 369
Henschen, A. 705
Herberhold, M. 82 [81]
Herdtweck, E. 132, 462, 466, 697, 787, 1263 [158, 462, 466, 687, 787, 1286]
Herges, R. 703 [610]
Herrmann, W. A. 73, 132, 462, 464, 466, 697, 787, 1263 [88, 158, 462, 464, 466, 687, 787, 1286]
Herrmann-Schönherr, O. 1249 [1300]
Herschbach, D. R. 1221 [1251]
Herzog, W. 483 [493]
Hettich, B. 139 [160]
Hey, E. 81 [61]
Hierholzer, B. 791 [811]
Higuchi, T. 1171 [1182]
Hiiro, T. 1187 [1221]
Hildebrand, T. 1262 [1325]
Hildenbrand, K. 446 [453]
Hinkelmann, K. 352 [373]
Hinrichs, R. 143 [137]
Hippe, D. 470 [459]
Hirs, C. H. W. 367
Hirthammer, M. 1246 [1276]
Hitchcock, P. B. 474 [497]
Ho, D. M. 135 [147]

Hoberg, H. 153, 571, 771 [141, 567, 799]
Hoferichter, R. 332 [345]
Hoffmann, H. M. R. 1015 [1047]
Hoffmann, R. 846 [871]
Hoffmann, R. W. 488, 1145 [503, 1196]
Hoffmann, V. T. 1006 [1036]
Höland, W. 527 [541]
Holdgrün, X. 1295 [1309]
Holdt, G. 151 [143]
Hollstein, W. 1287 [1279]
Hong, M. C. 897 [943]
Hopf, H. 232, 564, 580 [243, 594, 598]
Hoppe, D. 1034, 1145 [1079, 1196]
Hoppe, H.-U. 664 [692]
Hoppe, R. 706
Höweler, U. 238 [250]
Howell, J. A. 590
Huang, D. B. 897 [943]
Huber, B. 234, 338 [248, 354]
Huber, F. 906 [948]
Huber, W. 1290 [1305]
Hübner, T. 82 [81]
Hucker, J. 232 [243]
Hucknall, D. J. 269
Huffman, J. C. 135, 904, 915 [147, 937, 934]
Hüllmann, M. 477 [478]
Hummel, R.-P. 1150 [1180]
Humphrey, A. E. 589
Hünerbein, J. 779 [810]
Hung, D. T. 1184 [1197]
Hünig, S. 670, 672, 1281, 1283 [694, 695, 1322, 1323]
Hunkler, D. 452 [484]
Hupe, K.-P. 705
Huttner, G. 743 [765]

INDLEKOFER, G. 309 [312]
Irngartinger, H. 356 [356]
Issleib, K. 706
Iyoda, M. 559 [574]

JACKE, J. 885 [960]
Jahn, R. 356 [356]
Janda, P. 1021 [1065]
Janiak, C. 789 [788]
Janke, N. 1025 [1046]
Janoschek, R. 364, 1267, 1298 [374, 1312, 1332]
Jansen, M. 1098 [1136]
Jefferson, D. A. 676 [688]
Jenni, K. 153 [141]
Jeong, K.-S. 1244 [1297]
Jerrard, H. G. 938
Johnson, B. F. G. 676 [688]
Johnson, M. R. 678 [679]
Johnson, V. B. 1175 [1216]
Johnson, W. S. 1056
Jonas, K. 908 [957]
Jones, P. G. 1034 [1079]
Josel, H.-P. 241 [264]
Jung, G. 336, 1148 [343, 1180]
Jung, K. 464 [464]
Jutzi, P. 583 [563]

KAIM, W. 251, 1153 [257, 1178]
Kaiser, F.-J. 1163 [1199]
Kalcher, J. 364 [374]
Kalz, H.-J. 371 [381]
Kambe, N. 1187 [1221]
Kaminaka, M. 1171 [1182]
Kanellakopulos, B. 900 [929]
Kapoor, V. K. 159
Karcher, M. 763 [805]
Karsch, H. H. 673, 674 [703, 705]
Katakis, D. 1301
Kätker, H. 702 [714]
Kaub, J. 59 [59]
Kaufmann, D. 665 [682]
Kaulen, J. 773 [800]
Kaupp, G. 1280 [1327]
Kausch, M. 761 [795]
Kawaguchi, A. T. 1184 [1197]
Kawase, T. 559, 584 [574, 601]
Keim, W. 1012 [1042]
Keller, R. 483 [493]
Kendrick, R. D. 247 [241]
Keppeler, U. 344 [349]
Keryou, K. 918 [949]
Kessler, H. 888 [919]
Khemiss, A. K. 661 [711]
Kilminster, C. W. 1052
Kintzinger, J.-P. 661 [711]
Kirkland, A. 676 [688]
Kirmse, W. 570 [560]
Kissler, B. 1252 [1292]
Kitagawa, Y. 334 [366]
Kitzinger, A. I. 676 [688]
Klärner, F.-G. 1294 [1295]
Klaunzer, N. 1281 [1322]
Klebe, G. 78 [62]
Kleemann, G. 799 [808]
Klein, R. 403 [413]
Kleinermanns, K. 38 [38]
Kleinkauf, H. 367
Klement, U. 230, 1174 [268, 1176]
Klessinger, M. 238 [250]
Kliche, G. 349 [350]
Kling, A. 888 [919]
Klingler, O. 566 [579]
Klotzbücher, W. E. 885 [960]
Kluge, H. 664 [692]
Knaup, W. 248 [277]
Kneuper, H.-J. 132, 462, 464 [158, 462, 464]
Knoch, F. 1012 [1042]
Knölker, H.-J. 1035 [1067]
Knoll, F. 1256 [1299]
Knoll, K. 743 [765]
Knollmüller, M. 442 [467]
Knörzer, E. 551 [578]
Knözinger, H. 1050
Knunyants, I. L. 704
Kobayashi, N. 1021 [1065]
Koch, E. 545 [570]
Koch, H. 1188 [1201]
Koch, M. H. J. 551 [578]
Koch, P. 928 [909]
Koch, W. 140 [153]
Köcher, M. 931, 934 [912, 914]
Köhler, P. 1271 [1318]
Kohlmann, S. 1153 [1178]
Köhn, A. 482 [490]
Kohnke, F. H. 892 [941]
Kolar, C. 888 [919]
Koll, B. 347 [371]
Kölle, U. 567 [572]
Kölling, E. 580 [598]
Kolshorn, H. 1046 [1040]
Komoroski, R. A. 1301
König, W. A. 331 [362]
Kopf, J. 587 [569]
Korth, H.-G. 233 [246]
Koryta, J. 1302
Kottenhahn, M. 888 [919]
Koutecký, J. 170 [216]
Kowalczik, U. 1285 [1330]
Kowalczyk-Przewloka, T. 61 [82]
Krause, N. 580 [598]
Krebs, B. 139, 145, 1009 [160, 131, 1039]
Kreher, R. P. 1262 [1325]
Krepinsky, J. J. 1186 [1183]
Krestel, M. 1133 [1175]
Kreuder, W. 1249 [1300]
Krickemeyer, E. 1045 [1060]
Krongauz, V. 1178 [1204]
Krüger, C. 65, 146, 153, 563, 575, 666, 764, 771, 885, 908, 919, 1025, 1279 [72, 142, 141, 587, 583, 708, 798, 799, 960, 957, 953, 1046, 1303]
Krüger, G. 240 [245]
Krügerke, T. 799 [808]
Krull, M. 699 [707]
Krummel, G. 1290 [1305]
Kubiniok, S. 780 [820]
Kuckert, E. 563 [587]
Kühlein, K. 468 [470]
Kühnle, W. 480 [480]
Kulpe, J. 787 [787]
Kunz, H. 267, 294, 557 [269, 297, 595]
Küppers, H.-J. 250, 575 [253, 583]
Küppers, J. 1054
Kurreck, H. 345 [357]
Kvita, V. 790 [816]
Kynast, U. 681 [702]

LACHHEIN, S. 479 [475]
Lam, H. 1021 [1065]
Lange, A. 344 [349]
Langensee, P. 1291 [1306]
Langer, R. 256 [271]
Lanz, J. 1145 [1196]
Lappert, M. F. 592
Laube, T. 560 [580]
Laugier, J. 913 [958]
Lauterfeld, P. 146 [142]
Lebertz, H. 785 [785]
Lebrilla, C. B. 354 [352]
Lecht, R. 666 [708]
Lee, Y. T. 939 [967]
Leffers, W. 583 [563]
Lehmkuhl, H. 1279 [1303]
Lehn, J.-M. 266, 1266 [259, 1310]
Leigh, G. J. 474 [497]
Lentz, D. 921 [951]
Lerf, A. 110 [113]
Leumann, C. 261 [273]
Leupold, E. I. 468 [470]
Lever, A. B. P. 1021 [1065]
Levi-Montalcini, R. 707 [727]
Lex, J. 446, 928, 931, 1268 [455, 909, 912, 1277]
Leznoff, C. C. 1021 [1065]
Lichtenthaler, F. W. 1271 [1318]
Lidin, S. 1017 [1056]
Liebman, J. F. 1199
Lii, K.-H. 549 [576]
Limbach, H.-H. 247, 934 [241, 914]
Litterer, H. 468 [470]
Logan, D. E. 676 [688]
Lohray, B. B. 351 [359]
Lomölder, R. 1253 [1282]
Lonsky, R. 143 [137]
Losensky, H.-W. 901 [930]
Lottspeich, F. 705
Lucas, J. 340 [341]
Luger, P. 799 [808]
Luke, M. A. 768 [802]

MAAH, M. J. 474 [497]
Maas, G. 577, 1257 [585, 1328]
Mackie, A. G. 264 [237]
MacRory, P. P. 264 [237]
Madhavan, G. V. M. 1013 [1073]
Maercker, A. 972, 1032 [1002, 1075]
Maffi, S. 137 [149]
Mahlendorf, F. 352 [373]
Mahmoud, S. 229 [249]
Maier, G. 155, 256, 356, 1285 [152, 271, 356, 1330]
Maier, W. F. 452, 1182 [484, 1222]
Maigrot, N. 548 (804) [590]
Manojlović-Muir, L. 86 [79]
March, J. F. 1188 [1201]
Marcus, Y. 486
Märkl, G. 236, 1134 [255, 1214]
Marsch, M. 78, 696, 1287 [62, 706, 1279]
Marz, D. 462 [462]
Masamune, S. 584 [601]
Massa, W. 546, 696, 798, 1163 [559, 706, 790, 1199]
Masseyeff, R. 1299
Mastalsky, I. 345 [357]
Mathey, F. 275, 548 (804) [285, 590]
Mathis, G. 266 [259]
Mattay, J. 825 [849]
Mattes, R. 64 [74]
Matthes, K. E. 1162 [1195]
Mayer, K. K. 236 [255]
Mayr, H. 1029 [1059]
McAuliffe, C. A. 264 [237]
McEwen, A. B. 452 [484]
McNeill, D. B. 938
Means, C. M. 485 [476]
Meier, H. 1046 [1040]
Meissner, H. 228 [238]
Meli, A. 767 [821]
Menjón, B. 697 [687]
Mercando, P. 244 [252]
Merrill, E. W. 1056
Mestdagh, H. 1246 [1276]
Metternich, R. 1145 [1196]
Metzger, J. 336 [343]
Metzger, J. O. 479 [475]
Meyer, H. 546, 798 [559, 790]
Michaelis, R. 1026 [1049]
Michl, J. 170 [216]
Middle, F. A. 1056
Milchereit, A. 571 [567]
Milczarek, R. 908 [957]
Miller, J. S. 287 [332]
Millward, G. 918 [949]
Miranda, M. A. 797 [818]
Mißfeldt, M. 1165 [1210]
Miyoshi, N. 1187 [1221]
Mizoue, K. 1247 [1283]
Mizuno, Y. 1198
Modica, G. 137 [149]
Mohr, R. 332 [345]
Montoneri, E. 137 [149]
Moody, G. J. 890 [939]
Moo-Young, M. 588
Morawetz, H. 93, 270 [95, —]
Morley, S. D. 485 [476]
Mortensen, J. 457 [488]
Moskau, D. 156, 1212 [151, 1242]
Moskovits, M. 1050
Mosler, E. 551 [578]
Muir, K. W. 86 [79]
Mukai, T. 335 [367]
Müllen, K. 204, 1290, 1291 [192, 1305, 1306]
Müller, A. 1045 [1060]
Müller, B. 267 [269]
Müller, B. G. 688, 689, 1081 [685, 685, 1120]
Müller, G. 234, 338, 669, 673, 674 [248, 354, 683, 703, 705]
Müller, H. P. 359 [368]
Müller, U. 1026 [1049]
Müller, W. 256, 1285 [271, 1330]
Müller, W. M. 901 [930]
Münzel, N. 471 [471]
Murai, S. 1187 [1221]
Murata, I. 1247 [1283]
Murty, B. A. R. C. 451, 452, 455, 457 [482, 484, 486, 488]
Musso, H. 554, 1006 [588, 1036]

NAGEL, U. 1037 [1068]
Nakamura, A. 723 [745]
Nakamura, T. 1157 [1193]
Nehl, H. 1279 [1303]
Neidlein, R. 65 [72]
Nemetschek, T. 551 [578]
Nesemann, G. 367
Nesper, R. 1059 [1097]
Neugebauer, W. 587 [569]
Neukum, E. 483 [493]
Neumann, M. 1295 [1309]
Nevin, W. A. 1021 [1065]
Nicolaou, K. C. 1019 [1077]
Niecke, E. 1256 [1299]
Niedermann, H.-P. 1046 [1040]
Niedrach, L. W. 161 [183]
Nieger, M. 1256 [1299]
Nikolis, G. 937
Nixon, J. F. 474 [497]
Noe, C. R. 442 [467]
Nógrádi, M. 1053
Nöth, H, 1039 [1071]
Nuber, B. 575, 763, 924, 900, 1134 [583, 805, 927, 929, 1214]

OBERHAUSER, B. 442 [467]
Oberst, M. 1031 [1061]
Ochiai, H. 1157 [1193]
O'Connor, C. J. 549 [576]
Oda, M. 559 [574]
Oehlinger, G. 76 [69]
Oelhafen, P. 309 [312]
Oellerich, M. 1299
Oesterhelt, D. 580 [598]
Ogawa, A. 1187 [1221]
Ohmer, J. 148 [155]
Okubo, T. 765 [803]
Okuda, J. 466 [466]
Olivé, S. 369
Olti, F. 1057
Omae, I. 802
Oro, L. A. 444 [452]
Osborn, J. A. 1169 [1208]
Ostoja Starzewski, K. A. 63 [76]
Otterbach, A. 554 [588]
Owusu, R. K. 890 [939]

PAPE, H. 1057
Parker, D. 1162 [1195]
Parlar, H. 241 [264]
Parris, K. 1244 [1297]
Pascard, C. 661 [711]
Pasini, A. 615 [632]
Pattiasina, J. W. 330 [342]
Patton, A. T. 910 [921]
Patyk, A. 475 [495]
Paulus, W. 1188 [1201]
Penk, M. 1045 [1060]
Perathoner, S. 1266 [1310]
Peres, Y. 771 [799]
Peruzzini, M. 916 [955]
Peters, K. 780, 1165 [820, 1210]
Peyerimhoff, S. 470 [459]
Pfaendler, H. R. 1186 [1183]
Pfauntsch, J. 230 [268]
Pfeilsticker, K. 340 [341]
Philson, S. B. 1190 [1203]
Pickardt, J. 789 [788]
Plitzko, K.-D. 700 [715]
Pohl, S. 467, 583, 776, 912 [462, 563, 806, 945]
Polanyi, J. C. 952, 1298 [981, 1336]
Polk, M. 245 [239]
Poly, W. 1015 [1047]
Pomp, C. 924 [927]
Popall, M. 1158 [1220]
Pörschke, K.-R. 919, 1288 [953, 1321]
Postma, R. 140 [153]
Power, P. P. 1270 [1320]
Powietzka, B. 900 [929]
Pramod, K. 928 [909]
Preut, H. 906 [948]
Prinzbach, H. 451, 452, 455, 457, 566 [482, 484, 486, 488, 579]
Pritchard, R. G. 264 [237]
Pritzkow, H. 127, 781, 1259 [132, 789, 1294]
Puddephatt, R. J. 86 [79]
Puff, H. 470 [459]

QUABECK, U. 1023 [1054]
Quinkert, G. 61, 362 [82, 363]

RAABE, E. 146 [142]
Rabinovitz, M. 232 [243]
Ramphal, J. 1019 [1077]
Range, K.-J. 1174 [1176]
Rankin, D. W. H. 1197
Raston, C. L. 81, 592, 681 [61, —, 702]
Rattay, W, 1039 [1071]
Rau, F. 1174 [1176]
Rauenbusch, C. 702 [714]
Rebek, J., Jr. 1244 [1297]
Reber, G. 1146 [1189]
Reed, G. 1057
Reetz, M. T. 477, 592, 1028, 1141 [478, —, 1081, 1186]
Regitz, M. 83, 85, 764, 908, 1011, 1257 [65, 67, 798, 957, 1058, 1328]
Rehm, H.-J. 1057
Reichow, S. 1277 [1285]
Reiner, J. 774 [814]
Reinold, P. 672 [695]
Reinsch, M. 238 [250]
Reisenauer, H. P. 256, 1285 [271, 1330]
Reiser, O. 1277 [1285]
Rempp, P. 1056
Renger, G. 643 [660]
Rey, P. 913 [958]
Rheingold, A. L. 244 [252]
Ricard, L. 548 (804) [590]
Rice, S. B. 1155 [1172]
Richert, J.-L. 88 [77]
Riede, J. 673, 674 [703, 705]
Riemer, R. 784 [784]
Rihs, G. 668 [710]
Ringsdorf, H. 1178, 1249 [1204, 1300]
Robertson, G. B. 258, 260 [261, 262]

Robinson, C. W. 590
Roder, K. 686 [719]
Rohrer, H. 606 [622]
Rösch, W. 85, 1011 [67, 1058]
Roth, W. D. 452 [484]
Roth, W. R. 256, 1285 [271, 1330]
Rubow, M. 1029 [1059]
Rüchardt, C. 573, 770 [592, 807]
Ruisinger, B. 253 [266]
Ruiz-Pérez, C. 82 [81]
Ruska, E. 595 [611]
Russ, M. 1007 [1037]
Rüsseler, W. 908 [957]
Rüther, R. 906 [948]
Rylander, P. N. 593

SAAK, W. 467, 583, 776, 912 [462, 563, 806, 945]
Saalfrank, R. W. 1160 [1218]
Sabbatini, N. 1266 [1310]
Sadlej, J. 158
Sager, W. 557 [595]
Saitmacher, K. 470 [459]
Salzer, A. 704
Samhaber, W. 1055
Sander, W. 475 [495]
Sangwan, N. K. 896 [923]
Sansoni, B. 273
Sartor, K. 1143 [1188]
Sauter, H.-P. 790 [816]
Sauvage, J.-P. 661 [711]
Sax, A. F. 364 [374]
Schacht, H.-T. 352 [373]
Schacht, W. 665 [682]
Schade, C. 1029 [1059]
Schäfer, Adolf 462, 464, 466 [462, 464, 466]
Schäfer, Annemarie 766 [806]
Schäfer, H. J. 1026, 1253 [1049, 1282]
Schanzenbach, D. 267 [269]
Schauer, C. K. 255 [275]
Scheffold, R. 1300
Schenk, W. A. 98 [101]
Scherer, O. J. 59, 1153 [59, 1178]
Schindler, M. 761 [795]
Schlemper, H. 1167 [1212]
Schleyer, P. von R. 364, 452, 587, 761, 1267 [374, 484, 569, 795, 1312]
Schlichte, K. 1025 [1046]
Schlögl, R. 309 [312]
Schlund, R. 666, 1281 [708, 1322]
Schmalz, D. 1212 [1242]
Schmalz, H.-G. 61 [82]
Schmalz, P. 791 [811]
Schmickler, H. 931 [912]
Schmidbaur, H. 234, 338, 1146, 1148 [248, 354, 1189, 1191]
Schmidt, D. 1034 [1079]
Schmidt, H. 900 [929]
Schmidt, Martin 79 [64]
Schmidt, Max 887 [917]
Schmidt, R. R. 482, 793 [490, 813]
Schmidt, T. 1268 [1277]
Schmitz, A. 1141 [1186]
Schmuck, A. 134, 1180 [138, 1206]
Schneider, H.-J. 896 [923]
Schneider, K. 774 [814]
Schneider, R. 1029 [1059]
Schnering, H. G. von 349, 780, 1059, 1165 [350, 820, 1087, 1210]
Schöllhorn, R. 1188 [1201]
Schöllkopf, U. 143, 480, 683 [137, 480, 717]
Schöttmer, B. 555 [591]
Schötz, K. 761 [795]
Schreck, M. 449, 690 [474, 720]
Schröder, M. 250 [253]
Schröder, W. 919 [953]
Schröer, D. 1294 [1295]
Schubert, B. 587 [569]
Schuchmann, H.-P. 446 [453]
Schuhmann, W. 241 [264]
Schumann, H. 789 [788]
Schwager, H. 65, 67 [72, 73]
Schwarz, H. 140, 354, 805 [153, 352, 829]
Schwarz, M. 349 [350]
Schwarzensteiner, M.-L. 1039 [1071]
Schweig, A. 343, 471 [348, 471]
Schwesinger, R. 1164, 1165, 1167 [1209, 1210, 1212]
Seely, F. L. 1013 [1073]
Seevogel, K. 885 [960]
Seifart, K. H. 218 [206]
Seiler, P. 1175 [1216]
Seitz, G. 332, 1163 [345, 1199]
Seitz, T. 477, 1028 [478, 1081]
Self, V. A. 1042 [1050]
Sendhoff, N. 777 [794]
Seppelt, K. 134, 799, 1180 [138, 808, 1206]
Sermon, P. A. 918, 1042 [949, 1050]
Sessler, J. L. 678 [679]
Sextl, G. 76 [69]
Sheldrick, W. S. 1172 [1184]
Shimazaki, N. 335 [367]
Shin, J.-H. 564 [594,]
Shriver, D. F. 255 [275]
Siabalis, N. 779 [810]
Siebert, W. 781 [789]
Simon, A. 139, 579 [160, 602]
Simon, H. 128, 785 [139, 785]
Simon, W. 1009 [1039]
Singh, H. 159
Sipos, W. 1152 [1177]
Skopan, H. 128 [139]
Slawin, A. M. Z. 692, 693, 890, 892 [697, 698, 939, 941]
Sluyser, M. 591
Sonntag, C. von 446 [453]
Sonoda, N. 1187 [1221]
Spangenberg, B. 1133 [1175]
Spencer, N. 890 [939]
Spes, P. 1039 [1071]
Spiro, T. G. 487
Spiteller, G. 774 [814]
Spurr, P. R. 455 [486]
Spyroudis, S. 1246 [1276]
Staab, H. A. 460 [460]
Stadler, M. 1174 [1176]
Stahl, H. 794 [822]
Steffan, B. 586 [597]
Steglich, W. 586 [597]
Stella, S. 68 [84]
Steudel, R. 151 [143]
Stevermann, B. 256 [271]
Stezowski, J. J. 1034 [1079]
Stiehm, T. 329 [340]
Stoddart, J. F. 692, 693, 890, 892 [697, 698, 939, 941]
Stoppioni, P. 916 [955]
Streith, J. 668 [710]
Strunck, A. 687 [701]
Stütz, A. 320 [323]
Stüwe, H.-T. 331 [362]
Subramanian, S. 1192
Sugihara, Y. 1247 [1283]
Sustmann, R. 233, 256, 1285 [246, 271, 1330]
Sutherland, B. R. 135 [147]
Swarowsky, H. 1153 [1178]
TAKACS, J. M. 1013 [1073]
Tamaru, Y. 1157 [1193]
Tang, D. 1048 [1063]
Tarara, G. 1034, 1145 [1079, 1196]
Tasi, M. 685 [691]
Teichler, I. 931 [912]
Teles, J. H. 155 [152]
Teo, B. K. 897 [943]
Teo, B. K. 801
Terlouw, J. K. 140, 354, 805 [153, 352, 829]
Teuben, J. H. 330 [342]
Thanos, I. 785 [785]
Thiem, J. 555 [591]
Thomas, J. D. R. 890 [939]
Thomas, J. M. 918, 1048 [949, 1063]
Thomasson, R. 1017 [1056]
Tietze, L. F. 1295 [1309]
Timasheff, S. N. 367
Timmermann, R. 64 [74]
Tiripicchio, A. 444, 768 [452, 802]
Tiripicchio-Camellini, M. 444, 768 [452, 802]
Toda, T. 334, 335 [366, 367]
Töfke, S. 147 [134]
Toniolo, C. 1148 [1180]
Treacy, M. M. J. 1155 [1172]
Treber, J. 1025 [1046]
Treurnicht, I. 86 [79]
Trömel, M. 1007 [1037]
Tsay, Y.-H. 575, 771, 885, 919 [583, 799, 960, 953]
Tschamber, T. 668 [710]

UEDA, T. 1171 [1182]
Ugi, I. 703 [610]
Ulrich, D. R. 706
Uphoff, J. 357 [361]
Urland, W. 1275 [1316]

VAHRENKAMP, H. 352, 355, 572 [373, 353, 561]
van Baar, B. L. M. 140 [153]
van Bolhuis, F. 330 [342]
van de Heisteeg, B. J. J. 73 [88]
Van der Sluys, W. G. 904 [937]
van Eldik, R. 240, 1053 [245, —]
Veith, M. 1 [1]
Viguri, F. 444 [452]
Vincent, J. B. 915 [934]
Vizza, F. 767 [821]
Voelter, W. 705
Vogel, E. 928, 931, 934 [909, 912, 914]
Vogel, P. 274
Vogel, W. 527 [541]
Vogelbacher, U.-J. 85 [67]
Vögtle, F. 470, 777, 901 [459, 794, 930]
Völlenkle, H. 442 [467]
Vollhardt, K. P. C. 1035, 1246 [1067, 1276]
Volz, H. 564 [594]
Voss, H. 1280 [1327]
Vostrowsky, O. 784 [784]

WACHTER, J. 230 [268]
Wadepohl, H. 127, 1259 [132, 1294]
Wagner, F. E. 1148 [1191]
Wagner, H.-U. 1037, 1039 [1068, 1071]
Wagner, O. 1257 [1328]
Wagner, W. 462, 787 [462, 787]
Walberg, H.-J. 1045 [1060]
Wallmeier, H. 403 [413]
Walzer, E. 61 [82]

Wang, D. I. C. 590
Warwel, S. 702 [714]
Watanabe, M. 1171 [1182]
Webber, S. E. 1019 [1077]
Weber, J. 74 [68]
Weber, L. 1010 [1045]
Weber, T. 142 [146]
Weetman, J. 1143 [1188]
Wehle, D. 130 [135]
Wehrle, B. 247, 934 [241, 914]
Weidenbruch, M. 776 [806]
Weigmann, R. 923 [918]
Weinges, K. 1152 [1177]
Weinhold, F. 1175 [1216]
Weisman, G. R. 1175 [1216]
Weiss, E. 587 [569]
Weiss, J. 575, 924 [583, 927]
Weissbarth, K.-H. 777 [794]
Welch, G. R. 488
Wendorff, J. H. 1249 [1300]
Wengenmayer, F. 382 [392]
Werner, H. 248, 686 [277, 719]
Werner, U. 901 [930]
West, R. 1201 [1231]
White, A. H. 81, 681 [61, 702]
White, H. 785 [785]
Wickramasinghe, W. A. 258 [261]
Wieghardt, K. 250, 575, 924 [253, 583, 927]
Wieland, S. 240 [245]
Wilckens, M. 1034 [1079]
Wilk, A. 1009 [1039]
Wilke, G. 65, 67 [72, 73]
Williams, D. J. 692, 693, 890, 892, 1044 [697, 698, 939, 941, 1053]
Williams, K. 1244 [1297]
Willis, A. C. 258 [261]
Wingender, E. 218 [206]
Winpenny, R. E. P. 1044 [1053]
Wirth, U. 1160 [1218]
Witte, J. 63 [76]
Witzel, T. 233 [246]
Wokaun, A. 1192
Wolfrum, J. 38 [38]
Wolmershäuser, G. 1153 [1178]
Wörth, J. 452 [484]
Wucherer, E. J. 355 [353]
Wullbrandt, D. 483 [493]
Wünsch, M. 229 [249]
Würthwein, E.-U. 923 [918]
Wüster, H. 577 [585]
Wyckoff, H. W. 367

XAVIER, A. V. 90

YAKOBSON, G. G. 70
Yamamoto, H. 1247 [1283]
Yang, Z.-z. 360 [369]
Yannoni, C. S. 247 [241]
Yasuda, H. 91
Yasuda, H. 723 [745]
Yoshida, T. 1171 [1182]
Yoshida, Z. 1157 [1193]
Yu, D. 331 [362]

ZAHN, T. 236 [255]
Zanazzi, P. F. 680 [681]
Zarzycki, R. 692, 693 [697, 698]
Zhang, H. 897 [943]
Zhou, W. 1048 [1063]
Ziegler, M. L. 236, 763, 900, 1134 [255, 805, 929, 1214]
Ziegler, T. 458 [491]
Zimmermann, Helmuth 1160 [1218]
Zimmermann, Herbert 247 [241]
Zirnstein, M. A. 460 [460]
Zora, J. A. 474 [497]
Zuckerman, J. J. 1195
Zunino, F. 615 [632]
Zurmühlen, F. 83 [65]
Zwick, B. D. 910 [921]
Zybill, C. 669 [683]

SUBJECT INDEX

(R) = Review Article (C) = Short Communication (B) = Book Review (L) = Correspondence

ABSOLUTE CONFIGURATION, The absolute configuration of the ant alarm pheromone manicone (C) 784

Acenaphthene, Cerium(IV)-catalyzed single electron transfer (SET) on acenaphthene and 1,4-dihydronaphtho-[1,8-*d,e*][1,2]diazepine: chemical evidence for distinct radical cations (C) 797

Active sites, Chemical modification of enzymes. Active site studies (B) 1301

Addition, Formation of diiridium(II) complexes by photoassisted oxidative-addition reactions: structure of a stable binuclear iodo(iodomethyl)iridium(II) complex (C) 444

Oxidative addition of hydrogen telluride to organometallic fragments (C) 132

Unsaturated molecules containing main group metals (R) 1

1,6-Addition, Unusual 1,6-addition of a carbenoid (C)72

Adenine receptors, Molecular recognition: stacking interactions influence Watson-Crick vs. Hoogsteen base-pairing in a model for adenine receptors (C) 1244

Adsorption and curvature in highly dealuminated zeolites (C) 1017

A-Frame cluster, New $AuPt_2$ A-frame cluster complexes (C) 86

Alcohols, Inversion of the configuration of secondary alcohols via isourea ethers prepared in situ (C) 773

Aldoketene dimers, Mycoloylpeptides and other lipopeptide adjuvants from higher aldoketene dimers (C) 336

Aldol reaction, Stereoselective aldol reactions with α-unsubstituted chiral enolates (R) 24

Alkali-metal cyclopentadienide, Structure of a crystalline alkali-metal cyclopentadienide (C) 583

Alkali metals, Ether cleavage with organoalkali-metal compounds and alkali metals (R) 972

Alkanoates, Reduction of 2-enoates and alkanoates with carbon monoxide or formate, viologens, and *clostridium thermoaceticum* to saturated acids and unsaturated and saturated alcohols (C) 785

Alkene complexes, Diene, alkyne, alkene, and alkyl complexes of early transition metals: structures and synthetic applications in organic and polymer chemistry (R) 723

α-Alkoxyaldehydes, The first direct evidence for a Cram chelate (C) 477

α-Alkoxyketones, The first direct evidence for a Cram chelate (C) 477

Alkylaluminum cations: synthesis and structure of $[Al(2\text{-}C(SiMe_3)_2C_5H_4N)_2][AlCl_4]$ (C) 681

Alkylation, Control of the relative electrophilicity of alkylating agents by variation of the Lewis acid concentration (C) 1029

Alkylation of aromatic compounds, Stereoselective alkylation of aromatic compounds with threonine trifluoromethanesulfonates (C) 142

Alkyl complexes, Diene, alkyne, alkene, and alkyl complexes of early transition metals: structures and synthetic applications in organic and polymer chemistry (R) 723

Alkyl radicals, The effect of solvent on the stability of mero-substituted alkyl radicals (C) 770

Alkyne complexes, Diene, alkyne, alkene, and alkyl complexes of early transition metals: structures and synthetic applications in organic and polymer chemistry (R) 723

Allenes, Generation and interception of 1-oxa-3,4-cyclohexadiene (C) 690

Trimethylenemethane complexes of Cr, Mo, and W by novel methylenation of allenes with carbene complexes; cyclopentanes by [3+2] cycloaddition of trimethylenemethane complexes to allenes (C) 357

Allenylidene ligands, Alkyne complexes of rhenium in medium oxidation states: synthesis and molecular structure of a rhenium(V)–allenylidene complex (C) 1263

Allylamines, Allylamine derivatives—a new class of active substances in antifungal chemotherapy (R) 320

Allylcyclopentadienylpalladium, Reactions of $(\eta^3\text{-allyl})(\eta^5\text{-cyclopentadienyl})$palladium with cyclopropabenzenes (C) 67

Allylic anions, Regioselective protonation of allylic anions (C) 1281

Allylic ethers, Unusual ligand directed regioselectivity in the iron catalyzed cross coupling of allylic ethers to 2-substituted 1,3-dienes (C) 1013

Allylmetal compounds, Crystal structure of the η^1-allyl-Grignard compound bis(allylmagnesium chloride-TMEDA) (C) 696

Allylzinc compounds, High-resolution CP-MAS ^{13}C-NMR spectra of allylzinc compounds—structural similarities and differences in the solid state and in solution (C) 1279

Aluminum compounds, Alkylaluminum cations: synthesis and structure of $[Al(2\text{-}C(SiMe_3)_2C_5H_4N)_2][AlCl_4]$ (C) 681

Stabilization of the $[AlMe_2]^{\oplus}$ cation by crown ethers (C) 485

Amalgams, Square Hg_4 clusters in the compound CsHg (C) 687

Amavadin, an example for selective binding of vanadium in nature: studies of its complexation chemistry and a new structural proposal (C) 545

α-Amino acids, Asymmetric synthesis of cyclic α-amino acids by the bislactim ether method (C) 143

α-Amino-γ-nitrocarboxylic esters, Asymmetric synthesis of α-amino-γ-nitrocarboxylic esters by the bislactim ether method (C) 480

Amino acids, Diastereoselective Strecker synthesis of α-aminonitriles on carbohydrate templates (C) 557

β-Amino alcohols, Stereoselective synthesis of β-amino alcohols from optically active α-amino acids (C) 1141

Amino(imino)phosphanes, $(Me_3Si)_2N\text{–}P{=}NSiMe_3$ as educt for electron-rich phosphorus-nitrogen ligands (C) 59

Analysis, ^{2}H,^{2}H-COSY and ^{2}H,^{2}H,^{13}C-RELAY NMR experiments for the analysis of deuteriated compounds (C) 156

Instrumentelle Multielementanalyse (B) 273

Analytical methods, Direct identification of the carbon skeleton of organic compounds using double quantum coherence ^{13}C-NMR spectroscopy. The INADEQUATE pulse sequence (R) 625

in human toxicology (B) 1051

Nuclear quadrupole interaction and time-resolved perturbed γ-γ-angular correlation spectroscopy: applications in chemistry, materials science, and biophysical chemistry (R) 110

The generation and characterization of molecules by neutralization-reionization mass spectrometry (NRMS) (R) 805

The practice of quantitative gel electrophoresis (B) 370

Angular correlation spectroscopy, Nuclear quadrupole interaction and time-resolved perturbed γ-γ-angular correlation spectroscopy: applications in chemistry, materials science, and biophysical chemistry (R) 110

Annulenes, A new class of organozirconium(IV) compounds: alkyl derivatives of tetramethyltetraazadibenzo[14]annulenatozirconium(IV) (C) 70

Anthracyclinone ring C synthesis via chelate carbene complexes (C) 1158

Antifungal chemotherapy, Allylamine derivatives—a new class of active substances in antifungal chemotherapy (R) 320

Antimony compounds, Nonaphenyltristiboxane-1,5-diyl disulfonates (C) 906

$[Ph_4P]_2[Sb_2I_8]$: weak interactions between phenyl groups of the cation and antimony atoms of the anion (C) 467

Antitumor agents, New cisplatin analogues — on the way to better antitumor agents (R) 615

Arene adducts, $[Ph_4P]_2[Sb_2I_8]$: weak interactions between phenyl groups of the cation and antimony atoms of the anion (C) 467

Arene complexes, Arene adducts with weak interactions: hexaethylbenzene–bis(tribromoarsane) (C) 234

Arene complexes with weak interactions: a macrocyclic tris(arene) complex of gallium(I) with ν^{18} coordination (C) 338

Azulene as unusual η^6-ligand and as $\eta^6{:}\eta^4$-bridge in Mo-complexes (C) 147

$[CH_3C_6H_5BiCl_2][AlCl_4]$ and $[(CH_3)_6C_6BiCl_2][AlCl_4]$—compounds containing η^6-arene-complexed $BiCl_2^{\oplus}$ units (C) 74

$[\{(C_5H_5)Co\}_3(C_6H_5CH{=}CHCH_3)]$, an organometallic cluster with a face-bridging arene ligand (C) 1259

Electron delocalization in diruthenium complexes of polycyclic arenes (C) 700

Arenes, Benzene and linearly annelated arenes as dienophiles in Diels–Alder reactions with inverse electron demand (C) 332

Deep-colored, through-conjugated multitriphenylmethylium ions (C) 794

Selective molecular recognition and separation of isomeric and partially hydrogenated arenes (C) 901

Arenium ions, Mono- and diarenium ions of [2.2]paracyclophanes (C) 564

Aromaticity, Annelated isoindoles with 18π electrons (C) 1262

Back to the structure of benzene (L) 1298

[2.2](1,4)Benzo[*g*]chrysenoparacyclophane dianion: a novel, paratropic, double-layered carbanion (C) 232

Concerning the structure of benzene (C) 782

Cyclohepta[*a*]phenalene: a highly electron—donating nonalternant hydrocarbon (C) 1247

2,6-Diaza-*s*-indacenes (C) 1037

Dicyclopropa[*a,c*]naphthalene: a compound capable of existence? (C) 577

Propellanes of the glycoluril series and bridged tetrazocines (C) 1039

Synthesis of tricyclo[5.2.0.0^{1,3}]nona-4,6,8-triene, a norcaradiene structure constrained by the antiaromaticity of cyclobutadiene (C) 559
Aromatic nitration at the encounter rate in the gas phase (C) 1177
Arsenic bromides, Arene adducts with weak interactions: hexaethylbenzene-bis(tribromoarsane) (C) 234
Arsenic compounds, $[As_3Br_{12}]^{3-}$ and $[As_8I_{28}]^{4-}$ — structurally novel, discrete halogenoarsenate(III) ions (C) 1172
Arsenic iodides, Structure of triphenylarsane diiodide, $[Ph_3As \cdot I_2]$, a compound formed in the thermal decomposition of $[Mn(OAsPh_3)_3I_2(SO_2)_2]$ (C) 264
Arsenic-titanium compounds, Synthesis of the four-membered metallacycle $[Cp_2Ti(AsPh)_3]$ via the in situ reduction of $[Cp_2TiCl_2]$ (C) 244
Arsinosulfur diimides, $As_4S_5N_{10}$—A diaminosulfane derivative with two bicyclic arsino sulfur diimides (C) 82
Arsoles, 1,1'-Diarsaferrocene (C) 229
α-Arylglycine esters, Optically active α-arylglycine esters by Friedel-Crafts alkylation with the chiral cation of the bislactim ether of *cyclo*-(L-Val-Gly) (C) 683
(+)-Aspicilin, Total synthesis of the enantiomerically pure lichen macrolide (+)-aspicilin (C) 362
Asteranes, Diasterane (tricyclo[3.1.1.1^{2,4}]octane) (C) 554
Nonacyclo[10.8.0.0^{2,11}.0^{4,9}.0^{4,19}.0^{6,17}.0^{7,16}.0^{9,14}.0^{14,19}]icosane, a double tetraasterane (C) 1006
Asymmetric Diels-Alder reactions, High stereoselectivity in Lewis-acid-catalyzed and uncatalyzed Diels-Alder reactions of the fumarate of (S)-ethyl lactate (C) 1143
Asymmetric synthesis of α-amino-γ-nitrocarboxylic esters by the bislactim ether method (C) 480
of cyclic α-amino acids by the bislactim ether method (C) 143
Optically active α-arylglycine esters by Friedel-Crafts alkylation with the chiral cation of the bislactim ether of *cyclo*-(L-Val-Gly) (C) 683
Azaalkenylidene complexes, A novel route to azaalkenylidene-metal complexes (C) 248
2-Azabut-1-en-3-ynes, First synthesis of *N*-methylene-ynamines (2-azabut-1-en-3-ynes) (C) 923
Azatriphosphete, A 3,7-diaza-1,2,4,5,6,8-hexaphosphatricyclo[4.2.0.0^{2,5}]octane, a [2+2] dimer of a 1,2-dihydro-1-azatriphosphete containing a P_4 structure (C) 1256
Azides, [4+2] Cycloadditions of 2,3-diazido-1,3-butadienes: a novel entry to vicinal vinyl diazides and 1,4-dicyano compounds (C) 879
The pyrolysis of azides in the gas phase (R) 504
Azoalkene-nitrene cleavage on an Fe_3-cluster (C) 355
Azo compounds, Azo cope rearrangements of nonstabilized azo compounds (C) 672
Azo cope rearrangements of nonstabilized azo compounds (C) 672
Azo coupling, Diazo coupling of nortricyclene(tricyclo[2.2.1.0^{2,6}]heptane)-1-diazonium ions (C) 570
Azo/nitrene addition, Unusually stable *cis,cis*-trialkyltriaziridines by azo/nitrene addition (C) 566
Azulene as unusual η^6-ligand and as η^6:η^4-bridge in Mo-complexes (C) 147

BACTERIORHODOPSIN, Regulation of the 6-s equilibrium conformation of retinal in bacteriorhodopsin by substitution at C-5; 5-methoxy- and 5-ethylretinalbacteriorhodopsin (C) 580
Base-pairing, Molecular recognition: stacking interactions influence Watson-Crick vs. Hoogsteen base-pairing in a model for adenine receptors (C) 1244
Bases, Novel, very strongly basic, pentacyclic "proton sponges" with vinamidine structure (C) 1165
Peralkylated polyaminophosphazenes—extremely strong, neutral nitrogen bases (C) 1167
Tricyclic 2,4-diaminovinamidines—readily accessible, very strong CHN bases (C) 1164
Belts, Molecular belts and collars in the making: a hexaepoxyoctacosahydro[12]-cyclacene derivative (C) 892
Benzene, Back to the structure of benzene (L) 1298
Concerning the structure of benzene (C) 782
Benzoborole, The first synthesis of a benzoborole (C) 665
Bergmeyer, Methods of enzymatic analysis. Vol. VIII. Metabolites 3: Lipids, amino acids, and relate compounds (B) 272
Vol. IX. Proteins and peptides (B) 368
Vol. X: Antigens and antibodies 1. Vol. XI: Antigens and antibodies 2. Vol. XII: Drugs and pesticides (B) 1299
Bicycloalkylcarboxylic acids, Anodic Grob fragmentation of bicycloalkylcarboxylic acids to specifically disubstituted cycloalkenes (C) 1026
Bicyclotetrasilanes, Bond stretch isomerism in bicyclo[1.1.0]tetrasilanes. Contrasts between strained silicon and carbon ring systems (C) 364
Bilayer membranes, Lactosylceramides with unsaturated fatty acids — synthesis and use in the generation of bilayer membranes (C) 793
Bimetallic macrocyclic polymer structures, Novel bimetallic macrocyclic polymer structures incorporating deprotonated 2-pyrrolidone bridges: the crystal structures of $[\{Hg_2Cu(C_4H_6NO)_4\}X_2]_n$ ($X = NO_3$ or ClO_4) (C) 1044
Binuclear complexes, The synthesis and catalytic properties of some open-sided binuclear complexes of Rh^1: the structure of $[Rh_2(CO)_2(CH_3CN)_2\{CH(PPh_2)_3\}](CF_3SO_3)_2$ (C) 1169
Biocatalysts, A biocatalyst for the preparation of (*R*)- and (*S*)-2-hydroxycarboxylic acids (C) 128
Biochemistry, High-performance liquid chromatography in biochemistry (B) 705
Bioglass ceramics, The development of bioglass ceramics for medical applications (R) 527
Bioinorganic chemistry, Frontiers in bioinorganic chemistry (B) 90
Biological macromolecules, Methods in enzymology. Vols 114 and 115. Diffraction methods for biological macromolecules (B) 367
Biological recognition, Synthesis of glycopeptides, partial structures of biological recognition components (R) 294
Biological reduction, Reduction of 2-enoates and alkanoates with carbon monoxide or formate, viologens, and *clostridium thermoaceticum* to saturated acids and unsaturated and saturated alcohols (C) 785
Biomimetic synthesis, Chemistry of pyrrocorphins: biomimetic regioselectivity of *C*-methylation at the ligand periphery of magnesium(II) uropyrrocorphinate(type I)-octanitriles (C) 261
of a twofold *N,N'*-bridged porphyrinogen (C) 64
Biotechnology. A comprehensive treatise in 8 volumes. Vol. 4: microbial products II (B) 1057
Comprehensive biotechnology. The principles, applications and regulations of biotechnology in industry, agriculture and medicine (B) 588
Mikrobiologische und biochemische Verfahrenstechnik; eine Einführung (B) 1055
Biphenylenes with strongly distorted trapezoidal four-membered ring (C) 470
Bipyridyl complexes, Photoisomerization of bis(bipyridyl)rhodium(III) complexes; synthesis of *trans*-$[Rh(bpy)_2YCl]^{n\oplus}$, Y = Cl, H_2O (C) 240
Bishomo-aromaticity, Propellanes of the glycoluril series and bridged tetrazocines (C) 1039
Bislactim ether method, Asymmetric synthesis of α-amino-γ-nitrocarboxylic esters by the bislactim ether method (C) 480
Optically active α-arylglycine esters by Friedel-Crafts alkylation with the chiral cation of the bislactim ether of *cyclo*-(L-Val-Gly) (C) 683
Bismuth(III) chlorides, $[CH_3C_6H_5BiCl_2][AlCl_4]$ and $[(CH_3)_6C_6BiCl_2][AlCl_4]$—compounds containing η^6-arene-complexed $BiCl_2^{\oplus}$ units (C) 74
Bismuth compounds, Structure and color of pentaphenylbismuth (C) 1180
Bissecododecahedradienes, One- and two-electron oxidations of pagodanes and bissecododecahedradienes: unusually persistent radical cations (C) 457
Bissecododecahedraenes, unusual hyperstable olefins (C) 455
Bissetone, Proof of the (*S,S*) configuration of (−)-bissetone by synthesis from D-glucose (C) 1271
Bis(trimethylsilyl)methyl phenyl sulfone, X-ray structure analysis of the Li_2-compound of bis(trimethylsilyl)methyl phenyl sulfone; structural units of an α-sulfonyl- and a complex-stabilized *ortho*-sulfonyl carbanion (C) 1287
Bond angles, Biphenylenes with strongly distorted trapezoidal four-membered ring (C) 470
Bonding concepts, Homoatomic d^{10}-d^{10} interactions: their effects on structure and chemical and physical properties (R) 1098
Bond stretch isomerism in bicyclo[1.1.0]tetrasilanes. Contrasts between strained silicon and carbon ring systems (C) 364
Borazine-analogue, Synthesis and X-ray structure of $(2,4,6\text{-}Me_3C_6H_2BPC_6H_{11})_3$: a boron-phosphorus analogue of borazine (C) 1270
Boron compounds, Synthesis and structure of a 2,5-dihydro-1*H*-1,2,5-phosphadiborole derivative (C) 781
The first synthesis of a benzoborole (C) 665
Boron-Oxygen compounds, Cooperative effects in the phase transformation of triethylcyclotriboroxane (C) 245
Boron-phosphorus compounds, Synthesis and X-ray structure of $(2,4,6\text{-}Me_3C_6H_2BPC_6H_{11})_3$: a boron-phosphorus analogue of borazine (C) 1270
Bridging ligands, A mixed-metal cluster with two quadruply-bridging carbonyl ligands (C) 685
$[\{(C_5H_5)Co\}_3(C_6H_5CH{=}CHCH_3)]$, an organometallic cluster with a face-bridging arene ligand (C) 1259
Dinuclear complexes of gold(I) containing bridging cyclometalated arylphosphane or arylarsane ligands (C) 258
1,8-Naphthalene-linked cofacial dimeric phthalocyanines (C) 1021
RP-Bridged metal carbonyl clusters: synthesis, properties, and reactions (R) 743
Sulfur oxides as ligands in coordination compounds (R) 98
Tetranuclear mixed-valence manganese complexes with reduced TCNE or TCNQ as η^4-bridging ligands (C) 251
Butterfly structure, Synthesis and structure of $[(PPh_3)_2N][Fe_3Mn(CO)_{12}(\mu_4\text{-}O)]$: a butterfly oxo cluster (C) 255
tert-Butylethynyllithium, Tetrameric and dodecameric *tert*-butylethynyllithium: a

novel aggregation principle in organolithium compounds (C) 587

CAGE COMPOUNDS, $[Ag_4(SCH_2C_6H_4CH_3S)_3]^{2-}$, a novel polynuclear silver thiolate with trigonal-planar coordination of all silver atoms and a central $[Ag_4S_6]$-cage (C) 145
Macrobicyclic polyethers as second sphere ligands for tetraammineplatinum(II) (C) 693
Nonacyclo[10.8.0.0^{2,11}.0^{4,9}.0^{4,19}.0^{6,17}.0^{7,16}.0^{9,14}.0^{14,19}]icosane, a double tetraasterane (C) 1006
Second sphere coordination of tetraammineplatinum(II) by a macropolycyclic crown ether bisamide receptor (C) 692
Selective molecular recognition and separation of isomeric and partially hydrogenated arenes (C) 901
Synthesis and chirality of sixfold-bridged triple-decker phanes (C) 777
Unsaturated molecules containing main group metals (R) 1

Calcium antagonists, Substituted α-pyrones as starting compounds for the synthesis of 4,4-disubstituted 1,4-dihydropyridines (C) 790

Captodative substitution, A test for synergetic captodative radical stabilization (C) 573

Carbanions, [2.2](1,4)Benzo[*g*]chrysenoparacyclophane dianion: a novel, paratropic, double-layered carbanion (C) 232
Enantioselective protonation of carbanions with chiral proton sources (C) 1283
New reductive transformations of unsaturated cyclic hydrocarbons (R) 204

Carbene additions, Apparently nonstereospecific dihalocarbene addition—an explanation (C) 329

Carbene complexes, Nitrogen heterocycles from carbene complexes and alkenyl isocyanides (C) 563
Trimethylenemethane complexes of Cr, Mo, and W by novel methylenation of allenes with carbene complexes; cyclopentanes by [3+2] cycloaddition of trimethylenemethane complexes to allenes (C) 357
Vanadium carbene complexes by reaction of (diene)metallocenes with $[CpV(CO)_4]$ (C) 666

Carbene-like chemistry, The development of a carbene-like chemistry with terminal phosphinidene complexes (R) 275

Carbenes, Conversion of η^4-bound cyclopentadiene into the complexed carbene cyclopentadienylidene (C) 127
Reactions of 2,2,4,4-tetramethyl-3-methylenecyclobutylidene; thermal rearrangements of a 2-methylenebicyclo[2.1.0]-pentane (C) 1260

Carbenium ions, Control of the relative electrophilicity of alkylating agents by variation of the Lewis acid concentration (C) 1029

Carbenoid, Unusual 1,6-addition of a carbenoid (C) 72

Carbocations, Carbocation chemistry (B) 274
Crystal structure analysis of the 1,2,4,7-*anti*-tetramethyl-2-norbornyl cation: an unsymmetrically bridged carbocation (C) 560

Carbohydrate matrices, Diastereoselective Diels-Alder reaction on carbohydrate matrices (C) 267

Carbon-carbon bond formation, CC-linkages of ethene with CO_2 on an iron(0) complex—synthesis and crystal structure analysis of $[(PEt_3)_2Fe(C_2H_4)_2]$ (C) 153
Coupling of cyclometalated phenylphosphanes in dinuclear gold(II)-complexes (C) 260
Generation of β-, γ-, δ-, ε-, and ζ-zinc ketones and their transition-metal-catalyzed reactions with carbon electrophiles (C) 1157
Low-temperature photolysis of peracetylated dodecanoyl peroxides of tartaric acid and D-gluconic acid in the solid state—a diastereoselective radical coupling (C) 1253
Radicals in organic synthesis: formation of carbon-carbon bonds (B) 369
Regio- and stereoselective carbosulfenylation of olefins (C) 1028
Shortened C–C bonds and antiplanar O=C–O–H torsion angles in 1,4-cubanedicarboxylic acid (C) 447
Stereoselective aldol reactions with α-unsubstituted chiral enolates (R) 24
Unusual ligand directed regioselectivity in the iron catalyzed cross coupling of allylic ethers to 2-substituted 1,3-dienes (C) 1013

Carbon dioxide, Formation of oxazolidinones and oxazinanones by reaction of allylamines and of homoallylamines with carbon dioxide and iodine via intramolecular cyclization (C) 334
Nickel(0)-catalyzed production of a functionalized cyclopentanecarboxylic acid from 1,3-butadiene and CO_2 (C) 571

Carbonic acid, Thermolysis of NH_4HCO_3—a simple route to the formation of free carbonic acid (H_2CO_3) in the gas phase (C) 354

Carbon-sulfur, Bond cleavage in a π-thiophene ruthenium complex (C) 909

Carbon-supported nickel catalysts, Decarbonylation on carbon-supported nickel catalysts (C) 461

Carbon-tin double bond, A stable stannaethene (C) 546

Carbonyl complexes, RP-Bridged metal carbonyl clusters: synthesis, properties, and reactions (R) 743

Carbosilanes (R) 1111

Carbosulfenylation, Regio- and stereoselective carbosulfenylation of olefins (C) 1028

Carboxylic acids, CC-linkages of ethene with CO_2 on an iron(0) complex—synthesis and crystal structure analysis of $[(PEt_3)_2Fe(C_2H_4)_2]$ (C) 153

Catalysis, A new 1,3-diphosphaallylnickel complex for the polymerization of ethene (C) 1012
A 1-oxa-2-nickela-5-cyclopentanone from ethene and carbon dioxide: preparation, structure, and reactivity (C) 771
Control of the molecular weight of polyethene in syntheses with bis(ylide)nickel catalysts (C) 63
Coupling of two ethyne molecules at a nickel center to form a nickelacyclopentadiene complex (C) 1288
C–S Bond cleavage in a π-thiophene ruthenium complex (C) 909
Directed homogeneous hydrogenation (R) 190
Homogeneous catalysis with compounds of rhodium and iridium (B) 271
Metal clusters (B) 1050
Metal clusters in catalysis (B) 1050
The synthesis and catalytic properties of some open-sided binuclear complexes of Rh^{I}: the structure of $[Rh_2(CO)_2(CH_3CN)_2\{CH(PPh_2)_3\}](CF_3SO_3)_2$ (C) 1169

Catalysts, A biocatalyst for the preparation of (*R*)- and (*S*)-2-hydroxycarboxylic acids (C) 128
A novel heterobimetallic asymmetric hydrogenation catalyst based upon a chiral rhenium template containing two phosphido substituents (C) 910
Catalytic dehydrogenation of cyclohexene on silica overlayer films (C) 1182
Emission of microparticles from automotive sources—X-ray photoelectron spectroscopy in environmental analysis (R) 309
IR Emission analysis of temperature profiles in Pt/SiO_2 catalysts during exothermic reactions (C) 1042
Organometallic rhodium(III) complexes as catalysts for the photoreduction of protons to hydrogen on colloidal TiO_2 (C) 567

Catenates, Molecular structure of a [3]-catenate: curling up of the interlocked system by interaction between the two copper complex subunits (C) 661

Cations, Alkylaluminum cations: synthesis and structure of $[Al(2\text{-}C(SiMe_3)_2C_5H_4N)_2][AlCl_4]$ (C) 681

Ceramics, Science of ceramic chemical processing (B) 706
The development of bioglass ceramics for medical applications (R) 527
The importance of chemistry in the development of high-performance ceramics (R) 371

Ceramides, Lactosylceramides with unsaturated fatty acids — synthesis and use in the generation of bilayer membranes (C) 793

Cerium(IV)-catalysis, Cerium(IV)-catalyzed single electron transfer (SET) on acenaphthene and 1,4-dihydronaphtho-[1,8-*d,e*]-[1,2]diazepine: chemical evidence for distinct radical cations (C) 797

Charge transfer and radical ions in photochemistry (R) 825

Charge-transfer complexes, Control of the electronic structure of organic conductors as exemplified by [NMP][TCNQ] charge-transfer complexes (R) 287

Charge-transfer interaction, Noncovalent bonding interactions between tetraphenylborate anions and paraquat and diquat dications (C) 890

Chelate complexes, Novel rhenium(V) carbonato and sulfato chelate complexes: synthesis and investigation of molecular dynamics by ^{17}O-NMR spectroscopy (C) 464

Chemical bond, Homoatomic d^{10}–d^{10} interactions: their effects on structure and chemical and physical properties (R) 1098

Chemical bonding, Superconductivity—a new classification of the chemical bonding in the solid (C) 1275

Chemical evolution, Aspects of chemical evolution (B) 937

Chemical processing, Science of ceramic chemical processing (B) 706

Chiral auxiliaries, Diastereoselective Strecker synthesis of α-aminonitriles on carbohydrate templates (C) 557

Chiral complexes, The mechanism of substitution reactions at $[LRe(NO)(CO)(CH_3)]^{\oplus}$ in acid solution and the structure of $[\{LRe(NO)(CO)\}_2(\mu\text{-}CH_2OCH_2)]I_2$ (L = 1,4,7-triazacyclononane) (C) 924

Chiral recognition, Stereoelectronic effects and chiral recognition: a natural system of relationships between chiral compounds based on selectivities in the formation of acetals (C) 442

Chlorins, 2,3-Dihydroporphycene—an analogue of chlorin (C) 931

CHN bases, Tricyclic 2,4-diaminovinamidines—readily accessible, very strong CHN bases (C) 1164

C–H···O hydrogen bonds, Observation of an eclipsed C_{sp^3}–CH_3 bond in a tricyclic orthoamide; experimental and theoretical evidence for C–H···O hydrogen bonds (C) 1175

Chromatographic separation of higher polythionates $S_nO_6^{2\ominus}$ (n = 3 ... 22) and their detection in cultures of *Thiobacillus ferroxidans*; molecular composition of bacterial sulfur secretions (C) 151

Chromatography, Affinity chromatography: a practical approach (B) 1056

CIDNP, Photo-CIDNP in the vacuum-UV: di-*tert*-butyl ether and 2,2,5,5-tetramethyltetrahydrofuran in aqueous solution (C) 446

Cisplatin analogues, New cisplatin analogues — on the way to better antitumor agents (R) 615
α-Cleavage, MNDOC calculations of the potential surfaces for photochemical α-cleavage (C) 238
Cleavage of water, A new photosynthesis-like system for the light-induced reduction of water to molecular hydrogen (C) 241
Cluster chemistry, Isoelectronic relationships in cluster chemistry: nucleophilic addition to a vinylidene ligand (C) 572
Clusters, Azoalkane-nitrene cleavage on an Fe_3-cluster (C) 355
Cluster of clusters: structure of the 37-atom cluster $[(p\text{-}Tol_3P)_{12}Au_{18}Ag_{19}Br_{11}]^{2\oplus}$ and a novel series of supraclusters based on vertex-sharing icosahedra (C) 897
Heterometallic polyhydride raft formation: a comparison of syntheses using alkoxides of copper and gold (C) 135
Metal clusters (B) 1050
Metal clusters in catalysis (B) 1050
Mixed-metal cluster formation by carbonylmetalate-induced Pt–P bond cleavage in $[PtCl_2(Ph_2PCH_2PPh_2]$ (C) 88
$[\{(C_5H_5)Co\}_3(C_6H_5CH{=}CHCH_3)]$, an organometallic cluster with a face-bridging arene ligand (C) 1259
New $AuPt_2$ A-frame cluster complexes (C) 86
Novel Ni-clusters with Se and PR_3 (R=Ph, Et) as ligands (C) 148
Reactions of $[Pd_2(\mu\text{-dppm})_2Cl_2]$ with electrophilic complexes of copper and gold. Synthesis of the Pd_4 cluster $[Pd_4(\mu\text{-}Cl)_2(\mu\text{-dppm})_4](PF_6)_2\cdot 2(CH_3)_2CO$ (C) 768
RP-Bridged metal carbonyl clusters: synthesis, properties, and reactions (R) 743
Salicylate-mediated assembly of the discrete mixed-valence nonanuclear manganese complex $[Mn_9O_4(O_2CPh)_8(sal)_4(salH)_2(py)_4]$ ($salH_2$ = salicylic acid, py = pyridine) 915
Spherical mixed-valence $[V_{15}O_{36}]^{5\ominus}$, an example from an unusual cluster family (C) 1045
Square Hg_4 clusters in the compound CsHg (C) 687
Synthesis and structure of $[(PPh_3)_2N][Fe_3Mn(CO)_{12}(\mu_4\text{-}O)]$: a butterfly oxo cluster (C) 255
^{13}C-NMR spectroscopy, High-resolution CP-MAS ^{13}C-NMR spectra of allylzinc compounds—structural similarities and differences in the solid state and in solution (C) 1279
Cobalt clusters, A triple decker sandwich structure by reaction of cyclopentadienylbis(ethylene)cobalt with carbodiimides: an unusual cyclopentadienylcobalt oligomer (C) 68
"Two-electron reduction" of phosphane-substituted tricobalt clusters—evidence for a 17-electron intermediate in the dissociative ETC ligand substitution (C) 352
Cobalt compounds, Cobalt-mediated [2+2+2]cycloadditions of alkynes to the imidazole 4,5-double bond. First Synthesis of the 3*a*,7*a*-dihydrobenzimidazole nucleus and its preliminary chemistry including a novel quinoline construction (C) 1035
Conversion of η^4-bound cyclopentadiene into the complexed carbene cyclopentadienylidene (C) 127
1,8-Naphthalene-linked cofacial dimeric phthalocyanines (C) 1021
2,3,9,10-Tetrakis(trimethylsilyl)[5]phenylene. Synthesis via regiospecific cobalt-catalyzed cocyclization of 1,6-bis(triisopropylsilyl)-1,3,5-hexatriyne (C) 1246
Cobalt(II)-ions, Highly polarizing Co^{2+} ions from $[Co_2(CO)_8]$ and pyridine in hydrocarbons: synthesis and structure of $[\{Co_3(CO)_{10}\}_2\{Co(py)_4\}]$ and $[(Co)_4CoCo(py)_3][Co(CO)_4]$ (C) 680
Cobaltocenium, $[\{Co(Cp)_2\}\{CuI_2\}]_n$ (n = 3, 4), cobaltocenium iodocuprates(I) with unusual anion structures (C) 927
Cocyclization, 2,3,9,10-tetrakis(trimethylsilyl)[5]phenylene. Synthesis via regiospecific cobalt-catalyzed cocyclization of 1,6-bis(triisopropylsilyl)-1,3,5-hexatriyne (C) 1246
Coin-metal fluorides, Fluorides of copper, silver, gold, and palladium (R) 1081
Collagen fibers, Structural dynamics of collagen fibers cross-linked with isocyanates; application of synchrotron radiation in macromolecular chemistry (C) 551
Collars, Molecular belts and collars in the making: a hexaepoxyoctacosahydro[12]-cyclacene derivative (C) 892
Colloidal metals, Colloidal bimetallic catalysts: Pt-Au (C) 918
The morphology and microstructure of colloidal silver and gold (C) 676
Comprehensive biotechnology. The principles, applications and regulations of biotechnology in industry, agriculture and medicine (B) 588
Computer-assisted molecular design (CAMD)—an overview (R) 403
Conductivity, Control of the electronic structure of organic conductors as exemplified by [NMP][TCNQ] charge-transfer complexes (R) 287
Superconductivity—a chemical phenomenon? (C) 579
(+)-Confertin, Total synthesis of the pseudoguaianolide (+)-confertin (C) 61
Configuration, Inversion of the configuration of secondary alcohols via isourea ethers prepared in situ (C) 773
Proof of the (*S*,*S*) configuration of (−)-bissetone by synthesis from D-glucose (C) 1271
The absolute configuration of the ant alarm pheromone manicone (C) 784
Configurational stability, Estimation of the configurational stability of chiral organometallic reagents (C) 1145
Configuration analysis, Sequential configuration analysis of peptides (C) 331
Conformation, Observation of an eclipsed C_{sp^3}–CH_3 bond in a tricyclic orthoamide; experimental and theoretical evidence for C–H···O hydrogen bonds (C) 1175
Regulation of the 6-s equilibrium conformation of retinal in bacteriorhodopsin by substitution at C-5; 5-methoxy- and 5-ethylretinalbacteriorhodopsin (C) 580
Conformational Analysis, Dibenzo[*fg*,*mn*]-octalene and cycloocta[*def*]phenanthrene. New models for the conformational analysis of biphenyl systems (C) 1291
Conformational transitions between enantiomeric 3_{10}-helices (C) 1150
Conjugation, Deep-colored, through-conjugated multitriphenylmethylium ions (C) 794
Relay conjugation via twisted six- and seven-membered rings (C) 1252
The dependence of intramolecular electron transfer on structure in a spiro compound containing two cyclooctatetraene moieties (C) 1290
Coordination, Alkylaluminum cations: synthesis and structure of $[Al(2\text{-}C(SiMe_3)_2\text{-}C_5H_4N)_2][AlCl_4]$ (C) 681
Conversion of η^4-bound cyclopentadiene into the complexed carbene cyclopentadienylidene (C) 127
Fluorides of copper, silver, gold, and palladium (R) 1081
High-pressure LiGe with layers containing two- and four-coordinate germanium atoms (C) 76
Macrobicyclic polyethers as second sphere ligands for tetraammineplatinum(II) (C) 693
Novel bimetallic macrocyclic polymer structures incorporating deprotonated 2-pyrrolidone bridges: the crystal structures of $[\{Hg_2Cu(C_4H_6NO)_4\}X_2]_n$ (X = NO_3 or ClO_4) (C) 1044
Novel Ni-clusters with Se and PR_3 (R=Ph, Et) as ligands (C) 148
Second sphere coordination of tetraammineplatinum(II) by a macropolycyclic crown ether bisamide receptor (C) 692
Simultaneous primary and secondary coordination of a neutral guest within a macrocyclic complex of rhodium(III) (C) 1162
Structure of triphenylarsanediiodine, $[Ph_3As\cdot I_2]$, a compound formed in the thermal decomposition of $[Mn(OAsPh_3)_3\text{-}I_2(SO_2)_2]$ (C) 264
Sulfur oxides as ligands in coordination compounds (R) 98
Tetrameric and dodecameric *tert*-butylethynyllithium: a novel aggregation principle in organolithium compounds (C) 587
s-Tetrazine as ligand for monomeric and bridged macrocyclic metal complexes (C) 344
Cope rearrangements, Azo cope rearrangements of nonstabilized azo compounds (C) 672
Proton-controlled equilibration between $[4^+ + 2]$ and $[4 + 2^+]$ cycloadducts: a characteristic example for the aberrant Diels-Alder reactions between two 1,3-dienes (C) 670
Copolymer, The copolymer of 2,6-pyridinedimethanethiol and 1,4-benzenedimethanethiol (C) 137
Copper compounds, $FCu[AuF_4]$, an unusual copper(II) fluoroaurate(III) (C) 688
$[\{Co(Cp)_2\}\{CuI_2\}]_n$ (n = 3, 4), cobaltocenium iodocuprates(I) with unusual anion structures (C) 927
Reactions of $[Pd_2(\mu\text{-dppm})_2Cl_2]$ with electrophilic complexes of copper and gold. Synthesis of the Pd_4 cluster $[Pd_4(\mu\text{-}Cl)_2(\mu\text{-dppm})_4](PF_6)_2\cdot 2(CH_3)_2CO$ (C) 768
Coronanes, Pentacyclo[11.3.0.0^{1,5}.0^{5,9}.0^{9,13}]-hexadecane ([4.5]coronane) (C) 1023
Heptacyclo[19.3.0.0^{1,5}.0^{5,9}.0^{9,13}.0^{13,17}.0^{17,21}]-tetracosane ([6.5]coronane) (C) 130
Correspondence, Questions of assignment (L) 703
CP-MAS ^{13}C-NMR spectroscopy, High-resolution CP-MAS ^{13}C-NMR spectra of allylzinc compounds—structural similarities and differences in the solid state and in solution (C) 1279
Cram chelate, The first direct evidence for a Cram chelate (C) 477
Cross-linking, Structural dynamics of collagen fibers cross-linked with isocyanates; application of synchrotron radiation in macromolecular chemistry (C) 551
Crown ethers, 1D and 2D NMR investigations of the jump mechanism of Co^{II} ions in [12]crown-4 stacks (C) 228
Noncovalent bonding interactions between tetraphenylborate anions and paraquat and diquat dications (C) 890
Stabilization of the $[AlMe_2]^{\oplus}$ cation by crown ethers (C) 485
Crown thioether complexes of Ag^I and Cu^I: the crystal structures of $[\{Ag_3L_2\}\{AgL_2\}](ClO_4)_4$ and [LCuI] (L = 1,4,7-Trithiacyclononane (C) 575
Cryptates, Energy transfer luminescence of europium(III) and terbium(III) cryptates of macrobicyclic polypyridine ligands (C) 266
Luminescence probes: the $Eu^{3\oplus}$ and $Tb^{3\oplus}$ cryptates of polypyridine macrobicyclic ligands (C) 1266
1,4-Cubanedicarboxylic acid, Shortened C–C bonds and antiplanar O=C–O–H torsion angles in 1,4-cubanedicarboxylic acid (C) 447
Cubane-like frameworks, $[Fe_4Te_4(TePh)_4]^{3\ominus}$, the first telluride-tellurolate complex (C) 1009
$[(\eta^5\text{-}C_5Me_5)_2Ti_2P_6]$, a distorted dimetallaphosphacubane (C) 1153
$Cs_3Mo_5P_6O_{25}$: a novel molybdenum phosphate containing a cubane-like Mo_4O_4

cluster with six molybdenum–molybdenum bonds (C) 549
Cumulenes, Synthesis and properties of 1-cycloheptatrienylidene-2-cyclopentadienylideneethylene derivatives (C) 335
Cuprates, $[\{Co(Cp)_2\}\{CuI_2\}]_n$ (n = 3, 4), cobaltocenium iodocuprates(I) with unusual anion structures (C) 927
Curvature, Adsorption and curvature in highly dealuminated zeolites (C) 1017
How nature adapts chemical structures to curved surfaces (R) 1059
Cyanohydrin synthesis, Enzyme-catalyzed cyanohydrin synthesis in organic solvents (C) 458
Cyanotriphenylphosphoranylidenemethanide Synthesis of nitriles via the ylide anion of sodium cyanotriphenylphosphoranylidenemethanide (C) 79
Cyclization, Formation of oxazolidinones and oxazinanones by reaction of allylamines and of homoallylamines with carbon dioxide and iodine via intramolecular cyclization (C) 334
Methyl (*E*)-2-(1-aryl-4,5-dihydro-1*H*-tetrazol-5-ylidene)-2-cyanoacetate from methyl 3,3-diazido-2-cyanoacrylate and primary aromatic amines (C) 1160
Cycloadditions, Cobalt-mediated [2+2+2]-cycloadditions of alkynes to the imidazole 4,5-double bond. First Synthesis of the 3*a*, 7*a*-dihydrobenzimidazole nucleus and its preliminary chemistry including a novel quinoline construction (C) 1035
[1+4] Cycloaddition of a diphosphene to acrolein: synthesis and structure of a dihydro-1,2λ^5-oxaphosphole with an exocyclic P=P bond (C) 1010
[4+2] Cycloadditions of 2,3-diazido-1,3-butadienes: a novel entry to vicinal vinyl diazides and 1,4-dicyano compounds (C) 879
Proton-controlled equilibration between $[4^+ + 2]$ and $[4 + 2^+]$ cycloadducts: a characteristic example for the aberrant Diels–Alder reactions between two 1,3-dienes (C) 670
Trimethylenemethane complexes of Cr, Mo, and W by novel methylenation of allenes with carbene complexes; cyclopentanes by [3+2] cycloaddition of trimethylenemethane complexes to allenes (C) 357
Cycloalkenes, Anodic Grob fragmentation of bicycloalkylcarboxylic acids to specifically disubstituted cycloalkenes (C) 1026
Cycloannelation, New reductive transformations of unsaturated cyclic hydrocarbons (R) 204
Cyclobutafuran, Dihydrocyclobutafuran (C) 471
β-Cyclodextrin, Changes of stereoselectivity in Diels–Alder reactions by hydrophobic solvent effects and by β-cyclodextrin (C) 896
Cyclohepta[*a*]phenalene: a highly electron-donating nonalternant hydrocarbon (C) 1247
1-Cycloheptatrienylidene-2-cyclopentadienylideneethylenes, Synthesis and properties of 1-cycloheptatrienylidene-2-cyclopentadienylideneethylene derivatives (C) 335
1,2-Cyclohexadiene, 1,2,3,5,8,8a-Hexahydronaphthalene from 1,2-cyclohexadiene (C) 449
Cycloocta[*def*]phenanthrene, New models for the conformational analysis of biphenyl systems (C) 1291
Cyclooligomerization, Coupling of two ethyne molecules at a nickel center to form a nickelacyclopentadiene complex (C) 1288
Cyclopentadienides, Structure of a crystalline alkali-metal cyclopentadienide (C) 583
Cyclopentadienylidene, Conversion of η^4-bound cyclopentadiene into the complexed carbene cyclopentadienylidene (C) 127
Cyclopentanecarboxylic acid, Nickel(0)-catalyzed production of a functionalized cyclopentanecarboxylic acid from 1,3-butadiene and CO_2 (C) 571
Cyclopentanediyl, 2,2-Dimethyl-4,5-dimethylene-1,3-cyclopentanediyl (C) 1285
Cyclopentanes, A novel route to cyclopentane derivatives: a radical chain reaction (C) 1152
Stereocontrolled formation of annelated cyclopentanes by intramolecular hetero-Diels–Alder reaction. Synthesis of deoxyloganin from citronellal (C) 1295
Trimethylenemethane complexes of Cr, Mo, and W by novel methylenation of allenes with carbene complexes; cyclopentanes by [3+2] cycloaddition of trimethylenemethane complexes to allenes (C) 357
Cyclophosphanes, P_8iPr_4—the first tricyclo[3.2.1.0^{2,4}]octaphosphane (C) 347
Polyphosphorus compounds—new results and perspectives (R) 419
$P_8tBu_6O_6$—a highly oxidized cyclophosphane with intact P framework (C) 348
Cyclpropabenzenes, Reactions of (η^3-allyl)(η^5-cyclopentadienyl)palladium with cyclopropabenzenes (C) 67
Cyclopropapyridine, Synthesis and structure of a cyclopropapyridine (C) 668
Cyclotrimerization, Metal-promoted cyclotrimerization of a λ^3-phosphaalkyne: formation of a molybdenum-coordinated 1,3,5-triphosphabenzene (C) 907
Metal-promoted cyclotrimerization of a λ^3-phosphaalkyne: formation of vanadium-complexed valence isomers of a 1,3,5-triphosphabenzene (C) 908
DEBYE SCREENING LENGTH, The role of Debye screening length in ordered arrays of cylindrical nickel dimethylglyoxime particles (C) 765
Decarbonylation on carbon-supported nickel catalysts (C) 461
1,3-Dehydro-5,7-adamantanediyl dication, Four-center two-electron bonding in a tetrahedral topology. Experimental realization of three-dimensional homoaromaticity in the 1,3-dehydro-5,7-adamantanediyl dication (C) 761
Dehydrogenation, Catalytic dehydrogenation of cyclohexene on silica overlayer films (C) 1182
Deltate, Trithiodeltate: a new, aromatic thioxocarbon dianion (C) 1163
Deoxyhexoses, Enantioselective synthesis of methylfuranosides of unnatural 3,6-dideoxy-3-methylaldohexoses from lactates by homoaldol reactions (C) 1034
Deoxyloganin, Stereocontrolled formation of annelated cyclopentanes by intramolecular hetero-Diels–Alder reaction. Synthesis of deoxyloganin from citronellal (C) 1295
2-Deoxy sugars, Synthesis of 2-deoxy sugars (C) 233
Deuteriated compounds, $^2H,^2H$-COSY and $^2H,^2H,^{13}C$-RELAY NMR experiments for the analysis of deuteriated compounds (C) 156
Dewar-Phosphinine, Isomerization reactions in the system Dewar-phosphinine/phosphaprismane/phosphabenzvalene/phosphinine (C) 85
Diaminosulfanes, $As_4S_5N_{10}$—A diaminosulfane derivative with two bicyclic arsinosulfur diimides (C) 82
2,4-Diaminovinamidines, Tricyclic 2,4-diaminovinamidines—readily accessible, very strong CHN bases (C) 1164
1,1'-Diarsaferrocene (C) 229
Diasterane (tricyclo[3.1.1.1^{2,4}]octane) (C) 554
Diastereoselective Diels–Alder reaction on carbohydrate matrices (C) 267
Diastereoselective radical coupling, Low-temperature photolysis of peracetylated dodecanoyl peroxides of tartaric acid and D-gluconic acid in the solid state—a diastereoselective radical coupling (C) 1253
Diastereoselectivity, Totally synthetic routes to the higher monosaccharides (R) 15
Transition state π-solvation by aromatic rings: an electronic contribution to Diels–Alder reaction diastereoselectivity (C) 1184
Diazahexaphosphatricyclooctane, A 3,7-diaza-1,2,4,5,6,8-hexaphosphatricyclo[4.2.0-0^{2,5}]octane, a [2+2] dimer of a 1,2-dihydro-1-azatriphosphete containing a P_4 structure (C) 1256
2,6-Diaza-*s*-indacenes (C) 1037
2,5-Diazapentalenes (C) 552
Diazido-2-cyanoacrylate, Methyl (*E*)-2-(1-aryl-4,5-dihydro-1*H*-tetrazol-5-ylidene)-2-cyanoacetate from methyl 3,3-diazido-2-cyanoacrylate and primary aromatic amines (C) 1160
Dibenzo[*fg,mn*]octalene and cycloocta[*def*]-phenanthrene. New models for the conformational analysis of biphenyl systems (C) 1291
Di-*tert*-butyl ether, Photo-CIDNP in the vacuum-UV: di-*tert*-butyl ether and 2,2,5,5-tetramethyltetrahydrofuran in aqueous solution (C) 446
Dichroism, Structure and color of pentaphenylbismuth (C) 1180
Dictionary, A dictionary of scientific units (B) 938
1,4-Dicyano compounds, [4+2] Cycloadditions of 2,3-diazido-1,3-butadienes: a novel entry to vicinal vinyl diazides and 1,4-dicyano compounds (C) 879
Dicyclopropa[*a,c*]naphthalene: a compound capable of existence? (C) 577
Diels-Alder reactions, A non-stereospecific Diels–Alder reaction (C) 1046
Benzene and linearly annelated arenes as dienophiles in Diels–Alder reactions with inverse electron demand (C) 332
Changes of stereoselectivity in Diels–Alder reactions by hydrophobic solvent effects and by β-cyclodextrin (C) 896
Diastereoselective Diels–Alder reaction on carbohydrate matrices (C) 267
High stereoselectivity in Lewis-acid-catalyzed and uncatalyzed Diels–Alder reactions of the fumarate of (S)-ethyl lactate (C) 1143
New lead structures by Diels–Alder reactions of streptazolin with naphthoquinones (C) 664
Proton-controlled equilibration between $[4^+ + 2]$ and $[4 + 2^+]$ cycloadducts: a characteristic example for the aberrant Diels–Alder reactions between two 1,3-dienes (C) 670
Transition state π-solvation by aromatic rings: an electronic contribution to Diels–Alder reaction diastereoselectivity (C) 1184
Diene complexes, Diene, alkyne, alkene, and alkyl complexes of early transition metals: structures and synthetic applications in organic and polymer chemistry (R) 723
Dienes, Stereoselective synthesis of (*E*)-3-methylene-4-alken-2-ones from aldehydes and methyl vinyl ketone and their spontaneous dimerization (C) 1015
Unusual ligand directed regioselectivity in the iron catalyzed cross coupling of allylic ethers to 2-substituted 1,3-dienes (C) 1013
Dienophiles, Benzene and linearly annelated arenes as dienophiles in Diels–Alder reactions with inverse electron demand (C) 332
Di-*Grignard compounds and metallacycles* (R) 990
Dihalocarbene additions, Apparently non-

stereospecific dihalocarbene addition—an explanation (C) 329
3*a*,7*a*-Dihydrobenzimidazole, Cobalt-mediated [2+2+2] cycloadditions of alkynes to the imidazole 4,5-double bond. First Synthesis of the 3*a*,7*a*-dihydrobenzimidazole nucleus and its preliminary chemistry including a novel quinoline construction (C) 1035
Dihydrocyclobutafuran (C) 471
1,4-Dihydronaphtho-[1,8-*d*,*e*][1,2]diazepine, Cerium(IV)-catalyzed single electron transfer (SET) on acenaphthene and 1,4-dihydronaphtho-[1,8-*d*,*e*][1,2]diazepine: chemical evidence for distinct radical cations (C) 797
1,4-Dihydropyridines, Substituted α-pyrones as starting compounds for the synthesis of 4,4-disubstituted 1,4-dihydropyridines (C) 790
Dilithioethylene, *cis*- and *trans*-1,2-Dilithioethylene (C) 1032
Dimanganese heptoxide, The crystal structure of Mn_2O_7 (C) 139
for the selective oxidation of organic substrates (C) 1007
Dimerization, Macrocyclic dienes by metathetic dimerization of cycloheptene and cyclooctene on Re_2O_7/Al_2O_3 (C) 702
of 1,6-dithiacyclodeca-3,8-diyne in the presence of cobalt complexes. A simple synthesis of a [2.2](2,5)thiophenophane derivative (C) 763
Preparation and structure of $[Mo_4(OMe)_2(OiPr)_{10}]$; comments on why $[W_2(OiPr)_6]$ dimerizes, whereas $[Mo_2(OiPr)_6]$ does not (C) 904
Stereoselective synthesis of (*E*)-3-methylene-4-alken-2-ones from aldehydes and methyl vinyl ketone and their spontaneous dimerization (C) 1015
2,2-Dimethyl-4,5-dimethylene-1,3-cyclopentanediyl (C) 1285
Dioxetanes, A psoralen-substituted dioxetane as DNA intercalator for photogenotoxic studies (C) 796
Photooxidation of 2,5-dimethyl-2,3,4-hexatriene—matrix isolation of a trisdioxetane (C) 475
Diphosphaallylnickel complex, A new 1,3-diphosphaallylnickel complex for the polymerization of ethene (C) 1012
1,4-Diphospha-1,3-butadienes (C) 779
Diphosphene, [1+4] Cycloaddition of a diphosphene to acrolein: synthesis and structure of a dihydro-1,2λ^5-oxaphosphole with an exocyclic P=P bond (C) 1010
Diphosphetes, A new low-temperature synthesis of 1,2-dihydro-1,2-diphosphetes (C) 548
A new low-temperature synthesis of 1,2-dihydro-1,2-diphosphetes (C) 548 (804)
Dipyrrolo[1,2-*a*:2′,1′-*c*]quinoxalines: A novel heterocyclic system (C) 1280
Diquat, Noncovalent bonding interactions between tetraphenylborate anions and paraquat and diquat dications (C) 890
Diradicals, 2,2-Dimethyl-4,5-dimethylene-1,3-cyclopentanediyl (C) 1285
Neutral and charged biradicals, zwitterions, funnels in S_1, and proton translocation: their role in photochemistry, photophysics, and vision (R) 170
Reactions of 2,2,4,4-tetramethyl-3-methylenecyclobutylidene; thermal rearrangements of a 2-methylenebicicyclo[2.1.0]-pentane (C) 1260
The diradical 2,3,5,6-tetramethylene-1,4-cyclohexanediyl ("1,2,4,5-tetramethylenebenzene") (C) 256
Discotic compounds, The "Wheel of Mainz" as a liquid crystal?—Structural variation and mesophase properties of trimeric discotic compounds (C) 1249
1,2-Diselenete and 1,2-thiaselenete (C) 343
Disilenes, Chemistry of the silicon-silicon double bond (R) 1201
Synthesis and characterization of tetrakis[bis(trimethylsilyl)methyl]disilene (C) 584
Disproportionation, Highly polarizing Co^{2+} ions from $[Co_2(CO)_8]$ and pyridine in hydrocarbons: synthesis and structure of $[\{Co_3(CO)_{10}\}_2\{Co(py)_4\}]$ and $[(Co)_4CoCo(py)_3][Co(CO)_4]$ (C) 680
Redox disproportionation of Ge^{II} compounds: synthesis and structure of $[(Me_3Si)C(PMe_2)_2]_2GeCl_2$ and $[\mu\text{-}\{(Me_3Si)C(PMe_2)_2\}]_2Ge_2$ (C) 673
Distortion, Biphenylenes with strongly distorted trapezoidal four-membered ring (C) 470
Disulfur, 5,5-Dimethyl-1,2-dithia-3,7-diselenacycloheptane—a storable source of disulfur, S_2 (C) 887
1,6-Dithiacyclodeca-3,8-diyne, Dimerization of 1,6-dithiacyclodeca-3,8-diyne in the presence of cobalt complexes. A simple synthesis of a [2.2](2,5)thiophenophane derivative (C) 763
Dititanahexaphosphacubane, $[(\eta^5\text{-}C_5Me_5)_2Ti_2P_6]$, a distorted dimetallaphosphacubane (C) 1153
DNA intercalator, A psoralen-substituted dioxetane as DNA intercalator for photogenotoxic studies (C) 796
2D-NMR Spectroscopy, Modern NMR techniques for chemistry research (B) 1192
Modern techniques in high resolution FT NMR (B) 1192
Nuclear magnetic resonance. Basic principles (B) 1192
Principles of nuclear magnetic resonance in one and two dimensions (B) 1192
Dodecahedradienes, One- and two-electron oxidations of pagodanes and bissecododecahedradienes: unusually persistent radical cations (C) 457
Dodecahedraenes, Bissecododecahedraenes, unusual hyperstable olefins (C) 455
Dodecahedranes from [1.1.1.1]pagodanes (C) 452
The pagodane route to dodecahedranes—thermal, reductive, and oxidative transformations of pagodanes (C) 451
Donor-acceptor complexes, $[\{\mu\text{-}[(Me_3Si)C(PMe_2)_2]\}_2Ge_2\}_2GeCl_2$, a germanediyl-donor germanediyl-acceptor complex containing a mixed-valent Ge_5 chain (C) 674
Double-bond localization, The influence of substituents on double-bond localization e.g. in *s*-indacene (C) 360
Double proton transfer, Kinetic ^{15}N-CPMAS-NMR study of a double proton transfer in a crystalline malonaldehyde diimine derivative (C) 247
Drugs, New cisplatin analogues — on the way to better antitumor agents (R) 615
New lead structures by Diels-Alder reactions of streptazolin with naphthoquinones (C) 664
Dynamics, Dynamic processes on the IR time scale: coalescence of CO stretching vibrational bands in $[(\eta^4\text{-diene})Fe(CO)_3]$ complexes (C) 885

EFFECT OF SOLVENT, The effect of solvent on the stability of mero-substituted alkyl radicals (C) 770
Eicosapentaenoic acid, Stereocontrolled total synthesis of lipoxins A_5 and B_5 (C) 1019
Electrocatalysis, Electrocatalytic deposition of polypyrrole (C) 1031
Electrochemistry, Anodic Grob fragmentation of bicycloalkylcarboxylic acids to specifically disubstituted cycloalkenes (C) 1026
Geschichte der Elektrochemie (B) 160
1,8-Naphthalene-linked cofacial dimeric phthalocyanines (C) 1021
Principles of electrochemistry (B) 1302
Electrocyclization, 1,5-Electrocyclization in homofuran, homopyrrole, and homothiophene (C) 1294
Electrodes for potential measurements in aqueous systems at high temperatures and pressures (R) 161
Electron delocalization in diruthenium complexes of polycyclic arenes (C) 700
Electron donor, Cyclohepta[*a*]phenalene: a highly electron-donating nonalternant hydrocarbon (C) 1247
Electron microscopy, Imaging oxygen vacancies in superconducting $YBa_2Cu_3O_{7-\delta}$ by high resolution electron microscopy (C) 1048
Scanning tunneling microscopy - from birth to adolescence (Nobel lecture) (R) 606
The development of the electron microscope and of electron microscopy (Nobel lecture) (R) 595
Electron transfer, The dependence of intramolecular electron transfer on structure in a spiro compound containing two cyclooctatetraene moieties (C) 1290
Electron transport, Control of the electronic structure of organic conductors as exemplified by [NMP][TCNQ] charge-transfer complexes (R) 287
Electrophilicity, Control of the relative electrophilicity of alkylating agents by variation of the Lewis acid concentration (C) 1029
Elementary chemical processes, Molecular beam studies of elementary chemical processes (Nobel lecture) (R) 939
Molecular dynamics of elementary chemical reactions (Nobel Lecture) (R) 1221
Some concepts in reaction dynamics (Nobel lecture) (R) 952 (1302)
Element-element bonds, $[\{\mu\text{-}[(Me_3Si)C(PMe_2)_2]\}_2Ge_2\}_2GeCl_2$, a germanediyl-donor germanediyl-acceptor complex containing a mixed-valent Ge_5 chain (C) 674
Pentabenzylcyclopentadienylthallium(I): synthesis and structure of a "dimeric" organothallium compound with Tl-Tl interaction (C) 789
Redox disproportionation of Ge^{II} compounds: synthesis and structure of $[(Me_3Si)C(PMe_2)_2]_2GeCl_2$ and $[\mu\text{-}\{(Me_3Si)C(PMe_2)_2\}]_2Ge_2$ (C) 673
Elimination, Glycolate and thioglycolate complexes of rhenium and their oxidative elimination of ethylene and of glycol (C) 462
Emission of microparticles from automotive sources—X-ray photoelectron spectroscopy in environmental analysis (R) 309
Emission analysis, IR Emission analysis of temperature profiles in Pt/SiO_2 catalysts during exothermic reactions (C) 1042
Enantioselective protonation of carbanions with chiral proton sources (C) 1283
Enantioselectivity, Enantioselective synthesis of α-trialkylsilyl ketones and aldehydes (C) 351
Enantiotopomerization, Conformational transitions between enantiomeric 3_{10}-helices (C) 1150
ENDOR investigation, First ENDOR investigations of biologically relevant organic radicals in reversed micelles (C) 345
ENDOR spectroscopy, The spin distribution in ion pairs of 1-aminoanthraquinone radical anion and alkali-metal cations (C) 791
Energy transfer luminescence of europium(III) and terbium(III) cryptates of macrobicyclic polypyridine ligands (C) 266
Enoates, Reduction of 2-enoates and alkanoates with carbon monoxide or formate, viologens, and *clostridium thermoaceticum* to saturated acids and unsaturated and saturated alcohols (C) 785
Environmental chemistry, Emission of microparticles from automotive sources—X-ray photoelectron spectroscopy in environmental analysis (R) 309

Enzymatic analysis, Methods of enzymatic analysis. Vol. VIII. Metabolites 3: lipids, amino acids, and related compounds (B) 272
Methods of enzymatic analysis. Vol. IX. Proteins and peptides (B) 368
Methods of enzymatic analysis. Vol. X: Antigens and antibodies 1. Vol. XI: Antigens and antibodies 2. Vol. XII: Drugs and pesticides. Cumulated subject index (B) 1299
Enzyme catalysis, Enzyme-Catalyzed cyanohydrin synthesis in organic solvents (C) 458
Enzymes, A biocatalyst for the preparation of (*R*)- and (*S*)-2-hydroxycarboxylic acids (C) 128
Chemical modification of enzymes. Active site studies (B) 1301
IR Spectroscopic determination of the enzyme content of carrier-fixed enzymes (C) 483
Molybdenum enzymes (B) 487
Organized multienzyme systems: catalytic properties (B) 488
Enzymology, Methods in enzymology. Vols. 114 and 115. Diffractin methods for biological macromolecules (B) 367
Epidermal growth factor (Nobel lecture) (R) 717
Epitaxicity, Reaction of Sn_9^{4-} with single crystal Au: textured fiber epitaxial growth of AuSn at room temperature (C) 1155
Ethene, A new 1,3-diphosphaallylnickel complex for the polymerization of ethene (C) 1012
Ether cleavage with organo-alkali-metal compounds and alkali metals (R) 972
Ethylene complexes, Olefinic C=C double bond coordination to a M≡M triple bond: bis(η^2-ethylene)hexakis(neopentyloxy)ditungsten (C) 903
Ethylene elimination, Glycolate and thioglycolate complexes of rhenium and their oxidative elimination of ethylene and of glycol (C) 462
Europium compounds, Energy transfer luminescence of europium(III) and terbium(III) cryptates of macrobicyclic polypyridine ligands (C) 266
EXAFS: basic principles and data analysis (B) 801

FECAPENTAENE-14, Natural fecapentaene-14 and one fecapentaene-12 component are all-*trans* stereoisomers (C) 1186
Fischer–Tropsch synthesis, Hydride abstraction from $[C_6H_6Os(CO)(CH_3)_2]$: does a metal-bound methyl group migrate preferentially to a CO or to a CH_2 ligand? (C) 686
Synthesis and structure of the formaldehyde complex $[(tmeda)Ni(C_2H_4)(H_2CO)]$ (C) 919
Fluorides of copper, silver, gold, and palladium (R) 1081
Fluoro compounds, $Ag[MF_6]_2$ (M = Nb, Ta), ternary fluorides of divalent silver (C) 689
$FCu[AuF_4]$, an unusual copper(II) fluoroaurate(III) (C) 688
Inorganic solid fluorides. Chemistry and physics (B) 803
Preparation of $F_4S=CH-COF$ by isomerization of $F_5S-CH=C=O$ (C) 799
Trifluoromethyl isocyanide as a synthetic building block—reaction with trifluoroacetic acid and with hexafluoroacetone (C) 921
Fluorometry, The fluorometric determination of thymine glycol as criterion of the treatment of foodstuffs (biological material) with ionizing radiation (C) 340
Fluoroorganic compounds, Syntheses of fluoroorganic compounds (B) 704
Fluorosulfur compounds, Sulfur pentafluoride cyanate, $F_5S-O-C\equiv N$ (C) 134
Foodstuffs, The fluorometric determination of thymine glycol as criterion of the treatment of foodstuffs (biological material) with ionizing radiation (C) 340
Formaldehyde complexes, Synthesis and structure of the formaldehyde complex $[(tmeda)Ni(C_2H_4)(H_2CO)]$ (C) 919
Fragmentation, Anodic Grob fragmentation of bicycloalkylcarboxylic acids to specifically disubstituted cycloalkenes (C) 1026
Friedel–Crafts alkylation, Optically active α-arylglycine esters by Friedel–Crafts alkylation with the chiral cation of the bislactim ether of *cyclo*-(L-Val-Gly) (C) 683
Frontier orbitals, How chemistry and physics meet in the solid state (R) 846
Fulvalene complexes, Dinuclear fulvalene complexes of tri- and tetravalent zirconium (C) 697
Fulvene complexes, Titanium hydride formation through hydrogen transfer from 2-methylpyridine to a titanium fulvene compound; the first structurally characterized terminal titanium hydride (C) 330

GADOLINIUM COMPOUNDS, Structure and magnetic properties of a gadolinium hexafluoroacetylacetonate adduct with the radical 4,4,5,5-tetramethyl-2-phenyl-4,5-dihydro-1*H*-imidazole 3-oxide 1-oxyl (C) 913
Gallium compounds, Arene complexes with weak interactions: a macrocyclic tris(arene) complex of gallium(I) with η^{18} coordination (C) 338
Gas-inclusion crystals of tetra-*tert*-butyltetrahedrane and its deformation density (C) 356
Gas-phase pyrolysis, 1,2-Diselenete and 1,2-thiaselenete (C) 343
The pyrolysis of azides in the gas phase (R) 504
Gel electrophoresis, The practice of quantitative gel electrophoresis (B) 370
Gene recognition, Transcription in eukaryotes—the role of transcription complexes and their components (R) 218
Genetic engineering with plants (R) 382
Genotoxic studies, A psoralen-substituted dioxetane as DNA intercalator for photogenotoxic studies (C) 796
Germaethenes, Stable germaethenes (C) 798
Germanides, High-pressure LiGe with layers containing two- and four-coordinate germanium atoms (C) 76
Germanium compounds, $[\{\mu\text{-}[(Me_3Si)C(PMe_2)_2]\}_2Ge_2]_2GeCl_2$, a germanediyl-donor germanediyl-acceptor complex containing a mixed-valent Ge_5 chain (C) 674
Redox disproportionation of Ge^{II} compounds: synthesis and structure of $[(Me_3Si)C(PMe_2)_2]_2GeCl_2$ and $[\mu\text{-}\{(Me_3Si)C(PMe_2)_2\}]_2Ge_2$ (C) 673
Glycol, Glycolate and thioglycolate complexes of rhenium and their oxidative elimination of ethylene and of glycol (C) 462
Glycopeptides, Synthesis of glycopeptides, partial structures of biological recognition components (R) 294
O-(α-Glyco)peptides, Synthesis of *O*-(α-glyco)peptides by the *N*-iodosuccinimide procedure (C) 888
Glycosphingolipids, Lactosylceramides with unsaturated fatty acids — synthesis and use in the generation of bilayer membranes (C) 793
β-Glycosylation in 2-deoxysaccharides: convergent synthesis of the oligosaccharides of mithramycin (C) 555
Glycosyl isocyanide dichlorides—novel synthetic building blocks in sugar chemistry (C) 359
Gold, The morphology and microstructure of colloidal silver and gold (C) 676
Gold compounds, Cluster of clusters: structure of the 37-atom cluster $[(p\text{-}Tol_3P)_{12}Au_{18}Ag_{19}Br_{11}]^{2\oplus}$ and a novel series of supraclusters based on vertex-sharing icosahedra (C) 897
Coupling of cyclometalated phenylphosphanes in dinuclear gold(II)-complexes (C) 260
Dinuclear complexes of gold(I) containing bridging cyclometalated arylphosphane or arylarsane ligands (C) 258
$FCu[AuF_4]$, an unusual copper(II) fluoroaurate(III) (C) 688
Gold-tin compounds, Reaction of Sn_9^{4-} with single crystal Au: textured fiber epitaxial growth of AuSn at room temperature (C) 1155
Isovalent and mixed-valent ylide complexes of gold: the synthesis of trinuclear compounds having double paddlewheel structure (C) 1146
New $AuPt_2$ A-frame cluster complexes (C) 86
Graphite, Two different intercalate structures in the intercalation compounds of graphite with perfluorobutanesulfonic acid (C) 253
Grignard compounds, Crystal structure of the η^1-allyl-Grignard compound bis(allylmagnesium chloride-TMEDA) (C) 696
Di-Grignard compounds and metallacycles (R) 990
9,10-(1′-Magnesiapropano)-9,10-dihydroanthracene, synthesis, structure, and reactivity (C) 1025
Grob fragmentation, Anodic Grob fragmentation of bicycloalkylcarboxylic acids to specifically disubstituted cycloalkenes (C) 1026
Growth factors, Epidermal growth factor (Nobel lecture) (R) 717
The nerve growth factor: 35 years later (Nobel lecture) (R) 707

HALOPHOSPHORANES, Iodophosphonium salts with unusual properties and a structural alternative for halophosphoranes (C) 912
β-Halothiophenes, Preparation of β-halothiophenes by isomerization of α-halothiophenes on zeolite catalysts (C) 468
3_{10}-Helices, Conformational transitions between enantiomeric 3_{10}-helices (C) 1150
Heptoses, Totally synthetic routes to the higher monosaccharides (R) 15
Heteroallenes, Metathesis of CS_2-like heteroallenes on 1,1-dithio complexes of rhodium(III) (C) 767
Heteroannulenes, The synthesis of 1,3- and 1,4-phenylene-linked bisquinone-substituted porphyrin dimers (C) 678
Heteroarenes, 2,3-Dihydroporphycene—an analogue of chlorin (C) 931
Metal-promoted cyclotrimerization of a λ^3-phosphaalkyne: formation of a molybdenum-coordinated 1,3,5-triphosphabenzene (C) 907
Noncovalent bonding interactions between tetraphenylborate anions and paraquat and diquat dications (C) 890
Quino[7,8-*h*]quinoline, a new type of "proton sponge" (C) 460
Synthesis and structure of a cyclopropapyridine (C) 668
2,7,12,17-Tetrapropylporphycene—counterpart of octaethylporphyrin in the porphycene series (C) 928
The first synthesis of a benzoborole (C) 665
Heterocycles, Bis(η^5-cyclopentadienyl)-1,3-diphosphabicyclo[1.1.0]butane-2,4-diylzirconium: a simple synthesis of an unusual molecule (C) 764
1,4-Diphospha-1,3-butadienes (C) 779
Dipyrrolo[1,2-*a*:2′,1′-*c*]quinoxalines: A novel heterocyclic system (C) 1280
Nitrogen heterocycles from carbene complexes and alkenyl isocyanides (C) 563
Phosphasilirenes, three-membered rings containing PC double bonds (C) 776
Synthesis and structure of a 2,5-dihydro-

1*H*-1,2,5-phosphadiborole derivative (C) 781
Hetero-Dewar-benzenes, Metal-promoted cyclotrimerization of a λ^3-phosphaalkyne: formation of vanadium-complexed valence isomers of a 1,3,5-triphosphabenzene (C) 908
Hetero-Diels-Alder reaction, Stereocontrolled formation of annelated cyclopentanes by intramolecular hetero-Diels-Alder reaction. Synthesis of deoxyloganin from citronellal (C) 1295
Heterometallic clusters, Heterometallic polyhydride raft formation: a comparison of syntheses using alkoxides of copper and gold (C) 135
Mixed-metal cluster formation by carbonylmetalate-induced Pt-P bond cleavage in $[PtCl_2(Ph_2PCH_2PPh_2)]$ (C) 88
Synthesis and structure of $[(PPh_3)_2N][Fe_3Mn(CO)_{12}(\mu_4\text{-}O)]$: a butterfly oxo cluster (C) 255
Heteropolycycles, Reaction of phosphinines with diazoalkanes: diphosphachiropteradienes by intramolecular, ionic 5s+5s [6+4] cycloaddition (C) 236
Heteroprismanes, Metal-promoted cyclotrimerization of a λ^3-phosphaalkyne formation of vanadium-complexed valence isomers of a 1,3,5-triphosphabenzene (C) 908
Hexacarbonylzirconate(2−), $[Zr(CO)_6]^{2-}$: the first binary carbonyl complex of zirconium (C) 1190
Hexafluoroacetone, Trifluoromethyl isocyanide as a synthetic building block—reaction with trifluoroacetic acid and with hexafluoroacetone (C) 921
1,2,3,5,8,8a-Hexahydronaphthalene from 1,2-cyclohexadiene (C) 449
Hexatriyne, 2,3,9,10-tetrakis(trimethylsilyl)-[5]phenylene. Synthesis via regiospecific cobalt-catalyzed cocyclization of 1,6-bis-(triisopropylsilyl)-1,3,5-hexatriyne (C) 1246
High-performance liquid chromatography in biochemistry (B) 705
Practice of high-performance liquid chromatography (B) 705
High pressure chemistry, Electrodes for potential measurements in aqueous systems at high temperatures and pressures (R) 161
High-pressure synthesis and crystal structure of neodymium(III) oxide peroxide, $Nd_2O_2(O_2)$ (C) 1174
Inorganic high pressure chemistry. Kinetics and mechanisms (B) 1053
High temperature chemistry, Electrodes for potential measurements in aqueous systems at high temperatures and pressures (R) 161
History of chemistry, Difficulties in the emergence of the polymer concept—an essay (R) 93
Geschichte der Elektrochemie (B) 160
Ostwalds Klassiker der exakten Wissenschaften 265. Jacobus Henricus van't Hoff: Studien zur chemischen Dynamik (études de dynamique chimique) 1884 (B) 936
Polymers. The origins and growth of a science (B) 270
The development of the electron microscope and of electron microscopy (Nobel lecture) (R) 595
Schrödinger. Centenary celebration of a polymath (B) 1052
Homoaldol reaction, Enantioselective synthesis of methylfuranosides of unnatural 3,6-dideoxy-3-methylaldohexoses from lactates by homoaldol reactions (C) 1034
Homoaromaticity, Four-center two-electron bonding in a tetrahedral topology. Experimental realization of three-dimensional homoaromaticity in the 1,3-dehydro-5,7-adamantanediyl dication (C) 761
Homofuran, 1,5-Electrocyclization in homofuran, homopyrrole, and homothiophene (C) 1294
Homogeneous catalysis with compounds of rhodium and iridium (B) 271
Homopyrrole, 1,5-Electrocyclization in homofuran, homopyrrole, and homothiophene (C) 1294
Homothiophene, 1,5-Electrocyclization in homofuran, homopyrrole, and homothiophene (C) 1294
Hopping conduction in solids (B) 92
Houben-Weyl, Methoden der Organischen Chemie. Vol. E 18/Parts 1 and 2; Vol. XIII/9a and XIII/9b (B) 1196
Hydride abstraction from $[C_6H_6Os(CO)(CH_3)_2]$: does a metal-bound methyl group migrate preferentially to a CO or to a CH_2 ligand? (C) 686
Hydrido complexes, Heterometallic polyhydride raft formation: a comparison of syntheses using alkoxides of copper and gold (C) 135
Hydrocarbon combustion, Chemistry of hydrocarbon combustion (B) 269
Hydrodesulfurization, C-S Bond cleavage in a π-thiophene ruthenium complex (C) 909
Hydrogenation, A novel heterobimetallic asymmetric hydrogenation catalyst based upon a chiral rhenium template containing two phosphido substituents (C) 910
Directed homogeneous hydrogenation (R) 190
Hydrogenation methods (B) 593
Hydrogen bonds, Observation of an eclipsed $C_{sp^3}\text{-}CH_3$ bond in a tricyclic orthoamide; experimental and theoretical evidence for C-H···O hydrogen bonds (C) 1175
Hydrogen production, Organometallic rhodium(III) complexes as catalysts for the photoreduction of protons to hydrogen on colloidal TiO_2 (C) 567
Hydrogen telluride, Oxidative addition of hydrogen telluride to organometallic fragments (C) 132
2-Hydroxycarboxylic acids, A biocatalyst for the preparation of (*R*)- and (*S*)-2-hydroxycarboxylic acids (C) 128
Hyperstable olefins, Bissecododecahedraenes, unusual hyperstable olefins (C) 455

ICOSAPEPTIDES, Structure elucidation of a new icosapeptide from human semen (C) 774
Iminophosphanes, Imino-, phosphoranylidene-, and sulfuranylidenephosphanes by 1,3-silyl migration (C) 83
Inadequate, Direct identification of the carbon skeleton of organic compounds using double quantum coherence ^{13}C-NMR spectroscopy. The INADEQUATE pulse sequence (R) 625
s-Indacenes, 2,6-Diaza-*s*-indacenes (C) 1037
The influence of substituents on double-bond localization e.g. in *s*-indacene (C) 360
Inorganic chemistry, Inorganic reactions and methods. Vol. 1: The formation of bonds to hydrogen (part 1), Vol. 15: Electron-transfer and electrochemical reactions (B) 1195
Mechanisms of inorganic reactions (B) 1301
Interactions, Homoatomic d^{10}–d^{10} interactions: their effects on structure and chemical and physical properties (R) 1098
Molecular recognition: stacking interactions influence Watson-Crick vs. Hoogsteen base-pairing in a model for adenine receptors (C) 1244
Relay conjugation via twisted six- and seven-membered rings (C) 1252
Intercalation compounds, Two different intercalate structures in the intercalation compounds of graphite with perfluorobutanesulfonic acid (C) 253
Interfaces, Chemistry and structure at interfaces: new laser and optical techniques (B) 1198
Inversion of the configuration of secondary alcohols via isourea ethers prepared in situ (C) 773
Iodocuprates, $[\{Co(Cp)_2\}\{CuI_2\}]_n$ (n = 3, 4), cobaltocenium iodocuprates(I) with unusual anion structures (C) 927
Iodophosphonium salts with unusual properties and a structural alternative for halophosphoranes (C) 912
Iodoselenides, Synthesis and structure of a stable iodoselenide (C) 780
N-Iodosuccinimide, Synthesis of *O*-(α-glyco)peptides by the *N*-iodosuccinimide procedure (C) 888
Ion pairs, The spin distribution in ion pairs of 1-aminoanthraquinone radical anion and alkali-metal cations (C) 791
Ion solvation (B) 486
IR emission analysis of temperature profiles in Pt/SiO_2 catalysts during exothermic reactions (C) 1042
Iridium compounds, Formation of diiridium(II) complexes by photoassisted oxidative-addition reactions: structure of a stable binuclear iodo(iodomethyl)iridium(II) complex (C) 444
Iron catalysts, CC-linkages of ethene with CO_2 on an iron(0) complex—synthesis and crystal structure analysis of $[(PEt_3)_2Fe(C_2H_4)_2]$ (C) 153
Iron compounds, Dynamic processes on the IR time scale: coalescence of CO stretching vibrational bands in $[(\eta^4\text{-diene})Fe(CO)_3]$ complexes (C) 885
Synthesis and structure of $[(OC)_4Fe{=}Si(OtBu)_2{\cdot}HMPT]$, a donor-stabilized silanediyl ("silylene") complex (C) 669
IR Spectroscopy, Dynamic processes on the IR time scale: coalescence of CO stretching vibrational bands in $[(\eta^4\text{-diene})Fe(CO)_3]$ complexes (C) 885
IR-Spectroscopic determination of the enzyme content of carrier-fixed enzymes (C) 483
Isocyanide dichlorides, Glycosyl isocyanide dichlorides—novel synthetic building blocks in sugar chemistry (C) 359
Isocyanides, Nitrogen heterocycles from carbene complexes and alkenyl isocyanides (C) 563
Trifluoromethyl isocyanide as a synthetic building block—reaction with trifluoroacetic acid and with hexafluoroacetone (C) 921
Isoindoles, Annelated isoindoles with 18π electrons (C) 1262
Isomerization, Isomerization reactions in the system Dewar-phosphinine/phosphaprismane/phosphabenzvalene/phosphinine (C) 85
Photoisomerization of stilbazolium chromophores with potential nonlinear optical applications (C) 341
Preparation of β-halothiophenes by isomerization of α-halothiophenes on zeolite catalysts (C) 468

KINETICS, Control of the relative electrophilicity of alkylating agents by variation of the Lewis acid concentration (C) 1029
1D and 2D NMR investigations of the jump mechanism of Co^{II} ions in [12]crown-4 stacks (C) 228
Kinetic ^{15}N-CPMAS-NMR study of a double proton transfer in a crystalline malonaldehyde diimine derivative (C) 247

LANTHANOID COMPOUNDS, Luminescence probes: the $Eu^{3\oplus}$- and $Tb^{3\oplus}$-cryptates of polypyridine macrobicyclic ligands (C) 1266
Laser chemistry—What is its current status? (R) 38

Lead structures, New lead structures by Diels-Alder reactions of streptazolin with naphthoquinones (C) 664
Ligands, Alkyne complexes of rhenium in medium oxidation states: synthesis and molecular structure of a rhenium(V)–allenylidene complex (C) 1263
Crown thioether complexes of Ag^{I} and Cu^{I}: the crystal structures of $[\{Ag_3L_3\}\{AgL_2\}](ClO_4)_4$ and [LCuI] (L = 1,4,7-trithiacyclononane) (C) 575
Mo^{II} and Mo^{0} complexes of 3,3,7,7,11,11,15,15-octamethyl-1,5,9,13-tetrathiacyclohexadecane (C) 1171
Lipoxins, Stereocontrolled total synthesis of lipoxins A_5 and B_5 (C) 1019
Liquid crystals, Liquid crystalline polymers (R) 816
Photo- and thermochromic liquid crystal polysiloxanes (C) 1178
The "Wheel of Mainz" as a liquid crystal?—Structural variation and mesophase properties of trimeric discotic compounds (C) 1249
Lithium compounds, *cis*- and *trans*-1,2-Dilithioethylene (C) 1032
Lithium germanide, High-pressure LiGe with layers containing two- and four-coordinate germanium atoms (C) 76
Tetrameric and dodecameric *tert*-butylethynyllithium: a novel aggregation principle in organolithium compounds (C) 587
X-ray structure analysis of the Li_2-compound of bis(trimethylsilyl)methyl phenyl sulfone; structural units of an α-sulfonyl- and a complex-stabilized *ortho*-sulfonyl carbanion (C) 1287
Lithium-tellurium exchange: a new entry to organolithium compounds (C) 1187
Loganin, Stereocontrolled formation of annelated cyclopentanes by intramolecular hetero-Diels-Alder reaction. Synthesis of deoxyloganin from citronellal (C) 1295
Low-temperature photolysis of peracetylated dodecanoyl peroxides of tartaric acid and D-gluconic acid in the solid state—a diastereoselective radical coupling (C) 1253
LSI mass spectrometry, Structure elucidation of a new icosapeptide from human semen (C) 774
Luminescence, Energy transfer luminescence of europium(III) and terbium(III) cryptates of macrobicyclic polypyridine ligands (C) 266
Luminescence probes: the $Eu^{3\oplus}$ and $Tb^{3\oplus}$ cryptates of polypyridine macrobicyclic ligands (C) 1266
Lysine, Precipitates with β-pleated sheet structure by mixing aqueous solutions of helical poly(D-lysine) and poly(L-lysine) (C) 699

MACROBICYCLES, Luminescence probes: the $Eu^{3\oplus}$ and $Tb^{3\oplus}$ cryptates of polypyridine macrobicyclic ligands (C) 1266
Macrobicyclic polyethers as second sphere ligands for tetraammineplatinum(II) (C) 693
Macrocycles, A new class of organozirconium(IV) compounds: alkyl derivatives of tetramethyltetraazadibenzo[14]annulenatozirconium(IV) (C) 70
Arene complexes with weak interactions: a macrocyclic tris(arene) complex of gallium(I) with η^{18} coordination (C) 338
Mo^{II} and Mo^{0} complexes of 3,3,7,7,11,11,15,15-octamethyl-1,5,9,13-tetrathiacyclohexadecane (C) 1171
Molecular structure of a [3]-catenate: curling up of the interlocked system by interaction between the two copper complex subunits (C) 661
Novel bimetallic macrocyclic polymer structures incorporating deprotonated 2-pyrrolidone bridges: the crystal structures of $[\{Hg_2Cu(C_4H_6NO)_4\}X_2]_n$ (X = NO_3 or ClO_4) (C) 1044
Simultaneous primary and secondary coordination of a neutral guest within a macrocyclic complex of rhodium(III) (C) 1162
Stabilization of the $[AlMe_2]^{\oplus}$ cation by crown ethers (C) 485
s-Tetrazine as ligand for monomeric and bridged macrocyclic metal complexes (C) 344
The synthesis of 1,3- and 1,4-phenylene-linked bisquinone-substituted porphyrin dimers (C) 678
Macrocyclic dienes by metathetic dimerization of cycloheptene and cyclooctene on Re_2O_7/Al_2O_3 (C) 702
Macrolides, Total synthesis of the enantiomerically pure lichen macrolide (+)-aspicilin (C) 362
Macropolycycles, Second sphere coordination of tetraammineplatinum(II) by a macropolycyclic crown ether bisamide receptor (C) 692
Selective molecular recognition and separation of isomeric and partially hydrogenated arenes (C) 901
Magnesium compounds, Chemistry of pyrrocorphins: biomimetic regioselectivity of *C*-methylation at the ligand periphery of magnesium(II) uropyrrocorphinate(type I)-octanitriles (C) 261
Crystal structure of the η^{1}-allyl-Grignard compound bis(allylmagnesium chloride-TMEDA) (C) 696
9,10-(1'-Magnesiapropano)-9,10-dihydroanthracene, synthesis, structure, and reactivity (C) 1025
Magnesium phosphides—Synthesis and structure of $[Mg(PHPh)_2(tmeda)]$ (C) 81
Main-group elements, Chemie der Hauptgruppenelemente - Stand und Erwartung (B) 802
Main-group metals, $[\{\mu\text{-}[(Me_3Si)C(PMe_2)_2]\}_2Ge_2]_2GeCl_2$, a germanediyl-donor germanediyl-acceptor complex containing a mixed-valent Ge_5 chain (C) 674
Redox disproportionation of Ge^{II} compounds: synthesis and structure of $[(Me_3Si)C(PMe_2)_2]_2GeCl_2$ and $[\mu\text{-}\{(Me_3Si)C(PMe_2)_2\}]_2Ge_2$ (C) 673
Mainz Wheel, The "Wheel of Mainz" as a liquid crystal?—Structural variation and mesophase properties of trimeric discotic compounds (C) 1249
Manganese compounds, Dimanganese heptoxide for the selective oxidation of organic substrates (C) 1007
Salicylate-mediated assembly of the discrete mixed-valence nonanuclear manganese complex $[Mn_9O_4(O_2CPh)_8(sal)_4(salH)_2(py)_4]$ ($salH_2$ = salicylic acid, py = pyridine) 915
(2,2,8,8-Tetramethyl-5-oxa-4,6-diphospha-3,6-nonadiene)tetrakis[dicarbonyl(methylcyclopentadienyl)manganese], the first complexed bis(phosphavinyl)ether (C) 900
Tetranuclear mixed-valence manganese complexes with reduced TCNE or TCNQ as η^{4}-bridging ligands (C) 251
The crystal structure of Mn_2O_7 (C) 139
Manicone, The absolute configuration of the ant alarm pheromone manicone (C) 784
Mass spectrometry, Gaseous ion chemistry and mass spectrometry (B) 1055
Structure elucidation of a new icosapeptide from human semen (C) 774
The generation and characterization of molecules by neutralization-reionization mass spectrometry (NRMS) (R) 805
Materials science, Control of the electronic structure of organic conductors as exemplified by [NMP][TCNQ] charge-transfer complexes (R) 287
Nuclear quadrupole interaction and time-resolved perturbed γ-γ-angular correlation spectroscopy: applications in chemistry, materials science, and biophysical chemistry (R) 110
The development of bioglass ceramics for medical applications (R) 527
The importance of chemistry in the development of high-performance ceramics (R) 371
Medical applications, The development of bioglass ceramics for medical applications (R) 527
Medicinal chemistry research in India (B) 159
Membranes, Lactosylceramides with unsaturated fatty acids — synthesis and use in the generation of bilayer membranes (C) 793
Mercury compounds, Square Hg_4 clusters in the compound CsHg (C) 687
Mero-stabilization, The effect of solvent on the stability of mero-substituted alkyl radicals (C) 770
Metabolite formation, Regulation of secondary metabolite formation. Proceedings of the sixteenth workshop conference, Hoechst, Gracht castle, May 12–16, 1985 (B) 367
Metallacycles, A 1-oxa-2-nickela-5-cyclopentanone from ethene and carbon dioxide: preparation, structure, and reactivity (C) 771
Di-Grignard compounds and metallacycles (R) 990
First four-membered metallacycles of Rhenium (C) 73
Reactions of (η^{3}-allyl)(η^{5}-cyclopentadienyl)palladium with cyclopropabenzenes (C) 67
Synthesis of the four-membered metallacycle $[Cp_2Ti(AsPh)_3]$ via the in situ reduction of $[Cp_2TiCl_2]$ (C) 244
Unsaturated molecules containing main group metals (R) 1
Metalloproteins, Pt. 1: Metal proteins with redox roles, Pt. 2: Metal proteins with non-redox roles (B) 91
Metathesis, Macrocyclic dienes by metathetic dimerization of cycloheptene and cyclooctene on Re_2O_7/Al_2O_3 (C) 702
of CS_2-like heteroallenes on 1,1-dithio complexes of rhodium(III) (C) 767
(*E*)-3-Methylene-4-alken-2-ones, Stereoselective synthesis of (*E*)-3-methylene-4-alken-2-ones from aldehydes and methyl vinyl ketone and their spontaneous dimerization (C) 1015
2-Methylenebicyclo[2.1.0]pentane, Reactions of 2,2,4,4-Tetramethyl-3-methylenecyclobutylidene; thermal rearrangements of a 2-methylenebicyclo[2.1.0]pentane (C) 1260
N-Methylene-ynamines, First synthesis of *N*-methylene-ynamines (2-azabut-1-en-3-ynes) (C) 923
Micelles, First ENDOR investigations of biologically relevant organic radicals in reversed micelles (C) 345
Microparticles, Emission of microparticles from automotive sources—X-ray photoelectron spectroscopy in environmental analysis (R) 309
Mithramycin, β-Glycosylation in 2-deoxysaccharides: convergent synthesis of the oligosaccharides of mithramycin (C) 555
Mixed-metal clusters, A mixed-metal cluster with two quadruply-bridging carbonyl ligands (C) 685
Mixed-metal cluster formation by carbonylmetalate-induced Pt-P bond cleavage in $[PtCl_2(Ph_2PCH_2PPh_2]$ (C) 88
Mixed-valence compounds, Electron delocalization in diruthenium complexes of polycyclic arenes (C) 700
Isovalent and mixed-valent ylide complexes of gold: the synthesis of trinuclear compounds having double paddlewheel structure (C) 1146
$[\{\mu\text{-}[(Me_3Si)C(PMe_2)_2]\}_2Ge_2]_2GeCl_2$, a germanediyl-donor germanediyl-acceptor complex containing a mixed-valent Ge_5 chain (C) 674

1,8-Naphthalene-linked cofacial dimeric phthalocyanines (C) 1021
Salicylate-mediated assembly of the discrete mixed-valence nonanuclear manganese complex $[Mn_9O_4(O_2CPh)_8(sal)_4(salH)_2(py)_4]$ ($salH_2$ = salicylic acid, py = pyridine) 915
Spherical mixed-valence $[V_{15}O_{36}]^{5\ominus}$, an example from an unusual cluster family (C) 1045
The recoil-free fraction of the γ resonance in ^{197}Au Mössbauer spectroscopy; findings from measurements of polynuclear, mixed-valent ylide complexes (C) 1148
MNDOC calculations of the potential surfaces for photochemical α-cleavage (C) 238
Molecular beam studies of elementary chemical processes (Nobel lecture) (R) 939
Molecular design, Computer-assisted molecular design (CAMD)—an overview (R) 403
Molecular dynamics, Novel rhenium(V) carbonato and sulfato chelate complexes: synthesis and investigation of molecular dynamics by ^{17}O-NMR spectroscopy (C) 464
Molecular dynamics of elementary chemical reactions (Nobel Lecture) (R) 1221
Molecular metals, Polystannanes $Ph_3Sn-(tBu_2Sn)_n-SnPh_3$ (n = 1–4): a route to molecular metals? (C) 1255
Molecular recognition, Selective molecular recognition and separation of isomeric and partially hydrogenated arenes (C) 901
Stacking interactions influence Watson-Crick vs. Hoogsteen base-pairing in a model for adenine receptors (C) 1244
Molecular structure and energetics. Vol. 1: Chemical bonding models; Vol. 3: Studies of organic molecules (B) 1199
Molybdenum compounds, A mixed-metal cluster with two quadruply-bridging carbonyl ligands (C) 685
$Cs_3Mo_5P_6O_{25}$: a novel molybdenum phosphate containing a cubane-like Mo_4O_4 cluster with six molybdenum–molybdenum bonds (C) 549
Mo^{II} and Mo^0 complexes of 3,3,7,7,11,11,15,15-octamethyl-1,5,9,13-tetrathiacyclohexadecane (C) 1171
Preparation and structure of $[Mo_4(OMe)_2(OiPr)_{10}]$: comments on why $[W_2(OiPr)_6]$ dimerizes, whereas $[Mo_2(OiPr)_6]$ does not (C) 904
Synthesis and structure of $[(C_5Me_5)_2Mo_2S_4 \cdot SO_3]$: concerning the oxidation of sulfur ligands in transition-metal complexes (C) 230
Monosaccharides, Totally synthetic routes to the higher monosaccharides (R) 15
Morphology, The morphology and microstructure of colloidal silver and gold (C) 676
The role of Debye screening length in ordered arrays of cylindrical nickel dimethylglyoxime particles (C) 765
Mössbauer spectroscopy, The recoil-free fraction of the γ resonance in ^{197}Au Mössbauer spectroscopy; findings from measurements of polynuclear, mixed-valent ylide complexes (C) 1148
Multicenter bonding, Four-center two-electron bonding in a tetrahedral topology. Experimental realization of three-dimensional homoaromaticity in the 1,3-dehydro-5,7-adamantanediyl dication (C) 761
Multienzyme systems, Organized multienzyme systems: catalytic properties (B) 488
Multitriphenylmethylium ions, Deep-colored, through-conjugated multitriphenylmethylium ions (C) 794
Mutagens, Natural fecapentaene-14 and one fecapentaene-12 component are all-*trans* stereoisomers (C) 1186
Mycoloylpeptides and other lipopeptide adjuvants from higher aldoketene dimers (C) 336
Mycoses, Allylamine derivatives—a new class of active substances in antifungal chemotherapy (R) 320

NAFTIFINE, Allylamine derivatives—a new class of active substances in antifungal chemotherapy (R) 320
Natural products, Amavadin, an example for selective binding of vanadium in nature: studies of its complexation chemistry and a new structural proposal (C) 545
Metalloproteins. Pt. 1: Metal proteins with redox roles. Pt. 2: Metal proteins with non-redox roles (B) 91
Mycoloylpeptides and other lipopeptide adjuvants from higher aldoketene dimers (C) 336
Natural fecapentaene-14 and one fecapentaene-12 component are all-*trans* stereoisomers (C) 1186
Proof of the (*S,S*) configuration of (−)-bissetone by synthesis from D-glucose (C) 1271
Stereocontrolled formation of annelated cyclopentanes by intramolecular hetero-Diels–Alder reaction. Synthesis of deoxyloganin from citronellal (C) 1295
Stereoselective syntheses of building blocks with three consecutive stereogenic centers: important precursors of polyketide natural products (R) 489
Synthesis of 2-deoxy sugars (C) 233
Synthesis of valienamine (C) 482
The chemistry of the plasmodial pigments of the slime mold *Fuligo septica* (myxomycetes) (C) 586
Totally synthetic routes to the higher monosaccharides (R) 15
Total synthesis of the pseudoguaianolide (+)-confertin (C) 61
^{15}N-CPMAS-NMR spectroscopy study of the problem of NH tautomerism in crystalline porphine and porphycene (C) 934
Neighboring group effects, Regio- and stereoselective carbosulfenylation of olefins (C) 1028
Neodymium(III) oxide peroxide, High-pressure synthesis and crystal structure of neodymium(III) oxide peroxide, $Nd_2O_2(O_2)$ (C) 1174
Nerve growth factor, The nerve growth factor: 35 years later (Nobel lecture) (R) 707
Neutralization-reionization mass spectrometry, The generation and characterization of molecules by neutralization-reionization mass spectrometry (NRMS) (R) 805
Nickelacyclopentadiene, Coupling of two ethyne molecules at a nickel center to form a nickelacyclopentadiene complex (C) 1288
Nickelatricyclo[4.1.1.$0^{1,6}$]octadienes, Nickel complexes with a propellane structure (C) 65
Nickel compounds, A 1-oxa-2-nickela-5-cyclopentanone from ethene and carbon dioxide: preparation, structure, and reactivity (C) 771
Novel Ni-clusters with Se and PR_3 (R = Ph, Et) as ligands (C) 148
Synthesis and structure of compounds containing ditellurium *side-on* bonded to nickel complex fragments (C) 916
Synthesis and structure of the formaldehyde complex $[(tmeda)Ni(C_2H_4)(H_2CO)]$ (C) 919
Nickel dimethylglyoxime, The role of Debye screening length in ordered arrays of cylindrical nickel dimethylglyoxime particles (C) 765
Niobium compounds, $Ag[MF_6]_2$ (M = Nb, Ta), ternary fluorides of divalent silver (C) 689
Nitration, Aromatic nitration at the encounter rate in the gas phase (C) 1177
Nitrenes, The pyrolysis of azides in the gas phase (R) 504
Unusually stable *cis,cis*-trialkyltriaziridines by azo/nitrene addition (C) 566
Nitrile oxides, Isolation and photoisomerization of simply substituted nitrile oxides (C) 155
Nitriles, Synthesis of nitriles via the ylide anion of sodium cyanotriphenylphosphoranylidenemethanide (C) 79
Nitrobenzyllithium·ethanol, Crystal structure of $[\alpha$-nitrobenzyllithium·ethanol$]_n$; a lithium nitronate–ethanol interaction (C) 78
Nitrogen bases, Peralkylated polyaminophosphazenes—extremely strong, neutral nitrogen bases (C) 1167
Nitrogen compounds, [4 + 2] Cycloadditions of 2,3-diazido-1,3-butadienes: a novel entry to vicinal vinyl diazides and 1,4-dicyano compounds (C) 879
Nitrogen heterocycles from carbene complexes and alkenyl isocyanides (C) 563
Nitrogen homocycles, Unusually stable *cis,cis*-trialkyltriaziridines by azo/nitrene addition (C) 566
Nitronate–ethanol interaction, Crystal structure of $[\alpha$-nitrobenzyllithium·ethanol$]_n$; a lithium nitronate–ethanol interaction (C) 78
Nitroxyl radicals, Structure and magnetic properties of a gadolinium hexafluoroacetylacetonate adduct with the radical 4,4,5,5-tetramethyl-2-phenyl-4,5-dihydro-1*H*-imidazole 3-oxide 1-oxyl (C) 913
NMR of solids, Transient techniques in NMR of solids. An introduction to theory and practice (B) 1053
NMR Spectroscopy, 1D and 2D NMR investigations of the jump mechanism of Co^{II} ions in [12]crown-4 stacks (C) 228
Direct identification of the carbon skeleton of organic compounds using double quantum coherence ^{13}C-NMR spectroscopy. The INADEQUATE pulse sequence (R) 625
^{2}H,^{2}H-COSY and ^{2}H,^{2}H,^{13}C-RELAY NMR experiments for the analysis of deuteriated compounds (C) 156
High resolution NMR spectroscopy of synthetic polymers in bulk (B) 1301
Kinetic ^{15}N-CPMAS-NMR study of a double proton transfer in a crystalline malonaldehyde diimine derivative (C) 247
Modern NMR spectroscopy of organolithium compounds (R) 1212
Modern NMR techniques for chemistry research (B) 1192
Modern techniques in high resolution FT NMR (B) 1192
^{15}N-CPMAS-NMR study of the problem of NH tautomerism in crystalline porphine and porphycene (C) 934
Nuclear magnetic resonance. Basic principles (B) 1192
Principles of nuclear magnetic resonance in one and two dimensions (B) 1192
Nobel lecture, Epidermal growth factor (Nobel lecture) (R) 717
Molecular beam studies of elementary chemical processes (Nobel lecture) (R) 939
Molecular dynamics of elementary chemical reactions (Nobel lecture) (R) 1221
Scanning tunneling microscopy – from birth to adolescence (Nobel lecture) (R) 606
Some concepts in reaction dynamics (Nobel lecture) (R) 952 (1302)
The development of the electron microscope and of electron microscopy (Nobel lecture) (R) 595
The nerve growth factor: 35 years later (Nobel lecture) (R) 707
Nonacyclo[10.8.0.0^{2,11}.0^{4,9}.0^{4,19}.0^{6,17}.0^{7,16}-0^{9,14}.0^{14,19}]icosane, a double tetraasterane (C) 1006
Nonbenzenoid aromatic compounds, Synthesis and properties of 1-cycloheptatrien-

ylidene-2-cyclopentadienylideneethylene derivatives (C) 335
Nonclassical carbocations, Crystal structure analysis of the 1,2,4,7-*anti*-tetramethyl-2-norbornyl cation: an unsymmetrically bridged carbocation (C) 560
Nonlinear optical properties, Photoisomerization of stilbazolium chromophores with potential nonlinear optical applications (C) 341
Norbornyl cation, Crystal structure analysis of the 1,2,4,7-*anti*-tetramethyl-2-norbornyl cation: an unsymmetrically bridged carbocation (C) 560
Norcaradiene, Synthesis of tricyclo[5.2.0.0^{1,3}]nona-4,6,8-triene, a norcaradiene structure constrained by the antiaromaticity of cyclobutadiene (C) 559
Norcaradiene/tropylidene equilibrium, Valence isomerization between 1-phosphanorcaradienes and 1-phospha-2*H*-tropylidenes (2*H*-phosphepines) (C) 1134
Nortricyclene-diazonium ions, Diazo coupling of nortricyclene(tricyclo[2.2.1.0^{2,6}]-heptane)-1-diazonium ions (C) 570
NRMS, The generation and characterization of molecules by neutralization-reionization mass spectrometry (NRMS) (R) 805
Nuclear quadrupole interaction and time-resolved perturbed γ-γ-angular correlation spectroscopy: applications in chemistry, materials science, and biophysical chemistry (R) 110
Nucleic acids, The organic chemistry of nucleic acids (B) 1198
Nucleophilic addition, Isoelectronic relationships in cluster chemistry: nucleophilic addition to a vinylidene ligand (C) 572

OLEFIN METATHESIS and ring-opening polymerization of cyclo-olefins (B) 270
Concerning the role of organotin compounds in olefin metathesis: synthesis, structure, and lewis acidity of [(η^5-C_5Me_5)CH_3ReCl_3] (C) 466
Oligosaccharides, β-Glycosylation in 2-deoxysaccharides: convergent synthesis of the oligosaccharides of mithramycin (C) 555
Opto-electronics, Liquid crystalline polymers (R) 816
Organic chemistry, Houben-Weyl, Methoden der Organischen Chemie. Vol. *E 18*/Parts 1 and 2; Vol. XIII/9a and Vol. XIII/9b (B) 1196
Organische Chemie (B) 271
Organic conductors, Control of the electronic structure of organic conductors as exemplified by [NMP][TCNQ] charge-transfer complexes (R) 287
Organo-alkali metal compounds, Ether cleavage with organo-alkali metal compounds and alkali metals (R) 972
Organo-hafnium compounds, Chemistry of organo-zirconium and -hafnium compounds (B) 592
Organolithium compounds, Lithium-tellurium exchange: a new entry to organolithium compounds (C) 1187
Modern NMR spectroscopy of organolithium compounds (R) 1212
Organometallic chemistry, An introduction to organometallic chemistry (B) 704
Organometallic compounds, Organometallic intramolecular-coordination compounds (B) 802
Organometallic oligomers, A triple decker sandwich structure by reaction of cyclopentadienylbis(ethylene)cobalt with carbodiimides: an unusual cyclopentadienylcobalt oligomer (C) 68
Organotitanium reagents in organic synthesis (B) 592
Organo-zirconium compounds, Chemistry of organo-zirconium and -hafnium compounds (B) 592
Osmium compounds, A novel route to azaalkenylidene-metal complexes (C) 248
Overlayer catalysts, Catalytic dehydrogenation of cyclohexene on silica overlayer films (C) 1182
1-Oxa-3,4-cyclohexadiene, Generation and interception of 1-oxa-3,4-cyclohexadiene (C) 690
Oxaphosphole, [1 + 4] Cycloaddition of a diphosphene to acrolein: synthesis and structure of a dihydro-1,2λ^5-oxaphosphole with an exocyclic P=P bond (C) 1010
Oxazinanones, Formation of oxazolidinones and oxazinanones by reaction of allylamines and of homoallylamines with carbon dioxide and iodine via intramolecular cyclization (C) 334
Oxazolidinones, Formation of oxazolidinones and oxazinanones by reaction of allylamines and of homoallylamines with carbon dioxide and iodine via intramolecular cyclization (C) 334
Oxidation, Dimanganese heptoxide for the selective oxidation of organic substrates (C) 1007
Methods for the oxidation of organic compounds. Alkanes, alkenes, alkynes, and arenes (B) 593
One- and two-electron oxidations of pagodanes and bissecododecahedradienes; unusually persistent radical cations (C) 457
Synthesis and structure of [$(C_5Me_5)_2$-$Mo_2S_4 \cdot SO_3$]: concerning the oxidation of sulfur ligands in transition-metal complexes (C) 230
Oxidative elimination, Glycolate and thioglycolate complexes of rhenium and their oxidative elimination of ethylene and of glycol (C) 462
Oxirene, CO_2 elimination from vinylene carbonate radical anions and charge reversal in $C_2H_2O^{\ominus\ominus}$: reactions involving the radical anion and cation of oxirene? (C) 140
Oxygen vacancies, Imaging oxygen vacancies in superconducting $YBa_2Cu_3O_{7-\delta}$ by high resolution electron microscopy (C) 1048

PAGODANES, Dodecahedranes from [1.1.1.1]pagodanes (C) 452
One- and two-electron oxidations of pagodanes and bissecododecahedradienes: unusually persistent radical cations (C) 457
The pagodane route to dodecahedranes—thermal, reductive, and oxidative transformations of pagodanes (C) 451
Palladium compounds, Reactions of [Pd_2(μ-dppm)$_2Cl_2$] with electrophilic complexes of copper and gold. Synthesis of the Pd_4 cluster [Pd_4(μ-Cl)$_2$(μ-dppm)$_4$]$(PF_6)_2 \cdot 2(CH_3)_2CO$ (C) 768
Palladium reagents in organic synthesis (B) 593
Paracyclophanedienes, A facile, general entry to bridge-annelated [2.2]paracyclophanedienes (C) 1277
Paracyclophanes, Mono- and diarenium ions from [2.2]paracyclophanes (C) 564
Paraquat, Noncovalent bonding interactions between tetraphenylborate anions and paraquat and diquat dications (C) 890
Pentacyclo[11.3.0.0^{1,5}.0^{5,9}.0^{9,13}]hexadecane, ([4.5]coronane) (C) 1023
Pentaphenylbismuth, Structure and color of pentaphenylbismuth (C) 1180
Pentaphosphaferrocenes, [(η^5-P_5)Fe(η^5-C_5Me_5)], a pentaphosphaferrocene derivative (C) 59
Pentasila[1.1.1]propellane. Predictions concerning structure, bonding, and strain energy (C) 1267
Peptides, Conformational transitions between enantiomeric 3_{10}-helices (C) 1150
Sequential configuration analysis of peptides (C) 331
Structure elucidation of a new icosapeptide from human semen (C) 774
Synthesis of *O*-(α-glyco)peptides by the *N*-iodosuccinimide procedure (C) 888
Pericyclic reactions, Electrocyclic opening of 2,3-benzo- and 2,3;7,8-dibenzobicyclo-[4.2.0]octa-2,4,7-triene; benzoannelated transition states (C) 1268
Periodic minimal surface, Adsorption and curvature in highly dealuminated zeolites (C) 1017
Periodic potential surfaces, How nature adapts chemical structures to curved surfaces (R) 1059
Persistency, One- and two-electron oxidations of pagodanes and bissecododecahedradienes: unusually persistent radical cations (C) 457
Phanes, A facile, general entry to bridge-annelated [2.2]paracyclophanedienes (C) 1277
[2.2](1,4)Benzo[*g*]chrysenoparacyclophane dianion: a novel, paratropic, double-layered carbanion (C) 232
Mono- and diarenium ions from [2.2]paracyclophanes (C) 564
Synthesis and chirality of sixfold-bridged triple-decker phanes (C) 777
Phase-transfer catalysis, Apparently nonstereospecific dihalocarbene addition—an explanation (C) 329
Phase transformation, Cooperative effects in the phase transformation of triethylcyclotriboroxane (C) 245
Pheromones, The absolute configuration of the ant alarm pheromone manicone (C) 784
Phosgene, Triphosgene, a crystalline phosgene substitute (C) 894
Phosphaalkyne complexes, First examples of complexes containing η^1-bonded phosphaalkynes - synthesis and crystal and molecular structure of *trans*-[Mo(AdC$\equiv$P)$_2$($Et_2PCH_2CH_2PEt_2$)$_2$] (Ad=adamantyl) (C) 474
Phosphaalkynes, Mono- and Diphosphatricyclo[3.2.1.0^{2,7}]oct-3-enes: synthesis from 1,3- and 1,4-dienes and a stable phosphaalkyne (C) 1011
(2,2,8,8-Tetramethyl-5-oxa-4,6-diphospha-3,6-nonadiene)tetrakis[dicarbonyl(methylcyclopentadienyl)manganese], the first complexed bis(phosphavinyl)ether (C) 900
λ^3-Phosphaalkynes, Metal-promoted cyclotrimerization of a λ^3-phosphaalkyne formation of a molybdenum-coordinated 1,3,5-triphosphabenzene (C) 907
Metal-promoted cyclotrimerization of a λ^3-phosphaalkyne: formation of vanadium-complexed valence isomers of a 1,3,5-triphosphabenzene (C) 908
Phosphabenzvalene, Isomerization reactions in the system Dewar-phosphinine/phosphaprismane/phosphabenzvalene/phosphinine (C) 85
Phosphadiboroles, Synthesis and structure of a 2,5-dihydro-1*H*-1,2,5-phosphadiborole derivative (C) 781
Phosphanediyl complexes, The development of a carbene-like chemistry with terminal phosphinidene complexes (R) 275
Phosphanes, Imino-, phosphoranylidene-, and sulfuranylidenephosphanes by 1,3-silyl migration (C) 83
1-Phosphanorcaradienes, Valence isomerization between 1-phosphanorcaradienes and 1-phospha-2*H*-tropylidenes (2*H*-phosphepines) (C) 1134
Phosphaprismane, Isomerization reactions in the system Dewar-phosphinine/phosphaprismane/phosphabenzvalene/phosphinine (C) 85
Phosphasilirenes, three-membered rings containing PC double bonds (C) 776
Phosphatricyclooctenes, Mono- and Diphosphatricyclo[3.2.1.0^{2,7}]oct-3-enes: synthesis from 1,3- and 1,4-dienes and a stable phosphaalkyne (C) 1011

Phosphavinyl ethers, (2,2,8,8-Tetramethyl-5-oxa-4,6-diphospha-3,6-nonadiene)tetrakis[dicarbonyl(methylcyclopentadienyl)-manganese], the first complexed bis(phosphavinyl)ether (C) 900
Phosphazenes, Peralkylated polyaminophosphazenes—extremely strong, neutral nitrogen bases (C) 1167
2*H*-Phosphepines, Valence isomerization between 1-phosphanorcaradienes and 1-phospha-2*H*-tropylidenes (2*H*-phosphepines) (C) 1134
Phosphinidene complexes, The development of a carbene-like chemistry with terminal phosphinidene complexes (R) 275
Phosphinines, Isomerization reactions in the system Dewar-phosphinine/phosphaprismane/phosphabenzvalene/phosphinine (C) 85
Reaction of phosphinines with diazoalkanes: diphosphachiropteradienes by intramolecular, ionic 5s + 5s [6 + 4] cycloaddition (C) 236
Phosphirene, The first 2*H*-phosphirene (C) 1257
Phosphonium salts, Iodophosphonium salts with unusual properties and a structural alternative for halophosphoranes (C) 912
Phosphoranes, Iodophosphonium salts with unusual properties and a structural alternative for halophosphoranes (C) 912
Phosphoranylidenephosphanes, Imino-, phosphoranylidene-, and sulfuranylidenephosphanes by 1,3-silyl migration (C) 83
Phosphorus compounds, A new low-temperature synthesis of 1,2-dihydro-1,2-diphosphetes (C) 548
1,4-Diphospha-1,3-butadienes (C) 779
Polyphosphorus compounds—new results and perspectives (R) 419
Phosphorus homocycles, $[(\eta^5\text{-}P_5)Fe(\eta^5\text{-}C_5Me_5)]$, a pentaphosphaferrocene derivative (C) 59
P_8iPr_4—the first tricyclo[3.2.1.$0^{2,4}$]octaphosphane (C) 347
$P_8tBu_6O_6$—a highly oxidized cyclophosphane with intact P framework (C) 348
Phosphorus ligands, A novel heterobimetallic asymmetric hydrogenation catalyst based upon a chiral rhenium template containing two phosphido substituents (C) 910
Bis(η^5-cyclopentadienyl)-1,3-diphosphabicyclo[1.1.0]butane-2,4-diylzirconium: a simple synthesis of an unusual molecule (C) 764
RP-Bridged metal carbonyl clusters: synthesis, properties, and reactions (R) 743
Phosphorus-nitrogen compounds, A 3,7-diaza-1,2,4,5,6,8-hexaphosphatricyclo-[4.2.0.$0^{2,5}$]octane, a [2 + 2] dimer of a 1,2-dihydro-1-azatriphosphete containing a P_4 structure (C) 1256
Phosphorus-nitrogen ligands, $(Me_3Si)_2N\text{-}P{=}NSiMe_3$ as educt for electron-rich phosphorus-nitrogen ligands (C) 59
Phosphorus-phosphorus double bond, [1 + 4] Cycloaddition of a diphosphene to acrolein: synthesis and structure of a dihydro-1,2λ^5-oxaphosphole with an exocyclic P=P bond (C) 1010
Phosphorus-titanium compounds, $[(\eta^5\text{-}C_5Me_5)_2Ti_2P_6]$, a distorted dimetallaphosphacubane (C) 1153
Photochemistry, Charge transfer and radical ions in photochemistry (R) 825
Formation of diiridium(II) complexes by photoassisted oxidative-addition reactions: structure of a stable binuclear iodo(iodomethyl)iridium(II) complex (C) 444
Photochromic behavior, Photo- and thermochromic liquid crystal polysiloxanes (C) 1178
Photo-CIDNP in the vacuum-UV: di-*tert*-butyl ether and 2,2,5,5-tetramethyltetrahydrofuran in aqueous solution (C) 446
Photoelectron spectroscopy, Emission of microparticles from automotive sources—X-ray photoelectron spectroscopy in environmental analysis (R) 309
Photoisomerization, Isolation and photoisomerization of simply substituted nitrile oxides (C) 155
of bis(bipyridyl)rhodium (III) complexes; synthesis of *trans*-$[Rh(bpy)_2YCl]^{n\oplus}$, Y = Cl, H_2O (C) 240
of stilbazolium chromophores with potential nonlinear optical applications (C) 341
Unusual photoisomerization of a cyclic sulfonamide (C) 146
Photolysis, Low-temperature photolysis of peracetylated dodecanoyl peroxides of tartaric acid and D-gluconic acid in the solid state—a diastereoselective radical coupling (C) 1253
Photooxidation of 2,5-dimethyl-2,3,4-hexatriene—matrix isolation of a trisdioxetane (C) 475
Photoreduction, Organometallic rhodium(III) complexes as catalysts for the photoreduction of protons to hydrogen on colloidal TiO_2 (C) 567
Photosynthesis, A new photosynthesis-like system for the light-induced reduction of water to molecular hydrogen (C) 241
The synthesis of 1,3- and 1,4-phenylene-linked bisquinone-substituted porphyrin dimers (C) 678
Phthalocyanine derivatives, 1,8-Naphthalene-linked cofacial dimeric phthalocyanines (C) 1021
Plant breeding, Genetic engineering with plants (R) 382
Platinum compounds, Macrobicyclic polyethers as second sphere ligands for tetraammineplatinum(II) (C) 693
Mixed-metal cluster formation by carbonylmetalate-induced Pt-P bond cleavage in $[PtCl_2(Ph_2PCH_2PPh_2)]$ (C) 88
New $AuPt_2$ A-frame cluster complexes (C) 86
New cisplatin analogues — on the way to better antitumor agents (R) 615
Second sphere coordination of tetraammineplatinum(II) by a macropolycyclic crown ether bisamide receptor (C) 692
Platinum-gold sols, Colloidal bimetallic catalysts: Pt-Au (C) 918
β-Pleated sheet structure, Precipitates with β-pleated sheet structure by mixing aqueous solutions of helical poly(D-lysine) and poly(L-lysine) (C) 699
Poisonous gas, The poisonous cloud, chemical warfare in the first world war (B) 90
Polyaminophosphazenes, Peralkylated polyaminophosphazenes—extremely strong, neutral nitrogen bases (C) 1167
Polycycles, [2.2](1,4)Benzo[*g*]chrysenoparacyclophane dianion: a novel, paratropic, double-layered carbanion (C) 232
Cyclohepta[*a*]phenalene: a highly electron-donating nonalternant hydrocarbon (C) 1247
2,3-Dihydroporphycene—an analogue of chlorin (C) 931
Dimerization of 1,6-dithiacyclodeca-3,8-diyne in the presence of cobalt complexes. A simple synthesis of a [2.2](2,5)thiophenophane derivative (C) 763
Electrocyclic opening of 2,3-benzo and 2,3;7,8-dibenzobicyclo[4.2.0]octa-2,4,7-triene; benzoannelated transition states (C) 1268
Heptacyclo[19.3.0.$0^{1,5}$.$0^{5,9}$.$0^{9,13}$.$0^{13,17}$.$0^{17,21}$]tetracosane ([6.5]coronane) (C) 130
Molecular belts and collars in the making: a hexaepoxyoctacosahydro[12]cyclacene derivative (C) 892
New reductive transformations of unsaturated cyclic hydrocarbons (R) 204
Reaction of phosphinines with diazoalkanes: diphosphachiropteradienes by intramolecular, ionic 5s + 5s [6 + 4] cycloaddition (C) 236
2,7,12,17-Tetrapropylporphycene—counterpart of octaethylporphyrin in the porphycene series (C) 928
The dependence of intramolecular electron transfer on structure in a spiro compound containing two cyclooctatetraene moieties (C) 1290
Polyethene, Control of the molecular weight of polyethene in syntheses with bis(ylide)nickel catalysts (C) 63
Polyketides, Stereoselective syntheses of building blocks with three consecutive stereogenic centers: important precursors of polyketide natural products (R) 489
Polylysine, Precipitates with β-pleated sheet structure by mixing aqueous solutions of helical poly(D-lysine) and poly(L-lysine) (C) 699
Polymer chemistry, Diene, alkyne, alkene, and alkyl complexes of early transition metals: structures and synthetic applications in organic and polymer chemistry (R) 723
Polymer concept, Difficulties in the emergence of the polymer concept—an essay (R) 93
Polymer foams, Integral/Structural polymer foams. Technology, properties and applications (B) 369
Polymerization, Control of the molecular weight of polyethene in syntheses with bis(ylide)nickel catalysts (C) 63
Olefin metathesis and ring-opening polymerization of cyclo-olefins (B) 270
Plasma polymerization (B) 91
Polymerization of ethene, A new 1,3-diphosphaallylnickel complex for the polymerization of ethene (C) 1012
The copolymer of 2,6-pyridinedimethanethiol and 1,4-benzenedimethanethiol (C) 137
Polymers, High resolution NMR spectroscopy of synthetic polymers in bulk (B) 1301
Liquid crystalline polymers (R) 816
Polymer synthesis (B) 1056
Structural dynamic of collagen fibers cross-linked with isocyanates; application of synchrotron radiation in macromolecular chemistry (C) 551
The origins and growth of a science (B) 270
Polynuclear complexes, Novel bimetallic macrocyclic polymer structures incorporating deprotonated 2-pyrrolidone bridges: the crystal structures of $[\{Hg_2Cu(C_4H_6NO)_4\}X_2]_n$ (X = NO_3 or ClO_4) (C) 1044
Polyphosphorus compounds—new results and perspectives (R) 419
P_8iPr_4—the first tricyclo[3.2.1.$0^{2,4}$]octaphosphane (C) 347
$P_8tBu_6O_6$—a highly oxidized cyclophosphane with intact P framework (C) 348
Polypyridine ligands, Energy transfer luminescence of europium(III) and terbium(III) cryptates of macrobicyclic polypyridine ligands (C) 266
Luminescence probes: the $Eu^{3\oplus}$ and $Tb^{3\oplus}$ cryptates of polypyridine macrobicyclic ligands (C) 1266
Polypyrrole, Electrocatalytic deposition of polypyrrole (C) 1031
Polysiloxanes, Photo- and thermochromic liquid crystal polysiloxanes (C) 1178
Polystannanes, $Ph_3Sn\text{-}(tBu_2Sn)_n\text{-}SnPh_3$ (n = 1–4): a route to molecular metals? (C) 1255
Polythioethers, Mo^{II} and Mo^0 complexes of 3,3,7,7,11,11,15,15-octamethyl-1,5,9,13-tetrathiacyclohexadecane (C) 1171
Polythionates, Chromatographic separation of higher polythionates $S_nO_6^{2\ominus}$ (n = 3...22) and their detection in cultures of *Thiobacillus ferrooxidans*; molecular composition of bacterial sulfur secretions (C) 151
Porphines, ^{15}N-CPMAS-NMR study of the problem of NH tautomerism in crystalline porphine and porphycene (C) 934
Porphycenes, 2,3-Dihydroporphycene—an analogue of chlorin (C) 931

^{15}N-CPMAS-NMR study of the problem of NH tautomerism in crystalline porphine and porphycene (C) 934
2,7,12,17-Tetrapropylporphycene—counterpart of octaethylporphyrin in the porphycene series (C) 928
Porphyrin dimers, The synthesis of 1,3- and 1,4-phenylene-linked bisquinone-substituted porphyrin dimers (C) 678
Porphyrins, A new photosynthesis-like system for the light-induced reduction of water to molecular hydrogen (C) 241
2,7,12,17-Tetrapropylporphycene—counterpart of octaethylporphyrin in the porphycene series (C) 928
Porphyrinogens, Biomimetic synthesis of a twofold *N,N'*-bridged porphyrinogen (C) 64
Precipitates with β-pleated sheet structure by mixing aqueous solutions of helical poly(D-lysine) and poly(L-lysine) (C) 699
Propellanes of the glycoluril series and bridged tetrazocines (C) 1039
Propellane Structure, Nickel complexes with a propellane structure (C) 65
Pentasila[1.1.1]propellane. Predictions concerning structure, bonding, and strain energy (C) 1267
Reactions of (η^3-allyl)(η^5-cyclopentadienyl)palladium with cyclopropabenzenes (C) 67
Protective group methods, Synthesis of glycopeptides, partial structures of biological recognition components (R) 294
Proteins, The nerve growth factor: 35 years later (Nobel lecture) (R) 707
Protonation, Enantioselective protonation of carbanions with chiral proton sources (C) 1283
Regioselective protonation of allylic anions (C) 1281
Proton sponges, Quino[7,8-*h*]quinoline, a new type of "proton sponge" (C) 460
Novel, very strongly basic, pentacyclic "proton sponges" with vinamidine structure (C) 1165
Proton transfer, Kinetic ^{15}N-CPMAS-NMR study of a double proton transfer in a crystalline malonaldehyde diimine derivative (C) 247
Pseudoguaianolide, Total synthesis of the pseudoguaianolide (+)-confertin (C) 61
Psoralen, A psoralen-substituted dioxetane as DNA intercalator for photogenotoxic studies (C) 796
Pyridinedimethanethiol, The copolymer of 2,6-pyridinedimethanethiol and 1,4-benzenedimethanethiol (C) 137
Pyrolysis, The pyrolysis of azides in the gas phase (R) 504
α-Pyrones, Substituted α-pyrones as starting compounds for the synthesis of 4,4-disubstituted 1,4-dihydropyridines (C) 790
Pyrrocorphins, Chemistry of pyrrocorphins: biomimetic regioselectivity of *C*-methylation at the ligand periphery of magnesium(II) uropyrrocorphinate(type I)octanitriles (C) 261

QUANTUM CHEMISTRY, A handbook of computational chemistry (B) 158
Back to the structure of benzene (L) 1298
Bond stretch isomerism in bicyclo[1.1.0]tetrasilanes. Contrasts between strained silicon and carbon ring systems (C) 364
Computer-assisted molecular design (CAMD)—an overview (R) 403
MNDOC calculations of the potential surfaces for photochemical α-cleavage (C) 238
Neutral and charged biradicals, zwitterions, funnels in S_1, and proton translocation: their role in photochemistry, photophysics, and vision (R) 170
Pentasila[1.1.1]propellane. Predictions concerning structure, bonding, and strain energy (C) 1267
Semi-empirical methods of quantum chemistry (B) 158
Quinoline derivatives, Cobalt-mediated [2+2+2]cycloadditions of alkynes to the imidazole 4,5-double bond. First Synthesis of the 3*a*,7*a*-dihydrobenzimidazole nucleus and its preliminary chemistry including a novel quinoline construction (C) 1035
Quino[7,8-*h*]quinoline, a new type of "proton sponge" (C) 460

RADICAL ANIONS, The spin distribution in ion pairs of 1-aminoanthraquinone radical anion and alkali-metal cations (C) 791
Radical cations, Cerium(IV)-catalyzed single electron transfer (SET) on acenaphthene and 1,4-dihydronaphtho-[1,8-*d*, *e*][1,2]diazepine: chemical evidence for distinct radical cations (C) 797
One- and two-electron oxidations of pagodanes and bissecododecahedradienes: unusually persistent radical cations (C) 457
Radical chain reaction, A novel route to cyclopentane derivatives: a radical chain reaction (C) 1152
Radical ions, Charge transfer and radical ions in photochemistry (R) 825
CO_2 elimination from vinylene carbonate radical anions and charge reversal in $C_2H_2O^{\ominus\ominus}$: reactions involving the radical anion and cation of oxirene? (C) 140
Radical reactions, Influence of H-donor and temperature on the stereoselectivity of radical reactions (C) 479
Radicals, A test for synergetic captodative radical stabilization (C) 573
First ENDOR investigations of biologically relevant organic radicals in reversed micelles (C) 345
Low-temperature photolysis of peracetylated dodecanoyl peroxides of tartaric acid and D-gluconic acid in the solid state—a diastereoselective radical coupling (C) 1253
Structure and magnetic properties of a gadolinium hexafluoroacetylacetonate adduct with the radical 4,4,5,5-tetramethyl-2-phenyl-4,5-dihydro-1*H*-imidazole 3-oxide 1-oxyl (C) 913
The effect of solvent on the stability of mero-substituted alkyl radicals (C) 770
Radicals in organic synthesis: formation of carbon-carbon bonds (B) 369
Raft structure, Heterometallic polyhydride raft formation: a comparison of syntheses using alkoxides of copper and gold (C) 135
Raman spectrum of the tetrasilatetrahedrane anion Si_4^{4-} (C) 349
Reaction dynamics, Molecular beam studies of elementary chemical processes (Nobel lecture) (R) 939
Molecular dynamics of elementary chemical reactions (Nobel lecture) (R) 1221
Some concepts in reaction dynamics (Nobel lecture) (R) 952 (1302)
Reaction mechanisms, A non-stereospecific Diels–Alder reaction (C) 1046
Aromatic nitration at the encounter rate in the gas phase (C) 1177
Hydride abstraction from $[C_6H_6Os(CO)(CH_3)_2]$: does a metal-bound methyl group migrate preferentially to a CO or to a CH_2 ligand? (C) 686
Reactive intermediates, 1,2,3,5,8,8a-Hexahydronaphthalene from 1,2-cyclohexadiene (C) 449
Rearrangements, Electrocyclic opening of 2,3-benzo and 2,3;7,8-dibenzobicyclo-[4.2.0]octa-2,4,7-triene; benzoannelated transition states (C) 1268
Heptacyclo[19.3.0.0^{1,5}.0^{5,9}.0^{9,13}.0^{13,17}.0^{17,21}]-tetracosane ([6.5]coronane) (C) 130
Reactions of 2,2,4,4-tetramethyl-3-methylenecyclobutylidene; thermal rearrangements of a 2-methylenebicyclo[2.1.0]-pentane (C) 1260
Reduction, A new photosynthesis-like system for the light-induced reduction of water to molecular hydrogen (C) 241
New reductive transformations of unsaturated cyclic hydrocarbons (R) 204
of 2-enoates and alkanoates with carbon monoxide or formate, viologens, and *clostridium thermoaceticum* to saturated acids and unsaturated and saturated alcohols (C) 785
Regioselective protonation of allylic anions (C) 1281
Regioselectivity, Totally synthetic routes to the higher monosaccharides (R) 15
Unusual ligand directed regioselectivity in the iron catalyzed cross coupling of allylic ethers to 2-substituted 1,3-dienes (C) 1013
Relative electrophilicity, Control of the relative electrophilicity of alkylating agents by variation of the Lewis acid concentration (C) 1029
Relay conjugation via twisted six- and seven-membered rings (C) 1252
Retinal, Regulation of the 6-s equilibrium conformation of retinal in bacteriorhodopsin by substitution at C-5; 5-methoxy- and 5-ethylretinalbacteriorhodopsin (C) 580
Reversed micelles, First ENDOR investigations of biologically relevant organic radicals in reversed micelles (C) 345
Rhenium compounds, Alkyne complexes of rhenium in medium oxidation states: synthesis and molecular structure of a rhenium(V)—allenylidene complex (C) 1263
A novel heterobimetallic asymmetric hydrogenation catalyst based upon a chiral rhenium template containing two phosphido substituents (C) 910
Concerning the role of organotin compounds in olefin metathesis: synthesis, structure, and Lewis acidity of $[(\eta^5\text{-}C_5Me_5)CH_3ReCl_3]$ (C) 466
First four-membered metallacycles of rhenium (C) 73
Glycolate and thioglycolate complexes of rhenium and their oxidative elimination of ethylene and of glycol (C) 462
$[(\eta^5\text{-}C_5Me_5(Re(CH_3)_4]$, the first organorhenium(V) compound without heteroatom ligands (C) 787
Novel rhenium(V) carbonato and sulfato chelate complexes: synthesis and investigation of molecular dynamics by ^{17}O-NMR spectroscopy (C) 464
Oxidative addition of hydrogen telluride to organometallic fragments (C) 132
The mechanism of substitution reactions at $[LRe(NO)(CO)(CH_3)]^{\oplus}$ in acid solution and the structure of $[\{LRe(NO)(CO)\}_2(\mu\text{-}CH_2OCH_2)]I_2$ (L = 1,4,7-triazacyclononane) (C) 924
Rhodium compounds, Metathesis of CS_2-like heteroallenes on 1,1-dithio complexes of rhodium(III) (C) 767
Organometallic rhodium(III) complexes as catalysts for the photoreduction of protons to hydrogen on colloidal TiO_2 (C) 567
Photoisomerization of bis(bipyridyl)rhodium (III) complexes; synthesis of *trans*-$[Rh(bpy)_2YCl]^{n\oplus}$, Y = Cl, H_2O (C) 240
Simultaneous primary and secondary coordination of a neutral guest within a macrocyclic complex of rhodium(III) (C) 1162
The synthesis and catalytic properties of some open-sided binuclear complexes of Rh^I: the structure of $[Rh_2(CO)_2(CH_3CN)_2\{CH(PPh_2)_3\}](CF_3SO_3)_2$ (C) 1169
Ring opening, Electrocyclic opening of 2,3-benzo and 2,3;7,8-dibenzobicyclo[4.2.0]-octa-2,4,7-triene; benzoannelated transition states (C) 1268
Ruthenium compounds, A mixed-metal

cluster with two quadruply-bridging carbonyl ligands (C) 685
C–S bond cleavage in a π-thiophene ruthenium complex (C) 909
Electron delocalization in diruthenium complexes of polycyclic arenes (C) 700
Synthesis and crystal structure of the homoleptic thioether ruthenium complex [Ru(1,4,7-trithiacyclononane)$_2$]-(BPh$_4$)$_2$·2 Me$_2$SO (C) 250

SANDWICH COMPLEX, Structure of a crystalline alkali-metal cyclopentadienide (C) 583
Scanning tunneling microscopy, Scanning tunneling microscopy - from birth to adolescence (Nobel lecture) (R) 606
Schrödinger. Centenary celebration of a polymath (B) 1052
Scientific units, A dictionary of scientific units (B) 938
Selenide ligands, Novel Ni-clusters with Se and PR$_3$ (R=Ph, Et) as ligands (C) 148
Selenium compounds, 5,5-Dimethyl-1,2-dithia-3,7-diselenacycloheptane—a storable source of disulfur, S$_2$ (C) 887
1,2-Diselenete and 1,2-thiaselenete (C) 343
Synthesis and structure of a stable iodoselenide (C) 780
Shortened C–C bonds and antiplanar O=C–O–H torsion angles in 1,4-cubanedicarboxylic acid (C) 447
Side-on complexes, Synthesis and structure of compounds containing ditellurium side-on bonded to nickel complex fragments (C) 916
Silanediyl complexes, Synthesis and structure of [(OC)$_4$Fe=Si(O*t*Bu)$_2$·HMPT], a donor-stabilized silanediyl ("silylene") complex (C) 669
Silicides, Raman spectrum of the tetrasilatetrahedrane anion Si$_4^{4-}$ (C) 349
Silicon compounds, Bond stretch isomerism in bicyclo[1.1.0]tetrasilanes. Contrasts between strained silicon and carbon ring systems (C) 364
Carbosilanes (R) 1111
Phosphasilirenes, three-membered rings containing PC double bonds (C) 776
Silicon-silicon double bond, Chemistry of the silicon-silicon double bond (R) 1201
Synthesis and characterization of tetrakis[bis(trimethylsilyl)methyl]disilene (C) 584
Silver, The morphology and microstructure of colloidal silver and gold (C) 676
Silver compounds, Ag[MF$_6$]$_2$ (M=Nb, Ta), ternary fluorides of divalent silver (C) 689
[Ag$_4$(SCH$_2$C$_6$H$_4$CH$_2$S)$_3$]$^{2-}$, a novel polynuclear silver thiolate with trigonal-planar coordination of all silver atoms and a central [Ag$_4$S$_6$]-cage (C) 145
Cluster of clusters: structure of the 37-atom cluster [(*p*-Tol$_3$P)$_{12}$Au$_{18}$Ag$_{19}$Br$_{11}$]$^{2\oplus}$ and a novel series of supraclusters based on vertex-sharing icosahedra (C) 897
Silylene complexes, Synthesis and structure of [(OC)$_4$Fe=Si(O*t*Bu)$_2$·HMPT], a donor-stabilized silanediyl ("silylene") complex (C) 669
Single electron transfer, Cerium(IV)-catalyzed single electron transfer (SET) on acenaphthene and 1,4-dihydronaphtho-[1,8-*d*,*e*][1,2]diazepine: chemical evidence for distinct radical cations (C) 797
Slime mold, The chemistry of the plasmodial pigments of the slime mold *Fuligo septica* (myxomycetes) (C) 586
Solar energy, A new photosynthesis-like system for the light-induced reduction of water to molecular hydrogen (C) 241
Biological exploitation of solar energy by photosynthetic water splitting (R) 643
Solid-state chemistry, A new mechanism for superconductivity (C) 1273
Control of the superconducting properties of YBa$_2$Cu$_3$O$_7$ by topotactic redox reactions (C) 1188
Fluorides of copper, silver, gold, and palladium (R) 1081
Homoatomic d^{10}–d^{10} interactions: their effects on structure and chemical and physical properties (R) 1098
How chemistry and physics meet in the solid state (R) 846
How nature adapts chemical structures to curved surfaces (R) 1059
Superconductivity—a new classification of the chemical bonding in the solid (C) 1275
Solid-state physics, How chemistry and physics meet in the solid state (R) 846
π-Solvation, Transition state π-solvation by aromatic rings: an electronic contribution to Diels–Alder reaction diastereoselectivity (C) 1184
Solvent effects, Changes of stereoselectivity in Diels–Alder reactions by hydrophobic solvent effects and by β-cyclodextrin (C) 896
The effect of solvent on the stability of mero-substituted alkyl radicals (C) 770
Solvophobicity, Changes of stereoselectivity in Diels–Alder reactions by hydrophobic solvent effects and by β-cyclodextrin (C) 896
Spectroscopy, EXAFS: basic principles and data analysis (B) 801
Nuclear quadrupole interaction and time-resolved perturbed γ-γ-angular correlation spectroscopy: applications in chemistry, materials science, and biophysical chemistry (R) 110
Spin distribution, The spin distribution in ion pairs of 1-aminoanthraquinone radical anion and alkali-metal cations (C) 791
Spirobi(bicyclo[6.3.0]undeca-2,4,6,8-tetraene), The dependence of intramolecular electron transfer on structure in a spiro compound containing two cyclooctatetraene moieties (C) 1290
Spiro compounds, Heptacyclo[19.3.0.0^{1,5}.0^{5,9}.0^{9,13}.0^{13,17}.0^{17,21}]tetracosane ([6.5]coronane) (C) 130
Stabilization, A test for synergetic captodative radical stabilization (C) 573
The effect of solvent on the stability of mero-substituted alkyl radicals (C) 770
Stacking interactions, Molecular recognition: stacking interactions influence Watson-Crick vs. Hoogsteen base-pairing in a model for adenine receptors (C) 1244
Stannaethenes, A stable stannaethene (C) 546
Stereoelectronic effects and chiral recognition: a natural system of relationships between chiral compounds based on selectivities in the formation of acetals (C) 442
Stereoselective aldol reaction, Stereoselective aldol reactions with α-unsubstituted chiral enolates (R) 24
Stereoselective alkylation of aromatic compounds with threonine trifluoromethanesulfonates (C) 142
Stereoselective synthesis, Estimation of the configurational stability of chiral organometallic reagents (C) 1145
of building blocks with three consecutive stereogenic centers: important precursors of polyketide natural products (R) 489
Stereoselective synthesis (B) 1053
Stereoselectivity, Changes of stereoselectivity in Diels–Alder reactions by hydrophobic solvent effects and by β-cyclodextrin (C) 896
Directed homogeneous hydrogenation (R) 190
Influence of H-donor and temperature on the stereoselectivity of radical reactions (C) 479
Stereospecificity, A non-stereospecific Diels–Alder reaction (C) 1046
Steroids, Interaction of steroid hormone receptors with DNA (B) 591
Stiboxanes, Nonaphenyltristiboxane-1,5-diyl disulfonates (C) 906
Stilbazolium chromophores, Photoisomerization of stilbazolium chromophores with potential nonlinear optical applications (C) 341
Strain, Dicyclopropa[*a*,*c*]naphthalene: a compound capable of existence? (C) 577
Strain energy, Pentasila[1.1.1]propellane. Predictions concerning structure, bonding, and strain energy (C) 1267
Strecker synthesis, Diastereoselective Strecker synthesis of α-aminonitriles on carbohydrate templates (C) 557
Streptazolin, New lead structures by Diels–Alder reactions of streptazolin with naphthoquinones (C) 664
Structural chemistry, How nature adapts chemical structures to curved surfaces (R) 1059
Structural methods in inorganic chemistry (B) 1197
Structure, Back to the structure of benzene (L) 1298
Concerning the structure of benzene (C) 782
Structure determination, Direct identification of the carbon skeleton of organic compounds using double quantum coherence ^{13}C-NMR spectroscopy. The INADEQUATE pulse sequence (R) 625
Structural dynamics of collagen fibers cross-linked with isocyanates; application of synchrotron radiation in macromolecular chemistry (C) 551
Substituent effects, A test for synergetic captodative radical stabilization (C) 573
Substitution, The mechanism of substitution reactions at [LRe(NO)(CO)(CH$_3$)]$^{\oplus}$ in acid solution and the structure of [{LRe(NO)(CO)}$_2$(μ-CH$_2$OCH$_2$)]I$_2$ (L = 1,4,7-triazacyclononane) (C) 924
Sugar chemistry, Glycosyl isocyanide dichlorides—novel synthetic building blocks in sugar chemistry (C) 359
Sulfenes, A sulfene umpolung (C) 1133
Sulfonamides, Unusual photoisomerization of a cyclic sulfonamide (C) 146
Sulfones, X-ray structure analysis of the Li$_2$-compound of bis(trimethylsilyl)methyl phenyl sulfone; structural units of an α-sulfonyl- and a complex-stabilized *ortho*-sulfonyl carbanion (C) 1287
Sulfonyl carbanions, X-ray structure analysis of the Li$_2$-compound of bis(trimethylsilyl)methyl phenyl sulfone; structural units of an α-sulfonyl- and a complex-stabilized *ortho*-sulfonyl carbanion (C) 1287
Sulfuranylidenephosphanes, Imino-, phosphoranylidene-, and sulfuranylidenephosphanes by 1,3-silyl migration (C) 83
Sulfur bacteria, Chromatographic separation of higher polythionates S$_n$O$_6^{2\ominus}$ (n=3...22) and their detection in cultures of *Thiobacillus ferrooxidans*; molecular composition of bacterial sulfur secretions (C) 151
Sulfur compounds, Chromatographic separation of higher polythionates S$_n$O$_6^{2\ominus}$ (n=3...22) and their detection in cultures of *Thiobacillus ferrooxidans*; molecular composition of bacterial sulfur secretions (C) 151
Dimerization of 1,6-dithiacyclodeca-3,8-diyne in the presence of cobalt complexes. A simple synthesis of a [2.2](2,5)thiophenophane derivative (C) 763
5,5-Dimethyl-1,2-dithia-3,7-diselenacycloheptane—a storable source of disulfur, S$_2$ (C) 887
The copolymer of 2,6-pyridinedimethanethiol and 1,4-benzenedimethanethiol (C) 137
Sulfur ligands, [Ag$_4$(SCH$_2$C$_6$H$_4$CH$_2$S)$_3$]$^{2-}$, a novel polynuclear silver thiolate with trig-

onal-planar coordination of all silver atoms and a central $[Ag_4S_6]$-cage (C) 145
Metathesis of CS_2-like heteroallenes on 1,1-dithio complexes of rhodium(III) (C) 767
Synthesis and structure of $[(C_5Me_5)_2Mo_2S_4 \cdot SO_3]$: concerning the oxidation of sulfur ligands in transition-metal complexes (C) 230
Sulfur oxides as ligands in coordination compounds (R) 98
Sulfur pentafluoride cyanate, $F_5S-O-C\equiv N$ (C) 134
Sulphur fluor compounds, Preparation of $F_4S=CH-COF$ by isomerization of $F_5S-CH=C=O$ (C) 799
Superconduction, Control of the superconducting properties of $YBa_2Cu_3O_7$ by topotactic redox reactions (C) 1188
Imaging oxygen vacancies in superconducting $YBa_2Cu_3O_{7-\delta}$ by high resolution electron microscopy (C) 1048
Superconductivity—a chemical phenomenon? (C) 579
—a new classification of the chemical bonding in the solid (C) 1275
A new mechanism for superconductivity (C) 1273
Supersandwich complex, Structure of a crystalline alkali-metal cyclopentadienide (C) 583
Supraclusters, Cluster of clusters: structure of the 37-atom cluster $[(p\text{-}Tol_3P)_{12}Au_{18}Ag_{19}Br_{11}]^{2\oplus}$ and a novel series of supraclusters based on vertex-sharing icosahedra (C) 897
Surface chemistry, Low energy electrons and surface chemistry (B) 1054
Surface reactions, Decarbonylation on carbon-supported nickel catalysts (C) 461
Reaction of Sn_9^{4-} with single crystal Au: textured fiber epitaxial growth of AuSn at room temperature (C) 1155
Synthetic methods, Directed homogeneous hydrogenation (R) 190
Modern synthetic methods 1986. Vol. 4 (B) 1300
New reductive transformations of unsaturated cyclic hydrocarbons (R) 204
Stereoselective aldol reactions with α-unsubstituted chiral enolates (R) 24
Stereoselective syntheses of building blocks with three consecutive stereogenic centers: important precursors of polyketide natural products (R) 489
Synthesis of glycopeptides, partial structures of biological recognition components (R) 294
Totally synthetic routes to the higher monosaccharides (R) 15

TANTALUM COMPOUNDS, $Ag[MF_6]_2$ (M = Nb, Ta), ternary fluorides of divalent silver (C) 689
Tautomerism, ^{15}N-CPMAS-NMR study of the problem of NH tautomerism in crystalline porphine and porphycene (C) 934
Telluride-tellurolate complex, $[Fe_4Te_4(TePh)_4]^{3\ominus}$, the first telluride-tellurolate complex (C) 1009
Tellurium ligands, Synthesis and structure of compounds containing ditellurium *side-on* bonded to nickel complex fragments (C) 916
Temperature profiles, IR Emission analysis of temperature profiles in Pt/SiO_2 catalysts during exothermic reactions (C) 1042
Tetra-*tert*-butyltetrahedrane, Gas-inclusion crystals of tetra-*tert*-butyltetrahedrane and its deformation density (C) 356
Tetrahedrane, Gas-inclusion crystals of tetra-*tert*-butyltetrahedrane and its deformation density (C) 356
2,3,9,10-Tetrakis(trimethylsilyl)[5]phenylene. Synthesis via regiospecific cobalt-catalyzed cocyclization of 1,6-bis(triisopropylsilyl)-1,3,5-hexatriyne (C) 1246
Tetramethylene cyclohexanediyl, The diradical 2,3,5,6-tetramethylene-1,4-cyclohexanediyl ("1,2,4,5-tetramethylenebenzene") (C) 256
2,2,4,4-Tetramethyl-3-methylenecyclobutylidene, Reactions of 2,2,4,4-tetramethyl-3-methylenecyclobutylidene; thermal rearrangements of a 2-methylenebicyclo-[2.1.0]pentane (C) 1260
2,2,5,5-Tetramethyltetrahydrofuran, Photo-CIDNP in the vacuum-UV: di-*tert*-butyl ether and 2,2,5,5-tetramethyltetrahydrofuran in aqueous solution (C) 446
Tetrasilatetrahedrane anion, Raman spectrum of the tetrasilatetrahedrane anion Si_4^{4-} (C) 349
s-Tetrazine as ligand for monomeric and bridged macrocyclic metal complexes (C) 344
Tetrazocines, Propellanes of the glycoluril series and bridged tetrazocines (C) 1039
Tetrazole derivatives, Methyl (*E*)-2-(1-aryl-4,5-dihydro-1*H*-tetrazol-5-ylidene)-2-cyanoacetate from methyl 3,3-diazido-2-cyanoacrylate and primary aromatic amines (C) 1160
Thallium compounds, Pentabenzylcyclopentadienylthallium(I): synthesis and structure of a "dimeric" organothallium compound with Tl-Tl interaction (C) 789
Theoretical chemistry, Concerning the structure of benzene (C) 782
How chemistry and physics meet in the solid state (R) 846
Thermochromic behavior, Photo- and thermochromic liquid crystal polysiloxanes (C) 1178
Thermodynamics, Computer-aided chemical thermodynamics of gases and liquids—theory, models, programs (B) 1057
Thermolysis of NH_4HCO_3—a simple route to the formation of free carbonic acid (H_2CO_3) in the gas phase (C) 354
1,2-Thiaselenete, 1,2-Diselenete and 1,2-thiaselenete (C) 343
Thioether complexes, Synthesis and crystal structure of the homoleptic thioether ruthenium complex $[Ru(1,4,7\text{-trithiacyclononane})_2](BPh_4)_2 \cdot 2\,Me_2SO$ (C) 250
Thiophene complexes, C-S Bond cleavage in a π-thiophene ruthenium complex (C) 909
Thioxocarbon dianion, Trithiodeltate: a new, aromatic thioxocarbon dianion (C) 1163
Threonine trifluoromethanesulfonates, Stereoselective alkylation of aromatic compounds with threonine trifluoromethanesulfonates (C) 142
Thymine glycol, The fluorometric determination of thymine glycol as criterion of the treatment of foodstuffs (biological material) with ionizing radiation (C) 340
Tin compounds, Concerning the role of organotin compounds in olefin metathesis: synthesis, structure, and Lewis acidity of $[(\eta^5\text{-}C_5Me_5)CH_3ReCl_3]$ (C) 466
Polystannanes $Ph_3Sn-(tBu_2Sn)_n-SnPh_3$ (n = 1–4): a route to molecular metals? (C) 1255
Titanium hydride formation through hydrogen transfer from 2-methylpyridine to a titanium fulvene compound; the first structurally characterized terminal titanium hydride (C) 330
Topotactic redox reactions, Control of the superconducting properties of $YBa_2Cu_3O_7$ by topotactic redox reactions (C) 1188
Total synthesis of the enantiomerically pure lichen macrolide (+)-aspicilin (C) 362
Toxicology, Analytical methods in human toxicology (B) 1051
Trace analysis. Spectroscopic methods for molecules (B) 1052
Transcription in eukaryotes—the role of transcription complexes and their components (R) 218
Transition metal complexes, Diene, alkyne, alkene, and alkyl complexes of early transition metals: structures and synthetic applications in organic and polymer chemistry (R) 723
s-Tetrazine as ligand for monomeric and bridged macrocyclic metal complexes (C) 344
The development of a carbene-like chemistry with terminal phosphinidene complexes (R) 275
Transition states, Electrocyclic opening of 2,3-benzo and 2,3;7,8-dibenzobicyclo-[4.2.0]octa-2,4,7-triene; benzoannelated transition states (C) 1268
Transmission electron microscopy, Reaction of Sn_9^{4-} with single crystal Au: textured fiber epitaxial growth of AuSn at room temperature (C) 1155
α-Trialkylsilylaldehydes, Enantioselective synthesis of α-trialkylsilyl ketones and aldehydes (C) 351
α-Trialkylsilyl ketones, Enantioselective synthesis of α-trialkylsilyl ketones and aldehydes (C) 351
Triaziridines, Unusually stable *cis,cis*-trialkyltriaziridines by azo/nitrene addition (C) 566
Tricycloheptane-1-diazonium ions, Diazo coupling of nortricyclene(tricyclo-$[2.2.1.0^{2,6}]$heptane)-1-diazonium ions (C) 570
Tricyclononatriene, Synthesis of tricyclo-$[5.2.0.0^{1,3}]$nona-4,6,8-triene, a norcaradiene structure constrained by the antiaromaticity of cyclobutadiene (C) 559
Tricyclooctane, Diasterane (tricyclo-$[3.1.1.1^{2,4}]$octane) (C) 554
Tricyclooctaphosphane, P_8iPr_4—the first tricyclo$[3.2.1.0^{2,4}]$octaphosphane (C) 347
Trifluoroacetic acid, Trifluoromethyl isocyanide as a synthetic building block—reaction with trifluoroacetic acid and with hexafluoroacetone (C) 921
Trifluoromethyl isocyanide as a synthetic building block—reaction with trifluoroacetic acid and with hexafluoroacetone (C) 921
Trimethylenemethane complexes of Cr, Mo, and W by novel methylenation of allenes with carbene complexes; cyclopentanes by [3+2] cycloaddition of trimethylenemethane complexes to allenes (C) 357
Triphenylarsane diiodide, Structure of triphenylarsane diiodide, $[Ph_3As \cdot I_2]$, a compound formed in the thermal decomposition of $[Mn(OAsPh_3)_3I_2(SO_2)_2]$ (C) 264
Triphenylmethylium, Deep-colored, through-conjugated multitriphenylmethylium ions (C) 794
Triphosgene, a crystalline phosgene substitute (C) 894
1,3,5-Triphosphabenzene, Metal-promoted cyclotrimerization of a λ^3-phosphaalkyne: formation of a molybdenum-coordinated 1,3,5-triphosphabenzene (C) 907
Metal-promoted cyclotrimerization of a λ^3-phosphaalkyne: formation of vanadium-complexed valence isomers of a 1,3,5-triphosphabenzene (C) 908
Triphosphatriborinane, Synthesis and X-ray structure of $(2,4,6\text{-}Me_3C_6H_2BPC_6H_{11})_3$: a boron-phosphorus analogue of borazine (C) 1270
Triple bond, Olefinic C=C double bond coordination to a M≡M triple bond: bis(η^2-ethylene)hexakis(neopentyloxy)ditungsten (C) 903
Triple-decker phanes, Synthesis and chirality of sixfold-bridged triple-decker phanes (C) 777
Triple decker sandwich structure, A triple decker sandwich structure by reaction of cyclopentadienylbis(ethylene)cobalt with carbodiimides: an unusual cyclopentadienylcobalt oligomer (C) 68
Trisdioxetane, Photooxidation of 2,5-dimethyl-2,3,4-hexatriene—matrix isolation of a trisdioxetane (C) 475

Trithiacyclononane, Crown thioether complexes of Ag^I and Cu^I: the crystal structures of $[\{Ag_3L_3\}\{AgL_2\}](ClO_4)_4$ and $[LCuI]$ (L = 1,4,7-Trithiacyclononane) (C) 575
Trithiodeltate: a new, aromatic thioxocarbon dianion (C) 1163
Tungsten compounds, Olefinic C=C double bond coordination to a M≡M triple bond: bis(η^2-ethylene)hexakis(neopentyloxy)ditungsten (C) 903
The first 2*H*-phosphirene (C) 1257
Two-electron reduction, "Two-electron reduction" of phosphane-substituted tricobalt clusters—evidence for a 17-electron intermediate in the dissociative ETC ligand substitution (C) 352

UMPOLUNG, A sulfene umpolung (C) 1133
Unsaturation, Molecular belts and collars in the making: a hexaepoxyoctacosahydro-[12]cyclacene derivative (C) 892
New reductive transformations of unsaturated cyclic hydrocarbons (R) 204
Unsaturated molecules containing main group metals (R) 1
Unstable compounds, Generation and interception of 1-oxa-3,4-cyclohexadiene (C) 690
The generation and characterization of molecules by neutralization-reionization mass spectrometry (NRMS) (R) 805

VALENCE ISOMERISM, Metal-promoted cyclotrimerization of a λ^3-phosphaalkyne formation of vanadium-complexed valence isomers of a 1,3,5-triphosphabenzene (C) 908
Valence isomerization between 1-phosphanorcaradienes and 1-phospha-2*H*-tropylidenes (2*H*-phosphepines) (C) 1134
Valienamine, Synthesis of valienamine (C) 482
Vanadium compounds, Amavadin, an example for selective binding of vanadium in nature: studies of its complexation chemistry and a new structural proposal (C) 545
Spherical mixed-valence $[V_{15}O_{36}]^{5\ominus}$, an example from an unusual cluster family (C) 1045
Vanadium carbene complexes by reaction of (diene)metallocenes with $[CpV(CO)_4]$ (C) 666
Vinamidines, Novel, very strongly basic, pentacyclic "proton sponges" with vinamidine structure (C) 1165
Tricyclic 2,4-diaminovinamidines—readily accessible, very strong CHN bases (C) 1164
Vinyl diazides, [4+2] Cycloadditions of 2,3-diazido-1,3-butadienes: a novel entry to vicinal vinyl diazides and 1,4-dicyano compounds (C) 879
Vinylene carbonate, CO_2 elimination from vinylene carbonate radical anions and charge reversal in $C_2H_2O^{\odot\ominus}$: reactions involving the radical anion and cation of oxirene? (C) 140
Vinylidene ligands, Isoelectronic relationships in cluster chemistry: nucleophilic addition to a vinylidene ligand (C) 572
Viologens, Reduction of 2-enoates and alkanoates with carbon monoxide or formate, viologens, and *clostridium thermoaceticum* to saturated acids and unsaturated and saturated alcohols (C) 785

WATER SPLITTING, Biological exploitation of solar energy by photosynthetic water splitting (R) 643

X-RAY PHOTOELECTRON SPECTROSCOPY, Emission of microparticles from automotive sources—X-ray photoelectron spectroscopy in environmental analysis (R) 309

YLIDE COMPLEXES, Isovalent and mixed-valent ylide complexes of gold: the synthesis of trinuclear compounds having double paddlewheel structure (C) 1146
The recoil-free fraction of the γ resonance in ^{197}Au Mössbauer spectroscopy; findings from measurements of polynuclear, mixed-valent ylide complexes (C) 1148
Ylides, 1,5-Electrocyclization in homofuran, homopyrrole, and homothiophene (C) 1294
Synthesis of nitriles via the ylide anion of sodium cyanotriphenylphosphoranylidenemethanide (C) 79
Ynamines, First synthesis of *N*-methyleneynamines (2-azabut-1-en-3-ynes) (C) 923

ZEOLITE CATALYSTS, Preparation of β-halothiophenes by isomerization of α-halothiophenes on zeolite catalysts (C) 468
Zeolites, Adsorption and curvature in highly dealuminated zeolites (C) 1017
Zinc compounds, High-resolution CP-MAS ^{13}C-NMR spectra of allylzinc compounds—structural similarities and differences in the solid state and in solution (C) 1279
Zinc ketones, Generation of β-, γ-, δ-, ε-, and ζ-zinc ketones and their transition-metal-catalyzed reactions with carbon electrophiles (C) 1157
Zirconium compounds, A new class of organozirconium(IV) compounds: alkyl derivatives of tetramethyltetraazadibenzo-[14]annulenatozirconium(IV) (C) 70
Bis(η^5-cyclopentadienyl)-1,3-diphosphabicyclo[1.1.0]butane-2,4-diylzirconium: a simple synthesis of an unusual molecule (C) 764
Dinuclear fulvalene complexes of tri- and tetravalent zirconium (C) 697
Hexacarbonylzirconate(2−), $[Zr(CO)_6]^{2-}$: the first binary carbonyl complex of zirconium (C) 1190
Zwitterions, Neutral and charged biradicals, zwitterions, funnels in S_1, and proton translocation: their role in photochemistry, photophysics, and vision (R) 170